

VERHANDLUNGEN

der Deutschen Physikalischen Gesellschaft

3/2023

DPG-Frühjahrstagung der DPG DPG Spring Meeting

of the Condensed Matter Section (SKM)
with its Divisions

- Biological Physics
- Chemical and Polymer Physics
- Crystalline Solids and their Microstructure
- Dynamics and Statistical Physics
- Low Temperature Physics
- Magnetism
- Metal and Material Physics
- Physics of Socio-economics Systems
- Semiconductor Physics
- Surface Science
- Thin Films
- Vacuum Science and Technology

as well as the Working Groups

- Equal Opportunities
- Industry and Business
- Young DPG
- Young Leaders in Physics

Symposia

Tutorials

Exhibition of Scientific Instruments and Literature

Dresden

26 - 31 March 2023

DPG-Frühjahrstagung
(DPG Spring Meeting)
of the Condensed Matter Section (SKM)

together with the Working Groups

Equal Opportunities; Industry and Business, Young DPG, Young Leaders in Physics

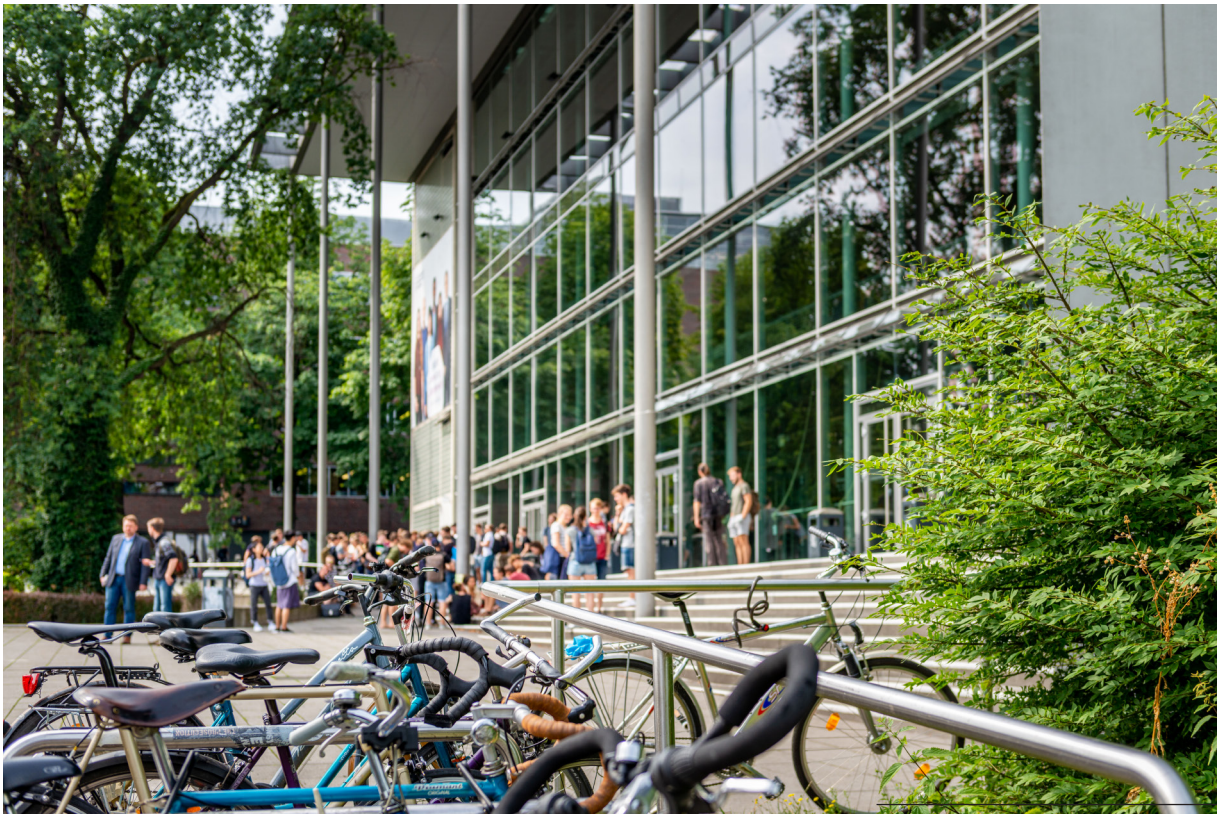


Foto: Crispin-Iven Mokry

26 – 31 March 2023
Technische Universität Dresden

Verhandlungen der Deutschen Physikalischen Gesellschaft (ISSN 2751-0522 [Online])
Reihe VI, Band 58 (2023)
Zitertitel: Verhandl. DPG (VI) 58, 3/2023
Erscheinungsweise: Jährlich 3 - 6 Online-Hefte, je nach Bedarf

Verantwortlich für den Inhalt:
Dr. Bernhard Nunner, DPG e. V., Hauptstraße 5, 53604 Bad Honnef
Telefon: +49 (0)2224 9232-0, Telefax: +49 (0)2224 9232-50
© Deutsche Physikalische Gesellschaft e. V., 53604 Bad Honnef

Content

Greeting	5
Organisation	
Organiser	6
Local Organiser	6
Scientific Organisation	
Chair of the Condensed Matter Section	6
Chairs of the Participating Divisions of the DPG	6
Chairs of the Participating Working Groups of the DPG	6
Symposia	6
Conference Information	
Conference Venue	9
Conference Office / Information Desk	9
Lecture Rooms	9
DPG-App	9
Presentation	10
Oral Presentation	10
Poster Presentation	10
Notice Board	10
General Information	
Internet	10
Message Board	11
Public Working Area	11
Cloakroom	11
Lost and Found Property	11
Catering	
Coffee Breaks	11
Snacks	11
Lunch	11
Events	
Public Evening Lecture.....	12
Welcome Evening	12
Opening of the Conference	12
EinsteinSlam	12
Ceremonial Session with Award Ceremony	12
Job Market	13
Exhibition of Scientific Instruments and Literature	13
Scientific Bar Hopping	13
jDPG Pub Crawl	13
Video Competition: Physics in the Future	13
Wilhelm and Else Heraeus Communication Programme	14
Members' Assemblies of the Divisions	14
CO ₂ Compensation for the DPG Conferences	14
Acknowledgement	14
SAY CHEESE!	14
Disclaimer of Liability	14
Sponsors	15
Synopsis of the Daily Programme	17
Plenary Talks	50
Prize Talks	52

Plenary Special Talks	53
Tutorials	55
Symposia	
Dynamics of Opinion Formation – From Quorum Sensing to Polarization (SYOF)	58
SKM Dissertation Prize 2023 (SYSD)	60
Green Magnets for Efficient Energy Conversion (SYGM)	62
Physics of Fluctuating Paths (SYFP)	64
Ultrafast Excitation Pathways of Quantum Materials (SYUE)	66
Topology in Quantum and Classical Physics – From Topological Insulators to Active Matter (SYQC)	68
Real-Time Measurements of Quantum Dynamics (SYQD).....	70
Topological Superconductor-Magnet Heterostructures (SYTS)	72
Physics of van der Waals 2D Heterostructures (SYHS)	74
Programme of the Divisions of SKM	
BP Biological Physics	76
CPP Chemical and Polymer Physics	135
DS Thin Films	194
DY Dynamic and Statistical Physics	217
HL Semiconductor Physics	277
KFM Crystalline Solids and their Microstructure	357
MA Magnetism	381
MM Metal and Material Physics	461
O Surface Science	512
SOE Physics of Socio-economic Systems	637
TT Low Temperature Physics	652
VA Vacuum Science and Technology	764
Working Groups	
AIW Industry and Business	767
AKC Equal Opportunities	769
Index of Authors	771
Index of Exhibitors	809
Exhibition Maps	818
Timetable of the Conference	820
Campus Map	821



Leading for Tomorrow

Physikerinnen und Physiker in
Führungspositionen?

Trotz oder *wegen* Physikstudiums?

Wirtschaft oder
Wissenschaftsmanagement?

Ist das überhaupt was
für *mich?*

Mehrtägige Intensivworkshops und Learning Expedition

Bewerbung möglich vom 1. bis 31. März 2023

Mehr Informationen und
die Möglichkeit zur Bewerbung:
leading-for-tomorrow.dpg-physik.de



Greeting

Dear Participants,

Welcome to the DPG-Frühjahrstagung (DPG Spring Meeting) of the Condensed Matter Section (SKM) with the participating divisions and working groups involved on the campus of the Technische Universität Dresden (TUD).

I am very pleased that with our DPG-Frühjahrstagungen (DPG Spring Meetings), even more so in presence, we can once again set a widely visible and public sign for the outstanding importance of basic research for scientific and societal progress. Basic research is indispensable for tackling the major societal challenges. Above all a sustainable energy supply with regard to climate change with its dramatic consequences for all life on our planet. On the other hand, the spring conferences are probably the most important instrument of the DPG to enable as many scientists as possible, especially young scientists, to participate in a cross-border, international and peaceful scientific exchange.

The last year has shown us with full force how important and by no means self-evident such a necessary and international exchange is, how vulnerable our world order is and how quickly a change can take place that even threatens the existence of countries. Therefore, it is the special responsibility of the DPG – guided by the values in our DPG Statutes, our compass – to stand up for freedom, tolerance, truthfulness and dignity in science and to act in awareness that we are particularly responsible for shaping the whole of human life: Especially and particularly in troubled times!

The DPG conference at the TUD plays an outstanding role for peaceful international scientific exchange and discourse as well as for the perception and appreciation of the work of the DPG. I would therefore like to thank all those involved for their great commitment to the success of this conference.

My special thanks go to the Technische Universität Dresden (TUD) for its hospitality and support. I would like to sincerely thank the Wilhelm and Else Heraeus Foundation for once again generously supporting all DPG Spring Meetings. My great appreciation goes to the participating divisions and working groups for a great programme.

I would especially like to thank the Local Organising Committee, Prof. Jochen Geck, Technische Universität Dresden (TUD), Institute of solid state and material physics (IFMP), and his entire team.

For the support of all DPG-Frühjahrstagungen (DPG Spring Meetings), my special thanks go to the DPG Head Office.

A handwritten signature in black ink, appearing to read 'Joachim Ullrich', written in a cursive style.

Prof. Dr. Joachim Ullrich
President
Deutsche Physikalische Gesellschaft e.V.

Organisation

Organiser

Deutsche Physikalische Gesellschaft e.V.
Hauptstraße 5, 53604 Bad Honnef
Phone +49 (0)2224 9232-0
Fax +49 (0)2224 9232-50
Email dpg@dpg-physik.de
Homepage www.dpg-physik.de

Local Organiser

Prof. Dr. Jochen Geck
Technische Universität Dresden
Institut für Festkörper- und Materialphysik
Haeckelstraße 3, 01062 Dresden
Phone +49 (0) 351 463 37589
Email jochen.geck@tu-dresden.de

Scientific Organisation

Chair of the Condensed Matter Section (SKM)

Prof. Dr. Martin Wolf
Fritz-Haber-Institut der MPG
Abt. Physikalische Chemie
Faradayweg 4-6, 14195 Berlin
Phone +49 (0) 30 84135 111
Email wolf@fhi-berlin.mpg.de

Chairs of the Participating Divisions of the DPG:

(BP)	Biological Physics	–	Prof. Dr. Joachim Rädler (raedler@lmu.de)
(CPP)	Chemical and Polymer Physics	–	Prof. Dr. Hans-Jürgen Butt (butt@mpip-mainz.mpg.de)
(DS)	Thin Films	–	Prof. Dr. Stefan Krischok (stefan.krischok@tu-ilmenau.de)
(DY)	Dynamics and Statistical Physics	–	Prof. Dr. Markus Bär (markus.baer@ptb.de)
(HL)	Semiconductor Physics	–	Prof. Dr. Axel Lorke (axel.lorke@uni-due.de)
(KFM)	Crystalline Solids and their Microstructure	–	J. Prof. Dr. Anna Grünebohm (anna.gruenebohm@rub.de)
(MA)	Magnetism	–	Prof. Dr. Heiko Wende (heiko.wende@uni-due.de)
(MM)	Metal and Material Physics	–	Prof. Dr. Christian Elsässer (christian.elsaesser@iwf.fraunhofer.de)
(O)	Surface Science	–	Prof. Dr. Ulrich Höfer (ulrich.hoefel@physik.uni-marburg.de)
(SOE)	Physics of Socio-economic Systems	–	Dr. Philipp Hövel (phoewel@physik.tu-berlin.de)
(TT)	Low Temperature Physics	–	Prof. Dr. Elke Scheer (elke.scheer@uni-konstanz.de)
(VA)	Vacuum Science and Technology	–	Dr.-Ing. Stylianos Varoutis (stylianos.varoutis@kit.edu)

Chairs of the Participating Working Groups

(AGYouLeap)	Young Leaders in Physics	–	Dr. Tobias Heindel (tobias.heindel@tu-berlin.de) Dr. Doris Reiter (doris.reiter@tu-dortmund.de)
(AKC)	Equal Opportunities	–	OSTr Agnes Sandner (akc@dpg-physik.de)
(AIW)	Industry and Business	–	Dr. Udo Weigelt (weigelt@grunecker.de)
(AKJDPG)	Young DPG	–	Vivienne Leidel (leidel@jdpdg.de)

Symposia

SYFP	–	Physics of Fluctuating Paths
SYGM	–	Green Magnets for Efficient Energy Conversion
SYHS	–	Physics of van der Waals 2D Heterostructures
SYOF	–	Dynamics of Opinion Formation – From Quorum Sensing to Polarization
SYQC	–	Topology in Quantum and Classical Physics – From Topological Insulators to Active Matter

- SYQD – Real-Time Measurements of Quantum Dynamics
- SYSD – SKM Dissertation Prize 2023
- SYTS – Topological Superconductor-Magnet Heterostructures
- SYUE – Ultrafast Excitation Pathways of Quantum Materials

Organisation of the Exhibition of Scientific Instruments and Literature

DPG-Ausstellungs-, Kongreß- und Verwaltungsgesellschaft mbH

Hauptstraße 5, 53604 Bad Honnef

Phone +49 (0)2224 9232-0

Fax +49 (0)2224 9232-50

Email dpg@dpg-physik.de

Website www.dpg-gmbh.de

Programme

The scientific programme consists of **4.134** contributions:

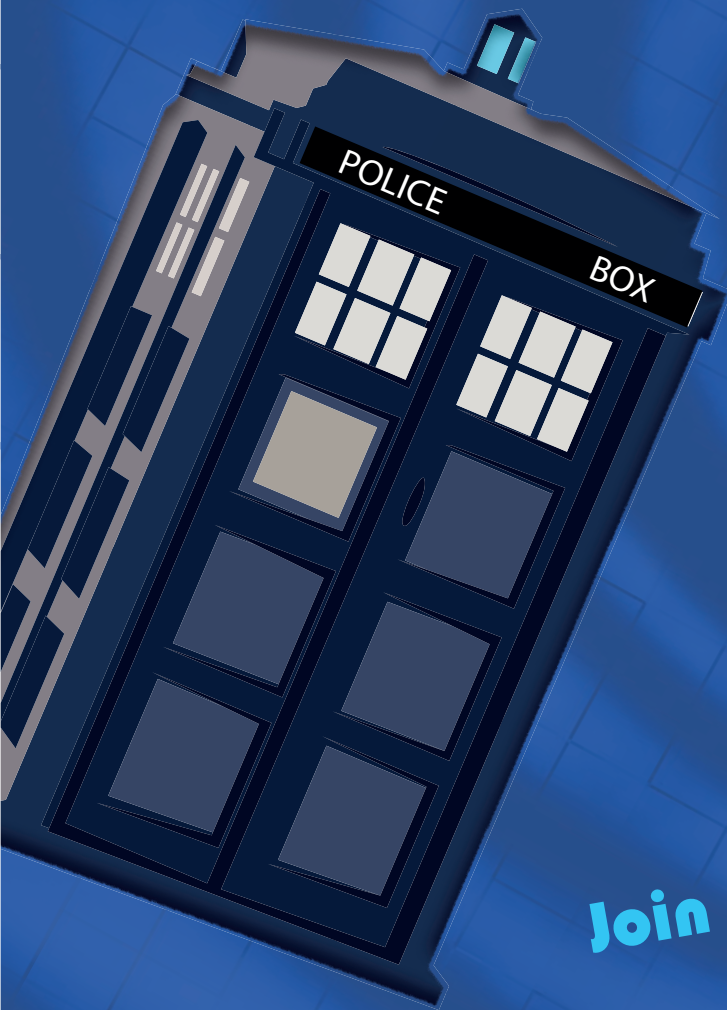
11	Plenary Talks
1	Evening Talk
5	Prize Talks
1	Ceremonial Talk
5	Lunch Talks
211	Invited Talks
54	Topical Talks
2667	Contributions
7	Tutorials
1169	Posters
3	Discussions

The programme stated in this document corresponds to the status from February 10, 2023 and will not be updated!

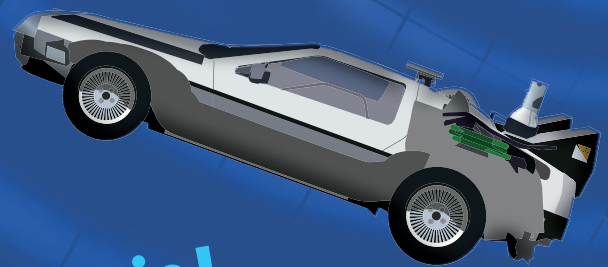
Video Contest:

Physics in the Future

March 27-31, 2023



What are the major challenges for physics in the future?
Which research areas will come into focus?
Or will time travel even be possible?



Join in and win!

What will the physics of the future look like and what will it be used for?

Share your vision with us!

The aim of this video competition is to bring together all kinds of different ideas for the future of physics. Even without a Police Box or a converted DeLorean, the competition promises numerous exciting answers. Tell us your vision – only time will tell if it comes true.

More information:

www.skm23.dpg-tagungen.de/veranstaltungen/wettbewerb

Information for Participants

The conference will be held March 26 – 31, 2023.

1. Conference Information

1.1 Conference Venue

Technische Universität Dresden
Campus Südvorstadt
Bergstraße 64
01069 Dresden

The central activities like registration etc. will take place in the Lecture Hall Center (HSZ) of the TU Dresden (Bergstraße 64). For a detailed map of the campus and the buildings please see end of this document. The position of the lecture rooms on the campus can be found at the campus navigator of TU Dresden <https://navigator.tu-dresden.de/> or the DPG-App (see 1.3.1).

1.2 Conference Office / Information Desk

The conference office and the information desk are located in the Lecture Hall Center, HSZ E01.

		Registration	Information Desk
Sunday	March 26	15:00 – 19:00	15:00 – 20:00
Monday	March 27	08:00 – 18:00	08:00 – 20:00
Tuesday	March 28	08:00 – 16:00	08:00 – 18:00
Wednesday	March 29	08:00 – 16:00	08:00 – 18:00
Thursday	March 30	08:00 – 16:00	08:00 – 18:00
Friday	March 31	08:00 – 12:00	08:00 – 15:00

You will receive your name tag, a receipt for your conference fee, the Login-Password for using WLAN (WiFi) as well as food and drink vouchers for the Welcome Evening (Sunday 18:30-21:30). The name tag must be worn visibly during the entire conference.

Please note: This year, no conference ticket for public transportation is included in the conference pass. We kindly ask you to buy a ticket yourself if you need it (the DVB one-week ticket price level A1 Dresden tariff zone at the normal price for 22,90 EUR is transferable, i.e. it is not personal).

The organisers, staff of the conference desk and student assistants will be identifiable by colored name tags and T-shirts. Please contact them if you have any questions. Do not hesitate to come to the information desk and inquire about all necessary information concerning the conference, orientation in Dresden, accommodation, restaurants, going out and cultural events.

1.3 Lecture Rooms

The lecture rooms will be signposted by abbreviations for the respective buildings and the room number. The campus map and location of the buildings are printed at the end of this document.

Abbr. Building (see also: <https://navigator.tu-dresden.de/>)

BAR	Barkhausen-Bau	REC	Rechnagel-Bau
CHE	Chemiegebäude (Chemistry Building)	SCH	Georg-Schumann-Bau
GER	von-Gerber-Bau	Tents	Tents behind the Lecture Hall Center / Exhibition
GÖR	Görges-Bau	TOE	Toepler-Bau
HSZ	Hörsaalzentrum (Lecture Hall Center)	TRE	Trefftz-Bau
MER	Merkel-Bau	WIL	Willers-Bau
MOL	Mollier-Bau	ZEU	Zeuner-Bau
POT	Gerhard-Potthoff-Bau		

1.3.1 With the DPG-App through the Spring Meetings!

With the app you can find out not only about the conference programme but also about the venue and exhibitors at the industry and book exhibition. With the help of new functions such as “What’s going on now?” or the building plan overview it is now even easier to find your way around on site. Download the free “DPG Spring Meetings” app for Android or iOS now!

1.4 Presentation

Scientific presentations will be held either orally or by poster. Presentations with a German abstract will be given in German.

1.4.1 Oral Presentation

Lecturers are requested to provide their presentations electronically. All lecture rooms are equipped with a projector ("beamer") mainly with HDMI input. Overhead Presenters are not available.

Laptops must be provided by the speakers as well as all associated adapters (e.g. HDMI to VGA, Apple-adapter). Furthermore, the presentation should be recorded onto a USB stick as back-up in PDF or Power Point format.

All laptops must be set up and connected with the data projector before the start of the respective session. All rooms will be opened at latest 30 minutes prior to the lecture. Speakers are requested to be in the lecture room at least 20 minutes prior to the start of the session*, to report to the chairperson as well as the technical staff, to ensure that the laptops handshake with the beamer, and to receive a brief introduction to the equipment in the lecture room.

** In HSZ 01, HSZ 02, HSZ 03 and HSZ 04 it is recommended to transfer the presentation on the day before the lecture or on Monday morning.*

1.4.2 Poster Presentation

Sites for poster sessions are named and located as follows:

P1A	Tent A behind the Lecture Hall Center (Exhibition Tent)
P2/EG	Lecture Hall Center (HSZ): foyer
P2/10G	HSZ: 1st floor (hallway)
P2/20G	HSZ: 2nd floor (hallway)
P2/30G	HSZ: 3rd floor (hallway)
P2/40G	HSZ: 4th floor (hallway)
P3	Chemiegebäude (Chemistry Building (CHE)) in the foyer

Posters must fit within a rectangle 90 cm wide and 120 cm high (DIN A0), portrait format!

The poster boards will be marked with the number according to the scientific programme. Authors are asked to mount their poster when the poster board is prepared with the corresponding poster number. Usually this will be arranged in the morning, or one hour before the session when there are several poster sessions per day. Each poster should display the number according to the scientific programme.

For the mounting of the poster please use the prepared "power strips" at the poster frame or contact the available student staff. Please make sure to use only power strips for mounting the poster (residue-free removing). The presenting authors should be at hand for discussion at their poster during at least half of the poster session and should note this time at the poster.

The posters have to be removed after the poster session. Any posters remaining on display walls after the poster session will be removed and disposed of without requesting your permission. The conference management accepts no liability for the posters.

1.5 Notice Board

All changes to the conference programme (i.e. cancellation of presentations, change of rooms, etc.) will be continuously updated on the notice board of the conference website. All upcoming changes are also taken into account in the regular updates of the electronic version of the conference programme which is available in different formats (sorted by publication date, filterable by conference parts and as an rss-feed). Please use the form <https://skm23.dpg-tagungen.de/programm/notice-board-form> to notify changes or cancellations.

2. General Information

2.1 Internet

EDUROAM

The TU Dresden is member of the eduroam-network. Users from eduroam institutions, who have registered for eduroam, can use WLAN at the TU Dresden without local registration in Dresden. Eduroam in Dresden is possible with WLAN SSID eduroam.

WLAN in the buildings of TU-Campus

For internet access at TU Dresden, please use your individual login-password on your registration document. Please search for and connect to the network named „VPN/WEB“. If this network isn't shown in the list of available networks, the access isn't possible. After you have been connected, please visit any website with your browser to get redirected to the login page of the network. Enter your username and password and click on „Login“. Afterwards you should be able to access the internet. This connection is not encrypted.

2.2 Message Board

Important general information about TU Dresden and the city of Dresden is displayed on a message board in the foyer of the Lecture Hall Center (HSZ). Alterations of the scientific programme however will be announced via the conference website "Notice Board".

2.3 Public Working Area

Public working rooms where you can work on your laptop are located in CHE 184 and GER 007.

2.4 Cloakroom

A guarded cloakroom is located in the basement of the Lecture Hall Centre (HSZ). The opening hours are as follows:

Sunday	March 26	15:00 – 21:30
Monday	March 27	08:00 – 21:30
Tuesday	March 28	08:00 – 20:30
Wednesday	March 29	08:00 – 20:30
Thursday	March 30	08:00 – 22:00
Friday	March 31	08:00 – 14:00

2.5 Lost and Found Property

You can bring found items to the Lecture Hall Center, room E03 (next to the information desk). There you can also get your lost property back.

3. Catering

3.1 Coffee Breaks

Coffee and tea are offered for free during the breaks in nearly all conference locations (see also in the legend of the campus map). You want to actively contribute to protect our climate and environment? Then please bring your own cup or use your paper cup several times. Thank you!

3.2 Snacks

You can get coffee, tea, refreshments and snacks as indicated in the campus map at the:

- Tent B behind the Lecture Hall center Monday to Thursday, 08:00 – 19:00; Friday 08:00 – 14:00
- „Grill-Cube“ next to the exhibition Tent B Monday to Friday, 09:00 – 15:00
- Restaurant of the Leibniz-Institute IFW Dresden Monday to Friday, 08:00 – 15:00
- „insgrüne coffeebar“ in the Georg-Schumann-Bau (SCH) Monday to Friday, 10:00 – 15:00
- Cafeteria & Mensa "Alte Mensa", Mommsenstraße 13 Monday to Thursday, 08:00 – 16:00; Friday 08:00 – 15:00
- Cafeteria & Mensa Zeltschlösschen, Nürnberger Str. 55 Monday to Friday, 08:00 – 15:30
- Cafeteria & Mensa Siedepunkt, Zellescher Weg 17 Monday to Friday, 11:00 – 15:00

as well as at Bergstr. 68 „FIRAT-Kebab-Haus“ and Münchner Str. „DERSIM-Dürüm-Kebab-Haus“ and bakery „Möbius“.

3.3 Lunch

The Mensa Zeltschlösschen, Mensa Siedepunkt and the Mensa Mommsenstraße offer plenty of opportunities for lunch at moderate prices (self-payment). The IFW restaurant offers regular meals for a limited number of conference participants.

Please note: Only cash payment is possible in all mensas (no cards!).

4. Events

4.1 Public Evening Lecture

Sunday, March 26, 18:30 – 20:00, HSZ 01 (Audimax, in German language)

Prof. Dr. Ricarda Winkelmann, Potsdam Institute for Climate Impact Research (PIK) will speak about „Kipp-Punkte im Klimasystem: Vorboten aus dem polaren Eis“. All conference participants and the interested public are welcome.

4.2 Welcome Evening

On Sunday, March 26, 18:30 – 21:30 the Welcome Evening will be held in the Tent A. Small food, beer and soft drinks will be served. Do not miss the opportunity to register (15:00 – 19:00) before the official beginning of the conference and to meet people in an informal atmosphere. When registering for the conference you will receive your badge and food and drink vouchers for the Welcome Evening. Please wear your badge which you have received at the registration.

4.3 Opening of the Conference

A short opening address will be given by the chair of the Condensed Matter Section (SKM) on Monday, March 27 from 8:25 until 8:30 in HSZ 01 (Audimax).

4.4 EinsteinSlam

Monday, March 27, 20:00, HSZ 01 (Audimax)

EinsteinSlam is the competitive art of making complex science accessible to a broad audience. There are just 10 minutes for every attendee to present his/her self-made performance. The event will finish with a public poll in order to evaluate if a particular contribution was either instructive and amusing or rather should have never been performed. All presentations will be given in German. For more information please refer to www.einstein-slam.de.

4.5 Ceremonial Session with Award Ceremony

On Tuesday, March 28, at 15:30 the Ceremonial Session with Award Ceremony will take place in HSZ 01 (Audimax). The programme is as follows:

Music

„Viviendo Trio“

Welcome

Prof. Dr. Jochen Geck, TU Dresden
Local Organiser

Prof. Dr. Ronald Tetzlaff, Prorector for Research at the Technical University of Dresden
Chief Officer Technologietransfer und Internationalisierung

Speech

Dr. Lutz Schröter
Vice-President of the Deutsche Physikalische Gesellschaft

Music

Award Ceremony

Walter-Schottky-Prize 2023

to Dr. Kai-Qiang Lin, Universität Regensburg

Gaede-Prize 2023

to Dr. Benjamin Stadtmüller, TU Kaiserslautern und Johannes Gutenberg-Universität Mainz

Dissertation Prize of the Condensed Matter Section 2023

(The Laureate will be announced after the SKM-Dissertations-Prize Symposium)

Ceremonial Lecture

Prof. Dr. Metin Tolan, Universität Göttingen
„Die Star Trek Physik – Warum die Enterprise nur 158 kg wiegt und andere galaktische Erkenntnisse“

4.6 Job Market

During the conference, various companies and organisations will present their working fields and career opportunities to all interested participants. The presentations will last for about 30 minutes plus discussion and will take place in Room HSZ 405 (Tuesday-Thursday). For additional information and contacts refer to the information board close to the conference office.

Programme:

Tuesday, March 28

- 11:30 – 12:30 **neocx GmbH & Trace Tronic GmbH**
Tracetronic / neocx: Automate Everything – speeding up software testing in the automotive industry
- 12:45 – 13:45 **Ritzenhoefer GmbH**
Transformation Consulting – #impact23
- 14:00 – 15:00 **Wiley VCH-Verlag GmbH**
Physiker:innen im Wissenschaftsverlag

Wednesday, March 29

- 11:30 – 12:30 **Bundesamt für Sicherheit in der Informationstechnik**
Aus der Physik in die IT-Sicherheit – Karriere beim BSI
- 12:45 – 13:45 **Trumpf Lasersystems for Semiconductor Manufacturing GmbH**
TRUMPF Lasersystems for EUV Lithography – Enabler für das digitale Zeitalter gesucht
- 14:00 – 15:00 **Basycon Unternehmensberatung GmbH**
Aus der Wissenschaft in die Beratung
- 15:15 – 16:15 **ZEISS**
Am Herzschlag der Digitalisierung: Forschung & Entwicklung in der Halbleiterfertigungstechnik

Thursday, March 30

- 11:30 – 12:30 **Horn & Company Financial Services GmbH**
Horn & Company – Gewinne Einblicke in unsere Projekte zu Data Analytics, Big Data und Künstlicher Intelligenz und lerne unseren Beratungsansatz kennen!
- 14:00 – 15:00 **d-fine GmbH**
Einblicke in die Beratungspraxis bei d-fine – Projekte im Bankensektor

4.7 Exhibition of Scientific Instruments and Literature

From Tuesday to Thursday there will be an exhibition of Scientific Instruments and Literature. The exhibition will take place in the Lecture Hall Center (Foyer) and the nearby exhibition tent A. More than 130 companies (see list of exhibitors at the end of this document) will present their products. Opening hours are from 09:30 to 18:00 (Thursday until 16:00). All conference participants are welcome to attend the exhibition. The entrance is free.

4.8 Scientific Bar Hopping

On Tuesday, March 28, a scientific Bar Hopping will take place in cooperation with the jDPG, the student council Dresden and the Studiclubs of Dresden.

At a Scientific Bar Hopping scientists have the opportunity to communicate their research to an interested public. General comprehensibility is a must. The intimate atmosphere of the venues helps the public to overcome fears of contact with the researchers. After all, follow-up questions are explicitly encouraged. Spread over several Studiclubs in Dresden, several talks happen in parallel. Further details will be announced on the event website <https://scientific-barhopping.stura.tu-dresden.de/>.

4.9 jDPG Pub Crawl

On Wednesday evening, the young DPG invites to a pub crawl through Dresden. Next to the opportunity to be on a move outside and network with others, the members of the local regional group will tell about the Dresden physics, the life in the city and other facts worth knowing. Further details will be announced on the website of the conference.

4.10 Video competition: Physics in the Future

The public and also the physics community have various imaginations of how physics will look like in the future and what physics will be needed for in the future. The aim of this video competition is to bring together these different views

and ideas for the “future of physics”. Even without a modified DeLorean and flux capacitor, the competition will bring to light many exciting answers. Time will show which ones will come true.

A Video box will be available from Monday to Friday in Tent A (exhibition tent) to help you easily participate in the video competition. Take part and tell us what you think about “physics in the future”.

5. Wilhelm and Else Heraeus Communication Programme

Important notes for participants who apply for a grant of the Wilhelm and Else Heraeus Foundation:

At the beginning of the conference you will receive an identification form at the conference office. The participation in the conference must be certified by the conference desk. You have the possibility to leave this certificate by the staff members of the DPG (recommended!) in the conference office or submit it to the DPG head office (DPG-Geschäftsstelle, Hauptstr. 5, 53604 Bad Honnef, Germany) by April 14, 2023 at the latest.

For more detailed information refer to <https://skm23.dpg-tagungen.de/registrierung/weh>.

The Deutsche Physikalische Gesellschaft thanks the Wilhelm and Else Heraeus Foundation for the generous financial support of young academic talents. We hope that young physicists will continue to seize the offered opportunity for active scientific communication at scientific conferences. A total of about 37,800 young academics were supported by this programme so far.

6. Members’ Assemblies of the Divisions and Working Groups

During the DPG Spring Meeting, Members’ Assemblies of the divisions and working groups take place. Please refer to the scientific programme for the time and place of the meetings.

7. CO₂ compensation for the DPG conferences

By decision of the Executive Board, the DPG will compensate for fossil CO₂ emissions resulting from mobility for DPG conferences and committee meetings.

8. Acknowledgement

The organisers want to thank

- the Wilhelm and Else Heraeus Foundation, Hanau
- the TU Dresden
- the official sponsors of the DPG-Frühjahrstagung (refer to page 15)

for supporting the conference and all staff, who make the conference possible.

9. SAY CHEESE!

The DPG Spring Meetings are basically public to the press. Please note: On behalf of DPG, photos and videos will be recorded during the Spring Meetings. In the context of public relations, these recordings (as the case may be) will be published on our website, in social media or within prints of the DPG for example.

10. Disclaimer of liability

Participants are asked to look carefully after their wardrobe, valuables, laptops, and other belongings. The organisers are not liable.

Sponsors of the DPG Spring Meeting Dresden

Main Sponsors:



Sponsors



Industrietag 2023

„Karrieren für Physikerinnen und Physiker in Industrie und Wirtschaft“

im Rahmen der DPG-Frühjahrstagung an der Universität Dresden

„Physikerinnen und Physiker sind in unzähligen Branchen und Berufsgruppen gefragt. Sie werden gerne in Führungs- und Managementpositionen aufgrund hoher Problemlösekompetenz häufig eingesetzt.“

Wie vielseitig die Möglichkeiten für Physikerinnen und Physiker sind, soll exemplarisch an fünf Karrieren gezeigt werden, die unterschiedlicher nicht sein können und alle eines gemeinsam haben: alle Vortragenden sind Physikerinnen oder Physiker.“

Mit Vorträgen von:

Prof. Dr. Joachim Rädler

CeNs (Centre For Nanoscience), LMU München

Dr. Diana Nanova

Customer Engineering Manager, Google Cloud

Dr. Udo Weigelt

LL.M., Patentanwalt und Partner in der Kanzlei Grünecker Patent- und Rechtsanwälte, München

Dr. Oliver de Haas

CEO und Gründer von evico, Dresden

Dr. Charles Majer

Digital Portfolio Expert, Siemens Healthineers

Mittwoch,
29. März 2023,
13:45 - 17:30 Uhr
IAP/HKB
Raum 1.11.

Synopsis of the Daily Programme

Sunday, March 26, 2023

TUT

Tutorials

16:00	HSZ 01	TUT 1	Physics Meets Machine Learning
16:00	HSZ 01	TUT 1.1	Machine Learning for Quantum Technologies •Florian Marquardt
16:45	HSZ 01	TUT 1.2	The Unreasonable Effectiveness of Gaussians in the Theory of Deep Neural Networks •Zohar Ringel
17:30	HSZ 01	TUT 1.3	Computing learning curves for large machine learning models using the replica approach •Manfred Opper
16:00	HSZ 02	TUT 2	Stochastic Processes of Opinion Formation
16:00	HSZ 02	TUT 2.1	Bounded Confidence Revisited: What We Overlooked, Underestimated, and Got Wrong •Rainer Hegselmann
16:45	HSZ 02	TUT 2.2	When intuition fails: the complex effects of assimilative and repulsive influence on opinion polarization •Michael Maes
17:30	HSZ 02	TUT 2.3	How growing connectivity and self-organization changes opinion dynamics •Philipp Lorenz-Spreen
16:00	HSZ 03	TUT 3	Hands-on tutorial on workflows for materials science simulation
16:00	HSZ 03	TUT 3.1	Hands-on tutorial on workflows for materials science simulations •Jörg Neugebauer
16:00	HSZ 04	TUT 4	Strategic elements and sustainability
16:00	HSZ 04	TUT 4.1	Making better batteries? – From Li-ion to Na-ion batteries •Philipp Adelhelm
16:30	HSZ 04	TUT 4.2	Sustainable Thermoelectric Materials Predicted by Data Mining and Machine Learning •Kornelius Nielsch
17:00	HSZ 04	TUT 4.3	Design strategies for electrocatalysts – an electrochemist’s perspective •Kristina Tschulik
17:30	HSZ 04	TUT 4.4	Green magnetic materials for efficient energy, transport and cooling applications •Oliver Gutfleisch

Public Evening Talk (*free entrance*)

18:30	HSZ 01	PSV I	Kipp-Punkte im Klimasystem: Vorboten aus dem polaren Eis •Ricarda Winkelmann
-------	--------	-------	---

18:30	Tent A	Welcome Evening (<i>for registered participants</i>)
-------	--------	---

Monday, March 27, 2023

08:25	HSZ 01		Opening
			Plenary Talks
08:30	HSZ 01	PLV I	Spin-Photon Interfaces and Their Applications •Mete Atatuere
14:00	HSZ 01	PLV II	New directions in electromagnetic field mapping in materials in the transmission electron microscope •Rafal E. Dunin-Borkowski
14:00	HSZ 02	PLV III	Microgels at Interfaces •Regine von Klitzing
			Lunch Talk, Discussion
13:15	HSZ 02	PSV II	Patentanwalt, Verfahren zu dessen Herstellung und Verwendung eines Patentanwalts •Carina Ehrig
13:15	HSZ 03	PSV III	Talking about different career paths into Academia •Alexander Osterkorn, Christoph Kastl, Anna Grünebohm, and Amelie Heuer-Jungemann

SYOF

			Symposium
09:30	HSZ 01	SYOF 1	Dynamics of Opinion Formation – from Quorum Sensing to Polarization
			Invited Talks
09:30	HSZ 01	SYOF 1.1	Towards understanding of the social hysteresis – insights from statistical physics •Katarzyna Sznajd-Weron
10:00	HSZ 01	SYOF 1.2	Polarization in attitude distributions from surveys and models of continuous opinion dynamics •Jan Lorenz
10:30	HSZ 01	SYOF 1.3	Collective patterns and stable misunderstandings in networks striving for consensus without a common value system •Johannes Falk
11:15	HSZ 01	SYOF 1.4	A yet undetected cognitive bias, revealed by opinion dynamics simulations •Guillaume Deffuant
11:45	HSZ 01	SYOF 1.5	Extreme switches in kinetic exchange models of opinion. •Parongama Sen

SYSD

			Symposium
09:30	HSZ 04	SYSD 1	SKM Dissertation Prize
			Invited Talks
09:30	HSZ 04	SYSD 1.1	Diffusion of antibodies in solution: from individual proteins to phase separation domains •Anita Girelli
10:00	HSZ 04	SYSD 1.2	Intermediate Filament Mechanics Across Scales •Anna V. Schepers
10:30	HSZ 04	SYSD 1.3	Ultrafast Probing and Coherent Vibrational Control of a Surface Structural Phase Transition •Jan Gerrit Horstmann
11:00	HSZ 04	SYSD 1.4	Electro-active metasurfaces employing metal-to-insulator phase transitions •Julian Karst
11:30	HSZ 04	SYSD 1.5	The role of unconventional symmetries in the dynamics of many-body systems •Pablo Sala

Monday, March 27, 2023

SYGM

			Symposium
15:00	HSZ 01	SYGM 1	Green Magnets for Efficient Energy Conversion
			Invited Talks
15:00	HSZ 01	SYGM 1.1	Data mining protocols for functional magnetic materials •Olle Eriksson
15:30	HSZ 01	SYGM 1.2	High performance permanent magnets; elements criticality, new demands, and extrinsic magnetic properties •Hossein Sepehri-Amin
16:00	HSZ 01	SYGM 1.3	Magnetic shape memory Heuslers: microstructure-related effects on the martensitic transformation •Franca Albertini
16:45	HSZ 01	SYGM 1.4	Thin film combinatorial studies of hard magnetic materials •Nora Dempsey
17:15	HSZ 01	SYGM 1.5	Magnetocaloric materials for energy-efficient thermal control systems •Victorino Franco

BP

			Invited Talks
11:15	BAR Schö	BP 1.7	Cell-free expression of membrane proteins and control of their spatial organization in synthetic lipid membranes •Jan Steinkühler
09:30	TOE 317	BP 2.1	Emergent properties in motile active matter •Roland G. Winkler
10:30	BAR 0106	BP 3.5	Resolving gating and allosteric modulation in ion channels through simulations and small-angle neutron scattering •Erik Lindahl
15:00	TOE 317	BP 5.1	Repurposing nucleic acids as high-resolution force sensors: From fundamental mechanotransduction to translational biophysics •Khalid Salaita
16:15	BAR 0106	BP 6.5	Mechanical and electrical properties of bacterial biofilms modulate antibiotic tolerance •Berenike Maier
			Sessions
09:30	BAR Schö	BP 1	Membranes, Vesicles, Synthetic Cells
09:30	TOE 317	BP 2	Active Matter I
09:30	BAR 0106	BP 3	Computational Biophysics I
15:00	BAR Schö	BP 4	Tissue Mechanics I
15:00	TOE 317	BP 5	Focus Session NanoAgents
15:00	BAR 0106	BP 6	Bacterial Mechanics
15:00	ZEU 160	BP 7	Active Matter II

CPP

			Invited Talks
09:30	GÖR 226	CPP 1.1	Strategies for advancing the performance of organic photovoltaics •Thomas Anthopoulos
11:30	GÖR 226	CPP 1.7	Lost in translation? Transport resistance in organic solar cells •Carsten Deibel
09:30	MER 02	CPP 2.1	Molecular Theories meet Explainable Machine Learning – Novel Concepts for Advanced Drug Formulations •Jens Smiatek
15:00	GÖR 226	CPP 11.1	Quantifying the potential of organic solar cells using luminescence measurements and modelling •Jenny Nelson
15:00	MER 02	CPP 12.1	Adaptive Resolution Simulations: Past, Present and Open (Boundaries) Future •Robinson Cortes-Huerto

Monday, March 27, 2023

CPP

15:00	ZEU 255	CPP 13.1	Nanocomposites and polymer thin films: from gas phase synthesis to functional applications •Franz Faupel
Sessions			
09:30	GÖR 226	CPP 1	Focus: Organic Solar Cells Based on Non-fullerene Acceptors: Loss Mechanism and Options for Above 20 % Efficiencies I
09:30	MER 02	CPP 2	Modeling and Simulation of Soft Matter I
09:30	ZEU 255	CPP 3	Hydrogels and Microgels
09:30	TOE 317	CPP 4	Active Matter I
09:30	POT 81	CPP 5	2D Materials I
09:30	POT 251	CPP 6	Perovskite and photovoltaics I
09:30	POT 361	CPP 7	Organic Semiconductors
10:45	ZEU 255	CPP 8	Responsive and Adaptive Systems
11:30	SCH A 315	CPP 9	Organic Thin Films, Organic-Inorganic Interfaces
14:30	POT 106	CPP 10	Instrumentation and Methods for Micro- and Nanoanalysis
15:00	GÖR 226	CPP 11	Focus: Organic Solar Cells Based on Non-fullerene Acceptors: Loss Mechanism and Options for Above 20 % Efficiencies II
15:00	MER 02	CPP 12	Modeling and Simulation of Soft Matter II
15:00	ZEU 255	CPP 13	Composites and Functional Polymer Hybrids
15:00	ZEU 160	CPP 14	Active Matter II
15:00	POT 81	CPP 15	2D Materials II
15:00	GER 39	CPP 16	Nanostructures at Surfaces
18:00	P3	CPP 17	Poster Session I

DS

Sessions			
09:30	SCH A 316	DS 1	2D Materials and their Heterostructures I: Graphene
11:30	SCH A 316	DS 2	2D Materials and their Heterostructures II: h-BN and WSe ₂
11:30	SCH A 315	DS 3	Organic Thin Films, Organic-Inorganic Interfaces
15:30	SCH A 316	DS 4	Thin Film Properties I

DY

Invited Talks			
09:30	MOL 213	DY 5.1	Extreme events, entropies and instantons for turbulence and water waves •Joachim Peinke
12:30	ZEU 250	DY 8.1	Novel phenomena and analysis methods in oscillator networks: higher-order interactions, higher-order averaging, and inference •Hiroshi Kori
16:30	ZEU 160	DY 10.6	Long-range communications enable the hierarchical self-organization of active matter •Igor Aronson
15:00	ZEU 250	DY 11.1	The challenge of structured disorder in statistical physics •Marc Mezard
15:30	ZEU 250	DY 11.2	The emergence of concepts in shallow neural-networks •Elena Agliari
16:00	ZEU 250	DY 11.3	Adaptive Kernel Approaches to Feature Learning in Deep Neural Networks •Zohar Ringel
17:00	ZEU 250	DY 11.5	Analysing the dynamics of message passing algorithms •Manfred Opper
17:30	ZEU 250	DY 11.6	Deep Learning Theory Beyond the Kernel Limit •Cengiz Pehlevan
Sessions			
09:30	HSZ 03	DY 2	Focus Session: Physics Meets ML I – Machine Learning for Complex Quantum Systems
09:30	TOE 317	DY 3	Active Matter I

Monday, March 27, 2023

DY

09:30	ZEU 250	DY 4	Pattern Formation, Delay and Nonlinear Stochastic Systems
09:30	MOL 213	DY 5	Fluid Physics: Turbulence and Convection
10:00	ZEU 160	DY 6	Statistical Physics: General I
10:00	ZEU 147	DY 7	Granular Matter and Contact Dynamics
12:30	ZEU 250	DY 8	Invited Talk: Dynamics of Networks
14:00	MOL 213	DY 9	Quantum Dynamics, Decoherence and Quantum Information
15:00	ZEU 160	DY 10	Active Matter II
15:00	ZEU 250	DY 11	Focus Session: Physics Meets ML II – Understanding Machine Learning as Complex Interacting Systems

HL

Invited Talks			
09:30	POT 151	HL 3.1	Schrödinger cat states of a 16-microgram mechanical oscillator •Yiwen Chu
10:00	POT 151	HL 3.2	High-fidelity quantum information processing with spins and phonons •Peter Rabl
11:30	POT 151	HL 3.5	Control of spin centers in silicon carbide using acoustic fields •Alberto Hernández-Mínguez
17:30	POT 81	HL 8.9	Time-resolved optical spectroscopy of 3R-stacked MoS ₂ •Swarup Deb
15:00	POT 361	HL 9.1	Spin and valley lifetime in graphene quantum dots •Guido Burkard
15:30	POT 361	HL 9.2	Microscopic modelling of electrostatically induced bilayer graphene quantum dots •Angelika Knothe
16:45	POT 361	HL 9.4	Single-shot spin and valley Pauli blockade read-out in bilayer graphene quantum dots •Chuyao Tong
17:15	POT 361	HL 9.5	Particle-hole symmetry protects spin-valley blockade in graphene quantum dots •Christian Volk
15:00	POT 151	HL 10.1	Surface Acoustic Wave Cavity Optomechanics with 2D Materials •Galan Moody
15:30	POT 151	HL 10.2	Phononic Microresonators Coupled by Surface Acoustic Waves •Sarah Benchabane

Sessions			
09:30	POT 81	HL 1	2D Materials I
09:30	POT 361	HL 2	Organic Semiconductors
09:30	POT 151	HL 3	Focus Session: Progress in Hybrid Phononic Quantum Technologies I
09:30	POT 251	HL 4	Perovskite and photovoltaics I
10:00	POT 112	HL 5	Heterostructures, interfaces and surfaces
10:30	TRE Ma	HL 6	Focus Session: Frontiers of Electronic-Structure Theory III
13:00	P2/EG	HL 7	Poster I
15:00	POT 81	HL 8	2D Materials II
15:00	POT 361	HL 9	Focus Session: Graphene quantum dots
15:00	POT 151	HL 10	Focus Session: Progress in Hybrid Phononic Quantum Technologies II
15:00	POT 251	HL 11	Quantum transport and quantum Hall effects I
15:00	POT 112	HL 12	Semiconductor lasers I
15:00	TRE Ma	HL 13	Focus Session: Frontiers of Electronic-Structure Theory II

KFM

Invited Talks			
09:00	POT 51	KFM 1.1	Investigations of multiferroic behavior within domains and domain walls of a multiferroic Aurivillius phase system •Lynette Keeney
10:45	POT 51	KFM 1.5	Domains or no Domains in Wurtzite-Type Ferroelectrics •Simon Fichtner

Monday, March 27, 2023

KFM

14:30	POT 51	KFM 2.1	Formation of conducting channels along of dislocations in SrTiO ₃ •Christian Rodenbücher
15:55	POT 51	KFM 2.4	Plastic properties of MgO: Insights from numerical modeling •Philippe Carrez
Sessions			
09:00	POT 51	KFM 1	Focus: Domains and Domainwalls in (Multi)Ferroics I
14:30	POT 51	KFM 2	Focus: Dislocations in Ceramics: Mechanics, Structures and Functionality
14:30	POT 106	KFM 3	Instrumentation and Methods for Micro- and Nanoanalysis

MA

Invited Talks			
09:30	HSZ 02	MA 2.1	Two-dimensional Skyrmions in the real three-dimensional world •Nikolai Kiselev
15:00	HSZ 04	MA 8.1	Optical control of antiferromagnetism •Christian Tzschaschel
Sessions			
09:30	HSZ 02	MA 2	Skyrmions I
09:30	HSZ 401	MA 3	Magnetic Materials for Efficient Energy Conversion
09:30	HSZ 403	MA 4	Spin Transport and Orbitronics, Spin-Hall Effects
09:30	POT 6	MA 5	Thin Films: Magnetic Coupling Phenomena / Exchange Bias
14:30	POT 51	MA 6	Focus: Dislocations in Ceramics: Mechanics, Structures and Functionality
15:00	HSZ 02	MA 7	Computational Magnetism
15:00	HSZ 04	MA 8	Ultrafast Magnetization Effects I
15:00	HSZ 401	MA 9	Cooperative Phenomena: Spin Structures and Magnetic Phase Transitions
15:00	HSZ 403	MA 10	Topological Insulators
15:00	POT 6	MA 11	Non-Skyrmionic Magnetic Textures I

MM

Invited Talks, Topical Talks			
09:30	SCH A 251	MM 2.1	Function follows form: on tailoring functional materials via microstructural design •Erica Lilleodden
10:15	SCH A 216	MM 4.1	Crack and dislocations interactions: coupling DDD and XFEM •Marc Fivel
10:45	SCH A 216	MM 4.2	multiscale studies on the fracture behaviors of body centered cubic metal •Yinan Cui
11:45	SCH A 216	MM 4.4	Capturing Micromechanical Crack Tip Stress States and Toughening Plasticity in 2D and 3D •Thomas E. J. Edwards
15:00	SCH A 251	MM 7.1	Molecular dynamics simulations of shock waves in alloys: Interplay of defects and phase transition •Nina Merkert
15:45	SCH A 216	MM 9.1	Modeling of grain boundary embrittlement phenomena in metallic materials •Lorenz Romaner
Sessions			
09:30	SCH A 251	MM 2	Invited Talk: Lilleodden
10:15	SCH A 251	MM 3	Development of Computational Methods: Evaporation, Growth and Oxidation – Density Functional, Tight Binding
10:15	SCH A 216	MM 4	Topical Session: Fundamentals of Fracture – Micromechanical Fracture Experiments
10:15	SCH A 215	MM 5	Materials in Energy Conversion: Mechanical Properties and Solid State Batteries
10:15	SCH A 118	MM 6	Transport in Materials: Ion, Charge and Heat Transport
15:00	SCH A 251	MM 7	Invited Talk: Merkert
15:45	SCH A 251	MM 8	Development of Computational Methods: Diverse Topics and Machine Learning
15:45	SCH A 216	MM 9	Topical Session: Fundamentals of Fracture – Interface Fracture

Monday, March 27, 2023

MM

15:45	SCH A 215	MM 10	Materials for Storage and Conversion of Energy: New Storage Materials
17:00	SCH A 215	MM 11	Functional Materials: Performance, Reliability and Degradation
18:15	P2/OG1+2	MM 12	Poster I

O

Invited Talk, Topical Talks

09:30	TRE Phy	O 1.1	From surface structure to exciton evolution: a many-body theoretical perspective •Sivan Refaely-Abramson
10:30	GER 38	O 5.1	Highly charged, slow and swift ions interacting with surfaces and 2D materials •Marika Schleberger
11:30	GER 38	O 5.4	A contactless single-step process for simultaneous nanoscale patterning and cleaning of large-area graphene •Tuan Tran
10:30	REC C 213	O 7.1	Superconductivity in atom-by-atom crafted quantum corrals •Lucas Schneider
11:00	TRE Ma	O 9.3	Large-scale machine-learning assisted discovery and characterization of materials •Miguel Alexandre Lopes Marques
15:00	CHE 89	O 10.1	Photoemission Orbital Tomography: Imaging Molecular Wave Functions in Reciprocal and Real Space •F. S. Tautz
15:00	GER 38	O 13.1	Space weathering of planetary surfaces •Peter Wurz
15:45	TRE Phy	O 16.4	Microscopic insight into non-equilibrium dynamics through time-resolved x-ray absorption spectroscopy •Andrea Eschenlohr
15:00	TRE Ma	O 17.1	Coupled-cluster theory for complex solids made ready •Andreas Grüneis

Sessions

09:30	TRE Phy	O 1	Overview Talk Sivan Refaely-Abramson
10:30	CHE 89	O 2	Organic Molecules on Inorganic Substrates I: Electronic, Optical and Other Properties I
10:30	CHE 91	O 3	Metal Substrates: Adsorption and Reaction of Small Molecules I
10:30	GER 37	O 4	Tribology: Surfaces and Nanostructures
10:30	GER 38	O 5	Focus Session: Ion Beam Interaction with Surfaces and 2D Materials I
10:30	GER 39	O 6	New Methods: Experiments and Theory
10:30	REC C 213	O 7	Spins on Surfaces at the Atomic Scale I
10:30	TRE Phy	O 8	Ultrafast Electron Dynamics at Surface and Interfaces I
10:30	TRE Ma	O 9	Focus Session: Frontiers of Electronic-Structure Theory I
15:00	CHE 89	O 10	Organic Molecules on Inorganic Substrates II: Electronic, Optical and Other Properties II
15:00	CHE 91	O 11	Surface Reactions
15:00	GER 37	O 12	Scanning Probe Techniques: Method Development I
15:00	GER 38	O 13	Focus Session: Ion Beam Interaction with Surfaces and 2D Materials II
15:00	GER 39	O 14	Nanostructures at Surfaces
15:00	REC C 213	O 15	Spins on Surfaces at the Atomic Scale II
15:00	TRE Phy	O 16	Ultrafast Electron Dynamics at Surface and Interfaces II
15:00	TRE Ma	O 17	Focus Session: Frontiers of Electronic-Structure Theory II
18:00	P2/EG	O 18	Poster: 2D Materials I
18:00	P2/EG	O 19	Poster: Ultrafast Electron Dynamics at Surface and Interfaces I
18:00	P2/EG	O 20	Poster: Spins and Magnetism at Surfaces
18:00	P2/EG	O 21	Poster: Scanning Probe Techniques
18:00	P2/EG	O 22	Poster Session: Organic Molecules on Inorganic Substrates I
18:00	P2/EG	O 23	Poster: Surface Reactions
18:00	P2/EG	O 24	Poster: Ion Beam Interaction with Surfaces and Interfaces
18:00	P2/EG	O 25	Poster: Metal Substrates
18:00	P2/EG	O 26	Poster: New Methods

Monday, March 27, 2023

SOE

			Invited Talks
15:10	HSZ 03	SOE 3.1	Initial Progress on the Science of Science •Dashun Wang (Laureate of the SOE-Young Scientist Award 2023)
16:00	HSZ 03	SOE 3.2	Complexity science can address marginalization in society and algorithms •Fariba Karimi (Laureate of the SOE-Young Scientist Award 2023)
			Sessions
12:30	ZEU 250	SOE 2	Invited Talk: Dynamics of Networks
15:00	HSZ 03	SOE 3	Award Session: Young Scientist Award for Socio- and Econophysics (YSA)
17:00	P2/OG2	SOE 4	Poster

TT

			Invited Talks
09:30	HSZ 03	TT 2.1	Enhanced variational Monte Carlo for Rydberg atom arrays •Stefanie Czischek
10:00	HSZ 03	TT 2.2	Data mining the output of quantum simulators – from critical behavior to algorithmic complexity •Marcello Dalmonte
10:30	HSZ 03	TT 2.3	Reinforcement learning for quantum technologies •Florian Marquardt
11:00	HSZ 03	TT 2.4	Machine learning of phase transition •Christof Weitenberg
15:00	HSZ 103	TT 8.1	Molecules on a superconductor: Inducing magnetism and resonance-enhanced vibrational spectroscopy •Richard Berndt
17:15	HSZ 304	TT 17.3	Noise signatures of anyon statistics and Andreev scattering in the $\nu = 1/3$ fractional quantum Hall regime •Anne Anthore
			Sessions
09:30	HSZ 03	TT 2	Focus Session: Physics Meets ML I – Machine Learning for Complex Quantum Systems
09:30	HSZ 103	TT 3	Superconductivity: Properties and Electronic Structure
09:30	HSZ 201	TT 4	f-Electron Systems and Heavy Fermions I
09:30	HSZ 204	TT 5	Correlated Electrons: Method Development
09:30	HSZ 304	TT 6	Topological Semimetals
09:30	HSZ 403	TT 7	Spin Transport and Orbitronics, Spin-Hall Effects
15:00	HSZ 103	TT 8	Yu-Shiba-Rusinov Systems
15:00	HSZ 201	TT 9	f-Electron Systems and Heavy Fermions II
15:00	HSZ 204	TT 10	Correlated Electrons: Other Materials
15:00	HSZ 304	TT 11	Spintronics, Spin-calorics and Magnetotransport
15:00	HSZ 403	TT 12	Topological Insulators
15:00	ZEU 250	TT 13	Focus Session: Physics Meets ML II – Understanding Machine Learning as Complex Interacting Systems
15:00	POT 361	TT 14	Focus Session: Graphene Quantum Dots
15:00	POT 251	TT 15	Quantum Transport and Quantum Hall Effects I
15:00	P2/OG4	TT 16	Poster: Transport
16:45	HSZ 304	TT 17	Topology: Quantum Hall Systems
17:15	HSZ 201	TT 18	Nano- and Optomechanics

VA

			Sessions
09:30	HSZ 301	VA 1	Vacuum Technology: New Developments and Applications
14:00	P2/OG2	VA 2	Vacuum Technology: New Developments and Applications – Poster

20:00 HSZ 01 **EinsteinSlam**

Ceremonial Session with Award Ceremony

Deutsche Physikalische Gesellschaft

Award Ceremony

Walter-Schottky-Prize 2023

to Dr. Kai-Qiang Lin
Universität Regensburg

Gaede-Prize 2023

to Dr. Benjamin Stadtmüller, TU Kaiserslautern and
Johannes Gutenberg-Universität Mainz

Dissertation Prize of the Condensed Matter Section (SKM)

(The award winner will be selected after the
Dissertation Award Symposium SYSD)

Ceremonial Lecture

Prof. Dr. Metin Tolan, Universität Göttingen

*„Die Star Trek Physik – Warum die Enterprise nur 158 kg wiegt
und andere galaktische Erkenntnisse“*

Tuesday, March 28, 2023, 15:30

HSZ 01 (Audimax)

Deutsche Physikalische Gesellschaft



Tuesday, March 28, 2023

			Plenary Talk
08:30	HSZ 01	PLV IV	Stochastic thermodynamics: From concepts to model-free inference •Udo Seifert
			Prize Talk
13:15	HSZ 01	PRV I	Seeing is believing: Nonlinear optics on ferroic materials •Manfred Fiebig (Laureate of the Stern-Gerlach-Medal 2023)
			Ceremonial Talk, Lunch Talks
13:15	HSZ 02	PSV IV	Berufswege für Physiker in Elektrotechnik, Unternehmensberatung und IT •Philipp Dedié
13:15	HSZ 03	PSV V	Research Funding by the DFG – Insights into the Decision Process •Michael Mößle
15:30	HSZ 01		Ceremonial Session with Award Ceremony and Ceremonial Lecture
		PSV VI	Die Star Trek Physik – Warum die Enterprise nur 158 kg wiegt und andere galaktische Erkenntnisse •Metin Tolan

SYFP

			Symposium
09:30	HSZ 01	SYFP 1	Physics of Fluctuating Paths
			Invited Talks
09:30	HSZ 01	SYFP 1.1	Time at which a stochastic process achieves its maximum •Satya Majumdar
10:00	HSZ 01	SYFP 1.2	Fluctuations and molecule-spanning dynamics of single Hsp90 proteins on timescales from nanoseconds to days •Thorsten Hugel
10:30	HSZ 01	SYFP 1.3	Path reweighting for Langevin dynamics •Bettina Keller
11:15	HSZ 01	SYFP 1.4	Out-of-equilibrium dynamics of trapped Brownian particles •Raul A. Rica
11:45	HSZ 01	SYFP 1.5	Thermodynamics of Clocks •Patrick Pietzonka

BP

			Invited Talks
10:45	BAR Schö	BP 8.5	Microtubule Lattice Dynamics •Laura Schaedel
09:30	BAR 0106	BP 10.1	Protein evolution in sequence landscapes: from data to models and back •Martin Weigt
			Sessions
09:30	BAR Schö	BP 8	Cell Mechanics I
09:30	TOE 317	BP 9	Active Matter III
09:30	BAR 0106	BP 10	Evolution and Origin of Life
12:30	P1	BP 11	Poster Session I

CPP

			Invited Talks
09:30	MER 02	CPP 19.1	Multiscale Model of Flow-Induced Crystallization in Polymers •Gregory Rutledge
09:30	ZEU 255	CPP 20.1	Granular Matter Rheology – fluid-/solid-like behavior and state-transitions •Stefan Luding

Tuesday, March 28, 2023

CPP

Sessions

09:30	GÖR 226	CPP 18	Organic Electronics and Photovoltaics I
09:30	MER 02	CPP 19	Crystallization, Nucleation and Self-Assembly
09:30	ZEU 255	CPP 20	Polymer and Molecular Dynamics, Friction and Rheology
09:30	TOE 317	CPP 21	Active Matter III
09:30	POT 81	CPP 22	2D Materials III
09:30	POT 112	CPP 23	Optical Properties
10:00	MOL 213	CPP 24	Complex Fluids and Soft Matter I
12:00	HSZ 201	CPP 25	Molecular Electronics and Photonics
14:00	MER 02	CPP 26	Electrical, Dielectrical and Optical Properties of Thin Films
14:00	ZEU 147	CPP 27	Glasses and Glass Transition I

DS

Invited Talk

09:30	SCH A 316	DS 5.1	Operando infrared studies of confined water and protons in MXene •Mailis Lounasvuori
-------	-----------	--------	---

Sessions

09:30	SCH A 316	DS 5	2D Materials and their Heterostructures III
10:00	SCH A 315	DS 6	Thin Film Properties II
11:15	SCH A 316	DS 7	2D Materials and their Heterostructures IV
11:30	SCH A 315	DS 8	Thin Film Properties III

DY

Invited Talk

09:30	MOL 213	DY 14.1	Unraveling structural and dynamical features in glassy fluids using machine learning •Laura Filion
-------	---------	---------	---

Sessions

09:30	HSZ 204	DY 12	Nonequilibrium Quantum Many-Body Systems I
09:30	TOE 317	DY 13	Active Matter III
09:30	MOL 213	DY 14	Invited Talk: Machine Learning and Complex Fluids
09:30	ZEU 260	DY 15	Physics of Contagion Processes I
10:00	MOL 213	DY 16	Complex Fluids and Soft Matter
10:00	ZEU 160	DY 17	Machine Learning in Dynamics and Statistical Physics I
10:00	ZEU 147	DY 18	Nonlinear Dynamics, Synchronization and Chaos
10:00	ZEU 260	DY 19	Physics of Contagion Processes II
11:00	ZEU 260	DY 20	Networks: From Topology to Dynamics I
14:00	MOL 213	DY 21	Quantum Chaos and Coherent Dynamics
14:00	ZEU 160	DY 22	Machine Learning in Dynamics and Statistical Physics II
14:00	ZEU 250	DY 23	Statistical Physics: General II
14:00	ZEU 147	DY 24	Glasses and Glass Transition

HL

Sessions

09:30	POT 81	HL 14	2D Materials III
09:30	POT 361	HL 15	Spin phenomena in semiconductors
09:30	POT 151	HL 16	Quantum dots: Transport
09:30	POT 251	HL 17	THz and MIR physics in semiconductors
09:30	POT 112	HL 18	Optical Properties
09:30	GÖR 226	HL 19	Organic Electronics and Photovoltaics I
10:30	TRE Ma	HL 20	Focus Session: Frontiers of Electronic-Structure Theory I
11:00	POT 361	HL 21	Thermal properties

Tuesday, March 28, 2023

KFM

09:00	POT 51	KFM 4.1	Invited Talk Towards spatially resolved measurements of thermal transport and electrocaloric effects at the nanoscale in ferroelectric materials •Raymond McQuaid
09:00	POT 51	KFM 4	Sessions Focus: Domains and Domainwalls in (Multi)Ferroic II Thin Film Properties Poster
10:00	SCH A 315	KFM 5	
17:00	P3	KFM 6	

MA

09:30	HSZ 04	MA 14.1	Invited Talk Antiferromagnetism-driven two-dimensional topological nodal-point superconductivity •Roberto Lo Conte
09:30	HSZ 02	MA 12	Sessions Skyrmions II Focus Session: New Perspectives for Adiabatic Demagnetization Refrigeration in the Kelvin and sub-Kelvin Range Surface Magnetism INNOMAG e.V. Prizes 2023 (Diplom-/Master and Ph.D. Thesis) Magnonics Thin Films: Magnetic Anisotropy Functional Antiferromagnetism I Molecular Magnetism I Spintronics (other effects) Spin-Dependent Phenomena in 2D Terahertz Spintronics Poster Magnetism I
09:30	HSZ 03	MA 13	
09:30	HSZ 04	MA 14	
09:30	HSZ 401	MA 15	
09:30	HSZ 403	MA 16	
09:30	POT 6	MA 17	
15:00	HSZ 02	MA 18	
15:00	HSZ 04	MA 19	
15:00	HSZ 401	MA 20	
15:00	HSZ 403	MA 21	
15:00	POT 6	MA 22	
17:00	P1	MA 23	

MM

09:30	SCH A 251	MM 13.1	Invited Talks Exploring the Slow Dynamics of Interfaces and Glasses via Markov State Models •Chad Sinclair
10:15	SCH A 216	MM 15.1	
09:30	SCH A 251	MM 13	Sessions Invited Talk: Sinclair Development of Computational Methods: Thermodynamics and Local Chemistry, Electronic Structure Topical Session: Fundamentals of Fracture – Atomistic Studies of Fracture Energy Conversion Phase Transformations: Microstructural Transformations Transport in Materials: Metals, Alloys and Oxides Development of Computational Methods: Simulation Methods – Theory Topical Session: Fundamentals of Fracture – Microstructure Impact on Fracture (Experiments) Materials for Storage and Conversion of Energy: Energy Conversion Mechanical Properties and Alloy Design: Porous and Nanostructured Materials Poster II
10:15	SCH A 251	MM 14	
10:15	SCH A 216	MM 15	
10:15	SCH A 215	MM 16	
10:15	SCH A 118	MM 17	
11:30	SCH A 118	MM 18	
14:15	SCH A 251	MM 19	
14:15	SCH A 216	MM 20	
14:15	SCH A 215	MM 21	
14:15	SCH A 118	MM 22	
18:15	P2/OG1+2	MM 23	

Tuesday, March 28, 2023

O**Invited Talk, Topical Talks**

09:30	TRE Phy	O 27.1	Dive right in! Molecular insights into electrochemical surface science •Katrin F. Domke
10:30	GER 38	O 31.1	Ultra-low energy ion implantation of two-dimensional materials •Hans Hofsäss
10:30	REC C 213	O 33.1	Fermi liquids, Luttinger integrals, topological invariants ... and magnetic molecules •Rok Zitko
11:45	TRE Phy	O 34.6	Photoemission orbital tomography for excitons •Peter Puschnig
11:15	TRE Ma	O 35.4	Towards low-scaling GW calculations for 2D materials •Jan Wilhelm

Sessions

09:30	TRE Phy	O 27	Overview Talk Katrin Domke
10:30	CHE 89	O 28	Organic Molecules on Inorganic Substrates III: Adsorption and Growth I
10:30	CHE 91	O 29	Supported Nanoclusters: Structure, Reactions and Catalysis
10:30	GER 37	O 30	2D Materials I: Electronic Structure
10:30	GER 38	O 31	Focus Session: Ion Beam Interaction with Surfaces and 2D Materials III
10:30	GER 39	O 32	Semiconductor Substrates
10:30	REC C 213	O 33	Spins on Surfaces at the Atomic Scale III
10:30	TRE Phy	O 34	Ultrafast Electron Dynamics at Surface and Interfaces III
10:30	TRE Ma	O 35	Focus Session: Frontiers of Electronic-Structure Theory III
18:00	P2/EG	O 36	Poster: 2D Materials II
18:00	P2/EG	O 37	Poster: Ultrafast Electron Dynamics at Surface and Interfaces II
18:00	P2/EG	O 38	Poster: Organic Molecules on Inorganic Substrates II
18:00	P2/EG	O 39	Poster Session: Heterogeneous Catalysis and Surface Dynamics
18:00	P2/EG	O 40	Poster: Semiconductor Substrates
18:00	P2/EG	O 41	Poster: Supported Nanoclusters
18:00	P2/EG	O 42	Poster: Nanostructures at Surfaces
18:00	P2/EG	O 43	Poster: Plasmonics and Nanooptics I

SOE**Invited Talk**

09:30	ZEU 260	SOE 5.1	Digital Pandemology – Is that physics? •Dirk Brockmann
-------	---------	---------	---

Sessions

09:30	ZEU 260	SOE 5	Physics of Contagion Processes I
10:00	ZEU 260	SOE 6	Physics of Contagion Processes II
11:00	ZEU 260	SOE 7	Networks: From Topology to Dynamics I
14:00	ZEU 260	SOE 8	Semantic Networks, Language and Culture

TT**Invited Talks**

09:30	HSZ 03	TT 19.1	Self-cooling molecular spin quantum processors •Marco Evangelisti
10:00	HSZ 03	TT 19.2	Triangular rare-earth borates for milli-Kelvin adiabatic demagnetization refrigeration •Philipp Gegenwart
10:30	HSZ 03	TT 19.3	A millikelvin scanning tunnelling microscope in ultra-high vacuum with adiabatic demagnetisation refrigeration •Ruslan Temirov
11:15	HSZ 03	TT 19.4	ADR cryostats in low temperature physics and their applications •Doreen Wernicke
11:45	HSZ 03	TT 19.5	Frustrated dipolar materials for low-temperature magnetic refrigeration •Mike Zhitomirsky

Tuesday, March 28, 2023

TT

11:00	HSZ 204	TT 22.6	Higgs spectroscopy of superconductors in nonequilibrium •Dirk Manske
Sessions			
09:30	HSZ 03	TT 19	Focus Session: New Perspectives for Adiabatic Demagnetization Refrigeration in the Kelvin and sub-Kelvin Range
09:30	HSZ 103	TT 20	Superconductivity: Tunnelling and Josephson Junctions
09:30	HSZ 201	TT 21	Correlated Electrons: Electronic Structure Calculations
09:30	HSZ 204	TT 22	Nonequilibrium Quantum Many-Body Systems I
09:30	HSZ 304	TT 23	Kagome Systems
09:30	POT 151	TT 24	Quantum Dots: Transport
12:00	HSZ 201	TT 25	Molecular Electronics and Photonics
14:00	HSZ 304	TT 26	Members' Assembly

AKC

Invited Talks			
10:30	ZEU 250	AKC 1.1	The tragic destiny of Mileva Marić Einstein •Pauline Gagnon
11:30	ZEU 250	AKC 1.2	Physik-Projekt-Tage – Ein Workshop für Schülerinnen der Oberstufe •Anna Benecke
12:00	ZEU 250	AKC 1.3	Belonging – a key to success in STEM?! •Barbara M. Gordalla
Sessions			
10:30	ZEU 250	AKC 1	AKC
12:30	ZEU 250	AKC 2	Women in Physics Lunch

09:30 Foyer HSZ / Tent A **Exhibition of Scientific Instruments and Literature**

Job Market			
11:30	HSZ 405		neocx GmbH & Trace Tronic GmbH <i>"Tracetrionic / neocx: Automate Everything – speeding up software testing in the automotive industry"</i>
12:45	HSZ 405		Ritzenhoefer GmbH <i>"Transformation Consulting – #impact23"</i>
14:00	HSZ 405		Wiley-VCH Verlag GmbH <i>"Physiker:innen im Wissenschaftsverlag"</i>

Wednesday, March 29, 2023

			Plenary Talks
08:30	HSZ 01	PLV V	Advances in Ultrafast Electron Microscopy •Claus Ropers
14:00	HSZ 01	PLV VI	Topological defects in active and living matter •M Cristina Marchetti
14:00	HSZ 02	PLV VII	Ferroelectric and multiferroic domain walls for nanotechnology •Dennis Meier
			Prize Talk
13:15	HSZ 01	PRV II	Towards chemical and optical band structure engineering in molecular-based heterostructures •Benjamin Stadtmueller (Laureate of the Gaede-Prize 2023)
			Lunch Talk, Discussion
13:15	HSZ 02	PSV VII	Vom Physiker zum (erfolgreichen) Unternehmer der Plasway-Technologies GmbH •Stephan Wege
13:15	HSZ 03	PSV VIII	Vielfalt der Wissenschaftskommunikation •Ulrich Bleyer, Nicolas Wöhrle und Peter Kohl

SYUE

			Symposium
09:30	HSZ 01	SYUE 1	Ultrafast Excitation Pathways of Quantum Materials
			Invited Talks
09:30	HSZ 01	SYUE 1.1	Dynamics and control in quantum materials using multi-terahertz spectroscopy •Richard Averitt
10:00	HSZ 01	SYUE 1.2	Assessing the nonthermal phonon populations in 2D materials with femtosecond electron diffuse scattering •Hélène Seiler
10:30	HSZ 01	SYUE 1.3	Exciting potentials – Exploring the realms of ultrafast phase transitions •Laurenz Rettig
11:15	HSZ 01	SYUE 1.4	Sub-cycle multidimensional spectroscopy of strongly correlated materials •Olga Smirnova
11:45	HSZ 01	SYUE 1.5	Witnessing many-body entanglement in light-driven quantum materials •Matteo Mitrano
12:15	HSZ 01	SYUE 1.6	Optical responses of photoexcited materials: from parametric amplification to photoinduced superconductivity •Eugene Demler

SYQC

			Symposium
15:00	HSZ 01	SYQC 1	Topology in Quantum and Classical Physics – From Topological Insulators to Active Matter
			Invited Talks
15:00	HSZ 01	SYQC 1.1	Topological magnetic whirls for computing •Karin Everschor-Sitte
15:30	HSZ 01	SYQC 1.2	Topological waves from solids to geo/astrophysical flows •Pierre Delplace
16:00	HSZ 01	SYQC 1.3	Topological Phase Transitions in Population Dynamics •Erwin Frey
16:45	HSZ 01	SYQC 1.4	Topological invariants protect robust chiral currents in active matter •Evelyn Tang
17:15	HSZ 01	SYQC 1.5	Topological defects in biological active matter •Amin Doostmohammadi

Wednesday, March 29, 2023

BP**Invited Talks**

10:15	TOE 317	BP 12.4	Materials properties of bacterial biofilms. •Cécile M. Bidan
09:30	BAR 0106	BP 13.1	Biological signal processes across scales •Steffen Rulands
11:15	BAR 0106	BP 16.1	Systems biophysics of bacterial response to cell wall-targeting antibiotics •Rosalind Allen

Sessions

09:30	TOE 317	BP 12	Biopolymers and Biomaterials
09:30	BAR 0106	BP 13	Signaling, Biological Networks
09:30	ZEU 160	BP 14	Focus Session: From Inter-individual Variability to Heterogeneous Group Dynamics and Disorder in Active Matter
10:30	BAR Schö	BP 15	Tissue Mechanics II
11:15	BAR 0106	BP 16	Systems Biophysics
15:00	BAR 0106	BP 17	Protein Structure and Dynamics
15:00	ZEU 250	BP 18	Biologically Inspired Statistical Physics
16:30	MER 02	BP 19	Biopolymers, Biomaterials and Bioinspired Functional Materials
18:00	BAR Schö	BP 20	Members' Assembly

CPP**Invited Talk**

09:30	MER 02	CPP 29.1	Imaging mineral-water interfaces with atomic force microscopy •Angelika Kühnle
-------	--------	----------	---

Sessions

09:30	GÖR 226	CPP 28	Molecular Electronics and Excited State Properties
09:30	MER 02	CPP 29	Interfaces and Thin Films
09:30	TOE 317	CPP 30	Biopolymers and Biomaterials I
09:30	ZEU 160	CPP 31	Focus Session: From Inter-individual Variability to Heterogeneous Group Dynamics and Disorder in Active Matter
09:30	POT 81	CPP 32	2D Materials IV
09:30	POT 251	CPP 33	Perovskite and photovoltaics II
10:00	ZEU 147	CPP 34	Wetting, Droplets and Microfluidics I
11:00	P1	CPP 35	Poster Session II
15:00	GÖR 226	CPP 36	Organic Electronics and Photovoltaics II
15:00	MER 02	CPP 37	Nanostructures, Nanostructuring and Nanosized Soft Matter
15:00	MOL 213	CPP 38	Microswimmers and Fluid Physics of Life
15:00	ZEU 160	CPP 39	Focus Session: Physics of Fluctuating Paths
15:00	GER 37	CPP 40	2D Materials V: Growth, Structure and Substrate Interaction
16:30	MER 02	CPP 41	Biopolymers, Biomaterials and Bioinspired Functional Materials II

DS**Invited Talk**

09:30	SCH A 316	DS 9.1	Flüssigphasen-Elektrochemie im Ultrahochvakuum unter XPS-Kontrolle •Frank Endres
-------	-----------	--------	---

Sessions

09:30	SCH A 316	DS 9	Layer Properties I
11:00	SCH A 316	DS 10	Layer Properties II
11:00	SCH A 315	DS 11	Thin Film Application
17:00	P3	DS 12	Poster

DY**Invited Talks**

09:30	MOL 213	DY 25.1	Many-body localization from Hilbert- and real-space points of view •Ivan Khaymovich
-------	---------	---------	--

Wednesday, March 29, 2023

DY

09:30	ZEU 160	DY 26.1	More is different: High-throughput 3D tracking reveals bacterial navigation strategies •Katja Taute
10:00	ZEU 160	DY 26.2	Variability and heterogeneity in natural swarms •Gil Ariel
11:15	ZEU 160	DY 26.5	Superstatistical Analysis and Modelling of Complex Dynamical Systems •Claus Metzner
09:30	ZEU 250	DY 27.1	Evolution in changing environments and driven disordered systems •Joachim Krug

Sessions

09:30	MOL 213	DY 25	Many-Body Quantum Dynamics
09:30	ZEU 160	DY 26	Focus Session: From Inter-individual Variability to Heterogeneous Group Dynamics and Disorder in Active Matter
09:30	ZEU 250	DY 27	Statistical Physics: Far From Equilibrium I
09:30	ZEU 260	DY 28	Focus Session: Critical Transitions in Society, Economy, and Nature
10:00	ZEU 147	DY 29	Wetting, Droplets and Microfluidics
15:00	HSZ 204	DY 30	Nonequilibrium Quantum Many-Body Systems II
15:00	MOL 213	DY 31	Microswimmers and Fluid Physics of Life
15:00	ZEU 160	DY 32	Focus Session: Physics of Fluctuating Paths
15:00	ZEU 250	DY 33	Biologically Inspired Statistical Physics
16:45	ZEU 250	DY 34	Statistical Physics: Far From Equilibrium II

HL

Invited Talks

09:30	POT 361	HL 23.1	Vertical-cavity surface-emitting lasers – this is the way •Å. Haglund
10:00	POT 361	HL 23.2	Towards GaN-based diode lasers with narrow linewidth and high reliability •Sven Einfeldt
10:30	POT 361	HL 23.3	Use of wafer patterning for new functionalities of InGaN light emitters •Anna Kafar
09:30	POT 251	HL 25.1	Interfaces in perovskite optoelectronics: role of energy level alignment and interface chemistry •Selina Olthof
15:00	POT 81	HL 27.1	experimentamus! Forschendes Lernen von Physik und Chemie in der Grundschule •Sebastian Schlücker
16:00	POT 81	HL 27.4	Under the Microscope – spotlighting materials and nano science •Svenja Lohmann
17:00	POT 81	HL 27.5	Phyphox – A pocketful of physics •Christoph Stampfer
18:00	POT 81	HL 27.8	Physics for school and the public at the LMU •Dr. Cecilia Scorza-Lesch
15:00	POT 361	HL 28.1	Fabrication of AlGaIn-based UV-B laser diodes on lattice-relaxed high-quality AlGaIn •Motoaki Iwaya
15:30	POT 361	HL 28.2	Breakthrough technologies to realize room-temperature continuous-wave deep-ultraviolet laser diodes •Maki Kushimoto

Sessions

09:30	POT 81	HL 22	2D Materials IV
09:30	POT 361	HL 23	Focus Session: Breakthroughs in wide-bandgap semiconductor laser diodes I
09:30	POT 151	HL 24	Quantum dots: Optics
09:30	POT 251	HL 25	Perovskite and photovoltaics II
10:30	TRE Ma	HL 26	Focus Session: Frontiers of Electronic-Structure Theory IV
15:00	POT 81	HL 27	Focus Session: Wissenschaftskommunikation / Outreach
15:00	POT 361	HL 28	Focus Session: Breakthroughs in wide-bandgap semiconductor laser diodes II
15:00	POT 151	HL 29	Materials and devices for quantum technology I
15:00	POT 251	HL 30	Quantum transport and quantum Hall effects II

Wednesday, March 29, 2023

				HL
15:00	TRE Ma	HL 31	Focus Session: Frontiers of Electronic-Structure Theory V	
15:00	GÖR 226	HL 32	Organic Electronics and Photovoltaics II	
17:00	P1	HL 33	Poster II	

KFM				
Invited Talks				
09:00	POT 51	KFM 7.1	Novel device integration – combining bottom-up and topdown approaches •Artur Erbe	
11:05	POT 51	KFM 7.6	4D meso-scale electronics for next generation medical tools and electronic skins •Daniil Karnauschenko	
Sessions				
09:00	POT 51	KFM 7	Focus: High-resolution Lithography and 3D Patterning	
14:00	POT 51	KFM 8	Diamond and related dielectric materials	
09:00	POT 106	KFM 9	Microscopy and Tomography with X-ray Photons, Electrons, Ions and Positron	

MA				
Invited Talks				
09:30	HSZ 04	MA 25.1	MAGNOTHERM – One way to start a deep tech spin-off from research •Max Fries	
10:00	HSZ 04	MA 25.2	Spin-Ion Technologies: taking the research from a lab to a start-up company •Dafiné Ravelosona	
10:30	HSZ 04	MA 25.3	MagREEsources: the green Rare Earth Magnet company •Sophie Rivoirard	
11:00	HSZ 04	MA 25.4	THATec Innovation – we automate your lab •Thomas Sebastian	
11:30	HSZ 04	MA 25.5	Kiutra: Magnetic refrigeration for science and technology •Alexander Regnat	
09:30	HSZ 401	MA 26.1	The self-induced spin glass: the perplexing magnetism of elemental neodymium •Alexander Khajetoorians	
15:00	HSZ 02	MA 30.1	Femto- phono- magnetism •Sangeeta Sharma	
15:30	HSZ 02	MA 30.2	Spin-switchable molecules in interaction with their environment. •Cyrille Barreteau	
16:15	HSZ 02	MA 30.3	Yep, real photodoping. •Julia Stähler	
16:45	HSZ 02	MA 30.4	Probing ultrafast magnetization thanks to ultrashort soft X-ray pulses •Emmanuelle Jal	
Sessions				
09:30	HSZ 02	MA 24	Molecular Magnetism II	
09:30	HSZ 04	MA 25	Focus Session: Startups in Magnetism	
09:30	HSZ 401	MA 26	Non-Skyrmionic Magnetic Textures II	
09:30	HSZ 403	MA 27	Electron Theory of Magnetism and Correlations	
09:30	POT 6	MA 28	Bulk Materials: Soft and Hard Permanent Magnets	
11:30	HSZ 02	MA 29	Neuromorphic Magnetism / Magnetic Logic	
15:00	HSZ 02	MA 30	PhD Focus Session: Non-equilibrium dynamics in theory and experiment	
15:00	HSZ 04	MA 31	Functional Antiferromagnetism II	
15:00	HSZ 401	MA 32	Magnetic Imaging Techniques I	
15:00	HSZ 403	MA 33	Frustrated Magnets I	

MM				
Invited Talks, Topical Talks				
09:30	SCH A 251	MM 24.1	Characterization of hydrogen effect on mechanical properties of metals at different length scales •Afrooz Barnoush	

Wednesday, March 29, 2023

MM

15:00	SCH A 251	MM 30.1	Direct observations of grain boundary phase transformations in metallic alloys •Christian Liebscher
15:45	SCH A 216	MM 32.1	Defect phase diagrams: Concepts, computational approaches and applications •Jörg Neugebauer
18:00	SCH A 216	MM 32.8	Towards a Rigorous Theory of Grain Boundary Segregation in Polycrystals •Christopher Schuh
Sessions			
09:30	SCH A 251	MM 24	Invited Talk: Barnoush
10:15	SCH A 251	MM 25	Development of Computational Methods: Crystal Structure and Properties
10:15	SCH A 216	MM 26	Interface Controlled Properties and Nanomaterials: Grain Boundaries and Stability, Spectroscopy and Interatomic Potentials
10:15	SCH A 215	MM 27	Hydrogen in Materials
10:15	SCH A 118	MM 28	Liquid and Amorphous Metals
11:45	SCH A 251	MM 29	Data Driven Materials Science: Big Data and Work Flows – Electronic Structure
15:00	SCH A 251	MM 30	Invited Talk: Liebscher
15:45	SCH A 251	MM 31	Data Driven Materials Science: Big Data and Work Flows – Machine Learning
15:45	SCH A 216	MM 32	Topical Session: Defect Phases I
15:45	SCH A 215	MM 33	Topical Session: Fundamentals of Fracture – Amorphous Metals
18:45	SCH A 251	MM 34	Members' Assembly

O**Invited Talk, Topical Talks**

09:30	TRE Phy	O 44.1	Spins on Surfaces: A Gateway to the Quantum World •Christian R. Ast
10:45	CHE 89	O 45.2	Single-molecule reactions performed and characterized using atomic force microscopy •Leo Gross
10:30	GER 38	O 48.1	Surface functionalization of semiconductors: Introducing spectroscopic labels, monolayer control for ultra-shallow doping, and providing surface passivation for atomically-precise processes •Andrew Teplyakov
11:15	GER 38	O 48.3	Growth of organic monolayers on Si(111) •Martin Franz
11:15	TRE Phy	O 52.4	Modeling and Design of Single-Atom Alloy Catalysts •Mie Andersen
10:45	TRE Ma	O 53.2	TREX: an integrated HPC software platform for quantum Monte Carlo calculations •Claudia Filippi
15:00	CHE 89	O 54.1	Peering into interfacial water by qPlus-based atomic force microscopy •Ying Jiang
16:15	CHE 89	O 54.5	AFM with the qPlus sensor: An ideal tool for oxide surface science •Ulrike Diebold
16:15	CHE 91	O 55.6	Towards Understanding and Controlling On-Surface Reactions and Self-Assembly Mechanisms •Daniel Ebeling
15:00	GER 38	O 57.1	Incorporation of arsenic into silicon (001) and germanium (001) for atomic-scale device fabrication. •Steven R. Schofield
15:45	GER 38	O 57.3	Semiconductor surface chemistry towards hybrid interfaces with ab initio approaches •Ralf Tonner-Zech
15:30	WIL A317	O 58.3	Phase-locked photon-electron interaction without a laser •Nahid Talebi
15:00	REC C 213	O 59.1	Interplay of Inversion Symmetry Breaking and Spin-Orbit Coupling •Maximilian Ünzelmann
16:15	TRE Ma	O 61.5	Challenges in modelling correlated electronic matter •Roser Valenti

Wednesday, March 29, 2023

O**Sessions**

09:30	TRE Phy	O 44	Overview Talk Christian Ast
10:30	CHE 89	O 45	Focus Session: Scanning Probe Microscopy with Quartz Sensors I
10:30	CHE 91	O 46	Electron-Driven Processes at Surfaces and Interfaces
10:30	GER 37	O 47	2D Materials II: Growth, Structure and Substrate Interaction I
10:30	GER 38	O 48	Focus Session: Semiconductor Surface Chemistry – from Reaction Mechanisms to Well-Ordered Interfaces I
10:30	WIL A317	O 49	Plasmonics and Nanooptics I: Fabrication and Application
10:30	REC C 213	O 50	Spins on Surfaces at the Atomic Scale IV
11:30	REC C 213	O 51	Surface Magnetism
10:30	TRE Phy	O 52	Heterogeneous Catalysis and Surface Dynamics I
10:30	TRE Ma	O 53	Focus Session: Frontiers of Electronic-Structure Theory IV
15:00	CHE 89	O 54	Focus Session: Scanning Probe Microscopy with Quartz Sensors II
15:00	CHE 91	O 55	Organic Molecules on Inorganic Substrates IV: Adsorption and Growth II
15:00	GER 37	O 56	2D Materials III: Growth, Structure and Substrate Interaction II
15:00	GER 38	O 57	Focus Session: Semiconductor Surface Chemistry – from Reaction Mechanisms to Well-Ordered Interfaces II
15:00	WIL A317	O 58	Plasmonics and Nanooptics II: Light-Matter Interaction and Spectroscopy I
15:00	REC C 213	O 59	Electronic Structure of Surfaces I
15:00	TRE Phy	O 60	Solid-Liquid Interfaces I: Structure and Spectroscopy
15:00	TRE Ma	O 61	Focus Session: Frontiers of Electronic-Structure Theory V
15:00	POT 81	O 62	Focus Session: Wissenschaftskommunikation / Outreach
18:00	P2/EG	O 63	Poster: Data Management
18:00	P2/EG	O 64	Poster: Graphene
18:00	P2/EG	O 65	Poster: Topology and Symmetry-Protected Materials
18:00	P2/EG	O 66	Poster: Scanning Probe Microscopy with Quartz Sensors
18:00	P2/EG	O 67	Poster: Electronic Structure of Surfaces
18:00	P2/EG	O 68	Poster: Oxide and Insulator Surfaces
18:00	P2/EG	O 69	Poster: Solid-Liquid Interfaces
18:00	P2/EG	O 70	Poster: Plasmonics and Nanooptics II

SOE**Topical Talks**

09:30	ZEU 260	SOE 9.1	Many universality classes in an interface model restricted to non-negative heights •Peter Grassberger
10:00	ZEU 260	SOE 9.2	Nonequilibrium phase transitions and critical behavior in networks •Eckehard Schöll
10:45	ZEU 260	SOE 9.3	Critical transition to monsoon: statistical physics principles of monsoon forecasting •Elena Surovyatkina

Sessions

09:30	ZEU 260	SOE 9	Focus Session: Critical Transitions in Society, Economy, and Nature
15:00	ZEU 260	SOE 10	Traffic Dynamics, Urban and Regional Systems I
16:45	ZEU 260	SOE 11	Traffic Dynamics, Urban and Regional Systems II
18:30	ZEU 260	SOE 12	Members' Assembly

TT**Invited Talks**

09:30	HSZ 03	TT 27.1	Superconducting diode effect in Rashba superlattice •Teruo Ono
10:00	HSZ 03	TT 27.2	Quasiparticle-based and Cooper-pair based superconducting diodes •Maria Spies
10:30	HSZ 03	TT 27.3	Non-reciprocal superconductivity and the field free Josephson diode •Mazhar Ali
10:45	HSZ 103	TT 28.6	Studying the Fulde-Ferrell-Larkin-Ovchinnikov order parameter in quasi-2D organic superconductors •Tommy Kotte

Wednesday, March 29, 2023

TT

15:00	HSZ 03	TT 35.1	Strongly correlated excitons in atomic double layers •Phuong Nguyen
15:30	HSZ 03	TT 35.2	The Quantum Twisting Microscope •Shahal Ilani
16:00	HSZ 03	TT 35.3	Light-driven phenomena in two-dimensional and correlated quantum materials •Angel Rubio
16:45	HSZ 03	TT 35.4	Cascade of transitions in twisted and non-twisted graphene layers within the van Hove scenario •Laura Classen
17:15	HSZ 03	TT 35.5	Topology and strong correlation: From twisted bilayer graphene to the boundary zeros of Mott insulators •Giorgio Sangiovanni
15:00	HSZ 304	TT 39.1	Sensing and control of MHz photons with microwave photon-pressure •Daniel Bothner

Sessions

09:30	HSZ 03	TT 27	Focus Session: Unconventional Transport Phenomena in Low-Dimensional Superconducting Heterostructures
09:30	HSZ 103	TT 28	Unconventional Superconductors
09:30	HSZ 201	TT 29	Frustrated Magnets: General
09:30	HSZ 204	TT 30	Complex Oxides
09:30	HSZ 304	TT 31	Topology: Majorana Physics
09:30	GÖR 226	TT 32	Molecular Electronics and Excited State Properties
09:30	MOL 213	TT 33	Many-Body Quantum Dynamics
11:30	HSZ 103	TT 34	Fe-based Superconductors
15:00	HSZ 03	TT 35	Focus Session: Correlations in Moiré Quantum Matter I
15:00	HSZ 103	TT 36	Topological Insulators
15:00	HSZ 201	TT 37	Ruthenates
15:00	HSZ 204	TT 38	Nonequilibrium Quantum Many-Body Systems II
15:00	HSZ 304	TT 39	Superconducting Electronics
15:00	POT 81	TT 40	Focus Session: Wissenschaftskommunikation / Outreach
15:00	POT 251	TT 41	Quantum Transport and Quantum Hall Effects II
15:00	P2/OG2	TT 42	Poster: Correlated Electrons I
15:00	P2/OG3	TT 43	Poster: Correlated Electrons II

AIW

Invited Talks

13:45	KRO 1.11	AIW 1.1	Als Physiker*in Krankenhäuser digitalisieren? Klar doch! •Charles Ludwig Majer
14:15	KRO 1.11	AIW 1.2	From the Lab to Customer Engineering at Google – the Unconventional Career Path of an Experimental Physicist •Diana Nanova
14:45	KRO 1.11	AIW 1.3	Von der Promotion zur eigenen Firma •Oliver de Haas
15:30	KRO 1.11	AIW 2.1	How start-ups and alumni networks enrich young scientist's career options •Joachim Rädler
16:00	KRO 1.11	AIW 2.2	Karrieremöglichkeiten für Physikerinnen und Physiker auf dem Gebiet des Gewerblichen Rechtsschutzes •Udo Weigelt

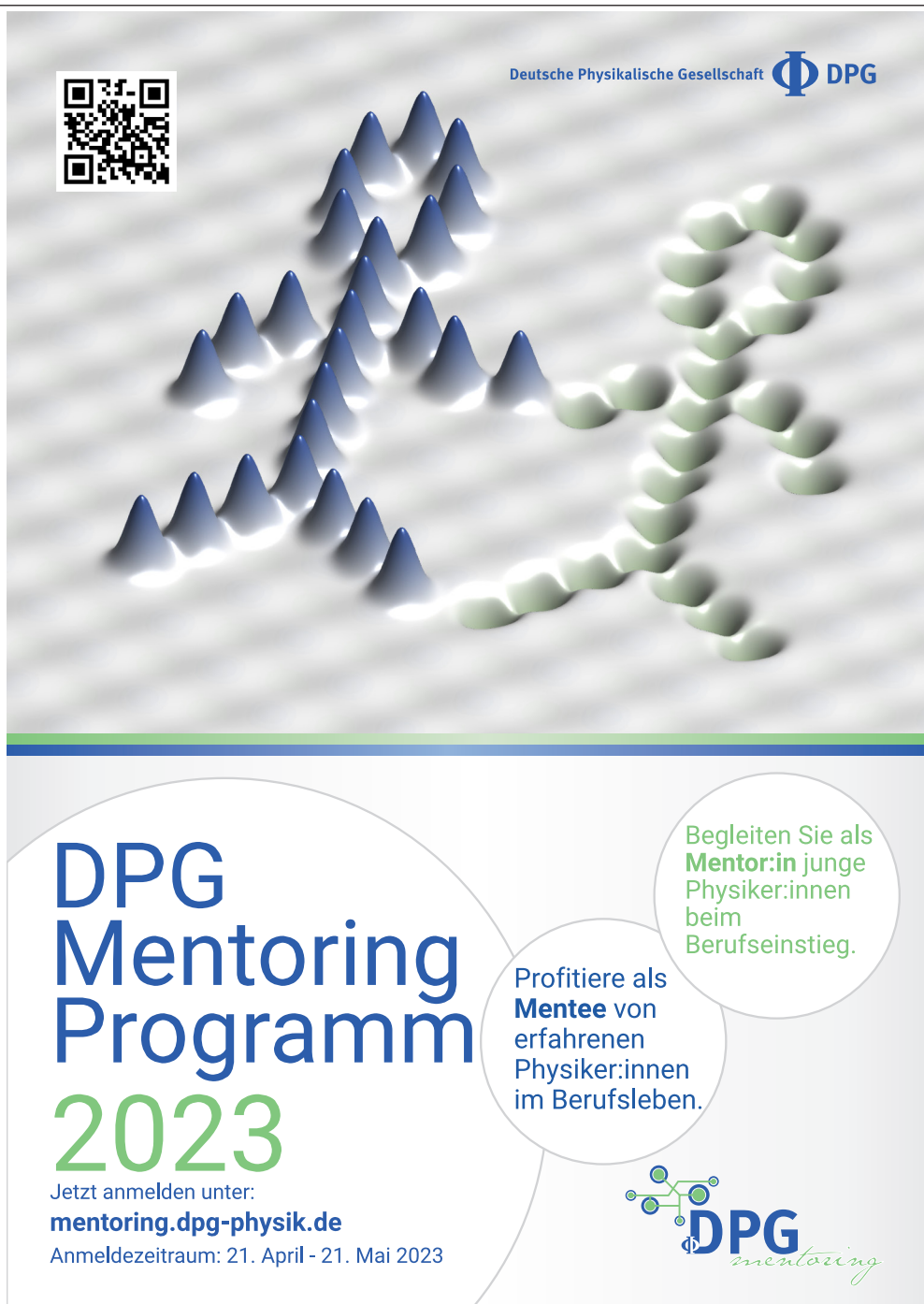
Sessions

13:45	KRO 1.11	AIW 1	AIW Industrietag I
15:30	KRO 1.11	AIW 2	AIW Industrietag II
16:45	KRO 1.11	AIW 3	Podiumsdiskussion
17:30	KRO 1.11	AIW 4	Gemütlicher Ausklang mit Networking bei Bier & Brezn

09:30	Foyer HSZ / Tent A	Exhibition of Scientific Instruments and Literature	
-------	--------------------	--	--

Wednesday, March 29, 2023

11:30	HSZ 405	Job Market Bundesamt für Sicherheit in der Informationstechnik <i>"Aus der Physik in die IT-Sicherheit – Karriere beim BSI"</i>
12:45	HSZ 405	Trumpf Lasersystems for Semiconductor Manufacturing GmbH <i>"TRUMPF Lasersystems for EUV Lithography – Enabler für das digitale Zeitalter gesucht"</i>
14:00	HSZ 405	Basycon Unternehmensberatung GmbH <i>"Aus der Wissenschaft in die Beratung"</i>
15:15	HSZ 405	ZEISS <i>"Am Herzschlag der Digitalisierung: Forschung & Entwicklung in der Halbleiterfertigungstechnik"</i>



The graphic features a QR code in the top left corner. The background is a grayscale image of a surface with blue and green peaks. In the top right, it says "Deutsche Physikalische Gesellschaft Φ DPG". The main text "DPG Mentoring Programm 2023" is in large blue and green letters. Below it, it says "Jetzt anmelden unter: mentoring.dpg-physik.de" and "Anmeldezeitraum: 21. April - 21. Mai 2023". Two speech bubbles contain the text: "Begleiten Sie als **Mentor:in** junge Physiker:innen beim Berufseinstieg." and "Profitiere als **Mentee** von erfahrenen Physiker:innen im Berufsleben." The DPG logo with "mentoring" is in the bottom right.

Deutsche Physikalische Gesellschaft Φ DPG

DPG
Mentoring
Programm
2023

Jetzt anmelden unter:
mentoring.dpg-physik.de
Anmeldezeitraum: 21. April - 21. Mai 2023

Begleiten Sie als **Mentor:in** junge Physiker:innen beim Berufseinstieg.

Profitiere als **Mentee** von erfahrenen Physiker:innen im Berufsleben.

Φ **DPG**
mentoring

Thursday, March 30, 2023

			Plenary Talks
08:30	HSZ 01	PLV VIII	Nanomechanics: Tunes of the nanoguitar •Eva Weig
14:00	HSZ 01	PLV IX	Metal Halide Perovskites for Photovoltaic Applications •Laura Herz
14:00	HSZ 02	PLV X	Single-electron-spin-resonance detection by microwave photon counting •Patrice Bertet
			Prize Talk
13:15	HSZ 01	PRV III	High-lying excitons and excitonic quantum interference in 2D semiconductors •Kai-Qiang Lin (Laureate of the Walter-Schottky-Prize 2023)
			Lunch Talk, Discussion
13:15	HSZ 02	PSV IX	Working as a Physicist in the Microelectronic Industry •Matthias U. Lehr
13:15	HSZ 03	PSV X	NFDI and FAIR research data: benefit or burden? Laurenz Rettig, Heiko B. Weber, and •Martin Aeschlimann

SYQD

			Symposium
09:30	HSZ 01	SYQD 1	Real-Time Measurements of Quantum Dynamics
			Invited Talks
09:30	HSZ 01	SYQD 1.1	Real-time measurement and control of spin dynamics in quantum dots •Seigo Tarucha
10:00	HSZ 01	SYQD 1.2	Quantum Dot arrays for Quantum Information Transfer •Gloria Platero
10:30	HSZ 01	SYQD 1.3	Optical Detection of Real-Time Quantum Dynamics in Quantum Dots •Martin Geller
11:30	HSZ 01	SYQD 1.4	Cooper Pair Splitting in Real-Time •Christian Flindt
12:00	HSZ 01	SYQD 1.5	Trajectory-based detection in stochastic and quantum thermodynamics •Jukka Pekola

SYTS

			Symposium
15:00	HSZ 01	SYTS 1	Topological Superconductor-Magnet Heterostructures
			Invited Talks
15:00	HSZ 01	SYTS 1.1	Blending of superconductivity and magnetism via topological solitons •Christos Panagopoulos
15:30	HSZ 01	SYTS 1.2	Topological landscaping in magnet-superconductor heterostructures •Sebastián A. Díaz
16:00	HSZ 01	SYTS 1.3	Experimental study of minigaps and end states in bottom-up designed multi-orbital Shiba chains •Jens Wiebe
16:45	HSZ 01	SYTS 1.4	Quantum spins and hybridization in artificially-constructed chains of magnetic adatoms on superconducting 2H-NbSe ₂ •Katharina J. Franke
17:15	HSZ 01	SYTS 1.5	Braiding of Majorana zero modes •Stephan Rachel

BP

			Invited Talks
11:15	BAR Schö	BP 21.7	Visualizing the inner life of microbes •Ulrike Endesfelder

Thursday, March 30, 2023

BP

10:30	TOE 317	BP 22.5	Statistical Physics of Spatially Organized Catalytic Particles •Ulrich Gerland
09:30	BAR 0106	BP 23.1	Conformational dynamics of SARS-CoV-2 spike protein modulates the binding affinity to ACE2 •Felix Rico
15:00	TOE 317	BP 26.1	Decoding Molecular Plasticity in the Dark Proteome of the Nuclear Transport Machinery •Edward Lemke

Sessions

09:30	BAR Schö	BP 21	Bioimaging
09:30	TOE 317	BP 22	Statistical Physics of Biological Systems I
09:30	BAR 0106	BP 23	Single Molecule Biophysics
09:30	ZEU 160	BP 24	Active Matter IV
15:00	BAR Schö	BP 25	Cell Mechanics II
15:00	TOE 317	BP 26	Focus Session mRNA Physics
15:00	BAR 0106	BP 27	Computational Biophysics II
18:00	P2/EG	BP 28	Poster Session II

CPP

15:00	ZEU 255	CPP 53.1	Invited Talk Aqueous nanoclusters govern ionic transport in dense polymer membranes •Joachim Dzubiella
-------	---------	----------	---

Sessions

09:00	POT 51	CPP 42	Battery Materials
09:30	GÖR 226	CPP 43	Organic Electronics and Photovoltaics III
09:30	MER 02	CPP 44	Wetting, Fluidics and Liquids at Interfaces and Surfaces II
09:30	ZEU 255	CPP 45	Emerging Topics in Chemical and Polymer Physics, New Instruments and Methods
09:30	ZEU 160	CPP 46	Active Matter IV
09:30	POT 81	CPP 47	2D Materials VI
10:15	SCH A 251	CPP 48	Data Driven Materials Science: Big Data and Work Flows – Microstructure-Property-Relationships
10:30	GER 37	CPP 49	2D Materials VII: Heterostructures
12:15	ZEU 255	CPP 50	Glasses and Glas Transition II
15:00	GÖR 226	CPP 51	Hybrid and Perovskite Photovoltaics III
15:00	MER 02	CPP 52	Wetting, Fluidics and Liquids at Interfaces and Surfaces III
15:00	ZEU 255	CPP 53	Charged Soft Matter, Polyelectrolytes and Ionic Liquid
16:30	MER 02	CPP 54	2D Materials VIII
18:00	MER 02	CPP 55	Members' Assembly

DS**Invited Talks**

09:30	SCH A 316	DS 13.1	Towards Catalytic Applications of Infrared Laser Polarimetry •Andreas Furchner
11:15	SCH A 316	DS 15.1	In-Situ Optical Investigation of Electrochemically Induced Conformational Changes at Solid Liquid Interfaces: A Source of new Electronic States •Christoph Cobet
16:15	SCH A 316	DS 17.1	In-situ optical spectroscopy on electrochemical interfaces: From OER electrocatalysts to "smart" electro-switchable interfaces •Martin Rabe
16:45	SCH A 316	DS 17.2	The physics of low symmetry semiconductors: Gallium oxide for the future of green energy as example •Mathias Schubert
17:15	SCH A 316	DS 17.3	Spectroscopic ellipsometry studies of optical constants in highly excited semiconductors •Stefan Zollner

Thursday, March 30, 2023

DS**Sessions**

09:30	SCH A 316	DS 13	Optical Analysis of Thin Films I
09:30	SCH A 315	DS 14	Thin Oxides and Oxide Layers
11:15	SCH A 316	DS 15	Optical Analysis of Thin Films II
11:30	SCH A 315	DS 16	Thermoelectric and Phase Change Materials; Layer Deposition
16:15	SCH A 316	DS 17	Optical Analysis of Thin Films III
18:00	SCH A 315	DS 18	Members' Assembly

DY**Invited Talks**

11:00	MOL 213	DY 37.6	Power law error growth rates – a dynamical mechanism for a strictly finite prediction horizon in weather forecasts •Holger Kantz
09:30	ZEU 160	DY 38.1	Acoustically propelled nano- and microparticles: From fundamentals to applications •Raphael Wittkowski

Sessions

09:30	TOE 317	DY 35	Statistical Physics of Biological Systems I
09:30	MER 02	DY 36	Wetting, Fluidics and Liquids at Interfaces and Surfaces I
09:30	MOL 213	DY 37	Data Analytics of Complex Dynamical Systems
09:30	ZEU 160	DY 38	Active Matter IV
09:30	ZEU 260	DY 39	Networks: From Topology to Dynamics II
10:00	ZEU 250	DY 40	Stochastic Thermodynamics
10:00	ZEU 260	DY 41	Networks: From Topology to Dynamics III
13:00	P1	DY 42	Poster: Active Matter, Soft Matter, Fluids
13:00	P1	DY 43	Poster: Quantum Dynamics and Many-Body Systems
13:00	P1	DY 44	Poster: Statistical Physics
13:00	P1	DY 45	Poster: Nonlinear Dynamics, Pattern Formation and Networks
13:00	P1	DY 46	Poster: Machine Learning and Data Analytics
15:00	MER 02	DY 47	Wetting, Fluidics and Liquids at Interfaces and Surfaces II
15:00	MOL 213	DY 48	Dynamics and Chaos in Many-Body Systems I
15:00	ZEU 160	DY 49	Critical Phenomena and Phase Transitions
15:00	ZEU 260	DY 50	Evolutionary Game Theory
18:00	ZEU 160	DY 51	Members' Assembly

HL**Invited Talks**

09:30	POT 361	HL 35.1	Quantum Dynamics of Polarons in Doped Semiconductor Monolayers •Xiaoqin Elaine Li
10:00	POT 361	HL 35.2	Impact of phonons on time-resolved optical signals from excitons •Doris E. Reiter
10:30	POT 361	HL 35.3	Hot-Exciton Quantum Dynamics in Zero-Dimensional Structures •Alfred Leitenstorfer
12:00	POT 361	HL 35.6	Ultrafast dynamics and wave mixing at excitonic resonances in atomically thin semiconductors •Andreas Knorr
12:30	POT 361	HL 35.7	Spontaneous parametric down-conversion in semiconductor metasurfaces •Maria Chekhova
15:00	POT 251	HL 43.1	Superradiance as a witness to multipartite entanglement •Frederik Lohof

Sessions

09:30	POT 81	HL 34	2D Materials V
09:30	POT 361	HL 35	Focus Session: Transient multi-wave mixing on excitonic resonances
09:30	POT 151	HL 36	Transport properties
09:30	POT 251	HL 37	Materials and devices for quantum technology II

Thursday, March 30, 2023

HL

09:30	POT 6	HL 38	Functional semiconductors for renewable energy solutions I
09:30	GÖR 226	HL 39	Organic Electronics and Photovoltaics III
10:30	TRE Ma	HL 40	Focus Session: Frontiers of Electronic-Structure Theory VI
15:00	POT 81	HL 41	Oxide Semiconductors I: Ga ₂ O ₃
15:00	POT 151	HL 42	Quantum dots: Growth
15:00	POT 251	HL 43	Semiconductor lasers II
15:00	POT 112	HL 44	Nitrides: Devices
15:00	POT 6	HL 45	Functional semiconductors for renewable energy solutions II
18:00	POT 6	HL 46	Members' Assembly

KFM

Sessions

09:00	POT 51	KFM 10	Battery Materials
14:00	POT 51	KFM 11	Crystal Structure Defects / Real Structure / Microstructure
18:00	POT 51	KFM 12	Members' Assembly
10:00	POT 106	KFM 13	Polar Oxide Crystals and Solid Solutions I
14:00	POT 106	KFM 14	Polar Oxide Crystals and Solid Solutions II

MA

Invited Talks

09:30	HSZ 02	MA 34.1	Polarized phonons carry angular momentum in ultrafast demagnetization •Peter Baum
10:00	HSZ 02	MA 34.2	Spin-phonon coupling in ordered magnets: origin and consequences •Akashdeep Kamra
10:30	HSZ 02	MA 34.3	Magnon-mechanics in high overtone acoustic resonators •Hans Huebl
11:15	HSZ 02	MA 34.4	Cavity Magnomechanics: Harnessing the Magnomechanical Coupling for Applications in the Microwave and Optical Regimes •Silvia Viola Kusminskiy
11:45	HSZ 02	MA 34.5	Coherent spin-wave transport in an antiferromagnet •Andrea Caviglia
15:00	HSZ 02	MA 41.1	Altermagnetism and spin symmetries •Libor Šmejkal
15:30	HSZ 02	MA 41.2	Spontaneous Hall effect in Mn ₅ Si ₃ altermagnet •H. Reichlova
16:30	HSZ 02	MA 41.5	Generation of tilted spin-current by the collinear antiferromagnet RuO ₂ •Arnab Bose
17:00	HSZ 02	MA 41.6	First-principles studies on the anomalous transport properties of ferromagnets, antiferromagnets, and altermagnets •Wanxiang Feng
17:30	HSZ 02	MA 41.7	Insight into chemical and magnetotransport properties of epitaxial α-Fe ₂ O ₃ /Pt bilayers •Anna Koziol-Rachwał

Sessions

09:30	HSZ 02	MA 34	Focus Session: Spin-Phonon Coupling
09:30	HSZ 04	MA 35	Skyrmions III
09:30	HSZ 401	MA 36	Magnetic Particles / Clusters
09:30	HSZ 403	MA 37	Magnetic Heuslers
11:30	HSZ 401	MA 38	Micro- and Nanostructured Magnetic Materials
11:30	HSZ 403	MA 39	Weyl Semimetals
14:00	P2/EG	MA 40	Poster Magnetism II
15:00	HSZ 02	MA 41	Focus Session: Altermagnetism: Transport, Optics, Excitations
15:00	HSZ 04	MA 42	Caloric Effects in Ferromagnetic Materials
15:00	HSZ 401	MA 43	Magnetic Imaging Techniques II
15:00	HSZ 403	MA 44	Frustrated Magnets II
18:00	HSZ 04	MA 45	Members' Assembly

			Topical Talks
09:30	SCH A 251	MM 35.1	Configuration entropy and sample size effect on glass transition temperature •Yannick Champion
10:15	SCH A 216	MM 37.1	Structural and chemical atomic complexity of lattice defects – From defect phase diagrams to properties of intermetallics •Sandra Korte-Kerzel
11:45	SCH A 216	MM 37.5	Density-based Grain Boundary Phase Diagrams •Reza Darvishi Kamachali
10:15	SCH A 215	MM 38.1	The Fundamental physics of the onset of frictional motion: How does friction start? •Jay Fineberg
15:45	SCH A 216	MM 41.1	Entropy in grain boundary segregation •Pavel Lejcek
			Sessions
09:30	SCH A 251	MM 35	Invited Talk: Champion
10:15	SCH A 251	MM 36	Data Driven Materials Science: Big Data and Work Flows – Microstructure-Property-Relationships
10:15	SCH A 216	MM 37	Topical Session: Defect Phases II
10:15	SCH A 215	MM 38	Topical Session: Fundamentals of Fracture – Fracture Experiments
11:45	SCH A 215	MM 39	Phase Transformations: Simulation and Machine Learning
15:45	SCH A 251	MM 40	Mechanical Properties and Alloy Design
15:45	SCH A 216	MM 41	Topical Session: Defect Phases III
15:45	SCH A 215	MM 42	Interface Controlled Properties and Nanomaterials: Nanoporous Materials and Nanolaminates

			Invited Talk, Topical Talks
09:30	TRE Phy	O 71.1	Surface dynamics under reaction conditions •Edvin Lundgren
10:30	GER 38	O 75.1	Ultrafast nano-imaging: probing quantum dynamics in space and time •Markus Raschke
11:45	GER 38	O 75.5	Lightwave-driven scanning tunneling microscopy and spectroscopy at the atomic scale •Vedran Jelic
11:00	TRE Ma	O 79.3	New Opportunities for First Principles Simulations of Thousands of Atoms Using Linear Scaling Density Functional Theory •Laura Ratcliff
15:30	CHE 89	O 80.3	Topological Plasmonics and Plasmonic Twistronics: Skyrmions, Merons, Quasicrystals, and Skyrmion Bags •Harald Giessen
15:00	GER 38	O 83.1	Imaging ultrafast electron dynamics in isolated nanoparticles •Daniela Rupp
16:15	GER 38	O 83.5	Ultrafast coherent manipulation of free electrons via quantum interaction with shaped optical fields •Giovanni Maria Vanacore
15:00	WIL A317	O 84.1	Introducing a FAIR research data management infrastructure for experimental condensed matter physics data •Christoph Koch
17:00	WIL A317	O 84.7	Open Research Data for Photons and Neutrons: Applications in surface scattering and machine learning •Linus Pithan
15:30	TRE Phy	O 86.3	Novel concepts to simulate electrified liquid/solid interfaces from first principles •Stefan Wippermann
15:00	TRE Ma	O 87.1	Quartz-sensor detection for single-electron tunneling spectroscopy •Jascha Repp

Thursday, March 30, 2023

O

16:15	TRE Ma	O 87.5	Application of atomic force microscopy with quartz sensors to quantum states in graphene and related twisted heterostructures •Joseph Strosio
Sessions			
09:30	TRE Phy	O 71	Overview Talk Edvin Lundgren
10:30	CHE 89	O 72	Gerhard Ertl Young Investigator Award Competition
10:30	CHE 91	O 73	Metal Substrates: Adsorption and Reaction of Small Molecules II
10:30	GER 37	O 74	2D Materials IV: Heterostructures
10:30	GER 38	O 75	Focus Session: Ultrafast Dynamics in Nanostructures I
10:30	WIL A317	O 76	Plasmonics and Nanooptics III: Light-Matter Interaction and Spectroscopy II
10:30	REC C 213	O 77	Scanning Probe Techniques: Method Development II
10:30	TRE Phy	O 78	Heterogeneous Catalysis and Surface Dynamics II
10:30	TRE Ma	O 79	Focus Session: Frontiers of Electronic-Structure Theory VI
15:00	CHE 89	O 80	Plasmonics and Nanooptics IV: Light-Matter Interaction and Spectroscopy III
15:00	CHE 91	O 81	Oxide and Insulator Surfaces I: Adsorption and Reaction of Small Molecules
15:00	GER 37	O 82	Graphene I: Adsorption, Intercalation and Doping
15:00	GER 38	O 83	Focus Session: Ultrafast Dynamics in Nanostructures II
15:00	WIL A317	O 84	Focus Session: Making Experimental Data F.A.I.R. – New Concepts for Research Data Management I
15:00	REC C 213	O 85	Electronic Structure of Surfaces II
15:00	TRE Phy	O 86	Solid-Liquid Interfaces II: Reactions and Electrochemistry I
15:00	TRE Ma	O 87	Focus Session: Scanning Probe Microscopy with Quartz Sensors III
19:00	HSZ 01	O 88	Members' Assembly
19:30	HSZ 01	O 89	Post-Deadline Session

SOE

Invited Talk			
09:30	ZEU 260	SOE 14.1	Networks in space and time – Exploring the physics in graph learning •Ingo Scholtes
Sessions			
09:30	MOL 213	SOE 13	Data Analytics of Complex Dynamical Systems
09:30	ZEU 260	SOE 14	Networks: From Topology to Dynamics II
10:00	ZEU 260	SOE 15	Networks: From Topology to Dynamics III
11:00	ZEU 260	SOE 16	Collective Dynamics in Animal and Human Societies
15:00	ZEU 260	SOE 17	Evolutionary Game Theory
15:30	ZEU 260	SOE 18	Social Systems, Opinion and Group Dynamics I
16:45	ZEU 260	SOE 19	Social Systems, Opinion and Group Dynamics II

TT

Invited Talks			
09:30	HSZ 03	TT 44.1	Atomic-scale insights to lattice and electronic structure in superconducting nickelates •Berit Goodge
10:00	HSZ 03	TT 44.2	Nickelate and cuprate superconductors: Similar yet different •Vamshi Mohan Katukuri
10:30	HSZ 03	TT 44.3	Superconducting instabilities in strongly-correlated infinite-layer nickelates •Andreas Kreisel
11:15	HSZ 03	TT 44.4	Infinite-layer nickelate thin films: From synthesis to spectroscopy •Daniele Preziosi
11:45	HSZ 03	TT 44.5	Superconducting layered square-planar nickelates: Synthesis, properties, and progress •Grace Pan
Sessions			
09:30	HSZ 03	TT 44	Focus Session: Superconducting Nickelates I
09:30	HSZ 103	TT 45	Correlated Electrons: 1D Theory

Thursday, March 30, 2023

TT

09:30	HSZ 201	TT 46	Frustrated Magnets: Spin Liquids
09:30	HSZ 204	TT 47	Quantum-Critical Phenomena
09:30	HSZ 304	TT 48	Topological Superconductors
11:30	HSZ 304	TT 49	Quantum Coherence and Quantum Information Systems I
15:00	HSZ 03	TT 50	Focus Session: Superconducting Nickelates II
15:00	HSZ 103	TT 51	Correlated Electrons: Charge Order
15:00	HSZ 201	TT 52	Frustrated Magnets: Strong Spin-Orbit Coupling
15:00	HSZ 204	TT 53	Graphene
15:00	HSZ 304	TT 54	Quantum Coherence and Quantum Information Systems II
15:00	MOL 213	TT 55	Dynamics and Chaos in Many-Body Systems I
15:00	WIL A317	TT 56	Focus Session: Making Experimental Data F.A.I.R. – New Concepts for Research Data Management I
15:00	P2/OG2	TT 57	Poster: Superconductivity I
15:00	P2/OG3	TT 58	Poster: Superconductivity II
15:00	P2/OG4	TT 59	Poster Session: Topology
17:15	HSZ 03	TT 60	Quantum Dots, Quantum Wires, Point Contacts
17:45	HSZ 201	TT 61	Focus Session: Correlations in Moiré Quantum Matter II

09:30 Foyer HSZ / Tent A **Exhibition of Scientific Instruments and Literature**

11:30	HSZ 405	Job Market Horn & Company Financial Services GmbH <i>"Horn & Company – Gewinne Einblicke in unsere Projekte zu Data Analytics, Big Data und Künstlicher Intelligenz und lerne unseren Beratungsansatz kennen!"</i>
14:00	HSZ 405	d-fine GmbH <i>"Einblicke in die Beratungspraxis bei d-fine – Projekte im Bankensektor"</i>

Friday, March 31, 2023

08:30	HSZ 01	PLV XI	Plenary Talk Physics in Nanopores: From Data storage to DNA/RNA analysis •Ulrich Keyser
-------	--------	--------	--

SYHS

09:30	HSZ 01	SYHS 1	Symposium Physics of van der Waals 2D Heterostructures
09:30	HSZ 01	SYHS 1.1	Invited Talks Novel moiré excitons and ultrafast optical dynamics in van der Waals 2D heterostructures •Steven G. Louie
10:00	HSZ 01	SYHS 1.2	Interaction induced magnetism in 2D semiconductor moiré superlattices •Xiaodong Xu
10:30	HSZ 01	SYHS 1.3	Ions in tight places: intercalation and transport of ions in van der Waals heterostructures •Irina Grigorieva
11:15	HSZ 01	SYHS 1.4	Spin-orbit proximity in van der Waals heterostructures •Felix Casanova
11:45	HSZ 01	SYHS 1.5	Plethora of many-body ground states in magic angle twisted bilayer graphene •Dmitri Efetov

BP

09:30	TOE 317	BP 30.1	Invited Talks Experiments on Active Polymer-Like Worms •Antoine Deblais
12:15	HSZ 03	BP 32.1	Closing Topical Talk The physical regulation of brain development •Kristian Franze
09:30	BAR Schö	BP 29	Sessions Statistical Physics of Biological Systems II
09:30	TOE 317	BP 30	Active Matter V
10:00	BAR 0106	BP 31	Cell Mechanics III
12:15	HSZ 03	BP 32	Closing Topical Talk Kristian Franze

CPP

09:30	GÖR 226	CPP 56.1	Invited Talks Self-assembled optical metamaterials •Ullrich Steiner
11:30	GÖR 226	CPP 56.7	Simulating quantum systems with plasmonic waveguide arrays •Stefan Linden
12:00	GÖR 226	CPP 56.8	single molecule detection on a smartphone microscope enabled by DNA origami biosensors •Philip Tinnefeld
09:30	MER 02	CPP 57.1	Chiral transport of active and passive colloids •Anke Lindner
09:30	ZEU 255	CPP 58.1	Studies of polymer thermosets using scattering techniques •Mats Johansson
09:30	GÖR 226	CPP 56	Sessions Focus: Self-Assembly of Plasmonic Nanostructures
09:30	MER 02	CPP 57	Complex Fluids and Colloids, Micelles and Vesicles II
09:30	ZEU 255	CPP 58	Polymer Networks and Elastomers
09:30	TOE 317	CPP 59	Active Matter V
12:15	HSZ 03	CPP 60	Closing Plenary Talk

Friday, March 31, 2023

DY

10:30 ZEU 160 DY 56.5
Invited Talk
Transport and self-organization in living fluids
•Matthias Weiss

Sessions
09:30 BAR Schö DY 52 Statistical Physics of Biological Systems II
09:30 TOE 317 DY 53 Active Matter V
09:30 MER 02 DY 54 Complex Fluids and Colloids, Micelles and Vesicles
09:30 MOL 213 DY 55 Dynamics and Chaos in Many-Body Systems II
09:30 ZEU 160 DY 56 Brownian Motion and Anomalous Diffusion
09:30 ZEU 250 DY 57 Networks: From Topology to Dynamics IV

HL

Sessions
09:30 POT 81 HL 47 Oxide Semiconductors II
09:30 POT 361 HL 48 Ultra-fast Phenomena
09:30 POT 151 HL 49 Quantum dots: Devices
09:30 POT 251 HL 50 Materials and devices for quantum technology III
09:30 POT 112 HL 51 Nitrides: Preparation and Characterization
09:30 GÖR 226 HL 52 Focus: Self-Assembly of Plasmonic Nanostructures

MA

Sessions
09:30 HSZ 02 MA 46 Ultrafast Magnetization Effects II
09:30 HSZ 04 MA 47 Skyrmions IV
09:30 HSZ 401 MA 48 Magnetic Instrumentation and Characterization
09:30 HSZ 403 MA 49 Magnetic Information Technology, Recording, Sensing
09:30 POT 6 MA 50 Magnetic Domain Walls (non-skyrmionic)

O

Invited Talks, Topical Talks
09:30 TRE Phy O 90.1 Molecular Surfaces With a Twist: Magnetochiral Asymmetries and Topological Self-Assembly
•Karl-Heinz Ernst
09:30 WIL A317 O 95.1 FAIRifying ARPES: a Route to Open Data & Data Analytics
•Ralph Ernstorfer
11:15 WIL A317 O 95.7 Electronic Lab Notebooks in Teaching and Implications on Science
•Michael Krieger
11:15 TRE Ma O 97.4 Heteroatom-substituted and three-dimensional nanocarbon materials studied with low temperature STM and qPlus AFM
•Shigeki Kawai

Closing Overview Talk
13:15 HSZ 03 O 98.1 Surfaces go topological – third generation 2D quantum materials
•Ralph Claessen

Sessions
09:30 TRE Phy O 90 Overview Talk Karl-Heinz Ernst
10:30 CHE 89 O 91 Plasmonics and Nanooptics V: Waveguides and Antennas
10:30 CHE 91 O 92 Oxide and Insulator Surfaces II: Structure, Epitaxy and Growth
10:30 GER 37 O 93 Graphene II: Electronic Structure and Growth
10:30 GER 38 O 94 Topology and Symmetry-Protected Materials
09:30 WIL A317 O 95 Focus Session: Making Experimental Data F.A.I.R. – New Concepts for Research Data Management II
10:30 TRE Phy O 96 Solid-Liquid Interfaces III: Reactions and Electrochemistry II
10:30 TRE Ma O 97 Focus Session: Scanning Probe Microscopy with Quartz Sensors IV
13:15 HSZ 03 O 98 Closing Overview Talk Ralph Claessen

Friday, March 31, 2023

SOE

09:30 ZEU 260 SOE 21.1 **Invited Talk**
Marginal Stability and Excess volatility in firm networks
•Jean-Philippe Bouchaud

Sessions
09:30 ZEU 250 SOE 20 Networks: From Topology to Dynamics IV
09:30 ZEU 260 SOE 21 Financial Markets and Risk Management I
10:00 ZEU 260 SOE 22 Financial Markets and Risk Management II
11:00 ZEU 260 SOE 23 Economic Models

TT

09:30 HSZ 304 TT 66.1 **Invited Talk**
Towards ultrasensitive calorimetric detection in superconducting quantum circuits
•Bayan Karimi

Sessions
09:30 HSZ 03 TT 62 Ultrafast Dynamics of Light-Driven Systems
09:30 HSZ 103 TT 63 Superconductivity: Theory
09:30 HSZ 201 TT 64 Topology: Other Topics
09:30 HSZ 204 TT 65 Correlated Electrons: Other Theoretical Topics
09:30 HSZ 304 TT 66 Cryogenic Detectors
09:30 MOL 213 TT 67 Dynamics and Chaos in Many-Body Systems II
09:30 WIL A317 TT 68 Focus Session: Making Experimental Data F.A.I.R. – New Concepts for Research Data Management II

62. Wochenendseminar „Physiker:innen im Beruf“

Der Übergang von der Hochschule in die **berufliche Karriere** fällt vielen nicht leicht: Die Möglichkeiten und Aufgabengebiete sind vielfältig - und wer kennt schon nach Studium oder Promotion die verschiedenen Anforderungen und Arbeitsabläufe?

Das Seminar bietet durch **Erfahrungsberichte** etablierter Physiker:innen sowie junger Berufsanfänger:innen Orientierung. Die 15 Vortragenden repräsentieren ganz verschiedene Arbeitsgebiete und zeigen damit das breite **Einsatzspektrum** von Physikerinnen und Physikern.

Neben den Vorträgen bietet der gemütliche Lichtenbergkeller des Physikzentrums Bad Honnef ein ideales Forum, mit den Vortragenden am Abend **in kleiner Runde offen** zu **diskutieren** und Erfahrungen zu sammeln.

Zielgruppe:

Physikstudierende ab Bachelor bis zur Promotion. Max. 80 Personen.

5. bis 7. Mai 2023

Physikzentrum Bad Honnef

Weitere Infos und Anmeldung: www.pib.dpg-physik.de

Sessions

– Plenary Talks –

Plenary Talk PLV I Mon 8:30 HSZ 01
Spin-Photon Interfaces and Their Applications — •METE ATATUERE — University of Cambridge

Optically active spins in solids are often considered prime candidates for scalable and feasible quantum-optical devices. Numerous material platforms including diamond, semiconductors, and atomically thin layered materials are investigated, where each platform brings their own advantages along with their challenges. I will highlight the common challenges and the ways forward for some of the promising systems for applications in quantum networks and quantum sensing.

Plenary Talk PLV II Mon 14:00 HSZ 01
New directions in electromagnetic field mapping in materials in the transmission electron microscope — •RAFAL E. DUNIN-BORKOWSKI — Ernst Ruska-Centre for Microscopy and Spectroscopy with Electrons, Forschungszentrum Jülich, 52425 Jülich, Germany

Transmission electron microscopy has been revolutionized in recent years, both by the introduction of new hardware such field-emission electron guns, aberration correctors and in situ stages and by the development of new techniques that take advantage of increased computational speed and the ability to control and automate modern electron microscopes. In this talk, I will describe how electron microscopy can be used to obtain quantitative information about not only local variations in microstructure and composition in materials, but also magnetic fields and charge density distributions with close-to-atomic spatial resolution. When combined with model-based iterative reconstruction, electron tomography and in situ techniques, this information can be obtained quantitatively, in three dimensions, as a function of temperature, with high temporal resolution and in the presence of applied fields, light and reactive gases. I will present results obtained from studies of magnetization distributions in individual magnetic nanocrystals and three-dimensional magnetic solitons in geometrically-confined structures, from measurements of electric fields in nanoscale materials and from studies of electron-light-matter interactions. I will conclude with a personal perspective on directions for the future development of transmission electron microscopy, which may require radical changes to the design of electron microscopes.

Plenary Talk PLV III Mon 14:00 HSZ 02
Microgels at Interfaces — •REGINE VON KLITZING — Institute for Condensed Matter Physics, TU Darmstadt, Germany

Rupturing foams (and emulsions) on demand is a big challenge for many applications. One strategy is to use stimuli-responsive surface-active polymer particles as stabilizers. Here we use thermosensitive microgel particles which show an LCST-like volume phase transition. In order to understand their impact on foam stabilisation it is important to get deeper insight into different length scales of the foams, i.e. from adsorption of microgels at the air/water interface studied by scanning force microscopy (AFM), via forces across microscopic foam lamellas measured with a thin film pressure balance and foam bubbles to macroscopic foams stabilized by PNIPAM microgels. The foam structure is investigated by small angle neutron scattering (SANS). The deformation of the microgels plays an important role for the stabilisation mechanism and is related to their inner structure (studied by SANS), the swelling behaviour and nanomechanical and nanorheological properties that are investigated by dynamic indentation with an AFM tip. The combination of these studies on different length scales almost completes the picture about the stabilisation ability of microgels and might be transferred to other types of colloidal dispersions.

Plenary Talk PLV IV Tue 8:30 HSZ 01
Stochastic thermodynamics: From concepts to model-free inference — •UDO SEIFERT — II. Institut für Theoretische Physik, Universität Stuttgart

Stochastic thermodynamics provides a universal framework for analyzing nano- and micro-sized non-equilibrium systems. Prominent examples are single molecules, molecular machines, colloidal particles in time-dependent laser traps and biochemical networks. Thermodynamic notions like work, heat and entropy can be identified on the level of individual fluctuating trajectories. They obey universal relations like the fluctuation theorem.

Thermodynamic inference as a general strategy uses consistency constraints derived from stochastic thermodynamics to infer otherwise hidden properties of non-equilibrium systems. As a paradigm for thermodynamic inference, the thermodynamic uncertainty relation discovered in 2015 provides a lower bound on the entropy production through measurements of the dispersion of any current in the system. Likewise, it quantifies the cost of temporal precision for biomolecular processes and provides a model-free bound on the thermodynamic efficiency of molecular motors and microscopic heat engines.

Plenary Talk PLV V Wed 8:30 HSZ 01
Advances in Ultrafast Electron Microscopy — •CLAUS ROPERS — Max-Planck Institute for Multidisciplinary Sciences, Göttingen — University of Göttingen

Providing the most detailed views of atomic-scale structure and composition, Transmission Electron Microscopy (TEM) serves as an indispensable tool for structural biology and materials science. The combination of electron microscopy with pulsed electrical or optical stimuli allows for the study of transient phenomena, involving magnetization dynamics, strain evolution and structural phase transformations. Ultrafast transmission electron microscopy (UTEM) is a pump-probe technique, in which non-equilibrium processes can be tracked with simultaneous femtosecond temporal and nanometer spatial resolutions.

This talk will cover recent developments and applications in UTEM based on laser-triggered field emitters, including the real-space and diffractive probing of a structural phase transition. Moreover, the mechanisms involved in free-electron beams interacting with optical fields at photonic structures will be discussed, emphasizing quantum effects. In particular, recent progress in the coupling of electron beams to integrated photonic structures will be presented. Finally, harnessing developments in event-based electron spectroscopy, we demonstrate the preparation and characterization of electron-photon and electron-electron pair states.

Plenary Talk PLV VI Wed 14:00 HSZ 01
Topological defects in active and living matter — •M CRISTINA MARCHETTI — University of California Santa Barbara, USA

Topological defects play a central role in the physics of many materials, including magnets, superconductors and liquid crystals. In oriented active fluids defect acquire a new life as spontaneous local currents turn them into self-propelled particles that drive chaotic flows. There is growing evidence that living systems may exploit this relation between structure and dynamics and use defects to localize stress or perform specific functions. The intimate connection between defect textures and active flow suggests that properties of active materials can be engineered by controlling defects. In this talk I will describe our work on formulating the dynamics of active topological defects as particle-like excitations, their role in driving the turbulent-like dynamics of active liquid crystals, and recent approaches to manipulate the defect dynamics in both space and time.

Plenary Talk PLV VII Wed 14:00 HSZ 02
Ferroelectric and multiferroic domain walls for nanotechnology — •DENNIS MEIER — Department of Materials Science and Engineering, NTNU Norwegian University of Science and Technology — Center for Quantum Spintronics, Department of Physics, NTNU Norwegian University of Science and Technology

Ferroelectric and multiferroic domain walls have emerged as a new type of functional interface. Because of their distinct symmetry and chemical environment, the domain walls offer a wide variety of functional electric and magnetic properties, representing excellent 2D components for the development of more agile next-generation nanotechnology. In my talk, I will discuss fundamental key properties of domain walls in ferroics and how the field of domain wall nanoelectronics evolved from classical device ideas to advanced concepts, where the walls themselves are used as ultra-small electronic components. I will conclude with a discussion of open experimental challenges and newly discovered domain-wall phenomena that may play an important role in future directions of the field.

Plenary Talk PLV VIII Thu 8:30 HSZ 01
Nanomechanics: Tunes of the nanoguitar — •EVA WEIG — Technical University of Munich, Garching, Germany

Nanomechanical resonators - freely suspended, vibrating nanostructures - show great promise as versatile elements in hybrid nanosystems, as sensors or signal transducers both in the classical and in the quantum realm. Here I will focus on nanomechanical string resonators. These seemingly simple devices exhibit remarkably large room temperature quality factors and enable electrostatic control. Nanostrings are thus an ideal testbed to explore a variety of dynamical phenomena. I will review recent progress in controlling the coherent as well as the nonlinear dynamics of nanostring resonators. This includes the realization of a nanomechanical two-mode system mimicking the coherent dynamics of a quantum two-level system, and novel insights into squeezing and frequency comb generation.

Plenary Talk PLV IX Thu 14:00 HSZ 01
Metal Halide Perovskites for Photovoltaic Applications — •LAURA HERZ — University of Oxford, Department of Physics, Parks Road, Oxford OX1 3PU, U.K.

Organic-inorganic metal halide perovskites have emerged as attractive materials for solar cells with power-conversion efficiencies now exceeding 25%. This talk

will provide an overview of our work unravelling the fundamental processes that have enabled these materials to be such efficient light-harvesters and charge collectors, examining e.g. fundamental mechanisms underpinning charge-carrier mobility and recombination. Our analysis of intrinsic photophysical parameters opens the promise of targeted material design for solar energy harvesting, based on readily accessible parameters, such as band structure, phonon frequencies and the dielectric function.

We further discuss a range of remaining challenges and opportunities relating to material microstructure, ionic migration and toxicity. We examine how the optoelectronic properties of hybrid perovskites are governed by their nanostructure and structural phases. In the context of silicon-perovskite tandem cells, we discuss the peculiar mechanisms underlying detrimental halide segregation in mixed iodide-bromide lead perovskites with desirable electronic band gaps near 1.8eV. We further outline the challenges and rewards of lead-free metal halide perovskites and their structural derivatives.

Plenary Talk

PLV X Thu 14:00 HSZ 02

Single-electron-spin-resonance detection by microwave photon counting —

•PATRICE BERTET¹, ZHIREN WANG¹, LEO BALEMBOIS¹, ERIC BILLAUD¹, MILOS RANCIC¹, MARIANNE LE DANTEC¹, THIERRY CHANELIERE², ALBAN FERRIER³, PHILIPPE GOLDNER³, SYLVAIN BERTAINA⁴, DENIS VION¹, DANIEL ESTEVE¹, and EMMANUEL FLURIN¹ — ¹Université Paris-Saclay, Gif-sur-Yvette, France — ²Université Grenoble-Alpes, Grenoble, France — ³Université PSL, Paris, France — ⁴Université Aix-Marseille, Marseille, France

We report a new method for single-electron-spin-resonance spectroscopy at millikelvin temperatures. It consists in measuring the spin fluorescence signal at microwave frequencies using a microwave photon counter based on a superconducting transmon qubit. In our experiment, individual paramagnetic erbium ions in a scheelite crystal of CaWO₄ are magnetically coupled to a small-mode-volume, high-quality factor superconducting microwave resonator to enhance their radiative decay rate. We detect the microwave photon spontaneously emit-

ted by a spin following its excitation with a signal-to-noise ratio of 1.9 in one second integration time. Coherence times up to 3 ms are measured, limited by the spin radiative lifetime. The method applies to arbitrary paramagnetic species with long enough non-radiative relaxation time, and offers large detection volumes (10 μm³); as such, it may find applications in magnetic resonance and quantum computing.

Plenary Talk

PLV XI Fri 8:30 HSZ 01

Physics in Nanopores: From Data storage to DNA/RNA analysis — •ULRICH KEYSER — Cavendish Laboratory, University of Cambridge, JJ Thomson Ave, Cambridge, CB3 0HE, UK

DNA and RNA are the molecules of life. Their sequence encodes the blueprints from cells to viruses. Both polymers store information in their three-dimensional structure.

RNA and DNA are often analysed by translocating single molecules through small holes known as nanopores. An accurate understanding of the translocation dynamics is essential for the read out of polymer structure, including the localization of binding sites or sequences. Here we use synthetic nanopores and nanostructured DNA molecules to directly measure the velocity profile of driven polymer translocation through synthetic nanopores. We adjust nanopore geometry and translocation direction to resolve individual nanostructures only 7 nm apart and with a surface-to-surface gap distance of 2 nm. We then discuss the potential and challenges of our super-resolution nanopore sensing for future DNA data storage.

In the second part of the talk, we use our insights on polymer dynamics in nanopore confinement to analyse RNA molecules. We identify target RNA through making distinct three-dimensional structures with designed RNA:DNA interactions. Finally, we highlight multiplexed detection of RNA viruses - like SARS-CoV-2 and its variants - as one exciting application of nanopore sensing and DNA nanotechnology.

Sessions

– Prize Talks –

Prize Talk

PRV I Tue 13:15 HSZ 01

Seeing is believing: Nonlinear optics on ferroic materials — •MANFRED FIEBIG — Dept. of Materials, ETH Zurich, Switzerland — Laureate of the Stern-Gerlach-Medal 2023

For millennia, ferromagnetism was the only form of ferroic order known to humankind. Now, however, a large variety of magnetic, electrical and mechanical types of ferroic phenomena is discussed. All of these all have one property in common: The ferroic ordering breaks the symmetry of the host material. Non-linear optical processes are very sensitive to these symmetry changes. Even its simplest representative, doubling of the frequency of the light or "second harmonic generation" (SHG), therefore couples to the ferroic order parameter and accesses important features of the ferroic state that are often inaccessible to non-optical techniques. Novel ferroic states like ferroitoroidicity as a spontaneous order of magnetic whirls can thus be probed. Ultrafast processes can be resolved — how fast can a magnetic state be switched? In particular, the coexistence of different types of ferroic order in a material can be imaged by SHG. Thus, SHG became an invaluable tool for resolving the magnetoelectric coupling of domains in multiferroics as materials uniting magnetic and ferroelectric order. In my talk I will give an overview of the most important milestones in the classification of (multi-)ferroic materials by nonlinear optics. I will discuss basic questions such as the search for yet unknown types of ferroic order and correlations. I will also address highly application-relevant issues such as the use of SHG for tracking the emergence of ferroic order in thin films in-situ, during the growth process. A not-too-serious concept for "magnetoelectric teleportation" will conclude the lecture.

Prize Talk

PRV II Wed 13:15 HSZ 01

Towards chemical and optical band structure engineering in molecular-based heterostructures — •BENJAMIN STADTMUELLER — Department of Physics and Research Center OPTIMAS, TU Kaiserslautern, 67663 Kaiserslautern, Germany — Institute of Physics, JGU Mainz, 55128 Mainz, Germany — Laureate of the Gaede-Prize 2023

Optical excitations with femtosecond light pulses offer the intriguing opportunity to control material properties on ever-shorter timescales down to the duration of the optical excitation itself. One of the most promising ways to reduce the timescale of the ultrafast material response is to exploit optical-induced spin and charge transfer processes that can directly act on the material's band structure

and its population. In this presentation, I will introduce molecular-based heterostructures as a highly intriguing platform to chemically and optically tailor charge and spin carrier functionalities on the nanoscale. Using time-, spin- and momentum-resolved photoemission with fs-XUV radiation, I will first demonstrate that optical excitation of charge transfer states in molecular materials can instantaneously alter the local energy level alignment within the molecular film on ultrafast timescales [1,2]. This approach can be transferred to heterostructures between molecular and 2D semiconductors where it allows us to transiently uncover the otherwise hidden spin polarization of the prototypical layered semiconductor WSe₂. These findings will open new avenues for optical controlling and functionalizing spin phenomena in molecular-based heterostructures on ultrafast timescales. [1] Nat. Commun. 10, 1470 (2019), [2] J. Electron. Spectros. Relat. Phenomena 252, 147110 (2021).

Prize Talk

PRV III Thu 13:15 HSZ 01

High-lying excitons and excitonic quantum interference in 2D semiconductors — •KAI-QIANG LIN — Department of Physics, University of Regensburg, Regensburg, Germany — College of Chemistry and Chemical Engineering, Xiamen University, Xiamen, China — Laureate of the Walter-Schottky-Prize 2023

Two dimensional semiconductors such as transition-metal dichalcogenide (TMDC) monolayers show a wealth of exciton physics. We present the existence of a novel excitonic species, the high-lying exciton (HX), in TMDC monolayers with almost twice the energy of the band-edge A-exciton but with a linewidth as narrow as that of band-edge excitons. The HX is populated through momentum-selective optical excitation in the K-valleys, and is identified experimentally in upconverted photoluminescence and theoretically in ab initio GW-BSE calculations. These calculations show that the HX is comprised of electrons of negative effective mass. The coincidence of such high-lying excitonic species at around twice the energy of band-edge excitons gives rise to a well-defined excitonic three-level system, which enables quantum-interference phenomenon revealed in optical second-harmonic generation. We show that the temporal dynamics in such a three-level system can be probed through time-resolved sum-frequency generation and four-wave mixing. The HXs can also be tuned over a wide range by twisting and Stark effect in bilayer WSe₂, which gives control over the excitonic quantum interference and the corresponding optical nonlinearities. Finally, we show how an electrical gate can be used to tune excitonic quantum interference in a monolayer TMDC transistor device by forming triions.

Sessions

– Ceremonial, Lunch, Evening Talks and Discussions –

Evening Talk

PSV I Sun 18:30 HSZ 01

Kipp-Punkte im Klimasystem: Vorboten aus dem polaren Eis — •RICARDA WINKELMANN — Potsdam Institute for Climate Impact Research, Member of the Leibniz Association, Germany — Institute of Physics and Astronomy, University of Potsdam, Germany

Der kälteste, der windigste, der trockenste Ort der Welt: Die Antarktis ist ein Ort der Extreme. Der Kontinent am Südpol ist von einem gigantischen Eisschild bedeckt, der Millionen von Jahre alt und in einigen Gebieten mehr als 4.000 m dick ist. Würde das gesamte Eis der Antarktis abschmelzen, hätte das einen globalen Meeresspiegelanstieg von etwa 58 m zur Folge.

Trotz dieser gewaltigen Ausmaße ist der antarktische Eisschild besonders anfällig gegenüber Klimaänderungen – über die vergangenen Jahrzehnte hat insbesondere die Westantarktis beschleunigt Eis verloren. Aufgrund von sich gegenseitig verstärkenden Wechselwirkungen zwischen Eis, Atmosphäre und Ozean steigt mit zunehmender globaler Erwärmung das Risiko, dass Kipp-Punkte in der Antarktis ausgelöst werden: Ist eine kritische Temperaturschwelle erst einmal überschritten, könnte dies zu einem selbsttragenden und möglicherweise irreversiblen Eisverlust in Teilen der West- und Ostantarktis führen.

In diesem Vortrag werden die zugrundeliegenden physikalischen Prozesse und die Risiken solcher dynamischer Instabilitäten genauer beleuchtet, sowie die daraus resultierenden Auswirkungen auf den Anstieg des Meeresspiegels und unser globales Klima – nicht nur in den kommenden Jahrzehnten, sondern für die nächsten Jahrhunderte und darüber hinaus.

Lunch Talk

PSV II Mon 13:15 HSZ 02

Patentanwalt, Verfahren zu dessen Herstellung und Verwendung eines Patentanwalts — •CARINA EHRIG — Kailuweit & Uhlemann Patentanwälte Partnerschaft mbB, Bambergstraße 49, 01187 Dresden

Wie wird man Patentanwalt? Und wie sieht der Arbeitsalltag im Patentwesen aus? Der Vortrag gibt einen Überblick über die Ausbildung und die Arbeit im gewerblichen Rechtsschutz. Die Arbeit als Patentanwalt ist abwechslungsreich und spannend. Als Übersetzer zwischen Technik und Recht sind insbesondere Physiker gefragt und geeignet, da sie in der Lage sind, sich schnell in neue, komplexe und interdisziplinäre Sachverhalte einzuarbeiten. Der Weg zum fertigen Anwalt hingegen birgt noch so manche Herausforderung, auf die im Vortrag eingegangen wird.

Discussion

PSV III Mon 13:15 HSZ 03

Talking about different career paths into Academia — •ALEXANDER OSTERKORN¹, CHRISTOPH KASTL², ANNA GRÜNEBOHM², and AMELIE HEUERJUNGEMANN² — ¹JDPG — ²AGyouLeaP

On the way to a position in academia, nowadays several career paths are available. After the PhD, people usually go through a PostDoc phase and then take the next qualification step. For the latter, besides the more established Habilitation, one can become for example a Junior-Professor or an independent group leader funded by third-party funding like an Emmy-Noether fellowship. We want to discuss with people who followed these different career paths about their experiences and viewpoints on their career path. The panel discussion will be moderated by Alexander Osterkorn from jDPG and on the panel we are happy to welcome the AGyouLeaP members Christoph Kastl (Habilitation, TU München), Anna Grünebohm (Junior-Professor, Ruhr-Universität Bochum) and Amelie Heuer-Jungemann (Emmy-Noether Group Leader, Max-Planck Institut für Biochemie).

Lunch Talk

PSV IV Tue 13:15 HSZ 02

Berufswege für Physiker in Elektrotechnik, Unternehmensberatung und IT — •PHILIPP DEDIÉ — PhDSoft-Ingenieure GmbH, Hartriegelweg 12B, 38112 Braunschweig

Ich berichte aus meinem eigenen beruflichen Werdegang zu Berufswegen für Physiker in den Bereichen elektrische Energiespeicher und -wandler, Unternehmensberatung in der Automobilbranche und Informationstechnologie branchenübergreifend. Dazu gebe ich aktuelle Tätigkeitsbeispiele aus der IT in verschiedenen Branchen und Unternehmensgrößen von Startup über KMU bis Großunternehmen.

Lunch Talk

PSV V Tue 13:15 HSZ 03

Research Funding by the DFG – Insights into the Decision Process — •MICHAEL MÖSSLE¹, MARIO BOMERS¹, JOANNA KOWALSKA¹, CHRISTIAN HAHN¹, and SARAH KÖSTER² — ¹Deutsche Forschungsgemeinschaft, Bonn — ²Institute for X-Ray Physics, Universität Göttingen

The German Research Foundation (DFG) is one of the largest research funding organizations in Germany. It is self-governed by the scientific community and

offers a broad range of funding opportunities from individual grants to larger coordinated programmes. The talk will give an overview of the DFG funding schemes and the bodies involved in the decision process, in particular the elected review boards. Also, we will attempt to give some first-hand insights into the review and decision process from the perspective of the DFG head office and a current review board member.

Ceremonial Talk

PSV VI Tue 16:30 HSZ 01

Die Star Trek Physik – Warum die Enterprise nur 158 kg wiegt und andere galaktische Erkenntnisse — •METIN TOLAN — Georg-August-Universität Göttingen

Die Serie Star Trek wurde 1966 im amerikanischen Fernsehen gestartet und nach Anlaufschwierigkeiten zur erfolgreichsten Serie überhaupt. Dazu beigetragen hat sicher auch die Beschreibung physikalischer Sachverhalte. In diesem Vortrag werden verschiedene Beispiele aus der klassischen und der Quantenphysik gezeigt und durchgerechnet. Ein physikalisch vorgebildetes Publikum wird dabei sicher nicht überfordert.

Lunch Talk

PSV VII Wed 13:15 HSZ 02

Vom Physiker zum (erfolgreichen) Unternehmer der Plasway-Technologies GmbH — •STEPHAN WEGE — Plasway-Technologies GmbH, 01728 Bannewitz, Heinrich-Heine Str. 2b

Werdegang Herr Stephan Wege: Vom Studium über die Erfahrungen in der Industrie und eine Kurzübersicht der Plasway-Technologies GmbH. Neben einer guten fachlichen Ausbildung (Diplom in Physik) sind Themen wie die Führung von Personal sowie gute Kenntnisse im Projektmanagement und Planung sehr wichtig. Die Darstellung der Arbeit auf einer höheren Managementebene bis hin zu Gesprächen mit Banken und Fördermittelgebern gehören schon fast zum täglichen Geschäft. Es werden viele öffentliche Fördermittel angeboten. Die Formulare sind eine zu große Herausforderung. Externe kostenpflichtige Berater können helfen. Ab einem gewissen Zeitpunkt können auch externe Investoren hilfreich sein. Die Erstellung eines Businessplanes ist hilfreich für die eigene Transparenz und wird von den Banken vorausgesetzt. Basiswissen im Steuer- Handels- und Finanzrecht sind ebenfalls sehr hilfreich. Ein guter Steuerberater ist unerlässlich. Die Rechtsform der zukünftigen Firma sollte man sich gut überlegen (GmbH, GbR). Welcher Standort ist günstig? Werbung für die Außendarstellung von großem Vorteil (Homepage, Visitenkarten, Filme, Flyer). Aber auch über Themen soziale Absicherung sollte man frühzeitig nachdenken. Das Wichtigste zum Schluss: Eine positive Einstellung zu einer 80 Stunden-Woche ist offensichtlich. Eine hohe Frustrationstoleranz gegenüber den Behörden und vor allem dem Finanzamt und auch der IHK sind selbstverständlich. Warum das Ganze? Es macht sehr viel Spaß.

Discussion

PSV VIII Wed 13:15 HSZ 03

Vielfalt der Wissenschaftskommunikation — •ULRICH BLEYER¹, NICOLAS WÖHRI² und PETER KOHL² — ¹Urania Berlin (a.D), 10787 Berlin — ²Universität Duisburg-Essen, 47048 Duisburg

Gerade Physiker:innen sind durch den Anwendungsbezug ihrer Arbeit gefragt, wenn es um Wissenschaftskommunikation geht, z.B. bei transformativen Themen wie Quantenkryptographie, alten und neuen Energietechniken oder dem Klimawandel. Wir brauchen zielgruppenspezifische Kommunikation, die interaktiv und dialogorientiert ist. Dabei geht es nicht nur um die reinen Forschungsergebnisse, sondern auch darum, Prozesse und Methoden von wissenschaftlicher Arbeit transparent abzubilden – eine Aufgabe, die prinzipiell alle Forschenden übernehmen können. In dieser Veranstaltung soll zunächst die Bedeutung und die Vielfalt von Methoden der Öffentlichkeitsarbeit aus Sicht der DPG durch zwei erfahrene Akteure dargestellt werden. Zum einen die Berliner Gesellschaft Urania, die mit dem Ziel gegründet wurde wissenschaftliche Erkenntnisse auch einem Laienpublikum zugänglich zu machen. Zum anderen die 'Junge DPG' die beispielsweise den 'Einsteinclam' und andere Formate – bei DPG-Veranstaltungen und darüber hinaus – veranstaltet. Anschließend werden in einer Focus-Session erfolgreiche Projekte der Wissenschaftskommunikation aus dem Bereich der Festkörperphysik vorgestellt. In ihrer Gesamtheit sollen sie das Spektrum der Wissenschaftskommunikation, auch im Hinblick auf den benötigten Aufwand, aufzeigen, Methoden für unterschiedliche Zielgruppen vorstellen und Hinweise geben, wie man bei Interesse konkret mit der Kommunikation beginnen kann.

Lunch Talk

PSV IX Thu 13:15 HSZ 02

Working as a Physicist in the Microelectronic Industry — •MATTHIAS U. LEHR — Globalfoundries Dresden, Germany

This talk describes the career path from a PhD work in basic research towards a technical manager position in the microelectronic industry. The variety of tasks

and different options for the personal development in a big high-tech company are discussed. It will be shown what is needed in terms of technical expertise as well as personal behavior to become successful as a physicist in a challenging, competitive and international environment.

Discussion

PSV X Thu 13:15 HSZ 03

NFDI and FAIR research data: benefit or burden? — LAURENZ RETTIG¹, HEIKO B. WEBER², and •MARTIN AESCHLIMANN³ — ¹Fritz Haber Institute of the MPG, Berlin, Germany — ²Friedrich-Alexander-Universität Erlangen, Germany — ³TU Kaiserslautern, Germany

Big data is becoming an ever more important resource for future research, especially for data-driven research fields and artificial intelligence. This is certainly also true for research data in solid state physics, which, however, are so far nei-

ther homogeneously structured nor openly accessible. The necessary requirements have been cast into the FAIR (findable, accessible, interoperable, reusable) principles, which provide a guideline for suitable data infrastructures. Given the growing demand from society, policymakers, and research funding agencies for open access to research data as well as metadata, researchers face a variety of questions and challenges:

How does the requirement for FAIR data influence daily laboratory routines? What reservations, what (e.g. legal) limitations do exist, and what is the meaning of FAIR, if corresponding (meta-) data standards or their documentation are (still) lacking? Are researchers willing and able to share data? These topics are at the focus of this discussion forum with invited speakers from research and funding agencies, followed by a dialogue with the audience.

Invited and Contributed Talks

TUT 1: Physics Meets Machine Learning (joint session DY/TUT/TT)

Machine learning has revolutionized many application fields such as computer vision and natural language processing. In physics there is a growing interest in using machine learning to enhance the analysis of experimental data and to devise and optimize experiments or numerical simulations. On the other hand physicists use their intuition and methods from statistical physics and complex systems theory to better understand the working principles of modern machine learning methods. This tutorial session introduces some subfields within this area and the basic methods involved.

Organized by Sabine Andergassen (Tübingen), Martin Gärtner (Heidelberg), Moritz Helias (Jülich), and Markus Schmitt (Cologne)

Time: Sunday 16:00–18:15

Location: HSZ 01

Tutorial TUT 1.1 Sun 16:00 HSZ 01

Machine Learning for Quantum Technologies — •FLORIAN MARQUARDT — Max Planck Institute for the Science of Light and Friedrich-Alexander Universität Erlangen-Nürnberg, Erlangen, Germany

Machine learning is revolutionizing science and technology. In the past few years, it has become clear that it promises significant benefits as well for the development of quantum technologies. In this tutorial I will first give a brief introduction to neural networks. I will then discuss a number of areas and examples in which machine learning is being successfully applied in this context. These include measurement data analysis and quantum state representation, approximate quantum dynamics, parameter estimation, discovering strategies for hardware-level quantum control, the optimization of quantum circuits, and the discovery of quantum experiments, discrete quantum feedback strategies, and quantum error correction protocols.

Reference: "Artificial intelligence and machine learning for quantum technologies", M. Krenn, J. Landgraf, T. Foesel, and F. Marquardt, Phys. Rev. A 107, 010101 (2023).

Tutorial TUT 1.2 Sun 16:45 HSZ 01

The Unreasonable Effectiveness of Gaussians in the Theory of Deep Neural Networks — •ZOHAR RINGEL — Racah Institute of Physics, Hebrew University in Jerusalem

Physical Sciences are in many ways the success story of explaining fundamental phenomena using simple math [1]. The fact that physical phenomena could be arranged in that manner is remarkable. Yet this simplicity does not necessarily carry over to life sciences or data sciences. Indeed prominent authors have argued against our desire to rely on neat mathematical structures when analyzing big data [2].

In the past half-decade several results have emerged which balance mathematical simplicity with data-induced complexity. These could be seen as a middle ground between the above juxtaposing views. The common divider here is the use of Gaussian distributions as approximants of various different quanti-

ties in deep neural networks (DNNs). Specifically these Gaussians emerge when describing outputs of DNNs with random weights, outputs of trained DNNs at random times, outputs of fixed DNNs over random input data, and fluctuations of hidden DNN pre-activations. In this tutorial I will present these quantities, provide arguments supporting their Gaussianity, and outline several theoretical implications.

[1] The Unreasonable Effectiveness of Mathematics in the Natural Sciences. Wigner (1960)

[2] The Unreasonable Effectiveness of Data. Halevy, Norvig, Pereira (2009)

Tutorial TUT 1.3 Sun 17:30 HSZ 01

Computing learning curves for large machine learning models using the replica approach — •MANFRED OPPER — Inst. für Softwaretechnik und Theor. Informatik, TU Berlin — Centre for Systems Modelling and Quantitative Biomedicine, University of Birmingham, UK

Methods of statistical physics have been used for a long time to mathematically analyse the typical performance of machine learning models in the limit where both the number of data and the number of parameters (such as network weights) is large. By defining Boltzmann-Gibbs probability distributions over parameters where the cost function of the machine learning problem plays the role of a hamiltonian, one can derive analytical expressions for training errors and generalisation errors using the corresponding partition functions and free energies in terms of a usually small number of order parameters.

Since the models depend on a set of random data to be learnt, additional appropriate statistical (so-called quenched) averages of free energies over this 'disorder' have to be performed. The replica approach is a prominent analytical tool from the statistical physics of disordered systems to solve this nontrivial technical challenge.

In this tutorial I will give an introduction to this approach. Starting with an explicit calculation for simple single layer perceptrons, I will then argue how the method can be applied to more complex problems such as kernel machines (support vector machines and Gaussian processes) and multilayer networks.

TUT 2: Stochastic Processes of Opinion Formation (joint session SOE/TUT)

Time: Sunday 16:00–18:15

Location: HSZ 02

Tutorial TUT 2.1 Sun 16:00 HSZ 02

Bounded Confidence Revisited: What We Overlooked, Underestimated, and Got Wrong — •RAINER HEGSELMANN — Frankfurt School of Finance & Management, 60322 Frankfurt, Adickesallee 32-34

The talk will discuss the so called bounded confidence model (BC-model, for short). The model is very simple: Period by period, all agents average over all opinions that are not further away from their actual opinion than a given distance Epsilon, their *bound of confidence*.

The simplicity of the model is deceptive. Two decades ago, Ulrich Krause and me published an analysis of the model in which we overlooked completely a decisive feature of our model: For increasing values of Epsilon, our analysis back then suggests smooth transitions in the model's behavior. But in fact, the transitions are wild, chaotic, and non-monotonic.

In my talk I will present a new type of approach in which everything we overlooked at the time becomes directly obvious and, in a sense, unmissable. Key component of the new approach is an algorithm that identifies, exactly and exhaustively, all bounds of confidence, that make a difference. We get a list that, then, allows direct checks for wild behavior exhaustive of all possible cases. That is a good news. But it is accompanied by a bad one: The algorithm that does

the work, requires an absolutely exact fractional arithmetic with integers of arbitrary length. As a consequence, we have to pay a price in terms of computational speed.

Tutorial TUT 2.2 Sun 16:45 HSZ 02

When intuition fails: the complex effects of assimilative and repulsive influence on opinion polarization — •MICHAEL MAES¹, ANDREAS FLACHE², SHUO LIU³, and HAOXIANG XIA³ — ¹Karlsruhe Institute of Technology, Karlsruhe, Germany — ²University of Groningen, Groningen, The Netherlands — ³Dalian University of Technology, Dalian, China

There is a debate about whether personalized services of social-media platforms contribute to the rise of bipolarization of political opinions. On the one hand, it is argued that personalized services of online social networks generate filter bubbles limiting contact between users who disagree. This reduces opportunities for assimilative social influence between users from different camps and prevents opinion convergence. On the other hand, empirical research also indicated that exposing users to content from the opposite political spectrum can activate the counter-part of assimilative influence, repulsive influence. Fostering contact that leads to opinion assimilation and limiting contacts likely to induce repulsive interactions, it has been concluded, may therefore prevent bipolarization.

We demonstrate that these conclusions fail to capture the complexity that assimilative and repulsive influence generate in social networks. Sometimes, more assimilative influence can actually lead to more and not less opinion bipolarization. Likewise, increasing the exposure of users to like-minded individuals sometimes intensifies opinion polarization.

Tutorial TUT 2.3 Sun 17:30 HSZ 02
How growing connectivity and self-organization changes opinion dynamics — •PHILIPP LORENZ-SPREEN — Center for Adaptive Rationality, Max Planck Institute for Human Development, Berlin, Germany

Information technology has made various aspects of our lives more dynamic and self-organized. Connections with others can be made across spatial and socio-demographic boundaries and undone with the click of a button. Since the famous six degrees of separation, networks seem much more connected; Face-

book reports 3.5 degrees of separation on its friendship graph. Yet there have been repeated reports of segregated, homophilic network structures and related trends of increasing polarization on most online platforms. The mechanism that could resolve this apparent paradox may lie behind the question of whether we change our opinions according to our friends or whether we change our friends according to our opinions. We have recently proposed that an agent's opinion changes as a process of mutual reinforcement within clusters of shared attitudes and a coevolution of the associated network structure that dynamically adapts to changing opinions and follows a probability distribution governed by homophily. This combination helps explain the potential emergence of increasing polarization even as connectivity increases. Moreover, extending this model to multiple dimensions of topics can explain the empirical observation of increasing alignment of issues, where opinions become increasingly correlated within ideological clusters.

TUT 3: Hands-on tutorial on workflows for materials science simulation (joint session MM/TUT)

Time: Sunday 16:00–18:00

Location: HSZ 03

Tutorial TUT 3.1 Sun 16:00 HSZ 03
Hands-on tutorial on workflows for materials science simulations — •JÖRG NEUGEBAUER¹, TILMANN HICKEL¹, and RALF DRAUTZ² — ¹Max-Planck-Institut für Eisenforschung, Düsseldorf — ²ICAMS, Ruhr-Universität Bochum

Advanced computational simulations in materials science have reached a maturity that allows one to accurately describe and predict materials properties and processes. The underlying simulation tasks often involve several different models and software that requires expert knowledge to set up a project and to vary input parameters. The accompanying increasing complexity of simulation protocols means that the workflow along the simulation chain becomes an integral part

of research. Effective workflow management therefore is important for efficient research and transparent and reproducible results.

In this hands-on tutorial we will provide an interactive hands-on introduction into managing workflows with pyiron (www.pyiron.org). Pyiron is an integrated development environment for materials science built on python and Jupyter notebooks that may be used for a wide variety of simulation tasks, from rapid prototyping to high performance computing. The tutorial will first give a general introduction to using pyiron, with a focus on atomistic simulation tasks. In the second part of the tutorial, the training and validation of machine learning potentials from reference density functional calculations will provide a real-life application example.

TUT 4: Strategic elements and sustainability (joint session MA/TUT)

Our appetite for resources is insatiable. The path to a climate-neutral society and economy requires the increasingly intensive use of strategy metals such as lithium, cobalt, nickel, but also the group of rare earth elements. This major transformation is not possible without the sustainable use of these so-called critical elements along the entire value chain. In the Tutorial "Strategic elements and sustainability", we have four eminent speakers looking in this context at new developments in batteries, catalysis, thermoelectrics and magnetism.

Organizers: Oliver Gutfleisch (TU Darmstadt) and Heiko Wende (U. Duisburg-Essen).

Time: Sunday 16:00–18:00

Location: HSZ 04

Invited Talk TUT 4.1 Sun 16:00 HSZ 04
Making better batteries? – From Li-ion to Na-ion batteries — •PHILIPP ADELHELM — Humboldt-University Berlin, Berlin, Germany — Helmholtz-Zentrum Berlin, Berlin, Germany

The shift to electromobility is one of the most important transformations currently taking place in our society. This is associated with a sharp increase in battery production, which on the one hand opens up new opportunities, but on the other hand also has a massive impact on raw material supply and supply chains. In addition, new large markets are emerging, such as stationary energy supply or mobile robotics. Lithium-ion batteries are currently the most attractive technology for this. However, due to the large demand for batteries and the different application scenarios, other technologies are also being pursued. Sodium ion batteries can be produced on the same production lines as lithium ion batteries and are therefore considered a "drop-in" technology. The aim here is to replace not only costly lithium but also other expensive elements such as nickel or copper. Work is therefore being done worldwide on a cell chemistry for sodium ion batteries that works almost as well as lithium ion technology, but at the same time is cheaper and more readily available, or has other specific advantages. The tutorial gives an introduction to sodium ion technology. The motivation and state-of-the-art are explained in more detail and material aspects are discussed. In particular, the question is addressed which electrode materials are promising for sodium ion batteries, what is needed to achieve further progress and what actually happens when lithium ions are replaced by sodium ions in a battery.

Invited Talk TUT 4.2 Sun 16:30 HSZ 04
Sustainable Thermoelectric Materials Predicted by Data Mining and Machine Learning — •KORNELIUS NIELSCH — Leibniz Institute of Solid States and Materials Research, Dresden, Germany — Institute of Materials Research at TU Dresden, Germany — Institute of Applied Physics at TU Dresden, Germany

Generating electricity from temperature differences has proven itself in space. Thanks to this technology, the Voyager probes launched in 1977 are still sending

signals today. In the meantime, the car industry and ship producers have become interested in thermoelectrics. The combustion of fossil fuels produces exhaust gas that is up to 1300 °C hot. Modern thermoelectric materials are continuously expanding the fields of thermoelectric applications. The experimental search for new thermoelectric materials remains largely restricted to a limited number of successful chemical and structural families, such as chalcogenides, skutterudites and zintl phases. In principle, computational tools such as density functional theory (DFT) offer the possibility of directing experimental synthesis efforts towards very different chemical structures. In practice, however, predicting thermoelectric properties based on first principles remains a difficult endeavour, and experimental researchers do not usually use computations directly to drive their own synthesis efforts. Strategies to bridge this practical gap between experimental requirements and computational tools will be discussed and presented in this tutorial talk. Ref: Energy Environ. Sci. 14, 3559 (2021) and Advanced Theory and Simulations 5, 2200351 (2022)

Invited Talk TUT 4.3 Sun 17:00 HSZ 04
Design strategies for electrocatalysts – an electrochemist's perspective — •KRISTINA TSCHULIK — Ruhr-Universität Bochum, Faculty for Chemistry and Biochemistry, Chair for Electrochemistry and Nanoscale Materials — Max-Planck-Institut für Eisenforschung GmbH, Max-Planck-Straße 1, 40237 Düsseldorf

The aim to produce highly active, selective, and long-lived electrocatalysts by design drives major research efforts toward gaining fundamental understanding of the relationship between material properties and their catalytic performance. Surface characterization tools enable to assess atomic scale information on the complexity of electrocatalyst materials. Advancing electrochemical methodologies to adequately characterize such systems was less of a research focus point. In this tutorials, we shed light on the ability to gain fundamental insights into electrocatalysis and establish design strategies based on these. Concepts on how to improve mass transport, e.g. by exploiting magnetic fields are highlighted in this

respect. Particular attention is paid to deriving design strategies for nanoelectrocatalysts, which is often impeded, as structural and physical material properties are buried in electrochemical data of whole electrodes. Thus, a second major approach focuses on overcoming this difference in the considered level of complexity by methods of single-entity electrochemistry. The gained understanding of intrinsic catalyst performance will ultimately allow us to advance design concepts to transforming "pre-catalysts" in the foreseeable future.

Invited Talk

TUT 4.4 Sun 17:30 HSZ 04

Green magnetic materials for efficient energy, transport and cooling applications — •OLIVER GUTFLEISCH — TU Darmstadt, Material Science, Functional Materials

High performance hard and soft magnets are key components of energy-related technologies, such as direct drive wind turbines and e-mobility. They are also important in robotics and automatization, sensors, actuators, and information

technology. The magnetocaloric effect (MCE) is the key for new and disruptive solid state-based refrigeration. Magnetic hysteresis and its inherent energy product characterise the performance of all magnetic materials. In the 60th position of the periodic table of elements is neodymium - an element that belongs to the rare earth-lanthanides and essential for the above applications. Basic material requirements, figure of merits, demand and supply, criticality of strategic elements and their recycling are explained for both permanent magnets and magnetocalorics referring to the benchmark materials NdFeB and LaFeSi. Every battery needs a magnet. 95% of electric vehicles utilize rare earth magnet-based drive motors, the quantities required global will grow from 5.000 t in 2019 to about 40.000 - 70.000 t per anno in 2030. The material history of neodymium is exciting and complex; monopolistic mining in China under ruinous conditions is just as problematic as our dependence on it. How "green" are the metals for renewable technologies? Who pays which price for it, and when?

Symposium Dynamics of Opinion Formation – From Quorum Sensing to Polarization (SYOF)

jointly organised by
the Physics of Socio-economic Systems Division (SOE),
the Dynamics and Statistical Physics Division (DY),
and the Biological Physics Division (BP)

Karoline Wiesner
Department of Physics and Astronomy
University of Potsdam
Germany
karoline.wiesner@uni-potsdam.de

Sven Banisch
Institute of Technology Futures
Karlsruhe Institute of Technology
Germany
sven.banisch@universecity.de

Jens Christian Claussen
Institute of Technology Futures
University of Birmingham
United Kingdom
j.c.claussen@bham.ac.uk

Quorum sensing is a widespread biological mechanism through which cells can exchange information and achieve a consensus state – hence a pre-social opinion formation process. In societies, opinion formation is a complex dynamical process that can, depending on the voting system and social interactions, lead to polarized societies or multi-parties systems. This symposium focuses on the dynamical processes underlying this opinion formation, the influence of the underlying topology of the opinion space (binary/Ising, Potts, continuous, higher-dimensional) and the resulting phase transitions.

Overview of Invited Talks and Sessions

(Lecture hall HSZ 01)

Invited Talks

SYOF 1.1	Mon	9:30–10:00	HSZ 01	Towards understanding of the social hysteresis – insights from statistical physics — •KATARZYNA SZNAJD-WERON
SYOF 1.2	Mon	10:00–10:30	HSZ 01	Polarization in attitude distributions from surveys and models of continuous opinion dynamics — •JAN LORENZ, MARTIN GESTEFELD
SYOF 1.3	Mon	10:30–11:00	HSZ 01	Collective patterns and stable misunderstandings in networks striving for consensus without a common value system — •JOHANNES FALK, EDWIN EICHLER, KATJA WINDT, MARC-THORSTEN HÜTT
SYOF 1.4	Mon	11:15–11:45	HSZ 01	A yet undetected cognitive bias, revealed by opinion dynamics simulations — •GUILLAUME DEFFUANT
SYOF 1.5	Mon	11:45–12:15	HSZ 01	Extreme switches in kinetic exchange models of opinion. — •PARONGAMA SEN, KATHAKALI BISWAS

Sessions

SYOF 1.1–1.5	Mon	9:30–12:15	HSZ 01	Dynamics of Opinion Formation – From Quorum Sensing to Polarization
--------------	-----	------------	--------	--

Sessions

– Invited Talks –

SYOF 1: Dynamics of Opinion Formation – From Quorum Sensing to Polarization

Time: Monday 9:30–12:15

Location: HSZ 01

Invited Talk

SYOF 1.1 Mon 9:30 HSZ 01

Towards understanding of the social hysteresis – insights from statistical physics — •KATARZYNA SZNAJD-WERON — Wrocław University of Science and Technology, Wrocław, Poland

Hysteresis and tipping points are common features found in many complex social and psychological systems. For example, empirical studies suggest that public opinion demonstrates both of these phenomena, where it appears to be unresponsive to change (related to hysteresis) and then suddenly shifts abruptly at the tipping point. Hysteresis is used in social science to explain the inflexibility of change and is seen as a slow response of society to new issues, even when they are acknowledged by experts. From a statistical physics point of view, hysteresis is associated with first-order (discontinuous) phase transitions. This has led us to investigate what factors promote discontinuous phase transitions in models of opinion dynamics. We have been working on this subject for the last 10 years, focusing mainly on the q-voter model which is particularly attractive both from a theoretical and social point of view. In the first part of the lecture I will briefly review these results, and discuss which results are particularly relevant from the point of view of social sciences.

Someone might ask why physicists are concerned with social systems. Probably the first answer that comes to mind is that the methods and concepts of statistical physics can also be useful in the social sciences. But is feedback possible? During the lecture I will show that result obtained within the model originally proposed to describe social opinion dynamics can go beyond the state of the art in physics.

Invited Talk

SYOF 1.2 Mon 10:00 HSZ 01

Polarization in attitude distributions from surveys and models of continuous opinion dynamics — •JAN LORENZ and MARTIN GESTEFELD — Constructor University (formerly Jacobs University), Bremen, Germany

Empirical attitude distributions from the European Social Survey often have non-trivial shapes with varying degrees of polarization. We analyze a large sample of 4,155 attitude distribution from various European countries and topics like left-right self-placement, European unification, and the cultural implications of migrations (and several others) for years between 2002 to 2018. All opinion distributions are built on questions with an 11-point quasi-continuous scale. Even in this one-dimensional setting, measuring polarization has many aspects, but not all are empirically relevant. Many distributions have up to five modes with modes: Two at both extremes, one in the center, and two off-center. We specify a measurement model for these opinion distributions and use it to decompose polarization. Finally, we discuss to what extent an opinion dynamics model with individual attitude change functions from psychological theory can replicate the empirically observed attitude distributions as stable outcomes.

Invited Talk

SYOF 1.3 Mon 10:30 HSZ 01

Collective patterns and stable misunderstandings in networks striving for consensus without a common value system — •JOHANNES FALK¹, EDWIN EICHLER^{2,3}, KATJA WINDT^{3,1}, and MARC-THORSTEN HÜTT¹ — ¹Constructor University, Bremen, Germany — ²EICHLER Consulting AG, Weggis, Switzerland — ³SMS Group GmbH, Düsseldorf, Germany

Collective phenomena in systems of interacting agents have helped us understand diverse social, ecological and biological observations. The corresponding explanations are challenged by incorrect information processing. In particular, the models typically assume a shared understanding of signals or a common

truth or value system, i.e., an agreement on whether the measurement or perception of information is right or wrong. It is an open question whether a collective consensus can emerge without these conditions. We introduce a model of interacting agents that strive for consensus, however, each with only a subjective perception of the world. We do not presuppose a definition of right or wrong and the actors can hence not distinguish between correct and incorrect observations. Depending on how responsive the agents are to changing their world-view we observe a transition between an unordered phase of individuals that are not able to communicate and a phase of an emerging shared signalling framework. We find that there are two types of convention-aligned clusters: one, where all social actors in the cluster have the same set of conventions, and one, where neighbouring actors have different but compatible conventions (stable misunderstandings). [1] Sci Rep 12, 3028 (2022)

15 min. break

Invited Talk

SYOF 1.4 Mon 11:15 HSZ 01

A yet undetected cognitive bias, revealed by opinion dynamics simulations — •GUILLAUME DEFFUANT — Université Clermont Auvergne, INRAE, UR LISC, Aubière, France

In the first part of the talk, I consider a recent opinion dynamics model in which the agents hold opinions about each other. The simulations of this model show surprising patterns. When agents do not gossip, the average opinion tends to increase and then to remain at a high value. When agents gossip, the average opinion tends to decrease and then to stabilise at a negative value. The mathematical analysis shows that a positive bias on the self-evaluation appears in the model and plays a crucial role in the pattern emergence. In the second part of the talk, I present an experiment that provides evidence supporting the existence of a similar positive bias in human subjects. I argue that this bias is different from the well-known positive bias from self-enhancement and was yet undetected.

Invited Talk

SYOF 1.5 Mon 11:45 HSZ 01

Extreme switches in kinetic exchange models of opinion. — •PARONGAMA SEN¹ and KATHAKALI BISWAS² — ¹Department of Physics, University of Calcutta, 92 APC Road, Kolkata 700009, India — ²Department of Physics, Victoria Institution, 78B APC Road, Kolkata 700009, India

We consider a kinetic exchange opinion formation model, where the opinions can take three discrete values represented by $\pm 1, 0$. Such states may represent the support for two candidates/parties and a neutral opinion or three different ideologies where ± 1 correspond to radically different ones. We take a finite probability to switch from $+1$ to -1 and vice versa, which is usually not considered in similar models studied earlier. Except for initially completely disordered states, consensus states are reached for this model in general. Subsequently, a noise is incorporated by making the interactions both positive and negative. An order-disorder phase transition is obtained for this two parameter model. We discuss the critical properties and dynamical behaviour of the model in a mean field approach where results can be obtained analytically. Although the effect of the negative interactions is stronger, the extreme switches alone determine the nature of the disordered phase. As the extreme switches are allowed with larger probability, the system tends to a polarisation. For the maximum possible extreme switch, the system becomes identical to a two state voter model after a transient time.

Symposium SKM Dissertation Prize 2023 (SYSD)

jointly organised by
the divisions of the Condensed Matter Section (SKM)

Sarah Köster
Georg-August-Universität Göttingen
Friedrich-Hund-Platz 1
37077 Göttingen
sarah.koester@uni-goettingen.de

The divisions belonging to the Condensed Matter Section (SKM) of the DPG annually award the SKM Dissertation Prize. The prize acknowledges outstanding research during the PhD work in the research areas of SKM completed in 2021 or 2022, and its excellent oral presentation. Based on nominations, a jury consisting of the chairpersons of all SKM divisions has selected five finalists for the award to present their work in this symposium. The winner will be selected after the symposium and publicly announced Tuesday, March 28th in the afternoon during the ceremonial session.

Overview of Invited Talks and Sessions

(Lecture hall HSZ 04)

Invited Talks

SYSD 1.1	Mon	9:30–10:00	HSZ 04	Diffusion of antibodies in solution: from individual proteins to phase separation domains — •ANITA GIRELLI
SYSD 1.2	Mon	10:00–10:30	HSZ 04	Intermediate Filament Mechanics Across Scales — •ANNA V. SCHEPERS
SYSD 1.3	Mon	10:30–11:00	HSZ 04	Ultrafast Probing and Coherent Vibrational Control of a Surface Structural Phase Transition — •JAN GERRIT HORSTMANN
SYSD 1.4	Mon	11:00–11:30	HSZ 04	Electro-active metasurfaces employing metal-to-insulator phase transitions — •JULIAN KARST
SYSD 1.5	Mon	11:30–12:00	HSZ 04	The role of unconventional symmetries in the dynamics of many-body systems — •PABLO SALA

Sessions

SYSD 1.1–1.5	Mon	9:30–12:00	HSZ 04	SKM Dissertation Prize
--------------	-----	------------	--------	-------------------------------

Sessions

– Invited Talks –

SYSD 1: SKM Dissertation Prize

Time: Monday 9:30–12:00

Location: HSZ 04

Invited Talk SYSD 1.1 Mon 9:30 HSZ 04**Diffusion of antibodies in solution: from individual proteins to phase separation domains** — •ANITA GIRELLI — Universität Tübingen, Tübingen, Germany — Stockholm University, Stockholm, Sweden

We investigated the diffusion of a model system for liquid-liquid phase separation (LLPS), which is a biological mechanism for the formation of intracellular organelles. The solution of γ -globulin and PEG spontaneously separates and reaches a gel state due to the high concentration of the more concentrated of the two phases. The hierarchy of motions requires to probe the sample from nanometers to micrometers and time scales from picoseconds to hundreds of seconds. We achieved this by combining light, neutron, and X-ray scattering. At LLPS domains length scale, X-ray photon correlation spectroscopy (XPCS) reveals correlation functions which show typical characteristics of ballistic motion as seen for colloidal gels [1]. The experimental results are compared with simulated data based on the Cahn-Hilliard equation. Qualitative comparability is obtained by adding a strong dependence of the protein mobility on protein concentration. The validity of this assumption is confirmed by probing the diffusion on the protein length scale and below with neutron quasi-elastic scattering and XPCS [2,3]. The combination of Neutron Spin Echo and XPCS allows to access the diffusion at protein length scale over 10 orders of magnitude.

[1] Girelli et al., PRL 126 (13), 2021. [2] Girelli et al., Mol. Pharm. 18 (11), 2021. [3] Reiser et al., Nat. Comm., 13,2022.

Invited Talk SYSD 1.2 Mon 10:00 HSZ 04**Intermediate Filament Mechanics Across Scales** — •ANNA V. SCHEPERS — Rosalind Franklin Institute and University of Oxford, UK — Georg-August University Göttingen, DE

The mechanical properties of cells are largely determined by the cytoskeleton, an intricate and complex structure formed by protein filaments, motor proteins, and crosslinkers. The three main types of protein filaments are microtubules, actin filaments, and intermediate filaments (IFs). Whereas microtubules and actin filaments are exceptionally conserved, the family of IFs is diverse. The variety of IF proteins is potentially linked to the various mechanics of different cell types. We combined studies of IF mechanics on different time scales and in systems of increasing complexity, from single filaments to networks in cells. This multiscale approach allows us to interpret observations from simplified system while adding increasing physiological context in subsequent experiments. We focussed on the tunability of IF mechanics by environmental cues. In a series of experiments, including single filament stretching measurements and filament-filament interaction measurements with optical tweezers, microrheology, and cell stretching, we characterised how electrostatic and hydrophobic interactions provide mechanisms by which the IF cytoskeleton can be tuned. The studies revealed how small changes influence IF mechanics on multiple scales. In combination with simulations, we characterised how charge shifts alter single filament mechanics. Such insights provide a deeper understanding of the mechanisms by which cells can maintain their integrity and mechanically adapt to their environment.

Invited Talk SYSD 1.3 Mon 10:30 HSZ 04**Ultrafast Probing and Coherent Vibrational Control of a Surface Structural Phase Transition** — •JAN GERRIT HORSTMANN — Max Planck Institute for Multidisciplinary Sciences, Göttingen, Germany — Dept. of Materials, ETH Zürich, Zürich, Switzerland

The desire to exert active optical control over matter is a unifying theme across multiple scientific fields. In femtochemistry, multi-pulse optical excitation schemes exploit coherences in decisive electronic and vibrational degrees of freedom of molecules to influence the efficiencies of chemical reactions. The application of this concept to solid-state systems is, however, complicated by, e.g., the high electronic and vibrational density of states, or couplings to an external heat

bath. In this respect, low-dimensional and strongly correlated systems represent a promising intermediate between molecules and bulk solids, with phase transitions assuming the role of a ‘reaction’.

In this talk, I report on the coherent vibrational control of a metal-insulator structural phase transition in a quasi-one-dimensional surface system, namely, atomic indium wires on the (111) surface of silicon. By analogy with repeatedly pushing a child on a swing, we use timed sequences of femtosecond light pulses to manipulate the amplitudes of key phonon modes connecting the insulating and metallic phases, thereby steering the system across the transition state. Our results confirm the applicability of coherent control tactics from femtochemistry to solids, creating not only strong conceptual links between the two fields, but also providing a new handle to switch the chemical and physical functionalities of materials on ultrafast time scales.

Invited Talk SYSD 1.4 Mon 11:00 HSZ 04**Electro-active metasurfaces employing metal-to-insulator phase transitions** — •JULIAN KARST — 4th Physics Institute and Research Center SCoPE, University of Stuttgart, Germany

Functional and active plasmonic nanostructures and metasurfaces are at the heart of emerging and novel optical technologies as they allow to confine and actively manipulate light on very small length scales. Ultimately, they will contribute to the miniaturization of existing and novel optical devices necessary in a great variety of different fields. They include but are not limited to new display and projection technologies for augmented and virtual reality, dynamic 3D holography devices or miniaturized LiDAR (Light Detection and Ranging) approaches. I will introduce and give an in-depth analysis of our novel approaches for such functional and active plasmonic systems and metasurfaces, utilizing metal-to-insulator phase change materials. In particular, I will highlight nanoantennas and metasurfaces from metallic polymers which can be electrically switched in the infrared spectral range via CMOS-compatible voltages. This concept is based on an electrically driven metal-to-insulator phase transition and allows me to demonstrate, on the one hand, metasurfaces for ultra-high-contrast active beam switching. On the other hand, I realize an electro-active metaobjective comprising metalenses-on-demand. By using gel electrolytes, the presented metadevices can even be integrated into state-of-the-art on-chip electro-optic components.

Invited Talk SYSD 1.5 Mon 11:30 HSZ 04**The role of unconventional symmetries in the dynamics of many-body systems** — •PABLO SALA — California Institute of Technology (Caltech), Pasadena, United States

Symmetries are essential to classify equilibrium phases of matter and to explain how thermal equilibrium is attained. In this talk, we explore the role that certain unconventional symmetries play in the dynamics of many-body systems.

To begin with, we show that the conservation of a charge and its associated dipole moment leads to a provable fragmentation of the Hilbert space into exponentially many disconnected sectors. In turn, this can translate into non-vanishing bulk correlators and the existence of localized among other unexpected phenomena. In general, we find that this conservation leads to novel universal hydrodynamic behavior, which can coexist with initial states that avoid thermalization, hence providing examples of weak ergodicity breaking.

We then show that dipole-conserving models become good approximations of strongly-tilted interacting systems. In fact, the high level of control of current experimental platforms makes these phenomena accessible to present-day experiments. We use our previous insights to analyze experimental results obtained via ultracold atoms, where the system is observed to remain localized at accessible times.

We conclude by revisiting the notion of symmetry from a broader perspective. In particular, we inquire about what spatially-modulated symmetries a system can have, providing a novel approach to realize some of them.

Symposium Green Magnets for Efficient Energy Conversion (SYGM)

jointly organised by
the Magnetism Division (MA) and
the Metal and Material Physics Division (MM)

Oliver Gutfleisch
Technical University of Darmstadt
Materials Science
Alarich-Weiss-Str. 16
64287 Darmstadt
oliver.gutfleisch@tu-darmstadt.de

Michael Farle
University Duisburg-Essen
Faculty of Physics
Lotharstr. 1
47057 Duisburg
michael.farle@uni-due.de

Ever increasing demands for efficient, low cost energy conversion require the development of new materials, which can be used in e-mobility, power generation, robotics and refrigeration. The class of magnetic materials covers all of these technologies; in fact hard and soft magnets as well as caloric materials are often overlooked key enablers of a net-zero CO₂ emission scenario. In e-mobility, every battery needs a magnet, i.e. either the mass of the battery is reduced or the range is extended when highly efficient hard and soft magnets are employed in motor and generator. The complexity of magnetostructural phase transitions offers ample opportunities to design (magneto-)caloric and elastic properties for efficient, climate friendly future cooling technologies, smart actuators and soft magnetic robotics.

Overview of Invited Talks and Sessions

(Lecture hall HSZ 01)

Invited Talks

SYGM 1.1	Mon	15:00–15:30	HSZ 01	Data mining protocols for functional magnetic materials — •OLLE ERIKSSON
SYGM 1.2	Mon	15:30–16:00	HSZ 01	High performance permanent magnets; elements criticality, new demands, and extrinsic magnetic properties — •HOSSEIN SEPEHRI-AMIN, XIN TANG, TADAKATSU OHKUBO, KAZUHIRO HONO
SYGM 1.3	Mon	16:00–16:30	HSZ 01	Magnetic shape memory Heuslers: microstructure-related effects on the martensitic transformation — •FRANCA ALBERTINI
SYGM 1.4	Mon	16:45–17:15	HSZ 01	Thin film combinatorial studies of hard magnetic materials — •NORA DEMPSEY
SYGM 1.5	Mon	17:15–17:45	HSZ 01	Magnetocaloric materials for energy-efficient thermal control systems — •VICTORINO FRANCO, AUN N. KHAN, JORGE REVUELTA-LOSADA, ÁLVARO DÍAZ-GARCÍA, LUIS M. MORENO-RAMÍREZ, JIA YAN LAW

Sessions

SYGM 1.1–1.5	Mon	15:00–17:45	HSZ 01	Green Magnets for Efficient Energy Conversion
--------------	-----	-------------	--------	--

Sessions

– Invited Talks –

SYGM 1: Green Magnets for Efficient Energy Conversion

Time: Monday 15:00–17:45

Location: HSZ 01

Invited Talk SYGM 1.1 Mon 15:00 HSZ 01**Data mining protocols for functional magnetic materials** — •OLLE ERIKSSON — Uppsala University, Uppsala, Sweden

Theory of functional magnetic materials for use in permanent magnet applications or for magneto caloric cooling is described in this presentation. Using a high-throughput approach of calculations based on density functional theory together with a data-mining algorithm, several new rare-earth-free permanent magnets are reported. An interesting set of elements is found for materials containing 3d and p-elements, in particular Fe₂C, Mn₂MoB₄, and Mn₂WB₄. For these systems doping protocols were also investigated and, in particular, (Fe_{0.75}X_{0.25})₂C (X = Mn, Cr, V, and Ti), Mn₂XB₄ (X = Mo and W) along with Mn₂(X_{0.5}Y_{0.5})B₄ (X, Y = Mo, W, Ta, Cr) are suggested here as promising permanent magnets. Screening algorithms for magneto caloric materials are also discussed, and promising compounds will be presented.

Invited Talk SYGM 1.2 Mon 15:30 HSZ 01**High performance permanent magnets; elements criticality, new demands, and extrinsic magnetic properties** — •HOSSEIN SEPEHRI-AMIN, XIN TANG, TADAKATSU OHKUBO, and KAZUHIRO HONO — National Institute for Materials Science, Tsukuba, Japan

Permanent magnets are widely used in the green energy conversions and they play an important role toward realization of carbon neutrality. In order to maintain sustainable production of permanent magnets in a long term, efforts are required to eliminate the permanent magnets* reliance on critical elements such as Dy and to diverge rare-earth usage while maintaining sufficiently large coercivity and energy product in the magnets. we will first present our research efforts on development of high coercivity Dy-free Nd-Fe-B magnets for applications in traction motor of hybrid/electric vehicles and generator of wind turbines. We will demonstrate how grain boundary/interface engineering in the hot-deformed Nd-Fe-B magnets has led to a large coercivity of 2.5 T, remanent magnetization of 1.32 T and excellent thermal stability of coercivity. In the second part of the talk, the potential of Fe-rich SmFe₁₂-based magnets and the current challenges to realize these materials as new permanent magnets will be discussed. we will show our recent success in realizing a sufficiently large coercivity of 1.0 T in rare-earth lean SmFe₁₂-based anisotropic sintered magnets assisted by machine learning. Based on detailed microstructure characterizations, modeled thin films, and micromagnetic simulations, we will discuss the optimum microstructure which can lead to a larger coercivity and remanent magnetization in the SmFe₁₂-based magnets.

Invited Talk SYGM 1.3 Mon 16:00 HSZ 01**Magnetic shape memory Heuslers: microstructure-related effects on the martensitic transformation** — •FRANCA ALBERTINI — Institute of Materials for Electronics and Magnetism (IMEM) - CNR, Parma, Italy

The vast family of magnetic shape memory Heuslers provides an extended playground of physical properties. The interplay between a martensitic transformation and magnetically ordered states gives rise to a series of functional properties that can be exploited in different technological sectors, among which solid state refrigeration, thermomagnetic generation, and robotics. Their excellent responsiveness to external fields, i.e. magnetic field, pressure and stress and their combined application, makes them promising for multifunctional exploitation. On the other hand, the hysteretic character of the martensitic transformation limits the performances of these materials in cyclic operations. In my talk I report some recent results on micro and nanoscale materials obtained by different fabrication methods, i.e. epitaxial thin films, micro/nanostructures obtained by

lithographic techniques, and mechanically-milled particles. Thin films and micro/nanostructures are of particular interest not only for the realisation of miniaturised devices, but also for providing insights into the magneto-structural coupling at the different length scales. The talk will focus on microstructure tuning and microstructure-related effects on the martensitic transformation, in view of the fully exploitation of this class of materials in caloric and smart applications.

15 min. break**Invited Talk** SYGM 1.4 Mon 16:45 HSZ 01**Thin film combinatorial studies of hard magnetic materials** — •NORA DEMPSEY — Univ. Grenoble Alpes, CNRS, Grenoble INP, Institut NEEL, 38000 Grenoble, France

Combinatorial thin film studies are used for the screening and optimization of a range of functional materials. The basic idea is to produce compositionally graded films, to allow high throughput characterisation of materials properties as a function of composition, as well as other processing parameters such as deposition temperature and post-deposition annealing conditions. This approach holds much potential for the development of green magnets for efficient energy conversion. In particular, it can be used to study the effect of element substitution in Rare Earth - Transition Metal hard magnetic phases, so as to reduce dependence on critical rare earth elements.

In this talk I will present both recent [1] and on-going studies of compositionally graded hard magnetic materials produced by sputtering asymmetric targets or co-sputtering of multiple targets followed by annealing under different conditions. I will discuss the influence of composition and processing parameters on structural and magnetic properties, as probed using high throughput scanning mode characterisation tools (EDX, XRD and MOKE). I will finish up by presenting future prospects for such studies, in particular when combined with ab-initio calculations on the one hand and machine learning on the other.

[1] Y. Hong et al., *J. Mater. Res. Technol.* 18 (2022) 1245**Invited Talk** SYGM 1.5 Mon 17:15 HSZ 01**Magnetocaloric materials for energy-efficient thermal control systems** — •VICTORINO FRANCO, AUN N. KHAN, JORGE REVUELTA-LOSADA, ÁLVARO DÍAZ-GARCÍA, LUIS M. MORENO-RAMÍREZ, and JIA YAN LAW — University of Seville, Spain

Energy efficient and environmentally friendly thermal management have a direct impact on the sustainability of our way of life, with magnetocaloric refrigeration being promising for achieving a greener cooling technology [1]. However, appliances are not yet on the consumer market due to relevant limitations of the active materials. In addition to applications point of view, the effect can be used to perform studies of phase transitions. Focusing on rare earth free materials, two new types of have a promising future: high entropy alloys and materials for additive manufacturing. We will present a novel fabrication procedure for obtaining homogeneous composite filaments for additive manufacturing and we will demonstrate that the magnetocaloric response of the fillers is not affected by the manufacturing procedure [2]. We will also highlight magnetocaloric high-entropy alloys, for which new compositions have allowed to close the gap between traditional HEA and high-performing magnetocaloric materials [3,4].

[1] V. Franco et al., *Progress in Materials Science* 93 (2018) 112; [2] Á. Díaz-García et al., *Composites Communications* 35 (2022) 101352; [3] J.Y. Law et al., *APL Materials* 9, (2021) 080702; [4] J.Y. Law et al., *Journal of Materials Research* (2022). <https://doi.org/10.1557/s43578-022-00712-0>

Symposium Physics of Fluctuating Paths (SYFP)

jointly organised by
the Dynamics and Statistical Physics Division (DY),
the Chemical and Polymer Physics Division (CPP), and
the Biological Physics Division (BP)

Aljaz Godec
Forschungsgruppe Mathematische
Biophysik
Max Planck Institut für
multidisziplinäre Naturwissenschaften
Am Fassberg 11
37077 Göttingen
agodec@mpinat.mpg.de

Udo Seifert
II. Institut für Theoretische Physik
Universität Stuttgart
Pfaffenwaldring 57
70550 Stuttgart
useifert@theo2.physik.uni-stuttgart.de

Peter Sollich
Institut für Theoretische Physik
Georg-August-Universität Göttingen
Friedrich-Hund-Platz 1
37077 Göttingen
peter.sollich@uni-goettingen.de

State-of-the-art experiments probe physical observables, such as heat, work or entropy production, empirical densities and currents, on the level of individual, stochastic paths. Such experiments are typically analysed by averaging along a limited number of individual realisations, which leads to substantial uncertainties in estimates. The systematic sample-to-sample fluctuations of such path-observables encode important information about the underlying, microscopic dynamical processes and are therefore a frontier of experimental, theoretical, and computational physics. Recently there has been a surge in the development and applications of path-based concepts across many fields of physics, which are surveyed in this symposium.

Overview of Invited Talks and Sessions

(Lecture hall HSZ01)

Invited Talks

SYFP 1.1	Tue	9:30–10:00	HSZ 01	Time at which a stochastic process achieves its maximum — •SATYA MAJUMDAR
SYFP 1.2	Tue	10:00–10:30	HSZ 01	Fluctuations and molecule-spanning dynamics of single Hsp90 proteins on timescales from nanoseconds to days — •THORSTEN HUGEL
SYFP 1.3	Tue	10:30–11:00	HSZ 01	Path reweighting for Langevin dynamics — •BETTINA KELLER
SYFP 1.4	Tue	11:15–11:45	HSZ 01	Out-of-equilibrium dynamics of trapped Brownian particles — •RAUL A. RICA
SYFP 1.5	Tue	11:45–12:15	HSZ 01	Thermodynamics of Clocks — •PATRICK PIETZONKA

Sessions

SYFP 1.1–1.5	Tue	9:30–12:15	HSZ 01	Physics of Fluctuating Paths
--------------	-----	------------	--------	-------------------------------------

Sessions

– Invited Talks –

SYFP 1: Physics of Fluctuating Paths

Time: Tuesday 9:30–12:15

Location: HSZ 01

Invited Talk

SYFP 1.1 Tue 9:30 HSZ 01

Time at which a stochastic process achieves its maximum — •SATYA MAJUMDAR — Lptms, Université Paris-Saclay, Bat 530, Rue André Rivière, Orsay 91405, France

For any stochastic time-series of duration T , the time t_{\max} at which the process achieves its maximum is an important observable. For example, for a stock price over a trading period T , one would like to sell the stock at the time when the price is maximal. I'll discuss the statistics of t_{\max} for a variety of stochastic processes. In particular, for several stationary processes, both in and out of equilibrium systems, we show that the distribution of t_{\max} over $[0, T]$ exhibits a universal and interesting edge behavior (near 0 and T).

Invited Talk

SYFP 1.2 Tue 10:00 HSZ 01

Fluctuations and molecule-spanning dynamics of single Hsp90 proteins on timescales from nanoseconds to days — •THORSTEN HUGEL — Institute of Physical Chemistry, University of Freiburg, Germany — Signalling research centers BIOS and CIBSS, University of Freiburg, Germany — Cluster of Excellence livMatS @ FIT, University of Freiburg, Germany

Protein dynamics have been investigated on a wide range of timescales. Nano- and picosecond dynamics have been assigned to local fluctuations, while slower dynamics have been attributed to larger conformational changes. However, it is largely unknown how local fluctuations can lead to global changes and on which timescales the proteins dynamics are ergodic and if they show ageing. These questions become even more challenging if ATP hydrolysis is involved.

Here we set out to understand the fluctuations and conformational dynamics in the molecular machine and heat shock protein Hsp90. Therefore, we measure the dynamics of single Hsp90s on timescales from nanoseconds to days with a combination of single-molecule fluorescence, Neutron scattering and Plasmon resonance supported by MD simulations.

I will show that molecule-spanning dynamics on the 100 ns timescale likely precede hierarchical allosteric processes on slower timescales. Then the very good statistic on the even slower conformational dynamics allows us to discuss directionality, ergodicity and ageing in this fascinating ATP fueled molecular machine.

Invited Talk

SYFP 1.3 Tue 10:30 HSZ 01

Path reweighting for Langevin dynamics — •BETTINA KELLER — Freie Universität Berlin, Berlin, Germany

Transition processes in molecular dynamics are investigated by simulating the molecular dynamics as underdamped Langevin dynamics on a high-dimensional energy surface. The accuracy of the rate estimates depends critically on the number of transitions observed in the simulated trajectories. However, the relevant molecular timescales are often beyond the reach of molecular simulations - even when the simulation is conducted on a supercomputer. Slow molecular processes include formation of molecular complexes, transitions through membranes, or phase transitions in crystalline materials. By biasing the potential energy one can sample transitions of rare events, but the rate estimates are distorted. Path reweighting techniques [1, 2] unbiased the rate estimates by explicitly calculating the path probability density in the original and biased potential, and thus enable us to characterize slow molecular processes. While the path probability density for overdamped Langevin dynamics is well-documented, little information is available on the path probability densities for underdamped Langevin dynam-

ics [3]. This hampers the use of path reweighting in molecular simulations. I will focus on Langevin integrators constructed via the operator splitting technique, and derive their path probability density. An important intermediate result is the single-step transition probability which maps a point in state space to another point in state space. The image of this function determines whether the integrator can be used (efficiently) for path reweighting. I will demonstrate the results on model potentials and molecular examples.

[1] Luca Donati and Bettina G Keller. Girsanov reweighting for metadynamics simulations. *The Journal of Chemical Physics*, 149(7):072335, 2018.

[2] Luca Donati, Marcus Weber, and Bettina G Keller. A review of Girsanov reweighting and of square root approximation for building molecular Markov state models. *Journal of Mathematical Physics*, 63(12):123306, 2022.

[3] Stefanie Kieninger and Bettina G Keller. Path probability ratios for Langevin dynamics exact and approximate. *The Journal of Chemical Physics*, 154(9):094102, 2021.

15 min. break

Invited Talk

SYFP 1.4 Tue 11:15 HSZ 01

Out-of-equilibrium dynamics of trapped Brownian particles — •RAUL A. RICA — Universidad de Granada, Granada (Spain)

Micro and nanoparticles can be individually manipulated by different trapping mechanisms, among which optical tweezers and Paul traps are the most extended approaches. Trapped particles are subject to Brownian motion due to collisions with the molecules of the dispersing medium. Once trapped, the particles can be driven out of equilibrium under the action of external fields, giving rise to very rich dynamics. In this talk, we will discuss some of our work with trapped nanoparticles dispersed in different media, including water, air, and vacuum. We will present recent experimental results demonstrating the occurrence of anomalous relaxation processes, time asymmetries, and bistability with trapped particles.

Invited Talk

SYFP 1.5 Tue 11:45 HSZ 01

Thermodynamics of Clocks — •PATRICK PIETZONKA — Max Planck Institute for the Physics of Complex Systems, Dresden, Germany

The thermodynamic uncertainty relation (TUR) establishes a seemingly universal trade-off between cost and precision for classical non-equilibrium systems in a steady state. Applied to clocks subject to thermal noise, it states that the product of the energy used for the driving and the squared relative uncertainty of the displayed time is always greater than $2k_B T$. The TUR has been proven for models based on Markov jump dynamics or overdamped Brownian motion. It had also been conjectured to hold for underdamped Brownian dynamics, i.e., systems where inertia plays a role. This conjecture can now be disproven. I will present a counterexample that is inspired by a pendulum clock, consisting of an underdamped oscillator and a discrete counter, with thermal noise accounted for in both degrees of freedom. As it turns out analytically, this classic design principle of a clock allows one to overcome the bounds on precision set by the TUR. Beyond the minimal model, I also show numerically that the TUR can be broken in a fully continuous model with two underdamped degrees of freedom. Finally, I present a new bound valid for time-symmetric observables, which shows that for overdamped systems there is a minimal cost for producing a precise sequence of "ticks".

Symposium Ultrafast Excitation Pathways of Quantum Materials (SYUE)

jointly organised by
the Surface Science Division (O),
the Low Temperature Physics Division (TT), and
the Thin Films Division (DS)

Michael Sentef
University of Bristol, UK
Tyndall Avenue
Bristol BS8 1TL
michael.sentef@bristol.ac.uk

Martin Eckstein
University of Hamburg
Notkestraße 9-11
22607 Hamburg
martin.eckstein@uni-hamburg.de

Ultrafast laser experiments provide avenues to utilizing ultrafast light-matter interaction to control macroscopic properties of quantum materials. While conventional photo-induced processes in condensed matter often rely on ultrafast laser heating, there are intriguing pathways towards emergent macroscopic properties in quantum materials that are inherently non-thermal in nature. The mechanisms behind such pathways include transient modifications of the free-energy landscape by population redistributions, the dynamical modification of coupling strengths, and coherent light-matter dressing via Floquet engineering. This symposium brings together leading researchers in the field to showcase experimental and theoretical progress and discuss new avenues.

Overview of Invited Talks and Sessions

(Lecture hall HSZ 01)

Invited Talks

SYUE 1.1	Wed	9:30–10:00	HSZ 01	Dynamics and control in quantum materials using multi-terahertz spectroscopy — •RICHARD AVERITT
SYUE 1.2	Wed	10:00–10:30	HSZ 01	Accessing the nonthermal phonon populations in 2D materials with femtosecond electron diffuse scattering — •HÉLÈNE SEILER, MARIOS ZACHARIAS, DANIELA ZAHN, PATRICK-NIGEL HILDEBRANDT, THOMAS VASILEIADIS, YOAV WILLIAM WINDSOR, YINGPENG QI, CHRISTIAN CARBOGNO, CLAUDIA DRAXL, RALPH ERNSTORFER, FABIO CARUSO
SYUE 1.3	Wed	10:30–11:00	HSZ 01	Exciting potentials – Exploring the realms of ultrafast phase transitions — •LAURENZ RETTIG
SYUE 1.4	Wed	11:15–11:45	HSZ 01	Sub-cycle multidimensional spectroscopy of strongly correlated materials — VIKTOR VALMISPILD, EVGENY GORELOV, MARTIN ECKSTEIN, ALEXANDER LICHTENSTEIN, HIDEO AOKI, MIKHAIL KATSNELSON, MISHA IVANOV, •OLGA SMIRNOVA
SYUE 1.5	Wed	11:45–12:15	HSZ 01	Witnessing many-body entanglement in light-driven quantum materials — •MATTEO MITRANO, DENITSA BAYKUSHEVA, MONA KALTHOFF, DAMIAN HOFMANN, MARTIN CLAASSEN, DANTE KENNES, MICHAEL SENTEF
SYUE 1.6	Wed	12:15–12:45	HSZ 01	Optical responses of photoexcited materials: from parametric amplification to photoinduced superconductivity — •EUGENE DEMLER

Sessions

SYUE 1.1–1.6	Wed	9:30–12:45	HSZ 01	Ultrafast Excitation Pathways of Quantum Materials
--------------	-----	------------	--------	---

Sessions

– Invited Talks –

SYUE 1: Ultrafast Excitation Pathways of Quantum Materials

Time: Wednesday 9:30–12:45

Location: HSZ 01

Invited Talk SYUE 1.1 Wed 9:30 HSZ 01

Dynamics and control in quantum materials using multi-terahertz spectroscopy — •RICHARD AVERITT — UC San Diego, Department of Physics
Dynamics and control of quantum materials using light has emerged as a frontier research area. There are numerous possibilities to investigate including photoinduced metastability, creating non-equilibrium states with emergent properties, driving coherent many-body dynamics, or impulsively driving an order parameter to investigate the nonlinear *optical* response which can encode properties not evident with linear optical probes. In this vein, terahertz to mid-infrared spectroscopy is a particularly useful probe of low energy electrostatics in quantum materials in both the static and dynamic limits. I will present examples from my research group. This includes: (i) Efficient coherent magnon generation in the Mott insulator Sr_2IrO_4 using sub-gap circularly polarized mid-IR pulses. (ii) Gentle photoexcitation of the putative excitonic insulator Ta_2NiSe_5 resulting in stimulated nonlinear parametric terahertz generation that serves as a reporter of the excitonic condensate and its coupling to phonons.

Invited Talk SYUE 1.2 Wed 10:00 HSZ 01

Accessing the nonthermal phonon populations in 2D materials with femtosecond electron diffuse scattering — •HÉLÈNE SEILER^{1,2}, MARIOS ZACHARIAS^{1,3}, DANIELA ZAHN¹, PATRICK-NIGEL HILDEBRANDT¹, THOMAS VASILEIADIS¹, YOAV WILLIAM WINDSOR^{1,4}, YINGPENG QI¹, CHRISTIAN CARBOGNO¹, CLAUDIA DRAXL⁵, RALPH ERNSTORFER^{1,4}, and FABIO CARUSO⁶ — ¹Fritz-Haber-Institut der Max-Planck-Gesellschaft, Berlin, Germany — ²Freie Universität Berlin, Berlin, Germany — ³INSA de Rennes, 35708 Rennes, France — ⁴Technische Universität Berlin, Berlin, Germany — ⁵Humboldt-Universität zu Berlin, Berlin, Germany — ⁶Christian-Albrechts-Universität zu Kiel, Kiel, Germany

Femtosecond electron diffuse scattering (FEDS) is a powerful technique to access nonthermal phonon populations in photo-excited materials. We perform FEDS experiments to study the microscopic energy flow in two prototypical 2D materials, black phosphorus and MoS_2 . The experiments are complemented by first-principles calculations of the coupled electron-phonon dynamics based on the time-dependent Boltzmann equations. We also introduce an efficient first-principles methodology for the calculation of the all-phonon inelastic scattering in solids, and demonstrate its broad applicability to other 2D materials. Our joint experimental-theoretical approach provides a detailed picture of nonthermal phonons in photo-excited materials.

Invited Talk SYUE 1.3 Wed 10:30 HSZ 01

Exciting potentials – Exploring the realms of ultrafast phase transitions — •LAURENZ RETTIG — Fritz Haber Institute of the Max Planck Society, Berlin, Germany

Phase transitions, ubiquitous in nature, are characterized by breaking of characteristic material symmetries, which can be described by an order parameter. The phase of a material is then determined by the shape and the minima of the free energy surface. While in thermal equilibrium, a system occupies the phase space close to these minima, and phase transitions occur as function of thermodynamic state variables, ultrafast laser excitation allows modifying the energy surfaces on timescales faster than the response time of the system, thereby driving ultrafast phase transitions, and triggering coherent dynamics within the transient energy surfaces. This approach not only provides information about the microscopic couplings behind a phase transition, but also allows for coherent manipulation of material properties.

In my talk, I will discuss recent experiments employing time- and angle-resolved photoemission spectroscopy (trARPES), unearthing rich dynamics of photoinduced phase transitions in prototypical charge-density wave materials, including a transition into a hidden, metastable state.

15 min. break

Invited Talk SYUE 1.4 Wed 11:15 HSZ 01

Sub-cycle multidimensional spectroscopy of strongly correlated materials — VIKTOR VALMISPILD³, EVGENY GORELOV³, MARTIN ECKSTEIN⁶, ALEXANDER LICHTENSTEIN^{4,5}, HIDEO AOKI⁷, MIKHAIL KATSNELSON⁸, MISHA IVANOV^{1,9}, and •OLGA SMIRNOVA^{1,2} — ¹Max-Born-Institut Berlin — ²Technische Universität Berlin — ³European XFEL, Germany — ⁴Institute of Theoretical Physics, University of Hamburg — ⁵The Hamburg Centre for Ultrafast Imaging — ⁶Department of Physics, University of Erlangen-Nuremberg — ⁷National Institute of Advanced Industrial Science and Technology (AIST), Japan — ⁸Institute for Molecules and Materials, Radboud University, — ⁹Department of Physics, Imperial College London

Strongly correlated solids are extremely complex and fascinating quantum systems, where new states continue to emerge and where interaction with light may trigger interplay between them. In this interplay, sub-laser cycle electron response is particularly attractive as a tool for ultrafast manipulation of matter at PHz scale.

We introduce a new type of non-linear multidimensional spectroscopy, which allows us to unravel the sub-cycle dynamics of strongly correlated systems interacting with few-cycle infrared pulses and the complex interplay between different correlated states evolving on the sub-femtosecond time-scale. We use laser-driven two-dimensional Hubbard model to resolve sub-cycle transitions between Mott-insulating and metallic states, and follow pathways of charge and energy flow leading to final non-equilibrium state stabilized by correlations after the end of the laser pulse.

Invited Talk SYUE 1.5 Wed 11:45 HSZ 01

Witnessing many-body entanglement in light-driven quantum materials — •MATTEO MITRANO¹, DENITSA BAYKUSHEVA¹, MONA KALTHOFF², DAMIAN HOFMANN², MARTIN CLAASSEN³, DANTE KENNEDY^{2,4}, and MICHAEL SENTER² — ¹Department of Physics, Harvard University, Cambridge, Massachusetts 02138, USA — ²Max Planck Institute for the Structure and Dynamics of Matter, Center for Free-Electron Laser Science (CFEL), Luruper Chaussee 149, 22761 Hamburg, Germany — ³Department of Physics and Astronomy, University of Pennsylvania, Philadelphia, PA 19104, USA — ⁴Institut für Theorie der Statistischen Physik, RWTH Aachen University, 52056 Aachen, Germany and JARA-Fundamentals of Future Information Technology, 52056 Aachen, Germany

Many-body entanglement in condensed matter systems can be diagnosed from equilibrium response functions through the use of entanglement witnesses and operator-specific quantum bounds. Here, we investigate the applicability of this approach for detecting entangled states in quantum systems driven out of equilibrium. We use a multipartite entanglement witness, the quantum Fisher information, to study the dynamics of a paradigmatic fermion chain undergoing a time-dependent change of the Coulomb interaction. Our results show that the quantum Fisher information is able to witness distinct signatures of multipartite entanglement both near and far from equilibrium that are robust against decoherence. We discuss implications of these findings for probing entanglement in light-driven quantum materials with time-resolved optical and x-ray scattering methods.

Invited Talk SYUE 1.6 Wed 12:15 HSZ 01

Optical responses of photoexcited materials: from parametric amplification to photoinduced superconductivity — •EUGENE DEMLER — ETH, Zurich, Switzerland

Optical drives at terahertz and mid-infrared frequencies in quantum materials are commonly used to explore the nonlinear dynamics of interacting many-body systems. Recent experiments demonstrated several surprising optical properties of transient states induced by driving, including the appearance of photo-induced edges in the reflectivity, enhancement of reflectivity, and even light amplification. I will show that many of these unusual properties can be understood from the general perspective of reflectivity from Floquet materials, in which pump-induced oscillations of a collective mode lead to parametric generation of excitation pairs. This analysis predicts a universal phase diagram of drive induced features in reflectivity, which evidence a competition between driving and dissipation. I will argue that this mechanism explains several recent experimental observations, including photoinduced superconductivity in the pseudogap phase of high T_c cuprates.

Symposium Topology in Quantum and Classical Physics – From Topological Insulators to Active Matter (SYQC)

jointly organised by
the Biological Physics Division (BP),
the Low Temperature Physics Division (TT), and
the Dynamics and Statistical Physics Division (DY)

Magdalena Marganska
Theoretische Physik
Universität Regensburg
Universitätsstraße 31
93053 Regensburg
magdalena.marganska@physik.uni-regensburg.de

Antoine Venaille
Laboratoire de Physique
ENS de Lyon
46 allée d'Italie
69007 Lyon, France
antoine.venaille@ens-lyon.fr

The field of solid state physics, especially of material physics, has grown vigorously thanks to the discovery of topological protection and the universality of topological notions in many solid state systems. These ideas, rooted in the low temperature physics, have since expanded into other domains of physics, even into bio- and geophysics. The topological defects in bacterial colonies and tissues decide the life and death of cells; topological modes arise in active matter on curved surfaces; equatorial waves form at the boundary between two regions with opposite sign of the Coriolis force. It is fascinating that topological ideas flourish even in the chaotic environments of living matter and Earth systems. The aim of this symposium is to bring together the speakers and audience from the seemingly disparate fields of biological and low temperature physics, to explore together the mathematical connection between these two domains.

Overview of Invited Talks and Sessions

(Lecture hall HSZ 01)

Invited Talks

SYQC 1.1	Wed	15:00–15:30	HSZ 01	Topological magnetic whirls for computing — •KARIN EVERSCHOR-SITTE
SYQC 1.2	Wed	15:30–16:00	HSZ 01	Topological waves from solids to geo/astrophysical flows — •PIERRE DELPLACE, ANTOINE VENAILLE, NICOLAS PEREZ, GUILLAUME LAIBE, ARMAND LECLERC, MANOLIS PERROT, BRAD MARSTON
SYQC 1.3	Wed	16:00–16:30	HSZ 01	Topological Phase Transitions in Population Dynamics — •ERWIN FREY
SYQC 1.4	Wed	16:45–17:15	HSZ 01	Topological invariants protect robust chiral currents in active matter — •EVELYN TANG
SYQC 1.5	Wed	17:15–17:45	HSZ 01	Topological defects in biological active matter — •AMIN DOOSTMOHAMMADI

Sessions

SYQC 1.1–1.5	Wed	15:00–17:45	HSZ 01	Topology in Quantum and Classical Physics – From Topological Insulators to Active Matter
--------------	-----	-------------	--------	---

Sessions

– Invited Talks –

SYQC 1: Topology in Quantum and Classical Physics – From Topological Insulators to Active Matter

Time: Wednesday 15:00–17:45

Location: HSZ 01

Invited Talk SYQC 1.1 Wed 15:00 HSZ 01

Topological magnetic whirls for computing — •KARIN EVERSCHOR-SITTE — Faculty of Physics and Center for Nanointegration Duisburg-Essen, University of Duisburg-Essen, 47057 Duisburg, Germany

Novel computational paradigms in combination with suitable hardware solutions are required to overcome the limitations of our state-of-the-art computer technology. In this talk, I focus on the potential of magnetic whirls – so-called skyrmions – for computing.

Skyrmions are topologically stable whirls that occur in various areas of physics and were discovered by Tony Skyrme in the 1960s in particle physics. Skyrmions occurring in magnetic systems were first observed experimentally in 2009. Within a decade, the field of magnetic skyrmions has become a very active area of research, with the aim of exploiting the topological properties of the magnetic whirl-like particles for spintronics applications. For example, the peculiar twist of the magnetization in skyrmions leads to a very efficient coupling to electric currents and allows for "banana kicks" analogous to those in soccer. More recently, magnetic skyrmions have become the focus of unconventional computing schemes such as reservoir computing.

Invited Talk SYQC 1.2 Wed 15:30 HSZ 01

Topological waves from solids to geo/astrophysical flows — •PIERRE DELPLACE¹, ANTOINE VENAILLE¹, NICOLAS PEREZ^{1,2}, GUILLAUME LAIBE², ARMAND LECLERC², MANOLIS PERROT¹, and BRAD MARSTON³ — ¹CNRS, Laboratory of Physics, ENS de Lyon, France — ²CRAL, ENS de Lyon France — ³Brown University

Robust uni-directional edge modes are the hallmark of Chern insulators, a peculiar kind of topological insulators. Such topological states have been engineered in various platforms, from quantum solids to various classical analogs in photonics, acoustics and mechanics. Remarkably, such chiral modes also exist in continuous media encountered in nature. This is the case of oceanic and atmospheric equatorial waves that only propagate their energy eastward. This remarkable property, that triggers the El Niño southern oscillations and impacts the climate over the globe, has a topological interpretation somehow similar to Chern insulators. Maybe more importantly, such topological tools actually also allow the prediction of previously unnoticed waves in strongly stratified fluids that might be observable e.g. in stars.

Invited Talk SYQC 1.3 Wed 16:00 HSZ 01

Topological Phase Transitions in Population Dynamics — •ERWIN FREY — LMU Muenchen, Theresienstrasse 37, 80333 Muenchen, Germany

In this talk, I discuss how topological phases determine the behavior of nonlinear dynamical systems that arise, for example, in population dynamics. We have shown that topological phases can be realized with the antisymmetric Lotka-Volterra equation (ALVE). It governs, for example, the evolutionary dynamics of zero-sum games, such as the rock-paper-scissors game [1]. It also describes the condensation of non-interacting bosons in driven-dissipative setups [2]. We have shown that robust polarization emerges at the chain's edge for the ALVE, defined on a one-dimensional chain of rock-paper-scissors cycles [3]. The system undergoes a transition from left to right polarization as the control parameter passes through a critical value. We found that the polarization states are topological phases and that this transition is indeed a topological phase transition. Remarkably, this phase transition falls into symmetry class D within the

"ten-fold way" classification scheme of gapped free-fermion systems. Beyond the observation of topological phases in the ALVE, it might be possible to generalize the approach of our work to other dynamical systems in biological physics whose attractors are nonlinear oscillators or limit cycles.

[1] J. Knebel, T. Krüger, M. F. Weber, and E. Frey, *Phys. Rev. Lett.* **110**, 168106 (2013). [2] J. Knebel, M. F. Weber, T. Krüger, and E. Frey, *Nature Communications* **6**, 6977 (2015). [3] J. Knebel, P. M. Geiger, and E. Frey, *Phys. Rev. Lett.* **125**, 258301 (2020).

15 min. break

Invited Talk SYQC 1.4 Wed 16:45 HSZ 01

Topological invariants protect robust chiral currents in active matter — •EVELYN TANG — Rice University, Houston, USA

Living and active systems exhibit various emergent dynamics necessary for system regulation, growth, and motility. However, how robust dynamics arises from stochastic components remains unclear. Towards understanding this, I develop topological theories that support robust edge currents, effectively reducing the system dynamics to a lower-dimensional subspace. In particular, I will introduce stochastic networks in molecular configuration space that can model different systems from a circadian clock to the stochastic dynamics of cytoskeletal filaments. The edge localization results in new properties, e.g., the clock demonstrates increased precision with simultaneously decreased cost. These out-of-equilibrium systems further possess uniquely non-Hermitian features such as exceptional points and vorticity. More broadly, my work provides a blueprint for the design and control of novel and robust function in correlated and active systems.

Invited Talk SYQC 1.5 Wed 17:15 HSZ 01

Topological defects in biological active matter — •AMIN DOOSTMOHAMMADI — Niels Bohr Institute, University of Copenhagen, Copenhagen, Denmark

The spontaneous emergence of collective flows is a generic property of active fluids and often leads to chaotic flow patterns characterized by topological defects [1]. I will first discuss two examples of these collective features helping us understand biological processes: (i) to explain the tortoise & hare story in bacterial competition: how motility of *Pseudomonas aeruginosa* bacteria leads to a slower invasion of bacteria colonies, which are individually faster [2], and (ii) how self-propelled defects lead to finding an unanticipated mechanism for cell death [3,4]. I will then discuss various strategies to tame, otherwise chaotic, active flows, showing how hydrodynamic screening of active flows can act as a robust way of controlling and guiding active particles into dynamically ordered coherent structures. I will also explain how combining hydrodynamics with topological constraints can lead to further control of exotic morphologies of active shells [6].

[1] A. Amiri, R. Mueller, and A. Doostmohammadi, *J. Phys. A.* (2021).

[2] O. J. Meacock et al., *Nat. Phys.* (2021).

[3] T. N. Saw et al., *Nature.* (2017).

[4] R. Mueller, J. M. Yeomans, and A. Doostmohammadi, *Phys. Rev. Lett.* (2019).

[6] L. Metselaar, J. M. Yeomans, and A. Doostmohammadi, *Phys. Rev. Lett.* (2019).

Symposium Real-Time Measurements of Quantum Dynamics (SYQD)

jointly organised by
the Semiconductor Physics Division (HL),
the Magnetism Division (MA), and
the Low Temperature Physics Division (TT)

Jürgen König
Theoretische Physik
Universität Duisburg-Essen
Lotharstr. 1
47048 Duisburg
koenig@thp.uni-due.de

Rolf Haug
Leibniz Universität Hannover
Institut für Festkörperphysik
Appelstraße 2
30167 Hannover
haug@nano.uni-hannover.de

Time-resolved studies of quantum systems are the key to understanding quantum dynamics at its core. The real-time measurement of individual quantum jumps yields maximal physical insight. This includes electrical and optical detection schemes to monitor individual quantum jumps in nanoscopic devices. It is, furthermore, a prerequisite for coherent control of quantum states and can be used to optimise devices for metrological applications. The symposium is meant to report on recent experimental progress in performing real-time measurements of quantum dynamics, to present recently-developed theoretical methods for analyzing measured data, and to highlight recent successful examples of accessing quantum dynamics via real-time measurements.

Overview of Invited Talks and Sessions

(Lecture hall HSZ 01)

Invited Talks

SYQD 1.1	Thu	9:30–10:00	HSZ 01	Real-time measurement and control of spin dynamics in quantum dots — •SEIGO TARUCHA
SYQD 1.2	Thu	10:00–10:30	HSZ 01	Quantum Dot arrays for Quantum Information Transfer — •GLORIA PLATERO, DAVID FERNANDEZ-FERNANDEZ, JUAN ZURITA
SYQD 1.3	Thu	10:30–11:00	HSZ 01	Optical Detection of Real-Time Quantum Dynamics in Quantum Dots — •MARTIN GELLER, JENS KERSKI, ERIC KLEINHERBERS, JÜRGEN KÖNIG, ANNIKA KURZMANN, PIA LOCHNER, AXEL LORKE, ARNE LUDWIG, HENDRIK MANNEL, PHILIPP STEGMANN, ANDREAS WIECK, MARCEL ZÖLLNER
SYQD 1.4	Thu	11:30–12:00	HSZ 01	Cooper Pair Splitting in Real-Time — •CHRISTIAN FLINDT
SYQD 1.5	Thu	12:00–12:30	HSZ 01	Trajectory-based detection in stochastic and quantum thermodynamics — •JUKKA PEKOLA

Sessions

SYQD 1.1–1.5	Thu	9:30–12:30	HSZ 01	Real-Time Measurements of Quantum Dynamics
--------------	-----	------------	--------	---

Sessions

– Invited Talks –

SYQD 1: Real-Time Measurements of Quantum Dynamics

Time: Thursday 9:30–12:30

Location: HSZ 01

Invited Talk SYQD 1.1 Thu 9:30 HSZ 01**Real-time measurement and control of spin dynamics in quantum dots** — •SEIGO TARUCHA — Center for Emergent Matter Science and Quantum Computing, RIKEN, Wako, Saitama 351-0198, Japan

The progress of quantum information technologies using semiconductor quantum dots has provided novel methods to control and detect quantum dynamics of single electron spins. The quantum information unit (qubit) is prepared using a concept of electron spin resonance and the qubit dynamics is dependent on dephasing or fluctuations of the resonance frequency through interactions with electromagnetic environment. In this talk I will first show experiments on real-time measurements of fluctuating frequencies of the respective spins and exchange-coupled two spins in a double quantum dot. The quantum dot is made in natural Si and also isotopically purified ^{28}Si , which have different magnetic environments of nuclear spins. We use Ramsey interference sequence to derive the auto- and cross-power spectral density of the fluctuating resonance frequencies and address the influences from magnetic and charge noise in the respective quantum dots. We find an evident cross-correlation between two spins arising from the charge noise and devise a model of two-level fluctuators to account for the cross-correlation. Lastly I will show feedback control to suppress the influence on the spin dynamics from the environment.

Invited Talk SYQD 1.2 Thu 10:00 HSZ 01**Quantum Dot arrays for Quantum Information Transfer** — •GLORIA PLATERO, DAVID FERNANDEZ-FERNANDEZ, and JUAN ZURITA — Instituto de Ciencia de Materiales de Madrid (CSIC), Spain

The fabrication and control of semiconductor quantum dot arrays open the possibility to use these systems as quantum links, for transferring quantum information between distant sites, an indispensable part of large-scale quantum information processing. In this talk I will discuss different pulse-based protocols to transfer spin holes between edges of a quantum dot chain with high fidelity. I will show how the spin polarization of the transferred holes can be controlled by tuning the ratio between the SOC and the spin conserving tunneling rate [1]. Also, I will discuss how to transfer entangled hole spin qubits between edge dots. Our theoretical results suggest the feasibility of quantum dot arrays as high-fidelity quantum buses to distribute information between distant sites and perform one qubit gates in parallel.

An alternative way to transfer information between distant sites is mediated by protected topological edge states. I will discuss the long-range particle dynamics mediated by edge states in different quantum dot array configurations [2], which opens a new avenue for quantum state transfer protocols in low dimensional topological lattices.

[1] D. Fernández-Fernández et al., Phys. Rev. App., in press; D. Fernández-Fernández et al., submitted. [2] J. Zurita, C. E. Creffield, G. Platero, Quantum, 5, 591 (2021); *ibid*, submitted.

Invited Talk SYQD 1.3 Thu 10:30 HSZ 01

Optical Detection of Real-Time Quantum Dynamics in Quantum Dots — •MARTIN GELLER¹, JENS KERSKI¹, ERIC KLEINHERBERS¹, JÜRGEN KÖNIG¹, ANNIKA KURZMANN², PIA LOCHNER¹, AXEL LORKE¹, ARNE LUDWIG³, HENDRIK MANDEL¹, PHILIPP STEGMANN¹, ANDREAS WIECK³, and MARCEL ZÖLLNER¹ — ¹Faculty of Physics, University of Duisburg-Essen, 47057 Duisburg, Germany — ²2nd Institute of Physics and JARA-FIT, RWTH Aachen University, 52074 Aachen, Germany — ³Applied Solid State Physics, Ruhr-University, 44780 Bochum, Germany

Recording every single quantum event in a real-time measurement gives the maximum information of a dynamical quantum system. The obtained time traces can be used in a statistical evaluation to get a deep understanding about the underlying physical mechanisms. We use a self-assembled quantum dot coupled to a reservoir in combination with resonant optical excitation to study phenomena such as electron tunneling [1] and Auger recombination [2] with a time resolution down to single quantum events. The resulting telegraph signal is evaluated by full counting statistics to obtain deep insights into the spin and charge dynamics, where we use factorial cumulants as a very sensitive statistical tool to reduce the influence of statistical and systematic errors [3]. We show that factorial cumulants together with optical excitation push the limits in the detection and analysis of random telegraph data.

[1] Kurzmann et al., PRL 122, 247403 (2019). [2] Lochner, et al. Nano Lett. 20, 1631 (2020). [3] Kleinherbers et al., PRL 128, 087701 (2022).

30 min. break**Invited Talk** SYQD 1.4 Thu 11:30 HSZ 01**Cooper Pair Splitting in Real-Time** — •CHRISTIAN FLINDT — Department of Applied Physics, Aalto University, Finland

Cooper pair splitters are promising candidates for generating spin-entangled electrons. By splitting the Cooper pairs in a superconductor into different normal-state leads, spin-entanglement between spatially separated electrons can be achieved. In this talk, I will give an overview of our recent works on Cooper pair splitters [1-5]. I will discuss our proposal for observing and characterizing the splitting of Cooper pairs in real-time as well as its experimental realization [2,3]. I will then go on to talk about two proposals for controlling the splitting of Cooper pairs using time-dependent gate voltages [4]. Finally, if time allows, I will discuss how an entanglement witness can be formulated in terms of current cross-correlation measurements, which makes it possible to detect the entanglement of the split Cooper pairs [5].

[1] N. Walldorf, F. Brange, C. Padurariu, and CF, Phys. Rev. B **101**, 205422 (2020)

[2] N. Walldorf, C. Padurariu, A.-P. Jauho, and CF, Phys. Rev. Lett. **120**, 087701 (2018)

[3] A. Ranni, F. Brange, E. T. Mannila, CF, and V. F. Maisi, Nat. Commun. **12**, 6358 (2021)

[4] F. Brange, K. Prech, and CF, Phys. Rev. Lett. **127**, 237701 (2021)

[5] M. Tam, CF, and F. Brange, Phys. Rev. B **104**, 245425 (2021)

Invited Talk SYQD 1.5 Thu 12:00 HSZ 01**Trajectory-based detection in stochastic and quantum thermodynamics** — •JUKKA PEKOLA — Aalto University, Helsinki, FINLAND

I start by discussing the relation between jump trajectories and stochastic thermodynamics when applied to electrons and photons in quantum circuits. After that I describe our experiments on electron counting and calorimetry for trajectory analysis. In the theoretical part I discuss the calorimetric detection of single microwave photons in circuit QED setups.

References: [1] Jukka P. Pekola and Bayan Karimi, Rev. Mod. Phys. 93, 041001 (2021). [2] J. P. Pekola and I. M. Khaymovich, Annu. Rev. Condens. Matter 10, 193 (2019). [3] Bayan Karimi and Jukka P. Pekola, Phys. Rev. Lett. 124, 170601 (2020); Phys. Rev. X 12, 011026 (2022).

Symposium Topological Superconductor-Magnet Heterostructures (SYTS)

jointly organised by
the Low Temperature Physics Division (TT),
the Magnetism Division (MA), and
the Metal and Material Physics Division (MM)

Ilya Eremin
Ruhr-Universität Bochum
Theoretische Physik III
Universitätsstraße 150
44801 Bochum
Ilya.Eremin@rub.de

Karin Everschor-Sitte
Universität Duisburg-Essen
Fakultät für Physik
Lotharstraße 1
47057 Duisburg
karin.everschor-sitte@uni-due.de

Wulf Wulfhchel
KIT Karlsruhe
Physikalisches Institut
Wolfgang-Gaede-Str. 1
76131 Karlsruhe
wulf.wulfhchel@kit.edu

Superconductivity and magnetism have been usually regarded, in a rather pessimistic sense, as antagonistic. Nevertheless, phenomena arising from the competition between them have captivated physicists for almost a century. Nowadays, we are at the verge of a paradigm shift where we can embrace the synergy between superconductivity and magnetism. In fact, owing to recent advances in sample fabrication together with guiding principles from topology, it is now possible to engineer novel superconductor-magnet hybrid systems. These are unique platforms for exotic topological states whose fascinating properties can be exploited, for example, for topological quantum computing. The goal of this symposium is to bring together the community of this burgeoning field to strengthen the communication line between theorists and experimentalists from various divisions, to collaboratively identify challenges and set the research agenda for the coming years.

Overview of Invited Talks and Sessions

(Lecture hall HSZ 01)

Invited Talks

SYTS 1.1	Thu	15:00–15:30	HSZ 01	Blending of superconductivity and magnetism via topological solitons — •CHRISTOS PANAGOPOULOS
SYTS 1.2	Thu	15:30–16:00	HSZ 01	Topological landscaping in magnet-superconductor heterostructures — •SEBASTIÁN A. DÍAZ
SYTS 1.3	Thu	16:00–16:30	HSZ 01	Experimental study of minigaps and end states in bottom-up designed multi-orbital Shiba chains — •JENS WIEBE
SYTS 1.4	Thu	16:45–17:15	HSZ 01	Quantum spins and hybridization in artificially-constructed chains of magnetic adatoms on superconducting 2H-NbSe₂ — •KATHARINA J. FRANKE
SYTS 1.5	Thu	17:15–17:45	HSZ 01	Braiding of Majorana zero modes — •STEPHAN RACHEL

Sessions

SYTS 1.1–1.5	Thu	15:00–17:45	HSZ 01	Topological Superconductor-Magnet Heterostructures
--------------	-----	-------------	--------	---

Sessions

– Invited Talks –

SYTS 1: Topological Superconductor-Magnet Heterostructures

Time: Thursday 15:00–17:45

Location: HSZ 01

Invited Talk SYTS 1.1 Thu 15:00 HSZ 01**Blending of superconductivity and magnetism via topological solitons** —

•CHRISTOS PANAGOPOULOS — Nanyang Technological University, Singapore
 Topological solitons and quantum mechanics have been intertwined for the past 60 years. Even before the term soliton had been coined, Abrikosov theory predicted the formation of vortices in the phase field of superconductors, an exemplar exposition of macroscopic quantum coherence. Recent work shows that solitons are in fact a timely and promising platform for quantum operations. I will demonstrate the viability of using spin topology to influence a superconductor at selective length scales through a completely new material architecture namely, a stack of magnets and a superconductor that shows stable vortices above elongated chiral spin textures, as well as isolated skyrmions. This is an ideal geometry for fluxions and chiral superconductivity, as well as quantum processes such as non-perturbative, non-contact Majorana braiding.

Invited Talk SYTS 1.2 Thu 15:30 HSZ 01**Topological landscaping in magnet-superconductor heterostructures** —

•SEBASTIÁN A. DÍAZ — University of Duisburg-Essen, Duisburg, Germany
 Magnet-superconductor heterostructures, due to the rich interplay between their adjacent order parameters, are fertile grounds for novel topological phenomena. Our theoretical studies demonstrate that topological defects in the magnetic order parameter lend themselves as versatile tools to landscape the superconducting order and its topological excitations. A chain of antiferromagnetic skyrmions induces topological superconductivity and supports Majorana bound states - the building blocks of topological quantum computing [1]. Ferromagnetic skyrmions coupled to superconducting vortices form a bound pair that can be used to braid Majorana bound states [2]. These findings strongly suggest that magnet-superconductor heterostructures are ideal arenas to further explore how magnetism and superconductivity influence each other to engineer and manipulate their order parameters and topological excitations.

[1] S. A. Díaz et al., Phys. Rev. B 104, 214501 (2021)

[2] J. Nothhelfer et al., Phys. Rev. B 105, 224509 (2022)

Invited Talk SYTS 1.3 Thu 16:00 HSZ 01**Experimental study of minigaps and end states in bottom-up designed multi-orbital Shiba chains** —

•JENS WIEBE — Universität Hamburg, Department of Physics, 20355 Hamburg, Germany

Chains of transition-metal atoms on *s*-wave superconductors evoke multi-orbital Shiba bands inside the gap of the substrate. If a spin-orbit coupled band overlaps with the Fermi energy, a topologically nontrivial minigap may open up which can potentially host Majorana bound states at the chain's ends. We study atom-by-atom fabricated chains with respect to such phenomena [1]. Most recent strategies in order to increase the width of topological minigaps [2,3] and experimental methods to decide on the Majorana nature of close-to-zero-energy end states [4] will be presented.

Funding by the DFG via the Cluster of Excellence "Advanced Imaging of Matter" (EXC 2056-project ID 390715994) and via the SFB-925-project 170620586 is acknowledged

[1] L. Schneider et al., Nature Physics 17, 943 (2021)

[2] P. Beck et al., arXiv:2205.10062 [cond-mat.supr-con] (2022)

[3] P. Beck et al., arXiv:2205.10073 [cond-mat.supr-con] (2022)

[4] L. Schneider et al., arXiv:2211.00561v1 [cond-mat.supr-con]

15 min. break**Invited Talk** SYTS 1.4 Thu 16:45 HSZ 01**Quantum spins and hybridization in artificially-constructed chains of magnetic adatoms on superconducting 2H-NbSe₂** — •KATHARINA J. FRANKE — Freie Universität Berlin, Berlin, Germany

Magnetic adatom chains on superconducting substrates are promising platforms for topological superconductivity and Majorana zero modes. Signatures of these have been found in densely packed chains with direct exchange interaction among the adatoms. Theoretical predictions suggest chains, where the atoms are sufficiently far spaced that direct hybridization of their *d* orbitals is negligible, but close enough for substrate-mediated interactions, as an alternative platform.

We build such chains from individual Fe atoms on a 2H-NbSe₂ substrate using the tip of a scanning tunneling microscope. In each step we track the evolution of the Yu-Shiba-Rusinov (YSR) states. We find signatures of quantum-spin behavior and YSR band formation consistent with ferromagnetic coupling [1,2].

[1] E. Liebhaber, L. M. Rütten, G. Reecht, J. F. Steiner, S. Rohlf, K. Rossnagel, F. von Oppen, K. J. Franke, Nat. Commun. 13, 2160 (2022)

[2] J. F. Steiner, C. Mora, K. J. Franke, F. von Oppen, Phys. Rev. Lett. 128, 036801 (2022)

Invited Talk SYTS 1.5 Thu 17:15 HSZ 01**Braiding of Majorana zero modes** — •STEPHAN RACHEL — School of Physics, University of Melbourne, Australia

There has been tremendous experimental progress in recent years in establishing magnet-superconductor hybrid (MSH) systems as a promising platform for Majorana physics.

In the first part of this talk, I will discuss MSH structures with Re or Nb as a superconducting substrate, and Fe or Mn as magnetic adatoms. In particular, I will illustrate the theoretical challenges to simulate and understand the topological superconductivity and their concomitant Majorana modes in such materials

In the second part of this talk, I will explain our first steps to investigate the braiding of Majorana zero modes. In particular, I will focus on braiding errors which can be introduced from sources such as quasiparticle poisoning and Majorana hybridization, and how these error rates behave in a full quasiparticle background.

Symposium Physics of van der Waals 2D Heterostructures (SYHS)

jointly organised by
 the Low Temperature Physics Division (TT),
 the Semiconductor Physics Division (HL),
 the Surface Science Division (O),
 the Magnetism Division (MA), and
 the Thin Films Division (DS)

Christoph Stampfer
 RWTH Aachen University
 II. Physikalisches Institut
 Templergraben 55
 52062 Aachen
 stampfer@physik.rwth-aachen.de

Jaroslav Fabian
 Universität Regensburg
 Institut I – Theoretische Physik
 Universitätsstraße 31
 93053 Regensburg
 jaroslav.fabian@ur.de

Van der Waals heterostructures based on 2D layered materials provide an exciting platform to engineer and control electronic, transport, optical properties, spin, and magnetic properties. Many exciting phenomena have been reported in stacked materials coupled by weak van der Waals interactions. Perhaps most spectacular are strong correlations and superconductivity in graphene and transition-metal dichalcogenides multilayers. Also in the exciton physics, there is a trend towards investigating signatures of many-body effects. New directions of research include searches for novel topological states, investigations of spin and magnetic proximity effects, strain physics, or studying magnetic excitations. The aim of this symposium is to present an overview of some of the recent developments in this field by leading experts in this forefront area of condensed matter physics.

Overview of Invited Talks and Sessions

(Lecture hall HSZ 01)

Invited Talks

SYHS 1.1	Fri	9:30–10:00	HSZ 01	Novel moiré excitons and ultrafast optical dynamics in van der Waals 2D heterostructures — •STEVEN G. LOUIE
SYHS 1.2	Fri	10:00–10:30	HSZ 01	Interaction induced magnetism in 2D semiconductor moiré superlattices — •XIAODONG XU
SYHS 1.3	Fri	10:30–11:00	HSZ 01	Ions in tight places: intercalation and transport of ions in van der Waals heterostructures — •IRINA GRIGORIEVA
SYHS 1.4	Fri	11:15–11:45	HSZ 01	Spin-orbit proximity in van der Waals heterostructures — •FELIX CASANOVA
SYHS 1.5	Fri	11:45–12:15	HSZ 01	Plethora of many-body ground states in magic angle twisted bilayer graphene — •DMITRI EFETOV

Sessions

SYHS 1.1–1.5	Fri	9:30–12:15	HSZ 01	Physics of van der Waals 2D Heterostructures
--------------	-----	------------	--------	---

Sessions

– Invited Talks –

SYHS 1: Physics of van der Waals 2D Heterostructures

Time: Friday 9:30–12:15

Location: HSZ 01

Invited Talk SYHS 1.1 Fri 9:30 HSZ 01**Novel moiré excitons and ultrafast optical dynamics in van der Waals 2D heterostructures** — •STEVEN G. LOUIE — Physics Dept, University of California, Berkeley, and Lawrence Berkeley National Lab, Berkeley, CA, USA

Recent experiments have revealed signatures of novel exciton states and intriguing pump-probe optical responses in van der Waals 2D heterostructures. But their microscopic nature remains to be fully understood. We perform ab initio GW-Bethe Salpeter equation calculations and discover a rich diversity of excitonic states in these moiré systems. In rotationally aligned WSe₂/WS₂ heterobilayer, we find some excitons of a modulated Wannier character and others of a previously unidentified intralayer charge-transfer character. In 57.7° twisted bilayer WS₂, we discover layer-hybridized excitons with in-plane charge transfer character. Many of the theoretical predictions are confirmed by experiments. Ultrafast optical dynamics in 2D heterostructures is also of fundamental and practical interest. We discover a new many-body mechanism for ultrafast photoexcited dynamics in pump-probe measurement of the optical response of transition metal dichalcogenide heterobilayers. We show that coupling between the intralayer and interlayer excitons dominates the measured ultrafast dynamics, conceptually different from a previously believed picture of single-particle charge transfer between layers. These studies are made possible with the development of two new methods that allow for the ab initio calculations of the excitonic physics and optical response of systems with thousands of atoms in the unit cell and in the time domain.

Invited Talk SYHS 1.2 Fri 10:00 HSZ 01**Interaction induced magnetism in 2D semiconductor moiré superlattices** — •XIAODONG XU — Department of Physics, Department of Materials Science and Engineering, University of Washington, Seattle, USA

Many-body interactions between carriers lie at the heart of correlated physics. The ability to tune such interactions would open the possibility to access and control complex electronic phase diagrams on demand. Recently, moiré superlattices formed by two-dimensional materials have emerged as a promising platform for quantum engineering such phenomena. In this talk, I will present a systematic study of the emergent magnetic interactions (both antiferromagnetic and ferromagnetic) in strongly correlated transition metal dichalcogenides moiré superlattices. I will show that the combination of doping, electric field, and optical excitation provide dynamic controls of the moiré many-body Hamiltonian.

Invited Talk SYHS 1.3 Fri 10:30 HSZ 01**Ions in tight places: intercalation and transport of ions in van der Waals heterostructures** — •IRINA GRIGORIEVA — University of Manchester, UK

Understanding and control of ion transport through angstrom-scale channels and capillaries is important in diverse technological fields, from sieving and separation to Li ion batteries and energy storage. I will review our recent work on using few-layer graphene as a model system for understanding ion intercalation in layered crystals and on ion transport through designer nanochannels made by van der Waals assembly. It allowed us to answer such questions as what limits the Li ion storage capacity of bilayer graphene, whether protons can fit into the interlayer space in van der Waals crystals, and why protons can diffuse through monolayer water while no other ions can.

15 min. break**Invited Talk** SYHS 1.4 Fri 11:15 HSZ 01**Spin-orbit proximity in van der Waals heterostructures** — •FELIX CASANOVA — CIC nanoGUNE, Donostia, Basque Country

Transition metal dichalcogenides (TMD) can be used to enhance the spin-orbit coupling of graphene, leading to new spin transport channels with unprecedented spin textures [1]. We have optimized bilayer graphene/WSe₂ van der Waals heterostructures to achieve magnetic-field-free spin precession. Remarkably, the sign of the precessing spin polarization can be tuned electrically by back-gate voltage and drift current [2], being the first realization of a spin field-effect transistor at room temperature in a diffusive system, a long-awaited goal.

The spin-orbit proximity in graphene/TMD van der Waals heterostructures also leads to spin-to-charge conversion (SCC) of spins along z due to spin Hall effect (SHE), which was first observed by our group using MoS₂ as the TMD [3]. The combination of long-distance spin transport and SHE in the same material gives rise to an unprecedented figure of merit (product of spin Hall angle and spin diffusion length) of 40 nm in graphene proximitized with WSe₂, which is also gate tunable [4]. Finally, we demonstrate SCC of spins oriented in all three directions (x, y, and z) in graphene/NbSe₂ heterostructure, due to spin-orbit proximity and broken symmetry at the twisted graphene/NbSe₂ interface [5].

[1] Gmitra and Fabian, Phys. Rev. B 93, 155104 (2016)

[2] Ingla-Aynés et al., Phys. Rev. Lett. 127, 047202 (2021)

[3] Safeer et al., Nano Lett. 19, 1074 (2019)

[4] Herling et al., APL Mater. 8, 071103 (2020)

[5] Ingla-Aynés et al., 2D Mater. 9, 045001 (2022)

Invited Talk SYHS 1.5 Fri 11:45 HSZ 01**Plethora of many-body ground states in magic angle twisted bilayer graphene** — •DMITRI EFETOV — LMU Munich, Germany

Twist-angle engineering of 2D materials has led to the recent discoveries of novel many-body ground states in moiré systems such as correlated insulators, unconventional superconductivity, strange metals, orbital magnetism and topologically nontrivial phases. These systems are clean and tuneable, where all phases can coexist in a single device, which opens up enormous possibilities to address key questions about the nature of correlation induced superconductivity and topology, and allows to create entirely novel quantum phases with enhanced interactions. In this talk we will introduce some of the main concepts underlying these systems, concentrating on magic angle twisted bilayer graphene (MATBG) and show how symmetry-broken states emerge at all integer electron fillings [1]. We further will discuss recent experiments including screened interactions [2], Chern insulators [3], magnetic Josephson junctions [4], quantum criticality [5], re-entrant correlated insulators at high magnetic fields [6], Dirac spectroscopy of correlated states in magic angle trilayers and discuss some of the avenues for novel quantum sensing applications [8].

[1] Nature, 574, 653 (2019)

[2] Nature, 583, 375 (2020)

[3] Nature Physics, 17, 710 (2021)

[4] arXiv:2110.01067 (2021)

[5] Nature Physics, 18, 633 (2022)

[6] PRL 128, 217701 (2022)

[7] Nature Materials, in press (2022)

[8] Nano Letters, 22, 6465 (2022)

Biological Physics Division Fachverband Biologische Physik (BP)

Joachim Rädler
Lehrstuhl Physik weicher Materie
Fakultät für Physik
Ludwig-Maximilians-Universität München
Geschwister-Scholl-Platz 1
80539 München
raedler@lmu.de

Overview of Invited Talks and Sessions

(Lecture halls BAR Schö, TOE 317, and BAR 0106; Poster P1 and P2/EG)

Invited Talks

BP 1.7	Mon	11:15–11:45	BAR Schö	Cell-free expression of membrane proteins and control of their spatial organization in synthetic lipid membranes — •JAN STEINKÜHLER
BP 2.1	Mon	9:30–10:00	TOE 317	Emergent properties in motile active matter — •ROLAND G. WINKLER
BP 3.5	Mon	10:30–11:00	BAR 0106	Resolving gating and allosteric modulation in ion channels through simulations and small-angle neutron scattering — •ERIK LINDAHL
BP 5.1	Mon	15:00–15:30	TOE 317	Repurposing nucleic acids as high-resolution force sensors: From fundamental mechanotransduction to translational biophysics — •KHALID SALAITA
BP 6.5	Mon	16:15–16:45	BAR 0106	Mechanical and electrical properties of bacterial biofilms modulate antibiotic tolerance — •BERENIKE MAIER
BP 8.5	Tue	10:45–11:15	BAR Schö	Microtubule Lattice Dynamics — SUBHAM BISWAS, RAHUL GROVER, CORDULA REUTHER, MONA GRÜNEWALD, STEFAN DIEZ, •LAURA SCHAEDEL
BP 10.1	Tue	9:30–10:00	BAR 0106	Protein evolution in sequence landscapes: from data to models and back — •MARTIN WEIGT
BP 12.4	Wed	10:15–10:45	TOE 317	Materials properties of bacterial biofilms. — •CÉCILE M. BIDAN
BP 13.1	Wed	9:30–10:00	BAR 0106	Biological signal processes across scales — •STEFFEN RULANDS
BP 16.1	Wed	11:15–11:45	BAR 0106	Systems biophysics of bacterial response to cell wall-targeting antibiotics — REBECCA BROUWERS, SHARAREH TAVADDOD, LEONARDO MANCINI, JACOB BIBOY, ELIZABETH TATHAM, PIETRO CICUTA, WALDEMAR VOLLMER, •ROSALIND ALLEN
BP 21.7	Thu	11:15–11:45	BAR Schö	Visualizing the inner life of microbes — •ULRIKE ENDESFELDER
BP 22.5	Thu	10:30–11:00	TOE 317	Statistical Physics of Spatially Organized Catalytic Particles — •ULRICH GERLAND
BP 23.1	Thu	9:30–10:00	BAR 0106	Conformational dynamics of SARS-CoV-2 spike protein modulates the binding affinity to ACE2 — FIDAN SUMBUL, CLAIRE VALOTTEAU, PRITHWIDIP SAHA, IGNACIO FERNANDEZ, ANNALISA MEOLA, EDUARD BAQUERO, DOROTA KOSTRZ, JAMES R PORTMAN, FRANÇOIS STRANSKY, PABLO GUARDADO CALVO, CHARLIE GOSSE, TERENCE STRICK, FELIX REY, •FELIX RICO
BP 26.1	Thu	15:00–15:30	TOE 317	Decoding Molecular Plasticity in the Dark Proteome of the Nuclear Transport Machinery — •EDWARD LEMKE
BP 30.1	Fri	9:30–10:00	TOE 317	Experiments on Active Polymer-Like Worms — •ANTOINE DEBLAIS, DANIEL BONN, SANDER WOUTERSEN
BP 32.1	Fri	12:15–13:00	HSZ 03	The physical regulation of brain development — •KRISTIAN FRANZE

Invited Talks of the joint Symposium Dynamics of Opinion Formation – From Quorum Sensing to Polarization (SYOF)

See SYOF for the full program of the symposium.

SYOF 1.1	Mon	9:30–10:00	HSZ 01	Towards understanding of the social hysteresis – insights from statistical physics — •KATARZYNA SZNAJD-WERON
SYOF 1.2	Mon	10:00–10:30	HSZ 01	Polarization in attitude distributions from surveys and models of continuous opinion dynamics — •JAN LORENZ, MARTIN GESTEFELD

SYOF 1.3	Mon	10:30–11:00	HSZ 01	Collective patterns and stable misunderstandings in networks striving for consensus without a common value system — •JOHANNES FALK, EDWIN EICHLER, KATJA WINDT, MARC-THORSTEN HÜTT
SYOF 1.4	Mon	11:15–11:45	HSZ 01	A yet undetected cognitive bias, revealed by opinion dynamics simulations — •GUILLAUME DEFFUANT
SYOF 1.5	Mon	11:45–12:15	HSZ 01	Extreme switches in kinetic exchange models of opinion. — •PARONGAMA SEN, KATHAKALI BISWAS

Invited Talks of the joint Symposium SKM Dissertation Prize 2023 (SYSD)

See SYSD for the full program of the symposium.

SYSD 1.1	Mon	9:30–10:00	HSZ 04	Diffusion of antibodies in solution: from individual proteins to phase separation domains — •ANITA GIRELLI
SYSD 1.2	Mon	10:00–10:30	HSZ 04	Intermediate Filament Mechanics Across Scales — •ANNA V. SCHEPERS
SYSD 1.3	Mon	10:30–11:00	HSZ 04	Ultrafast Probing and Coherent Vibrational Control of a Surface Structural Phase Transition — •JAN GERRIT HORSTMANN
SYSD 1.4	Mon	11:00–11:30	HSZ 04	Electro-active metasurfaces employing metal-to-insulator phase transitions — •JULIAN KARST
SYSD 1.5	Mon	11:30–12:00	HSZ 04	The role of unconventional symmetries in the dynamics of many-body systems — •PABLO SALA

Invited Talks of the joint Symposium Physics of Fluctuating Paths (SYFP)

See SYFP for the full program of the symposium.

SYFP 1.1	Tue	9:30–10:00	HSZ 01	Time at which a stochastic process achieves its maximum — •SATYA MAJUMDAR
SYFP 1.2	Tue	10:00–10:30	HSZ 01	Fluctuations and molecule-spanning dynamics of single Hsp90 proteins on timescales from nanoseconds to days — •THORSTEN HUGEL
SYFP 1.3	Tue	10:30–11:00	HSZ 01	Path reweighting for Langevin dynamics — •BETTINA KELLER
SYFP 1.4	Tue	11:15–11:45	HSZ 01	Out-of-equilibrium dynamics of trapped Brownian particles — •RAUL A. RICA
SYFP 1.5	Tue	11:45–12:15	HSZ 01	Thermodynamics of Clocks — •PATRICK PIETZONKA

Invited Talks of the joint Symposium Topology in Quantum and Classical Physics – From Topological Insulators to Active Matter (SYQC)

See SYQC for the full program of the symposium.

SYQC 1.1	Wed	15:00–15:30	HSZ 01	Topological magnetic whirls for computing — •KARIN EVERSCHOR-SITTE
SYQC 1.2	Wed	15:30–16:00	HSZ 01	Topological waves from solids to geo/astrophysical flows — •PIERRE DELPLACE, ANTOINE VENAILLE, NICOLAS PEREZ, GUILLAUME LAIBE, ARMAND LECLERC, MANOLIS PERROT, BRAD MARSTON
SYQC 1.3	Wed	16:00–16:30	HSZ 01	Topological Phase Transitions in Population Dynamics — •ERWIN FREY
SYQC 1.4	Wed	16:45–17:15	HSZ 01	Topological invariants protect robust chiral currents in active matter — •EVELYN TANG
SYQC 1.5	Wed	17:15–17:45	HSZ 01	Topological defects in biological active matter — •AMIN DOOSTMOHAMMADI

Sessions

BP 1.1–1.12	Mon	9:30–13:00	BAR Schö	Membranes, Vesicles, Synthetic Cells
BP 2.1–2.12	Mon	9:30–13:00	TOE 317	Active Matter I (joint session BP/PPP/DY)
BP 3.1–3.12	Mon	9:30–13:00	BAR 0106	Computational Biophysics I
BP 4.1–4.9	Mon	15:00–17:30	BAR Schö	Tissue Mechanics I
BP 5.1–5.8	Mon	15:00–17:30	TOE 317	Focus Session NanoAgents
BP 6.1–6.7	Mon	15:00–17:15	BAR 0106	Bacterial Mechanics
BP 7.1–7.11	Mon	15:00–18:15	ZEU 160	Active Matter II (joint session DY/BP/PPP)
BP 8.1–8.11	Tue	9:30–13:00	BAR Schö	Cell Mechanics I
BP 9.1–9.11	Tue	9:30–12:30	TOE 317	Active Matter III (joint session BP/PPP/DY)
BP 10.1–10.9	Tue	9:30–12:15	BAR 0106	Evolution and Origin of Life
BP 11.1–11.78	Tue	12:30–15:30	P1	Poster Session I

BP 12.1–12.12	Wed	9:30–13:00	TOE 317	Biopolymers and Biomaterials (joint session BP/CPP)
BP 13.1–13.5	Wed	9:30–11:00	BAR 0106	Signaling, Biological Networks
BP 14.1–14.10	Wed	9:30–13:00	ZEU 160	Focus Session: From Inter-individual Variability to Heterogeneous Group Dynamics and Disorder in Active Matter (joint session DY/BP/CPP)
BP 15.1–15.6	Wed	10:30–12:15	BAR Schö	Tissue Mechanics II
BP 16.1–16.6	Wed	11:15–13:00	BAR 0106	Systems Biophysics
BP 17.1–17.9	Wed	15:00–17:30	BAR 0106	Protein Structure and Dynamics
BP 18.1–18.6	Wed	15:00–16:30	ZEU 250	Biologically Inspired Statistical Physics (joint session DY/BP)
BP 19.1–19.6	Wed	16:30–18:00	MER 02	Biopolymers, Biomaterials and Bioinspired Functional Materials (joint session CPP/BP)
BP 20	Wed	18:00–19:00	BAR Schö	Members' Assembly
BP 21.1–21.12	Thu	9:30–13:00	BAR Schö	Bioimaging
BP 22.1–22.12	Thu	9:30–13:00	TOE 317	Statistical Physics of Biological Systems I (joint session BP/DY)
BP 23.1–23.12	Thu	9:30–13:00	BAR 0106	Single Molecule Biophysics
BP 24.1–24.12	Thu	9:30–13:00	ZEU 160	Active Matter IV (joint session DY/BP/CPP)
BP 25.1–25.9	Thu	15:00–17:30	BAR Schö	Cell Mechanics II
BP 26.1–26.8	Thu	15:00–17:30	TOE 317	Focus Session mRNA Physics
BP 27.1–27.9	Thu	15:00–17:30	BAR 0106	Computational Biophysics II
BP 28.1–28.58	Thu	18:00–20:00	P2/EG	Poster Session II
BP 29.1–29.9	Fri	9:30–12:00	BAR Schö	Statistical Physics of Biological Systems II (joint session BP/DY)
BP 30.1–30.8	Fri	9:30–12:00	TOE 317	Active Matter V (joint session BP/CPP/DY)
BP 31.1–31.7	Fri	10:00–12:00	BAR 0106	Cell Mechanics III
BP 32.1–32.1	Fri	12:15–13:00	HSZ 03	Closing Plenary Talk (joint session BP/CPP)

Members' Assembly of the Biological Physics Division

Wed 18:00–19:00 BAR Schö

Sessions

– Invited Talks, Contributed Talks, and Posters –

BP 1: Membranes, Vesicles, Synthetic Cells

Time: Monday 9:30–13:00

Location: BAR Schö

BP 1.1 Mon 9:30 BAR Schö

Bottom-up assembly of a synthetic glycocalyx on lipid vesicles — •KEVIN JAHNKE and DAVID A. WEITZ — Harvard University, Cambridge, MA, USA

The glycocalyx serves as physicochemical barrier that increases cellular rigidity and as interface for chemical cues to guide cell-cell communication. However, while preliminary results highlight the importance of the glycocalyx, the biophysical functioning remained elusive and mostly untested due to the complexity within natural cells. Recent advances in the membrane functionalization of giant unilamellar vesicles (GUVs) with macromolecules like DNA and proteins (Jahnke et al., ACS Nano 2022; Jahnke et al. Nat. Commun. 2021) pave the way for a systematic investigation of glycocalyx properties within a fully-controlled environment. Here, we engineer biomimetic glycocalyces to understand their effect on the biophysical properties of GUVs. The synthetic glycocalyx consists of polysaccharides functionalized with cholesterol that self-assemble in the lipid membrane. We employ fluorescence recovery after photobleaching and micropipette aspiration to assess the changes in diffusion and membrane rigidity of glycocalyx-decorated GUVs. The control over the type of polysaccharide, its molecular weight and density on the vesicle enable us to design and study a variety of synthetic glycocalyces. Additionally, we compare them to other common vesicle functionalizations like polyethyleneglycol and explore their potential for carbohydrate-specific adhesion. This work underpins bottom-up glycocalyx engineering as important tool for cellular biophysics and biotechnological applications.

BP 1.2 Mon 9:45 BAR Schö

Surface-induced phase separation of reconstituted nascent integrin clusters

— •CHIAO-PENG HSU¹, JONAS ARETZ², REINHARD FÄSSLER², and ANDREAS BAUSCH¹ — ¹Center for Functional Protein Assemblies and Lehrstuhl für Zellbiophysik (E27), Physics Department, Technische Universität München, Garching, Germany — ²Max Planck Institute of Biochemistry, Martinsried, Germany

Integrin adhesion complexes are essential membrane-associated cellular compartments for multi-cellular life. While biomolecular condensates organize specific functions in cells, cell membranes can regulate the positions and dynamics of many biomolecular condensates. Yet, the role played by membrane surfaces in the formation of initial integrin adhesion complexes still needs to be fully understood. Here, we report that phosphoinositides containing lipid membranes induce minimal integrin adhesion condensates composed of integrin β tails, kindlin, talin, paxillin, and FAK at physiological ionic strengths and protein concentrations. We show that the presence of phosphoinositides is key to enriching kindlin and talin on the membrane, forming first nascent integrin complexes, which in turn are necessary to further nucleate condensates. These results demonstrate that the biophysical properties of lipid membranes are key for inducing specific membrane-associated condensates throughout the cell.

BP 1.3 Mon 10:00 BAR Schö

Small-Angle and Inelastic Neutron Scattering from Polydisperse Oligolamellar Vesicles Containing Glycolipids — •LUKAS BANGE¹, INGO HOFFMANN², and EMANUEL SCHNECK¹

— ¹Institute for Condensed Matter Physics, Technical University Darmstadt, Germany — ²Institut Laue-Langevin, Grenoble, France

Glycolipids are known to stabilize biomembrane multilayers through preferential sugar-sugar interactions that act as weak transient membrane crosslinkers [1, 2]. We use small-angle and inelastic neutron scattering on oligolamellar phospholipid vesicles containing defined glycolipid fractions in order to elucidate the influence of glycolipids on membrane mechanics and dynamics. Small-angle neutron scattering (SANS) reveals that the oligolamellar vesicles (OLVs) obtained by extrusion are polydisperse with regard to the number of lamellae, n , which renders the interpretation of the inelastic neutron spin echo (NSE) data [3] non-trivial. To overcome this problem, we propose a method to model the NSE data in a rigorous fashion based on the obtained histograms of n and on their q -dependent intensity-weighted contribution. This procedure yields meaningful values for the bending rigidity of individual lipid membranes and insights into the mechanical coupling between adjacent membrane lamellae, including the effect of the glycolipids.

References [1] Latza, Demé, Schneck, Biophys J., 2020, Volume 118, 7, P1602-1611 [2] Kav et al, Front. Mol. Biosci., 2021, 8, 754645 [3] Hoffmann, Hoffmann, Farago, Prevost, Gradzielski, J. Chem. Phys., 2018, 148, 104901

BP 1.4 Mon 10:15 BAR Schö

Controlling phase separations and reaction kinetics in microfluidically trapped droplets — •SEBASTIAN W. KRAUSS, PAULA GIRONES PAYA, and MATTHIAS WEISS

— Experimental Physics I, University of Bayreuth, Germany

Droplet-based microfluidics is an efficient and versatile tool to study biomimetic reactions and self-organization in selected geometries and small volumes. It is also frequently used to perform high-throughput experiments, e.g. as selection platforms for directed evolution or for personalised medicine. While elaborate techniques are available for the production of picoliter-sized droplets, there is an increasing demand for subsequent manipulation and control of the droplet interior after production. Here we report on a straightforward method to rapidly and reversibly adjust the size of single to several hundred double-emulsion droplets in a microfluidic sieve by varying the osmotic pressure, leading to a change in concentration of enclosed molecules. We show that this approach allows for driving reversible demixing transitions of a biomimetic binary fluid which can be used to control the kinetics of enclosed enzymatic reactions. We also show that changing droplet sizes can be exploited for a reversible denaturing of double-stranded DNA, which may eventually allow for an osmotically driven PCR in small droplets.

BP 1.5 Mon 10:30 BAR Schö

Predicting membrane turnover during cytokinesis — •FELIX FREY¹ and TIMON IDEMA²

— ¹Institute of Science and Technology Austria, Klosterneuburg, Austria — ²Department of Bionanoscience, Kavli Institute of Nanoscience, Delft University of Technology, Delft, The Netherlands

When animal cells divide, they split into two equal parts. Since the volume of the cell is typically conserved during cell division, the projected area of the cell membrane has to increase to allow for the change of shape. The membrane area is controlled by exocytosis, resulting in an increase in membrane area and its counterpart endocytosis, resulting in a decrease in membrane area. However, it is unclear how exo- and endocytosis need to adapt to enable successful division. To address this question, we developed a kinetic model in which membrane gain and loss depend on membrane curvature and tension [1]. We apply this model to a series of calculated vesicle shapes, which we take as a proxy for the shape of dividing cells. We find that the ratio of membrane gain and loss changes non-monotonically during cytokinesis due to the complex interplay between membrane area and shape. Our results suggest that controlling membrane turnover is critical for the successful division of both biological and artificial cells. [1] Felix Frey and Timon Idema, Phys. Rev. E 106, 024401 (2022).

BP 1.6 Mon 10:45 BAR Schö

Antimicrobial peptides: Revealing the Penetration Mechanism of Melittin in the Outer Membrane of Gram-Negative Bacteria — •JUSTUS C. STEPHANI¹, LUCA GERHARDS¹, ILIA A. SOLOV'YOV¹, and IZABELLA BRAND²

— ¹Dept. of Physics, Carl von Ossietzky Universität, Germany — ²Dept. of Chemistry, Carl von Ossietzky Universität Oldenburg, Germany

Studying the interaction between antimicrobial peptides (AMPs) and bacterial membranes might aid to find new treatments against bacterial pathogens and even drug-resistant bacteria. The AMP melittin can target the complex structure of a cell membrane leading to membrane permeabilization via hole formation or disruption. We report on the results of electrochemical experiments, aided by modern, all-atom molecular dynamics simulations that reveal the role of lipopolysaccharides (LPS) in the outer membrane of gram-negative bacteria in melittin binding and penetration. We demonstrate that certain amino acid residues play a key role in the binding of melittin to the membrane and thereby stabilizing and preserving the confirmation of the peptide. With a combined method of polarization modulation infrared reflection-absorption spectroscopy (PM IRRAS) and the statistical analysis of C=O bond orientation in the peptide, we determine the orientation of melittin on the membrane and observed penetration of the N-Terminus of the peptide into the membrane and a formation of hydrogen bonds between the N-Terminus and carboxylate and phosphate of the LPS.

15 min. break**Invited Talk**

BP 1.7 Mon 11:15 BAR Schö

Cell-free expression of membrane proteins and control of their spatial organization in synthetic lipid membranes — •JAN STEINKÜHLER

— Northwestern University, Evanston, USA — Georg-August-Universität Göttingen, Germany

Cell-free expression (CFE) is a powerful tool for synthesizing proteins outside of living cells, including membrane proteins. In this talk, we will discuss the factors that affect the yield of synthesized membrane proteins in CFE systems, including ribosome stalling and the balance between peptide-membrane association and peptide aggregation rates. We will also present a quantitative kinetic model that can be used to rationalize the engineering of protein N-terminal domain sequences and membrane composition for improved membrane protein synthesis. In addition to covering the synthesis of natural membrane proteins, we will show how CFE of de novo membrane protein designs can be used to study the role of membrane-protein hydrophobic mismatch in protein integration and organization in synthetic lipid membranes. [DOI:10.1101/2022.06.01.494374]. Our findings provide insight into protein organization in biological membranes and a framework for building up of synthetic cell membranes with new functions.

BP 1.8 Mon 11:45 BAR Schö

Entry of Microparticles into Giant Lipid Vesicles Induced by Optical Force — •FESSLER FLORENT, SHARMA VAIBHAV, MULLER PIERRE, THALMANN FABRICE, MARQUES CARLOS, and STOCCO ANTONIO — Institut Charles Sadron, Strasbourg, France

Interactions between micro- or nano-sized objects and lipid membranes are crucial in many processes such as entry of viruses in host cells, microplastics pollution, drug delivery or biomedical imaging. Here, we investigated the physical principles of particle crossing of lipid membranes using microparticles and giant unilamellar vesicles (GUVs) in the absence of strong irreversible binding and for low membrane tensions. In these conditions, we observed that organic as well as inorganic particles can always penetrate inside GUVs provided that an external picoNewton force is applied. In the limit of a vanishing particle-membrane affinity, we pointed out the role of membrane area reservoirs and showed that a force barrier minimum exists when the particle size is comparable to the bendocapillary length.

BP 1.9 Mon 12:00 BAR Schö

Simulating transient pores in hemifused membranes — •RUSSELL SPENCER and MARCUS MÜLLER — Georg-August Universität Göttingen, Institute for Theoretical Physics, 37077 Göttingen, Germany

Transportation of material from one side of a hemifused membrane to another can be facilitated through the formation of transient pores, which open, allow the material to pass and then close. One important example of this occurs in the 'kiss and run' (KAR) mechanism for transporting material from inside a vesicle in a cell to outside of the cell. The vesicle first fuses with the membrane, forming a hemifusion diaphragm (HD). A pore then opens in the HD allowing the material out, then the pore closes and the vesicle detaches. This process occurs in the release of neurotransmitters from a synapse into the post-synaptic cleft. This work uses self-consistent field theory and the string method to calculate the minimum free energy path for membrane fusion and the opening and closing of the transient pore. We also study the effects of proteins, which facilitate the process by altering the thermodynamics of pore formation.

BP 1.10 Mon 12:15 BAR Schö

Lipid movement in monolayers at the air/water interface: hydrodynamic coupling to the subphase — FLORIAN GELLERT, HEIKO AHRENS, and •CHRISTIANE A. HELM — Institute of Physics, University of Greifswald, Germany

Domain nucleation and growth in the liquid expanded/liquid condensed

(LE/LC) phase transition in erucic acid monolayers at the air/water interface is studied. Dendritic domains are observed at high compression speeds and seaweed domains at low compression speeds. The different domain types are distinguished by fractal dimension, tip width, and the spacing of the side arms. A local, normalized supersaturation describes the hydrodynamic coupling of lipids in the LE phase moving towards the domain border to subphase movement. The coupling differs for the growth regimes. Additionally, the shape and symmetry of the domains are affected by barrier movement. The downstream side of the domains grows faster than the upstream side, as shown by directionality diagrams and FFTs. We suggest that the flow direction disturbs the diffusion direction of the lipids within the LE phase but not the coupling to the subphase.

BP 1.11 Mon 12:30 BAR Schö

X-ray studies of bidirectional switching in phospholipid membranes containing photoswitchable glycolipids — •SVENJA C. HÖVELMANN^{1,2,3}, JONAS E. WARIAS¹, RAJENDRA P. GRRI¹, JULE KUHN¹, KARIN HANSEN¹, LUKAS PETERSDORF¹, NICOLAS HAYEN¹, PHILIPP JORDT¹, ANDREA SARTORI¹, CHEN SHEN³, FRANZISKA REISE⁴, OLAF M. MAGNUSSEN¹, THISBE K. LINDHORST⁴, and BRIDGET M. MURPHY^{1,3} — ¹Institute of Experimental and Applied Physics, Kiel, Germany — ²Deutsches Elektronen-Synchrotron DESY, Hamburg, Germany — ³Ruprecht Haensel Laboratory, Kiel, Germany — ⁴Otto Diels Institute of Organic Chemistry, Kiel, Germany

Lipid molecules not only play an essential role in the structure and geometry in biomembranes but also in the functionality and self-assembly of membrane proteins and channels. Their dynamic is under intense investigation owing to their applications in biosensor engineering and drug delivery. To understand the interaction between lipid and functional molecules, we investigate photoswitchable glycoconjugates embedded in a 1,2-dipalmitoyl-phosphatidylcholine (DPPC) model systems in the form of Langmuir films and vesicles. The glycoconjugates change reversibly between their trans- and cis-conformation by illumination with visible and UV light inducing a reversible change in the surrounding molecular arrangement. These structural changes, their evolution and time scales are characterised with multiple measurement techniques including X-ray scattering. Studies performed on mixed monolayers and vesicles with varying glycoconjugates identify bidirectional switching in the in DPPC monolayers.

BP 1.12 Mon 12:45 BAR Schö

Structure/Friction relationship in solid supported phospholipid layers — •SWEN HELSTROFFER, PIERRE MULLER, and THIERRY CHARITAT — Institute Charles Sadron, Strasbourg, France

Stacks of phospholipid bilayers adsorbed on biological rubbing surfaces lubricate remarkably well under severe conditions. However, the energy dissipation pathway allowing ultra low friction is still unknown. To elucidate the mechanism, we propose here to study an experimental model consisting of hydrated phospholipid layers deposited at the air/solid interface. Our system presents a well-controlled geometry in which we can fine-tune the hydration level of the lipid heads. By combining neutron reflectometry and ellipsometry studies with macroscopic tribology experiments, we demonstrated a negative correlation between hydration and friction coefficient. Using the Eyring model, we obtained microscopic activation volumes characteristic of slip. Our results suggest that the hydration level is a key parameter for lubrication. We believe that the sliding plane is located in the confined water layers.

BP 2: Active Matter I (joint session BP/PP/DY)

Time: Monday 9:30–13:00

Location: TOE 317

Invited Talk

BP 2.1 Mon 9:30 TOE 317

Emergent properties in motile active matter — •ROLAND G. WINKLER — Theoretical Physics of Living Matter (IBI-5/IAS-2), Forschungszentrum Jülich, Jülich Motile active matter systems, ranging from assemblies of bacteria, self-organized bio-polymers such as the cytoskeleton of living cells, to schools of fish and flocks of birds, exhibit intriguing emerging structural and dynamical out-of-equilibrium properties, even with reminiscence to classical turbulence. Their spatiotemporal dynamics is controlled by the propulsion of the active agents in combination with various direct interactions. The latter are typically anisotropic and emerge from different sources, such as elongated agent shapes, intrinsic flexibility and constraints, microswimmer flow fields etc. By analytical theory and mesoscale simulations, we study the physical aspects of motile active matter, ranging from propulsion of bacteria and linear filaments to large-scale collective properties of active agents, and unravel its generic features. Studies on individual polymers reveal fundamental differences in their dynamical and conformational properties depending on their propulsion mechanism, which is illustrated for polymers either tangentially driven or composed of active Brownian particles. In the latter case, hydrodynamic interactions additionally affect the conformational properties, in contrast to passive polymers. Moreover, hydrodynamic

interactions determine the activity-induced phase behavior. For spherical microswimmers (squirmers), hydrodynamics suppresses motility-induced phase separation, but enhances collective turbulent-like large-scale flows.

BP 2.2 Mon 10:00 TOE 317

High-resolution mapping of odd fluctuations and oscillations in living chiral crystals — •JINGHUI LIU^{1,2}, LISA LIN¹, YUCHAO CHEN¹, YU-CHEN CHAO¹, and NIKTA FAKHRI¹ — ¹Department of Physics, Massachusetts Institute of Technology — ²Center for Systems Biology Dresden

It has been shown that active crystals formed by self-assembling clusters of swimming starfish embryos exhibit signatures of odd mechanics, such as self-sustained chiral waves. How are these observed chiral waves and oscillations actuated and how their dynamics couple to the formation and dissolution of the living chiral crystal? Here, we report the use of vibrational mode decomposition to dissect various non-equilibrium phases of the crystal dynamics. By analyzing embryo cluster trajectories over the time course of crystal formation and dissolution, we identify the spatial modes responsible for the collective actuation of an oscillatory active crystal both in spontaneous and mechanically excited conditions. We also report a direct extraction of dispersion relation from fluctuations

of confined crystals to infer odd elastic moduli. Taken together, our results unveil the complex spatiotemporal origin of mechanical waves in non-reciprocal materials and provide insight on the design principles of collective phases of active metamaterials.

BP 2.3 Mon 10:15 TOE 317

Self-organized chemotaxis of coupled cell populations — •MEHMET CAN UCAR and EDOUARD HANNEZO — Institute of Science and Technology Austria, Am Campus 1, 3400 Klosterneuburg, Austria

Many processes in development and disease such as tissue morphogenesis, cancer invasion and immune response rely on collective directional movement of cells. In a wide array of systems this collective motility is driven locally by self-generated chemokine or stiffness gradients, as opposed to pre-patterned, global guidance cues. While recent studies have explored migration mechanisms of a single species of cells, the role of self-generated gradients navigating multiple cell types remains largely untested. Here we address this issue by introducing a theoretical framework for self-organized guidance of chemotactically coupled cell populations. Combining analytical theory and simulations with experiments on immune cell populations, we discover a diverse spectrum of collective migration patterns controlled by single-cell properties. We find that differential chemotactic sensitivity leads to efficient colocalization of distinct cell types, and show that this coupling also depends on the geometry and initial configuration of the dynamical system. We finally outline conditions for robust, sustained multicellular interactions relevant for physiological settings such as during immune response.

BP 2.4 Mon 10:30 TOE 317

Geometry-induced patterns in collective cell migration — •DAVID BRÜCKNER — Institute of Science and Technology, Am Campus 1, 3400 Klosterneuburg, Austria

The coordinated migration of cell collectives is increasingly well understood at the level of large two-dimensional confluent monolayers. However, many physiological migration processes rely on small polarized cell clusters and their responses to external confining geometries, such as 2D channels and 3D curved environments. How active motion and cell-cell interactions interplay with such external boundaries remains poorly understood. I will discuss how external geometries can induce patterns in collective cell migration, using two examples. First, we show that the migration efficiency of 2D confined cell clusters is determined by the contact geometry of cell-cell contacts that are either parallel or perpendicular to the direction of migration. Our minimal active matter model reveals how cell-cell interactions determine a geometry-dependent supracellular stress field that controls this response to external boundaries. Secondly, we show how the interplay of curvature and active flocking dynamics of 3D cell spheroids induces a collective mode of cell migration manifesting as a propagating velocity wave. Together, these approaches provide a conceptual framework to understand how cell-cell interactions interplay with 2D and 3D geometries to determine the emergent dynamics of collective cell migration.

BP 2.5 Mon 10:45 TOE 317

Shape primed AC-electrophoretic microrobots — •FLORIAN KATZMEIER and FRIEDRICH C. SIMMEL — Technical University of Munich, Munich, Germany

Second-order electrokinetic flow around colloidal particles caused by concentration polarization electro-osmosis can be utilized to controllably move asymmetric particle dimers in AC electrical fields. To demonstrate this actuation mechanism, we created particle dimers from micron-sized silica spheres with sizes 1.01 μm and 2.12 μm by connecting them with DNA linker molecules. The dimers can be steered along arbitrarily chosen paths within a 2D plane by controlling the direction of the AC electric field in a fluidic chamber with the joystick of a gamepad. Further utilizing induced dipole-dipole interactions, we demonstrate that particle dimers can be used to controllably pick up monomeric particles and release them at any desired position, and also to assemble several particles into groups. Systematic experiments exploring the dependence of the movement direction and velocity on buffer composition, frequency, and field strength further elucidate the underlying physical mechanism, and provide operational parameter ranges for our micro robotic swimmers which we termed 'SPACE-bots'.

15 min. break

BP 2.6 Mon 11:15 TOE 317

Rodrolls: self-rolling rods powered by light and chemical gradients — •ANN ROSNA GEORGE¹, MARTIN WITTMANN², ANTONIO STOCÇO¹, IGOR M. KULIĆ¹, and JULIANE SIMMCHEN² — ¹CNRS, Institute Charles Sadron, Strasbourg, France — ²Physical chemistry, TU Dresden, Germany

The self-rolling motion upon spontaneous symmetry breaking is demonstrated by certain rod-shaped microorganisms like viruses. Hence it is imperative that we understand the mechanism of this symmetry breaking triggering the active rolling motion. This behaviour has also been demonstrated on the macroscopic scale by rod-like objects. It is very interesting to try and replicate this on a microscopic scale. The main aim of the project is to create a new class of active rods that exhibit rolling activity under chemical and optical gradients. To achieve this,

it is important to understand the mechanism of activity of rod-like objects under chemical and optical stimuli.

Experiments conducted using silica Janus rods with a Platinum layer in an aqueous solution of H₂O₂ give interesting results and exhibit different kinds of activity when parameters like concentration of H₂O₂ and aspect ratio of rods are changed. Under specific conditions, particles are capable of switching their direction of motion. Experiments done using rods covered in gold nanoparticles under an optical gradient also reveal promising results of being able to make the rods roll upon providing sufficient energy to break the symmetry and fine-tuning certain parameters.

BP 2.7 Mon 11:30 TOE 317

Active Nematic Multipoles: Flow Responses and the Dynamics of Defects and Colloids — •ALEXANDER J. H. HOUSTON^{1,2} and GARETH P. ALEXANDER^{1,3} —

¹Department of Physics, Gibbet Hill Road, University of Warwick, Coventry, CV4 7AL, United Kingdom — ²Department of Physics, University of York, Heslington, York YO10 5DD, United Kingdom — ³Centre for Complexity Science, Zeeman Building, University of Warwick, Coventry, CV4 7AL, United Kingdom

Two fundamental questions in active nematics are how to extract useful work from their non-equilibrium dynamics and how to extend the topological defect-based description of dynamics that has proved useful in two dimensions to three dimensions, in which the defects form geometrically-complex loops. We introduce a general description of localised distortions in active nematics using the framework of 'active nematic multipoles'. We give the Stokesian flows for arbitrary multipoles in terms of differentiation of a fundamental flow response and describe them explicitly up to quadrupole order. This allows the identification of the dipolar and quadrupolar distortions that generate self-propulsion and self-rotation respectively and serves as a guide for the design of arbitrary flow responses. Our results can be applied to both defect loops in three-dimensional active nematics and to systems with colloidal inclusions. They reveal the geometry-dependence of the self-dynamics of defect loops and provide insights into how colloids might be designed to achieve propulsive or rotational dynamics, and more generally for the extraction of work from active nematics.

BP 2.8 Mon 11:45 TOE 317

Structure and Dynamics of Active Polymer — •SUNIL PRATAP SINGH — Indian Institute of Science Education and Research Bhopal, India, 462066

In this talk we are going to present structural and dynamical properties of a self-propelled filament using coarse-grained Brownian dynamics simulations. We consider two kinds of self-propulsion force on polymers, in case one force is applied tangent to the filament and in another model direction of active force is considered to be random. Case one shows that chain's stiffness and radius of gyration monotonically decrease. Moreover, the radius of gyration of the filament shows universal scaling for various bending rigidities with flexure number. In the latter model, where monomers are assumed to be active Brownian particle (ABP), displays a non-monotonic behaviour of end-to-end distance with activity strength. We will discuss here the role of many-body interactions on its structure and relaxation behavior. Additional we talk about the rheological behavior of chain under linear shear-flow. Our simulations reveal that active polymer's zero-shear viscosity varies in non-monotonic fashion with the active noise. More-importantly the viscosity decreases in the intermediate regime, that is followed by an increase in the more extensive Pe regime. We attribute the decrease of the zero-shear viscosity in the intermediate regime is due to many-body interactions among chain monomers.

BP 2.9 Mon 12:00 TOE 317

Pumping, Mixing, and Signal Transmission in Active Pores — •GONCALO ANTUNES^{1,2,3}, PAOLO MALGARETTI^{1,2,3}, SIEGFRIED DIETRICH^{2,3}, and JENS HARTING^{1,4} — ¹Helmholtz-Institut Erlangen-Nürnberg für Erneuerbare Energien (IEK-11), Forschungszentrum Jülich, Cauer Str. 1, 91058 Erlangen, Germany — ²Max-Planck-Institut für Intelligente Systeme, Heisenbergstr. 3, 70569 Stuttgart, Germany — ³IV. Institut für Theoretische Physik, Universität Stuttgart, Pfaffenwaldring 57, 70569 Stuttgart, Germany — ⁴Department Chemie- und Bioingenieurwesen und Department Physik, Friedrich-Alexander-Universität Erlangen-Nürnberg, Fürther Straße 248, 90429 Nürnberg, Germany

Much attention is currently being given to the problem of manipulating fluids at the microscale, with successful applications to fields such as 3D fabrication and biomedical research. An intriguing technique to manipulate fluid flows in a pore is diffusioosmosis. We show both numerically and analytically that a corrugated catalytic pore can act as a micropump even when it is fore-aft symmetric. This phenomenology is possible due to a spontaneous symmetry breaking which occurs when advection rather than diffusion is the dominant mechanism of solute transport. Relaxing the condition of Stokes flow leads to unsteady flow, and persistent oscillations with a tunable frequency appear. We further include the inverse chemical reaction that consumes solute and introduces an additional timescale. Finally, we find that the flow may lose its axial symmetry and hence promote mixing in the low Reynolds number regime.

BP 2.10 Mon 12:15 TOE 317

Interacting particles in an activity landscape — •ADAM WYSOCKI¹, ANIL KUMAR DASANNA^{1,2}, and HEIKO RIEGER^{1,2} — ¹Department of Theoretical Physics and Center for Biophysics, Saarland University, Saarbrücken, Germany — ²INM-Leibniz Institute for New Materials, Saarbrücken, Germany

We study interacting active Brownian particles (ABPs) with a space-dependent swim velocity. We find that, although an equation of state exists, a mechanical equilibrium does not apply to ABPs in activity landscapes. The pressure imbalance originates in the flux of polar order across the interface between regions of different activity. An active-passive patch system is mainly controlled by the smallest global density for which the passive patch can be close packed. Below this density a critical point does not exist and the system splits continuously into a dense passive and a dilute active phase with increasing activity. Above this density and for sufficiently high activity the active phase may start to phase separate into a gas and a liquid phase caused by the same mechanism as motility-induced phase separation of ABPs with a homogeneous swim velocity.

BP 2.11 Mon 12:30 TOE 317

Active phase fluctuations of Chlamydomonas axonemes — •ABHIMANYU SHARMA¹, BENJAMIN M. FRIEDRICH², and VEIKKO F. GEYER¹ — ¹B CUBE - Center for Molecular Bioengineering, TU Dresden, Dresden, Germany — ²Cluster of Excellence Physics of Life, TU Dresden, Dresden, Germany

Cilia and eukaryotic flagella generate periodic beat patterns by the activity of dynein motors. Earlier studies revealed active fluctuations in the ciliary beat arising presumably from small number fluctuations in the collective dynamics of the molecular motors that drive the beat. A theoretical model of the beating cilium as a system of coupled motors predicts that the fluctuations measured in terms of the quality factor of the oscillations scale with the number of beat-generating-motors.

To measure those fluctuations experimentally, we use in situ reactivated axonemes, the mechanical core of motile cilia isolated from the green alga Chlamy-

domonas. To modulate the number of motors in beating axonemes, we make use of motor mutants or partially extract molecular motors biochemically.

Using shape mode analysis and limit-cycle reconstruction, we characterize the phase fluctuations in the beat and report for the first time the relation between beat parameters and the motor number in Chlamydomonas axonemes. We experimentally infer scaling relations for the beat frequency, mean beat amplitude, and the quality factor. Further, using mass spectrometry, we identify specific dynein motors and infer their role in regulating the beat fluctuations.

BP 2.12 Mon 12:45 TOE 317

Lattice dynamics of pulsating active particles — •ALESSANDRO MANACORDA and ÉTIENNE FODOR — University of Luxembourg

Cells in epithelial tissues can drastically deform their shapes and volume giving rise to collective behavior such as size oscillation and wave propagation. These phenomena have a striking impact in many biological contexts such as embryonic development, cardiac arrhythmias and uterine contraction.

The theoretical models describing the emergence of contractile waves so far consider the cells as motile particles, where activity is represented by self-propulsion; however this ingredient is questionable in dense systems where particles barely move. We therefore introduce a novel class of active matter where the activity is the ability to change an internal degree of freedom at the single-particle level e.g. particles' size. The collective behavior of active particles is investigated in a lattice model, where the interplay between pulsation and synchronization gives rise to emergent behavior such as wave propagation. Fluctuating hydrodynamic equations can be obtained from microscopic dynamics and their predictive power is shown in comparison with numerical simulations.

We highlight the minimal ingredients needed for the complex behavior above-mentioned and point out future directions in the growing field of pulsating active matter.

BP 3: Computational Biophysics I

Time: Monday 9:30–13:00

Location: BAR 0106

BP 3.1 Mon 9:30 BAR 0106

Elucidating the Binding Process of a Disordered Protein to a Membrane Containing Ionic Lipids via Atomistic Simulations: a Case Study of LKB1 — •AZADEH ALAVIZARGAR and ANDREAS HEUER — Institute of Physical Chemistry, University of Muenster, Corrensstr. 28/30, 48149 Muenster, Germany

Liver kinase LKB1 is a serine/threonine kinase, which apart from playing a significant role in many biological processes such as cell proliferation and polarity, it functions also as a downregulator in tumors. In this work, we probe the significance of phosphatidic acid (PA) lipids as well as the poly-basic region for the binding of the C-terminus of the protein to the membrane, using molecular dynamics simulations. It was revealed that PA lipids are essential for the protein-membrane binding and that the mutation of the first three lysine residues does not abolish the binding. We specifically show the details of the protein-membrane binding at the atomic resolution using various amount of PA lipids in the membrane. Importantly, it was also found that the protein-membrane binding is dynamic and gives rise to structural changes of the protein as a result of the interaction and the accumulation of PA lipids in the membrane, which is beyond the accessible resolution in the corresponding experiments. Furthermore, we quantified the significance of each polar amino acid in the poly-basic region of the protein. These results provide important insights into the understanding and mechanism of the interaction of disordered proteins with membranes including ionic lipids.

BP 3.2 Mon 9:45 BAR 0106

Migration of oxygen in the human bc1 complex and the behavior of QH2 and Q cofactors inside it — •KATARINA KRETSCHMER, MALENA KOTTKE, and ILIA SOLOV'YOV — Institute of Physics, University of Oldenburg, Oldenburg, Germany

The dimeric bc1-complex embedded in the inner membrane of mitochondria is a relevant part of the respiratory chain in a mitochondrial cell of eukaryotes. Through different electron transfers that include oxidation and reduction reactions of the substrate molecules at the Qo- and Qi-site in this protein complex, it contributes to the metabolic system of the cell. Specifically, the complex facilitates proton transfers across the membrane to maintain an electrostatic potential, which is in turn used to drive ATP synthesis. This molecular machinery, however, is suspected to be a source of superoxide and is believed to be one of the factors in cellular aging.

Through molecular dynamics simulations, we have investigated the migration of molecular oxygen in the bc1-complex in order to identify possible reaction sites that could lead to superoxide formation. The investigation follows an earlier study of the bc1-complex from Rhodospirillum rubrum and reveals several

important differences. Specifically, we investigate further into the behavior of the cofactors Ubiquinol (QH2) and Ubiquinone (Q) in both monomers in the bc1-complex and determine the oxygen diffusion pathways that could lead to the sites where O2 could be efficiently converted to superoxide, thereby disturbing the regular functioning of the bc1-complex.

BP 3.3 Mon 10:00 BAR 0106

On the road to cellular digital twins of in vivo tumors — •ERIC BEHLE¹, JULIAN HEROLD², and ALEXANDER SCHUG¹ — ¹NIC Research Group Computational Structural Biology, Jülich Supercomputing Centre, Jülich Research Center, Jülich, Germany — ²Steinbuch Centre for Computing, KIT, Karlsruhe

To this day, cancer remains an insufficiently understood disease plaguing humanity. In particular, the mechanisms driving tumor invasion still require extensive study. Current investigations address collective cellular behavior within tumors, which leads to solid or fluid tissue dynamics. Furthermore, the extracellular matrix (ECM) has come into focus as a driving force facilitating invasion. To complement the experimental studies, computational models are employed, and advances in computational power within HPC systems have enabled the simulation of macroscopic tissue arrangements. We hereby present our work using Cells in Silico (CiS), a high performance framework for large-scale tissue simulation previously developed by us. CiS is capable of simulating tissues composed of tens of millions of cells, while accurately representing many physical and biological properties. Our ultimate aim is to build a cellular digital twin of an in vivo tumor. Unfortunately, current in vivo measurement methods lack the required resolution for directly parameterizing our simulations. Therefore, we aim to parameterize CiS via a bottom-up approach, utilizing experimental data from multiple in vitro systems. We focused our first studies on tumor spheroids, a main workhorse of tumor analysis. Towards this, we developed a novel method to compare spatial features of spheroids in 3D.

BP 3.4 Mon 10:15 BAR 0106

Resolving hierarchical interactions of proteins in phase-separated condensates by multi-scale simulations — •LUKAS STELZL^{1,2,3}, KUMAR GAURAV^{1,2,3}, XIAOFEI PING^{1,2,3}, ARYA CHANGIARATH SIVADASAN^{1,2,3}, RENÉ KETTING³, and DOROTHEE DORMANN^{3,4} — ¹Institute of Physics, JGU Mainz, Germany — ²Faculty of Biology, JGU Mainz, Germany — ³IMB Mainz, Germany — ⁴Institute of Molecular Physiology, JGU Mainz, Germany

Liquid-liquid phase separation and the resulting phase-separated condensates of proteins help to organize cellular processes in time and space. At same time, dysregulation of phase separation is implicated in the development of neurodegenerative diseases. Using particle-based multi-scale simulations we are elucidating

how phase-separated condensates can provide for specific molecular recognition and thus cellular regulation and how this specificity is lost in diseases. With simulations we are elucidating how a hierarchy of interactions such as strong interactions of folded domains and weak and multivalent interactions between disordered regions of proteins determine phase behavior. With our multi-scale methods we can simulate condensates with atomic resolution and resolve molecular details of "sticker"-sticker interactions, their kinetics and how these provide for specific recognition and cellular function. We also show how mutations and biochemical modifications can shift the conformational equilibria of proteins and their interactions in phase-separated condensates and favor the formation of toxic aggregates in neurodegenerative diseases.

Invited Talk

BP 3.5 Mon 10:30 BAR 0106

Resolving gating and allosteric modulation in ion channels through simulations and small-angle neutron scattering — •ERIK LINDAHL — Dept. Biophysics & Biochemistry, Science for Life Laboratory, Stockholm University
Pentameric ligand-gated ion channels (pLGICs) perform electrochemical signal transduction in organisms ranging from bacteria to humans. In addition to their normal gating cycle, pLGICs are highly sensitive to allosteric modulation where small compounds such as barbiturates, benzodiazepines or alcohols influence the gating kinetics by binding in separate sites, either in the transmembrane or extracellular domain. Despite a wealth of new experimental structures, it has been challenging to understand the gating kinetics, in particular since the channels rapidly undergo transitions to a desensitized nonconducting state rapidly after opening. I will present our recent combined experimental and computational work on a number of prokaryotic and eukaryotic pLGICs from the team, and how we are trying to combine low-resolution experimental techniques such as SANS (small-angle neutron scattering) with simulations to model channels under realistic conditions. In addition, I will show how we have been able to resolve structures in all separate functional states, their state-specific interactions with lipids, and not least how we are beginning to understand the properties of the desensitized state.

15 min. break

BP 3.6 Mon 11:15 BAR 0106

Clustering Molecular Dynamics Trajectories using Density and Flux — •JAYASHRITA DEBNATH¹ and GERHARD HUMMER^{1,2} — ¹Max Planck Institute of Biophysics, Frankfurt am Main, Germany — ²Goethe University, Frankfurt am Main, Germany

Molecular dynamics (MD) simulations are a powerful tool for studying a wide range of molecular systems and processes, with applications ranging from materials science to biology and medicine. Analyzing these simulations often involves finding a low-dimensional representation of the trajectory data and clustering the sampled configurations into kinetically relevant metastable states. The steady growth in the time and length scales of MD simulations, and in the complexity of their molecular systems, necessitates the development of new analysis tools that do not rely entirely on chemical or physical intuition. Here, we propose a neural network based unsupervised algorithm that can identify states using the static and dynamic information encoded in the trajectories. The network identifies metastable states by modeling a probability distribution of the data in a reduced dimensional space and learns the state boundaries by minimizing the flux between states. Furthermore, it can learn the optimal number of states from single long equilibrium trajectories or multiple short ones. After demonstrating the effectiveness of this method for a toy potential, we apply it to trypsin-benzamidine unbinding as a model of drug binding kinetics, to and folding-unfolding transitions of the villin headpiece subdomain.

BP 3.7 Mon 11:30 BAR 0106

Enhancing Traction-Force Microscopy with Machine Learning — •FELIX S. KRATZ, LARS MÖLLERHERM, and JAN KIERFELD — TU Dortmund University, Germany

Traction patterns of adherent cells provide important information on their interaction with the environment, cell migration or tissue patterns and morphogenesis. Traction Force Microscopy is a method aimed at revealing these traction patterns for adherent cells on engineered substrates with known constitutive elastic properties from deformation information obtained from substrate images. Conventionally, the substrate deformation information is processed by numerical algorithms of varying complexity to give the corresponding traction field via solution of an ill-posed inverse elastic problem. We explore the capabilities of a deep convolutional neural network as a computationally more efficient and robust approach to solve this inversion problem. We develop a general purpose training process based on collections of circular force patches as synthetic training data, which can be subjected to different noise levels for additional robustness. The performance and the robustness of our approach against noise is systematically characterized for synthetic data, artificial cell models and real cell images, which are subjected to different noise levels. A comparison to state-of-the-art Bayesian Fourier transform traction cytometry reveals the precision, robustness, and speed improvements achieved by our approach, leading to an acceleration of Traction Force Microscopy methods in practical applications.

BP 3.8 Mon 11:45 BAR 0106

Finding pathways in molecular dynamics simulations using machine learning and graph methods — •STEFFEN WOLF¹, MIRIAM JÄGER¹, VICTOR TÄNZEL¹, SIMON BRAY^{1,2}, MATTHIAS POST¹, and GERHARD STOCK¹ — ¹Biomolecular Dynamics, Institute of Physics, University of Freiburg, 79104 Freiburg, Germany — ²Bioinformatics Group, Institute of Informatics, University of Freiburg, 79110 Freiburg, Germany

Understanding the mechanisms of biomolecular systems and complexes, e.g., of protein-ligand (un)binding, requires the understanding of paths such systems take between metastable states. In MD simulation data, paths are usually not observable per se, but need to be inferred from simulation trajectories. Here we present novel approaches to cluster trajectories according to similarities. These approaches include neighbor-nets allowing to correct for input data ambiguity [1] and an unsupervised learning approach employing only a single free parameter [2]. We demonstrate how such clusters of trajectories correspond to pathways, and how the approaches help in the identification of reaction coordinates for a considered process. Last, we present a theoretical framework how potentials of mean force can be calculated for individual pathways, and how these potentials and kinetics along paths can be combined into a comprehensive complete free energy profile and process kinetics.

[1] Bray, S., Tänzels, V. & Wolf, S. *J. Chem. Inf. Model.* 62, 4591-4604 (2022).
[2] Diez, G., Nagel, D. & Stock, G. *J. Chem. Theory Comput.* 18, 5079-5088 (2022).

BP 3.9 Mon 12:00 BAR 0106

Artificial Intelligence for Molecular Mechanism Discovery — •HENDRIK JUNG¹, ROBERTO COVINO², A ARJUN³, CHRISTIAN LEITOLD⁴, PETER G BOLHUIS³, CHRISTOPH DELLAGO⁴, and GERHARD HUMMER¹ — ¹Max Planck Institute of Biophysics, Frankfurt, Germany — ²Frankfurt Institute for Advanced Studies, Frankfurt, Germany — ³University of Amsterdam, Amsterdam, The Netherlands — ⁴University of Vienna, Vienna, Austria

We present a machine learning algorithm to extract the mechanism of collective molecular phenomena from computer simulations. The algorithm combines transition path sampling (TPS), deep learning (DL), and statistical inference to simultaneously enhance the sampling and understanding of complex molecular reorganizations without human intervention. TPS is a Markov Chain Monte Carlo method in trajectory space that samples the rare transition trajectories connecting meta-stable states. In our algorithm a DL model is selecting the configurations from which the new trial trajectories are generated using shooting moves, i.e., the trajectories are propagated according to the physical model of the simulated system. By iteratively training on the outcomes of the shooting moves, the model simultaneously increases the efficiency of the rare-event sampling and gradually reveals the underlying mechanism of the transition. In a second step we distill the knowledge about the transition encoded in the DL model into a simplified mathematical expression. With this algorithm we study a diverse set of molecular systems ranging from the association of ions in solution to the oligomerization of a transmembrane alpha helix dimer.

BP 3.10 Mon 12:15 BAR 0106

MD simulations of *n*-alkanes in a phospholipid bilayer: CHARMM36 vs. Slipids — •ANIKA WURL and TIAGO FERREIRA — Institute of Physics, Martin-Luther Universität Halle-Wittenberg

The incorporation of *n*-alkanes into phospholipid bilayers is a convenient starting point for studying the molecular behavior of linear, (purely) hydrophobic molecules in lipid membranes. Here, we perform atomistic molecular dynamics simulations using two state-of-the-art lipid force fields, CHARMM36 [1] and Slipids [2], to systematically investigate how the miscibility of *n*-alkanes in dipalmitoylphosphatidylcholine (DPPC) bilayers depends on alkane chain length. The two force fields show a distinct behavior: Slipids simulations predict an effect of chain length on miscibility, while for CHARMM36 simulations this is not the case for the alkanes studied. A comparison with ²H NMR spectra shows that the accuracy of the two force fields is dependent on alkane length. CHARMM36 performs well for the shorter chains, while Slipids models the longer alkanes better. Slipids chains are more flexible, due to reduced electrostatic 1-4 interactions compared to CHARMM36. By scaling these 1-4 interactions, CHARMM36 can be adapted to model longer alkanes and lipid acyl tails better. The presented results are of general interest for future studies of other long and flexible hydrophobic molecules inside lipid membrane environments, and show that *n*-alkane/lipid mixtures should be taken into account for optimization of force fields designed to model lipid membranes. [1] Jämbeck et al.; *J Phys Chem B* 2012, 116, 3164-3179 [2] Klauda et al.; *J Phys Chem B* 2010, 114, 7830-7843

BP 3.11 Mon 12:30 BAR 0106

Scission criteria upon proteins X-ray absorption — •CARLOS ORTIZ-MAHECHA¹, LUCAS SCHWOB², SADIYA BARI², and ROBERT MEISSNER^{1,3} — ¹Technische Universität Hamburg, Hamburg, Germany — ²Deutsches Elektronen-Synchrotron, Hamburg, Germany — ³Helmholtz-Zentrum Hereon, Geesthacht, Germany

Dynamic protonation in a protein lead to conformational changes which could be studied by challenging near-edge X-ray absorption mass spectrometry (NEX-

AMS) experiments and computationally expensive quantum mechanical (QM) calculations. Less demanding assessment is essential for interpreting the underlying electronic density changes in proteins. Those density changes in the amino acid (AA) non-covalent environment are evaluated by *in-silico* X-ray spectra and their chemical-physical properties by the pair interaction energy decomposition analysis (PIEDA) method. In order to represent a protein X-ray absorption spectra as a summation of their smaller protein fragments X-ray spectra, we first assess its electronic neighboring influence to establish a scission criteria. For that, we propose a pattern involving the change of excited-state transition energy probability in a two-body AA localized density population and the charge transfer energy change from PIEDA as a function of the non-covalent interaction distance. In this way using this criteria, the X-ray absorption spectra of proteins could potentially be represented as a composition of X-ray spectra of their smaller fragments, which would be computationally more efficient.

BP 3.12 Mon 12:45 BAR 0106

Fluid deformable surfaces, the influence of surface viscosity in fluid membranes — VEIT KRAUSE and AXEL VOIGT — Institute of Scientific Computing, Technische Universität Dresden, Germany

We consider a fluid-solid duality of membranes, with in-plane fluid properties and out-of-plane solid (bending) properties. In such systems any tangential flow induces shape deformations and any change in morphology induces tangential flow. This numerically challenging surface problem is solved by surface finite elements and we explore the dynamics towards equilibrium states in various settings, ranging from transitions from biconcave to dumbbell shapes, coarsening of two-component surface fluids under the influence of curvature and wrinkling in fluid membranes.

BP 4: Tissue Mechanics I

Time: Monday 15:00–17:30

Location: BAR Schö

BP 4.1 Mon 15:00 BAR Schö

Nonlinear and active rheology of cell tissues — CHARLIE DUCLUT^{1,2}, JORIS PAIJMANS², MANDAR M. INAMDAR³, CARL D. MODES⁴, and FRANK JÜLICHER² — ¹Laboratoire Physico-Chimie Curie, Paris, France — ²Max Planck Institute for the Physics of Complex Systems, Dresden, Germany — ³Indian Institute of Technology Bombay, Mumbai, India — ⁴Max Planck Institute for Molecular Cell Biology and Genetics, Dresden, Germany

Tissues are assemblies of large numbers of cells which form a soft active material. In amorphous solids as in tissues, neighbour exchanges (or T1 transitions) can relax local stresses and allow the material to flow. In tissues, in addition to these passive events, energy consumption at the microscopic level allows cells to perform active neighbour exchanges that can shape the tissue into a prescribed geometry. In my talk, I will consider an anisotropic vertex model to study T1 rearrangements in polygonal cellular networks. I will consider two different physical realizations of the active anisotropic stresses, that can be both observed in experiments: (i) anisotropic bond tension and (ii) anisotropic cell stress. Interestingly, the two types of active stress lead to patterns of relative orientation of T1 transitions and cell elongation that are different. Using the lens of a continuum description of the tissue as an anisotropic active material, I will discuss the energetics of the dynamic tissue and express the energy balance in terms of internal elastic energy, mechanical work, chemical work and heat. This allows us to define active T1 transitions that can perform mechanical work while consuming chemical energy.

BP 4.2 Mon 15:15 BAR Schö

Hydraulic and osmotic control of lumen coarsening — MATHIEU LE VERGE SERANDOUR^{1,2} and HERVÉ TURLIER² — ¹School of Natural Sciences, Technical University of Munich, Germany — ²Center for Interdisciplinary Research in Biology, Collège de France, PSL Research University, Paris, France

The blastocoel formation is a keystone in the morphogenesis of the pre-implantation mammalian embryo, yet the physical mechanism for its emergence remained unclear. The blastocoel is a fluid-filled cavity (or lumen) that positions the first axis of symmetry of the embryo. We showed that, in the mouse embryo, the blastocoel results from micron-sized lumens, nucleating at the adhesive basolateral side of embryonic cells and coarsening in a process akin to Ostwald ripening. We investigate the collective dynamics of a one-dimensional chain of lumens as a minimal model for the blastocoel formation, taking the osmotic effects into account. We include the permeation of water and osmolyte through the cellular membrane. We show that the coarsening of the chain is reminiscent of dewetting films, with a scaling law for the number of lumens controlled by a screening length associated with water permeation, while the influence of osmotic inhomogeneities remains limited. Finally, we consider active osmolyte pumping that may rescue the chain from collapse. We find a new scaling law controlled by active pumping emerging from the coalescence of lumens, which may also direct the position of the final lumen.

BP 4.3 Mon 15:30 BAR Schö

Mechanical Properties of the Premature Lung — JONAS NAUMANN¹, NICKLAS KOPPE¹, ULRICH THOME², MANDY LAUBE², and MAREIKE ZINK¹ — ¹Research Group Biotechnology & Biomedicine, Peter Debye Institute for Soft Matter Physics, Leipzig University, 04103 Leipzig, Germany — ²Center for Pediatric Research Leipzig, Department of Pediatrics, Division of Neonatology, Leipzig University, 04103 Leipzig, Germany

Premature infants are often reliant on mechanical ventilation to survive. However, prolonged ventilation and associated mechanical stress may cause subsequent pulmonary diseases of the immature lung. To study the mechanical properties of fetal rat lungs on macroscopic scale, we performed rheology experiments under compression and tension using different velocities. Fetal lung tissue

showed a hyperelastic behavior and became significantly stiffer with increasing deformation velocities. In fact, fetal lung tissue under compression showed clear viscoelastic features even for small strains. A higher Young's modulus of fetal lungs compared to adult controls clearly pointed towards altered tissue characteristics. In addition, the influence of a hydrostatic pressure difference on the electrophysiology of primary fetal distal lung epithelial cells was investigated on microscopic scale. We observed a strong impact of hydrostatic pressure on the activity of the epithelial sodium channel and the sodium-potassium pump. Vectorial sodium transport, crucial for alveolar fluid clearance, was significantly impaired.

BP 4.4 Mon 15:45 BAR Schö

'Forcing' changes in health and disease: New access into bioengineered skeletal muscle mechanics for preclinical screening — ARNE HOFEMEIER^{1,2}, TILL MUENKER², MARIAM RISTAU², TIMO BETZ², and WOLFRAM ZIMMERMANN¹ — ¹University Medical Center, Göttingen, Germany — ²Third Institute of Physics, Göttingen, Germany

Mechanical properties of skeletal muscles are tightly related to proper functionality, which makes experimental access to the biomechanics of skeletal muscle tissue essential to advance our understanding of muscle function, development and disease. Recently devised *in vitro* culture systems allow for raising 3D muscle tissues using single cells from patients. However, these systems are inherently incompatible with high resolution microscopy and precise mechanical in-plate measurements. Here, we present a new chamber design that allows real-time high resolution 3D microscopy and non-invasive quantification of global contractile forces and tissue tension during muscle formation. Surprisingly, we found that bioengineered muscles, derived from patients suffering from Duchenne muscular dystrophy, develop under higher tension although they appear weaker upon stimulation. Duchenne is caused by loss of a membrane linker protein, dystrophin, which we therefore dedicate an important novel role as a molecular tension sensor. Testing an individualized gene therapy for a subset of Duchenne patients, we were able to demonstrate that not just the contractile strength of the bioengineered muscles was restored, but also the elevated tissue tension was decreased again.

15 min. break

BP 4.5 Mon 16:15 BAR Schö

Harnessing active viscoelasticity for synthetic epithelial morphogenesis — NIMESH RAMESH CHAHARE^{1,2}, ADAM OUZERI², TOM GOLDE¹, THOMAS WILSON^{1,3}, PERE ROCA-CUSACHS¹, MARINO ARROYO^{2,3}, and XAVIER TREPAT^{1,4} — ¹Institute for Bioengineering of Catalonia, Barcelona, Spain — ²Universitat Politècnica de Catalunya, Barcelona, Spain — ³Centre Internacional de Mètodes Numèrics en Enginyeria, Barcelona, Spain — ⁴Institució Catalana de Recerca i Estudis Avançats, Barcelona, Spain

Epithelial sheets are active viscoelastic materials that form specialized 3D structures suited to their physiological roles, such as branched alveoli in the lungs, tubes in the kidney, and villi in the intestine. How epithelial shape arises from active viscoelasticity and luminal pressure remains poorly understood. Here we developed a microfluidic setup to engineer 3D epithelial tissues with controlled shape and pressure. Through this approach, we subject the tissues to a range of lumen pressures at different rates and probe the relation between strain and tension in different regimes. Slow pressure changes relative to the timescales of actin dynamics allow the tissue to accommodate large strain variations. However, under sudden pressure reductions, the tissue buckles and folds to store excess tissue area. This behavior is well captured by a 3D computational model that incorporates the turnover, viscoelasticity, and contractility of the actomyosin cortex. Informed by this model, we harness the active behavior of the cell cortex to pat-

tern epithelial folds by rationally directed buckling. Our study establishes a new approach to engineering epithelial morphogenetic events.

BP 4.6 Mon 16:30 BAR Schö

Continuum Mechanics of Cell Intercalation in *Tribolium* — •MARYAM SETOUDEH^{1,2,3} and PIERRE A. HAAS^{1,2,3} — ¹Max Planck Institute for the Physics of Complex Systems, Nöthnitzer Straße 38, 01187 Dresden, Germany — ²Max Planck Institute of Molecular Cell Biology and Genetics, Pfotenhauerstraße 108, 01307 Dresden, Germany — ³Center for Systems Biology Dresden, Pfotenhauerstraße 108, 01307 Dresden, Germany

Deformations of tissues during development often involve cell intercalations and cell neighbour exchanges, but a general continuum description of such plastic rearrangements in tissues is still lacking.

Here, we combine morphoelasticity and plasticity theory to develop a continuum framework of tissue mechanics combining cell intercalations, intrinsic deformations such as tissue contraction, and elastic deformations of the tissue.

We apply our theory to the development of the beetle *Tribolium* [1] during which a layer of cells, the serosa, closes over the embryo. Cells deintercalate from the rim of the serosa into its bulk, thus reducing the number of cells at the boundary and closing the serosa. This is associated with actomyosin contraction at the rim of the serosa [1].

We model this process by the axisymmetric closure of a circular hole in a flat elastic sheet contracting near the hole. Our analytical and numerical results show how intercalation reduces the contraction required for serosa closure and hint at the importance of an additional force exerted by the embryo at the rim of the serosa.

[1] Jain *et al.*, Nat. Commun. **11**, 5604 (2020)

BP 4.7 Mon 16:45 BAR Schö

Tracking and comprehending single cell dynamics in *Drosophila* dorsal closure using machine learning — •DANIEL HÄRTTER^{1,3}, YUXI LONG², JANICE CRAWFORD², DANIEL P. KIEHART², and CHRISTOPH F. SCHMIDT¹ — ¹Department of Physics and Soft Matter Center, Duke University, USA — ²Department of Biology, Duke University, USA — ³Department of Pharmacology and Toxicology, Göttingen University Medical Center

Dorsal closure in *Drosophila melanogaster* embryos is a key model system for cell sheet morphogenesis and wound healing. We pursue a data-driven approach to understand the emergence of organized behavior on tissue level from the stochastic dynamics of single cells across scales. We developed DeepTissue, a deep-learning-based algorithm to automatically and robustly detect and temporally track various single cell features: cell shapes, cell junction lengths, myosin intensities, and tissue topology. Epithelial cells in dorsal closure exhibit oscillations and contribute to progressive cell sheet movements, while showing a large variability in individual shapes, dynamics, and fates. Based on high-quality

multi-parametric trajectories of 1000s of single cells, we use unsupervised machine learning techniques to detect and classify behavioral and structural phenotypes. Further we study how the behavior of single cells throughout closure is driven by deterministic and/or stochastic factors, with the aim to predict singular cell ingress events.

BP 4.8 Mon 17:00 BAR Schö

The role of intermediate filaments in stress resistance in 3D epithelial structures — •TOM GOLDE¹, MARCO PENSALFINI², NIMESH CHAHARE¹, MARINO ARROYO^{1,2}, and XAVIER TREPAT^{1,3,4} — ¹IBEC, Barcelona, Spain — ²UPC, Barcelona, Spain — ³UB, Barcelona, Spain — ⁴ICREA, Barcelona, Spain

The safety belt hypothesis states that IFs are protecting cells from large and rapid deformations. However, typical experiments for stretching epithelial tissues only reach maximum strains of around 0.3. We developed a microfluidic device where an epithelial monolayer is grown on a porous surface with circular low adhesion zones. Upon applying hydrostatic pressure, the monolayer delaminates into a spherical cap (dome), generating tissue strains of more than 1 while individual cells are stretched up to strains of 9. We can image these 3D epithelial domes with high resolution, determine the tissue tension via Laplace law, and control the rate of inflation and deflation.

Using this approach with MDCK cells, we observed a striking reorganization of the keratin IF rim-and-spoke network into a central knot with thick, radially oriented bundles. Previous results by us and others hereby indicate a crucial role of actin-IF interactions. To better understand the mechanical principles of such transitions, we developed a multiscale computational model that simulates the interactions of keratin IFs with the nucleus, desmosomes, and the actin cortex. Combining experiments and simulations, we can now conclusively test the safety belt hypothesis in controlled and unparallelled large 3D tissue deformations

BP 4.9 Mon 17:15 BAR Schö

Instabilities in hexanematic models of epithelia — •JOSEP-MARIA ARMENGOL-COLLADO, LIVIO CARENZA, and LUCA GIOMI — Instituut-Lorentz, Leiden Institute of Physics, Universiteit Leiden, P.O. Box 9506, 2300 RA Leiden, The Netherlands

Epithelial tissues, whose study remain fundamental to understand processes such as cancer progression, have revealed to exhibit multiscale orientational order. While the large scale dynamics is ruled by the nematic symmetry, hexatic order instead controls the behaviour of small clusters of cells. By considering a hydrodynamic approach, we investigate the stability of hexanematic liquid crystals identifying the role of activity and flow alignment in the generation of spontaneous flows, which also reflect the interplay between different length scales. We finally address possible consequences when confining such a fluid in a channel, connecting this phenomenology with recent observations of metastatic cell invasion.

BP 5: Focus Session NanoAgents

Time: Monday 15:00–17:30

Location: TOE 317

Invited Talk

BP 5.1 Mon 15:00 TOE 317

Repurposing nucleic acids as high-resolution force sensors: From fundamental mechanotransduction to translational biophysics — •KHALID SALAITA — Emory University, Department of Chemistry, Atlanta, Georgia, USA

Cells are highly dynamic structures that are constantly converting chemical energy into mechanical work to pull and push on one another and on their surroundings. These pulls and pushes are mediated by tiny molecular forces at the scale of tens of piconewtons. For context, 7 pN applied a distance of 1 nm is ~1 kcal/mol. Nonetheless, these forces can have profound biochemical consequences. For example, the rapidly fluctuating forces between immune cells and their targets can drastically tune immune response and function. Despite the importance of mechanics there are limited methods to study forces at the molecular scale and particularly within living cells.

In this talk, I will discuss my group's efforts at addressing this gap in knowledge by developing tools to map the molecular forces applied by cells. I will describe the development of a suite of DNA tension probes which offer significant improvements in S/N and lead to enhanced spatial and temporal resolution. I will also describe a series of force-triggered reactions that enable signal amplification. Fluorescence polarization spectroscopy and super-resolution imaging offer the highest resolution maps of cell traction forces reported to date. Finally, armed with these new tools, I will describe the advent of translational mechanobiology where we predict the bleeding risk in patients by measuring the mechanical activity of their platelet adhesion receptors.

BP 5.2 Mon 15:30 TOE 317

Remodelling DNA filaments for bottom-up synthetic biology — •MAJA ILLIG¹, KEVIN JAHNKE^{1,2}, MARLENE SCHEFFOLD¹, HAUKE DRECHSLER³, STEFAN DIEZ³, and KERSTIN GÖPFRICH¹ — ¹MPI for Medical Research, Heidelberg,

Germany — ²Harvard University, School of Engineering and Applied Sciences (SEAS), Cambridge, MA, USA — ³TU Dresden, Center for Molecular Bioengineering (B CUBE), Dresden, Germany

The control of filamentous cytoskeletal systems is one of the dedicated aims of bottom-up synthetic biology to engineer self-dividing synthetic cells and equip them with mechanical cell-to-cell communication pathways. A molecular engineering approach to achieve specific functionality from the nanoscale to the microscale requires programmability in order to design self-assembly.

This work reinforces how DNA nanotechnology paves the way to create biocompatible nanostructures that can mimic cellular entities. Here, we demonstrate the remodelling of entirely synthetic filaments made from DNA nanotubes: (i) Towards bottom-up synthetic cell division, we can rationally design a ring structure made from bundled filaments. We can control the ring formation by engineering of a synthetic crosslinking peptide and we further constrict the ring diameter by external triggers. (ii) Towards mechanotactic synthetic cells, a transmembrane signalling pathway enables the reconfiguration of the cytoskeleton made from DNA filaments. The stimulus-induced clustering of transmembrane entities results in mechanical remodelling of the internal DNA cytoskeleton (Jahnke, Illig *et al.* Biorxiv 2022).

BP 5.3 Mon 15:45 TOE 317

Einfluss von Kohlenstoff-Nanoteilchen auf die Funktion von Lysosomen — •CARLA SPRENGEL, CATHRIN NOLLMANN, LENA BERNING, THOMAS LENZ, BJÖRN STORK und THOMAS HEINZEL — Heinrich-Heine-Universität Düsseldorf Die Verwendung von Nanopartikeln als Wirkstoffträger in Drug Delivery Systemen gewinnt besonders bei der Tumortherapie an Bedeutung. Die zielgenaue Medikamentenfreisetzung in pathologischen Zellen könnte bei gleichbleibender therapeutischer Wirkung starke Nebenwirkungen durch Schädigung gesunder

Zellen vermeiden. Kohlenstoff-Nanopartikel (CNDs) eignen sich aufgrund ihrer Fluoreszenzeigenschaften, geringen Zytotoxizität und Möglichkeit zur Funktionalisierung besonders gut als Carrier für ein solches Drug Deliver System. Durch die Fluoreszenz der CNDs im blauen Bereich nach UV-Anregung können die CNDs in Zellen nachgewiesen werden und auf zellulärer Ebene lokalisiert werden. Bisherige Untersuchungen zeigen, dass die CNDs über Endozytose in die Zelle aufgenommen und in den Endosomen und Lysosomen angelagert werden. Da wichtige metabolische Prozesse wie die Autophagie abhängig von Lysosomen sind, werden die Auswirkungen der CNDs auf diese lysosomalen Prozesse mittels verschiedener Methoden untersucht und diskutiert.

BP 5.4 Mon 16:00 TOE 317

Aufnahme von Kohlenstoff-Nanopartikeln in humane AML-Zellen im Vergleich zu primären hämatopoetischen Zellen — •CATHRIN NOLLMANN¹, THOMAS HEINZEL¹ und RAINER HAAS² — ¹Institut für Physik der kondensierten Materie, Heinrich-Heine-Universität, Düsseldorf, Deutschland — ²Klinik für Hämatologie, Onkologie und Klinische Immunologie, Universitätsklinikum Düsseldorf, Deutschland

Kohlenstoff-Nanopartikel (CNDs) sind eine vielversprechende Klasse von Nanopartikeln. Diese kohlenstoffbasierten, nanometergroßen Partikel bieten ein breites Spektrum potenzieller biomedizinischer Anwendungen wie Bioimaging, Krebsdiagnostik und Drug-Delivery. Im Zusammenhang mit Drug Delivery ist eine selektive Aufnahme durch maligne Zellen entscheidend. Unser Ziel war es zu untersuchen, ob es ein unterschiedliches Aufnahmeverhalten von AML-Zellen im Vergleich zu primären hämatopoetischen Zellen gibt. Dazu wurden aus Zitronensäure und Diethylentriamin hergestellte CNDs 24 Stunden lang mit Zellen von fünf Patienten mit de novo AML und primären hämatopoetischen Zellen von drei gesunden Spendern inkubiert. Die differentielle Aufnahme der CNDs wurde mittels Durchflusszytometrie und monoklonalen Antikörpern untersucht. [1]

[1] C. Nollmann et al., Uptake of carbon nanodots into human AML cells in comparison to primary hematopoietic cells, *RSC Adv.*, (11), pp. 26303-26310, 2021.

15 min. break

BP 5.5 Mon 16:30 TOE 317

DNA origami agents for the efficient treatment of solid tumors — •JOHANN MORITZ WECK¹, MERVE-ZEYNEP KESICI¹, CORNELIA MONZEL², and AMELIE HEUER-JUNGEMANN¹ — ¹Max Planck Institut für Biochemie, Am Klopferspitz 18, 82152 Martinsried — ²Heinrich Heine Universität Düsseldorf, Universitätsstraße 1, 40225 Düsseldorf

We previously used DNA origami as a platform to pre-cluster Fas ligands (FasL) of the tumor necrosis factor receptor superfamily (TNFRSF) with nanometer precision in varying patterns and presented those to HeLa cells in a 2D cell culture model. We found up to a 100x increase of potency upon pre-clustering FasL in hexagonal geometries, a high sensitivity towards inter-ligand distance and a dependency on linker rigidity. In order to use this knowledge for the advancement of TNRSF ligand-based therapeutics, we investigated the interactions of DNA origami nanoagents with solid tumors. Certain aspects of cancer cell biology, such as the complex biological environment of solid tumors cannot be efficiently simulated in regular 2D cell culture systems. Using a 3D tumor spheroid model, we here show that FasL-DNA origami nanoagents are able to strongly affect the growth of 3D tumor spheroids. Partial dissolution of 3D tumoroids is observed after exposure to the nanoagents. We provide insights into DNA origami tumor spheroid penetration ability as well as a threshold like behavior of signaling initiation, and design rules for nanomaterial based therapeutics.

BP 5.6 Mon 16:45 TOE 317

Monitoring the Switching dynamics of Photolipid Membranes with Plasmonic Nanorods — •JINHUA ZHANG, FRANCIS SCHUKNECHT, LUDWIG HABERMANN, ALEXANDER PATTIS, STEFANIE PRITZL, and THEOBALD LOHMÜLLER — Chair for Photonics and Optoelectronics, Nano-Institute Munich, Department of Physics, Ludwig-Maximilians-Universität, Königinstraße 10, 80539 Munich, Germany

Photoswitchable lipids (i.e. photolipids) are intriguing nanoagents for controlling lipid membrane properties with light. However, analyzing the switching dynamics in a single lipid bilayer locally and in situ is challenging due to a lack of sensitive tools for detecting the very small changes in membrane thickness (< 1 nm). Here, we demonstrate a new approach to monitor the photoisomerization of photolipid membranes on the nanoscale via plasmonic sensing.

In our experiment, gold nanorods are deposited on a glass substrate and coated with a supported photolipid bilayer. The photosensitive azobenzene group in the lipid tails is switched between a trans and cis form by an illumination sequence with UV and blue light, while scattering spectra of individual nanorods are simultaneously measured. We find that the photoisomerization process of azobenzene leads to a reversible shift of the nanorod's plasmon resonance over many switching cycles. Our study shows that single nanorods may thus be used as sensitive probes to study isomerization dynamics and photostationary states of photolipid bilayer membranes within nanoscale environments.

BP 5.7 Mon 17:00 TOE 317

Bio-inspired Magnetic Nanoprobes For Subcellular Manipulation Studies in Single Cells — •ANDREAS NEUSCH¹, IULIA NOVOSELOVA¹, LIESA ZITZKE¹, SARAH SADIK¹, MICHAEL FARLE², ULF WIEDWALD², and CORNELIA MONZEL¹ — ¹Heinrich-Heine-University, Düsseldorf — ²University of Duisburg-Essen, Duisburg

Probing and manipulating biological functions requires tools to target and modify the proteins involved in the respective process. In recent years Magnetogenetics emerged as an approach where magnetic nanoparticles (MNPs) and external magnetic fields are used to realize such manipulation (Lisse et al., *Adv. Mater.*, 29, 1700189 (2017)). The advantages of this combination lies within the deep tissue penetration of magnetic fields and the possibility to apply stimuli on nanoscales leading to spatial redistribution, force application, or heat generation of proteins. However, a precise active perturbation requires MNPs to be monodisperse, biocompatible, tunable with regard to their magnetic properties, as well as exhibiting a modifiable molecular shell (Monzel et al., *Chem. Sci.* 8, 7330-7338 (2017)). Here, we synthesize a bioinspired semisynthetic MNP - Magnetoferritin (MFT) -, which fulfils these demands. MFT is based on the globular iron storage protein complex ferritin that converts iron ions to a ferrihydrite core but can be synthetically loaded with a magnetic iron oxide core (Novoselova et al., *Nanomaterials*, 11, 2267 (2021)). MFT was chemically, physically and magnetically characterized both in vitro and in vivo. We demonstrate how MFT can be used to target proteins on living cells as well as to spatially manipulate MFTs in a single cell environment.

BP 5.8 Mon 17:15 TOE 317

Precise micro-manipulations via multiplexed feedback-controlled thermoviscous flows — •ELENA ERBEN¹, NICOLA MAGHELLI¹, WEIDA LIAO², ANTONIO MINOPOLI¹, ERIC LAUGA², and MORITZ KREYSING¹ — ¹Max Planck Institute of Molecular Cell Biology and Genetics, Dresden, Germany — ²DAMTP, University of Cambridge, UK

Methods for precise micro-manipulation are highly relevant for many problems in biological research such as cell patterning and controlled droplet fusion. Thermoviscous flows [1] hold great potential for manipulations in biological systems since they can be induced optically and enable non-invasive in-vivo perturbations [2]. Recently, we developed a novel optofluidic manipulation method based on feedback-controlled thermoviscous flows. This technique facilitates the automatic positioning of a single micro-particle, with a precision of up to 24 nm [3]. Our approach can be multiplexed to the parallel manipulation of multiple particles, thus facilitating dynamic micropatterning. Furthermore, we found that positioning of multiple particles can be greatly accelerated by leveraging highly complex flow patterns that result from multiplexing. We anticipate that combining our approach with elaborate theoretical modelling will increase the precision and speed of this manipulation method even more, facilitating translation onto applications in the life sciences and beyond.

[1] Weinert et al. *Phys. Rev. Lett.* 2008; [2] Mittasch et al. *Nat. Cell Biol.* 2018; [3] Erben et al. *Opt. Express* 2021.

BP 6: Bacterial Mechanics

Time: Monday 15:00–17:15

Location: BAR 0106

BP 6.1 Mon 15:00 BAR 0106

Antigenic variation modulates attractive forces between bacteria and affects antibiotic tolerance — •ISABELLE WIELERT^{1,3}, SEBASTIAN KRAUS-RÖMER^{1,3}, PAUL HIGGINS^{2,3}, and BERENIKE MAIER^{1,3} — ¹Institute for Biological Physics, University of Cologne, Germany — ²Institute for Medical Microbiology, Immunology and Hygiene, University of Cologne, Germany — ³Center for Molecular Medicine Cologne

Type 4 pili (T4P) are multifunctional surface exposed polymers involved in adhesion, force generation, surface motility, aggregation and act as major antigens. During antigenic variation, the human pathogen *Neisseria gonorrhoeae* varies the primary structure of the pilin, the major subunit of the T4P fibre, to escape from immune surveillance. But it is unclear how pilin antigenic variation impacts other T4P functions. We addressed this question by replacing the pilin of a laboratory strain by pilins from various clinical isolates. By performing dual

laser trap experiments, we found that the pilin variant strains clustered into two groups with different attractive forces. Variants with interaction forces exceeding 40 pN formed colonies while weakly interacting bacteria retained a planktonic lifestyle. All pilin variants supported surface motility, yet the planktonic variants moved faster. Previous studies indicated that bacterial aggregation results in higher tolerance against antibiotic treatment. To test whether pilin antigenic variation affects tolerance, we carried out bacterial survival assays and showed that indeed colony-forming variants are more tolerant. We conclude that pilin variation enhances bacterial fitness beyond immune escape.

BP 6.2 Mon 15:15 BAR 0106

Stress anisotropy in confined populations of growing rods — JONAS ISENSEE^{1,2}, LUKAS HUPE^{1,2}, RAMIN GOLESTANIAN^{1,2,3}, and PHILIP BITTIHN^{1,2} — ¹Max Planck Institute for Dynamics and Self-Organization, Göttingen, Germany — ²Institute for the Dynamics of Complex Systems, Göttingen University — ³Rudolf Peierls Centre for Theoretical Physics, University of Oxford, UK

A central feature of living matter is its ability to grow and multiply. The mechanical activity associated with growth produces both macroscopic flows shaped by confinement, and striking self-organization phenomena, such as orientational order and alignment, which are particularly prominent in populations of rod-shaped bacteria due to their nematic properties. However, how active stresses, passive mechanical interactions and flow-induced effects interact to give rise to global alignment patterns remains elusive. Here, we study in silico colonies of growing rod-shaped particles confined in channel-like geometries. A spatially resolved analysis of the stress tensor reveals a strong relationship between near-perfect alignment and an inversion of stress anisotropy for particles with large length-to-width ratios. In quantitative agreement with an asymptotic theory, strong alignment can lead to a decoupling of active and passive stresses parallel and perpendicular to the growth axis, respectively. We demonstrate the robustness of these effects to perturbations and for weaker confinement. Our results illustrate the complexity arising from the inherent coupling between nematic order and active stresses in growing active matter, modulated by geometric and configurational constraints due to confinement.

BP 6.3 Mon 15:30 BAR 0106

Magnetic fields help magnetotactic bacteria navigate complex environments — AGNESE CODUTTI^{1,2}, MOHAMMAD CHARSOOGHI¹, KONRAD MARX³, ELISA CERDA-DONATE¹, OMAR MUNOZ³, PAUL ZASLANSKY¹, VITALI TELEZKI³, TOM ROBINSON¹, DAMIEN FAIVRE^{1,4}, and STEFAN KLUMPP³ — ¹MPI of Colloids and Interfaces, Potsdam — ²TU Munich — ³University of Göttingen — ⁴Aix-Marseille Université, CEA, CNRS, BIAM, Saint Paul lez Durance, France
To study swimming of magnetotactic bacteria in a near-realistic sediment environment resembling those in their natural habitat, we produced microfluidic channels that contained sediment-mimicking obstacles. These obstacle channels were produced based on microCT reconstructions of sediment samples. We characterized the swimming of magnetotactic bacteria through these channels and found that swimming throughput was highest for intermediate magnetic fields. This observation was confirmed by extensive computer simulations using an active Brownian particle model, parameterized based on experimental trajectories. The simulations indicate that swimming at strong field is impeded by the trapping of bacteria in corners that require transient swimming against the magnetic field for escape. At weak fields, the direction of swimming is almost random, making the process inefficient as well. We confirmed the trapping effect in our experiments and showed that lowering the field strength allows the bacteria to escape.

BP 6.4 Mon 15:45 BAR 0106

Mechanical strain sensing and growth of rod-shaped *Escherichia coli* independent of cell wall synthesis — LARS RENNER¹, FELIX WONG², ARIEL AMIR², YUKI KITAHARA³, and SVEN VAN TEEFFELN³ — ¹Leibniz Institute of Polymer Research, Dresden — ²Harvard University, Cambridge, USA — ³Université de Montréal, Canada

One of the central questions in bacterial cell biology is how specific shapes evolved and are maintained. It is remarkable how bacteria can precisely control the cellular processes regulating cell shape. However, many of the underlying biophysical cues are largely unknown. We set out to understand how mechanical stress affects rod-shape maintenance. Specifically, we combine microfabrication tools and mathematical modelling to identify a stress-based mechanism that regulates shape in rods. We then examined the influence of the biomolec-

ular machinery that builds the cell wall and found that rod-shaped cells retain the ability to expand their envelopes differentially in response to locally varying mechanical forces. Thus, cell-wall cleaving enzymes appear to represent an alternative pathway for coupling cell envelope growth to mechanical forces that is distinct from cell wall insertion.

15 min. break

Invited Talk

BP 6.5 Mon 16:15 BAR 0106

Mechanical and electrical properties of bacterial biofilms modulate antibiotic tolerance — BERENIKE MAIER — Institute for Biological Physics and Center for Molecular Medicine Cologne, University of Cologne

Aggregation into colonies and biofilms can enhance bacterial survivability under antibiotic treatment. Yet, the transition between the life as an individual cell and life within a biofilm is poorly understood. We investigate this transition using the human pathogen *Neisseria gonorrhoeae* (gonococcus). Within minutes, these bacteria self-assemble into spherical colonies comprising thousands of cells. We show that freshly assembled colonies are reminiscent of liquid droplets whose viscosity can be tuned by the pilus-mediated attractive force between bacterial cells. The viscosity correlates with antibiotic tolerance. Next to mechanical properties, we investigate the electrical properties of gonococcal colonies. We show that once the colonies have reached a critical size, the membrane polarization transitions from uncorrelated to collective dynamics. The spatial polarization pattern correlates with patterns of distinct growth rates and antibiotic tolerance. In summary, both mechanical and electrical properties of bacterial colonies affect survivability under external stresses.

BP 6.6 Mon 16:45 BAR 0106

Acclimatization of filamentous cyanobacteria to light and pH - from individual to colony-scale — FRANZISKA PAPPENFUSS, SARAH HAEGER, MAXIMILIAN KURJAHN, ANTARAN DEKA, and STEFAN KARPITSCHKA — MPI for Dynamics and Self-Organization, Göttingen, Germany

Photoautotrophic cyanobacteria contribute about 10 % to the net primary production of earth's biosphere. Acclimatization to fluctuating environmental conditions supported their sustained existence over a few billion years, but the underlying mechanisms remain elusive. Here, we investigate three species of filamentous cyanobacteria, cultivated for three weeks at different light-intensities (0.25-8 μ E) and pH buffered to specific values between 6.8-8.4 or unbuffered. During cultivation, micro-scale parameters like the abundance of photopigments and the velocity of single filaments as well as macro-scale parameters like growth rate, pH and colony morphology were tracked. In unbuffered cultures, pH varies between 6.5-10, depending on light driven photosynthesis. Filaments start to aggregate at high densities but mainly independent of illumination and pH. Neither is the growth rate influenced by pH, however it is positively correlated to illumination. Nevertheless, in some species, pH seems to influence the filament gliding velocity and photopigmentation. Thus, our investigations show that pH is not only a consequence of the photosynthetic activity, but also influences the acclimatization of the cyanobacteria in a regulating feedback mechanism.

BP 6.7 Mon 17:00 BAR 0106

Molecular Dynamics Simulation of the Polymer Layering on the Surface Layer Proteins of *Methanosarcina acetivorans* — JONATHAN HUNGERLAND¹, AITOLKYN S. UAL², PO-HENG LEE³, and ILIA A. SOLOV'YOV¹ — ¹Dept of Physics, University of Oldenburg — ²Dept of Chemistry, Gumilyov Eurasian National University — ³Dept of Civil and Environmental Engineering, Imperial College London

The archaea of the type *Methanosarcina* can produce Methane in an efficient, anaerobic, symbiotic process with *Geobacter metallireducens*. Their symbiosis is a so-called direct interspecies electron transfer (DIET), which is not limited by diffusion and has potential application in prospective energetically net-positive, anaerobic waste-water treatment. However, the mechanisms underlying DIET are yet unclear. The *Methanosarcina* species that coat themselves in layers of Methanochondroitin polymers were found to be capable of DIET. Therefore, the polymers might be crucial for the DIET of *Methanosarcina* species. The performed molecular dynamics simulations generate an atomistic picture of the Methanochondroitin layers accounting for the porous surface layer proteins aiming to suggest potential charge-transfer mechanisms into the cell and might reveal the role of the surface layer pores.

BP 7: Active Matter II (joint session DY/BP/ CPP)

Time: Monday 15:00–18:15

Location: ZEU 160

BP 7.1 Mon 15:00 ZEU 160

Chiral motion of actively driven objects in discrete steps towards a remote target — •ANDREAS M. MENZEL — Otto-von-Guericke-Universität Magdeburg, Magdeburg, Germany

We address the motion of chiral actively driven objects that move in discrete steps on a flat substrate [1]. While closed polygon-shaped trajectories are found in the case of unperturbed motion, the dynamics becomes surprisingly rich and nonlinear, if the objects additionally head for a fixed remote target. In that situation, cycloidal-like, straight, zigzag-type, doubled zigzag, quadrupled zigzag, and further period-doubled types of trajectory emerge, besides chaotic behavior. Additionally, we investigate the motion of crowds of such objects under explicit mutual alignment interaction. In the absence of fluctuations, collective orientational ordering occurs also in the chaotic regime, in combination with spatial gathering of the particles. Conversely, fluctuations and polydispersity in target alignment counteract orientational ordering. Our results may apply to various types of actively driven objects, for instance, light-responsive bacteria, laser-controlled colloidal particles, or hoppers on vibrated substrates.

[1] A. M. Menzel, resubmitted.

BP 7.2 Mon 15:15 ZEU 160

Polar flocks with discretized directions: the active clock model approaching the Vicsek model — •MATTHIEU MANGEAT, SWARNAJIT CHATTERJEE, and HEIKO RIEGER — Universität des Saarlandes, Saarbrücken, Germany

We study the off-lattice two-dimensional q -state active clock model (ACM) [EPL **138**, 41001 (2022)] as a natural discretization of the Vicsek model (VM) [PRL **75**, 1226 (1995)] describing flocking. The ACM consists of particles able to move in the plane in a discrete set of q equidistant angular directions, as in the active Potts model (APM) [EPL **130**, 66001 (2020); PRE **102**, 042601 (2020)], with a local alignment interaction inspired by the ferromagnetic equilibrium clock model. A collective motion emerges at high densities and low noise. We compute phase diagrams of the ACM and explore the flocking dynamics in the region, in which the high-density (polar liquid) phase coexists with the low-density (gas) phase. We find that for a small number of directions, the flocking transition of the ACM has the same phenomenology as the APM, including macrophase separation and reorientation transition from transversal to longitudinal band motion as a function of the particle self-propulsion velocity. For a larger number of directions, the flocking transition in the ACM becomes equivalent to the one of the VM and displays microphase separation and only transverse bands, i.e. no reorientation transition. Concomitantly also the transition of the $q \rightarrow \infty$ limit of the ACM, the active XY model, is in the same universality class as the VM. We also construct a coarse-grained hydrodynamic description akin to the VM.

BP 7.3 Mon 15:30 ZEU 160

Tracer-induced temperature difference in motility-induced phase separation — •LUKAS HECHT, IRIS DONG, and BENNO LIEBCHEN — Institut für Physik kondensierter Materie, Technische Universität Darmstadt, Hochschulstr. 8, D-64289 Darmstadt, Germany

Previous studies of overdamped active Brownian particles (ABPs) mixed with passive tracers have shown that self-propulsion can induce motility-induced phase separation (MIPS) for large enough particle density and self-propulsion speed [1]. Here, we present our study on overdamped ABPs mixed with inertial passive tracers. We show that MIPS features different kinetic temperatures in the dense and the dilute phase if the passive tracers are sufficiently heavy (inertial). Remarkably, unlike for underdamped ABPs [2,3], neither the overdamped ABPs nor the passive tracers alone would feature such a temperature difference in coexisting phases. The observed temperature difference is accompanied by a violation of the equipartition theorem and strongly depends on the self-propulsion speed and the particle density. This allows us to tune the temperature difference from a cold dense and hot dilute phase to the counterintuitive opposite case in which the dense phase is hotter than the dilute phase. These findings open a route to create active materials with a persistent temperature profile by inserting active particles and tuning their self-propulsion speed accordingly.

[1] J. Stenhammar et al., Phys. Rev. Lett. **114**, 018301 (2015).

[2] S. Mandal et al., Phys. Rev. Lett. **123**, 228001 (2019).

[3] L. Hecht et al., Phys. Rev. Lett. **129**, 178001 (2022).

BP 7.4 Mon 15:45 ZEU 160

Collective motion in two-dimensional colloidal systems with effective (active) self-propulsion due to time-delayed feedback — •ROBIN A. KOPP and SABINE H. L. KLAPP — ITP, TU Berlin, Berlin, Germany

In recent years, delayed feedback in colloidal systems has become an active and promising field of study [1,2], key topics being history dependence and the manipulation of transport properties. Here we study the dynamics of a two-dimensional colloidal suspension, subject to time-delayed feedback, where time-

delayed feedback can be interpreted as a mechanism of effective self-propulsion, i.e., activity [3]. To this end we perform overdamped Brownian dynamics simulations, where the particles interact through a Weeks-Chandler-Andersen potential. Furthermore, each particle is subject to a Gaussian, repulsive feedback potential, that depends on the difference of the particle position at the current time, and at an earlier time. We observe and quantitatively study the emergence of dynamical clustering and collective motion characterized by a nonzero mean velocity and provide a possible explanation for the underlying mechanism combining single-particle and mean-field-like effects.

[1] S. A. M. Loos, and S. H. L. Klapp, Scientific Reports **9**, 2491 (2019)

[2] M. A. Fernandez-Rodriguez et al., Nature Communications **11**, 4223 (2020)

[3] R. A. Kopp and S. H. L. Klapp, arXiv:2210.03182 (2022)

BP 7.5 Mon 16:00 ZEU 160

Inverted Sedimentation of Active Particles in Unbiased ac Fields — •JOSÉ CARLOS UREÑA MARCOS and BENNO LIEBCHEN — Institut für Physik Kondensierter Materie, TU Darmstadt, Darmstadt, Germany

Biological microswimmers can steer autonomously and use this ability to perform sophisticated tasks. Synthetic microswimmers do not yet reach the same degree of autonomy, and need to be controlled externally if they are to carry out tasks such as targeted cargo delivery or microsurgery. While much progress has been made recently to control their motion based on external forces or gradients, e.g. in light intensity, which have a well-defined direction or bias, little is known about how to steer APs in situations where no permanent bias can be realized.

Here, we show that ac fields with a vanishing time average provide an alternative route to steering APs. We exemplify this route for inertial APs in a gravitational field, observing that a substantial fraction of them persistently travels in the upward direction upon switching on the ac field, resulting in an inverted sedimentation profile at the top wall of a confining container. Our results offer a generic control principle which could be used in the future to steer active motion, to direct collective behaviors and to purify mixtures.

15 min. break

Invited Talk

BP 7.6 Mon 16:30 ZEU 160

Long-range communications enable the hierarchical self-organization of active matter — •IGOR ARONSON¹, ALEXANDER ZIEPKE², IVAN MARYSHEV², and ERWIN FREY² — ¹Pennsylvania State University, USA — ²Ludwig-Maximilians-University, Munich, Germany

The most distinct markers of life are the ability to move (locomotion), consume energy (metabolism), process information, and form multi-cellular aggregates. Many biological systems exhibit long-range signaling strategies for evolutionary advantage. We explore the multi-scale self-organization of interacting self-propelled agents that locally process information transmitted by chemical signals. The communication capacity dramatically expands their ability to form complex structures, allowing them to self-organize through a series of collective dynamical states at multiple hierarchical levels.

The consequent study shows that information exchange by acoustic waves between the self-propelled units creates a slew of multifunctional structures. Each unit is equipped with an acoustic emitter and a detector in this realization. The swimmers respond to the resulting acoustic field by adjusting their emission frequency and migrating toward the strongest signal. We find self-organized structures with different morphology, including snake-like self-propelled entities, localized aggregates, and spinning vortices. Our results provide insights into the design principles of communicating active particles capable of performing complex tasks.

BP 7.7 Mon 17:00 ZEU 160

Arrested by heating — •CORINNA C. MAASS^{1,2}, PRASHANTH RAMESH^{2,1}, and MAZIYAR JALAAL³ — ¹University of Twente, Enschede, Netherlands — ²MPI for Dynamics and Self-organization, Göttingen, Germany — ³Universiteit van Amsterdam, Amsterdam, Netherlands

Active droplets are a class of microswimmers driven by chemical reactions at the droplet interface. Typically, the activity is powered by an advection-diffusion instability in the chemohydrodynamic fields around the droplet that is characterized by the Péclet number Pe of chemical transport. With increasing Pe , higher hydrodynamic modes at the interface cause the droplet to transition from inactivity, to steady, to reorienting, to fully unsteady motion. Here, we demonstrate that it is possible to change Pe reversibly and in situ by thermally activated changes in the chemical environment, and thereby to control the motility of the droplet.

BP 7.8 Mon 17:15 ZEU 160

Chiral active particles with non-reciprocal couplings: results from particle-based simulations — •KIM L. KREIENKAMP and SABINE H. L. KLAPP — Technische Universität Berlin, Germany

Non-reciprocal interactions manifest their drastic impact on the collective dynamics of active matter systems by changing, for example, the general type of observed instabilities [1] and leading to time-dependent states [2,3]. In particular, the combination of non-reciprocity and chirality in terms of intrinsically rotating chiral active particles (“circle swimmers”) reveals intriguing non-trivial time-dependent collective dynamics [1].

After having developed an understanding of the collective dynamics on the continuum level in previous work [1], we here present first results of particle-based simulations of chiral active particle systems with non-reciprocal alignment couplings. Indeed, quantitative predictions from continuum approaches are somewhat limited by the approximations made during the coarse-graining process. Thus, the first goal of our particle-based simulations is to explore the validity of the previously obtained continuum results regarding the overall state diagram. Second, we aim at investigating microscopic aspects of the various time-dependent states. Finally, we discuss possibilities to characterize the thermodynamic behavior of the non-reciprocal chiral system based on the stochastic trajectories obtained in particle-resolved simulations.

[1] K. L. Kreienkamp and S. H. L. Klapp, *New J. Phys.* (2022).

[2] M. Fruchart et al., *Nature* 592, 363 (2021).

[3] Z. You et al., *PNAS* 117, 19767 (2020).

BP 7.9 Mon 17:30 ZEU 160

Lattice-induced freezing in active systems unveils dynamic crystallites with square ordering — •ARITRA K. MUKHOPADHYAY¹, PETER SCHMELCHER^{2,3}, and BENNO LIEBCHEN¹ — ¹Technische Universität Darmstadt, 64289 Darmstadt, Germany. — ²Zentrum für Optische Quantentechnologien, Universität Hamburg, Luruper Chaussee 149, 22761 Hamburg, Germany. — ³The Hamburg Centre for Ultrafast Imaging, Universität Hamburg, Luruper Chaussee 149, 22761 Hamburg, Germany.

Active matter, comprising self-propelled particles like bacteria, colloidal microswimmers, or granular microflyers is currently attracting enormous attention for its ability to self-organize into complex nonequilibrium structures. In this work, we report on a new state of dynamic active crystallites, which occurs when exposing active particles to a spatially periodic potential. These crystallites require activity to emerge, adopt the structure of the underlying lattice (e.g.

square rather than hexagonal close packing), and are continuously in motion. This new phase unifies the structural properties of crystals with the dynamical properties of disordered fluids. Our work thus unveils a route to creating a new state of active materials with an intrinsic structure that can be externally controlled.

BP 7.10 Mon 17:45 ZEU 160

Shape-dependent collective motion: cohesive groups and cargo transport of colloidal rods — PHILIPP STENGELE, •ANTON LÜDERS, and PETER NIELABA — Universität Konstanz, Konstanz, Deutschland

In active toy model systems where colloids interact via predefined social interaction rules as well as steric collisions, the shape of the individual particles strongly influences emerging collective behavior. We study this based on two example systems using Brownian dynamics simulations (without hydrodynamic interactions). Firstly, we investigate a simple perception model in which colloidal rods move actively if predefined visual stimuli exceed a certain threshold. Here, we find an aspect ratio range where the rods form a dilute cohesive group with a time-independent particle distribution. If the aspect ratio surpasses this range, the rods slowly drift apart. Secondly, we look into the cargo capture and transport of a passive rod using a dense swarm of active spheres which form a hexagonal cage with a cavity for the cargo. Again, the aspect ratio of the rod proves to be crucial, as we find geometric restrictions that must be met to stabilize the cavity. Our work underlines that the shape (here, the aspect ratio) of the particles in active matter systems must be carefully considered while defining interaction rules to perform specific tasks.

BP 7.11 Mon 18:00 ZEU 160

Active Chiral Nematics — •RÜDIGER KÜRSTEN^{1,2,3} and DEMIAN LEVIS^{1,2} — ¹Departament de Física de la Matèria Condensada, Universitat de Barcelona, Barcelona, Spain — ²Universitat de Barcelona Institute of Complex Systems (UBICS), Barcelona, Spain — ³Institut für Physik, Universität Greifswald, Greifswald, Germany

We study inherently chiral self-propelled particles in two dimensions that are subjected to nematic alignment interactions and rotational noise. By means of both, homogeneous and spatially resolved mean field theory we identify various different flocking states. We confirm the presence of the predicted phases using agent-based simulations. We emphasize that special care has to be taken within the simulations in order to avoid artifacts. We present a non-standard simulation technique in order to avoid those artifacts.

BP 8: Cell Mechanics I

Time: Tuesday 9:30–13:00

Location: BAR Schö

BP 8.1 Tue 9:30 BAR Schö

Chiral flows can drive pattern formation in viscoelastic surfaces — •ELOY DE KINKELDER^{1,2}, ELISABETH FISCHER-FRIEDRICH^{3,4}, and SEBASTIAN ALAND^{1,2} — ¹TU Bergakademie Freiberg, Freiberg, Germany — ²HTW Dresden, Dresden, Germany — ³TU Dresden, Dresden, Germany — ⁴BIOTEC, Dresden, Germany

During division in animal cells, the actomyosin cortex has been found to exhibit counter-rotating cortical flows along the axis of division. These are also known as chiral flows. Notably, the chiral flows were shown to influence cellular rearrangements and drive the left-right symmetry breaking in developing organisms. At the current state, no numerical simulations have been done to study the influence of chiral flows on the cell cortex shape. To deepen the insight on that matter, we present here a numerical study of an axi-symmetric viscoelastic surface embedded in a viscous fluid. On this surface we impose a generic counter rotating force field to investigate its influence on the surface shape and material transport. Notably, we find that a large areal relaxation time results in flows towards the equator of the surface. These flows assist the transport of a surface concentration during the forming of a contractile ring. Accordingly, we show that chiral forces by themselves can drive pattern formation and stabilise contractile rings at the equator.

BP 8.2 Tue 9:45 BAR Schö

Neutrophil mechanotransduction during durotaxis — •FATEMEH ABBASI¹, MATTHIAS BRANDT², and TIMO BETZ¹ — ¹Third Institute of Physics, Biophysics, Georg August University Göttingen — ²Institute of Cell Biology, ZMBE, University of Münster

In Vivo, cells experience complex tissue environments with various chemical and physical features. 3D confinement is one of the major physical obstacles for cells in their natural environment. Neutrophils are among the most abundant immune cells in our body, which have to cope with various physical constrictions on their way from production to the infection site. In addition to confinement, the stiffness of the microenvironment is another mechanical feature these rapidly moving cells are exposed to. Neutrophils experience various tissue stiffness, from 1 kPa (bone marrow) to 20 MPa (bone). Previous studies have demonstrated that

these cells are responsive to their microenvironment stiffness by adjusting their adhesion and spreading. Based on this knowledge we decided to combine confinement and stiffness change and investigate the impact of 3D stiffness gradient on cell behaviour and migration, a fact called durotaxis. We hypothesized that stiffness gradient might be a triggering factor of neutrophil migration toward the infection site. We confine neutrophils in between 2 layers of polyacrylamide hydrogels with 2 different stiffness and keep this distance stable for the desired period of time to investigate cell mechanotransduction during durotaxis from different points of view. Our preliminary results regarding the neutrophil durotaxis show a surprising and transient force peak on the soft substrate during cell shifting.

BP 8.3 Tue 10:00 BAR Schö

Red blood cell lingering modulates hematocrit distribution in the microcirculation — •YAZDAN RASHIDI¹, GRETA SIMONATO², QI ZHOU³, THOMAS JOHN¹, ALEXANDER KIHM¹, MOHAMMED BENDAOU¹, TIMM KRUEGER³, MIGUEL O. BERNABEU³, LARS KAESTNER¹, MATTIAS W. LASCHKE², MICHAEL D. MENDER², CHRISTIAN WAGNER¹, and ALEXIS DARRAS¹ — ¹Experimental Physics, Saarland University, 66123 Saarbruecken, Germany — ²Institute for Clinical and Experimental Surgery, Saarland University, 66421 Homburg, Germany — ³School of Engineering, University of Edinburgh, Edinburgh EH9 3FD, United Kingdom

The distribution of red blood cells (RBCs) in the microcirculation determines how oxygen is delivered to tissues and organs. This process relies on the partitioning of RBCs at successive microvascular bifurcations. It is known that RBCs partition disproportionately to the blood flow rate, therefore leading to heterogeneity of the hematocrit in microvessels. Usually, downstream of a bifurcation, the vessel branch with a higher fraction of blood flow receives a higher fraction of RBC flux.

However, deviations from this phase-separation law have been observed in recent works. Here, we quantify how the microscopic behavior of RBCs lingering influences their partitioning, through combined in vivo experiments and in silico simulations. We quantify the cell lingering at capillary-level bifurcations and

demonstrate that it correlates with deviations from the phase-separation process from established empirical predictions by Pries et al.

BP 8.4 Tue 10:15 BAR Schö

Mechanical fingerprint of the intra-cellular space — •TILL M. MUENKER, BART E. VOS, and TIMO BETZ — University of Göttingen, Göttingen, Germany

Many important cellular functions such as organelle positioning and internal cargo transport are dependent on the viscoelastic intracellular mechanical properties of cells. A range of different mechanical models has been proposed to describe these properties. Whilst simple models such as Maxwell or Kelvin-Voigt models don't seem sufficient to capture the full complexity of cells, more elaborate models like generalized Kelvin-Voigt models require a huge number of parameters. This hinders the comparison and interpretation of experimental findings. Further, from a physics perspective, cells are systems out of thermodynamic equilibrium, permanently consuming metabolic energy to carry out mechanical work. The level of "non-equilibrium" can be proposed as an indicator for cell type, cell state or even diseases. To determine both, the viscoelastic properties and the cellular activity, we use optical tweezers based active and passive microrheology in a diverse group of 9 different cell-types. Surprisingly, despite differences in origin and function, the complex moduli of all cell types can be described using a 4 parameter based fractional Kelvin-Voigt model. Additionally, the frequency dependent activity can be described with a simple power law. This approach allows to reduce those complex and frequency dependent properties down to a fingerprint of 6 parameter. Further principal component analysis shows that only 2 of them may be sufficient to characterize the mechanical intracellular state.

15 min. break

Invited Talk

BP 8.5 Tue 10:45 BAR Schö

Microtubule Lattice Dynamics — SUBHAM BISWAS¹, RAHUL GROVER², COR-DULA REUTHER², MONA GRÜNEWALD¹, STEFAN DIEZ², and •LAURA SCHAEDEL¹ — ¹Saarland University, Saarbrücken, Germany — ²TU Dresden, Germany

Microtubules are dynamic cytoskeletal filaments that grow and shrink by subunit addition or removal at their tips. In contrast, the microtubule lattice far from the tips was long considered to be static. The discovery of subunit loss and incorporation along the lattice far from the tips - termed lattice dynamics - led to a paradigm shift and revealed a new dimension of microtubule dynamics.

Microtubule lattice dynamics occur in vitro as well as in living cells and contribute to microtubule organization and resilience to mechanical stress. Yet, it is largely unknown which cellular mechanisms are involved in their regulation. Recent discoveries suggest that microtubule-associated proteins (MAPs), which control a variety of properties of intracellular microtubules, are a key factor in the regulation of lattice dynamics. Here, we take a closer look at MAP-regulated microtubule lattice dynamics.

BP 8.6 Tue 11:15 BAR Schö

Force generation in human blood platelets by filamentous actomyosin structures — •ANNA ZELENA¹, JOHANNES BLUMBERG², ULRICH S. SCHWARZ², and SARAH KÖSTER¹ — ¹Institute for X-Ray Physics, Georg-August-University of Göttingen, Germany — ²Institute for Theoretical Physics, University of Heidelberg, Germany

Blood platelets are central elements of the blood clotting response after wounding. Upon vessel damage, they adhere to the surrounding matrix of the vessel and contract the emerging blood clot, thus helping to restore normal blood flow. The blood clotting function of platelets has been shown to be directly connected to their mechanics and cytoskeletal organization. The reorganization of the platelet cytoskeleton during spreading occurs within minutes and leads to the formation of contractile actomyosin bundles, but it is not known how this structure formation corresponds to force generation. In this study, we combine fluorescence imaging of the actin structures with traction force measurements in a time-resolved manner. We find that force generation is localized in few hotspots, which spatially align very closely with the visualized end points of the fibrous actin structures and do not change much with time. Moreover we show that force generation is a very robust mechanism independent of changes in the amount of added thrombin in solution or fibrinogen coverage on the substrate, suggesting that force generation after platelet activation is a threshold phenomenon that ensures reliable blood clot contraction in diverse environments.

BP 8.7 Tue 11:30 BAR Schö

How to build muscle? Sarcomeric pattern formation by non-local interactions — •FRANCINE KOLLEY^{1,2}, CLARA SIDOR³, FRANK SCHNORRER³, and BENJAMIN M. FRIEDRICH^{1,2} — ¹Physics of Life, TU Dresden — ²cfaed, TU Dresden — ³IBDM, Aix Marseille University

Striated muscles drive all voluntary movements and are highly organized in crystal-like structures, comprising different filament types on a micrometer scale. The specific size of a sarcomere is set by the giant protein titin. Titin links the molecular motor myosin in the middle of a sarcomere to the so-called Z-disc, which is rich in actin crosslinkers at the sarcomere boundary. Despite the impor-

tance of the repeated structures of these sarcomeres for muscle functionality, it is poorly understood how they self-assemble during muscles development. To investigate this question, we introduce theoretical models based on putative mechanism. We can show with a minimal Mean-field model that a non-local interaction between the key proteins is sufficient for the emergence of periodic patterns. Agent-based simulations of this model reveal the influence of small-number fluctuations. We can expand this model to include additional properties, such as different myosin bindings or the catch-bond behavior of the Z-disc crosslinker α -actinin. In addition, from analyzing images of the *Drosophila* flight muscles during early developmental stages, provided by Schnorrer Lab, we are able to identify α -actinin and titin as the first proteins forming periodic patterns with myosin, while actin follows later, constraining possible models.

15 min. break

BP 8.8 Tue 12:00 BAR Schö

Impact of oxidative stress on the mechanical properties of isolated mitochondria — •YESASWINI KOMARAGIRI^{1,2}, MUZAFFAR H PANHWAR^{1,2}, BOB FREGIN^{1,2}, GAYATRI JAGIRDAR³, CARMEN WOLKE³, STEFANIE SPIEGLER^{1,2}, and OLIVER OTTO^{1,2} — ¹Institut für Physik, Universität Greifswald, Friedrich-Ludwig-Jahn-Str. 15a, 17489 Greifswald, Germany — ²DZHK, Greifswald, Universitätsmedizin Greifswald, Fleischmannstr. 42, 17489 Greifswald, Germany — ³Universitätsmedizin Greifswald, Ferdinand-Sauerbruch-Strasse, 17475 Greifswald, Germany

Mitochondria are essential in various physiological processes, including the homeostasis of reactive oxygen species (ROS) as key intracellular signaling molecules. While it is already established that mechanical properties are a crucial parameter in characterizing and comprehending biological systems such as cells and tissues, little is known about the significance of organelle mechanics for cell function. Here, we demonstrate the application of real-time fluorescence and deformability cytometry for the label-free and high-throughput analysis of mitochondria isolated from C6 glial cells. Our data on several thousands of viable mitochondria indicate that their deformation is shear stress dependent. We studied the effect of exogenously and endogenously generated ROS on mitochondria mechanics in two proof-of-concept studies. Under both conditions, we observed a decrease in size while the deformation increased relative to a control condition. The results suggest a general biophysical mechanism of how mitochondria respond to oxidative stress.

BP 8.9 Tue 12:15 BAR Schö

New applications for the direct method in 3D traction force microscopy — •JOHANNES BLUMBERG^{1,2}, SIMON BRAUBURGER^{1,2}, and ULRICH SCHWARZ^{1,2} — ¹Institute for Theoretical Physics, Heidelberg University — ²Bioquant, Heidelberg University

Traction force microscopy (TFM) estimates the mechanical forces of cells adhering to an elastic substrate by measuring by the movement of embedded marker beads. It has become a standard tool to study the mechanobiology of single cells or cell monolayers on flat two-dimensional (2D) substrates, but three-dimensional (3D) setups provide new challenges. Although the inverse method of force inference by minimization of a loss function has become the standard method for 2D TFM, for 3D TFM the direct method of directly calculating stress and surface traction from strain becomes an attractive alternative, for example when performing 3D TFM with elastic beads in organisms, tumor spheroids or organoids. We explain how this method works in practice and how it compares to the inverse method.

BP 8.10 Tue 12:30 BAR Schö

Profilin Regulating the Polymerisation Velocity of Actin — •LINA HEYDENREICH and JAN KIERFELD — TU Dortmund University, 44227 Dortmund, Germany F-Actin, as a part of the cytoskeleton, drives crucial biological processes like cell motility, where the control of the polymerisation speed is essential. Experiments in [1] show a maximal polymerisation speed of F-actin at high concentrations of profilin and actin.

We present a kinetic model of F-actin growth in the presence of profilin and obtain an exact result for the mean growth velocity which is in agreement with stochastic simulations, and explains the experimental data. The maximal growth speed is limited by the release rate of profilin from filamentous actin. In the limit where nearly all actin monomers are bound to profilin, the polymerisation speed follows the Michaelis-Menten kinetics.

By analysing the presented model, we can examine the influence of an external force and the influence of profilin on the fluctuations and precision of the polymerisation. Additionally we can give constraints on the concentrations to obtain a saturation of the growth velocity.

[1] Johanna Funk et al. "Profilin and formin constitute a pacemaker system for robust actin filament growth". eLife 8 (2019), e50963

BP 8.11 Tue 12:45 BAR Schö

Development of a platform for accessing the membrane tension of cells in microchannels — •ERIC SÜNDERMANN, BOB FREGIN, DOREEN BIEDENWEG, STEFANIE SPIEGLER, and OLIVER OTTO — ZIK HIKE, University of Greifswald, Greifswald, Germany

The development of high-throughput methods for cell mechanical research is becoming increasingly important in biology, medicine and physics as the analysis of large samples opens up possibilities for basic science and clinical use. Currently, various techniques are available, but hardly any can discriminate between membrane and bulk contributions to the mechanical properties of a cell.

Here, we combined deformability cytometry with fluorescence lifetime imag-

ing microscopy (FLIM) to study the response of membrane tension to hydrodynamic stress. Myeloid precursor cells were first stained with Flipper-TR[®], a fluorescent dye with a lifetime proportional to the membrane tension, and then flushed through the constriction of a microfluidic chip, where they deform under a shear stress. Under steady-state conditions, our data shows that the membrane tension of cells increases with increasing hydrodynamic stress, as expected. Exposing cells to methyl- β -cyclodextrin to reduce the amount of cholesterol in the cell membrane leads to a reduction in membrane tension while the bulk Young's modulus is not affected.

These results highlight the potential of microfluidic technologies to quantify the contribution of different cell components to its overall mechanical phenotype.

BP 9: Active Matter III (joint session BP/ CPP/DY)

Time: Tuesday 9:30–12:30

Location: TOE 317

BP 9.1 Tue 9:30 TOE 317

Gliding motility and reorientation of flagellated microbes on curved surfaces — •ALEXANDROS FRAGKOPOULOS¹, NICOLAS FARES^{1,2}, and OLIVER BÄUMCHEN¹ — ¹University of Bayreuth, Experimental Physics V, 95447 Bayreuth, Germany — ²University of Bordeaux, CNRS, LOMA, UMR 5798, 33400 Talence, France

The model organism *Chlamydomonas reinhardtii*, a unicellular biflagellated microalga, can adhere and colonize almost any surface under particular light conditions. Once the cells attach to a surface, an intraflagellar transport machinery translocates the cell body along the flagella, which are oriented in a 180° configuration. This motion is known as gliding motility. Even though the cells firmly adhere to surfaces, they are able to reorient through different physical mechanisms [1]. With the use of the orientation autocorrelation function, we find that cells exhibit large reorientation events shortly after their initial attachment to a surface, while at longer time scales they are primarily constrained to 1D motion. On cylindrical surfaces, the large reorientations cause the cells to predominantly align in the direction of the minimum principle curvature. We quantify the curvature-induced alignment using the nematic order parameter and reveal that the minimum surface curvature required for cell alignment is comparable to the static flagella curvature.

[1] S. Till, et al., *Phys. Rev. Res.*, (Accepted)

BP 9.2 Tue 9:45 TOE 317

Efficiency of navigation strategies for active particles — •LORENZO PIRO¹, RAMIN GOLESTANIAN^{1,2}, and BENOIT MAHAULT¹ — ¹Max Planck Institute for Dynamics and Self-Organization, Göttingen, Germany — ²Rudolf Peierls Centre for Theoretical Physics, University of Oxford, Oxford, United Kingdom

Optimal navigation in complex environments is a problem with multiple applications ranging from designing efficient search strategies to engineering microscopic cargo delivery. When motion happens in presence of strong external forces, route optimization is particularly important as active particles may encounter trapping regions that would substantially slow down their progress.

Here, considering a self-propelled agent moving at a constant speed, we study the efficiency of Zermelo's classical solution. Investigating both cases of motion on the plane and on curved surfaces, we focus on the regime where the external force exceeds self-propulsion in finite regions. There, we show that, despite the fact that most trajectories following the trivial policy of going straight get arrested, the Zermelo policy allows for a comprehensive exploration of the environment.

However, our results also indicate an increased sensitivity of the Zermelo strategy to initial conditions, which limits its robustness and long-time efficiency, particularly in presence of fluctuations. These results suggest an interesting trade-off between exploration efficiency and stability for the design of control strategies to be implemented in real systems.

BP 9.3 Tue 10:00 TOE 317

Run with the Brownian Hare, Hunt with the Deterministic Hounds — •DAVIDE BERNARDI¹ and BENJAMIN LINDNER^{2,3} — ¹Italian Institute of Technology, Ferrara, Italy — ²Bernstein Center for Computational Neuroscience, Berlin, Germany — ³Institut für Physik, Humboldt-Universität zu Berlin

Pursuit and evasion are vital to most animal species and play an important role in many human activities. Traditionally, chase-and-escape models have been studied in the framework of game theory, or in detailed models that can be studied only through numerical simulations and that lack generalization power.

Here, we present analytic results for the mean time and energy used by a pack of deterministic hounds to capture a prey that undergoes Brownian diffusion. Depending on the number of chasers, we find that the mean capture time as a function of the prey's diffusion coefficient can be monotonically increasing, decreasing, or attain a minimum at a finite value. Furthermore, an optimal speed and number of chasing hounds exist, that depend on the baseline power consumption and drag coefficient of each chaser.

The present model can be seen as an analytically tractable basis for the theoretician's perspective on the growing field of smart microswimmers and autonomous robots.

BP 9.4 Tue 10:15 TOE 317

Function of Morphodynamics in Foraging *Physarum polycephalum* — •LISA SCHICK¹, MIRNA KRAMAR², and KAREN ALIM¹ — ¹School of Natural Sciences, Technical University of Munich, Germany — ²Institute Curie, Paris, France

How network-forming fungi structure and reorganize their network morphology and thereby the carbon flows in the soil is key to understanding climate - yet hidden from us due to the long time scales of network dynamics and the soil itself. Here, the network-forming slime mold *Physarum polycephalum* serves as a model of network dynamics of a foraging network-forming life. We follow and quantify the network migration velocity and morphology of foraging *P. polycephalum*. We identify three distinct morphological states characterized by network compactness and density of moving fronts. Estimating the energetic cost of distinct states, we find that morphological variability allows the organism to balance the energetic costs of foraging and search strategy. Our observations allow us to project how resource availability might shift the balance and thereby affect network extension in foraging network-forming organisms.

BP 9.5 Tue 10:30 TOE 317

Unraveling the migratory behavior of a large single-celled organism — •LUCAS TRÖGER, FLORIAN GOIRAND, and KAREN ALIM — School of Natural Sciences, Technical University of Munich, Germany

Many cells face search problems, such as finding food, conspecifics, or shelter, and different search strategies can provide different chances for success. In contrast to most single-celled organisms the slime mold *Physarum polycephalum* forms a giant network-shaped cell while foraging for food. Which advantage does the giant cell at the verge to multicellularity provide? We experimentally investigate and quantify the long-time migratory behavior of small networks of *P. polycephalum* in the absence and in the presence of food, and develop a simple mechanistic model that successfully describes its migration. We find that *P. polycephalum* performs a run-and-tumble-like motion modified by self-avoidance to achieve superdiffusive migration. Furthermore, it tunes its short-time dynamics in order to adapt to environments with different amounts of available nutrients, while its long-time dynamics remain unchanged. This work shows how *P. polycephalum* controls the inherent stochasticity of its movement by simple rules, which may represent an evolutionary advantage.

15 min. break

BP 9.6 Tue 11:00 TOE 317

Controlling active turbulence by activity patterns — •ARGHAVAN PARTOVIFARD, JOSUA GRAWITTER, and HOLGER STARK — Institute of Theoretical Physics, Technische Universität Berlin, Hardenbergstraße 36, 10623 Berlin, Germany

Active fluids exhibit spontaneous and chaotic flow patterns which are known as active turbulence [1]. One of the current challenges in active matter is controlling and harnessing these flow patterns for powering processes at small scales [2]. As a simple realization of an active fluid, we consider a semi-dilute solution of active rods and study it within a numerical simulation of the governing equations that are formulated in terms of velocity and the orientational order tensor parameter fields.

We find that for a solution of pusher active rods there is a critical magnitude of activity above which the initially isotropic solution develops locally varying nematic order and turbulent-like fluid flow. Aiming to control the turbulent flow state, we pattern the activity with a square lattice of circular inactivity spots. We find that for a specific range of lattice parameters the flow field develops lanes of unidirectional flow with alternating directions while between them a row of corotating vortexes emerges; We call this state the laning state and it is multi-stable since different realizations of the random initial state of rods lead to dif-

ferent configurations of the laning state with various widths of the lanes. In this state, the director field develops nematic domains oriented toward the Leslie angle with respect to the flow.

- [1] Wensink *et al.*, Proc. Natl. Acad. Sci. **109**, 14308-14313 (2012)
 [2] Bowick *et al.*, Phys. Rev. X **12**, 010501 (2022)

BP 9.7 Tue 11:15 TOE 317

Active matter: From spontaneous to controlled phenomena. — •DANIEL PEARCE — University of Geneva

Active matter is the study of materials able to move themselves. During this talk I will discuss how we can take advantage of the interplay between topological defects, geometry and topology to exercise control over active materials. By studying active nematic fluids on a curved surface, we can influence the position and orientation of topological defects according to their charge. This means specific nematic textures can be generated. By studying active contractile actomyosin gels, it is possible to show that only active topological defects with charge +1 can generate curvature, and the sign is related to the phase of the defect. This frees the process from the constraints of the Poincaré-Hopf theorem and allows complex surfaces to be generated. This is demonstrated by recreating the shape of a freshwater hydra from the positions of the topological defects

BP 9.8 Tue 11:30 TOE 317

Nucleation of chemically active droplets — •NOAH ZIETHEN and DAVID ZWICKER — Max Planck Institute for Dynamics and Self-Organization, Göttingen, Germany

Liquid-liquid phase separation emerged as a crucial organizing principle inside biological cells giving rise to a plethora of intracellular compartments. Unique to the cellular context, these condensates can consist of only a few hundred molecules and are affected by non-equilibrium processes. In particular, active chemical conversion between condensate material and proteins in the surrounding cytoplasm can control multiple aspects of the condensates. Yet, it is unclear how these reactions affect the spontaneous nucleation and dissolution associated with low particle numbers. Here, we investigate the influence of chemical reactions on the bistable region of active droplets using a stochastic field theory. We find an effective increase in the energy barrier and thus decelerated transitions between the homogeneous and the droplet state. Using classical nucleation theory, we approximate the full dynamics by diffusion in a free energy potential described by an analytical expression only depending on droplet radius and reaction rate. This analogy also allows us to determine the equivalence of the binodal line, so we can propose an extension of the equilibrium phase diagram to capture driven chemical reactions. Cells might use these effects to control the nucleation of intracellular droplets.

BP 9.9 Tue 11:45 TOE 317

Hydrodynamic description and transport coefficients in a model of active cellular aggregates — •SUBHADIP CHAKRABORTI^{1,2} and VASILY ZABURDAEV^{1,2} — ¹Friedrich-Alexander-Universität Erlangen-Nürnberg, Erlangen, Germany — ²Max-Planck-Zentrum für Physik und Medizin, Erlangen, Germany

Complex multicellular aggregates consisting of a large number of interacting cells are ubiquitous in biology, ranging from bacterial biofilms to organoids, cell spheroids, and tumors. We consider colonies of *N. gonorrhoeae* bacteria as a prototypical example of cells that use retractile cell appendages to actively interact with a substrate and with each other. We construct a microscopic model on a 1D lattice taking into account the non-equilibrium bacterial motility driven by two crucial forces – cell-substrate and cell-cell interactions. We observe a

phase transition from a homogeneous state to a clustered state upon tuning the density and activity parameters. Using macroscopic fluctuation theory (MFT), we analytically derive hydrodynamics for the model system and calculate two density-dependent transport coefficients – the bulk-diffusion coefficient and the conductivity. The behavior of these transport coefficients successfully explains the non-equilibrium phase transition. We support our analytical findings with the results obtained numerically. Our theory provides a general framework for studying the non-equilibrium collective behavior of other dense cellular aggregates also, in the context of dynamics and their transport properties.

BP 9.10 Tue 12:00 TOE 317

Flocking of unfriendly species: The two-species Vicsek model — •SWARNAJIT CHATTERJEE¹, MATTHIEU MANGEAT¹, CHUL-UNG WOO², HEIKO RIEGER¹, and JAE DONG NOH² — ¹Saarland University, Saarbrücken, Germany — ²University of Seoul, Seoul, Korea

We consider the two-species Vicsek model (TSVM) consisting of two kinds of self-propelled particles, A and B, that tend to align with particles from the same species and to anti-align with the other. The model shows a flocking transition that is reminiscent of the original Vicsek model [1]: it has a liquid-gas phase transition and displays micro-phase separation in the coexistence region where multiple dense liquid bands propagate in a gaseous background. The novel feature of the TSVM is the existence of two kinds of bands, one composed of mainly A-particles and one mainly of B-particles and the appearance of two dynamical states in the coexistence region: the PF (parallel flocking) state in which all bands of the two species propagate in the same direction, and the APF (anti-parallel flocking) state in which the bands of species A and species B move in opposite directions. When PF and APF states exist in the low-density part of the coexistence region they perform stochastic transitions from one to the other. The system size dependence of the transition frequency and dwell times shows a pronounced crossover that is determined by the ratio of the band width and the longitudinal system size. Our work paves the way for studying multispecies models with heterogeneous alignment interactions.

[1] T. Vicsek, A. Czirók, E. Ben-Jacob, I. Cohen, and O. Shochet, Phys. Rev. Lett. **75**, 1226 (1995).

BP 9.11 Tue 12:15 TOE 317

Two-potential model for molecular motors — •SOPHIE KLEMPAHN and HELMUT SCHIESEL — Cluster of Excellence Physics of Life, Technical University of Dresden, Germany

Molecular motors are highly efficient biological machines, which drive systems away from equilibrium and realise key biological processes. For the description of the molecular motor action, discrete jump processes as well as energy barriers with height differences can be used. However, these models are based on symmetric conditions or unidirectional motion and therefore do not capture real biological systems with fuel gradients or where the motion is not unidirectional. To predict the effect of molecular motors on the density distribution of cargo particles in one dimension, we introduce a two potential model. This model represents the cargo particles as active particles, in which the binding of molecular motors to the cargo particle causes the active part of motion. Furthermore, we use two different energy landscapes for jumps to the left or right side, to include motors moving back- and forward, asymmetric environment or two different molecular motors acting on the same cargo particle in different directions. The solution of a master equation with different energy landscapes for jumps to the left and right side results in specific extremal points in the probability density of the cargo particles and shows a ratchet effect in case of periodic potentials.

BP 10: Evolution and Origin of Life

Time: Tuesday 9:30–12:15

Location: BAR 0106

Invited Talk

BP 10.1 Tue 9:30 BAR 0106

Protein evolution in sequence landscapes: from data to models and back — •MARTIN WEIGT — Sorbonne University, Paris, France

In the course of evolution, proteins diversify their sequences via mutations, while keeping their 3D structure and biological functions remarkably conserved. Modern sequence databases provide us with increasingly large samples for this sequence diversity. In my talk, I will describe how these samples can be used to infer data-driven protein sequence landscapes, using approaches borrowed from statistical physics or machine learning. In turn, we can model the interplay between mutation and selection in protein evolution as a stochastic process in these landscapes. I will illustrate these ideas in three examples: (i) the prediction of the effect of individual mutations in proteins, (ii) the modeling of experimental protein evolution, and (iii) the statistical design of artificial but functional proteins.

BP 10.2 Tue 10:00 BAR 0106

Non-equilibrium approaches to the origin of life — THOMAS MATREUX¹, PAULA AIKILA¹, CORINNA KUFNER², DOMINIK BUCHER³, ALMUTH SCHMID¹, WOLFGANG ZINTH¹, DIETER BRAUN¹, and •CHRISTOF MAST¹ — ¹LMU, Munich, Germany — ²Harvard, Cambridge, USA — ³TUM, Munich, Germany

Life is an out-of-equilibrium process, so its emergence must also have been decisively shaped and driven by the non-equilibrium systems present 4 billion years ago. We investigated how simple heat fluxes through geological networks of interconnected chambers created chemical niches from complex mixtures of prebiotically relevant substances, each with different prevailing concentration ratios. These "micro-labs" could thus enable a wide variety of prebiotic reactions and massively increase their yield and selectivity compared to bulk systems. We further measured the sequence selectivity of UV radiation on pseudo-genomes built from subsets of codon sequences. Comparison with existing chronologies for codon and amino acid evolution suggests the importance of UV light as a selection pressure during the evolution of early life.

BP 10.3 Tue 10:15 BAR 0106

Unpredictable repeatability in evolutionary dynamics — •SUMAN DAS and JOACHIM KRUG — Institute for Biophysics, University of Cologne, Germany

Biological evolution proceeds through occurrence and fixation of mutations. But how repeatable are evolutionary trajectories? Is the evolution of specific well-adapted genotypes largely a matter of chance, or should we expect the same genotypes to evolve repeatedly? The answer depends in part on the probability distribution of mutational effect sizes. Repeatability is itself a random variable, and for light-tailed distributions it converges to its mean value in the limit of a large number of available mutations. However, for heavy-tailed distributions, we show that the repeatability is much higher but the distribution remains broad, and consequently the repeatability cannot be predicted based on the distribution. This non-self averaging effect is similar to those observed in certain disordered systems, and arises from the fact that the fixation process is dominated by a few mutations even in the limit of infinite mutation number. We discuss the behavior in various heavy-tailed regimes, and illustrate it with applications to empirical data on drug resistance evolution.

REF: S G Das and J Krug (2022). Unpredictable repeatability in molecular evolution. *Proceedings of the National Academy of Sciences*, 119(39):e2209373119.

BP 10.4 Tue 10:30 BAR 0106

Kinetics of Information Content in a Virtual Circular Genome — •LUDWIG BURGER, TOBIAS THUN, and ULRICH GERLAND — Technical University of Munich

We study the kinetics of information content in an ensemble of oligonucleotides that undergo hybridization, dehybridization, non-enzymatic templated ligation and single-strand cleavage. The stability of hybridized complexes depends on the sequence because the dehybridization rate depends on the free hybridization energy. Mismatches are possible, but they lead to a thermodynamic and kinetic penalty. The information that is supposed to be "stored" in the ensemble is a circular genome as well as its complementary strand. Therefore, the oligonucleotides in the initial ensemble are chosen such that every element in the ensemble is part of the true genomic sequence. In most investigated scenarios, the initial ensemble loses its information content and no information amplification can be observed. Depending on the choice of ligation and cleavage rate, the loss of information can be driven by cleavage or ligation. Information loss by ligation is caused by templated ligation processes that produce long strands that do not resemble the true genomic sequence. This is the case if the hybridization site is too short or contains too many mismatches to guarantee correct alignment of template and ligated strands. Even though information amplification appears to be difficult to achieve, the timescale of information loss can be extended by tuning the hybridization energy or the concentration of short oligomers.

15 min. break

BP 10.5 Tue 11:00 BAR 0106

Evolutionary rescue of resistant mutants is governed by a balance between radial expansion and selection in compact populations — SERHII AIF^{1,2}, NICO APPOLD^{1,2}, LUCAS KAMPMANN³, OSKAR HALLATSCHER^{3,4}, and •JONA KAYSER^{1,2} — ¹MPI für die Physik des Lichts, Erlangen, Germany — ²MPZ für Physik und Medizin, Erlangen, Germany — ³University of California, Berkeley, USA — ⁴Leipzig University, Leipzig, Germany

Mutation-mediated treatment resistance is one of the primary challenges for modern antibiotic and anti-cancer therapy. Yet, how slower-growing resistant lineages may escape purifying selection via continued evolution is still unclear. Here, we introduce a system of fluorescence-coupled synthetic mutations to track the entire evolutionary trajectory of thousands of resistant lineages in expanding yeast colonies. We uncover that an underlying quasi-stable equilibrium between the opposing forces of radial expansion and natural selection, a phenomenon we term inflation-selection balance, enhances the evolutionary rescue of resistant lineages. Tailored computational models and agent-based simulations corroborate the fundamental nature of the observed effects and demonstrate the potential impact on drug resistance evolution in cancer. The described phenomena should be considered when predicting multi-step evolutionary dynamics in any mechanically compact cellular population, including pathogenic microbial biofilms and solid tumors. The insights gained will be especially valuable for the quantitative understanding of response to treatment, including emerging evolution-based therapy strategies.

BP 10.6 Tue 11:15 BAR 0106

Heat flows drive ionic and pH gradients — •THOMAS MATREUX¹, ALMUTH SCHMID¹, PAULA AIKKILA¹, KRISTIAN LE VAY², JOHANNES RAITH³, BERNHARD ALTANER³, BETTINA SCHEU⁴, ULRICH GERLAND³, HANNES MUTSCHLER², DIETER BRAUN¹, and CHRISTOF B. MAST¹ — ¹Systems Biophysics, LMU Munich, Germany — ²Biomimetic systems, TU Dortmund, Germany — ³Physics of Complex Biosystems, TU Munich, Germany — ⁴Earth and Environmental Sciences, LMU Munich, Germany

The first steps in the emergence of life on Earth occurred on rocks and their constituent phases with a feedstock of simple molecules. Our aim is to combine this background with physical non-equilibria such as thermal gradients, offering unique opportunities for molecular selection on all levels.

In this scenario, ions leached from mineral samples are selectively accumulated by heat flows through water-filled fractures. In contrast to up-concentration by dehydration or freezing, this actively alters the Magnesium:Sodium ratio to an extent that permits key ribozyme activities.

Simple mixtures of formic acid and sodium hydroxide, exposed to thermal gradients, drive pH gradients which can be understood and predicted by a separation of timescales. Such proton gradients can locally acid-dissolve Apatite, a presumably abundant phosphate mineral that is close to insoluble at physiological pH. By thermal fractionation, significant concentrations of phosphate are provided at neutral pH.

BP 10.7 Tue 11:30 BAR 0106

Evolution Mechanics: a Framework of Hierarchy Formation in Evolving Systems — •YUNUS SEVINCHAN — Science of Intelligence Cluster, Technische Universität Berlin, Berlin, Germany — Institute for Theoretical Biology, Humboldt-Universität zu Berlin, Berlin, Germany — Institute of Environmental Physics, Universität Heidelberg, Heidelberg, Germany

The structures we observe around us are of a wide diversity and complexity, ranging from simple cells to intricate ecosystems and human societies. The question how these hierarchically modularized structures can arise from simpler ones is of central importance when desiring to understand our world.

I present the Evolution Mechanics framework [1] which aims to find a concise description of the mechanisms by which evolutionary systems unfold into hierarchically organized modules. Key elements of this conceptual framework are a so-called Self-Replicator and a set of processes that need to occur in order for an Evolutionary Transition in Individuality to take place, thus leading to a new hierarchical level. While inspired by the evolution of biological life, Evolution Mechanics is abstracted from it and takes a more general perspective, providing a consistent language to address the fundamental processes giving rise to the complexity we observe.

[1]: Yunus Sevinchan. Dissertation, 2021. *Evolution Mechanics and Perspectives on Food Web Ecology*. Heidelberg University Library. DOI: 10.11588/heidok.00030750

BP 10.8 Tue 11:45 BAR 0106

Sequence distributions in coexisting phases — •IVAR SVALHEIM HAUGERUD¹, GIACOMO BARTOLUCCI², and CHRISTOPH A. WEBER¹ — ¹University of Augsburg, Augsburg, Germany — ²Max Planck Institute for the Physics of Complex Systems, Dresden, Germany

Phase separation, sequence, and length distributions of heteropolymers such as RNA and DNA are essential in regulating functions and spatial organization in living cells and at the molecular origin of life. Here, we theoretically investigate the interplay between phase separation, polymer sequence, and length at non-dilute conditions. To this end, we developed a thermodynamic description for the reversible polymerization of different monomeric units. In the model, polymers can grow, shrink and phase separate from each other and the solvent. We show that growth in length facilitates phase separation already at low concentrations. Our key finding is that the distribution of sequences is entirely different in each phase. These results suggest that condensed phases can act as hubs for functionalities that rely on the sequence-specificity of RNA or DNA.

BP 10.9 Tue 12:00 BAR 0106

Controlling Alkaline Vent Morphologies in Microfluidic Models by pH and Fluid Flow — •MAXIMILIAN WEINGART¹, SIYU CHEN², CLARA DONAT², DIETER BRAUN¹, and KAREN ALIM² — ¹Systems Biophysics, Ludwig-Maximilians Universität München, Amalienstraße 54, 80799 München, Germany — ²CPA and Department of Biosciences, School of Natural Sciences, Technische Universität München, Ernst-Otto-Fischer-Straße 8, 85748 Garching b. München, Germany

Alkaline vents provide the unique chemical composition for the precipitation of alkaline fluids in acidic, metal-ion containing ocean water, thereby providing the necessary gradients to drive molecular reactions at the origin of life. Yet, the 3D chimney-like structure of vents pre-vents any visualization of potentially reaction fueling gradients. Here, we develop a microfluidic model of alkaline vents permitting spatio-temporal visualization of precipitate formation and morphology. Varying concentration and inflow rate of an alkaline solution into a flat microfluidic-chamber pre-filled with an acidic Fe(II)-solution we observe a diverse set of precipitate morphologies. Visualizing the pre-precipitation pattern we identify for which physical parameter vent morphologies allow for gradients in pH and molecular composition to arise. We establish our microfluidic model as a framework to investigate the potential of gradients across a permeable boundary for early compartmentalisation and molecular reactions at the Origin of life. The 2D microfluidic alkaline vent model shows that disordered precipitate morphologies allow for the formation of strong pH gradients.

BP 11: Poster Session I

Time: Tuesday 12:30–15:30

Location: P1

BP 11.1 Tue 12:30 P1

Reinforcement Learning: Optimizing Target-search in a homogeneous environment — •HARPREET KAUR, MICHELE CARAGLIO, and THOMAS FRANOSCH — Institute for Theoretical Physics, Universität Innsbruck, Innsbruck, Austria.

The target-search problem is an interdisciplinary problem comprising several scales, ranging from bacteria looking for food to robots collecting garbage. Generally, in target search we make decisions in an uncertain and often complex environment with the aim of finding a target as efficiently as possible. The key feature that efficient searching agents have in common is the ability to self-propel. Being able to develop efficient search strategies is crucial, as the time needed to discover a target is often a limiting resource. Here, we address the problem of how a smart microswimmer finds a randomly located target in a homogeneous environment by resorting on machine-learning techniques, particularly Reinforcement Learning. We aim to show that learned strategies are optimal and enable minimization of the search time. Also, our work will provide a better understanding of bacteria behavior and biological foraging.

BP 11.2 Tue 12:30 P1

A study of bacteria entrapment using multiparticle collision dynamics — •PIERRE MARTIN and HOLGER STARK — Technische Universität, Berlin, Germany

The purpose of the current study is to investigate entrapment of bacteria near surfaces. Mechanisms to control trapping of bacteria near solid surfaces is of utmost interest to many medical and biotechnological applications. Trapping leads to enhanced attachment, facilitates the proliferation of cells and ultimately the formation of bacterial biofilms on the surface. Bacteria such as *Escherichia coli* (*E. coli*) propel themselves by rotating a bundle of helical flagella. They can change direction by reversing the rotation of a flagella, a process known as tumbling. The motion of bacteria near surfaces induces hydrodynamic interactions with the substrate, aligning the cell almost parallel to the surface. This creates an attractive force from the bacteria to the surface, moving and trapping the bacteria along it.

We currently implement a realistic model of *E. coli* including its tumbling motion within a computer code where we couple it to fluid flow at low Reynolds numbers. The fluid flow is simulated using the method of multi-particle collision dynamics, an efficient solver of the Navier-Stokes equations. Our first goal is to simulate non-tumbling numerical strain of *E. coli* under shear flow. We will analyse the importance of rheotaxis and Jefferey orbits for near surfaces motility and trapping.

BP 11.3 Tue 12:30 P1

Collective dynamics of multicellular systems in curved geometries — •TOM BRANDSTÄTTER^{1,2}, DAVID BRÜCKNER³, YU LONG HAN⁴, RICARD ALERT⁵, MING GUO⁴, and CHASE BROEDERSZ^{1,2} — ¹Arnold-Sommerfeld-Center for Theoretical Physics, Ludwig-Maximilians-Universität München — ²Department of Physics and Astronomy, Vrije Universiteit Amsterdam — ³Institute of Science and Technology Austria — ⁴Department of Mechanical Engineering, Massachusetts Institute of Technology — ⁵Max Planck Institute for the Physics of Complex Systems

The multicellular organization of diverse systems, including embryos, intestines, and tumors relies on coordinated cell migration in curved environments. In these settings, cells establish supracellular patterns of motion, including collective rotation and invasion. While such collective modes are increasingly well understood in 2D flat systems, the consequences of geometrical and topological constraints on collective cell migration in 3D curved tissues are largely unknown. Here, we discover a collective mode of cell migration in rotating spherical tissues manifesting as a propagating single-wavelength velocity wave. This wave is accompanied by a pattern of incompressible cellular flow across the spheroid surface featuring topological defects. Using a minimal active particle model, we reveal that this collective mode originates from the active flocking behavior of a cell layer confined to a curved surface. Our results identify curvature-induced velocity waves as a generic active matter mode, impacting the dynamical organization of 3D curved tissues.

BP 11.4 Tue 12:30 P1

Self-propulsion of Janus particles at small laser powers and the impact of salt — •FRANZISKA BRAUN and REGINE VON KLITZING — Institute for Condensed Matter Physics, Technische Universität Darmstadt, D-64289 Darmstadt

The anisotropy in the architecture allows Janus particles to create an out-of-equilibrium state around the particle in the solvent, which is a necessary condition for triggering self-propulsion. One possible propulsion mechanism is thermophoretic self-propulsion. When laser light ($\lambda = 532$ nm) illuminates a gold-capped particle, a local temperature gradient is generated along the particle surface due to surface plasmon excitation of the gold cap. This gradient perturbs the equilibrium conditions of the surrounding medium and leads to self-propulsion.

This contribution focuses on an intensive study of the self-propulsion behavior of self-thermophoretic Janus particles. For this purpose, the movement of the Janus particles is tracked in real-time with dark-field microscopy (DFM). First, the thermophoretic velocity of Au-PS particles is investigated focusing on very low laser powers below 10 mW. Surprisingly, the study shows a deviation of the thermophoretic velocity from the expected linear behavior in the low laser power regime. Secondly, the influence of salt ions on the self-propulsion behavior of such Au-PS particles is described.

BP 11.5 Tue 12:30 P1

An omnipresent material that still surprises: Anomalous stress relaxation of polydimethylsiloxane (PDMS) — PHILIPP LACH, ERDEM BONDAN, PIERRE-LOUIS CRAMER, NAN XUE, ROBERT W. STYLE, STEFANIE HEYDEN, •CHARLOTTE LORENZ, and ERIC R. DUFRESNE — Department of Materials, ETH Zürich, Vladimir-Prelog-Weg 1-5/10, 8093 Zürich, Switzerland

Polydimethylsiloxane (PDMS) is an elastomer which finds ubiquitous use as a model system in experimental settings, as well as in engineering applications. It is easy to fabricate and tune over a large stiffness range. Recent applications in soft robotics have stimulated a closer look at its mechanical properties. Here, we report anomalous responses of PDMS networks to deformation. In one set of experiments, PDMS becomes stiffer after repeated cycles of deformation. In another, PDMS has a non-monotonic stress relaxation in response to a step-strain. Together, these results suggest a mechano-chemical coupling in PDMS where deformed networks are capable of forming new cross-links.

BP 11.6 Tue 12:30 P1

Complex formation between Polyethylenimine and mRNA — •JONAS LEHNEN¹, GIOVANNI SETTANNI², and FRIEDRIKE SCHMID¹ — ¹KOMET 1, Institute of Physics, JGU Mainz, Germany — ²Faculty of Physics and Astronomy, Ruhr University Bochum, Germany

Messenger RNA vaccines have proven invaluable in the fight against the COVID-19 pandemic. Among the vehicles for non-viral gene delivery Polyethylenimine (PEI) has attracted attention due to its high transfection efficiency. PEI binds to negatively charged mRNA forming polyplexes. These are nanoparticles (NP) of different sizes, depending on the pH used for their assembly as well as salt, PEI and RNA concentration. Small NP have been shown to be critical for high transfection efficiency. We use coarse-grained molecular dynamics simulations to examine the effects of the various factors determining polyplex size and gain a better understanding of the processes involved in their formation, with a special interest on the effects of PEI concentrations way above the amount necessary to neutralize the mRNA, following up on recent experimental results. Experimental and atomistic simulation data were used to tune our model with the aim of finding the mechanism responsible for controlling the size of NPs and give a description of the formation process.

BP 11.7 Tue 12:30 P1

Long-Term Stability, Biocompatibility and Magnetization of Suspensions of Isolated Bacterial Magnetosomes — F. MICKOLEIT¹, C. JÖRKE², •R. RICHTER³, S. ROSENFELDT⁴, S. MARKERT¹, I. REHBERG³, A. S. SCHENK⁵, O. BÄUMCHEN³, D. SCHÜLER¹, and J. H. CLEMENT² — ¹Dept. Microbiology, University of Bayreuth, D-95447 Bayreuth, Germany — ²Dept. Hematology and Medical Oncology, Jena University Hospital, D-07747 Jena, Germany — ³Experimental Physics V, University of Bayreuth, D-95447 Bayreuth, Germany — ⁴Physical Chemistry I, University of Bayreuth, D-95447 Bayreuth, Germany — ⁵Physical Chemistry - Colloidal Systems, University of Bayreuth, D-95447 Bayreuth, Germany

Magnetosomes are magnetic nanoparticles biosynthesized by magnetotactic bacteria. Due to a genetically strictly controlled biomineralization process, the ensuing magnetosomes have been envisioned as agents for biomedical and clinical applications. In the present work, we examine the stability parameters of magnetosomes isolated from *Magnetospirillum gryphiswaldense* upon storage as a suspension in a buffer solution at 4°C and N₂ atmosphere for one year in the absence of antibiotics. The magnetic potency, measured by the saturation magnetization of the particle suspension [1], drops by 2/3 within this year - about ten times slower than at ambient air and room temperature. The particle size distribution, the integrity of the surrounding magnetosome membrane, the colloidal stability, and the biocompatibility turn out to be not severely affected by long-term storage. — [1] Mickoleit F., et al. (2018). ACS Appl. Mater. Interfaces 10(44), 37898.

BP 11.8 Tue 12:30 P1

The change of DNA radiation damage upon hydration: In-situ observations by near-ambient-pressure XPS — •MARC BENJAMIN HAHN¹, PAUL M. DIETRICH², and JÖRG RADNIK¹ — ¹undesanstalt für Materialforschung und -prüfung, Berlin, Germany. — ²SPECS Surface Nano Analysis GmbH, Berlin, Germany

X-ray photoelectron-spectroscopy (XPS) allows simultaneous irradiation and damage monitoring. Although water radiolysis is essential for radiation damage, all previous XPS studies were performed in vacuum. [1] Here we present near-ambient-pressure XPS experiments to directly measure DNA damage under water atmosphere. They permit in-situ monitoring of the effects of radicals on fully hydrated double-stranded DNA. Our results allow us to distinguish direct damage, by photons and secondary low-energy electrons (LEE), from damage by hydroxyl radicals or hydration induced modifications of damage pathways. The exposure of dry DNA to x-rays leads to strand-breaks at the sugar-phosphate backbone, while deoxyribose and nucleobases are less affected. In contrast, a strong increase of DNA damage is observed in water, where OH-radicals are produced. In consequence, base damage and base release become predominant, even though the number of strand-breaks increases further. [1] Hahn, M.B., Dietrich, P.M. & Radnik, J. In situ monitoring of the influence of water on DNA radiation damage by near-ambient pressure X-ray photoelectron spectroscopy. *Commun Chem* 4, 50 (2021).

BP 11.9 Tue 12:30 P1

A NAP-XPS-study on X-ray radiation damage: Chemical changes to Gene-V Protein — •DOROTHEA C HALLIER^{1,2,3}, JÖRG RADNIK², PAUL M DIETRICH⁴, HARALD SEITZ^{1,3}, and MARC BENJAMIN HAHN² — ¹Fraunhofer Institute for Cell Therapy and Immunology, Branch Bioanalytics and Bioprocesses, Potsdam, Germany — ²Federal Institute for Materials Research and Testing BAM Berlin, Berlin, Germany — ³University of Potsdam, Institute for Biochemistry and Biology, Potsdam Germany — ⁴SPECS Surface Nano Analysis GmbH, Berlin, Germany

Single-stranded DNA-binding proteins such as Gene-V Protein (G5P/GVP) are involved in maintaining the DNA metabolism after exposure to ionizing radiation, i.e. after radiation therapy in cancer treatment. X-ray photoelectron spectroscopy (XPS) was used to analyze the chemical damage of ionizing radiation to G5P itself. Direct and indirect damage was detected through combined vacuum XPS and near-ambient pressure (NAP) XPS measurements under water and nitrogen atmosphere. The x-ray irradiation leads to degradation i.e. via dehydrogenation, decarboxylation, dehydration and deamination. A strong increase of protein damage was observed in water as compared to vacuum.

BP 11.10 Tue 12:30 P1

FTIR and SRE spectra analysis for supported lipids bilayers (SLB's) with dry incorporation of Gramicidin A — •D. SAAVEDRA¹, N. MORAGA¹, N. GOMEZ-VIERLING¹, M. CISTERNAS², R. RODRIGUEZ², S. ROJAS², and U.G. VOLKMANN¹ — ¹Institute of Physics and CIEN-UC, Pontificia Universidad Catolica de Chile — ²School of Industrial Engineering, Universidad de Valparaiso, Santiago, Chile A dry method for SLB's assembling was developed in our group, without use of solvents and in vacuum [1], with the aim of synthesizing stable platforms for biosensors. For characterization, FTIR spectrum was analyzed for the detection of functional groups of DPPC and DSPC phospholipids in the range of 800 - 4000 1/cm. Using the SRE spectrum of DPPC and DSPC, their phase transitions were studied as a function of temperature. The SLB's/Gramicidin interaction at different concentrations were analyzed in order to optimize the growth of the biomolecules. These results would allow to evaluate the use of spin-probes in Gramicidin for the study of ion channel formation [2] and as a prototype for insertion of larger proteins.

Fondecyt 1180939 (UGV), ANID doctoral grants (NM and NGV) and ANID SIA SA77210032 (MC and SR).

[1] M. A. Cisternas, et al., *Int. J. Mol. Sci.* 21 (18), (2020) 6819.[2] Dzikovski, B.G., et al., *J. Phys. Chem. B* 2011, 115(1), 176-185.

BP 11.11 Tue 12:30 P1

Detection of Gramicidin by DPH fluorescence technique in supported phospholipids bilayers (SLB's) on SiO2 substrate — •D. SAAVEDRA¹, M. SOTO-ARRIAZA², N. MORAGA¹, N. GOMEZ-VIERLING¹, M. CISTERNAS³, and U.G. VOLKMANN¹ — ¹Institute of Physics and CIEN-UC, Pontificia Universidad Catolica de Chile — ²Faculty of Medicine and Science, Universidad San Sebastian, Santiago, Chile — ³School of Industrial Engineering, Universidad de Valparaiso, Santiago, Chile

An unconventional method to manufacture supported lipid bilayers (SLB's) was developed in our laboratory: without solvents, dry [1,2] and in the absence of gases, with the aim of synthesizing stable biosensor platforms. In this work we use our physical fabrication method for the incorporation of specific signal transmitters that have selective sensitivity.

The fluorescence emission spectra of Gramicidin, with DPH as extrinsic probe and fluorescence resonant energy transfer (FRET) techniques, seeks to detect its incorporation into the SLB's.

A series of samples were prepared in absence and presence of Gramicidin and the extrinsic probe DPH. Detection was realized using a single time-correlated spectrofluorimeters photon counting (TCSPC).

Fondecyt 1180939 (UGV), ANID doctoral grants (NM and NGV).

[1] Cisternas Fruns, M. A. (2021). Ph.D. Thesis, PUC, Chile. <https://repositorio.uc.cl/handle/11534/60584>.[2] M. A. Cisternas, et al., *Int. J. Mol. Sci.* 21 (18), (2020) 6819.

BP 11.12 Tue 12:30 P1

Homogenization of DPPC films deposited from the gas phase onto silicon substrates — •N. MORAGA¹, D. SAAVEDRA¹, N. GOMEZ-VIERLING¹, M. CISTERNAS², M.J. RETAMAL³, and U.G. VOLKMANN¹ — ¹Institute of Physics and CIEN-UC, Pontificia Universidad Catolica de Chile, Santiago, Chile — ²School of Industrial Engineering, Universidad de Valparaiso, Santiago, Chile — ³Engineering Faculty, Universidad Finis Terrae, Santiago, Chile

Supported lipid bilayers (SLBs) are stable structures that allow us to gain insight into the physical behavior of cell membranes through thin film characterization techniques. In this work, DPPC SLBs are made through Physical Vapor Deposition (PVD) technique on silicon substrates without using any solvent [1]. The film thickness was monitored in situ by high-resolution ellipsometry. The DPPC deposition rate, substrate temperature during deposition and post deposition membrane annealing temperature in vacuum and in dry air are used as parameters. Homogeneity of the phospholipid bilayer is observed through the topographical analysis and Young modulus by AFM. Lower deposition rates and a slight increase of substrate temperature led to more homogeneous films. The right annealing temperature and time further improve membrane quality to favor protein insertion [2].

Fondecyt 1180939 (UGV) and ANID doctoral grants (NM and NGV)

[1] M. A. Cisternas, et al., *Int. J. Mol. Sci.* 21 (18), (2020) 6819.[2] Dzikovski, B.G., et al., *J Phys Chem B* 2011, 115(1), 176-185.

BP 11.13 Tue 12:30 P1

Foam-like properties of bundled polymer networks — •LUKAS PAUL WEISE, TOBIAS ALEXANDER KAMPFMAN, and JAN KIERFELD — TU Dortmund University, Germany

We simulate systems of mutually attractive semiflexible harmonic chain polymers in quasi-two dimensions with the event chain algorithm. An isotropic initialization of the system evolves into a network of densely packed bundles of polymers. The resulting structure aims to minimize the overall bundle length which gives rise to properties reminiscent of foams. We examine the applicability of laws and relations characterizing the structure of foams to the bundled polymer networks in order to assess to what extent the networks behave foam-like. The dynamics of the bundled networks are found to be very sensitive with respect to details of the polymer interactions via friction terms albeit qualitative resemblance to foams remains.

BP 11.14 Tue 12:30 P1

Self-assembled Peptides Structure Mediated by Solid Interfaces. — •LEILA SAHEBMOHAMMADI¹, REGINE VON KLITZING¹, MARKUS MEZGER², and POL BESENIUS³ — ¹Soft Matter at Interfaces, Department of Physics, Technical University of Darmstadt, Hochschulstraße 8, 64289 Darmstadt, Germany — ²Dynamics of condensed systems, Faculty of Physics, Universität Wien, Währinger Straße 38-42, 1090 Wien, Austria — ³Department of Chemistry, Johannes Gutenberg-Universität Mainz, Duesbergweg 10-14D-55128 Mainz, Germany

In situ QCM-D reveal a layer-by-layer absorption of the oppositely charged peptides, forming a multilayer. The total amount of adsorbing peptides is derived by the adsorbed temperature and increases with increasing temperature. Exposure to high or low pH (12 or 2) removes the peptide stacks apparently due to reduced electrostatic interaction. AFM result shows the distribution pattern is nanorod-like. These experiments prove stable switchable blocks on the surface that can carry biological and colloidal materials.

BP 11.15 Tue 12:30 P1

Investigations of the Fusion Process of Lipid-Based Nanoparticles with Model Endosomal Membranes Using Coarse-Grained Molecular Dynamics Simulations — •THOMAS KOLBE¹, FRIEDERIKE SCHMID¹, and GIOVANNI SETTANNI^{1,2} — ¹Physics Department, Johannes Gutenberg University Mainz — ²Faculty of Physics and Astronomy, Ruhr University Bochum

Lipid based nanoparticles have proven to be viable choices for the delivery of genetic material inside a living organism. Compared to the more traditionally used non-pathogenic viruses they attract through potentially much lower costs and milder effects on the immune system. Yet, the exact mechanisms of the endosomal escape - the process with which the delivered drug enters the cell - requires more thorough examination. We simulate the related fusion of a DNA-lipid based nanoparticle with a model endosomal membrane, using coarse-grained molecular dynamics to gain more insights into the underlying processes. By modeling the drop of the system's pH in the various stages of the endosome with different degrees of ionization in our nanoparticle, we can see that the better part of transfections happen at a late stage, confirming that cationic lipids are a main driver of the transfection process. Further, we observe that the size and structure of the nanoparticles have substantial influence on the transfection efficiency.

BP 11.16 Tue 12:30 P1

Machine Learning Guided RNA Contact Prediction — •UTKARSH UPADHYAY¹, OSKAR TAUBERT², CHRISTIAN FABER³, and ALEXANDER SCHUG⁴ — ¹Forschungszentrum Jülich, Jülich, Germany — ²Karlsruher Institut für Technologie, Karlsruhe, Germany — ³Forschungszentrum Jülich, Jülich, Germany — ⁴Forschungszentrum Jülich, Jülich, Germany

For around 50 years, the primary focus of genomic research has been the development of efficient and accurate methods to predict the structure of proteins, which led to the birth of better sequencing techniques and databases. About 98% of the human genome (RNA, DNA) during this action was overlooked.

RNA is not merely a messenger for making proteins, in the past few years, studies have revealed the existence of many non-coding RNAs which catalyze various biological processes; to gain detailed insights into these roles, we require the appropriate structure. Recent years have led to breakthroughs in protein structure prediction via Deep Learning. The scarcity of RNA structures, however, makes a direct transfer of these methods impossible.

We predict contact maps as a proxy to understand and predict RNA structure, they provide a minimal representation of the structure. We have worked on methods that took accuracy from 47% (DCA) to 77% (CoCoNet) and now to 87% (Barnacle). Further, we are trying to create more efficient neural networks for working with limited data, using statistical physics and ML techniques, to substantially reduce the sequence-structure gap for RNA.

BP 11.17 Tue 12:30 P1

Neighbor list artifacts in molecular dynamics simulations — •HYUNTAE KIM — Max Planck Institute for Biophysics — International Max Planck Research School on Cellular Biophysics

Molecular dynamics simulations are widely used in biophysics. To aid non-expert users, most simulation packages provide default values for key input parameters. We found that the default setting of the neighbor list cut-off rlist in the GROMACS package is not sufficient to prevent various artifacts in certain systems. Beyond an already known significant energy drift, we observed catastrophic box deformations of large membrane systems with a semi-isotropically coupled Parrinello Rahman (PR) barostat, rapid oscillations in the pressure, and asymmetric deformations of the box shape. We traced the cause of these artifacts to infrequent neighbor-list updates resulting in missed long-range Lennard-Jones interactions that are systematically attractive. We find that for the small molecular systems commonly simulated, these effects tend to be masked. We present measures to diagnose the problem and guidelines for practitioners.

BP 11.18 Tue 12:30 P1

Sequential resource-sharing speeds up replication in *Plasmodium falciparum* — •PATRICK BINDER^{1,2}, SEVERINA KLAUS³, MARKUS GANTER³, ULRICH S. SCHWARZ², THOMAS HÖFER¹, and NILS B. BECKER¹ — ¹German Cancer Research Center (DKFZ), Heidelberg — ²Institute for Theoretical Physics and BioQuant, Heidelberg University — ³Center for Infectious Diseases, Heidelberg University Hospital

The malaria-causing pathogen *Plasmodium falciparum* is a eukaryotic parasite with a complex life cycle that includes proliferation within red blood cells. After invasion of a red blood cell, the parasite undergoes several rounds of nuclear division and after two days releases around 20 daughter parasites. Although nuclei reside in a shared cytoplasm, using fluorescent imaging, we observe that these cycles desynchronize during multiplication, and do so more rapidly than expected for independent nuclei. To explain the observed asynchrony, we introduce a branching model for allocation of a shared enzyme to the different nuclei. The model encompasses parallel and sequential DNA replication modes. We find that when the shared enzyme is limiting, a sequential replication utilizes resources more efficiently than parallel, which result in faster completion of nuclear multiplication. Overall, our findings suggest that *Plasmodium falciparum* has evolved optimal resource utilization by exploiting a sequential sharing of replication machinery.

BP 11.19 Tue 12:30 P1

Semantic Segmentation for Single Particle Tracking in Noisy Data — •MATTIAS LUBER, MOHAMMAD AMIN ESKANDARI, and TIMO BETZ — Third Institute of Physics - University of Göttingen

The quantitative analysis of particle motion critically depends on the quality of particle trajectory detection. Especially the position detection of particles in fluorescence microscopy images is an important task faced in biophysics. Trajectories are used to study processes like intra-cellular transport, protein diffusion within and through membranes and the reconstruction of force fields driving the particle motion. In such settings, high spatial and temporal resolution are desired. However, in practice those factors have contradictory measurement requirements. High temporal resolution requires short exposure times, which limits the photon budget and thus lead to low signal to noise ratios. This work proposes an approach to reconstruct the particle position from noisy images by applying U-NET based deep learning models to fluorescence microscopy images. Further it is shown that this method can successfully track particles with shorter exposure times, compared to traditional approaches.

BP 11.20 Tue 12:30 P1

Mathematical modelling of *Nippostrongylus brasiliensis* helminth infection: from single worm motility to tissue load dynamics — •SOHAM MUKHOPADHYAY¹, JONATHAN POLLOCK², DAVID VOEHRINGER², and VASILY ZABURDAEV¹ — ¹Max-Planck-Zentrum für Physik und Medizin, Erlangen, Germany — ²Department of Infection Biology, University Hospital Erlangen, Friedrich-Alexander University Erlangen-Nuremberg, Germany

Helminth infections affect a large proportion of the world's population and cause significant morbidity. There are no vaccines against helminths, and the mechanisms by which the body fights off helminth infections are not well-understood. To better understand the immune system response we aim to develop a mathematical model describing the helminth load in different organs of the host as a function of time. As an experimental system, we use murine helminth infection by *N. brasiliensis* worms, where primary, secondary, and infections of mice with altered immune systems could be studied. We model the progression of infection as a system of coupled, time-delayed equations which allow us to link the larvae starting the infection on the skin of mice to the number of eggs shed to the environment by adult worms from the intestine and compare the predictions of the model to the data. For a more microscopic insight into the behaviour of larvae at different developmental stages we carry out biophysical characterisation of larval motility in in vitro settings. Combining these results we aim to achieve a quantitative description of the infection progression in the host.

BP 11.21 Tue 12:30 P1

RNA G-quadruplex folding is a multi-pathway process with a variety of short-lived intermediate states — •MARIJANA UGRINA¹, INES BURKHART², DIANA MÜLLER², HARALD SCHWALBE², and NADINE SCHWIERZ¹ — ¹University of Augsburg, Augsburg, Germany — ²Goethe University, Frankfurt am Main, Germany

The folding kinetics of regulatory RNAs is crucial for their function. Here, we provide molecular insights into the folding pathways of a G-quadruplex from telomeric repeat-containing RNA by combining all-atom molecular dynamics and coarse-grained simulations with circular dichroism experiments. The ion atmosphere surrounding the highly charged quadruplex plays a crucial role in folding. To correctly capture the electric double-layer in implicit solvent coarse-grained simulations, we develop a matching procedure based on all-atom simulations in explicit water. This procedure allows us to provide quantitative agreement between the experiments and simulations as judged by the number of native contacts at different salt concentrations and temperatures. Folding of the quadruplex is on the timescale of minutes and the coarse-grained simulations using the three-interactions site model are therefore ideal to resolve the folding pathways and intermediate states. The results reveal that the folding is sequential with each pathway passing through two transient, on-pathway intermediates: A hairpin and a triplex or double hairpin state. Since these intermediates are degenerate with at two to four alternative conformations per state, quadruplex folding is a multi-pathway process with high conformational entropy.

BP 11.22 Tue 12:30 P1

OCTOPOS.jl: A user-friendly tool for synonymous genetic code optimization — •SIMON CHRIST¹, JAN-HENDRIK TRÖSEMEIER², CHRISTEL KAMP², and SOPHIA RUDORF¹ — ¹Leibniz Universität, Hannover — ²Paul-Ehrlich-Institut, Langen

Synonymous genetic code optimization takes advantage of the fact that aminoacids can be encoded by different nucleotid triplets. It attempts to influence the translation process by synonymous substitutions to alter characteristics such as the protein expression.

OCTOPOS.jl is the reimplementation of the java desktop application OCTOPOS in the julia programming language as a web application.

OCTOPOS combines detailed mechanistic mathematical modeling of in-vivo protein synthesis with machine learning to predict protein expression levels based on codon choice and can generate optimized synonymous mRNA sequences for enhanced heterologous gene expression in different host organisms.

The aim of this reimplementation is to enhance the accessibility of this tool for the community.

BP 11.23 Tue 12:30 P1

Self-regulation of mRNA expression via LNP-based incoherent feed-forward loops — •JUDITH A. MÜLLER and JOACHIM O. RÄDLER — Ludwig-Maximilians-Universität, Munich

Lipid Nanoparticles (LNPs) have revolutionized the delivery of nucleic acid to living cells, including messenger RNAs (mRNAs) and small non-coding RNAs. However, at the single cell level, delivery of LNPs is heterogeneous and the expression level and timing is poorly controlled. A frequently occurring motif in natural gene regulation are incoherent feedforward loops (iFFLs) consisting of simultaneous initiation of activating transcription factors and down-regulating micro-RNAs. Here we realize lipid nanoparticles containing iFFL by ratiometric codelivery of eGFP coding mRNA and eGFP targeting siRNA. We find faster and more homogenous expression in eGFP time courses using Live Imaging on Single Cell Arrays (LISCA). The steady states levels show power law decrease

as a function of siRNA/RNA ratio. Our approach demonstrates self-regulated expression via iFFL-LNP based genetic programs.

BP 11.24 Tue 12:30 P1

How not to lose spikes: inference methods for spike-count neurons — •TOBIAS KÜHN and ULISSE FERRARI — Institut de la Vision, Sorbonne Université, INSERM, CNRS, F-75012 Paris

Maximum-entropy models have been successfully applied to neuronal data stemming from diverse areas like cortex, hippocampus or the retina. Despite this success, it features the major drawback of being restricted to describing every neuron to be in one out of two states: in a given time bin, either there was at least one spike or not. This property does not only limit the statistics that can be matched, but also prevents capturing the neurons' behavior when the firing rate is high, that is when the amount of transmitted information is large. The spike-count model we are suggesting provides a solution to both of these caveats. We are assuming the single-neuron probability distribution to be given in Boltzmann form with energy functions of the shape $E(n) = h \cdot n + J \cdot n^2 + \epsilon \cdot n^3 + \mathcal{O}(n \ln(n))$, where n is the spike count in the respective time bin and ϵ is a small negative hyper parameter guaranteeing that the probability is well-defined for all J . To account for pairwise covariances, we extend the independent neuron case by including an Ising-like interaction term that couples neurons in the network. To infer the model parameters, we develop Monte-Carlo and mean-field methods. We are confident that these techniques will prove useful in the further investigation of neuronal data, in particular in the search for second-order phase transitions.

BP 11.25 Tue 12:30 P1

Parameter Optimization for 1D-0D Coupled Blood Flow Models: Physics-Informed Neural Networks versus Kernel Methods — •TOBIAS KÖPPL¹, BENEDIKT HOOK^{1,3}, and GABRIELE SANTIN² — ¹Technische Universität München, School of Computation, Information and Technology — ²Digital Society Research Center, Fondazione Bruno Kessler, Italy — ³Support by Computing Facilities of Leibniz-Rechenzentrum München

The understanding of blood perfusion of organs is essential to improve motion therapy. Here, numerical simulations of the blood flow on the human arteries network have already come up to augment in-vivo measured data. A common approach is the coupled 1D-0D hydrodynamic model combining the simplified incompressible Navier-Stokes equations with the Windkessel model. Fine-tuning the free model parameters such as the resistance and capacity is computationally expensive so it is beneficial to find a simpler surrogate. To this purpose we apply two different machine-learning techniques: physics-informed neural networks and kernel-based methods. The first simultaneously minimizes the quadratic loss to existent reference data and the residuals of a physical system of differential equations by a neural network. The second builds a model from kernel functions and is purely data-driven. We refine these approaches to predict the blood pressure from the 1D-0D model in a single vessel at varying resistance, capacity and heart beat, sampled over time and space. Comparing them in terms of the training and test error and their run time, we conclude that they are equally applicable to be now integrated into quantum optimization.

BP 11.26 Tue 12:30 P1

From in vitro to in silico: a pipeline for the generation of 3D-cell culture simulations from real image data — ELINA NÜRNBERG^{1,2,3}, FELIX ROMER¹, •MARIO VITACOLONNA^{2,3}, RÜDIGER RUDOLF^{2,3}, and SIMEON SAUER¹ — ¹Institut für mathematisch-naturwissenschaftliche Grundlagen, Mannheim University of Applied Sciences, Mannheim, Germany — ²Institute of Molecular and Cell Biology, Mannheim University of Applied Sciences, Mannheim, Germany — ³Center for Mass Spectrometry and Optical Spectroscopy, Mannheim University of Applied Sciences, Mannheim, Germany

Immunofluorescence labelling, optical tissue clearing and confocal laser scanning microscopy enable the visualization of whole, intact 3D-cell culture models on a single cell level, without loss of 3D spatial information. However, a manual extraction of quantitative information from the entire sample is cumbersome and often only performed on a subset of the data. Moreover, due to lack of computational resources, appropriate statistical methods or theoretical models, this data is often analyzed only qualitatively. In order to overcome these obstacles and improve exploitation of available data beyond quantitative image analysis, we propose a 3D-image analysis pipeline, consisting of image segmentation and 3D-feature extraction to gain quantitative information on cell morphology and protein distribution. Subsequently, this information is used to statistically define prototypical cell types, which are implemented into a basic 3D simulation based on the cellular potts model, which aims to recreate in-silico the in-vitro 3D cell culture, and which can be further adapted to specific research questions.

BP 11.27 Tue 12:30 P1

Determinants of lipid-based nanoparticle structure and stability investigated using molecular dynamics simulations — •JONAS PAULUS¹ and GIOVANNI SETTANNI^{1,2} — ¹Department of Physics, Johannes Gutenberg University Mainz, Germany — ²Faculty of Physics and Astronomy, Ruhr University Bochum, Germany

mRNA-based therapeutics represent an effective tool to fight several diseases including viral infections, as demonstrated by the COVID-19 vaccination campaign, and cancer. To protect the mRNA from the harsh conditions in a human body, the polyanion is packed into a lipid-based nanoparticle (LNP). This delivery vehicle, although effective, still presents some problems like strict storage requirements, low fraction of successfully delivered mRNA as well as undesirable reactions in some patients. The source of these problems as well as solution approaches are topic of a promising research field. Here we use molecular dynamics simulations to provide a characterization of the internal structure of LNPs and lipid-based nanomaterials for the delivery of RNA. In particular we measure how several observables obtained from different lipid formulations, like the flexibility of bilayers, the tendency to phase separation, the pattern of interactions or behavior under different pH values are related to experimentally measured physico-chemical characteristics as well as to the transfection efficiency. Such structural information could help design more effective lipid formulations for mRNA delivery.

BP 11.28 Tue 12:30 P1

On European Robin cryptochrome 4 interaction with membranes — •MAJA HANIC¹, MARTA MAJEWSKA², IZABELLA BRAND², and ILIA SOLOV'YOV^{1,3,4} — ¹Department of Physics, Carl von Ossietzky University of Oldenburg, Carl-von-Ossietzky Straße 9-11, 26129, Oldenburg, Germany — ²Department of Chemistry, Carl von Ossietzky University of Oldenburg, Carl-von-Ossietzky Straße 9-11, D-26111, Oldenburg, Germany — ³Research Centre for Neurosensory Sciences, Carl von Ossietzky University of Oldenburg, Carl-von-Ossietzky Straße 9-11, 26111, Oldenburg, Germany — ⁴Department of Physics, Center for Nanoscale Dynamics (CENAD), Carl von Ossietzky University of Oldenburg, Ammerländer Heerstr. 114-118, 26129 Oldenburg

Since the 19th century it was postulated that migratory birds use the geomagnetic field for navigation. Exactly how a migratory bird is able to migrate long distances has become a scientific interdisciplinary question. Recently, cryptochrome 4a from night-migratory songbird European Robin (ErCry4) has been expressed and shown to be sensitive to magnetic field. The sensitivity of ErCry4 to the Earth's magnetic field could be explained by uniform alignment of the ErCry4 protein in bird's eye cells. The possible interaction of ErCry4a with the model membrane mimicking the one found in the outer part of the cone cells was investigated both experimentally and computationally. The experimental and computational results indicate that the ErCry4 does interact with the model lipid membrane. This is the first known observation that ErCry4 interacts with a cell membrane, which could be a key step for ErCry4 to propagate the signal as a magnetoreceptor.

BP 11.29 Tue 12:30 P1

Heat flows through rock cracks purify >50 building blocks of life — •PAULA AIKKILA, THOMAS MATREUX, DIETER BRAUN, and CHRISTOF MAST — Systems Biophysics, LMU Munich, Germany

A crucial step during the origins of life is the emergence of biopolymer building blocks. However, the optimal reaction pathways for their formation usually require feedstocks of pure reactants and defined purification and mixing steps to suppress unwanted side reactions and allow for high product yields. We show that heat flows through thin crack-like compartments purify complex mixtures of prebiotically relevant building blocks with high selectivity by bringing together geomaterials, chemistry and microfluidics in a realistic environment. This non-equilibrium process differentially enriches prebiotically relevant building blocks, and distinguishes even mass-identical molecules. Using the experimentally determined thermophoretic properties, we model geologically plausible networks of connected heat flow compartments. Our results show how geologically driven non-equilibrium could purify compounds and implement downstream mixing for the origin of life.

BP 11.30 Tue 12:30 P1

Theory of adaptation to a moving optimum — •SAKSHI PAHUJANI and JOACHIM KRUG — Institute for Biological Physics, University of Cologne, Zùlpicher Straße 77, D-50937 Köln, Germany

We study the evolution of a polygenic trait under changing environment using a theory of adaptation formulated by Michael Kopp and Joachim Hermisson [1]. This theory treats the changing environment as a fitness optimum moving in the phenotypic space. Within this framework, we work with the assumption of instantaneous fixation of beneficial mutations. Consequentially, we view adaptation as a walk in the phenotypic space, the dynamics of which are governed by the selection coefficient and the dimensionless speed of the optimum. We investigate the conditions pertaining to the existence of a stationary distribution of the phenotypic lag of the population from the optimum and the dependence of the distribution of adaptive substitutions on the distribution of phenotypic effect sizes available to the population. Further, we go beyond the linear dependence of the optimum on time to non-linear dependencies and incorporate this into the theory to answer questions about the time until first passage through a fitness threshold which potentially leads to the extinction of the population.

[1] Michael Kopp, Joachim Hermisson, genetics.108.099820 (2009)

BP 11.31 Tue 12:30 P1

(De)hydration can speed up chemical process — IVAR HAUGERUD, •PRANAY JAISWAL, and CHRISTOPH WEBER — Mesoscopic Physics of Life, Institute of Physics, Universitätsstr. 1, Augsburg, Germany

Under early earth conditions, wet-dry cycles and phase separated droplets are separately believed to facilitate chemical processes. Recent experimental studies suggest that chemical reactions can accelerate when subject to non-equilibrium conditions of hydration or dehydration. We develop a theoretical model studying the interplay between wet-dry cycles, phase separation, and chemical processes. We find that hydration and dehydration can significantly increase chemical reaction rates and are further magnified with increasing oscillation amplitudes. Repeated cycles keep the system out of equilibrium, allowing for persistent chemical activity. Furthermore, resonance behaviour in the cycle frequency maximizes the chemical turnover. Our findings show under what conditions the physics of wet-dry cycles could have accelerated chemical reactions in prebiotic soups, similar to enzymes in living cells.

BP 11.32 Tue 12:30 P1

Spontaneous engulfment of microparticles by giant unilamellar vesicles — •CLÉMENT MARQUE and ANTONIO STOCCO — Institut Charles Sadron, Strasbourg, France

Giant unilamellar vesicles (GUVs) are micrometer sized concentric phospholipid bilayers, containing an aqueous medium and constituting simple and controllable model systems to study interaction mechanisms of cells. Adhesion, membrane tension and bending are involved in the engulfment of microparticles and a balance between these contributions is necessary to observe particle wrapping by a GUV membrane. In this context, we mimic the particle endocytosis process by using two types of (1 - 2 microns diameter) colloids interacting with GUVs: uniform silica microparticles and Janus microparticles, half coated with gold nanoparticles (10 - 100 nm) and fabricated by a bottom-up microfluidic self-assembly approach. For this purpose, we aim at controlling particle engulfment in absence of any applied external force. By tuning only membrane properties, we define the critical parameters to observe spontaneous engulfment of microparticles by GUVs. We focus our attention on membrane tension, membrane spontaneous curvature and lipid composition. Membrane spontaneous curvature is tuned by addition of salt, adsorbing onto the outer bilayer surface. Membrane composition is adjusted, as well, to tune lipid fluidity, and membrane surface charge. Finally, Janus microparticle-vesicle interaction will be investigated in out of equilibrium conditions when microparticles are able to self-propel and impart an effective force on the membrane by light exploiting the photothermal properties of gold nanoparticles.

BP 11.33 Tue 12:30 P1

Impact of biomolecular condensates on endocytosis — •TYLER HARMON¹, MAX FERRIN², and FRANK JÜLICHER³ — ¹Leibniz Institute for Polymer Research, Dresden, Germany — ²University of California, Berkeley, USA — ³Max Planck Institute for the Physics of Complex Systems

Endocytosis is a mechanism that cells use to import material from outside the cell without allowing it immediate access to the cytoplasm. This process involves a section of a cell membrane that is folded inward and then separated into a membrane coated sphere containing the cargo called a vesicle. The process involves recruiting many different protein components to the membrane. We model this recruitment as the formation of a small droplet (biomolecular condensate) located on the membrane. We show using a theoretical model that the presence of a droplet has two major impacts. It creates an additional barrier to initializing endocytosis and it accelerates the process once started. Importantly, the magnitude of this barrier is reduced as droplets get larger. Taken together, droplets are ideal for improving the robustness of endocytosis. It provides a natural checkpoint where cells can ensure they are ready to proceed with endocytosis and, once started, helps ensure that it doesn't stop halfway.

BP 11.34 Tue 12:30 P1

Investigation of thermal fluctuations and elastic properties of lipid bilayers via molecular dynamics simulations — •CLARA RICKHOFF, AZADEH ALAVIZARGAR, and ANDREAS HEUER — Institute of Physical Chemistry, University Münster, Münster, Germany

As cell membranes consist to a large part of a lipid bilayer and are essential for living cells by forming a barrier between different compartments of cells, which needs to be stable on the one hand but also ductile for processes like cell division on the other hand, the mechanical properties of lipid bilayers are of interest for a better understanding of the behaviour of cell membranes. One important quantity is the bending modulus, which can be extracted from the thermal fluctuation of the bilayer in an equilibrium state and thus from molecular dynamics simulations (MD simulations) and generally can be, due to similar length and time scales, also compared to neutron spin echo spectroscopy (NSE).

In this work, we first performed atomistic MD simulations on a pure DMPC-system and a DPPC-system in order to compare the resulting bending modulus and effective bending modulus with available data from literature. Those simulations were then compared with the results of coarse-grained MD-simulations

(CG-simulations), which offer the possibility to examine larger systems and also investigate the impact of transmembrane domains on those quantities.

BP 11.35 Tue 12:30 P1

phospholipids diffusion on the surface of model lipid droplets — •SHIMA ASFIA, RALF SEEMANN, and JEAN-BAPTISTE FLEURY — Universität des Saarlandes, Experimental Physics and Center for Biophysics, 66123 Saarbrücken, Germany
Lipid droplets (LD) are organelles localized in the membrane of the Endoplasmic Reticulum (ER) that play an important role in metabolic functions. Many studies have focused on the biophysical properties of these LDs. However, despite numerous efforts, we are lacking information on the mobility of phospholipids on the LDs surface, although they may play a key role in the protein distribution. In this article, we developed a microfluidic setup that allows the formation of a triolein*buffer interface decorated with a phospholipid monolayer. Using this setup, we measured the motility of phospholipid molecules by performing Fluorescent Recovery After Photobleaching (FRAP) experiments for different lipidic compositions. The results of the FRAP measurements reveal that the motility of phospholipids is controlled by the monolayer packing decorating the interface [1].

[1]S. Asfia, R. Seemann and J-B. Fleury, BBA-Biomembranes, 1865, 1 (2023).

BP 11.36 Tue 12:30 P1

SAXS measurements during polychromatic illumination of photoswitching in azobenzene lipid vesicles — •MATTHIAS LÖSCHE¹, BENEDIKT BAUMGARTNER², BENJAMIN AJANOVIC¹, OLIVER THORN-SESHOLD², and BERT NICKEL¹ — ¹Faculty of Physics and CeNS, Ludwig-Maximilians-Universität München, Geschwister-Scholl-Platz 1, Munich 80539, Germany — ²Department of Pharmacy, Ludwig-Maximilians-Universität München, Butenandtstraße 5-13, Munich 81377, Germany

Photoswitchable molecules are envisioned to be used in the field of nanomedicine. Here we study photoswitchable azobenzene lipids which switch to predominantly cis-state at 365 nm wavelength illumination and to trans-state at 465 nm illumination. The conformational change of the lipid induces different vesicle membrane thicknesses, which can be read out by small-angle x-ray scattering, as established by us before. What is not yet known is how azobenzene lipid vesicles behave when irradiated at other wavelengths. We illuminate lipid vesicles with 16 different wavelengths (generated by high-power LEDs) which cover the whole visible light region. We follow the kinetics of the switching process by SAXS. This establishes an action spectrum that correlates the different photostationary states with illumination wavelength.

BP 11.37 Tue 12:30 P1

Two-photon 3D laser printing inside synthetic cells — •TOBIAS ABELE^{1,2}, TOBIAS MESSER³, KEVIN JAHNKE^{1,2}, MARC HIPPLER³, MARTIN BASTMEYER³, MARTIN WEGENER³, and KERSTIN GÖPFRICH^{1,2} — ¹Max Planck Institute for Medical Research, Heidelberg, Germany — ²Heidelberg University, Heidelberg, Germany — ³Karlsruhe Institute of Technology, Karlsruhe, Germany

Towards the ambitious goal of manufacturing synthetic cells from the bottom up, various cellular components have already been reconstituted inside of lipid vesicles. However, the deterministic positioning of these components inside the compartment has remained elusive. Here, by using two-photon 3D laser printing, 2D and 3D hydrogel architectures were manufactured with high precision and nearly arbitrary shape inside of preformed giant unilamellar lipid vesicles (GUVs). The required water-soluble photoresist is brought into the GUVs by diffusion in a single mixing step. Crucially, femtosecond two-photon printing inside the compartment does not destroy the GUVs. Beyond this proof-of-principle demonstration, early functional architectures were realized. In particular, a transmembrane structure acting as a pore was 3D printed, thereby allowing for the transport of biological cargo, including DNA, into the synthetic compartment. These experiments show that two-photon 3D laser microprinting can be an important addition to the existing toolbox of synthetic biology.

BP 11.38 Tue 12:30 P1

Self-patterning of polyelectrolyte multilayer films: the roles of PSS molecular weight, the top layer, and post-preparation treatment — AMIR AZINFAR and •CHRISTIANE A. HELM — Institute of Physics, University of Greifswald, Germany

The self-patterning of thin films is relevant both for fundamental research and applications. We investigate polyelectrolyte multilayer films made from poly(diallyldimethylammonium) and poly(styrene sulfonate) (PDADMA/PSS). Various PSS with low molecular weight were used. Invariably, the film thickness increases exponentially with the number of deposited PDADMA/PSS bilayers. The separation and height of the domains increase significantly with each deposited PDADMA/PSS bilayer, as AFM images show. At the end of the exponential growth regime, either a parabolic (and then a linear) or a linear growth regime follows, depending on the selected PSS molecular weight. In the non-exponential growth regimes, the domain separation changes less during film growth than in the exponential growth regime.

PSS is more strongly bound to the film than PDADMA. PSS-terminated films show the same domain distance in water and air. However, when PDADMA-

terminated films are dried, the domain distance in the air increases while the domain height decreases, causing a reduction in total area. In the air, the surface energy is greater than in water, and a highly textured surface costs a lot of energy. We propose the changed surface pattern is attributable to energy minimization. Furthermore, the domains are stable when exposed to 1 M NaCl solution but shrink in 2 M NaCl.

BP 11.39 Tue 12:30 P1

Membranes with large phospholipid asymmetries — •MARTIN GIRARD — Max-Planck-Institut für Polymerforschung, Ackermannweg 10, 55128 Mainz
Plasma membranes in cells are asymmetric, an observation that dates 40 years. Recent observations suggest that these membranes present large lipid number asymmetries, with almost twice as many phospholipids on one of the leaflet than the other. Simulations provide an excellent avenue to probe behavior of these membranes. Here, I discuss the behavior of such membranes, in particular with respect to chemical asymmetries in the membrane. The work required to establish the phospholipid number asymmetry is also discussed, a quantity that is directly related to the work done on lipids by the so-called flippases and floppases proteins responsible for asymmetry homeostasis.

BP 11.40 Tue 12:30 P1

Wetting-effects of liquid-liquid condensates on lipid membranes — CHAE YEON KANG, YOOHYUN CHANG, and •KATJA ZIESKE — Max Planck Institute for the Science of Light, Erlangen

Liquid-liquid condensates are supramolecular assemblies of proteins and RNA molecules and have been studied extensively, due to their ability to spatially structure cells and to spatially confine biological reactions. However, little is known about the interactions of liquid-liquid condensates with lipid membranes and the consequences of these interactions on cellular length scales.

Here, we used a cell-free bottom-up approach to reconstitute liquid-liquid condensates at lipid membranes. Our results demonstrate how lipid membranes and liquid-liquid condensates interact under various experimental conditions and point towards an important role of wetting-effects in intracellular organization.

BP 11.41 Tue 12:30 P1

A preparative mass spectrometer to deposit intact large native protein complexes — •PAUL FREMDLING¹, TIM K. ESSER¹, BODHISATTWA SAHA¹, ALEXANDER A. MAKAROV^{2,3}, KYLE L. FORT², MARIA REINHARDT-SZYBA², JOSEPH GAULT¹, and STEPHAN RAUSCHENBACH^{1,4} — ¹Chemistry Research Laboratory, University of Oxford, 12 Mansfield Road, Oxford OX1 3TA, UK — ²Thermo Fisher Scientific, Bremen, 28199, D — ³Bijvoet Center for Biomolecular Research, University of Utrecht, Padualaan 8, 3584 CH Utrecht, NL — ⁴MPI for Solid State Research, Heisenbergstrasse 1, Stuttgart, 70569, D

Electrospray ion-beam deposition (ES-IBD) is a tool to study structure and reactivity of nonvolatile molecules. It ionises molecules gently, purifies and deposits them onto a substrate. In combination with imaging techniques, direct structural information can be obtained.

There are only a small number of custom ES-IBD instruments worldwide, with no commercial ones. We present a module that adds ion-beam deposition capabilities to a commercial MS (Thermo Scientific™ Q Exactive™ UHMR).

We characterise beam intensity, landing-energy control, and deposition spot size for a broad range of molecules. In combination with atomic force microscopy (AFM) and transmission electron microscopy (TEM), we distinguish near-native from unfolded proteins and show retention of native shape of protein assemblies after dehydration and deposition. Further, we use an enzymatic assay to quantify activity of a non-covalent protein complex after deposition on a dry surface.

BP 11.42 Tue 12:30 P1

Tracking the Electron Transfer Cascade in European Robin Cryptochrome 4 Mutants — •DANIEL TIMMER¹, ANDERS FREDERIKSEN¹, DANIEL C. LÜNEMANN¹, ANITTA R. THOMAS¹, JINGJING XU¹, RABEA BARTÖLKE¹, JESSICA SCHMIDT¹, TOMAS KUBAR², ANTONIETTA DE SIO¹, ILIA A. SOLOV'YOV¹, HENRIK MOURITSEN¹, and CHRISTOPH LIENAU¹ — ¹University of Oldenburg, Germany — ²Karlsruhe Institute of Technology, Germany

The ability of some birds to sense weak earth-strength magnetic fields for navigation is thought to rely on the quantum mechanical radical pair (RP) mechanism [1]. Here, cryptochrome proteins, located in the birds retina, can undergo consecutive electron transfers after blue light photo-excitation of a bound flavin chromophore with a nearby chain of four tryptophan amino acid residues. This leads to the formation of a long-lived RP, which can interconvert between the singlet and triplet state due to hyperfine interactions. Spin-selective signaling state populations can eventually be influenced via a weak external magnetic field [1]. Using pump-probe spectroscopy on wildtype cryptochrome protein of the European robin and a series of mutants, where we selectively blocked the electron transfer along the chain with redox-inactive phenylalanine, we are able to track RP formation step by step and extract the electron transfer times and yields [1]. Our experimental study is supported by theoretical modeling of the electron

transfer cascade using a mixed quantum mechanical/molecular mechanical approach. [1]: Xu, Jingjing, et al., Nature 594.7864, 535-540 (2021). [2]: Timmer, Daniel, et al., arXiv preprint arXiv:2205.10393 (2022).

BP 11.43 Tue 12:30 P1

Nonlinear Transmission of FUS Protein Solution at 0.5 THz — •QUANG MINH THAI¹, IGOR ILYAKOV², MANTHAN RAJ¹, DANIEL DORNBUSCH², ATIQA ARSHAD², THALES DE OLIVEIRA², MARCUS JAHNEL^{1,3}, JAN-CHRISTOPH DEINERT², ALEXEY PONOMARYOV², SERGEY KOVALEV², and ELLEN M. ADAMS^{1,2} — ¹Cluster of Excellence Physics of Life (PoL), TU Dresden, Dresden, Germany — ²Helmholtz-Zentrum Dresden-Rossendorf (HZDR), Dresden, Germany — ³Center for Molecular and Cellular Bioengineering, Biotechnology Center, TU Dresden, Dresden, Germany

Water possesses strong absorption in the THz range due to intermolecular vibrational modes in a network of hydrogen-bonded water molecules. Its THz response is also sensitive to the coupling of water to other molecules, i.e. the hydration shell of a protein. Probing the nonlinear properties of hydration water can provide insight into protein solvent dynamics, and in the case of intrinsically disordered proteins, its subsequent role in the liquid-liquid phase separation (LLPS). Such characterization at low THz frequencies (< 3 THz) remains yet limited, due to the scarcity of brilliant light sources in this range. Here, we present the nonlinear characterization at 0.5 THz of water and FUS protein solution in a liquid transmission cell, using a THz time-domain spectroscopy (THz-TDS) setup with the TELBE free electron laser source at HZDR. Our results show that the nonlinear absorption and refractive indices of the FUS protein solution differ from that of water, indicating a perturbed hydrogen bonding network.

BP 11.44 Tue 12:30 P1

Bio-SAXS of Single-Stranded DNA-Binding Proteins: Radiation Protection by the Compatible Solute Ectoine — •MARC BENJAMIN HAHN¹, DOROTHEA C. HALLIER^{1,2,3}, GLEN J. SMALES^{2,3}, and HARALD SEITZ¹ — ¹Bundesanstalt für Materialforschung und prüfung (BAM), 12205 Berlin, Germany — ²Fraunhofer Institute for Cell Therapy and Immunology, Branch Bioanalytics and Bioprocesses (IZI-BB), 14476 Potsdam, Germany — ³Universität Potsdam, Institut für Biochemie und Biologie, 14476 Potsdam, Germany

Small-angle X-ray scattering (SAXS) can be used for structural determination of biological macromolecules and polymers in their native states. To improve the reliability of such experiments, the reduction of radiation damage occurring from exposure to X-rays is needed. One method, is the use of scavenger molecules that protect macromolecules against radicals produced by radiation exposure. In this study we investigate the feasibility to apply the compatible solute, osmolyte and radiation protector Ectoine (THP(B)) as a scavenger throughout SAXS measurements of single-stranded DNA-binding protein Gene-V Protein (G5P/GVP). Therefore we monitor the radiation induced changes of G5P during bio-SAXS. The resulting microscopic energy-damage relation was determined by particle scattering simulations with TOPAS/Geant4. The results are interpreted in terms of radical scavenging as well as post-irradiation effects, related to preferential-exclusion from the protein surface. Thus, Ectoine provides an non-disturbing way to improve structure-determination of proteins via bio-SAXS in future studies.

BP 11.45 Tue 12:30 P1

Molecular Dynamics Simulations of Large Proteins in Vacuum and during Surface Adsorption — •ALPCAN ÖNÜR^{1,2}, TIM K. ESSER², CHRISTOPH GLOBISCH¹, CHRISTINE PETER¹, and STEPHAN RAUSCHENBACH^{2,3} — ¹Departement of Chemistry, University of Konstanz, Konstanz, Germany — ²Departement of Chemistry, University of Oxford, Oxford, UK — ³Max Planck Institute for Solid State Research, Stuttgart, Germany

Knowledge of protein structures is crucial for biological and medical research in for instance metabolism, drug discovery and diseases. Cryogenic electron microscopy (cryo-EM) recently became a dominant method of protein structure determination. One of the main challenges with cryo-EM measurements lies in the protein preparation with many pitfalls which can destroy the native structure of proteins due to surface effects. The combination of electrospray ion beam deposition (ESIBD) and native mass-spectrometry creates chemically selective cryo-EM samples. This method has the potential to overcome many conventional cryo-EM sample preparations. However, the native ESIBD-CryoEM approach prepares and images dehydrated gas-phase proteins, which have collided with a surface. This can affect the native protein fold and hence influence the cryo-EM obtained structure, for instance reducing the resolution or inducing deviations. In this work we will present first steps towards understanding structural changes of proteins in electrospray ion beams, after surface interactions, and during dehydration in ultra-high vacuum by utilizing molecular dynamics simulations.

BP 11.46 Tue 12:30 P1

Dynamics of Tau protein studied with X-ray photon correlation spectroscopy (XPCS) — •SEBASTIAN RETZBACH¹, NIMMI DAS ANTHUPARAMBIL^{2,5}, ANITA GIRELLI³, KEVIN POUNOT⁴, SONJA TIMMERMANN², MAXIMILIAN D. SENFT¹, MARVIN KOWALSKI², MICHELLE DARGASZ², NAFISA BEGAM¹, FABIAN WESTERMEIER⁵, ANASTASIA RAGULSKAYA¹, FAJUN ZHANG¹, CHRISTIAN GUTT², and FRANK SCHREIBER¹ — ¹Universität Tübingen, Germany — ²Universität Siegen, Germany — ³Stockholm University, Sweden — ⁴ESRF, Grenoble, France — ⁵DESY, Hamburg, Germany

Proteins exhibit a rich phase behavior, including the formation of amyloid fibrils, which have been linked to many diseases, e.g. Alzheimer's disease. Understanding the dynamics and the structural changes of the Alzheimer associated, amyloid fibril forming, protein Tau. After inducing the fibrillation with Heparin, at a Tau concentration of 100 mg/ml, and waiting for 22 hours, a fractal structure with a characteristic length of around 200 nm has evolved. The dynamics exhibited ballistic behavior that show similarities to the dynamics in gels.

[1] A. Girelli et al. (2021) Phys Rev Lett 126, 138004.

BP 11.47 Tue 12:30 P1

Upconversion-nanoparticle optical trapping for ultraresolution motor protein measurements — •ALEKSANDR KOSTAREV and ERIK SCHÄFFER — Universität Tübingen, ZMBP, Tübingen, Deutschland

Molecular machines are essential for many cellular processes. For example, kinesin motor proteins transport cargo along microtubule cytoskeletal filaments. The stepping and force generation of single motors can be measured using optical tweezers. However, the spatiotemporal resolution achieved with common optical tweezers probes is insufficient to detect fast steps in particular at low forces. To improve the resolution, nanoparticles are required as optical tweezers probes. Upconversion nanoparticles trapped near resonance of their electric susceptibility have the highest reported trapping efficiency and are chemically stable. Yet, they have not been used for biophysical measurements. To use them, we have integrated a near-resonance trapping laser, detector, and laser steering system in an optical tweezers system. Calibration measurements show that the upconversion nanoparticles indeed have a very high trapping efficiency when trapped with a laser near resonance compared to off-resonance trapping. Once functionalized with the motors, trapping experiments will shed light on how weak kinesin motors step and diffuse on microtubules. In the long term, upconversion-nanoparticle optical trapping will improve the spatiotemporal resolution of optical tweezers and shed light on the working mechanism of a wide range of molecular machines.

BP 11.48 Tue 12:30 P1

Diffusive anchorage of molecular motors facilitates robust cargo transport — •RACHELE CATALANO¹, GINA A. MONZON MONZON^{1,2}, RAHUL GROVER¹, LUDGER SANTEN², and STEFAN DIEZ^{1,3} — ¹B CUBE - Center for Molecular Bioengineering, TU Dresden — ²Center for Biophysics, Department of Physics, Saarland University — ³Cluster of Excellence Physics of Life, TU Dresden

Intracellular transport of vesicles and organelles is carried out by teams of molecular motor proteins moving cargo along polar intracellular filaments. Multiple motors are coupled to each other via a fluid membrane that allows motors to diffuse along the cargo surface. How the number of involved motors and the diffusivity of motors on the cargo surface influence such transport is not well understood. Here we use a combined experimental and theoretical approach to investigate the impact of motor number and motor-cargo interaction on the motility parameters of kinesin-driven cargoes moving along microtubules. We found that the velocities of cargoes with highly diffusive motors decrease with an increase in motor number. Cargoes with non-diffusively bound motors moved with velocities independent of the motor number. Numerical simulations reveal that diffusive motor-cargo binding results in higher numbers of microtubule-bound motors, which increases steric hindrance associated with cargo slow down. Additionally, the higher number of microtubule bound motors enhances cargo run length and increases transport robustness. Our results demonstrate that loose mechanical coupling of multiple motors by diffusive membrane anchorage leads to robust transport at the cost of lower velocity.

BP 11.49 Tue 12:30 P1

Amplified self-stabilization of cell adhesions under load — •JULIA MÜLLNER^{1,2} and BENEDIKT SABASS^{1,2} — ¹Institute for Infectious Diseases and Zoonoses, Department of Veterinary Sciences, LMU München — ²Department of Physics, LMU München

Cell adhesion is crucial for the structural organization of living organisms. Experimentally, it was found that planar cell-matrix adhesions respond to an increase in shear force by growing in size in order to maintain structural stability. As part of this process, the protein vinculin binds to force-activated binding sites

of talin and to actin, thereby strengthening the cluster. However, it is not fully understood how mechanical forces induce adhesion molecules to drive adhesion growth. We present a minimalist model to explore the dynamics of an adhesion cluster under shear force. The system is reduced to a single adapter molecule species (talin) that can undergo conformational changes when being stretched. As in an open system, molecules are exchanged between a reservoir and the adhesion cluster. To account for adhesion growth upon molecule unfolding, we expand the reservoir rate to be proportional to the number of unfolded molecules. Simulation results show that the number of adhesion bonds rises with increasing shear force, as seen in experiments. A state diagram is constructed, delineating regimes of adhesion stabilization from unbounded growth and adhesion rupture. An analytical mean-field model yields solutions that are in good agreement with the simulation results. Overall, we describe and characterize a mechanism that amplifies self-stabilization of cellular adhesions under load.

BP 11.50 Tue 12:30 P1

Is sensory adaptation generally limited by the energy-speed-accuracy trade-off? — •VANSI KHARBANDA^{1,2} and BENEDIKT SABASS^{1,2} — ¹Institute for Infectious Diseases and Zoonoses, Department of Veterinary Sciences, LMU München — ²Department of Physics, LMU München

Sensory adaptation is vital to all living organisms. An adaptive sensory system can be modelled as a stochastic, nonlinear feedback network. Using a generic framework, we study the accuracy of adaptive mechanisms and its energetic cost. Recently, it has been suggested that the steady-state dissipation rate associated to maintenance of an adaptive state increases logarithmically with the adaptation accuracy. We present results that demonstrate that this logarithmic scaling does not hold generally, but appears to be linear when the state of the system is close to the phase-space boundaries. Our numerical results also suggest that boundaries in the phase space of system variables limit the capacity of the system to dissipate. Moreover, we conjecture a new empirical expression relating the steady-state dissipation rate and the strength of the input signal if the state lies in the vicinity of the boundaries. Finally, the combined adaptation accuracy of two linearly coupled systems is studied. We show that a coupling of the outputs of the systems deteriorates the overall adaptation accuracy while the associated energy cost is also reduced. In contrast, a coupling of the control elements reduces the dissipation rate without compromising on the adaptation accuracy.

BP 11.51 Tue 12:30 P1

Three-compartment model describes coarsening of biomolecular condensates in Meiosis — •MARCEL ERNST and DAVID ZWICKER — Max Planck Institute for Dynamics and Self-Organization, Göttingen, Germany

During meiosis, crossovers between the female and male chromosomes mix genetic information. Experimental observations consistently reveal two key findings: First, the number of crossovers per chromosome is at least one and usually small, between one and three. Second, there is crossover interference, which prevents nearby crossovers on a single chromosome. A recently suggested model proposes biomolecular condensates that coarsen by exchanging material along chromosomes to determine crossovers. We extend this model by including the exchange with the surrounding nucleoplasm, leading to a three-compartment model. We validate the model by comparing numerical results with various experimental data in Arabidopsis. In particular, we explain the behavior of a mutant without the axial structure linking the chromosome pairs. Moreover, we derive scaling laws, analogous to Lifshitz-Slyozov-Wagner theory, predicting the final number of crossovers, and their spatial structure as a function of coarsening time, chromosome length, and the initial amount of material. In summary, our model reveals how meiotic crossovers are regulated in wild-type and in mutants.

BP 11.52 Tue 12:30 P1

Investigation on the learning ability of the single-celled slime mould *P. polycephalum* — •ADRIAN BÜCHL, LISA SCHICK, and KAREN ALIM — School of Natural Sciences, Technical University of Munich, Germany

The slime mould *Physarum polycephalum* is well known for its ability to store information and perform complex problem-solving despite being just a single, gigantic, network-shaped cell. Yet, can we consider such complex behaviour learning? Using bright-field microscopy observations we investigate how *P. polycephalum* networks react to repetitive negative blue light stimuli. We vary stimuli duration and the concentration of the growth medium in the substrate to probe how training time and migration speed impact *P. polycephalum*'s ability to follow trained behaviour.

BP 11.53 Tue 12:30 P1

Can iron-phthalocyanines, Fe-Pc, on CrI3 imitate active site of hemoglobin? — •CIHAN BACAŞIZ and MARIA FYTA — Computational Biotechnology, RWTH Aachen University, Aachen, Germany

The metallo-phthalocyanines (M-Pc) molecules are studied for their chemical, magnetic, and optoelectronic properties. They can function in a wide range of applications, such as gas sensors, field effect transistors, organic light-emitting diodes, and data storage devices. More specifically, the core of iron-phthalocyanines (Fe-Pc) resembles structurally the active site of hemoglobin

(heme), which is responsible of holding the oxygen and carbon dioxide. Motivated by this potential, we have studied the oxygen-capture and -release properties of Fe-Pc on top of magnetic monolayer CrI₃ using first-principle simulations. The interplay between the magnetic properties of Fe-Pc on CrI₃ and its chemical activity are investigated. It is found that the surface effects on the molecule accompanied with the magnetic interactions between Fe and Cr atoms can be used to manipulate - even control - the oxygen capture-release properties of Fe-Pc.

BP 11.54 Tue 12:30 P1

Band formation of red blood cells by density gradient centrifugation — •LUCA DAVID HASTENTEUFEL, FELIX MILAN MAURER, and CHRISTIAN WAGNER — Experimentalphysik, Universität des Saarlandes, Saarbrücken

Percoll is a commercial density medium consisting of coated silica particles, which show a non-toxicity to cells and low surface charge. Nowadays, Percoll is the standard medium for density separation of erythrocytes, leukocytes and other subcellular particles. The distribution of red blood cells after centrifugation in a self-forming Percoll gradient is characterized by a heterogeneous structure of discrete bands. We established a one dimensional particle model and a set of experiments to show that band formation is caused by aggregation. We also developed a continuum model describing the development of the RBC volumetric density under influence of a pair interaction. It shows also discrete solutions in the shape of band patterns. Understanding the band patterns gives information on the aggregation energy and disease severeness.

BP 11.55 Tue 12:30 P1

Exploiting Onsager regression in passive measurements to reveal active mechanics of living systems — TILL MUENKER, GABRIEL KNOTZ, MATTHIAS KRÜGER, and •TIMO BETZ — Faculty of Physics, Georg-August-University Göttingen

Understanding life is arguably among the most complex scientific problems faced in modern research. From a physics perspective, living systems are complex dynamic entities that operate far from thermodynamic equilibrium. This active, non-equilibrium behaviour, with its constant hunger for energy, allows life to overcome the dispersing forces of entropy, and hence drives cellular organisation and dynamics at the micrometer scale. Unfortunately, most analysis methods provided by the powerful toolbox of statistical mechanics cannot be used in such non-equilibrium situations, forcing researchers to use sophisticated and often invasive approaches to study the mechanistic processes inside living organisms. Inspired by Onsager's regression hypothesis, we introduce here a Mean Back Relaxation (MBR) observable, which detects active motion in purely passive measurements of particle fluctuations. The MBR, which is based on three point probabilities, is theoretically and experimentally shown to exhibit markers of non-equilibrium, i.e., of detailed balance breaking dynamics. We furthermore observe an astonishing relation between the MBR and the effective non-equilibrium energy in living cellular systems. This is used to successfully predict the viscoelastic response function and the complex shear modulus from a purely passive approach, hence opening the door for rapid and simple passive mechanics measurements even in active systems.

BP 11.56 Tue 12:30 P1

Theory of rheology and aging of protein condensates — •RYOTA TAKAKI¹, LOUISE JAWERTH², MARKO POPOVIC¹, and FRANK JÜLICHER¹ — ¹Max Planck Institute for the Physics of Complex Systems — ²Leiden University

Biological polymeric materials form liquid droplets through liquid-liquid phase separation, referred to as biological condensates. Although the material properties of biological condensates are deemed to play essential roles in cellular functions, quantitative studies of condensates' rheology became available very recently. Particularly the experiments found the glass-like material property of condensates, showing slow relaxation, termed "aging" in the glass field. In this study, we develop a rheological model of biological condensates from the physical pictures: diffusion and stochastic binding of proteins inside condensates. We obtain the constitutive equation for the material property of protein condensates showing aging behavior observed in experiments. We elucidate how aging manifests in the experimental observations in microrheology, both in active and passive rheology. We develop a novel method for active rheology to compute the time-dependent property of aging materials. We derive generalized fluctuation-response relations to bridge the mean squared displacement of diffusing elements inside aging Maxwell fluid to the time-dependent material properties, which can be used in passive rheology.

BP 11.57 Tue 12:30 P1

Mitochondrial dynamics control cellular anti-viral responses in the innate immune system — •FELIX J. MEIGEL¹ and STEFFEN RULANDS^{2,1,3} — ¹MPI for the Physics of Complex Systems, Dresden, Germany — ²Arnold Sommerfeld Center for Theoretical Physics, Department of Physics, Ludwig-Maximilians-Universität, München, Germany — ³Center for Systems Biology Dresden, Germany

The inflammation response of mammalian cells to infection with RNA viruses (e.g. coronaviruses or influenza A) is mediated by the signaling pathway around

the protein MAVS. For an efficient inflammation response, MAVS proteins need to form large homo-oligomers on the mitochondrial membrane. Here, we discuss how mitochondrial fusion and fission assists the formation of large membrane-bound protein aggregates by inducing density fluctuations among mitochondria. We demonstrate how the dynamic compartmentalization of the protein aggregation dynamics by steady organelle fusion and fission qualitatively alters the extreme value statistics of the aggregate size distribution beyond a limit set by the Vigil-Ziff criterion. We develop a thermodynamic framework, that allows us to assess under which conditions dynamic compartmentalization affects the aggregate size distribution and facilitates the formation of large aggregates. In this work, we not only emphasize the importance of mitochondrial dynamics for efficient immune responses but also introduce a framework to discuss the non-equilibrium thermodynamics of multi-scale systems in the context of dynamic compartmentalization.

BP 11.58 Tue 12:30 P1

Monodominance in tropical forests: modelling the influences of biological mechanisms on cluster formation — •JULIA MEYER¹, PIA BACKMANN², and ALEXANDER K. HARTMANN¹ — ¹Institute of Physics, University of Oldenburg, Germany — ²University of Leipzig, Germany

Monodominance in tropical forests describes the formation of patches dominated by a single tree species, i.e., *clusters*, in an otherwise highly species-rich forest. The reasons for its emergence are not fully understood yet, probably multiple causes exist [1], depending on the specific forest.

Recently, a statistical-mechanics model was introduced [2] which allowed for an analysis of the cluster formation process. A phase transition between a non-percolating and a monodominated percolating phase could be observed, and analyzed by finite-size scaling techniques. The properties of this system, such as the morphology of clusters, are quite distinct from standard percolation. Here, we numerically [3] further investigate extensions of the model by including different biological mechanisms, like shade tolerance, that are believed to potentially favor monodominance. We analyze how the properties of this phase transition change for the modified model.

[1] K. S.-H. Peh, S.L. Lewis, and J. Lloyd, *J. Ecol.* **99**, 891 (2011).

[2] M. Kazmierczak et al., *J. R. Soc. Interface* **13**, 20160123 (2016).

[3] A.K. Hartmann, *Big practical Guide to Computer Simulations* (World Scientific, 2015).

BP 11.59 Tue 12:30 P1

Phase segregation and microemulsion module of DNA oligo based nano-motifs — •RAKESH CHATTERJEE¹, MAI P. TRAN², YANNIK DREHER², JULIUS FICHTLER², KEVIN JAHNKE², XENIA TSCHURIKOW³, AARON GADZEKO³, LENNART HILBERT³, KERSTIN GÖPFRICH², and VASILY ZABURDAEV¹ — ¹Friedrich-Alexander- Universität Erlangen-Nürnberg, Germany — ²Max Planck Institute for Medical Research, Heidelberg, Germany — ³Karlsruhe Institute of Technology, Karlsruhe, Germany

DNA can be used as a programmable material by designing the base sequences to drive self-assembly. The technology of forming macromolecular droplets through sequence design of DNA-like biopolymers could provide insights into the mechanisms of liquid-like droplet formation via liquid-liquid phase separation. In two experimental setups we study how the process of phase segregation of two motifs is affected by confinement and how the dispersal of the aggregated phase is controlled by addition of amphiphiles. To quantify this process theoretically we use a versatile lattice-gas model in two dimensions with cross-shaped particles that can closely mimic the shape of synthetic nano-motifs and their interaction valencies as well as account for their translational and rotational diffusion. With our numerical results we can recapitulate the observed effects of the slowing down phase segregation in confinement and the dose response of the aggregate dispersal by addition of amphiphile components.

BP 11.60 Tue 12:30 P1

Delay time of erythrocyte sedimentation rate — •JAN FISCHER, THOMAS JOHN, LARS KAESTNER, CHRISTIAN WAGNER, and ALEXIS DARRAS — Experimental Physics, Saarland University; D-66123 Saarbrücken, Germany

In many suspensions of microscopic particles, ranging from cosmetic creams to food dough to oil paints, the suspended state is only transient. Indeed, unless the densities of particles and fluid are perfectly matched, gravity eventually separates the two phases. In many practical cases with a high concentration of particles, this separation happens as a sudden "collapse" after a long period (sometimes months or years) where no separation was observed. This phenomenon actually defines the life span of many practical products.

Our group recently demonstrated that red blood cells (aka erythrocytes) follow the same behavior on short time scales. This has practical application, since their average sedimentation rate is used as a medical parameter. However, while it is known that the collapse delay time has an intrinsic random component for thermal suspensions, it is not clear whether it is the case for red cells, which are mainly athermal.

For the first time, we characterized the variability of the delay time for a given suspension of red blood cells. Moreover, the influence of various parameters

unique to red blood cells, such as cell shape and rigidity, has been studied and correlated with the microstructure of the red blood cells aggregates.

BP 11.61 Tue 12:30 P1

Modeling of protein condensates — •KATHRIN HERTÄG and JOSHUA ROBINSON — ITP4, Stuttgart, Deutschland

Phase separation in systems driven away from thermal equilibrium has recently attracted substantial interest, in particular for motile active matter and protein condensates in cells. The latter are characterized by a finite size that can be stable *in vivo* over the whole cell cycle while *in vitro* the same proteins undergo conventional phase separation that coarsens towards a fully phase-separated state. The physical processes that control the condensate size are largely unexplored. Here we apply methods from active liquid theory to study and assess possible mechanisms.

BP 11.62 Tue 12:30 P1

Cumulative refractoriness in Calcium signaling — •LUKAS RAMLOW¹, MARTIN FALCKE^{1,2}, and BENJAMIN LINDNER¹ — ¹Physics Department of Humboldt University, Berlin, Germany — ²Max Delbrück Center for Molecular Medicine, Berlin, Germany

Stochastic spiking and adaptation are two essential features of calcium signaling. The stochasticity stems from the punctate calcium release from the ER into the cytosol by IP3R channel clusters. The adaptation is due to the depletion and slow replenishment of the ER. To capture calcium spike generation, we adopt the popular stochastic adaptive integral-and-fire (IF) model from neuroscience. Our model describes i) activity of IP3R clusters and ii) dynamics of the global calcium concentrations in the cytosol and ER. Cluster activity is modeled by a Markov chain, capturing the puff. The calcium concentrations are described by a two-variable IF model driven by the puff current. While it has been known for decades that the activity of IP3R clusters is random, a method to derive the noise acting on the cytosolic calcium is lacking. We close this gap using a time scale separation to approximate the puffing current by a white Gaussian noise with analytically accessible intensity. This results in a nonlinear IF model with and multiplicative noise. Assuming fast replenishment the IF model generates a renewal spike train and we can derive analytical expressions for the mean and coefficient of variation of the interspike interval (ISI). Taking into account ER depletion, the model displays cumulative refractoriness and can be used to infer otherwise inaccessible parameters from experimental data.

BP 11.63 Tue 12:30 P1

Protein induced lipid demixing in homogeneous membranes — •PIOTR NOWAKOWSKI^{1,2}, BERND HENNING STUMPF³, ANA-SUNČANA SMITH^{1,3}, and ANNA MACIOLEK^{2,4} — ¹Institut Ruđer Bošković, Zagreb, Croatia — ²Max Planck Institute for Intelligent Systems, Stuttgart, Germany — ³Friedrich-Alexander-Universität Erlangen-Nürnberg, Erlangen, Germany — ⁴Instytut Chemii Fizycznej Polskiej Akademii Nauk, Warszawa, Poland

We study a model of a lipid bilayer membrane with two order parameters: the chemical composition described using the Gaussian model and the spatial configuration described with the elastic deformation model of a membrane with a finite thickness, or equivalently, for an adherent membrane. We assume a linear coupling between the two order parameters. Using the exact solution, we calculate the correlation functions and order parameters profiles. We also study the domains that form around inclusions on the membrane. We propose and compare several distinct ways to quantify the size of such domains. Despite of its simplicity, the model has many interesting features like Fisher-Widom line and two distinct critical regions.

BP 11.64 Tue 12:30 P1

Self-organized criticality in animal collectives — •YUNUS SEVINCHAN^{1,2}, DAVID BIERBACH^{1,3,4}, LUIS GÓMEZ-NAVA^{1,2}, JENS KRAUSE^{1,3,4}, and PAWEŁ ROMANCZUK^{1,2} — ¹Science of Intelligence, TU Berlin, Berlin, Germany — ²Institute for Theoretical Biology, HU Berlin, Berlin, Germany — ³Leibniz-Institute of Freshwater Ecology and Inland Fisheries, Berlin, Germany — ⁴Thaer-Institute, HU Berlin, Berlin, Germany

Collective biological systems – such as animal groups or neuronal networks – are presumed to operate at or near so-called critical points at which they exhibit maximal sensitivity towards environmental cues. We have studied large fish shoals of sulphur mollies (*Poecilia sulphuraria*) which perform collective diving cascades as a response to predation. We previously found these shoals to operate close to criticality, allowing near-optimal propagation of information through the collective [1]. By analyzing a large video dataset of surface waves originating as a response to bird attacks or various synthetic stimuli, we relate wave characteristics to the macroscopic state of the shoal and varying environmental contexts. These results help in better understanding the fundamental mechanisms allowing collectives to self-tune their distance to criticality and navigate the robustness-sensitivity tradeoff.

[1]: L. Gómez-Nava, RT. Lange, PP. Klamsler, J. Lukas, L. Arias-Rodriguez, D. Bierbach, J. Krause, H. Sprekeler, and P. Romanczuk: *Fish shoals maximize sensitivity towards external cues and show optimal information spread at criticality*. Nature Physics (accepted), 2022

BP 11.65 Tue 12:30 P1

Electro-thermodynamics of coacervate interfaces — •ARGHYA MAJEE¹, CHRISTOPH A. WEBER², and FRANK JÜLICHER^{1,3,4} — ¹Max Planck Institute for the Physics of Complex Systems, Dresden, Germany — ²Institute of Physics, University of Augsburg, Germany — ³Center for Systems Biology Dresden, Germany — ⁴Cluster of Excellence Physics of Life, TU Dresden, Germany

Biological condensates are assemblies of proteins and nucleic acid that provide biochemical compartments in the cell. Such condensates can form by coacervation since many condensate components are charged and condensate properties vary with salt concentration. While the thermodynamic description based on short ranged interactions is well established, a theory accounting for the role of electrostatic interactions in the presence of salt is lacking. Here, we propose an electro-thermodynamic theory of such systems taking into account the role of electrostatics. We find that two or even more charged layers can form at the interface, where charge neutrality is locally not obeyed. Depending on the values of parameters, such charge profiles and associated electrostatic potential profiles imply either reflection or attraction of single molecules diffusing across the interface. Such interface properties could also account for a varying tendency of droplets to fuse and be of relevance for chemical reactions inside biological condensates by selectively recruiting reacting components by charge.

BP 11.66 Tue 12:30 P1

Mean-field theory for fibrillar aggregation and nematic-isotropic phase separation — •KAFA ALAMEH^{1,2} and CHRISTOPH WEBER¹ — ¹Mesoscopic Physics of Life, Institute of Physics, Universitätsstr. 1, Augsburg, Germany — ²Center for Systems Biology Dresden, Pfotenhauerstr. 108, 01307 Dresden, Germany

Cells use droplet-like compartments to spatially organize their interior into sub-compartments, known as membrane-less organelles. Such organelles are liquid condensates and provide distinct physical environments for chemical processes. Recently, it has been shown that various proteins with beta-sheet structures, such as FUS, are involved in protein aggregation diseases such as ALS and Alzheimer's. Moreover, FUS-rich condensates were shown to undergo aberrant “phase transition,” leading to fibrillar, solid-like aggregates. Several theoretical studies have focused on how phase-separated compartments affect the irreversible aggregation of dilute monomers; however, the interplay between aggregation and phase separation at non-dilute conditions remains elusive. Such conditions are particularly relevant at the condensate interface, where aggregates are often nucleated and enriched. Here, we propose a mean-field theory accounting for the interplay between aggregation, condensate formation, and phase transition at condensate interfaces. We find a rich phase behavior; three coexisting phases differing in density and the degree of order: disordered-dilute, disordered-dense, and nematic-dense phases. Our theory suggests the possibility of finding ordered membrane-less organelles in regulatory pathways of neurodegenerative diseases.

BP 11.67 Tue 12:30 P1

Density fluctuation analysis of living matter — •CONRAD MÖCKEL^{1,2,3}, KYOOHYUN KIM^{1,2}, ABIN BISWAS^{1,2,4}, SIMONE REBER⁴, VASILY ZABURDAEV^{1,2,5}, and JOCHEN GUCK^{1,2,3} — ¹Max Planck Institute for the Science of Light, 91058 Erlangen, Germany — ²Max Planck Zentrum für Physik und Medizin, 91058 Erlangen, Germany — ³Department of Physics, Friedrich-Alexander-Universität Erlangen-Nürnberg, 91054 Erlangen, Germany — ⁴IRI Life Sciences, Humboldt-Universität zu Berlin, 10115 Berlin, Germany — ⁵Department of Biology, Mathematics in Life Sciences, Friedrich-Alexander-Universität Erlangen-Nürnberg, 91054 Erlangen, Germany

The characterisation of the dynamical properties of living matter plays an important role in unraveling its complexity. Here we present the combination of quantitative phase imaging with differential dynamic microscopy in order to probe and evaluate its inherent density fluctuations. By employing theoretical models, this approach allows for the determination of the time- and length scale dependent viscoelastic properties of optically transparent systems as demonstrated for high speed supernatant (HSS) *Xenopus laevis* egg extract. We find that HSS exhibits distinct dynamics at two time scales which can be explained by diffusion in a diffusing potential.

BP 11.68 Tue 12:30 P1

Optimal navigation of smart active particles in complex landscapes — •MISCHA PUTZKE and HOLGER STARK — Technische Universität Berlin, Institut für Theoretische Physik, Straße des 17. Juni 135, 10623 Berlin, Germany

The field of active matter, and in particular microswimmers, is finding more and more applications. Synthetic microswimmers are potentially used for microsurgery and the targeted transport of drugs and genes. This requires smart active particles that can process information.

The mentioned applications require the optimal navigation in complex environments where the self-propelled microswimmer only changes its orientation but not its velocity. Machine learning is often used to solve optimization problems. We employ Q-learning to train the agent to move towards a target while it receives information about the direction and distance of the target. To model the smart active particle we use Langevin dynamics.

We show that the microswimmer with its limited information is able to navigate in complex landscapes such as potential barriers and wells but also in vortical flow and find the fastest trajectories. We also show that the navigation optimization is stable against thermal fluctuations by including thermal noise in the orientation during training. For potential wells and vortical flow, it can also be observed that during training not the entire set of existing trajectories is covered by the microswimmer, thus optimal solutions can remain hidden.

BP 11.69 Tue 12:30 P1

Evaluation of nanoparticle resistance development of microorganisms — •STEFANIE SCHUBA, JULIAN SCHÜTT, JÜRGEN FASSBENDER, and DENYS MAKAROV — Helmholtz-Zentrum Dresden-Rossendorf

Over the last century, antibiotics against bacterial infections have led to increased life expectancy and quality of people worldwide. Yet the WHO has brought attention to the increasing resistance development of bacterial pathogens against antibiotics - many bacteria are already multi-resistant. In the search of alternatives to classical antibiotics, nanotechnology and nanoparticles (NP) are moving into the focus of scientific research. Particular attention is paid to the Nano-silver (Ag-NP), which has experienced an immense upswing in recent years and is used in many medical products such as wound dressings or consumer products. However, are Ag-NPs safe for health and environment? To tackle this challenge, conventional methods have been used to explore nanoparticle resistance. Conversely, these methods have proven to be limited in terms of labor, cost, and statistical power. In our work, we intend to overcome these barriers by developing a droplet-based microfluidic analytical platform as a tool to elucidate the impact and biological influence of nanoparticles on living microorganisms with high statistical evaluation and detection efficiency. This method allows the separation of bacteria into single droplets, the generation of individual bioreactors, and the screening of the bacterial metabolism in the presence of Ag-NP.

BP 11.70 Tue 12:30 P1

Traffic Slowdown by Antibiotics — •JOHANNES KEISERS, LUCA CIANDRINI, and PHILIPPE FUCHS — Centre De Structurale Biologie (CBS), Montpellier, France The transcription and translation process are amongst the most fundamental processes in biology. In both processes, the flow of RNAP or ribosomes determines the biosynthesis rate. Here, we model this flow with a unidimensional traffic model called the Totally Asymmetric Simple Exclusion Process or TASEP. In particular, we are interested in understanding the role of ribosome pausing states induced by sublethal doses of antibiotics. These pausing states give further insights in the dynamics between different antibiotics and the translation process. The final goal is to model how antibiotics change the translation rate by adding a pausing state to the ribosomes and extend the previously derived solution to the open boundary case.

BP 11.71 Tue 12:30 P1

The Influence of pegRNA Variations on Prime Editing Kinetics — •NATHALIE SCHÄFFLER¹, JULIAN GEILENKEUSER², DONG-JIUNN JEFFERY TRUONG², GIL WESTMEYER², and JOACHIM RÄDLER¹ — ¹LMU München, Deutschland — ²ISBM, Helmholtz-Zentrum München, Deutschland

A key development in recent CRISPR technology is the "Search and Replace" system, also called Prime Editing (PE). Right now, the optimization of this is an active research field, which could lead to interesting new possibilities like approaches for biocomputing. However, current studies focus primarily on end-point measurements with FACS.

In our research we compare different pegRNA variations and their editing efficiency via collective and single cell timescale measurements. We transfect a HEK293T cell line, which stably expresses a blue shifted mGreenLantern (bs-mGL), with the two PE components: pegRNA and Cas9-complex. With this, the cells gain the ability to edit their bsmGL DNA back to the original green mGL sequence. We track the fluorescence-time courses of this signal with Live-cell Imaging of Single Cell Arrays (LISCA) and use kinetic rate equations to better understand the defining processes in the timing of those edits.

This allows us to have a closer look into the kinetics of PE.

BP 11.72 Tue 12:30 P1

Steady-state operation of a cell-free genetic band-detection circuit — •ANNA C. JÄKEL, LUKAS AUFINGER, and FRIEDRICH C. SIMMEL — Technical University of Munich, Munich, Germany

Synthetic gene networks have been used extensively to explore principles of biological pattern formation as they play a decisive role during biological growth and development processes. Here, we report on a bottom-up approach to design and analyze a cell-free genetic circuit based on an incoherent feed forward loop (IFFL-2), which is expected to produce a three-stripe pattern in response to an input gradient. In our work, we first simulated the behavior of the circuit and explored relevant parameters using a genetic algorithm. We then tested our circuit in a bacterial cell-free gene expression system and found that our circuit is only functional under non-equilibrium conditions in microfluidic ring reactors, whereas it fails to perform in bulk experiments in closed reactors. Hence, we concluded that non-equilibrium conditions are of necessity to establish the double-repression cascade which was the essential element of the genetic circuit.

We used six neighboring ring reactors to establish a 'virtual' morphogen gradient by supplying the reactors with decreasing amounts of the transcription factor sigma28, corresponding to the different positions within an exponential morphogen gradient. We finally demonstrated that our IFFL-2 circuit, when operated in the microfluidic system, shows the correct gene expression response that is required for stripe-formation in a spatial context.

BP 11.73 Tue 12:30 P1

Steady-state operation of a cell-free genetic band-detection circuit — •ANNA C. JÄKEL, LUKAS AUFINGER, and FRIEDRICH C. SIMMEL — Technical University of Munich, Munich, Germany

Synthetic gene networks have been used extensively to explore principles of biological pattern formation as they play a decisive role during biological growth and development processes.

Here, we report on a bottom-up approach to design and analyze a cell-free genetic circuit based on an incoherent feed forward loop (IFFL-2), which is expected to produce a three-stripe pattern in response to an input gradient. In our work, we first simulated the behavior of the circuit and explored relevant parameters using a genetic algorithm. We then tested our circuit in a bacterial cell-free gene expression system and found that our circuit is only functional under non-equilibrium conditions in microfluidic ring reactors, whereas it fails to perform in bulk experiments in closed reactors. Hence, we concluded that non-equilibrium conditions are of necessity to establish the double-repression cascade which was the essential element of the genetic circuit. We used six neighboring ring reactors to establish a 'virtual' morphogen gradient by supplying the reactors with decreasing amounts of the transcription factor sigma28, corresponding to the different positions within an exponential morphogen gradient.

We finally demonstrated that our IFFL-2 circuit, when operated in the microfluidic system, shows the correct gene expression response that is required for stripe-formation in a spatial context.

BP 11.74 Tue 12:30 P1

A first approach for mimicking guided axon-growth by electrical circuits — •BAKR AL BEATTIE, SEBASTIAN JENDERNY, KARLHEINZ OCHS, and DENNIS MICHAELIS — Ruhr University Bochum, Chair of Digital Communication Systems, Bochum, Germany

The self-organization aspect of electrical circuits mimicking neuronal networks often only focuses on synapses. Besides the adjustment of synaptic coupling strength, the guidance of growing axons is another important principle for the biological wiring process of neurons. In particular, guidance cues determine the growth direction and thus which neurons interconnect with each other. Up to now, only mathematical models of this process exist. Our aim hence is to provide an ideal electrical circuit mimicking fundamental principles of guided axon growth. For this purpose, we use memristors in combination with sensors. Here, the sensors represent the sensing of guidance cues, while the memristors form the non-volatile signal transmission paths. We then develop a corresponding wave digital model to verify our circuit approach.

BP 11.75 Tue 12:30 P1

Mimicking axon-growth by a bio-inspired memristive circuit — SEBASTIAN JENDERNY, •BAKR AL BEATTIE, and KARLHEINZ OCHS — Ruhr University Bochum, Chair of Digital Communication Systems, Bochum, Germany

Hardware implementations of neuronal networks are already very powerful. In terms of e.g. energy efficiency, however, they are still far inferior to biological neuronal networks. For this purpose, a better understanding of the general principles that shape these networks can contribute to the development of improved electrical circuits. One principle often neglected is the growing of axons, which has, up to now, only been considered for technical abstract circuit realizations. In this context, our aim is to develop a more bio-inspired circuit model mimicking axon growth in a way that can be compared to the biological process. To this end, we utilize Morris-Lecar oscillators as axon segments and memristors for implementing the growth mechanism. A wave digital emulation then successfully verifies our circuit approach for an axon growth example taken from biology.

BP 11.76 Tue 12:30 P1

RNA Contact Prediction by Data Efficient Deep Learning — •OSKAR TAUBERT¹, FABRICE LEHR², ALINA BAZAROVA^{3,4}, CHRISTIAN FABER³, PHILIPP KNECHTGES², MARIE WEIEL^{1,4}, CHARLOTTE DEBUS^{1,4}, DANIEL COQUELIN^{1,4}, ACHIM BASERMANN², ACHIM STREIT¹, STEFAN KESSELHEIM^{3,4}, MARKUS GÖTZ^{1,4}, and ALEXANDER SCHUG³ — ¹Karlsruhe Institute of Technology, Karlsruhe, Germany — ²Deutsches Zentrum für Luft- und Raumfahrt, Köln, Germany — ³Forschungszentrum Jülich, Jülich, Germany — ⁴Helmholtz AI

On the path to full understanding of the structure-function relationship or even design of RNA, structure prediction would offer an intriguing complement to experimental efforts. Any deep learning on RNA structure, however, is hampered by the sparsity of labeled training data. Utilizing the limited data available, we here focus on predicting spatial adjacencies (*contact maps*) as a proxy for 3D

structure. We explore the space of self-supervised learning for RNA multiple sequence alignments and focus on downstream contact prediction from latent attention maps.

Boosted decision trees in particular prove an advancement in contact prediction quality that can be further enhanced by finetuning the pretrained backbone. We name our model BARNACLE. Our conceptual advance is reflected by a considerable increase of precision and other metrics for contact prediction, thus promising to decrease the sequence-structure gap for RNA.

BP 11.77 Tue 12:30 P1

Influence of Contact Map Topology on RNA Structure Prediction — •CHRISTIAN FABER and ALEXANDER SCHUG — Forschungszentrum Jülich, Germany

The available sequence data of RNA molecules have highly increased in the past years. Unfortunately, while computational power is still under exponential growth, the computer prediction quality from sequence to final structure is still inferior to the labour intensive experimental work. Therefore, various attempts have been made to improve computer generated structure predictions.

Although an end-to-end procedure has been developed for proteins in the form of AlphaFold2, such a breakthrough is not yet available for RNA molecules. The current strategy entails two steps: (i) predicting potential contacts in the form of a contact maps from evolutionary data, and (ii) simulating the molecule with a physical force field while using the contact map as restraint. However, the quality of the structure prediction crucially depends on the quality of the contact map.

Until now, only the proportion of true positive contacts was considered as a quality characteristic. We propose to also include the distribution of these con-

tacts, and have done so in our recent studies. We observed that the distribution into clusters (typical for ML) leads to poor results. Therefore, we propose a new quality criterion for contact maps that can be easily incorporated into existing ML algorithms. We have introduced this criterion into Barnacle, a recent, very strong ML algorithm especially designed for RNA contact prediction.

BP 11.78 Tue 12:30 P1

Combined cell and nanoparticle models for TOPAS to study radiation dose enhancement by Monte-Carlo based particle scattering Simulations — •MARC BENJAMIN HAHN¹ and JULIAN MATEO ZUTTA VILLATE² — ¹Bundesanstalt für Materialforschung und -prüfung, 12205 Berlin, Germany — ²Pontificia Universidad Javeriana, Bogota, Colombia

Dose enhancement by gold nanoparticles (AuNP) increases the biological effectiveness of radiation damage in biomolecules and tissue. To apply them effectively during cancer therapy their influence on the locally delivered dose has to be determined.[1] Hereby, the AuNP locations strongly influence the energy deposit in the nucleus, mitochondria, membrane and the cytosol of the targeted cells. In this work, two newly developed continuous and discrete-geometric models for simulations of AuNP in cells are presented.[2] We apply the presented models in Monte-Carlo particle scattering simulations to characterize the energy deposit in cell organelles by radioactive ¹⁹⁸AuNP. They emit beta and gamma rays and are therefore considered for applications with solid tumors. Differences in local dose enhancement between randomly distributed and nucleus targeted nanoparticles are compared. Hereby nucleus targeted nanoparticles showed a strong local dose enhancement in the radio sensitive nucleus.[1] J.M. Zutta Villate and M.B. Hahn, Eur. Phys. J. D. 73 (2019) 95. [2] M.B. Hahn and J.M. Zutta Villate, Sci Rep 11 (2021) 6721.

BP 12: Biopolymers and Biomaterials (joint session BP/PPP)

Time: Wednesday 9:30–13:00

Location: TOE 317

BP 12.1 Wed 9:30 TOE 317

Interaction of laminin and brain cells with ion implanted titania nanotube scaffolds — •JAN FRENZEL^{1,2,3}, ASTRID KUPFERER^{1,2}, and STEFAN MAYR^{1,2} — ¹Leibniz Institute of Surface Engineering (IOM), 04318 Leipzig, Germany — ²Division of Surface Physics, Faculty of Physics and Earth Sciences, Leipzig University — ³Research Group Biotechnology and Biomedicine, Faculty of Physics and Earth Sciences, Leipzig University

Brain-machine interfaces enable symptomatic treatment of neurodegenerative diseases by modulating neural activities and enjoy great popularity when brain tissue is assessed ex vivo. However, current-use interface materials are troubled by numerous challenges concerning loss of long-term adhesion, rejection reactions, and glial scarring. We show that ion-implanted titania nanotube scaffolds (TNS) are a promising candidate for dealing with these issues because they combine high biocompatibility with adequate electrical conductivity. Based on our experiments, we explain how changes in the adsorption of laminin and the viability/adhesion of neurons and glial cells caused by ion implantation can be described by alterations in surface characteristics. The high neuron viability observed on all TNS, but suppressed glial cell formation on implanted TNS, demonstrates the potential as a future interface material. We acknowledge funding by SMWK (100331694). Reference: Frenzel et al., *Nanomaterials* 2022, 12, 3858. <https://doi.org/10.3390/nano12213858>

BP 12.2 Wed 9:45 TOE 317

Fiber-based femtosecond 3D printing — •CLAUDIA IMIOLCZYK¹, ANDY STEINMANN¹, MORITZ FLÖSS¹, ZHEN WANG¹, MICHAEL HEYMANN², ANDREA TOULOUSE³, and HARALD GIESSEN¹ — ¹4th Physics Institute, Research Center SCoPE, University of Stuttgart, Pfaffenwaldring 57, 70569 Stuttgart, Germany — ²Institute of Biomaterials and Biomolecular Systems, University of Stuttgart, Pfaffenwaldring 57, 70569 Stuttgart, Germany — ³Institute of Applied Optics, Research Center SCoPE, University of Stuttgart, Pfaffenwaldring 9, 70569 Stuttgart, Germany

Ultrashort laser pulses are often used in medical applications, for instance for soft-tissue surgeries. However, the progress on using such laser pulses for tissue structuring is rather marginal so far. Therefore, we aim to realize an endoscopic fiber-based femtosecond 3D printer to minimally invasively surgically repair organ damage on a micrometer scale. For this, high-power femtosecond laser pulses are required, in order to 3D print desired geometries with a microfluidic bio-ink using two-photon-lithography. We utilize ruled reflective diffraction gratings to pre-chirp laser pulses, as dispersion in optical fibers broadens these femtosecond laser pulses. We report on measurements of pulse duration, spectrum, compression, and nonlinear effects. These resulting 3D printed structures should be colonized with endogenous cells, analogous to the extracellular matrix. This could open a new area of endoscopic 3D printing of biomaterials inside the human body to revolutionize plastic micro-surgery, such as repairing defects in the heart of embryos or even repairs behind the eardrum at the auditory ossicles.

BP 12.3 Wed 10:00 TOE 317

DNA-encoded viscoelastic matrices for cell and organoid culture — •ELISHA KRIEG — Leibniz-Institut für Polymerforschung Dresden e.V. — Technische Universität Dresden

The recent advances in mechanobiology and the physics of life have driven an immense interest in mechanically programmable viscoelastic materials for cell and organoid culture. Here I describe a class of soft hydrogels based on novel DNA libraries that self-assemble with synthetic polymers.[1] This dynamic DNA-based matrix (DyNAtrix) provides computationally predictable, systematic, and independent control over key cell-instructive properties by merely changing DNA sequence information without affecting the compositional features of the system. This approach enables: (1) thermodynamic and kinetic control over network formation; (2) adjustable heat activation for the homogeneous embedding of mammalian cells; and (3) dynamic tuning of stress relaxation times to precisely recapitulate the mechanical characteristics of living tissues. DyNAtrix is self-healing, printable, exhibits high stability, cyto- and hemocompatibility, and controllable degradation. DyNAtrix-based 3D cultures of human mesenchymal stromal cells, pluripotent stem cells, canine kidney cysts, and placental organoids exhibit high viability, proliferation, and morphogenesis over several days to weeks. DyNAtrix thus represents a programmable and versatile precision matrix, paving the way for advanced approaches to biomechanics, biophysics, and tissue engineering.

[1] Peng et al. *bioRxiv* 2022, DOI:10.1101/2022.10.08.510936

Invited Talk

BP 12.4 Wed 10:15 TOE 317

Materials properties of bacterial biofilms. — •CÉCILE M. BIDAN — Max Planck Institute of Colloids and Interfaces, Department of Biomaterials, Potsdam, Germany

As bio-sourced materials are raising interest for their sustainability, using bacteria to produce biofilms made of a protein and polysaccharide matrix has become a new strategy to make engineered living materials with various functionalities. Our group contributes to this emerging field by clarifying how bacteria adapt biofilm materials properties to the environment. For this, we culture *E. coli* producing curli amyloid and phosphoethanolamine-cellulose fibers on nutritive agar substrates with varying physico-chemical properties and study the growth, morphology and mechanical properties of the resulting biofilms. We demonstrated that changing the properties of the agar substrate with polyelectrolyte coatings or by varying the water content the bulk properties of the agar affects *E. coli* biofilm growth, morphology and mechanical properties. We also used *E. coli* producing only amyloid fibers and focus on the matrix structural and functional changes at the molecular scale. To assess the contribution of each matrix component to the macroscopic biofilm materials properties, we compared the characteristics of biofilms produced by a collection of *E. coli* mutants differing in the matrix they produce. The results indicate that *E. coli* biofilm matrix is a composite made of rigid and brittle curli amyloid fibers assembled within a mesh of soft and adhesive phosphoethanolamine-cellulose fibers. Finally, we

explored how treating biofilms with ionic solutions can help tuning further their properties.

BP 12.5 Wed 10:45 TOE 317

The migration and search behavior of immune cells — REZA SHAEBANI and •FRANZISKA LAUTENSCHLÄGER — Saarland University, Saarbrücken

Immune cells have a variety of tasks in the body. For example, dendritic cells act as the *sentinels* searching for pathogens. For this search, the cells need to scan a certain area in an effective way. Here, we investigate how cells optimize the search of such area. We have shown before that all cell types show a correlation of migration speed and persistence [1]. We later found that cells which strongly correlate these two parameters are particularly good at searching objects [2]. Interestingly, we found that cells do not keep the memory of their speed as long as the memory of their persistence [3]. Now, we investigate how we can disturb this migration and search behavior, preferable by altering the cytoskeleton [4].

1.*Maiuri, P., et al., Actin flows mediate a universal coupling between cell speed and cell persistence. *Cell*, 2015. 161(2): p. 374-86. 2.*Shaebani, M.R., et al., Persistence-Speed Coupling Enhances the Search Efficiency of Migrating Immune Cells. *Phys Rev Lett*, 2020. 125(26): p. 268102. 3.*Shaebani, M.R., M. Piel, and F. Lautenschläger, Distinct Speed and Direction Memories of Migrating Cells Diversify Their Possible Search Strategies. arXiv. 4.*Shaebani, M.R., et al., Vimentin provides target search efficiency and mechanical resilience for dendritic cell migration. *bioRxiv*, 2020: p. 2020.12.18.423401.

BP 12.6 Wed 11:00 TOE 317

Molecular motors from a 3D perspective: how do kinesins organize microtubules? — •LAURA MEISSNER¹, JONAS BOSCHE², LUDGER SANTEN², and STEFAN DIEZ^{1,3,4} — ¹B CUBE - Center for Molecular Bioengineering, TU Dresden, Dresden, Germany — ²Center for Biophysics, Department of Physics, Saarland University, Saarbrücken, Germany — ³Cluster of Excellence Physics of Life, TU Dresden, Dresden, Germany — ⁴Max Planck Institute of Molecular Cell Biology and Genetics, Dresden, Germany

Kinesins are ubiquitous motor proteins that are essential for intracellular transport processes. In addition, several kinesins act within the mitotic spindle by sliding and crosslinking microtubules. Some of those kinesins not only move longitudinally on the microtubule filament but also display an axial component in their motion. So far, the effect of this axial motion on motility and force generation within the mitotic spindle has not been explored deeply. Using a 3D motility assay, we show that the antagonistic motor proteins kinesin-5 and kinesin-14 drive the rotation of microtubules around each other. We characterize their motility parameters, including velocity and pitch. Further, we determine the extension of the motors, which reveals the conformation of the motors in microtubule overlaps. To investigate the rotational force (torque) that the motors could produce during microtubule sliding, we developed a microtubule coiling assay. Here, both kinesin-5 and kinesin-14 bent and coiled microtubules, indicative of the generation of significant torque. We hypothesize that this behavior serves to organize spindle fibers and to provide robustness to the spindle.

15 min. break

BP 12.7 Wed 11:30 TOE 317

3D stimulated Raman spectral imaging of water dynamics associated with pectin-glycocalyx entanglement — •MORITZ FLOESS¹, TOBIAS STEINLE¹, FLORIAN WERNER¹, YUNSHAN WANG¹, WILLI L. WAGNER², VERENA STEINLE², BETTY S. LIU³, YIFAN ZHENG³, STEVEN J. MENTZER³, and HARALD GIESSEN¹ — ¹4th Physics Institute, University of Stuttgart, Pfaffenwaldring 57, 70569 Stuttgart, Germany — ²Department of Diagnostic and Interventional Radiology, University Hospital of Heidelberg, Im Neuenheimer Feld 420, 69120 Heidelberg, Germany — ³Laboratory of Adaptive and Regenerative Biology, Brigham & Women's Hospital, Harvard Medical School, Boston MA

Pectin, a heteropolysaccharide, is an ideal biomaterial for medical applications such as serosal wound healing and visceral tissue repair. It forms strong mechanical bonds with the underlying tissue. The extraordinary adhesive properties of pectin on organ surfaces are highly water-dependent and most likely result from a microstructural entanglement of pectin polysaccharide chains with the similarly textured glycocalyx, a glycoprotein coat, covering mammalian cell surfaces. We employ label-free 3D stimulated Raman scattering (SRS) microscopy to investigate the hydrophilicity of pectin hydrogel without the altering effects of sample fixation, dehydration, or tissue staining. In particular, we quantify the time scales, on which two different hydration mechanisms take place. Furthermore, the transition zone between pectin and porcine serosal tissue is imaged to obtain quantitative insights into the entanglement between pectin and mammalian glycocalyx.

BP 12.8 Wed 11:45 TOE 317

Quantifying optomechanical properties of phase separated protein condensates — •TIMON BECK¹, LIZE VAN DER LINDEN², RAIMUND SCHLÜSSLER², KYOOHYUN KIM¹, SIMON ALBERTI², and JOCHEN GUCK¹ — ¹Max Planck Institute for the Science of Light, Erlangen, Germany — ²Biotec TU Dresden, Dresden, Germany

The organization of intracellular material is a complex task and cells have different strategies for compartmentalization. One way is the formation of membrane-less organelles that are involved, for example, in metabolic control and DNA repair. The underlying process of phase separation and percolation is tightly controlled by many parameters as temperature, ion and protein concentration, as well as crowding conditions. Changes in these parameters have an impact on the intermolecular interactions and accordingly tune optical and viscoelastic characteristics of the condensates. Despite the dynamic development of the research field in the last years, there is a lack of tools to quantitatively measure such physical properties. A combination of Brillouin microscopy with quantitative phase imaging, providing information about refractive index and density, gives access to a set of optical and mechanical quantities and in particular the longitudinal modulus. By varying temperature and ion conditions, we were able to tune intermolecular interactions within phase separated protein droplets and found that the introduced variations are reflected in the optomechanical properties of the condensates.

BP 12.9 Wed 12:00 TOE 317

Confinement-induced fractionation and liquid-liquid phase separation of polymer mixtures — •ARASH NIKOUBASHMAN¹ and MIHO YANAGISAWA² — ¹Institute of Physics, JGU Mainz, Germany — ²Graduate School of Science, The University of Tokyo, Japan

The formation of (bio)molecular condensates via liquid-liquid phase separation in cells has received increasing attention, as these coacervates play important functional and regulatory roles within biological systems. However, the majority of studies focused on the behavior of pure systems in bulk solutions, thus neglecting confinement effects and the interplay between the numerous molecules present in cells. To advance our knowledge, we perform simulations of binary polymer mixtures in droplets, considering both monodisperse and polydisperse molecular weight distributions for the longer polymer species. We find that confinement induces a spatial separation of the polymers by length, with the shorter ones moving to the droplet surface. This partitioning causes a distinct increase of the local polymer concentration in the droplet center, which is more pronounced in polydisperse systems. Consequently, the systems exhibit liquid-liquid phase separation at average polymer concentrations where bulk systems are still in the one-phase regime.

BP 12.10 Wed 12:15 TOE 317

Branching morphogenesis in the silica cell wall of diatoms — •IAROSLAV BABENKO^{1,2,3}, BENJAMIN M. FRIEDRICH^{1,2}, and NILS KRÖGER^{1,3} — ¹Cluster of Excellence Physics of Life, TU Dresden, 01062 Dresden, Germany. — ²Center of Advancing Electronics Dresden, TU Dresden, 01062 Dresden, Germany. — ³Center for Molecular and Cellular Bioengineering, 01307 Dresden, Germany.

Diatoms live in a glass house: these common single-celled algae fascinated evolutionary biologists, chemical engineers and inspired artists for their ability to produce intricately nano- and micropatterned silica shells. The valve of the cell wall is formed in a planar intracellular compartment termed silica deposition vesicles (SDVs). The physical mechanism that guides the self-assembly of species-specific silica patterns is unknown. Here, we address this question by studying the formation of the silica rib patterns in the cell wall of the model diatom *Thalassiosira pseudonana* by combining theory and electron microscopy of nascent silica valves. We propose a minimal model of branching morphogenesis based on a non classical Turing reaction-diffusion system to quantitatively account for the time course of experimentally observed rib patterns. We introduce a novel mechanism of branching morphogenesis, which relies on a transition from soluble to insoluble silica phases inside the SDV and the concurrent release of an inhibitor that hinders this transition. Moreover, our minimal model is capable of producing a wide range of rib patterns, suggesting that this model may be applicable for describing branching morphogenesis in other diatom species and potentially, in other organisms.

BP 12.11 Wed 12:30 TOE 317

Reimplementing the formation and dispersal of transcriptional clusters with synthetic DNA-nanomotifs and Langevin-dynamics simulations — •AARON GADZEKPO¹, XENIA TSCHURIKOW¹, MAI TRAN², RAKESH CHATTERJEE^{3,4}, VASILY ZABURDAEV^{3,4}, KERSTIN GÖPFRICH², and LENNART HILBERT¹ — ¹Karlsruhe Institute of Technology — ²Max Planck Institute for Medical Research — ³Max Planck Zentrum für Physik und Medizin — ⁴Friedrich-Alexander Universität Erlangen-Nürnberg

Spatial organisation of the genome is emerging as a crucial aspect of gene transcription. In pluripotent cells, self-interacting molecular factors, such as RNA polymerase II, form microphase-separated domains, which become increasingly dispersed due to amphiphilic effects of newly transcribed genes. To under-

stand the principles that lead to this behaviour, we designed synthetic DNA-nanomotifs that form droplets due to self-interaction and allow for the addition of an amphiphilic tail of thymines. Time-lapse microscopy, titration experiments and analysis of the resulting distributions of droplet properties demonstrate that the synthetic system reproduces the dispersal of phase-separated domains found for increasing transcription levels. Simulations based on Langevin-dynamics equally reproduce this behaviour after tuning interaction strengths and number ratios. Our findings illustrate how model-guided design of DNA-based systems can elucidate the mechanisms that control spatio-temporal compartmentalisation in cells.

BP 12.12 Wed 12:45 TOE 317

Partition complex structure can arise from sliding and bridging of ParB dimers — •LARA CONNOLLEY¹, LUCAS SCHNABEL², MARTIN THANBICHLER², and SEAN MURRAY¹ — ¹Max Planck Institute for Terrestrial Microbiology, Marburg, Germany — ²University of Marburg, Marburg, Germany

Chromosome segregation is vital for cell replication and in many bacteria is controlled by the ParABS system. A key part of this machinery is the association of ParB proteins to the parS-containing centromeric region to form the partition complex. Despite much work, the formation and structure of this nucleoprotein complex has remained unclear. It was recently discovered that CTP binding allows ParB dimers to entrap and slide along the DNA, as well as leading to more efficient condensation through ParB-mediated DNA bridging. Here, we use semi-flexible polymer simulations to show how these properties of sliding and bridging can explain partition complex formation. We find that transient ParB bridges can organise the DNA into either a globular state or into hairpins and helical structures, depending on the bridge lifetime. Upon coupling with stochastic sliding simulations to form a unified sliding and bridging model, we find that short-lived ParB bridges do not hinder ParB sliding and the model can reproduce both the ParB binding profile and the condensation of the nucleoprotein complex. Overall, our model clarifies the mechanism of partition complex formation and predicts its fine structure.

BP 13: Signaling, Biological Networks

Time: Wednesday 9:30–11:00

Location: BAR 0106

Invited Talk

BP 13.1 Wed 9:30 BAR 0106

Biological signal processes across scales — •STEFFEN RULANDS — Ludwig-Maximilians Universität München, Arnold Sommerfeld Center for theoretical Physics, Theresienstr. 37, 80333 München — Max-Planck-Institute for theoretical Physics, Nöthnitzer Str. 38, 01187 Dresden

In contrast to many physical systems, biological systems have the remarkable architecture of being organized into a spatial hierarchy of non-equilibrium processes: from molecules embedded into sub-cellular compartments to cells interacting in tissues. In my talk, I will show how biological systems manipulate the transmission of noise and information between and across these scales in order to perform biological functions. By combining theory and experiments I will first describe a general theory describing the propagation of noise and signals in multi-scale non-equilibrium systems. I will then apply these insights to show how cells make use of the propagation of fluctuations on the subcellular scale to perform biological signal processing: by establishing a low-pass filter of concentration fluctuations in the regulation of cell death and by facilitating a gelation phase transition in the innate immune response.

BP 13.2 Wed 10:00 BAR 0106

Protein Dynamics in the Complex Physical Environment of the Synapse — •SIMON DANNENBERG, SARAH MOHAMMADINEJAD, and STEFAN KLUMPP — Institut für Dynamik komplexer Systeme Georg-August-Universität Göttingen, Göttingen, Germany

The synapse is a complex environment that is densely packed with proteins and has an internal geometry structured by membranes. This affects the mobility of proteins involved in signal transmission and hence, their availability at corresponding reaction sides.

In our work we use dynamic Monte Carlo simulations to investigate the influence of different physical features of the synapse on protein mobility. The simulations are parameterized by mobility measurements via FRAP experiments. Our approach revealed an unexpectedly high sensitivity of the experiments on the geometry of the synapses as well as dependence of protein fluxes on synaptic features such as axon diameter and synapse size.

BP 13.3 Wed 10:15 BAR 0106

How can a single neuron influence behavior? Hints from integrate-and-fire network models — •DAVIDE BERNARDI¹ and BENJAMIN LINDNER^{2,3} — ¹Italian Institute of Technology, Ferrara, Italy — ²Bernstein Center for Computational Neuroscience, Berlin, Germany — ³Institut für Physik, Humboldt-Universität zu Berlin

Recent experiments challenge the established view that only large neuronal populations can reliably encode information, as is argued on the basis of the large noise and chaotic dynamics of cortical networks. One striking example is that awake rats can be trained to respond to the stimulation of a single cell in the barrel cortex. Here, this problem is framed theoretically by studying how the stimulation of a single neuron can be detected in large networks of integrate-and-fire neurons.

Combining numerical simulations and analytical calculations, we illustrate a simple strategy to detect the single neuron stimulation in the activity of a readout subpopulation or in a second network, which is both more realistic and more efficient. Furthermore, a readout network tuned to approximate a differentiator circuit can detect the single-neuron stimulation in a more biologically detailed

model. In this case, the detection probability increases significantly upon injection of an irregular current, in agreement with experiments.

Our models show how inhibitory synapses could make it possible for the sensitivity to single-neuron perturbation to coexist with a stable asynchronous spontaneous activity, that is, through a mild selective imbalance in the topological (spatial) and temporal sense.

BP 13.4 Wed 10:30 BAR 0106

Towards statistical models of activity recordings from stem cell derived neuronal networks — •SEBASTIAN WILLENBERG¹, ELIJAH R. SHELTON¹, PAULINA M. WYSMOLEK², FILIPPO D. KIESSLER¹, ACHIM BRINKOP¹, and FRIEDHELM SERWANE^{1,2,3} — ¹Faculty of Physics and CeNS, LMU, Munich, Germany — ²MPI for Medical Research, Heidelberg, Germany — ³Munich Cluster for Systems Neurology, Munich, Germany

Analysis of neuronal activity is the key to understanding the principles of brain circuitry. Theoretical models have been applied on many different scales, ranging from the analysis of single neuron activity to the collective behaviour of large groups of neurons. Models from statistical physics describe the behaviour of networks across spatial and temporal scales with a minimal amount of parameters. Until now, those models have mainly been applied to datasets recorded via 2D electrode arrays. This makes accessing 3D network morphology challenging. I will present our first steps applying statistical models to neuronal recordings of stem cell derived neuronal networks obtained using lightsheet¹ or confocal microscopy. To model the collective firing we map single neuron activity to two states and apply a maximum entropy model to calculate the entropy and energy following the approach of Tkačik et al.². Using this approach, we seek a minimal model describing the firing activity which allows us to understand and predict the collective behaviour of *in vitro* neuronal networks.

1: Wysmolek et al., Sci Rep 12, 20420, 2022

2: Tkačik et al., PNAS 112, 11508, 2015

BP 13.5 Wed 10:45 BAR 0106

Inference of dynamical networks connectivity with Recurrent Neural Networks — •PABLO ROJAS, MARIE KEMPKES, and MARTIN E GARCIA — Theoretical Physics, University of Kassel, Germany

The inference of directed links in networks of interacting systems is a problem spanning many disciplines. Systems out of equilibrium represent a special case, where samples are not independent but structured as timeseries. In this context, Recurrent Neural Networks (RNN) have attracted recent attention, due to their ability to learn dynamical systems from sequences. We introduce a method to infer connectivity of a network from the timeseries of its nodes, using a RNN based on Reservoir Computing (RC). We show how modifications of the standard RC architecture enable a reliable computation of the existence of links between nodes. While the method does not require information about the underlying mathematical model, its performance is further improved if the selection of hyperparameters is roughly informed by knowledge about the system. The method is illustrated with examples from different complex systems, ranging from networks of chaotic Lorenz attractors to biological neurons. Using simulations of these systems, we demonstrate its power and limitations under a variety of conditions, such as noise levels, delayed interactions, size of the network and hidden variables.

BP 14: Focus Session: From Inter-individual Variability to Heterogeneous Group Dynamics and Disorder in Active Matter (joint session DY/BP/ CPP)

The study of active particle dynamics has developed into a vibrant field of multidisciplinary research, including such diverse systems as bacterial colonies, cellular self-organization, synthetic colloids and microrobots as well as macroscopic systems like locusts, flocks of birds, schools of fish or pedestrians. Whereas many studies in the past focused either on the random transport of individual particles or on the interplay of temporal fluctuations (noise) and interactions (velocity alignment or attraction/repulsion), there is now an increasing interest in the question how structural disorder and inter-individual variability, i.e., different motility characteristics of individuals, shape the active particle dynamics and emergent pattern formation of groups. The presence of structural or quenched disorder raises furthermore the immediate question how to bridge data and models based on (short time) tracking data, given the simultaneous presence of temporal fluctuations. With this focus session, we aim at bringing researchers from statistical physics and biophysics together to discuss this interdisciplinary topic and exchange ideas on common challenges arising in different application areas.

Organized by Robert Großmann (Potsdam)

Time: Wednesday 9:30–13:00

Location: ZEU 160

See DY 26 for details of this session.

BP 15: Tissue Mechanics II

Time: Wednesday 10:30–12:15

Location: BAR Schö

BP 15.1 Wed 10:30 BAR Schö

Hydrostatic pressure and lateral actomyosin tension control stretch and tension of the basement membrane in epithelia — •KARLA YANIN GUERRA SANTILLAN^{1,3}, ELISABETH FISCHER-FRIEDRICH^{1,2}, and CHRISTIAN KARLA YANIN^{1,3} — ¹Cluster of Excellence Physics of Life, Technische Universität Dresden, Dresden, Germany. — ²Biotechnology Center, TU Dresden, Tatzberg, 01307 Dresden, Germany — ³School of Science, Technische Universität Dresden, Dresden, Germany

The shaping of epithelial tissues into functional organs often depends on asymmetries in mechanical tension present at the apical and basal sides of cells. Contraction of an actomyosin meshwork underlying the apical side of cells is known to generate apical tension. The basal side of cells is also associated with an actomyosin meshwork, but it is, in addition, connected to a specialized extracellular matrix, the basement membrane. However, how basal tension is generated, and the role of the basement membrane in this process, are often disregarded and not well understood. Here, using atomic force microscopy, we measure mechanical tension in the basal surface of the wing disc epithelium of *Drosophila*. We find that basal tension depends crucially on the basement membrane with additional contributions of the actomyosin cytoskeleton. Further, performing localized optogenetic activation of actomyosin contractility and osmotic shocks, we deduce that elastic basement membrane stretch is generated by intracellular hydrostatic pressure and lateral actomyosin contractility.

BP 15.2 Wed 10:45 BAR Schö

Noisy growth and buckling in soft tissues — •RAHUL G. RAMACHANDRAN¹, RICARD ALERT^{1,2}, and PIERRE A. HAAS^{1,2,3} — ¹Max Planck Institute for the Physics of Complex System, 01187 Dresden, Germany — ²Center for Systems Biology Dresden, 01307 Dresden, Germany — ³Max Planck Institute of Molecular Cell Biology and Genetics, 01307 Dresden, Germany

The generation of curved tissue shapes such as the villi of the gut or the gyrations of the brain has been associated with buckling instabilities that release elastic stresses accumulated by constrained growth. However, most mechanical theories for these morphogenetic processes assume homogeneous growth and mechanical properties, while these parameters often exhibit strong fluctuations in biological systems. Here, we therefore study a minimal mechanical model of these fluctuations: We analyze the buckling of a growing, neo-Hookean rod through nonlinear finite-element simulations. Fluctuations are introduced as spatial inhomogeneities of the growth tensor and the material parameters. Our results show that stronger growth fluctuations promote buckling by decreasing the buckling threshold. We interpret these results using strain energy distribution from homogenous, patterned and random growth simulations and validate them using analytical calculations.

BP 15.3 Wed 11:00 BAR Schö

Viscoelastic measurements in glioblastoma-infiltrated cerebral organoids — •MICHAEL FRISCHMANN¹, ELIJAH SHELTON¹, SOFIA KALPAZIDOU², JOVICA NINKOVIC^{2,3}, and FRIEDHELM SERWANE^{1,3} — ¹Faculty of Physics and Center for NanoScience, LMU Munich, Germany — ²Biomedical Center, LMU Munich, Germany — ³Munich Cluster for Systems Neurology, Munich, Germany

The glioblastoma is a malignant neuroepithelial brain tumor with median survival rates of a few months without treatment. One reason is the rapid infiltrative

growth with active destruction of brain tissue and the resulting necrotic debris. Glioblastomas are well described from a molecular biology perspective. However, little is known about their mechanical properties which directly affect the tumor's ability to spread into adjacent tissues. I will present measurements of mechanical properties of glioblastoma and its surrounding tissue. To study tumor biophysics in an accessible in vitro system, we use cerebral organoids grown from induced pluripotent stem cells (iPSCs) with implanted glioblastoma cells. To determine the mechanical properties of the tumor and its microenvironment, we use magnetic microdroplets that we inject into the tissue via microneedles. Actuated by a homogeneous magnetic field, the droplet deforms and its deformation is recorded via a confocal microscope. The dynamic deformation is used to infer the viscoelastic properties of physiological and pathological tissue, as well as boundary regions. The recorded data allows us to establish a viscoelastic model of glioblastoma and to develop a mechanical understanding how brain tumors infiltrate their environment.

15 min. break

BP 15.4 Wed 11:30 BAR Schö

Density-dependent active flow transition of biological tissues — •MATHIEU DEDENON^{1,2}, CARLES BLANCH-MERCADER³, and KARSTEN KRUSE^{1,2} — ¹Department of Biochemistry, University of Geneva, 1211 Geneva, Switzerland — ²Department of Theoretical Physics, University of Geneva, 1211 Geneva, Switzerland — ³Laboratoire Physico-Chimie Curie, Institut Curie, Université PSL, Sorbonne Université, CNRS UMR168, Paris, France

Biological tissues of elongated cells can spontaneously flow thanks to active stresses, as predicted by 2D generalized hydrodynamics. This effect has been recently confirmed experimentally with confined C2C12 myoblasts.

Under circular confinement, those cells are observed to undergo tissue rotation at confluence. Cells have maximal orientational order at the disc periphery, forming a spiral +1 topological defect. However at a later stage, cell density increases and the tissue ceases rotational motion. This transition is accompanied by a reorientation of cells along the radial direction, transforming the +1 defect into a static aster.

To understand density-dependent spiral-aster transitions, we generalize the previously used 2D polar active fluid description to incorporate a generic passive coupling between cell density and polarity fields. Using symmetry arguments, several energy terms are allowed and we explore systematically how such couplings affect the spontaneous flow transition, under which conditions they promote a spiral-aster transition. This work shows that collective motion is not only driven by tissue active stress but is also sensitive to cell density.

BP 15.5 Wed 11:45 BAR Schö

Capturing the mechanosensitivity of cell proliferation in models of epithelium — •MAXIME HUBERT¹, KEVIN HÖLLRING¹, LOVRO NUIĆ², LUKA ROGIĆ², SARA KALIMAN¹, SIMONE GEHRER¹, FLORIAN REHFELDT^{3,4}, and ANA-SUNČANA SMITH^{1,2} — ¹FAU Erlangen-Nürnberg, Erlangen, Germany — ²Ruder Bošković Institute, Zagreb, Croatia — ³University of Göttingen, Göttingen, Germany — ⁴University of Bayreuth, Bayreuth, Germany

The proliferation of epithelial cells, the process of cell growth and cell division, is affected by the mechanical properties of the surrounding environment. While

an extensive literature covers single cell mechanoresponse, information about tissue-wide mechanoresponse are scarce. It is only known that high cell density restricts proliferation and eventually leads to homeostasis. In this presentation, we aim at completing the existing literature by addressing the role of both cell density and extracellular stiffness in the proliferation of cells in epithelial monolayer. Using MDCK-II epithelial tissues stained with EdU we are able to measure the fraction of dividing cells at a given cell density and quantify mechanoresponse. We build a cell-level theory of proliferation based on a two-population description which is compared successfully to the experiments and implemented into simulations. Using experiments and simulations, we also address the role of proliferation in the large scale growth of tissues. A tissue-scale theory of epithelial growth based on the cell-level findings is finally presented. This work provides a first step towards a complete description of proliferation at the tissue scale and its influence on its compartmentalization.

BP 15.6 Wed 12:00 BAR Schö

Quantitative 3D live-imaging of self-organisation in embryonic organoids — •VALENTIN DUNSING, SHAM TLLI, CLAIRE CHARDÈS, LÉO GUIGNARD, and PIERRE-FRANÇOIS LENNE — IBDM & CENTURI, Aix-Marseille University/CNRS, Marseille, France

BP 16: Systems Biophysics

Time: Wednesday 11:15–13:00

Location: BAR 0106

Invited Talk

BP 16.1 Wed 11:15 BAR 0106

Systems biophysics of bacterial response to cell wall-targeting antibiotics — REBECCA BROUWERS¹, SHARAREH TAVADDOD¹, LEONARDO MANCINI², JACOB BIBOY³, ELIZABETH TATHAM¹, PIETRO CICUTA², WALDEMAR VOLLMER³, and •ROSALIND ALLEN^{1,4} — ¹School of Physics & Astronomy, University of Edinburgh, Edinburgh, UK — ²Cavendish Laboratory, University of Cambridge, Cambridge, UK — ³Centre for Bacterial Cell Biology, University of Newcastle, Newcastle, UK — ⁴Theoretical Microbial Ecology, Faculty of Biological Sciences, University of Jena, Germany

Antibiotics are central in modern medicine, yet bacterial infections are increasingly becoming resistant to antibiotics. To use antibiotics more effectively, we need to understand better how they work. We have used a combination of microbiological and biophysical experiments, and theoretical modelling, to probe how the antibiotic mecillinam, which targets bacterial cell wall synthesis, kills the bacterium *Escherichia coli*. Comparing killing dynamics under conditions of rich and poor nutrients we conclude that the balance between the rates of creation of cell surface area and volume plays a crucial role in the fate of cells when exposed to this antibiotic.

BP 16.2 Wed 11:45 BAR 0106

Cell size distribution: an analytical comparison between lineage and population experiments — •ARTHUR GENTHON — ESPCI, Université PSL, Paris, France (until december 2022) — Max Planck Institute for the Physics of Complex Systems, Dresden, Germany (from january 2023)

In the past decade, new microfluidic devices, like the mother machine, have been designed to monitor single lineages of cells for many generations with great precision. In classical bulk cultures where full populations are grown, cells with high reproductive success lead to larger populations of offsprings, while no such selection effect is present in single-lineage experiments. Quantifying the statistical bias between these two families of experiments is at the basis of a universal notion of natural selection, which can be defined for any branching tree, not just in cell biology. In this work, we thus compute analytical lineage-population biases for the cell size distribution, in the context of size-controlled cells. The role of stochasticity, both in single-cell growth and in volume partitioning at division, is explored, and we show how it can cancel the lineage-population bias. In addition, in simple cases we show how we can learn the laws of cell growth and division from mother machine steady state size distributions. The parameters of the model, such as the single-cell growth rate, the strength of the size control or the asymmetry of division are obtained by fitting analytical distributions to *Escherichia coli* data.

BP 16.3 Wed 12:00 BAR 0106

Tuning pattern formation of *E. coli* Min proteins *in vivo* — ZIYUAN REN¹, •HENRIK WEYER², LAESCHKIR WÜRTHNER², ERWIN FREY², and SUCKJOON JUN¹ — ¹Department of Physics & Section of Molecular Biology, Division of Biological Sciences, University of California San Diego, 9500 Gilman Dr. La Jolla, CA 92093, USA — ²Arnold Sommerfeld Center for Theoretical Physics and Center for NanoScience, Department of Physics, Ludwig-Maximilians-Universität München, Theresienstraße 37, D-80333 München, Germany

The Min protein system of *Escherichia coli* bacteria is crucial for their proliferation. The Min proteins ensure symmetric cell division by positioning the cell-division machinery at midcell. This spatial templating is achieved by the

The emergence of asymmetries within a mass of equivalent cells is the starting event in the development of embryos, resulting in the formation of the main body axes. Despite its fundamental role, the mechanisms that induce symmetry breaking remain largely unknown because they are difficult to probe *in vivo*, particularly in mammalian embryos. A promising *in vitro* model to study such mechanisms are embryonic organoids, which undergo gastrulation-like movements similar to those observed in embryos. We aim to use live imaging to disentangle the interplay between signaling, cell differentiation and mechanics underlying self-organized symmetry breaking. Currently available imaging platforms are limited to low-throughput 3D or high-throughput 2D imaging. To overcome this limitation, we establish multi-view single-objective lightsheet microscopy, allowing us to image tens of organoids over hours to days with cellular resolution and sufficient temporal sampling to track cells in 3D. We present ongoing efforts using deep learning based segmentation and quantitative image analysis to correlate cellular dynamics and rearrangements with the expression of key differentiation markers during polarization of aggregates. We thereby analyze how spatially localized expression domains and collective cell movements establish symmetry breaking. Finally, we analyze the variability of spatiotemporal patterns across multiple specimen.

self-organized pole-to-pole oscillation of the Min proteins, suppressing FtsZ ring formation at the cell poles. We experimentally study the robustness of Min pattern formation under changes in the total protein content of MinD and MinE by genetically modifying their expression in live *E. coli* bacteria. This uncovers a remarkable robustness of Min patterns *in vivo* comparable with previous findings *in vitro*. Moreover, this study reveals that the protein concentrations determine the pattern type, and both standing-wave and traveling-wave patterns form in filamentous cells. We show that the same reaction-diffusion model based on the conformational switch of MinE introduced earlier for the *in vitro* system explains both the robustness and the pattern characteristics *in vivo*. Thus, common principles underlie Min pattern formation *in vivo* and *in vitro*.

BP 16.4 Wed 12:15 BAR 0106

Stochastic dynamics of cell shape during cellular state transitions — •WOLFRAM PÖNISCH¹, ISKRA YANAKIEVA¹, AKI STUBB², GUILLAUME SALBREUX³, and EWA PALUCH¹ — ¹Dept. of Physiology, Development and Neuroscience, University of Cambridge, Cambridge, UK — ²Stem Cells and Metabolism Research Program, University of Helsinki, Helsinki, Finland — ³Dept. of Genetics and Evolution, University of Geneva, Geneva, Switzerland

The development of an organism is characterized by a series of cellular state transitions where cells become increasingly specialized. Such state transitions are often accompanied by morphological changes and there are strong indications of coupling between a cell's shape and state. Here, we present a pipeline to quantify and analyse cell shapes as cells undergo the epithelial-to-mesenchymal transition (EMT). We apply our analysis pipeline to study how shape and fate are coupled during the EMT of MDCK cells. We confirm that cell morphology is closely associated with the state: While epithelial cells display spherical shapes, mesenchymal cells undergo spreading. After defining the distinct cellular shapes corresponding to cell states, we study how exactly the morphological features of a cell evolve during EMT. To this aim, we investigate trajectories of the morphological features of individual cells in a low-dimensional morphospace and describe the evolution of cellular shape as a Langevin process, allowing us to entangle the role of deterministic and stochastic morphogenetic forces. By integrating morphometric analysis into studies of cell state transitions, we aim to better understand the crosstalk between cell state and shape.

BP 16.5 Wed 12:30 BAR 0106

Sensitivity of Boolean attractors to small network changes and implications for the inference of microbial interaction networks — •JYOTI JYOTI and MARC-THORSTEN HÜTT — Jacobs university, Bremen, Germany

Sensitivity of dynamics on graphs under small topological changes has been studied for diverse types of dynamics and in relation with a wide range of applications. Here we extend this direction of research by studying (and deciphering) the change of attractors in Boolean threshold dynamics under single and multiple edge switches. By evaluating differences in attractor sets, we can, with high accuracy, predict the structural change in the network. This is of high relevance for network inference, e.g., inferring microbial interactions from abundance patterns: Current approaches, where interaction networks are inferred from attractors [1], often fail to provide networks, which in turn can reproduce the initial attractor set. Evaluating the differences in attractor sets (initial set vs. the one produced by the inferred network) and estimating topological differences from

them can pave the way towards better inference algorithms. We briefly discuss the implications of our findings for microbiome analyses.

[1] Claussen, J. C., Skieciwienė, J., Wang, J., Rausch, P., Karlsen, T. H., Lieb, W., Baines, J. F., Franke, A., and Hütt, M.-Th. (2017). Boolean analysis reveals systematic interactions among low-abundance species in the human gut microbiome. *PLoS Computational Biology*, 13(6):e1005361.

BP 16.6 Wed 12:45 BAR 0106

Information storage allows for optimal adaptation in chemical signalling networks out-of-equilibrium — •DANIEL MARIA BUSIELLO¹ and GIORGIO NICOLETTI² — ¹Max Planck Institute for the Physics of Complex Systems, Germany — ²University of Padua, Italy

Living systems process information and exhibit dynamical adaptation. We propose a chemical model for sensing that encompasses only necessary ingredients: energy consumption, information storage, and negative feedback. Indeed, equilibrium constraints limit the efficiency of information processing, and storage is

an unavoidable energy-consuming step to exploit information. Our model architecture is informed by experimental observations that found negative feedback to be ubiquitous. We show that the presence of information storage and negative feedback leads to finite-time memory, essential for dynamical adaptation. Surprisingly, adaptation is associated with both an increase in the mutual information between external and internal variables and a reduction of dissipation in the internal chemical processes. This twofold advantage comes at an energetic cost. By simultaneously optimising energy consumption and information processing features, we find that far-from-equilibrium sensing dominates in the low-noise regime. Finally, we employ our model to shed light on the adaptation of neurons in zebrafish larvae subjected to periodic visual stimuli. We find striking similarities between predicted and observed behaviours, quantifying dissipation and information-processing performance. Our theory provides a stepping stone towards the idea of highlighting crucial ingredients for information processing starting from a chemical description.

BP 17: Protein Structure and Dynamics

Time: Wednesday 15:00–17:30

Location: BAR 0106

BP 17.1 Wed 15:00 BAR 0106

Computational Approaches to Liquid-Liquid Phase Separation of Partially Disordered RS-Proteins — •YANNICK WITZKY¹, STEPHAN HOBE², ANDREAS WACHTER², ARASH NIKOUBASHMAN¹, and FRIEDERIKE SCHMID¹ — ¹Institute of Physics, Johannes Gutenberg University — ²Institute for Molecular Physiology, Johannes Gutenberg University

RS-proteins are a class of proteins that contribute to light-activated gene regulation (via an alternative splicing mechanism) in plant morphogenesis. It has been hypothesized that liquid-liquid phase separation (LLPS) plays an important role for the regulation mechanism. Studying these proteins is challenging because they contain both intrinsically disordered regions (IDRs) - which presumably control the LLPS - as well as folded domains that contain the functionally important RNA binding sites. Here we use and compare different coarse-grained models to study the condensation and phase behavior of RS proteins: Commonly used IDP models [1,2] as well as the structure predictive UNRES model [3]. We specifically focus on the on the single-chain conformations, phase behavior and the accessibility of RNA binding site.

[1] Tesei et al. (2022) *Open Research Europe*, 2(94), 94.

[2] Rizuan et al. (2022) *J Chem Inf Model* 62(18), 4474-4485.

[3] Sieradzan et al. (2019) *J. Phys. Chem. B*, 123, 27, 5721-572

BP 17.2 Wed 15:15 BAR 0106

Key Role of the Solvent in Driving Liquid-Liquid Phase Separation — •ELLEN ADAMS^{1,2}, JONAS AHLERS³, VERIAN BADER³, SIMONE PEZZOTTI³, KONSTANZE WINKHOFFER³, JÖRG TATZELT³, and MARTINA HAVENITH³ — ¹Technische Universität Dresden — ²Hemholtz Zentrum Dresden Rossendorf — ³Ruhr Universität Bochum

In recent years the importance of the aqueous solvent in influencing protein structure, function, and dynamics has been recognized. Coupling of water molecules to the protein surface creates an interfacial region in which water molecules within this region have distinctly different properties than bulk water. Yet, the structure and dynamics within this interfacial region are still not easy to access experimentally. Terahertz (THz) spectroscopy has been shown to be a powerful tool to investigate solvent dynamics in bulk solutions and is directly sensitive to changes in the low frequency collective intermolecular hydrogen-bonding vibrations of water. Here the role of solvation dynamics in the liquid-liquid phase separation (LLPS) of the intrinsically disordered protein fused in sarcoma (FUS) is probed. Characterization of the hydrogen bonding network reveals that water solvating hydrophobic groups is stripped away in the membrane-less FUS biomolecular condensates. Additionally, water left inside of the biomolecular condensates is highly constrained, indicative of a population of bound hydration water. These results uncover the vital role of hydration water in LLPS: the entropically favorable release of unfavorable hydration water serves as a driving force for LLPS.

BP 17.3 Wed 15:30 BAR 0106

Local structure and dynamics of water molecules in FUS protein molecular condensates. — DANIEL CHAVEZ ROJAS¹, JOSEPH RUDZINSKI^{1,2}, and MARTIN GIRARD¹ — ¹Max Planck Institute for Polymer Research, Mainz, Germany — ²Institut für Physik, Humboldt-Universität zu Berlin, Berlin, Germany

There is evidence that molecular condensates of the FUS protein play a role in the development of some neurodegenerative diseases like ALS. For this reason, understanding the molecular mechanism by which these condensates form at an atomistic level is of therapeutic interest. However, the molecular structure and water-protein interactions of these condensates is poorly understood. In this work, we utilize a multi-scale approach to generate FUS condensates at a suffi-

cient scale with a coarse-grained model, followed by investigation of the atomic scale with shorter, fully-atomistic molecular dynamics simulations. As a result, we are able to efficiently characterize water-protein hydrogen bonding interactions, contacts, and water ordering around the individual amino acids of FUS proteins in the condensate versus in solution. The characterization of water-protein and protein-protein structure provides insights about the driving forces that promote the formation of these molecular condensates.

BP 17.4 Wed 15:45 BAR 0106

Structural dynamics of the intrinsically disordered SNARE proteins at the membrane interface: Recent insights by NMR spectroscopy — TOBIAS STIEF^{1,2}, MIRKO KRAUS^{1,2}, KATHARINA VORMANN^{1,2}, REINHARD JAHN³, ANGEL PEREZ-LARA⁴, and •NILS-ALEXANDER LAKOMEK^{1,2} — ¹Forschungszentrum Jülich, Jülich, Germany — ²Heinrich-Heine-Universität, Düsseldorf, Germany — ³Max Planck Institute for Multidisciplinary Sciences, Göttingen, Germany — ⁴University of Granada, Granada, Spain

SNARE proteins play a crucial role during neurotransmitter release by eliciting the fusion of the synaptic vesicle membrane with the presynaptic plasma membrane. In their pre-fusion state, the SNARE proteins are intrinsically disordered. They do not exhibit a well-defined structure and show high internal flexibility, being membrane-anchored. However, the mode of interaction between the SNARE proteins and the lipid membrane needs to be better understood.

We use the SNARE proteins as a model system for developing novel NMR methods to characterize the inner and conformational dynamics of intrinsically disordered proteins interacting with lipid membranes or being membrane-anchored. Therefore, we address a large range of timescales, from pico- to milliseconds, employing both solution NMR and solid-state NMR methods. The aim is to better describe the conformational space of intrinsically disordered proteins at the lipid membrane interface. At the conference, we will present recent (unpublished) insights into the structural dynamics of the SNARE protein synaptobrevin-2 at the lipid membrane interface.

BP 17.5 Wed 16:00 BAR 0106

Single-chain and condensed-state behavior of intrinsically disordered nuclear proteins in bulk and confinement — •JANKA BAUER¹, LUKAS STELZL^{1,2,3}, DOROTHEE DORMANN^{2,3}, and ARASH NIKOUBASHMAN¹ — ¹Institute of Physics, JGU Mainz, Germany — ²Biocenter, Institute of Molecular Physiology, JGU Mainz, Germany — ³Institute of Molecular Biology, Mainz, Germany

The liquid-liquid phase separation of intrinsically disordered proteins plays an integral part for the formation of membraneless organelles in cells, which in turn have key functional and regulatory roles. To better understand the complex relation between the sequence and self-assembly of these heteropolymers, we perform molecular simulations of the low-complexity domains of heterogeneous nuclear ribonucleoprotein A1 (hnRNPA1) and Fused in Sarcoma (FUS). For hnRNPA1, we systematically analyze how the conformation and phase behavior are affected by the number of aromatic residues within the examined sequences in both single-chain and condensed state simulations. Our observations strongly support the hypothesis that aromatic residues play a dominant role for condensation, which is further corroborated by a detailed analysis of the intermolecular contacts. To mimic more closely conditions prevalent in cellular environments, we perform simulations of hnRNPA1 and FUS in spherical confinement, where we systematically vary the fraction of the crowding agent polyethylene glycol.

15 min. break

BP 17.6 Wed 16:30 BAR 0106

Efficiency and selectivity in the self-assembly of SAS-6 rings on a surface — •SANTIAGO GOMEZ MELO¹, DENNIS WÖRTHMÜLLER¹, PIERRE GÖNCZY², NICCOLO BANTERLE³, and ULRICH SCHWARZ¹ — ¹Heidelberg University, Heidelberg, Germany — ²EPFL, Lausanne, Switzerland — ³EMBL, Heidelberg, Germany

Centrioles are large cylindrical structures that organize various microtubule-based processes in cells, including the formation of cilia and spindles. Their characteristic nine-fold symmetry results from rings that are formed by dimers of the protein SAS-6. Recently it was observed that the self-assembly of SAS-6 rings is strongly facilitated on a surface. Moreover, a fraction of non-canonical symmetries (i.e., different from nine) was observed. To better understand the factors that determine the efficiency and selectivity of this process, we have performed Brownian Dynamics computer simulations with patchy particles, in which we varied interaction energies and angular binding range. For weak interaction energies and large angular range, we find that the assembly kinetics can be described well by the coagulation-fragmentation equations in the reaction-limited approximation. In contrast, large interaction energies and small angular range lead to kinetic trapping and diffusion-limited assembly. Comparison with experimental data suggests that the SAS-6 system combines a weak binding energy with a small angular range in order to avoid kinetic trapping and favor the desired nine-fold symmetry.

BP 17.7 Wed 16:45 BAR 0106

Alphafold predicts the most complex protein knot and composite protein knots — MAARTEN BREMS¹, ROBERT RUNKEL¹, TODD YEATES², and •PETER VIRNAU¹ — ¹Institut für Physik, Staudingerweg 9, JGU Mainz — ²UCLA-DOE Institute for Genomics and Proteomics, University of California Los Angeles (USA)

The computer artificial intelligence system AlphaFold has recently predicted previously unknown three-dimensional structures of thousands of proteins. Focusing on the subset with high-confidence scores, we algorithmically analyze these predictions for cases where the protein backbone exhibits rare topological complexity, i.e. knotting. Amongst others, we discovered a 7_1 -knot, the most topologically complex knot ever found in a protein, as well as several 6-crossing composite knots comprised of two methyltransferase or carbonic anhydrase domains, each containing a simple trefoil knot [1]. These deeply embedded composite knots occur evidently by gene duplication and interconnection of knotted dimers. Finally, we report two new five-crossing knots including the first 5_1 -knot. Our list of analyzed structures forms the basis for future experimental studies to confirm these novel knotted topologies and to explore their complex folding mechanisms.

[1] M. Brems et al, Protein Science 31(8), e4380 (2022).

BP 17.8 Wed 17:00 BAR 0106

Multi-state Unfolding Processes: Discrimination of protein domains by urea-induced thermal shift — •JI YOUNG YANG^{1,2,3}, OLIVER BURKERT², BORIS MIZAIKOFF¹, and JENS SMIAŁEK^{3,4} — ¹Institute for Analytical and Bioanalytical Chemistry, University of Ulm, Ulm, Germany — ²Boehringer Ingelheim Pharma GmbH & Co. KG, Analytical Development Biologicals, Biberach(Riss), Germany — ³Boehringer Ingelheim Pharma GmbH & Co. KG, Development NCE, Biberach (Riss), Germany — ⁴Institute for Computational Physics, University of Stuttgart, Stuttgart, Germany

Co-solute induced molecular denaturation and aggregation mechanisms related to stability changes for multi-domain proteins like mAbs are often hard to monitor experimentally. In addition, a thorough theoretical explanation is often missing. We performed intrinsic fluorescence (IF) measurements of monoclonal antibody (mAb) samples for different aqueous urea concentrations under thermal denaturation. Our results show that the denaturing effect of urea on individual mAb domains can be explained by linear mapping of the thermal shifting curve to the actual urea concentration. Notably, the achieved thermal shifting curves can be assigned to certain protein domains, which enables discrimination of overlapping denaturation processes. Our approach highlights the benefits of direct monitoring of co-solute effects on the conformational stability of mAb domains and its colloidal stability. We will discuss the experimental approach and present the corresponding outcomes in terms of the underlying molecular mechanisms.

BP 17.9 Wed 17:15 BAR 0106

X-ray damage to Gene-V Protein: NAP-XPS analysis of Chemical changes to Proteins in Water — •DOROTHEA C HALLIER^{1,2,3}, JÖRG RADNIK², PAUL M DIETRICH⁴, HARALD SEITZ^{1,3}, and MARC BENJAMIN HAHN² — ¹Fraunhofer Insitute for Cell Therapy and Immunology, Branch Bioanalytics and Bioprocesses, Potsdam, Germany — ²Federal Insitute for Materials Research and Testing BAM Berlin, Berlin, Germany — ³Univerity of Potsdam, Institute for Biochemistry and Biology, Potsdam Germany — ⁴SPECS Surface Nano Analysis GmbH, Berlin, Germany

X-ray photoelectron spectroscopy (XPS) was used to analyze the chemical damage of ionizing radiation to a single-stranded DNA-binding protein: Gene-V Protein (G5P/GVP) and its most abundant amino acids (Alanine, Arginine, Cysteine, Glycine, Lysine, Methionine, Tyrosine). This protein plays a crucial role in maintaining the DNA metabolism, especially DNA replication, recombination and repair. Vacuum measurements were combined with near-ambient pressure (NAP) XPS measurements under water and nitrogen atmosphere to detect both direct and indirect radiation damage and corresponding damage pathways. The exposure of proteins and aminoacids to x-rays leads to degradation i.e. via dehydrogenation, decarboxylation, dehydration and deamination. A strong increase of protein damage was observed in water as compared to vacuum.

BP 18: Biologically Inspired Statistical Physics (joint session DY/BP)

Time: Wednesday 15:00–16:30

Location: ZEU 250

BP 18.1 Wed 15:00 ZEU 250

Comparison of fitting strategies to extract the diffusion coefficient in microrheological experiments — •STEN LEIPNITZ, CHRISTIAN WAGNER, and THOMAS JOHN — Experimental Physics, Saarland University, Saarbrücken

Tracking of small particles undergoing a Brownian motion in liquids is a widespread method in passive microrheology to extract the diffusion coefficient D , the viscosity of the sample respectively. The mean-squared displacement (MSD) is determined from particle positions as a function of the timelag $MSD(\tau) = \sigma_0^2 + 2nD\tau + v_{\text{drift}}^2 \tau^2$, where v_{drift} is a possible drift velocity and σ_0 is an offset due to position detection noise in experiments. We present: the extracted parameters depend strongly on the used number of fitting points in the MSD -relation. Surprisingly, considering only the beginning of the MSD -relation in the fitting procedure leads to the best expectation value of the diffusion coefficient. This is shown by numerical simulations of the Brownian motion as well as from experimental data.

BP 18.2 Wed 15:15 ZEU 250

Non-monotonic behavior of timescales of passage in heterogeneous media: Dependence on the nature of barriers — MOUMITA DASGUPTA¹, •SOUGATA GUHA², LEON ARMBRUSTER¹, DIBYENDU DAS², and MITHUN K. MITRA² — ¹Department of Physics, Augsburg University, USA — ²Department of Physics, IIT Bombay, India

Usually time of passage across a region may be expected to increase with the number of barriers along the path. Can this intuition fail depending on the special nature of the barrier? We study experimentally the transport of a robotic bug which navigates through a spatially patterned array of obstacles. Depending on the nature of the obstacles we call them either entropic or energetic barriers. For energetic barriers we find that the timescales of first passage vary non-

monotonically with the number of barriers, while for entropic barriers first passage times increase monotonically. We perform an exact analytic calculation to derive closed form solutions for the mean first passage time for different theoretical models of diffusion. Our analytic results capture this counter-intuitive non-monotonic behaviour for energetic barriers. We also show non-monotonic effective diffusivity in the case of energetic barriers. Finally, using numerical simulations, we show this non-monotonic behaviour for energetic barriers continues to hold true for super-diffusive transport. These results may be relevant for timescales of intra-cellular biological processes.

BP 18.3 Wed 15:30 ZEU 250

Phase behavior and finite-size effects in biology — •FELIX HERRMANN, BURKHARD DUENWEG, and MARTIN GIRARD — Max-Planck Institut fuer Polymerforschung (MPI-P), Mainz, Germany

Phase behavior observed in biology remains puzzling. For instance, the plasma membrane of cells exhibits signs of criticality, as it is controlled to remain near a demixing point. This membrane contains thousand of components, and it is largely unclear how its composition is controlled. Beyond this, one can ask whether cells should obey the traditional thermodynamic picture, given their small size, large number of components and the presence of non-equilibrium processes.

Here, we study toy systems, lattice models containing many (>30) components. We show that these systems exhibit strong finite-size effects. These manifest as behavior that appears similar to traditional critical behavior, but vanish logarithmically with system size. We examine scaling laws, and whether traditional paradigms from macroscopic thermodynamics can be broken in such systems.

BP 18.4 Wed 15:45 ZEU 250

Hierarchical interactions in complex ecosystems — •LYLE POLEY¹, JOSEPH W. BARON³, and TOBIAS GALLA^{1,2} — ¹Theoretical Physics, Department of Physics and Astronomy, School of Natural Sciences, The University of Manchester, Manchester M13 9PL, UK — ²Instituto de Física Interdisciplinar y Sistemas Complejos IFISC (CSIC-UIB), 07122 Palma de Mallorca, Spain — ³Laboratoire de Physique Statistique, École Normale Supérieure (ENS), Paris Sciences et Lettres (PSL) Research University, Sorbonne Université, 75005 Paris, France

In the analysis of complex ecosystems it is common to use random interaction coefficients, often assumed to be such that all species are statistically equivalent. We relax this assumption by imposing hierarchical inter-species interactions, which we incorporate into a generalised Lotka-Volterra dynamical system. These interactions impose a hierarchy in the community. Species benefit more, on average, from interactions with species below them in the hierarchy than from interactions with those above.

Using analytical tools from the theory of disordered systems, most notably path-integrals and dynamic mean-field theory, we demonstrate that a stronger hierarchy stabilises the community by reducing the number of species in the surviving community. We will also show that the probability of survival for a given species is dependent on its position in the hierarchy.

Reference: Poley L, Baron J W and Galla T Generalised Lotka-Volterra model with hierarchical interactions 2022 arXiv:2208.01569

BP 18.5 Wed 16:00 ZEU 250

Quantifying information content in continuous attractor networks — •TOBIAS KÜHN^{1,2} and RÉMI MONASSON¹ — ¹Laboratoire de Physique de l'École Normale Supérieure, ENS, Université PSL, CNRS, Sorbonne Université, Université Paris Cité, F-75005 Paris — ²Institut de la Vision, Sorbonne Université, INSERM, CNRS, F-75012 Paris

Attractor networks are a theme with long tradition to model information storage in the brain. Continuous attractor neural networks (CANN), in particular, have been employed to describe the storage of information about space and orientation. However, it stays controversial how useful this paradigm really is to explain

actual processes, for example the representation of space in grid and place cells in the entorhinal cortex and the hippocampus, respectively.

A common criticism is that the disorder present in the connections might deteriorate the system's capability to reliably preserve the information of a certain pattern. In order to investigate if this criticism is valid, a measure is needed to objectively quantify the information content of a given neural network. Using the replica-trick, we compute the Fisher information for a network receiving space-dependent input whose connections are composed of a distance-dependent and a disordered component. We observe that the decay of the Fisher information is slow for not too large disorder strength, indicating that CANNs have a regime in which the advantageous effects of connectivity on information storage outweigh the detrimental ones.

BP 18.6 Wed 16:15 ZEU 250

Gift of gab: Probing the limits of dynamic concentration-sensing across a network of communicating cells — •MOHAMMADREZA BAHADORIAN^{1,2}, CHRISTOPH ZECHNER^{1,2,3}, and CARL D. MODES^{1,2,3} — ¹Max Planck Institut für Molecular Cell Biology and Genetics (MPI-CBG), 01307 Dresden, Germany — ²Center for Systems Biology Dresden (CSBD), 01307 Dresden, Germany — ³Cluster of Excellence Physics of Life, TU Dresden, 01069 Dresden, Germany

Many systems in biology and other sciences employ collaborative, collective communication strategies for improved efficiency and adaptive benefit. One such paradigm of particular interest is the community estimation of a dynamic signal, when, for example, an epithelial tissue of cells must decide whether to react to a given dynamic external concentration of stress-signaling molecules. At the level of dynamic cellular communication, however, it remains unknown what effect, if any, arises from communication beyond the mean field level. What are the limits and benefits to communication across a network of neighbor interactions? What is the role of Poissonian versus super-Poissonian dynamics in such a setting? How does the particular topology of connections impact the collective estimation and that of the individual participating cells? In this article we construct a robust and general framework of signal estimation over continuous-time Markov chains in order to address and answer these questions.

BP 19: Biopolymers, Biomaterials and Bioinspired Functional Materials (joint session CPP/BP)

Time: Wednesday 16:30–18:00

Location: MER 02

BP 19.1 Wed 16:30 MER 02

Low-Temperature and Water-Based Biotemplating of Nanostructured Foam-Like Titania Films using β -Lactoglobulin — •JULIAN E. HEGER¹, WEI CHEN¹, SHANSHAN YIN¹, NIAN LI¹, VOLKER KÖRSTGENS¹, CALVIN J. BRETT^{2,3}, WIEBKE OHM², STEPHAN V. ROTH^{2,3}, and PETER MÜLLER-BUSCHBAUM^{1,4} — ¹TUM School of Natural Sciences, Chair for Functional Materials, Garching, Germany — ²DESY, Hamburg, Germany — ³Royal Institute of Technology KTH, Stockholm, Sweden — ⁴MLZ, TUM, Garching, Germany

Energy-related applications such as solar cells, batteries, and the photocatalytic production of hydrogen are broadly built up on titania nanostructures. A tailored titania morphology is necessary to match the required charge diffusion lengths and the crystallinity beneficial for efficient performance. In the context of large-scale fabrication, the aspect of sustainability becomes essential. Biopolymer templating based on β -Lactoglobulin (β -lg) and spray deposition promotes low-temperature and water-based synthesis of nanostructured, crystalline, foam-like titania films. During spray deposition, the β -lg biopolymer matrix sterically directs the titania morphology. Afterwards, the biotemplate is removed by UV-light exposure. To understand the kinetics of film formation during the spray deposition on the nano and crystalline length scale, we simultaneously perform in situ grazing-incidence small-angle and wide-angle X-ray scattering (GISAXS/GIWAXS). Together with scanning electron microscopy (SEM), the results explain the role of β -lg as a biotemplate.

BP 19.2 Wed 16:45 MER 02

Structural changes in cellulose nanofibril-colloid hybrid films during humidity cycling — •STEPHAN V. ROTH^{1,2}, CALVIN J. BRETT^{1,2}, ALEXANDROS ALEXAKIS², LUCAS P. KREUZER³, MARTIN MANSSON², SARAH ROGERS⁴, EVA MALMSTRÖM², PETER MÜLLER-BUSCHBAUM^{3,5}, and L. DANIEL SÖDERBERG² — ¹Deutsches Elektronen-Synchrotron DESY, Hamburg, Germany — ²KTH Royal Institute of Technology, Stockholm, Sweden — ³TUM School of Natural Sciences, Chair for Functional Materials, Garching — ⁴ISIS-STFC, Rutherford Appleton Laboratory, Chilton, Oxon OX11 0QX, UK — ⁵MLZ, TUM, Garching, Germany

Biocompatible cellulose nanofibrils (CNFs) are an ideal material for sustainable biomaterial templates. Combined with latex colloids, the resulting hybrid colloid-CNF functional materials are excellent candidates for bio-inspired structural colors. Due to the hydrophilic nature of CNFs, we investigate the stability against humidity cycling in terms of reversible/irreversible structural rearrangements. We applied depth sensitive grazing incidence small-angle neutron

scattering to evaluate the humidity-induced rearrangements in hybrid latex colloid:CNF templates in situ during cyclic humidification. After the first humidity cycle, a change in morphology on the scale of several 10 nm was observed, which is attributed to latex particles which diffused in the network and enlarged the pores of the network. The measured kinetics resolve the time- and depth-dependence of the differently sized colloids' penetration into the porous CNF network.

BP 19.3 Wed 17:00 MER 02

Fluorescence correlation spectroscopy for studying the aggregation of nanoplastics in model biofilm substances — •TOBIAS GUCKEISEN, ROZALIA ORGHICI, and SILKE RATHGEBER — Universität Koblenz, Deutschland

Nanoplastics in the environment are a growing problem. Pollutants can adhere to their surfaces and therefore be easily transported into the natural systems. Biofilms are found everywhere in the environment; they are formed by microbial communities that produce a matrix of extracellular polymeric substances. The interaction between nanoplastics and biofilms can lead to aggregation and sedimentation of nanoparticles and determines the transport and fate of nanoplastics. A better understanding of the transport and fate of nanoplastics is important to improve our ability to predict risks associated with these ubiquitous contaminants. In this project, we use fluorescence correlation spectroscopy (FCS) to study the aggregation and interactions of nanoplastics with model biofilm substances. Protein-polysaccharide mixing ratio and pH-dependent aggregation studies show that it is crucial to consider correlative effects between multiple biofilm components to better understand the impact biofilms have on nanoplastic aggregation. Biofilm model systems with only one component, as commonly considered, may lead to an incorrect assessment of the tendency to aggregation.

BP 19.4 Wed 17:15 MER 02

Ensemble inequivalence and negative extensibility in a wormlike chain with fluctuating bending stiffness — •PANAYOTIS BENETATOS — Department of Physics, Kyungpook National University, Republic of Korea

Many semiflexible polymers exhibit fluctuations in the local bending stiffness along their contour. This may be due to intrinsic conformational changes (e.g., denaturation bubble formation in double stranded DNA or helix-coil transition in polypeptides) or to the reversible adsorption and desorption of molecules from the polymer's environment. In this presentation, we analyse the tensile elasticity of a strongly stretched wormlike chain which consists of N concatenated segments, where each segment can be in one of two states, A and B, which differ

in bending stiffness. We call this model the reversible wormlike chain (rWLC) model. In the Gibbs (fixed-force, isotensional) ensemble, we obtain analytic expressions for the force-expression relation and the mean fraction of B segments. We show that, under certain conditions, there is a tension-induced crossover from a mostly A to a mostly B rWLC. In the Helmholtz (fixed-extension, isometric) ensemble, we obtain analytic expressions up to a summation. We show that, for finite N, there is marked ensemble inequivalence. Remarkably, in the Helmholtz ensemble, the rWLC can exhibit negative extensibility and multiple peaks.

BP 19.5 Wed 17:30 MER 02

Aging and compressed exponential stress relaxation in mechanoresponsive hydrogels — •GEONHO SONG^{1,2}, WOUTER ELLENBROEK³, and KERSTIN BLANK^{1,2} — ¹Johannes Kepler University Linz, Linz, Austria — ²Max Planck Institute of Colloids and Interfaces, Potsdam, Germany — ³Eindhoven University of Technology, Eindhoven, The Netherlands

Biological materials, such as the extracellular matrix (ECM), are viscoelastic and exhibit stress relaxation. Stress relaxation in the ECM is linked to cellular behavior and needs to be considered as a design parameter when developing bioinspired materials for cell culture and tissue engineering. Here, we introduce a collagen-inspired hydrogel with tunable crosslink kinetics. We utilize collagen-mimetic peptides with controlled association and dissociation rates to crosslink star-shaped polyethylene glycol. We show that ultraslow crosslink dissociation rates cause a distinctive relaxation behavior that is reminiscent of soft glassy ma-

terials, showing out-of-equilibrium properties. In particular, subjecting the networks to a sequence of pre-stress and aging causes uncommon compressed exponential relaxation. This unique phenomenon has previously only been reported for a small number of soft glassy systems where compressed exponential relaxation was related to ultraslow dynamics that prohibited the release of internal stresses. In such systems, slow crosslink dissociation delays network relaxation until an external trigger is applied. In future work, we aim to investigate the interplay between locally generated stresses, such as cellular traction forces, and network relaxation properties.

BP 19.6 Wed 17:45 MER 02

Nonaffinity controls critical slowing down and rheology near the onset of rigidity — •ABHINAV SHARMA¹, JORDAN SHIVERS², and FRED MACKINTOSH² — ¹Leibniz institute for polymer research, Dresden — ²Rice University, Houston, Texas

Fluid-immersed networks and dense suspensions often reside near a boundary between soft (or fluid-like) and rigid (or solid-like) mechanical regimes. This boundary can be crossed either by varying the concentration or by deformation. Near the onset or loss of rigidity, dissipation-limiting nonaffine rearrangements dominate the macroscopic viscoelastic response, giving rise to diverging relaxation times and power-law rheology. Here, we derive a simple relationship between nonaffinity and excess viscosity in fluid-immersed amorphous materials. We then demonstrate this relationship and its rheological consequences in simulations of stress relaxation in strained filament networks and dense suspensions.

BP 20: Members' Assembly

Time: Wednesday 18:00–19:00

Location: BAR Schö

All members of the Biological Physics Division are invited to participate.

BP 21: Bioimaging

Time: Thursday 9:30–13:00

Location: BAR Schö

BP 21.1 Thu 9:30 BAR Schö

Imaging DNA-Origami with Low Energy Electron Holography — •MORITZ EDTE¹, HANNAH OCHNER¹, LUIGI MALAVOLTI¹, and KLAUS KERN^{1,2} — ¹Max-Planck-Institute for Solid State Research, Stuttgart, Germany — ²École Polytechnique Fédérale de Lausanne, Lausanne, Switzerland

Our low-energy electron holography (LEEH) approach makes use of a coherent low-energy electron wave (energies in the range of 50 to 150 eV) for imaging biomolecules with high contrast [1]. Hence, the method allows true single-molecule imaging of large three-dimensional molecules and can map conformational variability of flexible molecules [2]. I will show LEEH measurements of individual DNA-Origami molecules on single layer graphene, demonstrating that LEEH is capable of imaging this class of molecules without introducing perceptible structural changes on the time scale of the measurements and on the spatial scale defined by our current resolution limit.

[1] J.-N. Longchamp, et al., PNAS, 2017, 114, 1474-1479. [2] H. Ochner, et al., PNAS, 2021, 118, e2112651118

BP 21.2 Thu 9:45 BAR Schö

Spectral and nanolocal discrimination of crosslinked from single fibrillar actin using mid-IR photoinduced force microscopy (PiF-IR) — JESVIN JOSEPH^{1,2}, DIJO MOONNUKANDATHIL JOSEPH^{1,2}, LUKAS SPANTZEL^{2,3}, KATHARINA REGLINSKI^{1,2}, CHRISTOPH KRAFFT^{1,2}, CHRISTIAN EGGELE^{1,2}, RAINER HEINTZMANN^{1,2}, MICHAEL BÖRSCH^{2,3}, and •DANIELA TÄUBER^{1,2} — ¹Leibniz Institute of Photonic Technology, Jena — ²Friedrich Schiller University Jena — ³Jena University Hospital, Jena, Germany

Fibrillar actin is one of the major structural components in cells. Consequently, pathogenic alterations in cell functionality may be revealed by monitoring the re-arrangement of F-actin. However, discriminating protein aggregation in the range below 10 nm is challenging even by high resolution fluorescence microscopy. This gap can be addressed by recently developed mid-IR photo-induced force microscopy (PiF-IR). PiF-IR spectra obtained from fibrillar and monomeric actin match the corresponding FTIR spectra. The high spectral resolution of PiF-IR provides simplified access to IR spectroscopic signatures from secondary protein structure. The intensity of bands at 1655 cm⁻¹ and 1685 cm⁻¹ associated to α -helices and intermolecular β -sheets, respectively, varied within the scan image. Furthermore, PiF-IR hyperspectra obtained from single fibrillar actin appear more homogeneous than those from cross-linked F-actin. These first results are very promising for using PiF-IR to discriminate F-actin structures to study pathogenic alterations in cells and tissue ex vivo.

BP 21.3 Thu 10:00 BAR Schö

Cryo-EM samples of gas-phase purified protein assemblies using native electrospray ion-beam deposition (ES-IBD) — •TIM ESSER¹, LUKAS ERIKSSON², PAUL FREMDLING², and STEPHAN RAUSCHENBACH² — ¹Thermo Fisher Scientific, 1 Boundary Park, Hemel Hempstead, HP2 7GE, UK — ²Department of Chemistry, University of Oxford, Oxford OX1 3TF, UK

Combining native mass spectrometry (MS) with cryo electron microscopy (cryo-EM) allows to correlate information on homogeneity, stoichiometry, shape, and interactions of native protein complexes, complementary to high-resolution protein structures. Cryo-EM samples are conventionally made by coating TEM grids with a protein-containing solution, blotting, and plunge freezing in liquid ethane, quenching proteins in their native state, embedded in ultra-thin films of vitreous ice. Reliable sample preparation remains a major challenge, in particular for heterogeneous samples. Here we demonstrate mass-selective cryo-EM sample preparation via native electrospray ion-beam deposition (ES-IBD), as a direct link between native MS and cryo-EM. Protein complexes are brought into the gas phase, mass-selected, and deposited on TEM grids with thin carbon films at defined temperature. By controlling interactions in solution, gas-phase, and on the surface, we probe protein conformations between native solution-phase and native-like gas-phase structures. We show sub-nanometer EM density maps obtained using native ES-IBD and discuss its potential to extend the scope of cryo-EM in structural biology.

BP 21.4 Thu 10:15 BAR Schö

CRISPR activation screen to improve the optical properties of living tissues — •SUSAN WAGNER, VENKAT KRISHNASWAMY, KAUSHIKARAM SUBRAMANIAN, HEIKE PETZOLD, BENJAMIN SEELBINDER, RICO BARSACCHI, and MORITZ KREYSING — Max Planck Institute of Molecular Cell Biology and Genetics, Dresden, Germany

Today, optical microscopes deliver unprecedented resolution allowing discoveries down to the molecular level. Nevertheless, optical access of living biological samples by microscopes is usually restricted to the outer most surface owing to tissue-induced light scattering.

Using directed evolution, we successfully improved the optical properties of mammalian cells. We aim to fully understand this optical plasticity of cells, and genetically clear living mammalian tissues by targeting responsible genes. We are conducting a genome-wide CRISPR activation screen to find genes which confer transparency. This contribution seeks to report on progress, challenges, and opportunities of this technology for biophotonics research, and more generally its potential towards a system level understanding of cellular biophysics.

As a next step, we are investigating how improved optical properties of individual cells influence the optical properties of 3D cell clusters, such as spheroids,

using interspersed external fluorescent microspheres to quantify unbiased imaging quality.

Understanding the full potential of the optical plasticity of a tissue bears the potential of providing us with a broad toolkit, so that different genetic strategies can be applied depending on the specific nature of the various biological samples.

BP 21.5 Thu 10:30 BAR Schö

Optical characterization of biological material across scales using interferometric microscopy — •DANIEL MIDTVEDET — Department of Physics, University of Gothenburg

The physicochemical properties, such as size, mass, and composition, of biological matter generally impact its function. However, quantitative characterization of these parameters across the many length-, time-, and mass scales relevant for biology is challenging. Interferometric imaging techniques, such as holographic imaging and interferometric scattering microscopy (iSCAT), provide quantitative measurements of the light scattering properties of biological objects, and are promising techniques for achieving such characterization. However, although iSCAT provides exquisite sensitivity, quantitatively relating the measured signal to physicochemical properties is straightforward only for small (Rayleigh) scatterers. The holographic signal, on the other hand, can be quantified across arbitrary length scale, but due to poor signal-to-noise ratio it is typically restricted to particles larger than the illuminating wavelength. In this talk, I will showcase some of our recent results combining interferometric imaging techniques with deep learning, enabling pushing the limit of mass quantification in holographic imaging toward the Rayleigh limit, thereby bridging a gap in optical characterization of small particles. With our technique, we are able to characterize biological matter across four orders of magnitude in length, four order of magnitude in time, and ten orders of magnitude in mass. I will highlight the key steps that have enabled us to make this development, and discuss its potential impact on life science research.

BP 21.6 Thu 10:45 BAR Schö

Adaptive optics in Confocal microscopy and Fluorescence correlation spectroscopy — •JULIUS TRAUTMANN, PHILIPP KELLNER, and CHRISTIAN EGGELING — Institute for Applied Optics and Biophysics, Friedrich-Schiller University Jena, Philosophenweg 7, 07743 Jena

For more than three decades adaptive optics have been widely used in astronomical applications, but only in recent years it has established itself as an important feature for high resolution microscopy. The ability to correct for optical aberrations can be useful for any kind of setup but it proved particularly useful when imaging samples with inhomogeneous refractive index structures such as cells and especially cell tissue.

The most established adaptive optic elements include deformable mirrors (DMs) and spatial light modulators (SLMs) which can dynamically correct for aberrations.

This talk will cover the basic idea of including a deformable mirror (DM) in a confocal microscope within a fluorescence correlation spectroscopy (FCS) setup. A comparison of placing the deformable mirror in the excitation or detection beam path will take place.

15 min. break

Invited Talk

BP 21.7 Thu 11:15 BAR Schö

Visualizing the inner life of microbes — •ULRIKE ENDESFELDER — Institute for Microbiology and Biotechnology, Bonn University, Germany

Microbes, as unicellular organisms, are crucial model systems for the study of cellular mechanisms and functions. With the advent of modern fluorescence microscopy techniques, we can now visualize the inner workings of microbes at the molecular level, e.g. the dynamics of single molecules and the molecular architecture of sub-cellular structures. By quantifying the molecular characteristics of microbes *in vivo*, we thus can create detailed, spatially and temporally resolved maps of their molecular makeup, allowing us to understand the dynamic heterogeneity and sub-populations at the sub-cellular level. In this talk, I will discuss the potential of single-molecule biophysical approaches for microbiology, using examples from our own research and outlining our future visions.

BP 21.8 Thu 11:45 BAR Schö

A Minimal Model of CD95 Signal Initiation Revealed by Advanced Molecular-Sensitive Imaging — •NINA BARTELS¹, NICOLAAS TM VAN DER VOORT², CLAUS AM SEIDEL², and CORNELIA MONZEL¹ — ¹Experimental Medical Physics, Heinrich-Heine University, Düsseldorf, Germany — ²Molecular Physical Chemistry, Heinrich-Heine University, Düsseldorf, Germany

The spatio-temporal organization and dynamic interactions of receptors in the plasma membrane are fundamental for our mechanistic understanding of cell signal initiation. A paradigm of a cell signal initiation process is the ligand-induced oligomerization of TNF (tumor necrosis factor) receptor CD95 in the signaling pathway for apoptosis. Here, we scrutinize proposed CD95 oligomerization models in the cell plasma membrane by applying a molecular sensitive imaging toolkit with up to nanometric resolution including time-resolved FRET

spectroscopy, confocal Photobleaching Step Analysis, STED microscopy, and FCS. Covering a wide range of parameters, CD95 interactions are probed over the whole dynamic range from μ s to hours, molecular to cellular scales, and with particular focus on quantifying molecular concentrations. Our multiscale study reveals a minimal oligomerization model to trigger apoptosis efficiently, where only ~8-17% CD95 monomers assemble into dimers/trimers after ligand binding. Further, we highlight the importance of combining complementary techniques for a full understanding of transient and potentially localized processes such as a cell signal initiation.

see also <https://doi.org/10.1101/2022.11.29.518370>

BP 21.9 Thu 12:00 BAR Schö

Investigating human lung tissue by propagation-based phase-contrast X-ray tomography — •JAKOB REICHMANN¹, STIJN VERLEDEN², MARK KÜHNEL³, JAN-CHRISTOPHER KAMP³, LAVINIA NEUBERT³, JAN-HENDRIK MÜLLER¹, THANH QUYNH BUI¹, DANNY JONIGK³, and TIM SALDITT¹ — ¹Institute for X-ray Physics, University of Göttingen, Friedrich-Hund-Platz 1, 37077 Göttingen — ²Anatomy and Research Centre, University of Antwerp, Universiteitsplein 1, 2610 Wilrijk, Belgium — ³Institute of Pathology, Hannover Medical School, Carl-Neuberg-Straße 1, 30625 Hannover

The lung is a perfect example of how the function of an organ is enabled by its three-dimensional structure, here formed by intricate and intertwined networks of ventilation and vasculature. In this work we study the structure of lung tissues over multiple scales down to the sub-cellular level by phase-contrast computed tomography (PCCT). We show how human lung tissues with their largely air-filled compartments and small vessels can be imaged non-destructively with a scalable, isotropic resolution and quantitative density. Three-dimensional reconstructions with varied voxel sizes down to 130nm are obtained by advanced phase retrieval and tomographic reconstruction, shedding light on the three-dimensional cytoarchitecture. Morphometric parameters are extracted by automated image processing, and used to quantify the degree of pathological alterations. This offers unique potential to extend histology and pathohistology to study e.g. SARS-CoV-2 infected tissue or other lung degrading diseases such as COPD or cystic fibrosis, as we show with first applications of the method.

BP 21.10 Thu 12:15 BAR Schö

Dynamic allometry of nuclei and cell size in early embryos of a model organism — ROLF FICKENTSCHER¹, TOMOKO OZAWA², AKATSUKI KIMURA², and •MATTHIAS WEISS¹ — ¹Experimental Physics I, University of Bayreuth, Germany — ²Cell Architecture Laboratory, National Institute of Genetics, Mishima, Japan

Allometric relations between two observables are a widespread phenomenon in biology. The volume of nuclei, for example, has frequently been reported to be linearly related to the cell volume, but also conflicting, sublinear power-law correlations have been reported. Given that nuclei are vital organelles that harbor and maintain the cells' DNA, an understanding of the allometric scaling of nuclear volumes, which eventually defines the concentration and accessibility of chromatin, is of high interest. Using the model organism *Caenorhabditis elegans*, we show here that the allometry between cell and nucleus volumes is a dynamically adapting phenomenon with an asymptotic linear scaling. The adaption rate of the nucleus volume also scales with cell size. Our experimental data are well captured by a simple and supposedly generic model based on a diffusion-limited liberation of chromatin sites which drives decompaction and hence nucleus growth. Extrapolating our results to the general case of growing and proliferating cells suggests an isometric scaling of cell and nucleus volumes as the generic case.

BP 21.11 Thu 12:30 BAR Schö

Mechanical and electrophysiological recordings of neural organoids — ELIJAH SHELTON¹, PAULINA WYSMOLEK², FILIPPO KIESSLER¹, ACHIM BRINKOP¹, SEBASTIAN WILLENBERG¹, MICHAEL FRISCHMANN¹, and •FRIEDHELM SERWANE^{1,2,3} — ¹Faculty of Physics & CeNS, LMU Munich, Germany — ²MPI for Medical Research, Heidelberg, Germany — ³Munich Cluster for Systems Neurology, Munich, Germany

Stem-cell derived organoids have made the exploration of neuronal network function accessible *in vitro* and are now allowing disease modelling. Both biochemical and mechanical signals, such as the elastic modulus, modulate the underlying behaviour of neurons to connect to networks. My group is developing tools for the mechanical and electrophysiological characterization of neuronal organoids. I will present a minimal-complexity setup for 3D imaging of their network activity (Wysmolek et al., Sci Rep 12, 20420, 2022). To extract Ca-signals we combine a lightsheet microscope as an add-on to a standard inverted microscope with computational tools. We created a 3D connectivity map by imaging spontaneous activity. As a next step, we apply statistical models to characterize the network behaviour. Changes in the tissue mechanical properties are one biophysical hallmark of tumour formation *in vivo*. We map the mechanical properties of tumor-forming cerebral organoids using ferrofluid droplets as mechanical actuators. Our measurements performed in neural organoids could inform researchers about the interaction between mechanics and function in the central nervous system.

BP 21.12 Thu 12:45 BAR Schö

Multi-scale X-Ray phase contrast tomography from the whole cochlea to single cells — •JANNIS JUSTUS SCHAEPER¹, CHRISTOPH KAMPSHOFF², BETTINA WOLF², DANIEL KEPPELER², TOBIAS MOSER², and TIM SALDITT¹ — ¹Institut für Röntgenphysik, Georg-August-Universität Göttingen — ²InnerEarLab, Universitätsmedizin Göttingen

The cochlea is the receptor organ of the inner ear which transduces sound into neuronal activity. Both fundamental aspects of signal transduction and neurophysiology as well as biomedical research (implant technology, hearing loss and disorders) require 3D imaging techniques capable to quantify the micro-anatomy (1).

We present multi-scale 3D imaging of small-animal cochleae by X-ray phase-

contrast tomography (XPCT) using both synchrotron radiation (SR) and lab μ -CT to assess the morphology of the cochlea, orientation of cochlear implants (CIs), and the number and density of spiral ganglion neurons (SGNs). Due to optimization in sample preparation, image acquisition and phase retrieval we achieve high contrast for unstained soft tissue. Without extensive sample preparation, shape and volume of every SGN in the entire organ can be identified. In the high-resolution PC-CT, and in the parallel beam, we reach cellular resolution in the organ of Corti. Lab μ -CT is suitable to analyze cochlear morphology and to assess the correct positioning of CIs and resulting (non-)optimal signal transduction.

(1) Keppeler et al. (2021), PNAS 118(18), e2014472118 (2) Schaeper et al. (2022), Proc. SPIE 12242

BP 22: Statistical Physics of Biological Systems I (joint session BP/DY)

Time: Thursday 9:30–13:00

Location: TOE 317

BP 22.1 Thu 9:30 TOE 317

Reduced stochastic models of drifting assemblies in plastic neuronal networks — •SVEN GOEDEKE, CHRISTIAN KLOS, YAROSLAV FELIPE KALLE KOSSIO, and RAOUL-MARTIN MEMMESHEIMER — University of Bonn, Bonn, Germany

In a standard model, associative memories are represented by assemblies of strongly interconnected neurons. It has recently been proposed that these assemblies are not static but drift freely in neural circuits. On the level of single neurons, assembly drift is reflected by characteristic dynamics: relatively long times of stable assembly membership interspersed with fast transitions. How can we mechanistically understand these dynamics? Here we answer this question by proposing simplified, reduced models. We first construct a random walk model for neuron transitions between assemblies based on the statistics of synaptic weight changes measured in simulations of spiking neural networks exhibiting assembly drift. It shows that neuron transitions between assemblies can be understood as noise-activated switching between metastable states. The random walk's potential landscape and inhomogeneous noise strength induce metastability and thus support assembly maintenance in the presence of ongoing fluctuations. In a second step, we derive an effective random walk model from first principles. In this model, a neuron spikes at a fixed background rate and with an input weight-dependent probability when its current or another assembly reactivates. The approach can be applied generally to networks of drifting assemblies, irrespective of the employed neuron and plasticity models.

BP 22.2 Thu 9:45 TOE 317

Fluctuation-dissipation relations for spiking neurons — •BENJAMIN LINDNER — Bernstein Center for Computational Neuroscience Berlin, Philippstr. 13, Haus 2, 10115 Berlin, Germany — Physics Department of Humboldt University Berlin, Newtonstr. 15, 12489 Berlin, Germany

Spontaneous fluctuations and stimulus response are essential features of neural functioning but how they are connected is poorly understood. I derive fluctuation-dissipation relations (FDR) between the spontaneous spike and voltage correlations and the firing rate susceptibility for i) the leaky integrate-and-fire (IF) model with white noise; ii) an IF model with arbitrary voltage dependence, an adaptation current, and correlated noise. The FDRs can be used to derive thus far unknown statistics analytically [model (i)] or the otherwise inaccessible intrinsic noise statistics [model (ii)].

BP 22.3 Thu 10:00 TOE 317

Current fluctuations in nanopores: origin and breakdown of 1/f noise — •PAUL ROBIN, MATHIEU LIZEE, ALESSANDRO SIRIA, and LYDÉRIC BOCQUET — ENS, Université PSL, CNRS, Sorbonne Université, Université Paris-Cité, Paris, France

Ion transport through nanometric pores is key to many biological processes, from osmoregulation to neurotransmission, yet this process is known to occur under strong fluctuations. The power spectrum of this current noise is known to scale like $1/f$ at low frequency, according to the long-standing yet empirical Hooge law. Modelling attempts generally rely on complex assumptions such as self-organized criticality or microscopic disorder - in contrast with the apparent universality of $1/f$ pink noise. In this talk, I will present a simple theoretical model accounting for the presence of $1/f$ fluctuations in ionic currents through nanopores regardless of their microscopic structure. In particular, I will show how pink noise can emerge from diffusive processes alone, rather than necessitating complex conductance switching mechanisms. This prediction also explains why pink noise can be observed for frequencies much lower than that of microscopic processes. Lastly, I will discuss under which conditions this description is expected to break down. Notably, chemical processes on the pore's walls can alter ion dynamics and slow down diffusion, leading to memory effects and deviations to Hooge's law. I will compare these predictions to experimental data on artificial nanofluidic pores with various surface properties and reactivities.

BP 22.4 Thu 10:15 TOE 317

Selective alignment force in schooling fish linked to leader-follower interactions given by relative speeds of neighbours — •ANDREU PUY¹, PALINA BARTASHEVICH^{2,3}, and PAWEŁ ROMANCUK^{2,3} — ¹Departament de Física, Universitat Politècnica de Catalunya, Barcelona, Spain — ²Institute for Theoretical Biology, Humboldt-Universität zu Berlin, Germany — ³Excellence Cluster Science of Intelligence, Technische Universität Berlin, Germany

Collective motion is commonly assumed to emerge when individuals in a group interact with neighbours via some combination of attraction, repulsion and alignment forces. Alignment has been the most elusive and controversial force to study in experimental setups, with previous works differing about its existence. Here we revisit the topic by introducing a force map technique depending on the relative velocities of neighbours. In contrast to commonly used force maps, our technique demonstrates evidence for experimental data of schooling fish of a selective alignment force when individuals move at slower speeds than their neighbours and an antialignment force when they move at higher speeds. We employ a simple model with alignment to demonstrate the validity and robustness of the proposed force map. Including a selective interaction where individuals only interact with faster neighbours allowed us to reproduce the alignment interactions in the experimental data. Finally, we link this idea to leader-follower interactions, justifying that faster individuals act as leaders with respect to their neighbours.

Invited Talk

BP 22.5 Thu 10:30 TOE 317

Statistical Physics of Spatially Organized Catalytic Particles — •ULRICH GERLAND — Technical University of Munich, Germany

Catalytic particles are spatially organized in a number of biological systems across different length scales, from enzyme complexes to metabolically coupled cells. Despite operating on different scales, these systems all feature localized reactions involving partially hindered diffusive transport, which is determined by the collective arrangement of the catalysts. We explore how different arrangements affect the interplay between the reaction and transport dynamics, which ultimately determines the flux through the reaction pathway. Two fundamental trade-offs arise, the first between efficient inter-catalyst transport and the depletion of substrate, and the second between steric confinement of intermediate products and the accessibility of catalysts to substrate. We find that the question of optimal catalyst arrangements generalizes the well-known Thomson problem of electrostatics [1]. Furthermore, we map the problem of optimally arranging enzymes to an economic investment problem, which helps to formulate and understand a possible design principle for synthetic biomolecular systems [2].

[1] F. Hinzpeter, F. Tostevin, A. Buchner, and U. Gerland (2022), Trade-offs and design principles in the spatial organization of catalytic particles, *Nature Phys.* 18, 203-211.

[2] G. Giunta, F. Tostevin, S. Tanase-Nicola, and U. Gerland (2022), Optimal spatial allocation of enzymes as an investment problem, *Commun. Phys.* 5, 319.

15 min. break

BP 22.6 Thu 11:15 TOE 317

Collective Dynamics of Multi-Scale Interacting Complex Systems — •FABRIZIO OLMEDA^{1,2} and STEFFEN RULANDS^{1,3} — ¹Max Planck Institute for the Physics of Complex Systems, Dresden, Germany — ²IST Austria, Vienna, Austria — ³Ludwigs-Maximilians-Universität München, Arnold Sommerfeld Center for Theoretical Physics, Munich, Germany

Understanding the conditions under which complex systems are stable is pivotal for understanding their response to perturbations. Theoretical work has shown that for global interactions between components a minimal complex system is stable if the standard deviation of linearised interaction rates is sufficiently small. In biological systems, which often contain a small number of important and in-

interactions are mediated by diffusing agents, stochasticity and non-locality may influence stability. Here, we generalise these results to stochastic, spatial systems with interaction on multiple length scales. Starting from a microscopic description we derive a coarse-grained field theory and identify a transition between a regime defined by giant density fluctuations and one exhibiting a spatial instability with a finite wave length. The latter is suppressed by non-reciprocity in the interactions between components. Our work provides a rigorous framework to infer collective dynamics and stability in complex systems, with applications ranging from ecosystems to morphogenesis.

BP 22.7 Thu 11:30 TOE 317

Physical mechanism of erythrocytes sedimentation rate — •ALEXIS DARRAS, THOMAS JOHN, LARS KAESTNER, and CHRISTIAN WAGNER — Experimental Physics, Saarland University; D-66123 Saarbrücken, Germany

Red blood cells (or erythrocytes) sedimentation rate (ESR) is a physical parameter of blood which is often checked in medical diagnosis. It is indeed well known that in case of inflammation, the increase in fibrinogen and other proteins induces a higher ESR.

Until recently, researchers thought that the increase of fibrinogen accelerates the ESR by creating bigger aggregates of red blood cells (RBC). Fibrinogen is indeed an aggregation agent of RBCs, and bigger aggregates tend to sediment faster in Stokes regime. However, modeling the ESR measurements with this hypothesis is challenging and often requires physical assumptions specific to this system.

Besides, modern colloidal science has shown that attractive particles, in suspensions with a high volume fraction, form percolating aggregates, as wide as the container. The sedimentation of those colloids then follows a so-called "colloidal gel collapse" regime, governed by the geometry of the percolating aggregate acting as a porous material. In this talk, we show that RBCs actually follow the same behavior. We also demonstrate that a porous-material model naturally leads to an efficient description of the RBC sedimentation, which also provides a long-sought dependency of the ESR as a function of the initial RBC volume fraction (i.e. the hematocrit).

BP 22.8 Thu 11:45 TOE 317

Stochastic wavelength selection and pattern fixation — •TOM BURKART^{1,2}, ANASTASIA PETROVA^{2,3}, LAESCHKIR WÜRTHNER^{1,2}, CLAUDIA VEIGEL^{2,3}, and ERWIN FREY^{1,2,4} — ¹Arnold Sommerfeld Center for Theoretical Physics (ASC), Department of Physics, LMU München, Munich, Germany — ²Center for NanoScience, LMU München, Munich, Germany — ³Department of Cellular Physiology, Biomedical Center (BMC), LMU München, Planegg-Martinsried, Germany — ⁴Max Planck School Matter to Life, Munich, Germany

Biological pattern-forming processes are typically driven by a chemical fuel (out-of-equilibrium systems) or by a relaxation towards a thermodynamic equilibrium (phase separation). In these cases, pattern wavelength selection results from translational shifts of high-density regions and mass redistribution in between such regions. Here, we study how a pattern with a characteristic wavelength can form when high-density regions can only grow, but neither mass redistribution nor translation are allowed. The corresponding wavelength selection mechanism relies on thermal fluctuations, irreversible fixation of randomly occurring high-density regions, and long-ranged interactions between these regions. To model the density dynamics and the long-ranged interaction, we derive a set of reaction-diffusion equations from a free energy functional. In addition, we derive the statistics of pattern wavelengths from order statistics, emphasising the stochastic nature of the underlying mechanism. Our results constitute an alternative path to pattern formation next to out-of-equilibrium dynamics and phase separation processes.

BP 22.9 Thu 12:00 TOE 317

Control of non-equilibrium chemical reactions via phase separation — •SUDARSHANA LAHA^{1,2}, JONATHAN BAUERMANN^{1,2}, TYLER S. HARMON³, FRANK JÜLICHER^{1,2}, THOMAS C.T. MICHAELS⁴, and CHRISTOPH A. WEBER⁵ — ¹Max Planck Institute for the Physics of Complex Systems Dresden, Germany — ²Center for Systems Biology Dresden, Germany — ³IFW Dresden, Germany — ⁴ETH Zürich, Switzerland — ⁵Institute of Physics, University of Augsburg, Germany

Fuel-driven out-of-equilibrium chemical reactions are spatially organized using compartments in living cells. To what extent the properties of chemical reactions are altered by the compartments relative to homogeneous systems and the underlying physical principles are less explored. Here, we derive a theoretical framework to study such chemical reactions in the presence of compartments. We highlight the different governing kinetic equations for the reactants in diffusion-limited and reaction-limited regimes. We show that for two-state

transition processes, the turnover of the product can be significantly affected in the limit of infinitely fast diffusion of the components. We can further derive the optimal compartment volume analytically which shows how phase separation parameters can affect the turnover. We further observe that the initial rate can be strongly modified for enzymatic and nucleation processes. These aspects allow us to understand better the control of such processes and exemplify the role of enzymes in compartments to speed up the reaction. This understanding is crucial for synthetically designing of cells as compartments and establishing communication between them.

BP 22.10 Thu 12:15 TOE 317

Microphase separation of living cells — •FRANÇOIS DETCHEVERRY, ADRIEN CARRÈRE, JOSEPH D'ALESSANDRO, OLIVIER COCHET-ESCARTIN, JULIE HESNARD, NASSER GHAZI, CHARLOTTE RIVIÈRE, CHRISTOPHE ANJARD, and JEAN-PAUL RIEU — University of Lyon, Université Claude Bernard Lyon 1, CNRS, Institut Lumière Matière, F-69622, VILLEURBANNE, France

Self-organization of cells is key to a variety of biological systems and physical concepts inspired from condensed matter have proven essential in understanding some of their properties. Here we demonstrate that microphase separation, long known in polymeric materials and other inert systems, has a natural counterpart in living cells. When placed below a millimetric film of liquid nutritive medium, a quasi two-dimensional population of *Dictyostelium discoideum* cells spontaneously self-assembles into compact domains. Their typical size of 100 μm is governed by a balance between competing interactions: an adhesion which acts as a short-range attraction and promotes aggregation, and an effective long-range repulsion stemming from aerotaxis in near anoxic condition. We present a combination of experimental data, analytical modelling and cell-based simulations that all support this scenario. Our findings establish a generic mechanism for self-organization of living cells and highlight oxygen regulation as an emergent organizing principle for biological matter.

[Preprint: bioRxiv <https://doi.org/10.1101/2022.05.25.493184>]

BP 22.11 Thu 12:30 TOE 317

Hydration and crowding effects on SOD1 sequestration into FUS biocondensates — LUIS ENRIQUE CORONAS¹, EMELINE LABORIE², STEPAN TIMR², FABIO STERPONE², and •GIANCARLO FRANZESE^{1,3} — ¹Interdisciplinary and Statistical Physics Section—Department of Condensed Matter Physics, Physics & Institute of Nanoscience and Nanotechnology (IN2UB), Universitat de Barcelona, Barcelona, Spain — ²CNRS Laboratoire de Biochimie Théorique, Institut de Biologie Physico-Chimique, Université Paris Denis Diderot, Paris, France — ³Max Planck Institut für Physik Komplexer Systeme, Dresden, Germany

Superoxide Dismutase 1 (SOD1) is a protein related to amyotrophic lateral sclerosis that, under Heat Stress (HS), is sequestered into Stress Granules in vivo and Fused in Sarcoma (FUS) biomolecular condensates in vitro. Experiments show that an in vitro cytomimetic medium, using Bovine Serum Albumin (BSA) as crowder, decreases the SOD1 partition coefficient (PC) even after 60 min of HS. Implicit-water OPEP simulations show no preferential interactions of SOD1 with BSA. Here, by combining the OPEP with a coarse-grained water model, accounting for water contributions to the interactions in large biological systems, we show that SOD1 has one preferred associative state in FUS but three in BSA, whose transition rates and residency times are controlled by their hydration. We conclude that the SOD1 PC's decrease in FUS condensate, when BSA crowders are present, is due to the hydration entropy increase in BSA, a mechanism possibly relevant also in vivo.

BP 22.12 Thu 12:45 TOE 317

Stochastic heat production in phase-separated systems out of equilibrium — •KATHRIN LAXHUBER, JONATHAN BAUERMANN, and FRANK JÜLICHER — Max Planck Institute for the Physics of Complex Systems, Dresden, Germany

Phase-separated multi-component systems in the presence of chemical reactions provide interesting examples of non-equilibrium systems. We complement the dynamics of phase separation by a heat transport equation which is coupled to diffusive matter transport. On a microscopic scale, fluctuations become relevant, which we include by developing a stochastic lattice model that we link to the macroscopic continuum dynamics. We then implement this model in a kinetic Monte Carlo simulation of spatial flows of energy and matter as well as local reactions. By coupling to reservoirs or by fueling reactions, a system can be driven out of equilibrium. Using a toy system of a single phase-separated droplet, we discuss how temperature fluctuations affect the droplets' dynamics and the noise in the system. We furthermore show how the fluxes due to the driving give rise to a stochastic production of latent heat and reaction heat. The systems we discuss serve as models for biological condensates and the study of energetics in cells.

BP 23: Single Molecule Biophysics

Time: Thursday 9:30–13:00

Location: BAR 0106

Invited Talk

BP 23.1 Thu 9:30 BAR 0106

Conformational dynamics of SARS-CoV-2 spike protein modulates the binding affinity to ACE2 — FIDAN SUMBUL¹, CLAIRE VALOTTEAU¹, PRITHWIDIP SAHA¹, IGNACIO FERNANDEZ², ANNALISA MEOLA², EDUARD BAQUERO², DOROTA KOSTRZ³, JAMES R PORTMAN³, FRANÇOIS STRANSKY³, PABLO GUARDADO CALVO², CHARLIE GOSSE³, TERENCE STRICK³, FELIX REY², and •FELIX RICO¹ — ¹Aix-Marseille Univ, CNRS, INSERM, LAI, CENTURI, Marseille, France — ²Institut Pasteur, Department of Virology, CNRS UMR 3569, Paris France — ³Ecole Normale Supérieure, Institut de Biologie, CNRS, INSERM, PSL, Paris, France

SARS-CoV-2 spike protein (S) interacts with angiotensin-converting enzyme 2 (ACE2) to enter host cells. Protein S forms a homotrimer with three receptor-binding domains (RBD) adopting open and closed conformations. The (un)binding of S to ACE2 may be affected by these conformational dynamics. Here, we used single molecule force spectroscopy to probe the binding strength and affinity of the S-trimer/ACE2 interaction and high-speed atomic force microscopy (HS-AFM) to visualize the RBD opening dynamics of S-trimers. HS-AFM imaging revealed dynamic S-trimers with the three RBDs stochastically and independently switching between open and closed conformations. This modulates binding to ACE2 of S-trimers, but not unbinding. Experimental opening rates and a simple conformational binding model explain the modulation of the binding affinity. Our results shed light on the molecular basis of coronavirus infection.

BP 23.2 Thu 10:00 BAR 0106

ion-specific DNA adsorption at mica mediated by monovalent and divalent metal cations — •IBRAHIM MOHD¹, MAX LALLEMANG², BIZAN N BALZER², and IBRAHIM MOHD¹ — ¹University of Augsburg, 86159 Augsburg, Germany — ²universitätsstraße 1

Ion mediated attraction between biomolecules and solid substrates plays a crucial role in a broad range of biotechnological applications. In this work, we combine molecular dynamics simulations and single-molecule atomic force microscopy experiments to characterise the desorption properties of single-stranded DNA at mica surface mediated by the alkali and alkaline earth metal ions Li⁺, Na⁺, K⁺, Cs⁺, Mg²⁺ and Ca²⁺. Our results show that both monovalent and divalent ions induce an attractive interaction between DNA and the negatively charged mica surface. DNA adhesion is caused by two effects: Firstly, ion-specific adsorption of the monovalent cations compensates the negative charge and induces a long-ranged attraction. In addition, the surface adsorbed cations form inner-sphere contacts with the oxygen atoms of the DNA backbone. Both effects depend on the type of cation: Cs⁺ and K⁺ ions lead to loosely associated DNA with high surface mobility and low rupture forces. Na⁺, Li⁺, and divalent ions lead to a stronger association of DNA with low surface mobility and high rupture forces. By comparing the force-extension curve shapes from experiments and simulations we could provide atomistic insights into the desorption mechanisms and identify the dominant interactions involved in the desorption process.

BP 23.3 Thu 10:15 BAR 0106

Understanding the molecular determinants of chitin-protein interactions in the arthropod cuticle - a single-molecule approach — •AYESHA TALIB^{1,2}, YAEL POLITI², and KERSTIN G. BLANK^{1,3} — ¹Max Planck Institute of Colloids and Interfaces, Potsdam, Germany — ²Technische Universität Dresden, CMCB, B CUBE, Dresden, Germany — ³Johannes Kepler Universität, Institute of Experimental Physics, Linz, Austria

In the cuticle of arthropods, structural proteins and chitin fibers form a composite material with anisotropic mechanical properties. The molecular parameters that define the chitin-protein interaction are largely unknown. To answer the fundamental question of what controls cuticle mechanical properties, a molecular strategy is employed that integrates protein engineering with single-molecule force spectroscopy. Chitin binding domains (CBDs) from the spider *Cupiennius salei* have been identified and expressed recombinantly to qualitatively and quantitatively compare the strength of the protein-chitin interaction. For one CBD present in all spider tissues, we investigated the three partly overlapping consensus motifs RR-1, RR-2 and CB-4. Pull-down assays and single-molecule force spectroscopy suggest that the shortest RR-1 motif does not bind to chitin, whereas similar binding strength is observed for the longer sequences RR-2 and CB-4. We observe a fast dissociation rate, suggesting that CBDs facilitate energy dissipation upon deformation. Our ultimate goal is to correlate molecular properties with the mechanical function of the composite and to synthesize artificial analogues with tunable mechanical properties.

BP 23.4 Thu 10:30 BAR 0106

Complex unfolding, refolding and DNA association of the relaxase TrwC — •CÉSAR AUGUSTO QUINTANA-CATAÑO¹, •MIRIAM SCHRAMM¹, EKATERINA VOROBESKAIA¹, ANDREAS HARTMANN¹, and MICHAEL SCHLIERF^{1,2} — ¹B

CUBE - Center for Molecular Bioengineering, TU Dresden, Germany — ²Cluster of Excellence Physics of Life, TU Dresden, Germany

Referred as "bacterial sex", bacterial conjugation is a process in which a donor cell transfers DNA to a recipient cell. Conjugation is a main driver for spreading of antibiotic resistance genes. The relaxase TrwC associated to the type 4 secretion system is a multi-domain model enzyme essential for bacterial conjugation. It serves multiple purposes: DNA recognition, nicking and unwinding in the donor cell; and re-ligation of ssDNA in the receptor cell. For this last step a mechanical unfoldase denatures TrwC, which then refolds in the receptor cell. TrwC is a multi-domain protein consisting of 966 amino acids with a 55 amino acids long intrinsically disordered C-terminus. Here, we studied unfolding and folding mechanics of TrwC using single-molecule magnetic tweezers force spectroscopy. We show that the subdomains of TrwC unfold at distinct, different force regimes ranging from ~10 pN to 90 pN and TrwC refolds in a complex multistep reaction. Using our data, we can quantify the folding energetics of TrwC. We have further discovered complex DNA binding events of monomers and dimers using fluorescence correlation spectroscopy, allowing us to build a model of DNA association. We anticipate that our data helps to understand a key enzyme of DNA conjugation and its multifold activities.

BP 23.5 Thu 10:45 BAR 0106

Superpower behavior of the budding yeast kinesin-8 — •ANITA JANNASCH, BRENT FIELDEN, MICHAEL BUGIEL, and ERIK SCHÄFFER — Universität Tübingen

Kinesin-8 motor proteins can regulate microtubule dynamics and their length. Furthermore, they can crosslink microtubules and slide them relative to each other. These properties make the motor important for cell division. The budding yeast kinesin-8, Kip3, depolymerizes microtubule in a collective, force and length-dependent manner. The latter is due to the motor's very high processivity. Recently, we found that contrary to the depolymerization activity of multiple motors, a single Kip3 motor stabilizes microtubules. Compared to conventional kinesin, Kip3 is more than 10x slower and can generate about a 5x lower maximum force suggesting that it is a low power motor. Surprisingly, using high-precision optical tweezers, we observed that single Kip3 bound via a nanobody to optically trapped microspheres occasionally moved about 6x faster generating 3x higher forces compared to its usual behavior. This superpower behavior is almost comparable to conventional kinesin, but it is unclear whether it is related to one of its biological functions. The nanobody coupling also reduced the compliance of the system and thereby improved the spatiotemporal resolution. With the improved resolution, we were able to detect 4-nm mechanical substeps of the motor. In the long term, a better understanding of the various talents of Kip3 on the molecular level will have implications for cell division and associated diseases.

BP 23.6 Thu 11:00 BAR 0106

Thermodynamic inference for molecular motor models based on non-invasive conditioned waiting-time measurements — •BENJAMIN ERTEL, JANN VAN DER MEER, and UDO SEIFERT — II. Institut für Theoretische Physik, Universität Stuttgart, 70550 Stuttgart, Germany

Molecular motors are one example of biophysical systems operating far from equilibrium. For the description of their dynamics in motor-bead assays, three classes of models have been proposed. The first class, discrete Markov networks, emphasizes the configurational changes of the motor where the bead enters the transition rates. The second class of models focuses on the motion of the bead, which is described by an overdamped Langevin equation. The third class of models, hybrid motor-bead complexes, describes the full dynamics of the motor-bead assay by combining discrete and continuous models from the two previous classes. In this work, we develop a thermodynamic inference scheme that can be used to distinguish qualitatively between the different classes of models. Since this inference scheme is based on the observation of waiting times for conditioned transitions of the bead trajectory only, it is non-invasive and operationally accessible in experiments. Various characteristics of the motor, like its driving affinity, can be inferred without further information. We have obtained these results through analytical derivations and extensive numerical calculations.

15 min. break

BP 23.7 Thu 11:30 BAR 0106

Metal-protein-metal junctions: electron transport and mechanical deformation — •LINDA ANGELA ZOTTI — Departamento de Física Teórica de la Materia Condensada, Universidad Autónoma de Madrid, 28049 Madrid, Spain

Proteins have proven to be promising candidates for molecular electronics, showing in some cases much higher conductance than one would naively expect from their size. In particular, the blue-copper azurin extracted from *Pseudomonas aeruginosa* has been the subject of many experimental studies, al-

though the exact electron-transport mechanism is still under debate. Here I will present our efforts towards understanding the origin of such interesting effects from a theoretical perspective, analyzing both the electronic structure and the geometrical arrangement [1-6].

References [1] M. P. Ruiz et al. , J. Am. Chem. Soc. 139, 43, 15337 (2017). [2] C. Romero Muñoz, M. Ortega, J.G Vilhena, I. Diéz Pérez, R. Pérez, J. C. Cuevas, L. A. Zotti, Phys. Chem. Phys., 20, 30392 (2018). [3] C. Romero Muñoz, M. Ortega, J.G Vilhena, I. Diéz Pérez, R. Pérez, J. C. Cuevas, L. A. Zotti, Biomolecules, 9(9), 506 (2019). [4] C. Romero Muñoz, M. Ortega, J.G Vilhena, I. Diéz Pérez, R. Pérez, J. C. Cuevas, L. A. Zotti, J.Phys.Chem.C 125 (3), 1693 (2021). [5] C. Romero Muñoz, M. Ortega, J.G Vilhena, R. Pérez, J. C. Cuevas, L. A. Zotti, Appl. Sci. 11 (9), 3732 (2021). [6] C. Romero Muñoz, J.G Vilhena, R. Pérez, J. C. Cuevas, L. A. Zotti, Front. Phys. 10:950929. doi: 10.3389/fphy.2022.950929 (2022).

BP 23.8 Thu 11:45 BAR 0106

A variance sum rule and its entropy production estimation — •IVAN DI TERLIZZI^{1,2}, MARTA GIRONELLA³, MARCO BAIESI³, and FELIX RITORT² — ¹Max Planck Institute for the Physocxs of complex systems — ²University of Padua — ³University of Barcelona

Nonequilibrium steady states, from the planetary scale to biological processes, are characterized by entropy production via energy dissipation to the environment, which is often challenging to measure. A novel variance sum rule sets a new resource for exploiting fluctuations to measure physical quantities in stochastic systems. In particular, we focus on the formula it gives for estimating the entropy production rate from trajectories of positions and forces. We describe this method with analytically solvable models and we show its robustness and usefulness in practical applications to experimental data. By introducing a model-dependent fitting procedure, the method is also adapted to deal with conditions where not all degrees of freedom are experimentally accessible. For example, by analysing traces of flickering red blood cells, we obtain estimates of the entropy production rate in line with values obtained with totally different thermodynamic techniques.

BP 23.9 Thu 12:00 BAR 0106

Lattice defect sites accelerate microtubule severing by spastin — •CORDULA REUTHER¹, PAULA SANTOS-OTTE¹, RAHUL GROVER¹, and STEFAN DIEZ^{1,2,3} — ¹B CUBE - Center for Molecular Bioengineering, TU Dresden, Dresden, Germany — ²Cluster of Excellence Physics of Life, TU Dresden, Dresden, Germany — ³Max Planck Institute of Molecular Cell Biology and Genetics, Dresden, Germany

Length regulation of microtubules and their organization into complex arrays occurs through the activity of polymerases, depolymerases as well as severing enzymes such as katanin and spastin. The latter hexamerize on the microtubule lattice, pull out single tubulin dimers in an ATP-dependent manner and eventually generate internal breaks in the microtubule. For both enzymes it was shown that the severing activity is regulated by tubulin posttranslational modifications. So far, however, only katanin has been reported to exhibit a lattice-defect- or crossover-sensing activity. Here, we determined whether lattice defects in GMPCPP-stabilized microtubules also affect the severing activity by spastin. In controlled in vitro assays we characterized microtubules with defects next to control microtubules. Defect sites were introduced either through specific polymerization conditions or by end-to-end annealing of microtubules. We found that (i) the presence of defects accelerated the onset of the severing process and (ii) severing occurred twice as often in microtubule segments with defect sites as compared to random lattice segments. Furthermore, we quantified the correlation of the fluorescence signal of GFP-labelled spastin along the microtubule lattice to the severing sites as a function of time.

BP 23.10 Thu 12:15 BAR 0106

Keratin filament mechanics and energy dissipation are determined by metal-like plasticity — •CHARLOTTA LORENZ¹, JOHANNA FORSTING¹, ROBERT W. STYLE², STEFAN KLUMPP³, and SARAH KÖSTER¹ — ¹Institute for X-Ray Physics, University of Göttingen, Friedrich-Hund-Platz 1, 37077 Göttingen, Germany

— ²Department of Materials, ETH Zürich, Vladimir-Prelog-Weg 1-5/10, 8093 Zürich, Switzerland — ³Institute for the Dynamics of Complex Systems, University of Göttingen, Friedrich-Hund-Platz 1, 37077 Göttingen, Germany

Cell mechanics is determined by an intracellular biopolymer network, including intermediate filaments that are expressed in a cell-type specific manner. A prominent pair of intermediate filaments are keratin and vimentin as the epithelial-to-mesenchymal transition is associated with a switch from keratin to vimentin. The transition coincides with a change in cellular mechanics, and thus dynamic properties of the cells. This observation raises the question of how the mechanical properties already differ on the single filament level. Here we use optical tweezers and a computational model to compare the stretching and dissipation behavior of the two filament types. We find that keratin and vimentin filaments behave in opposite ways: keratin filaments elongate, but retain their stiffness, whereas vimentin filaments soften, but retain their length. This finding is explained by fundamentally different ways to dissipate energy: viscous subunits sliding within keratin filaments and non-equilibrium α helix unfolding in vimentin filaments.

BP 23.11 Thu 12:30 BAR 0106

The single-strand annealing protein RAD52 can form a stable nucleoprotein filament — •CAROLINA CARRASCO¹, LAURA MURAS¹, TOBIAS JACHOWSKI¹, SIVARAMAN SUBRAMANIAM², FRANCIS STEWART², and ERIK SCHÄFFER¹ — ¹Center for Plant Molecular Biology (ZMBP), University of Tübingen, Tübingen, Germany — ²Department of Genomics, Biotechnology Center, TU Dresden, Dresden, Germany

Genome maintenance requires the repair of DNA double-strand breaks. It can be mediated among others by the single-strand annealing. RAD52 proteins form rings that are thought to promote the annealing. How RAD52 interacts with and anneals DNA strands remains unclear. We have investigated the dynamic interaction of RAD52 with DNA by force spectroscopy using optical tweezers. Upon stretching single DNA molecules in the presence of RAD52, we have observed elongation steps in DNA extension that are consistent with either dissociation, unwrapping, or opening of individual DNA-bound rings. Upon relaxation, reverse steps of similar amplitude were detected. Under constant force, step sizes were uniform. Surprisingly, the disruption forces followed a gamma distribution suggesting that the RAD52-DNA dissociation process consists of multiple stochastic steps. Successive stretch-relax cycles at high forces promoted DNA softening and a melting-force increase because of an intercalation and sealing mechanism on DNA. The final DNA-RAD52 hysteresis-free nucleoprotein filament is consistent with a flexible helical structure in which RAD52 monomers, and not rings, mediate strand annealing.

BP 23.12 Thu 12:45 BAR 0106

Assessing biomolecular interactions across scales using optical tweezers — •ROMAN RENGER, NICHOLAS LUZZIETTI, and PHILIPP RAUCH — Paalbergweg 3, 1105 AG Amsterdam, Netherlands

Biological processes involving proteins interacting with nucleic acids, cell membranes or cytoskeletal filaments are key to cell metabolism and hence to life in general. Detailed insights into these processes provide essential information for understanding the molecular basis of physiology and the pathological conditions that develop when such processes go awry. The next scientific breakthrough consists in the direct, real-time observations and measurements of the most fundamental mechanisms involved in biology. Single-molecule technologies offer a powerful opportunity to meet these challenges and to study dynamic protein function and activity in real-time and at the single-molecule level. Here, we present our efforts for further enabling discoveries in the field of biology and biophysics using the combination of optical tweezers with correlative fluorescence microscopy (widefield, TIRF, confocal and STED) and label-free Interference Reflection Microscopy (IRM). We present several examples in which our technology has enhanced the understanding of basic biological phenomena, ranging from protein structure to intracellular organization. Furthermore, we show that advances in hybrid single-molecule methods can be turned into an easy-to-use and stable instrument that has the ability to open up new avenues in many research areas.

BP 24: Active Matter IV (joint session DY/BP/CPP)

Time: Thursday 9:30–13:00

Location: ZEU 160

Invited Talk

BP 24.1 Thu 9:30 ZEU 160

Acoustically propelled nano- and microparticles: From fundamentals to applications — •RAPHAEL WITTKOWSKI — Institut für Theoretische Physik, Center for Soft Nanoscience, Westfälische Wilhelms-Universität Münster, 48149 Münster, Germany

Among the existing types of artificial active colloidal particles, acoustically propelled nano- and microparticles have a particularly high potential for future ap-

plications in fields like medicine and materials science. However, despite intensive research on this type of motile particles in recent years, the understanding of their properties is still very limited. A reason for the limited understanding is that the previous research has mostly been experimental and that it is difficult to study the dependence of certain system parameters on the propulsion of the particles in experiments since the parameters can often not be varied independently of the other parameters and in ranges of reasonable size. In this talk, I will give

an overview about our theoretical investigation of the properties of acoustically propelled nano- and microparticles and the challenges that remain for future research.

Funded by the Deutsche Forschungsgemeinschaft (DFG) - 283183152 (WI 4170/3).

BP 24.2 Thu 10:00 ZEU 160

Force on probe in a confined active fluid — SHUVOJIT PAUL¹, ASHREYA JAYARAM², N NARINDER¹, THOMAS SPECK², and CLEMENS BECHINGER¹ — ¹Fachbereich Physik, Universität Konstanz, 78464 Konstanz, Germany — ²Institut für Physik, Johannes Gutenberg-Universität Mainz, 55128 Mainz, Germany

When immersed in a dispersion of smaller "depletants", a colloidal particle experiences depletion forces in the presence of another colloidal particle or under confinement. While the nature of these forces is well-established for passive systems, much less is known about the consequence of making the depletants self-propelled or "active". In this work, we consider a large, optically trapped probe under circular confinement surrounded by smaller active Janus particles. We find that the force experienced by the probe varies non-monotonically as the distance between the colloid and the confinement is increased. To rationalize this observation, we relate the measured force to the active stress and, subsequently, to the microstructure of the surrounding active fluid. Going beyond synthetic active matter, our work could shed light on the organization of intracellular entities in biological systems.

BP 24.3 Thu 10:15 ZEU 160

Symmetry-breaking refractive index profiles as a propulsion mechanism for active Brownian particles — JULIAN JEGGLE¹, MATTHIAS RÜSCHENBAUM², CORNELIA DENZ², and RAPHAEL WITTKOWSKI¹ — ¹Institut für Theoretische Physik, Center for Soft Nanoscience, Westfälische Wilhelms-Universität Münster, 48149 Münster, Germany — ²Institut für Angewandte Physik, Westfälische Wilhelms-Universität Münster, 48149 Münster, Germany

Active Brownian particles (ABPs) have been realized with various propulsion mechanisms such as self-diffusiophoresis, self-electrophoresis or acoustic scattering. Typically, these mechanisms induce flow fields around the particles that represent a deviation from the "pure" ABP model. Here, we present a novel implementation of ABPs in the form of transparent microswimmers with a symmetry-breaking refractive index gradient. Utilizing the momentum transfer associated with light refraction as the driving force induces no flow fields beyond Stokes flow. Unlike optothermally driven particles, this archetype of ABPs also allows for sensitivity to the phase and polarization of the driving light field thus improving the spatio-temporal control of light-based propulsion mechanisms. Using non-light-absorbing particles enables bulk volume systems and allows the introduction of feedback loops, therefore making this approach a promising foundation for adaptive matter systems.

**Funded by the Deutsche Forschungsgemeinschaft (DFG) - Project-ID 433682494 - SFB 1459*

BP 24.4 Thu 10:30 ZEU 160

The interaction-expansion method: a systematic derivation strategy for active field theories — MICHAEL TE VRUGT^{1,2}, JENS BICKMANN^{1,2}, STEPHAN BRÖKER^{1,2}, TOBIAS FROHOFF-HÜLSMANN¹, EYAL HEIFETZ³, MICHAEL E. CATES⁴, UWE THIELE^{1,5,6}, and RAPHAEL WITTKOWSKI^{1,2,5} — ¹Institut für Theoretische Physik, Westfälische Wilhelms-Universität Münster, 48149 Münster, Germany — ²SoN, Westfälische Wilhelms-Universität Münster — ³Porter School of the Environment and Earth Sciences, Tel Aviv University, 69978 Tel Aviv, Israel — ⁴DAMTP, Centre for Mathematical Sciences, University of Cambridge, Cambridge CB3 0WA, United Kingdom — ⁵CeNoS, Westfälische Wilhelms-Universität Münster — ⁶CMTC, Westfälische Wilhelms-Universität Münster

Field-theoretical models have made enormous contributions to our understanding of the collective dynamics of active matter. In this contribution, we introduce the interaction-expansion method (IEM) [1], which allows for a systematic derivation of active field theories from the microscopic dynamics of individual particles. We then discuss some recent applications of the IEM to particles with orientation-dependent propulsion speed [2] and particles with inertia [3].

[1] M. te Vrugt et al., in preparation (2022)

[2] S. Bröker et al., arXiv:2210.13357 (2022)

[3] M. te Vrugt et al., Nature Communications (provisionally accepted), arXiv:2204.03018 (2022)

**Funded by the Deutsche Forschungsgemeinschaft (DFG)-283183152*

BP 24.5 Thu 10:45 ZEU 160

Entropy production in active turbulence — BYJESH NALINI RADHAKRISHNAN, THOMAS SCHMIDT, and ETIENNE FODOR — Department of physics and material science, University of Luxembourg

Active particles like bacteria and sperm cells sustain a continuous intake and dissipation of energy. Consequently, they are intrinsically out of equilibrium which leads to a non-vanishing entropy production rate (EPR) even in steady states.

Quantifying how the EPR varies in different collective phases is crucial in developing a thermodynamic framework for active matter. In this work, we look at the EPR in active turbulence. We use Active Model H, a continuum model for active particles in a momentum-conserving fluid, to study turbulence in contractile scalar active systems. We measure the local EPR in numerical simulations, which unveils the role of the noise and activity parameters on the EPR in active turbulent systems.

15 min. break

BP 24.6 Thu 11:15 ZEU 160

Phase transitions in multicomponent active matter: a quantitative kinetic theory — JAKOB MIHATSCH¹, THOMAS IHLE¹, RÜDIGER KÜRSTEN², and HORST-HOLGER BOLTZ¹ — ¹Institute for Physics, University of Greifswald, Greifswald, Germany — ²Departament de Física de la Matèria Condensada, University of Barcelona, Barcelona, Spain

We consider a multicomponent model of self-propelled particles with Kuramoto-type alignment interactions. Starting from the N-particle Fokker-Planck equation we observe that the usual factorization Ansatz of the probability density, often called Molecular Chaos approximation, predicts a relaxation behavior which qualitatively disagrees with agent-based simulations. Therefore, we develop a kinetic theory which takes the time-evolution of the two-particle correlation function explicitly into account, i.e. goes beyond the mean-field approximation. We show that this theory predicts the relaxation behavior of the system as well as the order-disorder transition with high precision in certain parameter ranges. In particular, the dependence of the transition threshold on the particle speed is predicted correctly.

BP 24.7 Thu 11:30 ZEU 160

Emergent collective behaviour due to virtual interactions between robotic swimmers — SAMUDRAJIT THAPA^{1,2}, BAT-EL PINCHASIK^{1,3}, and YAIR SHOKEF^{1,2,3} — ¹School of Mechanical Engineering, Tel Aviv University, Tel Aviv 69978, Israel — ²Sackler Center for Computational Molecular and Materials Science, Tel Aviv University, Tel Aviv 69978, Israel — ³Center for the Physics and Chemistry of Living Systems, Tel Aviv University, 69978, Tel Aviv, Israel

Many organisms in nature use local interactions to realize global collective behaviour. Here we study how simple two body distance-based interactions between active Brownian particles results in collective motion. The interactions are not physical but virtual, wherein each particle senses the presence of other particles nearby and changes its behaviour accordingly. We study the radial distribution function to quantify the emergent interactions for both social and anti-social behaviour. Using Langevin dynamics simulations, we discover that under certain conditions positive correlations of the motion can emerge even in the case of anti-social behaviour. Our results might be potentially useful for designing robotic swimmers that can swim collectively just based on sensing the distance to their neighbours.

BP 24.8 Thu 11:45 ZEU 160

Kinetic Event-Chain Algorithm for Active Matter — NICO SCHAFFRATH, THEVASHANGAR SATHIYANESAN, TOBIAS KAMPMANN, and JAN KIERFELD — Physics Department, TU Dortmund University, 44221 Dortmund, Germany

We present a cluster kinetic Monte-Carlo algorithm for active matter systems of self-propelled hard particles. The kinetic event-chain algorithm is based on the event-chain Monte-Carlo method and is applied to active hard disks in two dimensions. The algorithm assigns Monte-Carlo moves of active disks a mean time based on the mean and variance of the move length in force direction. This time is used to perform diffusional rotation of their propulsion force. We show that the algorithm reproduces the motility induced phase separated region in the phase diagram of hard disks correctly and efficiently.

BP 24.9 Thu 12:00 ZEU 160

Emergent pattern formation in communicating active matter — ROBERT GROSSMANN¹, ZAHRA MOKHTARI², ROBERT I.A. PATTERSON³, and FELIX HÖFLING^{2,4} — ¹Institut für Physik und Astronomie, Universität Potsdam — ²Institut für Mathematik, Freie Universität Berlin — ³WIAs Berlin — ⁴Zuse Institut Berlin

Inspired by trail formation as observed in colonies of driver ants, for example, we study ensembles of agent particles that communicate via deposition and sensing of pheromones. These chemical traces are produced by the agents themselves and encode their current position and walking direction. Other agents passing by will then tend to align with the orientation inscribed in the pheromone traces. In the limit of short pheromone lifetime, the dynamics of this system reduces to the seminal Vicsek model and, thus, yields the formation of transversally moving bands. In the opposite limit, the effective agent-agent interaction represents a form of delayed feedback and yields the spontaneous formation of macroscopic, persistent trails, which are followed and reinforced by the agents [New J. Phys. 24 013012 (2022)]. In this talk, we present large-scale simulations of the agent model and establish the phase diagram as function of the lifetime of pheromones. We rationalize our findings by analyzing mean-field equations that are systemati-

cally derived from the stochastic particle model. Combining numerical solutions of these order parameter equations and a linear stability analysis, we show how transversal bands, common in the Vicsek model, are destabilized, giving rise to the formation of “longitudinal” trails, pointing in the mean direction of motion.

BP 24.10 Thu 12:15 ZEU 160

Binary Mixture of Deforming Particles — •YIWEI ZHANG, ALESSANDRO MANACORDA, and ETIENNE FODOR — DPhyMS, University of Luxembourg, Luxembourg, Luxembourg

Phase separation occurs in miscible liquids where components have distinct properties. In reactors, components undergo stochastic change in their properties which affect the liquid composition. While phase separation and reaction-diffusion have already been studied extensively as separate ingredients, how they combine in non-ideal reactors remains poorly understood. To bridge this gap, we consider repulsive particles with fluctuating size subject to one-body landscape and nonequilibrium synchronisation. The landscape features minima which, regarding size as reaction coordinate, distinguish three states: Particles with finite size, either A- or B-type, and point particles. In this context, synchronisation penalizes A particles in B-rich phases, and vice versa, so that the system eventually accommodates a uniform state. We report the phase diagram depending on the stability of each state and the corresponding particle sizes. Combining hydrodynamic and phenomenological arguments, we recapitulate how metastability regulates the interplay between synchronisation and repulsion. Our results reveal the role of nonequilibrium kinetic factors at play in non-ideal reaction-diffusion systems.

BP 24.11 Thu 12:30 ZEU 160

Self-organization of model catalytic cycles — •VINCENT OUAZAN-REBOUL¹, JAIME AGUDO-CANALEJO¹, and RAMIN GOLESTANIAN^{1,2} — ¹Max Planck Institute for Dynamics and Self-Organization, Am Fassberg 17, D-37077, Göttingen, Germany — ²Rudolf Peierls Centre for Theoretical Physics, University of Oxford, OX1 3PU, Oxford, UK

We study analytically and numerically a model metabolic cycle composed of an arbitrary number of species of catalytically active particles. Each species converts a substrate into a product, the latter being used as the substrate by the next

species in the cycle. Through a combination of catalytic activity and chemotactic mobility, the catalytic particles develop effective interactions with particles belonging to neighbouring species in the cycle. These interactions, being fully out-of-equilibrium, show some unusual features, in particular being non-reciprocal. We find that such model metabolic cycles are able to self-organize through a macroscopic instability, with a strong dependence on the characteristics of the cycle. For instance, cycles containing an even number of species are able to minimize repulsion between their component particles by aggregating all even-numbered species in one cluster, and all odd-numbered species in another. Such a grouping is not possible if the cycle contains an odd number of species, which can lead to oscillatory steady states in the case of chasing interactions.

BP 24.12 Thu 12:45 ZEU 160

Reentrant condensation transition in a model of driven scalar active matter with diffusivity edge — BERX JONAS², •BOSE ARITRA¹, MAHAULT BENOIT¹, and GOLESTANIAN RAMIN^{1,3} — ¹Max Planck Institute for Dynamics and Self-Organization, 37077 Göttingen, Germany — ²Institute for Theoretical Physics, KU Leuven, B-3001 Leuven, Belgium — ³Rudolf Peierls Centre for Theoretical Physics, University of Oxford, Oxford OX1 3PU, United Kingdom

A class of scalar active matter for which the effective diffusivity vanishes beyond a certain density threshold, hereby referred to as diffusivity edge, triggers the formation of a condensate when confined in a harmonic potential. The condensation transition exhibits remarkable similarities with a Bose-Einstein Condensation (BEC). Here we study the effect of a diffusivity edge in a system of scalar active matter confined by a periodic potential and driven by an external force.

We find that this system shows qualitatively distinct stationary regimes depending on the amplitude of the driving force with respect to the potential barrier. For small driving, the diffusivity edge induces a condensation analogous to the BEC-like transition reported for the nondriven case, which is characterised by a density-independent steady state current. Conversely, large external forces lead to a qualitatively different phase diagram where condensation is not possible below a density threshold and the associated transition at moderate densities above the threshold the transition is reentrant due to the existence of a subsequent evaporation transition at low effective temperatures.

BP 25: Cell Mechanics II

Time: Thursday 15:00–17:30

Location: BAR Schö

BP 25.1 Thu 15:00 BAR Schö

Nuclear mechanics probed by optical tweezers-based active microrheology — •BART VOS¹, TILL MÜNCKER¹, IVAN AVILOV², PETER LENART², and TIMO BETZ¹ — ¹Third Institute of Physics, University of Göttingen, Göttingen, Germany — ²Max Planck Institute for Biophysical Chemistry, Göttingen, Germany

Mechanics play a crucial role in a wide range of cellular processes, from differentiation to division and metastatic invasion. Consequently, the mechanical properties of the cytoskeleton, providing shape, motility and mechanical stability to the cell, have been extensively studied. However, remarkably little is known about the mechanical environment within the nucleus of a cell, and fundamental questions remain unanswered, such as the role of nuclear actin or the sudden “freezing” of the cell during cellular division that prevents diffusion or active mixing of the nucleus and the cytoplasm.

To address these questions, we perform optical tweezers-based microrheology in the cellular nucleus. Microrheology has proven to be a suitable tool for intracellular mechanical measurements, as it enables local, non-invasive measurements. However, although the cytoskeleton has been extensively studied this way, the cell nucleus has not been investigated, mainly due to difficulties with inserting appropriate probe particles. By using starfish oocytes that have larger dimensions than most other cell types, we are able to perform microinjection of micrometer-sized particles. We observe viscoelastic behavior of the nucleoplasm that is profoundly different from the cytoskeleton. In addition, we mechanically follow the oocyte during meiotic cell division.

BP 25.2 Thu 15:15 BAR Schö

Mechanosensitive binding of filamins in the actin cytoskeleton of live cells — •VALENTIN RUFFINE and ELISABETH FISCHER-FRIEDRICH — DFG Cluster of Excellence Physics of Life, Technische Universität Dresden, Dresden, Germany
Filamins A and B are cross-linkers of the actin cytoskeleton expressed in a wide range of human cell types. In particular, filamins are crucial in actin cytoskeleton interactions with the extracellular matrix and therefore are major molecular players in cartilage and bone development. Filamins form dimers which can bind and cross-link two actin filaments and thus contribute to the mechanical integrity of cytoskeletal structures such as the actin cortex. Myosin-generated contractile tension in the actin cortex is likely translated into a tensile force on the filamin-actin bonds in cross-linking filamins. Filamin binding to actin is transient with unbinding events after a characteristic bond lifetime. This en-

ables large reorganizations of the cytoskeleton at longer timescales. However, tensile force in filamin-actin bonds may affect their unbinding kinetics. Here, we study the binding dynamics of filamins A and B to actin, in the cortex of mitotic HeLa cells. With a set-up combining a confocal and an atomic force microscope, we measure how changes in contractile tension in the actin cortex change filamin binding dynamics. Our results suggest a substantial increase of the lifetime of filamin-actin bonds under increased tensile force. This behavior is termed “catch-binding” and may act as a fast rescue mechanism that prevents rupture of filamin-containing actin cytoskeletal structures upon sudden tension increase.

BP 25.3 Thu 15:30 BAR Schö

T-cell migration: Improving searching efficiency by targeting Microtubules — •GALIA MONTALVO^{1,2,3}, BIN QU^{3,4}, and FRANZISKA LAUTENSCHLÄGER^{1,2,3} — ¹University of Saarland, Department of Experimental Physics — ²University of Saarland, Center for Biophysics — ³Biophysics, Center for Integrative Physiology and Molecular Medicine (CIPMM), School of Medicine — ⁴Leibniz Institute for New Materials

Cytotoxic T lymphocytes (CTLs) are the key players in the adaptive immune system to eliminate tumor cells. Proper mobility in three-dimensional environments is a prerequisite for CTLs to execute their killing function and the cytoskeleton plays a central role in CTL migration in 3D. In dense matrices, migration and the consequent killing efficiency of CTLs is greatly impaired. Interestingly, we observed that in 3D matrices, CTLs go through narrow quasi-1D channels. Manufactured micro-channels are a recently emerged promising tool with well-defined parameters to investigate cell migration in 1D. In this project, we characterize MTs as a major cytoskeletal component regulating the migration of CTLs in micro-fabricated environments and in dense collagen matrices. To this end, we expose CTLs to MTs disturbing drugs. We studied the mechanics of treated cells and described the role of actin in the observed stiffness increase after MT depolymerization. Our main conclusion is that searching efficiency and killing capacity of CTLs is enhanced after MT depolymerization through stiffness increase.

BP 25.4 Thu 15:45 BAR Schö

Global membrane tension is independent of polyacrylamide substrate stiffness — •EVA KREYSING¹, JEFFREY MCHUGH^{1,2}, SARAH FOSTER^{1,3}, KURT ANDRESEN⁴, RYAN GREENHALGH¹, EVA PILLAI^{1,5}, ANDREA DIMITRICOPOULUS¹, ULRICH KEYSER¹, and KRISTIAN FRANZE^{1,6} — ¹University of Cambridge, UK — ²Collège de France, Paris — ³University of Tübingen; Germany — ⁴Gettysburg College, USA — ⁵EMBL Heidelberg, Germany — ⁶University Erlangen/Nürnberg, Germany

Cellular processes such as cell migration or axonal pathfinding have been shown to depend strongly on mechanical properties of the cell's environment such as stiffness. It has been shown that Piezo1 is one of the mechanosensitive ion channels that contributes to such behaviour. It is hypothesised that Piezo1 is activated by changes in membrane tension. This raises the question whether membrane tension is influenced by stiffness of the cell's environment. We measured membrane tension as a function of substrate stiffness in different cell types with optical tweezers. To our surprise, we found that global membrane tension is independent of substrate stiffness in the physiological range. However, we found strong differences between membrane tension on compliant substrates and glass substrates. To explain these observations, this work introduces a toy model for substrate, membrane and cortex interaction.

BP 25.5 Thu 16:00 BAR Schö

Self-stabilization of cell adhesions under load — •BENEDIKT SABASS — LMU München

Mechanical loading generally weakens adhesive structures and eventually leads to their rupture. However, biological systems can adapt to loads by strengthening adhesions, which is essential for maintaining the integrity of tissue and whole organisms. Inspired by cellular focal adhesions, we discuss generic, molecular mechanisms that enable adhesions to harness applied loads for self-stabilization through adhesion growth. The mechanisms are based on conformation changes of adhesion molecules that are dynamically exchanged with a reservoir. Tangential loading drives the occupation of some states out of equilibrium, which, for thermodynamic reasons, leads to association of further molecules with the cluster. The self-stabilization principle can be realized in many ways in complex adhesion-state networks and we show how it naturally occurs in cellular adhesions involving the adaptor proteins talin and vinculin.

Braeutigam, A., Simsek, A.N., Gompper, G., and Sabass, B., Nature Communications 13(1):1-9, 2022

15 min. break

BP 25.6 Thu 16:30 BAR Schö

Unraveling the light activation of flagellar adhesiveness in *Chlamydomonas* — •RODRIGO CATALAN^{1,2}, ANTOINE GIROT^{1,2}, ALEXANDROS FRAGKOPOULOS^{1,2}, SIMON KELTERBORN³, DARIUS RAUCH³, OLGA BAIDUKOVA³, PETER HEGEMANN³, and OLIVER BÄUMCHEN^{1,2} — ¹Max Planck Institute for Dynamics and Self-Organization (MPIDS), 37077 Göttingen, Germany — ²University of Bayreuth, Experimental Physics V, 95447 Bayreuth, Germany — ³Humboldt University Berlin, Institute of Biology, 10115 Berlin, Germany

Photoreceptors are essential constituents of photoactive microbes and control several biological processes, such as circadian life cycle, sexual reproduction and phototaxis. *Chlamydomonas reinhardtii*, a unicellular model organism to study light-activated microbial functionalities, exhibits light-switchable flagellar adhesion to surfaces upon blue-light exposure [Kreis *et al.*, Nature Physics 2018]. Using single-cell micropipette force spectroscopy, we compare the adhesion forces of wild-type (WT) cells and several blue-light photoreceptor-deletion mutants. We find that the wavelength response of flagellar adhesion forces in WT cells resembles the absorption spectrum of plant cryptochrome (pCRY) and animal cryptochrome (aCRY) photoreceptors. We further assess the involvement of pCRY and aCRY photoreceptors in the light-switchable adhesion of *C. reinhardtii* by means of adsorption experiments [Catalan *et al.*, arXiv:2208.01338] at the population level using photoreceptor-deletion mutants lacking either one or both CRYs.

BP 25.7 Thu 16:45 BAR Schö

Chromatin and Nucleocytoplasmic Transport Control the Nuclear Biophysical Properties during Assembly in Egg Extracts — •OMAR MUÑOZ^{1,2}, ABIN BISWAS^{1,4}, KYOOHYUN KIM^{1,3}, SIMONE REBER⁴, JOCHEN GUCK^{1,3}, and

VASILY ZABURDAEV^{1,2} — ¹Max-Planck-Zentrum für Physik und Medizin — ²Department of Biology, Friedrich-Alexander-Universität Erlangen-Nürnberg — ³Max Planck Institute for the Science of Light — ⁴IRI Life Sciences, Humboldt-Universität zu Berlin

Biophysical properties of the cell nucleus are important for various cellular processes from migration to stress responses, but largely are still not well understood. One fundamental example is the mass density: we observed that the nuclear mass density consistently displays a lower value than its cytoplasmic counterpart for a wide range of species, which is surprising given that it contains the highly compacted genetic material. To understand the mechanisms behind this, we measured volume and mass density of growing nuclei reconstituted in *Xenopus* egg extracts. Our results identified nucleocytoplasmic transport and chromatin as the main determinants for the dry mass and volume of then nucleus, and suggest a coupling of chromatin with nucleocytoplasmic transport. We propose a theoretical model informed by experiments, which incorporates active transport of proteins and balance of colloid osmotic pressure and an entropic polymer pressure exerted by chromatin. With only a few adjustable parameters, our model can fully describe the nuclear volume and mass dynamics as observed in the experiments.

BP 25.8 Thu 17:00 BAR Schö

Dyneins, unite! How a weak motor protein can drive efficient transport of large cargoes — •SIMON WIELAND^{1,2}, CHRISTINA STEININGER¹, DAVID E. GITSCHIER¹, MARIUS M. KAISER¹, WOLFGANG GROSS¹, ABDULLAH R. CHAUDHARY³, JANA RITSCHAR⁴, CHRISTIAN LAFORSCH², ADAM G. HENDRICKS³, and HOLGER KRESS¹ — ¹Biological Physics, University of Bayreuth, Germany — ²Animal Ecology I, University of Bayreuth, Germany — ³Department of Bioengineering, McGill University, Montreal, Canada — ⁴Laboratory of Molecular Parasitology, University of Bayreuth, Germany

To promote robust transport of organelles, dyneins need to work together to overcome intracellular drag forces and opposing forces of kinesins. However, current models of dynein cooperativity cannot explain how dyneins produce very high forces to power transport of large organelles with diameters of several microns. Here, we show that many dynein teams interact with multiple microtubules to drive efficient transport of large organelles. We measured retrograde transport forces of phagosomes with diameters of 1-5 μm . These forces were adapted to the cytoplasmic viscosity, enabling equally fast transport of all phagosomes. Furthermore, we labeled and quantified dyneins on isolated phagosomes. By modeling the distribution of microtubules around the phagosomes we linked the observed transport forces to the corresponding dynein numbers. We show that both dynein's cooperativity and size-dependent interactions of organelles with microtubules contribute to the production of high collective transport forces.

BP 25.9 Thu 17:15 BAR Schö

The formation of microtentacles — •LUCINA KAINKA¹, REZA SHAEBAN^{2,3}, KATHI KAISER¹, LUDGER SANTEN^{2,3}, and FRANZISKA LAUTENSCHLÄGER^{1,3} — ¹Department of Experimental Physics, Saarland University, Saarbrücken, Germany — ²Department of Theoretical Physics, Saarland University, Saarbrücken, Germany — ³Center for Biophysics, Saarland University, Saarbrücken, Germany

It is widely assumed that cellular stiffness decreases during cancer progression, and this is mainly attributed to changes in their actin cortex properties. It has recently been proposed that a weakened actin cortex enables the formation of so called microtentacles. Microtentacles are microtubule-based membrane protrusions that are formed by circulating tumor cells. It is assumed that microtentacles promote reattachment of circulating tumor cells to the tissue and the escape from the blood stream. In this study, we aim to understand how the actin cortex structure changes during cancer progression to enable microtentacle formation. We further ask how microtubules generate forces to protrude the cell membrane. In our experiments, we use noncancer RPE-1 cells as a model system. By treating these cells with actin affecting compounds while they are in suspension, they form microtentacles. We further can control the number and length of microtentacles by varying the concentration of compounds applied. We analyze the actin cortex and microtubule network in these cells with fluorescence and scanning electron microscopy. We further study the microtubule dynamics inside microtentacles by fluorescence recovery after photobleaching (FRAP).

BP 26: Focus Session mRNA Physics

Time: Thursday 15:00–17:30

Location: TOE 317

Invited Talk

BP 26.1 Thu 15:00 TOE 317

Decoding Molecular Plasticity in the Dark Proteome of the Nuclear Transport Machinery — •EDWARD LEMKE — JGU & IMB Mainz, GE

The mechanisms by which intrinsically disordered proteins (IDPs) engage in rapid and highly selective binding is a subject of considerable interest and repre-

sents a central paradigm to nuclear pore complex (NPC) function. Nuclear transport receptors (NTRs) can move small proteins and mRNA through the central channel of the NPC which is filled with hundreds of phenylalanine-glycine-rich nucleoporins (FG-Nups) reaching millimolar concentrations with elusive conformational plasticity. We have now developed a semi-synthetic strategy to equip

the living cell with up to three genetic codes and label FG-Nups inside functional NPCs site-specifically with small FRET probes. This allowed us to develop an experimental approach and use fluorescent lifetime imaging microscopy (FLIM) to directly decipher the plasticity of FG-Nups. Our study enabled a conformational look on the densely packed IDPs in the sub-resolution (roughly (50 nm)³ small cavity) cavity of the NPC. We extracted the scaling exponent, which directly describes the conformations of FG-Nups at their functional status as well as the solvent quality in the cellular and even inner NPC environment. Pairing our data with coarse grained simulations enabled us to complement the missing half of protein mass that due to its dynamics are not present in even the most recent electron tomograms of the NPC.

BP 26.2 Thu 15:30 TOE 317

Decomposition of ensemble fluorescence signals from translation experiments and simulations — •NADIN HAASE, SIMON CHRIST, and SOPHIA RUDORF — Institute of Cell Biology and Biophysics, Leibniz University Hannover, Germany

Proteins are major components of cells and perform all kinds of tasks essential for survival. Those parts of the DNA that contain blueprints for the synthesis of proteins are transcribed to messenger RNA (mRNA). Complex biomolecular machines called ribosomes translate the mRNA by assembling the corresponding building blocks of proteins, the amino acids. This process can be studied by in-vitro ensemble experiments through monitoring time-dependent output signals such as fluorescence time traces, where the ensemble signal is a superposition of the individual signals from all molecules in the reaction. However, translation is a stochastic process and thus even for initially synchronized reactions the ensemble signal may not reflect the features in the individual signals, especially on longer time scales. Here we present an approach to decompose the ensemble signal to reveal hidden information about the individual steps of the translation process. We explore the limits of this method and study the conditions under which a meaningful solution can be gathered.

BP 26.3 Thu 15:45 TOE 317

Creating an evolution machine with 2-3-cyclic RNA — •DIETER BRAUN — Systems Biophysics, Ludwig Maximilian University Munich

For life to start, a simple physical non-equilibrium mechanism combined with a most robust chemistry of a few molecules had to reach the regime of Darwinian molecular evolution. We found RNA oligomerization and templated ligation from very mildly activated RNA with 2-3-cyclic phosphates [1], with wet-dry cycling at heated air-water interfaces [2]. The oligomerization operated at elevated pH 9-10 without added salts at temperatures between 4-40°C and created oligomers of all four bases with 15 percent yield. It operated in a water-poor 'dry' state. Replication was possible with templated ligation and showed with only 1mM MgCl₂ a strongly base-selective templated ligation with 25 percent yield. If catalytic conditions to recycle the hydrolytically opened 2-3-cyclic phosphate from linear 2 prime or 3 prime endings would be found, the reaction would operate indefinitely without feeding in a thermal gradient setting. We will show preliminary experiments for local feeding, vesiculation and protein expression in the same setting. The experiments suggest a most simple scenario for the emergence of life from only two nucleotide molecules, implemented in an early Earth volcanic setting under a CO₂ atmosphere. It showcases how physics and chemistry could have acted together in a geologically abundant microfluidic setting to create Darwinian evolution.

[1] ChemSystemsChem doi.org/10.1002/syst.202200026 (2022)

[2] Nature Physics doi.org/10.1038/s41567-022-01516-z (2022)

BP 26.4 Thu 16:00 TOE 317

RNA G-quadruplex folding is a multi-pathway process with a variety of short-lived intermediate states — •MARIJANA UGRINA¹, INES BURKHART², DIANA MÜLLER², HARALD SCHWALBE², and NADINE SCHWIERZ¹ — ¹University of Augsburg, Augsburg, Germany — ²Goethe University, Frankfurt am Main, Germany

The folding kinetics of regulatory RNAs is crucial for their function. Here, we provide molecular insights into the folding pathways of a G-quadruplex from telomeric repeat-containing RNA by combining all-atom molecular dynamics and coarse-grained simulations with circular dichroism experiments. The ion atmosphere surrounding the highly charged quadruplex plays a crucial role in folding. To correctly capture the electric double-layer in implicit solvent coarse-grained simulations, we develop a matching procedure based on all-atom simulations in explicit water. This procedure allows us to provide quantitative agreement between the experiments and simulations as judged by the number of native contacts at different salt concentrations and temperatures. Folding of the quadruplex is on the timescale of minutes and the coarse-grained simulations using the three-interactions site model are therefore ideal to resolve the folding pathways and intermediate states. The results reveal that the folding is sequential with each pathway passing through two transient, on-pathway intermediates: A hairpin and a triplex or double hairpin state. Since these intermediates are degenerate with at two to four alternative conformations per state, quadruplex folding is a multi-pathway process with high conformational entropy.

15 min. break

BP 26.5 Thu 16:30 TOE 317

Codon position-specific engineering of translation kinetics — JUDITH MÜLLER¹, GERLINDE SCHWAKE¹, ANITA REISER¹, DANIEL WOSCHÉE¹, ZAHRA ALIREZAEIZANJANI³, JOACHIM RÄDLER¹, and •SOPHIA RUDORF² — ¹Faculty of Physics, Ludwig Maximilian University of Munich — ²Faculty of Natural Sciences, Leibniz University Hannover — ³independent researcher

Recently, we introduced Live Imaging on Single Cell Arrays (LISCA), which combines time-lapse microscopy of single cells on microstructured surfaces with automated image analysis. LISCA enables us to observe and analyze the time-evolution of protein expression in hundreds of individual cells in parallel. Here, we combine LISCA with our software OCTOPOS, which simulates ribosome movement on the ORF and is used to generate reporter genes with varying ribosome speeds and densities. We predict and monitor the translation kinetics of synonymous variants of eGFP to determine mRNA functional lifetimes and translation rates with high accuracy in single lung tissue cells. Our approach allows us to study how provoked ribosome jams on specific positions within the ORF influence mRNA stability, thus linking ribosome dynamics and mRNA biophysics.

BP 26.6 Thu 16:45 TOE 317

The pH dependent phase transition in lipid nanoparticle cores leads to changes of protein expression in single cells — •JULIAN PHILIPP and JOACHIM RÄDLER — LMU, Munich, Germany

Lipid nanoparticles developed into the most powerful delivery platform for mRNA-based vaccination and therapies. In general, LNPs are particles exhibiting PEG-lipid and DSPC at the surface and ionizable lipid, cholesterol and mRNA in the core. However, the pH dependent changes induced by ionizable lipids in the context of endosomal release are little understood. In particular the ionizable lipids MC3, KC2 and DLin are known to exhibit remarkably different efficacy despite similar pK values. Here, we study the structural response of ionizable lipids with cholesterol as a function of pH using synchrotron X-ray scattering. All three core phases exhibit a sequence of ordered mesophases in the range of pH 7 to 4, beginning with an isotropic swollen phase above their pK value. Lowering the pH reveals transitions to inverse micellar *P6₃/mmc / Fd3m*, inverse hexagonal *H_{II}* and bicontinuous cubic *Pn3m* phases. If polyA, as mRNA surrogate, is added to the core phases, coexistence of pure lipid phases and condensed nucleic acid lipid *H_{II}* phase occurs. We show that the observed core structures are consistent with the SAXS scattering of mRNA containing core phases and full LNP. The difference in structural features of DLin versus MC3 and KC2 phases is also consistent with the delayed onset and reduced level of GFP expression observed in single cell time courses after transfection with DLin LNPs compared to MC3/KC2. We conclude that pH dependent core phase transitions trigger endosomal release.

BP 26.7 Thu 17:00 TOE 317

pH-dependent behavior of ionizable cationic lipids in mRNA-carrying lipoplexes investigated by molecular dynamics simulations — •GIOVANNI SETTANNI^{1,2}, WOLFGANG BRILL³, HEINRICH HAAS³, and FRIEDRIKE SCHMID¹ — ¹Department of Physics, Johannes Gutenberg University Mainz, Germany — ²Faculty of Physics and Astronomy, Ruhr University Bochum, Germany — ³BioNTech SE, Mainz, Germany

Lipid-based nanoparticles and lipoplexes are successful nanocarriers for mRNA-based therapies. The molecular structure of these assemblies is still not fully understood. Lipoplexes including the ionizable lipid 2-dioleoyloxy-N,N-dimethyl-3-aminopropane (DODMA), under specific conditions, have a pH-dependent lamellar structure, where lipid bilayers are separated by mRNA-rich layers. Here, the structure and dynamics of these lipoplexes are investigated at varying pH and mRNA concentration using multiscale molecular dynamics simulations [1]. It is observed that the interaction between DODMA and RNA is slightly attractive only at low pH levels. This results into a pH-dependent relocation of the RNA inside the multilayers, from bilayer's surface at low pH to a more uniform distribution inside the hydrophilic slabs at high pH. Also, at high pH, DODMA lipids shift toward the hydrophobic part of the bilayer, thus increasing their leaflet-flipping rate, a phenomenon which may ultimately affect the fusion process of the lipoplex with the endosomal membrane.

[1] Settanni, G., Brill, W., Haas, H. and Schmid, F. (2022), *Macromol. Rapid Commun.* 43:2100683. <https://doi.org/10.1002/marc.202100683>

BP 26.8 Thu 17:15 TOE 317

Charge and structural properties of transfection lipid layers adsorbing mRNA — •MIRIAM GRAVA¹, IBRAHIM MOHD^{2,3}, JULIO PUSTERLA¹, JULIAN PHILIPP⁴, JOACHIM RÄDLER⁴, OLAF SOLTWEDEL¹, NADINE SCHWIERZ^{2,3}, HEINRICH HAAS⁵, and EMANUEL SCHNECK¹ — ¹Technische Universität Darmstadt, Germany — ²University of Augsburg, Germany — ³Max-Planck-Institute of Biophysics, Frankfurt am Main, Germany — ⁴Ludwig-Maximilians-Universität München, Germany — ⁵BioNTech Corporation, Mainz, Germany

Some of the most effective COVID-19 vaccines are based on cationic lipid-based delivery systems for messenger RNA (mRNA), a promising technology for a

broader use in biomedical applications. Its efficiency depends on pH variations and ionic conditions of the bulk phase. We combine x-ray scattering and x-ray fluorescence on monolayers of positively chargeable transfection lipid mixtures with atomistic molecular dynamics (MD) simulations in order to determine their pH-dependent structural properties and the protonation degree. While the experiments yield electron density profiles and surface charge densities, the

MD simulations yield the area per molecule, the conformation of different lipid species, and the counter-ion distributions. The analysis of experimental and simulation data provides detailed information on the transfection lipid layer characteristics. We applied the same experimental techniques to transfection lipid layers before and after mRNA adsorption, which yields insights into the structure of the adsorbed layers and the interfacial electrostatic balance.

BP 27: Computational Biophysics II

Time: Thursday 15:00–17:30

Location: BAR 0106

BP 27.1 Thu 15:00 BAR 0106

Spectral signatures of excess-proton waiting and transfer-path dynamics — •FLORIAN BRÜNIG¹, MANUEL RAMMLER¹, ELLEN ADAMS², MARTINA HAVENITH², and ROLAND NETZ¹ — ¹Freie Universität Berlin, Department of Physics, 14195 Berlin, Germany — ²Ruhr-Universität Bochum, Department of Physical Chemistry II, 44780 Bochum, Germany

Signatures of solvated excess protons in infrared difference absorption spectra, such as the continuum band between the water bend and stretch bands, have been experimentally known for a long time and have recently been used to analyze protonation dynamics in photoactive proteins. However, the theoretical basis for linking spectral signatures with the microscopic proton-transfer mechanism so far relied on normal-mode analysis.

We analyze the excess-proton dynamics in ab initio molecular-dynamics simulations of aqueous hydrochloric acid solutions by trajectory-decomposition techniques. The continuum band is shown to be due to normal-mode oscillations of temporary H_3O^+ complexes. The actual proton transfer between two water molecules, which for large water separations involves crossing of a barrier and thus is not a normal mode, is characterized by two time scales: Firstly, the waiting time for transfer to occur, which leads to a broad weak shoulder around 100 cm^{-1} , consistent with our experimental THz spectra. Secondly, the mean duration of a transfer event, which produces a rather well-defined spectral contribution around 1200 cm^{-1} and agrees in location and width with previous experimental spectra.

BP 27.2 Thu 15:15 BAR 0106

Lipid-based nanomaterials for RNA delivery investigated using molecular dynamics simulations — •DAVID NOEL ZIMMER¹ and GIOVANNI SETTANNI^{1,2} — ¹Physics Department University of Mainz — ²Faculty of Physics and Astronomy Ruhr University Bochum

Lipid-based nanoparticles (LNP) are one of the most effective carriers in mRNA therapeutics. They are made of a mixture of ionizable, helper, and pegylated lipids encapsulating mRNA. While peg tends to remain on the surface of the nanoparticle, the structure of the core has not yet been well characterized. Experimental data point to a relative lack of order. The lipid composition of the formulation plays a key role in determining the effectiveness of the nano carrier. Small changes in the chemical structure of ionizable and helper lipids dramatically affect the efficiency of mRNA transfection. LNPs based on DLinDMA and DLinDAP, two ionizable lipids, showed significantly different transfection efficiencies, notwithstanding the very small difference in structure. Here, using a multiscale modeling approach, the behavior of lipid formulations based on these two lipids, cholesterol and DSPC or DOPE is examined aiming to provide an understanding of the interactions of lipids and mRNA. The simulations show that, despite DLinDAP binding affinity for mRNA is larger than DLinDMA, the overall interaction of the whole lipid formulation containing DLinDAP with mRNA is weaker, resulting in a larger average distance of the mRNA from the lipid bilayer. This shows that chemical optimization based only on mRNA-ionizable lipid interactions may not be sufficient for the development of more effective lipid formulations for RNA delivery.

BP 27.3 Thu 15:30 BAR 0106

Toehold-Mediated Strand Displacement in Random Sequence Pools — •THOMAS MAYER, LUKAS OESINGHAUS, and FRIEDRICH SIMMEL — School of Natural Sciences, Department of Bioscience, TU Munich, D-85748 Garching, Germany

Toehold-mediated strand displacement (TMSD) has been used extensively for molecular sensing and computing in DNA-based molecular circuits. As these circuits grow in complexity, sequence similarity between components can lead to cross-talk causing leak, altered kinetics, or even circuit failure. For small circuits, such unwanted interactions can be designed against. In environments containing a huge number of sequences, this becomes infeasible. Therefore, a general understanding of the impact of sequence backgrounds on TMSD reactions is of great interest. Here, we investigate the impact of random DNA sequences on TMSD circuits. We begin by studying individual interfering strands and use the obtained data to build machine learning models that estimate kinetics. We then investigate the influence of pools of random strands and find that the kinetics are determined by only a small subpopulation of strongly interacting strands.

Consequently, their behavior can be mimicked by a small collection of such strands. Finally, we compare two established and a novel technique that speed up TMSD reactions in random sequence pools: a threeletter alphabet, protection of toeholds by intramolecular secondary structure, or by an additional blocking strand. We expect that our insights will be useful for the construction of TMSD circuits that are robust to molecular noise.

BP 27.4 Thu 15:45 BAR 0106

comparison of molecular dynamics simulations and neutron reflectivity experiments reveals strengths and weaknesses of current force fields for ionizable Dlin-MC3-DMA lipids — •IBRAHIM MOHD^{1,3}, JENNIFER GILBERT², MARCEL HEINZ³, TOMMY NYLANDER², and NADINE SCHWIERZ^{1,3} — ¹University of Augsburg, 86159 Augsburg, Germany — ²Lund University, SE-22100 Lund, Sweden — ³Max-Planck-Institute of Biophysics, 60438 Frankfurt am Main, Germany

Dlin-MC3-DMA (MC3) is one the most promising ionisable lipid for designing lipid nanoparticles (LNPs), which are used as drug delivery agents. Here, we provide force field parameters for cationic and neutral MC3 compatible with the AMBER Lipid17 force field. Subsequently, we carefully assess the accuracy of the current and existing MC3 force fields by providing a direct comparison to neutron reflectivity experiments of mixed lipid bilayers consisting of MC3 and DOPC at different pH. At low pH (cationic MC3) and at high pH (neutral MC3) the newly developed MC3 parameters in combination with AMBER Lipid17 for DOPC give excellent agreement with the experiments compared to existing MC3 models. With the currently parametrized MC3 parameters we are able to simulate MC3 containing LNPs in atomistic details and gain insights into the effect of pH and RNA cargo on the LNP structure. Combining molecular dynamics simulations, neutron reflectivity experiments and other scattering techniques is therefore a valuable step to drive the advancement of accurate atomistic force fields and to unravel the detailed structure of LNPs.

BP 27.5 Thu 16:00 BAR 0106

Simulation-based Parameter Inference for Large Scale Tumor Simulations — •JULIAN HEROLD¹, ERIC BEHLE², and ALEXANDER SCHUG² — ¹Karlsruhe Institute of Technology, Karlsruhe, Deutschland — ²Jülich Supercomputing Center, Jülich, Deutschland

While clinical imaging of tissues focuses on macroscopic tumors, many experiments investigate only small clusters of cells. We aim on providing a scale-bridging link by performing large scale tissue simulations. We employ highly parallelized code in an HPC setting to simulate mm-sized virtual tissues such as embryogenetic zebrafish tissue or breastcancer tumors with more than a million μm -resolved individual cells. We deploy Cells in Silico (CiS), which combines a cellular potts model with an agent based layer and is thus capable of accurately representing many physical and biological properties, such as individual cell shapes, cell division, cell motility, interactions with the extra-cellular matrix etc.

Using a model with such a strong representational capacity poses the task of adjusting a large number of parameters to reproduce experimental findings. Prior work has attempted to characterize the similarity between experimental and simulated data by extracting different features and using statistical tests to establish a distance measure. This work highlights how this difficult task can be circumvented by training neural networks to distinguish between experimental and simulated data while simultaneously optimizing the model parameters to maximize the error rate of the network.

15 min. break

BP 27.6 Thu 16:30 BAR 0106

Effects of chromatin fibers characteristics on cohesin mediated loop architecture — •AYMEN ATTOU, TILO ZÜLSKE, and GERO WEDEMANN — University of Applied Sciences Stralsund, System Engineering and Information Management, 18435 Stralsund, Germany

The spatial organization of DNA in eucaryotes starts at nucleosome chains forming chromatin loops that can cluster together establishing fundamental units called topologically associating domains (TADs). TADs are an important factor for gene regulation by facilitation or repressing long range contacts in the

genome. Those loops are formed and held together by a ring-shaped protein complex called cohesin together with the effect of CTCF. A loop has a residence time of several minutes. To clarify the spatial structure of a loop, we established a coarse-grained computer model of chromatin with a resolution of single nucleosomes integrating potentials describing CTCF and cohesin. We performed Metropolis Monte Carlo simulations combined with replica exchange procedure with regular spaced nucleosomes and experimentally determined nucleosome positions in presence of cohesin-CTCF as well as depleted systems as control for different loop sizes. We studied differences in the spatial structure and of contacts probabilities of different domains, what allowed us to understand the role of cohesin and CTCF, and their impact on the 3D structure of chromatin. This study also allowed clarifying how nucleosome positions can impact the conformations of the chromatin loops during the residence time of the loop anchor, with presumed consequences for transcriptional activity.

BP 27.7 Thu 16:45 BAR 0106

Theoretical investigations on enzyme-plasma interactions in the context of plasma-driven biocatalysis — •HANNA-FRIEDERIKE POGGEMANN, BJÖRN KIRCHHOFF, TIMO JACOB, and CHRISTOPH JUNG — Ulm University, Institute of Electrochemistry, D-89069 Ulm

Biocatalysis is an emerging field that has several advantages over classical catalysis. The use of enzymes as catalysts is not only more environmentally friendly, but also has potential to be more efficient than the conventional approach in industrial applications. Plasma-assisted biocatalysis is a specific subsection of this field, where a plasma source is used to provide a constant supply of the enzyme co-substrate H_2O_2 that drives the catalytic reaction. However, the use of plasma presents some challenges. The plasma species can alter the structure of the enzyme leading to changes in the catalytic reaction pathway or even deactivation of the enzyme. In a theoretical multiscale approach, we address the questions of how the plasma interacts with the enzyme and how this alters the catalytic reaction. To this end, we use reactive molecular dynamics simulations to investigate possible structural changes of the enzyme by plasma species. We also perform QM/MM hybrid simulations to further investigate the reaction pathway of the enzyme AaeUPO.

BP 27.8 Thu 17:00 BAR 0106

Diffusive properties in simulations of polydisperse sphere mixtures mimicking the inside of a cell — •FRANK HIRSCHMANN¹, HENDER LOPEZ², FELIX ROOSEN-RUNGE³, and MARTIN OETTEL¹ — ¹Institute for Applied Physics, Uni-

versity of Tübingen, Germany — ²School of Physics and Optometric & Clinical Sciences, Technological University Dublin, Ireland — ³Department of Biomedical Sciences and Biofilms-Research Center for Biointerfaces (BRCB), Malmö University, Sweden

The interiors of living cells contain a multitude of different-sized biomacromolecules at relatively high packing fractions. Diffusivity and transport properties in such crowded environments are highly influenced by hydrodynamic interactions. Thus, the time needed for proteins to come into contact with each other within the cell is determined by a complex interplay of polydispersity, size-distribution and crowding. In order to analyze such systems theoretically, we employ Brownian Dynamics (BD) simulations of polydisperse mixtures of hard spheres. Using results of Stokesian dynamics we approximate hydrodynamic interactions in our BD simulations by a simple multiplicative ansatz (equivalent to a hydrodynamic "renormalization" of the Brownian short-time diffusivity), which allows us to access the long-time limit of our system. We investigate resulting diffusion constants and survival probabilities, exhibiting non-trivial behavior.

BP 27.9 Thu 17:15 BAR 0106

Unwrapping trajectories of constant-pressure molecular dynamics simulations — •JAKOB TÓMAS BULLERJAHN¹, SÖREN VON BÜLOW², JÉRÔME HÉNIN³, and GERHARD HUMMER^{1,4} — ¹Department of Theoretical Biophysics, Max Planck Institute of Biophysics, Frankfurt am Main, Germany — ²Linderstrøm-Lang Centre for Protein Science, Department of Biology, University of Copenhagen, Copenhagen, Denmark — ³Laboratoire de Biochimie Théorique, Institut de Biologie Physico-Chimique, CNRS, Paris, France — ⁴Institute of Biophysics, Goethe University Frankfurt, Frankfurt am Main, Germany

In molecular dynamics simulations at constant pressure, the size and shape of the periodic simulation box fluctuate with time. Special care is thus required when a particle trajectory is unwrapped from a projection into the central box under periodic boundary conditions into a trajectory in full three-dimensional space, e.g., for the calculation of diffusion coefficients. Here, we review and compare different schemes proposed for trajectory unwrapping, and specify the respective rewinding scheme to put an unwrapped trajectory back into the central box. On this basis, we then identify a scheme in which the wrapped and unwrapped trajectory are mutually consistent and in which the statistical properties of the trajectory are preserved. We conclude with advice on best practice for the consistent unwrapping of constant-pressure simulation trajectories.

BP 28: Poster Session II

Time: Thursday 18:00–20:00

Location: P2/EG

BP 28.1 Thu 18:00 P2/EG

X-Ray Phase-Contrast Tomography Imaging of Single Cells Using an Optical Stretcher — •JAN-PHILIPP BURCHERT¹, ROLAND STANGE², MADLEEN BUSSE³, TIM SALDITT¹, and SARAH KÖSTER¹ — ¹Institute for X-Ray Physics, University of Göttingen — ²RS Zelltechnik GmbH, Schöllnach — ³Department of Physics and Munich School of Biomedical Engineering, Technical University of Munich X-rays penetrate deep into matter and allow us to image structures with high spatial resolution, which makes them attractive for investigating individual biological cells. Here, we combine x-ray phase-contrast tomography with an x-ray compatible optical stretcher to image single cells in solution, thus in their physiological environment, and avoid the need for freezing, drying or embedding of the samples. The cells are trapped in a contact-free manner in a fixed position by the optical stretcher and are probed by the x-ray beam. The microfluidic flow sets the cells in slow rotational motion, which enables tomographic imaging. We apply this combination of techniques to unfixed and fixed NIH3T3 fibroblasts, which are partially stained with an x-ray contrast agent. The experimental data show that we can acquire images of these cells with our setup. Moreover, the comparison of the different preparations and two beam energies will improve the image quality in future experiments.

BP 28.2 Thu 18:00 P2/EG

Scanning small angle x-ray scattering of hydrated, keratin-rich cells in flow environment — •BORAM YU¹, SOPHIE-CHARLOTTE AUGUST¹, PETER LULEY¹, MANFRED BURGERHAMMER², and SARAH KÖSTER¹ — ¹Institute for X-Ray Physics, University of Göttingen, Germany — ²European Synchrotron Radiation Facility (ESRF), Grenoble, France Intermediate filaments (IFs), one of the three main components of the cytoskeleton, form a network that contributes to cell mechanics. Thus, collecting structural information about IF networks in their physiological setting, i.e., in whole living cells, is crucial. We study mammalian cells expressing cytokeratin, which forms bundle structures. To obtain this information, we use scanning small angle x-ray scattering (SAXS), as it provides both real space overview images with moderate resolution and reciprocal space information with a high resolution.

X-ray imaging of cells in aqueous state is challenging as their electron density contrast is low, and pronounced radiation damage and radiation-induced gas formation occurs. For this reason, we used a dedicated flow sample chamber that minimizes the thickness of liquid layer in the beam path and serves to exchange liquid continuously during scanning. Despite weak contrast and short exposure times, we are able to retrieve the local main orientation of subcellular structures, thus demonstrating how scanning SAXS offers valuable information from fixed-hydrated cells in liquid flow.

BP 28.3 Thu 18:00 P2/EG

Comparative investigation of differently prepared porcine retinal pigment epithelium (RPE) cells using mid-IR photo-induced force microscopy (PiF-IR) — •JESVIN JOSEPH^{1,2}, ROBIN SCHNEIDER¹, ROWENA SIMON³, and DANIELA TÄUBER^{1,2,4} — ¹Heintzmann Lab, Leibniz Institute of Photonic Technology, Jena — ²Institute of Physical Chemistry & Abbe Center of Photonics, Friedrich-Schiller-University Jena — ³Department of Ophthalmology, University Hospital Jena — ⁴Institute of Solid State Physics, Friedrich Schiller University Jena, Germany

Age-related loss of sight caused by macular degeneration (AMD) is monitored in clinical health care using fundus autofluorescence, which investigates variations in the autofluorescence signal stemming from the retinal pigment epithelium (RPE)[1]. Nanolocal chemical characterization of RPE cells and pigment granules could deepen the understanding of involved cellular processes. Nanoinfrared imaging methods can provide chemical information at a lateral resolution below 10 nm[2]. We used PiF-IR to investigate externally grown porcine RPE cells, which were dried in varied conditions. First results show spectral variations obtained from cells dried at room temperature and at 37°C. We compare these spectra to PiF-IR and conventional FTIR spectra obtained from plain retinal pigment chemicals. Funding by Profil Line Light, project pintXsum, FSU Jena, is acknowledged. [1] Schultz, R., Schwanengel, L., Klemm, M., Meller, D. & Hammer, M. *Acta Ophthalmologica* (2021). [2] Luo, X. Xue, Y.; Wu, J.; Cai, W.; Täuber, et al. *Applied Physics Letters* DOI: 10.1063/5.0128850.

BP 28.4 Thu 18:00 P2/EG

Redirecting the early embryogenesis of *Caenorhabditis elegans* by altering mechanical cues — •VINCENT BORNE and MATTHIAS WEISS — Experimental Physics I, University of Bayreuth, Universitätsstr. 30, D-95447 Bayreuth, Germany

During early development, somatic and germline precursor cells of the model organism *Caenorhabditis elegans* undergo an apparently pre-determined and robust division scheme, suggesting early embryogenesis to run on autopilot. While the role of biochemical signaling in embryogenesis has long been recognized, the influence of mechanical forces for proper cell arrangement has been revealed only recently. Aiming at challenging the robustness of the organismal development mechanically, we have flattened the embryo to induce altered positioning and division timing of cells. Indeed, upon a controlled squeezing between two coverslips, the outer boundary of the embryo remained intact but cytokinesis was seen to be compromised, i.e. normal development came to a full stop. Surprisingly, nuclei still underwent division, resulting in multinucleated cells or even a syncytium-like state with up to 60 nuclei. In this state, we have monitored the growth of nuclei and their division timing. Despite the total failure of cell division, both observables are in line with experimental data and theoretical descriptions obtained from unperturbed embryos. Our results highlight how some key features for correct embryonic development prevail even under mechanically stressful conditions.

BP 28.5 Thu 18:00 P2/EG

Microfluidics-based analysis of the mobility and migration pattern of *Trypanosoma brucei* — •HANNES WUNDERLICH¹, LUCAS BREHM², JANA RITSCHAR², SEBASTIAN KRAUSS¹, KLAUS ERSFELD², and MATTHIAS WEISS¹ — ¹Experimental Physics I, University of Bayreuth, Germany — ²Molecular Parasitology, University of Bayreuth, Germany

Trypanosoma brucei is a unicellular parasite that causes the African sleeping sickness after entering the human bloodstream via the bite of an infected tsetse fly. Active spiral movement of trypanosomes, mediated by the beating of a microtubule-driven cell-body attached flagellum, is crucial to evade the hosts immune response, i.e. swimming is a matter of survival for trypanosomes. Beyond the flagellum, microtubules also form a highly ordered, subpellicular array beneath the cell membrane, hence determining the effective elasticity of the parasite and its propulsion via the flagellum. Using soft lithography to produce well-defined two-dimensional chambers and using a temperature controlled environment, we have optimized cell tracking, shape determination, and subsequent analyses. As a result, we find that wild-type and mutant strains with altered post-translational modifications of microtubules not only feature different phenotypes but also show distinct mobility patterns, e.g. a strain-dependent swimming velocity and intermittency of swimming (run-and-tumble phases).

BP 28.6 Thu 18:00 P2/EG

2D polarization fluorescence imaging (2DPOLIM) - Evaluation of depolarization artifacts in fixed four channel detection — •YUNHAO MEI^{1,2}, ASAD HAFEEZ^{1,2}, YUTONG WANG^{1,2}, MOHAMMAD SOLTANINEZHAD^{1,2}, RAINER HEINTZMANN^{1,2}, and DANIELA TÄUBER^{1,2} — ¹Heintzmann Lab, Leibniz Institute of Photonic Technology, Jena — ²Institute of Physical Chemistry & Abbe Center of Photonics, Friedrich-Schiller-University Jena, Germany

Fluorescence polarization and anisotropy measurements are widely used in Diagnostics and Imaging in the Life Sciences. Most common is the use of linearly polarized excitation together with two-channel detection of linear polarization parallel and perpendicular to the polarization in excitation. However, when applied to anisotropic samples, the result may depend on the lab frame in respect to structural alignments within the sample, which can be prevented by collecting the sample fluorescence in more polarization angles[1]. We designed a four-channel detection for evaluating Förster Resonance Energy Transfer between similar fluorescence labels, the so-called homo-FRET or emFRET. The quantitative discrimination of FRET via tiny changes in polarization resolved fluorescence intensities requires highly sensitive cameras and well-designed and calibrated detection channels. Wire grids provide high-quality polarization properties when used in normal incidence in transmission but may introduce depolarization when implemented tilted in respect to the optical axis. We studied several possible arrangements and compared the introduced depolarizations. [1] R. Camacho et al. Adv. Mater. 2019, 1805671.

BP 28.7 Thu 18:00 P2/EG

Monitoring actomyosin flows in early *Caenorhabditis elegans* embryos by lightsheet microscopy — •IVANA JEREMIC and MATTHIAS WEISS — University of Bayreuth, Bayreuth, Germany

Symmetry breaking, i.e. the formation of body axes, is crucial for embryonic development as it guides the formation of highly organized tissues and consequently assures proper maturation of the organism. A convenient model system for studying such events is *Caenorhabditis elegans* since all body axes are fully defined already in the 8-cell stage of the embryo. Confocal fluorescence imaging on *C. elegans* has revealed that chiral mechanical forces, generated by the actomyosin cortex, play an important role in the left-right symmetry breaking. Con-

focal imaging, however, requires a gentle flattening of the embryo to allow for a full three-dimensional assessment of the embryo. Yet, even a gentle squeezing of the embryo can already delay cell divisions and subsequently lead to altered cell positions, suggesting that also the symmetry-breaking action of the actomyosin cortex can be affected. Using a custom-made lightsheet microscope that does not require any squeezing of the embryo, we have monitored actomyosin flows in the early embryo in three dimensions over time. Preliminary data from these experiments suggest that the previously observed chiral forces are even enhanced under these unconfined conditions.

BP 28.8 Thu 18:00 P2/EG

Organelle organization and dynamics in cells on soft substrates — •PAULA GIRONES PAYA, FLORIAN REHFELDT, and MATTHIAS WEISS — Experimental Physics I, University of Bayreuth, Germany

The interior of eukaryotic cells features a highly organized and dynamically evolving set of compartments (organelles), e.g. mitochondria, the endoplasmic reticulum, or the nucleus. How these organelles self-organize to arrive at an arrangement that is beneficial for a cell is still poorly understood. Numerous studies have monitored organelle morphologies and dynamics in well-characterized culture cells grown on rigid substrates, e.g. glass coverslips. In real life, however, cells are situated in soft tissues with an elastic modulus that is five to six orders of magnitude lower. On soft substrates, actin-based stress fibers are less pronounced, and consequently cell morphologies are considerably less flattened by tensile forces, suggesting that also organelle arrangement and dynamics is altered. Here, we compare results of mitochondrial dynamics, cell nucleus volumes, and the exchange kinetics for diffusively driven transport between the nucleoplasm and the cytoplasm of cells on soft and rigid substrates.

BP 28.9 Thu 18:00 P2/EG

Quantifying Molecular Mobility, Abundance and Interactions by Fluorescence Correlation Spectroscopy — •JANA SÜTTERLIN¹, KATHARINA REGLINSKI^{1,2,3}, FRANCISCO PÁEZ LARIOS^{1,2}, and CHRISTIAN EGGELING^{1,2} — ¹Institut für angewandte Optik und Biophysik, Friedrich-Schiller Universität Jena, Jena, Deutschland — ²Leibniz-Institut für photonische Technologien e.V., Jena, Deutschland — ³Universitätsklinikum Jena, Jena, Deutschland

Since many biological functions rely on molecular interactions, knowledge about molecular mobility and diffusional processes are key to understand cellular signalling. To gain the desired insights, it is of utmost importance to develop and apply live-cell compatible approaches for diffusional investigations. Fluorescence Correlation Spectroscopy (FCS) is a powerful technique that enables the quantification of these dynamics.

This poster will provide an outline on how to utilise parameters acquired from FCS and dual-colour Fluorescence Cross-Correlation Spectroscopy (DC-FCCS) to quantify diffusion characteristics of particles in aqueous environments. This way, an examination of diffusional behaviour influenced by various binding conditions can be carried out.

FCS study about the peroxisomal import receptor PEX5 in live HEK cells is shown to elucidate its molecular interaction dynamics within the cytosol. Thereby the potential of FCS is exploited, highlighting its non-invasive, live-cell compatible properties. Ensuring proper function of organelles and cells, PEX5 transports cargo proteins featuring a targeting sequence, which need to be imported into peroxisomes.

BP 28.10 Thu 18:00 P2/EG

Evolution of the crowded state of cells as seen by FRET — •AVIJIT KUNDU and MATTHIAS WEISS — Experimentalphysik I, Universität Bayreuth, Universitätsstraße 30 95447 Bayreuth

Cells are the basic units of all living organisms. Somewhat surprisingly, however, virtually all cells feature very similar and high degrees of macromolecular crowding, with total concentrations of more than 100 mg/ml, irrespective of the species from which the cell is taken. Macromolecular crowding plays a key role in many biophysical processes and it can even alter biochemical cues by changing the binding kinetics or the steady-state fraction of associated states, suggesting that cells need to actively maintain their crowding state. Using a FRET sensor that reports on the local crowdedness in living cells, we have explored how individual cells can re-adapt their crowding state after a perturbation. Using a stepwise change of the osmotic pressure, we find that cells react rapidly to the external perturbation but aim at a relaxation back to the native state over time scales of minutes to hours.

BP 28.11 Thu 18:00 P2/EG

3D light-sheet microscopy of contracting skeletal muscle tissue — •LAURA STRAMPE, ARNE HOFEMEIER, PAUL MAIER, JAN HUISKEN, and TIMO BETZ — Third Institute of Physics - Biophysics, Georg August Universität, Göttingen

Skeletal muscle makes up the majority of human muscle tissue. Its contraction allows for controlled movements of the body, as well as being essential for maintaining posture. To understand the global and local forces at play during such contractions, occurring on the time scale of seconds, a 3D high-speed, high-resolution imaging method is necessary. We present a protocol for rais-

ing biomimetic muscle tissue anchored between two flexible mm-sized post. A full contraction cycle can be recorded through the synchronization of periodic electric stimuli and image acquisition using a custom build Flamingo light-sheet microscope. This enables us to study a wide range of questions including the influence of local contractile forces on muscle stem cell activation and contractile sarcomere dynamics.

BP 28.12 Thu 18:00 P2/EG

Screening for Pharmacologically Enhanced Tissues for Optical Microscopy. — •VENKAT RAGHAVAN KRISHNASWAMY, SUSAN WAGNER, RICO BARSACCHI, and MORITZ KREYSING — Max Planck Institute of Molecular Cell Biology and Genetics, Dresden, Germany.

Our ability to observe the complexity of a living tissue under a light microscope is heavily impeded by the inherent light-scattering properties of the biological tissues. But remarkably some living tissues are highly transparent in nature, e.g., human retina, certain deep-sea creatures, etc. Comprehending and replicating the mechanisms by which tissue transparency is attained would unleash the full capabilities of optical microscopes. Here, we propose to unravel the molecular basis of tissue transparency in three-dimensional tissues using the immense potential of high-throughput screening and large-content image analysis tools. Specifically, we used active pharmacological compounds to screen for pathways that impact light-scattering properties in spheroids of human colorectal carcinoma cell line (HCT116). Randomly integrated multifluorescent beads within the spheroids served as an extrinsic readout factor and a conventional chemical-based clearing method was used as a positive control for assessing the optical properties of the tissue. The image analysis pipeline constructed to measure the intensities of the beads through the Z-sections clearly distinguishes cleared from uncleared spheroids. Overall, a robust assay was developed which would be employed on larger screens, to rapidly identify compounds and, further, signaling pathways that regulate the molecular mechanisms of tissue transparency.

BP 28.13 Thu 18:00 P2/EG

Imaging of vital mitochondria using Scanning Ion Conductance Microscopy (SICM) and electron microscopy methods — •ERIC LIEBERWIRTH¹, CHRISTIAN VÖLKNER¹, REGINA LANGE¹, ANJA SCHAEFER², MAGDALENA OTTE², MARCUS FRANK³, KEVIN OLDENBURG⁴, INGO BARKE¹, SIMONE BALTRUSCH², and SYLVIA SPELLER¹ — ¹University of Rostock, Institute of Physics — ²Rostock University Medical Center, Institute for Medical Biochemistry and Molecular Biology — ³Rostock University Medical Center, Medical Biology and Electron Microscopy Center — ⁴University of Rostock, Center for Interdisciplinary Electron Microscopy MV

Mitochondria are enclosed by a double membrane. While the inner membrane with many insertions creates a large surface for the respiratory chain complexes, the outer one mediates fusion, fission and degradation of the organelles in the network. In this process, pole-like interaction sites develop, which impact the surface of the outer membrane. Scanning Ion Conductance Microscopy (SICM) allows the outer membrane of immobilized vital mitochondria to be measured in a buffer solution with a spatial resolution of about 50 nm and a height resolution of a few nanometers. The outer membrane shows dynamic height fluctuations as well as spatial height variations depending on the medium. Transmembrane proteins can be made visible when labelled with nanoscopic gold particles. A complementary study of SICM topographies, Scanning Electron Microscopy (SEM) and in situ liquid Transmission Electron Microscopy (TEM) images gives insight into the spatial distribution of internal and membrane-bound structures.

BP 28.14 Thu 18:00 P2/EG

Imaging Soft-Landed DNA-Aggregates — •ISABELLE LEGGE, JOVANA PEPIC, TIM ESSER, MÁRKÓ GRABARICS, and STEPHAN RAUSCHENBACH — Department of Chemistry, University of Oxford, Oxford, United Kingdom

Deoxyribose nucleic acid (DNA) is involved in important biological processes including replication, encoding information and gene expression. The helical structure of DNA double strands is well known but the superstructure of more complex assemblies such as DNA origami can be challenging to characterise by averaging techniques. Therefore, a versatile, yet practical, sample preparation technique is needed to make DNA-based molecules accessible to high-resolution, single-molecule imaging by atomic force microscopy (AFM) or transmission electron microscopy (TEM). Here, we use electrospray ion-beam deposition (ESIBD) to produce clean samples of single- and double-stranded DNA or DNA origami to enable AFM and TEM imaging, providing information on structure, conformation and revealing the mechanical properties. We discuss the advantages and limitations of this approach to improve the understanding of the function of these molecules.

BP 28.15 Thu 18:00 P2/EG

A backward-mode optical-resolution photoacoustic microscope for functional 3D imaging — •ELISABETH BAUMANN^{1,2}, ULRIKE POHLE³, THOMAS ALLEN⁴, HOLGER GERHARDT^{1,2}, and JAN LAUFER³ — ¹MDC, Berlin, DE — ²Charité, Berlin, DE — ³MLU, Halle, DE — ⁴UCL, London, UK

Optical-resolution photoacoustic microscopy (OR-PAM) is a biomedical imaging technique with great potential for preclinical studies of the vasculature. It can be used to obtain spatially resolved information on parameters like the blood flow speed and blood oxygen saturation. However, for many in vivo applications, backward-mode operation of the OR-PAM system is required for which conventional piezoelectric ultrasound sensors are at a disadvantage as they need to be placed far away from the signal source. Here, we present an all-optical, backward-mode OR-PAM system that fulfils the requirements for functional imaging of the vasculature. The system incorporates a novel planar Fabry-Pérot (FP) ultrasound sensor, which is transparent to the excitation light and can be placed immediately adjacent to the sample.

To demonstrate the morphological imaging capabilities of the system, we performed 3D imaging in vitro of a leaf skeleton phantom and in vivo of a zebrafish embryo in raster-scanning mode. To be able to resolve blood flow, a fast continuous-scanning mode was established and validated in imaging phantoms. To show the capabilities of the system to image blood oxygen saturation, a Raman laser was set up for multi-wavelength excitation OR-PAM of ink phantoms.

BP 28.16 Thu 18:00 P2/EG

Imaging Symmetry-Dependent Behavior of Orbital Angular Momentum Entangled States — •JUAN NICOLAS CLARO RODRIGUEZ^{1,2} and ROBERTO RAMIREZ ALARCON¹ — ¹Centro de Investigaciones en Óptica, 37150 León-Guanajuato, México — ²Paderborn University, 33098 Germany

Orbital angular momentum (OAM) is a degree of freedom of photons, promising for many high-dimensional quantum applications. By tuning the symmetry of OAM states using dove prisms and measuring spatially resolved interference properties, we find that fringes are produced depending on the type of the state symmetry and propose an application to achieve twice the contrast in quantum optical coherence tomography. This technique also permits high-resolution microscopy of photo-sensitive tissue.

BP 28.17 Thu 18:00 P2/EG

Quantitative imaging of Caenorhabditis elegans dauer larvae during cryptobiotic transition — •KYOOHYUN KIM¹, VAMSHIDHAR N. GADE^{2,3}, TEYMURAS V. KURZCHALIA², and JOCHEN GUCK¹ — ¹Max Planck Institute for the Science of Light, Erlangen, Germany — ²Max Planck Institute of Molecular Cell Biology and Genetics, Dresden, Germany — ³Institute of Biochemistry, ETH Zürich, Zürich, Switzerland

Caenorhabditis elegans can survive harsh environments by entering dauer diapause with reduced metabolic activity and distinct structural changes. We employed optical diffraction tomography (ODT) to quantitatively measure the transitions of mass density distribution inside living C. elegans larvae in the reproductive and diapause stages. ODT revealed that the mass density of C. elegans larvae increased upon entry into dauer diapause, and surprisingly, the harshly desiccated dauer larvae exhibited very high refractive index values ($n \sim 1.5$). Moreover, mutants that are sensitive to desiccation displayed structural abnormalities in the anhydrobiotic state that were not observable by conventional microscopy. Our findings open a door to quantitatively understanding the importance of material properties of an organism on the verge of life and death.

BP 28.18 Thu 18:00 P2/EG

Shaping the embryo: blastoderm stress maps reveal early mechanical symmetry breaking — •ALEJANDRO JURADO JIMÉNEZ, LEON LETTERMANN, BERNHARD WALLMEYER, and TIMO BETZ — Drittes Physikalisches Institut, Georg-August-Universität Göttingen

In this work we present a hydrodynamical analysis of early Zebrafish development which aims to understand the mechanical state of the tissue leading to its first symmetry breaking during epiboly: the shield formation. A full mechanical characterization of the blastoderm is achieved using a combination of Light-Sheet microscopy and state-of-the-art cell tracking of the cells nuclei, viscosity measurements and polyacrylamide beads as force sensors. The extraction of stress maps in the tissue is possible thanks to a custom-made software for the analysis of the bead deformation, which is presented here a versatile tool for similar stress analyses in other biological samples.

Our experimental analysis of the mechanical state of the embryo is supported and expanded by a model-driven extraction of the stress fields using NeuronODEs. The NODEs system only necessitates the velocity field on the blastoderm to solve the hydrodynamic problem, optimizing up to 10^5 parameters and retrieving a full dynamical description of the embryo. Both the experimental and numerical analyses expose a stress asymmetry prior and during the shield formation, from which we can learn more about the mechanical origin of the first embryonal symmetry breaking.

BP 28.19 Thu 18:00 P2/EG

Radial growth and the impact of stress on the cell division plane in the hypocotyl — •MATHIAS HÖFLER and KAREN ALIM — School of Natural Sciences, Technical University of Munich, Germany

The morphogenesis of plant tissue is a reliably stable and efficient process, yet individual cell shape and growth underlie high variance. Theory and experiment

show that there is a mechanical and biochemical feedback loop for plant tissue development. In fact, mechanical stresses have a pronounced effect on microtubule orientation in the tissue, thereby changing the mechanical properties and leading to anisotropic cell growth. Here, we study the effect of cell mechanics, stress patterns and feedback mechanisms on the bidirectional radial growth of the plant hypocotyl. We furthermore study the connection between mechanical stresses and the choice of cell division plane orientation. We seek to unveil the minimal biophysical requirements and relevant forces to achieve the experimentally observed morphologies. Our results show that inhomogeneous growth generates distinct stress patterns in the tissue. Introducing cell division along the direction of maximum stress furthermore gives us a first perspective on how radial growth morphologies emerge.

BP 28.20 Thu 18:00 P2/EG

3D Traction Force Microscopy on engineered blood vessels — •KARIM AJMAIL, FATEMEH MIRZAPOUR, and KAREN ALIM — School of Natural Sciences, Technical University of Munich, Germany

The endothelium lines the walls of every blood vessel the human body. By virtue of their strategic position the endothelium has to withstand a plethora of mechanical cues including shear stress, circumferential strain as well as pressure exerted by the blood flow. Therefore, the mechanobiology of endothelial cells is a particularly pivotal part for the functionality of this tissue. However, the immense complexity of the vasculature necessitates *in vitro* systems that can uncouple and measure these various effects. Although *in vitro* approaches greatly enhanced our understanding of endothelial complexity, a mechanical characterization of endothelial systems is missing so far. Here, we employ 3D Traction Force Microscopy (TFM) as state-of-the-art method to measure cellular forces in physiologically relevant environments. In particular, we use 3D TFM to measure forces in a perfusable engineered blood vessel embedded in a fibrin hydrogel. Further, the effect of different stationary as well as pulsatile flow patterns on the mechanical response of the cells is investigated. We propose 3D TFM as an additional readout parameter in future human-on-a-chip applications for a quantitative mechanical characterization of the tissue.

BP 28.21 Thu 18:00 P2/EG

Tissue tension during zebrafish development — •MING HONG LU^{1,2}, ALEJANDRO JURADO¹, LEON LETTERMANN^{1,3}, and TIMO BETZ^{1,2} — ¹3rd Institute of Physics - Biophysics, University of Göttingen — ²Max Planck School Matter to Life — ³Institute for Theoretical Physics, Heidelberg University

Understanding the morphogenesis during development is one of the emerging fields where the interaction between developmental and tissue biology with biophysics has provided a series of new insights into nature's physical working principles. In particular, during embryonic development of zebrafish, cells in the blastoderm exhibit collective migration towards the yolk in a process known as epiboly, while simultaneously shield formation and gastrulation break symmetry preceding tissue differentiation. These elegantly robust processes are facilitated by both biochemical and mechanical interactions.

To determine how mechanical tissue stresses contribute to these interactions, we use photoablation to externally break symmetry by severing connections in the enveloping layer and record the subsequent population redistribution using light sheet microscopy of the whole embryonic volume. From the analysis of the nuclei trajectories, we noted that the epiboly process is highly robust and mostly unaffected by the damage, during which there is a convergent motion of cells towards an azimuthal angle (orthogonal to the direction of epiboly) that forms the future spine. Ablations can transiently disrupt this convergence dependent on the developmental time at which the damage is introduced.

BP 28.22 Thu 18:00 P2/EG

A 3D Voronoi vertex model for fluid transport in lumenogenesis — •ANNE MATERNE¹, CHARLIE DUCLUT^{1,2}, QUENTIN VAGNE^{1,3,4}, PIETRO INCARDONA^{3,5,6}, IVO F. SBALZARINI^{3,5,7,8}, and FRANK JÜLICHER^{1,3,8} — ¹Max Planck Institute for the Physics of Complex Systems, Dresden, Germany — ²Laboratoire Physico-Chimie Curie, Paris, France — ³Center for Systems Biology Dresden, Germany — ⁴Department of Genetics and Evolution, Université de Genève, Switzerland — ⁵Faculty of Computer Science, TU Dresden, Germany — ⁶Institute for Genomic Statistics and Bioinformatics, Universität Bonn, Germany — ⁷Max Planck Institute of Molecular Cell Biology and Genetics, Dresden, Germany — ⁸Cluster of Excellence Physics of Life, TU Dresden, Germany

In many systems, cells collectively organise to build complex structures. In particular, in certain developmental processes the formation of a fluid-filled cavity called a lumen plays a crucial role. Various mechanisms, for example programmed cell death, are known to initiate lumen formation. However, in order to sustain lumenogenesis, cells must collectively transport water and ions into the newly forming cavity. Here, we present a 3D Voronoi vertex model to study this collective transport process at cellular resolution. Our approach involves a substantial extension of the typical Voronoi work function minimisation procedures to account for the hydraulic and mechanical mechanisms in cell volume regulation and for pressure-driven flows. Fully-parallelised and efficient for systems with many cells, our procedure allows us to study the dynamics of lumenogenesis in complex geometries.

BP 28.23 Thu 18:00 P2/EG

Dystrophin as a tension regulator in human skeletal muscles — •MARIAM RISTAU¹, ARNE HOFEMEIER^{1,2}, and TIMO BETZ¹ — ¹Third Institute of Physics - Biophysics, Georg-August-University Göttingen, Germany — ²ZMBE - Institute of Cell Biology, University of Münster, Germany

Skeletal muscles are associated with contraction, movement and force generation. They are important for maintaining posture and maintaining bone and joint stability. Muscular dystrophies such as Duchenne muscular dystrophy (DMD) result in progressive weakening of skeletal muscles. DMD is caused by the loss of the protein dystrophin which is thought to stabilize and protect muscle fibers from injury. In the progression of the disease, damaged muscle fibers degrade, muscle mass is lost and greater functional impairments develop. We have studied the contractile potential of myoblasts and reconstituted tissue derived from healthy and DMD patients, and found that they were mechanically different in muscle tension and contractility. DMD derived myoblasts exhibited an overall weaker contractility compared to healthy derived myoblasts. In contrast, DMD derived myoblasts showed an overall higher muscle tension, suggesting that dystrophin may function as a tension regulator in skeletal muscles. In order to rule out the possibility that these findings are due to patient variability we intend to establish a genetic model in which we knockout dystrophin with the CRISPR/Cas9 system in healthy myoblasts and rescue dystrophin in DMD myoblasts by integrating micro-dystrophins (μ Dys).

BP 28.24 Thu 18:00 P2/EG

Influence of vimentin intermediate filaments on microtubules in cells — •ANNA BLOB¹, ROMAN DAVID VENTZKE^{1,2}, THOMAS GIACOMO NIES², AXEL MUNK², LAURA SCHAEDEL³, and SARAH KÖSTER¹ — ¹Institute for X-Ray Physics, University of Göttingen — ²Institute for Mathematical Stochastics, University of Göttingen — ³Center for Biophysics, Saarland University

The cytoskeleton in eucaryotic cells is an intricate network of three different filamentous proteins: microtubules, actin filaments and intermediate filaments. They are essential for the mechanical properties of a cell as well as intracellular transport and division. Each filament type has its own unique features, and, in particular, microtubules, can withstand large compressive forces and show characteristic buckling and bending behavior that is still not fully understood. There is evidence for important interactions between cytoskeletal filaments: vimentin intermediate filaments stabilize microtubules *in vitro* and can template the microtubule network in migrating cells. Following up on this idea, we are interested in the influence of vimentin networks on microtubule mechanics. Investigating how the bending of microtubules depends on both the microtubule network itself and the vimentin network will improve our understanding of the mechanical consequences of the interaction within and between these filament systems. We compare microtubule networks in vimentin-knockout and wild-type mouse fibroblasts on micropatterns. We find that the local curvature of microtubules depends on the cellular region and increases with both increasing microtubule density and increasing vimentin density.

BP 28.25 Thu 18:00 P2/EG

Interactions between synaptic vesicles and cytoskeletal filaments — •TIAGO MIMOSO, TYZIAN SCHMIDT, and SARAH KÖSTER — Institute for X-Ray Physics, University of Göttingen, Germany

Signal transmission of neurons occurs both electrically and chemically. The chemical signal is transported by synaptic vesicles (SVs) from one cell to another via the synaptic cleft to the adjacent neuron. Thus, these SVs are found in the synapse, within the so-called synaptic bouton. Here, the SVs are surrounded by cytoskeletal filaments, including dynamic microtubules that undergo rapid assembly and disassembly. There are studies that suggest an interactions between SVs and the cytoskeletal filaments, however the exact mechanisms remain unknown. Therefore, we now ask the question of whether SVs and microtubules interact and what influence the presence of SVs has on the growth rate, disassembly rate, catastrophe frequency and rescue frequency of the microtubules. We employ a reconstituted *in vitro* system and image the dynamic microtubules by total internal reflection fluorescence (TIRF) microscopy. We use a novel and fast data analysis technique based on a neural network to segment the microtubules in the microscopy pictures. This method provides the advantage of being applicable also curved microtubules and yields results that are comparable to the commonly used manual analysis method.

BP 28.26 Thu 18:00 P2/EG

Burst Mode Characteristics of an Ultrasonic Transducer for Treatment of Cancer Cells — •REBECCA KAMPMANN¹, BIRTE SEHLMAYER¹, CLAUDIUS SCHEIDEMANN², TOBIAS HEMSEL², and MATHIAS GETZLAFF¹ — ¹Institute of Applied Physics, Düsseldorf University — ²Dynamics and Mechatronics, Paderborn University

Head and neck squamous cell carcinoma cells and oral keratinocytes have different cell mechanics and because of that they have different natural frequencies. This characteristic is used to selectively destroy cancer cells.

For this purpose, ultrasonic waves at a resonant frequency of 90kHz were used in burst mode to achieve the largest possible deflection of the ultrasonic trans-

ducer. The ultrasonic actuators were electrically excited using a flexible ultrasonic generator developed by ATHENA Technologie Beratung GmbH, Paderborn. Investigation of the active current, which is proportional to the transducer tip velocity, showed that the active current depends on the set active time. If the active time is too low, the active current is not able to reach the desired target current. The longitudinal deflection of the ultrasonic probe in burst mode is comparable to the one in continuous mode. The setpoint current amplitude and the active time are decisive parameters. In addition, the transverse deflection was investigated, showing that this vibration is larger than the longitudinal one.

BP 28.27 Thu 18:00 P2/EG

Burst Mode of Ultrasonic Resonant Oscillations for Stimulation and Destruction of Tumor Cells — •BIRTE SEHLMAYER¹, REBECCA KAMPMANN¹, CLAUDIUS SCHEIDEMANN², TOBIAS HEMSEL², and MATHIAS GETZLAFF¹ — ¹Applied Physics, Düsseldorf University — ²Dynamics and Mechatronics, Paderborn University

Different types of cancer, such as prostate carcinomas, are nowadays already treated with the ultrasound-based therapy HIFU (high intensity focused ultrasound). The healthy cells, which are located in the irradiation field, cannot be spared in this process. The elasticity differences between cancer cells and healthy cells strongly influence their stimulation frequency. LIPUS (low intensity pulsed ultrasound) is used to selectively stimulate and destroy cancer cells close to their own natural frequency, while sparing locally adjacent healthy cells.

Here we report new findings on the maximum oscillation amplitude of an ultrasound unit in burst mode. In burst mode, there is only a signal output during the active times. The ultrasonic actuators were electrically excited using a flexible ultrasonic generator developed by ATHENA Technologie Beratung GmbH, Paderborn. The excitation of the ultrasonic unit was varied by setting the targets current amplitude and the active time. Regarding the characteristic stimulation frequency of tumor cells, the frequency spectrum and frequency filters are discussed. In addition to the longitudinal deflection amplitude, an oscillation in the transverse direction was observed. Finally, the transverse oscillation behavior is investigated in relation to half-wave synthesis.

BP 28.28 Thu 18:00 P2/EG

Cytoskeletal Networks in Cells Under Strain — •RUTH MEYER¹, ANNA V. SCHEPERS¹, PETER LULEY¹, JONATHAN BODENSCHATZ², AMAURY PEREZ TIRADO², ANDREAS JANSHOFF², and SARAH KÖSTER¹ — ¹Institute for X-Ray Physics, University of Göttingen — ²Institute for Physical Chemistry, University of Göttingen

The cytoskeleton of eukaryotes consists of three types of filaments: F-actin, microtubules and intermediate filaments (IFs). In contrast to microtubules and actin filaments, IFs are expressed in a cell-type specific manner, and keratins are found in epithelial cells. In certain cell types, the keratin filaments form a layer close to the membrane which may be referred to as an "IF-cortex". Furthermore, it is hypothesized that this IF-cortex arranges with radial spokes in a "rim-and-spokes" structure in epithelia. Based on this hypothesis, IFs and actin filaments might add complementary mechanical properties to the cortex. It was previously shown that single IFs remain undamaged even at high strains. We now ask the question of whether this unique force-extension behavior of single IFs is also relevant in the filament network within a cell. We designed an equibiaxial stretcher that can apply high strains to the cells. This setup is combined with fluorescence and atomic force microscopy enabling simultaneously imaging of the cells and measuring their stiffness during stretching. By quantitatively analyzing the force indentation curves and the microscopy images, we analyze the structure and the mechanical properties of actin and IF networks close to the cell membrane.

BP 28.29 Thu 18:00 P2/EG

Exploring cell-cell interactions inferred from trajectories in two-site arrays — •EMILY BRIEGER¹, TOM BRANDSTÄTTER², GEORG LADURNER¹, CHASE P. BROEDERSZ², and JOACHIM O. RÄDLER¹ — ¹LMU, Munich, Germany — ²VU Amsterdam, Amsterdam, Netherlands

Collective cell migration is a fundamental aspect to a variety of physiological processes. The migratory dynamics of these collective processes rely on cell-cell interactions that are depending on complex molecular mechanisms, such as cadherin dependent pathways. In previous work we studied the interaction behavior of two cells migrating on dumbbell-like micropattern. This geometry enforces repeated head-to-head collisions of cells and allows the distinction of interacting and noninteracting events. In this framework non-cancerous MCF10A cells and cancerous MDA-MB-231 cells clearly differ in their effective adhesion and friction terms derived from quantitative theoretical analysis. Here we use this data-driven approach to study how specific molecular alterations of surface proteins change cell-cell interactions in different cell lines. Blocking of E-cadherin and Ephrin A2 via antibodies yield distinct shifts in cell behavior space. Likewise knockouts that prevent cells from using their usual communication pathways alter the adhesive and frictional interactions. We show that the analysis yields insight into the role of E-Cadherin and Ephrin A2 in frictional and adhesive interactions as well as repulsive response known as contact inhibition of locomotion.

BP 28.30 Thu 18:00 P2/EG

A high-throughput pipeline for morphological and functional analysis of cardiomyocytes — DANIEL HÄRTTER^{1,2}, •LARA HAUKE¹, WOLFRAM-HUBERTUS ZIMMERMANN¹, and CHRISTOPH F. SCHMIDT² — ¹Institute of Pharmacology and Toxicology, University Medical Center Göttingen, Germany — ²Department of Physics, Duke University, Durham, NC, USA

Cardiomyopathies, diseases of the heart muscle, affect 1 in 500 adults in Western countries. Nevertheless, reliable knowledge about disease onset and pathogenesis is lacking. To develop effective treatment options for patients, a dynamic and quantitative understanding of cardiomyopathies is needed. We developed an assay in which individual stem-cell derived heart cells of a fluorescent sarcomere reporter cell line grow in a heart-like environment - while allowing for automated high-resolution and high-frame-rate imaging - using micropatterned polyacrylamide acid (PAA) gels. We analyze the time-course of cell morphology and function upon drug-induced or genetic interventions with our deep-learning-based SarcAsM (Sarcomere Analysis Multitool) software. The resulting multiparametric functional and structural trajectories of cardiac muscle cells can be used to gain novel dynamical perspectives on the time-course and interplay of structure and function in health and disease and might contribute to the discovery of novel treatments.

BP 28.31 Thu 18:00 P2/EG

A mechanical bottom-up approach of memory formation in *Physarum polycephalum* — •MATHIEU LE VERGE SERANDOUR and KAREN ALIM — School of Natural Sciences, Technical University of Munich, Germany

Understanding the emergence of memory in artificial or living complex systems is a considerable challenge: its origin, possibly an interplay of physics, genetics, or signaling, has not yet been elucidated. *Physarum polycephalum*, a unicellular organism organized as a two-dimensional tubular network, exhibits hallmarks of memory formation: its adaptive morphology encodes the location of past stimuli. We propose to investigate memory formation with a bottom-up approach focusing on the physical mechanisms of vascular morphology adaptation. First, we study the mechanical properties of *Physarum* by microrheology. We measure the viscoelasticity of the network's tubes and protrusions, and the change in stiffness or viscosity exposed to external stimuli, such as light or food. At the macroscopic scale, we study the dynamics of pruning of the network and its remodeling. We find an exponential decrease in the number of tubes reproduced by a toy model based on network hierarchy. These two complementary approaches will allow us to build a solid basis for establishing physical principles to characterize information encoding and memory emergence in *Physarum polycephalum*.

BP 28.32 Thu 18:00 P2/EG

Viscoelastic response of vimentin intermediate filament networks measured via optical tweezers-based active microrheology — •KAAN ÜRGÜP¹, ANNA V. SCHEPERS², and SARAH KÖSTER¹ — ¹Institute for X-Ray Physics, Universität Göttingen, Germany — ²Rosalind Franklin Institute and Kennedy Institute of Rheumatology, University of Oxford, UK

The microscale mechanics of the intermediate filament (IF) cytoskeleton are relevant for many cellular processes. The properties of the IF network have been shown to influence cell motility, migration and organelle transport. On the molecular level, an IF monomer is composed of amino acids that lead to α -helical domains in the center, flanked by non-helical domains. Multiple monomers assemble laterally to unit-length-filaments and longitudinally to mature filaments. Vimentin is the most abundant IF protein in humans. Single vimentin filaments show a loading-rate dependent behavior, which can be attributed to the unfolding of α -helical structures into disordered structures and β -sheets when high strains are applied. What is unclear, however, is whether this nonlinear behavior is relevant in cellular vimentin networks. In this work, we measure strain and relaxation dynamics of *in vitro* vimentin networks via optical tweezers in the nonlinear regime. We use an active-passive calibration method based on the Onsager theorem. We measure the nonlinear response to different oscillation amplitudes, which correspond to different strains applied to the network. Our setup allows us to investigate whether the nonlinear behavior of the single filaments is preserved on the network scale.

BP 28.33 Thu 18:00 P2/EG

Traction force microscopy quantifies the contractility of laminopathic cardiomyocytes — •VALENTINA KUHN^{1,2}, CHRISTINA GOSS^{1,3}, AISTE LIUTKUTE², ANNA ZELENA¹, ULRICH S. SCHWARZ³, NIELS VOIGT², and SARAH KÖSTER¹ — ¹Institute for X-Ray Physics, University of Göttingen, Germany — ²Institute of Pharmacology and Toxicology, University Medical Center Göttingen, Germany — ³Institute for Theoretical Physics, University of Heidelberg, Germany

Cardiomyocytes generate the contractile forces in the intact heart. In their nuclear lamina, cardiomyocytes express lamins A and C, a type of intermediate filament proteins that are encoded by the *LMNA* gene and are important for both genetic regulation and cytoskeletal organization. Patients with pathogenic *LMNA* mutations typically suffer from diseases characterized by altered cardiomyocyte contractile behavior, leading to high sudden cardiac death rates. So far, no detailed mechanistic explanation nor specific therapies are available. Cardiomy-

ocytes derived from induced pluripotent stem cells (iPSC-CMs) are powerful *in vitro* models to study the mechanisms underlying cardiomyopathies. We combine traction force microscopy with fluorescence imaging of the actin structures in a time-resolved manner on a single cell level. The experiment is conducted by seeding iPSC-CMs on elastic substrates featuring fibronectin micropatterns, which regularize their geometry for imaging while simulating physiological conditions. Thus, we can quantify the altered contractility of iPSC-CMs with the R331Q LMNA mutation in comparison with wild-type cells.

BP 28.34 Thu 18:00 P2/EG

Cell migration on micropatterns - how regular is the motion of different cell types? — •ANNIKA A. VOGLER, SEBASTIAN W. KRAUSS, RADHAKRISHNAN A. VEETIL, FLORIAN REHFELDT, and MATTHIAS WEISS — Experimental Physics I, University of Bayreuth, Germany

During processes like embryonic development, wound healing, or cancer metastasis, cells are often migrating in complex and obstacle-rich environments. Microstructured surfaces offer a versatile opportunity to model such environments and study cell migration under controlled conditions. Recent studies on cells that migrate in fairly simple two-state micropatterns have revealed, for example, a rich and nonlinear migration dynamics [1]. Following up on this study, we have explored the migration dynamics of non-cancerous MCF-12A cells on simple dumbbell patterns in comparison to malignant MDA-MB-231 cells. As a result, we observed that MCF-12A cells exhibit a strikingly more regular migration pattern while trajectories of cancerous cells appeared more stochastic. In particular, the path of non-tumorigenic cells was mainly focused on the edges of the pattern whereas malignant cells explored the whole available adhesion area. These results suggest differences in how the external environment is perceived by the internal biochemical state of cells.

[1] Brueckner, Fink, Schreiber et al., Nat. Phys. 15, 595 (2019)

BP 28.35 Thu 18:00 P2/EG

Cell Shape and Tension alter Focal Adhesion Structure — CAROLIN GRANDY¹, FABIAN PORT¹, •JONAS PFEIL¹, MARIANA AZEVEDO GONZALEZ OLIVA², MASSIMO VASSALLI², and KAY-EBERHARD GOTTSCHALK¹ — ¹Universität Ulm, Institut für experimentelle Physik, Ulm, Germany — ²University of Glasgow, James Watt School of Engineering, Glasgow, United Kingdom

Cells are anchored to the extracellular matrix via the focal adhesion complex. It also serves as a sensor for force transduction. We analyse the effect of tension on the location of key focal adhesion proteins vinculin, paxillin and actin. We use micropatterning on gold surfaces to manipulate the cell shape, to create focal adhesions at specific cell areas, and to perform metal-induced energy transfer (MIET) measurements on the patterned cells. We use drugs influencing the cellular motor protein myosin or mechanosensitive ion channels to get deeper insight into focal adhesions at different tension states. We show here that in particular actin is affected by the rationally tuned force balance. Blocking mechanosensitive ion channels has a particularly high influence on the actin and focal adhesion architecture, resulting in larger focal adhesions with elevated paxillin and vinculin and strongly lowered actin stress fibres. Our results can be explained by a balance of adhesion tension with cellular tension together with ion channel-controlled focal adhesion homeostasis, where high cellular tension leads to an elevation of vinculin and actin, while high adhesion tension lowers these proteins.

BP 28.36 Thu 18:00 P2/EG

Interactions of cytoskeletal elements during phagocytosis in macrophages. — •ERBARA GJANA¹ and FRANZISKA LAUTENSCHLÄGER^{1,2} — ¹Department of Physics, Saarland University, Saarbrücken, Germany — ²Center for Physics, Saarland University, Saarbrücken, Germany

The structure of cells is realized via their cytoskeleton - a polymer network inside cells. It is the main component of structural integrity and it shapes cells. The cytoskeleton is involved in many active cellular activities that includes cell division, migration, and phagocytosis. In macrophages, we know that actin - one protein of the cytoskeleton * plays an important role during phagocytosis. In my project, I work on understanding how actin is involved in sensing the object which needs to be phagocytosed.

Particularly, I study the effect of the physical properties such as form, size and stiffness of the objects. Therefore, I am varying the stiffness of objects, e.g. I use gelatine beads, latex beads and polystyrene beads and investigate how these are phagocytosed with the help of actin. Through different microscopy methods (epi-fluorescence, confocal) I will be able to image the process of phagocytosis. Till now, we have established phagocytosis protocols with macrophages derived from the cell line HL60. For a better biological fit I am now shifting to THP1 derived macrophages. This will help me to understand questions such as how macrophages distinguish between dead cells (ei. Dead RBCs), cell debris, and healthy cells. Also, we collaborate with theoreticians to build general mathematical model of phagocytosis.

BP 28.37 Thu 18:00 P2/EG

Micromechanics of spherical cellular aggregates — •ANTOINE GIROT^{1,2}, MARCIN MAKOWSKI², MARCO RIVETTI², CHRISTIAN KREIS², ALEXANDROS FRAGKOPOULOS^{1,2}, MATILDA BACKHOLM³, and OLIVER BÄUMCHEN^{1,2} — ¹University of Bayreuth, Experimental Physics V, 95447 Bayreuth, Germany — ²Max Planck Institute for Dynamics and Self-Organization (MPIDS), 37077 Göttingen, Germany — ³Aalto University School of Science, Department of Applied Physics, 02150 Espoo, Finland

Understanding the rich dynamics of biophysical processes, such as pathogenic tissue development and morphogenesis, requires a proper mechanical characterization of multicellular aggregates. Spherical aggregates often serve as model systems, yet, they cannot be readily characterized with conventional techniques that are optimized for single cells. In this presentation, we report on *Volvox globator*, a natural cellular aggregate that is composed of hundreds of bi-flagellated cells forming a spherical monolayer filled with mucilage. We employ *in vivo* micropipette force measurements combined with optical detection to simultaneously measure the force response and the deformation of this living aggregate. We show that the micromechanics of *Volvox* can be described by a model coupling elasticity and viscosity, which allows to extract the mechanical properties. We find that the viscous component exhibits a shear-thinning behavior, that can be properly described by implementing a power-law fluid model, while the elasticity of the aggregate depends on its size.

BP 28.38 Thu 18:00 P2/EG

The influence of calcium on the structure of the actin cortex in cell monolayers and single cells — •CHRISTOPH ANTON¹, LUCINA KAINKA¹, SANDRA IDEN², and FRANZISKA LAUTENSCHLÄGER^{1,3} — ¹Department of Physics, Saarland University, Saarbrücken, Germany — ²Center of Human and Molecular Biology (ZHMB), Saarland University, Homburg, Germany — ³Center for Biophysics, Saarland University, Saarbrücken, Germany

We recently showed that adhesion to a substrate, mediated via integrins, causes significant changes to the structure, mechanics and dynamics of the cellular actin cortex. In tissues, however, cells additionally form cell-cell junctions. Therefore, we investigate how the structure of the actin cortex of healthy and cancerous epithelial cell lines is affected by the transition from single cells to cell monolayers. One important step during this transition is the formation of cell-cell junctions, such as the cadherin-based adherens junctions. These junctions are dependent on the presence of calcium ions. In our work, we varied the extracellular calcium concentration to investigate the effect of cadherin-mediated adhesion and other calcium-based cellular processes on the actin cortex. We used scanning electron microscopy (SEM) to visualize the actin cortex. We applied our filament network tracing algorithm to the SEM images to quantify the structural properties of the actin cortex, such as the mesh hole area. By comparing the cortex parameters of cells within a monolayer with the cortex parameters of isolated cells we plan to characterize the structural changes that are induced by cell-cell contacts and extracellular calcium concentrations.

BP 28.39 Thu 18:00 P2/EG

Motility of adherent cells on structured surfaces at elevated viscosities — •RADHAKRISHNAN ADIYODI VEETIL, SEBASTIAN W. KRAUSS, ANNIKA A. VOGLER, FLORIAN REHFELDT, and MATTHIAS WEISS — Experimental Physics I, University of Bayreuth, Germany

Cell motility is sensitive to the viscosity of the surrounding medium, suggesting that such external cues can trigger cells to switch gears. Indeed, it has been recently reported that elevated viscosities can induce significant changes in cell area, cell migration speed and focal adhesion turn over [1]. Here, we have followed up on these experiments by monitoring the viscosity-dependent migration of different cell types on microstructured surfaces, e.g. cell hopping of cancerous and non-cancerous cells in dumbbell patterns. Our data suggest that altering viscosity can markedly alter the migration dynamics of cells on microstructured surfaces.

[1] Pittman, Iu, Li et al., Nat. Phys. 18, 1112 (2022)

BP 28.40 Thu 18:00 P2/EG

Coordination of information in *Physarum polycephalum* — •KASPAR WACHINGER¹, JOHNNY TONG¹, NICO SCHRAMMA², SIYU CHEN¹, and KAREN ALM¹ — ¹School of Natural Sciences, Technical University of Munich, Germany — ²Faculty of Science, University of Amsterdam, The Netherlands

Physarum polycephalum is a network-structured, single-cell organism with thousands of nuclei that can sense and adapt to its environment. To understand how *P. polycephalum* maintains efficient gene expression, it is necessary to understand the coordinated intracellular transport of nuclei within its structure. Microinjecting several fluorescent dsDNA markers into the tubes of *P. polycephalum* allows *in vivo* imaging of nuclei and their dynamics: Nuclei can either be trapped in the more solid wall cortex or follow the oscillatory cytoplasmic streaming. We investigate the flow-driven behaviours of nuclei in functionally different regions of *P. polycephalum*'s network and motivate a hypothesis of inter-nuclei communication far past the degradation distance of mRNA.

BP 28.41 Thu 18:00 P2/EG

FilamentSensor 2.0: An open-source modular toolbox for 2D/3D cytoskeletal filament tracking — LARA HAUKE¹, ANDREAS PRIMESSNIG¹, EMESE ZAVODSZKY¹, and FLORIAN REHFELDT² — ¹Institute of Pharmacology and Toxicology, University Medical Center Göttingen, Germany — ²Experimental Physics I, University of Bayreuth, Germany

Cytoskeletal pattern formation and structural dynamics are key to a variety of biological functions and a detailed and quantitative analysis yields insight into finely tuned and well-balanced homeostasis and potential pathological alterations. High content life cell imaging of fluorescently labeled cytoskeletal elements under physiological conditions is nowadays state-of-the-art and can record time lapse data for detailed experimental studies. However, systematic quantification of structures and in particular the dynamics (i.e. frame-to-frame tracking) are essential. Here, an unbiased, quantitative, and robust analysis workflow that can be highly automatized is needed. For this purpose we upgraded and expanded our fiber detection algorithm FilamentSensor [1] to the FilamentSensor 2.0 [2] toolbox, allowing for automatic detection and segmentation of fibrous structures and the extraction of relevant data (center of mass, length, width, orientation, curvature) in real-time as well as tracking of these objects over time and cell event monitoring. Furthermore, we offer the Focal Adhesion Filament Cross-correlation Kit (FAFCK) [3] for automated correlation with point-like structures. [1] B. Eltzner, et al., PLoS One, 2015 [2] L. Hauke, et al., PLoS One, under review [3] L. Hauke, et al., PLoS One, 2021

BP 28.42 Thu 18:00 P2/EG

Mechanically induced Bioluminescence - from single cells to glowing sea — NICO SCHRAMMA¹, HUGO FRANÇA^{1,2}, and MAZIYAR JALAAL¹ — ¹Van der Waals-Zeeman Institute, University of Amsterdam, Amsterdam, Netherlands — ²Instituto de Ciências Matemáticas e Computação, Universidade de São Paulo, São Carlos, Brazil

The ability of single-celled organisms to sense mechanical cues is of high importance for their migration, navigation and survival in their ever-changing environment. However, studying single-cell mechano-sensing under dynamic mechanical conditions is complicated. For this reason, the bioluminescent marine algae *Pyrocystis lunula* is a particularly interesting organism: mechanical stimuli trigger them to release a flash of blue light, which is mostly known from the bioluminescent tide, turning the sea into a mysterious pale blue shimmering. Combining mechanical tests on single cells with dynamics of millions of bioluminescent algae in a wave impact experiment and computational fluid mechanics we find and test general relations describing macroscopic (fluid)mechanical cues with bioluminescence. Our research paves the way towards a better understanding of mechanosensation of algae and plants, but may also lead to applications of bioluminescent organisms as “living force sensors”.

BP 28.43 Thu 18:00 P2/EG

Predicting optimal optogenetic control of cell migration with an active gel model — OLIVER M. DROZDOWSKI, FALKO ZIEBERT, and ULRICH S. SCHWARZ — Institute for Theoretical Physics and BioQuant, Heidelberg University, 69120 Heidelberg, Germany

Cell motility is one of the hallmarks of life and often results from flow in the actin cytoskeleton that is driven by actin polymerization at the front and myosin II motor contractility at the back. The standard model to describe such flows is active gel theory, in which myosin II contractility enters as active stress. Advancements in optogenetic tools have sparked interest in controlling these flows externally and consequently also motility.

Recently we have shown that bistability between motile and sessile states emerges in a one-dimensional active gel model if the myosin II motors are modeled as a supercritical van der Waals fluid [1]. We now incorporate optogenetic perturbations into this description and consider two experimentally accessible protocols for migration control - localized contractility perturbations and global upregulation of contraction. We find that the local protocol permits full external control. Global upregulation reliably leads to irreversible motility initiation, but does not allow for full control. Our results agree with recent experiments on cell migration in microchannels and reconcile experimental observations of local versus global regulatory mechanisms.

[1] O. M. Drozdowski, F. Ziebert, U. S. Schwarz, arXiv:2206.05915 (2022).

BP 28.44 Thu 18:00 P2/EG

Nuclei trafficking dynamics in Physarum polycephalum — JOHNNY TONG, KASPAR WACHINGER, NICO SCHRAMMA, and KAREN ALIM — School of Natural Sciences, Technical University of Munich, Germany

Synthetic organism and organs house up to thousands of nuclei within a single envelope, often shaped into a complex network architecture. How are nuclei able to efficiently exchange signals over long distances? To understand how synthetic coordinate gene expression, intracellular transport within these networks is key. *Physarum polycephalum* is an ideal syncytia model as its network-shaped body is a single multinucleated cell which can sense and adapt to its environment in a short time scale and a long length scale. Here, nuclei are trapped in the tube walls or advected by the oscillatory cytoplasmic streaming.

We investigate its flow-driven dynamics and mechanochemical behaviors using image-based methods, including particle tracking and velocimetry, to analyze the nuclei trafficking. We also utilize the thousands of nuclei to propose a new technique akin to traction force microscopy. By analyzing the fluctuations of nuclei trapped in the actomyosin cortex, we can probe the change of mechanical properties due to external stimuli, such as food, substrate stiffness, and light. Our techniques may be applied to other systems to unveil the mechanisms of long-range genetic communication within network-shaped organisms like fungi.

BP 28.45 Thu 18:00 P2/EG

Super-resolved Imaging of Cellular Traction Forces — ARMINA MORTAZAVI, JIANFEI JIAN, and BENEDIKT SABASS — Ludwig Maximilian University of Munich, Munich, Germany

Traction force microscopy (TFM) is a well-established method that enables the measurement of forces that are exerted by adherent cells to an underlying substrate. We aim to enhance the spatial resolution of TFM by using stochastic optical reconstruction microscopy in total internal reflection mode. To measure the substrate deformations below adherent cells, we employ DNA-based FluoroCubes that each carries multiple, spontaneously blinking, fluorescent dye molecules. Grafting of these new fluorescent probes to the top surface of Polydimethylsiloxane gels and using RGD peptides as the smallest ligands representative of extracellular matrix allows us to measure the forces generated by individual focal adhesion sites. The proposed method in principle allows one to extend traction force microscopy to lengthscales below 100 micrometers and can therefore help to unravel the mechanobiology of highly localized cell-physiological processes.

BP 28.46 Thu 18:00 P2/EG

Length distributions of microtubules with a multistep catastrophe mechanism — FELIX SCHWIETERT, LINA HEYDENREICH, and JAN KIERFELD — TU Dortmund University, 44227 Dortmund, Germany

Regarding the experimental observation that microtubule catastrophe can be described as a multistep process, we extend the Dogterom-Leibler model for dynamic instability in order to discuss the effect that such a multistep catastrophe mechanism has on the distribution of microtubule lengths in the two regimes of bounded and unbounded growth. We show that in the former case the steady state length distribution is non-exponential and has a lighter tail if multiple steps are required to undergo a catastrophe. If rescue events are possible, we detect a maximum in the distribution, i.e., the microtubule has a most probable length greater than zero. In the regime of unbounded growth, the length distribution converges to a Gaussian distribution whose variance decreases with the number of catastrophe steps. All results are verified by stochastic simulations.

BP 28.47 Thu 18:00 P2/EG

Bridging the gap between surface flows and motility patterns of malaria parasites — LEON LETTERMANN¹, MIRKO SINGER², FALKO ZIEBERT¹, FRIEDRICH FRISCHKNECHT², and ULRICH S. SCHWARZ¹ — ¹I TP & Bioquant, Heidelberg University — ²CIID, Heidelberg University

Malaria is one of the most devastating infectious diseases and transmitted from mosquitos to humans by so-called Plasmodium sporozoites, which move by gliding motility. Myosin motors move actin filaments below the plasma membrane, which leads to surface flows of adhesins that are anchored into the plasma membrane. How this surface flow is converted into the complicated motility patterns observed in experiments is not clear. Here we introduce a theoretical model that bridges this gap. The coupling between surface flow and substrate is modeled by a system of reversible adhesion bonds. We numerically solve the resulting system of ordinary differential equations and find a rich variety of motility patterns, including the circular and helical paths observed in experiments. This allows us to estimate likely patterns of surface flows, which are hard to measure experimentally.

BP 28.48 Thu 18:00 P2/EG

Stem Cell Dynamics in Tissues — JOHANNES C. KRÄMER, GERHARD GOMPPER, and JENS ELGETI — Theoretical Physics of Living Matter (IBI-5/IAS-2), Forschungszentrum Jülich, Jülich, Germany

The renewal of epidermal tissue relies on a few stem cells dividing asymmetrically, and a cascade of transient amplifying cells resulting in the necessary cell mass of terminally differentiated cells. We integrated this process in the two-particle growth model, and find that this simple process results in very interesting dynamic features: Stem cells repel each other in the tissue bulk and are thus found rather isolated in the tissue.

Simulating just two isolated stem cells, we construct the probability density function to find two stem cells in a given distance, and observe a reduced probability to find stem cells close to each other. To understand this repulsive mechanism better, we apply equilibrium methods to construct an effective interaction potential. Although a massive simplification it allows us describe the repulsive interaction in a simple fashion. Thermal colloid simulations, where particles interact via the effective interaction, are consistent with simulations of bulk tissues.

Our findings may contribute to better understand the cancer stem cell hypothesis. Here, cancerous growth is assumed to emerge from few stem cell like cancer cells, which might evade being targeted by therapy. However, the cancer stem cells are difficult to observe – maybe because they get separated by this mechanism.

BP 28.49 Thu 18:00 P2/EG

On multistability and constitutive relations of cell motion on Fibronectin lanes — •JOHANNES CLEMENS JULIUS HEYN¹, BEHNAM AMIRI², CHRISTOPH SCHREIBER¹, MARTIN FALCKE^{2,3}, and JOACHIM OSKAR RÄDLER¹ — ¹Ludwig-Maximilians-Universität München — ²Max Delbrück Center for Molecular Medicine in the Helmholtz Association — ³Humboldt Universität zu Berlin
Migration of eukaryotic cells is a fundamental process for embryonic development, wound healing, immune responses, and tumour metastasis. Experiments on 2d migration show a broad spectrum of morphodynamic features for many cell types. Cells exhibit distinct motile states: They are spread or moving and either steady or oscillatory and they display spontaneous transition between those states. Here, we present a study of the motion of MDA-MB-231 cells on 1d Fibronectin (FN) microlanes and group the migratory behaviour into four discrete states. A high-throughput setup allows to quantitatively analyse state transitions for a broad range of FN densities. We develop a biophysical model based on the force balance at the protrusion edge, the noisy clutch of retrograde flow and a response function to integrin signalling. The model reproduces cell states, characteristics of oscillations and state probabilities in very good agreement with our experimental data. The statistics of trajectories and theory suggests an adhesion related mechanism that not only explains multistability but also the well-known biphasic adhesion-velocity relation and the universal correlation between speed and persistence (UCSP).

BP 28.50 Thu 18:00 P2/EG

Single-molecule tracking in dense images — •JIANFEI JIANG^{1,2}, ARMINA MORTAZAVI^{1,2}, and BENEDIKT SABASS^{1,2} — ¹Institute for Infectious Diseases and Zoonoses, Department of Veterinary Sciences, LMU München — ²Department of Physics, LMU München

Traction force microscopy (TFM) quantifies cellular traction forces on a surface. The technique is based on measuring the deformations in the substrate. A standard implementation of TFM involves using first particle image velocimetry (PIV) to measure the two-dimensional deformations. Subsequently, a force reconstruction algorithm calculates the traction field based on PIV measurements. The spatial resolution of TFM can be improved by using smaller-sized fluorescent particles embedded in the substrate. To this end, we develop a new technique that combines TFM with Stochastic Optical Reconstruction Microscopy (STORM). Using STORM, we can record the positions of FluoroCubes (~ 6nm) that are densely distributed in the substrate. Here, we propose a new single-molecule tracking algorithm to acquire fine-grained displacement fields. We first use PIV with large-sized fluorescent beads (~ 40nm) to obtain coarse-grained displacement fields, which helps us to estimate the displacement of each FluoroCube. Then, the tracking process is formulated as a linear assignment problem, where we implement the Hungarian algorithm to minimize the overall deviation from PIV estimations. The particle tracking algorithm is parallelized by dividing the image into smaller subimages to reduce computation time. The tracking results enable us to build a high-resolution displacement field for force reconstruction.

BP 28.51 Thu 18:00 P2/EG

Reconstituting a polymer hydrogel that mimics intracellular viscoelastic properties — •DORIAN MARX, BART VOS, and TIMO BETZ — 3. Institute of Physics, Faculty of Physics, Georg-August-University Göttingen

Throughout the years numerous models were developed that describe the mechanical response of cells to deformations. However, all models, both classic and modern, are phenomenological, that is, they lack a connection of their parameters to the real physical system, making them hard to interpret. Furthermore, the strongest argument for a particular model so far is how accurately it matches to measurements. While this is fine on a phenomenological level, a deeper understanding, e. g. why it fits, is missing. This also holds for the fractional Kelvin-Voigt model (fKVM) that is composed of two complex power-laws and was shown to fit a range of different cells very well.

To connect the fit parameters of the fKVM to the physical system we opt for a bottom-up approach by using a passive viscoelastic polymer with constituents that have analogs in cells. After confirming that the fKVM accurately fits this system, we focus on finding "the most cell-like" parameter set. Varying the composition of the gel (e. g. via the cross-linker concentration) allows us to directly connect properties of the physical system to model parameters. With this, we are now able to formulate hypotheses that can be checked in live cells, giving a quantitative handle for connecting the real world biophysics to rheological models.

BP 28.52 Thu 18:00 P2/EG

Does Size Matter? Actin filament length in cell migration — •CARSTEN ALEXANDER BALTES¹, DIVYENDU GOUD THALLA¹, and FRANZISKA LAUTENSCHLÄGER^{1,2} — ¹Experimental Physics, Saarland University, Saarbrücken, Germany — ²Center for Biophysics, Saarbrücken, Germany

The ability to perform cellular locomotion is crucial for a large variety of tasks. This includes the search and chase of immunecells for pathogens as well as the search for food and the reorganisation of cells in tissue development. The cytoskeleton protein actin is particularly important for migration of eucaryotic cells. It is involved in the formation of filopodia and creates a retrograde flow from the leading edge towards the back of the cell, both of which allow them to move forward. Alteration of the actin network therefore might have an impact of the migratory behavior of cells. Here I am going to present the effects of elongated actin filaments on migrating RPE-1 cells. I will show that cells, migrating either on 1D fibronectin lines or on a fibronectin coated surface, displayed a reduction of migration speed, while keeping their persistence. They also occupy a larger area when allowed to spread freely and express a higher amount of focal adhesions. The change in migration speed vanishes when we put those cells under confinement in PDMS microchannels. Taking those facts together we propose that the length of actin filaments is important for cell migration. However further research is needed to fully understand the importance regarding the different migration modes cells can take depending on the surrounding environment.

BP 28.53 Thu 18:00 P2/EG

From Shape to Function of Sampling Resident Tissue Macrophages — •MIRIAM SCHNITZERLEIN¹, ANJA WEGNER², STEFAN UDERHARDT², and VASILY ZABURDAEV¹ — ¹Department of Biology, Friedrich-Alexander-Universität Erlangen-Nürnberg and Max-Planck-Zentrum für Physik und Medizin, Erlangen, Germany — ²Department of Internal Medicine 3 - Rheumatology and Immunology, Friedrich-Alexander-Universität Erlangen-Nürnberg and Universitätsklinikum Erlangen, Germany

Mammalian tissues are permanently subjected to various stresses - be it pathogens, dead cells and related waste products or injuries like micro-lesions - which have to be resolved properly to prevent inflammations and maintain tissue homeostasis. To detect such incidents, sessile resident-tissue macrophages (RTMs) persistently sample their surroundings by seemingly random extension and retraction of their protrusions. Quantifying these sampling dynamics over time and comparing RTM behaviour under different conditions can uncover certain patterns or strategies in RTM sampling, which will then help us to understand how RTMs ensure tissue homeostasis. In this project, we have employed a high-resolution intravital imaging protocol to generate movies of RTM sampling dynamics *in vivo*. Next we have built an image processing pipeline to assess cell dynamics via its shape, the curvature and displacement of the cell membrane as well as the movement of the cell protrusions over time. Such detailed measurements enable differentiating physiological states of RTMs, and will help to build a quantitative mathematical model for RTM protrusion dynamics.

BP 28.54 Thu 18:00 P2/EG

The energy cost of membrane-cortex deformation in phagocytosis of different sized pathogens — •MEHDI AIT YAHIA and RHODA JOY HAWKINS — University of Sheffield

During their lifetime macrophages (a type of white blood cell) defend against infection in biological organisms by moving and interacting with micrometer sized pathogens. Interactions include phagocytosis which is the engulfment of pathogens by the cell deforming around the target. We model the physical description of the deformation of the membrane and cortex composition based on the energy of bending and stretching. For the bending energy we use the Helfrich energy for an elastic membrane in terms of its elastic moduli and curvature. The stretching energy is a function of the moduli and the extra surface needed to engulf the target object. We consider different methods to obtain the elastic moduli including the possibility of exocytosis modifying the surface area. The bending energy is expected to be smaller for larger objects since the curvature is inversely proportional to the radius. On the contrary the stretching energy is expected to increase for a larger object. We minimize the sum of these two energies with respect to the radius to find an optimum size for phagocytosis. We compare our theoretical predictions with data from simulations and experiments on macrophages engulfing beads of different sizes and the fungal pathogen *Cryptococcus*.

BP 28.55 Thu 18:00 P2/EG

We can see you think: Towards label-free imaging of action potentials — •ANDRII TRELIN¹, HEIKO LEMCKE², SOPHIE KUSSAUER², CHRISTIAN RIMMBACH², ROBERT DAVID², and FRIEDEMANN REINHARD¹ — ¹Institute for Physics, University of Rostock — ²Department of Cardiac Surgery, Rostock University Medical Center

The ability to directly observe neuronal communication like propagation of action potentials (AP) is crucial for the understanding of biological neural networks such as the mammalian brain. Existing methods either cannot access cells

deep inside tissue (microelectrode arrays) or are not suitable for observing cells over long time periods (fluorescence). We are developing a novel method of AP imaging, based on the fact that the propagation of an AP through a neural network is accompanied by tiny movements due to various processes, including an increase of cell volume, a change of membrane tension, and others. Although movements happen on a nm scale, i.e. beyond the resolution of classical microscopy, theoretical estimates show that detection of these movements is possible by performing high-speed video recording of the cell and combining information from multiple pixels. The sensitivity can be amplified by employing a suitable optical setup, e.g. interferometric microscope. In this poster, we present the design of the experimental setup and share some of the results obtained in the project. Additionally, we will discuss the development of algorithms, capable of extracting cell movement information from high-speed videos. These include simple statistical analysis of videos, decomposition methods such as PCA, as well as machine learning approaches.

BP 28.56 Thu 18:00 P2/EG

Classifying single cells by their motion — •ANTON KLIMEK¹, DEBASMITA MONDAL², PRERNA SHARMA², and ROLAND NETZ¹ — ¹Freie Universität Berlin, Germany — ²Indian Institute of Science, Bangalore, India

We present a method to differentiate cells solely by their trajectories based on the generalized Langevin equation and apply it to distinguish two differently swimming types of strongly confined microalgae *Chlamydomonas reinhardtii* cells with an accuracy of 100%. The model we use is suggested by the data and succeeds to describe the motion on the single cell level. By a simple fit we can extract model parameters for individual cells and subsequently perform an unbiased cluster analysis to determine the number of different cell types in the population and obtain an assignment of every cell to one of the types. Additionally, the model suggested by the data includes information on the underlying processes leading to the observed patterns of motion, which in the case of our *Chlamydomonas reinhardtii* data could hint towards a harmonic coupling between the cell nucleus and the flagellar propulsion apparatus. As it still remains a challenge to classify cells on the single cell level, the presented method to distinguish cells with as little information as their trajectories might have important implications in biology and medicine.

BP 28.57 Thu 18:00 P2/EG

The role of vimentin in endothelial cells under flow — •JULIA KRAXNER^{1,2}, WOLFGANG GIESE^{1,2}, and HOLGER GERHARDT^{1,2} — ¹Integrative Vascular Biology, Max Delbrück Center for Molecular Medicine in the Helmholtz Association (MDC) — ²German Center for Cardiovascular Research (DZHK), partnersite Berlin

Vascular endothelial cells (VECs) compose the inner layer of blood vessels where they need to be able to constantly sense, withstand and adapt to varying mechanical stresses. For the sensing and adaptation to mechanical stress cytoskeletal proteins, i.e. actin, microtubules and intermediate filaments, play an important role. Here, we focus on vimentin which is the most abundant intermediate filament in VECs. These cells are constantly exposed to shear stress and they respond to the flow by polarizing and aligning in direction of flow. We investigate the role of vimentin in this flow response by exposing VECs to shear stress in vitro. Furthermore, experiments under flow reveal an increase of specific phosphorylation sites in vimentin. We study the role of these specific phosphorylation sites on the mechanotransduction. Therefore, we want to combine traction force microscopy under flow with mutations in vimentin which inhibit phosphorylation of specific sites. Additionally, we plan on tuning the substrate stiffness to study the effect of tissue mechanics observed in aging of the vascular system and possible effects on mechanotransduction. These insights have the potential to improve our understanding of the complex mechanism of mechanotransduction in VECs.

BP 28.58 Thu 18:00 P2/EG

Optical Stretcher for Adherent Cells — •ALEXANDER JANIK, TOBIAS NECKER-NUSS, and OTHMAR MARTI — Institute of Experimental Physics, Ulm University
The characterization of cellular viscoelastic properties by utilizing the interface force arising from a laser beam shining through the cell has proven to be a valuable method for suspended cells, e.g. red blood cells.

The work presented here is based on the same phenomenon. A laser locally pulls the membrane of an adherent cell upwards, while the displacement is detected by off-axis interferometry. In proof-of-concept measurements, it is shown, that this contact-free method is sensitive enough to determine the complex shear modulus of stiff adherent NIH-3T3 cells. Laser power and wavelength are chosen to minimize heating induced softening.

BP 29: Statistical Physics of Biological Systems II (joint session BP/DY)

Time: Friday 9:30–12:00

Location: BAR Schö

BP 29.1 Fri 9:30 BAR Schö

Evolutionary optimization of multicomponent phase separation — •DAVID ZWICKER¹ and LIEDEWIJ LAAN² — ¹MPI-DS, Göttingen, Germany — ²TU Delft, The Netherlands

Biological cells use passive phase separation to segregate different biomolecules into various condensates. Since the molecular interactions determine the number of distinct condensates and their composition, they have likely been optimized evolutionarily for robust segregation. To study this, I will present a numerical method that efficiently determines coexisting phases in multicomponent liquids and use it in evolutionary optimization experiments. I will demonstrate that the optimized interactions lead to a precise number of different condensates, even if the overall composition varies. Consequently, adjusting microscopic interactions leads to stable emergent behaviors in these complex systems.

BP 29.2 Fri 9:45 BAR Schö

Kinetics of droplet sizes in non-conserved emulsions — •JACQUELINE JANSSEN¹, FRANK JÜLICHER¹, and CHRISTOPH A. WEBER² — ¹Max Planck Institute for the Physics of Complex Systems — ²University of Augsburg

Droplets form via phase separation and coexist with a dilute phase that is composed of droplet material of lower concentration. Many droplets in an emulsion undergo coarsening to the thermal equilibrium state that corresponds to a single droplet in a finite system. In passive emulsions, where the total amount of droplet material is conserved, the average radius grows as a function $t^{1/3}$ in time, and the droplet size distribution function broadens. Here we consider emulsions for which the total droplet material is not conserved, e.g. material is supplied by a chemical reaction or external reservoirs. We calculate the kinetics of droplet sizes and show that there is a switch from coarsening to narrowing of the size distribution upon material supply. Regulation of droplet sizes by material supply could be relevant for biomolecular condensates in living cells.

BP 29.3 Fri 10:00 BAR Schö

Dynamics of vesicle clusters studied by passive x-ray microrheology — •TITUS CZAJKA¹, CHARLOTTE NEUHAUS¹, JETTE ALFKEN¹, MORITZ STAMMER¹, YURIY CHUSHKIN², DIEGO PONTONI², CHRISTIAN HOFFMANN³, DRAGOMIR MILOVANOVIC³, and TIM SALDITT¹ — ¹Institut für X-ray Physics, Georg-August-Universität Göttingen, Germany — ²ESRF, Grenoble, France — ³Laboratory of Molecular Neuroscience, DZNE, Berlin, Germany

Inferring the viscoelastic properties of a complex fluid from the dynamics of suspended tracer particles is a common method to perform rheological measurements where a direct measurement of the constituents of the system is not possible or impractical. The previously observed pool formation of vesicles induced by divalent salts or the protein synapsin I is a case in point. One would like to know how the mobility of a single (tracer) particle changes in a dense pool as compared to a homogeneous vesicle suspension. Here we used x-ray correlation spectroscopy (XPCS) to measure silica nanoparticles immersed in a complex biomolecular fluid composed of small unilamellar vesicles and CaCl_2 , or SUVs and Synapsin-Ia protein, both in buffer solution. While the former system leads to irregular clusters, the latter has been observed to form protein induced vesicle pools, suggesting a liquid-liquid phase separation. Analysis of the photon correlation functions reveals the presence of different timescales, which we attribute to the free diffusive motion of the tracer particles and the motion of the tracer particles that interact with the cluster.

BP 29.4 Fri 10:15 BAR Schö

A stereotypical sequence of condensation and dispersal of RNA polymerase II clusters during stem cell differentiation — •TIM KLINGBERG¹, IRINA WACHTER², AGNIESZKA PANCHOLI², ROSHAN PRIZAK², PRIYA KUMAR³, YOMNA GOHAR³, MARCEL SOBUCKI², ELISA KÄMMER², SÜHEYLA EROĞLU-KAYIKÇI², SYLVIA ERHARDT², CARMELO FERRAI³, VASILY ZABURDAEV¹, and LENNART HILBERT² — ¹Friedrich-Alexander-Universität Erlangen-Nürnberg — ²Karlsruher Institut für Technologie — ³Universitätsmedizin Göttingen

Most eukaryotic genes are transcribed by RNA polymerase II (Pol II). In stem cells, recruited Pol II forms prominent, long-lived clusters, which gradually disappear during differentiation, so that only smaller clusters remain. Here, we ask whether the loss of large Pol II clusters is a stereotypical transition that can be explained by changes in the Pol II transcriptional state during differentiation. We assess clusters by super-resolution microscopy in three different experimental models of differentiation. In all cases, Pol II clusters first become larger and rounder, then unfold, and finally split into small clusters. These shape changes are accompanied by changes of transcriptional activity of Pol II. Previous work suggests a surface-condensate model, where enhancer regions support Pol II cluster formation, and transcriptional activity disperses clusters. Using this theoretical model, we propose that the developmental changes in enhancer marks and transcriptional activity during differentiation are sufficient to define a stereotyped trajectory through a cluster shape space.

BP 29.5 Fri 10:30 BAR Schö

Anomalous dynamics of differentiated droplets — •XI CHEN¹, FRANK JÜLICHER², JENS-UWE SOMMER¹, and TYLER HARMON¹ — ¹Leibniz-Institut für Polymerforschung Dresden, Institut Theory der Polymere 01069 Dsdn — ²Max-Planck-Institut für Physik komplexer Systeme, 01187 Dresden

Membraneless compartments formed by liquid-liquid phase separation in cells behave like droplets and take part in various biological processes. The function of these droplets are largely dependent on their components. We previously showed with a theoretical model that droplets can undergo a differentiation process where a homogeneous population of droplets converts into two coexisting types of droplets. We proposed this allows droplet specialization similar to cell differentiation.

These differentiated droplets exhibit new features and anomalous dynamics. Like a normal droplet system where droplets ripen and merge into one big droplet, this differentiation can significantly accelerate this Ostwald ripening. This happens with the caveat that instead of ripening into one droplet, it ripens into two droplets of different types with a competing reverse Ostwald ripening process. Unexpectedly, these differentiated droplets divide and repel each other over long distances.

15 min. break

BP 29.6 Fri 11:00 BAR Schö

Microrheology of red blood cell cytosol — •THOMAS JOHN and CHRISTIAN WAGNER — Universität des Saarlandes, Saarbrücken

Tracking of small particles undergoing a Brownian motion is a widespread method in passive microrheology. Washed human red blood cells (RBC) are destroyed by ultrasound treatment to extract the cytosol, the hemoglobin and protein solution inside the cells. We use microrheology with sub-micrometer-sized particles to determine the viscosity of the cytosol. Since the cytosol is always diluted with an unknown amount of water due to the treatment, this small dilution has a huge impact on the viscosity. To circumvent this problem, we measured very accurately the mass density of every sample. However, the resulting density-viscosity relation is a strong monotonic increasing relation. In a separate experiment we determined the mass density distribution of individual intact RBCs in a continuous density gradient by centrifugation. Finally, we can present the probability density distribution of the viscosity in naturally distributed human RBCs.

BP 29.7 Fri 11:15 BAR Schö

Clonal dynamics at tissue interfaces — •RUSLAN MUKHAMADIAROV^{1,2}, MATTEO CIARCHI^{1,2}, FABRIZIO OLMEDA^{1,2}, and STEFFEN RULANDS^{1,2} — ¹Ludwig Maximilian University of Munich, München, Germany — ²Max Planck Institute for the Physics of Complex Systems, Dresden, Germany

Tissue morphogenesis relies on the spatial separation of different cell types. Understanding how cells regulate the positions of such interfaces is key to under-

standing the processes that occur during dysregulation, such as in cancer. Genetic tracing has become an important experimental tool in studying the regulation of cell behaviour. However, its use in both homeostatic and growing tissues is limited by the emergence of universal size distributions. Here, we show that the mechanisms of tissues interface regulation is reflected in cell-fate specific size distributions of genetically labelled cells, termed clones. Specifically, we show how interface fluctuations affect the size distributions of labelled clones and derive theoretical predictions for a range of biologically relevant scenarios that can be tested experimentally. We test our theoretical framework by stochastic simulations and analysis of live imaging experiments. By relating interface fluctuations to clone size distributions our work paves the way for using genetic tracing experiments to understand the mechanisms underlying tissue compartmentalization.

BP 29.8 Fri 11:30 BAR Schö

Multivalent binding proteins can drive collapse and reswelling of chromatin in confinement — •SOUGATA GUHA and MITHUN K. MITRA — Department of Physics, IIT Bombay, India

Collapsed conformations of chromatin have been long suspected of being mediated by interactions with multivalent binding proteins, which can bring together distant sections of the chromatin fiber. In this study, we use Langevin dynamics simulation of a coarse grained chromatin polymer to show that the role of binding proteins can be more nuanced than previously suspected. In particular, for chromatin polymer in confinement, entropic forces can drive reswelling of collapsed chromatin with increasing binder concentrations, and this reswelling transition happens at physiologically relevant binder concentrations. Both the extent of collapse, and also of reswelling depends on the strength of confinement. We also study the kinetics of collapse and reswelling and show that both processes occur in similar timescales. We characterise this reswelling of chromatin in biologically relevant regimes and discuss the non-trivial role of multivalent binding proteins in mediating the spatial organisation of the genome.

BP 29.9 Fri 11:45 BAR Schö

A possible application of the Physics of topological defects to oncology — •ANDY MANAPANY, LEILA MOUEDDENNE, SÉBASTIEN FUMERON, BERTRAND BERCHE, and LORIANE DIDIER — Université de Lorraine

We propose a numerical study of the thermal diffusion process in non-Euclidian geometry applied to biological active matter. Thanks to the similarities displayed by both nematic and cells in biological tissue, we aim to apply results derived from the study of diffusion processes around topological defects found in liquid crystals, in order to highlight the thermal response in the vicinity of certain disclination defects found in epithelial tissues. This work is motivated by the fact that these types of disclination defects, mainly "comet" and "trefoil" systematically appear during metastatic phases in some forms of aggressive cancers. Thus, a study of the thermal footprint in such mediums may give us information on the most efficient ways to perform thermal ablation targeted towards aforementioned cells while preserving healthy surrounding tissue.

BP 30: Active Matter V (joint session BP/PPP/DY)

Time: Friday 9:30–12:00

Location: TOE 317

Invited Talk

BP 30.1 Fri 9:30 TOE 317

Experiments on Active Polymer-Like Worms — •ANTOINE DEBLAIS¹, DANIEL BONN¹, and SANDER WOUTERSEN² — ¹Van der Waals-Zeeman Institute, Institute of Physics, University of Amsterdam, 1098XH Amsterdam, The Netherlands — ²Van't Hoff Institute for Molecular Sciences, University of Amsterdam, Science Park 904, 1098XH Amsterdam, The Netherlands

We propose a new 'active particle' system in which the particles are in fact polymer-like: the Tubifex tubifex or 'sludge' worm. I will discuss three recent experiments that highlight the richness of this active system. In the first experiment, we perform classical rheology experiments on this entangled polymer-like system. We find that the rheology is qualitatively similar to that of usual polymers, but, quantitatively, the (tunable) activity of the particle changes the flow properties. In a second experiment, we disperse the worm in a quasi-2D aquarium and observe their spontaneous aggregation to compact, highly entangled blobs; a process similar to polymer phase separation, and for which we observe power-law growth kinetics. We find that the phase separation of active polymer-like worms occurs through active motion and coalescence of the phase domains. This leads to a fundamentally different phase-separation mechanism, that may be unique to active polymers. Finally, in the remaining time, I will briefly show that we can efficiently separate by size and activity these living polymers using hydrodynamic chromatography techniques.

BP 30.2 Fri 10:00 TOE 317

Filamentous Cyanobacteria Aggregate at Light Boundaries — •MAXIMILIAN KURJAHN¹, LEILA ABBASPOUR¹, PHILIP BITTICH¹, RAMIN GOLESTANIAN^{1,2}, BENOÎT MAHAULT¹, and STEFAN KARPITSCHKA¹ — ¹Max Planck Institute for Dynamics and Self-Organization, Göttingen, Germany — ²Rudolf Peierls Centre for Theoretical Physics, University of Oxford, OX1 3PU, Oxford, UK

Filamentous cyanobacteria are among the oldest, yet still most abundant phototrophic prokaryotes on Earth, fixing vast amounts of atmospheric carbon by photosynthesis. Gliding motility, coupled to photophobic responses (direction reversals in response to light intensity gradients), are believed to drive accumulation in suitable light conditions. Here, we demonstrate that photosensitivity goes beyond simple accumulation: Super-filamentous aggregates, capable of collective mechanical action, form at the boundaries of illuminated regions and may, for instance, contract and detach from the substrate, once grown to a critical mass. We explore how the light pattern, in particular its boundary curvature, impacts aggregation. A minimal model of active rods captures the behavior qualitatively. The ecological impact of such behavior is still unclear, but may enable colonies to escape from saturated habitats by switching to a planktonic state.

BP 30.3 Fri 10:15 TOE 317

Odd dynamics of living chiral crystals — •TZER HAN TAN^{1,2,3,4}, ALEXANDER MIETKE^{4,5}, JUNANG LI⁴, YUCHAO CHEN⁴, HUGH HIGINBOTHAM⁴, PETER FOSTER⁴, SHREYAS GOKHALE⁴, JORN DUNKEL⁴, and NIKTA FAKHRI⁴ — ¹MPI-PKS, Dresden, Germany — ²MPI-CBG, Dresden, Germany — ³CSBD, Dresden, Germany — ⁴MIT, Cambridge, USA — ⁵University of Bristol, Bristol, UK

Active crystals are highly ordered structures that emerge from the self-organization of motile objects, and have been widely studied in synthetic and bacterial active matter. Whether persistent crystalline order can emerge in groups of autonomously developing multicellular organisms is currently unknown. Here we show that swimming starfish embryos spontaneously assemble into chiral crystals that span thousands of spinning organisms and persist for tens of hours. Combining experiments, theory and simulations, we demonstrate that the formation, dynamics and dissolution of these living crystals are controlled by the hydrodynamic properties and the natural development of embryos. Remarkably, living chiral crystals exhibit self-sustained chiral oscillations as well as various unconventional deformation response behaviours recently predicted for odd elastic materials. Our results provide direct experimental evidence for how non-reciprocal interactions between autonomous multicellular components may facilitate non-equilibrium phases of chiral active matter.

BP 30.4 Fri 10:30 TOE 317

Optimal collective durotaxis through active wetting — MACIÀ-ESTEVE PALLARÈS¹, IRINA PI-JAUMÀ², ISABELA CORINA FORTUNATO¹, VALERIA GRAZU³, MANUEL GÓMEZ-GONZÁLEZ¹, PERE ROCA-CUSACHS¹, JESUS DE LA FUENTE³, RICARD ALERT⁴, RAIMON SUNYER¹, JAUME CASADEMUNT², and XAVIER TREPAT¹ — ¹Institute for Bioengineering of Catalonia — ²University of Barcelona — ³Instituto de Nanociencia y Materiales de Argón — ⁴Max Planck Institute for the Physics of Complex Systems

The directed migration of cell clusters enables morphogenesis, wound healing and collective cancer invasion. Gradients of substrate stiffness are known to direct migration of cell clusters in a process called collective durotaxis, but underlying mechanisms remain unclear. Combining theory and experiments, we reveal a connection between collective durotaxis and the wetting properties of cell clusters. Our experiments show that durotaxis is non-monotonic with substrate stiffness, being optimal at intermediate stiffness. Modeling the cell clusters as active droplets, we explain this non-monotonic durotaxis in terms of a balance between active traction, tissue contractility, and surface tension. Finally, we show that the distribution of cluster displacements has a heavy tail, with infrequent but large cellular hops that contribute to durotactic migration. Our study demonstrates a physical mechanism of collective durotaxis based on the wetting properties of active droplets.

15 min. break

BP 30.5 Fri 11:00 TOE 317

Chlamydomonas axonemes twist during the beat — MARTIN STRIEGLER^{1,2}, BENJAMIN M. FRIEDRICH³, STEFAN DIEZ^{1,2,3}, and VEIKKO F. GEYER¹ — ¹B CUBE - Center for Molecular Bioengineering, TU Dresden, Dresden, Germany — ²Max Planck Institute of Molecular Cell Biology and Genetics, Dresden, Germany — ³Cluster of Excellence Physics of Life, TU Dresden, Dresden, Germany

Motile cilia are slender cell appendages that drive single cell locomotion and fluid transport across surfaces. The motility of cilia is generated by its inner core, the axoneme, which bends by the activity of dynein motor proteins. Generation of bending requires antagonistic dynein activity on opposing sides of the axoneme. How dyneins are activated antagonistically is unknown. Theoretical models propose dynein regulation by mechanical feedback, which entails structural deformations of the axoneme, but direct experimental evidence is missing. To study axonemal deformations during the beat, we purify and reactivate *Chlamydomonas reinhardtii* axonemes. Using defocused-high-speed-darkfield microscopy, we resolve the 3D waveforms with nanometer resolution on mil-

lisecond timescales. We find that asymmetric waveforms have a non-planar component, which is most pronounced during the recovery stroke. To generate non-planarity within the geometric constraints of the axoneme, twist is thought to be required. Using gold-nano-particles as probes attached to the outside of reactivated axonemes, we, for the first time, measure dynamic twisting deformations in reactivated axonemes. We hypothesize that these deformations are involved in controlling dynein motors generating the axonemal beat.

BP 30.6 Fri 11:15 TOE 317

Curvotaxis - the effect of curvature on cells and tissue — LEA HPPEL, JAN SICHKA, and AXEL VOIGT — Institute of Scientific Computing, Technische Universität Dresden, Germany

How do cells respond to curvature? Does curvature have an influence on cell shape and movement? What are the consequences for collective behaviour of interacting cells in tissue? We address these questions using a multiphase field model on different curved surfaces and compare the results with experimental data on pillars, in tubes and other surfaces. The results show a significant influence of curvature and the possibility to effectively model the observed phenomena with classical models and additional curvature terms.

BP 30.7 Fri 11:30 TOE 317

Onset of Homochirality in Cell Monolayers — LUDWIG A. HOFFMANN and LUCA GIOMI — Universiteit Leiden, Leiden, Netherlands

Chirality is a feature of many biological systems and much research has been focused on understanding the origin and implications of this property. Most famously, sugars and amino acids that are found in nature are homochiral, meaning that chiral symmetry is broken and only one of the two possible chiral states is ever observed. Perhaps less well-known, something similar is the case for certain types of cells too. They show chiral behavior and only one of the two possible chiral states is observed in nature. Understanding the origin of cellular chirality and what, if any, use or function it has in tissues and cellular dynamics is still an open problem and subject to much (recent) research. For example, cell chirality has already been shown to play an important role in drosophila morphogenesis.

BP 30.8 Fri 11:45 TOE 317

Dynamic instability of cytoplasmic compartments — MELISSA RINALDIN^{1,2} and JAN BRUGUÉS^{1,2} — ¹Max Planck Institute of Molecular Cell Biology and Genetics, Dresden, Germany — ²Cluster of Excellence Physics of Life, TU Dresden, Dresden, Germany

Early embryos are the epitome of self-organization. Following the cell cycle oscillator, their internal structure is continuously reorganized into precise patterns at remarkable speeds. For example, the mm-sized egg of the frog *Xenopus laevis* divides every 30 minutes into equally-sized cells. Physical processes such as autocatalytic growth, active transport, and reaction-diffusion can allow these embryos to keep up with fast cell cycle times, however, their understanding in early development remains largely elusive. Here, we present recent data from experiments of in vitro cytoplasmic extract obtained from frog eggs and exhibiting cell-free division. We show that the properties of the cell cycle oscillator regulate the pattern of cytoplasmic compartments. Specifically, by perturbing the oscillator, we establish that the interface of cytoplasmic compartments is unstable. We demonstrate that such instability arises from competing waves of autocatalytic microtubule growth, and can generate compartment fusion, strongly affecting the early embryonic pattern formation. Altogether, our results propose that the cell cycle oscillator plays a critical role in partitioning the cytoplasm of early embryos, keeping the dynamic instability of cytoplasmic compartments at bay.

BP 31: Cell Mechanics III

Time: Friday 10:00–12:00

Location: BAR 0106

BP 31.1 Fri 10:00 BAR 0106

Viscoelastic properties of cells under influence of drugs — HENRIK SIBONI^{1,2}, IVANA RUSESKA¹, LEONHARD GRILL², and ANDREAS ZIMMER¹ — ¹Pharmaceutical Technology & Biopharmacy, University of Graz, Austria — ²Single Molecule Chemistry, University of Graz, Austria

Nanoscale Drug Delivery Systems are an increasingly popular type of pharmaceutical treatment with the recent vaccines against COVID-19 being prime example. Here, we present our latest results in characterising preadipocyte cells when treated with protamine-miRNA nanoparticles. We employ Atomic Force Microscopy to perform force-indentation experiments in order to spatially resolve the elastic properties before and after drug treatment. Going further, we use force clamping and creep-relaxation in order to map the viscous properties as well. We then discuss the potential conclusions that can be drawn from this study and the pharmaceutical implications.

BP 31.2 Fri 10:15 BAR 0106

A mechano-osmotic feedback couples cell volume to the rate of cell deformation — LARISA VENKOVA^{1,2}, AMIT SINGH VISHEN³, SERGIO LEMBO⁴, NISHIT SRIVASTAVA^{1,2}, BAPTISTE DUCHAMP^{1,2}, ARTUR RUPPEL⁵, ALICE WILLIART^{1,2}, STÉPHANE VASSILOPOULOS⁶, ALEXANDRE DESLYS^{1,2}, J. M. GARCIA ARCOS^{1,2}, ALBA DIZ-MUÑOZ⁴, MARTIAL BALLAND⁵, J.-F. JOANNY³, DAMIEN CUVÉLIER^{1,2,6}, PIERRE SENS³, and MATTHIEU PIEL^{1,2} — ¹Institut Curie, PSL, CNRS, UMR 144, Paris, France — ²IPGG, PSL Research University, Paris, France — ³Institut Curie, PSL, CNRS, UMR 168, Paris, France — ⁴Cell Biology and Biophysics Unit, EMBL, Heidelberg, Germany — ⁵Laboratoire Interdisciplinaire de Physique, Grenoble, France — ⁶Sorbonne Université, Paris, France

Mechanics has been a central focus of physical biology in the past decade. In comparison, how cells manage their size is less understood. Here, we show that a parameter central to both the physics and the physiology of the cell, its volume, depends on a mechano-osmotic coupling. We found that cells change their volume depending on the rate at which they change shape, when they sponta-

neously spread or when they are externally deformed. Cells undergo slow deformation at constant volume, while fast deformation leads to volume loss. We propose a mechanosensitive pump and leak model to explain this phenomenon. This mechano-osmotic coupling defines a membrane tension homeostasis module constantly at work in cells, causing volume fluctuations associated with fast cell shape changes, with potential consequences on cellular physiology.

BP 31.3 Fri 10:30 BAR 0106

Viscoelastic characterization of biological cells in hyperbolic microfluidic channels — •FELIX REICHEL^{1,2} and JOCHEN GUCK^{1,2} — ¹Max Planck Institute for the Science of Light, Erlangen, Germany — ²Max-Planck-Zentrum für Physik und Medizin, Erlangen, Germany

Research over the last decades revealed that single-cell mechanical properties can serve as label-free markers of cell state and function and that mechanical changes are a sign of alterations in the cell's molecular composition. This led to the development of a number of microfluidics tools to rapidly measure the deformability and also the viscoelastic properties of cells. The quantification of the stresses, that cause the deformation of the cells in these channels, is often challenging and with that the derivation of a stress-strain relation for such a system becomes complex. Here, we used hyperbolic channels to create an extensional flow field where the acting stresses can be measured using calibration particles and yield a simple relationship between acting stress and resulting cell strain. We then used the setup to measure the Young's modulus and bulk viscosity of HL60 cells and blood cells over a wide range of time scales. Drug induced changes to the cell state could be measured by a change in cell mechanical properties. Our simple setup offers a straightforward measurement of the viscoelastic properties of cells and microscale soft particles.

BP 31.4 Fri 10:45 BAR 0106

Pancreatic cancer metastasis: mechanics and adhesion — •SHRUTI G. KULKARNI¹, MALGORZATA LEKKA², and MANFRED RADMACHER¹ — ¹Institute of Biophysics, University of Bremen, Otto-Hahn Allee 1, 28359 Bremen, Germany — ²Institute of Nuclear Physics PAN, Radzikowskiego 152, 31-342 Krakow, Poland

We use Atomic Force Microscopy (AFM) to characterise the mechanical properties of Pancreatic ductal adenocarcinoma (PDAC) cell lines from the primary tumour site (PANC1), and from liver (CFPAC1) and lymph node (Hs766T) metastases. AFM measures forces using the optical lever system. To measure their stiffness, cells were probed using a rectangular cantilever with a three-sided pyramidal tip. Apparent Young's modulus (E) and power-law exponent (α) can be calculated from the force curves. To probe the adhesive properties of the cells, a single cell was attached to functionalised triangular tipless cantilevers, and then pressed against a confluent layer of cells. When the cell-cantilever is retracted, the contact of the attached cell with the cell layer is broken. The detachment exerts force on the cantilever, and this signal is also recorded by and characterised from the retract curve. The adhesion of cancer cells was measured with self-cells (the same cell line) as well as with endothelial cells (EA.hy926). CFPAC1 cells soften in confluent layers, and have increased cell-cell interaction with endothelial cells as compared to self-cells. Hs766t have similar stiffness as both single cells and as a confluent layer, and have higher cell-cell interaction with self-cells than with endothelial cells.

15 min. break

BP 31.5 Fri 11:15 BAR 0106

Dynamics of confined cell migration in 3D micro-dumbbells — •STEFAN STÖBERL¹, JOHANNES FLOMMERSFELD², MAXIMILIAN M. KREFT¹, CHASE P. BROEDERSZ², and JOACHIM O. RÄDLER¹ — ¹Faculty of Physics and Center for NanoScience, Ludwig-Maximilians-University, Munich, Germany — ²Department of Physics and Astronomy, Vrije Universiteit Amsterdam, 1081 HV Amsterdam, The Netherlands

Cell migration plays a key role in physiological processes such as wound healing, cancer metastasis and immune response. In previous work we have studied the non-linear dynamics of single cells migrating between two surface-patterned adhesion sites guided by a bridging line. Here, we study the dynamics of MDA-MB-231 cells captured in three dimensional (3D) dumbbell-like micro cavities. The structures formed by photolithography of PEG-Norbornene hydrogels provide a soft and hence deformable frame, while cells attach and migrate on a fibronectin-coated bottom. We find that the dwell time of cells before transitioning is retarded when the width of the dumbbell constriction is narrowed below 10 μm . In this limit, deformation of the nucleus determines the time course of the repeated stochastic transitions. We measure the forces exerted by the nucleus parallel and perpendicular to the dumbbell channel walls using the displacement field of beads embedded near the 3D constriction. At the same time, the nuclear deformation is followed by confocal 4D imaging revealing an elongation and temporary decrease in nuclear volume during migration through confinement.

BP 31.6 Fri 11:30 BAR 0106

Geometry sensing by active flows: how the cell cortex can feel its shape — •JONAS NEIPEL and FRANK JÜLICHER — Max Planck Institute for the Physics of Complex Systems, Dresden, Germany

Morphogenesis often involves chemical patterns, e.g. defined by the concentration of signalling molecules, that specify the shape of a cell or tissue. The robustness of such processes with respect to perturbations can be enhanced by feedbacks where the generated shape impacts back on the formation of the chemical pattern. Here, we show that such shape sensing can result from the same forces that drive shape changes. We consider sheets of active matter, such as the cell cortex or a developing tissue layer, that behave as active fluid surfaces on long time scales. In these systems, forces drive flows within the surface that inevitably depend on the surface geometry of the surface. When molecules are advected by this flow, a pattern arises, reflecting the symmetries of the geometry. In particular, we show that viscous shear forces result in an effective friction force being proportional to the Gaussian curvature, such that patches of contractile stresses are advected towards regions of minimal Gaussian curvature. On a surface with spherical topology but elongated shape, this implies that a contractile ring such as the cytokinetic ring aligns perpendicularly to the long axis of the surface. Hence, the actomyosin cortex can drive alignment of the division axis with the long axis of the cell by a rotation of the entire cell, consistent with recent experiments.

BP 31.7 Fri 11:45 BAR 0106

Large area automated structural and mechanical analysis of developing cells and tissues — •JOERG BARNER, TANJA NEUMANN, ANDRÉ KÖRNIG, DIMITAR R. STAMOV, and HEIKO HASCHKE — JPK BioAFM Business, Bruker Nano GmbH, Am Studio 2D, 12489 Berlin, Germany

Active forces in biological systems define the interactions between single molecules, growing cells and developing tissues. Atomic force microscopy (AFM) can be successfully applied for comprehensive nano-mechanical characterization of such samples under near physiological conditions. Currently, the trend is to extend this by studying the mechanobiology of living cells while evaluating their structure and the interaction with their cell culture substrates.

We will demonstrate how cell spreading and migration in living KPG-7 fibroblasts and CHO cells, can be studied with high-speed AFM and associated with spatially resolved cytoskeletal reorganization events. We will further extend this with high-speed mechanical mapping of confluent cell layers, which in combination with optical tiling can be applied to automated analysis of large sample areas. As a tool for analyzing the complex cellular mechanobiology, we went beyond purely elastic models, and performed sine oscillations (up to 500 Hz, amplitude 5-60 nm) in Z while in contact with the surface to probe the frequency-dependent response of living fibroblasts.

BP 32: Closing Plenary Talk (joint session BP/ CPP)

Time: Friday 12:15–13:00

Location: HSZ 03

Invited Talk

BP 32.1 Fri 12:15 HSZ 03

The physical regulation of brain development — •KRISTIAN FRANZE — IMP, FAU Erlangen-Nürnberg — Max-Planck-Zentrum für Physik und Medizin, Erlangen — PDN, University of Cambridge

The brain is our most complex organ system. Billions of neurons form an intricate network that regulates all major body functions including thought and emotions. However, the brain is not always that complex. It originally starts off as a simple epithelium, i.e., a single layer of cuboid cells. Axons, which transmit information to other cells over large distances, are only formed during embryonic development. Their immense length - up to several meters in some large animals - comes with severe logistic challenges. For example, how is transport

of proteins and genetic information achieved from the nucleus, where the DNA is located, to the axon's distant end? And how does an axon growing through a crowded and dynamic environment know where to turn and where to connect? These questions have captured the imagination of neuroscientists for more than a century. However, despite tremendous progress in molecular biology and imaging technologies, many problems remain unresolved. Combining theory and experiments, we here identified how microtubules, which are polar polymers along which molecular motors transport cargo, orient uniformly along the axon to enable long-range transport, and how mechanical tissue properties regulate axon growth through the developing brain. Our results suggest that chemical and physical signals are integrated by neurons, and that their interaction is crucial for proper brain development and function.

Chemical and Polymer Physics Division Fachverband Chemische Physik und Polymerphysik (CPP)

Hans-Jürgen Butt
Max-Planck-Institut für
Polymerforschung
Ackermannweg 10
55128 Mainz
butt@mpip-mainz.mpg.de

Jens-Uwe Sommer
Leibniz-Institut für Polymerforschung
Dresden e.V.
Hohe Strasse 6
01069 Dresden
sommer@ipfdd.de

Stephan Roth
Deutsches Elektronen-Synchrotron
(DESY)
Notkestr. 85
22607 Hamburg
stephan.roth@desy.de

Overview of Invited Talks and Sessions

(Lecture halls GÖR 226, MER 02, and ZEU 255; Poster P3 and P1A)

Invited Talks

CPP 1.1	Mon	9:30–10:00	GÖR 226	Strategies for advancing the performance of organic photovoltaics — •THOMAS ANTHOPOULOS
CPP 1.7	Mon	11:30–12:00	GÖR 226	Lost in translation? Transport resistance in organic solar cells — •CARSTEN DEIBEL
CPP 2.1	Mon	9:30–10:00	MER 02	Molecular Theories meet Explainable Machine Learning – Novel Concepts for Advanced Drug Formulations — •JENS SMIATEK
CPP 11.1	Mon	15:00–15:30	GÖR 226	Quantifying the potential of organic solar cells using luminescence measurements and modelling — •JENNY NELSON
CPP 12.1	Mon	15:00–15:30	MER 02	Adaptive Resolution Simulations: Past, Present and Open (Boundaries) Future — LUIS A. BAPTISTA, MAURICIO SEVILLA, KURT KREMER, •ROBINSON CORTES-HUERTO
CPP 13.1	Mon	15:00–15:30	ZEU 255	Nanocomposites and polymer thin films: from gas phase synthesis to functional applications — •FRANZ FAUPEL, STEFAN SCHRÖDER, ALEXANDER VAHL, SALIH VEZIROGLU, CENK AKTAS, THOMAS STRUNSKUS
CPP 19.1	Tue	9:30–10:00	MER 02	Multiscale Model of Flow-Induced Crystallization in Polymers — DAVID NICHOLSON, MARAT ANDREEV, CHENMAY GANGAL, •GREGORY RUTLEDGE
CPP 20.1	Tue	9:30–10:00	ZEU 255	Granular Matter Rheology – fluid-/solid-like behavior and state-transitions — •STEFAN LUDING
CPP 29.1	Wed	9:30–10:00	MER 02	Imaging mineral-water interfaces with atomic force microscopy — •ANGELIKA KÜHNLE
CPP 53.1	Thu	15:00–15:30	ZEU 255	Aqueous nanoclusters govern ionic transport in dense polymer membranes — •JOACHIM DZUBIELLA
CPP 56.1	Fri	9:30–10:00	GÖR 226	Self-assembled optical metamaterials — •ULLRICH STEINER
CPP 56.7	Fri	11:30–12:00	GÖR 226	Simulating quantum systems with plasmonic waveguide arrays — •STEFAN LINDEN
CPP 56.8	Fri	12:00–12:30	GÖR 226	single molecule detection on a smartphone microscope enabled by DNA origami biosensors — •PHILIP TINNEFELD
CPP 57.1	Fri	9:30–10:00	MER 02	Chiral transport of active and passive colloids — •ANKE LINDNER, ANDREAS ZÖTTL, OLIVIA DU ROURE, ERIC CLEMENT, FRANCESCA TESSER, GUANGYING JING
CPP 58.1	Fri	9:30–10:00	ZEU 255	Studies of polymer thermosets using scattering techniques — •MATS JOHANSSON

Invited Talks of the joint Symposium SKM Dissertation Prize 2023 (SYSD)

See SYSD for the full program of the symposium.

SYSD 1.1	Mon	9:30–10:00	HSZ 04	Diffusion of antibodies in solution: from individual proteins to phase separation domains — •ANITA GIRELLI
SYSD 1.2	Mon	10:00–10:30	HSZ 04	Intermediate Filament Mechanics Across Scales — •ANNA V. SCHEPERS
SYSD 1.3	Mon	10:30–11:00	HSZ 04	Ultrafast Probing and Coherent Vibrational Control of a Surface Structural Phase Transition — •JAN GERRIT HORSTMANN
SYSD 1.4	Mon	11:00–11:30	HSZ 04	Electro-active metasurfaces employing metal-to-insulator phase transitions — •JULIAN KARST
SYSD 1.5	Mon	11:30–12:00	HSZ 04	The role of unconventional symmetries in the dynamics of many-body systems — •PABLO SALA

Invited Talks of the joint Symposium Physics of Fluctuating Paths (SYFP)

See SYFP for the full program of the symposium.

SYFP 1.1	Tue	9:30–10:00	HSZ 01	Time at which a stochastic process achieves its maximum — •SATYA MAJUMDAR
SYFP 1.2	Tue	10:00–10:30	HSZ 01	Fluctuations and molecule-spanning dynamics of single Hsp90 proteins on timescales from nanoseconds to days — •THORSTEN HUGEL
SYFP 1.3	Tue	10:30–11:00	HSZ 01	Path reweighting for Langevin dynamics — •BETTINA KELLER
SYFP 1.4	Tue	11:15–11:45	HSZ 01	Out-of-equilibrium dynamics of trapped Brownian particles — •RAUL A. RICA
SYFP 1.5	Tue	11:45–12:15	HSZ 01	Thermodynamics of Clocks — •PATRICK PIETZONKA

Sessions

CPP 1.1–1.11	Mon	9:30–13:00	GÖR 226	Focus: Organic Solar Cells Based on Non-fullerene Acceptors: Loss Mechanism and Options for Above 20 % Efficiencies I
CPP 2.1–2.12	Mon	9:30–13:00	MER 02	Modeling and Simulation of Soft Matter I
CPP 3.1–3.4	Mon	9:30–10:30	ZEU 255	Hydrogels and Microgels
CPP 4.1–4.12	Mon	9:30–13:00	TOE 317	Active Matter I (joint session BP/CPP/DY)
CPP 5.1–5.10	Mon	9:30–12:30	POT 81	2D Materials I (joint session HL/CPP)
CPP 6.1–6.10	Mon	9:30–12:30	POT 251	Perovskite and photovoltaics I (joint session HL/CPP)
CPP 7.1–7.6	Mon	9:30–11:15	POT 361	Organic Semiconductors (joint session HL/CPP)
CPP 8.1–8.8	Mon	10:45–13:00	ZEU 255	Responsive and Adaptive Systems
CPP 9.1–9.5	Mon	11:30–12:45	SCH A 315	Organic Thin Films, Organic-Inorganic Interfaces (joint session DS/CPP)
CPP 10.1–10.3	Mon	14:30–15:30	POT 106	Instrumentation and Methods for Micro- and Nanoanalysis (joint session KFM/CPP)
CPP 11.1–11.7	Mon	15:00–17:15	GÖR 226	Focus: Organic Solar Cells Based on Non-fullerene Acceptors: Loss Mechanism and Options for Above 20 % Efficiencies II
CPP 12.1–12.7	Mon	15:00–17:15	MER 02	Modeling and Simulation of Soft Matter II
CPP 13.1–13.10	Mon	15:00–18:00	ZEU 255	Composites and Functional Polymer Hybrids
CPP 14.1–14.11	Mon	15:00–18:15	ZEU 160	Active Matter II (joint session DY/BP/CPP)
CPP 15.1–15.10	Mon	15:00–18:15	POT 81	2D Materials II (joint session HL/CPP)
CPP 16.1–16.11	Mon	15:00–17:45	GER 39	Nanostructures at Surfaces (joint session O/CPP)
CPP 17.1–17.60	Mon	18:00–20:00	P3	Poster Session I
CPP 18.1–18.13	Tue	9:30–13:00	GÖR 226	Organic Electronics and Photovoltaics I (joint session CPP/HL)
CPP 19.1–19.12	Tue	9:30–13:00	MER 02	Crystallization, Nucleation and Self-Assembly
CPP 20.1–20.10	Tue	9:30–12:30	ZEU 255	Polymer and Molecular Dynamics, Friction and Rheology
CPP 21.1–21.11	Tue	9:30–12:30	TOE 317	Active Matter III (joint session BP/CPP/DY)
CPP 22.1–22.10	Tue	9:30–12:15	POT 81	2D Materials III (joint session HL/CPP)
CPP 23.1–23.12	Tue	9:30–13:00	POT 112	Optical Properties (joint session HL/CPP)
CPP 24.1–24.11	Tue	10:00–13:00	MOL 213	Complex Fluids and Soft Matter I (joint session DY/CPP)
CPP 25.1–25.4	Tue	12:00–13:00	HSZ 201	Molecular Electronics and Photonics (joint session TT/CPP)
CPP 26.1–26.3	Tue	14:00–14:45	MER 02	Electrical, Dielectrical and Optical Properties of Thin Films
CPP 27.1–27.4	Tue	14:00–15:00	ZEU 147	Glasses and Glass Transition I (joint session DY/CPP)
CPP 28.1–28.11	Wed	9:30–12:30	GÖR 226	Molecular Electronics and Excited State Properties (joint session CPP/TT)
CPP 29.1–29.11	Wed	9:30–12:45	MER 02	Interfaces and Thin Films
CPP 30.1–30.12	Wed	9:30–13:00	TOE 317	Biopolymers and Biomaterials I (joint session BP/CPP)
CPP 31.1–31.10	Wed	9:30–13:00	ZEU 160	Focus Session: From Inter-individual Variability to Heterogeneous Group Dynamics and Disorder in Active Matter (joint session DY/BP/CPP)
CPP 32.1–32.10	Wed	9:30–12:30	POT 81	2D Materials IV (joint session HL/CPP)
CPP 33.1–33.11	Wed	9:30–13:00	POT 251	Perovskite and photovoltaics II (joint session HL/CPP)
CPP 34.1–34.11	Wed	10:00–13:00	ZEU 147	Wetting, Droplets and Microfluidics I (joint session DY/CPP)
CPP 35.1–35.66	Wed	11:00–13:00	P1	Poster Session II
CPP 36.1–36.9	Wed	15:00–17:30	GÖR 226	Organic Electronics and Photovoltaics II (joint session CPP/HL)
CPP 37.1–37.5	Wed	15:00–16:15	MER 02	Nanostructures, Nanostructuring and Nanosized Soft Matter
CPP 38.1–38.12	Wed	15:00–18:15	MOL 213	Microswimmers and Fluid Physics of Life (joint session DY/CPP)
CPP 39.1–39.12	Wed	15:00–18:15	ZEU 160	Focus Session: Physics of Fluctuating Paths (joint session DY/CPP)
CPP 40.1–40.10	Wed	15:00–17:30	GER 37	2D Materials V: Growth, Structure and Substrate Interaction (joint session O/CPP)
CPP 41.1–41.6	Wed	16:30–18:00	MER 02	Biopolymers, Biomaterials and Bioinspired Functional Materials II (joint session CPP/BP)
CPP 42.1–42.10	Thu	9:00–12:35	POT 51	Battery Materials (joint session KFM/CPP)
CPP 43.1–43.11	Thu	9:30–12:30	GÖR 226	Organic Electronics and Photovoltaics III (joint session CPP/HL)

CPP 44.1–44.13	Thu	9:30–13:00	MER 02	Wetting, Fluidics and Liquids at Interfaces and Surfaces II (joint session CPP/DY)
CPP 45.1–45.9	Thu	9:30–12:00	ZEU 255	Emerging Topics in Chemical and Polymer Physics, New Instruments and Methods
CPP 46.1–46.12	Thu	9:30–13:00	ZEU 160	Active Matter IV (joint session DY/BP/CPP)
CPP 47.1–47.9	Thu	9:30–12:00	POT 81	2D Materials VI (joint session HL/CPP)
CPP 48.1–48.11	Thu	10:15–13:15	SCH A 251	Data Driven Materials Science: Big Data and Work Flows – Microstructure-Property-Relationships (joint session MM/CPP)
CPP 49.1–49.9	Thu	10:30–12:45	GER 37	2D Materials VII: Heterostructures (joint session O/CPP)
CPP 50.1–50.3	Thu	12:15–13:00	ZEU 255	Glasses and Glas Transition II
CPP 51.1–51.8	Thu	15:00–17:15	GÖR 226	Hybrid and Perovskite Photovoltaics III
CPP 52.1–52.5	Thu	15:00–16:15	MER 02	Wetting, Fluidics and Liquids at Interfaces and Surfaces III (joint session CPP/DY)
CPP 53.1–53.9	Thu	15:00–17:45	ZEU 255	Charged Soft Matter, Polyelectrolytes and Ionic Liquid
CPP 54.1–54.5	Thu	16:30–17:45	MER 02	2D Materials VIII
CPP 55	Thu	18:00–19:00	MER 02	Members' Assembly
CPP 56.1–56.8	Fri	9:30–12:30	GÖR 226	Focus: Self-Assembly of Plasmonic Nanostructures (joint session CPP/HL)
CPP 57.1–57.12	Fri	9:30–13:00	MER 02	Complex Fluids and Colloids, Micelles and Vesicles II (joint session CPP/DY)
CPP 58.1–58.7	Fri	9:30–11:30	ZEU 255	Polymer Networks and Elastomers
CPP 59.1–59.8	Fri	9:30–12:00	TOE 317	Active Matter V (joint session BP/CPP/DY)
CPP 60.1–60.1	Fri	12:15–13:00	HSZ 03	Closing Plenary Talk (joint session BP/CPP)

Members' Assembly of the Chemical and Polymer Physics Division

Thursday 18:00-19:00 MER 02

- Report of the current speaker team
- Election of the second deputy speaker
- Award of the poster prize of the CPP Division
- Miscellaneous

Sessions

– Invited Talks, Contributed Talks, and Posters –

CPP 1: Focus: Organic Solar Cells Based on Non-fullerene Acceptors: Loss Mechanism and Options for Above 20 % Efficiencies I

Organized by Dieter Neher and Christoph J. Brabec

Time: Monday 9:30–13:00

Location: GÖR 226

Invited Talk

CPP 1.1 Mon 9:30 GÖR 226

Strategies for advancing the performance of organic photovoltaics — •THOMAS ANTHOPOULOS — King Abdullah University of Science and Technology (KAUST), Thuwal 23955-6900, Kingdom of Saudi Arabia

The dramatic advances in the power conversion efficiency (PCE) of organic photovoltaics (OPVs) witnessed in recent years have been primarily driven by the development of new materials and the minimisation of performance losses associated with conventional cell architectures. This talk will discuss our recent OPV work, focusing on practical strategies for boosting cell performance. I will first discuss using low-dimensional charge-extracting interlayers and the numerous advantages of these innovative materials for next-generation OPVs. I will then present recent progress in using molecular dopants to improve the PCE of OPVs and how their combination with innovative interlayers can improve the material utilisation and circularity of the ensuing OPV cells without compromising their performance.

CPP 1.2 Mon 10:00 GÖR 226

Can Organic Solar Cells Beat the Near-Equilibrium Thermodynamic Limit? — TANVI UPRETI¹, •CONSTANTIN TORMANN², and MARTIJN KEMERINK^{1,2} — ¹Complex Materials and Devices, Department of Physics, Chemistry and Biology (IFM), Linköping University, Sweden — ²Institute for Molecular Systems Engineering and Advanced Materials, Heidelberg University, Germany

Switching to non-fullerene acceptors has led to an impressive increase in power conversion efficiencies (PCEs) of organic photovoltaic cells over the past decade. Despite this, the PCE of such devices is still below the near-equilibrium limit of the corresponding material, which is particularly evident from losses in the open-circuit voltage (Voc). A prominent yet incompletely understood loss channel affecting Voc is the thermalization of photogenerated charge carriers in the density of states, which is broadened by energetic disorder. In contrast to symmetric morphologies like classic bulk heterojunctions, morphologies with a gradient in the donor:acceptor ratio can mitigate this loss channel by rectifying the diffusive motion of the thermalizing photogenerated charge carriers. Here, we show by extensive numerical modelling how funnel-shaped donor and acceptor-rich domains in a phase-separated morphology promote directed transport of positive and negative charge carriers towards the anode and cathode, respectively. In such optimized funnel morphologies, this kinetic, nonequilibrium effect even allows one to surpass the near-equilibrium thermodynamic limit for the same active material in the absence of gradients.

CPP 1.3 Mon 10:15 GÖR 226

Transparent Conductive Electrodes: Figure of Merit Revisited for Photovoltaics — •HARALD HOPPE — Center for Energy and Environmental Chemistry Jena (CEEC Jena), Friedrich Schiller University Jena, Philosophenweg 7a, 07743 Jena, Germany — Laboratory of Organic and Macromolecular Chemistry (IOMC), Friedrich Schiller University Jena, Humboldtstrasse 10, 07743 Jena, Germany

Figure of Merits (FOMs) are meant to provide a simple means for assessing the suitability of a certain material for or compartments within devices in general. In case of photovoltaic devices, the role of the transparent conductive electrode is to allow as much as possible light to enter into the device as well as to enable current flow out of the device. Over the last 5 decades a number of FOMs were introduced based on several approaches. Here we present a rather novel, yet implicit approach for an FOM, which is highly suitable for photovoltaics, allowing to assess the potential photovoltaic performance quantitatively.

CPP 1.4 Mon 10:30 GÖR 226

Reconnoitering the impact of fluorination on both donor and non-fullerene acceptor in bulk heterojunction organic photovoltaics — •SHAHIDUL ALAM¹, JAFAR I. KHAN¹, VOJTECH NÁDAŽDÝ³, TOMÁŠ VÁRY³, AURELIEN D. SOKENG², MD MOIDUL ISLAM², CHRISTIAN FRIEBE², WEJDAN ALTHOBAITI², MARTIN HAGER², ULRICH S. SCHUBERT², CARSTEN DEIBEL⁴, DENIS ANDRIENKO⁵, FRÉDÉRIC LAQUAI¹, and HARALD HOPPE² — ¹KAUST Solar Center (KSC), Kingdom of Saudi Arabia — ²FSU Jena, Germany — ³Slovak Academy of Sciences, Bratislava — ⁴TU Chemnitz, Germany — ⁵MPIP, Mainz, Germany

Organic solar cells' performance can be often effectively improved through fluorination of the donor and/or non-fullerene acceptor (NFA). The end-group fluo-

ration of the well-known NFA ITIC yields further extension of the absorption spectrum to the near infrared, which results in an increment of the device's photocurrent as compared to the non-fluorinated version. Herein, ITIC and two fluorinated variants of ITIC (ITIC-2F* and ITIC-4F) were synthesized and systematically investigated the influence of end-group fluorination physicochemical properties, optical properties, and photovoltaic performance. Photovoltaic parameters are discussed in terms of exciton quenching, charge generation, charge dissociation, and recombination losses. Specifically, it is found that fluorinated acceptors control the devices' open circuit voltage. All the results shed light on the importance of the energy landscape and the quadrupole moment of acceptor beyond the underlying donor-acceptor interface.

CPP 1.5 Mon 10:45 GÖR 226

Synthesis and Characterization of Organic Heterojunction Model Interfaces — •HANBO YANG¹, JARVIST MOORE FROST¹, JENNY NELSON¹, and HUGO BRONSTEIN² — ¹Imperial College London, London, UK — ²Cambridge University, Cambridge, UK

Control of the molecular configuration at the interface of an organic heterojunction is key to the development of efficient optoelectronic devices. Due to the difficulty in characterizing these buried and (likely) disordered heterointerfaces the interfacial structure in most systems remains a mystery. Here, we demonstrate a novel synthetic strategy to design and control model interfaces, allowing for their detailed study in isolation from the bulk material. This is achieved by the synthesis of a donor polymer-non-fullerene acceptor 'through space' linked system, where the exact position and orientation of the moieties is completely controlled and we further showed that the kinetics of charge separation can be tuned using transient absorption spectroscopy and excited state calculations.

CPP 1.6 Mon 11:00 GÖR 226

Direct Determination of the Photogenerated Free Charge Carrier Luminescence in Organic Solar Cells via Transient Photoluminescence Measurements — •JARED FAISST, MATHIAS LIST, and ULI WÜRTEL — Fraunhofer ISE, Freiburg, Deutschland

Photoluminescence (PL) measurements have shown to be a valuable tool characterizing the optoelectronic properties of semiconductors. In organic solar cells, the PL measurement of free charge carriers is hindered by the strong and spectrally broad luminescence of non-dissociated local exciton recombination. Therefore, the PL of free charge carriers under steady state condition is not directly detectable. To overcome this problem, we make use of the vastly different lifetimes of local excitons (ps-ns) and free charge carriers (μ s). In this work, we present experimental time resolved PL data of a fullerene based D18:PC₇₁BM and two non-fullerene based D18:Y6 and PV-X plus organic solar cells and demonstrate the possibility to separate the luminescence of local excitons from the one of free charge carriers. We further show that the luminescence of the free charge carriers indeed correlates with the quasi-Fermi level splitting as expected. Hence, this novel measurement technique eventually allows to investigate free charge carriers in organic absorber layers directly. This is of great importance to further understand recombination mechanisms and degradation effects and to identify optimization potentials.

15 min. break**Invited Talk**

CPP 1.7 Mon 11:30 GÖR 226

Lost in translation? Transport resistance in organic solar cells — •CARSTEN DEIBEL — Institut für Physik, Technische Universität Chemnitz, 09126 Chemnitz, Germany

With the advent of non-fullerene acceptors, breaking the 20 % power conversion efficiency limit is within close reach for organic solar cells. Understanding the efficiency-limiting processes remains important.

I will discuss how losses in the fill factor can be due to the transport resistance, a voltage loss because of a low conductivity in the active layer. Its relevance for organic solar cells was only shown a half dozen years ago [1]. I will present transport resistance limiting different organic solar cell types, and then focus on fresh and thermally degraded PM6:Y6 solar cells (heated to 85°C, in the dark, under nitrogen atmosphere), a state-of-the-art system based on the non-fullerene Y6.

The increasing fill factor losses on this degradation path are because of the transport resistance [2]. The reason seems to be trap formation in the tail states, which decrease the active layer conductivity.

[1] U. Würfel, D. Neher, A. Spies, S. Albrecht, Nat. Commun. 6, 6951 (2015).

[2] C. Wöpke, C. Göhler, M. Saladina, X. Du, L. Nian, C. Greve, C. Zhu, K. M. Yallum, Y. J. Hofstetter, D. Becker-Koch, N. Li, T. Heumüller, I. Milekhin, D. R. T. Zahn, C. J. Brabec, N. Banerji, Y. Vaynzof, E. M. Herzog, R. C. I. MacKenzie, C. Deibel. Nat. Commun. 13, 3786 (2022).

CPP 1.8 Mon 12:00 GÖR 226

Thermal Degradation Mechanism in PM6: Y-series Acceptors Organic Solar Cells — •SI CHEN, JULIEN GORENFLOT, and LAQUAI FREDERIC — Abdullah University of Science and Technology Thuwal 23955-6900, Saudi Arabia

The stability issue is the core restriction for the application of organic solar cells (OSCs), and the study of the degradation mechanism of high-efficient PM6: Y-series systems is an urgent problem to be solved. We concluded one specific pathway of FF degradation for typical PM6:Y-series acceptors organic solar cells since FF changed most obviously after thermal aging. After developing several characterization measurements, including time-delayed collection field (TDCF), light intensity dependent measurements, etc. to study the photophysics of PM6:Y-series solar cells before and after thermal degradation, we can quantify FF degradation with field-dependent charge generation, non-geminate recombination, and transport resistance factors. The effect of transport resistance is quantified by the Suns-Voc method. The results show that the increase of charge transport resistance is the primary factor leading to FF degradation, which can be further explained by excessive phase separation with the information from GIWAXS and AFM. Our work can not only provide material design ideas for highly efficient and stable organic solar cells by figuring out the thermal degradation mechanism of PM6:Y-series organic solar cells but also come up with a new methodology to quantify the FF degradation of organic solar cells.

CPP 1.9 Mon 12:15 GÖR 226

Photophysics of Poly(3-hexylthiophene):Non-Fullerene Acceptor Based Organic Solar Cells — •WEJDAN ALTHOBAITI, JAFAR KHAN, JULIEN GORENFLOT, SHAHIDUL ALAM, GEORGE HARRISON, STEFAAN DE WOLF, and FRÉDÉRIC LAQUAI — King Abdullah University of Science and Technology (KAUST), KAUST Solar Center (KSC), Physical Sciences and Engineering Division (PSE), Saudi Arabia

Charge generation can proceed through two different paths in Bulk Heterojunction based organic solar cells which are electron transfer from donor to acceptor and hole transfer from acceptor to donor. These processes can be controlled by Electron Affinity (EA) offsets and Ionization Energy (IE) offsets, respectively. Understanding the relationship between the IE offsets, EA offsets between donor and acceptor materials, and the performance of OSCs could improve the charge generation efficiency. We characterized the impact of large IE and EA offsets on device performances and more precisely on the internal quantum efficiency (IQE) using a wide bandgap polymer donor which has shallow IE such as P3HT and Non Fullerene Acceptor (NFA). This provides a wide range of diagonal bandgap (IE of the donor and EA of the acceptor). Thus, enables us to find the relation between small diagonal bandgap and the decrease of the IQE in energy gap law framework. Low IQE while high exciton quenching observed can be ex-

plained due to charge recombination as our results demonstrated by geminate and non-geminate recombination.

CPP 1.10 Mon 12:30 GÖR 226

Efficient Nanoscale Exciton Transport in Non-fullerene Organic Solar Cells Enables Reduced Bimolecular Recombination of Free Charges — •DREW B. RILEY¹, OSKAR J. SANDBERG¹, NASIM ZARRABI¹, RYUN KIM², PAUL MEREDITH¹, and ARDALAN ARMIN¹ — ¹Swansea University, Swansea, Wales. — ²Cambridge University, Cambridge, UK

The origins of reduced bimolecular recombination in high efficiency OPV-based solar cells are debated, and mechanisms related to the charge-transfer (CT) state and free-carrier encounter dynamics have been proposed as underlying factors.[1] Further, it is expected that the CT-state dynamics is strongly influenced by exciton dynamics in low off-set blends.[2]

In this presentation I will explore the role exciton dynamics play in the charge generation and recombination processes. Specifically, I will introduce a photoluminescence-based probe to quantify the acceptor domain size in OPV blends. It will be shown that NFA-based blends form larger domains than fullerene-based systems but that this increase is unable to account for the observed non-Langevin recombination. Further, I will show that the reduction of bimolecular recombination is correlated with enhanced exciton dynamics within the NFA domains. This indicates that the processes responsible for efficient exciton transport also enable strongly non-Langevin recombination in high efficiency NFA-based solar cells with low energy offsets.

[1] A. Armin, et.al. AEM, 11, 2003570, 2021.

[2] A. Classen, et.al. Nat.Energy, 5,2020.

CPP 1.11 Mon 12:45 GÖR 226

Power-law density of states in organic solar cells revealed by the open-circuit voltage dependence of the ideality factor — •MARIA SALADINA¹, CHRISTOPHER WÖPKE¹, CLEMENS GÖHLER¹, IVAN RAMIREZ², OLGA GERDES², CHAO LIU^{3,4}, NING LI^{3,4,5}, THOMAS HEUMÜLLER^{3,4}, CHRISTOPH J. BRABEC^{3,4}, KARSTEN WALZER², MARTIN PFEIFFER², and CARSTEN DEIBEL¹ — ¹Technische Universität Chemnitz, Germany — ²Heliatek GmbH, Germany — ³FAU Erlangen-Nürnberg, Germany — ⁴Helmholtz Institute Erlangen-Nürnberg for Renewable Energy, Germany — ⁵South China University of Technology, China We determine the density of states (DOS) in disordered semiconductors via the diode ideality factor (n_{id}). We employ illumination intensity and temperature-dependent open-circuit voltage measurements. In amorphous silicon, we found that n_{id} only depends on the temperature, and can be explained by an exponential DOS distribution.

For the organic donor-acceptor solar cells, we find that n_{id} is not only temperature but also light intensity-dependent. The seemingly unsystematic dependence of n_{id} on the light intensity becomes systematic once the former is displayed in dependence of the open-circuit voltage, which is a means to sample the DOS distribution at a certain energetic depth. This evaluation approach leads to our central result: the DOS follows a power-law distribution over a broad range of energies. In particular, for the investigated organic solar cells under working conditions the DOS is best represented by the power-law, not a gaussian or exponential one.

CPP 2: Modeling and Simulation of Soft Matter I

Time: Monday 9:30–13:00

Location: MER 02

Invited Talk

CPP 2.1 Mon 9:30 MER 02

Molecular Theories meet Explainable Machine Learning - Novel Concepts for Advanced Drug Formulations — •JENS SMIA TEK — Institute for Computational Physics, University of Stuttgart, Germany — Boehringer Ingelheim Pharma GmbH & Co. KG, Biberach (Riss), Germany

Pharmaceutical processes and drug formulations are based on a variety of molecular mechanisms and principles. Significant advances have been made in recent years in terms of basic understanding. Despite these advances, a large number of mechanisms are not yet fully understood, which would be of great advantage, especially for the optimization of development processes as well as the quality and stability of drugs. In this talk I will present fundamental molecular theories of electronic interactions in solutions. Due to the large number of components and the complexity of the interactions, these theories can only be used for a qualitative understanding. However, by combining it with explainable machine learning, the basic molecular mechanisms can be identified and the corresponding thermodynamic properties of the solutions can be predicted. I will present some examples and discuss the underlying benefits and additional challenges for future developments.

CPP 2.2 Mon 10:00 MER 02

Revealing the relation between structure and dynamics using unsupervised machine learning — •MOUMITA MAITI¹, ANAND NARAYANAN KRISHNAMOORTHY², YOUSSEF MABROUK², DIDDO DIDDENS², and ANDREAS HEUER¹ — ¹Institute of Physical Chemistry, University of Münster, Corrensstrasse 28/30, 48149 Münster, Germany — ²Forschungszentrum Jülich GmbH, Helmholtz-Institute Münster (IEK-12), Corrensstraße 46, 48149 Münster, Germany

Molecular dynamics trajectories of Li-ions in electrolytes with different anions are analysed using an unsupervised machine learning algorithm to understand the relation between structure and dynamics. The trajectories are generated using a polarizable force-field model instead of the standard OPLS force-field, thereby generating excellent agreement of structural and dynamical properties with experiment. The high-dimensional feature space is constructed from the distances and angles between Li-ions and its neighbours, reflecting the structural information of local environments. It can be reasonably reduced to 2 dimensions using the dimension reduction algorithm umap. This is performed for a large number of Li-ions. After the mapping distinct clusters can be identified. Although they are based on structural properties, they also reflect different dynamical properties with respect to diffusivity and ion-correlations. We finally show how the total ionic conductivity can be expressed in terms of the structural information of the first solvation shell.

CPP 2.3 Mon 10:15 MER 02

Data reweighting in metadynamics simulations — TIMO SCHÄFER¹ and GIOVANNI SETTANNI^{1,2} — ¹Department of Physics, Johannes-Gutenberg University Mainz, Germany — ²Faculty of Physics and Astronomy, Ruhr University Bochum, Germany

The data collected along a metadynamics simulation can be used to recover information about the underlying unbiased system by means of a reweighting procedure. We analyze the behavior of several reweighting techniques in terms of the quality of the reconstruction of the underlying unbiased free energy landscape in the early stages of the simulation and propose a simple reweighting scheme that we relate to the other techniques. We show^[1] that the free energy landscape reconstructed from reweighted data can be more accurate than the negative bias potential depending on the reweighting technique, the stage of the simulation, and the adoption of well-tempered or standard metadynamics. While none of the tested reweighting techniques from the literature provides the most accurate results in all the analyzed situations, the one proposed here, in addition to helping simplifying the reweighting procedure, converges quickly and precisely to the underlying free energy surface in all the considered cases, thus allowing for an efficient use of limited simulation data.

[1] Schäfer TM, Settanni G. *J Chem Theory Comput.* 2020 Apr 14;16(4):2042-2052. doi: 10.1021/acs.jctc.9b0086

CPP 2.4 Mon 10:30 MER 02

findR: An automatized workflow from molecular dynamic simulation to quantum chemical methods for reaction discovery — GUNNAR SCHMITZ¹, ÖZLEM YÖNDER², VANESSA ANGENENT³, CHRISTOF HÄTTIG², and ROCHUS SCHMID³ — ¹Ruhr-Universität Bochum, Lehrstuhl für Theoretische Chemie II, Bochum, Germany, 44801 Bochum — ²Ruhr-Universität Bochum, Lehrstuhl für Theoretische Chemie I, Bochum, Germany, 44801 Bochum — ³Ruhr-Universität Bochum, Lehrstuhl für Anorganische Chemie II, Bochum, Germany, 44801 Bochum

Computer-guided reaction discovery is still an open issue, which will be vital for applications in science and industry. For this purpose, we present an automatized workflow that, starting from molecular dynamics simulations (MD), identifies reaction events based on graph theory, filters them, and prepares them for accurate quantum chemical calculations using e.g. Density Functional Theory (DFT) or Coupled Cluster methods. The capabilities of the automatized workflow are demonstrated by the example of simulations for the combustion of polycyclic aromatic hydrocarbons. A limiting factor of the reaction sampling by means of MD simulations is the required simulation time to observe reactions. In order to enhance this process, we compare different acceleration techniques like metadynamics and a nano reactor setup, in which a spherical confinement is combined with periodically applied forces directed to the simulation box center. We demonstrate that our workflow can be used to identify reactions without prior chemical knowledge and can give new insights into the combustion process.

CPP 2.5 Mon 10:45 MER 02

Data-driven analysis and prediction of the performance of cleansing solutions — TAKAHIRO YOKOYAMA¹, HIDEKI MIWAKE², RYUICHI NAKATAKE², NORIYOSHI ARAI¹, and ARASH NIKOUBASHMAN^{1,3} — ¹Department of Mechanical Engineering, Keio University, Yokohama, Japan — ²Research Institute, Fancl Corporation, Yokohama, Japan — ³Institute of Physics, JGU Mainz, Germany

Cleansing solutions are complex multi-component liquids, which are commonly used to wash excess sebum, dirt, and make-up cosmetics directly from the skin. Their formulations typically contain a large variety of ingredients, including surfactants, viscosity modifiers, and polyols to meet the desired product requirements, such as high skin compatibility, moisture retention, and long shelf life. The large number of different components makes it, however, challenging to understand and predict the physical properties of such cleansing solutions, since the majority of established theories have been developed for pure systems. Machine learning (ML) methods are promising methods to solve these kinds of problems, as they can reveal non-trivial trends and interactions between the various components. In this work, we predict the cleansing performance of a large number of formulations using various ML methods, such as random forest regression and (recurrent) neural networks. Although this work focuses primarily on cleansing solutions, the applied methodology should be transferable to predict the physical properties of other multi-component liquids as well.

CPP 2.6 Mon 11:00 MER 02

Multiscale Simulation Framework for the electromechanical behavior of PEDOT:PSS — STEFFEN KAMPMANN¹, ALEXANDER CROY², AREZOO DIANAT¹, and GIANAURELIO CUNIBERTI¹ — ¹Chair of Materials Science and Nanotechnology, Faculty of Mechanical Science and Engineering, TU Dresden, Dresden, Germany — ²Chair of Theoretical Chemistry, Faculty of Chemistry and Earth Sciences, Friedrich Schiller University Jena, Jena, Germany

Functional mechanically resilient polymer films, such as poly(3,4-ethylenedioxythiophene) polystyrene sulfonate (PEDOT:PSS), play an important role for strain gauges or organic light-emitting diode displays [1-3]. Typically, the respective material behavior results from an interplay of mechanisms

across multiple scales. The modeling and simulation workflow presented here enables the generation of disordered polymers and the linking of their mechanical and their electronic properties from the atomistic to the microscopic scale. In particular, we focus on the relationship between deformation and conductivity by combining density functional tight binding calculations, molecular dynamics simulations, and finite element calculations. The in-situ processing, evaluation as well as the exchange of the generated data across the simulation methods is performed using a Python framework which provides a computationally efficient assessment of material properties at different scales. Exemplarily, we present results for a strain gauge based on PEDOT:PSS. [1] R. Luo, et al., *Progress in Organic Coatings*, 162, 106593 (2022) [2] M. Cinquino et al., *JS: AMD*, 7, 1,100394 (2022) [3] L. Liu, et al., *Organic Electronics*, 89, 106047 (2021)

15 min. break

CPP 2.7 Mon 11:30 MER 02

Differentiable simulation for Solar Power Plants and beyond — STEFAN KESSELHEIM¹, MAX PARGMANN², and JAN EBERT¹ — ¹Forschungszentrum Jülich — ²German Aerospace Center (DLR)

In Solar Power Plants, temperatures sufficient for chemical processes or the generation of electrical power are created by reflecting sunlight with thousands of mirrors ("heliostats") to a surface ("the receiver"). In operation, the temperature distribution on the receiver is critical for the performance and must be optimized. The heliostats are never perfectly flat as due to budget constraints, the construction is not optimal. We have devised a method to infer the heliostat surface from the reflection of the sun. The technique is based on an implementation of a simulation in PyTorch, where the automatic differentiation engine is used to optimize the surface. The surface is modeled as by a Non-Uniform Rational B-Spline (NURBS) and the NURBS parameters are subject to optimization. Furthermore we employ a regularization technique to mitigate the appearing challenge of ambiguous solutions. Our approach makes efficient use of GPUs based on PyTorch's linear algebra engine. We believe our approach poses an interesting example of a fruitful interaction of techniques originating from Machine Learning and simulation, that can serve as an exciting example how to integrate simulation and experimental data, for example in biomolecular simulation.

CPP 2.8 Mon 11:45 MER 02

Simulation-based inference of single-molecule force-spectroscopy — ROBERTO COVINO^{1,2}, LARS DINGELDEIN¹, and PILAR COSSIO³ — ¹Frankfurt Institute for Advanced Studies, 60438 Frankfurt am Main, Germany — ²International Max Planck Research School on Cellular Biophysics, 60438 Frankfurt am Main, Germany — ³Center for Computational Mathematics and Biology, Flatiron Institute, 10010 New York, United States

Single-molecule force spectroscopy (smFS) is a powerful approach to studying molecular self-organization. However, the coupling of the molecule with the ever-present experimental device introduces artifacts, that complicates the interpretation of these experiments. Performing statistical inference to learn hidden molecular properties is challenging because these measurements produce non-Markovian time series, and even minimal models lead to intractable likelihoods. To overcome these challenges, we developed a computational framework built on novel statistical methods called simulation-based inference (SBI). SBI enabled us to directly estimate the Bayesian posterior, and extract reduced quantitative models from smFS, by encoding a mechanistic model into a simulator in combination with probabilistic deep learning. Using synthetic data, we could systematically disentangle the measurement of hidden molecular properties from experimental artifacts. The integration of physical models with machine-learning density estimation is general, transparent, easy to use, and broadly applicable to other types of biophysical experiments.

CPP 2.9 Mon 12:00 MER 02

Coarse-grained modelling of liquid-liquid and liquid-gas interfaces — JAKOB FILSER¹, HARALD OBERHOFER², CHRISTOPH SCHEURER¹, and KARSTEN REUTER¹ — ¹Fritz-Haber-Institut der MPG, Berlin, Germany — ²Chair for Theoretical Physics VII, University of Bayreuth

Modelling of dielectric interfaces remains a central challenge in computational chemistry. We present a new method to incorporate solvation effects into density-functional theory calculations of organic adsorbates at liquid-liquid and liquid-gas interfaces.

Simulating a large number of solvent molecules explicitly at first-principles level is generally not computationally tractable. We therefore resort to an implicit solvation approach, treating the solvent as a structureless dielectric continuum. Specifically, we advance the multipole-expansion method, in which we model the interface as the boundary of two semi-infinite media with different permittivity. Gauging the limiting behaviour for moving the solute from one bulk medium into the other is straightforward by referencing experimental transfer free energies. Complementary force-field level MD simulations with explicit solvent molecules are used as a reference for the behaviour at the interface. These calculations yield thermal distributions at atomic scale resolution, allowing for a fine assessment of the role of the solvent structure in the adsorption. In our im-

PLICIT method, we employ a model for the transition of free energy terms, such as the surface tension, between the two media, aimed at reproducing the above mentioned thermal distributions extracted from an atomistic solvent model.

CPP 2.10 Mon 12:15 MER 02

Geometrical frustration causes self-limiting assembly in systems of bipods — •ASWATHY MUTTATHUKATTIL and MICHAEL ENGEL — Institute for Multiscale Simulation, IZNF, Friedrich-Alexander Universität Erlangen-Nürnberg, 91058 Erlangen, Germany

Geometric frustration emerges in self-assembly if local interactions between building blocks are incompatible to form uniform (bulk) materials. Examples for geometrically frustrated assemblies with self-limiting size include protein filament bundles, twisted molecular crystals, bent core liquid-crystals and viral capsids. Despite of significant efforts to develop a general theory on geometrical frustration, it remains as a challenge to use it as a design principle to engineer finite-size equilibrium assemblies in soft matter. In this study, we control geometrical frustration deliberately and systematically in system of bipods to demonstrate self-limiting crystallization. Our minimal computational model consists of a central sphere that connect to two attractive rigid rods diametrically via a flexible hinge. Tuning the flexibility of the hinge and rod attraction, anisotropic fibrillar assemblies are observed. The fibrils do not grow wider than a fixed limit, which can be controlled by the misfit introduced by the radius of central sphere. Our model bipods can be realized in experiments as nanoparticles with tethered polymer bundles, partially unfolded polymer globules (including biopolymers like proteins) and organic molecules.

CPP 2.11 Mon 12:30 MER 02

Pair-Reaction Dynamics in Water: Competition of Memory, Potential-Shape and Inertial Effects — •FLORIAN BRÜNIG, JAN DALDROP, and ROLAND NETZ — Freie Universität Berlin, Department of Physics, 14195 Berlin, Germany

When described by a one-dimensional reaction coordinate, pair-reaction rates in a solvent depend, in addition to the potential barrier height and the friction coefficient, on the potential shape, the effective mass and the friction relaxation spectrum, but a rate theory that accurately accounts for all these effects does not exist. We show how to extract all parameters of the generalized Langevin equation (GLE) and in particular the friction memory function from molecular dynamics (MD) simulations of two prototypical pair reactions in water, the

dissociation of NaCl and of two methane molecules. Simulations of the GLE by Markovian embedding techniques accurately reproduce the pair-reaction kinetics from MD simulations without any fitting parameters, which confirms the accuracy of the approximative form of the GLE and of the parameter extraction techniques. By modification of the GLE parameters, we investigate the relative importance of memory, mass and potential-shape effects. Neglect of memory slows down NaCl and methane dissociation by roughly a factor of 2, neglect of mass accelerates reactions by a similar factor, the harmonic approximation of the potential shape gives rise to slight acceleration. This error cancellation explains why Kramers' theory, which neglects memory effects and treats the potential shape harmonically, describes reaction rates better than more sophisticated theories.

CPP 2.12 Mon 12:45 MER 02

The Crucial Role of Solvation Forces in the Steric Stabilization of Nanoplatelets — •NANNING PETERSEN, MARTIN GIRARD, ANDREAS RIEDINGER, and OMAR VALSSON — Max Planck Institute for Polymer Research, Ackermannweg 10, D-55128 Mainz

The precipitation of ligand coated cadmium selenide nanoplatelets is linked to the formation of nanoplatelet stacks. The exact nature of nanoplatelets' interaction is an open question, as the van der Waals attraction is too weak to be the cause of stack formation. CdSe nanoplatelets combine a large facet to particle size ratio, and a very dense ligand shell. Both features are in favor of interactions in the form of solvation forces.

We use coarse-grained molecular dynamics simulations of ligand coated nanoplatelets in different alkane solvents to investigate the role of solvation forces in nanoplatelet interactions [1]. We demonstrate that solvation forces resulting from solvent layering are sufficiently strong to stabilize nanoplatelet stacks. We examine the dependence of solvation forces on the nanoplatelets' ligand shell, size, and other parameters. In particular, we demonstrate that for sufficiently large nanoplatelets, solvation forces are proportional to the interacting facet area. We show that their strength is intrinsically tied to the softness of the ligand shell, depends on the isomer of the alkane solvent, and is increasing with the alkane molecule length.

[1] N. Petersen, M. Girard, A. Riedinger, and O. Valsson, ChemRxiv, doi:10.26434/chemrxiv-2022-mw1cs-v3 (2022), accepted for publication in Nano Letters

CPP 3: Hydrogels and Microgels

Time: Monday 9:30–10:30

Location: ZEU 255

CPP 3.1 Mon 9:30 ZEU 255

Acousto-responsive poly(N-isopropylacrylamide) microgels — •AMIN RAHIMZADEH, ATIEH RAZAVI, and REGINE VON KLITZING — Soft Matter at Interfaces, Department of Physics, Technical University of Darmstadt, Hochschulstraße 8, 64289 Darmstadt, Germany

In this work, we introduce a novel stimulus for Poly(N-isopropylacrylamide), known as PNIPAM, microgels. High-frequency ultrasonic waves provide the required energy for collapsing microgels while the solution temperature maintains below their volume phase transition temperature (VPTT). Ultrasound propagates through the liquid and its energy will be absorbed due to the liquid viscosity. A part of the energy will be absorbed due to the translational relaxation of the liquid molecules leading to the creation of a flow that is called acoustic streaming. Another part of the energy of the waves will be absorbed due to the rotational and vibrational relaxations of the liquid molecules. The former absorption is due to the dynamic viscosity and the latter is due to the bulk viscosity. We show that along with acoustic streaming, the absorbed energy due to the bulk viscosity provides the energy for breaking hydrogen bonds between the microgels and water molecules. The turbidity of the liquid is used as a way to visualize and quantify the energy absorption, by calculating the required energy for making the solution fully turbid. We use image processing to quantify the absorbed energy by the hydrogen bonds and investigate the effects of solution concentrations (0.2 wt.%, 1 wt.% and 5 wt.%), ultrasound amplitude and frequency.

CPP 3.2 Mon 9:45 ZEU 255

Swelling and nanophase separation of amphiphilic star polymer conetworks — •REINHARD SCHOLZ and MICHAEL LANG — Leibniz Institut für Polymerforschung, Hohe Str. 6, 01069 Dresden, Germany

Polymer conetworks consisting of complementary four functional stars coupled via complementary end groups are simulated within the framework of a lattice-based Monte Carlo algorithm. A classification of different stars reveals that the conetworks are dominated by ideal star configurations surrounded by four different bonding partners. In a good solvent, the simulation reproduces analytical scaling relations for swelling, modulus and residual bond orientation [1]. A selective solvent induces a phase separation between a swollen polymer phase and embedded clusters consisting of insoluble polymer stars. Due to the com-

plementary end groups, all elastically active chains cross the phase boundary, so that residual bond orientations correspond either to swollen conformations, collapsed stars, or bonds across the phase boundary with a particularly large component along the interface normal. Calculated pair distributions and scattering functions reveal that the length scale of phase separation depends only weakly on the concentration over a broad range of concentrations, $c^* < c < 6c^*$.

[1] M. Lang, R. Scholz, L. Löser, C. Bunk, N. Fribiczter, S. Seiffert, F. Böhme, and K. Saalwächter, Macromolecules 55, 5997 - 6014 (2022).

CPP 3.3 Mon 10:00 ZEU 255

How topology impacts magnetic and rheological properties of a suspension of magnetic nanogels — •IVAN NOVIKAU¹, ALLA DOBROSERDOVA², EKATERINA NOVAK², and SOFIA KANTOROVICH^{1,2} — ¹University of Vienna, Austria — ²Ekaterinburg, Russia

Hydrogels are soft materials, that attracted solid interest over the last 6 decades and are widely used in chemical, biomedical, and even civil engineering applications. Today, at the front edge of gels' realm stand out nanogels, often additionally functionalization, for instance, by magnetic nanoparticles.

Given the magnetic nanogels (MNG's) size, typical time and velocity scales involved in their nanofluidics, experimental characterization of the systems is difficult. Here, we use molecular dynamics (MD) simulations in conjunction with the Lattice-Boltzmann (LB) scheme in order to describe how the MNG topology affects the rheological and magnetic properties of their suspensions.

We study in detail how the shape and magnetization of a single MNG are affected by the distribution of crosslinkers: uniform, with a displaced centre of mass, with Gaussian distribution from the centre to the periphery and reverse. The impact of a topology in a combination with an external magnetic field on MNG's viscoelastic and magnetic characteristics of the suspensions is also explored.

CPP 3.4 Mon 10:15 ZEU 255

Incorporation of Hydrophilic Microgels at Water in Oil Emulsion stabilized by Hydrophobic Nanospheres — •SEBASTIAN STOCK, CARINA SCHNEIDER, LUCA MIRAU, FRANZISKA BRAUN, and REGINE VON KLITZING — TU Darmstadt, Darmstadt, Germany

For particle-stabilized emulsions (Pickering emulsions, PEs), the affinity of the particular stabilizers to one or the other liquid decides about the resulting emulsion type - either oil in water (o/w) or water in oil (w/o). Besides specific exceptions, hydrophilic microgel particles (MGs) are only able to stabilize o/w emulsions. However, the w/o emulsion type is preferable in a multitude of applications ranging from the food industry over medicine towards interfacial catalysis. We solved this problem by using well-characterized, hydrophobic, positively charged, spherical silica particles (SNs) and hydrophilic, positively charged PNI-

PAM MGs to stabilize water in 1-dodecene emulsions simultaneously. Using these thoroughly characterized model particles allows deep insights into the interplay between soft and solid particles at the interface and the structure formation of the PEs. The interaction between different kinds of particles was studied on a Langmuir trough in combination with AFM measurements. The observable structure formation at the interface of the Langmuir Trough could explain the particle assembly at the droplet interfaces in PEs.

CPP 4: Active Matter I (joint session BP/CPP/DY)

Time: Monday 9:30–13:00

Location: TOE 317

See BP 2 for details of this session.

CPP 5: 2D Materials I (joint session HL/CPP)

Time: Monday 9:30–12:30

Location: POT 81

See HL 1 for details of this session.

CPP 6: Perovskite and photovoltaics I (joint session HL/CPP)

Time: Monday 9:30–12:30

Location: POT 251

See HL 4 for details of this session.

CPP 7: Organic Semiconductors (joint session HL/CPP)

Time: Monday 9:30–11:15

Location: POT 361

See HL 2 for details of this session.

CPP 8: Responsive and Adaptive Systems

Time: Monday 10:45–13:00

Location: ZEU 255

CPP 8.1 Mon 10:45 ZEU 255

Spreading drops of volatile oil induce long range thickness gradients in swelling hydrophobic polymer brush layers — •ÖZLEM KAP¹, SIMON HARTMANN², HARMEN HOEK¹, IGOR SIRETANU¹, SISSI DE BEER³, UWE THIELE², and FRIDER MUGELE¹ — ¹University of Twente, Physics of Complex Fluids, PO Box 217, 7500 AE Enschede (NL) — ²Westfälische-Wilhelms-Universität Münster, Wilhelm-Klemm-Str. 9, 48149 Münster (D) — ³University of Twente, Sustainable Polymer Chem., PO Box 217, 7500 AE Enschede (NL)

Polymer brush layers are responsive materials that swell in contact with good solvents and their vapors. We combined optical experiments and numerical calculations based on gradient dynamics of a free energy density to study how fluid flow and solvent diffusion control the macroscopic spreading of (weakly) volatile oil drops and the swelling kinetics of an underlying hydrophobic polymer brush layer. The macroscopic spreading dynamics follow algebraic law with an exponent of 1/6, yet the spreading drops are found to be surrounded by halos of partially swollen polymer brushes. The width of the halos reaches values of hundreds of micrometers wide within hours to days, with thickness variations ranging from the dry thickness up to a maximum swelling ratio of ~4 close to the contact line. The halo profiles display long-living non-equilibrium steady state configurations that are controlled by the competition of two transport mechanisms, solvent diffusion through the polymer brush layer and through the vapor phase.

CPP 8.2 Mon 11:00 ZEU 255

Effect of architecture in thermoresponsive hydrogels from PEG-based tri- and tetrablock terpolymers — •FEIFEI ZHENG¹, WENQI XU¹, EIRINI MELAMPIANAKI¹, ANNA P. CONSTANTINO², THEONI K. GEORGIU², and CHRISTINE M. PAPADAKIS¹ — ¹TUM School of Natural Sciences, Technical University of Munich, Garching, Germany — ²Department of Materials, Imperial College, London, UK

Thermogels are an exciting class of stimuli-responsive materials with many promising applications ranging from the medical field to additive manufacturing. The mechanical properties in the gel state strongly depending on the architecture of the polymer [1]. Here, we address an ABC triblock terpolymer and a BABC tetrablock terpolymer consisting of the hydrophilic oligo(ethylene gly-

col) methyl ether methacrylate (OEGMA, A), hydrophobic *n*-butyl methacrylate (BuMA, B), and thermoresponsive di(ethylene glycol) methyl ether methacrylate (DEGMA, C). The results from dynamic light scattering on dilute solutions show that the hydrodynamic radii of the micelles formed by both, ABC and of BABC, increase strongly above 25 °C, and the solutions feature a cloud point, i.e. aggregation of the micelles sets in. By synchrotron small-angle X-ray scattering, we found that, ABC and BABC form elongated and spherical micelles, respectively. Forward scattering attributed to large aggregates is observed at temperatures above the cloud point for both terpolymers.

[1] A. P. Constantinou et al., *Macromolecules*, 2021, 54, 1943.

15 min. break

CPP 8.3 Mon 11:30 ZEU 255

Hydration Water Dynamics in a Thermoresponsive Polymer Solution Under Pressure — BART-JAN NIEBUUR¹, BAHAR YAZDANSHENAS¹, FEIFEI ZHENG¹, WIEBKE LOHSTROH², MARCELL WOLF², MARIE-SOUSAI APPAVOU³, MICHAELA ZAMPONI³, ALFONS SCHULTE⁴, and •CHRISTINE M. PAPADAKIS¹ — ¹Technical University of Munich, TUM School of Natural Sciences, Garching, Germany — ²Technical University of Munich, Heinz Maier-Leibnitz Zentrum (MLZ), Garching, Germany — ³Jülich Centre for Neutron Science (JCNS) at MLZ, Garching, Germany — ⁴University of Central Florida, Department of Physics, Orlando FL, U.S.A.

The water dynamics is key to functionality and phase behavior of synthetic and biological polymers. We investigate the dynamic behavior of hydration water in a concentrated aqueous solution of the thermoresponsive polymer poly(*N*-isopropyl acrylamide) (PNIPAM) in dependence on temperature and pressure employing quasi-elastic neutron scattering (QENS) [1]. The susceptibility spectra reveal the relaxation peak of the hydration water in addition to the known dynamic processes of bulk water. We find that the dehydration process at the phase transition depends strongly on pressure. Using perdeuterated PNIPAM along with QENS allows us to suppress the signal of the chain segments and to identify and characterize the behavior of the different types of bound water at the phase transition.

1. B.-J. Niebuur, W. Lohstroh, M.-S. Appavou, A. Schulte, C. M. Papadakis, *Macromolecules* 2019, 52, 1942.

CPP 8.4 Mon 11:45 ZEU 255

Topology Impact on nanoscale hydration of polymer brushes — •APOSTOLOS VAGIAS¹, ANDREW NELSON², PEIXI WANG³, JULIJA REITENBACH³, CHRISTINA GEIGER³, LUCAS PHILIPP KREUZER^{1,3}, THOMAS SAERBECK⁴, ROBERT CUBITT⁴, EDMONDO MARIA BENETTI⁵, and PETER MÜLLER-BUSCHBAUM^{1,3} — ¹MLZ, TUM, Garching — ²ANSTO, Sydney, Australia — ³TUM School of Natural Sciences, Chair for Functional Materials, Garching — ⁴ILL, Grenoble, France — ⁵Polymer Surfaces Group, University of Padova, Padova, Italy

Polymer brushes have demonstrated growing interest during last years, in particular in combination with exposure to aqueous environment. By utilizing time-of-flight neutron reflectometry (ToF-NR), we correlate the swelling properties of hydrophilic cyclic grafted polymer brushes to their thermodynamics. Cyclic brushes exhibit more compact conformations with lower roughness compared to their linear analogues, due to the absence of dangling chain ends extending at the interface. In addition, due to increased interchain steric repulsions, cyclic brushes feature larger swelling ratios at the same composition and comparable molar mass. Moreover, the two topologies exhibit differences in ageing, upon repetitive swelling/drying cycles. We present a case where current Flory-like expressions breakdown in the explanation of the experimental observations.

CPP 8.5 Mon 12:00 ZEU 255

Spiropyran/Merocyanine Amphiphile in Various Solvents: A Joint Experimental-Theoretical Approach to Photophysical Properties — VLADYSLAV SAVCHENKO¹, NINO LOMADZE², SVETLANA SANTER², and •OLGA GUSKOVA¹ — ¹IPF Dresden — ²University of Potsdam

This joint experimental-theoretical work explains the negative photochromism of spiropyran-containing (SP) amphiphile aqueous solutions. Experiments demonstrate that the orange-red merocyanine (MC) form becomes thermodynamically more stable in water, and both UV and vis stimuli lead to the partial or complete photobleaching of the solution. The explanation of this phenomenon is given on the basis of DFT calculations and MD simulations. The latter reveal that stabilization of MC in water proceeds with the energy of ca. 70 kJ/mol, and that the Helmholtz free energy of hydration of MC form is 100 kJ/mol lower. The explanation of such a difference lies in the molecular properties of the MC. The presence of three charged groups on the periphery of a flat MC backbone stimulates its self-assembly in water ending up with the formation of elongated associates with stack-like building blocks. Our quantitative evaluation of the hydrophilicity switching in SP/MC containing surfactants may prompt the search for new systems, including colloidal and polymeric ones, aiming at remote tuning of their morphology, which could give new promising shapes and patterns for the needs of modern nanotechnology. This work is supported by DFG, grant GU1510/5-1. [1] Savchenko V., et al. Int. J. Mol. Sci. 2022, 23(19), 11535

CPP 8.6 Mon 12:15 ZEU 255

Mechanochemistry: a theoretical and experimental interplay — •MICHAEL WALTER, Wafa MAFTUHIN, and POOJA BHAT — Albert-Ludwigs-Universität Freiburg, Freiburg i. Br., Germany

Mechanochromic polymers are intriguing materials that allow to sense force of specimens under load. The connection between macroscopic stress and the forces acting on the molecular level is still elusive and covalently incorporated molecular mechanochromophores promise to shed light on this connection. Most mechanochromic systems rely on covalent bond scission with optically distinct *on* and *off* states. Bond rupture is induced by temperature fluctuations involving force dependent barriers. We show that these barriers are fully determined by the dissociation energy and the maximal force the potential can withstand, which allows for a re-interpretation of the Eyring-Zhurkov-Bell length

Δx^\ddagger and the expressions going beyond.

We furthermore present and analyse the concept of mechanochromic donor-acceptor (DA) torsional springs that allows for a continuous mapping of molecular forces to photoluminescence wavelengths. The mechanically induced deflection from equilibrium geometry of the DA spring is theoretically predicted and reveals forces of 1 nN on the molecular level. Our theoretical analysis demonstrates a thiophene ring flip as the major part of the overall mechanochromic response within a related ansa-DAD spring at forces as low as 27 pN. Such micromechanical motion gives access to sensing of tiny forces and expands both sensitivity and the force range of conformational mechanochromophores.

CPP 8.7 Mon 12:30 ZEU 255

Humidity & Electrochemical Switching of Mixed Conducting Polymer Films — •SABINE LUDWIGS — IPOC - Functional Polymers, Institute of Polymer Chemistry, University of Stuttgart

Though electrochemistry of conducting polymers is a rather old topic(1), only recently conducting polymers have received renewed attention as inherently mixed-ionic-electronic conductors for a number of emerging switchable technologies including actuators, wetting on surfaces and electrically switchable metasurfaces. One of the work-horses of the community remains poly(ethylenedioxythiophene) :poly(styrenesulfonate) (PEDOT:PSS). While typically known as synthetic metal with application as transparent flexible electrodes, the material is a mixed conductor and shows ionic conductivity which is strongly affected by humidity.(2) The humidity dependence of the PSS polyelectrolyte phase together with the electroactive nature of the PEDOT can be used to create multifunctional and multiresponsive materials and films. A recent example from my group is the preparation of intelligent humidity-triggered bilayer actuators whose bending behavior (curvature) can be explained by the humidity-dependent mechanical behavior of the constituents.(3) In collaboration with the Giessen Group the electrochemical stimuli were further used to switch nanoantennas on and off between the metallic and the insulating state.(4)

Ref: (1) Chemical Reviews 2010, 110, 4724.(2) ACS Applied Materials & Interfaces, 2020, 12, 6742. (3) Advanced Materials 2021, 202007982. (4) Science 2021, 374, 612.

CPP 8.8 Mon 12:45 ZEU 255

Stimuli-responsive high aspect ratio surfaces for wetting studies — •GISSELA CONSTANTE¹, INDRA APSITE¹, PAUL AUERBACH², SEBASTIAN ALAND³, DENNIS SCHÖNFELD³, THORSTEN PRETSCH³, PAVEL MILKIN¹, and LEONID IONOV^{1,4} — ¹Uni Bayreuth, Bayreuth, Germany — ²HTW Dresden, Dresden, Germany — ³Fraunhofer IAP, Postdam, Germany — ⁴BPI, Bayreuth, Germany

The fabrication of switchable surfaces has been of interest in several fields such as biotechnology, industry, and others. The selection of materials and methods is crucial to provide proper control on the tunable surface. In this research, an exceptionally high aspect ratio lamellar surface topography was fabricated by melt-electrowriting of microfibers of a shape-memory thermo-responsive polyurethane. Two different types of stimuli: temperature and light exposition were applied to modify the mechanical properties and by it the deformation and recovery of the original surface. Wetting studies showed that the deformation of the high aspect ratio lamellar surface can be tuned not only manually, but as well by a liquid droplet. This behavior is controlled by variation of temperature conducted by direct heating/cooling or by exposure to light when the lamellae were stained with black ink. The liquid in combination with thermo-responsive topography presents a new type of wetting behavior. This feature opens the possibility to apply such topographies for the design of smart elements for microfluidic devices, for example, smart valves.

CPP 9: Organic Thin Films, Organic-Inorganic Interfaces (joint session DS/CPP)

Time: Monday 11:30–12:45

Location: SCH A 315

See DS 3 for details of this session.

CPP 10: Instrumentation and Methods for Micro- and Nanoanalysis (joint session KFM/CPP)

Chair: Prof. Dr. Theo A. Scherer (KIT Karlsruhe)

Time: Monday 14:30–15:30

Location: POT 106

See KFM 3 for details of this session.

CPP 11: Focus: Organic Solar Cells Based on Non-fullerene Acceptors: Loss Mechanism and Options for Above 20 % Efficiencies II

Organized by Dieter Neher and Christoph J. Brabec

Time: Monday 15:00–17:15

Location: GÖR 226

Invited Talk CPP 11.1 Mon 15:00 GÖR 226

Quantifying the potential of organic solar cells using luminescence measurements and modelling — •JENNY NELSON — Department of Physics, Imperial College London, SW7 2AZ, UK

In a molecular photovoltaic device, charge separation and energy conversion result from the evolution of a photogenerated exciton into a charge separated state, in competition with recombination to ground. Recently, new molecular materials have increased power conversion efficiency to approach 20%. To make further advances, we need to understand and isolate the effects of chemical structure, molecular packing, energetics and disorder on the competition between charge separation and recombination and hence on device efficiency. Electro- and photoluminescence have proved to be valuable tools to probe the energy and dynamics of excited states involved in photoinduced charge separation, and indirectly of the structure of molecular interfaces. Combined with other spectroscopic techniques, electrical measurements and modelling, luminescence can help us to understand how chemical and physical structure control the basic mechanisms in photovoltaic conversion. We show how such an approach can be used to study the properties and role of charge transfer states, the impact of structural and energetic disorder and to infer structure-property relationships. We apply a computational model that integrates the molecular charge transfer process with a one-dimensional drift-diffusion simulation to interpret experimental measurements and explore the effects of parameters on device performance. We consider the ultimate limits placed on solar to electric conversion by the molecular nature of the materials.

CPP 11.2 Mon 15:30 GÖR 226

Increasing the ionization offset to increase the quantum efficiency in non-fullerene acceptor based organic solar cells: How far can we go? — •JULIEN GORENFLOT, WEJDAN ALSUFYANI, MARYAM ALQURASHI, SRI HARISH KUMAR PALETI, ANIRUDH SHARMA, DERYA BARAN, and FRÉDÉRIC LAQUAI — KAUST Solar Center, King Abdullah University of Science and Technology, Thuwal, Kingdom of Saudi Arabia

Molecular engineering offers a virtually unlimited number of unique semiconductors for organic photovoltaics applications, that can be tailored to adapt specific needs, but only a handful of combinations enables to reach state-of-the-art efficiencies. Rules are thus strongly needed to guide the design of promising systems. A recently unraveled rule is that the electron acceptor molecule requires an ionization energy 0.5 eV deeper than that of the electron donor to overcome the bending of the energy levels at the donor acceptor heterojunction interface, maximizing the charge transfer, hence the cell's quantum efficiency. Here we study the energy losses associated to this ΔIE increase. Based on 30+ blends, we show that those losses remain minimal up to an offset of 0.7 eV. We then use electroluminescence spectroscopy to evaluate the charge transfer state energy (E_{CT}) and find that this low energy losses range is associated to E_{CT} remaining at most similar to the NFA's optical bandgap ($E_{g,NFA}$), while further ΔIE increase pulls E_{CT} below $E_{g,NFA}$, accordingly decreasing V_{OC} . We finally study the evolution of the fill factor (FF) within this maximum quantum efficiency – minimal energy losses ΔIE range.

CPP 11.3 Mon 15:45 GÖR 226

The excess energy optimum to minimize recombination losses in organic solar cells — •CLEMENS GÖHLER, ALEXANDER FLAMM, and MARTIJN KEMERINK — Institute for Molecular Systems Engineering and Advanced Materials, Universität Heidelberg, Im Neunheimer Feld 225, 69120 Heidelberg

Semiconductor blends that incorporate non-fullerene acceptors (NFA) have pushed organic solar cells to efficiency records based on an established principle: enhancing the generation yield of free charge carriers from tightly bound molecular excitations via interfacial charge transfer between donor and acceptor phases. Their success can in huge parts be attributed to an increase of the photocurrent; however, in comparison to less-effective systems, NFA blends possess a similar overall absorbance and lack the distinct low-energy absorption typically associated with charge transfer (CT) excitons.

The increased charge carrier densities are thus based on reduced recombination yields. As further improvements of the photocurrent are necessary to reach higher efficiencies, a thorough understanding of the mechanisms behind the cut in recombination losses compared to fullerene solar cells is invaluable. To contribute, we have investigated recombination signatures of both systems with respect to the available excess energy by combining field and excitation dependent electro-optical absorption spectroscopy in the steady state and close to solar cell working conditions with kinetic Monte-Carlo simulations. Our findings indicate towards an optimal excess energy which minimizes non-geminate recombination in CT processes.

CPP 11.4 Mon 16:00 GÖR 226

On the impact of the energy level offset on carrier recombination in organic non-fullerene acceptor-based solar cells — •NURLAN TOKMOLDIN¹, BOWEN SUN¹, FLORIANA MORUZZI², OBAID ALQAHTANI³, BRIAN COLLINS³, IAIN McCULLOCH², DIETER NEHER¹, and SAFA SHOAEI¹ — ¹University of Potsdam, Potsdam-Golm, Germany — ²University of Oxford, Oxford, UK — ³Washington State University, Pullman, USA

The energetic offset between the highest occupied molecular orbital (HOMO) levels of the donor and acceptor components of the organic photovoltaic (OPV) blends is well-known to affect the efficiency of the singlet exciton (S1) dissociation into separated charges (CS) via the charge-transfer (CT) state, however the impact of this offset on bimolecular recombination of free charge carriers has not been explored. In this study, using three different non-fullerene acceptors Y6, ITIC and o-IDBTR, blended with the same donor polymer PM6, we demonstrate that, apart from reducing the driving force for charge generation, diminishing HOMO-HOMO energy offset also activates exciton reformation as a channel for bimolecular recombination of free charges. This is accompanied by the rise in the respective bimolecular recombination coefficient, which in turn influences the device fill-factor. Using the comparison between PM6:ITIC and PM6:o-IDBTR, we show that neither morphology, nor carrier mobilities can on their own explain the observed difference in performance, signaling the importance of the energy landscape in controlling the OPV device efficiency, both through generation and recombination of charge carriers.

15 min. break

CPP 11.5 Mon 16:30 GÖR 226

Relating free charge carrier generation and field induced photoluminescence quenching in a non-fullerene-based organic blend with a low energy offset — •MANASI PRANAV¹, THOMAS HULTZSCH¹, BOWEN SUN¹, RONG WANG², SAFA SHOAEI¹, LARRY LÜER², CHRISTOPH BRABEC², and DIETER NEHER¹ — ¹Institute of Physics and Astronomy, University of Potsdam, 14476 Germany — ²Institute of Materials for Electronics and Energy Technology (i-MEET), Friedrich-Alexander-Universität Erlangen-Nürnberg Martensstrasse 7, 91058 Erlangen, Germany

Many studies currently target the process of free charge carrier generation and recombination in relation to the energy level offset in organic blends based on non-fullerene acceptors (NFA). Here, we add to this discussion with a focus on the NFA Y5, characterized by a smaller highest occupied molecular orbital offset in PM6:Y5 compared to PM6:Y6, despite molecular similarity between Y5 and Y6. We find that the PM6:Y5 blend exhibits a pronounced field-dependence of free charge generation, as measured with the time-delayed collection field (TDCF) technique. We verify this with a new arbitrary-waveform TDCF technique that provides finer control over the time-delay parameters. In addition to this, we also observe a surprisingly pronounced effect of the electric field on both the steady state photoluminescence (PL) intensity and the transient PL lifetime. These results indicate that the field dependence of photo-current, free charge carrier generation and PL quenching in this low-offset system are governed by the same mechanism: likely field-induced exciton dissociation.

CPP 11.6 Mon 16:45 GÖR 226

Field Dependent Exciton Dissociation in Single-Component Organic Non-fullerene Acceptor Solar Cells — •FLURIN EISNER, MOHAMMED AZZOUI, and JENNY NELSON — Blakett Laboratory, Imperial College London, South Kensington, SW7 2AZ, UK

Improvements in the molecular design of non-fullerene acceptors (NFAs) has almost doubled the power-conversion efficiency (PCE) of organic photovoltaics in the last 5 years, from 11 to 19%. However, the exact molecular reasons behind why some acceptors (e.g. Y-series) perform better than others (e.g. ITIC-series) remain unclear. Interestingly, recent studies have shown that some of the most efficient non-fullerene acceptors can achieve relatively high charge-generation efficiency in the absence of a donor-acceptor interface, challenging the current understanding of how photogenerated excitons dissociate into free charges in organic solar cells.

Here, we study the charge-generation processes in a series of NFA molecules in single-component devices, including A-DA*D-A-type acceptors (e.g. Y6) and A-D-A type acceptors (e.g. ITIC) using optoelectronic and spectroscopy characterisation methods under strong applied fields and at different temperatures. By combining experimental results with molecular and device-level calculations, we link exciton and charge dissociation efficiency in NFA films to molecular pa-

rameters such as reorganisation energy and electronic coupling. We use this to suggest how to design materials with both higher single-component device performance and how to improve heterojunction device performance beyond 20% PCE.

CPP 11.7 Mon 17:00 GÖR 226

Triplet Excitons and associated Efficiency-Limiting Pathways in NFA-based Organic Solar Cell Blends — JEANNINE GRÜNE^{1,2}, GIACOMO LONDI³, ALEXANDER J. GILLET², YOANN OLIVIER³, VLADIMIR DYAKONOV¹, and •ANDREAS SPERLICH¹ — ¹Experimental Physics 6, Julius Maximilian University of Würzburg, Germany — ²Cavendish Laboratory, University of Cambridge, UK — ³Laboratory for Computational Modeling of Functional Materials, Université de Namur, Belgium

Organic solar cells (OSC) have made great progress in recent years, but are now reaching a performance plateau. Triplet states are known to adversely affect efficiency by opening a channel for non-radiative recombination pathways. Here, we use the complementary spin-sensitive methods of photoluminescence detected magnetic resonance (PLDMR) and transient electron paramagnetic resonance (trEPR) corroborated by transient absorption and quantum-chemical calculations to unravel exciton pathways in OSC blends employing the (non-) halogenated polymer donors PBDB-T, PM6 and PM7 together with NFAs Y6 and Y7. We reveal that all blends form triplet excitons on the NFA populated via non-geminate hole back transfer and, in blends with halogenated donors, also by spin-orbit coupling driven intersystem crossing. Identifying these triplet formation pathways in all tested solar cell absorber films highlights the untapped potential for improved charge generation to further increase efficiencies.

CPP 12: Modeling and Simulation of Soft Matter II

Time: Monday 15:00–17:15

Location: MER 02

Invited Talk

CPP 12.1 Mon 15:00 MER 02

Adaptive Resolution Simulations: Past, Present and Open (Boundaries) Future — LUIS A. BAPTISTA, MAURICIO SEVILLA, KURT KREMER, and •ROBINSON CORTES-HUERTO — Max-Planck-Institut für Polymerforschung, Mainz, Deutschland

Soft-matter systems challenge computational methods because interactions spanning a wide range of lengths and time scales require a multiscale approach capable of describing open systems and non-equilibrium conditions. Nonetheless, a high-resolution method is often only necessary to describe a relatively small portion of the system, embedded in a less detailed environment or even a particle reservoir. In this context, the adaptive resolution simulation (AdResS) method provides a seamless interpolation between high- and low-resolution descriptions: both concurrently present within the simulation box in a thermodynamically consistent framework.

In this talk, we introduce the AdResS method and present a few applications as a multiscale simulation protocol. By reducing the complexity of the low-resolution model and describing it as an ideal gas, it is practically possible to control the chemical potential of the system. In this context, we show extensions of AdResS as an efficient method to compute chemical potentials and solvation free energies in complex molecular systems. We also discuss its recent development into an open-boundary method to perform grand canonical and non-equilibrium molecular dynamics simulations. Finally, we examine possible extensions and challenges of developing the method into an open adaptive QM/MM approach.

CPP 12.2 Mon 15:30 MER 02

Chirality propagation across length scales: the case of knots in helical polymers — YAN ZHAO¹, JAN ROTHÖRL², POL BESENIUS³, PETER VIRNAU², and •KOSTAS DAOULAS¹ — ¹Max Planck Institute for Polymer Research, Mainz, Germany — ²Department of Physics, Johannes Gutenberg University, Mainz, Germany — ³Department of Chemistry, Johannes Gutenberg University, Mainz, Germany

We use computer simulations to investigate the effect of helicity in isolated polymers on the topological chirality of their knots. Polymers are described by worm-like chains (WLC), where chiral coupling between segments promotes helical conformations. The sign and magnitude of the coupling coefficient u determine the sense and strength of helicity. The excluded volume is adjusted via the radius R of a hard sphere placed at each WLC segment. Open and compact helices are, respectively, obtained for R that is zero or smaller than the length of the WLC bond, and R that is a few times larger than the bond length. We perform Monte Carlo sampling of polymer conformations for u spanning a broad range of values, from achiral polymers to polymers with well-developed helices. First, we demonstrate that the coil-helix transition in our model is not a phase transition but a crossover. Next, we perform statistical analysis of knotted polymer conformations and demonstrate that the sense of polymer helicity, left- or right-handed, influences the handedness of molecular knots and identify a generic mechanism that underlies this effect.

CPP 12.3 Mon 15:45 MER 02

Dynamics of the Rouse-mode distribution of a Gaussian chain in an external field and connection to spinodal decomposition — •DAVID STEFFEN¹, JÖRG RÖTTLER², and MARCUS MÜLLER¹ — ¹Institut für Theoretische Physik, Georg-August-Universität, 37077 Göttingen, Germany — ²Department of Physics and Astronomy and Stewart Blusson Quantum Matter Institute, University of British Columbia, Vancouver, British Columbia V6T 1Z1, Canada

The current description of spinodal decomposition of a homopolymer blend via dynamic self-consistent field theory (D-SCFT) is based on the density of the monomers and uses a time-independent Onsager coefficient. This is sufficient for long wavevectors where the dynamics can be solely described by the diffu-

sion of the center of mass. On small timescales and for larger wavevectors the dynamic is influenced by subdiffusive processes inside the chain. Therefore, a more microscopic description is needed. In this work, we provide an analytical solution for the time-dependent Rouse-mode distribution of a single chain in a weak external field. The time-dependent monomer density can then be obtained via a projection from the Rouse-mode distribution. Although different Rouse-mode distributions yield the same monomer density, an accurate description of the dynamics of the density requires the more microscopic description via the Rouse-modes distribution. This technique can be extended to the spinodal decomposition of a binary homopolymer melt. We compare the analytical results for the density and the Rouse-mode distribution to Monte-Carlo simulations of Gaussian chains.

CPP 12.4 Mon 16:00 MER 02

Simulation of diblock-copolymer membrane fabrication — •NIKLAS BLAGOJEVIC und MARCUS MÜLLER — Universität Göttingen, Institut für Theoretische Physik

Diblock copolymers can be used to create integral asymmetric membranes used for ultrafiltration purposes – for example water purification. The combination of evaporation-induced self assembly (EISA) and non-solvent induced phase separation (NIPS) is a promising way for efficient membrane fabrication. The importance of different time- and length-scales makes it difficult to investigate the influence of processing parameters and molecular architecture in experiments. We use a coarse-grained particle based model in conjunction with the Single-Chain in Mean Field (SCMF) algorithm to simulate membrane fabrication with EISA and SNIPS to understand how the membrane structure is formed and how it can be tailored by different processing parameters and varying molecular architecture. For example, we find that nonsolvent macrovoids in the membrane substructure coarsen with an increasing distance into the membrane, while an increasing incompatibility between nonsolvent and polymer leads to more narrow and straight macrovoids.

15 min. break

CPP 12.5 Mon 16:30 MER 02

Salt effects on N-isopropylacrylamide in aqueous solutions. Experimental measurements, Kirkwood-Buff theory and computer simulation — JAKUB POLÁK, •DANIEL ONDO, and JAN HEYDA — Department of Physical Chemistry, University of Chemistry and Technology, Prague, Technická 5, 166 28 Prague 6, Czech Republic

In this work, we investigate salt-specific effects on N-isopropylacrylamide (NiPAM) by means of densimetry and vapor pressure osmometry, employing family of sodium and guanidinium salts from low NiPAM concentration up to the solubility limit. Employing Kirkwood-Buff (KB) theory, complete set of effective pair interactions, KB-integrals, at any composition are determined, serving as a bridge to well calibrated molecular dynamics (MD) simulation. All atom MD simulations were used in direct analogy to the experiments and volumetric properties determined. For the first time, in-silico vapor pressure osmometry experiment was performed and excess osmolality evaluated from ternary structure. Finally, we establish a strong correlation between salt effect on NiPAM hydration and the salting-out ability of studied salts.

CPP 12.6 Mon 16:45 MER 02

Evaporation-induced confinement assembly of functional terpolymer microparticles — •ELIAS M. ZIRDEHI¹, MANUEL TRÖMER², ANDRÉ H. GRÖSCHEL², and ARASH NIKOUBASHMAN¹ — ¹Institute of Physics, Johannes Gutenberg University Mainz — ²Institute of Physical Chemistry, University of Münster

Evaporation-induced confinement assembly of terpolymers is an effective technique for fabricating internally structured microparticles (MPs). The wide range

of usable building blocks allows for a large variety of MPs, but poses also an immense challenge due to the staggering amount of process parameters, which cannot be explored through experiments alone. Therefore, we performed dissipative particle dynamics simulations of a bead-spring model to study the directed assembly of triblock copolymers in evaporating droplets. We developed a semi-grand canonical simulation approach, where droplet particles in the vapor phase are periodically removed to drive evaporation at constant flux. In this model, the evaporation rate is controlled by the frequency and the number of particle removal. The resulting shrinking of the droplet was in excellent agreement with theory and experiments. We then implemented this procedure to investigate how the final morphology of terpolymer MPs is influenced by the evaporation rate as well as surfactant type. Finally, the possibility of altering the morphology tailored for specific applications by adding homopolymers will be discussed.

CPP 12.7 Mon 17:00 MER 02

Wavenumber dependent viscosity of a system of particles coupled dissipatively to a Lattice Boltzmann fluid — •JOYDIP CHAUDHURI¹ and BURKHARD DÜNWEG^{1,2} — ¹Max Planck Institute for Polymer Research, Ackermannweg 10, 55128 Mainz, Germany — ²Department of Chemical and Biological Engineering, Monash University, Clayton, Victoria 3800, Australia

We consider a particle based Molecular Dynamics (MD) system coupled dissipatively to a stochastic Lattice Boltzmann (LB) fluid. The employed force coupling method is dissipative which means that the velocity of an MD particle is damped with respect to the velocity of the LB fluid interpolated to the position of the particle. The present study explores the viscosity response of such a coupled LBMD system due to a sinusoidally varying external force. The analytic theory for that system is based upon a two-fluid model, whose predictions are well corroborated by numerical tests. Except for the respective viscosities of the two uncoupled fluids, the total viscosity of the coupled system depends on a hydrodynamic screening length associated with the Stokes coupling parameter, the mass density ratio, and the wavenumber of the applied external force. In the asymptotic long-wavelength limit, the total viscosity is just the sum of the two input viscosities. This behavior deviates significantly from the well known Einstein prediction for dilute colloidal dispersions, and this is due to the different type of particle-fluid coupling.

CPP 13: Composites and Functional Polymer Hybrids

Time: Monday 15:00–18:00

Location: ZEU 255

Invited Talk

CPP 13.1 Mon 15:00 ZEU 255

Nanocomposites and polymer thin films: from gas phase synthesis to functional applications — •FRANZ FAUPEL, STEFAN SCHRÖDER, ALEXANDER VAHL, SALIH VEZIROGLU, CENK AKTAS, and THOMAS STRUNSKUS — Chair for Multi-component Materials, Faculty of Engineering, Kiel University, Kiel, Germany
Highly filled particulate metal-dielectric nanocomposites films have unique functional properties with hosts of applications. To explore collective interactions between the particles, we control the particle separation on the nm scale by employing vapor phase deposition, which is a scalable approach permitting, inter alia, excellent control of the filling factor. For deposition of functional polymer thin films, we have recently used initiated chemical vapor deposition (iCVD) to avoid decomposition of the functional groups. Examples include highly stable electrets for electret microphones and magnetoelectric sensors, 3D superhydrophobic coatings, nanoscale gradient copolymers, and strain-invariant conductors for soft robotics. For the fabrication of the nanocomposites, the nanoparticles can form during gas phase co-deposition via self-organization or by means of high-rate gas aggregation cluster sources, which provide independent control of filling factor and size as well as in situ monitoring and control of composition. Recent examples of nanocomposites range from plasmonic meta-materials through photoswitchable molecular plasmonic systems to memristors and memsensors for neuromorphic electronics. We also explored nanoscale synergetic effects of plasmonics and photocatalysis, e.g. for photoinduced enhanced Raman spectroscopy (PIERS).

CPP 13.2 Mon 15:30 ZEU 255

Rheological optimization of filler packings using micro scale simulations — •OLIVER ROSER^{1,2}, ANDREAS GRIESINGER³, and OTHMAR MARTI² — ¹Center for Heat Management (ZFW), Stuttgart — ²Institute of Experimental Physics, Ulm University — ³Baden-Wuerttemberg Cooperative State University (DHBW) Stuttgart

In a wide range of applications, polymers are modified with granular fillers to improve thermal or electric conductivity. The higher the amount of filler, the higher the conductivity. However, the attainable conductivity is restricted by processing limitations as the amount of filler also affects the composites viscosity. Only a clever combination of filler with multimodal size distributions can shift this limit and allow for higher amounts of filler without significant viscosity increase. The effect of multimodal packing structures on viscosity has already been investigated in several experimental and numerical studies, however common calculation techniques are mainly restricted to spherical and equal-sized filler particles. We extended common approaches with new packing simulations, considering the actual size distribution and shape of different filler materials. We implemented numerical packing optimization to find the best filler compositions for highly filled polymers with up to 80 v%. In this talk we will introduce the new packing simulations and their use for packing optimizations and present the acquired results and experimental validations.

CPP 13.3 Mon 15:45 ZEU 255

Increasing the Electrical Conductivity of Polymer Thin Films for Thermoelectric Applications — •MARIE SIEGERT¹, MARKUS HÖNIG², MICHAEL SOMMER², and JENS PFLAUM^{1,3} — ¹University of Würzburg — ²Chemnitz University of Technology — ³ZAE Bayern

Thermoelectric generators based on sustainable, low-cost organic materials harbor great potential for waste heat recovery. Polymer thin films in particular can be easily upscaled to meet industrial standards and display aptly low thermal conductivity κ , but lack high electrical conductivity σ . However, the augmentation of σ imposes a major challenge as an increase in charge carrier concentration is usually accompanied by an unintentional decrease of the Seebeck coefficient S , which is detrimental for efficient thermoelectrics. Hence, we compare two possible strategies to enhance the charge carrier transport in such disordered systems. Firstly, doped polymer thin films utilizing the temperature activated n-type dopant TAM have been characterized regarding their thermoelectric properties. Secondly, composite films have been investigated, combining well studied polymers with metallic additives. Both approaches will be evaluated with respect to the enhancement in σ and the underlying transport mechanisms. First estimations of the resulting power factors indicate future strategies to further refine the electronic properties and thus, the thermoelectric figure of merit. The Deutsche Bundesstiftung Umwelt (DBU) is acknowledged for financial support.

CPP 13.4 Mon 16:00 ZEU 255

Conductivity of filled diblock copolymer systems. — •ALEXANDER CHERVANYOV — Institut für Theoretische Physik, Westfälische Wilhelms-Universität Münster, Münster, Germany

The reported work looks into the effect of stimuli-induced morphological changes in the composite consisting of insulating diblock copolymers (DBC) and conductive nanoparticles (NP) on the conductivity of this composite. The relation between the nano-structure of the described composite and its conductivity is studied by developing and making use of the multiscale computational approach. This approach relies on the consistent phase-field model of DBC, Monte-Carlo simulations of the filler distribution in DBC, and the resistor network model of the composite conductivity. The dependencies of the conductivity on the temperature of the composite, DBC morphology, and the affinities of fillers for copolymer blocks are studied in detail. In particular, the order-disorder transition in the host DBC system is found to be accompanied by the conductor-insulator transition in the filler network. The order-order transition between the lamella and cylindrical microphases of DBC proves to co-occur with a spike of the composite conductivity caused by restructuring of the conductive filler network.

15 min. break

CPP 13.5 Mon 16:30 ZEU 255

Modeling micro-structure evolution and its impact on moduli in magnetoactive elastomers — •MEHRAN ROGHANI, DIRK ROMEIS, and MARINA SAPHIANNIKOVA — Leibniz-Institut für Polymerforschung Dresden, Germany

Magneto Active Elastomers (MAEs) are field-controllable composites made of micron-sized, magnetizable particles embedded into a soft elastomeric matrix. These materials show a strong coupling between their mechanical properties and an applied magnetic field. The coupling can be directly related to magnetic interactions between the particles, which lead to the evolution of microstructure under the field. In the case of initially isotropic MAEs, this micro-structure evolution results in chains forming from the magnetized particles. This in turn causes

a huge increase in the mechanical moduli along the field direction, leading to anisotropic behavior. We consider a transversely isotropic material model for the mechanics, and magnetic interactions are taken into account by the dipolar mean field approach. To couple the mechanical and magnetic effects, a restructuring parameter is introduced which is a function of material magnetization and moduli. This modeling approach improves our understanding of how microstructure evolution affects magnetically induced material deformation and stiffness. The first predictions are in good agreement with experimental results available in the literature. We thank the DFG for financial support through RTG-2430.

CPP 13.6 Mon 16:45 ZEU 255

Magneto-active elastomers: From composite structure to effective susceptibility — •DIRK ROMEIS and MARINA SAPHIANIKOVA — Leibniz-Institute of Polymer Research Dresden e.V.

Embedding magnetizable particles into elastic polymer network yields a field-controllable material known as magneto-active elastomer (MAE). In order to describe macroscopic samples of such composite material it is useful to develop an effective macro-continuum model. Based on the dipole approximation, we derive analytic relations for the effective magnetization behavior in MAEs, spanning from linear to saturation regime, for isotropic and anisotropic particle arrangements. In the limiting case of linear magnetics and isotropic distributions we reproduce an expression known from previous works. Accordingly, we believe that the present homogenization scheme provides a general description of the effective magnetic behavior with high practical relevance also in case of anisotropic distributions and beyond the linear magnetization. For a given particle arrangement and magnetization model on microscale, the solutions are obtained with low computational effort. Furthermore, the present formulation can be directly implemented into a macroscopic material model for a composite sample of specified shape. It turns out, that an anisotropic particle distribution has an equivalent effect as an anisometric sample shape.

CPP 13.7 Mon 17:00 ZEU 255

Tuning the thermal conductivity of magnetic gels and elastomers — GUSTAV J. L. JÄGER, •LUKAS FISCHER, TYLER LUTZ, and ANDREAS M. MENZEL — Institut für Physik, Otto-von-Guericke-Universität Magdeburg, Magdeburg, Germany
When an external magnetic field is applied to magnetic gels or elastomers—composite materials consisting of magnetic or magnetizable particles inside an elastic matrix—these materials typically exhibit interesting deformational (magnetostrictive) responses or changes in rheological properties (magnetorheological effect).

We study how the induced magnetic interactions lead to an internal restructuring of the magnetic particles, mainly the formation of particle chains along the direction of the external magnetic field. This behavior is not only connected to the aforementioned effects, it can also change the thermal conductivity of the magnetic gels and elastomers, which we focus on here. We analyze this phenomenon numerically for 2D mesoscopic (particle-resolved) models of magnetic gels and elastomers [1], thus characterizing thin elastic films and membranes.

Our results indicate significant magnetically induced changes in the thermal conductivity. The influence of several parameters on this effect is investigated, such as the density and number of magnetizable particles, the amplitude of their magnetization, and the aspect ratio of the systems. Similar changes in the electric conductivity of magnetic gels and elastomers are expected.

[1] G. J. L. Jäger, L. Fischer, T. Lutz, A. M. Menzel, *J. Phys.: Condens. Matter* **34**, 485101 (2022).

CPP 13.8 Mon 17:15 ZEU 255

Morphology evolution and nanoparticle localization in printed hybrid nanoparticle-diblock copolymer thin films investigated by in situ GISAXS — •CHRISTOPHER R. EVERETT¹, GUANGJIU PAN¹, MANUEL A. REUS¹, DAVID KOSBAHN¹, FRANK HARTMANN², MARTIN BITSCH², MATTHIAS OPEL³, MARKUS GALLET², MATTHIAS SCHWARTZKOPF⁴, and PETER MÜLLER-BUSCHBAUM^{1,5} — ¹TUM, TUM School of Natural Sciences, Chair for Functional Materials, 85748

Garching — ²Saarland University, LS Polymer Chemistry, 66123 Saarbrücken — ³Walther-Meißner-Institut, Bayerische Akademie der Wissenschaften, 85748 Garching — ⁴DESY, 22607 Hamburg — ⁵MLZ, TUM, 85748 Garching

The diblock copolymer (DBC) PS-*b*-PMMA forms films with periodic ordered nanostructures that can act as scaffolds for inorganic magnetic nanoparticles. These films have application as magnetic sensors and in magnetic data storage devices. Film formation and the resulting magnetic properties both depend on the localization of the nanoparticles in the DBC domains. In this investigation, ultra-high molecular weight PS-*b*-PMMA films containing two types of nanoparticles, cobalt ferrite and nickel, are fabricated by a slot-die coating technique. Grazing incidence small-angle X-ray scattering (GISAXS) is used to monitor in situ the morphological evolution of the DBC films and nanoparticle segregation in the films during the deposition and drying process. The magnetic properties of the hybrid films are investigated with a SQUID magnetometer.

CPP 13.9 Mon 17:30 ZEU 255

Tunable mesoporous zinc titanate films via diblock copolymer-directed cooperative self-assembly and a sol-gel technique — •YANAN LI¹, NIAN LI¹, SHANSHAN YIN¹, CONSTANTIN HARDER², YUSUF BULUT², APOSTOLOS VAGIAS³, STEPHAN V. ROTH^{2,4}, and PETER MÜLLER-BUSCHBAUM^{1,3} — ¹TUM School of Natural Sciences, Chair for Functional Materials, 85748 Garching, Germany — ²DESY, 22607 Hamburg, Germany — ³MLZ, TUM, 85748 Garching, Germany — ⁴Department of Fiber and Polymer Technology, KTH, SE-100 44 Stockholm, Sweden

Mesoporous ordered films have broad applications ranging from sensors to supercapacitors and biodevices due to their large specific surface area and pore accessibility of their porous nanostructures. Here, we investigate the evolution and formation mechanisms of morphologies of mesoporous zinc titanate films obtained by changing the ratio of two inorganic precursors after calcining hybrid films consisting of organic-inorganic materials. The amphiphilic diblock copolymer self-assembles into micelles in a mixture of N,N-dimethylformamid/hydrogen chloride playing the role as structure directing template. The inorganic precursors are loaded in the micellar shell due to hydrogen bonds between PEO and precursors. We combine a sol-gel route with a spin coating to prepare hybrid films, and investigate the influence of the different weight fractions of precursors and polymer concentration on the film morphologies. The inner and surface morphologies of the hybrid films are characterized using grazing incidence small-angle X-ray scattering and scanning electronic microscopy, respectively.

CPP 13.10 Mon 17:45 ZEU 255

Gold Nanoparticle/Polymer Brushes Composites: Controlling the Structure via Ion-Specific Effects — •PHILIPP RITZERT and REGINE V. KLITZING — Institute for Condensed Matter Physics, TU Darmstadt, Hochschulstr. 8, 64289 Darmstadt, Germany

Nanocomposite materials based on inorganic gold nanoparticle (AuNP) inclusions inside an organic matrix (e.g. polymer brushes) are employed in various fields: medical technology, catalysis, materials engineering. Combining the properties of both material classes facilitates high versatility of mechanical, optical and chemical properties, while simultaneously covering obvious drawbacks, e.g. stability of one compound. To provide the wide range of applications, nanocomposite materials usually require a specific internal structure. Yet, the understanding of the formation of internal structure and control over formation process is still lacking. Therefore, we aim to provide an approach to manufacture nanocomposite materials with controlled structure. Our model system utilizes various sodium salts (anion: F, Cl, Br, I, SCN) as stimuli for the assembly of citrate-capped gold nanoparticles in a poly-(N-isopropylacrylamide) brush. In a first step, we characterize the effect of sodium salts on pure AuNP suspensions. In a second step, we investigate adsorption parameters of AuNPs from suspension to brush, e.g. adsorption time. The third step involves the structure control of the composite materials with the characterized stimuli. Optical measurements reveal distinct differences between the sodium ions and concentration dependent aging behaviour.

CPP 14: Active Matter II (joint session DY/BP/CPP)

Time: Monday 15:00–18:15

Location: ZEU 160

See DY 10 for details of this session.

CPP 15: 2D Materials II (joint session HL/CPP)

Time: Monday 15:00–18:15

Location: POT 81

See HL 8 for details of this session.

CPP 16: Nanostructures at Surfaces (joint session O/CPP)

Time: Monday 15:00–17:45

Location: GER 39

See O 14 for details of this session.

CPP 17: Poster Session I

Topics: Focus: Self-Assembly of Plasmonic Nanostructures (1-4); Molecular Electronics and Excited State Properties (5-10); Organic Electronics and Photovoltaics (11-30); Hybrid and Perovskite Photovoltaics (31-44); Charged Soft Matter, Polyelectrolytes and Ionic Liquids (45-48); Interfaces and Thin Films (49-57), 2D Materials (58-60).

Time: Monday 18:00–20:00

Location: P3

CPP 17.1 Mon 18:00 P3

Plasmonic behaviour of surface modifications of γ -AlOOH nanoparticles and their effect on the particles Hamaker constant — •DOROTHEE SILBERNAGL¹, MATEUSZ DUDZIAK¹, ANNA MARIA MANZONI¹, and HEINZ STURM^{1,2} — ¹Bundesanstalt für Materialforschung und -prüfung, Unter Den Eichen 87, 12205, Berlin, Germany — ²Institute for Machine Tools and Factory Operations (IWF), TU Berlin, Pascalstr. 8-9, 10587 Berlin, Germany

Boehmite (γ -AlOOH) nanoparticles (BNP, particle size appr. 14nm) are known for their extremely low Hamaker constant A, which results in low interparticle van der Waals forces. However, surface modified BNPs (modifications are acidic acid BNPA, lactic acid BNPL and stearic acid BNPS) exhibit a gradually increased Hamaker constant A and therefore increased interparticle van der Waals forces. This was measured by atomic force microscopy force distance curves (AFM FDC). For this experiment an unmodified BNP agglomerate of approximately 50nm diameter was attached to an AFM cantilever and measured against pressed BNPs without and with different surface modifications. This set-up provides a sphere/plane geometry, necessary to calculate the Hamaker constant A of each material pairing from the FDCs attractive regime. Electron energy loss spectroscopy (EELS) measurements in the low energy region (up to 80eV) of unmodified and surface modified BNPs were performed to understand the origin of the increased van der Waals forces. As a result, additional plasmon bands were found in the region below 10eV for surface modified BNPs, which contribute to the attractive forces between particles.

CPP 17.2 Mon 18:00 P3

Liquid phase (S)TEM of DNA origami gold nanoparticle hybrids — •A. ONG¹, D. POHL¹, T.K. JEONG^{2,3}, A. HEERWIG^{2,3}, M. MERTIG^{2,3}, and B. RELLINGHAUS¹ — ¹Dresden Center for Nanoanalysis (DCN), cfaed, TU Dresden, Germany. — ²Physical Chemistry, TU Dresden, Germany — ³Kurt-Schwabe-Institut für Mess- und Sensortechnik Meinsberg e.V., Germany

DNA origami pads with site-specific patterns of ssDNA are flexible molecular templates for gold nanoparticles to self-assemble into functional supracolloidal structures [1]. The structure-property relation of supracolloidal structures play a significant role in constructing novel materials with desired properties for application in devices [2]. However, this relation has not been adequately understood. The study focuses on investigating the self-assembly and kinetic processes in supracolloidal structures using (scanning) transmission electron microscopy [(S)TEM] both in vacuum and in the liquid phase. Images of gold nanoparticles attached to DNA origami were acquired under vacuum and in-situ in the liquid phase, highlighting the possibility of real-time visualizations at the nanometer scale in different environments. The measured distances between gold nanoparticles in liquid confirm the intended templating mechanism. Financial support by DFG through RTG 2767 and by the EU Horizon 2020 Research & Innovation Programme grant agreement no. 964248 is gratefully acknowledged.

[1] J. Zessin et al. Nano Lett. (2017)17, 5163.

[2] T. Woehl, ACS Nano (2019) 13, 12272.

CPP 17.3 Mon 18:00 P3

Probing photoluminescent polymers using plasmonic self-assembly — •ONIMA BISHIT^{1,3}, SEZER SEÇKIN¹, and TOBIAS KÖNIG^{1,2} — ¹Leibniz-Institut für Polymerforschung e.V., Hohe Straße 6, 01069 Dresden, Germany — ²Center for Advancing Electronics Dresden (cfaed), Technische Universität Dresden, 01062 Dresden, Germany — ³Department of Physics, Indian Institute of Technology Delhi, Hauz Khas, New Delhi, 110016, India

Surface Enhanced Raman Spectroscopy (SERS) is an advantageous and indispensable technique for detection and sensing applications. Although SERS substrates have been fabricated using several top-down approaches, these methods are limited by scalability, uniformity, and high instrumentation costs. Recent developments in template-assisted self-assembly (TASA) techniques have facilitated us to fabricate low-cost, scalable, and uniform gratings consisting of plasmonic nanoparticle chains. [König et al., Adv. Funct. Mater. 2021, 2105054] With the support of the finite-difference time-domain (FDTD) method, we have rationally designed the colloidal grating to benefit from the coherent interaction

between Rayleigh anomalies and various plasmon modes. We will combine these modes with the quantum emitter, which we used previously as an efficient gain component for optoelectronic devices. [König et al., Adv. Optical Mater. 2020, 2001280] Finally, we use this overlap of the plasmonic modes with the photoluminescence of the emitters for nonlinear effects such as lasing, strong coupling, and ultra-high SERS sensitivity.

CPP 17.4 Mon 18:00 P3

Influence of thermal effects on a combinatorial plasmonic nanostructure for bio-detection — •TIANFU GUAN¹, SUZHE LIANG¹, YUSUF BULUT^{1,2}, KRISTIAN RECK³, MATTHIAS SCHWARTZKOPF², JONAS DREWES³, THOMAS STRUNSKUS³, FRANZ FAUPEL FAUPEL³, STEPHAN V. ROTH^{2,4}, and PETER MÜLLER-BUSCHBAUM^{1,5} — ¹TUM School of Natural Sciences, Chair for Functional Materials, 85748 Garching, Germany — ²DESY, 22607 Hamburg, Germany — ³CAU, Chair for Multicomponent Materials, Faculty of Engineering, 24143 Kiel, Germany — ⁴Department of Fiber and Polymer Technology, KTH, SE-100 44 Stockholm, Sweden — ⁵MLZ, TUM, 85748 Garching, Germany

In recent decades, Au nanoparticles (NPs) have been utilized in a wide range of sensor applications, such as photodetection, bio-detection, and thermal-detection, because of their unique optical and chemical properties. Among the optical sensors, surface-enhanced Raman spectroscopy (SERS) has attracted extensive attention being used in the identification of unknown substances in analytical chemistry. In this work, we investigate in situ sputter deposition of Ag on highly ordered Au NPs substrates as probed by grazing incidence small angle X-ray scattering (GISAXS). In addition, we explore the effect of temperature on the silver growth kinetics on different sizes of Au NPs substrates. Furthermore, by correlating the growth steps of the composite Au/Ag nanostructures with their SERS performance, we obtain the plasmonic hot spot performance corresponding to the combined nanostructure.

CPP 17.5 Mon 18:00 P3

Understanding the Double Doping of Organic Semiconductors Via State Energy Renormalization upon Charging — •ROSS WARREN¹, EUNKYUNG CHO², HONG LI², JEAN-LUC BREDAS², and NORBERT KOCH^{1,3} — ¹Institut für Physik & IRIS Adlershof, Humboldt-Universität zu Berlin, 12489 Berlin, Germany — ²Department of Chemistry and Biochemistry, The University of Arizona, Tucson, Arizona 85721-0088, United States — ³Helmholtz-Zentrum Berlin für Materialien und Energie GmbH, 12489 Berlin, Germany

The double ionisation of dopants is a recent experimental observation that allows the doping efficiency to rise above 100%. This is exciting because high conductivities can be achieved with fewer dopant molecules, meaning less disruption to the resulting film's microstructure. However, the current models of doped organic semiconductors based on Fermi-Dirac statistics fail to explain the double ionization of dopants and also the analogous situation of bipolaron formation on a host polymer. Here, we address this shortcoming by considering the renormalization of the state energies upon electron transfer between host and p-dopant. We vary the model parameters - the reorganization energy and evolutions of ionization energies and electron affinities upon charging - and plot the fractions of doubly ionized, singly ionized, and neutral species. We find good agreement with experiment. Finally, we suggest that the state energy renormalization upon charging is the key parameter to be minimized for double ionization of dopants or maximized to avoid formation of bipolarons on the host.

CPP 17.6 Mon 18:00 P3

Temperature Dependent Photoluminescence of β -Phase Zinc Phthalocyanine Single Crystals — •KILIAN STRAUSS¹, LISA SCHRAUT-MAY¹, SEBASTIAN HAMMER^{1,2}, KILIAN FRANK³, BERT NICKEL³, and JENS PFLAUM¹ — ¹Experimental Physics VI, Julius-Maximilians-Universität of Würzburg — ²Department of Physics, Ludwig Maximilian University, Munich — ³Departments of Physics and Chemistry, McGill University, Montreal, Canada

The photophysical properties of organic crystals are strongly dependent on the interactions between the comprising molecules. We chose zinc phthalocyanine (ZnPc) in its crystallographic β -phase as a model system to investigate the ex-

citonic coupling as a function of crystallographic direction. For this purpose, we performed polarization dependent photoluminescence (PL) measurements from 5 K to 300 K on needle-shaped single crystals grown by horizontal vapour deposition. A gradual optical transition from a J- to H-aggregate like behavior occurs on cooling down to 100 K. Upon further cooling, we find the emergence of superradiant luminescence typical for exciton delocalization in J-aggregates. This optical transition is induced by an anisotropic thermal compression of the crystal lattice.

We thank the Bavarian Research Network SolTech for financial support.

CPP 17.7 Mon 18:00 P3

On the Parametrization of Exciton-Phonon Coupling Matrix Elements by Ab Initio Methods — •MAXIMILIAN FRANZ XAVER DORFNER and FRANK ORTMANN — Department of Chemistry, Technische Universität München, 85748 Garching b. München, Germany

The accurate description of optical or transport properties of organic semiconductors, such as small molecules or polymers requires, besides the electronic degrees of freedom, also the incorporation of the nuclear motion into the theoretical treatment. This is because in these materials the electrons and the core movement are significantly coupled to each other.

This interaction co-determines macroscopic observables, like absorption cross-sections, charge carrier mobilities, or electronic relaxation time-scales. Close to the equilibrium configuration, the interplay of the electronic degrees of freedom and the nuclei can be cast into the form of a Holstein-Peierls model. In this representation, the interaction is characterized by a set of coupling constants, which are typical for a given molecule and dictate behavior in a range around the equilibrium configuration.

Here we present a novel scheme and an implementation for the computation of these effective coupling constants based on the CP2K software package. We benchmark our implementation for a number of molecules and study their non-radiative electronic relaxation behavior by the use of a matrix product state approach.

CPP 17.8 Mon 18:00 P3

Unraveling Structural Dynamics in Excimer Formation Using Ultrafast Electron Diffraction — •SEBASTIAN HAMMER¹, LAURENZ KREMEYER¹, TRISTAN BRITT¹, MAXIMILIAN RÖDEL², SYED ALI HASSAN¹, JENS PFLAUM^{2,3}, and BRADLEY SIWICK¹ — ¹Departments for Physics and Chemistry, McGill University, Montreal, QC H3A 2K6, Canada — ²Experimental Physics VI, University of Würzburg, 97074 Würzburg — ³Bayerisches Zentrum für Angewandte Energieforschung (ZAE Bayern), 97074 Würzburg

Excimer formation, *i.e.* the formation of an excited dimer state which is accompanied by structural deformations in the local inter-molecular geometry, is a common phenomena in molecular solids and crucially determines the optoelectronic properties of the material. While the process is understood well on a theoretical level [1], direct observational evidence of the underlying structural dynamics are experimentally challenging.

In recent years, the technique of ultrafast electron diffraction (UED) has proven to be capable of unraveling the structural dynamics of molecular single crystals after photo-excitation [2]. Using the prototypical excimer system zinc-phthalocyanine in its crystallographic α -phase [3], we show that UED experiments on polycrystalline thin-films can disclose the structural dynamics accompanying excimer formation. We gratefully acknowledge funding from the DFG (Project 490894053).

[1] Bialas et al. *J. Chem. Phys. C*. **126** 4067-4081 (2022)

[2] Gao et al. *Nature*. **496** 343-346 (2013)

[3] Hammer et al., *Mater. Horiz.* (2022)

CPP 17.9 Mon 18:00 P3

Influence of Ligands and Linker on the Optoelectronic Properties of Phenazine-based Iron Spin-Crossover Complexes — •LYDIA PLOSS¹, FLORIAN DAUMANN², KONSTANTIN SCHÖTZ¹, GERALD HÖRNER², BIRGIT WEBER², and ANNA KÖHLER^{1,3} — ¹Experimental Physics II, University of Bayreuth — ²Anorganische Chemie IV, University of Bayreuth — ³Bayreuth Institute of Macromolecular Research, University of Bayreuth

Spin-crossover (SCO) complexes are a class of materials - typically organometallic complexes - whose electronic ground state can be switched between a high spin (HS) and a low spin (LS) state by external stimuli, *e.g.*, by varying the temperature. This possibility renders them promising candidates for applications such as molecular switches or sensors.

An easy way to read out sensors is, *e.g.*, by using photoluminescence (PL) spectroscopy. Recently, an iron-based SCO complex was found that shows PL in both spin states.¹ This is remarkable since most SCO complexes show PL in only one of the two spin states or are not luminescent at all. To understand what defines the optical properties of such compounds, we systematically vary ligands and linker molecules of the complexes and investigate their influence on the optical properties of the resulting complexes, using absorption and temperature-dependent PL spectroscopy.

¹Lochenie et al., *J. Am. Chem. Soc.* 2018, 140, 2, 700-709

CPP 17.10 Mon 18:00 P3

Multichromophore Macrocycles of Perylene Bisimide Dyes as Fluorescent OLED Emitters — •THEODOR KAISER¹, BJÖRN EWALD¹, ULRICH MÜLLER¹, PETER SPEST², MATTHIAS STOLTE², FRANK WÜRTHNER², and JENS PFLAUM¹ — ¹Experimental Physics VI, University of Würzburg — ²Institut für Organische Chemie and Center for Nanosystems Chemistry, University of Würzburg

While fluorescent organic emitters exhibit an efficient and bright singlet decay their efficiency in Organic Light Emitting Diodes (OLEDs) is limited by the lifetime and non-radiative loss pathway of triplet dark states. Therefore OLED applications are mainly based on phosphorescent emitters harvesting triplet excitons for light emission. In order to increase the efficiency of fluorescent OLEDs we present a novel approach for the chemical design of fluorescent emitters based on multichromophore macrocycles of perylene bisimide dyes (PBIs). By linking individual PBI chromophores in macrocyclic architectures, biexcitonic coupling can lead to an efficient transformation of triplet dark states by processes like triplet-triplet annihilation (TTA). This allows for an efficient bright electrical operation in OLED devices as the lifetime of dark states is drastically reduced. As recently reported by our groups trimeric perylene bisimides can even produce non-classical electrically driven single photon emission at room temperature [1], which has so far only been reported for phosphorescent emitters. Therefore these emitters offer new options for the application of strictly fluorescent materials in classical and non-classical OLED devices.

[1] Ulrich Müller et al., *Adv. Optical Mater* 2022, 10, 2200234.

CPP 17.11 Mon 18:00 P3

Investigation of Metal-Insulator Transitions in Organic Field-Effect Transistors of an n-Type Organic Semiconductor — •PAUL SCHLACHTER¹, MAXIMILIAN FRANK¹, MATTHIAS STOLTE², FRANK WÜRTHNER², and JENS PFLAUM^{1,3} — ¹Experimental Physics VI, University of Würzburg, 97074 Würzburg — ²Institut für Organische Chemie and Center for Nanosystems Chemistry, University of Würzburg, 97074 Würzburg — ³ZAE Bayern, 97074 Würzburg

Metal-insulator transitions in organic materials offer many exciting applications and are therefore gaining increasing scientific as well as technological interest. In this work, we aim to investigate electronic field-effect-induced phase transitions (semiconductor \rightarrow conductor \rightarrow insulator) in organic single crystals (especially Cl₂NDI [1]) of high electron mobility. The long-range order of their molecular entities in combination with a preferred (001) gliding plane geometry provides the pre-condition of a nearly defect-free interface for studying quasi-two-dimensional electron gas formations. For this purpose, we use an electrolyte as a top gate in addition to a dielectric conventional back gate. By simultaneously varying the bottom and top gate voltages, respectively, we aim to control the charge carrier density and thereby to gain deeper insights into Mott physics. First results on these efforts will be presented and evaluated with respect to the possible implementation in Mott field-effect transistors.

[1] Tao He et al., *Nat. Commun.* 2015, 6, 5954

CPP 17.12 Mon 18:00 P3

On the orientation mechanism of non-polar dyes in light-emitting guest-host systems — •BINH-MINH NGUYEN, MARKUS SCHMID, JOHANN KIRSCH, and WOLFGANG BRÜTTING — Experimental Physics IV, Institute of Physics, University of Augsburg, 86159 Augsburg, Germany

After many years of development, OLEDs have continuously been optimized to reach higher efficiency, for which the horizontal orientation of the emitter molecules is one of the dominant factors [1]. For the purpose of studying intrinsic orientation without electrostatic interaction, our work considers non-polar dyes, namely TTPA, BSBCz, DIP and DBP. While the emitter orientation has been studied in neat film as a basic approach, their behavior in guest-host systems has not been studied widely. In this work we focus on the correlation between emitter concentration and its orientation. With the results from experimental and simulation study, we also discuss the possible orientation mechanism of emitter molecules on the substrate surface in terms of molecular structure, possibility to form crystallites and the effective glass transition temperature of the guest-host system. We observe that isotropic structure of the emitter as well as the crystallized and aggregated molecules are not favorable for horizontal orientation. However, molecules having a rod-like structure have the tendency to arrange horizontally to the substrate. These results contribute to a further understanding of orientation of non-polar emitter molecules.

[1] Brütting et. al, *Physical Review Applied*, 2017, 8(3), 037001.

CPP 17.13 Mon 18:00 P3

Self-heating in OLED Lighting — •ANTON KIRCH^{1,2}, AXEL FISCHER¹, MATTHIAS LIERO³, JÜRGEN FUHRMANN³, ANNEGRET GLITZKY³, LUDVIG EDMAN², and SEBASTIAN REINEKE¹ — ¹Dresden Integrated Center for Applied Physics and Photonic Materials (IAPP), TU Dresden, Germany — ²Department of Physics, Umeå University, Sweden — ³Weierstrass Institute Berlin, Germany

For bright area light sources, such as OLED lighting tiles, the electric resistivity of transparent electrodes induces a non-uniform current distribution within the device. At high driving currents, the interaction between conductivity, heat, and power dissipation results in a positive electrothermal feedback loop, which dras-

tically exacerbates inhomogeneities in local device temperature and luminance.

Such nonlinear behavior induces unprecedented electrothermal effects that compromise the performance of bright area light sources. In this contribution, we present how Joule self-heating squeezes temperature and current into a tiny device region, while the remainder of the active area decreases in luminance (Switch-back effect) [1]. We further introduce how the dimension of the active area governs the current-voltage characteristics of the OLED and how two and even three stable operating branches develop (tristability) that can promote destructive incidences [2].

[1] Kirch et al., *Light: Science & Applications* 9, 5 (2020)

[2] Kirch et al., *Adv. Func. Mat.* 31, 47 (2021)

CPP 17.14 Mon 18:00 P3

Organic Photoconductors based on Rubrene Thin-Films — •JONAS SCHROEDER, RISHABH RISHABH, JOHANNES BENDUHN, and KARL LEO — Dresden Integrated Center for Applied Physics and Photonic Materials (IAPP) and Institute for Applied Physics, Technische Universität Dresden, Nöthnitzer Str. 61, 01187 Dresden, Germany

Thin films of organic semiconductors possess huge potential for large-scale industrial applications. However, the limited possibilities of crystal growth directly on the substrates often restrict device concepts but also achievable device performance. Here, we use vacuum-deposited rubrene in combination with a thermal post-treatment to fabricate different morphologies of polycrystalline thin films. To take advantage of the high in-plane mobility ($3 \text{ cm}^2 \text{ V}^{-1} \text{ s}^{-1}$) of the well-known orthorhombic rubrene phase in light detection applications, we employ photoconductive detectors in which the contacts are placed laterally on the sides of the active material. This allows for decoupling of the filtering of the incident light from the channel geometry and a photocurrent gain due to the natural imbalance of electron and hole mobilities in organic semiconductors. We show performance benchmarks of prototypical photoconductive organic photodetectors and relate these to the optical and electrical properties of the used rubrene thin films.

CPP 17.15 Mon 18:00 P3

Optimizing narrowband OPDs for wavelength range from 700 nm to 1100 nm — •FRED KRETSCHMER, LOUIS CONRAD WINKLER, JAKOB WOLANSKY, JOHANNES BENDUHN, and KARL LEO — Technische Universität Dresden, Dresden Integrated Center for Applied Physics and Photonic Materials (IAPP) and Institute of Applied Physics (IAP), Dresden, Germany

In recent years, organic photodetectors have attracted particular interest, due to their advantageous properties, such as cheap manufacturing costs and high performance, compared to inorganic devices. Particularly important is the narrowband photo-response, which enables the detection of small wavelength ranges, making optical filters obsolete and allowing miniature detector compositions. Narrowband spectroscopic sensors are an integral part of modern society, for example, in food quality monitoring, signal communication, or medical imaging.

In this contribution, microcavity-enhanced organic photodetectors in the visible and near-infrared wavelength range are investigated. For these devices, the active and transport layer thickness are varied and analysed for the donor material Rubrene and Spiro-MeO-TPD. Therefore, performance parameters such as the external quantum efficiency, the specific detectivity, the dark current, the response speed, and parasitic side effects are investigated and examined, leading to concrete device guidelines which can increase the performance of narrowband organic photodetectors. In a next step, we are planning to complement these detectors with infrared light-emitting diodes for a fully organic, spectroscopic sensing system.

CPP 17.16 Mon 18:00 P3

Humidity Stable Thermoelectric Hybrid Materials for A Self-Powered Sensing System — •SUO TU¹, TING TIAN¹, TIANXIAO XIAO¹, SHANSHAN YIN¹, JULIAN HEGER¹, GUANGJIU PAN¹, SHUIJIN HOU², ALIAKSANDR BANDARENKA², MATTHIAS SCHWARTZKOPF³, STEPHAN ROTH³, and PETER MÜLLER-BUSCHBAUM^{1,4} — ¹Technical University of Munich, TUM School of Natural Sciences, Department of Physics, Chair for Functional Materials, 85748 Garching — ²Technical University of Munich, TUM School of Natural Sciences, Department of Physics, Physik der Energiewandlung und -speicherung, 85748 Garching — ³DESY, 22607 Hamburg — ⁴MLZ, TUM, 85748 Garching

Highly sensitive and humidity-resistive detection of the most common physical stimuli is of primary importance for practical application in a real-time monitoring. Here, we report a simple yet effective strategy to achieve a highly humidity-stable hybrid composite that enables simultaneous and accurate pressure and temperature sensing in a single sensor. The improved electronic performance was due to the enhanced planarity of PEDOT and charge transfer between PEDOT:PSS and multi-walled carbon nanotubes (MWCNT) by strong π - π interaction. The preferred electronic pathway induced by robust morphology in the hybrid composite is responsible for the high humidity stability. These observations have been recognized by Grazing-incidence wide/small-angle X-ray scattering (GIWAXS/GISAXS), Raman, FTIR, and electrochemical impedance spectroscopy (EIS).

CPP 17.17 Mon 18:00 P3

New insights into the P3HT:PCBM bulk-heterojunction — •SHAHIDUL ALAM¹, CHRISTOPHER E. PETOUKHOFF¹, HAYA ALDOSARY¹, XINYU JIANG², TOMÁŠ VÁRY³, WEJDAN ALTHOBAITI¹, SANDRA P. GONZALEZ LOPEZ¹, WEJDAN ALSUFYANI¹, PETER MÜLLER-BUSCHBAUM², VOJTECH NÁDAŽDÝ⁴, HARALD HOPPE⁵, and FRÉDÉRIC LAQUAI¹ — ¹KAUST Solar Center (KSC), Kingdom of Saudi Arabia — ²TU Munich, Germany — ³STU Bratislava, Slovak Republic — ⁴Slovak Academy of Sciences, Bratislava, Slovak Republic — ⁵FSU Jena, Germany

Here, we studied the influence of thermal annealing on blends of well-known regio-random and regio-regular P3HT conjugated polymers and fullerene derivative [6,6]-phenyl-C60-butyric acid methyl ester (PC60BM). Several advanced microscopic and spectroscopic techniques were applied to investigate the thermal annealing effects on the structural, morphological, and energetic states, e.g., grazing-incidence wide-angle x-ray scattering, polarized light microscopy, hyperspectral photoluminescence spectroscopy, and photo-deflection spectroscopy. Furthermore, the blends' density of states (DOS) distribution was studied using energy resolved-electrochemical impedance spectroscopy. Coupled transfer matrix methods and drift-diffusion simulations were employed to see the impact of DOS on the solar cells' device parameters.

CPP 17.18 Mon 18:00 P3

Crystal Orientation and Surface Morphology in Thin Films of Poly-[3-(6-trifluorohexyl)thiophene] on Silicon and Graphene — •ALEXANDER MUCH¹, ROBERT KAHL¹, FLORIAN MEICHSNER², MUKUNDAN THELAKKAT², THOMAS THURN-ALBRECHT¹, and OLEKSANDR DOLYNCHUK¹ — ¹Experimental Polymer Physics, Martin Luther University Halle-Wittenberg — ²Applied Functional Polymers, University of Bayreuth

Semiconducting polymers gained much interest for use in electronic devices due to their easy processing from solution and mechanical flexibility. To improve the efficiency of organic electronic devices, it is crucial to understand and control the crystal orientation in thin films.

As recently found in films of poly-(3-hexylthiophene) (P3HT) on graphene, the interfaces to vacuum and graphene induce edge-on and face-on orientation, respectively [1]. We propose to influence the crystal orientation in polythiophenes by increasing the polarity of the end group of the side chains. Thereby, melt-crystallized thin films of poly-[3-(6-trifluorohexyl)thiophene] (P3CF3HT) studied by GIWAXS showed an increased and thickness-dependent tendency to face-on orientation not only on graphene, but also on silicon, which is inactive for P3HT. Furthermore, the film surface morphology probed by AFM strongly depends on the crystal orientation and the substrate. Our results validate the approach and open a pathway to control molecular orientation in polythiophenes.

[1] Dolynchuk et al., *Macromolecules* 54, 5429-5439, 2021

CPP 17.19 Mon 18:00 P3

Influence of amphiphilic additives on P3HT:PC60BM organic solar cells — •JOSE PRINCE MADALAIMUTHU^{1,2}, ZHUO XU^{1,2}, ULRICH S. SCHUBERT^{1,2}, and HARALD HOPPE^{1,2} — ¹Laboratory of Organic and Macromolecular Chemistry (IOMC), Friedrich Schiller University Jena, Humboldtstr. 10, D-07743 Jena, Germany — ²Center for Energy and Environmental Chemistry Jena (CEEC Jena), Friedrich Schiller University Jena, Philosophenweg 7a, D-07743 Jena, Germany

The mechanical stability of the layer stack is a significant barrier to the continued functioning of flexible OPVs. Delamination processes have the potential to significantly reduce photovoltaic performance. High-crystallinity polymers retain blend morphologies for a long time but yield brittle thin films. Amorphous polymers produce more flexible films but have less morphological stability. Device performance is associated with high crystallinity and superior charge carrier mobility. Furthermore, the elasticity required for mechanical stability is often improved with more amorphous polymers. This seems to split the necessary material characteristics in two. The objectives of the investigations are to improve mechanical resilience by lowering the tensile modulus and reducing crystallization by introducing tiny amounts of amphiphilic plasticizers. The effect of amphiphilic small molecule additions in donor-acceptor blends was investigated for toluene sulfonic acid (TSA) and then with a series of perylenes with systematically varying amphiphilicity. Enhancing the device's performance and long-term stability illustrates that the active layer's morphology can be regulated by the presence of amphiphilic additives.

CPP 17.20 Mon 18:00 P3

Enhanced air stability of green-solvent polymer solar cells with green-fluorescent polymer EH-P — •ZERUI LI¹, SERGEI VAGIN², KUN SUN¹, MORGAN LE DÜ¹, MANUEL A. REUS¹, and PETER MÜLLER-BUSCHBAUM^{1,3} — ¹Technical University of Munich, TUM School of Natural Sciences, Department of Physics, Chair for Functional Materials, James-Franck-Str. 1, 85748 Garching, Germany — ²Technical University of Munich, TUM School of Natural Sciences, Department of Chemistry, Chair of Macromolecular Chemistry, James-Franck-Str. 1, 85748 Garching, Germany — ³Technical University of Munich, MLZ, Lichtenbergstr. 1, 85748 Garching, Germany

The rapid development of materials has promoted that the efficiency of polymer solar cells (PSCs) reached over 20%, which is highly close to the application requirement. While the relative poor stability of PSCs slows down their commercial progress. Nowadays the research of stability in nitrogen or vacuum received much attention, while the inevitable contact of air would also cause undesirable effect on the device performance. Here, we select a green-solvent based material system PBDB-TF-T1:BTP-4F-12 as research model. Firstly the degradation of solar cells in air was observed and the mechanism was investigated. Then a green fluorescent polymer additive could EH-P was explored and it's found that it could improve the air-illumination stability of these solar cells. The doped solar cells shown obvious advantaged performance compared than reference ones after 24-hours-illumination in air. Such a material shows great potential in real application and provides guidance in exploring new additive.

CPP 17.21 Mon 18:00 P3

Calculation of intra-molecular transition rates depending on structural parameters with DFTB — •FABIAN TEICHERT, ROBIN SILLIGMANN, FLORIAN GÜNTHER, and ANGELA THRÄNHARDT — Institute of Physics, Chemnitz University of Technology, Chemnitz, Germany

Organic semiconductors become increasingly important for electronic applications. The large number of organic materials and their combinations make it useful to investigate properties like current-voltage characteristics using simulations in order to find suitable material combinations for applications. We investigate the transition rates of electrons between two organic molecules, especially between thiophene, zinc porphyrin and PCBM. For this, we calculate HOMO and LUMO states and energies, reorganisation energies and Hamiltonian coupling matrices with DFTB using the software dftb+. Based on these results, the transition rates are computed using Marcus theory for charge transfer. We present result for two systems: (1) two thiophene molecules and (2) zinc porphyrin and PCBM. We show reorganisation energies, Hamiltonian coupling constants and transition rates dependent on the structural configuration. E.g. the thiophene molecules are shifted and rotated against each other. The final goal of our work is to obtain the statistical distribution of all the results due to the statistical fluctuation of the structure. This is suitable as input for subsequent Monte-Carlo hopping simulations, which can be used to describe the large-scale transport of charges within organic materials for e.g. solar cell applications.

CPP 17.22 Mon 18:00 P3

Charge transfer characteristics of an optically-driven conjugated molecular system — VLADYSLAV SAVCHENKO and •OLGA GUSKOVA — IPF Dresden, Dresden, Germany

Recently [1], we have simulated E/Z isomers of two azobenzene-bithiophene (azo-bt) molecular switches in-between an anchoring surface and a gold STM tip. One of these switches has been previously synthesized [2], another one represents a structural isomer of [2], where azo and bt blocks have been swapped along the molecule. Here, we focus on the intermolecular charge transfer within chemisorbed monolayer because this aspect is still unexplored. First, DFT method is applied to define the reorganization energies for electron and hole transfer and the transfer integrals for stacked molecules using energy splitting in dimer approach. Further, the charge carrier mobility is evaluated. The results show, that the position of azo and bt favors either hopping of electrons or holes. For example, both isomers of the molecule with swapped blocks [1] are prone to the electron transfer, whereas for switch [2] the UV light stimulus toggles the main charge carrier from electron to hole. Interestingly, that molecule [2] possesses a non-zero mobility for the hopping distances $h < 0.5$ nm, which requires densely packed layers. On contrary, relatively high electron transfer is predicted for molecule [1] even for sparsely anchored switches (h ca. 1 nm); the UV light turns off the hole hopping at distances $h > 0.5$ nm as well. This work is supported by DFG, grant GU1510/5-1. [1] Savchenko V., Guskova O. Herald of TvSU. Series: Chem. 3(45) 2021, 7. [2] Karpe S., et al. Chem. Commun. 46, 2010, 3657.

CPP 17.23 Mon 18:00 P3

Critical Conditions in Transfer Matrix Methods — •REINHARD SIGEL — Independent Scientist, Markdorf, Germany

The propagation of light in a layered refractive index profile is well described by transfer matrix methods (TMMs) [1]. Critical conditions (CC) occur when the wave vector perpendicular to the layering becomes zero. This case can be encountered in a total reflection geometry. Conventional TMMs become singular for CC. We discuss the divergence of layer amplitudes when one approaches CC. It is furthermore elucidated, how this divergence shows up in different experiments. New types of basis functions for a TMM based on virtually linear functions to circumvent the singularity have been introduced recently [2].

[1] J. Lekner, *Theory of reflection of electromagnetic and particle waves*, Martinus Nijhoff Publisher, Dordrecht, 1987.

[2] R. Sigel, *Light Propagation in Layered Media in a Total Reflection Geometry: A Transfer Matrix Method Using Virtually Linear Basis Functions to Handle Critical Conditions*, J. Opt. Soc. Am. A, accepted.

CPP 17.24 Mon 18:00 P3

Surface doping of rubrene single crystals by molecular electron donors and acceptors — •CHRISTOS GATSIOS¹, ANDREAS OPITZ¹, SEBASTIAN HAMMER³, JENS PFLAUM³, YADONG ZHANG⁴, STEPHEN BARLOW⁴, SETH R. MARDER⁵, and NORBERT KOCH^{1,2} — ¹Institut für Physik & IRIS Adlershof, Humboldt-Universität zu Berlin, 12489 Berlin, Germany — ²Helmholtz-Zentrum Berlin für Materialien und Energie GmbH, 12489 Berlin, Germany — ³Experimentelle Physik VI, Julius-Maximilians-Universität Würzburg, 97074 Würzburg, Germany — ⁴Renewable and Sustainable Energy Institute (RASEI), University of Colorado, Boulder, CO 80309, USA — ⁵Renewable and Sustainable Energy Institute (RASEI), Department of Chemical and Biological Engineering, Department of Chemistry, and Materials Science and Engineering Program, University of Colorado, Boulder, CO 80309, USA

Molecular doping can be used as a method to control the electronic energy levels and charge carrier densities of the organic semiconductor via charge transfer interactions with electron-donating or electron-accepting molecules. This work seeks to understand the mechanisms of interface engineering by focusing on the surface doping of rubrene single-crystals by molecular electron donors (CoCp2) and acceptors (Mo(tfd-CO2Me)3). Our angle-resolved photoemission results show that deposition of molecular dopants on rubrene shifts the valence band with respect to the Fermi level, thus changing the p- (n-) character of the surface, while the electronic band parameters remain essentially unaffected.

CPP 17.25 Mon 18:00 P3

Electronic structure of singlet fission donor-acceptor complexes — •KARIN S. THALMANN¹, PEDRO B. COTO², and MICHAEL THOSS¹ — ¹Institute of Physics, University of Freiburg, Germany — ²Spanish National Research Council (CSIC), Madrid, Spain

Singlet fission (SF) is a photophysical process in molecular materials describing the spin-allowed conversion of a singlet exciton to two triplet excitons [1]. Due to its ability to multiply charge carriers and its potential usage in solar cells to circumvent the Shockley-Queisser limit [2,3], SF has received significant attention recently. For future applications in energy conversion, the molecule exhibiting SF has to be combined with an electron acceptor to extract the energy of the two triplet excitons. As an example, we consider the complex of two covalently linked diazadiborane chromophore units as the SF exhibiting donor and tetracyanoquinodimethane as the acceptor molecule. Using multireference perturbation theory techniques, we analyze the electronic structure of the complex, in particular the electronically excited states, which include locally excited, charge transfer, and multiexcitonic states. Furthermore, we study the influence of the acceptor on the electronic structure of the donor molecule.

[1] M. B. Smith, J. Michl, Chem. Rev. **110**, 6891 (2010).

[2] W. Shockley, H. J. Queisser, J. Appl. Phys. **32**, 510 (1961).

[3] A. J. Baldacchino et al., Chem. Phys. Rev. **3**, 021304 (2022).

CPP 17.26 Mon 18:00 P3

Recyclable-refabricated efficient solar cells with cellulose-based materials — •SHUXIAN XIONG^{1,2}, MARIE BETKER^{1,3}, BENEDIKT SOCHOR¹, CONSTANTIN HARDER^{1,2}, YUSUF BULUT^{1,2}, L. DANIEL SÖDERBERG³, PETER MÜLLER-BUSCHBAUM^{2,4}, and STEPHAN V. ROTH^{1,3} — ¹DESY, 22607 Hamburg, Germany — ²TUM School of Natural Sciences, Chair for Functional Materials, 85748 Garching, Germany — ³KTH Royal Institute of Technology, 10044 Stockholm, Sweden — ⁴MLZ, TUM, Garching, Germany

Cellulose-based nanomaterials are used in a variety of potential applications, particularly in green electronics and optoelectronic devices, due to their sustainability, low cost and the ease of chemical functionalization. For recycling and prefabrications of cellulose-based solar cells, we propose the fabrication of green, fully sprayed solar cells based. The electrode material using conductive inks laminated with cellulose is easy to fabricate in large-area solutions. Preferably chlorine-free solvents are used in the active layer, and solvent engineering and post-treatment are used to control the morphology and aggregation to achieve high performance and environmental recyclability. The solar cells are planned to be recycled using the most environmentally friendly physical and chemical methods. The solar cell materials should be recycled to the maximum extent possible, and the recycled materials are then used to refabricate the solar cells and evaluate them in terms of morphology and efficiency.

CPP 17.27 Mon 18:00 P3

Towards needleless Electrospinning of a non-toxic, textile Dye-sensitized solar cell — •MARIUS DOTTER — FH Bielefeld, University of Applied Sciences, Bielefeld, Deutschland

Photovoltaics can be used not only to feed energy into the power grid, but also to provide opportunities for applications on a smaller scale and for the autonomous supply of small electrical devices. In some cases, optimized efficiency can be dispensed with in favor of more cost-effective variants. Dye-sensitized solar cells (DSSC) offer a good option in this regard. They are also more effective indoors, because of a better conversion of stray light than semiconductor cells. Another idea is to make previously unused areas usable, with textiles such as tarpaulins, umbrellas and awnings being of particular interest. This niche, which has hardly

been used so far, is to be filled by a textile DSSC, relying on needleless electrospinning for the textile haptics. This process, in which a polymer solution is formed into fine nanofibers using high voltage, which are then arranged in a disordered manner to form a nanofiber mat, enables simple and industrially scalable production of the DSSC components with a textile feel. In addition, simple production with non-toxic materials can also enable later reuse or simple recycling. In this context, this poster shows the general concept and progress of the work on the front electrode, which is based on a currently submitted paper.

CPP 17.28 Mon 18:00 P3

Exploring the kinetics of pseudo-bilayer architecture formation during sequential deposition via slot die coating — •JINSHENG ZHANG¹ and PETER MÜLLER-BUSCHBAUM^{1,2} — ¹TUM School of Natural Sciences, Chair for Functional Materials, Garching — ²MLZ, TUM, Garching

Recently, organic solar cells have received increasing attention due to obvious advantages such as flexibility and being lightweight. Among the different types of structures of the active layer, typically planar and bulk heterojunction geometries are used, which introduces intrinsic shortcomings. The newly developed pseudo-bilayer structure can perfectly combine their strengths and circumvent the drawbacks. Unfortunately, most of the pseudo-bilayer are still prepared by spin coating and rarely by printing methods such as slot die coating. Besides these studies mainly focus on selecting solvents, adding third components and studying the vertical morphology. The kinetics of forming the pseudo-bilayer architecture with slot-die coating are still unknown. Here we select the donor acceptor system PM6 and Y6 and the solvents CB and CF. First, PM6 is printed on the substrate and then Y6 is printed on top of PM6. During the deposition, in situ GIWAXS, in situ GISAXS, and in situ UV-vis absorption is carried out to study the formation of the pseudo-bilayer.

CPP 17.29 Mon 18:00 P3

Flash-lamp processing of charge extraction layers for polymer solar cells — •AURELIEN SOKENG DJOUMESSI^{1,2}, JOSE PRINCE MADALAIMUTHU^{1,2}, SHAHIDUL ALAM^{1,2,3}, AMAN ANAND^{1,2}, ANASTASIA SICHWARDT^{1,2}, PETER FISCHER⁴, ROLAND RÖSCH^{1,2}, ULRICH S. SCHUBERT^{1,2}, and HARALD HOPPE^{1,2} — ¹Laboratory of Organic and Macromolecular Chemistry (IOMC), Friedrich Schiller University Jena, Humboldtstrasse 10, 07743 Jena, Germany — ²Center for Energy and Environmental Chemistry Jena (CEEC Jena), Friedrich Schiller University Jena, Philosophenweg 7a, 07743 Jena, Germany — ³King Abdullah University of Science and Technology (KAUST), KAUST Solar Center (KSC), Physical Sciences and Engineering Division (PSE), Material Science and Engineering Program (MSE), Thuwal 23955-6900, Kingdom of Saudi Arabia — ⁴Institute of Materials Engineering, Technical University of Ilmenau, Gustav-Kirchhoff-Str. 6, 98693 Ilmenau, Germany

Despite the benefits of thermal annealing (TA) in the fabrication of polymer solar cells, the high processing temperatures are not compatible with high throughput manufacturing techniques such as roll-to-roll, which commonly used flexible substrates. Therefore, techniques such as flash lamp annealing (FLA), which do not negatively affect the plastic substrate are needed. Herein, the FLA was successfully applied to PEDOT:PSS and SnO₂ films used as interfacial layers in PM6:Y6-based solar cells, yielding device performances comparable to or even better than the devices treated with TA on a hotplate. Even at prototype size, the FLA is clearly more energy-efficient than the TA.

CPP 17.30 Mon 18:00 P3

Validating novel solar cells in space — •LUKAS V. SPANIER¹, LENNART K. REB¹, MICHAEL BÖHMER², CHRISTOPH DREISSIGACKER³, ZERUI LI¹, EMANUEL ANWANDER¹, AHMED KRIFA², and PETER MÜLLER-BUSCHBAUM^{1,4} — ¹Technical University of Munich, TUM School of Natural Sciences, Department of Physics, Chair for Functional Materials, Garching, Germany — ²Technical University of Munich, TUM School of Natural Sciences, Department of Physics, Central Technology Laboratory, Garching, Germany — ³Institut für Materialphysik im Weltraum, Deutsches Zentrum für Luft- und Raumfahrt (DLR), Köln, Germany — ⁴Technical University of Munich, Heinz Maier-Leibnitz Zentrum (MLZ), Garching, Germany

The exploration of the outer solar system so far relied heavily on the use of scarce, highly radioactive plutonium stockpiles for power generation, as traditional solar cells have a too low power-to-mass ratio in low light environments to be suitable for those missions. Latest advances in organic and perovskite solar cells now open up the possibility of utilizing them on lightweight foils as photovoltaic solar sails for efficient power generation in low solar irradiation conditions.

We report the deployment of various organic and hybrid solar cell systems on a sounding rocket and their operation in outer space. We investigate the environmental influences during ascent, exposure to space, and reentry on the photovoltaic performance. We further study and compare the changes in morphology and optoelectronic behavior at various stages during the space mission, isolating different external impact factors.

CPP 17.31 Mon 18:00 P3

In situ study of superlattice self-assembly during slot-die coating of perovskite quantum dot films. — •DAVID P. KOSBAHN¹, MANUEL A. REUS¹, CHRISTOPHER R. EVERETT¹, GUANGJIU PAN¹, MATTHIAS SCHWARTZKOPF², STEPHAN V. ROTH^{2,3}, and PETER MÜLLER-BUSCHBAUM^{1,4} — ¹TUM School of Natural Sciences, Chair for Functional Materials, Garching — ²DESY, 22607 Hamburg — ³Department of Fibre and Polymer Technology, KTH, Stockholm, Sweden — ⁴MLZ, TUM, Garching

Research into quantum dots (QDs) of metal halide perovskites has become increasingly popular due to their stability and tunable optoelectronic properties. Their controllable surface chemistry and simple preparation make them a promising alternative to bulk perovskite solar cells. The power conversion efficiency of Cs_xFA_{1-x}PbI₃ QD solar cells has been steadily rising, up to a recent record efficiency of more than 16%. However, the alignment and self-assembly of the colloidal precursor into a superstructure during film fabrication via slot-die coating is not yet well-understood. In this work, we study the formation of perovskite QD films using in situ grazing-incidence X-ray scattering on different substrates and at different temperatures, to achieve a better understanding of the kinetic processes during solvent evaporation.

CPP 17.32 Mon 18:00 P3

Steady-State Microwave Conductivity (SSMC) on ionic liquid doped lead halide perovskites — •PATRICK DÖRFLINGER¹, YONG DING², MOHAMMAD KHAJA NAZEERUDDIN², and VLADIMIR DYAKONOV¹ — ¹Experimental Physics VI, Julius Maximilian University of Würzburg, 97074 Würzburg — ²Group for Molecular Engineering of Functional Materials, Institute of Chemical Sciences and Engineering, EPFL Valais, Sion 1950, Switzerland

Knowledge of the charge carrier lifetime and recombination behavior in perovskite solar cells is crucial, as non-radiative recombination processes still limit solar cell efficiencies. Here we present a technique to probe the charge carrier recombination. Of particular interest is the dominant charge carrier recombination pathway, which enables to quantify non-radiative recombination in the perovskite bulk. Furthermore, simultaneous photoluminescence measurements allow for estimating the doping density and determining the radiative efficiency at different charge carrier densities. As an example, the SSMC technique is applied to investigate the influence of ionic liquid additives, which are known to improve the stability of perovskite solar cells and the optoelectronic properties of perovskite absorbers.

CPP 17.33 Mon 18:00 P3

Giant Electrostriction in Lead Halide Perovskite MAPbI₃ Films as Measured with Double-Modulated Interferometry — •PHILIPP RAMMING¹, MARVIN MALCHAU², EMMA RAULAND¹, ANNA KÖHLER¹, and LOTHAR KADOR² — ¹Experimental Physics II, University of Bayreuth, Germany — ²Institute of Physics and BIME, University of Bayreuth, Germany

Hybrid lead halide perovskite semiconductor MAPbI₃ and similar materials have attracted much recent interest for photovoltaic devices. Upon application of moderate electrical fields, MAPbI₃ exhibits very large electrostriction effects. The thickness variation was measured with high precision using a double-modulation interferometer set-up. Phase modulation of the laser light and mechanical modulation of the interferometric path difference were employed. With field strengths on the order of 100 kV/cm, the relative thickness change of a polycrystalline film of 1 micron thickness can be as large as several per cent. The electrostriction varies with the square of the field strength; it is strongest at very low frequencies below one Hertz and decreases quickly at higher frequencies. The effect is compared to recently published data obtained on perovskite single crystals.

CPP 17.34 Mon 18:00 P3

First-principles study of the electronic and optical properties of perovskite solution precursors — •FREERK SCHÜTT¹, ANA M. VALENCIA^{1,2}, and CATERINA COCCHI^{1,2} — ¹Carl von Ossietzky Universität, Institut für Physik, Oldenburg, Germany — ²Humboldt-Universität zu Berlin und Iris Adlershof, Berlin, Germany

Metal halide perovskites have shown great promise for next-generation optoelectronic applications but the predominant employment of Pb poses a problem in terms of environmental sustainability of these compounds. Replacing Pb with Sn represents a viable solution, however, despite recent efforts in this direction [1], knowledge of Sn-based perovskites and precursors is to date still insufficient. In a first-principles work based on time-dependent density-functional theory coupled to the polarizable continuum model, we systematically investigate electronic and optical properties of SnI₂M₄ complexes, with M being common solvent molecules. We find that the structural, electronic, and optical properties are strongly affected by the choice of the solvent. By rationalising the behavior of 14 of such compounds even in comparison with lead-halide counterparts [2,3], we provide useful indications to complement experiments in the choice of the solvent molecules for SnI₂-based solution complexes and in their characterization towards the production of thin films [4].

[1] Di Girolamo et al., ACS Energy Lett. 6, 959 (2021). [2] Schier et al., Phys. Status Sol. B 258, 2100359 (2021). [3] Procida et al., PCCP 23, 21087 (2021). [4] Schütt et al., in preparation.

CPP 17.35 Mon 18:00 P3

In situ Grazing-Incidence Small-Angle X-ray Scattering Observation of TiOx Sputter Deposition on SnO2 Layer for Perovskite Solar Cells Application — •XIONGZHUO JIANG¹, ZHUIJUN XU¹, YUSUF BULUT^{1,2}, STEPHAN V. ROTH^{2,3}, and PETER MÜLLER-BUSCHBAUM^{1,4} — ¹TUM School of Natural Science, Chair for Functional Materials, 85748 Garching, Germany — ²Deutsches Elektronen-Synchrotron (DESY), 22607 Hamburg, Germany — ³Department of Fibre and Polymer Technology, KTH, Stockholm, Sweden — ⁴MLZ, TUM, 85748 Garching, Germany

It is crucial for the efficiency perovskite solar cells to promote the charge transport and suppress the non-radiation recombination in the hole blocking layer (HBL) and at the interface between the HBL and the active layer. Here, TiOx layers are deposited onto a SnO2 layer via sputter deposition at room temperature, forming a bilayer HBL. The structure evolution of TiOx during sputter deposition is investigated via in situ grazing-incidence small-angle X-ray scattering. After sputter deposition of TiOx with suitable thickness on the SnO2 layer, the bilayer HBL shows a suitable transmittance, smoother surface roughness, fewer surface defects and more suitable energy arrangement with active layer, and thus resulting in a lower trap-assisted recombination at the interface between the HBL and the active layer. With this SnO2/TiOx functional bilayer, the perovskite solar cells exhibit higher power conversion efficiencies than the unmodified SnO2 monolayer devices.

CPP 17.36 Mon 18:00 P3

Interfacial engineering via modifications of the electron blocking layer in PbS quantum dot solar cells — •TIMO PIECUCH¹, HUAYING ZHONG¹, and PETER MÜLLER-BUSCHBAUM^{1,2} — ¹TUM School of Natural Sciences, Chair for Functional Materials, Garching, Germany — ²MLZ, TUM, Garching, Germany

Colloidal quantum dot solar cells (CQDSCs) have received tremendous attention as next generation solar cells. Best performances up to 15% power conversion efficiency (PCE) have been achieved using lead sulfide quantum dots in a heterojunction cell architecture. PbS is especially efficient in the infrared region, and thus particularly interesting for future applications like space satellites. Research in the last years mainly has focused on improving the absorber layer and the hole blocking layer, but the potential by improving the electron blocking layer (EBL) has recently aroused increasing interest. In order to reduce interfacial charge carrier recombination and capture the large fraction of long wavelength photons at the EBL/active layer interface, the different interfacial energy-level offsets between EBL and absorber layer, tuned by the EBL-QDs size, are investigated using ultraviolet photoelectron spectroscopy (UPS) and absorption spectroscopy. Furthermore, the corresponding photovoltaic performances are characterized to demonstrate improved interfacial band alignment.

CPP 17.37 Mon 18:00 P3

PbS Quantum Dot Solar Cells for Space Applications — •JASPER EBEL¹, HUAYING ZHONG¹, and PETER MÜLLER-BUSCHBAUM^{1,2} — ¹TUM School of Natural Sciences, Chair for Functional Materials, Garching, Germany — ²MLZ, TUM, Garching, Germany

A key performance parameter for photovoltaics (PVs) on space missions is the power-to-weight ratio since launch costs increase drastically with the mass-to-orbit. During the last decades, several promising, light-weight and flexible alternatives to current silicon- and GaAs-based technology have emerged, such as perovskite, organic or colloidal quantum dot (CQD) based solar cells. Lead sulfide (PbS) CQD solar cells are especially interesting due to their easily size-tunable bandgap range in the infrared regime, allowing for the exploitation of previously unused parts of the solar spectrum. This in conjunction with ligand, solvent and interface-customizable opto-electronic properties makes QD solar cells a promising candidate for tandem solar cells reaching high efficiencies. Here, by mimicking heat and illumination cycles experienced in orbit, we analyse the performance and structural integrity of PbS CQD solar cells under lab conditions to explore the viability of their use for space applications. Repeating this experiment for various solvents, we test a range of devices to investigate their effects on the stability.

CPP 17.38 Mon 18:00 P3

Hybrid Energy Harvester Based on the Combination of Triboelectric Nanogenerator and PbS Quantum Dot Solar Cell — •TIANXIAO XIAO¹, WEI CHEN¹, WEI CAO¹, and PETER MÜLLER-BUSCHBAUM^{1,2} — ¹TUM School of Natural Sciences, Chair for Functional Materials, 85748 Garching, Germany — ²MLZ, TU München, 85748 Garching, Germany

Developing clean energy lies in the heart of sustainable development of human society. Triboelectric nanogenerator (TENG) originating from Maxwell's displacement current is a new type of energy harvester for harnessing ambient mechanical energy based on the coupling of triboelectrification and electrostatic induction effect. Compared with other counterparts, owing to the light-weight,

low-cost, and easy fabrication, TENG has become one of the most promising candidates in replacement of conventional fossil fuels and attracted worldwide attention in the past years. However, to further increase the energy harvesting efficiency and broaden application fields, integrating the TENG with other kinds of energy harvesters in one device is a possible way to meet these needs. In the present work, a TENG based hybrid energy harvester is designed and fabricated on the flexible polyethylene terephthalate (PET) substrate. This hybrid device consists of a single-electrode mode TENG component and a PbS quantum dot (QD) based solar cell component, which can harness both mechanical and solar energy from ambient environment to directly generate electricity.

CPP 17.39 Mon 18:00 P3

Improved surface passivation of AgBiS2 quantum dots for photovoltaic applications — •PETAR LOVRIC¹, HUAYING ZHONG¹, and PETER MÜLLER-BUSCHBAUM^{1,2} — ¹TUM School of Natural Sciences, Chair for Functional Materials, Garching, Germany — ²Heinz Maier-Leibnitz-Zentrum (MLZ), TUM, Garching, Germany

AgBiS2 colloidal quantum dots (QDs) are a non-toxic alternative for the commonly used PbS QDs for photovoltaic applications. Similar to its PbS QDs, they show great promise due to a tunable bandgap and solution processing, but what makes them stand out is the abundance of materials as well as a high absorption coefficient, which enables to greatly reduce the thickness of the active layer to around 35 nm. Additionally, studies have shown that they are more stable in water and can effectively harvest photons in the near-infrared part of the solar spectrum. One of major issue that impedes the development of AgBiS2 based photovoltaics is QD surface defects induced recombination losses. Here, we aim to improve the surface passivation of individual QDs and improve the charge transport in the QD films using surface ligand treatment with ZnI, mercapto-carboxylic acid (MPA) and TBAI as surface ligands. The optical and electrical properties of corresponding QDs films are characterized utilizing FTIR, XPS and UPS techniques, and further the corresponding device performances are investigated.

CPP 17.40 Mon 18:00 P3

Effect of ground state charge transfer and photoinduced charge separation on the energy level alignment at metal halide perovskite / organic charge transport layer interfaces — •LENNART FROHLOFF¹, FENGSHUO ZU¹, DONGGUEN SHIN¹, and NORBERT KOCH^{1,2} — ¹Institut für Physik & IRIS Adlershof, HU Berlin — ²Helmholtz-Zentrum Berlin

A proper energy level alignment at semiconductor interfaces is of paramount importance for realising high performance in perovskite solar cells. Therefore, we investigated the interface between a modern triple cation perovskite and a prototypical electron acceptor molecule in great detail. Strong band bending on both sides of the junction as well as negatively charged species of the organic molecule were evidenced by the means of photoemission spectroscopy, indicating a ground-state charge rearrangement across the interface. The band bending leads to significantly altered charge extraction offsets as compared to a hypothetical vacuum level alignment and flat band conditions. Additionally, we present direct evidence of a reversible reduction of the electron extraction offset under white light illumination as compared to the dark condition. The energy levels of the organic semiconductor were observed to rigidly shift to lower binding energy by up to 0.26 eV whilst the perovskite energy levels remain essentially unchanged. Consequently, we emphasise the necessity to determine the energy level alignment at interfaces involving perovskites not only in the electronic ground state but also under device operating conditions to allow for a reliable correlation to the performance of the device.

CPP 17.41 Mon 18:00 P3

Active layer aging for the fabricating durable perovskite solar cells with improved reproducibility — •YUQIN ZOU¹ and PETER MÜLLER-BUSCHBAUM^{1,2} — ¹TUM School of Natural Sciences, Chair for Functional Materials, Garching — ²MLZ, TUM, Garching

Solution processing of semiconductors is a highly promising approach for the fabrication of cost-effective electronic and optoelectronic devices. Although hybrid perovskites have potential in various device applications, challenges remain in the development of high-quality materials with simultaneously improved processing reproducibility and scalability. Here, we report a facile and practical aging treatment method to modulate crystal growth over the entire film to produces homogeneous films with high crystallinity, low defects and full-coverage. The resulting aged perovskite solar cells (PSCs) exhibits superior electronic properties: fast charge carrier transport, efficient charge extraction and low carrier recombination. The average power conversion efficiency (PCE) of MAPI-based PSCs greatly increase from 16.38% to 17.26% with high reproducibility. In addition, the aged PSCs maintain 80% of their initial PCE after 18 hours of operation under ambient and vacuum conditions, respectively, which illustrates their feasibility in scalable fabrication. Aging treatment effectively prevents the uneven performance and low reproducibility of PSCs arising from variations in the preparation environment (temperature, humidity). Thus, this method opens a new and effective avenue to improving the quality of perovskite films and photovoltaic devices in a scalable and reproducible manner.

CPP 17.42 Mon 18:00 P3

Investigating the Impact of Surfactants on Perovskite Film Formation Using In Situ Optical Spectroscopy — •TOBIAS SIEGERT, SIMON BIBERGER, KONSTANTIN SCHÖTZ, ANNA KÖHLER, and FABIAN PANZER — Soft Matter Optoelectronics (Experimental Physics II), University Bayreuth, Germany

Recent reports have shown that adding surfactants in the solution processing of halide perovskites, e.g. by blade-coating, can improve the morphology and optoelectronic properties of the resulting perovskite sample. In general, the crystallization processes of halide perovskites occurring during thin film formation largely determine the final film morphology. Thus, here we investigate the change in crystallization dynamics upon addition of surfactants to the precursor solution of halide perovskites. We monitor the film formation processes by multimodal optical in situ spectroscopy[1] to gain detailed insights about the film formation process of halide perovskites.[2-4] This finally allows us to elucidate the exact role and the impact of the presence of surfactants during solution processing on the crystallization behavior of the perovskite.

[1] Buchhorn, Wedler, Panzer. *J. Phys. Chem. A* 2018

[2] Chauhan, Zhong, Köhler, Panzer et al. *J. Mater. Chem. A*. 2020

[3] Schötz, Greve, Panzer et al. *Adv. Optical Mater.* 2021

[4] Biberger, Panzer et al. *J. Mater. Chem. A*. 2022

CPP 17.43 Mon 18:00 P3

Exploring the impact of nucleation seeds on the defect formation of printed hybrid perovskite films — •ALTANTULGA BUYAN-ARIVJIKH¹ and PETER MÜLLER-BUSCHBAUM^{1,2} — ¹TUM School of Natural Sciences, Chair for Functional Materials, Garching — ²MLZ, TUM, Garching

In the research of next-generation solar technologies, perovskite-based devices are prominent candidates due to their lucrative power conversion efficiencies and ease of fabrication. Such devices typically contain a polycrystalline perovskite layer grown via various coating methods. Due to the short timeframe of the growth process, the formation of defects is inevitable, leading to increased non-radiative recombination- and decreased extraction of photogenerated charge-carriers. One route to counteract the extensive formation of defects would be the addition of external seeds in the precursor solutions, leading to more controlled nucleation and improved crystallinity of the thin film. In this study, different nucleation seeds in the precursor solutions were used for the fabrication of polycrystalline perovskite thin films via slot-die coating. The effect of the seeds on the formation of defects in the film was explored via optical spectroscopical methods such as UV-vis & PL spectroscopy.

CPP 17.44 Mon 18:00 P3

In-situ observation of growth mechanisms during printing of 2D perovskite films — •KUN SUN¹, RENJUN GUO¹, LINUS F. HUBER¹, MANUEL A. REUS¹, JUNGUI ZHOU¹, MATTHIAS SCHWARTZKOPF², STEPHAN V. ROTH^{2,3}, and PETER MÜLLER-BUSCHBAUM^{1,4} — ¹TUM School of Natural Sciences, Chair for Functional Materials, 85748 Garching, Germany — ²DESY, 22607 Hamburg, Germany — ³Department of Fiber and Polymer Technology, KTH, SE-100 44 Stockholm, Sweden — ⁴MLZ, TUM, 85748 Garching, Germany

Two-dimensional (2D) metal halide perovskites have emerged as a promising candidate for perovskite solar cells (PSCs) due to their remarkable stability compared with their 3D counterparts. However, solution-based spin-coating as fabrication method is not adequate in terms of upscaling. In this regard, the slot-die coating technique, having minimal expenditure and low costs, is a well suitable upscaling method to speed up the commercialization of PSCs. Nevertheless, a fundamental understanding of the film formation during printing is yet not well understood, which causes printed solar cells to stay behind in device efficiencies. Here, we investigate the nucleation and growth of 2D perovskite films during slot-die coating with in-situ grazing incidence wide angle X-ray scattering (GIWAXS) in combination with photoluminescence (PL) during printing. In addition, the crystallite orientation and phase distribution of 2D perovskite containing different dimensionality are well elucidated.

CPP 17.45 Mon 18:00 P3

Design, fabrication and application of PEO-based solid polymer electrolytes for all-solid-state lithium batteries — •YINGYING YAN¹ and PETER MÜLLER-BUSCHBAUM^{1,2} — ¹TUM School of Natural Sciences, Chair for Functional Materials, Garching, Germany — ²Heinz Maier-Leibnitz-Zentrum (MLZ), TUM, Garching, Germany

All-solid-state lithium batteries (ASSLBs) have received extensive attention as one of the most promising power sources for flexible and wearable electronics, mainly because of their high flexibility, high energy density and reliable safety. However, the practical application of ASSLBs has been hindered by the poor interfacial stability and inferior ionic conductivity. Therefore, the exploration of advanced solid electrolytes with superior interfacial compatibility/ionic conductivity is an important research topic for all-solid-state batteries. Solid polymer electrolytes (SPEs) exhibit great potential in developing solid-state batteries, specifically for PEO and PEO-based derivatives, because of their superior interfacial compatibility, outstanding solubility against lithium salts, wide electrochemical windows and high ionic conductivity. At the same time, solid fillers,

as an important component in SPEs, play a crucial role in determining the overall electrochemical properties. As a consequence, we start from PEO-based materials and prepare SPEs by adding plastic additives and solid fillers with good structure. The electrochemical performance and structural stability of SPEs are elucidated by a combination of electrochemical characterization and morphological structural characterization.

CPP 17.46 Mon 18:00 P3

Study of PEO Composite Electrolyte in All-solid-state Lithium Batteries — •YUXIN LIANG¹, ZHUIJUN XU¹, KUN SUN¹, TIANFU GUAN¹, FABIAN A.C. APFELBECK¹, PAN DING², IAN SHARP², MATTHIAS SCHWARTZKOPF³, STEPHAN V. ROTH^{3,4}, and PETER MÜLLER-BUSCHBAUM^{1,5} — ¹TUM School of Natural Sciences, Chair for Functional Materials, Garching, Germany — ²TUM Walter Schottky Institute, Experimental Semiconductor Physics, Garching, Germany — ³DESY, 22607 Hamburg, Germany — ⁴KTH Royal Institute of Technology, Stockholm Sweden — ⁵MLZ, TUM, 85748 Garching

Lithium batteries (LBs) with composite electrolyte present good ionic conductivity, flexibility and intimate contact with electrodes. However, lithium dendrites will grow and the Coulombic efficiency (CE) will decrease with Li plating and stripping. Moreover, the poly(ethylene oxide) (PEO)-based electrolyte undergoes serious oxidation on the cathode side at high voltage and cause the battery collapse. Strategies have been applied to alleviate the abovementioned challenges, nevertheless, fundamental research on the degradation mechanism of the PEO electrolyte is still lacking. It is of great value to get a deeper understanding and therefore optimize the electrolyte for high voltage LBs. Herein, we select PEO/Al₂O₃ as composite electrode to understand the degradation process. The Li/cathode cells are assembled to observe the battery performance and grazing incidence wide-angle X-ray scattering (GIWAXS) is used to detect morphology changes of the electrolyte before and after cycling.

CPP 17.47 Mon 18:00 P3

Influence of Al₂O₃ concentration in poly(propylene carbonate) based solid polymer electrolyte — •THIEN AN PHAM^{1,2}, RALPH GILLES¹, and PETER MÜLLER-BUSCHBAUM^{1,2} — ¹MLZ, TUM, Garching, Germany — ²TUM School of Natural Sciences, Chair for Functional Materials, Garching, Germany

Solid polymer electrolytes (SPE) have emerged as promising electrolyte material group for all-solid-state batteries that allow the operation with Li metal anodes. Representing one of the main obstacles for Li metal anodes, Li dendrite growth can lead to short circuits which ultimately prevent the usage with liquid electrolytes. SPE offer higher mechanical stability compared to their liquid counterparts and thus, increase the general safety of Li metal batteries.

In this work, poly(propylene carbonate) based solid polymer electrolytes were synthesized with Lithium bis(trifluoromethanesulfonyl)imide (LiTFSI) as Li salt and varying Al₂O₃ concentrations via solution casting. The addition of Al₂O₃ has shown to increase the ionic conductivity of SPEs while simultaneously improve the mechanical stability. Furthermore, small angle X-ray scattering and FTIR were used to study the influence of Al₂O₃ on the structure of the SPE.

CPP 17.48 Mon 18:00 P3

Investigating Thermoelectric Properties of a Sodium-based, Solid Polymer-Electrolyte — •JULIAN-STEVEN SCHILLING, MAXIMILIAN FRANK, and JENS PFLAUM — Experimental Physics VI, University of Würzburg, 97074 Würzburg

Motivated by the large amount of available waste heat and the need to use energy more efficiently, the development of thermoelectric generators is becoming increasingly important. Their efficiency is characterized by the thermoelectric figure-of-merit z which includes the electrical conductivity σ , the thermal conductivity κ and the Seebeck coefficient S , respectively, and, at a given temperature T , is given by $zT = \frac{S^2 \sigma}{\kappa} T$. In contrast to electronic thermoelectric materials, ionic systems promise larger Seebeck coefficients due to lower mobility of the participating charge carriers. Therefore, ionic electrolytes based on organic polymers are of interest due to their expected good thermoelectric performance. In this work, first results on the thermoelectric properties of a methacrylate-based solid polymer electrolyte utilizing sodium as conducting salt are presented. By means of impedance spectroscopy in a frequency range from 100 mHz to 500 kHz we analyzed the mechanisms governing the electrical conductivity in the technologically relevant temperature range from 273K to 353K. Complementary, thermovoltage measurements as function of temperature enable the determination of the Seebeck coefficient and, together with impedance spectroscopy data, reveal strategies how the electronic and ionic transport properties can be modified by the respective salt concentration as well as by the ratio of different carbon-based additives.

CPP 17.49 Mon 18:00 P3

In-situ force measurements on a gold working electrode in lithium-ion electrolytes — •SABRINA KERZ, THOMAS TILGER, and REGINE VON KLITZING — Department of Physics, Technische Universität Darmstadt, Germany

Batteries have gained a great importance in recent years. They play a vital role in our every-day lives e.g. in mobile-devices and are an important pillar in the transition to renewable energies.

For these applications the solid electrolyte interface (SEI) at electrodes is of great interest. The Gouy-Chapman-Stern (CGS) model describes the interactions of the electrolyte with the charged electrode surface as an interplay between direct adsorption (Stern Layer) and a diffuse double layer. DLVO theory describes the diffuse double layer at the electrode's surface.

In-situ colloidal probe atomic force microscopy (CP-AFM) measures the force between a silica particle and the SEI. The obtained force curves are analyzed using DLVO theory. In a three-electrode setup different potentials are applied between a gold surface (working electrode) and a reference electrode. Thus, changes in the structure of the SEI with varying potentials and salt concentrations are examined.

CPP 17.50 Mon 18:00 P3

High-concentration Lithium-ion Electrolyte Overcomes the Challenges of High-temperature Lithium Batteries — •TIANLE ZHENG^{1,2}, YA-JUN CHENG², and PETER MÜLLER-BUSCHBAUM^{1,3} — ¹TUM School of Natural Sciences, Chair for Functional Materials, 85748 Garching, Germany — ²Ningbo Institute of Materials Technology & Engineering, CAS, Ningbo, 315201, P. R. China — ³TUM, MLZ, 85748 Garching, Germany

Conventional Li-ion batteries are severely constrained in high-temperature applications due to the low thermal stability of the electrolyte/electrode interface and electrolyte decomposition in the cell. Herein, we demonstrate a new electrolyte that achieves an excellent stable long-term cycling at 100 °C, well beyond the typical 60 °C limits of normal conventional Li-ion batteries. High concentrated lithium oxalylidifluoroborate (LiODFB) is selected as the lithium salt with a carefully designed high thermal stability solvent group. As a result, this unique high-concentration electrolyte can promote to form a stable and inorganic solid electrolyte interface layer on the electrode at elevated temperature, leading to improved performance in MCMB/Li and lithium iron phosphate (LFP)/Li half-cells, and achieve reversible capacities of 160 and 350 mA h/g, respectively, with Coulombic efficiencies > 99.3%. Subsequently, we further investigate the mechanism of high concentration LiODFB electrolytes by molecular dynamics simulations and XPS characterization techniques, exploring a new way for future high-temperature electrolytes.

CPP 17.51 Mon 18:00 P3

Morphology Control of Titanium Thin Films in a Low Temperature Process — •GUANGJIU PAN¹, SHANSHAN YIN¹, LINUS F. HUBER¹, CAROLINE EHGARTNER², NICOLA HÜSING², MATTHIAS SCHWARTZKOPF³, STEPHAN V. ROTH^{3,4}, and PETER MÜLLER-BUSCHBAUM^{1,5} — ¹TUM School of Natural Sciences, Chair for Functional Materials, 85748 Garching, Germany — ²Universität Salzburg, 5020 Salzburg, Austria — ³DESY, 22607 Hamburg, Germany — ⁴KTH Royal Institute of Technology, SE 100 44 Stockholm, Sweden — ⁵TUM, MLZ, 85748 Garching, Germany

A low-temperature routine to realize inorganic hole-blocking layers (HBLs) is important for the commercialization of perovskite solar cells. Fabricating HBLs at low temperature is energy-saving and compatible with flexible substrates. In this work, titania thin films are synthesized at low temperature (below 100 Celsius degree) with a polymer template sol-gel method based on the amphiphilic diblock copolymer polystyrene-*b*-polyethylene oxide (PS-*b*-PEO), in combination with selective incorporation of the titanium precursor ethylene glycol-modified titanate (EGMT). A joint process of UV treatment and water-vapor treatment is introduced to substitute the traditional high-temperature calcination. Morphology tailoring of titania thin films in the low-temperature process is achieved by managing phase separation of the polymer template. The surface morphologies of titania films are probed via scanning electron microscopy and GISAXS. The optical properties are examined with ultraviolet-visible spectroscopy and photoluminescence spectra.

CPP 17.52 Mon 18:00 P3

Bilayer formation in liquid-processed mono-functionalized BTBT films — TIM HAWLY, •ANDREAS SPÄTH, MANUEL JOHNSON, MARCUS HALIK, MINGJIAN WU, ERDMANN SPIECKER, and RAINER H. FINK — FAU Erlangen-Nürnberg, Erlangen, Germany

Two-dimensionally (2D) extended thin films of the p-type organic semiconductor C13-BTBT were fabricated by self-controlled growth at the water-toluene interface. Depicting a compound class originally developed for further functionalization and subsequent realization of self-assembled monolayers (SAMs) or their implementation into SAM-based organic field-effect transistors, the potent BTBT core unit commonly excels in high-quality structure formation as well as charge-transport characteristics. Utilizing various spectromicroscopic tools, we observe extraordinarily crystalline C13-BTBT films with a close to upright standing configuration of the BTBT backbone accounting for superior intermolecular orbital overlap. The well-defined morphology and internal structure of the film are underpinned by superior charge-transport parameters in corresponding OFETs. The inherently favorable membrane-like bilayer molecular arrangement is confirmed by the unambiguous representation of the unit cell as derived from STEM tomography. This study has been funded by the DFG within GRK 1896, the BMBF (contract 05K19WE2) and the Bavarian SolTECH initiative. [1] T. Hawly et al., ACS Adv. Energy Mat.(2022)/doi:10.1021/acsaem.2c01095

CPP 17.53 Mon 18:00 P3

Characterization of pure DbSeQ thin films and their multilayers with different semiconductor materials — •ANTON PYLYPENKO, ELENA CHULANOVA, ALEXANDER GERLACH, and FRANK SCHREIBER — Universität Tübingen, Auf der Morgenstelle 10, 72076 Tübingen, Germany

Organic semiconductor thin films are widely used in different areas of science and industry, especially for the manufacturing of organic optoelectronic devices. Bilayers of organic semiconductors are of high interest for research due to the possibility of increasing the advantages of blended materials [1]. Prospective candidates for these applications are derivatives of 2,1,3-benzothiadiazole, especially Dibenzoselenadiazoloquinoxaline (DbSeQ). The heavy atom has a strong impact on the spin-orbit coupling and thus the optical properties of the film. Understanding and investigating mechanisms of growth behavior is a key requirement for optimizing films.

We have investigated thin film growth and templating effects for various bilayers like DbSeQ:PIC or DbSeQ:DIP. The binary thin films are prepared by consistent evaporation of DbSeQ, DIP, and PIC on weakly interacting substrates under ultra-high vacuum conditions. Using ex-situ AFM, UV-VIS, and photoluminescence spectroscopies, X-ray reflectometry, and grazing-incidence wide-angle X-ray scattering, we have observed the morphology, structure, and crystallinity of bilayer films.

[1] A. Hinderhofer, F.Schreiber Chem Phys Chem (2012) 13 628

CPP 17.54 Mon 18:00 P3

Tunable morphologies in charged multiblock terpolymers in thin film geometry: effect of solvent vapor annealing — •BAHAR YAZDANSHENAS¹, FLORIAN A. JUNG¹, TIM BOHNEN¹, SINA ARIAE², DORTHE POSSELT², HEINZ AMENITSCH³, CONSTANTINOS TSITSILIANIS⁴, and CHRISTINE M. PAPADAKIS¹ — ¹Technische Universität München, TUM School of Natural Sciences, Soft Matter Physics group, Garching, Germany — ²Roskilde University, Department of Science and Environment, Roskilde, Denmark — ³Graz University of Technology, Institute of Inorganic Chemistry, Graz, Austria — ⁴University of Patras, Department of Chemical Engineering, Patras, Greece

Thin films of a pentablock terpolymer with an ABCBA architecture of two types of pH-responsive midblocks and short hydrophobic end blocks are investigated. As-prepared spin-coated films from different pH-values have previously shown highly tunable and non-monotonous behavior of the lateral structure sizes, based on the charge [1]. Here, we investigate further accessible morphologies by swelling the films in the vapors of solvents having different selectivity. Results from spectral reflectance, atomic force microscopy, and grazing-incidence small-angle X-ray scattering suggest that a solvent selective for the pH-responsive blocks leaves the nanostructures intact, while a nonselective solvent enables reorganization. Their vapor mixtures are also studied to potentially access further orientations and morphologies. In addition, an ABA triblock copolymer is investigated as a reference. [1] F. A. Jung, C. M. Papadakis et al., Adv. Funct. Mater. 2021, 31, 2102905.

CPP 17.55 Mon 18:00 P3

Computer simulations of liquids in extreme Confinement — •LUCA MUIGG¹, GERHARD JUNG², THOMAS FRANOSCH¹, and ROLF SCHILLING³ — ¹Institute for Theoretical physics, Universität Innsbruck, Innsbruck, Austria. — ²Laboratoire Charles Coulomb (L2C), Université de Montpellier, CNRS, 34095 Montpellier, France. — ³Institut für Physik, Johannes Gutenberg-Universität Mainz, Germany.

Computer simulations of a monodisperse hard-sphere liquid confined between two parallel hard walls of accessible width L are performed. By reducing the distance between the walls the two-dimensional limit $L \rightarrow 0$ is approached. An analysis of structural properties, such as the structure factor and the radial distribution function shows convergence to their two-dimensional counterparts, which is in agreement to the theoretical predictions. Furthermore an isobaric-like ensemble, with the slit width as an additional degree of freedom is introduced to study the behavior of the compressibility.

CPP 17.56 Mon 18:00 P3

Exploring the deposition conditions for formation of larger homogeneous colloidal arrays — •JOANNE NEUMANN, JAN RUBECK, ANDREI CHUMAKOV, and MATTHIAS SCHWARTZKOPF — DESY, Photon Science, Notkestr. 85, D-22607 Hamburg

Installing regular arrays on mesoscopic length scales plays an important role in nanotechnology to create uniform templates for sputter deposition or plasma treatments. Different techniques of self-assembly via solvent evaporation out of dispersions have been used to obtain highly ordered colloidal structures. We used spin-coating, Langmuir-Blodgett (LB) technique and spray-deposition, representing the most attractive tools for the formation of larger homogeneous colloidal arrays on plain substrates. Due to their different deposition and boundary conditions, the assembly behaviour of polystyrene nanoparticles varies, resulting in two-dimensional layers with LB-technique and a large variety of pattern by spray deposition. We present our first results from atomic force microscopy and microbeam grazing incidence small-angle x-ray scattering (GISAXS).

CPP 17.57 Mon 18:00 P3

Incorporation of Nanomaterials to Form Electrically Conductive Multilayers with the Layer-by-Layer Technique — •MUHAMMAD KHURRAM¹, SVEN NEUBER², ANNEKATRIN SILL³, and CHRISTIANE A. HELM⁴ — ¹muhammad.khurr@uni-greifswald.de — ²sven.neuber@uni-greifswald.de — ³annekatrin.sill@uni-greifswald.de — ⁴helm@uni-greifswald.de

Surface modification of an implant provides an adequate bio-interface and determines which promotes cell adhesion and proliferation. To promote healing, the coating should be electrically conductive. The Layer-by-Layer (LbL) method * sequential adsorption of oppositely charged macromolecules or nanoparticles - has become prominent in coating and functionalizing a surface. Polyelectrolytes show poor charge transfer capabilities; therefore, electrically conductive nanoparticles are essential. MXene nanoparticles are investigated. The MXene contains a high aspect ratio, functional groups, and good electrical conductivity. LbL films are built from polyanion MXene and polycation polydimethylammonium (PDADMA). In addition, the conductive and conjugated polymers poly(3,4-ethylene dioxathiophene):poly(styrene sulfonate) (PEDOT:PSS) is used because of their promising electrical properties. PDADMA is again the polycation. With the Atomic Force Microscope (AFM) film morphology and roughness are determined. Layer growth is monitored by UV-Vis Spectroscopy and ellipsometry. The electrical conductivity is determined with the two-point method.

CPP 17.58 Mon 18:00 P3

Band Gap Modification of 2D Covalent-Organic Frameworks (COFs) with Electron Rich and Electron Deficient Molecules — •LAURA FUCHS, KONRAD MERKEL, and FRANK ORTMANN — School of Natural Sciences, Technische Universität München

A new type of porous materials are covalent-organic frameworks (COFs), which are suitable candidates as active substances for solar cells due to their highly tunable physical and electronic properties. Introducing electron rich (donor) and electron deficient (acceptor) regions to the molecular structure of 2D-COFs has an significant influence on the energetic levels of the highest occupied (HOMOs) and lowest unoccupied molecular orbitals (LUMOs). We provide insights to construction principles for band gap modifications by comparing the nature of the effect of widely-known electron acceptor and donor molecules[1] on the frontier electronic levels, as well as their impact on the charge density distribution using ab initio calculations within the density functional theory (DFT).

[1]Chua, M. H., Zhu, Q., Tang, T., Shah, K. W., & Xu, J. (2019). Diversity of electron acceptor groups in donor-acceptor type electrochromic conjugated polymers. *Solar Energy Materials and Solar Cells*, 197, 32-75.

CPP 17.59 Mon 18:00 P3

From a Completely Different Angle: Exploring Twistoric Layered Materials with Atomic Force Microscopy — •ALEXANDER KLASSEN¹ and JAMES KERFOOT² — ¹Park Systems Europe GmbH Schildkroetstrasse 15,68199 Mannheim, Germany — ²Park Systems UK Limited, MediCity Nottingham Thane Road NG90 8BH, Nottingham, UK

Single atomic layer-based systems emerged as a promising class of materials with unique optical, mechanical, and electronic properties that could provide a pathway to novel applications.1,2 Their two-dimensional nature gives rise to a wide range of tunability since their functional properties do not only depend on the type of atoms and bonds within one plane but also on the strain, local defects, and interplay between adjacent layers.3,4 Here, we present Atomic Force Microscopy (AFM) based approaches as an ideal toolbox to map various functional properties of 2D materials and heterostructures on a nanometer scale. More specifically, by deterministically breaking and re-stacking single flakes of layered materials, we form homostructures of both hexagonal boron nitride (hBN) and molybdenum disulfide (MoS₂) Investigating ferroelectric superlattices on a hexagonal boron nitride bilayer on a graphene single layer, we can induce domain switching when applying a constant DC potential and study them via Piezoelectric Force Microscopy.5,6 We will show how conductive AFM (C-AFM) and Lateral Force Microscopy (LFM) allow imaging strain variations as distorted domains in both the current channel and the lateral force channel.

CPP 17.60 Mon 18:00 P3

Lieb lattice embedded in square polymer — •YINGYING ZHANG, MIROSLAV POLOŽIJ, and THOMAS HEINE — Faculty of Chemistry and Food Chemistry, TU Dresden, Dresden, Germany

Dirac cone and flat band are exotic band features, which attracted much attention in these years, in which the movement of charge carriers is massless fermions, leading to ultra-high carrier mobility and various quantum Hall effects. Structure in lieb lattice owns these two intriguing bands simultaneously, characterized by one dispersive Dirac band inserted with a flat band, which may give rise to many exotic quantum phenomena such as ferromagnetism, topological states, or superconductivity.

The theoretical TB model predicted that the idea lieb band requires rigorous lattice symmetry and zero next-nearest neighbor (NNN) hopping, making the lieb band rarely found in real materials except widely studied via TB model or photonic and cold-atom. There are only two synthesized structures with lieb band were reported.

Therefore, I studied a systematic square phthalocyanine COF with a defined length of linkers, showing that the lieb band is embedded in square polymer. The Pc-xBz COFs show how the band evolution between square and lieb is based on a series of structures with extending linkers. The band structure and charge density distribution are analyzed to further study the electronic properties. We also show that, by charge doping and atom replacement, the fermi level can be tailored to the lieb band position, making the structure intriguing and potential.

CPP 18: Organic Electronics and Photovoltaics I (joint session CPP/HL)

Time: Tuesday 9:30–13:00

Location: GÖR 226

CPP 18.1 Tue 9:30 GÖR 226

Use of a multiple hydride donor to achieve an n-doped polymer with high solvent resistance — FARZANEH SAEEDIFARD^{1,2}, DOMINIQUE LUNGWITZ³, ZI-DI YU⁴, SEBASTIAN SCHNEIDER⁵, AHMED E. MANSOUR^{3,6}, •ANDREAS OPITZ³, STEPHEN BARLOW^{1,2}, MICHAEL F. TONEY¹, JIAN PEI⁴, NORBERT KOCH^{3,6}, and SETH R. MARDER^{1,2} — ¹University of Colorado Boulder, US — ²Georgia Institute of Technology, Atlanta, US — ³Humboldt-Universität zu Berlin, Germany — ⁴Peking University, China — ⁵Stanford University, US — ⁶Helmholtz-Zentrum Berlin für Materialien und Energie GmbH, Germany

Insolubilization of doped semiconducting polymer layers can help to fabricate efficient multilayer solution-processed electronic and opto-electronic devices. Here, we present a promising technique to simultaneously n-dope and largely insolubilize conjugated polymer films using tetrakis[4-(1,3-dimethyl-2,3-dihydro-1H-benzo[d]imidazol-2-yl)phenoxy]methane (tetrakis-O-DMBI-H), which consists of four 2,3-dihydro-1H-benzimidazole (DMBI-H) n-dopant moieties covalently linked to one another. [1] Doping a thiophene-fused benzodifurandione-based oligo(*p*-phenylenevinylene)-*co*-thiophene polymer (TBDOPV-T) with tetrakis-O-DMBI-H results in a highly n-doped film with bulk conductivity of 15 S/cm. Optical absorption spectra reveal a film retention of ~93% after immersion in *o*-dichlorobenzene for 5 min. This is caused by multiple electrostatic interactions the multiple electrostatic interactions between each dopant tetra-cation and up to four nearby anionic doped polymer segments.

[1] F. Saeedifard et al., *ACS Appl. Mater. Interfaces* **14** (2022) 33598.

CPP 18.2 Tue 9:45 GÖR 226

Numerical Simulation of Crystallization Kinetics in Binary Mixtures for Organic Photovoltaic Applications — •MAXIME SIBER, OLIVIER RONSIN, and JENS HARTING — Helmholtz-Institute Erlangen-Nürnberg for Renewable Energies (HI-ERN), Germany

With the aim to understand the formation process of organic photoactive layers, and identify process-structure relationships in order to optimize their fabrication, a computational framework relying on the phase-field modelling approach has recently been developed. It is now sought to quantitatively compare numerical simulations of drying organic photovoltaic (OPV) films with corresponding experimental realizations.

Since the fabrication process involves the interplay of multiple physical phenomena, which separate characterization already is a challenging task from the simulative, as well as from the experimental side, this first study focusses on crystallization behaviour in isothermal, non-evaporating, binary OPV blends. In particular, this talk addresses crystalline structures that arise from different crystallization processes such as solution-triggered crystallization, diffusion-limited crystallization, or spinodal decomposition-assisted crystallization. Furthermore, crystallization kinetics quantified for several blend ratios and material parameters are also analyzed and compared. Finally, perspectives regarding validation against in-situ experiments and derivation of design rules for OPV film fabrication are also provided.

CPP 18.3 Tue 10:00 GÖR 226

Optical properties of perfluorotetracene (PFT) crystal polymorphs — ANA MARIA VALENCIA^{1,2} and CATERINA COCCHI^{1,2} — ¹Institut für Physik, Carl von Ossietzky Universität Oldenburg — ²Physics Dept., Humboldt-Universität zu Berlin und IRIS Adlershof

The family of perfluorinated acenes is gaining popularity among organic materials for optoelectronics. Since the electronic and optical properties of molecular solids are crucially dependent on their packing motifs, it is crucial to consider crystalline phases in the simulations to understand the structure-property relationships of these materials, especially regarding electronic correlations and excitations. Here, we investigate from first principles by means of density functional theory and many-body perturbation theory the electronic structure and the optical excitations of two crystal polymorphs of perfluorotetracene, considering for comparison tetracene and the corresponding isolated molecules. This way, we can assess the effects of fluorination as well as of the crystal periodicity. We find that the absorption spectra are only mildly influenced by the packing motif. However, our analysis gives insight into the exciton binding energies as well as the spatial distribution of the excitons. We inspect not only the first excitations but also the higher-energy ones, thus providing an all-around understanding of the optical excitations in these materials.

CPP 18.4 Tue 10:15 GÖR 226

Controlling long-range order in dip coated piezo- and ferroelectric molecular materials — ANDREY BUTKEVICH and MARTIJN KEMERINK — Institute for Molecular Systems Engineering and Advanced Materials, Im Neuenheimer Feld 225, 69120 Heidelberg, Germany

Organic piezo- and ferroelectrics are of great interest due to their tunable properties. However, the extensive procedures that are often required to achieve saturation polarization limit their possible applications. A so far unexplored possible solution is to pre-align the molecules during the deposition from solution. Here, we analyzed the effect of dip coating parameters on the alignment of multiple supramolecular piezo- and ferroelectrics. Dip coated films were characterized for different material concentrations and dip coating velocities. The investigation revealed that morphologies with strong alignment along the dip coating direction are formed for both material types. For ferroelectrics, the changes in the ferroelectric switching behavior of the resulting thin films were investigated. The ferroelectric switching was investigated using the double wave method, revealing that dip coating perpendicular to the electrodes leads to an almost perfect in-plane alignment of the supramolecular polymers, which was confirmed by X-ray diffraction. The observed switching behavior was comparable to films that were aligned via conventional field-annealing. Hence, dip coating enhanced the ferroelectric switching in the investigated molecules, which we anticipate can be directly transferable to other molecular ferroelectrics.

CPP 18.5 Tue 10:30 GÖR 226

In search of novel organic ferroelectrics — HEIKO MAGER — IMSEAM, Heidelberg University

The switchable polarization and concomitant pyroelectric and piezoelectric properties of ferroelectric materials enable a variety of applications, ranging from memory devices over thermal and mechanical sensors to energy harvesters. Although current applications are dominated by inorganic materials, organic ferroelectrics offer a flexible, cheap and possibly non-toxic and biodegradable alternative.

Here, we present experimental research on the ferroelectric-like behavior of the novel liquid crystalline molecule C₆H₆F₅O-C₃-Amide and its molecular derivatives. To screen for a possible para- to ferroelectric phase transitions, dielectric spectroscopy was employed. While the fer for ferroelectric materials characteristic Curie-Weiß behavior was not directly observed, features in the dielectric suggest a possible phase transition coinciding with a peak in differential scanning calorimetry traces.

Polarization hysteresis loops were obtained via double wave measurements and characteristic capacitance-voltage "butterfly" loops measured. Comparisons between the different molecular derivatives allow insights into the molecular groups relevant for the switching process.

CPP 18.6 Tue 10:45 GÖR 226

Implementation and simulation of drift-diffusion models for organic mixed conductor devices — ANDRES DAVID PEÑA UNIGARRO^{1,2} and FLORIAN STEFFEN GUNTHER^{2,3} — ¹Institute of physics, TU Chemnitz, Chemnitz, Germany — ²IFSC, University of São Paulo, Brazil — ³UNESP, Rio Claro, Brazil

Organic electrochemical transistors (OECTs) have emerged as potential transducers in applications that require the conversion of ion fluxes to electronic current. For the understanding of the fundamental mechanism in OECTs and OECT-based applications, as well as for their rational optimization, however, it is essential to have theoretical models that agree with experimentally measured device responds. Most of the existing OECT models consider that the ion flux from the electrolyte into the organic, semiconducting layer takes place only due to an electrical field. These models are efficient to describe the steady state operations of OECTs, but are rather limited when compared to transient behaviors.

Recently, more refined models which take a diffusion term into account, have been developed. The simplifications needed to use an analytical solution of the governing equation, however, reduces its generality, limiting the results to specific cases. In our work, we use numerical methods to solve the drift-diffusion equation in one dimension to overcome these limitations of the analytical solution. This allows us to go beyond the standard boundary conditions and to analyze the impact of other alterations.

CPP 18.7 Tue 11:00 GÖR 226

Noise in Organics Semiconductors and Devices — PRIYA VIJI, DOROTHEA SCHEUNEMANN, CONSTANTIN TORMANN, and MARTIJN KEMERINK — Institute for Molecular Systems Engineering and Advanced Materials, Heidelberg University, Germany

Noise, typically considered an unwanted signal in measurements, can also contain information about the charge kinetics in organic semiconductors. Since the corresponding devices often show high resistances and capacitances, the measurement of -albeit very small- current fluctuations via voltage noise is most suitable. To quantify this noise and to eliminate noise from other devices in the measurement line, a cross-correlation technique is implemented and applied to P3HT doped with varying concentrations of F4TCNQ. The results compare quantitatively with kinetic Monte Carlo simulations in which noise calculations were implemented. To understand the effect of the electric field on the charge carriers, disentangling noise in directions parallel and perpendicular to the electric field is essential. The direction perpendicular to the electric field does show a gradual increase at high electric fields, which matches the concept of an Effective Temperature, as described by Marianer and Shklovskii, in which the effects of electric field and lattice temperature are combined. In the direction of the electric field, an additional contribution due to shot noise is observed. However, its magnitude deviates from the theoretical prediction of shot noise, which can be quantified as a non-unity Fano-factor.

15 min. break

CPP 18.8 Tue 11:30 GÖR 226

Uniaxially Aligned Merocyanine Films by Graphene Nanoribbon Templated Growth — PHILIPP WEITKAMP, LUKAS BÖHNER, NORA GILDEMEISTER, DIRK HERTEL, and KLAUS MEERHOLZ — Physikalische Chemie, Universität zu Köln, Deutschland

We herein report the unique and novel approach of achieving a polycrystalline thin film consisting of uniaxially aligned domains by using 7-armchair graphene nanoribbon (7-aGNR) monolayers as van-der-Waals template. For this purpose, a merocyanine dye was evaporated on 7-aGNRs, transferred on quartz glass substrates. The alignment of the formed molecular aggregate along the GNR alignment direction was proven by polarisation dependent absorbance spectroscopy. The J- and H-transition, formed by the dye aggregate, were correlated with distinct axes of the crystal structure. By combining this correlation with polarisation dependent absorbance measurements and X-ray diffraction experiments we elucidated the three-dimensional structure of the formed aggregate thin film. The growth mode of these films was investigated as a function of the applied layer thickness. Atomic force microscopy-based morphology analysis and X-ray diffraction experiments were used to reveal the anisotropic on-surface crystallisation along the 7-aGNR long axes direction. Furthermore, we found that the delocalisation length of the aggregate increases with increasing in-plane order. Finally, we demonstrated that the in-plane alignment leads to an anisotropic charge carrier transport by implementing the templated merocyanine thin film as active layer in a top-gated organic field effect transistor.

CPP 18.9 Tue 11:45 GÖR 226

Investigation on organic light-emitting diodes, fabricated by a self-developed and highly automated physical vapor deposition system — FABIAN BINDER, MONA LÖTHER, PASCAL SCHADY, VLADIMIR DYAKONOV, and ANDREAS SPERLICH — Experimental Physics VI, Julius Maximilian University of Würzburg, 97074 Würzburg

Organic light emitting diodes (OLEDs) are most commonly produced in ultra-high vacuum by physical vapor deposition (PVD) of several organic and metallic layers on a carrier substrate. We developed an automated PVD system, mainly consisting of two vacuum chambers for organic and metal deposition, respectively. Stepper motors and sensor solutions ensure a smooth and precise positioning of the carrier substrate above the evaporation crucibles. The substrate is then rotated with a defined speed to achieve an even deposition of the material. In order to vapor-deposit material, a certain material-specific temperature range is required which is realized by a software-based temperature controller which manages the evaporation rate according to the user's specifications. A user interface facilitates planning of the desired OLED layer stack and provides information about the production progress. The capabilities of our new PVD system were tested by producing OLEDs based on multiple-resonance TADF emitters of the DABNA series. We performed electro-optical LJV-characterization and determined the devices' quantum efficiencies. The results of this investigation will enable us to optimize the production process with regard to evaporation rates and layer thicknesses.

CPP 18.10 Tue 12:00 GÖR 226

Improvement of electrical transport in organic semiconductor thin films by charge transfer doping — •HONGWON KIM¹, ANDREAS OPITZ², FLORIAN FENZL¹, and WOLFGANG BRÜTTING¹ — ¹Experimentalphysik IV, Institut für Physik, Universität Augsburg — ²Institut für Physik, Supramolekulare Systeme, HU zu Berlin

Charge carrier transport in organic semiconductor is based on the hopping mechanism. We have used in-situ charge transfer doping during film-growth to improve the electrical conductivity by simultaneously increasing the carrier density and reducing their thermal activation energy. By doping planar organic semiconductors, such as DBTTF, a-6T, and DIP, with strong acceptors (F6-TCNNQ & HATCN), hybridization of pi-orbitals occurs while generating new interphases (charge transfer complex, CTC). On the other hand, DBP, a non-planar molecule, forms an amorphous thin film without any CTC generation. To measure the characteristics of CTC, we used near-infrared transmission spectroscopy, which can detect the absorption peaks of CTCs and the energy gap. In addition, the activation energy is obtained from temperature-dependent conductivity measurements. We observe a correlation between the magnitude of the electrical conductivity and its activation energy, which can be ascribed to the binding energy of CTCs. Depending on the specific system, conductivity maxima are observed between 10 and 30% molar doping ratios.

CPP 18.11 Tue 12:15 GÖR 226

Electrical transport dynamics of conducting polymers in nanoconfinement — SUKANYA DAS and •K.S. NARAYAN — Chemistry and Physics of Materials Unit, Jawaharlal Nehru Centre for Advanced Scientific Research, Bengaluru-560064, India

Inherently disordered conducting polymers consist of different characteristic lengths, defect distribution over the polymer chains and their microstructural modifications can alter the transport properties significantly. The electrical transport of conducting polymers such as poly(3,4-ethylene dioxythiophene):poly(styrenesulfonate) PEDOT:PSS has shown conductivity enhancement when confined in an array of nanochannels in the form of alumina nanopillars. The transverse conductivity along the nanopillar axis, which is an otherwise suppressed quantity, increases nonlinearly by approximately three orders in magnitude as the diameter of the scaffold-channel is decreased to 20 nm, when measured at single nanochannel level as well as at bulk-macroscopic level. This suggests the major role of dimensions and geometry in eliciting efficient electrical transport. Similarly, more than 3 orders of conductivity increase have been shown by in-situ polymerized poly(3,4-ethylenedioxythiophene):tosylate within the nanochannels which has similar electronic backbone PEDOT but a different dopant environment. The microscopic insight into PEDOT:Tos has shown higher degree of crystallinity and ordering as compared to PEDOT:PSS nanochannels. We utilize this property of PEDOT:PSS to fabricate hybrid

organic-inorganic perovskite photodiode with efficient hole extraction and faster response times in the nanoconfined devices.

CPP 18.12 Tue 12:30 GÖR 226

In-situ spectro-electrochemistry of N-type conjugated organic systems for opto-electronic and electro-optic applications — •MEENAL KATARIA and SABINE LUDWIGS — IPOC-Functional Polymers, Institute of Polymer Chemistry, University of Stuttgart, Pfaffenwaldring 55, 70569 Stuttgart, Germany

This talk will highlight our ongoing research on in-situ spectroelectrochemistry. We are developing functional organic conjugated materials and devices for opto-electronic and electro-optic applications. Here, one of our aims is to utilize an in-situ spectroelectrochemical approach to calculate the energy levels of blends of donor polymers (e.g. PM6) and non-fullerene acceptors (e.g. Y6) utilized for high performance organic solar cells. For relevant device information it is important to have precise values of energy levels of the same blend systems as used in devices. Thus, our absorption assisted electrochemistry technique proved to be advantageous approach (1). In another research work discussing the effect of isomerism on conductivity of n-type polymers (e.g. P(NDI2OD-T2)), this above approach has been used to identify the redox states during electrochemical doping which helped to identify the charge transfer transport mechanism (2). In the last example, this technique has been utilized to calculate the frontier energy levels of push-pull D- π -A systems and to study the effect of acceptor strength on their energy levels (3).

Ref. (1) J. Mater. Chem. C 2022, 10, 11565. (2) Chem. Mater. 2019, 31, 3542. (3) Phys.Chem.Chem.Phys. 2020, 22, 2283.

CPP 18.13 Tue 12:45 GÖR 226

Delocalization Enhances Conductivity at High Doping Concentrations — •DENNIS DEREWJANKO¹, DOROTHEA SCHEUNEMANN¹, EMMY JÄRSVALL², ANNA I. HOFMANN², CHRISTIAN MÜLLER², and MARTIJN KEMERINK¹ — ¹IMSEAM, Heidelberg University, Im Neuenheimer Feld 225, 69120 Heidelberg, Germany — ²Department of Chemistry and Chemical Engineering, Chalmers University of Technology, 41296 Gothenburg, Sweden

Many p-type organic semiconductors are experimentally found to follow a universal power-law trend between conductivity and charge carrier concentration at practically relevant high doping levels. This behavior cannot consistently be explained by conventional charge transport models. Here, we develop a physically transparent model based on the combination of a tight binding model and a variable range hopping model to show that the observed power-law trend can be explained by consideration of an energy dependent localization length. The underlying cause is an energetic lifting of the charge carriers to partly delocalized states due to the rising Fermi energy level at high charge carrier concentration. At low charge carrier concentrations, the well-known Mott-Martens model is recovered.

CPP 19: Crystallization, Nucleation and Self-Assembly

Time: Tuesday 9:30–13:00

Location: MER 02

Invited Talk

CPP 19.1 Tue 9:30 MER 02

Multiscale Model of Flow-Induced Crystallization in Polymers — DAVID NICHOLSON, MARAT ANDREEV, CHENMAY GANGAL, and •GREGORY RUTLEDGE — Massachusetts Institute of Technology, Cambridge, MA USA

The structure and properties of a semicrystalline polymer depends sensitively on both its chemico-physical nature and the way it is processed. Flow-induced crystallization (FIC) is one such coupled phenomenon. Models of FIC in polymers must account for the effect of flow on crystallization kinetics, but also the effect of evolving crystallinity on the rheology of the flowing polymer melt. For the first part, atomistic nonequilibrium molecular dynamics (NEMD) simulations are used to characterize the nucleation of a new crystal phase from the polymer melt under homogeneous flow conditions. The kinetics of nucleation are characterized using a mean first-passage time analysis, and a model based on the orientational ordering of Kuhn segments is proposed. For the second part, a variation of the discrete slip-link model (DSM) is used for the rheology of entangled polymer melts that accounts for partial crystallinity through the introduction of crosslinked *bridge* and/or *dangling* segments between developing crystallites, combined with a suspension model to reflect the stiffening associated with a growing crystal phase. This dual-network/suspension model describes well the evolution of both viscoelasticity and crystallinity for a number of linear low-density polyethylenes, and affords a deeper understanding of the essential physics that underlie the coupling between fluid mechanics and phase change.

CPP 19.2 Tue 10:00 MER 02

Polyethylene crystallization induced by a solution-prefolded nucleus — •TIMUR SHAKIROV and WOLFGANG PAUL — University of Halle, Halle, Germany We present results of molecular dynamics simulations of an undercooled

polyethylene melt. We simulate a system of 2000 chains of 150 monomers each with the PYS force-field [1]. To initiate crystallization we insert in the melt a small two-chain nucleus (which we pre-fold in the vacuum) and cool down the system to 280 K. The crystalline lamella forms around the inserted nucleus during the cooling process and grows further at constant temperature. We characterize the growing crystallite by its average diameter (typical linear size in the cross-section perpendicular to the crystal director) and the height of the lamella (the averaged size along the crystal director). Both, diameter and height of lamella, grow during the entire simulation (~ 900 ns at the final temperature). A saturation of the growth is observed only as the crystallite reaches the surrounding spontaneously formed crystallites. Our analysis of the chain kinetics in the inner volume of the crystallite shows remaining chain mobility along the chain director. The distribution of short-time displacements of the inner-crystalline monomers has signatures of discrete jumps of a single bond length along the director of the crystal.

[1] W. Paul, D. Y. Yoon, and G. D. Smith, J. Chem. Phys. 103 (1995) 1702-1709.

CPP 19.3 Tue 10:15 MER 02

How to grow semicrystalline lamellae in MD simulations — WILLIAM FALL^{1,2}, JÖRG BASCHNAGEL¹, OLIVIER LHOST³, and •HENDRIK MEYER¹ — ¹Institut Charles Sadron, CNRS UPR22 and Université de Strasbourg, France — ²LPS Université Paris-Saclay, Orsay, France — ³TotalEnergies One Tech Belgium, Zone Industrielle C, 7181 Feluy, Belgium

To investigate the influence of short chain branches in the crystallization of high molecular weight polyethylene (PE) we adapted a united monomer model for molecular dynamics simulations. We showed recently that a small fraction of branches allows to control the lamellar thickness in the semicrystalline structures [Macromol 55 (2022) 8434]. This work is extended to bidisperse mixtures

of highly entangled C_{4000} and C_{400} with different branch distributions mimicking industrial PE morphologies. A self-seeding protocol is presented which allows to simulate the growth of well aligned lamella, and analyse morphological features. We thank TotalEnergies for funding and GENCI/IDRIS (Orsay) and CAIUS/HPC centre (Strasbourg).

CPP 19.4 Tue 10:30 MER 02

Crystallization precursors in polymer melt analyzed by machine learning

— •ATMIKA BHARDWAJ^{1,2}, MARCO WERNER¹, and JENS-UWE SOMMER^{1,2} — ¹Leibniz-Institut für Polymerforschung Dresden e. V., Hohe Str. 6, D-01069 Dresden, Germany — ²Institute for Theoretical Physics, Technische Universität Dresden, Zellescher Weg 17, D-01069 Dresden, Germany

Crystallization in polymers is a long-standing problem in both experimental and theoretical polymer science. The transition dynamics occurring in an undercooled polymer melt is a local environmental phenomenon rather than a property of individual particles (or monomers) and depends on subtle conformation patterns such as entanglements between the chains. We develop machine learning (ML) methods to study this non-equilibrium thermodynamic process. Upon recognizing the relevant parameter set to explore different phases during polymer crystallization, we investigate the spatial and temporal patterns of the precursor states that determine the nucleation sites. The objective is to recognize the precursors that stimulate crystal growth before the occurrence of such development.

CPP 19.5 Tue 10:45 MER 02

How entanglements determine the morphology of semicrystalline polymers — ZEFAN WANG, MAREEN SCHALLER, ALBRECHT PETZOLD, KAY SAALWÄCHTER, and •THOMAS THURN-ALBRECHT — Institut für Physik, Martin-Luther-Universität Halle-Wittenberg, 06099 Halle

Crystallization of polymers from entangled melts generally leads to the formation of semicrystalline materials with a nanoscopic lamellar morphology. Controlling this structure is key to the rational design of thermoplastic materials, but there is no consensus yet on the factors that control the thickness of the amorphous layers and therefore together with the crystal thickness the crystallinity. We here elucidate the effect of entanglements on the morphology in a series of model blends of high-molecular-weight polymers with unentangled oligomers leading to a reduced entanglement density in the melt as characterized by rheological measurements. Small-angle X-ray scattering experiments after isothermal crystallization reveal a reduced thickness of the amorphous layers, while the crystal thickness remains largely unaffected. A simple yet quantitative model without adjustable parameter is suggested, according to which the measured thickness of the amorphous layers adjusts itself in such a way that the entanglement concentration reaches a specific maximum value.

CPP 19.6 Tue 11:00 MER 02

Modelling Study of Reinforcement and Crack Formation in Strain-Crystallizing Elastomer Networks — •LENA TARRACH¹, REINHARD HENTSCHKE¹, and JAN WEILERT² — ¹Bergische Universität Wuppertal, Wuppertal, Germany — ²Covestro Deutschland AG, Leverkusen, Germany

A coarse-grained model has been developed to simulate reinforcement and crack formation in strain-crystallizing elastomer networks. This work is based on the model for strain-induced crystallization (SIC) proposed by Plagge and Hentschke [1], which here is extended for the investigation of rupture.

Generally, strain-crystallizing elastomer networks possess a higher tensile strength than non-crystallizing networks. Therefore, the force on the links, i.e. the polymer chains in the model network, is analyzed to define a critical force for their rupture. It is examined how structural parameters and parameters for the free energy of semi-crystalline links affect the tensile strength of strain-crystallizing networks compared to non-crystallizing networks. The variation of these parameters does not improve the tensile strength in both the 2D- and the 3D-case.

Thus, a critical crystallinity, which makes certain links unbreakable, is introduced to model the alignment of the polymer backbones along the stretching direction. The tensile strength of 2D- and 3D-networks is enhanced.

[1] Plagge, J. & Hentschke, R. Microphase Separation in Strain-Crystallizing Rubber. *Macromolecules* 54, 5629-5635. <https://doi.org/10.1021/acs.macromol.1c00757> (2021).

15 min. break

CPP 19.7 Tue 11:30 MER 02

New experimental setup to analyze structure formation in thermoplastic polymer melts

— •ANNA KATHARINA SAMBALE¹, ERIC EUCHLER¹, REGINE BOLDT¹, KAI UHLIG¹, LAURA NEUMANN¹, KONRAD SCHNEIDER¹, MATTHIAS SCHWARTZKOPF², STEPHAN ROTH^{2,3}, and MARKUS STOMMEL^{1,4} — ¹Leibniz-Institut fuer Polymerforschung, Dresden, Germany — ²Deutsches Elektronen Synchrotron DESY, Hamburg, Germany — ³KTH Royal Institute of Technology, Stockholm, Sweden — ⁴Technical University Dresden, Dresden, Germany

The microstructure of semi-crystalline thermoplastics is significantly influenced by the processing procedure and its parameters. Inhomogeneous shear and ex-

tensional flow fields occurring during processing can cause constraints to the chain conformations, which in turn lead to altered crystallization behavior. Although the influence of crystallization kinetics on the properties of the most commonly used polymers is considered to be sufficiently known, (local) conditions and parameters in commercially used melt processing technologies are not fully understood. We recently started to develop a new experimental setup to study structure formation in polymers induced by melt processing. The first results on the crystallization processes in quiescent polymer melts under isothermal conditions investigated by X-ray scattering measurements will be presented. In particular, time- and temperature-dependent crystallization of polylactic acid (PLA) and isotactic polypropylene (iPP) with different crystallization rates were examined and proved the concept of the experimental setup.

CPP 19.8 Tue 11:45 MER 02

The missing billions in hard sphere nucleation — SAHANA KALE, NIDHI JOSHI, and •HANS JOACHIM SCHÖPE — Universität Tübingen, Institut für angewandte Physik, Auf der Morgenstelle 10, 72076 Tübingen

Crystal nucleation in colloidal hard spheres is a longstanding research topic in colloidal science. Light scattering experiments as well as simulations have been carried out to determine key parameters characterizing the nucleation process and to get a microscopic picture of the fluid to crystal transformation. In these studies, results both differ and agree with each other. It is still unclear whether the large disagreement in the nucleation rate densities between the experiments and simulations are of physical nature or result from different data analyses. Using laser-scanning confocal microscopy and polarization microscopy we study crystal nucleation in colloidal hard spheres. The used systems have been characterized with extreme care to allow for meaningful comparison with other experiments and simulations. We present high quality data of the nucleation rate density and key parameters describing crystal nucleation. Analyzing the nucleation process we conclude that classical nucleation theory fails.

CPP 19.9 Tue 12:00 MER 02

Non-metallic quasicrystals minimize sphere packing energy — •MARTIN DULLE¹, VLADISLAVA FOKINA¹, THOMAS GRUHN², and STEPHAN FÖRSTER¹ — ¹Forschungszentrum Jülich, Jülich, Germany — ²Universität Bayreuth, Bayreuth, Germany

Quasicrystals are a peculiar state of order, which is fundamentally different from classical ordered crystalline states. Discovered in 1982 for metal alloys, they have in recent years also been reported for an increasing number of non-metallic materials.

Using MD-simulations we calculate the phase diagram of soft repulsive core/shell particles and find stability regions for seven different octagonal, decagonal, dodecagonal and icosahedral quasicrystals. We compare the structure and stability region of the dodecagonal phase with experiments on different polymer and nanoparticle systems and find quantitative agreement. We identify a new high density dodecagonal phase in a large number of reported non-metallic quasicrystalline systems including polymers, mesoporous silica, surfactants, BaTiO₃, TaTe and MnCrNiSi. All remaining reported non-metallic quasicrystals can be related to the other simulated quasicrystal types.

We geometrically derive all respective tilings and show how in-plane quasicrystalline order is combined with axial periodic order via the realization of certain gyro-elongated bipyramids. This geometrical arrangement minimizes sphere packing energy for certain length scale ratios and particle densities, irrespective of the absolute length scale, the type of interactions and chemical constituents.

CPP 19.10 Tue 12:15 MER 02

Controlling internal structure of colloidal supraparticles - crystalline to amorphous — •YASHRAJ WANI¹, MELIS YETKIN², MICHAEL KAPPL², HANS-JÜRGEN BUTT², and ARASH NIKOUBASHMAN¹ — ¹Institute of Physics, JGU Mainz, Germany — ²Max Planck Institute for Polymer Research, Mainz, Germany

Colloidal supraparticles made from smaller nanoparticles (NPs) are versatile materials whose properties can be tailored through the chemistry and ordering of their constituent NPs. Such supraparticles can be scalably fabricated using solvent-drying processes that assemble NPs inside liquid droplets. In charge stabilized dispersions, the interactions can be controlled by the salt concentration, which we systematically probed in experiments and simulations. In experiments at low salt concentrations, the dried supraparticles exhibited high crystalline order, whereas amorphous structures were found at high salinity. To understand this evaporation-induced structure formation, we first determined the interaction potentials between NPs via colloidal probe atomic force microscopy and dynamic light scattering experiments. Using these pair potentials, we carried out particle-based simulations to study the aggregation behavior in detail: At low salt concentrations, the effective NP-NP interactions remained purely repulsive until the end of drying, resulting in highly crystalline supraparticles. At higher salt concentrations, however, the electrostatic repulsion became screened, leading to the formation of small NP aggregates at early stages of drying, which then eventually merged into an amorphous supraparticles.

CPP 19.11 Tue 12:30 MER 02

Unravelling the synthesis of halide perovskite nanoplatelets by SAXS — •KILIAN FRANK¹, CAROLA LAMPE², ALEXANDER S. URBAN², and BERT NICKEL¹ — ¹Soft Condensed Matter Group and CeNS, Faculty of Physics, LMU Munich — ²Nanospectroscopy Group and CeNS, Nano-Institute, Faculty of Physics, LMU Munich

Halide perovskite nanoplatelets (NPLs) are a promising material for optoelectronic applications, such as LEDs and single photon emitters. While highly scalable and reliable ligand-assisted synthesis routes exist, a detailed structural understanding of the underlying pathways is lacking. We elucidate the processes of nucleation, growth, and superstructure assembly of CsPbBr₃ NPLs using in situ small-angle X-ray scattering (SAXS), total scattering (TS) and photoluminescence (PL) spectroscopy during the synthesis. Thereby we enable even better control of the platelet thickness on the monolayer level, and therefore of the emission wavelength, due to quantum confinement. For this purpose we built and used a specialized reaction cell for in situ synthesis at the beamlines P07 and P62 (PETRAIII, DESY, Hamburg). By SAXS analysis we follow the assembly of the constituents into a regular superstructure. In addition, we investigated the effect of post-synthetic treatment of the NPLs using the same setup to further enhance their optoelectronic properties. With our results we contribute to the development of assembly-based synthesis routes for size-tunable nanomaterials. Such materials are of particular interest to the perovskite community as building blocks for hierarchical structures.

CPP 19.12 Tue 12:45 MER 02

From protein adsorption to crystallization: a simultaneous real-time QCM-D and microscopy study — •HADRA BANKS, FURIO SURFARO, SIMON STORZ, ANNA MAISCHBERGER, CARA BUCHHOLZ, KAI-FLORIAN PASTRYK, ALEXANDER GERLACH, and FRANK SCHREIBER — University of Tübingen, Germany

Protein crystallization is widely investigated by employing a homogeneous nucleation approach; however, it is predicted that heterogeneous nucleation is energetically more favorable [1]. Nevertheless, only few experimental studies on the nucleation of protein crystals at surfaces are available, since this is a complex phenomenon and requires surface-sensitive techniques. Here, quartz crystal microbalance with dissipation monitoring (QCM-D), a real-time surface-sensitive technique, was employed simultaneously with optical microscopy to investigate protein adsorption and crystallization at a negatively charged surface. Human serum albumin (HSA) and β -lactoglobulin (BLG), in the presence of a trivalent salt, were used as model systems for the study of heterogeneous nucleation [2]. We found that their surface behavior during crystallization exhibit complex phenomena such as wetting transition, enhanced adsorption, and layer rearrangements. The results highlight the importance of the interaction between proteins and surfaces and how this can influence protein phase behavior.

[1] J. R. Espinosa et al., *Soft Matter* 15 (47), 9625-9631, 2019

[2] O. Matsarskaia et al., *ChemPhysChem* 21 (16), 1742-1767, 2020

CPP 20: Polymer and Molecular Dynamics, Friction and Rheology

Time: Tuesday 9:30–12:30

Location: ZEU 255

Invited Talk

CPP 20.1 Tue 9:30 ZEU 255

Granular Matter Rheology – fluid-/solid-like behavior and state-transitions — •STEFAN LUDING — University of Twente, NL

The dynamic and static behavior of particulate and granular matter (like sand, powder, suspended particles, often with a wide distribution of particle sizes) is of considerable interest in a wide range of industries and research disciplines. Special is that they can behave both solid-like and fluid-like, which is a challenge for both academia and industry. The related mechanisms/processes in particle systems are active at multiple scales (from nano-meters to meters), and explaining their multiple states, and transitions, will lead to a better understanding of natural disasters like avalanches or industrial problems like silo-failure.

To understand the fundamental micro-mechanics and -physics, one can use particle simulation methods. However, large-scale applications (due to their enormous particle numbers) have to be addressed by coarse-grained models or by continuum theory. For this, to derive constitutive rheology relations, so-called micro-macro transition methods are necessary, which translate particle positions, velocities and forces into density-, stress-, and strain-fields, which must be compatible with the balance equations for mass, momentum, and energy of continuum theory. Additional non-classical fields describe the micro-structure (fabric, force-chains) or the statistical fluctuations, before a universal granular rheology can be defined, involving state-transitions between the states, the so-called jamming/un-jamming transitions.

CPP 20.2 Tue 10:00 ZEU 255

Phase-Sensitive, Active Microrheology via Probe-Free Application of Thermoviscous Flows — •ILIYA STOEV, ELENA ERBEN, VENKAT KRISHNASWAMY, ANTONIO MINOPOLI, SUSAN WAGNER, BENJAMIN SEELBINDER, NICOLA MAGHELLI, and MORITZ KREYSING — Max Planck Institute of Molecular Cell Biology and Genetics, Pfotenhauerstraße 108, 01307, Dresden, Germany

We recently found how thermoviscous expansion phenomena give rise to a new, contactless particle trap that is characterised by a linear force-extension relationship and can therefore be employed in non-invasively measuring femtoNewton forces with thermally limited sensitivity. Our new force-measurement method is based on optically generated flows, thereby lifting prerequisites related to the probe material and resulting in only moderate heating at the position of the micromanipulated object. This methodology offers an appealing alternative to the use of optical tweezers in highly delicate samples and living systems. Next, we asked the question if our thermoviscous flows can be used to obtain more quantitative data and possibly demonstrate the equivalence between flow-driven and force-driven rheology in their ability to extract phase angles as a measure of relative mechanics. With our new flow-based and phase-sensitive microrheology, we provide access to the mechanics of highly viscous media, tenuous gels and even cellular cytoplasm. Further refinements of the method aim at multiplexing and removing the need for using fluorescent tags.

CPP 20.3 Tue 10:15 ZEU 255

Nanoscope Friction on Monolayer MoS₂ in Presence of Water Investigated with Molecular Dynamics — •MILJAN DAŠIĆ and IGOR STANKOVIĆ — Scientific Computing Laboratory, Center for the Study of Complex Systems, Institute of Physics Belgrade, University of Belgrade, Pregrevica 118, 11080 Belgrade, Serbia

We have implemented and applied a molecular dynamics (MD) simulation setup in order to study the nanoscopic friction on monolayer MoS₂ plate in the presence of different quantities of water. Our setup mimics a standard AFM experiment, including an amorphous SiO₂ probe, a monolayer crystalline MoS₂ plate, and water molecules in-between. Presence of water molecules matches experimental conditions of air humidity. We studied two different quantities of water: (1) *full water layer* - SiO₂ probe is fully immersed in water and surrounded by water molecules, and (2) *capillary water* - water forms a capillary around the SiO₂ probe, with lateral vacuum gaps. We conducted two modes of simulations: vertical approach of SiO₂ probe towards MoS₂ plate and lateral sliding of SiO₂ probe. There are always *trapped* water molecules in the gap between the probe and the plate; their number drops with the increase of temperature. We have obtained well-pronounced *stick-slip* friction loops; we found that an increase of the applied normal load leads to the more pronounced stick-slip behaviour, as seen in AFM experiments. The amount of water present in the studied nanoscopic tribosystem has a pronounced impact on the stick-slip frictional behaviour.

CPP 20.4 Tue 10:30 ZEU 255

Polymers of Intrinsic Microporosity - Molecular Mobility and Physical Aging Revisited by Dielectric Spectroscopy and X-Ray Scattering — •FARNAZ EMAMVERDI, GLEN JACOB SMALES, MARTIN BÖHNING, and ANDREAS SCHÖNHALS — Bundesanstalt für Materialforschung und -prüfung (BAM), Unter den Eichen 87, 12205 Berlin, Germany

The applications of polymers of intrinsic microporosity (PIMs) membranes are restrained by their strong tendency to physical aging. Aging phenomenon involves a significant loss of their good performance in gas separation technology. The initial microporous structure approach a denser state via local rearrangements, leading to a reduction of the permeability. In this work, the dielectric behavior of PIM-1 films and their behavior upon hating (aging) were revisited by isothermal frequency scans during different heating/cooling cycles over a broad temperature range between 133 K and 523 K. In addition, the obtained results were compared with data of samples that were annealed at ambient temperatures over different time scales. Multiple dielectric processes were observed: several relaxation processes due to local fluctuations and a Maxwell-Wagner-Sillars polarization effect related to microporosity. The temperature dependence of the rates of all processes follows the Arrhenius law where the estimated activation energy depends on the nature of the process. SAXS/WAXS patterns were measured as a function of temperature during heating/cooling in a temperature range corresponding to that covered by dielectric spectroscopy. The influence of the aging on the processes is discussed in detail.

CPP 20.5 Tue 10:45 ZEU 255

Viscoplastic Modeling of Surface Relief Grating Growth on Isotropic and Pre-oriented Azopolymer Films — TVERDOKHLEB NINA¹, LOEBNER SARAH², SAN-TER SVETLANA², and MARINA SAPHIANNIKOVA¹ — ¹Institute Theory of Polymers, Leibniz Institute of Polymer Research Dresden, 01069 Dresden, Germany — ²Institute of Physics and Astronomy, University of Potsdam, 14476 Potsdam, Germany

We report on solving two intriguing issues concerning the inscription of surface relief gratings within azopolymer thin films under irradiation with SS, PP and RL interference patterns. For this, we utilize the orientation approach and viscoplastic modeling in combination with experimental results, where the change in surface topography is acquired in-situ during irradiation with modulated light. First, the initial orientation state of polymer backbones is proved to be responsible for the contradictory experimental reports about the efficiency of the SS interference pattern. Different orientation states can influence not only the phase of SS grating but also its height, which is confirmed experimentally using special pre-treatments. Second, faster growth of gratings inscribed by the RL interference pattern is shown to be promoted by a weak photo-softening effect. Overall, the modeled results are in good agreement with the order of relative growth efficiency: RL-PP-SS.

CPP 20.6 Tue 11:00 ZEU 255

Equilibration of free-standing films of highly entangled polymer melts — HSIAO-PING HSU and KURT KREMER — Max-Planck-Institut für Polymerforschung, Ackermannweg 10, 55128, Mainz, Germany

Equilibrating confined and free-standing films of highly entangled polymer melts is a challenge for computer simulations. We approach this problem by first studying polymer melts based on a soft-sphere coarse-grained model confined between two walls. The distance of the walls is compatible with the simulation box of bulk melts in equilibrium, while periodic boundary conditions in the directions parallel to the walls are kept. Then we successively insert more fine grained polymer representations until the underlying microscopic details of the bead-spring model are reached. Tuning the wall potential, the monomer density of confined polymer melts in equilibrium is kept at bulk melt density even near the walls. Switching to another recently developed variant of the bead-spring model we can study melts at zero pressure [1] and study free-standing polymer films [2]. Furthermore, this also allows us to study free-standing films under strain and analyze the influence of entanglements on the local film morphology. [1] H.-P. Hsu, K. Kremer, J. Chem. Phys. 150, 091101 (2019); 150, 159902 (2019). [2] H.-P. Hsu, K. Kremer, J. Chem. Phys. 153, 144902 (2020); 156, 019901 (2022).

15 min. break

CPP 20.7 Tue 11:30 ZEU 255

A nanofluidic system based on cylindrical polymer brushes: molecular dynamics simulation and scaling theory — CHENG-WU LI — Leibniz-Institut für Polymerforschung Dresden, Germany

Using molecular dynamics simulations and scaling theory, we present a systematic study of the function of cylindrical nanopores which are decorated with polymer brushes. Our focus is on the regimes in which these systems are able to function as controllable (switchable) gates for bulky nanoparticles. In a slightly poorer solvent, closed cylindrical brushes facilitate the self-organized formation of droplets from a continuous flow of incoming nanoparticles. We analyze droplet formation and propagation by means of simple scaling arguments which are tested in the simulations. Polymer brushes in marginally poor solvents serve as a pressure feedback system, exhibit a collapse transition under the moderate pressure of the incident flow, without the need for additional external stimuli, and finally close spontaneously after droplet passage. Our results qualitatively demonstrate the control of polymer brushes over continuous fluids and droplet formation, and its effectiveness as a means of fluid control can be used to design nanofluidic rectification devices that operate reliably under moderate pressure.

CPP 20.8 Tue 11:45 ZEU 255

Polymer chain dynamics under shear studied by rheological NMR — ULRICH SCHELER — Leibniz-Institut für Polymerforschung Dresden e.V., Dresden, Germany

The NMR spin-lattice relaxation time T_2 is particularly sensitive to slow chain-segment motion in polymers, at least two components in the signal decay are observed, a faster relaxing component from chain segments of motion restricted by crosslinks or entanglements and a slower component associated with parts moving more freely. Ordering of the polymer chains under shear would result in restrictions for the segment motion and thus a shortening of T_2 , a loss of entanglements due to the shear results in a prolongation of T_2 . Rheological NMR combined external shear with NMR experiments. In a polymer melt of poly(dimethylsiloxane) under shear longer relaxation times are observed. Together with a reduction of the fraction of shorter T_2 this indicates the loss of entanglements is the dominating process for high molecular weight. In a new experimental setup both the amplitude and the frequency of the deformation are varied. It demonstrates that a minimum strain rate above 1000/s is required to observe the loss of entanglements. Combining pulsed-field-gradient (PFG) NMR with NMR imaging permits to measure flow pattern. After the turning point in oscillatory shear counterflow is observed when a fraction of the liquid at the static wall still is in initial flow direction while liquid in contact with the moving bob started in the new direction. At this time the velocity gradient drastically exceeds the velocity gradient at the point of maximum velocity representing a high shear rate.

CPP 20.9 Tue 12:00 ZEU 255

On the Relaxation Behavior of Linear Chains under Oscillatory Forces — RON DOCKHORN¹ and JENS-UWE SOMMER^{1,2} — ¹Leibniz-Institut für Polymerforschung Dresden e.V., D-01069 Dresden, Germany — ²Technische Universität Dresden, Institut für Theoretische Physik, D-01069 Dresden, Germany

We are studying the relaxation spectra and the force-extension behavior of linear chains under externally driven oscillatory periodic forces f in means of theory and simulations. An oscillatory force $f = f_0 + f_a \cdot \sin(\omega t)$ is applied on the chain ends and the response of the end-to-end-distance R as well as the relaxation time τ_R on the oscillatory frequency ω is investigated. An analytical expression for the end-to-end-distance $R(f)$ is derived by using the Rouse model and compared to simulations. The dissipated energy is calculated by the hysteresis loop $A = \oint dfR(f)$, which shows a characteristic maximum at $\omega\tau_R \approx 1$ for ideal chains independent of the applied force. Contrary, excluded volume chains show a force dependence on the relaxation time $\tau_R \sim f^{-0.3}$ as well as a shift on the hysteresis in the Pincus regime. Extensive computer simulations are performed to investigate the scaling properties utilizing the Bond-Fluctuation-Model. Furthermore, the relaxation behavior of different polymer architectures (ring polymer, 3₁-trefoil knot, two concatenate rings) are compared to the linear chain behavior. The theory and simulations suggests implications for dynamic experiments of biopolymer subject to external forces.

CPP 20.10 Tue 12:15 ZEU 255

Orientation Polarization Spectroscopy — FRIEDRICH KREMER, WYCLIFFE KIPNUSU, and MARKUS ANTON — Leipzig University, Peter Debye Institute for Soft Matter Physics, Linnéstr.5, 04103 Leipzig, Germany

The theory of orientation polarization and dielectric relaxation was developed by P. Debye more than 100 years ago. It is based on approximating a molecule by a sphere having one or more dipole moments. By that the detailed intra- and intermolecular interactions are explicitly not taken into consideration. In this contribution the principal limitations of the Debye approximation are discussed and novel experiments based on Quantum Cascade IR-Lasers are presented [1] which enable to determine the orientation polarization of selected molecular moieties for the example of the glass forming liquid glycerol. [1] Kremer, F. et al. Int. J. Mol. Sci. 23, 8254 (2022)

CPP 21: Active Matter III (joint session BP/CPP/DY)

Time: Tuesday 9:30–12:30

Location: TOE 317

See BP 9 for details of this session.

CPP 22: 2D Materials III (joint session HL/CPP)

Time: Tuesday 9:30–12:15

Location: POT 81

See HL 14 for details of this session.

CPP 23: Optical Properties (joint session HL/CPP)

Time: Tuesday 9:30–13:00

Location: POT 112

See HL 18 for details of this session.

CPP 24: Complex Fluids and Soft Matter I (joint session DY/CPP)

Time: Tuesday 10:00–13:00

Location: MOL 213

See DY 16 for details of this session.

CPP 25: Molecular Electronics and Photonics (joint session TT/CPP)

Time: Tuesday 12:00–13:00

Location: HSZ 201

See TT 25 for details of this session.

CPP 26: Electrical, Dielectrical and Optical Properties of Thin Films

Time: Tuesday 14:00–14:45

Location: MER 02

CPP 26.1 Tue 14:00 MER 02

Electronic and optical properties of thin film P3HT-based thermoelectrics

— •SIMON SCHRAAD^{1,2}, BENEDIKT SOCHOR¹, CONSTANTIN HARDER^{1,3}, PETER MÜLLER-BUSCHBAUM^{3,4}, TIM LAARMANN^{1,2}, and STEPHAN VOLKHER ROTH^{1,5} — ¹Deutsches Elektronen Synchrotron DESY, Notkestraße 85, 22607 Hamburg, Germany — ²University Hamburg, Mittelweg 177, 20148 Hamburg, Germany — ³MLZ, TUM, 85747 Garching, Germany — ⁴Research Neutron Source Heinz Maier-Leibnitz, Lichtenbergstraße 1, 85747 Garching, Germany — ⁵KTH Royal Institute of Technology, Teknikringen 56-58, Stockholm, Sweden

The polymer Poly(3-hexylthiophen-2,5-diyl) (P3HT) is widely considered in research of organic electronics. If doped with metal chlorides or nanoparticles, P3HT shows thermoelectric properties. Deposition of small gold domains inside the polymer films optimizes the charge transport properties and thermoelectric Seebeck-coefficient and hence the so-called figure of merit zT . There is usually an Au, P3HT intermixing layer near the surface, but implanting the dopant deep inside the organic films results in higher thermoelectric coefficients. P3HT and Poly(3-hexylthiophen-2,5-diyl)-block-poly(methyl methacrylate) (P3HT-b-PMMA) diblock copolymer derivatives were prepared by spray deposition and doped via chloroauric acid. Here, structural, optical and (thermo-)electrical properties were determined using AFM, ellipsometry as well as conductivity measurements. The results are a first step towards sprayed organic thermoelectric device, with great scalability potential in future industrial applications.

CPP 26.2 Tue 14:15 MER 02

On the way to sustainable photoluminescent tags — •HEIDI THOMAS, SHUAIFEI ZHU, SEBASTIAN SCHELLHAMMER, and SEBASTIAN REINEKE — IAPP, TU Dresden

Recently, by using amorphous purely organic systems, we have been able to develop transparent programmable luminescent tags (PLTs) which can be used for labelling application or data storage [1,2]. So far the system consists of a phosphorescent organic emitter embedded in poly(methyl methacrylate) on quartz substrate or flexible foil. An oxygen-blocking layer allows for the spatial control

of the phosphorescence of the system. The demand for sustainable solutions is high motivating the design of ecofriendly information storage. Here we present the investigation of suitable biocompatible and/or biodegradable polymers and emitters for their use in PLTs.

[1] Gmelch, M.; Thomas, H.; Fries, F.; Reineke, S. Programmable Transparent Organic Luminescent Tags. *Sci. Adv.* (2019).

[2] Gmelch, M.; Achenbach, T.; Tomkeviciene, A.; Reineke, S. High-Speed and Continuous-Wave Programmable Luminescent Tags Based on Exclusive Room Temperature Phosphorescence (RTP). *Adv. Sci.* (2021).

CPP 26.3 Tue 14:30 MER 02

Programmed Assembly of Dipolar Precursors into Porous, Crystalline Molecular Thin Films — •ALEXEI NEFEDOV¹, RITESH HALDAR¹, ZHIYUN XU¹, HANNES KÜHNER¹, DENNIS HOFMANN², DAVID GOLL², BENEDIKT SAPOTTA¹, STEFAN HECHT³, MARJAN KRSTIĆ¹, CARSTEN ROCKSTUHL¹, WOLFGANG WENZEL¹, STEFAN BRÄSE¹, PETRA TEGGERER², EGBERT ZOJER⁴, and CHRISTOF WÖLL¹ — ¹Karlsruhe Institute of Technology, Eggenstein-Leopoldshafen, Germany — ²Universität Heidelberg, Heidelberg, Germany — ³RWTH Aachen University, Aachen, Germany — ⁴Graz University of Technology, Graz, Austria

Liquid-phase, quasi-epitaxial growth has been used to stack asymmetric, dipolar organic compounds on inorganic substrates, permitting porous, crystalline molecular materials which lack inversion symmetry. This allows material fabrication with built-in electric fields. We describe a new programmed assembly strategy based on metal-organic frameworks (MOFs) that facilitates crystalline, non-centrosymmetric space groups for achiral compounds. Electric fields are integrated into crystalline, porous thin films with an orientation normal to the substrate. Changes in electrostatic potential are detected via core-level shifts of marker atoms on the MOF thin films and agree with theoretical results. The integration of built-in electric fields into molecular solids creates possibilities for band structure engineering to control the alignment of electronic levels in organic molecules and it may also be used to tune the transfer of charges from donors loaded via programmed assembly into MOF pores.

CPP 27: Glasses and Glass Transition I (joint session DY/CPP)

Time: Tuesday 14:00–15:00

Location: ZEU 147

See DY 24 for details of this session.

CPP 28: Molecular Electronics and Excited State Properties (joint session CPP/TT)

Time: Wednesday 9:30–12:30

Location: GÖR 226

CPP 28.1 Wed 9:30 GÖR 226

Strong Solvatochromism in a Two Metal Center Photocatalyst Molecule — •MIFTAHOSSURUR HAMIDI PUTRA¹ and AXEL GROSS^{1,2} — ¹Universität Ulm Institut für Theoretische Chemie Mez-Starck-Haus Oberberghof 7 89081 Ulm Deutschland — ²Helmholtz Institute Ulm (HIU) Electrochemical Energy Storage, 89069 Ulm, Deutschland

In the theoretical study presented here, we show that the electronic and optical properties of a molecular photocatalyst can strongly depend on the sol-

vent it is dissolved in [1]. Ground-state density functional theory and linear response time dependent density functional theory calculations are applied in order to investigate the influence of implicit solvents on the structural, electronic and optical properties of a two metal center molecular photocatalyst $[(\text{tbbpy})_2\text{Ru}(\text{tpphz})\text{PtI}_2]^{2+}$ (RuPtI_2) [2]. These calculations predict a significant dependence of the HOMO-LUMO gap of the photocatalyst on the dielectric constant of the solvent. We elucidate the electronic origins of this strong solvatochromic effect and sketch the consequences of these insights for the use of

photocatalysts in different environments.

[1] M. K. Nazeeruddin, S. M. Zakeeruddin, R. Humphry-Baker, M. Jirousek, P. Liska, N. Vlachopoulos, V. Shklover, C.-H. Fischer, M. Grätzel, *Inorg. Chem.* **38**, 6298-6305 (1999).

[2] M. G. Pfeffer, T. Kowacs, M. Wächtler, J. Guthmüller, B. Dietzek, J. G. Vos, S. Rau, *Angew. Chem.* **54**, 6627-6631 (2015).

CPP 28.2 Wed 9:45 GÖR 226

Dynamic Charge-Transport and Charge-Transfer Regimes for Electron-Phonon-Coupled Molecular Systems — •MICHEL PANHANS, SEBASTIAN HUTSCH, and FRANK ORTMANN — Department of Chemistry, TU München

Different approaches for charge transport in organic solids exist but they differ significantly in the described physics of the electron-phonon coupling. In our recent work, we investigate the charge-transfer dynamics, the fading of transient localization (TL) and the formation of polarons for a large range of vibration frequencies and temperatures in the phase space of the two-site Holstein model. The combined numerical and analytical method is based on the time-domain Kubo formula of electrical conductivity to describe the highly correlated electron-phonon dynamics from femtoseconds to very large time scales, reaching nanoseconds. We identify three charge-transport regimes, which are TL, soft gating, and polaron transport. Of particular interest is the built up of correlations between the electronic motion and the nuclei manifesting in the crossover between TL and polaron transport. We find, that the transition between these two limiting cases is seamless at all temperatures and all adiabatic ratios even for the low-frequency vibrational modes that were often considered to be frozen.

CPP 28.3 Wed 10:00 GÖR 226

Multichromophore Macrocycles of Perylene Bisimide Dyes as Fluorescent OLED Emitters — •BJÖRN EWALD¹, ULRICH MÜLLER¹, PETER SPENST², PHILIPP KAGERER¹, THEODOR KAISER¹, MATTHIAS STOLTE², FRANK WÜRTHNER², and JENS PFLAUM¹ — ¹Experimental Physics VI, University of Würzburg, 97074 Würzburg — ²Institut für Organische Chemie and Center for Nanosystems Chemistry, University of Würzburg, 97074 Würzburg

Highly efficient electroluminescence from Organic Light Emitting Diodes (OLEDs) is limited by the non-radiative character of triplet states for conventional fluorophores. While fluorescent emitters benefit from high radiative recombination rates on the order of 10^9 s^{-1} , they lack from dark triplet states with lifetimes up to several μs or ms. Here we elucidate the potential of perylene bisimide macrocycles as a novel class of fluorescent OLED emitters by applying photon-correlation studies. The correlation experiments unfold additional excitonic relaxation pathways shortening the dark state lifetime for the covalently linked perylene bisimide chromophores. A trimeric chemical design leads to efficient single-photon emission from optically excited thin film samples and even under electrical operation in OLEDs. To the best of our knowledge this is the first indication of electrically-driven single-photon emission from a fluorescent molecule [1]. Therefore we consider our work to constitute an important step towards the design of state-of-the-art fluorescent OLED emitters that might also feature a high potential for application in non-classical single-photon sources.

[1] Ulrich Müller et al., *Adv. Optical Mater.* 2022, 10, 2200234.

CPP 28.4 Wed 10:15 GÖR 226

A Tool Kit for Analyzing Emission Spectra of Multi-Molecular States — •SEBASTIAN HAMMER^{1,4}, THERESA LINDERL², KRISTOFER TVINGSTEDT¹, WOLFGANG BRUETTING², and JENS PFLAUM^{1,3} — ¹Experimental Physics VI, University of Würzburg, 97074 Würzburg — ²Institute of Physics, University of Augsburg, 86135 Augsburg, Germany — ³Bayerisches Zentrum für Angewandte Energieforschung (ZAE Bayern), 97074 Würzburg — ⁴Departments for Physics and Chemistry, McGill University, Montreal, Canada

The performance of opto-electronic devices is often crucially impacted by multi-molecular excited states such as charge-transfer (CT) states or excimers. Hence, the spectroscopic analysis of these states is a common tool in the characterization of such systems. Due to the many parameters at play full quantum mechanical interpretations are tedious and therefore the analysis is often performed on a phenomenological level only. Here we present a tool kit to analyze temperature dependent emission spectra using a Franck-Condon based approach with a single effective inter-molecular vibrational mode and discuss the implications of considering different potentials for the ground and excited state harmonic oscillators [1]. Finally, we show that fundamental parameters of the potential energy landscape can be extracted from temperature dependent steady state emission spectra using the example of a tetraphenylidibenzoperiflanthene: C_{60} CT heterostructure [2]. Funding from the DFG (Project 490894053) is gratefully acknowledged.

[1] Hammer et al., *Mater. Horiz.* (2022). doi: 10.1039/D2MH00829G

[2] Linderl et al., *Phys. Rev. Appl.* **13** 024061 (2020)

CPP 28.5 Wed 10:30 GÖR 226

Singlet Fission search in polyacene molecules in gas-phase and on rare-gas clusters using ab initio methods — •SELMANE FERCHANE and MICHAEL WALTER — Institute of Physics, University of Freiburg, Germany

Singlet fission (SF), is a spontaneous photo-excited splitting phenomenon. Where an organic chromophore dimer, converts its singlet exciton into a pair of triplet excitons. A great promise for future photon-to-current conversion of solar energy using organic materials with high efficiency. To get more insight into these processes of SF, we employed different ab initio theories and approaches in our investigation, namely, density functional theory (DFT), TD-DFT, MCTDH, and CASPT2/CASSCF. Since the spatial orientation is crucial to whether the molecule will go SF and the rate of it due to the orbital coupling of both molecules, based on recent studies. We calculate the most favorable orientation of the chromophores with the binding energies in the gas phase and adsorbed on Argon and Neon surfaces. Then we calculate the lowest-lying excited states that contribute to the singlet and triple transition plus the search for the possible conical intersection that crosses the surface potential energies.

CPP 28.6 Wed 10:45 GÖR 226

Template-Designed Organic Electronics — •KLAUS MEERHOLZ — Chemistry Department, University of Cologne, Greinstr. 4-6, 50939 Cologne, Germany

Worldwide, organic electronic devices such as OLEDs and solar cells have revolutionized the field of electronics; however, technological progress has been largely made by empirical research and development, while fundamental knowledge is often still incomplete.

This presentation will report results from the DFG-funded Research Training Group Template-Designed Organic Electronics addressing the question, how structural order influences the optoelectronic properties of pi-conjugated materials, and how these properties can be improved via the use of templates for the optimization of devices. Our approach spans all the way from the design of appropriate pi-conjugated molecular building blocks and surface-active templates, investigation of surfaces and interfaces by different spectroscopies, fabrication of optoelectronic devices, and finally theoretically modelling.

CPP 28.7 Wed 11:00 GÖR 226

Optically detected magnetic resonance of TADF OLED emitters — •PASCAL SCHADY, MONA LÖTHER, FABIAN BINDER, VLADIMIR DYAKONOV, and ANDREAS SPERLICH — Experimental Physics VI, Julius Maximilian University of Würzburg, 97074 Würzburg

Thermally activated delayed fluorescence (TADF) is an efficient triplet harvesting mechanism for organic light-emitting diodes (OLED). Molecular TADF Donor-Acceptor type emitters are limited by low reverse intersystem crossing (rISC) rates and broad spectra, making them less suitable for potential OLED devices. In contrast, so-called multiple resonance (MR) effect emitters, are very promising as they show narrowband emission, even for deep blue wavelengths. MR-TADF emitters consist mostly of planar and rigidly bound benzyl groups with boron and nitrogen substituents for HOMO and LUMO pinning. As a result, the exchange integral is small, therefore the energy gap between singlet and triplet states is low enough to efficiently populate emissive singlet states by up-converting long-lived triplet states via thermal excitation, even at room temperature. However, many MR-TADF materials, like the DABNA-series behave differently in solution or as a solid. We therefore are investigating the spin system of those emitters by optically detected magnetic resonance (ODMR) in order to shed light on spin-dependent efficiency limiting pathways and how to address them to improve future OLED devices.

15 min. break

CPP 28.8 Wed 11:30 GÖR 226

Influence of Fluorination on the Temperature Dependent Optical Transition in β -Phase ZnPc Single Crystals — •LISA SCHRAUT-MAY¹, KILIAN STRAUSS¹, SEBASTIAN HAMMER², KILIAN FRANK³, BERT NICKEL³, and JENS PFLAUM¹ — ¹Experimental Physics VI, University of Würzburg — ²Departments of Physics and Chemistry, McGill University, Montreal, Canada — ³Department of Physics, LMU Munich

The possibility of fluorination renders zinc phthalocyanine (ZnPc) an excellent model system to study the interplay between molecular packing and optoelectronic properties [1]. Here, we conduct temperature as well as polarisation dependent photoluminescence (PL) studies on β -phase ZnPc single crystals with different degrees of fluorination to modify the microscopic packing and, thus, the interaction between the molecules. For plain ZnPc an exceptionally sharp PL peak can be observed at temperatures below 100 K, which can be attributed to a superradiant enhancement [2]. Since this coherent coupling between several molecules strongly depends on the intermolecular spacing, we show, that this phenomenon can be steered by the fluorination of the molecules involved. We interpret the resulting PL signal and its temperature dependence in combination with X-ray studies by a model based on coupled excitons whose coupling is affected by the spatial anisotropy of the thermal contraction of the crystal lattice.

We thank the Bavarian research network SolTech for financial support. [1] Rödel et al., *J. Phys. Chem. C* (2022) [2] Hestand et al., *Chem. Rev.* (2018)

CPP 28.9 Wed 11:45 GÖR 226

Charge Delocalization and Vibronic Couplings in Quadrupolar Squaraine Dyes — DANIEL TIMMER¹, FULU ZHENG², MORITZ GITTINGER¹, THOMAS QUENZEL¹, DANIEL C. LÜNEMANN¹, KATRIN WINTE¹, YU ZHANG³, MOHAMED E. MADJET², JENNIFER ZABLOCKI⁴, ARNE LÜTZEN⁴, JIN-HUI ZHONG¹, ANTONIETTA DE SIO¹, THOMAS FRAUENHEIM², SERGEI TRETIAK³, and CHRISTOPH LIENAU¹ — ¹University of Oldenburg, Germany — ²University of Bremen, Germany — ³Los Alamos National Laboratory, USA — ⁴University of Bonn, Germany

Squaraines are prototypical quadrupolar charge-transfer chromophores. Their optical properties are often rationalized using an essential state model, predicting that optical transitions to the lowest excited state (S1) are one-photon allowed and to the next higher state (S2) are only two-photon-allowed and that vibronic coupling to high-frequency modes is greatly reduced. Here, we combine time-resolved spectroscopy techniques and quantum-chemical simulations to test and rationalize these predictions. We find the one-photon-allowed S1 and two-photon-allowed S2 states to be energetically well-separated. Also, we find small Huang-Rhys factors, especially for the high-frequency modes. The resulting concentration of the oscillator strength in a narrow spectral region around the S1 transition makes squaraines almost perfect optical two-level. Thus, these molecules and their aggregates are exceptionally interesting for e.g. strong coupling applications. [1]: Timmer, Daniel, et al., *J. Am. Chem. Soc.*, 144, 41, 19150-19162 (2022)

CPP 28.10 Wed 12:00 GÖR 226

In-operando observation of polaron formation in SAMFETs using NEXAFS spectroscopy — MANUEL JOHNSON, ANDREAS SPÄTH, BAOLIN ZHAO, MARCUS HALIK, and RAINER H. FINK — FAU Erlangen-Nürnberg, Erlangen, Germany

We present an in-operando near-edge x-ray absorption fine structure (NEXAFS) study on p-type BTBT-based self-assembled monolayer (BTBT-SAM) films. As a 2D-model system, the BTBT-SAM offers direct electron spectroscopic insight

into the active organic semiconductor layer without interfering bulk contributions. This optimized geometry allows for the first time the observation of polaronic states caused by charged species at the dielectric/organic interface using a core-level spectroscopic tool. Linear NEXAFS dichroism is employed to derive the molecular orientation of the BTBT subunit. In addition to the conventional C K-edge NEXAFS resonances, we observe modifications in the density of unoccupied states. The spectral changes are affected by the strength and polarity of the applied gate voltage. Furthermore, the related energies match the energy levels of polaronic states. Thus, we have clear indications to interpret the data in the context of polaron formation due to charge accumulation induced by the applied electric field in our ultrathin device. [1] The study has been funded by the DFG within GRK 1896 and the SolTECH initiative. [1] M. Johnson et al., *Appl. Phys. Lett.* 121 (2022) 183503.

CPP 28.11 Wed 12:15 GÖR 226

Machine learning for molecular design of organic molecules and reaction optimization — JULIA WESTERMAYR¹, REINHARD J. MAURER², and DETLEV BELDER³ — ¹Artificial Intelligence in Theoretical Chemistry Group, Leipzig University, Germany — ²Computational Surface Chemistry Group, University of Warwick, UK — ³Analytical Chemistry, Leipzig University, Germany

High-throughput screening of reaction conditions and electronic properties of molecules plays a crucial role in chemical industry and can be facilitated by automated workflows and machine learning. However, the high combinatorial complexity of the various parameters affecting molecular properties leaves unguided searches in chemical space highly inefficient and the optimization of reactions to synthesize these molecules often fails as theoretical protocols are usually decoupled from experiments. In this talk, we will show how predictive and generative deep learning models can be combined to theoretically design new molecules with potential relevance to organic electronics [1]. Further, we will present how these tools can be coupled with experiments to enable automated micro-laboratories [2] for targeted chemical synthesis. [1] JW et al. *Nat. Comp. Sci.* in press (2023). [2] R. J. Beulig et al., *Lab Chip* 17, 1996 (2017).

CPP 29: Interfaces and Thin Films

Time: Wednesday 9:30–12:45

Location: MER 02

Invited Talk

CPP 29.1 Wed 9:30 MER 02

Imaging mineral-water interfaces with atomic force microscopy — ANGELIKA KÜHNLE — Bielefeld University, Bielefeld, Germany

Mineral-water interfaces are omnipresent in nature and technology. Consequently, mineral-water interfaces play a decisive role in many fields, ranging from geochemistry, environmental science and biomineralization to catalysis and electrochemistry. A comprehensive understanding of the interaction of minerals with their surroundings requires the knowledge of the atomic surface structure including the hydration at the interface. In this respect, atomic force microscopy allows for gaining real-space, molecular-level information of the interfacial structure. In this presentation, silver iodide will be discussed as a prototypical example for an ice nucleating material. Silver iodide is a polar material, calling for a stabilization mechanism. So far, however, the stabilization mechanism is unknown. Our atomically resolved atomic force microscopy images reveal no indication for a surface reconstruction at the atomic scale, indicating that another mechanism seems to be at play.

CPP 29.2 Wed 10:00 MER 02

Template-Induced Growth of Sputter-Deposited Gold Nanoparticles on Ordered Porous TiO₂ Thin Films for SERS Sensors — SUZHE LIANG¹, TIANFU GUAN¹, SHANSHAN YIN¹, EVA KROIS², WEI CHEN¹, CHRISTOPHER R. EVERETT¹, JONAS DREWES³, THOMAS STRUNSKUS³, MARC GENSCHE^{1,4}, JAN RUBECK⁴, CHRISTOPH HAISCH², MATTHIAS SCHWARTZKOPF⁴, FRANZ FAUPEL³, STEPHAN V. ROTH^{4,5}, YA-JUN CHENG⁶, and PETER MÜLLER-BUSCHBAUM^{1,7} — ¹TUM School of Natural Sciences, Chair for Functional Materials, Garching — ²TUM School of Natural Sciences, Chair of Analytical Chemistry and Water Chemistry, Garching — ³LS Materialverbunde, Institut für Materialwissenschaft, CAU, Kiel — ⁴DESY, Hamburg — ⁵Department of Fibre and Polymer Technology, KTH, Stockholm, Sweden — ⁶Ningbo Institute of Materials Technology & Engineering, CAS, Ningbo, China — ⁷MLZ, TUM, Garching

Ordered porous gold/titanium dioxide (Au/TiO₂) hybrid nanostructured films are specifically interesting in large-scale applications using localized surface plasmon resonances (LSPRs) and surface-enhanced Raman scattering (SERS). We investigate the optical response of sputter-deposited Au/TiO₂ nanohybrid thin films with a focus on the plasmonic response and application as molecular sensors. To elucidate the origin of this behavior, we apply in situ grazing-incidence small-angle X-ray scattering (GISAXS) to investigate the growth kinetics of Au on a TiO₂ template during sputter deposition. The Raman intensity of deposited molecules, probed with rhodamine 6G (R6G), depends on the deposited gold thickness.

CPP 29.3 Wed 10:15 MER 02

Proteins as stabilizers for foam films: Untangling the different stabilizing effects — KEVIN GRÄFF, SEBASTIAN STOCK, LUCA MIRAU, SABINE BÜRGER, and REGINE VON KLITZING — Soft Matter at Interfaces, Technische Universität Darmstadt, Darmstadt, Germany

Macroscopic foams consist of foam films, which separate the single air bubbles from each other. Investigation of foam films is crucial to understand macroscopic foam properties such as foam stability. In order to untangle electrostatic, steric and network stabilization effects, we study and compare two globular proteins (β -lactoglobulin and bovine serum albumin) and a disordered, flexible protein (whole casein) at low ionic strengths with varying solution pH. Image intensity measurement allows to record spatially resolved disjoining pressure isotherms in a Thin Film Pressure Balance (TFPB). This reveals insights into the structure formation in inhomogeneous protein films. We introduce inhomogeneity tracking (feature-tracking) as a novel method to enable the measurement of interfacial mobility and stiffness of foam films. Around the isoelectric point, Newton Black Films form which are stable for the globular proteins while they are unstable for the disordered flexible one. This difference in film stability is explained by different characteristics of the network structures which is supported by findings in the bulk and at the surface of the respective protein solutions.

[1] Gräff, K. et al. (2022), Untangling effects of proteins as stabilizers for foam films, *Front. Soft. Matter* 2:1035377.

CPP 29.4 Wed 10:30 MER 02

Anomalous underscreening in concentrated aqueous electrolytes: myth or reality? — SARAVANA KUMAR¹, PETER CATS², IGOR SIRETANU¹, RENÉ VAN ROIJ², and FRIEDER MUGELE¹ — ¹Physics of Complex Fluids, Univ. Twente, Enschede, The Netherlands — ²Institute for Theoretical Physics, Utrecht Univ., Utrecht, The Netherlands

Recent surface forces apparatus experiments that measured the forces between two mica surfaces and a series of subsequent theoretical studies suggest the occurrence of universal underscreening in highly concentrated electrolyte solutions. We performed a set of systematic Atomic Force Spectroscopy measurements for aqueous salt solutions in a concentration range from 1 mM to 5 M using chloride salts of various alkali metals. Experiments were carried out using flat substrates and submicrometer-sized colloidal probes made of smooth oxidized silicon immersed in salt solutions at pH values of 6 and 9 and temperatures of 25 degC and 45 degC. While strong repulsive forces were observed for the smallest tip-sample separations, none of the conditions explored displayed any indication of anomalous long range electrostatic forces as reported for mica

surfaces. Instead, forces are universally dominated by attractive van der Waals interactions at tip-sample separations beyond approximately 2nm for salt concentrations of 1 M and higher. Complementary calculations based on classical density functional theory for the primitive model support these experimental observations and display a consistent decrease in screening length with increasing ion concentration.

CPP 29.5 Wed 10:45 MER 02

Layer-by-Layer Spray-deposition of Cellulose and Lignin — •SHOUZHENG CHEN^{1,2}, CONSTANTIN HARDER^{1,3}, IULIANA RIBCA⁴, LUCIANA PLUNTKE^{1,5}, MARKUS OBERTHUER⁵, MATS JOHANSSON⁴, JULIEN NAVARRO², and STEPHAN V. ROTH^{1,4} — ¹DESY, 22607 Hamburg, Germany — ²University Hamburg, 20146 Hamburg, Germany — ³TUM School of Natural Sciences, Chair for Functional Materials, 85748 Garching, Germany — ⁴KTH Royal Institute of Technology, 10044 Stockholm, Sweden — ⁵HAW, Department Design, 22087 Hamburg, Germany

Cellulose and lignin are the main chemical components of wood and can be further processed and purified into more valuable chemical raw materials such as cellulose nanofibrils (CNF), Kraft lignin and liginosulfonate. Using the idea of a bottom-up approach, CNF-Lignin composite films were prepared by layer-by-layer (LbL) spray-deposition with CNF and different lignins. CNFs provide a three-dimensional porous network structure, and lignin molecules are attached to the structure of CNF to form a homogeneous structure. In addition, Kraft lignin and lignin derivatives contain a large number of phenolic hydroxyl groups, which might be preferential for thermoelectricity. Thus, CNF-Lignin composite film is an ideal template for composite functional materials.

CPP 29.6 Wed 11:00 MER 02

Growth Kinetics and Molecular Mobility of the adsorbed Layer of Poly(bisphenol-A Carbonate) (PBAC), Polysulfone (PSU), and Poly(2-Vinyl Pyridine) (P2VP) — •HASSAN OMAR, PAULINA SZYMONIAK, ANDREAS HERTWIG, and ANDREAS SCHÖNHALS — Bundesanstalt für Materialforschung und -prüfung (BAM), Berlin, Germany

Interactions between a polymer and a substrate interface play a vital role in understanding the improvement in thin film material properties as well as serving as a model for nanocomposites. For any non-repulsive polymer-substrate interactions, polymer segments form an irreversibly adsorbed layer and show a slow-down in the glassy dynamics and thus an increase in the thermal glass transition temperature compared to the bulk-like values. The growth kinetics of the adsorbed layer obey a two-step mechanism: formation of immobilized layer with flat segmental conformations and a loosely bound layer with stretched chains pinned to the surface. Here the adsorbed layer was studied for: poly (bisphenol-A carbonate) (PBAC) and polysulfone (PSU), two bulky polymers containing a functional group (phenyl ring) in the backbone and compared to poly (2-vinyl pyridine) (P2VP), where the backbone is a vinyl-derivative and the functional group (pyridine) is in the side chain. The growth kinetics for PBAC and PSU were found to deviate from the well-known mechanism, observed for polymers such as P2VP. Atomic force microscopy and ellipsometry were used for this investigation and was additionally supported by broadband dielectric spectroscopy.

15 min. break

CPP 29.7 Wed 11:30 MER 02

Influence of heavy chalcogen atoms on structural arrangement and spectroscopic properties in molecular donor/acceptor thin film heterostructures — •ELENA CHULANOVA¹, ANTON PYLYPENKO¹, ALEXANDER GERLACH¹, JANNIKA LAUTH², and FRANK SCHREIBER¹ — ¹Institute for Applied Physics, University of Tübingen, 72076 Tübingen, Germany — ²Institute for Physical and Theoretical Chemistry, University of Tübingen, 72076 Tübingen, Germany

Organic semiconductors are widely used in optoelectronics due to their tunable electronic and structural properties. For many applications, the active layers consist of heterostructures and the details of the interaction between an electron donating and accepting moieties are the key factors for enhancing devices' efficiency. The chalcogenadiazole ring is a common acceptor core for organic chromophores and a variety of its condensed derivatives is known and used in this context. The presence of heavy chalcogens in the latter can impact the spin-orbit coupling and affect the optical properties. Here, we present a study on organic binary mixtures in thin films prepared by vacuum deposition, namely of dibenzochalcogenadiazolopyrazines as acceptors and known donors; i.e. diindenoperylene, pentacene, α -sexithiophene. The bulk heterojunction geometry was used with two materials mixed on the molecular level. We discuss the correlation between the mixing behavior of the molecules, and their structural and optical properties to obtain a systematic understanding of the processes occurring in molecular D-A systems based on 1,2,5-chalcogenadiazoles.

CPP 29.8 Wed 11:45 MER 02

The influence of increased kinetic energy of gold deposition onto polymers — •YUSUF BULUT^{1,2}, BENEDIKT SOCHOR¹, KRISTIAN RECK³, JONAS DREWES³, SUZHE LIANG², TIANFU GUAN², THOMAS STRUNSKUS³, FRANZ FAUPEL³, PETER MÜLLER-BUSCHBAUM^{2,4}, and STEPHAN V. ROTH^{1,5} — ¹DESY, 22607 Hamburg — ²TUM School of Natural Sciences, Chair for Functional Materials, 85748 Garching, Germany — ³CAU Kiel, Chair for Multicomponent Materials, Faculty of Engineering, 24143 Kiel — ⁴MLZ, TUM, 85748 Garching — ⁵KTH Royal Institute of Technology, Department of Fibre and Polymer Technology, SE-100 44 Stockholm

High Power impulse magnetron sputtering (HIPIMS) is a novel industrial relevant deposition technique enabling thin metal layers being coated onto polymers with increased adhesion and density. Compared to conventional direct current magnetron sputtering, no pre- and post-treatment is required to achieve these properties. So far there is no report discussing the nucleation and growth process during HIPIMS deposition. In this study, the polymer templates polystyrene (PS), poly-4-vinylpyridin (P4VP) and polystyrene sulfonicacid (PSS) are studied. Even though the polymers are very similar in their structure, it is expected that the distinct different functional moiety influence the kinetics of the initial growth stages of the gold layer. Results of simultaneous in situ grazing-incidence small angle X-ray scattering (GISAXS) and grazing incidence wide angle X-ray scattering (GIWAXS) are presented.

CPP 29.9 Wed 12:00 MER 02

Analysis of non-equilibrium thin film growth using X-ray photon correlation spectroscopy — •INGRID DAX¹, IVAN ZALUZHNYI¹, MICHAEL SPRUNG², and FRANK SCHREIBER¹ — ¹Universität Tübingen, Germany — ²Deutsches Elektronen-Synchrotron DESY, Hamburg, Germany

Thin film growth is a classic example of a non-equilibrium process in which a wide variety of functional properties can be obtained depending on the growth kinetics. Understanding the microscopic dynamics underlying the growth of molecular materials is an essential prerequisite for the rational design of complex structures and morphologies with controlled properties.

We perform in-situ X-ray experiments in grazing incidence geometry to follow the formation of thin film growth in real time, which reveals details of the dynamics during this process. This includes the adsorption of molecules on the substrate and the subsequent formation, realignment and diffusion of resulting molecular islands.

Specifically, we use modern coherent techniques based on X-ray photon correlation spectroscopy (XPCS). This resolves dynamics on the scale of 50-1000 nm, providing an unprecedented level of detail into the growth and diffusion of molecular islands during the growth process. We decompose our measurements into dynamic and kinetic time scales by comparing them to simulations, and interpret the results using established XPCS tools. This allows us to show that the time scales of a few 100 seconds are mainly due to kinetics, i.e., the growth of the islands.

CPP 29.10 Wed 12:15 MER 02

In situ GISAXS investigation of sputtering IZO thin film for optoelectronic applications — •HUAYING ZHONG¹, LUKAS V SPANIER¹, CHRISTOPHER R. EVERETT¹, XINYU JIANG¹, SHANSHAN YIN¹, MARLENE SOPHIE HÄRTEL², JIAHUAN ZHANG², BERTWIN BILGRIM OTTO SEIBERTZ³, MATTHIAS SCHWARTZKOPF⁴, STEPHAN V. ROTH^{4,5}, and PETER MÜLLER-BUSCHBAUM^{1,6} — ¹TUM School of Natural Sciences, Chair for Functional Materials, Garching, Germany — ²HZB, Solar Energy, Berlin, Germany — ³Department of technology for thin-film components, TU Berlin, Berlin, Germany — ⁴DESY, Hamburg, Germany — ⁵Department of Fibre and Polymer Technology, KTH, Stockholm, Sweden — ⁶MLZ, TUM, Garching, Germany

Transparent conducting oxide (TCO) thin films have been studied intensively for optoelectronic devices, such as photodetectors, photovoltaics and light emitting diodes (LEDs). Among the several TCO thin films, zinc doped indium oxide (IZO) has received much attention as interface layer in optoelectronic devices due to its excellent electrical conductivity, optical transmittance, high thermal/chemical stability, low cost and low deposition temperature. Here, ITO glass and spin coated ZnO on ITO glass are used as the templates for IZO thin film deposition via DC magnetron sputtering technique. The growth dynamics of IZO film on these two templates are respectively investigated via grazing small angle x-ray scattering (GISAXS) characterization, and the morphology and optoelectrical properties of final films are further investigated.

CPP 29.11 Wed 12:30 MER 02

Investigation of Mg(0001) and Mg(1010) surfaces in Grignard electrolytes by reflection anisotropy spectroscopy — •MARIO LÖW¹, HOLGER EUCHNER², and MATTHIAS M. MAY^{1,2} — ¹Universität Ulm, Institute of Theoretical Chemistry, 89081 Ulm, Germany — ²Universität Tübingen, Institute of Physical and Theoretical Chemistry, 72076 Tübingen, Germany

The high abundance and large volumetric capacity of the metal anode make rechargeable magnesium batteries potential candidates for future battery technologies. While understanding and controlling the electrode-electrolyte inter-

face is essential for battery performance, there is often little known about the underlying atomistic interface structure under operating conditions [1].

To address this issue for the case of Mg, we study single crystalline magnesium surfaces in contact with standard Grignard electrolytes and under applied potential [2]. We employ reflection anisotropy spectroscopy (RAS) as an optical, high-resolution technique for the operando investigation of the interfacial struc-

ture as a function of the applied electrode potential. The Mg-crystal surface is studied in various solvents and Grignard electrolytes during voltammetric cycling. Finally, we seek comparison to theoretical spectra obtained within the random phase approximation.

[1] Popovic, Jelena. *Nature Communications* 12.1 (2021): 1-5.

[2] Lu, Z., et al. *Journal of Electroanalytical Chemistry* 466.2 (1999): 203-217.

CPP 30: Biopolymers and Biomaterials I (joint session BP/CPP)

Time: Wednesday 9:30–13:00

Location: TOE 317

See BP 12 for details of this session.

CPP 31: Focus Session: From Inter-individual Variability to Heterogeneous Group Dynamics and Disorder in Active Matter (joint session DY/BP/CPP)

The study of active particle dynamics has developed into a vibrant field of multidisciplinary research, including such diverse systems as bacterial colonies, cellular self-organization, synthetic colloids and microrobots as well as macroscopic systems like locusts, flocks of birds, schools of fish or pedestrians. Whereas many studies in the past focused either on the random transport of individual particles or on the interplay of temporal fluctuations (noise) and interactions (velocity alignment or attraction/repulsion), there is now an increasing interest in the question how structural disorder and inter-individual variability, i.e., different motility characteristics of individuals, shape the active particle dynamics and emergent pattern formation of groups. The presence of structural or quenched disorder raises furthermore the immediate question how to bridge data and models based on (short time) tracking data, given the simultaneous presence of temporal fluctuations. With this focus session, we aim at bringing researchers from statistical physics and biophysics together to discuss this interdisciplinary topic and exchange ideas on common challenges arising in different application areas.

Organized by Robert Großmann (Potsdam)

Time: Wednesday 9:30–13:00

Location: ZEU 160

See DY 26 for details of this session.

CPP 32: 2D Materials IV (joint session HL/CPP)

Time: Wednesday 9:30–12:30

Location: POT 81

See HL 22 for details of this session.

CPP 33: Perovskite and photovoltaics II (joint session HL/CPP)

Time: Wednesday 9:30–13:00

Location: POT 251

See HL 25 for details of this session.

CPP 34: Wetting, Droplets and Microfluidics I (joint session DY/CPP)

Time: Wednesday 10:00–13:00

Location: ZEU 147

See DY 29 for details of this session.

CPP 35: Poster Session II

Topics: Biopolymers, Biomaterials and Bioinspired Functional Materials (1-5); Complex Fluids and Colloids, Micelles and Vesicles (6-13); Composites and Functional Polymer Hybrids (14-23); Crystallization, Nucleation and Self-Assembly (24-32); Emerging Topics in Chemical and Polymer Physics, New Instruments and Methods (33-41); Hydrogels and Microgels (42-44); Modeling and Simulation of Soft Matter (45-50); Nanostructures, Nanostructuring and Nanosized Soft Matter (51-52); Polymer and Molecular Dynamics, Friction and Rheology (53-57); Responsive and Adaptive Systems (58-61); Wetting, Fluidics and Liquids at Interfaces and Surfaces (62-66).

Time: Wednesday 11:00–13:00

Location: P1

CPP 35.1 Wed 11:00 P1
Stability of biobased coatings on textiles — •LUCIANA PLUNTKE^{1,2}, CON-STANTIN HARDER^{1,3}, SHOZHENG CHEN^{1,4}, IULIANA RIBCA⁵, NADJA KÖLPIN¹, MARKUS OBERTHÜR², PETER MÜLLER-BUSCHBAUM³, MATS JOHANSSON⁵, and STEPHAN V. ROTH^{1,5} — ¹DESY, 22607 Hamburg, Germany — ²HAW, 20999 Hamburg, Germany — ³TUM School of Natural Sciences, Department

of Physics, Chair for Functional Materials, 85748 Garching, Germany — ⁴University Hamburg, 20146 Hamburg, Germany — ⁵KTH Royal Institute of Technology, 10044 Stockholm, Sweden

Functionalizing textiles by spray-coating is in wide-spread use. Here, we focus on functional multi-layer protective coatings on light woven textile materials. The functionalization is achieved by spray-coating with bio-based materials.

We investigate the mechanical stability of these novel coatings and changes in the coating under external stress and standard abrasion conditions. Our aim is to determine the degree of stress that the coating can withstand under different types of mechanical stress until it loses its functionality. The results are important for implementing sustainable materials in the textile industry.

CPP 35.2 Wed 11:00 P1

In situ GISAXS printing of biotemplated titania nanostructures — •LINUS F. HUBER¹, MANUEL E. SCHEEL¹, STEPHAN V. ROTH³, and PETER MÜLLER-BUSCHBAUM^{1,2} — ¹Technical University of Munich, TUM School of Natural Sciences, Department of Physics, Chair for Functional Materials, James-Frank-Str. 1, 85748 Garching, Germany — ²MLZ, TUM, 85748 Garching — ³Deutsches Elektronen-Synchrotron (DESY), Notkestr. 85, 22607 Hamburg, Germany

Biotemplating is an effective method of nanostructuring hybrid inorganic-organic materials. This approach allows the tuning of material properties like porosity or domain sizes. Therefore, parameters like the electronic conductivity can be adjusted for different applications. In this work, differently structured Titania thin films are investigated for application in thermoelectric generators. Beta-lactoglobulin is a bovine whey protein that is used as a template during sol-gel synthesis. The Seebeck effect allows the conversion of waste heat into electrical energy. State of the art thermoelectric materials are rare, toxic and expensive. Biotemplated titania could provide a non-toxic and abundant alternative. To investigate the different titania morphologies, in situ GISAXS, GIWAXS and SEM are used. In situ GISAXS printing enables a time resolved investigation of the structure formation, domain sizes and domain distances. UV-Vis and PI are used to analyze differences in the optical properties of the thin films. These structural and optical changes are then correlated with measurements of the Seebeck coefficient and the electrical conductivity.

CPP 35.3 Wed 11:00 P1

A two-state Gaussian loop under tension: negative extensibility and ensemble inequivalence — •GEUNHO NOH and PANAYOTIS BENETATOS — Department of Physics, Kyungpook National University, Republic of Korea

Loop formation is commonly observed in biopolymers and, in many cases, the loop structure is transient. Some examples of this structural rearrangement are the formation of denaturation bubbles in double-stranded DNA and the transient DNA looping associated with gene regulation. Here, we study the conformational statistics and the elastic behavior of a flexible polymer under tension with a two-state structure: looped or unlooped. We analyze two cases. In the first, the loop can zip to form a double-stranded chain. In the second, the dangling ends of a chain can bind to form a loop. In each case, we investigate the force-extension relation of the two-state loop in both the Helmholtz and the Gibbs ensembles. We also extend the two-level system to a three-level Gaussian loop by introducing a third (intermediate) state. In contrast to the single Gaussian chain, the two- or three-level systems show qualitatively different tensile response and ensemble inequivalence. Interestingly they can have negative extensibility in the Helmholtz ensemble, and we point out that this is one of the simplest polymer models which exhibits such metamaterial-like behavior.

CPP 35.4 Wed 11:00 P1

Determination of the roast-dependent pore size in coffee beans using positron lifetime spectroscopy — •ADRIAN LANGREHR, VASSILY BURWITZ, LUCIAN MATHES, and CHRISTOPH HUGENSCHMIDT — Forschungs-Neutronenquelle Heinz Maier-Leibnitz (MLZ), Technische Universität München, Lichtenbergstr. 1, 85748 Garching, Germany

Positron Annihilation Lifetime Spectroscopy (PALS) is an established method to determine the type and concentration of open volume defects in crystals as well as to investigate the free volume in polymers. Using ²²Na as β^+ emitting radioisotope in the so-called "sandwich" geometry we present the capabilities of our four-detector setup with digital readout and signal processing. The efficient readout of this PAL spectrometer produces 12 lifetime spectra simultaneously. Our study encompasses the comparison of three different methods to combine information contained in these 12 spectra. To demonstrate a use case of a biomaterial we measured the positron lifetimes in coffee beans as a function of the degree of roasting. The application of the so-called Tao-Eldrup model allows us to study the influence of the roasting parameters on the mean pore size on the nanometer scale.

CPP 35.5 Wed 11:00 P1

Microgels for Enhanced Adsorption of Endothelial Cells on Artificial Networks — •SOURAJ MANDAL and REGINE VON KLITZING — Soft Matter at Interfaces, Department of Physics, Technical University of Darmstadt, Germany

Artificial 3-D supply networks can be applied as a transport system for oxygen and nutrients, which can promote vascularization for organ-like 3-D cell culture systems. In the human body, the inner surface of such networks (blood vessels) is lined with a layer of endothelial cells and they play a vital role in cell maturation and angiogenesis (formation of new blood vessels). So far, the attachment of endothelial cells on the surface of the artificial network system is not sufficient. Addressing this problem, this study focuses on designing a suitable mediator be-

tween the inner walls of the artificial network and endothelial cells, which should be mechanically stable to flows of nutrient solutions. Here we employ Poly(N-isopropylacrylamide) (PNIPAm) microgel (MG) as cell-culturing surface mediator. However, the main challenges are (i) ensuring the firm adhesion of MGs on the surface of the artificial polymeric network, and (ii) seeding endothelial cells on top of them. As a primary approach, we synthesized positively charged MGs to attach them on plasma-treated silicon (Si) and 3-D printed polymeric surfaces. MG particles are characterized by their Zeta potential and hydrodynamic radius. As a rapid fabrication technique, spin coating was used to deposit a thin polymeric layer of MG particles on the substrates. AFM analyses showed a stable adhesion of MG particles on the flat surfaces even upon water washing and mechanical stress.

CPP 35.6 Wed 11:00 P1

Depletion induced phase behavior and equilibrium clusters in charged BSA and HSA protein solutions — •MAXIMILIAN D. SENFT, FAJUN ZHANG, and FRANK SCHREIBER — Universität Tübingen, Germany

Understanding and predicting the phase behavior of proteins is an ongoing endeavor in many scientific research areas, including the pharmaceutical industry. In addition to crystallization, liquid-liquid phase separation and condensate formation, which includes equilibrium clusters, dense liquid droplets, fibrils, and gels, appear to be closely related to many pathological conditions. The formation of equilibrium protein clusters in solution requires an interaction potential with competing contributions, i.e., long-ranged repulsion and short ranged attraction. Bovine and human serum albumin (BSA and HSA) carry negative charges at neutral pH which provide a long-range electrostatic repulsion between proteins. The attractive potential can be generated via the depletion interactions introduced by the non-adsorbing polymer polyethylene glycol in protein solutions. By tuning the ionic strength, polymer size and concentration, the competing potential can be continuously adjusted, resulting in equilibrium protein clusters due to the subtle balance to the different contributions of the interaction potential. Having performed systematic small angle scattering measurements, on BSA and HSA, together with quantitative modeling combined with protein phase diagrams a better understanding of depletion induced protein phase behavior and cluster state can be provided.

CPP 35.7 Wed 11:00 P1

Purely elastic instability of semi-dilute polymer solutions in shear flow — PEGAH SHAKERI^{1,2}, •MICHAEL JUNG^{1,2}, and RALF SEEMANN^{1,2} — ¹Universität des Saarlandes, Saarbrücken, Germany — ²Max Planck-Institute for Dynamics and Self-Organization, Göttingen, Germany

Polymer solutions in the semi-dilute regime are of considerable industrial importance. The complex rheological properties of such highly viscoelastic fluids and the complexity of their flow characteristics, especially in curved geometries, require a thorough experimental characterization of the dynamics of such fluid flows. We experimentally investigate the flow of highly elastic polymer solutions above their overlap concentrations in a microfluidic serpentine channel using pressure measurements and particle image velocimetry. Our results show that the flow resistance increases significantly at high Weissenberg numbers but vanishing Reynolds numbers, indicating the occurrence of a purely elastic instability. We show that the onset of instability can be scaled by including shear-dependent rheological properties of the polymer solutions in the nonlinear stability analysis. As a result, a universal criterion as a function of normalized polymer concentration is provided for scaling the onset of pure elastic instability in the semi-dilute regime independent of the type and molecular weight of the polymer.

CPP 35.8 Wed 11:00 P1

Improved displacement efficiency in porous media by invasion of viscoelastic fluids — •MICHAEL JUNG^{1,2}, PEGAH SHAKERI^{1,2}, and RALF SEEMANN^{1,2} — ¹Universität des Saarlandes, Saarbrücken, Germany — ²Max Planck-Institute for Dynamics and Self-Organization, Göttingen, Germany

Improving the displacement efficiency of capillary entrapments in porous media by adding high molecular weight polymers to the invading phase has a variety of industrial applications. Apart from an increased viscosity contrast compared to water flooding, the flow of viscoelastic polymer solutions exhibits unstable flow behavior even at small Reynolds numbers, which can lead to an additional displacement mechanism of the capillary entrapments. We use a microfluidic approach to reveal the underlying mechanism of this enhanced displacement by first considering a random array of cylindrical posts to identify fundamental differences in displacement processes for elastic and non-elastic fluids. Then, to focus directly on displacement processes driven solely by elastic stresses and to exclude the effects of viscous stresses, we consider a single capillary entrapment connected to two symmetric serpentine channels. We show that the unique viscoelastic fluid features, such as the emergence of a significant first normal stress difference, combined with the curved flow geometry, lead to purely elastic instability and elastic secondary flow, which in turn generate the stresses required to overcome the capillary threshold and displace capillary entrapment.

CPP 35.9 Wed 11:00 P1

Supraparticles: Aggregation of colloids in evaporating dispersion drops — •MELIS YETKIN¹, YASHRAJ MANISH WANI², ARASH NIKOUBASHMAN², MICHAEL KAPPL¹, and HANS-JÜRGEN BUTT¹ — ¹Department of Physics at Interfaces, Max-Planck-Institute for Polymer Research, Germany — ²Institute of Physics, Johannes Gutenberg University Mainz, Germany

Evaporating dispersion drops from superamphiphobic surfaces opens a way to fabricate supraparticles (SPs) with complex structures. The structure formation can be controlled by tailoring the interaction forces between particles and process conditions. In this study, the structure of the SPs was investigated by tuning the shape of the primary building blocks and the process conditions. Ellipsoidal polystyrene (PS) particles of different aspect ratios were obtained by stretching a polymeric film of spherical particles above the glass transition temperature. Aqueous dispersion drops of the ellipsoidal particles were evaporated from silicone nanofilaments-based superamphiphobic surfaces under varying humidity conditions, during which the evaporation process was monitored by a camera. The interaction between the building blocks, and hence the final morphology of the SPs, were altered by the addition of surfactant sodium dodecyl sulfate (SDS). Control experiments with spherical PS building blocks were conducted in parallel. The study elucidated the effect of primary building block shape on the final morphology of supraparticles and the transition between a shape-dominated regime and an interaction-dominated regime.

CPP 35.10 Wed 11:00 P1

Temperature dependent measurements of the diffusion- and Soret-coefficient in a binary polystyrene/toluene mixture — •JANNIK KANTELHARDT and WERNER KÖHLER — Physikalisches Institut Universität Bayreuth, Germany

In this work we investigate the dependence of the diffusion- and Soret-coefficient in respect to different ambient temperatures with a temperature range from 10°C to 50°C in steps of 5°C. The here investigated system, a solution of polystyrene (PS) in toluene with a weight fraction of $c_{PS}=1\%$, has in a similar concentration also been used in the binary companion cell of the DCMIX4 microgravity campaign on ternary mixtures. Furthermore, binary and ternary polystyrene solutions are candidates for the forthcoming GIANT FLUCTUATIONS project of ESA for the investigation of non-equilibrium fluctuations under microgravity conditions.

The measurements were performed with a Thermal-Diffusion-Forced-Rayleigh-Scattering (TDFRS) setup. Through a writing beam a holographic grating is created inside the mixture where a small amount of an inert dye is added. The grating heats the sample periodically which leads to temperature gradients. Through the Soret-effect concentration gradients appear and both lead to changes in the refractive index. The signal is measured with a readout beam under Bragg diffraction.

CPP 35.11 Wed 11:00 P1

Diffusion, Thermodiffusion and turbidity of thermoresponsive Poly(N-acryloylglycinamide) in water. — •ROMAN REH¹, NIKOLA MAJSTOROVIC², SEEMA AGARWAL², and WERNER KÖHLER¹ — ¹Universität Bayreuth, Physikalisches Institut, Germany — ²Universität Bayreuth, Macromolecular Chemistry II, Germany

We report about measurements on Poly(N-acryloylglycinamide) (PNAGA) in aqueous solution. Diffusion-, Thermodiffusion- and Soretcoefficients were measured with the polymer in linear form and as a crosslinked microgel. Furthermore, temperature dependent measurements on turbidity were done with the linear polymer. Experiments on diffusion were performed with the Optical-Beam-Deflection technique where a vertical temperature gradient is applied to the sample and information about the time dependent distribution of temperature and concentration in the sample is gathered by recording the position of a laser beam, which traverses the sample and gets deflected. This is because the refractive index changes with temperature and concentration, which on its part changes due to thermodiffusion. Turbidity measurements show a UCST-behavior and a hysteresis in the temperature of the cloud point, depending on the direction of the temperature ramp, which is in accordance with results from literature. Thermodiffusion- and Soretcoefficients at different temperatures are described with an exponential Piazza function [S. Iacopini et al., Eur. Phys. J. E **19**, 59-67 (2006)] and are comparable for the linear polymer and the microgel, showing a systematical behaviour and a change in sign in the region of about 35 to 40 °C.

CPP 35.12 Wed 11:00 P1

Measurement of diffusion and thermodiffusion of polydisperse polymers by means of a compact optical beam deflection setup — •MAREIKE HAGER, ROMAN REH, and WERNER KÖHLER — Universität Bayreuth, Physikalisches Institut, Germany

We have performed diffusion and thermodiffusion experiments on solutions of polydisperse polymers by means of a newly developed double-pass optical beam deflection (OBD) instrument. The aim is to develop a model for the description of the multimodal OBD signals and to develop the technique into a method for polydispersity analysis. The double-pass OBD instrument utilizes a laser beam that is reflected behind the Soret cell and passes the sample volume a second

time. In the cell a vertical temperature gradient is applied that leads to thermodiffusion in the sample and, thus, to a concentration gradient and a gradient of the refractive index. The laser beam that traverses the cell twice is deflected and detected on a camera where the time dependent laser position is recorded. From the measured OBD signal the diffusion, thermodiffusion and Soret coefficients can be extracted. The multimodal time traces are evaluated with an adapted version of the CONTIN program for the solution of inverse problems. It is shown that diffusion coefficients extracted in this way agree with literature data. The results of the measurements of samples with two polymers of different sizes are in accordance with the results for the single components. Based on these results, polymers with a broad molar mass distribution can now be investigated.

CPP 35.13 Wed 11:00 P1

Mixture of magnetic and non-magnetic ellipsoids — •ELENA PYANZINA¹, ANNA AKISHEVA¹, TATYANA BELAYEVA¹, MARINA GUPALO¹, and SOFIA KANTOROVICH² — ¹Ekaterinburg, Russia — ²University of Vienna, Vienna, Austria

In this contribution, mixtures of magnetic and non-magnetic ellipsoids were studied. We chose systems with the ratio of the semi-axes equal to 3 and 5 and different concentrations, as well as the direction of the magnetic moment along the main axis. The ratios of magnetic and non-magnetic particles considered were as follows: 30/70, 50/50 and 70/30. The initial susceptibility of such systems was calculated since the magnetic response of the system is very important for various applications. It turned out that with an increase in the magnitude of the magnetic moment, a structural transition occurs in the system: first, the initial susceptibility increases, and then it becomes almost zero. This is because the basic state of elongated ellipsoids is an antiparallel pair, which becomes stable with an increase in the magnitude of the magnetic moment. And its total magnetic moment is quite small, and the susceptibility of such an object is much lower than that of a pair of particles with a head to tail orientation. The behavior of mixtures of ellipsoids with similar systems of magnetic disks (like ellipsoids with a magnetic moment perpendicular to the main axis) was also compared. It turned out that at large values of the magnetic moment, the disks form "stacks" in which the magnetic moments are directed head to tail, and ellipsoids form flat structures with a thickness of one ellipsoid, with an antiparallel orientation of the moments.

CPP 35.14 Wed 11:00 P1

Mesoporous polymers as electrode material in hybrid organic-inorganic lithium-ion batteries — •TOM WICKENHÄUSER¹, LUCAS UEBERRICKE², ANGELINA JOCIC², ERIK MISSELWITZ², ELISA THAUER¹, YUQUAN WU¹, MICHAEL MASTALERZ², MILAN KIVALA², and RÜDIGER KLINGELER¹ — ¹Kirchhoff Institute for Physics, Heidelberg University, Germany — ²Institute of Organic Chemistry, Heidelberg University, Germany

We report on the characterisation of mesoporous polymers as electrode materials in hybrid organic-inorganic lithium-ion batteries. In particular, dendritic pyrene tetraone (D-PTO) and triphenylamine (TPA) is investigated as cathode material and non-planar covalent carbon networks are studied as anode material in lithium half-cells. Cyclic voltammetry as well as galvanostatic cycling measurements were done to investigate on ionic and electric transport mechanisms. For redox active dendritic pyrene tetraone, the mesoporous character of the amorphous polymer is confirmed and the specific surface areas range up to nearly 700 m²g⁻¹. Galvanostatic cycling measurements show a specific capacity of 137 mAhg⁻¹ and a capacity retention of 86% after 50 cycles.

CPP 35.15 Wed 11:00 P1

Design, fabrication and nano-scale characterization of novel SEI layers — •ZHUIJUN XU¹, YAJUN CHENG², YONGGAO XIA², and PETER MÜLLER-BUSCHBAUM^{1,3} — ¹TUM School of Natural Sciences, Chair for Functional Materials, 85748 Garching, Germany — ²Ningbo Institute of Materials Technology and Engineering, Chinese Academy of Sciences, 315201, Ningbo, China — ³MLZ, TUM, 85748 Garching, Germany

Rechargeable lithium metal batteries have been recognized as one of the most promising energy storage devices due to their superior energy density. However, serious safety concerns and poor cyclability are challenges originating from an uncontrolled lithium dendrite growth and an unstable solid electrolyte interface (SEI) layer. SEI can be enhanced by synergetic additives in commercial electrolytes. Herein, amphiphilic block copolymers/inorganic materials-PS-b-PEO/LiNO₃ as additives, which bear some clear advantages including absorbing mechanical stress, conducting lithium ion and controlling the lithium dendrite growth, are mixed with commercial electrolytes and applied in the lithium metal battery. Remarkably, Li symmetric cells have a long-term cycling life over 300 h with a capacity of 3 mAh cm⁻². Moreover, full battery with lithium metal anode and LiFePO₄ exhibits a stable and high capacity of 138 mAh g⁻¹ at 1 C. With ex-situ scattering techniques or in-situ scattering studies, the structures of the surface modified lithium metal anodes and structure formation processes are studied.

CPP 35.16 Wed 11:00 P1

Less is more: tiny amounts of insoluble multi-functional microporous additive plays a big role in lithium secondary batteries — •RUOXUAN QI¹, PETER MÜLLER-BUSCHBAUM^{1,2}, and YA-JUN CHENG³ — ¹TUM School of Natural Sciences, Chair for Functional Materials, Garching, Germany — ²MLZ, TUM, Garching, Germany — ³NIMTE, CAS, Zhejiang Province, P. R. China

Binders play an important role in multi-component electrodes for rechargeable batteries, which suffer from poor electronic and ionic conductivity. Binder-free electrodes provide another way to resolve problems, where sophisticated structure construction is required. A new concept of electrode processing alternative to binder-containing and binder-free electrodes was established. A multi-functional PIM-1 (a polymer with intrinsic microporosity) additive was used instead of PVDF to form mechanically processable Li secondary battery cathodes. Due to its unique nanoporous structure built by the spiro-containing rigid aromatic polymer chain, only a tiny amount of PIM-1 in the LiNi_{0.8}Co_{0.1}Mn_{0.1}O₂ cathode is needed to retain good performance, far below the typical composition for PVDF. Homogeneous dispersion of carbon black is achieved by PIM-1, which stabilizes the electrode and increases the electronic conductivity. Different from PVDF, mechanical buffering by stiff PIM-1 yields crack-free electrodes after cycles. Moreover, an inorganic rich cathode-electrolyte interface layer is formed via a desolvation process promoted by PIM-1, because of its strong binding ability with lithium ions, which is beneficial for cyclic stability and rate capability.

CPP 35.17 Wed 11:00 P1

Positrons probe advanced and functionalized porous materials — •AHMED GAMAL ATTALLAH, ERIC HIRSCHMANN, MAIK BUTTERLING, MACIEJ OSKAR LIEDKE, and ANDREAS WAGNER — Institute of Radiation Physics, Helmholtz-Zentrum Dresden-Rossendorf

Positron annihilation lifetime spectroscopy (PALS) is an effective porosimetry technique complementing standard gas intrusion methods. PALS is able to detect open and closed pores, and resolve depth-dependent porosity. It can operate under variable pressures, temperatures, and atmospheres to monitor structural changes during in situ conditions. In this contribution, PALS results of various functionalized porous materials including polymer grating, structural changes in metal-organic-frameworks (MOFs), effect of additives in food ingredients (maltodextrin) on water uptake, and impact of modification of low-k dielectrics on stiffness will be presented. In polymer grafting, the mechanism of polymer grafting on MCM-48-type mesoporous silica nanoparticles forming core-shell composite structure is understood from PALS. Uniquely in MOFs, PALS was able to prove that the temperature-driven transformed metal-organic framework DUT-8(Ni) is still porous possessing closed porosity that is not accessible by other techniques. Sucrose in maltodextrin is the third topic where in situ humidity experiment during PALS revealed that adding 10 % sucrose to maltodextrins has a negligible effect on hygrocapacity at relative humidity > 50 %. Finally, the improved mechanical stability of low-k materials by adding methyl terminal groups that cause less interconnected pores has been verified by positron annihilation.

CPP 35.18 Wed 11:00 P1

Insights into the morphology-structure-property relationship of mesoporous ZnO films during humidity sensing — •TING TIAN¹, SHANSHAN YIN¹, SUO TU¹, APOSTOLOS VAGIAS², ANNA-LENA OECHSLE¹, TIANXIAO XIAO¹, SIGRID BERNSTORFF³, and PETER MÜLLER-BUSCHBAUM^{1,2} — ¹Technical University of Munich, TUM School of Natural Sciences, Department of Physics, Chair for Functional Materials, 85748 Garching — ²MLZ, TU München, 85748 Garching — ³Elettra-Sincrotrone Trieste S.C.p.A., Strada Statale 14 km 163.5, AREA Science Park, Basovizza, 34149 Trieste, Italy

Moisture can strongly influence the conductivity of ZnO semiconductors via the physisorption and chemisorption of water molecules on the ZnO surface. Mesoporous ZnO structures can facilitate the absorption process by providing a large surface area and active sites. However, little effort has been devoted yet to gain an in-depth understanding of the effect of water on the morphology and electrical property. In the present work, different mesoporous ZnO thin films were synthesized by exploiting different diblock copolymers. Benefiting from the different inorganic frameworks, these thin films show significantly different structural properties and defects density. To explore the morphology-structure-property relationship, in situ Fourier-transform infrared spectroscopy (FTIR) was used to confirm the water absorption. Simultaneously, in situ grazing-incidence small-angle X-ray scattering (GISAXS) measurements were performed to investigate the morphology evolution, and in situ electrochemical impedance spectroscopy (EIS) was used to monitor the conductivity changes.

CPP 35.19 Wed 11:00 P1

Morphology transformation pathway of block copolymer- directed cooperative self-assembly of ZnO hybrid films monitored in situ during slot-die coating — •TING TIAN¹, SHANSHAN YIN¹, SUO TU¹, CHRISTIAN L. WEINDL¹, KERSTIN S. WIENHOLD¹, SUZHE LIANG¹, MATTHIAS SCHWARTZKOPF², STEPHAN VOLKHER ROTH², and PETER MÜLLER-BUSCHBAUM^{1,3} — ¹Technical University

of Munich, TUM School of Natural Sciences, Department of Physics, Chair for Functional Materials, 85748 Garching — ²James-Franck-Str. 1 — ³MLZ, TUM, 85748 Garching

Co-assembly of diblock copolymers (DBC) and inorganic precursors that takes inspiration from the rich phase separation behavior of DBCs can enable the realization of a broad spectrum of functional nanostructures with the desired sizes. In a DBC assisted sol-gel chemistry approach with polystyrene-block-poly(ethylene oxide) and ZnO, hybrid films are formed with slot-die coating. Pure DBC films are printed as control. In situ grazing-incidence small-angle X-ray scattering (GISAXS) measurements are performed to investigate the self-assembly and co-assembly process during the film formation. Combining complementary ex situ characterizations, several distinct regimes are differentiated to describe the morphological transformations from the initially solvent-dispersed to the ultimately solidified films. The precursor reduces the degree of order, prevents crystallization of the poly(ethylene oxide) block, and introduces additional length scales in the hybrid films.

CPP 35.20 Wed 11:00 P1

Evaluation of different textile mount designs for printing on textiles in commercial SLA 3D printers for scientific investigation — •TIMO GROTHE¹, ELISE DIESTELHORST¹, JAN LUKAS STORCK¹, DANIEL KOSKE¹, NATALIE FRESE², and MARTIN WORTMANN² — ¹Faculty of Engineering and Mathematics, Bielefeld University of Applied Sciences, Interaktion 1,33619 Bielefeld, Germany — ²Faculty of Physics, Bielefeld University, Universitätsstraße 25, 33615 Bielefeld, Germany

The technology of 3D printing has already reached the commercial sector. But it is not only the industry that is interested in 3D printing; the scientific world is also investigating the possibilities of this multifaceted technology. Here, in addition to the fused deposition modeling (FDM) process, the cornerstone stereolithographic (SLA) process in particular has become the focus of scientific attention. Especially in combination with textiles, some unique composites with outstanding properties can be produced. In order to be able to print these in commercially available printers, some textile mounts were developed and their applicability as well as usability were investigated. Not only the printing result and the adhesion between resin and different textiles were investigated by abrasion tests, but also the application of the individual holders was evaluated. Finally, the produced composites were examined with a scanning helium ion microscope to show, in combination with the other examination methods, that both the textile-resin composites have exceptional abrasion resistance and that the textile holders make it much easier to produce them.

CPP 35.21 Wed 11:00 P1

Polymer Composite Films with Induced Structural Anisotropy for Thermoelectric Application — •CHRISTIAN GRADL¹, MARIE SIEGERT¹, and JENS PFLAUM^{1,2} — ¹Experimental Physics VI, University of Würzburg, 97074 Würzburg — ²ZAE Bayern, 97074 Würzburg

Thermoelectric generators offer a prospective opportunity to handle the increasing energy demand by utilizing waste heat. Organic thin films represent a promising candidate because of benefits like non-toxicity, cost-effectivity or versatile implementation. For an efficient thermoelectric device, the thermoelectric figure of merit $zT = \sigma S^2 T / \kappa$ needs to be high. So the Seebeck coefficient S and the electrical conductivity σ should achieve high values, whereas the thermal conductivity κ has to be low. Taking advantage of the intrinsically low κ , we combine the polymer PEDOT:PSS with additives like silver nanowires, the crystalline organic TTT₂I₃ or VO₂ needles, by which a higher σ is aspired without pronounced detriment of the Seebeck coefficient. TTT₂I₃ and VO₂ are fabricated via microspacing in-air sublimation. Controlled orientation of the additives induced by the substrate is a main topic of our research. Further we investigate the alignment of additives embedded in polymer thin films prepared via doctor-blading to improve the efficiency for thermoelectric application. The results on characterizing the electrical and thermal properties of the organic-metallic composites with respect to their anisotropy will be presented.

CPP 35.22 Wed 11:00 P1

Morphological studies in semicrystalline polymers and polymer nanocomposites using spin diffusion — •DORIT HARTMANN, ANNA NITSCHKE, YURY GOLITSYN, HORST SCHNEIDER, and KAY SAALWÄCHTER — Department of Physics / NMR Group, University of Halle, Betty-Heimann-Str. 7, 06120 Halle, Germany

ABSTRACT: The properties of synthetic polymers can be selectively modified by adding nanoparticles, which is why polymer nanocomposites have a wide range of applications. The interaction of the polymer chains with the surface of silica particles leads to the formation of a multiphase structure, characterized by a gradient of molecular dynamics. [1] Studies of polymer nanocomposites using spin diffusion (SD) experiments in conjunction with the numerical simulations have shown that the interphases exhibit complex morphology with dynamic heterogeneities. [2] In this work, we investigate the effect of magnetic field strength on spin diffusion in semicrystalline poly(ϵ -caprolactone) and a poly(2-vinyl pyridine)-silica nanocomposite. The experiments were performed at two

different field strengths of 0.47 T and 4.7 T (proton Larmor frequency of 20 MHz and 200 MHz, respectively) and were supported by spin diffusion calculations. In addition, this paper aims to provide an overview of the different data acquisition and analysis strategies for high- and low-field instruments. REFERENCES: [1] Horst Schneider, Kay Saalwächter, and Matthias Roos. *Macromol.* (2017), 50, 8598-8610. [2] Horst Schneider, Matthias Roos, Yury Golitsyn, Kerstin Steiner, and Kay Saalwächter. *Macromol. Rapid Commun.* (2021), 2100061.

CPP 35.23 Wed 11:00 P1

Two-step electrochemical Au nanoparticle formation in polyaniline — •BIN ZHAO and SEBASTIAN GUTSCH — institut für mikrosystemtechnik, freiburg, germany

In this study, we report on an electrochemical insertion of Au nanoparticles in polyaniline (PANI) using a two-step process. In the first step, tetrachloroaurate anions (AuCl_4^-) are attached on the protonated imine sites of PANI while holding the potential at +0.8 V. The applied electrochemical potential prevents any reduction of the PANI/ AuCl_4^- complex. After rinsing of excess AuCl_4^- , a controlled reduction is carried out via cyclic voltammetry. Therefore, we investigate the introduction of Au species into PANI via precise electrochemical control in a flow cell system. The PANI/Au composites are characterized using scanning electron microscopy (SEM) and Rutherford backscattering spectrometry (RBS) to quantify the amount of introduced Au. It is demonstrated that the PANI/ AuCl_4^- complex is not aggregating prior to the electrochemical reduction process. However, the controlled reduction of these PANI/Au complexes leads to the subsequent formation of Au nanoparticles, whose density and size dispersion depend on the Au loading in PANI. Furthermore, additional Au deposition cycles increase both the Au nanoparticle density and size. We propose a two-step growth model based on our experimental results. The results are discussed with respect to the formation of atomic Au clusters reported in previous works.

CPP 35.24 Wed 11:00 P1

Accelerating self-assembly of colloidal particles at air-water interface by laser induced heating of upconverting particle — •LOKESH CHINNAKANA MURUGA, GOKUL NALUPURACKAL, SRESTA ROY, SNIIGHADEV CHAKRABORTY, JAYESH GOSWAMI, and BASUDEV ROY — Indian Institute of Technology Madras, Chennai, India - 600036

Particles can be assembled at the air-water interface due to optically induced local heating. This induces convection currents in the water which brings particles to the surface. We improve the technique by employing an upconverting particle (UCP), which, when illuminated with 975 nm light, not only emits visible emission but also generates heat owing to the poor efficiency of the upconversion process. This induces strong convection currents which makes particles dispersed in the suspension assemble at the interface and immediately under the UCP. We show assembly of polystyrene particles of 1 μm diameter and diamonds of 500 nm diameter bearing Nitrogen-Vacancy (NV) centers around the UCP. We also show, for the first time, that the microdiamonds are assembled within about 30 nm at the bottom of the UCP by utilizing non-radiative energy transfer that reduces the lifetime of the 550 nm emission from about 90 μs to about 50 μs .

CPP 35.25 Wed 11:00 P1

Following the directed self-assembly of crystallizable block co oligomers via in situ AFM — •ALEXANDER MEINHARDT¹, PENG QI², IVAN MAXIMOV³, and THOMAS F. KELLER¹ — ¹Centre for X-ray and Nano Science (CXNS), Deutsches Elektronen-Synchrotron DESY, Hamburg, Germany — ²Paul Scherrer Institut, Villigen, Switzerland — ³Solid State Physics and NanoLund, Lund University, Lund, Sweden

Bottom up nanofabrication utilizing the molecular self-assembly of block co-oligomers with sub-10 nm domain sizes is widely discussed as a promising route for next generation photolithography. Double crystalline co-oligomers can be used to create well defined, high-fidelity nanostructures by controlling the competing driving forces microphase separation and crystallization. We report on the surface nanostructure formation and the temporal evolution during annealing of thin films of an amphiphilic double crystalline polyethylene-block-poly(ethylene oxide) co-oligomer (PE-b-PEO) on planar and patterned surfaces. On a planar Si surface we observed the self-assembly of PE-b-PEO into locally ordered lamellar surface structures extending over several micrometers. Directed self-assembly (DSA) of this PE-b-PEO system by physical guiding patterns can enable the formation of large scale nano-templates interesting for future applications. First DSA experiments indicate that the formed PE-b-PEO based surface nanostructures depend on the pitch of the guiding pattern. We furthermore aim to use in situ AFM to shed light on the pitch-dependent structural evolution during dedicated temperature-controlled annealing procedures.

CPP 35.26 Wed 11:00 P1

Intracrystalline dynamics of polybutylene succinate and poly(3-Hydroxybutyrate) — •MOHD AFIQ BIN ANUAR, YU QIANG, THOMAS THURN-ALBRECHT, and KAY SAALWÄCHTER — Institut für Physik, Martin-Luther-Universität Halle-Wittenberg, 06099 Halle, Germany

The dynamics behavior of polymers chain in crystal lamellae plays a critical role for its semicrystalline morphology [1, 2]. It is influenced by this intracrys-

talline dynamics (ICD) explaining the factors that limit its crystal thickness during isothermal crystallization. In this work, two different behaviours of semicrystalline polyesters, namely polybutylene succinate (PBS) and poly(3-Hydroxybutyrate) (P3HB), are discussed. A combination of nuclear magnetic resonance (NMR) techniques shows that isothermally crystallized PBS exhibit slow ICD longer than 1s which is similar to the reported crystal-fixed polymer, polycaprolactone [1]. Meanwhile, in P3HB crystal chain, the ICD with correlation jump motion around 0.5s/monomer at 120°C was detected. This is in contrast to previous reported [3] demonstrating a crystal-mobile behavior. Small-angle X-ray scattering measurement reveal that the P3HB crystal lamellae are significantly thicker than in PBS, confirming that P3HB and PBS can be classified as crystal-mobile and crystal-fixed, respectively. Details regarding morphology are shown in the poster.

References: [1] Schulz, M., et al., *Macromolecules* 2018, 51, 8377. [2] Schulz, M., et al., *Nat. Common.* 2022, 13, 1. [3] Xia, Z., et al., *Soft Matter* 2021, 17, 4195.

CPP 35.27 Wed 11:00 P1

Non-linear mechanical properties of polycaprolactone polymer/oligomer blends with defined entanglement density and crystalline thickness — •TONGHUA LIU, ALBRECHT PETZOLD, and THOMAS THURN-ALBRECHT — Von-Danckelmann-Platz 3, 06120, Halle(Saale)

The mechanical properties of semi-crystalline polymers are determined by the semi-crystalline morphology and the entanglements in the amorphous regions. Here we use polymer/oligomer blends to control the entanglement density independently of the crystallinity. This system is also used as a model to study effects on the non-linear mechanical properties. The aim of the project is to develop a quantitative method for the determination of the entanglement density in the amorphous region as well as to investigate its relation to yielding, modulus and strain hardening. The commonly used method is tensile testing, but cavitation and necking cannot be avoided. Instead, we use plane-strain compression tests, which allow the direct determination of the true stress and avoids problems like cavitation. A separation of viscous and elastic contributions can be achieved by inserting relaxation measurements during the deformation. Our preliminary results indicate a strong effect of the crystallinity on the modulus and yield stress. The relation between strain hardening and entanglement density will be discussed.

CPP 35.28 Wed 11:00 P1

New experimental methods for structure analysis of soft matter — •ERIC EUCHLER¹, ANNA KATHARINA SAMBALE¹, REGINE BOLDT¹, KAI UHLIG¹, LAURA NEUMANN¹, KONRAD SCHNEIDER¹, MATTHIAS SCHWARTZKOPF², STEPHAN ROTH^{2,3}, and MARKUS STOMMEL^{1,4} — ¹Leibniz-Institut fuer Polymerforschung, Dresden, Germany — ²Deutsches Elektronen Synchrotron DESY, Hamburg, Germany — ³KTH Royal Institute of Technology, Stockholm, Sweden — ⁴Technical University Dresden, Dresden, Germany

Recently developed stretching devices for synchrotron measurements are available to investigate deformation-induced phenomena, such as strain-induced crystallization in natural rubber or void formation in biological tissues, at quasi-static and impact loading. In addition to measurements in transmission, novel studies of thin layers on flexible substrates can be realized by performing in situ grazing-incidence (GI) experiments.

Beside structure analysis in solid parts, the flow-induced structure formation in polymer melts is of particular interest to better understand the impact of melt processing parameters on macroscopic material properties, such as Young's modulus and tensile strength. For this purpose, a new experimental setup has been designed and built to study time- and temperature-dependent structure evolution events in thermoplastics. Within a temperature-controlled flow channel, polymer melts can be monitored with a microfocus X-ray synchrotron beam and first results obtained for two different thermoplastic materials proofed the experimental concept under quiescent melt conditions.

CPP 35.29 Wed 11:00 P1

Towards experimental detection of crystallization in individualized polymer chains — •WING KIT OR, ALAA HASSAN, and MARTIN TRESS — Peter Debye Institute for Soft Matter Physics, Leipzig University, Leipzig, Germany

Although crystallization of polymers has been investigated since decades, it is not yet fully understood. One way to gain more insight is to study the difference between bulk polymer and confined polymer chains with focus on how crystallization characteristics change depending on the size and type of confinement. Until now, most studies have used confinement in thin films or nanopores but the approach to study crystallization and aggregation in individual chains was accessible only to computer simulations. Since detection of phase transitions in individual polymer chains poses a severe challenge to most experimental methods, the measurement of ensembles of individual chains is desirable. However, maintaining the individual character requires a sophisticated method to separate them. Here, we use block copolymer micelle lithography (BCML) to deposit a regular pattern of well-separated gold nanodots on a silicon substrate in order to chemically graft end-functionalized polymer chains on these nanodots to in-

dividualize them. Instead of common thermodynamic methods (which require considerably more sample material), we employ dielectric spectroscopy using a nanostructured electrode arrangement since it is much more sensitive. Albeit being typically considered a dynamics method, it also allows to examine density changes and thus phase transitions of polymers.

CPP 35.30 Wed 11:00 P1

Uniaxially Aligned Merocyanine Films by Graphene Nanoribbon Templated Growth — •PHILIPP WEITKAMP, NORA GILDEMEISTER, LUKAS BÖHNER, DIRK HERTEL, and KLAUS MEERHOLZ — Physikalisches Chemie, Universität zu Köln, Deutschland

We herein report the unique and novel approach of achieving a polycrystalline thin film consisting of uniaxially aligned domains by using 7-armchair graphene nanoribbon (7-aGNR) monolayers as van-der-Waals template. For this purpose, a merocyanine dye was evaporated on 7-aGNRs, transferred on quartz glass substrates. The alignment of the formed molecular aggregate along the GNR alignment direction was proven by polarisation dependent absorbance spectroscopy. The J- and H-transition, formed by the dye aggregate, were correlated with distinct axes of the crystal structure. By combining this correlation with polarisation dependent absorbance measurements and X-ray diffraction experiments we elucidated the three-dimensional structure of the formed aggregate thin film. The growth mode of these films was investigated as a function of the applied layer thickness. Atomic force microscopy-based morphology analysis and X-ray diffraction experiments were used to reveal the anisotropic on-surface crystallisation along the 7-aGNR long axes direction. Furthermore, we found that the delocalisation length of the aggregate increases with increasing in-plane order. Finally, we demonstrated that the in-plane alignment leads to an anisotropic charge carrier transport by implementing the templated merocyanine thin film as active layer in a top-gated organic field effect transistor.

CPP 35.31 Wed 11:00 P1

Long chain Polyamides: Influence of methylene sequence length and external forces on structural features — •RENE SÄTTLER^{1,2}, VARUN DANKE³, and MARIO BEINER^{1,2} — ¹Fraunhofer IMWS, Walter-Hülse-Str. 1, D-06120 Halle (Saale), — ²Martin-Luther-Universität Halle-Wittenberg, Naturwissenschaftliche Fakultät II, D-06099 Halle (Saale) — ³Evonik Operations GmbH, Research Development & Innovation, Paul-Baumann-Str. 1, D-45722 Marl

Crystallographic studies towards the influence of methylene sequence length on a series of even-even polyamides PA 10.n (with n = 12, 14, 16 and 18) are performed. Temperature-dependent X-ray diffraction measurements show that the triclinic α phase is the preferred phase at room temperature after slow cooling from melt. In PA 10.12 and PA 10.14 a reversible Brill transition to the (pseudo)hexagonal high temperature γ phase is observed. However, the Brill transition temperature is strongly dependent on n and shifting to higher temperatures with increasing methylene sequence length. For the two higher members a Brill transition is absent. The analysis of annealed, uniaxial oriented fibers reveals that the crystalline state achieved under ambient conditions is influenced by external forces. This is due to relatively small energetic differences between the α and β polymorphs. All the uniaxial oriented PA 10.n samples show a β polymorph which is most prominent for PA 10.12 and PA 10.14. The higher members show a mixture of the β polymorph superimposed with a certain fraction of the α polymorph.

CPP 35.32 Wed 11:00 P1

Bond order parameters in crystallization of short polymer chains in thin films: SAMC simulation — •EVGENIYA FILIMONOVA, TIMUR SHAKIROV, and VIKTOR IVANOV — Martin Luther University of Halle-Wittenberg, Institute of Physics, 06120, Halle (Saale), Germany

We study the crystallization of polymer melts in thin films using a coarse-grained model and stochastic approximation Monte Carlo (SAMC) simulation. Our goal is to reveal physical factors which are responsible for one of two possible scenarios of surface-induced polymer crystallization: heterogeneous nucleation or prefreezing. We have developed an approach that allows us to identify the translational and orientational local ordering by means of comparing our system configurations with reference crystalline structures of different symmetries. In addition to calculating the usual order parameters (Steinhardt parameters, common neighbors analysis, nematic order parameter, etc.), we suggested new order parameters based on scalar products of bonds between nearest neighbors. We observe a coexistence of an isotropic structure in the center of the film with ordered structures at the walls at intermediate values of energies (in microcanonical analysis). A change in the crystal structure accompanying a change in density at different energies is also shown. Financial support of the International Graduate School AGRIPOLY supported by the European Social Fund (ESF) and the Federal State Saxony-Anhalt is acknowledged.

CPP 35.33 Wed 11:00 P1

Investigating the thermodynamics and kinetics of catechin pyrolysis for environmentally friendly binders — •JAKOB KRAUS and JENS KORTUS — Institute of Theoretical Physics, TU Bergakademie Freiberg, Leipziger Str. 23, D-09599 Freiberg, Germany

The thermodynamics and kinetics of the pyrolysis of (+)-catechin, a building block of the condensed tannins found in recipes for sustainable binders, are evaluated at the CCSD(T) level and compared to other methods from quantum chemistry. Using the climbing image nudged elastic band method coupled with transition state optimization, minimum energy paths and highest-energy transition states are identified for the first two pyrolysis steps, a catechol splitoff with subsequent dehydrogenation. While the catechol splitoff path was very smooth, the dehydrogenation featured an additional transition state in the form of an OH group rotation. The combined reaction was judged endothermic in the range of 0 K to 1250 K, and exergonic at 1000 K and above. It is shown that the catechol splitoff is the rate-determining step of the pyrolysis of catechin, which is equivalent to kinetic inhibition at all investigated temperatures.

CPP 35.34 Wed 11:00 P1

Pyrolysis of ellagic acid - a thermodynamic and kinetic study by means of quantum chemistry — •PHILIP SCHÖNE, JAKOB KRAUS, and JENS KORTUS — TU Bergakademie Freiberg (Institut für Theoretische Physik) Leipziger Str. 23, 09599 Freiberg, Deutschland

By performing ab-initio calculations, thermodynamic and kinetic data on the pyrolysis of ellagic acid were computed. The reaction path consists of two decarboxylations and two hydrolyses. The pyrolysis of ellagic acid can take place via the formation of either hexahydroxydiphenic acid or urolithin m5. Using select DFT functionals and quantum chemical methods, data for each reaction were calculated between 0 K and 1200 K. The occurring decarboxylations were found to be very similar to each other, being exothermic and exergonic reactions that become increasingly so with rising temperature. The hydrolyses show the opposite behavior, being slightly endothermic and endergonic reactions that become increasingly so with rising temperature. With the help of the climbing image nudged elastic band method, mechanisms for all reactions could be proposed and highest energy transition states could be identified. For the decarboxylations, these represent H transfers from the carboxylic group to the neighboring C atom. For the hydrolyses, the highest energy transition states correspond to H transfers from water to the nascent carboxylic group. Moreover, the rate-determining steps in the pyrolysis of ellagic acid were determined, which are the hydrolyses of urolithin m5 and luteic acid.

CPP 35.35 Wed 11:00 P1

Transversal piezo-force-microscopy with the use of interdigitated electrodes — •MAXIMILIAN LITTERST, ANDREY BUTKEVICH, and MARTIJN KEMERINK — Institute for molecular systems engineering and advanced materials, Heidelberg, Germany

Piezoresponse force microscopy (PFM) is a simple method to measure the piezoelectric effect of many materials with an atomic force microscope (AFM). Usually, a voltage is applied between the tip and the substrate to trigger a vertical displacement of the material via the converse, longitudinal, piezoelectric effect, which results in a vertical displacement of the tip. The transversal piezoelectricity can result in a torsion of the tip, it is however often very difficult to find a direct connection between the two.

Here, we present how interdigitated electrodes (IDEs) can be used to apply an electric field in the film-plane, resulting in a vertical displacement of the film due to the converse, transversal, piezoelectric effect. In addition, the longitudinal component can be measured via the torsional tip motion. This does not only provide a direct way to measure the transverse piezoelectricity, but also opens new possibilities for the device preparation.

CPP 35.36 Wed 11:00 P1

Ca substitution instead of Sr in $\text{La}_{0.58}\text{Sr}_{0.4}\text{Co}_{0.2}\text{Fe}_{0.8}\text{O}_{3-\delta}$ as a cathode electrode for IT-SOFCs — •MAJID JAFARI¹, FATEMEH YADOLLAHI FARSAANI², NORBERT MENZLER³, CHRISTIAN LENSER⁴, and FABIAN GRIMM⁵ — ¹Plön, Germany — ²Isfahan university of technology, Isfahan, Iran — ³Forschungszentrum Jülich, Jülich, Germany — ⁴Forschungszentrum Jülich, Jülich, Germany — ⁵Forschungszentrum Jülich, Jülich, Germany

$\text{La}_{0.58}\text{Ca}_{0.4}\text{Co}_{0.2}\text{Fe}_{0.8}\text{O}_{3-\delta}$ (L58CCF) was synthesized and evaluated as a cathode electrode for intermediate temperature solid oxide fuel cells (IT-SOFC) based on the Y_2O_3 -stabilized ZrO_2 (YSZ) electrolyte. The effect of sintering temperature on the L58CCF performance was investigated. The best Area specific resistances (ASRs) for the L58CCF sintered at 950 °C were 1.218, 0.447, 0.228, 0.156, 0.099 $\Omega\cdot\text{cm}^2$ at 600, 650, 700, 750, 800 °C, respectively.

CPP 35.37 Wed 11:00 P1

Antiperovskites (Li_2Fe)ChO as cathode material for lithium-ion batteries and investigation of the reaction mechanism — •BOWEN DONG¹, LENNART SINGER¹, MOHAMED ABDULLAH ABDULLAH MOHAMED², SILKE HAMPEL², NICO GRÄSSLER², and RÜDIGER KLINGELER¹ — ¹Kirchhoff Institute for Physics, Heidelberg University, Germany — ²Leibniz Institute for Solid State and Materials Research (IFW) Dresden e.V., Germany

Due to its unique structure, antiperovskite (Li_2Fe)ChO (Ch = S, Se) have emerged as a promising Li-ion battery (LIB) cathode material with excellent rate capability and a good discharge capacity. We report synthesis of antiperovskites by a

direct ball-milling process and evaluate the phase stability, cycling performance, and rate performance. The effect of post-synthesis heat treatment on the resulting materials as well as on its battery performance is studied. Cyclic voltammetry studies reveal a high-voltage decomposition process which progressively yields the formation of Fe_xCh_y . Galvanostatic measurements exhibit outstanding electrochemical cycling performance of antiperovskite-based cathodes of 250 mAh/g at 0.1 C. Further, we suggest a route to avoid the progressing conversion of $(\text{Li}_2\text{Fe})\text{ChO}$ ($\text{Ch}=\text{S}, \text{Se}$) to Fe_xCh_y , which effectively improves the cell performance of antiperovskites.

CPP 35.38 Wed 11:00 P1

Rational Design of Novel Photoswitches with Generative Models — •ROBERT STROTHMANN, CHRISTIAN KUNKEL, JOHANNES MARGRAF, and KARSTEN REUTER — Fritz-Haber-Institut der MPG, Berlin, Germany

The sheer vastness of chemical spaces poses a daunting challenge to molecular discovery through high-throughput screening based on exhaustive sampling. Generative models (GMs) are an emerging machine learning (ML) approach that enables a more guided discovery. Implicitly learning chemical design rules from large reference data sets and suitable descriptors of a targeted functionality, GMs directly propose promising, yet diverse candidates.

Here we explore the use of GMs for the design of novel molecular photoswitches. In a first step, large general molecular databases are used to train a GM to generate chemically valid photoswitches. In a second step, the creation process needs to be conditioned towards performant switching capabilities. In the absence of sufficient corresponding experimental reference data, this conditioning is based on synthetic first-principles data. For that purpose computationally efficient descriptors are used in a multi-objective fashion to account for the desired key aspects of the switching process.

CPP 35.39 Wed 11:00 P1

Correlating molecular properties to nonlinear optical activity: Prerequisites for white light generation. — •FERDINAND ZIESE, LENA ALBOHN, KEVIN EBERHEIM, and SIMONE SANNA — Institut für Theoretische Physik Heinrich-Buff-Ring 16, 35392 Gießen, Germany

Recent studies have demonstrated white light generation from molecular clusters with adamantane-like cores and different ligands [1,2]. To understand the origin of this behavior, we have investigated structural, electronic, and (nonlinear) optical properties from first principles for isolated molecules and dimer structures [3]. In this contribution, we focus on the comparison between isolated molecules and molecular dimers. We correlate the structural and electronic properties with the optical response and investigate the effect of symmetry and heterogeneous composition.

[1] N. W. Rosemann, J. P. Eufner, A. Beyer, S. W. Koch, K. Volz, S. Dehnen, S. Chatterjee, *Science* 2016, 352, 1301

[2] N. W. Rosemann, J. P. Eufner, E. Dornsiepen, S. Chatterjee, S. Dehnen, *J. Am. Chem. Soc.* 2016 138 (50), 16224-16227

[3] S. Schwan, A. J. Achazi, F. Ziese, P. R. Schreiner, K. Volz, S. Dehnen, S. Sanna, D. Mollenhauer, *J. Comput. Chem.* 2022

CPP 35.40 Wed 11:00 P1

Effect of electron and laser irradiation on the structure of halogen substituted adamantane clusters — •LENA ALBOHN, SIMONE SANNA, KEVIN EBERHEIM, and FERDINAND ZIESE — Institut für Theoretische Physik Heinrich-Buff-Ring 16, 35392 Gießen, Germany

Functionalized adamantane molecular clusters are highly nonlinear optical materials which are able to convert infrared radiation into a directed emission supercontinuum. While the origin of the optical nonlinearity is still under debate, the amorphous habitus of the materials seems to be a prerequisite for the white-light generation.

Unfortunately, many adamantane-based or organotetrel clusters crystallize in an ordered structure characterized by intense second-harmonic generation instead of white-light emission. In order to render the molecular crystals amorphous, electron or laser irradiation has been suggested. In order to explain the mechanisms leading to the structural modification, we model electron or laser irradiation from first principles. Thereby, we employ halogen substituted adamantane clusters as a model system. Our calculations reveal that laser and electron irradiation have a similar effect on the compounds. Depending on the irradiation dose, intermolecular rearrangements as well as intramolecular deformations (photochemical rearrangement) may occur, thus facilitating the white-light emission.

CPP 35.41 Wed 11:00 P1

Structural properties of a semi-dilute suspensions of magnetic multi-core nanoparticles — •EKATERINA NOVAK¹, ANDREY KUZNETSOV², ELENA PYANZINA¹, MARINA GUPALO¹, TATYNA BELYAEVA¹, and SOFIA KANTOROVICH² — ¹Ekaterinburg, Russia — ²University of Vienna, Vienna, Austria

During the last thirty years, magnetic soft matter systems have become highly promising candidates for medical applications such as magnetic hyperthermia and magnetic drug targeting. The subject of this work, magnetic multicore nanoparticles (MMNPs), are rigid clusters of single-domain magnetic nanocrystals

(cores or grains) embedded in a polymer or other non-magnetic matrix. While the grains typically have a characteristic linear size of the order of 10 nm, the size of MMNPs can range from tens to a few hundred nanometers. Here, using Langevin dynamics computer simulations, we investigated diluted suspensions of MMNPs composed by grains, whose positions are fixed within the particle body, but their magnetic moments are free to rotate, corresponding to the grains with negligibly low magnetic anisotropy.

We calculated cluster size distributions and compared them to their counterparts in a system of single-domain magnetic nanoparticles. A drastic difference was found: for two MMNPs to aggregate they need to form a bridge a stable array of grains from both multicores that are connected via dipolar interactions. The more bridges the two MMNPs form, the more stable is their aggregate.

CPP 35.42 Wed 11:00 P1

Characterisation and transport within tetra-PEG*tetra-PCL amphiphilic end-linked polymer model networks — •LUCAS LÖSER¹, CAROLIN BUNK², FRANK BÖHME², and KAY SAALWÄCHTER¹ — ¹Inst. F. Physik * NMR, Martin-Luther-Universität Halle-Wittenberg, Halle/D — ²Leibnitz-Institut für Polymerforschung Dresden e.V., Hohe Str. 6, Dresden/D

A new approach for the synthesis of model-like amphiphilic co-networks is introduced, and their structure is analyzed by static 1H time-domain nuclear magnetic resonance (NMR) methods [1]. The hetero-complementary end-linking reaction of two well-defined star precursors [2] is implemented to obtain amphiphilic gels. We link PEG stars with hydrophobic poly- ϵ -caprolactone stars (tetra-PCL), resulting in the formation of an amphiphilic network. NMR is shown to be capable of distinguishing different chain species in the swollen PEG-PCL networks, allowing quantification of network connectivity defects arising from the end-linking reaction, as well as accurate quantification of inelastic material. The mesh size of the networks is studied by Pulsed-Field Gradient (PFG) NMR, using dextran as hydrophilic probe molecules for the network swollen in selective solvents. Furthermore, we performed measurements using small-angle x-ray scattering and 1H MAS recoupling NMR for information on the properties of the selectively swollen networks, e.g., estimates for the correlation length of PCL domains, and chem. shift-specific information about the chain dynamics. [1] Bunk et al.; *Macromolecules* 2022, 55, (15), 6573-6589 [2] Sakai, T. et al.; *Macromolecules* 2008, 41, (14), 5379-5384

CPP 35.43 Wed 11:00 P1

Hybrid hydrogel films for scalable H₂ production — •MORGAN LE DÛ¹, JULIJA REITENBACH¹, MANUEL A. REUS¹, KUN SUN¹, ZERUI LI¹, SIGRID BERNSTORFF², CRISTIANE HENSCHEL³, ANDRÉ LASCHWESKY³, CHRISTINE M. PAPADAKIS⁴, and PETER MÜLLER-BUSCHBAUM^{1,5} — ¹TUM School of Natural Sciences, Chair for Functional Materials, Garching, Germany — ²Elettra-Sincrotrone Trieste, Basovizza, Italy — ³Fraunhofer-Institut für Angewandte Polymerforschung, Potsdam-Golm, Germany — ⁴TUM School of Natural Sciences, Soft Matter Physics group, Garching, Germany — ⁵Heinz Maier-Leibnitz-Zentrum (MLZ), TUM, Garching, Germany

The water splitting reaction can produce hydrogen-based energy from solar radiation. A promising photocatalyst for this reaction is Pt loaded graphitic carbon nitride (g-CN). It shows a high H₂ evolution efficiency in aqueous solution. Previous works proposed to introduce hydrogels as host matrix and water storage to facilitate homogeneous spreading. This work aims to develop this system industrially scalable in a polymer thin film configuration. Poly(N-isopropylacrylamide) thin films exhibit good swelling capacity in water vapor atmosphere and appear suitable for a hybrid thin film system. A new isomer poly(N-vinylisobutyramide) seems also promising due to its higher lower critical solution temperature in aqueous solution. Therefore, a comparison of both polymers is based on in situ spectral reflectance and FT-IR measurements. The films have been spray coated to proceed grazing incident small angle x-ray scattering where g-CN/Pt blended polymer films microstructure was analysed under light irradiation.

CPP 35.44 Wed 11:00 P1

Effect of type of initiator and purification on the properties of thermo-responsive PNIPAM microgels — •JOANNE ZIMMER, SEBASTIAN STOCK, SOURAJ MANDAL, CARINA SCHNEIDER, LUCA MIRAU, and REGINE VON KLITZING — Soft Matter at Interfaces, Institute for Condensed Matter Physics, TU Darmstadt, Germany

Microgels (MG) are polymeric networks in the size range of micrometers boasting properties of both colloids and polymers. Depending on their composition MG can respond to external stimuli such as temperature or pH. An example of a thermo-responsive polymer is Poly(N-isopropylacrylamide) (PNIPAM). PNIPAM MG can be synthesized by surfactant-free precipitation polymerization comprising NIPAM monomers, the crosslinker N,N'-methylenebisacrylamide (BIS) and a radical initiator. Depending on the radical initiator, either negatively or positively charged MG are generated. The subject of this work is the evaluation of the MG charge on the thermo-responsive swelling behavior and elastic properties using Dynamic Light Scattering and Atomic Force Microscopy. In addition, the type of MG purification and its effect on the resulting MG proper-

ties is investigated. It was shown, that the presence of undesired low-molecular weight products strongly impacts the MG interfacial adsorption behavior what we wish to understand. In this regard, sufficient removal was only achieved if, apart from the standard purification via dialysis, subsequent centrifugation steps were carried-out. The MG bulk properties (hydrodynamic radius, Zeta-potential) remained unchanged before and after centrifugation.

CPP 35.45 Wed 11:00 P1

Diketopyrrolopyrroles on graphite: Carpets self-assembled via hydrogen bonding — MOUFDI HADJAB^{1,2}, VLADYSLAV SAVCHENKO², NINA TVERDOKHLEB², and •OLGA GUSKOVA² — ¹Mohamed Boudiaf University of M'sila, Algeria — ²IPF Dresden, Germany

We investigate the initial stages of the adsorption and thin-film formation of N-unsubstituted difuryl-diketopyrrolopyrroles (DPP) on graphite. Molecules in a particular conformational state (cis-cis, cis-trans or trans-trans) build the adsorption layers during in-silico self-assembly on surface through intermolecular hydrogen bonding. Here, the vacuum deposition of the molecules is reproduced in the all-atom MD setup [1]. We found out the formation of stable carpets made of molecular stripes. These carpets can be characterized as monomolecular layers in contrast to the structures, formed using droplet deposition [2]. The most stable stripes are made of cis-cis conformers, which is explained by stronger intermolecular hydrogen bonding. The stripe growth is accompanied by the reduction of the Eg gap. At the same time, the binding energy of the molecules does not show a clear dependence on the stripe length, which is a signature of the isodesmic self-assembly. Additionally, we quantify the intermolecular and the molecule/graphite energies for the hydrogen-bonded DPP molecules and compare the results with known experimental data. This work is supported by DFG, grant GU1510/5-1. [1] Guskova O.A., et al. J. Phys. Chem. C 2013, 117, 33, 17285. [2] Hadjab M., Guskova O. Herald of TvSU. Ser. Chem. 2021, 4, 46, 118.

CPP 35.46 Wed 11:00 P1

Ground- and excited-state properties of tetraphenyl compounds from first-principles calculations — •KEVIN EBERHEIM, LENA ALBOHN, FERDINAND ZIESE, CHRISTOF DUES, and SIMONE SANNA — Institut für Theoretische Physik and Center for Materials Research, Justus-Liebig-Universität Gießen, 35392 Gießen, Germany

Tetraphenyl compounds with formula $X(C_6H_5)_4$ (X being a tetravalent atom of the 14th group such as C, Si, Ge, Sn, Pb), crystallize either in a tetragonal crystalline structure or in an amorph phase [1]. Depending on their habitus, the compounds are characterized by very different optical properties. The molecular crystals are known for their second harmonic generation (SHG) properties, while the amorph phase is a white light emitter. Tetraphenyl molecules feature indeed the delocalized π -orbitals, which have been proposed as a prerequisite for the white-light generation [2]. In an attempt to understand the mechanisms related to the white light emission, we model the structural, electronic and vibrational properties of different $X(C_6H_5)_4$ structures within density functional theory. The calculated structural parameters closely reproduce the measured values, however vdW corrections are crucial for a correct description of the structural properties. This confirms that dispersion forces are responsible for the intermolecular bonds in the compound. Different implementations of the vdW forces lead to very similar results. Calculated vibrational properties are in agreement with measured Raman spectra. [1] A Kitaigorodsky, Molecular Crystals and Molecules, Acad. Press (1973). [2] Nils W. Rosemann et al., J. Am. Chem. Soc. 138, 16224 (2016), Science 352, 1301 (2016).

CPP 35.47 Wed 11:00 P1

Scaling Properties of Tree-like Self-Similar Polymers — •RON DOCKHORN¹ and JENS-UWE SOMMER^{1,2} — ¹Leibniz-Institut für Polymerforschung Dresden e.V., D-01069 Dresden, Germany — ²Technische Universität Dresden, Institut für Theoretische Physik, D-01069 Dresden, Germany

In this study, regular polymeric Vicsek- and T-fractals are compared to dendrimers in means of theory and simulations. Albeit all structures exhibit exponential growth both for the number of monomers inside the structures and also for the terminal groups their structural properties differ significantly. Computer simulations are performed to investigate the scaling properties of the tree-like self-similar polymers utilizing the Bond-Fluctuation-Model with the Metropolis method as well as with the Wang-Landau algorithm. The radius of gyration, the heat capacity and the θ -point of those systems is investigated to examine the coil-globule transition of the polymeric fractals. A mean field theory for the scaling exponent in different solvent regimes is applied and found in fair agreement to the simulation data. A cross-over from almost linear chain behavior to spherical shape is observed, which can be tuned by the intrinsic functionality of the building blocks. The polymeric fractals can be an alternative to dendrimers in the class of hyperbranched polymers.

CPP 35.48 Wed 11:00 P1

Statistical Analysis of the Dimerization of Polyglutamine Chains — •CHRISTIAN LAUER and WOLFGANG PAUL — Martin-Luther-Universität Halle-Wittenberg, Halle (Saale), Germany

We are presenting a numerical investigation of the dimerization of polyglutamine homo-peptides of varying length. We use the intermediate resolution protein model PRIME20 and study it with a flat-histogram type Monte Carlo simulation. This gives us access to the thermodynamic equilibrium of this model over the complete control parameter range, which for our simulations is the temperature. For densities comparable to typical in vitro experimental conditions we find that the aggregation and folding of the polyglutamine chains occur concurrently. However, as a function of chain length the sequence of establishment of intra- and intermolecular hydrogen bonding contacts changes. Chains longer than about $N = 24$ polyglutamine repeat units fold first and then aggregate. This agrees well with the experimental finding, that beyond $N = 24$ the single polyglutamine chain is the critical nucleus for the aggregation of amyloid fibrils. A finite size scaling of the ordering temperatures reveals that for this chain length (and longer chains) folding occurs at physiological (respectively larger) temperatures whereas shorter chains are disordered at physiological conditions.

CPP 35.49 Wed 11:00 P1

Construction of a polarizable force field for molecular dynamics simulation of a NaOTF Water-in-Salt electrolyte — •MAJID REZAEI, SUNG SAKONG, and AXEL GROSS — Institute of Theoretical Chemistry, Ulm University, 89069 Ulm, Germany

A NaOTF Water-in-Salt (WiS) electrolyte is modeled using classical molecular dynamics (MD) simulations. For this, four different force fields are employed to account for atomic polarization at different levels: a non-polarizable all-atom force field where the polarization effect is only implicitly included in the Van der Waals interaction parameters; the same force field with uniformly scaled ionic charges which, in a mean-field approximation, mimics electron polarization; a partially polarizable force field where ion polarization is explicitly accounted for via Drude oscillators while water is modeled by the non-polarizable SPC/E model; and a fully polarizable force field where the Drude oscillator model is used to account for both water and ion polarization. The primary goal of this study is to evaluate the simulation stability when using the above force fields and to investigate how the electrolyte properties are sensitive to the force field parameters. The results are then used to construct a force field that best reproduces the electrolyte properties obtained from ab initio molecular dynamics (AIMD) calculations. For this purpose, we use the partially polarizable model, which we believe is accurate enough to reproduce various properties of the studied electrolyte while the computational effort is affordable. The optimized force field will then be used to study the structure and dynamic properties of a NaOTF WiS solution under different conditions.

CPP 35.50 Wed 11:00 P1

Kirkwood-Buff theory approach towards cosolvent effects on single polymer chain collapse transition — •MARTIN MELČÁK, JAKUB SMUTEK, and JAN HEYDA — Department of Physical Chemistry, University of Chemistry and Technology, Prague, Technická 5, CZ-16628 Praha 6, Czech Republic

The so-called smart materials are unique for their ability to rapidly and fully reversibly change physical or chemical properties upon exposure to external stimuli, such as temperature, light, pH, or solvent quality. In this contribution, we have taken under focus the prominent example of thermoresponsive polymer, which conformation can be near critical temperature modulated by the addition of small doses of cosolvents. To reveal the microscopic origin of the thermodynamic effect, we employed coarse-grained molecular dynamics simulations of a single polymer chain in mixed solution. The studied model can effectively describe changes in polymer chain conformation as well as the responses of the local solution composition in polymer proximity. Utilizing this fact, we have described and analyzed system thermodynamics in the framework of Kirkwood-Buff theory, which combines the polymer and environmental perspective of cosolvent effect on the polymer transition. Within a single unifying concept, our model is thus capable to quantitatively describe cosolvent effects in three interaction regimes, namely: depleted, weakly binding, and bridging regime.

CPP 35.51 Wed 11:00 P1

Fabrication of Plasmonic Au Nanostructures for Electrocatalysis — •GINA ROSS and BJÖRN BRAUNSCHWEIG — Institut für Physikalische Chemie, WWU Münster, 48149 Münster, Germany

Nanosphere lithography (NSL) is a classical technique to fabricate reproducible 2D masks. These masks can be used to structure surfaces in a well-defined fashion. We have used spherical polystyrene (PS) particles to generate closed-packed hexagonal layers on a substrate surface that serves as a quasi 2D mask. The latter is subsequently coated with Au to fabricate Au nanopyramids which are received by dissolution of the PS particles. Their deposition as a mask was done with the Langmuir-Blodgett transfer at the air-water interface. For that a suspension of polystyrene particles was spread on the water subphase containing no additional salt or surfactant. The fraction of PS particles sinking into the bulk subphase was drastically reduced by a 1:1 suspension of water and ethanol, and by dispensing the PS suspension onto the air-water interface with a glass slide at an angle of 45° relative to the interface. Au deposition and mask removal with an ultrasonic bath led to the formation of Au nanopyramids. We expect the interaction of

these nanostructures with electromagnetic radiation to result in a local field enhancement which promises to improve chemical reactions sensitive to electric field gradients. For that reason we have investigated the ability of Au plasmonic structures to promote CO₂ electrocatalysis.

CPP 35.52 Wed 11:00 P1

Luminescence properties of Nd complexes and processing of photonic crystal structures — •MIRIAM GERSTEL¹, INGO KÖHNE², PAUL MERTIN³, BERND WITZIGMANN³, JOHANN PETER REITHMAIER¹, RUDOLF PIETSCHNIG², and MOHAMED BENYOUCEF¹ — ¹Institute of Nanostructure Technologies and Analytics — ²Institute of Chemistry, CINSaT, University of Kassel, Germany — ³EET Department, Friedrich-Alexander University of Erlangen-Nürnberg, Germany

Lanthanide ion luminescence exhibits characteristic narrow emission bands along with relatively long emission lifetimes which makes them attractive for applications in lighting, sensing, and display technologies. We investigate the optical characteristics of phosphonate ester-supported nitrite and chloride neodymium(III) complexes as solid bulk material and in solution. Optical properties of Nd complexes are determined by photoluminescence (PL) spectroscopy, which reveals emission bands of Nd(III) ions in the NIR region. PL measurements of equimolar solutions reveal information about the emission strength of the complexes with different ligand types. Temperature-dependent PL spectra enable the assignment of the emission lines observed around 880 nm. For light enhancement, molecules are immobilized on photonic crystal cavities (PhCs). The fabrication of PhCs by electron-beam lithography, inductively coupled plasma reactive ion etching and selective wet etching techniques is discussed. This work is supported by the state of Hesse in the frame of LOEWE priority project SmolBits and the DFG grant-BE 5778/4-1.

CPP 35.53 Wed 11:00 P1

Insights into structure and dynamics of polycaprolactone-based star-shaped polymer electrolytes from molecular dynamics simulations — •MIRKO FISCHER¹, DIDDO DIDDENS², and ANDREAS HEUER¹ — ¹Institute of Physical Chemistry, Westfälische Wilhelms-Universität Münster, Münster 48149, Germany — ²Forschungszentrum Jülich GmbH, Helmholtz Institute Münster, Münster 48149, Germany

Solid polymer electrolytes (SPEs) are promising candidates to substitute classical organic electrolytes in lithium-ion batteries, as they are chemically and mechanically more stable and have improved safety. However, they exhibit low ionic conductivity, which can be generally improved by developing novel polymer architectures. Experiments have shown that the biodegradable Grafted Cyclodextrin-Polycaprolactone (GCD-PCL) has higher transfer numbers than classical poly(ethylene oxide). In this work, we present results of molecular dynamics (MD) simulations to understand the ion transport in GCD-PCL. In order to directly compare our simulations with experiments, we used the time-temperature superposition of mean residence times and mean squared displacements of lithium ions to calculate the ionic conductivity at low temperatures, which would otherwise require larger time scales than are accessible through MD simulations.

CPP 35.54 Wed 11:00 P1

Organisation of Nanoparticles with Polymer Brushes: Computer Simulation Studies — •BHUVAN POUDEL, HSIAO-PING HSU, and KURT KREMER — Max Planck Institute for Polymer Research, Mainz, Germany

For polymer brushes containing nanoparticles, the interplay between concentration of nanoparticles and interaction between monomers and nanoparticles affects the ordering of nanoparticles and the structural and dynamical properties of the respective polymer brushes. We perform molecular dynamics simulations of polymer brushes based on the bead-spring model and treat nanoparticles as hard spheres with a diameter six times larger than the monomer size. Initially, nanoparticles are randomly distributed inside or above the polymer brushes. By tuning the attractive interaction between monomers and nanoparticles, we study the assembly of nanoparticles within the polymer brushes as a function of nanoparticle concentration. The appropriate choice of monomer-nanoparticle interaction and concentration of nanoparticles gives rise to a single (ordered) layers of nanoparticles whose equilibrium positions fluctuate within their diameters.

CPP 35.55 Wed 11:00 P1

Tribological Properties of Selected Vanadium Oxides Investigated with ReaxFF molecular dynamics — •MILJAN DAŠIĆ^{1,2}, ILIA PONOMAREV¹, TOMAŠ POLCAR¹, and PAOLO NICOLINI¹ — ¹Department of Control Engineering, Faculty of Electrical Engineering, Czech Technical University in Prague, Technicka 2, Prague 6, 16627, Czech Republic — ²Scientific Computing Laboratory, Center for the Study of Complex Systems, Institute of Physics Belgrade, University of Belgrade, Pregrevica 118, 11080 Belgrade, Serbia

Providing effective lubrication at high temperatures/pressures and in oxidative environments is relevant for various industrial applications, such as turbomachinery and cutting tools. Promising solutions are oxidation-resistant hard coatings consisting of binary or ternary films (e.g., Cr - N, Ti - N, Cr - Al - N,

Ti - Al - N) doped with vanadium. The amount of oxygen present in an oxidative environment can be varied, leading to different vanadium oxide stoichiometries. We investigated tribological performance of under-oxidized vanadium lubricants, selected based on available experiments. We conducted a *ReaxFF* molecular dynamics study on selected stoichiometries {V₂O₃, V₃O₅, V₈O₁₅, V₉O₁₇, VO₂} at elevated temperatures {600, 800, 1000} [K] and pressures {1, 2, 3, 4} [GPa]. Our tribosystem consists of two rigid V₂O₅ layers, and a vanadium oxide in-between. At a fixed temperature, we did not notice significant changes of the friction coefficient with stoichiometry. All considered stoichiometries provide effective lubrication. Our study is relevant and interesting for the design of vanadium doped oxidation-resistant hard coatings.

CPP 35.56 Wed 11:00 P1

interfacial rheology of PNIPAM aqueous solutions at air-water interface: effect of cross-linking and oscillation frequency — •ATIEH RAZAVI, REGINE VON KLITZING, and AMIN RAHIMZADEH — Hochschulstraße 8, 64289 Darmstadt, Germany

PNIPAM microgels are swollen and dispersible in water at temperatures below their VPTT. Microgels tend to adsorb at the liquid-air interface, thus reducing the surface tension. The degree of crosslinking influences the required time to reach the steady state. Higher cross-linker content results in a longer transient time in the order of several minutes (depending on the solution concentration). Upon the formation of a new interface, this transient time together with the mechanical properties of microgels play key roles in the interfacial elasticity of the air-water interface. The dynamic surface elasticity of aqueous solutions of PNIPAM has been measured by the oscillating barrier method as a function of time and concentration in different surface elongation frequencies. Results shows the apparent dilational elastic and loss moduli deduced from the pendant drop shape analysis at the air*water interface, as a function of pressure for the three cross-linking densities: 1, 5 and 10 mol%. In all cases, the apparent elastic modulus is much larger than the apparent loss modulus. The magnitude of the different elastic moduli goes through a maximum of elasticity for pressure values of about 15 mN/m. This behavior is a direct consequence of the particular structure of microgels, i.e. a dense and rigid core surrounded by a deformable shell made of dangling chains. The effect of oscillation frequency is still challenging and open question.

CPP 35.57 Wed 11:00 P1

Diffusion controlled pairwise associations of telechelic polymer chains — •MICHAEL LANG and RON DOCKHORN — Leibniz-Institut für Polymerforschung Dresden, Institut Theorie der Polymere, Hohe Straße 6, 01069 Dresden, Germany

We study the pairwise association of telechelic chains in polymer melts. We derive the life time distributions of open stickers that return to the same partner as before (return walks) and the life time distribution of open stickers that exchange their binding partners (exchange walks) for both entangled and non-entangled chains. These distributions contain the full information of the bond association dynamics and allow to develop a generalization of the law of mass action in the diffusion controlled limit. The model predictions are tested by Monte-Carlo simulations and compared with preceding work on associations in networks.

CPP 35.58 Wed 11:00 P1

Architecture effect on the behavior of gradient and triblock terpolymer OEGMA-BuMA-DEGMA — •WENQI XU¹, EIRINI MELAMPIANAKI¹, FEIFEI ZHENG¹, ANNA P. CONSTANTINO², THEONI K. GEORGIU², and CHRISTINE M. PAPADAKIS¹ — ¹TUM School of Natural Sciences, Technical University of Munich, Garching, Germany — ²Department of Materials, Imperial College, London, England

Triblock terpolymers with hydrophilic, hydrophobic, and thermoresponsive blocks feature micellization, aggregation, and gelation in response to temperature changes and are therefore promising in various biomedical applications [1]. Gradient terpolymers can serve as a cost-effective alternative. Here, we investigate a triblock and a gradient terpolymer composed of hydrophilic oligo(ethylene glycol) methyl ether methacrylate (OEGMA), hydrophobic *n*-butyl methacrylate (BuMA), and thermoresponsive di(ethylene glycol) methyl ether methacrylate (DEGMA). Dynamic light scattering and synchrotron small-angle X-ray scattering revealed that the gradient terpolymer forms spherical micelles, whereas the triblock terpolymer is apt to form elongated micelles. With increasing temperature, the former grow in radius and the latter in length, which may be due to the increasing hydrophobicity of the DEGMA block.

[1] A. P. Constantinou, L. Wang, S. Wang, T. K. Georgiou, *Polym. Chem.* 2022., doi: 10.1039/D2PY01097F

CPP 35.59 Wed 11:00 P1

Adaptive Air-Water Interfaces with Spiropyran and Arylazopyrazole Photo-switches — •MICHAEL HARDT and BJÖRN BRAUNSCHWEIG — University Münster, Center for Soft Nanoscience, 48149 Münster, Germany

Interfaces that respond to stimuli such as light or temperature are of great interest for new intelligent materials. Using molecular switches that respond to orthog-

onal triggers, the properties of fluid interfaces can be preconditioned and a low level of adaptivity can be integrated that extends the possibilities of soft matter interfaces beyond responsive functions.

In this contribution, we report on the adaptive behavior of air-water interfaces that are decorated by spiropyran (SP) and arylazopyrazole (AAP) photo-responsive surfactants. The SP surfactants increase their surface activity when irradiated with UV light that causes a ring-closure reaction. *E/Z* photo-isomerization of the AAP surfactants drives a substantial decrease in surface activity and thus desorption from the interface when the AAP surfactants are switched from their *E* to the *Z* state. In addition, at low pH the short thermal lifetime of the *Z* state as well as of the SP form offers the use of thermal relaxation as an alternative trigger, while also irradiation with green light can partially recover the initial properties. Interfacial properties and molecular kinetics were studied in detail using surface tensiometry and vibrational sum-frequency generation (SFG).

CPP 35.60 Wed 11:00 P1

A thermo- and photoresponsive polymer for schizophrenic switching of amphiphilic self-assembled micelles — •PEIRAN ZHANG¹, RENÉ STEINBRECHER², ANDRÉ LASCHEWSKY^{2,3}, PETER MÜLLER-BUSCHBAUM⁴, and CHRISTINE M. PAPADAKIS¹ — ¹Soft Matter Physics Group, TUM School of Natural Sciences, Technical University of Munich — ²Institute of Chemistry, University of Potsdam — ³Fraunhofer IAP, Potsdam-Golm — ⁴Chair for Functional Materials, TUM School of Natural Sciences, Technical University of Munich

Schizophrenic switching, namely the exchanging of hydrophilic and hydrophobic segment of an amphiphilic diblock copolymer, leads to self-assembly of micelles and inverse micelles, which can be used in the drug delivery application [1]. We aim to achieve such behavior by means of diblock copolymers composed of a thermo-responsive block with a fixed LCST (lower critical solution temperature) and a photo-responsive block with a tunable LCST, which is accomplished by cis-trans isomerization of the incorporated azobenzene group. As a first step, we use turbidimetry and dynamic light scattering (DLS) to investigate a homopolymer precursor with respect to the cloud point and the chain size in the cis- and trans-form of the azobenzene group, which is realized by 365 nm UV light and 470 nm blue light, respectively.

[1] C. M. Papadakis, P. Müller-Buschbaum, A. Laschewsky, Langmuir 2019, 35, 9660-9676.

CPP 35.61 Wed 11:00 P1

Effect of pressure on the micellar structure of PMMA-*b*-PNIPAM in aqueous solution — •PABLO A. ALVAREZ HERRERA¹, GEETHU P. MELEDAM¹, CRISTIANE HENSCHEL², LEONARDO CHIAPPISI³, ANDRÉ LASCHEWSKY², and CHRISTINE M. PAPADAKIS¹ — ¹TU München, School of Natural Sciences, Garching Germany — ²Universität Potsdam, Institut für Chemie, Potsdam-Golm, Germany — ³Institut Laue- Langevin, Grenoble, France

In aqueous solution, amphiphilic diblock copolymers consisting of a permanently hydrophobic and a thermo-responsive block self-assemble into core-shell micelles. In particular, poly(methyl methacrylate)-*b*-poly(*N*-isopropylacrylamide) (PMMA-*b*-PNIPAM) forms micelles featuring a hydrophobic PMMA core and a thermo-responsive PNIPAM shell. This phase transition can be also induced by changing the pressure. Here, we study the effect of pressure on the micellar structure of PMMA-*b*-PNIPAM in aqueous solution by small-angle neutron scattering (SANS). In temperature-resolved experiments, we find that the micellar shell strongly dehydrates after crossing the co-existence line at 0.1 MPa. At 75 MPa, on the contrary, it remains hydrated and the micelles are highly-correlated within the aggregates. We also characterized the micellar structure in a pressure-resolved experiment at 31.8 °C. In this case, we find that, after crossing the co-existence line, the micellar shell appreciably shrinks, even though it remains partially hydrated. We conclude that the micellar structure in the two-phase region strongly depends on pressure.

CPP 35.62 Wed 11:00 P1

Synthesis of diblock copolymer brush surfaces to control the adaptation time to water — •BENJAMIN LEIBAUER¹, ANDRES DE LOS SANTOS PEREIRA², OGNEN POP-GEORGIEVSKI², HANS-JÜRGEN BUTT¹, and RÜDIGER BERGER¹ — ¹Max-Planck institute for polymer research, Ackermannweg 10, 55128 Mainz — ²Institute of macromolecular chemistry cas, Heyrovskeho nam. 1888, 162 00, Praha 6

The Young's model describes the wetting behavior of an ideal surface. Recently, Butt et al. presented a model, which connects adaptation processes of the surface to dynamic contact angles. We developed an experimental setup, which allows measuring adaptation processes. The adaptation model was experimentally verified by Li et al. using surfaces coated with films of statistical copolymers. We synthesize polymer brush surfaces with the aim to control the adaptation time scale upon wetting and dewetting systematically. We used the surface-initiated atom transfer radical polymerization / ATRP to selectively synthesize diblock copolymer brushes. We prepared poly(2-hydroxyethyl methacrylate) (PHEMA) as a hydrophilic block from the surface and we grafted polystyrene (PS) as hydrophobic block on top of the PHEMA block. By regulating the architecture and thickness of the polymer brush we can tune surface adaption to wetting.

CPP 35.63 Wed 11:00 P1

Droplets sliding on compressed soft surfaces — •YOUCHUANG CHAO, HAN-SOL JEON, and STEFAN KARPITSCHKA — Max Planck Institute for Dynamics and Self-Organization, 37077 Göttingen, Germany

The motion of droplets on rigid substrates is mainly slowed up by the viscous dissipation inside the liquid phase. However, this does not hold for droplets sliding on soft substrates: viscoelastic dissipation inside solid phase now dominates the motion, leading to "viscoelastic breaking". A recent study revealed that droplets move anisotropically on soft, pre-stretched solids, which is incompatible with the classical visco-elastocapillary wetting theory. Here, we impose a compression rather than a stretch on the soft solid, and explore how pre-compression influences the droplet speed. Intriguingly, we observe a non-monotonic dependence of the sliding speed on the pre-strain: a minimal speed exists as the solid is consecutively compressed. This may enrich our current understanding of elastocapillarity, for instance, in tissue engineering where soft materials are frequently squeezed.

CPP 35.64 Wed 11:00 P1

Understanding wetting and drying of nanoporous media through optical and dilatometry experiments — •LAURA GALLARDO^{1,2,3}, JUAN SÁNCHEZ^{1,2,3}, YANNICK TETZNER^{1,2,3}, and PATRICK HUBER^{1,2,3} — ¹Institute of Materials Physics and Technology, Hamburg University of Technology, Germany — ²Photon Sciences, Deutsches Elektronen-Synchrotron DESY, Hamburg, Germany — ³Center for Hybrid Nanostructures CHyN, Hamburg University

While imbibition kinetics is well-understood in nanoporous materials [1], their drying dynamics is still under investigation [2]. In this study, we present time-dependent macroscopic dilatometry experiments on the deformation of nanoporous monoliths upon spontaneous, capillarity-driven infiltration of water as well as drying. During both processes, we find characteristic dynamical regimes that can be quantitatively described in terms of Laplace pressure effects and changes in the surface stress at the inner pore walls [3]. In the particular case of transparent nanoporous Vycor glass, additional imaging experiments are conducted, allowing direct optical access to the filling front. The observed wetting-drying dynamics are consistent with our analysis of the strain regimes. Our study demonstrates that it is possible to monitor the interplay of imbibition and drying dynamics by simple dilatometry measurements, provided proper humidity control. [1] Gruener, et al (2009), Phys. Rev. E Stat. Nonlin. Soft Matter Phys., 79(6). [2] Al-Madani, R. (2018), Conference paper: YUCOMAT2018. [3] Gor, G. Y., et al. (2017). Appl. Phys. Rev., 4(1), 011303

CPP 35.65 Wed 11:00 P1

Studying Solid-liquid Contact Charge Separation Dynamics using Mirror Charge — •PRAVASH BISTA¹, HANS-JÜRGEN BUTT¹, and STEFAN A.L WEBER^{1,2} — ¹Max-Planck-Institut für Polymer research Mainz — ²Johannes Gutenberg University of Mainz

Charge separation as water drops slide over a hydrophobic solid surface is a well known phenomenon (Slide electrification). Nevertheless, a macroscopic understanding of dynamics in solid-liquid contact charge separation is still incomplete. To address that, we introduce a method based on "mirror charge" detection to locally measure the change in surface charge density ($\Delta\sigma$). Here, we placed a grounded metal electrode parallel beneath the substrate. As a spontaneously charged drops move over a surface, they attract opposite charge in the metal electrode causing a flow of capacitive current. Analysing this current, we studied $\Delta\sigma$ dynamics with increasing slide length and drop number as multiple deionized water drops slid down the inclined hydrophobic surface (trichloro(1H,1H,2H,2H-perfluorooctyl)silane, PFOTS-functionalized glass). Using the results, we estimated a set of parameters to describe the $\Delta\sigma$ dynamics in slide electrification. Further, we used these parameters in a numerical simulation where we numerically reproduced the experimental results.

CPP 35.66 Wed 11:00 P1

Towards wetting on switchable and adaptive conducting polymer surfaces — •JUNQI LU¹, ALDILENE SANTOS FRANCA¹, NIKOLAOS KARADIMITRIOU², HOLGER STEEB², and SABINE LUDWIG¹ — ¹IPOC-Functional Polymers, Institute of Polymer Chemistry, University of Stuttgart, Germany — ²Institute of Mechanics (MIB) & SC SimTech, University of Stuttgart, Germany

Conducting polymers (CPs) are discussed in a huge variety of electronic devices including electrochromic windows, batteries, actuators and chemical-biology sensors, mainly because of switchable electronic and optical properties. Compared to other conducting materials, CPs have advantages of light-weight, low cost, non-toxicity, flexibility, easy processing, and low voltage operation. In our group, poly(3-hexylthiophene) (P3HT) and poly(3,4-ethylenedioxythiophene):poly(styrene sulfonate) (PEDOT:PSS) are mostly studied. In the case of P3HT, the doping states can be precisely controlled by electrochemical or chemical doping, which results e.g. in an increase of conductivity over 6 orders of magnitude with a maximum of 224 S/cm. [1] On the other hand, PEDOT: PSS can be controlled by electrochemical means, but also by humidity, as used e.g. for actuators. [2] In this contribution, we will show our preliminary data on the wetting behavior on such switchable and adaptive CP surfaces.

Ref.: [1] Chem. Mater. 2020, 32, 14, 6003; [2] Adv. Mater. 2021,33, 2007982

CPP 36: Organic Electronics and Photovoltaics II (joint session CPP/HL)

Time: Wednesday 15:00–17:30

Location: GÖR 226

CPP 36.1 Wed 15:00 GÖR 226

Charge-carrier dynamics across seven orders of magnitude in double-cable polymer-based single-component organic solar cells — •YAKUN HE^{1,2}, BINGZHE WANG¹, LARRY LUEER¹, DIRK GULDI¹, NING LI¹, and CHRISTOPH BRABEC¹ — ¹Friedrich-Alexander-Universität Erlangen-Nürnberg, Martensstrasse 7, 91058 Erlangen, Germany — ²KAUST Solar Center, King Abdullah University of Science and Technology, Thuwal 23955, Saudi Arabia

Single-component organic solar cells (SCOSCs) with intrinsically high stability have witnessed efficiencies from 2-3% to 6-11%. For boosting higher efficiencies of SCOSCs, essential information of charge-carrier dynamics as a function of microstructure is highly demanded, requesting systematical investigation on photophysics. In this work, for the first time, the charge-carrier dynamics of a representative double-cable polymer, which achieves efficiencies of over 6% as an active layer in SCOSCs, is investigated across seven orders of magnitude in time scale, from fs-ps TAS and ps-ns TRPL for probing charge generation to ns-us TAS for charge recombination. Specific emphasis is placed on understanding the impact of thermal post-treatment on the charge dissociation, transport, and recombination dynamics. By increasing the thermal annealing temperature, geminate recombination is reduced accompanied by more efficient charge dissociation and suppressed bimolecular recombination. Annealing the photoactive layer at 230 °C results in the highest photovoltaic performance correlating well with the findings from transient studies. This work intends to present a complete picture of the charge-carrier dynamics in SCOSCs.

CPP 36.2 Wed 15:15 GÖR 226

What determines the Recombination Order in Organic Solar Cells? — •KATHRIN BROCKER, JANA SEILER, DOROTHEA SCHEUNEMANN, CLEMENS GÖHLER, and MARTIJN KEMERINK — Institute for Molecular Systems Engineering and Advanced Materials, Heidelberg University

Organic Solar Cells provide an interesting and low-cost alternative to conventional inorganic photovoltaics. Upon illumination, excitons are created that separate into free electrons and holes at the donor-acceptor-interface and can be extracted to deliver electricity. The opposing loss mechanism is the recombination of charge carriers, which happens in the bulk both prior to and after charge separation. To understand these processes, the recombination order is crucially important. Experimentally, orders around or above 2 are typically found. Surprisingly, kinetic Monte Carlo (kMC) simulations that otherwise accurately reproduce experimental observations, yield values closer to 1. Here, we investigate the factors that might lead to higher recombination orders. Apart from the influence of morphology and contacts, special focus is laid on the effect of charge carrier delocalisation, which is shown to facilitate charge carrier separation and increase the fraction of bimolecular recombination. Simulation results are compared to experimental data obtained via the Steady State Bias Assisted Charge Extraction (BACE) method on P3HT:PCBM and PM6:Y6 solar cells.

CPP 36.3 Wed 15:30 GÖR 226

Modeling of the photoluminescence of geminate pairs using a hopping based Monte Carlo simulation — •MAIK SCHWUCHOW, ANGELA THRÄNHARDT, CARSTEN DEIBEL, and SYBILLE GEMMING — TU Chemnitz, Institut für Physik, 09126 Chemnitz, Deutschland

The investigation of the transport and recombination characteristics of optically excited charge carriers in organic materials is an on-going research topic. Studying the underlying effects is crucial for understanding and improving practical applications, e.g. organic solar cells (OSCs). A main step in the process of free charge carrier generation in OSCs is the formation of geminate pairs, so called charge transfer complexes, consisting of spatially separated, Coulomb-bound charges. The radiative recombination of geminate pairs yields a photoluminescence (PL) decay $\propto t^{-3/2}$ (t is time) on long time scales which arises due to a combination of thermally activated diffusion and attractive Coulomb interaction. While a continuous drift-diffusion model is able to theoretically explain this experimentally observed decay, weak molecular interaction and disorder are known to cause charge carrier localization. Therefore, a hopping model, based on tunneling between localized states, is usually more appropriate to describe charge transport in organic materials. We simulate the diffusion and recombination of hopping charge carriers using the Monte Carlo method and investigate the influence of different parameters, e.g. temperature and energetic disorder, on the PL data and the asymptotic slope.

CPP 36.4 Wed 15:45 GÖR 226

Time-consistent hopping, transient localization, and polarons - new insights and approaches for carrier transport in organic crystals — SEBASTIAN HUTSCH, MICHEL PANHANS, and •FRANK ORTMANN — Technische Universität München, Germany

Charge transport in organic semiconductors is affected by the complex interplay of electronic degrees of freedom and molecular vibrations. This is further

complicated due to the rich vibrational spectrum of these materials with mode energies covering two orders of magnitude. If the electronic coupling between molecules is small, hopping approaches are a popular choice to model charge transport for which we have recently derived a time-consistent hopping theory. [1]

Similarly, for high-mobility materials a recent improvement has been realized based on a mode-specific treatment of molecular vibrations. This leads to an unprecedented level of accuracy for the prediction of the carrier mobility for a large number of systems. [2] I will finally discuss physically motivated predictors with a very good correlation to the mobility and low computational costs.

[1] S. Hutsch, M. Panhans and F. Ortman, Phys. Rev. B. 104, 054306 (2021).

[2] S. Hutsch, M. Panhans and F. Ortman, npj Comput. Mater. 8, 228 (2022).

CPP 36.5 Wed 16:00 GÖR 226

Analysis of industrial viability for single-component organic solar cells — •YAKUN HE^{1,2}, NING LI¹, THOMAS HEUMÜLLER¹, JONAS WORTMANN¹, and CHRISTOPH BRABEC¹ — ¹Friedrich-Alexander-Universität Erlangen-Nürnberg, Martensstrasse 7, 91058 Erlangen, Germany — ²KAUST Solar Center, King Abdullah University of Science and Technology, Thuwal 23955, Saudi Arabia

Despite approaching 20% efficiency, organic solar cells still lag behind for industrial application. The industrial figure of merit (i-FOM) of OSCs is analyzed, including PCE, photostability, and synthetic complexity (SC) index. Single-component organic solar cells (SCOSCs) employing materials with donor and acceptor moieties chemically bonded within one molecule or polymer exhibit intrinsically high morphological stability. SCOSCs exhibit overall much higher i-FOM values than the corresponding bulk heterojunction OSCs, and the highest value reaches 0.3, which is even higher than the famous PM6:Y6, even though the PCE (8%) is only half of PM6:Y6. Synthetic complexity of SCOSCs is slightly higher than that of the corresponding BHJ OSCs due to extra synthetic step for connecting donor and acceptor moieties. This feature however overcomes the large-scale phase separation and stability issue. SCOSCs based on dyad 1 exhibit surprisingly high photostability under concentrated light (7.5 suns and 30 suns), corresponding to almost unchanged device stability up to 10,000 hours under 1-sun illumination. For realizing industrial application, SCOSCs have to achieve higher efficiencies, while BHJ should be developed with less complicated synthesis.

15 min. break

CPP 36.6 Wed 16:30 GÖR 226

Temperature-induced morphology changes at the organic-metal interface: effects on the structure, electronic and thermoelectric performance

— •BENEDIKT SOCHOR¹, YUSUF BULUT^{1,2}, MARIE BETKER^{1,3}, ANNA LENA OECHSLE², SIMON SCHRAAD^{1,4}, CHRISTOPHER R. EVERETT², CONSTANTIN HARDER^{1,2}, TZU-YEN HUANG^{5,6}, ANTON LE BRUN⁵, TIM LAARMANN^{1,4}, PETER MÜLLER-BUSCHBAUM^{2,7}, and STEPHAN V. ROTH^{1,3} — ¹Deutsches Elektronen-Synchrotron DESY, Notkestr. 85, 22607 Hamburg, Germany — ²TUM School of Natural Sciences, Chair for Functional Materials, James-Franck-Str. 1, 85748 Garching, Germany — ³KTH Royal Institute of Technology, Teknikringen 56-58, 100 44 Stockholm, Sweden — ⁴University Hamburg, Department of Physics, Notkestr. 85, 22607 Hamburg, Germany — ⁵ANSTO, New Illawarra Road, Lucas Heights, NSW 2234, Australia — ⁶NSRRC, 101 Hsin-Ann Road, Hsinchu Science Park, Hsinchu 30076, Taiwan — ⁷MLZ, TUM, Lichtenbergstr. 1, 85748 Garching, Germany

Flexible organic electronics are one of the most sought-after devices in the field of photovoltaics, sensors, or smart wearables. Here, the structure of the organic-metal interface and its modification potential are of utmost interest for future large-scale production. This study focuses on two semiconducting Poly(3-hexylthiophene-2,5-diyl) diblock variants, whose sprayed and doped thin films show excellent potential as thermoelectric generators. Using AFM, ellipsometry, *in situ* GISAXS/GIWAXS, and NR measurements, the structural changes of the polymer-gold interfaces were tracked during thermal annealing.

CPP 36.7 Wed 16:45 GÖR 226

Compatible solution-processed interface materials for improving the efficiency of organic solar cells

— •ZHUO XU^{1,2}, JOSE PRINCE MADALAIMUTHU^{1,2}, JOSEF BERND SLOWIK^{1,2}, RICO MEITZNER^{1,2}, AMAN ANAND^{1,2}, SHAHIDUL ALAM^{1,2,4}, HÉCTOR CORTE⁵, STEFFI STUMPF^{1,3}, ULRICH S. SCHUBERT^{1,2,3}, and HARALD HOPPE^{1,2} — ¹Laboratory of Organic and Macromolecular Chemistry, Friedrich Schiller University Jena, Germany. — ²Center for Energy and Environmental Chemistry Jena, Friedrich Schiller University Jena, Germany. — ³Jena Center for Soft Matter, Friedrich Schiller University Jena, Germany. — ⁴King Abdullah University of Science and Technology, KAUST Solar Center, Physical Sciences and Engineering Division, Material Science and Engineering Program, Thuwal, Kingdom of Saudi Arabia. — ⁵Nanosurf AG, Liestal, Switzerland.

The electron transport layer (ETL) is a key component for better performance and stability in OSCs. Herein, conjugated PDINO, sol-gel derivatized under stoichiometric TiO_x, and the same combination as the ETL was used to fabricate solution-processed PBDTTT-C-T:PC71BM-based OSCs. A hybrid of organic-inorganic ETL revealed less bimolecular and trap-assisted recombination than a single ETL of either material. Furthermore, the efficiency of devices using blend ETLs showed better performance in comparison to single ETLs in both fullerene and non-fullerene systems. This blending strategy has demonstrated beneficial consequences in device stability and efficiency, which will play a key role for future commercialization of OSCs.

CPP 36.8 Wed 17:00 GÖR 226

Influence of dye-doping on the nanostructure of the highly efficient PM6:Y6 solar cells — •ELISABETH ERBES^{1,2}, CONSTANTIN HARDER^{1,3}, BENEDIKT SOCHOR¹, SUSANN FRENZKE¹, NAIREETA BISWAS^{1,2}, JAN RUBEK¹, MATTHIAS SCHWARTZKOPF¹, VOLKER KÖRSTGENS³, PETER MÜLLER-BUSCHBAUM^{3,5}, STEPHAN V. ROTH^{1,4} und SIMONE TECHERT^{1,2} — ¹DESY, Hamburg, DE — ²Institute for X-ray Physics, Goettingen University, Goettingen, DE — ³TUM School of Natural Sciences, Chair for Functional Materials, Garching, Germany — ⁴KTH Royal Institute of Technology, Stockholm, SWE. — ⁵MLZ, TUM, Garching, DE

Organic solar cells based on the donor polymer PM6 and the acceptor Y6 give power conversion efficiencies (PCE) of 13-16% without any additives. The current study aims to investigate systematically the effect of doping PM6:Y6 with optical-light absorbing, electron transfer (ET) dyes. These pyrene-based dyes (PyxDMA) have inter- and intra-molecular charge transfer properties and a very high quantum yield. Also the absorption in the UV regime extends the absorption range of the PM6:Y6 system. The structural and morphological integrity of the dopants within the active layer were studied with grazing incidence X-ray scattering experiments. The analysis showed the intercalation and distri-

bution of the dyes within the PM6:Y6 matrix. The sprayed solar cell architecture Cu/PM6:Y6:PyxDMA/PEDOT:PSS/Au/ITO/Glass was used to measure the PCEs. Correlating these efficiencies with the molecular and nanostructural results allows explaining the changing PCE due to different doping levels of PyxDMA.

CPP 36.9 Wed 17:15 GÖR 226

Hydrogenated nanodiamonds as efficient electron extraction layers in organic solar cells — •AURELIEN SOKENG DJOUMESSI^{1,2}, ANASTASIA SICHWARDT^{1,2}, DARIA MILIAIEVA³, JAN ČERMÁK³, MAXIMILIAN SCHAAL⁴, FELIX OTTO⁴, ŠTĚPÁN STEHLÍK³, VOJTECH NÁDAŽDÝ⁶, TORSTEN FRITZ⁴, BOHUSLAV REZEK⁵, ULRICH S. SCHUBERT^{1,2}, and HARALD HOPPE^{1,2} — ¹Laboratory of Organic and Macromolecular Chemistry, Friedrich Schiller University Jena (IOMC), Jena, Germany — ²Center for Energy and Environmental Chemistry (CEEC), Friedrich Schiller University Jena, Jena, Germany — ³Institute of Physics, Czech Academy of Sciences, Prague 6, Czech Republic — ⁴Institute of Solid State Physics, Friedrich Schiller University Jena, Jena, Germany — ⁵Faculty of Electrical Engineering, Czech Technical University, Prague, Czech Republic — ⁶Institute of Physics, Slovak Academy of Sciences, Bratislava, Slovak Republic

Surface tunability is one property of nanodiamonds (NDs), which enables attachment of a range of functional groups on their surfaces. This may have a significant impact on NDs' electrical and optical characteristics and be helpful for charge extraction in solar cell devices. Herein, the surface chemistries of HPHT NDs modified by hydrogenation in a hydrogen atmosphere exhibit sp²-phases, which may help in improving the material's electrical conductivity and electron extraction when employed as an electron transport layer in PBDB-T:ITIC-based solar cells. The device performance was 7%, which differs only marginally from the outcomes of the state-of-the-art ETLs (ZnO, SnO₂).

CPP 37: Nanostructures, Nanostructuring and Nanosized Soft Matter

Time: Wednesday 15:00–16:15

Location: MER 02

CPP 37.1 Wed 15:00 MER 02

Structure and dynamics of a 1,4-polybutadiene melt in an alumina nanopore: A molecular dynamics study — •LAMA TANNOURY¹, MATHIEU SOLAR², and WOLFGANG PAUL¹ — ¹Martin-Luther-Universität Halle-Wittenberg — ²Université de Strasbourg

The study of the structure and dynamics of polymer melts confined by solid surfaces enhances our knowledge about the glass transition temperature as well as that of composite materials. It has been shown that conformations and dynamics of polymer melts confined to thin films and flat surfaces as well as cylindrical pores are altered in comparison with the bulk. The change in properties depends on several factors including but not limited to the geometry of confinement. In this research, we study the effects of both nanoscopic confinement and curvature on the dynamics and properties of a chemically realistic 1,4-polybutadiene (PBD) melt using Molecular Dynamics (MD) simulations. We investigate the density layering across the nanopore as well as the orientational ordering in the melt on both the segmental and chain scales. As for the dynamics, we show that the confinement creates an adsorbed layer that not only slows down the relaxation but also creates a third step not present in the bulk. The system has also been investigated by different experimental techniques, allowing for a comparison of our simulations to the experimental data.

CPP 37.2 Wed 15:15 MER 02

Toluene-mediated morphology transition of amphiphilic diblock copolymer templated Si/Ge/C thin films — •CHRISTIAN L. WEINDL¹, KEXIN WU¹, CHRISTIAN E. FAJMAN², CONSTANTIN HARDER³, BENEDIKT SOCHOR³, MATTHIAS SCHWARTZKOPF³, STEPHAN V. ROTH^{3,4}, THOMAS F. FÄSSLER², and PETER MÜLLER-BUSCHBAUM^{1,5} — ¹TUM School of Natural Sciences, Chair of Functional Materials, 85748 Garching — ²TUM School of Natural Sciences, Chair of Inorganic Chemistry with Focus on Novel Materials, 85748 Garching — ³DESY, 22607 Hamburg — ⁴Royal Institute of Technology KTH, 100 44 Stockholm — ⁵MLZ, TUM, 85748 Garching

The latest research has revealed promising results for silicon (Si) and germanium (Ge) as anode materials for lithium-ion batteries. These two group 14 semiconductors are considered auspicious additives in graphite anodes due to their high specific capacity (Si) and electron mobility (Ge). This study aims to synthesize a mesoporous Si/Ge/C structure over a wet chemical sol-gel approach with the structure-directing amphiphilic diblock copolymer PS-b-PEO and the Zintl cluster $K_{12}Si_xGe_{17-x}$. Furthermore, we added toluene as an additive to further induce the microphase separation. Real-space data as SEM will be discussed with the reciprocal-space analysis methods as grazing-incidence small/wide-angle x-ray scattering (GISAXS/GIWAXS). Finally, as an application, we will show the performance of these novel films as Li-ion battery anodes.

CPP 37.3 Wed 15:30 MER 02

Ultracompact Beam Deflector using Electrically Switchable Metallic Polymer Nanogratings — •YOHAN LEE, JULIAN KARST, MONIKA UBL, MARIO HENTSCHEL, and HARALD GIESSEN — 4th Physics Institute and Research Center SCoPE, University of Stuttgart, Pfaffenwaldring 57, 70569, Stuttgart, Germany

We introduce nanogratings from metallic polymers which show an electrochemically-driven optical metal-to-insulator transition. A key feature of the design is separately addressable electrodes to vary the superlattice period of the grating via the applied voltages. Thus, the proposed ultracompact beam deflectors can generate various angles.

CPP 37.4 Wed 15:45 MER 02

Molecular dynamics of superglassy polymers for gas separation by neutron scattering, dielectric spectroscopy, and calorimetry — •PAULINA SZYMONIAK¹, MOHAMED AEJAZ KOLMANGADI¹, REINER ZORN², and ANDREAS SCHÖNHALS¹ — ¹Bundesanstalt für Materialforschung und -prüfung, Berlin, Germany — ²Forschungszentrum Jülich, Jülich Centre for Neutron Science, Jülich, Germany

Janus polytricyclononenes (PTCN) with rigid backbones and flexible n-alkyl (n=propyl-decyl) are innovative materials that show potential in separating hydrocarbons. These superglassy polymers were designed to show an enhanced, controllable gas permeability via flexible alkyl side chains. PTCNs show nanophase separation between the alkyl side chains and the backbones with a distinct α -relaxation of the alkyl-rich nanophase found by broadband dielectric spectroscopy and temperature modulated DSC. Further, Janus PTCNs were studied by quasielastic neutron scattering (QENS) employing backscattering and time of flight instruments. For an overview of dynamic processes inelastic fixed window scans were performed showing segmental motions of alkyl-rich nanodomains and an additional low temperature relaxation, assigned to methyl group rotations. The molecular mobility was extracted from a combined analysis of backscattering and time of flight QENS data. The glass transition of the backbone-rich domains, which is beyond or near to the degradation of the materials, was evidenced by fast scanning calorimetry by decoupling it from decomposition, employing high heating rates.

CPP 37.5 Wed 16:00 MER 02

Size matters: Size Effects on Surface Chemistry and Raman Spectra of Sub-5 nm Oxidized High-Pressure High-Temperature and Detonation Nanodiamonds — •BERNHARD SCHUMMER¹ and ŠTEPÁN STEHLÍK² — ¹Fraunhofer Development Center X-ray Technology, 90768 F^{urth}, Germany — ²Institute of Physics of the Czech Academy of Sciences, 162 00 Prague 6, Czechia

Materials with very small dimensions of a few nanometers is of major importance for fundamental science as well as innovative applications. Those nanomaterials show different effects like quantum size effects, structural transformation or

phonon-confinement effects. It has been predicted theoretically that nanodiamonds (NDs) have a structural transformation and phonon-confinement effect below 3 nm in size. Here, we investigate how size effects the surface chemistry, microscopic structure, and Raman scattering of high-pressure high-temperature (HPHT) and detonation nanodiamonds (DNDs) between 2 to 3 nm. The particle size and particle size distribution (PSD) of those different fractions was ana-

lyzed with dynamic light scattering, analytical ultracentrifugation, small-angle X-ray scattering, X-ray diffraction, and transmission electron microscopy as complementary techniques. Comprehensive comparison of detonation and pure monocrystalline HPHT NDs reveals effects of diamond core size and defects, chemical and temperature (in)stability, and limitations of current phonon confinement models.

CPP 38: Microswimmers and Fluid Physics of Life (joint session DY/CPP)

Time: Wednesday 15:00–18:15

Location: MOL 213

See DY 31 for details of this session.

CPP 39: Focus Session: Physics of Fluctuating Paths (joint session DY/CPP)

State-of-the-art experiments probe physical observables, such as heat, work or entropy production, empirical densities and currents, on the level of individual, stochastic paths. Such experiments are typically analysed by averaging along a limited number of individual realisations, which leads to substantial uncertainties in estimates. The systematic sample-to-sample fluctuations of such path-observables encode important information about the underlying, microscopic dynamical processes and are therefore a frontier of experimental, theoretical, and computational physics. Recently there has been a surge in the development and applications of path-based concepts across many fields of physics. This focus session complements a symposium and contains contributed talks.

Organized by Aljaz Godec, Udo Seifert, and Peter Sollich

Time: Wednesday 15:00–18:15

Location: ZEU 160

See DY 32 for details of this session.

CPP 40: 2D Materials V: Growth, Structure and Substrate Interaction (joint session O/CPP)

Time: Wednesday 15:00–17:30

Location: GER 37

See O 56 for details of this session.

CPP 41: Biopolymers, Biomaterials and Bioinspired Functional Materials II (joint session CPP/BP)

Time: Wednesday 16:30–18:00

Location: MER 02

CPP 41.1 Wed 16:30 MER 02

Low-Temperature and Water-Based Biotemplating of Nanostructured Foam-Like Titania Films using β -Lactoglobulin — •JULIAN E. HEGER¹, WEI CHEN¹, SHANSHAN YIN¹, NIAN LI¹, VOLKER KÖRSTGENS¹, CALVIN J. BRETT^{2,3}, WIEBKE OHM², STEPHAN V. ROTH^{2,3}, and PETER MÜLLER-BUSCHBAUM^{1,4} — ¹TUM School of Natural Sciences, Chair for Functional Materials, Garching, Germany — ²DESY, Hamburg, Germany — ³Royal Institute of Technology KTH, Stockholm, Sweden — ⁴MLZ, TUM, Garching, Germany

Energy-related applications such as solar cells, batteries, and the photocatalytic production of hydrogen are broadly built up on titania nanostructures. A tailored titania morphology is necessary to match the required charge diffusion lengths and the crystallinity beneficial for efficient performance. In the context of large-scale fabrication, the aspect of sustainability becomes essential. Biopolymer templating based on β -Lactoglobulin (β -lg) and spray deposition promotes low-temperature and water-based synthesis of nanostructured, crystalline, foam-like titania films. During spray deposition, the β -lg biopolymer matrix sterically directs the titania morphology. Afterwards, the biotemplate is removed by UV-light exposure. To understand the kinetics of film formation during the spray deposition on the nano and crystalline length scale, we simultaneously perform in situ grazing-incidence small-angle and wide-angle X-ray scattering (GISAXS/GIWAXS). Together with scanning electron microscopy (SEM), the results explain the role of β -lg as a biotemplate.

CPP 41.2 Wed 16:45 MER 02

Structural changes in cellulose nanofibril-colloid hybrid films during humidity cycling — •STEPHAN V. ROTH^{1,2}, CALVIN J. BRETT^{1,2}, ALEXANDROS ALEXAKIS², LUCAS P. KREUZER³, MARTIN MANSSON², SARAH ROGERS⁴, EVA MALMSTRÖM², PETER MÜLLER-BUSCHBAUM^{3,5}, and L. DANIEL SÖDERBERG² — ¹Deutsches Elektronen-Synchrotron DESY, Hamburg, Germany — ²KTH Royal Institute of Technology, Stockholm, Sweden — ³TUM School of Natural Sciences, Chair for Functional Materials, Garching — ⁴ISIS-STFC, Rutherford Appleton Laboratory, Chilton, Oxon OX11 0QX, UK — ⁵MLZ, TUM, Garching, Germany

Biocompatible cellulose nanofibrils (CNFs) are an ideal material for sustainable biomaterial templates. Combined with latex colloids, the resulting hybrid colloid-CNF functional materials are excellent candidates for bio-inspired structural colors. Due to the hydrophilic nature of CNFs, we investigate the stability against humidity cycling in terms of reversible/irreversible structural rearrangements. We applied depth sensitive grazing incidence small-angle neutron scattering to evaluate the humidity-induced rearrangements in hybrid latex colloid:CNF templates in situ during cyclic humidification. After the first humidity cycle, a change in morphology on the scale of several 10 nm was observed, which is attributed to latex particles which diffused in the network and enlarged the pores of the network. The measured kinetics resolve the time- and depth-dependence of the differently sized colloids' penetration into the porous CNF network.

CPP 41.3 Wed 17:00 MER 02

Fluorescence correlation spectroscopy for studying the aggregation of nanoplastics in model biofilm substances — •TOBIAS GUCKEISEN, ROZALIA ORGHICI, and SILKE RATHGEBER — Universität Koblenz, Deutschland
Nanoplastics in the environment are a growing problem. Pollutants can adhere to their surfaces and therefore be easily transported into the natural systems. Biofilms are found everywhere in the environment; they are formed by microbial communities that produce a matrix of extracellular polymeric substances. The interaction between nanoplastics and biofilms can lead to aggregation and sedimentation of nanoparticles and determines the transport and fate of nanoplastics. A better understanding of the transport and fate of nanoplastics is important to improve our ability to predict risks associated with these ubiquitous contaminants. In this project, we use fluorescence correlation spectroscopy (FCS) to study the aggregation and interactions of nanoplastics with model biofilm substances. Protein-polysaccharide mixing ratio and pH-dependent aggregation studies show that it is crucial to consider correlative effects between multiple biofilm components to better understand the impact biofilms have on nanoplastic aggregation. Biofilm model systems with only one component, as commonly considered, may lead to an incorrect assessment of the tendency to aggregation.

CPP 41.4 Wed 17:15 MER 02

Ensemble inequivalence and negative extensibility in a wormlike chain with fluctuating bending stiffness — •PANAYOTIS BENETATOS — Department of Physics, Kyungpook National University, Republic of Korea

Many semiflexible polymers exhibit fluctuations in the local bending stiffness along their contour. This may be due to intrinsic conformational changes (e.g., denaturation bubble formation in double stranded DNA or helix-coil transition in polypeptides) or to the reversible adsorption and desorption of molecules from the polymer's environment. In this presentation, we analyse the tensile elasticity of a strongly stretched wormlike chain which consists of N concatenated segments, where each segment can be in one of two states, A and B, which differ in bending stiffness. We call this model the reversible wormlike chain (rWLC) model. In the Gibbs (fixed-force, isotensional) ensemble, we obtain analytic expressions for the force-extension relation and the mean fraction of B segments. We show that, under certain conditions, there is a tension-induced crossover from a mostly A to a mostly B rWLC. In the Helmholtz (fixed-extension, isometric) ensemble, we obtain analytic expressions up to a summation. We show that, for finite N , there is marked ensemble inequivalence. Remarkably, in the Helmholtz ensemble, the rWLC can exhibit negative extensibility and multiple peaks.

CPP 41.5 Wed 17:30 MER 02

Aging and compressed exponential stress relaxation in mechanoresponsive hydrogels — •GEONHO SONG^{1,2}, WOUTER ELLENBROEK³, and KERSTIN BLANK^{1,2} — ¹Johannes Kepler University Linz, Linz, Austria — ²Max Planck Institute of Colloids and Interfaces, Potsdam, Germany — ³Eindhoven University of Technology, Eindhoven, The Netherlands

Biological materials, such as the extracellular matrix (ECM), are viscoelastic and exhibit stress relaxation. Stress relaxation in the ECM is linked to cellular behav-

ior and needs to be considered as a design parameter when developing bioinspired materials for cell culture and tissue engineering. Here, we introduce a collagen-inspired hydrogel with tunable crosslink kinetics. We utilize collagen-mimetic peptides with controlled association and dissociation rates to crosslink star-shaped polyethylene glycol. We show that ultraslow crosslink dissociation rates cause a distinctive relaxation behavior that is reminiscent of soft glassy materials, showing out-of-equilibrium properties. In particular, subjecting the networks to a sequence of pre-stress and aging causes uncommon compressed exponential relaxation. This unique phenomenon has previously only been reported for a small number of soft glassy systems where compressed exponential relaxation was related to ultraslow dynamics that prohibited the release of internal stresses. In such systems, slow crosslink dissociation delays network relaxation until an external trigger is applied. In future work, we aim to investigate the interplay between locally generated stresses, such as cellular traction forces, and network relaxation properties.

CPP 41.6 Wed 17:45 MER 02

Nonaffinity controls critical slowing down and rheology near the onset of rigidity — •ABHINAV SHARMA¹, JORDAN SHIVERS², and FRED MACKINTOSH² — ¹Leibniz institute for polymer research, Dresden — ²Rice University, Houston, Texas

Fluid-immersed networks and dense suspensions often reside near a boundary between soft (or fluid-like) and rigid (or solid-like) mechanical regimes. This boundary can be crossed either by varying the concentration or by deformation. Near the onset or loss of rigidity, dissipation-limiting nonaffine rearrangements dominate the macroscopic viscoelastic response, giving rise to diverging relaxation times and power-law rheology. Here, we derive a simple relationship between nonaffinity and excess viscosity in fluid-immersed amorphous materials. We then demonstrate this relationship and its rheological consequences in simulations of stress relaxation in strained filament networks and dense suspensions.

CPP 42: Battery Materials (joint session KFM/CPP)

Chair: Prof. Dr. Anna Grünebohm (Ruhr-University Bochum)

Time: Thursday 9:00–12:35

Location: POT 51

See KFM 10 for details of this session.

CPP 43: Organic Electronics and Photovoltaics III (joint session CPP/HL)

Time: Thursday 9:30–12:30

Location: GÖR 226

CPP 43.1 Thu 9:30 GÖR 226

Determining exciton diffusion lengths in organic non-fullerene acceptors with Kinetic Monte Carlo Simulation — •WENCHAO YANG, SAFAKATH KARUTHEATH, CATHERINE CASTRO, JULIEN GORENFLOT, and FREDERIC LAQUAI — KAUST Solar Center, King Abdullah University of Science and Technology, Thuwal, Saudi Arabia

Optimal exciton diffusion length (L_D) is a key parameter for reducing losses during exciton to charge carrier conversion in organic solar cells (OSC). However, different research groups report contradicting numbers for the same non-fullerene acceptors (NFA) using different lifetimes to calculate L_D . In this work, in order to verify the measured L_D 's in NFAs (ITIC, IT4F, ITM and IT2Cl) using transient absorption (TA) spectroscopy, we employed the Kinetic Monte Carlo (KMC) method to simulate the exciton dynamics and calculate the corresponding L_D . With the assumption of Förster resonant energy transfer type exciton hopping rate in a cubic lattice, the TA decay kinetics under different fluences are reproduced by the KMC simulation, and the only free parameter: the energetic disorder σ is extracted. The use of the lifetime τ measured by time-resolved photoluminescence in neat NFA enables to reproduce the transients using more realistic σ values. The L_D 's in the NFAs are further calculated with the τ 's and found to be consistent with the experimental values. This work provides microscopic descriptions of exciton diffusion and more insight into the determination of L_D in organic semiconductors.

CPP 43.2 Thu 9:45 GÖR 226

A thorough analysis of conformational locking and related electrical properties in fluorinated thieno-quinoxalines — •MD MOIDUL ISLAM^{1,2}, ARTHUR MARKUS ANTON^{1,2,5}, SHAHIDUL ALAM⁶, RICO MEITZNER^{1,2}, CHRISTOS L. CHOCHOS^{3,4}, ULRICH S. SCHUBERT^{1,2}, and HARALD HOPPE^{1,2} — ¹Laboratory of Organic and Macromolecular Chemistry (IOMC), Friedrich Schiller University Jena, Jena, Germany — ²Center for Energy and Environmental Chemistry Jena (CEEC Jena), Friedrich Schiller University Jena, Jena, Germany — ³Institute of Chemical Biology, National Hellenic Research Foundation, Athens 11635, Greece — ⁴Advent Technologies SA, Patra, Greece — ⁵Peter Debye Institute for

Soft Matter Physics, Universität Leipzig, Leipzig, Germany — ⁶King Abdullah University of Science and Technology (KAUST), KAUST Solar Center (KSC), Physical Sciences and Engineering Division (PSE), Material Science and Engineering Program (MSE), Kingdom of Saudi Arabia

Thieno-quinoxaline derivatives with low band gaps are promising donor materials for organic solar cells. Therefore, investigations have been conducted on thieno-quinoxaline polymers with systematically varied fluorination sites. Cyclic voltammetry revealed that fluorination lowers both the HOMO as well as LUMO energy levels, whereas the size of photochromic units is affected through the particular kind of fluorination demonstrated by UV-Vis absorption spectra. Furthermore, excitation-emission mapping exposed excitation-independent and excitation-selective PL pathways.

CPP 43.3 Thu 10:00 GÖR 226

Orientation and Order of Molecular Subunits and Excited State Dynamics in a P3HT Bottlebrush Copolymer — •ARTHUR MARKUS ANTON^{1,2}, FRIEDRICH KREMER¹, JENNY CLARK², and FRANK CICHOS¹ — ¹Leipzig University, Peter Debye Institute for Soft Matter Physics, Linnéstr. 5, 04103 Leipzig, Germany — ²The University of Sheffield, Department of Physics and Astronomy, Hounsfield Rd, Sheffield S37RH, United Kingdom

Orientation and order at different length scales are believed to play a crucial role for the performance of organic semiconductor devices. Taking advantage of the material properties of *bottlebrush copolymers* and gain control of structure formation, a poly-(3-hexylthiophene) grafted copolymer has been studied [1]. In order to investigate the structure on the molecular scale the technique of *Infrared Transition Moment Orientational Analysis* (IR-TMOA) has been employed [2,3]. The absorbance of structure-related bands is evaluated depending on the inclination of the sample film (ϑ) and polarization of the IR light (φ). This combination then allows to determine the tensor of absorption separately for the respective molecular moieties and to deduce their orientation (Θ, Φ) relative to a sample-fixed coordinate system. In addition *transient absorption* measurements have been conducted. The dynamics of exciton and polaron formation and decay has been investigated and the derived results on the basis of the bottlebrush copoly-

mer are compared with results from linear P3HT. [1] Heinrich and Thelakkat, *J. Mater. Chem. C* 4 (2016) 5370 [2] Anton et al, *J. Am. Chem. Soc.* 137 (2015), 6434 [3] Anton et al, *Macromolecules* 49 (2016) 1798

CPP 43.4 Thu 10:15 GÖR 226

Utilizing High Gain and Spectral Narrowing for Near-Infrared Organic Photodetectors — •LOUIS CONRAD WINKLER¹, JONAS KUBLITSKI², JOHANNES BENDUHN¹, and KARL LEO¹ — ¹TU Dresden, Germany — ²Federal University of Technology Paraná UTFPR, Curitiba, Brazil

There is a multitude of applications for infrared photodetectors that demand high-volume fabrication, including blood oxygen determination, continued monitoring of food quality, control of industrial processes, and many more. Organic photodetectors (OPDs) have great potential to enrich today's photodetector market with their low-cost fabrication, flexible devices and tunable response. However, most studied organic semiconducting materials have neglectable absorption above 1000 nm. This contribution presents a donor-acceptor blend with a low-energy and broad charge-transfer (CT) feature. To overcome the inherent increase of charge carrier recombination of such low-energy systems, we introduce two photocurrent multiplication (PM) mechanisms. By embedding this OPD into an optical micro-cavity, a spectral response (SR) of 15 AW⁻¹ at 1095 nm is achieved. Furthermore, a very narrow response of only 18 nm makes this architecture ideal for spectroscopic resolved measurements that could be easily integrated into CMOS readout circuitry due to the optimization for operation under reverse bias.

CPP 43.5 Thu 10:30 GÖR 226

Realizing a high-performance, fully thermal-evaporated, blue narrowband organic photodetector — •TIANYI ZHANG, JOHANNES BENDUHN, and KARL LEO — Dresden Integrated Center for Applied Physics and Photonic Materials (IAPP) and Institute for Applied Physics, Technische Universität Dresden, Dresden, Germany

Organic photodetector (OPD) boasts of its tunable absorption window, mechanical flexibility, transparency, non-toxicity, facile processing, and cheaper cost. Recent development of high-performing polymers and small molecules further reveals its potential in numerous communication and biomedical applications. To realize visible light communication, commercially available inorganic photodetector usually incorporates additional optical filters, which further increases the complexity and cost of the sensing system. Therein, we demonstrate a blue absorbing organic photodetector with ultrahigh specific detectivity (D^*) approaching 10^{14} Jones. By employing a wide bandgap hole transporting layer BF-DPB with Rubrene:C₆₀ active layer, the absorption peaks at 450nm with an external quantum efficiency (EQE) of 50% at zero bias. The parasitic absorption renders the narrowband characteristic of the blends to span merely over the blue wavelength region. Upon BF-DPB incorporation, ultrafast responses are also observed at sub-microseconds. We conclude that the judicious choice of transporting layer is critical for achieving application-tailored properties, namely high speed or high D^* . To date, those values are among the best-reported blue OPDs.

CPP 43.6 Thu 10:45 GÖR 226

Investigation of high performance organic photodetectors based on single component photoactive layer — •JAKOB WOLANSKY¹, CEDRIC HOFFMANN², FELIX TALNACK³, MICHEL PANHANS⁴, DONATO SPOLTORRE⁵, STEFAN C.B. MANNSFELD³, FRANK ORTMANN⁴, NATALIE BANERJI², JOHANNES BENDUHN¹, and KARL LEO¹ — ¹IAPP, TU Dresden — ²University of Bern — ³Cfaed, TU Dresden — ⁴TU Munich — ⁵University of Parma

In organic semiconductor applications such as organic photovoltaics and photodetectors, an intermolecular interface with an energetic gradient between electron donating and accepting materials is usually required for efficiently generating charges. This driving force facilitates the dissociation of the photogenerated excitons. At the same time, this energy offset reduces the maximum possible open-circuit voltage, and the additional interface can act as a recombination site and increases the dark current. Therefore, single-component devices are extensively researched to overcome these drawbacks.

Here, we report on single-component devices that perform very well as organic photodetectors. By utilizing different device processing parameters and employing different interface layers, we optimized the device characteristics such as external quantum efficiency, dark current, and specific detectivities of more than $1e13$ Jones. Investigations of the morphology, combined with ultrafast transient absorption measurements, give insight into the charge generation mechanism in our material system.

CPP 43.7 Thu 11:00 GÖR 226

Reduced defect density in crystalline halide perovskite films via methylamine treatment for the application in photodetectors — •EMILIA ROSA SCHÜTZ¹, AZHAR FAKHARUDDIN¹, YENAL YALCINKAYA^{2,3}, EFRAIN OCHOA-MARTINEZ², SHANTI BIJANI⁵, ABD. RASHID BIN MOHD YUSOFF⁶, MARIA VASILOPOULOU⁷, TOBIAS SEEWALD¹, ULLRICH STEINER⁴, STEFAN WEBER^{2,3}, and LUKAS SCHMIDT-MENDE¹ — ¹University of Konstanz, Konstanz, Germany — ²Max Planck Institute for Polymer Research, Mainz, Germany — ³Johannes Gutenberg University Mainz, Mainz, Germany — ⁴Adolphe Merkle Institute, University of Fribourg,

Fribourg, Switzerland — ⁵Unidad de Nanotecnología, Centro de Supercomputador y Bioinnovación SCBI, Universidad de Málaga, Málaga, Spain — ⁶Pohang University of Science and Technology, Pohang, Republic of Korea — ⁷National Center for Scientific Research Demokritos, Attica, Greece

The quality of a perovskite layer strongly depends on the processing conditions. Consequently, the fabrication process is often complex, and reproducibility is a challenge. Our methylamine gas-based method is able to recrystallize perovskite layers of any given quality in a controlled way, leading to millimeter-sized domains. Crystallinity significantly increases upon methylamine treatment, and crystal growth follows a preferred orientation. Photoluminescence- and space-charge limited current measurements imply that the trap density decreases after recrystallization. When applied in photodetectors, the improved film quality of the recrystallized films leads to increased detectivities and shorter response times.

15 min. break

CPP 43.8 Thu 11:30 GÖR 226

Reducing Dark Current in Highly Ordered Rubrene:C₆₀ Heterojunctions for Organic Photodetectors — •ANNA-LENA HOFMANN¹, JAKOB WOLANSKY¹, LUCY WINKLER¹, MAX HERZOG¹, FELIX TALNACK², EVA BITTRICH³, JOHANNES BENDUHN¹, and KARL LEO¹ — ¹IAPP, TU Dresden, Dresden, Germany — ²Cfaed, Dresden, Germany — ³Leibniz-Institut für Polymerforschung Dresden e.V., Dresden, Germany

Vacuum-deposited rubrene can form highly ordered phases, demonstrating an exceptionally high charge carrier mobility for holes ($> 10 \text{ cm}^2 \text{ V}^{-1} \text{ s}^{-1}$) even in thin films. Depending on the post-treatment of our films, we can control different crystalline phases. For fast-response OPDs, the triclinic phase is very promising since it exhibits high hole mobility in the vertical direction. However, the high surface roughness is a key reason why these devices fall short in specific detectivity. In this work, we employ different strategies to reduce the impact of Ohmic shunts within the device to minimize the noise current of our devices. We characterize the morphology of our films and investigate the performance parameters of fully working devices. Finally, these characteristics are compared to rubrene's other two crystalline phases.

CPP 43.9 Thu 11:45 GÖR 226

Utilizing charge-transfer states for narrowband and highly sensitive photodetection — •JOHANNES BENDUHN, LOUIS CONRAD WINKLER, AWAIS SAWAR, JONAS KUBLITSKI, and KARL LEO — IAPP, TU Dresden, Germany

Near-infrared (NIR) spectroscopic material sensing has the potential to revolutionize many aspects of life, ranging from food control to material determination. However, currently available products are either too bulky or too expensive to be used in mobile customer applications. In this regard, organic photodetectors (OPDs) can open new perspectives due their cheap and versatile processing techniques. Nevertheless, the external quantum efficiency (EQE) as well as the specific detectivity of those devices in the NIR wavelength range are still lacking behind. In this contribution, we explore photomultiplication (PM) in fully vacuum deposited OPDs. Broadband devices achieve a maximum EQE of almost 2000 % at -10 V. Employing very sensitive measurement techniques as well as optical modelling of our devices, we are able to proof that the photomultiplication can take place even if weakly absorbing charge-transfer states are responsible for the photon harvesting. Employing a suitable donor-acceptor system as well as an optimized device architecture for photomultiplication and constructive interference in the NIR wavelength range, we achieve narrowband OPDs with the spectral response of more than 10 A W^{-1} at a wavelength of 1100 nm with full width at half maximum even below 20 nm. These results demonstrate the versatility of OPDs and their potential for spectroscopic material sensing.

CPP 43.10 Thu 12:00 GÖR 226

Design of Integrated All-Organic Oxygen Sensors — •TONI BÄRSCHNEIDER and SEBASTIAN REINEKE — Dresden Integrated Center for Applied Physics and Photonic Materials (IAPP), Technische Universität Dresden

Organic electronic devices, such as light-emitting diodes (OLEDs) and photodetectors (OPDs), are ideal for sensor applications because of their versatility and flexibility. Additionally, they can be easily fabricated on any substrate, making integrated sensor applications possible. This allows for easy miniaturization and cheap fabrication. Organic room temperature phosphorescence (RTP) materials are well suited for optical oxygen sensing because of their strong oxygen dependency.

In this work, we developed a monolithic all-organic oxygen sensor composed of a RTP sensing layer, an ultraviolet OLED as an excitation source, and a narrow bandwidth OPD for detection. The RTP sensing layer simultaneously shows fluorescence and phosphorescence at room temperature, which enables self-referencing to avoid photodegradation-caused distortion. Due to the long phosphorescence lifetime, sensing within the ultra-trace range is possible.

The presented sensors overcome drawbacks of current optical oxygen sensors, such as complexity, expensive read-out electronics, and a lack of possible miniaturization.

CPP 43.11 Thu 12:15 GÖR 226

Atomistic insights on the electrode material CuDEPP — •CHRISTOPH JUNG^{1,2} and TIMO JACOB^{1,2} — ¹Universität Ulm, Institut für Elektrochemie, Ulm, Germany — ²HIU, Ulm, Germany

Devices for electrical energy storage need to provide high energy yields as well as output power while at the same time guaranteeing safety, low costs and long operation times. The porphyrin CuDEPP [5,15-bis(ethyl)-10,20-diphenylporphyrinato]copper(II) is a promising electrode material for various battery systems both as anode or cathode. CuDEPP combines the positive properties of lithium ion batteries (high energy density) with those of a supercapacitor (fast electron release and absorption). While its functionality has been demon-

strated experimentally, there had been no atomistic information as to why CuDEPP expresses these interesting properties or how the incorporation of ions affects its structure. Starting with the smallest possible unit (i.e. a single molecule) we successively increased the spatial dimensionality of the structure by studying: a) di- and trimers, b) molecular stacking in a 1D chain, c) extending these chains to planar CuDEPP sheets and finally c) a three-dimensional extended polymer structure. Combining the individual results of the molecule, the chain, the plane and the extended polymer lead to a comprehensive and consecutive understanding of the CuDEPP system. Afterwards the insertion (or intercalation) of different ions (including Li, Mg and Na) has been studied. Based on the optimal ion intercalation structure, discharge voltage curves have been calculated and compared to experimental measurements.

CPP 44: Wetting, Fluidics and Liquids at Interfaces and Surfaces II (joint session CPP/DY)

Time: Thursday 9:30–13:00

Location: MER 02

CPP 44.1 Thu 9:30 MER 02

Dynamic wetting of concentrated granular suspensions — •REZA AZIZ-MALAYERI, PEYMAN ROSTAMI, and GÜNTER K. AUERNHAMMER — Leibniz-Institut für Polymerforschung Dresden e.V., Dresden, Germany

Concentrated granular suspensions are employed in a variety of processes where the contact line dynamics and internal structure of the suspension interact. The process can be characterized using individual particle analysis and average suspension descriptions. Along the contact line, particles interact with each other and the substrate, and the shear rate influence the suspension's non-Newtonian rheological behavior. In this study, we use fluorescently-labeled tracer particles in a refractive index-matched silica suspension. We track the motion of the tracer particles in the concentrated suspension with astigmatism particle tracking velocimetry (APT-V). Averaging over single tracks gives the flow profile in a droplet near the advancing contact line. In addition, side-view allows characterizing the drop shape. The behavior of high-concentration suspensions near contact lines differs significantly from that of simple liquids. Near the advancing contact line, we observe the fast-moving layering of suspensions close to the substrate, which is controlled by the suspension's rheology. Near the receding contact line, the suspension adheres to its previous layer and moves on top of it. Initially, there is an unsteady motion, which becomes stationary with time.

CPP 44.2 Thu 9:45 MER 02

Sliding drops: towards a universal law of friction — XIAOMEI LI¹, FRANCISCO BODZIONY², MARIANA YIN², HOLGER MARSHALL², RÜDIGER BERGER¹, and •HANS-JÜRGEN BUTT¹ — ¹Max Planck Institute for Polymer Research, Ackermannweg 10, 55128 Mainz — ²Computational Multiphase Flows, Technische Universität Darmstadt, Alarich-Weiss-Straße 10, 64287 Darmstadt

Liquid drops moving on tilted surfaces are an everyday phenomenon and are important for many industrial applications. Still, it is not possible to predict their velocity. To make a step forward in quantitative understanding, we measured the velocity U , width w , length, advancing Θ_a , and receding contact angle Θ_r of liquid drops sliding down inclined flat surfaces. By solving the equation of motion, we determined the friction force versus slide velocity for different hydrophobic surfaces. The friction force acting on moving drops of polar and non-polar liquids with viscosities ranging from 10^{-3} to 1 Pa s can empirically be described by $F_f(U) = F_0 + \mu w Ca^\alpha$ for the whole relevant velocity range. Here, $Ca = U\eta/\gamma$ is the capillary number, in which η is the viscosity and γ the surface tension of the liquid. The friction coefficient μ is in the range of 1 - 3 N/m for all liquid/surface combinations. For viscosities above 0.006 Pa s, we find $\alpha = 1.0$. Bulk and wedge viscous dissipation can fully account for the velocity-dependent friction force. These results were confirmed by direct numerical diffuse-interface simulations of the flow pattern inside sliding drops. We demonstrate that the Furmidge-Kawasaki equation, is also valid in the dynamic case.

CPP 44.3 Thu 10:00 MER 02

Spreading of soft elasto-viscoplastic droplets — •MAZIYAR JALAL¹, CASSIO OISHI¹, and HUGO FRANÇA^{1,2} — ¹Institute of Physics, University of Amsterdam, Amsterdam, The Netherlands — ²Sao Paulo State University, Sao Paulo, Brazil

The spreading under surface tension of a droplet of complex fluid with elastic and plastic properties is studied. Unlike Newtonian fluids, the droplet converges to a final equilibrium shape once the driving stresses inside the droplet fall below the critical yield stress. Scaling laws are presented for the final radius and complemented with an asymptotic analysis for shallow droplets. Moreover, numerical simulations using the volume-of-fluid method and an elasto-viscoplastic (EVP) constitutive law, and experiments with an aqueous solution of Carbopol, are presented.

CPP 44.4 Thu 10:15 MER 02

Stick-slip Contact Line Dynamics in Forced Wetting of Polymer Brushes — •DANIEL GREVE¹, SIMON HARTMANN¹, and UWE THIELE^{1,2} — ¹Institut für Theoretische Physik, WWU Münster — ²Center for Nonlinear Science (CeNoS), WWU Münster

We study the wetting of adaptive substrates using a mesoscopic hydrodynamic model for a liquid droplet on a polymer brush, refining the model in [1]. First, we show that Young's law still holds for the macroscopic equilibrium contact angle and that on the mesoscale a Neumann-type law governs the shape of the wetting ridge (comparable to the case of elastic substrates [2]). Further, we numerically examine the wetting ridge dynamics for a moving meniscus, i.e., we consider an "inverse Landau-Levich geometry" where a brush-covered plate is introduced into a bath. We find stick-slip motion in good qualitative agreement with experimental observations [3,4] and discuss criteria for the onset of the corresponding instability.

[1] U. Thiele and S. Hartmann, *Eur. Phys. J.-Spec. Top.*, 2020, 229, 1819-1832.[2] B. Andreotti and J. H. Snoeijer, *Annu. Rev. Fluid Mech.*, 2020, 52, 285-308.[3] S. Schubotz et al., *Adv. Colloid Interface Sci.*, 2021, 294, 102442.[4] L. Wan, X. Meng, Y. Yang, J. Tian and Z. Xu, *Sci. China Chem.*, 2010, 53, 183-189.

CPP 44.5 Thu 10:30 MER 02

Demixing of liquid PDMS during dewetting into the equilibrium state — •KHALIL REMINI¹, LEONIE SCHMELLER², DIRK PESCHKA², BARBARA WAGNER², and RALF SEEMANN¹ — ¹Experimental Physics, Saarland University, Saarbrücken, Germany — ²Weierstrass-Institute, Berlin University, Berlin, Germany

The study of micrometer-sized equilibrium droplets on elastic substrates is of great interest because, due to negligible gravity, other interactions such as elastic or capillary forces and their mutual influence can easily be investigated, so deviations from the expected behaviour at larger scales becomes visible. This applies in particular to soft solids like PDMS that are typically considered as ideal rubbers on the macro scale. Our experimental system is composed of liquid polystyrene (PS) droplets on a viscoelastic substrate consisting of cross-linked polydimethylsiloxane (PDMS) of different elasticities. Using atomic force microscopy (AFM), we analyse the topography of the materials and thus their contact angles with high precision, we also use AFM to demonstrate the existence of non-cross-linked liquid PDMS that migrates from the elastic PDMS toward the three-phase contact line TPCL to form a demixed liquid ring around the dewetted PS droplet. In that situation, on the nanometer distance around the TPCL, liquid PS meets liquid PDMS instead of being in direct contact with the soft solid PDMS. Further analysis allows us to say that this phenomenon also exists during the dewetting of liquid polystyrene in the same type of elastic solids.

CPP 44.6 Thu 10:45 MER 02

How droplets dry on stretched soft substrates — •BINYU ZHAO, YIXUAN DU, and GÜNTER K. AUERNHAMMER — Leibniz Institute of Polymer Research Dresden, Dresden 01069, Germany

Droplets evaporation on solid substrates is a ubiquitous phenomenon and relevant in many natural and industrial processes. Well known are the coffee-ring. Many studies have succeeded in promoting, suppressing or even reversing the formation of coffee-ring by using non-spherical particles, surfactants, patterned substrates, and so on.

Here, we show that a uniaxial stretching of soft substrates strongly controls the dynamics of droplet evaporation and particle deposition through controlling the contact line motion. Water droplet evaporates with an elongated non-circular contact line on the stretched substrates and switches the elongation direction during evaporation. The contact line evolution depends on the orientation of the contact line relative to the stretching direction. When nanoparticles are added into the liquid, the circular deposition pattern, i.e., the so-called coffee-ring, becomes elongated along the direction perpendicular to the stretching direction.

Particularly, such non-circular deposition pattern exhibits periodic height gradients along its rim. The finer structure of the pattern can be controlled by applying different stretching ratios to the soft substrate and thus are correlated to the anisotropic surface stresses near the contact line. The findings broaden our understanding of droplet wetting and evaporation on soft and anisotropic substrates, and open the way to reshaping the coffee-ring to allow anisotropic, non-circular patterning.

CPP 44.7 Thu 11:00 MER 02

Gradient dynamics model for sessile drop evaporation in a gap: from simple to applied scenarios — •SIMON HARTMANN¹, UWE THIELE¹, CHRISTIAN DIDDENS², and MAZIYAR JALAAL³ — ¹Institut für Theoretische Physik and Center for Nonlinear Science, Universität Münster — ²Physics of Fluids group, Max Planck Center Twente for Complex Fluid Dynamics, and J. M. Burgers Center for Fluid Dynamics, University of Twente — ³Van der Waals-Zeeman Institute, Institute of Physics, University of Amsterdam

We consider an evaporating drop of volatile partially wetting liquid on a rigid solid substrate. In addition, the setup is covered with a plate, forming a narrow gap with the substrate. First, we develop an efficient mesoscopic description of the liquid and vapor dynamics in a gradient dynamics form. It couples the diffusive dynamics of the vertically averaged vapour density in the narrow gap to an evolution equation for the drop profile. The dynamics is purely driven by a free energy functional that incorporates wetting, bulk and interface energies of the liquid as well as vapour entropy.

Subsequently, we employ numerical simulations to validate the model against both experiments and simulations based on Stokes equation. Finally, we show that the gradient dynamics approach allows for extensions of our model to cover more intricate scenarios, e.g., spreading drops of volatile liquid on polymer brushes or on porous media.

15 min. break

CPP 44.8 Thu 11:30 MER 02

Modeling the temporal evolution and stability of thin evaporating films for wafer surface processing — •MAX HUBER^{1,2,3}, XIAO HU^{1,2,3}, ANDREAS ZIENERT^{1,2,3}, and JÖRG SCHUSTER^{1,2,3} — ¹Fraunhofer Institute for Electronic Nano Systems ENAS, Technologie-Campus 3, 09126 Chemnitz, Germany — ²Center for Materials, Architectures and Integration of Nanomembranes (MAIN), Chemnitz University of Technology, Rosenbergstr. 6, 09126 Chemnitz, Germany — ³Center for Microtechnologies, Chemnitz University of Technology, Reichenhainer Str. 70, 09126 Chemnitz, Germany

Thin liquid films play a crucial role for many applications, e.g., coating, particle deposition, wafer bonding, and the cooling of electronic devices. As an example, we investigate the evaporation of thin water films on LiTaO₃. *Ab initio* density functional theory is used to calculate the Gibbs free energy of adsorption. These results are fitted to an expression of the Gibbs free energy which is derived from the disjoining pressure, consisting of molecular and structural components. In this way, the parameters for the disjoining pressure can be determined. A combination of literature-known models for spin drying and evaporation is used to analyze the temporal evolution of the water layer. The vapor above the water layer is modeled by diffusion and a mass balance is applied at the water-air interface. The results can be used to optimize the process time needed to reach the equilibrium thickness of the water layer. In addition, computational fluid dynamics simulations are utilized to investigate the evaporation in a wafer bond chamber during pump-down.

CPP 44.9 Thu 11:45 MER 02

Electrokinetic, electrochemical and electrostatic surface potentials of the pristine water liquid-vapor interface — •MAXIMILIAN R BECKER and ROLAND R NETZ — Freie Universität Berlin, Berlin, Germany

Although conceptually simple, the interface between liquid water and vapor displays rich behavior and is subject to intense experimental and theoretical investigations. Different definitions of the electrostatic surface potential as well as different calculation methods, each relevant for distinct experimental scenarios, lead to widely varying potential magnitudes. Here, based on density-functional-theory (DFT) molecular dynamics (MD) simulations, different surface potentials are evaluated and compared to force-field (FF) MD simulations. The laterally averaged electrostatic surface potential, accessible to electron holography, is dominated by the trace of the water molecular quadrupole moment and therefore differs strongly between DFT and FF MD. Thus, when predicting electrostatic potentials within water molecules DFT simulation methods need to be used. The electrochemical surface potential inside a neutral atom, relevant for ion transfer reactions and ion surface adsorption, is much smaller and depends specifically on the atom radius. Charge transfer between interfacial water molecules leads to a sizable surface potential as well. However, when probing electrokinetics by explicitly applying a lateral electric field in DFT-MD simulations, the electrokinetic zeta-potential turns out to be negligible. Thus, interfacial polarization charges from charge transfer between water molecules do not lead to a significant electrokinetic mobility.

CPP 44.10 Thu 12:00 MER 02

How Charges Separate at Moving Contact Lines — •AARON D. RATSCHOW¹, LISA S. BAUER¹, PRAVASH BISTA², STEFAN A. L. WEBER^{2,3}, HANS-JÜRGEN BUTT², and STEFFEN HARDT¹ — ¹Technische Universität Darmstadt, Darmstadt, Germany — ²Max Planck Institute for Polymer Research, Mainz, Germany — ³Johannes Gutenberg Universität, Mainz, Germany

Spontaneous charge accumulation in sliding drops is ubiquitous in nature and has been the subject of research activities for over two decades. Despite the growing number of experimental investigations in recent years, the physical mechanism behind the charging remains poorly understood. We identify the origin of charge separation as the dewetting of the immobilized part of the electric double layer (EDL) by the moving contact line. This layer of physically or chemically bound surface charges depends strongly on the local EDL structure, which is disturbed by the vicinity of the gas-liquid interface and the flow in the liquid. We summarize the physics of charge separation in an analytical model that predicts parametric dependencies on surface chemistry, wetting, and liquid properties. The results agree well with our experiments and numerical simulations and uncover decreasing charge separation with decreasing dynamic contact angle and increasing contact line velocity. Our findings reveal the universal mechanism of charge separation at moving contact lines, not limited to drops, with broad implications for the field of wetting.

CPP 44.11 Thu 12:15 MER 02

Beyond the plate capacitor: Calculating the full dielectric tensor for arbitrary system geometries — •DAVID EGGER, CHRISTOPH SCHEURER, and KARSTEN REUTER — Fritz Haber Institute of the Max Planck Society, Berlin, Germany

Realistic models for catalytic reactions at aqueous interfaces require a profound understanding of the electrostatic properties in the vicinity of the solvated catalytic complex, in particular for (photo-)electrochemical reactions with charged intermediates. However, explicit quantum mechanical simulations of these systems on the required length- and time-scales remain oftentimes out of reach. Coarse-graining the electrostatic response of the molecular solvent into a continuum dielectric, described by the dielectric permittivity tensor ϵ , can hence be a necessity. Existing coarse-graining protocols for ϵ typically assume a separation of the dielectric response parallel and perpendicular to the active interface. This approximation is equivalent to two decoupled sets of in-series plate capacitors and ignores potential non-zero off-diagonal elements in the ϵ tensor.

In this contribution, we present a comprehensive and general formalism to coarse-grain molecular solvents into a truly anisotropic ϵ beyond this approximation. We obtain the full, spatially resolved dielectric tensor for arbitrary system geometries with no prior assumptions on boundary conditions. Common bulk and slab formulas are obtained as special cases. The approach is applied exemplarily to bulk water, water-dichloroethane liquid-liquid interfaces, and solvated platinum nanoparticles following from Wulff constructions.

CPP 44.12 Thu 12:30 MER 02

Asymmetric Sessile Compound Drops — •JAN DIEKMANN and UWE THIELE — Westfälische Wilhelms-Universität, Münster, Germany

We consider compound drops of two immiscible liquids on a rigid solid substrate. Having established a mesoscopic model (amending [1]) consistent with the macroscopic description of [2,3], we show for one-dimensional (1D) substrates that asymmetric compound drops can be energetically favoured using continuation techniques. Furthermore, we investigate selected dewetting and coarsening processes and discuss emerging steady compound drops for two-dimensional (2D) substrates, thereby discussing the relation of 1D and 2D results.

[1] A. Pototsky et al., "Morphology changes in the evolution of liquid two-layer films". J. Chem. Phys. 122, 224711, 2005.

[2] L. Mahadevan, M. Adda-Bedia, and Y. Pomeau., "Four-phase merging in sessile compound drops". J. Fluid Mech. 451, 411-420, 2002.

[3] M. J. Neeson et al., "Compound sessile drops". Soft Matter 8, 11042-11050, 2012.

CPP 44.13 Thu 12:45 MER 02

Steering droplets on substrates with plane-wave wettability patterns and deformations — •JOSUA GRAWITTER and HOLGER STARK — Technische Universität Berlin, Institut für Theoretische Physik, StraÙe des 17. Juni 135, 10623 Berlin

Droplets are set in motion on substrates with a spatio-temporal wettability pattern as generated, for example, on light-switchable surfaces. To study such cases, we implement the boundary-element method to solve the governing Stokes equations for the fluid flow field inside and on the surface of a droplet and supplement it by Cox-Voinov friction for the dynamics of the contact line. One objective of our research is targeted microfluidic transport of such droplets. In earlier work we investigated how a droplet can be steered by imposing a wettability pattern on the substrate [Grawitter and Stark, Soft Matter 17, 2454 (2021)]. As a next step, we have recently extended our method to include substrates the height profile of which varies temporally in a prescribed manner.

We compare two cases: First, we investigate a droplet on substrates with planar-wave wettability pattern by varying the speed and wave length of the pattern. Second, we investigate a droplet on substrates with a planar-wave height profile. In both scenarios, for small wave velocities the droplet moves steadily

forward. In contrast, above a wave velocity the droplet performs steady oscillations. These speed oscillations correlate with oscillations in the shape of the droplet which decay linearly as a function of pattern speed.

CPP 45: Emerging Topics in Chemical and Polymer Physics, New Instruments and Methods

Time: Thursday 9:30–12:00

Location: ZEU 255

CPP 45.1 Thu 9:30 ZEU 255

Structural effects of many-body van der Waals interactions: from small molecules to polymers — •RAUL IAN SOSA, MARIO GALANTE, and ALEXANDRE TKATCHENKO — Department of Physics and Materials Science, University of Luxembourg, L-1511 Luxembourg City, Luxembourg.

Van der Waals (vdW) dispersion interactions are among the key determinants of structure, stability, and dynamics in a wide range of systems such as supramolecules, complex interfaces and low-dimensional nanostructures. Most commonly used approaches for incorporating vdW interactions in extended systems rely on pairwise approximations, neglecting the quantum many-body nature of molecular interactions [Quantum Chem. 114, 1157 (2014), Science. 350, 6257 (2015)]. Recent simulations which incorporate Many-Body Dispersion (MBD) show that a many-body description of van der Waals can be essential for properly describing extended molecules and molecular solids [Physical Review Letters. 108, 23 (2012)]. These effects often manifest themselves as increased ranges of interaction and collective dynamics in a way that is highly dependent on the molecular structure [Nat Comm. 11, 1651 (2020)]. Here we will present a systematic analysis on the impact that many-body interactions have on the range of van der Waals forces in polymers, one dimensional nanostructures and small molecules, making a particular emphasis on the structural dependence of such interactions.

CPP 45.2 Thu 9:45 ZEU 255

Bulk magneto-mechanical response of magnetic filaments in applied magnetic fields — •DENIZ MOSTARAC and SOFIA KANTOROVICH — Univesity of Vienna, Vienna, Austria

Incorporating magnetic nanoparticles within permanently cross-linked structures, opens up the possibility for synthesis of complex, highly magneto-responsive systems. Magnetic filaments (MFs) are polymer-like chains of magnetic, nano-sized colloids, and are a promising platform for engineering novel, magnetically controlled filtering and flow control elements in micro-fluidic devices. The interplay between central attraction forces, and anisotropic, dipolar interactions is the key factor when tuning the macroscopic response of MFs. In this contribution, we show that taking in to account nonlinear contributions to the magnetisation of super-paramagnetic colloids is essential to capture the bulk, magneto-mechanical response of MFs consisting of magnetisable colloids. In the presence of central attraction forces, we report substantial differences in the equilibrium structure of filament clusters, and the mechanical and magnetic response of filament suspensions, to static and time dependant magnetic fields. While on the level of a single filament, magneto-mechanical properties are in general more dependant on the crosslinking approach than on the magnetic nature of colloids, in bulk, the long-range nature of dipolar interactions in quasi-infinite systems makes up for a tremendous difference, and underlines the necessity of a sophisticated model of magnetic colloids that can be magnetised by the presence of magnetic and dipole fields.

CPP 45.3 Thu 10:00 ZEU 255

Improving the Electrochemically Assisted Surfactant Assembly of Vertically Aligned Mesoporous Silica Films — •GILLES MÖHL^{1,2}, SAMUEL FITCH², LI SHAO², JONATHAN RAWLE³, RALPH GILLES¹, GUY DENUAULT², TAUQIR NASIR², YISONG HAN⁴, RICHARD BEANLAND⁴, RUOMENG HUANG², YASIR NOORI², PHILIP BARTLETT², and ANDREW HECTOR² — ¹FRM II/TUM, München, Deutschland — ²UOS, Southampton, United Kingdom — ³Diamond Light Source, Harwell, United Kingdom — ⁴Warwick University, Coventry, United Kingdom

Mesoporous silica films are typically produced by evaporation-induced self-assembly (EISA), but vertical alignment of the pores to the substrate remains difficult. Hexagonal arrays of vertically aligned mesopores can be made by electrochemically assisted surfactant assembly (EASA). The self-assembly of a cationic surfactant (cetyltrimethylammonium bromide), which relies on the production of hydroxide species close to the substrate, also leads to the formation of spheroidal surface aggregates, limiting the obtainable film thickness to a few hundreds of nm. In this work, we show the results obtained from operando Grazing incidence small angle X-ray scattering (GISAXS) experiments done during the EASA of silica, following the evolution of the structure formation in real time with sub-second time resolution. We include the findings from operando pH measurements using an electrochemical microsensor, revealing the temporal evolution of the hydroxide concentration close to the electrode. This enabled

us to adapt the EASA protocol to reduce aggregate formation and increase film thickness.

CPP 45.4 Thu 10:15 ZEU 255

Pair-wise dependences of morphological descriptors provide fingerprint of pore structure in cellulose-based materials — •KARIN ZOJER¹, MATTHIAS NEUMANN², PHILLIP GRÄFENSTEINER², EDUARDO MACHADO CHARRY¹, ANDRE HILGER³, INGO MANKE³, ULRICH HIRN⁴, and VOLKER SCHMIDT² — ¹Institute of Solid State Physics, Graz University of Technology, Petersgasse 16, 8010 Graz, Austria — ²Institute of Stochastics, Ulm University, Helmholtzstrasse 18, 89069 Ulm, Germany — ³Institute of Applied Materials, Helmholtz-Zentrum Berlin für Materialien und Energie, Hahn-Meitner-Platz 1, 14109 Berlin, Germany — ⁴Institute of Bioproducts and Paper Technology, Graz University of Technology, Inffeldgasse 23, 8010 Graz, Austria

Predicting the macroscopic behavior of heterogeneous porous materials from their microscopic structure is formidably challenging, because local morphological microstructure descriptors markedly and erratically vary across a sample. We demonstrate how to quantify cross relationships between pore space-related descriptors and to use these relations to distinguish complex pore spaces at a glance, alike using fingerprints. The key idea is to map the actual microstructure on a multivariate probability distribution. The latter contains strongly compressed information to reproduce the spatial variations of selected properties and their pair-wise interdependencies. Using R-vine copulas, we will exemplarily construct such a distribution of the local morphological descriptors porosity, thickness, surface area per volume and pathway tortuosity for the measured microstructure of paper sheets.

CPP 45.5 Thu 10:30 ZEU 255

Ab initio cavity QED - modifying chemistry with strong light-matter interaction — •CHRISTIAN SCHÄFER^{1,2}, ENRICO RONCA³, JOHANNES FLICK^{4,5}, PRINEHA NARANG⁵, and ANGEL RUBIO^{2,4} — ¹Department of Microtechnology and Nanoscience, MC2, Chalmers University of Technology, 412 96 Göteborg, Sweden — ²Max Planck Institute for the Structure and Dynamics of Matter, Hamburg, Germany — ³Istituto per i Processi Chimico Fisici del CNR (IPCF-CNR), Via G. Moruzzi, 1, 56124, Pisa, Italy — ⁴Center for Computational Quantum Physics (CCQ), The Flatiron Institute, 162 Fifth Avenue, New York NY 10010, USA — ⁵John A. Paulson School of Engineering and Applied Sciences, Harvard University, Cambridge, Massachusetts 02138, USA

The alchemical dream of altering a given material on demand into something desirable is at the very heart of chemistry. Optical-Cavity environments provide a novel handle to non-intrusively control materials and chemistry. The self-consistent interaction between complex electromagnetic environments and realistic materials gave birth to a new discipline, sometimes referred to as 'ab initio QED', on the interface of condensed matter, chemistry and quantum optics.

I will provide a brief introduction into this newly emerged field and illustrate how chemical reactions can be controlled [1] with optical cavities.

[1] Schäfer, C., Flick, J., Ronca, E., Narang, P., and Rubio, A., arXiv:2104.12429 (2021).

CPP 45.6 Thu 10:45 ZEU 255

Structural Descriptors for Constructing High-Dimensional Neural Network Potentials — •MORITZ R. SCHÄFER^{1,2}, JONAS A. FINKLER³, STEFAN GOEDECKER³, and JÖRG BEHLER^{1,2} — ¹Lehrstuhl für Theoretische Chemie II, Ruhr-Universität Bochum, 44780 Bochum, Germany — ²Research Center Chemical Sciences and Sustainability, Research Alliance Ruhr, 44780 Bochum, Germany — ³Basel University, Department of Physics, Klingelbergstrasse 82, 4056 Basel, Switzerland

High-dimensional neural network potentials (HDNNPs) are a well established method to efficiently compute close-to ab initio-quality energies and forces for performing large-scale molecular dynamics simulations of complex systems. In this method, the total energy is constructed as a sum of environment-dependent atomic energy contributions. Also electrostatic interactions based on flexible atomic charges can be included. Both components crucially depend on the quality of the structural descriptors employed to characterize the local atomic environments. Here we investigate the combination of atom-centered symmetry functions with the recently proposed overlap matrix descriptor. Moreover, the advantages and disadvantages of both descriptors are discussed and illustrated for benchmark systems.

CPP 45.7 Thu 11:00 ZEU 255

Solving inverse transport problems across irregular interfaces of sorptive porous media via physics-informed neural networks — •ALEXANDRA SEREBRENNIKOVA and KARIN ZOJER — Institute of Solid State Physics, TU Graz, Petersgasse 16, 8010, Graz, Austria

We show how state of the art extended physics-informed neural networks serve us to solve inverse transport problems with jump conditions across irregular interfaces. This approach reveals the material constants which govern reactive diffusion of organic volatiles migrating across an interface between porous sorptive packaging and food media if we provide experimental data and a transport model.

In such scenarios, associated differential equations (PDE) imply jumps not only in the solution, but also in the solution gradient across interfaces. The idea is to use multiple NN to construct the solution; each NN approximates the solution function of the PDE associated to a domain within the defined interfaces. The networks are coupled across interfaces such that the boundary conditions are satisfied.

As NNs are required to fit underlying physics by minimizing PDE residuals, they are inherently suited to solve inverse problems for the parameters involved in the equations. As further benefit, the discretized experimental data can be represented with a continuous function which offers a meshfree and compact surrogate model for the solution function.

15 min. break

CPP 45.8 Thu 11:30 ZEU 255

Aging-driven compositional changes in Li-ion batteries — •DOMINIK PETZ^{1,2}, PETER MÜLLER-BUSCHBAUM^{1,2}, and ANATOLIY SENYSHYN¹ — ¹MLZ, TUM, Garching — ²TUM School of Natural Sciences, Chair of Functional Materials, Garching

Electrochemical cycling of lithium-ion batteries is supplemented by the active transport of lithium ions and electrons, which are exchanged between the cathode and anode material. Besides material properties, such exchange is facilitated

by the parameters of electrochemical cell like electrode dimensions and geometry, current density, temperature, etc. Such parameters are neither uniformly distributed nor static in general and, therefore, serve as a factor stabilizing heterogeneous states in Li-ion batteries typically reflected in the lithium concentration profiles in the electrodes. Thus, cell aging directly affects the distribution of the lithium-ions in the graphite anode of 18650-type lithium-ion batteries. Lithium heterogeneities (often reflected in loss of lithium inventory) are directly related to the electrolyte filling level. In order to quantify and correlate them simultaneously, a set of cells at different state-of-health was studied non-destructively using spatially resolved neutron powder diffraction. Experimental results unambiguously revealed changes of the lithium and electrolyte distribution versus cell state-of-health in a series of commercial 18650-type lithium-ion battery.

CPP 45.9 Thu 11:45 ZEU 255

Dedoping of PEDOT:PSS using amines to shift the threshold voltage in OECTs — •LAURA TEUERLE, RAKESH NAIR, HANS KLEEMANN, and KARL LEO — IAPP Dresden

With an increasing importance of organic semiconductors, due to their flexibility, transparency and possible biocompatibility, more applications and device classes emerge.

One of them - the organic electrochemical transistor (OECT) can be utilized in neuromorphic computing and printed digital logic. The most commonly used - PEDOT:PSS is a p-type semiconductor, which leads to normally-on type transistors. However, normally-off type devices are needed for a successful application in logic circuits.

We show that a chemical dedoping method involving amines leads to a shift in threshold voltage to zero and even negative in the corresponding devices.

Different processing methods for the dedoping process and device building are studied, which involve photolithography, inkjet printing and spraycoating.

Furthermore, IV measurements for device characterization were taken.

The results show that the studied chemical dedoping of -PEDOT:PSS can be a viable method to create normally-off type transistors for an application in logic circuits.

CPP 46: Active Matter IV (joint session DY/BP/CPP)

Time: Thursday 9:30–13:00

Location: ZEU 160

See DY 38 for details of this session.

CPP 47: 2D Materials VI (joint session HL/CPP)

Time: Thursday 9:30–12:00

Location: POT 81

See HL 34 for details of this session.

CPP 48: Data Driven Materials Science: Big Data and Work Flows – Microstructure-Property-Relationships (joint session MM/CPP)

Time: Thursday 10:15–13:15

Location: SCH A 251

See MM 36 for details of this session.

CPP 49: 2D Materials VII: Heterostructures (joint session O/CPP)

Time: Thursday 10:30–12:45

Location: GER 37

See O 74 for details of this session.

CPP 50: Glasses and Glas Transition II

Time: Thursday 12:15–13:00

Location: ZEU 255

CPP 50.1 Thu 12:15 ZEU 255

Analysis of glass transition for polymer melts using data-driven methods — •ATREYEE BANERJEE, HSIAO-PING HSU, KURT KREMER, and OLEKSANDRA KUKHARENKO — Max Planck Institute for Polymer Research, Ackermannweg 10, 55128 Mainz, Germany

Upon cooling, the dynamical properties of most polymer melt slow down exponentially leading to a glassy state without any drastic change in structure. While determining glass transition temperature and understanding the glass transition are important topics of current physical research, the properties in the glassy

state are crucial for their general applicability. The conventional ways to calculate glass transition temperature from simulation data of polymer melts rely on the fitting of high- vs. low-temperature branches of macroscopic properties such as volume or density and are sensitive to the choice of parameters. We propose a new data-driven approach based on the information about structural fluctuations in the chains to identify the glass transition temperature. Our data-driven approach utilizes high-resolution details accessible through molecular dynamics simulations and considers the structural information of individual chains. The method was tested for coarse-grained weakly semi-flexible polymer model sim-

ulations [1]. It is also applied to the all-atom acrylic polymer simulations with different lengths of side-chain residues.

[1] Atreyee Banerjee, Hsiao-Ping Hsu, Kurt Kremer, and Oleksandra Kukharenko, arXiv:2211.14220 (2022)

CPP 50.2 Thu 12:30 ZEU 255

Roughness Induced Rotational Slowdown near the Colloidal Glass Transition — BEYBIN ILHAN, MICHEL DUTTS, and •FRIEDER MUGELE — University of Twente, Physics of Complex Fluids group

Rotational diffusion of colloidal spheres has been studied rarely, in spite of its importance in the kinetics of many processes involving friction. While for smooth hard spheres, rotational diffusion gets impeded only weakly with increasing volume fraction, the picture changes drastically when surface roughness is introduced. We show this for a system of undeformable all-silica colloidal raspberries, studied with time-resolved 3D Confocal Scanning Laser Microscopy (CSLM).

We find that the strong surface roughness leads to a significantly lower maximum volume fraction, preceded by a broad concentration range in which the rotational Brownian motion changes signature from high-amplitude diffusive to low-amplitude rattling. This strong rotational slowdown occurs at significantly higher concentrations than for the translations, thus presenting a second glass transition.

In the regime where the Mean Squared Angular Displacement (MSAD) is subdiffusive, significant correlations are found between the translational and rotational motions. The drastic rotational slowdown occurs when the particle intersurface distance becomes comparable to the surface roughness amplitude. Currently, the number of contacts exceeds a critical value. This picture is supported by observations in a densely packed layer of raspberries at a smooth wall:

here significant rotational motions are found while the translations are almost completely frozen.

CPP 50.3 Thu 12:45 ZEU 255

When molecular heterogeneities matter: thermal expansion and relaxation time in polyalcohols — •MARTIN TRESS¹, JAN GABRIEL², and FRIEDRICH KREMER¹ — ¹Universität Leipzig, Leipzig, Germany — ²Roskilde University, Roskilde, Denmark

Structural relaxation in liquids is considered to depend directly on the available free volume. Many theoretical concepts of liquid dynamics and the glass transition approximate this molecular quantity using macroscopic density. However, particularly hydrogen (H-) bonding liquids defy proper description by these approaches (e.g. the failure of density-scaling in such materials). To study densification on molecular scale, we use infrared spectroscopy on a series of polyalcohols. By analyzing specific molecular vibrations and correlating them with interatomic bond lengths, the thermal expansion of several types of intramolecular covalent bonds and intermolecular H-bridges is quantified. Pronounced differences between intra- and intermolecular expansion verify the dominance of the latter. Surprisingly, the overall thermal expansion (i.e. cube root of inverse density) is even bigger than that of the strong H-bridges. This suggests that weak H-bridges dominate thermal expansion while strong ones must control structural relaxation, i.e. the glass transition. The method is validated by successfully describing the density of water based on extracted H-bridge lengths. Consequently, inhomogeneities on intra- and intermolecular scale can play distinct roles in densification and orientational relaxation and require a careful consideration in a comprehensive theoretical description. [Gabriel, Tress et al. J Chem Phys 154 (2021) 024503]

CPP 51: Hybrid and Perovskite Photovoltaics III

Time: Thursday 15:00–17:15

Location: GÖR 226

CPP 51.1 Thu 15:00 GÖR 226

Slot-die coating of nanocrystal and bulk perovskite thin films for photovoltaics — •MANUEL A. REUS¹, AHMED KRIFA¹, DAVID P. KOSBAHN¹, QUINTEN A. AKKERMAN², ALEXANDER BIEWALD³, LENNART K. REB¹, MATTHIAS SCHWARTZKOPF⁴, ANDREI CHUMAKOV⁴, STEPHAN V. ROTH⁴, ACHIM HARTSCHUH³, JOCHEN FELDMANN², and PETER MÜLLER-BUSCHBAUM^{1,5} — ¹TUM School of Natural Sciences, Chair for Functional Materials, Garching — ²Nano-Institut München und Fakultät für Physik, LMU München — ³Department Chemie und CeNS, LMU München — ⁴DESY, 22607 Hamburg — ⁵MLZ, TUM, Garching

Thin-film solar cells might offer large-scale and cheap production with highly tunable properties, e.g., semi-transparency, color, thickness, or flexibility. Slot-die coated nanocrystal and bulk hybrid perovskite thin films are significant for high-efficiency next-generation solar cell absorber materials. In this work, we show the feasibility of creating high-quality thin films of this material class by the easily scalable and roll-to-roll compatible deposition method of meniscus-guided slot-die coating. We use time-resolved grazing-incidence X-ray scattering to investigate the crystal structure, texture, and morphology of the printed thin films. We track the printing process in real-time and extract parameters describing the quality and kinetics of the printing process. We also present solar cell data with perovskite absorber layers printed from colloidal hybrid perovskite nanocrystal solution.

CPP 51.2 Thu 15:15 GÖR 226

Time-resolved structural changes in hybrid perovskites under illumination — •IVAN ZALUZHNYI¹, LINUS PITHAN¹, ALEXANDER HINDERHOFER¹, RUSTAM RYSOV², FABIAN PAULUS³, and FRANK SCHREIBER¹ — ¹Institute of applied physics, University of Tübingen, Tübingen, Germany — ²Deutsches Elektronen-Synchrotron DESY, Hamburg, Germany — ³Center for advancing electronics Dresden, Technical University of Dresden, Dresden, Germany

Hybrid perovskites with mixed halides are known to undergo phase segregation when illuminated by visible light. We used coherent X-ray diffraction at synchrotron sources to reveal the structural changes in the series of MAPbBr_(3-x)I_x perovskites illuminated with a white and blue light (broad spectrum and $\lambda \approx 450$ nm, respectively). The experimental data allow us to characterize the initial structure of the perovskite films, observe the changes during the illumination, and estimate the time scales over which these changes take place. Moreover, using x-ray photon correlation spectroscopy (XPCS), we can observe the movement of the domain walls and characterize the mobility of the halide ions. The obtained results allow us to better understand the microscopic mechanisms leading to the halide segregation.

CPP 51.3 Thu 15:30 GÖR 226

Investigation of defects inside of mixed halide perovskite solar cells — •PASCAL ROHRBECK¹, YENAL YALCINKAYA^{1,2}, and STEFAN A. L. WEBER^{1,2} — ¹Max Planck Institute for polymer research, department physics at interfaces, Ackermannweg 10, 55128 Mainz, Germany — ²Johannes Gutenberg University, Department of Physics, Staudingerweg 10, 55128 Mainz, Germany

Understanding the electron and ion dynamics is an important task for improving the lead halide perovskites and related devices. For this task, macroscopic measurement techniques are not sufficient. Therefore, nanoscale characterization methods can play an important role in studying perovskite solar cells. In this study, we investigate the spatial defect distribution in the vicinity of grain boundaries. We introduce local photovoltage, photovoltage decay, and defect mapping via time-resolved Kelvin probe force microscopy (tr-KPFM) methods. We are able to detect and localize areas of increased charge carrier recombination, ion migration, and defects. This will help to understand recombination losses and improve perovskite solar cells on the long run.

CPP 51.4 Thu 15:45 GÖR 226

Post-Flight Analysis of Space-Probed Perovskite and Organic Solar Cells by Means of Grazing-Incidence X-Ray-Scattering — •LENNART KLAUS REB¹, MICHAEL BÖHMER¹, BENJAMIN PREDESCHLY¹, SEBASTIAN GROTT¹, CHRISTIAN LUDWIG WEINDL¹, GORAN IVKOVIC IVANDEKIC¹, RENJUN GUO¹, LUKAS VIKTOR SPANIER¹, CHRISTOPH DREISSIGACKER², JÖRG DRESCHER², ROMAN GERNHÄUSER¹, ANDREAS MEYER², and PETER MÜLLER-BUSCHBAUM^{1,3} — ¹TU München, Garching, DE — ²Deutsches Zentrum für Luft- und Raumfahrt (DLR), Köln, DE — ³Heinz Maier-Leibnitz-Zentrum, Garching, DE

Thin-film perovskite and organic solar cells exhibit an exceptional power per mass that makes them particularly interesting for space applications. Recently, we launched perovskite and organic solar cells into space on a suborbital rocket flight for the first time [1, 2]. The rocket experiment enables post-flight characterization of the space-probed solar cells, based on Grazing-Incidence Small-Angle and Wide-Angle X-ray Scattering (GISAXS/GIWAXS) to investigate morphological and structural changes in the active layers. The morphology is altered slightly by the space flight and environmental conditions before and after the rocket launch; interestingly, the sole solar cell transport in nitrogen environment modified their active layers compared to the reference solar cells. The crystalline phase, however, does not reveal changes in any solar cell type. [1] L. Reb et al., Joule 4,1880-1892 (2020), doi.org/10.1016/j.joule.2020.07.004. [2] L. Reb et al., Rev. Sci. Instrum. 92 (2021), doi.org/10.1063/5.0047346.

CPP 51.5 Thu 16:00 GÖR 226

Simulation of the impact of processing conditions on the perovskite film morphology — •MARTIN MAJEWSKI, OLIVIER RONSIN, and JENS HARTING — Forschungszentrum Jülich GmbH, Helmholtz Institute Erlangen- Nürnberg (IEK-11), Dynamics of Complex Fluids and Interfaces, Cauerstraße 1, 91058 Erlangen, Germany

The solution-processed perovskite layer forms complex structures during drying. This morphology of the dry film heavily influences the efficiency of the final solar cell. The impact of the physical mechanisms on the morphology, like for example nucleation and evaporation rate, in a drying, crystallizing wet film is not really understood yet. Therefore a better understanding of the interplay of these phenomena is needed. We will present phase field simulations which are capable to describe the main physical processes like: evaporation, diffusion, spontaneous nucleation, crystal growth and advection, to investigate the impact of processing conditions on the final morphology of the perovskite film. Comparisons of the simulation to the theory will be presented. First simulations of drying solutions, including all physical phenomena, will be shown and compared to experiments.

15 min. break

CPP 51.6 Thu 16:30 GÖR 226

Influence of mesoporous-TiO₂ on mobile ion migration and charge extraction of perovskite solar cells — •PATRICK DÖRFLINGER¹, VALENTIN SCHMID¹, YONG DING², MOHAMMAD KHAJA NAZEERUDDIN², and VLADIMIR DYAKONOV¹ — ¹Experimental Physics VI, Julius Maximilian University of Würzburg, 97074 Würzburg — ²Group for Molecular Engineering of Functional Materials, Institute of Chemical Sciences and Engineering, EPFL Valais, Sion 1950, Switzerland

Hybrid lead halide perovskite solar cells have reached over 25% power conversion efficiency in the past years but still suffer from poor long term stability. Therefore, increasing attention is given to interfacial engineering. Especially the interplay of the transport layer with the perovskite layer is essential, determining various key properties like the ability of charge extraction or surface recombination. In this study, the potential of different mesoporous TiO₂ electron transport layers (ETL) with focus on the mobile ions is investigated. Therefore, concentration and diffusion of mobile ions, often linked to device degradation, is analyzed by measuring open-circuit voltage decay (OCVD). Furthermore, measuring the photoluminescence quenching efficiencies (PLQE) between open-circuit and short-circuit conditions of complete devices allows to study charge extraction and link the obtained results to device performance. These studies prove the advantage of using a mesoporous-TiO₂ layer made of single-crystalline nanoparticles as an ETL.

CPP 51.7 Thu 16:45 GÖR 226

Interferometric Bulk Access in Pump-Probe Microspectroscopy of MAPbBr₃ Crystals — •TOBIAS SEEWALD¹, ULRICH J. BAHNMÜLLER², SEBASTIAN POLARZ², and LUKAS SCHMIDT-MENDE¹ — ¹Department of Physics, University of Konstanz, Germany — ²Institute of Inorganic Chemistry, Leibnitz University Hannover, Germany

We present a microspectroscopic study on individual facets of MAPbBr₃ crystals synthesized via an aerosol method controlling the exposed lattice planes. Transient reflection and photoluminescence spectra collected from single few μm facets allow to correlate the findings to micromorphology and lattice termination. Internal reflection of the probe pulse is found to form Fabry-Pérot resonances in the sub-band gap spectral region, which sensitively respond to the modified refractive index upon photoexcitation. Comparing one- and two-photon pump absorption, the dynamics of bulk and surface states can be distinguished on ps timescales.

CPP 51.8 Thu 17:00 GÖR 226

An alternative non-invasive technique for studying hybrid perovskite solar cells' in-situ degradation — •CHIKEZIE WILLIAMS UGOKWE^{1,2}, ZEKARIAS TEKLU GEBREMICHAEL^{1,2}, KEHINDE OGUNMOYE^{1,2}, ULRICH S. SCHUBERT^{1,2}, and HARALD HOPPE^{1,2} — ¹Center for Energy and Environmental Chemistry Jena (CEEC Jena), Friedrich Schiller University Jena, Philosophenweg 7a, 07743 Jena, Germany — ²Laboratory of Organic and Macromolecular Chemistry (IOMC), Friedrich Schiller University Jena, Humboldtstrasse 10, 07743 Jena, Germany

The main obstacle to the commercialization of hybrid organic-inorganic perovskite (HOIP) solar cells is stability. Hence understanding degradation routes within the solar cell is essential. Traditional characterization methods have so far either monitored global properties, which precludes a better knowledge of local degradation processes, or induced some type of degradation, which conflates results in in-situ degradation studies of perovskite solar cells. In this paper, we describe a non-invasive technique for the in-situ analysis of the degradation of the active layer of an inverted HOIP solar cell. Utilizing the phenomenon of coherent light propagation in thin film layer stacks, we were able to see lead (II)iodide formation over time in a fully functional perovskite solar cell, which is an undeniable by-product of degradation. We were able to quantify the vertical distribution of the degradation product along the thickness of the active layer by using the measured reflectance of the entire solar cell as the input data for the optical modeling.

CPP 52: Wetting, Fluidics and Liquids at Interfaces and Surfaces III (joint session CPP/DY)

Time: Thursday 15:00–16:15

Location: MER 02

CPP 52.1 Thu 15:00 MER 02

Hierarchical superhydrophobic composite membrane for enhanced distillation with excellent fouling resistance — •PREXA SHAH¹, YOUNMIN HOU², MICHAEL KAPPL¹, and HANS JÜRGEN BUTT¹ — ¹Max-Planck-Institute for Polymer Research, Physics at Interfaces group, Ackermannweg 10, 55128 Mainz, Germany. — ²School of Power and Mechanical Engineering, Wuhan University, 430072, Wuhan, China.

In arid areas near the coast, seawater desalination has become an essential supply of clean water. As a result, energy-efficient desalination systems must be developed to avoid overburdening the restricted energy supply. Membrane distillation (MD) is gaining popularity as a hybrid thermal/membrane-based desalination approach that may use waste heat for small-scale desalination as well as treating high-salinity brines. The objective is now to maximize the distillation rate while avoiding membrane wetting and fouling. In this work, composite membranes with multiscale pore sizes are formed by depositing a thin layer of nano-porous nanofilaments over microporous membranes. Distillation performance and fouling resistance are explored utilizing low surface tension impurities, which might enhance the chance of membrane wetting. The resistance of protein adsorption to organic fouling is also examined. Our unique multiscale porous membranes outperform traditional hydrophobic membranes in terms of fouling resistance while achieving better distillation flow. This research shows how to optimize MD procedures for wastewater and saltwater treatment.

CPP 52.2 Thu 15:15 MER 02

Surface tension of cavitation bubbles — •MARINE BOSSERT¹, PANAYOTIS SPATHIS², PIERRE-ÉTIENNE WOLF², LAURENT CAGNON², ISABELLE TRIMAILLE³, and ÉTIENNE ROLLEY⁴ — ¹Institut of Materials Physics and Technology, Hamburg University of Technology, Germany — ²Institut Néel, Grenoble, France — ³Institut des NanoSciences de Paris, Paris, France — ⁴Laboratoire de Physique de l'École Normale Supérieure, Paris, France

The evaporation of a fluid contained in a porous material occurs by cavitation when the pores are connected to the outer gas reservoir through small constrictions. Using monolithic transparent porous samples, we have measured the cavitation rate J as a function of the departure from equilibrium for hexane at room temperature [1] and nitrogen over a wide temperature range.

When the radius of the critical nucleus R^* is large, our measurements are in agreement with the prediction of the Classical Nucleation Theory. However, when the thickness of the interface is not negligible compared to R^* , we find that J is much larger than predicted. We show that this shift can be accounted for if the liquid-vapor surface tension is allowed to depend on the interface curvature. This dependence is in reasonable agreement with Density Functional calculations for Lennard-Jones fluid, including the correction to second order in curvature.

[1] V. Doebele, et al, Phys. Rev. Lett. 125 (2020) 255701.

CPP 52.3 Thu 15:30 MER 02

Simulations for Wetting of Biomembranes — •MARCEL MOKBEL and SEBASTIAN ALAND — TU Bergakademie Freiberg, Freiberg, Germany

The dynamics of membranes, shells, and capsules in fluid flow has become an active research area in computational physics and computational biology. The small thickness of these elastic materials enables their efficient approximation as a hypersurface, which exhibits an elastic response to in-plane bending and out-of-plane stretching deformations. If such a closed thin shell is filled with (and/or surrounded by) multiple fluids, capillary forces on the contact line between the fluids and the shell may arise and force the shell to deform.

In this work, we present a novel Arbitrary Lagrangian-Eulerian (ALE) method to simulate such elastic surfaces immersed in Navier- Stokes fluids, which is combined with a phase field approach to model droplets inside and/or outside the surface. This method combines high accuracy with computational efficiency, since the grid is matched to the elastic surface and can therefore be resolved with relatively few grid points near the surface. We formulate elastic surface forces

and propose an evolving finite-element discretization. Several wetting test cases demonstrate the versatility of the proposed method. Examples are simulations of single or multiple droplets deforming a vesicle-like shell.

CPP 52.4 Thu 15:45 MER 02

Dilute suspensions of chemically active particles in thin liquid films — •TILMAN RICHTER, PAOLO MALGERETTI, and JENS HARTING — Helmholtz-Institut Erlangen-Nürnberg für erneuerbare Energien, Erlangen, Germany

Thin liquid films are important for many microfluidic applications such as printing or coating of e.g. printable electronics or photovoltaic cells as well as so called lab-on-a-chip devices. Also in catalysis at liquid interfaces thin film dynamics are important. It is well known that a thin film on a solid substrate can be unstable and droplet formation may arise.

The dynamics of thin liquid films and their instability has been the subject of intensive experimental, analytical, and numerical studies, the latter often based on the thin film equation. We propose a set of newly developed equations for the influence of chemical active colloids suspended in a thin liquid film based on the lubrication and Fick-Jacobs approximation. For this novel set of equations we perform a linear stability analysis (LSA) that reveals surprisingly interesting dynamics. We identify the subset of parameters for which the thin film becomes stable i.e. is not rupturing, as well as a variety of different dominating wave-modes. This allows us to control not only the stability but also the droplet size distribution after film rupture, as well as the time it takes for an initially flat film to rupture.

In order to assess the asymptotic state of the thin film, the LSA results are compared against numerical simulations using the Lattice Boltzmann method.

CPP 52.5 Thu 16:00 MER 02

Light properties and water resistant of combined sobrerol methacrylate cellulose thin films. — •CONSTANTIN HARDER^{1,2}, ALEXANDROS E. ALEXAKIS³, MARIE BETKER^{1,3}, YUSUF BULUT^{1,2}, BENEDIKT SOCHOR¹, HUAYING ZHONG², GUANGJIU PAN², MANUEL REUS², KORNELIYA GOORDEYEVA³, APOSTOLOS VAGIAS^{2,4}, DANIEL SÖDERBERG³, EVA MALMSTRÖM³, PETER MÜLLER-BUSCHBAUM^{2,4}, and STEPHAN V. ROTH^{1,3} — ¹DESY, 22607 Hamburg, Germany — ²TUM School of Natural Sciences, Chair for Functional Materials, 85748 Garching, Germany — ³KTH Royal Institute of Technology, 10044 Stockholm, Sweden — ⁴MLZ, TUM, 85748 Garching, Germany

Functionalization of porous materials in terms of optical, chemical and mechanical properties is achieved by applying fully wood-based layers materials. In this project, the refraction index, extinction coefficient and water adhesion properties of cellulose thin films combined with sobrerol methacrylate colloids are investigated together with their topography and morphology. Cellulose nanofibrils (CNF) are a hydrophilic material, and form networks during the drying with specific refraction index, extinction coefficient. Applying additional colloids, their optical properties and water-contact angle can be tuned. Hence, in order to produce water-resistant thin film, a combination of CNF and colloids is a perfect candidate.

CPP 53: Charged Soft Matter, Polyelectrolytes and Ionic Liquid

Time: Thursday 15:00–17:45

Location: ZEU 255

Invited Talk

CPP 53.1 Thu 15:00 ZEU 255

Aqueous nanoclusters govern ionic transport in dense polymer membranes — •JOACHIM DZUBIELLA — Physikalisches Institut, Universität Freiburg

Hydrated polymer materials with low water uptake exhibit a highly heterogeneous interior characterized by water clusters in the form of nanodroplets and nanochannels. Here, based on our recent insights from computer simulations, we argue that the water cluster structure has large implications for ionic transport and selective permeability in polymer membranes. Importantly, we demonstrate that the two key quantities for transport, the ion diffusion and the solvation free energy inside the polymer, are extremely sensitive to molecular details of the water clusters. In particular, we highlight the significance of water droplet interface potentials and the nature of hopping diffusion through transient water channels. These mechanisms can be harvested and fine-tuned and may optimize selectivity in ionic transport in a wide range of applications.

CPP 53.2 Thu 15:30 ZEU 255

Why weakly hydrated anions bind to polymers but not to monomers? — BRADLEY A. ROGERS¹, HALIL I. OKUR^{1,4}, CHUANYU YAN¹, TINGLU YANG¹, •JAN HEYDA², and PAUL S. CREMER^{1,3} — ¹Department of Chemistry, The Pennsylvania State University, University Park, PA, USA. — ²Department of Physical Chemistry, University of Chemistry and Technology, Prague, Dejvice, Czech Republic. — ³Department of Biochemistry and Molecular Biology, The Pennsylvania State University, University Park, PA, USA. — ⁴Present address: Department of Chemistry and National Nanotechnology Research Center (UNAM), Bilkent University, Ankara, Turkey.

Weakly hydrated anions help to solubilize hydrophobic macromolecules in aqueous solutions, but small molecules comprising the same chemical constituents precipitate out when exposed to these ions. Here, this apparent contradiction is resolved by systematically investigating the interactions of NaSCN with polyethylene oxide oligomers and polymers of varying molecular weight. A combination of spectroscopic and computational results reveals that SCN⁻ accumulates near the surface of polymers, but is excluded from monomers. This occurs because SCN⁻ preferentially binds to the centre of macromolecular chains, where the local water hydrogen-bonding network is disrupted. These findings suggest a link between ion-specific effects and theories addressing how hydrophobic hydration is modulated by the size and shape of a hydrophobic entity.

CPP 53.3 Thu 15:45 ZEU 255

Constrained Conductivity in Smallest Polymer Aggregates — •ALAA HASSAN, WING KIT OR, and MARTIN TRESS — Peter Debye Institute, Leipzig university

Detailed insight into material properties at the nanometric level is highly desired in advancing nanotechnology. In the past, Broadband Dielectric Spectroscopy (BDS) revealed altered dynamics of polymers confined to thin films or nanometric channels. However, little is known about the properties of individual polymer chains because of the extreme experimental challenge. We aim to investigate individualized polymer chains using nano-BDS by refining a nanostructured electrode setup and combining it with chemical surface modification. The latter involves depositing a very regular pattern of gold nanoparticles (AuNPs)

of well-controllable size and separation at the nanometer scale. These AuNPs act as anchors for chemical grafting-to of thiol-terminated polyethylene oxide (PEO). AFM is used to determine the volume of PEO grafted to each AuNP from which the average number chains are deduced. The successful implementation of this approach is confirmed by measuring the conductivity of separated PEO aggregates down to about five chains each. The conductivity of the isolated aggregates shows Arrhenius-like behavior in the whole temperature range, while in bulk, this is only seen below the glass transition. Additionally, the slope of the conductivity in the loss spectra is reduced in the aggregates, which suggests that intra-chain hopping dominates as opposed to inter-chain hopping in bulk. This might exemplify structural constraints that restrict charge mobility close to the surface.

CPP 53.4 Thu 16:00 ZEU 255

KCl modulated D2O Hydration and Subsequent Thermoresponsive Behavior of Poly(sulfobetaine)-Based Diblock Copolymer Thin Films — •PEIXI WANG¹, CHRISTINA GEIGER¹, JULIJA REITENBACH¹, APOSTOLOS VAGIAS⁵, ROBERT CUBITT², VIET HILDEBRAND³, ANDRÉ LASCHEWSKY³, CHRISTINE M. PAPADAKIS⁴, and PETER MÜLLER-BUSCHBAUM^{1,5} — ¹TUM School of Natural Sciences, Chair for Functional Materials, Garching — ²Institut Laue-Langevin, Grenoble — ³Fraunhofer-Institut für Angewandte Polymerforschung, Potsdam-Golm — ⁴TUM School of Natural Sciences, Soft Matter Physics, Garching — ⁵MLZ, TUM, Garching

The salt effect of KCl on D2O hydration and subsequent thermoresponsive behavior of diblock copolymer (DBC) thin films, which feature a short zwitterionic poly(4-((3-methacrylamidopropyl) dimethylammonio) butane-1-sulfonate) (PSBP) block and a long nonionic thermo-responsive poly(N-isopropylmethacrylamide) (PNIPMAM) block, is studied by in situ spectral reflectance (SR) and time-of-flight neutron reflectivity (ToF-NR) in combination with isotope sensitivity. The solvation-triggered phase transition upon D2O hydration and subsequent heating is probed in situ by Fourier transform infrared spectroscopy (FT-IR). Besides, the migration and/or aggregation of KCl domains inside the DBC thin films is also demonstrated by complementary methods, namely, X-ray reflectivity (XRR) and atomic force microscopy (AFM).

15 min. break

CPP 53.5 Thu 16:30 ZEU 255

Photoisomerization of Arylazopyrazole Surfactants Drives Property Changes of Polyelectrolyte/Surfactant Mixtures — •MICHAEL HARDT and BJÖRN BRAUNSCHWEIG — University Münster, Center for Soft Nanoscience, 48149 Münster, Germany

Polyelectrolyte/surfactant (P/S) mixtures are in most cases static in nature, which renders them invariable for property changes unless massive changes in pH or ionic strength are applied. We have shown that mixtures of cationic photoresponsive arylazopyrazole (AAP) surfactants with NaPSS exhibit substantial changes in particle size and electrophoretic mobility [1] that can be easily triggered by light irradiation.

Here, we present new information on PDADMAC polyelectrolyte mixtures with three anionic AAP surfactants that have H, butyl and octyl terminal groups. The E and Z configurations of the AAP photoswitches show substantially different hydrophobic interactions that drastically alter their binding affinity to the PDADMAC. Measurements of the electrophoretic mobility clearly indicate that the E/Z photoisomerization of AAP surfactants causes a charge reversal of the P/S aggregates, while for the H-AAP also larger P/S aggregates in the bulk solution can be dissolved by UV irradiation and formed again with green light. Vibrational sum-frequency generation (SFG) spectroscopy reveals that similar to the changes in the bulk, the charging state at the air-water interface can be reversibly tuned by the light conditions. This has interesting consequences for soft matter materials such as foams [1] and emulsions.

[1] Schnurbus et al., ACS Appl. Mater. Int. 2022, 14, 4656-4667.

CPP 53.6 Thu 16:45 ZEU 255

Grazing incidence x-ray scattering on lithium iron phosphate electrodes with polymer blend binders — •FABIAN A.C. APFELBECK¹, JULIAN E. HEGER¹, TIANFU GUAN¹, MATTHIAS SCHWARTZKOPF², STEPHAN V. ROTH^{2,3}, and PETER MÜLLER-BUSCHBAUM^{1,4} — ¹TUM School of Natural Sciences, Chair for Functional Materials, 85748 Garching — ²DESY, 22607 Hamburg — ³Royal Institute of Technology KTH, 100 44 Stockholm — ⁴MLZ, TU München, 85748 Garching
Lithium iron phosphate (LFP) is a widely used cathode for lithium ion batteries especially in vehicles due to its low cost, high safety, long cycle life and low toxicity. However, so far structural investigations are mainly limited to x-ray diffraction (XRD) techniques. In this project, we extend the investigation of these electrodes to grazing incidence techniques. Therefore, we study electrodes which consist of the active material lithium iron phosphate, carbon black as conducting agent and the polymeric binder polyvinylidene fluoride (PVDF). Additionally, we prepare several binder blends of the neutral PVDF and the single-ion conducting polymer poly(trifluoromethane) sulfonimide lithium styrene (PSTF-SiLi) since it is known, that a 1:1 wt% mixture of PVDF and a single-ion conducting polymer results in superior battery performance. We measure grazing incidence small/wide angle x-ray scattering (GISAXS/GIWAXS) and based on these data, we can understand the influence of the binder on the structure of the electrode. We can correlate ex-situ the morphological and structural data (GISAXS/GIWAXS) with electrochemical results (EIS).

CPP 53.7 Thu 17:00 ZEU 255

Comparative Study of Thermoelectric Transport Properties of Lithium- and Sodium-based Solid Polymer Electrolytes and their Tuning by Carbon-based Additives — •MAXIMILIAN FRANK, JULIAN-STEVEN SCHILLING, and JENS PFLAUM — Experimental Physics VI, University of Würzburg, 97074 Würzburg
Due to the high abundance of their atomic constituents, solution as well as easily scalable processing, and intrinsically low thermal conductivity, organic polymers have gained much attention for potential thermoelectric applications. In particular, ionic systems can generate significantly higher thermal voltages than electronic materials. In this work, we will compare our previous findings [1]

on the electrical and thermoelectric transport properties of a solution-processed methacrylate-based solid polymer electrolyte with new results obtained by variation of the conducting salt. Using impedance spectroscopy in a broad frequency range from 100 mHz to 510 kHz in a temperature range between 263 K and 353 K and by means of thermoelectric voltage measurements, we deduced the essential concentration-related differences in the application of LiTFSI and NaTFSI as conducting salts. As an extension, we demonstrate the possibility to efficiently tune the transport properties of these polymer electrolytes by carbon-based additives, which differ in their conductivity characteristics (semiconducting or metallic, 1D or 2D). A proof-of-concept thermoelectric generator verifies the functionality of our approach and substantiates the potential of mixed ionic and electronic materials for future TE applications. [1] M. Frank, J. Pflaum, *Adv. Funct. Mater.* 2022.

CPP 53.8 Thu 17:15 ZEU 255

Understanding Electron Hopping Mechanism in Organic Radical Batteries — •SOUVIK MITRA¹, ANDREAS HEUER², and DIDDO DIDDENS³ — ¹University of Muenster — ²University of Muenster — ³University of Muenster

In recent years, there has been an increasing interest in organic radical batteries (ORBs) due to their potentially high power density and availability of Cobalt free cathode materials [1]. Understanding charge transport in ORBs is still an open question due to the disordered behavior of the organic environment [2]. To understand the fundamental mechanism associated with charge hopping and ion transport we use reactive step MD (rs@md) [3]. The rs@md technique accounts for charge transfer reactions in classical MD simulation based on the rates of these reactions. We calculate these rates using the Marcus theory [4]. In this contribution, we explicitly study the Marcus curve for the TEMPO molecule (a very common redox component used in ORBs) in presence of various solvents and salts. We also study the Marcus coupling using quantum methods such as Frontier Molecular Orbital (FMO) [5] and Complete Active Space Self Consistent Field (CASSCF) [6] theories.

[1] Kemper et al., J. Phys. Chem. C 2014, 118, 17213-17220. [2] Kemper et al., J. Phys. Chem. C 2016, 120, 25639-25646. [3] Bidermann et al., J. Chem. Theory Comput. 2021, 17, 2, 1074-1085. [4] Marcus, R.A., J. Chem. Phys. 1956, 24, 5, 966-978. [5] Baumeier et al., Phys. Chem. Chem. Phys., 2010, 12, 36, 11103-11113. [6] Blancafort et al., J. Phys. Chem. C 2006, 110, 20, 6426-6432.

CPP 53.9 Thu 17:30 ZEU 255

Fluid ferroelectric nematic fibres — •ALEXANDER JAROSIK and ALEXEY EREMIN — Otto-von-Guericke Universität, Magdeburg, Germany

Nematics with a broken polar symmetry is one of the fascinating recent discoveries in soft matter. High spontaneous polarisation and the fluidity of the ferroelectric nematic NF phase make such materials attractive for future applications and interesting for fundamental research. We report the first example of metastable fluid fibres formed in the ferroelectric phase and characterise their polar and nonlinear optical properties. We discuss the filament stability in the frame of the polarisation-splay model of the ferroelectric nematic phase.

CPP 54: 2D Materials VIII

Time: Thursday 16:30–17:45

Location: MER 02

CPP 54.1 Thu 16:30 MER 02

Structure elucidation of 2D covalent organic frameworks — •MARYKE KOUYATE^{1,3}, KONRAD MERKEL¹, DOMINIK PASTOETTER², ALBRECHT LUDWIG WAENTIG², XINLIANG FENG², and FRANK ORTMANN¹ — ¹Technical University of Munich, Munich, Germany — ²TU Dresden, Dresden, Germany — ³Fritz Haber Institute of the Max Planck Society, Berlin, Germany

We determine the structure of novel 2D framework materials (known as 2D polymers or 2D COFs) that are based on Diquinoxalino[2,3-a:2'3'-c]phenazine (HATNA) vertex units and different linkers (naphthalene vs. pyrene). We simulate the unit cell parameters and stacking patterns with density functional theory. The studied COFs were synthesized and experimentally characterized by our collaborators. Our theoretical studies include extensive xyz scans to find the most energetically favorable stacking geometry. With the results of the xyz scans and the appropriate selection of the unit cell, good agreement is obtained with the experimental PXRD patterns, and individual XRD peaks can be assigned to specific in-plane or out-of-plane directions. Moreover, the simulated structures show a clear difference in the packing of the two COFs which are caused by differences in their linker units. This observation is also consistent with the differences in the experimental PXRD patterns. As a result, we can shed light on the actual cell parameters and stacking behavior.

CPP 54.2 Thu 16:45 MER 02

How to calculate electron-hole interaction efficiently in large covalent organic frameworks? — •KONRAD MERKEL and FRANK ORTMANN — TU München, School of Natural Sciences

Solving the Bethe-Salpeter equation for crystalline materials with many atoms per unit cell, such as covalent organic frameworks, is computationally very expensive and often not feasible. Established tools are usually not suitable for this class of materials because they have enormous memory requirements due to their large basis sets. An elegant solution is to use material-specific, tailored basis sets that allow a complete description with only a handful of basis functions and therefore require only a fraction of the computational resources. In our talk, we present a technique using Wannier functions as a suitable basis and computing Coulomb matrix elements in this basis. The fully parameterized exciton Hamiltonian is then solved using a linear scaling approach that allows efficient computation of spectral quantities such as the exciton DOS for materials with hundreds of atoms per unit cell.

CPP 54.3 Thu 17:00 MER 02

New Paradigm for Gas Sensing by Two-Dimensional Materials — •UDO SCHWINGENSCHLÖGL, VASUDEO BABAR, and SITANSH SHARMA — King Abdullah University of Science and Technology (KAUST), Physical Science and Engineering Division (PSE), Thuwal 23955-6900, Saudi Arabia

The adsorption behavior and electronic transport properties of CO and NH₃ molecules on para-C₃Si and meta-C₃Si monolayers are studied using first-principles calculations and the non-equilibrium Green's function method. The adsorption sites are determined along with their adsorption energies. It turns out that CO and NH₃ molecules physisorb on both monolayers. The current-voltage characteristics show that the para-C₃Si monolayer can be used to sense CO and NH₃ gases with high sensitivity. In contrast to other two-dimensional materi-

als, the sensing mechanism is not based on charge transfer but on the presence of Dirac states and their susceptibility to symmetry-breaking structural distortions. Journal Reference: J. Phys. Chem. C 123, 13104 (2019)

CPP 54.4 Thu 17:15 MER 02

Tunable gas permeation properties through sub-nanometer porous molecular thin carbon nanomembranes — •VLADISLAV STROGANOV¹, DANIEL HÜGER¹, TABATA NOETHEL¹, CHRISTOF NEUMANN¹, MONIKA KRUK², PIOTR CYGANIK², and ANDREY TURCHANIN¹ — ¹Friedrich Schiller University Jena, Jena, Germany — ²Jagiellonian University, Kraków, Poland

Molecular thin carbon nanomembranes (CNMs) are 1 nm thick nanosheets with sub-nanometer porosity combined with high mechanical and chemical stability. These properties make them promising for the next generation of filtration and gas separation technologies. Here we investigated influence of the structure of molecular precursors on the gas permeation properties of a series of CNMs. The CNMs were synthesized from self-assembled monolayers of biphenyl substituted carboxylic acids on silver substrate $C_6H_5 - C_6H_4 - (CH_2)_n - COO|Ag$ ($n = 2 - 6$) via the electron-irradiation induced cross-linking. We study for this homologous sequence of CNMs the permeation of He, D₂ and D₂O vapors as a function of temperature. We demonstrate that even a smallest variation of the number of $-CH_2-$ units leads to a significant change in the permeation which enables the molecular design of these nanomembranes for nanofiltration.

CPP 54.5 Thu 17:30 MER 02

Vapor Adsorption on CNMs studied with Infrared Spectroscopy — •JAKOB KREIE, PETR DEMENTYEV, NEITA KHAYYA, and ARMIN GÖLZHÄUSER — Physics of Supramolecular Systems and Surfaces, Bielefeld University, Germany

Carbon nanomembranes (CNM) are made by electron induced cross-linking of aromatic self-assembled monolayers. Previous studies show that CNM enable rapid transport of water vapor. This may be related to a strong adsorption of water molecules on the CNM surface. A spectroscopic setup for infrared measurements of vapor adsorption on CNMs is designed to investigate the adsorption on the surface under realistic conditions. For this purpose, a reaction chamber in a polarization-modulation infrared reflection absorption spectroscopy (PM IRAS) is connected to a vacuum system in order to be able to control the vapor environment.

First measurements are performed with a terphenyl-4-thiol carbon nanomembrane (TPT-CNMs). The results show that even low vapor pressures of heavy water are sufficient to achieve strong adsorption on the surface of the TPT-CNMs, which indicates a large influence of the surface effects on water transport through the membrane.

CPP 55: Members' Assembly

Report of the current Speaker team Election of the second deputy speaker Award of the poster Prize of the CPP Division Miscellaneous

Time: Thursday 18:00–19:00

Location: MER 02

All members of the Chemical and Polymer Physics Division are invited to participate.

CPP 56: Focus: Self-Assembly of Plasmonic Nanostructures (joint session CPP/HL)

Organized by Tobias A. F. König and Markus Lippitz

Time: Friday 9:30–12:30

Location: GÖR 226

Invited Talk

CPP 56.1 Fri 9:30 GÖR 226

Self-assembled optical metamaterials — •ULLRICH STEINER — Adolphe Merkle Institute, Chemin des Verdiers 4, 1700 Fribourg

The self-assembly of block-copolymers gives rise to numerous 2D and 3D morphologies with characteristic pattern sizes on the 10 nm length scale. These polymer structures can be transformed into plasmonic metals to fabricate 2D metasurfaces and 3D metamaterials. These plasmonic replicas have the appropriate structure sizes for the coupling of plasmon resonances to the visible light spectrum, yielding interesting optical materials.

This presentation will review recent progress in manufacturing and studying these materials and highlight interesting current developments.

CPP 56.2 Fri 10:00 GÖR 226

In Situ Monitoring of Self-Assembly and Plasmonic Shifts during the Growth of AgCu Alloy Nanostructures — •MATTHIAS SCHWARTZKOPF¹, ANDRÉ ROTHKIRCH¹, NIKO CARSTENS², THOMAS STRUNKUS², FRANZISKA C. LÖHRER³, SENLIN XIA³, VOLKER KÖRSTGENS³, PETER MÜLLER-BUSCHBAUM^{3,4}, FRANZ FAUPEL², and STEPHAN V. ROTH^{1,5} — ¹DESY, Notkestr. 85, D-22607 Hamburg — ²CAU zu Kiel, Kaiserstr.2, 24143 Kiel — ³TUM, James-Franck-Str. 1, D-85748 Garching — ⁴MLZ, Lichtenbergstr. 1, D-85748 Garching — ⁵KTH, Teknikringen 56-58, SE-100 44 Stockholm

While magnetron sputtering is a versatile routine method in industry for the deposition of large area metal and alloy coatings, it can be also used for the preparation of functional nanocomposites with e.g. adjustable optical properties [1]. We investigated in real-time the formation of supported silver, copper, and silver-copper-alloy nanoclusters during sputter deposition on poly(methyl methacrylate) by combining in situ surface-sensitive X-ray scattering with optical spectroscopy [2]. While following the transient growth morphologies, we quantify the early stages of phase separation at the nanoscale, track the shifts of surface plasmon resonances, and quantify the growth kinetics of the nanogranular layers at different thresholds. We are able to extract the influence of scaling effects on the nucleation and phase selection and demonstrate a route to tailor accurately the plasmon resonances of nanosized, polymer-supported clusters. [1] Faupel et al., Adv. Eng. Mater. 2010, 12, 12, 1177-1190. [2] Schwartzkopf et al., ACS Appl. Nano Mater. 2022, 5, 3, 3832-3842.

CPP 56.3 Fri 10:15 GÖR 226

What happens to bovine serum albumin in-between two gold nanoparticles and how this biomolecule defines the plasmonic effect? — NINA TVERDOKHLEB, •OLGA GUSKOVA, ZIWEI ZHOU, HOLGER MERLITZ, and VLADYSLAV SAVCHENKO — Leibniz-Institut für Polymerforschung Dresden e. V.

In experiments, spherical gold nanoparticles (NPs) covered by bovine serum albumin (BSA) create 1D Au-BSA nanoarrays on a polymer film. The external mechanical strain applied to the film leads to plasmon-coupled circular dichroism (PCCD) enhancement. To explain this phenomenon, we perform all-atom MD simulations of plasmonic nanostructures, representing BSA in-between two gold NPs. The following steps were undertaken: (1) BSA was adsorbed on the gold wall (a model of NP) in implicit water with optimization of its geometry; (2) the second mobile gold wall was approaching adsorbed protein until the distance between NPs reaches the experimentally measured value; (3) mimicking mechanical stretching mentioned above, an external tensile force applied on the second wall has induced the backbone stretching of the initially compressed BSA. This process is accompanied by the crucial growth of BSA dipole moment along the directional deformation, restructuring of the protein secondary structure from helices to coils upon compression (2), the reorientation of the charged amino-acid residues, and subsequent partial back-folding of the secondary structure elements upon stretching (3). We correlate an observed plasmonic effect in the 1D Au-BSA arrays to the changes in dipole moment and chirality of BSA.

CPP 56.4 Fri 10:30 GÖR 226

Uniform and sensitive Raman signal by self-assembled plasmonic nanoparticle gratings — •SEZER SEÇKIN¹ and TOBIAS A. F. KÖNIG^{1,2} — ¹Leibniz-Institut für Polymerforschung e.V., Hohe Straße 6, 01069 Dresden — ²Center for Advancing Electronics Dresden (cfaed), Technische Universität Dresden, 01062 Dresden

Despite recent advancements in this field, it is still challenging to manufacture SERS substrates that provide high sensitivity and uniformity over large areas. One can overcome this challenge by employing a colloidal approach such as directed self-assembly of plasmonic nanoparticles into ordered structures [König et al. Advanced Functional Materials 31.36 (2021): 2105054]. Here, we have produced highly ordered 1D plasmonic lattice structures by assembling nanoparticles of various sizes. With the help of the low optical loss of colloidal gratings, we studied the enhancement capabilities of the SERS substrates by the excitation of a fluorescent reporter Rhodamine 6G, at different wavelengths. We conducted the

polarization-dependent SERS enhancement by exciting colloidal gratings parallel and perpendicular to the polarization of the excitation lasers. Moreover, we studied the effect of the surface plasmon modes on the SERS enhancement at different orientations using the FDTD simulation. The mapping technique visually interpreted the SERS performances of other substrates, which supports the reproducibility and uniformity of the Raman signals over larger areas. Controlling the particle size while keeping the periodicity constant allows us to tune the SERS enhancement factor, which can be helpful for various sensing applications.

CPP 56.5 Fri 10:45 GÖR 226

Investigating Charge Transfers in Colloidal Photonic Crystal Slabs — •SWAGATO SARKAR¹ and TOBIAS A. F. KÖNIG^{1,2} — ¹Leibniz-Institut für Polymerforschung Dresden e.V., Institute of Physical Chemistry, Hohe Str. 6, 01069 Dresden, Germany — ²Center for Advancing Electronics Dresden (cfaed), Technische Universität Dresden, Helmholtzstraße 18, 01069 Dresden

The challenges of large-scale and low-loss plasmonic charge transfers are systematically investigated by optical designs with colloidal 1D plasmonic lattice structures. These plasmonic lattices are used as couplers to confine the incident energy into the underlying titanium dioxide layers, thus acting as colloidal photonic crystal (cPhC) slabs. Conventionally, photodetection is possible at energy levels close to the semiconductor bandgap; however, with the observed plasmonic-photonic hybrid modes, the extended solar spectrum can be used for energy harvesting. The photo-amplified current is measured locally with simple two-point contact on the centimeter-sized nanostructure by applying a bias voltage. The optical concepts for metallic grating composed of nanobars are extended for the first time to colloidal self-assembled gold nanoparticle (AuNP) chains to make large-scale charge injection accessible at a reasonable cost. Further, the possibility of photodetection by electric field vectors lying both along and perpendicular to the grating lines can be achieved by tuning the plasmonic grating periodicities.

CPP 56.6 Fri 11:00 GÖR 226

Self-assembled plasmonic metasurfaces for sensing and photocatalysis — •OLHA AFTENIEVA¹ and TOBIAS A.F. KÖNIG^{1,2} — ¹Leibniz-Institute for Polymer Research Dresden, Hohe Straße 6, 01169 Dresden, Germany — ²Center for Advancing Electronics Dresden (cfaed), Technische Universität Dresden, 01062 Dresden, Germany

Self-assembly of colloids allows for robust and tunable manufacturing over centimeter-scaled areas. Here we present the soft lithographic approach for creating plasmonic lattices and demonstrate their usage for sensing applications and photocatalysis. First, a particular case of collective out-of-plane resonant coupling is considered. Such resonances are excited solely under oblique illumination with transverse magnetic polarization and provide field enhancement in the area above the metasurface that is easily accessible to an analyte and is par-

ticularly sensitive to the changes in the refractive index. On the other hand, we realize imprinting of such periodic plasmonic lattices on functional substrates, including glass, silicon wafers, carbon, gold, semiconductor, or polymer thin films, illustrating the versatility of the colloidal approach. In particular, the combination of titanium dioxide thin waveguiding layers and plasmonic metasurface gives rise to narrow-bandwidth guided plasmon-polariton modes. Moreover, it induces the generation of hot charge carriers and enhances photocatalytic processes. Thus, colloidal self-assembly of plasmonic metasurfaces presents an application-oriented approach that is of potential use for optical sensors, photonic circuit applications, or hybrid device manufacturing.

15 min. break

CPP 56.7 Fri 11:30 GÖR 226

Simulating quantum systems with plasmonic waveguide arrays — •STEFAN LINDEN — Physikalisches Institut, Universität Bonn, 53115 Bonn

Coupled waveguides provide a powerful platform to simulate the evolution of quantum mechanical tight-binding systems in a classical wave environment. The basis for this is the mathematical equivalence between the time-dependent Schrödinger equation and the paraxial Helmholtz equation. In this presentation, we report on the observation of the Wannier-Stark ladder and Bloch oscillations in arrays of plasmonic waveguides with a propagation constant gradient acting as an effective external potential. Moreover, we show that Floquet engineering is a powerful method to tailor the topological properties of plasmonic waveguide arrays. In this context, we demonstrate that time-periodic modulation of dissipation can restore transport quantization in fast Thouless pumps and report on the observation of the anomalous Floquet topological π -mode at optical frequencies.

CPP 56.8 Fri 12:00 GÖR 226

single molecule detection on a smartphone microscope enabled by DNA origami biosensors — •PHILIP TINNEFELD — Department of Chemistry and Center for NanoScience, Ludwig-Maximilians-Universität München, Bute-
nandtstr. 5-13, 81377 München, Germany

DNA nanotechnology and especially the DNA origami technique allow well-defined assembly of optically active components and sensing units for novel biosensing approaches. We here demonstrate single-molecule detection on a battery driven smartphone microscope enabled by fluorescence enhancement with DNA origami nanoantennas. As further examples, we show DNA origami membrane sensors for curvature and membrane potentials. Finally, DNA origamis are used for a novel superresolution approach combining graphene energy transfer, pMINIFLUX and DNA PAINT that enables nanometric 3D superresolution close to the coverslip.

CPP 57: Complex Fluids and Colloids, Micelles and Vesicles II (joint session CPP/DY)

Time: Friday 9:30–13:00

Location: MER 02

CPP 57.1 Fri 9:30 MER 02

Chiral transport of active and passive colloids — •ANKE LINDNER¹, ANDREAS ZÖTTL², OLIVIA DU ROURE¹, ERIC CLEMENT¹, FRANCESCA TESSER¹, and GUANGYING JING³ — ¹PMMH-ESPCI, 10, rue Vauquelin, 75011 Paris, France — ²Faculty of Physics, University of Vienna, Kolingasse 14-16, 1090 Wien, Austria — ³School of Physics, Northwest University, Xi'an, 710127, China

Chirality-induced effects are at the origin of bacterial rheotaxis and particle drift in shear flows. Here we investigate such effects using a combination between experiments and theoretical modeling for two systems: E-coli bacteria and 3D printed micro-particles.

The micro-particles consist of a spherical head and a helical tail of different pitch and handedness. We investigate the chirality-induced reorientation dynamics using microfluidics and observe asymmetric orientation bistability perpendicular to the flow direction. We quantitatively explain our findings through a theoretical model without adjustable parameters considering particle elongation, chirality and head-heaviness, in very good agreement with experiments.

We then present a study of the transport of motile bacteria in shear flows. Experimentally, we obtain with high accuracy and for a large range of flow rates, the spatially resolved velocity and orientation distributions. They are in excellent agreement with the simulations of a kinematic model accounting for stochastic and microhydrodynamic properties and flagella chirality. In contrast to the micro-printed particles Brownian rotational noise plays a crucial role in bacterial rheotactic drift.

CPP 57.2 Fri 10:00 MER 02

Active and driven colloids interacting with vesicles — •ANTONIO STROCCO, VAIBHAV SHARMA, FLORENT FESSLER, and CARLOS MARQUES — Institut Charles Sadron, CNRS University of Strasbourg

When a colloid is close to a lipid giant vesicle, the interaction between the Brownian particle and the fluctuating soft membrane affects not only the particle motion but also the membrane properties. The membrane may change its shape to accommodate the particle and partial or complete engulfment may occur as a function of the energy of adhesion, membrane tension and bending. Furthermore, the interaction between a micrometric solid particle and a giant vesicle membrane may lead to complex dynamics when the system is driven out of equilibrium. Here, we report our efforts with self-propelled Janus colloids and with bare colloids under optical trapping to mimic complex dynamics such as particle endocytosis, the motion of a self-propelled particle confined to a spherical membrane, or the physics of particle engulfment by a membrane. In a wide range of experimental conditions, we have observed that a self-propelled Janus colloid is able to perform orbital motion around a giant vesicle remaining in a non-engulfment state. Still, the active particle is able to impart a force of the order of 0.01 pN on the vesicle, which is however too small to trigger particle engulfment. By applying external forces in the 1-100 pN range, we were able to observe engulfment of bare and Janus colloids by a giant vesicle.

CPP 57.3 Fri 10:15 MER 02

Universal Casimir interaction and its relevance for colloidal and biophysical systems — •TANJA SCHÖGER¹, BENJAMIN SPRENG², GERT-LUDWIG INGOLD¹, PAULO A. MAIA NETO³, and SERGE REYNAUD⁴ — ¹Universität Augsburg, Germany — ²University of California at Davis, USA — ³Universidade Federal do Rio de Janeiro, Brazil — ⁴Laboratoire Kastler Brossel, France

Colloidal systems and biophysical interfaces involve electrolytic environments where the Debye screening is extremely efficient. Therefore, it was thought that the interaction induced by electromagnetic fluctuations could not give rise to long-range forces in such systems. It has now been shown and experimentally

verified [1] that the contribution to the Casimir force or retarded van der Waals force induced by low-frequency transverse magnetic fluctuations is not screened. There thus exists a contribution to the long-range interaction between two objects in an electrolyte two orders of magnitude larger than previously thought at distances as small as one hundred nanometres.

For two dielectric microspheres in salted water at room temperature, the force becomes universal for sufficiently large distances, in that it depends solely on the geometrical parameters and not on dielectric functions. While in general, a significant numerical effort is required to determine the Casimir interaction [2], we have also derived approximate simple expressions [3] accurate enough for most practical applications. - [1] L. B. Pires et al., *Phys. Rev. Res.* 3 033037, (2021); [2] B. Spreng et al. *J. Chem. Phys.* 153, 024115 (2020); [3] T. Schoger et al., *Phys. Rev. Lett.* 128, 230602 (2022)

CPP 57.4 Fri 10:30 MER 02

Interparticle forces between real cement surfaces across aqueous and non-aqueous solvents — •SIMON BECKER and REGINE VON KLITZING — Soft Matter at Interfaces, TU Darmstadt, 64289 Darmstadt, Germany

Concrete and cement are highly abundant construction materials. Therefore, their flow behavior in early stages of processing is of great interest. By using chemical admixtures such as superplasticizers (e.g. polycarboxylate ethers - PCEs) their rheological performance can be enhanced. The rheology is governed by the forces between the particles and the forces between particles and the liquid phase.

The aim of this work is to map the force between cement surfaces across an electrolyte via colloidal probe atomic force microscopy (CP-AFM). Since cement hydrates in aqueous solutions the surface changes with time. The challenge is to disentangle different effects like hydration and roughness of the cement surfaces on the interaction. To prevent hydration of the cement the force measurements are conducted in ethanol solutions. For comparison the force measurements are carried out between two silica particles, between cement and silica as well as between cement and cement.

Furthermore, the time dependence of the cement surface due to hydration in water is mapped using tapping mode AFM. Moreover, the hydration time dependent interparticle force between cement surfaces is investigated in aqueous electrolyte solution with and without PCE to approach application related conditions.

CPP 57.5 Fri 10:45 MER 02

Structure and interaction of surface charged polymeric micelles — LINGSAM TEA, LUTZ WILLNER, •JÖRG STELLBRINK, and STEPHAN FÖRSTER — JCN-1, Forschungszentrum Jülich, 52425 Jülich, Germany

Soft colloids are ubiquitous in synthetic and biological matter and display macroscopically interesting structural and dynamical properties resulting from its hybrid microscopic structure. We established micelles formed by amphiphilic block copolymers as an easy and elegant model system to tailor colloidal softness [1].

In the present work, we introduce surface charges on n-alkyl-PEO-OH micelles resulting in electrostatic interactions in addition to the inherently present steric repulsion. These charges are precisely implemented by oxidation of only the terminal hydroxy group of the PEO block into a carboxy group. We studied intra- and interparticle structure by SANS over a broad range of concentrations, pH and ionic strength and demonstrate that the micellar form factor remains the same independent of the number of charges. However, in contrast to neutral micelles, the charged micelles typically reveal structure factor contributions even at very dilute concentration, arising from the here dominating long-range electrostatic repulsion. Structure factors in the liquid state are analyzed using competing effective interaction potentials. By increasing the concentration a liquid to crystal transition is observed for all systems, but for charged micelles at a much lower concentration compared to the uncharged micelles.

[1] S. Gupta et al., *Nanoscale*, 7 (2015) 13924.

CPP 57.6 Fri 11:00 MER 02

Structure and dynamics of concentrated suspensions of PMMA-PDMS core-shell particles — •JOEL DIAZ MAIER, PAUL TÜMMLER, and JOACHIM WAGNER — Institut für Chemie, Universität Rostock, 18051 Rostock, Germany

Sterically stabilized polymer particles with silicone based stabilizers find increasing interest as a novel colloidal model system with hard-sphere interactions. In this contribution, the largely unknown behavior of concentrated suspensions of PMMA-PDMS core-shell particles was investigated over a wide range of volume fractions employing static and dynamic light scattering experiments. Static structure factors extracted from scattered intensities are analyzed using integral equation theory. The wavevector-dependent short-time diffusion of the systems can be accurately described using $\delta\gamma$ -expansion, based on interpolated experimental structure factors as a direct input. All investigated structural and dynamical properties closely follow theoretical predictions for hard-sphere systems, proving the suitability of these colloidal particles as an easily accessible model system for hard spheres.

15 min. break

CPP 57.7 Fri 11:30 MER 02

Inverse ISAsomes in biocompatible oils - formulation and characterisation — •FLORIAN TRUMMER¹, OTTO GLATTER², and ANGELA CHEMELLI² — ¹Universität Stuttgart, Institut für Physikalische Chemie, Pfaffenwaldring 55, 70569 Stuttgart, Deutschland — ²Technische Universität Graz, Institut für Anorganische Chemie, Stremayrgasse 9, 8010 Graz, Österreich

In contrast to their more common counterparts in aqueous solutions, inverse ISAsomes (internally self-assembled somes/particles) are formulated as kinetically stabilised dispersions of hydrophilic, lyotropic liquid-crystalline phases in non-polar oils. This contribution reports on their formation in bio-compatible oils and their structural characterisation with Small Angle X-Ray Scattering (SAXS), Dynamic Light Scattering (DLS) and optical microscopy [1]. By using these methods, we were able to demonstrate the presence of inverse hexosomes, inverse micellar cubosomes (Fd3m) and an inverse emulsified microemulsion in squalane with a polyethylene glycol (PEG) alkyl ether as the primary surfactant forming the internal self-assembled phase, which was stabilised by hydrophobised silica nanoparticles. Furthermore, an emulsified L_1 -phase and inverse hexosomes were formed in triolein with the triblock-copolymer Pluronic P94 as the primary surfactant. In this case, stabilisation was achieved with a molecular stabiliser of type PEG-dipolyhydroxystearate. Finally, triolein was replaced with olive oil which also led to the successful formation of inverse hexosomes.

[1] Trummer, F., Glatter, O. & Chemelli, A. *Nanomaterials* 12, 1133 (2022)

CPP 57.8 Fri 11:45 MER 02

Anomalous Screening Behavior of Nanometer-Sized Ions — •THOMAS TILGER and REGINE VON KLITZING — Department of Physics, Technische Universität Darmstadt, Darmstadt, 64289, Germany

Natural colloidal dispersions have accompanied mankind in the form of blood or milk ever since. Besides this, artificial systems have gained a significant importance for our daily life during the last decades.

Therefore, it is of special interest to gain an understanding of which interparticle forces govern the stability of colloidal dispersions and how this stability can be tailored. The DLVO theory is a powerful framework to describe these interactions. While this description provides a good agreement with experimental data for small 1:1 electrolytes, larger deviations emerge for ions of higher valency and of larger dimensions. For a detailed examination of these border cases, we directly measure the forces between colloidal silica particles in aqueous electrolyte solutions containing nanometer-sized ions by the colloidal probe AFM (atomic force microscopy) technique.

Two different types of nano-ions were chosen as model systems, Keggin ions (silicotungstic acid, STA, a 1:4 system) and Terpyridine-Nickel-complexes with variable charge. Their electrostatic screening behavior reveals significant deviations between the calculated and measured ionic strengths, which indicates some unexpected phenomena.

CPP 57.9 Fri 12:00 MER 02

Charged, screened-charged and hard-sphere fluids studied by confocal microscopy, analytical theory and simulation. — SAHANA KALE, MARTIN OETTEL, and •HANS JOACHIM SCHÖPE — Universität Tübingen, Institut für angewandte Physik, Auf der Morgenstelle 10, 72076 Tübingen

We present a joint experimental and theoretical study investigating the fluid structure in direct and reciprocal space of PMMA particles dispersed in various solvents. Using decaline and CHB alone the structure can be well-described using PB-RMSA-Theory for monodisperse systems. Upon adding TBAB we observe that the surface charge can't be screened entirely. To model the fluid structure we use Monte Carlo simulations for a polydisperse hard core Yukawa System. Thus we get meaningful data for the effective charge and salt concentration. The results indicate behavior that is significantly different from HS. Surprisingly the situation is fundamentally different for particles dispersed in a mixture of decaline and TCE. Here all measured observables follow polydisperse Percus-Yevick theory.

CPP 57.10 Fri 12:15 MER 02

Bicontinuous Microemulsion in Porous Materials — •MARGARETHE DAHL¹, RENÉ HAVERKAMP², LARISSA DOLL¹, THOMAS HELLEWEG², and STEFAN WELLERT¹ — ¹Institut für Chemie, Technische Universität Berlin, Germany — ²Physikalische und Biophysikalische Chemie, Universität Bielefeld, Germany

While the bulk phase behavior of microemulsions has been intensively studied, the influence of a geometrical confinement has been widely neglected. Understanding the influence of geometrical restrictions yields both, fundamental insights and importance for applications, e.g. decontamination and enhanced oil recovery. In our study, controlled-pore silica glasses (CPGs) serve as confining matrices for bicontinuous microemulsions. Effects of the pore network and surface chemistry on phase behavior and structure of a model microemulsion are studied by using various CPGs with pore diameter between 75 – 1000 Å and ternary bicontinuous microemulsions (water/octane/ $C_{10}E_4$). The naturally hydrophilic surfaces of the CPGs were hydrophobically modified to analyze the

influence of the surface polarity. We use imaging techniques (cryo-SEM), small angle scattering (SANS, SAXS) with measurements of the advancing contact angles inside the hydrophilic and hydrophobically modified pores (Washburn approach) to explore the microemulsion phase structure in bulk and inside the pores. In this talk, the results of these combined experiments will be presented and discussed.

CPP 57.11 Fri 12:30 MER 02

Diffusion and thermodiffusion of polymers in mixed solvents — •DANIEL SOMMERMANN, JANNIK KANTELHARDT, and WERNER KÖHLER — Physikalisches Institut, Universität Bayreuth, Germany

We present experiments on diffusion and thermodiffusion of polymers in mixed solvents. So far, most works on thermodiffusion have dealt with binary systems or ternary mixtures of small molecules. Binary samples with polymers in solvents have been studied over both a broad concentration and polymer molar mass range. Only a few very recent experiments measured polymers in a binary solvent. In this work, samples made of polystyrene ($M_w = 4880 \text{ g/mol}$), toluene and cyclohexane have been analysed using multi-color optical beam deflection (OBD) and supporting single-color thermal diffusion forced Rayleigh scattering (TDFRS). While binary mixtures are readily characterized by one diffusion and one thermodiffusion coefficient, the number of coefficients increases to four plus two for ternaries. The measured signals show three well separated modes that can be assigned to the thermal diffusivity and the two eigenvalues of the mass diffusion matrix. We are particularly interested in the question, to what extent the dynamics of the large entity, the polymer, is coupled to the solvent-

solvent dynamics, both with respect to diffusion and thermodiffusion. A first analysis supports the picture of an effective solvent whose internal dynamics is decoupled from the one of the polymer.

CPP 57.12 Fri 12:45 MER 02

Dynamic susceptibility of magnetic nanoplatelet suspensions — •MARGARET ROSENBERG¹, SOFIA S. KANTOROVICH¹, and PHILIP J. CAMP² — ¹Department of Physics, University of Vienna, Vienna, 1090, Austria — ²School of Chemistry, The University of Edinburgh, David Brewster Road, Edinburgh EH9 3FJ, UK

Particle anisometry and anisotropy provide valuable control parameters to alter the self-assembly, and thermodynamic, rheological, and phase behaviour, of colloidal suspensions. This work is concerned with the dynamic magnetic susceptibility (DMS) of a ferrofluid with platelet-shaped anisotropic particles, which have a fixed out-of-plane dipole moment providing additional, magnetic anisometry. Such a colloidal suspensions is of particular interest as, above a threshold concentration, it exhibits a ferromagnetic nematic phase. Recent experimental work [1] has shown that the DMS spectrum exhibits multiple dynamical modes, suggesting that there might be clusters of particles with distinct rotational timescales. Using Brownian dynamics simulations, we explore the effects of varying nanoparticle concentration - and therefore microstructure - on the DMS, and explain the gap in relaxation times, and changes in the spectrum, that are observed experimentally.

[1] M. Küster et al., "Magnetic dynamics in suspensions of ferrimagnetic platelets", *Journal of Molecular Liquids*, Vol. 360, (2022), 119484

CPP 58: Polymer Networks and Elastomers

Time: Friday 9:30–11:30

Location: ZEU 255

Invited Talk

CPP 58.1 Fri 9:30 ZEU 255

Studies of polymer thermosets using scattering techniques — •MATS JOHANSSON — Department of Fibre & Polymer Technology, KTH Royal Institute of Technology, SE-100 44 Stockholm, Sweden

Thermoset polymers are complex macromolecular structures where the macroscopic properties depend on several different structural features such as crosslink density, rigidity on a molecular level, and internal secondary bond interactions. The final thermoset structure not only depend on the in-going monomers structure but also how these form the network i.e. the polymerization process. The presentation will describe how a combination of scattering techniques and traditional physical and chemical characterization techniques can reveal new insights on the structure / property relationship for thermoset polymers. It is moreover demonstrated that this approach also can be used to monitor the network formation in-situ i.e. how the structures evolves on a nanoscale during polymerization.

CPP 58.2 Fri 10:00 ZEU 255

Effect of π - π stacking interactions on mechanical properties of lignin-based thermosetting resins — •IULIANA RIBCA¹, BENEDIKT SOCHOR², MARIE BETKER^{1,2}, STEPHAN V. ROTH^{1,2}, MARTIN LAWOKO¹, MICHAEL A. R. MEIER^{3,4}, and MATS JOHANSSON¹ — ¹Department of Fibre and Polymer Technology, KTH Royal Institute of Technology, Stockholm, Sweden — ²Deutsches-Elektronen Synchrotron (DESY), Hamburg, Germany — ³Institute of Organic Chemistry (IOC), Materialwissenschaftliches Zentrum MZE, Karlsruhe Institute of Technology (KIT), Karlsruhe, Germany — ⁴Institute of Biological and Chemical Systems-Functional Molecular Systems (IBCS-FMS), Karlsruhe Institute of Technology (KIT), Eggenstein-Leopoldshafen, Germany

The transition towards a more sustainable global carbon economy can be achieved by replacing petroleum-based materials with bio-based alternatives. Lignin is the most abundant aromatic resource in nature and a largely unused by-product of the pulp and paper industry. It is considered a good replacement for fossil-based aromatics. One promising strategy for lignin valorization is to produce thermosetting resins. Further applications of these resins require the understanding of their physicochemical properties. An important role on these properties are playing π - π stacking interactions. Different configurations of π - π stacking interactions are favored between the lignin chains, due to the presence of aromatic rings. In this study, it was investigated the effect of π - π stacking interactions on mechanical properties of lignin-based thermosets by small and wide-angle X-ray scattering methods.

CPP 58.3 Fri 10:15 ZEU 255

Strain hardening of hydrogenated acrylonitrile butadiene rubber — •CHRISTOPH GÖGELEIN¹ and MARJAN HEMSTEDE - VAN URK² — ¹Arlanxco Deutschland GmbH, Kaiser-Wilhelm-Allee 40, 51369 Leverkusen — ²Arlanxco Netherlands B.V., Urmonderbaan 24, 6167 RD Geleen, The Netherlands
Therban hydrogenated acrylonitrile butadiene rubber (HNBR) is a specialty elastomer used in the automotive and oil and gas markets. It is well known that HNBR with acrylonitrile (ACN) contents above 39 wt% shows strain-induced

crystallization (SIC), caused by the crystallization of alternating ethylene-ACN units (Obrecht, 1986). For HNBR polymers with ACN contents lower than 36 wt%, crystallization occurs in longer ethylene units derived from hydrogenated butadiene sequences (Uschold & Finlay, 1974). Besides these well-established findings, there is an ongoing debate up to which temperature SIC occurs for HNBR (Narynbek Ulu, et al., 2017) (Shaw, 2019). Therefore, crystallization of the polymers was studied, using regular and isothermal differential scanning calorimetry at varying storage times. Furthermore, we investigated strain hardening behavior of HNBR networks with varying ACN contents from room temperature (RT) up to 100 °C, as well as at varying crosslink densities and filler loadings. Our results show that there is a significant strain hardening behavior for HNBR vulcanizates with high ACN content, i.e. for > 39 wt% ACN content. The effect is still observed at 60 °C, but not at 80 °C. Surprisingly, strain hardening doesn't enhance the fatigue lifetime for the samples under investigation.

CPP 58.4 Fri 10:30 ZEU 255

From Cellulose Model Surfaces to Elastic Papers — •CASSIA LUX, SABRINA KERZ, and REGINE VON KLITZING — Department of Physics, Technische Universität Darmstadt, Darmstadt, 64289, Germany

Paper is a hierarchical material based on cellulose which allows functionalization on different length scales. The resulting multilateral use is especially crucial with regard to reducing plastic use and waste and replacing it with renewable and biodegradable resources. A novelty in terms of mechanical robustness and controllable fluid mechanics are elastic papers, prepared through the functionalization of the paper fibers with elastomeric particles that concentrate at the fiber-fiber-crossing points. In order to study the particle adsorption, planar cellulose model surfaces are prepared to mimic the surface of a cellulose fiber. The elastomeric core shell particles have a pH-responsive polycation shell, and their adsorption to the negative charged cellulose surface is studied in dependence of e.g. pH-value. The question we address is how the properties of the cellulose surface and the particles affect the contact area between both, and what effect the adsorption has on the elastic behavior of the particles. A special focus is to resolve the core-shell structure of the particles by Indentation AFM.

CPP 58.5 Fri 10:45 ZEU 255

Structure, phase behavior and mechanical properties of the surface of amphiphilic co-polymer networks — •KEVIN HAGMANN¹, NORA FRIBICZER², SEBASTIAN SEIFFERT², CAROLIN BUNK³, FRANK BÖHME³, and REGINE VON KLITZING¹ — ¹Institute for Condensed Matter Physics, Technische Universität Darmstadt, D-64289 Darmstadt — ²Department of Chemistry, Johannes Gutenberg University Mainz, D-55128 Mainz — ³Leibniz-Institut für Polymerforschung Dresden e.V., D-01069 Dresden

The underlying study focuses on the structure, phase separation and mechanics of the surface of amphiphilic co-polymer networks (ACNs).[1] The amphiphilic networks are synthesized from tetrameric star-shaped polymers, combining tetra-poly(ethylene glycol) (hydrophilic) and tetra-poly(ϵ -caprolactone) (hydrophobic) to form a 3D gel network. The topology and near surface struc-

ture of the networks are studied with atomic force microscopy (AFM). We put special emphasis on AFM phase imaging under various solvent conditions to identify nanophase separation at the interface. Additionally, we like to present the relation between surface structure and swelling and the resulting mechanical and rheological properties laterally and orthogonally to the gel surface of ACNs. In order to evaluate heterogeneities and phase separation, the mechanical and rheological behavior at the interface of the ACNs will be presented on various length scales (nm - μm). The study shows that the environmental conditions have a strong effect on the gel structure and on nano/microrheological properties. [1] Haggmann et al.; *Polymers* 2022.

CPP 58.6 Fri 11:00 ZEU 255

A mean field model for reversible networks made of star polymers — •MICHAEL LANG¹, KIRAN SURESH KUMAR^{1,2}, and JENS-UWE SOMMER^{1,2} — ¹Leibniz-Institut für Polymerforschung Dresden, Institut Theorie der Polymere, Hohe Straße 6, 01069 Dresden, Germany — ²Institut für Theoretische Physik, Technische Universität Dresden, Zellescher Weg 17, 01069 Dresden, Germany We extend our recent approach [1] for linear equilibrium polymers with cyclization towards reversible networks made of star polymers. These model systems are particularly suited to test generalizations of the theory that account for the formation of cyclic network defects. Monte-Carlo simulation data and our mean field model demonstrate that the lack of pending loops in networks made by a hetero-complementary coupling of the stars leads to a pronounced shift of the position of the gel point of conventional networks towards lower concentrations. Larger cyclic structures in the networks, on the contrary, can develop a stabilizing effect on the network structure and can cause a reduction of the critical

concentration for gelation for a suitable set of system parameters. Remarkably, this leads then to the opposite effect of finite loops as known for conventional irreversible gels.

[1] Lang, M.; Kumar, K. S. *Macromolecules* 54 (2021) 7021, 10.1021/acs.macromol.1c00718.

CPP 58.7 Fri 11:15 ZEU 255

Thermal Conductivity of Semicrystalline Polymer Networks: Crystallinity or Cross-Linking? — •MANOJ KUMAR MAURYA¹, JAMES WU², MANJESH KUMAR SINGH¹, and DEBASHISH MUKHERJI² — ¹Department of Mechanical Engineering, Indian Institute of Technology Kanpur, Kanpur, UP 208016, India — ²Quantum Matter Institute, University of British Columbia, Vancouver, BC V6T 1Z4, Canada

Understanding the heat flow in polymers is at the onset of many developments in designing advanced functional materials. Here, however, amorphous linear polymers usually exhibit a very low thermal conductivity κ , often hindering their broad applications. In this context, two common routes to increase κ are via semicrystallinity and cross-linking. It can therefore be inferred that the combination of these two effects may result in a further increase of κ with respect to the systems where only one of these two effects is important. Using molecular dynamics simulations, we investigate κ in semicrystalline polymer networks. Contrary to a prior understanding, we show that a combination of cross-linking and crystallinity does not always increase κ . Instead, a delicate competition between the lattice periodicity, the cross-linker types, and the bond density dictates the tunability of κ in these complex macromolecular systems. These results are also compared with the existing experiments.

CPP 59: Active Matter V (joint session BP/CPP/DY)

Time: Friday 9:30–12:00

Location: TOE 317

See BP 30 for details of this session.

CPP 60: Closing Plenary Talk (joint session BP/CPP)

Time: Friday 12:15–13:00

Location: HSZ 03

See BP 32 for details of this session.

Thin Films Division Fachverband Dünne Schichten (DS)

Stefan Krischok
Technische Universität Ilmenau
Weimarer Straße 32
98693 Ilmenau
stefan.krischok@tu-ilmenau.de

Overview of Invited Talks and Sessions

(Lecture halls SCH A 315 and SCH A 316; Poster P3)

Gaede Prize Talk

PRV II Wed 13:15–13:45 HSZ 01 **Towards chemical and optical band structure engineering in molecular-based heterostructures** — •BENJAMIN STADTMUELLER

Invited Talks

DS 5.1	Tue	9:30–10:00	SCH A 316	<i>Operando</i> infrared studies of confined water and protons in MXene — •MAILIS LOUNASVUORI
DS 9.1	Wed	9:30–10:00	SCH A 316	Flüssigphasen-Elektrochemie im Ultrahochvakuum unter XPS-Kontrolle — •FRANK ENDRES
DS 13.1	Thu	9:30–10:00	SCH A 316	Towards Catalytic Applications of Infrared Laser Polarimetry — •ANDREAS FURCHNER, KARSTEN HINRICHS
DS 15.1	Thu	11:15–11:45	SCH A 316	In-Situ Optical Investigation of Electrochemically Induced Conformational Changes at Solid Liquid Interfaces: A Source of new Electronic States — •CHRISTOPH COBET
DS 17.1	Thu	16:15–16:45	SCH A 316	In-situ optical spectroscopy on electrochemical interfaces: From OER electrocatalysts to "smart" electro-switchable interfaces — •MARTIN RABE
DS 17.2	Thu	16:45–17:15	SCH A 316	The physics of low symmetry semiconductors: Gallium oxide for the future of green energy as example — •MATHIAS SCHUBERT
DS 17.3	Thu	17:15–17:45	SCH A 316	Spectroscopic ellipsometry studies of optical constants in highly excited semiconductors — •STEFAN ZOLLNER

Invited Talks of the joint Symposium SKM Dissertation Prize 2023 (SYSD)

See SYSD for the full program of the symposium.

SYSD 1.1	Mon	9:30–10:00	HSZ 04	Diffusion of antibodies in solution: from individual proteins to phase separation domains — •ANITA GIRELLI
SYSD 1.2	Mon	10:00–10:30	HSZ 04	Intermediate Filament Mechanics Across Scales — •ANNA V. SCHEPERS
SYSD 1.3	Mon	10:30–11:00	HSZ 04	Ultrafast Probing and Coherent Vibrational Control of a Surface Structural Phase Transition — •JAN GERRIT HORSTMANN
SYSD 1.4	Mon	11:00–11:30	HSZ 04	Electro-active metasurfaces employing metal-to-insulator phase transitions — •JULIAN KARST
SYSD 1.5	Mon	11:30–12:00	HSZ 04	The role of unconventional symmetries in the dynamics of many-body systems — •PABLO SALA

Invited Talks of the joint Symposium Ultrafast Excitation Pathways of Quantum Materials (SYUE)

See SYUE for the full program of the symposium.

SYUE 1.1	Wed	9:30–10:00	HSZ 01	Dynamics and control in quantum materials using multi-terahertz spectroscopy — •RICHARD AVERITT
SYUE 1.2	Wed	10:00–10:30	HSZ 01	Accessing the nonthermal phonon populations in 2D materials with femtosecond electron diffuse scattering — •HÉLÈNE SEILER
SYUE 1.3	Wed	10:30–11:00	HSZ 01	Exciting potentials – Exploring the realms of ultrafast phase transitions — •LAURENZ RETTIG
SYUE 1.4	Wed	11:15–11:45	HSZ 01	Sub-cycle multidimensional spectroscopy of strongly correlated materials — •OLGA SMIRNOVA
SYUE 1.5	Wed	11:45–12:15	HSZ 01	Witnessing many-body entanglement in light-driven quantum materials — •MATTEO MITRANO
SYUE 1.6	Wed	12:15–12:45	HSZ 01	Optical responses of photoexcited materials: from parametric amplification to photoinduced superconductivity — •EUGENE DEMLER

Invited Talks of the joint Symposium Physics of van der Waals 2D Heterostructures (SYHS)

See SYHS for the full program of the symposium.

SYHS 1.1	Fri	9:30–10:00	HSZ 01	Novel moiré excitons and ultrafast optical dynamics in van der Waals 2D heterostructures — •STEVEN G. LOUIE
SYHS 1.2	Fri	10:00–10:30	HSZ 01	Interaction induced magnetism in 2D semiconductor moiré superlattices — •XIAODONG XU
SYHS 1.3	Fri	10:30–11:00	HSZ 01	Ions in tight places: intercalation and transport of ions in van der Waals heterostructures — •IRINA GRIGORIEVA
SYHS 1.4	Fri	11:15–11:45	HSZ 01	Spin-orbit proximity in van der Waals heterostructures — •FELIX CASANOVA
SYHS 1.5	Fri	11:45–12:15	HSZ 01	Plethora of many-body ground states in magic angle twisted bilayer graphene — •DMITRI EFETOV

Sessions

DS 1.1–1.6	Mon	9:30–11:00	SCH A 316	2D Materials and their Heterostructures I: Graphene
DS 2.1–2.5	Mon	11:30–12:45	SCH A 316	2D Materials and their Heterostructures II: h-BN and WSe₂
DS 3.1–3.5	Mon	11:30–12:45	SCH A 315	Organic Thin Films, Organic-Inorganic Interfaces (joint session DS/ CPP)
DS 4.1–4.6	Mon	15:30–17:00	SCH A 316	Thin Film Properties I
DS 5.1–5.4	Tue	9:30–10:45	SCH A 316	2D Materials and their Heterostructures III
DS 6.1–6.4	Tue	10:00–11:00	SCH A 315	Thin Film Properties II (joint session DS/KFM)
DS 7.1–7.5	Tue	11:15–12:30	SCH A 316	2D Materials and their Heterostructures IV
DS 8.1–8.5	Tue	11:30–12:45	SCH A 315	Thin Film Properties III
DS 9.1–9.3	Wed	9:30–10:30	SCH A 316	Layer Properties I
DS 10.1–10.5	Wed	11:00–12:15	SCH A 316	Layer Properties II
DS 11.1–11.5	Wed	11:00–12:15	SCH A 315	Thin Film Application
DS 12.1–12.57	Wed	17:00–19:00	P3	Poster
DS 13.1–13.5	Thu	9:30–11:00	SCH A 316	Optical Analysis of Thin Films I
DS 14.1–14.7	Thu	9:30–11:15	SCH A 315	Thin Oxides and Oxide Layers
DS 15.1–15.5	Thu	11:15–12:45	SCH A 316	Optical Analysis of Thin Films II
DS 16.1–16.6	Thu	11:30–13:00	SCH A 315	Thermoelectric and Phase Change Materials; Layer Deposition
DS 17.1–17.3	Thu	16:15–17:45	SCH A 316	Optical Analysis of Thin Films III
DS 18	Thu	18:00–19:00	SCH A 315	Members' Assembly

Members' Assembly of the Thin Films Division

Thursday 18:00–19:00 SCH A 316

Sessions

– Invited Talks, Contributed Talks, and Posters –

DS 1: 2D Materials and their Heterostructures I: Graphene

Time: Monday 9:30–11:00

Location: SCH A 316

DS 1.1 Mon 9:30 SCH A 316

Atomistic and network models for graphene based macromaterials: role of intercalation, defects and dopants — •FLORIAN FUCHS^{1,2} and JÖRG SCHUSTER^{1,2} — ¹Fraunhofer Institute for Electronic Nano Systems (ENAS), Chemnitz, Germany — ²Center for Materials, Architectures and Integration of Nanomembranes (MAIN), Chemnitz University of Technology, Chemnitz, Germany

The excellent properties of graphene can be utilized in macroscopic conductor materials if the individual flakes are decoupled from each other, for example by misalignment of the lattices or by intercalation. Such materials are promising candidates to replace metals for numerous electrical conductor applications [1].

We show the results of a network model [2,3] which relates the structural arrangement and the properties of the individual graphene flakes to the macroscopically observed electrical conductivity. By this model we assess the properties of the macromaterial as a function of relevant parameters such as flake size, packing density, the graphene flake conductivity, and the interlayer conductance.

On the flake-level, intercalation, doping, and defect healing control the conductivity of the graphene-based macromaterial. We performed density functional theory calculations of these processes. In our presentation we discuss the impact on the material quality by focussing on the in-plane and the out-of-plane conductivity.

[1] J. Schuster et al., *Nano Express* 1, 020035 (2020)

[2] J. Schuster et al., *ACS Appl. Mater. Interfaces* 10, 43008 (2018)

[3] J. Schuster et al., *Comp. Mat. Science* 161, 364 (2019)

DS 1.2 Mon 9:45 SCH A 316

Post-processing on graphene field-effect transistors by critical point drying — •HAMID REZA RASOULI¹, DAVID KAISER¹, CHRISTOF NEUMANN¹, MARTHA FREY¹, GHAZALEH ESHAGHI¹, THOMAS WEIMANN², and ANDREY TURCHANIN¹ — ¹Institute of Physical Chemistry, Friedrich Schiller University Jena, 07743 Jena, Germany — ²Physikalisch-Technische Bundesanstalt (PTB), 38116 Braunschweig, Germany

We report on a critical point drying (CPD) technique with supercritical carbon dioxide (S-CO₂) as a post-processing step to enhance electrical performance of graphene field-effect transistors (GFETs). This technique is promising for integration into the industrial clean rooms environment and demonstrates high potential not only for GFETs but also for other electronic, photonic and optoelectronic devices based on 2D materials.

DS 1.3 Mon 10:00 SCH A 316

Intercalation of indenene in SiC/graphene interface — •CEDRIC SCHMITT^{1,2}, JONAS ERHARDT^{1,2}, TIEN-LIN LEE³, TIMUR KIM³, SIMON MOSER^{1,2}, and RALPH CLAESSEN^{1,2} — ¹Physikalisches Institut, Universität Würzburg, D-97074 Würzburg, Germany — ²Würzburg-Dresden Cluster of Excellence ct.qmat, Universität Würzburg, D-97074 Würzburg, Germany — ³Diamond Light Source, Harwell Science and Innovation Campus, Didcot, UK

In the search for new quantum materials, ultrathin metals are highly interesting as they push bulk properties to the 2D limit and foster novel quantum effects. Unfortunately, unprotected metals are prone to oxidation in air, making them useless for transport devices. Here, we report about a capping method for 2D materials via metal intercalation. In this process an atomic metal monolayer is sandwiched between a SiC substrate and a graphene buffer layer, thus forming freestanding graphene, which protects the intercalated layer against oxidation. Previous intercalation studies focused mainly identifying stable allotropes but lack a detailed investigation of metal coverage and oxidation. Here, we study the intercalation of indenene, a monolayer of indium, which is a novel quantum material [1]. First experiments indicate the indenene layer to remain intact upon air exposure, indeed pointing to an effective protective function of the overlayer graphene. Furthermore, we observe an enlarged In-Si bond distance, which is expected to have a larger non-trivial energy gap.

[1] M. Bauernfeind et al. *Nat. Commun.* 12, 5396 (2021)

DS 1.4 Mon 10:15 SCH A 316

Ultrafast photo-thermoelectric currents in graphene — •XIAOYI ZHOU, NINA PETTINGER, JOHANNES GRÖBMEYER, PHILIPP ZIMMERMANN, and ALEXANDER HOLLEITNER — Walter Schottky Institut and Physics Department, Technische Universität München, Germany

Graphene as an optoelectronic material has attracted significant attention due to its interesting properties such as fast charge carrier relaxation rates, broadband optical absorption and high carrier mobilities. We apply an ultrafast on-chip pump-probe photocurrent spectroscopy to demonstrate an immediate thermoelectric photocurrent after a femtosecond laser pulse. We demonstrate that gate-tunable graphene junctions can be integrated into THz-circuits, paving the way for graphene-based ultrafast photodetectors and switches.

DS 1.5 Mon 10:30 SCH A 316

Twist angle dependent proximity induced spin-orbit-coupling in graphene/TMDC and graphene/TI heterostructures — •THOMAS NAIMER¹, KLAUS ZOLLNER¹, MARTIN GMTIRA², and JAROSLAV FABIAN¹ — ¹Institute for Theoretical Physics, University of Regensburg, 93040 Regensburg, Germany — ²Institute of Physics, Pavol Jozef Safarik University in Kosice, 04001 Kosice, Slovakia

We investigate the proximity-induced spin-orbit coupling in twisted heterostructures of graphene/transition-metal dichalcogenides (MoS₂, WS₂, MoSe₂, and WSe₂) as well as graphene/topological insulators (Bi₂Se₃ and Bi₂Te₃) from first principles. We establish that, regardless of the twist angle, the band offsets between the Dirac point and the substrate bands vary linearly with the strain, which is necessary for defining commensurate supercells. This relation allows to identify the apparent zero-strain band offsets and find a compensating transverse electric field correcting for the strain. The resulting corrected band structure is then fitted around the Dirac point to an established spin-orbit Hamiltonian, yielding the twist angle dependencies of the spin-orbit couplings. While for most structures a mix of Rashba and valley-Zeeman spin-orbit coupling is present, we also witness the emergence of Kane-Mele spin-orbit coupling in graphene/topological insulator structures at 30° twist angle. This work was funded by the Elite Network of Bavaria, the Deutsche Forschungsgemeinschaft (DFG), SFB 1277, SPP 2244 and by the European Union Horizon 2020 Research and Innovation Program under contract number 881603 (Graphene Flagship). M.G. acknowledges VEGA 1/0105/20.

DS 1.6 Mon 10:45 SCH A 316

Mobile trions in two-dimensional hybrid perovskites — JONAS DAVID ZIEGLER¹, YEONGSU CHO², •SOPHIA TERRES¹, MATAN MENAHEM³, OMER YAFFE³, TAKASHI TANIGUCHI⁴, KENJI WATANABE⁴, TIMOTHY C. BERKELBACH², and ALEXEY CHERNIKOV¹ — ¹TU Dresden, Dresden, Deutschland — ²Columbia University, New York, USA — ³Weizmann Institute of Science, Rehovot, Israel — ⁴National Institute for Materials Science, Tsukuba, Japan

Two-dimensional hybrid perovskites represent natural quantum well systems composed of alternating organic and inorganic molecular layers. They combine an efficient coupling of electrons to a soft lattice with strong Coulomb interactions between the charge carriers. The latter leads to the formation of tightly bound excitons that determine the optical response of this class of materials. The interaction between excitons and free charge carriers, however, remains difficult to access in halide perovskites due to persistent challenges to introduce doping.

Here, we report experimental realization of electrically tunable, ultrathin two-dimensional perovskites, by combining them with hBN and multilayer graphene in field-effect transistor geometries. We demonstrate the formation of both negatively and positively charged exciton-electron complexes, known as trions with binding energies up to 46 meV. These values are a direct consequence of strong Coulomb interaction and scale with exciton binding energies, as demonstrated by theoretical calculations. The trions exhibit finite oscillator strength in absorption-like response, are localized at cryogenic temperatures, and exhibit thermally activated diffusion at 50 K.

DS 2: 2D Materials and their Heterostructures II: h-BN and WSe₂

Time: Monday 11:30–12:45

Location: SCH A 316

DS 2.1 Mon 11:30 SCH A 316

Engineering of exciton g-factors in van der Waals structures — •TOMASZ WOŹNIAK¹, PAULO FARIA JUNIOR², ANDREY CHAVES³, UMM-E-HANI ASGHAR⁴, and AGNIESZKA KUC⁵ — ¹Wrocław University of Science and Technology, Poland — ²Universitaet Regensburg, Germany — ³Universidade Federal do Ceara, Brazil — ⁴Jacobs Universitaet Bremen, Germany — ⁵Helmholtz-Zentrum Dresden-Rossendorf, Germany

We develop a fully ab-initio based calculation scheme for excitonic g-factors, which describe their energy dependence on external magnetic field, and apply it to 1L TMDs and MoSe₂/WSe₂ heterobilayers, obtaining excellent agreement with experiments [1]. We identify a series of magneto-PL peaks in 1L WS₂ based on the calculated g-factors of excitons, trions and biexcitons, as well as phonon replicas of the dark trion [2]. We explain the reduction of g-factor measured in MoSe₂/WS₂ by the spatial confinement of the intralayer moiré exciton [3]. We find a significant strain dependence of excitonic g-factors and dipole strengths in 1L TMDs. It allows to explain the strain-induced hybridization of direct and indirect excitons in WS₂ [4,5]. We investigate a new class of hexagonal materials with formula MSi₂Z₄ (M: Mo, W; Z: N, P, As, Sb), which are isosymmetric to 1L TMDs. We find a new set of circularly polarized excitonic transitions with high binding energies and large positive g-factors [6].

[1] Phys. Rev. B 101, 235408 (2020) [2] Nano Lett. 21, 2519 (2021) [3] Nano Lett. 21, 8641 (2022) [4] Phys. Rev. Lett. 129, 067402 (2022) [5] New J. Phys. 24, 083004 (2022) [6] arXiv:2210.10679 (2022)

DS 2.2 Mon 11:45 SCH A 316

Phase-locked photon-electron interaction without a laser applied to 2D Materials — •NAHID TALEBI¹, MASOUD TALEB¹, MARIO HENTSCHEL², KAI ROSSNAGEL¹, and HARALD GIESSEN² — ¹Institute for Experimental and Applied Physics, Kiel University, 24118 Kiel, Germany — ²4th Physics Institute and Research Center SCoPE, University of Stuttgart, 70569 Stuttgart, Germany

Ultrafast electron-photon spectroscopy in electron microscopes commonly requires ultrafast laser setups. Photoemission from an engineered electron source is used to generate pulsed electrons, interacting with a sample that is excited by the ultrafast laser pulse at a specified time delay. Here, we present an inverse approach based on cathodoluminescence spectroscopy to introduce internal radiation sources in an electron microscope. Our method is based on a sequential interaction of the electron beam with an electron-driven photon source (EDPHS) and the investigated sample. An electron-driven photon source in an electron microscope generates phase-locked photons that are mutually coherent with the near-field distribution of the swift electron. We demonstrate the mutual coherence between the radiations from the EDPHS and the sample by performing interferometry with a combined system of an EDPHS and a WSe₂ flake. Our method has the advantage of being simple, compact and operating with continuous electron beams. It will open the door to local electron-photon correlation spectroscopy of quantum materials, single photon systems, and coherent exciton-polaritonic samples with nanometric resolution.

DS 2.3 Mon 12:00 SCH A 316

Phase-locked photon-electron interaction without a laser applied to 2D Materials — •NAHID TALEBI — Institute for Experimental and Applied Physics, Kiel University, 24118 Kiel, Germany

Ultrafast electron-photon spectroscopy in electron microscopes commonly requires ultrafast laser setups. Photoemission from an engineered electron source is used to generate pulsed electrons, interacting with a sample that is excited by the ultrafast laser pulse at a specified time delay. Thus, developing an ultrafast electron microscope demands the exploitation of extrinsic laser excitations and complex synchronization schemes. Here, we present an inverse approach based

on cathodoluminescence spectroscopy to introduce internal radiation sources in an electron microscope. Our method is based on a sequential interaction of the electron beam with an electron-driven photon source (EDPHS) and the investigated sample. An electron-driven photon source in an electron microscope generates phase-locked photons that are mutually coherent with the near-field distribution of the swift electron. We demonstrate the mutual coherence between the radiations from the EDPHS and the sample by performing interferometry with a combined system of an EDPHS and a WSe₂ flake. Our method has the advantage of being simple, compact and operating with continuous electron beams. It will open the door to local electron-photon correlation spectroscopy of quantum materials, single photon systems, and coherent exciton-polaritonic samples with nanometric resolution.

DS 2.4 Mon 12:15 SCH A 316

Mobile interlayer excitons at the Mott transition in Moiré-free heterostructures — •EDITH WIETEK¹, MIKHAIL M. GLAZOV², MATTHIAS FLORIAN³, TAKASHI TANIGUCHI⁴, KENJI WATANABE⁴, ALEXANDER STEINHOFF⁵, and ALEXEY CHERNIKOV¹ — ¹Technische Universität Dresden — ²Sankt Petersburg — ³University of Michigan — ⁴NIMS, Ibaraki — ⁵Universität Bremen

Vertically stacked heterostructures of transition metal dichalcogenides present an exciting platform to study electronic and excitonic many-particle states. In this study we investigate propagation of excitons in these systems from low to very high densities to disentangle the effects of dipolar excitons from those stemming from moiré effects. We take advantage of hBN-encapsulated WSe₂/MoSe₂ heterostructures studied in the moiré-free limit of large, atomically reconstructed domains. Using ultrafast microscopy, we show that the interlayer excitons propagate freely even at cryogenic temperatures and low densities. At elevated exciton densities, we demonstrate that in addition to broadly assumed exciton-exciton repulsion, the non-linear increase of the diffusion coefficient also originates from efficient exciton-exciton annihilation. Remarkably, at the exciton ionization threshold of the Mott transition and beyond, we reveal a highly unusual regime of negative effective diffusion that persist for many 100's of ps after the excitation. This observation presents a particularly interesting case of non-equilibrium phenomena in composite many-particle systems, highlighting the rich physics of optical excitations in van der Waals heterostructures.

DS 2.5 Mon 12:30 SCH A 316

Atomic structures of single photon emitters in hexagonal boron nitride — •TJORBEN MATTHES¹, ANAND KUMAR¹, CHANAPROM CHOLSUK¹, and TOBIAS VOGL^{1,2} — ¹Institute of Applied Physics, Friedrich-Schiller-University Jena, Albert-Einstein-Straße 15, 07745 Jena — ²Fraunhofer-Institute for Applied Optics and Precision Engineering IOF, Albert-Einstein-Str. 7, 07745 Jena

Single photon emitters in solid-state crystals have received a lot of attention as building blocks for numerous quantum technology applications. Fluorescent defects in hexagonal boron nitride (hBN) stand out due to their high luminosity and robust operation at room temperature. The fabrication of identical emitters at pre-defined sites is still challenging, which hampers the integration of these defects in optical systems and electro-optical devices. Additionally, the atomic structure of many defects remain unclear or are subject to ambiguous guesswork. Here, we show an analysis on the atomic structures of defects we created by electron beam irradiation using a standard scanning electron microscope with deep sub-micron lateral precision. The emitters are created with a high yield and a reproducible spectrum peaking at 575 nm. We also present results on correlating crystal structure properties and polarization dynamics. Our results indicate that these emitters that all emitters are identical, which is a crucial advantage for the realization of quantum integrated devices, as well as for the identification of these fluorescent defects.

DS 3: Organic Thin Films, Organic-Inorganic Interfaces (joint session DS/PPP)

Time: Monday 11:30–12:45

Location: SCH A 315

DS 3.1 Mon 11:30 SCH A 315

Thickness dependency of the critical dose for beam-sensitive two-dimensional polymers — •DAVID MÜCKE¹, UTE KAISER¹, and HAOYUAN QI^{1,2} — ¹Central Facility of Material Science Electron Microscopy, Universität Ulm, 89081 Ulm, Germany — ²Center for Advancing Electronics Dresden (cfaed) & Faculty of Chemistry and Food Chemistry, Technische Universität Dresden, 01062 Dresden, Germany

For organic materials the achievable resolution in a TEM is limited by their resilience against electron irradiation. Due to that, increasing the critical dose of these sensitive materials is of highest importance. For layer stacked materials,

where the thickness is easily controllable, the thickness dependency of the critical dose is a key feature. Aimed at gathering a better understanding of this effect, in our study this dependency was examined in more detail. To achieve this, the critical dose of a triazine-based 2D polymer[1] was measured for a wide thickness range. The polymer samples, obtained by mechanical exfoliation, ranged from 15 nm to 85 nm thickness. To obtain the critical dose of the polymer, sequences of electron diffraction patterns with a dose of only 0.5 e⁻/Å² were obtained. The measurements revealed, that the critical dose for amorphization of this polymer is only 1-2 e⁻/Å², independent of sample thickness.

1. F. Hu, et al. J. Am. Chem. Soc. 143, 5636-5642 (2021).

DS 3.2 Mon 11:45 SCH A 315

Determining Anisotropic Effects in Strongly Coupled Metal Organic Hybrid Structures — •MAXIMILIAN RÖDEL¹, JINHONG KIM², MATTHIAS STOLTE², LUCA NILS PHILIPP³, MATTHIAS LEHMANN², FRANK WÜRTHNER², ROLAND MITRIC³, and JENS PFLAUM^{1,4} — ¹Experimental Physics VI, University of Würzburg — ²Institut für Organische Chemie and Center for Nanosystems Chemistry, University of Würzburg — ³Institut für Physikalische und Theoretische Chemie, University of Würzburg — ⁴Bavarian Center for Applied Energy Research, 97074 Würzburg

Coupling phenomena in metal organic hybrid structures enable unique possibilities to tune the properties of opto-electronic devices. Furthermore, the strong coupling between surface plasmons and excitons in organic semiconductors leads to novel hybrid states, which are termed plexcitons[1]. By means of a Kretschmann Set Up we investigate these plexcitonic states in oriented liquid crystalline perylene bisimide (PBI) thin films deposited via off-centered spin coating on gold surfaces which exhibiting J-type coupling [2]. The Alignment of the hydrogen-bonded PBI molecules and, thus, their transition dipoles results in long-range ordered films with a pronounced spatially anisotropy of structural and optical characteristics. These new states show a characteristic coupling strength of ≈ 27 meV. Understanding this directional correlation between molecular order and optical properties will enable new device concepts utilizing the presented opto-electronic directionality.

[1] Maximilian Rödel et al. J. Phys. Chem. C 2022, 126(8), 4163-4171

[2] Stefanie Herbst et al. Nat. Commun. 2018, 9(1), 2646-2654.

DS 3.3 Mon 12:00 SCH A 315

Long-term degradation in Blatter radical derivative thin films — •EWA NOWIK-BOLTYK, TOBIAS JUNGHÖFER, and MARIA BENEDETTA CASU — Universität Tübingen, Institut für Physikalische und Theoretische Chemie, Auf der Morgenstelle 18, D-72076 Tübingen, GERMANY

Materials with a radical site are strong candidates for ground-breaking applications from energy storage to quantum computing. In this framework, Blatter radical derivatives are very attractive due to their chemical stability. We focus on the latest insights regarding the fundamental mechanisms of radical thin film long-term degradation, by comparing two Blatter radical derivatives, using X-ray-based techniques, such as photoelectron spectroscopy and absorption spectroscopy. Our findings indicate that air exposure affects the chemical and magnetic properties of the thin films.

DS 3.4 Mon 12:15 SCH A 315

Controlled Thermal Deposition of Organic Diradicals — •TOBIAS JUNGHÖFER and MARIA BENEDETTA CASU — Institut für Physikalische und Theoretische Chemie, Eberhard Karls Universität Tübingen, Germany

Using X-ray photoelectron spectroscopy (XPS) and atomic force microscopy (AFM) we demonstrate that it is possible to evaporate diradicals in a controlled environment obtaining thin films in which the diradical character is preserved. However, evaporation represents a challenge. The presence of two radical sites makes the molecules more reactive also in the case of very stable single radicals. We have explored the parameters that play a role in this phenomenon. We found that the higher the formation energies of the crystal, the more difficult is the evaporation of intact radicals. Large delocalization of the unpaired electrons helps the diradical to stand evaporation. The evaporation of different diradicals can be successfully addressed considering our findings.

DS 3.5 Mon 12:30 SCH A 315

Interaction of cyanoacrylate thin films with copper (oxide) in different processing atmospheres — •PHILIPP MORITZ¹, OLIVER HÖFFT², LIENHARD WEGEWITZ¹, and WOLFGANG MAUS-FRIEDRICHS¹ — ¹Clausthal Centre of Material Technology, Clausthal University of Technology, Agricolastrasse 2, 38678 Clausthal-Zellerfeld — ²Institute of Electrochemistry, Clausthal University of Technology, Arnold-Sommerfeld-Strasse 6, 38678 Clausthal-Zellerfeld

The adhesive class of fast-curing cyanoacrylates plays an increasingly important role, especially in hybrid composites. However, the adhesion mechanism at the interface to the metal (oxide) substrates is not sufficiently understood.

To study the interactions, cyanoacrylate films of a few nm thickness are spin-coated onto metallic copper and copper oxide in (i) a normal air atmosphere and in (ii) an oxygen-free environment (O_2 partial pressure $< 10^{-20}$ mbar). The natively oxidized copper is deoxidized with a dielectric barrier discharge (DBD plasma) directly before the coating process.

Spectroscopic and microscopic methods are used to understand the underlying molecular interactions at the interface between cyanoacrylate and copper (oxide). The formation of hydrogen bonds as well as an ionic interaction can be observed. In addition, an influence of the oxide layer and the effects of the surrounding atmosphere can be seen.

Funded by the Deutsche Forschungsgemeinschaft (DFG, German Research Foundation) – Project-ID 394563137 – SFB 1368

DS 4: Thin Film Properties I

Time: Monday 15:30–17:00

Location: SCH A 316

DS 4.1 Mon 15:30 SCH A 316

Ultrafast laser induced structural motion in crystalline and amorphous gold — •OTHMANE BENHAYOUN¹, EMILIANO PRINCIPPI³, BERND BAUERHENNE¹, DMITRY S. IVANOV², and MARTIN E. GARCIA¹ — ¹University of Kassel, Theoretical physics II, Kassel, Germany — ²Moscow, Russia — ³Elettra-Sincrotrone Trieste S.C.p.A., Trieste, Italy

A recent Ultrafast Electron Diffraction (UED) experiment showed a time-dependent nonuniform compression and expansion of a monocrystalline gold foil. This led to the time modulation of the Au Bragg peaks in both height and width. The same effect is however not observed in polycrystalline gold. We thus perform Molecular Dynamics - Two Temperature Model (MD-TTM) simulations aiming to understand the results of the experiment. In our simulations, we obtain similar peak oscillations and determine the major mechanisms that lead to such lattice dynamics.

DS 4.2 Mon 15:45 SCH A 316

Co-electrodeposition of compositionally complex Co-Cr-Fe-Mo-Ni alloy thin films — •HONGSHUAI LI, MARTIN PETERLECHNER, and GERHARD WILDE — Institute of Materials Physics, University of Münster, Wilhelm-Klemm-Str. 10, 48149 Münster, Germany

A compositionally complex Co-Cr-Fe-Mo-Ni alloy with a face-centered cubic structure was successfully obtained by electrochemical deposition using a constant current density. An aqueous electrolyte with several additives was developed to accomplish the electrodeposition of films onto Cu substrates. The characterization reveals that the deposited films are metallic with a face-centered cubic structure, including impurities incorporated during deposition. In addition, mechanical tests were performed to study adhesion and hardness by nano-scratch tests and nanoindentation. Mechanical tests show a high hardness and nonetheless microscopically ductile behavior. The electrolytes developed in this study may be a promising approach for the electrodeposition of Co-Cr-Fe-Mo-Ni compositionally complex alloy coatings.

DS 4.3 Mon 16:00 SCH A 316

Thermally controlling the length of transition and alkali metal squarate wires — •EGZONA ISUFI NEZIRI^{1,2}, KARL-HEINZ ERNST^{1,2}, and CHRISTIAN WÄCKERLIN^{3,4} — ¹Empa, Swiss Federal Laboratories for Materials Science and Technology, 8600 Dübendorf, Switzerland — ²University of Zürich, 8006 Zürich, Switzerland — ³Paul Scherrer Institute, 5232 Villigen, Switzerland — ⁴EPFL, Swiss Federal Institute of Technology Lausanne, 1015 Lausanne, Switzerland

Low-dimensional metal-organic nanomaterials on surfaces can be engineered to yield promising, novel and highly customizable chemical/physical properties such as magnetism, electronic structure and catalytic properties. A variety of metal elements, including alkali, transition and even lanthanide metals have been used to direct the metal-organic assembly.

Here metal-organic structures obtained from squaric acid ($H_2C_4O_4$) molecules, co-deposited with K and Ni atoms on a hot Au(111) surface, are studied by XPS and STM. We find that both K and Ni lead to the formation of condensed arrays of wires, composed of M-squarate ($C_4O_4(2-)$). Controlling the length of these wires is possible by a thermally activated process: Ni-squarate wires tend to get longer at higher temperatures while K-squarate wires get shorter.

DS 4.4 Mon 16:15 SCH A 316

Deep learning-supported in-situ HRTEM experiments on single-layer carbon — •CHRISTOPHER LEIST¹, HAOUYUAN QI^{1,2}, and UTE KAISER¹ — ¹Central Facility Materials Science Electron Microscopy, Ulm University, 89081 Ulm, Germany — ²Faculty of Chemistry and Food Chemistry Dresden, Technische Universität Dresden, 01062 Dresden, Germany.

We perform in-situ experiments on single-layer carbon using the Cc/Cs-corrected low-voltage transmission electron microscope SALVE, resolving structure and dynamics down to the level of the single atom. These types of experiments create large amounts of data both in terms of numbers of individual images acquired and the amount of information per image. Conventional image analysis methods, e.g., handcrafted filter kernels, often require heavy user supervision and tremendous time cost, posing strong limitations on the data volume making them inconvenient for use in these experiments. Deep learning in the form of

convolutional neural networks offers a reliable and effective way to handle large amounts of complex image data. Using simulated data we train a modified U-Net like neural network to identify atom positions and their structure i.e. polygons while at the same time removing contaminated areas from the evaluation in real micrographs. Thus, gaining the ability for both largescale statistical evaluation and mapping atomically-resolved the material's transformation.

DS 4.5 Mon 16:30 SCH A 316

Microstructure and mechanical properties of Ta-Al-B coatings — •CHUN HU¹, SHUYAO LIN¹, MAXIMILIAN PODSEDNİK², ANDREAS LIMBECK², NIKOLA KOUTNÁ¹, and PAUL H. MAYRHOFER¹ — ¹Institute of Materials Science and Technology, TU Wien, Getreidemarkt 9, Vienna, A-1060, Austria — ²Institute of Chemical Technologies and Analytics, TU Wien, A-1060 Wien, Austria

Alloying is a simple yet powerful tool to tune properties of hard coatings. Here we report stoichiometry, microstructure and hardness evolution of Al-alloyed TaB₂-z coatings. Sputtering a stoichiometric TaB₂ target results in sub-stoichiometric TaB_{1.23} with a mixed hexagonal-TaB₂ (α -ALB₂-type) and orthorhombic TaB structure. Co-sputtering an ALB₂ target*with half the sputtering power density*increases the B content and strongly promotes the α -phase, while only little Al is incorporated (Ta_{0.997}Al_{0.003}B_{1.64}). The coating shows a small grain size and the overall highest hardness. Further increasing the ALB₂/TaB₂ sputter ratio allows for B/Metal ratios of 1.97 and 2.29 with Al metal-fractions up to 48 at%. These coatings are single- α -phased with a smooth surface but gradually decreased hardness due to the increased ALB₂-fraction. The structural evolutions are underpinned by ab initio calculations.

DS 4.6 Mon 16:45 SCH A 316

X-ray characterization of an above-RT bi-stable sublimable molecular spin-crossover Fe(II)-complex — •YAHYA SHUBBAK¹, MIGUEL GAVARA EDO², ARNO EHRESMANN¹, and EUGENIO CORONADO MIRALES² — ¹Institute of Physics & Center for Interdisciplinary Nanostructure Science and Technology (CINSA^T), University of Kassel, D-34132 Kassel — ²Institute of Molecular Science (ICMol), University of València, S-46980 Paterna

Spin crossover (SCO) molecules are a promising type of material that can undergo reversible switching between low-spin (LS)- and high-spin (HS)-states upon external stimuli (heat, light, pressure, etc.)[1], making them useful for information technology, data storage, and optoelectronics[2]. However, most SCO molecules need to be cooled significantly for this transition to be observable. We have investigated the hitherto unknown electronic structure of the complex molecule bis[hydrotris(1,2,4-triazol-1-yl)borate]iron(II) ([Fe(HB(tz)₃)₂])[3] capable of above-RT transition by XPS and XAS measurements, since the distinct electronic structure in both spin-states unmistakably prove the transition between them. [1]P. Gülich and H. A. Goodwin. Spin Crossover in Transition Metal Compounds I. Springer Berlin Heidelberg, May 2004. 356 pp. [2]E. P. Geest et al., Contactless Spin Switch Sensing by Chemo-Electric Gating of graphene. In: Advanced Materials (2020), p. 1903575. [3]S. Rat et al., Solvatomorphism and structural-spin crossover property relationship in bis[hydrotris(1,2,4-triazol-1-yl)borate]iron(ii). In: CrystEngComm 19.24 (2017).

DS 5: 2D Materials and their Heterostructures III

Time: Tuesday 9:30–10:45

Location: SCH A 316

Invited Talk

DS 5.1 Tue 9:30 SCH A 316

Operando infrared studies of confined water and protons in MXene — •MAILIS LOUNASVUORI — Helmholtz-Zentrum Berlin, Berlin, Germany
MXenes are a large family of 2-dimensional transition metal carbides, nitrides and carbonitrides with excellent potential for energy storage applications. Due to hydrophilic surfaces and weak attractive forces between the negatively charged layers, MXenes can retain significant amounts of water between the layers, and they can be intercalated with a variety of cations and molecules. Here, I will present our recent research efforts to apply *operando* infrared spectroscopy to probe the vibrational dynamics of water confined between Ti₃C₂ MXene sheets during electrochemical charging and discharging. Data for both lithium- and proton-containing electrolytes will be presented. Potential-dependent, reversible changes in the O-H stretching modes of confined water are observed that are specific to the cation. In acidic electrolyte, we observe a unique signature of confined hydrated protons which is not seen in the bulk.

DS 5.2 Tue 10:00 SCH A 316

Contact Printed Micro Circuit Boards - A Novel Platform for the Defect Free Integration of 2D Materials — •CHRISTIAN N. SAGGAU¹, SANAZ SHOKRI^{1,2}, YEJIN LEE^{1,2}, MICKEY MARTINI^{1,2}, TOMMASO CONFALONE¹, GENDA GU³, VALENTINA BROSCO⁴, DOMENICO MONTEMURRO⁵, VALERII M. VINOKUR⁶, KORNELIUS NIELSCH^{1,2,7}, and NICOLA POCCIA¹ — ¹Leibnitz Institute for Solid State and Materials Science Dresden, Dresden, Germany — ²Institute of Applied Physics, Technische Universität Dresden, Dresden, Germany — ³Condensed Matter Physics and Materials Science Department, Brookhaven National Laboratory, Upton, USA — ⁴Italian National Research Council, Institute for Complex Systems, Rome, Italy — ⁵Department of Physics, University of Naples Federico II, Naples, Italy — ⁶Terra Quantum AG, St. Gallen, Switzerland — ⁷Institute of Materials Science, Technische Universität Dresden, Dresden, Germany
The 2D cuprate superconductor BSCCO, promises upon integration with CMOS electronics, on-chip high temperature superconducting single photon detectors or quantum interference device (SQUID). Unfortunately, its properties degrade quickly if exposed to elevated temperatures, solvents, oxygen or water. Here we present Hall devices with a record thin film T_c of 91 K, which is identical to the bulk value of the crystal. Electrical contacts were established through transfer-printable circuits embedded in SiNx nanomembranes. The membrane encapsulates the material shielding it from the environment, while via contacts are used to form the electrical contacts.

DS 5.3 Tue 10:15 SCH A 316

Probing magnetic ordering in air stable iron-rich van der Waals minerals — •MUHAMMAD ZUBAIR KHAN¹, APOORVA SHARMA², SERGIO VALENCIA³, FLORIAN KRONAST³, OLEG E. PEIL⁴, GEORGETA SALVAN², CHRISTIAN TEICHERT¹, and ALEKSANDAR MATKOVIC¹ — ¹Institute of Physics, Montanuniversität Leoben, Austria. — ²Institute of Semiconductor Physics, Technische Universität Chemnitz, Germany. — ³Department of Spin and Topology in Quantum Materials, Helmholtz-Zentrum Berlin, Germany. — ⁴Materials Center Leoben, Austria.

We demonstrate magnetic ordering in Fe-rich two-dimensional (2D) phyllosilicates: annite, minnesotaite, and biotite. These van der Waals (vdW) minerals, incorporate local moment bearing iron (Fe) ions via magnesium (Mg) substitution. The phyllosilicate capping silicate/aluminate tetrahedral groups make monolayers air stable. Superconducting quantum interference device vibrating sample magnetometry (SQUID-VSM) was used probe long-range magnetic ordering in bulk. In-field magnetic force microscopy (MFM) confirmed the local magnetic moment at room temperature, present down to monolayers. X-ray photoelectron spectroscopy (XPS) were used to observe the Fe oxidation state and to establish a correlation with magnetic ordering. Further, magnetic ordering in thin flakes was probed via X-ray magnetic circular dichroism. Our study of Fe-bearing vdW minerals may drive the development for controllable synthesis of novel 2D magnetic insulators.

DS 5.4 Tue 10:30 SCH A 316

Anisotropic Spontaneous Magnetostriction in Fe_{3-x}GeTe₂ — •REINHARD K. KREMER and EVA BRÜCHER — MPI for Solid State Research, Stuttgart, Germany
By determining the lattice parameters as a function of temperature of the hexagonal van der Waals ferromagnet Fe_{2.93(2)}Ge_{1.02(3)}Te₂ we detect a spontaneous negative in-plane magnetostriction occurring below the Curie temperature. The spontaneous magnetostriction follows the square of the spontaneous magnetization and leads to an expansion of the hexagonal layers, and is clearly seen for the in-plane lattice parameter *a*, but less well pronounced perpendicular to the planes along *c*. Extrapolating to *T* → 0 K we obtain a saturation spontaneous magnetostriction of $\lambda_{sp,a}(T \rightarrow 0) = -214(6) \times 10^{-6}$ and a volume magnetostriction $\lambda_{sp,vol}(T \rightarrow 0) \approx -450 \times 10^{-6}$, indicating that the spontaneous magnetostriction along *c* is very small. The linear thermal expansion coefficients at 295 K of Fe_{2.93(2)}Ge_{1.02(3)}Te₂ amount to $13.9(1) \times 10^{-6} \text{ K}^{-1}$ and to $23.22(15) \times 10^{-6} \text{ K}^{-1}$ for the in-plane and out of plane direction, respectively, indicating in a linear volume thermal expansion coefficient of $51.0(2) \times 10^{-6}$.

DS 6: Thin Film Properties II (joint session DS/KFM)

Time: Tuesday 10:00–11:00

Location: SCH A 315

DS 6.1 Tue 10:00 SCH A 315

Defect nanostructure and its impact on magnetism of α -Cr₂O₃ thin films — •IHOR VEREMCHUK¹, OSKAR LIEDKE¹, PAVLO MAKUSHKO¹, TOBIAS KOSUB¹, NATASCHA HEDRICH², OLEKSANDR PYLYPOVSKIY¹, FABIAN GANSS¹, MAIK BUTTERLING¹, RENÉ HÜBNER¹, ERIC HIRSCHMANN¹, AHMED ATTALLAH¹, ANDREAS WAGNER¹, KAI WAGNER², BRENDAN SHIELDS², PATRICK MALETINSKY², JÜRGEN FASSBENDER¹, and DENYS MAKAROV¹ — ¹Helmholtz-Zentrum Dresden-Rossendorf e.V., Dresden, Germany — ²Department of Physics University of Basel, Switzerland

Thin films of the magnetoelectric insulator Cr₂O₃ are technologically relevant for energy-efficient magnetic memory devices controlled by electric fields. We experimentally investigated the defect nanostructure of 250-nm-thick Cr₂O₃ thin films prepared under different conditions on single crystals of Al₂O₃ (0001) and correlate it with the integral and local magnetic properties of the samples. Positron annihilation spectroscopy reveals that the Cr₂O₃ thin films are characterized by the presence of complex defects at grain boundaries, formed by groups of monovacancies, coexisting with monovacancies and dislocations. The defect nanostructure strongly affects the magnitude of the electrical readout. Furthermore, the presence of larger defects like grain boundaries has a strong influence on the pinning of magnetic domain walls in thin films. We show that the Néel temperature is hardly affected by the formed defects in a broad range of deposition parameters.

DS 6.2 Tue 10:15 SCH A 315

Dynamics of phase transition in Lead-free Ferroelectric thin films — •MALLIKA KHOSLA¹, JUTTA SCHWARZKOPF¹, DANIEL SCHMIDT², DANIEL HENSEL¹, and PETER GAAL^{1,2} — ¹Leibniz-Institut für Kristallzüchtung, Berlin, Germany — ²Tailored x-ray products, Hamburg, Germany

In this contribution, we monitor the dynamics of the phase transition in Potassium Sodium Niobate (KNaxNb1-xO3) by taking snapshots of the structure after optical excitation using pulsed synchrotron radiation in a pump-probe scheme. Our sample is a 50 nm KNaxNb1-x O3 film grown on 20 nm thin SrRuO3 on TbScO3 substrate. The low-temperature phase displays a hierarchical order of domains and superdomains on sub-100 nm and on few μ m length scales, respectively. First, we show that laser heating with 7 ns pulses has a similar effect locally in terms of structural rearrangement as static heating of the whole sample volume. However, in our localized excitation the transient phase transition required to transform a similar volume fraction of the sample in the high temperature phase is about 5 times higher compared to static heating. Comparison with finite-element simulations of heat-transport in our sample shows that the phase transition dynamics does not exactly follow the temperature evolution in the ferroelectric film. In addition, time-resolved diffraction imaging experiments reveal that the stability of a spatial domain morphology has a nonlinear dependence on the local laser-induced temperature. Our results indicate that it is essential to resolve both the temporal and spatial coordinate to monitor the equilibration path of such phase transition.

DS 7: 2D Materials and their Heterostructures IV

Time: Tuesday 11:15–12:30

Location: SCH A 316

DS 7.1 Tue 11:15 SCH A 316

THz-Light Canalization by means of Phonon Polaritons in 2D van der Waals Materials — •MAXIMILIAN OBST^{1,2}, TOBIAS NÖRENBERG^{1,2}, GONZALO ÁLVAREZ-PÉREZ³, THALES V.A.G. DE OLIVEIRA⁴, ALEXEY NIKITIN⁵, PABLO ALONSO-GONZÁLEZ³, J. MICHAEL KLOPF⁴, SUSANNE C. KEHR^{1,2}, and LUKAS M. ENG^{1,2} — ¹TU Dresden, Germany — ²Würzburg-Dresden Cluster of Excellence - EXC 2147 (ct.qmat), Germany — ³University of Oviedo, Spain — ⁴HZDR, Dresden, Germany — ⁵DIPC, Donostia-San Sebastian, Spain

Hyperbolic phonon polaritons (PhP) in anisotropic, 2D van der Waals materials present a promising platform to shrink THz optics into nm-sized volumes, as they enable ultra-high field confinement. Recently, controlled PhP dispersion tuneability was demonstrated at MIR wavelengths by vertically stacking two α -MoO₃-flakes under a well-defined twist-angle θ , introducing a topological transition, where PhPs propagate along one distinct direction (so-called 'canalized propagation')[1].

In this talk, we explore the THz dispersion tunability in twisted bilayer MoO₃ at frequencies ranging from $\nu = 8.28$ to 9.38 THz, for which the existence of hyperbolic PhP has been demonstrated recently [2], and where longer (THz) wavelengths make strong confinement even more desirable. We demonstrate the transition from hyperbolic to elliptic propagation of these PhPs by varying both θ and ν and report the very first observation of canalized PhPs in the THz spectral range, i.e., for $\nu = 8.67$ THz and $\theta = 50^\circ$.

DS 6.3 Tue 10:30 SCH A 315

Ferroelectric thin films studied by X-ray standing waves — •LE PHUONG HOANG¹, IRENA SPASOJEVIC², DAVID PESQUERA², GUSTAU CATALAN², KAI ROSSNAGEL^{3,5}, JÖRG ZEGENHAGEN⁴, TIEN-LIN LEE⁴, IVAN VARTANYANTS⁵, ANDREAS SCHERZ³, and GIUSEPPE MERCURIO¹ — ¹European XFEL, Schenefeld, Germany — ²Catalan Institute of Nanoscience and Nanotechnology, Barcelona, Spain — ³Christian-Albrechts-Universität zu Kiel, Kiel, Germany — ⁴Diamond Light Source, Didcot, UK — ⁵Deutsches Elektronen-Synchrotron DESY, Hamburg, Germany

We investigated the structural properties of ferroelectric BaTiO₃ thin films by X-ray standing waves with the goal to determine the atomic positions within the tetragonal unit cell in samples with different strain. Our samples consist of BaTiO₃ thin films grown by pulsed laser deposition (with a SrRuO₃ bottom electrode) on three different substrates SmScO₃, GdScO₃, DyScO₃ providing increasing compressive strain. All the samples were characterized by X-ray reflectivity (XRR) and reciprocal space mapping (RSM). We present X-ray photoelectron spectroscopy, X-ray diffraction and X-ray standing waves data measured at the Diamond Light Source that provide Ba and Ti atomic positions within the unit cells of sample surface. In this study we show a relation between atomic positions and compressive strain of ferroelectric BaTiO₃ thin films.

DS 6.4 Tue 10:45 SCH A 315

Exploring transition-metal substitution in FeSe₂ thin films formed by selenization at various temperatures — •LUQMAN MUSTAFA¹, ANDREAS KREYSSIG¹, JILL FORTMANN², AURELIJA MOCKUTE², ALAN SAVAN², ALFRED LUDWIG², and ANNA E. BÖHMER¹ — ¹Institute for Experimental Physics IV, Ruhr-Universität Bochum, Germany — ²Materials Discovery and Interfaces, Institute for Materials, Ruhr University Bochum, Germany

Transition-metal dichalcogenides with orthorhombic marcasite structure have been extensively studied for their applications in light energy conversion and photoelectrochemical devices. Lately this structure type has also gained interest for its magnetic properties as a candidate for the newly-predicted altermagnetic order.

Using combinatorial deposition and ex-situ selenization at 250°C, 350°C and 430°C, we have studied the substitution of iron with different TMs in (Fe,X)Se₂ thin films, (X= Co, Ni, Cr). This technique allowed to efficiently and quickly explore the possible ranges of substitution of TMs in this compound. We find that the marcasite structure of (Fe,Co)Se₂ forms with higher Co content when the selenization temperature is lower.

Our results represent an example for the agility of combinatorial deposition of thin films in exploring the phase diagrams of transition-metal dichalcogenides. It may be adapted for other systems, such as FeSb₂, and is therefore a unique tool to study a broad material family and its possible substitution ranges.

[1] G. Hu et al., *Nature* **582**, 209 (2020).[2] T.V.A.G. de Oliveira et al., *Adv. Mater.* **33**, 2005777 (2021).

DS 7.2 Tue 11:30 SCH A 316

Magnetically induced band splitting of the exfoliated antiferromagnet MnPS₃ revealed by temperature dependent μ -ARPES — •J. STRASDAS¹, B. PESTKA¹, M. RYBAK², A. K. BUDNIAK³, N. LEUTH¹, H. BOBAN⁴, I. COJOCARIU⁴, D. BARANOWSKI⁴, V. FEYER⁴, J. AVILA⁵, P. DUDIN⁵, Y. AMOUYAL⁶, L. PLUCINSKI⁴, E. LIFSHTIZ³, M. BIROWSKA⁷, and M. MORGENSTERN¹ — ¹II. Institute of Physics B and JARA-FIT, RWTH-Aachen University, Germany — ²Department of Semiconductor Materials Engineering Wroclaw University of Science and Technology, Poland — ³Schulich Faculty of Chemistry, Solid State Institute, Russell Berrie Nanotechnology Institute and Helen Diller Quantum Center, Technion, Israel Institute of Technology, Israel — ⁴Forschungszentrum Jülich, Peter Grünberg Institute (PGI-6), Germany — ⁵Synchrotron-SOLEIL, Université Paris-Saclay, France — ⁶Department of Materials Science and Engineering, Technion, Israel Institute of Technology — ⁷Institute of Theoretical Physics, University of Warsaw, Poland

We provide micron-scale angle-resolved photoelectron spectroscopy (μ -ARPES) of the exfoliated intralayer antiferromagnet (AFM) MnPS₃ above and below the Néel temperature in comparison with density functional theory (DFT) calculations. We demonstrate a splitting of parts of the Mn 3d_{2,2}-bands induced by the

AFM ordering in line with DFT results. Related changes of adjacent S 3p-bands indicate a competing FM superexchange contribution. This novel access to the electronic band structure is found to be transferable to other AFM MPX₃ materials (M: transition metal, P: phosphorus, X: chalcogenide).

DS 7.3 Tue 11:45 SCH A 316

Twistronics of high temperature superconductors — •NICOLA POCCIA — Leibniz Institute for Solid State and Materials Research Dresden (IFW-Dresden) Ideally, one would like to have quantum technologies that could work at higher temperature and at the same time show all the advantages of a twisted architecture as for example its revolutionary degree of electronic tunability. However, highly tunable superconductors that operate above liquid nitrogen are either not yet showed up using multi-layered graphene twisted heterostructures or the materials are very difficult to assemble in twisted heterostructures given their extreme sensitivity to the environmental conditions. Here we show a possible avenue towards the resolution of this problem, demonstrating how to engineer a new generation of the van der Waals heterostructures comprising atomically high temperature superconducting thin Bi₂Sr₂Ca_n-1Cu_nO_{2n+4} (where n = 1,2,3) crystals. The intended van der Waals constituent Bi₂Sr₂Ca_n-1Cu_nO_{2n+4} planes are twisted with respect to each other and make the Josephson junctions. We measure different quantum transport properties of the Josephson junctions in a wide range of twisted angles, indicating the high temperature superconducting topological nature of these systems. Finally, technological prospects on the realization of hybrid complex superconducting circuits will be given.

DS 7.4 Tue 12:00 SCH A 316

New magneto-polaron resonances in a monolayer of a transition metal dichalcogenide — CARLOS TRALLERO-GINER^{1,2}, DARÍO G. SANTIAGO-PÉREZ³, and •VLADIMIR M. FOMIN^{1,4} — ¹Institute for Integrative Nanosciences (IIN), Leibniz IFW Dresden, D-01069 Dresden — ²Havana University, Havana 10400, Cuba — ³Universidad Autónoma del Estado de Morelos, CP 62209, Cuernavaca,

Morelos, México — ⁴Moldova State University, MD-2009 Chişinău, Republic of Moldova

For transition metal dichalcogenide (TMD) semiconductors, the behavior of the magneto-polaron resonances (MPRs) is revealed as a function of the phonon symmetry inherent in the system. It is shown that the renormalized Landau energy levels are modified by the interplay of the long-range Pekar-Fröhlich (PF) and short-range deformation potential (DP) interactions. This interplay leads to a new series of MPRs involving the optical phonons at the center of the Brillouin zone. The coupling of the two Landau levels with the LO and A₁ optical phonon modes provokes resonant splittings of double avoided-crossing levels giving rise to three excitation branches. To explore the interplay between the MPR, the electron-phonon interactions (PF and DP) and the couplings between adjacent Landau levels, a full Green's function treatment for the evaluation of the energy and its life-time broadening is developed. A generalization of the two-level approach is performed for the description of the new MPR branches. The obtained results are a guideline for the magneto-optical experiments in TMDs, where three MPR peaks should be observable.

DS 7.5 Tue 12:15 SCH A 316

Light driven magnetic transitions in transition metal dichalcogenide heterobilayers — •MICHAEL VOGL¹, SWATI CHAUDHARY^{2,3,4}, and GREGORY FIETE^{3,4} — ¹Department of Physics, King Fahd University of Petroleum and Minerals, 31261 Dhahran, Saudi Arabia — ²Department of Physics, The University of Texas at Austin, Austin, Texas 78712, USA — ³Department of Physics, Northeastern University, Boston, Massachusetts 02115, USA — ⁴Department of Physics, Massachusetts Institute of Technology, Cambridge, Massachusetts 02139, USA

We study strongly correlated phases of twisted transition metal dichalcogenide heterobilayers (tTMDs) subject to a period drive. Specifically, we employ Floquet theory to investigate how for this family of materials different forms of light can induce various magnetic phase transitions.

DS 8: Thin Film Properties III

Time: Tuesday 11:30–12:45

Location: SCH A 315

DS 8.1 Tue 11:30 SCH A 315

Growth of Sc(x)Ga(1-x)N on 6H-SiC by plasma assisted molecular beam epitaxy — •FABIAN ULLMANN^{1,2}, AARON GIESS^{1,2}, and STEFAN KRISCHOK^{1,2} — ¹Institut für Physik, TU Ilmenau, Ehrenbergstraße 29, 98693 Ilmenau — ²Institut für Mikro- und Nanotechnologien, TU Ilmenau, Gustav-Kirchhoff-Straße 7, 98693 Ilmenau

ScGaN can occur in different crystal orientations. Most important are the wurtzite and the rocksalt formation. In dependency of the Scandium concentration a phase transition between these orientations can be found.

Plasma assisted molecular beam epitaxy (PAMBE) in combination with reflective high electron energy diffraction (RHEED) was performed to create layers with different Scandium concentrations within ScGaN. To determine the concentration of the grown layers X-ray photoelectron spectroscopy (XPS) was used in the same vacuum chamber. Additionally, the surfaces were investigated by atomic force microscopy (AFM, in-situ) and scanning electron microscope (SEM) to gain information about the morphology of the surfaces and to confirm the gained crystal orientations investigations with X-ray diffraction (XRD) were made.

DS 8.2 Tue 11:45 SCH A 315

α -FeGe₂ films on GaAs(001) substrates grown by MBE and solid-phase epitaxy — •MORITZ HANSEMANN, MICHAEL HANKE, ACHIM TRAMPERT, and JENS HERFORT — Paul-Drude-Institut für Festkörperelektronik, Berlin, Germany

Layered magnets show promising results towards advancements in the field of spintronics. Such materials exhibiting a ferro- and/or antiferromagnetic (FM/AFM) phases close to room temperature are especially on demand for future technologies.

Recently we discovered a novel metastable α -FeGe₂ phase sandwiched between two ferromagnetic Fe₃Si Heusler alloy metals. Comprehensive transmission electron microscopy (TEM) and X-ray diffraction (XRD) measurements revealed the layered structure and P4mm spacegroup, that is absent in bulk FeGe₂. By a combination of molecular beam and solid phase epitaxy we demonstrate the isolated growth of α -FeGe₂ on a GaAs(001) substrate. This is achieved by first growing Fe₃Si and covering it with amorphous Germanium in the thickness ratio of 1:3. Finally, a subsequent annealing forms the layered FeGe₂. Through a optimization of this process we are able to grow layers of extremely high quality with layer thicknesses down to 4 nm. The films are structurally characterized by atomic force microscopy, XRD, X-ray reflectivity and TEM measurements, which also demonstrate the importance of a smooth GaAs initial surface. First transport measurements showed metallic behavior and a ferromagnetic behavior at low temperatures.

DS 8.3 Tue 12:00 SCH A 315

Heteroepitaxial Growth of Ultrawide Bandgap Cubic Spinel Zn₂GeO₄ Thin Films by Pulsed Laser Deposition — •JINGJING YU, SIJUN LUO, and MARIUS GRUNDMANN — Felix Bloch Institute for Solid State Physics, Faculty of Physics and Earth Sciences, Universität Leipzig, 04103 Leipzig

It is significant to explore new ultrawide bandgap oxides thin films with a bandgap larger than 4 eV for potential applications in power electronics and deep-UV photodetectors. Cubic spinel Zn₂GeO₄ is a high-temperature and high-pressure phase which was originally synthesized at 1600 °C and 3 GPa. To date the experimental results on physical properties and thin film growth of cubic spinel Zn₂GeO₄ are not available. In this study, we report the heteroepitaxial growth of cubic spinel Zn₂GeO₄ thin films on cubic spinel MgAl₂O₄ single crystal substrates by using pulsed laser deposition at about 800 °C. Combining the analysis results from XRD 2theta-omega scans and rocking curves with the AFM surface morphologies, it is concluded that the oxygen partial pressure of around 0.05–0.10 mbar is optimal for growing high-quality Zn₂GeO₄ epitaxial thin films. Phi-scan results confirm the single-domain epitaxy of (100)-, (110)- and (111)-oriented Zn₂GeO₄ epitaxial thin films grown on (100), (110) and (111) MgAl₂O₄ substrates, respectively. The dielectric function of the cubic spinel Zn₂GeO₄ epitaxial thin films was measured by spectroscopic ellipsometry, indicating a bandgap energy greater than 4.5 eV. This work advances the fundamental research on ultrawide bandgap cubic spinel Zn₂GeO₄ epitaxial thin films.

DS 8.4 Tue 12:15 SCH A 315

Rutile CuTiO₂ alloy thin films: lowered growth temperature and retained optical properties. — •HAO LU^{1,2}, MARTIN BECKER^{1,2}, and PETER J. KLAR^{1,2} — ¹Institute of Experimental Physics I, Justus-Liebig-University, Giessen — ²Center for Materials Research (ZfM), Justus-Liebig-University, Giessen

Titanium dioxide (TiO₂) with a rutile structure and suitable bandgap may be advantageously employed as buffer layer and anti-reflection layer in VO₂-based smart windows coated on float glass by sputter deposition. The phase transition of the thermodynamically metastable phases, anatase and brookite, into the stable rutile phase occurs in pristine TiO₂ at temperatures about 600 °C, which is higher than the melting point of float glass. Hence, we need to significantly reduce the growth temperature of rutile TiO₂ in order to deposit it as the film on float glass substrates.

Cu doping has been reported as a means for achieving this goal. We study series of TiO₂:Cu thin-film samples deposited on float glass to assess the growth window for rutile TiO₂:Cu deposited at temperature below 600 °C. The samples are compared with reference TiO₂ thin-films deposited under the same conditions in terms of crystal structure and optical properties.

DS 8.5 Tue 12:30 SCH A 315

The challenge to grow β -(Al_xGa_{1-x})₂O₃ on (100) off-oriented β -Ga₂O₃ by MOVPE — •JANA REHM, TA-SHUN CHOU, ARUB AKHTAR, RAIMUND GRÜNEBERG, SAUD BIN-ANOOZ, and ANDREAS POPP — Leibniz-Institut für Kristallzüchtung, Max-Born-Str. 2, 12489 Berlin, Deutschland

Although immense progress in homoepitaxial thin film growth of β -Ga₂O₃ on different substrate orientations has been achieved, β -Ga₂O₃ based high-efficiency devices are still limited by the materials intrinsic low thermal conductivity and electron mobility. Increasing the bandgap by alloying β -Ga₂O₃ with Al₂O₃ opens up the possibility to overcome the materials restraints and realize

high-performance lateral β -(Al_xGa_{1-x})₂O₃/Ga₂O₃ heterostructure devices. It has been shown that the crystal orientation plays an important role in the Al incorporation limit and band offsets where the (100) orientation is predicted to be the most promising orientation exhibiting the highest critical thickness and incorporated Al content. The role of off-oriented (100) β -Ga₂O₃ substrates is suggested to achieve the full advantage of β -(Al_xGa_{1-x})₂O₃/Ga₂O₃ heterostructure with the benefit of potentially suppressing the formation of twin defects. For the first time, we report a comprehensive study on the growth of β -(Al_xGa_{1-x})₂O₃ on off-oriented (100) β -Ga₂O₃ substrates using MOVPE. The influence of different growth parameters on the morphology and Al incorporation are systematically investigated by HR-XRD and AFM.

DS 9: Layer Properties I

Time: Wednesday 9:30–10:30

Location: SCH A 316

Invited Talk

DS 9.1 Wed 9:30 SCH A 316

Flüssigphasen-Elektrochemie im Ultrahochvakuum unter XPS-Kontrolle — •FRANK ENDRES — Institut für Elektrochemie, TU Clausthal

Ionische Flüssigkeiten zeichnen sich durch zwei interessante Eigenschaften aus. Zum einen haben sie sehr weite sog. elektrochemische Fenster, die Untersuchungen ermöglichen, die insbesondere in wässrigen Elektrolyten nicht möglich sind. Zum anderen haben sie sehr geringe Dampfdrücke, die die Untersuchung ionischer Flüssigkeiten unter den Bedingungen eines Ultrahochvakuums ermöglichen. In diesem Beitrag werden nun beide Ansätze kombiniert, indem elektrochemische Prozesse in ionischen Flüssigkeiten im Ultrahochvakuum mittels Photoelektronenspektroskopie untersucht werden. Ein Einblick in die Prozesse bei der elektrochemischen Reduktion von Tantalverbindungen, in die Prozesse bei der elektrochemischen Oxidation von Gold sowie in Disproportionierungsreaktionen bei der Reduktion von Galliumverbindungen wird gegeben.

F. Krebs, O. Höfft, F. Endres, Applied Surface Science 155130 (2022)

Z. Liu, O. Höfft, A. Gödde, F. Endres, Journal of Physical Chemistry C 125 (2021) 26793*26800

Z. Liu, O. Höfft, F. Endres, Journal of Physical Chemistry C 125 (2021) 24589-24595

DS 9.2 Wed 10:00 SCH A 316

Oxide thickness-dependent resistive switching characteristics of Cu/HfO₂/Pt ECM devices — •TAEWOOK KIM¹, TOBIAS VOGEL¹, ESZTER PIROS¹, DESPINA NASIOU², NICO KAISER¹, PHILIPP SCHREYER¹, ROBERT WINKLER², ALEXANDER ZINTLER², ALEXEY ARZUMANOV¹, STEFAN PETZOLD¹, LEOPOLDO MOLINA-LUNA², and LAMBERT ALFF¹ — ¹Advanced Thin Film Technology Division, Institute of Materials Science, Technische Universität Darmstadt, Alarich-Weiss-Str. 2, 64287 Darmstadt, Germany — ²Advanced Electron Microscopy Division, Institute of Materials Science, Technische Universität Darmstadt, Alarich-Weiss-Str. 2, 64287 Darmstadt, Germany

This study investigates the resistive switching mechanism and electrical conduction mechanism of the Cu/HfO₂/Pt MIM (Metal-Insulator-Metal) structure. In this study, we investigated the resistance switching characteristics of Cu/HfO₂/Pt samples. Specifically, we focus on changes in resistive switching characteristics

as a function of oxide layer thickness. We noticed an interesting phenomenon of resistance switching property, that the reset switching occurs more sharply and abruptly in the sample with thick HfO₂ film. However, gradual reset is more dominant in the sample with thin HfO₂ film. Therefore, we devised the model (Thermally Assisted Electrochemical Mechanism) to explain the physical phenomenon. For better understanding, the conduction mechanism of Cu/HfO₂/Pt samples was also investigated. Cu/HfO₂/Pt has SCLC (Space Charge Limited Conduction) mechanism as the conduction mechanism. However, the mechanism is divided into several steps depending on the thickness of the oxide layer.

DS 9.3 Wed 10:15 SCH A 316

Substoichiometric conducting HfO_x phases as novel type of electrodes with a built-in oxygen vacancy reservoir for RRAM applications — •PHILIPP SCHREYER¹, NICO KAISER¹, ESZTER PIROS¹, TOBIAS VOGEL¹, TAEWOOK KIM¹, DESPINA NASIOU², LEOPOLDO MOLINA-LUNA², and LAMBERT ALFF¹ — ¹Advanced Thin Film Technology Division, TU Darmstadt, Alarich-Weiss-Str. 2, 64287 Darmstadt, Germany — ²Advanced Electron Microscopy Division, TU Darmstadt, Darmstadt, Germany

Hafnium oxide is an outstanding candidate as the active material in RRAM due to its performance and proven CMOS compatibility. In previous studies, we have shown that electrically conducting hafnium oxide phases can be stabilized by significant oxygen deficiency [1,2]. While so far only the physical properties of these structures have been investigated, we reproduced the phases in RRAM configuration to investigate the device properties. Resistive switching was found to be absent in all deficient in-vacuo processed samples. They show ohmic conduction, confirming the conducting nature of the substoichiometric phases. However, when exposed to air, a thin oxidized layer forms at the surface which stabilizes reliable resistive switching. Note that the oxidation process is self-limited leading to reproducible oxide thicknesses of a few nm. We suggest that the substoichiometric phases may act as second electrode with an oxygen vacancy reservoir that stabilizes oxygen vacancy filaments in ultrathin layers of near-stoichiometric HfO₂. [1] N. Kaiser et al., ACS Appl. Mater. Interfaces 14, 1290 (2022). [2] N. Kaiser, accepted. ACS Appl. Electron. Mater. (2023).

DS 10: Layer Properties II

Time: Wednesday 11:00–12:15

Location: SCH A 316

DS 10.1 Wed 11:00 SCH A 316

Electronic structure of epitaxial (Cr_{1-x}Mn_x)₂GaC thin films by X-ray absorption and optical spectroscopy — •IVAN TARASOV¹, ANDREI ROGALEV², FABRICE WILHELM², MICHAEL FARLE¹, and ULF WIEDWALD¹ — ¹Faculty of Physics and Center for Nanointegration (CENIDE), University of Duisburg-Essen, 47057 Duisburg, Germany — ²The European Synchrotron Radiation Facility (ESRF), 38000 Grenoble, France

Heteroepitaxial thin films of (Cr_{1-x}Mn_x)₂GaC MAX phase for x = of 0.13 - 1 were deposited on MgO(111), Al₂O₃(0001) and KAl₃Si₃O₁₀(001) substrates by pulsed laser deposition at T = 500-600 °C. X-ray absorption near edge spectroscopy (XANES) spectra were collected at the Mn K-edge, Cr K-edge and Ga K-edge. Evidence of chemical disorder associated with (Mn, Cr) is observed. The similarity of the Cr K-edge spectra to Mn, and the presence of a strong X-ray linear dichroism signal for the Mn K-edge, indicates that Mn is substitutional for Cr in the MAX phase hexagonal lattice. With increasing of Mn content additional features attributed to a cubic antiperovskite structure are observed. Simulations of the XANES spectra confirm the origin of X-ray linear dichroism observed in the sample, which is due to the inherent nanolaminated structure of the MAX phase.

Funding by the Deutsche Forschungsgemeinschaft (DFG) within CRC/TRR 270, project B02 (Project-ID 405553726) is gratefully acknowledged. We thank Martina Schmid (University of Duisburg-Essen) for assistance and providing access to the ellipsometer.

DS 10.2 Wed 11:15 SCH A 316

Perovskite-organic multiple quantum wells towards lasing — •TOBIAS ANTRACK¹, MARTIN KROLL¹, MARKAS SUDZIUS¹, CHANGSOON CHO¹, PAULIUS IMBRASAS¹, MIGUEL ALBALADEJO-SIGUAN¹, JOHANNES BENDUHN¹, LENA MERTEN², ALEXANDER HINDERHOFER², FRANK SCHREIBER², SEBASTIAN REINEKE¹, YANA VAYNZOF¹, and KARL LEO¹ — ¹IAPP, TU Dresden, Dresden, Germany — ²Institut für Angewandte Physik, Universität Tübingen, Tübingen, Germany

Metal halide perovskites are of high interest due to their excellent electro-optical properties. Their high damage threshold makes them of special interest for high-fluence applications like lasing devices, and the possibility of production by vacuum deposition is promising for future large-scale industrial production. This technique allows precise thickness control and, therefore, the production of multiple quantum wells (MQWs). Such structures result in high charge carrier con-

centration and enhanced electron-hole recombination, making them promising for high-performance and fine-tunable materials. This work presents a comprehensive study of the optical properties of vacuum-deposited CsPbBr₃ perovskite MQWs with organic (TPBi) barrier layers. Blue shifts in absorption and emission spectra with decreasing well width demonstrate quantum confinement and are confirmed by simulations. Additionally, the photoluminescence quantum yield increases by up to 32 times from bulk material to the thinnest well layers. Amplified spontaneous emission (ASE) measurements show very low thresholds down to 7.3 μJ cm⁻² for a perovskite thickness of 8.7 nm, which is significantly lower than previously observed for CsPbBr₃ thin films.

DS 10.3 Wed 11:30 SCH A 316

Defect-engineered magnetic field dependent optoelectronics of vanadium doped tungsten diselenide monolayers — •CHRISTIN MÄDLER^{1,2}, KATHARINA NISI^{1,2}, JONAS KIEMLE^{1,2}, LUKAS POWALLA³, ALESSIO SCAVUZZO³, TUAN DUNG NGUYEN^{4,5}, DINH LOC DUONG^{4,5}, MARKO BURGHARD³, ALEXANDER W. HOLLEITNER^{1,2}, and CHRISTOPH KASTL^{1,2} — ¹Walter Schottky Institut, Technical University of Munich, Am Coulombwall 4a, 85748 Garching, Germany — ²Munich Center of Quantum Science and Technology (MCQST), Schellingstrasse 4, 80799 Munich, Germany — ³Max-Planck-Institut für Festkörperforschung, Heisenbergstrasse 1, D-70569 Stuttgart, Germany — ⁴Center for Integrated Nanostructure Physics (CINAP), Institut für Basic Science (IBS), Suwon 16419, Republic of Korea — ⁵Department of Energy Science, Sungkyunkwan University, Suwon 16419, Republic of Korea

In this work, we investigate semiconducting WSe₂ monolayers, substitutionally doped with vanadium atoms, using low temperature luminescence and optoelectronic spectroscopy. V-dopants lead to a p-type doping character and an impurity-related emission ~ 160 meV below neutral exciton, both of which scale with the nominal percentage of vanadium dopants. Measurements using field-effect devices of 0.3% V-doped WSe₂ demonstrate bipolar carrier tunability. The doped monolayers display a clear magnetic hysteresis in photocurrent measurements for the studied range of carrier densities, whereas the valley polarization of the excitons reveals a non-linear g-factor without a magnetic hysteresis within the experimental uncertainty.

DS 10.4 Wed 11:45 SCH A 316

On the influence of the cation composition in reactively co-sputtered Ag_xCu_{1-x}I thin films: Characterization of electrical, optical and structural properties — •SOFIE VOGT, CHRISTIANE DETHLOFF, JORRIT BREDOW, TILLMANN STRALKA, HOLGER VON WENCKSTERN, and MARIUS GRUNDMANN — Universität Leipzig, Felix-Bloch-Institut, Germany

CuI and its alloys are promising transparent p-type materials for complementary transparent devices. Polycrystalline thin films exhibit hole mobilities of about 19 cm²V⁻¹s⁻¹, which is comparable to the electron mobility of commercially used indium-gallium-zinc-oxide thin films^[1,2]. It has been shown that alloying CuI with Ag leads to a transition from p-type material to n-type material for $x \approx 0.5$ ^[3]. This paves the way for Ag_xCu_{1-x}I/Ag_yCu_{1-y}I based homojunction diodes. We present reactively co-sputtered Ag_xCu_{1-x}I thin films in a range of 0.01 ≤ x ≤ 0.86. The thin films were deposited on glass substrates and crystallized in the γ-phase up to $x \leq 0.67$ and exhibit an additional AgI phase for higher Ag contents. An increase of the thin film resistivity from 2 × 10⁻⁴ Ωm to 30 Ωm was achieved by increasing the silver content from $x = 0.01$ to $x = 0.67$. All thin films are transparent in the visible light range and the expected decrease of the exciton binding energy up to $x \approx 0.5$ is observed, above which it remains constant.

[1] C. Yang *et al.*, ACS Appl. Electr. Mater., 2, 3627-3632, 2020.

[2] S. Yang *et al.*, IEEE Electron Device Lett., 32 (12), 1692-1694, 2011.

[3] A. Annadi *et al.*, Appl. Mater. Today, 20, 100703, 2020.

DS 10.5 Wed 12:00 SCH A 316

Novel Energy-Filtered Field Stop Technology For Highly Blocking IGBTs — •ROBERT KOCH¹, MARCEL GEROLD¹, SHAVKAT AKHMADALIEV², MICHAEL RÜB¹, and ELKE WENDLER³ — ¹Ernst-Abbe-Hochschule, Fachbereich SciTec, Jena, Germany — ²Helmholtz-Zentrum Dresden-Rossendorf, Dresden, Germany — ³Friedrich-Schiller-Universität, Physikalisch-Astronomische Fakultät, Jena, Germany

Insulated Gate Bipolar Transistors (IGBTs) require on the one hand adjustable switching behavior and on the other hand high blocking capability. The technology presented in this work aims at implementing continuous deep carrier profiles as field stop structures. We insert a micro-patterned silicon membrane (energy filter) into the primary ion beam. This broadens its energy spectrum in a well controlled way, allowing production of extended continuous profiles. The micro patterns are restricted to rectangular shapes, due to the KOH etching manufacturing process. This means, instead of using multiple implantation steps for field-stop formation, our approach results in tailored smooth profiles by using energy-filtered Hydrogen implantations in the range of 1500 to 2500 keV. The defect profiles generated by H-implantation, are transformed into hydrogen-related donors by annealing at 300 to 400 °C. The annealing efficiency is related to the implanted dose (10¹³ to 5 × 10¹⁵ cm⁻²), annealing temperature, hold time and the process gas composition (H₂ content 2%). The defect profiles caused by proton bombardment using an energy filter and subsequent annealing are analyzed by Spreading Resistance Profiling (SRP).

DS 11: Thin Film Application

Time: Wednesday 11:00–12:15

Location: SCH A 315

DS 11.1 Wed 11:00 SCH A 315

Resonante Mikrowellenabsorberschichten für Fusionsreaktoren — •ANDREAS HENTRICH — Universität Stuttgart

Um einen Fusionsreaktor zu betreiben wird ein Heizsystem benötigt, im Falle des ITERs ist das eine Mikrowellenheizung bei 170GHz. Dies impliziert aber direkt, dass entsprechende Absorber vorhanden sein müssen, die den extremen Bedingungen innerhalb eines Fusionsreaktors standhalten. Ebendiese wurden für den ITER in Form einer gemischten Metall-Oxid-Schicht realisiert. Da geläufige Mikrowellenabsorber platzintensiv sind, wurde ein resonanter Absorptionsmechanismus genutzt, was Absorptivitäten von über 90% bei Schichtdicken von rund 100μm ermöglicht.

Der Absorptionsmechanismus wurde sowohl im Modell als auch durch Messungen verifiziert und quantifiziert. Es wurden die Reflektivitäten von vier verschiedenen Materialsystemen winkel-, schichtdicken- und polarisationsabhängig bestimmt. Deren Materialeigenschaften wurden mit Hilfe der Modelle bestimmt und damit die Schichten hinsichtlich ihrer Absorptionseigenschaften optimiert.

DS 11.2 Wed 11:15 SCH A 315

The effect of photon recycling and back-grading on CIGS cell performance — •SEÇİL GÜLER^{1,2}, UWE RAU^{1,3}, and THOMAS KIRCHARTZ^{1,2} — ¹IEK-5 Photovoltaik, Forschungszentrum Jülich — ²NST and CENIDE, Universität Duisburg-Essen — ³Faculty of Electrical Engineering and Information Technology, RWTH Aachen University

Photon recycling, i.e. the reabsorption of photons created by radiative recombination within the solar cell, is the missing link between Shockley-Queisser model and classical diode theory. In order to determine the thermodynamic limits of solar cells, it is therefore necessary to consider the photon recycling process. This study aims at calculating the theoretical efficiency limits of Cu(In,Ga)Se₂ (CIGS) solar cells using 1-dimensional drift-diffusion solvers by including the effect of photon recycling and bandgap grading. Simulations of current-voltage curves were performed by changing limiting factors such as back grading, back sur-

face recombination velocity, electron and hole mobilities, and Shockley-Read-Hall (SRH) lifetime as well as the back reflection at the interface of the Mo/CIGS structure. We investigate under which circumstances photon recycling has a significant effect on device performance and study the optimum bandgap grading for different material properties.

DS 11.3 Wed 11:30 SCH A 315

Strategies to obtain chiral perovskites via surface modification — •MARKUS HEINDL^{1,2}, TIM KODALLE³, NATALIE FEHN², LENNART REB², SHANGPU LIU^{1,2}, CONSTANTIN HARDER^{2,4}, MAGED ABDELSAMIE³, LISSA EYRE^{2,5}, IAN SHARP², STEPHAN ROTH^{4,6}, PETER MÜLLER-BUSCHBAUM², ALEXANDER ÜRBAN⁷, ARAS KAROUZIAN², CAROLIN SUTTER-FELLA³, and FELIX DESCHLER¹ — ¹Heidelberg University, Heidelberg, Germany — ²Technical University of Munich, Garching, Germany — ³Lawrence Berkeley National Laboratory, Berkeley, USA — ⁴Deutsches Elektronen-Synchrotron (DESY), Hamburg, Germany — ⁵University of Cambridge, Cambridge, Great Britain — ⁶KTH Royal Institute of Technology, Stockholm, Schwede — ⁷Ludwig-Maximilians-Universität, Munich, Germany

The generation, manipulation and detection of light is a key requirement for a wide range of technologies. Thus, this field is in the constant focus of further technological advancement. Recent discoveries on the design of chiral metal-organic perovskites now promise cheap, sustainable materials for energy efficient generation and detection of polarized light. However, so far, the available pool of chiral perovskite materials is limited to a few one- and two-dimensional crystal structures.

Here, we present novel strategies to produce perovskite thin films with chiral surface modification directly. The resulting compound displays strong circular dichroism effects in the blue spectral region, which can be adjusted in their intensity by varying synthetic parameters. Furthermore, we perform an extensive structural investigation into the origin of these phenomena utilizing XRD and GIWAX experiments.

DS 11.4 Wed 11:45 SCH A 315

All-oxide thin-film varactors with Mn- and Ni-doped (Ba,Sr)TiO₃ for microwave applications — •YATING RUAN¹, STIPO MATIC², ALEXEY ARZUMANOV¹, PHILIPP KOMISSINSKIY¹, ROLF JAKOBY², and LAMBERT ALFF¹ — ¹Advanced Thin Film Technology, Institute of Materials Science, Technische Universität Darmstadt, Darmstadt, Germany — ²Microwave Engineering and Technology, Technische Universität Darmstadt, Darmstadt, Germany

With a trend toward miniaturization of modern electronics, tunable microelectronic devices operating over a wide range of frequencies are required for mobile communications, high-speed data connections with the upcoming 5G and Internet of Things (IoT) technologies.

Here we present all-oxide thin-film tuneable capacitors (varactors) with single-crystalline films of a tunable dielectric perovskite Ba_xSr_{1-x}TiO₃ (BST) doped with Mn and Ni, grown epitaxially by pulsed laser deposition on a highly conducting thin-film oxide SrMoO₃ bottom electrodes with a room-temperature resistivity of 30 μΩcm. A partial substitution of the tetravalent Ti at B-sites of the BST perovskite structure with Mn and Ni in a trivalent or divalent state decreases a concentration of oxygen vacancies in the BST, leading to a reduction of the leakage current density of the varactor by 5 orders of magnitude down to 1 A/m². The low leakage current allows the thickness of the BST layers to go below 50 nm, enabling varactors tunable with low voltages.

DS 11.5 Wed 12:00 SCH A 315

Finite Volume Modeling of Two-Dimensional Memristive Devices for Neuromorphic Computing — •BENJAMIN SPETZLER¹, DILARA ABDEL², and PATRICK FARRELL² — ¹Technische Universität Ilmenau, Ilmenau, Germany — ²Weierstrass Institute, Berlin, Germany

In recent years, memristive devices have shown considerable potential for realizing synaptic functionalities in neuromorphic computing systems. Here, we present numerical models to analyze the hysteretic behavior of memristive devices. A finite volume model self-consistently solves the semiconductor equations for the electrostatic potential and the quasi-Fermi levels of electrons and holes. Further, we include the dynamics of mobile dopants and briefly discuss the boundary conditions implemented for the calculation of the switching dynamics and the current-voltage characteristics. Simulations are compared with measurements on two-dimensional flake devices based on MoS₂. The results are used to validate the simulations and discuss the underlying switching mechanisms. Implications for the design of memristive devices are derived and discussed.

This work was partially funded by the Carl-Zeiss Foundation via the Project MemWerk and the German Research Foundation (DFG) through the Collaborative Research Centre CRC 1461 "Neurotronics - Bio-Inspired Information Pathway" as well as the Leibniz competition.

DS 12: Poster

Time: Wednesday 17:00–19:00

Location: P3

DS 12.1 Wed 17:00 P3

Growth and structural investigation of the SnBiTe stoichiometric series via MBE and TEM — •XIAO HOU¹, ABDUR REHMAN JALIL², DETLEV GRÜTZMACHER², CLAUS CLAUS MICHAEL SCHNEIDER¹, and LUKASZ PLUCINSKI¹ — ¹PGI-6, Forschungszentrum Jülich, Germany — ²PGI-9, Forschungszentrum Jülich, Germany

A topological phase transition (TPT) can be induced to engineer the band structure. This TPT is a fascinating, yet complex phenomenon in condensed matter research. Upon changing the stacking order of layers having different spin-orbit coupling (SOC) strengths, one can achieve a topological phase transition between trivial and nontrivial states [1,2]. Here, the Sn_xBi_yTe_z (SBT) stoichiometric series is a classical example, in which a stacking-dependent topological phase transformation group is explored.

The epitaxial growth of three distinct compositions i.e. SnBi₂Te₄, SnBi₄Te₇, Sn₂Bi₂Te₅ is conducted on Si (111) substrates via molecular beam epitaxy (MBE). X-ray diffraction (XRD) is employed to characterize the crystal quality of the grown thin films. We have also used advanced transmission electron microscopy (TEM) to investigate the stacking order. High-angle annular dark-field imaging provided detailed information about the crystallinity and atomic arrangements of the layer stacks and also of various types of structural defects in the thin films. The link between the stacking order and the topological characteristics requires further investigation that is ongoing.

[1] B.-J. Yang and N. Nagaosa, Nature Comm. 5, 4898 (2014). [2] R. Peng et al. Phys. Rev. B 101,115427 (2020).

DS 12.2 Wed 17:00 P3

Thin film growth characterization of a multipurpose physical vapor deposition apparatus with the goal of investigating tailored perpendicular magnetic anisotropy systems — •FLORIAN OTT, CHRISTIAN JANZEN, ARNE SCHRÖDER, and ARNO EHRESMANN — Institute of Physics, University of Kassel, D-34132 Kassel

In recent years, systems of multilayered (ML) magnetic thin films consisting of ferromagnetic transition metals (TM) with noble metallic spacers displaying perpendicular magnetic anisotropy (PMA) have gained increased interest for applications in magnetic particle transport [1], controlled domain movement [1,2] and sensor technologies [3]. These TM-based PMA systems may rely on the precise modulation of layer growth additionally to the already very low thickness requirements [1]. As a result, a precise control of the growth conditions is necessary in order to produce these systems. This work focuses on the characterization of growth conditions and parameters inside a multipurpose physical vapor deposition (PVD) apparatus with the ultimate goal of creating and investigating engineered TM-based PMA systems. [1] M Urbaniak, et al. Magnetization reversal of Co/Au multilayer stripes with keV-He⁺ ion bombardment induced coercivity. J. Phys. D: Appl. Phys. 48 (2015) 335003 (7pp) gradient, [2] A. Jarosz, et al. Magnetic domain propagation in Pt/Co/Pt micro wires with engineered coercivity gradients along and across the wire, Journal of Magnetism and Magnetic Materials, Volume 435 (2017) [3] M. Matczak, et al. Co/Au multilayers with graded magnetic anisotropy for magnetic field sensing. applied physics letters 100, 162402 (2012)

DS 12.3 Wed 17:00 P3

Strain and Lattice-Relaxation Effects of (Al,Ga)N/GaN Interfaces on 4D-STEM Signals — •FREDERIK OTTO, LAURA NIERMANN, TORE NIERMANN, and MICHAEL LEHMANN — Technical University of Berlin, Berlin, Germany

The immense increase in computation power over the past decades can be attributed to the decreasing size of semiconductor device structures. Preceding this trend, semiconductor research focuses on thin films and their interfaces with the surrounding substrate material.

At these interfaces of heterogeneous device structures, the atomic lattices are strained due to the mismatch of lattice constants of interfacing materials. Scanning-Transmission Electron-Microscopy (STEM) is capable of resolving strain at a nanometer scale, however, investigated specimens must be sufficiently thin to be electron transparent. For such thin specimens, the relaxation of the strained lattice at its surfaces cannot be neglected when measuring strain in an electron microscope.

Here, knowledge about the underlying strain and relaxation effects at the interface of (Al,Ga)N/GaN Quantum Wells (QWs) is obtained by comparing 4D-STEM measurements with simulations. By carefully choosing the experimental parameters, i.e., convergence angle and tilt, features of multiple scattering events are found in the measured diffraction discs perpendicular to the QW structure at every position of a 2D scanned area. These features are evaluated by comparison with corresponding simulations considering a strain field and relaxation effects as obtained from finite element calculations.

DS 12.4 Wed 17:00 P3

Comparative evaluation of EDS quantification methods for the analysis of Sc_xAl_{1-x}N films — •HAUKE HONIG¹, REBECCA PETRICH², LORENZ STEINACKER¹, YOUNES SLIMI², DANIEL GLÖSS³, STEPHAN BARTH³, HAGEN BARTZSCH³, RAPHAEL KUHNEN⁴, DIETMAR FRÜHAUF⁴, STEFAN KRISCHOK², and KATJA TONISCH² — ¹Technische Universität Ilmenau, Fachgebiet Werkstoffe der Elektrotechnik, IMN MacroNano[®], 98693 Ilmenau — ²Technische Universität Ilmenau, Fachgebiet Technische Physik I, IMN MacroNano[®], 98693 Ilmenau — ³Fraunhofer-Institut für Organische Elektronik, Elektronenstrahl- und Plasmatechnik FEP, 01277 Dresden, Germany — ⁴Endress+Hauser SE+Co. KG, TTD Technologieentwicklung, 79689 Maulburg, Germany

The quantitative analysis of Sc_xAl_{1-x}N films with energy dispersive x-ray spectroscopy (EDS) poses some challenges due to peak overlaps and the thin film character. Standard-free and standard-based methods are compared regarding their reliability for the quantification of the Sc-content in sputtered films with 0 ≤ x ≤ 0.35 and evaluated using reference samples that have been quantified with GDOES and EDS by Fraunhofer FEP. Therefore, parameters such as acceleration voltage, selection of standard materials and quantification models are considered. Theoretical spectrums generated with Monte-Carlo simulations are used to improve the selection of excitation energy in the small range between substrate influence and limits of the quantification models. The crystalline hexagonal structure is confirmed with XRD.

DS 12.5 Wed 17:00 P3

From Doping to Dilution: Local Chemistry and Collective Interactions of La in HfO₂ — •OLIVER REHM¹, THOMAS SZYJKA^{1,2}, LUTZ BAUMGARTEN², CLAUDIA RICHTER³, YURY MATVEYEV⁴, CHRISTOPH SCHLUETER⁴, THOMAS MIKOLAJICK^{3,5}, UWE SCHROEDER³, and MARTINA MÜLLER¹ — ¹Uni Konstanz, Konstanz, Germany — ²FZJ, Jülich, Germany — ³NaMLab, Dresden, Germany — ⁴DESY, Hamburg, Germany — ⁵TU Dresden, Dresden, Germany

HfO₂-based thin films exhibit huge potential for the next generation of non-volatile memory applications, such as FeRAM or FeFET. The application of HfO₂-based thin films as active ferroelectrics (FE) in these devices face reliability issues like wake-up, imprint, and fatigue. The FE phase of HfO₂ is the metastable orthorhombic structure, for which La doping is considered a promising route for stabilization.

La:HfO₂ samples were grown by ALD with a range of La doping, from 3.5% to 33%, i.e., from the doping to dilution level. We link the local chemistry at the La lattice sites with local and collective electronic properties of the La:HfO₂ matrix using HAXPES. The satellite structure of La 3d core level, the plasmonic excitation energies, and core-level rigid binding energy (BE) shifts are investigated. The emerging chemical phases and electronic properties are discussed as a function of La doping. From the evolution of the plasmon excitation energies and rigid BE shifts, it is concluded that electronic charge compensation by oxygen vacancies occurs for increasing La content.

[1] T. Szyjka, et al., Phys. Status Solidi RRL 2022, 16, 2100582

DS 12.6 Wed 17:00 P3

Molecular Dynamics - Two Temperature Model simulations of gold — •OTHMANE BENHAYOUN¹, EMILIANO PRINCIPPI³, BERND BAUERHENNE¹, DMITRY S. IVANOV², and MARTIN E. GARCIA¹ — ¹University of Kassel, Theoretical physics II, Kassel, Germany — ²Moscow, Russia — ³Elettra-Sincrotrone Trieste S.C.p.A., Trieste, Italy

We aim to explain the results obtained from a recent Ultrafast Electron Diffraction (UED) experiment that showed periodic oscillations in both height and width of the (311) Au diffraction peak. The same effect is however not observed in polycrystalline gold. We have thus performed Molecular Dynamics - Two Temperature Model (MD-TTM) simulations to model more than 11 million atoms, enabling us to understand the underlying physical processes. In our simulations, we obtain similar peak oscillations and determine the major mechanisms that lead to such lattice dynamics.

DS 12.7 Wed 17:00 P3

In situ X-Ray Total Scattering Investigation of Thermal Annealing in Fe-CoSiB Metallic Glass Films — •NICOLAS HAYEN¹, PHILIPP JORDT¹, LARS THORMÄHLEN², MATHIS MEWES¹, ANN-CHRISTIN DIPPEL³, OLOF GUTOWSKI³, NIKLAS WOLFF², LORENZ KIENLE², and BRIDGET MURPHY^{1,4} — ¹Institute of Experimental and Applied Physics, Kiel University, Germany — ²Institute of Material Sciences, Kiel University, Germany — ³Deutsches Elektronen-Synchrotron DESY, Hamburg, Germany — ⁴Ruprecht Haensel Laboratory, Kiel University, Germany

Thin films of the iron-based metallic glass (Fe_{0.9}Co_{0.1})₇₈Si₁₂B₁₀ (FeCoSiB) are seen as a promising candidate for technical applications in high sensitivity magnetic field sensors and have been utilized extensively within the CRC 1261 "Biomagnetic Sensing". Thermal annealing of these films leads to a decrease in quality of the desired magnetic properties depending on the parameters of the annealing process.

In situ grazing incidence high-energy x-ray total scattering experiments were used to investigate the onset of structural changes occurring in the material. Films of thickness ranging from 0.05 to 1 μm were investigated under varied annealing conditions with temperatures up to 700°C. From these measurements we were able to observe two separate crystallization phase transitions and the emergence of textured structures. Further analysis of the scattering from the amorphous phase may give further insight into the initial structural changes the material undergoes during annealing and their influence on magnetic properties.

DS 12.8 Wed 17:00 P3

Synthesis of structurally defined graphene nanoribbons: Peri-tetracene and its corresponding 1,1'-bitetracene precursor — •MAREN KLEIN^{1,2}, JOHN B. BAUER², MARIE WAGNER^{1,2}, HOLGER F. BETTINGER², THOMAS CHASSÉ¹, and HEIKO PEISERT¹ — ¹Institute of Physical and Theoretical Chemistry, University of Tübingen, Germany — ²Institute of Organic Chemistry, University of Tübingen, Germany

Band gap engineering of precise nanographenes has attracted much attention in the field of organic electronics as they show great electronic properties. One class of these promising nanographenes are acenes and their related peri-acenes. Acenes are linearly condensed polycyclic hydrocarbons whereas peri-acenes exhibit a two-dimensionally enlarged π system. As peri-acenes possess a diradical open-shell character, the synthesis is quite challenging. Here we demonstrate that peri-tetracene can be formed on-surface by annealing the deposited precursor molecule 1,1'-bitetracene on a Cu (111) surface. The unique 1,1'-bitetracene undergoes a surface-assisted cyclodehydrogenation which was investigated by

microscopic and spectroscopic techniques, as well as by DFT calculations. In the XAS spectra we could observe that the as-deposited molecule shows a vanishing intensity of π* transitions at normal incidence (90°), which indicates a planarization of the molecule already before annealing and an almost flat lying adsorption geometry.

DS 12.9 Wed 17:00 P3

Study of cadmium-based thin films obtained by pulsed laser deposition — •CRISTINA POSTOLACHI¹, GEORGIANA BULAI¹, SANDU CIBOTARU², ALEXANDRU COCEAN¹, BOGDANEL SILVESTRU MUNTEANU³, NICANOR CIMPOESU^{1,4}, SILVIA GAROFILDE¹, GEORGIANA COCEAN¹, IULIANA COCEAN¹, and SILVIU GURLUT¹ — ¹Alexandru Ioan Cuza University of Iasi, Faculty of Physics, Atmosphere Optics, Spectroscopy and Laser Laboratory (LOASL), 11 Carol I Bld. 700506 Iasi, Romania — ²Petru Poni Institute of Macromolecular Chemistry, Gr. Ghica Voda Alley, 41A, 700487 Iasi, Romania — ³Alexandru Ioan Cuza University of Iasi, Faculty of Physics, 11 Carol I Bld. 700506 Iasi, Romania — ⁴Gheorghe Asachi Technical University of Iasi, Faculty of Material Science and Engineering, 59A Mangeron Bld., Iasi, Romania

This study investigates the processes that occur when different chemical compounds of cadmium are mixed with selenium and are further used as targets for thin film growth by pulsed laser deposition. Here the interactions between these compounds in the laser induced plasma plume will be analyzed.

The aim of the investigation of the reactions that take place in the plasma plume at high vacuum is to obtain thin films of cadmium selenide. The thin films properties will be investigated with different techniques, such as Scanning Electron Microscopy coupled with Energy Dispersive Spectroscopy (SEM-EDX), X-ray Diffraction (XRD), profilometry, UV-VIS spectroscopy and others.

DS 12.10 Wed 17:00 P3

Fabrication of copper halide thin films by combinatorial PLD — •CHRISTOPHER WALTER, FELIX-FLORIAN DELATOWSKI, MICHAEL BAR, HOLGER VON WENCKSTERN, and MARIUS GRUNDMANN — Universität Leipzig, Felix Bloch Institute for Solid State Physics, Semiconductor Physics Group, Leipzig, Germany

Copper halides are promising p-type materials for transparent device applications due to their large direct band gaps ($E_g = 3-3.4 eV$) [1]. Here we present the deposition of copper halide thin films by combinatorial pulsed laser deposition (PLD) and discuss their structural, morphological and optical properties as a function of different growth parameters [2]. At ambient conditions, CuI crystallizes in the cubic zinc-blende structure. XRD shows <111>-orientation for CuI independent from the used substrate material. CuBr and CuCl grow polycrystalline with the same crystal structure as CuI. However, with the incorporation of low iodine concentration, the crystallinity improves significantly. We find that the thin films exhibit very smooth surfaces with a roughness of $R_{RMS} = 0.8-1.6 nm$ for the binary CuI, CuBr and CuCl systems under optimal parameters. Furthermore, using combinatorial PLD and a segmented target with one segment each of CuBr and CuI, ternary CuBr_xI_{1-x} alloys were grown. Based on the resulting locally varying composition, the influence on structural and optical properties can be directly observed.

[1] M. Grundmann *et al.* : phys. stat. sol. (a) 210, 9, 1671 (2013)

[2] H. von Wenckstern *et al.* : phys. stat. sol. (b) 257, 7, 1900626 (2019)

DS 12.11 Wed 17:00 P3

Electrical characterization of SnTe thin film topological crystalline insulator — •NEGIN BERYANI NEZAFAT, SEPIDEH IZADI, and GABI SCHIERNING — Department of physics, Experimental physics, Bielefeld University, 33615, Bielefeld, Germany

Topological crystalline insulators (TCIs) with gapless metallic states and protected carrier transport offer unique electrical features. Band structure of these materials consists of conventional parabolic band diagram together with linear surface transport. In this work, SnTe thin film as a promising TCI is considered to be our model system. Therewith, SnTe thin films with different thicknesses are deposited on silicon substrate using RF magnetron sputtering. The resulting morphology characterization for rock-salt SnTe crystalline thin film fulfills stoichiometric ratio. Electrical characterization including temperature dependent resistivity, magnetoresistance and Hall analysis are performed using Van der Pauw configuration. These findings introduce SnTe thin film as a promising candidate for technical applications such as device fabrication.

DS 12.12 Wed 17:00 P3

Current probe AFM measurements on reactively co-sputtered Ag_xCu_{1-x}I thin films — TILLMANN STRALKA, •SOFIE VOGT, CHRISTIANE DETHLOFF, JORRIT BREDOW, HOLGER VON WENCKSTERN, and MARIUS GRUNDMANN — Universität Leipzig, Felix-Bloch-Institut, Germany

CuI exhibits a high hole mobility of up to 44 cm²/Vs in bulk crystals and of about 19 cm²/Vs in polycrystalline thin films^[1,2]. This, combined with high transparency in the visible light range, renders CuI an interesting material for transparent complementary devices. However, grain boundary (GB) conduction is dominating electrical properties and might inhibit device performance^[3]. An-

nadi *et al.* showed that alloying with silver reduces the conductivity of $\text{Ag}_x\text{Cu}_{1-x}\text{I}$ thin films and even results in switching from p-type to n-type^[4].

We present topological and current probe (cp)-atomic force microscopy measurements on reactively sputtered $\text{Ag}_x\text{Cu}_{1-x}\text{I}$ thin films with silver contents from $x=0.1$ to $x=0.6$. A strong decrease of the grain size with increasing silver content is observed. In addition, a decrease of the overall surface current is observed, which agrees well with electrical bulk characterizations. For $x \geq 0.39$ we observed that the current from tip to sample is mainly injected at grain boundaries while for large Ag content the injected current at GBs is negligible.

^[1] D. Chen *et al.*, *Crystal Growth Design*, 10, 2057*2060, 2010.

^[2] C. Yang *et al.*, *ACS Appl. Electr. Mater.*, 2, 3627-3632, 2020.

^[3] Kneiß *et al.*, *Adv. Mater. Interfaces*, 5, 1701411, 2018.

^[4] A. Annadi *et al.*, *Appl. Mater. Today*, 20, 100703, 2020.

DS 12.13 Wed 17:00 P3

Analysis of the structural properties of $\text{Li}(\text{Ni}_{1/3}\text{Co}_{1/3}\text{Mn}_{1/3})\text{O}_{2-\delta}$ (NCM) thin film model cathodes — JULIUS KONSTANTIN DINTER and •MATTHIAS ELM — Center for Materials Research, Justus-Liebig-University Giessen Germany, Heinrich-Buff-Ring 16, 35392 Giessen

Lithium ion batteries often suffer from capacity fading due to undesired side reactions occurring at the cathode surface. To get a deeper understanding of these side reactions, 2D model system are necessary. For this purpose, NCM thin film cathodes were prepared via spin coating followed by annealing at high temperatures. Using these thin film cathodes allow us to perform various surface sensitive measurements such as Raman microscopy, AFM, ESM, SEM and EDX. As no additives are used, we are able to study the surface reaction occurring at the cathode active material in more detail using in-situ measurements. The results reveal structural changes of the surface accompanied by an increase of the cell resistance, which confirms the formation of an SEI. Furthermore, the electrochemical performance of thin films coated with Al_2O_3 using atomic layer deposition (ALD) were investigated. The analysis of the surface properties confirm that coating of the NCM-thin film suppresses the undesired surface reactions resulting in an improved long-term cycling stability.

DS 12.14 Wed 17:00 P3

Nanoscope Investigation of the Monolayer MoSe_2 - WSe_2 Lateral Heterostructures under Illumination — •ALEXANDER TURCHANIN¹, TOBIAS NÖRENBERG¹, ZIYANG GAN², ANTONY GEORGE², ANDREY TURCHANIN², SUSANNE C. KEHR^{1,3}, and LUKAS M. ENG^{1,3} — ¹TU Dresden — ²Friedrich Schiller University Jena — ³Wuerzburg-Dresden Cluster of Excellence - EXC 2147 (ct.qmat)

Transition metal dichalcogenides (TMDCs) such as MoSe_2 and WSe_2 , are inorganic semiconductor monolayers with great potential for integration into nanoscale devices. Monolayers of different TMDCs can be engineered into lateral or vertical heterostructures forming, e.g., 1D or 2D p-n junctions that strongly respond to light [1]. Here, lateral heterostructures of monolayer MoSe_2 and WSe_2 grown by chemical vapor deposition are studied at the nanometer length scale by Kelvin Probe Force Microscopy (KPFM) under visible to near-infrared light illumination, i.e. photon energies between 1.45 and 1.95 eV. This approach enables for the simultaneous recording of both the sample surface morphology and the local photoinduced surface potential. By employing the side-band KPFM demodulation [2], quantification of the local band-bending of this in-plane heterostructure is possible with superior sensitivity. Different alterations of the local surface potential are observed when choosing the light exposure above and below the individual TMDCs bandgap energies.

^[1] P.A. Markeev *et al.*, *J. Phys. Chem. C* **125**, 13551 (2021).

^[2] T. Wagner *et al.*, *Beilstein J. Nanotechnol.* **6**, 2193 (2015).

DS 12.15 Wed 17:00 P3

Electronic structure of MXenes determine from angle-resolved photoelectron spectroscopy — •WEI YAO¹, DONGQI LI^{1,2}, JONAS A. KRIEGER¹, MIHIR DATE¹, EMILY C. MCFARLANE¹, MINGHAO YU^{1,2}, XINLIANG FENG^{1,2}, and NIELS B.M. SCHRÖTER¹ — ¹Max-Planck Institute of Microstructure Physics, Halle (Saale), 06120, Germany — ²Center for Advancing Electronics Dresden (cfaed) and Faculty of Chemistry and Food Chemistry, TU Dresden, Dresden, 01062, Germany

Transition metal carbides, also known as MXenes, have been one of the most fascinating two-dimensional material systems beyond graphene. Chemical substitution of the transition metal elements and terminal function groups have resulted in versatile and tunable electronic, optical and mechanical properties, with applications in energy storage, multifunctional sensors, transparent and flexible electrodes, electromagnetic interference shielding, or hydrogen evolution reaction catalysis [1]. However, to reveal the origins of the MXenes' exceptional properties, a deeper understanding of their electronic structure is required. Here we report the first micro-focused angle-resolved photoemission spectroscopy (ARPES) measurements of single MXene flakes, which will reveal the influence of the chemical environment on the the single-particle electronic band structure, as well as many-body effects reflected in its spectral function.

[1]. A. VahidMohammadi, J. Rosen, and Y. Gogotsi. The world of two-dimensional carbides and nitrides (MXenes). *Science* **372**, eabf1581 (2021)

DS 12.16 Wed 17:00 P3

Mode-selective Raman Signal Enhancement in MoS_2/WS_2 Heterostructures — •ANNIKA BERGMANN¹, MUSTAFA HEMAID¹, RICO SCHWARTZ¹, ZIYANG GAN², ANTONY GEORGE², ANDREY TURCHANIN², and TOBIAS KORN¹ — ¹Institute of Physics, University of Rostock, Germany — ²Institute of Physical Chemistry, Friedrich Schiller University Jena, Germany

In the family of van der Waals materials, transition metal dichalcogenides (TMDCs) have attracted much attention in recent years. Stacking various TMDC materials forms heterostructures in which new phenomena, such as interlayer charge transfer and interlayer excitons [1] occur. However, for the observation of interlayer effects good contact between the constituent monolayers is crucial. Here, we investigate bilayer heterostructures that were formed by combining Chemical Vapor Deposition (CVD) grown MoS_2 and exfoliated WS_2 monolayers. Photoluminescence quenching is used as an indicator to evaluate the interlayer coupling. In addition, the out-of-plane (A_{1g}) phonon mode provides information on the interfacial contact [2]. We observe a selective enhancement of the WS_2 A_{1g} Raman mode in well-coupled MoS_2/WS_2 heterostructures compared to WS_2 monolayers or heterostructures with only poor contact. A systematic study of this phenomenon is presented to elucidate its microscopic origin.

[1] Fang *et al.*, *Proc. Natl. Acad. Sci. USA* **111** (2014)

[2] Zhou *et al.*, *ASC Nano* **8** (2014)

DS 12.17 Wed 17:00 P3

Exfoliation of 2D materials for nanooptics — •JAKOB WETZEL¹, MAXIMILIAN OBST^{1,2}, SUSANNE C. KEHR^{1,2}, and LUKAS M. ENG^{1,2} — ¹TU Dresden, Dresden, Germany — ²Würzburg-Dresden Cluster of Excellence - EXC 2147 (ct.qmat), Dresden, Germany

The desire for smaller and more energy efficient optical components leads to the necessity of light confinement below the diffraction limit. This can be achieved e.g. by phonon polaritons (PhPs) which are quasiparticles formed by the coupling of infrared photons with the optical phonons of a crystal. Particularly the related light confinement is enhanced when the PhPs are generated in anisotropic, 2D van der Waals materials such as MoO_3 and GeS [1, 2]. Therefore, flat and μm -sized nanosheets of such materials are required, which can be realized by mechanical exfoliation.

Here, we present an optimized exfoliation technique for MoO_3 and GeS resulting in the reproducible generation of 20 to 100 μm -sized flakes with a thickness of about 100 nm. We present a quick and easy to implement adaptation of the scotch-tape exfoliation technique as well as exemplary results based on optical microscopy images and atomic force microscopy.

[1] T.V.A.G de Oliveira *et al.*, *Adv. Mater.* **33**, 2005777 (2021).

[2] T. Nörenberg *et al.*, *ACS Nano*, published online (2022),

DOI: 10.1021/acsnano.2c05376.

DS 12.18 Wed 17:00 P3

hybrid resonant circuits with van der Waals materials — •HAOLIN JIN¹, GIUSEPPE SERPICO², CHRISTIAN N. SAGGAU², SANAZ SHOKRI², MICKEY MARTINI², YEJIN LEE², POYA YANG¹, SEBASTIAN SEIFERT¹, URI VOOL¹, and NICOLA POCCIA² — ¹Max Planck Institute for Chemical Physics of Solids, Dresden, Germany — ²Leibniz Institute for Solid State and Materials Science Dresden (IFW Dresden), Dresden, Germany

Van der Waals superconductors, especially heterostructures, are believed to exhibit novel superconducting phases. However, the standard measurement techniques designed for bulk superconductors are challenging to apply in 2D materials which cannot be grown in sufficient size and quality. Herein, we introduce an efficient method to explore the properties of 2D materials, by combining them into hybrid resonant circuits. The resonator can have a strong inductive interaction with a small-size superconducting sample, affecting its frequency response. However, creating superconducting contacts between the resonator and the 2D material is challenging, especially for air-sensitive materials where evaporation must be done in a protected glovebox. Here, we present a technique to make robust superconducting contacts to a 2D sample by using a flexible nanomembrane. The Niobium resonator circuit is fabricated on top of the nanomembrane, and via contacts connect it to the 2D materials. Through the circuit response, we can explore the properties of novel unconventional superconductors. Moreover, this hybrid circuit is a new type of quantum device for future quantum technology applications.

DS 12.19 Wed 17:00 P3

Phase transformations in few-layer transition metal phosphorus trichalcogenides studied by low-voltage TEM — •ALEXANDER STORM¹, JANIS KÖSTER¹, MAHDI ASL-GOHRBANI², SILVAN KRETSCHMER², TATIANA GORELIK¹, MICHAEL K. KINYANJUI¹, ARKADY KRASHENINNIKOV², and UTE KAISER¹ — ¹Central Facility Materials Science Electron Microscopy, Ulm University, 89081 Ulm, Germany, — ²Institute of Ion Beam Physics and Materials Research, Helmholtz-Zentrum Dresden-Rossendorf, 01328 Dresden, Germany,

In this work we study phase transformations in freestanding few-layer transition metal phosphorus trichalcogenides (TMPTs) induced by electron irradiation as well as thermal annealing in vacuum, using various analytical transmission elec-

tron microscopy techniques (TEM). In addition, our results are supported by ab-initio calculations.

We show that due to knock-on damage, first sulphur atoms are ejected in sulphur-based TMPTs at common TEM acceleration voltages (60kV - 300kV), which in turn leads to the formation of defects and strong modifications of the TMPT's properties [1]. For instance, we show that in few-layer MnPS₃ and MnPSe₃, stable, ultrathin α - and γ -MnS/MnSe phases are formed showing the reliability of this transformation in Mn based TMPTs. Eventually, we elucidate the emerging phases and transition temperatures for few-layer MnPS₃, MnPSe₃, FePS₃, FePSe₃, and NiPS₃ induced by thermal annealing.

[1] Köster, Storm et al., J. Phys. Chem. C, 126, 36, 15446 (2022).

DS 12.20 Wed 17:00 P3

Encapsulating high-temperature superconducting twisted van der Waals heterostructures blocks detrimental effects of disorder — •YEJIN LEE^{1,2}, MICKY MARTINI^{1,2}, TOMMASO CONFALONE¹, SANAZ SHOKRI^{1,2}, CHRISTIAN SAGGAU¹, DANIEL WOLF¹, GENDA GU³, KENJI WATANABE⁴, TAKASHI TANIGUCHI⁴, DOMENICO MONTEMURRO⁵, VALERII VINOKUR⁶, KORNELIUS NIELSCH^{1,2}, and NICOLA POCCIA¹ — ¹IFW Dresden, Dresden, Germany — ²TU Dresden, Dresden, Germany — ³Condensed Matter Physics and Materials Science Department, Brookhaven National Laboratory, NY, USA — ⁴NIMS, Tsukuba, Japan — ⁵University of Naples Federico II, Naples, Italy — ⁶Terra Quantum AG, Gallen, Switzerland

Van der Waals (vdW) heterostructures based on cuprate superconductors attract substantial interest of novel topological phases as well as technological applications. One of the hindrances for the progress is the detrimental effect of disorder on the properties of the vdW devices-based Josephson junctions. This work reports a novel method of fabricating twisted vdW heterostructures made of Bi₂Sr₂CuCaO_{8+x}, combining the employed cryogenic stacking using a solvent-free stencil mask technique and additionally covering the interface with insulating hexa boron nitride layers. We find that encapsulating the interface in the stacked systems overcomes detrimental effects of disorder providing highly coherent Josephson junction. This finding enables crucial improvement of its critical current and the T_c of the junctions up to their magnitudes in bulk intrinsic junctions.

DS 12.21 Wed 17:00 P3

In-situ formation of Mo₅Te₆ nanowire in single-layer 2H-MoTe₂ by annealing and electron irradiation — •JANIS KÖSTER¹, SILVAN KRETSCHMER², MICHAEL K. KINYANJUI¹, ALEXANDER STORM¹, FABIAN RASPER¹, ARKADY V. KRASHENINNIKOV², and UTE KAISER¹ — ¹Electron Microscopy of Materials Science, Ulm University, Albert Einstein Allee 11, 89081 Ulm, Germany — ²Institute of Ion Beam Physics and Materials Research, Helmholtz-Zentrum Dresden-Rossendorf, 01328 Dresden, Germany

Up to now, the fundamental understanding of transformations in 2D materials at the atomic scale are not fully characterized. Here, we demonstrate a route to locally transform freestanding single-layer (1H-) MoTe₂ [1] into 1D-Mo₅Te₆ nanowires [2] under electron beam irradiation and by heating. (HR)TEM at the Cc/Cs-corrected SALVE [3] microscope at 80 kV is used to analyse structural changes in the material. Combining the experimental data with the results of first-principles calculations, we explain energetics and stabilities of MoTe₂ monolayers and Mo₅Te₆ nanowires due to an interplay of electron-beam-induced energy input, atom ejection, and oxygen absorption. A detailed understanding of high-temperature solid-to-solid phase transformation in the 2D limit provides insights into the material's applicability for future device fabrication.

[1] J. Köster, et al. The Journal of Physical Chemistry C 125.24 (2021): 13601-13609.

[2] H. Kim, et al. Small 16.47 (2020): 2002849

[3] M. Linck, et al. Physical review letters 117.7 (2016): 076101

DS 12.22 Wed 17:00 P3

Structural and magnetic properties of two dimensional (2D) Fe_xGeTe₂ and Fe_xGaTe₂ grown by molecular beam epitaxy (MBE) — •ATEKELTE KASSA, HUA LV, NEHA AGRAWAL, MICHAEL HANKE, ABBES TAHRAOUI, MANFRED RAMSTEINER, and MARCELO LOPES — Paul-Drude-Institut für Festkörperelektronik, Leibniz Institut im Forschungsverbund Berlin e.V., Berlin, Germany

2D materials with intrinsic functionality showed importance in fundamental condensed-matter science and for the development of advanced technologies, where 2D ferromagnetic materials have raised interest for developing low-dimensional magnetic/spintronic devices. Yet maintaining 2D ferromagnetism at /above room temperature remains a challenge. This work presents our recent results on 2D ferromagnets of Fe_xGeTe₂ and Fe_xGaTe₂ (3 ≤ x ≤ 5) prepared using MBE. Films were grown at 300 °C using elemental fluxes of Fe, Ge (Ga), and Te on epitaxial graphene on SiC (0001). Epitaxial films with good structural quality were confirmed by reflection high-energy electron diffraction and X-ray Diffraction. Atomic force microscopy confirmed continuous and smooth surface growth. Raman spectroscopy results showed that the graphene layers remain structurally unaltered after MBE growth. Anomalous Hall effect investigations through Magneto-transport studies identified a perpendicular magneto anisotropy as well as a Curie temperature (T_c) above 300 K for both films with Fe

composition close to x=5. For Fe_xGaTe₂, T_c values around 380 K were obtained. These results make the studied ferromagnets promising for the development of novel spintronic devices based on 2D materials and heterostructures.

DS 12.23 Wed 17:00 P3

Towards engineering of tailored 2D single photon emitters (SPE) by encapsulating single dye molecules into few layer hexagonal boron nitride (hBN) — •NILS LE COUTRE, TIM VÖLZER, PAUL WEINBRENNER, LISA BÖHME, FRANZISKA FENNEL, TOBIAS KORN, STEFAN LOCHBRUNNER, and FRIEDEMANN REINHARD — University of Rostock, Rostock, Germany

We hypothesize that encapsulating dye molecules into multilayer hBN flakes overcomes photobleaching, for example by improved thermal conduction and airtight sealing. This would tackle one of the biggest barriers to the application of fluorescent dyes in various methods like optical nearfield microscopy or quantum sensing. I will present work to deposit dyes on exfoliated multilayer hBN flakes by different methods of physical vapor deposition (PVD) and liquid deposition, as well as initial studies on photostability by confocal microscopy. The large variety of available dye molecules will provide a rich toolbox for engineering of 2D SPEs, with greater flexibility than the limited set of intrinsic defects in 2D materials and bulk crystals.

DS 12.24 Wed 17:00 P3

Epitaxy and transfer of freestanding oxide perovskites — •JEREMY MALTITZ, DUC NGUYEN, ALEV YUVANC, JENS MARTIN, and JUTTA SCHWARZKOPF — Leibniz Institut für Kristallzüchtung, Max-Born-Str. 2, 12489 Berlin, Deutschland

Fabrication of artificial 3D heterostructures is of increasing interest for a broad range of application, such as flexible sensor, memristors, or electronic skins. Layer transfer of thin films has established a new paradigm of material assembly and design in context of 2D-van-der-Waals crystals. Recently, freestanding oxide perovskites have been achieved by introducing a perovskite-like sacrificial layer (Sr₃Al₂O₆) between substrate and functional film. In combination with layer transfer, the functional film can be placed on arbitrary substrates (e.g. silicon wafers). Additionally, two functional layers (same or different) can be stacked with the opportunity to create moiré patterns by rotating the layers with respect to each other. Therefore, the influence of PLD growth parameter and thickness of SrTiO₃/Sr₃Al₂O₆ heterostructures are studied to improve the quality of freestanding SrTiO₃ thin films. Furthermore, the solid-solution family of (Ba,Ca,Sr)3Al₂O₆ enables the possibility to tune the lattice parameter. This property was used to adjust the lattice parameter of the sacrificial layer to closely match the lattice parameter of SrTiO₃. With improved growth parameter and lattice matched sacrificial layer, the crackformation of the freestanding film was reduced, paving the path towards the stacking of freestanding thin films.

DS 12.25 Wed 17:00 P3

Characterization of structural and magnetic properties of SrRuO₃ thin films

— •VITOR DE OLIVEIRA LIMA¹, MAI HUSSEIN HAMED¹, CONNIE BEDNARSKI-MEINKE¹, MICHAEL FALEY², EMMANUEL KENTZINGER¹, and THOMAS BRÜCKEL¹ — ¹Jülich Centre for Neutron Science (JCNS-2) and Peter Grünberg Institute (PGI-4), JARA-FIT, Forschungszentrum Jülich GmbH, Germany. — ²Ernst Ruska-Centre for Microscopy and Spectroscopy with Electrons (ERC), Forschungszentrum Jülich GmbH, Germany.

Proximity effects in Ferromagnet/Superconductor Heterostructures (F/S-H) have demonstrated high potential for development of new devices for spintronic and quantum computing application. SrRuO₃ (SRO) has attracted much attention among transition metal oxides for being the only 4d oxide to show itinerant ferromagnetism and metallic conductivity. In this work, we are characterizing the crystal structure as well the magnetic properties of SRO thin films for further application in F/S-H with YBa₂Cu₃O_{7-x} superconducting films. The samples were prepared on STO (001) single crystals by High-Oxygen Pressure Sputtering. SRO thin films are epitaxial and have smooth surface. Magnetometry indicate that samples have out-of-plane magnetic anisotropy and paramagnetic-ferromagnetic transition at approximately 150 K, which corresponds to the SRO with Ru⁴⁺ Curie temperature, and two transitions at lower temperatures, that may be related to another Ru oxidation state. The samples stoichiometry will be further investigated by Rutherford Backscattering Spectroscopy.

DS 12.26 Wed 17:00 P3

Charge-to-spin conversion in the quasi-two-dimensional electron gas emerging at the doped interface between LiNbO₃ and LaAlO₃ — •IGOR MAZNICHENKO^{1,2}, SERGEY OSTANIN¹, INGRID MERTIG¹, and PAWEŁ BUCZEK² — ¹Institute of Physics, Martin Luther University Halle-Wittenberg, D-06099 Halle, Germany — ²Department of Engineering and Computer Sciences, Hamburg University of Applied Sciences, Berliner Tor 7, D-20099 Hamburg, Germany

We anticipate that the functional use of a solid electrolyte lithium niobate in LaAlO₃/LiNbO₃ heterostructure allows one to tune the quasi-two-dimensional electron gas (q2DEG) which emerges there. This phenomenon can be achieved by charging and discharging LiNbO₃. Here, on the basis of *ab initio* calculations of the hydrogen-doped LaAlO₃/LiNbO₃ interface, we demonstrate how the

q2DEG and its spin polarization appear. The out-of-plane electric polarization of $\text{LaAlO}_3/\text{LiNbO}_3$ forces the H dopants to accommodate at the Al-terminated interface. This results in the formation of the q2DEG, whose spatial extent is about 1.5 nm along the stacking direction.

DS 12.27 Wed 17:00 P3

Preparation of oxide ferroelectric membranes by epitaxial sacrificial layers — •JONAS WAWRA^{1,2}, ROBIN ADLUNG^{1,2}, KORNELIUS NIELSCH^{1,2}, and RUBEN HÜHNE¹ — ¹Institute for Metallic Materials, Leibniz IFW Dresden, Germany — ²Institute of Applied Physics, TU Dresden, Germany

Oxide ferroelectric thin films are used in a variety of applications due to their strong remnant polarization and excellent dielectric, piezoelectric and optoelectric properties. However, well performing and robust materials require a high crystalline quality and orientation, which is commonly achieved by growing the desired ceramic on comparably thick and rigid substrates at high temperatures. This procedure prohibits in most cases the incorporation in advanced organic heterostructures and limits their utilization in flexible devices. One idea to overcome the discrepancy between processing and implementation is the use of a sacrificial layer during growth, which allows to release the functional material as a thin membrane afterwards and enables a transfer to flexible substrates. Here, we present our approach by growing different fully epitaxial hetero-structures of $\text{La}_{0.7}\text{Sr}_{0.3}\text{MnO}_3$ (which can be wet-etched in a hydrochloric acid solution), conducting SrRuO_3 and ferroelectric $\text{Ba}_{1-x}\text{Sr}_x\text{TiO}_3$ on oxide single crystal substrates by pulsed laser deposition. Different sample architectures were used to obtain a diversity of membranes that allow us to study their microstructure and functional properties with methods like X-ray diffraction, scanning probe microscopy, dielectric and ferroelectric measurement techniques to compare them to similar films still clamped on a substrate.

DS 12.28 Wed 17:00 P3

Resistive switching and oscillations in NdNiO_3 and SmNiO_3 planar thin film devices — •FARNAZ TAHOUNI-BONAB¹, THEODOR LUIBRAND¹, CLARIBEL DOMÍNGUEZ², JENNIFER FOWLIE², STEFANO GARIGLIO², RODOLFO ROCCO³, SOUMEN BAG³, LORENZO FRATINO³, MARCELO ROZENBERG³, JEAN-MARC TRISCONI², REINHOLD KLEINER¹, DIETER KOELLE¹, JAVIER DEL VALLE², and STEFAN GUÉNON¹ — ¹Physikalisches Institut, Center for Quantum Science (CQ) an LISA⁺, Universität Tübingen, 72076 Tübingen, Germany — ²Department of Quantum Matter Physics, Université de Genève, 1211 Geneva, Switzerland — ³Université Paris-Saclay, CNRS, Laboratoire de Physique des Solides, 91405 Orsay, France

Recently, there has been growing interest in strongly correlated materials that undergo a temperature-driven insulator-to-metal transition in the emerging research field of neuromorphic computing. Of particular interest are resistive switching phenomena for emulating integrate-and-fire behavior or self-sustained oscillations for spike train generation. In this study, we used a combination of wide field microscopy and electrical transport measurements to investigate thin film devices of the charge transfer insulators NdNiO_3 and SmNiO_3 . Current-voltage characteristics and photomicrographs reveal resistive switching via an intermediate state with a blurry metallic filament. The intermediate state is accompanied by oscillations in the 10 kHz frequency range that have a characteristic saw-tooth shape indicative of a relaxation oscillator. The intermediate state can be suppressed by changing the slew rate of the current source.

DS 12.29 Wed 17:00 P3

Determining the brazeability of copper surfaces via spectroscopic ellipsometry — •FRIEDRICH BÜRGER, LIENHARD WEGEWITZ, and WOLFGANG MAUS-FRIEDRICH — Clausthal Centre of Material Technology, Clausthal University of Technology, Agricolastr. 2, 38678 Clausthal-Zellerfeld

In Brazing, surface conditions play a fundamental role in determining the joint strength. Not all changes of the surface, like thick oxide layers or oil films, may be immediately apparent and therefore will only be noticed when the brazing process failed. Since most methods of determining brazeability work by performing a brazing process and evaluating the results they can only be performed on samples. This does not represent variation of surfaces within a batch of material. To fill this gap a nondestructive method to determine brazeability is needed. Spectroscopic ellipsometry (SE) is an optical measurement method commonly used to characterize the optical properties of surfaces and thin films. To evaluate if SE can be used to distinguish surface states of copper surfaces that negatively impact the joint strength, different surfaces were prepared. The selected surface states were a reference condition, ground surfaces, oxidized surfaces and different oil films on the reference surface. Those surfaces were characterized by confocal laser scanning microscopy (CLSM) and X-Ray photoelectron spectroscopy (XPS) to determine their morphology and chemical composition. SE-measurements were performed subsequently. Except for the ground states all surfaces showed distinct features in their SE-spectra, suggesting identification via SE is possible.

DS 12.30 Wed 17:00 P3

Microscopic theory of X-ray absorption spectroscopy — •JORIS STURM, DOMINIK CHRISTIANSEN, MALTE SELIG, and ANDREAS KNORR — Institut für Theoretische Physik, Nichtlineare Optik und Quantenelektronik, Technische Universität Berlin, Hardenbergstr. 36, 10623 Berlin, Germany

X-ray absorption near-edge spectroscopy (XANES) and extended X-ray absorption fine structure (EXAFS) are two widely used methods to investigate the structure of solid states. [1,2,3].

In this contribution, we present a self-consistent Maxwell-Bloch approach based on Heisenberg equations of motion for a unified description of XANES and EXAFS for 2D solid-state materials and apply it to the exemplary material graphene. For XANES we reproduce the experimentally observed absorption peaks and polarization-dependent selection rules of the included orbitals. Furthermore, the rigorous treatment of the Bloch wave interference allows us to calculate the Fourier transformed EXAFS spectrum [2] predicting so far uninterpreted features which have not been assigned within point-scattering theory [1].

[1] Sayers, Dale E., et al., PRL 27 (1971): 1204

[2] Buades, Bárbara, et al., Optica 5 (2018): 502

[3] Chowdhury, M. T., R. Saito, and M. S. Dresselhaus, PRB 85 (2012): 115410.

DS 12.31 Wed 17:00 P3

Ultrafast vibrational dynamics of CH-stretch modes of surface adsorbates — •TIM LÄMMERZAHN, NELLI KREMER, and ECKART HASSELBRINK — University Duisburg-Essen

The understanding of energy transfer between different modes in one molecule, which is called internal vibrational energy redistribution (IVR), is crucial for further development in the field of rate theory and for applications in molecular electronics. As a model we study adsorbate monolayers of a single species using time-resolved two-color pump probe sum frequency spectroscopy.

Previously, we revealed that the coupling between valence vibrations is faster than a few ps and equilibrates with bending and torsion modes on a tens of ps time scale in fatty acid monolayers [1]. Now we moved on to conducting surfaces (e.g. gold) and used different terminated alkanethiols. Since gold surfaces exhibit a strong non-resonant (NR) signal, which is usually the dominant source of noise, we used the technique by Dlott et al. [2] to suppress the NR signal. Results from a study of alkylthiols with different headgroups on gold will be presented.

[1] M. Lackner, M. Hille, E. Hasselbrink, Phys. Chem. Lett. 11 (2019), 108-112.

[2] A. Lagutchev, S.A. Hambir, D.D. Dlott. J. Phys. Chem. C. 111 (2007), 13645-13647.

DS 12.32 Wed 17:00 P3

Dynamics of the response of thiol monolayers to rapid heating — •MATTHIAS LINKE and ECKART HASSELBRINK — Universität Duisburg-Essen, Germany

Energy transport between metal substrates and molecules as well as intramolecular energy transport between vibrations is still not well understood, even though systems such as thiols on gold were studied extensively. Self-assembled molecular films are an ideal model system such as their characterization attracted much interest over the last decades, especially in the field of nanotechnology. It is well established that thiols adsorb easily and reproducibly on gold substrates by self-assembly. Sum-frequency generation vibrational spectroscopy (SFGvS) can be used for characterization of such systems, since it is inherently sensitive to surface species, interfaces at which centrosymmetry is broken. We adsorbed different thiols on Au-surfaces and heated the substrate by focussing an additional 25 ps 532 nm laser beam on the backside of the sample. Absorption of the photons leads to temperature jumps in the metal which can be assessed by tracking the reflectivity changes of the sample. Tracking the spectral changes via SFGvS at different delays between the pump and probe pulses can be done to assess the temperature effects induced in the substrate and the molecules and time constants can be extracted. The effect of the probing of different head groups (NO_2 , CN , CH_3) and variation of the spacer group are studied in this work.

DS 12.33 Wed 17:00 P3

In-situ spectroscopic ellipsometry measurement and analysis of native SiO_2 behavior under different atmosphere and temperature — •YOUNES SLIMI^{1,2}, JANNIS WALDMANN¹, RÜDIGER SCHMID-GUND¹, and STEFAN KRISCHOK¹ — ¹Technische Universität Ilmenau, Fachgebiet Technische Physik I, Weimarer StraÙe 32, 98693 Ilmenau, Germany — ²Ferhat Abbas University, Institut of optics and precision mechanics, Optics and Applied Photonics laboratory 19000 Setif, Algeria

the most common wafer used in the semiconductor industry nowadays is silicon (Si), the latter oxidizes when left to its own devices. these silicon oxide layers' behavior was investigated using In-situ Spectroscopic ellipsometry to obtain optical constants and thin film thicknesses under different atmospheres (nitrogen, dry air) and temperatures. We found changes in the refractive index and thickness of the SiO_2 layer under different conditions due to oxidation and material ablation. These results are meant to be used as possible references for future Electrochemical cells for in-situ Spectroscopic ellipsometry measurement for water splitting devices.

DS 12.34 Wed 17:00 P3

Sprayed hybrid nanocellulose fibril-silver nanowire transparent electrodes — •MARIE BETKER^{1,2}, CONSTANTIN HARDER^{1,3}, ELISABETH ERBES^{1,4}, JULIAN HEGER³, ALEXANDROS E. ALEXAKIS^{2,5}, BENEDIKT SOCHOR¹, QING CHEN¹, MATTHIAS SCHWARTZKOPF¹, ANDREI CHUMAKOV¹, PETER MÜLLER-BUSCHBAUM^{3,6}, KONRAD SCHNEIDER⁷, SIMONE TECHERT¹, L. DANIEL SÖDERBERG^{2,5}, and STEPHAN V. ROTH¹ — ¹DESY, 22607 Hamburg — ²Fibre and Polymer Technology, KTH, 10044 Stockholm, Sweden — ³TUM School of Natural Sciences, Chair for Functional Materials, 85748 Garching — ⁴Institute for X-ray Physics, Goettingen University, 37077 Goettingen — ⁵WWSC, KTH, 10044 Stockholm, Sweden — ⁶MLZ, TUM, 85748 Garching — ⁷Leibniz-Institut für Polymerforschung Dresden e.V., Abteilung Werkstofftechnik, 01069 Dresden

The fabrication of sustainable, thin, and flexible electrical devices on an industrial scale will be an important challenge in the future. Nanocomposites, consisting of conductive nanoparticles like silver nanowires (AgNWs) and a sustainable matrix material like cellulose nanofibrils (CNFs), can meet these requirements. Here, we report on the nanoscale structure and the corresponding optoelectronic properties of a sprayed CNFs-AgNWs nanocomposite electrode. Adding CNF to the aqueous AgNW-based spray ink improves the dispersion and distribution of the AgNWs. This, and the cold-welding of the AgNW junctions enhance the conductivity of the electrode greatly. Finally, we demonstrate the electrode's high transmittance, resilience under multiple cycles of bending deformations, and its long-term stability.

DS 12.35 Wed 17:00 P3

Detecting nitrogen-vacancy-hydrogen centers on the nanoscale using nitrogen-vacancy centers as local sensors in CVD-diamond — •CHRISTOPH FINDLER, GERHARD WOLFF, KAROLINA SCHÜLE, RÉMI BLINDER, PRIYADHARSHINI BALASUBRAMANIAN, JOHANNES LANG, CHRISTIAN OSTERKAMP, and FEDOR JELEZKO — Institute for Quantum Optics, Ulm University, Albert-Einstein-Allee 11, D-89081 Ulm, Germany

The negatively-charged nitrogen-vacancy center (NV) in diamond has attracted a lot of attention in the field of quantum technologies as it shows coherence times up to milliseconds at room temperature and enables optical polarization and coherent control of the electron spin. Apart from NV centers, the spin bath in diamond grown by chemical vapor deposition (CVD) consists mainly of substitutional nitrogen (P1) and negatively charged nitrogen-vacancy-hydrogen (NVH) defects which are usually analyzed by electron paramagnetic resonance (EPR) spectroscopy. In nm-thick epitaxial layers, however, the total number of paramagnetic spins becomes eventually too low for state-of-the-art EPR spectrometers. This problem can be solved by switching to a confocal microscope and studying the NV centers optically. Here, we show that 15NV ensembles can be employed as local sensors to estimate the density of non-fluorescent 15NVH and P1 centers in 15N-doped (100)-diamond layers and even get insight into the spatial distribution and correlation of P1 and 15NVH on the micrometer scale using a wide-field microscope.

DS 12.36 Wed 17:00 P3

Tailoring Optical Properties in Transparent Highly Conducting Perovskites by Cationic Substitution — •MAHDAD MOHAMMADI, RUIWEN XIE, NILOOFAR HADAEGHI, ALDIN RADETINAC, ALEXEY ARZUMANOV, PHILIPP KOMISSINSKIY, HONGBIN ZHANG, and LAMBERT ALFF — Institute of Materials Science, Technische Universität Darmstadt

SrMoO₃, SrNbO₃, and SrVO₃ are remarkable highly conducting d^1 (V, Nb) or d^2 (Mo) perovskite metals with an intrinsically high transparency in the visible. A key scientific question is how the optical properties of these materials can be manipulated to make them suitable for application as transparent conductors and emergent plasmonics. In this work, it is demonstrated for the first time how $3d/4d$ cationic substitution in perovskites shifts the optical transition energy and plasma frequency. At the example of the solid solution SrV_{1-x}Mo_xO₃ we show that the absorption and reflection edges can be shifted to the edges of the visible, resulting in a material that has the potential to outperform ITO due to its extremely low sheet resistance. For $x = 0.5$, a resistivity of 32 *Ωcm (12 Ω/sq.) is paired with a transmittance above 84 % in the whole visible spectrum. Quantitative comparison between experiments and electronic structure calculations show that the shift of the plasma frequency is governed by the interplay of d -band filling and electronic correlations.

[1] M. Mohammadi *et al.*, "Tailoring Optical Properties in Transparent Highly Conducting Perovskites by Cationic Substitution", *Adv. Mater.* (2022), Accepted Author Manuscript 2206605

DS 12.37 Wed 17:00 P3

Influence of dielectric Layers on the optomechanical Properties of Polymer Membranes in a Fiber Cavity — •ANDREAS REUSS¹, STEFAN LINDEN¹, HANNES PFEIFER², LUKAS TENBRAKE², and ALEXANDER FASSBENDER¹ — ¹Physikalisches Institut, Universität Bonn, Germany — ²Institut für Angewandte Physik, Universität Bonn, Germany

Fiber cavities are an attractive platform for optomechanical experiments as they can combine direct fiber-coupled optical access, small cavity lengths, high op-

tical finesse, and an open resonator volume. Direct laser writing allows for a fast and flexible way to add polymer drums as mechanical resonators directly on the end facets of a fiber cavity. These membrane-in-the-middle systems show a rather large optomechanical coupling strength despite of the low reflectivity due to the maximized intensity differences on the two membrane interfaces. A disadvantage of direct laser written structures are the comparatively large mechanical losses of the used resist, which limit the mechanical quality factor of the membranes to several hundred at cryogenic temperatures. Therefore, we are interested how the deposition of different dielectric layers influences the optomechanical response of the polymer membranes. By using materials with high young's modulus, like MgF₂, we aim to reduce overall mechanical losses and therefore increase the optomechanical response.

DS 12.38 Wed 17:00 P3

IST 312 - an unconventional phase change material? — •MARIA HÄSER, PETER KERRES, SOPHIA WAHL, CARL-FRIEDRICH SCHÖN, and MATTHIAS WUTTIG — I. Physikalisches Institut (IA), RWTH Aachen University, 52056 Aachen Germany

Chalcogenide-based Phase Change Materials (PCM) are a prominent candidate for energy-efficient memory devices. This material class shows a significant difference in its optical properties between the amorphous and crystalline phases: The former phase shows more insulating characteristics. In contrast, the almost metallic properties characterise the crystalline state. However, enabling fast switching between insulators and a real metal would broaden the field of application of PCMs.

In this study, the unusual phase change material In₃SbTe₂ (IST) has been investigated, which shows a metallic-like behaviour in its crystalline phase. The dielectric functions of both phases were determined using optical measurements (FTIR, Ellipsometry). Additionally, DFT calculations and XRD measurements were performed to better understand the unusual property change.

DS 12.39 Wed 17:00 P3

Characterization of the interaction of acrylic polymers with gold and silica surfaces — •SASCHA JAN ZIMMERMANN, PHILIPP MORITZ, and WOLFGANG MAUS-FRIEDRICH — Clausthal Centre of Material Technology, Clausthal University of Technology, Agricolastr. 2, 38678 Clausthal-Zellerfeld

Adhesives play a key role in the 21st century. In particular, hybrid material composites can be joined in this way while saving weight. To advance this technology, a fundamental understanding of adhesive interactions, particularly to metal (oxide) substrates, is required.

In order to investigate these interactions, nanometer thin planar polymer films were deposited on the model substrates of silicon oxide and gold. This was done for the polymers poly(methyl methacrylate) and poly(glycidyl methacrylate) applying a spin coating process. X-ray photoelectron spectroscopy (XPS), Metastable Impact Electron Spectroscopy (MIES) and Ultraviolet photoelectron spectroscopy (UPS) were used to analyze the chemical interactions at the interface.

In the case of PMMA, the XPS measurements show the presence of a carboxylate ion, which indicates probable ionic interactions. A varying chemical shift and the changes in the MIES spectra indicate additional hydrogen bonds. In the case of PGMA, no interactions were detected by the applied measurement methods.

DS 12.40 Wed 17:00 P3

Photoinduced charge injection into single-layer WSe₂ via deposited dye molecules — •TIM VÖLZER^{1,2}, ALINA SCHUBERT^{1,2}, JULIAN SCHRÖBER¹, RICO SCHWARTZ¹, TOBIAS KORN^{1,2}, and STEFAN LOCHBRUNNER^{1,2} — ¹Institute of Physics, University of Rostock, Albert-Einstein-Str. 23, 18059 Rostock, Germany — ²Department "Life, Light and Matter", University of Rostock, Albert-Einstein-Str. 25, 18059 Rostock, Germany

The deposition of molecules allows the functionalization of 2D semiconductors as well as the fabrication of hybrid structures exhibiting charge separation after optical excitation that can be exploited in optoelectronic devices. Here, we investigate the charge transfer from optically excited molecules of the dye Perylene Orange (PO) into a monolayer of tungsten diselenide (1L-WSe₂) by means of low-temperature micro-photoluminescence spectroscopy: In comparison to the blank 1L-WSe₂, the proportion of charged trion versus neutral exciton emission is expected to change as the PO molecules are deposited and excited. In contrast, when reducing the pump photon energy below the PO absorption band, the emission spectrum would remain identical. Thus, we aim to control the light-induced charge injection into the WSe₂ by tuning the pump wavelength.

DS 12.41 Wed 17:00 P3

Theoretical insights into the monolayer adsorption and characterization of HB238 Merocyanine on Ag(100) surface — •RITU TOMAR, THOMAS BREDOW, ANNA KNY, and MORITZ SOKOLOWSKI — Clausius Institute of Physical and Theoretical Chemistry, University of Bonn, Germany

Merocyanines (MCs) are intriguing compounds that can be used as efficient absorbers for organic solar cells. We studied the adsorption of HB238 merocyanine on the surface of Ag (100) using STM and SPA-LEED experiments, which

suggested that HB238 self-organizes as chiral tetramers upon adsorption. The molecular structure was significantly different from the typical configuration in the bulk phases of HB238. It is critical to control the structure and morphology of mercyanine films to enhance light absorption and optimize their optoelectronic properties. Therefore, we performed quantum chemical calculations to corroborate our experimental findings. Initially, we screened the HB238 conformers and used the most stable structure to determine the optimal adsorption orientation of HB238 on the Ag surface using the semi-empirical method GFN1-XTB in DFTB+. HB238 preferentially adheres face-on to the Ag surface. Next, we optimized the tetramer models at the DFT level to analyze the assembly of chiral tetramers while maintaining supercell lattice constant values, as in the experiment. We then relaxed the HB238 molecules on the Ag 3-layer slab model and fixed the bottom two layers using the GGA method in VASP. However, rapid and effective system convergence was achieved only using the ASE/LBFGS optimization algorithm.

DS 12.42 Wed 17:00 P3

Modelling liquid flow through nanopores on the nanoscale — •RUSTAM DURDYEV¹, CHRISTIAN R. WICK¹, and ANA-SUNČANA SMITH^{1,2} — ¹Friedrich-Alexander-Universität Erlangen-Nürnberg, PULS Group, Institute for theoretical physics, Interdisciplinary Center for Nanostructured Films (IZNF), Cauerstrasse 3, 91058 Erlangen, Germany — ²Division of Physical Chemistry, Ruder Bošković Institute, Zagreb, Croatia

Liquid chromatography is one of the most important separation techniques and has proceeded mainly along empirical knowledge from the expansive collection of experimental data by using chromatographic methods, spectroscopic methods and technical innovations in column packing, particle technology and equipment design. However, a classic liquid chromatography column, is a cylinder densely packed with mesoporous silica particles whose surface has been mostly chemically modified. In this work, we investigated the physisorption of water to functionalized silica surfaces and hydrophilicity properties of surface by molecular dynamics simulations. We built on previously gathered knowledge on chromatography to establish a unified picture of stationary phase and solute mobility in liquid chromatography. In analogy to previous studies, we utilized a crystalline SBA-15 structure as starting point for our modeling approach. Furthermore, we investigate the effect of functionalization using different loadings with silanol group (Si-OH) and trimethylsilyl groups (O-Si-(CH₃)₃). With this strategy, we hope to understand the effect of functionalization of silica on the physisorption of water molecules at the nanometer scale.

DS 12.43 Wed 17:00 P3

Optimizing two-dimensional materials for biomolecule detection using machine learning techniques — •CALIN-ANDREI PANTIS-SIMUT^{1,2,3}, AMANDA TEODORA PREDA^{1,2,3}, NICOLAE FILIPOIU^{1,2}, and GEORGE ALEXANDRU NEMNES^{1,2,3} — ¹Horia Hulubei National Institute of Physics and Nuclear Engineering (IFIN-HH), Str. Reactorului no.30, P.O.BOX MG-6, Magurele, Romania — ²University of Bucharest, Faculty of Physics, 077125 Magurele-Ilfov, Romania — ³Research Institute of the University of Bucharest (ICUB), Sos. Panduri 90, Bucharest Romania.

The problem of correctly identifying the biomarkers associated with specific pathologies is of great interest nowadays for rapid diagnoses. The transport properties of different active layers like beta-arsenite, phosphorene, graphene, or Al-doped MoSe₂ were investigated in the presence of certain biomolecules. Additionally, predictions of biomolecular compounds with tunable gaps were reported as well as carbon nanotube-based. Our study brings a detailed analysis of 2D semiconductor heterostructures in contact with biomarkers of respiratory diseases, which exhibit large tunabilities in transport properties. As a first step, by using DFT simulations, the electronic properties of the systems are analyzed under different doping conditions and nanostructuring. In a second step, a large number of systems will be considered for transport calculations and the results will define the input for machine learning procedures. This involves the mapping between structural information and transport properties. In the end, an analysis of the sensor's limit of detection and regeneration is performed.

DS 12.44 Wed 17:00 P3

Microstructure investigation of pulsed laser deposited GeTe-Sb₂Te₃ heterostructures — •SONJA CREMER¹, LENNART VOSS², NILS BRAUN¹, LORENZ KIENLE², and ANDRIY LOTNYK^{1,3,4} — ¹Leibniz Institute of Surface Engineering, Leipzig — ²Faculty of Engineering, University of Kiel — ³Laboratory of Infrared Materials and Devices, Ningbo University — ⁴College of Physics and Optoelectronic Engineering, Harbin Engineering University

Heterostructured phase change materials are an auspicious candidate to overcome high power consumption and resistance drift, hindering the implementation of Ge-Sb-Te based thin films for neuromorphic computing. Aiming at future systematic performance improvement, the impact of deposition parameters on the microstructure of GeTe-Sb₂Te₃ heterostructures (HSs) was investigated. HSs were grown at RT onto SiO₂/Si by PLD. Combining advanced TEM with XRD the microstructure was investigated in-depth. Energy and number of laser pulses affect the layer thickness and composition. The low energy and number

of pulses lead to pronounced intermixing and hence to the formation of a single GeSb₂Te₄ layer. Besides, the local structure of the layers within the HS differs. While GeTe layers are amorphous, Sb₂Te₃ layers are polycrystalline and contain nanocrystals featured by varying sizes, defects and multiple phases. Thus, deposition parameters mainly affect the morphology and chemical composition of GeTe-Sb₂Te₃ HSs. However, the main factor influencing the crystallinity of the HS layers is the alloy itself. Financial support by the DFG (No. 445693080) is acknowledged. We thank A. Mill for assistance in FIB preparation.

DS 12.45 Wed 17:00 P3

Dynamics of ion beam-induced defects in phase-change materials investigated by in-situ optical measurements — •SEBASTIAN GRATZ, MARCEL BUCH, MARTIN HAUFERMANN, and CARSTEN RONNING — Institute of Solid State Physics, Friedrich-Schiller-Universität Jena, 07743 Jena, Germany

Phase-change materials (PCMs) provide the ability of reversible, repeatable and rapid switching between amorphous and crystalline states. These transformations are accompanied with drastic changes of the electrical and optical properties, which is already been used in rewritable optical data storage or phase-change electronic memory. The transitions can be triggered by external thermal, optical, or electrical stimuli. The most extensively studied PCMs are pseudo-binary (GeTe)_m(Sb₂Te₃)_n chalcogenide compounds (m, n being integer values), short GST. Ion irradiation was recently introduced to induce structural disorder and amorphize initially crystalline GST films. There are multiple studies that investigated the effect of defect engineering of GST compounds. However, there is still a lack of understanding of the dynamic effects, such as dynamic annealing of defects during the ion irradiation process. Furthermore, the direct impact of the specific GST stoichiometry on the ion-beam induced disorder has not been observed yet. Thus, we investigated the dynamics of defect formation for different GST stoichiometries, such as Ge₁Sb₂Te₄ (m=1, n=1), Ge₁Sb₄Te₇ (m=1, n=2), and Ge₂Sb₂Te₅ (m=2, n=1), via in-situ optical measurements during ion irradiation at different temperatures.

DS 12.46 Wed 17:00 P3

Preparation and characterization of Cu-Te phases using focused ion beam — •NILS BRAUN¹, VLADIMIR RODDATIS², AGNES MILL¹, SONJA CREMER¹, HAGEN BRYJA¹, LENNART VOSS³, LORENZ KIENLE³, and ANDRIY LOTNYK^{1,4,5} — ¹Leibniz Institute of Surface Engineering e.V. (IOM) — ²GFZ German Research Centre for Geosciences — ³Institute for Materials Science, Faculty of Engineering, University of Kiel — ⁴Laboratory of Infrared Materials and Devices, The Research Institute of Advanced Technologies, Ningbo University — ⁵College of Physics and Optoelectronic Engineering, Harbin Engineering University

In this work, we prepared different nanoscale Cu-Te phases from Cu - Sb₂Te₃ system using FIB. Copper chalcogenides have shown promising thermoelectric properties, e.g. high efficiency and tunability. Sb₂Te₃ thin layers are epitaxially grown on p-type Si (111) substrates and polycrystalline Sb₂Te₃ thin film are grown on a SiO₂ coated wafer using PLD. A standard cross-section FIB preparation method is used. Samples are investigated using advanced TEM methods and XRD. Dependent on beam current used during FIB lamella preparation and Sb₂Te₃ layer thickness, hole formation in the Cu layer, thickness change and chemical changes of the Sb₂Te₃ layers are observed. In specimen prepared from the heated samples Sb₂Te₃ and Cu-Te grains are found. In polycrystalline Sb₂Te₃ specimen the intercalation of Cu and formation of new Cu-Te phases is observed. We thank P. Hertel for magnetron sputtering. We acknowledge the financial support by the German Research Foundation (DFG 448667535).

DS 12.47 Wed 17:00 P3

Investigation of the insights of a TiN-PEALD process in a remote capacitively coupled plasma ALD reactor — •JAN BIEDINGER, JAN-MICHAEL SCHMALHORST, and GÜNTER REISS — Bielefeld University, Faculty of Physics, Germany Atomic Layer Deposition (ALD) is a deposition technique of great interest due to precise and reproducible layer control, large-area uniformity and conformal coating. As it bases on chemical surface reactions, it is important to understand the mechanism of an ALD process. In the presented study, the effect of different process parameters (temperature, plasma power, plasma pulse length, NH₃ flow, plasma pressure) was studied in a titaniumnitride (TiN) plasma-enhanced ALD process, consisting of sequential pulsing of tetrakis(dimethylamido)titanium (TDMAT) and a NH₃ plasma. X-ray reflectivity and 4-point probe measurements were performed to determine the growth rate, roughness, density and electrical resistivity of all TiN films, respectively. Additionally, Auger electron spectroscopy revealed information about the chemical composition. By combining in-situ mass spectrometry data, where plasma species as well as reaction products could be identified during the process, with these ex-situ results, the process could be described in more detail. During the NH₃ step, the release of dimethylamine groups was observed, which decreased gradually with time. This correlates with the decline of carbon content by increasing the NH₃ step time. Moreover, it was observed that the plasma species (hydrogen and nitrogen radicals) seems to be responsible for decreasing the oxygen content and hence, improving thin film quality.

DS 12.48 Wed 17:00 P3

Epitaxial growth of $\text{Ag}_x\text{Cu}_{1-x}\text{I}$ on Al_2O_3 (0001) — •E. KRÜGER¹, V. GOTTSCHALCH², G. BENNDORF¹, R. HILDEBRANDT¹, A.L. PEREIRA¹, M. BAR¹, E. ABO EL FADL¹, S. BLAUROCK², S. MERKER², C. STURM¹, M. GRUNDMANN¹, and H. KRAUTSCHEID² — ¹Universität Leipzig, Felix-Bloch-Institut für Festkörperphysik, Germany — ²Universität Leipzig, Institut für Anorganische Chemie, Germany

Copper iodide (CuI) and related alloy compounds are of great interest as suitable materials for applications in fully transparent optoelectronic devices. While CuI exhibits intrinsic p-type conductivity with excessive high hole densities typically around $10^{18} - 10^{19} \text{ cm}^{-3}$, it was recently shown that the carrier density can be strongly reduced for $\text{Ag}_x\text{Cu}_{1-x}\text{I}$ alloy and even n-type conductivity can be achieved for high Ag contents [1]. Here we present the epitaxial growth of $\text{Ag}_x\text{Cu}_{1-x}\text{I}$ thin films on Al_2O_3 (0001) substrates using sublimation technique [2]. We demonstrate that $\text{Ag}_x\text{Cu}_{1-x}\text{I}$ thin films with $x \leq 0.5$ exclusively exhibit the zincblende γ -phase, while a coexistence of zincblende γ - and wurtzite β -phases is observed for Ag-rich alloy compositions. In addition we provide the epitaxial relationships between the different $\text{Ag}_x\text{Cu}_{1-x}\text{I}$ phases and the Al_2O_3 substrate. Moreover, we present another deposition approach based on a solid-state reaction between CuI and AgI, which allows the preparation of single-phase γ - $\text{Ag}_x\text{Cu}_{1-x}\text{I}$ films up to $x = 0.7$.

[1] A. Annadi and H. Gong, Appl. Mater. Today **20**, 100703 (2020)

[2] E. Krüger et al., Phys. Stat. Solidi B (accepted)

DS 12.49 Wed 17:00 P3

Growth of CoO Thin Films for Application in Superconductor - Magnet Heterostructures — •AMY MCGLINCHY — Trinity College Dublin, Ireland

Cobalt monoxide, CoO, is an antiferromagnet (AF) with a Néel temperature of 293K. It is utilised to pin the magnetisation of Co layers via exchange bias and is employed in magnetic heterostructures. The interaction between ferromagnet (F) and AF layers is predicted to generate long-range spin-triplet superconductivity in F-S-AF heterostructures [1]. CoO is a good candidate for the AF due to its low Néel temperature, which facilitates in-field cooling through the transition improving magnetic homogeneity. For the most part, CoO is synthesized by the oxidation of Co thin films or using techniques such as spray pyrolysis and pulsed laser deposition. In this work, we focus on the growth of CoO by molecular beam epitaxy, investigating the crystalline quality of the CoO as a function of deposition conditions. We have optimised these conditions to grow single crystalline CoO(100) thin films on MgO(100) substrates. As a second step towards a F-S-AF heterostructure, we also investigate the superconducting properties of Nb grown on CoO films. Due to the proximity effect, the properties of the niobium - especially at low thickness relevant to heterostructures - will be influenced by the CoO magnetic and interface structure [2]. 1. L. G. Johnsen et al., Phys. Rev. B, **103**, L060505 (2021). 2. G. A. Bobkov et al., Phys. Rev. B, **106**, 144512 (2022).

DS 12.50 Wed 17:00 P3

Potential of La-doped SrTiO3 thin films grown by metal-organic vapor phase epitaxy for thermoelectric applications — •MOHAMED ABDELDAYEM¹, AYKUT BAKI¹, CARLOS MORALES SÁNCHEZ³, JAN INGO FLEGE³, DETLEF KLIMM¹, ANDREAS FIEDLER¹, OLIVER BIERWAGEN², and JUTTA SCHWARZKOPF¹ — ¹Leibniz Institut für Kristallzüchtung, Berlin, Germany — ²Paul Drude Institut für Festkörperelektronik, Berlin, Germany — ³Brandenburgische Technische Universität Cottbus, Brandenburg, Germany

Conversion of waste heat energy into electrical energy by exploiting the thermoelectric effect in solids promises a great contribution to energy harvesting concepts. However, most thermoelectric materials use toxic Pb or Te. Recently, La-doped SrTiO3 has gained a lot of interest as a potential candidate for thermoelectric devices for its good thermoelectric properties, chemical and thermal stability. In this paper, we report the homoepitaxial growth of La-doped SrTiO3 thin films by metalorganic vapor phase epitaxy (MOVPE) technique, which works at high oxygen partial pressures and offers upscaling potential for industry. The adjustment of charge carrier concentration, necessary for thermoelectric power factor optimization, was performed by introducing a defined amount of the metal-organic precursor La(tmhd)3 and tetraglyme to the liquid precursor solution. X-ray diffraction and atomic force microscopy verified a pure perovskite phase with high structural quality. The electrical conductivity increases linearly with the La concentration in the gas phase, which is attributed to the substitution of La+3 ions on the Sr+2 sites inferred from photoemission spectroscopy.

DS 12.51 Wed 17:00 P3

Ultrathin alumina membrane: A new opportunity for constructing stable sodium metal anodes — •JIAJIA QIU, CHANGFAN XU, HUAPING ZHAO, and YONG LEI — Fachgebiet Angewandte Nanophysik, Institut für Physik & IMN MacroNano, Technische Universität Ilmenau, 98693 Ilmenau, Germany

Unstable solid electrolyte interphase (SEI) remains a major bottleneck for sodium metal batteries due to the mossy or dendritic growth of Na in the repetitive stripping/plating process. Recently, nanostructured modification of Na and Al2O3 coatings have been reported as two effective solutions to address this is-

sue. Accordingly, with almost identical pore regularity and precisely controlled geometrical structure, ultrathin alumina membrane (UTAM) is utilized as a functional layer to effectively protect the Na anode of Na-metal batteries for the first time in this work. The mossy or dendritic growth of Na has been suppressed due to the UTAM protection, resulting in a uniform electrodeposition interface. UTAM significantly improved the Coulombic efficiency while avoiding short circuit risks. And it has the potential to be applied to other metal anodes. The novel design of a UTAM-protected metal Na anode may bring in new opportunities for next-generation high performance Na metal batteries.

DS 12.52 Wed 17:00 P3

Contact printed micro circuit boards for thermoelectric circuits in van der Waals high temperature twisted cuprate heterostructures — •SANAZ SHOKRI^{1,2}, CHRISTIAN N SAGGAU¹, KORNELIUS NIELSCH^{1,2}, and NICOLA POC CIA¹ — ¹Institute for Metallic Materials, IFW Dresden, Dresden, Germany, IFW Dresden — ²Institute for Materials Science, Dresden University of Technology

Recently, thermoelectric measurement has been established as an indicator of the topological nature of material due to its sensitivity to the Berry curvature. Nernst effect, which is defined as a generation of transverse electric field by a longitudinal temperature gradient in the presence of a magnetic field, in particular, is a powerful tool to investigate the area above superconductivity transition temperature where the transverse electrical signals become very small. Twisted $\text{Bi}_2\text{Sr}_2\text{CaCu}_2\text{O}_{8+\delta}$ (BSCCO) van der Waals heterostructures have exhibited topological superconductivity. Nevertheless, the BSCCO is too fragile to make a complex circuit like thermoelectric. Therefore, we developed the whole thermoelectric circuit like Seebeck and Nernst, embedded within inorganic SiN so called nanomembrane and transferred it on the optimally doped BSCCO flake inside the Ar-filled glovebox to encapsulate the BSCCO flakes and contact it at the same time. We used Pt as a heater and gold as the thermocouples and will calibrate our measurements based on the heat losses through a thermal insulating substrate and nanomembrane as well.

DS 12.53 Wed 17:00 P3

Preparation and characterization of Zn1-xMgxO thin films obtained by the aerosol deposition method for UV radiation detector — •VADIM MORARI — Technical University of Moldova, D. Ghitu Institute of Electronic Engineering and Nanotechnologies, Chisinau, Republic of Moldova

Zn1-xMgxO ternary oxide solutions with wide band gap were prepared by the aerosol spray deposition method [1] using zinc acetate and magnesium acetate as precursors. This technique offers the possibility of rapid deposition of homogeneous thin films with good electrical and optical properties. It is suitable for growing high-quality thin films on Si, quartz, glass or sapphire substrate, with relatively large areas at low cost due to vacuum-free equipment, low temperatures during deposition, low defect density and low environmental impact. The obtained thin films were characterized by scanning electron microscopy (SEM), energy dispersive X-Ray analysis (EDX), X-Ray Diffraction (XRD), Raman spectroscopy and optical absorption spectroscopy. The investigation of photosensitivity revealed that multilayer ZnMgO structures with different Mg content are more sensitive than single-layer films in a wide spectral range from visible to the ultraviolet (UV-C) radiation.

[1] Morari, V., et. All. Photosensitivity of heterostructures produced by aerosol deposition of ZnMgO thin films on Si substrates. In: Proceedings of SPIE - The International Society for Optical Engineering, vol. 11718, p. 1171818:1*8, (2020). <https://doi.org/10.1117/12.2571189>.

DS 12.54 Wed 17:00 P3

Heterostructure diodes based on reactively co-sputtered $\text{Ag}_x\text{Cu}_{1-x}\text{I}$ thin films — •JORRIT BREDOW, SOFIE VOGT, CHRISTIANE DETHLOFF, HOLGER VON WENCKSTERN, and MARIUS GRUNDMANN — Universität Leipzig, Felix-Bloch-Institut, Germany

Copper iodide (CuI) is a transparent p-type semiconductor that exhibits high hole mobilities of up to $25 \text{ cm}^2/\text{Vs}$ in polycrystalline thin films^[1]. This renders CuI an interesting candidate for the fabrication of transparent heterostructure diodes, such as p-CuI/n-ZnO^[2], or p-CuI/n-AgI^[3]. CuI further exhibits a low resistivity, which was shown to be increased with an increasing fraction of silver (Ag) in $\text{Ag}_x\text{Cu}_{1-x}\text{I}$ thin films^[4]. Moreover, a transition from p-type to n-type material of the $\text{Ag}_x\text{Cu}_{1-x}\text{I}$ thin films for $x \approx 0.5$ was observed^[4]. However, the $\text{Ag}_x\text{Cu}_{1-x}\text{I}$ thin films were prepared with the Bädiker method, i.e. the iodization of metallic $\text{Ag}_x\text{Cu}_{1-x}$ thin films.

We present transparent heterostructure diodes based on the ternary compound $\text{Ag}_x\text{Cu}_{1-x}\text{I}$. The $\text{Ag}_x\text{Cu}_{1-x}\text{I}$ thin films were deposited using reactive co-sputtering of metallic Cu and Ag in Ar and I atmosphere. The feasibility of pn-heterojunction diodes with varying silver content is presented.

[1] C. Yang et al., ACS Appl. Electr. Mater., **2**, 3627-3632, 2020.

[2] F.-L. Schein et al., Appl. Phys. Lett., **102**, 092109, 2013.

[3] J.-H. Cha and D.-Y. Jung, ACS Appl. Mater. Interfaces, **9**, 43807-43813, 2017.

[4] A. Annadi et al., Appl. Mater. Today, **20**, 100703, 2020.

DS 12.55 Wed 17:00 P3

SnTe topological insulator thin film for field-effect transistors — •SEPIDEH IZADI, NEGIN BERYANI NEZAFAT, and GABI SCHIERNING — Department of physics, Experimental physics, Bielefeld University, 33615, Bielefeld, Germany
Topological insulators (TIs) as a new class of quantum materials are one of the potential interests for device fabrication. The unique electrical characteristics of TIs arises from robust metallic states passing through the bulk semiconducting band gap within the material. These surface states with high electrical mobility are considered as an efficient factor regarding high performance transistor. We herein present SnTe topological insulator as a potential candidate for active layer in field-effect transistor (FET). In this work the results of SnTe transistor device fabrication is reported using bottom gate approach. Therewith, Si₃N₄ and Al₂O₃ are applied as gate insulating material which are deposited using magnetron sputtering and atomic layer deposition (ALD), respectively. The provided findings and analysis in this work paves the way for SnTe electrical device characterization.

DS 12.56 Wed 17:00 P3

Electric field induced laser-assisted polarization switching dynamics in ferroelectric thin films — •REKIKUA SAHILU ALEMAYEHU¹, MATTHIAS RÖSSLE², and MATIAS BAGRHEER^{1,2} — ¹Institute for Physics & Astronomy, University of Potsdam, Karl-Liebknecht-Str 24-25, 14476 Potsdam, Germany — ²Helmholtz Zentrum Berlin, Albert-Einstein-Str. 15, 12489 Berlin, Germany

Nucleation and growth of domains with opposite polarization moderates the electric field-induced polarization reversal process in ferroelectric materials. Accordingly, the domain wall velocity governs the timescale of polarization switching. Achieving the ultimate switching time in ferroelectrics is a fundamental

quest to improve the device response time. Here we show laser-assisted polarization switching dynamics in metal-ferroelectric-metal heterostructure via heat and strain waves induced by a femtosecond laser pulse.

DS 12.57 Wed 17:00 P3

Engineering Vertical Memristive Devices with TMDC Thin Films — •ANNA LINKENHEIL^{1,2}, THERESA SCHELER^{3,2}, OLE GRONENBERG⁴, HENDRIK GROSS⁴, MICHAELA BLUM^{3,2}, TZVETAN IVANOV^{1,2}, BENJAMIN SPETZLER¹, FRANK SCHWIERZ¹, PETER SCHAAF^{3,2}, LORENZ KIENLE⁴, and MARTIN ZIEGLER^{1,2} — ¹Micro- and Nanoelectronic Systems, Faculty of Electrical Engineering and Information Technology, TU Ilmenau, Ilmenau, Germany — ²Institute of Micro- and Nanotechnologies, MacroNano^o, TU Ilmenau, Ilmenau, Germany — ³Materials for Electrical Engineering and Electronics, Faculty of Electrical Engineering and Information Technology, TU Ilmenau, Ilmenau, Germany — ⁴Synthesis and Real Structure, Faculty of Engineering, Kiel University, Kiel, Germany

Transition metal dichalcogenides (TMDCs) represent a class of promising materials for memristive devices, which become increasingly important for emerging information processing approaches. In particular, homogeneous thin-films of few layers thickness have advantageous properties for memristive devices, such as excellent scaling behavior combined with the potential integration into planar wafer technology. Here, we assess the electrical properties of sputtered MoS₂ based devices and analyze the material. The devices were fabricated in a 4-inch wafer thin film technology, allowing for a systematic electrical investigation. Various electrode materials as well as oxidation treatments and their respective influences on device performance are evaluated using Transmission Electron Microscopy (TEM), revealing probable switching mechanisms and their origin.

DS 13: Optical Analysis of Thin Films I

Time: Thursday 9:30–11:00

Location: SCH A 316

Invited Talk

DS 13.1 Thu 9:30 SCH A 316

Towards Catalytic Applications of Infrared Laser Polarimetry — •ANDREAS FURCHNER¹ and KARSTEN HINRICHS² — ¹Helmholtz-Zentrum Berlin für Materialien und Energie GmbH, Division Energy and Information, Schwarzschildstraße 8, 12489 Berlin, Germany — ²Leibniz-Institut für Analytische Wissenschaften – ISAS – e.V.

Infrared (IR) polarimetry and ellipsometry are well-established non-destructive spectroscopic techniques for studying the refractive and absorptive properties of thin films and surfaces with monolayer sensitivity. This spectral range is particularly suited for investigating chemical composition, molecular interactions, anisotropy, conductivity, as well as changes and reactions at surfaces and interfaces.

The incorporation of quantum cascade lasers (QCLs) in novel IR polarimeter designs has pushed the boundaries of the achievable spatial and temporal resolution well into the sub-mm and sub-second range, respectively. Laser-based polarimeters thus enable hyperspectral and time-resolved amplitude-phase measurements with novel application potential. Probing individual laser pulses delivers time resolutions of 10 μs, spectral sweeps in 100 ms, and hyperspectral maps in minutes.

This presentation focuses on recent instrumental developments, such as the combination of QCLs with single-shot designs, that pave the way towards the application of IR laser polarimetry in thin-film catalysis. Here, surface reactions have to be studied *in situ* and *operando* in order to resolve the evolution of surface species and temporary adsorbates.

DS 13.2 Thu 10:00 SCH A 316

Large area functional thin film properties mapping using in-line hyperspectral imaging during roll-to-roll magnetron sputter deposition — FLORIAN GRUBER², PATRICK SCHLENZ¹, STEFFEN BIEDER⁴, ERIC SCHNEIDER⁴, JOLANTA SZELWICKA¹, JULIO HERNANDEZ³, CHRISTIAN STERNEMANN⁴, and •STEFFEN CORNELIUS¹ — ¹Fraunhofer FEP, Winterbergstrasse 28, 01277 Dresden, Germany — ²Fraunhofer IWS, Winterbergstrasse 28, 01277 Dresden, Germany — ³Norsk Elektro Optikk AS, Ostensjoveien 34, 0667, Oslo, Norway — ⁴Fakultät Physik/DELTA, Technische Universität Dortmund, August-Schmidt-Straße 1, 44227 Dortmund, Germany

Roll-to-roll (R2R) coating processes of flexible substrates are established for cost-efficient thin film functional materials production for applications like energy efficient windows and solar cells. However, even small variations of thickness and/or composition homogeneity may affect the final product performance. Due to the high throughput of coated surface area in R2R coating the ex-situ material characterization is very time consuming, often destructive and offers no possibility for in-situ process monitoring and/or quality control.

The NanoQI EU-H2020 project develops a powerful in-line technology combining hyperspectral imaging with X-ray reflectivity via a machine learning algorithms, enabling large area (0.5m x 100m) high resolution (<1mm) high speed

(m/min) thin film properties imaging. The combinatorial thickness mapping of a binary metal-oxide double layer (thickness up to 120nm) on PET substrate will be discussed in detail - aiming to achieve a thickness accuracy of only a few %.

DS 13.3 Thu 10:15 SCH A 316

Developing an open source ellipsometry analysis workflow — •FLORIAN DOBENER¹, MARIUS MÜLLER², CAROLA EMMINGER^{1,3}, CHRIS STURM³, TAMÁS HARASZTI⁴, MARIUS GRUNDMANN³, and SANDOR BROCKHAUSER¹ — ¹Department of Physics, Humboldt-Universität zu Berlin, Germany — ²Institute of Experimental Physics I, Justus-Liebig-University Giessen, Germany — ³Felix-Bloch Institut für Festkörperphysik, Universität Leipzig, Germany — ⁴DWI Leibniz Institute for Interactive Materials, Aachen, Germany

Optical and geometric characteristics of multilayer material stacks are not accessible from ellipsometric data in a direct way. The optical model applied to the data is the key, which allows understanding of these properties. Accordingly, there exist a lot of different software tools to construct such models, which vary in their model implementation and are often closed source. Comparing, reproducing and using data from literature can therefore be challenging. Here, we present the open source ellipsometry software pyElli. It implements specific dispersion models from manufacturers and from literature. Furthermore, it allows for easy construction of non-standard measurement tasks, e.g. combining different measurements or using uncommon measurement parameters. Together with the recent NeXus ellipsometry standard, the NOMAD research data management platform and its interactive Jupyter based toolkit, we show how pyElli contributes to an open ellipsometry workflow. This open workflow is a standardised and reproducible way of analysing ellipsometry data and adds to the goal of making ellipsometry data FAIR.

DS 13.4 Thu 10:30 SCH A 316

IR dual-comb polarimetry of anisotropic nanofibers — •KARSTEN HINRICHS¹, BRIANNA BLEVINS², ANDREAS FURCHNER³, NATARAJA SEKSHAR YADAVALLI², SERGIY MINKO², RAPHAEL HORVATH⁴, and MARKUS MANGOLD⁴ — ¹Leibniz-Institut für Analytische Wissenschaften – ISAS e.V., Schwarzschildstraße 8, 12489 Berlin, Germany — ²Department of Chemistry, The University of Georgia — ³Helmholtz-Zentrum Berlin für Materialien und Energie GmbH, Division Energy and Information, Schwarzschildstraße 8, 12489 Berlin, Germany — ⁴IRsweep AG, Laubisruetistrasse 44, 8712 Staefa, Switzerland

In this work an anisotropic nanofiber scaffold is investigated non-invasively under ambient conditions by infrared dual-comb polarimetry (IR - DCP). Amplitude and phase spectra at various azimuthal sample rotations are correlated with the orientation of characteristic vibrational transition dipole moments. IR - DCP is proven as a new method for the spectral analysis (here 1200 cm⁻¹ to 1300 cm⁻¹) of such anisotropic samples in very short measurement times (0.065 ms) at 1.4 cm⁻¹ spectral resolution. Such capabilities are in particular interesting for imaging applications, time resolved studies and hyperspectral spectroscopy

of anisotropic samples. In difference to classical ellipsometry which measures phase differences, IR - DCP can measure s- and p-polarized phases separately. We acknowledge financial support by the EU through EFRE 1.8/13 and the Horizon 2020 grant 820419 and by the BMBF through CatLab (03EW0015A/B).

DS 13.5 Thu 10:45 SCH A 316

Orientation in thin spider silk films at silicon substrates evidenced by dichroic FTIR spectroscopy — •MARTIN MÜLLER^{1,2}, MIRJAM HOFMAIER^{1,3}, SARAH LENTZ⁴, THOMAS SCHEIBEL⁴, and ANDREAS FERY^{1,3} — ¹Leibniz-Institut für Polymerforschung Dresden e.V., Institut für Physikalische Chemie und Physik der Polymere, Dresden, Germany — ²Technische Universität Dresden, Lehrstuhl für Makromolekulare Chemie, Dresden, Germany — ³Technische Universität Dresden, Lehrstuhl für Physikalische Chemie Polymerer Materialien, Dresden, Germany — ⁴Universität Bayreuth, Lehrstuhl für Biomaterialien, Bayreuth, Germany

Biomedically relevant spider silk films were deposited on unscratched and parallelly scratched silicon substrates and checked for conformation and orientation by dichroic transmission (T-) and ATR-FTIR spectroscopy. Films ($d=0-200$ nm) were casted from hexafluoroisopropanol solutions of recombinantly engineered spider silk proteins. Both FTIR methods revealed little β -sheet (<10%) and much disordered structure (>80%) from Amide I band analysis. Dichroic ratios R of Amide I components close to isotropic films were found by T- and ATR-FTIR indicating no orientation. Whereas, silk films after swelling in MeOH vapor revealed higher β -sheet (>30%) and lower disordered structure amounts (<60%). By T-FTIR isotropic R values of Amide I components assigned to antiparallel β -sheet were found indicating no in-plane orientation, while ATR-FTIR revealed R values significantly deviating from isotropy indicating out-of-plane orientation. Orientation was independent on scratching and increased decreasing d .

DS 14: Thin Oxides and Oxide Layers

Time: Thursday 9:30–11:15

Location: SCH A 315

DS 14.1 Thu 9:30 SCH A 315

Strain effects of the electronic and magnetic properties of thulium iron garnet films — •SIBYLLE GEMMING¹, GEORGETA SALVAN¹, APOORVA SHARMA¹, OANA T. CIUBOTARIU², and MANFRED ALBRECHT² — ¹Institute of Physics, TU Chemnitz — ²Institute of Physics, U Augsburg.

Rare earth iron garnets are magnetic insulators, in which two structurally distinct iron centers form sublattices, which couple antiferromagnetically. The overall magnetization of the compounds results from the alignment of the local magnetic moments of the 4f electrons at the rare earth sites and is sensitive to external effects such as temperature and strain. We performed gradient-corrected density-functional calculations including spin-orbit and correlation corrections to study the property-thickness relation of thin thulium iron garnet films that had been grown epitaxially under tensile strain on a doped gallium gadolinium garnet substrate. We could rationalize the observed growth modes for different film thicknesses with strain arguments and correlate it with the observed electronic properties (Funding: DFG, GE 1202/12-1)

DS 14.2 Thu 9:45 SCH A 315

Optoelectronic Properties of Al-doped ZnO Films Prepared by ALD and Flash Lamp Annealing — •GUOXIU ZHANG^{1,2}, OLIVER STEUER¹, YU CHENG¹, YI LI¹, KAIMAN LIN¹, SHENGQING ZHOU¹, YUFEI LIU^{2,3}, and SLAWOMIR PRUCNAL¹ — ¹Helmholtz-Zentrum Dresden-Rossendorf, Institute of Ion Beam Physics and Materials Research, Bautzner Landstrasse 400, Dresden, 01328, Germany — ²Key Laboratory of Optoelectronic Technology & Systems (Chongqing University), Ministry of Education, Chongqing 400044, China — ³Faculty of Science and Engineering, Swansea University, Swansea SA2 8PP, UK

Zinc oxide (ZnO) is a wide-band-gap semiconductor considered for transparent and flexible optoelectronics. Effective and controlled doping of ZnO can be realized by substitution Zn or O atoms with metal or non-metal elements like H, Al, Ga for n-type doping and e.g. group V elements for p-type doping. In this work, we have investigated the optoelectronic properties of *-doped ZnO with Al. 100 nm thick Al-doped ZnO (AZO) films were deposited on Si wafers by atomic layer deposition (ALD) varying the distance between Al-layers. After ALD process samples were annealed using ms-range flash lamp annealing (FLA) in either nitrogen or oxygen atmosphere. The highest carrier concentration estimated from Hall-effect measurements is $2.7 \cdot 10^{21}$ cm⁻³ and the resistivity is $8.8 \cdot 10^{-4}$ Ω cm, for AZO films where the Al*-layer is separated by 20-layers of Zn. In general annealing in N₂ atmosphere promotes n-type doping while annealing in O₂ leads to the formation of highly resistive films.

DS 14.3 Thu 10:00 SCH A 315

Strain Engineering of Buffer Layers: A Way to Overcome Film/Substrate Lattice Misfit — •PIA HENNING¹, ULRICH ROSS², KAREN STROH¹, VITALY BRUCHMANN-BAMBERG¹, and VASILY MOSHNYAGA¹ — ¹I. Physikalisches Institut, Georg-August-Universität Göttingen, Germany — ²Institut für Materialphysik, Georg-August-Universität Göttingen, Germany

A fundamental problem in thin film physics is the film/substrate lattice misfit and the related epitaxial strain. An especially important role plays stress for perovskite manganites, e.g. colossal magnetoresistive (La_{0.6}Pr_{0.4})_{0.7}Ca_{0.3}MnO₃ (LPCMO), yielding a suppression of the metal-insulator and ferromagnetic phase transition for LPCMO thin films grown on standard perovskite substrates, like SrTiO₃ (STO, tensile stress) and LaAlO₃ (LAO, compressive stress). We propose a route to engineer the strain via LAO buffers epitaxially grown on STO substrates by means of metalorganic aerosol deposition to obtain epitaxial stress-free LPCMO films. By changing the LAO thickness in the range $d_{LAO} \sim 2-35$ nm and precisely tuning the stress in it, an ideal lattice adjustment between LPCMO and LAO has been achieved. This allows us to grow stress-free epi-

taxial LPCMO/LAO/STO(100) thin and ultrathin ($d_{LPCMO} \sim 10$ nm) films with bulk properties. The structure and microstructure of these films as well as the stress distribution within layers was studied by X-ray diffraction and high resolution transmission electron microscopy. A generalization of this method on other film/buffer/substrate combinations has been proposed.

DS 14.4 Thu 10:15 SCH A 315

Transfer and Thermal Processing of Freestanding Oxide Membranes — •YU-JUNG WU, VARUN HARBOLA, SANDER SMINK, SARAH C. PARKS, and JOCHEN MANNHART — Max Planck Institute for Solid State Research, Heisenbergstraße 1, 70569 Stuttgart, Germany

Epitaxial films of complex oxides have gained interest due to their wide-ranging physical properties, including high-temperature superconductivity, magnetism, ferroelectricity, and multiferroicity. The conventionally grown single-crystalline oxide thin films are usually bound to their substrates, which imposes constraints on their properties and usage. Therefore, growth techniques have recently been developed that enable lifting-off freestanding complex oxide membranes by wet etching of oxide buffer layers. To achieve transfer of large-area oxide films, we have systematically studied growth and transfer of a variety of thin films, grown on aluminate and manganese wet-etchable buffer layers. Various oxide membranes were successfully transferred with good quality and up to 3x2 mm² area with minimal cracking. Furthermore, after thermal processing the stack of the transferred membrane on sapphire, the transferred membrane starts dewetting, yielding nanostructures. This work is not only expected to enable a wide range of oxide films to be transferred in high quality for fundamental studies and applications in oxide electronic devices but also serves as a starting point for crystalline nano-structuring of oxide materials.

DS 14.5 Thu 10:30 SCH A 315

Tungsten-oxide thin films characterized by Positron Annihilation Spectroscopy — •VASSILY VADIMOVITCH BURWITZ¹, ANNEMARIE KÄRCHER^{2,3}, LUCIAN MATHES¹, THOMAS SCHWARZ-SELINGER³, MAIK BUTTERLING⁴, ERIC HIRSCHMANN⁴, MACIEJ OSKAR LIEDKE⁴, ANDREAS WAGNER⁴, and CHRISTOPH HUGENSCHMIDT¹ — ¹Heinz Maier-Leibnitz Zentrum, TU München — ²TU München — ³Max-Planck-Institut für Plasmaphysik, Garching bei München — ⁴Helmholtz-Zentrum Dresden-Rossendorf, Institute of Radiation Physics

For future nuclear fusion reactors it is foreseen that tungsten is used as inner wall cladding. Understanding the formation and behaviour of radiation induced defects in tungsten is therefore important for their safe operation. Tungsten mono-crystal model systems are studied by positron annihilation Doppler-broadening spectroscopy (DBS) and positron annihilation lifetime spectroscopy (PALS) to foster the understanding of the type and evolution of these defects. Both methods are sensitive tools when examining the defect type and concentration. However, data obtained by either of these methods is influenced by any thin oxide film on the surface of a sample. Such a film is present on any tungsten sample exposed to air, therefore its effect on DBS and PALS results needs to be known for their correct interpretation. In this work we measured tungsten-oxide thin films grown by thermal and electro-chemical methods as well as by exposure to air by DBS and PALS. The DBS measurements were performed using a moderated β^+ emitter, the PALS measurements at an accelerator-based positron source.

DS 14.6 Thu 10:45 SCH A 315

Monitoring switching process in Fe_3O_4/STO heterostructures via in-situ instrument — •YIFAN XU¹, MAI HUSSEIN HAMED^{1,2}, CONNIE BEDNARSKI-MEINKE¹, ASMAA QDEMAT¹, STEFFEN TOBER¹, EMMANUEL KENTZINGER¹, OLEG PETRACIC¹, and THOMAS BRÜCKEL¹ — ¹Jülich Centre for Neutron Science (JCNS-2) and Peter Grünberg Institut (PGI-4), JARA-FIT, Forschungszentrum Jülich GmbH, 52425 Jülich, Germany — ²Faculty of Science, Helwan University, 11795 Cairo, Egypt

The ability to tune magnetic oxide phases via redox reactions across their heterointerfaces could lead to useful spintronic and memristive device applications. By applying a small electric field, oxidation/reduction occurs at the heterointerface and leads to a reversible phase transition. In this talk, we present the preparation and characterization of epitaxial Fe_3O_4 thin films grown on TiO_2 -terminated Nb:STO via pulsed laser deposition (PLD). Using magnetometry, we detect the Verwey transition; a strong indicator of the oxygen content in the Fe_3O_4 films. We observe the disappearance in the Verwey transition temperature with an applied positive electric field. This could be explained by oxygen diffusion through the interface which then leads to a reversible phase transition from Fe_3O_4 (magnetite) to $\gamma-Fe_2O_3$ (maghemite). Using ex-situ x-ray diffraction (XRD), we observe the structural transitions from (001) to (111) in the out-of-plane direction influenced by the applied voltage. Interestingly, by grazing-incidence small-angle X-ray scattering, we observe a change in the magnetite domain size for the sample after applying the electric field.

DS 14.7 Thu 11:00 SCH A 315

Engineering magnetic anisotropy by Rashba spin-orbit coupling in 3d-5d oxide heterostructures — •MEGHA VAGADIA, JAYA PRAKASH SAHOO, ANKIT KUMAR, SUMAN SARDAR, TEJAS TANK, and D.S. RANA — ¹Department of Physics, Indian Institute of Science Education and Research Bhopal, M.P. 462066, India
In recent times, Rashba spin-orbit coupling (SOC) has been successfully employed for the emergence of exotic phenomena at the quantum oxide interfaces. In these systems, the combined effect of charge transfer, broken symmetries, and SOC yields intriguing interfacial magnetism and transport properties. However, role of Rashba SOC, particularly without applied bias, in modulating magnetic anisotropy of oxide heterostructures is unexplored. Here, we provide insight into tuning transport phenomena by the charge transfer driven Rashba SOC in $CaMnO_3/CaIrO_3$ heterostructures. Rashba SOC remarkably enhances the anomalous Hall conductivity and reconstructs the Berry curvature. From the anisotropy magnetoresistance measurements, we demonstrate that Rashba SOC is instrumental in tailoring magnetic anisotropy where magnetization easy-axis rotates from the out-of-plane direction to the in-plane direction. The ability to tune Rashba SOC and resulting competing magnetic anisotropies provides a route to manipulate electronic band structure for the origin of non-trivial spin texture useful for spin-orbitronics applications.

DS 15: Optical Analysis of Thin Films II

Time: Thursday 11:15–12:45

Location: SCH A 316

Invited Talk

DS 15.1 Thu 11:15 SCH A 316

In-Situ Optical Investigation of Electrochemically Induced Conformational Changes at Solid Liquid Interfaces: A Source of new Electronic States — •CHRISTOPH COBET — Linz School of Education, Center for Surface- and Nanoanalytics (ZONA), Johannes Kepler University, Altenbergerstr 69, A-4040, Linz, Austria

The electrical potential between an electrolyte and a solid electrode, whether it is a metal, semiconductor, polymer or a bio-membrane, could induce considerable changes in the conformational appearance. In biological systems such conformation changes are well-known e.g. as a control element for the chemistry on one or both sides of a membrane. In periodically ordered thin films or at surfaces, one can observe conformation changes at the atomic length scale which could induce new electronic properties. The interfacial electrical potential is in all cases a very versatile control element. On the one hand, it allows to change the chemical formation potential over a huge range which is otherwise only accessible for example by rather extreme temperature or pressure differences. On the other hand, it offers a very precise control of the thermodynamic equilibrium conditions. With the help of in-situ optical methods like spectroscopic ellipsometry (SE) and reflection anisotropy spectroscopy (RAS), we could study the interplay of the potential induced charge accumulation, the conformational changes and the evolution of (self) localized electronic states. The mechanisms will be discussed by two examples: The electrochemical doping and formation of polarons in polymers and the formation of surface quantum well states at a metal-electrolyte interface.

DS 15.2 Thu 11:45 SCH A 316

Singlet fission and triplet dynamics in pentacene embedded in a surface-anchored metal-organic framework — •MARTIN RICHTER¹, ZHIYUN XU², PHILIPP LUDWIG³, PAVEL KOLESNICHENKO¹, UWE BUNZ³, CHRISTOF WÖLL², and PETRA TEGEDER¹ — ¹Physikalisch-Chemisches Institut, Universität Heidelberg — ²Institut für Funktionelle Grenzflächen, Karlsruher Institut für Technologie — ³Organisch-Chemisches Institut, Universität Heidelberg

It has been observed, that the rate of singlet fission in pentacene and the lifetime of the generated triplets strongly depend on the molecular arrangement.[1]

Here, a cofacial orientation of pentacene molecules is achieved by embedding them in a surface anchored metal-organic framework (SURMOF). Transient absorption spectroscopy has been used to analyze the ultrafast dynamics as well as long lived states after photoexcitation. The observed difference absorption spectra indicate, that after the initial excitation a singlet excited state generates a correlated triplet pair within a few picoseconds that retains singlet character. Subsequent dynamics show the formation of a long-lived species (47us) with triplet character. This exceeds by far the observed lifetime of triplets generated in pentacene thin films (10ns) and may enhance triplet harvesting capabilities in photovoltaic devices.[2]

1. Lubert-Perquel, D., Nat Commun. 2018, 9, 4222

2. Poletayev, A.D., Adv. Mater. 2014, 26, 919-924

DS 15.3 Thu 12:00 SCH A 316

Birefringence of orthorhombic $DyScO_3$: Towards a terahertz quarter-wave plate — •JINGWEN LI, CHIA-JUNG YANG, JANNIS LEHMANN, NIVES STRKALJ, MORGAN TRASSIN, MANFRED FIEBIG, and SHOYON PAL — D-MATL, ETH Zurich, Switzerland

The energy scale of THz light corresponds to plenty of the fundamental collective excitations in materials, such as phonons, magnons, and heavy fermions. This makes THz light an ideal tool to investigate the low-energy excitations and non-equilibrium processes in solid-state systems. With the growing interest in studying the aforementioned collective phenomena, manipulating the polarization of THz light becomes necessary. However, prevailing THz waveplates, such as quarter-wave plates (QWPs) for generating circularly polarized THz light, typically suffer from various problems, including bulky size, complex fabrication, or narrow working ranges. Here, we present a broadband THz QWP based on a 50- μm -thick (110)-cut orthorhombic $DyScO_3$ (DSO) crystal. We show a polarimetry measurement to verify the polarization of the output CP-THz light and prove that our DSO plate behaves like a QWP over a broad frequency range of 0.50-0.70 THz with a phase tolerance of $\pm 3\%$. We believe that our results expand the choices of broadband THz QWPs, as well as the possibilities of simple and compact achromatic THz QWPs by combining DSO crystals. Most importantly, as a common substrate for growing various thin films, DSO shows its potential as a compact built-in broadband THz waveplate for thin film research with circularly polarized THz light. [1]

[1] Appl. Phys. Lett. **118**, 223506 (2021).

DS 15.4 Thu 12:15 SCH A 316

Temperature Dependence of Coherent Phonon Oscillations in Metavalently Bonded Solids — •TIMO VESLIN¹, FELIX HOFF¹, JULIAN MERTENS¹, JONATHAN FRANK¹, and MATTHIAS WÜTTIG^{1,2,3} — ¹I. Institute of Physics (IA), RWTH Aachen University — ²Jülich-Aachen Research Alliance (JARA FIT and JARA HPC) — ³PGI 10 (Green IT), Forschungszentrum Jülich GmbH

Femtosecond optical pump probe measurements are carried out in order to detect changes in the reflectivity of the material response of MBE grown metavalently bonded (MVB) materials on sub-ps timescales. MVB differs significantly from metallic, ionic and covalent bonding. Examination of reflectivity changes due to the coherent phonon response provides insight into the ultrafast lattice dynamics and relaxation of MVB materials. To this end, the mechanism of dispersive excitation of coherent phonons (DECP) is used to analyse the highly symmetric A1 modes. The material response consists of the ultrafast carrier excitation and a slower carrier relaxation together with a damped harmonic phonon oscillation measured in the transient reflectivity trace. The temperature dependence of the frequency, lifetime and oscillation amplitude of the coherent phonon A1 mode in Sb_2Te_3 , $GeTe$ and Bismuth will be presented. This allows to identify phonon coupling effects and dephasing mechanisms, as well as the temperature dependence of phonon frequencies. Furthermore, the results are supported by optical and structural data recorded at room temperature. These measurements will help to better understand the MVB mechanism which governs phase change materials.

DS 15.5 Thu 12:30 SCH A 316

Identification of different polymorphs of a zone-cast perylene diimide derivative with low-frequency Raman and infrared scanning near-field microscopy

— •NADINE VON COELLN, CHRISTIAN HUCK, NIKLAS HERRMANN, PETRA TEGEDER, and JANA ZAUMSEIL — Institute of Physical Chemistry, Heidelberg University, Germany

Small-molecule organic semiconductors are prone to form multiple thin film polymorphs. As their charge transport characteristics may vary substantially, effective and fast polymorph characterization techniques are necessary. Here, zone-cast films of perfluorobutyl dicyanoperylene-carboxydiimide (PDIF-CN₂) were studied with X-ray diffraction (XRD), confocal low-frequency Raman mi-

croscopy and infrared scanning near-field microscopy (IR-SNOM). Based on low-frequency Raman spectra and XRD, two different thin film polymorphs of PDIF-CN₂ were identified, which form depending on the solvents used for deposition. While confocal Raman microscopy is limited in the spatial resolution of areas, the near-field infrared technique (IR-SNOM) offers the unique possibility of both infrared microscopy and spectroscopy with a spatial resolution down to ~10 nm. We demonstrate that it is possible to discriminate between neighboring crystalline regions of the two PDIF-CN₂ polymorphs by means of IR-SNOM using slight differences in IR absorption. As a non-destructive technique, IR-SNOM may even enable in-situ investigations of thin semiconducting films in functional devices.

DS 16: Thermoelectric and Phase Change Materials; Layer Deposition

Time: Thursday 11:30–13:00

Location: SCH A 315

DS 16.1 Thu 11:30 SCH A 315

A Multiscale Simulation Method for Deposition Processes: Micrometer-scale Off-Lattice Film Growth with Atomistic Precision— •ERIK E. LORENZ¹ and JÖRG SCHUSTER^{2,1} — ¹Center for Mikrotechnologien, Chemnitz University of Technology, Chemnitz, Germany — ²Fraunhofer Institute for Electronic Nano Systems ENAS, Chemnitz, Germany

We present a multiscale method for the simulation of thin film deposition processes such as PVD, CVD and ALD. By combining Kinetic Monte Carlo (KMC) methods for adsorption event sampling and Molecular Dynamics (MD) for adsorption simulation and nanostructure relaxation with a graph-based triangulating bulk-surface representation, fast and efficient highly-parallel surface growth simulations are facilitated.

The enhancement of KMC-MD coupling with a graph-based bulk-surface representation enables efficient subdomain decompositions, bulk KMC event insertions and removals, and the robust and constant-time update of connected subdomain. Using the same graph structure, the effects of further computational improvements such as incident particle ray tracing, surface diffusion and limited KMC time warping are shown.

We demonstrate the growth of atomistic copper seed layers on a Tantalum substrate for micrometer-scale electronic devices in parallelized simulation runs saturating over 1000 CPU cores, and compare it to established methods.

DS 16.2 Thu 11:45 SCH A 315

Characterization and optimization of MgZnO thin films with steep lateral composition gradient

— •LAURENZ THYEN, MAX KNEISS, HOLGER VON WENCKSTERN, and MARIUS GRUNDMANN — Universität Leipzig, Felix-Bloch-Institut für Festkörperphysik, Linnéstraße 5, 04103 Leipzig, Germany

The materials magnesium- and zinc-oxide have been widely investigated in the past. Corresponding step graded ternary alloy thin films of Mg_xZn_{1-x}O have been of great interest [1]. Pulsed laser deposition (PLD) has been used to grow laterally and vertically graded thin films [2]. The precise control of chemical composition is of great importance for possible applications. Additionally, in the course of miniaturization of electrical devices like wavelength-selective multi-channel UV photodetectors, a well-defined steep slope of the material gradient will be beneficial [3,4].

In this contribution the properties of Mg_xZn_{1-x}O thin films with lateral compositional gradient grown by pulsed laser deposition will be discussed. In order to obtain information about the material composition of the thin films, energy-dispersed X-ray spectroscopy, spatially resolved ellipsometry and micro-photoluminescence spectroscopy measurements have been conducted. Moreover, steep lateral gradients with a slope of up to 20 % Mg/mm were realized.

[1] Z. Zhang, *et al.* IEEE Journal Quantum Elec, 20.6, 106-111, (2014)[2] H. v. Wenckstern, *et al.* physica status solidi (b) 257.7 (2020)

[3] M. Grundmann, IEEE Transact. Elec. Dev. 66.1 (2018): 470-477

[4] M. Kneiß, *et al.* ACS Combinatorial Science 20.11 (2018): 643-652.

DS 16.3 Thu 12:00 SCH A 315

Physical properties of Ni_xCu_{1-x}I thin films deposited by magnetron co-sputtering

— •CHRISTIANE DETHLOFF, SOFIE VOGT, DANIEL SPLITH, HOLGER VON WENCKSTERN, and MARIUS GRUNDMANN — Felix-Bloch-Institut, Universität Leipzig, Deutschland

The highly conductive, p-type semiconductor CuI is subject to various doping approaches to tailor optical and electrical properties [1-4]. As recently shown [5], doping CuI with Ni reduces its high hole density of up to $2 \times 10^{19} \text{ cm}^{-3}$ [4]. After surpassing a threshold of 15 % Ni content, a carrier conversion, as observed by Annadi *et al.*, turns the Ni_xCu_{1-x}I alloy into an n-type semiconductor, which predestines Ni_xCu_{1-x}I to fabricate p-n-homojunctions.

We present our investigations regarding morphology, electrical and possible ferromagnetic properties of Ni_xCu_{1-x}I thin films with varying Ni contents. The deposition was conducted by reactive magnetron co-sputtering of metallic Cu and Ni in an iodine and argon atmosphere. X-ray and scanning electron mi-

croscopy as well as Hall-effect and conductivity measurements were used to investigate the thin films. First measurements yielded a low resistivity of $5 \times 10^{-3} \Omega \text{ m}$ for $x=0.035$.

[1] T. Jun *et al.*, Advanced materials 2018 30, e1706573[2] H. Wu *et al.*, Appl. Phys. Lett. 2021 118, 222107[3] P. Storm *et al.*, Phys. Status Solidi RRL. 2021 15, 2100214[4] A. Annadi *et al.*, Applied Materials Today. 2020 20, 100703[5] A. Annadi *et al.*, ACS applied materials & interfaces. 2020 12, 6048

DS 16.4 Thu 12:15 SCH A 315

Self-assembled droplet etching during semiconductor epitaxy for versatile quantum structures

— •CHRISTIAN HEYN, AHMED ALSHAIKH, and ROBERT BLICK — Center for Hybrid Nanostructures (CHyN), University of Hamburg

As a fundamental extension of conventional epitaxy, we describe the integration of self-assembled top-down strategies into the bottom-up molecular beam epitaxy (MBE) of semiconductor quantum structures (QS). The samples are fabricated using standard solid-source MBE without any additional equipment. Ga, Al, or In droplets are formed on a GaAs or AlGaAs surface driven by the minimization of surface and interface energies in Volmer-Weber mode. The metal droplets drill self-assembled nanoholes into the semiconductor surface which is called local droplet etching (LDE). Afterwards, the nanoholes are filled with a material different from the substrate for the generation of QS. This presentation discusses the general mechanism of LDE, the influence of the process parameters on the density, size, and shape of the resulting nanoholes, as well as an intermixing with substrate material. For LDE with Ga droplets on AlGaAs, a crystalline wall formed around a nanohole represents a GaAs quantum ring. Further strain-free QS are created by filling of nanoholes drilled using Al droplets in AlGaAs with GaAs. The size and shape of the resulting QS is controlled by the initial nanohole, the amount of deposited material for hole filling, and capillary. Examples are QS that are shaped like the shell of a cone and vertically coupled quantum dot molecules.

DS 16.5 Thu 12:30 SCH A 315

Interplay of Glass Dynamics and Crystallization Kinetics of Photonic Phase Change Materials Sb₂S₃ & Sb₂Se₃— •FELIX HOFF¹, JULIAN PRIES¹, MAXIMILIAN J. MÜLLER¹, ERIC N. LENSCHER¹, and MATTHIAS WUTTIG^{1,2,3} — ¹Institute of Physics (IA), RWTH Aachen University — ²Jülich-Aachen Research Alliance (JARA FIT and JARA HPC) — ³PGI 10 (Green IT), Forschungszentrum Jülich GmbH

Due to their large bandgaps, the chalcogenide phase-change materials (PCM) antimony sulfide Sb₂S₃ and antimony selenide Sb₂Se₃ are interesting for photonic applications in the visible and telecommunication wavelength range. They are promising for photonic integrated circuits or tunable metasurfaces. While recent literature focuses on the optical properties and the resulting applications, a systematic quantification of the amorphous glass phase, as well as its influence on the process of crystallization under different conditions, is missing. In this work, both the standard glass transition and fragility of antimony sulfide are presented and discussed. Sb₂S₃ is found to crystallize from the undercooled liquid phase for all technologically relevant heating rates spanning over six orders of magnitude. In contrast, Sb₂Se₃ appears to show a glass transition only for higher heating rates. This can be used to explain the unusual temperature dependence of its crystallization mechanism in thin films.

DS 16.6 Thu 12:45 SCH A 315

Seebeck coefficient inversion in highly doped organic semiconductors— •MORTEZA SHOKRANI¹, KAI XU², TERO-PETRI RUOKO², DOROTHEA SCHEUNEMANN¹, HASSAN ABDALLA², HENGDA SUN², CHI-YUAN YANG², YUTAPOOM PUTTISONG², NAGESH KOLHE³, JOSÉ SILVESTRE MENDOZA FIGUEROA², JONAS PEDERSEN², THOMAS EDERTH², WEIMIN CHEN², MAGNUS BERGGREN², SAMSON JENEKHE³, DANIELE FAZZI⁴, MARTIJN KEMERINK^{1,2}, and SIMONE FABIANO² — ¹Heidelberg University, Germany — ²Linköping University, Sweden — ³University of Washington, USA — ⁴University of Cologne, Germany

The investigation of the thermoelectric properties of organic semiconductors (OSC) with the aim of increasing their efficiency as active material in thermoelectric generators has attracted attention for the past years. The maximum efficiency of the energy conversion process in a thermoelectric material is set by zT , which is proportional to electrical conductivity and Seebeck coefficient (S) squared. A common way of increasing zT is by doping, which typically increases the charge carrier density and electrical conductivity, while decreasing S . The

sign of S is often used to determine the polarity of the majority charge carriers in OSC. In recent years, a surprising change in the sign of S has sometimes been observed to occur in highly doped OSC. Here, by combining conductivity and S measurements with kinetic Monte Carlo simulations, it is shown that density of state filling in combination with the opening of a hard Coulomb gap around the Fermi energy is responsible for the sign inversion

DS 17: Optical Analysis of Thin Films III

Time: Thursday 16:15–17:45

Location: SCH A 316

Invited Talk DS 17.1 Thu 16:15 SCH A 316
In-situ optical spectroscopy on electrochemical interfaces: From OER electrocatalysts to "smart" electro-switchable interfaces — •MARTIN RABE — Department of Interface Chemistry and Surface Engineering, Max-Planck-Institut für Eisenforschung GmbH, Max-Planck-Str. 1, 40237 Düsseldorf

We employ electrochemical in-situ optical spectroscopies, namely IR- and Raman-spectroscopy as well as UV/vis-spectroscopic ellipsometry to understand fundamental processes at electrolyte/solid interfaces. Here, different examples from our research will be presented and discussed. 1: Electrocatalytically active manganese and nickel oxides during the anodic oxygen evolution reaction (OER) were studied. The formation, phase transitions and dissolution processes in these metal oxides is shown to govern their activity and stabilities on metallic electrodes. These material properties play a major role for the improvement of electrocatalysts for the sluggish OER in hydrogen production by the electrochemical water splitting. 2: The impact of the electrochemical Ge-OH to Ge-H surface termination on germanium interfaces was studied, which is accompanied by a switching of the interface hydrophobicity. The formation of a hydrophobic gap at semiconductor/electrolyte interface gives access to study fundamental properties of the water solvation layers. Furthermore, it is shown how the macroscopic change of the hydrophobicity can be employed as a "smart" electro-switchable surface that allows to reversibly control the adsorption and orientation of bio-macromolecules, a process that is potentially useful for novel bio sensing applications.

Invited Talk DS 17.2 Thu 16:45 SCH A 316
The physics of low symmetry semiconductors: Gallium oxide for the future of green energy as example — •MATHIAS SCHUBERT — Department of Electrical and Computer Engineering, University of Nebraska-Lincoln, Lincoln, Nebraska 68588, USA — NanoLund and Solid State Physics, Lund University, 22100 Lund, Sweden

The physics of Gallium arsenide (zincblende structure) and Gallium nitride (wurtzite structure) led to disruptive technologies driven by extreme properties such as small effective mass, large direct bandgap, and piezoelectric polarization. Gallium reappears in a monoclinic crystal structure Oxide with enormous prospects for applications in power electronics for the future of green energy.

Numerous new phenomena hitherto unknown for traditional semiconductors occur in monoclinic symmetry semiconductors such as non-parallel phonon-plasmon scattering, hyperbolic shear polaritons, splitting of associated transverse and longitudinal phonon modes, non-degenerate highly anisotropic fundamental excitonic band-to-band transitions, directional band offsets, and complex defect spin interactions within the highly anisotropic host lattice. The influences of composition, strain, doping, and defects are discussed for Gallium oxide and related alloys, and special emphasis is given to new semiconductor physics, and consequences for thin film growth and device designs are pointed out. Methods such as generalized ellipsometry, the optical Hall effect, Terahertz electron paramagnetic resonance ellipsometry, and density functional perturbation theory computations are employed for characterization and analysis.

Invited Talk DS 17.3 Thu 17:15 SCH A 316
Spectroscopic ellipsometry studies of optical constants in highly excited semiconductors — •STEFAN ZOLLNER — New Mexico State University, Las Cruces, NM, USA

Spectroscopic ellipsometry is an optical reflection technique with polarized light. Most commonly, it is used to measure the thicknesses of thin-film layers, such as SiO_2 on Si. But it can also be used to study the energies and broadenings of elementary excitations in solids, such as electrons (band gaps, transport), infrared active phonons, and their interactions. We previously reported precision measurements of the complex refractive index of germanium near the direct band gap, which allowed us to compare our results quantitatively with theoretical predictions from Fermi's Golden Rule, based on k.p theory and including the excitonic interaction between electrons and holes. Going further, we can investigate how many-body effects impact the properties of electrons in highly excited semiconductors. Large carrier concentrations can be achieved through doping, thermal excitation of electron-hole pairs in small band-gap semiconductors, or optical excitation with ultrafast lasers. In this talk, I will report recent ellipsometry results for the temperature-dependent dielectric function of InSb near the direct band gap and the transient dielectric function of Ge near the E_1 and $E_1 + \Delta_1$ transitions from femtosecond pump-probe ellipsometry. I will also point out the theoretical approach needed to explain these data sets.

DS 18: Members' Assembly

Time: Thursday 18:00–19:00

Location: SCH A 315

All members of the Thin Films Division are invited to participate.

Dynamics and Statistical Physics Division Fachverband Dynamik und Statistische Physik (DY)

Markus Bär
Physikalisch-Technische Bundesanstalt
FB 8.4 - Modellierung und
Datenanalyse
Abbestraße 2 - 12
D-10587 Berlin
markus.baer@ptb.de

Carsten Beta
Biologische Physik
Institut für Physik und Astronomie
Universität Potsdam
Karl-Liebknecht-Str. 24/25
D-14476 Potsdam
beta@uni-potsdam.de

Walter Zimmermann
Theoretische Physik
Universität Bayreuth
Universitätsstrasse 30
D-95447 Bayreuth
walter.zimmermann@uni-bayreuth.de

The Dynamics and Statistical Physics Division covers theoretical and experimental activities in all areas of statistical physics, quantum dynamics and many-body systems, nonlinear dynamics and pattern formation, data analysis and machine learning as well as active matter, fluid physics, soft matter and complex fluids. The DY section has strong links and joint sessions with the sections of Biological Physics (BP), Chemical Physics and Polymers (CPP), Socio- and Econophysics (SOE), and Low Temperatures (TT).

Overview of Invited Talks and Sessions

(Lecture halls MOL213, ZEU147, ZEU160, and ZEU250; Poster P1)

Invited Talks

DY 2.1	Mon	9:30–10:00	HSZ 03	Enhanced variational Monte Carlo for Rydberg atom arrays — •STEFANIE CZISCHEK
DY 2.2	Mon	10:00–10:30	HSZ 03	Data mining the output of quantum simulators – from critical behavior to algorithmic complexity — •MARCELLO DALMONTE
DY 2.3	Mon	10:30–11:00	HSZ 03	Reinforcement learning for quantum technologies — •FLORIAN MARQUARDT
DY 2.4	Mon	11:00–11:30	HSZ 03	Machine learning of phase transition — •CHRISTOF WEITENBERG
DY 5.1	Mon	9:30–10:00	MOL 213	Extreme events, entropies and instantons for turbulence and water waves — •JOACHIM PEINKE, ANDRÉ FUCHS, MATTHIAS WÄCHTER
DY 8.1	Mon	12:30–13:00	ZEU 250	Novel phenomena and analysis methods in oscillator networks: higher-order interactions, higher-order averaging, and inference — •HIROSHI KORI
DY 10.6	Mon	16:30–17:00	ZEU 160	Long-range communications enable the hierarchical self-organization of active matter — •IGOR ARONSON, ALEXANDER ZIEPKE, IVAN MARYSHEV, ERWIN FREY
DY 11.1	Mon	15:00–15:30	ZEU 250	The challenge of structured disorder in statistical physics — •MARC MEZARD
DY 11.2	Mon	15:30–16:00	ZEU 250	The emergence of concepts in shallow neural-networks — •ELENA AGLIARI
DY 11.3	Mon	16:00–16:30	ZEU 250	Adaptive Kernel Approaches to Feature Learning in Deep Neural Networks — •ZOHAR RINGEL
DY 11.5	Mon	17:00–17:30	ZEU 250	Analysing the dynamics of message passing algorithms — •MANFRED OPPER, BURAK CAKMAK
DY 11.6	Mon	17:30–18:00	ZEU 250	Deep Learning Theory Beyond the Kernel Limit — •CENGİZ PEHLEVAN
DY 14.1	Tue	9:30–10:00	MOL 213	Unraveling structural and dynamical features in glassy fluids using machine learning — •LAURA FILION, FRANK SMALLENBURG, RINSKE ALKEMADE
DY 25.1	Wed	9:30–10:00	MOL 213	Many-body localization from Hilbert- and real-space points of view — •IVAN KHAYMOVICH, GIUSEPPE DE TOMASI, FRANK POLLMANN, SIMONE WARZEL
DY 26.1	Wed	9:30–10:00	ZEU 160	More is different: High-throughput 3D tracking reveals bacterial navigation strategies — •KATJA TAUTE
DY 26.2	Wed	10:00–10:30	ZEU 160	Variability and heterogeneity in natural swarms — •GIL ARIEL
DY 26.5	Wed	11:15–11:45	ZEU 160	Superstatistical Analysis and Modelling of Complex Dynamical Systems — •CLAUS METZNER, CHRISTOPH MARK, BEN FABRY, PATRICK KRAUSS, ACHIM SCHILLING, MAXIMILIAN TRAXDORF, HOLGER SCHULZE
DY 27.1	Wed	9:30–10:00	ZEU 250	Evolution in changing environments and driven disordered systems — •JOACHIM KRUG, SUMAN DAS, MUHITTIN MUNGAN
DY 37.6	Thu	11:00–11:30	MOL 213	Power law error growth rates – a dynamical mechanism for a strictly finite prediction horizon in weather forecasts — HYNEK BEDNAR, JONATHAN BRISCH, BURAK BUDANUR, •HOLGER KANTZ
DY 38.1	Thu	9:30–10:00	ZEU 160	Acoustically propelled nano- and microparticles: From fundamentals to applications — •RAPHAEL WITTKOWSKI
DY 56.5	Fri	10:30–11:00	ZEU 160	Transport and self-organization in living fluids — •MATTHIAS WEISS

Invited Talks of the joint Symposium Dynamics of Opinion Formation – From Quorum Sensing to Polarization (SYOF)

See SYOF for the full program of the symposium.

SYOF 1.1	Mon	9:30–10:00	HSZ 01	Towards understanding of the social hysteresis – insights from statistical physics — •KATARZYNA SZNAJD-WERON
SYOF 1.2	Mon	10:00–10:30	HSZ 01	Polarization in attitude distributions from surveys and models of continuous opinion dynamics — •JAN LORENZ, MARTIN GESTEFELD
SYOF 1.3	Mon	10:30–11:00	HSZ 01	Collective patterns and stable misunderstandings in networks striving for consensus without a common value system — •JOHANNES FALK, EDWIN EICHLER, KATJA WINDT, MARC-THORSTEN HÜTT
SYOF 1.4	Mon	11:15–11:45	HSZ 01	A yet undetected cognitive bias, revealed by opinion dynamics simulations — •GUILLAUME DEFFUANT
SYOF 1.5	Mon	11:45–12:15	HSZ 01	Extreme switches in kinetic exchange models of opinion. — •PARONGAMA SEN, KATHAKALI BISWAS

Invited Talks of the joint Symposium SKM Dissertation Prize 2023 (SYSD)

See SYSD for the full program of the symposium.

SYSD 1.1	Mon	9:30–10:00	HSZ 04	Diffusion of antibodies in solution: from individual proteins to phase separation domains — •ANITA GIRELLI
SYSD 1.2	Mon	10:00–10:30	HSZ 04	Intermediate Filament Mechanics Across Scales — •ANNA V. SCHEPERS
SYSD 1.3	Mon	10:30–11:00	HSZ 04	Ultrafast Probing and Coherent Vibrational Control of a Surface Structural Phase Transition — •JAN GERRIT HORSTMANN
SYSD 1.4	Mon	11:00–11:30	HSZ 04	Electro-active metasurfaces employing metal-to-insulator phase transitions — •JULIAN KARST
SYSD 1.5	Mon	11:30–12:00	HSZ 04	The role of unconventional symmetries in the dynamics of many-body systems — •PABLO SALA

Invited Talks of the joint Symposium Physics of Fluctuating Paths (SYFP)

See SYFP for the full program of the symposium.

SYFP 1.1	Tue	9:30–10:00	HSZ 01	Time at which a stochastic process achieves its maximum — •SATYA MAJUMDAR
SYFP 1.2	Tue	10:00–10:30	HSZ 01	Fluctuations and molecule-spanning dynamics of single Hsp90 proteins on timescales from nanoseconds to days — •THORSTEN HUGEL
SYFP 1.3	Tue	10:30–11:00	HSZ 01	Path reweighting for Langevin dynamics — •BETTINA KELLER
SYFP 1.4	Tue	11:15–11:45	HSZ 01	Out-of-equilibrium dynamics of trapped Brownian particles — •RAUL A. RICA
SYFP 1.5	Tue	11:45–12:15	HSZ 01	Thermodynamics of Clocks — •PATRICK PIETZONKA

Invited Talks of the joint Symposium Topology in Quantum and Classical Physics – From Topological Insulators to Active Matter (SYQC)

See SYQC for the full program of the symposium.

SYQC 1.1	Wed	15:00–15:30	HSZ 01	Topological magnetic whirls for computing — •KARIN EVERSCHOR-SITTE
SYQC 1.2	Wed	15:30–16:00	HSZ 01	Topological waves from solids to geo/astrophysical flows — •PIERRE DELPLACE, ANTOINE VENAILLE, NICOLAS PEREZ, GUILLAUME LAIBE, ARMAND LECLERC, MANOLIS PERROT, BRAD MARSTON
SYQC 1.3	Wed	16:00–16:30	HSZ 01	Topological Phase Transitions in Population Dynamics — •ERWIN FREY
SYQC 1.4	Wed	16:45–17:15	HSZ 01	Topological invariants protect robust chiral currents in active matter — •EVELYN TANG
SYQC 1.5	Wed	17:15–17:45	HSZ 01	Topological defects in biological active matter — •AMIN DOOSTMOHAMMADI

Sessions

DY 1.1–1.3	Sun	16:00–18:15	HSZ 01	Tutorial: Physics Meets Machine Learning (joint session DY/TUT/TT)
DY 2.1–2.9	Mon	9:30–13:00	HSZ 03	Focus Session: Physics Meets ML I – Machine Learning for Complex Quantum Systems (joint session TT/DY)
DY 3.1–3.12	Mon	9:30–13:00	TOE 317	Active Matter I (joint session BP/PPP/DY)
DY 4.1–4.11	Mon	9:30–12:30	ZEU 250	Pattern Formation, Delay and Nonlinear Stochastic Systems
DY 5.1–5.9	Mon	9:30–12:15	MOL 213	Fluid Physics: Turbulence and Convection
DY 6.1–6.11	Mon	10:00–13:00	ZEU 160	Statistical Physics: General I
DY 7.1–7.10	Mon	10:00–12:45	ZEU 147	Granular Matter and Contact Dynamics
DY 8.1–8.1	Mon	12:30–13:00	ZEU 250	Invited Talk: Dynamics of Networks (joint session DY/SOE)
DY 9.1–9.12	Mon	14:00–17:15	MOL 213	Quantum Dynamics, Decoherence and Quantum Information
DY 10.1–10.11	Mon	15:00–18:15	ZEU 160	Active Matter II (joint session DY/PPP/PPP)
DY 11.1–11.8	Mon	15:00–18:30	ZEU 250	Focus Session: Physics Meets ML II – Understanding Machine Learning as Complex Interacting Systems (joint session DY/TT)
DY 12.1–12.13	Tue	9:30–13:15	HSZ 204	Nonequilibrium Quantum Many-Body Systems I (joint session TT/DY)
DY 13.1–13.11	Tue	9:30–12:30	TOE 317	Active Matter III (joint session BP/PPP/DY)
DY 14.1–14.1	Tue	9:30–10:00	MOL 213	Invited Talk: Machine Learning and Complex Fluids
DY 15.1–15.1	Tue	9:30–10:00	ZEU 260	Physics of Contagion Processes I (joint session SOE/DY)
DY 16.1–16.11	Tue	10:00–13:00	MOL 213	Complex Fluids and Soft Matter (joint session DY/PPP)
DY 17.1–17.10	Tue	10:00–12:45	ZEU 160	Machine Learning in Dynamics and Statistical Physics I
DY 18.1–18.8	Tue	10:00–12:15	ZEU 147	Nonlinear Dynamics, Synchronization and Chaos
DY 19.1–19.3	Tue	10:00–10:45	ZEU 260	Physics of Contagion Processes II (joint session SOE/DY)
DY 20.1–20.5	Tue	11:00–12:15	ZEU 260	Networks: From Topology to Dynamics I (joint session SOE/DY)
DY 21.1–21.5	Tue	14:00–15:15	MOL 213	Quantum Chaos and Coherent Dynamics
DY 22.1–22.5	Tue	14:00–15:15	ZEU 160	Machine Learning in Dynamics and Statistical Physics II
DY 23.1–23.5	Tue	14:00–15:15	ZEU 250	Statistical Physics: General II
DY 24.1–24.4	Tue	14:00–15:00	ZEU 147	Glasses and Glass Transition (joint session DY/PPP)
DY 25.1–25.12	Wed	9:30–13:00	MOL 213	Many-Body Quantum Dynamics (joint session DY/TT)
DY 26.1–26.10	Wed	9:30–13:00	ZEU 160	Focus Session: From Inter-individual Variability to Heterogeneous Group Dynamics and Disorder in Active Matter (joint session DY/PPP/PPP)
DY 27.1–27.12	Wed	9:30–13:00	ZEU 250	Statistical Physics: Far From Equilibrium I
DY 28.1–28.5	Wed	9:30–11:45	ZEU 260	Focus Session: Critical Transitions in Society, Economy, and Nature (joint session SOE/DY)
DY 29.1–29.11	Wed	10:00–13:00	ZEU 147	Wetting, Droplets and Microfluidics (joint session DY/PPP)
DY 30.1–30.13	Wed	15:00–18:30	HSZ 204	Nonequilibrium Quantum Many-Body Systems II (joint session TT/DY)
DY 31.1–31.12	Wed	15:00–18:15	MOL 213	Microswimmers and Fluid Physics of Life (joint session DY/PPP)
DY 32.1–32.12	Wed	15:00–18:15	ZEU 160	Focus Session: Physics of Fluctuating Paths (joint session DY/PPP)
DY 33.1–33.6	Wed	15:00–16:30	ZEU 250	Biologically Inspired Statistical Physics (joint session DY/PPP)
DY 34.1–34.6	Wed	16:45–18:15	ZEU 250	Statistical Physics: Far From Equilibrium II
DY 35.1–35.12	Thu	9:30–13:00	TOE 317	Statistical Physics of Biological Systems I (joint session BP/DY)
DY 36.1–36.13	Thu	9:30–13:00	MER 02	Wetting, Fluidics and Liquids at Interfaces and Surfaces I (joint session PPP/DY)
DY 37.1–37.8	Thu	9:30–12:00	MOL 213	Data Analytics of Complex Dynamical Systems (joint session DY/SOE)
DY 38.1–38.12	Thu	9:30–13:00	ZEU 160	Active Matter IV (joint session DY/PPP/PPP)
DY 39.1–39.1	Thu	9:30–10:00	ZEU 260	Networks: From Topology to Dynamics II (joint session SOE/DY)
DY 40.1–40.9	Thu	10:00–12:30	ZEU 250	Stochastic Thermodynamics
DY 41.1–41.3	Thu	10:00–10:45	ZEU 260	Networks: From Topology to Dynamics III (joint session SOE/DY)
DY 42.1–42.17	Thu	13:00–16:00	P1	Poster: Active Matter, Soft Matter, Fluids
DY 43.1–43.22	Thu	13:00–16:00	P1	Poster: Quantum Dynamics and Many-Body Systems
DY 44.1–44.22	Thu	13:00–16:00	P1	Poster: Statistical Physics
DY 45.1–45.16	Thu	13:00–16:00	P1	Poster: Nonlinear Dynamics, Pattern Formation and Networks
DY 46.1–46.10	Thu	13:00–16:00	P1	Poster: Machine Learning and Data Analytics
DY 47.1–47.5	Thu	15:00–16:15	MER 02	Wetting, Fluidics and Liquids at Interfaces and Surfaces II (joint session PPP/DY)
DY 48.1–48.9	Thu	15:00–17:30	MOL 213	Dynamics and Chaos in Many-Body Systems I (joint session DY/TT)
DY 49.1–49.10	Thu	15:00–17:45	ZEU 160	Critical Phenomena and Phase Transitions
DY 50.1–50.2	Thu	15:00–15:30	ZEU 260	Evolutionary Game Theory (joint session SOE/DY)
DY 51	Thu	18:00–19:00	ZEU 160	Members' Assembly
DY 52.1–52.9	Fri	9:30–12:00	BAR Schö	Statistical Physics of Biological Systems II (joint session BP/DY)
DY 53.1–53.8	Fri	9:30–12:00	TOE 317	Active Matter V (joint session BP/PPP/DY)
DY 54.1–54.12	Fri	9:30–13:00	MER 02	Complex Fluids and Colloids, Micelles and Vesicles (joint session PPP/DY)
DY 55.1–55.11	Fri	9:30–12:30	MOL 213	Dynamics and Chaos in Many-Body Systems II (joint session DY/TT)

DY 56.1–56.11	Fri	9:30–12:45	ZEU 160	Brownian Motion and Anomalous Diffusion
DY 57.1–57.8	Fri	9:30–11:45	ZEU 250	Networks: From Topology to Dynamics IV (joint session DY/SOE)

Members' Assembly of the Dynamics and Statistical Physics Division

Thursday 18:00–19:00 ZEU 160

- Report
- Elections
- Future activities of DY
- Any other business

Sessions

– Invited Talks, Topical Talks, Tutorials, Contributed Talks, and Posters –

DY 1: Tutorial: Physics Meets Machine Learning (joint session DY/TUT/TT)

Machine learning has revolutionized many application fields such as computer vision and natural language processing. In physics there is a growing interest in using machine learning to enhance the analysis of experimental data and to devise and optimize experiments or numerical simulations. On the other hand physicists use their intuition and methods from statistical physics and complex systems theory to better understand the working principles of modern machine learning methods. This tutorial session introduces some subfields within this area and the basic methods involved.

Organized by Sabine Andergassen (Tübingen), Martin Gärtner (Heidelberg), Moritz Helias (Jülich), and Markus Schmitt (Cologne)

Time: Sunday 16:00–18:15

Location: HSZ 01

Tutorial DY 1.1 Sun 16:00 HSZ 01

Machine Learning for Quantum Technologies — •FLORIAN MARQUARDT — Max Planck Institute for the Science of Light and Friedrich-Alexander Universität Erlangen-Nürnberg, Erlangen, Germany

Machine learning is revolutionizing science and technology. In the past few years, it has become clear that it promises significant benefits as well for the development of quantum technologies. In this tutorial I will first give a brief introduction to neural networks. I will then discuss a number of areas and examples in which machine learning is being successfully applied in this context. These include measurement data analysis and quantum state representation, approximate quantum dynamics, parameter estimation, discovering strategies for hardware-level quantum control, the optimization of quantum circuits, and the discovery of quantum experiments, discrete quantum feedback strategies, and quantum error correction protocols.

Reference: "Artificial intelligence and machine learning for quantum technologies", M. Krenn, J. Landgraf, T. Foesel, and F. Marquardt, Phys. Rev. A 107, 010101 (2023).

Tutorial DY 1.2 Sun 16:45 HSZ 01

The Unreasonable Effectiveness of Gaussians in the Theory of Deep Neural Networks — •ZOHAR RINGEL — Racah Institute of Physics, Hebrew University in Jerusalem

Physical Sciences are in many ways the success story of explaining fundamental phenomena using simple math [1]. The fact that physical phenomena could be arranged in that manner is remarkable. Yet this simplicity does not necessarily carry over to life sciences or data sciences. Indeed prominent authors have argued against our desire to rely on neat mathematical structures when analyzing big data [2].

In the past half-decade several results have emerged which balance mathematical simplicity with data-induced complexity. These could be seen as a middle ground between the above juxtaposing views. The common divider here is the use of Gaussian distributions as approximants of various different quanti-

ties in deep neural networks (DNNs). Specifically these Gaussians emerge when describing outputs of DNNs with random weights, outputs of trained DNNs at random times, outputs of fixed DNNs over random input data, and fluctuations of hidden DNN pre-activations. In this tutorial I will present these quantities, provide arguments supporting their Gaussianity, and outline several theoretical implications.

[1] The Unreasonable Effectiveness of Mathematics in the Natural Sciences. Wigner (1960)

[2] The Unreasonable Effectiveness of Data. Halevy, Norvig, Pereira (2009)

Tutorial DY 1.3 Sun 17:30 HSZ 01

Computing learning curves for large machine learning models using the replica approach — •MANFRED OPPER — Inst. für Softwaretechnik und Theor. Informatik, TU Berlin — Centre for Systems Modelling and Quantitative Biomedicine, University of Birmingham, UK

Methods of statistical physics have been used for a long time to mathematically analyse the typical performance of machine learning models in the limit where both the number of data and the number of parameters (such as network weights) is large. By defining Boltzmann-Gibbs probability distributions over parameters where the cost function of the machine learning problem plays the role of a hamiltonian, one can derive analytical expressions for training errors and generalisation errors using the corresponding partition functions and free energies in terms of a usually small number of order parameters.

Since the models depend on a set of random data to be learnt, additional appropriate statistical (so-called quenched) averages of free energies over this 'disorder' have to be performed. The replica approach is a prominent analytical tool from the statistical physics of disordered systems to solve this nontrivial technical challenge.

In this tutorial I will give an introduction to this approach. Starting with an explicit calculation for simple single layer perceptrons, I will then argue how the method can be applied to more complex problems such as kernel machines (support vector machines and Gaussian processes) and multilayer networks.

DY 2: Focus Session: Physics Meets ML I – Machine Learning for Complex Quantum Systems (joint session TT/DY)

Modern machine learning methods open new perspectives on the high-dimensional data arising naturally in complex quantum systems. The applications range from the analysis of experimental observations over optimal control to the enhancement of numerical simulations in and out of equilibrium. This focus session brings together experts in the field to discuss recent progress and promising directions for future research.

Organizers: Markus Schmitt (University of Cologne), Martin Gärtner (University of Heidelberg)

Time: Monday 9:30–13:00

Location: HSZ 03

Invited Talk DY 2.1 Mon 9:30 HSZ 03

Enhanced variational Monte Carlo for Rydberg atom arrays — •STEFANIE CZISZEK — Department of Physics, University of Ottawa, Ottawa, Canada, K1N 6N6

Rydberg atom arrays are promising candidates for high-quality quantum computation and quantum simulation. However, long state preparation times limit the amount of measurement data that can be generated at reasonable timescales. This restriction directly affects the estimation of operator expectation values, as well as the reconstruction and characterization of quantum states.

Over the last years, neural networks have been explored as a powerful and systematically tuneable ansatz to represent quantum wave functions. Via tomographical state reconstruction, such numerical models can significantly reduce the amount of necessary measurements to accurately reconstruct operator expectation values. At the same time, neural networks can find ground state wave functions of given Hamiltonians via variational energy minimization.

While both approaches experience individual limitations, a combination of the two leads to a significant enhancement in the variational ground state search by naturally finding an improved network initialization from a limited amount

of measurement data. Additional specific modifications of the neural network model and its implementation can further optimize the performance of variational Monte Carlo simulations for Rydberg atom arrays and provide significant insights into their behaviour.

Invited Talk DY 2.2 Mon 10:00 HSZ 03
Data mining the output of quantum simulators – from critical behavior to algorithmic complexity — •MARCELLO DALMONTE — Abdus Salam International Centre for Theoretical Physics, Trieste (I)

Recent experiments with quantum simulators and noisy intermediate-scale quantum devices have demonstrated unparalleled capabilities of probing many-body wave functions, via directly probing them at the single quantum level via projective measurements. However, very little is known about to interpret and analyse such huge datasets. In this talk, I will show how it is possible to provide such characterisation of many-body quantum hardware via a direct and assumption-free data mining. The core idea of this programme is the fact that the output of quantum simulators and computers can be construed as a very high-dimensional manifold. Such manifold can be characterised via basic topological concepts, in particular, by their intrinsic dimension. Exploiting state of the art tools in non-parametric learning, I will discuss theoretical results for both classical and quantum many-body spin systems that illustrate how data structures undergo structural transitions whenever the underlying physical system does, and display universal (critical) behavior in both classical and quantum mechanical cases. I will conclude with remarks on the applicability of our theoretical framework to synthetic quantum systems (quantum simulators and quantum computers), and emphasize its potential to provide a direct, scalable measure of Kolmogorov complexity of output states.

Invited Talk DY 2.3 Mon 10:30 HSZ 03
Reinforcement learning for quantum technologies — •FLORIAN MARQUARDT — Max Planck Institute for the Science of Light and Friedrich-Alexander Universität Erlangen-Nürnberg, Erlangen, Germany

Complex quantum devices require sophisticated control. Discovering such control strategies from scratch with the help of machine learning will enable us to keep pace with the ever-increasing demands encountered when scaling up quantum computers. In this talk, I will describe how the field of reinforcement learning can deliver on this promise. I will present examples ranging from the optimization of quantum circuits to the model-based discovery of better quantum feedback strategies. Moreover, in a recent collaboration with our experimental colleagues, we could show how to train a novel latency-optimized neural network by reinforcement learning in an experiment, acting on a superconducting qubit in cycles of less than one microsecond.

Invited Talk DY 2.4 Mon 11:00 HSZ 03
Machine learning of phase transition — •CHRISTOF WEITENBERG — Universität Hamburg, Institut für Laserphysik, Hamburg, Germany

Machine learning is emerging as vital tool in many sciences. In quantum physics, notable examples are neural networks for the efficient representation of quantum many-body states and reinforcement learning of preparation and read-out routines. In this talk, I will present our results on machine learning of quantum phase transitions using classification techniques. This approach works very well even on noisy experimental data both with supervised and unsupervised machine learning, as we demonstrate for quantum simulators based on ultracold atoms. Next to the practical advantages, such techniques might in the future reveal phase transitions, for which conventional order parameters are not known.

15 min. break

DY 2.5 Mon 11:45 HSZ 03
Machine learning optimization of Majorana hybrid nanowires — •MATTHIAS THAMM and BERND ROSENOW — Institut für Theoretische Physik, Universität Leipzig

As the complexity of quantum systems such as quantum bit arrays increases, efforts to automate expensive tuning are increasingly worthwhile. We investigate machine learning based tuning of gate arrays using the CMA-ES algorithm for the case study of Majorana wires with strong disorder. We find that the algorithm is able to efficiently improve the topological signatures, learn intrinsic disorder profiles, and completely eliminate disorder effects. For example, with only 20 gates, it is possible to fully recover Majorana zero modes destroyed by disorder by optimizing gate voltages.

DY 2.6 Mon 12:00 HSZ 03
Model-independent learning of quantum phases of matter with quantum convolutional neural networks — •YU-JIE LIU¹, ADAM SMITH², MICHAEL KNAP¹, and FRANK POLLMANN¹ — ¹Technical University of Munich, 85748 Garching, Germany — ²University of Nottingham, Nottingham, NG7 2RD, UK

Quantum convolutional neural networks (QCNNs) have been introduced as classifiers for gapped quantum phases of matter. Here, we propose a model-independent protocol for training QCNNs to discover order parameters that are unchanged under phase-preserving perturbations. We initiate the training sequence with the fixed-point wavefunctions of the quantum phase and then add translation-invariant noise that respects the symmetries of the system to mask the fixed-point structure on short length scales. Without the translational invariance or other additional symmetries, we prove that a phase-classifying QCNN cannot exist. We illustrate this approach by training the QCNN on phases protected by time-reversal symmetry in one dimension, and test it on several time-reversal symmetric models exhibiting trivial, symmetry-breaking, and symmetry-protected topological order. The QCNN discovers a set of order parameters that identifies all three phases and accurately predicts the location of the phase boundary. The proposed protocol paves the way towards hardware-efficient training of quantum phase classifiers on a programmable quantum processor.

DY 2.7 Mon 12:15 HSZ 03
Simulating spectral functions of two-dimensional systems with neural quantum states — •TIAGO MENDES SANTOS¹, MARKUS SCHMITT², and MARKUS HEYL¹ — ¹University of Augsburg, Augsburg, Germany — ²Forschungszentrum Jülich, Jülich, Germany

Spectral functions are key tools to characterize and probe condensed matter systems. Simulating such quantities in interacting two-dimensional quantum matter is, however, still an outstanding challenge. This work presents a numerical approach to simulate spectral functions using Neural Quantum States. As the key aspect, our scheme leverages the flexibility of artificial-neural-network wave functions to access spectral properties by simulating the dynamics of localized excitations with the time-dependent variational Monte Carlo. For demonstration, we study the dynamical structure factor (DSF) of models describing two-dimensional quantum phase transitions, namely, the quantum Ising and a square-lattice Rydberg Atom Arrays model in a regime of parameters relevant to quantum simulators. When combined with deep network architectures whose number of variational parameters increase at a mild polynomial expense with the number of spins, we showcase that our approach reliably describes the DSF for unprecedented system sizes and time scales.

DY 2.8 Mon 12:30 HSZ 03
Efficient optimization of deep neural quantum states toward machine precision — •AO CHEN and MARKUS HEYL — Center for Electronic Correlations and Magnetism, University of Augsburg, 86135 Augsburg, Germany

Neural quantum states (NQSs) have emerged as a novel promising numerical method to solve the quantum many-body problem. However, it has remained a central challenge to train modern large-scale deep network architectures, which would be key to utilize the full power of NQSs and to make them competitive or superior to conventional numerical approaches. Here, we propose a minimum-step stochastic reconfiguration (MinSR) method that reduces the optimization complexity by orders of magnitude while keeping similar accuracy as compared to conventional stochastic reconfiguration. In this talk, I will show MinSR allows for an accurate training on unprecedentedly deep NQS with up to 64 layers and more than 10^5 parameters in the spin-1/2 Heisenberg J_1 - J_2 models on the square lattice. With limited numerical resources, partly obtained on single workstations, we find that this approach yields better variational energies as compared to existing NQS results and we further observe that the accuracy of our ground state calculations approaches different levels of machine precision on modern GPU and TPU hardware.

DY 2.9 Mon 12:45 HSZ 03
Time-dependent variational principle for quantum and classical dynamics — •MORITZ REH¹, MARKUS SCHMITT², and MARTIN GÄRTNER^{1,3,4} — ¹Kirchhoff-Institut für Physik, Universität Heidelberg, Im Neuenheimer Feld 227, 69120 Heidelberg, Germany — ²Institut für Theoretische Physik, Universität zu Köln, 50937 Köln, Germany — ³Physikalisches Institut, Universität Heidelberg, Im Neuenheimer Feld 226, 69120 Heidelberg, Germany — ⁴Institut für Theoretische Physik, Universität Heidelberg, Philosophenweg 16, 69120 Heidelberg, Germany

The solution of many-body quantum dynamics is a challenging feat due to the curse of dimensionality, hindering the exploration of dynamics beyond a mediocre number of qubits. Neural Networks can variationally approximate the state of interest and therefore present a promising tool as they allow to efficiently represent the quantum state at the expense of truncating the Hilbert space.

We present such a scheme that is aimed at solving dissipative quantum dynamics using a probabilistic framework, i.e. the so-called POVM-formalism and demonstrate it for spin chains of up to 40 spins. We then show that the generality of the approach allows us to translate this formalism directly to the case of partial differential equations in high dimensions, defeating the exponential growth of grid cells when adding dimensions.

DY 3: Active Matter I (joint session BP/PP/DY)

Time: Monday 9:30–13:00

Location: TOE 317

See BP 2 for details of this session.

DY 4: Pattern Formation, Delay and Nonlinear Stochastic Systems

Time: Monday 9:30–12:30

Location: ZEU 250

DY 4.1 Mon 9:30 ZEU 250

Spiral waves within a bistability parameter region of an excitable medium — •VLADIMIR ZYKOV and EBERHARD BODENSCHATZ — Max Plank Institute for Dynamics and Self-Organization, D-37077, Goettingen, Germany

Spiral waves are a well-known and intensively studied dynamic phenomenon in excitable media of various types. Most studies have considered an excitable medium with a single stable resting state. However, spiral waves can be maintained in an excitable medium with bistability. Our calculations, performed using the widely used Barkley model, clearly show that spiral waves in the bistability region exhibit unique properties. For example, a spiral wave can either rotate around a core that is in an unexcited state, or the tip of the spiral wave describes a circular trajectory located inside an excited region. The boundaries of the parameter regions with positive and negative cores have been defined numerically and analytically evaluated. It is also shown that the creation of a positive or *negative* core may depend on the initial conditions, which leads to hysteresis of spiral waves.

DY 4.2 Mon 9:45 ZEU 250

Band Pattern Formation in a Suspension of Red Blood Cells During Centrifugation in a Percoll Density Gradient — •FELIX MAURER, THOMAS JOHN, CHRISTIAN WAGNER, and ALEXIS DARRAS — Dynamics of Fluids, Experimental Physics, Saarland University, 66123 Saarbrücken, Germany

Percoll is a suspension of silica nanoparticles often used to establish density gradients and separate biological matter in centrifugation protocols. When red blood cells (RBCs) sediment in a Percoll medium, they form patterns of discrete bands. While this is a popular approach for RBC age separation, the mechanisms involved in band formation were unknown. In a series of experiments we could show that the formation of those patterns could be explained by cell aggregation. We developed a new continuum model to describe the volumetric RBC density under the influence of attractive pair interaction. Our numerical solutions are characterized by pattern formation and transitions between the equilibrium states depending on aggregation energy and initial volumetric RBC concentration.

DY 4.3 Mon 10:00 ZEU 250

A missing amplitude equation — •TOBIAS FROHOFF-HÜLSMANN¹ and UWE THIELE^{1,2} — ¹Institute of Theoretical Physics, WWU Münster — ²Center for Nonlinear Science (CeNoS), WWU Münster

Amplitude (or envelope) equations describe the spatiotemporal dynamics of the essential linear mode(s) in the vicinity of a stability threshold and represent universal equations for spatially extended systems [3]. They are determined by the type of linear instability, the symmetries and whether or not conservation laws are present [5, 6]. For systems without conservation laws these equations are well studied, e.g. the complex Ginzburg-Landau equation [1]. However, the presence of conservation laws is highly relevant for a wide spectrum of pattern forming systems, e.g. for certain reaction diffusion (RD) systems [2, 4]. Here, we review the basic types of linear instabilities in the presence of conservation laws and show that there are relevant cases for which the amplitude equation is still unknown. We focus on such a missing case and derive an amplitude equation relevant for practically important RD systems.

[1] I. S. Aranson and L. Kramer. *Rev. Mod. Phys.*, 74:99-143, 2002.[2] C. Beta, N. S. Gov, and A. Yochelis. *Cells*, 9:1533, 2020.[3] M. C. Cross and P. C. Hohenberg. *Rev. Mod. Phys.*, 65:851-1112, 1993.[4] J. Halatek and E. Frey. *Nature Phys.*, 14:507-514, 2018.[5] P. C. Matthews and S. M. Cox. *Nonlinearity*, 13:1293-1320, 2000.[6] F. Bergmann, L. Rapp, and W. Zimmermann. *Phys. Rev. E*, 98:020603, 2018.

DY 4.4 Mon 10:15 ZEU 250

The universal CHEOPS, the path to it, and applications — ANDRE FÖRTSCH and •WALTER ZIMMERMANN — Theoretische Physik, Universität Bayreuth

Solutions to fundamental questions in the field of nonequilibrium phase transitions are presented. What are the 'generic transport equations for oscillatory phase separation' (GTOPS) in systems described by conserved fields? GTOPS cover both classical and oscillatory phase separation. But what is the universal equation for oscillatory phase separation, i.e., the counterpart of the famous universal complex Ginzburg-Landau equation (cGLE) for an unconserved order parameter [1]? It is the 'Cahn-Hilliard model extended to oscillatory phase

separation' (CHEOPS) that includes the model in [2] as a special case. By generalizing methods from [3-6] CHEOPS is derived from GTOPS or even from a chemotaxis model for two species. Examples of surprising solutions of GTOPS and CHEOPS (patterns) are presented and some of them are also illustrated by a so-called minimal model (MIMO).

[1] I. Aranson, L. Kramer, *Rev. Mod. Phys.* 74, 99 (2002)[2] W. Zimmermann, *Physica A* 237, 575 (1997)[3] F. Bergmann et al., *Phys. Rev. E* 98, 020603(R) (2018)[4] L. Rapp et al., *Eur. Phys. J E* 42, 57 (2019)[5] F. Bergmann, W. Zimmermann, *PLoS ONE* 14, e0218328 (2019)[6] F. J. Thomsen, L. Rapp, F. Bergmann, W. Zimmermann, *New J. Phys.* (FT) 23, 042002 (2021)

DY 4.5 Mon 10:30 ZEU 250

Quasi-steady interface flows in simple reaction-diffusion systems — •TOBIAS ALEXANDER ROTH, HENRIK WEYER, and ERWIN FREY — Arnold Sommerfeld Center for Theoretical Physics and Center for NanoScience, Department of Physics, Ludwig-Maximilians-Universität München, München, Germany

Intracellular protein patterns are essential features of living systems. A well-studied framework for describing simple protein systems are 2-component reaction-diffusion systems that preserve mass (2cMCRD). These genuine non-equilibrium systems can not be written in terms of a variational approach: there is neither a free energy nor a classical surface tension. Interestingly, it was found that the long-term evolution of these reaction-diffusion systems, however, is phenomenologically similar to the interface dynamics of phase-separating thermodynamic systems.

Here we show that an interface line in 2cMCRD systems obeys a flow, that interpolates between two paradigmatic limits: the two-sided Mullins-Sekerka flow and the area-preserving geodesic curvature flow. This generalised flow conserves area and minimises the interface length. One can tune its character by the time scale of diffusive mass redistribution compared to reactive turnover.

15 min. break

DY 4.6 Mon 11:00 ZEU 250

Amplitude expansion of the phase-field crystal model on deformable surfaces — •LUCAS BENOIT-MARÉCHAL, MARCO SALVALAGLIO, INGO NITSCHKE, and AXEL VOIGT — Institute of Scientific Computing, TU Dresden, Dresden, Germany

The Phase Field Crystal (PFC) model describes lattices at diffusive timescales but atomic lengthscales, thus requiring subatomic resolution meshes. To remedy this restriction, the complex amplitude expansion (APFC) was developed, whereby the amplitude of the density fluctuations is modeled instead of the density itself, enabling simulations at mesoscales that retain atomistic features.

We extend the two-dimensional APFC model to include out-of-plane displacements in order to study the coupling between crystal defects and surface deformation, paving the way for applications such as the topological tuning of mechanical properties of crystalline sheets.

To validate our model, we compare representative settings with atomistic simulations from the PFC model and Molecular Dynamics and find, within certain limits that we discuss, excellent agreement between all models.

DY 4.7 Mon 11:15 ZEU 250

Laminar chaos in systems with quasiperiodic delay — •DAVID MÜLLER-BENDER¹ and GÜNTER RADONS^{1,2} — ¹Institute of Physics, Chemnitz University of Technology, 09107 Chemnitz, Germany — ²ICM - Institute for Mechanical and Industrial Engineering, 09117 Chemnitz, Germany

A new type of chaos called laminar chaos was found in singularly perturbed dynamical systems with periodic time-varying delay [Phys. Rev. Lett. 120, 084102 (2018)]. It is characterized by nearly constant laminar phases, which are periodically interrupted by irregular bursts, where the intensity levels of the laminar phases vary chaotically from phase to phase. In this paper, we demonstrate that laminar chaos can also be observed in systems with quasiperiodic delay, where we generalize the concept of conservative and dissipative delays to such systems. It turns out that the durations of the laminar phases vary quasiperiodically and follow the dynamics of a torus map in contrast to the periodic variation observed for periodic delay. Theoretical and numerical results indicate that introducing a quasiperiodic delay modulation into a time-delay system can lead to a giant re-

duction of the dimension of the chaotic attractors. By varying the mean delay and keeping other parameters fixed, we found that the Kaplan-Yorke dimension is modulated quasiperiodically over several orders of magnitudes, where the dynamics switches quasiperiodically between different types of high- and low-dimensional types of chaos.

Details can be found in the preprint [arXiv:2210.04706 (2022)].

DY 4.8 Mon 11:30 ZEU 250

Pulse generation in opto-electronic neurons with time-delayed feedback — •JONAS MAYER MARTINS¹, SVETLANA V. GUREVICH¹, and JULIEN JAVALOYES² — ¹Institute for Theoretical Physics, University of Münster, Wilhelm-Klemm-Str. 9 and Center for Nonlinear Science (CeNoS), University of Münster, Corrensstrasse 2, 48149 Münster, Germany — ²Departament de Física and IAC-3, Universitat de les Illes Balears, C/ Valldemossa km 7.5, 07122 Mallorca, Spain

We study a neuromorphic circuit composed of a nano resonant tunneling diode (RTD) operated in the excitable regime, where the diode generates, when triggered, an all-or-nothing electrical response pulse. This pulse is fed into a nano laser diode (LD), which in turn emits an optical pulse that is re-injected with time delay back into the RTD. Our theoretical analysis of this time-delayed optoelectronic nonlinear system describes how such neuron-like excitability can lead to sustained periodic pulsations due to the time-delayed feedback. We derive a bifurcation diagram through numerical continuation, unveiling the rich dynamics of the system. Furthermore, direct numerical simulations of the RTD-LD reveal emerging solitons that may serve as memory for information. Optoelectronic neurons like the RTD-LD are particularly interesting because they allow for fast computations at very low energy consumption and are therefore promising candidates for new computational architectures that mimic the brain.

DY 4.9 Mon 11:45 ZEU 250

Spontaneous vortex formation by microswimmers with retarded attractions — XIANGZUN WANG¹, •PIN-CHUAN CHEN², KLAUS KROY², VIKTOR HOLUBEC³, and FRANK CICHOS¹ — ¹Peter Debye Institute for Soft Matter Physics, Leipzig University, 04103 Leipzig, Germany — ²Institute for Theoretical Physics, Leipzig University, Postfach 100 920, 04009 Leipzig, Germany — ³Department of Macromolecular Physics, Faculty of Mathematics and Physics, Charles University, 18000 Prague, Czech Republic

In recent experiments done in the Molecular Nanophotonics Group in the Peter Debye Institute, thermophoretic microswimmers are observed to self-assemble into bi-stable orbital modes due to retarded attractive interactions.

A single agent which is attracted to an immobilized target with a time delay can be described by a time-local overdamped Langevin equation with a potential determined by time delay, and the transition in between the two stable modes is well predicted by Kramers' escape rate. Simulations of multiple agents attracted to one target also show that the collective behavior can be reduced to a one-agent description; however, the experiments (with up to 16 agents) show otherwise.

The discrepancy between the results are attributed to additional effects in experiments.

We further show results of extended simulations with larger number of agents, which demonstrate two transitions depending solely on the time delay.

DY 4.10 Mon 12:00 ZEU 250

Stochastic pH oscillator confined to lipid vesicles — •ARTHUR STRAUBE¹, STEFANIE WINKELMANN¹, and FELIX HÖFLING^{2,1} — ¹Zuse Institute Berlin — ²Institut für Mathematik, Freie Universität Berlin

We study an urea-urease-based pH oscillator confined to lipid vesicles serving as an open reactor [1,2]. In contrast to conventional pH oscillators in closed reactors, the exchange with the vesicle exterior periodically resets the pH clock that switches the system from acid to basic, resulting in self-sustained oscillations. Stochastic simulations for microscopically small vesicles predict a significant statistical variation of the oscillation period. Although the mean period remains remarkably robust for vesicle sizes down to nearly 200 nm, the periodicity of the rhythm is gradually destroyed for smaller vesicles [1]. We analyze the structure of the limit cycle, which controls the dynamics for giant vesicles and dominates the strongly stochastic oscillations in small vesicles of submicrometer size. We derive reduced two-variable models, amenable to analytic treatments, and show that the accuracy of predictions, including the period of oscillations, is highly sensitive to the choice of the reduction scheme [2]. The accurate description of a single pH oscillator is crucial for rationalizing experiments and understanding communication of vesicles and synchronization of rhythms.

[1] A. Straube, S. Winkelmann, C. Schütte, F. Höfling, *J. Phys. Chem. Lett.* **12**, 9888 (2021). [2] A. Straube, S. Winkelmann, F. Höfling, *ZIB Report 22-21* (2022), preprint (DOI: 10.12752/8817).

DY 4.11 Mon 12:15 ZEU 250

Sampling from the rule 150 fractal through an iterated stochastic process — •JENS CHRISTIAN CLAUSSEN — University of Birmingham, UK

A widely known, but surprising way of sampling points from the Sierpinski fractal is through an iterated stochastic process where in each time step one of three operators is applied, which can be interpreted from their number representation, or as a geometric operation. While the Sierpinski fractal can also be generated by the rule 90 elementary cellular automaton (ECA), the ECA rule 150 generates a fractal pattern with a 2-step self-similarity resembling a generalization of a Fibonacci iteration [1]. Here we show that the rule 150 fractal can be generated without a 2-step iteration. We introduce a set of 6 operators, which allow to generate the rule 150 fractal from a stochastic process. We show that these 6 operators can be reduced to 4 operators, by adding one operator to the 3 operators from the rule 90 case. The operators for the rule 150 can be interpreted both from their number representation and geometrically. Further each point of the rule 150 fractal can be represented by a any base-6 number, or by a 4-letter symbolic sequence with a grammar restriction.

[1] Jens Christian Clausen, *J. Math. Phys.* **49**, 062701 (2008)

DY 5: Fluid Physics: Turbulence and Convection

Time: Monday 9:30–12:15

Location: MOL 213

Invited Talk

DY 5.1 Mon 9:30 MOL 213

Extreme events, entropies and instantons for turbulence and water waves — •JOACHIM PEINKE, ANDRÉ FUCHS, and MATTHIAS WÄCHTER — Inst. of Physics, University of Oldenburg, Germany

Complex systems like turbulence and ocean waves can produce extreme events like large changes in wind speed or monster waves. It has long been debated whether coherent structures or special statistical properties are essential for the understanding. Here we show a comprehensive stochastic approach for Lagrangian and Eulerian turbulence, as well as, for waves, leading to a joint multi-point statistic. We consider cascade trajectories through scales as realizations of a stochastic Langevin process that can be deduced from data. Knowledge of the stochastic equations allows determination of the entropy production of each cascade trajectory. Trajectories with negative entropies are linked to large fluctuations like extreme wind speeds or monster waves. Thus entropy seems to select different structures. Furthermore, negative and positive entropy values are balanced by rigorous fluctuation theorems, so that extreme and normal fluctuations are mutually dependent. In this way the entropy concept links statistics with the coherent structure approach. Finally, trajectories concentrate around an optimal path, called instanton, which is the minimum of an effective action given by the estimated stochastic equations. Entropions, defined as instantons conditioned on fixed entropy values, pinpoint the trajectories responsible for the emergence of non-Gaussian statistics at small scales. *Ann. Rev. Cond. Matt. Phys.* **10**, 107-132 (2019), *EPL* **137**, 53001 (2022), *Phys. Rev. Lett.* **129**, 034502 (2022)

DY 5.2 Mon 10:00 MOL 213

Discrete and Continuous Symmetry Reduction for Minimal Parametrizations of Chaotic Fluid Flows — •SIMON KNEER and NAZMI BURAK BUDANUR — Max Planck Institute for the Physics of Complex Systems, Dresden, Germany

Mathematical laws that govern fluid motion preserve their shape under translation, rotation, and reflection of coordinates. Consequently, most hydrodynamic systems of interest exhibit a set of symmetries, the action of which on the fluid states commutes with the dynamics. In complex flows, typical non-laminar fluid states are not invariant under these symmetries. Thus, each solution of the system has many dynamically equivalent symmetry copies. For data-driven model reduction methods, such as undercomplete Autoencoders, this multiplicity is not desired since it results in an artificial inflation of the training data which does not yield any physical insight. We consider this problem in the sinusoidally-driven Navier-Stokes equations in two dimensions, i.e. Kolmogorov flow, which is symmetric under continuous translations as well as discrete rotations and reflections. We formulate a symmetry reduction that combines first Fourier mode slicing with invariant polynomials that yields a fully invariant formulation of the corresponding dynamical system. Through this symmetry reduction, we are able to find a minimal approximation to the inertial manifold of this system as well as ordinary differential equations on this manifold that describe the dynamics.

DY 5.3 Mon 10:15 MOL 213

Spontaneous symmetry breaking for extreme vorticity and strain in the three-dimensional Navier-Stokes equations — •TIMO SCHORLEPP¹, TOBIAS GRAFKE², SANDRA MAY³, and RAINER GRAUER¹ — ¹Institute for Theoretical Physics I, Ruhr-University Bochum, Germany — ²Mathematics Institute, University of Warwick, United Kingdom — ³Department of Mathematics, TU Dortmund University, Germany

We investigate the spatio-temporal structure of the most likely configurations realizing extremely high vorticity or strain in the stochastically forced three-dimensional incompressible Navier-Stokes equations. Most likely configurations are computed by numerically finding the highest probability velocity field realizing an extreme constraint as solution of a large optimization problem. High-vorticity configurations are identified as pinched vortex filaments with swirl, while high-strain configurations correspond to counter-rotating vortex rings. We additionally observe that the most likely configurations for vorticity and strain spontaneously break their rotational symmetry for extremely high observable values. Instanton calculus and large deviation theory allow us to show that these maximum likelihood realizations determine the tail probabilities of the observed quantities. In particular, we are able to demonstrate that artificially enforcing rotational symmetry for large strain configurations leads to a severe underestimate of their probability, as it is dominated in likelihood by an exponentially more likely symmetry-broken vortex-sheet configuration.

DY 5.4 Mon 10:30 MOL 213

Delayed onset in spanwise rotating compressible convection — •KEVIN LÜDEMANN and ANDREAS TILGNER — Institute for Astrophysics and Geophysics, Göttingen, Germany

We are investigating compressible convection with spanwise rotation in direct numerical simulations meaning that the direction of gravity and the axis of rotation are perpendicular to each other. This is a model for the equatorial region of gas planets like Jupiter or Earth's outer core. Both consist of compressible liquids ranging many orders of magnitude in density variations for Jupiter to about 20 percent of density changes for earth outer core. We are more interested in moderate density changes since those are realizable in laboratory experiment like the one performed in Lyon. From a parameter study in the number of density scale heights controlling the compressibility and the Ekman number controlling the global rate of rotation, we find that the onset of convection is delayed by compressibility and rotation. Additionally, a horizontal drift of the many slender convection rolls has been found at the onset for high rotation rates. An extensive study is presented highlighting these unforeseen results.

DY 5.5 Mon 10:45 MOL 213

Offshore wind: Evidence for two-dimensional turbulence and role of sea horizon — •SO-KUMNETH SIM¹, JOACHIM PEINKE², and PHILIPP MAASS¹ — ¹Fachbereich Physik, Universität Osnabrück, Germany — ²Institut für Physik & ForWind, Universität Oldenburg, Germany

We analyze offshore wind speeds with a time resolution of one second over a period of 20 months [1]. Wind speed power spectra show a scaling behavior that is governed by three- and two-dimensional turbulence [2]. The latter is observed for frequencies lower than a crossover frequency f_{2D} . An analysis of the third moment (third-order structure function) of wind speed fluctuations provides strong evidence of this transition to two-dimensional turbulence [3]. We argue that $f_{2D} \sim \bar{v}/d$, where \bar{v} is the mean wind speed and d the distance between the measurement device and the sea horizon. For the regime of two-dimensional turbulence, two scaling regimes are predicted, which originate from an inverse energy and an enstrophy cascade. Our results indicate that the scaling due to the inverse energy cascade occurs at low frequencies and is followed by the scaling of the enstrophy cascade at higher frequencies. This is in agreement with the theoretical prediction but contrary to earlier observations.

[1] S.-K. Sim, J. Peinke, P. Maass, arXiv:2203.07685 (2022).

[2] X. Larsén, S. Larsen, E. Petersen, *Boundary-Layer Meteorol.* 159, 349 (2016).

[3] R. Cerbus, P. Chakraborty, *Phys. Fluids* 299, 111110 (2017).

15 min. break

DY 5.6 Mon 11:15 MOL 213

Convective turbulent superstructures in Rayleigh-Benard convection — •HIUFAI YIK¹, STEPHAN WEISS^{1,2}, and EBERHARD BODENSCHATZ¹ — ¹Max Planck Institute for Dynamics and Self-Organization — ²Max Planck Center for Complex Fluid Dynamics

We report experimental results on turbulent superstructures in high-turbulence thermal convection. The 0.7 m high, 3.5 m wide and 0.35 m deep rectangular cell was installed in the Göttingen U-Boot and filled with sulphur hexafluoride at pressures up to 19 bar. Convection in this installation can be investigated up to Rayleigh numbers $Ra = 10^{13}$ at Prandtl numbers of about 0.8. More than 200 thermistors were distributed in the upper and lower plates for temperature and heat flux measurements, and 20 additional thermistors in the centre of the cell to measure the fluid temperature along the longitudinal axis. We report the results on turbulent superstructures and their dependence on heat transport and boundary conditions. For this purpose, the upper and lower plates of the convection cell were each divided into 4 sections, with an independent temperature control allowing both homogeneous and inhomogeneous temperature boundary conditions and the selection of different turbulent superstructures.

DY 5.7 Mon 11:30 MOL 213

Statistical field theory for a stochastic linear advection-stretching model for turbulence — LUKAS BENTKAMP, MAURIZIO CARBONE, and •MICHAEL WILCZEK — Theoretical Physics I, University of Bayreuth, 95440 Bayreuth

A major obstacle in developing a statistical field theory of turbulence is the analysis of the functional equations that govern the complete statistics of the flow field. Simplified models of turbulence may help to develop such a statistical framework. In this contribution, we discuss the stochastic linear advection and stretching of an incompressible passive vector field as a model for small-scale turbulence. The model encompasses non-Gaussian statistics due to an intermittent energy flux from large scales to small scales, thereby displaying hallmark features of turbulence. We explore this model using the Hopf functional formalism, which naturally leads to a decomposition of the complex non-Gaussian statistics into Gaussian sub-ensembles based on different realizations of advection and stretching.

This project has received funding from the European Research Council (ERC) under the European Union's Horizon 2020 research and innovation programme (Grant agreement No. 101001081).

DY 5.8 Mon 11:45 MOL 213

Description of laminar-turbulent transition of an airfoil boundary layer measured by differential image thermography using directed percolation theory — •TOM T. B. WESTER, JOACHIM PEINKE, and GERD GÜLKER — ForWind, University of Oldenburg, Institute of Physics, Oldenburg, Germany

Transition from laminar to turbulent flow is still a challenging problem. Recent studies indicate a good agreement when describing this phase transition with the directed percolation theory. This study presents a new experimental approach by means of differential image thermography (DIT) enabling to investigate this transition on the suction side of a heated airfoil. The results extend the applicability of the directed percolation theory to describe the transition on curves surfaces. The experimental effort allows for the first time an agreement between all three universal exponents of the (1+1)D directed percolation for such airfoil application. Furthermore, this study proves that the theory holds for a wide range of flows, as shown by the various conditions tested. Such a large parameter space was not covered in any examination so far. The findings underline the significance of percolation models in fluid mechanics and show that this theory can be used as a high precision tool for the problem of transition to turbulence.

DY 5.9 Mon 12:00 MOL 213

How to generate turbulence with highest Reynolds numbers in the wind tunnel — •LARS NEUHAUS, MICHAEL HÖLLING, and JOACHIM PEINKE — ForWind, University of Oldenburg, Institute of Physics, Oldenburg, Germany

In order to study objects like buildings, vehicles or wind turbines under the influence of wind fluctuations, the generation of laboratory flows that resemble atmospheric turbulence is of prime importance. This is where active grids come into play, allowing to excite the wind tunnel flow in a user-defined way. With a blockage induced flow design, it is possible to recreate atmospheric flows through their time series or to create single coherent structures such as gusts defined by industrial standards. In addition, it is possible to generate turbulence with large integral length scales through a random driving that follows a stochastic process. Velocity fluctuations with correlation lengths and thus integral scales much larger than the transverse dimensions of the wind tunnel can be generated. By combining active grid excitation with fan speed modulation, it is additionally possible to generate a flow characterized by an inertial range of four decades and an integral Reynolds number of $2 \cdot 10^7$. By a newly developed active grid it is furthermore possible to vary the turbulent properties over height to mimic height dependencies found in the atmosphere and also to generate a turbulent non-turbulent interface.

DY 6: Statistical Physics: General I

Time: Monday 10:00–13:00

Location: ZEU 160

DY 6.1 Mon 10:00 ZEU 160

Noether's theorem in statistical mechanics — •SOPHIE HERMANN and MATTHIAS SCHMIDT — Universität Bayreuth, Bayreuth, Deutschland

Noether's Theorem is familiar to most physicists due its fundamental role in linking the existence of conservation laws to the underlying symmetries of a physical system. Typically the systems are described in the particle-based context of classical mechanics or on the basis of field theory. We apply Noether's calculus of invariant variations to thermal systems, where fluctuations are paramount and one aims for a statistical mechanical description, both in and out of equilibrium. Generating functionals, such as the free energy, yield mechanical laws under continuous translational and rotational symmetry operations. The resulting global theorems express vanishing of total internal and total external forces and torques. Local sum rules interrelate density correlators, as well as static and time direct correlation functions via infinite hierarchies, including memory. We demonstrate that this approach is consistent with the earlier work in equilibrium, and that it enables one to go, with relative ease, beyond the sum rules that these authors formulated. For anisotropic particles, systematic coupling of orbital and spin motion is identified. The theory allows to shed new light on the spatio-temporal coupling of correlations in complex systems. We present novel exact and nontrivial identities that apply to time-dependent problems and driven and active fluids.

DY 6.2 Mon 10:15 ZEU 160

Mean-field brittle yielding of amorphous solids — •JACK T. PARLEY¹ and PETER SOLLICH^{1,2} — ¹Institut für Theoretische Physik, University of Göttingen, Friedrich-Hund-Platz 1, 37077 Göttingen, Germany — ²Department of Mathematics, King's College London, London WC2R 2LS, UK

We study the brittle yielding of athermal amorphous solids within the celebrated Hébraud-Lequeux mean-field elastoplastic model, which incorporates the sign-varying nature of Eshelby interactions as a Gaussian mechanical noise. As in finite-dimensional particle simulations, we find a critical value of the initial disorder, below which yielding in the limit of quasistatic shear becomes a discontinuous non-equilibrium transition. We find evidence that in this limit yielding cannot be described as a spinodal instability, in contrast to the behaviour found in driven random magnets or depinning-like models. At small but finite shear rates, we show that the tail exponents characterising the decay of the plastic yield rate function on either side of its peak at the transition are related to the athermal aging exponents. We finally derive analytically the scaling with shear rate of the peak susceptibility at the random critical point, and discuss the connection to avalanches in finite-size systems.

DY 6.3 Mon 10:30 ZEU 160

Bringing the power of Monte Carlo methods to long-range-interacting molecular systems — •PHILIPP HÖLLMER¹, A. C. MAGGS², and WERNER KRAUTH³ — ¹University of Bonn, Germany — ²ESPCI Paris, France — ³École normale supérieure de Paris, France

Molecular simulations are widespread in molecular sciences to study, e.g., protein folding. Here, chemical systems are modeled empirically by a set of atomic positions with parameterized interaction potentials. Nowadays, molecular-dynamics (MD) simulations are predominantly used to study long-range-interacting molecular systems because of their superior computational complexities and Newtonian dynamics when compared to traditional Markov-chain Monte Carlo (MCMC) simulations. We argue that both disadvantages of traditional reversible MCMC are overcome by event-chain Monte Carlo (ECMC), which is a family of non-reversible MCMC methods.

In this talk, we will explore how ECMC samples the equilibrium Boltzmann distribution exactly, although it uses non-equilibrium dynamics and never computes the total system potential. We will discuss how ECMC's sole restriction of the global-balance condition yields a great freedom to implement quickly decorrelating dynamics beyond Newtonian's dynamics of MD. Finally, we will demonstrate $\mathcal{O}(N \log N)$ scaling for ECMC's decorrelation of an N -body system of a commonly used long-range-interacting water model. This matches the performance of MD without ever discretizing time or space.

DY 6.4 Mon 10:45 ZEU 160

Virial coefficients of hard, anisotropic particles in two- to four-dimensional Euclidean spaces — •MARKUS KULOSSA, DANIEL WEIDIG, and JOACHIM WAGNER — Institut für Chemie, Universität Rostock, 18051 Rostock, Germany

We compare virial coefficients up to order eight for anisotropic, hard particles in two- to four-dimensional Euclidean spaces in dependence on their aspect ratio. The virial coefficients of both, convex shapes such as stadia, spherocylinders and hyperspherocylinders and concave shapes such as dumbbells in two to four dimensions are analyzed. Since the second virial coefficient of hard objects equals their mutual excluded D -dimensional volume per particle, analytically obtained expressions for the second virial coefficients serve as a test

for orientation-dependent overlap algorithms. In first approximation, a nearly universal dependence of reduced virial coefficients on the excess part of the mutual excluded volume is observed for third and higher order virial coefficients.

DY 6.5 Mon 11:00 ZEU 160

Geometric Bounds on the Power of Adiabatic Thermal Machines — •JOSHUA EGLINTON^{1,2} and KAY BRANDNER^{1,2} — ¹School of Physics and Astronomy, University of Nottingham, Nottingham NG7 2RD, United Kingdom — ²Centre for the Mathematical and Theoretical Physics of Quantum Non-equilibrium Systems, University of Nottingham, Nottingham NG7 2RD, United Kingdom

The laws of thermodynamics put fundamental bounds on the efficiencies of thermal machines. These Carnot bounds can typically be attained only if the machine is operated quasi-statically, which leads to vanishing power output. We present a new family of power-efficiency trade-off relations that imply a quadratic decay of power at Carnot efficiency, for devices operating between two fixed temperatures. Notably, these relations depend only on geometric quantities such as the thermodynamic length of the driving cycle and hold for essentially any thermodynamically consistent micro-dynamics such as classical Markov-jump processes, adiabatic Lindblad dynamics or coherent transport. This analysis is based on a new general scaling argument, with which we show that the efficiency of such devices reaches the Carnot bound only if heat-leaks between the baths can be fully suppressed. Furthermore, we find that their power is in fact determined by second-order terms in the temperature difference between the two baths, which are neglected in standard linear-response theory.

[1] - J. Eglinton and K. Brandner, Phys. Rev. E 105, L052102 (2022)

DY 6.6 Mon 11:15 ZEU 160

Hard rods on a 2D lattice system — •MICHAEL ZIMMERMANN — Universität Tübingen, Tübingen, Deutschland

An exact solution for the equilibrium density for a hard rod system on a 1D continuous system was found by Percus [1]. For lattice systems of hard rods, Lafuente and Cuesta established a method based on Rosenfeld's fundamental measure theory to find the exact solution in 1D and to extrapolate from this result to a density functional in higher dimensions [2,3]. But already in 2D theoretical properties differ from respective simulation results [4], such as the onset of demixing between rods of different orientation. In this talk we will discuss some possible extensions of the Lafuente-Cuesta functional for improving the excess free energy functional and for better approximations of density distributions in 2D hard rod lattice systems.

[1] Percus J. K. 1976 J. Stat. Phys. 15 505*11 [2] Rosenfeld Y. 1989 Phys. Rev. Lett. 63 980*3 [3] Lafuente L. and Cuesta J.A. 2002 J. Phys.: Condens. Matter 14 12079 [4] Oettel M., Klopotek M. et al 2016 J. Chem. Phys. 145 074902

15 min. break

DY 6.7 Mon 11:45 ZEU 160

Mean first-passage times of continuous-time random walkers determined through Wiener-Hopf integral equations — •MARCUS DAHLENBURG^{1,2} and GIANNI PAGNINI^{1,3} — ¹BCAM-Basque Center for Applied Mathematics, Alameda de Mazarredo 14, 48009 Bilbao, Basque Country, Spain — ²Institute for Physics & Astronomy, University of Potsdam, 14476 Potsdam, Germany — ³Ikerbasque-Basque Foundation for Science, Plaza Euskadi 5, 48009 Bilbao, Basque Country, Spain

Asymmetric continuous-time random walks in continuous-space characterised by waiting-times with finite mean and by jump-amplitudes with both finite mean and finite variance are governed by an advection-diffusion equations in the asymptotic limit. The mean first-passage time (MFPT) of such an advective-diffusive system on a halfline results to be finite when the advecting drift is in the direction of the boundary. In our investigation we derive an inhomogeneous Wiener-Hopf integral equation that allows to avoid approximated results in the asymptotic limits and leads indeed to the exact determination of the MFPT. This quantity depends on the average of the waiting-times only but it conserves the information about the whole distribution of the jump-amplitudes. Through the case study of asymmetric double-exponential distributions of the jump-amplitudes one may identifies a length-scale, that defines the transition from starting points near the boundary to starting points far-away from the boundary where the MFPT loses the information about the exact shape of the jump-amplitudes' distribution and only conserves their mean.

DY 6.8 Mon 12:00 ZEU 160

A combinatorial approach to the many-body density of levels and the Bethe approximation — •CAROLYN ECHTER, GEORG MAIER, JUAN-DIEGO URBINA, and KLAUS RICHTER — Institut für Theoretische Physik, Universität Regensburg, Regensburg, Germany

The Bethe formula, originally derived in [1] to estimate the density of levels of heavy nuclei, has become a widely used approximation for the many-body density of levels of a non-interacting fermionic system, appropriate for large numbers of particles and energies in a system-dependent range. Notably, in the case of equally spaced single-particle energy levels, it coincides with the asymptotic result for the number of unrestricted partitions of an integer known from analytic number theory [2]. An explanation is suggested by the combinatorics of distributing integer amounts of energy to particles obeying given statistics. We present a combinatorial derivation of the exact many-body density of levels for various particle statistics in the case of a constant single-particle density of states, thereby adding to existing discussions [3,4] and explaining the asymptotic agreement of Bethe's approximation with number theoretical partition functions. We compare numerically with semiclassical results and make suggestions towards a bosonic analogue of the Bethe formula based on our observations.

[1] H. A. Bethe, *Phys. Rev.* 50, 332-41 (1936). [2] G. H. Hardy, S. Ramanujan, *Proc. London Math. Soc.* (2) 17, 75-115 (1918). [3] F. C. Auluck, D. S. Kothari, *Math. Proc. Camb. Philos. Soc.* 42, 272-77 (1946). [4] A. Comtet, P. Leboeuf, S. N. Majumdar, *Phy. Rev. Lett.* 98, 070404 (2007).

DY 6.9 Mon 12:15 ZEU 160

Integral Equations in Statistical Mechanics: A Size-effect Study — •JOSE MAURICIO SEVILLA MORENO and ROBINSON CORTES-HUERTO — Max Planck Institute for Polymer Research, Ackermannweg 10, 55128 Mainz, Germany

Integral equations (IE) are in the core of statistical mechanics of liquids as they connect the local structure with thermodynamic properties as compressibility, activity coefficients and excess entropy. IE are normally defined in the grand canonical ensemble and calculated in the thermodynamic limit (TL). By contrast, computer simulations are performed with finite-size systems and mimic the TL using periodic boundary conditions (PBC). This proceeding introduces several finite-size contributions whose effects must be identified and corrected in order to approximate the simulation results to the TL. In this talk, we present a generic method to compute IE from molecular dynamics simulations. In our approach, we define finite-size IE, integrating them in Fourier space to trivially introduce PBC. This procedure allows us to identify and isolate ensemble, finite-volume domains and PBC effects and accurately obtain the corresponding thermodynamic quantities in the TL or artificially for any finite size system. To validate our method, we compute isothermal compressibilities, chemical potentials and excess entropies of simple liquids and liquid mixtures, including water and aqueous alcohol solutions, showing good agreement with results available in the literature.

DY 6.10 Mon 12:30 ZEU 160

A Multiscale Approach for Large-Scale Proton Dynamics Simulations — •CHRISTIAN DRESSLER¹ and DANIEL SEBASTIANI² — ¹TU Ilmenau, Institute of Physics, Theoretical Solid State Physics — ²MLU Halle-Wittenberg, Institute of Chemistry, Theoretical Chemistry

We present a multiscale simulation approach for the calculation of proton diffusion/conduction in disordered organic and inorganic materials. We combine quantum chemical calculations for elementary reactions between the ions and surrounding molecules with molecular dynamics simulations for the incorporation of local dynamical heterogeneities at the nanometer/nanosecond scale. Data from both levels are integrated in a stochastic propagation scheme (Monte Carlo or Markov matrix approach) for the simulation of proton transfer at much larger time and length scales. The approach allows for an atom-level resolution of ion dynamics with quantum chemical accuracy but with final length- and time-scales of micrometers and milliseconds. As a proof-of-principle simulation, we have computed the explicit dynamics of a non-equilibrium process in an 8 μm CsH_2PO_4 system during 5 ms. Finally, we demonstrate the application potential of the scheme by computing the proton conductivity of a nanostructured CsH_2PO_4 fuel cell membrane with respect to the porosity.

DY 6.11 Mon 12:45 ZEU 160

Population Annealing and the Role of Resampling in Population Annealing — •DENIS GESSERT^{1,2}, MARTIN WEIGEL³, and WOLFHARD JANKE¹ — ¹Institut für Theoretische Physik, Leipzig University, Postfach 100920, D-04009 Leipzig, Germany — ²Centre for Fluid and Complex Systems, Coventry University, Coventry CV1 5FB, United Kingdom — ³Institut für Physik, Technische Universität Chemnitz, D-09107 Chemnitz, Germany

Studying equilibrium properties of thermodynamic systems with rough free-energy landscapes particularly challenges standard Markov chain Monte Carlo techniques such as the Metropolis algorithm. Sampling can be improved by using generalized ensemble methods, one of which is Population Annealing (PA). Although PA is not expected to outperform its contenders in terms of time complexity, it is particularly well suited for parallel execution with no theoretical limit on the level of parallelism, which makes it a viable option on modern HPC.

In PA a population of replicas is collectively cooled down. At each temperature a population control step is carried out before applying some replica-independent update moves. This population control is realized by means of resampling. Here, we compare various different resampling methods and their performance in PA applications. Using the $d = 2$ Ising model as a benchmark system, we identify two resampling methods that appear preferable over the widely used multinomial resampling. Further, we point out when different resampling choices affect the statistical quality of the simulation outcome and obtain some model-independent guiding principles for the choice of PA parameters.

DY 7: Granular Matter and Contact Dynamics

Time: Monday 10:00–12:45

Location: ZEU 147

DY 7.1 Mon 10:00 ZEU 147

Collective dipole reorganization in magnetostructures — •WAFFLARD ADRIEN, VANDEWALLE NICOLAS, and OPSOMER ERIC — GRASP, Institut de Physique B5a, Université de Liège, Liège, BE

Playing with spherical neodymium magnets that you find in your favorite toy market is really addicting. By assuming they are uniformly magnetized, magnetic beads behave as point-like dipoles. For scientists, those inexpensive objects demonstrate how dipolar particles self-assemble into various structures ranging from 1D chains to 3D crystals. We show that magnetotubes and magnetocrystals can self-buckle, i.e. change their geometry, above a critical aspect ratio. The underlying dipolar ordering is found to exhibit a collective reorganization, altering the mechanical stability of the entire system. We identify the conditions in which these phenomena occur and conjecture that in chains, square or cubic magnetostructures, neighboring dipoles reorientate in order to form the longest possible chains. This suggests that a wide variety of magnetostructures, including well known stable structures, may collapse due to reorientation of dipoles.

DY 7.2 Mon 10:15 ZEU 147

How is the growth of ferromagnetic granular networks controlled by an orthogonal magnetic field? — MATTHIAS BIRSACK¹, •ALI LAKKIS¹, OKSANA BILOUS², PEDRO A. SANCHEZ², SOFIA S. KANTOROVICH², and REINHARD RICHTER¹ — ¹University of Bayreuth, Experimental Physics V, 95447 Bayreuth, Germany — ²Computational and Soft Matter Physics, Faculty of Physics, University of Vienna, 1090 Vienna, Austria

We are exploring in experiments the aggregation process in a shaken granular mixture of glass and magnetized steel beads, occurring in a horizontal vessel after the shaking amplitude is suddenly decreased. Then the magnetized beads form a transient network that coarsens in time into compact clusters, following

a viscoelastic phase separation [1]. A homogeneous magnetic field oriented in plane has been observed to "unknot" network structures orthogonal to the field [2]. Here we focus on the impact of a magnetic field B_z oriented orthogonally to the plain of the network. We measure the average number of neighbours $\bar{k}(t)$ and the efficiency $E(t)$ of the emerging networks. Both can be fitted by a logistic growth function for $B_z \in [0, 2]$ mT, unveiling that its characteristic time τ increases by about ten. Our results demonstrate that via dipole-dipole repulsion the field reduces the mobility of isolated steel beads, thus hindering the growth of the networks. The experimental results are compared with those of numerical simulations.

[1] A. Kögel, et al. *Soft Matter*, 14 (2018) 1001.

[2] P. A. Sánchez, J. Miller, S. S. Kantorovich, R. Richter, *J. Magn. Magn. Mater.*, 499 (2019) 166182.

DY 7.3 Mon 10:30 ZEU 147

Dynamic light scattering from single macroscopic particles — LISA KÜNSTLER¹, RAPHAEL KESSLER¹, MATTHIAS SPERL^{1,2}, and •PHILIP BORN¹ — ¹Institut für Materialphysik im Weltraum, Deutsches Zentrum für Luft- und Raumfahrt (DLR), 51170, Köln, Germany — ²Institut für Theoretische Physik, Universität zu Köln, 50937, Köln, Germany

Here we present a methodology to extract information from the fluctuations in light scattered from moving single granular particles. We first describe the experimental setup and the associated theoretical framework required to isolate contributions to the intensity autocorrelation function emerging from translational and from rotational particle motion [1]. We subsequently present an approach to extract the angular velocity and the translational speed of the granular particles from the light scattering data. The approach is applied to a small ensemble of granular particles in an hour-glass-like experiment to determine the granular temperature with a dynamic light scattering measurement. The results

indicate the next steps to be taken to eventually develop a thermometer for fluidized granular media based on dynamic light scattering.

[1] L. Dossow, R. Kessler, M. Sperl, & P. Born, Dynamic light scattering from single macroscopic particles. *Applied Optics*, 60(32), 10160-10167 (2021).

DY 7.4 Mon 10:45 ZEU 147

Shear jamming and free surface deformation enable reciprocal swimming in granular materials — •HONGYI XIAO, ACHIM SACK, and THORSTEN PÖSCHEL — Institute for Multiscale Simulations, Friedrich-Alexander-Universität Erlangen-Nürnberg, Cauerstraße 3, 91058 Erlangen, Germany

Swimming with reciprocal motion is desirable due to its simplicity, but it is prohibited in Newtonian fluids at low Reynolds number as stated by the scallop theorem. Such a constraint can be broken in fluids with complex rheology. In this study, we show that propulsion generation with reciprocal motion in granular materials is enabled by a prolonged hysteresis in the material response, which originates from a combination of jamming-induced material rigidity and plastic deformation of the free surface. Using both lab experiments and discrete element method simulations, a reciprocal swimmer mimicking a scallop was constructed and buried in a tank of polydisperse granular particles. The swimmer consists of two wings that open and close with geometrical and temporal symmetry. The resistive force, the swimmer's displacement, and the deformation of the free granular surface were measured. Results indicate that net propulsion force is generated when the swimmer is tethered, and net displacement is generated when the swimmer is released. Small amplitude oscillatory experiments confirm the existence of an elastic regime at small strains, and free surface deformation measurement reveals its influence at large strains. Furthermore, a secondary symmetry breaking mechanism due to a cooperative effect of the wings is also identified.

DY 7.5 Mon 11:00 ZEU 147

Phase space characterization of three-dimensional nucleation of glass spheres — •FRANK RIETZ^{1,2} and MATTHIAS SCHRÖTER² — ¹University of Magdeburg, Department of Nonlinear Phenomena — ²Max Planck Institute for Dynamics and Self-Organization (MPIDS), Göttingen

Packings of macroscopic spheres serve as a model system for studying atomic states. In many compactification protocols, the spheres do not form nuclei and remain in the state of random close packing. By cyclically shearing a packing of 50000 spheres, we can cross this boundary and observe a transition from a disordered to a crystallized state [1]. The three-dimensional temporal positions of the spheres are tracked by refractive index-matched scanning [2]. The description of disordered states and the nature of random close packing are open scientific problems. In our case, we describe the nucleation process by partitioning the packing into local groups of four touching spheres. These groups of spheres are tracked during the crystallization process and their contacts and relative orientation are recorded in a phase space diagram. By comparing the states before and after crystallization with the states that avoid crystallization, we show whether there are conditions under which the spheres statistically tend to crystallize.

[1] F. Rietz, C. Radin, H. L. Swinney, M. Schröter: Nucleation in sheared granular matter, *Phys. Rev. Lett.* 120, 055701 (2018)

[2] J. A. Dijkstra, F. Rietz, K. A. Lőrincz, M. van Hecke, W. Losert: Refractive index matched scanning of dense granular materials, *Rev. Sci. Instrum.* 83, 011301 (2012)

15 min. break

DY 7.6 Mon 11:30 ZEU 147

Non-convex particles under shear in a split bottom cell — •MAHDIEH MOHAMMADI¹, AHMED ASHOUR², DMITRY PUZYREV³, TORSTEN TRITTEL³, and RALF STANNARIUS³ — ¹Technische Hochschule Brandenburg — ²Future University of Egypt — ³Otto-von-Guericke-Universität Magdeburg

We study dynamical features of surface flow in the top layer of a granular bed containing non-convex tetrapod and hexapod particles in a split-bottom shear cell. Different heights of granular beds were prepared and examined. Based on Particle Image Velocimetry and Particle Tracking Velocimetry, angular and radial displacements of particles on the surface of the ensemble were derived in dependence on the number of rotations of the bottom disk. Stereoscopic measurements of surface fluctuations of the bed during shearing turn out to be a key factor in this study to characterize heap and sink formation phenomena, which are related to the secondary flow of the grain ensembles in the bulk. We acknowledge support of DPG with project STA 425/40 and DLR with project EVA (50WM2048), and stimulating discussion with K. Harth.

[1] Mahdiah Mohammadi, Dmitry Puzyrev, Torsten Trittel, and Ralf Stannarius, *Phys. Rev. E* 106, L052901 (2022).

DY 7.7 Mon 11:45 ZEU 147

Forces on obstacles suspended in flowing granular matter — •JING WANG¹, BO FAN², TIVADAR PONGÓ³, TAMÁS BÖRZSÖNYI², RAÚL CRUZ HIDALGO³, and RALF STANNARIUS¹ — ¹Institute of Physics, Otto von Guericke University Magdeburg, Magdeburg, Germany — ²Institute for Solid State Physics and Optics, Wigner Research Centre for Physics, Budapest, Hungary — ³Física y Matemática Aplicada, Facultad de Ciencias, Universidad de Navarra, Pamplona, Spain

We investigate the force on a spherical obstacle exerted by a flowing granular material. A sphere suspended in a discharging silo experiences mechanical forces both from the weight of the overlaying layers and from friction of the surrounding moving granular material. When the flow stops due to clogging of the silo, in experiments with hard frictional glass beads, the force on the obstacle remains exactly the same as during flow. In contrast, for nearly frictionless soft hydrogel particles the force decreased considerably after the flow stopped. The dependence of the total force on the obstacle diameter is qualitatively different for the two types of material: It grows quadratically with the sphere diameter of the obstacle for hydrogel spheres, while it grows much weaker, nearly linearly with the obstacle diameter, in a bed of hard frictional glass spheres.

DY 7.8 Mon 12:00 ZEU 147

Free cooling dynamics and energy partition in 3D granular gas mixtures — •DMITRY PUZYREV¹, ADRIAN NIEMANN¹, KIRSTEN HARTH^{2,3}, TORSTEN TRITTEL¹, and RALF STANNARIUS¹ — ¹Institute of Physics and MARS, Otto von Guericke University, 39106 Magdeburg — ²Department of Engineering, TH Brandenburg, 14770 Brandenburg an der Havel — ³MARS and MRTM, OVGU, 39106 Magdeburg

Granular gases are nonlinear systems that exhibit fascinating dynamical behavior far from equilibrium, including unusual cooling properties, clustering and violation of energy equipartition. Our study focuses on 3D microgravity experiments with dilute ensembles of rod-like particles and their mixtures. In drop tower experiments at ZARM, we studied granular cooling of mixtures of rods with two different diameters. The confirmation of Haff's equation [2] describing the energy decay is of particular interest. Experimental data analysis suggests different cooling rates, and the violation of energy equipartition between the rotational and translational degrees of freedom for the mixture components. Particle detection and tracking was performed with Machine Learning-aided approach [3]. The software will be available as a Python library that can be extended to other 3D and 2D particle tracking problems.

The authors acknowledge support from DLR in projects EVA (50WM2048) and VICKI (50WM2252).

References: [1] K. Harth et al., *Phys. Rev. Lett.*, 120 (2018), 214301 [2] P. K. Haff, *J. Fluid Mech.*, 134 (1983), 401-430 [3] Puzyrev et al., *Microgravity Sci. Technol.*, 32 (2020), 897

DY 7.9 Mon 12:15 ZEU 147

Effect of particle size on the suction mechanism in granular grippers — •ANGEL SANTAROSSA, OLFA D'ANGELO, ACHIM SACK, and THORSTEN PÖSCHEL — Institute for Multiscale Simulation, Friedrich-Alexander Universität Erlangen-Nürnberg, Cauerstraße 3, 91058 Erlangen, Germany

Granular grippers are highly adaptable soft actuators able to grasp objects of different shapes and sizes. They consist of an elastic membrane partially filled with a granulate. Their operating principle relies on the reversible jamming transition of granular materials. The filled membrane can be deformed and reshaped when pressed onto an object. When the air within the membrane is evacuated, the granulate hardens, creating forces to hold and manipulate the object. Three mechanisms contribute to the holding force of granular grippers: frictional forces, geometrical constraints, and suction effects. Using X-ray computed tomography, we link the activation of suction to the size of the particles. We show that a gripper filled with small particles (average diameter $d \approx 0.12$ mm) conforms to a high degree around the object than with larger particles (average diameter $d \approx 4$ mm), thus enabling the formation of air-tight seals. When the gripper is pulled off, simulating the lifting of an object, vacuum pressure is generated in the sealed cavity at the interface gripper-object. If the particles are too large, the gripper does not conform tightly enough around the object, leaving gaps at the interface gripper-object. These gaps prevent the creation of sealed vacuum cavities between the object and the gripper, impeding the suction mechanism from operating.

DY 7.10 Mon 12:30 ZEU 147

Visualization of flow dynamics for Poly-dispersed dense granular suspension in various sections of pipe — •HIMANSHU P PATEL and GÜNTER K AUERNHAMMER — Leibniz-Institut für Polymerforschung Dresden e. V., Hohe Straße 6, D-01069 Dresden, Germany

The study of flow dynamics in non-Newtonian media with polydispersed dense granular suspension, e.g., slurry, mud, concrete, still lacks quantification on the flow parameters linked to shear induced particle migration and insight about flow at center and at wall in closed pipes.

We developed transparent granular system that is a granular suspension of particles suspended in non-Newtonian media (particle volume fractions of 30%

to 48%) [1]. The non-Newtonian granular system has yield stress and plastic viscosity and is well index matched. The rheological characteristics of the model system is tunable through its composition of additives.

We analyze gravity-assisted continuous flow of millimetric sized particles. We perform tracking of flow at different sections of pipe. The flow analysis reveals understanding on the relaxation of such flow and the development of velocity

profile within the length of pipe, we observe this using camera at entry and exit of pipe and later a 3D setup to observe flow at near end of pipe. This gives quantitative values into the particle migration to understand the effect of polydispersity and particle flow.

[1] Auernhammer, Günter K., et al., *Materials & Design* (2020):108673

DY 8: Invited Talk: Dynamics of Networks (joint session DY/SOE)

Time: Monday 12:30–13:00

Location: ZEU 250

Invited Talk

DY 8.1 Mon 12:30 ZEU 250

Novel phenomena and analysis methods in oscillator networks: higher-order interactions, higher-order averaging, and inference — •HIROSHI KORI — The University of Tokyo, Japan

Synchronization of oscillator networks is essential for functionalization of systems. Examples include heart pacemaker, circadian clock, and locomotion, to name a few. In this talk, after reviewing a general background, I will present recent studies with an emphasis on novel phenomena and analysis techniques. (i) A network of three oscillators shows complex synchronization transitions when the

network structure or overall coupling intensity is varied [1]. The transition is analyzed using a higher-order averaging method. (ii) In the assembly of noisy oscillators with a three-body interaction, synchronized state appears only transiently and its persistent time increases exponentially with the interaction strength of three-body coupling. (iii) I will present our proposed inference methods of coupling intensity from spike data [2] and the phase from oscillatory time series [3].

[1] M. Kato, H. Kori, *PRE* (2023)

[2] F. Mori and H. Kori, *PNAS* (2022)

[3] A. Matsuki, H. Kori, R. Kobayashi. *arXiv* (2022)

DY 9: Quantum Dynamics, Decoherence and Quantum Information

Time: Monday 14:00–17:15

Location: MOL 213

DY 9.1 Mon 14:00 MOL 213

From Dual Unitarity to Generic Quantum Operator Spreading — •MICHAEL A. RAMPP, RODERICH MOESSNER, and PIETER W. CLAEYS — Max Planck Institute for the Physics of Complex Systems, 01187 Dresden, Germany

Dual-unitary circuits are paradigmatic examples of exactly solvable yet chaotic quantum many-body systems, but solvability naturally goes along with a degree of non-generic behaviour. By investigating the effect of weakly broken dual-unitarity on the spreading of local operators we study whether, and how, small deviations from dual-unitarity recover fully generic many-body dynamics. We present a discrete path-integral formula for the out-of-time-order correlator and use it to recover a butterfly velocity smaller than the light-cone velocity, $v_B < v_{LC}$, and a diffusively broadening operator front, two generic features of ergodic quantum spin chains absent in dual-unitary circuit dynamics. We find that the butterfly velocity and diffusion constant are determined by a small set of microscopic quantities and that the operator entanglement of the gates plays a crucial role.

DY 9.2 Mon 14:15 MOL 213

Harnessing the exponential Hilbert space dimension of quantum systems for reservoir computing — •NICLAS GÖTTING^{1,2}, FREDERIK LOHOF^{1,2}, and CHRISTOPHER GIES^{1,2} — ¹Institute for Theoretical Physics, University of Bremen, Bremen — ²Bremen Center for Computational Material Science, University of Bremen, Bremen

With the ever growing prevalence of machine learning in science and industry, the machine learning paradigm of reservoir computing has gained new attention. While classical reservoir computers have proven to be able to solve various prediction tasks by exploiting the complex dynamics of classical systems, their quantum counterparts are yet to be fully explored.

Coherent quantum systems exhibit properties like superposition and quantum entanglement, which in principle lead to an exponential scaling of the reservoir phase space dimension with respect to the number of quantum particles. The question arises if these quantum reservoir computers (QRCs) can energy and space efficiently outperform their classical analogues in complex prediction tasks.

As a first step we investigate the transverse-field Ising model as a QRC to find the link between the properties of the quantum network, the phase space dimension, and the performance of the QRC.

DY 9.3 Mon 14:30 MOL 213

Giant Residual Current from Ultrafast AC Driving of Bloch Electrons — •ADRIAN SEITH, JAN WILHELM, and FERDINAND EVERS — Institut für Theoretische Physik, Universität Regensburg

In recent experiments, residual currents were seen to survive long after the laser illumination has died out[1]. Motivated by a vision of a "light-wave electronics", the effect has been utilized to design a petahertz logical gate[2].

In this work, we theoretically study residual currents of Bloch electrons and demonstrate that residual currents can be as large as the maximum current during illumination.

Based on a perturbative expansion of the semiconductor-Bloch equations, we derive an analytical formula; it explains the strong dependence of residual cur-

rents on the model parameters and the laser pulse shape. In particular, our formula allows to optimize pulse shapes for maximizing the residual currents' magnitude reaching values order of magnitudes larger than observed in recent experiments.

[1] Higuchi et. al., *Nature* 550, 224 (2017)

[2] Boolakee et. al., *Nature* 605, 251 (2022)

DY 9.4 Mon 14:45 MOL 213

Time-local generator of non-Markovian quantum dynamics by iterating its memory kernel — MAARTEN WEGEWIJS¹, JAN VANBERG², and •KONSTANTIN NESTMANN² — ¹Peter Grünberg Institute, Forschungszentrum Jülich, Germany — ²Institute for Theory of Statistical Physics, RWTH Aachen University

The time-convolutionless generator (TCL) \mathcal{G} of a quantum master equation (QME) has been found to be the fixed point $\mathcal{G} = \mathcal{K}[\mathcal{G}]$ of the Nakajima-Zwanzig memory kernel \mathcal{K} of the equivalent QME with time-convolution^a. Here we investigate the calculation of \mathcal{G} by iterating \mathcal{K} directly in the stationary limit starting from any initial guess to construct approximations to the dynamics. We show that the local stability of the iteration is connected to the long-time dynamics using an extended but still tractable version of the dissipative Jaynes-Cummings model. The iteration automatically selects the asymptotically most relevant decay and oscillation frequency, providing a non-perturbative Markovian semigroup approximation. Linearization about the fixed point allows to extract the amplitude of this approximation in the full dynamics, providing a non-perturbative initial-slip correction. Around the strongly non-Markovian regime (non-CP divisibility) the iteration stability can be either lost, or, remarkably, enhanced, yielding an additional fixed point. The global iteration stability is counter-intuitive: convergence to the main locally stable fixed point is guaranteed by starting from an initial guess "far away" with frequencies in the "wrong", non-physical half-plane. ^aPhys. Rev. X 11, 021041 (2021), Phys. Rev. B 104, 155407 (2021) ^bSciPost Phys. 11, 053 (2021)

DY 9.5 Mon 15:00 MOL 213

Performance of quantum registers in diamond in the presence of spin impurities — •DOMINIK MAILE and JOACHIM ANKERHOLD — Institut für Complex Quantum Systems, Ulm University

The Nitrogen Vacancy Center in diamond coupled to addressable surrounding nuclear spins forms a versatile building block for future quantum technologies. While previous activities focused on sensing with only a single or very few spins in operation, recently multi-qubit registers have been successfully implemented for quantum information processing. Further progress requires a detailed understanding of the performance of quantum protocols for consecutive gate operations and thus, beyond established treatments for relaxation and dephasing. In this talk (see also [1]), we provide such an analysis for a small spin registers with up to four spins built out of NV and environmental constituents in presence of ensembles of interacting impurity spins. Adapting a cluster correlation expansion, we predict coherence properties as well as fidelities for GHZ- and Bell-gate operations. The influence of the volume density and the geometry of the spin-bath consisting of substitutional nitrogen atoms are also taken into account.

[1] D. Maile and J. Ankerhold, *arXiv:2211.06234*

DY 9.6 Mon 15:15 MOL 213

Quantum Zeno manipulation of quantum dots — NASER AHMADINIAZ¹, MARTIN PAUL GELLER², JÜRGEN KÖNIG², PETER KRATZER², AXEL LORKE², •GERNOT SCHALLER¹, and RALF SCHÜTZHOLD^{1,3} — ¹Helmholtz-Zentrum Dresden-Rossendorf, Bautzner Landstraße 400, 01328 Dresden, Germany — ²Fakultät für Physik und CENIDE, Universität Duisburg-Essen, Lotharstraße 1, 47057 Duisburg, Germany — ³Institut für Theoretische Physik, Technische Universität Dresden, 01062 Dresden, Germany

We investigate whether and how the quantum Zeno effect, i.e., the inhibition of quantum evolution by frequent measurements, can be employed to isolate a quantum dot from its surrounding electron reservoir. In contrast to the often studied case of tunneling between discrete levels, we consider the tunneling of an electron from a continuum reservoir to a discrete level in the dot. Realizing the quantum Zeno effect in this scenario can be much harder because the measurements should be repeated before the wave packet of the hole left behind in the reservoir moves away from the vicinity of the dot. Thus the required repetition rate could be lowered by having a flat band (with a slow group velocity) in resonance with the dot or a sufficiently small Fermi velocity or a strong external magnetic field. We also consider the anti-Zeno effect, i.e., how measurements can accelerate or enable quantum evolution.

[1] N. Ahmadianiaz *et al.*, Phys. Rev. Res. **4**, L032045 (2022).

15 min. break

DY 9.7 Mon 15:45 MOL 213

Winding Number Statistics for Parametric Chiral Random Matrices — •NICO HAHN¹, MARIO KIEBURG², OMRI GAT³, and THOMAS GUHR¹ — ¹University of Duisburg-Essen — ²University of Melbourne — ³The Hebrew University of Jerusalem

The winding number is a concept in complex analysis which has, in the presence of chiral symmetry, a physics interpretation as the topological invariant belonging to gapped phases of Fermions. We analytically study the statistical properties of this topological quantity. To this end, we set up a random matrix model for a chiral system with a parametric dependence. We address two chiral symmetry classes, the chiral unitary class without any further symmetries and the chiral symplectic class with additional time reversal symmetry. These classes are referred to as AIII and CII in the tenfold way of topological insulators and superconductors.

DY 9.8 Mon 16:00 MOL 213

Simulating Non-Markovian Qubit Dynamics on a Quantum Processor — •MIRKO ROSSINI, DOMINIK MAILE, JOACHIM ANKERHOLD, and BRECHT DONVIL — Institute for Complex Quantum Systems and IQST

We propose a novel scheme to simulate the open system dynamics of a qubit. We go beyond the completely positive framework and consider linear, trace and Hermiticity-preserving but not necessarily positivity-preserving evolution maps. We call these maps general dynamical maps. These maps naturally arise as the solution of general time-local master equations and for finite-dimensional systems they can always be decomposed as the difference between two completely positivity maps. We bring this difference into a form suitable for quantum simulation.

We illustrate our scheme by implementing two examples on IBMQ quantum processors: in the first example, we simulate the evolution of a general time local master equation both from an initial time when the evolution map is guaranteed to be completely positive and from an intermediate time when it is not. With our second example, we show that the simulation of non-completely positive maps gives the ability to recover the initial state of Lindbladian evolution.

DY 9.9 Mon 16:15 MOL 213

Quantum Non-Markovianity made simple through extended states — MENG XU¹, YAMING YAN², QIANG SHI², JOACHIM ANKERHOLD¹, and •JÜRGEN T. STOCKBURGER¹ — ¹Institute for Complex Quantum Systems and IQST, Ulm University — ²Beijing National Laboratory for Molecular Sciences, Chinese Academy of Sciences

We present a recent computational treatment of non-Markovianity [1] in open-system quantum dynamics. Focusing more on intrinsic timescales than on properties of a quantum channel and its generator, we extend the Hierarchical Equations of Motion (HEOM) approach through a highly efficient decomposition of environmental correlation functions into complex exponentials. Complex dynamics at ultralow temperatures and long reservoir timescales becomes tractable by this approach. We demonstrate that our version of the HEOM approach is closely related to an entire family of extended-state approaches, with our new approach being favored through a comparably low number of auxiliary dimen-

sions. The accurate reproduction of long-time algebraic tails in an open-system correlation function provides a benchmark result.

[1] M. Xu *et al.*, Phys. Rev. Lett. **129**, 230601 (2022).

DY 9.10 Mon 16:30 MOL 213

The Influence of Dynamical Phases on a Quantum Processor based Reservoir Computer — •BRECHT DONVIL, MIRKO ROSSINI, DOMINIK MAILE, and JOACHIM ANKERHOLD — ICQ and IQST, University of Ulm, Ulm, Germany

Reservoir computing is subbranch of machine learning where a physical system, the reservoir, is used to perform computational tasks instead of a large neural network which has to be trained. In the last years, quantum systems are being explored as potential reservoirs [1,2,3]. While most of the research has focussed on Ising spin systems, recently it was shown that also quantum processors can serve as reservoirs. The authors of [3] illustrated this fact by successfully implementing reservoir computing on an IMBQ quantum processor.

The dynamical phase of the reservoir can influence its performance on certain information processing tasks. For example, the authors of [2] found that the transverse-field Ising model performs best on examples of memory related tasks on the edge of the ergodic phase. The work I present here concerns quantum processor based reservoir computing as proposed in [3]. I consider simple circuit layout which is known to exhibit a dynamical phase transition between a localised and ergodic phase. I show the influence of the dynamical phase of the circuit on its information processing capacity and its performance as a readout device.

[1] K. Fujii and K. Nakajima, Phys. Rev. Applied **8**, 024030 (2017) [2] R. Martínez-Peña *et al.*, Phys. Rev. Lett. **127**, 100502 (2021)

[3] J. Chen *et al.*, Phys. Rev. Applied **14**, 024065 (2020)

DY 9.11 Mon 16:45 MOL 213

String order in measurement-induced symmetry-protected topological phases — •RAÚL MORRAL¹, FRANK POLLMANN^{1,3}, and IZABELLA LOVAS^{1,2} — ¹Department of Physics, TFK, Technische Universität München, James-Frank-Straße 1, D-85748 Garching, Germany — ²Kavli Institute for Theoretical Physics, University of California, Santa Barbara, CA 93106, USA — ³Munich Center for Quantum Science and Technology (MCQST), Schellingstr. 4, 80799 München, Germany

We study measurement-induced symmetry protected topological (SPT) order in a wide class of quantum random circuit models, by combining calculations within the stabilizer formalism with tensor network simulations. We construct a family of quantum random circuits, generating the out-of-equilibrium version of all generalized cluster models, and derive a set of non-local string order parameters to distinguish symmetry protected topological phases. We apply this framework to study the random circuit realization of the ZXZ cluster model, and use the string order parameter to demonstrate that the phase diagram is strikingly stable against extending the class of unitary gates in the circuit, from Clifford gates to Haar unitaries. We then turn to the ZXXX generalized cluster model, and demonstrate the coexistence of SPT order and spontaneous symmetry breaking, by relying on string order parameters and a connected correlation function. Our results pave the way to study the properties of a wide range SPT phases in quantum random circuit models with efficient tensor network methods.

DY 9.12 Mon 17:00 MOL 213

Quasiclassical and exact approaches to dissipative nonadiabatic quantum dynamics — •GRAZIANO AMATI¹, JOHAN RUNESON², and JEREM RICHARDSON³ — ¹Albert Ludwigs Universität Freiburg, Hermann Herder Str. 3, 79104 Freiburg, Germany — ²Physical and Theoretical Chemistry Laboratory, Oxford University, South Parks Road, Oxford, OX1 3QZ, UK — ³Laboratory of Physical Chemistry, ETH Zuerich, 8093 Zuerich, Switzerland

The study of many relevant processes in nature from photosynthesis, to radiation damage, to vision, depends on an accurate description of the electronic nonadiabatic dynamics. The brute-force simulation of nonadiabatic systems happens to be a computationally intensive task, given that the complexity of dynamic simulations scales exponentially with time and with the size of the system. Recently developed of 'spin mapping' approaches allow to recast a wide class of quantum nonadiabatic models onto quasiclassical systems of spins, whose dynamics exhibit a favorable linear or polynomial scaling in complexity. In my contribution I will firstly compare the accuracy in the long-time relaxation of several quasiclassical methods, borrowing ideas from classical ergodic theory. I will then discuss how to further improve the reliability of the long-time predictions of spin mapping techniques, by coupling these methods to the formalism of the non-Markovian generalized quantum master equation. I will then introduce the recent 'ellipsoid mapping' approach, a detailed-balance-preserving extension of spin mapping suited to study systems in thermal equilibrium.

DY 10: Active Matter II (joint session DY/BP/PPP)

Time: Monday 15:00–18:15

Location: ZEU 160

DY 10.1 Mon 15:00 ZEU 160

Chiral motion of actively driven objects in discrete steps towards a remote target — •ANDREAS M. MENZEL — Otto-von-Guericke-Universität Magdeburg, Magdeburg, Germany

We address the motion of chiral actively driven objects that move in discrete steps on a flat substrate [1]. While closed polygon-shaped trajectories are found in the case of unperturbed motion, the dynamics becomes surprisingly rich and nonlinear, if the objects additionally head for a fixed remote target. In that situation, cycloidal-like, straight, zigzag-type, doubled zigzag, quadrupled zigzag, and further period-doubled types of trajectory emerge, besides chaotic behavior. Additionally, we investigate the motion of crowds of such objects under explicit mutual alignment interaction. In the absence of fluctuations, collective orientational ordering occurs also in the chaotic regime, in combination with spatial gathering of the particles. Conversely, fluctuations and polydispersity in target alignment counteract orientational ordering. Our results may apply to various types of actively driven objects, for instance, light-responsive bacteria, laser-controlled colloidal particles, or hoppers on vibrated substrates.

[1] A. M. Menzel, resubmitted.

DY 10.2 Mon 15:15 ZEU 160

Polar flocks with discretized directions: the active clock model approaching the Vicsek model — •MATTHIEU MANGEAT, SWARNAJIT CHATTERJEE, and HEIKO RIEGER — Universität des Saarlandes, Saarbrücken, Germany

We study the off-lattice two-dimensional q -state active clock model (ACM) [EPL **138**, 41001 (2022)] as a natural discretization of the Vicsek model (VM) [PRL **75**, 1226 (1995)] describing flocking. The ACM consists of particles able to move in the plane in a discrete set of q equidistant angular directions, as in the active Potts model (APM) [EPL **130**, 66001 (2020); PRE **102**, 042601 (2020)], with a local alignment interaction inspired by the ferromagnetic equilibrium clock model. A collective motion emerges at high densities and low noise. We compute phase diagrams of the ACM and explore the flocking dynamics in the region, in which the high-density (polar liquid) phase coexists with the low-density (gas) phase. We find that for a small number of directions, the flocking transition of the ACM has the same phenomenology as the APM, including macrophase separation and reorientation transition from transversal to longitudinal band motion as a function of the particle self-propulsion velocity. For a larger number of directions, the flocking transition in the ACM becomes equivalent to the one of the VM and displays microphase separation and only transverse bands, i.e. no reorientation transition. Concomitantly also the transition of the $q \rightarrow \infty$ limit of the ACM, the active XY model, is in the same universality class as the VM. We also construct a coarse-grained hydrodynamic description akin to the VM.

DY 10.3 Mon 15:30 ZEU 160

Tracer-induced temperature difference in motility-induced phase separation — •LUKAS HECHT, IRIS DONG, and BENNO LIEBCHEN — Institut für Physik kondensierter Materie, Technische Universität Darmstadt, Hochschulstr. 8, D-64289 Darmstadt, Germany

Previous studies of overdamped active Brownian particles (ABPs) mixed with passive tracers have shown that self-propulsion can induce motility-induced phase separation (MIPS) for large enough particle density and self-propulsion speed [1]. Here, we present our study on overdamped ABPs mixed with inertial passive tracers. We show that MIPS features different kinetic temperatures in the dense and the dilute phase if the passive tracers are sufficiently heavy (inertial). Remarkably, unlike for underdamped ABPs [2,3], neither the overdamped ABPs nor the passive tracers alone would feature such a temperature difference in coexisting phases. The observed temperature difference is accompanied by a violation of the equipartition theorem and strongly depends on the self-propulsion speed and the particle density. This allows us to tune the temperature difference from a cold dense and hot dilute phase to the counterintuitive opposite case in which the dense phase is hotter than the dilute phase. These findings open a route to create active materials with a persistent temperature profile by inserting active particles and tuning their self-propulsion speed accordingly.

[1] J. Stenhammar et al., Phys. Rev. Lett. **114**, 018301 (2015).

[2] S. Mandal et al., Phys. Rev. Lett. **123**, 228001 (2019).

[3] L. Hecht et al., Phys. Rev. Lett. **129**, 178001 (2022).

DY 10.4 Mon 15:45 ZEU 160

Collective motion in two-dimensional colloidal systems with effective (active) self-propulsion due to time-delayed feedback — •ROBIN A. KOPP and SABINE H. L. KLAPP — ITP, TU Berlin, Berlin, Germany

In recent years, delayed feedback in colloidal systems has become an active and promising field of study [1,2], key topics being history dependence and the manipulation of transport properties. Here we study the dynamics of a two-dimensional colloidal suspension, subject to time-delayed feedback, where time-

delayed feedback can be interpreted as a mechanism of effective self-propulsion, i.e., activity [3]. To this end we perform overdamped Brownian dynamics simulations, where the particles interact through a Weeks-Chandler-Andersen potential. Furthermore, each particle is subject to a Gaussian, repulsive feedback potential, that depends on the difference of the particle position at the current time, and at an earlier time. We observe and quantitatively study the emergence of dynamical clustering and collective motion characterized by a nonzero mean velocity and provide a possible explanation for the underlying mechanism combining single-particle and mean-field-like effects.

[1] S. A. M. Loos, and S. H. L. Klapp, Scientific Reports **9**, 2491 (2019)

[2] M. A. Fernandez-Rodriguez et al., Nature Communications **11**, 4223 (2020)

[3] R. A. Kopp and S. H. L. Klapp, arXiv:2210.03182 (2022)

DY 10.5 Mon 16:00 ZEU 160

Inverted Sedimentation of Active Particles in Unbiased ac Fields — •JOSÉ CARLOS UREÑA MARCOS and BENNO LIEBCHEN — Institut für Physik Kondensierter Materie, TU Darmstadt, Darmstadt, Germany

Biological microswimmers can steer autonomously and use this ability to perform sophisticated tasks. Synthetic microswimmers do not yet reach the same degree of autonomy, and need to be controlled externally if they are to carry out tasks such as targeted cargo delivery or microsurgery. While much progress has been made recently to control their motion based on external forces or gradients, e.g. in light intensity, which have a well-defined direction or bias, little is known about how to steer APs in situations where no permanent bias can be realized.

Here, we show that ac fields with a vanishing time average provide an alternative route to steering APs. We exemplify this route for inertial APs in a gravitational field, observing that a substantial fraction of them persistently travels in the upward direction upon switching on the ac field, resulting in an inverted sedimentation profile at the top wall of a confining container. Our results offer a generic control principle which could be used in the future to steer active motion, to direct collective behaviors and to purify mixtures.

15 min. break

Invited Talk

DY 10.6 Mon 16:30 ZEU 160

Long-range communications enable the hierarchical self-organization of active matter — •IGOR ARONSON¹, ALEXANDER ZIEPKE², IVAN MARYSHEV², and ERWIN FREY² — ¹Pennsylvania State University, USA — ²Ludwig-Maximilians-University, Munich, Germany

The most distinct markers of life are the ability to move (locomotion), consume energy (metabolism), process information, and form multi-cellular aggregates. Many biological systems exhibit long-range signaling strategies for evolutionary advantage. We explore the multi-scale self-organization of interacting self-propelled agents that locally process information transmitted by chemical signals. The communication capacity dramatically expands their ability to form complex structures, allowing them to self-organize through a series of collective dynamical states at multiple hierarchical levels.

The consequent study shows that information exchange by acoustic waves between the self-propelled units creates a slew of multifunctional structures. Each unit is equipped with an acoustic emitter and a detector in this realization. The swarms respond to the resulting acoustic field by adjusting their emission frequency and migrating toward the strongest signal. We find self-organized structures with different morphology, including snake-like self-propelled entities, localized aggregates, and spinning vortices. Our results provide insights into the design principles of communicating active particles capable of performing complex tasks.

DY 10.7 Mon 17:00 ZEU 160

Arrested by heating — •CORINNA C. MAASS^{1,2}, PRASHANTH RAMESH^{2,1}, and MAZIYAR JALAAAL³ — ¹University of Twente, Enschede, Netherlands — ²MPI for Dynamics and Self-organization, Göttingen, Germany — ³Universiteit van Amsterdam, Amsterdam, Netherlands

Active droplets are a class of microswimmers driven by chemical reactions at the droplet interface. Typically, the activity is powered by an advection-diffusion instability in the chemohydrodynamic fields around the droplet that is characterized by the Péclet number Pe of chemical transport. With increasing Pe , higher hydrodynamic modes at the interface cause the droplet to transition from inactivity, to steady, to reorienting, to fully unsteady motion. Here, we demonstrate that it is possible to change Pe reversibly and in situ by thermally activated changes in the chemical environment, and thereby to control the motility of the droplet.

DY 10.8 Mon 17:15 ZEU 160

Chiral active particles with non-reciprocal couplings: results from particle-based simulations — •KIM L. KREIENKAMP and SABINE H. L. KLAPP — Technische Universität Berlin, Germany

Non-reciprocal interactions manifest their drastic impact on the collective dynamics of active matter systems by changing, for example, the general type of observed instabilities [1] and leading to time-dependent states [2,3]. In particular, the combination of non-reciprocity and chirality in terms of intrinsically rotating chiral active particles (“circle swimmers”) reveals intriguing non-trivial time-dependent collective dynamics [1].

After having developed an understanding of the collective dynamics on the continuum level in previous work [1], we here present first results of particle-based simulations of chiral active particle systems with non-reciprocal alignment couplings. Indeed, quantitative predictions from continuum approaches are somewhat limited by the approximations made during the coarse-graining process. Thus, the first goal of our particle-based simulations is to explore the validity of the previously obtained continuum results regarding the overall state diagram. Second, we aim at investigating microscopic aspects of the various time-dependent states. Finally, we discuss possibilities to characterize the thermodynamic behavior of the non-reciprocal chiral system based on the stochastic trajectories obtained in particle-resolved simulations.

[1] K. L. Kreienkamp and S. H. L. Klapp, *New J. Phys.* (2022).

[2] M. Fruchart et al., *Nature* 592, 363 (2021).

[3] Z. You et al., *PNAS* 117, 19767 (2020).

DY 10.9 Mon 17:30 ZEU 160

Lattice-induced freezing in active systems unveils dynamic crystallites with square ordering — •ARITRA K. MUKHOPADHYAY¹, PETER SCHMELCHER^{2,3}, and BENNO LIEBCHEN¹ — ¹Technische Universität Darmstadt, 64289 Darmstadt, Germany. — ²Zentrum für Optische Quantentechnologien, Universität Hamburg, Luruper Chaussee 149, 22761 Hamburg, Germany. — ³The Hamburg Centre for Ultrafast Imaging, Universität Hamburg, Luruper Chaussee 149, 22761 Hamburg, Germany.

Active matter, comprising self-propelled particles like bacteria, colloidal microswimmers, or granular microflyers is currently attracting enormous attention for its ability to self-organize into complex nonequilibrium structures. In this work, we report on a new state of dynamic active crystallites, which occurs when exposing active particles to a spatially periodic potential. These crystallites require activity to emerge, adopt the structure of the underlying lattice (e.g.

square rather than hexagonal close packing), and are continuously in motion. This new phase unifies the structural properties of crystals with the dynamical properties of disordered fluids. Our work thus unveils a route to creating a new state of active materials with an intrinsic structure that can be externally controlled.

DY 10.10 Mon 17:45 ZEU 160

Shape-dependent collective motion: cohesive groups and cargo transport of colloidal rods — PHILIPP STENGELE, •ANTON LÜDERS, and PETER NIELABA — Universität Konstanz, Konstanz, Deutschland

In active toy model systems where colloids interact via predefined social interaction rules as well as steric collisions, the shape of the individual particles strongly influences emerging collective behavior. We study this based on two example systems using Brownian dynamics simulations (without hydrodynamic interactions). Firstly, we investigate a simple perception model in which colloidal rods move actively if predefined visual stimuli exceed a certain threshold. Here, we find an aspect ratio range where the rods form a dilute cohesive group with a time-independent particle distribution. If the aspect ratio surpasses this range, the rods slowly drift apart. Secondly, we look into the cargo capture and transport of a passive rod using a dense swarm of active spheres which form a hexagonal cage with a cavity for the cargo. Again, the aspect ratio of the rod proves to be crucial, as we find geometric restrictions that must be met to stabilize the cavity. Our work underlines that the shape (here, the aspect ratio) of the particles in active matter systems must be carefully considered while defining interaction rules to perform specific tasks.

DY 10.11 Mon 18:00 ZEU 160

Active Chiral Nematics — •RÜDIGER KÜRSTEN^{1,2,3} and DEMIAN LEVIS^{1,2} — ¹Departament de Física de la Matèria Condensada, Universitat de Barcelona, Barcelona, Spain — ²Universitat de Barcelona Institute of Complex Systems (UBICS), Barcelona, Spain — ³Institut für Physik, Universität Greifswald, Greifswald, Germany

We study inherently chiral self-propelled particles in two dimensions that are subjected to nematic alignment interactions and rotational noise. By means of both, homogeneous and spatially resolved mean field theory we identify various different flocking states. We confirm the presence of the predicted phases using agent-based simulations. We emphasize that special care has to be taken within the simulations in order to avoid artifacts. We present a non-standard simulation technique in order to avoid those artifacts.

DY 11: Focus Session: Physics Meets ML II –

Understanding Machine Learning as Complex Interacting Systems (joint session DY/TT)

Machine-learning has recently entered and is now transforming many fields of science, enabling discoveries in a data-driven manner. As a scientific method, however, ML often lacks one defining feature: Explainability. We here seek discussions with pioneers in understanding, explaining, and improving machine learning methods from the point of view as a physical system of interacting elements. In fact, the history of approaching neuronal networks and problems of inference and learning as a problem of statistical physics has a long history, with a number of important discoveries early on. The close relation between spin glasses and neuronal networks are being currently exploited to address pressing questions, such as the remarkable generalization properties of neuronal networks despite their massive overparameterization and their behavior reminiscent of renormalization group transformations.

Organized by Sabine Andergassen (Tübingen) and Moritz Helias (Jülich)

Time: Monday 15:00–18:30

Location: ZEU 250

Invited Talk

DY 11.1 Mon 15:00 ZEU 250

The challenge of structured disorder in statistical physics — •MARC MEZARD — Bocconi University, Milano

Statistical physics offers many interesting tools to study machine learning. In most cases it needs to use a statistical ensemble of data. Most of the theoretical work has relied on unstructured data. Yet, the highly structured character of data used in training deep networks is a crucial ingredient of their performance. Modelling structured data, analyzing the learning and the generalization of deep networks trained on this data, are major challenges. This talk will describe several recent developments in this direction.

Invited Talk

DY 11.2 Mon 15:30 ZEU 250

The emergence of concepts in shallow neural-networks — •ELENA AGLIARI — Piazzale A. Moro 5, 00185 Roma

In the first part of the seminar I will introduce shallow neural-networks from a statistical-mechanics perspective, focusing on simple cases and on a naive scenario where information to be learnt is structureless. Then, inspired by biological information-processing, I will enrich the framework and make the network

able to successfully and cheaply handle structured datasets. Results presented are both analytical and numerical.

Invited Talk

DY 11.3 Mon 16:00 ZEU 250

Adaptive Kernel Approaches to Feature Learning in Deep Neural Networks — •ZOHAR RINGEL — Racah Institute of Physics, Hebrew University in Jerusalem
Following the ever-increasing role of deep neural networks (DNNs) in our world, a better theoretical understanding of these complex artificial objects is desirable. Some progress in this direction has been seen lately in the realm of infinitely overparameterized DNNs. The outputs of such trained DNNs behave essentially as multivariate Gaussians governed by a certain covariance matrix called the kernel. While such infinite DNNs share many similarities with the finite ones used in practice, various important discrepancies exist. Most notably the fixed kernels of such DNNs stand in contrast to feature learning effects observed in finite DNNs. Such effects are crucial as they are the key to understanding how DNNs process data. To accommodate such effects within the Gaussian/kernel viewpoint, various ideas have been put forward. Here I will provide a short overview of those efforts and then discuss in some detail a general set of equations we

developed for feature learning in fully trained/equilibrated DNNs. Interestingly, our approach shows that DNNs accommodate strong feature learning via mean-field effects while having decoupled layers and decoupled neurons within a layer. Furthermore, learning is achieved not by compression of information but rather by increasing neuron variance along label-relevant directions in function space.

DY 11.4 Mon 16:30 ZEU 250

Interpreting black-box ML with the help of physics — •MIRIAM KLOPOTEK — University of Stuttgart, SimTech Cluster of Excellence EXC 2075, Stuttgart, Germany

Complexity is an unavoidable part of systems with emergent or even so-called intelligent capabilities. Ultimately, it stems from the many microscopic constituents with multiple possible states, which introduces a vast space of degrees of freedom. This is true both for many-body systems as well as modern machine learning (ML) systems. Today, the latter suffer notoriously from the ‘black-box problem’, i.e. they are inherently opaque. We argue that an engagement with physics can offer deep insights ultimately for a theory of operation and thus an interpretation, as well as powerful ways to assess their reliability and shortcomings. We show some results for a case study with beta-variational autoencoders (β -VAEs) [1], which we trained on data from a well-characterized model system of hard rods confined to 2D lattices [2].

[1] D. P. Kingma and M. Welling, ICLR 2014. D. J. Rezende, S. Mohamed, and D. Wierstra, ICML 2014, p. 1278-1286.

[2] P. Quiring, M. Klopotek and M. Oettel, Phys. Rev. E 100, 012707 (2019).

15 min. break

Invited Talk

DY 11.5 Mon 17:00 ZEU 250

Analysing the dynamics of message passing algorithms — •MANFRED OPPER^{1,2} and BURAK ÇAKMAK¹ — ¹Institut für Softwaretechnik und Theoretische Informatik, Technische Universität Berlin, 10587, Germany — ²Centre for Systems Modelling and Quantitative Biomedicine, University of Birmingham, B15 2TT, United Kingdom

Message passing algorithms are deterministic methods which are designed for efficiently computing marginal statistics for probabilistic, Bayesian data models used in machine learning and statistics. Such algorithms have been developed in parallel within the machine learning and the statistical physics communities. They often provide highly accurate approximations at a much higher speed compared to exact Monte Carlo sampling. The fixed points of such algorithms can be analysed for high dimensional models (under the assumption of specific data distributions) using the replica method of statistical physics. In this talk we will focus on the dynamical properties of the algorithms. Applying dynamical functional techniques to the nonlinear dynamics, the degrees of freedom which interact via a random matrix can be decoupled in the limit of large systems resulting in exact stochastic single node dynamics. For general dynamical models, it is hard to further analyse this effective dynamics due to the occurrence of memory terms. Surprisingly, for message passing algorithms memory terms are absent and exact results for convergence rates and stability can be derived for specific data distributions.

Invited Talk

DY 11.6 Mon 17:30 ZEU 250

Deep Learning Theory Beyond the Kernel Limit — •CENGİZ PEHLEVAN — Harvard University, USA

Deep learning has emerged as a successful paradigm for solving challenging machine learning and computational problems across a variety of domains. However, theoretical understanding of the training and generalization of modern deep learning methods lags behind current practice. I will give an overview of our recent results in this domain, including a new theory that we derived by applying dynamical field theory to deep learning dynamics. This theory gives insight into internal representations learned by the network under different learning rules.

DY 11.7 Mon 18:00 ZEU 250

Solving the Bethe–Salpeter equation with exponential convergence — •MARKUS WALLERBERGER¹, HIROSHI SHINAOKA², and ANNA KAUCH¹ — ¹TU Wien, Vienna, Austria — ²Saitama University, Japan

The Bethe–Salpeter equation plays a crucial role in understanding the physics of correlated fermions, relating to optical excitations in solids as well as resonances in high-energy physics. Yet, it is notoriously difficult to control numerically, typically requiring an effort that scales polynomially with energy scales and accuracy. This puts many interesting systems out of computational reach.

Using the intermediate representation and sparse modeling for two-particle objects on the Matsubara axis, we develop an algorithm that solves the Bethe–Salpeter equation in $O(L^8)$ time with $O(L^4)$ memory, where L grows only logarithmically with inverse temperature, bandwidth, and desired accuracy. This opens the door for computations in hitherto inaccessible regimes. We benchmark the method on the Hubbard atom and on the multiorbital weak-coupling limit, where we observe the expected exponential convergence to the analytical results. We then showcase the method for a realistic impurity problem.

[1] M. Wallerberger et al., Phys. Rev. Research 3, 033168 (2021)

DY 11.8 Mon 18:15 ZEU 250

Making machines untangle the parquet equations — •SAMUEL BADR¹, ANNA KAUCH¹, HIROSHI SHINAOKA², KARSTEN HELD¹, and MARKUS WALLERBERGER¹ — ¹TU Wien, Vienna, Austria — ²Saitama University, Saitama, Japan

Diagrammatic theories at the two-particle level are increasingly important in understanding the subtle interplay of phenomena occurring in strongly correlated electron systems. The parquet equations are a centerpiece of many such theories, since they are the simplest unbiased topological classification of two-particle diagrams. However, due to their eponymous interlocking structure, the parquet equations are vexingly difficult to solve, requiring prohibitive amounts of memory.

We tackle this problem using the recently developed, machine learning inspired, techniques: firstly, the overcomplete intermediate representation, a highly compressed model for two-particle objects which is guaranteed to converge exponentially; secondly, a sparse set of Matsubara frequencies tailored to the structure of the parquet equations. This allows us to perform convolutions and frequency shifts at no loss of accuracy.

We benchmark our solver for the Hubbard atom, where we reproduce analytic results, and then showcase the solver for more extended systems.

DY 12: Nonequilibrium Quantum Many-Body Systems I (joint session TT/DY)

Time: Tuesday 9:30–13:15

Location: HSZ 204

See TT 22 for details of this session.

DY 13: Active Matter III (joint session BP/PPP/DY)

Time: Tuesday 9:30–12:30

Location: TOE 317

See BP 9 for details of this session.

DY 14: Invited Talk: Machine Learning and Complex Fluids

Time: Tuesday 9:30–10:00

Location: MOL 213

Invited Talk

DY 14.1 Tue 9:30 MOL 213

Unraveling structural and dynamical features in glassy fluids using machine learning — •LAURA FILION¹, FRANK SMALLENBURG², and RINSKE ALKEMADE¹ — ¹Debye Institute for Nanomaterials Science, Utrecht University, Netherlands — ²Laboratoire de physique des Solides, Université Paris-Saclay, France

Developments in machine learning (ML) have opened the door to fully new methods for studying phase transitions due to their ability to extremely efficiently identify complex patterns in systems of many particles. Applications of machine

learning techniques vary from the use of developing new ML-based order parameters for complex crystal structures, to locating phase transitions, to speeding up simulations. The rapid emergence of multiple applications of machine learning to statistical mechanics and materials science demonstrates that these techniques are destined to become an important tool for soft matter physics. In this talk, I will briefly present an overview of the work my group is doing on using ML to study soft matter systems, with a focus on how ML can be used to explore new connections between structure and dynamics in supercooled liquids.

In particular, I will present a strategy to fit the dynamics in glassy systems using advanced hierarchical order parameters combined with simple linear regression. Additionally, I will present a method for extracting the cage structure of a glassy

configuration, and demonstrate that this information significantly improves our ability to predict glassy dynamics over a broad range of time scales.

DY 15: Physics of Contagion Processes I (joint session SOE/DY)

Time: Tuesday 9:30–10:00

Location: ZEU 260

See SOE 5 for details of this session.

DY 16: Complex Fluids and Soft Matter (joint session DY/ CPP)

Time: Tuesday 10:00–13:00

Location: MOL 213

DY 16.1 Tue 10:00 MOL 213

How are mobility and friction related in viscoelastic fluids? — •JULIANA CASPERS¹, NIKOLAS DITZ², KARTHIKA KRISHNA KUMAR², FELIX GINOT², CLEMENS BECHINGER², MATTHIAS FUCHS², and MATTHIAS KRÜGER¹ — ¹Institute for Theoretical Physics, Georg-August Universität Göttingen, 37073 Göttingen, Germany — ²Fachbereich Physik, Universität Konstanz, 78457 Konstanz, Germany

The motion of a colloidal probe in a viscoelastic fluid is described by friction or mobility, depending on whether the probe is moving with a velocity or feeling a force. While the Einstein relation describes an inverse relationship valid for Newtonian solvents, both concepts are generalized to time-dependent memory kernels in viscoelastic fluids. We theoretically and experimentally investigate their relation by considering two observables: the recoil after releasing a probe that was moved through the fluid and the equilibrium mean squared displacement (MSD). Applying concepts of linear response theory, we generalize Einstein's relation and thereby relate recoil and MSD, which both provide access to the mobility kernel. With increasing concentration, however, MSD and recoil show distinct behaviors, rooted in different behaviors of the two kernels. Using two theoretical models, a linear two-bath particle model and hard spheres treated by mode-coupling theory, we find a Volterra relation between the two kernels, explaining differing timescales in friction and mobility kernels under variation of concentration.

DY 16.2 Tue 10:15 MOL 213

Can liquid-state theory predict jamming of hard particles? — •CARMINE ANZIVINO¹, MATHIAS CASIULIS², AMGAD MOUSSA³, STEFANO MARTINIANI², and ALESSIO ZACCONE¹ — ¹Department of Physics "A. Pontremoli", University of Milan, via Celoria 16, 20133 Milan, Italy — ²Center for Soft Matter Research, Department of Physics, New York University, New York 10003, USA — ³Syngenta AG, 4058 Basel, Switzerland

By generalizing the notion of maximally random jammed (MRJ) state [1,2] to that of MRJ-line, we show [3] that it is reasonable to assume the most random branch of jammed states to undergo crowding in a way qualitatively similar to an equilibrium liquid. We then prove that, for hard-sphere systems, liquid-state theories can be successfully used to estimate the RCP density, when the latter is identified with the densest isostatic point, i. e. the densest among the MRJ states with $z=6$.

Our finding is further enforced by the analysis of polydisperse systems. Either in the case of bidisperse and polydisperse hard spheres our prediction of the RCP density is in very good agreement with simulations, for a large values of size ratios and polydispersity.

[1] S. Toquato, T. M. Truskett, and P. G. Debenedetti, Phys. Rev. Lett. 84, 2064 (2000). [2] S. Torquato and F. H. Stillinger, Reviews of Modern Physics 82, 2633 (2010). [3] C. Anzivino, M. Casiulis, T. Zhang, A. S. Moussa, S. Martiniani and A. Zaccane, "Estimating RCP as the densest isostatic packing in bidisperse and polydisperse hard spheres", manuscript submitted (2022).

DY 16.3 Tue 10:30 MOL 213

2D crystals of squares and the tetraic phase — •PETER KEIM — Max-Planck-Institut für Dynamik und Selbstorganisation, Göttingen

Squares (5 micron edge-length) were manufactured from a photo-resist using a 3D nanoprinter (nanoscribe GT). In aqueous solution, particles sediment by gravity to a thin cover slide where they form a mono-layer of Brownian particles. The curvature of the cover slide can be adjusted from convex to concave, which allows to vary the area-density of the mono-layer from 700 to 1500 particles in the field of view. For low densities, the squares are free to diffuse and form a 2D fluid while for high densities they form a quadratic crystal. In analogy to 2D-melting by topological defects with an intermediate hexatic phase for isotropic particles (KTHNY-theory and Nobel-price 2016), a four-folded bond-order correlation function is used to resolve a tetratic phase with quasi-long-range orientational order but short rang translational order.

DY 16.4 Tue 10:45 MOL 213

Transient microrheology unveils the presence of two relaxation processes in viscoelastic fluids — •FÉLIX GINOT¹, JULIANA CASPERS², LUIS FRIEDER REINALTER¹, KARTHIKA KRISHNA KUMAR¹, MATTHIAS KRÜGER², and CLEMENS BECHINGER¹ — ¹Fachbereich Physik, Universität Konstanz, 78457 Konstanz, Germany — ²Institute for Theoretical Physics, Georg-August Universität Göttingen, 37073 Göttingen, Germany

We experimentally investigate the transient dynamics of a colloidal probe particle in a viscoelastic fluid after the driving force acting on the probe is suddenly removed. In this situation, the probe exhibits a strong backward recoil, with two distinct timescales. While the first timescale naturally originates from the viscoelastic properties of the fluid, the second timescale arises from the coupling between the probe and the bath. These experimental observations are in excellent agreement with a microscopic model which considers the probe particle to be coupled to two bath particles via harmonic springs. Interestingly, this model exhibits two sets of eigenmodes corresponding to reciprocal and non-reciprocal force conditions, and which can be experimentally confirmed in our experiments. We expect our findings to be relevant under conditions where particles are exposed to non-steady shear forces as this is encountered e.g. in microfluidic sorting devices or the intermittent motion of motile bacteria within their natural viscoelastic surroundings.

15 min. break

DY 16.5 Tue 11:15 MOL 213

Phason strain-free growth of quasicrystals based on purely local rules and without repair mechanism — STEFAN WOLF¹, MICHAEL ENGEL², and •MICHAEL SCHMIEDEBERG¹ — ¹Institute of Theoretical Physics, Friedrich-Alexander-Universität Erlangen-Nürnberg, 91058 Erlangen, Germany — ²Institute for Multiscale Simulation, Friedrich-Alexander-Universität Erlangen-Nürnberg, 91058 Erlangen, Germany

We introduce a simple model for the growth of colloidal quasicrystals where new particles are sequentially added according to specific local rules to the system in three dimensions. Subsequent changes to the particles are not allowed, i.e., no phasonic rearrangements can occur once a particle has been placed into the system. Our findings demonstrate that the purely local energetic rules are sufficient to obtain complex long-ranged order. Thus, phasonic rearrangements or fluctuations might be important to facilitate the formation of almost perfect quasicrystals [1-3] but they are not indispensable.

[1] C.V. Achim, M. Schmiedeberg, and H. Löwen, Phys. Rev. Lett. 112, 255501 (2014).

[2] A. Gemeinhardt, M. Martinsons, and M. Schmiedeberg, Eur. Phys. J. E 41, 126 (2018).

[3] K. Nagao, T. Inuzuka, K. Nishimoto, and K. Edagawa, Phys. Rev. Lett. 115, 075501 (2015).

DY 16.6 Tue 11:30 MOL 213

Magnus force on microscopic spinning objects moving through non-Markovian baths — XIN CAO¹, •DEBANKUR DAS², NIKLAS WINDBACHER¹, FELIX GINOT¹, MATTHIAS KRÜGER², and CLEMENS BECHINGER¹ — ¹Fachbereich Physik, University Konstanz, 78464 Konstanz, Germany — ²Institut für Theoretische Physik, Universität Göttingen, 37077 Göttingen Germany

When a spinning object moves through a fluid or air, its direction of motion becomes deflected due to the Magnus force that is perpendicular both to the moving direction and the spinning axis. Since the Magnus effect is caused by inertial effects within the surrounding medium, it should vanish at micro scales where viscous forces dominate over inertia. Recent experiments have observed the phenomenon similar to Magnus effect when a spinning colloids and there aggregates are externally driven through a viscoelastic fluid. Even though the deflection force shows a similar dependence on the spinning and translating velocity of the particles as in case of Magnus forces, its sign is reversed. Here, we

have developed a theory of such motions which does not rely on the inertial effects but caused explicitly by the memory effect of the viscoelastic fluid. To better elucidate our theory we corroborate our results with experiments. Our theory successfully captures the density relaxation timescales of the viscoelastic fluid. Further we proposed viable theoretical predictions which can be verified with further experiments.

DY 16.7 Tue 11:45 MOL 213

Preferential alignment of colloidal dumbbells with recoil direction — •KARTHIKA KRISHNA KUMAR¹, FÉLIX GINOT¹, JULIANA CASPERS², MATTHIAS KRÜGER², and CLEMENS BECHINGER¹ — ¹Fachbereich Physik, Universität Konstanz, Germany — ²Institute for Theoretical Physics, Georg-August Universität Göttingen, Germany

Unlike Newtonian fluids, viscoelastic fluids can store and dissipate energy on much longer timescales leading to non-Markovian dynamics. Hence, probing viscoelastic fluids using colloidal particles reveal complex dynamics in microscopic lengthscales. A consequence of this is the recoil behavior of a colloidal particle after dragging it through a viscoelastic fluid. In this work, we use a pair of colloidal particles stuck together due to depletion interactions forming a dumbbell-shaped structure. This gives the advantage of resolving the orientational component in addition to the translational components of the particle motion. Surprisingly, we report that the axis of the dumbbell tends to align with the direction of the motion during a recoil. The amplitude of this orientational component follows a non-linear trend even in the regime where translational recoil amplitudes show a linear increase with shear velocity. This behavior can no longer be explained by the linear two-bath particle model which is able to explain the bi-exponential translational recoils. Furthermore, the amplitude of this re-orientation increases with the initial angle at which the dumbbell is dragged. This points to an asymmetric distribution of elastic energy between the two particles of the dumbbell which might cause this effect.

DY 16.8 Tue 12:00 MOL 213

Entropic phase diagram of twisted convex particles — •POSHIKA GANDHI and ANJA KUHNHOLD — Institute of Physics, University of Freiburg, Germany

The field of liquid crystal simulations has, over the years, benefitted immensely from the study of purely entropy driven systems. Since Onsager's[1] predictions of the existence of a nematic phase in long rods, the list of known phases of hard rod-like particles has grown to include phases like smectics and cholesterics.

An important parameter in the formation of these phases is the particle shape anisotropy. By considering unusual particle shapes new phases can be discovered. Recently, Dussi and Dijkstra[2] showed the formation of stable chiral nematic phase in twisted polyhedral particles using only entropic interactions.

We used Monte Carlo NVT simulations to produce phase diagrams of a different class of twisted particles - convex triangular and rectangular prisms. The results show a host of previously undiscovered phases arising from the shape anisotropy parameters like twist angle and aspect ratios.

[1] Onsager, L., *Ann. N. Y. Acad. Sci.*, 51, 627 (1949).

[2] Dussi, S., Dijkstra, M., *Nat Commun.* 7, 11175 (2016).

DY 16.9 Tue 12:15 MOL 213

Optimizing the Structure of Acene Clusters — •PHILIPP ELSÄSSER and TANJA SCHILLING — Institute of Physics, University of Freiburg, Germany

In the production of organic solar cells, neutral acene cluster beams are used to create thin films. The molecules in these clusters can be arranged in various ways. Most types of acene molecules are quasi two dimensional with one long

axis - they prefer stacked or herring-bone structures. Additionally, the positions of the molecules in a cluster may vary. Thus, the exact way of how they arrange has a strong influence on the overall energy of the cluster.

We have investigated the structures of anthracene, tetracene, and pentacene clusters with up to 30 molecules. In order to find the configurations at the global minimum of the potential energy surface with respect to the positions of the atoms, we applied the Basin-Hopping Monte-Carlo (BH) algorithm to atoms described by the polymer-consistent force field - interface force field (PCFF-IFF). We studied for these cluster structures the relative stability between different sizes of clusters, as well as the accessibility of the global minimum at different temperatures.

DY 16.10 Tue 12:30 MOL 213

Ergodicity breaking in overpacked colloidal hard spheres — •HANS JOACHIM SCHÖPE — Universität Tübingen, Institut für angewandte Physik, Auf der Morgenstelle 10, 72076 Tübingen

The ergodic hypothesis is an essential prerequisite for the applicability of statistical mechanics in thermodynamic equilibrium. Direct experimental evidence of the validity of the ergodic hypothesis is extremely rare. Furthermore, the question arises to what extent - if at all - ergodicity exists in non-equilibrium. We have realized a novel dynamic light scattering experiment, which makes it possible to determine the probability distribution of relaxation-times in colloidal suspensions. We present here a systematic study of the relaxation-time distribution in colloidal hard spheres at the transition from equilibrium to non-equilibrium. In thermodynamic equilibrium, we can impressively confirm the ergodic hypothesis and show that the fluctuations are of a Gaussian nature. Out of equilibrium, we can detect non-Gaussian behavior, which increases rapidly with increasing undercooling (overpacking). The ergodic hypothesis is no longer fulfilled in non-equilibrium. Furthermore, we observe that the metastable fluid ages in the induction stage, the non-Gaussian fluctuations increase in the time before crystallization sets in. To what extent these fluctuations cause crystallization must be clarified in the future.

DY 16.11 Tue 12:45 MOL 213

Coacervates from a polyelectrolyte and a small polyion: preparation, phase behavior and theoretical modeling — LUCY CORIA-ORIUNDO¹, EUGENIA APUZZO², SANTIAGO HERRERA¹, MARCELO CEOLÍN², GABRIEL DEBAIS¹, FERNANDO BATTAGLINI¹, and •MARIO TAGLIAZUCCHI¹ — ¹Universidad de Buenos Aires, Bs.As., Argentina — ²Universidad Nacional de la Plata, Bs.As., Argentina.

A mixture of oppositely charged polyelectrolytes, under the proper experimental conditions, can undergo liquid-liquid phase separation. The resulting polymer-rich phase is usually known as polyelectrolyte coacervate. This work reports liquid coacervates composed of a small polyanion (ferricyanide) and branched poly(ethyleneimine) (BPEI), a polycation. The phase diagram of the system was measured as a function of the concentration of both components at fixed pH = 6 and a concentration of added NaCl of 0.5 M. The salt resistance of the coacervate was studied and it was found that the coacervate is stable up to [NaCl] = 1.35 M. The phase diagram and salt-resistance experiments were modeled with a statistical-thermodynamics formalism that models the association of the oppositely charged species as a pseudo-chemical-equilibrium. The model fits very well the experimental data and was used to analyze the differences between polymer-polymer and polymer-small ion coacervates. Finally, the diffusion coefficient of ferricyanide within the coacervated (measured with cyclic voltammetry) was shown to increase 10 times when the concentration of added NaCl was increased from 0 to 1.2 M.

DY 17: Machine Learning in Dynamics and Statistical Physics I

Time: Tuesday 10:00–12:45

Location: ZEU 160

DY 17.1 Tue 10:00 ZEU 160

On-the-fly adaptive sparse grids for coupling high-fidelity and coarse-grained models — •TOBIAS HÜLSER, SINA DORTAJ, and SEBASTIAN MATERA — Fritz-Haber-Institut der MPG, Berlin, Germany

Most simulations of continuum models require the repetitive evaluation of some non-linear functions. If the latter are only given by the outcome of some high-fidelity simulation, these evaluations can easily become the computational bottleneck of the coupled simulation. To overcome this limitation, computationally efficient machine-learning models have become popular as surrogates of the high-fidelity model in the continuum scale simulation. However, if the input dimension of these models is high, the training of the surrogate often requires infeasible numbers of simulations, the so-called curse of dimensionality. We present an on-the-fly adaptive sparse grids approach, which lifts these limitations. This exploits that, on the one hand, sparse grids are only mildly affected by the curse of dimensionality and allow for an adaptive, local error based training set design. On the other hand, we utilize that, during a continuum simulation, only a small low-dimensional subset of the high-dimensional input space of the

high-fidelity model is visited. We therefore construct the surrogate on the fly during the continuum simulation, only generating the high-fidelity data which is needed to interpolate this subset.

We demonstrate the approach on exemplary physical-chemical models from the field of heterogeneous catalysis. We find that our approach can significantly reduce the number of high-fidelity evaluations compared to the direct coupling.

DY 17.2 Tue 10:15 ZEU 160

Reservoir Computing using Active Matter Model Systems: A Physics Viewpoint — •MARIO U. GAIMANN and MIRIAM KLOPOTEK — Stuttgart Center for Simulation Science (SimTech), Cluster of Excellence EXC 2075, University of Stuttgart, Germany

Spatio-temporal prediction of chaotic systems is a challenging problem that is relevant for many fields (weather, finance, energy, and other dynamic systems). Recurrent neural networks and specifically neuron-based reservoir computing were previously used to approach this problem [1,2]. However, these learning systems are typically treated as black boxes, and do not incorporate reasoning

or analysis in terms of physical laws and dynamics. Here we study the non-equilibrium dynamics of simple active matter models serving as reservoir computing substrates [3]. This allows us to determine and interpret the state of our reservoir and relate the learning problem to other generic phenomena in statistical physics. With this knowledge we aim to understand optimal conditions for learning in relation to critical states and physical constraints.

[1] Tanaka, G. *et al.* (2019), *Neural Networks* **115**, 100-123.

[2] Nakajima, K. and Fischer, I. (2021). *Reservoir Computing*. Springer Singapore.

[3] Lyburn, T. *et al.* (2021), *Chaos* **31**(3), 033121.

DY 17.3 Tue 10:30 ZEU 160

Machine Learning Percolation: Does it understand the physics? — •DJÉNABOU BAYO^{1,2}, ANDREAS HONECKER², and RUDOLF A. RÖMER¹ — ¹Departement of Physics, University of Warwick, Coventry, CV47AL, United Kingdom — ²Laboratoire de Physique Théorique et Modélisation (LPTM) (CNRS UMR8089), CY Cergy Paris Université, 95302 Cergy-Pontoise, France
The percolation model is one of the simplest models in statistical physics displaying a phase transition at a critical site occupation probability p_c . The hallmark of the percolation transition is the emergence of a spanning cluster of connected neighboring sites across the lattice. Machine learning (ML) approaches to percolation have shown that the non-spanning ($p < p_c$) and the spanning ($p > p_c$) phases can be identified reasonably well with supervised deep learning (DL) strategies for classification based on convolutional neural networks (CNNs). Surprisingly, the role of the spanning cluster seems to be less prominent in such DL methods. Here, we show that CNNs, when trained with the site occupation probabilities p as labels, can classify not only the two phases $p < p_c$ and $p > p_c$, but also according to the many individual p 's. Nevertheless, the same CNNs struggle when trying to predict the emergence of the spanning cluster. Indeed, when we train with correlation lengths or the existence of the spanning cluster, the results suggest that the CNNs seem to rely mostly on the p 's as a proxy measure. This suggests that the essential physics of the spanning cluster is not actually what determines the DL results.

DY 17.4 Tue 10:45 ZEU 160

Bayesian deep learning for error estimation in the analysis of anomalous diffusion — •HENRIK SECKLER¹ and RALF METZLER^{1,2} — ¹Institute for Physics & Astronomy, University of Potsdam, 14476 Potsdam-Golm, Germany. — ²Asia Pacific Centre for Theoretical Physics, Pohang 37673, Republic of Korea
Modern single-particle-tracking techniques produce extensive time-series of diffusive motion in a wide variety of systems, from single-molecule motion in living-cells to movement ecology. The quest is to decipher the physical mechanisms encoded in the data and thus to better understand the probed systems. We here augment recently proposed machine-learning techniques for decoding anomalous-diffusion data to include an uncertainty estimate in addition to the predicted output. To avoid the Black-Box-Problem a Bayesian-Deep-Learning technique named Stochastic-Weight-Averaging-Gaussian is used to train models for both the classification of the diffusion model and the regression of the anomalous diffusion exponent of single-particle-trajectories. Evaluating their performance, we find that these models can achieve a well-calibrated error estimate while maintaining high prediction accuracies. In the analysis of the output uncertainty predictions we relate these to properties of the underlying diffusion models, thus providing insights into the learning process of the machine and the relevance of the output.

DY 17.5 Tue 11:00 ZEU 160

A machine learned classical density functional for orientational correlations in the Kern-Frenkel model for patchy particles — •ALESSANDRO SIMON^{1,2} and MARTIN OETTEL¹ — ¹Institute for Applied Physics, University of Tübingen, Germany — ²Max Planck Institute for Intelligent Systems, Tübingen, Germany
Models of patchy particles in a generic form (hard spheres decorated with a fixed number of attraction sites), possess an interesting phase behaviour, despite their apparent simplicity. This includes gel-formation and a vanishing fluid density at the gas-liquid coexistence, as the number of attractive patches and temperature is decreased. Using simulations of a symmetric four-patch model, we examine the orientational order of the particles and the effects of their tetrahedral symmetry on the expansion of density profiles and pair correlations in rotational invariants. Building on an existing classical density functional model which is formulated on the basis of Wertheim's theory for associating liquids and does not resolve orientational correlations [Stopper *et al.* *J. Chem. Phys.* **149**, 224503 (2018)], we construct an improved density functional using machine learning and show that it yields the correct orientation distribution in slit-like geometries.

15 min. break

DY 17.6 Tue 11:30 ZEU 160

Classification of Gel Networks using Graph Convolutional Neural Networks — •MATTHIAS GIMPERLEIN and MICHAEL SCHMIEDEBERG — FAU Erlangen-Nürnberg, Erlangen, Germany

The structural properties of gel networks are important for the mechanical properties of the corresponding gels. We analyze gel networks and their structure using a machine learning approach based on graph convolutional networks (GCN) employing only the local neighborhood of particles as input information.

Using these we define a GCN-Autoencoder to reconstruct adjacency matrices of networks and quantitatively analyze in which properties the prediction of the network differs from the original input. This includes analysis on the abstract graph level as well as on the real physical network level.

Furthermore we use GCNs to classify gel networks depending i.e. on the loop-sizes which are present in the network. Our goals include getting robust classification of strongly or weakly connected gel networks, predictions of minimal connecting structures and an insight how - according to an artificial intelligence - gel networks look like.

DY 17.7 Tue 11:45 ZEU 160

A 3-layer injection-locked multimode semiconductor laser neural network — •ELIZABETH ROBERTSON^{1,3}, ROMAIN LANCE², ANAS SKALLI², XAVIER PORTE², JANIK WOLTERS^{1,3}, and DANIEL BRUNNER² — ¹Deutsches Zentrum für Luft- und Raumfahrt, 12489 Berlin, Germany — ²Institut FEMTO-ST, Université Bourgogne Franche-Comté, CNRS UMR6174, Besançon, France — ³Technische Universität Berlin, Institut für Optik und Atomare Physik, 10623 Berlin, Germany
Optical hardware implementations of artificial neural networks (ANNs) have become a hot topic of research due to the inherent parallelism, potentially high speed and energy efficiency of optics [1]. Semiconductor laser networks are of specific interest as they are highly non-linear systems, which can be modulated at high throughput [2]. Previous work using spatial modes as nodes of an ANN, illustrated the use of multimode large area VCSELs for neural network computing in a fully parallel substrate, without pre- or post-processing [3,4]. We further expand this concept to a three-layer network consisting of mutually coupled multimode VCSELs, injection locked to a DFB laser. Here, information is fed into the network by modulating the injection laser, and boolean output weights are implemented using a digital micromirror device. We present an outline of the system, investigate its locking behavior and non-linear response. [1] Huang C. *et al.*, *Advances in Physics: X* **7**, 1 (2022) [2] Skalli A. *et al.*, *Opt. Mater. Express* **12**, 2395-2414 (2022) [3] Porte X. *et al.*, *J. Phys. Photonics* **3** 024017 (2021) [4] Skalli A. *et al.*, *Opt. Mater. Express* **12**, 2793-2804 (2022)

DY 17.8 Tue 12:00 ZEU 160

Efficiently compressed time series approximations — •PAUL WILHELM¹ and MARC TIMME^{1,2} — ¹Chair for Network Dynamics, Institute of Theoretical Physics and Center for Advancing Electronics Dresden (cfaed), TU Dresden, Germany — ²Lakeside Labs, Klagenfurt, Austria
Time series emerge from a broad range of applications, for instance as stock market pricing, electrocardiographic recordings or trajectories in chaotic dynamical systems. Long time series require an approximation scheme for compressing and storing, analyzing or predicting them.

How can we construct efficient approximations? Continuous, piecewise linear functions with variable knots that mark the end points of each segment are easy to handle and often used. However, fitting the knots is highly nonlinear and only feasible with a lucky initial guess. Here we propose a novel method that exploits repeating motifs in the data and thereby avoids fitting each knot independently, significantly accelerating the construction of the approximation.

Starting from the beginning of a time series, the method iteratively integrates subsequent data points. For each extension, it tries to reuse parts of the already existing function to approximate the yet uncovered data points. If successful, each motif is approximated only once and reused multiple times. As a result, the knots of the function are interdependent and can thus be represented in compact form. In contrast to deep neural networks that also find a piecewise linear approximation, our approach offers an efficient and explainable method and thereby a novel perspective onto why and how deep neural networks may work.

DY 17.9 Tue 12:15 ZEU 160

Active Learning Strategies for Molecular Dynamics with Machine-learned Potentials — •SHUBHAM SHARMA¹ and MARIANA ROSSI^{1,2} — ¹Max Planck Institute for the Structure and Dynamics of Matter, Hamburg, Germany — ²Fritz Haber Institute of the Max Planck Society, Berlin, Germany
Machine-learning potentials (MLPs) have allowed the efficient modelling of complex atomistic systems with ab-initio accuracy. Normally, the construction of sufficiently large and diverse reference datasets, using first-principles calculations, is a bottleneck for training. Therefore, several active-learning strategies have been proposed, which aim to make the training more efficient, especially when used together with molecular-dynamics techniques [1]. In this work, we explore building protocols for training sets of high-dimensional neural-network potentials (HDNNPs), targeting specifically weakly-bound condensed-phase systems. For that, we show how we can use and augment the committee-model framework within the i-PI code [2]. We show results for acene-based molecular crystals and discuss the advantages and limitations of different learning strategies to treat different crystal polymorphs, at various thermodynamic conditions. [1] C. Schran *et al.*, *J. Chem. Phys.* **153**, 104105 (2020). [2] V. Kapil *et al.*, *Comput. Phys. Commun.* **236**, 214 (2019).

DY 17.10 Tue 12:30 ZEU 160

Machine learning-based prediction of dynamical clustering in excited granular media — •SAI PREETHAM SATA, DMITRY PUZYREV, and RALF STANNARIUS — Institute of Physics and MARS, Otto von Guericke University Magdeburg, Universitätsplatz 2, D-39106 Magdeburg, Germany

Granular gases excited by external force tend to undergo gas-like to cluster transitions when the filling fraction of particles reaches sufficient value. In order to understand the clustering dynamics, experiments were performed in microgravity [1,2]. A numerical simulation model based on DEM is available. By varying geometrical and material parameters, a phase diagram is obtained. Cumulative distribution functions of the density profiles and uniform distribution profiles

are obtained and the maximum distance between these curves is compared to the Kolmogorov-Smirnov (KS) test threshold to detect gas-cluster transitions. We aim to predict the formation of dynamical clusters with the use of machine learning techniques as an alternative to DEM simulations, requiring much less computational effort. We confirm the reliability of the predictions for relatively well-studied spherical beads, with the perspective of analysis of clustering of more complicated particle shapes.

This study is supported by DLR projects VICKI and EVA (50WM2252 and 50WM2048)

References: [1] S. Aumaitre, et al. Review of Scientific Instruments 89, 075103 (2018) [2] M. Noirhomme et al. EPL 123, 14003 (2018) [3] Puzyrev, D., Fischer, D., Harth, K. et al., Sci Rep 11, 10621 (2021).

DY 18: Nonlinear Dynamics, Synchronization and Chaos

Time: Tuesday 10:00–12:15

Location: ZEU 147

DY 18.1 Tue 10:00 ZEU 147

Synchrony at Weak Coupling in the Complexified Kuramoto Model — •MORITZ THÜMLER¹, SHESHA G.M. SRINIVA², MALTE SCHRÖDER¹, and MARC TIMME^{1,3} — ¹Chair for Network Dynamics, Institute of Theoretical Physics & Center for Advancing Electronics Dresden (cfaed), TU Dresden — ²Institute of Physics and Material Sciences, Université du Luxembourg — ³Lakeside Labs, Klagenfurt, Austria

We present the finite-size Kuramoto model analytically continued from real to complex variables and analyze its collective dynamics. For strong coupling, synchrony appears through locked states that constitute attractors, as for the real-variable system. However, synchrony persists in the form of *complex locked states* for coupling strengths K below the transition $K^{(pl)}$ to classical *phase locking*. Where complex locked states are stable, their imaginary parts indicate which units belong to the locked population in the original, real-variable system. We uncover a second transition at $K' < K^{(pl)}$ below which complex locked states become linearly unstable yet still exist for arbitrarily small coupling strengths. The results open up a path towards a new field of network dynamics with variables complexified by analytic continuation.

DY 18.2 Tue 10:15 ZEU 147

Predicting tipping points in driven nonlinear systems — •GWENDOLYN QUASEBARTH¹, MORITZ THÜMLER¹, and MARC TIMME^{1,2} — ¹Chair for Network Dynamics, Institute for Theoretical Physics and Center for Advancing Electronics Dresden (cfaed), Technical University of Dresden, Dresden, Germany — ²Lakeside Labs, Lakeside B04b, Klagenfurt, Austria

Tipping points mark parameter values beyond which a system qualitatively changes its collective dynamics, often in undesired ways. Standard response theory for nonequilibrium nonlinear systems predicts local deviations around a stable fixed point via a polynomial in the amplitude ϵ of the driving signal. However, such standard response theories (of arbitrary order in ϵ) necessarily fail to predict nonequilibrium tipping points. Here, we propose a novel nonlinear response theory that overcomes the constraints of polynomial response theory of any order. We illustrate our findings in a class of sinusoidally driven damped nonlinear oscillators.

DY 18.3 Tue 10:30 ZEU 147

Pseudo-laminar chaos from on-off intermittency — •DAVID MÜLLER-BENDER¹, RAHIL N. VALANI², and GÜNTER RADONS^{1,3} — ¹Institute of Physics, Chemnitz University of Technology, 09107 Chemnitz, Germany — ²School of Mathematical Sciences, University of Adelaide, Adelaide, South Australia 5005, Australia — ³ICM - Institute for Mechanical and Industrial Engineering, 09117 Chemnitz, Germany

In finite-dimensional, chaotic, Lorenz-like wave-particle dynamical systems one can find diffusive trajectories, which share their appearance with that of laminar chaotic diffusion [Phys. Rev. Lett. 128, 074101 (2022)] known from delay systems with lag-time modulation. Applying, however, to such systems a test for laminar chaos, as proposed in [Phys. Rev. E 101, 032213 (2020)], these signals fail such test, thus leading to the notion of pseudo-laminar chaos. The latter can be interpreted as integrated periodically driven on-off intermittency. We demonstrate that, on a signal level, true laminar and pseudo-laminar chaos are hardly distinguishable in systems with and without dynamical noise. However, very pronounced differences become apparent when correlations of signals and increments are considered. We compare and contrast these properties of pseudo-laminar chaos with true laminar chaos.

Details can be found in the preprint [arXiv:2211.01278 (2022)].

DY 18.4 Tue 10:45 ZEU 147

Power-flow-based circuit synthesis of neuronal dynamics — •KARLHEINZ OCHS¹, SEBASTIAN JENDERNY¹, and PHILIPP HÖVEL² — ¹Ruhr-Universität Bochum, Germany — ²Christians-Albrechts-Universität zu Kiel, Germany

We present a modeling framework to study neuronal dynamics based on power-flow considerations. This is inspired by a circuit synthesis and analog electronics. Exemplified by the Hindmarsh-Rose model, we demonstrate that the proposed framework reproduces key characteristics of the dynamical model, including spiking and bursting behavior. This approach is a stepping stone towards the emulation of neuronal behavior on larger networks by means of analog circuits.

15 min. break

DY 18.5 Tue 11:15 ZEU 147

On the Correlation of Functionality and Lyapunov Stability in Oscillator-based Ising machines — •BAKR AL BEATTIE¹, MAXIMILIANE NOLL², HERMANN KOHLSTEDT², and KARLHEINZ OCHS¹ — ¹Ruhr-Universität Bochum, Lehrstuhl für digitale Kommunikationssysteme, Bochum, Deutschland — ²Christian-Albrechts-Universität zu Kiel, Lehrstuhl für Nanoelektronik, Kiel, Deutschland

Oscillator-based Ising machines are a promising analog approach for dealing with combinatorial optimization problems that are classified as NP (nondeterministic polynomial). The idea is to mimic the Ising model by coupling electrical oscillators that behave like the spins of the Ising model. Here, the coupling should somehow map the Ising Hamiltonian onto the energy of electrical system. With this contribution, we demonstrate numerical evidence demonstrating the correlation between the Ising machine's functionality and stability. We make use of the well-known Kuramoto model to describe a coupled oscillator network and show stability to be the key property that makes an Ising machine solve optimization problems. Furthermore, we give an answer to the question: when has an Ising machine finished solving a mapped problem?

DY 18.6 Tue 11:30 ZEU 147

Manifolds of equilibrium states in ensembles of globally coupled oscillators — •MICHAEL ZAKS — Humboldt Universität zu Berlin, Berlin, Germany

Global fields generated by ensembles of coupled oscillators are responsible for many unusual kinds of collective behavior. Among their most striking effects are existence of numerous constants of motion and a drastic reduction in the number of degrees of freedom. Here, we offer a simpler approach, restricted to the widespread situations in which the number of parameters defining the action of the global fields is smaller than the overall number of elements in the ensemble. In the phase space of such ensembles, high-dimensional manifolds composed of the equilibrium states can generically arise. Existence of these manifolds is not related to symmetries. In the simplest cases, such continua of steady states are attracting or repelling as a whole; in general, however, their stability with respect to transversal perturbations varies in the course of the motion along the manifold. Remarkably, the suggested mechanism does not require that all oscillators are identical: the sufficiently strong global field is able to counteract diversity among the ensemble units and halt the temporal evolution.

DY 18.7 Tue 11:45 ZEU 147

X-ray imaging of the sonoluminescent cavitation bubble collapse with single XFEL pulses — •HANNES PAUL HOEPE¹, ATIYEH AGHELMALEKI², JUAN MANUEL ROSSELLÓ³, MALTE VASSHOLZ¹, MARKUS OSTERHOFF¹, DANIEL SCHWARZ⁴, JOHANNES HAGEMANN⁴, ROBERT METTIN², ANDERS MADSEN⁵, and TIM SALDITT¹ — ¹Institute for X-ray Physics, Georg-August-University, Göttingen, Germany — ²Third Institute of Physics, Georg-August-University, Göttingen, Germany — ³Faculty of Mechanical Engineering, University of Ljubljana, Ljubljana, Slovenia — ⁴Center for X-ray and Nano Science, Deutsches Elektronen-Synchrotron DESY, Hamburg, Germany — ⁵European X-Ray Free-Electron Laser Facility, Schenefeld, Germany

We study the dynamics and in particular the collapse of a single cavitation bubble in water. A cavitation bubble is trapped and driven by an ultrasonic field leading to nonlinear radial oscillations. During its periodic collapses, extreme pressure and temperature is reached which can lead to the formation of a plasma

core and the emission of light. The fast evolving pressure, density and temperature distribution and the shape of the bubble during its collapse has so far only been accessible by simulations. Full-field X-ray phase contrast imaging provides quantitative information of the density distribution of the sample. Implemented at X-ray free-electron lasers, this enables the investigation of fast processes and extreme states of matter with a unique contrast. We present the evolution of the bubble's density profile during the sonoluminescent collapse and the current state of analysis.

DY 18.8 Tue 12:00 ZEU 147

Quantum synchronization in a network of dissipatively coupled linear oscillators — •JUAN MORENO¹, CHRISTOPHER W WÄCHTLER², and ALEXANDER EISFELD¹ — ¹Max Planck Institute for the Physics of Complex Systems, Dresden, Germany — ²Department of Physics, University of California Berkeley, CA, 94720-7300

Synchronization in classical systems has a long history and by now is a very well understood phenomenon. However, the question whether the classical notions of synchronization can be extended to the quantum regime has only recently been addressed in investigations of classically inspired models like quantum Van der Pol oscillators as well as models without classical analog. Inspired by the theoretical prediction that two-level atoms are able to synchronize even without interacting directly [1], we investigate a network of dissipatively coupled quantum harmonic oscillators. Within a mean-field approximation we find that the network is able to synchronize. For the fully quantum system described in terms of a Lindblad master equation we analyze various measures that have been proposed in the literature. Additionally, we investigate the Liouvillian spectrum in order to draw connections between the spectrum and the synchronization measures.

[1] PRA 101, 042121 (2020)

DY 19: Physics of Contagion Processes II (joint session SOE/DY)

Time: Tuesday 10:00–10:45

Location: ZEU 260

See SOE 6 for details of this session.

DY 20: Networks: From Topology to Dynamics I (joint session SOE/DY)

Time: Tuesday 11:00–12:15

Location: ZEU 260

See SOE 7 for details of this session.

DY 21: Quantum Chaos and Coherent Dynamics

Time: Tuesday 14:00–15:15

Location: MOL 213

DY 21.1 Tue 14:00 MOL 213

Bit-Flipping based on Stability Transition of Coupled Spins — •MAXIMILIAN F. I. KIELER and ARND BÄCKER — TU Dresden, Institut für Theoretische Physik, Dresden, Germany

A bipartite spin system is proposed for which a bit-flipping mechanism between two states is possible when the coupling is varied. The states correspond in the semiclassical limit to equilibrium points showing a stability transition from elliptic-elliptic stability to complex instability. Based on the classical system we find a universal scaling for the transfer time, which even applies in the deep quantum regime.

DY 21.2 Tue 14:15 MOL 213

New type of scarring in quantum chaotic scattering — •JAN ROBERT SCHMIDT and ROLAND KETZMERICK — TU Dresden, Institut für Theoretische Physik, Dresden, Germany

We study the three-disk scattering system, which is a paradigmatic example for quantum chaotic scattering. It is shown that any resonance state can be described by a product of a multifractal pattern of classical origin and universal, exponentially distributed fluctuations, as found for optical microcavities [1]. The first factor is determined by averaging resonance states with similar lifetime and is compared to an approximate conditionally-invariant measure from open chaotic maps [2]. A new type of scarring along ray segments, unrelated to periodic-orbit scarring, was recently observed in (partially open) optical microcavities [1]. Ray-segment scarring is just as well observed in the (fully open) three-disk system and has been overlooked for 30 years.

[1] R. Ketzmerick, K. Clauß, F. Fritzsche, and A. Bäcker, Phys. Rev. Lett. **129**, 193901 (2022).

[2] K. Clauß, M. J. Körber, A. Bäcker, and R. Ketzmerick, Phys. Rev. Lett. **121**, 074101 (2018).

DY 21.3 Tue 14:30 MOL 213

Manipulating light inside a microcavity with phase-space tailoring — YANJUN QIAN¹, HUI LIU¹, QI-TAO CAO¹, •JULIUS KULLIG², KEXIU RONG¹, CHENGWEI QIU³, JAN WIERSIG², QIHUANG GONG^{1,4}, JIANJUN CHEN⁵, and YUN-FENG XIAO^{1,4} — ¹Peking University, Beijing, China — ²Otto-von-Guericke-University Magdeburg, Magdeburg, Germany — ³National University of Singapore, Singapore, Singapore — ⁴Shanxi University, Taiyuan, China — ⁵Beijing Normal University, Beijing, China

We report on a novel powerful method for purposely manipulating light inside an optical microcavity. Via small absorptive, reflective or refractive elements embedded in the interior of the microcavity the photon transport is controlled in the phase space. Thus, phase-space tailoring allows for a spacial and temporal

control of the light confinement enabling a manipulation of the far-field emission pattern or the quality-factor.

DY 21.4 Tue 14:45 MOL 213

A spectral duality in graphs and microwave networks — •TOBIAS HOFMANN¹, JUNJIE LU², ULRICH KUHL^{1,2}, and HANS-JÜRGEN STÖCKMANN¹ — ¹Fachbereich Physik, Philipps-Universität Marburg, 35032 Marburg, Germany — ²Institut de Physique de Nice, CNRS, Université Côte d'Azur, 06108 Nice, France

Quantum graphs and their experimental counterparts, microwave networks, are ideally suited to study the spectral statistics of chaotic systems. The graph spectrum is obtained from the zeros of a secular determinant derived from energy and charge conservation. Depending on the boundary conditions at the vertices, there are Neumann and Dirichlet graphs. The first ones are realized in experiments, since the standard junctions connecting the bonds obey Neumann boundary conditions due to current conservation. On average, the corresponding Neumann and Dirichlet eigenvalues alternate as a function of the wave number, with the consequence that the Neumann spectrum is described by random matrix theory only locally, but adopts features of the interlacing Dirichlet spectrum for long-range correlations. Another spectral interlacing is found for the Green's function, which in contrast to the secular determinant is experimentally accessible. This is illustrated by microwave studies and numerics.

DY 21.5 Tue 15:00 MOL 213

Quantum Coherent Spin-Bath Dynamics and The Impact of Interactions on Quantum Memory Effects — •TOBIAS BOORMAN and BERND BRAUNECKER — University of St Andrews, St Andrews, United Kingdom

Using a robust theoretical framework, we systematically extract the joint-coherent dynamics of an impurity spin coupled to a strongly correlated material as the central process of a magnetic resonance. This framework enables a complete dynamical picture, extending beyond the usual high-temperature approximation that underpins the contemporary understanding of spin-bath decoherence, and allowing one to probe even further to the sub-thermal time regime, where quantum memory effects are the dominant feature. As a theoretically and experimentally accessible model of a strongly correlated conductor, we take the Luttinger liquid as a prototype to study how interactions alter the response of the bath to the impurity. Taken under the lens of the framework, we find that the joint quantum-coherent dynamics manifests itself as a rapid and seemingly instantaneous initial slip prior to the spin decoherence, whilst interactions within the bath play a role in modulating the amplitude and rate of this feature. We fit this understanding into a wider picture of magnetic resonance in interacting systems at intermediate temperatures, improving upon the known interaction-induced modifications of high-temperature approximations.

DY 22: Machine Learning in Dynamics and Statistical Physics II

Time: Tuesday 14:00–15:15

Location: ZEU 160

DY 22.1 Tue 14:00 ZEU 160

Reservoir Computing using Quantum Dot Lasers — •HUIFANG DONG, LINA JAURIGUE, and KATHY LÜDGE — Institute of Physik, Technische Universität Ilmenau, Weimarer Str. 32, 98684 Ilmenau, Germany.

Time-multiplexed reservoir computing is a machine-learning approach which is well suited for implementation using semiconductor lasers subject to optical feedback. In such a delay-based setup the feedback has two important roles; it directly influences the memory of the system and it generates the high dimensional transient dynamics needed for good computational performance [1]. However, commonly used and commercially available quantum well semiconductor lasers are dynamically very sensitive to optical feedback, which can make the implementation of such systems difficult. Implementation and on-chip integration of optical reservoir computing become feasible with quantum dot lasers, as they emit at the telecommunication wavelength and are less sensitive to unwanted reflections [2]. Using typical benchmark tasks for time series prediction we show that quantum dot lasers show good computing performance that can be further optimized by proper delay time tuning.

[1] T. Hülser, et al., *Opt. Mater. Express* 12, 3, 1214 (2022).

[2] C. Otto, et al., *Int. J. Bifurc. Chaos* 22, 10, 1250246 (2012).

DY 22.2 Tue 14:15 ZEU 160

Studying sequence property relationships with neural networks — •HUZAIFA SHABIR¹, JENS UWE SOMMER^{1,2}, and MARCO WERNER¹ — ¹Leibniz Institute for Polymer Research Dresden, Germany. — ²Technische Universität Dresden

In this work, we investigate the relationships between chemical sequence and property space for various sequence lengths with the help of neural networks (NN). Two different systems are investigated for this purpose: system I comprises copolymer sequences and their free energy of interaction with a lipid bilayer membrane. System II consists of metallic nanoparticle sequences and their plasmonic spectrum. We compare the performance of different neural network architectures such as feed-forward NNs and gated recurrent unit (GRU) networks in terms of their interpolation and extrapolation capacity between different sequence lengths. We show that the GRU is particularly suitable to transfer the learned patterns from smaller sequence lengths to enhance significantly the learning result for larger sequence lengths.

DY 22.3 Tue 14:30 ZEU 160

Modelling dynamic 3D-heat transfer for laser material processing using physics-informed neural networks (PINNs) — •MICHAEL MOECKEL and JORRIT VOIGT — TH Aschaffenburg, Würzburger Str. 45, 63743 Aschaffenburg

Machine learning (ML) algorithms are increasingly applied to fit complex models to empirical data and to predict on dynamical system behaviour. However, such models are not intrinsically protected from violating causality or other, well-understood physical laws. Black-box ML models offer limited interpretability. Extending ML models by including physical knowledge in the optimization procedure is known as physics-based and data-driven modelling. A promising recent development are physics informed neural networks (PINN), which en-

sure consistency to physical laws and measured data via appropriately designed optimization routines. Here we model the 3D time-dependent temperature profile following the passage of a laser focus at the surface of some material using PINNs. In this setting, we discuss aspects of numerically efficient training for PINNs, e.g. on a set of varying collocation points. The results from the PINN agree with finite element simulations, proving the suitability of the approach. The proposed models can be smoothly integrated in monitoring systems and naturally extend to the joint analysis of measurement data and dynamical behaviour encoded in governing equations.

DY 22.4 Tue 14:45 ZEU 160

Optical convolutional neural network with atomic nonlinearity — •MINGWEI YANG^{1,2}, ELIZABETH ROBERTSON^{1,2}, LUISA ESGUERRA^{1,2}, KURT BUSCH^{3,4}, and JANIK WOLTERS^{1,2} — ¹Deutsches Zentrum für Luft- und Raumfahrt, Institute of Optical Sensor Systems, Berlin, Germany. — ²Technische Universität Berlin, Berlin, Germany. — ³Humboldt-Universität zu Berlin, Institut für Physik, AG Theoretische Optik & Photonik, Berlin, Germany. — ⁴Max-Born-Institut, Berlin, Germany.

Due to their inherent parallelism, fast processing speeds and low energy consumption, free-space-optics implementations have been identified as an attractive possibility for analog computations of convolutions [1,2]. However, the efficient implementation of optical nonlinearities for such neural networks still remains challenging. In this work, we report on the realization and characterization of a three-layer optical convolutional neural network where the linear part is based on a 4f-imaging system and the optical nonlinearity is realized via the absorption profile of a cesium atomic vapor cell. This system classifies the handwritten digital dataset MNIST with 83.96% accuracy, which agrees well with corresponding simulations. [1] H. J. Caulfield and S. Dolev, *Why future supercomputing requires optics,* *Nat. Photonics* 4, 261*263 (2010). [2] M. Miscuglio, Z. Hu, S. Li, J. K. George, R. Capanna, H. Dalir, P. M. Bardet, P. Gupta, and V. J. Sorger, *Massively parallel amplitude-only fourier neural network,* *Optica* 7, 1812*1819 (2020).

DY 22.5 Tue 15:00 ZEU 160

Phase Diagram of the J_1 - J_2 Ising Model from Unsupervised Learning: Neural Networks vs Image Comparison — •BURAK ÇIVITCIOĞLU¹, ANDREAS HONECKER¹, and RUDOLF A. RÖMER² — ¹Laboratoire de Physique Théorique et Modélisation, CNRS UMR 8089, CY Cergy Paris Université, Cergy-Pontoise, France — ²Department of Physics, University of Warwick, Coventry, CV4 7AL, United Kingdom

Machine learning methods have been shown to be one of the novel approaches in identifying the phases and phase transitions in models of statistical physics. Here, we study the performance of unsupervised learning in the J_1 - J_2 Ising model. We benchmark the results for phase diagram reconstruction using variational autoencoders (VAEs) against straightforward image comparison. We show that such image comparison can result in accuracies that are akin to that of VAEs.

DY 23: Statistical Physics: General II

Time: Tuesday 14:00–15:15

Location: ZEU 250

DY 23.1 Tue 14:00 ZEU 250

Microscopic theory for the shear-induced structure distortion in concentrated suspensions of spherical colloids — •CARMINE ANZIVINO¹, FRANCESCO LEONE¹, LUCA BANETTA², MICHAEL S. MURILLO³, and ALESSIO ZACCONE¹ — ¹Department of Physics "A. Pontremoli", University of Milan, via Celoria 16, 20133 Milan, Italy — ²Department of Applied Science and Technology, Politecnico di Torino, Corso Duca degli Abruzzi 24, 10129, Turin, Italy — ³Department of Computational Mathematics, Science and Engineering, Michigan State University, East Lansing, Michigan 48824, USA

We combine an analytical solution of the Smoluchowski convection-diffusion equation that fully takes into account the boundary-layer structure, with generalized integral equations of the liquid state. We investigate the shear-induced structural distortion in suspensions of spherical colloids, in concentrated regimes of packing fraction so far explored only by means of numerical simulations [1].

For hard spheres, our findings are in very good parameter-free agreement with numerical data from literature [2]. In addition, our scheme predicts (for the first time) a consistent enhancement of the structure factor $S(k)$ at vanishing k , upon increasing the shear rate, which we argue may signal the onset of a shear-induced phase transition from the isotropic phase to a non-uniform one.

[1] L. Banetta, F. Leone, C. Anzivino, M.S. Murillo and A. Zaccone, *Phys. Rev. E* 106, 044610 (2022). [2] J.F. Morris and B. Katyal, *Physics of Fluids* 14, 1920 (2002).

DY 23.2 Tue 14:15 ZEU 250

Coupling of a particle-based solver to a fluctuating hydrodynamic reservoir through an adaptive resolution simulation approach — •ABBAS GHOLAMI², RUPERT KLEIN¹, and LUIGI DELLE SITE¹ — ¹Freie Universität Berlin, Berlin, Germany — ²Max Planck Institute for Polymer Research, Mainz, Germany

Adaptive Resolution Simulation (AdResS) is a multi-resolution approach for coupling different particle-based regions. In AdResS, a fully atomistic subregion (open system) is in contact with reservoirs of non-interacting particles through a small buffer region. In this approach, a thermostat and an external (thermodynamic) force are applied in the reservoir and buffer regions to ensure the same behaviour as the reference simulation. Coupling a particle-based domain with a continuum reservoir will significantly reduce computational costs while preserving satisfactory precision in different regions.

This work uses a novel algorithm to couple the AdResS particle-based simulator to a Navier-Stokes Landau-Lifshitz solver. The coupling algorithm suggests that the proper thermodynamic force for the AdResS simulation will be interpolated among a set of pre-calculated thermodynamic forces based on the resulting

continuum state at the interface region. On the other hand, to pass the information from the particle side to the continuum reservoir, the result of the AdResS simulation will apply to the corresponding continuum cells with proper interface values. The accuracy of this coupling algorithm is demonstrated through various numerical scenarios with different initial conditions.

DY 23.3 Tue 14:30 ZEU 250

The orientation field generated by a moving defect: multivalued solutions of the diffusion equation — •JACOPO ROMANO, BENOIT MAHAULT, and RAMIN GOLESTANIAN — Max Planck Institute for Dynamics and Self-Organization

Point-like topological defects are singular configurations that occur in a variety of in and out of equilibrium systems with two-dimensional orientational order. As they are associated with a nonzero circulation condition, the presence of defects induces a long-range perturbation of the orientation landscape around them. Their effective dynamics is thus generally described in terms of quasi-particles interacting through the orientation field they produce, which in the simplest setting is described by the diffusion equation. Due to the multivaluedness of the orientation field, its expression for a defect moving with an arbitrary trajectory cannot be obtained via simple techniques and is often approximated by that of a static defect. Here, we propose a solution to this problem that relies on particular gauge invariance properties of the proper multivalued field derivatives. Our approach allows to derive the exact expression for the orientation created by multiple moving defects, which we find to depend on their past trajectories and thus to be nonlocal in time. Performing various expansions in relevant regimes, we show how improved approximations with respect to the static defect solution can be obtained. Moreover, our results lead to so far unnoticed structures in the orientation field of moving defects which we discuss in light of existing experimental results.

DY 23.4 Tue 14:45 ZEU 250

Perturbative and Semiclassical Expansions in Quantum Thermodynamics Using a Modified Keldysh Contour — •SADEQ S. KADIJANI, VASCO CAVINA, MASSIMILIANO ESPOSITO, and THOMAS L. SCHMIDT — Department of Physics and Materials Science, University of Luxembourg, L-1511 Luxembourg, Luxembourg

Modified Keldysh contours are a versatile tool for calculating moment generating functions (MGFs) in the context of quantum thermodynamics and quantum transport theory, and are the backbone of both Green's functions (GFs) and path

integral approaches to open quantum systems. By using a different modification of the Keldysh contour, we will construct a perturbation expansion of the MGFs and discuss its semi-classical expansion. Using the symmetry property of the modified contour, we prove that the perturbative expansion obtained in this way satisfies the fluctuation theorem (FT) in every order of perturbation theory. We show that the contribution of the different diagrams can be added to obtain a general expression of the work statistics in terms of a sum of independent Poisson processes.

To further investigate the work MGF we apply the Feynman path integral techniques to the modified contour. In this way, the MGF can be written in terms of the action, which depends on the fields running on the modified contour. The action can be used to obtain a semiclassical expansion of the MGF, which is then used to compute explicitly the zeroth (classical) and the first quantum correction to the work MGF.

DY 23.5 Tue 15:00 ZEU 250

Effect of Frequency-Dependent Viscosity on Molecular Friction in Liquids — •HENRIK KIEFER¹, DOMENICO VITALI², BENJAMIN DALTON³, LAURA SCALFI⁴, and ROLAND NETZ⁵ — ¹Freie Universität Berlin, Department of Physics, Berlin, Germany — ²Freie Universität Berlin, Department of Physics, Berlin, Germany — ³Freie Universität Berlin, Department of Physics, Berlin, Germany — ⁴Freie Universität Berlin, Department of Physics, Berlin, Germany — ⁵Freie Universität Berlin, Department of Physics, Berlin, Germany

A fundamental problem in molecular dynamics is the relation between the frequency-dependent friction of a molecule in a liquid and the hydrodynamic properties of the liquid. We investigate this connection in the case of a water molecule moving in liquid water using all-atomistic molecular dynamics simulations and linear hydrodynamic theory. For this, we analytically calculate the frequency-dependent friction of a sphere with finite surface slip moving in a non-Newtonian compressible fluid by solving the linear transient Stokes equation, including frequency-dependent shear and volume viscosities, which are both determined from MD simulations of bulk liquid water. By fitting the effective sphere radius and the slip length, the frequency-dependent friction and velocity autocorrelation function from the transient Stokes equation and simulations quantitatively agree with the frequency-dependent friction of a single water molecule moving in liquid water, as defined by the generalized Langevin equation from MD simulation trajectories, provided accurate frequency-dependent viscosities are used.

DY 24: Glasses and Glass Transition (joint session DY/ CPP)

Time: Tuesday 14:00–15:00

Location: ZEU 147

DY 24.1 Tue 14:00 ZEU 147

Dynamical phase transitions in trap models and universality classes of aging — •DIEGO TAPIAS¹ and PETER SOLLICH^{1,2} — ¹Institute for Theoretical Physics, University of Göttingen, Germany — ²Department of Mathematics, King's College London, London, UK

We investigate how aging and driving by trajectory biasing interact in two mean field models of glassy dynamics, widely known as trap models. We show that similarly to kinetically constrained models, the equilibrium state of the unbiased system above the glass transition temperature is located at the coexistence of two dynamical phases (active and inactive). In contrast, below this temperature, we find two different nonequilibrium scenarios: energetic (or activated) aging that is destroyed by any dynamical bias towards low activity, which we call “fragile aging”, and entropic aging that is stable against the existence of such a dynamical bias, which we refer to as “robust aging”. We conjecture that these categories have broader relevance as universality classes for aging dynamics in glassy systems.

DY 24.2 Tue 14:15 ZEU 147

Fragile to strong crossover as general glassy feature — •ANSHUL DEEP SINGH PARMAR and ANDREAS HEUER — Institute of Physical Chemistry, University of Münster, Corrensstrasse 28/30, 48149 Münster, Germany

As a liquid is cooled below the melting temperature, the dynamics become increasingly sluggish with the degree of supercooling, known as fragility. The fundamental question is whether the liquid ceases to flow at some finite temperature, the material undergoing the glass transition, or dynamics diverge smoothly to zero temperature. This is a central question of pivotal importance for unraveling the nature of glass and theoretical understanding, concealing with astronomical long observation times.

We circumvent this infeasibility by taking advantage of swap Monte Carlo with multi-billion speedups for equilibration well beyond the glass transition. Our investigation of a wide range of system sizes and temperatures across the experimental glass transition unveils the nature of the energy landscape. We observe a notable deviation from the Gaussian nature of the potential-energy landscape. Rapid depletion of states is associated with the glassy bottom of the landscape,

unveiling the fragile to strong crossover is the general glassy behavior. Our result ultimately rules out the finite-temperature divergence and establishes the conceptualized Arrhenius description of the dynamics at low temperatures. Our findings are critical in advancing the investigation of glass in an experimental and theoretical framework.

DY 24.3 Tue 14:30 ZEU 147

A solution to the plasticity of glasses based on topological physics — •ALESSIO ZACCONE — Department of Physics, University of Milan, 20133 Milano, Italy

I will start by reviewing the microscopic theory of linear elasticity in amorphous solids which, from first-principles consideration of non-centrosymmetry in the particle contact environment, leads to mathematical predictions of elastic moduli in quantitative parameter-free agreement with numerical simulations of random jammed packings [1]. This theory fully accounts for the extra non-affine displacements which arise due to the lack of centrosymmetry in disordered solids. I will then show that non-affinity of particle motions gives rise to well-defined topological defects (dislocation-like topological defects, DTDs) which have recently been discovered in the displacement field of glasses [1] and later confirmed in [2]. The norm of the associated Burgers vector of these defects can be used as an accurate predictor of the onset of plastic flow and yielding of glasses, and, in combination with Schmid's law, it can explain the phenomenon of shear banding via self-organization of DTDs in slip systems at 45 degrees with respect to flow direction [4]. Broader implications of a unifying topological field theory of liquids and the glass transition will also be mentioned. [1] A. Zaccone and E. Scossa-Romano, Phys. Rev. B 83, 184205 (2011) [2] Z. W. Wu, Y. Chen, W.-H. Wang, W. Kob, L. Xu, arXiv:2209.02937 (2022)

DY 24.4 Tue 14:45 ZEU 147

Confinement induced relaxations and phase behavior of a nanoconfined ionic liquid crystal — •MOHAMED AEJAZ KOLMANGADI¹, ANDREAS SCHÖNHALS¹, LI ZHUOQING², and PATRICK HUBER² — ¹Bundesantalt für Materialforschung und -prüfung (BAM), Berlin, Germany — ²Technical University Hamburg TUHH and DESY

We investigate the molecular dynamics and electrical conductivity of a linear shaped guanidinium based ILC confined in self-ordered nano porous alumina

oxide membranes of pore size ranging from 180nm down to 25nm by employing broadband dielectric spectroscopy (BDS) and calorimetry. Calorimetric investigation reveals a complete suppression of the columnar - isotropic transition, while the plastic crystalline - columnar transition temperature decreases with inverse pore size and deviates from the Gibbs - Thomson equation. For the bulk case, BDS detects two relaxation modes in the crystalline phase, the gamma relaxation and the α_1 relaxation, and two relaxation modes in the columnar phase, the α_2 and α_3 relaxation. For the confined case, all relaxation modes slow down

compared to the bulk. However, for the least pore size (25 nm), the α_2 relaxation is absent. We discuss the possible molecular origins of the different relaxation modes observed. For the bulk ILC, a clear jump of 4 orders of magnitude in the absolute values of DC conductivity occurs at the transition from the plastic crystalline to hexagonal columnar phase, for the confined ILC, this transition is smooth. DC conductivity is reduced for the confined case, except for the 25nm, where the values is similar to the bulk.

DY 25: Many-Body Quantum Dynamics (joint session DY/TT)

Time: Wednesday 9:30–13:00

Location: MOL 213

Invited Talk

DY 25.1 Wed 9:30 MOL 213

Many-body localization from Hilbert- and real-space points of view — •IVAN KHAYMOVICH¹, GIUSEPPE DE TOMASI², FRANK POLLMANN³, and SIMONE WARZEL³ — ¹Nordic Institute for Theoretical Physics, Stockholm, Sweden — ²University of Illinois Urbana-Champaign, USA — ³Technical University Munich, Germany

Many-body localization (MBL), known as a generic mechanism to break quantum ergodicity, has been recently shown to be not the Hilbert-space Anderson localization. Instead, the MBL eigenstate occupies a fractal support [1-2], with extensive number of configurations. On the other hand, the well-established and accepted by the community picture of an emergent set of local integrals of motion [3] provides the structure of the MBL in the real space.

In this talk, I will provide the observable (later measured in the experiment [4]) which combines the fractality in the Hilbert space with the presence of local integrals of motion [2]. This observable, being the radial profile of the eigenstate over the Hamming distance, keeps the information about both the Hilbert-space fractal dimensions and the real-space localization lengths and uncovers the structure of these measures across the MBL transition. Phenomenological picture behind this behavior is consistent with the Kosterlitz-Thouless scenario of the MBL transition, suggested in the literature.

Literature: [1] N. Macé et al., PRL 123, 180601 (2019). [2] G. De Tomasi, I. M. Khaymovich et al. PRB 104, 024202 (2021). [3] Abanin et al., RMP 91, 021001 (2019). [4] Y. Yao et al arXiv:2211.05803.

DY 25.2 Wed 10:00 MOL 213

Bridging classical and quantum many-body information dynamics — •ANDREA PIZZI^{1,2}, DANIEL MALZ^{3,4}, ANDREAS NUNNENKAMP⁵, and JOHANNES KNOLLE^{6,4,7} — ¹Department of Physics, Harvard University, Cambridge 02138, Massachusetts, USA — ²Cavendish Laboratory, University of Cambridge, Cambridge CB3 0HE, United Kingdom — ³Max-Planck-Institute of Quantum Optics, Hans-Kopfermann-Str. 1, 85748 Garching, Germany — ⁴Munich Center for Quantum Science and Technology (MCQST), 80799 Munich, Germany — ⁵Faculty of Physics, University of Vienna, Boltzmanngasse 5, 1190 Vienna, Austria — ⁶Department of Physics, Technische Universität München, James-Frank-Str. 1, 85748 Garching, Germany — ⁷Blackett Laboratory, Imperial College London, London SW7 2AZ, United Kingdom

The fundamental question of how information spreads in closed quantum many-body systems is often addressed through the lens of the bipartite entanglement entropy. Among its most striking features are unbounded linear growth in the thermodynamic limit, asymptotic extensivity in finite-size systems, and measurement-induced phase transitions. Here, we show that these key qualitative features emerge naturally also for the classical bipartite mutual information, the natural classical analogue of the quantum entanglement entropy. Key for this observation is treating the classical many-body problem on par with the quantum one, that is, explicitly accounting for the exponentially large probability distribution. Our analysis is supported by extensive numerics on prototypical cellular automata and Hamiltonian systems.

DY 25.3 Wed 10:15 MOL 213

Performance boost of a collective qutrit refrigerator — •DMYTRO KOLISNYK¹ and GERNOT SCHALLER² — ¹Jacobs University Bremen, Campus Ring 1, 28759 Bremen, Germany — ²Helmholtz-Zentrum Dresden-Rossendorf, Bautzner Landstraße 400, 01328 Dresden, Germany

A single qutrit with transitions selectively driven by weakly-coupled reservoirs can implement one of the world's smallest refrigerators. We analyze the performance of N such fridges that are collectively coupled to the reservoirs. We observe a quantum boost, manifest in a quadratic scaling of the steady-state cooling current with N . As N grows further, the scaling reduces to linear, since the transitions responsible for the quantum boost become energetically unfavorable. Fine-tuned inter-qutrit interactions may be used to maintain the quantum boost for all N and also for not-perfectly collective scenarios.

[1] D. Kolisnyk and G. Schaller, Performance boost of a collective qutrit refrigerator, arXiv:2210.07844.

[2] M. Kloc, K. Meier, K. Hadjikyriakos, and G. Schaller, Superradiant Many-

Qubit Absorption Refrigerator, Phys. Rev. Applied 16, 044061 (2021).

[3] N. Linden, S. Popescu, and P. Skrzypczyk. How small can thermal machines be? The smallest possible refrigerator. Phys. Rev. Lett. 105:130401, 2010.

DY 25.4 Wed 10:30 MOL 213

Hidden Phase of the Spin-Boson Model — •FLORIAN OTTERPOHL^{1,2}, PETER NALBACH³, and MICHAEL THORWART^{2,4} — ¹Center for Computational Quantum Physics, Flatiron Institute, New York, New York 10010, USA — ²Institut für Theoretische Physik, Universität Hamburg, Notkestraße 9, 22607 Hamburg, Germany — ³Fachbereich Wirtschaft und Informationstechnik, Westfälische Hochschule, Münsterstraße 265 46397 Bocholt, Germany — ⁴The Hamburg Centre for Ultrafast Imaging, Luruper Chaussee 149, 22761 Hamburg, Germany

A quantum two-level system immersed in a sub-Ohmic bath experiences enhanced low-frequency quantum statistical fluctuations which render the nonequilibrium quantum dynamics highly non-Markovian. Upon using the numerically exact time-evolving matrix product operator approach, we investigate the phase diagram of the polarization dynamics. In addition to the known phases of damped coherent oscillatory dynamics and overdamped decay, we identify a new third region in the phase diagram for strong coupling showing an aperiodic behavior. We determine the corresponding phase boundaries. The dynamics of the quantum two-state system herein is not coherent by itself but slaved to the oscillatory bath dynamics.

DY 25.5 Wed 10:45 MOL 213

Exploring anomalies by many-body correlations — •KLAUS MORAWETZ — Münster University of Applied Sciences, Stegerwaldstrasse 39, 48565 Steinfurt, Germany — International Institute of Physics- UFRN, Campus Universitário Lagoa nova, 59078-970 Natal, Brazil

The quantum anomaly can be written alternatively into a form violating conservation laws or as non-gauge invariant currents seen explicitly on the example of chiral anomaly. By reinterpreting the many-body averaging, the connection to Pauli-Villars regularization is established which gives the anomalous term a new interpretation as arising from quantum fluctuations by many-body correlations at short distances. This is exemplified by using an effective many-body quantum potential which realizes quantum Slater sums by classical calculations. It is shown that these quantum potentials avoid the quantum anomaly but approaches the same anomalous result by many-body correlations. A measure for the quality of quantum potentials is suggested to describe these quantum fluctuations in the mean energy. Consequently quantum anomalies might be a short-cut way of single-particle field theory to account for many-body effects. This conjecture is also supported since the chiral anomaly can be derived by a completely conserving quantum kinetic theory. [Eur. Phys. J. B 92 (2019) 176, Phys. Lett. A 383 (2019) 1362, Phys. Status Solidi B (2021) 2100316]

DY 25.6 Wed 11:00 MOL 213

Non-Markovian Stochastic Schrödinger Equation: Matrix Product State Approach to the Hierarchy of Pure States — XING GAO¹, JIAJUN REN², ZHIGANG SHUAI², and •ALEXANDER EISFELD³ — ¹Sun Yat-sen University, Shenzhen, Guangdong, China — ²Tsinghua University, Beijing, China — ³MPI-PKS, Dresden

We derive a stochastic hierarchy of matrix product states (HOMPS) for non-Markovian dynamics in open quantum system at finite temperature, which is numerically exact and efficient. HOMPS is obtained from the stochastic hierarchy of pure states (HOPS) by expressing HOPS in terms of formal creation and annihilation operators. The resulting stochastic first order differential equation is then formulated in terms of matrix product states and matrix product operators. In this way the exponential complexity of HOPS can be reduced to scale polynomial with the number of particles. The validity and efficiency of HOMPS is demonstrated for the spin-boson model and long chains where each site is coupled to a structured, strongly non-Markovian environment.

[1] X. Gao, J. Ren, A. Eisfeld, Z. Shuai, Phys. Rev. A 105, L030202 (2022)

DY 25.7 Wed 11:15 MOL 213

ultrafast gap dynamics near the zone boundary in a cuprate superconductor — •QINDA GUO, MACIEJ DENDZIK, MAGNUS BERNTSEN, CONG LI, WANYU CHEN, YANG WANG, DIBYA PHUYAL, and OSCAR TJERNBERG — Department of Applied Physics, KTH Royal Institute of Technology, Hannes Alfvéns väg 12, 114 19 Stockholm, Sweden

The time- and angle- resolved photoemission spectroscopy (tr-ARPES) is a powerful technique to directly probe the ultrafast electron dynamics in the momentum space. Our recently developed narrow-bandwidth tr-ARPES setup enabled us to access the ultrafast dynamics of the quasiparticle population as well as the superconducting gap, in the whole surface Brillouin zone of the photoexcited cuprate superconductor (Bi2212). The results show non-trivial dynamics at the d-wave antinode and provide new insights into the enigma of the Cooper-pair formation process and condensation that takes place in the high-temperature cuprate superconductor.

15 min. break

DY 25.8 Wed 11:45 MOL 213

Controlling Many-Body Quantum Chaos — •LUKAS BERINGER¹, STEVEN TOMSOVIC^{1,2}, JUAN DIEGO URBINA¹, and KLAUS RICHTER¹ — ¹Institut für Theoretische Physik, Universität Regensburg, D-93040 Regensburg, Germany — ²Department of Physics and Astronomy, Washington State University, Pullman, WA USA

Targeting in classical chaos control problems makes optimal use of the system's exponential instabilities to direct a given initial state to a predetermined final target state. A generalization to chaotic quantum systems in the semiclassical regime is possible [1], but also requires controlling an initially localized evolving quantum state's spreading. A coherent procedure of this kind enables directing highly excited, far-out-of-equilibrium states from an initial to some final target quantum state. Such methods have been successfully developed and applied to initially minimum uncertainty wave packets in a quantum kicked rotor system. The aim of our work is to extend those procedures to bosonic many-body systems. More specifically, we demonstrate how to make a localized quantum initial state follow special chaotic mean-field solutions of a Bose-Hubbard system toward an arbitrary localized target final state.

[1] S. Tomsovic, J. D. Urbina, and Klaus Richter, Controlling Quantum Chaos: Optimal Coherent Targeting, arXiv:2211.07408

DY 25.9 Wed 12:00 MOL 213

Environment-induced decay dynamics of antiferromagnetic order in Mott-Hubbard systems — •GERNOT SCHALLER¹, FRIEDEMANN QUEISSER^{1,2}, NIKODEM SZPAK³, JÜRGEN KÖNIG³, and RALF SCHÜTZHOLD^{1,2} — ¹Helmholtz-Zentrum Dresden-Rossendorf, Bautzner Landstraße 400, 01328 Dresden, Germany — ²Institut für Theoretische Physik, Technische Universität Dresden, 01062 Dresden, Germany — ³Fakultät für Physik and CENIDE, Universität Duisburg-Essen, Lotharstraße 1, 47057 Duisburg, Germany

We study the dissipative Fermi-Hubbard model in the limit of weak tunneling and strong repulsive interactions, where each lattice site is tunnel-coupled to a Markovian fermionic bath. For cold baths at intermediate chemical potentials, the Mott insulator property remains stable and we find a fast relaxation of the particle number towards half filling. On longer time scales, we find that the antiferromagnetic order of the Mott-Néel ground state on bipartite lattices decays, even at zero temperature. For zero and nonzero temperatures, we quantify the different relaxation time scales by means of waiting time distributions, which

can be derived from an effective (non-Hermitian) Hamiltonian and obtain fully analytic expressions for the Fermi-Hubbard model on a tetramer ring.

[1] G. Schaller *et al.*, Phys. Rev. B **105**, 115139 (2022).

DY 25.10 Wed 12:15 MOL 213

Arrow of time concept based on properties of Lanczos coefficients — •CHRISTIAN BARTSCH, MATS H. LAMANN, ROBIN HEVELING, LARS KNIPSCHILD, JIAOZI WANG, ROBIN STEINIGEWEG, and JOCHEN GEMMER — Fachbereich Physik, Universität Osnabrück, Barbarastraße 7, DE-49076 Osnabrück

We introduce an arrow of time concept based on a specifically defined class of arrow of time functions (ATF) consisting of a limited number of Krylov space generating observables. These ATF'S are found to be essentially monotonously decaying in time which is measured by some quantifying parameter. The ATF'S are constructed to be upper bounds for pertinent autocorrelation functions. Employing certain features of the Lanczos coefficients and the wave package-like excitation moving on the Krylov chain, we find reasonable agreement with corresponding numerics.

DY 25.11 Wed 12:30 MOL 213

Fast Time-Evolution of Matrix-Product States using the QR decomposition — •JAKOB UNFRIED^{1,2}, JOHANNES HAUSCHILD¹, and FRANK POLLMANN^{1,2} — ¹Department of Physics, TFK, Technische Universität München, James-Frank-Straße 1, D-85748 Garching, Germany — ²Munich Center for Quantum Science and Technology (MCQST), Schellingstr. 4, 80799 München, Germany

Numerical simulations of quantum many-body dynamics in and out of equilibrium is essential for the understanding of a wide range of physical phenomena. Efficient matrix product state simulation techniques, such as time evolution block decimation (TEBD), are widely successful in extracting experimentally relevant signatures, such as dynamical correlation functions. We propose and benchmark a modified TEBD algorithm that uses a truncation scheme based on the QR decomposition instead of the singular value decomposition (SVD). The modification reduces the scaling with the dimension of the physical Hilbert space d from d^3 down to d^2 . Unlike the SVD, the QR decomposition allows for highly efficient implementations on GPU hardware. In a benchmark simulation of a global quench in a quantum clock model, we observe a speedup of orders of magnitude comparing the QR based scheme on a GPU to the SVD based TEBD on CPU.

DY 25.12 Wed 12:45 MOL 213

Simulating infinite temperature spin dynamics by a dynamic mean-field theory — •TIMO GRÄSSER¹, KRISTINE REZAI², ALEXANDER O. SUSHKOV², and GÖTZ S. UHRIG¹ — ¹Condensed Matter Theory, TU Dortmund University, Otto-Hahn Straße 4, 44221 Dortmund, Germany — ²Department of Physics, Boston University, Boston, MA 02215, USA

We develop a dynamic mean-field theory for spin systems at infinite temperature (spinDMFT) [1]. The idea is to replace the large environment of a spin by a dynamic mean-field which displays a random Gaussian temporal evolution. Its autocorrelations are self-consistently linked to the quantum mechanic expectation values of spin-spin correlations. This approach becomes exact in the limit of large lattice coordination numbers. We improve the approach by considering spin clusters quantum-mechanically (cluster spinDMFT). The extended model is able to describe dynamic spin correlations measured in recent experiments [2] where an inhomogeneous spin- $\frac{1}{2}$ ensemble on a diamond surface is probed using nitrogen-vacancy centers as sensors.

[1] T. Gräßer *et al.*, Phys. Rev. Research **3**, 043168 (2021).

[2] K. Rezaei *et al.*, arXiv:2207.10688 (2022).

DY 26: Focus Session: From Inter-individual Variability to Heterogeneous Group Dynamics and Disorder in Active Matter (joint session DY/BP/CP)

The study of active particle dynamics has developed into a vibrant field of multidisciplinary research, including such diverse systems as bacterial colonies, cellular self-organization, synthetic colloids and microrobots as well as macroscopic systems like locusts, flocks of birds, schools of fish or pedestrians. Whereas many studies in the past focused either on the random transport of individual particles or on the interplay of temporal fluctuations (noise) and interactions (velocity alignment or attraction/repulsion), there is now an increasing interest in the question how structural disorder and inter-individual variability, i.e., different motility characteristics of individuals, shape the active particle dynamics and emergent pattern formation of groups. The presence of structural or quenched disorder raises furthermore the immediate question how to bridge data and models based on (short time) tracking data, given the simultaneous presence of temporal fluctuations. With this focus session, we aim at bringing researchers from statistical physics and biophysics together to discuss this interdisciplinary topic and exchange ideas on common challenges arising in different application areas.

Organized by Robert Großmann (Potsdam)

Time: Wednesday 9:30–13:00

Location: ZEU 160

Invited Talk DY 26.1 Wed 9:30 ZEU 160

More is different: High-throughput 3D tracking reveals bacterial navigation strategies — •KATJA TAUTE — Rowland Institute at Harvard, Harvard University, Cambridge, MA, USA — Department of Biology, Microbiology, LMU München, 82152 Martinsried, Germany

How microbes navigate environmental chemical gradients has implications that range from health to climate. The behavioral mechanisms underlying chemotaxis are unknown for most species because of a lack of techniques capable of bridging scales from individual navigation behavior to the resulting population-level performance. We present a multiscale 3D chemotaxis assay that combines high-throughput 3D bacterial tracking with microfluidically created chemical gradients. Large datasets of 3D trajectories yield the statistical power required to assess chemotactic performance at the population scale, while simultaneously resolving the underlying 3D navigation behavior for every individual. Applying this technique to the well-studied model bacterium *Escherichia coli*, we uncover dramatic, previously unknown heterogeneity in chemotactic performance. We investigate the underlying behavioral mechanisms and discuss potential implications at the population level.

Invited Talk DY 26.2 Wed 10:00 ZEU 160

Variability and heterogeneity in natural swarms — •GIL ARIEL — Bar Ilan University, Ramat Gan, Israel

Collective motion of large-scale natural swarms, such as moving animal groups or expanding bacterial colonies, have been described as self-organized phenomena. Thus, it is clear that the observed macroscopic, coarse-grained swarm dynamics depend on the properties of the individuals of which it is composed. In nature, individuals are never identical, and may differ in practically every parameter. Hence, intra-group variability and its effect on the ability to form coordinated motion is of interest, both from theoretical and a biological points of view. In this talk, I will review and examine some of the fundamental properties of heterogeneous collectives in nature, with an emphasis on two widely-used model organisms - swarming bacteria and locusts. Theoretical attempts to explain the observed phenomena will be discussed in view of laboratory experiments, highlighting their successes and failures. While heterogeneity typically discourages collectivity, there are several natural examples where it has an opposite effect.

Effect of individual differences on the jamming transition in traffic flow —

•YI-CHIEH LAI and KUO-AN WU — Department of Physics, National Tsing Hua University, 30013 Hsinchu, Taiwan

The individual difference, particularly in drivers' distance perception, is introduced in the microscopic one-dimensional optimal velocity model to investigate its effect on the onset of the jamming instability seen in traffic systems. We show analytically and numerically that the individual difference helps to inhibit the traffic jam at high vehicle densities while it promotes jamming transition at low vehicle densities. In addition, the jamming mechanism is further investigated by tracking how the spatial disturbance travels through traffics. We find that the jamming instability is uniquely determined by the overall distribution of drivers' distance perception rather than the spatial ordering of vehicles. Finally, a generalized form of the optimal velocity function is considered to show the universality of the effect of the individual difference.

Distinct impacts of polar and nematic self-propulsion on active unjamming —

VARUN VENKATESH¹, •CHANDANA MONDAL², and AMIN DOOSTMOHAMMADI¹ — ¹Niels Bohr Institute, University of Copenhagen, Blegdamsvej 17, 2100 Copenhagen, Denmark — ²UGC-DAE CSR, University Campus, Khandwa Road, Indore 452017, India

We explore, by MD simulations, the jamming-unjamming transition in a dense system of active semiflexible filaments. In particular, we characterize the distinct impact of polar vs nematic driving for different filament rigidities and at varying densities. Our results show that high densities of dynamic active filaments can be achieved by only changing the nature of the active force, nematic or polar. Interestingly, while polar driving is more effective at unjamming the system at high densities below confluency, we find that at even higher densities, nematic driving enhances unjamming compared to its polar counterpart. The effect of varying the rigidity of filaments is also significantly different in the two cases: While for nematic driving, lowering the bending rigidity unjams the system, we find an intriguing reentrant jamming-unjamming-jamming transition for polar driving as the filament rigidity is lowered. While the first transition (unjamming) is driven by softening due to reduced rigidity, the second transition (jamming) is a cooperative effect of ordering and coincides with the emergence of nematic order in the system. Together, through a generic model of self-propelled flexible filaments, our results demonstrate how tuning the nature of self-propulsion and flexibility can be employed by active materials to achieve high densities without getting jammed.

15 min. break

Invited Talk DY 26.5 Wed 11:15 ZEU 160

Superstatistical Analysis and Modelling of Complex Dynamical Systems — •CLAUS METZNER^{1,2}, CHRISTOPH MARK², BEN FABRY², PATRICK KRAUSS¹, ACHIM SCHILLING¹, MAXIMILIAN TRAXDORF³, and HOLGER SCHULZE¹ — ¹Neuroscience Lab, University Hospital Erlangen, Germany — ²Biophysics Lab, Friedrich-Alexander Universität Erlangen-Nürnberg — ³Department of Otorhinolaryngology, Head and Neck Surgery, Paracelsus Medical University, Nuremberg, Germany

On longer time scales, complex systems often pass through different dynamical attractors and thus produce 'anomalous' distributions and correlations when analyzed with conventional statistical tools. We argue that the most appropriate way of describing such systems is by hierarchical multilevel models, in which the lowest level is a relatively simple random walk model that can generate the observed time series on short time scales, but which depends on latent hyperparameters that are themselves time-dependent and controlled by the higher levels of the model. First, our Bayesian method is introduced for the sequential inference of those gradual or abrupt parameter changes. We then review possible applications of the superstatistical framework in such diverse fields as biophysics, neuroscience, finance, or policy assessment. Finally, we discuss more recent extensions of the method for model selection and the use of machine learning models for estimating complex likelihood functions.

How to infer parameter distributions in heterogeneous populations of active particles —

•JAN ALBRECHT¹, ROBERT GROSSMANN¹, and MANFRED OPPER^{2,3} — ¹Institute of Physics and Astronomy, University of Potsdam, 14476 Potsdam, Germany — ²TU Berlin, Fakultät IV-MAR 4-2, Marchstraße 23, 10587 Berlin, Germany — ³Centre for Systems Modelling and Quantitative Biomedicine, University of Birmingham, B15 2TT, United Kingdom

Experiments with active particles, e.g., motile microorganisms like bacteria or amoebae, provide information about their position at discrete points in time. However, most active particle models, like active Ornstein-Uhlenbeck particles for example, are commonly described by first order stochastic differential equations for the velocity or force. This leads to a second order model in position posing challenges for parameter inference, because there is no general way to obtain a closed form expression for the likelihood of the parameters in terms of

those time-sampled trajectories. This would be needed to apply efficient Bayesian parameter estimation techniques. In this talk, we propose a filtering-like sequential method to address this problem. The likelihood is first expressed in terms of integrals over transition probabilities. Approximating the transition probability for small times makes these integrals analytically feasible, leading to a likelihood approximation that allows consistent parameter inference. Using a Bayesian approach, we furthermore show how to extend this framework to estimate the entire distribution of motility parameters in heterogeneous populations of particles efficiently.

DY 26.7 Wed 12:00 ZEU 160

Derivation and analysis of a phase field crystal model for a mixture of active and passive particles* — •MICHAEL TE VRUGT^{1,2}, MAX PHILIPP HOLL¹, ARON KOCH¹, RAPHAEL WITTKOWSKI^{1,2,3}, and UWE THIELE^{1,3,4} — ¹Institut für Theoretische Physik, Westfälische Wilhelms-Universität Münster, 48149 Münster, Germany — ²Center for Soft Nanoscience — ³Center for Nonlinear Science — ⁴Center for Multiscale Theory and Computation

We discuss an active phase field crystal (PFC) model that describes a mixture of active and passive particles [1]. First, a microscopic derivation from dynamical density functional theory is presented that includes a systematic treatment of the relevant orientational degrees of freedom. Of particular interest is the construction of the nonlinear and coupling terms. This allows for interesting insights into the microscopic justification of phenomenological constructions used in PFC models, the approximations required for obtaining them, and possible generalizations. Second, the derived model is investigated using linear stability analysis and nonlinear methods. It is found that the model allows for a rich nonlinear behavior with states ranging from steady periodic and localized states to various time-periodic states. The latter include standing, traveling, and modulated waves corresponding to spatially periodic and localized traveling, wiggling, and alternating peak patterns and their combinations.

[1] MtV et al., Modelling Simul. Mater. Sci. Eng. 30, 084001 (2022)

* Funded by the Deutsche Forschungsgemeinschaft (DFG)-WI 4170/3-1

DY 26.8 Wed 12:15 ZEU 160

Active Brownian Particles in a disordered motility environment — GIANNI JACUCCI¹, •DAVIDE BREONI², SANDRINE HEIJNEN³, HARTMUT LÖWEN², GIORGIO VOLPE³, and SYLVAIN GIGAN¹ — ¹Laboratoire Kastler-Brossel, Paris, France — ²HHU Universität, Düsseldorf, Germany — ³University College London, London, United Kingdom

The study of active matter, i.e. matter that consumes energy to perform actions, is fundamental to deepen the knowledge of living systems, as for example bacterial colonies or flocks of birds, and their collective behaviors. Complex environments, like the internal structure of a cell or a blood vessel, are of particular relevance in this field, as they provide a better description of the real-life settings typical of living matter.

In this work we study the effects of a disordered motility field on active Brownian particles, both in experiments and simulations. Experimentally, the motility

field is generated by applying a speckle light field to thermophoretic Janus particles, in our case silica colloids half-coated with a carbon layer, suspended in a critical mixture of water and 2,6-lutidine. We focus on the differences between the effects of respectively a homogeneous and a disordered motility field on the dynamics of the particles.

DY 26.9 Wed 12:30 ZEU 160

Characterization of spatial heterogeneities as influencing factors on the dynamics of confluent endothelial cell migration — •ANSELM HOHLSTAMM, ANDREAS DEUSSEN, STEPHAN SPEIER, and PETER DIETERICH — Institut für Physiologie, TU Dresden

Confluent endothelial cells are in perpetual movement. Their collective dynamics arises from the interplay of self-propelled motility and various distance-related cell interactions. However, an understanding of collective cell dynamics is complicated by large spatial heterogeneities and local cluster formations. It is the aim of this work to quantify and characterize their influence on the dynamics of cell migration. We used human umbilical vein endothelial cells, which were stained with a fluorescent dye and observed for 48 hours via time-lapse microscopy. With automated image segmentation we could track several 10.000 cells. Cell densities and mean squared velocities showed a heterogeneous spatial distribution with an inverse relation to each other. Higher cell densities also affected the strength of the velocity autocorrelation, whereas correlation times remained mostly stable during experiments. However, cell division increased the mean squared velocity without changing temporal correlations. In parallel, the mean squared displacement characterized regions with short superdiffusive phases in an aging, highly non-stationary system. In addition, local dynamics are coupled by long range spatial correlations. In summary, the dynamics of an entire endothelial layer is influenced by interactions of small heterogeneous regions. Next, we will use this approach to compare different endothelial cells.

DY 26.10 Wed 12:45 ZEU 160

Exploiting the unknown - Smart nutrient collection surpassing the run and tumble strategy — •MAHDI NASIRI, EDWIN LORAN, and BENNO LIEBCHEN — Institut für Physik kondensierter Materie, Technische Universität Darmstadt, Hochschulstraße 8, D-64289 Darmstadt, Germany

Throughout evolution, microorganisms have developed efficient strategies for locating nutrients and avoiding toxins in complex environments. Understanding their adaptive policies can provide new key insights for the development of smart artificial active particles. In this talk, we will present a novel method that uses deep reinforcement learning (DRL) to develop smart nutrient collection strategies for chemotactic active particles. Our method is complementary to our previous work which used DRL to explore optimal navigation [1] and is able to devise efficient survival strategies inside unknown and complex environments while only having access to local sensory data. We were also able to extract an interpretable model from the learned strategies which resemble striking similarities with the classical run and tumble motion.

[1] M. Nasiri, B. Liebchen, New J. Phys. 24, 073042 (2022).

DY 27: Statistical Physics: Far From Equilibrium I

Time: Wednesday 9:30–13:00

Location: ZEU 250

Invited Talk

DY 27.1 Wed 9:30 ZEU 250

Evolution in changing environments and driven disordered systems — •JOACHIM KRUG, SUMAN DAS, and MUHITIN MUNGAN — Institute for Biological Physics, University of Cologne, Köln, Germany

Biological evolution is governed by the fitness landscape, a map from the genetic sequence of an organism to its fitness. A fitness landscape depends on the organism's environment, and evolution in changing environments is still poorly understood. After introducing the concept of fitness landscapes and their mathematical description, the talk will focus on a particular model of antibiotic resistance evolution in bacteria [1]. Tradeoffs between adaptation to low and high concentration lead to a rugged landscape with an exponentially large number of fitness peaks. With evolutionary dynamics that follow fitness gradients, resistance evolution under slowly changing antibiotic concentration maps to the zero temperature dynamics of a disordered spin system [2]. Specifically, the set of genetic sequences that form a fitness peak at some concentration maps exactly to the metastable states in an equivalent Preisach system, a paradigmatic model of hysteresis in random magnets. Making use of the conceptual tool of state transition graphs developed in the context of driven disordered systems, we quantify the degree of genotypic and phenotypic reversibility in the response of the population to antibiotic concentration cycling.

[1] S.G. Das, S.O.L. Direito, B. Waclaw, R.J. Allen, J. Krug, eLife 9:e55155 (2020)

[2] S.G. Das, J. Krug, M. Mungan, Phys. Rev. X 12:031040 (2022)

DY 27.2 Wed 10:00 ZEU 250

Anomalous relaxation of density waves in a ring-exchange system — •PRANAY PATIL^{1,2}, MARKUS HEYL^{1,3}, and FABIEN ALET² — ¹Max-Planck Institute for the Physics of Complex Systems, Dresden, Germany — ²Laboratoire de Physique Théorique, Université de Toulouse, CNRS, UPS, France — ³Theoretical Physics III, Center for Electronic Correlations and Magnetism, Institute of Physics, University of Augsburg, 86135 Augsburg, Germany

We present the analysis of the slowing down exhibited by stochastic dynamics of a ring-exchange model on a square lattice, by means of numerical simulations. We find the preservation of coarse-grained memory of initial state of density-wave types for unexpectedly long times. This behavior is inconsistent with the prediction from a low frequency continuum theory developed by assuming a mean field solution. Through a detailed analysis of correlation functions of the dynamically active regions, we exhibit an unconventional transient long ranged structure formation in a direction which is featureless for the initial condition, and argue that its slow melting plays a crucial role in the slowing-down mechanism. We expect our results to be relevant also for the dynamics of quantum ring-exchange dynamics of hard-core bosons.

DY 27.3 Wed 10:15 ZEU 250

Colloidal monolayers: bridging the gap between two and three spatial dimensions — JOHANNES BLEIBEL¹, •ALVARO DOMÍNGUEZ¹, and MARTIN OETTEL² — ¹Univ. Sevilla, Spain — ²Univ. Tübingen

It is well established that, unlike for a three-dimensional fluid, particle interactions prevent the hydrodynamic transport coefficients from being defined for a

two-dimensional fluid due to the notorious “long-time tail” feature of the velocity autocorrelation.

A colloidal monolayer formed at a fluid interface builds a bridge between these two limiting cases, and it provides insight on the transition from three down to two spatial dimensions: the particle positions are constrained to a plane and the colloid thus resembles a two-dimensional fluid. But the exchange of particle momentum takes place in three-dimensional space through hydrodynamic interactions in the ambient fluid.

Here we study the colloidal diffusivity starting from the Smoluchowski equation. We show that the diffusivity exhibits an intermediate behavior between purely two-dimensional and fully three-dimensional fluid: on the one hand, Fick’s law, which pertains to *collective diffusion*, breaks down altogether, as confirmed experimentally. On the other hand, the coefficient of *self-diffusion* is finite, but the transitional nature of the monolayer shows up in a non-analytic dependence on the colloidal packing fraction, at odds with the case of a fully three-dimensional colloid.

DY 27.4 Wed 10:30 ZEU 250

Nonequilibrium mixture dynamics: A model for mobilities and its consequences — MARYAM AKABERIAN, •FILIPE THEWES, PETER SOLLICH, and MATTHIAS KRÜGER — Institut für Theoretische Physik, Georg-August-Universität Göttingen, Göttingen, Germany

Extending the famous Model B for the time evolution of a liquid mixture, we develop an approximate approach for the mobility matrix that couples the different mixture components. This approach is based on a single component fluid with particles that are artificially grouped into colors and the relevant parameters can be determined from experiments or numerical simulations. We identify two distinct regimes, corresponding to collective motion and inter-diffusion, respectively, and show how they emerge from the microscopic properties of the fluid. As a test scenario, we study the dynamics after a thermal quench, providing a number insights from a Gaussian theory. Specifically, for systems with two or three components, analytical results for the time evolution of the equal time correlation function compare well to results of Monte Carlo simulations of a lattice gas. A rich behavior is observed, including the possibility of fractionation.

DY 27.5 Wed 10:45 ZEU 250

Dynamical Renormalization Group Theory for Driven Systems — •NIKOS PAPANIKOLAOU and THOMAS SPECK — Institute of Theoretical Physics 4, University of Stuttgart, Stuttgart, Germany

Active matter describes nonequilibrium systems that are self-driven due to their microscopic dynamics. These systems pose a fundamental physics challenge by unveiling new phenomena, not present in equilibrium systems, such as the Motility Induced Phase Separation; formation of clusters in the absence of any attractive interactions. To study analytically nonequilibrium complex systems, the Renormalization Group (RG) theory has been successfully used to extract the phase diagram, to study its qualitative behavior, and to explore the critical properties in the different phases. In this project, we explore a variation of RG called Dynamical RG to study self-driven systems by directly applying the RG to dynamical field equations such as the KPZ equation or the Active Model B+ which describe the stochastic evolution of systems like the population of bacteria, interfaces, and neural networks.

DY 27.6 Wed 11:00 ZEU 250

Metastability as a Mechanism for Yielding in Amorphous Solids under Cyclic Shear — •MUHITTIN MUNGAN¹ and SRIKANTH SASTRY² — ¹Institute of Biological Physics, University of Cologne, Cologne, Germany — ²Jawaharlal Nehru Centre for Advanced Scientific Research, Bengaluru, India

We consider the yielding behavior of amorphous solids under cyclic shear deformation and show that it can be mapped into a random walk in a confining potential with an absorbing boundary. The resulting dynamics is governed by the first passage time into the absorbing state and suffices to capture the essential qualitative features recently observed in atomistic simulations of amorphous solids. Our results provide insight into the mechanism underlying yielding and its robustness. When the possibility of activated escape from absorbing states is added, it leads to a unique determination of a threshold energy and yield strain, suggesting thereby an appealing approach to understanding fatigue failure [1].

[1] M. Mungan and S. Sastry, Phys. Rev. Lett. 127 (2021) 248002

15 min. break

DY 27.7 Wed 11:30 ZEU 250

Tunable Brownian magneto heat pump — •IMAN ABDOLI¹, RENÉ WITTMANN², JOSEPH BRADER³, JENS-UWE SOMMER¹, HARTMUT LÖWEN², and ABHINAV SHARMA¹ — ¹Leibniz-Institut für Polymerforschung Dresden, 01069 Dresden, Germany — ²Heinrich-Heine-Universität Düsseldorf, 40225 Düsseldorf, Germany — ³Université de Fribourg, CH-1700 Fribourg, Switzerland

We propose a mesoscopic Brownian magneto heat pump made of a single charged Brownian particle that is steered by an external magnetic field. The particle is subjected to two thermal noises from two different heat sources. When

confined, the particle performs gyrating motion around a potential energy minimum. We show that such a magneto-gyrotor can be operated as both a heat engine and a refrigerator. The maximum power delivered by the engine and the performance of the refrigerator, namely the rate of heat transferred per unit external work, can be tuned and optimised by the applied magnetic field. Further tunability of the key properties of the engine, such as the direction of gyration and the torque exerted by the engine on the confining potential, is obtained by varying the strength and direction of the applied magnetic field. In principle, our predictions can be tested by experiments with colloidal particles and complex plasmas.

DY 27.8 Wed 11:45 ZEU 250

Work fluctuations in the harmonic Active Ornstein-Uhlenbeck particle model — •GIUSEPPE GONNELLA — Università degli Studi di Bari, Bari, Italy — Istituto Nazionale di Fisica Nucleare, sezione di Bari

Over the past few years great interest arose in providing a thermodynamic description of Active Matter Systems and an important emphasis was put on the Active Work study. The distribution of such an observable has been object of recent research[1] as possible singularities signal the occurrence of Dynamical Phase Transitions (DPTs)[2,3], in turn related to peculiar trajectory realisations.

Here we focus on a single harmonically trapped Active Ornstein-Uhlenbeck Particle and provide the analytic expression for the scaled cumulant generating function (SCGF) of the Active Work. Interestingly, we find the SCGF to be non-steep in many physical situations and we provide insight on the effect of relevant system parameters, such as the Peclet number, on the SCGF steepness through a phase diagram in the system parameter space. Through Legendre-Fenchel transform, the SCGF steepness is shown to lead to singular rate functions with linear tails, and ultimately to the occurrence of DPTs also in this system. We also investigate on the role of initial and final condition in producing the consequent anomalous trajectories.

[1] Semeraro M. et al, J Stat Mech, 2021

[2] Cagnetta F. et al., PRL, 2017

[3] Keta YE. et al., PRE, 2021

DY 27.9 Wed 12:00 ZEU 250

Non-thermal fixed points of universal sine-Gordon coarsening dynamics — PHILIPP HEINEN¹, ALEKSANDR N. MIKHEEV^{1,2}, CHRISTIAN-MARCEL SCHMIED¹, and •THOMAS GASENZER^{1,2} — ¹Kirchhoff-Institut für Physik, Universität Heidelberg, Im Neuenheimer Feld 227, 69120 Heidelberg — ²Institut für Theoretische Physik, Universität Heidelberg, Philosophenweg 16, 69120 Heidelberg

We examine coarsening of field-excitation patterns of the sine-Gordon (SG) model, in two and three spatial dimensions, identifying it as universal dynamics near non-thermal fixed points. The focus is set on the non-relativistic limit, governed by a Schrödinger-type equation with Bessel-function nonlinearity. The results of our classical statistical simulations suggest that, in contrast to wave turbulent cascades, in which the transport is local in momentum space, the coarsening is dominated by rather non-local processes corresponding to a spatial confinement in position space. The scaling analysis of a kinetic equation obtained with path-integral techniques corroborates this numerical observation and suggests that the non-locality is directly related to the slowness of the scaling in space and time. Our methods, which we expect to be applicable to more general types of models, could open a long-sought path to analytically describing universality classes behind domain coarsening and phase-ordering kinetics from first principles, which are usually modelled in a near-equilibrium setting by a phenomenological diffusion-type equation in combination with conservation laws.

DY 27.10 Wed 12:15 ZEU 250

Nonequilibrium probability currents in optically-driven colloidal suspensions — •SAMUDRAJIT THAPA^{1,2}, DANIEL ZARETZKY³, GRZEGORZ GRADZIUK⁴, CHASE BROEDERSZ^{4,5}, YAIR SHOKEF^{1,2,6}, and Yael ROICHMAN^{3,6,7} — ¹School of Mechanical Engineering, Tel Aviv University, Tel Aviv 69978, Israel — ²Sackler Center for Computational Molecular and Materials Science, Tel Aviv University, Tel Aviv 69978, Israel — ³School of Chemistry, Tel Aviv University, Tel Aviv 69978, Israel — ⁴Arnold Sommerfeld Center for Theoretical Physics, Ludwig Maximilians Universität München, Theresienstr. 37, 80333 Munich, Germany — ⁵Department of Physics and Astronomy, Vrije Universiteit Amsterdam, 1081 HV Amsterdam, The Netherlands — ⁶Center for the Physics and Chemistry of Living Systems, Tel Aviv University, 69978, Tel Aviv, Israel — ⁷School of Physics & Astronomy, Tel Aviv University, Tel Aviv 69978, Israel

In the absence of visible currents and prior knowledge, it is often hard to recognize athermal fluctuations. Probability currents provide such a measure in terms of the rate at which they enclose area in phase space. We measure this area enclosing rate for trapped colloidal particles, where only one particle is driven, and they interact hydrodynamically. By combining experiment, theory and simulation, we identify an optimal measurement protocol in terms of the relations between the different time scales in the system. Furthermore, we find that hydrodynamic interactions render the effect of athermal agitation more local than that of elastic interactions. This may have significant implications for the interpretation of fluctuations in biological systems.

DY 27.11 Wed 12:30 ZEU 250

A nonlinear fluctuation-dissipation theorem for Markovian systems — •BENJAMIN LINDNER^{1,2}, KIRSTEN ENGBRING², DIMA BORISKOVS³, and YAEL ROICHMAN³ — ¹Bernstein Center for Computational Neuroscience Berlin, Philippstr. 13, Haus 2, 10115 Berlin, Germany — ²Physics Department of Humboldt University Berlin, Newtonstr. 15, 12489 Berlin, Germany — ³The Raymond and Beverley School of Physics & Astronomy and The Raymond and Beverley School of Chemistry, Tel Aviv University, Tel Aviv 6997801, Israel

Fluctuation-Dissipation-Theorems (FDT) connect the internal spontaneous fluctuations of a system with its response to an external perturbation. In this work we propose a new nonlinear fluctuation-dissipation theorem as a test for Markovianity. Previously suggested FDTs are based on linear response and require a significant amount of measurements. However, the nonlinear relation holds for systems out of equilibrium, and for strong perturbations requiring significantly less data than the standard linear relation. We verify the nonlinear theorem for two theoretical model systems: a Brownian particle in a tilted periodic potential, and a harmonically bound particle. In addition, we apply our

formalism and test for Markovianity in an inherently out of equilibrium experimental system, based on self-propelled agents.

DY 27.12 Wed 12:45 ZEU 250

Heat capacity for a driven array of semiclassical dots — •PRITHA DOLAI and CHRISTIAN MAES — Instituut voor Theoretische Fysica, KU Leuven, Belgium

We analyze thermal properties for particle transport along an array of two-level systems. More specifically, we obtain analytic and numerical results for the heat capacity of a system of particles subject to mutual exclusion and to birth and death, driven around a ring by an external field. We find a zero-temperature phase transition as a function of the chemical potential of the environment, as shown by the divergence of the heat capacity at zero temperature. The non-vanishing of the heat capacity at absolute zero, violating the extended Third Law, is caused by a localization and corresponding delay in relaxation of excess heat. We also derive a regime of negative heat capacity indicating an anticorrelation between the temperature-dependence of the stationary occupation and the excess heat.

DY 28: Focus Session: Critical Transitions in Society, Economy, and Nature (joint session SOE/DY)

Organizers: Fakhteh Ghanbarnejad (Robert Koch-Institut), Diego Rybski (Potsdam Institute for Climate Impact Research)

Time: Wednesday 9:30–11:45

Location: ZEU 260

See SOE 9 for details of this session.

DY 29: Wetting, Droplets and Microfluidics (joint session DY/PPP)

Time: Wednesday 10:00–13:00

Location: ZEU 147

DY 29.1 Wed 10:00 ZEU 147

Crises and chaotic scattering in hydrodynamic pilot-wave experiments — GEORGE CHOUËIRI^{1,2}, BALACHANDRA SURI^{1,3}, JACK MERRIN¹, MAKSYM SERBYN¹, BJÖRN HOF¹, and •NAZMI BURAK BUDANUR^{1,4} — ¹Institute of Science and Technology Austria, 3400 Klosterneuburg, Austria — ²MIME Department, University of Toledo, Toledo, Ohio 43606, USA — ³Department of Mechanical Engineering, Indian Institute of Science, Bengaluru 560012, India — ⁴Max Planck Institute for the Physics of Complex Systems, 01187 Dresden, Germany

Theoretical foundations of chaos have been predominantly laid out for finite-dimensional dynamical systems, such as the three-body problem in classical mechanics and the Lorenz model in dissipative systems. In contrast, many real-world chaotic phenomena, e.g., weather, arise in systems with many (formally infinite) degrees of freedom, which limits direct quantitative analysis of such systems using chaos theory. In the present work, we demonstrate that the hydrodynamic pilot-wave systems offer a bridge between low- and high-dimensional chaotic phenomena by allowing for a systematic study of how the former connects to the latter. Specifically, we present experimental results, which show the formation of low-dimensional chaotic attractors upon destabilization of regular dynamics and a final transition to high-dimensional chaos via the merging of distinct chaotic regions through a crisis bifurcation. Moreover, we show that the post-crisis dynamics of the system can be rationalized as consecutive scatterings from the nonattracting chaotic sets with lifetimes following exponential distributions.

DY 29.2 Wed 10:15 ZEU 147

Chemically Active Wetting — •SUSANNE LIESE¹, XUEPING ZHAO², FRANK JÜLICHER³, and CHRISTOPH WEBER¹ — ¹Universität Augsburg, Augsburg, Germany — ²Xiamen University, Xiamen, China — ³MPI/PKS, Dresden, Germany

In living cells, wetting of condensed phases on membrane surfaces provides a mechanism for positioning biomolecules. Biomolecules are also able to bind to such membrane surfaces. In living cells, this binding is often chemically active as it is kept out of equilibrium by the supply of energy and matter. Here, we investigate how active binding on membranes affects the wetting of condensates. To this end, we derive the non-equilibrium thermodynamic theory of active wetting. We find that active binding significantly alters the wetting behavior leading to non-equilibrium steady states with condensate shapes reminiscent of a fried egg or a mushroom. We further show that such condensate shapes are determined by the strength of active binding in the dense and dilute phases, respectively. Strikingly, such condensate shapes can be explained by an electrostatic analogy where binding sinks and sources correspond to electrostatic dipoles along the triple line. Through this analogy, we can understand how fluxes at the triple line control the three-dimensional shape of condensates.

DY 29.3 Wed 10:30 ZEU 147

Stimuli-responsive high aspect ratio surfaces for wetting studies — •GISSELA CONSTANTE¹, INDRA APSITE¹, PAUL AUERBACH², SEBASTIAN ALAND², DENNIS SCHÖNFELD³, THORSTEN PRETSCH³, PAVEL MILKIN¹, and LEONID IONOV^{1,4} — ¹Uni Bayreuth, Bayreuth, Germany — ²HTW Dresden, Dresden, Germany — ³Fraunhofer IAP, Postdam, Germany — ⁴Bavarian Polymer Institute, Bayreuth, Germany

The fabrication of switchable surfaces has been of interest in different fields such as biotechnology, industry, robotics, and others. The fabrication of these shape-changing bioinspired surfaces is a challenge due to the limited availability of materials and methods. In this research, an exceptional high aspect ratio lamellar surface topography was fabricated by melt-electrowriting of microfibers of a shape-memory thermo-responsive polyurethane. Two different types of stimuli: temperature and light exposition were applied to modify the mechanical properties and by it the deformation and recovery of the original surface. Wetting studies showed that the deformation of the high aspect ratio lamellar surface can be tuned not only manually, but as well by a liquid droplet. This behavior is controlled by variation of temperature conducted by direct heating/cooling or by exposure to light when the lamellae were stained with black ink. The liquid in combination with thermo-responsive topography presents a new type of wetting behavior. This feature opens the possibility to apply such topographies for the design of smart elements for microfluidic devices, for example, smart valves.

DY 29.4 Wed 10:45 ZEU 147

A Study about Shock-Induced Spallation in Mono- and Nanocrystalline High-Entropy Alloys — •DANIEL THÜRMER¹, NINA MERKERT NÉE GUNKELMANN¹, SHITENG ZHAO², ORLANDO DELUIGI³, CAMELIA STAN⁴, IYAD ALHAFEZ⁵, HERBERT URBASSEK⁵, MARC MEYERS⁶, and EDUARDO BRINGA^{3,7} — ¹Institute of Applied Mechanics, Clausthal University of Applied Technology, Arnold-Sommerfeld-Str. 4, D-38678 Clausthal-Zellerfeld, Germany — ²School of Material Science and Engineering, Beihang University, 37 Xueyuan Rd, Haidian District, Beijing, China, 100191 — ³CONICET and Faculty of Engineering, University of Mendoza, Mendoza, 5500, Argentina — ⁴Advanced Light Source Facility, Lawrence Berkeley National Laboratory, One Cyclotron Road, Berkeley, CA 94720, United States — ⁵Physics Department and Research Center OPTIMAS, University Kaiserslautern, Erwin-Schrödinger-Str. 46, D-67663 Kaiserslautern, Germany — ⁶Mechanical and Aerospace Department, Univ. of California San Diego, La Jolla, CA 92093, United States — ⁷Centro de Nanotecnología Aplicada, Universidad Mayor, Santiago, Chile

High-entropy alloys are highly attractive for future applications in the technical field thanks to their incredible potential regarding mechanical properties. Although they are increasingly sparking interest for future usage, their general understanding is not yet complete. To further understand high-entropy alloys and their capabilities, we studied the influence of shock-induced spallation on mono- and nanocrystalline high-entropy alloys with varying grain sizes.

DY 29.5 Wed 11:00 ZEU 147

Instability of Active Fluid Interfaces in Microfluidics — •KUNTAL PATEL and HOLGER STARK — Institut für Theoretische Physik, Technische Universität Berlin, Berlin, Germany

In recent years, microfluidic lab-on-a-chip devices have emerged as efficient miniaturized flow control platforms. Specifically, the advent of nonlinear microfluidics has opened a new avenue for chemical and biomedical applications such as droplet formation and cell sorting. In this work, we integrate ideas from active matter into a microfluidic setting and try to understand the mechanism and practical relevance of resulting microfluidic flows.

The present setup consists of two vertically stacked fluid layers with identical densities but different viscosities, sandwiched between the walls of a microfluidic channel. The interface separating both fluids is initialized with uniformly distributed active particles, which induce force dipoles that generate flows in the adjacent fluids.

Our hybrid lattice-Boltzmann finite-difference simulations reveal that when we perturb the fluid interface covered with extensile force dipoles $\frac{1}{2}$, it eventually returns to its flat state irrespective of the strength of interfacial tension. In contrast, contractile force dipoles $\frac{1}{2}$ lead to activity-driven interfacial instability. However, such instability emerges only above a critical value of the activity, which is proportional to the interfacial tension. We further examine the mechanism of instability and quantify the effect of viscosity contrast and perturbation wavelength. Lastly, we demonstrate the systematic formation of droplets using the present interfacial instability.

DY 29.6 Wed 11:15 ZEU 147

Optically controlled micro-transport with reduced heating impact — •ANTONIO MINOPOLI, ELENA ERBEN, SUSAN WAGNER, and MORITZ KREYSING — Max Planck Institute of Molecular Cell Biology and Genetics, Dresden, Germany

Recently it was demonstrated that thermoviscous flows can be used to move the cytoplasm of cells and developing embryos. These laser-induced intracellular flows (aka FLUCS), reach velocities comparable with those occurring during early stages of embryogenesis. As a side effect, the laser scanning may also cause temperature gradients across the sample (1-3 Kelvins) that could give rise to out-of-equilibrium phenomena. Here, we demonstrate that exploiting symmetry relations during the laser scan, we disentangle heating and flows. Specifically, since the flow speeds depend on the repetition frequency rather than on the beam velocity, it is possible to accelerate the scanning of the primary scan pattern, effectively compressing the scan signal to occupy only a fraction of the original period, and allowing to complement the flow stimuli by flow-invariant heat stimuli. We introduce strategies to complement even complex primary scan patterns by secondary heating stimuli thereby yielding a near isothermal temperature distribution and still generating significant net flows. As we experimentally show, the resulting temperature distributions are near homogenous across the sample (standard deviations 5-10 times lower than those measured with standard FLUCS) and can therefore be better compensated for by ambient cooling. In the next future, ISO-FLUCS may become the new standard for optofluidic manipulations within biological systems.

15 min. break

DY 29.7 Wed 11:45 ZEU 147

3D passive non-mechanical microfluidic valves fabricated using grayscale lithography — •SEBASTIAN BOHM^{1,3}, HAI BINH PHI^{2,3}, ERICH RUNGE¹, LARS DITTRICH³, and STEFFEN STREHLE² — ¹TU Ilmenau, FG Theoretische Physik I — ²TU Ilmenau, FG Mikrosystemtechnik — ³5microns GmbH, 98693 Ilmenau

Passive non-mechanical valves represent a promising method for rectifying flows in micro- or nanofluidic systems [1]. They are very robust due to the absence of mechanical parts, easy to fabricate, and allow the implementation of efficient microfluidic systems such as micropumps [2,3]. However, with existing methods, the fabrication of fully three dimensional (3D) structured geometries is very hard to achieve. Here, a new and easy to implement method for the fabrication of three-dimensional valves is presented: Grayscale lithography followed by a proportional transfer with reactive ion etching is utilized to create 3D diffuser valves in silicon and glass substrates. We show that higher diodicities were achieved with 3D diffuser valves compared to conventional diffuser valves. These experimental findings correspond fit very well to the predictions of our numerical simulations. In combination with highly efficient optimization methods for two-dimensional Tesla valves, the fabrication of even more efficient 3D Tesla valves is hence now within reach.

[1] Bohm, S. et al.; *npg Microsystems & Nanoengineering* (8), 97 (2022)

[2] Bohm, S. et al.; *COMSOL Conference 2020 Europe*, 14-15. Oct. 2020 online

[3] Hoffmann, M. et al.; German patent DE112011104467 (2017)

DY 29.8 Wed 12:00 ZEU 147

Coalescence of nematic droplets in quasi 2D liquid crystal films — •CHRISTOPH KLOPP and RALF STANNARIUS — Otto von Guericke University, Institute of Physics

Coalescence of droplets is ubiquitous in nature and modern technology. Various experimental and theoretical studies explored droplet dynamics in three dimensions (3D) and on two-dimensional (2D) solid or liquid substrates, e.g. [1-4]. Here, we demonstrate coalescence experiments of isotropic and nematic droplets in quasi-2D liquids, viz. overheated smectic A freely suspended films. We investigated their dynamics experimentally and measured the shape deformation during the entire merging process using high-speed imaging and interferometry. This system is a unique example where the lubrication approximation can be directly applied, and the smectic membrane plays the role of a precursor film. Our studies reveal the scaling laws of the coalescence time depending on the droplet size and the material parameters. We also compared the dynamics of isotropic and nematic droplets and additionally analyzed the results based on an existing model for liquid lens coalescence on liquid and solid surfaces [4].

This study was supported by DLR with project 50WM2054 and by DFG with project STA 425/40.

References:

[1] J. D. Paulsen et al., *Nat. Commun.*, 5, 3182 (2014) [2] D. G. A. L. Aarts et al., *Phys. Rev. Lett.*, 95, 164503 (2005). [3] M. A. Hack et al., *Phys. Rev. Lett.* 124, 194502 [4] N. S. Shuravin et al., *Phys. Rev. E*, 99, 062702 (2019) [5] C. Klopp et al., *Langmuir*, 36, 10615 (2020)

DY 29.9 Wed 12:15 ZEU 147

effect of deposition method on the static contact angle of nanodroplets measured by AFM — •MOHAMMADALI HORMOZI and REGINE VON KLITZING — soft matter at interface, tu darmstadt, darmstadt, Germany

The wetting properties of substrates are often described by the static contact angle of a particular liquid. The contact angle depends on many parameters like substrate chemistry, liquid properties, and environment condition. In this study, we show that the method of depositing the liquid phase on the solid phase can play an important role for the static contact angle. For this purpose, microscale droplets of non-volatile liquids including Polyethylene Glycol (PEG200) and Squalane are deposited on the silanized substrate using four different methods. These methods are either based on nucleation (condensation and solvent exchange) or printing (inkjet and microcontact printing) of droplets. The contact angle of the microdroplets is scanned with an AFM and allows detailed analysis of the three phase contact line on a nm scale. The final static contact angle of the microdroplets is compared with the macroscopic contact angle determined by optical methods. Droplets formed via nucleation show smaller contact angle than printed ones. The latter ones were closer to the macroscopic contact angle. We will discuss this phenomenon.

DY 29.10 Wed 12:30 ZEU 147

Fingering contact propagation between a droplet and a thin liquid film — •KIRSTEN HARTH — Fachbereich Technik, TH Brandenburg — MRTM und MARS, Otto von Guericke Universität Magdeburg

When impacting droplets approach a hard plane substrate slowly, so that the Weber number is below approximately 5, a contact-less rebound will occur due to the entrainment of ambient gas. On slightly deformable and smooth spin-coated liquid films upon a rigid solid, this effect is more robust and may occur until slightly higher Weber numbers. Deformation of the thin film is usually ignored while it is proven to be present. The deformation amplitude depends on the impact dynamics as well as the thickness and viscosity of the surficial oil layer. At slightly higher impact velocities, i.e. slightly higher Weber numbers, delayed contact formation between the film liquid and the droplet occurs. Depending on the layer properties, interestingly, the contact line may be unstable displaying a fingering texture. Instability occurs independently of whether the drop and film liquid differ or not. We present and analyze this phenomenon.

DY 29.11 Wed 12:45 ZEU 147

Universality in One-Dimensional Breath Figures — •DANIEL DERNBACH, ADRIAN HÄUSSLER-MÖHRING, M MUHAMMAD, and JÜRGEN VOLLMER — Institut für Theoretische Physik, Universität Leipzig, Brüderstr. 16, D-04103 Leipzig, Germany

Patterns of droplets which condense upon substrates reveal self-similar features. They are described by a scaling theory with a non-trivial exponent that has been related to the fractal dimension of the scaling of the free area ("porosity") in between droplets. There is no agreement if this exponent is universal or affected by the dynamics. Here, we present numerical data that address the dependence of the asymptotic scaling of the porosity for hyper-spherical droplets growing on one-dimensional substrates. We vary the droplet dimension and interactions. For a given dimension the exponent is universal up to a critical range of interaction. For longer-ranged interactions the scaling depends on the dynamics.

DY 30: Nonequilibrium Quantum Many-Body Systems II (joint session TT/DY)

Time: Wednesday 15:00–18:30

Location: HSZ 204

See TT 38 for details of this session.

DY 31: Microswimmers and Fluid Physics of Life (joint session DY/PPP)

Time: Wednesday 15:00–18:15

Location: MOL 213

DY 31.1 Wed 15:00 MOL 213

Physics of gut motility governs digestion and bacterial growth — •AGNESE CODUTTI¹, JONAS CREMER², and KAREN ALIM¹ — ¹School of Natural Sciences, Technical University of Munich, Germany — ²Biology Department, Stanford University, USA

Malfunctioning of the small intestine contractility and the ensuing bacterial population therein are linked to a plethora of diseases. We, here, study how the small intestine's variety of contractility patterns impacts nutrient uptake and bacterial population [1]. Our analytical derivations in agreement with simulations identify flow velocity as the key control parameter of the nutrients uptake efficiency and bacterial growth, independently of the specifics of contractility patterns. Self-regulating flow velocity in response to the number of nutrients and bacteria in the gut allows for achieving 100% efficiency in nutrient uptake. Instead of the specifics of intestine contractility, our work points to the flow velocity and its variation in time within the intestine to prevent malfunctioning.

[1] Codutti A., Cremer J., Alim K., "Changing Flows Balance Nutrient Absorption and Bacterial Growth along the Gut" PRL 129, 138101 (2022)

DY 31.2 Wed 15:15 MOL 213

Turbulence induces clustering and arrested phase separation in polar active fluids — VASCO WORLITZER^{1,2}, GIL ARIEL², AVRAHAM BEER³, HOLGER STARK⁴, •MARKUS BÄR^{1,4}, and SEBASTIAN HEIDENREICH¹ — ¹Physikalisch-Technische Bundesanstalt, Berlin — ²Bar-Ilan University, Ramat Gan, Israel — ³Ben-Gurion University, Beer Sheva, Israel — ⁴Technische Universität Berlin

We study a novel phase of active polar fluids, which is characterized by the continuous creation and destruction of dense clusters due to self-sustained turbulence. This state arises due to the interplay between self-advection of the aligned swimmers and their defect topology. The typical cluster size is determined by the characteristic vortex size. Our results are obtained by investigating a continuum model of compressible polar active fluids [1], which incorporates typical experimental observations in bacterial suspensions [2], in particular a non-monotone dependence of speed on density.

[1] V. Worlitzer et al., *Soft Matter* 17, 10447-10457 (2021)

[2] A. Beer et al., *Communications Physics* 3, 66 (2020)

DY 31.3 Wed 15:30 MOL 213

Bacterial spreading in complex environments — •AGNIVA DATTA, SÖNKE BEIER, VERONIKA PFEIFER, ROBERT GROSSMANN, and CARSTEN BETA — Institute of Physics and Astronomy, University of Potsdam, Potsdam, Germany

Elucidating the principles of bacterial motility and navigation is key to understand many important phenomena such as the spreading of infectious diseases and the formation of biofilms. A prime challenge of swimming bacteria is to navigate in their habitat purposefully and efficiently, e.g., in the soil, which is a complex, structured environment. In this talk, we address the question of how bacterial navigation at the microscale relates to their large-scale spreading in heterogeneous environments. We combine experiments with the soil bacterium *Pseudomonas putida* with active particle modeling. In particular, the motility pattern of these bacteria in agar will be discussed with a focus on anomalous transport properties in disordered environments. In contrast to *E. coli*, our analysis reveals transient subdiffusion of bacteria in agar due to intermittent trapping, giving rise to a hop-and-trap dynamics with power-law distributed trap times.

DY 31.4 Wed 15:45 MOL 213

Minimum Entropy Production by Microswimmers with Internal Dissipation — •ANDREJ VILFAN, ABDALLAH DADDI-MOUSSA-IDER, BABAK NASOURI, and RAMIN GOLESTANIAN — Max Planck Institute for Dynamics and Self-Organization, Göttingen, Germany

Microswimmers are natural or artificial self-propelled microscale objects moving through a fluid at low Reynolds numbers. The entropy production of microswimmers, related to their dissipated power, consists of two contributions. The external dissipation takes place in the viscous fluid surrounding the microswimmer. Internal dissipation takes place in the propulsive layer on the swimmer's surface. We have previously shown that a lower bound on the external dissipation can be derived with the knowledge of drag coefficients of two bodies of the same shape, one with a no-slip and one with a perfect slip boundary condition [1]. Here, we show that our approach can be generalized to take into account the internal dissipation, which is often the dominant contribution. By combin-

ing the Helmholtz minimum dissipation theorem and the principle of linear superposition, we solve the combined minimum dissipation problem for different classes of swimmers including surface-driven viscous droplets, swimmers driven by tangential forces and swimmers driven by normal forces. We show that the minimum entropy production in suspensions of active microswimmers differs fundamentally from particles driven by external forces.

[1] B. Nasouri, A. Vilfan and R. Golestanian, *Phys. Rev. Lett.*, 126, 034503 (2021).

DY 31.5 Wed 16:00 MOL 213

Synchronization of model cilia by time-dependent elasto-hydrodynamics — •ALBERT VON KENNE¹, HOLGER STARK², and MARKUS BÄR¹ — ¹Physikalisch-Technische Bundesanstalt (PTB), 10587 Berlin — ²Technische Universität Berlin, 10623 Berlin

Collections of hair-like micro actuators known as cilia are employed in biology to pump extra cellular fluids at low Reynolds number conditions. Their collective dynamics exhibit synchronization and a large scale coordinated motion called metachronal waves. Typically, simple models that characterize the self-organization among hydrodynamically interacting cilia neglect the inertial forces in the fluid against the viscous forces. In this case, the mutual flows are determined instantaneously through the forces exerted by cilia. Consequentially synchronization requires a symmetry breaking external to hydrodynamics, that can come from elastic responses to flow perturbations (*T. Niedermayer et al., Chaos* 2008). Meanwhile, experiments show that inertial forces are significant in microscopic flow at the relevant scales (*D. Wei et al. Phys. Rev. Lett.* 2019). In this situation, the fluid response is explicitly time-dependent and hydrodynamic correlations can lead to synchronization (*M. Theers and R. Winkler, Phys. Rev.* 2013). We derived a simplified phase-oscillator model that describes the leading order coupling between cilia by elastic responses and hydrodynamic correlations. We show that its interrelations don't change the collective state qualitatively. However, the strength of coupling is always increased.

DY 31.6 Wed 16:15 MOL 213

Microswimming near a wedge — •ALEXANDER R. SPRENGER and ANDREAS M. MENZEL — Institut für Physik, Otto-von-Guericke-Universität Magdeburg, Universitätsplatz 2, D-39106 Magdeburg, Germany

Artificial and living microswimmer encounter a large variety of geometric confinements and surfaces in the biological world which alter their motion when nearby. Here, we study the low-Reynolds-number dynamics of a microswimmer enclosed by a wedge-shaped free-slip interface. For various opening angles of the wedge, we derive an exact solution for flow and pressure fields using the method of images. The active swimmer is represented in terms of a superposition of Stokes singularities. In this way, the hydrodynamic interactions between the swimmer and the confining interfaces are examined. In particular, we find attraction or repulsion by the wedge depending on the propulsion mechanism (pusher- or puller-type swimming strokes) and the opening angle of the wedge. For the dynamics of a microswimmer inside the wedge, we present a minimal model in terms of coupled Langevin equations for position and orientation. Our analytic results are evaluated for parameters inspired by common self-propelling microorganisms like *Escherichia coli*.

15 min. break

DY 31.7 Wed 16:45 MOL 213

Role of cohesion in the flow of active particles through bottlenecks — •TIMO KNIPPENBERG¹, ANTON LÜDERS¹, CELIA LOZANO², PETER NIELABA¹, and CLEMENS BECHINGER¹ — ¹Fachbereich Physik, Universität Konstanz, Germany — ²Bosonit, AI Department, La Rioja, Spain

Recently, many studies examined the intermittent flow of granular particles through bottleneck-shaped apertures. A common framework which describes the occurring flow statistics was empirically found for a wide range of such systems reaching from microscopic colloids and macroscopic grains up to sheep herds. However, similar studies with active matter are scarce and do merely consider steric agent interactions. Here, we experimentally and numerically study the flow of programmable, colloidal active Janus swimmers through bottlenecks. Our results confirm the applicability of the above-mentioned statistical framework of granular intermittent flow also on complex-interacting active microswimmers. Moreover, upon increasing the strength of interparticle cohe-

sion, we find a transition from an arch-dominated clogging regime to a cohesion-dominated regime where droplets form at the outlet. The flow-rate only weakly depends on the cohesion strength in the arch-dominated regime, which suggests that cohesion needs not necessarily to hinder particle flow through geometric constrictions or pores.

DY 31.8 Wed 17:00 MOL 213

Self-assembling meso-machines along liquid-air interfaces — •NICOLAS VANDEWALLE, MEGAN DELENS, and YLONA COLLARD — GRASP, University of Liege, B4000 Liege, Belgium

Magnetocapillary driven self-assembly allows us to create complex structures floating along a liquid-air interface. We show how these structures can be elaborated and how they can be triggered for locomotion. First, the pairwise capillary and magnetic interactions between floating objects are experimentally studied and rationalized through analogies with electrostatics. Then, the combination of capillary attraction and magnetic repulsion will lead to the spontaneous formation of a rich variety of floating structures. Placed in processing magnetic fields, those structures may behave like swimming ciliate organisms and start to move along the liquid-air interface. The conditions to obtain this magnetic powered locomotion are emphasized.

DY 31.9 Wed 17:15 MOL 213

Induced capillary dipoles in floating particle assemblies — •MEGAN DELENS, YLONA COLLARD, and NICOLAS VANDEWALLE — GRASP, Institut de Physique B5a, Université de Liège, Liège, BE

Capillary-driven self-assembly is a common fabrication method that consists in placing floating particles onto a liquid-air interface. The attractive capillary interaction between particles is due to the local deformations of the interface which can be described via so-called capillary charges. When the particles are spherical and far from each other, the menisci are planar circles and can be described by monopolar capillary charges. The capillary interaction is then approximately found by assuming that the charges carried by individual spheres may be linearly superposed. However, when particles are close together, we experimentally observed that the attraction is enhanced and becomes far more complex. Indeed, the contact lines start to tilt and the superposition principle no longer holds. For these situations, we propose to additionally consider induced capillary dipoles to describe the menisci, therefore, providing an extra attraction between particles at short distances. This effect is enhanced when particles have different sizes such that binary self-assemblies may reveal unusual local ordering.

DY 31.10 Wed 17:30 MOL 213

A Versatile Swarm of Individually Controlled Microparticles for Object Manipulation and Transport — •VEIT-LORENZ HEUTHE¹, EMANUELE PANIZON², and CLEMENS BECHINGER¹ — ¹Universität Konstanz, Konstanz, Germany — ²International Centre for Theoretical Physics, Trieste, Italy

Some tasks for robotic systems require many robots to cooperate, similar to ants that join their forces to carry large objects. On a macroscopic scale, many examples for such collective tasks exist, like robot swarms that can assemble objects. However, future potential applications like minimally invasive medicine call for miniaturization of such concepts. On the microscopic scale, one major challenge is the strong thermal noise, that demands for much more robust control. We use a reinforcement learning algorithm to individually steer microswimmers

in a swarm that can manipulate and transport a large object. Due to decentralized control, our multi robot system is highly flexible, scalable and robust. With this demonstration we take micro-robot swarms one step further on their way to become tools for manipulating microscopic objects.

DY 31.11 Wed 17:45 MOL 213

New insights into the mechanism of self-phoresis — •ALVARO DOMÍNGUEZ¹, MIHAIL POPESCU¹, and SIEGFRIED DIETRICH² — ¹Univ. Sevilla, Spain — ²MPI für Intelligente Systeme, Stuttgart

Chemophoresis describes the displacement of a particle in an ambient fluid due to a gradient in chemical composition. Classic phoresis can be understood through linear-response theory: in the presence of a sufficiently small gradient $(\nabla n)_{\text{ext}}$ in concentration, the phoretic velocity of the particle is $\mathbf{V} = \mathcal{L}_{\text{lin}}(\nabla n)_{\text{ext}}$, in terms of the phoretic coefficient \mathcal{L}_{lin} given by a Green-Kubo expression.

Self-phoretic particles induce a composition gradient $(\nabla n)_{\text{act}}$ through catalytic activity and provide a physical realization of artificial swimmers. Experimental observations are then customarily addressed as another instance of classic phoresis, $\mathbf{V} = \mathcal{L}_{\text{lin}}(\nabla n)_{\text{act}}$.

However, an additional role of the particle's chemical activity has been recently identified [1,2], namely, as responsible for a specific activity-induced response \mathcal{L}_{act} , so that one has to write

$$\mathbf{V} = (\mathcal{L}_{\text{lin}} + \mathcal{L}_{\text{act}})[(\nabla n)_{\text{ext}} + (\nabla n)_{\text{act}}]$$

in the more general scenario. This would mean a change in paradigm as it disproves the claim that "self-phoresis is phoresis in a self-induced gradient".

[1] A. Domínguez, M. Popescu, C. Rohwer, S. Dietrich, *Physical Review Letters*, **125**, 268002 (2020).

[2] A. Domínguez, M. Popescu, *Current Opinion in Colloid & Interface Science*, **61**, 101610 (2022).

DY 31.12 Wed 18:00 MOL 213

Oriental dynamics and rheology of active suspensions in viscoelastic media — •AKASH CHOUDHARY¹, SANKALP NAMBIAR², and HOLGER STARK¹ — ¹Institute of Theoretical Physics, Technische Universität Berlin, 10623 Berlin, Germany — ²KTH Royal Institute of Technology and Stockholm University, Stockholm 10691, Sweden

Active suspensions are systems of motile organisms or active filaments that are driven out of equilibrium through self-propulsion. This localized energy-work conversion imparts rich phenomenology and anomalous macroscale properties that are in stark contrast to passive suspensions and polymeric fluids. Motivated by the ubiquitous microbial systems in biological fluids, we analyse the impact of non-Newtonian fluids on the rheological response of active suspensions to steady shear flows.

We first study the suspension at an individual level and show that elongated pushers (representative of *E. coli*) and pullers (*C. reinhardtii*) exhibit diverse orbital dynamics in a weakly viscoelastic shear flow. We find that the active stresses not only modify the Jeffery orbits well-known from Newtonian fluids, but microswimmers can exhibit alignment and shear-plane rotation states. To analyze the impact of such behavior on the bulk rheological response, we study an ensemble of a dilute suspension of such swimmers in the presence of stochastic noise from bacterial tumbling and rotary diffusion. In comparison to Newtonian media, the polymeric elastic stresses substantially amplify the swimmer-induced viscosity, in particular, the superfluid transition observed in pusher solutions.

DY 32: Focus Session: Physics of Fluctuating Paths (joint session DY/ CPP)

State-of-the-art experiments probe physical observables, such as heat, work or entropy production, empirical densities and currents, on the level of individual, stochastic paths. Such experiments are typically analysed by averaging along a limited number of individual realisations, which leads to substantial uncertainties in estimates. The systematic sample-to-sample fluctuations of such path-observables encode important information about the underlying, microscopic dynamical processes and are therefore a frontier of experimental, theoretical, and computational physics. Recently there has been a surge in the development and applications of path-based concepts across many fields of physics. This focus session complements a symposium and contains contributed talks.

Organized by Aljaz Godec, Udo Seifert, and Peter Sollich

Time: Wednesday 15:00–18:15

Location: ZEU 160

DY 32.1 Wed 15:00 ZEU 160

Towards a stochastic thermodynamics of fields and tracers — •SARAH A.M. LOOS¹, DAVIDE VENTURELLI², BENJAMIN WALTER³, EDGAR ROLDAN⁴, and ANDREA GAMBASSI² — ¹DAMTP, University of Cambridge, Cambridge, UK — ²SISSA, Trieste, Italy — ³Imperial College London, UK — ⁴ICTP, Trieste, Italy

Many results of stochastic thermodynamics, including the close connection between entropy production and stochastic heat dissipation, rely on physical assumptions, e.g., break down if there is no clear separation into "fast equilibrium bath degrees of freedom" and "slow nonequilibrium degrees of freedom". In this talk, I will discuss some insights into thermodynamic notions of nonequilibrium

systems that do not fall into the usual paradigm of stochastic thermodynamics. In particular, we develop a thermodynamic description for systems consisting of tracer particles coupled to correlated scalar fields with thermal fluctuations in terms of trajectory-wise energy flows of the particle and the field, as well as the joint entropy production rate measured by path-probability ratios. As an illustration, we consider the case in which the particle is dragged by a harmonic trap through a complex medium described by a fluctuating Gaussian field. Using a perturbative approach, we uncover three dynamical regimes with distinct scaling behavior of the power and discuss the heat dissipation occurring within the field.

DY 32.2 Wed 15:15 ZEU 160

Fluctuation theorem for time reversal markers — •GABRIEL KNOTZ, TILL M. MUENKER, TIMO BETZ, and MATTHIAS KRÜGER — Fakultät für Physik, Georg-August-Universität, Göttingen, Germany

The analysis of particle trajectories is of high theoretical and experimental interest. Especially if hidden degrees are present, detecting broken detailed balance is a challenging task. We introduce and analyze a class of observables with certain symmetry properties under time reversal of trajectories that detect the breakage of detailed balance. Further, these observables fulfill a new form of fluctuation theorem and, under certain conditions, this fluctuation theorem provides bounds and relations for the total change in entropy. These findings are not limited to Markov or overdamped dynamics.

DY 32.3 Wed 15:30 ZEU 160

Necessity for Coarse Graining Empirical Densities and Currents in Continuous Space — •CAI DIEBALL and ALJAZ GODEC — Max Planck Institute for Multidisciplinary Sciences, Goettingen, Germany

We present general results on fluctuations and spatial correlations of the coarse-grained empirical density and current of diffusion in equilibrium or non-equilibrium steady states on all time scales. The time averaging and coarse graining hardwired in the definition of the functionals under consideration give rise to experimentally relevant but highly non-trivial statistics. We unravel a deep connection between current fluctuations and generalized time-reversal symmetry. We highlight the essential role of coarse graining in space from mathematical, thermodynamical, and experimental points of view. Spatial coarse graining is required to uncover salient features of currents that break detailed balance, and a thermodynamically "optimal" coarse graining ensures the most precise inference of dissipation. Defined without coarse graining, the fluctuations of empirical density and current are proven to diverge on all time scales in dimensions higher than one, which has far-reaching consequences for large-deviation limits in continuous space and for continuum limits of Markov-jump processes. Our findings provide new intuition about time-averaged observables and allow for a more efficient analysis of single-molecule experiments.

References: Phys. Rev. Lett. 129, 140601 (2022) and Phys. Rev. Research 4, 033243 (2022)

DY 32.4 Wed 15:45 ZEU 160

How Stickiness Can Speed Up Diffusion in Confined Systems — ARTHUR ALEXANDRE¹, MATTHIEU MANGEAT², •THOMAS GUÉRIN¹, and DAVID DEAN¹ — ¹Laboratoire Ondes et matière d'Aquitaine, CNRS/University of Bordeaux, F-33400 Talence, France — ²Center for Biophysics and Department for Theoretical Physics, Saarland University, D-66123 Saarbrücken, Germany

The paradigmatic model for heterogeneous media used in diffusion studies is built from reflecting obstacles and surfaces. It is well known that the crowding effect produced by these reflecting surfaces slows the dispersion of Brownian tracers. In this talk, using a general adsorption-desorption model with surface diffusion, we present an analytical theory showing that making surfaces or obstacles attractive can accelerate dispersion. In particular, we show that this enhancement of diffusion can exist even when the surface diffusion constant is smaller than that in the bulk. Even more remarkably, this enhancement effect occurs when the effective diffusion constant, when restricted to surfaces only, is lower than the effective diffusivity with purely reflecting boundaries. We give analytical formulas for this intriguing effect in periodic arrays of spheres as well as undulating microchannels. Our results are confirmed by numerical calculations and Monte Carlo simulations. [Ref: How Stickiness Can Speed Up Diffusion in Confined Systems, Phys Rev Lett 128 210601 (2022)]

DY 32.5 Wed 16:00 ZEU 160

From trajectories to models: data-driven approaches to decipher the stochastic dynamics of living systems — •PIERRE RONCERAY — Turing Centre for Living Systems, CINaM, CNRS, Aix-Marseille University, France

Stochastic differential equations are often used to model the dynamics of living systems, from Brownian motion at the molecular scale to the dynamics of cells and animals. How does one learn such models from experimental data? This task faces multiple challenges, from information-theoretical limitations to practical considerations. I will present a recent and ongoing effort to develop new methods to reconstruct such stochastic dynamical models from experimental data, with a focus on robustness and data efficiency. This provides a generic means to quantify complex behavior and unfold the underlying mechanisms of an apparently erratic trajectory.

DY 32.6 Wed 16:15 ZEU 160

Entropions as vibrational excitations in active solids — •LORENZO CAPRINI¹, UMBERTO MARINI BETTOLO MARCONI², ANDREA PUGLISI³, and HARTMUT LÖWEN¹ — ¹Heinrich-Heine-Universität Düsseldorf — ²Scuola di Scienze e Tecnologia, University of Camerino — ³Istituto dei Sistemi Complessi, CNR

We study the vibrational properties of non-equilibrium active crystals, i.e. solids formed by active particles, that are intrinsically out of equilibrium and governed by entropy production. As known in solid-state physics, equilibrium crystals are

characterized by basic collective excitations with thermal origins that are named phonons. In this talk, I will show that active crystals are described by additional vibrational excitations that we called 'entropions' because each of them represents a mode of spectral entropy production. Entropions coexist with phonons and dominate over them for large activity, i.e. when the solid is far from equilibrium, while they vanish in equilibrium conditions. Their existence can be verified in experiments on dense self-propelled colloidal Janus particles and granular active matter, as well as in living systems such as dense cell monolayers.

15 min. break

DY 32.7 Wed 16:45 ZEU 160

Inferring Fractional Processes Using Path Integrals — •JOHANNES A. KASSEL¹, BENJAMIN WALTER², and HOLGER KANTZ¹ — ¹Max Planck Institute for the Physics of Complex Systems, Dresden, Germany — ²Imperial College London, London, UK

We present a method for inferring overdamped nonlinear Langevin equations driven by multiplicative fractional Gaussian noise from single-trajectory time series. Constructing a maximum-likelihood estimator, we simultaneously infer the nonlinear deterministic force term and the space-dependent diffusion term. We illustrate our method using artificial time series. We observe that Markovian modeling of long-range correlated data leads to a substantial underestimation of the deterministic force term while for anti-correlated data it leads to an overestimation of the force term.

DY 32.8 Wed 17:00 ZEU 160

Kinetics of Imperfect Reactions for non-Markovian Random Walks — •TONI VIEIRA MENDES and THOMAS GUÉRIN — Laboratoire Ondes et Matière d'Aquitaine, Université de Bordeaux

Most transport influenced reactions between two random walkers are usually imperfect, i.e., they do not occur at first contact between the reactants. For such imperfect reactions, recent work has been made to determine the statistics of first reaction time for Markovian random walkers in confinement. However, a lot of physical random walks are actually non-Markovian, i.e., their movement in the future depend on the trajectory they have followed up to then, thus displaying memory effects. These memory effects can be seen, for example, for beads moving inside complex fluids where the force fields do not equilibrate instantly. In this contribution, we describe an analytical theory giving access to the mean reaction time for imperfect reactions for random walkers with memory in confinement. Our theory clearly shows that, contrary to the Markovian case, the reaction time is not the sum of the mean first passage time and the time to react once within reactive distance. We show that the results of our theory match the results of simulations for both one and two dimensions. Then, the equations are analytically solved in the limit of weakly non-Markovian processes. Remarkably, in the limit of weakly reactive targets for fractional Brownian Motion, we find that the mean reaction time displays a non-trivial scaling as a function of the reactivity.

DY 32.9 Wed 17:15 ZEU 160

Instantons and the Path to Intermittency in Turbulent Flows — •ANDRÉ FUCHS¹, CORENTIN HERBERT², JORAN ROLAND³, MATTHIAS WÄCHTER¹, FREDDY BOUCHET², and JOACHIM PEINKE¹ — ¹Institute of Physics and For-Wind, University of Oldenburg, Küppersweg 70, 26129 Oldenburg, Germany — ²Université de Lyon, Ens de Lyon, Université Claude Bernard, CNRS, Laboratoire de Physique, F-69364 Lyon, France — ³Université de Lille, CNRS, ONERA, Arts et Métiers Institute of Technology, Centrale Lille, UMR 9014 - LMFL - Laboratoire de Mécanique des fluides de Lille - Kampé de Fériet, F-59000 Lille, France

Processes leading to anomalous fluctuations in turbulent flows, referred to as intermittency, are still challenging. We consider cascade trajectories through scales as realizations of a stochastic Langevin process for which multiplicative noise is an intrinsic feature of the turbulent state. The trajectories are conditioned on their entropy exchange. Such selected trajectories concentrate around an optimal path, called instanton, which is the minimum of an effective action. The action is derived from the Langevin equation, estimated from measured data. In particular instantons with negative entropy pinpoint the trajectories responsible for the emergence of non-Gaussian statistics at small-scales.

DY 32.10 Wed 17:30 ZEU 160

A nonadiabatic generalized-dividing-surface instanton rate theory — •RHIANNON A. ZAROTIADIS, JOSEPH E. LAWRENCE, and JEREMY O. RICHARDSON — Lab. für Physikalische Chemie, ETH Zürich, Zürich, Switzerland.

The accurate prediction of quantum rate processes is fundamental to our understanding of chemical reactions, but exact calculations are extremely costly. To make them tractable many chemical processes are described within the Born-Oppenheimer (BO) approximation, which assumes strong coupling between the diabatic states, and BO instanton theory is known to capture nuclear quantum effects for these systems well [1]. Alternatively, some systems are better captured by Fermi's golden rule, which is appropriate in the opposite limit of weak coupling.

Nevertheless, many reactions are in neither of these two limits, and so a universal rate theory is desirable. We introduce a new nonadiabatic generalized-dividing-surface instanton approach rigorously derived from the flux-flux correlation function. Our new theory correctly recovers the weak- and strong-coupling limits and goes beyond existing, ad hoc attempts to describe general, nonadiabatic rate processes.

Instanton rate theories [1] have already resolved many longstanding discrepancies between experiment and theory [2] and this new rate theory will be key to address processes beyond their scope such as proton-coupled electron transfer reactions.

[1] Richardson, J. O., *Int. Rev. Phys. Chem.*, 2018, 37:2, 171-216.

[2] Zarotiadis, R. A., Fang, W., Richardson, J. O., *Phys. Chem. Chem. Phys.*, 2020, 22, 10687.

DY 32.11 Wed 17:45 ZEU 160

Sojourn probabilities for diffusive dynamics with state-dependent friction: Theory and experiment — ALICE THORNEYWORK^{1,2}, JANNES GLADROW^{2,3}, ULRICH F. KEYSER², RONOJOY ADHIKARI⁴, and •JULIAN KAPPLER^{4,5} — ¹Department of Chemistry, University of Oxford, Oxford, United Kingdom — ²Cavendish Laboratory, University of Cambridge, Cambridge, United Kingdom — ³Microsoft Research, Cambridge, United Kingdom — ⁴Department of Applied Mathematics and Theoretical Physics, Cambridge University, Cambridge, United Kingdom — ⁵Fakultät für Physik, Ludwig-Maximilians-Universität, München, Germany

The trajectories of diffusion processes are continuous but nondifferentiable, and each occurs with vanishing probability. This introduces a gap between theory, where path probabilities are used in many contexts, and experiment, where only events with nonzero probability are measurable. We bridge this gap by considering the sojourn probability, i.e. the probability for diffusive trajectories to remain

within a tube of small but finite radius around a smooth path. For systems with state-dependent diffusivity, we show that the sojourn probability is characterized by a functional that is different from all previously reported multiplicative-noise stochastic actions. We corroborate our theoretical results by comparison to experimentally measured sojourn probabilities for a colloidal particle in a corrugated microchannel. Our work directly connects the discussion of path probabilities for diffusive dynamics with state-dependent friction to physical observables.

DY 32.12 Wed 18:00 ZEU 160

Optimality of non-conservative driving in discrete systems — •JONAS FRITZ and UDO SEIFERT — II. Institut für Theoretische Physik, Universität Stuttgart, 70550 Stuttgart, Germany

A fundamental problem in stochastic thermodynamics is that of optimal driving. The goal is to drive a system from some specified initial state to a specified final state, while minimizing entropy production (or work performed) along the trajectory. As shown recently [1], the optimal protocol in a cyclical Markov network has a non-conservative force, i.e. non-zero cycle affinity, which is in contrast to continuous systems. However, the reduction in entropy production from such a non-conservative force has been numerically found to be at most on the order of 10^{-2} for the case of the three state cycle. We investigate why this is the case, by systematically varying step size and initial conditions numerically for the simple case of the three state cycle. Further, we try to maximize the improvement in entropy production through the non-conservative force. By increasing the number of states in the cycle, we find a possible improvement which is an order of magnitude larger than the previously known one. We attempt to find a lower bound for the possible improvement through non-conservative driving, by analyzing the scaling behavior of the underlying quantities.

[1] Benedikt Remlein and Udo Seifert, *Phys. Rev. E* 103, L050105

DY 33: Biologically Inspired Statistical Physics (joint session DY/BP)

Time: Wednesday 15:00–16:30

Location: ZEU 250

DY 33.1 Wed 15:00 ZEU 250

Comparison of fitting strategies to extract the diffusion coefficient in microrheological experiments — •STEN LEIPNITZ, CHRISTIAN WAGNER, and THOMAS JOHN — Experimental Physics, Saarland University, Saarbrücken

Tracking of small particles undergoing a Brownian motion in liquids is a widespread method in passive microrheology to extract the diffusion coefficient D , the viscosity of the sample respectively. The mean-squared displacement (MSD) is determined from particle positions as a function of the timelag $MSD(\tau) = \sigma_0^2 + 2nD\tau + v_{\text{drift}}^2\tau^2$, where v_{drift} is a possible drift velocity and σ_0 is an offset due to position detection noise in experiments. We present: the extracted parameters depend strongly on the used number of fitting points in the MSD -relation. Surprisingly, considering only the beginning of the MSD -relation in the fitting procedure leads to the best expectation value of the diffusion coefficient. This is shown by numerical simulations of the Brownian motion as well as from experimental data.

DY 33.2 Wed 15:15 ZEU 250

Non-monotonic behavior of timescales of passage in heterogeneous media: Dependence on the nature of barriers — MOUMITA DASGUPTA¹, •SOUGATA GUHA², LEON ARMBRUSTER¹, DIBYENDU DAS², and MITHUN K. MITRA² — ¹Department of Physics, Augsburg University, USA — ²Department of Physics, IIT Bombay, India

Usually time of passage across a region may be expected to increase with the number of barriers along the path. Can this intuition fail depending on the special nature of the barrier? We study experimentally the transport of a robotic bug which navigates through a spatially patterned array of obstacles. Depending on the nature of the obstacles we call them either entropic or energetic barriers. For energetic barriers we find that the timescales of first passage vary non-monotonically with the number of barriers, while for entropic barriers first passage times increase monotonically. We perform an exact analytic calculation to derive closed form solutions for the mean first passage time for different theoretical models of diffusion. Our analytic results capture this counter-intuitive non-monotonic behaviour for energetic barriers. We also show non-monotonic effective diffusivity in the case of energetic barriers. Finally, using numerical simulations, we show this non-monotonic behaviour for energetic barriers continues to hold true for super-diffusive transport. These results may be relevant for timescales of intra-cellular biological processes.

DY 33.3 Wed 15:30 ZEU 250

Phase behavior and finite-size effects in biology — •FELIX HERRMANN, BURKHARD DUENWEG, and MARTIN GIRARD — Max-Planck Institut fuer Polymerforschung (MPI-P), Mainz, Germany

Phase behavior observed in biology remains puzzling. For instance, the plasma membrane of cells exhibits signs of criticality, as it is controlled to remain near

a demixing point. This membrane contains thousand of components, and it is largely unclear how its composition is controlled. Beyond this, one can ask whether cells should obey the traditional thermodynamic picture, given their small size, large number of components and the presence of non-equilibrium processes.

Here, we study toy systems, lattice models containing many (>30) components. We show that these systems exhibit strong finite-size effects. These manifest as behavior that appears similar to traditional critical behavior, but vanish logarithmically with system size. We examine scaling laws, and whether traditional paradigms from macroscopic thermodynamics can be broken in such systems.

DY 33.4 Wed 15:45 ZEU 250

Hierarchical interactions in complex ecosystems — •LYLE POLEY¹, JOSEPH W. BARON³, and TOBIAS GALLA^{1,2} — ¹Theoretical Physics, Department of Physics and Astronomy, School of Natural Sciences, The University of Manchester, Manchester M13 9PL, UK — ²Instituto de Física Interdisciplinar y Sistemas Complejos IFISC (CSIC-UIB), 07122 Palma de Mallorca, Spain — ³Laboratoire de Physique Statistique, École Normale Supérieure (ENS), Paris Sciences et Lettres (PSL) Research University, Sorbonne Université, 75005 Paris, France

In the analysis of complex ecosystems it is common to use random interaction coefficients, often assumed to be such that all species are statistically equivalent. We relax this assumption by imposing hierarchical inter-species interactions, which we incorporate into a generalised Lotka-Volterra dynamical system. These interactions impose a hierarchy in the community. Species benefit more, on average, from interactions with species below them in the hierarchy than from interactions with those above.

Using analytical tools from the theory of disordered systems, most notably path-integrals and dynamic mean-field theory, we demonstrate that a stronger hierarchy stabilises the community by reducing the number of species in the surviving community. We will also show that the probability of survival for a given species is dependent on its position in the hierarchy.

Reference: Poley L, Baron J W and Galla T Generalised Lotka-Volterra model with hierarchical interactions 2022 arXiv:2208.01569

DY 33.5 Wed 16:00 ZEU 250

Quantifying information content in continuous attractor networks — •TOBIAS KÜHN^{1,2} and RÉMI MONASSON¹ — ¹Laboratoire de Physique de l'École Normale Supérieure, ENS, Université PSL, CNRS, Sorbonne Université, Université Paris Cité, F-75005 Paris — ²Institut de la Vision, Sorbonne Université, INSERM, CNRS, F-75012 Paris

Attractor networks are a theme with long tradition to model information storage in the brain. Continuous attractor neural networks (CANN), in particular, have been employed to describe the storage of information about space and orienta-

tion. However, it stays controversial how useful this paradigm really is to explain actual processes, for example the representation of space in grid and place cells in the entorhinal cortex and the hippocampus, respectively.

A common criticism is that the disorder present in the connections might deteriorate the system's capability to reliably preserve the information of a certain pattern. In order to investigate if this criticism is valid, a measure is needed to objectively quantify the information content of a given neural network. Using the replica-trick, we compute the Fisher information for a network receiving space-dependent input whose connections are composed of a distance-dependent and a disordered component. We observe that the decay of the Fisher information is slow for not too large disorder strength, indicating that CANNs have a regime in which the advantageous effects of connectivity on information storage outweigh the detrimental ones.

DY 33.6 Wed 16:15 ZEU 250

Gift of gab: Probing the limits of dynamic concentration-sensing across a network of communicating cells — •MOHAMMADREZA BAHADORIAN^{1,2}, CHRISTOPH ZECHNER^{1,2,3}, and CARL D. MODES^{1,2,3} — ¹Max Planck Institut

for Molecular Cell Biology and Genetics (MPI-CBG), 01307 Dresden, Germany — ²Center for Systems Biology Dresden (CSBD), 01307 Dresden, Germany — ³Cluster of Excellence Physics of Life, TU Dresden, 01069 Dresden, Germany

Many systems in biology and other sciences employ collaborative, collective communication strategies for improved efficiency and adaptive benefit. One such paradigm of particular interest is the community estimation of a dynamic signal, when, for example, an epithelial tissue of cells must decide whether to react to a given dynamic external concentration of stress-signaling molecules. At the level of dynamic cellular communication, however, it remains unknown what effect, if any, arises from communication beyond the mean field level. What are the limits and benefits to communication across a network of neighbor interactions? What is the role of Poissonian versus super-Poissonian dynamics in such a setting? How does the particular topology of connections impact the collective estimation and that of the individual participating cells? In this article we construct a robust and general framework of signal estimation over continuous-time Markov chains in order to address and answer these questions.

DY 34: Statistical Physics: Far From Equilibrium II

Time: Wednesday 16:45–18:15

Location: ZEU 250

DY 34.1 Wed 16:45 ZEU 250

Lane formation of colloidal particles driven by gravity — •MARC ISELE, KAY HOFMANN, and PETER NIELABA — Physics Department, University of Konstanz, Konstanz, Germany

Systems of particles that move with differing relative speeds as a counterpart to the movements of pedestrians and crowds have been shown to form a so-called lane structure. We simulate a quasi two dimensional system of two spherical particle types of different sizes driven by gravity. The particles are confined by hard walls orthogonal to the driving force and we employed Brownian Dynamics simulations (without hydrodynamic interactions). We found that the particles formed the well-known lane structure rather quickly. In this formation process the particles form slanted boundaries between the soon to be lanes which leads to regions of high and low densities. In the steady state we further found that the lanes closest to the hard walls were always occupied by the smaller particles (via something we call a funneling process). We also analyzed a wide variety of parameters giving us an optimized system for lane formation. Our work shows that the lane formation of driven particles is a phenomenon with a lot of different aspects that can depend heavily on the chosen system.

DY 34.2 Wed 17:00 ZEU 250

Time-reversal symmetries and equilibrium-like Langevin equations — •LOKRSHI PRAWAR DADHICHI and KLAUS KROY — ITP, Leipzig University, Brüderstraße 15, 04103, Leipzig

Graham has shown in Z. Physik B 26, 397-405 (1977) that a fluctuation-dissipation relation can be imposed on a class of non-equilibrium Markovian Langevin equations that admit a stationary solution of the corresponding Fokker-Planck equation. Here we show that the resulting equilibrium form of the Langevin equation is associated with a nonequilibrium Hamiltonian and ask how precisely the broken equilibrium condition manifests itself therein. We find that this Hamiltonian need not be time reversal invariant and that the "reactive" and "dissipative" fluxes lose their distinct time reversal symmetries. The anti-symmetric coupling matrix between forces and fluxes no longer originates from Poisson brackets and the "reactive" fluxes contribute to the ("housekeeping") entropy production, in the steady state. The time-reversal even and odd parts of the nonequilibrium Hamiltonian contribute in qualitatively different but physically instructive ways to the entropy. Finally, this structure gives rise to a new, physically pertinent instance of frenesy.

DY 34.3 Wed 17:15 ZEU 250

Quantum and classical contributions to entropy production in fermionic and bosonic Gaussian systems — •KRZYSZTOF PTASZYŃSKI^{1,2} and MASSIMILIANO ESPOSITO² — ¹Institute of Molecular Physics, Polish Academy of Sciences, Mariana Smoluchowskiego 17, 60-179 Poznań, Poland — ²Complex Systems and Statistical Mechanics, Physics and Materials Science Research Unit, University of Luxembourg, L-1511 Luxembourg, Luxembourg

As previously demonstrated, the entropy production – a key quantity characterizing the irreversibility of thermodynamic processes – is related to generation of correlations between degrees of freedom of the system and its thermal environment. The natural question appears whether such correlations are of a classical or a quantum nature, namely, whether they are accessible through measurements. We deal with this problem by investigating fermionic and bosonic Gaussian systems. It is shown that for fermions the entropy production is mostly quantum due to parity superselection rule which restricts the set of physically allowed

measurements to projections on the Fock states, which significantly limits the amount of classically accessible correlations. In contrast, in bosonic systems a much larger amount of correlations can be accessed through Gaussian measurements. Specifically, while quantum contribution may be important at low temperatures, in the high temperature limit the entropy production corresponds to purely classical position-momentum correlations.

DY 34.4 Wed 17:30 ZEU 250

Optimal power extraction from active particles with hidden states — •LUCA COCCONI^{1,2}, JACOB KNIGHT², and CONNOR ROBERTS² — ¹The Francis Crick Institute, London — ²Imperial College, London

We identify generic protocols achieving optimal power extraction from a single active particle subject to continuous feedback control under the assumption that the instantaneous velocity, but not the fluctuating self-propulsion velocity, is accessible to direct observation. Our Bayesian approach draws on the Onsager-Machlup path integral formalism and is exemplified in the cases of free run-and-tumble and active Ornstein-Uhlenbeck dynamics in one dimension. Such optimal protocols extract positive work even in models characterised by time-symmetric positional trajectories and thus vanishing informational entropy production rates. We argue that the theoretical bounds derived in this work are those against which the performance of realistic active matter engines should be compared.

DY 34.5 Wed 17:45 ZEU 250

Driving a first-order phase transformation by quenching the density: Unleashing hidden states — •MIRIAM KLOPOTEK¹, MARTIN OETTEL², and HANS JOACHIM SCHÖPE² — ¹University of Stuttgart, SimTech Cluster of Excellence EXC 2075, Stuttgart, Germany — ²University of Tübingen, Institute for Applied Physics, Tübingen, Germany

Abruptly increasing the number density, the primary order parameter of a many-particle system, is a basic mechanism to drive a first-order phase transition – elementary for athermal systems and thus for the solidification process from a fluid. A better-known experiment on thermal systems is quenching the temperature down to below the critical point, suddenly 'freezing out' the original degrees of freedom, whereafter the system densifies locally upon response. A density quench, in turn, intervenes directly and globally on the order parameter. A manifest example is thin film growth. As dynamical arrest is imminent, 'hidden' metastable states appear. We employ kinetic Monte Carlo simulations of a simple lattice model of sticky hard rods under quasi-2D confinement, gradually growing a full monolayer under different quench (growth) rates. The phenomenology is extremely rich: At least five distinct, non-classical phase transformation pathways are identified in this most simple model. They 'tile' a corresponding dynamical control diagram.

DY 34.6 Wed 18:00 ZEU 250

New phases and peculiar fluctuations in nonreciprocal systems — •SARAH LOOS — DAMTP, University of Cambridge, UK

Nonreciprocal interactions, i.e., interactions that violate the *actio=reactio* principle, occur in various biological and artificial nonequilibrium systems on a wide range of scales. For example, a bird in a flock may react to the movements of the bird in front of it, while the reverse interaction is zero, simply due to missing visual information. Recent research shows that the occurrence of such nonreciprocal interactions can have a dramatic impact on the self-organization of many-body systems [1], and on their thermodynamic properties [2]. In this talk, we

will consider a nonequilibrium lattice model with vision cone interactions [3], and show how the presence of nonreciprocal interactions can lead to the emergence of new phases and peculiar fluctuations.

[1] Fruchart, Non-reciprocal phase transitions, Nature (2021).

[2] S.A.M. Loos and S.H.L. Klapp, NJP 22, 123051 (2020).

[3] S.A.M. Loos, S.H.L. Klapp, and T. Martyneć, ArXiv:2206.10519 (2022).

DY 35: Statistical Physics of Biological Systems I (joint session BP/DY)

Time: Thursday 9:30–13:00

Location: TOE 317

See BP 22 for details of this session.

DY 36: Wetting, Fluidics and Liquids at Interfaces and Surfaces I (joint session CPP/DY)

Time: Thursday 9:30–13:00

Location: MER 02

See CPP 44 for details of this session.

DY 37: Data Analytics of Complex Dynamical Systems (joint session DY/SOE)

Time: Thursday 9:30–12:00

Location: MOL 213

DY 37.1 Thu 9:30 MOL 213

Reverse-engineering method for XPCS studies of non-equilibrium dynamics — •ANASTASIA RAGULSKAYA¹, VLADIMIR STAROSTIN¹, NAFISA BEGAM¹, ANITA GIRELLI¹, HENDRIK RAHMANN², MARIO REISER², FABIAN WESTERMEIER³, MICHAEL SPRUNG³, FAJUN ZHANG¹, CHRISTIAN GUTT², and FRANK SCHREIBER¹ — ¹Universität Tübingen, Germany — ²Universität Siegen, Germany — ³DESY, Germany

X-ray photon correlation spectroscopy (XPCS) is a powerful tool for the investigation of dynamics covering broad time and length scales [1]. For non-equilibrium states, the resulting time-dependent dynamic behavior can be described using the two-time correlation function (TTC), which often contains more interesting features than only the component along the diagonal, and cannot be easily interpreted via classical simulation methods. Here, a reverse-engineering (RE) approach is proposed based on particle-based simulations [1]. This approach is applied to XPCS measurements on a protein solution undergoing liquid-liquid phase separation. We demonstrate that the rich features of experimental TTCs can be well connected with the key control parameters including size distribution, concentration, viscosity, and mobility of domains. The dynamic information obtained from this RE analysis goes beyond existing theory. The RE approach established in this work is applicable to other processes such as film growth, domain coarsening, or phase transformations.

[1] A. Ragulska et al., IUCrJ 9 (2022), 439.

DY 37.2 Thu 9:45 MOL 213

Sensitivity of principal components to changes in the presence of non-stationarity — •HENRIK BETTE and THOMAS GUHR — Fakultät für Physik, Universität Duisburg-Essen, Duisburg, Deutschland

Non-stationarity affects the sensitivity of change detection in correlated systems described by sets of measurable variables. We study this by projecting onto different principal components. Non-stationarity is modeled as multiple normal states that exist in the system even before a change occurs. The studied changes occur in mean values, standard deviations or correlations of the variables. Monte Carlo simulations are performed to test the sensitivity for change detection with and without knowledge about the non-stationarity for different system dimensions and numbers of normal states. A comparison clearly shows that the knowledge about the non-stationarity of the system greatly improves change detection sensitivity for all principal components. This improvement is largest for those components that already provide the greatest possibility for change detection in the stationary case.

DY 37.3 Thu 10:00 MOL 213

Inferring partial differential equations from molecular dynamics simulations — •OLIVER MAI, TIM KROLL, UWE THIELE, and OLIVER KAMPS — Institute of Theoretical Physics and Center for Nonlinear Science, University of Münster

Although integral to scientific or engineering applications, deriving partial differential equations (PDEs) solely from experimental data proves quite challenging and in most cases relies on physical principles in addition to qualitative behaviour of the system. In the last decade various efforts based on empirical data have been put forth to supplement first-principle derivations in theoretical sciences. That is in place of or in addition to typical conservation laws or phenomenological observations, time series data has been used to yield analytic expressions to describe the spatio-temporal evolution of a given dynamical system. While there have been various improvements in the sparsity and interpretability of the results, we provide another approach to optimization using the predictive power of the estimation when integrating it. Additionally aggregated small scale

behaviour in macro- or mesoscopic experiments may exhibit unknown governing laws and as such a way for comparing data more directly to models derived in statistical physics may prove critical in furthering our understanding. To this end we study the application of system identification methods on molecular dynamics (MD) simulations.

DY 37.4 Thu 10:15 MOL 213

Reproducibility of analysis workflows in biomedical physics — •ALEXANDER SCHLEMMER^{1,4}, INGA KOTTLARZ^{1,2}, BALTASAR RÜCHARDT^{1,3,4}, ULRICH PARLITZ^{1,2,4}, and STEFAN LUTHER^{1,2,3,4} — ¹Max Planck Institute for Dynamics and Self-Organization, Göttingen, Germany — ²Institute for the Dynamics of Complex Systems, Georg-August-Universität Göttingen, Germany — ³Institute of Pharmacology and Toxicology, University Medical Center Göttingen, Germany — ⁴German Center for Cardiovascular Research (DZHK), Partner Site Göttingen, Germany

Sustainable and well-documented data analysis workflows are essential for effectiveness and reproducibility in data-intensive research. In our terminology, documentation includes method and algorithm descriptions as well as human- and machine-readable representations of parameters, initial conditions and data, versions and dependencies and a well-defined software execution environment.

In practice, many software frameworks for reproducibility fail to achieve a widespread adoption. Using examples from data analysis in cardiac research, we illustrate typical challenges and show, how simple guidelines - when implemented in a pragmatic way - can already lead to a high degree of documentation and reproducibility. Furthermore, we discuss the employment of containers and semantic data management which simplify reproducibility, findability and interoperability.

DY 37.5 Thu 10:30 MOL 213

Bayesian approach to anticipate critical transitions in complex systems — •MARTIN HESSLER^{1,2} and OLIVER KAMPS² — ¹Westfälische Wilhelms-Universität Münster, 48149 Münster — ²Center for Nonlinear Science, Westfälische Wilhelms-Universität Münster, 48149 Münster

Complex systems in nature, technology and society can undergo sudden transitions between system states with very different behaviour. In order to avoid undesired consequences of these tipping events, statistical measures have been proposed as leading indicators. They can give a hint of an ongoing bifurcation-induced (B-tipping) destabilization process. However, we present an alternative approach that is open-source available and more robust under numerous aspects. It assumes the dynamical system to be described by a Langevin equation. Starting from this stochastic description, we combine MCMC sampling, rolling window methods and Bayesian reasoning to derive the drift slope as an alternative early warning sign including credibility bands which make it easier to distinguish significant leading indicator trends prior to B-tipping. Furthermore, our approach provides information about an increasing noise level in a multi-stable system. This is an important information related to the Kramers escape rate of a noise-induced tipping (N-tipping) event. We show some results and discuss the method's potential to be applied in N-tipping scenarios and under more complex conditions like correlated non-Markovian or multiplicative noise. Finally, possible limitations and tasks of future research are mentioned.

15 min. break

Invited Talk

DY 37.6 Thu 11:00 MOL 213

Power law error growth rates – a dynamical mechanism for a strictly finite prediction horizon in weather forecasts — HYNEK BEDNAR^{1,2}, JONATHAN BRISCH¹, BURAK BUDANUR¹, and •HOLGER KANTZ¹ — ¹Max Planck Institute for the Physics of Complex Systems, Dresden, Germany — ²Dept. of Atmospheric Physics, Charles University, Prague, Czech Republic

While conventional chaotic systems have a finite positive Lyapunov exponent, physical arguments and observations suggest that the maximal Lyapunov exponent of the model equations of the atmosphere is the larger the smaller are the resolved spatial scales. Specifically, a power law divergence of the scale dependent error growth rate would translate into a strictly finite prediction horizon, since due to the divergence, additional accuracy of initial conditions is not translated into longer prediction times. We present conceptual toy models with such behavior, we show its presence in a more realistic spatially extended system with advective transport, and we present numerical results from turbulence simulations where the largest Lyapunov exponent scales as an inverse power of spatial resolution. The idea of a power law scale dependence of error growth rates and of a finite prediction horizon is also supported by re-analysis of numerical error growth experiments performed with an operational weather model. Altogether, this suggests that the prediction horizon of numerical weather prediction is strictly finite.

DY 37.7 Thu 11:30 MOL 213

Wave Digital Optimization of a Modified Compact Models of 1T-1R Random Resistive Access Memory Cells — •BAKR AL BEATTIE¹, MAX UHLMANN², GERHARD KAHMEN², and KARLHEINZ OCHS¹ — ¹Ruhr-Universität Bochum, Lehrstuhl für digitale Kommunikationssysteme, Bochum, Deutschland — ²Leibniz-Institut für innovative Mikroelektronik, Frankfurt (Oder), Deutschland

Random Resistive Access Memory (RRAM) cells are popular memristive devices that are commonly used in neuromorphic applications. In this context,

RRAM cells are usually utilized to embed synaptic plasticity, a property that is exhibited by biological synapses, into analog-based artificial neural networks. However, since RRAM-based technology has yet to reach a state of maturity, circuit designers are usually forced to make use of compact models to avoid dealing with device-to-device variabilities. The Stanford PKU model is a well-established compact model that has been developed to capture the dynamics of 1T-1R RRAM cells. In this contribution, we present a modified compact model, based on the Stanford PKU model, that takes more properties of real RRAM cells into account, such as the RESET voltage shift in multilevel devices. To demonstrate the capabilities of our model, we exploit the wave digital concept to apply a live parameter optimization, which fits the model parameters to a technologically reproducible device from the Leibniz Institute for High Performance Microelectronics (IHP).

DY 37.8 Thu 11:45 MOL 213

Discovering Causality and Coupling in high dimensional nonlinear dynamical systems — •TIM KROLL^{1,2} and OLIVER KAMPS² — ¹Westfälische Wilhelms-Universität Münster, 48149 Münster — ²Center for Nonlinear Science, Westfälische Wilhelms-Universität Münster, 48149 Münster

In this talk we present a method to infer causal relationships between observables from data of systems where the underlying dynamics are not known a priori. The method is based on the hypothesis that the system of interest can in principle be described by a set of coupled nonlinear ordinary differential equations. Following the work of Prusseit and Lehnertz in 2008 we can then determine the couplings between observables by integrating out all other observables. Since the estimation of the underlying dynamical system invokes the efficient representation in terms of polynomials the method can be applied also to high dimensional systems. We demonstrate the capabilities of the method by inferring the network structure of coupled Rössler-Attractors.

DY 38: Active Matter IV (joint session DY/BP/CPP)

Time: Thursday 9:30–13:00

Location: ZEU 160

Invited Talk

DY 38.1 Thu 9:30 ZEU 160

Acoustically propelled nano- and microparticles: From fundamentals to applications — •RAPHAEL WITTKOWSKI — Institut für Theoretische Physik, Center for Soft Nanoscience, Westfälische Wilhelms-Universität Münster, 48149 Münster, Germany

Among the existing types of artificial active colloidal particles, acoustically propelled nano- and microparticles have a particularly high potential for future applications in fields like medicine and materials science. However, despite intensive research on this type of motile particles in recent years, the understanding of their properties is still very limited. A reason for the limited understanding is that the previous research has mostly been experimental and that it is difficult to study the dependence of certain system parameters on the propulsion of the particles in experiments since the parameters can often not be varied independently of the other parameters and in ranges of reasonable size. In this talk, I will give an overview about our theoretical investigation of the properties of acoustically propelled nano- and microparticles and the challenges that remain for future research.

Funded by the Deutsche Forschungsgemeinschaft (DFG) – 283183152 (WI 4170/3).

DY 38.2 Thu 10:00 ZEU 160

Force on probe in a confined active fluid — SHUVOJIT PAUL¹, •ASHREYA JAYARAM², N NARINDER¹, THOMAS SPECK², and CLEMENS BECHINGER¹ — ¹Fachbereich Physik, Universität Konstanz, 78464 Konstanz, Germany — ²Institut für Physik, Johannes Gutenberg-Universität Mainz, 55128 Mainz, Germany

When immersed in a dispersion of smaller "depletants", a colloidal particle experiences depletion forces in the presence of another colloidal particle or under confinement. While the nature of these forces is well-established for passive systems, much less is known about the consequence of making the depletants self-propelled or "active". In this work, we consider a large, optically trapped probe under circular confinement surrounded by smaller active Janus particles. We find that the force experienced by the probe varies non-monotonically as the distance between the colloid and the confinement is increased. To rationalize this observation, we relate the measured force to the active stress and, subsequently, to the microstructure of the surrounding active fluid. Going beyond synthetic active matter, our work could shed light on the organization of intracellular entities in biological systems.

DY 38.3 Thu 10:15 ZEU 160

Symmetry-breaking refractive index profiles as a propulsion mechanism for active Brownian particles — •JULIAN JEGGLE¹, MATTHIAS RÜSCHENBAUM², CORNELIA DENZ², and RAPHAEL WITTKOWSKI¹ — ¹Institut für Theoretische Physik, Center for Soft Nanoscience, Westfälische Wilhelms-Universität Münster, 48149 Münster, Germany — ²Institut für Angewandte Physik, Westfälische Wilhelms-Universität Münster, 48149 Münster, Germany

Active Brownian particles (ABPs) have been realized with various propulsion mechanisms such as self-diffusiophoresis, self-electrophoresis or acoustic scattering. Typically, these mechanisms induce flow fields around the particles that represent a deviation from the "pure" ABP model. Here, we present a novel implementation of ABPs in the form of transparent microswimmers with a symmetry-breaking refractive index gradient. Utilizing the momentum transfer associated with light refraction as the driving force induces no flow fields beyond Stokes flow. Unlike optothermally driven particles, this archetype of ABPs also allows for sensitivity to the phase and polarization of the driving light field thus improving the spatio-temporal control of light-based propulsion mechanisms. Using non-light-absorbing particles enables bulk volume systems and allows the introduction of feedback loops, therefore making this approach a promising foundation for adaptive matter systems.

**Funded by the Deutsche Forschungsgemeinschaft (DFG) – Project-ID 433682494 – SFB 1459*

DY 38.4 Thu 10:30 ZEU 160

The interaction-expansion method: a systematic derivation strategy for active field theories — •MICHAEL TE VRUGT^{1,2}, JENS BICKMANN^{1,2}, STEPHAN BRÖKER^{1,2}, TOBIAS FROHOFF-HÜLSMANN¹, EYAL HEIFETZ³, MICHAEL E. CATES⁴, UWE THIELE^{1,5,6}, and RAPHAEL WITTKOWSKI^{1,2,5} — ¹Institut für Theoretische Physik, Westfälische Wilhelms-Universität Münster, 48149 Münster, Germany — ²SoN, Westfälische Wilhelms-Universität Münster — ³Porter School of the Environment and Earth Sciences, Tel Aviv University, 69978 Tel Aviv, Israel — ⁴DAMTP, Centre for Mathematical Sciences, University of Cambridge, Cambridge CB3 0WA, United Kingdom — ⁵CeNoS, Westfälische Wilhelms-Universität Münster — ⁶CMTC, Westfälische Wilhelms-Universität Münster

Field-theoretical models have made enormous contributions to our understanding of the collective dynamics of active matter. In this contribution, we introduce the interaction-expansion method (IEM) [1], which allows for a systematic derivation of active field theories from the microscopic dynamics of individual particles. We then discuss some recent applications of the IEM to particles with orientation-dependent propulsion speed [2] and particles with inertia [3].

[1] M. te Vrugt et al., in preparation (2022)

[2] S. Bröker et al., arXiv:2210.13357 (2022)

[3] M. te Vrugt et al., Nature Communications (provisionally accepted), arXiv:2204.03018 (2022)

* Funded by the Deutsche Forschungsgemeinschaft (DFG)-283183152

DY 38.5 Thu 10:45 ZEU 160

Entropy production in active turbulence — •BYJESH NALINI RADHAKRISHNAN, THOMAS SCHMIDT, and ETIENNE FODOR — Department of physics and material science, University of Luxembourg

Active particles like bacteria and sperm cells sustain a continuous intake and dissipation of energy. Consequently, they are intrinsically out of equilibrium which leads to a non-vanishing entropy production rate (EPR) even in steady states. Quantifying how the EPR varies in different collective phases is crucial in developing a thermodynamic framework for active matter. In this work, we look at the EPR in active turbulence. We use Active Model H, a continuum model for active particles in a momentum-conserving fluid, to study turbulence in contractile scalar active systems. We measure the local EPR in numerical simulations, which unveils the role of the noise and activity parameters on the EPR in active turbulent systems.

15 min. break

DY 38.6 Thu 11:15 ZEU 160

Phase transitions in multicomponent active matter: a quantitative kinetic theory — •JAKOB MIHATSCH¹, THOMAS IHLE¹, RÜDIGER KÜRSTEN², and HORST-HOLGER BOLTZ¹ — ¹Institute for Physics, University of Greifswald, Greifswald, Germany — ²Departament de Física de la Matèria Condensada, University of Barcelona, Barcelona, Spain

We consider a multicomponent model of self-propelled particles with Kuramoto-type alignment interactions. Starting from the N-particle Fokker-Planck equation we observe that the usual factorization Ansatz of the probability density, often called Molecular Chaos approximation, predicts a relaxation behavior which qualitatively disagrees with agent-based simulations. Therefore, we develop a kinetic theory which takes the time-evolution of the two-particle correlation function explicitly into account, i.e. goes beyond the mean-field approximation. We show that this theory predicts the relaxation behavior of the system as well as the order-disorder transition with high precision in certain parameter ranges. In particular, the dependence of the transition threshold on the particle speed is predicted correctly.

DY 38.7 Thu 11:30 ZEU 160

Emergent collective behaviour due to virtual interactions between robotic swimmers — •SAMUDRAJIT THAPA^{1,2}, BAT-EL PINCHASIK^{1,3}, and YAIR SHOKEF^{1,2,3} — ¹School of Mechanical Engineering, Tel Aviv University, Tel Aviv 69978, Israel — ²Sackler Center for Computational Molecular and Materials Science, Tel Aviv University, Tel Aviv 69978, Israel — ³Center for the Physics and Chemistry of Living Systems, Tel Aviv University, 69978, Tel Aviv, Israel

Many organisms in nature use local interactions to realize global collective behaviour. Here we study how simple two body distance-based interactions between active Brownian particles results in collective motion. The interactions are not physical but virtual, wherein each particle senses the presence of other particles nearby and changes its behaviour accordingly. We study the radial distribution function to quantify the emergent interactions for both social and anti-social behaviour. Using Langevin dynamics simulations, we discover that under certain conditions positive correlations of the motion can emerge even in the case of anti-social behaviour. Our results might be potentially useful for designing robotic swimmers that can swim collectively just based on sensing the distance to their neighbours.

DY 38.8 Thu 11:45 ZEU 160

Kinetic Event-Chain Algorithm for Active Matter — •NICO SCHAFFRATH, THEVASHANGAR SATHIYANESAN, TOBIAS KAMPMANN, and JAN KIERFELD — Physics Department, TU Dortmund University, 44221 Dortmund, Germany

We present a cluster kinetic Monte-Carlo algorithm for active matter systems of self-propelled hard particles. The kinetic event-chain algorithm is based on the event-chain Monte-Carlo method and is applied to active hard disks in two dimensions. The algorithm assigns Monte-Carlo moves of active disks a mean time based on the mean and variance of the move length in force direction. This time is used to perform diffusional rotation of their propulsion force. We show that the algorithm reproduces the motility induced phase separated region in the phase diagram of hard disks correctly and efficiently.

DY 38.9 Thu 12:00 ZEU 160

Emergent pattern formation in communicating active matter — •ROBERT GROSSMANN¹, ZAHRA MOKHTARI², ROBERT I.A. PATTERSON³, and FELIX HÖFLING^{2,4} — ¹Institut für Physik und Astronomie, Universität Potsdam — ²Institut für Mathematik, Freie Universität Berlin — ³WIAS Berlin — ⁴Zuse Institut Berlin

Inspired by trail formation as observed in colonies of driver ants, for example, we study ensembles of agent particles that communicate via deposition and sensing of pheromones. These chemical traces are produced by the agents themselves and encode their current position and walking direction. Other agents passing by will then tend to align with the orientation inscribed in the pheromone traces. In the limit of short pheromone lifetime, the dynamics of this system reduces to the seminal Vicsek model and, thus, yields the formation of transversally moving bands. In the opposite limit, the effective agent-agent interaction represents a form of delayed feedback and yields the spontaneous formation of macroscopic, persistent trails, which are followed and reinforced by the agents [New J. Phys. **24** 013012 (2022)]. In this talk, we present large-scale simulations of the agent model and establish the phase diagram as function of the lifetime of pheromones. We rationalize our findings by analyzing mean-field equations that are systematically derived from the stochastic particle model. Combining numerical solutions of these order parameter equations and a linear stability analysis, we show how transversal bands, common in the Vicsek model, are destabilized, giving rise to the formation of “longitudinal” trails, pointing in the mean direction of motion.

DY 38.10 Thu 12:15 ZEU 160

Binary Mixture of Deforming Particles — •YIWEI ZHANG, ALESSANDRO MANACORDA, and ETIENNE FODOR — DPhyMS, University of Luxembourg, Luxembourg, Luxembourg

Phase separation occurs in miscible liquids where components have distinct properties. In reactors, components undergo stochastic change in their properties which affect the liquid composition. While phase separation and reaction-diffusion have already been studied extensively as separate ingredients, how they combine in non-ideal reactors remains poorly understood. To bridge this gap, we consider repulsive particles with fluctuating size subject to one-body landscape and nonequilibrium synchronisation. The landscape features minima which, regarding size as reaction coordinate, distinguish three states: Particles with finite size, either A- or B-type, and point particles. In this context, synchronisation penalizes A particles in B-rich phases, and vice versa, so that the system eventually accommodates a uniform state. We report the phase diagram depending on the stability of each state and the corresponding particle sizes. Combining hydrodynamic and phenomenological arguments, we recapitulate how metastability regulates the interplay between synchronisation and repulsion. Our results reveal the role of nonequilibrium kinetic factors at play in non-ideal reaction-diffusion systems.

DY 38.11 Thu 12:30 ZEU 160

Self-organization of model catalytic cycles — •VINCENT OUAZAN-REBOUL¹, JAIME AGUDO-CANALEJO¹, and RAMIN GOLESTANIAN^{1,2} — ¹Max Planck Institute for Dynamics and Self-Organization, Am Fassberg 17, D-37077, Göttingen, Germany — ²Rudolf Peierls Centre for Theoretical Physics, University of Oxford, OX1 3PU, Oxford, UK

We study analytically and numerically a model metabolic cycle composed of an arbitrary number of species of catalytically active particles. Each species converts a substrate into a product, the latter being used as the substrate by the next species in the cycle. Through a combination of catalytic activity and chemotactic mobility, the catalytic particles develop effective interactions with particles belonging to neighbouring species in the cycle. These interactions, being fully out-of-equilibrium, show some unusual features, in particular being non-reciprocal. We find that such model metabolic cycles are able to self-organize through a macroscopic instability, with a strong dependence on the characteristics of the cycle. For instance, cycles containing an even number of species are able to minimize repulsion between their component particles by aggregating all even-numbered species in one cluster, and all odd-numbered species in another. Such a grouping is not possible if the cycle contains an odd number of species, which can lead to oscillatory steady states in the case of chasing interactions.

DY 38.12 Thu 12:45 ZEU 160

Reentrant condensation transition in a model of driven scalar active matter with diffusivity edge — BERX JONAS², •BOSE ARITRA¹, MAHAULT BENOIT¹, and GOLESTANIAN RAMIN^{1,3} — ¹Max Planck Institute for Dynamics and Self-Organization, 37077 Göttingen, Germany — ²Institute for Theoretical Physics, KU Leuven, B-3001 Leuven, Belgium — ³Rudolf Peierls Centre for Theoretical Physics, University of Oxford, Oxford OX1 3PU, United Kingdom

A class of scalar active matter for which the effective diffusivity vanishes beyond a certain density threshold, hereby referred to as diffusivity edge, triggers the formation of a condensate when confined in a harmonic potential. The condensation transition exhibits remarkable similarities with a Bose-Einstein Condensation (BEC). Here we study the effect of a diffusivity edge in a system of scalar active matter confined by a periodic potential and driven by an external force.

We find that this system shows qualitatively distinct stationary regimes depending on the amplitude of the driving force with respect to the potential barrier. For small driving, the diffusivity edge induces a condensation analogous to

the BEC-like transition reported for the nondriven case, which is characterised by a density-independent steady state current. Conversely, large external forces lead to a qualitatively different phase diagram where condensation is not possible

below a density threshold and the associated transition at moderate densities above the threshold the transition is reentrant due to the existence of a subsequent evaporation transition at low effective temperatures.

DY 39: Networks: From Topology to Dynamics II (joint session SOE/DY)

Time: Thursday 9:30–10:00

Location: ZEU 260

See SOE 14 for details of this session.

DY 40: Stochastic Thermodynamics

Time: Thursday 10:00–12:30

Location: ZEU 250

DY 40.1 Thu 10:00 ZEU 250

Optimized Work Protocols for the Higgs RNA-Model — •PETER WERNER and ALEXANDER K. HARTMANN — Institute of Physics, University of Oldenburg, Germany

When a system is driven from one state to another in a *finite* amount of time $t \in [0, \dots, \tau]$ by changing an external control parameter according to a protocol $\lambda(t)$, some work W is performed. Here $\langle W \rangle \geq \Delta F$ holds, where ΔF is the equilibrium free energy difference between initial and final states. The protocol $\lambda^*(t)$ minimizing the average amount of work is of interest, since it tightens the upper bound to ΔF . The optimum protocols of simple Brownian-particle systems exhibit distinct jumps especially at the beginning and end of the process [1,2] and it was speculated that these are a generic feature for arbitrary systems.

Here the *many-particle* Higgs RNA model [3] is considered, where work is performed by stretching the RNA through changing an external force. For this model, an exact calculation of the free-energy differences ΔF and the sampling of the equilibrium initial state can be performed in polynomial time. The work processes are realized by means of non-equilibrium Monte-Carlo simulations [4]. The optimum protocols are obtained numerically with the parallel-tempering approach. Also for this complex system, the optimum protocols exhibit distinct jumps at the beginning and end.

[1] T. Schmiedl and U. Seifert, Phys. Rev. Lett., **98**, 108301 (2007)

[2] H. Then and A. Engel, Phys. Rev. E **77**, 041105 (2008)

[3] P. G. Higgs, Phys. Rev. Lett., **76**, 704 (1996)

[4] P. Werner and A. K. Hartmann, Phys. Rev. E **104**, 034407 (2021)

DY 40.2 Thu 10:15 ZEU 250

Coherence of oscillations in the weak-noise limit — •BENEDIKT REMLEIN, VOLKER WEISSMANN, and UDO SEIFERT — II. Institut für Theoretische Physik, Universität Stuttgart, 70550 Stuttgart, Germany

In a noisy environment, oscillations lose their coherence, which can be characterized by a quality factor. We determine this quality factor for oscillations arising from a driven Fokker-Planck dynamics along a periodic one-dimensional potential analytically in the weak-noise limit. With this expression, we can prove for this continuum model the analog of an upper bound that has been conjectured for the coherence of oscillations in discrete Markov network models. We show that our approach can also be adapted to motion along a noisy two-dimensional limit cycle. Specifically, we apply our scheme to the noisy Stuart-Landau oscillator and the thermodynamically consistent Brusselator as a simple model for a chemical clock. Our approach thus complements the fairly sophisticated extant general framework based on techniques from Hamilton-Jacobi theory with which we compare our results numerically [1].

[1] B. Remlein, V. Weissmann, and U. Seifert, Phys. Rev. E **105**, 064101 (2022)

DY 40.3 Thu 10:30 ZEU 250

Work extraction potential for a single spin in equilibrium with a non-isotropic environment — •FELIX HARTMANN¹ and JANET ANDERS^{1,2} — ¹Institut für Physik und Astronomie, University of Potsdam, 14476 Potsdam, Germany — ²Department of Physics and Astronomy, University of Exeter, Stocker Road, Exeter EX4 4QL, UK

Thermal equilibrium properties of nanoscale systems deviate from standard macroscopic predictions due to a non-negligible coupling to the environment. For non-isotropic three-dimensional materials, we derive the mean force corrections to the equilibrium state of a single classical spin vector. The result is valid at arbitrary coupling strength.

Specifically, we consider cubic, orthorhombic, and monoclinic symmetries, and compare differences in their spin expectation values as a function of temperature. We underpin the correctness of the mean force state by evidencing its match to the steady state of the simulated non-Markovian spin dynamics. Our results show an explicit dependence on the symmetry of the material in which the spin is confined.

Further, we quantify how the mean force-generated inhomogeneities in the energy shells lead to a work extraction potential. Such inhomogeneities constitute a classical equivalent to quantum coherences.

DY 40.4 Thu 10:45 ZEU 250

Time-resolved statistics of snippets as general framework for model-free entropy estimators — •JANN VAN DER MEER, JULIUS DEGÜNTHER, and UDO SEIFERT — II. Institut für Theoretische Physik, Universität Stuttgart, 70550 Stuttgart

Irreversibility is commonly quantified by entropy production. An external observer can estimate it through measuring an observable that is antisymmetric under time-reversal like a current. We introduce a general framework that, inter alia, allows us to infer a lower bound on entropy production through measuring the time-resolved statistics of events with any symmetry under time-reversal, in particular, time-symmetric instantaneous events. We emphasize Markovianity as a property of certain events rather than of the full system and introduce an operationally accessible criterion for this weakened Markov property. Conceptually, the approach is based on snippets as particular sections of trajectories, for which a generalized detailed balance relation is discussed.

DY 40.5 Thu 11:00 ZEU 250

Anomalous relaxation from a non-equilibrium steady state: An isothermal analog of the Mpemba effect — •JULIUS DEGÜNTHER and UDO SEIFERT — II. Institut für Theoretische Physik, Universität Stuttgart, 70550 Stuttgart, Germany

The Mpemba effect denotes an anomalous relaxation phenomenon where a system initially at a hot temperature cools faster than a system that starts at a less elevated temperature. We introduce an isothermal analog of this effect for a system prepared in a non-equilibrium steady state that then relaxes towards equilibrium. Here, the driving strength, which determines the initial non-equilibrium steady state, takes the role of the temperature in the original version. As a paradigm, we consider a particle initially driven by a non-conservative force along a one-dimensional periodic potential. We show that for an asymmetric potential relaxation from a strongly driven initial state is faster than from a more weakly driven one at least for one of the two possible directions of driving. These results are first obtained through perturbation theory in the strength of the potential and then extended to potentials of arbitrary strength through topological arguments.

[1] Julius Degünther and Udo Seifert, EPL, **139** 4 (2022) 41002

15 min. break

DY 40.6 Thu 11:30 ZEU 250

Measurement phase transitions in the no-click limit as quantum phase transitions of a non-hermitean vacuum. — •CATERINA ZERBA^{1,2,3} and ALESSANDRO SILVA² — ¹Technical University of Munich, 85748 Garching, Germany — ²International School for Advanced Studies (SISSA), via Bonomea 265, 34136 Trieste, Italy — ³Università degli Studi di Trieste, via Alfonso Valerio 2, 34127 Trieste, Italy

We study dynamical phase transitions occurring in the stationary state of the dynamics of integrable many-body non-hermitian Hamiltonians, which can be either realized as a no-click limit of a stochastic Schrödinger equation or using spacetime duality of quantum circuits. In two specific models, the Transverse Field Ising Chain and the Long Range Kitaev Chain, we observe that the entanglement phase transitions occurring in the stationary state have the same nature as that occurring in the vacuum of the non-hermitian Hamiltonian: an area law phase when the imaginary part of the quasi-particle spectrum is gapped and a logarithmic growth for gapless imaginary spectrum. This observation suggests the possibility to generalize the area-law theorem to non-Hermitian Hamiltonians

DY 40.7 Thu 11:45 ZEU 250

Thermodynamics of growth in chemical reaction networks — •SHESHA GOPAL MAREHALLI SRINIVAS, FRANCESCO AVANZINI, and MASSIMILIANO ESPOSITO — Complex Systems and Statistical Mechanics, Department of Physics and Materials Science, University of Luxembourg, L-1511 Luxembourg

Open chemical reaction networks show a variety of complex dynamical behaviour such as chemical waves, oscillations, chaotic dynamics, multistability,

and so on. Progress in stochastic thermodynamics has enabled us to identify the energetic costs of these phenomena. However, very little attention has been paid to chemical growth. We will identify the necessary conditions under which open homogeneous CRNs evolving with mass action kinetics show asymptotic growth. Our main results show that growth with nonequilibrium abundances requires nonlinear CRNs with the influx of at least one species from the surrounding. Linear CRNs, on the other hand, can only grow with equilibrium abundances. Our results illustrate the important interplay between topology and the chemostatting procedure in determining the asymptotic dynamics of CRNs.

DY 40.8 Thu 12:00 ZEU 250

Irreversible fluctuations herald dynamical phases in non-Hermitian phase-field models — •THOMAS SUCHANEK¹, KLAUS KROY¹, and SARAH LOOS² — ¹Institut für Theoretische Physik, Universität Leipzig, Leipzig, Germany — ²DAMTP, University of Cambridge, Cambridge, United Kingdom

We study the time-reversal symmetry (TRS) breaking of fluctuations in phase-field models that exhibit dynamical phases. We focus on two typical scenarios in which dynamical phases can be born, namely, oscillatory instabilities and the recently uncovered \mathcal{PT} -symmetry breaking transitions in non-Hermitian systems [1] that are accompanied by Exceptional Points. Quantifying the TRS breaking by the informatic entropy production rate [2] and analytically investigating the zero noise limit, we find divergent behavior at both transitions. We discuss an example model of two nonreciprocally coupled Chan-Hilliard fields, and offer interpretations of the TRS breaking in terms of interface dynamics, the \mathcal{PT} -symmetry breaking and the amplification of dissipative noise near Exceptional Point transitions.

[1] M. Fruchart, R. Hanai, P. B. Littlewood, and V. Vitelli, Non-reciprocal phase transitions, *Nature* 592, 363-369 (2021).

[2] C.Nardini, E. Fodor, E. Tjhung, F. van Wijland, J. Tailleur, and M. E. Cates, Entropy production in field theories without time-reversal symmetry: Quantifying the non-equilibrium character of active matter, *Phys. Rev. X* 7, 021007 (2017).

DY 40.9 Thu 12:15 ZEU 250

Large deviations theory for noisy non-linear electronics — •ASHWIN GOPAL, MASSIMILIANO ESPOSITO, and NAHUEL FREITAS — University of Luxembourg, L-1511 Luxembourg, Luxembourg

The latest generations of transistors are nanoscale devices whose performance and reliability are limited by thermal noise in low-power applications. Therefore, developing efficient methods to compute the voltage and current fluctuations in such non-linear electronic circuits is essential. In this presentation, I will describe the large deviations approach to compute these fluctuations using the stochastic thermodynamic description of CMOS-based electronics (*Phys. Rev. B* 106, 155303). Starting from the thermodynamically consistent description of the charge transfer at a single electron level, I will then consider the macroscopic limit. This corresponds to scaling up the transistor's physical dimensions, resulting in an increase in the number of electrons on the conductors. In this limit, the thermal fluctuations satisfy a Large Deviations Principle which I will show is also remarkably precise in settings involving only a few tens of electrons, by comparing our results with Gillespie simulations and spectral methods. Traditional approaches, using the stationary Gaussian white noise, are recovered by resorting to an ad hoc diffusive approximation revealing their inconsistencies. To illustrate these findings, I will use the case study of the low-power CMOS inverter, or NOT gate, which is a basic primitive in electronic design. Finally, I will briefly comment on thermodynamic uncertainty (TUR) relations and information processing, in the context of such electronic circuits.

DY 41: Networks: From Topology to Dynamics III (joint session SOE/DY)

Time: Thursday 10:00–10:45

Location: ZEU 260

See SOE 15 for details of this session.

DY 42: Poster: Active Matter, Soft Matter, Fluids

Time: Thursday 13:00–16:00

Location: P1

DY 42.1 Thu 13:00 P1

Transition to mesoscale turbulence in an active fluid — •HENNING REINKEN¹, SEBASTIAN HEIDENREICH², MARKUS BÄR², and SABINE H.L. KLAPP¹ — ¹Technische Universität Berlin — ²Physikalisch-Technische Bundesanstalt

Microwimmer suspensions, a paradigmatic example of an active fluid, self-organize into complex spatio-temporal flow patterns, including regular vortex lattices and mesoscale turbulence, a highly dynamical state that exhibits a characteristic length scale. This work investigates the transition to this turbulent state using a continuum-theoretical approach for the effective microwimmer velocity field [1], where the dynamics is governed by the competition between relaxation to a regular vortex lattice and destabilization by nonlinear advection. For the unconstrained bulk flow, we show how to identify the onset of mesoscale turbulence analytically. To this end, we determine the linear stability of the vortex lattice state by explicitly taking into account the coupling between multiple modes via the nonlinear terms. Recent experiments [2] have also demonstrated how vortex lattices can be stabilized by small obstacles [3]. Using the continuum-theoretical approach, we further show numerically that the formation of these patterns exhibits features of a continuous second-order equilibrium phase transition in the 2D Ising universality class [4].

[1] Reinken et al., *Phys. Rev. E* 97, 022613 (2018)

[2] Nishiguchi et al., *Nat. Commun.* 9, 4486 (2018)

[3] Reinken et al., *Commun. Phys.* 3, 76 (2020)

[4] Reinken et al., *Phys. Rev. Lett.* 128, 048004 (2022)

DY 42.2 Thu 13:00 P1

Dynamics and clustering of active run-and-tumble particles on two-dimensional lattices — •LARS TORBJØRN STUTZER and PETER SOLLICH — Institut für Theoretische Physik, Georg-August Universität Göttingen

We study the dynamics of run-and-tumble particles on two-dimensional lattices, focusing on the effects of lattice geometry (square, triangular and hexagonal) and maximum occupation number n_{\max} per lattice site. We identify three phases in the stationary state: a cluster (C) phase with extensive clusters formed by motility-induced phase separation, which appears only for $n_{\max} \geq 2$; a gas (G) phase consisting of finite-sized clusters; and a new sponge (S) phase where small fluctuating clusters percolate. The nature of the transitions between these phases depend on lattice type and density. C-G transitions are mostly, but not always, first order, while C-S transitions are continuous. Single particle displacement

distributions become non-Gaussian at higher densities, with intermediate exponential tails. Considering finally the transient dynamics from a random initial condition, the time it takes for clustering to appear in the system is independent of the tumble rate α but grows with the lattice coordination number and (exponentially or stronger) with n_{\max} .

DY 42.3 Thu 13:00 P1

Pressure in inertial active particle systems with frictional contacts — •KAY-ROBERT DORMANN, LUKAS HECHT, and BENNO LIEBCHEN — Institut für Physik kondensierter Materie, Technische Universität Darmstadt, Hochschulstr. 8, 64289 Darmstadt, Germany

In systems of isotropic overdamped active Brownian particles (ABPs), the pressure is a state function [1]. It can be shown, that an equation of state (EOS) also exists, if the ABPs are inertial [2]. Here, we explore inertial active Brownian particles [3,4] with additional frictional contacts and find that no EOS exists. We attribute this to the fact that the rotational diffusion depends on density in the presence of frictional contacts.

The breakdown of the EOS due to frictional contacts has interesting implications: for example, when embedding a passive Janus-sphere, whose two hemispheres show a different stiffness, into an active bath, the sphere shows active Brownian motion. In addition, we find that frictional contacts and the associated breakdown of the EOS also have interesting implications for motility-induced phase separation as we will specify on the poster.

[1] A. P. Solon et al., *Phys. Rev. Lett.* 114, 198301 (2015).

[2] Y. Fily et al., *J. Phys. A Math. Theor.* 51, 044003 (2018).

[3] S. Mandal et al., *Phys. Rev. Lett.* 123, 228001 (2019).

[4] L. Hecht et al., *Phys. Rev. Lett.* 129, 178001 (2022).

DY 42.4 Thu 13:00 P1

Advanced Sampling Methods for Non-Equilibrium Particles — •THOMAS KIECHL, MICHELE CARAGLIO, and THOMAS FRANOSCH — Institute for Theoretical Physics, Universität Innsbruck, Innsbruck, Austria.

Active particles or microswimmers are capable of converting energy into directed motion - which is why they are classified as out-of-equilibrium systems. Microswimmers, such as bacteria or spermatozoa often find themselves in a *target search* situation, where the microswimmers have to make a transition from an initial area to a target area crossing complex environments. Transition Path

Theory, a rigorous statistical mechanics description of transition processes, can be generalized to characterize the target search problem. A simple way of modeling a complex environment for the microswimmer is via an external potential, in which the metastable initial position is separated from the target by an energy barrier. This makes the target search a *rare event*, in which the timescales of the fluctuations in the metastable states and the transition process are separated. Brute force simulations solving the equations of motion are inefficient due to this gap in timescales. The main result is that a more efficient sampling method, Transition Path Sampling (TPS), originally developed for rare transitions of passive systems, can be generalized to Run-and-Tumble systems. TPS is a Monte Carlo simulation of successful trajectories where the new trajectory is accepted according to a metropolis rule based on a path integral formulation.

DY 42.5 Thu 13:00 P1

Markov state modelling of self-assembling active triblock Janus particles — •SALMAN FARIZ NAVAS, JURI SCHUBERT, and SABINE H.L. KLAPP — ITP, Technische Universität Berlin, Germany

Active triblock Janus particles have been shown to form open-cell colloidal lattices in both experiments as well as simulations. Such structures are of particular interest owing to their novel optical and mechanical properties. However, the self-assembly of open-cell lattices is a multistep process involving the formation of many intermediate competing structures resulting in long time-scales.

Here, we develop a Markov State Model for a self-assembling active triblock Janus particle system [1] from particle resolved Brownian Dynamics simulations by reducing the continuous many particle dynamics into a discrete set of states [2],[3]. We use the local order parameters introduced in [4] to develop the discrete states. The transition probability matrix between these states can then be constructed using which, information regarding the metastable states, the relaxation times and the pathways relevant to the aggregation process can be extracted.

- [1] S. A. Mallory and A. Cacciuto, J. Am. Chem. Soc. 141, 2500 (2019).
 [2] J.-H. Prinz, H. Wu, M. Sarich, B. Keller, M. Senne, M. Held, J. D. Chodera, C. Schütte, and F. Noé, J. Chem. Phys. 134, 174105 (2011).
 [3] S.F. Navas and S.H.L. Klapp, in preparation.
 [4] H. Eslami, P. Sedaghat, and F. Müller-Plathe, Phys. Chem. Chem. Phys. 20, 27059 (2018).

DY 42.6 Thu 13:00 P1

Dynamics of an active agent subject to orientational resetting — •YANIS BAUCHE and CHRISTINA KURZTHALER — Max Planck Institute for the Physics of Complex Systems, Dresden, Germany

We study the dynamics of an active particle whose swimming direction is subject to rotational diffusion and a stochastic resetting mechanism. The latter allows for taking into account the particle's response to external stimuli.

We use renewal processes to model the reorientation mechanism of the active agent and provide analytical expressions for the characteristic function of the stochastic process and its low-order moments.

Finally, the interplay between rotational diffusion and resetting of the particle's orientation is quantified for different resetting distributions.

DY 42.7 Thu 13:00 P1

Adaptive microvascular remodeling under flow — FATEMEH MIRZAPOUR-SHAFIYI, •LEONIE KARR, and KAREN ALIM — School of Natural Sciences, Technische Universität München

Vessel morphology is adapted to minimise energetic costs of dissipation and homogenize flow transport in the network. Resource-deprived tissues produce chemotactic agents to induce vessel formation during development and in tissue homeostasis. The primitive, mesh-like vascular network formed initially through neovascularisation is highly ramified. Later, vascular network is normalised into a hemodynamically preferred tree-like structure. The normalisation process, termed vessel remodeling, leads to an organ-specific network architecture which better meets the metabolic needs of its surrounding tissue. As vessel growth and remodeling is found impaired in various disease states, several factors regulating vessel formation and branching morphology were identified over the past decades. However, while some of these factors have been undergoing clinical trials, their effects on transport properties of the altered vessel morphology are not fully elucidated yet. Establishing a perfusable human vasculature-on-a-chip (hVoC) model system, here we aim to investigate how vascular morphology correlates with flow field. Our hVoC model allows extensive quantitative analyses of network morphology and adaptive remodeling under fluid flow applied by a low-pressure syringe pump. Results of our analyses will contribute to the next generation therapeutics targeting vessel development.

DY 42.8 Thu 13:00 P1

Thermodynamics of active matter systems under coarse graining — •ROBIN BEBON and THOMAS SPECK — Institute for Theoretical Physics 4, University of Stuttgart, Heisenbergstraße 3, 70569 Stuttgart, Germany

Over the last decade, dynamic field theories have proven useful in the description of collective behavior and large-scale dynamics of active matter systems. However, despite their popularity, surprisingly little is known about how to capture

thermodynamics on the level of such hydrodynamic descriptions. This is partially due to the fact that common approaches, based on symmetry arguments and conservation laws, typically neglect degrees of freedom that play a crucial role in quantifying the system's energetics, e.g., the self-propulsion mechanism. To advance, we propose a bottom-up approach that starts with a thermodynamically consistent microscopic model of catalytic particles driven by a constant affinity and derive effective hydrodynamic equations via explicit coarse graining. To ensure that information of the self-propulsion mechanism and its energy consumption is preserved on the macro-scale, we introduce an additional field, which for the considered model tracks the local rate of successful chemical events. We find that, near equilibrium, particle current and chemical field couple linearly through their respective thermodynamic forces, closely resembling linear irreversible thermodynamics. This provides an access point to investigate the thermodynamic properties of our field theory and compare the results with their microscopic counterparts.

DY 42.9 Thu 13:00 P1

The Liquid-Glass-Jamming Rheology of Soft Active Particles — •ROLAND WIESE¹, KLAUS KROY¹, and DEMIAN LEVIS^{2,3} — ¹Institute for Theoretical Physics, Leipzig University, 04103 Leipzig, Germany — ²Departament de Física de la Materia Condensada, Facultat de Física, Universitat de Barcelona, Martí i Franquès 1, 08028 Barcelona, Spain — ³University of Barcelona Institute of Complex Systems (UBICS), Facultat de Física, Universitat de Barcelona, Martí i Franquès 1, 08028 Barcelona, Spain

We study the linear and nonlinear rheology of an active Brownian particle suspension at different densities. In the low density and low shear limits the flow is Newtonian. In this regime its linear response viscosity can be calculated via the Green-Kubo autocorrelation method and is found to scale with an effective temperature. In the nonlinear regime of high shearing rates shear thinning is observed universally for all parameters considered in our study. Above the critical density of the glass transition the dynamics becomes arrested, marked by the appearance of a finite yield stress. Increasing the self-propulsion of the active particles shifts the glass transition to higher densities by melting the amorphous solid. The yield stress enables us to construct a phase diagram in the spirit of jamming phase diagrams, but exchanging temperature with activity. For sufficiently high activities glassy physics becomes suppressed and the yield stress scales with a power law in the density, known from jammed granular materials.

DY 42.10 Thu 13:00 P1

Wetting of reflecting plates by an Active Brownian fluid — •MATTHIEU MANGEAT, SHAURI CHAKRABORTY, ADAM WYSOCKI, and HEIKO RIEGER — Universität des Saarlandes, Saarbrücken, Germany

We study, using interacting active Brownian particles (ABP), the wall-wetting mechanism of active sedimenting fluid. We consider a minimal model of active particles under gravitational field, inside a two-dimensional rectangular box. An accumulation of particles near the bottom wall is observed, as well as the wetting of vertical plates by the rise of active particles against the gravity, even without any attractive force within the system. We characterize this wall-wetting by the meniscus height, calculated from stationary density profile and depending on the inter-particle repulsion. The maximum wetting height depends super-linearly on active sedimentation length for interacting ABP, and linearly for non-interacting ABP. We also observe two large vortices concentrated close to the meniscus, due to the persistence motion of ABP against the gravity. Moreover, with non-interacting ABP, a current flow is present near the boundaries for which we propose a coarse-grained description.

DY 42.11 Thu 13:00 P1

Force-free Ratcheting in Static Activity Landscapes — •CONSTANTIN REIN¹, MARTIN KOLÁR², KLAUS KROY¹, and VIKTOR HOLUBEC² — ¹Leipzig University, Faculty of Physics and Earth Sciences, Institute for Theoretical Physics, Brüderstraße 16, 04081 Leipzig — ²Charles University, Faculty of Mathematics and Physics, Department of Macromolecular Physics, V Holešovičkách 2, CZ-180 00 Praha

We study the possibility of rectifying active Brownian motion solely using time-independent activity landscapes. We argue that, in one dimension, spatially asymmetric activity does not suffice to induce directed transport, unless the activity is modulated in time or an additional potential is used, whereas, in higher dimensions, static activity landscapes alone can induce ratcheting. The underlying principle is similar to the ratcheting induced by asymmetric obstacles in microswimmer baths: swimmers with suitable orientations get channeled, while the others get trapped in low-activity regions until they lost their orientation. For landscapes with wedge-shaped low-activity regions, we numerically found an average transport velocity of the order of 1% of the particle's swim speed.

DY 42.12 Thu 13:00 P1

The nature of non-phononic excitations in disordered systems — •WALTER SCHIRMACHER^{1,2}, MATTEO PAOLUZZI³, and GIANCARLO RUOCCO^{2,4} — ¹Universität Mainz, Mainz, Germany — ²Istituto Italiano di Tecnologia, Roma, Italy — ³Universitat de Barcelona, Barcelona, Spain — ⁴Università di Roma "La Sapienza", Roma, Italy

We theoretically and numerically investigate the nature of the non-phononic excitations appearing in the vibrational spectrum of disordered materials of small systems, which do not allow for low-frequency waves (phonons). Using heterogeneous-elasticity theory and a new generalization, we are able to distinguish between two types of non-phononic vibrational excitations of disordered materials (glasses). A first type (Type-I) arises beyond the boson peak due to strong scattering from the structural disorder. These excitations are similar to the eigenvectors of random matrices. In very small systems, in the absence of low-frequency waves, the spectrum exhibits a gap, which, in a marginal-stable situation, may extend to zero frequency and features a DOS proportional to the square of the frequency. In such small systems, in a more stable situation, a second type of non-phononic excitations (Type-II) appears, which involve rotational oscillations around local frozen-in stresses. The frequency spectrum of these Type-II excitations is related to the interaction potential in the regime, where the potential contributions are small, rendering the frequency dependence non-universal. The frequently observed frequency scaling with the fourth power is shown to be an artifact due to the smooth tapering of the potential cutoff in the simulations.

DY 42.13 Thu 13:00 P1

Glass Transition in Modulated Liquids — •ABOLFAZL AHMADIRAHMAT¹, MICHELE CARAGLIO¹, VINCENT KRAKOVIACK², and THOMAS FRANOSCH¹ — ¹Institut für Theoretische Physik, Universität Innsbruck, Technikerstraße 21A, A-6020 Innsbruck, Austria — ²Laboratoire de chimie, École normale supérieure de Lyon, 46 Allée d'Italie 69364 Lyon, Cedex 07, France

We have developed a theoretical description for the structural and dynamical properties of quasi-two-dimensional colloidal suspensions subject to periodic potentials using mode-coupling theory (MCT). We solve the MCT equations numerically for monodisperse hard disks modulated by a periodic external potential and, we show that the theory reduces to the conventional MCT equations of the glass transition for bulk systems if the external modulation vanishes. To do so, we elaborate numerical results for the long-time limits of suitably generalized intermediate scattering functions. We compare the nonergodicity parameter of a two-dimensional modulated liquid in zero modulation with the corresponding nonergodicity parameter for the bulk system in two dimensions.

DY 42.14 Thu 13:00 P1

Assembly of iron oxide nanocuboids directed by surface, ligand, and magnetic interactions — •SINDY J. RODRÍGUEZ SOTELO^{1,2}, MARIO C.G. PASEGGI JR.^{1,2}, CARLOS GARCÍA³, and IGOR STANKOVIĆ⁴ — ¹Instituto de Física del Litoral IFIS-CONICET, Santa Fe, Argentina — ²Facultad de Ingeniería Química, Universidad Nacional del Litoral UNL, Santa Fe, Argentina — ³Departamento de Física and Centro Científico Tecnológico de Valparaíso-CCTVal, Universidad Técnica Federico Santa María, Valparaíso, Chile — ⁴Scientific Computing Laboratory, Center for the Study of Complex Systems, Institute of Physics Belgrade, University of Belgrade, Serbia

The direction of the dipole moment in the magnetite spherical nanoparticles is unrelated to the morphology particle. For non-spherical particles, a coupling between particle form and magnetic moment direction might result in unexpected behaviours, especially when the moment is not aligned along a particle symmetry axis [1,2]. We introduce energy models accounting for the directionality and magnitude of the van der Waals and dipolar interactions as a function of the shape of the nanocubes, illustrating the importance of the directional dipolar forces for the formation of the nanocube clusters, the dominance of the van der Waals multi-body interactions and exclusion forces of ligands. We illustrate how minimal energy structures depend on the assembly size, shape of the particles, and the balance of surface and magnetic dipolar coupling.

[1] I. Stanković, *et al.* *Nanoscale* **12**, 19390, 2020.[2] L. Balcells *et al.* *Nanoscale* **11**, 14194, 2019.

DY 42.15 Thu 13:00 P1

Phase Behaviour of a Minimal Lattice Model with Chiral Interactions — •BOYI WANG^{1,2}, PATRICK PIETZONKA¹, and FRANK JÜLICHER^{1,3} — ¹Max Planck Institute for the Physics of Complex Systems, Dresden, Germany — ²Institute of Physics, Chinese Academy of Sciences, Beijing, China — ³Cluster of Excellence, Physics of Life, TU Dresden, Dresden, Germany

We introduce chiral interactions to a minimal lattice model based on the Ising model, adding second neighbour interactions that favour an L-shaped structure. We run Monte-Carlo simulations in equilibrium at low temperatures, and find two new ground states which exhibit chiral periodic tiling. We also study the phase behaviour analytically as a function of the strength of the chiral interaction and the external magnetic field. With number conservation, we observe the coexistence of chiral and achiral phases and the formation of droplets. Furthermore, we consider the role of chirality in this minimal lattice model with active driving forces.

DY 42.16 Thu 13:00 P1

Static and dynamical magnetic properties ferrofluid with ellipsoid-like nanoparticles — •VLADIMIR ZVEREV, ALLA DOBROSERDOVA, EKATERINA EKATERINA, ELENA PYANZINA, and ALEXEY IVANOV — Ekaterinburg, Russia

A system of magnetic ellipsoids with a point dipole at the particle center is considered. We take into account different shape's anisotropy and different positions of the magnetic moment inside the particle (parallel and perpendicular to the main axis of the ellipsoid). In order to study this system, molecular dynamics simulations are used. The ratio of the main semi-axis to the additional one was used as a measure of the particle anisotropy. In particular, we have studied the system in which the particles have magnetic moments, but there is no dipole-dipole interaction between them. As a result, the initial magnetic susceptibility (magnetic characteristic) and the radial distribution function (structural characteristic) were calculated. For the initial susceptibility, the data obtained in computer simulations differ from the Langevin magnetization (theoretical ideal case) within the statistical error. The data for the Radial Distribution Function (RDF) also match within the calculation error. The next stage of research was to take into account dipole-dipole interparticle interactions and also will be presented.

DY 42.17 Thu 13:00 P1

Hopping conduction in networks with site energy disorder — •QUINN EMILIA FISCHER, MARCO BOSI, and PHILIPP MAASS — Fachbereich Physik, Universität Osnabrück, Barabarastraße 7, D-49076 Osnabrück, Germany

Understanding conductivities due to hopping motion in disordered systems is an important problem with various applications ranging from electron transport in amorphous semiconductors to ion transport in glasses [1,2]. A prominent model is that of particle hopping on a lattice with random site energies, where each lattice site can be occupied by at most one particle. For this model, a theory has been proposed, where transport properties are determined by a mapping onto a random resistor network [3]. By comparison with extensive kinetic Monte Carlo simulations for different types of site energy distributions, we show that this theory gives good predictions for small and high particle concentrations but is less accurate for intermediate concentrations. We present a refined theory which takes into account nearest neighbour correlations between occupation numbers in current carrying nonequilibrium steady states. This theory yields an improved prediction of conductivities and their activation energies in very good agreement with the Monte Carlo results.

[1] M. Bosi, P. Maass, *J. Phys. Chem. C* **125** 6260 (2021).[2] M. Bosi, P. Maass, *Z. Phys. Chem.* **236**, 1055 (2022).[3] V. Ambegaokar, B. I. Halperin, *J. S. Langer*, *Phys. Rev. B* **4**, 2612 (1971).

DY 43: Poster: Quantum Dynamics and Many-Body Systems

Time: Thursday 13:00–16:00

Location: P1

DY 43.1 Thu 13:00 P1

applications of generalized coherent states in bosonic systems — •YULONG QIAO¹, FRANK GROSSMAN², and JOONSUK HUH³ — ¹Institute for theoretical physics, TU Dresden, 01062 Dresden, Germany — ²Institute for theoretical physics, TU Dresden, 01062 Dresden, Germany — ³Department of Chemistry, Sungkyunkwan University, Suwon 16419, Republic of Korea

Generalized coherent states (GCS) are found to be very useful for studying bosonic systems with a fixed number of particles, such as the Bose-Hubbard model and boson sampling. Firstly, we present the non-equilibrium dynamics of the Bose-Hubbard model based on the time-dependent variational principle [1]. Increasing the multiplicity of GCS leads to converged results quickly for weak interaction strength, which indicates that GCS are a well-suited basis in the superfluid phase. Secondly, we investigate the boson sampling problem whose input state is a Fock state. Using an exact expansion of the Fock state in terms of GCS,

we obtain the output state by means of a unitary rotation. By this process the total information is contained in a finite number of GCS. The specific structure of the GCS allows us to split the whole system into two parts easily and to study the entanglement entropy of the output state in detail [2].

[1] Y. Qiao and F. Grossmann, Exact variational dynamics of the multimode Bose-Hubbard model based on SU(M) coherent states, *Phys. Rev. A* **103**, 042209 (2021).

[2] Y. Qiao, J. Huh, F. Grossmann, Entanglement in the full state vector of boson sampling, arXiv:2210.09915 [quant-ph] (2022).

DY 43.2 Thu 13:00 P1

Coupling in Optical Microcavity-Arrays — •TOM RODEMUND and MARTINA HENTSCHEL — Department of Physics, University of Applied Sciences Chemnitz, Chemnitz, Germany

Optical microcavities capture light by total internal reflection in so-called whispering-gallery modes. Deformed disk-shaped microcavities, for example of Limaçon shape, allow one to keep high Q-factors while manipulating the far-field emission via the resonator geometry, thereby allowing for a wide range of applications from microlasers to sensors.

Coupling of several microdisk resonators enhances the possibilities to tame light considerably [1]. Depending on the number and distance of the coupled cavities, the far-field characteristics vary tremendously and can even be reversed [1]. Here, we investigate the underlying mechanisms. To this end we use phase-space methods and analyze the resonance wave functions in real space as well as the corresponding Husimi functions to characterize the coupling behavior. We employ ideas from ray-wave correspondence to deepen our insight by establishing a relation to the nonlinear light ray dynamics and its fingerprint in the Poincaré surface of section.

[1] J. Kreismann et al., Phys. Rev. Res. 1, 033171 (2019).

DY 43.3 Thu 13:00 P1

From Dual Unitarity to Generic Quantum Operator Spreading — •MICHAEL A. RAMPP, RODERICH MOESSNER, and PIETER W. CLAEYS — Max Planck Institute for the Physics of Complex Systems, 01187 Dresden, Germany

Dual-unitary circuits are paradigmatic examples of exactly solvable yet chaotic quantum many-body systems, but solvability naturally goes along with a degree of non-generic behaviour. By investigating the effect of weakly broken dual-unitarity on the spreading of local operators we study whether, and how, small deviations from dual-unitarity recover fully generic many-body dynamics. We present a discrete path-integral formula for the out-of-time-order correlator and use it to recover a butterfly velocity smaller than the light-cone velocity, $v_B < v_{LC}$, and a diffusively broadening operator front, two generic features of ergodic quantum spin chains absent in dual-unitary circuit dynamics. We find that the butterfly velocity and diffusion constant are determined by a small set of microscopic quantities and that the operator entanglement of the gates plays a crucial role.

DY 43.4 Thu 13:00 P1

Transmission of a single electron through a Berry ring — •KENMOE MASEIM BASSIS — Universitätsstraße 31, 93053, Regensburg — Prüfeningerstraße 121, 93049, Regensburg

A theoretical model of transmission and reflection of an electron with spin is proposed for a mesoscopic ring with rotating localized magnetic moment. This model may be realized in a pair of domain walls connecting two ferromagnetic domains with opposite magnetization. If the localized magnetic moment and the traveling spin is ferromagnetically coupled and if the localized moment rotates with opposite chirality in the double path, our system is formulated in the model of an emergent spin-orbit interaction in a ring. The scattering problem for the transmission spectrum of the traveling spin is solved both in a single-path and a double-path model. In the double path, the quantum-path interference changes dramatically the transmission spectrum due to the effect of the Berry phase. Specifically, the spin-flip transmission and reflection are both strictly forbidden.

DY 43.5 Thu 13:00 P1

Optimal route to quantum chaos in the Bose-Hubbard model — LUKAS PAUSCH^{1,2}, EDOARDO CARNIO^{2,3}, ANDREAS BUCHLEITNER^{2,3}, and •ALBERTO RODRÍGUEZ⁴ — ¹Département de Physique, Université de Liège, Belgium — ²Physikalisches Institut, Albert-Ludwigs-Universität Freiburg, Hermann-Herder-Straße 3, D-79104, Freiburg, Germany — ³EUCOR Centre for Quantum Science and Quantum Computing, Albert-Ludwigs-Universität Freiburg, Freiburg, Germany — ⁴Departamento de Física Fundamental, Universidad de Salamanca, E-37008 Salamanca, Spain

The dependence of the chaotic phase of the Bose-Hubbard Hamiltonian [1,2] on particle number N , system size L and particle density is investigated in terms of spectral and eigenstate features. We analyze the development of the chaotic phase as the limit of infinite Hilbert space dimension is approached along different directions, and show that the fastest route to chaos is the path at fixed density $n \leq 1$ [3]. The limit $N \rightarrow \infty$ at constant L leads to a slower convergence of the chaotic phase towards the random matrix theory benchmarks. In this case, from the distribution of the eigenstate generalized fractal dimensions, the ergodic phase becomes more distinguishable from random matrix theory for larger N , in a similar way as along trajectories at fixed density.

[1] L. Pausch et al., Phys. Rev. Lett. 126, 150601 (2021)

[2] L. Pausch et al., New J. Phys. 23, 123036 (2021)

[3] L. Pausch et al., J. Phys. A 55, 324002 (2022)

DY 43.6 Thu 13:00 P1

Chaotic resonance modes in optical microcavities — •FLORIAN LORENZ and ROLAND KETZMERICK — TU Dresden, Institut für Theoretische Physik, Dresden, Germany

Following a recently proposed conjecture, we show that resonance modes in dielectric cavities are a product of a conditionally invariant measure from classical dynamics and universal fluctuations [1]. The first factor describes the average of

modes with similar lifetime and has a multifractal structure which we resolve on very fine scales. It is approximately described by conditionally invariant measures from classical dynamics [1]. However, increasing the openness of a dielectric cavity (i.e. by investigating TE modes or a small refractive index) is a challenge to the construction of appropriate classical measures.

[1] R. Ketzmerick, K. Clauß, F. Fritzsche, and A. Bäcker, Chaotic resonance modes in dielectric cavities: Product of conditionally invariant measure and universal fluctuations, Phys. Rev. Lett. 129, 193901 (2022).

DY 43.7 Thu 13:00 P1

Classical and quantum escape dynamics in the vicinity of hyperbolic fixed points — •ALEXANDER HEMPEL, JONAS STÖBER, and ARND BÄCKER — TU Dresden, Institut für Theoretische Physik, Dresden, Germany

For an ensemble of orbits started in the vicinity of an inverse hyperbolic fixed point in the area-preserving standard map we find a slow, non-exponential decay of the survival probability. It turns out that this is governed by the geometry of the stable and unstable manifolds which form a partial barrier enclosing a resonance zone. An analysis of transit times through the resonance zone using the lobe dynamics of the partial barrier, including re-entrance of orbits, explains the non-exponential decay. Quantum mechanically, coherent states follow the classical behavior for remarkably long times.

DY 43.8 Thu 13:00 P1

Many-body localization in disordered Heisenberg-type spin chain models — •YILUN GAO and RUDOLF A. RÖMER — Department of Physics, University of Warwick, Coventry, CV4 7AL, UK

Disordered quantum systems have become an important research topic in modern condensed matter physics ever since the discovery of Anderson localization. The investigation of many-body localization in quantum interacting systems has received much recent attention following the increase of computational power and improvement in numerical methods. One of the standard models that has been studied is the disordered spin-1/2 Heisenberg chain. It was shown that there exists a phase transition from ergodic states to many-body localized states as the disorder is increased. Here, we focus on a variant of the model where the exchange couplings between neighboring spins are taken to be disordered. We calculate the consecutive-spectral-gap ratio and its probability distribution for different system sizes and disorders. The result is compared with the case when the disorder is onsite. We average over many disorder realizations. We also plot the sample-to-sample variance against disorder and system size as a further characteristic of the phases across the MBL transition.

DY 43.9 Thu 13:00 P1

Nonlinear magnetoelectric effects in class AIII 3D topological insulators — •NITHIN THOMAS, JAN WILHELM, and FERDINAND EVERS — Institute of Theoretical Physics, Regensburg University, D-93053 Regensburg, Germany

We investigate nonlinear magnetoelectric effects in class AIII 3D topological insulators[1]. Within the framework of a tight-binding model, we numerically observe a quadratic scaling of wrapping currents with the electric field strength. Starting with the theory of nonlinear Hall effect induced by Berry curvature dipole[2], we develop an analytic description of our numerical findings.

Shinsei Ryu et al 2010 New J. Phys. 12 065010 (2010) Inti Sodemann and Liang Fu, Phys. Rev. Lett. 115, 216806 (2015)

DY 43.10 Thu 13:00 P1

Flat band physics for dispersive bands — •JIE LIU¹, CARLO DANIELI², and RUDOLF A. RÖMER³ — ¹School of Physics and Optoelectronics, Xiangtan University, Xiangtan 411105, China — ²Department of Physics, University of Sapienza, Piazzale Aldo Moro 5, 00185 Rome, Italy — ³Department of Physics, University of Warwick, Coventry, CV4 7AL, United Kingdom

Lieb models provide a convenient test bed for the characterization of compactly localized states (CLS) in "flat" energy bands. The CLS have been discussed as potential candidates for information storage applications. However, they are typically sensitive to perturbations. Uncorrelated onsite disorder in most cases lifts the existence of CLS irrespective of the disorder strength and induces wave localization in flat band lattices. In certain cases, however, local symmetries within flat band lattices suggest local correlations in the onsite disorder which result in anomalous localization features. Here we make use of these ideas to propose an engineered "disorder" that allows to keep the compactness of the CLS while it at the same time changes half of the dispersive states to become more CLS-like. The work has potential applications for the many situations where flat-band physics has been shown to be relevant, effectively stabilizing the CLS.

DY 43.11 Thu 13:00 P1

Electron cavity optics in bilayer graphene billiards — •LUKAS SEEMANN¹, ANGELIKA KNOTHE², KLAUS RICHTER², and MARTINA HENTSCHEL¹ — ¹Technische Universität Chemnitz, D-09107 Chemnitz, Germany — ²Institut für Theoretische Physik, Universität Regensburg, 93040 Regensburg, Germany

Rapid developments in the field of 2D materials and their nanostructures make it possible to trap charge carriers with different dispersions in various confinement

geometries with a high degree of control. This progress now allows studying 2D electron optics phenomena enriched by the charge carriers' different electronic and topological properties compared to the photonic. Here, we demonstrate the differences induced by deviating from an isotropic dispersion relation by theoretically investigating cavities in gapped bilayer graphene characterized by the presence of a trigonally warped band structure [1]. We employ an approach based on ray-wave correspondence [2] and find dramatic deviations from the optical-case behavior with clear signatures in phase space. We show that the fermion optics characteristics can be conveniently tuned by gate voltages and illustrate the experimentally relevant consequences.

[1] C. Gold, A. Knothe, A. Kurzmann, A. Garcia-Ruiz, K. Watanabe, T. Taniguchi, V. Fal'ko, K. Ensslin, T. Ihn, *Phys. Rev. Lett.* 127, 046801 (2021).

[2] J.-K. Schrepfer, S. Chen, M.-H. Liu, K. Richter, and M. Hentschel, *Phys. Rev. B* 104, 155436 (2021).

DY 43.12 Thu 13:00 P1

Quantum many-body dynamics in two dimensions using tree tensor networks — •WLADISLAW KRINITINS¹, NIKLAS TAUSENDPFUND^{1,2}, MATTEO RIZZI^{1,2}, and MARKUS SCHMITT¹ — ¹Forschungszentrum, Jülich, Deutschland — ²Institut der Theoretischen Physik, Köln, Deutschland

Many body systems out of equilibrium are notoriously difficult to solve due to the rapid growth of entanglement with time. In particular the rapidly expanding possibilities to address 2-dimensional systems in quantum simulation turn a spotlight on the lack of reliable numerical methods in this regime. We explore an approach to solve the time dependence of 2-dimensional systems by applying the time-dependent variational principle (TDVP) to Tree Tensor Networks (TTNs). More specifically, this method is used to study non-ergodic dynamics in the quantum Ising model.

DY 43.13 Thu 13:00 P1

Numeric investigation of the Kibble-Zurek mechanism in 2D — •SEYEDEH PARYA KATOORANI, RALF SCHÜTZHOLD, NASER AHMADINIAZ, GERNOT SCHALLER, and FRIEDEMANN QUEISSER — Theoretical Physics (FWZ), HZDR, Dresden, Germany

The two-dimensional classical Ising model can be approximately implemented on a Si(100) surface, where the dimers are anisotropically coupled. In particular, the setup allows for time-dependent temperatures, where the Kibble-Zurek mechanism predicts topological defect formation while traversing the critical point at a finite rate. We numerically investigate the corresponding relaxation dynamics of a two-dimensional extended Ising model with diagonal couplings and time-dependent temperature.

DY 43.14 Thu 13:00 P1

Explicit expressions for stationary states of the Lindblad equation for a finite state space — •BERND MICHAEL FERNENGEL — TU Darmstadt, Darmstadt, Germany

The Gorini-Kossakowski-Sudarshan-Lindblad Equation is a quantum master equation describing the time evolution of quantum mechanical states. It is used to model open quantum systems. We give explicit expressions of stationary solutions of the Lindblad equation in the case of a finite state space, using the concept of state transition networks of Markov chains. Our treatment is based on the so-called quantum-jump unravelling, which is an ensemble of stochastic quantum trajectories, compatible with the Lindblad equation. A single such trajectory is a piecewise deterministic process, which is interrupted by stochastic jumps. We discuss differences to the classical case and conditions, under which the Lindblad equation is asymptotically stable.

DY 43.15 Thu 13:00 P1

Generic partial barriers to chaotic transport in 4D symplectic maps — •BENJAMIN HERTZSCH, ARND BÄCKER, and ROLAND KETZMERICK — TU Dresden, Institut für Theoretische Physik, Dresden, Germany

Chaotic transport in Hamiltonian systems is often restricted due to the presence of partial barriers, leading to a limited flux between different regions in phase space. Typically, the most restrictive partial barrier in a 2D symplectic map is based on a cantorus, the Cantor set remnants of a broken 1D torus. Recently, for a weakly coupled 4D symplectic map, a partial barrier based on a normally hyperbolic invariant manifold with the structure of a cantorus has been established. We investigate how this can be extended to a generic 4D map, where the most restrictive partial barriers are expected to lie on the most irrational slopes between resonance channels in frequency space.

DY 43.16 Thu 13:00 P1

Stability analysis of a periodically driven ultra-cold Bose gas — •LARISSA SCHWARZ, SIMON B. JÄGER, DIMO CLAUDE, IMKE SCHNEIDER, and SEBASTIAN EGGERT — Physics Department and Research Center OPTIMAS, Technische Universität Kaiserslautern, D-67663, Kaiserslautern, Germany

We theoretically study the dynamics of a Bose-Einstein condensate under periodic driving of the s-wave scattering length. In this setup, we first determine the stability of the condensate using Bogoliubov theory with time-periodic modulation. We find an exponential gain in the resonant k -modes due to a parameteric

amplification which leads to a rapid condensate depletion. These findings are compared with the simulation of the Gross-Pitaevskii equation which shows the formation of a density-wave pattern with the predicted k -wavevector. We extend the Bogoliubov theory by including non-linearities which result in an effective damping of the k -modes. This enables the creation of stable density-wave pattern below a critical driving strength. Moreover, above this critical driving strength we analyze simple non-quadratic models and find macroscopic and stable occupation of the resonant k -mode.

DY 43.17 Thu 13:00 P1

Energy-conserving adaptive partitioning QM/MM simulations — •MARVIN NYENHUIS^{1,2} and NIKOS DOLTSINIS^{1,2} — ¹Institute for Solid State Theory, University of Münster, Wilhelm-Klemm-Straße 10, 48149 Münster, Germany — ²Center for Multiscale Theory and Computation,, University of Münster, Wilhelm-Klemm-Straße 10, 48149 Münster, Germany

Bachmann and Doltsinis have recently proposed an energy-conserving adaptive partitioning method between two different atomistic representations based on an extended Hamiltonian, which switches the system from a potential energy surface V_1 to another potential V_2 . In this work, we develop this method further and implement it into the QM/MM molecular dynamics framework of the CP2K software package, enabling atoms travelling out of (or into) the QM region to adopt an MM (or QM) representation. For a test system consisting of a solvated sodium ion, we analyse the degree to which energy is conserved over a large number of switching events depending on the value chosen for the mass of the fictitious lambda particle. In addition, we investigate how this choice affects the switching speed and we seek the optimum mass that simultaneously ensures rapid switching and good energy conservation.

DY 43.18 Thu 13:00 P1

Classification of noisy spectra using machine learning — ARITRA MISHRA and •ALEXANDER EISEL — Max Planck Institute for the Physics of Complex Systems, Dresden, Germany

A general problem in quantum mechanics is to obtain information of the eigenstates from the experimentally measured data which consists inherent noises. For an example, in the case of molecular aggregates, the information about excitonic eigenstates is vitally important to understand their optical and transport properties [1,2].

We show that it is possible to reconstruct the underlying delocalised aggregate eigenfunctions from near-field spectra using convolution neural networks [3]. We also investigate convolution neural networks for an eigenstate based classification of the spectra, in the presence of noise. Each aggregate eigenstate, corresponds to a distinctly looking spectrum. Therefore, we can assign a class to each of the eigenstate. We find that the network is also able to classify the spectra of different noise strengths along with the one it has been trained for.

[1] X. Gao and A. Eisfeld, *J. Phys. Chem. Lett.* 9, 6003 (2018)

[2] S. Nayak, F. Zheng and A. Eisfeld, *J. Chem. Phys.* 155, 134701 (2021)

[3] F. Zheng, X. Gao and A. Eisfeld, *Phys. Rev. Lett.* 123, 163202 (2019)

DY 43.19 Thu 13:00 P1

Exact time local equations of quantum dissipation with minimal state space — •MENG XU¹, VASILII VADIMOV², MALTE KRUG¹, JÜRGEN T. STOCKBURGER¹, and JOACHIM ANKERHOLD¹ — ¹Institute for Complex Quantum Systems and IQST, Ulm University — ²QCD Labs, QTF Centre of Excellence, Aalto University, Finland

We present a minimal state space approach to unravel the Feynman path integral influence functional for open quantum system dynamics. The resulting time local evolution equation for the density in minimally extended state space is exact and in combination with tensor network methods, can be very efficiently propagated with very high precision also for long times [1]. It is capable to treat the full non-Markovian dynamics, regardless of low temperature, structured reservoir, and strong system-bath coupling. On a formal level, its intriguing structure allows to demonstrate that the new equation is closely related to an entire family of representations (Lindblad-type, Fokker-Planck-type). Alternative perturbative and non-perturbative formulations of quantum dissipation can be derived from it, with our new approach being favorable through a comparably low dimension of auxiliary dimensions. With the new platform at hand, lab-based high-precision simulations in parallel to actual experiments with, for example, superconducting qubits are within reach.

[1] M. Xu *et al.*, *Phys. Rev. Lett.* 129, 230601 (2022).

DY 43.20 Thu 13:00 P1

Training Restricted Boltzmann Machines for Spin-1 Quantum Magnets — •ABHIROOP LAHRI and MICHELE CASULA — IMPMC, Sorbonne Université, Paris, France

Neural Network Quantum states (NQS) have gained popularity in recent times for their ability to study quantum many-body systems. Restricted Boltzmann Machines (RBMs) have been quite successful in providing an accurate representation of the ground states of spin-1/2 quantum systems both in one and two dimensions. Based on recent studies of the spin-1 representation of RBMs using one-hot encoding and a quadratic energy function, we aim to test these ansätze

for spin-1 models in various configurations. We train the network parameters and investigate their behaviour to resolve the ground state of these systems.

DY 43.21 Thu 13:00 P1

Enhancement and suppression of charge transport in organic semiconductors under strong light-matter coupling — •SEBASTIAN STUMPER and JUNICHI OKAMOTO — University of Freiburg, Institute of Physics

We study a model of an organic semiconductor coupled to a cavity with variable disorder and electronic filling factors as well as dissipative effects. It represents a fermionic generalization of the Dicke model such that charges can move between lattice sites.

Different mechanisms are explored to explain experimentally observed conductivity enhancements in the strong coupling regime. These are either based on an increase of the charge mobility or of the charge density. Mobilities and the generalized inverse participation ratio, which characterizes localization, are accessible from various two- and four-point correlators that we obtain by a Lanczos technique. In agreement with several previous studies, we find that excitons are indeed delocalized under strong light-matter coupling and show an enormously increased mobility. The same is not true for electrons and holes.

Charge densities are increased by excitation of electrons to the upper band

through counter-rotating light-matter interaction terms. However, this is counteracted by the cavity-mediated formation of bound electron-hole states. We analyze the relative strengths of these processes under finite size scaling, and how the formation of bound states is affected by disorder and dephasing. In certain limits for an undoped system, the Dicke model is recovered.

DY 43.22 Thu 13:00 P1

Investigation of two-dimensional quantum billiards with mixed dynamics in microwave resonators — •LENNART ANDERSON and ANDREAS WIECK — Angewandte Festkörperphysik, Ruhr-Universität Bochum

Based on the analogy of the stationary Schrödinger equation and the Helmholtz equation for a flat electromagnetic resonator, two-dimensional quantum mushroom billiards are studied in the microwave regime. We give a practical approach, ranging from the construction process of the resonator to the eigenvalue statistics. I.e. the frequency spectrum is measured for different stem widths. The obtained nearest neighbour spacings are fitted with respect to three different distribution functions for systems with mixed dynamics respectively. The degrees of chaoticity are determined analytically, dependent on the stem width, and compared with the fitted data. The presented approach is of both conceptual and educational interest.

DY 44: Poster: Statistical Physics

Time: Thursday 13:00–16:00

Location: P1

DY 44.1 Thu 13:00 P1

Understanding probability and irreversibility in the Mori-Zwanzig projection operator formalism — •MICHAEL TE VRUGT — Institut für Theoretische Physik, Westfälische Wilhelms-Universität Münster, Center for Soft Nanoscience, Philosophisches Seminar, 48149 Münster, Germany

Explaining the emergence of stochastic irreversible macroscopic dynamics from time-reversible deterministic microscopic dynamics is one of the key problems in philosophy of physics. The Mori-Zwanzig (MZ) projection operator formalism, which is one of the most important methods of modern nonequilibrium statistical mechanics, allows for a systematic derivation of irreversible transport equations from reversible microdynamics and thus provides a useful framework for understanding this issue. However, discussions of the MZ formalism in philosophy of physics tend to focus on simple variants rather than on the more sophisticated ones used in modern physical research. In this work [1], I will close this gap by studying the problems of probability and irreversibility using the example of Grabert's time-dependent projection operator formalism. This allows to better understand how general proposals for understanding probability in statistical mechanics, namely (a) quantum approaches and (b) almost-objective probabilities, can be accommodated in the MZ formalism.

[1] European Journal for Philosophy of Science 12, 41 (2022)

DY 44.2 Thu 13:00 P1

Finite-temperature absorption spectrum of Al_2O_3 from first principles — •ANGELA F. HARPER¹, BARTOMEU MONSERRAT², and ANDREW J. MORRIS³ — ¹Fritz Haber Institute of the Max Planck Society, Berlin, Germany — ²University of Cambridge, UK — ³University of Birmingham, UK

Advancing the next generation of materials for solid-state devices requires an understanding of their underlying electronic structure. One such material is alumina (Al_2O_3), which is used to enhance performance in electronic devices from Li-ion batteries to perovskite solar cells and field effect transistors. By including phonon-assisted transitions within plane-wave DFT methods for calculating the X-ray absorption spectrum (XAS) we obtain the Al K-edge XAS at 300 K for two crystalline Al_2O_3 phases. The 300 K XAS reproduces the pre-edge peak for α - Al_2O_3 , which is not visible at the static-lattice level of approximation. The 300 K XAS for γ - Al_2O_3 correctly describes two out of the three experimental peaks. We show that the second peak arises from 1s to mixed *s-p* transitions and is absent in the 0 K XAS. The method presented here is generalizable to any element and absorption edge, and is a feasible way to calculate finite temperature spectroscopy for any crystalline material.

DY 44.3 Thu 13:00 P1

Potts model with invisible states on a scale-free network — •MARIANA KRASNITSKA^{1,2,3} and PETRO SARKANYCH^{1,2} — ¹ICMP, NAS of Ukraine, Lviv, Ukraine — ²L4 Collaboration Leipzig-Lorraine-Lviv-Coventry — ³Université de Lorraine, Nancy, France

Different models are proposed to understand magnetic phase transitions through the prism of competition between the energy and the entropy. One of such models is a $(q+r)$ -state Potts model with invisible states. This model introduces r invisible states such that if spin lies in one of them, it does not interact with the rest. We consider such a model using the mean-field approximation on an annealed scale-free network where the probability of a randomly chosen vertex having a given degree is governed by the power law with decay exponent

λ . Our results confirm that q , r and λ play a role of global parameters that influence the critical behaviour of the system. Depending on their values the phase diagram is divided into three regions with different critical behaviour. However, the topological influence, presented by the marginal value of $\lambda c(q)$, has proven to be dominant over the entropic one, governed by the number of invisible states r [arXiv:2211.14048].

DY 44.4 Thu 13:00 P1

Thermodynamics of $su(n)$ -symmetric integrable models and their continuum limit — •INGRYD PASSOS and ANDREAS KLÜMPER — Bergische Universität Wuppertal, Wuppertal, Germany

Traditionally the computation of the partition function of integrable quantum chains is achieved by means of the thermodynamic Bethe ansatz (TBA). On the other hand, an alternative formulation which relies on finite sets of nonlinear integral equations has been developed and successfully applied to seminal cases like for example the spin-1/2 Heisenberg chain, the supersymmetric t-J model and quantum chains with $su(3)$ and $su(4)$ invariance. This approach, known as the Quantum Transfer Matrix (QTM) method, allows for faster numerical computations and calculation of finite temperature correlation lengths. However, the derivation of these alternative equations was done in case by case studies in which by trial and error suitable auxiliary functions were identified. Another shortcoming of the QTM method is its applicability in the case of continuum integrable models. A way to circumvent this issue is to identify the proper lattice model from which the continuum model follows after a suitable scaling limit. This way, it is possible, for example, to determine the thermodynamics of multicomponent Bose gases from anisotropic spin chains. In this work we present a way to derive systematically finite sets of nonlinear integral equations for $su(n)$ -symmetric integrable lattice models and discuss a scaling limit of these equations in the case of the $su(3)$ -invariant anisotropic spin chain.

DY 44.5 Thu 13:00 P1

Simple-to-complex phase transition for longest increasing subsequences (Ulam's problem) — •TAMMO LENTSCH and ALEXANDER K. HARTMANN — Institute of Physics, University of Oldenburg, Germany

It is possible to calculate the LIS length L by efficient algorithms in polynomial time. Finding and analyzing LIS was first considered numerically in the 1950s by Stanislaw Ulam. The LIS problem has applications in bioinformatics and data analysis but is also studied in mathematics and statistical physics [1].

Recently, an algorithm to count the number of LIS [2] was extended to directly sample LIS [3]. The phase space where σ are random permutations was studied by calculating the distribution $P(q)$ of overlaps, revealing a complex structure similar to Replica Symmetry Breaking.

Here we consider the effect of randomly partially presorting σ with $O(n^\alpha)$ sorting steps. For sequences up to length $n = 8192$, we analyzed the LIS length L and $P(q)$. The results indicate a phase transition at a critical value α_c from $O(n)$ to $O(\sqrt{n})$ LIS length scaling and from simple to complex phase-space structure. [1] J. Börjes, H. Schawe, A.K. Hartmann, Phys. Rev. E **99**, 042104 (2019).

[2] P. Krabbe, H. Schawe, A.K. Hartmann, Phys. Rev. E **101**, 062109 (2020).

[3] P. Krabbe, H. Schawe, A.K. Hartmann, arXiv:2208.14955 (2022).

DY 44.6 Thu 13:00 P1

Nonergodicity of scaled fractional Brownian motion with nonlinear time and space clocks — •YINGJIE LIANG^{1,2}, WEI WANG², ANDREY G. CHERSTVY², and RALF METZLER^{2,3} — ¹Hohai University — ²University of Potsdam — ³Asia Pacific Center for Theoretical Physics

Experimental evidences show that diffusion processes are not always Brownian motion. It is anomalous diffusion with the mean squared displacement (MSD) being a power law in time, ultraslow diffusion with a logarithmic law, and superfast diffusion with an exponential law. To describe different types of non-Brownian motion in heterogeneous media, this study provides scaled fractional Brownian motion (SFBM) with nonlinear time and space clocks. In the Langevin system for the FBM running with a nonlinear time clock, i.e., the time scaled FBM, the real time is a temporal function of the original times in FBM. For the FBM running with a nonlinear space clock, i.e., the space scaled FBM, the real position is a nonlinear spatial function of the original positions in FBM. The nonergodicity properties of SFBM are quantified based on single particle trajectories of the fractional Brownian motion running with time and space clocks. The simulations are consistent with the general analytical results in specific values of the dominated parameters for the behaviors of the MSD, time averaged mean squared displacement (TAMSD) and aging. Potential applications of these results are encountered in diverse scientific fields, such as biophysical, soft matter and hydrology systems.

DY 44.7 Thu 13:00 P1

The Griffiths Phase: A Large Deviations Study — •LAMBERT MÜNSTER¹, MARTIN WEIGEL¹, and ALEXANDER K. HARTMANN² — ¹Institut für Physik, TU Chemnitz, 09107 Chemnitz, Germany — ²Institut für Physik, Carl von Ossietzky Universität Oldenburg, 26129 Oldenburg, Germany

For spin systems with quenched disorder, the Griffiths phase is the thermal region between the phase transition in the pure system and the corresponding transition in the disordered system. The standard example is a dilute ferromagnet, where a certain fraction of bonds is missing [1]. The physical behavior of this phase is characterized by large fluctuations in the order parameter which are visible in the tails of the distribution of the magnetic susceptibility. To directly investigate this property, we combine a large-deviation Monte Carlo sampling algorithm [2,3] with a Gaussian modified ensemble [4], thus allowing us to study the distribution of physical quantities on a much larger range of the support as compared to previous studies [5], i.e., in the region of exponential small probabilities. In addition to considering the susceptibility distribution we also study other observables such as the specific heat, thus shedding new light on this intriguing physical phenomenon.

- [1] A. J. Bray, Phys. Rev. Lett. **59**, 586 (1987).
- [2] A. K. Hartmann, Phys. Rev. E **65**, 056102 (2002).
- [3] A. K. Hartmann, Eur. Phys. J. B **84**, 627 (2011).
- [4] T. Neuhaus, J. S. Hager, Phys. Rev. E **74**, 036702 (2006).
- [5] K. Hukushima, Y. Iba, J. Phys. **95**, 012005 (2008).

DY 44.8 Thu 13:00 P1

Transport Properties of Brownian Particles: Analytical Results and Computer Simulations — •REGINA RUSCH¹, GERHARD JUNG², and THOMAS FRANOSCH¹ — ¹Institute for Theoretical Physics, Universität Innsbruck, Innsbruck, Austria. — ²Laboratoire Charles Coulomb (L2C), Université de Montpellier, CNRS, 34095 Montpellier, France.

The results of computer simulations for Brownian particles can be improved by using a novel noise cancellation algorithm, with which the velocity autocorrelation function (VACF) can be measured more precisely. The algorithm is based on the fact that the Brownian noise can be stored in computer simulations and thus the noise can be subtracted from a simulated trajectory. Doing this, a reduced motion of the particle due to interactions or an external force is obtained. It could be shown that the VACF of the reduced motion is connected with the original VACF up to a cross-correlation term, which is shown to be sufficiently small. For the system of a Brownian particle in a periodic step potential the noise cancellation algorithm decreases the error of the VACF by about one order of magnitude. A power-law decay in the VACF is found by employing Monte-Carlo simulations. We also present analytical results for the probability distribution of the particle position using the Bloch theorem. This enables us to compute further correlation functions such as the intermediate scattering function which is in quantitative agreement with simulations.

DY 44.9 Thu 13:00 P1

First passage time as thermodynamical parameter — •VASILY RYAZANOV — Institute for nuclear research NANU, Kiev, Ukraine

The first-passage time is proposed as an independent thermodynamic parameter of the statistical distribution that generalizes the Gibbs distribution. The thermodynamic parameter conjugated to the first-passage time is the same as the Laplace transform parameter of the first-passage time distribution in the partition function. The thermodynamic parameter conjugated to the first-passage time can be expressed in terms of the deviation of the entropy from the equilibrium value. Thus, all the moments of the distribution of the first passage time

expressed in terms of the deviation of the entropy from its equilibrium value and the external forces acting on the system. By changing the thermodynamic forces, you can change of the first passage time.

An analogy is drawn between version of non-equilibrium thermodynamics a distribution-based containing an additional thermodynamic first-passage time parameter, nonequilibrium statistical operator method and extended irreversible thermodynamics with flows as an additional thermodynamic parameter. Various conditions for the dependence of the distribution parameters of the first-passage time on the random value of energy, the first thermodynamic parameter, are considered. Expressions are obtained for the thermodynamic parameter, the conjugate of the first passage time through the entropy change, and for the average first passage time through the flows.

DY 44.10 Thu 13:00 P1

Stochastic dynamics with multiplicative noise under resetting — •TRIFCE SANDEV^{1,2,3}, LJUPCO KOCAREV^{1,3}, RALF METZLER^{2,4}, and ALEKSEI CHECHKIN^{2,5,6} — ¹Macedonian Academy of Sciences and Arts, Skopje, Macedonia — ²University of Potsdam, Germany — ³Ss. Cyril and Methodius University in Skopje, Macedonia — ⁴Asia Pacific Center for Theoretical Physics, Pohang, Republic of Korea — ⁵Wroclaw University of Science and Technology, Poland — ⁶Akhiezer Institute for Theoretical Physic, Kharkiv, Ukraine

We analyze different stochastic processes with multiplicative noise under resetting in non-homogeneous media. We use the subordination approach, which is a powerful technique for solving various diffusion and Fokker-Planck equations, to analyze the probability density functions and the mean squared displacements. Additionally, we show that such systems under stochastic resetting reach non-equilibrium stationary states. The transition to the non-equilibrium stationary states is analyzed in terms of the large deviation function, by employing the Laplace approximation of the integral in the renewal equation for the probability density of the process with resetting events.

- [1] T. Sandev, V. Domazetoski, L. Kocarev, R. Metzler, A. Chechkin, J. Phys. A: Math. Theor. **55**, 074003 (2022).
- [2] T. Sandev, L. Kocarev, R. Metzler, A. Chechkin, Chaos, Solitons & Fractals **156**, 112878 (2022).

DY 44.11 Thu 13:00 P1

Quench-Probe Setup as an Analyzer of Fractionalized Entanglement Spreading — •NICOLAS P. BAUER¹, JAN CARL BUDICH², BJÖRN TRAUZETTEL¹, and ALESSIO CALZONA³ — ¹Julius Maximilians Universität Würzburg, Würzburg, Germany — ²TU Dresden, Dresden, Germany — ³IQM Quantum Computers, München, Germany

We propose a novel spatially inhomogeneous setup for revealing quench-induced fractionalized excitations in entanglement dynamics. In this quench-probe setting, the region undergoing a quantum quench is tunnel-coupled to a static region, the probe. Subsequently, the time-dependent entanglement signatures of a tunable subset of excitations propagating to the probe are monitored. We exemplify the power of this generic approach by identifying a unique dynamical signature associated with the presence of an isolated Majorana zero mode in the post-quench Hamiltonian. In this case excitations emitted from the topological part of the system give rise to a fractionalized jump of $\log(2)/2$ in the entanglement entropy of the probe. This dynamical effect is highly sensitive to the localized nature of the Majorana zero mode, but does not require the preparation of a topological initial state.

DY 44.12 Thu 13:00 P1

Exploiting Skyrmion motion for computing — •ALESSANDRO PIGNEDOLI, BJÖRN DÖRSCHEL, and KARIN EVERSCHOR-SITTE — University of Duisburg-Essen, Duisburg, Germany

Brownian motion is a natural phenomenon that can be exploited for energy efficient computing. Here, an assemblage of simple parts evolves in an energetic labyrinth to a low energy state which is isomorphic to the desired solution of a computation [1]. Magnetic Skyrmions [2] are topologically stable magnetic whirls that have been shown to behave like interacting Brownian particles [3,4]. We use a Langevin model to describe and investigate the motion of Skyrmions by means of correlations and statistical observables to carry out Brownian computation. We show that besides the Brownian motion of individual Skyrmions, their interactions and external driving forces break ergodicity. This allows for a rapid convergence to the low-energy state of the system and thus solves the calculation faster.

- [1] C. H. Bennett, Int. J. Theor. Phys. **21**, 905 (1982) [2] K. Everschor-Sitte, J. Masell, R. M. Reeve and M. Kläui, J. Appl. Phys. **124**, 240901 (2018) [3] J. Závorka, et al. Nat. Nanotechnol. **14**, 658 (2019) [4] T. Nozaki, et al Appl. Phys. Lett. **114**, 012402 (2019)

DY 44.13 Thu 13:00 P1

A generalised rotational diffusion approach to modeling of the dielectric relaxation processes with resetting — •IRINA PETRESKA¹, LJUPCO PEJOV^{1,2}, TRIFCE SANDEV^{1,3,4}, LJUPCO KOCAREV^{1,3}, and RALF METZLER⁴ — ¹Ss. Cyril and Methodius University in Skopje, Macedonia — ²University of Stavanger,

Norway — ³Macedonian Academy of Sciences and Arts, Skopje, Macedonia — ⁴University of Potsdam, Germany

We consider the rotational diffusion equation with a generalised memory kernel in the context of dielectric relaxation processes in a medium composed of polar molecules. We give an overview of existing models on non-exponential relaxation and introduce an exponential resetting dynamic in the corresponding process, providing a detailed analysis of the autocorrelation function and complex susceptibility. It is shown that stochastic resetting leads to a saturation of the autocorrelation function to a constant value, in contrast to the case without resetting, for which it decays to zero. The behaviour of the autocorrelation function, as well as the complex susceptibility in the presence of resetting, confirms that the dielectric relaxation dynamics can be tuned by an appropriate choice of the resetting rate.

[1] I. Petreska, Lj. Pejov, T. Sandev, Lj. Kocarev and R. Metzler, *Fractal Fract.* **6**, 88 (2022).

DY 44.14 Thu 13:00 P1

Dividing Active Brownian Particles — •TILL WELKER and HOLGER STARK — Institut für Theoretische Physik, Technische Universität Berlin, Germany.

We aim to combine active motion with cell division to answer questions like: Does nutrient input induce clustering? How does a non-uniform nutrient distribution effects population dynamics?

To include cell division and death in the model of active Brownian particles, we propose a simple rule: *in a time interval dt , each particle has a probability $dt \cdot g(s)$ to divide and $dt \cdot d$ to die.* The growth rate g depends on the nutrient concentration s at the position of the bacterium and is described by the Monod function. The nutrient diffuses with the diffusion coefficient D_N . We add a source with steady input rate S_0 , in addition, each particle takes up nutrient with a rate $\gamma g(s)$.

The population dynamics strongly depends on nutrient diffusion: For large D_N , the population oscillates before reaching a steady population number N^* . For small D_N , the population is stronger damped and equilibrates quickly. N^* is independent of D_N , but the population fluctuation decreases for lower D_N due to the damping. The collective behavior is also influenced by the nutrient: First, for large D_N the swarm has a strongly asymmetric shape during the transient phase which then becomes symmetric in the steady state. Second, the swarm is less dense for larger D_N , but the relationship between spread of nutrient and bacteria is not linear.

We show that combining two key aspects of microbial life, mobility and growth, gives rise to interesting population and spatial dynamics.

DY 44.15 Thu 13:00 P1

Ornstein-Uhlenbeck process and generalizations: influence of comb geometry and stochastic resetting on the particle dynamics — •PETAR JOLAKOSKI¹, PECE TRAJANOVSKI¹, KIRIL ZELENKOVSKI¹, ALEXANDER IOMIN², LJUPCO KOCAREV^{1,4}, and TRIFCE SANDEV^{1,3,4} — ¹Macedonian Academy of Sciences and Arts, Skopje, Macedonia — ²Department of Physics, Technion, Haifa, Israel — ³University of Potsdam, Germany — ⁴Ss. Cyril and Methodius University in Skopje, Macedonia

The Ornstein-Uhlenbeck (O-U) process can be interpreted as a Brownian motion in a harmonic potential. The process is an established Gauss-Markov process that has a bounded variance and admits a stationary probability distribution, in contrast to the standard Brownian motion. Over time, the process tends to drift towards its mean function: such a process is called mean-reverting. Here, we study the effects of stochastic resetting on the O-U process and its generalizations which were hitherto unexplored. In particular, we investigate the dynamics with and without resetting on comb-like structures. For the studied specific 2D comb geometry, we compute the first moment, the non-equilibrium stationary state and the mean squared displacement, and find that the global resetting hinders the particle's transport in the two dimensions. Moreover, the two divergent forces, namely the resetting and the drift towards the mean, lead to compelling results both in the case of O-U process with resetting and its generalization on a 2D comb structure.

DY 44.16 Thu 13:00 P1

Theoretical design of Geometric Brownian Information Engine: Analysis of output work — •SYED YUNUS ALI, RAFNA RAFAEEK, and DEBASISH MONDAL — IIT Tirupati, Yerpedu, Andhrapradesh, India

We design a geometric Brownian information engine by considering overdamped Brownian particles inside a 2-D monolobal confinement with irregular width along the transport direction. Under such conditions, particles experience an effective entropic potential. We employ a feedback control protocol as an outcome of error-free position measurement. The protocol comprises three stages: measurement, feedback, and relaxation. We show that the upper bound of the achievable work shows a cross-over from $(5/3 - 2 \ln 2)k_B T$ to $k_B T/2$ when the system changes from an entropy-dominated regime to energy dominated one. Next, we determine the benchmarks for utilizing the available information in an output work and the optimum operating requisites for best work extraction in asymmetric feedback protocol. Transverse bias force (G) tunes the entropic con-

tribution in the effective potential and hence the equilibrium marginal probability distribution standard deviation (σ). We recognize that the amount of extracted work reaches a global maximum when $x_f = 2x_m$ with $x_m = 0.6\sigma$, irrespective of the extent of the entropic limitation.

1. S. Y. Ali, R. Rafeek, and D. Mondal, *J. Chem. Phys.* **156**, 014902 (2022).

2. R. Rafeek, S. Y. Ali, and D. Mondal (2022) (Under review).

DY 44.17 Thu 13:00 P1

Diffusion and order in mixed lattice gas of hard squares — NIKLAS RAAKE¹, •PIOTR NOWAKOWSKI², and ANA-SUNČANA SMITH^{1,2} — ¹Friedrich-Alexander-Universität Erlangen-Nürnberg, Erlangen, Germany — ²Institut Ruđer Bošković, Zagreb, Croatia

We study a lattice gas composed of hard square particles of 1×1 and 2×2 size (measured in lattice constant) undergoing Brownian motion on a two-dimensional square lattice. For different concentrations of both types of particles we determine numerically the diffusion coefficients and compare them with predictions of a model based on a persistent random walk with one or two step memory. Good agreement is observed only for very low and very high concentration of particles. The deviations present in between these regimes suggest that the correlations play an important role in the dynamics of the system.

Additionally, we introduce a configurational order parameter that characterizes clustering of bigger squares. This allows us to study the continuous transition between unordered liquid and ordered crystal phases.

DY 44.18 Thu 13:00 P1

Non-Markovian modeling of non-equilibrium fluctuations and dissipation in active viscoelastic biomatter — •AMIR ABBASI¹, ROLAND R. NETZ¹, and ALI NAJFI² — ¹Freie University of Berlin, Berlin, Germany — ²Institute for Research in Fundamental Sciences (IPM), Tehran, Iran

Viscoelastic gels such as permanently or transiently cross-linked networks of semiflexible polymers are important soft biological materials. The polymeric nature of such gels is responsible for their salient rheological properties, including their frequency-dependent response to external forces.

Here, based on a Hamiltonian that incorporates the elastic coupling between a tracer and active particles, we derive a generalized Langevin model for the non-equilibrium mechanical response of active viscoelastic biomatter. Our model accounts for the power-law viscoelastic response of the embedding polymeric network as well as for the non-equilibrium energy transfer between active and tracer particles. Our analytical expressions for the frequency-dependent response function and the positional autocorrelation function agree nicely with experimental data for red blood cells and actomyosin networks with and without ATP. The fitted effective active-particle temperature, elastic constants and effective friction coefficients of our model allow straightforward physical interpretation.

DY 44.19 Thu 13:00 P1

Ornstein-Uhlenbeck process on three dimensional comb structure under stochastic resetting — •PECE TRAJANOVSKI¹, PETAR JOLAKOSKI¹, KIRIL ZELENKOVSKI¹, ALEXANDER IOMIN², LJUPCO KOCAREV^{1,4}, and TRIFCE SANDEV^{1,3,4} — ¹Macedonian Academy of Sciences and Arts, Skopje, Macedonia — ²Department of Physics, Technion, Haifa, Israel — ³University of Potsdam, Germany — ⁴Ss. Cyril and Methodius University in Skopje, Macedonia

The Ornstein-Uhlenbeck (O-U) process is a generalised diffusion process, introduced as a model for the velocity of a particle undergoing a Brownian motion confined in harmonic potential. The process is a stationary, meaning that over time, it tends to drift towards its long-time mean function: such a process is called mean-reverting. Here, we investigate the influence of the three dimensional comb structure and the stochastic resetting on the particle dynamics governed by O-U processes along the backbone (x -direction) and the main fingers (y -direction) and standard Wiener process along the secondary fingers of the comb (z -direction). The explicit analytical expressions for the first moment and mean squared displacement along all three directions are calculated and confirmed numerically. The marginal probability density functions along all directions are simulated by using coupled Langevin equations for comb geometry.

DY 44.20 Thu 13:00 P1

Generalized molecular Stokes-Einstein and Stokes-Einstein-Debye relations including temperature-dependent slip and effective radius — •SINA ZENDEHROUD, JAN O. DALDROP, YANN VON HANSEN, and ROLAND R. NETZ — Freie Universität Berlin, Department of Physics, Arnimallee 14, 14195 Berlin, Germany

We perform molecular dynamics simulations of water at different temperatures and calculate the viscosities as well as the rotational and translational self-diffusion constants of water molecules in the lab frame and in the comoving coordinate frame of the molecules. Instead of interpreting the results as deviations from the Stokes-Einstein and Stokes-Einstein-Debye relations, we simultaneously determine the slip length and the effective hydrodynamic radius from the simulation data. We show that the viscosity dependence of the diffusion constants of water can be understood in terms of an almost constant effective radius and a pronounced temperature dependence of the slip length.

DY 44.21 Thu 13:00 P1

Energy transfer between the librational and the inter- and intramolecular vibrational modes of liquid water — •LOUIS LEHMANN and ROLAND NETZ — Fachbereich Physik, Freie Universität Berlin

The molecular dynamics of liquid water can be split into librational and inter- and intramolecular vibrational modes. By applying the Eckart decomposition scheme, the infrared absorption spectrum can be exactly decomposed into contributions from these different modes. The complete energy transfer network of the librational and inter- and intramolecular vibrational modes in liquid water is established based on the energy transfer rates determined from equilibrium molecular dynamics simulations with conventional and many-body force fields. The results are validated by comparison with non-equilibrium molecular dynamics simulations that mimic pump-probe experiments.

DY 44.22 Thu 13:00 P1

Domain Drift and Diffusion in Cell-Polarization Processes — •JOHANNES EWALD and JÜRGEN VOLLMEYER — Institute of Theoretical Physics, Universität Leipzig, Brüderstr. 16, D-04103 Leipzig, Germany

Cell polarization can be driven by the formation of signaling patterns on cell membranes. They can be modeled by two species of membrane proteins that can bind to cytosolic enzymes. The enzymes drive the conversion between cell membranes. These chemical reactions drive the coarsening of domains on the cell surface. Polarization amounts to the situation where the cell surface is covered by only two domains on opposing sides of the cell. Certain aspects of the domain coarsening are reminiscent to ripening of spin-up and spin-down domains in ferromagnets. In this analogy the conversion of membrane proteins takes the role of spin flips of the magnetic system. However, there are also distinct differences in the dynamics because the conversion is driven by a dissipative chemical reaction, while spin-flips arise due to thermal fluctuations. Based on the analytical solutions for domain drift and diffusion in the two models we will discuss differences and communalities of the processes.

DY 45: Poster: Nonlinear Dynamics, Pattern Formation and Networks

Time: Thursday 13:00–16:00

Location: P1

DY 45.1 Thu 13:00 P1

A systematic approximation scheme mapping systems with time delays to sets of ordinary differential equations — •DANIEL HENRIK NEVERMANN and CLAUDIUS GROS — Institut für Theoretische Physik, Goethe-Universität Frankfurt, Deutschland

Mathematically, delayed differential equations evolve in infinite dimensional state spaces. It is hence conceivable that time-delayed systems can be approximated by a set of $N + 1$ ordinary differential equations, with the trajectory of the primary variable converging to the solution of the original time-delayed system when $N \rightarrow \infty$. We show that this program can be carried out using sequences of time-delay kernels related to discrete gamma distributions.

We present several analytical and numerical results for the proposed approximation scheme, finding that the instability of fixed points due to increasing time delays is captured accurately already for $N \sim 10$. For the Mackey-Glass system we find that the locus of a limit-cycle doubling are recovered in good approximation only for substantially larger $N \sim 10^2 - 10^3$, with the transition to chaos requiring an even larger state space. In general, we find that relative approximation errors scale as $1/N$. In addition, we discuss how the approximation proposed can be applied to the case of distributed time delays.

It is in general an approximation to model a given experimental protocol by a dynamical system characterized by a single time delay T . Using a distribution of time delays peaked at T , with width $\sim 1/N$, can hence be argued to provide a more accurate description of real-world non-Markovian processes.

DY 45.2 Thu 13:00 P1

Preprocessing algorithms for the estimation of ordinary differential equation models with polynomial nonlinearities — •OLIVER STREBEL — Angelstr. 17, 75392 Deckenpfronn

The data analysis task of determining a model for an ordinary differential equation (ODE) system from given noisy solution data is addressed. Based on a previously published parameter estimation method for ODE models [1] four related model estimation algorithms were developed. The algorithms are tested for over 20 different polynomial ordinary equation systems comprising 60 equations at various noise levels. Two algorithms frequently compute the correct model [2]. They are compared to the prominent SINDy-family for those SINDy-algorithms that have simple default hyperparameters [3]. A novel and successful method for determining the parameter of Tikhonov regularization when calculating numerical differentials is also presented.

[1] O. Strebel: <http://dx.doi.org/10.1016/j.chaos.2013.08.015>

[2] O. Strebel: <https://osf.io/89djt/>

[3] S. Brunton et al: <http://dx.doi.org/10.1073/pnas.1517384113>

DY 45.3 Thu 13:00 P1

Testing Jump-Diffusion in Epileptic Brain Dynamics: Impact of Daily Rhythms — •JUTTA G. KURTH^{1,2}, KLAUS LEHNERTZ², and THORSTEN RINGS² — ¹Georg-August-Universität Göttingen — ²Rheinische Friedrich-Wilhelms-Universität Bonn

Stochastic approaches to complex dynamical systems have recently provided broader insights into spatial-temporal aspects of epileptic brain dynamics. Stochastic qualifiers based on higher-order Kramers-Moyal coefficients derived directly from time series data indicate improved differentiability between physiological and pathophysiological brain dynamics. It remains unclear, however, to what extent stochastic qualifiers of brain dynamics are affected by other endogenous and/or exogenous influencing factors. Addressing this issue, we investigate multi-day, multi-channel electroencephalographic recordings from a

subject with epilepsy. We apply a recently proposed criterion to differentiate between Langevin-type and jump-diffusion processes and observe the type of process most qualified to describe brain dynamics to change with time. Stochastic qualifiers of brain dynamics are strongly affected by endogenous and exogenous rhythms acting on various time scales* ranging from hours to days. Such influences would need to be taken into account when constructing evolution equations for the epileptic brain or other complex dynamical systems subject to external forcings.

Keywords: diffusion process; jump-diffusion process; time series analysis; brain; epilepsy; biological rhythms

DY 45.4 Thu 13:00 P1

Temporal localized states and square waves in semiconductor microresonators with strong time delayed feedback — •ELIAS R. KOCH^{1,2}, THOMAS SEIDEL¹, JULIEN JAVALOYES², and SVETLANA V. GUREVICH¹ — ¹Institute for Theoretical Physics, University of Münster, Wilhelm-Klemm-Str. 9, 48149 Münster, Germany — ²Departament de Física & IAC-3, Universitat de les Illes Balears, C/ Valldemossa km 7.5, 07122 Mallorca, Spain

Recent works demonstrated the promising potential of injected microresonators enclosed into external cavities as high-power, tunable sources of Frequency Combs in the near infra-red. It was shown that the natural modeling approach consists in using singularly perturbed time delayed systems. Departing from former studies that considered a single intensity dependent refractive index (i.e. Kerr nonlinearity) we explore in this contribution the impact of a semiconductor Quantum-Well as the nonlinear element. A first principle model for the optical response is employed which allows to explore the influence of the detuning with respect to the band-gap. We show that this extended model predicts the existence of a bistable set of bright and dark temporally localized states as well as square-waves, with a periodic of twice the delay in the case of antiresonant optical feedback.

Finally, in order to clarify the influence of the second and third order chromatic dispersion and of the frequency dependence of the quantum-well response, we perform a multiple time-scale analysis in the so-called good cavity limit. The resulting normal form PDE shows a good agreement with the original, first principle, time delayed model.

DY 45.5 Thu 13:00 P1

Antipersistent random walks in time-delayed systems — •TONY ALBERS¹, DAVID MÜLLER-BENDER¹, and GÜNTER RADONS^{1,2} — ¹Institute of Physics, Chemnitz University of Technology, Chemnitz, Germany — ²Institute for Mechanical and Industrial Engineering, Chemnitz, Germany

In this contribution, we show that the occurrence of chaotic diffusion in a typical class of time-delayed systems with linear instantaneous and nonlinear delayed term can be well described by an antipersistent random walk. We numerically investigate the dependence of all relevant quantities characterizing the random walk on the strength of the nonlinearity and on the delay. With the help of analytical considerations [1], we show that for a decreasing nonlinearity parameter the resulting dependence of the diffusion coefficient is well described by Markov processes of increasing order.

[1] Tony Albers, David Müller-Bender, and Günter Radons, Phys. Rev. E **105**, 064212 (2022)

DY 45.6 Thu 13:00 P1

Advection dependent pulse dynamics — •ADRIAN MISSELWITZ¹, SUSANNE LAFON², JEAN-DANIEL JULIEN², and KAREN ALIM^{1,2} — ¹School of Natural Sciences, Technische Universität München — ²Max-Planck-Institut für Dynamik und Selbstorganisation, Göttingen

Models of pulse formation in nerve conduction have provided manifold insight not only into neuronal dynamics but also the non-linear dynamics of pulse formation in general. Recent observation of neuronal electro-chemical pulses also driving mechanical deformation of the tubular neuronal wall and thereby generating ensuing cytoplasmic flow now question the impact of flow on the electro-chemical dynamics of pulse formation. We, here, theoretically investigate the classical Fitzhugh-Nagumo model now accounting for advective coupling between the pulse propagator typically describing membrane potential and here triggering mechanical deformations and, thus, governing flow magnitude, and the pulse controller, a chemical species advected with the ensuing fluid flow. Employing analytical calculations and numerical simulations we find, that advective coupling allows for a linear control of pulse width while leaving pulse velocity unchanged. We therefore uncover an independent control of pulse width by fluid flow coupling.

DY 45.7 Thu 13:00 P1

(Broken) gradient-dynamics description of reactive thin liquid films — •FLORIAN VOSS, FENNA STEGEMERTEN, and UWE THIELE — Institut für Theoretische Physik, Westfälische Wilhelms-Universität Münster, Wilhelm-Klemm-Str. 9, 48149 Münster, Germany

After reviewing the gradient dynamics formulation of chemical reactions, applied e.g. in [1] to reacting phase-separating systems, we apply the concept to thin liquid films and shallow drops that are either covered by reactive surfactants [2] or react with the solid substrate [3]. Next we discuss how the breaking of the variational form by imposed fluxes results in intricate spatio-temporal dynamics of the film/drop and reactant density profiles. As an example we consider a simple model for oscillatory behaviour in droplets of slime mould.

[1] D. Zwicker, *Current Opinion in Colloid & Interface Science*, 61, 101606 (2022),

[2] A. Pereira, P. M. J. Trevelyan, U. Thiele, and S. Kalliadasis, *Phys. Fluids* 19, 112102 (2007),

[3] K. John, M. Bär, and U. Thiele, *Eur. Phys. J. E* 18, 183 (2005).

DY 45.8 Thu 13:00 P1

Coupling short-range signaling and tissue mechanics for biological pattern formation — •VALÈRIA RIBELLES PÉREZ, STEPHAN KREMSEK, MAREIKE BOJER, SABINA ORAZOV, and ULRICH GERLAND — Physics Department, Technical University of Munich

Pattern formation phenomena are ubiquitous in natural and synthetic multicellular systems. Both mechanical forces and biochemical interactions between cells play key roles in tissue dynamics. While much is known about these physical and biochemical processes separately, their interplay is still poorly understood. Here, we focus on short-range signaling between cells, modelled by cellular automata, coupled to a vertex model incorporating mechanical interactions, to investigate patterning principles during tissue homeostasis and growth. We test the modelling framework in the context of salt-and-pepper-like patterns that arise for instance in epithelial tissues.

DY 45.9 Thu 13:00 P1

Robust, precise, and modular solutions to the French flag problem in two dimensions without global signaling — •LUKAS ZETT, STEPHAN KREMSEK, GABRIEL VERCELLI, and ULRICH GERLAND — Technical University of Munich

The formation of axial patterns with broad regions in multicellular systems has been conceptualized by Wolpert in his famous French flag problem. Both of Wolpert's proposed solutions, the balancing and gradient model, utilize long-range signaling between cells. Models relying on short-range signaling, based on cellular automata (CA) rules as modeling tool, have also computationally been shown to successfully solve the French flag problem in one dimension (1D). Here, we extend these models to two spatial dimensions (2D) to investigate whether the 1D solutions can be generalized to the 2D case and to search for novel solutions existing only in 2D. We dissect the 2D problem into two coupled, 1D pattern formation processes along and perpendicular to the axis of the French flag. Using evolutionary algorithms and consensus procedures as well as engineering approaches, CA dynamics which solve the French flag problem are found. We show that these solutions form more precise patterns and are in general more robust than their 1D counterparts, while still being able to scale with system size. Depending on the desired robustness and precision of the solution, different patterning modules along the two axes can be combined. Using the regulatory logics of these underlying modules could therefore serve as a basis for the design of synthetic patterning systems with a range of different specifications.

DY 45.10 Thu 13:00 P1

Kinetic Monte Carlo Model for Computing Functionalities in Nanoparticle Networks — •JONAS MENSING¹ and ANDREAS HEUER² — ¹Institut für Physikalische Chemie, WWU Münster — ²Institut für Physikalische Chemie, WWU Münster

We want to achieve reconfigurable computational functionality in a nanoparticle network for energy efficient machine learning applications. Previous research has shown that disordered networks of functionalized gold nanoparticles can be configured to behave like Boolean logic gates and binary classifiers. In this regard, gold nanoparticles serve as switchable single-electron transistors, while organic molecules connecting the nanoparticles act as tunable tunnel barriers. The resulting network is then placed within an array of electrodes that manipulate the charge and potential landscape of the network to evolve the system into its desired emergent functionality. In total, the network is able to mimic the mechanism of a brain-like neural network. The theoretical underpinning of these networks is investigated with a highly optimized physical model and subsequent simulations. The model is able to simulate the charge transport within the network stochastically, i.e. with a kinetic Monte Carlo approach. Requirements for various computing functionalities such as Boolean logic are examined. Besides graph theory and data-driven tools allow mapping network and electrode properties to the appearance of computational functionalities. The simulations are carried out in close comparison with corresponding experiments.

DY 45.11 Thu 13:00 P1

Randomised mixed labyrinth fractals — •JANETT PREHL¹, LIGIA LORETTA CRISTEA², and DANIEL DICK¹ — ¹Technische Universität Chemnitz, Chemnitz, Germany — ²Technische Universität Graz, Graz, Austria

Fractals, introduced by Benoit Mandelbrot in the early 1980s, allow the analysis of physical properties of natural geometries and structures in non-integer dimensions. It has been shown recently, that utilizing fractals structures, for instance for gas sensors made of carbon nanotubes increase their efficiency or give new insights to complex quantum phenomena. Here, we are interested how the effect of randomness, as observed in real materials, alter the topology and thus dynamics of the resulting fractal structures in comparison to the pure cases. We focus on a special class of Sierpinski carpets, i.e., the labyrinth fractals [1], that can be used for dendritic networks or porous materials. Therefore, we mix to fractal patterns, with different properties, i.e., shortest path and random walk dimension, randomly together at different mixing ratios. Surprisingly we found that even in cases where the initial patterns exhibit the same non-integer dimensions the resulting randomised fractals give a different property [2].

[1] L.L. Cristea and B. Steinsky, *Proc. Edinburgh Math. Soc.* 54.4 (2011) 329.

[2] J. Prehl, D. Dick, and L.L. Cristea, to be submitted to *Fractals* (2023).

DY 45.12 Thu 13:00 P1

How Can Cell-Like Inflated Shells Control Their Shape? — A Stability Analysis — •PAUL NEMEC and ULRICH GERLAND — Physics Department, Technical University of Munich

This work follows a long history of studying how biological organisms arrive at and maintain their shape [1]. Inspired by the question of how *E. coli* maintain their cylindrical shape during growth [2], we study the growth of pressurised cell-like structures. The model is this: a cell is an inflated elastic shell, where internal and fine grained details are neglected. Growth is the time evolution of the reference or undeformed configuration of the cell, which may depend on geometric and mechanical properties like curvature and stress. Growth must be local and invariant under translations and rotations of the entire cell. Under these constraints, how can cells robustly achieve simple target geometries like a sphere given arbitrarily perturbed initial conditions? This poster presents some initial insights.

[1] Goriely, A. *The Mathematics and Mechanics of Biological Growth*, Springer (2017).

[2] Amir, A., van Teeffelen, S. Getting into shape: How do rod-like bacteria control their geometry?. *Syst Synth Biol* 8, 227–235 (2014).

DY 45.13 Thu 13:00 P1

Stimulating self-optimisation of flow networks for transport — •SWARNAVO BASU and KAREN ALIM — School of Natural Sciences, Technical University of Munich, Germany

Flow transport in networks is ubiquitous in biology (e.g. blood vasculature) and engineering (e.g. porous media). Many biological networks are adaptive and can self-organise in response to external stimuli. They homogenise flow to achieve optimal perfusion and a uniform flow of chemicals across the network. In contrast, engineered networks of random media have heterogeneous flow velocity distributions across the network. Self-organising engineered networks that can homogenise flow will have many applications, ranging from microfluidic networks for cooling batteries and chemical reactors to *in vitro* vasculature for perfusing tissues and implants. We propose a model of a network whose tube radii can be controlled using periodic inflows of pulses of an eroding agent that erodes the network's walls. We observe that such networks self-organise in response to the eroding agent, leading to a homogenised flow. This provides a framework for engineering networks that can self-organise to achieve optimal perfusion.

DY 45.14 Thu 13:00 P1

Fixation probabilities in network structured meta-populations — •SEDIGHEH YAGOBI¹ and ARNE TRAUlsen² — ¹Max-Planck institute for evolutionary biology — ²Max-Planck Institute for Evolutionary Biology

The effect of population structure on evolutionary dynamics is a long-lasting research topic in evolutionary ecology and population genetics. Evolutionary graph theory is a popular approach to this problem, where individuals are located on the nodes of a network and can replace each other via the links. We study the effect of complex network structure on the fixation probability, but instead of networks of individuals, we model a network of sub-populations with a probability of migration between them. We ask how the structure of such a meta-population and the rate of migration affect the fixation probability. Many of the known results for networks of individuals carry over to meta-populations, in particular for regular networks or low symmetric migration probabilities. However, when patch sizes differ we find interesting deviations between structured meta-populations and networks of individuals. For example, a two patch structure with unequal population size suppresses selection for low migration probabilities.

DY 45.15 Thu 13:00 P1

Ising model with variable spin/agent strengths on graphs — MARIANA KRASNYSKA^{1,2,3}, YURIJ HOLOVATCH^{1,2,4}, •BERTRAND BERCHE^{2,3}, and RALPH KENNA^{2,4} — ¹ICMP, NAS of Ukraine, Lviv, Ukraine — ²L4 Collaboration Leipzig-Lorraine-Lviv-Coventry — ³Université de Lorraine, Nancy, France — ⁴Coventry University, UK

We consider a generalization of the Ising model in which individual spin strengths can vary [1]. The model describes the ordering in systems comprised of agents which, although matching in their binarity (i.e., maintaining the iconic Ising features of spin 'up/down', 'yes/no'), differ in their strengths. With inhomogeneous physical systems in mind, but also anticipating interdisciplinary applications, we present the model on graph structures of varying degrees of

complexity: complete graph, Erdős-Rényi graph, and on a scale-free network. This allows us to explore the interplay of two types of randomness: individual strengths of spins or agents and collective connectivity between them. We find the delicate interplay between variable properties of nodes and interactions between them leads to new universality classes.

[1] M. Krasnytska, B. Berche, Yu. Holovatch, R. Kenna, *J. Phys. Complex.*, 1 (2020) 035008; *Entropy*, 23(9) (2021) 1175.

DY 45.16 Thu 13:00 P1

Homeostatic plasticity in a minimal model for brain criticality — •MARCO SCHMIDT and STEFAN BORNHOLDT — Institut für Theoretische Physik, Universität Bremen

The 'criticality hypothesis' asserts that real-world neural networks operate near a critical phase transition. Experimental evidence exists and numerous models studying the possible underlying mechanisms accumulated during the last 20 years.

Early models based on simple threshold networks tune to a critical connectivity $K = 2$, which is not a realistic value when compared to real-world neural networks.

However, a phase transition in high degree threshold networks using the inhibition to excitation ratio as a control parameter does exist [1], as well as a corresponding self-organized critical toy model [2]. It features an adaptive threshold network, self-tuning to the critical inhibition to excitation ratio by using an activity based rewiring process that results in a highly clustered network and reaches criticality independent of K .

Here we present a new version of the model, incorporating a simple homeostatic plasticity mechanism as it appears in biological systems.

[1] L. Baumgarten, S. Bornholdt, *Critical excitation-inhibition balance in dense neural networks*, *Phys. Rev. E* 100, 010301 (2019).

[2] L. Baumgarten, S. Bornholdt, *A toy model for brain criticality: self-organized excitation/inhibition ratio and the role of network clustering*, arXiv:2202.03330.

DY 46: Poster: Machine Learning and Data Analytics

Time: Thursday 13:00–16:00

Location: P1

DY 46.1 Thu 13:00 P1

Time series analysis of loudness fluctuations in musical performances and psychophysical experiments — •BENJAMIN SCHULZ^{1,2}, CORENTIN NELIAS^{1,2}, and THEO GEISEL^{1,2,3} — ¹MPI for Dynamics and Self-Organization, Göttingen, Germany — ²Physics Dept., Georg-August University, Göttingen, Germany — ³Bernstein Center for Computational Neuroscience, Göttingen, Germany

Over the last decades, the study of fluctuations in musical time series showed power spectral densities that exhibit a $1/f^\beta$ -shape across certain frequency regions, indicating long range correlations. So far time series of pitch, rhythm, or timing were investigated across different musical epochs, composers and styles, showing a variety of β -values between 0 and 2. Whether the fluctuations of musical dynamics, or in other words loudness fluctuations, have similar spectral properties, is an open question, however. We have carried out in-depth studies of manually recorded data sets in different musical settings. A first set results from psychophysical tapping experiments. A second one consists of drum performances recorded in a musical environment. All participating musicians were professionals. The tapping and drumming data consistently show the clear occurrence of a $1/f^\beta$ -shape in the power spectral density. Furthermore, the presence of a metronome click in the tapping experiment leads to the strengthening of specific periodic structures in the loudness fluctuations and also seems to have an impact on the coefficient β .

DY 46.2 Thu 13:00 P1

Battery modeling: Fusing equivalent circuit models with data-driven surrogate modelling — •LIMEI JIN^{1,2}, FRANZ P. BERECK², JOSEF GRANWEHR², RÜDIGER-A. EICHEL², KARSTEN REUTER¹, and CHRISTOPH SCHEURER¹ — ¹Fritz-Haber-Institut der MPG, Berlin, Germany — ²IEK-9, Forschungszentrum Jülich, Jülich, Germany

Electrochemical impedance spectroscopy (EIS) is widely used to characterize electrochemical energy conversion systems. The traditional analysis with equivalent circuit models (ECM) has recently been augmented by a transform based distribution of relaxation times (DRT) analysis which allows one to reduce the ambiguity in the construction of ECMs and thus overfitting. Experimentally determined ECM parameters vary depending on operating conditions and the lifetime history of battery usage. Here we focus on State of Health (SOH) and State of Charge (SOC) as a basis for operando diagnosis and functionality optimization in the setting of fast-charging. Within pure ECM approaches, aging effects can only be represented to a limited extent, as aging is related to a variety of different factors whose impact on cell impedance are not sufficiently understood, yet. The highly complex interplay of factors motivates the development of data-driven Machine Learning (ML) models as a basis for future battery management sys-

tems. We present ML enabled ECMs based on experimental impedance analyses and a data-driven ML approach that computationally samples an abstract target space for classification and recognition of cells at vastly different SOC/SOH combinations.

DY 46.3 Thu 13:00 P1

Machine learning categorization of the Anderson model — •QUANGMINH BUI-LE and RUDOLF RÖMER — Department of Physics, University of Warwick, Coventry, CV4 7AL

Machine learning (ML) methods have been used to identify phase transitions of physical systems by categorizing systems based on the Ψ^2 values of their wave-functions into extended and localized states, which a model is then trained on in order to identify between the extended and localized states. Here we want to see if ML is powerful enough to categorize systems into even more specific groups by attempting to categorize Anderson model data into categories based on the disorder of the wave-function. We are using a PyTorch model to create a convolutional neural network using a ResNet18 model. This model will be trained on 3D Anderson model Ψ^2 values from 17 disorder values spanning a range of 15 to 18.

DY 46.4 Thu 13:00 P1

Neural-network based Monte Carlo Markov chain simulation of spin glasses — •MICHAEL ENGBERS and ALEXANDER K. HARTMANN — Carl von Ossietzky University, Oldenburg, Germany

Spin glasses exhibit a complex equilibrium and non-equilibrium behavior at low temperatures. The reason is the existence of an energy landscape with many local minima and high barriers. In computer simulations, this leads to long correlation times when investigating large systems. Due to this numerical hardness, the model has motivated the development of many new algorithmic approaches like generalized Wolff cluster algorithms, parallel tempering or genetic algorithms.

Recently, it has been shown that the application of generative neural networks can accelerate Monte Carlo simulations, also for simple spin models with apparently promising results.

Here, we use an autoregressive distribution estimator (NADE) to perform a Monte Carlo simulation of spin glasses [1]. We embedded the NADE into a Metropolis-Hastings Markov-chain approach, therefore ensuring detailed balance. We confirm previous results that the acceptance rates of the NADE approach surprisingly increase with decreasing temperature. Nevertheless, we show that crucial observables, such as the distribution of spin overlaps, indicate that this neural-network approach suffers from the lack of effective ergodicity.

[1] B. McNaughton, M.V. Milosević, A. Perali, and S. Pilati, *Phys. Rev. E* **101**, 053312 (2020).

DY 46.5 Thu 13:00 P1

Influence of mode-coupling on the information processing rate of Spin-VCSEL reservoir computer — •LUKAS MÜHLNICKEL, LINA JAURIGUE, and KATHY LÜDGE — Institut f. Physik, Technische Universität Ilmenau, Weimarer Str. 25, 98684 Ilmenau, Germany

The relative simplicity of reservoir computing, when comparing it to other machine learning methods, makes it suitable for efficient hardware implementation. The needed high dimensional reservoir dynamics can be provided by adding feedback to only one single nonlinear node, while driving the system with time multiplexed inputs. One promising realization utilizes the fast polarization dynamics of power efficient Spin-VCSELs. These fast field interactions are related to birefringence, dichroism and electron transition rates in the cavity material and occur on shorter time scales than the relaxation oscillations. Thus, compared to typical semiconductor lasers, much higher cutoff frequencies in the system response are observed for the Spin-VCSELs. We investigate the influence of these fast polarization oscillation dynamics on the reservoir performance when increasing data processing rates.

DY 46.6 Thu 13:00 P1

Deep learning-based clogging prediction in outflow of hard and soft grains — •SEDDIGHEH NIKIPAR, DMITRY PUZYREV, JING WANG, and RALF STANNARIUS — Institute of Physics and MARS, Otto von Guericke University Magdeburg, Universitätsplatz 2, D- 39106 Magdeburg, Germany

Studying the outflow of granular materials has been recognized as a challenging topic in physics due to their unexpected behavior, such as segregation, blockage, and other dynamical events [1]. In particular, the early detection of clogging during discharge of granular materials through narrow orifice in silo has significant challenges. In this work, the possibility of early prediction of clogging was investigated through implementation of image-based deep learning approach, which turns out to be a promising strategy to predict the time until the next clog [2]. For this purpose, experiments on discharge of mixtures of hard and soft spheres from a quasi-two dimensional (2D) silo have been conducted [3]. The image dataset of flowing particles was used to train the Convolutional Neural Networks of various architectures and to CNN-LSMT architecture specifically designed for time series analysis. The trained networks demonstrate considerable accuracy in clogging prediction.

This study is supported by DLR projects VICKI and EVA (50WM2252 and 50WM2048)

[1] Perge C, et al. Phys. Rev. E 85 021303 (2012) [2] Hanlan J, APS March Meeting, abstract id.M09.010 (2022) [3] J Wang, et al. Soft Matter, 17, 4282 (2021)

DY 46.7 Thu 13:00 P1

Optical reservoir computing with incoherent optical memory — •MINGWEI YANG^{1,2}, ELIZABETH ROBERTSON^{1,2}, LEON MESSNER^{1,3}, NORMAN VINCENZ EWALD¹, LUISA ESGUERRA^{1,2}, and JANIK WOLTERS^{1,2} — ¹Deutsches Zentrum für Luft- und Raumfahrt, Institute of Optical Sensor Systems, Berlin, Germany. — ²Technische Universität Berlin, Berlin, Germany. — ³Humboldt-Universität zu Berlin, Berlin, Germany.

Reservoir computing is a machine learning method that is particularly suited for dynamic data processing. A fixed reservoir projects the input information to a high-dimensional feature space, and only the readout weights need to be trained, allowing fast data processing with low energy consumption [1,2]. In this work, we demonstrate an optical reservoir computing using incoherent memory in a cesium vapor cell to predict time-series data. The information is stored in the reservoir by controlling the pump and probe process on the Cs D2 transitions. The coupling between the reservoir and both the input and output data is realized by acousto-optic modulators.

[1] G. Tanaka, T. Yamane, J. B. Héroux, R. Nakane, N. Kanazawa, S. Takeda, H. Numata, D. Nakano, and A. Hirose, *Recent advances in physical reservoir computing: A review*, Neural Networks 115, 100*123 (2019).

[2] L. Jaurigue, E. Robertson, J. Wolters, and K. Lüdge, *Photonic reservoir computing with non-linear memory cells: interplay between topology, delay and

delayed input,* in Emerging Topics in Artificial Intelligence (ETAI) 2022, vol. 12204 (SPIE, 2022), pp. 61*67.

DY 46.8 Thu 13:00 P1

Metadynamics Simulations of Chemical Reactions in Solution — •AZAD KIRSAN, SAGARMOY MANDAL, and BERND MEYER — Interdisciplinary Center for Molecular Materials and Computer Chemistry Center, FAU Erlangen-Nürnberg, Germany

For four important chemical reactions we have benchmarked two different methods for reconstructing the free energy surface (FES) and for estimating the free energy barrier from *ab initio* molecular dynamics (AIMD) simulations: standard metadynamics (MTD) and the recently introduced well-sliced metadynamics (WS-MTD) approach [1], which is a combination of umbrella sampling and MTD. The chosen reactions are a Diels-Alder reaction, an aromatic decarboxylation, an aromatic Claisen rearrangement, and the base-catalyzed hydrolysis of formamide. This selection includes a cycloaddition, an elimination, an intermolecular rearrangement, and an OH⁻ addition, thus covering a wide range of different reaction types and mechanisms. By utilizing our recently improved version of the CPMD code [2] it was possible to obtain many ns long trajectories of the reactions in the gas phase as well as in an explicitly included solvent.

[1] S. Awasthi, V. Kapil, N. Nair, J. Comput. Chem. 37 (2016) 1413

[2] T. Klöffel, G. Mathias, B. Meyer, Comput. Phys. Commun. 260 (2021) 107745

DY 46.9 Thu 13:00 P1

Analyzing Extreme Fluctuations of the Randomly Forced Nonlinear Schrödinger Equation via Large Deviation Theory — •SUMEJA BUREKOVIĆ¹, TOBIAS SCHÄFER², and RAINER GRAUER¹ — ¹Institute for Theoretical Physics I, Ruhr-University Bochum, Germany — ²Department of Mathematics, College of Staten Island, Staten Island, United States of America

Recently, the focusing nonlinear Schrödinger equation with additive noise has been proposed as a model for finite-time singularity mediated turbulence [1]. Among other findings, the authors of [1] show through direct numerical simulations that the statistics of quantities such as the energy dissipation rate and structure functions are intermittent. Here, in order to explain these observations and to quantify the effect of extreme fluctuations on the turbulence statistics, we employ methods from large deviation theory or instanton calculus [2]. In the first step, the probability density function or expectation for the quantities of interest is approximated by the Freidlin-Wentzell action of the large deviation minimizer or instanton. Additionally, our aim is to improve this approximation by taking into account Gaussian fluctuations around the instanton, harnessing the techniques of [3].

[1] Josserand, C., Pomeau, Y., & Rica, S. (2020). Phys. Rev. Fluid, 5(5), 054607.

[2] Grafke, T., Grauer, R., & Schäfer, T. (2015). J. Phys. A Math. Theor., 48(33), 333001. [3] Schorlepp, T., Grafke, T., & Grauer, R. (2021). J. Phys. A Math. Theor., 54(23), 235003.

DY 46.10 Thu 13:00 P1

Light propagation in media with electric and magnetic disorder: 3D Anderson localization — •WALTER SCHIRMACHER^{1,2}, THOMAS FRANOSCH³, MARCO LEONETTI^{1,4}, and GIANCARLO RUOCCO^{1,5} — ¹Istituto Italiano di Tecnologia, Roma, Italy — ²Universität Mainz, Mainz, Germany — ³Universität Innsbruck, Innsbruck, Austria — ⁴SLML, Consiglio Nazionale delle Ricerche, Roma, Italy — ⁵Università "La Sapienza", Roma Italy

We consider Maxwell's equations in a 3-dimensional material, in which both, the electric permittivity, as well as the magnetic permeability, fluctuate in space. Differently from all previous treatments, we transform the fields in such a way that the linear operator in the equations is manifestly Hermitian, in order to deal with a proper eigenvalue problem. We use an appropriate version of the Coherent-Potential approximation (CPA) to calculate the density of states and scattering-mean-free path. We find that in the presence of both electric and magnetic disorder the spectral range of Anderson localization appears to be much larger than in the case of electric (or magnetic) disorder only.

DY 47: Wetting, Fluidics and Liquids at Interfaces and Surfaces II (joint session CPP/DY)

Time: Thursday 15:00–16:15

Location: MER 02

See CPP 52 for details of this session.

DY 48: Dynamics and Chaos in Many-Body Systems I (joint session DY/TT)

Time: Thursday 15:00–17:30

Location: MOL 213

DY 48.1 Thu 15:00 MOL 213

Imperfect Many-Body Localization in Exchange-Disordered Isotropic Spin Chains — •JULIAN SIEGL and JOHN SCHLIEMANN — University of Regensburg

We study many-body localization in isotropic Heisenberg spin chains with the local exchange parameters being subject to quenched disorder. The Hamiltonian is invariant under global SU(2)-rotations and incorporates therefore a non-abelian symmetry. Systems of common spin length 1/2 and 1 are studied numerically using random matrix techniques. In both cases we find a transition from an ergodic phase at small disorder strength to an incompletely localized phase at stronger disorder. The transition is signaled by a maximum of the sample-to-sample variance of the averaged consecutive-gap ratio. The incompletely localized phase found here is distinguished from a fully localized system by the scaling behavior of the sample-to-sample variance.

DY 48.2 Thu 15:15 MOL 213

Magnetic Dipole Clusters - Resurrection of Catastrophe Machines — •INGO REHBERG and SIMEON VÖLKELE — Experimental Physics, University of Bayreuth

Hysteretic transitions between stable configurations of a hexagonal magnetic dipole cluster [1] are set in a broader context by revealing the nature of the corresponding instabilities [2]. Following the animation of this bifurcation scenario [3], we present an experimental setup where the height of the centre dipole serves as the bifurcation parameter. This catastrophe machine demonstrates the two instabilities forming the hysteresis loop, and it might provide a hint to the unresolved puzzle of the slowing down of one of the eigenmodes [4].

[1] Andrew D.P. Smith *et al.*, JMMM 549, 168991 (2022).[2] Simeon Völkel *et al.*, JMMM 559, 169520 (2022).[3] <https://doi.org/10.5281/zenodo.6380539> (18.5.2022).[4] Peter T. Haugen *et al.*, Chaos 32, 063108 (2022).

DY 48.3 Thu 15:30 MOL 213

Signatures of the interplay between chaos and local criticality on the dynamics of scrambling in many-body systems — FELIX MEIER¹, •MATHIAS STEINHUBER², JUAN DIEGO URBINA², DANIEL WALTNER¹, and THOMAS GUHR¹

— ¹University of Duisburg-Essen, Lotharstr. 1, 47048 Duisburg, Germany — ²University of Regensburg, Universitätsstr. 31, 93040 Regensburg, Germany

Fast scrambling, quantified by the exponential initial growth of Out-of-Time-Ordered-Correlators (OTOCs), is the ability to efficiently spread quantum correlations among the degrees of freedom of interacting systems, and constitutes a characteristic signature of local unstable dynamics. As such, it may equally manifest both in systems displaying chaos or even in integrable systems around criticality. We discuss the results from our recent publication [1], where we go beyond these two well-studied regimes with an exhaustive study of the interplay between local criticality and chaos. We address many-body systems with a well-defined classical (mean-field) limit, as coupled large spins and Bose-Hubbard chains, thus allowing for semiclassical analysis. Our aim is to investigate the dependence of the exponential growth of the OTOCs, defining the quantum Lyapunov exponent λ_q on quantities derived from the classical system with mixed phase space, specifically the local stability exponent of a fixed point λ_{loc} as well as the maximal Lyapunov exponent λ_r of the chaotic region around it.

[1] Meier, F., Steinhuber, M., Urbina, J. D., Waltner, D. & Guhr, T. arxiv:2211.12147

DY 48.4 Thu 15:45 MOL 213

Characterizing quantum chaoticity of kicked spin chains — •TABEA HERMANN, MAXIMILIAN F. I. KIELER, and ARND BÄCKER — TU Dresden, Institut für Theoretische Physik, Dresden, Germany

Quantum many body systems are commonly considered as quantum chaotic if their spectral statistics, such as the level spacing distribution, agree with those of random matrix theory. Using the example of the kicked Ising chain we demonstrate that even if both level spacing distribution and eigenvector statistics agree well with random matrix predictions, the entanglement entropy deviates from the expected Page curve. We propose a new measure of the effective spin interactions and obtain the corresponding random matrix result. By this the deviations of the entanglement entropy can be understood.

DY 48.5 Thu 16:00 MOL 213

Entanglement Characterization of Measurement-Induced Phase Transition in Fermionic Chains — •JIANGTIAN YAO^{1,2}, SEBASTIAN DIEHL¹, and MICHAEL BUCHHOLD¹ — ¹Institute for Theoretical Physics, University of Cologne, D-50937 Cologne, Germany — ²Max Planck Institute for the Physics of Complex Systems, 01187 Dresden, Germany

We report characterization of measurement-induced phase transition in Gaussian fermionic chains. We use various entanglement measures to characterize the two phases as well as the nature of the transition. Through a numerical study on the entanglement spectra, we observe closure of the entanglement gap in the

critical phase and relate the scaling of the closure to the effective central charge of the system. In addition, we numerically extract the effective Luttinger liquid parameter of the system and use it to characterize the critical phase. Lastly, we use the scaling behavior of the effective Luttinger liquid parameter as well as the Schmidt gap to estimate the critical point for the phase transition.

15 min. break

DY 48.6 Thu 16:30 MOL 213

Dynamical characterization of the chaotic phase in the Bose-Hubbard model

— DAVID PEÑA MURILLO and •ALBERTO RODRÍGUEZ — Departamento de Física Fundamental, Universidad de Salamanca, E-37008 Salamanca, Spain

We study the dynamical manifestation of the Bose-Hubbard model's chaotic phase [1] by analysing the temporal behaviour of connected two-point density correlations on experimentally accessible time scales up to a few hundred tunneling times. The time evolution of initial Mott states with unit density in systems including up to 17 bosons (Hilbert space dimension $\approx 10^9$) reveals that the chaotic phase can be unambiguously identified from the early time fluctuations of the considered observable around its equilibrium value [2]. The emergence of the chaotic phase is also seen to leave an imprint in the initial growth of the time signals. The possibility to discern specific features of this many-body chaotic phase, on top of the universal prediction of random-matrix theory, from these experimentally accessible measures is explored.

[1] L. Pausch *et al.*, Phys. Rev. Lett. 126, 150601 (2021)

[2] D. Peña Murillo, MSc Thesis, Universidad de Salamanca (2022)

DY 48.7 Thu 16:45 MOL 213

Universal Eigenvalue Distribution for Locally Interacting Quantum Systems

— •TOBIAS HELBIG, TOBIAS HOFMANN, RONNY THOMALE, and MARTIN GREITER — Institut für Theoretische Physik und Astrophysik, Universität Würzburg, D-97074 Würzburg, Germany

Wigner has shown [1] that the eigenvalue distribution of a Gaussian orthogonal or unitary ensemble of random matrices approaches a semicircle in the thermodynamic limit. Here, we show that the joint eigenvalue distribution of locally interacting quantum systems, that is, ensembles of finite dimensional subsystems with local interactions between them, approaches a Gaussian distribution as the number of subsystems is taken to infinity [2]. In the talk, we present our analytical results supported by numerical data and discuss possible implications of a Gaussian density of states for physical problems.

[1] E. P. Wigner. On the statistical distribution of the widths and spacings of nuclear resonance levels. *Mathematical Proceedings of the Cambridge Philosophical Society*, 47(4): 790-798 (1951).

[2] T. Hofmann, T. Helbig, R. Thomale, and M. Greiter. In preparation.

DY 48.8 Thu 17:00 MOL 213

Power-law decay of correlations after a global quench in the massive XXZ chain— •FLÁVIA BRAGA RAMOS¹, ANDREW URICHUK^{2,3}, IMKE SCHNEIDER¹, and JESKO SIRKER³ — ¹Fachbereich Physik und Research Center OPTIMAS, Technische Universität Kaiserslautern, Kaiserslautern, Germany — ²University of Manitoba, Winnipeg, Canada — ³Bergische Universität Wuppertal, Wuppertal, Germany

While there have been great advances in understanding the final equilibration of integrable systems after a quantum quench, relatively little is known about their precise relaxation towards the steady state. In this context, the XXZ chain provides a playground for the investigation of interaction effects in out-of-equilibrium properties of quantum many-body systems. We investigate the relaxation dynamics of equal-time correlations in the antiferromagnetic phase of the XXZ spin-1/2 chain following a global quantum quench of the anisotropy parameter. In particular, we focus on the relaxation dynamics starting from an initial Néel state. Using the exact solution of an effective free-fermion model, state-of-art density matrix renormalization group simulations, and the quench-action approach, we show that the late-time relaxation is characterized by a power-law decay $\sim t^{-3/2}$ independent of anisotropy. Overall, we find remarkable agreement in the results obtained from the distinct approaches.

DY 48.9 Thu 17:15 MOL 213

Universal correlations in chaotic many-body quantum states: lifting Berry's Random Wave Model into Fock space— RÉMY DUBERTRAND¹, JUAN-DIEGO URBINA², KLAUS RICHTER², and •FLORIAN SCHÖPPL² — ¹Department of Mathematics, Physics and Electrical Engineering, Northumbria University, NE1 8ST Newcastle upon Tyne, United Kingdom — ²Institut für Theoretische Physik, Universität Regensburg, 93040 Regensburg, Germany

Using a semiclassical analysis based on Berry's ansatz [1] we investigate the universal statistical features of eigenstate correlations in chaotic mesoscopic many-body quantum systems, focusing on Bose-Hubbard lattices, where the existence

of a classical (mean-field) limit allows for the use of many-body semiclassical methods [2]

For this, we first have to lift Berry's ansatz into the many-body space by expanding the microscopic correlations and the conjectured multivariate Gaussian distribution of expansion coefficients into the Fock space of quantum fields. Together with numerical evidence, which supports the extension to multi-point correlations of the known Gaussian distribution for a single expansion coefficient,

the universality of eigenstate correlations can be extended well beyond random matrix theory, where these correlations are absent. Our results bring the correlation backbone of eigenfunctions into a precise signature of quantum chaos in many-body mesoscopic systems.

- [1] M. V. Berry, *Journal of Physics A: Mathematical and General* **10**, 2083 (1977)
 [2] K. Richter, J.D. Urbina, and S. Tomsovic. "Semiclassical roots of universality in many-body quantum chaos," (2022)

DY 49: Critical Phenomena and Phase Transitions

Time: Thursday 15:00–17:45

Location: ZEU 160

DY 49.1 Thu 15:00 ZEU 160

Metastate analysis for two-dimensional Ising spin glasses — ALEXANDER K. HARTMANN¹ and A. PETER YOUNG² — ¹University of Oldenburg, Germany — ²University of California, Santa Cruz, USA

Spin glasses (SGs) are disordered magnetic systems which provide prototypical models for complex systems, including systems outside physics such as neural networks and machine-learning problems. For the two-dimensional (2d) case, exact numerical ground states (GSs) of large sizes can be obtained by polynomial-time graph-matching algorithms. Using these methods it was shown that 2d SGs exhibit a spin-glass ordered phase only at zero temperature, see e.g. [1]. Results from applying a modified version of the GS algorithm indicate that this phase is well described [2] by the so-called "droplet" theory, i.e., it has a simple structure. Here, we consider the *metastate* approach, which was introduced [3] to deal with the chaotic size-dependence of the spin-glass state. By studying a large range of sizes, we show convincingly that, in the thermodynamic limit, spin correlations in a local region are unaffected by the bonds far away, which is one of the main assumptions of the droplet picture.

[1] A.K. Hartmann and A.P. Young, *Phys. Rev. B* **64**, 180404 (2001).

[2] A.K. Hartmann and M.A. Moore, *Phys. Rev. Lett.* **90**, 127201 (2003).

[3] C.M. Newman and D.L. Stein, *J. Phys.: Condens. Matter* **15**, R1319 (2003).

DY 49.2 Thu 15:15 ZEU 160

On the criticality of structurally disordered magnets — MAXYM DUDKA^{1,2}, MARIANA KRASNYSKA^{1,2,3}, JUAN RUIZ-LORENZO^{4,5}, and YURIJ HOLOVATCH^{1,2,6} — ¹ICMP, NAS of Ukraine, Lviv, Ukraine — ²L4 Collaboration Leipzig-Lorraine-Lviv-Coventry, Europe — ³Université de Lorraine, Nancy, France — ⁴Universidad de Extremadura, Badajoz, Spain — ⁵BIFI, Zaragoza, Spain — ⁶Coventry University, Coventry, UK

We discuss the problem of influence of structural disorder on criticality. As a case study, we consider an impact of a weak quenched disorder on a magnetic phase transition. Usually, such an impact is analyzed for a two-component mixture (e.g. a solid solution of a magnet with its non-magnetic counterpart). A distinct feature of our analysis is consideration of changes in the magnetic phase transition when both components are magnets. To this end, we make use of a generalized Ising model suggested recently [M. Krasnytska et al., *J. Phys.: Complexity* **1** (2020) 035008] in a context of complex systems. We apply the field theoretical renormalization group approach to analyze its effective and asymptotic critical behaviour. We show that this is the structural disorder itself that causes changes in the universal critical behaviour, regardless of whether it has a form of a random mixture of magnetic and non-magnetic constituents or of two different magnetic compounds [M. Dudka et al., arXiv:2207.13655].

DY 49.3 Thu 15:30 ZEU 160

Non-Hermitian PT-symmetric Ising spin chains: novel quantum phases and quantum phase transitions — GRIGORY STARKOV, MIKHAIL FISTUL, and ILYA EREMIN — Ruhr-Universität Bochum, Bochum, Germany

A theoretical study of quantum phases and quantum phase transitions occurring in non-Hermitian PT-symmetric transverse-field Ising spin model. A non-Hermitian part of the Hamiltonian is implemented via imaginary staggered longitudinal magnetic field corresponding to a local staggered gain and loss terms, γ .

Using a numerical diagonalization of the Hamiltonian for spin chains of a finite size N accompanied by a scaling procedure for the coherence length ξ , a complete quantum phase diagram γ - J (J is an adjacent spins interaction strength) is established. We obtain two quantum phases for $J < 0$, i.e., PT-symmetry broken antiferromagnetic state and PT-symmetry preserved paramagnetic state, and the quantum phase transition line is the line of exception points. For $J > 0$ the PT-symmetry of the ground state is retained in a whole region of parameter space of J and γ , and a system shows two intriguing quantum phase transitions between ferromagnetic and paramagnetic states for a fixed parameter $\gamma > 1$.

The qualitative quantum phase diagram is derived in the framework of the Bethe-Peierls approximation that is in a good accord with numerically obtained results. The quantum phase diagram can be verified in the microwave transmission experiments allowing to identify the transitions between the first excited and the ground states.

DY 49.4 Thu 15:45 ZEU 160

Predictive percolation: assessing fire connectivity in California — OLIVIA HEMOND¹, DIEGO RYBSKI^{1,2,3}, ARIANI C. WARTENBERG^{1,4}, KATHERINE J. SIEGEL⁵, and VAN BUTSIC¹ — ¹Department of Environmental Science, Policy, and Management, University of California, Berkeley, Berkeley, CA, United States — ²Potsdam Institute for Climate Impact Research - PIK, Member of Leibniz Association, P.O. Box 601203, 14412 Potsdam, Germany — ³Complexity Science Hub Vienna, Josefstädterstrasse 39, A-1090 Vienna, Austria — ⁴Leibniz Centre for Agricultural Landscape Research, Eberswalder Str. 84, 15374 Müncheberg, Germany — ⁵Department of Ecology & Evolutionary Biology, University of Colorado, Boulder, CO, USA

Damages from wildfire are increasing globally. Analyzing historical California fire data from 1950-2019, we propose a new method to estimate the percolation threshold, which represents statewide connectivity of fire-affected habitats. We create grid realizations of burnt areas over various time spans, measure the critical distances, and explore analogies with continuum percolation to predict the percolation threshold. Fires within our study period trend towards but do not yet reach percolation. We calculate the percolation threshold to be 45.8% of the state's burnable area. Assuming fire patterns similar to the past seventy years, it would take 146.5 years, starting from 1950, to reach percolation across California. Within time periods shorter than 146 years, wildfire-affected areas are fragmented.

DY 49.5 Thu 16:00 ZEU 160

Determination of the nearest-neighbor interaction strength in VO₂ via fractal dimension analysis — JACOB HOLDER, DANIEL KAZENWADEL, PETER NIELABA, and PETER BAUM — Universität Konstanz, Konstanz, Deutschland

The Ising model is one of the simplest and well-established models to simulate phase transformations in complex materials. However, its most central constant, the interaction strength J between two nearest neighbors, is not directly related to any macroscopic material property and is therefore hard to obtain. Here we report how to obtain this basic constant by a fractal dimension analysis of measured domain structures. In the example of VO₂, a strongly correlated material with first-order metal-to-insulator transition close to room temperature, we obtain an interaction strength of 11 meV. In a two dimensional simplification, we find an effective value of 17 meV due to the reduced number of nearest neighbors. These results link the fundamental constants in the Ising model to measured quantities of bulk materials.

15 min. break

DY 49.6 Thu 16:30 ZEU 160

Global Speed Limit for Finite-Time Dynamical Phase Transition in Nonequilibrium Relaxation — KRISTIAN BLOM and ALJAZ GODEC — Max Planck Institute for Multidisciplinary Sciences, Göttingen, Germany

The nearest-neighbor interacting Ising model is a paradigm for classical many-body physics. Recent works unraveled an intriguing finite-time dynamical phase transition in the thermal relaxation of a mean field Curie-Weiss Ising model. This phase transition reflects a sudden switch in the dynamics, and manifests as a cusp in the probability density of magnetization. Its existence in systems with a finite range of interaction, however, remained unclear.

Employing the Bethe-Guggenheim approximation, which is exact on Bethe lattices, we demonstrate the finite-time dynamical phase transition in nearest-neighbor Ising systems for arbitrary quenches, including those within the two-phase coexisting region. Strikingly, for any given initial condition we prove and explain the existence of non-trivial speed limits for the dynamical phase transition and the relaxation of magnetization, which are absent in the mean field setting. Pair correlations, which are neglected in mean field theory, and trivial in the Curie-Weiss model, account for kinetic constraints due to frustrated local configurations, that give rise to a global speed limit.

Our findings may be relevant for optimizing ultrafast optical-switching ferromagnetic materials.

DY 49.7 Thu 16:45 ZEU 160

Crossover in the phase-coexistence between models with discrete and continuous variables — •FLORIAN KISCHEL, NILS CACI, and STEFAN WESSEL — RWTH Aachen University, Aachen, Germany

The relative weight of the distinct phases that coexist at a first-order phase transition in systems with discrete degrees of freedom is well understood. For example, in the q -state Potts model, it is characterized by a ratio $R = 1 : q$ of the disordered vs. ordered regions. In models with continuous variables on the other hand, this ratio is generally unknown. Several recent instances however suggest that it equals $R = 1 : I_O$, where I_O denotes the integral measure of the space of extremal states of the ordered phase. In order to explore the emergence of this integral measure, we examine a system that realizes a crossover from discrete to continuous variables and study the behavior of R at its phase-coexistence points. In particular, we consider a generalized n -state clock-model on a three-dimensional simple cubic lattice with both bilinear and biquadratic exchange interactions. In the large- n (XY) limit, this model is known to harbor a first-order thermal phase transition, as does the 3-state Potts model, to which the model reduces in the limit of $n = 3$. Here, we explore the phase-coexistence over the range of intermediate values of n using large-scale Monte Carlo simulations.

DY 49.8 Thu 17:00 ZEU 160

Partition function zeros in the 3D Blume-Capel model — •LEÏLA MOUËD-DENE — Laboratoire de Physique et Chimie Théoriques, Université de Lorraine, Vandoeuvre-lès-Nancy, France

The phase diagram of the three-dimensionnal Blume Capel model shows an ordered ferromagnetic phase and a disordered paramagnetic phase, separated by a transition line from second order to first order at the tricritical point (TCP). The universality class of the second-order line is the Ising class, while the tricritical universality class governs the behaviour of the critical exponents at the tricritical point. It is well known that the upper critical dimension is $d_{uc} = 3$ at the TCP, thus Mean Field exponents are expected, modified by logarithmic correction factor. We determine analytically the logarithmic-correction exponents - also universal - using RG for ϕ_6 model. The knowledge of the partition function zeros is a quite fundamental and powerful approach to study a phase transition. While the Fisher zeros and Lee-Yang zeros are well known to study the thermal exponent γ_t and magnetic exponent γ_h , we build a new type of zeros from the complex plane of the crystal field which leads to the crystal exponent γ_2 : the crystal field zeros. We study the leading and logarithmic-corrections exponents numerically from the partition function zeros and compare with the analytical results, and check if the scaling relations are verified.

DY 49.9 Thu 17:15 ZEU 160

Boundary critical behavior of the three-dimensional $O(N)$ universality class — •FRANCESCO PARISEN TOLDIN¹ and MAX A. METLITSKI² — ¹Institut für Theoretische Physik und Astrophysik, Universität Würzburg, Am Hubland, D-97074 Würzburg, Germany — ²Department of Physics, Massachusetts Institute of Technology, Cambridge, Massachusetts 02139, USA

It was recently realized that the three-dimensional $O(N)$ model exhibits an extraordinary surface universality class for a finite range of $N \geq 2$. We investigate the boundary critical behavior by means of high-precision Monte Carlo simulations of an improved model, where leading scaling corrections are suppressed. Contrary to simplified arguments on the bulk-surface phase diagram, and in line with a recent field-theoretical analysis, we find a special surface transition for $N = 3$, with unusual exponents, and an extraordinary phase with logarithmically decaying correlations. For a general N , the existence and universal properties of extraordinary phase are predicted to be controlled by certain amplitudes of the normal universality class, where one applies an explicit symmetry breaking field to the boundary. We extract these universal amplitudes by Monte Carlo simulations for $N = 2, 3$. Our results are in good agreement with direct Monte Carlo studies of the extraordinary universality class serving as a nontrivial quantitative check of the connection between the normal and extraordinary classes.

Ref.: F. Parisen Toldin, Phys. Rev. Lett. 126, 135701 (2021); F. Parisen Toldin, M. A. Metlitski, Phys. Rev. Lett. 128, 215701 (2022)

DY 49.10 Thu 17:30 ZEU 160

Critical phenomena in the two-dimensional dilute Baxter-Wu model — •ALEXANDROS VASILOPOULOS¹, NIKOLAOS G. FYTAS¹, MICHAEL AKRITIDIS¹, and MARTIN WEIGEL² — ¹Centre for Fluid and Complex Systems, Coventry University, Coventry CV1 5FB, United Kingdom — ²Institut für Physik, TU Chemnitz, 09107 Chemnitz, Germany

We study the question of universality in the two-dimensional spin-1 Baxter-Wu model in the presence of a crystal field Δ . We employ extensive numerical simulations consisting of various types, providing us with complementary results: Wang-Landau sampling at fixed values of Δ and a parallelized variant of the multicanonical approach performed at constant temperature T . A detailed finite-size scaling analysis in the regime of second-order phase transitions in the (Δ, T) phase diagram indicates that the transition belongs to the universality class of the four-state Potts model. Previous controversies with respect to the nature of the transition are discussed and attributed to the presence of strong finite-size effects, especially as one approaches the pentacritical point of the model. Lastly, to facilitate the study of $\Delta > 0$, where the two previous methods become increasingly inhibitory, a hybrid algorithm consisting of both a cluster and a single-spin-flip update was implemented and tested.

DY 50: Evolutionary Game Theory (joint session SOE/DY)

Time: Thursday 15:00–15:30

Location: ZEU 260

See SOE 17 for details of this session.

DY 51: Members' Assembly

Agenda: Report, Elections, Future Activities of DY, Any other bussiness

Time: Thursday 18:00–19:00

Location: ZEU 160

All members of the Dynamics and Statistical Physics Division are invited to participate.

DY 52: Statistical Physics of Biological Systems II (joint session BP/DY)

Time: Friday 9:30–12:00

Location: BAR Schö

See BP 29 for details of this session.

DY 53: Active Matter V (joint session BP/PPP/DY)

Time: Friday 9:30–12:00

Location: TOE 317

See BP 30 for details of this session.

DY 54: Complex Fluids and Colloids, Micelles and Vesicles (joint session CPP/DY)

Time: Friday 9:30–13:00

Location: MER 02

See CPP 57 for details of this session.

DY 55: Dynamics and Chaos in Many-Body Systems II (joint session DY/TT)

Time: Friday 9:30–12:30

Location: MOL 213

DY 55.1 Fri 9:30 MOL 213

Towards a more fundamental understanding of eigenstate thermalization — •TOBIAS HOFMANN, TOBIAS HELBIG, RONNY THOMALE, and MARTIN GREITER — Institut für Theoretische Physik und Astrophysik, Universität Würzburg, 97074 Würzburg, Germany

We explore several venues how eigenstate thermalization may be understood on a more fundamental level. In particular, we report on extensive numerical work in spin systems with random interactions, where a small subsystem is subject to thermalization. We discuss possible directions towards an understanding of our numerical results.

DY 55.2 Fri 9:45 MOL 213

Spectral Response of Disorder-Free Localized Lattice Gauge Theories — •NILOTPAL CHAKRABORTY¹, MARKUS HEYL^{1,2}, PETR KARPOV¹, and RODERICH MOESSNER¹ — ¹Max Planck Institute for Physics of Complex Systems, Dresden — ²University of Augsburg

We show that certain lattice gauge theories exhibiting disorder-free localization have a characteristic response in spatially averaged spectral functions: a few sharp peaks combined with vanishing response in the zero frequency limit. This reflects the discrete spectra of small clusters of kinetically active regions formed in such gauge theories when they fragment into spatially finite clusters in the localized phase due to the presence of static charges. We obtain the transverse component of the dynamic structure factor, which is probed by neutron scattering experiments, deep in this phase from a combination of analytical estimates and a numerical cluster expansion. We also show that local spectral functions of large finite clusters host discrete peaks whose positions agree with our analytical estimates. Further, information spreading, diagnosed by an unequal time commutator, halts due to real space fragmentation. Our results can be used to distinguish the disorder-free localized phase from conventional paramagnetic counterparts in those frustrated magnets which might realize such an emergent gauge theory.

DY 55.3 Fri 10:00 MOL 213

Chaos in the three-site Bose-Hubbard model - classical vs quantum — •GORAN NAKERST¹ and MASUDUL HAQUE^{1,2} — ¹Institut für Theoretische Physik, Technische Universität Dresden, D-01062 Dresden, Germany — ²Max-Planck-Institut für Physik komplexer Systeme, D-01187 Dresden, Germany

We consider a quantum many-body system - the Bose-Hubbard system on three sites - which has a classical limit, and which is neither strongly chaotic nor integrable but rather shows a mixture of the two types of behavior. We compare quantum measures of chaos (eigenvalue statistics and eigenvector structure) in the quantum system, with classical measures of chaos (Lyapunov exponents) in the corresponding classical system. As a function of energy and interaction strength, we demonstrate a strong overall correspondence between the two cases. In contrast to both strongly chaotic and integrable systems, the largest Lyapunov exponent is shown to be a multi-valued function of energy.

DY 55.4 Fri 10:15 MOL 213

Many-Body Dwell-time and Density of States — •GEORG MAIER, CAROLYN ECHTER, JUAN-DIEGO URBINA, and KLAUS RICHTER — Universität Regensburg, Regensburg, Germany

Many body systems with a large number of degrees of freedom are usually described by statistical physics on the theoretical side while experiments usually relay on scattering (e.g. particle physics). Is it possible to relate scattering and statistical physics, or to measure scattering-related observables which directly relate to quantities of statistical physics? At least for single particle systems a close relation exists between the well known Wigner-Smith delay time in scattering theory and the density of states of the scattering system.

I will present a novel ansatz relating a many-body version of dwell-/Wigner-Smith delay time and many body density of states based on the famous Birman-Krein-Friedel-Lloyd formula connecting scattering theory and statistical observables in the many-body context. This formalism could provide answers to a wide variety of interesting questions, e.g. can we observe the effect of interactions (or even the emergence of chaos) through the lens of the dwell-time? Another interesting point is the roll of particle statistics on dwell-time meaning e.g. does it take longer for a particle to leave a fermionic or bosonic system?. I will present our analytical and numerical results on these questions.

DY 55.5 Fri 10:30 MOL 213

Dynamical correlations and domain wall relocalisation in transverse field Ising chains — •PHILIPPE SUCHSLAND¹, BENOÎT DOUÇOT², VEDIKA KHEMANI³, and RODERICH MOESSNER¹ — ¹Max Planck Institute for the Physics of Complex Systems, Nöthnitzer Str. 38, 01187 Dresden, Germany — ²LPTHE, UMR 7589, CNRS and Sorbonne Université, 75252 Paris Cedex 05, France — ³Department of Physics, Stanford University, Stanford, California 94305, USA

We study order parameters and out-of-time-ordered correlators (OTOCs) for a wide variety of transverse field Ising chains: classical and quantum, clean and disordered, integrable and generic. The setting we consider is that of a quantum quench. We find a remarkably rich phenomenology, ranging from stable periodic to signals decaying with varying rates. This variety is due to a complex interplay of dynamical constraints (imposed by integrability and symmetry) which thermalisation is subject to. In particular, a process we term dynamical domain wall relocalisation provides a long-lived signal in the clean, integrable case, which can be degraded by the addition of disorder even without interactions. Our results shed light on a proposal to use an OTOC specifically as a local dynamical diagnostic of a quantum phase transition even when evaluated in a state with an energy density corresponding to the paramagnetic phase.

15 min. break

DY 55.6 Fri 11:00 MOL 213

Time evolution at the quantum-critical point of the sawtooth chain — •JANNIS ECKSELER, FLORIAN JOHANNESMANN, and JÜRGEN SCHNACK — Fakultät für Physik, Universität Bielefeld, Postfach 100131, D-33501 Bielefeld, Germany

It is known for the antiferromagnetic sawtooth chain with Heisenberg interactions to develop a flat band at the quantum-critical point of $J_1 = 2J_2$, where J_1 is the exchange interaction between nearest neighbors and J_2 the interaction at the base of the triangles [1]. We investigate the time evolution of several observables of the sawtooth chain, especially near that point and in particular in view of their equilibration properties. [1] J. Schulenburg, A. Honecker, J. Schnack, J. Richter, H.-J. Schmidt, Phys. Rev. Lett. 88 (2002) 167207

DY 55.7 Fri 11:15 MOL 213

Quantum Noise as a Symmetry-Breaking Field — •PAUL McCLARTY¹, BEATRIZ DIAS², DOMAGOJ PERKOVIC³, MASUDUL HAQUE⁴, and PEDRO RIBEIRO⁵ — ¹MPI PKS, Dresden, Germany — ²TU Munich, Garching, Germany — ³Cavendish Lab, University of Cambridge, UK — ⁴TU Dresden, Germany — ⁵IST, Lisbon, Portugal

We investigate the effect of quantum noise on the measurement-induced quantum phase transition in monitored random quantum circuits. Using the efficient simulability of random Clifford circuits, we find that the transition is broadened into a crossover and that the phase diagram as a function of projective measurements and noise exhibits several distinct regimes. We show that a mapping to a classical statistical mechanics problem accounts for the main features of the random circuit phase diagram. The bulk noise maps to an explicit permutation symmetry breaking coupling; this symmetry is spontaneously broken when the noise is switched off. These results have implications for the realization of entanglement transitions in noisy quantum circuits.

DY 55.8 Fri 11:30 MOL 213

Finite-size prethermal behavior at the chaos-to-integrable transition — •JOHANNES DIEPLINGER¹ and SOUMYA BERA² — ¹Institute of Theoretical Physics, University of Regensburg, D-93040 Germany — ²Department of Physics, Indian Institute of Technology Bombay, Mumbai 400076, India

We investigate the dynamics of the complex Sachdev-Ye-Kitaev model complemented with a single particle hopping term, leading to a chaos-to-integrable transition of the eigenstates. We determine the dynamics close to the transition via the density-density correlator, where we observe a prethermal plateau in the ergodic phase. This indicates a finite time localised behavior up to an interaction-dependent thermalization time scale. This time scale is quantified as $t_{th} \propto 2^{\alpha/\sqrt{\lambda}}$ as a function of the relative interaction strength λ . The results are validated by investigating the time-dependent structure of the time-evolved wave functions in the Fock space.

DY 55.9 Fri 11:45 MOL 213

Quasiparticle Description of Entanglement Growth — •MOLLY GIBBINS, BRUNO BERTINI, and ADAM SMITH — University of Nottingham

The quasiparticle picture of entanglement is a novel way to describe a feature unique to quantum many-body systems. Recent research has found excellent agreement of this description with numeric results: a description that had been shown to hold for the general family of Rényi entanglement entropies, for different classes of quench and different geometries of the boundary across which entanglement develops.

The aim of this project is to develop a quasiparticle description of the entanglement growth in free-fermionic systems with translational invariance in both 1D and 2D. The propagation of quasiparticles across this cut will respect this translational invariance and it is expected that the entanglement generated between these particles will be in very good agreement with the exact solution for these systems.

DY 55.10 Fri 12:00 MOL 213

Excitation Transport in Molecular Aggregates with Thermal Motion — •RITESH PANT and SEBASTIAN WÜSTER — Indian institute of science education and research, Bhopal, India

Molecular aggregates can under certain conditions transport electronic excitation energy over large distances due to the long range dipole-dipole interactions. These interactions are also the characteristics of Rydberg aggregates which have been proved as the quantum simulators for molecular aggregates. An idea that naturally arises in Rydberg aggregates, is adiabatic excitation transport through atomic motion, where slow motion of the atoms combined with excitation transport can result in efficient and guided transport of the excitation from one end of an atomic chain to the other. Based on the analogy between Rydberg and Molecular aggregates, in ref. [1] we explore whether the adiabatic excitation transport can play a functional role in molecular aggregates in the absence of intra-molecular vibrations. But because the transport is partially adiabatic and because it involves transitions between non-eigenstates, it is challenging to estimate the adiabaticity of transport in molecular aggregates. Hence, in ref [2] we established a measure to quantify the adiabatic character of quantum transitions in general. Next, the effect of intramolecular vibrations is included by extending our calculation for excitation transport to an open-quantum- system technique [3].

[1] R. Pant and S. Wüster, *Physical Chemistry Chemical Physics* 22, 21169 (2020). [2] R. Pant, et al., <https://arxiv.org/abs/2007.10707>. [3] R. Pant, et al., (Manuscript in preparation)

DY 55.11 Fri 12:15 MOL 213

Tailoring the Phonon Environment of Embedded Rydberg Aggregates — •SIDHARTH RAMMOHAN¹, SEBASTIAN WÜSTER¹, and ALEXANDER EISFELD² — ¹IISER Bhopal, Madhya Pradesh, India — ²MPIPKS, Dresden, Germany

State-of-the-art experiments can controllably create Rydberg atoms inside a Bose-Einstein condensate (BEC) such that the Rydberg electron orbital volume contains many neutral atoms, which can be tuned, resulting in electron-atom scattering events [1]. In my talk, I will discuss the physics of the interaction and corresponding dynamics of a single or multiple Rydberg atoms in two internal electronic states embedded inside a BEC, to assess their utility for controlled studies of decoherence and quantum simulations of excitation transport similar to photosynthetic light-harvesting. We initially developed a theoretical framework to calculate the open quantum system input parameters for a single Rydberg atom, possibly in two internal states, in BEC and then for a chain of Rydberg atoms, forming an aggregate [2]. The electron-atom interactions lead to Rydberg-BEC coupling, creating phonons in the BEC. Using the spin-boson model with the calculated parameters, we then examine the decoherence and the Non-Markovian features of a Rydberg atom in a superposition, resulting from the interaction with the environment [3]. The scenario with a single Rydberg atom is then extended to the aggregate case, allowing us to set up dynamics similar to those found in light-harvesting complexes. Ref:1. J. B. Balewski, et al; *Nature* 502 664 (2013).2. S. Rammohan, et al; *PRA* 103, 063307 (2021).3. S. Rammohan, et al; *PRA* 104, L060202 (2021).

DY 56: Brownian Motion and Anomalous Diffusion

Time: Friday 9:30–12:45

Location: ZEU 160

DY 56.1 Fri 9:30 ZEU 160

Odd Diffusion of Interacting Particles — •ERIK KALZ¹, HIDDE DERK VUIJK², IMAN ABDOLI², JENS-UWE SOMMER^{2,3}, HARTMUT LÖWEN⁴, RALF METZLER¹, and ABHINAV SHARMA^{2,3} — ¹Universität Potsdam, Institut für Physik und Astronomie — ²Leibniz-Institut für Polymerforschung Dresden, Institut Theorie der Polymere — ³Technische Universität Dresden, Institut für Theoretische Physik — ⁴Heinrich Heine-Universität Düsseldorf, Institut für Theoretische Physik II: Weiche Materie

It is generally believed that collisions of particles reduce the self-diffusion coefficient, closely related to autocorrelation functions, which are assumed to decay monotonously in the overdamped limit. We show that these beliefs are only limiting cases in odd-diffusive systems, which are characterized by diffusion tensors with antisymmetric offdiagonal elements. We show that in the dilute limit, particle interactions can reduce, unalter and even enhance the self-diffusion. The underlying particle dynamics thereby can be captured by the force autocorrelation function. We show that this autocorrelation function exhibits a variety of behaviour: (a) even in the dilute limit where collisions are rare, the correlation can become negative, (b) despite the overdamped dynamics, the force autocorrelation can exhibit temporal oscillations and (c) the long-time power-law decay of the force autocorrelation depends on the odd-diffusion parameter. Odd diffusivity, therefore, shines new light on fundamental beliefs in overdamped systems.

Kalz, Erik, et al. Collisions enhance self-diffusion in odd-diffusive systems. *Physical Review Letters* 129.9 (2022): 090601.

DY 56.2 Fri 9:45 ZEU 160

Bounding Uncertainty of Empirical First-Passage Times of Reversible Markov Processes — •RICK BEBON and ALJAZ GODEC — Max Planck Institute for Multidisciplinary Sciences, Göttingen, Germany

First-passage phenomena are ubiquitous in nature and are at the heart of, e.g. reaction kinetics, cell signaling, gene regulation, foraging behavior of animals, and stock option dynamics. Whereas theoretical studies typically focus on predicting statistics for a given process, practical applications often aim at inferring, e.g. mean first-passage times (i.e. inverse kinetic rates) from experimental or simulation data. The inference of mean first-passage times is challenging because only a small number of realizations is usually available, in turn leading to high uncertainties and non-Gaussian errors. We derive universal concentration inequalities for first-passage times of ergodic reversible Markov processes on discrete and continuous-state spaces. For a sample of $n \geq 1$ independent realizations of the first-passage process, we prove a Cramér-Chernoff-type bound on the probability that the inferred sample mean deviates from the true mean first-passage time by more than any given amount. We further construct reliable non-asymptotic estimation guarantees, such as confidence intervals valid for all sample sizes n . Our findings allow for a rigorous uncertainty quantification of inferred first-passage times and lay grounds for a systematic understanding of finite-sample effects avoiding asymptotic approximations or biases due to prior-distribution assumptions.

DY 56.3 Fri 10:00 ZEU 160

Single-trajectory spectral analysis as a criterion of anomalous diffusion — •VITTORIA SPOSINI — University of Vienna, Austria

The departure of the spreading dynamics of diffusing particles from the traditional law of Brownian-motion is a signature feature of a large number of complex soft-matter and biological systems. This anomalous diffusion can emerge due to a variety of physical mechanisms, e.g., trapping interactions or the viscoelasticity of the environment. Demonstrating that a system exhibits normal- or anomalous-diffusion is highly desirable for a vast host of applications. In this talk I will present a criterion for anomalous-diffusion based on the method of power-spectral analysis of single trajectories. The robustness of this criterion is studied for trajectories of fractional-Brownian-motion, a ubiquitous stochastic process for the description of anomalous-diffusion, in the presence of two types of measurement errors. In particular, I will report results from various tests on surrogate data in absence or presence of additional positional noise demonstrating the efficacy of this method in practical contexts.

[1] V Sposini, D Krapf, E Marinari, R Sunyer, F Ritort, F Taheri, C Selhuber-Unkel, R Benelli, M Weiss, R Metzler & G Oshanin, *Comms. Phys.* 5, 305 (2022).

DY 56.4 Fri 10:15 ZEU 160

Apparent anomalous diffusion and non-Gaussian distributions in a simple mobile-immobile transport model with poissonian switching — •TIMO J. DOERRIES¹, ALEKSEI V. CHECHKIN^{1,2,3}, and RALF METZLER¹ — ¹Institute of Physics & Astronomy, University of Potsdam, Germany — ²Faculty of Pure and Applied Mathematics, Hugo Steinhaus Center, Wrocław University of Science and Technology, Wrocław, Poland — ³Akhiezer Institute for Theoretical Physics National Science Center "Kharkiv Institute of Physics and Technology", Kharkiv, Ukraine

We analyse mobile-immobile transport of particles that switch between mobile and immobile states with finite rates. Despite this seemingly simple assumption of Poissonian switching we unveil rich transport dynamics including significant transient anomalous diffusion and non-Gaussian displacement distributions. Our discussion is based on experimental parameters for tau proteins in neuronal cells, but the results obtained here are expected to be of relevance for a broad class of processes in complex systems. Concretely, we obtain that when the mean binding time is significantly longer than the mean mobile time, transient anomalous diffusion is observed at short and intermediate time scales, with a strong dependence on the fraction of initially mobile and immobile particles. We unveil a Laplace distribution of particle displacements at relevant intermediate time scales and the mean squared displacement of mobile tracers displays a plateau. Adding advection to the mobile phase, corresponding to a biosensor with flow, generates a cubic regime of the MSD for high Péclet numbers.

Invited Talk

DY 56.5 Fri 10:30 ZEU 160

Transport and self-organization in living fluids — •MATTHIAS WEISS — Experimental Physics I, University of Bayreuth, Bayreuth, Germany

Intracellular fluids, e.g. the eukariotic cytoplasm, are crowded with a plethora of macromolecules, bearing similarities to semidilute polymer solutions. Since

many of the macromolecules are actively driven by ATP hydrolysis, these crowded living fluids are also equipped with genuine non-equilibrium properties. Using model systems from culture cells to extracts, we have explored fluctuation-driven transport and the self-organized formation of compartments in living fluids. As a result, we have observed via extensive single-particle tracking experiments that the generic mode of motion in the cytoplasm appears to be a driven, anti-persistent, and partially intermittent fractional Brownian motion process. On larger length scales, we have observed that a spontaneous, ATP-driven compartmentalization in cell extracts without priming template structures, features geometric properties and a dynamic coarse-graining like two-dimensional foams. Altogether, our experimental observations suggest that fluctuation-driven transport and self-organized space compartmentalization in living biofluids are well captured by few but robust physico-chemical principles.

15 min. break

DY 56.6 Fri 11:15 ZEU 160

Brownian solitons in periodic structures — •ALEXANDER P. ANTONOV¹, ARTEM RYABOV², and PHILIPP MAASS¹ — ¹Fachbereich Physik, Universität Osnabrück, Osnabrück, Germany — ²Charles University, Faculty of Mathematics and Physics, Department of Macromolecular Physics, Prague, Czech Republic. Solitons are known in systems with inertia as waves propagating without dispersion due to nonlinear effects. We show that solitons can occur in the absence of inertia for fully overdamped Brownian dynamics of hard spheres in periodic potentials at high particle densities [1,2]. The solitons manifest themselves as periodic sequences of different particle assemblies moving even in the zero-noise limit, where transport of single particles is not possible. To uncover the hard sphere dynamics at zero noise, a new simulation technique has been developed that can be applied for arbitrary external force fields [3]. At low temperature, the solitons give rise to particle currents appearing in band-like structures around certain particle diameters. At high temperatures, currents occur for all particle diameters. The variation of the current magnitudes with particle diameter and driving force reflects the inherent soliton formation.

[1] A. P. Antonov, A. Ryabov, P. Maass, Phys. Rev. Lett. 129, 080601 (2022).

[2] A. P. Antonov, D. Vorač, A. Ryabov, P. Maass, New J. Phys 24, 093020 (2022).

[3] A. P. Antonov, S. Schweers, A. Ryabov, P. Maass, Phys. Rev. E 106, 054606 (2022).

DY 56.7 Fri 11:30 ZEU 160

Large beam X-ray Photon Correlation Spectroscopy — •FABIAN WESTERMEIER, NIMMI DAS A, VIJAY KARTIK, ZHE REN, WOJCIECH ROSEKER, RUSTAM RYSOV, DANIEL WESCHKE, HAN XU, and MICHAEL SPRUNG — Deutsches Elektronen-Synchrotron DESY, Hamburg, Germany

The Coherence Applications Beamline P10 at PETRA III is dedicated to coherent X-ray scattering experiments such as X-ray Photon Correlation Spectroscopy (XPCS) and Coherent Diffraction Imaging (CDI). In an XPCS experiment, either the speckle visibility or the temporal changes of a series of scattering patterns are used to measure the dynamics of a sample.

At beamline P10, two 12 m long experimental hutches (EH1 and EH2) house various experimental setups. Among them, two setups are optimized to perform XPCS experiments. One of them is a SAXS/WAXS instrument, where the detector can be translated between 0° and 30° at a sample to detector distance of 5 m. This setup also offers the possibility to use a range of different focal sizes to adjust to the needs of the experiment. The other configuration is an ultra-small angle X-ray scattering (USAXS) setup, where the detector is positioned at a sample to detector distance of around 21 m. This long pathway allows it to use a large fraction of the coherent flux in an unfocused X-ray beam, while providing a fairly strong speckle visibility. Exemplary experimental results obtained at both setups will be shown illustrating the possibilities of XPCS at the beamline.

DY 56.8 Fri 11:45 ZEU 160

Dynamic finite size correction reveals the long-time hydrodynamic tail of liquid water from molecular dynamics simulations — •LAURA SCALFI, DOMENICO VITALI, and ROLAND R. NETZ — Fachbereich Physik, Freie Universität Berlin, Arnimallee 14, 14195 Berlin, Germany

Finite-size effects in molecular dynamics simulations with periodic boundary conditions have significant effects on computed static and dynamic properties. We study the effect of periodic boundary conditions on the friction memory function and on velocity autocorrelation functions of a particle in a liquid using hydrodynamic theory and molecular dynamics simulations. We show that

for liquid water, the long-time decay of these functions is significantly affected by hydrodynamic finite-size effects so that the long-time power law tails are not visible for standard simulation box sizes. We develop an analytical correction scheme that corrects for hydrodynamic finite-size effects. Using this correction scheme, the long-time power-law tails of the friction memory and the velocity autocorrelation functions are clearly revealed even for relatively small simulation box sizes. Our developed method generally allows the accurate determination of the long-time behavior of time-dependent response functions from molecular dynamics simulations.

DY 56.9 Fri 12:00 ZEU 160

Fractional anomalous diffusion and Non-Darcian flow in geological system — •QING WEI — Institute for Physics and Astronomy, University of Potsdam, 14476 Potsdam-Golm, Germany

With the non-Darcian flow and anomalous diffusion in low-permeability porous media as research subjects, the analytical models of non-Darcian flow as well as diffusive transport in low-permeability porous media was investigated by invoking the fractional calculus theory. Using the fractional derivatives with different kernel, fractional diffusion models are proposed to describe radionuclide anomalous transport in geological repository systems. On the basis of Darcy's law, the memory effectiveness deduced by solid-fluid interaction is depicted by fractional derivative approach, and a fractional Swartzendruber model is proposed for the description of low velocity non-Darcian flow in porous media.

DY 56.10 Fri 12:15 ZEU 160

Universal hyper-scaling relations, power-law tails, and data analysis for strong anomalous diffusion — •JÜRGEN VOLLMER¹, LAMBERTO RONDONI², CLAUDIO GIBERTI³, and CARLOS MEJÍA-MONASTERIO⁴ — ¹Inst. Theor. Physik, Univ. Leipzig, 04103 Leipzig, Germany — ²Dept. Math. Sc., Politecnico di Torino, 10129 Torino, Italy — ³Dept. Scienze e Metodi dell'Ingegneria, Univ. Modena e Reggio E., 42100 Reggio E., Italy — ⁴School of Agric. Food and Biosys. Eng., Techn. Univ. Madrid, 28040 Madrid, Spain

Strong anomalous diffusion is often characterized by a piecewise-linear spectrum of the moments of displacement. The spectrum is characterized by slopes ξ and ζ for small and large moments, respectively, and by the critical moment α of the crossover. Higher moments are asymptotically dominated by ballistic excursions; lower moments correspond to weak anomalous diffusion. We argue that ξ and ζ characterize the asymptotic scaling of the bulk and the tails of the distribution, respectively. Asymptotic theory is adopted to match the behaviors at intermediate scales. The resulting constraint entails that strong anomalous diffusion emerges if the distribution has algebraic tails, and it relates α to the corresponding power law. Our theory provides the leading-order corrections to the asymptotic power-law behavior. This insight allows us to point out sources of (at times) severe systematic errors in numerical estimates of the moments of displacement. Rather than fitting exponents we devise a robust scheme to determine ξ , ζ and α . The findings are supported by numerical and analytical results on different models exhibiting strong anomalous diffusion.

DY 56.11 Fri 12:30 ZEU 160

Bio-hybrid colloidal transport of beads on cell monolayers — LARA BORT, SETAREH SHARIFI PANAHI, •ROBERT GROSSMANN, and CARSTEN BETA — Institute of Physics and Astronomy, University of Potsdam, Potsdam, Germany

The erratic motion of Brownian particles at the mesoscale, driven by collisions with the surrounding fluid particles, is the paradigm of random colloidal transport within a passive environment. In this work, we describe the transport of polystyrene micro-beads whose motion is driven by a monolayer of motile cells. We use cells of the social amoeba *Dictyostelium discoideum*, which is a widely used model organism for actin-driven motility of adherent eukaryotic cells, including neutrophils and cancer cells. Given the non-specific adhesion of our model organism, the binding of such micro-cargo to the cell membrane does not require any surface-functionalization – the physical link between cargo and carrier is established spontaneously. As a particle gets in contact with a cell, it adheres to the cell membrane and is then subjected to active forces exerted by cells. The dynamics of micro-beads reveals linear scaling of the ensemble-averaged mean-square displacement and, notably, non-Gaussian displacement distributions. We rationalize these findings by assuming that each colloidal particle effectively performs normal Brownian motion, but the diffusion coefficients vary within the ensemble due to cell-to-cell variability. This superstatistics allows to reproduce the statistical features of the long-time dynamics of colloids, subject to the active cellular forces. It serves as a first step to better understand the targeted transport of foreign objects in dense tissues.

DY 57: Networks: From Topology to Dynamics IV (joint session DY/SOE)

Time: Friday 9:30–11:45

Location: ZEU 250

DY 57.1 Fri 9:30 ZEU 250

Efficient integration of short-range models on complex networks — •JEFFREY KELLING^{1,2}, GÉZA ÓDOR³, LILLA BARANCSUK³, SHENGFENG DENG³, BÁLINT HARTMANN³, and SYBILLE GEMMING² — ¹Chemnitz University of Technology, Chemnitz, Germany — ²Helmholtz-Zentrum Dresden - Rossendorf, Dresden, Germany — ³Centre for Energy Research, Budapest, Hungary

Complex, hierarchical or random network topologies can give rise to unique behavior in many physical models. We study dynamical synchronization behavior in Kuramoto models on power grids and brain connectomes with millions of connections and $\mathcal{O}(100k)$ nodes. At these scales it is crucial to use the sparsity when computing derivatives, which, due to the random network structure, makes employing modern parallel hardware tricky. Here, we present our approach to numerically solving large systems ordinary differential equations on random directed graphs, where we focus on the computationally expensive task of computing derivatives and leave the common integration step to the `boost::odeint` library. Our application can utilize both parallel CPUs and GPUs. We also provide an overview of our results on human and fly brain connectomes as well as failure cascades in power grids and provide a measure of the advantage gained from our computational optimization efforts.

DY 57.2 Fri 9:45 ZEU 250

Discovering hidden layers in quantum graphs — ŁUKASZ GAJEWSKI, •JULIAN SIENKIEWICZ, and JANUSZ HOŁYST — Faculty of Physics, Warsaw University of Technology, Warsaw, Poland

Finding hidden layers in complex networks is an important and nontrivial problem in modern science. We explore the framework of quantum graphs to determine whether concealed parts of a multilayer system exist and, if so, their extent, i.e., how many unknown layers are there. Assuming that the only information available is the time evolution of wave propagation on a single layer of a network, it is indeed possible to uncover that which is hidden by merely observing the dynamics. We present evidence on both synthetic and real-world networks that the frequency spectrum of the wave dynamics can express distinct features in the form of additional frequency peaks. These peaks exhibit dependence on the number of layers taking part in the propagation and thus allowing for the extraction of said number. We show that, in fact, with sufficient observation time, one can fully reconstruct the row-normalized adjacency matrix spectrum. We compare our propositions to a machine learning approach using a wave packet signature method modified for the purposes of multilayer systems.

DY 57.3 Fri 10:00 ZEU 250

Dynamic network modelling of tumor disease and sepsis — •ECKEHARD SCHÖLL^{1,2,3}, JAKUB SAWICKI^{1,2}, RICO BERNER^{1,4}, FENJA DRAUSCHKE¹, MORITZ ALKOEFER¹, ECKHARDT SCHNEIDER⁵, and THOMAS LÖSER⁵ — ¹Institut für Theoretische Physik, TU Berlin — ²Potsdam Institute for Climate Impact Research — ³Bernstein Center for Computational Neuroscience Berlin — ⁴Institut für Physik, HU Berlin — ⁵Institut LOESER, Wettiner Straße 6, 04105 Leipzig

We introduce a novel functional model for tumor disease and sepsis within the framework of complex networks [1,2]. Both diseases are treated in a unified way centered on their effect on the innate immune system. We propose an adaptively coupled two-layer network model of phase oscillators based upon the interaction of parenchymal cells (organ tissue) and immune cells, respectively, and the co-evolutionary dynamics of parenchymal, immune cells, and cytokines. The interaction and information exchange via cytokines between the cells of the parenchyma and the innate immune system is modeled by adaptive coupling weights. The emergent complex collective dynamics is represented with a few fundamental control parameters. Concepts and methods of nonlinear dynamical systems and networks theory, such as partial synchronization and clustering, as well as numerical and statistical methods are applied to describe physiological and pathological states. [1] Sawicki, J., Berner, R., Löser, T., and Schöll, E., *Front. Netw. Physiol.* 1, 730385 (2022). [2] Berner, R., Sawicki, J., Thiele, M., Löser, T. and Schöll, E., *Front. Netw. Physiol.* 2, 904480 (2022).

DY 57.4 Fri 10:15 ZEU 250

Automated chemical reaction network discovery for the simulation of long-timescale degradation of materials — •JOE GILKES¹, MARK STORR², REINHARD J. MAURER¹, and SCOTT HABERSHON¹ — ¹University of Warwick, United Kingdom — ²AWE plc, United Kingdom

Degradation of organic materials such as polymers occurs over time scales of years and involves rare reaction events over an expansive network of elementary processes. Building such networks in order to predict the degradation pathways of these materials requires tackling combinatorially large chemical spaces, and propagating these networks in time becomes considerably more difficult as network size increases. Predicting overall rates by which materials break down requires accurate calculations of the energetic barriers of thousands of elementary reaction steps, which also comes with a substantial computational cost. We

present a software framework written in the Julia language for automatically traversing chemical reaction space with an approach that iteratively expands the reaction network through successive re-evaluation of degradation products. We couple this with a machine learning model to predict activation energies. The result is a workflow that can swiftly sample reaction space to create computationally efficient molecular breakdown networks, and then run simulations to predict the long-term stability of these species under a range of environmental conditions. We demonstrate this approach for the example of polyethylene degradation.

UK Ministry of Defence * Crown Owned Copyright 2022/AWE

15 min. break

DY 57.5 Fri 10:45 ZEU 250

Exact statistical mechanics of spin models on networks — •KONSTANTIN KLEMM — IFISC (CSIC-UIB), Mallorca, Spain

Biological, social, and technical systems are modeled as discrete entities interacting through a network. Predicting these systems' behaviour thus involves the computationally difficult task of solving dynamics on a given complex network. Although networks of interest typically have an abundance of short cycles influencing dynamics, existing computational methods build on the assumption that short cycles are small structural corrections, thus making a *locally tree-like* approximation. Here we show that exact and efficient prediction, exemplified by the Ising and spin glass models, is possible for many networks. We exploit *globally tree-like* structure in the sense of small tree-width. The full manuscript is available at <https://arxiv.org/abs/2111.04766>.

DY 57.6 Fri 11:00 ZEU 250

Network meta-analysis: A statistical physics perspective — ANNABEL L. DAVIES¹ and •TOBIAS GALLA² — ¹Bristol Medical School, University of Bristol, Bristol BS8 2PS, UK — ²IFISC, Instituto de Física Interdisciplinar y Sistemas Complejos (CSIC-UIB), Campus Universitat de les Illes Balears, 07122 Palma de Mallorca, Spain

Network meta-analysis (NMA) is a technique used in medical statistics to combine evidence from multiple medical trials. In particular it allows one to compare treatments that have not been tested directly against each other in a trial. NMA defines an inference and information processing problem on a network of treatment options and trials connecting the treatments. In this talk I will briefly outline the 'NMA problem', and I will then describe how statistical physics can offer useful ideas and tools for this area, including from the theory of complex networks, stochastic modelling and simulation techniques [1]. In particular I will present an analogy we recently established between NMA and random walks on networks [2], and which improves existing algorithms for the estimation of 'proportion contributions' – that is the importance of any one element in the network for the comparison of any two given treatment options. One main aim of the talk is to attract physicists to this timely, interesting and worthwhile area of research.

[1] Annabel L Davies and Tobias Galla, *J. Stat. Mech.* (2022) 11R001[2] Annabel L Davies, Theodoros Papakonstantinou, Adriani Nikolakopoulou, Gerta Rücker, Tobias Galla, *Statistics in Medicine*, 41 (2022) 2091

DY 57.7 Fri 11:15 ZEU 250

Controlling the coarsening dynamics of ferrogranular networks by means of a vertical magnetic field — •OKSANA BILOUS¹, PEDRO SÁNCHEZ¹, MATTHIAS BIESSACK², ALI LAKKIS², REINHARD RICHTER², and SOFIA KANTOROVICH¹ — ¹University of Vienna — ²University of Bayreuth

In nature, phase transitions of various nature are significant and often lead to abrupt changes in the macroscopic properties of the material. Here, we address the question if a viscoelastic phase separation (VPS), proposed in 2000 by Hajime Tanaka for dynamically asymmetric mixtures, scales up for a shaken mixture of steel and glass spheres, i.e. for a so-called ferrogranulate when an external magnetic field is applied perpendicular to the plane in which the system is confined. In this contribution we focus on computer simulation. We calculated magnetization, dipolar and steric energies, radial distribution functions, the average number of neighbours and the efficiency of the emerging networks as functions of the simulation time and the values of the external vertical magnetic fields. Our results demonstrate that the network formation can be inhibited by the field perpendicular to the sample via dipole-dipole repulsion the field. These results are qualitatively confirmed by the experimental data.

DY 57.8 Fri 11:30 ZEU 250

Controlling the coarsening dynamics of ferrogranular networks by means of a vertical magnetic field — •OKSANA BILOUS¹, PEDRO SÁNCHEZ¹, MATTHIAS BIERSACK², ALI LAKKIS², REINHARD RICHTER², and SOFIA KANTOROVICH¹ — ¹Computational and Soft Matter Physics, Faculty of Physics, University of Vienna, 1090 Vienna, Austria — ²University of Bayreuth, Experimental Physics V, 95447 Bayreuth, Germany

In nature, phase transitions of various nature are significant and often lead to abrupt changes in the macroscopic properties of the material. Here, we address the question if a viscoelastic phase separation (VPS), proposed in 2000 by Hajime

Tanaka for dynamically asymmetric mixtures, scales up for a shaken mixture of steel and glass spheres, i.e. for a so-called ferrogranulate when an external magnetic field is applied perpendicular to the plane in which the system is confined. In this contribution we focus on computer simulation. We calculated magnetization, dipolar and steric energies, radial distribution functions, the average number of neighbours and the efficiency of the emerging networks as functions of the simulation time and the values of the external vertical magnetic fields. Our results demonstrate that the network formation can be inhibited by the field perpendicular to the sample via dipole-dipole repulsion the field. These results are qualitatively confirmed by the experimental data.

Semiconductor Physics Division Fachverband Halbleiterphysik (HL)

Axel Lorke
University Duisburg-Essen
Lotharstr. 1
47048 Duisburg
axel.lorke@uni-due.de

Overview of Invited Talks and Sessions

(Lecture halls POT 6, POT 81, POT 112, POT 151, POT 251, and POT 361; Poster P1 and P2/EG)

Plenary Talks of the Semiconductor Physics Division

PLV I	Mon	8:30– 9:15	HSZ 01	Spin-Photon Interfaces and Their Applications — •METE ATATUERE
PLV VIII	Thu	8:30– 9:15	HSZ 01	Nanomechanics: Tunes of the nanoguitar — •EVA WEIG
PLV IX	Thu	14:00–14:45	HSZ 01	Metal Halide Perovskites for Photovoltaic Applications — •LAURA HERZ

Invited Talks

HL 3.1	Mon	9:30–10:00	POT 151	Schrödinger cat states of a 16-microgram mechanical oscillator — •YIWEN CHU, MARIUS BILD, MATTEO FADEL, YU YANG, UWE VON LÜPKE, PHILLIP MARTIN, ALESSANDRO BRUNO
HL 3.2	Mon	10:00–10:30	POT 151	High-fidelity quantum information processing with spins and phonons — •PETER RABL
HL 3.5	Mon	11:30–12:00	POT 151	Control of spin centers in silicon carbide using acoustic fields — •ALBERTO HERNÁNDEZ-MÍNGUEZ
HL 8.9	Mon	17:30–18:00	POT 81	Time-resolved optical spectroscopy of 3R-stacked MoS₂ — •SWARUP DEB, MICHAEL KEMPF, RICO SCHWARTZ, TOBIAS KORN
HL 9.1	Mon	15:00–15:30	POT 361	Spin and valley lifetime in graphene quantum dots — •GUIDO BURKARD
HL 9.2	Mon	15:30–16:00	POT 361	Microscopic modelling of electrostatically induced bilayer graphene quantum dots — •ANGELIKA KNOTHE
HL 9.4	Mon	16:45–17:15	POT 361	Single-shot spin and valley Pauli blockade read-out in bilayer graphene quantum dots — •CHUYAO TONG, REBEKKA GARREIS, WISTER WEI HUANG, ANNIKA KURZMANN, JOCELYN TERLE, SAMUEL JELE, KENJI WATANABE, TAKASHI TANIGUCHI, THOMAS IHN, KLAUS ENSSLIN
HL 9.5	Mon	17:15–17:45	POT 361	Particle-hole symmetry protects spin-valley blockade in graphene quantum dots — •CHRISTIAN VOLK, LUCA BANSZERUS, SAMUEL MÖLLER, KATRIN HECKER, EIKE ICKING, KENJI WATANABE, TAKASHI TANIGUCHI, FABIAN HASSLER, CHRISTOPH STAMPFER
HL 10.1	Mon	15:00–15:30	POT 151	Surface Acoustic Wave Cavity Optomechanics with 2D Materials — •GALAN MOODY
HL 10.2	Mon	15:30–16:00	POT 151	Phononic Microresonators Coupled by Surface Acoustic Waves — •SARAH BENCHABANE, MACIEJ BARANSKI, FENG GAO, OLIVIER GAIFFE, VALÉRIE SOUMANN, ROLAND SALUT, ABDELKRIM KHELIF
HL 23.1	Wed	9:30–10:00	POT 361	Vertical-cavity surface-emitting lasers – this is the way — •Å. HAGLUND, G. CARDINALI, L. PERSSON, F. HJORT, J. ENSLIN, E. TORRES, C. KUHN, S. GRAUPETER, M. GRIGOLETTO, M. A. BERGMANN, N. PROKOP, M. GUTTMANN, L. SULMONI, N. LOBO PLOCH, M. COBET, T. KOLBE, J. GUSTAVSSON, F. NIPPERT, I. HÄUSLER, M. R. WAGNER, J. CIERS, T. WERNICKE, M. KNEISL
HL 23.2	Wed	10:00–10:30	POT 361	Towards GaN-based diode lasers with narrow linewidth and high reliability — •SVEN EINFELDT, ERIK FREIER, JI-HYE KANG, HANS WENZEL, ANNA MOGILATENKO, JOHANNES GLAAB, ASMAA ABOU-SHEWARIB, VEIT HOFFMANN, JOHANNES ENSLIN, MARTIN GUTTMANN, SAAD MAKHLADI, JÖRG FRICKE, OLAF BROX, MATHIAS MATALLA, MARIA NORMAN-REINER, CHRISTOPH STÖLMACKER, MARKUS WEYERS, LUCA SULMONI, MICHAEL KNEISSL, LUKAS UHLIG, ULRICH T. SCHWARZ

HL 23.3	Wed	10:30–11:00	POT 361	Use of wafer patterning for new functionalities of InGaN light emitters — •ANNA KAFAR, RYOTA ISHII, ATSUSHI SAKAKI, KIRAN SABA, CONNY BECHT, SZYMON GRZANKA, ULRICH SCHWARZ, MITSURU FUNATO, YOICHI KAWAKAMI, PIOTR PERLIN
HL 25.1	Wed	9:30–10:00	POT 251	Interfaces in perovskite optoelectronics: role of energy level alignment and interface chemistry — •SELINA OLTHOF
HL 27.1	Wed	15:00–15:30	POT 81	experimentamus! Forschendes Lernen von Physik und Chemie in der Grundschule — •SEBASTIAN SCHLÜCKER
HL 27.4	Wed	16:00–16:30	POT 81	Under the Microscope - spotlighting materials and nano science — •SVENJA LOHMANN, PRANOTI KSHIRSAGAR
HL 27.5	Wed	17:00–17:30	POT 81	Phyphox - A pocketful of physics — •CHRISTOPH STAMPFER
HL 27.8	Wed	18:00–18:30	POT 81	Physics for school and the public at the LMU — •DR. CECILIA SCORZA-LESCH
HL 28.1	Wed	15:00–15:30	POT 361	Fabrication of AlGaIn-based UV-B laser diodes on lattice-relaxed high-quality AlGaIn — •MOTOAKI IWAYA, SHO IWAYAMA, TETSUYA TAKEUCHI, SATOSHI KAMIYAMA, HIDEITO MIYAKE
HL 28.2	Wed	15:30–16:00	POT 361	Breakthrough technologies to realize room-temperature continuous-wave deep-ultraviolet laser diodes — •MAKI KUSHIMOTO
HL 35.1	Thu	9:30–10:00	POT 361	Quantum Dynamics of Polarons in Doped Semiconductor Monolayers — •XIAOQIN ELAINE LI, DI HUANG
HL 35.2	Thu	10:00–10:30	POT 361	Impact of phonons on time-resolved optical signals from excitons — •DORIS E. REITER
HL 35.3	Thu	10:30–11:00	POT 361	Hot-Exciton Quantum Dynamics in Zero-Dimensional Structures — •ALFRED LEITENSTORFER
HL 35.6	Thu	12:00–12:30	POT 361	Ultrafast dynamics and wave mixing at excitonic resonances in atomically thin semiconductors — •ANDREAS KNORR, DOMINIK CHRISTIANSEN, FLORIAN KATSCH, MANUEL KATZER, MALTE SELIG
HL 35.7	Thu	12:30–13:00	POT 361	Spontaneous parametric down-conversion in semiconductor metasurfaces — •MARIA CHEKHOVA
HL 43.1	Thu	15:00–15:30	POT 251	Superradiance as a witness to multipartite entanglement — •FREDERIK LOHOE, CHRISTOPHER GIES

Invited Talks of the joint Symposium SKM Dissertation Prize 2023 (SYSD)

See SYSD for the full program of the symposium.

SYSD 1.1	Mon	9:30–10:00	HSZ 04	Diffusion of antibodies in solution: from individual proteins to phase separation domains — •ANITA GIRELLI
SYSD 1.2	Mon	10:00–10:30	HSZ 04	Intermediate Filament Mechanics Across Scales — •ANNA V. SCHEPERS
SYSD 1.3	Mon	10:30–11:00	HSZ 04	Ultrafast Probing and Coherent Vibrational Control of a Surface Structural Phase Transition — •JAN GERRIT HORSTMANN
SYSD 1.4	Mon	11:00–11:30	HSZ 04	Electro-active metasurfaces employing metal-to-insulator phase transitions — •JULIAN KARST
SYSD 1.5	Mon	11:30–12:00	HSZ 04	The role of unconventional symmetries in the dynamics of many-body systems — •PABLO SALA

Invited Talks of the joint Symposium Real-Time Measurements of Quantum Dynamics (SYQD)

See SYQD for the full program of the symposium.

SYQD 1.1	Thu	9:30–10:00	HSZ 01	Real-time measurement and control of spin dynamics in quantum dots — •SEIGO TARUCHA
SYQD 1.2	Thu	10:00–10:30	HSZ 01	Quantum Dot arrays for Quantum Information Transfer — •GLORIA PLATERO, DAVID FERNANDEZ-FERNANDEZ, JUAN ZURITA
SYQD 1.3	Thu	10:30–11:00	HSZ 01	Optical Detection of Real-Time Quantum Dynamics in Quantum Dots — •MARTIN GELLER, JENS KERSKI, ERIC KLEINHERBERS, JÜRGEN KÖNIG, ANNIKA KURZMANN, PIA LOCHNER, AXEL LORKE, ARNE LUDWIG, HENDRIK MANNEL, PHILIPP STEGMANN, ANDREAS WIECK, MARCEL ZÖLLNER
SYQD 1.4	Thu	11:30–12:00	HSZ 01	Cooper Pair Splitting in Real-Time — •CHRISTIAN FLINDT
SYQD 1.5	Thu	12:00–12:30	HSZ 01	Trajectory-based detection in stochastic and quantum thermodynamics — •JUKKA PEKOLA

Invited Talks of the joint Symposium Physics of van der Waals 2D Heterostructures (SYHS)

See SYHS for the full program of the symposium.

SYHS 1.1	Fri	9:30–10:00	HSZ 01	Novel moiré excitons and ultrafast optical dynamics in van der Waals 2D heterostructures — •STEVEN G. LOUIE
SYHS 1.2	Fri	10:00–10:30	HSZ 01	Interaction induced magnetism in 2D semiconductor moiré superlattices — •XIAODONG XU
SYHS 1.3	Fri	10:30–11:00	HSZ 01	Ions in tight places: intercalation and transport of ions in van der Waals heterostructures — •IRINA GRIGORIEVA
SYHS 1.4	Fri	11:15–11:45	HSZ 01	Spin-orbit proximity in van der Waals heterostructures — •FELIX CASANOVA
SYHS 1.5	Fri	11:45–12:15	HSZ 01	Plethora of many-body ground states in magic angle twisted bilayer graphene — •DMITRI EFETOV

Sessions

HL 1.1–1.10	Mon	9:30–12:30	POT 81	2D Materials I (joint session HL/CPP)
HL 2.1–2.6	Mon	9:30–11:15	POT 361	Organic Semiconductors (joint session HL/CPP)
HL 3.1–3.9	Mon	9:30–13:00	POT 151	Focus Session: Progress in Hybrid Phononic Quantum Technologies I
HL 4.1–4.10	Mon	9:30–12:30	POT 251	Perovskite and photovoltaics I (joint session HL/CPP)
HL 5.1–5.5	Mon	10:00–11:15	POT 112	Heterostructures, interfaces and surfaces
HL 6.1–6.8	Mon	10:30–13:00	TRE Ma	Focus Session: Frontiers of Electronic-Structure Theory III (joint session O/HL)
HL 7.1–7.66	Mon	13:00–15:00	P2/EG	Poster I
HL 8.1–8.10	Mon	15:00–18:15	POT 81	2D Materials II (joint session HL/CPP)
HL 9.1–9.5	Mon	15:00–17:45	POT 361	Focus Session: Graphene quantum dots (joint session HL/TT)
HL 10.1–10.10	Mon	15:00–18:30	POT 151	Focus Session: Progress in Hybrid Phononic Quantum Technologies II
HL 11.1–11.7	Mon	15:00–17:15	POT 251	Quantum transport and quantum Hall effects I (joint session HL/TT)
HL 12.1–12.7	Mon	15:00–17:15	POT 112	Semiconductor lasers I
HL 13.1–13.7	Mon	15:00–17:15	TRE Ma	Focus Session: Frontiers of Electronic-Structure Theory II (joint session O/HL)
HL 14.1–14.10	Tue	9:30–12:15	POT 81	2D Materials III (joint session HL/CPP)
HL 15.1–15.4	Tue	9:30–10:30	POT 361	Spin phenomena in semiconductors
HL 16.1–16.9	Tue	9:30–12:15	POT 151	Quantum dots: Transport (joint session HL/TT)
HL 17.1–17.11	Tue	9:30–12:45	POT 251	THz and MIR physics in semiconductors
HL 18.1–18.12	Tue	9:30–13:00	POT 112	Optical Properties (joint session HL/CPP)
HL 19.1–19.13	Tue	9:30–13:00	GÖR 226	Organic Electronics and Photovoltaics I (joint session CPP/HL)
HL 20.1–20.7	Tue	10:30–12:45	TRE Ma	Focus Session: Frontiers of Electronic-Structure Theory I (joint session O/HL)
HL 21.1–21.3	Tue	11:00–11:45	POT 361	Thermal properties
HL 22.1–22.10	Wed	9:30–12:30	POT 81	2D Materials IV (joint session HL/CPP)
HL 23.1–23.6	Wed	9:30–12:15	POT 361	Focus Session: Breakthroughs in wide-bandgap semiconductor laser diodes I
HL 24.1–24.13	Wed	9:30–13:15	POT 151	Quantum dots: Optics
HL 25.1–25.11	Wed	9:30–13:00	POT 251	Perovskite and photovoltaics II (joint session HL/CPP)
HL 26.1–26.8	Wed	10:30–13:00	TRE Ma	Focus Session: Frontiers of Electronic-Structure Theory IV (joint session O/HL)
HL 27.1–27.8	Wed	15:00–18:30	POT 81	Focus Session: Wissenschaftskommunikation / Outreach (joint session HL/O/TT)
HL 28.1–28.5	Wed	15:00–16:45	POT 361	Focus Session: Breakthroughs in wide-bandgap semiconductor laser diodes II
HL 29.1–29.10	Wed	15:00–18:00	POT 151	Materials and devices for quantum technology I
HL 30.1–30.6	Wed	15:00–17:00	POT 251	Quantum transport and quantum Hall effects II (joint session HL/TT)
HL 31.1–31.8	Wed	15:00–17:30	TRE Ma	Focus Session: Frontiers of Electronic-Structure Theory V (joint session O/HL)
HL 32.1–32.9	Wed	15:00–17:30	GÖR 226	Organic Electronics and Photovoltaics II (joint session CPP/HL)
HL 33.1–33.62	Wed	17:00–19:00	P1	Poster II
HL 34.1–34.9	Thu	9:30–12:00	POT 81	2D Materials V (joint session HL/CPP)
HL 35.1–35.9	Thu	9:30–13:30	POT 361	Focus Session: Transient multi-wave mixing on excitonic resonances
HL 36.1–36.7	Thu	9:30–11:45	POT 151	Transport properties
HL 37.1–37.9	Thu	9:30–12:15	POT 251	Materials and devices for quantum technology II
HL 38.1–38.7	Thu	9:30–11:45	POT 6	Functional semiconductors for renewable energy solutions I
HL 39.1–39.11	Thu	9:30–12:30	GÖR 226	Organic Electronics and Photovoltaics III (joint session CPP/HL)

HL 40.1–40.7	Thu	10:30–12:45	TRE Ma	Focus Session: Frontiers of Electronic-Structure Theory VI (joint session O/HL)
HL 41.1–41.7	Thu	15:00–17:00	POT 81	Oxide Semiconductors I: Ga₂O₃
HL 42.1–42.7	Thu	15:00–17:15	POT 151	Quantum dots: Growth
HL 43.1–43.6	Thu	15:00–16:45	POT 251	Semiconductor lasers II
HL 44.1–44.7	Thu	15:00–17:00	POT 112	Nitrides: Devices
HL 45.1–45.7	Thu	15:00–17:15	POT 6	Functional semiconductors for renewable energy solutions II
HL 46	Thu	18:00–19:00	POT 6	Members' Assembly
HL 47.1–47.7	Fri	9:30–11:30	POT 81	Oxide Semiconductors II
HL 48.1–48.9	Fri	9:30–12:00	POT 361	Ultra-fast Phenomena
HL 49.1–49.7	Fri	9:30–11:45	POT 151	Quantum dots: Devices
HL 50.1–50.12	Fri	9:30–13:00	POT 251	Materials and devices for quantum technology III
HL 51.1–51.10	Fri	9:30–12:15	POT 112	Nitrides: Preparation and Characterization
HL 52.1–52.8	Fri	9:30–12:30	GÖR 226	Focus: Self-Assembly of Plasmonic Nanostructures (joint session CPP/HL)

Mitgliederversammlung / Members' Assembly of the Semiconductor Physics Division

Donnerstag 18:00–19:00 POT6

Alle Mitglieder des Fachverbands Halbleiterphysik sind herzlich willkommen / All members of the Semiconductor Physics Division are invited to participate.

- Bericht
- Wahl der Fachverbandsleitung
- Informationen zur Frühjahrstagung 2024
- Verschiedenes

Sessions

– Invited Talks, Topical Talks, Contributed Talks, and Posters –

HL 1: 2D Materials I (joint session HL/CPP)

Time: Monday 9:30–12:30

Location: POT 81

HL 1.1 Mon 9:30 POT 81

Spin-valley physics in strained transition metal dichalcogenides monolayers — •PAULO E. FARIA JUNIOR¹, KLAUS ZOLLNER¹, TOMASZ WOŹNIAK², MARCIN KURPAS³, MARTIN GMTIRA⁴, and JAROSLAV FABIAN¹ — ¹University of Regensburg, Regensburg, Germany — ²Wroclaw University of Science and Technology, Wroclaw, Poland — ³University of Silesia, Chorzów, Poland — ⁴Pavol Jozef Šafárik University in Košice, Košice, Slovakia

Transition metal dichalcogenides (TMDCs) are ideal candidates to explore the manifestation of spin-valley physics under external stimuli. Here, we investigate the influence of strain on the spin, orbital angular momenta and g-factors of monolayer TMDCs within first principles[1]. Our calculations reveal the behavior of direct exciton g-factors under the isolated impact of strain: tensile (compressive) strain increases (decreases) the absolute value of g-factors. Strain variations of 1% modify the bright (A and B) exciton g-factors by 0.3 (0.2) for W (Mo) based compounds and the dark exciton g-factors by 0.5 (0.3) for W (Mo) compounds, suggesting that strain can be responsible for g-factor fluctuations observed experimentally. We complete our analysis for the Gamma and Q valleys, revealing that the spin degree of freedom dominates. This fundamental microscopic insight into the role of strain in the spin-valley physics of TMDCs is crucial to understand recent experiments[2,3]. [1] Faria Junior et al., NJP 24, 083004 (2022). [2] Covre, Faria Junior et al., Nanoscale 14, 5758 (2022). [3] Blundo, Faria Junior et al., PRL 129, 067402 (2022). Funding: DFG SFB 1277, SPP 2244.

HL 1.2 Mon 9:45 POT 81

A bright single-photon source based on a WSe₂ monolayer in an open cavity — •VICTOR MITRYAKHIN¹, HANGYONG SHAN¹, JENS-CHRISTIAN DRAWER¹, SVEN STEPHAN¹, MARTIN SILIES², FALK EILENBERGER³, CARLOS ANTÓN-SOLANAS¹, MARTIN ESMANN¹, and CHRISTIAN SCHNEIDER¹ — ¹Carl von Ossietzky Universität Oldenburg, 26129 Oldenburg, Germany — ²Hochschule Emden/Leer, 26723 Emden, Germany — ³Friedrich-Schiller-Universität Jena, 07745 Jena, Germany

Single photon sources based on crystalline defects present in transition-metal dichalcogenide monolayers, 2D atomically thin direct-bandgap semiconductors, have recently emerged as a promising platform for realization of and use in quantum communication and information processing.

In this work, we investigate the properties of single photon emission from a single exciton in a WSe₂ monolayer weakly coupled to an asymmetric plano-concave microcavity consisting of freely movable mirrors in 3 directions. In this regard, it enables us for an in-situ control of the properties of the emission and the extraction efficiency of single photons in the device.

We report a highly bright and linearly polarized single photon source with source brightness exceeding 70 % under saturation conditions, polarization degree of 98.4 ± 1.3 % and high photon purity noted by the second-order correlation $g^{(2)}(0)$ value of 0.047 ± 0.007 , measured in Hanbury-Brown-Twist type of a setup.

HL 1.3 Mon 10:00 POT 81

Strong coupling of excitons in a WS₂-monolayer coupled to a silver nanogroove array — •YUHAO ZHANG¹, HANS-JOACHIM SCHILL^{1,2}, STEPHAN IRSEN², and STEFAN LINDEN¹ — ¹Physikalisches Institut, Universität Bonn — ²Center of Advanced European Studies and Research (caesar)

In this work, we report on room-temperature interaction of a WS₂ monolayer with a tapered nanogroove array milled into monocrystalline silver flake. The bare nanogroove array features three polariton branches resulting from the coupling of localized surface plasmon modes (LSPR) in the nanogrooves and propagation surface plasmon modes (SPP). The linewidth of the lower plasmon polariton branch critically depends on the geometry of the nanogrooves. When a WS₂ monolayer is deposited on the nanogroove array with optimized damping, the reflection spectra show an avoided crossing of the exciton mode and the lower plasmon polariton branch with a Rabi splitting of 38.7 meV indicating strong exciton-plasmon polariton coupling.

HL 1.4 Mon 10:15 POT 81

Theory of exciton localization in TMDCs using metal nanoparticles — •ROBERT SALZWEDEL¹, LARA GRETEN¹, STEFAN SCHMIDT¹, CHELSEA CARLSON², STEPHEN HUGHES², MALTE SELIG¹, and ANDREAS KNORR¹ — ¹Institut für Theoretische Physik, Nichtlineare Optik und Quantenelektronik, Technische Universität Berlin, Berlin, Germany — ²Department of Physics, Queen's University, Kingston, Ontario, Canada

In recent years, monolayers of transition metal dichalcogenides (TMDCs) have attracted considerable attention due to their strong Coulomb and light-matter interactions, leading to tightly bound excitons with large optical oscillator strength. Due to the finite thickness of the monolayers, these excitons are very sensitive to the environment, which allows their properties to be tailored, e.g., by functionalization with molecules or metal nanoparticles (MNPs) [1,2].

We present a theory based on a self-consistent solution of Maxwell's and Bloch equations to analytically study a coupled system of MNP plasmons and TMDC excitons. For the combined system, we identify an effective eigenvalue equation that governs the center of mass motion of the dressed excitons in a plasmon-induced potential. Examination of the ensuing plexcitonic equation reveals the existence of bound states, which we interpret as excitons localized in the external potential. The appearance of these bound states in this potential is an indicator of strong coupling between excitons and plasmons.

[1] Carlson et al. (2021). PRB, 104(12), 125424.

[2] Denning et al. (2022). PRB, 105(8), 085306.

15 min. break

HL 1.5 Mon 10:45 POT 81

Electronic effects of non-uniformly strained 2D TMDCs — •MOHAMMADREZA DAQIQSHIRAZI and THOMAS BRUMME — Chair of Theoretical Chemistry, Technische Universität Dresden, Bergstraße 66c, 01069 Dresden, Germany

Strain plays an important role in most 2D materials since there is a strong influence of the strain state on the relative band alignment of different valleys in the electronic band structure. The effects of non-uniform strain on the properties of 2D materials are scarcely studied theoretically, even if in experiments a lot of different structures can be found in which a spatial varying strain state is present such as wrinkles or folds. Here, we are investigating how such non-uniform strain influences the electronic properties of the prototypical 2D materials WSe₂ and MoS₂. We study nanoscale wrinkles and nanotubes in detail and discuss important differences in the strain distribution and magnitude, also to understand if nanotubes could be used as a model system for non-uniformly strained systems. Using Density Functional Theory we find that the inclusion of spin-orbit interaction is crucial to correctly predict the changes in the band structure of wrinkled 2D materials as the non-uniform strain changes the symmetry compared to a flat layer. This introduces a strong Rashba-like splitting of the valence-band maximum near the Γ point. The situation complicates even more with the addition of an extra layer forming a bilayer or a heterobilayer. The spatial varying band alignments in wrinkled multilayers can lead to new inter-layer excitons which are confined to certain regions of the system.

HL 1.6 Mon 11:00 POT 81

Optical properties of monolayer ReSe₂ and ReS₂ — •THORSTEN DEILMANN — Institute of Solid State Theory, University of Münster, Germany

Rhenium-based transition metal dichalcogenides unite the fascinating characteristics of the confined in-plane physics with their reduced crystal symmetry. This paves the way for polarization-sensitive applications, such as optical logic circuits operating in the infrared spectral region.

Here, we investigate the doping-dependent optical properties of ReSe₂ and ReS₂ from first principles. Besides strong excitonic effects, recent experimental studies have reported three-particle states (i.e. trions) with trion binding energies of more than 100 meV [1,2]. Using our ab initio methods we are able to predict neutral and charged properties and find much smaller binding energies compared to experiment.

[1] Advanced Functional Materials, 10, 1905961 (2019)

[2] Applied Physics Letters 119, 113103 (2021)

HL 1.7 Mon 11:15 POT 81

Evaluating Atomically Thin Single-Photon Sources for Quantum Key Distribution — •TIMM GAO¹, MARTIN V. HELVERSEN¹, CARLOS ANTÓN-SOLANAS², CHRISTIAN SCHNEIDER², and TOBIAS HEINDEL¹ — ¹Institut für Festkörperphysik, Technische Universität Berlin, 10623 Berlin, Germany — ²Institut für Physik, Carl von Ossietzky Universität Oldenburg, 26111 Oldenburg, Germany

Quantum light sources are considered key building blocks for future quantum communication networks. In recent years, atomic monolayers of transition metal dichalcogenides (TMDCs) emerged as a promising material platform for the development of compact quantum light sources. In this work, we evaluate for

the first time the performance of a single-photon source (SPS) based on a strain engineered WSe₂ monolayer [1] for applications in quantum key distribution (QKD) [2]. Employed in a QKD-testbed emulating the BB84 protocol, an anti-bunching of $g^{(2)}(0) = 0.127 \pm 0.001$ and a raw key rate of up to (66.95 ± 0.10) kHz make this source competitive with previous SPS based QKD experiments using quantum dot based SPSs. Furthermore, we exploit routines for the performance optimization previously applied to quantum dot based single-photon sources [2]. Our work represents an important step towards the application of TMDC-based devices in quantum technologies.

[1] L. Tripathi et al., ACS Photonics 5, 1919-1926 (2018)

[2] T. Gao et al., arXiv:2204.06427 (2022)

[3] T. Kupko et al., npj Quantum Information 6, 29 (2020)

HL 1.8 Mon 11:30 POT 81

Theory of Thermalization of Excitons at Elevated Densities in Atomically Thin Semiconductors — •MANUEL KATZER, ANDREAS KNORR, and MALTE SELIG — Nichtlineare Optik und Quantenelektronik, Technische Universität Berlin, Hardenbergstr. 36, 10623 Berlin, Germany

Atomically thin semiconductors exhibit tightly bound electron-hole pairs which stimulated exciton research in recent years [1]. So far, many studies focused on the understanding of exciton dynamics in the limit of very dilute systems. Recent experimental findings [2] raised the question of the excitonic thermalization behaviour for densities above this dilute, classical limit. Due to the co-bosonic nature of excitons [3], we find both bosonic but also fermionic contributions to the thermalization, with the fermionic Pauli blocking effects being dominant for a broad range of parameters. Based on a Heisenberg equation of motion ansatz [4], we discuss the first order of non-linear exciton-phonon interaction exceeding the classical Boltzmann scattering limit, in order to analyze the character of the exciton thermalization at elevated excitation densities.

[1] Wang et al. RMP 90, 021001 (2018).

[2] Sigl et al. PRR 2 (4), 042044 (2020).

[3] Katsch et al., PRL 124 25 257402 (2020).

[4] Selig et al. PRR, 1, 022007 (2019).

15 min. break

HL 1.9 Mon 12:00 POT 81

Strong exciton-plasmon coupling in hybrids of 2D semiconductors and plasmonic crystals — •LARA GRETEN¹, ROBERT SALZWEDEL¹, STEPHEN HUGHES², MALTE SELIG¹, and ANDREAS KNORR¹ — ¹Institut für Theoretische Physik, Nichtlineare Optik und Quantenelektronik, Technische Universität Berlin, Germany — ²Department of Physics, Queen's University, Kingston, Canada

Monolayers of transition metal dichalcogenides (TMDCs) are direct-gap semiconductors that exhibit tightly bound excitons with pronounced optical amplitudes. Thus, they are promising for various optoelectronic applications and an excellent material to investigate excitons. Another material with a large optical amplitude is a plasmonic crystal - arrays of metal nanoparticles - which supports collective plasmon modes, and yields amplification of the electric fields on the nano-scale.

Here, we theoretically consider exciton-plasmon coupling in a hybrid structure of a TMDC layer interacting with a plasmonic crystal with a 2d lattice. Our study reveals a hybridization of plasmons and initially momentum dark excitons. In addition, we find an excitonic mode with negligible coupling to the plasmonic near field, emitting undisturbed radiation into the far field. To connect to related experiments, we compute the scattered light in the near- and far-field explicitly and identify signatures of strong exciton-plasmon coupling with a Rabi splitting of more than 100 meV. We also find that the uncoupled exciton mode results in a third peak at the undisturbed exciton energy.

HL 1.10 Mon 12:15 POT 81

Enhancement of Light Emission in Hexagonal Boron Nitride Structures — •FELIX SCHAUMBURG, MARCEL ZÖLLNER, VASILIS DERGIANLIS, STEPHAN SLEZIONA, MARIKA SCHLEBERGER, AXEL LORKE, MARTIN GELLER, and GÜNTHER PRINZ — Faculty of Physics and CENIDE, University Duisburg-Essen, Germany

Optical spectroscopy, especially Raman- and photoluminescence (PL)-spectroscopy, is commonly used to study the optical properties of 2D materials. In order to obtain the highest Raman/PL-signals, it is important to reduce the reflection of the excitation laser.

We studied a number of exfoliated hexagonal Boron Nitride (hBN) flakes with different thicknesses on a Si substrate with a 300 nm SiO₂ top layer. By changing the hBN layer thickness, we found a specific thickness, where all Raman signals (from Si, SiO₂ and hBN) showed maximum intensity, whereas the backscattered laser light was suppressed. To explain the increased intensities, we calculated the reflectivity and transmissivity of the full layer system (air, hBN, SiO₂, Si) for different hBN layer thicknesses and for different excitation wavelengths (457 nm, 532 nm, 633 nm), using the transfer-matrix-algorithm. To compare theory with experiment, we performed Raman measurements with the 3 different wavelengths on different flakes and determined their thicknesses with AFM-measurements.

Our results are in good agreement with theory and show that it is possible to choose the best flakes for spectroscopy, just by looking at their color in an optical microscope. This also allows us to easily find good flakes for observation of efficient single defect emission.

HL 2: Organic Semiconductors (joint session HL/CPP)

Time: Monday 9:30–11:15

Location: POT 361

HL 2.1 Mon 9:30 POT 361

Field-induced Seebeck voltage in disordered semiconductors — •ANTON KOMPATSCHER and MARTIJN KEMERINK — IMSEAM, University Heidelberg

For disordered semiconductors it is theorized that finite electric fields can heat up the charge carrier distribution to effective temperatures that can significantly exceed the lattice temperature. Here, we argue that this effective temperature should be able to efficiently drive a thermoelectric generator (TEG) based on the Seebeck effect. (1) Utilizing kinetic Monte-Carlo simulations we were able to show similar results when driving a TEG with temperature or field. As a model system we choose the Seebeck ratchet introduced by Büttiker, replacing temperature- with field-driven effective temperature modulation. This allowed us to compare the current predicted by theory with the simulation currents resulting in good functional agreement. Effective temperature drive offers interesting advantages. Since only the electron distribution but not the lattice itself is heated, one of the mayor loss channels in TEG, lattice thermal conductivity, can be suppressed. Additionally, there is no need for n- and p-type materials (nor for heat exchangers) and a single material is sufficient. The main issue for concrete realization lies in the very high necessary field strengths at which effective temperature becomes relevant and that somehow need to be coupled into the TEG.

1. "On the concept of an effective temperature Seebeck ratchet", Appl. Phys. Lett. 119, 023303 (2021) <https://doi.org/10.1063/5.0052116>

HL 2.2 Mon 9:45 POT 361

Momentum dependent investigation of electronic excitations in β -metal-phthalocyanines — •LOUIS PHILIP DOCTOR and MARTIN KNUPFER — Leibniz-Institut für Festkörper- und Werkstoffforschung Dresden, Helmholtzstraße 20, 01069 Dresden

This work presents an investigation of the electronic excitations of β -metal-phthalocyanines. We prepared 120 nm thick thin films by physical vapour deposition, which afterwards underwent an annealing process. Infrared spectroscopy

revealed that the annealed films were in the β -phase. The films were further characterised in the visible regime. The prominent feature in this regime is the Q-band, which consists of four peaks arising from the HOMO to LUMO transition split by solid state effects. Furthermore the dispersion of the Q-band was measured using electron energy loss spectroscopy. We found a complex momentum dependent behaviour. Most interesting is the negative dispersion of the lowest lying excitation, which also has a tremendous effect on the performance of optoelectronic devices. This redshift partially correlates with the intermolecular distance and the charge carrier transfer integrals. The latter were determined by a theoretical model, which describes the interaction of Frenkel and charge transfer excitons in metal-phthalocyanines. Our results clearly indicate a prominent influence of charge transfer excitons to the lowest electronic excitations.

HL 2.3 Mon 10:00 POT 361

Photovoltaic and nonlinear optical properties of complex self-assembled liquid crystal structures — •AHMAD MURAD¹, ALEXEY EREMIN¹, MARTIN FENEBERG¹, MAXIMILIAN BAUMANN², MATTHIAS LEHMANN², and MOHAMED ALAASAR³ — ¹Otto-von-guericke-Universität, Magdeburg, Deutschland — ²Julius-Maximilians-Universität Würzburg — ³Martin Luther University Halle-Wittenberg, Halle (Saale),

We explore conducting and photovoltaic properties in a series of two classes of semiconducting liquid crystals. BTBT-derived polycatenary mesogens doped with fullerenes show helical network phases exhibiting a strong photovoltaic effect in a broad range of light spectrum from UV to VIS. The second class is star-shaped mesogens with subphthalocyanine core that forms self-assembled ferroelectric columnar phases. We characterise the polar order using polarisation-resolved measurements of Second Harmonic Generation (SHG). Dynamical SHG studies provide information about the switching rates and the stability of the ferroelectric states. The photovoltaic effect is demonstrated under UV exposure.

HL 2.4 Mon 10:15 POT 361

What's special about Y6; working mechanism of Neat Y6 organic solar cell — •ELIFNAZ SAGLAMKAYA¹, ARTEM MUSIENKO², MOHAMMAD SAEED SHADABROO¹, BOWEN SUN¹, SREELAKSHMI CHANDRABOSE³, GIULIA LO GERFO M.⁴, NIEK F. VAN HULST⁴, DIETER NEHER³, and SAFA SHOAE¹ — ¹University of Potsdam Disordered Semiconductor Optoelectronics Karl-Liebkecht-Strasse 24-25 14476 Potsdam-Golm — ²Department Novel Materials and Interfaces for Photovoltaic Solar Cells, Helmholtz-Zentrum Berlin für Materialien und Energie, Kekuléstraße 5, 12489 Berlin, Germany — ³University of Potsdam Physik und Optoelektronik weicher Materie Karl-Liebkecht-Straße 24-25 14476 Potsdam-Golm — ⁴Institut de Ciencies Fotoniques, The Barcelona Institute of Science and Technology, 08860 Castelldefels, Barcelona, Spain

In this study, we analyse the working mechanism of single component small molecule acceptor Y6 solar cells with power conversion efficiencies reaching up to 4.5% and short circuit currents up to 8.4 mAcm⁻². Using Hall effect, photo-Hall, and photoinduced absorption (PIA) measurements, we show that the charge photo-generation occurs in the bulk of Y6. With the aid of space charge limited current (SCLC) measurements we show that Y6 has an ambipolar charge carrier mobility. Our data shows that the limiting factor for the power conversion efficiency is fast charge recombination, which can be suppressed in presence of the transport layers, or modifying the morphology with a solvent additive.

15 min. break

HL 2.5 Mon 10:45 POT 361

Ultrastrong light-matter coupling of J-aggregated squaraine in a room temperature open cavity — •CHRISTOPH BENNENHEI¹, LUKAS LACKNER¹, MORITZ GITTINGER¹, HEIKO KNOPF², FALK EILENBERGER², JENNIFER ZABLOCKI³, ARNE LÜTZEN³, MARTIN SILIES¹, CHRISTOPH LIENAU¹, MARTIN ESMANN¹, and CHRISTIAN SCHNEIDER¹ — ¹Institute of Physics, University of Oldenburg — ²Fraunhofer-Institute for Applied Optics and Precision Engineering IOF, Jena — ³Kekulé Institute of Organic Chemistry and Biochemistry, University of Bonn

Organic molecule exciton-polaritons in artificial lattices are an emerging plat-

form to emulate complex electronic Hamiltonians at ambient conditions. We present J-aggregated squaraine dye (SQ) thin films [1] as a promising candidate for exciton-polaritons in optical cavities due to the high oscillator strength and tunable resonance. Using white light reflection spectroscopy, we demonstrate tunable ultrastrong coupling of light to the SQ thin film in an open cavity at room temperature [2] which we support by transfer matrix calculations. In ongoing experiments, we introduce structured photonic lattices to the open cavity to investigate the coupling of the polaritons to tailored potential landscapes. [1] M. Schulz, et al., Nat Commun 9, 2413 (2018). [2] L. Lackner, et al., Nat Commun 12, 4933 (2021).

HL 2.6 Mon 11:00 POT 361

Room-temperature polariton lasing in anisotropic optical microcavities — •CHRISTOPH BENNENHEI¹, NILS KUNTE¹, MARTI STRUVE¹, HEIKO KNOPF², FALK EILENBERGER², JÜRGEN OHMER³, UTZ FISCHER³, MARTIN ESMANN¹, and CHRISTIAN SCHNEIDER¹ — ¹Institute for Physics, Universität Oldenburg, Germany — ²Fraunhofer-Institute for Applied Optics and Precision Engineering IOF, Jena, Germany — ³Department of Biochemistry, Universität Würzburg, Germany

Organic molecule exciton-polaritons in artificial photonic potentials are an emerging platform to emulate electronic Hamiltonians at ambient conditions and for realizing low-threshold microlasers. In this work, we probe the polarization of polariton lasing in microcavities composed of dielectric Bragg reflectors with anisotropic indentations, enclosing the fluorescent protein mCherry. This material has been previously presented as a promising material for room-temperature polariton condensation [1,2]. Here, we experimentally show that lasing above the threshold differs distinctly for the two linearly polarized, energetically non-degenerate cavity eigenmodes. This effect leads to a drastic increase in the degree of linear polarization for the coherent photoluminescence emitted from the cavity. Our devices have relevant applications both for new types of polarized coherent light sources on chip and for accessing additional degrees of freedom in the emulation of topological electronic lattice Hamiltonians at room temperature.

[1] S. Betzold et al. ACS Photonics 7, 384 (2020).

[2] M. Dusel et al. Nano Lett. 21, 6398 (2021).

HL 3: Focus Session: Progress in Hybrid Phononic Quantum Technologies I

Phonons, the quanta of lattice vibrations, are the fundamental excitations in a crystal and couple to literally any type of excitation in a solid. This universal coupling makes them ideally suited for hybrid quantum architectures which synergistically harness the strengths of its components and at the same time mitigate individual shortcomings. For chip-based hybrid quantum devices, phonons are particularly attractive because they can be routed in integrated circuits with very little dissipation over macroscopic distances in the solid state or confined in small mode volume phononic cavities. Although the research of phonons has a long-lasting history, only recently important breakthroughs were made that will unleash the full potential of acoustic waves in quantum technologies. For example, the rapid progress in the development of surface acoustic wave resonators now allows to generate desired phonon quantum states which promotes the field of quantum acoustics.

Organized by Hubert J. Krenner and Daniel Wigger

Time: Monday 9:30–13:00

Location: POT 151

Invited Talk

HL 3.1 Mon 9:30 POT 151

Schrödinger cat states of a 16-microgram mechanical oscillator — •YIWEN CHU^{1,2}, MARIUS BILD^{1,2}, MATTEO FADEL^{1,2}, YU YANG^{1,2}, UWE VON LÜPKE^{1,2}, PHILLIP MARTIN^{1,2}, and ALESSANDRO BRUNO^{1,2} — ¹Department of Physics, ETH Zürich — ²Quantum Center, ETH Zürich

While the principle of superposition in quantum physics is routinely validated for microscopic systems, it is still unclear why we do not observe macroscopic objects to be in superpositions of states that can be distinguished by some classical property. I will present our experiments that harness the resonant Jaynes-Cummings interaction between a high overtone resonator mode of a bulk acoustic wave resonator and a superconducting qubit to demonstrate the preparation of Schrödinger cat states of motion. In such a state, the constituent atoms oscillate in a superposition of two opposite phases with an effective oscillating mass of 16 micrograms. Making use of the circuit quantum acoustodynamics toolbox we have developed, we furthermore show control over amplitudes and phases of the created Schrödinger cat states, and investigate their decoherence dynamics by observing the disappearance of Wigner negativities. Our results can find applications in continuous variable quantum information processing and in fundamental investigations of quantum mechanics in massive systems.

Invited Talk

HL 3.2 Mon 10:00 POT 151

High-fidelity quantum information processing with spins and phonons — •PETER RABL — Atominstitut, TU Wien, Stadionallee 2, 1020 Wien, Austria — Physik-Department, Technische Universität München, 85748 Garching, Germany — Walther-Meißner-Institut, Bayerische Akademie der Wissenschaften, 85748 Garching, Germany

Phonons in solids are usually uncontrolled and therefore represent one of the main sources of decoherence for many solid-state quantum systems. However, when appropriately designed, isolated mechanical modes offer fascinating new opportunities for engineering coherent interactions between systems that cannot be coupled efficiently otherwise. In this talk, I will discuss the prospects of this approach for engineering phonon-mediated quantum gate operations between spin qubits associated with SiV defect centers in a diamond phononic crystal. Specifically, I will show how the application of continuous spin-echo techniques can substantially boost the coherence times in this system and suppress gate errors below 10⁻⁴ for experimentally realistic noise parameters. Therefore, although the field is still in its infancy, this analysis outlines a realistic path toward moderate- and large-scale quantum devices with spins and phonons, at a level of control that is comparable to other leading quantum-technology platforms.

HL 3.3 Mon 10:30 POT 151

Acoustically-induced pseudo-gauge fields and anomalous transport phenomena in graphene — •PAI ZHAO¹, LARS TIEMANN¹, LEV MOUROKH², VADIM M. KOVALEV³, and ROBERT H. BLICK¹ — ¹University of Hamburg, Germany — ²Department of Physics, Queens College, New York, USA — ³Novosibirsk, Russia

One of many remarkable consequences of the low-energy Dirac description of graphene is the emergence of synthetic gauge fields under lattice deformation that affect the carrier dynamics. We show that acoustically stimulated carrier transport in graphene at 4 Kelvin signals the presence of artificial gauge fields through the build-up of a transversal voltage at zero magnetic field. We fabricated a gate-tunable, large-scale CVD graphene Hall bar on a hybrid piezoelectric LiNbO₃ on insulator substrate. An interdigitated transducer launches a surface acoustic wave (SAW) that acoustically accelerates the carriers in the graphene. At zero magnetic field, we observe large anomalous acoustically-induced synthetic Hall voltages up to 200 μ V, depending on the carrier type, concentration and SAW power. The synthetic Hall voltage can modulate a conventional Hall voltage arising in a large external magnetic field [1]. Our observation is consistent with studies of strain-induced pseudo-gauge fields [2-4].

[1] P. Zhao et al., *Phys. Rev. Lett.* 128, 256601 (2022); [2] N. Levy et al., *Science* 329, 544 (2010); [3] F. Guinea, M. I. Katsnelson and A. K. Geim, *Nat. Phys.* 6, 30 (2010); [4] M. Oliva-Leyva and G. G. Naumis, *J. Phys.: Condens. Matter* 28, 025301 (2015).

HL 3.4 Mon 10:45 POT 151

On-chip waveguides for hypersound with planar semiconductor optical microcavities — ANTONIO CRESPO-POVEDA, •ALEXANDER KUZNETSOV, ALBERTO HERNÁNDEZ-MÍNGUEZ, ABBES TAHRAOUI, KLAUS BIERMANN, and PAULO SANTOS — Paul Drude Institute for Solid State Electronics, Berlin, Germany

In solid-state systems, coherent oscillations of the atomic lattice (phonons) couple to the majority of elementary excitations. This motivates studies that aim at creating phonon-based interfaces between photons and quantum systems. In this work, we show piezoelectric excitation of 6 GHz hypersound in a buried (Al,Ga)As planar waveguide. Acoustic echo spectroscopy reveals that phonons propagate over mm-long distances. Furthermore, the waveguide contains quantum wells and is embedded into an optical microcavity. The strong-coupling between nIR photons and excitons leads to the formation of light-matter quasiparticles – polaritons. Due to the excitonic component, polaritons act as a sensitive local optical probe for gAPs. Thus, we demonstrated a conversion of microwave signals to guided hypersound with the subsequent polariton-mediated transduction to photons. In a broad context, the results are important for the remote coherent control of optoelectronic resonances and the realization of the on-chip phonon circuitry and a microwave-to-optical interface.

30 min. break

Invited Talk

HL 3.5 Mon 11:30 POT 151

Control of spin centers in silicon carbide using acoustic fields — •ALBERTO HERNÁNDEZ-MÍNGUEZ — Paul-Drude-Institut für Festkörperelektronik, Leibniz-Institut im Forschungsverbund Berlin e.V., Berlin, Germany

Atom-like color centers in solids are attractive for applications in quantum technologies because their spin states exhibit long coherence times and can be controlled by optical, microwave and acoustic fields. In this contribution, we report on acoustically driven spin transitions in silicon vacancy centers in SiC. Specifically, we use the dynamic strain of surface acoustic waves to selectively excite room-temperature spin transitions with magnetic quantum number differences of ± 1 and ± 2 in the absence of external microwave fields [1]. Compared to the ground states, spin levels in the optically accessible excited states possess even stronger interaction with acoustic vibrations, thus giving rise to novel and, so far, largely unexploited physical phenomena. A remarkable example is the acoustically induced coherent spin trapping [2], which consists in the quenching of the optically detected spin resonance due to the precession of the spin around the same axis in both ground and excited states. Our findings provide new opportunities for the coherent control of spin qubits with dynamic strain fields that can lead towards the realization of future spin-acoustic quantum devices.

[1] A. Hernández-Mínguez et al., *Phys. Rev. Lett.* 125, 107702 (2020)

[2] A. Hernández-Mínguez et al., *Sci. Adv.* 7, eabj5030 (2021)

HL 3.6 Mon 12:00 POT 151

Storage and retrieval of telecom single photons from a semiconductor quantum dot in a rubidium ORCA memory — •LUKAS WAGNER¹, SARAH THOMAS², CORNELIUS NAWRATH¹, SIMONE LUCA PORTALUPI¹, PATRICK LEDINGHAM³, IAN WALMSLEY², and PETER MICHLER¹ — ¹Institut für Halbleitertechnik und Funktionelle Grenzflächen (IHFG), Center for Integrated Quantum Science and Technology (IQST) and SCoPE, University of Stuttgart, Allmandring 3, 70569 Stuttgart, Germany — ²Faculty of Natural Sciences, Department of Physics, Imperial College London, Imperial College Rd, South Kensington Campus, London SW7 2AZ, United Kingdom — ³Department of Physics and Astronomy, University of Southampton, Southampton SO17 1BJ, United Kingdom

Photons are highly attractive as carriers of information thanks to their propagation at the speed of light and their low interaction with matter. Furthermore, various implementations of photonic quantum technologies will strongly benefit from the possibility of storing quantum information. Indeed, quantum memories would allow synchronizing the arrival time of multiple photons. Semiconductor quantum dots (QDs) are highly attractive as sources of quantum light. Atomic vapors are known as a very powerful platform to realize on-demand storage and retrieval of light. For these reasons a hybrid quantum system combining these two elements was for long sought after. Here, we will report on our progress to interface single photons from an In(Ga)As QD emitting at telecom wavelength with a rubidium off-resonance cascaded absorption (ORCA) quantum memory.

HL 3.7 Mon 12:15 POT 151

Excitation and read-out of macroscopic mechanical motion by phase-modulated optical driving of a single-photon emitter — •THILO HAHN¹, JACEK KASPRZAK², ORTWIN HESS³, TILMANN KUHN¹, and DANIEL WIGGER³ — ¹Institute of Solid State Theory, University of Münster, Germany — ²Université Grenoble Alpes, CNRS, France — ³School of Physics, Trinity College Dublin, Ireland

Resonance phenomena provide an access to drive inert systems out of equilibrium by applying a periodic force. In this contribution we will investigate a hybrid quantum system consisting of a single photon emitter (SPE) that is on the one hand coupled to a single phonon mode, e.g., in the form of a mechanic resonator, and on the other hand driven by a laser field. To convert a series of laser pulses into a measurable displacement of the phonon mode, originally a synchronization between the pulse repetition and the mode frequency was suggested [2] and demonstrated. Here, we discuss a different excitation scheme that is adapted from the heterodyne four-wave mixing (FWM) technique: We consider a series of pulse pairs which drives the phonons into a far displaced quasi-coherent state by tuning the harmonically oscillating phase relation within the pulse pairs in resonance with the phonons. Conversely, the optical properties of the SPE are dynamically affected by the phonon motion. Conveniently this can directly be measured by the FWM signal emitted by the SPE in order to detect the mechanical motion. Consequently, we combine resonant driving and read-out in a single method. [1] *Phys. Rev. A* 90, 023818 (2014) [2] *Nat. Nanotechnol.* 16, 283 (2021)

HL 3.8 Mon 12:30 POT 151

Imaging surface acoustic waves on 2D materials using atomic force microscopy — •MINGYUN YUAN¹, ALBERTO HERNÁNDEZ-MÍNGUEZ¹, IGOR AHARONOVICH², and PAULO V. SANTOS¹ — ¹Paul-Drude-Institut für Festkörperelektronik, Leibniz-Institut im Forschungsverbund Berlin e.V., Berlin, Germany — ²School of Mathematical and Physical Sciences, University of Technology Sydney, Ultimo, Australia

There is an increasing interest in coupling the dynamic strain of surface acoustic waves (SAWs) to electronic excitations in 2D-material-based nanostructures to acoustically manipulate their optoelectronic properties. While optical phenomena in 2D nanostructures can be conveniently mapped by photoluminescence, local probing of mechanical properties remains challenging. This task can, nevertheless, be assisted by high-frequency (GHz) SAWs, which are particularly suitable for probing very thin objects due to their micron-size wavelengths and their confinement near the surface. Here, we use atomic force microscopy (AFM) to image SAWs propagating along a LiNbO₃ acoustic resonator containing a multilayer hexagonal Boron Nitride (hBN) flake irradiated with Ar ions to create color centers. The high spatial resolution of AFM enables us to investigate the SAW strain transferred to the flake. We observe spatial inhomogeneities, revealing that the strain transferred to 2D materials can exhibit large spatial fluctuations. Possible mechanisms that affect the coupling will be discussed. Our method demonstrates a straight-forward way to characterize dynamic strain fields in hybrid SAW/2D-material systems.

HL 3.9 Mon 12:45 POT 151

Effect of helium ion implantation on nanomechanical resonators in 3C-SiC — •NAGESH SHAMRAO JAGTAP^{1,2}, YANNICK KLASS³, FELIX DAVID³, PHILIPP BREDOL³, EVA WEIG³, MANFRED HELM^{1,2}, GEORGY ASTAKHOV¹, and ARTUR ERBE^{1,2} — ¹Helmholtz-Zentrum Dresden - Rossendorf, Institute of Ion Beam Physics and Materials Research, Dresden — ²TU Dresden — ³Technical University of Munich, Chair of Nano and Quantum Sensors, Munich

Silicon carbide (SiC) is a suitable candidate for nanoelectromechanical systems due to its superior mechanical properties. It is also an interesting material platform to study the coupling of mechanical modes with localized spins associated with irradiation-induced defects. Such a spin-mechanical system can be used for quantum sensing applications [1]. The nanomechanical resonators in 3C-SiC are fabricated by standard semiconductor processing techniques such as electron beam lithography and reactive ion etching. They are characterized using Fabry-Pérot interferometer. In the preliminary experiments, we focus on the material modification by helium ion broad beam implantation on strained 3C-SiC resonators. The effect of varying fluence on resonance frequencies and quality factors is studied (see contribution of Philipp Bredol).

[1] A. V. Poshakinskiy, G. V. Astakhov, Optically detected spin-mechanical resonance in silicon carbide membranes, *PRB* 100 094104 (2019)

HL 4: Perovskite and photovoltaics I (joint session HL/CPP)

Time: Monday 9:30–12:30

Location: POT 251

HL 4.1 Mon 9:30 POT 251

Bandgap engineering of two-step processed perovskite top cells for application in perovskite-based tandem photovoltaics — •RONJA PAPPENBERGER^{1,2}, ALEXANDER DIERCKS², AHMED FARAG^{1,2}, PAUL FASSL^{1,2}, and ULRICH W. PAETZOLD^{1,2} — ¹Institut für Mikrostrukturtechnologie, KIT, Germany — ²Lichttechnisches Institut, KIT, Germany

Tandem solar cells offer a promising concept of raising the efficiency of silicon solar cells above the theoretical limit of 29%. In this context, silicon is supplemented by a wide-bandgap perovskite top solar cell to make better use of the solar spectrum. Perovskite solar cells come into play given their favorable optoelectronic quality and tunable bandgap. Textured-front perovskite silicon tandem solar cells currently promise the highest energy yield for modules in the field. To avoid shunting, ensure high efficiency and economic production of the perovskite on the μm -sized pyramids, a conformal growth of the perovskite layer as well as a sufficient layer thickness are necessary. A two-step method - containing a separate deposition of the PbI_2 and the organic cations - enables high film quality, flexibility in choice of component/solution and the possibility of up-scaling. Here, we investigate different strategies of increasing the bandgap of the perovskite. Thereby the location of the added bromine - cation solution and/or PbI_2 solution - is critical. With our approach, the device performance - PCE of 17.2%, FF of 76% and V_{oc} of 1.156 V ($E_g \approx 1.64$ eV) - and film quality can be maintained. Furthermore, the effect of an increasing bandgap in combination with planar/textured silicon bottom cells is studied.

HL 4.2 Mon 9:45 POT 251

Application of plasma enhanced atomic layer deposition process of alumina on perovskite film boosts efficiency of solar cells — •MALGORZATA KOT¹, MAYANK KEDIA², PAUL PLATE³, LUDWIG MARTH³, KARSTEN HENKEL¹, and JAN INGO FLEGE¹ — ¹Applied Physics and Semiconductor Spectroscopy, BTU Cottbus-Senftenberg, Konrad-Zuse-Strasse 1, 03046 Cottbus, Germany — ²Institut fuer Photovoltaik Universitaet Stuttgart, Pfaffenwaldring 47, 70569 Stuttgart, Germany — ³SENTECH Instruments GmbH, Schwarzschildstraße 2, 12489 Berlin, Germany

It is assumed that plasma-enhanced atomic layer deposition (PEALD) cannot be used to prepare thin films on sensitive organic-inorganic perovskites because the plasma destroys the perovskite film and thus deteriorates its photophysical properties. Here, we prove that using an appropriate geometry of the ALD system (SENTECH SI PEALD system) and suitable process parameters it is possible to coat perovskites with alumina by PEALD. Spectromicroscopy followed by electrical characterisation reveal that as long as the PEALD process is not optimized (too long plasma pulses) one gets degradation of the perovskite as well as dissociation of the created iodine pentoxide (during PEALD) under light that causes a valence band maximum (VBM) shift to the Fermi level and thus significantly decreases the solar cell efficiency. However, once the PEALD process parameters are optimized, no VBM shift is observed. Moreover, the solar cell efficiency depends inversely on process temperature and layer thickness.

HL 4.3 Mon 10:00 POT 251

Tuning Crystallization for Highly Efficient Perovskite Silicon Tandem Solar Cells — •MOHAMED MAHMOUD^{1,2}, OUSSAMA ER-RAJI^{1,2}, PATRICIA SCHULZE¹, ANNA JULIANE BORCHERT^{1,2}, and ANDREAS W. BETT^{1,2} — ¹Fraunhofer ISE — ²University of Freiburg

Perovskite solar cells have the advantages of a strong absorption edge, defect tolerance, and potential cheap production due to easy production methods such as spin coating or slot-die coating as a highly scalable production method. In the industry, double-sided textured (micro-meter sized pyramid) silicon is commonly produced to decrease reflection losses and improve light trapping. Solution-based processing methods of perovskite on top of the textured Si showed low conformality, which resulted in shunts and non-working solar cells. To overcome this issue, the hybrid route was developed, in which inorganic precursors are co-evaporated using the thermal vapor deposition technique and then organic precursors are spin-coated followed by a thermal annealing. By doing that, high conformality of perovskite thin films on top of the textured silicon is achieved. However, the resulting perovskite grain size is rather low, which can lower the bulk quality. In this work, various additives were used to increase the grain size, and their working mechanisms were studied. In addition, we study the consequences of different grain sizes at the tandem level with respect to device efficiency as well as stability. Moreover, using the thermodynamics fundamentals of crystallization, we hypothesize for the first time a common general explanation for the working mechanism of all the different additives used.

HL 4.4 Mon 10:15 POT 251

Efficient Modeling Workflow for Accurate Electronic Structures of Hybrid Perovskites — JULIAN GEBHARDT^{1,2}, •WEI WEI^{1,2}, and CHRISTIAN ELSÄSSER^{1,2,3} — ¹Fraunhofer IWM, 79108 Freiburg — ²Cluster of Excellence livMatS, University of Freiburg — ³Freiburg Materials Research Center, University of Freiburg

Hybrid organic-inorganic halide perovskites are the most promising photovoltaic absorber materials to substitute or complement silicon in high-efficiency solar cells. These hybrid materials are often constrained by their low stability and critical elements like lead. Computational high-throughput screening studies, based on solid-state electronic-structure theory, are useful to identify promising substitute materials with targeted properties. In this work, we present an efficient computational approach based on density-functional theory, which is suitable to predict band gaps for arbitrary compounds reliably and in good quantitative agreement with experimental band gap data for known compounds. This approach is described and demonstrated for the building blocks of one of the most promising hybrid perovskites, namely, $(\text{HC}(\text{NH}_2)_2)_x\text{Cs}_{1-x}\text{Pb}(\text{I}, \text{Br}_{1-y})_3$, with x and y varied between zero and one.

J. G. et al. *J. Phys. Chem. C* **2021** 125, 18597.

HL 4.5 Mon 10:30 POT 251

Photon Management for Ultrathin Solar Cells: Enabling Waveguide Modes by Structured Back Contact — •MERVE DEMIR, THOMAS SCHNEIDER, TORSTEN HÖLSCHER, HEIKO KEMPA, and ROLAND SCHEER — Martin-Luther-Universität Halle-Wittenberg, Germany

The recent research based on $\text{Cu}(\text{In,Ga})\text{Se}_2$ (CIGSe) solar cells is focused on thinning down the absorber layer to enable less material consumption and cost effective large scale production. However, having ultra-thin CIGSe solar cells with absorber layer thickness in sub-micron level brings the cost of limited absorption of solar spectra and hence leads to lower energy conversion efficiencies. This problem can be overcome by the cell architecture including functional back contact elements for the enhancement of optical absorption. In this contribution, ultrathin CIGSe solar cells with 500 nm thick absorber layer were combined with nano-textured SiO_2 back contacts together with aluminum back mirror. With this cell design, it is aimed to have increased power conversion efficiency for ultra-thin CIGSe solar cells due to enhanced absorption of long wavelength region photons. The solar cell parameters were extracted and compared with the conventional CIGSe back contact, flat molybdenum, to reveal the effects of functional back contact. The experimental findings on quantum efficiency measurements prove the positive effects of having highly reflective and textured back contact. Furthermore, the growth of CIGSe on textured substrates was examined throughout cross section cuts by scanning electron microscopy and energy dispersive X-ray diffraction.

30 min. break

HL 4.6 Mon 11:15 POT 251

Employing three-dimension structure analysis: digital twin for studying grain boundary effects in thin film solar cells — •CHANG-YUN SONG¹, MATTHIAS MAIBERG¹, HEIKO KEMPA¹, ALI GHOLINIA², WOLFRAM WITTE³, DIMITRIOS HARISKOS³, DANIEL ABOU-RAS⁴, and ROLAND SCHEER¹ — ¹Martin-Luther-University Halle-Wittenberg, Halle, D — ²University of Manchester, Manchester, UK — ³Zentrum für Sonnenenergie- und Wasserstoff-Forschung, Stuttgart, D — ⁴Helmholtz-Zentrum Berlin, Berlin, D

Grain boundaries (GBs) in polycrystalline $\text{Cu}(\text{In,Ga})\text{Se}_2$ (CIGSe), are believed to be one of the performance limiting factors of current record efficiency CIGSe solar cells. Numerous simulation studies have been conducted to unveil their effects. Most simulations, however, have been done within two-dimensions (2D), thereby presumably using the simplified GBs shapes. In this study, we thus present a realistic three-dimensional (3D) GB model for a high-efficiency CIGSe layer. To this end, a combination of electron backscatter diffraction and focused ion beam was applied to obtain 3D data of the CIGSe layer, which then allowed the reconstruction of the 3D grain structure into a computer model. By using the computer model as input for 3D optoelectronic simulations, we study the electronic effects of GBs on the high-efficiency solar cell under investigation bulk parameter values for the simulations were obtained through a combination of simulation and experiments, such that the solar cell is consistently described. As an outcome, the 3D simulations confirm that the effect of GB was indeed underestimated in earlier conventional 2D simulations.

HL 4.7 Mon 11:30 POT 251

Interface Engineering to reduce non-radiative recombination losses at the perovskite/C60 interface in monolithic perovskite silicon tandem solar cells — •JOHANNA MODES, PATRICIA S. C. SCHULZE, KAITLYN MC MULLIN, MARYAM-SADAT HEYDARIAN, CHRISTOPH MESSMER, JULIANE BORCHERT, and ANDREAS BETT — Fraunhofer ISE

Metal halide perovskites have emerged in recent years as a promising absorber material for solar cells with the potential to combine high power conversion efficiency with low production costs. However, significant non-radiative charge carrier recombination occurs at the perovskite interface to the contacts, thus preventing the full potential of the solar cell from being exploited. Photoluminescence quantum yield measurements clearly show that the Quasi-Fermi level splitting is reduced by evaporation of the electron contact C60 onto perovskites, leading to limited open-circuit voltage in devices. In recent literature, as well as in our investigations, different passivation layers are deposited between perovskite and the electron contact to reduce non-radiative recombination and to improve the open-circuit voltage. This is on the one hand pursued by increasing the selectivity at the contacts through field effects and band alignment and secondly by reducing defects at the interface through chemical passivation.

HL 4.8 Mon 11:45 POT 251

Spontaneous Polarization in NaNbO₃ — •KISUNG KANG¹, SAUD BIN ANOOZ², JUTTA SCHWARZKOPF², MATTHIAS SCHEFFLER¹, and CHRISTIAN CARBOGNO¹ — ¹The NOMAD Laboratory at the FHI of the Max-Planck-Gesellschaft and IRIS-Adlershof of the Humboldt-Universität zu Berlin — ²Leibniz-Institut für Kristallzüchtung (IKZ)

The perovskite NaNbO₃ is regarded as a promising lead-free piezoelectric material, also because its polarization properties can be further tailored via strain engineering. [1] In thin films, lattice strain can be incorporated by the heteroepitaxial growth on lattice mismatch. By tuning the epitaxial strain in the films, different polymorphs with distinctively different polarization strength and orientation can be realized [2, 3]. We investigate this question by using density-functional theory at the semi-local level of theory, which we carefully validate with hybrid-functional calculations. By this means, we compute the spontaneous polarization for ten phases of NaNbO₃ as a function of stress and strain. In line with experiments, we confirm that the monoclinic *Pm* phase features a non-vanishing in-plane polarization, the orientation of which is independent of the strain. Conversely, the polarization direction of the orthorhombic *Pmc*₂ phase depends on the applied tensile strain. We analyze the underlying electronic and atomistic mechanism and discuss how the relevant properties are influenced by phase transformations.

[1] N. Bein, *et al.*, *Phys. Rev. Mater.* **6**, 084404 (2022).

[2] J. Schwarzkopf, *et al.*, *J. Appl. Cryst.* **45**, 1015 (2012).

[3] S. B. Anooz, *et al.*, *Appl. Phys. Lett.* **120**, 202901 (2022).

HL 4.9 Mon 12:00 POT 251

Peculiar bond length dependence and its impact on the band gap bowing in (Ag,Cu)(In,Ga)Se₂ thin film alloys — •HANS H. FALK¹, STEFANIE ECKNER¹, KONRAD RITTER¹, SERGIU LEVCENKO¹, TIMO PFEIFFELMANN¹, EDMUND WELTER², JES LARSEN³, WILLIAM N. SHAFARMAN⁴, and CLAUDIA S. SCHNOHR¹ — ¹Felix Bloch Institute for Solid State Physics, Leipzig University, Germany — ²Deutsches Elektronen-Synchrotron DESY, Germany — ³Department of Materials Science and Engineering, Uppsala University, Sweden — ⁴Department of Materials Science and Engineering, University of Delaware, USA

Incorporation of Ag into Cu(In,Ga)Se₂ thin film solar cells improves several of their properties. However, with increasing Ag content, the band gap of (Ag,Cu)GaSe₂ increases even though the lattice expands and the Ga-Se bond length is predicted to decrease. This is counterintuitive, since in other chalcopyrite alloys all bond lengths increase and the band gap decreases as the lattice expands. Therefore, we studied the element-specific average bond lengths of (Ag,Cu)GaSe₂, (Ag,Cu)InSe₂ and Ag(In,Ga)Se₂ using X-ray absorption spectroscopy for thin films grown on Mo-coated soda lime glass by a single stage co-evaporation process. As predicted, the Ga-Se bond length decreases with increasing Ag content in (Ag,Cu)GaSe₂. While the In-Se bond length of (Ag,Cu)InSe₂ shows the same behavior, Ag(In,Ga)Se₂ exhibits a dependence similar to that of Cu(In,Ga)Se₂, demonstrating that the peculiar behavior is related to mixing the group-I lattice site. Using the bond lengths we model the anion positions and estimate their effect on the band gap bowing.

HL 4.10 Mon 12:15 POT 251

Fast diffusion of spin polarized excitons in bulk lead halide perovskites — •SERGIU ANGHEL¹, DMITRI R. YAKOVLEV¹, DMITRY N. DIRIN², MAKSYM V. KOVALENKO², MANFRED BAYER¹, and MARKUS BETZ¹ — ¹Experimentelle Physik 2, Technische Universität Dortmund, Otto-Hahn-Straße 4a, D-44227 Dortmund, Germany — ²Laboratory of Inorganic Chemistry, Department of Chemistry and Applied Biosciences, ETH Zürich, Zürich CH-8093, Switzerland

We investigate the spin diffusion of the free "hot" excitons in FA_{0.9}Cs_{0.1}PbI_{2.8}Br_{0.2} bulk lead halide perovskite crystal at cryogenic temperatures by employing ultrafast time- and spatial-resolved magneto-optical Kerr microscopy. We measure the spin diffusion coefficient (D_s) of the free excitons of $D_s \sim 50 \text{ cm}^2/\text{s}$, which is a very surprising outcome, especially in the light of the recent results obtained on bulk or two-dimensional perovskites [1,2], where D_s is at least two orders of magnitude lower. D_s shows a roughly linear dependence on pump energy whereas the dependence on pump power is much more intricate - after a certain pump power threshold we observe an anomalous, nonlinear spatial dependence of D_s . We discuss our findings in view of efficient exciton-phonon coupling and Auger processes.

[1] A. Baldwin, G. Delpont, K. Leng, R. Chahbazian, K. Galkowski, K. P. Loh, and S. D. Stranks, *J. Phys. Chem. Lett.* **12**, 4003 (2021). [2] S. D. Stranks, G. E. Eperon, G. Grancini, C. Menelaou, M. J. P. Alcocer, T. Leijtens, L. M. Herz, A. Petrozza, and H. J. Snaith, *Science* **342**, 341 (2013).

HL 5: Heterostructures, interfaces and surfaces

Time: Monday 10:00–11:15

Location: POT 112

HL 5.1 Mon 10:00 POT 112

Time-resolved analysis of propagating exciton-polariton condensates in photonic potential landscapes. — •CHRISTIAN G. MAYER, PHILIPP GAGEL, SIMON BETZOLD, TRISTAN H. HARDER, MONIKA EMMERLING, ADRIANA WOLF, FAUZIA JABEEN, SVEN HÖFLING, and SEBASTIAN KLEMBT — Technische Physik, RCCM and Würzburg-Dresden Cluster of Excellence ct.qmat, University of Würzburg, Germany

Confining photons in a Fabry-Perot microcavity and coupling them strongly to excitons leads to the formation of hybrid matter-light particles named exciton-polaritons (polaritons). Owing to their bosonic statistics, they undergo a phase transition above a critical density to a dynamic condensate via stimulated scattering. Polaritons have quite long diffusion length compared to excitons because of their lower effective mass inherited by their photonic fraction. Propagation effects of a polariton condensate take place on a time scale of a few picoseconds and are caused by the repulsive potential facilitated by the matter fraction due to polariton-exciton and polariton-polariton interactions. By varying the light-matter composition of the polariton condensate, we investigate changes in the propagation properties such as velocity and length.

Using electron beam lithography, we spatially confine propagating polaritons in waveguides, as well as in resonator lattices supporting quantum valley Hall modes. Using a streak camera, the propagation of the polariton condensate is measured in a variety of confined structures and systems.

HL 5.2 Mon 10:15 POT 112

Tackling the band ordering problem for transport calculations in strained semiconductors: A $\mathbf{k} \times \mathbf{p}$ perspective — •DANIEL FRITSCH¹, COSTANZA L. MANGANELLI², CHRISTIAN MERDON¹, and PATRICIO FARRELL¹ — ¹Weierstrass Institute for Applied Analysis and Stochastics, Mohrenstr. 39, 10117 Berlin, Germany — ²IHP Leibniz-Institute for High Performance Microelectronics, Im Technologiepark 25, 15236 Frankfurt (Oder), Germany

A reliable determination of band energies in strained semiconductor heterostructures is indispensable for subsequent transport calculations. However, one crucial problem is presently hidden within the change in valence band ordering due to intrinsically occurring strain in semiconductor heterostructures, nanowires, or quantum dots.

In order to tackle this problem, we present a numerical algorithm based on the Bir-Pikus $\mathbf{k} \times \mathbf{p}$ Hamiltonian, that takes into account additional wavevector dependent properties, e.g. the effective mass tensor, to identify the nature of the valence bands. It provides the necessary connection between arbitrary strain profiles for semiconductor nanostructures calculated by means of a finite element method [1] and transport calculations employing a drift diffusion model [2].

The new algorithm is applied to example strain profiles, e.g. biaxial and uniaxial strain, and results are compared to earlier theoretical and experimental findings.

[1] GradientRobustMultiPhysics.jl (10.5281/zenodo.7217591).

[2] ChargeTransport.jl (10.5281/zenodo.7124161).

HL 5.3 Mon 10:30 POT 112

Improved growth of unstrained HgTe quantum well on InAs — •MAHITOSH BISWAS^{1,2}, HARTMUT BUHMANN^{1,2}, and LAURENS W. MOLENKAMP^{1,2} — ¹Institute for Topological Insulators, Universität Würzburg, 97074 Würzburg, Germany — ²Physikalisches Institut (EP3), Universität Würzburg, 97074 Würzburg, Germany

HgTe turned out to be a prototype material for investigations of transport properties in topological insulator materials. The material system also demonstrated its versatility when compressive strain is applied, resulting in Weyl and Kane semimetal states. It has been shown that the strain can be controlled sufficiently by the period of a CdZnTe/CdTe superlattices grown on a doped GaAs substrate. However, these strained and/or strained layers exhibit a rather high surface roughness which makes them unsuitable for sub-micrometer device fabrication or local probe measurement techniques. Here we show that CdZnTe/CdTe superlattices grown on doped InAs improve the situation significantly. Surface roughness is about three times lower compared with GaAs. These observations are confirmed by TEM measurements which monitor dislocations originating at the III-V/III-VI semiconductor interface. Magneto-transport measurements reveal that the doped substrate can be used as a highly efficient back gate. Carrier variations between $2 \times 10^{11} \text{ cm}^{-2}$ (electron) and $-2 \times 10^{11} \text{ cm}^{-2}$ (hole) are observed for a medium $\pm 10 \text{ V}$ gate range. These results manifest a (big) step forward toward the fabrication of functional top and back gated devices on topological materials.

HL 5.4 Mon 10:45 POT 112

Band alignment of thin strontium germanate layer on silicon from *ab initio* — •TOMÁŠ RAUCH^{1,2}, PAVEL MARTON^{3,4}, SILVANA BOTTI^{1,2}, and JIŘÍ HLINKA³ — ¹Institut für Festkörpertheorie und -optik, Friedrich-Schiller-Universität Jena, Germany — ²European Theoretical Spectroscopy Facility — ³Institute of Physics of the Czech Academy of Sciences, Praha, Czech Republic — ⁴Institute of Mechatronics and Computer Engineering, Technical University of Liberec, Czech Republic

Silicon is one of the most used materials for optoelectronic applications. In photo-catalytic cells for hydrogen evolution reaction, Si must be capped by a

protective layer, additionally allowing the photo-excited electrons to travel to the device surface. It has been demonstrated, that SrTiO₃ (STO) can fulfill these two functions [1].

In this work, we studied SrGeO₃ (SGO) as an alternative to STO, using density-functional theory. We calculated the structural properties of a chosen prototypical SGO/Si(001) interface and studied its electronic structure, focusing on the band offsets between Si and SGO. We found a metallic type-III interface with occupied conduction bands of SGO and a charge transfer from Si to SGO. Aligning the local band edges of the thin SGO layer with the redox potentials allows us to conclude that the SGO/Si interface should be suitable for water reduction.

We acknowledge funding by the Czech Science Foundation (project no. 21-20110K) and by the Volkswagen Foundation (project “dandelion”).

[1] Li Ji et al., Nat. Nanotechnol. **10**, 84 (2015)

HL 5.5 Mon 11:00 POT 112

Evolution of vacancy like defects in heavily doped GaAs — •MACIEJ OSKAR LIEDKE¹, SLAWOMIR PRUCNAL², MAIK BUTTERLING¹, JUANMEI DUAN², ERIC HIRSCHMANN¹, MAO WANG², MANFRED HELM², SHENGQIANG ZHOU², and ANDREAS WAGNER¹ — ¹Institute for Radiation Physics, Helmholtz-Zentrum Dresden - Rossendorf, Dresden, Germany — ²Institute for Ion Beam Physics, Helmholtz-Zentrum Dresden - Rossendorf, Dresden, Germany

The effect of intense pulsed laser melting and flash lamp annealing on defects distribution and activation efficiency in chalcogenide-implanted GaAs was investigated by means of positron annihilation spectroscopy and transport measurements. Using positrons as a sensitive probe of open volumes and dedicated DFT calculations, we will highlight the capability of nanosecond pulsed laser melting to control the type and density of defect complexes, e.g. S or Te substituting As atoms associated to Ga vacancy, playing a crucial role for donor deactivation. The distribution of defects and carriers will be discussed regarding the depth distribution of implanted elements and the solidification velocity during recrystallization.

HL 6: Focus Session: Frontiers of Electronic-Structure Theory III (joint session O/HL)

Electronic-structure calculations, based on density-functional theory (DFT) and methodology beyond, are getting increasingly involved as they face the following challenges: First, investigations of modern materials typically require large unit cells, owing to complex crystal structures, mixed compositions, internal interfaces, etc. Second, at the same time, they often require advanced methods, including hybrid functionals of DFT, Green-function techniques from many-body perturbation theory (MBPT), high-level wavefunction-based methods like coupled-cluster (CC) theory, or quantum Monte-Carlo simulations. All these methods should ideally be implemented in scientific software that is running efficiently on modern supercomputers. With both methodology and computer architectures exhibiting increasing complexity, collaborative development and shared tools, including ready-to-use libraries and codes, are becoming indispensable. This interdisciplinary symposium covers recent progress in the broad area of electron-structure methods and highly-sophisticated tools that enable the entire community to explore most exciting materials from different perspectives to either predict peculiar features or get insight into measured counterparts.

Organizers: Claudia Draxl (HU Berlin), Dorothea Golze (TU Dresden), Xavier Gonze (U Louvain), and Andris Gulans (U Latvia)

Time: Monday 10:30–13:00

Location: TRE Ma

HL 6.1 Mon 10:30 TRE Ma

Testing the hell out of DFT codes with virtual oxides — EMANUELE BOSONI¹, •STEFAN COTTENIER², and GIOVANNI PIZZI³ — ¹ICMAB-CSIC, Spain — ²Ghent University, Belgium — ³EPFL, Switzerland

If you use DFT to predict a property of a crystal, how confident can you be that the prediction is computed in a bug-free way? And if your DFT-code uses pseudopotentials, can you trust that the pseudopotential does not modify your predictions? Answering such questions has been the goal of a study a few years ago, in which 71 unary crystals were examined in exactly the same way by 40 different DFT methods and codes [DOI 10.1126/science.aad3000]. In a next step, a consortium of 41 scientists (*) has done a similar exercise for a much larger pool of crystals: all elements of the periodic table up to Z=96, each in 10 different crystal structures, 6 of them being (virtual) oxides that sample a range of chemical bond types and 4 being unary crystals that sample low to high coordination environments. In this presentation, we will discuss the reasons to choose these crystals, the different quality criteria by which results can be compared, we will demonstrate how this exercise leads to more precise and more trustworthy pseudopotential libraries, and we will show how this data set is shared with the community in order to foster better-tested codes and pseudopotentials for all.

(*) Unfortunately the size of this abstract does not allow to mention them all.

HL 6.2 Mon 10:45 TRE Ma

High-throughput absorption spectra obtained by beyond-DFT workflows — •FABIAN PESCHEL, ALEXANDER BUCCHERI, and CLAUDIA DRAXL — Institut für Physik and IRIS Adlershof, Humboldt-Universität zu Berlin, Berlin, Germany

Fully converging *ab initio* calculations can be a challenging task, in particular when it comes to excited states, which require multiple ground-state calculations for different physical quantities. In this work, we aim at computing highly precise absorption spectra by employing the Bethe-Salpeter equation of many-body perturbation theory, as implemented in the all-electron full-potential package `exciting` [1,2]. To obtain benchmark data for a wide range of material classes, we have developed workflows where Python tools automatically create input files, start calculations, and evaluate results. For each material, all relevant input parameters, such as the number of k-points for the Brillouin-zone sampling, basis-set cutoff and the number of unoccupied states, are varied until the targeted convergence criteria are reached. With the help of a workflow manager, the calculations can be executed in a high-throughput fashion on a high-performance computing cluster. We demonstrate our approach with core-level spectra of elemental and binary solids, and provide an in-depth analysis of the obtained data. This work is carried out in the framework of the NOMAD Center of Excellence [3] and the CRC FONDA [4].

- [1] A. Gulans et al., *J. Phys. Condens. Matter* **26**, 363202 (2014)
 [2] C. Vorwerk, B. Aurich, C. Cocchi, C. Draxl, *Electron. Struct.* **1**, 037001 (2019)
 [3] <https://nomad-coe.eu>
 [4] <https://fonda.hu-berlin.de>

Topical Talk

HL 6.3 Mon 11:00 TRE Ma

Large-scale machine-learning assisted discovery and characterization of materials — •MIGUEL ALEXANDRE LOPES MARQUES — Institut für Physik Martin-Luther-Universität Halle-Wittenberg, Halle (Saale), Germany

In this talk we discuss our recent attempts to discover, characterize, and understand inorganic compounds using ab initio approaches accelerated by machine learning. We start by motivating why the search for new materials is nowadays one of the most pressing technological problems. Then we summarize our recent work in using crystal-graph attention neural networks for the prediction of materials properties. To train these networks, we curated a dataset of over 2 million density-functional calculations with consistent calculation parameters. Combining the data and the newly developed networks we have already scanned more than two thousand prototypes spanning a space of more than one billion materials and identified tens of thousands of theoretically stable compounds. We then discuss how simple, interpretable machine learning approaches can be used to understand complex material properties, such as the transition temperature of superconductors. Finally, we speculate which role machine learning will have in the future of materials science.

15 min. break

HL 6.4 Mon 11:45 TRE Ma

Predicting the electronic structure at any length scale with machine learning — •ATTILA CANGI — Helmholtz-Zentrum Dresden-Rossendorf, Görlitz, Germany

The properties of electrons in matter are of fundamental importance. They give rise to virtually all molecular and material properties and determine the physics at play in objects ranging from semiconductor devices to the interior of giant gas planets. Calculations rely primarily on density functional theory (DFT), which has become the principal method for predicting the electronic structure of matter. While DFT calculations have proven to be very useful, their computational scaling limits them to small systems. We have developed a scalable machine learning framework for predicting the electronic structure on any length scale [1,2,3]. It shows up to three orders of magnitude speedup on systems where DFT is tractable and, more importantly, enables predictions on scales where DFT calculations are infeasible. Our work demonstrates how machine learning circumvents a long-standing computational bottleneck and advances science to frontiers intractable with any current solutions.

- [1] J. A. Ellis, L. Fiedler, G. A. Popoola, N. A. Modine, J. A. Stephens, A. P. Thompson, A. Cangi, S. Rajamanickam, *Phys. Rev. B* **104**, 035120 (2021). [2] L. Fiedler, N. Hoffmann, P. Mohammed, G. A. Popoola, T. Yovell, V. Oles, J. A. Ellis, S. Rajamanickam, A. Cangi, *Mach. Learn.: Sci. Technol.* **3** 045008 (2022). [3] L. Fiedler, N. A. Modine, S. Schmerler, D. J. Vogel, G. A. Popoola, A. P. Thompson, S. Rajamanickam, A. Cangi, arXiv:2210.11343 (2022).

HL 6.5 Mon 12:00 TRE Ma

Demonstrating temperature transferability of neural network models replacing modern density functional theory — •LENZ FIEDLER and ATTILA CANGI — Helmholtz-Zentrum Dresden-Rossendorf / CASUS

Due to its balance between accuracy and computational cost, Density Functional Theory (DFT) is one of the most important computational methods within materials science and chemistry. However, current research efforts such as the modeling of matter under extreme conditions demand the application of DFT to larger length scales as well as higher temperatures. Such investigations are currently prohibited due to the computational scaling of DFT.

We have recently introduced a machine-learning workflow that replaces modern DFT calculations [1,2,3]. This workflow uses neural networks to predict the electronic structure locally. We show that by employing such an approach, models can be trained to predict the electronic structure of matter across temperature ranges. This paves the way for large-scale simulations of thermodynamically

sampled observables relevant to modeling technologically important phenomena such as radiation damage in fusion reactor walls.

- [1] J. A. Ellis et al., *Phys. Rev. B* **104**, 035120
 [2] L. Fiedler et al., *Mach. Learn.: Sci. Technol.*, **3** 045008
 [3] L. Fiedler et al., arXiv:2210.11343

HL 6.6 Mon 12:15 TRE Ma

Pure non-local machine-learned density functional theory for electron correlation — •JOHANNES T. MARGRAF — Fritz-Haber-Institut der MPG, Berlin, Germany

Density-functional theory (DFT) is a rigorous and (in principle) exact framework for the description of the ground state properties of atoms, molecules and solids based on their electron density. While computationally efficient density-functional approximations (DFAs) have become essential tools in computational chemistry, their (semi-)local treatment of electron correlation has a number of well-known pathologies, e.g. related to electron self-interaction. Here, we present a type of machine-learning (ML) based DFA (termed Kernel Density Functional Approximation, KDFA) that is pure, non-local and transferable, and can be efficiently trained with fully quantitative reference methods. The functionals retain the mean-field computational cost of common DFAs and are shown to be applicable to non-covalent, ionic and covalent interactions, as well as across different system sizes.

HL 6.7 Mon 12:30 TRE Ma

Predicting the response of the electron density to electric field using machine learning — •ALAN LEWIS and MARIANA ROSSI — MPI for Structure and Dynamics of Materials, Hamburg, Germany

The response of the electron density of a molecule or material to a homogeneous electric field defines its dielectric constant, along with its Raman and sum-frequency spectrum. We present a local and transferable machine learning approach capable of predicting the density response of molecules and periodic system on the same footing. This uses a very similar framework to that of the SALTED method recently introduced by these authors,[1,2] requiring only a small modification to the λ -SOAP descriptors used to represent the atomic environments. This allows us to predict the density response of liquid water to a field applied in each Cartesian direction from a single machine learning model. The tensorial dielectric constant can then be derived from this predicted density response, dramatically reducing the computational cost of calculating these properties relative to the standard approach of using density functional perturbation theory. We discuss the transferability of the model to different phases, and demonstrate the extrapolative power of this approach.

- [1] Lewis, Grisafi, Ceriotti, Rossi, *JCTC* **17**, 11, 7203 (2021)
 [2] Grisafi, Lewis, Rossi, Ceriotti, accepted *JCTC* (2022)

HL 6.8 Mon 12:45 TRE Ma

Analysis of Batching Methods in Graph Neural Network Models for Materials Science — •DANIEL SPECKHARD, TIM BECHTEL, JONATHAN GODWIN, and CLAUDIA DRAXL — Humboldt-Universität zu Berlin, Physics Department and IRIS Adlershof, Berlin, Germany

Graph neural network (GNN) based models have shown promising results for materials science [1]. These models often contain millions of parameters, and like other big-data based models, require only a portion of the entire training dataset to be fed as a mini-batch to update model parameters. The effect of batching on the computational requirements of training and model performance has been thoroughly explored for neural networks [2] but not yet for GNNs. We explore two different types of mini-batching methods for graph based models, static batching and dynamic batching. We use the Jraph library built on JAX to perform our experiments where we compare the two batching processes for two data-sets, the QM9 dataset of small molecules and the AFLOW materials database [3]. We show that dynamic batching offers significant improvements in terms of computational requirements for training. We also present results on the effect of the batch size and batching method on model performance.

- [1] T. Xie et al., *Physical Review Letters*, **120**, 14 (2018).
 [2] M. Li et al., *Proceedings of the 20th ACM SIGKDD* (2014).
 [3] S. Curtarolo et al., *Comp. Mat. Science*, **58**, 227-235 (2012).

HL 7: Poster I

Topics:

- Functional semiconductors for renewable energy solutions
- Heterostructures, interfaces and surfaces
- Optical properties
- Organic semiconductors
- Perovskite and photovoltaics
- Quantum dots and wires

Time: Monday 13:00–15:00

Location: P2/EG

HL 7.1 Mon 13:00 P2/EG

Investigation of the P-line in indium doped silicon with low temperature photoluminescence by applying an illumination and annealing cycle — •DOMINIK BRATEK, KATHARINA PEH, KEVIN LAUER, DIRK SCHULZE, STEFAN KRISCHOK, AARON FLÖTOTTO, and ROBIN MÜLLER — Institut für Physik, Technische Universität Ilmenau, Weimarer Str. 32, 98693 Ilmenau, Germany

In recent years a photoluminescent feature called P-line is of rising interest for the current research [1,2,3] and, in combination with the so called ASiSii-defect model, may lead to an explanation of the infamous light induced degradation (LID) process in indium doped silicon [2,3]. In this contribution we show studies of indium implanted silicon by using low temperature photoluminescence (LTPL) spectroscopy. We investigate the LID cycle and its influence on the P-line and show a possibility to explain the observed behavior by the proposed energy diagram of the ASiSii-defect. In addition we present activation energies, determined during these investigations, which can be associated to ASiSii-defect transitions. [1] K. Terashima and T. Matsuda, Japanese Journal of Applied Physics 41 Part 1, No. 3A (2002). [2] K. Lauer, C. Möller, D. Schulze, and C. Ahrens, AIP Advances 5, 017101 (2015). [3] K. Lauer, C. Möller, C. Teßmann, D. Schulze and N. V. Abrosimov, physica status solidi, c 14.5 (2017).

HL 7.2 Mon 13:00 P2/EG

Investigation of the influence of light-induced degradation on boron-doped silicon — •ROBIN LARS BENEDIKT MÜLLER, KATHARINA PEH, KEVIN LAUER, DIRK SCHULZE, STEFAN KRISCHOK, DOMINIK BRATEK, and AARON FLÖTOTTO — TU Ilmenau

For Si-based devices like solar cells or radiation detectors, the light-induced degradation (LID) in doped Czochralski Si is a profound issue. A reasonable explanation for the appearing LID process is the so-called ASi-Sii defect model [1,2], whose possible defect configuration manifests itself in indium-doped silicon by the appearance of the so-called P-line in the spectrum of low-temperature photoluminescence (LTPL) [3]. Comparatively, boron-doped Si does not exhibit a equivalent line, instead showing near the associated energy only the well-known electron-hole liquid (EHL) luminescence [4]. Therefore we investigate the influence of various treatments such as illumination, annealing or quenching on the LTPL spectrum of different boron-doped Si samples with emphasis on the behavior of the EHL. Additionally we present EPR studies on the impact of these treatments. [1]: Möller, C. et al., (2013), Light-induced degradation in indium-doped silicon. Phys. Status Solidi RRL, 7: 461-464 [2]: Möller, C. et al., ASi-Sii-defect Model of Light-induced Degradation in Silicon, Energy Procedia, Volume 55, 2014, Pages 559-563 [3]: Lauer, K. et al., "Identification of photoluminescence P line in indium doped silicon as InSi-Sii defect", AIP Advances 5, 017101 (2015) [4]: Peh, K. et al., Low-Temperature Photoluminescence Investigation of Light-Induced Degradation in Boron-Doped CZ Silicon. Phys. Status Solidi A, 219: 2200180.

HL 7.3 Mon 13:00 P2/EG

Atomic layer deposition of iron titanate for use as a photoanode — •NINA MILLER^{1,2}, RYAN KISSLINGER^{1,2}, and IAN SHARP^{1,2} — ¹Walter Schottky Institut Technical University of Munich — ²Physics Department, TUM School of Natural Sciences, Technical University of Munich, Garching, Germany

TiO₂ is of significant importance in the field of energy research. However, to develop it for artificial photosynthesis, the band gap of TiO₂, which is 3.2 eV and consequently absorbs only ultraviolet light, must be paired with a material capable of absorbing visible light. Here, we experimentally explore the effect of depositing thin films of hematite (α -Fe₂O₃) on nanostructured TiO₂ using atomic layer deposition, with a further high-temperature annealing step to produce visible-light absorbing iron titanate (Fe₂TiO₅). Iron titanate may allow enhance charge transfer at the photoanode surface, and serve as a visible light absorbing layer. Furthermore, the TiO₂ nanotube arrays used as the substrate during atomic layer deposition can orthogonalize light absorption with respect to charge separation, leading to enhanced photocatalytic conversion during solar water splitting.

HL 7.4 Mon 13:00 P2/EG

Polaron Transport in BiVO₄ — •SVEN DOLL, TIM RIETH, DAVID VOGL, VIKTORIA F. KUNZELMANN, IAN D. SHARP, and MARTIN S. BRANDT — Walter Schottky Institut and School of Natural Sciences, Technische Universität München, 85748 Garching

Bismuth vanadate (BiVO₄) is a promising photoelectrode material for solar-to-fuel conversion. This semiconductor is particularly interesting considering its strong visible light absorption, efficient charge carrier separation, and favorable quasi-Fermi-level alignment with relevant redox potentials. However, temperature-dependent photoconductivity measurements indicate thermally-activated hopping transport of small polarons, with transport barriers of several hundred meV. To gain further insight into charge carrier transport and the nature of these polaronic states, we explore whether the hopping of the small polarons in BiVO₄ is spin-dependent using electrically detected magnetic resonance. Since such spin-dependent signals are known (e.g., from similar experiments on doped crystalline silicon) to critically depend on the charge carrier density, we evaluate the possibility to use the persistent photoconductivity of BiVO₄ to tune the polaron density. This technique may provide valuable insights into the microscopic transport processes in modern photoelectrodes used for energy conversion. This work was supported by the DFG under Germany's Excellence Strategy - EXC 2089/1 - 390776260.

HL 7.5 Mon 13:00 P2/EG

In silico tuning the properties of inorganic-organic hybrid systems — •MOHAMMED EL AMINE MILOUDI and OLIVER KÜHN — Institute of Physics, Rostock University, Albert-Einstein-Str. 23-24 18059 Rostock

Two-dimensional (2D) materials are expanding the range of processes that can be studied in two dimensions as well as in van der Waals (vdW) heterostructures. Integrating organic molecules into these systems has enormous potential because nature offers a finite number of 2D materials. Still, an almost unlimited range of molecules can be tailored and synthesized with predictable properties. Organic compounds are widely known for their high absorption with low mobility and charge stability, whereas inorganic compounds have comparatively low absorption with excellent charge transport properties. Thus, the formation of vdW heterostructures that combines an inorganic compound with organic molecules potentially offers the advantages of both. Molybdenum disulfide (MoS₂), one of the transition-metal dichalcogenides (TMDs), is one of the most exciting 2D semiconductors holding promises for potential applications in transistors, optoelectronics, and catalysis. Perylenes are widely used dyes whose optical properties can be tuned by chemical modification of the perylene core. Here we report on a systematic study of the structural, electronic, and optical properties of MoS₂/perylene hybrid systems by means of density functional theory. Using different perylenes (perylene orange, perylene diimide, and perylene red) highlights the extent to which property tuning can be achieved in the hybrid system.

HL 7.6 Mon 13:00 P2/EG

Epitaxial growth of GaN buffer layers on Si(111) by reactive magnetron sputtering — •RALF BORGMANN, FLORIAN HÖRICH, JÜRGEN BLÄSING, ANJA DEMPEWOLF, FRANK BERTRAM, JÜRGEN CHRISTEN, GORDON SCHMIDT, PETER VEIT, ANDRÉ STRITTMATTER, and ARMIN DADGAR — Otto-von-Guericke-Universität Magdeburg, FNW-IfP, Universitätsplatz 2, 39106 Magdeburg

GaN is a key material typically grown by MOVPE for high-voltage electronic devices. Reactive sputter epitaxy is an alternative to MOVPE, potentially offering much lower growth cost. Recently, we achieved high quality AlN layers on Si(111) [1] on which (Al,Ga)N layers can be grown. We present study on the effects of ammonia flow and growth temperature on GaN layer quality using MOVPE-grown GaN templates, high purity gases and targets. At T_{growth} ~705 °C and an ammonia flow of ~20 sccm, GaN shows a smooth surface and XRD (0002) ω -FWHMs around 340 arcsec. AlGa_xN layers can be grown in a large composition range by Al- and Ga- co-sputtering resulting in very smooth surfaces. A sputtered 1.4 μ m thick AlN/AlGa_xN/GaN layer stack on Si(111) shows high resistivity and a vertical breakdown field strength >2.5 MV/cm, ideal as buffer for transistor devices. [1] F. Hörich et al., Journal of Crystal Growth 571, 126250 (2021)

HL 7.7 Mon 13:00 P2/EG

Molybdenum disulfide/diselenide deposition by radio frequency sputtering towards facile integration as heterojunction — •OSCAR ALBERTO LOPEZ GALAN^{1,2}, MANUEL RAMOS³, and TORBEN BOLL¹ — ¹Institute of Applied Materials (IAM-WK), Karlsruhe Institute of Technology (KIT), Eggenstein-Leopoldshafen, Germany — ²Institute of Nanotechnology (INT), Karlsruhe Institute of Technology (KIT), Eggenstein-Leopoldshafen, Germany — ³Instituto de Ingeniería y Tecnología, Universidad Autónoma de Ciudad Juárez (UACJ), Ciudad Juárez, Mexico

The fabrication of heterojunctions using transition metal dichalcogenides remains a fundamental challenge in solid-state technology. In this work, we studied vertical MoS₂/MoSe₂ heterojunctions deposited by radio frequency sputtering at 3 thicknesses, 300 nm, 500 nm, and 600 nm. We found a dependency between thickness and crystal structure; the sample with a total thickness of 500 nm presents a crystal size of 64 nm while the thinner and thicker samples appear amorphous. Scanning electron microscopy and Raman spectroscopy reveal the presence of MoS₂ and MoSe₂ distinctly. Measurements by atom probe tomography indicate that MoS₂ and MoSe₂ are not having a sharp interface. This may influence the electrical performance of the device since dangling bonds and lattice mismatch between MoS₂ and MoSe₂ limit the charge carriers flow. Density functional calculations reveal a type-I heterojunction, with a reduced band gap of ~1.0 eV and a potential alignment of 0.5 eV.

HL 7.8 Mon 13:00 P2/EG

Atomic structure of As-modified Si(100) surfaces prepared in CVD ambience — MANALI NANDY¹, AGNIESZKA PASZUK¹, OLEKSANDR ROMANYUK², •CHRIS YANNIC BOHLEMANN¹, AARON FLÖTOTTO³, AARON GIESS¹, PETER KLEINSCHMIDT¹, IVAN GORDEEV², JANA HOUDKOVA², ERICH RUNGE³, and THOMAS HANNAPPEL¹ — ¹Fundamentals of Energy Materials, Institute of Physics, Ilmenau University of Technology, Ilmenau, Germany — ²Institute of Physics, Academy of Sciences of the Czech Republic, Prague, Czech Republic — ³Theoretical Physics 1, Institute of Physics, Ilmenau University of Technology, Ilmenau, Germany

For highly efficient III-V-on-Si devices, a low-defect III-V nucleation and a sharp interface are prerequisites. Stabilization of Si surfaces by arsenic is a promising technological step allowing to grow As-based III-V epitaxial layers in consecutive process steps. Here, we study the atomic structure of Si(100) surfaces prepared in As-rich ambience utilizing MOCVD. Arsenic was supplied either directly via the precursor (TBAs) or indirectly as background As₄. The Si(100):As surfaces were analysed with a multitude of techniques such as STM, LEED, AR-XPS and FTIR after contamination-free transfer to ultra-high vacuum. The experimental results are supported by *ab initio* density functional theory (DFT) calculations. STM scans provide atomic-scale details of As-stabilized Si(100) surface structure consisting of rows of predominately asymmetric dimers. DFT simulations revealed a new stable structure with asymmetric As-Si-H dimers. The presence of hydrogen on the surface was confirmed by FTIR.

HL 7.9 Mon 13:00 P2/EG

Preparation of P- and III-rich GaInP (100) with subsequential water & oxygen exposure — •DAVID OSTHEIMER, MOHAMMAD AMIN ZARE POUR, SAHAR SHEKARABI, AGNIESZKA PASZUK, and THOMAS HANNAPPEL — Technische Universität Ilmenau, Ilmenau, Deutschland

III/V semiconductor multi-junction photoelectrochemical cells enable, either direct or indirect solar-to-fuel conversion with highest efficiencies to date, as their tunable bandgap enables optimal use of the solar spectrum. In tandem devices, GaInP has an appropriate bandgap for a top photoabsorber or a transparent, charge selective contact (window layer). A detailed understanding of the reactions at the semiconductor/electrolyte heterointerface is crucial to tailor the semiconductor surface appropriately to avoid trapping of the photogenerated charge carriers and reduce corrosion. Here, we study interaction of oxygen and water with the mixed-dimer, group-III-rich and phosphorus-rich GaInP (100) surface by combining *in situ* optical spectroscopy and *in situ* photoelectron spectroscopy. The GaInP(100) surfaces were prepared by metal-organic chemical vapor deposition. The surface reconstruction of the as-prepared samples and after exposure was investigated by low energy electron diffraction. We find that the surface reconstruction of the GaInP(100) significantly affects its interaction with water. P-rich GaInP(100) surface shows much higher stability compared to the group-III-rich.

HL 7.10 Mon 13:00 P2/EG

Band energy diagrams of n-GaInP/n-AlInP(100) surfaces and heterointerfaces — •MOHAMMAD AMIN ZARE POUR¹, OLEKSANDR ROMANYUK², DOMINIK C. MORITZ³, AGNIESZKA PASZUK¹, CLÉMENT MAHEU³, SAHAR SHEKARABI¹, KAI DANIEL HANKE¹, DAVID OSTHEIMER¹, THOMAS MAYER³, JAN P. HOFMANN³, WOLFRAM JAEGERMANN³, and THOMAS HANNAPPEL¹ — ¹Technische Universität Ilmenau, Ilmenau, Germany — ²Institute of Physics of the Czech Academy of Sciences, Prague, Czech Republic — ³Technical University of Darmstadt, Darmstadt, Germany

n-AlInP(100) charge selective contacts are commonly grown on n-p GaInP(100) top absorbers in high-efficiency III-V multijunction solar or photoelectrochemi-

cal cells. Understanding the atomic and electronic properties of the GaInP/AlInP heterointerface is crucial for the reduction of photocurrent losses in multijunction devices. We investigated chemical composition and electronic properties of n-GaInP/n-AlInP heterostructures by X-ray photoelectron spectroscopy (XPS). 1-50 nm thick n-AlInP(100) epitaxial layers were grown on n-GaInP(100) buffer layer on n-GaAs(100) substrates by metal organic vapor phase epitaxy. We observed (2x2)/(c(4x2)) low-energy electron diffraction patterns on both AlInP(100) and GaInP(100) as-prepared surfaces. An upward surface band bending probably caused by localized mid-gap electronic states was observed. Pinning of the Fermi level by localized electronic states remained in n-GaInP/n-AlInP heterostructures. A valence band offset of +0.2 eV was derived by XPS and band diagram models for the n-n junctions were suggested.

HL 7.11 Mon 13:00 P2/EG

GaAs/PEDOT:PSS Hybrid Solar Cell Improvement by the Incorporation of Ternary Quantum Dots — •ALEXANDER EHM¹, OLEKSANDR SELYSHCHEV¹, SERHIY KONDRATENKO², and DIETRICH R. T. ZAHN¹ — ¹Semiconductor Physics, TU Chemnitz, Chemnitz D-09107, Germany — ²Taras Shevchenko National University of Kyiv, 01601 Kyiv, Ukraine

Colloidal quantum dots (QD) have gained much interest over recent years due to their absorption and photoluminescence properties, which can be tuned by varying the particle size. Among these, ternary In-based chalcogenide QDs possess the advantage of low toxicity, making them more environmentally friendly candidates for the application in solar harvesting devices for green energy production.

As a prove of concept, colloidal AgInS and CuInS QDs [1] are deposited on n-GaAs(100) substrates in order to incorporate them in hybrid GaAs/PEDOT:PSS solar cells. The deposition is verified and analysed by X-ray photoemission and optical spectroscopy methods as well as atomic force microscopy. A significantly enhanced power conversion efficiency of such solar cells modified by colloidal QDs compared to the devices without QDs is shown by current density-voltage measurements under AM1.5 equivalent illumination.

[1] A. Raevskaya et al., J. Phys. Chem. C 2017, 121, 9032

HL 7.12 Mon 13:00 P2/EG

One-dimensional topological interface states: a novel approach for optical pressure sensors — •JAKOB LINDENTHAL^{1,2}, ANTON WIDULLA¹, JOHANNES BENDUHN¹, and KARL LEO^{1,2} — ¹Dresden Integrated Center for Applied Physics and Photonic Materials, Technische Universität Dresden — ²ct.qmat - Würzburg-Dresden Cluster of Excellence

The research field of nano-optics in connection with topological photonics has quickly evolved over the past decade. Topological considerations in the design of photonic systems open a wide range of possibilities for disorder protection and electric field alignment optimisation. Different material systems and topological setups are discussed in the context of pressure-sensitive nano-optical resonators, demonstrating a novel, highly versatile pressure sensor concept. The demonstrated system combines a compressible optical microcavity with an organic absorber material, which allows highly sensitive pressure-dependent tuning of the mode intensity. The contribution features modelling and characterisation results for systems with different topologies, showing pathways to significant topology-induced sensitivity enhancement. The use of coupled cavities is shown to provide additional sensing information with potential for industrial implementation.

HL 7.13 Mon 13:00 P2/EG

Electric-field-induced second harmonic generation in amorphous materials for hybrid photonic structures — •LAURIDS WARDENBERG, BENITO BUNK, and JÖRG SCHILLING — Martin-Luther-Universität Halle-Wittenberg, Halle (Saale), Germany

We investigate electric-field-induced second harmonic generation (EFISH) on different amorphous materials, e.g. a-Si and As₂S₃ films. These materials have sizeable $\chi^{(3)}$ values but a vanishing $\chi^{(2)}$ due to their amorphous structure. Applying a dc-voltage we gain the ability to create a quasi- $\chi^{(2)}$ and perform second order nonlinear optical processes. The possibility to manipulate value and polarity of the created quasi- $\chi^{(2)}$ allows an unprecedented control over these second order wavelength conversion processes. Introducing a way to electrically modulate and switch this nonlinearity, is of high practical interest for the realization of nonlinear active hybrid photonic structures.

Since EFISH is strongly associated with the $\chi^{(3)}$, we use the z-scan technique to determine the real and the imaginary parts of the $\chi^{(3)}$ of the investigated films. Subsequently chromium contacts were deposited on the films and electric fields up to 10⁵ V/m were applied. Our voltage and intensity dependent SHG measurements show a quadratic dependence on input intensity and applied DC field, which is a clear indicator for EFISH. The nonlinear optical measurements are mainly performed at a wavelength of 1030 nm using a femtosecond laser system supplying 200 fs pulses at a repetition rate of 1 kHz. Additional measurements at wavelengths above 1200 nm, which are of interest for silicon photonics, will be demonstrated as well.

HL 7.14 Mon 13:00 P2/EG

Excitons in lithium niobate and their impact on non-linear optical properties — •AGNIESZKA KOZUB, WOLF GERO SCHMIDT, and UWE GERSTMANN — Universität Paderborn, Department Physik, 33095 Paderborn, Germany

The influence of self-trapped and vacancy-trapped excitons on the lithium niobate (LiNbO₃, LN) dielectric function and nonlinear susceptibility is calculated based on density-functional theory. The PBE0 hybrid functional is used for the description of electron exchange and correlation. The dielectric function is obtained by solving the Bethe-Salpeter equation. This yields an absorption peak at 2.6 eV, in perfect agreement with experiment [1]. The second- and third order nonlinear susceptibility tensors are obtained from a Berry-phase formulation of the dynamical polarization. A strong enhancement of the susceptibilities for photon energies in the band gap region is noted to arise from localized excitons.

[1] L.E. HALLIBURTON, K.L. SWEENEY and C.Y. CHEN, Nuclear Instruments and Methods in Physics Research B1 344-347 (1984)

HL 7.15 Mon 13:00 P2/EG

Structured Gradient Index Silicon (Oxy)Nitride Layers for Antireflection in Silicon Solar Cells — •FLORIAN DAMERAU¹, MARIA GAUDIG¹, RALF WEHRSPORN¹, PRERAK DHAWAN², CARSTEN ROCKSTUHL², and ALEXANDER SPRAFKE¹ — ¹Institute of Physics, Martin Luther University Halle-Wittenberg, Heinrich-Damerow-Str. 4, 06120 Halle (Saale), Germany — ²Institute of Theoretical Solid State Physics, Karlsruhe Institute of Technology, 76131 Karlsruhe, Germany

The frontside of crystalline silicon (c-Si) solar cells oftentimes is micro- or nanotextured to increase light in-coupling, and thus conversion efficiency. Current state-of-the-art textures comprise micron sized pyramidal structures, whereas future ultrathin c-Si solar cells demand new approaches such as submicron nanophotonic structures. However, directly nanotexturing the Si surface degrades its electronic properties strongly, such that a possible gain in absorption does not necessarily translate into an increased conversion efficiency. In this work, we aim to maintain the electronic properties of a planar c-Si interface by leaving it intact but place a nanophotonic structure on top. This structure consists of a nanostructured SiO_xN_y layer. Moreover, changing the stoichiometry (x,y) during deposition enables us to smoothly vary its refractive index between $n \approx 1.5 - 3.0$. Inspired by transformation optics, we aim to mimic the optical properties of strongly non-planar textures such as black silicon by a planar layer of smoothly varying spatial-dependant refractive index. In this contribution we will present experimental results on the microstructure as well as on the optical properties of our fabricated structures.

HL 7.16 Mon 13:00 P2/EG

Exciton-polariton emission in copper halides — •E. KRÜGER¹, S. MERKER², S. BLAUROCK², R. HILDEBRANDT¹, A.L. PEREIRA¹, L. KÄFERSTEIN¹, H. KRAUTSCHEID², M. GRUNDMANN¹, and C. STURM¹ — ¹Universität Leipzig, Felix-Bloch-Institut für Festkörperphysik, Germany — ²Universität Leipzig, Institut für Anorganische Chemie, Germany

Copper halides (CuI, CuBr, and CuCl) have recently attracted research interest since they combine intrinsic p-type conductivity with large bandgaps (3.1 eV - 3.4 eV) and high exciton binding energies (62 meV - 190 meV), making them promising candidates for applications in transparent optoelectronics [1].

Here, we present an overview of the optical properties of solution grown Cu-halide bulk single crystals, focusing especially on spectral- and time-resolved measurements of the near-band-edge luminescence for temperatures between 10 K and room temperature. The line shape of the emission lines at low temperatures is interpreted in terms of exciton-polaritons and their dispersion relation [2]. The different decay characteristics of free and localized states are explained by their coupled interaction. In addition to observation of an anomalous temperature-dependent bandgap shift to higher energies with increasing temperature we present in detail the temperature-dependent decay characteristics of the polariton emission and discuss the corresponding relaxation mechanisms.

[1] M. Grundmann et al., pss (a) **210**, 1671 (2013)

[2] E. Krüger et al., APL Mater. **9**, 121102 (2021)

HL 7.17 Mon 13:00 P2/EG

Persistent spectral holeburning of the donor-bound exciton transition in ultra-pure ²⁸Si:P — •NICO EGGELING¹, MICHAEL OESTREICH¹, EDUARD SAUTER¹, JENS HUEBNER¹, and N. V. ABROSIMOV² — ¹Leibniz Universität Hannover, Germany — ²IKZ Berlin, Germany

We utilize persistent spectral hole burning to determine the origin of dynamic and static spectral broadening of the donor-bound exciton transition in ultra-pure ²⁸Si:P with 99.995% isotopic enrichment [1]. From time-dependent measurements of the spectral hole width and frequency shift we try to determine the impact of donor-acceptor interaction on the spectral transition broadening. The donor-acceptor pair recombination is on the order of seconds in the investigated sample with a donor concentration of $1.2 \times 10^{15} \text{ cm}^{-3}$ and an acceptor concentration of $4.6(10) \times 10^{13} \text{ cm}^{-3}$. We expect to observe an impact of the recombination dynamics on the measured frequency and width of spectral holes. These results could lead to a better understanding of spin initialization for

donors in ²⁸Si:P, which are a promising candidate for quantum computation [2]. [1] Sauter, E., Abrosimov, N. V., Hübner, J., & Oestreich, M., Phys. Rev. Lett. **126**(13), 137402 (2021).

[2] Morello, A. et al., Adv. Quant. Tech. **3**(11), 2000005 (2020).

HL 7.18 Mon 13:00 P2/EG

Manipulating the luminescence of a rare-earth doped spacer — •SÖREN LERNER¹, FRANCESCO VITALE¹, THOMAS SIEFKE², UWE ZEITNER^{2,3}, and CARSTEN RONNING¹ — ¹Institute of Solid State Physics, Friedrich-Schiller Universität, Helmholtzweg 3, 07743 Jena, Germany — ²Institute of Applied Physics, Friedrich Schiller Universität, Albert-Einstein-Straße 15, 07745 Jena, Germany — ³Fraunhofer Institute for Applied Optics and Precision Engineering IOF, Albert-Einstein-Straße 7, 07745 Jena, Germany

The coupling of rare-earth elements with surface plasmon polaritons can lead to a change of their emission properties. We implant rare-earth elements in a nanometric silica spacer on top of an aluminum layer by ion beam implantation. The luminescence properties of such systems were examined by photo- and cathodoluminescence measurements. Placing zinc oxide nanowires on top of this two-layer system allows for additional coupling with surface plasmon polaritons, which generate a high electric field density in the spacer layer. The respective effects and the possibilities of tailoring the emission will be discussed.

HL 7.19 Mon 13:00 P2/EG

Coupling of Excitons and Plasmons with Phonons in Raman scattering for CuI — •R. HILDEBRANDT¹, S. BLAUROCK², H. KRAUTSCHEID², M. GRUNDMANN¹, and C. STURM¹ — ¹Universität Leipzig, Felix Bloch Institute for Solid State Physics, Germany — ²Universität Leipzig, Institute of Inorganic Chemistry, Germany

CuI is an intrinsic p-type with potential for opto-electronic applications. Via resonance effects, various of its fundamental properties may be accessed. For CuI we investigate phonon-exciton- and phonon-plasmon-interactions by Raman spectroscopy.

We present Raman spectra with excitation wavelength of 532 nm, 355 nm and 325 nm for single crystals and thin films. Each excitation wavelength indicates different fundamental Raman scattering processes. With 532 nm fundamental modes as well as second order Raman signals are observed and analyzed [1]. For doped samples with $p = 10^{18} \text{ cm}^{-3}$, phonon-plasmon coupling is observed which is compared with Hall measurements. By 355 nm excitation, slightly above the bandgap, a phonon damped-plasmon mode coupling modifies the Raman spectra [2]. Finally with a 325 nm a transition close to $E_g + \Delta_0$, indicates a cascade exciton scattering process. This is dominated by the Fröhlich interaction and n-LO overtones up to $n = 7$ are observed [3]. For each excitation wavelength, an overview of possible applications and possible limits for CuI is shown.

[1] J. Birman, J. Phys. Rev., **131**, 1489, 1963.

[2] A. Mlayah et al., J. Appl. Phys., **69**, 4064, 1991.

[3] Y. Zhang, J. Semicond., **40**, 091102, 2019.

HL 7.20 Mon 13:00 P2/EG

Raman spectra of CuI alloys with Ag and Br — •A.L. PEREIRA¹, R. HILDEBRANDT¹, J. BREDOW¹, C. DETHLOFF¹, V. GOTTSCHALCH², S. VOGT¹, H. KRAUTSCHEID², M. GRUNDMANN¹, and C. STURM¹ — ¹Universität Leipzig, Felix Bloch Institute for Solid State Physics, 04103 Leipzig, Germany — ²Universität Leipzig, Institute of Inorganic Chemistry, 04103 Leipzig, Germany

CuI is a p-type semiconductor with a wide band gap of 3.1 eV that has potential for (opto-) electronic applications [1]. By alloying CuI with isoelectronic Ag or Br its properties such as e.g. the charge carrier concentration, lattice constant or band gap can be tuned.

We present our investigations on CuI alloys and their phonon properties with Raman spectroscopy. Ag_xCu_{1-x}I and CuBr_xI_{1-x} (both $0 \leq x \leq 1$) thin films were produced with various deposition techniques such as solid-state reaction, close distance sublimation, sputter deposition and pulsed laser deposition. Raman spectroscopy measurements were conducted at low temperatures and the phonon modes were analyzed regarding their energetic position, broadening and intensity. This was supported by an oscillator strength model [2]. The Cu(Br,I) alloy revealed a nonlinear dependence of the Raman shift on the composition. In the (Ag,Cu)I alloy an apparent three-mode behavior due to a defect mode was observed and characterized.

[1] E. Krüger, et al., Appl. Phys. Lett. **113**, 172102, 2018.

[2] G. Livescu, et al., J. Phys. C: Solid State Phys. **19** 2663, 1986.

HL 7.21 Mon 13:00 P2/EG

Excited-state properties of PbWO4 from ab initio calculations — •ATHER AHMAD and KAI-THOMAS BRINKMANN — II. Phys. Inst. Gießen

Fast response, high density and radiation hardness make lead tungstate (PbWO₄ or PWO) a well suited scintillator for an electromagnetic calorimeter. Lead tungstate crystals are already used as working material in various experiments, e.g. the CMS at the LHC in CERN. New generation crystals (PWO-II) with improved properties were developed for the PANDA experiment at FAIR in Darmstadt. To reduce absorption of the scintillation light within the crystals,

the lead tungstate is doped with Lanthanum and Yttrium. This results in a change of the electronic and optical properties.

In order to assess the functionality of the calorimeter, we first need to analyse these electronic and optical properties of lead tungstate. In our work, we investigate these properties of lead tungstate containing different impurities and defects with ab initio calculations to derive its radiation hardness and scintillation mechanism.

This project is supported by HFHF and HGS-hire

HL 7.22 Mon 13:00 P2/EG

Multiphoton absorption induced photoluminescence in CuI — •ANDREAS MÜLLER¹, SEBASTIAN HENN¹, EVGENY KRÜGER¹, STEFFEN BLAUROCK², HARALD KRAUTSCHEID², MARIUS GRUNDMANN¹, and CHRIS STURM¹ — ¹Felix-Bloch-Institut für Festkörperphysik, Universität Leipzig, Linnéstr. 5, 04103 Leipzig, Germany — ²Institut für Anorganische Chemie, Universität Leipzig, Johannisallee 29, 04103 Leipzig, Germany

Two- and three-photon absorption induced photoluminescence (2PAPL, 3PAPL) are nonlinear optical processes useful for energy upconversion or, in contrast to near-to-the-surface single-photon absorption, excitation within the bulk material.

In this work, we report on low temperature (30 K) 2PAPL and 3PAPL in transparent conducting CuI crystals ($E_g = 3.1$ eV), analyzed employing excitation energy and density-dependent, steady-state, and time-resolved photoluminescence. Using an excitation energy that corresponds to half of the bandgap energy, the observed intensity dependence on the excitation power shows an almost parabolic behavior. By a further reduction of the photon energy, the cubic contribution of the excitation power on the intensity increases, and for low excitation energies, an almost cubic behavior is obtained. We describe the experimental findings, taking into account the sum of the two- and three-photon transition rates and including the Gaussian spectral intensity distribution of the laser. Through this analysis, the ratio of the cross-sections for the two- and three-photon absorption is estimated to be 10^{-5} cm²/s.

HL 7.23 Mon 13:00 P2/EG

Optical properties of the organic semiconductor Dimethylantranthiophene (DMADT) — •ANNCHARLOTT KÜSBER and MARTIN KNUPFER — IFW Dresden, Helmholtz Straße 20, D-01069 Dresden, Germany

This work presents an analysis of the optical properties of anti- and syndimethylantranthiophene. We have produced 120 nm thick thin films by physical vapour deposition. Using optical spectroscopy, we were able to characterize the films in the visible range. Davydov splitting, due to the existence of two molecules in the unit cell, was observed. Besides that, we measured the exciton dispersion by using electron energy-loss spectroscopy. There we found a positive dispersion of the lowest lying excitation. Comparing the measured values and the calculated coupling strengths, we came to the conclusion that both materials are very weak J-aggregates and that charge transfer exciton coupling is the dominant process and determines the delocalization of the lowest lying excitations.

HL 7.24 Mon 13:00 P2/EG

Highly dipolar molecule on single crystals: Impact of chemical affinity on the interface formation — •BARIS ÖCAL and SELINA OLTHOF — Department of Chemistry, University of Cologne, Greinstraße 4-6, 50939 Cologne, Germany Merocyanines are functional dyes with interesting electronic properties due to their resonant structure between charged and uncharged states. Their bandgap can be widely tuned via the donor and acceptor strength, which makes them interesting as active material in organic-based solar cells, especially since they show very strong absorption. Their physical properties can be further improved by ordering them. The ordering of the molecules is closely related to initial growth on the substrate underneath and interaction between this substrate and molecule. In my work, I investigate the effect of substrate/molecule and molecule/molecule interactions on the electronic structure by photoelectron spectroscopy methods. Highly dipolar HB238 merocyanine has been chosen to observe the chemical interaction and its effect of the charge states of the molecule easier. Surfaces such as SiC/graphene, Au(100), Ag(100) and Cu(100) are used as templating substrates due to their different chemical affinity and ordered structure. Thickness dependent X-ray Photoelectron Spectroscopy (XPS) measurements helps us to understand the chemical effect of substrate on the charge states, while Ultraviolet Photoelectron Spectroscopy (UPS) measurement gives information on the molecular phase changes such as dimerization, orientation change. We find that chemical interaction of the substrate significantly affects molecule/molecule interaction.

HL 7.25 Mon 13:00 P2/EG

Spontaneous orientation polarization in phosphine oxides and how to control it — •ALBIN CAKAJ, MARKUS SCHMID, ALEXANDER HOFMANN, and WOLFGANG BRÜTTING — Institut für Physik, Universität Augsburg, Germany

The orientation of small organic molecules in amorphous thin films prepared by vapor-deposition is an important aspect in further improvement of organic semi-

conductor devices. This feature can influence the optical and electrical properties of organic light emitting diodes (OLEDs) drastically. Due to their asymmetric molecular structure, microscopic properties like the permanent dipole moment (PDM) can show preferential alignment and lead to a macroscopic film polarization in the organic layer. This so-called spontaneous orientation polarization (SOP) affects the charge injection and accumulation behaviour in a device. In our studies, we investigated the electrical and optical orientation of a group of organic molecules, characterized by P=O double bonds, and how to control it by their design and the film-growth conditions. Many of these phosphine oxides have a large PDM, due to a strong electronegative oxygen. However, the magnitude of their SOP is often affected by the presence of multiple molecular conformers. Thus, using less polar species with only one P=O bond yields superior performance with record-high SOP of up to 160mV/nm, even though optical measurements hint to almost no preferred orientation on average.

HL 7.26 Mon 13:00 P2/EG

Impact of solution processing on the photophysical properties of TADF emitters — •KONSTANTIN RAUSCH, RISHABH SAXENA, and ANNA KÖHLER — Soft matter Optoelectronics, University of Bayreuth, Germany

Continuous innovation of thermally activated delayed fluorescence (TADF) compounds has led to the rapid development of these materials as emitters in efficient vacuum-deposited organic light emitting diodes (OLEDs). However, the cost of device fabrication, inefficient use of materials and limitation on pixel size are some detracting features of vacuum-deposition. An alternative cost- and materials-efficient fabrication technique is solution processing. In this regard, it is important to understand the impact of different processing conditions, such as varying solvents and host materials, on the photophysical properties of TADF emitters. In general, a donor-acceptor (D-A) strategy is adopted for the chemical design of TADF emitters. Recent studies suggest that conformational flexibility associated with the D-A dihedral angle leads to a distribution of reverse intersystem crossing rates (k_{RISC}); a parameter that determines the efficiency of the TADF process. In this study, we perform inverse Laplace transform fitting of emission decay, obtained using time-resolved photoluminescence measurements, to extract this distribution. Furthermore, we investigate the impact of different film-preparation methods (spin-coating and evaporation), matrix polarity and conformational rigidity of TADF emitter on the RISC rate distribution with an aim to optimize the performance of solution-processed TADF OLEDs.

HL 7.27 Mon 13:00 P2/EG

single molecule spectroscopy of emitters in hexagonal boron nitride(hBN) — •OSAMA FAROOQI and KLAS LINDFORS — department of chemistry, university of cologne

Efficient interaction of light with atoms or molecules has been found crucial in the study of materials that can be used in the development of high-speed communication devices [1]. The central goal of this project is to observe and investigate the light emission and absorption processes in heterostructures of two- and one-dimensional materials and single emitter molecules.

Previously, single terrylene diimide (TDI) molecules on glass substrate have been investigated using single molecule spectroscopy. In order to address the problem of stability of the molecules, hBN is used to encapsulate emitter molecules to avoid chemical reactions with the ambient environment. The preliminary data of time traces of triisopropylsilyl pentacene (TIPS-pentacene) molecules encapsulated in hBN flakes shows that the molecules do not get photobleached over 1 hour at room temperature. However, fast photoblinking was observed in the time traces of the molecules. The cause of fast photoblinking could be the interaction of the molecules with close-by two-level systems, which appears to be related to hBN flakes.

Reference [1] Toninelli, C. et al. Single organic molecules for photonic quantum technologies. Nat. Mater. 1-14 (2021).

HL 7.28 Mon 13:00 P2/EG

Electronic and optical properties of p-type delafossite transparent conducting oxides: Density Functional Theory calculations — •MOUFDI HADJAB^{1,2} and OLGA GUSKOVA² — ¹Mohamed Boudiaf University of Msila, Msila, Algeria — ²IPF Dresden, Germany

Transparent conducting oxides (TCO) possessing high optical transparency and electrical conductivity have been studied widely due to their applications in optoelectronics. Delafossite materials with chemical formula AIBIII₂O₂ are among the promising p-type TCOs. In this study, we have investigated physical properties of three novel semiconductors to address some problems related to the photovoltaic industry. The structural, electronic and optical properties of delafossite transparent conducting oxides CuMO₂ have been studied using the Full-Potential Linearized Augmented Plan Wave method based on DFT as implemented in Wien2k computational code. The LDA and PBE generalized gradient approximation have been utilized as the exchange-correlation term for calculating the structural and electronic parameters. Moreover, Tran-Blaha modified Beck-Johnson potential has been used to achieve better degree of accuracy in calculations of the electronic and optical properties. The observations have been compared with published theoretical and experimental data. The ternary de-

lafossite transparent conducting oxide compounds can be considered as an alternative material in photovoltaic applications.

HL 7.29 Mon 13:00 P2/EG

Simulating multi-component target ablation: A new pulsed laser deposition technique — •ARNE JÖRNS, HOLGER VON WENCKSTERN, and MARIUS GRUNDMANN — University of Leipzig, Felix Bloch Institute for Solid State Physics, Semiconductor Physics Group

Laterally and radially segmented targets allow the fabrication of functional thin films with lateral and vertical composition spreads, respectively [1]. The latter also enables the creation of material libraries consisting of homogeneous thin films with discrete material composition. However, fabrication of such targets is technically demanding with respect to powder blending, insufficient hardening or thermic decomposition due to deviating sintering temperatures of the source powders for the respective segments.

In this work we present a new target design and deposition technique for pulsed laser deposition in order to create vertical composition spreads as well as discrete composition material libraries but bypassing the above mentioned drawbacks. Simulations for the expected material contents will be presented. Then, experimentally determined elemental distributions and growth rates are compared to calculated values. Electrical and optical properties of samples obtained by such techniques will be reported.

[1] H. von Wenckstern et al., Phys. Status Solidi 2020, 257, 1900626

HL 7.30 Mon 13:00 P2/EG

Wide bandgap aeromaterials and prospects for their applications — •VLADIMIR CIOBANU, TUDOR BRANISTE, EDUARD MONAICO, and ION TIGINYANU — National Center for Materials Study and Testing, Technical University of Moldova, Chisinau, Moldova

We report on the fabrication of aeromaterials based on GaN, Ga₂O₃, TiO₂ and Zn₂TiO₄ using hydride vapor phase epitaxy (HVPE) or Atomic Layer Deposition (ALD) approaches. The fabrication process is based on growth of the preferred material on sacrificial templates consisting of interconnected ZnO microtraps. During the epitaxial growth of GaN at high temperatures and corrosive environment, the ZnO is etched away and, consequently, hollow microtraps with the wall thickness of the tubes in the range of 20 - 100 nm are obtained. Further, GaN can be transformed into Ga₂O₃ through an annealing process at temperature as high as 800 °C. Alternatively, ALD approach is used to fabricate aero-TiO₂ or aero-Zn₂TiO₄ materials using sacrificial ZnO templates.

The fabricated materials demonstrated new interesting properties: aero-GaN exhibits good electromagnetic shielding in X-band and THz region, on the other hand aero-Ga₂O₃ is completely transparent at GHz and THz frequencies, up to 3 THz. We also established that aero-GaN is characterized by dual hydrophilic-hydrophobic behavior. This phenomenon enabled one to demonstrate novel liquid marbles. Due to high active surface area of developed aero-Ga₂O₃ decorated with noble metal nanodots, aero-TiO₂ and aero-Zn₂TiO₄, these materials are shown to be promising for photocatalytic applications.

HL 7.31 Mon 13:00 P2/EG

Graded Zn_xMg_{1-x}O layers as building blocks for ultra-compact wavemeters — PHILIPP FIRME, •CHRISTOPH BRUNHUBER, LUKAS TREFFLICH, PETER SCHLUPP, DANIEL SPLITH, HOLGER VON WENCKSTERN, CHRIS STURM, and MARIUS GRUNDMANN — Universität Leipzig, Felix Bloch Institute for Solid State Physics, 04103 Leipzig, Germany

Recently, a new design for a monolithic, ultra-compact wavemeter was proposed, which can be used in a wide spectral range [1]. The building blocks of this wavemeter are two vertically stacked, photosensitive layers, separated by a transparent, insulating layer. In order to achieve a spectral sensitivity, the top layer must consist of a material with a vertical absorption gradient. Here, we discuss the suitability of vertically graded Zn_xMg_{1-x}O layers as top layer of such an ultra-compact wavemeter with wurtzite photosensitive ZnO layer as backside. The layers were deposited by pulsed laser deposition, using a vertical continuous composition spread (VCCS-PLD) technique. In doing so, we were able to achieve out-of-plane composition gradients from $x = 1.0$ up to $x \approx 0.5$. XRD $2\theta - \omega$ -scans do not indicate a phase separation, and confirm the wurtzite phase. The Mg incorporation was also confirmed by photoluminescence spectroscopy. The suitability of the films as building blocks for the wavemeter was tested by photocurrent measurements. By radiation with monochromatic light of different wavelengths, a response similar to the theoretically calculated one [1] is obtained.

[1] M. Grundmann. Phys. Stat. Sol. A 215, 1800651 (2018)

HL 7.32 Mon 13:00 P2/EG

Synthesis of bismuth ferrite hollow spheres and their application in the photocatalytic degradation of dyes — •VALERIA SANCHEZ¹, THOMAS CADENBACH², ALEXIS DEBUT³, KARLA VIZUETE³, and MARIA J. BENITEZ¹ — ¹Departamento de Física, Facultad de Ciencias, Escuela Politécnica Nacional, Ladrón de Guevara E11-253, Quito, Ecuador — ²Colegio de Ciencias e Ingenierías, Universidad San Francisco de Quito, Diego de Robles y Vía Inter-

ceánica, Quito, Ecuador — ³Centro de Nanociencia y Nanotecnología, Universidad de las Fuerzas Armadas ESPE, Av. Gral. Rumiñahui s/n, Sangolquí, Ecuador

In this work, we show the synthesis and application of next generation semiconductor photocatalysts, i.e. GdxBi_{1-x}FeO₃ ($x = 0, 0.05, 0.10, 0.15$) hollow spheres which function as both, an advanced adsorption material and photocatalytic active semiconductor. The presented spheres were prepared by two distinct novel synthetic protocols, i.e. via a citric acid/urea/ethylene glycol assisted hydrothermal method and via an evaporation induced self-assembly strategy. In both cases, we study the mechanism of formation of phase pure GdxBi_{1-x}FeO₃ hollow spheres with a narrow size distribution by varying synthetic conditions such concentration, temperature and treatment time. The samples were characterized by X-ray powder diffraction, scanning electron microscopy and UV-vis diffuse reflectance spectroscopy. All synthesized materials were applied in the photocatalytic degradation of dyes under visible light irradiation. The photocatalysts show superior efficiencies which outperformed previously reported BiFeO₃ materials.

HL 7.33 Mon 13:00 P2/EG

Monitoring Phase Transitions in (Hot-)Pressed FAPbI₃ Films by In-Situ Reflection Measurements — •LORENZ KIEL¹, CHRISTINA WITT¹, KONSTANTIN SCHÖTZ¹, NICO LEUPOLD², RALF MOOS², ANNA KÖHLER¹, and FABIAN PANZER¹ — ¹Soft Matter Optoelectronics, University of Bayreuth, Bayreuth 95440, Germany — ²Department of Functional Materials, University of Bayreuth, Bayreuth 95440, Germany

In recent years, a remarkable increase in efficiencies of halide perovskite-based solar cells has been achieved. Record cells on laboratory scale, realized with the perovskite formamidinium lead iodide (FAPbI₃), are now competing with established silicon devices.[1] However, phase stability of FAPbI₃ is still challenging as the photoactive black α -phase is prone to degrade in the inactive yellow δ -phase or intermediate orange and red phases.[2, 3] To address this issue, we evaluate the temperature and pressure dependence of occurring phase transitions using in-situ reflection measurements during (hot-)pressing δ -FAPbI₃ powder, and analyze associated strain in the resulting thick films. We show that for our powder based thick films the phase transitions occur at significantly lower pressure and temperature compared to literature reports. The correlation of these parameters with resulting film properties like film morphology suggests strain to be decisive for the phase transition and phase stability.

[1] Jeong et al. Nature 2021, 592.

[2] Cordero et al. Nanomaterials 2021, 11.

[3] Cordero et al. J. Phys. Chem. C 2020, 124.

HL 7.34 Mon 13:00 P2/EG

Phase diagram of two-dimensional ferroelectric large polarons — •FLORIAN KLUBENSCHIEDL, GEORGIOS KOUTENTAKIS, and MIKHAIL LEMESHKO — Institute of Science and Technology Austria (ISTA), Am Campus 1, 3400 Klosterneuburg, Austria

We present a minimal, coarse-grained, two-dimensional model of charge transport in lead halide perovskites, which provides an intuitive explanation for the recently proposed formation of ferroelectric large polarons [1]. The phase-diagram analysis reveals the presence of three phases characterized by the distinct order of the molecular dipole moments which is strongly dependent on the tunneling anisotropy of the carriers. The most striking outcome is the formation of ferroelectric domains that amplify the anisotropy in the carrier tunneling dynamics which has been argued to lead to improved optoelectronic properties. These results provide the groundwork for realizing a top-down approach for understanding the complex carrier dynamics in hybrid organic-inorganic perovskites.

[1] F. Wang, Y. Fu, M. E. Ziffer, Y. Dai, S. F. Maehrlein, and X.-Y. Zhu. Journal of the American Chemical Society 2021 143 (1), 5-16. DOI: 10.1021/jacs.0c10943

HL 7.35 Mon 13:00 P2/EG

Optical spectroscopy on hBN-encapsulated perovskites — •LISA BÖHME, EUGEN KLEIN, RICO SCHWARTZ, CHRISTIAN KLINKE, and TOBIAS KORN — University of Rostock, Institute of Physics, 18059 Rostock, Germany

Perovskites shows promising optoelectronic properties that can be used in a wide range of technologies. For example, they play a central role in the development of more efficient and low-cost solar cells and are also used in LED or low-threshold lasers. However, they pose experimental challenges that need to be solved: perovskites degrade in contact with air and lose their attractive properties. A possibility to avoid this is encapsulation in hexagonal Boron Nitride (hBN). We have examined how lead-halogen perovskites with organic ligands can be encapsulated and whether they retain their stability. We use the Scotch-Tape method to exfoliate hBN crystals and deposit perovskite crystals on top using drop casting. To check the successful encapsulation of the perovskites, photoluminescence measurements were taken over different time periods and at different temperatures. Our measurements showed that the fully encapsulated perovskites remained stable for more than ten days.

HL 7.36 Mon 13:00 P2/EG

Reflection Electron Energy Loss Spectroscopy of Organic and Perovskite Semiconductors — •SEREN DILARA ÖZ and SELINA OLTROFF — Department of Chemistry, University of Cologne, Greinstraße 4-6, 50939 Cologne, Germany
The analysis of fundamental semiconductor properties, such as energy level positions and bandgaps, are important to enhance our understanding of these materials and to further improve their performance in applications. In this context, many spectroscopic tools such as ultraviolet photoelectron spectroscopy or UV-vis measurements are exploited. In this project, we explore the use of reflection electron energy loss spectroscopy (REELS) which is a rarely used technique in order to investigate the surface density of states (DOS) and bandgap of organic and perovskite based semiconductor materials.

This measurement technique records the energy loss due to inelastic electron scattering processes which excites electronic transitions. It presents an intriguing technique to gain insights on the joint valence and conduction band density of states over a wide energy range. Due to the extreme surface sensitivity, the band gap of ultra-thin layers can be accessed.

In this work, we try to understand the observed energy loss spectra in order to establish guidelines to investigate surface properties of semiconductor materials. For that reason, information gathered using REELS are compared to UPS, IPES, and UV-vis measurements. Our results show that the REELS technique can be used as an effective tool to explore surface properties of perovskite and organic semiconductors.

HL 7.37 Mon 13:00 P2/EG

Combinatorial synthesis of BaZrS₃ thin films: Influence of off-stoichiometry on optoelectronic and electronic properties — •ADRIANA RÖTTGER, MARIN RUSU, HANNES HEMPEL, DANIEL ABOU-RAS, ORESTIS KARALIS, İBRAHİM SIMSEK, and THOMAS UNOLD — Helmholtz-Zentrum Berlin für Materialien und Energie, Berlin, Deutschland

The chalcogenide perovskite BaZrS₃ is composed of earth-abundant elements and has potential applications for photovoltaic energy conversion. In this work, compositionally graded BaZrS₃ thin films are synthesized from oxide precursors deposited by pulsed laser deposition. The compositional gradient in a range of $0.8 < [\text{Ba}]/[\text{Zr}] < 1.3$ enables a high throughput characterization approach of structural, optical and optoelectronic properties. Sulfurization was performed in a tube furnace using H₂S in Ar gas at 1000°C. For all the examined compositions, BaZrS₃ forms as the main phase. Under Ba excess, Ruddlesden-Popper phases Ba₃Zr₂S₇ and Ba₄Zr₃S₁₀ emerge, while excess Zr forms ZrO₂ on the Zr-rich side. Optical absorption spectroscopy mapping shows that the band-gap energy exhibits a minimum at $1.0 < [\text{Ba}]/[\text{Zr}] < 1.1$ and ranges from 1.65 to 2.1 eV. Analysis of the optical constants n and k by ellipsometry mapping verified this trend. Low-temperature photoluminescence spectroscopy revealed deep defect states present for all compositions. Using time-resolved photoluminescence spectroscopy and optical -pump-terahertz probe spectroscopy, we found longer carrier lifetimes on the Ba-rich side, while the Zr-rich side features a higher mobility of charge carriers.

HL 7.38 Mon 13:00 P2/EG

Defect tolerance of halide perovskites solar absorbers via machine learning — •ANOOP K. CHANDRAN¹, CHRISTOPH FRIEDRICH¹, UWE RAU², STEFAN BLÜGEL¹, THOMAS KIRCHARTZ², and IRENE AGUILERA³ — ¹Peter Grünberg Institute and Institute for Advanced Simulation, Forschungszentrum Jülich, Germany — ²IEK5-Photovoltaik, Forschungszentrum Jülich, Germany — ³Institute of Physics, University of Amsterdam, The Netherlands

The deformation potential measures the changes in the bandgap of materials upon compression of the bonds, which helps to identify the bonding or anti-bonding nature of the valence and conduction bands. Previous works indicate that the bonding or anti-bonding nature impacts a material's tendency to exhibit shallow or deep intrinsic defect levels. Our high-throughput search is based on all-electron density functional theory calculations. Among 1173 studied halide perovskites, only 18% present a favourable anti-bonding valence band. We also establish the calculation of the deformation potential as an effective way to determine the bonding or anti-bonding nature near the band edges. However, subsequent supercell calculations reveal no explicit connection between the nature of the band edges and the defect tolerance. Deep learning neural networks require large datasets. To overcome this limitation, we devised a novel approach for the one-shot binary classification of the deformation potentials. Instead of learning to classify a single material, the network learns the similarity or the difference between two materials.

HL 7.39 Mon 13:00 P2/EG

Dressed-state analysis of two-color excitation schemes — •THOMAS BRACHT^{1,2}, TIM SEIDELMANN³, YUSUF KARLI⁴, FLORIAN KAPPE⁴, VIKAS REMESH⁴, GREGOR WEIHS⁴, VOLLRATH MARTIN AXT³, and DORIS E. REITER² — ¹Institut für Festkörpertheorie, WWU Münster, DE — ²Condensed Matter Theory, TU Dortmund, DE — ³Theoretische Physik III, Universität Bayreuth, DE — ⁴Institut für Experimentalphysik, Universität Innsbruck, AT

For coherent control of a few-level quantum emitter, typically pulses with an energy resonant to the transition energy are used, which requires sophisticated

filtering of the signal. However, two-color excitation protocols were recently employed to circumvent the necessity for filtering.

Here I present an analysis of two-color excitation schemes, using the laser dressed states of the system. It can be shown, that the two-color excitation approach can be understood as a driving of transitions between the dressed states. We investigate how these transitions depend on the pulse parameters and explain how the different combinations of laser energies can excite the system. In addition to the results for a simple two-level system (2LS), we consider a three-level exciton-biexciton system (3LS) that is typically found in semiconductor quantum dots and often used to generate entangled photon pairs. While in the 2LS, we can give clear conditions for the applicability, in the 3LS, due to strong state mixing, the conditions are less obvious. Nonetheless, we can find regimes of parameters to drive the system into either the exciton or the biexciton in the 3LS.

HL 7.40 Mon 13:00 P2/EG

Controlling the dimensions of top-down GaN nanowire ensembles via self-assembled metal islands — •ROSE MARY JOSE, JINGXUAN KANG, MIRIAM OLIVA, THOMAS AUZELLE, ABBES TAHRAOUI, OLIVER BRANDT, and LUTZ GEELHAAR — Paul-Drude-Institut für Festkörperelektronik, 10117 Berlin, Germany
The large surface-to-volume ratio of semiconductor nanowires and their potential for enhanced light absorption are attractive for photoelectrochemical applications. In this context, large-scale nanowire arrays are needed. For top-down fabrication, a scalable and rapid way to form a nano-island mask is the dewetting of a metal film.

In this work, we study how Pt films evolve upon thermal treatment into nano-islands which serve as a shadow mask for the top-down etching of GaN nanowire ensembles. To gain control over the nano-island ensembles' dimensions, we explore variations of the annealing conditions, Pt film thickness, and the surface energy by investigating Pt dewetting on GaN, SiN_x, and SiO_x surfaces. The islands' size and density are determined by the initial Pt film thickness. However, nano-island diameter and spacing are coupled by a fixed ratio. Therefore, individually controlling the spacing between nano-islands and their diameter is challenging in this approach.

Nanowire arrays are fabricated using Pt dewetting masks by plasma etching followed by KOH wet etching. The resulting nanowires' dimensions are consistent with those of the original nano-islands. In our experiments, diameters in the range 30 nm-200 nm and lengths of 500-1000 nm are demonstrated.

HL 7.41 Mon 13:00 P2/EG

Investigation of SiNWs [100] and [111] applying DFT with doping — •NEDHAL AL-NUAIMI, HILSER FLORIAN, and GEMMING SIBYLLE — Chemnitz University of Technology, Chemnitz (Germany)

We present an ab initio study of Silicon nanowires (SiNW) with p-type impurities (doping) of Boron (B) and n-type impurities of Phosphorus (P) using Abinit and VESTA Software. We compare total energy and band dispersion in the [100] and [111] directions with that of pure bulk (semiconductor) silicon. The resulting band structure shows metallic behaviour due to additional states within the band gap. Furthermore dangling bonds lead to localized surface states without dispersion. Saturating these states can cause shifts in the electrostatic potential and may be used to tune the sensing properties of SiNWs.

HL 7.42 Mon 13:00 P2/EG

Growth and characterisation of local droplet etched InAs quantum dots in an InGaAs matrix — •NIKOLAI SPITZER, HANS-GEORG BABIN, ANDREAS WIECK, and ARNE LUDWIG — Ruhr-Universität Bochum, Lehrstuhl für Angewandte Festkörperphysik, Universitätsstraße 150, 44801 Bochum

We present a new local droplet etching (LDE) method for selforganized InGaAs quantum dots (QDs). We use gallium droplets to etch on an InGaAs matrix layer and fill the nanoholes with InAs. The impact of the indium concentration in the InGaAs-layer and of the deposited InAs amount after etching is investigated by atomic force microscopy and photoluminescence spectroscopy.

HL 7.43 Mon 13:00 P2/EG

Enhancement of Quantum Dot Emission in the Telecom C-Band via Photonic Micro Cavities — •RAPHAEL JOOS, CHRISTIAN RUPP, SASCHA KOLATSCHEK, STEPHANIE BAUER, CORNELIUS NAWRATH, ROBERT SITTIG, PONRAJ VIJAYAN, MICHAEL JETTER, SIMONE LUCA PORTALUPI, and PETER MICHLER — Institut für Halbleitertechnik und Funktionelle Grenzflächen (IHFG), Center for Integrated Quantum Science and Technology (IQST) and SCoPE, Universität Stuttgart, Allmandring 3, 70569 Stuttgart, Germany

Potential quantum technology applications such as quantum communication rely on the availability of carrier of quantum information. For that matter single-photons can be utilized as „flying-qubits“ imprinting information in their polarization state. For these applications it is beneficial to operate at the telecom C-band which offers reduced dispersion and minimum loss in optical fibers. In the recent years InAs quantum dots (QDs) have shown to be capable of emission of single and entangled photons in the telecom C-band. However, as-grown QD structures have limited collection efficiency of the emitted light due to total internal reflection. To tackle this issue photonic cavity structures can be employed

which can enhance the photon extraction efficiency and decrease the decay time due to the underlying Purcell effect. While there are different approaches to photonic structures ranging from planar cavities to Gaussian micro lenses, this work mainly deals with circular Bragg grating structures. These offer high collection efficiency in a broadband manner as well as a cavity spectrum which potentially allows simultaneous Purcell enhancement of exciton and biexciton.

HL 7.44 Mon 13:00 P2/EG

Voronoi-Cell Analysis of Density Modulated InAs Quantum Dots — •PETER ZAJAC¹, NIKOLAI BART^{1,2}, CHRISTIAN DANGEL², KAI MÜLLER³, ANDREAS D. WIECK¹, JONATHAN FINLEY², and ARNE LUDWIG¹ — ¹Ruhr-Universität Bochum, Universitätsstraße 150, 44801 Bochum, Germany — ²Walter Schottky Institut and Physik Department, Technische Universität München, Am Coulombwall 4, 85748 Garching, Germany — ³Walter Schottky Institut and Department of Electrical and Computer Engineering, Technische Universität München, Am Coulombwall 4, 85748 Garching, Germany

InAs quantum dots (QDs) grown by molecular beam epitaxy exhibit a density modulation upon growth on top of a GaAs gradient layer [1]. The local variation of the nucleation probability is ascribed to the roughness of the underlying GaAs layer. It is of interest to study the QD formation on such a surface under the scope of the capture-zone model [2]. Here, the results of AFM data analysis with focus on correlations between Voronoi cell areas and QD size parameters such as height and volume are presented.

[1] Bart, N., Dangel, C. et al. Wafer-scale epitaxial modulation of quantum dot density. *Nat. Commun.* **13**, 1663 (2022).

[2] Löbl, Matthias C., et al. Correlations between optical properties and Voronoi-cell area of quantum dots. *Phys. Rev. B* **100**, 155402 (2019).

HL 7.45 Mon 13:00 P2/EG

Enhancing the extraction efficiency of photons from low intensity decay processes with solid immersion lenses — •PATRICIA KALLERT¹, BJÖRN JONAS², EVA SCHÖLL¹, TIM LANGER¹, DIRK REUTER¹, ARTUR ZRENNER¹, and KLAUS D. JÖNS¹ — ¹hqpd lab, PhoQS Institute and Department of Physics, Paderborn University, Germany — ²Photonic Quantum Engineering Group, Walter Schottky Institute, and Department for Electrical and Computer Engineering, Technical University of Munich, Germany

Single photons are basic building blocks for photon-based quantum technologies, such as quantum computation and communication concepts. A promising source offering high single-photon purity and indistinguishability are semiconductor quantum dots in photodiodes. A major drawback of this platform is the low extraction efficiency. Due to the refractive index mismatch of the semiconductor and the surrounding environment, total internal reflection occurs already for very small angles of incidence on the interface. In this study, the enhancement capability and the practical limits of using solid immersion lenses of hemispherical and Weierstrass geometry are investigated and compared. The hemispherical lens is insusceptible to misalignment but offers a mediocre enhancement in collection efficiency. In contrast, the Weierstrass geometry is sensitive to nonperfect alignment but improves the extraction by a factor of up to 2.9. Avoiding the need of the fabrication of complex structures as micropillars and other cavities, consequently, we can triple the detection of photons from low-intensity decay processes.

HL 7.46 Mon 13:00 P2/EG

Magnetic Field-Dependence of the Auger Recombination Rate in a Self-Assembled Quantum Dot — •FABIO RIMEK¹, HENDRIK MANNEL¹, MARCEL ZÖLLNER¹, ARNE LUDWIG², ANDREAS D. WIECK², AXEL LORKE¹, and MARTIN GELLER¹ — ¹Faculty of Physics and CENIDE, University Duisburg-Essen, Germany — ²Chair of Applied Solid State Physics, Ruhr-University Bochum, Germany

A quantum dot (QD) is an ideal system to study electron-electron interaction in a confined nanostructure [1]. The Auger recombination is a special case, where the recombination energy is transferred to a third charge carrier that leaves the dot [2] or is excited to a higher energy level. Therefore, the Auger effect destroys the radiative recombination of the charged exciton (trion) - an effect, which should be minimized for future applications that use spin states as stationary qubits, which can be transferred to photons via the QD trion transition. In this work, we investigate how the Auger rate is affected by an external magnetic field, applied perpendicular to the plane of the dots. In the magnetic field, the trion transition of a QD is no longer spin degenerate and splits up. We use two-color, time-resolved resonance fluorescence to investigate the quenching of the trion recombination due to the Auger effect. Two color excitation allows us to excite two quantum dot transitions (both trions or one trion and one exciton) and neglect spin relaxation as well as spin-flip Raman scattering. This ensures that we can directly measure the Auger and the tunneling rate of an electron into the dot.

[1] A. Kurzmann et al., *Nano Lett.* **16**, 3367-3372 (2016).

[2] P. Lochner et al., *Nano Lett.* **20**, 1631-1636 (2020).

HL 7.47 Mon 13:00 P2/EG

Towards solid-state quantum emitters strongly coupled to crossed nanobeam cavities — •JAN-GABRIEL HARTEL, OSCAR CAMACHO IBARRA, and KLAUS D. JÖNS — hqpd lab, PhoQS Institute and Department of Physics, Paderborn University, Germany

The strong coupling regime of quantum electrodynamics, theoretically described via the Jaynes-Cummings model, offers insight into purely quantum mechanical effects in the interaction of a two-level system and a single mode light field. An extension of this model to the interaction of a two-level system with two resonant modes yields the possibility of free exchange of the excitation between the light modes as well as subsequent applications in quantum gates. While the fundamental case has been experimentally studied, the realization of this extension has proven to be elusive due to the technological challenges of fabricating a stable coupled cavity system.

In this work, we seek to approach this realization by exploring nanofabrication of on-chip crossed nanobeam cavity systems, realized via Bragg mirrors. We numerically explore heuristic extensions of existing design recipes for 1D nanobeam cavities, based on the creation of a localized defect mode. We emphasize the challenges of conserving high Q-factors at the specified resonance frequency while minimizing coupling between the crossed cavities, developing novel design ideas.

HL 7.48 Mon 13:00 P2/EG

Towards frequency-converted polarization-entangled photon pairs from semiconductor quantum dots — •TIM STROBEL¹, ANDRE BISQUERRA¹, TOBIAS BAUER², NAND LAL SHARMA³, MARLON SCHÄFER², STEFAN KAZMAIER¹, CORNELIUS NAWRATH¹, LUKAS WAGNER¹, ANKITA CHOUDHARY³, MICHAEL JETTER¹, CASPAR HOPFMANN³, CHRISTOPH BECHER², SIMONE L. PORTALUPI¹, and PETER MICHLER¹ — ¹Institut für Halbleitertechnik und Funktionelle Grenzflächen, Center for Integrated Science and Technology (IQST) and SCOPE, University of Stuttgart, Allmandring 3, 70569 Stuttgart, Germany — ²Fachrichtung Physik, Universität des Saarlandes, Campus E2.6, 66123 Saarbrücken, Germany — ³Institute for Integrative Nanosciences, Leibniz IFW Dresden, Helmholtzstraße 20, 01069 Dresden, Germany

Fiber-based distribution of entangled, single photon pairs is a key requirement for future developments of terrestrial quantum networks. Quantum repeater schemes at telecom wavelengths can overcome the restriction set by fiber transmission losses over long distances. In this context semiconductor quantum dots (QDs) are promising candidates as deterministic sources of on-demand polarization-entangled photon pairs. Here, we investigate photons emitted via the biexciton-exciton cascade of GaAs QDs grown via Al droplet etching and integrated into a GaP solid immersion lens. To be compatible with existing fiber network infrastructures, quantum frequency conversion is employed to convert the QD emission from 780nm to telecom wavelengths.

HL 7.49 Mon 13:00 P2/EG

Strongly driven germanium qubit — •BASHAB DEY and JOHN SCHLIEMANN — Institute for Theoretical Physics, University of Regensburg, Regensburg, Germany

Hole qubits in germanium heterostructures are promising candidates for coherent control and manipulation of the spin degree of freedom by electric dipole spin resonance. The suppression of contact hyperfine interaction due to p-type character of the holes, possibility of nuclear-spin free isotopes and absence of valley degeneracies in germanium are favourable for sustaining longer spin coherence and relaxation times in these qubits. We study the time dynamics of a germanium qubit confined laterally by a parabolic potential and strongly driven by coherent circularly polarized radiation in presence of p-cubic Rashba spin-orbit coupling and perpendicular magnetic field. We calculate the transition rates between the lowest (Zeeman-split) levels of the qubit using Floquet theory. We observe peculiar beating patterns in the Rabi oscillations which depend on the strength of the driving field. When the driving frequency is resonant with Zeeman gap, the maxima of the oscillations is a decreasing function of driving amplitude which is in contrast to that of a harmonically driven two-level system. Furthermore, the time period of oscillations, time interval between the beating nodes and the number of oscillations between the nodes also decrease with the radiation amplitude.

HL 7.50 Mon 13:00 P2/EG

Swing-Up Dynamics in Quantum Dot Cavity Systems — •NILS HEINISCH, NIKOLAS KÖCHER, DAVID BAUCH, and STEFAN SCHUMACHER — Physics Department and CeOPP, Paderborn University, Germany

In this work, we further investigate the recently proposed [1] and experimentally demonstrated [2] SUPER-scheme (Swing-UP of the quantum EmitteR population). In the SUPER-scheme optical excitation of a quantum emitter is achieved using two off-resonant red-detuned Gaussian pulses. Here, we expand the studies to quantum dot cavity systems and aim for high quality photons, generated during the decay process following the excitation. After successful proof-of-principle studies with a two-level system, we present the successful single-photon and photon-pair generation using the SUPER-scheme for excitation of diamond-

shaped exciton-biexciton quantum dot model systems. For a more realistic simulation we also take phonons into account. For all systems studied it can be concluded that a cavity neither hinders the swing-up process nor degrades the quality of the generated photons which is in contrast to excitation schemes using resonant Gaussian pulses. [1] T. K. Bracht et al., PRX Quantum 2, 040354 (2021). [2] Y. Karli et al., Nano Letters 22, 6567 (2022).

HL 7.51 Mon 13:00 P2/EG

Time-Resolved Wave-Function Mapping in Self-Assembled Quantum Qots — •JENS KERSKI¹, DANIEL HECKER¹, NELSON CREUTZBURG¹, ARNE LUDWIG², ANDREAS D. WIECK², MARTIN GELLER¹, and AXEL LORKE¹ — ¹Faculty of Physics and CENIDE, University of Duisburg-Essen, Germany — ²Chair of Applied Solid State Physics, Ruhr-University Bochum, Germany

The static and dynamic properties of self-assembled quantum dots (QDs) are often modeled using the QD's single particle wavefunctions. Although this approximation is very successful, the influence of the electron-electron interaction on the few-particle wave-functions and their nonequilibrium dynamics has not yet been studied in detail.

We investigate an ensemble of InAs/GaAs QDs, embedded in a high electron mobility transistor. The QDs are tunnel-coupled to a two-dimensional electron gas (2DEG). By applying a voltage pulse to the gate, we induce charge carriers from the 2DEG to tunnel into targeted quantum dot states. We monitor the temporal evolution of the conductivity σ_{2D} of the 2DEG, which is sensitive to the transfer of charge into the QDs. A rate-equation-based evaluation of σ_{2D} allows us to separate tunneling processes into different equilibrium or non-equilibrium QD states. We use an in-plane magnetic field perpendicular to the tunneling direction for wave-function mapping [1, 2] of the quantum dot states. This allows us to study the shape and dynamics of the (excited) electron states.

[1] W. Lei et al., Phys. Rev. Lett. 105, 176804 (2010).

[2] D. Zhou et al. J. Appl. Phys. 134, 064401 (2022).

HL 7.52 Mon 13:00 P2/EG

Development and deterministic nanofabrication of quantum dot based single-photon sources with emission in the 780 nm-930 nm range — •DINARA BASHAROVA¹, STEPHAN REITZENSTEIN¹, SVEN RODT¹, CASPAR HOPFMANN², NAND LAL SHARMA², NORMEN AULER³, and DIRK REUTER³ — ¹Institute of Solid State Physics, Technische Universität Berlin, D-10623 Berlin, Germany — ²Leibniz Institute for Solid State and Materials Research Dresden, 01069 Dresden, Germany — ³Center of Optoelectronics and Photonics, Universität Paderborn, 33098 Paderborn, Germany

Important goals of quantum technology are to demonstrate the elementary building blocks of a quantum repeater and to integrate them into the infrastructure of a quantum network. A network of quantum repeaters allows the distribution of quantum entanglement, thereby enabling secure exchange of information between multiple parties. To implement such building blocks, we use semiconductor heterostructures (HS) with GaAs quantum dots (QDs) integrated into circular Bragg gratings (CBG). GaAs QDs are excellent single-photon emitters with almost negligible multi-photon emission probability and photon extraction efficiencies exceeding 60%. For this purpose, we deterministically integrate QDs on structures with back-side distributed Bragg reflector and in hybrid approach with backside Au mirror for comparison. In-situ electron beam lithography (EBL) is an ideal technique for deterministic fabrication of such QD-based quantum light sources. The fabricated QDs are characterized by microphotoluminescence and quantum optical spectroscopy.

HL 7.53 Mon 13:00 P2/EG

Fabrication of electrically controllable quantum dots in PIN diodes integrated within circular Bragg gratings — •SETTHANAT WIJITPATIMA¹, NORMEN AULER², SVEN RODT¹, DIRK REUTER², and STEPHAN REITZENSTEIN¹ — ¹Institute of Solid-State Physics, Technische Universität Berlin, D-10623 Berlin, Germany — ²Center of Optoelectronics and Photonics, Universität Paderborn, 33098 Paderborn, Germany

A quantum repeater is one emerging device of the decade that has been promised to play a crucial role in quantum communication. To produce an ideal quantum light source with high single-photon purity, nanophotonic structures must be fabricated on self-organized semiconductor quantum dots, which pose challenges due to their random occurrences and requirements of exact spatial and spectral integration. In addition to nanophotonic enhancement, such devices can be designed to allow an electrical manipulation of the excitonic state of quantum dots. Here, we propose a design that allows electrical controls via a PIN diode integrated within circular Bragg gratings (CBGs). Numerical simulations are done to optimize the design to yield the photon extraction efficiency (PEE) of 0.69 at N.A.=0.8. The deterministic fabrication is done with the use of cathodoluminescence (CL) scans and electron beam epitaxy (EBL), and the fabricated devices are characterized by electric-field dependent micro-photoluminescence (μ PL) measurements.

HL 7.54 Mon 13:00 P2/EG

Patterned growth of vertical zinc oxide nanowires on sputtered zinc oxide thin films — •JAN BÖHMNER, LUKAS JÄGER, ALEXANDER KOCH, and CARSTEN RONNING — Institute of Solid State Physics, Friedrich Schiller University Jena, Max-Wien-Platz 1, 07743 Jena

Because of the wide band of zinc oxide, ZnO nanowires have promising applications in short wavelength optoelectronics, like building photodetectors or laser emitters using nanowire arrays. ZnO nanowires can be easily grown by vapor transport techniques in a high temperature furnace on silicon substrates utilizing the vapor-solid-liquid (VLS) mechanism. However, the nanowires produced in this way typically show random orientations and often overlap each other. A pre-deposited thin film of aluminum doped zinc oxide (Al:ZnO or AZO) by RF sputtering on the substrate creates a polycrystalline ZnO surface with a preferred orientation, on which the nanowires can grow epitaxially. The ZnO nanowires grown this way are almost all orientated perpendicular to the substrate surface resulting in vertical/upstanding nanowires. By now patterning the pre-deposited AZO thin films, selective area growth (SAG) of nanowires is possible. In this contribution, we will discuss our growth results and our goal to control the exact position of nanowire growth to create ordered nanowire arrays.

HL 7.55 Mon 13:00 P2/EG

Energy transfer between Si quantum dots and protoporphyrin molecules as a function of distance, orientation and size — •ATHANASIOS KOLIOGIORGOS¹ and TOMAS POLCAR² — ¹Department of Condensed Matter Physics, Faculty of Mathematics and Physics, Charles University, Prague, Czech Republic — ²Department of Control Engineering, Faculty of Electrical Engineering, Czech Technical University in Prague, Czech Republic

Organic molecules such as protoporphyrin IX (PPIX) can be attached to bulk or nanostructured silicon to enhance its optical and electronic properties. In this study, the interaction between PPIX molecules (donor) and Si nanocrystals (acceptor) up to 2.5 nm for varying distances and orientations is studied by DFT, semi-empirical and TDDFT methods. Simulations show an effect on electronic structure, indicative of electron charge transfer in parallel orientation and very small distances and non-electron energy transfer for different orientations and larger distances. An absorption-emission spectral overlap is observed. We use the Transition Density Cube method to calculate the electronic couplings and energy transfer rates between donor and acceptor. The Si quantum dots with the smallest size yield larger couplings than the larger nanocrystals. The coupling is enhanced by adding a plasmon nanoparticle as a bridge between donor and acceptor. Results using Au nanoparticles show increased energy transfer rates up to four orders of magnitude and lower distance dependence.

HL 7.56 Mon 13:00 P2/EG

The internal photoeffect from a single solid-state quantum emitter: Excitation energy and band-structure dependence — •B. MAIB¹, M. ZÖLLNER¹, F. RIMEK¹, P. LOCHNER¹, H. MANNEL¹, A.D. WIECK², A. LUDWIG², A. LORKE¹, and M. GELLER¹ — ¹University of Duisburg-Essen and CENIDE, Germany — ²Ruhr-University Bochum, Germany

The coherence time is one of the limiting factors for using single quantum emitters, like self-assembled quantum dots, in future applications of quantum information processing. Besides spin and charge noise [1] the physical limits are given by the Auger recombination [2] and an internal photoeffect [3] that is present even for resonant excitation.

We have studied in detail the photoeffect in a single self-assembled quantum dot for different energies of a non-resonant laser that excites a single electron from the bound quantum dot state into the continuum of the conduction band. These measurements are realized by time-resolved two-color resonance fluorescence (RF) excitation. The first resonant laser drives the exciton transition, while the second pulsed laser simultaneously excites the photoelectron to the final state in the conduction band, caused by the internal photoeffect.

The results can be used to reduce the internal photoeffect and therefore suppress the photoemission, which would increase the coherence time in such a single photon emitter even under resonant excitation.

[1] A. V. Kuhlmann, Nature Physics, 9, 570-575 (2013).

[2] A. Kurzmann, Nano Letters 16, 3367-3372 (2016).

[3] P. Lochner, Phys. Rev. B, 103, 075426 (2021).

HL 7.57 Mon 13:00 P2/EG

Calibrating Photoluminescence Yield for Quantum emitters in Planar Photonic Heterostructures — •TIMO KRUCK, HANS-GEORG BABIN, ANDREAS D. WIECK, and ARNE LUDWIG — Ruhr-Universität-Bochum; Lehrstuhl für angewandte Festkörperphysik, Bochum, Deutschland

When performing photoluminescence (PL) measurements the spectral intensity of the emitted radiation strongly depends on the dielectric structure surrounding the quantum emitter. Here we show a method for calibrating PL measurements to obtain the unaltered spectrum of the optically active medium [1]. For this purpose, the spectral reflectivity and the wavelength dependent standing wave field are used. The reflectivity, which is determined by reflectometer measurements, and a simulation based on the transfer matrix method are used to compensate

for the true layer thickness. This is then used to calculate the standing wave field, the outcoupling efficiency and the quantum yield. To validate the method, the calibrated spectra are compared with cleaved-edge PL measurements where the QDs are excited from the side and the light is also collected from the side.

[1] Babin et al.; *Nanomaterials* 2021, 11(10), 2703;

HL 7.58 Mon 13:00 P2/EG

Nanowire-based light absorber patterning for artificial photosynthesis — •JULIANE KOCH¹, JIAJIA QIU², PETER KLEINSCHMIDT¹, HUAPING ZHAO², YONG LEI², and THOMAS HANNAPPEL¹ — ¹TU Ilmenau, Institute for Physics, Fundamentals of energy materials, Ilmenau, Germany — ²TU Ilmenau, Institute for Physics, Applied nanophysics, Ilmenau, Germany

Due to the increased degrees of freedom in device structures and properties, III-V nanowires (NWs) have been predicted to outperform planar devices. In the context of energy conversion in solar cells and photoelectrochemical devices, the kinetics and transport behavior of different charge carriers in light absorbers are closely related to the selected materials and their shape. A key factor for commercially relevant development is the enhanced light absorption, in particular in a uniform NW array, combined with lower costs and material usage (e.g. of III-Vs) for nanowire-based light absorbers. This may ultimately require fabrication techniques with homogenous patterning over a large range. In this work we demonstrate the fabrication techniques for creation of a NW array and key requirements during MOVPE NW growth. By applying a surface patterning technique with anodic aluminum oxide (AAO) templates, arrays of gold droplets can be deposited on a surface, which acts as a catalyst for NW growth during metalorganic vapor phase epitaxy (MOVPE). Under defined process parameters vertical III-V semiconductor NW can be achieved via vapor-liquid-solid (VLS) growth in a horizontal MOVPE system.

HL 7.59 Mon 13:00 P2/EG

Enhancing spatial resolution for terahertz waveform near-field microscopy — •FABIAN BRÜTTING, MORITZ HEINDL, and GEORG HERINK — Experimental Physics VIII, University of Bayreuth, Germany

The quantum confined Stark-effect induces field-driven modulations in the optical transitions of quantum emitters. Harnessing this ultrafast interaction in colloidal quantum dots enables us to image THz near-field waveforms with fluorescence microscopy in the visible spectrum [1]. The spatial resolution of fluorescence microscopy is principally not diffraction-limited and can be extended to the few-nanometer scale using super-resolution techniques such as stimulated emission depletion (STED) microscopy. The efficient depletion of quantum dot emission presents a key requirement [2]. In this contribution, we present our investigations on the STED process in the quantum dots employed as field-probes in the luminescence-based Quantum-probe field microscopy (QFIM) scheme.

[1] Heindl, M. B. et al., *Ultrafast imaging of terahertz electric waveforms using quantum dots*. *Light Sci. Appl.* 11, 5 (2022).

[2] Hanne, J. et al., *STED nanoscopy with fluorescent quantum dots*. *Nat. Comm.* 6, 7127 (2015).

HL 7.60 Mon 13:00 P2/EG

Investigation of the biexciton decay in semiconductor In(Ga)As/GaAs quantum dots — •CHRISTOPHER BUCHHOLZ, SEBASTIAN KREHS, and ARTUR ZRENNER — Universität Paderborn, Paderborn, Deutschland

The biexciton-exciton cascade is a widely used promising emission mechanism in quantum dots for generating entangled photon pairs with high fidelity. An often overlooked critical parameter for the quality of the emitted photons is the different lifetimes of electron and hole. Since the lifetimes of excitonic states can be influenced via external electrical fields (quantum confined stark effect), we studied this parameter in Schottky-contacted GaAs heterostructures. We approached this challenge by placing the quantum dots at different distances to the n-contact, 40 nm and 80 nm, respectively. The quantum dots were first characterized by voltage-dependant photoluminescence (PLV) measurements under above-band excitation and further investigated by photocurrent spectroscopy (PC) under resonant excitation and PLV under two-photon excitation (TPE). From the resonances in the PC measurements, the electron lifetime was extracted, whereas the TPE measurements showed the occurrence of the biexciton and charged exciton states as a function of the voltage. The results suggest that an increased distance to the n-contact leads to a decreased tunneling rate of electrons into the quantum dot. At the same time, the tunneling from the quantum dot is not affected.

HL 7.61 Mon 13:00 P2/EG

Influence of the quantum dot geometry on higher excited states — •JAN KASPARI and DORIS E. REITER — Condensed Matter Theory, TU Dortmund, Otto-Hahn-Straße 4, 44227 Dortmund

The energetic structure and absorption spectra of semiconductor quantum dots are strongly dependent on the dot geometry. In particular the higher excited states, typically denoted as p- or d-shell, can become highly mixed and depend strongly on the specific dot. We derive a theoretical model to describe higher excited quantum dot states based on the envelope function approximation. The four-band Luttinger theory as well as the direct and short-range Coulomb in-

teractions are treated within a configuration interaction approach. The quantum dot confinement is approximated by an anisotropic harmonic potential. We show that a variation of the size of a cylindrical symmetric quantum leads to energetic shifts of higher excited quantum dot states. Breaking this cylindrical symmetry significantly alters the absorption spectrum as further energy splittings in the energetic structure appear and state mixtures change which results in differences of oscillator strengths of some peaks. Our results give insight into the quantum dot energy structure especially for higher excited states, which become relevant in radiative Auger processes or for ultrafast quantum logic operations.

HL 7.62 Mon 13:00 P2/EG

Towards remote on-chip two-photon interference in gallium arsenide based-photonic integrated circuits — •ULRICH PFISTER¹, MORITZ SPEIDEL¹, FLORIAN HORNING¹, STEPHANIE BAUER¹, ROBERT SITTING¹, ERIC REUTTER², MICHAEL JETTER¹, SIMONE L. PORTALUPI¹, JÜRGEN WEIS², and PETER MICHLER¹ — ¹Institut für Halbleiter und Funktionelle Grenzflächen (IHFG), Center for Integrated Quantum Science and Technology (IQST) and SCoPE, University of Stuttgart, Allmandring 3, Germany — ²Max-Planck-Institut für Festkörperforschung (MPI), University of Stuttgart, Heisenbergstraße 1, Germany

InGaAs quantum dots (QDs) are a promising source of single and indistinguishable photons for the on-chip realization of two-photon interference (TPI) with remote QDs. One of the challenges is the inhomogeneously distributed emission frequency of the QDs, which makes frequency tuning necessary. We show that strain-induced emission frequency tuning is applicable for ridge waveguides and it can be considered a promising step towards remote on-chip TPI [1]. Additionally, a successful TPI with one single QD and an on-chip multimode interference beamsplitter as a part of a Mach-Zehnder interferometer has been realized and the feasibility of remote on-chip TPI with MOVPE-grown InGaAs QDs is discussed.

[1] Hepp, S. et al., *Appl. Phys. Lett.* 117, 254002 (2020)

HL 7.63 Mon 13:00 P2/EG

Quantum frequency conversion of entangled photon pair from GaAs Quantum dot to Sn-vacancy center in Diamond — •ANKITA CHOUDHARY, TIM POKART, NAND LAL SHARMA, MORITZ LANGER, and CASPAR HOPFMANN — Institute for Integrative Nanosciences, Leibniz IFW Dresden, Helmholtzstraße 20, 01069 Dresden, Germany

The distribution of entangled photons in future long-distance quantum networks requires both on-demand and high-fidelity entangled photon pair generation as well as their temporary storage in low dephasing quantum memory systems. While GaAs quantum dots have proven to be excellent entangled photon pair sources, this system suffers from strong dephasing of its spin qubits. Diamond color centers on the other hand are excellent quantum memories, but not ideal entangled photon pair sources. In order to combine the complementary properties of both material system in a hybrid quantum network approach, the efficient conversion between the operating photon energies without the loss of quantum information using quantum frequency conversion is required. In this study we present quantum frequency conversion from 780nm to 619nm, i.e. from GaAs quantum dot emission to the zero-phonon line of the diamond Sn vacancy center, using sum frequency generation in a periodically poled lithium niobate crystal and an infrared laser pump of about 3 * μm wavelength. We find that a conversion efficiency of at least 25% can be achieved.

HL 7.64 Mon 13:00 P2/EG

Design of circular Bragg resonators in the telecom band for efficient emission of entangled and indistinguishable photons from semiconductor quantum dots — •DUSTIN SIEBERT, DAVID BAUCH, KLAUS D. JÖNS, STEFAN SCHUMACHER, and JENS FÖRSTNER — Electrical Engineering Department, Physics Department, CeOPP and PhoQS, Paderborn University, Germany

The generation of indistinguishable and entangled photons via the biexciton-exciton cascade in semiconductor quantum dots can be tailored by a photonic environment providing an increased emission rate through the Purcell effect and a cavity feedback [1,2].

Circular Bragg resonators exhibit exactly these properties and enable good collection efficiency over a large bandwidth. We developed an optimization strategy based on a two-step process. First, we use a batch of 2D electromagnetic simulations within Bayesian global optimization and finally polish the optimum through Nelder-Mead local optimization based on full 3D simulations.

The optical properties obtained are then used within a quantum mechanical simulation of the carrier dynamics in the semiconductor quantum dots including phonon interaction [3]. After optimization, we achieve a tremendous enhancement of the indistinguishability of the emitted photons even considering that real structures might suffer fabrication imperfections.

[1] E. Schöll, et al., *Phys. Rev. Lett.* 125, 233605 (2020) [2] F. Sbresny, et al., *Phys. Rev. Lett.* 128, 093603 (2022) [3] D. Bauch et al., *Phys. Rev. B* 104, 085308 (2021)

HL 7.65 Mon 13:00 P2/EG

Origin of Antibunching in Resonance Fluorescence — •LUKAS HANSCHKE¹, EVA SCHÖLL¹, EDUARDO ZUBIZARRETA CASALENGUA^{2,3}, MELINA PETER⁴, AILTON GARCIA JR.⁴, SAIMON F. COVRE DA SILVA⁴, SANTANU MANNA⁴, ARMANDO RASTELLI⁴, KAI MÜLLER⁵, FABRICE P. LAUSSY³, ELENA DEL VALLE², and KLAUS D. JÖNS¹ — ¹PhoQS, CeOPP, and Department of Physics, Paderborn University — ²Departamento de Física Teórica de la Materia Condensada, Universidad Autónoma de Madrid — ³Faculty of Science and Engineering, University of Wolverhampton — ⁴Institute of Semiconductor and Solid State Physics, Johannes Kepler University Linz — ⁵Walter Schottky Institute, Technical University of Munich

Resonance fluorescence, the coherent emission of a quantum two-level system under weak resonant driving, exhibits sub-natural linewidth and inherits the coherence properties of the excitation laser. While previous experiments suggest that this emission also maintains antibunched, our results prove recent theoretical insights into the origin of the antibunching and the underlying interplay between the coherent and incoherent emission of the quantum system. This allows us to specifically manipulate the composition of the resonance fluorescence by frequency filtering and interference with the excitation laser field to enable single photons with sub-natural linewidth [PRL 123, 170402 (2020)].

HL 7.66 Mon 13:00 P2/EG

Near Fourier-Transform Limited Blinking Free Quantum Dots — •EVA SCHÖLL¹, LUKAS HANSCHKE¹, MELINA PETER², AILTON GARCIA JR.², PATRICIA KALLERT¹, FRANCESCO SALUSTI¹, SAIMON FILIPE COVRE DA SILVA², SANTANU MANNA², ARMANDO RASTELLI², and KLAUS D. JÖNS¹ — ¹PhoQS, CeOPP, and Department of Physics, Paderborn University, Warburger Straße 100, 33098 Paderborn, Germany — ²Institute of Semiconductor and Solid State Physics, Johannes Kepler University Linz, 4040 Linz, Austria

Tailored quantum light sources are crucial building blocks for applications in quantum technologies. Al droplet etched GaAs Quantum Dots are promising candidates for such sources, as they show very good characteristics for example in terms of single-photon purity, indistinguishability on short time scales and entanglement fidelity. However, these QDs usually exhibit an unstable charge environment, which leads to reduced coherence on long time scales, broadened linewidths and blinking. Embedding the QDs into a p-i-n diode structure enables energy tuning via the Stark effect and stabilizes the charge environment. Here we demonstrate a solid-state single-photon source with no signs of blinking on up to ms time scales and near Fourier-transform limited linewidths. This opens up possibilities for experiments for a fundamentally deeper understanding of quantum level schemes and realization towards a quantum network, where quantum interference between separate sources is required.

HL 8: 2D Materials II (joint session HL/CPP)

Time: Monday 15:00–18:15

Location: POT 81

HL 8.1 Mon 15:00 POT 81

Twist- and gate-tunable valley splitting in TMDC/CrI₃ heterostructures — •KLAUS ZOLLNER, PAULO E. FARIA JUNIOR, and JAROSLAV FABIAN — Institute of Theoretical Physics, University of Regensburg, 93053 Regensburg, Germany
Van der Waals heterostructures composed of twisted monolayers promise great tunability of electronic, optical, and magnetic properties. Twistronics has already demonstrated its potential in tuning proximity spin-orbit and exchange coupling in graphene-based heterostructures [1,2]. In this talk, we present the strong manipulation of the valley splitting upon twisting and gating in TMDC/CrI₃ heterostructures [3]. In particular, upon twisting from 0° to 30°, the proximity-induced TMDC valence band edge exchange splitting can be reversed (–2 to 2 meV), while the TMDC conduction band edge exchange splitting remains nearly constant (–3 meV). Further giant tunability (few meV) of the proximity exchange coupling is provided by a transverse electric field. Consequently, twisting and gating then allow to tailor the valley splitting of the first intralayer exciton peak in the range of 0 to 12 meV in WSe₂/CrI₃, which is equivalent to gigantic external magnetic fields of up to about 60 Tesla.

This work was supported by DFG SFB 1277, DFG SPP 2244, and the EU Horizon 2020 Research and Innovation Program (Graphene Flagship).

[1] K. Zollner and J. Fabian, *Phys. Rev. Lett.* 128, 106401 (2022).

[2] Lee *et al.*, *Phys. Rev. B* 106, 165420 (2022).

[3] K. Zollner, P. E. F. Junior, J. Fabian, arXiv:2210.13794 (2022).

HL 8.2 Mon 15:15 POT 81

Giant Enhancement of Interlayer Exciton Luminescence in WSe₂/WSe₂/MoSe₂ in Heterotrillayers. — •CHIRAG PALEKAR, CHING-WEN SHIH, IMAD LIMAME, BÁRBARA ROSA, and STEPHAN REITZENSTEIN — Institute of Solid State Physics, Technische Universität Berlin, D-10623 Berlin, Germany
TMDC heterolayers have gained lot on interest as a promising platform to study intricate many-body physics phenomena. Here we observe giant enhancement of interlayer exciton PL in a WSe₂/WSe₂/MoSe₂ heterotrillayers (HTL) system prepared by employing exfoliation and dry transfer method. The IX exciton forming at the heterojunction in the HTL region exhibits 10-fold increase in PL yield when compared to HBL region on the same sample. Such an enhancement can be attributed to the close to 0° twist angle between stacked WSe₂ homobilayers providing smaller interlayer separation and hybridization in the WSe₂ band structure, which in turn results in an efficient charge transfer. Further, PLE and reflection contrast reveal the twist angle dependence of the enhancement factor in such type II HTL systems as the large twist angle between WSe₂ homobilayers (57°) results in only up to 10% percent enhancement of IX PL in the HTL region when compared with the HBL. This fundamental study of excitons in the HTL system deepens the current understanding of physics of twisted TMDC heterostructures and paves the way for future experiments and theoretical work.

HL 8.3 Mon 15:30 POT 81

Photoluminescence tuning in hybrid devices of monolayer transition metal dichalcogenides and rylene dyes — •THERESA KUECHLE¹, GERGELY KNORR², KALINA PENEVA², and GIANCARLO SOAVI¹ — ¹Institute of Solid State Physics, Friedrich Schiller University Jena, Helmholtzweg 5, 07743 Jena, Germany — ²Institute of Organic Chemistry and Macromolecular Chemistry, Friedrich Schiller University Jena, Lessingstraße 8, 07743 Jena, Germany

Monolayer transition metal dichalcogenides (TMDs) are direct gap semiconductors that hold great promise for applications in nanoscale photonics and optoelectronic devices. A viable path for the development of devices with advanced functionalities and tunable properties is the integration with other nanoscale systems such as nanowires [1] and molecules [2]. Here, we realize hybrid devices based on TMDs and rylene dyes and study their optical properties via steady state photoluminescence. Preliminary results show that the PL emission in hybrid structures of WS₂/CN₄PMI can be quenched by a factor of 3, in the case of WSe₂/CN₄PMI by 300. We tentatively assign this variation to a different band alignment in the two heterostructures and to the interplay between charge transfer (in type II) and energy transfer (in type I). Future experiments including ultrafast pump-probe spectroscopy of pristine and hybrid systems as well as hybridization of different (tunable) molecules will further elucidate the role of band alignment in the ultrafast charge and energy transfer processes at the nanoscale.

[1] Kim *et al.*, *ACS Nano* 14, 9, 4323 (2020)

[2] Park *et al.*, *Adv. Mat. Interfaces* 8, 12, 2100215 (2021)

HL 8.4 Mon 15:45 POT 81

Coherence of interlayer exciton ensembles in MoSe₂/WSe₂ heterobilayers — •CHRISTOS PASPALIDES¹, MIRCO TROUE¹, JOHANNES FIGUEIREDO¹, LUKAS SIGL¹, MANUEL KATZER², MALTE SELIG², ANDREAS KNORR², URSULA WURSTBAUER³, and ALEXANDER HOLLEITNER¹ — ¹TU Munich — ²Technische Universität Berlin — ³University of Münster

Transition metal dichalcogenides exhibit strong light-matter interactions, which suggests them to be ideal candidates for novel 2D optoelectronic applications. Corresponding van der Waals heterostacks allow the excitation and formation of long-lived interlayer excitons [1]. We present coherence measurements of the ground state in such interlayer exciton ensembles by performing Michelson-Morley interferometry over a wide range of exciton density and temperature [2]. Moreover, we discuss the expansion dynamics of the interlayer excitons presumably driven by dipole-dipole interactions. The presented work paves the way towards a detailed understanding of excitonic many-body quantum phenomena in two-dimensional materials [3].

[1] B. Miller *et al.*, *Nano Letters* 17, 5229 (2017).

[2] M. Troue and J. Figueiredo, *et al* (2023).

[3] L. Sigl *et al.*, Signatures of a degenerate many-body state of interlayer excitons in a van der Waals heterostack, *Phys. Rev. Res.* 2, 042044 (2020).

15 min. break

HL 8.5 Mon 16:15 POT 81

Theoretical description of interlayer excitons in TMD homobilayers — •RUVEN HÜBNER¹, ALEXANDER STEINHOFF¹, and MATTHIAS FLORIAN² — ¹Institut für Theoretische Physik, Universität Bremen, Bremen, Germany — ²University of Michigan, Dept. of Electrical Engineering and Computer Science, Ann Arbor, MI, USA

In recent years, interlayer excitons in bilayers of transition metal dichalcogenides (TMDs) have received a rapid increase in attention. On the one hand, they feature the main characteristics of conventional excitons in the corresponding monolayers, namely an absorption spectrum in the optical regime combined with a high binding energy. On the other hand, they differ to such intralayer

excitons by a massively increased life time, a non-zero dipole moment in the out-of-plane direction and a strong sensitivity to material combination as well as stacking arrangement of adjacent monolayers. In this talk we focus on special excitonic properties inside TMD homobilayers that are particularly demanding from a theoretical point of view. In this context we discuss moiré excitons in twisted bilayers as well as high-lying excitons and trions at around twice the band gap energy arising within a highly non-parabolic band dispersion.

HL 8.6 Mon 16:30 POT 81

Raman signature of interlayer coupling and lattice dynamics in 2D TMDCs — •YANG PAN^{1,2} and DIETRICH R. T. ZAHN^{1,2} — ¹Semiconductor Physics, Institute of Physics, Chemnitz University of Technology, Chemnitz, Germany — ²Center for Materials, Architectures, and Integration of Nanomembranes (MAIN), Chemnitz University of Technology, Chemnitz, Germany

Vertical stacking of two-dimensional (2D) homo- and heterostructures are intriguing research objects, as they are essential for fundamental studies and a key towards 2D device applications. It is paramount to understand the interlayer coupling in 2D materials and to find a fast yet precise characteristic signature. In this work, we report on a Raman fingerprint of interlayer coupling in 2D transition metal dichalcogenides (TMDCs). We observed that the out-of-plane B_{2g} vibrational mode is absent when two monolayers form a vertical stack yet remain uncoupled but emerges after strong coupling. Using systematic Raman, photoluminescence (PL), and atomic force microscopy (AFM) studies of WSe_2/WSe_2 homo-bilayers and $MoSe_2/WSe_2$ hetero-bilayers, we conclude that the B_{2g} vibrational mode is a distinct Raman fingerprint of interlayer coupling in 2D TMDCs. Our further investigations confirmed its applicability on twisted 2D homo- and hetero-bilayers. Our results propose an easy, fast, precise, and reliable measure to evaluate the interlayer coupling and twisting angles in 2D TMDCs.

HL 8.7 Mon 16:45 POT 81

Correlated states of moiré interlayer excitons in twisted transition metal dichalcogenide heterostructures — •NILS-ERIK SCHÜTTE¹, NICLAS GÖTTING^{1,2}, FREDERIK LOHOF^{1,2}, and CHRISTOPHER GIES^{1,2} — ¹Institute for Theoretical Physics, University of Bremen, Bremen — ²Bremen Center for Computational Material Science, University of Bremen, Bremen

Stacking two transition metal dichalcogenide (TMD) monolayers on top of each other with a small relative twist yields a moiré pattern with a long lattice period. Quasiparticles perceive the resulting band-structure modulation as a potential landscape, making it possible to consider moiré heterostructures as a realization of a Bose-Hubbard model in a semiconductor material.

We address the question in how far correlated states of moiré excitons can emerge and study their phase transition behavior in relation to the twist angle between both monolayers. Expanding on previous results [1], we discuss the effect of nearest-neighbor interaction that gives rise to a variety of different phases, such as inhomogeneous insulating and supersolid phases. Special attention is paid to the possibility of local atomic reconstructions that are now known to occur at small twist angles.

[1] Götting et al., Phys. Rev. B 105, 165419 (2022)

HL 8.8 Mon 17:00 POT 81

Electronic structures of twisted bilayer graphene and tungsten diselenide investigated by transferable tight-binding-models — •XIAOYU LIU, STEFAN BLÜGEL, and HYUN-JUNG KIM — Peter Grünberg Institut and Institute for Advanced Simulation, Forschungszentrum Jülich and JARA, D-52425 Jülich, Germany

HL 9: Focus Session: Graphene quantum dots (joint session HL/TT)

Quantum dots have emerged as one of the contenders for a future quantum information processor. Bilayer graphene is now established as a material that allows high quality bi-polar Coulomb blockade measurement, time-dependent transport measurements and first relaxation time measurements. In contrast to the more conventional GaAs and Si-based systems, several exiting and unexpected observations in graphene have been explained by the peculiar graphene bandstructure, which is gate-tunable, the additional valley degree of freedom, and spin-valley coupling.

Organized by Klaus Ensslin

Time: Monday 15:00–17:45

Location: POT 361

Invited Talk

HL 9.1 Mon 15:00 POT 361

Spin and valley lifetime in graphene quantum dots — •GUIDO BURKARD — University of Konstanz, Germany

Graphene with its low nuclear spin density and weak spin-orbit coupling allows for long electron spin relaxation and coherence times. The spin and valley degrees of freedom of localized electrons can therefore be seen as potential embodiments of classical or quantum bits for computation. However, the formation of localized states in quantum dots requires some form of bandgap engineering, and the mechanisms for spin and valley relaxation have not been completely un-

derstood so far. Bilayer graphene has an electrically controllable bandgap that allows for the formation of quantum dots. We present general theoretical considerations regarding the formation of quantum dots in graphene and report on recent progress in understanding the relevant physical mechanisms of spin and valley relaxation in electrostatically gated bilayer graphene quantum dots.

Hyun-Jung Kim acknowledges support by the AvH Foundation.

15 min. break

Invited Talk

HL 8.9 Mon 17:30 POT 81

Time-resolved optical spectroscopy of 3R-stacked MoS_2 — •SWARUP DEB, MICHAEL KEMPF, RICO SCHWARTZ, and TOBIAS KORN — Institute of Physics, Rostock University

Manipulation of in-plane rotational and out-of-plane stacking symmetry in engineered two-dimensional (2D) crystals has provided means to realize a variety of exotic phases in extremely thin structures. The emergence of out-of-plane ferroelectricity in rhombohedrally-stacked 2D materials, such as boron nitride and transition metal dichalcogenides (TMDs), is a recent addition to this, but so far, most research on rhombohedrally stacked (3R) TMDs focussed on bilayer units.

Here, we present a systematic study of low-temperature absorption, differential reflectivity, and Kerr rotation in 3R-stacked MoS_2 as a function of thickness, aiming to probe the effects of ferroelectricity and interlayer charge transfer on ground-state exciton properties, valley and photocarrier dynamics. We observe clear signatures of an energetic splitting of the A exciton, as well as valley and energy relaxation dynamics on a few-ps timescale.

HL 8.10 Mon 18:00 POT 81

Constructing minimal tight-binding models for twisted TMDC bilayers — •MICHAEL WINTER, DOMINIK BENNER, and TIM WEHLING — I. Institute of Theoretical Physics, Universität Hamburg, Notkestraße 9-11, 22607 Hamburg, Germany

Transition metal dichalcogenides bilayers attract considerable attention within the last years due to the wide range of observable correlation effects, e.g. superconductivity, exciton condensation and there-like. One possible parameter to tune these phenomena is the twist angle between the two layers.

We study the electronic structure of twisted transition metal dichalcogenides from ab initio DFT calculations and subsequent Wannier construction on untwisted snapshots of commensurate structures. By choosing a subspace of only three Wannier orbitals per transition metal, we construct a minimal model for the description of twisted bilayers.

derstood so far. Bilayer graphene has an electrically controllable bandgap that allows for the formation of quantum dots. We present general theoretical considerations regarding the formation of quantum dots in graphene and report on recent progress in understanding the relevant physical mechanisms of spin and valley relaxation in electrostatically gated bilayer graphene quantum dots.

Invited Talk

HL 9.2 Mon 15:30 POT 361

Microscopic modelling of electrostatically induced bilayer graphene quantum dots — •ANGELIKA KNOTHE — Institut für Theoretische Physik, Universität Regensburg, D-93040 Regensburg, Germany

Quantum nanostructures, e.g., quantum wires and quantum dots, are needed for applications in quantum information processing devices, such as transistors or qubits. In gapped bilayer graphene, one can confine charge carriers purely electrostatically, inducing smooth confinement potentials and thereby limiting edge-induced perturbances while allowing gate-defined control of the confined structure. In this talk, I will give an overview of our recent contributions toward the theoretical modelling of gate-defined bilayer graphene quantum dots, taking into account microscopic details of the material properties and the confinement. As an outlook, I will point towards current and future challenges in describing coupled bilayer graphene nanostructures, e.g., setups with multiple bilayer graphene quantum dots.

HL 9.3 Mon 16:00 POT 361

Valley relaxation in a single-electron bilayer graphene quantum dot — •LIN WANG and GUIDO BURKARD — Department of Physics, University of Konstanz, D-78457, Germany

Bernal-stacked bilayer graphene (BLG) has a tunable gap controlled by an out-of-plane electric field. This makes BLG a possible candidate to form quantum dots (QDs) via quantum confinement. Spin-based qubits in BLG QDs have received great attention due to outstanding spin-coherence properties. Very recently, long spin relaxation times of a single-electron state in BLG QDs was reported [1,2]. In addition to spin, valley pseudospin is another degree of freedom in BLG. The two valleys experience opposite Berry curvatures and associated magnetic moments via an out-of-plane electric field. This provides a promising way to control valleys and further establish valley qubits. To assess the potential of valley qubits, the valley relaxation time is a crucial parameter since it directly limits the lifetime of encoded information. Here, we investigate the valley relaxation in a single-electron BLG QD due to intervalley coupling assisted by (i) $1/f$ charge noise and (ii) electron-phonon couplings arising from the deformation potential and bond-length change. Our calculation shows that valley relaxation time decreases with a power law dependence as a function of magnetic field, which is in a good agreement with very recent experiment.

References: [1] L. Banszerus, K. Hecker, S. Möller, E. Icking, K. Watanabe, T. Taniguchi, C. Volk and C. Stampfer, *Nat. Commun.* 13, 3637 (2022). [2] Lisa Maria Gächter et al., *PRX Quantum* 3, 020343 (2022).

30 min. break

Invited Talk

HL 9.4 Mon 16:45 POT 361

Single-shot spin and valley Pauli blockade read-out in bilayer graphene quantum dots — •CHUYAO TONG¹, REBEKKA GARREIS¹, WISTER WEI HUANG², ANNIKA KURZMANN^{1,2}, JOCELYN TERLE¹, SAMUEL JELE¹, KENJI WATANABE³, TAKASHI TANIGUCHI³, THOMAS IHN¹, and KLAUS ENSSLIN¹ — ¹ETH Zurich,

CH-8093 Zurich, Switzerland — ²RWTH Aachen University, Aachen, 52074, Germany — ³National Institute for Materials Science, 1-1 Namiki, Tsukuba 305-0044, Japan

In bilayer graphene quantum dots, apart from spins up and down, the additional valley degree of freedom K^- and K^+ gives rise to an unconventional single-dot two-carrier ground state: spin-triplet valley-singlet, altering the canonical even-odd double dot Pauli spin blockade picture. This ground state can be switched to a spin-singlet valley-triplet by a perpendicular magnetic field, allowing us to switch between valley-blockade at low, and spin-blockade at higher magnetic field for the two-carrier Pauli blockade (1,1) to (0,2). We employ charge sensing technology and perform single-shot Pauli blockade read-out at the two field regimes, probing characteristic relaxation times T_1 between spin or valley-triplet and -singlet. The spin- T_1 is measured to be up to 60ms, drastically decreasing with increasing inter-dot tunnel coupling and corroborating with recent experiments performed with single-dot Elzerman read-out. Moreover, we observe exceedingly long valley T_1 longer than 500ms, robust with inter-dot tunnel coupling. These promisingly long spin- and valley T_1 herald for long-living spin and valley bilayer graphene quantum dot qubits.

Invited Talk

HL 9.5 Mon 17:15 POT 361

Particle-hole symmetry protects spin-valley blockade in graphene quantum dots — •CHRISTIAN VOLK^{1,2}, LUCA BANSZERUS^{1,2}, SAMUEL MÖLLER^{1,2}, KATRIN HECKER^{1,2}, EIKE ICKING^{1,2}, KENJI WATANABE³, TAKASHI TANIGUCHI⁴, FABIAN HASSLER⁵, and CHRISTOPH STAMPFER^{1,2} — ¹JARA-FIT and 2nd Institute of Physics, RWTH Aachen University — ²Peter Grünberg Institute (PGI-9), Forschungszentrum Jülich — ³Research Center for Functional Materials, NIMS, Tsukuba, Japan — ⁴International Center for Materials Nanoarchitectonics, NIMS, Tsukuba, Japan — ⁵JARA-Institute for Quantum Information, RWTH Aachen University

Particle-hole symmetry plays an important role for the characterization of topological phases in solid-state systems. Graphene is a prime example of a gapless particle-hole symmetric system. The intrinsic Kane-Mele spin-orbit coupling in graphene leads to a lifting of the spin-valley degeneracy and renders graphene a topological insulator in a quantum spin-Hall phase while preserving particle-hole symmetry.

Here, we show that the Kane-Mele spin-orbit gap leads to a lifting of the spin-valley degeneracy in bilayer graphene quantum dots, resulting in Kramer's doublets with different ordering for electron and hole states preserving particle-hole symmetry. We observe the creation of single electron-hole pairs with opposite quantum numbers and use the electron-hole symmetry to achieve a protected spin-valley blockade in electron-hole double quantum dots. The latter will allow spin-to-charge and valley-to-charge conversion, which is essential for the operation of spin and valley qubits.

HL 10: Focus Session: Progress in Hybrid Phononic Quantum Technologies II

Time: Monday 15:00–18:30

Location: POT 151

Invited Talk

HL 10.1 Mon 15:00 POT 151

Surface Acoustic Wave Cavity Optomechanics with 2D Materials — •GALAN MOODY — University of California, Santa Barbara, CA, USA

Surface acoustic waves (SAWs) are a versatile tool for coherently interfacing with a variety of solid-state quantum systems spanning microwave to optical frequencies, including superconducting qubits, spins, and quantum emitters. In this presentation, I will discuss our progress on integrating 2D material quantum emitters with planar lithium niobate SAW resonators driven by superconducting electronics. Using steady-state photoluminescence spectroscopy and time-resolved single-photon counting, we map the temporal dynamics of modulated 2D emitters under coupling to different SAW cavity modes, showing energy-level splitting consistent with strong deformation potential coupling. We leverage the large anisotropic strain from the SAW to modulate the exciton and biexciton fine-structure splitting of 2D semiconductors, which may find applications for on-demand entangled photon-pair generation from 2D materials. I will conclude with a discussion on the prospects and outlook for SAW cavity optomechanics with 2D quantum emitters for high-speed single-photon modulators, efficient transducers, compact sensors, and exploring quantum electro-optomechanics with 2D materials.

Invited Talk

HL 10.2 Mon 15:30 POT 151

Phononic Microresonators Coupled by Surface Acoustic Waves — •SARAH BENCHABANE, MACIEJ BARANSKI, FENG GAO, OLIVIER GAIFFE, VALÉRIE SOUMANN, ROLAND SALUT, and ABDELKRIM KHELIF — FEMTO-ST, CNRS, Université Bourgogne-Franche-Comté, Besançon, France.

The implementation of scalable phononic circuits has become an appealing prospect in view of increasing the versatility of electro-acoustic devices for radio-frequency signal processing. Recent demonstrations have made convincing steps

towards this objective by proposing phononic architectures inspired by photonic integrated circuits or combining the rich dynamics of micro- and nano-electromechanical (M/NEMS) resonators with propagating elastic waves. In this work, we propose to exploit the interaction between surface acoustic waves (SAW) and locally-resonant, micron-scale mechanical resonators in order to achieve coherent driving of the resonator motion with SAW and, reciprocally, to control the elastic energy distribution at a deep sub-wavelength scale. Optical measurements by laser scanning interferometry allows retrieving both the resonator frequency response and mode shape, hence enabling direct observation of the vectorial nature of the interaction. We investigate the proposed physical system both in the linear and non-linear regimes and reveal that the elastic field behavior can be further controlled through resonator-to-resonator coupling, leading to a variety of interaction schemes. The proposed devices illustrate the potential of SAW-based architectures for the implementation of high-frequency phononic-NEMS circuits.

HL 10.3 Mon 16:00 POT 151

On-chip generation and dynamic piezo-optomechanical rotation of single photons — •MATTHIAS WEISS^{1,2}, DOMINIK D. BÜHLER³, ANTONIO CRESPO-POVEDA⁴, EMELINE D. S. NYSTEN^{1,2}, JONATHAN J. FINLEY⁵, KAI MÜLLER^{5,6}, PAULO V. SANTOS⁴, MAURICIO M. DE LIMA JR.³, and HUBERT J. KRENNER^{1,2} — ¹Physikalisches Institut, WWU Münster, Germany — ²Institut für Physik, Universität Augsburg — ³Materials Science Institute, University of Valencia, Spain — ⁴Paul-Drude Institute for Solid State Electronics, Berlin, Germany — ⁵Walter Schottky Institut, TU München, Germany — ⁶Department of Electrical and Computer Engineering, TU München, Germany

Integrated photonic circuits are key components for photonic quantum technologies and for the implementation of chip-based quantum devices. Future applications demand flexible architectures to overcome common limitations of

many current devices, for instance the lack of tuneability or built-in quantum light sources.

Here, we report on a dynamically reconfigurable integrated photonic circuit comprising integrated quantum dots (QDs), a Mach-Zehnder interferometer (MZI) and surface acoustic wave (SAW) transducers directly fabricated on a monolithic semiconductor platform. We demonstrate on-chip single photon generation by the QD and its sub-nanosecond dynamic on-chip control, enabling dynamic single photon routing with frequencies exceeding one gigahertz.

Bühler, D.D., Weiß, M., Crespo-Poveda, A. et al. Nat Commun 13, 6998 (2022)

HL 10.4 Mon 16:15 POT 151

Towards room temperature polaromechanics — •ISMAEL D.P. EMBID, ALEXANDER S. KUZNETSOV, KLAUS BIERMANN, and PAULO V. SANTOS — Paul-Drude-Institut für Festkörperelektronik, Leibniz-Institut im Forschungsverbund Berlin e.V., Berlin, Germany

Microcavity exciton-polaritons have emerged as a promising platform for novel solid-state devices ranging from low threshold lasers to quantum and classical simulators. The transition to a polariton condensate at high particle densities with long (ns) temporal coherence and enhanced sensitivity to vibrations has opened the way for polariton-based optomechanics in the GHz frequency domain [1]. Such highly coherent states have, however, so far been observed only at low temperatures (10K). Here, we show that long coherences can be maintained by confining the polariton condensates within μm -sized intracavity traps in (Al,Ga)As microcavities. In particular, we demonstrate temporal coherences in the GHz range up to temperatures exceeding 77K. Furthermore, we show that these condensates can be non-adiabatically modulated at these temperatures by electrically injected GHz phonons, leading to the formation of several phonon side bands. These results enable the generation of GHz optical frequency combs tunable by the electrical power, a relevant feature for the precise control of quantum states.

1. Kuznetsov et al., arXiv:2210.14331v1

30 min. break

HL 10.5 Mon 17:00 POT 151

Readout of phonon statistics via resonance fluorescence of a single photon emitter — •DANIEL GROLL¹, THILO HAHN¹, ORTWIN HESS², PAWEŁ MACHNIKOWSKI³, TILMANN KUHN¹, and DANIEL WIGGER² — ¹Institute of Solid State Theory, University of Münster, Germany — ²School of Physics, Trinity College Dublin, Ireland — ³Department of Theoretical Physics, Wrocław University of Science and Technology, Poland

Single photon emitters in a solid state environment are inevitably coupled to phonon modes of the host material. On the one hand, decoherence induced by this coupling is often detrimental for harnessing the full potential of such emitters. On the other hand, this interaction in principle allows for control of the emitter not only optically, but also acoustically. Hybrid systems, comprised of optical, acoustic and excitonic components thus offer a high degree of flexibility by making use of all available interaction channels.

We consider here a single photon emitter located inside a phononic resonator and driven by an external laser. We derive analytical expressions for the resonance fluorescence (RF) spectrum, depending explicitly on the quantum statistics of the resonator mode. We show that, in principle, the statistics of the phonon mode can be determined from a given RF spectrum using our analytical model. We thus establish a simple and direct connection between the optical and acoustic components of such a hybrid system, paving the way for using single photon emitters as quantum transducers between the optical and acoustic domain.

HL 10.6 Mon 17:15 POT 151

Dry processing of high Q 3C-silicon carbide nanostring resonators — •FELIX DAVID, PHILIPP BREDOL, EVA WEIG, and YANNICK KLASS — Technical University of Munich, Chair of Nano and Quantum Sensors, 85748 Munich, Germany We fabricate string resonators from strongly stressed 3C-silicon carbide (SiC) grown on a silicon substrate. In the conventional fabrication process, we do electron-beam lithography with PMMA to define a metallic hard mask for the subsequent dry-etching step via a liftoff process. This requires some wet-chemical process steps, which can destroy our samples. Here we describe an alternative process, which avoids all wet-chemical process steps to enable superior quality. It involves the use of a negative electron-beam resist as an etch mask, as well as the completely reactive-ion etching-based release of the nanostrings. The dry-processed nanostrings can be fabricated with a high yield and exhibit high mechanical quality factors at room temperature.

HL 10.7 Mon 17:30 POT 151

Acousto-optoelectric spectroscopy on transition metal dichalcogenide monolayers with surface acoustic waves — MATTHIAS WEISS^{1,2}, BENJAMIN MAYER¹, TOBIAS PETZAK², CLEMENS STROBL¹, •EMELINE NYSTEN^{1,2}, URSULA WURSTBAUER¹, and HUBERT KRENNER^{1,2} — ¹Physikalisches Institut, WWU Münster, Germany — ²Lehrstuhl für Experimentalphysik 1, Universität Augsburg, Germany

Surface acoustic waves have proven to be a useful tool for the control of semiconductor nanostructures optical properties and the dynamical transport of charge carriers [1,2,3]. For instance, SAW spectroscopy was already used to probe the electrical transport inside CVD-grown MoS₂ on LiNbO₃ in a contact-free manner [1]. In this work, we integrated transition metal dichalcogenide monolayer flakes into LiNbO₃ surface acoustic wave devices through a classical exfoliation process. The impact of the SAW on the photoluminescence of the monolayer was systematically studied. The results show a clear increase in the photoluminescence intensity of the monolayer as well as a SAW-periodic modulation which can be linked to the SAW-controlled diffusion of the excitons inside the monolayer.

[1] Nature Communications 6:8593 (2015)

[2] Nano Letters 19:8701-8707 (2019)

[3] IEEE Transactions on Quantum Engineering 3:1-17 (2022)

HL 10.8 Mon 17:45 POT 151

Strongly Stressed 3C-SiC Nanostring Resonators With High Quality Factors — •PHILIPP BREDOL¹, YANNICK KLASS¹, FELIX DAVID¹, EVA WEIG¹, NAGESH S. JAPTAP^{2,3}, MANFRED HELM^{2,3}, GEORGY ASTAKHOV², and ARTUR ERBE^{2,3} — ¹Technical University of Munich, Chair of Nano and Quantum Sensors, 85748 Munich, Germany — ²Helmholtz-Zentrum Dresden-Rossendorf, Institute of Ion Beam Physics and Materials Research, 01328 Dresden, Germany — ³Dresden University of Technology, 01062 Dresden, Germany

Strongly stressed SiC nanostring resonators are a promising platform for sensing applications. SiC is mechanically, chemically, and thermally robust and process compatible with many Si technologies. Mechanical quality factors in the 10⁵ range are achieved at room temperature with devices of $\approx 70 \times 1 \mu\text{m}^2$ footprint.

Because the mechanical quality factor often determines sensitivity and resolution of nanomechanical sensors, the understanding of mechanical loss mechanisms is important for possible applications. In this contribution we show how to separate intrinsic material losses and dissipation dilution effects by analyzing mechanical response spectra. We apply these methods to analyze how He⁺ irradiation damage affects the mechanical properties of SiC nanostring resonators (see contribution of Nagesh S. Jagtap).

HL 10.9 Mon 18:00 POT 151

Coupling single electrons and photons at photonic-chip based microresonators — •ARMIN FEIST^{1,2}, GUANHAO HUANG^{3,4}, GERMAINE AREND^{1,2}, YUJIA YANG^{3,4}, JAN-WILKE HENKE^{1,2}, ARSLAN SAJID RAJA^{3,4}, F. JASMIN KAPPERT^{1,2}, RUI NING WANG^{3,4}, HUGO LOURENÇO-MARTINS^{1,2}, QIU ZHERU^{3,4}, JUNQIU LIU^{1,2}, OFER KFIR^{3,4}, TOBIAS J. KIPPENBERG^{3,4}, and CLAUS ROPERS^{1,2} — ¹MPI for Multidisciplinary Sciences, Göttingen, Germany — ²4th Physical Institute, University of Göttingen, Germany — ³Institute of Physics, Swiss Federal Institute of Technology Lausanne, Switzerland — ⁴Center for Quantum Science and Engineering, Swiss Federal Institute of Technology Lausanne, Switzerland

Integrated photonics facilitates control over fundamental light-matter interactions in manifold quantum systems. Extending these capabilities to electron beams [1] fosters free-electron quantum optics.

Here, we show the coupling of single electrons and photons at a high-Q integrated photonic microresonator [2]. Spontaneous scattering at empty resonator modes creates electron-photon pair states [3], enabling single-particle heralding schemes and noise-suppressed mode imaging. This provides a pathway toward novel hybrid quantum technology with entangled electrons and photons, as well as the capability for quantum-enhanced electron imaging and Fock-state photon sources.

[1] J.-W. Henke *et al.*, Nature **600**, 653 (2021).

[2] A. Feist *et al.*, Science. **377**, 777 (2022).

[3] X. Bendaña *et al.*, Nano Lett. **11**, 5099 (2011).

HL 10.10 Mon 18:15 POT 151

Brillouin scattering selection rules in polarization-sensitive photonic resonators — ANNE RODRIGUEZ¹, PRIYA PRIYA¹, EDSON CARDOZO¹, ABDELMOUNAIM HAROURI¹, ISABELLE SAGNES¹, FLORIAN PASTIER², MARTINA MORASSI¹, ARISTIDE LEMAÎTRE¹, LOIC LANCO¹, •MARTIN ESMANN^{1,3}, and DANIEL LANZILLOTTI-KIMURA¹ — ¹Université Paris-Saclay, CNRS, Centre de Nanosciences et de Nanotechnologies, Palaiseau, France — ²Quandela SAS, Palaiseau, France — ³Institut für Physik, Universität Oldenburg, Germany

Spontaneous Brillouin scattering in bulk crystalline solids is governed by intrinsic selection rules which lock the relative polarization of excitation laser and Brillouin signal. In this work, we independently manipulate the polarization states of the two, using polarization-sensitive optical resonances in elliptical micropillars [1,2].

The induced wavelength-dependent polarization rotation [3] enables a polarization-based filtering technique [4]. We employ it to experimentally detect acoustic phonon resonances with frequencies in the range of 20-100 GHz, difficult to access with both standard Brillouin and Raman spectroscopy techniques. The strong modification of selection rules extends to any optical system with polarization-sensitive modes: plasmonic resonators, photonic crystals,

birefringent micro- and nanostructures. It is thus relevant for applications in optomechanical, optoelectronic, and quantum optics devices [1,2].

[1] H. Wang et al. Nat. Phot. 13, 770 (2019). [2] S. Gerhard et al. PRB 100, 115305 (2019). [3] B. Gayral et al. APL 72, 1421 (1998). [4] A. Rodriguez et al. arXiv:2209.12659 (2022).

HL 11: Quantum transport and quantum Hall effects I (joint session HL/TT)

Time: Monday 15:00–17:15

Location: POT 251

HL 11.1 Mon 15:00 POT 251

Local Chern patches and networks of chiral modes in quantum Hall phases with spatial magnetic field profiles. — •SURAJ HEGDE and TOBIAS MENG — Institute of Theoretical Physics and Würzburg-Dresden Cluster of Excellence ct.qmat, Technische Universität Dresden, 01069 Dresden, Germany.

Transport experiments on curved Hall bars show a variety of non-trivial transport signatures. Motivated by these experiments, we develop a model that accounts for various features in multi-terminal Hall bar measurements and perform numerical simulations using KWANT. We model the effect of curvature of the sample through spatial variation of the magnetic field profile and find that it results in patches of quantum Hall phases characterised by different local Chern markers. We find that most of the transverse and longitudinal transport can be understood in terms of local Chern patches and an intricate interplay of chiral modes at the interface of different patches. We also show that the spatial magnetic field textures could provide a novel platform to engineer lattices formed by networks of chiral modes.

HL 11.2 Mon 15:15 POT 251

Effect of the external fields in high Chern number quantum anomalous Hall insulators — •YURIKO BABA^{1,2}, FRANCISCO DOMÍNGUEZ-ADAME¹, and RAFAEL A. MOLINA-FERÁNDEZ² — ¹GISC, Departamento de Física de Materiales, Universidad Complutense, E-28040 Madrid, Spain — ²Instituto de Estructura de la Materia, IEM-CSIC, E-28006 Madrid, Spain

Multilayer structures consisting of alternating magnetic and undoped topological insulator layers have been proved so far to be a convenient platform for creating a quantum Anomalous Hall state with a high Chern number [1]. However, in previous proposals, the Chern number can only be tuned by varying the doping concentration or the width of the magnetic topological insulator TI layers. This restricts the applications of the dissipationless chiral edge currents in electronics, since the number of conducting channels remains fixed. In this work, we propose a way of varying the Chern number at will by means of an external electric field applied along the stacking direction. The electric field generates the hybridization of the inverted bands, generating new topological channels. In this way, the number of Chern states can be tuned externally in the sample, without the need of modifying the number and width of the layers or the doping level. We showed that this effect can be uncovered by the variation of the transverse conductance as a function of the electric field at constant injection energy at the Fermi level. [2]

[1] Zhao, Y. F. et al., Nature, 588 (2020) 419

[2] arXiv:2208.03585

HL 11.3 Mon 15:30 POT 251

Novel thermo-electric transport channel in the conformal limit of tilted Weyl semimetals — THORVALD BALLESTAD¹, ALBERTO CORTIJO², MARIA VOZMEDIANO³, and •ALIREZA QAIUMZADEH¹ — ¹Center for Quantum Spintronics, Norwegian University of Science and Technology, Trondheim, Norway — ²Universidad Autónoma de Madrid, Madrid, Spain — ³Instituto de Ciencia de Materiales de Madrid, CSIC, Madrid, Spain

Recently, a new contribution to the Nernst current was proposed in 3D Dirac and Weyl semimetals, originated from quantum conformal anomaly [1,2]. In the present study, we analyze the effect of the tilt on the transverse thermo-electric coefficient of Weyl semimetals in the conformal limit, i.e., zero temperature and zero chemical potential. Using the Kubo formalism, we find a non-monotonic behavior of the thermoelectric conductivity as a function of the tilt perpendicular to the magnetic field, and a linear behavior when the tilt is aligned to the magnetic field. An "axial Nernst" current is generated in inversion symmetric materials when the tilt vector has a projection in the direction of the magnetic field. This analysis will help in the design and interpretation of thermo-electric transport experiments in recently discovered topological quantum materials [3].

[1] M. N. Chernodub et al, Phys. Rev. Lett. 120, 206601 (2018). [2] V. Arjona et al, Phys. Rev. B 99, 235123 (2019). [3] T. M Ballestad, A. Cortijo, M. A. H. Vozmediano, A. Qaiumzadeh, arXiv:2209.14331 (2022).

HL 11.4 Mon 15:45 POT 251

Selective scattering between counter-propagating edge states in a topological insulator — •MENG HAO^{1,2}, LI-XIAN WANG^{1,2}, FABIAN SCHMITT^{1,2}, HARTMUT BUHMANN^{1,2}, and LAURENS W. MOLENKAMP^{1,2} — ¹Institute for Topological Insulators, Würzburg, Germany — ²Physikalisches Institut (EP III) Würzburg University, Würzburg, Germany

The quantum Hall state, known by its dissipationless nature, comprises chiral edge states in a two-dimensional electron gas (2DEG). In the ordinary quantum Hall effect, all edge states propagate in the same direction, populated equally. Thus, they are immune to inter-edge-state scattering. In contrast, counter-propagating edge states, populated unequally, are naturally sensitive to the scattering process. However, a realization of this scenario so far was only possible by stacked layers of high-mobility 2DEGs, e.g., quantum wells or graphene. Here we realize the counter-propagating edge states in a three-dimensional topological insulator controlled by top and bottom gates. Surprisingly, the counter-propagating edge states prove to scatter into each other selectively. Our first attempt shows that this inter-edge-state scattering occurs exclusively between Landau levels with the same Landau index. We further propose a cross bar equipped with split-gates to determine the selection rule of scattering and scattering parameters unambiguously. Following this proposal, we will show some preliminary results and report our experimental advances.

30 min. break

HL 11.5 Mon 16:30 POT 251

Edge modes, Hall conductivity and topological features of a dice lattice: Fate of flat bands under strain — •SAYAN MONDAL and SAURABH BASU — Indian Institute of Technology Guwahati

We study the topological properties of a dice lattice, which has three atoms per unit cell (A, B, and C). In addition, the bands are systematically deformed via the introduction of anisotropy among the nearest neighbour (NN) hoppings in two distinct ways. In the first case, we apply the uniaxial strain, which alters the NN hoppings (between the sublattices A-B and B-C) along the direction of applied strain. While in the second case, we selectively tune the NN hopping between A and B sublattices which may be achieved by a controlled chemical pressure. The first case yields the Chern insulating lobes in the phase diagram with $C = \pm 2$ till a certain critical anisotropy, where the spectral gap vanishes. The quantized plateau in the anomalous Hall conductivity and the pair of chiral edge modes at each edge of a ribbon support the obtained values of the Chern numbers. Whereas, the second case (selective strain) shows distorted flat band in the dispersion spectrum, which alters the gap-closing condition as compared to the case of uniaxial strain. Also, the Chern insulating lobes in the phase diagram and the Hall conductivity have distinct features compared to the case above. However, in both cases, topological phase transitions take place which is demonstrated via the Chern number changing discontinuously from ± 2 to zero across the gap-closing transitions.

HL 11.6 Mon 16:45 POT 251

Structure-imposed electronic topology in graphene nanoribbons — •FLORIAN ARNOLD¹, TSAI-JUNG LIU¹, AGNIESZKA KUC², and THOMAS HEINE^{1,2,3} — ¹Technische Universität Dresden, Dresden, Germany — ²HZDR, Leipzig, Germany — ³Yonsei University, Seoul, Republic of Korea

Zigzag graphene nanoribbons (ZGNR) can be transformed into new structure types by removing terminal carbon atoms in a regular pattern. When a single atom is removed on each zigzag edge so-called cove-edged ZGNR (ZGNR-C) are created, while removing multiple atoms results in gulf-edged ZGNR (ZGNR-G). In our seminal work, we demonstrated the direct structure-electronic structure relation based on the structural parameters that unambiguously characterize ZGNR-C. This allowed to create a scheme that classifies their electronic state, i.e., if they are metallic, topological insulators or trivial semiconductors, and to find an empirical formula for the band gap of the semiconducting ribbons. Since then, we were able to expand this description to ZGNR-G systems where the chemical space of possible structures increases further due to the variable size of the gulf edges. With this, we give guidance to realize new graphene nanoribbon heterojunctions hosting topological states and investigate the transport properties of exemplary systems.

HL 11.7 Mon 17:00 POT 251

Massive and topological surface states in strained HgTe and evidence for parity anomaly — •WOUTER BEUGELING^{1,2}, LIXIAN WANG^{1,2}, DAVID M. MAHLER^{1,2}, VALENTIN L. MÜLLER^{1,2}, EWELINA M. HANKIEWICZ³, HARTMUT BUHMANN^{1,2}, and LAURENS W. MOLENKAMP^{1,2} — ¹Institute for Topological Insulators, Würzburg, Germany — ²Physikalisches Institut (EP III), Würzburg University, Würzburg, Germany — ³Institute for Theoretical Physics and Astrophysics (TP IV), Würzburg University, Würzburg, Germany

The idea that band inversion in a narrow-gap material can lead to Dirac-type surface states was noted by Volkov and Pankratov in the 1980's. Only about two decades later, it was realized that the surface states of topological insulators are

the gapless Dirac states predicted by them. The massive Volkov-Pankratov states received much less attention. They are pulled from the bulk in a sufficiently large electric field and are topologically trivial. Until recently, direct evidence in the form of transport measurements was elusive.

From our magneto-transport experiments on a three-dimensional topological insulator heterostructure (strained HgTe), we demonstrate the coexistence of massless and massive Volkov-Pankratov states. The well-developed Hall quantization in the n- and the p-type regime is due to the topological surface state and the massive Volkov-Pankratov states, respectively, as confirmed by k-p theory. In a second series of experiments, we find a remarkable re-entrant quantum Hall effect in the p-type regime, which we can trace to spectral asymmetry, a salient manifestation of parity anomaly in a solid-state system.

HL 12: Semiconductor lasers I

Time: Monday 15:00–17:15

Location: POT 112

HL 12.1 Mon 15:00 POT 112

Adjustment of the active region on an InGaAsP VECSEL around 760nm for red pumping — •REBECCA RÜHLE, MARIUS GROSSMANN, MICHAEL JETTER, and PETER MICHLER — Institut für Halbleitertechnik und Funktionelle Grenzflächen, Center for Integrated Quantum Science and Technology (IQST) and SCoPE, Universität Stuttgart, Allmandring 3, 70569 Stuttgart, Germany

The quantum defect between the emission and the pump wavelength of vertical external-cavity surface-emitting lasers (VECSEL) has a huge impact on the performance of the structure. Especially to improve the thermal behavior, a longer wavelength pump laser is favorable. For the InGaAsP quantum well (QW) VECSEL with an emission wavelength at around 760nm, a pump laser at 675nm is preferable to one at 532nm. But the QWs are embedded in GaInP-barriers, thus are transparent for the pump light and the pump efficiency is rather small. To overcome this the composition of the GaInP can be changed so that the barrier again can absorb the pump light. The effects of adjusting the barrier in the active region and the performance of the VECSELs have now been investigated in detail. Photoluminescence and laser output power measurements were performed to compare the behavior of the different structures. A further study was carried out to evaluate the effect of the different gallium to indium ratio in the crystal structure on the surface roughness of the device.

HL 12.2 Mon 15:15 POT 112

Cavity effects in hybrid resonators embedding InGaAs quantum dots — •KARTIK GAUR, SARTHAK TRIPATHI, IMAD LIMAME, CHING-WEN SHIH, CHIRAG PALEKAR, SVEN RODT, and STEPHAN REITZENSTEIN — Institut für Festkörperphysik, Technische Universität Berlin, Germany

InGaAs quantum dots (QDs) embedded in microcavities based on highly reflective distributed Bragg reflectors (DBRs) allow for the development of high Q-factor, low mode volume micropillar cavities which feature high light-matter interaction. This makes them almost ideal candidates for quantum light sources and high- β microlasers. However, epitaxially grown GaAs/AlAs DBRs suffer from relatively low refractive index contrast, and often high absorption of the optical pumping laser. Here, we propose replacing the upper III-V DBR with dielectric DBR based on $\lambda/4$ -thick layers of SiO₂ and Si₃N₄ deposited using plasma-enhanced chemical vapor deposition. Numerical simulations are carried out to optimize the fabrication parameters and subsequently validate the optical properties. The MOCVD-grown InGaAs QD active region is integrated in the central one- λ GaAs cavity on top of the bottom DBR with 33 Al_{0.2}Ga_{0.8}As/Al_{0.9}Ga_{0.1}As mirror pairs, followed by electron beam lithography processing step to define photonic defects for lateral mode confinement. Such defects in the form of microlenses are created using a SiO₂ hard mask and wet chemical etching. We then deposit dielectric top DBR consisting of 15 $\lambda/4$ -thick SiO₂ and Si₃N₄ mirror pairs. The final structure is investigated via low-temperature micro-photoluminescence.

HL 12.3 Mon 15:30 POT 112

Latest developments on membrane external-cavity surface-emitting lasers (MECSELs) — •HERMANN KAHLE^{1,2}, PATRIK RAJALA², PHILIPP TATAR-MATHES², and MIRCEA GUINA² — ¹Institute for Photonic Quantum Systems (PhoQS), Department of Physics, Paderborn University, Warburger Straße 100, 33098 Paderborn, Germany — ²Optoelectronics Research Centre (ORC), Physics Unit / Photonics, Tampere University, Korkeakoulunkatu 3, 33720 Tampere, Finland

MECSELs have experienced a rapid progress in recent years. Based on the membrane geometry of MECSELs, an intrinsically excellent beam quality is one important benefit of this new vertically emitting kind of lasers. The most important recent progress, like continuous wave broadband tuning ($\Delta\lambda_{FWHM} \approx 70$ nm around $\lambda_0 = 985$ nm) and anti-resonant gain membrane design will be discussed.

HL 12.4 Mon 15:45 POT 112

Membrane saturable absorber mirror (MESAM) in a red-emitting VECSEL for the generation of stable ultrashort pulses — •ANA ĆUTUK, MARIUS GROSSMANN, MICHAEL JETTER, and PETER MICHLER — Institut für Halbleitertechnik und Funktionelle Grenzflächen, Center for Integrated Quantum Science and Technology (IQST) and SCoPE, Universität Stuttgart, Allmandring 3, 70569 Stuttgart

Optically-pumped semiconductor disk lasers, also known as vertical external-cavity surface-emitting lasers (VECSELs), provide several advantageous properties like near-diffraction-limited beam profile and the flexibility to add optical components inside the laser cavity and thereby modify the laser characteristics. One example is the semiconductor saturable absorber mirror (SESAM), a monolithic semiconductor structure consisting of a saturable absorber region on top of a distributed Bragg reflector (DBR). However, the epitaxial growth of SESAMs can be limited by the DBR design, making it difficult to fabricate pulsed lasers with wavelengths within spectral gaps. We demonstrate a membrane saturable absorber mirror (MESAM) which overcomes the growth restrictions of the DBR. A membrane containing the active region only is combined with a dielectric mirror and thus simulates a SESAM with an increased flexibility in design. We compare the dynamic properties of a SESAM- and MESAM-mode-locked VECSEL. With both devices we obtain fundamental mode locking with pulse durations in the ps-range.

30 min. break

HL 12.5 Mon 16:30 POT 112

AlGaInP-based VECSELs with grating waveguide structures — •PETER GIERSS¹, ANA ĆUTUK¹, MAXIM LEYZNER², UWE BRAUCH², MARWAN ABDOU AHMED², MICHAEL JETTER¹, THOMAS GRAF², and PETER MICHLER¹ — ¹Institut für Halbleitertechnik und Funktionelle Grenzflächen, Center for Integrated Quantum Science and Technology (IQST) and SCoPE, Universität Stuttgart, Allmandring 3, 70569 Stuttgart — ²Institut für Strahlwerkzeuge, Universität Stuttgart, Pfaffenwaldring 43, 70569 Stuttgart

Vertical external-cavity surface-emitting lasers (VECSELs) provide several superior properties like a near-diffraction beam profile and the flexibility to add optical components inside the cavity for further tailoring of the laser parameters. However, the heat generated by the pump laser within the active region proves to be a limiting factor for achieving higher output powers. This is mainly due to the poor thermal conductivity of the thick distributed Bragg reflector (DBR), which could be overcome by placing a heatspreader right next to the active region.

In this contribution, we present our recent progress in the development of an AlGaInP-VECSEL based on a grating waveguide structure (GWS). Excluding the DBR and adding a heatspreader instead improves the heat removal from the gain region while the guided-mode resonances from the GWS should provide good coupling of the pump and laser field and a high reflectivity to replace the function of the DBR. Our current research focuses on the fabrication and characterization of the high-contrast grating on top of a gain membrane.

HL 12.6 Mon 16:45 POT 112

Manipulating the emission characteristics of VCSEL in the red spectral range with polymer microlenses and etched surface reliefs — FARNAZ KHAMSEH, •LENA ENGEL, MICHAEL ZIMMER, SERGEJ VOLLMER, MICHAEL JETTER, and PETER MICHLER — Institut für Halbleitertechnik und Funktionelle Grenzflächen, Center for Integrated Quantum Science and Technology (IQST) and SCoPE, Universität Stuttgart, Allmandring 3, 70569 Stuttgart

Vertical-cavity surface-emitting lasers (VCSELs) are promising candidates for various applications like sensing, printing and data transfer due to their low power consumption and the possibility of arranging them in arrays. Especially in the red spectral range around 660nm VCSEL are interesting for example in

biomedical applications. However, their implementation is often hampered as light is emitted under an angle of divergence of 10° for single mode operation and higher order transverse modes are emitted especially for higher output power operation, further increasing the divergence and limiting the fiber coupling efficiency. Thus, the aim of this work is to improve the emission characteristics of red emitting VCSELs. Therefore, polymer microlenses for beam collimation are integrated directly on the VCSEL surface. Their ideal geometry and the tolerances for the alignment relative to the oxide aperture are thoroughly investigated utilizing ray-optics simulations. Additionally, etched surface reliefs are used to suppress the emission of higher order modes via a spatial modulation of the top mirror loss.

HL 12.7 Mon 17:00 POT 112

Multifold lasing threshold reduction of optically pumped micropillar lasers with low-absorbing $\text{Al}_{0.2}\text{Ga}_{0.8}\text{As}/\text{Al}_{0.9}\text{Ga}_{0.1}\text{As}$ distributed Bragg reflectors — •CHING-WEN SHIH¹, IMAD LIMAME¹, CHIRAG PALEKAR¹, SEBASTIAN KRÜGER¹, ARIS KOULAS-SIMOS¹, DANIEL BRUNNER², and STEPHAN REITZENSTEIN¹ —

¹Institut für Festkörperphysik, Technische Universität Berlin, Berlin, Germany — ²Département d'Optique P. M. Duffieux, Institut FEMTO-ST, Université Bourgogne-Franche-Comté CNRS UMR 6174, Besançon, France

Micropillar photonic devices, where the active layers are in an optical cavity sandwiched between epitaxially grown dielectric Bragg mirrors (DBRs), are one of the fundamental elements to study cavity quantum electrodynamics and to enable devices for quantum technology applications. Here, we report on the experimental realization of multifold lasing threshold reduction of optically pumped micropillar lasers by simply replacing the commonly used GaAs/ $\text{Al}_{0.9}\text{Ga}_{0.1}\text{As}$ DBRs with low-absorbing $\text{Al}_{0.2}\text{Ga}_{0.8}\text{As}/\text{Al}_{0.9}\text{Ga}_{0.1}\text{As}$ DBRs, which minimizes the DBRs absorption of the optical pump power. In pump-wavelength-dependent I/O measurements, we demonstrate that the incorporation of 20% Al content in the DBRs opens an optical pumping window from the absorption edge of $\text{Al}_{0.2}\text{Ga}_{0.8}\text{As}$ at 700 nm to the one of GaAs at 820 nm, where the excitation laser light can effectively reach the GaAs cavity above its bandgap while remaining transparent to the DBRs, resulting in high power conversion efficiency, low lasing threshold, and high thermal stability.

HL 13: Focus Session: Frontiers of Electronic-Structure Theory II (joint session O/HL)

Time: Monday 15:00–17:15

Location: TRE Ma

Topical Talk

HL 13.1 Mon 15:00 TRE Ma

Coupled-cluster theory for complex solids made ready — •ANDREAS GRÜNEIS — TU Wien, Institute for Theoretical Physics, Wiedner Hauptstraße 8-10/136, 1040 Vienna, Austria

This talk will review recent progress in applying periodic coupled-cluster theory, which has the potential to achieve a systematically improvable level of accuracy, to solids and surfaces. We will discuss novel techniques that reduce the computational cost by accelerating the convergence of calculated properties towards the complete basis set as well as the thermodynamic limit. The newly developed techniques have been implemented in the free and open source simulation software Cc4s that is interfaced to a growing number of widely-used electronic structure theory codes. These developments have enabled an increasing number of ab initio studies and allowed for assessing the level of accuracy of coupled-cluster theory by comparing to experimental findings as well as quantum Monte Carlo results. The presented applications will cover a wide range of materials science problems including the study of phase diagrams, molecule-surface interactions and properties of defects.

HL 13.2 Mon 15:30 TRE Ma

Speedup of structural optimisations using hybrid functionals: Case studies for energy materials — •DANIEL FRITSCHE — Weierstrass Institute for Applied Analysis and Stochastics, Mohrenstr. 39, 10117 Berlin, Germany — Helmholtz-Zentrum Berlin für Materialien und Energie, Hahn-Meitner-Platz 1, Berlin, 14109, Germany

First-principles calculations based on density functional theory have been established as de facto standard for computational materials investigations. Depending on the size of the unit cell, for every material of interest a suitable choice for the unknown exchange and correlation functional has to be made; taking not only into account the desired accuracy, but also the available computational resources.

In recent years, a promising combination of two approaches emerged, starting from a structural relaxation based on a simpler (semi)local functional, supplemented by a single shot hybrid functional calculation. Here, we propose a new method for combining different levels of exchange and correlation functional for structural relaxations.

In a first benchmarking step, this new method will be applied to various sets of promising energy materials, where full hybrid functional calculations are available, with a main focus on the performance of this new approach on the structural properties and the required computational resources. In a second step, this new approach will be applied to materials, which up-to-now have not been accessible to hybrid functional calculations due to the required computational resources. All the presented results on the structural, electronic, and optical properties will be critically discussed alongside experimental findings.

HL 13.3 Mon 15:45 TRE Ma

All-Electron Large-Scale Hybrid Density Functional Simulations — FLORIAN MERZ¹, ANDREAS MAREK², •SEBASTIAN KOKOTT³, CHRISTIAN CARBOGNO³, YI YAO³, MARIANA ROSSI⁴, MARKUS RAMPP², MATTHIAS SCHEFFLER³, and VOLKER BLUM⁵ — ¹Lenovo HPC Innovation Center, Stuttgart — ²Max Planck Computing and Data Facility, Garching — ³The NOMAD Laboratory at the FHI-MPG and IRIS-Adlershof HU, Berlin — ⁴MPI for the Structure and Dynamics of Matter, Hamburg — ⁵Duke University, North Carolina, USA

The localized resolution-of-identity approach [1] enables $O(N)$ hybrid density functional simulations and, thus, the computation of accurate electronic prop-

erties of large scale atomistic models in the range of ten thousands of atoms in *FHI-aims* [2]. In this range, parallelization and memory requirements of the exact exchange part, and the evaluation of the Hartree potential remain challenging. The solution of the generalized eigenvalue problem with direct eigensolvers like ELPA [3] naturally becomes a bottleneck due to $O(N^3)$ scaling. In this work, we present recent algorithmic advances for the exact exchange part and the evaluation of the Hartree potential, as well as optimizations of the ELPA library. We systematically perform benchmark tests on CPU and GPU-accelerated architectures covering inorganic solids, large molecules, and organic crystals with up to 50,000 atoms.

[1] Ihrig *et al.*, *New J. Phys.* **17**, (2015).

[2] Levchenko *et al.*, *Comp. Phys. Commun.* **192**, (2015).

[3] Marek *et al.*, *J. Phys. Condens. Matter* **26**, (2014).

15 min. break

HL 13.4 Mon 16:15 TRE Ma

A Koopman's compliant exchange correlation potential for semiconductors — •MICHAEL LORKE¹, PETER DEAK², and THOMAS FRAUENHEIM² — ¹Institute for Theoretical Physics, University of Bremen, Otto-Hahn-Allee 1, Bremen, 28359, Germany — ²BCCMS, University of Bremen, Germany

Density functional theory is the workhorse of theoretical materials investigations. Due to the shortcoming of (semi-)local exchange correlation potentials, hybrid functionals have been established for practical calculations to describe surfaces, molecular adsorption, and defects. These functionals operate by mixing between semi-local and Hartree-Fock exchange semi-empirically. However, their parameters have to be optimized for every material separately. To treat materials with a more physics driven approach and without the need of parameter optimization is possible with many-body approaches like GW, but at an immense increase in computational costs and without the access to total energies and hence geometry optimization. We propose a novel exchange correlation potential[1] for semiconductor materials, that is based on physical properties of the underlying microscopic screening. We demonstrate that it reproduces the low temperature band gap of several materials. Moreover it respects the required linearity condition of the total energy with the fractional occupation number, as expressed by the generalized Koopman's theorem. We also show that this novel functional can be used as a kernel in linear response TDDFT to reproduce excitonic effects in optical spectra [1] *Physical Review B* 102 (23), 235168 (2020)

HL 13.5 Mon 16:30 TRE Ma

Accurate and efficient treatment of spin-orbit coupling via second variation employing local orbital basis functions — •HANNAH KLEINE¹, ANDRIS GULANS², SVEN LUBECK¹, CECILIA VONA¹, and CLAUDIA DRAXL¹ — ¹Institut für Physik and IRIS Adlershof, Humboldt-Universität zu Berlin — ²Department of Physics, University of Latvia

Spin-orbit-coupling (SOC) effects can significantly change the properties of materials containing heavy elements, mostly by introducing shifts and splittings in the band structure. Including SOC effects in density-functional-theory (DFT) calculations can be challenging. In the linearized augmented planewaves plus local orbitals (LAPW+LO) method, SOC is treated as a perturbation and solved by a second variational (SV) scheme where eigenvectors of the scalar-relativistic Kohn-Sham Hamiltonian are used as basis functions for the SO-coupled problem. For certain materials, especially those with strong SOC effects, many SV basis functions are required which leads to high computational costs. By adding

LOs to the SV basis, we are able to drastically reduce the basis-set size and thus the computational cost. We implement this approach in the all-electron full-potential computer package exciting [1] and combine it with the use of relativistic LOs to achieve high accuracy results for a variety of different materials.

[1] A. Gulans et al., *J. Phys. Condens. Matter* 26, 363202 (2014).

HL 13.6 Mon 16:45 TRE Ma

Exact sum-rule approach to polarizability and asymptotic van der Waals functionals – derivation of exact benchmarks — •ALBERTO AMBROSETTI¹, JOHN DOBSON², MATTEO RICCI¹, and PIER LUIGI SILVESTRELLI¹ — ¹Dipartimento di Fisica e Astronomia, Università degli Studi di Padova, via Marzolo 8, 35131, Padova, Italy — ²Nanoscale Science and Technology Centre, Griffith University, Nathan, Queensland 4111, Australia

Using a sum-rule approach we develop an exact theoretical framework for polarizability and asymptotic van der Waals correlation energy functionals of isolated objects[1]. The functionals require only monomer groundstate properties as input. Functional evaluation proceeds via solution of a single position-space differential equation, without the usual summations over excited states or frequency integrations. Explicit functional forms are reported for reference physical systems, including atomic hydrogen and single electrons subject to harmonic confinement, and immersed in a spherical-well potential. Direct comparison with the popular Vydrov-van Voorhis density functional shows that this performs best when density decay occurs at atomic scales. The adopted sum-rule approach implies general validity of our theory, enabling exact benchmarking of van der Waals density functionals, and direct inspection of the subtle long-range correlation effects that constitute a major challenge for approximate (semi-)local

density functionals.

[1] M Ricci, PL Silvestrelli, JF Dobson, A Ambrosetti *J. Phys. Chem. Lett.* 13, 8298-8304

HL 13.7 Mon 17:00 TRE Ma

Interacting electrons and bosons in the doubly screened $G\bar{W}$ approximation — •YAROSLAV PAVLYUKH — Department of Theoretical Physics, Wrocław University of Science and Technology

In Ref. [1] we built on the Generalized Kadanoff-Baym Ansatz for electrons and bosons to map a broad class of nonequilibrium Green's function theories onto a coupled system of ordinary differential equations with linear time-scaling. Available methods to treat e - e correlations include GW [2], T -matrix and Faddeev, while e - b correlations are described by Ehrenfest and second-order diagrams in the e - b coupling [3].

In this work we present a substantial advance in the treatment of correlations, requiring no extra computational cost and preserving all conserving properties. Specifically, we include the effects of dynamical screening due to *both* e - e and e - b interactions ($G\bar{W}$ approximation). The $G\bar{W}$ extension opens the door to a wealth of phenomena ranging from carrier relaxation and exciton recombination to molecular charge migration and transfer in optical or plasmonic cavities.

[1] Y. Pavlyukh, E. Perfetto, D. Karlsson, R. van Leeuwen, and G. Stefanucci, *Phys. Rev. B* 105, 125134 (2022).

[2] E. Perfetto, Y. Pavlyukh, and G. Stefanucci, *Phys. Rev. Lett.* 128, 016801 (2022).

[3] D. Karlsson, R. van Leeuwen, Y. Pavlyukh, E. Perfetto, and G. Stefanucci, *Phys. Rev. Lett.* 127, 036402 (2021).

HL 14: 2D Materials III (joint session HL/CPP)

Time: Tuesday 9:30–12:15

Location: POT 81

HL 14.1 Tue 9:30 POT 81

Sub-THz detection in two dimensional systems and CVD graphene heterostructures — FRANZISKA LINSS¹, VINCENT STRENZKE¹, PAI ZHAO¹, CHITHRA S. SHARMA¹, LARS TIEMANN¹, •QIN HUA², and ROBERT H. BLICK¹ — ¹Center for Hybrid Nanostructures, Universität Hamburg, Luruper Chaussee 149, 22761 Hamburg, Germany — ²Suzhou Institute of Nanotech and Nanobionics (SINANO) of the Chinese Academy of Sciences (CAS), China

Electromagnetic radiation in the THz range can induce surface plasmons, i.e., a collective motion of electrons, in graphene-based devices. We fabricated a field-effect-transistor with asymmetric dual-grating gates (ADGG) to detect sub-THz radiation using large-scale graphene that was synthesized by chemical vapor deposition (CVD). The CVD graphene sheet is encapsulated between two flakes of hBN and placed on a highly doped Si wafer that acts as a back gate. The ADGG was structured on the top hBN flake. The control of the carrier concentration via electrostatic gates is crucial to match the resonance condition of the plasmons. The sample was characterized by sweeping the top gate voltage from -1 V to 2 V and the charge neutrality point was reached at a top gate voltage of 0.87 V at 4.2 Kelvin. Furthermore, we used a high electron mobility transistor (HEMT) to detect THz radiation, where the detection mechanism is based on a mixing with a reference radiation in a nonlinear medium. In this device, we can demonstrate sub-THz radiation at room temperature.

HL 14.2 Tue 9:45 POT 81

Theory of non-local Andreev reflection through Andreev molecular states in graphene Josephson junctions — •ANDOR KORMÁNYOS¹, EDUÁRD ZSURKA¹, NOEL PLASZKÓ¹, and PÉTER RAKYTA^{1,2} — ¹Department of Physics of Complex Systems, Eotvos Lorand University, Budapest, Hungary — ²Wigner Research Center for Physics, 29-33 Konkoly-Thege Miklos Str., H-1121 Budapest, Hungary

We propose that a device composed of two vertically stacked monolayer graphene Josephson junctions can be used for Cooper pair splitting. The hybridization of the Andreev bound states of the two Josephson junction can facilitate non-local transport in this normal-superconductor hybrid structure, which we study by calculating the non-local differential conductance. Assuming that one of the graphene layers is electron and the other is hole doped, we find that the non-local Andreev reflection can dominate the differential conductance of the system. Our setup does not require the precise control of junction length, doping, or superconducting phase difference, which could be an important advantage for experimental realization.

HL 14.3 Tue 10:00 POT 81

Quantum Hall measurements near electric field controlled Lifshitz transitions in trigonally warped bilayer graphene — •MARTIN STATZ, ANNA SEILER, JONAS PÖHLS, MORITZ KNAK, FRANCESCA FARLORSI, and THOMAS WEITZ — 1st Physical Institute, Faculty of Physics, University of Göttingen, Friedrich-Hund-Platz 1, Göttingen 37077, Germany

Various spontaneous symmetry broken phases such as Stoner ferromagnetism, spin-polarized superconductivity, a quantum anomalous Hall octet and a topologically non-trivial Wigner-Hall crystal phase have recently been reported in bilayer graphene (BLG) [1]. Since these interaction-driven phenomena are dictated by the ratio of the Coulomb and kinetic energy of carriers, they can be promoted by the formation of flat bands and a divergent density of states (DoS) near Lifshitz transitions (LT). Trigonally warped BLG at low vertical displacement fields (D-field) and carrier densities ($\sim 10^{11} \text{ cm}^{-2}$) displays one centre and three off-centre Dirac cones in each valley, and therefore offers a rich playground for correlated phases (CP) and changes in the Fermi surface topology by inducing charge density and D-field driven LT. Here, we report on quantum Hall measurements near charge density and D-field driven LT in trigonally warped BLG encapsulated in hexagonal boron-nitride in a dual-gated architecture with graphite contacts and graphite gates at 10 mK. We further outline our status on the temperature dependence of several CP in the aforementioned regimes.

[1] Seiler, A.M. et al. *Nature* 608, 298-302 (2022)

HL 14.4 Tue 10:15 POT 81

Tuning electronic properties of graphene with a transferred ultrathin Ga_2O_3 encapsulation — MATTHEW GEBERT¹, •SEMONTI BHATTACHARYYA², CHRISTOPHER BOUNDS¹, NITU SYED^{3,4}, TORBEN DAENEKE⁴, and MICHAEL S. FUHRER¹ — ¹School of Physics and Astronomy, Monash University, Melbourne — ²Leiden Institute of Physics, Leiden University, Leiden — ³School of Physics, The University of Melbourne, Parkville, Melbourne — ⁴School of Engineering, RMIT University, Melbourne

Although graphene holds immense potential for future electronics and spintronics, it is tricky to find a suitable large-area encapsulation layer for graphene that enhances its properties. In this talk, I will demonstrate a large-area passivation layer for graphene by mechanical transfer of ultrathin Ga_2O_3 synthesized on the surface of liquid Ga metal.¹

Electrical measurements of millimetre-scale passivated and bare CVD graphene on SiO_2 substrate indicate that the passivated graphene maintains its high field effect mobility, desirable for applications. Surprisingly, the temperature-dependent resistivity is reduced in our passivated graphene over a range of temperatures below 230 K, due to the interplay of screening of the remote optical phonon modes of the SiO_2 by the high dielectric constant of Ga_2O_3 , and the relatively high characteristic phonon frequencies of Ga_2O_3 . Raman spectroscopy and electrical measurements indicate that Ga_2O_3 passivation also protects graphene from further processing such as plasma-enhanced atomic layer deposition of Al_2O_3 .

Gebert, Bhattacharyya et al, *Nano Lett.* <https://doi.org/10.1021/acs.nanolett.2c03492>

HL 14.5 Tue 10:30 POT 81

Hopping transport in ultraclean dual graphite gated bilayer graphene — •DAVID ALEXANDER DAREK EMMERICH¹, EIKE THOMAS ICKING^{1,2}, PHILIPP SCHMIDT^{1,2}, FRANK VOLMER^{1,3}, KENJI WATANABE⁴, TAKASHI TANIGUCHI⁵, BERND BESCHOTEN¹, and CHRISTOPH STAMPFER^{1,2} — ¹RWTH Aachen University, Germany — ²Forschungszentrum Jülich, Germany — ³AMO GmbH, Advanced Microelectronic Center Aachen (AMICA), Germany — ⁴Research Center for Functional Material, Japan — ⁵International Center for Materials Nanoarchitectonics, Japan

Bernal-stacked bilayer graphene (BLG) is a material that has a unique property: BLG is intrinsically a semimetal, but becomes a semiconductor under the application of an out-of-plane displacement field. This controlled opening of a gate-tunable band gap makes it a promising material for realizing highly-tunable transistors and photodetectors. The limiting factor of BLG-based devices is disorder. Only by using graphitic bottom gates a true band insulating state was achieved in BLG, which exhibits a clean gap opening with faint signs of residual disorder. Using finite bias spectroscopy, we show that BLG devices with graphitic top and bottom gate electrodes exhibit extremely low disorder. We perform transport measurements down to the sub-Kelvin regime and analyse the temperature-dependent transport behaviour. For small displacement fields, where gap and disorder are expected to be of the same order of magnitude, the low-temperature hopping transport data are investigated concerning the dominant hopping mechanism.

15 min. break

HL 14.6 Tue 11:00 POT 81

high responsivity monolayer MoS₂ photodetectors on cyclic olefin copolymer-passivated SiO₂ gate dielectric — •EMAD NAJAFIDEHGHANI¹, SIRRI BATUHAN KALKAN², ZIYANG GAN¹, JAN DREWNIOK², MICHAEL F LICHTENEGGER², UWE HÜBNER³, ALEXANDER S URBAN², ANTONY GEORGE¹, BERT NICKEL², and ANDREY TURCHANIN¹ — ¹Friedrich Schiller University Jena, Institute of Physical Chemistry, Jena — ²Ludwig Maximilian University of Munich, Faculty of Physics, Munich — ³Leibniz Institute of Photonic Technology (IPHT), Jena

2D material-based photodetectors attracted significant research interest due to their high responsivity, flexibility and transparency. However, the trap states present at the surface of SiO₂ gate dielectrics diminishes the performance of 2D material-based photodetectors. To reduce the detrimental effect of SiO₂ surface traps, an ultrathin film (5 nm) of cyclic olefin copolymer (COC) layer is employed as a surface passivator. Due to the reduction of the interface trap density, the photoresponsivity of the MoS₂ devices on passivated SiO₂ is enhanced by four orders of magnitude compared to non-passivated MoS₂ devices. Under optimized conditions a record photoresponsivity of 3×10^7 A/W in combination with a short response time is observed. Our findings show that the ultrathin COC passivation of the gate dielectric enables to probe exciting properties of the atomically thin 2D semiconductors.

HL 14.7 Tue 11:15 POT 81

Atomic layer deposition of horizontal and vertical MoS₂/WS₂ heterostructures — •CHRISTIAN TESSAREK, TIM GRIEB, ANDREAS ROSENAUER, and MARTIN EICKHOFF — Institut für Festkörperphysik, Universität Bremen

Beyond the properties of single two-dimensional (2D) layers, heterostructures made of 2D transition metal dichalcogenides promise new properties based on moiré physics and interlayer excitons.

Vertical and horizontal MoS₂ and WS₂ heterostructures were grown by atomic layer deposition (ALD) and analyzed by Raman and photoluminescence spectroscopy. The influence of the the ALD growth sequence, i.e. MoS₂/WS₂ vs. WS₂/MoS₂, was investigated. Elemental distribution of Mo and W in a horizontal heterostructure was studied by high resolution transmission electron microscopy and energy-dispersive X-ray spectroscopy. Additional high temperature annealing was performed to improve the structural and optical properties of the layers.

HL 14.8 Tue 11:30 POT 81

Fully automated platform for 2D material flake detection using real-time machine learning techniques — •JAN-LUCAS USLU, TAOUFIQ OUAJ, BERND BESCHOTEN, LUTZ WALDECKER, and CHRISTOPH STAMPFER — JARA-FIT and 2nd Institute of Physics A, RWTH Aachen University, Aachen, Germany

As of today, most of fundamental experimental 2D material research is based on mechanically exfoliated flakes, finding suitable flakes for the fabrication of van der Waal heterostructures is time-consuming and time-critical part requiring expert knowledge and manpower.

In order to mitigate this problem, we demonstrate a simple and robust real time-capable algorithm based on Gaussian mixture models, a machine learning technique, to allow for a fast automated search of exfoliated flakes of different 2D materials in a single run with an automated microscope setup to analyze batches of exfoliated material.

The algorithm solves the task of automatically detecting various flakes on Si++/SiO₂ wafer dices, allows to index the location and segmentation of each flake and provides metrics such as size, thickness and shape.

The algorithm is evaluated on more than 500.000 images of different 2D materials including graphene and multilayer graphene, hexagonal boron nitride, transition metal dichalcogenides and 2D magnets.

HL 14.9 Tue 11:45 POT 81

CVD Growth of Hexagonal Boron Nitride on CMOS-compatible Substrates

— •MAX FRANCK¹, JAREK DABROWSKI¹, MARKUS ANDREAS SCHUBERT¹, WALTER BATISTA PESSOA², DOMINIQUE VIGNAUD², LUC HENRARD³, CHRISTIAN WENGER^{1,4}, and MINDAUGAS LUKOSIUS¹ — ¹IHP - Leibniz-Institut für innovative Mikroelektronik, Im Technologiepark 25, 15236 Frankfurt (Oder), Germany — ²University Lille, CNRS, Centrale Lille, JUNIA ISEN, University Polytechnique Hauts de France, UMR 8520-IEMN F-59000 Lille, France — ³Department of Physics, Namur Institute of Structured Materials, University of Namur, Rue de Bruxelles 61, 5000 Namur, Belgium — ⁴Semiconductor Materials, BTU Cottbus-Senftenberg, Platz der Deutschen Einheit 1, 03046 Cottbus, Germany

Hexagonal boron nitride (hBN) is a two-dimensional insulator with a range of promising applications, including DUV optoelectronics and protection layers for high-mobility graphene. Most commonly, high-quality hBN is grown via CVD on catalytic transition metal substrates. However, the hBN films require transfer to CMOS-compatible substrates, which leaves residual metal contaminations at concentrations unacceptable for Si technology integration.[1] Therefore, growth of hBN thin films directly on CMOS-compatible substrates, such as Si, Ge or dielectrics, is desirable. We present recent results regarding CVD synthesis of well-oriented, few-layer hBN films on such substrates using borazine as a single-source precursor. Morphology and crystalline quality were characterized using XPS, AFM, Raman spectroscopy and TEM. [1] G. Lupina, J. Kitzmann, et al. ACS Nano 2015, 9, 4776-4785.

HL 14.10 Tue 12:00 POT 81

Microwave plasma driven 2H-1T phase modulation of WSe₂ for improving NO₂ gas sensing performance — •YU DUAN^{1,2}, SAM ZHANG², HUAPING ZHAO¹, and YONG LEI¹ — ¹Fachgebiet Angewandte Nanophysik, Institut für Physik & IMN MacroNano, Technische Universität Ilmenau, 98693 Ilmenau, Germany — ²Center for Advanced Thin Films and Devices, School of Materials and Energy, Southwest University, Chongqing, 400715, China

Transition metal dichalcogenides (TMDs) have been widely used in recent years for gas sensors. Herein, we constructed a simple microwave plasma device by modifying a home microwave oven for surface treatment of WSe₂. A 1T/2H hybrid phase structure was constructed by phase modulation and Se vacancies were introduced to effectively enhance its gas sensing performance. The sample after 60 s of treatment exhibited high response (52.24%), fast response rate (49.8 s), short recovery time (14.9 mins), and outstanding stability and selectivity for 1 ppm NO₂ at room temperature. In addition, molecular model of the microwave plasma-treated sample is proposed, leading to the intrinsic mechanism of its performance enhancement. It is demonstrated that microwave plasma treatment is a promising method to enhance the gas sensing performance of TMDs.

Transition metal dichalcogenides (TMDs) have been widely used in recent years for gas sensors. Herein, we constructed a simple microwave plasma device by modifying a home microwave oven for surface treatment of WSe₂. A 1T/2H hybrid phase structure was constructed by phase modulation and Se vacancies were introduced to effectively enhance its gas sensing performance. The sample after 60 s of treatment exhibited high response (52.24%), fast response rate (49.8 s), short recovery time (14.9 mins), and outstanding stability and selectivity for 1 ppm NO₂ at room temperature. In addition, molecular model of the microwave plasma-treated sample is proposed, leading to the intrinsic mechanism of its performance enhancement. It is demonstrated that microwave plasma treatment is a promising method to enhance the gas sensing performance of TMDs.

HL 15: Spin phenomena in semiconductors

Time: Tuesday 9:30–10:30

Location: POT 361

HL 15.1 Tue 9:30 POT 361

Photoexcited charge carrier and spin dynamics in methylammonium lead bromide doped by magnetic transition metals. — •STANISLAV BODNAR, JONATHAN ZERHOCH, SHANGPU LIU, ANDRII SHCHERBAKOV, and FELIX DESCHLER — PCI, Universität Heidelberg, Im Neuenheimer Feld 253, 69120 Heidelberg

One of the most challenging tasks for LED applications is emitting 100% polarized light from the device. Typically, this is achieved by introducing an addi-

tional layer of polarization filter which leads to losing half of the light intensity. To overcome this issue, one has to find a system with a high degree of photoluminescence (PL) polarization. A promising approach here is using magnetic metal doping in combination with a highly efficient semiconductor. We have chosen to use transient absorption (TA) spectroscopy at cryogenic temperatures to investigate changes in the optical properties induced by magnetic metal doping in CH₃NH₃PbBr₃ since it gives spectral information about the energies of electronic states and dynamic properties of the photoexcited carriers. We find a change in the main ground state bleach (GSB) peak position in

doped $\text{CH}_3\text{NH}_3\text{PbBr}_3$, which depends on the transition metal used. The main GSB peak of pure $\text{CH}_3\text{NH}_3\text{PbBr}_3$ at 4 K is at 2.32 eV. Doping $\text{CH}_3\text{NH}_3\text{PbBr}_3$ with Mn leads to a shift of the main peak to lower energies by 0.04 eV. The modifications of the TA spectra are associated with changes in the bandgap energy, which is the result of doping-induced lattice expansion. Additionally, we observed changes in the spin lifetime by an order of magnitude which could be associated with modification of the Rashba field.

HL 15.2 Tue 9:45 POT 361

Mode locking of hole spin coherences in $\text{CsPb}(\text{Cl},\text{Br})_3$ perovskite nanocrystals — •ERIK KIRSTEIN¹, NATALIA E. KOPTOVA¹, DMITRI R. YAKOVLEV^{1,2,3}, EVGENY A. ZHUKOV^{1,2}, ELENA V. KOLOBKOVA^{4,5}, MARIA S. KUZNETSOVA⁶, VASILY V. BELYKH³, IRINA A. YUGOVA⁶, MIKHAIL M. GLAZOV², MANFRED BAYER¹, and ALEX GREILICH¹ — ¹Experimental Physics 2, Department of Physics, TU Dortmund, 44227 Dortmund, Germany — ²St. Petersburg, Russia — ³Moscow, Russia — ⁴St. Petersburg, Russia — ⁵St. Petersburg, Russia — ⁶St. Petersburg, Russia

The spin physics of perovskite nanocrystals is attracting increasing attention, both for fundamental studies and spintronic applications. Here, stable $\text{CsPb}(\text{Cl}_{0.5}\text{Br}_{0.5})_3$ lead halide perovskite nanocrystals embedded in a fluorophosphate glass matrix are studied by time-resolved optical spectroscopy to unravel the coherent spin dynamics of holes and their interaction with nuclear spins of the ²⁰⁷Pb isotope. We demonstrate the spin mode locking effect and nuclear induced frequency focussing leading to the synchronization of the hole spin Larmor precession frequencies of the nanocrystal ensemble.

HL 15.3 Tue 10:00 POT 361

Spin-flip Raman scattering on resident electrons and holes in two-dimensional $(\text{PEA})_2\text{PbI}_4$ perovskites — •CAROLIN HARKORT¹, DENNIS KUDLACIK¹, NATALIA E. KOPTOVA¹, DMITRI R. YAKOVLEV¹, MAREK KARZEL¹, ERIK KIRSTEIN¹, OLEH HORDIICHUK^{2,3}, MAKSYM V. KOVALENKO^{2,3}, and MANFRED BAYER¹ — ¹Experimentelle Physik 2, Technische Universität Dortmund, 44221 Dortmund — ²Laboratory of Inorganic Chemistry, Department of Chemistry and Applied Biosciences, ETH Zürich, CH-8093 Zürich, Switzerland —

³Laboratory for Thin Films and Photovoltaics, Empa-Swiss Federal Laboratories for Materials Science and Technology, CH-8600 Dübendorf, Switzerland

Two-dimensional lead halide perovskites are promising material systems for photovoltaic and optoelectronic applications. They are attractive for optical control of carrier spins due to an increased chemical stability compared to bulk lead halide perovskites. With the technique of Spin-flip Raman scattering we investigated in 2D Ruddlesden-Popper type $(\text{PEA})_2\text{PbI}_4$ perovskites the Zeeman splitting of carrier spins, resident electrons and holes, that can be detected through the exciton emission. The Landé-factors of these electrons and holes and their anisotropy are measured at a low temperature of 2 K. We show that the hole Zeeman splitting is affected by the Overhauser field resulting from the dynamic nuclear polarization which allows us to define the sign of the hole Landé-factor. In this structure the Overhauser field has a maximum value of 600 mT.

HL 15.4 Tue 10:15 POT 361

Microscopic origin of the effective spin-spin interaction in a semiconductor quantum dot ensemble — FREDRIK VONHOFF^{1,2}, ANDREAS FISCHER¹, •KIRA DELTENRE¹, and FRITHJOF B. ANDERS¹ — ¹Department of Physics, TU Dortmund University, D-44227 Dortmund — ²Department of Physics, Technical University of Munich, D-85748 Garching

We present a microscopic model for a singly charged quantum dot (QD) ensemble to reveal the origin of the long-range effective interaction between the electron spins in the QDs. Wilson's numerical renormalization group (NRG) is used to calculate the magnitude and the spatial dependency of the RKKY interaction mediated by the growth-induced wetting layer.

Using the NRG results obtained from realistic parameters as input for a semi-classical simulation for a large QD ensemble, we demonstrate that the experimentally reported phase shifts in the coherent spin dynamics between single and two-color laser pumping can be reproduced by our model [1], solving a longstanding open problem of the microscopic origin of the inter-QD electron spin-spin interaction.

[1] F. Vonhoff, A. Fischer, K. Deltenre, and F. B. Anders, Phys. Rev. Lett. **129**, 167701 (2022)

HL 16: Quantum dots: Transport (joint session HL/TT)

Time: Tuesday 9:30–12:15

Location: POT 151

HL 16.1 Tue 9:30 POT 151

Contact formation analysis of nickel to SiGeOI to form Nickel-Germanosilicide using Flash lamp annealing — •MUHAMMAD MOAZZAM KHAN¹, SLAWOMIR PRUCNAL¹, and YORDAN M. GEORGIEV^{1,2} — ¹Institute of Ion Beam Physics and Materials Research, Helmholtz-Zentrum Dresden-Rossendorf, Bautzner Landstraße 400, D-01328 Dresden, Germany — ²Institute of Electronics at the Bulgarian Academy of Sciences, 72, Tzarigradsko chaussee blvd, 1784-Sofia, Bulgaria

In CMOS technology, parasitic source/drain (S/D) resistance becomes more crucial in determining the overall device performance as the device dimensions get smaller. The contact resistance dominates this parasitic S/D resistance to a great extent, which limits the drive current. In order to have minimal impact on electrical performance, the contact should have linear Current-Voltage characteristics and negligible resistance in comparison to the device resistance. When replacing silicon with silicon-germanium as a channel material in future devices, it is necessary to investigate the contact formation mechanism in order to develop suitable contacts for energy-efficient devices. In this work, we are investigating metal semiconductor contact formation on SiGeOI using flash lamp annealing and studying their properties using structural and electrical characterization.

HL 16.2 Tue 9:45 POT 151

Predicting charge density maps in 2D nanostructures with machine learning techniques — •AMANDA TEODORA PREDA^{1,2,3}, CALIN ANDREI PANTIS-SIMUT^{1,2,3}, NICOLAE FILIPOIU^{2,3}, LUCIAN ION², ANDREI MANOLESCU⁴, and GEORGE ALEXANDRU NEMNES^{1,2,3} — ¹Research Institute of the University of Bucharest (ICUB), Sos. Panduri 90, Bucharest, Romania — ²University of Bucharest, Faculty of Physics, 077125 Magurele-Ilfov, Romania — ³Horia Hulubei National Institute for Physics and Nuclear Engineering, 077126 Magurele-Ilfov, Romania — ⁴Department of Engineering, Reykjavik University, Menntavegur 1, IS-102 Reykjavik, Iceland

Machine learning (ML) models have the potential to significantly improve and assist the design process of nanodevices that require precise control of the quantum states.

For 2D nanoelectronic structures, charge and spin densities are relevant observables and are also suited for ML techniques which employ image processing. The model systems that we considered are two dimensional quantum dots with multiple electrons and random confinement potentials. With convolutional neural networks, we built a ML model to predict whether a configuration displays

singlet-triplet transitions in the ground state. For image translation problems, we used models based on conditional generative adversarial networks in order to predict the charge density distribution for arbitrary interacting systems taking as input either the non-interacting cases or just the shape of the confining potential.

HL 16.3 Tue 10:00 POT 151

Mesoscopic transport properties of individually prepared GaN-nanowire field-effect transistors — •HANNES HERGERT^{1,2}, MATTHIAS T. ELM^{1,2,3}, and PETER J. KLAR¹ — ¹Institute of Experimental Physics I, Giessen, Germany — ²Center for Materials Research, Giessen, Germany — ³Institute of Physical Chemistry, Giessen, Germany

In order to keep the optimization of transistors within Moore's law new material systems as well as new transistor concepts such as GaN-nanowire field effect transistors (NW-FET) are needed. In this work we characterize the electrical transport properties of single NW-FET. Furthermore, we are able to obtain a deeper understanding of the mesoscopic transport processes. Unintentionally doped GaN-nanowires were fabricated using molecular-beam-epitaxy and device fabrication was performed by a combination of different lithographic methods and atomic layer deposition. After an annealing process the nanowire's resistance shows an ohmic behaviour. Electrical transport measurements were performed between 2 and 280 K. The investigated NW-FET exhibits a transfer characteristic identical to those of classical field-effect transistors. We show that the electrical transport is dominated by two transport processes: a transport within a metal-like impurity band at low temperatures and a hopping process at higher temperatures. Furthermore we were able to identify universal conductance fluctuations at temperatures below 140 K, which arise from the shift of the Fermi level when applying a topgate voltage.

HL 16.4 Tue 10:15 POT 151

Multi-Channel Kondo Effect in Few-Electron Quantum Dots — •OLFA DANI¹, JOHANNES C. BAYER¹, TIMO WAGNER¹, GERTRUD ZWICKNAGL², and ROLF J. HAUG¹ — ¹Institut für Festkörperphysik, Leibniz Universität Hannover, Germany — ²Institut für Mathematische Physik, Technische Universität Braunschweig, Germany

The Kondo effect is a many particle entangled system, that involves the interaction between a localized spin in the quantum dot and free electrons in the electron reservoirs. This entanglement can be calculated using simplifying assumptions concerning the electronic structure of the quantum dot.

In this work we investigate a quantum dot device formed electrostatically in a two-dimensional electron gas using top-gates. A quantum point contact is used as a sensitive charge detector to detect single-electrons tunneling through the system. This enables us to know the exact number of electrons in the quantum dot (Ne). By changing the applied gate voltage, we are able to control Ne.

A Zero-bias anomaly is observed for a strong coupling to the leads and possible symmetrical tunnel barriers. This Kondo resonance appears for successive Ne showing a deviation from the conjectured odd-even behavior. The Kondo resonance is strongest for Ne=9 and displays a particle-hole symmetry for Ne =7,...,11. It is absent for Ne =6 and Ne = 12. These observations indicate the influence of the shell structure [1] of the electronic states in the quantum dot where orbital degeneracy is present.

[1] L. P. Kouwenhoven, et. al., Rep. Prog. Phys. 64, 701-736 (2001).

HL 16.5 Tue 10:30 POT 151

Highly Conductive Silicon Nanowires by Modulation-Doping via Aluminum-Induced Acceptor States in an SiO₂-shell — •DANIEL HILLER¹, INGMAR RATSCHINSKI¹, SOUNDARYA NAGARAJAN², JENS TROMMER², THOMAS MIKOLAJICK^{2,3}, and DIRK KÖNIG⁴ — ¹Institute of Applied Physics, TU Bergakademie Freiberg, Germany — ²Nanoelectronic Materials Laboratory gGmbH, Dresden, Germany — ³Institute of Semiconductors and Microsystems, TU Dresden, Germany — ⁴Integrated Materials Design Lab, ANU, Canberra, Australia

Silicon nanowires (Si NWs) enable maximum gate control over the source-drain current when configured in a gate-all-around FET-architecture. However, Si NWs with few nm in diameter suffer from severe difficulties with efficient impurity doping due to a multitude of physical and technological problems (diffusion, dielectric and quantum confinement, statistics of small numbers, etc.). Here, we present a novel doping concept for Si NWs comparable to the modulation doping approach of III-V semiconductors. Based on results from density functional theory (DFT) calculations, we use Al-doped SiO₂ shells around the Si NWs, which contain unoccupied Al-induced acceptor states that are energetically located below the Si valence band edge. These states can capture electrons from the Si, creating free holes as majority charge carriers [1-5]. In this presentation, recent results from the experimental realization of this concept on Si NWs are shown. We demonstrate that modulation doping using SiO₂:Al-shells allows for several orders of magnitude lower resistances when compared to undoped SiO₂-shells. [1] D. König et al., Sci. Rep. 7, 46703 (2017)

30 min. break

HL 16.6 Tue 11:15 POT 151

Carrier dynamics in quantum-dot tunnel-injection structures: microscopic theory and experiment — •MICHAEL LORKE¹, IGOR KHANONKIN², STEPHAN MICHAEL¹, JOHANN PETER REITHMAIER³, GADI EISENSTEIN², and FRANK JAHNKE¹ — ¹Institute for Theoretical Physics, University of Bremen, Otto-Hahn-Allee 1, Bremen, 28359, Germany — ²Electrical Engineering Department and Rus- sel Berrie Nanotechnology Institute, Technion, Haifa, 32000, Israel — ³Technische Physik, Institute of Nanostructure Technologies and Analytics, Center of Interdisciplinary Nanostructure Science and Technology (CINSaT), University of Kassel, Kassel, 34132, Germany

Among the challenges for the next generation of semiconductor lasers is the enhancement of their modulation speed to satisfy the need for higher data transfer rates. For this purpose, tunnel injection lasers are an appealing concept, as they promise improved modulation rates and better temperature stability. Moreover, they eliminate a major detrimental effect of quantum dot lasers, which is the gain nonlinearity caused by hot carriers. It is shown in this work how the aforementioned improvements depend on the design of tunnel-injection devices. We perform a theory-experiment comparison on scattering times in tunnel injection devices to highlight the importance of alignment between the injector well and the quantum dot ensemble. It is shown how differences in the coupling to the injector quantum well caused by the alignment lead to scattering times into the quantum dot ensemble that vary by an order of magnitude.

HL 16.7 Tue 11:30 POT 151

Electron transport through a quantum dot in controlled heat bath environment — •HATEF GHANNADI MARAGHEH, JOHANNES C. BAYER, and ROLF J. HAUG — Institute for Solid State Physics, Leibniz Universität Hannover, Appelstraße 2, 30167 Hannover, Germany

For optimizing any device, amongst them semiconductor-based qubit, one has to understand the effects of the environment on them. In this sort of devices, not just quantum states of the channel but also the state of the particles is affected [1-3]. The device consists of split-gate quantum dot in a GaAs/AlGaAs heterostructure. The temperature of the measurement ranged from 49.9 mK to 800 mK.

There have been several works on explaining how electron transport through the quantum dot system would behave for different temperatures [4-5]. As the temperature changes, the Fermi distribution of the lead*s changes. This influenced the conductivity of the dot since in the presence of the bias voltage the transport window gets altered. Besides, depending on the presence of energy levels in the transfer window, the conductivity is manipulated by changing the temperature. For low temperatures, due to the local density of states and coupling of the barrier gates to the leads, fluctuations start to emerge.

[1]*K. C. Nowack et al, Science 318, 1430-1433 (2007)

[2]*Pioro-Ladrière, et al, Nature Physics 4, 776*779 (2008)

[3]*Jan K Kühne, et al, physica status solidi (b) 256(6) (2019)

[4]*E. B. Foxman, et al, Phys. Rev. B 47, 10020(R) (1993)

[5]*O. Dani, et al, Communications Physics 5 (1), 1-7 (2022)

HL 16.8 Tue 11:45 POT 151

Manipulation of temporal correlations in single-electron tunneling — •JOHANNES C. BAYER, ADRIAN SCHMIDT, TIMO WAGNER, and ROLF J. HAUG — Institut für Festkörperphysik, Leibniz Universität Hannover

Precisely timed single-particle operations are of critical importance for quantum technologies operating at fixed clock cycles. A detailed understanding of the interplay between an external drive and the response of the single-particle source is essential for achieving and improving the accuracy in the time domain. We here demonstrate a high level of control over the time domain of a driven single electron transistor (SET). Using a gate defined quantum dot connected to a highly sensitive charge detector [1] allows detecting electrons tunneling into and out of the SET in real-time [2, 3]. The tunneling rates of such devices are controllable by gate voltages. We drive the SET by modulating gate voltages periodically in time and use time-dependent tunneling rates [2] and waiting time distributions [4] to analyze the impact of the driving parameters on temporal correlations in the tunneling times.

[1] J. C. Bayer, T. Wagner, E. P. Rugeramigabo and R. J. Haug, Ann. Phys. 531, 1800393 (2019)

[2] T. Wagner, P. Talkner, J. C. Bayer, E. P. Rugeramigabo, P. Hänggi and R. J. Haug, Nat. Phys. 15, 330-334 (2019)

[3] R. Hussein, S. Kohler, J. C. Bayer, T. Wagner and R. J. Haug, Phys. Rev. Lett. 125, 206801 (2020)

[4] F. Brange, A. Schmidt, J. C. Bayer, T. Wagner, C. Flindt and R. J. Haug, Sci. Adv. 7, eabe0793 (2021)

HL 16.9 Tue 12:00 POT 151

Scalable integrated readout electronics for semiconductor quantum dots — •JONAS BÜHLER¹, ARUN ASHOK¹, LAMMERT DUIMPANS¹, PATRICK VLIEX¹, CHRISTIAN GREWING¹, ANDRÉ ZAMBANINI¹, and STEFAN VAN WAASEN^{1,2} — ¹Central Institute of Engineering, Electronics and Analytics, Electronics Systems (ZEA-2) Forschungszentrum Jülich GmbH, 52428 Jülich, Germany — ²Faculty of Engineering, Communication Systems, University Duisburg-Essen, 47057 Duisburg, Germany

Quantum computing is one of the promising candidates to overcome the limitations of *classical* computing, e.g. von Neumann architecture. Nowadays much progress has been made on the implementation of scalable qubits. This work focuses on semiconductor qubits, which need operating temperatures near 0 K. Room temperature electronics for control and readout, which are limiting the bandwidth and the scalability due to parasitic elements and heat conduction, are still widely used. Some progress has been made to integrate the qubit control and readout in the direct vicinity of the qubit at cryogenic temperatures. Especially readout electronics still have a limited scalability because of circuit size and power consumption. This work tries to overcome those limitations by comparing different readout architectures and implement a multiplexed and integrated readout circuit with lower area and power consumption. This integrated circuit in a 22nm FD-SOI technology will be placed on top of scalable quantum computing architectures and therefore might be a crucial step on the way to a multi-million qubit quantum computer.

HL 17: THz and MIR physics in semiconductors

Time: Tuesday 9:30–12:45

Location: POT 251

HL 17.1 Tue 9:30 POT 251

Terahertz-induced anomalous currents after optical excitation of excitons in quantum wells — •CONG NGO¹, SHEKHAR PRIYADARSHI², HUYNH THANH DUC³, MARK BIELER², and TORSTEN MEIER¹ — ¹Department of Physics, Paderborn University, Warburger Strasse 100, D-33098 Paderborn, Germany — ²Physikalisch-Technische Bundesanstalt, 38116 Braunschweig, Germany — ³Institute of Applied Mechanics and Informatics, VAST, 1 Mac Dinh Chi, District 1, Ho Chi Minh City, Vietnam

We study transient anomalous currents in GaAs quantum wells by solving the multi-band semiconductor Bloch equations in the length gauge, including excitonic effects and carrier longitudinal-optical and acoustic phonons scattering process. The band structure is obtained by diagonalizing a 14-band $\mathbf{k} \cdot \mathbf{p}$ model within the envelope function approximation. To solve the random phase problem originating from the numerical diagonalization of the band structure model, we apply a smoothing gauge transformation [1]. Our numerical results show quite strong anomalous currents appear for optical excitation near the excitonic resonances and simultaneous Terahertz excitation. The current transients oscillate with a frequency corresponding to the inverse of the energy difference between the 1s and 2s exciton states. The numerical results including excitons are in good agreement with experiments [2].

[1] L. H. Thong, C. Ngo, H. T. Duc, X. Song, and T. Meier, *Phys. Rev. B* **103**, 085201 (2021).

[2] S. Priyadarshi, K. Pierz, and M. Bieler, *Phys. Rev. Lett.* **115**, 257401 (2015).

HL 17.2 Tue 9:45 POT 251

Generation of THz vortex beams and interferometric determination of their topological charge — •SAMUEL W. PINNOCK, SEULKI ROH, TOBIAS BIESNER, ARTEM V. PRONIN, and MARTIN DRESSEL — 1. Physikalisches Institut, Universität Stuttgart, 70569 Stuttgart, Germany

We developed and demonstrated the efficacy of 3D printed spiral phase plates for the generation of vortex THz beams with orbital angular momenta $\ell = \pm 1$ and $\ell = \pm 2$. The vortex beam generation was confirmed by means of frequency-domain transmission spectroscopy. The topological charge of the vortex beams was determined via phase-sensitive Mach-Zehnder interferometry, which enabled the superposition of a vortex beam with ℓ and its conjugate beam with $-\ell$. The resulting interference patterns were found to be consistent with the expected intensity distributions for a given ℓ , which provides strong confirmation of the spatial phase structure of the generated vortex beams in the THz regime. Such THz vortex beams could be used in spectroscopic studies of optical transitions with $\Delta\ell \neq 0$ in different condensed-matter systems, including semiconductors and topological materials.

HL 17.3 Tue 10:00 POT 251

Ultrafast Terahertz-Wave Emission from Photoconductive Antenna Arrays and Spin Emitters — •OSAMA HATEM¹, THALES V. A. G. DE OLIVEIRA², SUSANNE C. KEHR¹, and LUKAS M. ENG^{1,3} — ¹Institute of Applied Physics, Technische Universität Dresden, 01062 Dresden, Germany — ²Institute of Ion Beam Physics and Materials Research, Helmholtz-Zentrum Dresden-Rossendorf, 01328 Dresden, Germany — ³ct.qmat: Würzburg-Dresden Cluster of Excellence - EXC 2147, Technische Universität Dresden, Dresden, Germany

For long time, terahertz (THz) radiation (0.1 THz to 10 THz) was little used in science and technology owing to the lack of efficient terahertz sources and detectors. However, recent advances in laser technology and semiconductors industry sparked the interest in exploring this spectral range further. Recently, THz radiation has shown great importance in a wide range of potential applications including THz time-domain spectroscopy and imaging [1-2].

In this work, we report the emission of THz waves from GaAs photoconductive antenna arrays and Fe/Pt spin emitters upon excitation with femtosecond laser pulses at 800 nm. THz waves with bandwidth of 0.1- 5 THz and SNR > 500 below 1 THz were measured. Moreover, detection of THz waves by electro-optic sampling was investigated using ZnTe, GaP, and GaSe crystals of varying thickness. The results are of great significance for THz nanoscopy and imaging applications.

[1] M. Schall et al., *Int. J. Infrared Millim. Waves* **20**, 595-604 (1999). [2] O. Hatem, *J. Opt. Soc. Am. B* **36**, 1144-1149 (2019).

HL 17.4 Tue 10:15 POT 251

Characterization of semiconductors and their properties using terahertz TDS and the Drude-Lorentz model — •JOSHUA HENNIG^{1,2}, JENS KLIER¹, STEFAN DURAN¹, KUEI-SHEN HSU³, ANTE HIRSCH⁴, CHRISTIAN RÖDER³, JAN BEYER³, FRANZISKA BEYER⁴, GEORG VON FREYMAN^{1,2}, and DANIEL MOLTER¹ — ¹Center for Materials Characterization and Testing, Fraunhofer ITWM, Kaiserslautern — ²Department of Physics and Research Center Optimas, Technische Universität Kaiserslautern (TUK), Kaiserslautern — ³Institut für Ange-

wandte Physik, TU Bergakademie Freiberg, Freiberg — ⁴Department of Crystal Growth, Fraunhofer IISB, Freiberg

Semiconductors play an important role in our modern world enabling many of the technological advancements. Therefore, it is of vital interest for an ever-growing industry as well as scientifically to find techniques to characterize optical and electrical properties such as the refractive index as well as the resistivity of these materials. Here, first steps in such characterizations using terahertz time-domain spectroscopy, a nondestructive technology proven to be capable of these challenging tasks, are shown. First, measurements performed on silicon, one of the most commonly used semiconductors, are evaluated to show the measurement principle and confirm the Drude-Lorentz model to be suitable to describe the charge carrier behavior. Next, samples of silicon carbide, an important semiconductor material with applications e.g. in power electronics are examined. The knowledge of these important semiconductor properties can be helpful in quality checks in the production process and any future work with those materials.

HL 17.5 Tue 10:30 POT 251

Interband cascade infrared photodetectors based on Ga-free InAs/InAsSb superlattice absorbers — •ANDREAS BADER¹, FLORIAN ROTHMAYR², NABEEL KHAN², FAUZIA JABEEN¹, JOHANNES KOETH², SVEN HÖFLING¹, and FABIAN HARTMANN¹ — ¹Technische Physik, Physikalisches Institut und Würzburg-Dresden Cluster of Excellence ct.qmat, Am Hubland, D-97074 Würzburg, Germany — ²nanoplus Nanosystems and Technologies GmbH, Oberer Kirschberg 4, D-97218 Gerbrunn, Germany

We present results on interband cascade infrared photodetectors (ICIP) based on Ga-free InAs/InAsSb superlattice (SL) absorbers. An alternative extraction path of photogenerated carriers is required when substituting the more standard InAs/Ga(In)Sb SL absorbers for Ga-free SLs. The device operates in the photovoltaic mode in the mid infrared spectral range with cut-off wavelengths between around 6.5 μm at 100 K and 9 μm at RT. At elevated temperatures, features of negative-differential-conductance (NDC) emerge. Under illumination, these NDC features can supply gain in the device leading to a peak responsivity of 0.45 A/W at room temperature. At 300 K the zero-bias detectivity D^* of the presented device is around 1×10^8 Jones which compares well to similar ICIPs based on InAs/GaSb SL absorbers.

HL 17.6 Tue 10:45 POT 251

Assessment of epitaxially grown p-doped InAs on undoped GaSb exhibiting terahertz emission — •CYRIL SALANG¹, DEAN VON JOHARI NARAG¹, ROMMEL JAGUS¹, GERALD ANGELO CATINDIG², MAE AGATHA TUMANGUIL¹, ALEXANDER DE LOS REYES², IVAN CEDRICK VERONA², HANNAH BARDOLAZA², ARMANDO SOMINTAC², ELMER ESTACIO², and ARNEL SALVADOR² — ¹Materials Science and Engineering Program, University of the Philippines Diliman, Philippines — ²National Institute of Physics, University of the Philippines Diliman, Philippines

A p-InAs/undoped-GaSb thin film was grown via molecular beam epitaxy. The 260 Å p-InAs was grown on 260 nm undoped InAs over 10 periods of InGaAs(3 nm)/GaAs(3 nm) superlattice to minimize the surface roughness prior to the p-InAs growth. Three periods of 20-nm undoped GaAs/260-nm undoped InAs served as a buffer with growth interruption applied on the first 2 mins of deposition of each GaAs and InAs layer. X-ray diffraction shows a peak at $2\theta \sim 61^\circ$ corresponding to InAs. The sample's resistance was measured to be 43 Ω . The terahertz (THz) emission was evaluated using 1.55 μm femtosecond laser excitation in reflection geometry. The current sample emits at ~ 20 times lower THz intensity compared to that of a previously investigated $1 \pm 0.4 \mu\text{m}$ p-InAs/n-GaSb sample possibly due to the lesser thickness leading to a lower photo-Dember response, and differing crystal qualities from the different growth processes. Nonetheless, exploring growth techniques for producing thin InAs films is desired to realize photoconductive antennas for transmission geometry.

30 min. break

HL 17.7 Tue 11:30 POT 251

Coherent State Steering in Condensed Matter Systems with Strong Light-Matter Engineering — •MICHAEL SPENCER, JOANNA URBAN, MAXAMILLIAN FRENZEL, and SEBASTIAN MAEHRLEIN — Department of Physical Chemistry, Fritz Haber Institute of the Max Planck Society, Faradayweg 4-6, 14195 Berlin, Germany

Physical properties of materials are derived largely from their chemical constituents, structural arrangement, and local properties such as temperature and dielectric environment. Next-generation materials science is increasingly focused on manipulation of structural properties in order to access material properties on-demand, in search of emergent, enhanced, or even hidden states of matter. One such method to transiently modify crystalline materials is the application of intense terahertz (THz) laser pulses. These pulses allow for resonant

and selective excitation of infrared-active vibrational modes (phonons) of a crystal, allowing for coherent and ultrafast modulation of condensed-matter system properties. With the introduction of an electromagnetic cavity, the subsequent enhancement of this light-matter interaction between the intense THz radiation and the phonons will provide expanded control over excited-state steering, allowing access to exotic, transient states of matter. I will present our steps towards first realizations of such strongly-coupled light-matter interactions of phonons in crystalline materials within the THz frequency range. In addition, I will discuss our novel measurement techniques for the detection of strong light-matter interactions, where we utilize the unique technical capabilities of terahertz time-domain spectroscopy.

HL 17.8 Tue 11:45 POT 251

Terahertz cyclotron emission from HgTe QWs — •S. GEBERT^{1,2}, C. CONSEJO¹, S. RUFFENACH¹, J. TORRES², B. JOUAULT¹, and F. TEPPE¹ — ¹Laboratoire Charles Coulomb (L2C), UMR 5221 CNRS, Université de Montpellier, F-34095 Montpellier, France — ²Institut d'Electronique et des Systèmes (IES), UMR 5214 CNRS, Université de Montpellier, F-34095 Montpellier, France

Motivated by the emergence of graphene, several concepts for Landau-level (LL) lasers, tunable by a magnetic field over the whole terahertz (THz) frequency range, have been proposed. One hoped in particular was, that the non-equidistance of the LLs from Dirac fermions could efficiently suppress the non-radiative Auger recombination, which typically prevails over the radiative recombination. However, despite this non-equidistance an unfavorable non-radiative process still persists in Landau-quantized graphene, and no cyclotron emission from Dirac fermions has yet been reported. To eliminate this last non-radiative process, it is sufficient to slightly modify the dispersion of the Landau levels, e.g. by opening a small gap in the linear band structure. A proven example of such gapped graphene-like materials are HgTe quantum wells (QWs) close to the topological phase transition. We here experimentally demonstrate spontaneous Landau emission from Dirac fermions in such HgTe QWs, where the emission is tunable between 0.5 THz and 3 THz by both the magnetic field and the carrier concentration [1].

[1] S. Gebert et al., Nat. Photon. (accepted); preprint is available at doi.org/10.21203/rs.3.rs-1630601/v1

HL 17.9 Tue 12:00 POT 251

Coherent phonon dynamics in quasi-2D perovskites probed by THz-induced Kerr effect — •JOANNA M. URBAN¹, MARIE CHERASSE^{1,2}, MAXIMILIAN FRENZEL¹, MICHAEL SPENCER¹, GAELLE TRIPPE-ALLARD³, EMMANUELLE DELEPORTE³, LUCA PERFETTI², MARTIN WOLF¹, and SEBASTIAN F. MAEHRLEIN¹ — ¹FHI of the Max Planck Society, Faradayweg 4-6, 14195 Berlin, Germany — ²LSI, Palaiseau, France — ³Université Paris-Saclay, LuMIn, Gif-sur-Yvette, France

2D hybrid organic-inorganic perovskites (HOIP) are self-assembled multiple quantum well structures, formed by metal halide octahedral layers alternating with large organic spacer cations. They combine the intriguing properties of the 3D HOIP polar, anharmonic lattice with optoelectronic properties arising due to low dimensionality. We study a family of 2D HOIPs in the Ruddlesden-Popper phase (PEA)₂(MA)_{n-1}Pb_nI_{3n+1} (n=1,2,3). Using intense, close to single-cycle THz fields we excite coherent optical phonons and probe the lattice dynamics via THz-induced Kerr effect (TKE). Strikingly, we observe long-lived coherent

phonon oscillations at room temperature. Comparison with static Raman spectroscopy results as well as the measured fluence and temperature dependence confirm that the observed features in the 0.5-3 THz range correspond to Raman-active modes of the inorganic sublattice, excited via a nonlinear driving process. The nontrivial azimuthal angle dependence of the TKE signal can be explained considering the crystal structure and the symmetry of the Raman modes using the $\chi^{(3)}$ nonlinear susceptibility tensor formalism.

HL 17.10 Tue 12:15 POT 251

Optically excited charge-carrier dynamics in the antiferromagnetic semiconductor MnTe — •CHANGQING ZHU¹, PATRICK PILCH¹, ANNEKE REINOLD¹, GUNTHER SPRINGHOLZ², MIRKO CINCHETTI¹, and ZHE WANG¹ — ¹TU Dortmund University, Germany — ²Johannes Kepler University of Linz, Austria

Room-temperature antiferromagnetic semiconductors are very interesting for possible spintronic applications. With a long-range antiferromagnetic order ($T_N = 307$ K) at room temperature, the hexagonal α -MnTe is a relevant candidate for those applications. Here we report on time-resolved measurements of ultrafast dynamics of optically excited charge carriers in α -MnTe thin film, by optical pump - optical probe and optical pump - THz probe spectroscopic techniques at room temperature. In contrast to a phononic oscillation mode at 5.3 THz as observed by 2.4 eV pump [1], our studies with an 1.5 eV pump pulse cannot reveal the optical phonon mode but rather low-energy acoustic phonon-like behavior at high pump fluence. Moreover, nonlinear dependence on pump fluence is observed both in our optical and terahertz probes, for a pump fluence above ~ 2.0 mJ/cm². This indicates a different physical mechanism than in the previous studies. The observed relaxation processes can be associated to electron-hole recombination and electron-phonon scattering.

[1] D. Bossini et al. Phys. Rev. B 104, 224424 (2021).

HL 17.11 Tue 12:30 POT 251

Time-resolved nanospectroscopy on Si-doped GaAs-InGaAs core-shell nanowires — •ANDREI LUFERAU^{1,2}, MAXIMILIAN OBST², SUSANNE KEHR², LUKAS ENG², STEPHAN WINNERL¹, ALEXEJ PASHKIN¹, EMMANOUIL DIMAKIS¹, and MANFRED HELM¹ — ¹Helmholtz-Zentrum Dresden-Rossendorf, Dresden, Germany — ²Institute of Applied Physics, Technische Universität Dresden, Dresden, Germany

High-quality epitaxial nanowires (NWs) based on III-V semiconductors offer the possibility to fabricate ultrafast optical devices due to their direct bandgap and the high electron mobility. Contactless investigation of photoexcited carriers within single NWs is enabled by optical-pump THz-probe scanning near-field optical microscopy (SNOM) experiment. Here we report on first THz-pump MIR-probe SNOM studies on Si-doped GaAs-InGaAs core-shell NWs utilizing THz radiation from the free-electron laser FELBE. The experiment was carried out with SNOM setup from Neaspec equipped with nanoFTIR module, where a broadband MIR source (5-15 μ m) serves as a probe. Upon intraband THz-pump (25 μ m) we observed a red shift of amplitude and phase of the NW plasma resonance, while control interband optical pumping (780nm) induced a blue shift of the resonance, and in both cases an exponential decay with a time constant of 4-5ps is seen. We attribute the blue shift to the contribution of photogenerated carriers. The red shift is assigned to the heating of the electrons in the conduction band and the subsequent increase of the effective mass in the nonparabolic Γ -valley due to high peak electric fields of THz pulses.

HL 18: Optical Properties (joint session HL/ CPP)

Time: Tuesday 9:30-13:00

Location: POT 112

HL 18.1 Tue 9:30 POT 112

Can Ge and Si be optoelectronic materials: Hexagonal polytypes — •MARTIN KELLER¹, ABDERREZAK BELABBES^{1,2}, JÜRGEN FURTHMÜLLER¹, FRIEDHELM BECHSTEDT¹, and SILVANA BOTTI¹ — ¹Friedrich-Schiller-Universität Jena, Institut für Festkörpertechnik und -optik, Max-Wien-Platz 1, 07743 Jena, Germany — ²Department of Physics, Sultan Qaboos University, P.O. Box 36, PC 123, Muscat, Oman

The group IV elements silicon and germanium crystallize in cubic diamond structure under ambient conditions and feature indirect bandgaps. Therefore they cannot emit light efficiently and are not applicable in active optoelectronic devices. Under high pressure, however, as well as using different growth techniques, several Si and Ge polymorphs, including hexagonal polytypes, have been observed. Lonsdaleite Ge as well as Ge-rich hexagonal alloys have even been found to have a direct bandgap and strongly emit light with varying frequency. Thus hexagonal systems have become of great interest for potential optical emitters that may be integratable with CMOS technology. We have performed extensive ab initio studies of the energetic, structural, elastic and electronic properties as well as the strengths of some dipole transitions of the hexagonal Si and Ge polytypes 2H, 4H and 6H using Density Functional Theory and approximate quasiparticle treatments, and trends between the different geometries are anal-

ysed. The results for cubic and hexagonal Si and Ge agree excellently with existing experimental findings. The electronic structures point to promising optical properties.

HL 18.2 Tue 9:45 POT 112

Many-body effects in the mid-infrared dielectric function of InSb from 80 to 800 K — MELISSA RIVERO ARIAS, CESY ZAMARRIPA, JADEN LOVE, CARLOS ARMENTA, CAROLA EMMINGER, SONAM YADAV, and •STEFAN ZOLLNER — New Mexico State University, Las Cruces, NM, USA

We describe measurements of the mid-infrared dielectric function of bulk InSb near the direct band gap using Fourier-transform infrared spectroscopic ellipsometry from 80 to 800 K in an ultra-high vacuum cryostat. Indium antimonide is the zinc blende compound semiconductor with the smallest direct band gap ($E_0=0.18$ eV at 300 K) due to its heavy elements and the large resulting spin-orbit splitting and Darwin shifts. The band gap is extracted from the dielectric function by fitting with a parametric oscillator model. It decreases from 80 to 450 K following a Bose-Einstein model, then remains constant up to 550 K, and increases again at the highest temperatures. This is explained with a thermal Burstein-Moss shift: The onset of optical absorption increases as electron-hole pairs are thermally excited at the highest temperatures. The intrinsic car-

rier concentration determined from the Drude tail in the ellipsometry spectra agrees qualitatively with temperature-dependent Hall experiments and calculations based on degenerate Fermi-Dirac statistics.

HL 18.3 Tue 10:00 POT 112

Polarized Raman scattering study of epitaxially grown GeSn layers with various Sn content — •AGNIESZKA ANNA CORLEY-WICIAK¹, OMAR CONCEPCIÓN², MARVIN HARTWIG ZOELLNER¹, DETLEV GRÜTZMACHER², DAN BUCA², GIOVANNI CAPELLINI^{1,3}, and DAVIDE SPIRITO¹ — ¹IHP Leibniz-Institut für innovative Mikroelektronik, Im Technologiepark 25, 15236 Frankfurt (Oder), Germany — ²Peter Grünberg Institute 9 (PGI-9) and JARA-Fundamentals of Future Information Technologies — ³Dipartimento di Scienze, Università Roma Tre, V.le G. Marconi 446, 00146 Roma, Italy

Ge_{1-x}Sn_x alloys are an excellent candidate for developing mid-infrared light sources integrated with CMOS technology. The challenges in the controlled growth with high crystal quality have highlighted the peculiarity of these alloys, which can be monitored by their vibrational properties. To this purpose, Raman spectroscopy is an effective experimental method to determine these properties, as this technique is non-destructive, contactless, fast, and locally resolved. We use Raman scattering with different polarization configurations to investigate Ge_{1-x}Sn_x (0.05 ≤ x ≤ 0.14) alloys grown by Chemical Vapour Deposition on Ge/Si virtual substrates. Measurements were performed in backscattering geometry with parallel and cross polarizations. In this way, we identify multiple components in the vibrational modes and how they deviate from simplified models. Our results will help to understand the fundamental properties of Ge_{1-x}Sn_x alloys to enable fast assessment for their applications in optoelectronic and thermoelectric.

HL 18.4 Tue 10:15 POT 112

Eigenmodes and Polarization Structure of Coupled Elliptical Microcavities — •JOHANNES DÜRETH¹, SIMON BETZOLD¹, MONIKA EMMERLING¹, ANTONINA BIEGANOWSKA², JÜRGEN OHMER³, UTZ FISCHER³, SVEN HÖFLING¹, and SEBASTIAN KLEMBT¹ — ¹Technische Physik, RCCM and Würzburg-Dresden Cluster of Excellence ct.qmat, University of Würzburg, Germany — ²Faculty of Problems of Fundamental Technology, Department of Experimental Physics, Laboratory for Optical Spectroscopy of Nanostructures, Wrocław, Poland — ³Department of Biochemistry, University of Würzburg, Germany

Elliptical potentials give rise to a set of eigenmodes called Ince-Gaussian modes. Contrary to hemispherical potentials, the geometric shape leads to a mode splitting of the otherwise degenerate fundamental mode. Theoretically, this behaviour can be exploited to realize interesting topological phenomena like non-reciprocal transport, the non-hermitian skin-effect or engineer artificial gauge fields. On the way to an experimental implementation of such systems, the singular building blocks of these photonic potentials - single and coupled elliptical potentials - have to be experimentally studied.

Here we present an investigation of the mode splitting and polarisation in single elliptical microcavities, as well as an examination of the coupling between differently angled ellipses.

15 min. break

HL 18.5 Tue 10:45 POT 112

Optical properties of Ag_xCu_{1-x}I alloy thin films — •E. KRÜGER¹, M. SEIFERT², V. GOTTSCHALCH³, H. KRAUTSCHEID³, C.S. SCHNOHR¹, S. BOTTI², M. GRUNDMANN¹, and C. STURM¹ — ¹Universität Leipzig, Felix-Bloch-Institut für Festkörperphysik, Germany — ²Friedrich-Schiller-Universität Jena, Institut für Festkörpertheorie und Optik, Germany — ³Universität Leipzig, Institut für Anorganische Chemie, Germany

Copper iodide (CuI) is a promising wide bandgap semiconductor for applications in transparent optoelectronic devices. In this context, the specific tuning of electrical and optical properties, which can potentially be achieved with ternary alloys such as CuBr_xI_{1-x} [1] and Ag_xCu_{1-x}I [2], is crucial for the development of novel CuI-based devices. In particular, Ag_xCu_{1-x}I is of great interest because the intrinsic conductivity changes from p-type to n-type with increasing Ag content.

Here we present the bandgap energy and spin-orbit splitting in Ag_xCu_{1-x}I alloys as a function of alloy composition and temperature, studied by a combination of experimental and computational methods. The non-linear bandgap dependence on Ag content can be described by a quadratic bowing parameter of 0.54 eV and is dominated by charge carrier redistribution effects in the presence of unequal element-specific bond lengths. The slight increase of the spin-orbit splitting from 640 meV for CuI to about 790 meV for AgI is discussed in terms of decreasing p-d hybridization of the valence bands at the Γ -point.

[1] N. Yamada et al., Adv. Funct. Mater. **30**, 2003096 (2020)

[2] A. Annadi and H. Gong, Appl. Mater. Today **20**, 100703 (2020)

HL 18.6 Tue 11:00 POT 112

Multipole theory of optical spatial dispersion in crystals — •ÓSCAR POZO — Centro de Física de Materiales, Universidad del País Vasco, 20018 San Sebastián, Spain

Natural optical activity is the paradigmatic example of an effect originating in the weak spatial inhomogeneity of the electromagnetic field on the atomic scale. In molecules, such effects are well described by the multipole theory of electromagnetism, where the coupling to light is treated semiclassically beyond the electric-dipole approximation. That theory has two shortcomings: it is limited to bounded systems, and its building blocks - the multipole transition moments - are origin dependent. In this work, we recast the multipole theory in a translationally-invariant form that remains valid for periodic crystals. Working in the independent-particle approximation, we introduce 'intrinsic' multipole transition moments that are origin independent and transform covariantly under gauge transformations of the Bloch eigenstates. Electric-dipole transitions are given by the interbank Berry connection, while magnetic-dipole and electric-quadrupole transitions are described by matrix generalizations of the intrinsic magnetic moment and quantum metric. In addition to multipole-like terms, the response of crystals at first order in the wave vector of light contains band-dispersion terms that have no counterpart in molecular theories. The rotatory-strength sum rule for crystals is found to be equivalent to the topological constraint for a vanishing chiral magnetic effect in equilibrium, and the formalism is validated by numerical tight-binding calculations.

HL 18.7 Tue 11:15 POT 112

Predicting bandgap in strain-engineered multinary III-V semiconductors — •BADAL MONDAL and RALF TONNER-ZECH — Wilhelm-Ostwald-Institut für Physikalische und Theoretische Chemie, Universität Leipzig, 04103 Leipzig, Germany

The tuning of the type and size of bandgaps of III-V semiconductors is a major goal for optoelectronic applications. Varying the relative composition of several III- or V-components in compound semiconductors is one of the major approaches here. Alternatively, straining the system can be used to modify the bandgaps. By combining these two approaches, bandgaps can be tuned over a wide range of values, and direct or indirect semiconductors can be designed. However, an optimal choice of composition and strain to a target bandgap requires complete material-specific composition, strain, and bandgap knowledge. Exploring the vast chemical space of all possible combinations of III- and V-elements with variation in composition and strain is experimentally not feasible. We thus developed a density-functional-theory-based predictive computational approach for such an exhaustive exploration. This enabled us to construct the 'bandgap phase diagram' [1] by mapping the bandgap in terms of its magnitude and nature over the whole composition-strain space. Further, we have developed efficient machine-learning models to accelerate such mapping. We will show the application to binary [2], ternary and quaternary material combinations and the possible impact on device design.

[1] <https://bmondal94.github.io/Bandgap-Phase-Diagram>, 2022

[2] <https://arxiv.org/abs/2208.10596>

HL 18.8 Tue 11:30 POT 112

GeSn vertical p/n photodetectors formed by 2-step ion implantation — •SHUYU WEN^{1,2}, SAIF SHAIKH¹, OLIVER STEUER¹, YONDER BERENCEN¹, SLAWOMIR PRUCNAL¹, and SHENGQIANG ZHOU¹ — ¹Helmholtz-Zentrum Dresden-Rossendorf, Institute of Ion Beam Physics and Materials Research, Dresden, Germany — ²Institute of Semiconductors, Chinese Academy of Sciences, Beijing, China

Germanium (Ge) is a promising material in integrated circuit (IC) due to the high mobility of hole carrier and highly compatibility in the Si-base IC technology. However, the indirect band structure of Ge leads to the low radiative recombination efficiency, limiting the application in opto-electronics. Alloying Ge with Tin (Sn) is a promising method to obtain energy band modification even to a direct band. Here, high quality Ge_{0.97}Sn_{0.03} and Ge_{0.955}Sn_{0.045} alloy is obtained by CMOS-compatible ion implantation method. Tensile strain leads by Sn alloying and damage recovery after Flash annealing (FLA) are characterized by Raman and XRD measurements. A subsequently phosphors implantation is applied to obtain vertical pn photodetectors (PD). The device shows an extended spectral response comparing with commercial Ge PD. This work provides a new CMOS-compatible method to fabricate photodetectors in short-wave infrared.

15 min. break

HL 18.9 Tue 12:00 POT 112

Interplay between strain, Sn content and temperature in GeSn-based optoelectronic devices — •IGNATI ZAITSEV¹, AGNIESZKA A. CORLEY-WICIAK¹, DAN BUCA², OMAR CONCEPCIÓN², MICHELE VIRGILIO³, GIOVANNI CAPELLINI^{1,4}, COSTANZA L. MANGANELLI¹, and DAVIDE SPIRITO¹ — ¹IHP - Leibniz-Institut für innovative Mikroelektronik, Frankfurt (Oder), Germany — ²PGI 9, Jülich, Germany — ³Università di Pisa, Pisa, Italy — ⁴Università Roma Tre, Roma, Italy

Several works have shown the subtle interplay between thermomechanical strain, Sn content and band occupation in optoelectronic devices based on CMOS-integratable group-IV materials (Ge, SiGe, SiGeSn). This is especially the case when temperature plays a key role, e.g. devices operating at cryo-

genic temperature or in presence of high power. Here we provide a theoretical-experimental approach combining 3D FEM calculations, Raman and photoluminescence spectroscopy to fully capture the influence of mechanical and thermo-mechanical features on the optical properties. We apply this method to strained GeSn microdisks, a device geometry aimed at laser in the MIR range. With the presented methods, we can develop a thorough guidelines for the assessment and design of integrated light emitters.

HL 18.10 Tue 12:15 POT 112

Excitons in MoS₂ bilayers under pressure — •JAN-HAUKE GRAALMANN¹, PAUL STEEGER², ROBERT SCHMIDT², STEFFEN MICHAELIS DE VASCONCELLOS², RUDOLF BRATSCHITSCH², and MICHAEL ROHLFING¹ — ¹Institute of Solid State Theory, University of Münster, 48149 Münster, Germany — ²Institute of Physics, University of Münster, 48149 Münster, Germany

Theoretical and experimental studies have shown that the optical spectrum of the MoS₂ bilayer changes under pressure.

Our theoretical investigations are based on DFT, *GdW* and the Bethe-Salpeter equation. For the specific stress conditions of the experiment, our calculations show an effective shift of the excitation energies of the A exciton towards higher energies with increasing pressure. This behaviour can be explained with an approximately constant direct band gap at the K point while the binding energy decreases. Due to a growing valence band splitting for increasing pressures, the interlayer exciton shows a smaller shift. These results are substantiated by measurements using a piston type diamond anvil cell (DAC) to create pressures in the GPa range.

The reason for only small changes of the fundamental band gap is a significant influence of interlayer interaction. The effect of a decreasing gap by biaxial lateral shrinking of each single layer under an external pressure gets counterbalanced by the reduction of the interlayer distance. Furthermore, the real space distribution shows an increased interlayer character for the A and interlayer exciton under pressure.

HL 18.11 Tue 12:30 POT 112

Optical properties of a vacancy-related complex in 4H-SiC — •MAXIMILIAN SCHOBER¹, NICOLAS JUNGWIRTH¹, TAKUMA KOBAYASHI², JOHANNES A. F. LEHMEYER², MICHAEL KRIEGER², HEIKO B. WEBER², and MICHEL BOCKSTEDTE¹ — ¹Institute for Theoretical Physics, Johannes Kepler University Linz, Austria — ²Lst. f. Angewandte Physik, Friedrich-Alexander-University Erlangen-Nürnberg, Germany

SiC is host to multiple color centers, such as the silicon vacancy, the divancy, and the carbon antisite-vacancy complex, with relevant applications as qubits, single photon sources and in quantum metrology. Recently, the carbon di-vacancy-antisite complex was identified as an annealing product of vacancy related defects [1], and is expected to feature favorable properties for quantum technology. The presence of strongly localized silicon and carbon dangling bonds points to rich photo- and spin physics that has so far not been explored in detail. In this work we probe the basal and axial configurations of $V_C C_{Si} V_C$ for their electronic-, optical- and radiative properties using a theoretical framework of hybrid density functional and many body approaches. We obtain the principal transitions, as well as the associated static- and transition dipole moments of the relevant charge states. Our results suggest a tentative identification of the carbon di-vacancy-antisite with the temperature-stable (TS) center [2].

[1] E. M. Y. Lee *et al.*, Nat. Commun. 12, 63 (2021).

[2] M. Rühl, C. Ott, S. Götzinger, M. Krieger, H. B. Weber, Appl. Phys. Lett. 113, 122102 (2018).

HL 18.12 Tue 12:45 POT 112

Defects or Dots – what semiconductor physics can bring into optical super-resolution imaging — •PHILIPP KELLNER¹, JANA SÜTTERLIN¹, PAUL KONRAD², ANDREAS SPERLICH², and CHRISTIAN EGGELING^{1,3} — ¹Institut für angewandte Optik und Biophysik, FSU Jena, Philosophenweg 7, 07743 Jena — ²Physikalisches Institut, Julius-Maximilians Universität Würzburg, Am Hubland, 97074 Würzburg — ³Institut für physikalische Hochtechnologie, Albert-Einstein-Straße 9, 07745 Jena

Super-resolved optical microscopy is a widely used tool throughout the medicine and biology community. Mostly and routinely done with organic dyes super-resolution imaging has led to various insights into cell structures and diffusional dynamics. The fundamental problem occurring with organic dyes is their rather dim brightness and their lack of photostability paired with photo-toxicity. This presentation will shed light on novel semi-conductor-based chromophores, like NV-centers in diamond, defects in hBN and CdTe quantum dots, and their use in optical nanoscale sensing schemes like StED-imaging or fluorescence correlation microscopy.

HL 19: Organic Electronics and Photovoltaics I (joint session CPP/HL)

Time: Tuesday 9:30–13:00

Location: GÖR 226

See CPP 18 for details of this session.

HL 20: Focus Session: Frontiers of Electronic-Structure Theory I (joint session O/HL)

Time: Tuesday 10:30–12:45

Location: TRE Ma

HL 20.1 Tue 10:30 TRE Ma

Two-component GW implementation for molecular valence excitations — •QINGLONG LIU, RAMÓN L. PANADÉS-BARRUETA, and DOROTHEA GOLZE — Chair of Theoretical Chemistry, Technische Universität Dresden, 01062 Dresden, Germany

We present an all-electron *GW* implementation for the computation of charged molecular excitations, that includes scalar relativistic effects and spin-orbit coupling (SOC). Our method is based on a two-component (2c) approach, which can process 2c spinors and their corresponding eigenvalues from different levels of theory. The relativistic input for our 2c *GW* calculation is obtained in two ways: One approach is a non-self-consistent second variation SOC scheme, i.e. a scalar relativistic (SR) calculation is performed followed by an expansion of the spinors on top of the SR eigenvectors [1]. Another approach is the spinors and their eigenvalues are obtained by running a self-consistent relativistic DFT calculation with the X2C method [2]. Our algorithm has been implemented in the FHI-aims program package, which is based on numeric atom-centered orbitals (NAOs). In our 2c *GW* algorithm we combine the all-electron NAO scheme with the resolution of the identity technique based on the Coulomb metric (RI-V) and use the analytical continuation to evaluate the G_0W_0 self energy. We present results for the numerical validation of our implementation and for the influence of the relativistic input (second variation SOC vs X2C) on the valence excitations of small heavy molecules.

[1] W. Huhn and V. Blum, Phys. Rev. Materials 1, 033803 (2017)

[2] M. Iliaš and T. Saue, J. Chem. Phys. 126, 064102 (2007)

HL 20.2 Tue 10:45 TRE Ma

Screened potential in two-dimensional GW calculations within the LAPW framework — •BEN ALEX, SVEN LUBECK, and CLAUDIA DRAXL — Physics Department and IRIS Adlershof, Humboldt-Universität zu Berlin, Berlin, Germany To calculate two-dimensional (2D) materials in a three-dimensional periodic code, one has to consider periodically repeated layers. The calculation of quasi-particle energies for 2D materials within the *GW* approximation requires the introduction of a 2D cutoff for the Coulomb potential as the layers would otherwise interact with each other. This cutoff leads to a stronger q dependence of the dielectric function around $q = 0$ which requires much denser sampling of the first Brillouin zone. In order to address this issue, an analytic expression for the dielectric function was previously derived for a plane-wave basis [1]. This expression is then integrated numerically in a small region around $q = 0$. The goal of this work is to adapt this technique to the linearized augmented planewave + local-orbital (LAPW+lo) basis as implemented in the full-potential all-electron code *exciting*. We show that also in our case, we obtain a significant computational speedup. Furthermore, this approach is compared with an approach where the dielectric function is interpolated to a denser q -grid.

[1] F. A. Rasmussen *et al.*, Phys Rev B 94, 155406 (2016).

HL 20.3 Tue 11:00 TRE Ma

GW multipole approach for the frequency description of the dielectric screening — •CLAUDIA CARDOSO¹, DARIO A. LEON², ANDREA FERRETTI¹, DANIELE VARSANO¹, and ELISA MOLINARI¹ — ¹S3 Centre, Istituto Nanoscienze, CNR, 41125, Modena (Italy) — ²Department of Mechanical Engineering and Technology Management, Norwegian University of Life Sciences, 1430, Ås (Norway)

In the present work, we discuss a numerical approach for GW calculations that takes into account the frequency dependence of the screening via a multi-pole approximation (MPA), an accurate and efficient alternative to current full-frequency methods, that overcomes several limitations of the plasmon pole approximation (PPA).

MPA was recently developed and validated for semiconductors[1]. We now extend the use of MPA to metallic systems by optimizing the frequency sampling for these class of materials and propose a simple method to include the zero q limit of the intra-band contributions. The good agreement between MPA and full frequency results for the calculations of quasi-particle energies, polarizability, self-energy and spectral functions in different metallic systems confirms the accuracy and computational efficiency of the method. Finally, we discuss the physical interpretation of the MPA poles through a comparison with experimental electron energy loss spectra for Cu.

[1] D. A. Leon, C. Cardoso, T. Chiarotti, D. Varsano, E. Molinari, A. Ferretti, Phys. Rev. B 104, 115157

Topical Talk

HL 20.4 Tue 11:15 TRE Ma

Towards low-scaling GW calculations for 2D materials — •JAN WILHELM — Institute of Theoretical Physics, University of Regensburg

Semiconducting two-dimensional materials are an ideal platform to study excitons thanks to the strong exciton binding energy and good experimental accessibility of the excitons. The GW+Bethe-Salpeter approach (GW+BSE) has been successful in analyzing excitons in single-layer 2D materials [1], but the application of GW+BSE is challenging for 2D double layers and moiré structures [2]. This is because the large unit cells in these structures contain hundreds to thousands of atoms, resulting in a high computational cost for GW+BSE calculations. In this talk, I will present a low-scaling GW algorithm for 2D materials that potentially allows for the inclusion of more than a thousand atoms in the simulation [3]. This algorithm is based on localized basis functions and can handle periodic boundary conditions and the divergence of Coulomb interactions in the Brillouin zone. I will present first benchmark calculations.

[1] D. Y. Qiu, F. H. da Jornada, S. G. Louie, PRL 111, 216805 (2013). [2] Nat. Phys. 17, 720 (2021), Nature 608, 499 (2022), Science 376, 406 (2022), Nature 603, 247 (2022). [3] J. Wilhelm, D. Golze, L. Talirz, J. Hutter, C. Pignedoli, JPCL 9, 306 (2018), J. Wilhelm, P. Seewald, D. Golze, JCTC 17, 1662 (2021).

15 min. break

HL 20.5 Tue 12:00 TRE Ma

Accelerating core-level GW calculations by combining the contour deformation with the analytic continuation of W — •RAMÓN L. PANADÉS BARRUETA and DOROTHEA GOLZE — Theoretische Chemie, Technische Universität Dresden, Bergstr. 66c, 01062 Dresden, Deutschland

Many-body methods, like the GW approximation, have recently proven to be a highly effective tool for computing core-level excitations [1]. In particular, the contour deformation (CD) is an efficient, scalable and numerically stable approach that has enabled core-level calculations on systems up to 100 atoms [2]. In this work, we reduce the scaling of CD applied to core-levels from $O(N^5)$ to $O(N^4)$, using an analytic continuation of the screened Coulomb interaction W [3]. The new method (CD-WAC) has been implemented in FHI-aims. CD-WAC has been extensively tested on well established benchmark sets like the GW100 and the CORE65, reporting MAEs of less than 5 meV with respect to

CD. The theoretical scaling has been confirmed by performing scaling experiments on large acene chains and amorphous carbon. Speedups of 5 times have been attained with CD-WAC for the largest systems.

[1] D. Golze, M. Dvorak, and P. Rinke. Front. Chem., 7:377, 2019.

[2] D. Golze, J. Wilhelm, M.J. Van Setten, and P. Rinke. J. Chem. Theory Comput., 14(9):4856-4869, 2018.

[3] I. Duchemin and X. Blase. J. Chem. Theory Comput., 16(3):1742-1756, 2020.

HL 20.6 Tue 12:15 TRE Ma

Many-Body Effects of Metals Investigated by Means of the GW Method — •ZIMO ZHOU, NAKIB PROTIK, and CLAUDIA DRAXL — Institut für Physik and IRIS Adlershof, Humboldt-Universität zu Berlin, Berlin, Germany

Even if semilocal exchange-correlation functionals of density-functional theory (DFT) can capture the overall band structure of many metals well, they fail to obtain the correct position of the d-bands. This leads, for instance, to the underestimation of the interband absorption onset in the corresponding optical spectra as shown for a set of elemental metals [1]. In this work, we provide a systematic investigation of the quasi-particle band structure and the optical properties of this set of materials. To this extent, the self-energy corrections to the DFT results are computed by the GW approach of many-body perturbation theory as implemented in the full-potential all-electron code exciting [2,3]. We show that the optical absorption spectra based on these quasi-particle bands remedy the shortcomings of semi-local DFT, accurately reproducing the experimental counterparts.

[1] W. S. M. Werner, K. Glantschnig, and C. Ambrosch-Draxl, J. Phys. Chem. Ref. Data 38, 1013 (2009). [2] A. Gulans, S. Kontur, C. Meisenbichler, D. Nabok, P. Pavone, S. Rigamonti, S. Sagmeister, U. Werner, and C. Draxl, J. Phys: Condens. Matter 26, 363202 (2014). [3] D. Nabok, A. Gulans, and C. Draxl, Phys. Rev. B 94, 035418 (2016).

HL 20.7 Tue 12:30 TRE Ma

Separable Resolution-of-Identity in an all-electron numeric atom-centered basis set framework — •FRANCISCO DELESMA¹, DOROTHEA GOLZE², and PATRICK RINKE¹ — ¹Department of Applied Physics, Aalto University, Espoo, Finland — ²Faculty of Chemistry and Food Chemistry, Technische Universität Dresden, Dresden, Germany

The resolution-of-identity (RI) is a common way in quantum chemistry and computational materials science to reduce the computational cost of two-electron Coulomb integrals, another central entity in computational quantum mechanics. In 2019, Duchemin and Blase proposed the separable-RI approach [1], which preserves the accuracy of the standard, global RI method with the Coulomb metric (RI-V) and permits the formulation of cubic-scaling random-phase approximation (RPA) and Green's function based GW approaches.

In this work, we present the first implementation of the separable-RI in an all-electron numeric atom-centered orbital framework. Separable-RI is implemented in the FHI-aims code [2] and optimized for massively parallel execution. We extend the separable-RI framework beyond the original Hartree-Fock (HF) and GW implementations of Duchemin and Blase to MP2 and RPA, SOSEX and CCSD. Our separable-RI total energies and GW quasiparticle energies for the Thiel test set of small organic molecules reproduce the exact two-electron Coulomb integral calculations within 1 meV or better.

[1] I. Duchemin and X. Blase, J. Chem. Phys. 150, 174120 (2019)

[2] V. Blum, et al, Comput. Phys. Commun. 180, 2175, (2009)

HL 21: Thermal properties

Time: Tuesday 11:00–11:45

Location: POT 361

HL 21.1 Tue 11:00 POT 361

Wigner thermal transport in rare-earth zirconates and their solid solutions — •ANEES PAZHEDATH¹, LORENZO BASTONERO¹, NICOLA MARZARI^{1,2}, and MICHELE SIMONCELLI³ — ¹U Bremen Excellence Chair, Bremen Center for Computational Materials Science, and MAPEX Center for Materials and Processes, University of Bremen, D-28359 Bremen, Germany — ²Theory and Simulation of Materials (THEOS), and National Centre for Computational Design and Discovery of Novel Materials (MARVEL), École Polytechnique Fédérale de Lausanne, Lausanne, Switzerland — ³Cavendish Laboratory, Theory of Condensed Matter Group, University of Cambridge, England

Anharmonicity and disorder are both limiting factors for heat transport, and understanding how their interplay determines thermal conductivity is crucial to devise design strategies for thermal barrier coatings (TBC). Rare-earth (RE) zirconates are prospective TBC materials, owing to their strong anharmonicity and disorder tunable through alloying. Here, we use the Wigner transport equation in conjunction with state-of-the-art first-principles simulations to elucidate the microscopic physics underlying thermal transport in solid solutions of RE-zirconates, analyzing solutions of $\text{La}_2\text{Zr}_2\text{O}_7$ and $\text{Yb}_2\text{Zr}_2\text{O}_7$ as a paradigmatic

test case. This work deepens our understanding on how the interplay between disorder and anharmonicity affects thermal transport in complex crystals with glass-like conductivity, also extending the reach of first-principles simulations to the description of thermal transport in RE-zirconate solid solutions

HL 21.2 Tue 11:15 POT 361

The Influence of Anharmonicity on Negative Thermal Expansion of α -Sn — •REINHARD K. KREMER¹, PAWEEL T. JOCHYM², JAN LAZEWSKI², ANDRZEJ PTOK², PRZEMYSŁAW PIEKARZ², ANDRZEJ M. OLÉS³, and EVA BRÜCHER¹ — ¹MPI for Solid State Research, Stuttgart, Germany — ²Institute of Nuclear Physics, Polish Academy of Sciences, Krakow, Poland — ³Institute of Theoretical Physics, Jagiellonian University, Krakow, Poland

The lattice vibrational properties of α -Sn (gray tin) were investigated experimentally by temperature dependent x-ray diffraction and theoretically by density functional theory calculations. Similar to the other elements of group IV, α -Sn exhibits a lattice anomaly at low temperatures and negative thermal expansion, with a minimum at ~ 27 K and a magnitude three times larger than in Si. Influence of anharmonic effects up to 4th order potential terms on the phonon dispersion relations, the lattice parameters, and the thermal expansion coefficient

have been tested. The performed analysis gives an excellent agreement with experiment when quartic potential terms are included in the theory. We point out that negative thermal expansion in α -Sn is not driven by anharmonicity of interatomic potential. This resolves the long-standing puzzle in the thermal behavior of α -Sn.

HL 21.3 Tue 11:30 POT 361

Origin of thermal anisotropy in monoclinic β -Ga₂O₃ — •MARKUS R. WAGNER^{1,2}, BENJAMIN M. JANZEN², ZBIGNIEW GALAZKA³, BARTLOMIEJ GRACZYKOWSKI⁴, KAI XU⁵, RICARDO RURALI⁵, and JUAN SEBASTIAN REPARAZ⁵ — ¹Paul-Drude-Institut für Festkörperelektronik, Berlin, Germany — ²Technische Universität Berlin, Germany — ³Leibniz-Institut für Kristallzüchtung, Berlin, Germany — ⁴Faculty of Physics, Adam Mickiewicz University, Poland — ⁵Institut de Ciència de Materials de Barcelona, ICMAB-CSIC, Spain

We present a comprehensive all-optical contact-free investigation of the anisotropy of GHz and THz phonon-mediated material properties in β -Ga₂O₃. The full thermal conductivity tensor is determined by a newly developed all-optical experimental technique that enables sub-degree angular resolution in the measurement of the in-plane anisotropy of the thermal conductivity based on anisotropic frequency-domain thermoreflectance. Using this novel approach we determine the in-plane anisotropy of the thermal conductivity and its anisotropy ratio with high precision. The anisotropy of the sound velocity, elasticity, and Young modulus is measured by polarized, angular-resolved Brillouin light scattering of GHz acoustic phonons. Based on the experimental anisotropy maps of acoustic phonon velocities and thermal conductivity in combination with calculations of the phonon density of states and phonon lifetimes, we discuss the individual contributions of phonon velocities and phonon lifetimes to the anisotropy of the thermal conductivity.

HL 22: 2D Materials IV (joint session HL/CPP)

Time: Wednesday 9:30–12:30

Location: POT 81

HL 22.1 Wed 9:30 POT 81

Nonlinear optical characterization of atomically thin layers of the transition metal dichalcogenides WSe₂ and MoS₂ — •HENRY VOLKER HÜBSCHMANN¹, GERHARD BERTH¹, IOANNIS CALTZIDIS¹, KATHARINA BURGHOLZER², ALBERTA BONANNI², and KLAUS D. JÖNS¹ — ¹Department of Physics, Paderborn University, 33098 Paderborn, Germany — ²Institute of Semiconductor and Solid State Physics, Johannes Kepler University Linz, 4040 Linz, Austria

In the field of quantum technologies functional 2D-structures based on transition metal dichalcogenides like WSe₂ and MoS₂ represent a novel material platform due to their specific optical and electronic properties. In contrast to semimetallic graphene they feature an electronic band gap and a strong spin-orbit coupling. Applications of such layered 2D-materials in functional structures are to be found within photonics, spinorbitronics or nanoelectronics. In this work we present our fundamental nonlinear study on mechanically exfoliated atomically thin layers of the semiconductors WSe₂ and MoS₂. In this context, the second harmonic generation was determined for both van der Waals layered material systems as a function of the layer number. The respective nonlinear behavior was proven by a power-dependent characterization and supplemented by polarimetric analysis. Nonlinear imaging of the flakes was successfully performed by confocal SH-microscopy. In a further step the oxidation of MoS₂ layered systems was analyzed, here it was shown that for an even number of layers the oxidation leads to a break of their centrosymmetric structure, which is manifested in the clear presence of a relatively strong second harmonic signal.

HL 22.2 Wed 9:45 POT 81

Single Photon Emitters in hBN via ultra-low energy helium ion implantation — •PROKHOR TKHOR^{1,2}, MINH BUI^{1,2}, RENU RANI¹, THORSTEN BRAZDA¹, and BEATA E. KARDYNAŁ^{1,2} — ¹Peter Grünberg Institut-9, Forschungszentrum Jülich, Jülich — ²Department of Physics, RWTH Aachen, Aachen

Properties of heterostructures of transition metal dichalcogenides depend strongly on the moiré lattice configuration and on the strength of coupling between the constituent monolayers. The first one can be controlled by the lattice constant of the constituent monolayers and their relative orientation, while the latter can be tuned by changing the spacing between them. In this contribution, we study a heterostructure of monolayers of WSe₂/hBN/WSe₂ with a moiré potential periodicity of around 5 nm. The insertion of a monolayer of hBN between the two WSe₂ monolayers results in a weak coupling between them. We discuss the results of the measurements of the dependence of the photoluminescence on the doping and electric field in this system. In this system the lowest intralayer excitonic states are optically spin-forbidden and at low electron concentration the effect of the moiré potential on scattering of electrons and excitons dominates the optical signal masking the effect of correlations. Further, we discuss the observed non-monotonic charge shifts between the monolayers as a function of applied electric field.

HL 22.3 Wed 10:00 POT 81

Thin hexagonal boron nitride in the deep-UV: The pursuit of single photon emitters and their properties — •NILS BERNHARDT¹, LUKA CHOI¹, FELIX NIPPERT¹, ANGUS GENTLE², MILOS TOT², and MARKUS R. WAGNER^{1,3} — ¹Technische Universität Berlin, Berlin, Germany — ²University of Technology Sydney, Sydney, Australia — ³Paul-Drude-Institut, Berlin, Germany

Interest in hexagonal boron nitride (hBN) continues to grow in optoelectronics with the discovery of an increasing number of quantum emitters in all spectral ranges. The wide band gap and chemical stability inherent to this material encourage hBN as a semiconductor substrate, while the possibility of reliably fabricating thin films entails unusual and unique properties. Consequently, room-temperature defect quantum emitters with reproducible emission prop-

erties from the UV to the near-IR can be engineered for applications such as quantum communication.

In this work, we investigate the recently observed luminescence of hBN at 4.1eV with a pulsed, frequency-tripled titanium-sapphire laser at 240nm. Experimental methods such as photoluminescence spectroscopy and time-resolved fluorescence spectroscopy are utilized alongside a Hanbury Brown and Twiss interferometer for correlation measurements in the deep UV as a means to identify single-photon emitters. Through this approach, we are able to establish a scientific basis for further investigation into the UV emission of hBN.

HL 22.4 Wed 10:15 POT 81

Electrical control of excitonic complexes in MoSe₂ homobilayers — •BÁRBARA ROSA¹, CHIRAG PALEKAR¹, ALISSON CADORE², YUHUI YANG¹, ARIS KOULASIMOS¹, SEFAATTIN TONGAY³, and STEPHAN REITZENSTEIN¹ — ¹Institut für Festkörperphysik, Technische Universität Berlin, Berlin, Germany — ²Brazilian Nanotechnology National Laboratory, Campinas, Brazil — ³School for Engineering of Matter, Transport and Energy, Arizona State University, Tempe, USA

Effects of periodic Moiré potential in transition metal dichalcogenides (TMDs) bilayers are directly controlled by the twist angle between the monolayers. Novel features arising from intra- and interlayer excitons, such as their ultrafast formation and charger transfer, long population recombination lifetimes, and binding energy of dozens of meVs, turn TMD heterostructures into an attractive device for the study and manipulation of optical and transport properties via electrical fields. Moreover, such effects may appear even more pronounced at twisted homobilayers, since the absence of lattice mismatch promotes the appearance of larger Moiré superlattices. In this work, we explore the ability to control excitonic complexes in MoSe₂/MoSe₂ twisted bilayers (t-BLs) by performing gate-dependent microphotoluminescence (μ PL) spectroscopy at room temperature. We observe the energy tunability of several meVs occurring at the emission of excitonic complexes derived from the t-BL region. In addition, other effects, such as the emergence of new excitonic features, are observed through μ PL spectroscopy at cryogenic temperatures.

15 min. break

HL 22.5 Wed 10:45 POT 81

Tailoring Coulomb interactions in WS₂-graphene heterostructures — •DAVID TEBBE¹, MARC SCHÜTTE¹, KENJI WATANABE², TAKASHI TANIGUCHI³, CHRISTOPH STAMPFER¹, BERND BESCHOTEN¹, and LUTZ WALDECKER¹ — ¹2nd Institute of Physics A, RWTH Aachen University — ²Research Center for Functional Materials, Japan — ³International Center for Materials Nanoarchitectonics, Japan

The exciton binding energy and the quasiparticle bandgap in two dimensional semiconductors depend on their dielectric environment.

We investigate the screening of Coulomb interactions in heterostructures of WS₂ and graphene, separated through thin spacer layers of hexagonal boron nitride (hBN). By using hBN spacers from one to 16 atomic layers, we experimentally determine the tuning of the exciton binding energy and the quasiparticle bandgap as a function of the WS₂-to-graphene interlayer spacing.

This change in both energies is well described by a one over distance dependence, which is consistent with a screening arising from an image charge induced by the graphene layer.

Additionally, by doping the graphene with a graphitic back gate, we show that the ability of the graphene to screen Coulomb interactions in neighbouring layers is strongly modified. We determine the change in screening strength to be approximately 20% at room temperature, demonstrating that Coulomb-interactions in WS₂ can be modified in-situ without changing the doping level of the material itself.

HL 22.6 Wed 11:00 POT 81

Evidence for equilibrium exciton condensation in monolayer WTe₂ — •MASSIMO RONTANI — CNR-NANO, Modena, Italy

We present evidence [1] that the two-dimensional bulk of monolayer WTe₂ contains electrons and holes bound by Coulomb attraction, excitons, that spontaneously form in thermal equilibrium. On cooling from room temperature to 100 K, the conductivity develops a V-shaped dependence on electrostatic doping, while the chemical potential develops a step at the neutral point. These features are much sharper than is possible in an independent-electron picture, but they can be accounted for if electrons and holes interact strongly and are paired in equilibrium. Our calculations from first principles show that the exciton binding energy is larger than 100 meV and the radius as small as 4 nm, explaining their formation at high temperature and doping levels. Below 100 K, more strongly insulating behaviour is seen, suggesting that a charge-ordered state forms. The observed absence of charge density waves in this state is surprising within an excitonic insulator picture, but we show that it can be explained by the symmetries of the exciton wavefunction. Therefore, in addition to being a topological insulator, monolayer WTe₂ exhibits strong correlations over a wide temperature range.

This work is done in collaboration with Elisa Molinari, Daniele Varsano, Samaneh Ataei, Maurizia Palumbo, Bosong Sun, David Cobden. It is partially funded by MUR PRIN2017 No. 2017BZPKSZ EXC-INS and MaX EU Center of Excellence.

[1] B. Sun et al., *Nature Physics* 18, 94-99 (2022).

HL 22.7 Wed 11:15 POT 81

Charge and exciton quenching at defect states in TMDC-graphene heterostructures — •DANIEL HERNANGÓMEZ-PÉREZ¹, AMIR KLEINER¹, ANDREA DONARINI², and SIVAN REFAELY-ABRAMSON¹ — ¹Department of Molecular Chemistry and Materials Science, Weizmann Institute of Science, 7610001 Rehovot, Israel — ²Institute for Theoretical Physics, University of Regensburg, 93040 Regensburg, Germany

In recent years, studies of charge transfer and excitonic properties of van der Waals heterostructures have revealed a fertile research arena, spanning Coulomb blockade physics [1], ultrafast interlayer charge separation [2] or graphene-quenched photoluminescence [3]. We theoretically study charge transfer and excitonic properties in XS₂-graphene (X = W, Mo) heterobilayers with monoatomic chalcogen vacancies [4-5]. We discuss the impact of the subgap defect-based features in the microscopic dynamics, as well as the interplay between spatial symmetries and the spin degree of freedom through the spin-orbit interaction. Finally, we report the electronic and optical properties computed by many-body perturbation theory and show how defects and graphene alter the absorption properties of the TMDC due to a combination of folding, commensuration and impact of defect in-gap energy bands.

[1] N. Papadopoulos, *et al.* *Phys. Rev. B* 101, 165303 (2020). [2] S. Aeschlimann, *et al.* *Science Advances* 6 (20)(2020). [3] E. Lorchat, *et al.*, *Nat. Nano.* 15, 283 (2020). [4] D. Hernangómez-Pérez, A. Donarini, and S. Refaely-Abramson, arXiv:2209.14420. [5] D. Hernangómez-Pérez, A. Kleiner, and S. Refaely-Abramson (in preparation).

15 min. break

HL 22.8 Wed 11:45 POT 81

The influence of anisotropy on excitons in magnetic semiconductors — •MARIE-CHRISTIN HEISSENBÜTTEL, THORSTEN DEILMANN, and MICHAEL ROHLFING — Institute of Solid State Theory, University of Münster, Germany

Understanding the peculiar interrelation between crystal structure, magnetic properties and light-matter interaction in semiconducting two-dimensional-like magnets is of fundamental interest. From our ab-initio GW/Bethe-Salpeter equation calculations, we are able to examine electronic and excitonic properties on the same footing.

Because of its large crystal anisotropy combined with in-plane ferromagnetism, the van-der-Waals stacked CrSBr has recently come to the fore e.g. to study correlated phenomena. Due to the unique interplay of anisotropy, two-dimensional magnetism and optoelectronic properties resulting in a quantum confinement, we observe very flat dispersions, different effective masses and a quasi-1D behaviour of excitons within a monolayer of CrSBr [1]. Moreover, we find that the Rydberg series of two excitonic states is intricately modified by the different extension of the wavefunctions within momentum space.

[1] <https://arxiv.org/abs/2205.13456>

HL 22.9 Wed 12:00 POT 81

From MoSe₂ to MoS₂ and everything in-between — •JENNIFER SCHMEINK, VLADISLAV MUSYTSCHUK, NICOLAS HILLE, ERIK POLLMANN, PETER KRATZER, and MARIKA SCHLEBERGER — Universität Duisburg-Essen, Fakultät für Physik, Germany

Asymmetrical, or Janus transition metal dichalcogenide (TMDC) monolayers such as MoS₂ are a current hot topic in the field of two-dimensional (2D) materials due to their unique properties. The most common approach of fabrication is to start off from one of the two base TMDCs' monolayer and selectively substitute the top-most layer of chalcogen atoms with another kind. However, if the substitution is partial, the resulting material resembles more an alloy than a Janus-type structure. These in-between materials show their own interesting features, as they allow for example a fluid optical band-gap tuning from that of MoSe₂ at 1.54 eV over 1.70 eV for MoS₂ up to 1.84 eV of MoS₂. In my talk I want to show off the varying optical and electronic properties of these MoS₂(1-x)Se_{2x} (0 ≤ x ≤ 1) structures with a special focus on the Janus-type MoS₂ monolayer. This talk will explore the fascinating question of what lies in between.

HL 22.10 Wed 12:15 POT 81

Optimized Irradiation Protocol for Quantum Sensors in Hexagonal Boron Nitride — •PAUL KONRAD¹, ANDREAS GOTTSCHOLL¹, ANDREAS SPERLICH¹, IGOR AHARONOVICH², and VLADIMIR DYAKONOV¹ — ¹Experimental Physics 6, Julius-Maximilians-University of Würzburg, 97074 Würzburg — ²School of Mathematics and Physical Sciences, University of Technology Sydney, Ultimo, NSW 2007, Australia

Colour centres in solid-state materials show great potential in quantum information technology and sensing applications. The lately discovered negatively charged boron vacancy (V_B^-) in hexagonal boron nitride (hBN)^[1] has shown that the defect exhibits a spin-triplet ground state with spin-dependent photoluminescence. The system can be exploited in terms of its application as temperature, magnetic field, and pressure sensor^[2,3] which extends the already known applications of e.g. NV-centers in diamond not only due to its 2D character but also by highly improved temperature sensing especially at low temperatures.

Here we present an irradiation protocol for creation of V_B^- by nitrogen ions, leading to optimized spin relaxation parameters and therefore improving quantum metrology limits. We also present tremendous improvement of ODMR contrast showing hyperfine interaction on flakes of down to 80nm thickness.

[1] Gottscholl et al., *Nat. Mat.*, **19**, 5, 540 (2020).

[2] Gottscholl et al., *Sci. Adv.*, **7** (14), eabf3630 (2021).

[3] Gottscholl et al., *Nat. Commun.*, **12**, 4480 (2021).

HL 23: Focus Session: Breakthroughs in wide-bandgap semiconductor laser diodes I

Recently, a number of significant breakthroughs have taken place in the area of wide-bandgap semiconductor laser diodes. The exploration of the limits of III-nitride materials, the improved understanding of the optical and electronic properties allowed to push the lasing wavelength towards the UV-B and UV-C spectral range with AlGaIn-based laser diodes emitting at record short wavelength near 270 nm and 300 nm. In addition, advanced designs and fabrication technologies have led to the realization of novel devices in the blue-violet and even UV spectral range such as low-threshold VCSELs, narrow-linewidth GaN-based DFB laser diodes and photonic crystal lasers. In this focus session we will review these recent developments and discuss the future challenges and application for these devices.

Organized by Tim Wernicke, Ulrich Schwarz, and Michael Kneissl

Time: Wednesday 9:30–12:15

Location: POT 361

Invited Talk HL 23.1 Wed 9:30 POT 361

Vertical-cavity surface-emitting lasers – this is the way — •Å. HAGLUND¹, G. CARDINALI², L. PERSSON¹, F. HJORT¹, J. ENSLIN², E. TORRES¹, C. KUHN², S. GRAUPETER², M. GRIGOLETTO², M. A. BERGMANN¹, N. PROKOP², M. GUTTMANN², L. SULMONI², N. LOBO PLOCH³, M. COBET², T. KOLBE³, J. GUSTAVSSON¹, F. NIPPERT², I. HÄUSLER², M. R. WAGNER², J. CIERS¹, T. WERNICKE², and M. KNEISL^{2,3} — ¹Chalmers University of Technology, Göteborg, Sweden — ²Technische Universität Berlin, Berlin — ³FBH, Berlin

In recent years, there has been tremendous improvement in the performance of blue-emitting vertical-cavity surface-emitting lasers (VCSELs). Ultraviolet (UV)B (280–320 nm) and UVC (<280 nm) VCSELs have also been demonstrated, but so far only under optical pumping. All VCSELs require high reflectivity mirrors with an accurate cavity length control, but there is today no consensus on which is the best approach to realize this. We will summarize state of the art and then go into depth on our concept which is based upon using all-dielectric distributed Bragg reflectors where substrate removal is achieved by selective electrochemical etching. This approach has enabled the world's first UVB VCSEL at 310 nm. It also gives access to both sides of the cavity which allows for detuning postgrowth with drastically reduced lasing thresholds as well as an athermalized lasing wavelength. Thus, we believe that - this is the way - for nitride VCSELs. As a first step towards electrically injected UV VCSELs, we will demonstrate resonant cavity light emitting diodes with tunnel junctions.

Invited Talk HL 23.2 Wed 10:00 POT 361

Towards GaN-based diode lasers with narrow linewidth and high reliability — •SVEN EINFELDT¹, ERIK FREIER¹, JI-HYE KANG¹, HANS WENZEL¹, ANNA MOGILATENKO¹, JOHANNES GLAAB¹, ASMAA ABOU-SHEWARIB¹, VEIT HOFFMANN¹, JOHANNES ENSLIN¹, MARTIN GUTTMANN¹, SAAD MAKHLADI¹, JÖRG FRICKE¹, OLAF BROX¹, MATHIAS MATALLA¹, MARIA NORMAN-REINER¹, CHRISTOPH STÖLMACKER¹, MARKUS WEYERS¹, LUCA SULMONI², MICHAEL KNEISL², LUKAS UHLIG³, and ULRICH T. SCHWARZ³ — ¹Ferdinand-Braun-Institut (FBH), Berlin, Germany — ²Technische Universität Berlin, Institut für Festkörperphysik, Berlin, Germany — ³Technische Universität Chemnitz, Institut für Physik, Chemnitz, Germany

Various applications require GaN-based diode lasers that not only operate in single-mode at well-defined wavelengths, but also exhibit a small linewidth and high reliability. Single-mode operation can be achieved via the distributed feedback (DFB) or distributed Bragg reflector (DBR) laser design, i.e. monolithic integration of gratings in the chip. We present here the current state of the art in fabrication technology and properties of DFB and DBR diode lasers with high-order laterally coupled surface gratings. These include continuous wave single-mode operation at room temperature with an optical power of up to 20 mW (DBR) and 70 mW (DFB), respectively, and spectral half widths of about 20 pm. We also show results of selected studies on the reliability of GaN-based lasers, in particular on the stability of the operating voltage, the evolution of spatial inhomogeneities in the current distribution in the chip, and the stability of the facets.

Invited Talk HL 23.3 Wed 10:30 POT 361

Use of wafer patterning for new functionalities of InGaIn light emitters — •ANNA KAFAR^{1,2}, RYOTA ISHII³, ATSUSHI SAKAKI⁴, KIRAN SABA¹, CONNY BECHT⁵, SZYMON GRZANKA^{1,2}, ULRICH SCHWARZ⁵, MITSURU FUNATO³, YOICHI KAWAKAMI³, and PIOTR PERLIN^{1,2} — ¹Institute of High Pressure Physics PAS, Warsaw, Poland — ²TopGaIn Ltd., Warsaw, Poland — ³Kyoto University, Kyoto, Japan — ⁴Nichia Corporation, Tokushima, Japan — ⁵Chemnitz University of Technology, Chemnitz, Germany

In this work we present the use of patterning of bulk GaN substrates to control the growth of InGaIn layers by metalorganic vapour-phase epitaxy. We demonstrate that using local change of substrate miscut, it is possible to obtain a spatial shift of emission energy of above 25 nm. Synchrotron radiation microbeam X-ray diffraction reveals that a significant change of In content in the QWs is possible between 9% and 18%. This approach can be used for example in fabri-

cation of micro-arrays of laser diodes with different lasing wavelength. Another application is the fabrication of superluminescent diodes with broadened emission spectra by utilizing a profile of indium content along the device waveguide. Furthermore, we use the same concept to demonstrate monolithic light-guides integrated with laser diodes on the same wafer and fabricated based on the same epitaxy. We also study the possibility to use substrate patterning in a form of micro strips and discs regions of improved quality InGaIn which can be used for fabrication of the active regions of the micro LEDs and laser diodes.

30 min. break

HL 23.4 Wed 11:30 POT 361

Time-dependent intensity and wavelength dynamics of blue laser diodes with wide quantum wells — •JANNINA TEPASS¹, LUKAS UHLIG¹, MATEUSZ HAJDEL², GRZEGORZ MUZIOL², and ULRICH THEODOR SCHWARZ¹ — ¹Institute of Physics, Chemnitz University of Technology, Chemnitz, Germany — ²Institute of High Pressure Physics, Polish Academy of Sciences, Poland

In this study, thick quantum wells with two different thicknesses of 10.4 nm and 25 nm are analyzed. The very low overlap of the electron and hole wavefunction in such QWs due to the quantum confined Stark effect would indicate inefficient devices. However, it has been shown that thick QWs can be more effective and achieve high optical gain. This can be explained by the electric field screening that leads to a high overlap of the excited electron and hole states, which enable lasing. In this work, a pulsed electrical excitation scheme is used in which carrier injection at forward voltage is largely separated from carrier recombination at zero or reverse voltage. Due to this effect, the interplay between the piezoelectric field and the built-in potential on the charge carrier recombination in dependence on an external bias voltage can be observed. In particular, a sharp increase in the radiative recombination rate after the trailing edge of the driving pulse is observed, as well as a wavelength shift.

HL 23.5 Wed 11:45 POT 361

Single-mode lasing in optically pumped UVB VCSELs with circular relief structures — •GIULIA CARDINALI¹, FILIP HJORT², JOHANNES ENSLIN¹, MUNISE COBET¹, MICHAEL A. BERGMANN², JOHAN GUSTAVSSON², JOACHIM CIERS², TIM KOLBE³, FELIX NIPPERT¹, MARKUS R. WAGNER¹, TIM WERNICKE¹, ÅSA HAGLUND², and MICHAEL KNEISL^{1,3} — ¹Institute of Solid State Physics, Technische Universität Berlin, Berlin, Germany — ²Department of Microtechnology and Nanoscience, Chalmers University of Technology, Gothenburg, Sweden — ³Ferdinand-Braun-Institut (FBH), Berlin, Germany

Extending the emission wavelength of vertical-cavity surface-emitting lasers (VCSELs) in the ultraviolet (UV) range would allow advances in many applications, e.g. in medical diagnostics, material curing, and sterilization. UV VCSELs have been demonstrated only under optical pumping and they suffer from strong filamentation (i.e. spatially inhomogeneous emission), resulting in multimode lasing. In this work, we study the emission characteristic of optically pumped UVB VCSELs with circular reliefs dry-etched on the bottom cavity. Single-mode lasing near 312 nm was achieved for VCSELs with 25 nm-deep reliefs with diameters smaller than 5 μm , when pumped up to 80 MW/cm². Here, the lateral size of the cavity was reduced below the dimension of one filament. VCSELs with 5 nm-deep reliefs did not show single mode lasing. 50 nm-deep structures did not lase for diameters below 6 μm . The higher thresholds in this sample are due to defect generation in the quantum-well by the dry etching, which was confirmed by time-resolved photoluminescence measurements of the carrier lifetimes.

HL 23.6 Wed 12:00 POT 361

Use of wafer patterning for new functionalities of InGaIn light emitters — •ANNA KAFAR^{1,2}, KIRAN SABA¹, RYOTA ISHII³, ATSUSHI SAKAKI⁴, SZYMON GRZANKA^{1,2}, CONNY BECHT⁵, ULRICH SCHWARZ⁵, MITSURU FUNATO³, YOICHI KAWAKAMI³, and PIOTR PERLIN^{1,2} — ¹Institute of High Pressure Physics PAS, Warsaw, Poland — ²TopGaIn Ltd., Warsaw, Poland — ³Kyoto University, Kyoto, Japan — ⁴Nichia Corporation, Tokushima, Japan — ⁵Chemnitz University of Technology, Chemnitz, Germany

In this work we present the use of patterning of bulk GaN substrates to control the growth of InGaN layers by metalorganic vapour-phase epitaxy. We demonstrate that using local change of substrate miscut, it is possible to obtain a spatial shift of emission energy of above 25 nm. Synchrotron radiation microbeam X-ray diffraction reveals that a significant change of In content in the QWs is possible * between 9% and 18%. This approach can be used for example in fabrication of micro-arrays of laser diodes with different lasing wavelength. Another

application is the fabrication of superluminescent diodes with broadened emission spectra by utilizing a profile of indium content along the device waveguide. Furthermore, we use the same concept to demonstrate monolithic light-guides integrated with laser diodes on the same wafer and fabricated based on the same epitaxy. We also study the possibility to use substrate patterning in a form of micro strips and discs regions of improved quality InGaN which can be used for fabrication of the active regions of the micro LEDs and laser diodes.

HL 24: Quantum dots: Optics

Time: Wednesday 9:30–13:15

Location: POT 151

HL 24.1 Wed 9:30 POT 151

Raman spectroscopic structure analysis of colloidal semiconductor core-shell quantum dots for the achievement of near-unity quantum efficiency — •SANDRA ZECH^{1,2}, SONJA KROHN², HANNES VAN AVERMAET³, ZEGGER HENS³, JAN STEFFEN NIEHAUS⁴, JANINA MAULTZSCH¹, and HOLGER LANGE² — ¹Department of Physics, Friedrich-Alexander-Universität Erlangen-Nürnberg, Erlangen, Germany — ²Institute of Physical Chemistry, University of Hamburg, Hamburg, Germany — ³Physics and Chemistry of Nanostructures, Ghent University, Ghent, Belgium — ⁴Fraunhofer IPA Center for Applied Nano-Technology CAN, Hamburg, Germany

State of the art applications of quantum dots (QDs) require near-unity photoluminescence quantum yield (PLQY). This demand is rarely achieved and therefore the synthesis process is under constant optimization and nanocrystals consisting of a core with one or more shells of different materials are paving the way to achieve high PLQY. As those components have diverse lattice parameters, the induction of strain within the QDs is inevitable. Recently, we applied Raman spectroscopy for in depth structure characterization and a strain minimization approach to optimize the synthesis of InP/ZnSe/ZnS QDs towards near-unity PLQY. A similar effect plays a role in CdSe/CdS QDs when aiming for high PLQY. In these QDs, the formation of an alloyed interface between the CdSe core and CdS shell is assumed. By Raman spectroscopy, we are able to monitor the formation of these alloyed domains for different QD parameters and correlate it with the PLQY.

HL 24.2 Wed 9:45 POT 151

Collective Excitation of Spatio-Spectrally Distinct Quantum Dots Enabled by Chirped Pulses — •FLORIAN KAPPE¹, YUSUF KARLI¹, THOMAS BRACHT², SAIMON COVRE DA SILVA³, TIM SEIDELMANN⁴, VOLLRATH MARTIN AXT⁴, ARMANDO RASTELLI³, GREGOR WEIHS¹, DORIS REITER^{2,5}, and VIKAS REMESH¹ — ¹Institute für Experimentalphysik, Universität Innsbruck, Innsbruck, Austria — ²Institut für Festkörpertheorie, WWU Münster, Münster, Germany — ³Institute of Semiconductor and Solid State Physics, Johannes Kepler University Linz, Linz, Austria — ⁴Theoretische Physik III, Universität Bayreuth, Bayreuth, Germany — ⁵Condensed Matter Theory, TU Dortmund, Dortmund, Germany

To boost the communication rate in quantum communication devices, it is desirable to have an ensemble of single photon sources that can be collectively excited, despite their spectral variability. Rabi rotation, the most popular method for resonant excitation of the quantum dot, cannot assure a highly efficient state preparation, due to its sensitivity to the excitation parameters. Here, we demonstrate the robustness of Adiabatic Rapid Passage, using chirped laser pulses and collectively excite biexciton states [1] in energetically and spatially distinct quantum dots. We also demonstrate a regime of phonon contribution that widens the detuning range. Being able to generate high-purity photons from spatially multiplexed quantum dot sources with high efficiency is a big step towards the implementation of high photon rate quantum key distribution protocols. [1] Kappe et al, <https://arxiv.org/abs/2209.08972> (in peer review)

HL 24.3 Wed 10:00 POT 151

Prospects of atomic vapor-based storage of single photons emitted by a deterministically fabricated quantum dot device — •AVIJIT BARUA¹, BENJAMIN MAASS², NORMAN VINCENZ EWALD², SUK-IN PARK³, SUNG-YUL PARK³, JIN-DONG SONG³, JANIK WOLTERS², and STEPHAN REITZENSTEIN¹ — ¹Technische Universität Berlin, Berlin, Germany — ²German Aerospace Center (DLR), Berlin, Germany — ³Korea Institute of Science and Technology, Seoul, Republic of Korea

Semiconductor quantum dots (QDs) are extensively investigated as single-photon sources for applications in photonic quantum technology. Here, we develop bright and strain-tunable QD single-photon sources at the Cs D1 transition wavelength and explore the storage ability of semiconductor QD in atomic quantum memories. The devices are designed and numerically optimized to maximize extraction efficiency using the finite element method. By considering circular Bragg resonators with integrated QDs and Au-backside mirror, we numerically demonstrate a photon extraction efficiency of 65% and a Purcell factor of 0.72. In the experimental development, we implement in-situ electron-beam lithography to precisely integrate selected single QDs at 894 nm in such struc-

tures to create bright single-photon sources. The emission from the developed quantum devices is studied by means of photon autocorrelation measurements. Furthermore, we explore the prospects of interfacing the QD single photons with a vapor-based quantum memory by employing a ladder-type EIT configuration that allows for low-noise storage and retrieval at high repetition rates.

HL 24.4 Wed 10:15 POT 151

Double pulse excitation schemes for enhanced multiphoton interference — •YUSUF KARLI¹, FLORIAN KAPPE¹, JULIAN MUNZBERG¹, THOMAS BRACHT², SAIMON COVRE DA SILVA³, ARMANDO RASTELLI³, DORIS REITER^{2,4}, ROBERT KEIL¹, VIKAS REMESH¹, and GREGOR WEIHS¹ — ¹Institute für Experimentalphysik, Universität Innsbruck, Innsbruck, Austria — ²Institut für Festkörpertheorie, WWU Münster, Münster, Germany — ³Institute of Semiconductor and Solid State Physics, Johannes Kepler University Linz, Linz, Austria — ⁴Condensed Matter Theory, TU Dortmund, Dortmund, Germany

High-efficiency generation multiphoton states is an important prerequisite for linear quantum computing applications. Semiconductor quantum dots are high-brightness sources of highly indistinguishable single photons, which can then be used to generate multiphoton states via active temporal-to-spatial demultiplexing. Resonant s-shell excitation is the most popular method to generate high-indistinguishability single photons from a quantum dot [1], however, at the cost of brightness from cross-polarization filtering. Here, we advocate the versatility of novel double-pulse excitation schemes by demonstrating an 8-fold enhancement in four-photon coincidence rates.

[1] APL Photonics 7.7 (2022)

HL 24.5 Wed 10:30 POT 151

Towards deterministic generation of time-bin entangled photons from GaAs quantum dots — •FLORIAN KAPPE¹, YUSUF KARLI¹, THOMAS BRACHT², SAIMON COVRE DA SILVA³, ARMANDO RASTELLI³, VIKAS REMESH¹, DORIS REITER^{2,4}, and FLORIAN KAPPE¹ — ¹Institut für Experimentalphysik, Universität Innsbruck, Innsbruck, Austria — ²Institut für Festkörpertheorie, WWU Münster, Münster, Germany — ³Institute of Semiconductor and Solid State Physics, Johannes Kepler University Linz, Linz, Austria — ⁴Condensed Matter Theory, TU Dortmund, Dortmund, Germany

Semiconductor quantum dots are bright, on-demand single photon sources suitable for realising quantum communication devices. Here, we present our first results towards the deterministic generation of time-bin entangled photon states via dark exciton states from GaAs/AlGaAs quantum dots. Our schemes employ chirped laser pulses and an external magnetic field that enables the coupling of bright and dark exciton states in the quantum dot [1,2]. Based on numerical methods we analyze the quantum dot dynamics and state preparation fidelity and identify that the preparation schemes are quite robust against the phonon influence.

[1] Phys. Rev. B. 92(20), (2015).

[2] Phys. Rev. B 104.7 (2021).

HL 24.6 Wed 10:45 POT 151

Generation of indistinguishable and entangled photons at telecom frequencies using tailored cavity designs — •DAVID BAUCH, DUSTIN SIEBERT, JENS FÖRSTNER, KLAUS D. JÖNS, and STEFAN SCHUMACHER — Department of Physics, Electrical Engineering and CeOPP, Paderborn University, Germany

The commonly utilized biexciton-exciton cascade yields photons with intrinsically limited indistinguishability [1]. By tuning the biexciton-exciton lifetime ratio, large increases in single photon indistinguishability can be achieved [1,2]. Using the cavity-induced Purcell enhancement is a simple method for radiative lifetime tuning. Employing a circular Bragg reflector at telecom wavelengths for suitable quantum dots allows for a Purcell enhanced biexciton-exciton transition, while still maintaining high extraction efficiency for the exciton-ground state transition. The decreased lifetime of the biexciton results in a faster emission of then indistinguishable single photons. Here, we demonstrate this effect numerically and determine the theoretically required parameters for the biexciton-exciton transition to yield highly indistinguishable single photons, which are also entangled with their exciton-ground state emission counterpart. We guide our calculations using Maxwell simulations for the cavity design, allowing for

close-to real-life system predictions. Our simulation demonstrates the robust increase of the indistinguishability of the emitted photons even when accounting for electron-phonon coupling at low temperatures.

[1] E. Schöll, et al., *Physical Review Letters* 125, 233605 (2020) [2] F. Sbresny, et al., *Physical Review Letters* 128, 093603 (2022)

HL 24.7 Wed 11:00 POT 151

Exciton diffusion in a quantum dot ensemble — •KAROL KAWA and PAWEŁ MACHNIKOWSKI — Wrocław University of Science and Technology, 50-370 Wrocław, Poland

We study theoretically Förster transfer [1] of an exciton in an ensemble of quantum dots (QDs) randomly distributed on a circular mesa. In such a system energy transfer was observed experimentally within a spatially resolved photoluminescence spectroscopy [2]. The analytical form of Förster coupling in the general ensemble of quantum dipole emitters is known [3–5]. It is a sum of three power-law terms diminishing with distance, each multiplied by an oscillating factor. The fundamental transition energy in each QD is randomized. We solve the equation of motion for the density matrix using the stochastic simulation method with a given exciton decay rate. Then, we present the evolution of the exciton mean square displacement (MSD) from the initially excited QD. It runs in three time stages. First, a ballistic motion, followed by a standard diffusion, which ends at saturation. Using an approximate analytical approach [6], we provide formulas that qualitatively reproduce all stages of the MSD.

[1] T. Förster, *Ann. Phys.*, 437, 55 (1948)

[2] F.V. de Sales et al., *Phys. Rev. B* 70, 235318 (2004)

[3] M.J. Stephen, *J. Chem. Phys.* 40, 669 (1964)

[4] R.H. Lehmburg, *Phys. Rev. A* 2, 883 (1970)

[5] F. Miftasani and P. Machnikowski, *Phys. Rev. B* 93, 075311 (2016)

[6] K. Kawa and P. Machnikowski, *Phys. Rev. B* 102, 174203 (2020)

30 min. break

HL 24.8 Wed 11:45 POT 151

Preparation of spin qubits in droplet-etched GaAs quantum dots using quasi-resonant excitation — •CASPAR HOPFMANN¹, NAND LAL SHARMA¹, WEIJIE NIE¹, ROBERT KEIL¹, FEI DING², and OLIVER G. SCHMIDT^{1,3,4} — ¹Institute for Integrative Nanosciences, IFW Dresden, Helmholtzstr. 20, 01069 Dresden — ²Institut für Festkörperphysik, Leibniz Universität Hannover, Appelstr. 2, 30167 Hannover — ³Material Systems for Nanoelectronics, Technische Universität Chemnitz, 09107 Chemnitz — ⁴Nanophysics, Faculty of Physics and Würzburg-Dresden Cluster of Excellence ct.qmat, TU Dresden, 01062 Dresden

Optically accessible quantum memories are fundamental for implementations of quantum networks as they facilitate the synchronization required for schemes of long-distance quantum information exchange. In order to use GaAs quantum dots, which so far has proven to be bright on-demand sources of entangled photon pairs, deterministic preparation of specific spin states is necessary. We present a comprehensive study on heralded spin preparation employing excited state resonances of droplet etched GaAs quantum dots. By observation of excitation spectra for a range of fundamental excitonic transitions the properties of different quantum dot energy levels, i.e. shells, are revealed. The innovative use of polarization-resolved excitation and detection in the context of quasi-resonant excitation spectroscopy of quantum dots greatly simplifies the determination of the spin preparation fidelities. By employing this method, spin preparation fidelities of quantum dot ground states of up to 85 % are found.

HL 24.9 Wed 12:00 POT 151

Effect of tunnel barrier thickness on optical properties of GaAs quantum dots embedded in Schottky diode structures — •NAND LAL SHARMA¹, MORITZ LANGER¹, ANKITA CHOUDHARY¹, OLIVER G. SCHMIDT², and CASPAR HOPFMANN¹ — ¹Institute for Integrative Nanosciences, IFW Dresden, Helmholtzstrasse 20, 01069 Dresden, Germany — ²Material Systems for Nanoelectronics, Technical University Chemnitz, 09107 Chemnitz, Germany

GaAs quantum dots (QDs) are promising candidates for on demand generation of single and entangled photon pair sources for quantum communication applications. In these QDs, the charge stability and optical linewidth depend on the solid-state environment, which can be controlled by embedding them in a diode structure [1]. In this work we investigate the effect of tunnel barrier thickness on the optical properties of droplet etched GaAs/AlGaAs QDs [2], embedded in Schottky diode structures. The QD photoluminescence from different charge states is controlled by application of an external bias. The effects of quantum dot charging, quantum confined Stark effect and photon coherence are investigated as a function of tunnel barrier thickness.

HL 24.10 Wed 12:15 POT 151

Size-dependence of the Auger process in self-assembled quantum dots — •HENDRIK MANNEL¹, MARCEL ZÖLLNER¹, FABIO RIMEK¹, ARNE LUDWIG², ANDREAS WIECK², MARTIN GELLER¹, and AXEL LORKE¹ — ¹Faculty of Physics and CENIDE, University of Duisburg-Essen, Duisburg, Germany — ²Chair of Applied Solid State Physics, Ruhr-University Bochum, Germany

Auger recombination is a non-radiative process, where the recombination energy of an electron-hole pair is transferred to a third charge carrier. In nanostructured materials, it is a common effect especially in colloidal quantum dots (QD), where short Auger recombination times $\tau_{Au} < 1$ ns quench the radiative recombination. In self-assembled QDs, an Auger recombination rate of $\tau_{Au} \approx 1$ ms has been observed [1].

We use resonance fluorescence to measure the Auger rate of differently sized self-assembled QDs having exciton recombination energies in the range of 920 to 980 nm [2]. The dots are charged with one electron before driving the trion transition to observe the quenching of this transition time-resolved on the investigated sample structure without a wetting layer.

Independently we can change the charge carrier occupation of the dot by gate voltage-dependent electron tunneling from the reservoir. This is a step to further understand the Auger effect and hopefully suppress this unwanted effect in future application of quantum information processing.

[1]*A. Kurzmann et al., *Nano Lett.* 16, 3367 (2016). [2]*M. Löbl et al., *Commun. Phys.* 2, 93 (2019).

HL 24.11 Wed 12:30 POT 151

Single Mode Coupled Emission of Resonant Excited GaAs Quantum Dots — •MARTIN KERNBACH^{1,2}, JULIAN SILLER¹, SOPHIA FUCHS¹, and ANDREAS W. SCHELL^{1,2} — ¹Leibniz Universität Hannover, Deutschland — ²Physikalisch-Technische Bundesanstalt, Braunschweig, Deutschland

Quantum technologies like computing, QKD, or sensing demand for deterministic bright sources of single indistinguishable photons. In order to provide quantum light of isolated systems properly usable for quantum information science, an efficient excitation and extensive collection in a single mode is required. Single molecules and cavity confined quantum dots are convenient sources. The coupling to the excited state is maximized on resonance, but challenges the usability of the emitter due to the costs for the separation of the optical excitation mode from the mode of emission. A temporal, spacial, spectral, or combined method for separation is typically used. Here we present a realization of a single emitter under resonant excitation in a confocal setup coupled into a single mode fiber with the emission mode filtered by polarization. So far, a free beam is directed on the objective mounted with the scanning stages on a 1 m long stick in a liquid helium reservoir. For resonant cw excitation of GaAs semiconductor quantum dots a SNR of polarization suppression up to 100 and count rates of 280 kcps are archived by using a collecting lens with NA 0.68 only. Under this scheme further investigations regarding the blinking behavior are possible as well as probing alternative emitters like single molecules.

HL 24.12 Wed 12:45 POT 151

The role of charge transfer for light emission from excitonic complexes in a single quantum emitter — •MARCEL ZÖLLNER¹, FABIO RIMEK¹, HENDRIK MANNEL¹, ANDREAS D. WIECK², ARNE LUDWIG², MARTIN GELLER¹, and AXEL LORKE¹ — ¹University of Duisburg-Essen, Germany — ²Ruhr-University Bochum, Germany

Due to the non-radiative Auger recombination in self-assembled quantum dots [1], the light emission of the trion X^- is reduced. However, for devices and statistical analyses, such as random telegraph signals, the amount of quantum dot photons is of great importance.

With time-resolved resonance fluorescence (RF) measurements, we investigate a comparatively small quantum dot, where we can tune the rate of the electron tunneling from the back contact into the quantum dot by increasing the gate voltage. This results in an up to two orders of magnitude higher trion intensity. Due to the large gate voltages (i.e. energetically strongly tilted conduction band) the electrons can easily overcome the tunnel barrier. Thus, the electron tunneling becomes the dominant effect and charges the quantum dot significantly faster than the Auger effect can discharge it.

Our results indicate that thin tunneling barriers, which can quickly equilibrate states in a quantum dot, make its radiative recombination more resilient against spurious charge transfer (Auger, electron capture, internal photoemission). However, this improvement goes along with a short coherence time.

[1] P. Lochner et al., *Phys. Rev. B* 103, 075426 (2021).

HL 24.13 Wed 13:00 POT 151

Single photon source in a topological cavity — JONATHAN JURKAT¹, SEBASTIAN KLEMBT¹, MARCO DE GREGORIO¹, •MORITZ MEINECKE¹, QUIRIN BUCHINGER¹, TRISTAN HADER¹, JOHANNES BEIERLEIN¹, OLEG EGOROV³, MONIKA EMMERLING¹, CONSTANTIN KRAUSE¹, CHRISTIAN SCHNEIDER², TOBIAS HUBER-LOYOLA¹, and SVEN HÖFLING¹ — ¹Technische Physik, Physikalisches Institut und Würzburg-Dresden Cluster of Excellence ct.qmat, Universität Würzburg, 97074 Würzburg, Germany — ²Lehrstuhl für Physik, Universität Oldenburg, 26129 Oldenburg, Germany — ³Lehrstuhl für Kondensierte Materie, Theorie und Optik, Friedrich-Schiller-Universität Jena, 07743 Jena, Germany

The introduction of topological physics into the field of photonics has led to the development of photonic devices endowed with robustness against structural and photonic disorder. While a range of platforms have been successfully implemented demonstrating topological protection of light in the classical do-

main, the implementation of quantum light sources in photonic devices harnessing topologically non-trivial resonances is largely unexplored. Here, we demonstrate a single photon source based on a single semiconductor quantum dot coupled to a topologically non-trivial Su-Schrieffer-Heeger (SSH) cavity mode. We

provide an in-depth study of Purcell enhancement for this topological quantum light source and demonstrate its emission of non-classical light on demand. Our approach is a promising step towards the application of topological cavities in quantum photonics.

HL 25: Perovskite and photovoltaics II (joint session HL/ CPP)

Time: Wednesday 9:30–13:00

Location: POT 251

Invited Talk

HL 25.1 Wed 9:30 POT 251

Interfaces in perovskite optoelectronics: role of energy level alignment and interface chemistry — •SELINA OLTTHOF — Universität zu Köln, Institut für Physikalische Chemie

Optoelectronic devices, such as perovskite solar cells, are typically multi-layer stacks in which the absorber layer is sandwiched between metal oxide and/or organic transport layers in order to facilitate charge extraction or ensure charge selectivity. As the perovskite absorber layer has been extensively optimized in the past years, the awareness is rising that device efficiency and stability is limited by the interfaces present in the device. However, in perovskite-based devices, the role of this energy level alignment remains to be elusive and rather inconclusive studies can be found in literature, which I will briefly outline. More important for the device seems to be the perovskite composition at the interface which can be significantly influenced by chemical reactions taking place, in particular next to metal oxides. I will summarize our work on a variety of metal oxides in which we use photoelectron spectroscopy to analyze which components are responsible for the strong interface chemistry. We show that the reactivity strongly depends on the choice of perovskite and that different metal oxides show fundamentally different reaction/degradation pathways. Intriguingly, we are able to introduce surface treatments which change the surface defect density and thereby affect the degree of perovskite degradation significantly.

HL 25.2 Wed 10:00 POT 251

Silver-nanoclusters and -vacancies influence the optical properties of Cs₂AgBiCl₆ nanocrystals — •FEI HE¹, YIYOU WANG¹, QUINTEN A. AKKERMAN¹, MARKUS DÖBLINGER², AMRITA DEY¹, and JOCHEN FELDMANN¹ — ¹Chair for Photonics and Optoelectronics, Nano-Institute Munich and Department of Physics, Ludwig-Maximilians-Universität, Königinstraße 10, 80539 Munich, Germany — ²Department of Chemistry, Ludwig-Maximilians-Universität München, Butenandtstrasse 5-13 (E), 81377 München, Germany

Though being indirect semiconductors Cesium-Silver-Bismuth-Halides (so-called double perovskites) have attracted much attention as a non-toxic alternative to Lead Halide Perovskites. Novel applications for solar cells and X-ray detectors have already been developed.

Here, we report on the successful synthesis of spherical Cs₂AgBiCl₆ nanocrystals showing good stability and characteristic photoluminescent spectra. In transmission electron microscopy (TEM) images we observe Ag-clusters on the surface of the nanocrystals. It is known that silver ions are easily reduced into metallic Ag leading to silver vacancies in the double perovskite material and probably to Ag-clusters on the surface. We discuss how silver-nanoclusters and -vacancies influence the luminescent behavior of the double perovskite nanocrystals and explain possible microscopic origins.

HL 25.3 Wed 10:15 POT 251

Accelerating research on solar cell materials with NOMAD — •JOSE MARQUEZ¹, LAURI HIMANEN¹, MARKUS SCHEIDGEN¹, CLAUDIA DRAXL¹, JENS HAUCH², CHRISTOPH BRABEC², and THOMAS UNOLD³ — ¹Humboldt Universität zu Berlin — ²Helmholtz Institute Erlangen-Nürnberg for Renewable Energy — ³Helmholtz-Zentrum Berlin

New solar cell technologies need decades to overcome the 20% power conversion efficiency threshold needed to make them commercially viable. With thousands of possible chemical compositions for new absorber layer materials and an unlimited number of possible device architectures, it becomes impossible to navigate this material space without the help of data science. To radically accelerate and democratize this development process, FAIR data management activities involving experimental solar cell data are needed. The NOMAD Laboratory (<https://nomad-lab.eu>) is a platform and open-source software driven by the NFDI consortium FAIRmat (<https://fairmat-nfdi.eu>) for making materials-science data FAIR. We show how the NOMAD infrastructure is evolving to support this task in the context of solar cells, demonstrated by an app for visualizing and searching rich and AI-ready experimental big solar cell data. NOMAD also provides an electronic lab notebook (ELN) which can be customized by research labs for AI-ready data/metadata entry, transfer, and processing in a FAIR-database context.

HL 25.4 Wed 10:30 POT 251

Interdiffusion of Cu(In,Ga)Se₂ and Ag(In,Ga)Se₂ investigated by In-Situ X-Ray Diffraction — •JULIA HORSTMANN¹, ROLAND MAINZ², KARSTEN ALBE³, HEIKO KEMPA¹, TORSTEN HÖLSCHER¹, and ROLAND SCHEER¹ — ¹Martin-Luther-Universität Halle-Wittenberg, Germany — ²Helmholtz-Zentrum Berlin, Germany — ³Technische Universität Darmstadt, Germany

The partial substitution of Ag with Cu in the chalcopyrite-based absorber of thin film solar cells is a promising approach towards higher power conversion efficiencies. The resulting (Ag,Cu)(In,Ga)Se₂ (ACIGSe) alloy achieves a bandgap widening up to 0.2 eV, increased grain growth and a lower melting temperature. The latter might reduce structural defects and therefore recombination losses in the absorber. This is favorable especially for wide-bandgap solar cells, used as top subcells in tandem devices, whose device performance is mainly limited by deep defects. To gain a better understanding of the diffusion on the (I) sublattice, we experimentally explored the interdiffusion of Cu(In,Ga)Se₂ and Ag(In,Ga)Se₂ layers by in-situ X-ray diffraction (IS-XRD) and glow discharge optical emission spectroscopy. Besides the positive aspects of Ag-alloying, thermodynamic simulations have shown a miscibility gap for temperatures between 100°C and 400°C. It is theoretically proposed, that ACIGSe with a high Ga content and with a [Ag]/([Ag]+[Cu]) ratio between 0.25 and 0.75 decomposes into Ag-rich and Ag-poor phases. We have studied the phase stability of Ga-free and Ga-rich samples using IS-XRD during post-annealing processes.

HL 25.5 Wed 10:45 POT 251

NiO in perovskite solar cells: a peculiar interplay of degradation, passivation and device performance — •JOHN MOHANRAJ¹, BIPASA SAMANTA², MAYTAL CASPARY TOROKAR², and SELINA OLTTHOF¹ — ¹University of Cologne, 50939 Cologne, Germany — ²Technion - IIT, Haifa, 3200003 Israel

The degradative interactions at the NiO/perovskite interface are notorious in the perovskite community as they lead to significant Voc and stability losses in p-i-n type perovskite solar cells (PSCs). So far, various Lewis bases have been introduced at this interface to passivate the metal oxide surface defects. Despite this process being successful in minimizing Voc and stability losses in PSCs, in-depth understanding of surface passivation and consequent suppression of the chemical processes at the NiO/perovskite interface are still elusive. This calls for a comprehensive surface investigation. To address these issues, we investigated solution processed NiO surfaces, their treatment with a series of passivating compounds, and the interface towards MAPbI₃ in order to systematically probe the interface stability. Our methods include X-ray and UV photoelectron spectroscopy (XPS/UPS), XRD, SEM and UV-Vis absorption techniques. In parallel, first principle DFT calculations on differently treated NiO/MAPbI₃ interfaces were carried out. These complementary investigations reveal changes in surface composition of the treated NiO and help us to suggest possible mechanisms for the degradative interactions. Finally, PSCs were fabricated using the stabilized NiO interfaces, and the impact on photovoltaic characteristics and device stability have been investigated.

30 min. break

HL 25.6 Wed 11:30 POT 251

Resonant coupling of spin-flip excitations with phonons in BiFeO₃ — •ASEEM RAJAN KSHIRSAGAR and SVEN REICHARDT — Department of Physics and Material Science, University of Luxembourg, Luxembourg

BiFeO₃ is a technologically relevant multiferroic perovskite. While a vast literature exists on its electronic, optical, and multiferroic properties, some of its optically active electronic excitations remain to be understood or have been interpreted in ambiguous ways. This applies in particular to features below the absorption onset that feature prominently in resonant Raman scattering [1]. Here we present a detailed study of the electronic structure and resonant Raman spectrum of BiFeO₃ from first principles. Using many-body perturbation theory on top of density functional theory, we first analyze and characterize its optical absorption spectrum in terms of excitons and atomic orbitals, focusing in particular on spin-flip excitations that are strongly localized. We then use the state-of-the-art method for the ab initio calculation of resonant Raman intensities [2,3] to analyze the resonant coupling of these finite-spin excitations with phonons. Our results show that these only weakly optically active excitations still leave a clear imprint on the resonant Raman spectrum, making the latter an even more powerful tool to probe "darker" electronic excitations.

- [1] M. C. Weber, et al. Phys. Rev. B, 93, 125204 (2016).
 [2] S. Reichardt and L. Wirtz, Phys. Rev. B, 99, 174312 (2019).
 [3] S. Reichardt and L. Wirtz, Sci. Adv., 6, eabb5915 (2020).

HL 25.7 Wed 11:45 POT 251

Coherent Phonons in Halide Perovskite Nanocrystals — •JULIAN GEORG MANN¹, FEI HE¹, QUINTEN AKKERMAN¹, TUSHAR DEBNATH², and JOCHEN FELDMANN¹ — ¹Chair for Photonics and Optoelectronics, Nano-Institute Munich and Department of Physics, Ludwig-Maximilians-Universität (LMU), Königinstr. 10, 80539 Munich, Germany — ²Centre for Nanotechnology, Indian Institute of Technology Guwahati, Guwahati-781039

Halide perovskite nanocrystals are gaining increasing attention in contemporary research due to their promising performance in both light-emitting and solar technologies. We recently showed that photoexcitation of halide-perovskite nanocrystals with ultrashort laser pulses produces coherent phonons (Nat. Comm. 12, 2629 (2021)). We report femtosecond pump-probe spectroscopy studies on the formation and dynamics of coherent phonons in formamidopyne lead-halide (FAPbX₃) nanocrystals in terms of higher harmonic vibrational modes. In addition, we investigate the dynamics of vibrational wave packets in spherical Cs₂AgBiBr₆ double perovskite nanocrystals. Here, we observe that optically launched vibrational wave-packets alter spectral positions of excitonic resonances or oscillator strength of particular electronic transitions. Our results show that electron-phonon couplings (polaronic effects) need to be considered to fully understand the optoelectronic properties of halide-perovskite semiconductors.

HL 25.8 Wed 12:00 POT 251

Phonon-driven Intra-exciton Rabi Oscillations in Halide Perovskites — •KATRIN WINTE¹, XUAN TRUNG NGUYEN¹, DANIEL TIMMER¹, DAVID CERATTI², CATERINA COCCHI¹, MICHAEL LORKE³, FRANK JAHNKE³, DAVID CAHEN², CHRISTOPH LIENAU¹, and ANTONIETTA DE STO¹ — ¹University of Oldenburg, Germany — ²Weizmann Institute of Science, Israel — ³University of Bremen, Germany

There is increasing consensus that in halide perovskites (HaPs) the interaction of electronic excitations with the phonon modes of their flexible polar lattice is crucial for the unique optoelectronic and transport properties of these materials. Here we show that coherent low frequency phonon of the lead-halide lattice induce Rabi oscillations between 1s and 2p excitons in CsPbBr₃ crystals. Ultrafast two-dimensional electronic spectroscopy reveals an excitonic peak structure oscillating with a 100-fs period up to 2 ps at 20 K. This frequency does not match any phonon modes of the crystals. Only after 2 ps, slow coherent phonon oscillations dominate the dynamics. We rationalize these findings as off-resonant intra-exciton Rabi oscillations induced by the Pb-Br phonon fields of the HaP crystals. We show that the slow motion of Pb-Br sublattice induces electric fields at THz frequencies that are sufficiently strong to drive off-resonant population oscillations between 1s and 2s excitons. Model simulation of the nonlinear optical response support this interpretation. This goes beyond prevailing models for the electron-phonon coupling in HaPs. It suggests that the coupling of characteristic low frequency phonon to intra-exciton transitions may be the key to control their anharmonic response.

HL 25.9 Wed 12:15 POT 251

Determining (almost) all optoelectronic properties of halide perovskites by transient photoluminescence — •HANNES HEMPEL¹, MARTIN STOLTERFOHT², FANGYUAN YE², and THOMAS UNOLD¹ — ¹Helmholtz Zentrum Berlin, Germany — ²Institute of Physics and Astronomy, University of Potsdam, Germany

Time-resolved photoluminescence (trPL) is probably the most common technique to quantify lifetimes of photogenerated charge carriers in semiconductors. However, the usual fitting of exponential decays to estimate lifetimes is a rather crude phenomenological approach since it ignores quenching processes that are not connected to carrier recombination and disregards the absolute amplitude

of the luminescence. Here, we present an analysis of injection-dependent absolute trPL transients of bare triple-cation lead halide perovskite thin films. The presented analysis reveals a doping concentration of 3x10¹³cm⁻³ and a charge carrier mobility of 0.8 cm²/Vs, which are confirmed by Hall measurements. Further, we determine the injection-dependence of external radiative lifetimes, of the external radiative coefficient, and of the effective charge carrier lifetime. Based on the properties, an implied current-voltage curve is constructed that reveals the potential performance of the material in solar cell. Our trPL-based approach agrees well with the results of injection-dependent photoluminescence quantum yield measurements. However, it is superior in attributing losses, e.g. in the radiative ideality factor or the implied open circuit voltage, to the internal optoelectronic properties and thereby indicates the path to overcome these losses.

HL 25.10 Wed 12:30 POT 251

Characterization of optoelectronic properties of CsSnI₃ perovskite thin film as a function of chemical composition. — •FATIMA AKHUNDOVA, HANNES HEMPEL, MARIN RUSU, ELIF HÜSAM, MARCUS BÄR, and THOMAS UNOLD — Helmholtz-Zentrum Berlin

The performance of lead-based halide perovskites as a next generation solar cell rises every year, however toxicity of Pb is a major obstacle for commercialization. Tin is the immediate substitute for Pb in perovskite crystal structure as both metals possess the same electronic configuration. However, Sn-perovskite solar cells have significantly lower efficiencies which is partially caused by poor stability of Sn(II). We report a systematic study of structural and optoelectronic properties of co-evaporated CsSnI₃ thin films with regard to lateral compositional gradient. Elemental compositions are confirmed by X-ray fluorescence and X-ray photoelectron spectroscopy techniques. Grazing-incidence X-ray diffraction reveals orthorhombic gamma phase with different preferred orientation for the excess Sn and Cs content. Moreover, Cs-rich regions shows better phase stability than the Sn-rich parts which undergo a phase transition to non-perovskite phase. The optical band gap, work function, and ionization energy are measured as a function of the Cs:Sn ratio to characterize the band diagram. The photoluminescence quantum yield, the charge carrier lifetime and mobility present these properties are rather robust against changes in composition. Our work emphasizes the impact of chemical composition on optoelectronic properties of Sn-based perovskites and demonstrates agile strategy for compositional engineering in materials research.

HL 25.11 Wed 12:45 POT 251

FAIR Cesium Lead Halide Perovskites Data by High-Throughput Investigation of Co-Evaporated Combinatorial Libraries — •HAMPUS NÄSSTRÖM¹, PASCAL BEBLO², FATIMA AKHUNDOVA², OLEKSANDRA SHARGAIEVA², JOSE A. MARQUEZ¹, HANNES HEMPEL², ANDREA ALBINO¹, SEBASTIAN BRÜCKNER¹, CLAUDIA DRAXL¹, EVA UNGER², and THOMAS UNOLD² — ¹Humboldt-Universität zu Berlin — ²Helmholtz-Zentrum Berlin

Artificial intelligence presents new possibilities in experimental materials research but typically require large well-characterized datasets. High-throughput technologies, including combinatorial synthesis, provide one method for obtaining such datasets. In this work, we show how such a dataset can be created through combinatorial co-evaporation and high-throughput characterization of Cs_yPb_{1-y}(Br_xI_{1-x})_{2-y} perovskites. The evaporated films were investigated with a multitude of contact-less characterization methods such as hyperspectral photoluminescence imaging, time-resolved photoluminescence mapping, and grazing-incidence wide-angle X-ray scattering mapping. The results were combined to estimate the potential of the material in terms of the photovoltaic power conversion efficiency as a function of the Cs to Pb and Br to I ratio. Finally, a generalized data schema for combinatorial thin films was developed, and the data of the 3456 individual samples was disseminated in a Findable, Accessible, Interoperable and Reusable (FAIR) way within the Novel Materials Discovery (NOMAD) laboratory (nomad-lab.eu) that is operated by the NFDI consortium FAIRmat (fairmat-nfdi.eu).

HL 26: Focus Session: Frontiers of Electronic-Structure Theory IV (joint session O/HL)

Time: Wednesday 10:30–13:00

Location: TRE Ma

HL 26.1 Wed 10:30 TRE Ma

A systematic DFT+U and Quantum Monte Carlo benchmark of magnetic two-dimensional (2D) CrX₃ (X = I, Br, Cl, F) — •DANIEL WINES, KAMAL CHOUDHARY, and FRANCESCA TAVAZZA — Materials Science and Engineering Division, National Institute of Standards and Technology (NIST), Gaithersburg, MD 20899, USA

The search for two-dimensional (2D) magnetic materials has attracted a great deal of attention because of the experimental synthesis of 2D CrI₃, which has a measured Curie temperature of 45 K. Often times, these monolayers have a higher degree of electron correlation and require more sophisticated methods

beyond density functional theory (DFT). Diffusion Monte Carlo (DMC) is a correlated electronic structure method that has been demonstrated successful for a wide variety of systems, since it has a weaker dependence on the Hubbard parameter (U) and density functional. In this study we designed a workflow that combines DFT+U and DMC in order to treat 2D correlated magnetic systems. We chose monolayer CrX₃ (X = I, Br, Cl, F), with a stronger focus on CrI₃ and CrBr₃, as a case study due to the fact that they have been experimentally realized and have a finite critical temperature. With this DFT+U and DMC workflow and the analytical method of Torelli and Olsen, we estimated an upper bound of 43.56 K for the T_c of CrI₃ and 20.78 K for the T_c of CrBr₃, in addition to analyzing

the spin densities and magnetic properties with DMC and DFT+U. We expect that running this workflow for a well-known material class will aid in the future discovery and characterization of lesser known and more complex correlated 2D magnetic materials.

Topical Talk

HL 26.2 Wed 10:45 TRE Ma
TREX: an integrated HPC software platform for quantum Monte Carlo calculations — •CLAUDIA FILIPPI — University of Twente, Enschede, The Netherlands

I will present the software development strategy and current achievements of the European Center of Excellence TREX “Targeting Real chemical accuracy at the EXascale” [1]. TREX focuses on methods at the high-end in the accuracy ladder of electronic structure approaches and, in particular, on quantum Monte Carlo methods which are uniquely positioned to fully exploit the massive parallelism of upcoming architectures. The main objective of TREX is the development of a user-friendly and open-source software suite, which integrates quantum Monte Carlo codes within an interoperable, high-performance platform. Core of our software efforts is the creation of the following two libraries:

TREXIO: A common I/O library and file format for easily exchanging data between applications, facilitating high-throughput computing workflows [2];

QMCKl: A library of computational kernels, written together by quantum Monte Carlo and HPC experts, to perform common CPU-intensive quantum Monte Carlo tasks [3].

[1] <https://trex-coe.eu>

[2] <https://github.com/trex-coe/trexio>

[3] <https://trex-coe.github.io/qmckl>

HL 26.3 Wed 11:15 TRE Ma

Exciton-phonon coupling in luminescence of indirect band-gap materials

— MATTEO ZANFROGNI^{1,2}, FULVIO PALEARI¹, DANIELE VARSANO¹, and •LUDGER WIRTZ³ — ¹Centro S3, CNR-Istituto Nanoscienze, Modena, Italy — ²Università di Modena e Reggio Emilia, Modena, Italy — ³Department of Physics and Materials Science, University of Luxembourg, Luxembourg

Layered, quasi-2D materials, such as hexagonal boron nitride (hBN) are known to display very strong excitonic effects due to the concentration of excitons in two dimensions and due to the relatively weak dielectric screening. If the band-gap of the material is indirect, the dispersion of the lowest lying exciton can have a minimum at a finite wave vector q . Upon absorption of a photon and excitation to a vertical ($q=0$) exciton, the system will relax to the finite- q exciton. Luminescence then entails the absorption/emission of a phonon with wave vector q . We present a computational approach for phonon-assisted luminescence in the presence of strong excitonic effects using two approaches: (i) a finite-displacement approach for the exciton-phonon coupling and (ii) a diagrammatic approach, calculating the q -dependent exciton-phonon coupling from the exciton eigenvectors and electron/hole-phonon scattering matrix elements. We show that the methodology quantitatively explains recent measurements of different stackings of BN layers. [1]

[1] A. Plaud, I. Stenger, F. Fossard, L. Sponza, L. Schué, F. Ducastelle, A. Loiseau, J. Barjon, to be published.

HL 26.4 Wed 11:30 TRE Ma

A combined G_0W_0 /BSE scheme of characterizing photoexcitations in hydroxylated rutile $\text{TiO}_2(110)$

— •SAVIO LARICCHIA, ANDREA FERRETTI, DANIELE VARSANO, and CLAUDIA CARDOSO — Centro S3, CNR-Istituto Nanoscienze, 41125 Modena, Italy

In reduced TiO_2 , electronic transitions originating from polaronic excess electrons in surface-localized band-gap states (BGS) are known to contribute to the photoabsorption and to the photocatalytic response of TiO_2 in the visible region. Recent state-selective studies using two-photon photoemission (2PPE) spectroscopy have also identified an alternative photoexcitation mechanism contributing to the photoabsorption of the reduced surface (110) of rutile TiO_2 . This process involves $d-d$ excitations from BGS arising from surface and subsurface defects, including bridging hydroxyls and oxygen vacancies. Density Functional Theory (DFT) has been used to determine the character of the electronic excited states involved in a $d_{12g}-d_{12g}$ transitions, but its accuracy is questioned by its theoretical framework: DFT is in principle exact for ground state systems and does not describe interacting photogenerated electron-hole pairs, i.e. the excitons. This has highlighted the need to move beyond the DFT formalism, by working within a many-body perturbation theory (MBPT) framework. It will be shown how a G_0W_0 method, combined with the solution of the Bethe-Salpeter equation (BSE), provides a powerful tool for characterizing from first principles the optical excitations from BGS identified by 2PPE experiments on hydroxylated $\text{TiO}_2(110)$.

15 min. break

HL 26.5 Wed 12:00 TRE Ma

Scaling the Way for All-Electron XPS Simulations to Calculate Absolute Binding Energies of Surface Superstructures

— •DYLAN MORGAN¹, SAM HALL¹, BENEDIKT KLEIN^{1,2}, MATTHEW STOODLEY^{1,2}, and REINHARD MAURER¹ — ¹Department of Chemistry, University of Warwick, United Kingdom — ²Diamond Light Source, Harwell Science and Innovation Campus, United Kingdom

First principles simulations of x-ray photoemission spectroscopy (XPS) and near-edge x-ray absorption fine-structure (NEXAFS) crucially support the assignment of surface spectra composed of many overlapping signatures. Core-level constrained Density Functional Theory calculations based on the Δ -SCF method are commonly used to predict relative XPS binding energy (BE) shifts but often fail to predict absolute BEs. The all-electron numeric atomic orbital code FHI-aims enables an accurate prediction of absolute BEs, but the legacy code lacked computational scalability to address large systems and robustness with respect to localisation of the core hole. We present a redesign of the core-hole constrained code in FHI-aims that delivers improvements to the scalability and robustness of core-hole constrained calculations in FHI-aims. We demonstrate the improved scaling behaviour and employ the new code to simulate core-level spectroscopic fingerprints of graphene moire superstructures. The code refactorisation forms the basis to expand the code towards improved core hole localisation methods and the rigorous treatment of relativistic effects for core-level spectra beyond the 1s shell.

HL 26.6 Wed 12:15 TRE Ma

Efficient diagonalization of BSE electron-hole Hamiltonian using group theory

— •JÖRN STÖHLER^{1,2}, DMITRII NABOK¹, STEFAN BLÜGEL¹, and CHRISTOPH FRIEDRICH¹ — ¹Peter Grünberg Institut and Institute for Advanced Simulation, Forschungszentrum Jülich, Germany — ²RWTH Aachen University, Germany

The Bethe-Salpeter equation (BSE) is the state-of-the-art method for the calculation of optical absorption and electron-energy loss spectra including excitonic effects. We solve the BSE by diagonalizing an effective electron-hole Hamiltonian. Often, a high number of k -points is needed to converge the BSE spectra, which leads to a large size of the Hamiltonian matrix and makes its diagonalization very expensive. In this work [1], we use the full spatial symmetry group to transform the electron-hole product basis into a symmetry-adapted product basis, which brings the Hamiltonian into a block-diagonal form and speeds up the subsequent diagonalization. The basis transformation is sparse and causes little overhead. We provide an implementation of our method in the FLAPW code Spex and demonstrate speedups of 36, 52, 12 for Si, BN, and monolayer MoS_2 , respectively.

We acknowledge financial support by MaX CoE funded by the EU through H2020-INFRAEDI-2018 (project: GA 824143).

[1] J. Stöhler, C. Friedrich, *Unpublished*

HL 26.7 Wed 12:30 TRE Ma

Excitonic effects on quadratic optical photoresponse tensors of semiconductors

— •PEIO GARCIA-GORICELAYA¹ and JULEN IBAÑEZ-AZPIROZ^{1,2} — ¹Centro de Física de Materiales, University of the Basque Country UPV/EHU, Spain — ²IKERBASQUE Basque Foundation for Science, Spain

We present a general ab initio scheme for including many-body excitonic effects in the non-linear optical photoresponse up to second order. Our practical implementation starts from the length-gauge formulation of the single-particle non-interacting optical photoresponse tensors [1] that are efficiently calculated using Wannier interpolation [2]. Subsequently, excitonic corrections are included in the many-body interacting current-density response tensors by means of Dyson-like equations derived within TD-CDFT. These equations allow a natural connection with the formalism of the single-particle picture and the Wannier-interpolation scheme respecting the tensorial character of the response. We employ this scheme to assess the impact of excitonic effects on several quadratic optical processes as the second-harmonic generation and the shift-current bulk photovoltaic effect in technologically appealing semiconductors.

Funding provided by the European Union's Horizon 2020 research and innovation programme under the European Research Council(ERC) grant agreement No 946629.

[1] J. E. Sipe and A. I. Shkrebtii, *Phys. Rev. B* 61, 5337 (2000).

[2] G. Pizzi et al., *J. Phys. Cond.Matt.* 32, 165902 (2020)

HL 26.8 Wed 12:45 TRE Ma

Electronic and optical properties of CoFe_2O_4 from density functional theory calculations, including many-body effects

— •SHOHREH RAFIEZADEH¹, VIJAYA BEGUM-HUDE^{1,2}, and ROSSITZA PENTCHEVA¹ — ¹Department of Physics University of Duisburg-Essen, Germany — ²University of Illinois at Urbana-Champaign, USA

CoFe_2O_4 is a ferrimagnetic semiconductor that finds application as an anode material in photocatalytic water splitting. We present a comprehensive study of the electronic and optical properties of bulk CoFe_2O_4 using density functional theory calculations and many-body perturbation theory to clarify the broad range of reported band gaps both experimentally (0.55-4.1 eV)[1] and theoret-

cally (0.9-1.90 eV). Starting with different exchange-correlation functionals, we obtain a direct band gap of 1.38 [PBE+($U=4$ eV)], 1.69 eV [SCAN+($U=3$ eV)], and an indirect gap of 2.02 eV (HSE06). Including quasiparticle corrections within G_0W_0 enhances and renders indirect band gaps for all functionals of 1.78, 1.95 and 2.17 eV, respectively. Excitonic effects are accounted for by solving the Bethe Salpeter equation and result in the lowest threshold for optical transitions

at 1.50 eV (SCAN) and 1.61 eV (HSE06), followed by peaks at ~ 2.0 , 3.5 and 5.0 eV, in agreement with experiment highlighting the importance of electron-hole interactions. Support by DFG- within CRC/TRR 247, project B04, and computational time at MagniUDE is gratefully acknowledged. [1] S. Singh and N. Khare, *Sci. Rep.* **8**, 6522 (2018).

HL 27: Focus Session: Wissenschaftskommunikation / Outreach (joint session HL/O/TT)

Im wissenschaftlichen Umfeld wird Maßnahmen der Öffentlichkeitsarbeit eine zunehmend größere Bedeutung zugemessen, - aus der Gesellschaft heraus und auch durch die großen Fördereinrichtungen und die DPG. Dabei geht es nicht nur um die Ergebnisse der Forschung, sondern auch darum, Prozesse und Methoden von wissenschaftlicher Arbeit transparent abzubilden – eine Aufgabe, die prinzipiell alle Forschenden übernehmen können. In diesem Symposium sollen erfolgreiche Projekte der Wissenschaftskommunikation, insbesondere aus dem Bereich der Festkörperphysik, vorgestellt werden. In ihrer Gesamtheit sollen sie das Spektrum der Wissenschaftskommunikation hinsichtlich des finanziellen und zeitlichen Aufwands aufzeigen und Methoden für unterschiedliche Zielgruppen vorstellen.

So dient diese Session sowohl als Ideengeber und Inspiration als auch als eine Art Netzwerk-Treffen zum Austausch über die Wissenschaftskommunikation in unterschiedlichen Kontexten.

Time: Wednesday 15:00–18:30

Location: POT 81

Invited Talk

HL 27.1 Wed 15:00 POT 81

experimentamus! Forschendes Lernen von Physik und Chemie in der Grundschule — •SEBASTIAN SCHLÜCKER — Universität Duisburg-Essen, Campus Essen

Der Sachunterricht in der Primarstufe ist ein Konglomerat aus allen Natur- und Gesellschaftswissenschaften, erst in der Sekundarstufe findet eine Aufspaltung in die einzelnen Fächer statt. Zudem unterrichten viele Grundschul-Lehrkräfte fachfremd. Auch der Zeitaufwand für die Vorbereitung von Experimenten ist nicht unerheblich. Wie also kann man trotz dieser Hürden kindgerechte physikalische und chemische Experimente bereits in der Grundschule einführen?

Ich berichte aus 10 Jahren Erfahrung mit dem Projekt experimentamus!. Dabei handelt es sich um einen Kanon aus ca. 40 Experimenten für die Klassen 2 bis 4, welcher die Themen Licht, Wärme, Magnetismus, Wasser, Luft, Feuer und Elektrizität mit einem kindgerechten Alltagsbezug abdeckt. Anstelle des darlegenden Lernens wird auf das Forschende Lernen gesetzt: Frage - Hypothese - Experiment - Beobachtung - Erklärung; diese fünf Stationen des wissenschaftlichen Erkenntnisprozesses werden immer wieder durchlaufen. Ganz im Sinne Martin Wagenscheins wird dabei nach der exemplarischen und sokratischen Methode vorgegangen. Die praktische Implementierung umfasst 1. Materialkisten für alle Themen, 2. kompakte und leicht verständliche Informationshefter für die Lehrkräfte, sowie 3. Lernheftchen für alle SuS. Am Ende möchte ich über Erfahrungen und Herausforderungen im Rahmen dieses Projektes berichten und Ideen für eine mögliche weitere Verbreitung vorstellen.

HL 27.2 Wed 15:30 POT 81

Internal interfaces - goals and realisation of a scientific image film — •ULRICH HÖFER^{1,2} and MICHAEL DÜRR^{2,3} — ¹Fachbereich Physik, Philipps-Universität Marburg — ²SFB 1083, www.internal-interfaces.de — ³Institut für Angewandte Physik, Justus-Liebig-Universität Giessen, Germany

Funded by the German Science Foundation (DFG), a professional film maker has produced an image film about the research conducted in the Collaborative Research Center SFB 1083 "Structure and Dynamics of Internal Interfaces". The six-minute video clip takes the non-specialist on a journey down to atomic scale to show the progress at the forefront of research at solid/solid interfaces. It is not a demanding educational film. Rather, it is a visually stunning piece that looks like science fiction taken straight out of a movie, with tracking shots that take the viewer down to the nanometer scale, with flights through luminous molecules, exotic excitons, and space-filling laser labs. The film also has a very impressive soundtrack. Gustav Holst's (1874-1934) composition "The Planets" was re-orchestrated especially for this film. It is available on the youtube channel of the DFG (<https://www.youtube.com/watch?v=-mDt0NzHrc>). Visitors of Chemikum Marburg can watch the German version on a 4K OLED screen, a device actually based on microscopic processes at interfaces investigated by SFB 1083. The idea behind the creation of a professional film, its conceptual design and the necessary steps towards its realization will be outlined.

HL 27.3 Wed 15:45 POT 81

Outreach activities of SFB 1083 @ Chemikum Marburg — •CHRISTOP WEGSCHEID-GERLACH, LUISE CLERES, INA BUDDÉ, KARL-HEINZ MUTH, and MARION ENSSLE — Chemikum Marburg / SFB1083

The diffusion of concepts, methods, and visions of the SFB 1083 on Structure and Dynamics of Internal Interfaces into the general public is our general goal. To this end project Ö makes use of the institution Chemikum Marburg e.V., whose

basic idea is to fascinate the public excited about natural sciences. The experiments offered here, stand for chemical, biological, pharmaceutical, and physical subjects related with daily phenomena or beyond. We will give an overview about the introduction of basic ideas and methods of SFB 1083 to the public as well as the institution Chemikum Marburg. The contents of the individual offers, such as experiments within the regular workspace, the workshops for the Girls' Day and the compilation of special workshops that are offered to give high-school students an understanding of the research content of the SFB 1083 are presented. An additional topic is the linking of basic research to applications for regenerative energy resources. Hydrogen fuel cells are well-known to the general public and rely on functional internal interfaces. An additional workshop which was prepared in cooperation with the district Marburg-Biedenkopf gives an overview about production, storage, and application of hydrogen as a new energy resource. We will also share various occasions at Chemikum Marburg where further outreach activities represent SFB 1083.

Invited Talk

HL 27.4 Wed 16:00 POT 81

Under the Microscope – spotlighting materials and nano science — •SVENJA LOHMANN and PRANOTI KSHIRSAGAR — The Science Talk, Germany

Real Scientists Nano is a science communication project dedicated to materials and nano science. Despite the widespread relevance of materials science to everyday life, we feel that dedicated science communication in this area is much rarer than in other fields. Our aim is to provide a platform for active materials and nano scientists to directly communicate their science and life as a scientist to the public. The use of social media thereby provides a very low threshold to science communication as basically the only requirement is to have an account. We have the goal to showcase the scientific community in all its diversity, and so far (12/2022) had guest scientists from more than 30 countries of origin as well as various fields and career stages. The two main pillars of the Real Scientists Nano project are the @RealSci_Nano Twitter account and the Under the Microscope podcast. Our guest scientists are interviewed for one podcast episode, and subsequently get to tweet from the account for one week following the rotation curation concept. We let curating scientist decide for themselves what they would like to tweet about. The form and content therefore vary greatly. Many of our scientists report from their everyday life, and are for example live-tweeting from a conference, uploading videos or photos from the lab or sending the occasional "stuck in meetings, will return later" tweet. Science communication on social media thus gives the opportunity to open a direct and real-time window into the scientist's life.

30 min. break

Invited Talk

HL 27.5 Wed 17:00 POT 81

Phyphox – A pocketful of physics — •CHRISTOPH STAMPFER — JARA-FIT and 2nd Institute of Physics, RWTH Aachen University, Germany — Peter Grünberg Institute (PGI-9), Forschungszentrum Jülich, Germany

Most smartphones are used to make phone calls, to write short messages, surf the Internet or check e-mails. However, they can do much more: With the help of the integrated sensors and the free app "phyphox" (abbreviation for Physical Phone Experiments), pupils, students, and teachers and interested others can independently perform and develop physics experiments. For example, the app can use the accelerometer to record pendulum movements and determine the rotational acceleration in a salad spinner, or the air pressure sensor to deter-

mine time-resolved differences in altitude and thus the speed of an elevator. The didactic potential of the app is great, as the students are picked up on ground that is very familiar and attractive to them (smartphones) and are introduced to experimental natural sciences in a playful way and with an extremely low barrier (zero cost, i.e. only one click away). The app helps to get students excited about scientific and technical questions and contexts at an early age. The app is available free of charge for Android and iOS (more information can be found at www.phyphox.org). In my presentation, I will go into the concept of phyphox, introduce the range of functions and show a number of application examples.

HL 27.6 Wed 17:30 POT 81

Chair PR representative as a doctoral student's secondary task: A field report — •PAULA M. WEBER, FELIX FRIEDRICH, and MANUEL SEITZ — Physikalisches Institut, Experimentelle Physik II, Universität Würzburg, Am Hubland, D-97074 Würzburg, Germany

Especially in recent years, it has become more important to communicate one's scientific work and methods to the public in order to show that in the scientific world, knowledge can only be created through research and the scientific process. Yet, extra time besides research is often limited and it is thus difficult to get into science communication. In this talk, I would like to present how PhD students can use their interest in science communication to benefit their own research group as a part-time PR representative.

In the first part of my talk, I will report on our efforts to attract new bachelor and master students. This advertising is focused on an audience with a scientific background, such that lab tours and advertising posters may contain scientific language and references. The second part is about communication with the general public, who usually know physics from their school days. Here, I will report on how we presented our research activities at the Night of Science in Physics and at the "Highlights der Physik" in Würzburg.

Working part-time as a PR representative could encourage doctoral students to try their hand at science communication and develop the associated communication skills.

HL 27.7 Wed 17:45 POT 81

Real or Fake - A format in science communication that encourages critical thinking — •TOBIAS LÖFFLER — Institut für Angewandte Physik Düsseldorf

The outreach format "Real or Fake" aims to train the audience in an critical approach to credible-sounding facts.

It is aimed at the general public and specifically at young people. At the same time, it offers an easy introduction for scientists to audience-oriented communication of science on stage. The format can be performed in front of a live audience or as an interactive online event. It has been proven to work as implemented into science festivals, nights of sciences, as a public individual event and also as part of events with constrained settings - such as outreach events at schools or as part of conferences.

"Real or Fake" was developed in 2017 by scientists around the Berlin March for Science who later founded Besserwissen e.V. with the goal to promote the format and support new organisers. I do cooperate with them since 2019 and have organized more than ten "Real or Fake" events since then.

In my talk, I will present the concept and its origins, give an overview of successful events and show what to do and what support one can get, if one wants to organize a "Real or Fake" event.

Invited Talk

HL 27.8 Wed 18:00 POT 81

Physics for school and the public at the LMU — •DR. CECILIA SCORZA-LESCH — Fakultät für Physik der LMU, München

Germany lives from research and technology. Physics, as the basis of all empirical sciences and technologies, has a very special, fundamental role to play. The Faculty of Physics at LMU, the largest in Germany, comprises nine research areas, three centres and two excellence clusters. In this talk we will present the approach we use to successfully communicate our various topics of modern research, the role of physics in our daily lives and in the fight against global warming to the schools and the public in a participatory way.

HL 28: Focus Session: Breakthroughs in wide-bandgap semiconductor laser diodes II

Time: Wednesday 15:00–16:45

Location: POT 361

Invited Talk

HL 28.1 Wed 15:00 POT 361

Fabrication of AlGa_N-based UV-B laser diodes on lattice-relaxed high-quality AlGa_N — •MOTOAKI IWAYA¹, SHO IWAYAMA^{1,2}, TETSUYA TAKEUCHI¹, SATOSHI KAMIYAMA¹, and HIDETO MIYAKE² — ¹Meijo Univ., Nagoya, Japan — ²Mie Univ., Tsu, Japan

Recently, AlGa_N-based ultraviolet (UV) light-emitting devices have been achieving remarkable performance. Highly efficient UV light-emitting diodes are finding applications in many fields, such as water and air sterilization. Meanwhile, room-temperature oscillation of laser diodes in the UV-C and UV-B region has also been realized in recent years by current injection. In this presentation, we show our realization of UV-B laser diode. To realize UV-B laser diodes, it is essential to fabricate them on lattice-relaxed AlGa_N because the lattice mismatch between AlN and AlGa_N active layers is at least 1.2%. We have obtained various methods for improving the quality of lattice-relaxed AlGa_N, and would like to report on the methods and effects. As specific methods to fabricate lattice-relaxed high-quality AlGa_N, we explain AlGa_N fabricated by the spontaneous nucleation method and the AlN nanopillar method. We will also discuss the correlation between lattice defects such as dislocations, V-shaped pits, and hillocks and device properties. And we would like to present the characteristics of UV-B laser diodes fabricated on such AlGa_N templates.

Invited Talk

HL 28.2 Wed 15:30 POT 361

Breakthrough technologies to realize room-temperature continuous-wave deep-ultraviolet laser diodes — •MAKI KUSHIMOTO — Nagoya University, Nagoya, Japan

AlGa_N-based UVC laser diodes operating at wavelengths are expected to be a low-cost, environmentally friendly, and highly efficient laser light source for a variety of applications. Although the pulsed operation of AlGa_N-based laser diodes at UV-C wavelengths has been confirmed in the previous studies, continuous wave lasing without cooling was difficult because of the high operating voltage. In this study, we further reduced the threshold gain by improving the optical confinement and improved the threshold current density while lowering drive voltage by modification of device designs. The new design improved the optical confinement factor to the quantum wells from 4% to 6%, which has led to a significant reduction in threshold current density. Furthermore, a reduction in threshold voltage was achieved by reducing the lateral distance between the n- and p-electrodes by tapering the sides of the LD mesa. In the conventional structure, the presence of process-induced crystal defects forced a distance between the n and p electrodes, which was a major factor in increasing the operating voltage. This tapered mesa performs the role of suppressing crystal defects by

controlling shear stress of mesa edge. As a result, room temperature CW lasing at a wavelength of 274 nm with a threshold current density of 4.2 kA/cm² and a voltage of 8.7 V was successfully achieved.

HL 28.3 Wed 16:00 POT 361

Spectral dynamics of lateral modes and filaments in InGa_N broad-ridge laser diodes — •LUKAS UHLIG¹, DOMINIC J. KUNZMANN¹, ANNA KAFAR^{2,3}, SZYMON GRZANKA^{2,3}, PIOTR PERLIN^{2,3}, and ULRICH T. SCHWARZ¹ — ¹Chemnitz University of Technology, Chemnitz, Germany — ²Institute of High Pressure Physics, Polish Academy of Sciences, Warsaw, Poland — ³Top-GaN Ltd., Warsaw, Poland. Blue InGa_N broad-ridge laser diodes are versatile, efficient, and compact high power emitters, which are demanded for copper welding, white light generation, and other applications. Compared with standard narrow-ridge laser diodes, in case of the broad-ridge devices the ridge width is increased from around 2 μm to tens of micrometers, leading to lateral multi-mode operation or filamentation.

We investigate a series of devices with ridge widths from 2.4 μm to 20 μm and study their lateral-spectral-temporal behavior as well as high-resolution spectra. With increasing ridge width, we observe the transition from lateral single-mode to multi-mode operation and in the case of the 20 μm wide ridge, filamentation occurs. In the multi-mode regime, the dynamic onset behavior as well as the spectral-lateral mode distribution are governed by competition of lateral and longitudinal modes for gain. Filaments form in the case of strong nonlinear interaction between intensity, charge carrier density, temperature, and refractive index. Using high-resolution spectroscopy, we can clearly differentiate between different lateral modes, which occur in parallel and form multiple longitudinal mode combs.

HL 28.4 Wed 16:15 POT 361

Temperature dependent electroluminescence studies of the carrier transport in multi colour deep ultraviolet light emitting diodes — •JAKOB HÖPFNER¹, FLORIAN KÜHL¹, MARCEL SCHILLING¹, ANTON MUHN¹, GREGOR HOFMANN², FRIEDHARD RÖMER², TIM WERNICKE¹, BERND WITZIGMANN², and MICHAEL KNEISSL¹ — ¹Technische Universität Berlin, Institute of Solid State Physics, Berlin, Germany — ²Lehrstuhl für Optoelektronik, Department EEI, Friedrich-Alexander-Universität, Erlangen-Nürnberg, German

Earlier studies have shown that a drop in current injection efficiency (CIE) is partly responsible for the poor external quantum efficiencies (EQE) of AlGa_N-based deep ultraviolet light emitting diodes (DUV-LEDs). In particular, the hole injection and the carrier distribution in the AlGa_N multi quantum well (MQW) active region is not well understood. In order to get a better insight we have

performed temperature dependent electroluminescence (EL) investigations of three-fold AlGaIn MQW LEDs with two of the QWs emitting at 233 nm and one QW emitting at 250 nm. In addition, the position of the 250 nm QW with the MQW structure was varied. From temperature dependent EL measurements we observe a strong shift in the intensity distribution over wavelength and temperature. We were able to correlate this with a change in the hole injection into the different QWs suggesting an efficient hole transport over the barriers between the QWs at room temperature. These experimental results are also supported by devices simulations and enable us to further improve the LED heterostructure.

HL 28.5 Wed 16:30 POT 361

265 nm LEDs and laser heterostructures with p-type distributed polarization doping AlGaIn layers — •MASSIMO GRIGOLETTO^{1,2}, SARINA GRAUPETER¹, VERENA MONTAG¹, JAKOB HÖPFNER¹, LUCA SULMONI¹, TIM WERNICKE¹, and MICHAEL KNEISSL^{1,2} — ¹Technische Universität Berlin, Institute of Solid State Physics, 10623 Berlin, Germany — ²Ferdinand-Braun-Institut (FBH), Berlin, Germany

Efficient hole injection in AlGaIn-based LEDs and lasers emitting in the ultra-violet (UV) spectral range remains a great challenge. Distributed polarization doped (DPD) p-type AlGaIn heterostructures have been developed to overcome this hurdle. By introducing a constant piezoelectric polarization charge along compositionally graded Al_xGa_{1-x}N layers a high density of free hole carriers can be established even in the absence of Mg dopants. In this study we have investigated the influence of the DPD design on the structural properties and electro-optic characteristics of AlGaIn-based LEDs and laser heterostructures emitting near 265 nm. For efficient hole injection p-type Al_xGa_{1-x}N layers with different Al gradients and thickness have been incorporated and grown by metal organic vapor phase epitaxy. On-wafer measurements of UV-LEDs exhibit forward voltages of 6 V at a dc current of 20 mA and output power of 1 mW comparable to conventionally Mg-doped heterostructures. The LEDs could be operated at high current densities up to 12 kA/cm² in pulsed mode, which shows the DPD is a promising approach for achieving low resistance p-type AlGaIn layers with high Al mole fractions.

HL 29: Materials and devices for quantum technology I

Time: Wednesday 15:00–18:00

Location: POT 151

HL 29.1 Wed 15:00 POT 151

Mapping of the local valley splitting in a Si/SiGe qubit shuttle device — •BINGJIE CHEN¹, MATS VOLMER¹, TOM STRUCK¹, RAN XUE¹, INGA SEIDLER¹, JOACHIM KNOCH² und LARS R. SCHREIBER¹ — ¹JARA-FIT Institute for Quantum Information, Forschungszentrum Jülich GmbH and RWTH Aachen University, Germany — ²Institut für Halbleitertechnik, RWTH Aachen University, Germany

Qubits based on the electron spin in gate-defined ²⁸Si/SiGe quantum dots (QD) are one of the major candidates for the quantum information processing. Due to weak spin-orbit coupling and low hyperfine interaction, their fidelity threshold for quantum error correction is reached. However, valley-state excitations [1-3] have implications for spin dephasing during qubit shuttling [4]. In our experiment, we map the valley splitting energy (E_{VS}) originating from the quantum well confinement at different locations of a qubit shuttle device [5]. We measure their orbital splitting and spin-polarization as a function of various electron fillings and magnetic fields [6]. We fit the local singlet-triplet splitting energy as a lower boundary of the relevant E_{VS} , which is distributed in a range of 11...73 μ eV. The correlation length is approximately the QD size and small dependence on the electric field perpendicular to the quantum well is found. [1]Dodson, J.P. et al., arXiv:2103.14702. [2]McJunkin, T. et al., Phys. Rev. B 104, 085406. [3]Hollman, A. et al., Phys. Rev. Applied 13, 034068. [4]Langrock, V. et al., arXiv:2202.11793. [5]Seidler, I. et al., npj Quantum Inf. 8, 100. [6]Friessen, M. et al., Phys. Rev. B 75, 115318. This work has been funded by the German Research Foundation (DFG) within the project KN 545/28-1.

HL 29.2 Wed 15:15 POT 151

Accessing broad-band quantum dynamics in the low photon regime — •MARKUS SIFFT¹, A. KURZMANN², J. KERSKI², R. SCHOTT¹, A. LUDWIG¹, A. D. WIECK¹, A. LORKE², M. GELLER², and D. HÄGELE¹ — ¹Ruhr University Bochum, Germany — ²Faculty of Physics and CENIDE, University of Duisburg-Essen, Germany

The analysis of quantum dynamics from measurement records $z(t)$ poses a fundamental challenge in many fields of science and engineering. Measurement records are notoriously difficult to analyze due to inherent or additional background noise, loss of e.g., probe photons, and finite measurement times. We recently introduced quantum polyspectra as a tool to analyze $z(t)$ in terms of higher order spectra whose shapes can be predicted within a quantum master equation approach [1,2]. Here, we solve the problem of analyzing the blinking (charging) dynamics of a semiconductor quantum dot in the regime of low photon rates or high photon loss [3]. The usual telegraph noise of binned photon click events changes to rare single clicks in case of high photon loss. Fitting theoretical quantum polyspectra to their measured counterparts gives full access to the in- and out-tunneling rates γ_{in} , γ_{out} of electrons despite low average photon rates $\gamma_p \ll \gamma_{in} + \gamma_{out}$. We demonstrate the successful evaluation of tunneling rates at up to 99.9 % loss of photons surpassing a previous scheme that handled a 98 % loss using the same data. [1] Hägele et al., PRB 98, 205143 (2018), [2] Siffit et al., PRR 3, 033123 (2021), [3] Siffit et al., arXiv:2109.05862

HL 29.3 Wed 15:30 POT 151

Generation of V_{Si} color centers in 4H-SiC using He and Li focused ion beam — •CHRISTIAN GOBERT¹, SHRAVAN KUMAR PARTHASARATHY¹, FEDOR HRUNSKI², ROLAND NAGY², and PATRICK BERWIAN¹ — ¹Fraunhofer Institute for Integrated Systems and Device Technology (IISB), 91058 Erlangen, Germany — ²Group of Applied Quantum Technologies, University Erlangen-Nuremberg (FAU), 91058 Erlangen, Germany

The silicon vacancy (V_{Si}) color center in 4H-SiC is a promising candidate as a qubit for quantum sensing, communication, and computing, due to its excellent spin and optical properties^{1,2}, scalability and mature semiconductor technology platform³. V_{Si} color centers can be fabricated by means of high energetic irradiation, e.g., using electrons, ions, neutrons, or laser pulses⁴. In this contribution, we report on a direct comparison of 3 different irradiation techniques, i.e. He-Li- and electron irradiation, for the first time on the very same sample material. Characterization is accomplished using confocal photoluminescence (PL) measurements on two perpendicular crystal orientations. We investigate the optical and spin properties of generated V_{Si} color centers and employ PL mappings to judge the scalability of the irradiation technique. To evaluate the quality of the generated V_{Si} color centers, PL excitation spectroscopy (PLE) is applied.

[1] R. Nagy et al., Nat. Commun. 10, 1954 (2019)

[2] R. Nagy et al., Appl. Phys. Lett. 118, 144003 (2021)

[3] C. Babin et al., Nat. Mater. 21, 67-73 (2022)

[4] S. Castelletto, A. Boretti, J. Phys.: Photonics 2 (2020) 022001

HL 29.4 Wed 15:45 POT 151

1.*Quantum Vector Magnetometry of Magnetic Nanoparticles in Living Tissue — •ANDRE POINTNER¹, PHILIPP KUNZE², REGINE SCHNEIDER-STOCK², BERNHARD FRIEDRICH³, CHRISTOPH ALEXIOU³, RAINER TIETZE³, and ROLAND NAGY¹ — ¹Chair of Electron Devices, FAU Erlangen-Nuremberg — ²Experimental Tumor Pathology, University Hospital Erlangen — ³Experimental Oncology and Nanomedicine, University Hospital Erlangen

Developing an understanding of the underlying processes of cancer dissemination is to this day a pressing topic in medical research, due to the lack of observation techniques capable of resolving single cell behavior in living tissue. Widefield imaging with ensembles of nitrogen-vacancy centers (NV-Centers) in diamond as a quantum sensor allows the observation of individual cells by mapping selectively attached superparamagnetic iron oxide nanoparticles (SPIONs) on cells of interest. Application of a magnetic bias field results in a magnetic dipole emitted by the SPIONs, which adds onto the known bias field. The magnetic field causes a lift of the degeneracy of the NV-Centers spin states. Evaluating the spin transitions via optically detected magnetic resonance (ODMR) and comparison to the ground state hamiltonian enables the reconstruction of the magnetic field vector. By applying this measurement scheme pixelwise to a sequence of widefield images of the diamond sample, we calculate the corresponding dipole vector for the SPIONs and map the resulting magnetic field over the field of view. This enables single cell tracking in living tissue inside a homemade integrated widefield microscope over the span of multiple days.

HL 29.5 Wed 16:00 POT 151

Fabrication and pre-characterization of 10 μ m long single-electron shuttling devices. — •MAX BEER¹, RAN XUE¹, INGA SEIDLER¹, JIHI-SIAN TU², LINO VISSER¹, HENDRIK BLUHM¹, and LARS R. SCHREIBER¹ — ¹JARA-FIT Institute for Quantum Information, Forschungszentrum Jülich GmbH and RWTH Aachen University, Aachen, Germany — ²Helmholtz Nano Facility (HNF), Forschungszentrum Jülich, Jülich, Germany

The electron-spin in gate-defined quantum dots in a Si/SiGe quantum well is one of the most promising qubits for scalable quantum computing. Scalability can be achieved by coherent coupling such as conveyor-mode single electron-spin shuttling [1]. Aiming at a shuttle distance of 10 μ m, we fabricate a shuttling device with three patterned metal-gate layers forming an array of >140 gates. Al₂O₃ deposited by atomic layer deposition (ALD) isolates the gates, but also induces potential disorder in the quantum well. This disorder can be reduced by

minimizing the oxid thickness [1]. We investigate two strategies: (I) Reduction of oxide thickness towards the ALD limit and (II) replacement of MOS-gates with Pd-Si Schottky-gates wherever applicable. Shuttling devices are selected by a transport measurement-protocol operating at 4.2 K on single electron transistors, which are operated as charge sensors for electron shuttling at 10 mK [2].

[1] Langrock, V. *et al.*, arXiv: 2202.11793 (2022).

[2] Seidler, I. *et al.*, npj Quantum Inf. 8: 100 (2022).

Work funded by the DFG under project number EXC 2004/1-390534769.

30 min. break

HL 29.6 Wed 16:45 POT 151

Coupling of solid-state quantum emitters to low-loss plasmonic waveguides — •PAUL STEINMANN, HANS-JOACHIM SCHILL, and STEFAN LINDEN — Physikalisches Institut, Universität Bonn, Nussallee 12, 53115 Bonn, Germany Plasmonic waveguides with integrated single photon emitters (SPEs) offer an attractive platform for nanophotonic quantum circuit applications. Here, we report on the coupling of strain-induced SPEs in an MoSe₂ monolayer to low-loss plasmonic waveguides. For this purpose, we used electron beam lithography with the negative-tone resist Medusa82 to fabricate dielectric-loaded surface plasmon polariton waveguides (DLSPWs) on top of a chemically prepared monocrystalline silver platelet. Additional gratings placed at the ends of the waveguides serve as in- and out-coupling structures. An MoSe₂ monolayer was deposited on the centre of one of the waveguides by a dry-transfer technique. Operating at 4 Kelvin, surface plasmon polaritons (SPPs) are launched by a green laser at the in-coupling port of the waveguide. The SPPs travel through the waveguide and lead to the excitation of the monolayer. In addition to the exciton and trion signal, we observe sharp emission lines that we attribute to strain-induced trap states. The second-order correlation function of one of the spectrally filtered emission lines was measured with an HBT setup. The measured value $g(2)(0)=0.4$ indicates the single-photon nature of the emitter. Our findings indicate that TMDC monolayers can be used as integrated SPEs in efficient plasmonic circuits, and thus further pave the way towards plasmonic-based single photon networks.

HL 29.7 Wed 17:00 POT 151

Sensing of electrolytes with nitrogen-vacancy centers in nanodiamonds — •MAXIMILIAN HOLLENDONNER^{1,2}, SANCHAR SHARMA², DURGA DASARI³, SILVIA VIOLA KUSMINSKIY^{2,4}, and ROLAND NAGY¹ — ¹Chair of Electron Devices, Friedrich-Alexander-Universität Erlangen-Nürnberg, Germany — ²Max Planck Institute for the Science of Light, Staudtstraße 2, Erlangen, Germany — ³3rd Institute of Physics, University of Stuttgart and Institute for Quantum Science and Technology (IQST), Stuttgart, Germany — ⁴Institute for Theoretical Solid State Physics, RWTH Aachen University, Aachen, Germany

Today's batteries suffer from performance losses with increasing cell age which is caused by irreversible degradation processes at a molecular level. To understand these processes, it is important to measure them *in-situ* and *in-operando*. Up to now there exists no sensor which can perform this task with sub-micrometer resolution. We propose to use nanodiamonds containing single NV-centers as such sensors inside the liquid electrolyte of a battery. It has been shown that NV-centers are excellent electric field sensors [1,2]. From theoretical considerations we found out that by performing repeated FID pulse sequences it is not only possible to measure the electric field components generated by the ions inside the electrolyte but also the local ionic concentrations at the position of the nanodiamond with nanometer-resolution.

Sources: [1] F. Dolde *et al.*, *Nature Phys* 7, 459-463 (2011) [2] J. Michl *et al.*, *Nano Lett.* 2019, 19, 8, 4904-4910

HL 29.8 Wed 17:15 POT 151

Interplay of Pauli Blockade with Electron-Photon Coupling in Quantum Dots — •FLORIAN GINZEL and GUIDO BURKARD — Department of Physics, University of Konstanz, D-78457 Konstanz, Germany

Both quantum transport measurements in the Pauli blockade regime and microwave cavity transmission measurements are important tools for spin-qubit readout and characterization. In our work [1] we theoretically investigate how a double quantum dot in a transport setup interacts with a coupled microwave resonator while the current through the DQD is rectified by Pauli blockade. We show that the output field of the resonator can be used to infer the leakage current and thus obtain insight into the blockade mechanisms without additional components such as charge or current sensors for each dot. In the case double quantum dot realized in silicon, we show how the valley quasi-degeneracy can impose limitations on this scheme. We also demonstrate that a large number of unknown double quantum dot parameters including (but not limited to) the valley splitting can be estimated from the resonator response simultaneous to a transport experiment, providing more detailed knowledge about the microscopic environment of the dots. Furthermore, we describe and quantify a back-action of the resonator photons on the steady state leakage current.

[1] F. Ginzler and G. Burkard, arxiv:2210.02982 (2022)

HL 29.9 Wed 17:30 POT 151

Structural and electrical characterization of the InAs/CdSe core/shell NWs — •MANE KALAJYAN¹, MARVIN MARCO JANSEN^{1,2}, NILS VON DEN DRIESCH³, ERIK ZIMMERMANN¹, NATALIYA DEMARINA⁴, ANTON FAUSTMANN¹, GERRIT BEHNER¹, CHRISTOPH KRAUSE¹, BENJAMIN BENNEMANN¹, JAN KARTHEIN¹, DETLEV GRÜTZMACHER^{1,3}, THOMAS SCHÄPERS¹, and ALEXANDER PAWLIS^{1,3} — ¹Peter Grünberg Institut (PGI-9), Forschungszentrum Jülich, Jülich, Germany — ²Eindhoven University of Technology, Eindhoven, Netherlands — ³Peter Grünberg Institut (PGI-10), Forschungszentrum Jülich, Jülich, Germany — ⁴Peter Grünberg Institut (PGI-2), Forschungszentrum Jülich, Jülich, Germany InAs nanowires (NWs) are a well-known basis for field-effect transistors (FETs), light-emitting diodes and lasers, quantum devices and biosensors. The larger band gap material CdSe, having a negligible lattice mismatch to InAs, allows for tailoring the conductive channel at the CdSe/InAs core/shell interface, thus making CdSe an excellent candidate for the InAs surface states passivation.

Here, we present the fabrication, structural, and electrical characterization of a unique InAs/CdSe core/shell NW system. The interface between the core and the shell is proven to be flawless by means of HR-TEM micrographs. Moreover, electrical characterization reveals a high-mobility two-dimensional transport channel in the InAs core. Finally, magnetotransport measurements show clear signs of weak antilocalization. These results make the novel InAs/CdSe hybrid NWs a promising basis for the quantum device applications.

HL 29.10 Wed 17:45 POT 151

Electrical excitation of color centers in phosphorus-doped diamond Schottky diodes — •FLORIAN SLEDZ¹, IGOR A. KHRAMTSOV², ASSEGD M. FLATAE¹, STEFANO LAGOMARSINO¹, NAVID SOLTANI¹, SHANNON S. NICLEY³, ROZITA ROUZBAHANI³, PAULIUS POBEDINSKAS³, KEN HAENEN³, JIN QUN⁴, XIN JIANG⁴, PAUL KIENITZ⁵, PETER HARING BOLIVAR⁵, DMITRY YU. FEDYANIN², and MARIO AGIO¹ — ¹Laboratory of Nano-Optics, University of Siegen, Germany — ²Moscow, Russian Federation — ³Institute for Materials Research (IMO) & IMOMEC, Hasselt University & IMEC vzw, Belgium — ⁴Institute of Materials Engineering, University of Siegen, Germany — ⁵Institute of Graphene-based Nanotechnology, University of Siegen, Germany

A robust single-photon source operating upon electrical injection at ambient condition is desirable for quantum technologies. Silicon-vacancy color centers in diamond are promising candidates as their emission is concentrated in a narrow zero-phonon line with a short excited-state lifetime of ~1 ns. Creating the color centers in n-type diamond (phosphorus-doped) allows the implementation of a Schottky-diode configuration. This provides a simpler approach than the traditional complex diamond semiconductor junctions e.g., p-i-n. Selective optical excitation allows addressing of single silicon-vacancy color centers while suppressing background from mainly nitrogen-vacancy defects created during Si ion implantation. This paves a way for the realization of the predicted bright electroluminescence of color centers.

HL 30: Quantum transport and quantum Hall effects II (joint session HL/TT)

Time: Wednesday 15:00–17:00

Location: POT 251

HL 30.1 Wed 15:00 POT 251

Aharonov-Bohm-type oscillations in phase-pure core/shell GaAs/InAs nanowires — •FARAH BASARIC^{1,2}, ANTON FAUSTMANN^{1,2}, ERIK ZIMMERMANN^{1,2}, GERRIT BEHNER^{1,2}, ALEXANDER PAWLIS^{1,2}, CHRISTOPH KRAUSE^{1,2}, HANS LÜTH^{1,2}, DETLEV GRÜTZMACHER^{1,2}, and THOMAS SCHÄPERS^{1,2} — ¹Peter Grünberg Institut (PGI-9), Forschungszentrum Jülich, 52425 Jülich, Germany — ²JARA-Fundamentals of Future Information Technology, Jülich-Aachen Research Alliance, Forschungszentrum Jülich and RWTH Aachen University, Germany

Epitaxially grown phase-pure GaAs/InAs core/shell nanowires offer uniformity in their electrical, mechanical and optical properties due to the absence of a crystallographic disorder. Magnetotransport measurements were carried out at variable temperatures and for different gate voltages, under an applied in-plane magnetic field. Pronounced Aharonov-Bohm-type oscillations in the conductance are observed for this nanowire type. In measurements at different gate voltages, significantly higher oscillation amplitudes are observed in comparison to the corresponding measurements on polymorphic core/shell nanowires. Furthermore, measurements at different temperatures show robustness of these

oscillations against high temperatures as a result of reduced disorder. Finally, strong indications of a quasi-ballistic transport regime could be recognized for the phase-pure nanowire type. Obtained results indicate a strong effect of disorder reduction in GaAs/InAs nanowire transport properties, manifested in superior transport properties.

HL 30.2 Wed 15:15 POT 251

Spin valves based on bilayer graphene quantum point contacts — •EIKE ICKING^{1,2}, CHRISTIAN VOLK^{1,2}, CHRISTOPHER SCHATTAUER³, LUCA BANSZERUS^{1,2}, KENJI WATANABE⁴, TAKASHI TANIGUCHI⁵, FLORIAN LIBISCH³, BERND BESCHOTEN¹, and CHRISTOPH STAMPFER^{1,2} — ¹RWTH Aachen University, Germany — ²Forschungszentrum Jülich, Germany — ³TU Vienna, Austria — ⁴Research Center for Functional Material, Japan — ⁵International Center for Materials Nanoarchitectonics, Japan

Bernal bilayer graphene (BLG) is a unique material as it allows opening and electrostatically tuning a sizeable band gap by applying a perpendicular electric field. Recently, charge carriers have been confined successfully in one dimension to form quantum point contacts (QPC) based on split gates separated by a channel of a few hundred nanometers. Moreover, spin-polarized quantum transport through such structures has been demonstrated up to $6 e^2/h$ using a high in-plane magnetic field. The threshold magnetic field at which the lowest modes become spin-polarized depends on the subband spacing and thus on the width of the split gate channel. In this work, we combine two QPCs of different geometric widths, resulting in different threshold magnetic fields, to spin-polarize the first QPC and use it as a filter for the second QPC. In particular, we report on a spin-valve achieving spin-polarized channels with a total conductance of up to $10 e^2/h$.

HL 30.3 Wed 15:30 POT 251

Optical and electrical tuning between the normal insulating and topological insulating phase of InAs/GaSb bilayer quantum wells — •MANUEL MEYER¹, TOBIAS FÄHNDRICH¹, SEBASTIAN SCHMID¹, SEBASTIAN GEBERT¹, GERALD BASTARD^{1,2}, FABIAN HARTMANN¹, and SVEN HÖFLING¹ — ¹Technische Physik, Physikalisches Institut und Würzburg-Dresden Cluster of Excellence ct.qmat, Am Hubland, D-97074 Würzburg, Germany — ²Physics Department, École Normale Supérieure, PSL 24 rue Lhomond, 75005 Paris, France

Topological insulators (TI) based on InAs/GaSb bilayer quantum wells (BQW) are appealing due to their rich phase diagram with a TI and normal insulating (NI) phase[1]. The switching between both phases can be achieved by external electric fields using a top and back gate (TG and BG)[2]. However, especially a fully functional BG is difficult to realize in antimonides due to leakage issues. To overcome this bottleneck we present another tuning knob using optical excitation to switch from the NI to the TI phase over the TI gap[3]. By monitoring the charge carrier densities we can identify the hybridized band structure and in-plane magnetic field measurements evidence the TI gap. Furthermore, a top-gated sample is investigated. Without a back gate we find properties from both phases for magnetotransport measurements which points to a mixing of NI and TI states. This is further indicated by the resistance peak evolutions with temperature for both samples.

[1] C. Liu et al., PRL 100, 236601 (2008)

[2] F. Qu et al., PRL 115, 036803 (2015)

[3] G. Knebl et al., PRB 98, 041301(R) (2018)

30 min. break

HL 30.4 Wed 16:15 POT 251

Transport in high mobility HgTe heterostructures — •MICHAEL KICK, LENA FÜRST, JOHANNES KLEINLEIN, SAQUIB SHAMIM, HARTMUT BUHMANN, and LAURENS W. MOLENKAMP — Experimentelle Physik III, Physikalisches Institut, Universität Würzburg, Am Hubland, 97074 Würzburg, Germany

HL 31: Focus Session: Frontiers of Electronic-Structure Theory V (joint session O/HL)

Time: Wednesday 15:00–17:30

Location: TRE Ma

HL 31.1 Wed 15:00 TRE Ma

Phase transitions in the two-dimensional Su-Schrieffer-Heeger model — •CHANGAN LI¹, SONGBO ZHANG², SANGJUN CHOI¹, JAN BUDICH³, and BJÖRN TRAUZETTEL¹ — ¹Institute for theoretical physics and astrophysics, University of Würzburg, Würzburg, Germany — ²Department of Physics, University of Zürich, Winterthurerstrasse 190 8057, Zürich, Switzerland — ³Institute of Theoretical Physics, Technische Universität Dresden, 01062 Dresden, Germany

The 2D Su-Schrieffer-Heeger (SSH) model is endowed with rich topological physics. First we show that the random flux can induce a metal-band insulator transition in the 2D SSH, thus reporting the first example of such a transition. Remarkably, we find that the resulting insulating phase can even be a higher-order topological insulator with zero-energy corner modes and fractional cor-

The Fractional Quantum Hall Effect (FQHE) has not yet been observed in the material system of HgTe. Due to recent progress in MBE growth, routinely charge carrier mobilities of HgTe heterostructures of over $\mu > 1 \cdot 10^6 \text{ cm}^2/\text{Vs}$ are obtained which is in the same order of magnitude as in the first reported experimental observation of the FQHE in GaAs/GaAlAs heterostructures. This opens up new prospects for transport investigations into the long time still open question of fractional states in this material system.

In 2-dimensional HgTe quantum wells, transport measurements show well pronounced quantum Hall plateaus for all filling factors, but no indication of any fractional state. High magnetic field measurements show a prolonged $\nu = 1$ plateau and a transition to an insulating state. Intriguingly, the $\nu = 1$ plateau exhibits a transition to an insulating state for filling factor $\nu = 1/2$.

Another possibility to observe the FQHE in HgTe is provided by the 2D surface states of a 3D topological insulator. High mobility layers, $\mu > 1 \cdot 10^6 \text{ cm}^2/\text{Vs}$, of tensile strained HgTe are subject of extensive magneto-transport investigations. First results reveal a good and detailed correspondence to recent k.p band structure calculations for non-interacting electron systems.

HL 30.5 Wed 16:30 POT 251

Electron Density Depended Giant Negative Magnetoresistance — •LINA BOCKHORN and ROLF J. HAUG — Institut für Festkörperphysik, Leibniz Universität Hannover, 30167 Hannover, Germany

Ultra-high mobility two-dimensional electron gases not only show an increasing number of new fractional filling factors, but also an astonishing robust negative magnetoresistance at zero magnetic field [1 -5]. The theoretical description of this negative magnetoresistance is still an open issue due to its complex dependencies on several parameters.

The behavior of the giant negative magnetoresistance is affected by different scattering events, e. g. interface roughness, oval defects, background impurities and remote ionized impurities, which leads to a strong dependence on different parameters. Here, we take a closer look on the temperature dependence of the giant negative magnetoresistance for different electron densities. At low temperatures we observe the predicted temperature dependence of $T^{1/2}$ [6].

[1] L. Bockhorn et al., Phys. Rev. B 83, 113301 (2011).

[2] A. T. Hatke et al., Phys. Rev. B 85, 081304 (2012).

[3] R. G. Mani et al., Scientific Reports 3, 2747 (2013).

[4] L. Bockhorn et al., Phys. Rev. B 90, 165434 (2014).

[5] L. Bockhorn et al., Appl. Phys. Lett. 108, 092103 (2016).

[6] I. V. Gornyi et al., Phys. Rev. B. 69, 045313 (2004).

HL 30.6 Wed 16:45 POT 251

Massless Dirac fermions on a space-time lattice with a topologically protected Dirac cone — •MICHAL PACHOLSKI¹, ALVARO DONÍS VELA³, GAL LEMUT³, JAKUB TWORZYDŁO², and CARLO BEENAKKER³ — ¹Max Planck Institute for the Physics of Complex Systems, Dresden, Germany — ²Warsaw University, Warsaw, Poland — ³Lorentz Institute, Leiden, The Netherlands

The symmetries that protect massless Dirac fermions from a gap opening may become ineffective if the Dirac equation is discretized in space and time, either because of scattering between multiple Dirac cones in the Brillouin zone (fermion doubling) or because of singularities at zone boundaries. Here we introduce an implementation of Dirac fermions on a space-time lattice that removes both obstructions. The quasi-energy band structure has a tangent dispersion with a single Dirac cone that cannot be gapped without breaking both time-reversal and chiral symmetries. We show that this topological protection is absent in the familiar single-cone discretization with a linear sawtooth dispersion, as a consequence of the fact that there the time-evolution operator is discontinuous at Brillouin zone boundaries.

ner charges. Employing both level statistics and finite-size scaling analysis, we characterize the metal-band insulator transition and numerically extract its critical exponent. By proposing another inclined 2D SSH model, a deformed one, we show that a pair of Dirac points protected by space-time inversion symmetry appear in the semimetallic phase. Interestingly, the locations of these Dirac points are not pinned to any high-symmetry points of the Brillouin zone but highly tunable through parameter modulations. Moreover, the merging of two Dirac points undergoes a topological phase transition, which leads to either an anisotropic topological insulating phase or a nodal-line metallic phase.

HL 31.2 Wed 15:15 TRE Ma

Ab initio embedding approach for carbon defects in hexagonal boron nitride: A new platform to probe environmental screening — •DANIS BADRTDINOV¹, MAGDALENA GRZESZCZYK², ALEXANDER HAMPEL³, CYRUS DREYER^{3,4}, MACIEJ KOPERSKI², and MALTE RÖNSNER¹ — ¹Radboud University, Nijmegen, The Netherlands — ²National University of Singapore, Singapore — ³Flatiron Institute, USA — ⁴Stony Brook University, USA

Correlated defects in layered van der Waals hosts hold high promises for realizing quantum technologies, as they allow for various possibilities to control defect properties, e.g., via altering the host thickness or by changing the substrate material. A quantitative description of the defect ground and excited states taking the details of the impurity environment into account is, however, a considerable challenge for conventional density-functional theory (DFT) based methods as the impurities might be correlated and dielectric environmental screening is not fully accounted for in DFT. To tackle these challenges we apply and extend an embedding approach that treat the defect states within exact many-body theory, while DFT is used as a starting point to describe the bulk host material. We study various carbon defects embedded in hexagonal boron nitride (hBN), allowing us to disentangle all mechanisms responsible for the alteration of defect properties including modifications to the impurity structure and changes in the environmental screening upon thinning down the hBN host. Our new embedding approach paves the way for improved identification of defects in layered materials and to tailor their properties.

HL 31.3 Wed 15:30 TRE Ma

Nonequilibrium electron dynamics in a two-sites Hubbard model — •JAKUB WRONOWICZ and YAROSLAV PAVLYUKH — Department of Theoretical Physics, Wrocław University of Science and Technology

Electron dynamics in a two-sites Hubbard model is studied using the nonequilibrium Green's function approach using formalism developed in [1]. We focus on the electron dynamics arising in the adiabatic switching scenario. Many-body approximations are classified according to the channel of the Bethe-Salpeter equation in which electronic correlations are explicitly treated. They give rise to the so-called second Born, T -matrix and GW approximations. In each of these cases, the model is reduced to a system of ordinary differential equations, which resemble equations of motion for a driven harmonic oscillator with time-dependent frequencies. We discuss transient solutions for the off-diagonal density matrix. Analytical result for the steady state in second Born approximation is compared with the exact solution. It is further shown numerically that in the large Hubbard- U limit the T -matrix in the particle-hole channel and spin-adapted GW approximations converge to the same solution.

[1] Y. Pavlyukh, E. Perfetto, and G. Stefanucci, *Photoinduced dynamics of organic molecules using nonequilibrium Green's functions with second-Born, GW, T-matrix, and three-particle correlations*, Phys. Rev. B **104**, 035124 (2021).

HL 31.4 Wed 15:45 TRE Ma

Time-linear quantum transport simulations with correlated nonequilibrium Green's functions — •RIKU TUOVINEN¹, YAROSLAV PAVLYUKH², ENRICO PERFETTO³, and GIANLUCA STEFANUCCI³ — ¹Department of Physics, Nanoscience Center, University of Jyväskylä, Finland — ²Department of Theoretical Physics, Wrocław University of Science and Technology, Poland — ³Dipartimento di Fisica, Università di Roma Tor Vergata, Italy

We present a time-linear scaling method for open and correlated quantum systems. The method inherits from many-body theory [1] the possibility of selecting the most relevant scattering processes, thereby paving the way for real-time characterizations of correlated ultrafast phenomena in quantum transport. The open system dynamics is described in terms of an embedding correlator from which the transient current can be calculated via the Meir-Wingreen formula [2]. We efficiently implement the method through a combination with recent time-linear schemes for closed systems [3]. Electron-electron and electron-phonon interactions can be treated on equal footing while preserving all fundamental conservation laws. We employ the method by studying transport of correlated electron-hole pairs in semiconductors [4].

[1] G. Stefanucci and R. van Leeuwen, *Nonequilibrium Many-Body Theory of Quantum Systems* (CUP 2013).

[2] Y. Meir and N. S. Wingreen, PRL **68**, 2512 (1992).

[3] N. Schlünzen, J.-P. Joost, and M. Bonitz, PRL **124** (2020) 076601.

[4] R. Tuovinen, Y. Pavlyukh, E. Perfetto, and G. Stefanucci, arXiv:2211.15635 (2022).

15 min. break

Topical Talk

HL 31.5 Wed 16:15 TRE Ma

Challenges in modelling correlated electronic matter — •ROSER VALENTI — Institute of Theoretical Physics, Goethe University Frankfurt, Frankfurt, Germany

The microscopic modelling of correlated electronic matter from first principles poses a fundamental theoretical challenge due to the many-body character of the systems. In recent years there have been a few internationally coordinated efforts in theoretical method development to generate a common platform of benchmarked software tools including dynamical mean field theory and extensions.

In this talk I will present some of the challenges we face in such an endeavour and illustrate them with some examples on models and materials.

Funding from the DFG through QUAST FOR 5249-449872909 is acknowledged.

HL 31.6 Wed 16:45 TRE Ma

Electron-Phonon Interactions from DFPT within an All-Electron Framework — •SEBASTIAN TILLACK, PASQUALE PAVONE, and CLAUDIA DRAXL — Humboldt-Universität zu Berlin and IRIS Adlershof, 12489 Berlin, Germany

The interplay between electrons and the motions of nuclei in solids, described in terms of phonons, play a crucial role in the modeling of functional materials, particularly for understanding temperature dependent effects. We present an implementation of density-functional perturbation theory (DFPT) within a full-potential all-electron framework as implemented in the code `exciting` [1]. Our implementation allows one to compute phonons as well as the linear response to external electric fields. We use DFPT calculations to study lattice vibrations and electron-phonon interactions (EPIs) by means of many-body perturbation theory in β -Ga₂O₃. The electron self-energy contribution is computed as a function of temperature from which various properties such as quasi-particle energies, electron linewidths, and spectral functions are derived. We further incorporate many-body electron-electron interactions described by the GW method. Beyond that, our work creates the foundation for a fully *ab initio* study of the effect of EPIs on optical excitations.

[1] A. Gulans, et al. J. Phys.: Condens. Matter **26**, 363202 (2014).

HL 31.7 Wed 17:00 TRE Ma

Calculation of phonon spectra with the FLAPW method using Density Functional Perturbation Theory — •ALEXANDER NEUKIRCHEN, CHRISTIAN-ROMAN GERHORST, GREGOR MICHALICEK, DANIEL WORTMANN, GUSTAV BIHLMAYER, and STEFAN BLÜGEL — Peter Grünberg Institute and Institute for Advanced Simulation, Forschungszentrum Jülich and JARA, 52425 Jülich, Germany

Computing phonons applying density functional perturbation theory (DFPT) within all-electron DFT methods is a well-known challenge due to the displacement of muffin-tin spheres and sphere-centered basis functions. In this talk, we present our current results of the phonon dispersion based on our implementation of the DFPT approach in the FLEUR code [1] (www.flapw.de), an implementation of the full-potential linearized augmented plane wave (FLAPW) method. We highlight the good agreement of our preliminary results with phonon dispersions obtained with the finite displacement method for which the FLEUR code has been combined with the phonopy tool (www.phonopy.github.io/phonopy/). We discuss the numerical challenges involved in calculating meV quantities on top of large ground state energies typical for all-electron methods and how we addressed them.

This work has been supported by the Helmholtz Postdoc Programme (VHPD-022) and by the MaX Center of Excellence funded by the EU through the H2020-INFRAEDI-2018-1 767 (Grant No. 824143).

[1] A. Neukirchen, C.-R. Gerhorst, D. A. Klüppelberg, M. Betzinger, D. Wortmann, G. Michalicek, G. Bihlmayer, S. Blügel, to be published.

HL 31.8 Wed 17:15 TRE Ma

Electron-phonon interaction using a localized Gaussian basis set — •GERRIT JOHANNES MANN, THORSTEN DEILMANN, and MICHAEL ROHLFING — Institute of Solid State Theory, University of Münster, Germany

Electron-phonon interaction is a crucial mechanism in solid state physics that is responsible for a multitude of phenomena. However, in electronic structure calculations it is usually neglected. We developed an *ab-initio* implementation on top of density functional theory that combines finite differences calculations with the perturbative Allen-Heine-Cardona framework in order to calculate the temperature-dependent renormalization of the electronic bandstructure due to electron-phonon interaction using a basis set of localized Gaussian orbitals.

This implementation circumvents the limiting problems of previous implementations while maintaining a good agreement with the literature. The calculated Fan-Migdal zero-point renormalization of the direct band gap of silicon amounts to about 15 meV compared to 20 meV in the literature. Also the temperature-dependence of the renormalization agrees similarly well.

HL 32: Organic Electronics and Photovoltaics II (joint session CPP/HL)

Time: Wednesday 15:00–17:30

Location: GÖR 226

See CPP 36 for details of this session.

HL 33: Poster II

Topics:

- 2D semiconductors and van der Waals heterostructures
- Focus Session: Graphene quantum dots
- Materials and devices for quantum technology
- Nitrides: Devices
- Nitrides: Preparation and characterization
- Quantum transport and quantum Hall effects
- Semiconductor lasers
- Spin phenomena in semiconductors
- THz and MIR physics in semiconductors
- Transport properties
- Ultra-fast phenomena

Time: Wednesday 17:00–19:00

Location: P1

HL 33.1 Wed 17:00 P1

Pump-probe spectroscopy on a MoSe₂ monolayer — •MAX WEGERHOFF and STEFAN LINDEN — Physikalisches Institut, Universität Bonn, Nussallee 12, 53115 Bonn, Germany

TMDC monolayers are atomically thin semiconductor materials, which, due to their reduced dimensionality and crystal structure, possess unique optical properties. In particular, they host bound electron-hole pairs, so-called excitons, with binding energies of several 100 meV.

Here, we report on pump-probe spectroscopy on excitons in a MoSe₂ monolayer encapsulated in h-BN. We use spectrally broad probe pulses and a spectrometer to measure the transient differential reflectivity spectra. Based on a mode-locked Ti:Sa laser, a temporal resolution of down to 400fs is achieved. A frequency-doubled OPO can be used to generate non-resonant pump pulses in the visible wavelength range. Furthermore, probe pulses with a bandwidth of up to 70nm can be generated via supercontinuum generation in a photonic crystal fiber. The experiments are performed at 4K in a helium-flow cryostat.

Within the first few picosecond after the pump pulse, we observe a blueshift of the exciton resonance. This shift depends on the wavelength of the pump pulses as well as the polarization of the pump- and probe pulses. Further experiments with an electrically gated heterostructure to control the doping of the monolayer are in progress.

HL 33.2 Wed 17:00 P1

A Model Study of the Phonon-Impact on Absorption Spectra of Moiré Exciton-Polaritons — •KEVIN JÜRGENS¹, DANIEL WIGGER², and TILMANN KUHN¹ — ¹Institute of Solid State Theory, University of Münster, Germany — ²School of Physics, Trinity College Dublin, Ireland

The interaction of multiple quantum emitters coupled to a resonant optical field can produce interesting collective behavior. Twisted bilayers of transition metal dichalcogenides are a class of materials, where localized quantum emitters, in this case moiré excitons, can occur. According to their strong localization at the minima of the moiré potential, these excitons have a relatively flat band structure. If the heterostructure is placed into an optical cavity, all excitons interact with the same mode of the resonator, leading to the formation of exciton-polaritons which can interact with lattice vibrations.

We model the moiré excitons in the limit of small densities as bosonic particles that couple to a single quantized cavity mode, resulting in lower and upper polariton states. In addition, each exciton is coupled to the same acoustic phonon bath. The interaction with phonons leads to inter- and intraband transitions between the two polariton branches that strongly depend on the curvature of the polariton dispersion.

We calculate absorption spectra and discuss the influence of phonons on the spectral shape and peak positions, and systematically study the influence of the band structures curvature.

HL 33.3 Wed 17:00 P1

Nonlinear optical processes in the layered magnetic semiconductor CrSBr — •MINJIANG DAN¹, PAUL HERRMANN¹, JULIAN KLEIN², ZDENEK SOFER³, and GIANCARLO SOAVI¹ — ¹Institute of Solid State Physics, Friedrich Schiller University Jena, Jena, Germany — ²Department of Materials Science and Engineer-

ing, Massachusetts Institute of Technology, Cambridge, USA — ³Department of Inorganic Chemistry, University of Chemistry and Technology Prague, 166 28 Prague 6, Czech Republic

CrSBr has recently emerged as a new member in the family of layered magnetic materials, with the distinct advantages compared to CrI₃ of being stable in air and having a high Néel temperature in the bulk form. Recently polarization-resolved Second Harmonic Generation (SHG) has been employed to reveal the layer-dependent magnetic order and symmetry in multilayer CrSBr [1]. In this work, we use nonlinear optical spectroscopy, i.e. SHG and Third Harmonic Generation (THG) and two photon absorption, to investigate the electronic and excitonic resonances in few-layer and bulk CrSBr as a function of the lattice temperature which, modulates the magnetic properties of the material. Our results show large enhancement (>100) in the SHG and THG for specific wavelengths and range of temperatures, pointing towards the existence of resonances from the magnetic dipole response of the system. This sheds light on the excited state landscape of this new material and offers viable insights towards its application in spintronic, magnonic and opto-electronic devices.

[1] Lee *et al.*, *Nano Letters* **21**, 8, 3511-3517 (2021)

HL 33.4 Wed 17:00 P1

The Impact of Inert Conditions During the Fabrication Process on the Optical Properties of MoS₂ Monolayers — •ALINA SCHUBERT¹, MICHAEL KEMPF¹, RICO SCHWARTZ¹, PATRICIA GANT², FELIX CARRASCOSO², CARMEN MUNUERA², ANDRES CASTELLANOS-GOMEZ², and TOBIAS KORN¹ — ¹Institut für Physik, Universität Rostock, Rostock, Germany — ²Instituto de Ciencia de los Materiales de Madrid, Madrid, Spain

Transition-metal dichalcogenides (TMDCs) are layered materials that can be thinned down to monolayers. The optical properties of these flakes depend strongly on the cleanliness of the surfaces. Transferring TMDCs with PDMS is simple to perform and allows the fabrication of large monolayers [1]. The objective of this work was to improve the methodology so that sample quality is enhanced without reducing the yield or increasing the effort required for production. For this purpose, a statistic of 20 monolayers was set up, which were half transferred to a SiO₂ substrate at ambient conditions and half transferred in a glovebox [2]. All samples were characterised by photoluminescence (PL) spectroscopy at room temperature and ~4 K. By examining the exciton and trion features in the spectra, it could be shown that only the small difference in the transfer process results in changes of the optical properties that can be attributed to a higher sample quality of the samples produced in the glovebox.

[1] Castellanos-Gomez, A. *et al.* *2D Mater.* **1** (2014)

[2] Gant, P. *et al.* *2D Mater.* **7** (2020)

HL 33.5 Wed 17:00 P1

Stokes shift of twisted bilayer WSe₂ — •ZHAO LIU¹, YANG PAN^{1,2}, and DIETRICH R. T. ZAHN^{1,2} — ¹Semiconductor Physics, Institute of Physics, Chemnitz University of Technology, Chemnitz, Germany — ²Center for Materials, Architectures, and Integration of Nanomembranes (MAIN), Chemnitz University of Technology, Chemnitz, Germany

Transition metal dichalcogenides (TMDCs) with a typical layered structure have exceptional optical properties exhibiting a characteristic absorption and emis-

sion at excitonic resonances. The weak van der Waals (vdW) interlayer coupling nature enables the possibility of artificial staking, leading to homo- and heterostructures formation. It was demonstrated in our previous work that the optical properties can be strongly modified by the twisting angle.

Here, WSe₂ monolayers (MLs) were obtained by mechanical exfoliation, which were then transferred onto sapphire substrates by a tear-and-stack method to form twisted homo-bilayers with a precision of 0.08°. We then performed optical transmission and photoluminescence (PL) experiments on monolayers, intrinsic bilayers and twisted bilayers to determine the Stokes shift values on a full period (0°-60°) of twisted bilayer WSe₂.

HL 33.6 Wed 17:00 P1

Transport and optical characterization of electrically contacted monolayer TMDCs — •JAN-NIKLAS HEIDKAMP, JOHANNES KRAUSE, SWARUP DEB, RICO SCHWARTZ, and TOBIAS KORN — Institute of Physics, University of Rostock, Rostock, Germany

Since Graphene was introduced in 2004, there has been a great interest in other 2D materials as well. Among the most studied is the group of semiconducting transition metal dichalcogenides (TMDCs). The band structure of these crystals changes from an indirect gap in the bulk to a direct gap in the monolayer limit. Herein, a method for contacting monolayer flakes using photolithography and lift-off processes is showcased. Electrical contacts are pre-defined on SiO₂ substrates and thereafter, TMDC flakes are deposited using a deterministic transfer technique. Flakes of the TMDC WS₂ contacted in this way are characterized via gate-dependent photoluminescence measurements and I-V curves.

HL 33.7 Wed 17:00 P1

Enhancing photoluminescence and Raman signals in TMDC monolayers via plasmonic nanostructures — •JOHANNES KRAUSE, ANNIKA BERGMANN, JAN-NIKLAS HEIDKAMP, RICO SCHWARTZ, and TOBIAS KORN — Institute of physics, university of Rostock, Rostock, Germany

Novel 2D thin film materials garnered a great interest in recent years. The family of Transition metal dichalcogenides (TMDCs) among those materials is especially appealing because of the indirect-direct bandgap transition and the possibility to stack different composites of the TMDCs on top of each other to achieve so called heterostructures. Herein, we present a technique to define nanostructures on a SiO₂ wafer using thermal scanning probe lithography. Further, we deposit individual TMDC monolayer flakes on top of the metallized structures via the deterministic transfer technique. We characterize our flakes utilizing photoluminescence and Raman measurements, reporting major enhancements effects (~10x) in PL and minor enhancement (~3x) in Raman signals.

HL 33.8 Wed 17:00 P1

Investigation of structural and electronic properties of monolayered MoS₂ and graphene compared to the MoS₂/graphene heterostructure — •ATEEB SHABAN¹, NEBAHAT BULUT², JAKOB KRAUS², FRANZ SELBMANN¹, JENS KORTUS², and YVONNE JOSEPH¹ — ¹TU Bergakademie Freiberg, Institute of Electronic and Sensor Materials, Germany — ²TU Bergakademie Freiberg, Institute of Theoretical Physics, Germany

Graphene and other 2D materials have been shown to have interesting structural and electronic properties. Transition metal dichalcogenides such as molybdenum disulfide (MoS₂) and tungsten diselenide (WSe₂) have tunable bandgaps that change from indirect to direct when decreasing the number of layers. This property allows for applications such as transistors and sensors. On the other hand, graphene is an ideal channel material. It is used as an electronic sensor in field-effect transistors due to the high sensitivity toward the change in the surrounding environment. These remarkable electronic and structural properties of graphene, being highly susceptible and conductive, have reignited the interest in 2D materials. Subsequently, building variable stacks of 2D van-der-Waals (vdW) structures can open the possibility of designing materials with specific properties across various chemistry's and systems.

In this theoretical work, we analyze and review the properties of MoS₂ and graphene individually and study their cumulative effect on the electronic and structural properties of the MoS₂/graphene vdW heterostructure using density functional theory.

HL 33.9 Wed 17:00 P1

Rapid hyperspectral imaging of transition metal dichalcogenides and their heterostructures — •MARC SCHÜTTE, DAVID TEBBE, CHRISTOPH STAMPFER, BERND BESCHOTEN, and LUTZ WALDECKER — 2nd Institute of Physics A, RWTH Aachen University, Aachen, Germany

Transition Metal Dichalcogenides are two-dimensional semiconductors with many interesting properties for optical applications, such as direct bandgaps in the visible spectral region or optically addressable inequivalent valleys. It is well known, however, that their optical properties can vary spatially by local changes of dielectric screening, doping or strain. Here, we present a measurement setup capable of performing photoluminescence and reflection contrast measurements of 2D heterostructures approximately twenty times faster compared to scanning a focal spot over the sample. The setup is based on simultaneously taking spec-

tra along a line with an imaging spectrometer (push-broom technique), which enables the measurement of multiple spectra simultaneously. The speed of the technique allows for taking images in multidimensional sweeps of parameters, such as gate voltages or magnetic fields.

In this way, the measurements can be conducted by imaging sample regions up to the full size of the heterostructure for each sweep. This allows to distinguish inhomogeneities and enhances the statistical relevance of the data.

HL 33.10 Wed 17:00 P1

Black phosphorus field-effect transistors and its application — •ZAHRA FEKRI¹, HIMANI ARORA¹, VICTORIA CONSTANCE KÖST², JENS ZSCHARSCHUCH¹, KRZYSZTOF NIEWEGLOWSKI², KENJI WATANABE³, TAKASHI TANIGUCHI⁴, MANFRED HELM^{1,2}, KARLHEINZ BOCK², and ARTUR ERBE^{1,2} — ¹Helmholtz Zentrum Dresden Rossendorf, Dresden, Germany — ²Technische Universität Dresden, Dresden, Germany — ³Research Center for Functional Materials, National Institute for Materials Science, Tsukuba, Japan — ⁴International Center for Materials Nanoarchitectonics, National Institute for Materials Science, Tsukuba, Japan

Black phosphorus (BP) has been known as a more favorable material in many applications compared to other 2D materials due to its exceptional properties. However, its sensitivity to air species has restricted its integration into active devices. In this work, we used a few nm thickness BP for developing field-effect transistors (FETs). Lithography-free via-encapsulation scheme allows us to fabricate fully-encapsulated BP-based field-effect transistors and perform reliable electrical measurements. Based on our results, we find that the electronic properties of the via-encapsulated BP FETs are significantly improved compared to unencapsulated devices. We further demonstrated a gas-sensing performance based on the BP FET. Our Preliminary result shows the promising potential of BP for applications in advanced gas-sensing technology.

HL 33.11 Wed 17:00 P1

Stationary and Time-Resolved Luminescence of Organic-Dye/transition metal dichalcogenide Heterostructures — •JULIAN SCHRÖER, TIM VÖLZER, ALINA SCHUBERT, RICO SCHWARTZ, STEPHAN LOCHBRUNNER, and TOBIAS KORN — University of Rostock, Institute of Physics

Thin layers of organic molecules and layered semiconductors build a new compound material with manifolds of interesting applications. The optoelectronic properties of these heterostructures strongly depend on the chosen compounds. Via stationary and time-resolved photoluminescence experiments, we investigate samples of Perylene-Orange (PO) deposited on top of single-layer tungsten diselenide. This joint material exhibits a type-II band alignment, enabling charge transfer processes between the two material layers. Here, we aim to reveal the temperature dependent dynamics of the charge transfer processes. Our work paves the way for a deeper understanding of organic/inorganic heterointerfaces and the functionalization of organics and TMD's in optoelectronic devices.

HL 33.12 Wed 17:00 P1

Quantum transport in twisted bilayer graphene supermoiré heterostructures — ALEXANDER ROTHSTEIN¹, ROBIN DOLLEMAN¹, CHRISTOPH SCHATTAUER², ANTHONY ACHTERMANN¹, STEFAN TRELLENKAMP³, FLORIAN LENTZ³, KENJI WATANABE⁴, TAKASHI TANIGUCHI⁵, DANTE KENNES⁶, FLORIAN LIBISCH², BERND BESCHOTEN¹, and CHRISTOPH STAMPFER¹ — ¹2nd Institute of Physics, RWTH Aachen University, Germany — ²Institute for Theoretical Physics, TU Wien, Austria — ³Helmholtz Nano Facility, Forschungszentrum Jülich, Germany — ⁴Research Center for Functional Materials, National for Material Science, 1-1 Namiki, Japan — ⁵International Center for Materials Nanoarchitectonics, National Institute for Materials Science, 1-1 Namiki, Japan — ⁶Institute for Theory of Statistical Physics, RWTH Aachen University, and Jara Fundamentals of Future Information Technology, Germany

Twisted bilayer graphene hosts a plethora of correlated quantum phenomena, such as superconductivity, correlated insulators and strange metal phases. The unprecedented in-situ gate-tunability of the system allows the study the underlying physics in detail by means of quantum transport experiments. The microscopic details of the van-der-Waals heterostructure, like the presence of competing moiré lattices, heavily influence the exact characteristics of the device. Here, we investigate different conductance regimes in near-magic angle twisted bilayer graphene devices, focusing on the insulating states. We are able to identify the presence of super-moiré lattices in our devices from magneto-transport experiments and compare our results with theory.

HL 33.13 Wed 17:00 P1

Ultrathin 2D gallium selenide devices for optoelectronics — •MARCO N. DEMBECKI, SIMON BERNÖCKER, MICHELE BISSOLO, EUGENIO ZALLO, and JONATHAN J. FINLEY — Walter Schottky Institute and TUM School of Natural Sciences, Technische Universität München, Am Coulombwall 4, Garching, Germany

The post-transition metal chalcogenides (PTMC, M = [In, Ga], C = [S, Se, Te]) are a group of semiconducting layered materials with a widely tunable band gap and direct-indirect band gap crossover in the few-layer limit. Type II band alignment of PTMC heterostructures makes them good candidates as photoabsorbers [1].

Among PTMCs, GaSe holds promise for optoelectronics, nonlinear optics, and terahertz (THz) generation but its usefulness for devices is inhibited by strong susceptibility to oxidation. Here, we report on the fabrication of dual gated-FET based on fully hBN-encapsulated GaSe multilayers. To preserve the intrinsic properties of the gallium selenide, the encapsulation process was carried out in a controlled nitrogen atmosphere. The gate electrodes are made from few-layer graphene to allow for an optoelectronic investigation. Electrical transport measurements are carried out and a roadmap for future optoelectronic devices will be discussed.

[1] Arora, H., and Erbe, A. Recent progress in contact, mobility, and encapsulation engineering of InSe and GaSe. *InfoMat*, 3 (6), 662-693, (2021)

HL 33.14 Wed 17:00 P1

Towards thermoelectric transport measurements in dual-gated bilayer graphene — •MORITZ KNAAK, MARTIN STATZ, and THOMAS WEITZ — 1st Physical Institute, Faculty of Physics, University of Göttingen, Friedrich-Hund-Platz 1, Göttingen 37077, Germany

The ratio of the thermal voltage to the corresponding temperature difference is defined as the Seebeck coefficient. As a transport coefficient due to its relation to the density of states (DoS) and its underlying link between entropy and charge transport, the Seebeck coefficient can help to better understand materials with interesting DoS and/or phase transitions. One of these materials is trigonally warped bilayer graphene (BLG), in which Lifshitz transitions can be induced by tuning an out-of plane electric field or the charge carrier density. Near these transitions the DoS is high and electron-electron interaction becomes important. To gain further insights into the emerging correlated phases near these Lifshitz transitions [1] and quantify the changes in the DoS, we measure the thermoelectric voltage and local temperature difference to extract the Seebeck coefficient. For that we combine a hexagonal boron nitride encapsulated, dual-gated BLG device with graphite gates and contacts together with an on-chip heater next to the BLG. The source and drain contacts are simultaneously used as 4-point-probe on-chip resistance thermometers to determine the local temperature differences. The devices are fabricated utilizing the dry transfer method, e-beam lithography, thermal evaporation of contact leads as well as reactive ion etching.

[1] Seiler, A.M. et al. *Nature* 608, 298-302 (2022)

HL 33.15 Wed 17:00 P1

Niobium-Doping of Atomically Thin Molybdenum Disulfide for Optoelectronic Applications — •OSAMAH KHARSAH, STEPHAN SLEZIONA, and MARIKA SCHLEBERGER — Universität Duisburg-Essen, Fakultät für Physik and CENIDE, Germany

Two-dimensional materials are predicted to become a very important disruptive technology, opening the door to a plethora of applications across many fields, especially in the field of optoelectronics. Among these materials, atomically thin molybdenum disulfide (MoS₂) has distinguished itself owing to its electronic properties, good thermal stability, and mechanical durability. However, its intrinsic strong n-type conductivity hinders its implementation. Overcoming this hurdle would allow MoS₂ to be used in structures such as p-n junctions either on its own or in tandem with other 2D materials, with the goal of fabricating the next generation of optoelectronic devices. One approach that could solve this problem is substitutional doping to controllably p-dope MoS₂. We report on the direct growth of niobium-doped monolayer MoS₂, which was characterized by Raman- and photoluminescence spectroscopy. Field-effect transistors, with the as-grown Nb-doped MoS₂, showed n-type transport behavior. After annealing the material in a sulfur atmosphere, this switched to an ambipolar transport behavior, which we attribute to the activation of Nb-doping sites. In addition, the hysteresis of this device exhibited a decrease of 4 orders of magnitude, indicating that the influence of intrinsic defects has been remedied by the annealing process.

HL 33.16 Wed 17:00 P1

Towards strong coupling of confined excitons to a fiber-based microcavity — •MORITZ SCHARFSTÄDT, MICHAEL KÖHL, and ANDREA BERGSCHNEIDER — Physikalisches Institut, Universität Bonn, Wegelerstraße 8, 53115 Bonn, Germany

Excitons in monolayer transition-metal dichalcogenides (TMD) exhibit large oscillator strengths and hence are well-suited for strong light-matter coupling. While for free excitons strong coupling to photonic cavities has been demonstrated in numerous experiments, nonlinearities in those systems are relatively weak. The recently demonstrated quantum confinement of excitons to length scales of about 20nm is a promising route towards enhancing nonlinearities [1].

We want to realize confined excitons with the prospect of embedding them into a high-finesse microcavity and reach the strong coupling regime. To confine the excitons in transverse direction and tune their energy, we develop a specific electric gate configuration. Our microcavity will be fiber-based and tunable at cryogenic temperatures. With this platform we aim for the realization of a quantum emitter in a cavity by harvesting the enhanced nonlinearity combined with a cavity-enabled photon blockade.

[1] Thureja et al., *Nature* 606, 298-304 (2022)

HL 33.17 Wed 17:00 P1

Photon assisted tunneling in bilayer graphene double quantum dots — •TOBIAS DEUSSEN¹, K. HECKER^{1,2}, L. BANSZERUS^{1,2}, A. SCHÄPERS¹, A. PETERS¹, S. MÖLLER^{1,2}, E. ICKING^{1,2}, K. WATANABE³, T. TANIGUCHI⁴, C. VOLK^{1,2}, and C. STAMPFER^{1,2} — ¹JARA-FIT & 2nd Institute of Physics, RWTH Aachen — ²Peter Grünberg Institute, Forschungszentrum Jülich — ³RCFM, NIMS, Japan — ⁴MANA, NIMS, Japan

Spin qubits in semiconductor quantum dots (QDs) are attractive candidates for solid state quantum computation. Singlet-triplet qubits, where the logical qubits are encoded in a two-electron spin system in double quantum dots (DQDs), turned out to be of special interest. In such systems, control over the interdot tunnel coupling and, hence, the exchange interaction is essential. Bilayer graphene (BLG) is an attractive host material for spin qubits due to its small spin-orbit and hyperfine interaction and its gate voltage controllable band gap. Only recently, it has become possible to confine single electrons in BLG QDs and to understand their spin and valley texture. However, microwave manipulation has not been demonstrated, so far. Here, we perform photon-assisted tunneling (PAT) spectroscopy, which relies on resonant microwave excitation of electrons across the interdot transition. We extract a lower bound for charge dephasing, T₂^{*}, of about 350 ps. In power-dependent measurements, we explore multi-photon processes. We use PAT as a probe for the interdot tunnel coupling in BLG DQDs and can control and measure the interdot tunnel coupling in a range of several GHz which is suitable for qubit operations.

HL 33.18 Wed 17:00 P1

Coherent coupling dynamics between excitonic complexes in a MoSe₂ monolayer — •DANIEL WIGGER¹, ALEKSANDER RODEK², THILO HAHN³, JAMES HOWARTH⁴, TAKASHI TANIGUCHI⁵, KENJI WATANABE⁵, MAREK POTEMSKI^{2,6}, PIOTR KOSSACKI², and JACEK KASPRZAK^{2,7} — ¹School of Physics, Trinity College Dublin, Ireland — ²Faculty of Physics, University of Warsaw, Poland — ³Institute of Solid State Theory, University of Münster, Germany — ⁴National Graphene Institute, University of Manchester, UK — ⁵National Institute for Materials Science, Tsukuba, Japan — ⁶Laboratoire National des Champs Magnétiques Intenses, CNRS-UGA-UPS-INSA-EMFL, Grenoble, France — ⁷Université Grenoble Alpes, CNRS, France

In modern heterostructures of layered van der Waals materials that combine graphene, hBN, and TMDCs it is possible to deterministically control the density of free charge carriers in a TMDC monolayer. With this approach and the ultrafast nonlinear four-wave mixing (FWM) spectroscopy technique we study the coherent coupling dynamics between neutral and charged excitons in a MoSe₂ monolayer. We demonstrate that the so-called Raman coherence between the two exciton species leads to characteristic quantum beats in the FWM signal. By exploiting 2D-FWM spectra, we can conclude that the bias dependent change of dipole strength between the exciton types is not sufficient to explain the experimental findings. Therefore, we conclude that the tuning of the free carrier density directly affects the coherent coupling between neutral and charged excitons.

HL 33.19 Wed 17:00 P1

Resonant Excitation and Resonant Photoluminescence Detection of Silicon Vacancy Centers in 4H Silicon Carbide for Single Photon Emission — •FEDOR HRUNSKI¹, MIKE GERD GEORG KÖSTLER¹, SHRAVAN KUMAR PARTHASARATHY^{2,1}, MAXIMILIAN HOLLENDONNER¹, ANDRE POINTNER¹, CHRISTIAN GOBERT², DANIEL SCHELLER¹, and NAGY ROLAND¹ — ¹Chair of Electron Devices (LEB), Friedrich-Alexander-University, Erlangen, Germany — ²Fraunhofer Institute for Integrated Systems and Device Technology (IISB), Erlangen, Germany

For today, quantum networks deal with the task of entangling several qubits with each other over a larger distance. Therefore, the resonant excitation of the qubits and the resonant detection of emitted photons by them appears to be an essential component of such a network for coherent spin state control. This work hereby deals with the resonant single photon detection of fluorescence, which is emitted by resonantly excited V₂ color centers in 4H-SiC. Therefore, a diode laser modulated by an electro-optical modulator performs a pulsed resonant excitation at one of the A₁ or A₂ spin-conservative optical transitions, while the emitted photons are detected by a superconducting single photon detector. However, due to the chromatic equality of the excitation photons and fluorescent photons, they are distinguished by their polarization.

HL 33.20 Wed 17:00 P1

A standalone fiber-based quantum sensor using ensembles of NV-Centers in diamond — •BENJAMIN POHL, ANDRE POINTNER, and ROLAND NAGY — Chair of Electron Devices, FAU Erlangen-Nuremberg

Though NV-Center magnetometry with diamonds is widely spread in scientific research, it is rarely used in an industrial context. In order to reduce the complexity of the required hardware we fixate the diamond on the tip of a fiber and miniaturize the system so all the required components can be included in a standalone device for magnetic field determination. The measurement is performed with ensembles of NV-Centers used as an optically controlled quantum sensor in

a confocal setup. Determination of the magnetic field is achieved through optical detected magnetic resonance (ODMR). In the presence of a local magnetic field, the four orientations of the NV-Centers in the diamond crystal results in up to four different Zeeman splits, which allows the evaluation of the local magnetic field vector. The resulting sensitivity to magnetic fields is strongly dependent on the number of collected signal photons on the detector. Therefore, to increase the sensitivity, the collection efficiency is crucial. Detection of the collected photons is realized by an integrated photodiode and the signal is evaluated by a field programmable gate array (FPGA) which also controls the measurement hardware. Such a standalone device will enable measurements in various environments and provide a system for users without insight to optics or quantum technology, thus greatly extending the possible applications for NV-Centers as quantum sensors.

HL 33.21 Wed 17:00 P1

Realization of remote entanglement using vacancy-centers in 4H-SiC — •MICHAEL BARON¹, MAXIMILIAN HOLLENDONNER¹, FEDOR HRUNSKI¹, DANIEL SCHELLER¹, ANDRE POINTNER¹, SHRAVAN KUMAR PARTHASARATHY², and ROLAND NAGY¹ — ¹Chair of Electron Devices FAU — ²Fraunhofer Institute for Integrated Systems and Device Technology IISB

The overall performance of quantum applications, such as quantum sensors, quantum tokens and optical quantum computers, can be highly improved by realizing a quantum network in which these constituents are connected. The emerging field of quantum technologies based on color centers in silicon carbide (SiC) will play an important part in the realization of such distributed quantum networks. As a physical platform silicon vacancy centers inside 4H SiC offer numerous advantages, such as low electrical field sensitivity making the system robust against stray fields, high photon yield in the Zero-Phonon-Line, good spin-coherence time and an already well-matured industrial fabrication knowledge for SiC. My research is concerned with the technical implementation and realization of a heralded single-photon entanglement protocol using V2 silicon vacancy centers in 4H-SiC. The experiment employs two such vacancies residing in independently operated cryostats separated by 2 meters, which are connected in an interferometer-like setup. This allows the creation of entanglement between both V2 centers and thus the creation of a quantum network based on these color centers.

HL 33.22 Wed 17:00 P1

Towards an integrated nanophotonic and electronic spin platform in 4H-SiC — •DANIEL SCHELLER¹, DANIEL HÄUPL², LIN JIN³, CHRISTIAN GOBERT⁴, JAN-NIK SCHWARBERG¹, JÖRG SCHULZE¹, NICOLAS JOLY², WOLFRAM PERNICE³, and ROLAND NAGY¹ — ¹Chair of Electron Devices, Friedrich-Alexander-University Erlangen-Nuremberg, Erlangen, Germany — ²Max-Planck-Institut für die science of light, Erlangen, Germany — ³Responsive Nanosystems, University of Münster, Münster, Germany — ⁴Fraunhofer IISB, Erlangen, Germany

The solid state spin system of negatively charged silicon vacancies (V_{Si}) V2 in 4H-SiC shows high spectral stability and excellent spin coherence times required for efficient quantum processing. Moreover, silicon carbide provides standardized semiconductor processes enabling the implementation of integrated quantum photonics. However, high-fidelity spin photon coupling and low-loss chip-to-fiber interfaces are necessary to improve experimental rates and, thus, the performance of quantum devices. Recently, high coupling efficiencies of emitted photons from the VSi color center into angle-etched SiC waveguides have been predicted which can be further enhanced by photonic crystal cavities. Further, a low-loss optical interface from on-chip diamond tapered waveguides to tapered optical fibers was shown. Our goal is to combine these properties and implement single VSi color centers into nanophotonic SiC waveguides coupled to tapered fibers for realizing the on-chip entanglement of color centers and two locally separated quantum registers.

HL 33.23 Wed 17:00 P1

Towards Silicon Vacancy centers based quantum repeaters for a distributed quantum computing network in 4H-SiC — •MAXIMILIAN HOLLENDONNER¹, FEDOR HRUNSKI¹, ANDRE POINTNER¹, SHRAVAN KUMAR PARTHASARATHY^{2,1}, CHRISTIAN GOBERT², DANIEL SCHELLER¹, and ROLAND NAGY¹ — ¹Chair of Electron Devices, Friedrich-Alexander-Universität Erlangen-Nürnberg, Germany — ²Fraunhofer Institute for Integrated Systems and Device Technology IISB, Schottkystraße 10, Erlangen, Germany

For the successful integration of quantum technological systems, like for instance optical quantum computers and quantum sensors [1] into a quantum internet of things it is vital to have quantum repeaters which mediate the exchange of information between various quantum nodes. Due to its excellent optical and spin properties [2], the V₂ silicon vacancy center in 4H-SiC is a promising platform for this task. Within this project we aim at building an interferometer in which after a first 50/50 beam splitter, two single V₂ centers separated by 2 meters are excited by 916nm photons. The single photon emitted by one of the two color centers then enters a second beam splitter, which effectively removes the which-path information and therefore creates a maximally entangled Bell state [3]. Successful demonstration of this entanglement between these two V₂ centers will be a vital step towards realization of a quantum internet of things.

Sources: [1] J. R. Maze *et al.*, *Nature* **455**, 644-647 (2008) [2] R. Nagy *et al.*, *Nat Commun* **10**, 1954 (2019) [3] P. C. Humphreys *et al.*, *Nature* **558**, 268-273 (2018)

HL 33.24 Wed 17:00 P1

On the positioning accuracy of single quantum emitters in photonic nano-structures embedded through in-situ electron beam lithography — •JAN DONGES, JOHANNES SCHALL, IMAD LIMAME, CHING-WEN SHIH, SVEN RODT, and STEPHAN REITZENSTEIN — Technische Universität Berlin, Hardenbergstr. 36, 10623 Berlin

The precise integration of single quantum emitters at the target position inside of photonic nano-structures is of utmost importance for their optimum performance. Differences between simulated photon extraction efficiencies and experimentally determined values are often at least partially contributed to a spatial misalignment of the emitter. This is a reasonable assumption considering that for instance in the case of Bullseye cavities simulations yield that the efficiency can drop more than 50% just in case of a 50nm misplacement between structure and emitter. The main problem with this approach so far has been that there is no direct way of determining the emitter position inside the structure. Therefore, all statements about the position were based indirectly on results of photoluminescence (PL) experiments. Here, we present a solution for this issue. Through the simultaneous measurement of the structure via cathodoluminescence and electron microscopy we can directly determine the emitter position inside a photonic structure with. Furthermore, this approach enables us to make a clear statement about the positioning accuracy of in-situ electron beam lithography.

HL 33.25 Wed 17:00 P1

Quantum Polyspectra for an uncompromising and universal evaluation of quantum measurements — •MARKUS SIFFT and DANIEL HÄGELE — Ruhr University Bochum, Faculty of Physics and Astronomy, Experimental Physics VI (AG), Germany

The analysis of a continuous measurement record $z(t)$ poses a fundamental challenge in quantum measurement theory. Different approaches have been used in the past as records can, e.g., exhibit predominantly Gaussian noise, telegraph noise, or clicks at random times. This poster summarizes our latest findings that show that quantum measurements from all cases above can be analyzed in terms of higher-order temporal correlations of the detector output $z(t)$ and be related to the Liouvillian of the measured quantum system. The comparison of temporal correlations via so called quantum polyspectra is based on expressions derived without approximation from the stochastic master equation [1] and automatized without the need for manual post-processing of the detector output. This allows for fitting of system parameters like e.g., tunneling rates in a quantum transport experiment [2]. The very general stochastic master equation approach includes coherent quantum dynamics, environmental damping, and measurement backaction at arbitrary measurement strength. This enables a systematic evaluation of quantum measurements from the realms of conventional spin noise spectroscopy, quantum transport experiments, and, as our newest finding, ultra-weak measurements with stochastically arriving single photons [3]. [1] Hägele *et al.*, PRB **98**, 205143 (2018), [2] Siffit *et al.*, PRR **3**, 033123 (2021), [3] Siffit *et al.*, arXiv:2109.05862

HL 33.26 Wed 17:00 P1

Detection of half-vortices in confined polariton condensates — •YANNIK BRUNE, BERND BERGER, and MARC ASSMANN — Department of Physics, TU Dortmund, Germany

A half-vortex describes a rotating quantum fluid carrying a spin dependent topological charge. Theory predicts half-vortices as solutions of the spin dependent GPE. We experimentally demonstrate the existence of half-vortices in an all optical circular confined polariton condensate. Therefore we excite a polariton microcavity across the threshold using a ringlike excitation profile and observe the polariton emission. Finally, we measure the topological charge of the condensate state, using spin filtered OAM sorting [1], and thereby confirm its half vortex character.

[1] Berger *et al.*, Optics Express **26**(24):32248 (2018)

HL 33.27 Wed 17:00 P1

Adaptive Bayesian estimation of an Overhauser field gradient — •JACOB BENESTAD¹, JAN KRZYWDA², EVERT VAN NIEUWENBURG^{2,3}, FABRIZIO BERRITTA³, TORBJØRN RASMUSSEN³, ANASUA CHATTERJEE³, FERDINAND KUEMMETH³, and JEROEN DANON¹ — ¹Center for Quantum Spintronics, Norwegian University of Science and Technology, Norway — ²Leiden Institute of Advanced Computer Science, Leiden University, The Netherlands — ³Center for Quantum Devices, University of Copenhagen, Denmark

Slow fluctuations of the Overhauser field gradient are an important source for decoherence in singlet-triplet spin qubits hosted in type III-V semiconductors. Single-shot Ramsey experiments are well suited for Bayesian inference of the Overhauser gradient, where smart experiment design and prior knowledge can be leveraged to increase the information gain of a new measurement. This has led to the development of adaptive schemes, where between each measurement

one attempts to determine the optimal next experiment in order to gain the most possible information about an Overhauser field gradient before the qubit decoheres. A real-time exact treatment of this problem at each step is difficult to achieve in an experimental setting. However an approximate treatment using only Gaussian distributions has been shown to give an exponential reduction of the distribution variance and would require only tracking two parameters. We propose a modification of this scheme that should make it more robust for gradients distributed around a mean of zero by evaluating the squared values and performing the Bayesian update scheme on the resulting chi-square distribution.

HL 33.28 Wed 17:00 P1

Zero-phonon line and electron-phonon coupling of the NV center in cubic silicon carbide: first-principles calculations — •TIMUR BIKTAGIROV¹, HANS JÜRGEN VON BARDELEBEN², JEAN-LOUIS CANTIN², WOLF GERO SCHMIDT¹, and UWE GERSTMANN¹ — ¹Universität Paderborn, Paderborn, Germany — ²Sorbonne Université, Paris, France

The nitrogen-vacancy (NV) center in cubic silicon carbide (3C polytype), the analog of the NV center in diamond, has recently emerged as a solid-state qubit with competitive properties and significant technological advantages [1, 2]. Most applications of NV centers are based on optical spectroscopy of the zero-phonon line (ZPL) and the analysis of the spin states. Thus, we use density functional theory (DFT) calculations to provide thorough insight into the ZPL and the related magneto-optical properties of this center. In the case of NV in diamond, the ZPL is known to be in the visible spectral range [3]. In contrast, we identify the ZPL of the NV center in 3C-SiC at 1289 nm (within the telecom O-band), which is more suitable for device applications due to low transmission losses in optical waveguides. An analysis of the measured phonon sideband reveals the Huang-Rhys factor of 2.85 and the Debye-Waller factor of 5.8 %. Along with exceptionally long low-temperature spin-lattice relaxation times [2], these properties make NV in 3C-SiC a strong competitor for qubit applications.

1. S. A. Zargaleh et al., Phys. Rev. B 98, 165203 (2018).
2. H. J. Von Bardeleben et al., Nano Lett. 21, 8119-8125 (2021).
3. M. W. Doherty et al., Phys. Rep. 528, 1-45 (2013).

HL 33.29 Wed 17:00 P1

Design of a microwave resonator for coherent nuclear spin control of ¹³C and ²⁹Si isotopes near V₂ color centers in 4H-SiC at cryogenic temperatures — •JAN PHILIPP AHNFELDT¹, FEDOR HRUNSKI¹, SHRAVAN KUMAR PARTHASARATHY^{1,2}, MAXIMILIAN HOLLENDONNER¹, DANIEL SCHELLER¹, ANDRE POINTNER¹, and ROLAND NAGY¹ — ¹Chair of Electron Devices, FAU Erlangen-Nürnberg, Erlangen, Germany — ²Fraunhofer Institute for Integrated Systems and Device Technology (IISB), Erlangen, Germany

One step to meaningful quantum technologies is to scale up the currently developed ones. This can be done by parallelizing several quantum systems through a quantum network. Therefore it is crucial that the network contains quantum memory nodes in which the quantum system used has a long coherence time. This can be ensured by the nuclear spin of the ¹³C or ²⁹Si isotopes surrounding a silicon vacancy in 4H-SiC. However, due to the low gyromagnetic ratio of a nuclear spin a large magnetic flux is needed for the spin control. Accordingly, a large RF power with a frequency in the upper kHz domain is required. Because the power dissipation causes problems when upscaling these systems, it is important to improve the spin control's efficiency. Hence, a resonator creating a standing magnetic wave polarized perpendicular to the quantization axis of the vacancy seems to be a promising approach. Since it must operate at room and cryogenic temperatures, the resonator must be mechanically stable and needs a wide bandwidth. Therefore, several resonators are investigated which could meet these requirements in a small package of a few cubic centimeters.

HL 33.30 Wed 17:00 P1

Optical Beamsplitter for Orbital Angular Momentum Modes — •REBECCA ASCHWANDEN¹, BERNHARD REINEKE², LINGLING HUANG³, KLAUS D. JÖNS¹, TIM BARTLEY¹, and THOMAS ZENTGRAF¹ — ¹Department of Physics, Paderborn University, Paderborn, Germany — ²Institute for Photonic Quantum Systems PhoQS, Paderborn University, Paderborn, Germany — ³Beijing Institute of Technology, Beijing, China

Metasurfaces consist of periodically arranged antennas of subwavelength dimensions that allow for specifically engineered functionalities and interaction with the incident light beam. They cannot only be used to replace conventional bulk optical elements but also to provide new functionalities. Here, we present the design and fabrication of a dielectric metasurface acting as a beamsplitter with multiple output ports for orbital angular momentum (OAM) states. The dielectric metasurface consists of silicon nanofins which are fabricated by electron beam lithography and etching. We show that the metasurface splits the beam containing a superposition of OAM states into four spatially separated output directions.

HL 33.31 Wed 17:00 P1

Integration of free-standing GaAs nanobeam cavities hosting InAs/GaAs QD with LNOI waveguides — •OSCAR CAMACHO IBARRA, IOANNIS CALTZIDIS, MARC SARTISON, and KLAUS D. JÖNS — Paderborn University, Paderborn, Germany

Monolithic integration is the most straightforward approach to incorporate single photon emitters and photonic integrated circuits (PICs). However, this approach limits you to the optical properties of the chosen material platform. Furthermore, the current best emitters on monolithic integration are randomly positioned [1]. Based on this context, hybrid integration, despite also requiring localization, stands out, in this approach different materials are integrated into one PIC, allowing one to exploit the advantages of each different material system (whether they are optical properties of the material or the emitters properties). In our work, we seek to hybridly integrate InAs/GaAs quantum dots embedded in nanobeam cavities with LNOI waveguides. To achieve this, we chose a transfer printing method [2] to place the nanobeam cavities (hosting the emitters) on top of the LNOI waveguides. Therefore, we report on the current progress and challenges for localization and nanofabrication of the free-standing nanobeam cavities.

[1] Marc Sartison et al, Scalable integration of quantum emitters into photonic integrated circuits, Mater. Quantum. Technol. 2 023002, 2022.

[2] Ryota Katsumi et al, Transfer-printed single-photon sources coupled to wire waveguides, Optica Vol. 5, No. 6, 2022.

HL 33.32 Wed 17:00 P1

Observation of quantum Zeno effects for localized spins — •VITALIE NEDELEA — Experimentelle Physik 2, Technische Universität Dortmund, 44221 Dortmund, Germany

One of the main dephasing mechanisms for the localized carrier spins in semiconductors is the coupling to the fluctuating nuclear spin environment. Here we present an experimental observation on the effects of the quantum back action under pulsed optical measurements of spin ensemble and demonstrate that the nuclei-induced spin relaxation can be influenced. We show that the fast measurements freeze the spin dynamics and increase the effective spin relaxation time, the so-called quantum Zeno effect. Furthermore, we demonstrate that if the measurement rate is comparable with the spin precession frequency in the effective magnetic field, the spin relaxation rate increases and becomes faster than in the absence of the measurements, an effect known as the quantum antiZeno effect. A theory describing both regimes allows us to extract the system parameters and the strength of the quantum back action.

HL 33.33 Wed 17:00 P1

On-demand strain-induced recombination dynamics in semiconductor quantum wells — DANIEL HENSEL¹, DANIEL SCHMIDT³, FARIBA HATAMI², and •PETER GAAL^{1,3} — ¹Leibniz-Institut für Kristallzüchtung, 12489 Berlin — ²Humboldt Universität zu Berlin, 12489 Berlin — ³TXproducts UG, 22547 Hamburg

Today's technology enables the fabrication of semiconductor structures with a high control over the electronic states. New technologies emerged from the manipulation of these states. To gain full control over the quantum state encrypted in a particle one must control both its lifetime and its coherence. Tailored transient strain pulses provide a new tool for the manipulation of nanoscale quantum objects. The strain-induced deformation of the crystal lattice manipulates the electronic bandstructure via deformation potential coupling. A convenient method to administer strain pulses to a sample are so-called surface acoustic waves (SAW). They are generated electronically by interdigitated circuits (IDT). The experimental control is limited by the ability to generate arbitrary lattice deformations on timescales short compared to the quantum decoherence. The photoacoustic method allows controlling the spatial and temporal shape of the optical excitation and thus shapes the strain pulse. In consequence, arbitrary SAWs can be generated on ultrafast timescales. Time-resolved photoluminescence (TRPL) spectroscopy is used to monitor the strain-induced change in electronic bandstructure. The control of the efficiency of radiative transitions of excitons through the applied strain could be the missing step for the realization of a fast on-demand single photon source.

HL 33.34 Wed 17:00 P1

Fiber-based Open Cavity: a tailored solution for Solid-state Quantum Emitters and their characterization. — •FRANCESCO SALUSTI¹, LUKAS HANSCHKE¹, EVA SCHÖLL¹, JONATHAN NOE², MANUEL NUTZ², MICHAEL FÖRG², THOMAS HÜMMER², and KLAUS D. JÖNS¹ — ¹PhoQS, CeOPP, and Department of Physics, Paderborn University, 33098 Paderborn, Germany — ²Qlibri GmbH, 80337 Munich, Germany and Fakultät für Physik, Ludwig-Maximilians-Universität, 80799 Munich, Germany

For the realization of bright and reliable quantum light emitters, the integration of these emitters into cavity structures represents an elegant solution. However, in many cases, the fabrication of such photonic structure requires remarkable efforts to precisely match the position and the emission wavelength of the emitter with respect to the cavity mode. The required level of control of the materials, size, and positioning makes the realization of a practical cavity resource intensive. Recent works have demonstrated the possibility to take advantage of open cavities to easily tailor the cavity around the specifications of individual emitters, such as 2D flakes and quantum dots. In our collaboration between industry and academia, we show that it is possible to take advantage of a fiber-based de-

vice to realize a tunable cavity at room and cryogenic temperature. In addition to the advantages of in-situ tuning of an optical resonator to specific emitter resonances, the high finesse of the system enables spatially resolved measurements of the absorption coefficient from oxidized 2D material.

HL 33.35 Wed 17:00 P1

Monolithic, heterogeneous and hybrid Integration of quantum emitters — •MARC SARTISON, OSCAR CAMACHO IBARRA, IOANNIS CALTZIDIS, DIRK REUTER, and KLAUS D JÖNS — Institute for Photonic Quantum Systems, Center for Optoelectronics and Photonics Paderborn, and Department of Physics, Paderborn University, 33098 Paderborn, Germany

Modern integrated quantum photonic devices can be built out of a variety of material platforms like Lithium-Niobate on insulator (LNOI), Silicon-Nitride or Silicon with different kinds of quantum emitters like quantum dots, NV centres or emitters hosted in 2D materials. Exploiting the unique material properties several integration approaches were realized that can coarsely be categorized and belong to one of the following types: Monolithic, heterogeneous, and hybrid integration. In our work we give an overview of the different integration methods and compare them in terms of yield and scalability. We discuss the advantages and disadvantages of monolithic, heterogeneous and hybrid integration methods and provide a perspective on the upcoming challenges to realize scalable systems with high yield.

[M. Sartison et al, Mater. Quantum. Technol. 2 023002 (2022)]

HL 33.36 Wed 17:00 P1

Electrical Stark tuning of multiple waveguides with integrated quantum dots — •YUHUI YANG¹, SHULUN LI^{1,2}, JOHANNES SCHALL¹, CHIRAG PALEKAR¹, LÉO ROCHE¹, HANQING LIU², SVEN RODT¹, HAIQIAO NI², ZHICHUAN NIU², and STEPHEN REITZENSTEIN¹ — ¹Institut für Festkörperphysik, TU Berlin, 10623 Germany — ²Institute of Semiconductors, CAS, 100083, China

Self-assembled quantum dots (QDs) are promising candidates for future photonic quantum technologies owing to their close-to-ideal quantum properties. However, the random spectral and spatial distribution of single QD complicates the controlled integration of single QD into photonic structures using standard nano-processing technologies such as standard electron beam lithography and makes upscaling to complex quantum circuits practically impossible. We overcome these technical issues by combining cryogenic cathodoluminescence (CL) mapping for spectrally selected integration of QDs and the quantum-confined Stark effect for spectral fine-tuning. Two spectrally similar self-assembled QDs in a p-i-n diode membrane are pre-selected and are deterministically integrated into the hybrid structure waveguides using marker-based electron beam lithography. Moreover, the gate voltage-dependent micro photoluminescence spectra reveal the achievement for tuning individual QD in waveguide systems and spectrally overlying them together. Our work demonstrates the high potential of deterministic quantum device processing for the scalable fabrication of complex quantum integrated circuits with multiple single-photon emitters as an attractive platform for future quantum technologies.

HL 33.37 Wed 17:00 P1

Electrical Stark tuning of multiple waveguides with integrated quantum dots — •YUHUI YANG¹, SHULUN LI^{1,2}, JOHANNES SCHALL¹, CHIRAG PALEKAR¹, LÉO ROCHE¹, HANQING LIU², SVEN RODT¹, HAIQIAO NI², ZHICHUAN NIU², and STEPHEN REITZENSTEIN¹ — ¹Institut für Festkörperphysik, TU Berlin, 10623 Germany — ²Institute of Semiconductors, CAS, 100083, China

Self-assembled quantum dots (QDs) are promising candidates for future photonic quantum technologies owing to their close-to-ideal quantum properties. However, the random spectral and spatial distribution of single QD complicates the controlled integration of single QD into photonic structures using standard nano-processing technologies such as standard electron beam lithography and makes upscaling to complex quantum circuits practically impossible. We overcome these technical issues by combining cryogenic cathodoluminescence (CL) mapping for spectrally selected integration of QDs and the quantum-confined Stark effect for spectral fine-tuning. Two spectrally similar self-assembled QDs in a p-i-n diode membrane are pre-selected and are deterministically integrated into the hybrid structure waveguides using marker-based electron beam lithography. Moreover, the gate voltage-dependent micro photoluminescence spectra reveal the achievement for tuning individual QD in waveguide systems and spectrally overlying them together. Our work demonstrates the high potential of deterministic quantum device processing for the scalable fabrication of complex quantum integrated circuits with multiple single-photon emitters as an attractive platform for future quantum technologies.

HL 33.38 Wed 17:00 P1

Donor Spins in Compressively Strained Silicon — •BASAK CIGDEM ÖZCAN, DAVID VOGL, and MARTIN S. BRANDT — Walter Schottky Institut and School of Natural Sciences, Technische Universität München, 85748 Garching, Germany Silicon doped with donors is a promising system for quantum computing applications due to long coherence times, fast spin control and the possibility of scaling as well as integration with conventional microelectronics. In order to achieve

long coherence times, coupling to other nuclear spins should be avoided. This is achieved by using isotopically purified Si-28 samples, which is the naturally more abundant isotope without nuclear spin. The conventional architecture to conduct measurements on doped Si-28 involves the placement of control and read-out gate structures on top of the sample. Such additional structures cause strain near the donors, which makes it important to understand the effect of strain on their spin properties. To study this under controlled strain conditions, we utilize a no-contact capacitive read-out scheme, where optical excitation of donor-bound excitons (DBE) followed by an Auger recombination facilitates spin-dependent excitation, spin polarization and spin-state read-out. Combining infrared optical excitation and microwave pulses, we perform electron nuclear double resonance (ENDOR) experiments, with which we achieve coherent control of nuclear spins of the donors. Here, we investigate the strain-dependent shift of DBE resonance frequencies under uniaxial compressive stress. We acknowledge the financial support of MCQST.

HL 33.39 Wed 17:00 P1

Application of low-cost visible light LEDs in avalanche mode as sensitive photoreceivers in a plastic optical fiber data transmission system — •HEINZ-CHRISTOPH NEITZERT — Dept. of Industrial Engineering (DIIN) Salerno University Fisciano, Italy

Commercial low-cost light emitting diodes have been tested as photoreceivers without and with applied reverse bias voltage. In particular the possibility to operate the devices in the breakdown regime as sensitive avalanche photodiodes has been successfully tested. High photogain amplification at relatively low breakdown voltage values has been observed. Based on this possibility to operate the LEDs efficiently not only as emitters but also as photoreceivers, a simple half-duplex bidirectional optical transmission scheme, which is based on the plastic-optical-fiber (POF) as transmission medium and green LEDs as receiving/emitting elements has been developed. The choice of the green wavelength range gives the possibility to operate the system at the minimum absorption of the plastic optical fiber

HL 33.40 Wed 17:00 P1

High Resolution Spectroscopy for (Al,In)GaN Laser Diodes — •DOMINIC J. KUNZMANN, RAPHAEL KOHLSTEDT, and ULRICH T. SCHWARZ — TU Chemnitz, 09126 Chemnitz, Germany

We investigate laser diodes based on the (Al,In)GaN material system with the help of high-resolution spectroscopy. Therefore, we use two setups, one with a grating spectrometer and a Fabry-Pérot-Interferometer. The grating spectrometer is used to measure the longitudinal mode spectra above and below the threshold current. Below the threshold we perform Hakki-Paoli gain spectroscopy to obtain the internal losses of laser diodes which is getting even more challenging, when the diodes get better and the losses smaller. Above the threshold wavelength shifts with current and temperature can be observed and with these shifts the thermal resistance is available. Additionally for broad ridge high power laser diodes the interplay of different longitudinal mode combs is investigated with the high-resolution spectrometer. The Fabry-Pérot-Interferometer enables us to go to even higher resolutions and to verify single mode behavior of laser sources and to observe much smaller wavelength shifts.

HL 33.41 Wed 17:00 P1

Indium incorporation in thin c-plane GaInN/GaN quantum wells grown via plasma-assisted molecular beam epitaxy — •FAROUK ALJASEM, HEIKO BREMERS, UWE ROSSOW, and ANDREAS HANGLEITER — Institut für Angewandte Physik & Laboratory for Emerging Nanometrology, Technische Universität Braunschweig, Germany

This work aims to investigate the physical mechanisms of the incorporation of indium atoms in GaInN QW structures with an emphasis on interface properties by growing thin GaInN multiple quantum wells. A comparison of the obtained results using MBE with the results from the previous work using MOVPE offers more information about indium incorporation mechanisms. As well known, the flux of the activated nitrogen in the plasma-assisted molecular beam epitaxy (PAMBE) is independent of the growth temperature. This feature enables the growth of GaInN MQWs at low temperatures and in different growth regimes compared to MOVPE. Fivefold thin GaInN/GaN MQWs are grown via PAMBE in the c-direction using MOVPE-grown GaN templates on sapphire as substrates. The GaInN/GaN MQW samples were grown at different growth temperatures with various III/V ratios and QW thicknesses. MQW thickness ranged between less than half a c-lattice constant and 2 nm with no significant relaxation. To provide a precise understanding of the physical processes during the growth process of GaInN monolayers, the samples were characterized using HR-XRD, AFM, HR-TEM and CW-PL.

HL 33.42 Wed 17:00 P1

Temperature dependent Raman spectroscopy on GaN:Si — •CHRISTINA HARMS, JONA GRÜMBEL, MARTIN FENEBERG, and RÜDIGER GOLDHAHN — Institut für Physik, Otto-von-Guericke-Universität Magdeburg, Germany GaN structures are of high interest for optical and electronic applications in current research projects. We investigate the Raman excitations of hexagonal bulk

GaN:Si under temperature variation from 80 K up to 300 K. Seven samples with carrier concentrations ranging between 10^{12} - 10^{19} cm⁻³ were measured using laser excitation of 532 nm. It is shown, that within room temperature measurements both coupled phonon-plasmon-modes (LPP_±) are visible and follow the prediction of polaritonic excitations. Under variation of temperature the LPP₊ mode shows a weak frequency shift with elevated temperature or remains unaffected for low carrier concentrations. Surprisingly, the LPP₋ mode shifts towards lower frequencies with increasing temperatures for all samples, which contradicts previous assumptions. A qualitative description of the results and possible interpretations will be presented. Additionally, we also investigated the temperature dependent FWHM of the LPP_± mode and the E₂ phonon mode. Here, both behaviours match the theoretical and experimental previous research.

HL 33.43 Wed 17:00 P1

Indium incorporation during GaInN quantum well growth: role of underlayer surface morphology — •RODRIGO DE VASCONCELOS LOURENÇO^{1,2}, UWE ROSSOW¹, PHILIPP HORENBURG¹, HEIKO BREMERS^{1,2}, and ANDREAS HANGLEITER^{1,2} — ¹Institute of Applied Physics, Technische Universität Braunschweig, Germany — ²Laboratory for Emerging Nanometrology, Technische Universität Braunschweig, Germany

The control of Indium incorporation is a key factor for the optoelectronic devices in the visible and near UV spectral region. The luminescence efficiency of such devices has been improved by the so-called underlayer, i.e the layer grown just before the active region. We investigate the surface morphology as function of the underlayer (UL) composed of GaN or InAlN. For GaN UL, we find extended, very smooth terraces separated by macrosteps in a range of growth temperature from 770 to 950 °C. Additionally, morphologies associated to the Ehrlich-Schwöbel barrier are not observed. On the other hand, for InAlN UL lattice matched to GaN, evidence for nuclei forming at step edges is observed, which may be due to lower surface mobility of Al compared to Ga or In. In the next step, we want to understand how the underlayer morphology affects the Indium incorporation of GaInN quantum wells.

HL 33.44 Wed 17:00 P1

The impact of laser lift-off on the optical properties of InGaN/GaN LEDs — •STEFAN WOLTER, STEFFEN BORNEMANN, HENDRIK SPENDE, and ANDREAS WAAG — Institut für Halbleitertechnik, Technische Universität Braunschweig, 38106 Braunschweig

InGaN/GaN LEDs are typically grown on sapphire, but sapphire is a disadvantageous material when it comes to electrical or thermal conductivity. This limits the performance, when the LED structure is processed into a device. For this reason, it is useful to transfer the LED structure to another carrier after growth, which can be achieved by laser lift-off (LLO). In this process, a pulsed laser beam is focused on the sapphire/GaN interface, leading to absorption of the laser photons in the GaN layer and subsequent decomposition of GaN near the interface resulting in detachment of the GaN film from sapphire. The usage of ultra short laser pulses can reduce the required laser fluence compared to nanosecond pulses, but has the disadvantage of penetrating deep into the LED structure and possibly even reaching the active region. This leads to a change in the characteristic properties of the LED, which is investigated in this study. For this purpose, in-house grown blue InGaN/GaN LEDs are investigated before and after LLO, which was conducted with sub-bandgap (520 nm) and above-bandgap (347 nm) laser light at a pulse width of 0.4 ps. Temperature-dependent photoluminescence experiments in the temperature range of 6 K to 295 K indicate that the maximum internal quantum efficiency decreases by at least 10 % after LLO. Furthermore, LLO can have an impact on the localization strength of the carriers inside the active region.

HL 33.45 Wed 17:00 P1

Characterization of a semiconductor microstructure analogous to a Venturi pump — •SEVERIN KRÜGER, FABIAN LIEDTKE, PETER ZAJAC, ANDREAS WIECK, ARNE LUDWIG, and ULRICH KUNZE — Ruhr-Universität Bochum, Universitätsstraße 150, 44801 Bochum, Germany

Micro-structuring a high-mobility two-dimensional electron gas allows investigation of the ballistic transport regime for electrons. The electrons in the examined channel structures show edge effects like a minimal resistance at finite currents [1]. Furthermore, the electrons show hydrodynamical behavior and can create a rectifying voltage at the narrow channel, similar to the Venturi-effect [2]. Here, first results of measurements regarding the Venturi analogon with different channel sizes, gate voltages and source-drain currents are presented.

[1] Gurzhi, R.N.: "Minimum of Resistance in Impurity-free conductors" *Soviet Phys. JETP* 17, 521-522 (1963).

[2] Szelong, M.: "Ballistische und hydrodynamische Vollwellengleichrichtung in nanoskaligen elektronischen GaAs/AlGaAs-Kreuzstrukturen" *Dissertation, Ruhr-Universität Bochum* (2017).

HL 33.46 Wed 17:00 P1

Novel approach to real-space renormalization group analysis of the quantum Hall effect — •NATHAN SHAW and RUDOLF A. RÖMER — Department of Physics, University of Warwick, Coventry, CV4 7AL, UK

Consensus on the value of the critical exponent ν of the plateau-to-plateau transitions in the quantum Hall effect has not yet been achieved. Recent work has highlighted a discrepancy between field theory based predictions and numerical high-precision estimates. A necessarily approximate real-space renormalization group (RG) approach to the Chalker-Coddington model has previously been shown to suggest a critical exponent of $\nu \approx 2.3$. However, most recent numerical estimations suggest that $\nu = 2.58(3)$. In this study, we experiment with varying the analytical form of the scattering matrix elements with the goal of increasing the numerical stability of the fixed point distribution constructed by the RG flow. Using this improved distribution, we recalculate the critical exponent with higher accuracy.

HL 33.47 Wed 17:00 P1

Epitaxial growth of high-density short wavelength InGaAs QDs for low-threshold VCSELs — •SARTHAK TRIPATHI, KARTIK GAUR, CHING-WEN SHIH, IMAD LIMAME, SVEN RODT, and STEPHAN REITZENSTEIN — Inst. for Solid State Phys., Technical Univ. of Berlin, Germany

Self-assembled growth of InGaAs quantum dots by MOCVD is used to form the active region of low-threshold vertical-cavity surface-emitting lasers (VCSELs). In our work, we optimize the QD gain medium for room-temperature lasing at 935-955 nm which is attractive for gas sensing applications. Multiple layers of high-density InGaAs quantum dots are stacked in order to maximize the modal gain. The density of dislocations and point defects in QD heterostructures is strongly reduced by annealing which enables a significant reduction of the spacer thickness (thinner active region) between stacked QD layers without forfeiting their crystalline quality. Surface characterization is performed using atomic force microscopy AFM to determine the QD density. Moreover, during growth optimization photoluminescence studies are conducted to evaluate the optical properties of single and stacked layers of QD emitting in the target wavelength range. In future, the resulting QDs will be integrated in an active region embedded VCSELs with monolithically integrated high contrast grating (MHCG) hybrid structure.

HL 33.48 Wed 17:00 P1

Simulation and fabrication of a WS₂-nanobeam cavity with a MoSe₂ monolayer as active material — •ARIS KOULAS-SIMOS¹, BÁRBARA ROSA¹, CHIRAG PALEKAR¹, LÉO ROCHE¹, YANG YUHUI¹, FELIX BINKOWSKI², SVEN BURGER^{2,3}, BATTULGA MUNKHBAT⁴, and STEPHAN REITZENSTEIN¹ — ¹Institut für Festkörperphysik, Technische Universität Berlin, 10623 Berlin, Germany — ²Zuse Institute Berlin (ZIB), 14195 Berlin, Germany — ³JCMwave GmbH, D-14050 Berlin, Germany — ⁴Department of Electrical and Photonics Engineering, Technical University of Denmark, 2800 Kongens Lyngby, Denmark

Transition metal dichalcogenides (TMDCs) exhibit extraordinary optical, electrical, and mechanical properties that can be easily tailored for novel integrated photonic applications. Different TMDCs can be combined to form novel nanostructures with highly interesting complex dynamics. Here, we report on the simulation and fabrication of a WS₂-nanobeam cavity with a MoSe₂ monolayer (ML) as active material. Utilizing a FEM eigenfrequency solver, cavity simulations are performed on a 3D stripe of WS₂ with a finite periodic air hole arrangement. The calculated eigenmodes exhibit high Q-factors and tight mode confinement with mode volumes near the fundamental diffraction limit after parameter optimization. The final parameter set is employed in the fabrication process of WS₂-nanobeam cavities with a MoSe₂ ML embedded in them. This work paves further the way toward the realization of novel nanolaser devices consisting purely of TMDC materials.

HL 33.49 Wed 17:00 P1

Design and optimization of Monolithic High Contrast Grating for tuneable quantum dot VCSEL arrays — •FLORIANA LAUDANI¹, MIKOŁAJ JANCZAK², BARTOSZ KAMIŃSKI³, NIELS HEERMEIER¹, ANNA MUSIAŁ³, GRZEGORZ SEK³, TOMASZ CZYSZANOWSKI², SVEN RODT¹, and STEPHAN REITZENSTEIN¹ — ¹Institute of Solid State Physics, Technische Universität Berlin, 10623 Berlin, Germany — ²Institute of Physics, Lodz University of Technology, 90-924 Łódź, Poland — ³Department of Experimental Physics, Wrocław University of Science and Technology, 50-370 Wrocław, Poland

Water vapor measurements are essential for industrial applications to ensure a qualitative processing and control chain and require gas sensors with short response times in a broad wavelength range. In contrast to standard vertical-cavity surface-emitting lasers (VCSELs), devices with monolithically integrated high contrast gratings (MHCGs) can provide a high flexibility with respect to the emission wavelength. We compare reflectivity measurements and theoretical results on GaAs-based MHCGs for a target wavelength around 940 nm. A numerical model based on Plane-Wave Admittance Method solving set of Maxwell equations was used to search for optimal geometric parameters for effective device optimization, allowing a controlled parameter tuning through-

out the fabrication process based on high-resolution electron-beam lithography. Since MHCs can be custom designed before fabrication, they offer great potential for realizing on-chip tuneable VCSEL arrays, e.g. in a variety of short-range communication systems.

HL 33.50 Wed 17:00 P1

In-plane coupling between a WGM micropillar laser and a ridge waveguide — •LÉO ROCHE¹, IMAD LIMAME¹, CHING-WEN SHIH¹, ARIS KOULAS-SIMOS¹, YUHUI YANG¹, SVEN BURGER², and STEPHAN REITZENSTEIN¹ — ¹Institut für Festkörperphysik (TUB), Berlin, Germany — ²JCMwave GmbH, Berlin, Germany

Integrated quantum photonic circuits (IQPCs) are very promising candidates for scalable and flexible on-chip quantum computation and quantum communication hardware. One critical requirement for their realization is the scalable integration of on-demand indistinguishable single-photon emitters. This is potentially possible through the resonant excitation of an integrated QD in a waveguide by means of an on-chip integrated coherent light microlaser. Towards this goal, we investigate the coupling and lasing properties of coherent light laterally emitted from a whispering gallery mode (WGM) type micropillar laser evanescently coupled to a single mode ridge waveguide. Using finite element method (FEM) simulations, we predict the pillar dimensions allowing for lasing modes in the typical emission wavelength of InGaAs QD (930nm) and investigate the coupling efficiency and the Q-factor of the pillar-waveguide system for different angular mode number, pillar-waveguide air gap distances and interface types (point-like or pulley coupling). The III-V semiconductor type nanostructures composed of a GaAs cavity with InGaAs QDs and distributed Bragg reflectors are processed using high-resolution electron beam lithography. Simulation predictions and micro-photoluminescence spectroscopy performed on the nanoprocessed devices are compared and discussed.

HL 33.51 Wed 17:00 P1

Relativistic calculation of hyperfine splittings of hydrogen-like atoms with finite-size nuclei — •KATHARINA LORENA FRANZKE, WOLF GERO SCHMIDT, and UWE GERSTMANN — Paderborn University, Warburger Str. 100, 33098 Paderborn

The hyperfine splittings of spin qubits play an important role in quantum information and spintronics application. They allow for readout of the spin qubits, while simultaneously being the dominant mechanism for the detrimental spin decoherence. Their exact knowledge is thus of prior relevance. In this work we show that the formula of Blügel et al. [1] also holds in the full relativistic regime even if finite-size structure of the nuclei are taken into account. For this purpose, different models for the nuclear charge and spin distributions are compared analytically. The calculated hyperfine splittings of H-like alkali atoms up to ¹³³Cs show a good agreement for all nuclei models. For the real one-electron systems ¹H, ²H, ³H, ³He⁺ they are also in very good agreement with available experimental data. Deviations of DFT-predicted hyperfine splittings from experiment are thus actually due to the use of the frozen-core approximation and limitations of the exchange-correlation (XC) functional.

[1] S. Blügel et al., *Hyperfine fields of 3d and 4d impurities in nickel*. Physical Review B 35, 3271 (1987).

HL 33.52 Wed 17:00 P1

Calculation of zero-field splitting in high-spin defects in semiconductors — •TIMUR BIKTAGIROV, WOLF GERO SCHMIDT, and UWE GERSTMANN — Universität Paderborn, Paderborn, Germany

High-spin defects in semiconductors represent an attractive class of potential solid-state qubits [1]. One of their key spectroscopic fingerprints is the splitting of their spin sublevels in the absence of external magnetic fields. Here we discuss recent progress and open challenges in the theoretical prediction of this zero-field splitting [2, 3].

1. J. R. Weber et al., PNAS 107, 8513-8518 (2010).
2. T. B. Biktagirov and U. Gerstmann, Phys. Rev. Research 2, 023071 (2020).
3. T. B. Biktagirov et al., Phys. Rev. Research 2, 022024 (2020).

HL 33.53 Wed 17:00 P1

Electro-optic response function of thin Quartz for sampling of high-field THz pulses — •MAXIMILIAN FRENZEL, MICHAEL S. SPENCER, and SEBASTIAN F. MAEHRLEIN — Fritz Haber Institute of the Max Planck Society, Faradayweg 4-6, 14195 Berlin, Germany

As high-field THz sources are currently getting more broadly employed, it becomes increasingly important to characterize intense single-cycle THz fields (> 1 MV/cm) in amplitude and phase without saturation or nonlinearities in the electro-optic detection. After previous attempts of spectrally neutral attenuation, z-cut α -Quartz has been recently found as a suitable electro-optic sampling (EOS) crystal. Nevertheless, its accurate response function, which allows the THz electric field to be exactly determined from the measured EOS signal, is still missing. Here, we employ intense THz fields (0.5 - 4 THz) generated via optical rectification in LiNbO₃ to measure EOS in Quartz of various thicknesses between 30 and 150 μ m. We find that both EOS peak amplitude and signal shape are significantly thickness-dependent. By modeling the Quartz EOS detector re-

sponse function, we find good agreement between parameter free theory and experiment, thus explaining the measured thickness dependence. Our work will therefore allow accurate measurement of intense THz electric fields wherever conventional EOS materials are facing saturation effects.

HL 33.54 Wed 17:00 P1

Fourier Transform Infrared Spectroscopy of Quantum Dot and Bragg Mirror Layers in Semiconductor Heterostructures — •NIKOLAJ LEHL, ANDREAS WIECK, NATHAN JUKAM, and AMAR ALOK — Lehrstuhl für Angewandte Festkörperphysik, Ruhr-Universität Bochum, Deutschland

A purposefully designed distributed Bragg reflector (DBR) in a semiconductor heterostructure improves this device's photon yield gathered from its quantum dot (QD) layer. In this master thesis the transmission spectra of such semiconductor heterostructure samples are taken using Fourier-transform infrared spectroscopy (FTIR). The molecular beam epitaxy (MBE) grown gallium arsenide (GaAs) based samples include indium arsenide (InAs) QDs, and DBRs made of sequences of GaAs layers and aluminium arsenide (AlAs) layers. The DBR stopband measurements are taken in the near-infrared (NIR) and mid-infrared (MIR) region, in vacuum, under room temperature. Furthermore, it is planned to investigate the QD intersubband transitions implied in the far-infrared (FIR) transmission spectra as a function of applied voltage at liquid nitrogen and liquid helium temperatures. All acquired spectra are compared to the devices' simulated spectra, in order to make a conclusion on the initially expected growth rates and the growth rates resulting from the measurements.

HL 33.55 Wed 17:00 P1

MIR Time-Domain Ellipsometry via 2D Electrooptic Sampling — •LEONA NEST, MICHAEL SCOTT SPENCER, MARTIN WOLF, and SEBASTIAN MAEHRLEIN — Fritz Haber Institute of the Max Planck Society, Department of Physical Chemistry, Faradayweg 4-6, 14195 Berlin, Germany

Terahertz time-domain spectroscopy (THz-TDS) has been established as a powerful tool in fundamental material science as it allows to measure conductivities, dielectric functions, and related phase transitions in e.g. semiconductors, topological insulators, and high-temperature superconductors. Moreover, THz-TDS is well suited to investigate ultrafast, and thus non-equilibrium, quasi-particle dynamics in such solid-state systems. The time-resolved detection of the electric field provides direct access to complex-valued static and transient material properties. Here, we extend this technique to additionally measure the temporal evolution of the field's polarization for direct determination of complex tensorial material responses. Operating our time-domain ellipsometer in the mid-Infrared (MIR, 15-40 THz) enables anisotropic transmittivity or reflectivity studies in a spectral region where fundamental resonances such as phonons can be found. As a benchmark system, we extract the complex-valued dielectric tensor components of y-cut α -quartz in the vicinity of its anisotropic 21 THz and 24 THz phonon resonances. Good agreement with free-electron-laser-based studies shows that we developed a versatile table-top time-domain ellipsometer that will be used to also measure non-equilibrium tensorial properties in the near future.

HL 33.56 Wed 17:00 P1

Comprehensive model for the thermoelectric properties of two-dimensional carbon nanotube networks — •ADITYA DASH, DOROTHEA SCHEUNEMANN, and MARTIJN KEMERINK — Institute for Molecular Systems Engineering and Advanced Materials, Heidelberg University, Im Neuenheimer Feld 225, 69120 Heidelberg, Germany.

Networks of semiconducting single-walled carbon nanotubes (SWCNTs) are interesting thermoelectric materials due to the interplay between CNT and network properties. Here we present a unified model to explain the charge and energy transport in SWCNT networks. We used the steady-state master equation for the random resistor network containing both the intra- and inter-tube resistances, as defined through their 1D density of states that is modulated by static Gaussian disorder. The tube resistance dependence on the carrier density and disorder is described through the Landauer formalism. Electrical and thermoelectric properties of the network were obtained by solving Kirchhoff's laws through a modified nodal analysis, where we used the Boltzmann transport formalism to obtain the conductivity, Seebeck coefficient, and electronic contribution to the thermal conductivity. The model provides a consistent description of previously published experimental data for temperature and carrier density-dependent conductivities and Seebeck coefficients, with energetic disorder being the main factor explaining observed mobility upswing with carrier concentration. For lower disorder, the Lorentz factor obtained from simulation is in accordance with the Wiedemann-Franz law. Suppressed disorder and lattice thermal conductivity can be a key to higher zT.

HL 33.57 Wed 17:00 P1

Electric field assisted transport in photodiodes studied by EBIC and STEM — •LENNART NOLTE¹, CHRISTOPH FLATHMANN¹, TOBIAS MEYER², and MICHAEL SEIBT¹ — ¹IV. Physical Institute, University of Goettingen, Germany — ²Institute for Materials Physics, University of Goettingen, Germany

P-i-n diodes consist of an intrinsic layer sandwiched between an n- and p-doped layer. Due to lack of carriers in the intrinsic layer, it shows a high Ohmic resistance and realizes more extended depletion zones compared to a typical p-n junction. This makes p-i-n-diodes particularly interesting for high frequency and high voltage electronic applications in addition to photo detection. In this study, we perform electron beam induced current (EBIC) investigations in cross-section geometry combined with scanning transmission electron microscopy (STEM) in order to study electric field assisted diffusion of excess carriers on a nanometer scale under well-defined experimental conditions. Special focus will be on carrier recombination at surfaces produced by focused ion beam (FIB) preparation.

HL 33.58 Wed 17:00 P1

Investigating the influence of stoichiometry-fluctuations on the electronic properties of ultra-scaled HBTs — •DANIEL DICK^{1,3}, JÖRG SCHUSTER^{1,2,3}, FLORIAN FUCHS^{2,3}, and SBYLLE GEMMING^{3,4} — ¹Center for Microtechnologies, Chemnitz University of Technology, Chemnitz, Germany — ²Fraunhofer Institute for Electronic Nano Systems (ENAS), Chemnitz, Germany — ³Center for Materials, Architectures and Integration of Nanomembranes (MAIN), Chemnitz University of Technology, Chemnitz, Germany — ⁴Institute of Physics, Chemnitz University of Technology, Chemnitz, Germany

Silicon-germanium (SiGe) heterojunction bipolar transistors (HBTs) have found widespread use in high-frequency applications. Scaling of the HBT base layer thickness to 5 nm and below makes an atomistic treatment indispensable as fluctuations of dopant concentrations play a bigger role.

We investigate the effect of scaling on properties such as band gap and carrier effective mass and obtain effective material parameters for use in simulations at a larger scale. The use of semi-empirical methods such as extended Hückel theory enables us to simulate a large number of permutations of the atomic structure and study statistical variation of its properties while first-principles methods such as density functional theory allow us to verify the results. Finally, using the non-equilibrium Green's function method we investigate the effect of alloy and phonon scattering on transport through such a layer.

HL 33.59 Wed 17:00 P1

Investigation of Transport Phenomena Through Functionalized Single Molecules Using Liquid Mechanically Controllable Break Junctions — •HARPREET SONDI — FWIO-T, Helmholtz-Zentrum Dresden-Rossendorf, Dresden, Germany

The creation of molecular components for use as electronic devices has made enormous progress. In order to advance the field further toward realistic electronic concepts, methods for the controlled modification of the conducting properties of the molecules contacted by metallic electrodes need to be further developed. Here a comprehensive study of charge transport in a class of molecules that allows modifications by introducing metal center/side chain groups into organic structures is presented. Single molecules are electrically contacted and characterized in order to understand the role of the metal center/side chain groups in the conductance mechanism through the molecular junctions. It is shown that the presence of single metal ions/side chain groups modifies the energy levels and the coupling of the molecules to the electrical contacts, and that these modifications lead to systematic variations in the statistical behavior of transport properties of the molecular junctions.

HL 33.60 Wed 17:00 P1

Time-gated coherent two-dimensional spectroscopy on the nanoscale — •LUIA BRENNEIS, JULIAN LÜTTIG, MATTHIAS HENSEN, and TOBIAS BRIKNER — Institut für Physikalische und Theoretische Chemie, Universität Würzburg, Am Hubland, 97074 Würzburg

The observation of the temporal dynamics of excitons, i.e., electron-hole pairs, is essential for the understanding of fundamental phenomena in nature, e.g., photosynthesis [1]. The method of optical two-dimensional (2D) spectroscopy has proven to be particularly suitable for this purpose. For example, electronic cou-

plings and energy transport phenomena can be directly revealed as cross peaks in a 2D spectrum, i.e., a correlation spectrum of excitation and probe frequency as a function of time. To additionally decipher the spatial dynamics of a system in a nanostructured environment beyond the optical diffraction limit, we have combined 2D spectroscopy with photoemission electron microscopy to realize coherent "2D nanoscopy" [2,3]. Here, using coupled molecular dimers in numerical simulations, we investigate the potential of 2D nanoscopy. In particular, we show how the exciton and biexciton dynamics can be disentangled by resolving the kinetic energy spectrum of photoemitted electrons and by realizing a time gate using an additional ionization pulse.

[1] T. Brixner et al., *Nature* **434**, 625-628 (2005).

[2] M. Aeschlimann et al., *Science* **333**, 1724 (2011).

[3] S. Pres et al., *Nat. Phys.* (2022) (accepted).

HL 33.61 Wed 17:00 P1

Negative thermal expansion in HgTe/CdTe heterostructures on ultrafast timescales — •MARC HERZOG¹, MATTHIAS RÖSSLE², JAN-ETIENNE PUDELL³, MAXIMILIAN MATTERN¹, LUKAS LUNCZER⁴, CLAUD SCHUMACHER¹, HARTMUT BUHMANN¹, LAURENZ MOLENKAMP¹, and MATIAS BARGHEER^{2,3} — ¹Institut für Physik und Astronomie, Universität Potsdam, Germany — ²Helmholtz-Zentrum Berlin, Germany — ³European XFEL, Germany — ⁴Physikalisches Institut EP3, Universität Würzburg, Germany

Materials that would exhibit an ultrafast negative thermal expansion (NTE) are desirable to generate ultrashort and high-amplitude acoustic waves as unconventional stimulus e.g. in the context of nonlinear acoustics or magnetoelectric effects. Both semimetallic HgTe and semiconducting CdTe exhibit pronounced NTE behaviour in thermal equilibrium below their Debye temperatures $\Theta_D \approx 150$ K owing to a negative Grüneisen parameter and correspondingly negative stress by transverse acoustic (TA) phonons.

Using ultrafast x-ray diffraction we investigate the coherent (sound) and incoherent (heat) lattice response in HgTe thin films on a CdTe substrate to ultrashort laser pulse excitation. While above Θ_D both materials exclusively expand upon excitation, below Θ_D a pronounced NTE is observed. However, the time scale for this NTE to develop is a few 100 ps suggesting a slow excitation of the TA modes. At few-ps time scales, however, a strong expansion of HgTe prevails at all measured excitation densities indicating a fast and dominant positive stress due to non-TA phonon modes and/or hot carriers.

HL 33.62 Wed 17:00 P1

h-BN as a protective encapsulation layer for monolayer graphene — •V. CALVI¹, M. BARNES¹, M. BUSCEMA¹, D. WEHENKEL¹, I.M.N. GROOT², and R. VAN RIJN¹ — ¹Applied Nanolayers B.V., Feldmannweg 17, 2628 CD Delft, The Netherlands — ²Leiden Institute of Chemistry, Leiden University, P.O. Box 9502, 2300 RA Leiden, The Netherlands

Graphene surface contamination by polymer residues used in the graphene processing is a key problem for certain device applications. PMMA is used for graphene transfer from a growth substrate to a target substrate. Transfer process leaves polymer residues on the graphene monolayer which causes p-doping. Technique used for the removal of polymer residue is annealing in different gas or vacuum atmospheres. Annealing in oxygen rich environment effectively removes polymer residue, but at the same time also causes damage to the graphene monolayer.

We have investigated stacking a monolayer of h-BN on top of a monolayer of graphene prior to transfer of the graphene. In this way the polymer necessary for the transfer only has direct contact with the surface of the h-BN and graphene would be protected in this way. We compared the damage and cleanliness to both bare graphene and stacked h-BN/graphene by Raman spectroscopy and AFM. We tested different annealing temperatures between 100°C and 500°C and found that the graphene is indeed protected from damage from the annealing process by covering it with a layer of h-BN. At the same time, we were able to show that polymer residue is effectively removed at the higher annealing temperatures.

HL 34: 2D Materials V (joint session HL/CPP)

Time: Thursday 9:30–12:00

Location: POT 81

HL 34.1 Thu 9:30 POT 81

Negative differential resistance with ultra-high peak-to-valley current ratio in tunnel diodes based on two-dimensional cold metals — •ERSOY SASIOGLU and INGRID MERTIG — Martin-Luther-Universität Halle-Wittenberg, Institut für Physik, 06120 Halle (Saale)

The negative differential resistance (NDR) effect is of great interest for future memory and logic circuit applications. We propose a novel semiconductor-free NDR tunnel diode concept with ultra-high peak-to-valley current ratio (PVCR) [1]. Our proposed NDR diode consists of two cold metal electrodes separated by a thin insulating tunnel barrier. The NDR effect stems from the unique electronic

band structure of the cold metal electrodes, i.e., the width of the isolated metallic bands around the Fermi level as well as the energy gaps separating higher- and lower-lying bands determine the current-voltage characteristics and PVCR value of the tunnel diode. By proper choice of the cold metal electrodes either Λ -type or N-type NDR effect can be obtained. We employ the nonequilibrium Green's function method combined with density functional theory to demonstrate the NDR characteristics of the proposed diode based on two-dimensional NbS₂/h-BN/NbS₂ vertical and AlI₂/MgI₂/AlI₂ planar heterojunctions. For the lateral tunnel diode, we obtain a Λ -type NDR effect with an ultra-high PVCR value of 10¹⁶ at room temperature, while the vertical tunnel diode exhibits a

conventional N-type NDR effect with a smaller PVCR value of about 10^4 . The proposed concept provides a semiconductor-free solution for NDR devices to achieve desired I - V characteristics.

[1] Ersoy Şaşıoğlu and Ingrid Mertig, arXiv:2207.02593 (2022).

HL 34.2 Thu 9:45 POT 81

Electrical contact engineering on 2D material through ion implantation and flash lamp annealing — •KAIMAN LIN^{1,2}, YI LI², MANFRED HELM², SHENGQIANG ZHOU², YAPING DAN¹, and SLAWOMIR PRUCNAL² — ¹University of Michigan-Shanghai Jiao Tong University Joint Institute, Shanghai Jiao Tong University, 20024 Shanghai, P. R. China — ²Institute of Ion Beam Physics and Materials Research, Helmholtz-Zentrum Dresden-Rossendorf, 01328 Dresden, Germany
In recent years, 2D material-based nanodevices have been extensively studied and exhibit highly competitive performance compared with conventional bulk semiconductors. Before they can be fully integrated with existing Si-based technology or offer new platform for novel nanoelectronics, some challenges must be solved. One of the key challenges in 2D devices is the large Schottky barrier at the 2D/metal interface, which limits the charge carrier injection from metal to 2D channel. In this paper, we propose a novel method, which exploits the top metal electrode as the capping layer during the ion implantation process, followed by ms-range flash lamp annealing to repair the defects caused by ion implantation and to activate dopants. Our approach allows to realize effective doping at the interface between multilayer 2D materials and metal electrodes and simultaneously minimize the defect concentration created during the ion implantation process. As a result, the ohmic contact between 2D material and metal electrodes will be realized.

HL 34.3 Thu 10:00 POT 81

Impact of free carriers on exciton and trion diffusion in monolayer WSe₂ — •MARZIA CUCCU¹, KOLOMAN WAGNER¹, ZAKHAR A. IAKOVLEV², JONAS D. ZIEGLER¹, TAKASHI TANIGUCHI³, KENJI WATANABE³, MIKHAIL M. GLAZOV², and ALEXEY CHERNIKOV¹ — ¹TU Dresden, Dresden, Germany — ²St. Petersburg, Russia — ³National Institute for Materials Science, Tsukuba, Japan
In monolayer transition metal dichalcogenides excitons are tightly bound, mobile at room and cryogenic temperatures, and interact strongly with free charge carriers. However, the role of the exciton-electron interaction in the context of exciton propagation remains unclear. Here, we address this question by demonstrating diffusion of excitons in hBN-encapsulated WSe₂ in the presence of a continuously tunable Fermi sea. Using ultrafast microscopy, we reveal a non-monotonic dependence of the exciton diffusion coefficient on the charge carrier density in both electron- and hole-doped regimes. We identify distinct regimes of elastic scattering and quasiparticle formation determining exciton diffusion and highlight the importance of treating exciton-electron scattering in the presence of additional energy and momentum dissipation via phonons. We further show that trions remain mobile even at low temperatures down to 5 K, with an effective trion mobility up to 3000 cm²/(Vs).

HL 34.4 Thu 10:15 POT 81

Electrical Characterization of Thin ZrSe₃ Films — •LARS THOLE¹, CHRISTOPHER BELKE¹, SONJA LOCMELIS², PETER BEHRENS², and ROLF J. HAUG¹ — ¹Institut für Festkörperphysik, Leibniz Universität Hannover, 30167 Hannover, Germany — ²Institut für Anorganische Chemie, Leibniz Universität Hannover, 30167 Hannover, Germany

Two dimensional materials have been of great interest in the past years, because of their huge potential for new applications [1]. While graphene has been extensively researched, a lot of other materials have emerged. One of the most notable groups are the transition metal chalcogenides because of their variety of different compounds. Among these the lesser known transition metal trichalcogenides show unique properties [2].

Here, we have researched the transition metal trichalcogenide ZrSe₃ [3]. Its bulk material was produced by a chemical vapor transport method and was then exfoliated to obtain thin films. Electrical measurements show a band gap of 0.6 eV which increases for thinner samples. The material is shown to be an n-type semiconductor by transistor measurements and a mean free path of about 103 nm was determined by looking at different samples with varying thicknesses.

[1] A. K. Geim, I. V. Grigorieva, Nature, 499, 419-425 (2013).

[2] J. O. Island et al., 2D Materials, 4, 0220033 (2017).

[3] L. Thole et al., ACS Omega, 7, 39913 (2022).

HL 34.5 Thu 10:30 POT 81

Electrically active deep defects in 2D vdW semiconductors — •MICHELE BISSOLO¹, RONGXIN LI¹, MASAKO OGURA², SVITLANA POLESYA², HUBERT EBERT², EUGENIO ZALLO¹, GREGOR KOBLMÜLLER¹, and JONATHAN J. FINLEY¹ — ¹Walter Schottky Institute and TUM School of Natural Sciences, Technical University of Munich, Am Coulombwall 4, 85748 Garching, Germany — ²Department of Chemistry/Phys. Chemistry, LMU Munich, Butenandtstrasse 11, 81377 Munich, Germany

Mid-gap defect states in semiconductors can both potentially degrade the performance of (opto)electronic devices and simultaneously act as a platform for

technologies such as (photo)catalysis and quantum computing. Characterizing the electrically active mid-gap defects in the emerging class of 2D van-der-Waals materials is thus a necessary step in the development of future 2D-based devices. Here, we employ Deep Level Transient Spectroscopy (DLTS) techniques to directly probe deep defects in transition metal dichalcogenides (TMDCs) and group-III monochalcogenides (III-MCs), which have recently gained traction in "more-than-Moore", low-power and renewable energy device applications. Unlike transmission electron or scanning tunneling microscopies, DLTS is both a non-destructive and bulk sensitive technique that provides multiple information on the electronically active defect states, such as concentration, energy and capture cross section. DLTS spectra are collected from few-layer MoS₂, MoSe₂ and GaSe Schottky diodes in the 10-300 K temperature range with 10 mK stability, and the properties and role of the observed defects are discussed.

15 min. break

HL 34.6 Thu 11:00 POT 81

Ionic based gate control of insulator-to-metal phase transitions on ZrS₂ — •JOSE GUIMARAES^{1,2}, DORSA FARTAB¹, MARCUS SCHMIDT¹, and HAIJING ZHANG¹ — ¹Max Planck Institute for Chemical Physics of Solids, 01187 Dresden, Germany — ²School of Physics and Astronomy, University of St Andrews, St Andrews KY16 9SS, UK

The possibility of tuning the properties of solids, such as their carrier density, allows for the amplification of their potential: In the context of 2D materials, ionic liquid gating provides a highly efficient doping alternative to traditional chemical doping.

Transitional metal dichalcogenides (TMDCs) have emerged as a potential 2D replacement for silicon in many technological applications, however their carrier mobility needs to be vastly increased. Ionic liquid gating enables carrier concentrations of the order of 10^{14} carriers per cm² in certain TMDCs, moreover, it allows for the emergence of unique physical phenomena, such as ambipolar behaviour. To realize transistor applications, materials that can be easily switched between p-type and n-type by applying an electric field are essential to minimize circuit size.

Here, an overview of the ionic liquid gating technique is given, including device fabrication and characterization methods, focusing on the TMDCs: ZrS₂ and ZrSe₂. Being ZrSe₂ an oxygen sensitive material, a method of estimating its thickness by its optical image is discussed. Furthermore, experimental efforts reporting ambipolar behaviour in ZrS₂ for the first time are presented.

HL 34.7 Thu 11:15 POT 81

Lattice reconstruction in twisted transition metal dichalcogenide heterobilayers — •WEI LI, THOMAS BRUMME, and THOMAS HEINE — TU Dresden, Dresden, Germany

Twisted heterostructures of 2D crystals have resulted in a series of high-impact contributions to condensed matter physics, most prominently flat bands and superconductivity in twisted bilayer graphene. But also two-dimensional crystals beyond graphene, such as transition metal dichalcogenides, show strong proximity effects that are affected by twisting. Here, we systematically investigate the structural impact of twist angles on transition metal dichalcogenide van der Waals heterobilayers consisting of MoS₂, WS₂, MoSe₂ and WSe₂ monolayers. We find that the significant lattice reconstruction involving in- and out-of-plane displacements strongly depends on the twist angle: from a continuous variation of local stacking alignment at large twist angles to a soliton-domain structure at small twist angles. Especially, starting from either 2H or 3R stacking, two different critical twist angles exist, above which the two constituting layers show dramatically asymmetrical corrugation, in contrast to the symmetry-preserving out-of-plane deformation in twisted homobilayers. We reveal that the development of either the corrugation or the soliton-domain results from the competition between strain energy cost and van der Waals energy gain. Our calculations show that van der Waals heterobilayers develop, besides the well-investigated moiré structures, also systems with large areas of special local stackings arranged in a superlattice, suggesting intriguing electronic properties of these systems.

HL 34.8 Thu 11:30 POT 81

Pump Probe Signatures of Interlayer Excitons in TMDC Heterostructures — •HENRY MITTENZWEY¹, MANUEL KATZER¹, BENJAMIN KAISER², VERONICA POLICHT³, OLEG DOGADOV³, STEFANO DAL CONTE³, GIULIO CERULLO³, ANDREAS KNORR¹, and MALTE SELIG¹ — ¹Institut für Theoretische Physik, Nichtlineare Optik und Quantenelektronik, Technische Universität Berlin, Hardenbergstr. 36, 10623 Berlin, Germany — ²Zuse Institute Berlin, Takustraße 7, 14195 Berlin, Germany — ³Dipartimento di Fisica, Politecnico di Milano, I-20133 Milano, Italy

TMDC heterobilayers are promising candidates for novel optoelectronic applications, since they exhibit long-lived excitonic states with spatially separated electrons and holes located in different layers. The relaxation dynamics of these interlayer excitons and their interplay with intralayer excitons are still under investigation.

Here, we present a microscopic description for the phonon and tunneling induced formation and relaxation of intra- and interlayer excitons in a MoSe₂/WSe₂ stack. Based on the microscopic dynamics we calculate the pump probe signal for intra- and interlayer transition and their population dynamics including hot exciton bottleneck effects and unbound interlayer occupations.

HL 34.9 Thu 11:45 POT 81

Microscopic picture of interlayer exciton-phonon coupling — MURALIDHAR NALABOTHULA, LUDGER WIRTZ, and SVEN REICHARDT — University of Luxembourg, Luxembourg

Excitons play a key role for opto-electronic applications of 2D heterostructures. They also can strongly couple to phonons as evidenced by their imprint on resonant Raman scattering intensities [1,2]. In 2D heterostructures, this sort of strong coupling and its signature Raman scattering offers an ideal setting to learn about exciton-phonon coupling both within and across material layers. Here we

focus on the example of monolayer WSe₂ and hBN. Its Raman spectrum features the normally silent out-of-plane optical phonon mode of hBN that becomes active due to symmetry breaking and - most curiously - very strongly enhanced due to resonant exciton-phonon scattering [1]. While the resonant scattering pathways have been identified as involving excitons in WSe₂ that couple to the phonons in hBN [1], a microscopic understanding of this interlayer exciton-phonon coupling is still missing. We provide such understanding using the state-of-the-art method for the computation for resonant Raman scattering intensities [2,3], which allows a detailed atomistic and quantum mechanical dissection of the Raman scattering process. Supplemented by a classical picture, our work sheds light on the microscopic mechanism behind exciton-phonon coupling in 2D heterostructures.

[1] C. Jin, et al. Nat. Phys., 13, 127-131, (2017).

[2] S. Reichardt and L. Wirtz. Sci. Adv. 6, eabb5915, (2020).

[3] S. Reichardt and L. Wirtz. Phys. Rev. B 99, 174312, (2019).

HL 35: Focus Session: Transient multi-wave mixing on excitonic resonances

Coherent nonlinear optical spectroscopy and, in particular, transient multi-wave mixing processes provide valuable information for basic research in material science and applications in photonics and quantum technology. It allows one to obtain detailed information about the energy structure and dynamic evolution of quantum systems including excited states which is not possible via linear optical spectroscopy and gives direct access to higher-order correlations among the elementary optical excitations. In addition, multi-wave mixing processes can be used as a powerful tool to coherently control the electronic states of the system and to generate non-classical states of light, which is appealing for the implementation in quantum information devices. Importantly for these studies is that excitons possess high oscillator strength which leads to a significant increase of higher-order mixing under resonant excitation with ultrashort optical pulses. This session will focus on multi-wave mixing processes as a unique tool to uncover the fascinating physics of excitons and many-body correlations in emerging materials such as transition metal dichalcogenides and perovskites and establish novel approaches for the coherent control of excitonic quantum systems with classical and quantum light.

Organized by I.A. Akimov and T. Meier

Time: Thursday 9:30–13:30

Location: POT 361

Invited Talk

HL 35.1 Thu 9:30 POT 361

Quantum Dynamics of Polarons in Doped Semiconductor Monolayers — XIAOQIN ELAINE LI¹ and DI HUANG² — ¹Physics Department, University of Texas at Austin, Austin, TX, U.S.A. — ²Physic Department, Tongji University, Shanghai, China

When mobile impurities are introduced and coupled to a Fermi sea, new quasiparticles known as Fermi polarons are formed. We study Fermi polarons in two dimensional systems, where many questions and debates regarding their nature persist. The model systems we investigate are doped MoSe₂ and WSe₂ monolayers. In MoSe₂, we find the observed attractive and repulsive polaron energy splitting and the quantum dynamics of attractive polarons agree with the predictions of a simple theory. As the doping density increases, the quantum dephasing of the attractive polarons remains constant, indicative of stable quasiparticles, while the repulsive polaron dephasing rate increases nearly quadratically. In WSe₂, two distinct species of attractive polarons exist, singlet and triplet polarons. The singlet (triplet) dynamics are mediated by the Fermi seas in the same (opposite) valley. A long-lived valley polarization component is found and likely related to a reservoir of dark states.

Invited Talk

HL 35.2 Thu 10:00 POT 361

Impact of phonons on time-resolved optical signals from excitons — DORIS E. REITER — Condensed Matter Theory, TU Dortmund, 44221 Dortmund

A major difference between optical manipulation of atoms and excitons in semiconductors is the interaction of the latter with the vibrational modes of the solid, i.e., the phonons. In particular in nanostructures like quantum dots, the interaction with acoustic phonons is non-monotonous as function of energy, yielding interesting phenomena like phonon sidebands, reappearance of Rabi rotations or phonon-assisted state preparation. When a quantum dot is optically driven exhibiting Rabi oscillations of the exciton, the pure dephasing-type electron-phonon interaction results in polaron formation accompanied by the emission of phonon wave packets. While for the occupation, the phonon influence leads to an exponential damping, optical multi-wave mixing experiments are more sensitive to the quantum dot polarization. Here, the phonons cannot be described by a simple damping, but their interaction can be understood as a relaxation into the lower dressed state. In this talk, we use a simple model of phonons [1] to discuss their impact on time-resolved optical signals in semiconductor quantum dots. We consider the impact of phonon on continuous wave excitation in a pump-probe configuration [1] and on optical photon echo signals, where the model is in excellent agreement with experiments [2]. Ref: [1] Ann. Phys. 533, 2100086 (2021) [2] PRB 106, 205408 (2022).

Invited Talk

HL 35.3 Thu 10:30 POT 361

Hot-Exciton Quantum Dynamics in Zero-Dimensional Structures — ALFRED LEITENSTORFER — Department of Physics and Center for Applied Photonics, University of Konstanz, Germany

Electronic quantum processes in intrinsic dimensions of time and space are investigated with femtosecond transient transmission spectroscopy of individual II-VI quantum dots. With our experiments, we are aiming at single-photon amplification for the ultimate control of the quantum statistics of ultrashort light pulses [1]. In these systems, the elementary dynamics of charges and spins is dominated by fundamental aspects such as Coulomb correlations and the Pauli principle [2]. Harnessing a pump-probe microscope optimized for single-electron sensitivity at cryogenic temperatures and high magnetic fields [3], we find extremely asymmetric relaxation characteristics in valence and conduction bands where e.g. femtosecond quantum kinetics of hole-phonon coupling is compatible with persistent spin coherence of hot excitons [4].

[1] F. Sotier et al., Nature Phys. 5, 352 (2009)

[2] C. Hinz et al., Phys. Rev. B97, 045302 (2018)

[3] C. Traum et al., Rev. Sci. Instr. 90, 123003 (2019)

[4] P. Henzler et al., Phys. Rev. Lett. 126, 067402 (2021)

HL 35.4 Thu 11:00 POT 361

Multi-wave mixing applied to explore and control the coherent dynamics of ensembles of semiconductor quantum dots — HENDRIK ROSE¹, STEFAN GRISARD², ARTUR V. TRIFONOV², RILANA REICHHARDT², DORIS E. REITER³, MATTHIAS REICHEL¹, CHRISTIAN SCHNEIDER^{4,5}, MARTIN KAMP⁴, SVEN HÖFLING⁴, MANFRED BAYER², ILYA A. AKIMOV², and TORSTEN MEIER¹ — ¹Paderborn University, Department of Physics & Institute for Photonic Quantum Systems (PhoQS), 33098 Paderborn, Germany — ²Experimentelle Physik 2, Technische Universität Dortmund, 44221 Dortmund, Germany — ³Condensed Matter Theory, Technische Universität Dortmund, 44221 Dortmund, Germany — ⁴Technische Physik, Universität Würzburg, 97074 Würzburg, Germany — ⁵Institute of Physics, University of Oldenburg, 26129 Oldenburg, Germany

Multi-wave mixing provides various possibilities to investigate the ultrafast dynamics of semiconductors. Here, we focus on ensembles of quantum dots where the nonlinear dynamics leads to emission in the form of photon echoes. We show that photon echoes can be temporally controlled by the application of multi-wave mixing [1] and furthermore demonstrate that a damping mechanism based on the spatial shape of the applied laser pulses can be circumvented by pulse shaping [2].

- [1] A. N. Kosarev, H. Rose, et al., *Commun. Phys.* **3**, 228 (2020).
 [2] S. Grisard, H. Rose, et al., *Phys. Rev. B* **106**, 205408 (2022).

HL 35.5 Thu 11:15 POT 361

Four-wave mixing at excitonic resonances in the telecom spectral range — •SEBASTIAN KLIMMER¹, ARTEM SINELNIK^{1,2}, MUHAMMAD HUSSAIN¹, ISABELLE STAUBE^{1,2}, HABIB ROSTAMI³, and GIANCARLO SOAVI¹ — ¹Institute of Solid State Physics, Friedrich Schiller University Jena, Germany — ²Institute of Applied Physics, Friedrich Schiller University Jena, Germany — ³Nordita, KTH Royal Institute of Technology and Stockholm University, Sweden

Over the last few decades, nonlinear optical (NLO) processes have become a pillar for novel photonic devices. In particular, four-wave mixing (FWM) effects can be used to generate quantum optical states of light, such as entangled photons. Transition metal dichalcogenides (TMDs) offer significant advantages compared to conventional nonlinear materials, as their strong light-matter interaction and ease of integration into existing photonic platforms[1] make them perfect for enhancing the performance of integrated NLO devices. In addition, their atomic thickness softens phase matching limits, providing a virtually unlimited bandwidth for FWM[2]. This could be exploited to entangle photons from various spectral regions, making them an ideal source for quantum imaging applications[3]. In this work, we study broadband and exciton enhanced FWM in the telecom spectral range in MoS₂, highlighting the capability of TMDs for integrated photonics and communication applications.

- [1] He, J. *et al.*, *Nano Lett.* **21**, 7, 2709-2718 (2021)
 [2] Trovatiello, C. *et al.*, *Nat. Photonics.* **15**, 6-10 (2021)
 [3] Gilaberte Basset, M. *et al.*, *Laser Photonics Rev.* **13**, 10 (2019)

30 min. break

Invited Talk

HL 35.6 Thu 12:00 POT 361

Ultrafast dynamics and wave mixing at excitonic resonances in atomically thin semiconductors — •ANDREAS KNORR, DOMINIK CHRISTIANSEN, FLORIAN KATSCH, MANUEL KATZER, and MALTE SELIG — Technische Universität Berlin Atomically thin semiconductors constitute an ideal playground for exciton physics in two dimensions. This involves optically accessible (bright) as well as spin- or momentum-forbidden (dark) excitonic states including intravalley and intervalley excitations. The nonlinear, coherent exciton and wave mixing dynamics induced by short light pulses result from the interplay of strong intrinsic exciton-exciton and exciton-phonon interactions and can be described in a many body Heisenberg equation of motion formalism. Here, we present applications of the theory to:

- exciton-exciton scattering and biexcitons in wave mixing,
- exciton wave function dynamics in time resolved ARPES,
- control of nonlinear excitonic Rabi-oscillations, and
- limits of the boson description of excitons.

Invited Talk

HL 35.7 Thu 12:30 POT 361

Spontaneous parametric down-conversion in semiconductor metasurfaces — •MARIA CHEKHOVA — Max-Planck Institute for the Science of Light, Erlangen, Germany — Friedrich-Alexander Universität Erlangen-Nürnberg Spontaneous parametric down-conversion (SPDC) is the most efficient way to generate pairs of entangled photons for quantum photonics applications such as quantum communication, quantum imaging and sensing, and quantum metrology. Today, several groups are trying to implement SPDC on nanoscale quasi-2D platforms, such as subwavelength crystalline layers and metasurfaces. These ultrathin sources have numerous advantages. They are integrable, ultrafast, ultra-

broadband and, most importantly, multifunctional. Metasurfaces, in addition, can enhance the rate of photon pair generation due to their *geometric* resonances.

In my talk I will show our recent results on the generation of photon pairs in metasurfaces made of gallium arsenide and gallium phosphide. The metasurfaces are structured to support bound states in the continuum (also known as Fano) resonances, with the quality factors Q reaching several hundred. The resonances enhance the spontaneous emission of pairs by a factor on the order of Q if the frequency of one of the photons coincides with the resonance. Due to the ultrasmall thickness of such sources, SPDC can be pumped slightly above their bandgap without considerable effect of absorption. The inevitably high level of photoluminescence can be overcome by time-resolved registration of photon pairs.

HL 35.8 Thu 13:00 POT 361

Time-resolved four-wave mixing spectroscopy of excitons in a FA_{0.9}Cs_{0.1}PbI_{2.8}Br_{0.2} perovskite crystal — •STEFAN GRISARD¹, ARTUR V. TRIFONOV¹, DMITRY N. DIRIN^{2,3}, MAKSYM V. KOVALENKO^{2,3}, ILYA A. AKIMOV¹, DMITRI R. YAKOVLEV¹, and MANFRED BAYER¹ — ¹Experimentelle Physik 2, Technische Universität Dortmund — ²Institute of Inorganic Chemistry, Department of Chemistry and Applied Bioscience, ETH Zürich — ³Laboratory for Thin Films and Photovoltaics, Empa-Swiss Federal Laboratories for Materials Science and Technology

Formamidinium lead triiodide (FAPbI₃) shows outstanding characteristics for future photovoltaic or light emitting devices, suffers however from poor phase stability. Additives such as cesium and bromine help to improve the phase stability, but possibly increase the localization of the charge carriers. In this work, we present time resolved four-wave mixing spectroscopy as a versatile tool to investigate the coherent optical properties of a FA_{0.9}Cs_{0.1}PbI_{2.8}Br_{0.2} crystal. At low temperatures of 1.5K, the coherent optical response is represented by photon echoes due to the strong inhomogeneous broadening of exciton resonances. We find that the coherence time T_2 is surprisingly long (≈ 100 ps), comparable with the lifetime T_1 . The spectral dependence of T_2 and T_1 indicate the importance of carrier localization.

HL 35.9 Thu 13:15 POT 361

Multi-photon pump probe of magnetic-field-induced quantum beats in Cu₂O — •NIKITA V. SIVERIN, ANDREAS FARENBRUCH, DIETMAR FRÖHLICH, DMITRI R. YAKOVLEV and MANFRED BAYER — TU Dortmund, Dortmund, Germany

Multi-photon processes such as second harmonic generation are suitable for the investigation of exciton symmetries by analyzing the linear polarization angles of the incoming and the outgoing light. We use difference frequency generation (DFG) with two-photon as the optical technique. The initial laser pulse excites an exciton population by a two-photon excitation process. Probe pulse stimulates a DFG photon. Delaying the second pulse in time enables us the measurement of exciton coherence times and quantum beats between several states. There is also an additional degree of freedom compared to the SHG technique in the polarization of the emission channel. We measure the coherence time of yellow series in Cu₂O. By applying a magnetic field up to 10T in Voigt geometry the 1S orthoexciton splits into three states denoted by the quantum number $M = -1, 0, 1$. We observe a beating between these three states. By a selection of the linear polarization setting in the emission channel one can deliberately choose to detect single-frequency beats between the $M=+1$ and $M=-1$, triple-frequency beats between all three states or only the $M=0$ state without beats. Beat frequencies scale with magnetic field strength.

HL 36: Transport properties

Time: Thursday 9:30–11:45

Location: POT 151

HL 36.1 Thu 9:30 POT 151

Charge carrier mobilities in 2D covalent organic frameworks — •ELIF UNSAL¹, ALEXANDER CROY², ALESSANDRO PECCHIA³, AREZOO DIANAT¹, RAFAEL GUTIERREZ¹, and GIANAURELIO CUNIBERTI¹ — ¹Institute for Materials Science and Nanotechnology, TU Dresden, Dresden, Germany. — ²Institute of Physical Chemistry, FSU Jena, Germany. — ³CNR-ISMN, Rome, Italy 2D COFs are functional porous crystalline structures, which have high chemical and thermal stabilities. Having tunable chemistry and structures are their major properties which make 2D COFs attractive for wide range of applications, such as electro-catalysis, gas storage, and optoelectronic applications[Xiao Feng, 2012, *Chem. Soc. Rev.*]. Despite the intensive studies on 2D COFs, charge transport properties of most of these materials are still unknown. Here, we present a new approach based on DFTB calculations of the phonon-limited mobility in 2D COFs. We are modelling charge transport properties by combining state-of-the-art electron-phonon coupling calculations and semiclassical Boltzmann transport theory. We are using our own code DFTBephy whose implementation

is based on DFTB+ [Marcus Elstner et al. 1998, *Phys. Rev. B: Condens. Matter Mater. Phys.*; Marcus Elstner, 2007, *J. Phys. Chem. A*] and phonopy [Atsushi Togo, 2015, *Scr. Mater.*] and it interfaces with BoltzTrap2 [Georg K. H. Madsen, 2018, *Comput. Phys. Commun.*] to calculate transport properties. Our results are benchmarked against state-of-the-art EPW [Samuel Ponce, 2016, *Comput. Phys. Comm.*] calculations.

HL 36.2 Thu 9:45 POT 151

Active Dopant Sites in Hyperdoped Si and Ge Investigated by Photoemission — •MORITZ HOESCH¹, MAO WANG², SLAWOMIR PRUCNAL², SHENGQIANG ZHOU², OLENA FEDCHENKO³, CHRISTOPH SCHLÜTER¹, KATYA MEDJANIK³, SERGEY BABENKOV³, ANCA CIOBANU¹, DMITRII POTOROCHIN^{1,4}, SANJOY MAHATHA^{1,5}, MARKUS SCHOLZ¹, QUYNH NGUYEN⁶, AIMO WINKELMANN⁷, H.-J. ELMERS³, and GERD SCHÖNHENSE³ — ¹DESY Photon Science, Hamburg, Germany — ²Helmholtz-Zentrum Dresden-Rossendorf, Germany — ³JGU, Institut für Physik, Mainz, Germany — ⁴TU Bergakademie Freiberg, Germany —

⁵UGC-DAE, Indore, India — ⁶SLAC, Menlo Park, USA — ⁷AGH University of Kraków, Poland

Hyperdoping of silicon and germanium, with dopant concentration well above the thermal solubility limit, is achieved by ion implantation followed by pulsed laser or flash lamp annealing. Here, we probe the materials by photoemission spectroscopy thus revealing the metallic carriers in the valence region as well as core level shifts of the dopant species. The samples are p-doped Ge:Ga and n-doped Si:Te, both well into the metallic regime. The latter shows non-saturating growth of the free carrier concentration with increasing doping [1]. We present experimental determinations of the Fermi surfaces of these materials by soft x-ray ARPES as well as geometrical structure measurements by photoelectron diffraction [2,3].

[1] M. Wang et al. Phys. Rev. Appl. 11 054039 (2019). [2] O. Fedchenko et al NJP 21, 113031 (2019); [3] O. Fedchenko et al NJP 22, 103002 (2020).

HL 36.3 Thu 10:00 POT 151

Rapid Electronic Transport Predictions via the Kubo-Greenwood Formalism — •FLORIAN FIEBIG, MATTHIAS SCHEFFLER, and CHRISTIAN CARBOGNO — The NOMAD Laboratory at the FHI of the Max-Planck-Gesellschaft and IRIS-Adlershof of the Humboldt-Universität zu Berlin

For the first-principles evaluation of electronic heat and charge transport coefficients, the Kubo-Greenwood (KG) formalism [1] represents a more general and accurate alternative to perturbative approaches, [2] since it naturally incorporates all orders of anharmonic and vibronic effects. In practice, however, KG calculations come with a prohibitive computational cost, since ordered crystalline materials typically require both dense reciprocal-space \mathbf{k} -grids for the electronic degrees of freedom and large real-space supercells for the vibrational ones. In this work, we propose an adaptive, KG-specific scheme for the \mathbf{k} -space sampling that alleviates this issue. It enables the use of very coarse \mathbf{k} -grids during the self-consistency cycle, whereas very dense \mathbf{k} -grids are used for the evaluation of the KG formula, but only for those Brillouin-zone regions that contribute to the conductivities. As demonstrated for Silicon, this massively reduces the involved computational cost, and hence paves the way towards affordable, fully anharmonic predictions of electronic heat and charge transport coefficients.

[1] B. Holst, M. French, and R. Redmer, Phys. Rev. B **83**, 235120 (2011).

[2] S. Poncá, E. R. Margine, and F. Giustino, Phys. Rev. B **97**, 121201 (2018).

HL 36.4 Thu 10:15 POT 151

Semiconductor to Semimetal Transition in Bi-based Core-Shell Nanowires — MAXIMILIAN KOCKERT¹, RÜDIGER MITDANK¹, MAHNI MÜLLER¹, HONGJAE MOON², JONGMIN KIM², WOYOUNG LEE², and •SASKIA FISCHER¹ — ¹Humboldt-Univ. zu Berlin, Germany — ²Yonsei Univ., Seoul, Korea

The full-thermoelectric characterization of individual core/shell Bi-based nanowires is presented. Compressive strain induced by a TiO₂ shell can lead to a band opening increasing the absolute Seebeck coefficient by up to 30 percent compared to bulk at room temperature [1]. If the strain exceeds the elastic limit the semimetallic state is recovered due to the lattice relaxation. The influence of strain on the temperature dependence of the electrical conductivity, the absolute Seebeck coefficient and the thermal conductivity of bismuth/titanium dioxide (Bi/TiO₂) nanowires with different diameters was measured and compared to bismuth (Bi) and bismuth/tellurium (Bi/Te) nanowires and bismuth bulk. Different nano-contacting methods are discussed.

[1] M. Kockert, et al., Nanoscale Advances **3** (2021) 263

30 min. break

HL 36.5 Thu 11:00 POT 151

Comprehensive model for the thermoelectric properties of two-dimensional carbon nanotube networks — •ADITYA DASH, DOROTHEA SCHEUNEMANN, and MARTIJN KEMERINK — Institute for Molecular Systems Engineering and Advanced Materials, Heidelberg University, Im Neuenheimer Feld 225, 69120 Heidelberg, Germany.

Networks of semiconducting single-walled carbon nanotubes (SWCNTs) are interesting thermoelectric materials due to the interplay between CNT and net-

work properties. Here we present a unified model to explain the charge and energy transport in SWCNT networks. We used the steady-state master equation for the random resistor network containing both the intra- and inter-tube resistances, as defined through their 1D density of states that is modulated by static Gaussian disorder. The tube resistance dependence on the carrier density and disorder is described through the Landauer formalism. Electrical and thermoelectric properties of the network were obtained by solving Kirchhoff's laws through a modified nodal analysis, where we used the Boltzmann transport formalism to obtain the conductivity, Seebeck coefficient, and electronic contribution to the thermal conductivity. The model provides a consistent description of previously published experimental data for temperature and carrier density-dependent conductivities and Seebeck coefficients, with energetic disorder being the main factor explaining observed mobility upswing with carrier concentration. For lower disorder, the Lorentz factor obtained from simulation is in accordance with the Wiedemann-Franz law. Suppressed disorder and lattice thermal conductivity can be a key to higher zT.

HL 36.6 Thu 11:15 POT 151

Thermal mapping of a c-plane oriented GaN membrane — •MAHMOUD ELHAJHASAN¹, ISABELL HÜLLEN¹, WILKEN SEEMANN¹, JEAN-FRANÇOIS CARLIN², IAN ROUSSEAU², NICOLAS GRANDJEAN², and GORDON CALLEN¹ — ¹Institute of Solid State Physics, University of Bremen, Germany — ²Institute of Solid State Physics, École Polytechnique Fédérale de Lausanne (EPFL), Switzerland

The thermal characterization of modern semiconductor membranes commonly employed for photonic devices like nanobeam lasers (1D) or photonic crystals (2D), often lacks spatial resolution and appropriate quantification of local temperatures. However exactly these two points are relevant for the detection of e.g., thermal anisotropies, heat leakage, and interfaces providing thermal resistance.

In this contribution, Raman thermometry employing one laser beam (1LRT) is used to quantify the thermal conductivity κ of 250-nm-thick, state-of-the-art, c-plane wurtzite GaN membranes. The same membranes are then probed by two laser Raman thermometry (2LRT) to map the temperature distribution caused by a heating laser via a second probe laser. From such a map, κ is extracted for all in-plane crystal directions, yielding a thermal anisotropy in the c-plane of GaN. Comparing this direct, sub- μm spatially resolved imaging technique to classical Fourier simulations reveals a significant divergence at the heating laser spot pointing to non-diffusive phonon transport.

In conclusion, our comparison of 1LRT and 2LRT measurements provides insight into the applicability of each technique to determine the thermal conductivity of photonic membranes.

HL 36.7 Thu 11:30 POT 151

Tunable preferable orientation of α -FeSi₂ crystallites on silicon surfaces — •TATIANA SMOLIAROVA, IVAN TARASOV, and ULF WIEDWALD — Faculty of Physics and Center for Nanointegration (CENIDE), University of Duisburg-Essen, 47057, Duisburg, Germany

Nowadays, one of the most important applications of silicon (Si) and Si-based functional materials is microelectronics. Silicon forms compounds in the form of solid solutions or intermetallic compounds * silicides. Metallic α -FeSi₂ phase can be used as a contact material to silicon or to the semiconducting β FeSi₂ phase with good ohmic characteristics.

In this work, we discuss the growth of α -FeSi₂ submicron-size crystallites on gold-activated and gold-free p-Si(001), p-Si(110) and p-Si(111) surfaces via molecular beam and reactive epitaxy. The study reveals that the surfactant-assisted mediated epitaxy regulates morphology and the preferable orientation relationship (OR) of the crystallites to Si. According to the X-ray diffraction, strongly preferable ORs are α -FeSi₂(001)//Si(001), α -FeSi₂(001)//Si(111), α -FeSi₂(001)//Si(110) for gold-activated and α -FeSi₂(111)//Si(001), α -FeSi₂(211)//Si(110), α -FeSi₂(112)//Si(111) for gold-free Si substrates. Thus, the orientation control of fabricated α -FeSi₂ crystallites can be used for tuning electron transport across the metal/semiconductor interface.

We acknowledge Ivan Yakovlev and Ivan Nemtcev (Krasnoyarsk, Russia) for assistance in sample preparation.

HL 37: Materials and devices for quantum technology II

Time: Thursday 9:30–12:15

Location: POT 251

HL 37.1 Thu 9:30 POT 251

Long-range shuttling of single electron by Si/SiGe conveyor — •RAN XUE¹, MAX BEER¹, JIHI-SIAN TU², SIMON HUMPHOHL¹, INGA SEIDLER¹, TOM STRÜCK¹, TOBIAS HANGLEITER¹, HENDRIK BLUM¹, and LARS R SCHREIBER¹ — ¹JARA-FIT Institute for Quantum Information, Forschungszentrum Jülich GmbH and RWTH Aachen University, Aachen, Germany — ²Helmholtz Nano Facility (HNF), Forschungszentrum Jülich, Jülich, Germany

Electrostatically confined electrons are promising candidates for spin-qubits due to their long coherence in ²⁸Si/SiGe. To scale up qubit numbers and integrate control electronics, we propose to use a 10 μm long quantum bus (QuBus), which requires four control lines independent of the shuttle distance. Providing a propagating sinusoidal potential in a gate-defined 1D channel, adiabatic movement of a quantum dot filled by a single electron representing the qubit has achieved a shuttling fidelity of $99.4 \pm 0.02\%$ in a 420 nm long QuBus [1]. Here, we propose and demonstrate the tomography of a single electron shuttling process on

a scaled-up 10 μm long QuBus. The electron is shuttled forth and back over micrometer-scale by a time-reversible pulse composed by only four sine-waves. Our tomography measures the shuttling fidelity and detects shuttling failures such as electron tunneling across pockets of the sinusoidal shuttling potential due to local potential disorder [2].

[1] Seidler, I. *et al.*, npj Quantum Inf. 8: 100 (2022).

[2] Langrock, V. *et al.*, arXiv: 2202.11793 (2022).

Work funded by the DFG under project number EXC 2004/1-390534769.

HL 37.2 Thu 9:45 POT 251

Telecom C-band photon emission from (In,Ga)As quantum dots generated by filling nanoholes in In_{0.52}Al_{0.48}As layers — •DENNIS DEUTSCH, CHRISTOPHER HENRIK BUCHHOLZ, KLAUS JÖNS, and DIRK REUTER — Universität Paderborn, Warburger Str. 100, 33098 Paderborn

Quantum communication technology requires sources for the on-demand generation of entangled photon pairs, preferably in the optical C-band for long-haul fiber-based communication. Quantum dots grown on InP substrates seem to be an ideal candidate: Here photon pairs can be generated from the biexciton-exciton cascade with emission wavelengths around 1.55 μm . However, the conventional approach of Stranski-Krastanov grown InAs quantum dots leads to several challenges related to the strain driven growth. In this study we report on an alternative approach allowing for unstrained quantum dots by filling of local droplet etched (LDE) nanoholes. The quantum dots are embedded in an In_{0.52}Al_{0.48}As matrix lattice-matched to the InP substrate and grown by molecular beam epitaxy. We show detailed investigations of the hole morphology measured by atomic force microscopy. Statistical analysis of nanoholes shows promising symmetry for a good number of them when etched at optimized temperatures. Furthermore, we see that filling of the holes with In_{0.53}Ga_{0.48}As works under the right growth conditions. By capping the filled holes and performing photoluminescence measurements we observe emission in the O-band up into the C-band depending on the filling height of the nanoholes.

HL 37.3 Thu 10:00 POT 251

Scalable Quantum Memory Nodes using nuclear spins in Silicon Carbide — •SHRAVAN KUMAR PARTHASARATHY^{1,2}, BIRGIT KALLINGER¹, FLORIAN KAISER^{3,4}, PATRICK BERWIAN¹, DURGA DASARI^{3,4}, JOCHEN FRIEDRICH¹, and ROLAND NAGY² — ¹Fraunhofer Institute for Integrated Systems and Device Technology (IISB), Erlangen, Germany — ²Chair of Electron Devices, Friedrich-Alexander-Universität Erlangen-Nürnberg (FAU), Erlangen, Germany — ³3rd Institute of Physics and Stuttgart Research Center of Photonic Engineering (SCoPE), University of Stuttgart, 70569 Stuttgart, Germany — ⁴Center for Integrated Quantum Science and Technology (IQST), Germany

The ultimate motivation of my project is to address the possibility of building a quantum analogue of Internet of Things in order to improve the standards of quantum information processing. A distributed quantum computing network which is capable of achieving this goal, would require large sets of memory nodes. The challenge in this field has been in realizing such memory nodes with features for scalable quantum computing. Solid state spins in 4H-Silicon Carbide (4H-SiC) provides a suitable platform in achieving this goal wherein a controlled generation of highly coherent qubit registers using nuclear spins (¹³C or ²⁹Si) and silicon vacancy color centers (V_{Si}^- center) are possible. A numerical model is hence established in order to investigate the influence of material or experimental parameters on number of such controllable nuclear spins. This study would be helpful in finding the optimal parameters to maximize qubits in Quantum Memory Nodes.

HL 37.4 Thu 10:15 POT 251

Coherent Conveyor Mode Shuttling of Electrons and their Spin — •TOBIAS OFFERMANN, TOM STRUCK, LINO VISSER, MATS VOLMER, RAN XUE, HENDRIK BLUHM, and LARS R. SCHREIBER — JARA-FIT Institute for Quantum Information, Forschungszentrum Jülich GmbH and RWTH Aachen University, Aachen, Germany

A missing key technology for scaling up electron spin qubits in ²⁸Si/SiGe is a coherent medium-range coupling between two qubits. It would enable a sparse-qubit architecture and makes space for signal-line fan-out and cryogenic electronics tiles integrated on the qubit chip. We present an approach named *conveyor-mode shuttling*, which relies on physically transporting the electron by a propagating wave-potential with simple input signals across an electrostatically defined quantum-channel [1,2]. We will introduce high fidelity single electron shuttling at a velocity high enough to reduce the shuttling time well below the typical spin-dephasing time of natural silicon. We show initialisation of the shuttle device on one end by two electrons in a spin-singlet. Shuttling only one of these electrons, we generate a separated Einstein-Podolsky-Rosen spin-pair. Combining the electrons by shuttling again, we detect their spin-singlet fraction by Pauli-spin blockade and explore the spin-coherence of the shuttling process.

[1] Seidler, I. *et al.*, npj Quantum Inf. 8: 100 (2022).

[2] Langrock, V. *et al.*, arXiv: 2202.11793 (2022).

Work funded by the DFG under project number EXC 2004/1- 390534769.

HL 37.5 Thu 10:30 POT 251

Prospects for electrically controlled, directly fiber-coupled circular Bragg gratings as high performance quantum light sources — •LUCAS RICKERT¹, FRIDTJOF BETZ², MATTHIAS PLOCK², SVEN BURGER^{2,3}, and TOBIAS HEINDEL¹ — ¹Institut für Festkörperphysik, Technische Universität Berlin, Hardenbergstraße 36, 10623 Berlin, Germany — ²Zuse Institute Berlin, Takustraße 7, 14195 Berlin, Germany — ³JCMwave GmbH, Bolivarallee 22, 14050 Berlin, Germany

Semiconductor quantum dots in (hybrid) circular Bragg gratings (hCBGs) have shown seminal performances as bright sources of indistinguishable entangled photons at wavelengths below 900 nm and have also shown significant boosts in performances for telecom wavelength single photons sources. To fully harness their potential for photonic quantum technologies, a direct coupling to single mode fibers (SMFs) for robust quantum light sources as well as designs with gate-contacts allowing for electrical control of the embedded emitters charge environment and spectral Stark-tuning is desirable. In this contribution, we present hCBG-based designs enabling electrical control, which are numerically optimized to show >85% direct fiber coupling efficiencies to SMFs, and Purcell enhancements >20 at operation wavelengths for 930 nm, 1310 nm and 1550 nm respectively. We investigated extensively the impact on performance of deviations in the fabrication using machine-learning algorithms, and show our recent progress in the experimental realization of directly fiber-coupled hCBG single photon sources.

30 min. break

HL 37.6 Thu 11:15 POT 251

X-ray nanobeam measurements of nanoscale elastic strain in electron shuttling devices — •CEDRIC CORLEY-WICIAK¹, MARVIN H. ZOELLNER¹, IGNATI ZAITSEV¹, COSTANZA L. MANGANELLI¹, EDOARDO ZATTERIN², KETAN ANAND¹, AGNIESZKA A. CORLEY-WICIAK¹, FELIX REICHMANN¹, YUJI YAMAMOTO¹, MICHELE VIRGILIO³, LARS SCHREIBER⁴, WOLFRAM LANGHEINRICH⁵, CARSTEN RICHTER⁶, and GIOVANNI CAPELLINI^{1,7} — ¹IHP, Frankfurt (Oder), Germany — ²ESRF, Grenoble, France — ³Department of Physics, Università di Pisa, Italy — ⁴JARA Institute, RWTH Aachen University, Germany — ⁵Infineon Technologies Dresden GmbH und Co.KG, Germany — ⁶IKZ, Berlin, Germany — ⁷Dipartimento di Scienze, Università Roma Tre, Italy

Recently, spin qubits housed in electrostatic quantum dots in epitaxial Si/SiGe heterostructures have evolved by the demonstration of multi-qubit algorithms. One key requirement for realizing arrays of qubits with shared gate control is highly homogenous lattice strain in the Si quantum well (QW) hosting the qubits. We leverage Scanning X-ray Diffraction Microscopy (SXDM), performed at the beamline ID01/ESRF, to map the strain tensor around several fully CMOS compatible electron shuttling devices for qubit interconnection (QuBus). We observe local modulations of the lattice strain by several 10^{-4} , which are translated into spatially resolved profiles for the energy of the conduction band valley state, showing local fluctuations > 1meV. Thus, our results demonstrate that material inhomogeneities must be considered in the design for scaled quantum processors.

HL 37.7 Thu 11:30 POT 251

Quantum optimal control for conveyor-mode single-electron shuttling in Si/SiGe — •ALESSANDRO DAVID¹, VEIT LANGROCK², JULIAN D. TESKE³, LARS R. SCHREIBER³, HENDRIK BLUHM³, TOMMASO CALARCO¹, and FELIX MOTZOL¹ — ¹Institute of Quantum Control (PGI-8), Forschungszentrum Jülich GmbH, Jülich, Germany — ²Institute of Theoretical Nanoelectronics (PGI-2), JARA-FIT Institute for Quantum Information, Forschungszentrum Jülich GmbH, Jülich, Germany — ³JARA-FIT Institute for Quantum Information, Forschungszentrum Jülich GmbH and RWTH Aachen University, Aachen, Germany

A quantum bus (QuBus) is a promising candidate for the scalability of spin-qubits quantum computers. We consider a gated Si/SiGe quantum well capable of shuttling electrons smoothly by a translating confining potential (conveyor-mode). Dephasing coupling with valley degree of freedom and geometry of the quantum well dictate a maximum shuttling speed to keep the electron state adiabatically in the ground state and avoid excitation of the valley state. In this work we use the position of the electron as a control parameter and we optimise the trajectory of the electron to show how the electron can be shuttled faster and with lower infidelity compared to the adiabatic regime.

HL 37.8 Thu 11:45 POT 251

Determination of optical dipole orientation of quantum emitters in monolayer MoS₂ — •ANNA HERRMANN, KATJA BARTHELMI, LUKAS SIGL, MIRCO TROUE, THOMAS KLOKKERS, JONATHAN FINLEY, CHRISTOPH KASTL, and ALEXANDER HOLLEITNER — Walter Schottky Institut and Physics Department, Technische Universität München, Am Coulombwall 4a, Garching bei München, Germany

Single photon emitters in 2D materials are interesting for applications in quantum science and technology. Recently, we demonstrated that defect-based single photon emitters can be site-selectively generated in monolayer MoS₂ van der Waals heterostacks by a focused beam of helium ions with an overall positioning

accuracy below 10 nm. The emitters show a luminescence with narrow emission lines around 1.75 eV. To determine the optical dipole orientation of the emitters we discuss the far-field photoluminescence intensity distribution of the defect emission in a back-focal plane geometry. The data is compared to simulations by an analytical model, which describes the dipolar emission pattern in the dielectric environment of the heterostructure. The demonstrated approach allows determining the relative contributions for in- and out-of-plane transition dipole moments of quantum emitters.

HL 37.9 Thu 12:00 POT 251

Interface control of valley splitting in Si-based heterostructures — •JONAS R F LIMA^{1,2} and GUIDO BURKARD¹ — ¹Department of Physics, University of Konstanz, D-78457 Konstanz, Germany — ²Departamento de Física, Universidade Federal Rural de Pernambuco, 52171-900, Recife, PE, Brazil

HL 38: Functional semiconductors for renewable energy solutions I

Time: Thursday 9:30–11:45

Location: POT 6

HL 38.1 Thu 9:30 POT 6

Energy landscape of B-Si defects calculated by DFT for modelling light-induced degradation in silicon — •AARON FLÖTOTTO¹, WICHARD J.D. BEENKEN¹, KEVIN LAUER^{1,2}, and ERICH RUNGE¹ — ¹Technische Universität Ilmenau, Institut für Physik, Ilmenau, Germany — ²CiS Forschungsinstitut für Mikrosensorik GmbH, Erfurt, Germany

Boron is a technologically highly relevant p-dopant of silicon. Often, boron does not simply replace a silicon atom, but forms a B-Si pair that shares one lattice site. Several metastable pair configurations exist, with boron being closer to either a more substitutional or a more interstitial position. Using DFT, we calculated all neutral and charged metastable configurations of these defects and – using the Nudged Elastic Band algorithm – the minimal-energy paths between them. The resulting energy minima, barrier heights, and conversion rates will be discussed within the A_{Si-Si_i} model for light-induced degradation (LiD) as suggested by K. Lauer et al. [1].

[1] for a recent review, see: K. Lauer, K. Peh, D. Schulze, T. Ortlev, E. Runge, and S. Krischok, "The A_{Si-Si_i} Defect Model of Light-Induced Degradation (LiD) in Silicon", *phys. status solidi A* 219, 2200099 (2022), <https://doi.org/10.1002/pssa.202200099>

HL 38.2 Thu 9:45 POT 6

Nanoscale characterization for understanding performance limitations in water splitting photoelectrodes — LUKAS WOLZ¹, HARISHANKAR BALAKRISHNAN², GUANDA ZHOU¹, IAN SHARP¹, ACHIM HARTSCHUH², and •JOHANNA EICHHORN¹ — ¹Walter Schottky Institute, TU München, Am Coulombwall 4, 85748 Garching, Germany — ²Department of Chemistry, LMU München, Butenandtstr. 5-13, 81377 Munich, Germany

Economically viable systems for photoelectrochemical water splitting are often based of polycrystalline or nanostructured semiconductor thin films. Their nano- to micrometer properties often control critical processes, such as efficiency and stability, of the macroscale system.

Here, we aim at resolving local heterogeneities and at elucidating their effect on light-driven processes of BiVO₄ thin films using a correlative nanoscale approach. Scanning nearfield infrared microscopy shows varying absorption from VO₄ stretching modes across the film which correlates with local photoconductivity heterogeneities revealed by photoconductive atomic force microscopy. Furthermore, local temperature-dependent current-voltage spectroscopy in controlled gas environment shows that the low intrinsic bulk conductivity limits the electron transport [1], and that adsorbed oxygen acts as surface trap states for electrons [2]. Overall, combining insights from different nanoscale techniques generates a comprehensive picture of charge transport and transfer at the nanoscale, which provides the foundation for the rational design of durable and efficient solar fuel devices.

[1] *Nat. Commun.* 2597 (2018) [2] *ACS Interfaces*, 10, 35129 (2018)

HL 38.3 Thu 10:00 POT 6

Calibration of low temperature photoluminescence of boron doped silicon with increased temperature precision — •KATHARINA PEH¹, AARON FLÖTOTTO¹, KEVIN LAUER^{1,2}, DIRK SCHULZE¹, and STEFAN KRISCHOK¹ — ¹TU Ilmenau, Institut für Physik und Institut für Mikro- und Nanotechnologien, 98693 Ilmenau, Germany — ²CiS Forschungsinstitut für Mikrosensorik GmbH, Konrad-Zuse-Str. 14, 99099 Erfurt, Germany

Low-temperature photoluminescence spectroscopy (LTPL) enables the determination of the dopant concentration of shallow impurities in silicon. We present a method which allows the determination of the boron concentration in silicon in a range from 10^{11} cm^{-3} to 10^{17} cm^{-3} at temperatures from 4.2 to 20 K with increased temperature accuracy. This method requires only one calibration function for the photoluminescence intensity ratio $I_{B_{TO(BE)}}/I_{I_{TO(FE)}}$. We obtain the

The spin of electrons is a natural two-level system that works as an excellent qubit. The control of the spin of isolated electrons in silicon-based heterostructures is very promising for high performance and scalable qubits. To achieve this, it is very important to predict and control the valley splitting in this system, since a very fast qubit relaxation is obtained, for instance, when the valley splitting becomes equal to the qubit Zeeman splitting. For this reason, different works have investigated the valley splitting in silicon spin qubits, both experimentally and theoretically. In this work we used the effective mass theory, which enables us to obtain the electron envelope function, to predict the valley splitting of silicon-based heterostructures, where we consider fluctuations in the interfaces of the heterostructure. We obtain how the valley splitting can be tuned by the width of the interfaces and compare our results with results obtained by other methods.

measurement temperature from the intrinsic silicon photoluminescence line of free excitons ($I_{TO(FE)}$) using a fitting method, which distinguishes the *TO* and *LO* components of the free exciton peak. The determined calibration function is $I_{B_{TO(BE)}}/I_{I_{TO(FE)}} = (5.8 \pm 0.08) \cdot 10^{-18} \text{ cm}^3 \cdot c_{boron} \cdot e^{(56.7 \pm 0.7 \text{ K})/T}$. The obtained exciton binding energy to boron, $E_b = 4.9 \pm 0.1 \text{ meV}$, agrees well with literature data.

HL 38.4 Thu 10:15 POT 6

Coaxial Nanowire-in-Nanopore Arrays Enabling Anti-Agglomeration and Reliable Length Retention — •CHENGZHAN YAN, HUAPING ZHAO, and YONG LEI — Fachgebiet Angewandte Nanophysik, Institut für Physik & IMN Macro-Nano, Technische Universität Ilmenau, 98693 Ilmenau, Germany.

Nanowire arrays, a typical one-dimensional (1D) nanostructure used in energy storage systems, have significantly improved the electrochemical performance by optimizing the active material distribution and promoting the charge transport kinetics in energy storage systems. Notably, nanowire arrays with well-defined arrangements and high aspect ratios are of particular interest. To this end, one prevailing strategy is to combine ordered templates with wet chemical techniques. However, nanowires with high aspect ratios have a more severe tendency to agglomerate because of uneven capillary forces, which leads to poor arrangement reliability and degrades the electrochemical performance. Herein, the ultra-thin honeycomb alumina nanopores are constructed to ensure the structural stability of nanowire arrays, achieving a reliable quadrupling of the length. Based on the integrated nanowire-in-nanopore architecture, MnO₂ and polypyrrole are further electrodeposited on these free-standing nanowires to form vertically aligned core-shell 1D nanostructure arrays as cathodes and anodes for micro-supercapacitors (MSCs). Attributed to the high specific surface area and low charge diffusion resistance, these MSCs attain remarkably improved energy density, rate performance and lifespan.

30 min. break

HL 38.5 Thu 11:00 POT 6

Tails states, Voc loss and semiconductor compensation — •SUSANNE SIEBENTRITT and OMAR RAMIREZ — University of Luxembourg, Laboratory for Photovoltaics

It has been shown for many solar cell absorbers that Voc loss correlates with the Urbach energy, which describes the decay of tail states into the band gap. In chalcopyrites it was furthermore observed that heavy alkali postdeposition treatments reduce both: Urbach energy and Voc loss. This behaviour has been attributed to passivation of grain boundaries. However, recently we have shown, that alkali treatment in single crystalline films without grain boundaries also leads to a reduction of Voc loss and Urbach energies. This behaviour can be traced back to a reduced compensation by increasing the doping level. It is to be expected that a similar mechanism plays a role in polycrystalline films. Part of the dependence of the Voc loss on Urbach energy can be attributed to radiative and non-radiative recombination in and through tail states. However, the dependence is stronger than would be expected from the increased recombination. We now understand that this is due to a simultaneous effect: increasing doping increases Voc and decreases tail states. Thus we propose, that one effect of heavy alkali treatment is due to the observed increase of Na doping inside the grains, because it increases the net-doping, reduces tail states and thereby reduces radiative and non-radiative recombination. All this increases Voc.

HL 38.6 Thu 11:15 POT 6

Dependence of the activation energy of light-induced degradation (LID) in silicon on the illumination intensity — •KEVIN LAUER^{1,2}, KATHARINA PEH¹, DIRK SCHULZE¹, and STEFAN KRISCHOK¹ — ¹Technische Universität Ilmenau, Institut für Physik und Institut für Mikro- und Nanotechnologien, Ilmenau, Germany — ²CIS Forschungsinstitut für Mikrosensorik GmbH, Erfurt, Germany

It was found that the activation energy of the dissociation process of the acceptor-iron defects (A_{Si-Fe}) in silicon depends on the illumination intensity.[1] This implies that besides the thermal energy an additional supply of energy due to e.g. carrier recombination is possible in that defect reaction. To check whether this is also the case for the slow process of the light-induced degradation (LID) in silicon,[2] which can be explained by acceptor-silicon defects (A_{Si-Si}).[3] We measured the activation energy for the slow LID process for different illumination intensities. No impact of the illumination intensity on the activation energy of the slow LID process could be found indicating a pure thermally activated process.

[1] K. Lauer, C. Möller, D. Debbih, M. Auge, and D. Schulze, *Solid State Phenom.* 242, 230 (2015).

[2] J. Lindroos and H. Savin, *Sol. Energy Mater. Sol. Cells* 147, 115 (2016).

[3] K. Lauer, K. Peh, D. Schulze, T. Ortlepp, E. Runge, and S. Krischok, *Phys. Status Solidi A* 219, 2200099 (2022).

HL 38.7 Thu 11:30 POT 6

Photoelectrochemical Catalyst Deposition on III-V Semiconductor Surfaces for Direct Solar Water Splitting — •ERICA SCHMITT, MORITZ KÖLBACH, MARGOT GUIDAT, MARCO FLIEG, MAX NUSSHÖR, ANNA-LENA RENZ, and MATTHIAS MAY — Universität Tübingen, Institute of Physical and Theoretical Chemistry, Tübingen, Germany

The conversion of solar electrical energy to chemical energy by the generation of hydrogen is believed to play a key role in the transition towards a sustainable energy system. One approach to generate sustainable hydrogen is the use of III-V photoelectrodes in a highly efficient photoelectrochemical water splitting device. Such fully integrated, monolithic systems have a potentially lower balance of system cost compared to more conventional decoupled PV-electrolysis approaches and have already shown to be highly efficient [1].

The III-V semiconductor-electrolyte interface plays a crucial role in the performance of a photoelectrochemical device. Our work focuses on the photoelectrochemical modification of the semiconductor surface with a suitable catalyst and its stabilization in the harsh environment of an acidic electrolyte under operating conditions while also understanding the underlying physicochemical processes. We present an optimized functionalization process to increase the solar-to-hydrogen efficiency and stability of a photoelectrochemical cell, as well as the electrochemical and spectroscopical characterization using, among other methods, reflection anisotropy spectroscopy. [1] May, M., Lewerenz, HJ., Lackner, D. et al., *Nat. Commun.* 6, 8286 (2015).

HL 39: Organic Electronics and Photovoltaics III (joint session CPP/HL)

Time: Thursday 9:30–12:30

Location: GÖR 226

See CPP 43 for details of this session.

HL 40: Focus Session: Frontiers of Electronic-Structure Theory VI (joint session O/HL)

Time: Thursday 10:30–12:45

Location: TRE Ma

HL 40.1 Thu 10:30 TRE Ma

Nailing down charge-density-wave phase-transition temperatures with downfolding approaches — •ARNE SCHOBERT¹, JAN BERGES², MICHAEL SENTEF³, ERIK VAN LOON⁴, SERGEY BRENER¹, MARIANA ROSSI³, and TIM WEHLING¹ — ¹University of Hamburg, Germany — ²University of Bremen, Germany — ³MPSD, Hamburg, Germany — ⁴Lund University, Sweden

The coupled dynamics of electrons and nuclei is an extremely complex problem of relevance to multiple branches of sciences. *Ab initio* molecular dynamics (AIMD) simulations are often challenging — especially in large systems, on long time scales, in non-equilibrium or in presence of strong correlation. We can overcome these problems by mapping the full *ab initio* density functional theory (DFT) Hamiltonian onto a low-energy lattice model through downfolding. Three different downfolding strategies based on constraining, unscreening and combinations thereof are compared. The best performing model, which properly accounts for anharmonicity, is combined with path integral molecular dynamics (PIMD). This allows us to nail down the transition temperatures of charge-density waves — for instance in 1H-TaS₂.

HL 40.2 Thu 10:45 TRE Ma

Structural and electronic properties of the Ba₈Au_xGe_{46-x} clathrate: an *ab initio* study with cluster expansion — •PETER WEBER, SANTIAGO RIGAMONTI, and CLAUDIA DRAXL — Humboldt-Universität zu Berlin, Berlin, Germany

Intermetallic clathrate materials are promising candidates for high-efficiency thermoelectric applications as they can reach very low thermal conductivity. These materials possess a cage-like structure containing guest atoms. Their electronic properties can be tailored by exploiting the idea of the phonon-glass-electron-crystal which allows for reaching a large figure of merit. We study the compound Ba₈Au_xGe_{46-x} ($0 \leq x \leq 8$), which has raised interest due to its glass-like thermal conductivity [1]. Using the Zintl concept, a semiconducting state is expected to occur at the charge-balanced composition corresponding to $x=5.33$. This composition requires a supercell of at least 3 unit cells (162 atoms) which makes a direct *ab initio* study challenging. We tackle this problem by using the cluster expansion method combined with density-functional theory calculations. In this way, we are able to find the atomic ground-state configurations, together with various properties at different temperatures and gold content. These include lattice constants, bond lengths, site occupancies, as well as band gaps and band structures which are compared with available experimental data.

[1] P.-F. Lory, *et al.* *Nature Communications* 8, 491 (2017).

Topical Talk

HL 40.3 Thu 11:00 TRE Ma

New Opportunities for First Principles Simulations of Thousands of Atoms Using Linear Scaling Density Functional Theory — •LAURA RATCLIFF — University of Bristol, Bristol, United Kingdom

Density-functional theory (DFT) is routinely used to simulate a wide variety of materials and properties, however, standard implementations are cubic scaling with the number of atoms, limiting the system sizes which can be treated. This motivated the development of alternative implementations of DFT, which exploit the nearsightedness principle by using a localised description of the system, leading to algorithms with linear scaling (LS) cost which can treat large systems containing tens of thousands of atoms. One approach, which is implemented in the wavelet-based BigDFT code, uses localised orbitals, also known as support functions, which are optimised to reflect their local chemical environment, and thus constitute an accurate minimal basis set. Beyond reduced computational cost, the localised support function description also facilitates additional developments, such as the ability to automate a fragment-based description. In this talk we will present the formalism behind LS-BigDFT, including some examples of the new types of systems and analyses which are opened up by the ability to treat such large systems. We will also describe recent developments in PyBigDFT, a python-based interface which aims to simplify the usage of LS-BigDFT for complex systems and workflows.

15 min. break

HL 40.4 Thu 11:45 TRE Ma

Fully Anharmonic Electronic Transport Coefficients from Temperature-dependent Spectral Functions — •JINGKAI QUAN, MATTHIAS SCHEFFLER, and CHRISTIAN CARBOGNO — The NOMAD Laboratory at the FHI of the Max-Planck-Gesellschaft and IRIS-Adlershof of the Humboldt-Universität zu Berlin The combination of *ab initio* molecular dynamics (aiMD) and band-structure unfolding techniques provides a non-perturbative route to obtain temperature-dependent spectral functions. [1] In contrast to commonly employed perturbative approaches [2], this technique accounts for all orders of anharmonic and vibronic couplings. Building on this non-perturbative formalisms, we here present an approach to obtain electronic transport coefficient such as the electrical conductivity using Kubo's formulation of the fluctuation-dissipation theorem. By this means, all relevant quantities, including electron lifetimes, are obtained from the unfolded, self-consistent wave functions computed during the aiMD runs. We critically benchmark the approach against existing perturbative data for harmonic systems, carefully analyzing to which extent short- and long-range couplings are captured with increasing supercell size. Furthermore, we demonstrate

the advantages of the proposed approach for strongly anharmonic systems, for which perturbative approaches become unreliable.

[1] M. Zacharias, M. Scheffler, and C. Carbogno, *Phys. Rev. B* **102**, 045126 (2020).

[2] F. Giustino, *Rev. Mod. Phys.* **89**, 015003 (2017).

HL 40.5 Thu 12:00 TRE Ma

Accurate prediction of vibrational spectra for solid state systems from ab initio molecular dynamics — •EKIN ESME BAS, THOMAS HEINE, and DOROTHEA GOLZE — Chair of Theoretical Chemistry, Technische Universität Dresden, 01062 Dresden, Germany

We present a highly accurate computational method to calculate vibrational spectra for solid state materials, primarily for covalent-organic frameworks (COFs). IR and Raman spectra are important tools that are frequently used for material characterization. However, the experimental spectra are often difficult to interpret without aid from theory. The computation of IR and Raman spectra is usually based on the harmonic approximation where molecular vibrations can be determined as normal modes from the second derivatives of the electronic energy with respect to the coordinates. Although this method is more straightforward and computationally less expensive, anharmonic modes cannot be captured. Thus, we employ an AIMD (ab initio molecular dynamics) based approach to include vibrational anharmonicities. Power, IR and Raman spectra can then be calculated via a Fourier transformation of the time correlation functions of velocities, dipole moments and polarizability tensors, respectively [1]. We discuss different approaches to compute dipole moments and polarizabilities. We present the power, IR and Raman spectra we calculated for COF-1, and we compare our AIMD based approach to the spectra obtained via harmonic approximation and experiment.

[1] M. Thomas, M. Brehm, R. Fligg, P. Vöhringer, B. Kirchner. *Phys. Chem. Chem. Phys.*, 6608-6622, 5, 2013.

HL 40.6 Thu 12:15 TRE Ma

Anharmonic Fingerprints from THz Modes of Polyacene Crystals — •PAOLO LAZZARONI, SHUBHAM SHARMA, and MARIANA ROSSI — Max Planck Institute for the Structure and Dynamics of Matter, Hamburg, Germany

Organic molecular crystals exhibit strong lattice anharmonicity, especially in

the collective motions that are governed by intermolecular interactions and lie in the low-frequency THz range [1]. Inspired by recent observations that the polarization-orientation (PO) Raman spectra can give exquisite insight into the anharmonic couplings between modes [2], we devise a first-principles framework that can reproduce, explain and give quantitative insight into the type and strengths of mode coupling. This framework is based on machine-learned potentials and polarizability tensors trained on *ab initio* molecular dynamics trajectories [3]. We obtain results through the time-correlation formalism for PO Raman signals, retaining the full anharmonic nature of the potential, and perform a novel analysis of effective temperature-dependent mode couplings from our trajectories. [1] M. Asher *et al.*, *Adv. Mater.* **32**, 1908028 (2020) [2] N. Benshalom *et al.*, arXiv:2204.12528 (2022) [3] N. Raimbault *et al.*, *New J. Phys.* **21** 105001 (2019)

HL 40.7 Thu 12:30 TRE Ma

A first-principles Newns-Anderson chemisorption function applied to ultra-fast electron transfer — •SIMIAM GHAN¹, ELIAS DIESEN¹, CHRISTIAN KUNKEL¹, KARSTEN REUTER¹, and HARALD OBERHOFER² — ¹Fritz-Haber-Institut der MPG, Berlin, Germany. — ²University of Bayreuth, Bayreuth, Germany

We offer a method to calculate the electronic couplings H_{ad} between an adsorbate and substrate in an ab-initio fashion. The couplings are acquired by projection of the Kohn-Sham Hamiltonian onto a diabatic basis[1]. By averaging over the Brillouin Zone, it becomes possible to calculate a convergent chemisorption function of Newns and Anderson[2], which gives the energetic broadening of an adsorbate frontier orbital upon adsorption. This broadening corresponds to the experimentally-observable lifetime of an electron in the state, which we confirm for the case of core-excited $Ar^*(2p_{3/2}^{-1}4s)$ atoms on a number of transition metal surfaces[3].

We find that the (tunneling) model captures and elucidates aspects of energy-dependence, spin, phase cancellation and k-space in the electron transfer process, in particular suggesting a significant role played by the surface d-bands. Given the prevalence of electronic couplings - and the chemisorption function - in theoretical models, we discuss potential for further applications.

[1] S. Ghan *et al.*, *J. Chem. Theory Comput.* **16**, 7431 (2020).

[2] D. Newns, *Phys. Rev.* **178**, 3, 1123 (1969).

[3] F. Blobner *et al.*, *Phys. Rev. Lett.* **112**, 086801 (2014).

HL 41: Oxide Semiconductors I: Ga₂O₃

Time: Thursday 15:00–17:00

Location: POT 81

HL 41.1 Thu 15:00 POT 81

Thermal Conductivities of Ga₂O₃ Polymorphs: Analysis of Anharmonicity and Anisotropy — •SHUO ZHAO, MATTHIAS SCHEFFLER, and CHRISTIAN CARBOGNO — The NOMAD Laboratory at the FHI of the Max-Planck-Gesellschaft and IRIS-Adlershof of the Humboldt-Universität zu Berlin

Gallium oxide (Ga₂O₃) is an ultra-wide bandgap material with substantial potential for electronics, e.g., in field effect transistors [1]. In this context, an atomistic understanding of its heat transport characteristics is essential for thermal management. For this purpose, we compute the lattice thermal conductivity of the α -, β -, and κ -polymorphs of Ga₂O₃ using the *ab initio* Green-Kubo formalism [2,3] that incorporates all orders of anharmonic effects via first-principle molecular dynamics. We discuss the role of anharmonic effects for the different polymorphs and investigate their influence on the anisotropy of the conductivity tensor. Our results provide guiding rules for maximizing and minimizing thermal transport in thin Ga₂O₃ films.

[1] M. Higashiwaki, *et al.*, *Appl. Phys. Lett.* **100**, 013504 (2012).

[2] C. Carbogno, R. Ramprasad, and M. Scheffler, *Phys. Rev. Lett.* **118**, 175901 (2017).

[3] F. Knoop, M. Scheffler, and C. Carbogno, arXiv:2209.01139 (2022).

HL 41.2 Thu 15:15 POT 81

Strain-induced polymorph conversion in gallium oxide via focused ion beam irradiation — •UMUTCAN BEKTAS, PAUL CHEKHONIN, and GREGOR HLAWACEK — Insitute of Ion Beam Physics and Materials Research, Helmholtz-Zentrum Dresden-Rossendorf, 01328 Dresden, Germany

Monoclinic β -Ga₂O₃ is chemically and thermally the most stable compound compared to its other polymorphs. It is a promising semiconductor material for power electronics, optoelectronics, and batteries. However, controlling the metastable polymorph phases is challenging, and the fabrication technology at the nanoscale is immature. Our goal is to understand and control the polymorph conversion, so we can establish new fabrication methods of single-phase polymorph coatings, buried layers, multilayers, and different nanostructures in gallium oxide.

Under ion beam irradiation, most semiconductors show transformation from crystalline to amorphous structure due to ion beam induced damage. However, it is observed that, this transformation is suppressed in gallium oxide, and a poly-

morph conversion is observed instead. Here, we use Gallium and Neon focused ion beams (FIB) from different sources (GFIS, LMIS) to create local strain and induce the polymorph transition. After irradiation, characterization of the exposed areas was conducted by electron backscatter diffraction (EBSD) and atomic force microscopy (AFM). First results indicate that the strain created by the FIB irradiation leads to a local transformation of beta gallium oxide to another polymorph.

HL 41.3 Thu 15:30 POT 81

Comparative Study of Temperature-dependent Bandgap Transitions in Ga₂O₃ Polymorphs — •BENJAMIN MORITZ JANZEN¹, MARCELLA NAOMI MARGGRAF¹, MORITZ MEISSNER¹, NILS BERNHARDT¹, CONRAD VALENTIN HARTUNG¹, NIMA HAJIZADEH¹, FELIX NIPPERT¹, and MARKUS RAPHAEL WAGNER^{1,2} — ¹Technische Universität Berlin, Institute of Solid State Physics, Germany — ²Paul-Drude-Institut für Festkörperelektronik, Leibniz-Institut im Forschungsverbund Berlin e.V., Germany

We employ a combined experimental-theoretical study to investigate the electronic bandgap transitions in Ga₂O₃ polymorphs as a function of the sample temperature. For this purpose, we apply temperature-dependent UV photoluminescence excitation (PLE) spectroscopy for the β -, κ -, α - and γ -polymorphs in the temperature range between 5 and 300 K and compare the obtained bandgap values with room temperature measurements of the dielectric function as determined by spectroscopic ellipsometry. The obtained temperature dependencies are discussed in conjunction with DFT calculations regarding the effects of electron-phonon coupling.

HL 41.4 Thu 15:45 POT 81

Anisotropic IR active phonon modes and fundamental direct band-to-band transitions in α -(Al_xGa_{1-x})₂O₃ alloys grown by MOCVD — •ELIAS KLUTH¹, A F M ANHAR UDDIN BHUIYAN², LINGYU MENG², HONGPING ZHAO², RÜDIGER GOLDHAHN¹, and MARTIN FENEBERG¹ — ¹Institut für Physik, Otto-von-Guericke-Universität Magdeburg, Germany — ²Department of Electrical and Computer Engineering, The Ohio State University, Columbus, Ohio, USA

The corundum-like Ga₂O₃ polymorph α -Ga₂O₃ is of high research interest as it allows bandgap-engineering by alloying e.g. with α -Al₂O₃, α -In₂O₃, α -Ti₂O₃ and similar materials. Since the corundum-like crystal structure is anisotropic, a direction dependent investigation of the material properties is crucial. m-

plane α -(Al_xGa_{1-x})₂O₃ thin film samples up to $x=0.76$, grown on m-plane sapphire substrate by MOCVD have been investigated by infrared (IR) and visible-ultraviolet (UV) spectroscopic ellipsometry. IR ellipsometry yields the anisotropic IR active phonons and their shift to higher wavenumbers with increasing x . Furthermore, with UV ellipsometry, we find the anisotropic dielectric functions up to 6.6eV and the shift of the fundamental direct band-to-band transitions with increasing x . We report an anisotropic bowing parameter for α -(Al_xGa_{1-x})₂O₃ of $b_{\text{ord}}=2.7\text{eV}$ and $b_{\text{extra}}=2.5\text{eV}$.

15 min. break

HL 41.5 Thu 16:15 POT 81

Adsorption enhanced photocatalytic degradation of Rhodamine B using GdxBi1-xFeO3@SBA-15 (x= 0, 0.05, 0.10, 0.15) nanocomposites under visible light irradiation — •THOMAS CADENBACH¹ and MARIA JOSE BENITEZ² — ¹Universidad San Francisco de Quito, Quito, Ecuador — ²Escuela Politecnica Nacional, Quito, Ecuador

In the present work show that very high removal efficiency of a variety of organic pollutants by GdxBi1-xFeO3@SBA-15 nanocomposites ($x = 0, 0.05, 0.10, 0.15$) under visible light irradiation. Specifically, we study the photocatalytic degradation of dyes using the above nanocomposite materials, with pore volume loadings of 5-25%. We compare the obtained catalytic results for the nanocomposite materials to monodisperse BiFeO3 nanoparticles with a particle diameter of 5.5 nm. We find that the best removal performance is achieved by a 10 vol% Gd0.05Bi0.95FeO3@SBA-15 sample, shown by a complete dye degradation in approximately 3h using extremely low concentrations of the actual active photocatalyst. The superior efficiencies of the nanocomposites, which outperformed their parent compounds, i.e. GdxBi1-xFeO3 nanoparticles as well as unfilled SBA-15, are attributable to a synergistic adsorption enhanced photocatalytic degradation process. The possible mechanism in the photodegradation process was investigated and discussed on the basis of trapping experiments.

HL 41.6 Thu 16:30 POT 81

Electrical and thermal transport properties of ZnGa2O4 — JOHANNES BOY¹, RÜDIGER MITDANK¹, ZBIGNIEW GALAZKA², and •SASKIA FISCHER¹ — ¹Novel Materials Group, Humboldt- Univ. zu Berlin, Germany — ²Leibniz-Institute of Crystal Growth, Berlin, Germany

The first full experimental determination of the low-temperature electrical, thermo-electrical [1] and thermal properties [2] of novel highly pure single crystalline ZnGa₂O₄ is reported. The temperature-dependences of the charge carrier density, mobility, and Seebeck coefficient including phonon drag are discussed between 10 K and 310 K. The thermal conductivity and diffusivity were determined by the so-called 2ω -method. At room temperature the electrical conductivity is 286 S/cm, the mobility 55 cm²/Vs, the Seebeck coefficient 125 $\mu\text{V}/\text{K}$ and the thermal conductivity is 22.9 W/mK. For temperatures above 100 K the phonon transport is limited by phonon Umklapp scattering. At lower temperatures boundary scattering at lattice defects limits the thermal conductivity to 95 W/mK. Therefore, if the cause of boundary scattering is reduced or eliminated, the thermal conductivity of ZnGa₂O₄ may be increased at low temperatures.

[1] J. Boy, *et al.*, AIP Advances 10, 055005 (2020) [2] J. Boy, *et al.*, Materials Research Express 9, 065902 (2022).

HL 41.7 Thu 16:45 POT 81

Temperature- and Polarisation- Dependant Photoluminescence Excitation Spectroscopy of β -Ga₂O₃ — •MORITZ MEISSNER¹, NILS BERNHARD¹, FELIX NIPPERT¹, BENJAMIN M. JANZEN¹, CONRAD V. HARTUNG¹, ZBIGNIEW GALAZKA², and MARKUS R. WAGNER^{1,3} — ¹Technische Universität Berlin, Institute of Solid State Physics, Berlin, Germany — ²Leibniz-Institut für Kristallzüchtung, Berlin, Germany — ³Paul-Drude-Institut für Festkörperelektronik, Berlin, Germany

The anisotropic, ultra-wide bandgap semiconductor β -Ga₂O₃ represents a promising candidate for applications in high power electronics. The high anisotropy of the monoclinic crystal structure and the formation of self-trapped excitons has made a precise determination of the bandgap parameters a challenging endeavor. In this work, we apply polarization- and temperature-dependent photoluminescence excitation spectroscopy (PLE) measurements to study the anisotropy of the optical bandgap transitions. The temperature dependence of the PLE spectra between 5K and 300K provides information on the strength of the electron-phonon coupling and zero temperature bandgap energies along the principal axes of the material. The measurements were performed on the three crystal planes (100), (010) and (001) prepared and polished from the same single bulk crystal grown by the Czochralski method. Our results are discussed in comparison with absorption, transmission, and reflectance spectroscopy data in the literature.

HL 42: Quantum dots: Growth

Time: Thursday 15:00–17:15

Location: POT 151

HL 42.1 Thu 15:00 POT 151

Cone-shell quantum structures with tunable wave functions — •CHRISTIAN HEYN, AHMED ALSHAIKH, KRISTIAN DENEKE, and ROBERT BLICK — Center for Hybrid Nanostructures (CHyN), University of Hamburg

We discuss the tailoring of the wave functions (WF) in strain-free GaAs quantum structures (QS) fabricated using self-assembled local droplet etching (LDE) during molecular beam epitaxy (MBE). Here, Al droplets are deposited on an AlGaAs surface and drill nanoholes with tunable shape and size. Subsequently, the holes are filled with GaAs to form strain-free QS. Dependent on the process parameters, the QS have the shape of a cone or of a cone-shell. In particular the low-density (about $1 \times 10^7 \text{ cm}^{-2}$) cone-shell QS (CSQS) demonstrate sharp excitonic lines with linewidth down to 25 μeV , a precise control of the emission wavelength from 680...810 nm by the nanohole filling level, a neutral exciton fine-structure splitting below 5 μeV , and nearly perfect single photon emission. To tune the WF in CSQS, a vertical electric field is applied which causes a strong charge-carrier separation. The resulting Stark shift is measured using micro-photoluminescence (PL). In combination with simulation results the optical data allow the determination of the QS size and shape. In addition, simulations indicate the transformation of either the electron or the hole WF into a quantum ring. As a further consequence of the field-induced charge-carrier separation, simulations of the exciton-recombination lifetimes predict a variability from nanoseconds up to milliseconds. This suggests CSQS for applications in the field of light storage

HL 42.2 Thu 15:15 POT 151

DNA Origami for low-dimensional electronics — •BORJA RODRIGUEZ-BAREA¹, SHIMA JAZAVANDI-GHAMSARI¹, MADHURI CHENNUR¹, ARCHANA JAIN¹, TURKAN BAYRAK¹, JINGJING YE², RALF SEIDEL², and ARTUR ERBE¹ — ¹Institute of Ion Beam Physics and Material Science, Helmholtz-Zentrum Dresden-Rossendorf, Germany — ²Peter Debye Institute for Soft Matter Physics, Universität Leipzig, Germany

The increasing demand for energy-efficient products gave rise to electronic fabs looking for new green manufacturing processes. Bottom-up techniques have the potential to reduce economic and environmental costs due to implementing low-dimensional materials with unique properties.

We demonstrated the formation of low-dimensional metallic nanostructures based on the DNA origami technique, which can be considered as building blocks for electronic circuits. DNA templates are used as molds to guide the placement and growth of the metallic 1D nanowires. This solution-based and high-resolution nanofabrication technique complements other nanolithography techniques such as electron-beam lithography and thermal scanning probe lithography. Thus, the shape of the nanostructures can be controlled and measured.

Electronic transport on these assemblies is non-ohmic and deteriorates at low temperatures. Temperature-dependent charge transport measurements reveal the dominating mechanisms along these wires.

HL 42.3 Thu 15:30 POT 151

1D Nanowires on DNA mold-based template — •MADHURI CHENNUR¹, BORJA RODRIGUEZ-BAREA¹, JAZAVANDI-GHAMSARI SHIMA¹, ARCHANA JAIN¹, TURKAN BAYRAK¹, ULRICH KEMPER², JINGJING YE², CHRISTOPH HADLICH², RALF SEIDEL², and ARTUR ERBE¹ — ¹Institute of Ion Beam Physics and Material Science, HZDR — ²Peter Debye Institute for Soft Matter Physics, Universität Leipzig, Germany

Sensors have a fundamental role in improving the world around us. For increasing sensitivity and faster response, new bottom-up approaches are required. DNA nanotechnology allows the creation of nanostructure arrays that can serve the purpose.

We study the controlled growth of 1D metallic nanostructures using DNA origami templates. The DNA nanomolds are folded via staples to obtain the desired conformation. The functionalized template provides the active site for a localized seed nanoparticle attachment, thus allowing metallization by electroless plating. We report continuous Pd and Au 1D nanowires based on this method.

The conductance of the assembled nanostructures through two-probe measurements was investigated. Different origami templates lead to diverse metal morphologies, which influence electronic properties. Temperature-dependent measurements determined the transport mechanism of these nanowires, proving the first step toward an electronic nanosensor.

HL 42.4 Thu 15:45 POT 151

Maximizing Homogeneity of GaAs LDE-QDs on Full Wafer Scale — •HANS-GEORG BABIN, TIMO KRUCK, ANDREAS D. WIECK, and ARNE LUDWIG — Lehrstuhl für angewandte Festkörperphysik, Ruhr-Universität Bochum, Deutschland

Local droplet etched GaAs quantum dots (LDE-QDs) are a promising candidate for excellent single and entangled photon sources. [1] Taking further steps towards application, this requires structures of increasing complexity, engineering the electronic and photonic environments of the QDs. [2] In previous studies, we showed how properties of GaAs LDE-QDs can be modulate, containing both 737 nm and 795 nm QDs on a single wafer. [3]

However, in device mass production, for example for creating larger quantum networks, it can also be intriguing to maximize the useable area of the produced wafer. This means for the QDs, that the ensemble should be of high homogeneity locally, but also on global wafer scale. Due to the short deposition times of material during LDE this can be challenging due to intrinsic inhomogeneities. We overcome these problems by matching the substrate rotation time with the material deposition time. With this method we receive light emitting QDs on over 96 % of the wafer, with 86 % of the wafer emitting between 792 nm and 802 nm (peak-center). The mean ensemble FWHM of the QD emission is as low as (11.3±0.4) meV.

[1] Huber, Daniel et al., Nat. Commun. 8 (1), S. 15506 (2017).

[2] Zhai, Liang et al. Nat. Commun. 11 (1), S. 4745 (2020).

[3] Babin et al.; J. Cryst. Growth 591, S. 126713 (2022)

30 min. break

HL 42.5 Thu 16:30 POT 151

Wafer-Scale Epitaxial Modulation of Quantum Dot Density — •NIKOLAI BART^{1,2}, CHRISTIAN DANGEL², PETER ZAJAC¹, NIKOLAI SPITZER¹, MARCEL SCHMIDT¹, KAI MUELLER^{2,3}, ANDREAS D. WIECK¹, JONATHAN FINLEY², and ARNE LUDWIG¹ — ¹Ruhr-Universität Bochum, Lehrstuhl fuer Angewandte Festkoerperphysik, Universitaetsstraße 150, 44801 Bochum, Germany — ²Walter Schottky Institut und Physik Department, Technische Universitaet Muenchen, Am Coulombwall 4, 85748 Garching, Germany — ³Walter Schottky Institut und Department of Electrical and Computer Engineering, Technische Universitaet Muenchen, Am Coulombwall 4, 85748 Garching, Germany

The effect of nanoscale surface roughness on the nucleation of self-assembled InAs quantum dots (QD) is investigated with photoluminescence spectroscopy and atomic force microscopy. We show in-situ control of the roughness modulation by common epitaxial layer-by-layer growth, leaving alternating atomically smooth (rough) surfaces for integer (fractional) completion of a monolayer. We report significant differences in both PL intensity and QD surface density at the critical threshold of nucleation. By varying the underlying GaAs thickness gradients, we create and control 1- and 2-dimensional density modulation patterns on entire 3-inch wafers with modulation periods between a few mm and down to hundreds of μm and densities between 1 and 10 QDs/ μm^2 .

Bart, N., Dangel, C. et al. Wafer-scale epitaxial modulation of quantum dot density. *Nat Commun* 13, 1633 (2022).

HL 43: Semiconductor lasers II

Time: Thursday 15:00–16:45

Location: POT 251

Invited Talk

HL 43.1 Thu 15:00 POT 251

Superradiance as a witness to multipartite entanglement — •FREDERIK LOHOF^{1,2} and CHRISTOPHER GIES^{1,2} — ¹Institute for Theoretical Physics, University of Bremen, Bremen — ²BCCMS, University of Bremen, Bremen

Generation and detection of entanglement is at the forefront of most quantum information technologies. There is a plethora of techniques that reveal entanglement on the basis of only partial information about the underlying quantum state including, in particular, entanglement witnesses. Superradiance refers to the phenomenon of highly synchronized photon emission from an ensemble of quantum emitters that is caused by correlations among the individual particles and has been connected to the presence of multipartite entangled states. We investigate this connection in a quantitative way and discuss the question, whether or not signatures of superradiance from semiconductor nanolasers, e.g. as revealed by photon-correlation measurements, can be interpreted as a witness to detect entanglement in the underlying state of the emitters.

HL 43.2 Thu 15:30 POT 251

Towards a quantum dot based semiconductor optical amplifier for sensing applications in the telecom O-band — •PHILIPP NOACK, MICHAEL ZIMMER, SERGEJ VOLLMER, MICHAEL JETTER, and PETER MICHLER — Universität Stuttgart, IHFG

Optical methods for gas sensing are of great interest in recent technologies. To facilitate the optical detection of gases, a swept laser source can be realized through

HL 42.6 Thu 16:45 POT 151

Statistical Analysis of the Spatial Distribution of MBE Grown InAs Quantum Dots on GaAs(100) — •NORMEN AULER, AKSHAY KUMAR VERMA, ZIYANG ZHANG, and DIRK REUTER — Universität Paderborn, Warburger Str. 100, 33098 Paderborn

Self-assembled InAs quantum dots (QDs) have been intensively studied as model systems for strong three-dimensional confinement over decades and gained considerable interest for applications in quantum technology. The growth by molecular beam epitaxy has been widely studied. In this contribution, we discuss the spatial distribution of InAs QDs grown by solid source molecular beam epitaxy on a GaAs(100) surface for different QD densities. Therefore, we determine the distribution of nearest-neighbor distances from atomic force microscope (AFM) images and compare them to simulated random distributions. We find good agreement under the assumption of a "denuded" zone of ca. 40 nm around each quantum dot center. This means that the QDs are basically randomly distributed as one would expect from the statistical nature of the nucleation process. The diameter of the denuded zone can either be interpreted as the average geometrical diameter of the QDs or the geometrical diameter plus a small distance due to a repelling interaction between QDs mediated by the strain field. We cannot decide this from our experimental data because AFM overestimates the geometrical diameter. For very low quantum dot densities as often required for single dot experiments, it is very difficult to obtain experimental data with statistical significance, whereas simulations can give insight into the spatial distribution.

HL 42.7 Thu 17:00 POT 151

Controlled MOF Growth on Functionalized Carbon Nanotubes — •MARVIN J. DZINNIK¹, NECMETTIN E. AKMAZ¹, ADRIAN HANNEBAUER², PETER BEHRENS², and ROLF J. HAUG¹ — ¹Leibniz Universität Hannover, Institut für Festkörperphysik, Appelstraße 2, 30167 Hannover, Germany — ²Leibniz Universität Hannover, Institut für Anorganische Chemie, Callinstraße 9, 30167 Hannover, Germany

The class of metal organic frameworks (MOFs) is continuously growing. These materials consist of inorganic building blocks, held together by organic linker molecules. Schulze *et al.* [1] showed that adding functionalized multi-walled carbon nanotubes (MWCNTs) to a UiO-66 synthesis drastically decreased the nucleation time. The MOFs preferably grow on the MWCNT until they fully encapsulate it. We demonstrate a mechanism to spatially control the UiO-66 MOF growth on individual carbon nanotubes and deplete the encapsulation. The MWCNTs are drop-casted on a silicon dioxide surface and then locally modified. The samples are then submerged in the synthesis solution. This process leads to a growth of MOF crystals on the MWCNT surface leaving the modified areas depleted. With this method we are able to define lines free of MOF on the length of a single MWCNT down to several hundred nanometres for example to electrically contact the tubes ends.

[1] Schulze, H. A., et al. Electrically Conducting Nanocomposites of Carbon Nanotubes and Metal-Organic Frameworks with Strong Interactions between the two Components. *ChemNanoMat*, 5(9), (2019), 1159-1169.

a semiconductor optical amplifier (SOA) and a tunable MEMS filter.

MOVPE grown quantum dots (QDs) are a prime candidate for providing gain in such a SOA system because of fast charge carrier recovery times and broad gain spectrum created by the statistical distribution of QD sizes.

To this end, we grow InGaAs QDs on a GaAs substrate. We control the growth parameters, such as material flow and growth time, to produce QDs at high densities. We incorporate a dots-in-well structure to shift the emission into the telecom O-band and to improve charge carrier confinement. To provide sufficient gain in a broad spectrum, we especially investigate the properties of vertically stacked QD layers.

After the optimization of the gain structure we perform optical simulations to find the electric field modes of edge-emitting laser structures. Then we incorporate the investigated QDs into electrically pumped edge-emitting structures and characterize the net modal absorption and net modal gain spectra of the devices as antecedent of the SOA.

HL 43.3 Thu 15:45 POT 251

Optical and quantum optical studies of feedback induced chaotic emission in bimodal VCSELs — •ARIS KOULAS-SIMOS, TIMO WILLBURGER, NIELS HERMEIER, CHING-WEN SHIH, IMAD LIMAME, JAMES LOTT, and STEPHAN REITZENSTEIN — Institut für Festkörperphysik, Technische Universität Berlin, 10623 Berlin, Germany

Vertical Cavity Surface Emitting Lasers (VCSELs) have proven to be a key building block for commercial applications in data communication, automotive sys-

tems and sensing as well as for novel complex neuromorphic photonic platforms. Here, we report on signatures of chaotic emission in bimodal GaAs-based quantum well VCSELs subject to delayed optical feedback. In excitation power-dependent microelectroluminescence studies, a clear lasing transition is evident for the strong mode reflected in the strong s-shape form of the I/O-curve accompanied by an abrupt linewidth narrowing, in contrast to the weak mode which exhibits intensity saturation and rollover at high injection currents. In power-dependent photon autocorrelation measurements, super thermal bunching is observed with $g^{(2)}(0)$ reaching values of 3. Revival peaks with a period equal to the round trip time of the external cavity emerge, indicating that the chaotic emission is induced from the optical feedback. This is further validated from signatures of chaotic emission, directly observed in single-shot intensity measurements with a streak camera.

HL 43.4 Thu 16:00 POT 251

Monolithic 850 nm VCSEL Array for QKD via the decoy state protocol — •MICHAEL ZIMMER, MORITZ BIRKHOFF, MICHAEL JETTER, and PETER MICHLER — Institut für Halbleitertechnik und Funktionelle Grenzflächen, Center for Integrated Quantum Science and Technology (IQST) and SCoPE, University of Stuttgart, Allmandring 3, 70569 Stuttgart.

In recent years, the need for secure data communication has increased. Here, the usage of quantum key distribution (QKD) offers fundamental advantages over classical key distribution. However, despite its high level of security, QKD comes along with numerous challenges regarding the application of single photons. In this view, the decoy state protocol offers the possibility to implement QKD using classical light sources such as semiconductor lasers. Here, we present an approach for the realization of a monolithic 850 nm eight VCSEL array capable for QKD via the BB84 and decoy state protocol. Growth of the VCSEL structure takes place by metal-organic vapor-phase epitaxy (MOVPE) on a GaAs substrate. In order to obtain defined light polarization states, each VCSEL features an integrated polarization grating in its light emission window. To allow for operation in the GHz-regime and hence a high key rate generation, the VCSELs are arranged in a co-planar contact design. Electro-optical device characteristics regarding light polarization and high frequency operation are presented.

HL 43.5 Thu 16:15 POT 251

In-situ EBL fabrication of highly homogeneous micropillar laser arrays based on InGaAs quantum dots for neuromorphic computing — •IMAD LIMAME¹, CHING-WEN SHIH¹, SVEN RODT¹, DANIEL BRUNNER², and STEPHAN REITZENSTEIN¹ — ¹Technical Univ. of Berlin, Germany — ²Univ. Bourgogne Franche-Comté, France

As classical computers are reaching their limit, especially in novel fields such as machine learning and artificial intelligence, cost-effective hardware platforms, and new computing architectures are needed. We combine reservoir computing with a nanophotonic platform in an all-optical computing architecture, taking inspiration from neuroscience. Our approach aims to utilize diffractive coupling between 900 micropillars to create a large-scale processing reservoir. Due to the high number of microlasers and the use of a spatial light modulator, laser arrays with low lasing threshold powers and high spectral homogeneity are required. We develop the necessary nanophotonic platform by optimized growth and in-situ electron beam lithography (EBL) fabrication of micropillar laser arrays. The MOCVD growth focuses on increasing the optical gain of the InGaAs quantum dots, used as the gain medium and on the design of the microresonator to decrease the lasing threshold. The realized devices feature thresholds as low as 20 μ W. In the second phase, low temperature in-situ EBL is performed. In this process, first a CL map is recorded to determine the local resonance of the planar microcavity before micropillar with suitable diameter to match a target wavelength are patterned by electron beam lithography. Finally, the resulting micropillar array is investigated via photoluminescence.

HL 43.6 Thu 16:30 POT 251

Multimode lasing in a microdisk nanolaser — •M. L. DRECHSLER¹, F. NIPPERT², L. SUNG-MIN CHOI², M. R. WAGNER², P. BOUCAUD³, S. REITZENSTEIN², and FRANK JAHNKE¹ — ¹Institute for Theoretical Physics, University of Bremen, Bremen, Germany — ²Institute of Solid State Physics, Technische Universität Berlin, Berlin, Germany — ³CRHEA, Université Côte d'Azur, 06560 Valbonne, France

We investigate the quantum emission properties of a GaN-based microdisk nanolasers with a diameter of 2 μ m and β -factor close to unity, pushing the device in the regime of strongly reduced laser threshold. A quantum optical semiconductor laser model based on the cluster expansion technique is used to describe the pump-power dependent emission with one consistent set of material parameters, thereby identifying laser action. Photon correlations quantified by $g^{(1)}(\tau)$ and $g^{(2)}(\tau)$ are an essential tool for this research. Information about the energy spectrum and the detection characteristics of photons is encoded in them. In this device we observe multimode lasing. We show that the mode coupling between well-separated resonator modes has a significant influence on the emission characteristics. Furthermore, we analyze what influence the mode couplings have on photon correlations.

HL 44: Nitrides: Devices

Time: Thursday 15:00–17:00

Location: POT 112

HL 44.1 Thu 15:00 POT 112

Highly doped GaN:Ge/GaN:Mg tunnel junctions for novel GaN-based optoelectronic devices — •CHRISTOPH BERGER, ARMIN DADGAR, and ANDRÉ STRITTMATTER — Otto-von-Guericke-Universität Magdeburg

We report on low resistive GaN-based tunnel junctions (TJs) implemented into optoelectronic devices grown by metalorganic vapor phase epitaxy. Very high donor concentrations, which are mandatory for low-resistive TJs, are achieved by using germanium instead of commonly used silicon. Fabricated TJ-LEDs show an increased light output by more than 60 % in comparison to conventional LEDs employing indium tin oxide contacts while exhibiting a comparable differential resistance of $1.2 \times 10^{-2} \Omega \text{cm}^2$ at a current density of 100 A/cm² and no voltage penalty by the TJ. Higher light output is attributed to a better light extraction efficiency due to V-pits formed within the GaN:Ge layer. We currently apply such tunnel-junctions in edge-emitting laser diodes as well as in vertical-cavity surface-emitting lasers. Furthermore, we will demonstrate cascaded LEDs featuring three tunnel junctions and three pn-junctions stacked on top of each other. Overgrowth of the lower LED sections affects their radiative efficiencies. We investigate different annealing concepts for acceptor activation but also the impact of annealing on the radiative recombination in the InGaN active regions.

HL 44.2 Thu 15:15 POT 112

Mitigating damage induced by strongly ionising radiation in nitride layered structures — •MIGUEL C. SEQUEIRA¹, MAMOUR SALL², FLYURA DJURABEKOVA³, KAI NORDLUND³, ISABELLE MONNET², CLARA GRYGIEL², CHRISTIAN WETZEL⁴, and KATHARINA LORENZ⁵ — ¹HZDR, Dresden, Germany — ²CIMAP, Caen, France — ³University of Helsinki, Finland — ⁴RPI, New York, USA — ⁵INESC-MN, & IST-Universidade de Lisboa, Portugal

Group-III nitrides are well-known for their high radiation resistance, which brings them to extreme radiation environments. GaN is known for having a high resistance to strongly ionising radiation, such as Swift Heavy Ions (SHI) [1,2]. However, the behaviour of other nitrides under this radiation is not well

understood especially when in layered structures (e.g. InGaN/GaN in LED). Here, we inspect how InGaN/GaN quantum wells (QW) resist SHI. We solve the Two-Temperature Model (TTM) using Finite Element Methods to show how the high electronic conductivity of InGaN in a QW acts as a heat sink, reducing the intensity of the ion-induced thermal spike in the entire InGaN/GaN structure. Combining TTM-Molecular Dynamics simulations and Transmission Electron Microscopy images show that the presence of QW significantly decreases the overall radiation damage in a device. The results presented here can lead to new radiation damage mitigation techniques, predict functional changes in devices under long radiation exposure, and ultimately improve device design.

[1] M. C. Sequeira et al., Communications Physics (2021); [2] M. C. Sequeira et al., Small (2022)

HL 44.3 Thu 15:30 POT 112

A guide on designing high performance porous GaN DBRs — •MATTHIAS HOORMANN^{1,2}, FREDERIK LÜSSMANN^{1,2}, FLORIAN MEIERHOFER^{1,2}, JANA HARTMANN^{1,2}, and ANDREAS WAAG^{1,2} — ¹Institute of Semiconductor Technology, Technische Universität Braunschweig, Hans-Sommer-Str. 66, 38106 Braunschweig, Germany — ²Laboratory for Emerging Nanometrology (LENA), Technische Universität Braunschweig, Langer Kamp 6, 38106 Braunschweig, Germany

Recently, porous GaN etching has gained significant attention, due to its broad variety of convenient applications for optoelectronic devices. Specifically, the introduction of nanoporous layers enables the quasi-epitaxial growth of low refractive index GaN-based compounds for applications such as vertical DBR mirror structures.

Whilst classical DBRs are designed in order to satisfy the quarter-wavelength-condition, porous GaN DBRs are subject to a competition between porosity and optimal constructive interference from the layer thicknesses. It is vital to understand the influence of the porosity, as deviations from typical DBR designs might be advantageous for the device performance as inferred from simulations.

In this contribution, we investigate the influence of different designs and etching parameters on the optical performance of a defined layer structure. Particularly, the interdependency between the etched porosity and the design porosity with respect to the optical device performance is investigated. To determine the porosity, a combination of optical measurements, simulations and a gravimetric approach is used.

HL 44.4 Thu 15:45 POT 112

PL enhancement from Mie resonant silicon-rich-nitride nano-disks — •KRISHNA KOUNDINYA UPADHYAYULA and JÖRG SCHILLING — Martin Luther Universität Halle-Wittenberg, Halle

PECVD grown silicon-rich-nitride (SRN) exhibits refractive indices up to 3.5 and a broad luminescence in the visible up to near IR wavelengths making it a viable candidate for a photonic platform for bio-sensing at the therapeutic window. After a fundamental study on the origin of this photoluminescence (PL) in SRN using spectral and time resolved PL, we demonstrate the impact of Mie resonances on the luminescence by fabricating single Mie resonant SRN nano-disks with sizes on the order of a few 100nm. Comparing the measured PL-spectra with theoretically modelled transmission and emission spectra from finite element simulations, the observed PL-peaks could be attributed to the coupling of the emitters to electric dipole, magnetic dipole and higher order multipole Mie resonances. Furthermore, we created 2D periodic arrays of such SRN-Mie resonators with periods between 300-500nm and an absolute size of 100nm² using interference lithography. The fabricated arrays exhibited an up to 27x enhancement of the room-temperature PL compared to that of an unstructured sample increasing further up 54x after hydrogen passivation. Tuning the structure parameters, we identify the remaining impact of the individual Mie-resonances in the spectra and the features caused by the grating/Bragg-resonances of the collective photonic crystal structure. Ongoing time resolved measurements will elucidate the impact of Purcell enhancement on the observed PL due to the Mie resonances.

15 min. break

HL 44.5 Thu 16:15 POT 112

UVC-LEDs grown on HTA-AIN templates with low dislocation densities and high Si doping for strain management — •TIM MAMPE¹, SARINA GRAUPETER¹, GIULIA CARDINALI¹, SYLVIA HAGEDORN², TIM WERNICKE¹, MARKUS WEYERS², and MICHAEL KNEISSL^{1,2} — ¹Technische Universität Berlin, Institute of Solid State Physics, Hardenbergstraße 36, 10623 Berlin, Germany — ²Ferdinand-Braun-Institut (FBH), Gustav-Kirchhoff-Straße 4, 12489 Berlin, Germany
High temperature annealing (HTA) of AlN layers reduces the threading dislocation density of such layers on sapphire substrates below 10⁹ cm⁻² enabling UVC-LEDs with improved efficiencies. However, the HTA AlN-layers are under high compressive strain after cooling down, which can lead to strain relaxation

and defect formation during further LED heterostructure growth. The in-plane lattice constant can be increased by growing a Si-doped AlN layer on HTA-AlN. In this work we investigate the influence of such an AlN:Si-layer on the growth of UVC-LEDs emitting at 265nm on AlN/sapphire substrates with silicon doped as well as undoped AlN layer and different sapphire offcut angles (0.1°, 0.2°, 0.5°). We will discuss the morphology as well as the strain state of AlN and AlGaN layers as well as the electro-optical properties of multi quantum-well (MQW) and LED structures.

HL 44.6 Thu 16:30 POT 112

Intensity fluctuations of infrared and green photodiodes at constant current and its correlation with voltage fluctuations — •DANYLO BOHOMOLOV and ULRICH T. SCHWARZ — Chemnitz University of Technology, Chemnitz, Germany
One important issue for display and sensing applications in LEDs is the fluctuation of light intensity over time. The physical reasons behind this are not fully understood yet, e.g. defect-related blinking is discussed. In addition, it is known that the noise of these devices has a strong correlation with their lifetime. Consequently, the noise of the infrared and green micro-LEDs will be measured here, after which the similarity of their behaviour will be investigated. Standard derivation and corner frequency between flicker noise and thermal noise are chosen as the main comparison parameters. For this purpose, their spectral power density of intensity fluctuations of the emitted light at constant current is investigated. We use a linear controlled precision current source. A large area Si photodiode with amplification capability is used as detector, and the signal is measured using a low-noise transimpedance amplifier and a 24-bit analog-to-digital converter. In parallel, the voltage of the LED is measured to correlate fluctuations in voltage and intensity. We observe oscillations in the frequency range from 1 Hz to 15 kHz. The first measurements of the infrared LEDs showed the presence of 1/f and Johnson-Nyquist noise in this frequency range as expected.

HL 44.7 Thu 16:45 POT 112

Theoretical improvement of 40% in efficiency of AlGaN UV LED using evolution strategies optimization algorithm — •LUCIE LEGUAY and ANDREI SCHLIWA — Institute of Solid-State Physics, Technische Universität Berlin, Hardenbergstr. 36, 10623 Berlin

Nowadays, LED light sources can be found in many technologies ranging from smart lamps to high-quality screen displays. In particular, ultraviolet (UV) LED light can be used to sterilise surfaces and food, to purify air and water and to detect gas and diseases.

However, the nitride-based existing technology is still lacking efficiency. One way to enhance the performance of such devices is to improve their design with optimization algorithms such as evolutionary algorithms which are inspired by biological evolution.

We report an increase of 40% in the theoretical internal quantum efficiency (IQE) of an AlGaN UV-emitting multiple quantum well nanostructure using an evolution strategies algorithm paired with the simulation software nextnano++.

HL 45: Functional semiconductors for renewable energy solutions II

Time: Thursday 15:00–17:15

Location: POT 6

HL 45.1 Thu 15:00 POT 6

Engineering interfaces in multilayer photoanodes for stable and efficient solar energy conversion — •KATARINA-SOPHIE FLASHAR, MATTHIAS KUHL, GABRIEL GRÖTZNER, LAURA WAGNER, LUKAS WOLZ, ALEX HENNING, IAN D. SHARP, and JOHANNA EICHHORN — Walter Schottky Institute and Physics Department, Technical University Munich, Am Coulombwall 4, 85748 Garching, Germany

Photoelectrochemical (PEC) energy conversion is a promising approach for the direct conversion of solar energy into storable chemical fuels. In this context, tantalum nitride (Ta₃N₅) has attracted considerable interest due to a theoretical photocurrent density limit of 12.9 mA*cm⁻² and a theoretical solar-to-hydrogen conversion efficiency of 15% under AM 1.5G illumination. However, currently Ta₃N₅ photoelectrodes suffer from poor stability, such as oxidative decomposition, under the harsh PEC operation conditions. To overcome these limitations, we investigate the protection of Ta₃N₅ photoelectrodes with ultra-thin catalyst layers deposited via plasma-enhanced atomic layer deposition. In these multilayer architectures, the metal oxide catalyst decreases the activation energy, provides active sites for water oxidation, and promotes charge extraction of photogenerated holes. Here, we use a combination of spectroscopic and microscopic methods to elucidate the impact on interfacial energetics, defect properties, charge transport, recombination, and catalytic reactions. The gained understanding of interfacial properties is applied to design efficient interfaces between semiconductor photoelectrodes and functional catalyst coatings for the realization of highly stable and efficient PEC systems.

HL 45.2 Thu 15:15 POT 6

Discovery of multi-anion antiperovskite as promising thermoelectric materials by computational screening — •DAN HAN¹, BONAN ZHU², KIERAN B. SPOONER², STEFAN S RUDEL¹, WOLFGANG SCHNICK¹, THOMAS BEIN¹, DAVID O. SCANLON², and HUBERT EBERT¹ — ¹Department of Chemistry, University of Munich, Germany — ²Department of Chemistry, University College London, United Kingdom

The thermoelectric performance of existing perovskites lags far behind the state-of-the-art thermoelectric materials such as SnSe, PbTe and Bi₂Te₃. Despite halide perovskites showing promising thermoelectric properties, namely, high Seebeck coefficients and ultralow thermal conductivities, their thermoelectric performance is significantly restricted by low electrical conductivities. Here, we explore new multi-anion antiperovskites by global structure searches, and demonstrate their phase stability by first-principles calculations. Ca₆NFSn₂ and Sr₆NFSn₂ exhibit decent Seebeck coefficients and ultralow lattice thermal conductivities (< 1 W m⁻¹ K⁻¹). The weak chemical bonding between the heavy-atom cage-rattler Sn and alkaline-earth metal (Ca and Sr) inducing low-frequency optical modes coupling with heat carrying acoustic phonons in combination with strong bond anharmonicity give rise to ultralow lattice thermal conductivities. Notably, Ca₆NFSn₂ and Sr₆NFSn₂ show remarkably larger electrical conductivities compared to halide perovskite CsSnI₃. Our exploration of multi-anion antiperovskites X₆NFSn₂ (X = Ca, Sr) realizes the "phonon-glass, electron-crystal" concept within perovskite structures.

HL 45.3 Thu 15:30 POT 6

Template realized well-defined nanostructures for energy storage and conversion — •MO SHA, HUAPING ZHAO, and YONG LEI — Fachgebiet Angewandte Nanophysik, Institut für Physik & IMN MacroNano, Technische Universität Ilmenau, 98693 Ilmenau, Germany

Template-based technique provides a perfect approach to realize well-defined arrayed nanostructures within large-scale. We have developed nanostructuring techniques mainly using anodic aluminum oxide templates for fabricating functional nanostructures. The obtained well-defined nanostructures possess large-scale arrayed configuration, high structural density, perfect regularity and cost-effectiveness, and are highly desirable for constructing different nano-devices especially for energy storage and conversion applications, including rechargeable sodium-ion and potassium-ion batteries, supercapacitors, and photo electrochemical devices. The device performances demonstrated that the obtained nanostructures benefit these applications through the precise control over the structural features enabled by the geometrical characteristics of the templates. Refs: Nat Commun, 2022, 13 (1), 2435; Adv Energy Mater, 2021, 11 (15), 2001537. Nat Commun 2020, 11 (1), 299; Nat Nanotechnology, 2017, 12 (3), 244.

HL 45.4 Thu 15:45 POT 6

Optical and Photocatalytic Properties of BiVO₄ Nanoplatelets — •PHILIPP BOOTZ¹, BHARATI DEBNATH¹, KILIAN FRANK², MARKUS DÖBLINGER³, BERT NICKEL², JACEK STOLARCZYK⁴, and JOCHEN FELDMANN¹ — ¹Chair for Photonics and Optoelectronics, Nano-Institute Munich, Physics Department, Ludwig Maximilians Universität (LMU), 80539 Munich, Germany — ²Chair for Soft Condensed Matter, 80539 Munich, Germany — ³Chair for Functional Nanosystems (Prof. Bein), Department Physical Chemistry, 81377 Munich, Germany — ⁴Smoluchowski Institute of Physics, Jagiellonian University, 30-348 Krakow, Poland

Bismuth vanadate (BiVO₄) with a bandgap of about 2.4 to 3.1 eV is known as one of the best water-oxidizing semiconductors in the field of photocatalysis. It is a material which can crystallize in three different phases - orthorhombic, tetragonal and monoclinic - and is often used as thin films or micron-sized crystals. In this study, we report a novel solvothermal synthesis method to obtain colloidal BiVO₄ nanoplatelets with a lateral size of less than 30 nm. We have performed X-ray diffraction and transmission electron microscopy measurements for their structural characterization. We compare the linear optical properties of the nanoplatelets with their three-dimensional pendants and discuss the microscopic origins for the observed differences. Finally, we present the results of photocatalytic experiments, where a gas chromatograph is used to measure the produced oxygen from water during illumination with light.

30 min. break

HL 45.5 Thu 16:30 POT 6

beneficial impact of KF post-deposition treatment on optical diode factor and non-radiative recombination of CIGSe absorbers — •SEVAN GHARABEIKI, MOHIT SOOD, VALENTINA SERRANO ESCALANTE, TAOWEN WANG, and SUSANNE SIEBENTRITT — Department of Physics and Materials Science, University of Luxembourg, 4422 Belvaux, Luxembourg

The efficiency of the solar cells depends on the open circuit voltage (VOC), short circuit current (JSC), and fill factor (FF) which in turn depends on the diode factor. The quasi-Fermi level splitting (QFLS) is the upper limit for VOC and the optical diode factor (ODF) is the lower limit of the diode factor. It has been long known that post-deposition treatment (PDT) with heavy alkalis has a beneficial impact on CIGSe solar cells. An increase in the hole concentration, decrease

in non-radiative recombination, and surface passivation have been reported by many studies. We present the effect of the KF PDT on the CIGSe absorbers with different deposition temperature. Our study shows that the KF PDT increases the (QFLS) and decreases non-radiative recombination for the samples deposited on soda lime glass with high deposition temperature. For the samples with low deposition temperature, the improvement in QFLS is mainly due to an increase in doping level. A combination of QFLS, lifetime and capacitive-voltage measurements were conducted to separate the doping effect from the non-radiative recombination effect. We propose that high concentration of Na is required to get the full effect of KF PDT, i.e. increase in the doping and decrease in the non-radiative recombination.

HL 45.6 Thu 16:45 POT 6

Tuning optical properties of graphitic carbon nitrides for photocatalytic applications — •JULIAN HIRSCHMANN¹, BHARATI DEBNATH¹, MATTHIAS KESTLER¹, KILIAN FRANK², BERT NICKEL², and JOCHEN FELDMANN¹ — ¹Chair for Photonics and Optoelectronics, Nano-Institute Munich and Department of Physics, Ludwig Maximilians Universität (LMU) — ²Chair for Experimental Physics Prof. Rädler, Department of Physics, Ludwig Maximilians Universität (LMU)

In the field of photocatalysis, graphitic carbon nitrides have proven to be a promising and cost-effective material. The organic graphene like material built from heptazine or triazole rings enable various photocatalytic applications such as hydrogen evolution and ammonia production.

Graphitic carbon nitrides have a two-dimensional sheet-like structure, which is advantageous for photocatalytic applications. Our refined synthesis process provides a simple way to obtain nanosheets of different thicknesses and varying π -conjugation areas. Their impact on the optical properties such as absorption and photoluminescence are presented. The results are compared with recently published electronic band structure calculations and with more molecularly based exciton models. Finally, photocatalytic measurements have been carried out and the obtained efficiencies are compared with our data from time-integrated and time-resolved optical experiments.

HL 45.7 Thu 17:00 POT 6

Functionalization of TiO₂ thin films with gold nanoparticles aiming at plasmonic photocatalysis — •NARMINA O. BALAYEVA^{1,2}, LU HE¹, DIETRICH R.T. ZAHN^{1,2}, and TERESA I. MADEIRA^{1,2} — ¹Semiconductor Physics, Institute of Physics, Chemnitz University of Technology, Reichenhainer Str. 70, 09126 Chemnitz, Germany — ²Research Center for Materials, Architectures and Integration of Nanomembranes (MAIN), Chemnitz University of Technology, Rosenbergstraße 6, 09126 Chemnitz, Germany

Developing novel photocatalytic systems with improved charge separation that can exploit visible light is of great interest. Here, we investigated the functionalization of anatase TiO₂ thin films with gold nanoparticles (Au NPs) for enhanced photocatalytic activity. The LSPR effect of Au NPs is studied by depositing them either on top of or embedding them beneath TiO₂ thin films or mixing them homogeneously into the precursor solution before the films are prepared using the spin-coating technique. An amount of Au NPs relative to TiO₂ (0.01 wt% - 1 wt%) was employed to study the effect of photocatalytic degradation of acetone using an FTIR-based gas photo-reactor chamber with a set of 6 cool white light-emitting diodes (LED). The structure and morphology of the Au/TiO₂ films were characterized with different techniques, i.e., Raman spectroscopy and X-ray diffraction (XRD), X-ray reflectivity (XRR), scanning electron microscopy (SEM), as well as atomic force microscopy (AFM). Spectroscopic ellipsometry (SE) was used for a complementary analysis of thickness, roughness, and, in addition, dielectric properties of the thin films.

HL 46: Members' Assembly

Themen unter anderem:

- Bericht
- Wahl der Fachverbandsleitung
- Informationen zur Frühjahrstagung 2024
- Verschiedenes

Time: Thursday 18:00–19:00

Location: POT 6

All members of the Semiconductor Physics Division are invited to participate.

HL 47: Oxide Semiconductors II

Time: Friday 9:30–11:30

Location: POT 81

HL 47.1 Fri 9:30 POT 81

Origin of Resistive Switching in SrTiO₃ — •WAHIB AGGOUNE¹, CHRISTIAN CARBOGNO¹, MARTIN ALBRECHT², and MATTHIAS SCHEFFLER¹ — ¹The NOMAD Laboratory at the FHI of the Max-Planck-Gesellschaft and IRIS-Adlershof of the Humboldt-Universität zu Berlin. — ²Leibniz-Institut für Kristallzüchtung, 12489 Berlin.

Memristors may play a key role for the next generation of non-volatile memory devices. They are typically realized using materials that allow to switch between a low- and a high-resistance state. This effect has been recently observed in SrTiO₃ thin films, whereby a pronounced dependence of the switching properties on the growth conditions was found [1,2]. To shed light on the underlying atomistic mechanisms, we performed density-functional theory calculations and carefully analyzed the critical effects of different exchange-correlation functionals. We explored the most stable defects (vacancies, interstitial, substitutional) under Ti-rich conditions. The study reveals that the formation of a Ti_{Sr} antisite defect is energetically favorable and also induces a spontaneous polarization. It can be further stabilized by an additional nearby Sr-vacancy (Ti_{Sr}+V_{Sr}). Furthermore, such a defect complex increases the observed polarization. We discuss these results with respect to the experimentally observed resistive switching by analyzing the electronic properties and the polarization as well as the energy barriers for switching it.

[1] A. Baki, *et al.*, *Sci. Rep.* **11**, 7497 (2021).

[2] K. Klyukin, *et al.*, *Phys. Rev. B* **95**, 035301 (2017).

HL 47.2 Fri 9:45 POT 81

Second harmonic generation of blue series excitons in Cu₂O — •ANDREAS FARENBRUCH¹, DIETMAR FRÖHLICH¹, HEINRICH STOLZ², DMITRI R. YAKOVLEV^{1,3}, and MANFRED BAYER^{1,3} — ¹Experimentelle Physik 2, TU Dortmund, Dortmund, Germany — ²Institut für Physik, Universität Rostock, Rostock, Germany — ³St. Petersburg, Russia

Excitons are Coulomb-bound complexes of electrons and holes in semiconductors with a discrete hydrogen-like energy series. The yellow exciton series in Cu₂O involves excitations between the highest valence and lowest conduction band and it presents an ideal platform for investigations of exciton physics with Rydberg states up to a principal quantum number of n=28. Excitations, that involve the same valence band but the second lowest conduction band belong to the so-called blue series. Access in linear optical spectroscopy to these states is hard to achieve due to the high absorption in this spectral range. Optical second harmonic generation (SHG) is therefore a suitable investigation method. By analyzing the measured polarization dependence of the SHG signal and comparing it with group theoretical simulations, the magneto-Stark and Zeeman effects are identified as the SHG mechanisms involved. The 1S, 2S and 2P excitons and magneto-excitons up to n=8 in magnetic fields up to 10 T are detected. By analyzing their magnetic-field shift and polariton effect, key properties such as the energies of the exciton resonances, the Rydberg energy, the band gap, the reduced exciton mass, the anisotropy of the conduction band mass and the exciton radius are obtained for the blue exciton series.

HL 47.3 Fri 10:00 POT 81

Electrical and thermoelectrical properties of the two-dimensional electron gas in polar discontinuity doped BaSnO₃/LaInO₃ heterostructure — •FAZEEL ZOHAI, GEORG HOFFMANN, and OLIVER BIERWAGEN — Paul-Drude-Institut für Festkörperelektronik, Hausvogteiplatz 7, Berlin, Germany

Transparent semiconducting oxides (TSOs) are key players for opto-electronic devices, among which high frequency applications benefit from electrical properties of two-dimensional electron gases (2DEGs). In this contribution we demonstrate the electrical and thermoelectric properties of the 2DEG at the interface between a nonpolar perovskite oxide BaSnO₃ and a polar perovskite oxide LaInO₃, grown by plasma assisted molecular beam epitaxy. The electrical and thermoelectric properties are analyzed using Seebeck measurements and van der Pauw-Hall measurements. Integrating the charge carrier concentrations from both measurements, we were able to deduce the thickness of the charge carrier system.

HL 47.4 Fri 10:15 POT 81

Analysis of thickness distributions for combinatorial pulsed laser deposition — •CLEMENS PETERSEN, HOLGER VON WENCKSTERN, and MARIUS GRUNDMANN — Universität Leipzig Felix-Bloch-Institut, Leipzig, Deutschland

Recently combinatorial deposition methods have increasingly gained scientists' attention, due to the high experimental throughput and resource-wise efficiency they offer in materials discovery. This enables fast screening of material properties of multinary material systems using just a single sample. By employing pulsed laser deposition with our segmented target approach [1] we successfully realized the deposition of α -(Al_xGa_{1-x})₂O₃ with continuous composition spread over the whole composition range on a single 2-inch sapphire wafer [2]. Accom-

panied by the usage of high-throughput measurements such as spectroscopic ellipsometry and x-ray diffraction, the characterization of the material systems' physical properties with high chemical resolution and comparably low efforts becomes feasible. By employing the plasma plume expansion model suggested by Anisimov *et al.* [3] and the resulting spatial material-deposition distribution we calculate binary growth rates as function of position enabling us to predict film thickness and composition locally. Thereby the deposition of group III sesquioxides can be described exceptionally well. We further show that the binary distributions can be used to predict the combinatorial deposition of ternary alloys with high precision. [1] H. von Wenckstern *et al.*, *pss(b)*, Vol. 257, 1900626 [2] A. Hassa *et al.*, *pss(b)*, Vol. 258, 2000394 [3] S. I. Anisimov *et al.*, *Phys. rev. B*, Vol 48, 12076.

15 min. break

HL 47.5 Fri 10:45 POT 81

Cloud in cell scheme based stochastic modelling of BiFeO₃ memristor for circuit simulations — •SAHITYA YARRAGOLLA¹, NAN DU^{2,3}, TORBEN HEMKE¹, XIANYUE ZHAO^{2,3}, ZIANG CHEN², and THOMAS MUSSENBROCK¹ — ¹Chair of Applied Electrodynamics and Plasma Technology, Ruhr University Bochum, Germany — ²Institute for Solid State Physics, Friedrich Schiller University Jena, Jena, Germany — ³Department of Quantum Detection, Leibniz Institute of Photonic Technology, Jena, Germany

In recent years, analog memristive devices have been extensively investigated for neuromorphic computing and hardware security applications. It is found that these devices show excellent properties such as long retention time, intrinsic stochasticity, and fast switching. However, the switching mechanism in these devices from the physics point of view is still under discussion. Therefore, in this work, we focus mainly on understanding the resistive switching based on the transport of oxygen vacancies in the interface-type Au/BiFeO₃ (BFO)/Pt/Ti memristive devices using a 1D cloud-in-a-cell model. The proposed model combines the advantages of both 1D concentrated and 3D distributed models in a single model. The model is stochastic and computationally less expensive, making it suitable for circuit simulations. The calculated *I-V* characteristics of BFO memristor using the proposed are in excellent agreement with the experimental results. Furthermore, the response of the BFO memristor to changes in electrical properties, temperature and retention characteristics are analyzed, and the results show reasonable agreement with experimental findings.

HL 47.6 Fri 11:00 POT 81

Comparing processing strategies for Indium oxide field-effect transistors — •FABIAN SCHÖPPACH, CLEMENS PETERSEN, HOLGER VON WENCKSTERN, and MARIUS GRUNDMANN — Felix Bloch Institute for Solid State Physics, Universität Leipzig, Germany

Indium oxide (In₂O₃) combines promising physical properties such as high carrier mobility and transparency in the visible. However, due to its tendency to form an electron accumulation layer on its surface (SEAL), the use of In₂O₃ in active devices is generally difficult. We use the published strategies, compensating Mg doping [1] and oxygen plasma treatment [2], to suppress SEAL formation and allow the films to be used in FET devices. In addition, In₂O₃ as sesquioxide is a very robust material that resists classical patterning processes such as wet chemical etching.

We identified two different fabrication strategies to structure our films laterally: Plasma-assisted etching and using a wet-chemical soluble sacrificial layer. In this work, both strategies are compared regarding additionally necessary processing steps and the final devices' performance. We used In₂O₃ films grown by pulsed laser deposition. For the source and drain contacts, gold was deposited via inert ambient sputtering. Schottky gate diodes were fabricated in a reactive sputtering process, which is a prerequisite for obtaining electrically rectifying contacts to In₂O₃ [3].

[1] SCHMIDT, *et al.* *physica status solidi (b)* 252.10, 2304–2308 (2015)

[2] MICHEL, *et al.* *ACS Appl. Mater. Interf.* **11**, 27073–27087 (2019)

[3] VON WENCKSTERN, *et al.* *APL Materials* **2.4**, 046104 (2014)

HL 47.7 Fri 11:15 POT 81

Charge carrier diffusion and localization in metal oxide photoabsorbers — •HANNES HEMPEL, MARKUS SCHLEUNING, KLAUS SCHWARZBURG, RAINER EICHBERGER, ROEL VAN DE KROL, MORITZ KÖLBACH, FATWA F. ABDI, and DENNIS FRIEDRICH — Helmholtz-Zentrum Berlin, Germany

Long diffusion lengths of photo-excited charge carriers are crucial for high power conversion efficiencies of photoelectrochemical and photovoltaic devices. However, in metal oxides effects such as (multiple-)trapping, carrier localization and polaron formation can lead to time-varying mobilities and lifetimes that are not accounted for in the conventional analysis. Therefore, here, a generalized analysis is presented that determines the diffusion length directly from the

integral of a photoconductivity transient, regardless of the nature of carrier relaxation. This approach is presented on amorphous silicon, a prototype of disordered materials, and BiVO₄, one of the most studied photoanode materials for solar water splitting. Our generalized analysis allows monitoring the temporal evolution of the charge carrier displacement, which converges for both materials after ~100 ns to a diffusion length of a few tens of nanometers. For BiVO₄, the

obtained diffusion length is significantly shorter than the typical thin film thickness, which rationalizes the photocurrent loss in the corresponding photoelectrochemical device. Finally, we probe several metal other prominent metal oxide photoabsorbers, namely Fe₂O₃, FeVO₄, CuFeO₂, α -SnWO₄, BaSnO₃, and CuBi₂O₄, and find signs of carrier localization on the nanometer scale, which limits the charge carrier diffusion.

HL 48: Ultra-fast Phenomena

Time: Friday 9:30–12:00

Location: POT 361

HL 48.1 Fri 9:30 POT 361

Characterizing the nonadiabatic tunneling dynamics in solid-state high harmonic generation — •RUIXIN ZUO¹, XIAOHONG SONG², SHUAI BEN², WEIFENG YANG², and TORSTEN MEIER¹ — ¹Department of Physics, Paderborn University, Warburger Str. 100, D-33098 Paderborn, Germany — ²School of Science, Hainan University, Hainan 570288, China

Tunneling is a fundamental quantum process which may result from light-matter interaction. High-harmonic radiation, as an ultrafast phenomenon initiated by the tunneling excitation, carries information about the electronic dynamics in the classically forbidden region. We introduce a quantum trajectory analysis to identify the underlying quantum dynamics governing solid-state high harmonics which improves the understanding of neighboring-atoms collisions [1]. It is revealed that properties of the electron-hole pairs when emerging in the classically allowed region like the group velocity and the relative displacement are dictated by the nonadiabaticity of tunnel ionization and are crucial in determining the subsequent propagation and radiation. Furthermore, we show that the two-color high harmonic spectroscopy validates the quantum trajectory analysis and enables us to probe the tunneling dynamics in strongly driven solid-state systems.

[1] R. Zuo, A. Trautmann, G. Wang, W.-R. Hannes, S. Yang, X. Song, T. Meier, M. Ciappina, H. T. Duc, and W. Yang, Neighboring atom collisions in solid-state high harmonic generation, *Ultrafast Science* **2021**, 9861923 (2021).

HL 48.2 Fri 9:45 POT 361

Compact, CEP-stable, few-cycle OPCPA for single attosecond pulse generation — •BASTIAN MANSCHWETUS, FILIPPO CAMPI, THOMAS BRAATZ, SEBASTIAN STAROSIELEC, JAN-HEYE BUSS, MICHAEL SCHULZ, and ROBERT RIEDEL — Class 5 Photonics, Hamburg, Germany

Attosecond technology paved the way for studying ultrafast electronic processes in atoms, molecules, solids, and complex many body systems. Carrier envelope phase (CEP) stabilization in the few-cycle regime is a key enabler of this technology. A crucial step forward is the demonstration of high-repetition rate optical parametric chirped-pulse amplifier (OPCPA) systems for the generation of phase-stable few-cycle, μ J-level driver pulses for high-harmonic-generation (HHG). In this work, we present an OPCPA providing white light seeded, actively controlled CEP stable, 9 fs pulses around 900 nm center wavelength with 30 μ J pulse energy as a high-harmonic driver for attosecond experiments at 200 kHz repetition rate.

HL 48.3 Fri 10:00 POT 361

Transient Optical Property Changes in Semimetals with Strong Electron-Phonon Coupling — •FABIAN THIEMANN¹, GERMÁN SCIAINI², ALEXANDER KASSEN¹, TYLER LOTT², and MICHAEL HORN-VON HOEGEN¹ — ¹University of Duisburg-Essen, Lotharstr. 1, 47057 Duisburg, Germany — ²University of Waterloo, 200 University Avenue West, Waterloo, ON N2L 3G1, Canada

Group V semimetals, such as bismuth used in this study, are well known for their strong electron-phonon coupling due to the inherent Peierls distortion of their lattice. In particular, the displacively excited coherent A_{1g} phonon mode plays an important role in ultrafast studies on Bi. With knowledge of the excitation density we used a series of thin Bi films on Si(111) to reconstruct the transient dielectric function in an all optical pump-probe experiment. Though we only access the first half ps of dynamics, we separate the contributions from the excited carrier system and the coherent atomic motion. Our results suggest that we can describe the changes in optical properties caused by the non-equilibrium distribution of carriers still similar to a thermal dependency in equilibrium. In the regime of high excitation densities, we no longer can use the two-band Raman susceptibility approach to describe changes caused by the coherent phonons. We suggest that the light scattering is greatly enhanced by the excited carriers and that recently proposed band shifts in the time domain mainly define this part of changes of the dielectric function.

HL 48.4 Fri 10:15 POT 361

Ultrafast optical control of polariton energy in an organic semiconductor microcavity — •K.E. MCGHEE^{1,2}, M. GUIZZARDI³, R. JAYAPRAKASH¹, K. GEORGIOU^{1,4}, G. CERULLO^{3,5}, T. JESSEWITSCH⁶, A. ZASEDATELEV⁷, U. SCHERF⁶, T. VIRGLI⁵, P.G. LAGOUDAKIS⁷, and D.G. LIDZEY¹ — ¹University of Sheffield, UK — ²Universität Leipzig, Germany — ³Politecnico di Milano, Italy — ⁴University of Cyprus, Cyprus — ⁵Istituto di Fotonica e Nanotecnologia-CNR, Italy — ⁶Universität Wuppertal, Germany — ⁷University of Southampton, UK

Exciton-polariton condensates are of great interest due to their potential applications in polariton logic devices, nonlinear photonic integrated circuits and quantum simulators. In this work, we have fabricated polariton microcavities designed to allow the dynamic trapping and manipulation of such condensates using ultrashort laser pulses. Using transient pump-probe spectroscopy, we have saturated the electronic transition of a weakly-coupled dye in a cavity containing a second strongly-coupled dye. In doing so, we alter the cavity effective refractive index and therefore the position of the lower polariton branch. We demonstrate a maximum blueshift of this mode of 12 meV, dependent on the pump fluence, and show that this effect is ultrafast, with switch 'on' and 'off' times of less than 1 ps. Utilising this controllable energy shift, it should be possible to dynamically 'write' energy barriers into organic polariton microcavities without affecting the coupling strength. This would allow important studies on interacting polariton condensates for the development of next generation quantum devices.

HL 48.5 Fri 10:30 POT 361

Imaging nanoscale electron dynamics with extreme ultraviolet radiation — •HUNG-TZU CHANG¹, SERGEY ZAYKO¹, JAKOB HAGEN¹, MURAT SIVIS^{1,2}, and CLAUD ROPERS^{1,2} — ¹Max Planck Institute for Multidisciplinary Sciences, 37077 Goettingen, Germany — ²4th Physical Institute, University of Goettingen, 37077 Goettingen, Germany

Non-equilibrium electronic processes such as electron thermalization, ballistic transport, and spin diffusion, occur at femtosecond time- and nanometer length-scales. While ultrafast spectroscopic methods can trace the temporal evolution of electronic states [1], capturing those dynamics in real space remains challenging. Here we demonstrate time-resolved coherent diffractive imaging using a table-top extreme ultraviolet (EUV) source based on high harmonic generation [2,3], where the sample is first excited by a near-infrared pump pulse and probed with core-level absorption induced by a time-delayed EUV pulse. The valence electron dynamics can be retrieved from the spatially resolved changes of the EUV field amplitude and phase exiting the sample after localized photoexcitation. This technique provides nanometer spatial resolution in addition to the time resolution and element specificity of femtosecond table-top core-level spectroscopy, and paves the way for further understanding of the mechanisms of photophysical processes in condensed matter.

[1] Chang et al., *Phys. Rev. B* **103**(6), 064305 (2021). [2] Kfir et al., *Sci. Adv.* **3**(12), eaao4641 (2017). [3] Zayko et al., *Nat. Commun.* **12**(1), 6337 (2021)

15 min. break

HL 48.6 Fri 11:00 POT 361

Coherent-to-incoherent crossover of photoexcited electron-phonon dynamics in 2D materials — •ENRICO PERFETTO^{1,2} and GIANLUCA STEFANUCCI^{1,2} — ¹Dipartimento di Fisica, Università di Roma Tor Vergata, Via della Ricerca Scientifica 1, 00133 Rome, Italy — ²INFN, Sezione di Roma Tor Vergata, Via della Ricerca Scientifica 1, 00133 Rome, Italy

We present a first principles nonequilibrium Green's function approach to describe the carrier and nuclear dynamics of 2D materials. Our scheme is based on the simultaneous propagation of the electronic and phononic degrees of freedom and includes the GW, Ehrenfest, and Fan-Migdal self-energies. The method scales linearly with the propagation time, and allows to describe in a conserving fashion the retarded Coulomb screening and the cooling dynamics of hot carriers via phonon emission. Numerical results are provided for a monolayer MoS₂ photo-excited above the gap. The intra-valley scattering is responsible for an ultrafast carriers migration toward the band edges already during pumping. Intervalley scattering occurs on a longer timescale, of the order of a few hundreds of femtoseconds. At high carrier density the energy exchange between electrons

and phonons is very efficient, leading to a sizable increase of the lattice temperature within one picosecond. During this process the electronic coherence is lost. The lattice coherence, instead, survives for much longer. Several hundreds of femtoseconds after the dephasing of the electronic polarization the nuclear displacements still exhibit undamped oscillations.

HL 48.7 Fri 11:15 POT 361

Coherent versus incoherent excitons: Stability, time-dependent ARPES spectrum and Floquet topological phases — •GIANLUCA STEFANUCCI^{1,2} and ENRICO PERFETTO^{1,2} — ¹Dipartimento di Fisica, Università di Roma Tor Vergata, Via della Ricerca Scientifica 1, 00133 Rome, Italy — ²INFN, Sezione di Roma Tor Vergata, Via della Ricerca Scientifica 1, 00133 Rome, Italy

We consider a band insulator turning into a nonequilibrium (NEQ) exciton superfluid (XS) after resonant pumping. The NEQ-XS is characterized by self-sustained coherent oscillations of the superfluid condensate. We show that the ARPES spectrum from long probe pulses features a subgap excitonic sideband; it originates from the condensate-dressing of the conduction states and it has an intensity proportional to the excitonic wavefunction squared [PRB94, 245303 (2016); PRM3, 124601 (2019)]. Reducing the probe duration below the condensate period the ARPES signal becomes periodic in the impinging time of the probe [PRB101, 041201(R)(2020)]. The stability of the NEQ-XS as the conduction density grows is jeopardized by the increased screening efficiency of the looser excitons. Nonetheless, a proper nonequilibrium self-consistent treatment of screening indicates that NEQ-XS is stable up to relatively high densities [PRB102, 085203 (2020)]. We also show that a p-wave NEQ-XS at high enough density undergoes a Floquet topological transition [PRL125, 106401 (2020)]. Phonon-induced decoherence eventually transforms the XS phase into an incoherent exciton-polaron fluid. During this process the excitonic sideband broadens and red-shifts (Stokes shift) [PRB103, 245103 (2021)]

HL 48.8 Fri 11:30 POT 361

Intermolecular conical intersections in acceptor-donor-acceptor aggregated molecules — •SOMAYEH SOURI¹, KATRIN WINTE¹, ANTONIETTA DE SIO¹, CHRISTOPH LIENAU¹, ELENA MENA-OSTERITZ³, PETER BÄUERLE², TERESA KRAUS³, FULU ZHENG², MOHAMED MADJET², and SERGEI TRETIAK⁴ — ¹University of Oldenburg, Germany — ²University of Bremen, Germany — ³Ulm University, Germany — ⁴Los Alamos National Laboratory, USA

In molecules, strong coupling between electronic excitations and vibrational modes may result in conical intersections (CoIns) of multidimensional potential energy surfaces. At CoIns different electronic states cross and couple strongly via vibrational modes. This results in large nonadiabatic couplings violating the Born-Oppenheimer approximation. While CoIns are ubiquitous in molecules, not much is known about their occurrence and relevance for intermolecular ultrafast energy and charge transfer dynamics in the solid state. Here, we reveal the existence of intermolecular CoIns in thin films of aggregated acceptor-donor-acceptor-type oligomers by ultrafast two-dimensional electronic spectroscopy (2DES). The 2DES maps show a grid-like peak pattern at early times, followed by a rapid reduction of the peak spacings which transforms into a featureless map after only ~40 fs. We take this abrupt change in the 2DES maps as clear evidence for the passage of the optically launched vibrational wave packet through the intermolecular CoIn in the thin films. Our results, which are confirmed by simulations, suggest new opportunities for guiding the coherent flow of energy and charge in solid-state nanostructures.

HL 48.9 Fri 11:45 POT 361

Potential signatures of hydrodynamic transport captured by THz high harmonic generation — •TIM PRIESSNITZ¹, THALES DE OLIVEIRA², LIWEN FENG^{1,3}, MIN-JAE KIM^{1,3}, SERGEY KOVALEV², BERNHARD KEIMER¹, and STEFAN KAISER^{1,3} — ¹Max-Planck Institute for Solid State Research, 70569 Stuttgart, Germany — ²Helmholtz-Zentrum Dresden-Rossendorf, 01328 Dresden, Germany — ³Institute of Solid State and Materials Physics, Technical University Dresden, 01069 Dresden, Germany

Terahertz high harmonic generation (THz HHG) is a common property of nonlinear systems. Recently it has been used to investigate fundamental principles that govern transport and nonlinear dynamics in novel quantum materials like graphene or Dirac semimetals. However, these studies have not yet been successfully extended to low temperatures where hydrodynamic effects come into play. Optical phenomena such as THz HHG are proposed to provide a more efficient way to probe hydrodynamic effects than previously studied DC transport measurements, which identified the delafossite PdCoO₂ as a candidate to observe such properties. Here, we report on THz HHG in thin films of PdCoO₂ at low temperatures and we will discuss potential signatures of hydrodynamics, contributing to the ongoing puzzle of low-temperature origins of THz HHG.

HL 49: Quantum dots: Devices

Time: Friday 9:30–11:45

Location: POT 151

HL 49.1 Fri 9:30 POT 151

Gate-based protocol simulations for quantum repeaters using quantum-dot molecules in switchable electric fields — •STEFFEN WILKSEN, FREDERIK LOHOF, and CHRISTOPHER GIES — Institute for Theoretical Physics, University of Bremen, Bremen, Germany

Semiconductor quantum dots provide a promising platform for applications in quantum information technologies, such as quantum repeaters, which enable secure quantum communication over long distances. Two quantum dots, separated by a small tunnelling layer, form a so-called quantum dot molecule (QDM), which exhibits properties similar to classical molecules. Their energy levels can be tuned by applying an external electric field, thereby allowing to perform gate operations. We consider QDMs in switchable electric fields towards quantum-repeater realizations. The time dependence that arises from performing gate operations requires a careful treatment of the system-bath interaction. We treat the QDM as an open quantum system using an explicitly time-dependent Redfield master equation approach, accounting for the time dependence of the interaction rates beyond more simple Lindblad approaches. Based on our approach, we investigate the adiabatic and non-adiabatic behaviour of the system for different switching speeds and determine achievable execution times for gate operations with currently existing QDMs.

HL 49.2 Fri 9:45 POT 151

Heterogeneous integration of telecom c-band emitting quantum dots on silicon photonics platform by adhesive bonding — •PONRAJ VIJAYAN, FIONA BRAUN, MICHAEL JETTER, and PETER MICHLER — Institut für Halbleitertechnik und Funktionelle Grenzflächen, Universität Stuttgart, Germany

Silicon photonics for telecommunications applications has garnered much attention recently. The optical transparency and the large refractive index contrast of silicon in the telecommunication wavelengths allow the implementation of high-density photonic integrated circuits. The drawback of silicon photonics is that there is no native light source due to the indirect band-gap nature of silicon. Integration of III-V material, which offers outstanding optical emission properties, on silicon provides a potential solution. The direct growth of III-V materials on silicon is the most desired approach because it is economically favourable. However, it is challenging because of large lattice mismatch between

the III-V materials and silicon. An alternate approach for large-scale integration is through heterogeneous integration of thin III-V membrane using adhesive bonding technique. For such integration, it is crucial to have a robust bonding procedure which provides a uniform bonding layer with a desired thickness for efficient light coupling between III-V active layer and the silicon photonic platform. Our group has previously developed InAs QD/InGaAs MMB/GaAs substrate structures for long-distance optical fiber applications [3]. Here, we report on the route to integrate the telecom C-band emitting InAs QD on silicon photonic platform using adhesive bonding.

HL 49.3 Fri 10:00 POT 151

Investigation of optical properties of open-fiber cavities embedding semiconductor quantum dots emitting in the telecom O-band — •NAM TRAN¹, JULIAN MAISCH¹, JONAS GRAMMEL², JULIA WECKER¹, THOMAS HERZOG¹, ROBERT SITTIG¹, PONRAJ VIJAYAN¹, MICHAEL JETTER¹, SIMONE L. PORTALUPI¹, DAVID HUNGER², and PETER MICHLER¹ — ¹Institut für Halbleitertechnik und Funktionelle Grenzflächen, Center for Integrated Quantum Science and Technology (IQST) and SCoPE, University of Stuttgart, Stuttgart, Germany — ²Physikalisches Institut, Karlsruher Institut für Technologie (KIT), Karlsruhe, Germany

Single photon sources operating at telecom wavelength play a central role in quantum information, in particular when long-distance implementations are targeted. Highly promising candidates are semiconductor quantum dots (QD). Cavity quantum electrodynamics is often used to tailor the emission properties and, in case of photon sources, enhance their performances. However, limiting factors like spatial and spectral mismatch can be detrimental to the cavity-emitter interaction. Using tunable fiber cavities can overcome these limitations. Additionally, since the fiber coupling is intrinsically given in these cavities the integration into the already existing fiber network is facilitated. Here, we made a thorough investigation of the optical properties of open fiber cavities embedding semiconductor QDs emitting in the telecom O-band. Moreover, deterministic positioning of individual QDs enables the comparison of the optical properties within and outside the cavity.

HL 49.4 Fri 10:15 POT 151

Higher order effective coefficients in Ge/Si core/shell nanowire devices — •SEBASTIAN MILES^{1,2}, PIOTR ROZEK^{1,2}, MERT BOZKURT^{1,2}, DÁNIEL VARJAS³, and MICHAEL WIMMER^{1,2} — ¹QuTech, Delft University of Technology, Delft 2600 GA, The Netherlands — ²Kavli Institute of Nanoscience, Delft University of Technology, Delft 2600 GA, The Netherlands — ³Max-Planck-Institut für Physik komplexer Systeme, 01187 Dresden, Germany

Germanium based nanowires are prominent platforms in mesoscopic physics because of their tunable spin-orbit interaction. This property makes them an interesting candidate for hole-qubit devices or as a platform for Majoranas. Hence, a good understanding of effective models for the relevant degrees of freedom in these devices is of great importance. We revisit the subject of effective Hamiltonians and effective coefficients for efficient nano-device control in Ge/Si core/shell semiconductor nanowires from a perturbation theory perspective. We elaborate on relevant terms and present numerical and semi-analytical results of Lowdin perturbation theory to second order. We discuss the consequences of higher order terms on the effective models of interest for device applications.

30 min. break

HL 49.5 Fri 11:00 POT 151

Interfacing Semiconductor Quantum Dots with Photonic Wire Bonds — •MARCO DE GREGORIO¹, SHANGXUAN YU^{2,3}, DONALD WITT^{2,3}, BECKY LIN^{2,3}, MATTHEW MITCHELL², TOBIAS HUBER-LOYOLA¹, LUKAS CHROSTOWSKI^{2,3}, JEFF F. YOUNG^{2,4}, ANDREAS PFENNING^{1,2}, and SVEN HÖFLING¹ — ¹Lehrstuhl für Technische Physik, Julius-Maximilians-Universität Würzburg, Am Hubland, D-97074 Würzburg, Germany — ²Stewart Blusson Quantum Matter Institute, University of British Columbia, Vancouver, British Columbia V6T 1Z4, Canada — ³Department of Electrical and Computer Engineering, University of British Columbia, Vancouver, British Columbia V6T 1Z4, Canada — ⁴Department of Physics and Astronomy, University of British Columbia, Vancouver, British Columbia V6T 1Z1, Canada

We present first experimental results of an alternative extraction technique of single photons emitted by semiconductor quantum dots. For this purpose, a photonic wire bond is directly attached to the end facet of a waveguide containing In(Ga)As semiconductor quantum dots grown by molecular beam epitaxy and connected to a single-mode optical fiber. We perform above-band and optical resonant excitation of the quantum dot and find that in this configuration, cross-polarization filtering of the single photons can be avoided, while measuring a steady stream of single-photons in fiber. The coupling efficiency can be further improved by optimized mode matching between photonic wire bond and waveguide.

HL 49.6 Fri 11:15 POT 151

Deterministically fabricated InAs quantum dot based single-photon sources at telecom wavelengths — •MONICA PENGERLA¹, ALKAALES MOHANAD², RANBIR KAUR², JAN DONGES¹, LUCAS BREMER¹, JOHANNES SCHALL¹, SVEN RODT¹, MOHAMED BENYOUCER², and STEPHAN REITZENSTEIN¹ — ¹Institut für Festkörperphysik, Technische Universität Berlin, Hardenbergstraße 36, D-10623 Berlin, Germany — ²Institute of Nanostructure Technologies and Analytics (INA), Center for Interdisciplinary Nanostructure Science and Technology (CINSaT), University of Kassel, Heinrich-Plett-Str. 40, 34132 Kassel, Germany

Quantum dot (QD) based single-photon sources are key elements of photonic quantum networks. Most interesting are sources emitting at telecom wavelengths to enable long distance fiber-based quantum communication. Here, we report on deterministically fabricated single-photon sources based on InAs QDs grown on InP substrate. Numerical simulations of such QD heterostructures with backside distributed Bragg reflector reveal photon extraction efficiency exceeding 50% when QDs are integrated into mesa or circular Bragg grating structures. A state-of-the-art electron beam lithography (EBL) system with integrated low temperature cathode luminescence (CL) system allows us to perform in-situ EBL at telecom wavelengths. For noisy CL maps, an advanced approach for machine learning enhanced in-situ EBL to enhance the maps at telecom wavelengths for better integration of QDs into photonic structures is used. Micro-photoluminescence studies reveal the optical properties of the fabricated quantum devices.

HL 49.7 Fri 11:30 POT 151

GaSb Quantum Dots as Emitters of Telecom S-Band Single Photons — •JOHANNES MICHL¹, GIORA PENIAKOV², ANDREAS PFENNING¹, JOONAS HILSKA², ABHIROOP CHELLU², TEEMU HAKKARAINEN², TOBIAS HUBER-LOYOLA¹, MIRCEA GUINA², and SVEN HÖFLING¹ — ¹Technische Physik, Julius-Maximilians-Universität Würzburg, Germany — ²Physics Unit / Photonics Faculty of Engineering and Natural Sciences, Tampere University, Finland

Over the last few years, several semiconductor quantum dot (QD) material platforms like In(Ga)As/ GaAs and InAs/InP have emerged as resources for non-classical light and spin-photon interfaces in the telecom wavelength range. However, there is not much data on the optical and spin properties of GaSb QDs, despite it being a physically rich system. For example, it is possible to switch between direct and indirect bandgap by controlling the size of the quantum dots. Moreover, due to reduced strain, it is expected to have less quadrupole nuclear interaction resulting in enhanced spin dephasing times, similar to what was recently observed in GaAs QDs in AlGaAs. Here, we investigate the (quantum-) optical properties of GaSb quantum dots which are fabricated by filling droplet-etched nanoholes in an AlGaSb matrix and exhibit photoluminescence (PL) with a narrow linewidth in the telecom S-band. We perform polarization resolved magneto-PL studies to investigate charge complexes in our sample and perform correlation measurements to evaluate the use of GaSb quantum dots as a source of indistinguishable single photons.

HL 50: Materials and devices for quantum technology III

Time: Friday 9:30–13:00

Location: POT 251

HL 50.1 Fri 9:30 POT 251

3D magnetic resonance tomography of nitrogen vacancy centers with sub-10nm resolution — •MOHAMMAD T AMAWI^{1,2}, ANDRII TRELIN¹, YOU HUANG¹, GEORG BRAUNBECK², FRANCESCO POGGIALI¹, and FRIEDEMANN REINHARD¹ — ¹Institute for Physics, Quantum Technology, University of Rostock, Germany — ²Physics Department, Technical University of Munich, Germany

We present a device for three-dimensional magnetic resonance tomography with nanoscale resolution, and apply it to image the spatial position of a nitrogen-vacancy center (NV) cluster in bulk diamond. Three orthogonal magnetic field gradients, generated from currents in microfabricated gold conductors, are used to create a position-specific Larmor frequency of the NV ground state spins. Measuring this frequency by pulsed optical-microwave spectroscopy, we determine the position of each NV center in 3D.

I will report on fabrication of the device, based on a liftoff process and maskless lithography, as well as the geometry required to create three orthogonal magnetic fields. The measurement protocol for 3D imaging will be discussed, as well as hardware and software means to reduce the shot-to-shot field variation, caused by electrical noise, down to 0.1%. This level of stability enabled us to demonstrate 3D imaging with around 5 nm spatial resolution. I will conclude with an outlook addressing how the resolution can be further improved by reducing the dimensions of the micro wires, and how it could be extended to image spins deposited on the diamond surface.

[1] Arai, K. et al. Nat. Nanotechnol. 10 (2015)

HL 50.2 Fri 9:45 POT 251

3D printing as an enabling tool for quantum technologies — •PAVEL RUCHKA¹, KSENIA WEBER¹, SINA HAMMER², CARLOS JIMENEZ³, SIMON THIELE³, JOHANNES DROZELLA³, TIM LANGEN², ALOIS HERKOMMER³, and HARALD GIESSEN¹ — ¹4th Physics Institute, Research Center SCoPE and Center for Integrated Quantum Science and Technology, Universität Stuttgart, Pfaffenwaldring 57, 70569 Stuttgart, Germany — ²5th Physics Institute and Center for Integrated Quantum Science and Technology, Universität Stuttgart, Pfaffenwaldring 57, 70569 Stuttgart, Germany — ³Institute of Applied Optics (ITO) and Research Center SCoPE, University of Stuttgart, Pfaffenwaldring 9, 70569 Stuttgart, Germany

Nowadays, a lot of effort is given to making quantum technologies more usable for day-to-day life. This involves many aspects, such as developing quantum computers with a large number of qubits, creating quantum gates with high fidelity, and establishing a large-scale communication links with quantum repeaters. Miniaturizing such quantum devices remains nevertheless a highly relevant issue. For this, the 2-photon polymerization (2PP) based 3D printing comes in handy. In this talk, we present several miniature 3D printed optical and mechanical components, which enable the optical trapping of atoms and coupling quantum emitters and detectors to fibers or chips. These devices have an exceptionally compact footprint and a comparably high efficiency. With the ease of production of such components, 2PP can be scaled for the future requirements of highly compact and efficient quantum devices.

HL 50.3 Fri 10:00 POT 251

Spatially controlled fabrication of telecom single-photon emitters in Si by focused ion beam implantation — •NICO KLINGNER¹, MICHAEL HOLLENBACH^{1,2}, NAGESH JAGTAP¹, LOTHAR BISCHOFF¹, CIARAN FOWLEY¹, ULRICH KENTSCH¹, GREGOR HLAWACEK¹, ARTUR ERBE¹, NIKOLAY ABROSIMOV³, MANFRED HELM¹, YONDER BERENCEN¹, and GEORGY ASTAKHOV¹ — ¹Helmholtz-Zentrum Dresden-Rossendorf, Institute of Ion Beam Physics and Materials Research, 01328 Dresden, Germany — ²Technische Universität Dresden, 01062 Dresden, Germany — ³Leibniz-Institut für Kristallzüchtung (IKZ), 12489 Berlin, Germany

Single photon emitters (SPE) are the starting point and foundation for future photonic quantum technologies. We present the laterally controlled fabrication of single G and W centers in silicon that emit in the telecom O-band. We utilized home built gold-silicon liquid metal alloy ion sources (LMAIS) in a focused ion beam (FIB) system to perform mask-free implantation of 40 keV Si ions from 6 to 500 ions per spot. Analysis and confirmation of SPEs has been done in a home-built cryo-photoluminescence setup. We will demonstrate a success rate of more than 50% and upscaling to wafer-scale. We will also provide an insight and overview on the LMAIS technology and an outlook on other potential applications of FIB implantation. arXiv:2204.13173

HL 50.4 Fri 10:15 POT 251

Plasma studies by optical emission spectroscopy for phosphorus doped diamond — •FELIX HOFFMANN¹, NICOLA LANG¹, PHILIPP REINKE², PETER KNITTEL¹, and VOLKER CIMALLA¹ — ¹Fraunhofer Institute for Applied Solid State Physics, Tullastraße 72, D-79108 Freiburg, Germany — ²Quantum Brilliance GmbH, Industriestraße 4, D-70565 Stuttgart, Germany

While p-doping of diamond by Boron is a well-controlled process, n-doping by Phosphorus (P) remains challenging due to its low solubility and big covalent radius in comparison to carbon. The control of plasma conditions and the understanding of its influence on growth parameter is crucial for single crystal diamond growth by microwave plasma assisted chemical vapor deposition (MPCVD) [1]. Hydrogen-methane plasmas with dopant-carrier gases have been analyzed with respect to kinetic gas temperature (of the C2 band) and radical concentration by optical emission spectroscopy (OES) under various experimental conditions such as excitation power, operating pressure and gas concentrations [2]. Here we present results of P-doped diamond growth using the carrier gas trimethylphosphine (TMP) and point out the influence of TMP on plasma properties and its relation to growth parameter of P-doped {111} diamond grown by MPCVD.

[1] V. Mortet et al. *Diamond and Related Materials*, 2022, 124, 108928

[2] Mikhail Aleksandrovich Lobaev et al. *Phys. Status Solidi A*, 2019, 216, 1900234

HL 50.5 Fri 10:30 POT 251

Modifying dipole selection rules in cuprous oxide Rydberg excitons — •ANNIKA NEUBAUER and HARALD GIESSEN — 4th Physics Institute, University of Stuttgart

Excitons in cuprous oxide have large binding energies, which implies that different principal quantum number state excitons can be created as they are energetically not spaced too closely to each other nor to the ionization continuum. High principal quantum number Rydberg excitons in cuprous oxide are macroscopic quantum systems with spatial extensions in the several hundreds of nm up to several μm range. This implies, that excitation with a focused light beam leads to a large overlap of light and matter wavefunctions and should lead to an enhanced optical transition.

We are going to show that the dipole selection rules in cuprous oxide Rydberg excitons can be manipulated via excitation with orbital angular momentum light or via the quadrupole field of plasmonic antennas. Both such light fields possess a strong field gradient or an additional angular momentum. This way, different angular momentum quantum number state excitons can be switched on and off, which is attractive for quantum state engineering. The mesoscopic size of cuprous oxide Rydberg excitons also implies that already μm -sized structures lead to mesoscopic quantum size effects. This can be advantageous for the realization of quantum technologies, such as optical switching applications, based on cuprous oxide Rydberg excitons.

HL 50.6 Fri 10:45 POT 251

Strong coupling of a single quantum dot to a tunable plasmonic nanogap antenna at room temperature using a novel scanning probe technique — •MICHAEL A. BECKER¹, HSUAN-WEI LIU^{1,2}, BURAK GURLEK^{1,2}, KORENOBU MATSUZAKI¹, RANDHIR KUMAR¹, STEPHAN GÖTZINGER^{2,1}, and VAHID SANDOGHDAR^{1,2} — ¹Max Planck Institute for the Science of Light, Staudtstr. 2, 91058 Erlangen, Germany — ²Friedrich Alexander University of Erlangen-Nürnberg, Schloßplatz 4, 91054 Erlangen, Germany

In the strong coupling regime of cavity quantum electrodynamics, the spectrum of an isolated quantum system hybridizes with a mode of a resonator. At room temperature, coupling to the environment leads to a fast dephasing of the transition dipole, and strong near-field enhancements in plasmonic nanoantenna ge-

ometries need to be exploited to reach the strong light-matter coupling regime. For an efficient coupling, the antennas need to be placed within a few nanometer with respect to the individual emitters. Here, we exploit our novel and simple press-roll scanning probe technique (PROscan) capable of performing high-precision optical near-field measurements with remarkable stability. We demonstrate an open nanogap antenna that can be tuned in resonance with the exciton transition of a single quantum dot. With this approach, we drive the system from the weak to the strong light-matter coupling regime, evidenced by a vacuum Rabi splitting. Our results elucidate the complex interplay between the nanoantenna's mode volume and the physics of its eigenmode.

30 min. break

HL 50.7 Fri 11:30 POT 251

Optimal quantum control of Si/SiGe spin qubits in a Quantum bus architecture — •AKSHAY MENON PAZHEDATH¹, ALESSANDRO DAVID¹, LARS R. SCHREIBER², HENDRIK BLUHM², TOMMASO CALARCO¹, and FELIX MOTZOI¹ — ¹Peter Grünberg Institute-Quantum Control (PGI-8), Forschungszentrum Jülich GmbH, Germany — ²JARA-FIT Institute for Quantum Information, Forschungszentrum Jülich GmbH and RWTH Aachen University, Germany

Quantum bus architecture based on electron spin-shuttling is a promising candidate for scalable quantum computing, as the number of control lines required to control the spin remains constant irrespective of the length of the device. A gated Si/SiGe quantum well with a carefully placed micro-magnet acts as an addressable qubit system in such an architecture. We investigate the feasibility of performing single qubit operations using optimal quantum control techniques. Spin decoherence due to interaction with the valley degree of freedom in the Si/SiGe heterostructure is identified as a potential decay mechanism and optimal pulses are engineered to maximize single qubit state transfer and unitary operation fidelities, so that the operations are compliant with the fault tolerant error threshold.

HL 50.8 Fri 11:45 POT 251

Generating spatially distributed entanglement as a resource for novel quantum computing paradigms on a platform of coupled microcavities — •MARC BOSTELMANN, STEFFEN WILKSEN, FREDERIK LOHOF, and CHRISTOPHER GIES — Institute for Theoretical Physics and Bremen Center for Computational Material Science, University of Bremen, Bremen, Germany

Spatially distributed entanglement is important for the realization of novel quantum-photonics applications in quantum computing and quantum machine learning. We consider photonic arrays made from quantum emitters in optically coupled microcavities as hardware platform for entanglement generation. These offer a large degree of tunability with the possibility of site-selective optical excitation. We present a scalable numerical scheme for the determination of excitation parameters to generate different classes of multipartite entangled states, and a quantum bath engineering approach to create entanglement in the steady-state [arXiv:2211.13639].

HL 50.9 Fri 12:00 POT 251

Towards the Development of Cryogenic Integrated Power Management Units — •ALFONSO RAFAEL CABRERA GALICIA — Forschungszentrum Jülich GmbH Wilhelm-Johnen-Straße 52428 Jülich

Integrated Circuits (ICs) in cryogenic environments are expected to allow the development of scalable quantum computers consisting of thousands of physical quantum bits (qubits). However, since these ICs require undistorted power supply for optimal performance, the development of Power Management Units (PMUs) capable of cryogenic operation is also needed for the quantum computing systems scalability. To develop such PMUs, it is necessary to understand the cryogenic electrical behavior of its components. Therefore, this talk will present the measurement results obtained from an exploratory cryogenic DC characterization of some of the passive and active components belonging to a commercial 22nm FDSOI IC technology.

HL 50.10 Fri 12:15 POT 251

Physical Integration of Cryogenic Control Electronic Together with a Spin Qubit Sample at mK Temperatures — •LEA-MARIE SCHRECKENBERG¹, PATRICK VLEEX¹, RENÉ OTTEN², and STEFAN VAN WAASEN^{1,3} — ¹Central Institute of Engineering, Electronics and Analytics, Electronic Systems, Forschungszentrum Jülich GmbH, Jülich, Germany — ²JARA Institute for Quantum Information, Forschungszentrum Jülich GmbH and RWTH Aachen University, Aachen, Germany — ³Faculty of Engineering, Communication Systems, University of Duisburg-Essen, Germany

A universal quantum computer requires the control and read out of millions of physical quantum bits (qubits). Due to wiring limitation in current state-of-the-art dilution refrigerators scaling up to millions of qubits with room-temperature electronics is challenging. Integrated Circuits (ICs) operating next to the qubits will help solving this scalability problem but require novel approaches for cryogenic circuits. This talk will focus on the physical design layer of the integration of a custom-designed 65nm CMOS low-power digital to analog converter (DAC)

for qubit bias together with a spin qubit sample. In total, eight DAC channels are integrated at the mixing chamber stage of a dilution refrigerator and are operated at milli-kelvin temperatures. Additionally, engineering aspects regarding the sample space setup, cryostat wiring and the tight density are pointed out.

HL 50.11 Fri 12:30 POT 251

Design of power efficient digital low-dropout circuit for quantum computers — •SWASTHIK BAJE SHANKARAKRISHNA BHAT¹, ALFONSO RAFAEL CABRERA GALICIA¹, ARUN ASHOK¹, PATRICK VLIEX¹, ANDRE ZAMBANINI¹, CHRISTIAN GREWING¹, and STEFAN VAN WAASEN^{1,2} — ¹Forschungszentrum Jülich GmbH, Germany — ²Universität Duisburg-Essen

Quantum computing is an approach to enable new computing paradigms with qubits as the computing elements that require individual tuning. A limitation in current setups is the number of controllable qubits. To scale the number of qubits, a close integration of control circuits close to the qubits in the cryogenic environment is required. However, to deal with these cryostats* minimal thermal power budget, ultra-low power dissipation is required, also for biasing circuits.

This contribution presents the design and simulation results of a power-efficient digital low-dropout regulator developed with a commercial 22nm FD-SOI technology. It is expected that the circuit will enable on-chip biasing for future quantum computers based on Cryogenic Electronics operating at 4 K. Unlike its Analog counterpart integrated Digital LDO is not prone to process and mismatches delivering high efficiency at the same time The circuit concept and the system model investigation performed via Matlab-Simulink will be showed, as well as the expected circuit performance.

HL 51: Nitrides: Preparation and Characterization

Time: Friday 9:30–12:15

Location: POT 112

HL 51.1 Fri 9:30 POT 112

High resistive buffer layers by Fermi-level engineering — •ARMIN DADGAR, RALF BORGMANN, and ANDRÉ STRITTMATTER — Otto-von-Guericke-Universität Magdeburg, FNW-IfP, Universitätsplatz 2, 39106 Magdeburg

We present a novel method to increase the resistivity of semiconductor buffer layers by aligning the Fermi level using a donor and an acceptor dopant of which one preferentially is a deep level placed in the lower (acceptor) or upper (donor) half of the energy band-gap. Potential doping sequences in GaN were simulated by nextnano software showing that the average Fermi-level position of alternately donor and acceptor doped layers can be shifted to the midgap position. This shift decreases the free carrier concentration and increases the resistivity as demonstrated for GaN:C / GaN:Si layer stacks. In structures grown by metalorganic vapor phase epitaxy, less charging and hysteresis effects are observed upon polarity changing between electrical contacts placed at surface and substrate. Also, the reduced total deep level concentration improves resistivity under electron and hole injection and the overall breakdown voltage by more than 20 %.

HL 51.2 Fri 9:45 POT 112

YOLO-assisted object detection of dislocation-related pits on GaN surfaces using generative adversarial networks — •MAHDI KHALILI HEZARJARIBI^{1,2}, UWE ROSSOW^{1,2}, HEIKO BREMERS^{1,2}, and ANDREAS HANGLEITER^{1,2} — ¹Institute of Applied Physics, Technische Universität Braunschweig, Germany — ²Laboratory for Emerging Nanometrology, Technische Universität Braunschweig, Germany

In this paper, we present a model for detecting dislocation-related pits on GaN surfaces using SEM images, which strongly relies on the use of synthetic image generation. Pits mark dislocations in the layers and are widely used to assess crystalline quality; therefore, a considerable amount of images containing pits have to be evaluated. For this purpose, a Deep Learning (DL) algorithm is employed to achieve objective results, which are detecting the pits, and hence the dislocations, in SEM images. In order to train the algorithm to efficiently detect the objects, we need a host of SEM images containing pits in multiple sizes, numbers, formations, and noises. Due to the complexity of the microscopic structures and the lack of enough images, we incorporated a group of powerful algorithms called Generative Adversarial Networks to create artificial fake images just like real images and feed them, together with our real images, to our dataset to enrich the volume of the dataset. In the next stage, the YOLO algorithm (version 5) has been employed as the core deep learning algorithm for the object detection process using the above-mentioned dataset to train the network. A minimum average confidence of 86% for detecting real objects has been realized, corresponding to a high probability of detection.

HL 51.3 Fri 10:00 POT 112

Molecular beam epitaxy growth study and characterization of HoN thin films — •ANNA MELENDEZ-SANS¹, VANDA M. PEREIRA¹, CHUN-FU CHANG¹, CHANG-YANG KUO^{1,2,3}, CHIEN-TE CHEN², LIU HAO TJENG¹, and SIMONE G.

HL 50.12 Fri 12:45 POT 251

Design of Ultra-Low Power High Speed Communication Interface From Cryogenic to Room Temperature Electronics — •EGE ONAT, JONAS BÜHLER, CHRISTIAN GREWING, and STEFAN VAN WAASEN — Central Institute of Engineering, Electronics and Analytics, ZEA-2: Electronic Systems, Forschungszentrum Jülich GmbH

The objective of this research is to transfer high-speed data from deep cryogenic temperatures to room temperature while aiming for the lowest achievable power consumption in the cryostat. Quantum computers are operated inside dilution refrigerators under deep cryogenic temperatures and they need additional circuitry to ensure fault-free operations. Heating of the qubits caused by additional electronics degrades the system performance. Due to the limited power budget of the dilution refrigerators, each circuit should be designed considering power consumption. In contrast, the higher temperature stage can manage a higher power budget than the stage with the qubits. In this research, low-power data transmission methods for quantum computer applications are investigated and an asymmetric communication interface is designed and implemented. To achieve the asymmetric interface, only a varactor is placed into the cryogenic stage. To measure the capacitance on the room temperature stage, a capacitance readout circuitry is designed. It converts the capacitance into a measurable output such as voltage, frequency, or digital data. By implementing this interface, the data is carried on capacitance rather than voltages, which minimizes the power consumption at the transmitter compared to widely implemented communication interfaces.

ALTENDORF¹ — ¹Max Planck Institute for Chemical Physics of Solids, Dresden, Germany — ²National Synchrotron Radiation Research Center, Hsinchu, Taiwan — ³Department of Electrophysics, National Yang Ming Chiao Tung University, Hsinchu, Taiwan

Rare earth nitrides show potential for a wide range of applications due to their strong magnetic moment and semiconducting behavior. However, their synthesis and characterization has proven challenging since they rapidly oxidize when exposed to ambient conditions. Thanks to continuous developments in UHV-based thin film growth methods it is possible to grow high quality rare earth nitride films and, through the characterization of these, gain better insight into these compounds.

Whilst there have been many reports on GdN and SmN, not much is yet known about HoN. Now we present a systematic growth study on HoN thin films synthesized by molecular beam epitaxy (MBE), and using different substrates (MgO, LaAlO₃) and growth conditions (substrate temperatures and Nitrogen-gas pressure). These films were subsequently characterized using *in situ* techniques (Reflection high-energy electron diffraction, X-ray absorption and photoelectron spectroscopy) and *ex situ* techniques (X-ray diffraction, Superconducting quantum interference device) in order to evaluate their crystalline, electronic and magnetic structure.

HL 51.4 Fri 10:15 POT 112

Theoretical study on the (Al_xSc_{1-x})N random alloy — •JAN M. WAACK^{1,2}, MARKUS KREMER^{1,2}, MICHAEL CZERNER^{1,2}, and CHRISTIAN HEILIGER^{1,2} — ¹Institut für theoretische Physik, Justus-Liebig-Universität Gießen, Germany — ²Center for Materials Research (LaMa), Justus-Liebig-Universität Gießen, Germany

Aluminium scandium nitride (Al_xSc_{1-x}N, (Al,Sc)N or AlScN) is a random alloy. As such, the calculation of physical properties requires specific methods such as the coherent potential approximation (CPA)[1] and special quasi-random structures (SQS)[2]. We compare the CPA in the framework of the atomic sphere approximation (ASA) Korringa-Kohn-Rostoker (KKR) density functional theory (DFT) with the SQS using the plane-wave pseudopotential DFT to calculate the lattice parameters and electronic band structures of the face-centered cubic phase of Al_xSc_{1-x}N (with 0 ≤ x ≤ 1).

Using the low computational cost LDA-1/2 quasiparticle method [3] to calculate the electronic band structures within SQS and CPA, we present the first implementation of LDA-1/2 within the KKR DFT. We find that both the lattice parameter and the indirect band gap deviate from Vegard's law.

[1] C. Franz, M. Czerner, and C. Heiliger, Phys. Rev. B 88, 94421 (2013). <https://doi.org/10.1103/PhysRevB.88.094421>

[2] A. Zunger, S.-H. Wei, L. G. Ferreira, and J. E. Bernard, Phys. Rev. Lett. 65, 353 (1990). <https://doi.org/10.1103/PhysRevLett.65.353>

[3] L. G. Ferreira, M. Marques, and L. K. Teles, Phys. Rev. B 78, 125116 (2008). <https://doi.org/10.1103/PhysRevB.78.125116>

HL 51.5 Fri 10:30 POT 112

Thermal Transport in c-plane GaN Membranes Studied by Raman Thermometry — •WILKEN SEEMANN¹, JOACHIM CIERS², ISABELL HÜLLEN¹, MAHMOUD ELHAJHASAN¹, JEAN-FRANÇOIS CARLIN³, NICOLAS GRANDJEAN³, ÅSA HAGLUND², and GORDON CALLEN¹ — ¹Institute of Solid State Physics, University of Bremen, Germany — ²Department of Microtechnology and Nanoscience, Chalmers University of Technology, Gothenburg, Sweden — ³Institute of Physics, École Polytechnique Fédérale de Lausanne (EPFL), Switzerland

Heating during operation often limits the lifetime or stability of semiconductor devices, like laser structures, e.g., via defect formation or by affecting the refractive index. Understanding how thermal energy is dissipated from the active region of such structures is therefore an important step towards device optimization.

We analyze the in-plane thermal transport in GaN-based membranes. The temperature is probed by the shift and width of Raman modes under heating with a UV laser. This allows for a non-contact characterization without the need for additional processing steps.

By varying the membrane undercutting process, we can tune the membrane bottom facet roughness and porosity to study their impact on thermal conductivity κ , due to phonon boundary scattering. A reduction of κ is a sign of phonon frequency filtering, which is a first step towards engineering the phonon dispersion relation in GaN membranes. Controlling this effect, e.g., via the position and sizes of pores, might enable thermal concepts to locally reduce temperature rises.

15 min. break

HL 51.6 Fri 11:00 POT 112

SmN thin films: MBE-growth and spectroscopy studies — •VANDA M. PEREIRA¹, ANNA MELENDEZ-SANS¹, CHUN-FU CHANG¹, CHANG-YANG KUO^{1,2,3}, CHIEN-TE CHEN², LIU HAO TJENG¹, and SIMONE G. ALTENDORF¹ — ¹Max Planck Institute for Chemical Physics of Solids, Dresden, Germany — ²National Synchrotron Radiation Research Center, Hsinchu, Taiwan — ³Department of Electrophysics, National Yang Ming Chiao Tung University, Hsinchu, Taiwan

Although the rare earth nitrides have been in the scientific scene for many decades, their poor stoichiometry and reactivity in ambient conditions have severely conditioned their progress. It has been only rather recently that studies on thin films have started to unveil some of their unique characteristics and solve decades-old controversies, but there are still significant gaps left to explore.

Recent studies on the ferromagnetic semiconductor SmN suggest that the 4f bands are involved in electron transport and are crucial to the observed superconductivity in nitrogen-vacancy doped samples. Nevertheless, more concrete experimental evidence is needed.

Here we present a systematic study of SmN thin films grown by molecular beam epitaxy, exploring their crystalline quality and composition as the growth parameters (substrate temperature and nitrogen pressure) are varied. The films were characterized *in situ* making use of photoemission and x-ray absorption spectroscopies, thereby allowing to reliably gain more insight into the electronic structure of this material.

HL 51.7 Fri 11:15 POT 112

Growth of ScN and AlScN by reactive sputter epitaxy — •FLORIAN HÖRICH, CHRISTOPHER LÜTTICH, RALF BORGMANN, JÜRGEN BLÄSING, ANDRÉ STRITTMATTER, and ARMIN DADGAR — Otto-von-Guericke University

Spontaneous polarization fields induced by a strained AlGaIn/GaN layer structure lead to high-density two-dimensional electron gases which are key to current high-power and high-frequency transistor devices. Recent theoretical and experimental data demonstrated an even higher two-dimensional electron density when AlScN is used [1]. Up to now, growth of Sc-containing materials by conventional MOVPE is hampered by the lack of a suitable Sc precursor. Reactive sputter epitaxy using metallic Al and Sc targets together with ammonia or molecular nitrogen has the potential to fabricate high quality layers at low cost. We will discuss principle growth parameters such as temperature and nucleation conditions for ScN and AlScN on bare Si(111) substrates and on MOVPE grown GaN templates. A large impact of growth temperature is observed on crystal structure and surface morphology. Single-phase crystalline material is obtained at temperatures > 800 °C. We find different optimum nucleation conditions for both kind of substrate surfaces. Growth on bare Si(111) surfaces with an initial metallic Sc thickness equivalent to <1 nm drastically improves crystallinity.

For the GaN(0001) template surface, such sequence has no impact. Additionally, sputtering of AlScN and ScN with ammonia results in better structural quality than with nitrogen.

[1] I. Streicher, et. al. Phys. Status Solidi RRL 2200387

HL 51.8 Fri 11:30 POT 112

On the variation of PL intensity in GaInN/GaN quantum wells with different cladding thicknesses — •NICO WAGNER¹, SHAWUTIJANG SIDIKEJIANG^{1,2}, PHILIPP HENNING^{1,2}, RODRIGO DE VASCONCELLOS LOURENÇO^{1,2}, HEIKO BREMERS¹, UWE ROSSOW^{1,2}, and ANDREAS HANGLEITER^{1,2} — ¹Institute of Applied Physics, Technische Universität Braunschweig, Germany — ²Laboratory for Emerging Nanometrology, Braunschweig, Germany

The absolute internal quantum efficiency (IQE) of GaInN/GaN quantum wells (QW) at low temperature can be determined using time-resolved photoluminescence (PL) measurements. If the IQE is 100 %, the PL intensity under steady state conditions is expected to be the same for all samples. We can verify that for some samples, but others show different intensities. It turns out that the difference varies for different cladding thicknesses, i.e. the layer between the QW and air. In this work, we present a model calculating the allowed modes inside the sample assuming that all the light is emitted into them if we have 100 % IQE. Due to the small critical angle, it is important to determine the small ratio of intensity, which is coupled out and detected. The result yields an oscillating behavior as a function of the cladding thickness and shows a good agreement with the measured samples. It is important to note that this is a consequence of the Purcell effect, i.e. that spontaneous emission depends on the optical environment.

HL 51.9 Fri 11:45 POT 112

Optical properties of ScN films grown by HVPE and sputter epitaxy — •JONA GRÜMBEL¹, YUICHI OSHIMA², CHRISTOPHER LÜTTICH¹, ARMIN DADGAR¹, MARTIN FENEBERG¹, and RÜDIGER GOLDHAHN¹ — ¹Institut für Physik, Otto-von-Guericke-Universität, Universitätsplatz 2, 39106 Magdeburg — ²Environment and Energy Materials Research Division, National Institute for Materials Science, 1-1 Namiki, Tsukuba, Ibaraki 305-0044, Japan

We investigate the optical properties of rocksalt structured ScN films using spectroscopic ellipsometry and Raman spectroscopy. Two different sets of samples were used for our measurements: (I) ca. 300nm thick ScN grown by sputter epitaxy and (II) 0.4µm up to 40µm thick ScN grown by HVPE. The HVPE grown ScN exhibits a very good crystalline structure, so the carrier concentration varies around 10^{18} cm^{-3} - 10^{19} cm^{-3} , while for ScN grown by sputter epitaxy the carrier concentrations can reach 10^{22} cm^{-3} or more. Therefrom we obtain detailed information about their impact on optical properties, such as optical transitions, optical phonon modes or luminescence. Using spectroscopic ellipsometry we arrive at the dielectric function of ScN from 0.04eV to 6.5eV. Detailed analysis yields the main transitions regarding to direct bandgaps at X- and Γ-point as it was already shown in earlier theoretical works. Surprisingly, we observe characteristic peaks in a Raman scattering measurement, although first order Raman scattering is forbidden in rocksalt structured crystals. Detailed discussion and a possible interpretation will be presented as well as ScN materials parameters calculated from our measurements.

HL 51.10 Fri 12:00 POT 112

Temperature dependent spectroscopic ellipsometry on cubic GaN — •JONAS ROSE¹, ELIAS BARON¹, RÜDIGER GOLDHAHN¹, MICHAEL DEPPE², DONAT J. AS², and MARTIN FENEBERG¹ — ¹Institut für Physik, Otto-von-Guericke-Universität Magdeburg, Germany — ²Department Physik, Universität Paderborn, Germany

Cubic Galliumnitride (c-GaN) is a promising material for designing and fabricating efficient optoelectronic devices, such as green LEDs, and can potentially replace hexagonal GaN for certain applications due to its lack of internal polarization fields. Therefore, the knowledge and control of the optical properties is essential. Recently, several breakthroughs regarding crystal quality of c-GaN have been achieved by utilizing 3C-SiC as a substrate material. We present our investigation of thin film c-GaN deposited by plasma-assisted molecular beam epitaxy on 3C-SiC/Si substrates in (001) orientation. Temperature dependent spectroscopic ellipsometry between 80 and 300 K yields the optical properties (dielectric function, DF) in this temperature range. Hereby, the influence of the excitonic contribution to the DF is of special interest. Using Elliott's model, we describe the lineshape of the DF around the absorption onset. The obtained transition energies follow Pässler's temperature dependent model. Degenerately doped samples up to 10^{20} cm^{-3} are investigated as well. A free-carrier dependent behaviour of the absorption onset is observed and explained for different temperatures.

HL 52: Focus: Self-Assembly of Plasmonic Nanostructures (joint session CPP/HL)

Organized by Tobias A. F. König and Markus Lippitz

Time: Friday 9:30–12:30

Location: GÖR 226

See CPP 56 for details of this session.

Crystalline Solids and their Microstructure Division Fachverband Kristalline Festkörper und deren Mikrostruktur (KFM)

Anna Grünebohm
Experimental Physics 5
Ruhr-Universität Bochum
Universitätsstraße 150
44801 Bochum
anna.gruenebohm@rub.de

Overview of Invited Talks and Sessions

(Lecture halls POT 51 and POT 106; Poster P3)

Invited Talks

KFM 1.1	Mon	9:00– 9:30	POT 51	Investigations of multiferroic behavior within domains and domain walls of a multiferroic Aurivillius phase system — •LYNETTE KEENEY
KFM 1.5	Mon	10:45–11:15	POT 51	Domains or no Domains in Wurtzite-Type Ferroelectrics — •SIMON FICHTNER, NIKLAS WOLFF, TOM-NIKLAS KREUTZER, GEORG SCHÖNWEGER, ADRIAN PETRARU, HERMANN KOHLSTEDT, LORENZ KIENLE, FABIAN LOFINK
KFM 2.1	Mon	14:30–15:00	POT 51	Formation of conducting channels along of dislocations in SrTiO₃ — •CHRISTIAN RODENBÜCHER, KRISTOF SZOT, GUSTAV BIHLMAYER, CARSTEN KORTE
KFM 2.4	Mon	15:55–16:25	POT 51	Plastic properties of MgO : Insights from numerical modeling — •PHILIPPE CARREZ
KFM 4.1	Tue	9:00– 9:30	POT 51	Towards spatially resolved measurements of thermal transport and electrocaloric effects at the nanoscale in ferroelectric materials — REBECCA KELLY, OLIVIA BAXTER, FRAN KURNIA, AMIT KUMAR, MARTY GREGG, •RAYMOND MCQUAID
KFM 7.1	Wed	9:00– 9:30	POT 51	Novel device integration – combining bottom-up and topdown approaches — •ARTUR ERBE
KFM 7.6	Wed	11:05–11:35	POT 51	4D meso-scale electronics for next generation medical tools and electronic skins — •DANIIL KARNAUSCHENKO

Invited Talks of the joint Symposium SKM Dissertation Prize 2023 (SYSD)

See SYSD for the full program of the symposium.

SYSD 1.1	Mon	9:30–10:00	HSZ 04	Diffusion of antibodies in solution: from individual proteins to phase separation domains — •ANITA GIRELLI
SYSD 1.2	Mon	10:00–10:30	HSZ 04	Intermediate Filament Mechanics Across Scales — •ANNA V. SCHEPERS
SYSD 1.3	Mon	10:30–11:00	HSZ 04	Ultrafast Probing and Coherent Vibrational Control of a Surface Structural Phase Transition — •JAN GERRIT HORSTMANN
SYSD 1.4	Mon	11:00–11:30	HSZ 04	Electro-active metasurfaces employing metal-to-insulator phase transitions — •JULIAN KARST
SYSD 1.5	Mon	11:30–12:00	HSZ 04	The role of unconventional symmetries in the dynamics of many-body systems — •PABLO SALA

Sessions

KFM 1.1–1.8	Mon	9:00–12:15	POT 51	Focus: Domains and Domainwalls in (Multi)Ferroics I
KFM 2.1–2.6	Mon	14:30–17:05	POT 51	Focus: Dislocations in Ceramics: Mechanics, Structures and Functionality (joint session KFM/MA)
KFM 3.1–3.3	Mon	14:30–15:30	POT 106	Instrumentation and Methods for Micro- and Nanoanalysis (joint session KFM/PPP)
KFM 4.1–4.10	Tue	9:00–13:10	POT 51	Focus: Domains and Domainwalls in (Multi)Ferroic II
KFM 5.1–5.4	Tue	10:00–11:00	SCH A 315	Thin Film Properties (joint session DS/KFM)
KFM 6.1–6.46	Tue	17:00–19:00	P3	Poster
KFM 7.1–7.9	Wed	9:00–12:35	POT 51	Focus: High-resolution Lithography and 3D Patterning

KFM 8.1–8.9	Wed	14:00–17:15	POT 51	Diamond and related dielectric materials
KFM 9.1–9.12	Wed	9:00–13:15	POT 106	Microscopy and Tomography with X-ray Photons, Electrons, Ions and Positron
KFM 10.1–10.10	Thu	9:00–12:35	POT 51	Battery Materials (joint session KFM/ CPP)
KFM 11.1–11.11	Thu	14:00–17:55	POT 51	Crystal Structure Defects / Real Structure / Microstructure
KFM 12	Thu	18:00–19:00	POT 51	Members' Assembly
KFM 13.1–13.7	Thu	10:00–12:35	POT 106	Polar Oxide Crystals and Solid Solutions I
KFM 14.1–14.7	Thu	14:00–16:35	POT 106	Polar Oxide Crystals and Solid Solutions II

Members' Assembly of the Crystalline Solids and their Microstructure Division

Thu 18:00–19:00 POT 51

Sessions

– Invited Talks, Contributed Talks, and Posters –

KFM 1: Focus: Domains and Domainwalls in (Multi)Ferroics I

The focus session is dedicated to advanced nanoscale characterization, property engineering, and modelling methods of (multi)ferroic materials. Typical examples may include ferroic domain walls, microstructural levers, or strain effects. Further, applications in novel nanoelectronic devices and nano-related engineering concepts for macroscopic properties of multiferroics are of interest.

Chair: Dr. Jan Schultheiß (University of Augsburg)

Time: Monday 9:00–12:15

Location: POT 51

Invited Talk

KFM 1.1 Mon 9:00 POT 51

Investigations of multiferroic behavior within domains and domain walls of a multiferroic Aurivillius phase system — •LYNETTE KEENEY — Tyndall National Institute, University College Cork, Lee Maltings Complex, Dyke Parade, Cork, Ireland, T12 R5CP

Single-phase multiferroics intertwine ferroelectric and ferromagnetic properties, providing novel ways to manipulate data and store information and provide opportunities for exploring new chemistry and physics. In recent years, my team reported the design of a room temperature multiferroic material with an Aurivillius phase structure demonstrating reversible magnetoelectric switching of ferroelectric domains under the influence of a cycled magnetic field. Our previous work used atomic structure determinations of preferred cation locations to advance comprehension of key mechanisms governing ferromagnetism within multiferroic domains. In this presentation, I will discuss fundamental electronic characteristics at differing bonding environments within this complex layered system. We reveal how crystal field splitting of the titanium cation is influenced by its position within the Aurivillius unit cell, correlating with the extent of tetragonal distortion, octahedral tilting and ferroelectric polarisation within the domains. I will discuss how electrostatic strain and elastic energy variations close to bismuth oxide interfaces and defect regions are not only influential in promoting magnetic cation partitioning and multiferroic behaviour, these also influence the formation of exotic charged domain walls and polar vortex domain walls, further initiating technology prospects for this intriguing multiferroic system.

KFM 1.2 Mon 9:30 POT 51

Understanding sensitivity of ferroelectric domain walls to atmospheric parameters — •LEONIE RICHARZ¹, JAN SCHULTHEISS^{1,2}, EDITH BOURRET³, ZEWU YAN^{3,4}, ANTONIUS T.J. VAN HELVOORT¹, and DENNIS MEIER¹ — ¹NTNU Norwegian University of Science and Technology, Trondheim, Norway — ²University of Augsburg, Augsburg, Germany — ³Lawrence Berkeley National Laboratory, Berkeley, CA, USA — ⁴ETH Zurich, Zurich, Switzerland

Ferroelectric domain walls are natural interfaces, separating volumes with different orientation of the spontaneous polarization. The walls can develop completely different electronic properties than the surrounding domains. In ferroelectric oxides, oxygen off-stoichiometry is an additional versatile control parameter, reflected by neutral ferroelectric domain walls in hexagonal manganites: Depending on the oxygen content, their conductance varies from insulating to conducting.

In this work, we change the conductance state of neutral ferroelectric domain walls in high-quality Er(Mn,Ti)O₃ single crystals from insulating to conducting by annealing the samples in reducing conditions, e.g., nitrogen. The process can be reversed by annealing under oxidizing conditions, reflecting the outstanding chemical flexibility of the domain walls. The sensitivity to off-stoichiometry can be exploited to utilize the domain walls for sensing applications.

Our results provide new insight into the impact of environmental parameters on the electronic domain wall properties. This is of interest for the development of atmospheric sensors, adding a new direction to the field of domain wall nanotechnology.

KFM 1.3 Mon 9:50 POT 51

Thermal and elastic stability of acceptor dopants in BaTiO₃ — •ARIS DIMOU¹, ALDO RAELIARIJAONA², R. E. COHEN², and ANNA GRÜNEBOHM¹ — ¹Interdisciplinary Center for Advanced Materials Simulation (ICAMS) and Center for Interface-Dominated High-performance Materials (ZGH), Ruhr-University Bochum, Germany — ²Extreme Materials Initiative, Earth and Planets Laboratory, Carnegie Institution for Science, Washington, DC 20015-1305, USA

The presence of defects, such as vacancies and aliovalent substitutions significantly impacts the functional properties of ferroelectric materials. Defect dipoles formed by acceptor dopants and oxygen vacancies have gained interest after the

demonstration of superlattice, reversible piezoelectric [1], and electrocaloric [2] responses. But so far a deep understanding of their stability is missing.

We compare the thermal stability of Fe, Cu, and Mn dopants, and explore the impact of biaxial strain on the defect stability by density functional theory and *ab-initio* molecular dynamics. We found the largest barrier for the $Cu_{Ti} - V_O$ defect complexes, and exhibit the enhanced barrier height under compressive biaxial strain.

[1] X. Ren, Nature Materials, 3(2):91-94, 2004

[2] A. Grünebohm et al., Phys. Rev. B, 93(13):134101, 2016

KFM 1.4 Mon 10:10 POT 51

Probing hidden order in ferroelectric oxide thin films with single crystal diffuse X-ray scattering — •JOOHEE BANG¹, NIVES STRKALJ², MARTIN SAROTT¹, MORGAN TRASSIN¹, and THOMAS WEBER¹ — ¹Department of Materials Science, ETH Zurich, Zurich, Switzerland — ²Department of Materials Science and Metallurgy, Cambridge University, Cambridge, United Kingdom

Ferroelectric thin films have attracted great attention for its rich applications in energy-efficient electronic devices because of functional properties such as high dielectric constants and electrically switchable polarization. Recently, ferroelectric oxide superlattices with complex topologies such as long-range vortex-antivortex arrays of polarization have garnered much interest as they hold promise for alternative device configurations for microelectronics [1]. Here, we report on a newly discovered local order state in ferroelectric superlattices using a complete three-dimensional diffuse X-ray scattering data, which was collected by taking advantage of high-energy synchrotron X-rays in ultra-small grazing incidence geometry. The data was analyzed with the 3D-deltaPDF method [2], which not only gives a three-dimensional view of the disorder, but also the access to weak disorder that was previously not accessible. This work will contribute to understanding structure-property correlations of ferroelectric oxide superlattices and lay groundwork for developing a novel solid-state characterization technique.

[1] Yadav et al., Nature 530, 206; S. Das et al., Nature 568, 2019

[2] Weber and Simonov, Z. Kristallogr. 227, 2012

15 min. break

Invited Talk

KFM 1.5 Mon 10:45 POT 51

Domains or no Domains in Wurtzite-Type Ferroelectrics — •SIMON FICHTNER^{1,2}, NIKLAS WOLFF¹, TOM-NIKLAS KREUTZER², GEORG SCHÖNWEGER^{1,2}, ADRIAN PETRARU¹, HERMANN KOHLSTEDT¹, LORENZ KIENLE¹, and FABIAN LOFINK^{1,2} — ¹Faculty on Engineering, Christian Albrechts University, Kiel, Germany — ²Fraunhofer ISIT, Itzehoe, Germany

For decades, the wurtzite structure served as a posterchild for pyroelectric, i.e. spontaneously polarized materials which are yet not ferroelectric. The resulting inability to control the dipole ordering after synthesis has largely limited research on wurtzite-type polarization domains and -walls to their suppression. Therefore, the growth of single domain materials of defined polarity has been one of the ultimate goals for the main applications of wurtzite-type semiconductors in the fields of MEMS, RF-, power- and optoelectronics.

Today though, the discovery of ferroelectricity in wurtzite-type solid solutions promises unprecedented possibilities in terms of reconfigurable polarization control in wurtzite-type materials, but also creates the necessity for renewed scientific attention to the domains and -walls of this structure. This contribution aims to provide a vantage point for this attention by giving a glimpse into the literature on this subject and by reporting on our preliminary experimental work on domains in wurtzite-type ferroelectrics. Regarding the latter, transmission electron and piezoelectric force microscopy next to chemical anisotropy studies allow us to draw first conclusions regarding the nucleation, coalescence and distribution of domains in this particular material class.

KFM 1.6 Mon 11:15 POT 51

The role of interfacial stress on the polarization stability of lead-free relaxor ceramics — •JULIA GLAUM^{1,2}, YOOUN HEO², MATIAS ACOSTA³, PANKAJ SHARMA², JAN SEIDEL², and MANUEL HINTERSTEIN^{2,4} — ¹NTNU, Trondheim, Norway — ²UNSW Australia, Sydney, Australia — ³TU Darmstadt, Darmstadt, Germany — ⁴KIT, Karlsruhe, Germany

The unique structural, dielectric and electromechanical properties displayed by canonical relaxor systems, make these materials fascinating objects for fundamental studies as well as for industrial applications. Contributors to these unique properties are the multiple crystallographic phases present simultaneously even in individual grains, as well as the ferroelectric-relaxor phase transformation, which can become reversible in the vicinity of the transition temperature.

Here, we report on the thermal evolution of the crystallographic phases in a (Bi_{1/2}Na_{1/2})TiO₃-BaTiO₃ relaxor ceramic. This system exhibits two polar phases, with the minority phase embedded into the majority phase. While the majority phase retains a stable poling state with increasing temperature up to the transition to the relaxor state, a gradual de-texturization of the poling state is observed for the minority phase over the whole temperature range. The surface domain structure decays already at significantly lower temperatures than expected from bulk observations. Development of interfacial stresses between majority and minority phases and differences in local stress state between surface and bulk are discussed as driving factors of the phase transition dynamics.

KFM 1.7 Mon 11:35 POT 51

Effect of strain on the 3D domain structure of hexagonal manganites — NELLY NATSCH, •AARON MERLIN MÜLLER, AMADÉ BORTIS, MANFRED FIEBIG, and THOMAS LOTTERMOSER — Department of Materials, ETH Zurich, 8093 Zurich, Switzerland

We simulate and visualize the three-dimensional domain structure of strained hexagonal manganites. Due to the improper nature of their ferroelectric order, hexagonal manganites exhibit unconventional vortex domain patterns. In 3D, these vortex domain patterns are characterized by vortex lines, which are 1D topological defects that form arbitrarily oriented loops in bulk materials. We

show that when strain is applied in the ab-plane, the domains exhibit an additional stripe-like order that is oriented perpendicular to the ab-plane. In addition, we show that the strain also acts on the vortex lines, forcing them to form closed loops aligned in the same plane as the domain walls. In our simulations, we observe two types of loops: one type that expands and another type that contracts and collapses. We relate both the formation of the stripe-like domains and the evolution of the vortex-line loops to a force acting directly on the vortex lines which is induced by the applied strain. Our numerical investigation is performed with a phase-field model to simulate the domain structure in three dimensions using a Landau-free-energy expansion.

KFM 1.8 Mon 11:55 POT 51

Tracing property-determining structural alterations via scanning electron diffraction — •URSULA LUDACKA¹, JIALI HE¹, EMIL FRANG CHRISTIANSEN¹, SHUYU QIN², MANUEL ZAHN^{1,6}, ZEWU YAN^{3,4}, EDITH BOURRET⁴, ANTONIUS VAN HELVOORT¹, JOSHUA AGAR^{2,5}, and DENNIS MEIER¹ — ¹NTNU, Trondheim, Norway — ²Lehigh University, Bethlehem, USA — ³ETH Zurich, Zurich, Switzerland — ⁴Lawrence Berkeley National Laboratory, Berkeley, USA — ⁵Drexel University, PA, USA — ⁶Augsburg University, Germany

Ferroelectricity originates from polar displacements of lattice atoms, suggesting a one-to-one correlation between electronic and structural properties at the atomic level. Scanning electron diffraction (SED), a subcategory of 4D-STEM, in combination with direct electron detection (DED) is a powerful tool for probing functional properties on the atomic scale. We demonstrate the potential and opportunities of this innovative SED approach using improper ferroelectric ErMnO₃, an ideal model system as its basic ferroelectric properties, such as local conductivity changes and atomic-scale structure are well understood. By utilizing a convolutional neural network on the SED dataset, we can deconvolve intrinsic scattering phenomena on the atomic level (ferroelectric domains and domain walls) from extrinsic scattering phenomena, such as thickness, bending, or scan distortions. Our results on this topic contain new insights into atomic scale property-structure relations for ferroelectrics. However, the gained knowledge is applicable to complex oxides in general.

KFM 2: Focus: Dislocations in Ceramics: Mechanics, Structures and Functionality (joint session KFM/MA)

Contrasting the common (mis)belief that ceramics are brittle, a new horizon of dislocation engineering in ceramics is being revealed, where dislocations are used to harness the mechanical and electro-functional properties. This session will bring together researchers who are interested in dislocations in ceramics, covering experiments and simulations, to stimulate new ideas for dislocation-based mechanics, characterization, and functionality in ceramics.

Chair: Dr. Xufei Fang (TU Darmstadt), Dr. Till Frömling (TU Darmstadt)

Time: Monday 14:30–17:05

Location: POT 51

Invited Talk

KFM 2.1 Mon 14:30 POT 51

Formation of conducting channels along of dislocations in SrTiO₃ — •CHRISTIAN RODENBÜCHER¹, KRISTOF SZOT², GUSTAV BIHLMAYER³, and CARSTEN KORTE¹ — ¹Forschungszentrum Jülich GmbH, Institute of Energy and Climate Research (IEK-14) — ²University of Silesia, Institute of Physics, 41-500 Chorzów, Poland — ³Forschungszentrum Jülich GmbH, Peter Grünberg Institut (PGI-1), 52425 Jülich, Germany

SrTiO₃ has become one of the most extensively studied metal oxides due to its exceptional electronic properties, which hold promising potential for applications in energy conversion and electronics. A key feature of SrTiO₃ is that its electronic transport properties are closely related to oxygen nonstoichiometry, which can be manipulated via redox reactions. Our nanoscale investigations on crystals and ceramics employing imaging techniques such as local-conductivity atomic force microscopy (LC-AFM) reveal that the reduction process is highly complex and heterogeneous on the nanoscale. Along extended defects such as dislocations there are easy reduction sites where oxygen vacancies are preferentially generated. In this way, filaments with high conductivity evolve around the dislocations in the originally insulating matrix and act as nanoscale short circuits. Upon application of mechanical stress, these filaments can even be moved through the crystal together with the dislocations. These findings not only can explain failure mechanisms in solid oxide electrolytes, but also raise fundamental questions regarding the mechanisms of electronic transport and superconductivity in self-doped transition metal oxides.

KFM 2.2 Mon 15:00 POT 51

Dislocation engineering in oxides at room temperature: understanding the competition between plasticity and cracking — •XUFEI FANG — Technical University of Darmstadt, Alarich-Weiss-Str. 2, 64287 Darmstadt, Germany

Dislocations in ceramic oxides are drawing increasing attention owing to their promising physical properties, such as dislocation-tuned electrical conductivity,

thermal conductivity, and electro-mechanical properties. However, due to the brittleness of most oxides at room temperature, it remains a great challenge to engineer dislocations without forming cracks, which is a prerequisite for harnessing the functionalities. Here, we demonstrate dislocations can be effectively introduced into various ceramic oxides (SrTiO₃, BaTiO₃, KNbO₃, TiO₂) at room temperature by using nanoindentation pop-in stop tests. Interestingly, we find a size-dependent competition between purely dislocation-dominated plastic deformation under a critical tip radius and a concurrent appearance of cracks and dislocations when the tip radius is larger than a certain value. We further extend the deformation scale up to the millimeter regime and identify a reversal of the above size-dependent competition. We will address the underlying mechanisms by examining the dislocation nucleation, multiplication, and motion individually to shed new light on the dislocation mechanics in oxides, particularly at room temperature. Last but not least, the dislocation-tuned electrical and thermal conductivity will be briefly showcased using our developed methods for dislocation engineering.

KFM 2.3 Mon 15:20 POT 51

Tuning dislocations in ferroelectric oxides by cyclic Indentation: dislocation toughening, domain fragmentation and phase stabilisation — •OLIVER PREUSS, FANGPING ZHUO, ENRICO BRUDER, CHRISTIAN MINNERT, JÜRGEN RÖDEL, and XUFEI FANG — Department of Materials and Earth Sciences, Alarich-Weiss-Str. 2, 64287 Darmstadt, Technical University of Darmstadt

In light of the growing research interest in dislocation-tuned functionality in ceramics, promising proofs-of-concept have been most recently demonstrated enhanced ferroelectric properties, electrical conductivity, and superconductivity. Yet introducing dislocations into brittle ceramics remains a grand challenge, especially at room temperature. Here, we demonstrate a simple method using a large Brinell indenter to cyclically indent the sample surface to tune the dislocation densities over 4 orders of magnitude (from 10¹⁰ m⁻² up to 10¹⁴ m⁻²) in

single-crystal KNbO_3 . A large, crack-free plastic zone (200 μm in diameter) is achieved on the sample surface at room temperature. More interestingly, both damage tolerance and fracture toughness have been improved. The interactions between dislocations and other microstructure features are examined in detail by optical microscopy, electron channelling contrast imaging, piezoresponse force microscopy methods and μ -Raman spectroscopy to shed light on the impact of dislocations on the mechanical properties as well as microstructural evolution. Our findings open new questions that may raise interest for further studies in ductile ceramics such as dislocation-domain wall interaction, domain wall fragmentation and strain-induced phase stabilisation.

15 min. break

Invited Talk

KFM 2.4 Mon 15:55 POT 51

Plastic properties of MgO : Insights from numerical modeling — •PHILIPPE CARREZ — Université de Lille, F-59000 Lille, France

Plastic properties of crystalline materials depend not only on the nature of the defects present in the crystal but also and more substantially on their mobilities and mutual interactions. This is typically the case for the creep properties of magnesium oxide (MgO), which has been the subject of numerous investigations over the years. Yet, the atomistic details of dislocation-point defects, dislocation-dislocation or dislocation-grain boundary interactions remain poorly described.

Nowadays, numerical modeling offers the possibility of modeling mechanical properties from the description of the elementary mechanisms of plasticity. As an example, we will discuss the interaction between $1/2\langle 110 \rangle\{110\}$ dislocations and point defects in MgO . We will show how the edge dislocation core, within a region across the glide planes that expands over several Burgers vector, is a sink for vacancies, and thus enhances the pipe diffusion at moderate temperature. At higher temperature, point-defect absorption or emission along the dislocation lines allow the dislocation climb mechanism and can impact creep properties of MgO . We will thus show how atomic-scale simulations can elucidate the atomic configurations of the various jog configurations structure and give access to their formation energies.

KFM 2.5 Mon 16:25 POT 51

Dislocation-tuned Schottky barrier in oxide ceramics — •MEHRZAD SOLEIMANY^{1,2}, TILL FRÖMLING¹, LUKAS PORZ¹, ENRICO BRUDER¹, MARIN ALEXE², and JÜRGEN RÖDEL¹ — ¹Department of Materials and Earth Sciences, Technical University of Darmstadt, 64287 Darmstadt, Germany — ²Department of Physics, University of Warwick, CV4 7AL Coventry, UK

For decades manipulation of interfaces and point defects in semiconductors have been the main focus of scientists for tuning the functional properties of materials. However, dislocations which are considered as one-dimensional defects, have not only been neglected but also tried to be avoided due to the assumption that they degrade desired properties of semiconductors. Nevertheless, it has recently been shown that this speculation can be challenged and dislocations can even be used to tune the thermal, electrical, and ferroelectric properties of materials, especially when they are introduced in high densities. In this work dislocation densities higher than $4 \times 10^{13} \text{ m}^{-2}$ were introduced in a large volume of the n-type and p-type SrTiO_3 by mechanical deformation and cyclic loading. That has been confirmed via sample thinning and electron channelling contrast imaging. Utilizing electrochemical impedance spectroscopy and DC electrical measurements, we showed that based on doping, dislocations can reduce the Schottky barrier in the n-type SrTiO_3 by a factor of seven and can increase that by a factor of three in the p-type one.

KFM 2.6 Mon 16:45 POT 51

Tailoring ceramic functional properties of YSZ with dislocations — •TILL FRÖMLING, QAISAR MUHAMMAD, and JÜRGEN RÖDEL — ¹Division of Nonmetallic-Inorganic Materials, Department of Materials and Earth Sciences, Technical University of Darmstadt, Alarich-Weiss-Str. 2, Darmstadt 64287, Germany

The defect chemistry of zirconia is usually modified by doping with high levels of yttrium. This induces a very high oxygen vacancy concentration which is responsible for the excellent ionic conductivity. There is a high demand for even better oxygen conductors because this would benefit applications like solid oxide fuel cells and solid state electrolyzers. Nevertheless, a limit has been reached concerning the doping strategy. Therefore, we suggest to use dislocations as one-dimensional defects. These have so far been mostly disregarded as defects for modification of functional properties but are finding increasing attention recently. However, ceramics are generally brittle and thus not easily plastically deformable. Besides the difficulty of introducing dislocations into ceramics, their exact influence on functional properties is still unclear. Our investigations of yttria-stabilized zirconia show that mechanically introduced dislocations can enhance ionic conductivity significantly. This illustrates the opportunity to tune ceramics beyond what can be achieved by chemical doping.

KFM 3: Instrumentation and Methods for Micro- and Nanoanalysis (joint session KFM/ CPP)

Chair: Prof. Dr. Theo A. Scherer (KIT Karlsruhe)

Time: Monday 14:30–15:30

Location: POT 106

KFM 3.1 Mon 14:30 POT 106

The Hitchhiker's Guide to BCARS on Solid-State Single Crystals — •FRANZ HEMPEL¹, LUKAS KÖNIG¹, FEDERICO VERNUCCIO², DARIO POLLI², GIULIO CERULLO², MICHAEL RÜSING¹, and LUKAS MATTHIAS ENG^{1,3} — ¹Institut für Angewandte Physik, TU Dresden, 01187 Dresden, Germany — ²Physics Department, Politecnico di Milano, 20133 Milano, Italy — ³ct.qmat: Dresden-Würzburg Cluster of Excellence - EXC 2147, TU Dresden, 01062 Dresden, Germany

Broadband coherent anti-Stokes Raman scattering (BCARS) is an advanced Raman spectroscopy technique that offers high-speed hyperspectral imaging and is so far widely applied in the biomedical field. For crystalline materials and their high-precision analysis, however, additional aspects of phase-matching, scattering direction, and background removal delicately need to be taken into account. To prove the reproducibility of BCARS results and pinpoint setup-related influences, we have performed a comparison study using (a) two different setups, and (b) comparing transmission with epi-detection BCARS experiments. A broad set of solid-state crystalline materials with increasing complexity was analyzed, achieving comparable, background-free spectra. Also, each machine allows the specification of optimum laser and setup parameters for inspecting the different samples.

KFM 3.2 Mon 14:50 POT 106

Novel techniques for low-energy positron beam diagnostics. — •FRANCESCO GUATIERI, MICHAEL BERGHOLD, and MICHAEL ZIMMERMANN — Heinz Maier-Leibnitz Zentrum (MLZ), Technical University of Munich, Lichtenbergstr. 1, 85748 Garching, Germany

Modern surface analysis techniques based on low-energy positron annihilation require the use of a stable, focused and intense particle beam. Although several techniques are available to beam scientists to measure position, shape and inten-

sity of a positron beam, each comes with its own limitations either in terms of precision, cost or measurement time. We will present two innovative techniques to detect low-energy positrons with the goal of performing beam optimization, each of which improves onto the previous state of the art.

KFM 3.3 Mon 15:10 POT 106

Accessible electron microscopy: Adding an EELS workflow to the ChemiTEM project — •DANIELA RAMERMANN, JULIA MENTEN, ELISABETH H. WOLF, and WALID HETABA — Max-Planck-Institut für Chemische Energiekonversion, Mülheim an der Ruhr

Transmission electron microscopy is a versatile tool for the investigation of micro- and nanostructures as well as chemical and electronic properties. However, TEM experts are needed to perform the majority of analytic measurements, which represents a bottleneck in the throughput of research. To broaden access to TEM investigations for every scientist, the ChemiTEM project[1] has developed workflows for the most used techniques (HRTEM, STEM, EDX). These are implemented in an app and guide the user through every step after only a basic training.

Now a workflow for EELS measurements has been added: For the three most used measurement scenarios, assessing sample thickness, elemental mapping and oxidation state determination, a decision-tree based workflow has been created. A prerequisite is the STEM alignment from the ChemiTEM app. A set of questions about the sample evaluates if EELS measurements using the workflow are possible or a TEM expert is needed. Step-by-step instructions guarantee a standardised measurement and data quality. The workflow can be easily adapted to other microscopes and makes EELS based techniques available to a broader community.

[1] Hetaba et al., Chemistry-Methods, 1, 401-407, <https://doi.org/10.1002/cmt.202100001>

KFM 4: Focus: Domains and Domainwalls in (Multi)Ferroic II

Chair: Prof. Dr. Lukas Eng (TU Dresden)

Time: Tuesday 9:00–13:10

Location: POT 51

Invited Talk

KFM 4.1 Tue 9:00 POT 51

Towards spatially resolved measurements of thermal transport and electrocaloric effects at the nanoscale in ferroelectric materials — REBECCA KELLY, OLIVIA BAXTER, FRAN KURNIA, AMIT KUMAR, MARTY GREGG, and •RAYMOND MCQUAID — School of Mathematics and Physics, Queen's University Belfast, Belfast, U.K.

Scanning Thermal Microscopy (S_{Th}M) is a promising Atomic Force Microscopy technique for mapping the thermal properties of materials at the nanoscale. In this talk, I will discuss how S_{Th}M could be a powerful tool for studying the role of microstructure on heat flow in ferroelectric materials.

Interest in using ferroic domain boundaries to enable active control of heat flow has been steadily growing over the last decade. However, direct, spatially resolved measurements of domain wall thermal transport have yet to be reported. In the first part of the talk, I will describe our S_{Th}M based approach to map spatial variations in thermal conductivity associated with microstructural inhomogeneity. We map the contrast in thermal response of the electrode/dielectric layers of a multilayer ceramic capacitor (MLCC) to demonstrate proof of principle thermal imaging and then use this approach to investigate the thermal transport properties of conducting domain walls in LiNbO₃.

In the second part of the talk, I will discuss how S_{Th}M can be adapted to measure electric field induced temperature changes in electrocaloric materials with sub-micron spatial resolution. Using our approach, 2D spatially resolved maps of electrocaloric heating and cooling can be generated, here demonstrated in a BaTiO₃ based MLCC.

KFM 4.2 Tue 9:30 POT 51

Real time polarization monitoring during growth for the design of artificial layered ferroelectrics — •IPEK EFE¹, ELZBIETA GRADAUSKAITE¹, ALEXANDER VOGEL², MARTA D. ROSSELL², MANFRED FIEBIG¹, and MORGAN TRASSIN¹ — ¹Department of Materials, ETH Zurich, Switzerland — ²Electron Microscopy Center, Empa, Switzerland

Increasing the complexity of unit cells of ferroelectric oxides beyond the standard perovskite building block supports exotic functionalities such as superconductivity, magnetoresistance, and ferroelectricity. However, integrating complex crystal structures into epitaxial design is challenging, and routes to precisely monitor the non-perovskite systems have yet to be established. Here, we directly access the polarization dynamics of the layered ferroelectric model system Aurivillius Bi₅FeTi₃O₁₅ films during growth using in-situ optical second harmonic generation (ISHG). We identify the characteristic Aurivillius antipolar ordering of the dipoles along the growth direction, which leads to an oscillating intensity of the ISHG signal during the layer-by-layer deposition. In combination with reflection high-energy electron diffraction monitoring, we show how the polarization orientation of the films consistently changes from out-of-plane during the growth of perovskite blocks, to fully in-plane upon the completion of the unit cell with the fluorite-like (Bi₂O₂)²⁺ planes. We demonstrate how direct access to structure-dependent polarization dynamics during growth enables the development of novel layered systems incorporating various functional perovskite blocks into the Aurivillius structure.

KFM 4.3 Tue 9:50 POT 51

3D mapping of grain boundary chemistry in ferroelectrics — •KASPER HUNNESTAD, JAN SCHULTHEISS, ANDERS MATHISEN, CONSTANTINOS HATZOGLOU, ANTONIUS HELVOORT, and DENNIS MEIER — Norwegian University of Science and Technology (NTNU), 7491 Trondheim, Norway

In this work, we study the impact of polar order on the local chemistry of charged grain boundaries, which naturally form in polycrystalline pyro- and ferroelectric materials during processing. Analogous to ferroelectric domain walls, these interfaces can develop new physical properties, representing intriguing functional 2D systems. Understanding the origin of the emergent interfacial phenomena, however, is a challenging task, requiring high-resolution imaging of the atomic-scale structure.

Here, we apply atom probe tomography (APT) to study the local chemistry at grain boundaries in ferroelectrics. APT combines high chemical sensitivity and accuracy with three-dimensional spatial resolution, allowing to map and quantify otherwise inaccessible changes in chemical composition. In our polycrystalline model system, ErMnO₃, we consistently find an enrichment of erbium and a depletion of oxygen at the grain boundaries. This trend occurs independently of the local charge state of each grain boundary and is unexpected as it implies a local violation of charge neutrality. Our results provide new insight into the defect chemistry at the grain boundaries in polar materials, suggesting pathways for local property engineering in ferroelectric oxides via grain-boundary-selective doping.

15 min. break

KFM 4.4 Tue 10:25 POT 51

Impact of defect dipoles on ferroelectric domain-walls motion — •SHENG-HAN TENG and ANNA GRÜNEBOHM — Interdisciplinary Centre for Advanced Materials Simulation (ICAMS) and Center for Interface-Dominated High Performance Materials (ZGH), Ruhr-University Bochum, Germany

Defect dipoles can alter the polarization switching and the dynamics of domain walls in ferroelectrics [1, 2], which may result in internal bias fields, domain-wall pinning [3] and bowing. In this work, we use *ab initio* based molecular dynamics simulations based on the effective Hamiltonian method [4, 5] to investigate the impact of defect dipoles on the domain-walls motion of tetragonal and orthorhombic phases in BaTiO₃. We find that the internal bias induced by defect dipoles may modify the potential energy landscape and leads to a completely different migration path for domain switching, which can pin and possibly even accelerate domain-wall motion.

[1] X. Ren, *Nat. Mater.* **3**, 91-94 (2004)[2] A. Grünebohm, M. Marathe, R. Khachatryan, R. Schiedung, D. C. Lupascu, and V. V. Shvartsman, *J. Phys.: Condens. Matter* **34**, 073002 (2021)[3] A. Dimou, P. Hirel, and A. Grünebohm, *Phys. Rev. B* **106**, 094104 (2022)[4] W. Zhong, D. Vanderbilt, and K. M. Rabe, *Phys. Rev. B* **52**, 6301-6312 (1995)[5] T. Nishimatsu, M. Iwamoto, Y. Kawazoe, and U. V. Waghmare, *Phys. Rev. B* **82**, 134106 (2010)

KFM 4.5 Tue 10:45 POT 51

Revealing hidden ferroelectric domain walls in sub-surface regions and their electronic properties via non-destructive conductance mapping — •JIALI HE¹, MANUEL ZAHN^{1,2}, LEONIE RICHAZ¹, URSULA LUDACKA¹, ERIK D. ROEDE¹, ZEWU YAN^{3,4}, EDITH BOURRET⁴, ISTVÁN KÉZSMÁRKI², and DENNIS MEIER¹ — ¹NTNU Norwegian University of Science and Technology, Norway — ²Universität Augsburg, Germany — ³ETH Zurich, Switzerland — ⁴Lawrence Berkeley National Laboratory, USA

Ferroelectric domain walls hold great promise for next-generation nanoelectronics. In particular, charged domain walls in improper ferroelectrics have triggered conceptually new application strategies. Although it is known that the electronic properties of domain walls are determined by their charge state, orientation, and curvature, non-destructive measurements of these parameters remain a major challenge. We investigate the correlation between electronic surface properties and hidden ferroelectric domain walls in ErMnO₃. By recording conductance maps using scanning electron microscopy (SEM) and conductive atomic force microscopy (CAFM) in combination with FIB-nanostructuring, we reveal that domain walls in surface-near regions give rise to distinct variations in surface contrast. The findings are rationalized in a simplified model, linking the contrast variations to the local charged state of the hidden domain walls, their orientation and distance from the surface. Our work introduces novel strategies to analyze the physical properties of ferroelectric domain walls in surface-near regions with nanoscale resolution in a non-destructive way.

KFM 4.6 Tue 11:05 POT 51

Electronic transport at pristine neutral ferroelectric domain walls in lead titanate — •SABINE KÖRBE¹ and CHRISTOPHE ADESS² — ¹Institute of Condensed Matter Theory and Optics, Friedrich Schiller University Jena, Germany — ²Institut Lumière Matière, Université Claude Bernard Lyon I, France

Ferroelectric domain walls are intrinsic interfaces that form spontaneously in ferroelectric materials, such as, for example, perovskite oxides. Whereas the ferroelectric perovskite oxide itself is an insulator, ferroelectric domain walls can be electrically conductive, as numerous experiments on different perovskite oxides have shown. This domain-wall conduction could serve, e.g., for charge-carrier transport in future photovoltaic absorbers. We investigated, using *ab initio* calculations based on Green's functions, the electronic transport along and through neutral ferroelectric domain walls in the prototype ferroelectric perovskite oxide PbTiO₃, and determined how the domain walls change the electronic transmission of bulk PbTiO₃ and the I-V curves of an ultrathin metal/perovskite/metal sandwich structure. We find that pristine neutral domain walls have a moderate effect on electronic transmission and I-V curve (within about one order of magnitude), much smaller than the experimentally measured conductivity increase at the walls by several orders of magnitude. We suggest that the measured conductivity increase does not directly originate in the electronic structure of the pristine neutral domain walls, but is caused by secondary effects, such as the accumulation of free charge carriers and/or the segregation of charged defects at the walls.

15 min. break

KFM 4.7 Tue 11:40 POT 51

Ferrielectric phase boundaries in antiferroelectric lead zirconate — •GUSTAU CATALAN¹, KRYSZTIAN ROLEDER², and YING LIU³ — ¹ICREA and ICN2, Barcelona, Catalonia — ²Institute of Physics, University of Silesia in Katowice, Katowice, Poland — ³ICN2-Institut Català de Nanociència i Nanotecnologia, Barcelona, Catalonia

When antiferroelectric PbZrO₃ is cooled down from the paraelectric phase, antiferroelectric domains nucleate and grow until they coalesce. Adjacent antiferroelectric domains can differ in the phase sequence of the antipolar arrangement, meaning that there is a polar discontinuity at the domain wall, also known as translational boundary or antiphase boundary. Using high resolution transmission electron microscopy, we have characterized such phase boundaries. We find that their internal structure is ferrielectric, with a basic unit cell that can be described as having two dipoles ion one direction and one in the antiparallel direction. We also find that such translational boundaries can cluster together, forming stripe domains of an incipient ferrielectric phase that can moreover be internally switched. We therefore propose that antiphase boundaries can act as the seed for a low-temperature ferrielectric phase that has been theoretically predicted and which might explain the remnant polarization sometimes observed as triple hysteresis loops in nominally antiferroelectric lead zirconate.

KFM 4.8 Tue 12:10 POT 51

Field Effect Transistor employing the static negative capacitance of a ferroelectric nano-domain nucleus — •PAVEL MOKRY¹, VIT KOSINA¹, and TOMAS SLUKA² — ¹Faculty of Mechatronics, Informatics and Interdisciplinary Studies, Technical University of Liberec, Liberec, Czech Republic — ²CREAL SA, Ecublens, Switzerland

Miniaturization of conventional field effect transistors (FETs) approaches the fundamental limits beyond which opening and closing the transistor channel require such a gate voltage swing, which causes an unacceptable increase in heat generation. This problem could be reduced by placing a ferroelectric layer between the FET gate electrode and the channel. In this ferroelectric-semiconductor sandwich structure, the gate voltage can be amplified due to the negative capacitance regime of ferroelectrics. However, the original idea of using a bulk ferroelectric for voltage amplification suffers several difficulties. In this work, we provide phase-field simulations of a system that provides static negative capacitance from a nano-domain nucleus. We model the nucleus of a ferroelectric domain with reversed polarization produced by applying the voltage on a small gate electrode. We show that such a nano-domain nucleus represents a reversible system, which follows a unique path during electrical cycling and inevitably crosses a higher energy state characterized by negative static differential capacitance. Phase-field simulations confirm the robustness of this concept offering conveniently small effective negative capacitance and its compatibility with FET technology.

KFM 4.9 Tue 12:30 POT 51

Novel functionalities at twin domain crossings — •KUMARA CORDERO-EDWARDS^{1,2}, PHILIPPE TÜCKMANTEL², IAROSLAV GAPONENKO², SAHAR SAREMI³, LANE MARTIN^{3,4}, and PATRYCJA PARUCH² — ¹Institut Català de Nanociència i Nanotecnologia, Barcelona, Catalonia. — ²DQMP, University of Geneva, Geneva, Switzerland — ³Department of Materials Science and Engineering, University of California, Berkeley, USA. — ⁴Materials Sciences Division, Lawrence Berkeley National Laboratory, Berkeley, USA.

In ferroelectrics, domain walls (DWs) are thin interfaces separating regions with different orientations of electric polarization. These interfaces can present physical properties quite different from the surrounding domains, allowing them to be used as active components in future device applications. Recent studies of DWs using scanning probe microscopy (SPM) have focused on mapping their response to different parameters in order to understand their structure-property relationships. In particular, the role of high strain gradients present at ferroelectric twins has been shown to enhance their electrical conduction and can lead to complex rotational polarization textures.

Here, I will present our investigation of ferroelastic twin domains in epitaxial PbTiO₃ thin films grown on SrTiO₃, explored with SPM. Our results suggest a complex polarization structure around the twin domains, which present an unusual and distinct lateral PFM signal, associated with a distinct current signature. Moreover, twin domain crossings show a unique mechanical response distinct from the surrounding ferroelectric phase, and enhanced electrical conduction.

KFM 4.10 Tue 12:50 POT 51

Three-dimensional imaging of ferroelectric domains using digital holographic tomography — •PAVEL MOKRY^{1,2}, MAREK MACH^{1,2}, PAVEL PSOTA¹, and KAREL ZIDEK¹ — ¹Faculty of Mechatronics, Informatics and Interdisciplinary Studies, Technical University of Liberec, Liberec, Czech Republic — ²Institute of Plasma Physics of the Czech Academy of Sciences, Prague, Czech Republic

The formation and evolution of domain patterns in ferroelectrics are fascinating physical phenomena, which determine to a large extent, the macroscopic properties of ferroelectric samples. Therefore, imaging of ferroelectric domains belongs to the essential characterization techniques of ferroelectric materials. This work demonstrates the three-dimensional (3D) imaging of ferroelectric domains using Digital Holographic Tomography (DHT). Our method is based on the construction of the Digital Holographic Microscope, which allows taking several images of the domain pattern projections from different directions. The 3D image of the ferroelectric domain pattern is then numerically reconstructed using our original method called Curvilinear Filtered Back-projection. Our experimental method has been demonstrated by imagining the domain structure in periodically poled lithium niobate single crystals. The developed method allows fast and accurate 3D observations of ferroelectric domain structures in the whole volume of the ferroelectric single crystals on the centimeter scale. The recent DHM and DHT systems, which allow high-resolution optical imaging and on-chip optical imaging of ferroelectric domain patterns, are demonstrated and discussed.

KFM 5: Thin Film Properties (joint session DS/KFM)

Time: Tuesday 10:00–11:00

Location: SCH A 315

See DS 6 for details of this session.

KFM 6: Poster

Time: Tuesday 17:00–19:00

Location: P3

KFM 6.1 Tue 17:00 P3

Electrochemical performance of KTiOAsO₄ (KTA) from density functional theory — •ADRIANA BOCCHINI, UWE GERSTMANN, TIM BARTLEY, HANS-GEORG STEINRÜCK, GERALD HENKEL, and WOLF GERO SCHMIDT — Universität Paderborn, 33095 Paderborn, Germany

The potassium titanil phosphate (KTiOPO₄, KTP) family has been recently suggested as a promising electrode for alkali-ion batteries [1-3]. Here, we present a study [4] based on density functional theory (DFT) that investigates the electrochemical performance of potassium titanil arsenate (KTiOAsO₄, KTA) as an electrode for potassium-ion batteries (KIBs). K-deficient K_{1-x}TiOAsO₄ ($x = 0.0-1.0$) and K-doped KTiOAsO₄K_x ($x = 0.0-0.5$) is used to model cathode and anode materials, respectively. We show that KTA combines high average working voltages (up to 3.8 V) with a modest volume expansion (shrinkage) upon K (de)intercalation (both below 8%). Nudged elastic band (NEB) calculations are performed to investigate the (de)intercalation dynamics. It is shown that the most favorable K-ion (K-vacancy) diffusion path is located along the [001] di-

rection and is characterized by activation energies lower 0.5 eV. Our results thus suggest a new application of the well-established KTA photonic crystal.

- [1] Huang et al., J. Phys. Lett. 12, 2721 (2021)
- [2] Huang et al., J. Chem. Phys. 156, 204702 (2022)
- [3] Fedotov et al., Chem. Mater. 26, 411 (2016)
- [4] Bocchini et al., Phys. Rev. Materials 6, 105401 (2022)

KFM 6.2 Tue 17:00 P3

Lithium vacancies concentration in LiNbO₃ from first principles — •CHRISTA FINK, FELIX BERNHARDT, and SIMONE SANNA — Justus-Liebig-University, Giessen, Germany

Lithium niobate is known as a crystalline material with ferroelectric, piezoelectric, photorefractive, and electro-optical properties and therefore has multiple applications. One of the intrinsic point defects of LiNbO₃, the negatively charged Lithium vacancy V_{Li}^{\prime} , is studied in this contribution from first principles. The isolated defect is investigated using density functional theory to calculate the

temperature dependency of the defect concentration of Lithium vacancies in LiNbO_3 crystals. The defect concentration can be calculated assuming an Arrhenius behavior where the activation energy is given by the Gibbs energy of defect formation. The Gibbs energy itself is a sum of several terms which are all depending on temperature. Since *ab initio* calculations are always performed at $T = 0$ K, a special formalism is used which allows adding a temperature dependency to the standard *ab initio* calculations. This formalism includes several approaches to take temperature into account. In addition, finite-size effects due to computational limitations need to be considered during the calculation of defect formation energies and formation entropies.

KFM 6.3 Tue 17:00 P3

Modelling of CARS — •LEONARD M. VERHOFF and SIMONE SANNA — Institute for theoretical physics, Giessen, Germany

Coherent anti-stokes Raman spectroscopy (CARS) is a widely used method for material characterization which has been recently extended to crystalline solids. Even though it relies on the same vibrational modes as Raman spectroscopy, it yields a much stronger output signal. Being a third order, non-linear optical process, it depends on the material's $\chi^{(3)}$ tensor.

In this contribution, we report on our theoretical modelling of the CARS-signal. In particular, we model the generation of the signal beam by solving the underlying differential equations resulting from Maxwell's equations numerically for LiNbO_3 , to extract a frequency-dependent amplitude that is also measured in experiments. The $\chi^{(3)}$ tensor is calculated from first principles using density functional theory before. Exploiting the symmetry of LiNbO_3 crystals, lower order non-linear optical effects can be neglected.

The partial differential equations defining the signal beam are further simplified by assuming plane waves for all involved lasers, including the pump, Stokes and probe beam and explicitly using a specific scattering geometry.

KFM 6.4 Tue 17:00 P3

Composition dependent optical properties of $\text{LiNb}_{1-x}\text{Ta}_x\text{O}_3$ solid solutions — •FELIX BERNHARDT, FLORIAN PFEIFFER, and SIMONE SANNA — Justus-Liebig-Universität, Gießen, Germany

Lithium niobate (LN) and lithium tantalate (LT) are ferroelectric crystals with a wide range of applications, extending from piezoelectric sensors [1] to integrated photonics [2]. Their structural similarities enable their combination to $\text{LiNb}_{1-x}\text{Ta}_x\text{O}_3$ (LNT) solid solutions. As the optical absorption edge of these alloys depend on their composition, one can determine the crystal composition non destructively, e.g. by optical spectroscopy.

Here, we use special quasi-random structures (SQS) to simulate LNT crystals with different compositions. These structures mimic an ideal random alloy, even when periodic boundary conditions are employed.

We calculate the first order dielectric tensor of LNT for different Ta concentrations by using density functional theory (DFT) and the independent particle approximation (IPA). Furthermore, we employ the Bethe-Salpeter equation (BSE) on top of quasi-particle calculations in GW-approximation for pure LN and LT to model excitonic effects.

Our calculations show a clear dependence on the absorption edge with respect to the Nb/Ta ratio of the LNT crystals. The inclusion of quasi-particle effects significantly shifts the absorption edge to higher energies. Our results are in good agreement to experimental data.

[1] M. Xu et al., ACS Appl. Mater. Interfaces, 9, 40, (2017) [2] W. Sohler et al., Optics & Photonics News, 19, 1, (2008) [3] A. van de Walle et al., Calphad, 42, 13-18 (2013)

KFM 6.5 Tue 17:00 P3

Hybrid Functionals for Periodic Systems in the Density Functional Tight-Binding Method — •TAMMO VAN DER HEIDE¹, BÁLINT ARADI¹, BENJAMIN HOURAHINE², THOMAS FRAUENHEIM¹, and THOMAS NIEHAUS³ — ¹BCCMS, Univ. of Bremen, Bremen, Germany — ²SUPA, Dep. of Physics, The Univ. of Strathclyde, Glasgow, G4 0NG, UK — ³Institut Lumière Matière, Univ. Lyon, Univ. Claude Bernard Lyon 1, CNRS, Villeurbanne, France

Screened range-separated hybrid (SRSH) functionals within generalized Kohn-Sham density functional theory (GKS-DFT) have been shown to restore the correct $1/(re)$ asymptotic decay of the screened Coulomb interaction in a dielectric environment (ϵ). Major achievements of SRSH include an improved description of optical properties and correct prediction of polarization-induced fundamental gap renormalization in molecular crystals. The density functional tight-binding method (DFTB) is an approximate DFT that bridges the gap between first principles methods and empirical schemes. While RSH have already been accessible for molecular systems, effort has been made to generalize the theoretical foundation to extended systems beyond the Γ -point. For treating the periodic Fock exchange and its integrable singularity in reciprocal space, we resort to techniques successfully employed by DFT. Starting from the first principles Fock operator, we derive suitable expressions for the DFTB method, using standard integral approximations and their efficient implementation in the DFTB+ software package. Convergence behavior is investigated and demonstrated for the infinite acene series as well as 2D and 3D materials.

KFM 6.6 Tue 17:00 P3

Vibrational and optical properties of LiNbO_3 and LiTaO_3 under uniaxial stress — •MIKE PIONTECK¹, EKTA SINGH², SVEN REITZIG², MICHAEL LANGE², MICHAEL RÜSING², LUKAS ENG², and SIMONE SANNA¹ — ¹Justus-Liebig-Universität Gießen, Germany — ²Technische Universität Dresden, Germany

In ferroelectrics, the bulk material and the domain walls differ strongly in their vibrational and optical properties. X-ray measurements have shown that the domain walls of LiNbO_3 and LiTaO_3 exhibit the structure of compressed bulk material [1]. Consequently, the knowledge of the Raman frequencies as well as the optical response of the bulk material as a function of stress can help to characterize the domain walls.

Our work provides, for the first time, a theoretical description of phonon frequencies under uniaxial stress along Cartesian axes using density functional theory (DFT). The calculations show a roughly linear dependence of the Raman frequencies on the applied stress, which is confirmed by corresponding Raman measurements. This behavior is very similar for LiNbO_3 and LiTaO_3 crystals. In particular, the E_{TO_5} and TO_6 modes show a strong dependence on uniaxial stress in the x and y direction. As the strain reduces the symmetry of the crystal, we predict degeneracy lifting for the E modes. In addition, we have calculated the linear and nonlinear optical behavior of LiNbO_3 . In particular, this includes the second (SHG) and third harmonic generation (THG) coefficients as a function of the applied uniaxial strain. [1] M. Rüsing et al., Phys. Rev. Mat. 2, 103801 (2018).

KFM 6.7 Tue 17:00 P3

Direct growth of iron-based compounds as anodes for potassium ion storage — •ZIDONG WANG, HUAPING ZHAO, and YONG LEI — Fachgebiet Angewandte Nanophysik, Institut für Physik & IMN MacroNano, Technische Universität Ilmenau, 98693 Ilmenau, Germany

Potassium-ion electrochemical energy storage technologies have received much attention in recent years as an alternative to lithium-based energy storage technologies. Iron-based compounds, as a typical transition metal compound, have attracted much attention because of their low cost and high capacity as an anode of batteries. However, poor electrical conductivity and structural instability, which are common in transition metal compounds, hinder their further application in potassium-based energy storage technologies. In this work, the conductivity of electrodes was improved by a strategy of growing iron-based compounds directly on carbon papers, eliminating the binding agent in conventional preparation methods. Also, the directly grown active material can effectively reduce agglomeration during charging and discharging, thus enhancing the stability. The results show that this direct growth strategy can effectively improve the electrochemical potassium ion storage performance of iron-based compounds as a promising high-performance anode.

KFM 6.8 Tue 17:00 P3

Fabrication of reproducible, conductive domain walls in lithium niobate — •JULIUS RATZENBERGER^{1,2}, IULIJA KISELEVA¹, PETER HEGARTY¹, ZEESHAN AMBER¹, MICHAEL RÜSING¹, and LUKAS ENG^{1,2} — ¹Institut für Angewandte Physik, Technische Universität Dresden, 01062 Dresden, Germany — ²ct.qmat: Dresden-Würzburg Cluster of Excellence–EXC 2147, TU Dresden, 01062 Dresden, Germany

In recent years, extensive research on conductive domain walls (CDW) in lithium niobate as possible building blocks for nanoelectronic circuits has been carried out. However, a fundamental understanding of the relationship between poling, and the properties of highly-conductive domains has been missing so to date.

In this work, we systematically investigate the various poling parameters in order to come up with a recipe of how to reproducibly fabricate conductive, hexagonal domains into lithium niobate single crystals. Furthermore, by optimizing the relevant parameters, the CDW is reproducibly enhanced when following the work of Godau et al. [1]. To gain a deeper understanding into the formation of highly-conductive DWs, we apply 3D second-harmonic generation (SHG) microscopy [2] for direct real-space visualization. Our findings provide key insights into the formation of CDW in lithium niobate single crystals.

[1] Ch. Godau et al., ACS Nano 11, 5 (2017).

[2] T. Kämpfe et al., Phys. Rev. B, 89, 035314 (2014).

KFM 6.9 Tue 17:00 P3

Photo-induced transport properties in ferroelectric lithium niobate single crystals and their domain walls — •L. L. DING¹, E. BEYREUTHER¹, K. KEMPF¹, M. RÜSING¹, and L. M. ENG^{1,2} — ¹Institut für Angewandte Physik, TU Dresden, Nöthnitzer Straße 61, 01187 Dresden, Germany — ²ct.qmat: Dresden-Würzburg Cluster of Excellence - EXC 2147, TU Dresden, 01062 Dresden, Germany

Ferroelectric materials exhibit a spontaneous and stable dielectric polarization, resulting in a variable assembly of domain and domain wall (DW) structures, that have received continuous attention[1]. Furthermore, the multifield-controlled electrical transport offers many prospects for the vivid application of ferroelectrics into electronic devices, such as ferroelectric sensors, memories,

even synaptic circuits[2]. Notably, (external) control of the electronic transport through photons is very desirable since being non-invasive and ultrafast, but has been studied only sparsely. In particular, polarization switching of domains and DWs, bandgap modulation, or DW dynamics, all are susceptible to the photon-electron interaction, thus need fundamental clarifications and profound investigations. Here, we combine scanning probe techniques with analyzing the impact of light irradiation onto lithium niobate (domains and) DWs, and vary both intensity and wavelength to probe the local conductivity. This ansatz thus will improve our in-depth knowledge on the local band structure and energy level distribution within DWs, and will lay the foundation to design integrated electro-optical components thereof. [1] D. Meier, et al., Nat. Rev. Mater. 7, 157 (2022) [2] Z. D. Luo, et al., ACS Nano 14, 746 (2020)

KFM 6.10 Tue 17:00 P3

Thermal Conductivity of CVT Grown FeS₂ Crystals Measured by Optothermal Raman Method — •AYBERK ÖZDEN¹, ESTEBAN ZUÑIGA PUELLES^{2,3}, JENS KORTUS¹, ROMAN GUMENIUK², and CAMELIU HIMCINSCHI¹ — ¹Institut für Theoretische Physik, TU Bergakademie Freiberg, Leipziger Str. 23, 09599 Freiberg, Germany — ²Institut für Experimentelle Physik, TU Bergakademie Freiberg, Leipziger Str. 23, 09599 Freiberg, Germany — ³Max-Planck-Institut für Chemische Physik fester Stoffe, Nöthnitzer Str. 40, 01187 Dresden, Germany

In this study, natural mineral and needle-like pyrite crystals grown by chemical vapour transport were selected as model systems and their thermal conductivities were obtained by the optothermal Raman (OTR) method [1]. It is shown that the bulk model used accurately detects differences in the thermal conductivities of mineral and CVT crystals. This difference is attributed to point defects, such as sulphur vacancies or impurity doping. Balkanski-Klemens model analysis showed that three-phonon scattering of Ag and Eg modes and lattice thermal expansion are the dominant anharmonic contributions, while four-phonon scattering is negligible in pyrite-FeS₂. Thus, OTR not only provides an easy access to the thermal conductivity of single crystals in their most native form but also sheds light on the underlying phonon scattering mechanisms.

[1]A. Özden, E. Zuñiga-Puelles, J. Kortus, R. Gumeniuk, C. Himcinschi, J. Raman Spectrosc., DOI:10.1002/jrs.6456.

KFM 6.11 Tue 17:00 P3

Dynamics of the electrocaloric effect in ferroelectric materials — •JAN FISCHER, DANIEL HÄGELE, and JÖRG RUDOLPH — Ruhr-Universität Bochum, Germany

Ferroelectric materials are promising candidates for sustainable and environmentally friendly cooling applications due to their electrocaloric effect (ECE). The reversible temperature change ΔT results from a change of polarization P under adiabatic conditions. However, direct studies of the adiabatic temperature change are experimentally challenging. The vast majority of previous studies has used either indirect methods or slow temperature sensors. Systematic studies of dynamics of the ECE down to short timescales are completely missing.

Here, we present a direct and contactless method to study the dynamics $\Delta T(t)$ of the ECE with mK temperature resolution and μ s temporal resolution via the infrared emission of the sample.^{1,2} The simultaneous recording of applied electric field $E(t)$ and polarization $P(t)$ transients gives further the opportunity to correlate the caloric with the dielectric properties thus opening new perspectives for a fundamental understanding. The technique also allows for measurements faster than the heat exchange between sample and environment achieving adiabatic conditions. Our method is applicable to a wide range of materials and requires no sophisticated sample processing.

We present measurements on different materials ranging from bulk ferroelectrics over complex relaxor ferroelectrics to thin polymer films.

¹ J., Döntgen, et al., Applied Physics Letters 106, 3 (2015)

² J., Döntgen, et al., Energy Technology 6, 8 (2018)

KFM 6.12 Tue 17:00 P3

Fabrication steps for realization of quantum tokens — •MIRIAM MENDOZA DELGADO¹, JULIA HEUPEL¹, JAN THIEME², JOHANN PETER REITHMAIER¹, KILIAN SINGER², and CYRIL POPOV¹ — ¹Institute of Nanostructure Technologies and Analytics (INA), Center of Interdisciplinary Nanostructure Science and Technology (CINsaT), University of Kassel, Germany — ²Institute of Physics, Center of Interdisciplinary Nanostructure Science and Technology (CINsaT), University of Kassel, Germany

Nitrogen-vacancy (NV) color centers in diamond are fluorescent defects which possess "atom-like" properties and can be implemented as single photon sources with high optical stability and quantum yield, even at room temperature. Furthermore, the coherent electron spin of NV can be used as a long lived qubit which can be applied in quantum information technology, e.g. in quantum repeaters or tokens. In order to enhance the photon emission from NV centers and the collection efficiency, they should be incorporated in photonic structures, like nanopillars. The aim of the current work is the fabrication of diamond nanopillars incorporated with NVs and integrated with microwave antennas and electrodes, for the realization of quantum tokens. The fabrication of arrays of monocrystalline diamond nanopillars with diameters between 150 nm and 250

nm, 1 μ m height and center-to-center distance of 10 μ m consisted of their definition by electron beam lithography and subsequent inductively coupled plasma reactive ion etching with oxygen. Different techniques are implemented for the creation of NVs, which can affect both their density and properties.

KFM 6.13 Tue 17:00 P3

Engineering of Dendrite-Free and Activity-Enhanced Dual-Functional Electrodes for High-Energy Na-CO₂ Batteries — •CHANGFAN XU, HUAPING ZHAO, and YONG LEI — Fachgebiet Angewandte Nanophysik, Institut für Physik & IMN MacroNano, Technische Universität Ilmenau, 98693 Ilmenau, Germany

Constructing suitable multifunctional electrodes for dendrite-free anodes and kinetics-enhanced CO₂ cathodes is considered one of the most important ways to further advance the practical application of Na-CO₂ batteries. Herein, Ru nanoparticles grown on carbon paper (RuCP) are rationally designed and employed as both Na anode and CO₂ cathode in Na-CO₂ batteries. The outstanding electrical conductivity, superior sodiophilicity, and high catalytic activity of RuCP electrodes can simultaneously contribute to homogenous Na⁺ distribution and dendrite-free sodium structure, and strengthen discharge and charging kinetics. The morphological evolution confirms uniform deposition of Na on RuCP anode with dense and flat interfaces, delivering enhanced Coulombic efficiency and cycling stability. Meanwhile, Na-CO₂ batteries with RuCP cathode demonstrates low overpotentials and excellent cycling stability. Significantly, excellent electrochemical properties are obtained in the full battery (RuCP@Na || RuCP), laying the foundation for practical applications of Na-CO₂ batteries.

KFM 6.14 Tue 17:00 P3

Material dependent differences in spectroscopic changes of the transient reflectivity on ultrashort timescales — JONATHAN FRANK, JULIAN MERTENS, FELIX HOFF, and •MATTHIAS WUTTIG — 1. Institute of Physics (IA), RWTH Aachen University, Aachen, Germany

Optical spectroscopy is a well-established technique to characterize solids. It can be utilized to distinguish different types of chemical bonding, i.e. separate solids which employ metallic, ionic and covalent bonding. We have tried to understand if these differences in bonding are still visible if the materials are excited with femto-second laser pulses. Femtosecond pump-probe spectroscopy experiments at a fixed pump-pulse wavelength were carried out in an isotropic detection scheme, to investigate the wavelength dependent reflectivity changes of optically excited samples on sub-ps timescales for wavelengths ranging from the visible to the near infrared. The measurements were carried out on various pure metals, chiral topological semimetals and semiconductors. The reflectivity changes, for a given material, vary greatly in duration and magnitude, depending on the probe wavelength. Furthermore, while an initial decrease in the transient reflectivity may be observed at one probe wavelength, an increase may be measured with another. This behavior is intrinsically linked to the excitation of carriers, their subsequent relaxation and their interaction with the lattice. The results for different materials are presented and compared, and trends within a material group evaluated. A possible link to emergent properties, conductivity and dielectric function, is discussed.

KFM 6.15 Tue 17:00 P3

Comparison of Infrared and Raman active phonon modes in Lithium Niobate — •SOHAM GHARAT¹, SUSANNE KEHR¹, MICHAEL RÜSING¹, and LUKAS M ENG^{1,2} — ¹Institut für Angewandte Physik, TU Dresden, Nöthnitzer Straße 61, 01187 Dresden, Germany — ²ct.qmat: Dresden-Würzburg Cluster of Excellence - EXC 2147, TU Dresden, 01062 Dresden, Germany

The isostructural crystal of Lithium niobate is among the most widely used single-crystalline ferroelectric crystal with applications ranging from nonlinear optics [1] and high-speed electro-optic modulators, to high-frequency electronic filters [2]. In this work, we investigate the Lithium niobate crystal using both Raman spectroscopy and Fourier transform infrared spectroscopy (FTIR) [3]. We focus on consistently assigning the phonons in this material system using the two techniques in order to characterize and compare all these vibrational modes and their associated optical response. This work hence serves as a basis for the future study of nanoscopic features in this material, i.e. especially domain walls, by means of nano-FTIR and micro-Raman spectroscopy [4].

[1] D. Zhu et al., Adv. Opt. Phot. 12, 242 (2021); <https://doi.org/10.1364/AOP411024>. [2] C. Wang et al., Nature 562, 101 (2018); <https://doi.org/10.1038/s41586-018-0551-y>. [3] S. Margueron et al., J. Appl. Phys 111,104105 (2012). <https://doi.org/10.1063/1.4716001>. [4] M. Rüsing et al., Phys. Rev. Mater. 2, 103801 (2018); <https://doi.org/10.1103/PhysRevMaterials.2.103801>.

KFM 6.16 Tue 17:00 P3

Control of structure and morphology of LiNi_{0.8}Co_{0.1}Mn_{0.1} powder before and after calcination — •SLAHEDDINE JABRI¹, MARKUS ROJER², GEORG GARNWEITNER^{2,3}, MARKUS ETZKORN^{1,3}, and UTA SCHLICKUM^{1,3} — ¹Institute of Applied Physics, Technische Universität Braunschweig, 38106 Braunschweig, Germany — ²Institute for Particle Technology, Technische Universität Braunschweig, 38104 Braunschweig, Germany — ³Laboratory for Emerging Nanometrology (LENA), Technische Universität Braunschweig, 38106 Braunschweig, Germany

The demand of high energy density of lithium battery cells has strongly increased in the last years to enable long-range electric vehicle applications. Nowadays one focus lies on the optimization of the material composition of LiNi_{0.8}Co_{0.1}Mn_{0.1} (NMC811) as the promotor cathode material, which has the advantage of high specific capacity. However, the synthesis of high quality NMC811 material is still difficult due to its structure and thermal instability. Here, the NMC811 powder is prepared from acetate precursors in a cheaper and more environmentally synthesis procedure. The structure and the morphology of pre-calcinated and calcinated NMC811 were investigated using (cross section) Scanning Electron Microscopy (FIB-SEM) and Raman Spectroscopy. Beside the internal structure of single particles, this study provides information about the impurities present in the powder. In addition, the result shows that a compact and ordered layered rhombohedral phase structure of the NMC811 powder is obtained after annealing to 800 and 850 °C.

KFM 6.17 Tue 17:00 P3

RbTiPO₄F: A novel electrode material? — •YINGJIE XIE, UWE GERSTMANN, WOLF GERO SCHMIDT, and ADRIANA BOCCHINI — Universität Paderborn, 33095 Paderborn, Germany

The development of renewable forms of energy goes hand in hand with the search for efficient energy storages. Battery technologies based on metal ions heavier than Li are discussed as a greener, more efficient, and less expensive energy storage alternative to lithium-ions in batteries. However, because of the larger ionic radii, new electrode materials are required to guarantee, e.g., high energy densities, a fast ion (de)intercalation, and a robust long-term operation. In this context, many recent studies indicate the potassium titanyl phosphate (KTiOPO₄, KTP) family as a promising electrode in alkali-ion batteries [1-4].

Here, we investigate the suitability of RbTiPO₄F as a cathode for Rb-ion batteries using density functional theory (DFT). Particular attention is paid to the average voltages and the volume shrinkage caused by the deintercalation of Rb atoms from the crystal.

[1] Fedotov et al., Chem. Mater. 26, 411 (2016)

[2] Fedotov et al., J. Mater. Chem. 6, 14420 (2018)

[3] Huang et al., J. Phys. Lett. 12, 2721 (2021)

[4] Bocchini et al., Phys. Rev. Materials 6, 105401 (2022)

KFM 6.18 Tue 17:00 P3

Nonlinear optical interactions in confined nanostructures — •ZEESHAN HUSAIN AMBER¹, KAI JÜRGEN SPYCHALA², BORIS KOPPITZ¹, LUKAS M ENG^{1,3}, and MICHAEL RÜSING¹ — ¹Institut für Angewandte Physik, TU Dresden, Nöthnitzer Straße 61, 01187 Dresden, Germany — ²Department of Physics, University of Paderborn, Warburger Straße 100, 33098 Paderborn, Germany — ³ct.qmat: Dresden-Würzburg Cluster of Excellence - EXC 2147, TU Dresden, 01062 Dresden, Germany

Nonlinear optical (NLO) micro-spectroscopy is a very powerful tool for both investigating the material properties and noninvasively visualizing domains and domain walls in ferroelectric materials [1]. Thin film materials are usually supported on substrates leading to interference and reflection related phenomena during spectroscopy, which make interpretation of experimental results particularly challenging. Here, we report on Second Harmonic (SH) and Third Harmonic (TH) generation experiments on wedge-shaped samples cut out from 5%Mg-doped congruent Lithium niobate single crystals, and compare these findings with numerical [2] and semi-analytical simulations. We find that thin-film interference, reflection and phase matching strongly affect the signal strength in SH/TH generation. The excellent agreement between the simulated and experimental data shows that rigorous theoretical analysis can help identifying genuine material properties through systematically varied sample and setup parameters during NLO analysis.

[1] M. Ruesing et al., J. Appl. Phys. 126,114105 (2019). [2] Z.H. Amber et al., J. Appl. Phys. 130,133102 (2021).

KFM 6.19 Tue 17:00 P3

Quantitative electrical characterization of conductive ferroelectric domain walls in LiNbO₃ — •MANUEL ZAHN^{1,2}, ELKE BEYREUTHER¹, IULIA KISELEVA¹, AHMED S. LOTFY¹, MICHAEL RÜSING¹, and LUKAS M. ENG^{1,3} — ¹Institut für Angewandte Physik, Technische Universität Dresden, 01187 Dresden — ²Experimentalphysik V, Zentrum für Elektronische Korrelation und Magnetismus, Universität Augsburg, 86135 Augsburg — ³ct.qmat: Dresden-Würzburg Cluster of Excellence - EXC 2147, Technische Universität Dresden, 01187 Dresden

Ferroelectric domain wall (DW) conductance can be divided into two separate mechanisms, (a) the injection/ejection of charge carriers across the Schottky barrier formed at the (metal-)electrode-DW junction and (b) the transport of those charge carriers along the DW. Current-voltage (I-U) characteristics recorded at variable temperatures from LiNbO₃ DWs are clearly able to differentiate between these two contributions and, moreover, allow us to directly quantify the physical parameters relevant for the two mechanisms (a) and (b) mentioned above. These are, e.g., the resistance of the DW, as well as the saturation current, the ideality factor, and the Schottky barrier height of electrode/DW junction, moreover the activation energies needed to initiate the thermally activated hopping transport along DWs. We will show that this electronic transport along LiNbO₃ DWs can be elegantly viewed and interpreted in an adapted semiconductor picture based on a double-diode/double-resistor equivalent circuit model.

KFM 6.20 Tue 17:00 P3

The impact of Schottky barriers when electrically contacting conductive domain-walls in lithium niobate single crystals — •IULIA KISELEVA¹, ULIANA YAKHNEVYCH², JULIUS RATZENBERGER¹, MANUEL ZAHN^{1,3}, ELKE BEYREUTHER¹, MICHAEL RÜSING¹, HOLGER FRITZE², and LUKAS M. ENG^{1,4} — ¹Institut für Angewandte Physik, TU Dresden, Nöthnitzer Straße 61, 01187 Dresden, Germany — ²Institut für Energieforschung und Physikalische Technologien, TU Clausthal, Am Stollen 19 B, Goslar, 38640, Germany — ³Experimentalphysik V, Universität Augsburg — ⁴ct.qmat: Dresden-Würzburg Cluster of Excellence - EXC 2147, TU Dresden, 01062 Dresden, Germany

Conductive domain walls (DWs) in lithium niobate are promising constituents for applications in nanoelectronics, due to their high conductance and ability to be created quasi-on-will through high-voltage poling. However, electrically contacting the DWs leads to the formation of a Schottky barrier between the DW and the electrode material. In this work, we study a variety of different factors affecting the electronic transport across the barrier, e.g. the electrode material, the quality of the lithium niobate surface, and the influence of the applied voltages during the DW conductivity-enhancement procedure. It was found that all these factors have a significant influence on the Schottky barrier formation; moreover, the bulk structure of the DWs is also influenced by the interface's state. Our results demonstrate the importance of reproducible sample surface conditions and identifying promising directions for implementing improved DW conductivity.

KFM 6.21 Tue 17:00 P3

Time-resolved reflectivity measurements of Sb₂Se₃:Bi₂Se₃ alloys and Sb₂S₃ as studied by an ultrafast Optical Tester — •RAMON PFEIFFER, MAXIMILIAN MÜLLER, ERIC LENSER, and MATTHIAS WUTTIG — Institute of Physics (IA), RWTH Aachen University, 52074 Aachen, Germany

Laser-induced crystallization at a wavelength of 658 nm of alloys of Sb₂Se₃:Bi₂Se₃ has shown that the minimum crystallization time decreases with increasing Bi₂Se₃ content. This is, however, also accompanied by a reduction of the reflectance change upon crystallization. For higher Sb₂Se₃ contents, on the contrary, a slow and stochastic crystallization process was observed. Since Sb₂Se₃ has a much higher absorption coefficient at shorter wavelength, more efficient switching is expected with a blue laser diode. A similar consideration is made for Sb₂S₃ where hardly any light is absorbed below wavelength of about 600 nm. As a blue laser setup is much closer to the absorption maximum of Sb₂S₃, a better energy input is expected. For this reason, in our optical phase change tester, a blue laser diode (405 nm) has been implemented to investigate the materials mentioned above.

KFM 6.22 Tue 17:00 P3

Simulation Study of the Multi-beam Ptychography Optics and Setup Optimization — •TANG LI, MIKHAIL LYUBOMIRSKIY, and MARTIN SEYRICH — Deutsches Elektronen-Synchrotron DESY, Notkestraße 85, 22607 Hamburg, Germany

Ptychography is a robust computational iterative phase retrieval imaging method using overlapping constraints to decouple the probe and object information. It has the ability to obtain nanometer resolution with a small probe size and efficient overlapping. However, for single beam ptychography, it is inefficient beam usage, where almost 99% of the photon flux is wasted, and time-consuming to collect a nanometer resolution dataset with a large field of view (FOV). Therefore, we propose using a developed multi-beam ptychography (MBP) to relax the sample size limitation and scan duration. The feasible FOV scales with the number of parallel beams.

Although, we demonstrate the feasibility of using six coded probes to reconstruct the sample successfully. It is still not clear what is the up limit for the probe number and the least requirements of the difference between the probes that we still can decouple the probe contribution from the diffraction pattern. Hence these boundaries are explored in this work. It focuses on the forward simulation framework using the MBP setup and investigates the influence of different physical parameters, such as probe distance, probe difference, probe number, noise level influence, etc. This work provides a feasible parametric design for MBP optical and experimental setup, and it also opens the way to further development.

KFM 6.23 Tue 17:00 P3

Loss tangent measurements on an extremely large diamond disc for Brewster angle windows — •ANDREAS MEIER¹, GAETANO AIELLO¹, THEO SCHERER¹, SABINE SCHRECK¹, DIRK STRAUSS¹, CHRISTOPH WILD², and ECKHARD WÖRNER² — ¹Karlsruhe Institute of Technology, Hermann-von-Helmholtz-Platz 1, 76344 Eggenstein-Leopoldshafen, Germany — ²Diamond Materials GmbH, Hans-Bunte-Straße 19, 79108 Freiburg, Germany

Advanced Electron Cyclotron heating systems for future fusion reactors, such as DEMO, are designed for multi-frequency operation. The favored output window concept of the high power microwave beam is the Brewster angle setup, but it requires a disc diameter of 180 mm for the 67.2° angle and the 63.5 mm waveguide. In addition, a thickness of approximately 2 mm is needed to achieve the proper mechanical stability. State of the art microwave plasma reactors are not capable of growing discs of such a size. The maximum available diameter of a polycrystalline CVD diamond disc suited to microwave applications is currently 140 mm.

An extremely large diamond disc with a diameter of 180 mm for RF transmission application was produced by the industrial partner Diamond Materials GmbH. High-resolution loss tangent measurements for several areas of this disc have been realized by using a spherical resonator.

KFM 6.24 Tue 17:00 P3

Analysis of Structural Materials with Coincident Doppler Broadening Spectroscopy Using New Evaluation Software — •LEON CHRYSOS, VASSILY BURWITZ, and CHRISTOPH HUGENSCHMIDT — Heinz Maier-Leibnitz Zentrum (MLZ), Technical University of Munich, Lichtenbergstr. 1, Garching, Germany
Coincident Doppler Broadening Spectroscopy (CDBS) of the 511 keV electron positron annihilation line not only provides defect sensitive studies of materials, but also elemental signatures at the positron annihilation site. This enables the analysis of foreign atoms in the host matrix, vacancy-solute complexes and precipitates in solids. Using a new data analysis software several structural materials were evaluated at the recently upgraded CDB spectrometer at the NEutron induced POSitron source MUniCh (NEPOMUC). The most important features of the software will be explained. The functionality of the experiment and analysis software will be evaluated using several structural materials including AlCu alloys and W single crystals.

KFM 6.25 Tue 17:00 P3

Improved thermoelectric properties of SnSe through forming a phase employing metavalent bonding — •NAN LIN, YUAN YU, TANMOY GHOSH, and MATTHIAS WUTTIG — I. Physikalisches Institut (IA), RWTH Aachen University

SnSe only shows high ZT values above 750 K when the structure transforms from the asymmetrical Pnma phase to the higher symmetrical Cmcm phase. As a typical IV-VI compound bonded by p-state electrons, the Cmcm phase SnSe with an improved symmetry is expected to show the same chemical bonding with other rock-salt IV-VI compounds, which could be responsible for its excellent thermoelectric performance. Yet, it is challenging to stabilize the Cmcm phase at room temperature to characterize the bonding indicators. We successfully obtained the high-symmetry rock-salt SnSe phase by growing (SnSe)_{0.67}(AgSbTe₂)_{0.33} (SnSe)_{0.67}(AgBiTe₂)_{0.33}, (SnSe)_{0.67}(AgBiSe₂)_{0.33}, and (SnSe)_{0.5}(AgSbSe₂)_{0.5} alloys in a Bridgman oven. All cubic SnSe alloys show a unique portfolio of properties including a high optical dielectric constant, a large Born effective charge, and abnormal bond-breaking behavior in laser assisted atom probe tomography. All these characteristics are indicative of the metavalent bonding mechanism while are not found in the pristine SnSe. Concomitantly, zT increases from near 0.1 for the Pnma SnSe to about 1.0 for all the Fm -3m SnSe phases. Our work demonstrates that metavalent bonding could be the origin of many special properties of SnSe including the excellent thermoelectric performance.

KFM 6.26 Tue 17:00 P3

Highly-ordered Ni nanoarrays as an effect current collector for dendrite-free sodium metal batteries — •MO SHA, HUAPING ZHAO, and YONG LEI — Fachgebiet Angewandte Nanophysik, Institut für Physik & IMN MacroNano, Technische Universität Ilmenau, 98693 Ilmenau, Germany

Sodium metal batteries (SMBs) are attracting extensive attention for energy storage field due to its intrinsic high theoretical capacity and low redox potential, as well as its low cost and broad sources. Nevertheless, the inevitable side reactions and uncontrollable dendrite growth block its practical application. 3D confinement strategy demonstrates great potential for stabilizing the Na anode owing to its optimized ion/electron transportation, lower deposition overpotential, and structural stability. A technique via anodized alumina oxide (AAO) templates is an advanced preparation technique to fabricate various 3D nanostructures. Here, a 3D Ni nano-arrays nanostructure was fabricated with highly-ordered structure, which provides a greater specific surface area, reduces local current density and inhibits of Na dendrite formation. Due to the unique 3D nanostructure, dendrite-free Na deposition and superior electrochemical performance improvements in SMBs have been realized.

KFM 6.27 Tue 17:00 P3

Local control of ferromagnetic domain patterns via structural ordering — •AHMED SAMIR LOTFY, LUKAS KUERTEN, YOOUN HEO, ELZBIETA GRADAUSKAITE, MORGAN TRASSIN, and MANFRED FIEBIG — Department of materials, ETH Zürich, Zürich, Switzerland

Controlling domain patterns is closely linked to device functionalities in logic applications. However, the means to engineer domain locations are scarce so far, limiting this functionality. The recent utilization of substrate topography to pre-define the ferroelectric domain patterns by engineering the substrate step spacing via different miscut angles motivates our investigation for a similar control mechanism over ferromagnetic domain patterns. Neodymium gallate (NGO) is our substrate of choice because it is the only oxide among the lanthanide gallates with no structural phase transitions in a very extended temperature range (12-1773K). Therefore, La_{0.7}Sr_{0.3}MnO₃ (LSMO) films grown on NGO substrates exhibiting substrate steps were also investigated for such a correlation between the substrate topography and the ferromagnetic domain patterns in LSMO. Strikingly our results show an identical domain pattern to the substrate steps. This correlation might result from the ferroelastic nature of LSMO and could be utilized for ultrahigh-density memory devices.

KFM 6.28 Tue 17:00 P3

How to employ advanced innovation tools to advance soft X-ray nanolithography — •ANDREAS SPÄTH — Institut für Nanotechnologie und korrelative Mikroskopie (INAM) gGmbH, 91301 Forchheim, Germany — Physikalische Chemie II, Friedrich-Alexander-Universität Erlangen-Nürnberg, 91058 Erlangen, Germany

The Theory of Inventive Problem Solving is becoming increasingly significant in technical engineering and design. The present work illustrates the potential of its most common tools to advance instrumentation in soft X-ray microscopy and nanolithography. The initial setup designed for Focused X-ray Beam Induced Deposition is analyzed in-depth by function modelling to identify harmful or defective interactions between components. These problematic interactions are tracked back to root causes by cause-effect chain analysis. Root causes are often disguised technical or physical contradictions. TRIZ employs abstract innovation principles to solve such contradictions after they are categorized based on the nature of conflicting parameters. Another approach is to transfer harmful/defective interactions into a substance-field model of the problem that can be addressed by suitable substance-field models of potential solutions. The analysis yielded ideas for a significantly improved FXBID setup. The project benefited from funding by DFG (grant SP 1775/1-1).

KFM 6.29 Tue 17:00 P3

X-ray near-edge absorption spectroscopy and X-ray diffraction on thin AlCrVYN films — •ERIC SCHNEIDER¹, NICOLA THIERING¹, MICHAEL PAULUS¹, FINN ONTRUP², NELSON FILIPE LOPES DIAS², and DAVID KOKALJ² — ¹Fakultät Physik/DELTA TU Dortmund, 44221 Dortmund, Deutschland — ²Fakultät Maschinenbau TU Dortmund, Dortmund, Deutschland

In materials science tool coatings are optimized for use at elevated process temperatures. AlCrVYN thin films are promising candidates in this area, as vanadium can form so called Magnéli phases, which reduce the coefficient of friction. The aim of this project is to gain a fundamental understanding of the dependence between deposition parameters, layer structure and oxidation behavior of AlCrVYN coatings. For this purpose, the coating systems were deposited on a WC-Co composite substrate by a hybrid procedure of DC sputtering and high-energy pulse magnetron sputtering (HiPIMS). In addition, different cathode-target combinations will be tested to determine their influence on the structure of the thin films. For the investigation of the samples we used synchrotron radiation at beamline BL9 and BL10 of the synchrotron radiation source DELTA (Dortmund, Germany) to perform XRD and XANES measurements. The samples were annealed ex situ in an oven to temperatures up to 1000°C to study their oxidation behavior. Depending on the process parameters, different oxidation behaviour and residual stresses present in the samples were observed. We thank DELTA for providing synchrotron radiation. This work was supported by the DFG via TO 169/21-1.

KFM 6.30 Tue 17:00 P3

Combine circular economy with analytical facilities, instruments and know-how — •ERIC HIRSCHMANN, MAIK BUTTERLING, MACIEJ OSKAR LIEDKE, AHMED GAMAL ATTALLAH, and ANDREAS WAGNER — Zentrum Dresden-Rossendorf, Dresden, Germany

As part of the ReMade@ARI (REcyclable MAterials DEvelopment at Analytical Reserach Infrastructures) project of the Horizon Europe program, we present the Positron Research Infrastructure (pELBE) at the ELBE linear accelerator of the HZDR. pELBE is a collection of methods and instruments that can characterize defects, determine open volumes and investigate open or closed microporous systems using positron annihilation spectroscopy. The ReMade@ARI project is committed to foster the development of innovative, sustainable materials for key components in a wide range of sectors including electronics, batteries, vehicles, construction, packaging, plastics, textiles and food. The project aims to simplify

the use of large-scale research facilities at HZDR or other European sites for both academic and industrial players in the circular economy. The poster will provide a closer look at the outline of the project as well as the positron research infrastructure (pELBE) at HZDR.

KFM 6.31 Tue 17:00 P3

Growth and characterization of $\text{Ni}_{37}\text{Co}_{13}\text{Mn}_{33}\text{Ti}_{17}$ single crystals — •DAVID KOCH¹, BENEDIKT BECKMANN¹, GAVIN VAUGHAN², OLIVER GUTFLEISCH¹, and WOLFGANG DONNER¹ — ¹Institute of Material Science, Darmstadt, Germany — ²European Synchrotron Radiation Facility, Grenoble, France

Since 2015 the „all-d-Heusler“ material $\text{Ni}(\text{Co})\text{MnTi}$ is object of interest due to its magneto-functional applications linked to a martensitic phase transition, like solid state cooling and magnetic shape memory effect. Nevertheless, for many characterization methods single crystals are necessary but not reported in literature so far. Here we report on the growth and preparation of $\text{Ni}_{37}\text{Co}_{13}\text{Mn}_{33}\text{Ti}_{17}$ single crystals based on anomalous grain growth. The resulting single crystals are several mm in size, can be used for various experiments and show a reversible martensitic phase transition around 200 K. Here, the samples are characterized using magnetometry and various laboratory single crystal diffraction experiments. In addition, we use high energy synchrotron experiments to improve the dynamic intensity range and to reconstruct the whole reciprocal space.

KFM 6.32 Tue 17:00 P3

Metavalent Bonding empowers the High Thermoelectric Performance in Bi_2Te_3 -based Alloys — •YINGHAO TAO — I.Physikalisches Institut of RWTH Aachen

Bi-Te-based alloys show outstanding thermoelectric performance near room temperature due to the large Seebeck coefficient, high electrical conductivity, and low thermal conductivity. Even though the excellent properties of these alloys have been recognised for decades, the origin of these favorable characteristics has not been fully revealed. Very recently, a special combination of properties has been found in group IV-VI and V2-VI3 compounds due to an unconventional bonding mechanism, coined metavalent bonding (MVB). Bi_2Te_3 -based alloys also utilize MVB. This raises the question of whether the excellent thermoelectric performance stems from the MVB. In this work, we have prepared single-crystal $\text{Bi}_x\text{Sb}_{1-x}\text{Te}_3$ ($x=0.5, 0.6, 0.7$) samples by Bridgman oven and then measured the transport properties by thermal transport option (TTO) in PPMS. We have also measured the optical properties and the bond-breaking behavior of these compounds using Fourier-transform infrared spectroscopy (FTIR) and atom probe tomography, respectively. These methods prove the metavalent bonding nature in these compounds. Finally, we relate the favorable transport properties to the close relationship between chemical bonding and the electronic band structure. Metavalent compounds are characterized by a large valley degeneracy, a small band effective mass, and strong phonon anharmonicity. All of these attributes lead to high thermoelectric performance.

KFM 6.33 Tue 17:00 P3

First X-ray diffraction measurement from high pressure hydrostatic cells for X-ray scattering applications — •KEVIN LEHNINGER, ERIC SCHNEIDER, JAQUELINE SAVELKOULS, MICHAEL PAULUS, and CHRISTIAN STERNEMANN — Fakultät Physik/DELTA, Technische Universität Dortmund, 44221 Dortmund, Germany Small-angle and wide-angle X-ray scattering (SAXS/WAXS) at moderate pressures are of increasing importance for the investigation of e.g. protein denaturation or stimulus-responsive materials. One of the experimental challenges is the precise pressure control in the pressure range up to 10 kbar while separating the sample volume from the pressure-transmitting medium. To this end, we present two dedicated hydrostatic high pressure cells designed for use at the beamlines BL2 and BL9 of the synchrotron radiation source DELTA, which use water for pressure transmission, and show first measured diffractograms of gold and potassium bromide. The WAXS cell with an opening angle of 60 degrees allows a sample volume with a cross-sectional area of one square millimetre to be exposed to a maximum pressure of 5000 bar. The sample volume is enclosed in a flexible capillary tube capillary tube, which is located between two diamond windows and can have a maximum diameter of 1.5 mm. The SAXS cell can be operated up to a pressure of 10kbar and an opening angle of 20 degrees. Here, the sample volume is contained in a cylinder sealed with polyimide film which is screwed into the high-pressure cell via a sliding system.

KFM 6.34 Tue 17:00 P3

Optical and Spin Properties of NV Center Ensembles in Diamond Nano-Pillars — •KSENIYA VOLKOVA¹, JULIA HEUPEL², SERGEI TROFIMOV¹, FRIDTJOF BETZ³, RÉMI COLOM³, ROWAN W. MACQUEEN¹, SAPIDA AKHUNDZADA⁴, MEIKE REGINKA⁴, ARNO EHRESMANN⁴, JOHANN PETER REITHMAIER², SVEN BURGER³, CYRIL POPOV², and BORIS NAYDENOV¹ — ¹ASPIN, Helmholtz-Zentrum Berlin, Germany — ²INA, CINSaT, University of Kassel, Kassel, Germany — ³Zuse Institute Berlin, Berlin, Germany — ⁴IP, CINSaT, University of Kassel, Kassel, Germany

Nitrogen-vacancy (NV) centers in diamond integrated in nano-pillars could be used as tips for scanning probe for magnetic field imaging with high sensitiv-

ity and nano-scale spatial resolution. We present the fabrication of diamond nano-pillars with diameters up to 1000 nm in type Ib diamonds with two crystal orientations [100] and [111] using electron beam lithography and inductively coupled plasma reactive ion etching. The NV centers ensembles were created by 6 keV-He ion bombardment and subsequent annealing. Estimated numbers of NVs per pillar to be 4300 ± 300 and 520 ± 120 for the [100] and [111] samples, respectively. Lifetime measurements of the NV's excited state showed two time constants with average values of $\tau_1 \approx 2$ ns and $\tau_2 \approx 8$ ns, which are shorter than a single NV center in a bulk crystal. This is probably due to interaction with defects created by the helium ion bombardment and substitutional nitrogen. Optically detected magnetic resonance contrast was about 5% and average coherence times are T_2 [100] = 420 ± 40 ns, T_2 [111] = 560 ± 50 ns.

KFM 6.35 Tue 17:00 P3

High-speed domain wall imaging using broadband coherent anti-Stokes Raman scattering — •ROBIN BUSCHBECK¹, FRANZ HEMPEL¹, SVEN REITZIG¹, JULIUS RATZENBERGER¹, LUKAS KÖNIG¹, PETER ANDREW HEGARTY¹, ZEESHAN HUSSAIN AMBER¹, MICHAEL RÜSING¹, and LUKAS ENG^{1,2} — ¹Institut für Angewandte Physik, TU Dresden, Nöthnitzer Straße 61, 01187 Dresden, Germany — ²ct.qmat: Dresden-Würzburg Cluster of Excellence - EXC 2147, TU Dresden, 01062 Dresden, Germany

Spontaneous Raman spectroscopy (SR) is a broadly used and versatile method for the analysis of structures in crystalline materials, such as strain distributions or ferroelectric domain walls. A large disadvantage of this technique are the high acquisition times of up to several seconds per data point to visualize these structures. In this work, we demonstrate the use of a promising alternative, broadband coherent anti-Stokes Raman scattering (B-CARS) and compare this technique with SR at the example of poled Lithium niobate. We demonstrate a more than resulting in a 100 times higher signal-to noise ratio, while maintaining similar intensities. These results promise the use of B-CARS for high-speed spectral imaging in the context of solid-state materials, such as ferroelectrics and their domain walls.

KFM 6.36 Tue 17:00 P3

Low Temperature combined Confocal/AFM microscope for photoluminescence and magnetic resonance experiments — •ELIZAVETA STARYKH, MICHAEL DOTAN, and BORIS NAYDENOV — Helmholtz-Zentrum Berlin für Materialien und Energie, Berlin, Germany

Measuring small magnetic fields emanating from spins or magnetic nanoparticles, both with high spectral resolution and under diverse conditions has always been an ambitious task. Nanoscale magnetic imaging using nitrogen-vacancy (NV) colour centres in diamond has been proven to be a reliable method due to their unique properties and ability to be effectively manipulated by external magnetic fields. With laser light, it is possible to both initialize and read out the NV spin state, thereby non-destructively determining the magnetic profile of the sample.

With recent developments in technology, it is now possible to fabricate single NVs on the tip of an AFM cantilever and measure a magnetic field map from a sample. Due to the NVs' high sensitivity and susceptibility to the external environment, precise control of many parameters must be observed.

To combine different techniques to perform such complex experiments, we built a confocal setup on top of an attoCUBE closed-cycle cryogenic system. With optical access at the top, microwave and radio frequency control, AFM cantilever and separate temperature control for magnets and sample volume, we can now access a wide range of physical properties of solid-state materials.

KFM 6.37 Tue 17:00 P3

Interatomic Potential for Laser-Excited NV-Centers in Diamond — •MALWIN XIBRAKU, BERND BAUERHENNE, and MARTIN E. GARCIA — Universität Kassel, Heinrich-Plett-Straße 40, 34132 Kassel, Germany

Nitrogen-vacancy-centers (NV-centers) are of interest for quantum computing, sensing and encryption. However, the fabrication of NV-centers is quite challenging. Recently, we have proposed a new fabrication method in which N atoms and vacancies far from each other find each other after femtosecond laser excitation. We simulated this method in a diamond bulk cell, consisting of 288 atoms, using density-functional-theory (DFT) and observed, that it works at very high laser excitations. To include surface effects and consider the electron-phonon coupling it is necessary to perform large-scale molecular-dynamics-simulations, with millions of atoms. This is only possible using an interatomic potential, which respects the excitation of the electrons by considering the electronic temperature T_e . Here, we present a T_e -dependent interatomic potential for laser-excited NV-centers in diamond, which was developed from a large DFT-data set, widely covering the phase space of the system.

KFM 6.38 Tue 17:00 P3

Combined Confocal-AFM setup — •SERGEI TROFIMOV, KLAUS LIPS, and BORIS NAYDENOV — BerlinJoint EPR Laboratory and Department Spins in Energy Conversion and Quantum Information Science (ASPIN), Helmholtz-Zentrum Berlin für Materialien und Energie, Berlin, Germany

Single nitrogen-vacancy (NV) centers in diamond can be utilized for magnetic field sensing with high spatial resolution and high sensitivity. It is even possible to detect spin ensembles or magnetic nanoparticles if they are placed in the vicinity of an NV center. However, precise positioning of such structures is challenging. To tackle this problem AFM cantilevers can be utilized. One can move nanoparticles with a cantilever or attach them to it in order to bring them close to an NV center.

To conduct these experiments a Confocal-AFM setup based on a Park Systems NX12 AFM was built. This setup allows to place a cantilever in the vicinity of an NV center in a diamond sample using a moving sample stage and obtain luminescence maps with laser scanning technique using a set of galvo-mirrors.

To test the setup a diamond plate with NV centers was used to visualize magnetic field lines of a ferromagnetic cantilever. It was shown that the technique can be also applied to image and separately address NV centers that are as close as 10 nm apart. The maximum measured magnetic field strength was 146 ± 2 G when an NV center was 180 ± 10 nm away from the cantilever. A magnetic field gradient at this distance was estimated to be 0.3 G/nm.

KFM 6.39 Tue 17:00 P3

Investigation of ferroelectricity in $BaTiO_3$ -relaxors by PFM — •PHILIPP MÜNZER¹, MARKUS KRATZER¹, CHRISTIAN MAIER³, KLAUS REICHMANN³, MARCO DELUCA², and CHRISTIAN TEICHERT¹ — ¹Institute of Physics, Montanuniversität Leoben, Leoben, Austria

— ²Materials Center Leoben, Leoben, Austria

— ³Institute for Chemistry and Technology of Materials, Graz, Austria

$BaTiO_3$ relaxor systems are promising materials for energy storage applications in microelectronic devices. These lead-free dielectrics are thermally stable and suitable for high-temperature operation due to their broad and high permittivity response and low electric coercivity. The relaxor behaviour can be achieved by homo- or heterovalent substitution of Ti^{4+} ions in the perovskite cell, which disrupts the long-range ferroelectric order. We investigated the presence of ferroelectricity in homovalent (Zr^{4+}) and heterovalent (Nb^{5+}) substituted polycrystalline $BaTiO_3$ systems utilizing Piezoresponse Force Microscopy (PFM). We used Single-Frequency-PFM to image the domain structure of the relaxors and conducted polarization switching with a biased tip. Furthermore, local hysteresis loops were recorded utilizing Switching-Spectroscopy-PFM. The results indicate that the grade of ferroelectric disruption is strongly dependent on the amount and type of substitutes.

KFM 6.40 Tue 17:00 P3

Synthesis of depth confined nitrogen vacancy centers in diamond — •KAROLINA SCHÜLE¹, CHRISTOPH FINDLER^{1,2}, JOHANNES LANG^{1,2}, and FEDOR JELEZKO^{1,3} — ¹Institute for Quantum Optics, Ulm University, Ulm, Germany — ²Diatope GmbH, Ummendorf, Germany — ³Center for Integrated Quantum Science and Technology (IQST), Ulm

The negatively charged nitrogen-vacancy center (NV) is a paramagnetic defect ($S=1$) in diamond which shows coherence times T_2 up to milliseconds even at room temperature. The NV is a promising candidate for quantum applications as its spin state can be initialized, read out optically, and manipulated by a microwave field. One way to fabricate NV centers is ion implantation where nitrogen is added into a single crystal diamond layer followed by an annealing process. The depth of the implanted nitrogen can be adjusted by the implantation energy. Larger kinetic energies are leading to deeper NV centers. At the same time, however, the depth distribution gets also broader limiting the degree of depth confinement. This contradicts the goal of homogeneous properties of the NVs beneficial for e.g. NMR applications. Using the method of indirect overgrowth, where implanted nitrogen is buried below a nanometer-thin capping layer of diamond. The resulting depth of the NV centers is decoupled from the implantation ion energy. Here, we show outstanding depth confinement resulting in single NVs which are located at a depth of around 20 nm confined in a range of approx. 1.4 nm. These NV centers are exhibiting a T_2 up to $\sim 100 \mu s$.

KFM 6.41 Tue 17:00 P3

Multiphoton imaging of ferroelectric domain structures by means of tunable, high energy fs-pulses — •FIETE BREER¹, FELIX KODDE¹, LAURA VITTADELLO¹, JAN KLENEN¹, MICHAEL RUESING², and MIRCO IMLAU¹ — ¹Inst. Physics, Barbarastr. 7, Osnabrück Univ. — ²Inst. Applied Physics, Nöthnitzer Str. 61, Techn. Univ. Dresden

Multiphoton imaging is a powerful tool for the analysis of polar oxide crystals and has been recently used to reveal previously not expected topologies present in ferroelectric domain walls [https://arxiv.org/abs/2207.01307]. In addition to non-linear optical effects, the system-specific parameters of the optical measuring arrangement in the microscope also determines the detected measurement signals. This includes, for example, the collimation of the infrared excitation light, the direction between excitation and detection, but also the apertures in the beam path of the confocal beam geometry and, therefore, require careful consideration when interpreting experimental results. In this work a Tunable hIGH EnerGy (TIGER) multiphoton microscope [Vittadello et al., Nanomaterials 11, 3193 (2021)] pumped by high energy fs-laser pulses from an optical parametric

amplifier allowing for widefield SHG is used to study ferroelectric domain structures. The results are comparatively evaluated for different measurement setups, discussed and possible consequences for the interpretation of the origin of the SHG signal from widefield and scanning modes are presented. Funded by the DFG (project IM 37/12-1, FOR 5044 and RU 2474/1-1).

KFM 6.42 Tue 17:00 P3

Small-polaron dynamics in lithium niobate tantalate solid solutions studied by means of fs-pump, cw-probe spectroscopy — •NIKLAS DÖMER¹, ANTON PFANNSTIEL¹, MIRCO IMLAU¹, and STEFFEN GANSCHOW² — ¹Inst. Physics, Barbarastr. 7, Osnabrück Univ. — ²Leibniz-Institut für Kristallzüchtung (IKZ), Berlin

The inspection of transport and recombination dynamics of optically generated small polarons with strong coupling enables far-reaching insight into the electronic and microscopic (defect) structure of polar oxide crystals using macroscopic measures. Here, we use the absorption cross-section of small polarons to relate fs-pulse induced transient absorption with the temporal evolution of small polaron number densities, i.e. with the 3D hopping transport of small polarons within a lattice with intrinsic defect structure. For the first time, fs-pump continuous-wave probe spectroscopy is applied to lithium niobate tantalate (LNT, $LiNb_xTa_{1-x}O_3$ with $0 \leq x \leq 1$) solid solutions. Remarkably, a two-step decay with lifetimes in the order of microseconds and minutes is uncovered, which has not been observed in the widely studied edge compositions lithium niobate (LN, $x=1$) and lithium tantalate (LT, $x=0$). This finding is studied over the entire composition range ($0 \leq x \leq 1$) at distinct wavelengths according to the maxima of small polaron absorption features. A microscopic model based on the simultaneous presence of two types of intrinsic antisite defect centers, Nb_{Li} and Ta_{Li} , is deduced to explain two different polaron decay channels. Financial support by the DFG (project IM 37/12-1 and GA 2403/7-1, FOR 5044).

KFM 6.43 Tue 17:00 P3

UV-triggered polymerisation of photosensitive resins via harmonic emission of Bariumtitanate nanocrystals — •EUGEN WOLF and MIRCO IMLAU — Institute of Physics, Barbarastr. 7, Osnabrück University

Ultraviolet-photosensitive resins are important in various industrial applications like laser-based 3D printing or fibre-reinforced polymers. Spatially localized polymerization becomes possible using laser light at photon energies that are adjusted to the absorption features of the corresponding photoinitiator. A drawback of this approach, however, is the transmission loss of the incident UV light, so that it can be applied only for polymerization of surfaces or thin volumes. To overcome this limitation, the use of infrared light in combination with nanoscaled photocatalytic containers in the resin has been proposed. In this contribution, we present an alternative approach based on the use of harmonic nanocrystals, i.e. to convert the incident infrared to the UV region deep inside the resin. For this purpose, commercially available Bariumtitanate nanocrystals and a regeneratively amplified fs-laser system are used. Remarkably, a high reproducibility of the polymerization process as a function of the light propagation coordinate is uncovered. Furthermore, our setup allows for the inspection of the dynamics and shape of the liquid-solid phase front for different laser parameters. We discuss our results taking a simplified model for nonlinear optical emission of nanoparticles stochastically distributed in the resin into account.

KFM 6.44 Tue 17:00 P3

Optical damage and hologram recording in as-grown Lithium-Niobate-Tantalate solid solutions — •SÖREN DOMKE¹, BJOERN BOURDON¹, STEFFEN GANSCHOW², and MIRCO IMLAU¹ — ¹Institute of Physics, Barbarastr. 7, Osnabrück Univ. — ²Leibniz-Institut für Kristallzüchtung (IKZ), Berlin

Lithium niobate tantalate (LNT, $LiNb_xTa_{1-x}O_3$ with $0 \leq x \leq 1$) solid solutions provide a promising material platform for nonlinear-photonics due to the ability for tuning the optical and electrical properties via composition. However, so far, very little is known about the (nonlinear) optical characteristics and intrinsic defect structure of LNT compared to its edge compositions lithium niobate (LN, $x=1$) and lithium tantalate (LT, $x=0$). In this respect, the presence of optical damage, i.e. the transient change of the index of refraction by the action of an incident light beam, is of particular importance as it drastically degrades the components' usability, but can also be used for wave-mixing applications. Originally discovered in LN, we report of our observations of a comparable nonlinear optical phenomenon in nominally undoped LNT samples and present the results of our systematic studies using the recording and reconstruction of elementary holographic gratings. As a particular feature of our finding, the phenomenon shows a transient behavior with a lifetime in the order of tens of hours that can only be erased using white light illumination and/or thermal treatment. The results are discussed in the framework of the photorefractive effect and an intrinsic defect model. Financial support by the DFG (projects IM37/12-1, GA 2403/7-1, FOR 5044).

KFM 6.45 Tue 17:00 P3

Laser induced damage threshold (LIDT) of additively manufactured components in photonics — •MORITZ HUESMANN, YANNIC TOSCHKE, and MIRCO IMLAU — Institute of Physics, Osnabrück University, Germany

Nowadays, desktop additive manufacturing technologies, e.g., 3D-printing based on thermoplastics (filaments), are widely available. They are increasingly finding their way into research laboratories in photonics due to the possibility to manufacture optomechanical components, such as versatile optical adapters, optomechanical mounts and sample holders. While the mechanical properties of the thermoplastics have been studied intensively in literature, nearly nothing is known about the laser damage threshold (LIDT) of these materials. Without this knowledge, the use in optical setups is limited to laser beams with moderate to low average power for safety reasons. In the second step, the damage threshold for PLA and PETG of different color was systematically determined under the exposure with intense femtosecond and nanosecond laser pulses. We discuss the determined LIDT values in the framework of applications in photonics, but also analyze the photophysical processes of the laser-induced damages based on a detailed topographic inspection. Financial support by the BMBF within Open Photonik Pro (project 13N15230, optocubes).

KFM 6.46 Tue 17:00 P3

Temperature dependence of the optical band gap of LNT solid solutions (20–330 K) — •T. HEHEMANN¹, A. PFANNSTIEL¹, S. SANNA², N. SYVOROTKA³, K.-D. BECKER⁴, S. GANSCHOW⁵, and M. IMLAU¹ — ¹Inst. Phys., Osnabrück Univ. — ²Inst. Phys., Univ. Giessen — ³Inst. Energy Res., TU Clausthal — ⁴Inst. Phys. Theo. Chem., TU Braunschweig — ⁵Leibniz-Inst. f. Kristallzüchtung, Berlin

Lithium niobate tantalate solid solutions (LNT, $\text{LiNb}_x\text{Ta}_{1-x}\text{O}_3$ with $0 \leq x \leq 1$) represent a promising class of polar oxide materials for photonics due to their favourable linear & nonlinear optical, but also photoelectrical properties. A mandatory basic requirement for customised optical applications is the (precise) knowledge of the optical band edge energy $E_{\text{gap}}^{\text{opt}}$. While $E_{\text{gap}}^{\text{opt}}$ and its relation to the intrinsic defect structure has been well investigated for the edge compositions LiNbO_3 (LN, $x=1$) and LiTaO_3 (LT, $x=0$), nearly nothing is reported for LNT in literature, so far. In particular, there are no data available for the important low temperature region 20–330 K. We here present temperature dependent absorption spectra of LNT in the vicinity of the optical band edge covering the entire composition range ($0 \leq x \leq 1$). The analysis of the data set follows the established fitting routines and reveals, both the composition and temperature dependent shifts of $E_{\text{gap}}^{\text{opt}}(x, T)$. The former is discussed in the framework of the intrinsic defect structure, while the latter is related with the properties of the electronic structure. All findings are compared with respective shifts widely reported for LN and LT. Financial support by the DFG (projects IM 37/12-1, SA 1948/3-1, FR 1301/40-1, GA 2403/7-1 of the FOR 5044)

KFM 7: Focus: High-resolution Lithography and 3D Patterning

While high-resolution 2D lithography and structuring is relatively matured and also widely applied in industrial processes, work on its 3D variant is mostly focusing on fundamental aspects and process development. At the lower edge of possible 3D feature dimensions, certainly methods such as focused electron beam induced deposition (FEBID), non-linear multi-photon-laser lithography and thermal scanning probe lithography techniques are required. This session will discuss most of these dedicated 3D methods in detail. For the fabrication of complex 2D and 2.5D patterns, advanced electron beam and X-ray methods are continuously developed further. In addition, new methods such as high resolution Talbot lithography for relatively large areas are already entering industrial maturity. This session will also discuss some of the latest developments in this field of binary lithography.

Chair: Dr. Frank Heyroth (Martin-Luther-Universität Halle)

Time: Wednesday 9:00–12:35

Location: POT 51

Invited Talk

KFM 7.1 Wed 9:00 POT 51

Novel device integration – combining bottom-up and topdown approaches — •ARTUR ERBE — Helmholtz-Zentrum Dresden-Rossendorf, Dresden, Germany — TU Dresden, Germany

Scaling electronic devices to smallest structure sizes well below 10nm will require novel developments for the fabrication of single components. Smallest functional devices can be assembled using chemical methods leading to, e.g., single molecules with electronic functionalities. Reliable contacting of single molecules using metallic contacts is, however, an extremely challenging task that has not been solved so far. We have therefore developed techniques that use self-assembly to create conducting nanostructures to create small, self-assembled circuits that can then be contacted reliably using standard lithographic methods. In this talk, we will show how DNA Origamis can be used for the self-assembly of metallic nanowires, which are contacted using electron beam lithography and electrically characterized. Self-assembly can be used to integrate semiconductor nanoparticles or single molecules for building nanodevices. Further integration of such nanostructures into standard silicon electronics may for example be achieved by connecting these nanodevices to silicon nanowires or transistors based on 2-dimensional materials. We have therefore developed reconfigurable transistors based on these materials using electron beam lithography and further processing (i.e. using a classical top-down approach), which are reconfigurable. With the combination of these transistors with self-assembled nanostructures, a large variety of electronic nanocircuits can be constructed in future applications.

KFM 7.2 Wed 9:30 POT 51

Optical properties of photoresists for femtosecond 3D printing: Refractive index, extinction, luminescence - dose dependence, aging, heat treatment and comparison between 1-photon and 2-photon exposure — •MICHAEL SCHMID, DOMINIK LUDESCHER, and HARALD GIESSEN — 4th Physics Institute and Research Center SCoPE, University of Stuttgart, Pfaffenwaldring 57, 70569 Stuttgart, Germany

Femtosecond 3D printing has emerged as an important technology for manufacturing nano- and microscopic optical devices and elements. Detailed knowledge of the dispersion in the visible and near-infrared spectral range is crucial for the design of these optical elements. Here, we provide refractive index measurements for different UV-doses, aging times, heat treatment and 2-photon exposed structures for the photoresists IP-S, IP-Dip, IP-L, OrmoComp, IP-Visio, and IP-n162. We use a modified and automated Pulfrich refractometer setup, utilizing

critical angles of total internal reflection with an accuracy of $5 \cdot 10^{-4}$ in the visible and near-infrared spectral range. We compare Cauchy and Sellmeier fits to the dispersion curves and also give Abbe numbers and Schott Catalog numbers of the almost entirely polymerized resists. Additionally, we provide quantitative extinction and luminescence measurements for all photoresists.

KFM 7.3 Wed 9:50 POT 51

3D direct laser writing of miniature optical apertures with highly absorptive photoresist — •MICHAEL SCHMID^{1,2}, ANDREA TOULOUSE^{2,3}, SIMON THIELE^{2,3,4}, SIMON MANGOLD^{1,2}, ALOIS HERKOMMER^{2,3}, and HARALD GIESSEN^{1,2} — ¹4th Physics Institute, University of Stuttgart, Pfaffenwaldring 57, 70569 Stuttgart, Germany — ²Research Center SCoPE, University of Stuttgart, Pfaffenwaldring 57, 70569 Stuttgart, Germany — ³Institute of Applied Optics (ITO), University of Stuttgart, Pfaffenwaldring 9, 70569 Stuttgart, Germany — ⁴Printoptix GmbH, Johannesstraße 11, 70176 Stuttgart

In recent years, 3D direct laser writing and its possible application developed rapidly. Different complex micro-optical systems have been demonstrated, such as multi-lens objectives. However, it is still challenging to integrate microscopic apertures to these systems. We present a novel approach to create 3D direct laser written apertures using an opaque material suitable for 2-photon lithography. This way, it is possible to integrate microscopic apertures into 3D printed micro-optical systems improving the imaging quality. We demonstrate this potential by combining 3D printed black apertures with singlet lenses made of the commonly used photoresist IP-S. A significant contrast improvement of the imaging is achieved. Furthermore, due to the absorption coefficient, it is possible to create thin lenses with the black material enabling the fabrication of optical lens and aperture in one step.

KFM 7.4 Wed 10:10 POT 51

Self-Folding micro cubes of laser-cut templates — •PIERRE LORENZ¹, YE YU², RONALD FRANZ³, JOACHIM ZAJADACZ¹, MARTIN EHRHARDT¹, ROBERT KIRCHNER², GREGORY LECRIVAIN³, and KLAUS ZIMMER¹ — ¹Leibniz Institute of Surface Engineering, Permoserstr. 15, Leipzig, 04318, Germany — ²Institute of Semiconductor and Microsystems, TU Dresden, Nöthnitzer Straße 64, Dresden, 01187, Germany — ³Helmholtz-Zentrum Dresden-Rossendorf, Institut für Fluidodynamik, Bautzner Landstraße 400, Dresden, 01328, Germany

3D microstructures exhibit manifold applications with compact system integration in mind. Especially self-folding processes of laser-cut 2D templates allow for

fast, flexible, and cost-effective fabrication of 3D structures. A UV ps laser was used for the laser cut of polyimide foil-based 2D templates. Two different folding concepts were tested: water-droplet self-folding and vacuum micro forming (VMF). The VMF concept is based on an array of cavities in a Teflon plate, which work similarly to deep drawing as a guide for the VMF of the 2D templates. In the water-droplet concept, a water droplet was added by a tweezer with a defined volume resulting in self-folding due to the surface tension. Both concepts allow the well-defined folding of sub-mm cubes after optimization of the 2D template geometry. Especially the VMF allows a parallelization and miniaturization of the folding process, which was monitored and analyzed by high-speed imaging.

KFM 7.5 Wed 10:30 POT 51

High resolution and process stability tests on new HSQ based resists — •NICOLAS KUNZFELD and AXEL RUDZINSKI — Raith GmbH, Konrad-Adenauer-Allee 8, 44263 Dortmund, Germany

Many new resist providers for hydrogen silsesquioxane (HSQ) based high resolution e-Beam-resist emerged on the market in the last few years.

Until now, the experience with these new resists regarding resolution capabilities, process stability and long term behaviour is very limited.

To expand the experience with these resist, further testing based on statistical methods like a process capability evaluation based on the CpK-Value is required.

This work presents the latest high resolution, process capability and long term stability tests of these HSQ-based resists provided by different resist suppliers.

We achieved isolated single pixel lines with sub 6 nm line width with a CpK-Value of 1 and were also able to get a first impression about the resist behaviour over a time frame of almost 30 days.

15 min. break

Invited Talk

KFM 7.6 Wed 11:05 POT 51

4D meso-scale electronics for next generation medical tools and electronic skins — •DANIIL KARNAUSCHENKO — Research Center MAIN, Technical University Chemnitz, Rosenbergstr. 6, 09126 Chemnitz, Germany

State-of-art mesoscale systems for IoT, e-skins or smart-dust applications, medical or commercial products are essentially 3D architectures, whose geometry plays vital role when providing communication, sensing, actuation and power management functions. Conventional components carrying electronic functions are static, functionally heterogeneous and spatially separated requiring nontrivial sequential assembly and packaging procedures, which hinder further miniaturization and development of next generation mesoscale systems. 3D self-assembled architectures are envisioned to become a driving force for 3D electronic devices designed, microfabricated and self-assembled from planar thin-film structures and self-organized electronic components. Dynamic (4D) parallel assembly operating at mesoscale (1 μm - 1 mm) allows offers improved performance while reducing overall manufacturing complexity of devices and components by harnessing the relative ease in which it can produce mesoscopic 3D geometries i.e. origami folded structures and "Swiss-roll" architectures. These architectures and benefits will lead to tighter a system integration e.g. electronic skins and medical tools made out of electronic components including active matrix, capacitors, power sources, coils, sensors, actuators and antennas with reduced costs fabricated from a single wafer.

KFM 7.7 Wed 11:35 POT 51

Two-Photon Polymerization Lithography Structures Characterized via Raman Spectroscopy and Nanoindentation — •SEVERIN SCHWEIGER^{1,2}, TIM SCHULZE^{1,2}, PETER REINIG¹, SIMON SCHLIPF³, and HARALD SCHENK^{1,2} — ¹Fraunhofer Institute for Photonic Microsystems, Maria-Reiche-Str. 2, Dresden, Germany, 01109 — ²Brandenburg University of Technology, Platz der Deutschen Einheit 1, Cottbus, Germany, 03046 — ³Fraunhofer Institute for Ceramic Technologies and Systems, Maria-Reiche-Str. 2, Dresden, Germany, 01109

Additive manufacturing using two-photon polymerization (TPP) lithography has gathered interest in industry and research. Parameter sweeps of cuboid structures fabricated using TPP lithography were investigated to find dependent mechanical material properties across the parameters of the laser power and scan speed. Raman spectroscopy and micro- or nanoindentation were used on the cuboids to find the degree of conversion (DC) of monomer to polymer and the Youngs modulus (E), respectively. The DC and E found for the photoresist IP-Dip was 20 % to 45 % and 1 to 2.1 GPa, respectively. These results were compared to reports found in the literature. The DC and E found for the photoresist IP-Q, was 53 % to 80 % and 0.5 to 1.3 GPa, respectively. The properties found for IP-Q are the current state of knowledge for this photoresist. Many structures fabricated via TPP and based on IP-Q can benefit from this knowledge and the customizability of the material. Examples are evaluated and discussed in the presentation.

KFM 7.8 Wed 11:55 POT 51

Dry film resists: A promising material class for micro-/acoustofluidic chip fabrication — •ANDREAS WINKLER — Group "Acoustic Microsystems", IFW Dresden, Helmholtz str. 20, 01069 Dresden, Germany

Dry film resists (DFRs) promise low-cost and greener microfabrication, and can partly replace conventional technologies for microstructure fabrication being associated with high-energy demands and intense use of toxic and climate-active chemicals. Due to their mechanical stability and superior film thickness homogeneity, DFRs also outperform spin-on resists, such as SU-8, as structural materials, especially when high-resolved two- and three-dimensional architectures are required such as the case in acoustofluidic chip devices. We investigated various dry film resists in the recent years for their suitability in micro-/acoustofluidic applications. While in general their performance was found to be highly promising and also allowed completely new solutions, properties of commercially available DFRs can vary strongly between individual products and even product charges, and literature on - as well as description of - these materials is still scarce. Here, we introduce this relatively young material class and present selected results regarding technically important effects and limitations, optical properties and performance in acoustofluidic cell separation and aerosol generation.

KFM 7.9 Wed 12:15 POT 51

Artificial Intelligence for high resolution multi-photon lithography — •JULIAN HERING-STRATEMEIER¹, SVEN ENNS^{1,2}, NICOLAS LANG¹, and GEORG VON FREYMAN^{1,2,3} — ¹Physics Department and State Research Centre OPTIMAS, TUK, 67663 Kaiserslautern, Germany — ²Opti-Cal GmbH, 67663 Kaiserslautern, Germany — ³Fraunhofer Institute for Industrial Mathematics ITWM, 67663 Kaiserslautern, Germany

Multi-photon lithography, a.k.a. direct laser writing (DLW), is one of today's most flexible high resolution 3D additive manufacturing technologies. Nevertheless, there are fundamental restrictions, limiting its resolution and structure-conformity: First, the shape of the polymerization-triggering laser focus limits the minimal volume that gets solidified (voxel). Hence, laser focus shape distorting optical aberrations within the beam path worsen the quality of the 3D printed outcome. Second, the physico-chemical properties of the photo resins influence the sharpness and extensions of single voxels, and, therefore, the 3D printed structure quality and resolution as well. Here, we show very first steps (i) towards a fast algorithm for predicting those error-loaded structures. Moreover, we use artificial intelligence (ii) to correct for optical aberrations within the beam path and (iii) to pre-compensate for the photo resin's outcome-worsening properties. Especially correcting aberrations is crucial for, e.g., extending DLW to high resolution STED-inspired DLW which is analogue to the well-known and Nobel price awarded STED-microscopy.

KFM 8: Diamond and related dielectric materials

In this session the basics of NV-centers and other defects in diamond were presented. The influence to applications in different fields are obvious. So, there is an influence on dielectric properties of diamond, used e.g. in high power microwave components for fusion applications in the GHz to THz frequency range. Biological diamond applications and applications in quantum photonics are also considered in this field of diamond and related materials.

Chair: Prof. Dr. Theo A. Scherer (KIT Karlsruhe)

Time: Wednesday 14:00–17:15

Location: POT 51

KFM 8.1 Wed 14:00 POT 51

Optimal Control for Quantum Sensing with NV Centers in Diamond — •MATTHIAS MÜLLER — Forschungszentrum Jülich GmbH

Diamond based quantum technology is a fast emerging field with both scientific and technological importance. The performance relies on unique features

like superposition and entanglement and depends on sophisticated mechanisms of control to perform the desired tasks. Quantum Optimal Control (QOC) has proven to be a powerful tool to accomplish this task. I will give a brief overview on the use of QOC for quantum sensing with NV centers in diamond and report on recent applications.

[1] P. Rembold et al., AVS Quantum Sci. 2, 024701 (2020) [2] M.M. Müller et al., Sci. Rep. 8, 14278 (2018) [3] N. Oshnik et al., Phys. Rev. A 106, 013107 (2022) [4] A. Marshall et al., arXiv:2112.15021 (2022)

KFM 8.2 Wed 14:20 POT 51

Influence of N defects on dielectric properties of diamond — •THEO SCHERER — KIT Karlsruhe

Atomistic structures and elastic and dielectric properties including first simulations of loss tangent, $\tan \delta$ of diamond with small nitrogen impurities can be calculated using the first principles methods. The effect of a single nitrogen substitutional atom on the Raman and IR absorbance spectra is analyzed and compared with other calculations. It is shown that nitrogen defects do not affect $\tan \delta$ at far IR region used in diamond windows in fusion reactors for plasma heating and stabilization.

KFM 8.3 Wed 14:40 POT 51

Technical application of CVD Diamond windows in fusion reactor heating systems. — •PETER SPÄH — KIT, Institute for applied materials, Karlsruhe

The application of CVD diamond windows in fusion experiments often comes along with challenging design requirements. Diamond windows and associated components must be protected properly from harsh environmental conditions. This is particularly the case for the future demonstration power plant reactor (EU DEMO), where sensitive applications shall operate under severe conditions in terms of heat, mechanical loads and radiation.

For the EU DEMO, an EC Heating and Current Drive System (ECH&CD) is under development, where CVD diamond windows together with microwave reflectors (mitre-bends and mirrors), corrugated waveguides, waveguide switches, shutter valves and confinement barrier feed-throughs, will be precisely integrated into a millimetre wave power transmission system. The entire system is installed into massive launching components and reactor building structures. The design takes into account mechanical integrity, dissipation of heat by powerful cooling systems, radiation shielding and the capability to be serviced and maintained by remote handling procedures.

This talk presents the conceptual design and integration of the ECH&CD launching system into the EU DEMO fusion power plant.

KFM 8.4 Wed 15:00 POT 51

Fabrication and Characterization of Thin Single-Crystal Diamond Membranes for Quantum Photonics — •JULIA HEUPEL¹, MAXIMILLIAN PALLMANN², JOHANN P. REITHMAIER¹, DAVID HUNGER², and CYRIL POPOV¹ — ¹Institute of Nanostructure Technologies and Analytics (INA), University of Kassel, Heinrich-Plett-Str. 40, 34132 Kassel, Germany — ²Physikalisches Institut, Karlsruher Institute für Technologie (KIT), Wolfgang-Gaede-Str.1, 76131 Karlsruhe, Germany

Due to its exceptional physical and chemical characteristics, single-crystal diamond (SCD) in a form of thin membranes is a promising material for the fabrication of high-quality photonic devices and for envisioned applications in quantum information technologies (QIT). In order to structure SCD membranes with a good quality and thickness of few micrometer or below, it is important to minimize defects originating from polishing (e.g., grooves and pits) or etching procedures (e.g., micro-masking effect). Here we report on the fabrication of thin SCD membranes, exhibiting a low surface roughness down to 0.2 nm by means of inductively coupled plasma reactive ion etching (ICP-RIE). A significant roughness reduction was achieved by using distinct Ar/Cl₂ etching recipes as a planarization step before the actual structuring process. These planarized SCD membranes are successfully bonded via van der Waals forces on plane cavity mirrors and optically characterized in a fiber-based Fabry-Pérot microcavity regarding their mode structure and finesse.

KFM 8.5 Wed 15:20 POT 51

Enhanced protein immobilization by nanostructuring of UNCD surface

— •DANIEL MERKER¹, DANIELA BERTINETTI², ROLF MERZ³, MICHAEL KOPNARSKI³, FRIEDRICH W. HERBERG², JOHANN P. REITHMAIER¹, and CYRIL POPOV¹ — ¹Institute of Nanostructure Technologies and Analytics (INA), Center for Interdisciplinary Nanostructure Science and Technology (CINSA-T), University of Kassel, Germany — ²Department of Biochemistry, CINSA-T, University of Kassel, Germany — ³Institut für Oberflächen- und Schichtanalytik GmbH, Kaiserslautern, Germany

Investigations of molecular mechanisms related to the formation of the inner clock require detection of coupling factors, e.g. secreted neuropeptides, that mediate synchronization. In this work we study the application of ultrananocrystalline diamond (UNCD) as biosensor for detection of such coupling factors. The crucial part is the feasibility of protein immobilization on UNCD surfaces. From all investigated coupling routes only photochemical attachment of alkenes gave acceptable results when the green fluorescent protein (GFP) was immobilized. A process to create nanostructures was developed to increase the effective surface for protein immobilization. Both functionalization and structuring have beneficial effects on immobilization performance, but especially in combination the immobilization efficacy increases significantly. Lastly, the immobilization of different binding proteins against GFP - antibodies, nanobodies, DARPin - was

investigated, with the last two showing promising results for high specificity and affinity capture of target molecules in a future UNCD biosensor.

15 min. break

KFM 8.6 Wed 15:55 POT 51

Numerical analyses of CVD diamond windows in high power microwave applications — •GAETANO AIELLO¹, ANDREAS MEIER¹, HEINRICH PETER LAQUA², THEO SCHERER¹, SABINE SCHRECK¹, and DIRK STRAUSS¹ — ¹Karlsruhe Institute of Technology, Institute for Applied Materials, 76021 Karlsruhe, Germany — ²Max Planck Institute for Plasma Physics (IPP), 17491 Greifswald, Germany

Nuclear fusion reactors require electron cyclotron heating and current drive (ECH&CD) systems for plasma heating and stabilization. Chemical vapor deposition (CVD) polycrystalline diamond windows on both the torus and gyrotron sides of the reactors act as confinement and/or vacuum boundaries allowing the transmission of high-power microwave beams. For example, the beam power scenarios of 1.5 MW and 2 MW are the current targets considered respectively in Wendelstein 7-X and European DEMO fusion machines. In this work, with reference to both reactors, the numerical analyses required to verify the thermal and structural performance of the windows are discussed. Experimental measurements of loss tangent in diamond provided inputs for the numerical analyses. Sensitivity studies of the windows with respect to loss tangent and other parameters were also carried out to check the temperature reserve margins of the design.

KFM 8.7 Wed 16:15 POT 51

Simulation study of LC superconducting microresonators for diamond characterization — •FRANCESCO MAZZOCCHI, DIRK STRAUSS, and THEO SCHERER — Karlsruhe Institute of Technology KIT IAM-AWP, Eggenstein-Leopoldshafen, Germany

The development of high optical quality, ultra-low losses single crystal diamond windows is paramount for the realization of future nuclear fusion facilities like DEMO, given the foresaw increase in power of microwave ECRH systems. Precise determination of the dielectric characteristics (ϵ_r and $\tan \delta$) of these innovative materials have so far relied on techniques involving Fabry-Perot microwave open resonators in various configurations. High Q, superconducting thin film resonators can be effectively used to determine dielectric characteristics of extremely low losses materials like single- and poly-crystalline diamond. Their extremely high-quality factors allow for a substantial increase in resolution in the determination of these parameters when compared to state-of-the-art Fabry Perot open resonators. We hereby report a detailed simulation study of the chosen resonators configurations (Lumped Elements and Circular) that lead to the final design of the devices.

KFM 8.8 Wed 16:35 POT 51

CVD Diamond Disks for ITER ECH windows - dielectric loss characterization and optical inspection — •SABINE SCHRECK¹, GAETANO AIELLO¹, PABLO ESTEBNEZ², ANDREAS MEIER¹, THEO SCHERER¹, DIRK STRAUSS¹, CHRISTOPH WILD³, and ECKHARD WOERNER³ — ¹Karlsruhe Institute of Technology, Institute for Applied Materials, 76021 Karlsruhe, Germany — ²Fusion for Energy, 08019 Barcelona, Spain — ³Diamond Materials, 79108 Freiburg, Germany

Diamond disks with a diameter of 70 mm and a thickness of 1.11 mm will be installed into windows of the Electron Cyclotron Heating and Current Drive System (EC-HCD) of the fusion reactor ITER. The bare disks, manufactured by a microwave plasma assisted chemical vapor deposition process, need to ensure high mechanical stability, thermal conductivity and transmission of MW-class microwave beams. Factory acceptance tests of the disks produced by Diamond Materials include a check of dimensional properties and a determination of its dielectric loss. The loss characterization and the comparison with the respective specifications is performed at KIT using dedicated Fabry-Perot resonators, that allow the measurement of the loss tangent at the disk centre and a mapping of it over the disk area. An optical inspection with a digital microscope completes the examination. More than 60 diamond disks need to be qualified prior to their integration into the window assemblies and the application in the ITER EC-system. The disk qualification activities are performed within a contract between F4E and KIT and the talk will present the current status.

KFM 8.9 Wed 16:55 POT 51

CVD Diamond Windows for Electron Cyclotron Resonant Heating in Fusion — •DIRK STRAUSS, GAETANO AIELLO, ANDREAS MEIER, THEO SCHERER, and SABINE SCHRECK — aKarlsruhe Institute of Technology, Institute for Applied Materials, Hermann-von-Helmholtz-Platz 1, 76344 Eggenstein-Leopoldshafen, Germany

Electron cyclotron resonant heating (ECRH) in nuclear fusion combines the injection of multi megawatt power with the possibility to focus the millimeter wave beam to small spot sizes of few centimeters. The ECRH allows efficient plasma heating as well as localized current drive for magneto-hydrodynamic stabilization of e.g. neoclassical tearing modes that create local magnetic islands with a fast loss of plasma confinement. One of the key challenges for high power ECRH systems is the provision of suitable confinement windows.

The low loss tangent, high thermal conductivity and outstanding mechanical properties qualify diamond as the state of the art material for high power millimeter wave heating systems in nuclear fusion devices. Artificial diamond disks are grown by CVD in diameters up to 180mm, sufficient for the usual waveguide diameters.

The principles of ECRH systems will be presented with a focus on the permittivity of diamond, which determines the loss tangent and suitable disk thickness. Further concepts and status for small and broadband windows for frequencies of 100-240GHz and beam powers up to 2MW will be discussed.

KFM 9: Microscopy and Tomography with X-ray Photons, Electrons, Ions and Positron

Chair: Prof. Dr. Theo A. Scherer (KIT Karlsruhe)

Time: Wednesday 9:00–13:15

Location: POT 106

KFM 9.1 Wed 9:00 POT 106

FePX₃ (X: S, Se): A stable new 2D material for water splitting — •HAFIZ MUHAMMAD ZEESHAN¹, SANDHYA SHARMA¹, ELENA VOLOSHINA^{1,2}, and YURIY DEDKOV^{1,2} — ¹Centre of Excellence ENSEMBLE3 Sp.z.o.o., Wolczynska Str. 133, 01-919 Warsaw, Poland. — ²Department of Physics, Shanghai University, 99 Shangda Road, 200444 Shanghai, P. R. China.

The interaction of high-quality transition metal trichalcogenides (TMTs) single crystals FePX₃ (X: S, Se) with water molecules is studied using NEXAFS and XPS in a wide range of temperature and partial pressure of H₂O. The physisorption nature of interaction between H₂O and FePX₃ is found at low temperatures and relatively small concentrations of water molecules, that is supported by the DFT results. When temperature of the FePX₃ samples and partial pressure of H₂O are increased, the interaction at the interface is defined by two competing processes - adsorption of molecules at high partial pressure of H₂O and desorption of molecules due to the increased surface mobility and physisorption nature of interaction. Our intensive XPS/NEXAFS experiments accompanied by DFT calculations bring new understanding on the interaction of H₂O with surface of a new class of 2D materials, TMTs, pointing to their stability and reactivity, that is important for further applications in different areas, like sensing and catalysis.

KFM 9.2 Wed 9:20 POT 106

Solving complex nanostructures with ptychographic atomic electron tomography — •PHILIPP PELZ — Institute for Micro- and Nanostructure Research, Friedrich-Alexander Universitaet Erlangen, Cauerstr. 3, 91058 Erlangen

Knowledge of the three-dimensional atomic structure of natural and manufactured materials allows us to calculate their physical properties and deduce their function from first principles. Phase-contrast electron microscopy methods like ptychography are ideally suited to solve the 3D atomic structure of nanomaterials containing light and heavy elements. We perform mixed-state electron ptychography from 34.5 million diffraction patterns to reconstruct a high-resolution tilt series of a double wall-carbon nanotube (DW-CNT), encapsulating a complex ZrTe sandwich structure. Class averaging of the resulting reconstructions and subpixel localization of the atomic peaks in the reconstructed volume reveals the complex three-dimensional atomic structure of the core-shell heterostructure with 17 picometer precision.

KFM 9.3 Wed 9:40 POT 106

Status and Upgrades of the Beam Facility at the High-Intensity Positron Source NEPOMUC — •CHRISTOPH HUGENSCHMIDT — Forschungs-Neutronenquelle Heinz Maier-Leibnitz (MLZ), Technische Universität München, Lichtenbergstr. 1, 85748 Garching, Germany

The bright low-energy positron beam provided by the neutron induced positron source in Munich (NEPOMUC) at FRM II is used in a large variety of experiments in materials science, condensed matter and surface physics as well as in fundamental research, e.g., for the creation of a positron-electron pair plasma. Within this contribution, an overview of the current status and developments of the positron beam facility with its instrumentation is given. Plans for the installation of a buffer gas trap for the creation of high-density positron pulses as well as ideas for increasing the performance of the remoderated positron beam are elucidated. The upgrades of the positron beam instruments (i) Coincident Doppler-Broadening Spectrometer (CDBS) using a scanning positron micro beam, (ii) instrument for the 2D measurement of the Angular Correlation of Annihilation Radiation (2D-ACAR), and (iii) the surface spectrometer are highlighted. Finally, the planned extension of the positron beam facility and the future operation of positron beam experiments in the experimental hall East are presented.

KFM 9.4 Wed 10:00 POT 106

Optimising the scintillator geometry for positron annihilation spectroscopy - A GEANT4 Simulation — •DOMINIK BORAS — Chair of chemical technology and material synthesis, Würzburg, Germany

To better understand the efficiency and the role of backscattering events of a Positron annihilation lifetime spectrometer, a GEANT4 simulation of the atomic processes is conducted. The gamma quanta from the radioactive decay of ²²Na and from the annihilation positron are detected by a scintillator-photomultiplier combination. In the basic setup of the simulation, as scintillation material plastic

BC422Q- 0.5wt.% was used due to its good energy resolution. Different geometries of the scintillator (box, cone, pyramid and tube) were simulated and their influence on the detection efficiency and the instrument resolution function was investigated. Furthermore, the influence of the measured sample material (density, atomic number) on the scattering of gamma quanta was considered.

KFM 9.5 Wed 10:20 POT 106

Formation and time dynamics of hydrogen-induced vacancies in nickel — •MAIK BUTTERLING¹, LUCA CHIARI², MASANORI FUJINAMI², MACIEJ OSKAR LIEDKE¹, ERIC HIRSCHMANN¹, AHMED GAMAL ATTALLAH¹, and ANDREAS WAGNER¹ — ¹Institute for Radiation Physics, Helmholtz-Zentrum Dresden-Rossendorf, Dresden, Germany — ²Department of Applied Chemistry and Biotechnology, Chiba University, 1-33 Yayoi, Inage, Chiba 263-8522, Japan

The formation of hydrogen-induced defects in nickel was investigated by positron annihilation lifetime spectroscopy and the time dynamics of those defects during room temperature aging was tracked with an unprecedented time resolution of the order of minutes using an ultrahigh-flux slow positron beam. Those measurements showed the formation of a large number of atomic vacancies simply by hydrogen addition at room temperature. It could be proved that they were monovacancy-level defects and that hydrogen was trapped and bound to those vacancies during the hydrogen charge. Room temperature aging, i.e. below the stage III temperature in Ni, and the concomitant hydrogen desorption induced the agglomeration of those monovacancies into large vacancy clusters which remained even after all the hydrogen had desorbed and hydrides had disappeared.

These results [1] constitute the first empirical evidence that vacancy-hydrogen complexes are induced in Ni only by hydrogen charging and demonstrate that hydrogen has a primary role in the formation and stabilization of vacancies even at room temperature.

[1] L. Chiari, et al., Acta Materialia 219(2021), 117264

KFM 9.6 Wed 10:40 POT 106

Electron tomography analysis of Ge/SiGe asymmetrically coupled quantum wells — •EKATERINA PAYSEN¹, GIOVANNI CAPELLINI^{2,3}, and ACHIM TRAMPERT¹ — ¹Paul-Drude-Institut für Festkörperelektronik, Leibniz-Institut im Forschungsverbund Berlin e.V., Berlin, Germany — ²IHP - Leibniz-Institut für innovative Mikroelektronik, Frankfurt (Oder), Germany — ³Dipartimento di Scienze, Università degli Studi Roma Tre, Roma, Italy

We present a method for the three-dimensional (3D) characterisation of the morphology and chemical intermixing of buried interfaces in a Ge/SiGe asymmetrically coupled quantum well structure applying electron tomography method based on high-angle annular dark-field (HAADF) scanning transmission electron microscopy. For this purpose, a needle-shaped specimen with a diameter of a few 100 nanometres is prepared with a focused ion beam, from which a tilt series of HAADF projections is recorded. Subsequently, the series is used to calculate a complete 3D image or tomogram of the specimen with the simultaneous iterative reconstruction technique. The analysis of iso-concentration surfaces enables a quantitative determination of morphological quantities such as the root mean square roughness and lateral correlation length individually for each interface. Subnanometre-thin cross-sections from the tomogram are used to measure the chemical interface width with the highest spatial resolution. An advantage of this method is thus the investigation of the interfaces as 3D entities in their buried state on a length scale of a few 100 nanometres without the projection problem.

15 min. break

KFM 9.7 Wed 11:15 POT 106

Weak-signal extraction enabled by deep-neural-network denoising of diffraction data — •JENS OPLIGER¹, MICHAEL MARCO DENNER¹, JULIA KÜSPERT¹, QISI WANG¹, OLEH IVASHKO², ANN-CHRISTIN DIPPEL², MARTIN VON ZIMMERMANN², FABIAN DONAT NATTERER¹, MARK HANNES FISCHER¹, TITUS NEUPERT¹, and JOHAN CHANG¹ — ¹Physik-Institut, Universität Zürich, Winterthurerstrasse 190, CH-8057 Zürich, Switzerland — ²Deutsches Elektronen-Synchrotron DESY, Notkerstrasse 85, 22607 Hamburg, Germany

Removal or cancellation of noise has wide-spread applications for imaging and acoustics. In every-day-life applications, denoising may even include generative aspects which are unfaithful to the ground truth. For scientific applications, however, denoising must reproduce the ground truth accurately. We show how data can be denoised via a deep convolutional neural network such that weak signals appear with quantitative accuracy. In particular, we study X-ray diffraction on crystalline materials. We demonstrate that weak signals stemming from charge ordering, insignificant in the noisy data, become visible and accurate in the denoised data. This success is enabled by supervised training of a deep neural network with pairs of measured low- and high-noise data. This way, the neural network learns about the statistical properties of the noise. We demonstrate that using artificial noise (such as Poisson and Gaussian) does not yield such quantitatively accurate results. Our approach thus illustrates a practical strategy for noise filtering that can be applied to challenging acquisition problems.

KFM 9.8 Wed 11:35 POT 106

Positron beams for materials research — •ANDREAS WAGNER¹, MAIK BUTTERLING¹, AHMED GAMAL ELSHERIF¹, ERIC HIRSCHMANN¹, MACIEJ OSKAR LIEDKE¹, and REINHARD KRAUSE-REHBERG² — ¹Institute for Radiation Physics, Helmholtz-Zentrum Dresden-Rossendorf, Dresden, Germany — ²Martin-Luther-Universität Halle-Wittenberg, Dept. of Physics, 06099 Halle/Saale, Germany

The Helmholtz-Center Dresden - Rossendorf operates several user beamlines for materials research using positron-annihilation energy and lifetime spectroscopy. The superconducting electron linear accelerator ELBE drives several secondary beams including hard X-ray production from electron-bremsstrahlung, which serves as an intense source of positrons by means of pair production. The Monoenergetic Positron Source MePS [1] utilizes positrons with variable kinetic energies ranging from 0.5 to 18 keV for depth profiling of atomic defects and porosities on nm-scales in thin films. High timing resolutions ($\sigma t \approx 100$ ps) at high average rates (105 s⁻¹) and adjustable beam repetition rates allow performing high-throughput experiments. The MePS facility has partly been funded by the Federal Ministry of Education and Research (BMBF) with the grant PosiAnalyse (05K2013). AIDA was funded by the Impulse- und Networking fund of the Helmholtz-Association (FKZ VH-VI-442 Memriox) and by the Helmholtz Energy Materials Characterization Platform. [1] A. Wagner, et al., AIP Conference Proceedings, 1970, 040003 (2018).

KFM 9.9 Wed 11:55 POT 106

Strain Distribution in Au/ZnO Microstructures for bio-magnetic sensing utilizing Scanning X-Ray Nano Diffraction and Coherent X-Ray Diffraction Imaging — •PHILIPP JORDT¹, NIKLAS WOLFF¹, STJEPAN HRKAC², JORIT GRÖTTRUP¹, SINDU SHREE¹, DI WANG³, ANTON DAVYDOK⁴, CHRISTINA KRYWKA^{4,1}, ROSS HARDER⁵, CHRISTIAN KÜBEL³, OLEG SHPYRKO², RAINER ADELUNG¹, OLAF MAGNUSSEN¹, LORENZ KIENLE¹, and BRIDGET MURPHY¹ — ¹Kiel University, Germany — ²UCSD, USA — ³KNME, KIT, Germany — ⁴Hereon, Germany — ⁵XSD, ANL, USA

Magnetic field sensors based on piezoelectric and magnetostrictive materials are a possible path to a new generation of sensors, capable of detecting bio-magnetic fields from human physiology at room temperature in an unshielded environment. A huge hurdle are the very low field strengths of these signals. One approach to further enhance the sensitivity is employing the piezotronic effect, which arises from the combination of a piezoelectric material and a Schottky contact. Here, a study on the strain distribution in ZnO nano and micro-rods coated with gold is presented. Scanning X-ray nano diffraction mapped the 2 dimensional strain distribution across 30-50 μm rods together with insitu current-voltage curves. It is demonstrated that the gold coating and the resulting Schottky contact has a direct impact on the lattice parameters in vicinity of the Au/ZnO interface and further, that the crystal quality of the ZnO is immensely influential on the properties of the Schottky contact. The full 3D strain distribution inside a 1 μm rod was characterized by coherent X-ray diffraction imaging.

KFM 9.10 Wed 12:15 POT 106

Correlation of Mechanical Stress and the Positron Lifetime in Aluminum Alloys — •LUCIAN MATHES¹, VASSILY VADIMOVITCH BURWITZ¹, ADRIAN LANGREHR¹, MAIK BUTTERLING², MACIEJ OSKAR LIEDKE², ERIC HIRSCHMANN², ANDREAS WAGNER², and CHRISTOPH HUGENSCHMIDT¹ — ¹Heinz Maier-Leibnitz Zentrum, TU München — ²Helmholtz-Zentrum Dresden-Rossendorf, Institute of Radiation Physics

Positron annihilation lifetime spectroscopy (PALS) is a sensitive technique to analyze the type and concentration of lattice defects on an atomic level. We applied ex-situ and in-situ PALS to plastically deformed technical Al and Al alloys. Thereby we are able to observe the creation and evolution of stress-induced defects in the region beyond the elastic Hook regime of the specimen. The in-situ bulk measurements were performed using a β^+ emitter in a new experimental setup combining tensile tests and PALS at TUM that also allows for investigation of the reversible elastic deformation of samples. The depth-dependent positron lifetime was measured ex-situ at the accelerator-based positron source MEPS at ELBE. For each sample we recorded the tensile stress, and the corresponding stress-strain curves. This allows us to determine the relation between applied stress, strain and mean positron lifetime. Within this contribution, we also discuss the evolution of the defect population with increasing deformation by examining the intensity change of the different positron lifetime components found in the PALS spectra.

KFM 9.11 Wed 12:35 POT 106

Start-to-end simulations of partially coherent X-ray imaging experiments at synchrotron beamlines — •MARTIN SEYRICH — Deutsches Elektronen-Synchrotron DESY, Centre for X-ray and Nano Science CXNS, Hamburg, Germany

In the last decade, coherent X-ray imaging techniques, such as ptychography and holography, have grown a large user base at third and fourth generation X-ray light sources. In contrast to conventional microscopy techniques, coherent imaging techniques do not directly project an image on a detector. Instead, the image of the object is retrieved algorithmically from interference patterns, usually under the assumption of a fully coherent illumination.

Real X-ray sources are not perfectly coherent, they can be simulated as stochastic sources emitting an ensemble of waves. These waves can be propagated from the source through the entire beamline ending at the detector. The simulated interference patterns can then be treated with the same phase retrieval algorithms as experimental data.

Here, we present our extensions to existing established simulation software (OASYS / SRW) that permit the user to perform such start-to-end simulations with relative ease. We will present simulated data sets of ptychographic and holographic experiments, and discuss the computational demands of such simulations.

KFM 9.12 Wed 12:55 POT 106

Illumination corrected X-ray near-field microscopy — •THEA ENGLER^{1,2}, JOHANNES HAGEMANN¹, CHRISTIAN G. SCHROER^{1,2}, and MATHIAS TRABS³ — ¹Deutsches Elektronen-Synchrotron, DESY, Germany — ²Universität Hamburg, Germany — ³Karlsruhe Institut of Technology, KIT, Germany

At synchrotron facilities, such as Petra III at DESY, small objects (μm) can be imaged with X-ray propagation-based phase-contrast imaging, i.e. near-field holography (NFH).

Reaching high resolution involves the use of nano-focusing optics. The imperfections of these optics cause aberrations in the illumination of the object and also upon further propagation in the measured hologram of the object. To correct the hologram for these artifacts, a flat-field correction must be applied. Considering a temporally stable beam, the hologram is divided by an empty-beam image, i.e. an image of the illumination without the object. With the common flat-field correction, the hologram is not fully corrected for the illumination function since the division is performed only in intensities in the detector plane.

Instead, the division of illumination and object should be performed in terms of complex wavefields in the sample plane, where the object transmission function physically interacts with the illumination function. Using a simulated dataset, we develop an algorithmic scheme using the recently proposed refractive formulation to take the illumination during the phase retrieval process properly into account.

KFM 10: Battery Materials (joint session KFM/ CPP)

Chair: Prof. Dr. Anna Grünebohm (Ruhr-University Bochum)

Time: Thursday 9:00–12:35

Location: POT 51

KFM 10.1 Thu 9:00 POT 51

Materialanalyse von NMC111 Kathodenmaterial aus recycelten Lithium-Ionen-Batterien mittels XRD, AFM und EDX/REM — •CLAUDIA SCHÖBERL, HANNO KÄSS und STEPHAN APPEL — Hochschule Esslingen, Kanalstraße 33, 73728 Esslingen, Deutschland

In einem industriellen Recyclingverfahren für Lithium-Ionen-Batterien wird Kathodenmaterial von der Trägerfolie mit Wasser abgestrahlt und getrocknet. In einem an der Hochschule Esslingen laufenden Forschungsprojekt wird die so gewonnene Schwarzmasse, die hauptsächlich aus NMC111 besteht, mittels Röntgendiffraktometrie (XRD), Rasterelektronenmikroskopie (REM) und elementanalytischen Methoden untersucht, um Hinweise auf die chemische Zusammensetzung und auf strukturelle Veränderungen zu erhalten. Ziel ist es unter anderem, passende Auswahlkriterien für die Qualität des Recyclingmaterials zu definieren, das nach Verarbeitung erneut in Lithium-Ionen-Batterien eingesetzt werden soll. Dazu zählen, neben dem Rest-Bindemittelgehalt, der Kohlenstoffanteil sowie der Anteil an Fremdelementen wie Kupfer und Aluminium. Das wiedergewonnene, recycelte Aktivmaterial wird bei einem Projektpartner zur Herstellung neuer Kathodenfolien verwendet, die in einer Messzelle elektrisch charakterisiert werden. Mittels Rasterkraftmikroskopie (AFM) werden diese neu präparierten Kathodenfolien an der Hochschule Esslingen untersucht. Mit Hilfe eines speziellen Messmodus, der quantitativen nanoskaligen mechanischen Charakterisierung, wird insbesondere die Korrelation von Strukturmerkmalen und mechanischen Eigenschaften überprüft.

KFM 10.2 Thu 9:20 POT 51

Structural response in NCA-type battery cathodes — •TOBIAS HÖLDERLE^{1,2}, PETER MÜLLER-BUSCHBAUM^{1,2}, and ANATOLIY SENYSHYN² — ¹TUM School of Natural Sciences, Chair for Functional Materials, Garching, Germany — ²MLZ, TUM, Garching, Germany

Battery-powered electric drivetrains in electric vehicles (EVs) are heavily limited and constrained to the performance of the energy storage device, i.e. battery. Batteries with higher power/energy densities, capacities, and cycling life are needed to increase EVs' performance and reduce greenhouse gas emissions. Mixed high nickel content $\text{Li}_x\text{Ni}_{0.8}\text{Co}_{0.15}\text{Al}_{0.05}\text{O}_2$ (NCA) cathode material is one of a few today that simultaneously possess high energy and power densities at lower costs. However, NCA materials suffer from poor thermal stability and limited power density. They display capacity fading/efficiency loss due to antisite defects (cation mixing) in their structure, actively discussed in literature. In order to address the issue of cation mixing, a systematic ex-situ neutron powder diffraction study was done for a series of electrochemically delithiated NCA cathodes. The collected set of structural data was modeled using full-profile Rietveld method and results were discussed in line with observed electrochemical behavior. It is observed that lithium occupancies showed a decreasing character upon charging, independent from transition metal occupancies and indicating an absence of antisite defects (cation mixing) in the commercial NCA material during cell operation.

KFM 10.3 Thu 9:40 POT 51

Dynamic structure evolution of extensively de-lithiated high voltage spinel LNMO — NICOLA JOBST¹, •NEELIMA PAUL², PREMYSL BERAN^{3,4}, MARILENA MANCINI¹, RALPH GILLES², MARGRET WOHLFAHRT-MEHRENS¹, and PETER AXMANN¹ — ¹Accumulators Materials Research (ECM), ZSW Cen-tre for Solar Energy and Hydrogen Research Baden-Württemberg, DE-89081 Ulm, Germany — ²Heinz Maier-Leibnitz Zentrum (MLZ), Technische Universität München, DE-85747 Garching, Germany — ³Nuclear Physics Institute CAS, CZ-25068 Rez, Czech Republic — ⁴European Spallation Source ERIC, Box 176, SE-221 00 Lund, Sweden

High voltage spinel is one of the most promising next-generation cobalt-free cathode materials for Li-ion batteries. Besides the typical compositional range of $\text{Li}_x\text{Ni}_0.5\text{Mn}_1.5\text{O}_4$ $0 < x < 1$ in the voltage window 4.90 to 3.00 V, additional 1.5 mol of Li per formula unit can be introduced into the structure, in an extended voltage range to 1.50 V. Theoretically, this leads to significant increase of the specific energy from 690 to 1190 Wh/kg. However, utilization of the extended potential window leads to rapid capacity fading, voltage polarization that lack a comprehensive explanation. In this work, we conducted potentiostatic entropy-metry, operando XRD and neutron diffraction on the ordered stoichiometric spinel $\text{Li}_x\text{Ni}_0.5\text{Mn}_1.5\text{O}_4$ within $0 < x < 2.5$ in order to understand the dynamic structure evolution and correlate it with the voltage profile. We were able to provide a conclusive explanation for the additional voltage step at 2.10 V, the sloping voltage profile below 1.80 V, and the additional voltage step at ~ 3.80 V.

KFM 10.4 Thu 10:00 POT 51

Computational Screening of Oxide Perovskites as Insertion-Type Cathode Material — •JOHANNES DÖHN¹ and AXEL GROSS^{1,2} — ¹Institute of Theoretical Chemistry, Ulm University, Germany — ²Helmholtz Institute Ulm, Germany

The intermittency of wind and solar power - the solely sustainable energy sources which are considered to be abundantly available - leaves only one consequence: For the transition towards renewable energy systems, efficient and reliable storage technologies are needed. Batteries are one of the most widely used storage devices but current technology based on the transfer of Li-ions faces several challenges including their dependence on critical materials with respect to both, scarcity and toxicity.

In our contribution we will discuss atomic-scale investigations of potential future battery materials carried out using density functional theory (DFT). We employed a high-throughput approach in order to screen the well known material class of oxide perovskites as insertion-type cathode materials and we derived several crucial battery properties including voltage and theoretical energy density for in total 280 compounds. For those candidate materials with promising properties, we evaluated additional features such as the voltage profile and diffusion barriers for ionic transport.

Such in silico investigations significantly narrow down the potential materials space for experimental coworkers and thereby contribute to finding green, cheap and reliable devices for energy storage.

KFM 10.5 Thu 10:20 POT 51

Construction of cobalt oxyhydroxide nanosheets with rich oxygen vacancies as high-performance Lithium-ion Battery anodes — •YONGHUAN FU^{1,2}, HUAPING ZHAO¹, JIANHONG LIU², and YONG LEI¹ — ¹Fachgebiet Angewandte Nanophysik, Institut für Physik & IMN MacroNano, Technische Universität Ilmenau, 98693 Ilmenau, Germany — ²Graphene Composite Research Center, College of Chemistry and Environmental Engineering, Shenzhen University, Shenzhen, P. R. China

Cobalt oxyhydroxide (CoOOH) is a promising anode material for lithium-ion batteries (LIBs) due to its high electronic conductivity and theoretical specific capacity. Herein, CoOOH nanosheets are successfully obtained using a facile one-pot method, and a hierarchical nanoporous structure is formed by oxidizing cobalt hydroxide (Co(OH)₂) in NaOH and (NH₄)₂S₂O₈ solution. The CoOOH anode shows better electrochemical performance compared to Co(OH)₂ and Co₃O₄ electrodes when applied to LIBs. The hierarchical nanoporous structure and high electronic conductivity of the CoOOH anode contribute to its outstanding initial discharge capacity, high initial coulombic efficiency, and excellent cyclability. Experiments and density functional theory (DFT) calculations confirmed that the high ICE and prominent rate capability of the nanosheets could be ascribed to the rapid and complete conversion reaction of CoOOH upon lithiation/delithiation facilitated by hydroxyl groups and oxygen vacancies. This study provides new insights into the structure-property relationship of transition-metal oxyhydroxide anode materials for LIBs.

KFM 10.6 Thu 10:40 POT 51

The dielectric behaviour of lithium intercalated graphite anodes - as a function of the state of charge — •SIMON ANNIÉS, CHIARA PANOSSETTI, and CHRISTOPH SCHEURER — Fritz Haber Institut Berlin

The dielectric behaviour of battery materials is a crucial piece of information for understanding atomistic mechanics and modelling diffusion- and charging processes. However, for the most common anode material in today's lithium ion batteries (lithium intercalated graphite), literature results regarding this property are sparse, conflicting and only available for graphite, i.e. the empty state of charge (SOC).

Utilizing our recently developed DFTB parametrization [1] which is based on a machine-learned repulsive potential, we are - for the first time - able to compute the dielectric behaviour of lithium intercalated graphite for the entire range of charge from 0% to 100% - finding a linear dependency from around $\epsilon_r=7$ at 0% SOC to around 25 at 100% SOC. We achieve this by sampling the Coulomb interactions between pairs of Li-ions and vacancies in large cells with varying intercalant concentrations in the adjacent layers.

Our results agree with experiments in the limit of "empty" graphite, as well as for (bilayer-) graphene, which we consider a validation of our approach. With this, we lay an important piece of foundation for the understanding and multi-scale modelling of entire charging and discharging cycles of graphite anodes in Li-ion batteries.

[1] Anniés, Simon, et al., Materials 14.21 (2021): 6633.

KFM 10.7 Thu 11:00 POT 51

Hypothetical t-LGPO as a good ionic conductor, and the influence of Li core electrons on diffusion — GIULIANA MATERZANINI¹, NICOLA MARZARI^{2,3}, and GIAN-MARCO RIGNANESE¹ — ¹Modelling Division, Universite catholique de Louvain, 1348 Louvain-la-Neuve, Belgium — ²Theory and Simulations of Materials (THEOS), Ecole Polytechnique Federale de Lausanne, CH-1015 Lausanne, Switzerland — ³National Centre for Computational Design and Discovery of Novel Materials (MARVEL), Ecole Polytechnique Federale de Lausanne, CH-1015 Lausanne, Switzerland

Following the computationally found high Li-ion conductivity in tetragonal Li₁₀GeP₂O₁₂ (t-LGPO), we study here the role of Li core electrons on Li diffusion in this hypothetical superionic material. We calculate Li diffusivity from two sets of Car-Parrinello canonical molecular dynamics simulations, one using Li pseudopotential with all electrons (1s2s1), and one with just one electron (2s1). The Arrhenius plots show a marked influence of the Li 1s electrons on the Li-ion diffusivity in t-LGPO, being the diffusion coefficient at 600 K one order of magnitude larger, and the activation barrier between 600 and 1200 K 1.5 times smaller, for the Li all-electrons with respect to the Li one-electron calculations. Similar sets of simulations performed for the analogue sulfide material, tetragonal Li₁₀GeP₂S₁₂ (LGPS), show, oppositely, that for LGPS the influence of Li 1s electrons on Li diffusivity is minimal. The different response of Li mobility to the explicit treatment of 1s electrons reveals fundamental differences in the ionic conductivity mechanism in these two classes of materials.

15 min. break

KFM 10.8 Thu 11:35 POT 51

Sodiation-induced reactivation of micro-nano flower for ultra-long cycling life sodium-ion batteries — YULIAN DONG, HUAPING ZHAO, and YONG LEI — Fachgebiet Angewandte Nanophysik, Institut für Physik & IMN MacroNano, Technische Universität Ilmenau, 98693 Ilmenau, Germany

A rational micro-nano hierarchical structure is demonstrated to prolong the cycle life of sodium-ion batteries (SIBs) by relieving the volume expansion and preventing active material agglomeration. In this work, micro-nano flower 3D-VS_x was fabricated as an anode electrode for SIBs. The advanced features of micro-nano flower and the unique crystal structures of NiAs-type vanadium sulfides synergistically contribute to enhancing the electrochemical kinetics of 3D-VS_x, and finally achieved remarking electrochemical performances with an ultra-high capacity (961.4 mAh/g at 2 A/g) and an ultra-long cyclability (more than 1500 cycles). Furthermore, ex situ X-ray diffraction, Raman, and SEM bring to light a gradual reactivation process of 3D-VS_x for sodium storage. Fortunately, upon reactivation, the electrochemical impedance of the 3D-VS_x anode gradually weakens, and the diffusion-controlled charge storage mode further dominates compared to the capacitively-controlled mode, all of which facilitate the 3D-VS_x to maintain a stable sodium storage capability. This work presents a general approach for preparing super-high specific capacity and rate capacity electrode materials for further improving the SIBs performance.

KFM 10.9 Thu 11:55 POT 51

Sodium diffusion mechanism in NASICON solid electrolyte materials studied via quasi-elastic neutron scattering — IVANA PIVARNÍKOVÁ^{1,2}, STEFAN SEIDLMEYER¹, MARTIN FINSTERBUSCH³, GERALD DÜCK³, NIINA JALARVO⁴, PETER MÜLLER-BUSCHBAUM^{1,2}, and RALPH GILLES¹ — ¹TUM, MLZ, Garching, Germany — ²TUM School of Natural Sciences, Chair for Functional Materials, Garching, Germany — ³FZJ, IEK-1, Jülich, Germany — ⁴ORNL, Oak Ridge, TN, USA

The sodium superionic conductor materials, also known as NASICON, have been a widely studied class of solid electrolytes for Na-ion based all-solid-state batteries. The aim of this work is to clarify the reason for extremely high conductivity exhibited by Na_{1+x}Zr₂SixP_{3-x}O₁₂ (0-x-3) and to explain the role of the monoclinic to rhombohedral phase transition for the material with x=2.4, which supposedly occurs at around 170°C. We also investigate the overall temperature dependence of the ionic conductivity in the temperature range of 297-640K. The quasi-elastic neutron scattering (QENS) is used to measure the spatial and temporal dynamic properties of diffusion of Na-ions in the crystal structure. The Na-ion diffusion mechanism can be described by the right choice of the diffusion model. Important parameters, such as diffusion coefficients, activation energies, jump distances between the occupation sites and residence times are extracted from the measured and modelled QENS data. Temperature dependent X-ray diffraction data have been obtained and analysed in order to confirm the results obtained from the QENS data.

KFM 10.10 Thu 12:15 POT 51

3D flower-like MnV₁₂O₃₁ center dot 10H₂O as a high-capacity and long-lifespan cathode material for aqueous zinc-ion batteries — YAN RAN¹, YUDE WANG², HUAPING ZHAO¹, and YONG LEI¹ — ¹Fachgebiet Angewandte Nanophysik, Institut für Physik & IMN MacroNano, Technische Universität Ilmenau, 98693 Ilmenau, Germany — ²Yunnan Key Laboratory of Carbon Neutrality and Green Low-carbon Technologies, Yunnan University, 650091 Kunming, China

In this work, MnV₁₂O₃₁ center dot 10H₂O (MnVO) synthesized via one-step hydrothermal method is proposed as a promising cathode material for AZIBs. Because its stable layered structure and hierarchical morphology provide a large layer space for rapid ion transports, this material exhibits a high specific capacity (433 mAh g⁻¹ at 0.1 A g⁻¹), outstanding long-term cyclability (5000 cycles at current density of 3 A g⁻¹), and sufficient energy density (454.65 Wh kg⁻¹). To illustrate the intercalation mechanism, ex-situ X-ray diffraction (XRD), Fourier transform infrared spectroscopy (FTIR), and X-ray photoelectron spectroscopy (XPS) are adopted, uncovering a H⁺/Zn²⁺ dual-cation co-intercalation processes. Besides, density functional theory (DFT) calculation analysis shows that MnVO has a delocalized electron cloud and the diffusion energy barrier of Zn²⁺ in MnVO is low, which promotes the Zn²⁺ transport and, consequently, improves the reversibility of the battery upon deep cycling. The results provide key and enlightening insights for the design of high-performance vanadium-oxide-based cathode materials for AZIBs.

KFM 11: Crystal Structure Defects / Real Structure / Microstructure

Chair: Prof. Dr. Theo A. Scherer (KIT Karlsruhe)

Time: Thursday 14:00–17:55

Location: POT 51

KFM 11.1 Thu 14:00 POT 51

eutectic: a game changer — SANDHYA SHARMA¹, HAFIZ MUHAMMAD ZEESHAN¹, ELENA VOLOSHINA^{1,2}, and YURIY DEDKOV^{1,2} — ¹Centre of Excellence ENSEMBLE3 Sp. z o. o., Wolczynska Str. 133, 01-919 Warsaw, Poland — ²Department of Physics, Shanghai University, 99 Shangda Road, 200444 Shanghai, P.R. China

The world of semiconductors has drastically improved the lifestyle due to its versatile applications. The demand for new efficient semiconductors is increasing day by day, giving birth to the idea of new synthesis methods. Many synthesis techniques have been utilized to engineer band gap of semiconductors to achieve higher efficiency. Here, a perspective on the importance of semiconductor eutectic materials has been presented as one of the future potential candidates, along with the micro (μ) pulling method (as a synthesis method for semiconductor eutectic materials) that not only control factors effecting the devices but also provides variety of options for band gap modification. The efficiency of the present devices in comparison with the eutectic composites has been made, showing the semiconductor eutectic materials as a better candidate for future devices.

KFM 11.2 Thu 14:20 POT 51

Determining the Crystallization Mechanism in Optical Switching Experiments with Electron Backscatter Diffraction — MAXIMILIAN MÜLLER and MATTHIAS WUTTIG — I. Institute of Physics (IA), Aachen, Germany

To tailor phase-change materials for computing and data storage applications unraveling the contribution of nucleation and crystal growth to crystallization is essential. Usually, these processes are studied at low temperatures. Subsequently, from the temperature dependence of both processes at low temperature, the role of these processes at high temperatures is extrapolated. This is inherently dangerous if the underlying processes do not follow Boltzmann kinetics.

In this study, crystallization was achieved by short laser pulses with pulse lengths between a few ns to several μ s. Afterwards, the resulting grain structure was analyzed by different techniques, including atomic force microscopy and Electron Backscatter Diffraction (EBSD). The grain size distribution is determined by these experiments which helps disentangling the processes of nucleation and growth. Significant differences are observed concerning the nucleation of different compounds. Trends for the nucleation and growth rate as a function of stoichiometry are analyzed and explained based upon systematic changes in bonding.

KFM 11.3 Thu 14:40 POT 51

Vacancies in Prussian White Cathode Materials employing Positron Annihilation Spectroscopy — DOMINIK BORAS¹, IDA NIELSEN², ALEXANDER BUCKEL³, TORE ERICSSON², LENNART HÄGGSTRÖM², TORSTEN E.M. STAAB¹, and WILLIAM R. BRANT² — ¹Institute for Functional Materials and Biofabrication, Julius-Maximilians Universität Würzburg, 97070 Würzburg, Röntgenring

11 — ²Department of Chemistry - Ångström Laboratory, Uppsala University, Box 538, SE-751 21 Uppsala, Sweden — ³Altris AB, Kungsgatan 70b, SE-753 18 Uppsala, Sweden

We are presenting a novel attempt to characterise Prussian blue analogues. Prussian White samples have been synthesized with different sodium content and, then, characterized by common methods (ICP-OES, TG, SEM) but also by Mössbauer spectroscopy. We prepared three different sample states: fully and half-sodiated as well as de-sodiated. As a new method positron annihilation lifetime spectroscopy (PALS) has been applied to characterize the different samples states. We can state that the methods of PALS gives reasonable results for Prussian White with varying sodium and water content. The relative intensity of the longer positron lifetime component (405ps) is increasing with decreasing sodium content, which is an indication that the positron "sees" less of the open crystal channels filled by movable ions, since those become more and more occupied by intercalated Na-atoms. This first attempt aims to present the potential of PALS to characterise Prussian Blue analogue materials with respect to defects and occupation of its crystal channels by movable ions.

KFM 11.4 Thu 15:00 POT 51

Disorder engineering for symmetry lowering in Prussian Blue analogues (PBAs) — •YEVHENIIA KHOLINA, THOMAS WEBER, and ARKADIY SIMONOV — ETH Zürich, Switzerland, Department of Materials, Laboratory for Multifunctional Ferroic Materials

A simple consequence of Neumann's principle is that certain properties can exist in crystals with a certain symmetry. As a result, a lot of materials engineering is focused on designing particular symmetries, which allow the properties of interest. In oxide perovskites as well as their molecular analogues, control of crystal symmetry is achieved by octahedral tilts and cation ordering. In this work we show an alternative way of symmetry lowering, using disorder. We focus on Mn[Co] PBA with the chemical composition $Mn[Co(CN)_6]_{2/3}$. These crystals have 1/3 of $Co(CN)_6$ sites vacant. The structure of such PBAs is believed to be cubic with space group $Fm\bar{3}m$. However, the optical measurements indicate that the crystal is twinned and an actual structure has tetragonal symmetry or lower. We collect single-crystal x-ray diffuse scattering from untwinned crystal to probe the local structure and quantitatively characterise defect distribution, using 3D- Δ PDF analysis. The symmetry of the local structure is reduced to tetragonal by local vacancies ordering. The vacancies have stronger correlation along c direction. Such asymmetry is formed because the crystal is growing in this direction. This means the symmetry can be lowered by choosing a specific direction of the crystal growth. We believe this result can be applied to other disordered crystalline materials and be an effective way to lower the symmetry for properties design.

KFM 11.5 Thu 15:20 POT 51

Single crystal growth of the Mott insulator BaCoS₂: structure and hole doping — •HANEEN ABUSHAMMALA, TESLIN THOMAS, ANDREAS KRYSSIG, and ANNA BOEHMER — Experimentalphysik IV, Ruhr-Universitaet Bochum, Universitaetsstrasse 150, 44801 Bochum, Germany

The quasi-2D BaCoS₂ is a Mott insulator with a stripe-like antiferromagnetic ordering at $T_N=290$ K. Both chemical doping or hydrostatic pressure drive the system into a paramagnetic metallic phase. Interestingly, there is no structural transition at the metal-insulator transition of this phase, which offers ideal conditions to investigate the Mott transition in a model multiband system [1].

Nevertheless, BaCoS₂ remains little studied, and the interplay of electronic and structural features is still unclear. High-quality single crystals are needed to elucidate this issue. The synthesis of single-crystalline BaCoS₂ is challenging owing to its metastability, with a decomposition into Ba₂CoS₃, CoS and S below 850°C. The BaCoS₂ phase can only be obtained via quenching from high temperature. Moreover, BaCoS₂ melts incongruently, which calls for a flux growth method necessitating separation of the crystals from the flux by the end of the growth. We have successfully grown single crystals of pure and the hole-doped BaCoS₂ using a self-flux method with high-temperature flux separation and quench. The structural and anisotropic electrical transport properties are determined and discussed.

[1] Abushammala, Lenz, Baptiste, Casula, Klein and Gauzzi, in preparation (2022).

KFM 11.6 Thu 15:40 POT 51

Monitoring the S-phase formation in an high-purity Al-Cu-Mg alloy by truncation during heating-up — •TORSTEN E.M. STAAB, DOMINIK BORAS, SEBASTIAN BREITFELDER, and TIMO STROBL — IFB, Julius-Maximilians Universität Würzburg, 97070 Würzburg, Röntgenring 11

We are presenting a novel attempt to combine in-situ and ex-situ measurements for aluminum alloys. As a model alloy we have chosen an Al-1.7Cu-1.3Mg (at.%) alloy, which has been cast from high purity elements (5N5 Al, 4N Cu and 4N Mg). As basic method DSC (heating ramp: 5 K/min) has been employed to determine different states during S-phase formation: onset, maximum of the exothermal peak, end of exothermal reaction. Sample states were frozen-in by an abrupt truncation of the heating ramp (5 K/min), i.e. cooling quickly to room

temperature. So, the current sample state is frozen-in. After truncation all samples have been measured without further preparation by X-ray diffraction (XRD) and positron annihilation lifetime spectroscopy (PALS). Thus we could correlate exactly different sample states, which is impossible by conventional experiments, i.e. heating to a certain temperature and then holding a certain time. This paves the way to investigate defined and comparable sample states by methods, which require an extensive sample preparation, like TEM or 3DAP, and in-situ methods like DSC or XRD at synchrotron beamlines.

15 min. break

KFM 11.7 Thu 16:15 POT 51

Local structure of titanite CaTiSiO₅ — •ARKADIY SIMONOV — ETH Zürich, Zürich, Switzerland

Titanite, CaTiSiO₅, is a multifunctional nesosilicate mineral which recently received attention as a material for building tunable capacitors and oscillators. Near 500K titanite shows a nonlinear dielectric response with positive dielectric tunability and thus its dielectric susceptibility can be efficiently controlled using a voltage bias, moreover capacitors made of this material have unusually low dielectric losses and thus high quality factor [1]. The origin of such a good performance is not currently understood, but one hypothesis is that it is related to an unusual locally antipolar disordered structure which is observed in titanite above 500K in the paraelectric $A2/a$ phase.

In this work we present the analysis of the local structure of titanite in the $A2/a$ phase. We use single crystal diffuse scattering as our probe and analyze it using a non-parametric method based on three dimensional difference pair distribution function (3D- Δ PDF) refinement. We show that despite the $A2/a$ structure is on average paraelectric, locally it is antipolar. It shows Ti^{4+} displacements which have strong ferro correlations along the b direction and weak locally anti-ferro correlations in a and c directions. Such locally antipolar structure can provide a crossover path for the low temperature $P2_1/a$ structure under applied electric field and thus explain the low dielectric losses observed in this material.

[1] Murata, T., Asaka, T., Hirose, S. (2021). J. Am. Cer. Soc. 104(11), 5794-5802.

KFM 11.8 Thu 16:35 POT 51

Pfaffian invariant identifies magnetic obstructed atomic insulators — •DANIEL VARJAS^{1,2,3,4}, ISIDORA ARAYA DAY^{3,4}, ANASTASIA VARENTCOVA³, and ANTON R. AKHMEROV³ — ¹Max Planck Institute for the Physics of Complex Systems, Nöthnitzer Straße 38, 01187 Dresden, Germany — ²Department of Physics, Stockholm University, AlbaNova University Center, 106 91 Stockholm, Sweden — ³QuTech, Delft University of Technology, Delft 2600 GA, The Netherlands — ⁴Kavli Institute of Nanoscience, Delft University of Technology, P.O. Box 4056, 2600 GA Delft, The Netherlands

We derive a Z_4 topological invariant that extends beyond symmetry eigenvalues and Wilson loops and classifies two-dimensional insulators with a C_4T symmetry. To formulate this invariant, we consider an irreducible Brillouin zone and constrain the spectrum of the open Wilson lines that compose its boundary. We fix the gauge ambiguity of the Wilson lines by using the Pfaffian at high symmetry momenta. As a result, we distinguish the four C_4T -protected atomic insulators, each of which is adiabatically connected to a different atomic limit. We establish the correspondence between the invariant and the obstructed phases by constructing both the atomic limit Hamiltonians and a C_4T -symmetric model that interpolates between them. The phase diagram shows that C_4T insulators allow ± 1 and 2 changes of the invariant, where the latter is overlooked by symmetry indicators.

KFM 11.9 Thu 16:55 POT 51

Probing Centrosymmetry of Emergent Materials by Convergent Beam Electron Diffraction — •S. SUBAKTI^{1,2}, Y. WANG³, A. CHAKRABORTY⁴, A.K. SRIVASTAVA⁴, D. WOLF¹, T. DOERT³, M. RUCK³, S.S.P. PARKIN⁴, B. BÜCHNER^{1,2}, and A. LUBK¹ — ¹Leibniz Institute for Solid State and Materials Research Dresden, Helmholtzstraße 20, 01069 Dresden, Germany — ²Institut für Festkörperphysik, TU Dresden, D-01062 Dresden, Germany — ³Faculty of Chemistry and Food Chemistry, Technische Universität Dresden, 01062 Dresden, Germany — ⁴Department for Nano-Systems from Ions, Spins, and Electrons (NISE), Max Planck Institute of Microstructure Physics, Weinberg 2, D-06120 Halle(Saale), Germany

Many exotic physics present in materials, such as chiral magnetic textures, hinges on the (non)existence of centrosymmetry. Consequently unambiguous structural determination beyond x-ray diffraction (XRD), which is to a certain extent blind to centrosymmetry, is indispensable. Here, we present structural investigation of two emergent quantum materials, namely Fe₃GeTe₂ and Rh₂NiSb, by means of convergent beam electron diffraction (CBED). Analyzing the diffraction group symmetries of the CBED patterns in combination with extinction rules and results from XRD analysis, we conclude the space group of these materials. Importantly, both phases are non-centrosymmetric, suggesting possible presence of chiral magnetic textures and multiferroicity.

KFM 11.10 Thu 17:15 POT 51

Nonsymmorphic chiral symmetry and solitons in the Rice-Mele model — •EDWARD MCCANN — Lancaster University, Lancaster, United Kingdom

The charge-density-wave (CDW) phase of the Rice-Mele model in one dimension has alternating onsite energies and constant nearest-neighbor hopping parameters. The chiral symmetry of the CDW wave phase is nonsymmorphic, resulting in a breaking of the bulk topology by an end or a texture in the alternating energies. We consider the presence of solitons (textures in position space separating two degenerate ground states) in finite systems with open boundary conditions. We identify the parameter range under which an atomically-sharp soliton in the CDW phase supports a localized state which lies within the band gap, and we calculate the expectation value of the nonsymmorphic chiral operator for this state, and the soliton electric charge [1]. Finally, we discuss other models with similar, nonsymmorphic nonspatial symmetries.

[1] R. E. J. Allen et al, Phys. Rev. B 106, 165409 (2022).

KFM 11.11 Thu 17:35 POT 51

The Initial Molecular Interactions in the Course of Enthalpy Relaxation and Nucleation in Polyethylene terephthalate (PET) as Monitored by Combined Nanocalorimetry and FTIR Spectroscopy — •WYCLIFFE KIPNUSU¹, EVGENY ZHURAVLEV², CHRISTOPH SCHICK^{2,3}, and FRIEDRICH KREMER¹ — ¹Peter Debye Institute for Soft Matter Physics, Leipzig University, Linnestr. 5, 04103, Leipzig, Germany — ²Universität Rostock Institute of Physics, Albert-Einstein_str. 23-24, Rostock, DE 18051, Germany — ³Kazan, Russia

Fast scanning calorimetry (FSC) and Fourier transform infrared (FTIR) spectroscopy are combined to trace for the same sample the evolution of the calorimetric properties and of the intra- and inter-molecular interactions in polyethylene terephthalate (PET). FSC enables to rapidly quench the sample to amorphous state and to monitor nucleation and crystal growth at isothermal conditions. By Determining the difference IR spectra between a quenched and an annealed sample unravels the the intra- and inter-molecular interactions in detail; (i) as first response already during enthalpy relaxation, the far reaching Coulomb interactions between the polar C=O moieties are active; (ii) in contrast, the ethylene unit and the aromatic ring show a response only, if homogeneous nucleation sets in, while the COC moiety remains uninfluenced; (iii) a hierarchy is observed in the sequence of the response of the different molecular moieties.

KFM 12: Members' Assembly

Time: Thursday 18:00–19:00

Location: POT 51

All members of the Crystalline Solids and their Microstructure Division are invited to participate.**KFM 13: Polar Oxide Crystals and Solid Solutions I**

Chair: Prof. Dr. Holger Fritze (TU Clausthal)

Time: Thursday 10:00–12:35

Location: POT 106

KFM 13.1 Thu 10:00 POT 106

Polaronic structures in LiNbO₃ and LiTaO₃ modelled from first principles — •NILS ANDRE SCHÄFER and SIMONE SANNA — Institute for Theoretical Physics, Justus Liebig University Giessen, Germany

Polaronic defects impact among other properties the optical response of LiNbO₃ (LN). Changes in their optical properties are of interest for the applications of LN in optoelectronics. These are relatively well known in LN but in LiTaO₃ (LT) less so. In order to improve our knowledge of polaronic structures in LT, we modeled polarons in LN and LT from first principles using the DFT+U method as implemented in VASP.

We explore different microscopic polaronic structures in both polar oxides with respect to changes in their electronic band structures and optical properties, especially with respect to Jahn-Teller distortions. Similarities and differences between different polaronic defects and both compounds are discussed as well.

KFM 13.2 Thu 10:20 POT 106

Crystal growth and thermal analysis of Li(Nb,Ta)O₃ solid solutions — •UMAR BASHIR GANIE — IKZ, Berlin

This work presents the growth and thermal analysis of Lithium Niobate Tantalate (Li(Nb,Ta)O₃, LNT) single crystals for different LiTaO₃ (LT) mole fractions (xLT), (xLT = nLT/(nLT+nLN)). Our crystal growth experiments show that growth of LNT single crystal over the entire LT mole fraction is not only possible but can be achieved with weaker constituent segregation and therefore higher degree of homogeneity than considered previously. Our differential thermal analysis (DTA) measurements show that the melting temperature increases with increasing fraction of LT and follow the behavior of a (pseudo)binary phase diagram as published previously [1]. Thorough evaluation of the DTA results allows to propose an improved version of the LN-LT phase diagram that is not only thermodynamically stringent but also allows to explain the component distribution observed in LNT single crystals and to design growth experiments yielding crystals of higher homogeneity. We also performed specific heat capacity measurements of single crystals of LNT solid solutions. The aim was to investigate the variation of ferroelectric Curie temperature with composition. We observed that the ferroelectric Curie temperature decreases linearly with growing Ta composition in the LNT solid solution crystals.

KFM 13.3 Thu 10:40 POT 106

Hydrogen Diffusion in LiNbO₃ and LiTaO₃ — •KOFAHL CLAUDIA¹, DÖRRER LARS¹, SUHAK YURIY², YAKHNEVYCH ULIANA², FRITZE HOLGER², and SCHMIDT HARALD^{1,3} — ¹Institut für Metallurgie, AG Festkörperkinetik, TU Clausthal, Germany — ²Institut für Energieforschung und Physikalische Technologien, TU Clausthal, Germany — ³Clausthaler Zentrum für Materialtechnik, TU Clausthal, Germany

LiNbO₃ and LiTaO₃ crystals are technologically important polar metal oxides with exceptional combinations of ferroelectric, piezoelectric, acoustic, optical and ion conductivity properties. The presence and diffusion of H in these materials has an important influence on the materials properties, reducing optical damage, increasing optical birefringence and changing ionic conductivity. The diffusion mechanism is unclear up to now. Therefore, it is of particular interest to study the diffusion of hydrogen. For this purpose, we use two different analytical methods, SIMS (Secondary Ion Mass Spectroscopy) and IRS (Infrared Spectroscopy). For the SIMS measurements, the crystals are loaded with high amounts of H by means of proton-exchange and the redistribution of H is monitored after post-annealing. In contrast, for the IRS experiments, only hydrogen of about 300 ppm, which is introduced by crystal growth in air, is replaced by deuterium during exchange anneals in D₂O. The measured diffusion coefficients of the two methods differ from each other, but are higher than Li diffusivities as given in literature. The activation energies are similar. Possible reasons for the differences are discussed.

KFM 13.4 Thu 11:00 POT 106

Acoustic loss in Lithium Niobate-Lithium Tantalate solid solutions with different Nb/Ta ratios at temperatures up to 900°C — •ULIANA YAKHNEVYCH¹, CLAUDIA KOFAHL², STEPAN HURSKYY¹, STEFFEN GANSCHOW³, YURIY SUHAK¹, HARALD SCHMIDT², and HOLGER FRITZE¹ — ¹Institute of Energy Research and Physical Technologies, Clausthal University of Technology, Germany — ²Institute of Metallurgy, Clausthal University of Technology, Germany — ³Leibniz-Institut für Kristallzüchtung, Berlin, Germany

Lithium niobate-lithium tantalate solid solutions (LNT) are poorly studied materials in modern materials science, which must be seen in the light that they can combine the advantages of the edge compounds lithium niobate (LN) and lithium tantalate (LT). These crystals are expected to exhibit high piezoelectric coefficients and thermal stability. This work focuses on comparing the Q-factor of LN, LT, and LNT as well as on the analysis of loss contributions in samples. Electromechanical losses of the samples were determined using two different approaches, namely noncontacting resonant ringdown spectroscopy and resonant piezoelectric spectroscopy using Pt electrodes. LNT thickness-shear mode (TSM) acoustic resonators exhibit significantly lower loss than LN. The study of the acoustic loss in LNT resonators operated in the TSM showed strong frequency dependent loss increases at temperatures above 450°C. The loss was modelled using independent materials data. Based on the modelling, the above-mentioned loss above 450°C is associated with a conductivity-induced piezoelectric/carrier relaxation mechanism governed by Li migration.

15 min. break

KFM 13.5 Thu 11:35 POT 106

High-temperature stability of electrical and acoustic properties of congruent and near stoichiometric single crystalline LiNbO₃, LiTaO₃ and LiNb_{0.94}Ta_{0.06}O₃ — •YURIY SUHAK¹, STEPAN HURSKYY¹, ULIANA YAKHNEVYCH¹, FATIMA EL AZZOZI¹, CLAUDIA KOFÄHL², HARALD SCHMIDT², STEFFEN GANSCHOW³, KLAUS-DIETER BECKER⁴, and HOLGER FRITZE¹ — ¹Institute for Energy Research and Physical Technologies, Clausthal University of Technology, Goslar, Germany — ²Institute of Metallurgy, Clausthal University of Technology, Clausthal-Zellerfeld, Germany — ³Leibniz Institut für Kristallzüchtung, Berlin, Germany. — ⁴Braunschweig University of Technology, Braunschweig, Germany

It is known that the intrinsic properties of LiNbO₃, LiTaO₃ and, consequently, of Li(Nb,Ta)O₃ solid solutions are strongly dependent on lithium stoichiometry. In current work the electrical and acoustic properties of congruent and near-stoichiometric single crystalline Li(Nb,Ta)O₃ are studied as a function of temperature by means of impedance spectroscopy and resonant piezoelectric spectroscopy, respectively. The preparation of near-stoichiometric samples was performed by vapor transport equilibration technique (VTE). It is shown, that VTE-treated samples generally exhibit lower conductivity and lower acoustic loss, which implies better thermal stability. The latter was examined by a long-term measurement of electrical conductivity at 500 °C in air. After about 330 hours of uninterrupted thermal treatment the conductivity of a congruent LiNb_{0.94}Ta_{0.06}O₃ specimen was found to decrease only for about 3 %.

KFM 13.6 Thu 11:55 POT 106

A high-temperature optical spectroscopy study of lithium niobate, LiNbO₃ — •KLAUS-DIETER BECKER¹, JIANMIN SHI¹, PIOTR GACZYNSKI¹, MISHA SINDER², ULIANA YAKHNEVYCH³, NATALIA SYVOROTKA³, YURIY SUHAK³, STEFFEN GANSCHOW⁴, and HOLGER FRITZE³ — ¹Institute of Physical and Theoretical Chemistry, TU Braunschweig, Braunschweig, Germany — ²Materials Engineering Department, Ben Gurion University of the Negev, Beer-Sheva, Israel — ³Institute for Energy Research and Physical Technologies, TU Clausthal, Goslar, Germany — ⁴Leibniz Institut für Kristallzüchtung, Berlin, Germany

Optical absorption spectra of chemically reduced LiNbO₃ (LN) show broad bands in the vis and NIR region which have been attributed to various types

of electron small polarons. At 1000 °C, spectra are dominated by an absorption band at 0.9 eV due to free small polarons, i.e. to electrons localized on niobium ions on regular sites. Band intensity has been found to follow a power-law dependence on oxygen partial pressure PO₂ of the form (PO₂)^m with m = -0.23(+/-)0.02. This m-value is in excellent agreement with the value of -1/4 predicted from point defect thermodynamics of the chemical redox model of LN. The experimental kinetics of reduction and oxidation following a rapid change in oxygen partial pressure have been found to provide a novel route to diffusion of lithium vacancies at high temperatures as well as to that of lithium ions in LN.

KFM 13.7 Thu 12:15 POT 106

Looking undercover - Probing subsurface properties by Piezoresponse force microscopy (PFM) — •MATTHIAS ROEPER¹, SAMUEL D. SEDDON¹, LILI DING¹, MICHAEL RÜSING¹, and LUKAS M. ENG^{1,2} — ¹Institut für Angewandte Physik, TU Dresden, Nöthnitzer Straße 61, 01187 Dresden, Germany — ²ct.qmat: Dresden-Würzburg Cluster of Excellence - EXC 2147, TU Dresden, 01062 Dresden, Germany

Piezoresponse force microscopy (PFM) is one of the most widespread methods for investigating and visualizing ferroelectric domain structures at the nanometer length scale, even along all 3 dimensions (3D) [1]. PFM couples to the local dielectric displacement that is present near the sample surface, and hence is also sensitively probing into the bulk of the sample under investigation, i.e. into a subsurface volume with penetration d [2]. In this work, we systematically analyze in both theory and experiment, the contrast and depth resolution capabilities of PFM as a function of the various relevant experimental parameters. PFM tool properties such as the tip radius, ac driving voltage, and ac frequency were optimized, while equally dedicated sample structures incorporating (known) buried features, i.e. ferroelectric domain walls, fabricated into the bulk host at a distance d below the surface, were analyzed. Our finding allow to accurately adjust the image contrast to a certain penetration depth d, and thus quantify those local features with high precision.

[1] L. M. Eng et al., Appl. Phys. Lett. 74, 233 (1999) [2] F. Johann et al., Appl. Phys. Lett. 94, 172904 (2009)

KFM 14: Polar Oxide Crystals and Solid Solutions II

Chair: Prof. Dr. Holger Fritze (TU Clausthal)

Time: Thursday 14:00–16:35

Location: POT 106

KFM 14.1 Thu 14:00 POT 106

Domain wall current in lithium niobate single crystals at temperatures up to 370 °C — •U. YAKHNEVYCH¹, M. KUNZMER¹, I. KISELEVA², J. GÖSSEL², J. RATZENBERGER², M. RÜSING², L.M. ENG^{2,3}, and H. FRITZE¹ — ¹Institut für Energieforschung und Physikalische Technologien, TU Clausthal, Am Stollen 19 B, Goslar, 38640, Germany — ²Institut für Angewandte Physik, TU Dresden, Nöthnitzer Straße 61, 01187 Dresden, Germany — ³Dresden-Würzburg Cluster of Excellence - EXC 2147, TU Dresden, 01062 Dresden, Germany

Lithium niobate (LN) ferroelectric crystals with an artificially formed domain structure are widely used in novel electronic devices. So far, a complete picture of the electrical transport mechanism at domain walls is still missing, including its high temperature behavior. This work focuses on the determination of the domain wall conductivity from room temperature up to 370 °C. Using 5%MgO:LN, conductive DWs are prepared and enhanced following the procedure by Godau et al. [1]. Direct current measurements using an electrometer amplifier and impedance spectroscopy are applied to locally map the temperature-dependent DW current. A strong dependence of the electrical conductivity on temperature is observed. The activation energy shows distinct values for low-to-medium and high temperatures, respectively, reaching values of ~0.1 eV and ~0.15 eV. For further analysis, the obtained samples should be measured at even higher temperatures. [1] C. Godau, T. Kämpfe, A. Thiessen et al. ACS Nano 11, 5, 4816-4824 (2017). <https://doi.org/10.1021/acsnano.7b01199>

KFM 14.2 Thu 14:20 POT 106

Ferroelectric domains and domain walls under uniaxial stress * A case study in lithium niobate — EKTA SINGH¹, HENRIK BECCARD¹, MICHAEL LANGE¹, SVEN REITZIG¹, ZEESHAN H. AMBER¹, CLIFFORD W. HICKS³, JULIUS RATZENBERGER^{1,2}, •MICHAEL RÜSING¹, and LUKAS M. ENG^{1,2} — ¹Institut für Angewandte Physik, TU Dresden, Nöthnitzer Straße 61, 01187 Dresden, Germany — ²ct.qmat: Dresden-Würzburg Cluster of Excellence - EXC 2147, TU Dresden, 01062 Dresden, Germany — ³School of Physics and Astronomy, University of Birmingham, Birmingham B15 2TT, United Kingdom

In material science, mechanical strain has an influence on a multitude of material properties. For ferroelectrics, strain can be achieved via standard techniques, such as lattice-mismatched epitaxial growth of thin films, or hydrostatic

pressure. However, these methods are either limited to specific material combinations or non-local investigation techniques. Here, we present an alternative approach [1] to study bulk crystals under the influence of uniaxial strain, using a piezo-actuator-based device that is compatible with various local probe techniques. To demonstrate the operation we present the influence of strain on the vibrational properties probed via micro-Raman spectroscopy [1], as well as the influence of strain on the local conductivity of ferroelectric domain walls probed by scanning conductance microscopy [2]. [1] E. Singh et al, arXiv:2210.14120 (2022). [2] E. Singh et al, Phys. Rev. B 106,144103 (2022).

KFM 14.3 Thu 14:40 POT 106

Hall effect in conductive ferroelectric domain walls in BaTiO₃ — HENRIK BECCARD¹, ELKE BEYREUTHER¹, MICHAEL RÜSING¹, BENJAMIN KIRBUS¹, EKTA SINGH¹, •SAMUEL SEDDON¹, PETR BEDNYAKOV², JIRI HLINKA², and LUKAS M. ENG^{1,3} — ¹Institut für Angewandte Physik, TU Dresden, Nöthnitzer Straße 61, 01187 Dresden, Germany — ²Institute of Physics, Academy of Sciences of the Czech Republic, Na Slovance 2, 18221 Praha 8, CZR — ³ct.qmat: Dresden-Würzburg Cluster of Excellence - EXC 2147, TU Dresden, 01062 Dresden, Germany

Two dimensional (2D) electronic systems are essential in cutting-edge nano-electronic research. Here, conductive ferroelectric domain walls (DWs) are experiencing a concerted research effort for the last decade. Much of the research, however, did focus onto measuring and tuning the electrical DW conductivity [1], with very little investigations reporting on the very fundamental DW properties such as charge carrier density and mobility. Here, we adapted the 4-point van der Pauw [2] geometry to probe these 2D sheets of ferroelectric DWs in BaTiO₃, and were able to determine the aforementioned properties. We find large electron mobilities of 400 cm² (Vs)⁻¹ and decent electron densities [3]. Not only are these results by themselves novel, but also perfectly demonstrate the power of this simple methodology to quantify the charge carrier properties in any low-dimensional system.

[1] C. Godau, et al., ACS Nano 11, 4816 (2017)

[2] L. J. Van der Pauw, Philips Tech Rev 20, 220-224 (1958)

[3] H. Beccard, et al., ACS Appl. Nano Mater. 7, 8717-8722 (2022)

KFM 14.4 Thu 15:00 POT 106

Thin Patterned Lithium Niobate Metasurfaces by Parallel Additive Capillary Stamping of Aqueous Precursor Solutions — •JAN KLENEN¹, FATIH ALARSLAN², LAURA VITTADELLO¹, MARTIN STEINHART², and MIRCO IMLAU¹ — ¹Department of Physics, Osnabrück University, Germany — ²Institute of Chemistry of New Materials, Osnabrück University, Germany

Optical metasurfaces are a rapidly evolving field in the aim to miniaturize optical functionalities and integrated photonics [A. Fedotova et al., *ACS Photonics* **2022**]. However, the large-scale application is still challenging as the preparation of such metasurfaces, i.e., by mechano-chemical wafer thinning or lithographic patterning, is usually complex, time-consuming, and expensive. We try to address this problem and present a novel method of metasurface patterning based on parallel additive capillary stamping of LiNbO₃ on an ITO substrate [F. Alarслан et al., *Advanced Engineering Materials* **2021**, 24(6)]. This technique offers the advantage of rapid, easily customizable and cheap structuring of layers with thicknesses on the order of 100 nm. Nonlinear optical investigations performed with the TIGER microscope show a homogeneous second harmonic generation (SHG) of the surface coinciding with the LiNbO₃ film structured by hexagonally arranged macropores. The additional implementation of gold nanoparticles at the position of the macropores allows for a drastic enhancement of the SHG by exploiting plasmonic resonances. Financial support by the ERC (project 646742 INCANA) and DFG (projects IM 37/12-1, FOR 5044 and INST 190/165-1) is gratefully acknowledged.

15 min. break

KFM 14.5 Thu 15:35 POT 106

Optical nonlinearities of lithium tantalate solid solutions — •MIRCO IMLAU, TOBIAS HEHEMANN, SÖREN DOMKE, NIKLAS DÖMER, FIETE BREER, FELIX KODDE, JAN KLEENEN, ANTON PFANNSTIEL, and LAURA VITTADELLO — Institute of Physics, Osnabrück University

Optical nonlinearities of optical materials, i.e. the nonlinear material response to incident electromagnetic radiation, are the fundamental physical basis for a number of components in nonlinear photonics, such as nonlinear optical Kerr lenses, saturable absorbers or frequency converters. The properties of optical nonlinearities are closely related to the electronic and atomic structure of the material systems used. Against this background, lithium niobate tantalate (LNT, LiNb_xTa_{1-x}O₃ with 0 ≤ x ≤ 1) solid solutions are promising because the edge compounds themselves (LN, x=1 and LT, x=0) are already extensively used in photonics' components, but especially because the nonlinear optical properties of LNT may be tailored to the specific requirements of the application via composition. We here present the state-of-the-art knowledge of our studies on optical nonlinearities of LNT over the entire composition range, both, for quasi-instantaneous nonlinear responses (absorption & nonlinear index, frequency conversion) and transient responses (time-resolved transient absorption on the temporal multiscale from femtoseconds to seconds & transient index dynamics). The findings are discussed in the framework of emerging applications in (nano-)photonics, particularly for laser systems of the next generation, and will be compared with LN and LT. Financial support by the DFG (project IM 37/12-1, FOR 5044).

KFM 14.6 Thu 15:55 POT 106

Small polaron absorption centers in lithium niobate-tantalate solid solutions — •ANTON PFANNSTIEL¹, SIMONE SANNA², YURIY SUHAK³, and STEFFEN GANSCHOW⁴ — ¹Inst. Physics, Osnabrück University — ²Inst. Theoretical Physics, University of Gießen — ³Inst. Energy Research, Technical university of Clausthal — ⁴Leibniz-Institut für Kristallzüchtung (IKZ), Berlin

The study of small polarons in ferroelectric lithium niobate (LN) enabled the understanding of various physical phenomena on a microscopic level, like photo-induced coloration or conductivity and led to the formulation of a robust model of polaronic localization centers and energies [O. F. Schirmer *et al* 2009 J Phys.: Condens. Matter **21** 123201]. So far, for lithium tantalate (LT) and the solid solution, lithium niobate-tantalate (LNT) a respective small polaron model is missing in literature.

For this purpose, this study provides polaron self localization energies for LN, LT and LNT crystals of various composition. Thermally reduced crystals are optically bleached at cryogenic temperatures. The resulting small polaron absorption bands are identified through transmission spectroscopy and modeled within the framework of small polaron absorption theory. The determined polaron energies are interpreted against the background of the known defect models for LN and LT but also in conjunction with ab-initio modeling results for carrier self-localization. Financial support by the DFG [projects IM 37/12-1, SA 1948/3-1, SU 1261/1-1, GA 2403/7-1, FOR5044] is gratefully acknowledged.

KFM 14.7 Thu 16:15 POT 106

Nonlinear diffuse fs-pulse reflectometry adopted to LNT solid solutions — •F. KODDE¹, L. VITTADELLO¹, J. KLENEN¹, K. KOEMPE², V. HREB³, D. SUGAK³, V. SYDORCHUK⁴, U. YAKHNEVYCH⁵, and M. IMLAU¹ — ¹Institute of Physics, Barbarastr. 7, Osnabrück University — ²Department of Biology and Chemistry, Barbarastr. 11, Osnabrück University — ³Department of Semiconductor Electronics, Bandery Str. 12, Lviv Polytechnic National University, 79013 Lviv, Ukraine — ⁴Institute for Sorption and Problems of Endoecology, NASU, 13 Gen. Naumov St., 03164 Kyiv, Ukraine — ⁵Institute of Energy Research and Physical Technologies, Am Stollen 19B, TU Clausthal

Nonlinear diffuse fs-pulse reflectometry is a powerful tool to analyze the spontaneous polarization of polar oxide nano-crystals [Kijatkin *et al.*, *Photonics* **4**, 11 (2017)]. It profits from the absence of a phase-matching condition for frequency conversion. We present our systematic investigations at the example of nanocrystals of LiNb_{1-x}Ta_xO₃ (LNT) solid solutions [Vasylechko *et al.*, *Crystals* **11**, 755 (2021)], that show a disappearance of the birefringence if the temperature is precisely adjusted [Wood *et al.*, *J. Phys.: Condens. Mat.* **20**, 235237 (2008)]. Accordingly, we have extended the experimental setup by a temperature controlled pellet holder and determined the harmonic ratio as a function of composition, i.e. Li/Ta-ratio. We find both, a characteristic maximum of the harmonic ratio, and a dependence of the maximum on the composition. Financially supported by the DFG and BMBF [project IM 37/12-1, FOR5044, BMBF, FKZ: 01DK20009].

Magnetism Division Fachverband Magnetismus (MA)

Heiko Wende
Universität Duisburg-Essen
Fakultät für Physik
Lotharstr. 1
D-47048 Duisburg
heiko.wende@uni-due.de

Overview of Invited Talks and Sessions

(Lecture halls HSZ 02, HSZ 04, HSZ 401, HSZ 403, and POT 6; Poster P1 and P2/EG)

Invited Talks

MA 1.1	Sun	16:00–16:30	HSZ 04	Making better batteries? – From Li-ion to Na-ion batteries — •PHILIPP ADELHELM
MA 1.2	Sun	16:30–17:00	HSZ 04	Sustainable Thermoelectric Materials Predicted by Data Mining and Machine Learning — •KORNELIUS NIELSCH
MA 1.3	Sun	17:00–17:30	HSZ 04	Design strategies for electrocatalysts – an electrochemist’s perspective — •KRISTINA TSCHULIK
MA 1.4	Sun	17:30–18:00	HSZ 04	Green magnetic materials for efficient energy, transport and cooling applications — •OLIVER GUTFLEISCH
MA 2.1	Mon	9:30–10:00	HSZ 02	Two-dimensional Skyrmions in the real three-dimensional world — •NIKOLAI KISELEV
MA 8.1	Mon	15:00–15:30	HSZ 04	Optical control of antiferromagnetism — •CHRISTIAN TZSCHASCHEL
MA 14.1	Tue	9:30–10:00	HSZ 04	Antiferromagnetism-driven two-dimensional topological nodal-point superconductivity — •ROBERTO LO CONTE, MACIEJ BAZARNIK, ERIC MASCOT, KRISZTIÁN PALOTÁS, LEVENTE RÓZSA, LÁSZLÓ SZUNYOGH, ANDRÉ KUBETZKA, DIRK K. MORR, KIRSTEN VON BERGMANN, ROLAND WIESENDANGER
MA 25.1	Wed	9:30–10:00	HSZ 04	MAGNOTHERM – One way to start a deep tech spin-off from research — •MAX FRIES
MA 25.2	Wed	10:00–10:30	HSZ 04	Spin-Ion Technologies : taking the research from a lab to a start-up company — •DAFINÉ RAVELOSONA
MA 25.3	Wed	10:30–11:00	HSZ 04	MagREEsources : the green Rare Earth Magnet company — •SOPHIE RIVOIRARD, ERICK PETIT
MA 25.4	Wed	11:00–11:30	HSZ 04	THATec Innovation – we automate your lab — •THOMAS SEBASTIAN
MA 25.5	Wed	11:30–12:00	HSZ 04	Kiutra: Magnetic refrigeration for science and technology — •ALEXANDER REGNAT, JAN SPALLEK, TOMEK SCHULZ, CHRISTIAN PFLEIDERER
MA 26.1	Wed	9:30–10:00	HSZ 401	The self-induced spin glass: the perplexing magnetism of elemental neodymium — •ALEXANDER KHAJETOORIAN
MA 30.1	Wed	15:00–15:30	HSZ 02	Femto- phono- magnetism — •SANGEETA SHARMA
MA 30.2	Wed	15:30–16:00	HSZ 02	Spin-switchable molecules in interaction with their environment. — •CYRILLE BARRETEAU
MA 30.3	Wed	16:15–16:45	HSZ 02	Yep, real photodoping. — LUKAS GIERSTER, •JULIA STÄHLER
MA 30.4	Wed	16:45–17:15	HSZ 02	Probing ultrafast magnetization thanks to ultrashort soft X-ray pulses — •EMMANUELLE JAL
MA 34.1	Thu	9:30–10:00	HSZ 02	Polarized phonons carry angular momentum in ultrafast demagnetization — •PETER BAUM
MA 34.2	Thu	10:00–10:30	HSZ 02	Spin-phonon coupling in ordered magnets: origin and consequences — •AKASHDEEP KAMRA
MA 34.3	Thu	10:30–11:00	HSZ 02	Magnon-mechanics in high overtone acoustic resonators — •HANS HUEBL
MA 34.4	Thu	11:15–11:45	HSZ 02	Cavity Magnomechanics: Harnessing the Magnomechanical Coupling for Applications in the Microwave and Optical Regimes — •SILVIA VIOLA KUSMINSKIY
MA 34.5	Thu	11:45–12:15	HSZ 02	Coherent spin-wave transport in an antiferromagnet — •ANDREA CAVIGLIA
MA 41.1	Thu	15:00–15:30	HSZ 02	Altermagnetism and spin symmetries — •LIBOR ŠMEJKAL

MA 41.2	Thu	15:30–16:00	HSZ 02	Spontaneous Hall effect in Mn₅Si₃ altermagnet — •H. REICHOVA, R. LOPES SEEGER, R. GONZÁLEZ-HERNÁNDEZ, I. KOUTA, R. SCHLITZ, D. KRIEGNER, P. RITZINGER, M. LAMMEL, M. LEIVISKA, V. PETRICEK, E. SCHMORANZEROVA, A. BADURA, A. THOMAS, V. BALTZ, L. MICHEZ, J. SINOVA, S.T.B. GOENNENWEIN, T. JUNGWIRTH, L. SMEJKAL
MA 41.5	Thu	16:30–17:00	HSZ 02	Generation of tilted spin-current by the collinear antiferromagnet RuO₂ — •ARNAB BOSE
MA 41.6	Thu	17:00–17:30	HSZ 02	First-principles studies on the anomalous transport properties of ferromagnets, antiferromagnets, and altermagnets — •WANXIANG FENG
MA 41.7	Thu	17:30–18:00	HSZ 02	Insight into chemical and magnetotransport properties of epitaxial α-Fe₂O₃/Pt bilayers — •ANNA KOZIOŁ-RACHWAŁ, NATALIA KWIATEK, WITOLD SKOWROŃSKI, KRZYSZTOF GROCHOT, JAROSŁAW KANAK, EWA MADEJ, KINGA FREINDL, JÓZEF KORZECKI, NIKA SPIRIDIS

Invited Talks of the joint Symposium SKM Dissertation Prize 2023 (SYSD)

See SYSD for the full program of the symposium.

SYSD 1.1	Mon	9:30–10:00	HSZ 04	Diffusion of antibodies in solution: from individual proteins to phase separation domains — •ANITA GIRELLI
SYSD 1.2	Mon	10:00–10:30	HSZ 04	Intermediate Filament Mechanics Across Scales — •ANNA V. SCHEPERS
SYSD 1.3	Mon	10:30–11:00	HSZ 04	Ultrafast Probing and Coherent Vibrational Control of a Surface Structural Phase Transition — •JAN GERRIT HORSTMANN
SYSD 1.4	Mon	11:00–11:30	HSZ 04	Electro-active metasurfaces employing metal-to-insulator phase transitions — •JULIAN KARST
SYSD 1.5	Mon	11:30–12:00	HSZ 04	The role of unconventional symmetries in the dynamics of many-body systems — •PABLO SALA

Invited Talks of the joint Symposium Green Magnets for Efficient Energy Conversion (SYGM)

See SYGM for the full program of the symposium.

SYGM 1.1	Mon	15:00–15:30	HSZ 01	Data mining protocols for functional magnetic materials — •OLLE ERIKSSON
SYGM 1.2	Mon	15:30–16:00	HSZ 01	High performance permanent magnets; elements criticality, new demands, and extrinsic magnetic properties — •HOSSEIN SEPEHRI-AMIN, XIN TANG, TADAKATSU OHKUBO, KAZUHIRO HONO
SYGM 1.3	Mon	16:00–16:30	HSZ 01	Magnetic shape memory Heuslers: microstructure-related effects on the martensitic transformation — •FRANCA ALBERTINI
SYGM 1.4	Mon	16:45–17:15	HSZ 01	Thin film combinatorial studies of hard magnetic materials — •NORA DEMPSEY
SYGM 1.5	Mon	17:15–17:45	HSZ 01	Magnetocaloric materials for energy-efficient thermal control systems — •VICTORINO FRANCO, AUN N. KHAN, JORGE REVUELTA-LOSADA, ÁLVARO DÍAZ-GARCÍA, LUIS M. MORENO-RAMÍREZ, JIA YAN LAW

Invited Talks of the joint Symposium Real-Time Measurements of Quantum Dynamics (SYQD)

See SYQD for the full program of the symposium.

SYQD 1.1	Thu	9:30–10:00	HSZ 01	Real-time measurement and control of spin dynamics in quantum dots — •SEIGO TARUCHA
SYQD 1.2	Thu	10:00–10:30	HSZ 01	Quantum Dot arrays for Quantum Information Transfer — •GLORIA PLATERO, DAVID FERNANDEZ-FERNANDEZ, JUAN ZURITA
SYQD 1.3	Thu	10:30–11:00	HSZ 01	Optical Detection of Real-Time Quantum Dynamics in Quantum Dots — •MARTIN GELLER, JENS KERSKI, ERIC KLEINHERBERS, JÜRGEN KÖNIG, ANNIKA KURZMANN, PIA LOCHNER, AXEL LORKE, ARNE LUDWIG, HENDRIK MANNEL, PHILIPP STEGMANN, ANDREAS WIECK, MARCEL ZÖLLNER
SYQD 1.4	Thu	11:30–12:00	HSZ 01	Cooper Pair Splitting in Real-Time — •CHRISTIAN FLINDT
SYQD 1.5	Thu	12:00–12:30	HSZ 01	Trajectory-based detection in stochastic and quantum thermodynamics — •JUKKA PEKOLA

Invited Talks of the joint Symposium Topological Superconductor-Magnet Heterostructures (SYTS)

See SYTS for the full program of the symposium.

SYTS 1.1	Thu	15:00–15:30	HSZ 01	Blending of superconductivity and magnetism via topological solitons — •CHRISTOS PANAGOPOULOS
SYTS 1.2	Thu	15:30–16:00	HSZ 01	Topological landscaping in magnet-superconductor heterostructures — •SEBASTIÁN A. DÍAZ
SYTS 1.3	Thu	16:00–16:30	HSZ 01	Experimental study of minigaps and end states in bottom-up designed multi-orbital Shiba chains — •JENS WIEBE
SYTS 1.4	Thu	16:45–17:15	HSZ 01	Quantum spins and hybridization in artificially-constructed chains of magnetic adatoms on superconducting 2H-NbSe₂ — •KATHARINA J. FRANKE
SYTS 1.5	Thu	17:15–17:45	HSZ 01	Braiding of Majorana zero modes — •STEPHAN RACHEL

Invited Talks of the joint Symposium Physics of van der Waals 2D Heterostructures (SYHS)

See SYHS for the full program of the symposium.

SYHS 1.1	Fri	9:30–10:00	HSZ 01	Novel moiré excitons and ultrafast optical dynamics in van der Waals 2D heterostructures — •STEVEN G. LOUIE
SYHS 1.2	Fri	10:00–10:30	HSZ 01	Interaction induced magnetism in 2D semiconductor moiré superlattices — •XIAODONG XU
SYHS 1.3	Fri	10:30–11:00	HSZ 01	Ions in tight places: intercalation and transport of ions in van der Waals heterostructures — •IRINA GRIGORIEVA
SYHS 1.4	Fri	11:15–11:45	HSZ 01	Spin-orbit proximity in van der Waals heterostructures — •FELIX CASANOVA
SYHS 1.5	Fri	11:45–12:15	HSZ 01	Plethora of many-body ground states in magic angle twisted bilayer graphene — •DMITRI EFETOV

Sessions

MA 1.1–1.4	Sun	16:00–18:00	HSZ 04	Tutorial: Strategic elements and sustainability (joint session MA/TUT)
MA 2.1–2.8	Mon	9:30–12:00	HSZ 02	Skyrmions I
MA 3.1–3.11	Mon	9:30–12:30	HSZ 401	Magnetic Materials for Efficient Energy Conversion
MA 4.1–4.14	Mon	9:30–13:00	HSZ 403	Spin Transport and Orbitronics, Spin-Hall Effects (joint session MA/TT)
MA 5.1–5.6	Mon	9:30–11:00	POT 6	Thin Films: Magnetic Coupling Phenomena / Exchange Bias
MA 6.1–6.6	Mon	14:30–17:05	POT 51	Focus: Dislocations in Ceramics: Mechanics, Structures and Functionality (joint session KFM/MA)
MA 7.1–7.12	Mon	15:00–18:00	HSZ 02	Computational Magnetism
MA 8.1–8.11	Mon	15:00–18:00	HSZ 04	Ultrafast Magnetization Effects I
MA 9.1–9.10	Mon	15:00–17:45	HSZ 401	Cooperative Phenomena: Spin Structures and Magnetic Phase Transitions
MA 10.1–10.8	Mon	15:00–17:15	HSZ 403	Topological Insulators (joint session MA/TT)
MA 11.1–11.6	Mon	15:00–16:45	POT 6	Non-Skyrmionic Magnetic Textures I
MA 12.1–12.8	Tue	9:30–11:30	HSZ 02	Skyrmions II
MA 13.1–13.9	Tue	9:30–13:15	HSZ 03	Focus Session: New Perspectives for Adiabatic Demagnetization Refrigeration in the Kelvin and sub-Kelvin Range (joint session TT/MA)
MA 14.1–14.7	Tue	9:30–11:45	HSZ 04	Surface Magnetism
MA 15.1–15.5	Tue	9:30–11:50	HSZ 401	INNOMAG e.V. Prizes 2023 (Diplom-/Master and Ph.D. Thesis)
MA 16.1–16.9	Tue	9:30–12:00	HSZ 403	Magnonics
MA 17.1–17.6	Tue	9:30–11:00	POT 6	Thin Films: Magnetic Anisotropy
MA 18.1–18.8	Tue	15:00–17:15	HSZ 02	Functional Antiferromagnetism I
MA 19.1–19.7	Tue	15:00–17:00	HSZ 04	Molecular Magnetism I
MA 20.1–20.10	Tue	15:00–17:45	HSZ 401	Spintronics (other effects)
MA 21.1–21.8	Tue	15:00–17:15	HSZ 403	Spin-Dependent Phenomena in 2D
MA 22.1–22.5	Tue	15:00–16:15	POT 6	Terahertz Spintronics
MA 23.1–23.80	Tue	17:00–19:00	P1	Poster Magnetism I
MA 24.1–24.6	Wed	9:30–11:00	HSZ 02	Molecular Magnetism II
MA 25.1–25.5	Wed	9:30–12:30	HSZ 04	Focus Session: Startups in Magnetism
MA 26.1–26.6	Wed	9:30–11:30	HSZ 401	Non-Skyrmionic Magnetic Textures II
MA 27.1–27.7	Wed	9:30–11:30	HSZ 403	Electron Theory of Magnetism and Correlations
MA 28.1–28.5	Wed	9:30–10:45	POT 6	Bulk Materials: Soft and Hard Permanent Magnets
MA 29.1–29.5	Wed	11:30–12:45	HSZ 02	Neuromorphic Magnetism / Magnetic Logic
MA 30.1–30.4	Wed	15:00–18:00	HSZ 02	PhD Focus Session: Non-equilibrium dynamics in theory and experiment

MA 31.1–31.8	Wed	15:00–17:15	HSZ 04	Functional Antiferromagnetism II
MA 32.1–32.6	Wed	15:00–16:30	HSZ 401	Magnetic Imaging Techniques I
MA 33.1–33.8	Wed	15:00–17:15	HSZ 403	Frustrated Magnets I
MA 34.1–34.8	Thu	9:30–13:00	HSZ 02	Focus Session: Spin-Phonon Coupling
MA 35.1–35.9	Thu	9:30–12:00	HSZ 04	Skyrmions III
MA 36.1–36.6	Thu	9:30–11:00	HSZ 401	Magnetic Particles / Clusters
MA 37.1–37.6	Thu	9:30–11:00	HSZ 403	Magnetic Heuslers
MA 38.1–38.5	Thu	11:30–12:45	HSZ 401	Micro- and Nanostructured Magnetic Materials
MA 39.1–39.5	Thu	11:30–12:45	HSZ 403	Weyl Semimetals
MA 40.1–40.66	Thu	14:00–16:00	P2/EG	Poster Magnetism II
MA 41.1–41.7	Thu	15:00–18:00	HSZ 02	Focus Session: Altermagnetism: Transport, Optics, Excitations
MA 42.1–42.10	Thu	15:00–17:45	HSZ 04	Caloric Effects in Ferromagnetic Materials
MA 43.1–43.7	Thu	15:00–16:45	HSZ 401	Magnetic Imaging Techniques II
MA 44.1–44.9	Thu	15:00–17:30	HSZ 403	Frustrated Magnets II
MA 45	Thu	18:00–19:00	HSZ 04	Members' Assembly
MA 46.1–46.13	Fri	9:30–12:45	HSZ 02	Ultrafast Magnetization Effects II
MA 47.1–47.11	Fri	9:30–12:30	HSZ 04	Skyrmions IV
MA 48.1–48.8	Fri	9:30–11:45	HSZ 401	Magnetic Instrumentation and Characterization
MA 49.1–49.8	Fri	9:30–11:45	HSZ 403	Magnetic Information Technology, Recording, Sensing
MA 50.1–50.7	Fri	9:30–11:15	POT 6	Magnetic Domain Walls (non-skyrmionic)

Members' Assembly of the Magnetism Division

Thu 18:00–19:00 HSZ 04

Sessions

– Invited Talks, Contributed Talks, and Posters –

MA 1: Tutorial: Strategic elements and sustainability (joint session MA/TUT)

Our appetite for resources is insatiable. The path to a climate-neutral society and economy requires the increasingly intensive use of strategy metals such as lithium, cobalt, nickel, but also the group of rare earth elements. This major transformation is not possible without the sustainable use of these so-called critical elements along the entire value chain. In the Tutorial "Strategic elements and sustainability", we have four eminent speakers looking in this context at new developments in batteries, catalysis, thermoelectrics and magnetism.

Organizers: Oliver Gutfleisch (TU Darmstadt) and Heiko Wende (U. Duisburg-Essen).

Time: Sunday 16:00–18:00

Location: HSZ 04

Invited Talk

MA 1.1 Sun 16:00 HSZ 04

Making better batteries? – From Li-ion to Na-ion batteries — •PHILIPP ADELHELM — Humboldt-University Berlin, Berlin, Germany — Helmholtz-Zentrum Berlin, Berlin, Germany

The shift to electromobility is one of the most important transformations currently taking place in our society. This is associated with a sharp increase in battery production, which on the one hand opens up new opportunities, but on the other hand also has a massive impact on raw material supply and supply chains. In addition, new large markets are emerging, such as stationary energy supply or mobile robotics. Lithium-ion batteries are currently the most attractive technology for this. However, due to the large demand for batteries and the different application scenarios, other technologies are also being pursued. Sodium ion batteries can be produced on the same production lines as lithium ion batteries and are therefore considered a "drop-in" technology. The aim here is to replace not only costly lithium but also other expensive elements such as nickel or copper. Work is therefore being done worldwide on a cell chemistry for sodium ion batteries that works almost as well as lithium ion technology, but at the same time is cheaper and more readily available, or has other specific advantages. The tutorial gives an introduction to sodium ion technology. The motivation and state-of-the-art are explained in more detail and material aspects are discussed. In particular, the question is addressed which electrode materials are promising for sodium ion batteries, what is needed to achieve further progress and what actually happens when lithium ions are replaced by sodium ions in a battery.

Invited Talk

MA 1.2 Sun 16:30 HSZ 04

Sustainable Thermoelectric Materials Predicted by Data Mining and Machine Learning — •KORNELIUS NIELSCH — Leibniz Institute of Solid States and Materials Research, Dresden, Germany — Institute of Materials Research at TU Dresden, Germany — Institute of Applied Physics at TU Dresden, Germany

Generating electricity from temperature differences has proven itself in space. Thanks to this technology, the Voyager probes launched in 1977 are still sending signals today. In the meantime, the car industry and ship producers have become interested in thermoelectrics. The combustion of fossil fuels produces exhaust gas that is up to 1300 °C hot. Modern thermoelectric materials are continuously expanding the fields of thermoelectric applications. The experimental search for new thermoelectric materials remains largely restricted to a limited number of successful chemical and structural families, such as chalcogenides, skutterudites and zintl phases. In principle, computational tools such as density functional theory (DFT) offer the possibility of directing experimental synthesis efforts towards very different chemical structures. In practice, however, predicting thermoelectric properties based on first principles remains a difficult endeavour, and experimental researchers do not usually use computations directly to drive their own synthesis efforts. Strategies to bridge this practical gap between experimental requirements and computational tools will be discussed and presented in this tutorial talk. Ref: Energy Environ. Sci. 14, 3559 (2021) and Advanced Theory and Simulations 5, 2200351 (2022)

Invited Talk

MA 1.3 Sun 17:00 HSZ 04

Design strategies for electrocatalysts – an electrochemist's perspective — •KRISTINA TSCHULIK — Ruhr-Universität Bochum, Faculty for Chemistry and Biochemistry, Chair for Electrochemistry and Nanoscale Materials — Max-Planck-Institut für Eisenforschung GmbH, Max-Planck-Straße 1, 40237 Düsseldorf

The aim to produce highly active, selective, and long-lived electrocatalysts by design drives major research efforts toward gaining fundamental understanding of the relationship between material properties and their catalytic performance. Surface characterization tools enable to assess atomic scale information on the complexity of electrocatalyst materials. Advancing electrochemical methodologies to adequately characterize such systems was less of a research focus point. In this tutorial, we shed light on the ability to gain fundamental insights into electrocatalysis and establish design strategies based on these. Concepts on how to improve mass transport, e.g. by exploiting magnetic fields are highlighted in this respect. Particular attention is paid to deriving design strategies for nanoelectrocatalysts, which is often impeded, as structural and physical material properties are buried in electrochemical data of whole electrodes. Thus, a second major approach focuses on overcoming this difference in the considered level of complexity by methods of single-entity electrochemistry. The gained understanding of intrinsic catalyst performance will ultimately allow us to advance design concepts to transforming "pre-catalysts" in the foreseeable future.

Invited Talk

MA 1.4 Sun 17:30 HSZ 04

Green magnetic materials for efficient energy, transport and cooling applications — •OLIVER GUTFLEISCH — TU Darmstadt, Material Science, Functional Materials

High performance hard and soft magnets are key components of energy-related technologies, such as direct drive wind turbines and e-mobility. They are also important in robotics and automatization, sensors, actuators, and information technology. The magnetocaloric effect (MCE) is the key for new and disruptive solid state-based refrigeration. Magnetic hysteresis and its inherent energy product characterise the performance of all magnetic materials. In the 60th position of the periodic table of elements is neodymium - an element that belongs to the rare earth-lanthanides and essential for the above applications. Basic material requirements, figure of merits, demand and supply, criticality of strategic elements and their recycling are explained for both permanent magnets and magnetocalorics referring to the benchmark materials NdFeB and LaFeSi. Every battery needs a magnet. 95% of electric vehicles utilize rare earth magnet-based drive motors, the quantities required global will grow from 5.000 t in 2019 to about 40.000 - 70.000 t per anno in 2030. The material history of neodymium is exciting and complex; monopolistic mining in China under ruinous conditions is just as problematic as our dependence on it. How "green" are the metals for renewable technologies? Who pays which price for it, and when?

MA 2: Skyrmions I

Time: Monday 9:30–12:00

Location: HSZ 02

Invited Talk

MA 2.1 Mon 9:30 HSZ 02

Two-dimensional Skyrmions in the real three-dimensional world — •NIKOLAI KISELEV — Institute for Advanced Simulation and Peter Grünberg Institute, Forschungszentrum Jülich, 52425 Jülich Germany

Chiral skyrmions (CSs) emerging in noncentrosymmetric magnetic crystals are a prominent example of topological magnetic solitons – objects possessing properties of ordinary particles. In three-dimensional (3D) bulk samples, CSs usually

form vortex-like strings penetrating the whole sample. Although CSs emerge as 3D objects, the two-dimensional (2D) model of a chiral magnet still represents a powerful tool for the theoretical study of CSs. In this talk, I'll present an overview of those phenomena predicted by the 2D model that found its experimental confirmation. In particular, I'll discuss the diversity of CSs with arbitrary topological charge [1] – skyrmions bags, the effect of turning skyrmions inside out [2], and the related phenomenon of skyrmion-antiskyrmion coexistence [3].

The discussion of the above phenomena is supported by a high-resolution transmission electron microscopy experiment. As an illustration of a phenomenon that cannot be described in a simplified 2D model, I'll present the theoretical and experimental study of so-called skyrmion braiding – the emergence of superstructures of skyrmion strings that wind around one another [4].

[1] F. N. Rybakov & N. S. Kiselev, *Phys. Rev. B* 99, 064437 (2019). [2] V. M. Kuchkin & N. S. Kiselev, *Phys. Rev. B* 101, 064408 (2020). [3] F. Zheng et al., *Nature Phys.* (2022) 18, 863 (2022). [4] F. Zheng et al., *Nature Commun.* 12, 5316 (2021).

MA 2.2 Mon 10:00 HSZ 02

Comparing Thiele-model computer simulations and experiments of skyrmion interactions and lattice formation — •JAN ROTHÖRL¹, YUQING GE^{1,2}, MAARTEN A. BREMS¹, RAPHAEL GRUBER¹, MATHIAS KLÄUI¹, and PETER VIRNAU¹ — ¹Institut für Physik, Johannes Gutenberg-Universität Mainz — ²Department of Physics, Chalmers University of Technology, Göteborg, Sweden
Magnetic skyrmions in thin films are often described as quasi-particles evolving according to the Thiele equation. Due to their effective 2D nature, their phase behavior can be compared to phase transitions described by the KTHNY theory. To allow for this analysis, we compare experimental and simulation results for skyrmion lattice formation [1] and determine skyrmion-skyrmion interaction potentials using the Iterative Boltzmann Inversion method [2]. These resulting potentials are then compared to the work describing the dependence of the kind of 2D phase transition on the shape of particle interactions [3].

[1] Zázvorka et al., *Adv. Funct. Mater.* 30 (46), 2004037 (2020). [2] Ge et al., arXiv:2110.14333 [cond-mat.mtrl-sci] (2021). [3] Kapfer, Krauth, *Phys. Rev. Lett.* 114 (3), 035702 (2015).

MA 2.3 Mon 10:15 HSZ 02

Machine learning based skyrmion detection with Kerr microscopy data — ISAAC LABRIE-BOULAY¹, THOMAS WINKLER¹, DANIEL FRANZEN², •KILIAN LEUTNER¹, ALENA ROMANOVA¹, HANS FANGOHR^{3,4}, and MATHIAS KLÄUI¹ — ¹Johannes Gutenberg University, Mainz, Institute of Physics, Staudinger Weg 7, Germany — ²Johannes Gutenberg University, Mainz, Institute of Informatics, Staudinger Weg 9, Germany — ³Max-Planck Institute for the Structure and Dynamics of Matter, Luruper Chaussee 149, 22761 Hamburg, Germany — ⁴University of Southampton, SO17 1BJ, Southampton, United Kingdom

Magnetic skyrmions are topologically stabilized quasi-particles and are a potential enabler for unconventional computing devices [1]. A common method for detecting skyrmions is to use a Kerr microscope. Experimental data is affected by noise, low contrast, intensity gradients, or defects. Therefore, manual data treatment is necessary to evaluate the observations. To automatize Kerr microscopy data analysis, we have used a special type of convolutional neural network, called U-Net, to determine the shapes and positions of skyrmions [2]. Different methods were used to optimize the classification and to detect the skyrmions quickly with high reliability and to minimize manual work [3]. Our approach can also be extended to other magnetic structures, such as stripe domains or vortices.

[1] Klaus Raab et al., *Nat. Commun.* 13, 6982 (2022)
[2] Olaf Ronneberger et al., arXiv:1505.04597 [cs.CV] (2015)
[3] Isaac Labrie-Boulay et al. (in preparation)

MA 2.4 Mon 10:30 HSZ 02

Topological Hall effect in Pd/Fe/Ir(111) induced by electron scattering on magnetic skyrmions — •ADAMANTIA KOSMA¹, PHILIPP RÜSSMANN^{2,3}, STEFAN BLÜGEL³, and PHIVOS MAVROPOULOS¹ — ¹Department of Physics, National and Kapodistrian University of Athens, Panepistimioupolis 15784, Athens, Greece — ²Institute for Theoretical Physics and Astrophysics, University of Würzburg, 97074 Würzburg, Germany — ³Peter Grünberg Institut and Institute for Advanced Simulation, Forschungszentrum Jülich and JARA, 52425 Jülich, Germany

This work comprises an ab-initio computational study of the topological Hall effect (THE) arising from magnetic skyrmions [1], which are formed in ultrathin films Pd/Fe/Ir(111) [2]. The investigation of the THE in these systems is of great importance, as it provides a way of electrically detecting magnetic skyrmions. We analyse the resistivity and the Hall angle of the system, which are calculated employing the non-collinear spin-density-functional theory within the full-potential relativistic Korringa-Kohn-Rostoker (KKR) Green function method combined with the semiclassical Boltzmann transport equation [3,4]. We discuss the dependence of the THE on additional electron scattering, modelled as random disorder broadening. Our findings predict a strong dependence of the topological Hall angle on the degree of disorder of a sample. [1] D. MacCarriello et al., *Nature Nanotechnology*, vol. 13, 233-237 (2018). [2] N. Romming et al., *Science*, vol. 341, 6146, 2013. [3] <https://jukkr.fz-juelich.de/>. [4] A. Kosma et al., *Phys. Rev. B*, vol. 102, 144424.

15 min. break

MA 2.5 Mon 11:00 HSZ 02

Observation of the sliding mode of the magnetic texture in Fe/Ir(111) — •WULF WULFHEKEL¹, HUNG-HSIANG HANG¹, LOUISE DESPLAT², VOLODYMYR KRAVCHUK¹, MARIE HERVÉ³, TIMOFEY BALASHOV⁴, PHILIPP MARKUS¹, MARKUS GARST¹, and BERTRAND DUPÉ⁵ — ¹Karlsruhe Institute of Technology, Karlsruhe — ²IPCMS, Université de Strasbourg, Strasbourg — ³Université Sorbonne, Paris — ⁴RWTH Aachen, Aachen — ⁵Université de Liège, Liège

The fourfold non-collinear spin texture of Fe on the sixfold surface of Ir(111) is known to be incommensurate along one of the diagonals of the unit cell, while it is commensurate along the other. As the periodicity of the spin texture is only a few atoms, the magnetic energy of the structure experiences the atomic lattice rather strongly. Theoretically, the sliding mode of the spin texture with respect to the crystal lattice becomes gapped in the commensurate direction while it stays soft along the incommensurate one. We report on a combined theoretical and experimental study of the sliding mode along the soft direction excited by microwave fields in the junction of a spin-polarized STM.

MA 2.6 Mon 11:15 HSZ 02

Chemical pressure tuning of a skyrmion lattice with giant topological Hall effect — •LEONIE SPITZ^{1,2}, MAX HIRSCHBERGER¹, SHANG GAO¹, TARO NAKAJIMA^{1,3}, CHRISTIAN PFELEDERER², TAKA-HISA ARIMA^{1,4}, and YOSHINORI TOKURA¹ — ¹RIKEN CEMS, Wakoshi, Saitama 351-0198, Japan — ²Physik-Department, Technical University of Munich, 85748 Garching, Germany — ³Institute for Solid State Physics, University of Tokyo, Kashiwa 277-8581, Japan — ⁴Department of Advanced Materials Science, University of Tokyo, Kashiwa, Chiba 277-8561, Japan

A skyrmion lattice accompanied by a large topological Hall effect was found in the centrosymmetric frustrated triangular lattice magnet Gd₂PdSi₃ [1]. In contrast to non-centrosymmetric compounds, the skyrmion spin-vortices are not stabilized by the Dzyaloshinskii-Moriya interaction, but rather by exchange frustration and the Ruderman-Kittel-Kasuya-Yosida interaction [2,3]. The nanometer-scale size of the skyrmions is a further novelty giving rise to a large emergent magnetic field. We study the effect of isoelectronic doping on Gd₂PdSi₃ to gain a deeper understanding of the material's magnetic and electronic properties. Via alloying we manipulate the lattice constants and polytypism of the structure [4]. We report the impact of chemical pressure tuning on the magnetic order and the topological Hall effect.

[1] T. Kurumaji, et al., *Science* 365, 914-918 (2019); [2] T. Okubo, et al., *Phys. Rev. Lett.* 108, 017206 (2012); [3] A. O. Leonov, et al., *Nat. Commun.* 6, 8275 (2015); [4] L. Spitz, et al., *J. Am. Chem. Soc.* 144, 16866-16871 (2022).

MA 2.7 Mon 11:30 HSZ 02

Relationship of charge and spin density waves in the skyrmion compound EuGa₂Al₂ — •STEVEN GEBEL¹, JAIME MOYA², JOCHEN GECK¹, and MAREIN RAHN³ — ¹Institute for Solid State and Materials Physics, Technical University of Dresden, 01062 Dresden, Germany — ²Department of Physics and Astronomy, Rice University, Houston, TX, 77005, USA

The interplay of spin and charge density waves (SDW/CDW) in rare earth intermetallics is a matter of great interest, since it may reveal a recipe of how to tailor an antiferromagnet to yield certain topological properties. The centrosymmetric skyrmion host series Eu(Ga,Al)₄ provides an ideal setting to explore this scenario: The electronic structure can be tuned by chemical and hydrostatic pressure, which induces CDWs, which, in turn, determine a landscape of frustrated itinerant electronic correlations. To clarify the origin and character of such nesting instabilities, we studied subtle structural variations with temperature and pressure, and related them to density functional structure calculations. As magnetic structure determinations of more members of the series become available, this may explain exactly which factors toggle the magnetism's topological character.

MA 2.8 Mon 11:45 HSZ 02

Influence of interlayer Dzyaloshinskii-Moriya interactions on magnetic textures — •ELENA VEDMEDENKO — University of Hamburg

An overview of magnet/non-magnetic metal/magnet trilayers with strong interlayer Dzyaloshinskii-Moriya interactions promoting out-of-plane as well as in-plane chirality between the magnetic layers will be presented [1-2]. Magnetic structuring in systems with the interlayer as well as intralayer Dzyaloshinskii-Moriya interactions will be discussed. An emphasis on the topological stability of those objects will be made.

1. A. Fernandez-Pacheco, E. Y. Vedmedenko et al., Symmetry-breaking interlayer Dzyaloshinskii* Moriya interactions in synthetic antiferromagnets, *Nature Mat.* 18, 679 (2019)

2. J. A. Arregi, P. Riego, A. Berger, and E. Y. Vedmedenko, Large Interlayer Dzyaloshinskii-Moriya interactions across Ag-layers, submitted.

MA 3: Magnetic Materials for Efficient Energy Conversion

Time: Monday 9:30–12:30

Location: HSZ 401

MA 3.1 Mon 9:30 HSZ 401

Voltage-driven giant modulation of magnetism in ferro- and ferri-magnetic alloys — •XINGLONG YE^{1,2}, HARISH SINGH¹, HONGBIN ZHANG¹, HOLGER GESSWEIN³, REDA CHELLALI², RALF WITTE², ALAN MOLINARI², KONSTANTIN SKOKOV¹, OLIVER GUTFLEISCH¹, HORST HAHN², and ROBERT KRUK² — ¹Department of Material Science, Technical University Darmstadt — ²Institute of Nanotechnology, Karlsruhe Institute of Technology — ³Institute of Applied Materials, Karlsruhe Institute of Technology

Controlling magnetism and magnetic properties by small voltages have become one of the core research topics vigorously pursued in magnetoelectric actuation, spintronics and data storage. In magnetically-ordered metals and alloys, however, the voltage effect is usually limited to the scale of atomic layers due to strong electric-field screening. Here, we propose to control their magnetism and magnetic properties by electrochemically-driven insertion/extraction of hydrogen atoms in interstitial sites. Using this approach, we have tuned the magnetocrystalline anisotropy and coercivity of SmCo₅ with micrometer-sized particles by more than 1 T by applying voltages as low as 1 V. Consequently, a voltage-assisted and -controlled magnetization reversal has been achieved at room temperature for the first time in permanent magnets. Furthermore, we will show that our electrochemically-driven hydrogen charging can switch the perpendicular anisotropy to in-plane anisotropy in ferrimagnetic thin films with high anisotropy energy, which further exemplifies the universality of our approach in controlling magnetism of rare earth - containing materials.

MA 3.2 Mon 9:45 HSZ 401

Additive Manufacturing of (Pr,Nd)-Fe-Cu-B Permanent Magnets — •JIANING LIU¹, RUIWEN XIE², ALEX AUBERT¹, LUKAS SCHÄFER¹, HOLGER MERSCHROTH³, JANA HARBIG³, YING YANG⁴, PHILIPP GABRIEL⁴, ANNA ZIEFUSS⁴, STEFAN BARCIKOWSKI⁴, MATTHIAS WEIGOLD³, HONGBIN ZHANG², OLIVER GUTFLEISCH¹, and KONSTANTIN SKOKOV¹ — ¹Functional Materials, Technical University of Darmstadt — ²Theory of Magnetic Materials, Technical University of Darmstadt — ³Institute of Production Management, Technology and Machine Tools, Technical University of Darmstadt — ⁴Technical Chemistry I, University of Duisburg-Essen

Additive Manufacturing (AM) of permanent magnets is a new and challenging field in material science and engineering. To obtain a microstructure necessary for high coercivity is by no means straightforward, especially after fast cooling in Laser Powder Bed Fusion (L-PBF). In order to achieve the desired microstructure and hard magnetic properties, we propose the Pr-Fe-Cu-B as a new useful reference alloy system and compare with its Nd-based counterpart. Our studies describe the L-PBF and the subsequent annealing optimization in order to understand the newly established coercivity mechanism. Specifically, we explore the 6-13-1-type grain boundary phase and grow single crystals to understand its magnetism, supported by DFT calculations. Furthermore, grain boundary engineering with nanoparticles shows great potential on grain refinement and uniaxial grain growth during re-solidification during L-PBF. We acknowledge the support of the Collaborative Research Centre/Transregio 270 HoMMage.

MA 3.3 Mon 10:00 HSZ 401

Simultaneous measurements of X-ray absorption, diffraction and bulk properties in HoCo₂ — •KATHARINA OLLEFS¹, GABRIEL GOMEZ-ESLAVA¹, ALEX AUBERT², KONSTANTIN SKOKOV², ALEXEY KARPENKOV², OLIVER GUTFLEISCH², FABRICE WILHELM³, ANDREI ROGALEV³, DAMIAN GÜNZING¹, JOHANNA LILL¹, BENEDIKT EGGERT¹, and HEIKO WENDE¹ — ¹Faculty of Physics and CENIDE, University Duisburg-Essen, Germany — ²Functional Materials, Technical University Darmstadt, Germany — ³European Synchrotron Radiation Facility, France

Bulk properties and atomistic/local parameters determined by X-ray Absorption Spectroscopy (XAS) or scattering are typically measured on different samples (such as powder) with the same composition. Together with the influence of the different sample environments in different setups this prevents a direct correlation of microscopic and macroscopic observations, especially for materials exhibiting dramatic changes of their properties around phase transitions. Here we present the ULMAG [1] set up. To demonstrate the capability of our technique we measured, a polycrystalline HoCo₂ sample. We show the magnetic field dependence of X-ray Magnetic Circular Dichroism (XMCD), stray field, longitudinal and transversal strain and sample temperature. Furthermore we demonstrate the capability to measure XAS/XMCD and diffraction on a single grain inside this material. [1] Aubert, Alex, et al. IEEE Transactions on Instrumentation and Measurement 71 (2022): 1-9. Supported by the DFG CRC TRR 270 HoMMage, the BMBF project ULMAG and the ESRF by beamtime allocation.

MA 3.4 Mon 10:15 HSZ 401

A thorough TEM investigation of B2 ordered FeRh (50/50) alloy — •ESMAEL ADABIFIROOZJAEI¹, NAGAARJHUNA KANI^{1,2}, ROBERT WINKLER¹, TIANSHU JIANG¹, OSCAR RECALDE¹, ALEXANDER ZINTLER¹, ALISA CHIRKOVA², KONSTANTIN SKOKOV², OLIVER GUTFLEISCH², and LEOPOLDO MOLINA LUNA¹ — ¹Advanced Electron Microscopy, Department of Materials- and Earth Sciences, Technical University of Darmstadt, Germany — ²Functional Materials, Department of Materials- and Earth Sciences, Technical University of Darmstadt, Darmstadt, Germany

Fe₅₀Rh₅₀ alloys are known to have a B2 structure with an antiferromagnetic to ferromagnetic transition at near room temperature. Since this alloy can be considered as betta alloy (CdAu, TiNi, Fe-C, etc), it is expected to present a pre-martensite structure followed by a martensite structure upon cooling at cryogenic temperature. The martensite was also predicted by extensive first principal calculations. However, so far, no evidence has been given regarding the formation of either pre-martensite or martensite structures in the Fe₅₀Rh₅₀ alloy. Here, we use various TEM techniques (including CTEM, HRTEM, STEM (HAADF), and EDS) to investigate the FeRh 50/50 alloy and demonstrate that although the structure of the alloy matches the B2 BCC structure, there is systematic modulation along certain reflexes (100 and 110). We believe that the existence of such ordered modulation along certain directions are indicative of a pre-martensite structure.

MA 3.5 Mon 10:30 HSZ 401

Shaping and functionalizing of Gd for a magnetocaloric cooling application — •LUKAS BEYER^{1,2}, BRUNO WEISE¹, JULIA KRISTIN HUFENBACH^{1,2}, and JENS FREUDENBERGER^{1,2} — ¹Leibniz IFW Dresden, Institute for Complex Materials, Helmholtzstr. 20, 01069, Dresden, Germany — ²TU Bergakademie Freiberg, Institute of Materials Science, Gustav-Zeuner-Str. 5, 09599, Freiberg, Germany

Magnetic refrigeration based on the magnetocaloric effect aims to substitute conventional cooling solutions, still, shaping and use of magnetocaloric materials remains challenging [1]. A combination with so-called thermal switches could improve the heat transport resulting in higher operating frequencies and therefore, an increase in the power density of magnetic cooling [2]. This could be beneficial for battery thermal management systems [3]. In this work we studied the influence of mechanical deformation on Gd while producing Gd-substrates that could be combined with fast thermal switches by ElectroWetting On Dielectric. We prepared Gd-substrates via cold-rolling and strip casting and investigated these in regards of sufficient surface quality and substrate dimensions. Heat treatments have been performed to restore the magnetocaloric effect after deformation. By means of magnetic and heat-capacity measurements we calculated the isothermal entropy and adiabatic temperature change and proved the recovery of the magnetocaloric effect in Gd-substrates. [1] J. S. Brown, et al.; Appl. Therm. Eng. 64 (2014). [2] A. Kitanovski, et al.; Int. J. Refrig. 33 (2010). [3] J. Kim et al.; Appl. Therm. Eng. 149 (2019).

MA 3.6 Mon 10:45 HSZ 401

Large Room Temperature Anomalous Transverse Thermoelectric Effect in Kagome Antiferromagnet YMn₆Sn₆ — •SUBHAJIT ROYCHOWDHURY¹, ANDREW M. OCHS², SATYA N. GUIN¹, KARTIK SAMANTA¹, JONATHAN NOKY¹, CHANDRA SHEKHAR¹, MAIA G. VERGNIORY¹, JOSHUA E. GOLDBERGER², and CLAUDIA FELSER¹ — ¹Max Planck Institute for Chemical Physics of Solids, 01187 Dresden, Germany — ²The Ohio State University, Columbus, 43210 Ohio, United States

Kagome magnets possess several novel non-trivial topological features owing to the strong correlation between topology and magnetism, that extends to their applications in the field of thermoelectricity. Conventional thermoelectric (TE) devices use the Seebeck effect to convert heat into electrical energy. In contrast, transverse thermoelectric devices based on the Nernst effect are attracting recent attention due to their unique transverse geometry, which uses a single material to eliminate the need for a multitude of electrical connections compared to conventional TE devices. In this study, we obtain a large anomalous transverse thermoelectric effect of ~ 2 microV K⁻¹ at room temperature in a kagome antiferromagnet YMn₆Sn₆ single crystal. The obtained value is larger than that of state-of-the-art canted antiferromagnetic (AFM) materials and comparable with ferromagnetic systems. The large anomalous Nernst effect (ANE) can be attributed to the net Berry curvature near the Fermi level.

15 min. break

MA 3.7 Mon 11:15 HSZ 401

Tailoring of thermal hysteresis in Ni-Mn-Sn shape memory alloys via microstructure design — •FRANZISKA SCHEIBEL¹, CHRISTIAN LAUHOFF², JOHANNES PUY¹, DAVID KOCH¹, PHILIPP KROOSS², THOMAS NIENDORF², and OLIVER GUTFLEISCH¹ — ¹Technische Universität Darmstadt, Darmstadt, Germany — ²Universität Kassel, Kassel, Germany

Ferromagnetic shape memory alloys (FSMA) like Ni-Mn-Sn undergo a magneto-structural transition and show giant multicaloric properties. Thus, these materials are excellent for caloric refrigeration as an energy efficient, environmentally friendly and safe alternative for vapor compression cooling. However, tailoring of the inherent thermal hysteresis is essential for material development [1].

The hysteresis can be influenced by the microstructure (grain configuration and size, texture, defects, or internal stress) [2]. In this study, the grain size and arrangement have been modified by powder-based processing using spark-plasma sintering and additive manufacturing technique to tailor both the microstructure and the thermal hysteresis at the same time. The understanding of the relation between grain-size, texture, grain arrangement and multiple external stimuli is essential to develop materials with first-order magneto-structural transition transformation for multicaloric cooling.

This work was supported by the ERC Advanced Grant "Cool Innov" and the SFB-TRR270 "HoMMage".

[1] F. Scheibel et al., Energy Technol. 6, 1397 (2018)

[2] O. Gutfleisch et al., Phil. Trans. R. Soc. A 374: 20150308 (2016)

MA 3.8 Mon 11:30 HSZ 401

Impact of disorder on the vibrational and magnetic properties of Ni-Mn-(Sn,In) Heusler alloys — •OLGA N. MIROSHKINA¹, BENEDIKT EGGERT¹, JOHANNA LILL¹, BENEDIKT BECKMANN², DAVID KOCH², KATHARINA OLLEFS¹, FRANCESCO CUGINI³, MASSIMO SOLZI³, MOJMIR ŠOŠ⁴, MARTIN FRIÁK⁴, OLIVER GUTFLEISCH², HEIKO WENDE¹, and MARKUS E. GRUNER¹ — ¹University of Duisburg-Essen, Duisburg, Germany — ²Technical University of Darmstadt, Darmstadt, Germany — ³University of Parma, Parma, Italy — ⁴Czech Academy of Sciences, Brno, Czech Republic

Ni-Mn-Z with Z=In,Sn Heuslers are promising magnetocaloric systems to be employed in the magnetic cooling devices. In this respect, it is important to understand the influence of the main group element on the vibrational and magnetic properties of these materials. By combining large-scale density functional theory calculations with ¹¹⁹Sn-NRIXS and Mössbauer spectroscopy, we disentangled the vibrational contributions of the Sn atoms in Ni₂MnSn. We found the evidence that inversion of optical modes at Γ involving the displacement of Ni and the heavier Z atoms predicted previously for other Ni-Mn-based Heuslers is also a property of Ni₂MnSn, while deviation between experimental spectra and simulations might be explained by site-disorder [1]. In turn, the variation of Z in combination with chemical disorder can be employed to control the magnetization of the transition metal sublattice [2]. This work is funded by DFG within CRC/TRR 270.

[1] O.N. Miroshkina, B. Eggert et al., PRB (accepted) (2022).

[2] F. Cugini et al., PRB 105, 174434 (2022).

MA 3.9 Mon 11:45 HSZ 401

Tailoring thermal hysteresis and microstructure of Ni-Mn-based Heusler alloys for multicaloric cooling applications — •ANDREAS TAUBEL¹, FRANZISKA SCHEIBEL¹, LUKAS PFEUFFER¹, BENEDIKT BECKMANN¹, NAVID SHAYANFAR¹, TINO GOTTSCHALL², KONSTANTIN SKOKOV¹, and OLIVER GUTFLEISCH¹ — ¹TUDarmstadt, Material Science, 64287 Darmstadt — ²Dresden High Magnetic Field Laboratory (HLD-EMFL), HZDR, 01328 Dresden

Refrigeration based on the magnetocaloric effect (MCE) attracts a lot of attention since it can be more energy efficient and environmentally friendly than current vapor compression technology. The concept uses a solid-state magnetic material that heats up and cools down cyclically when exposed to a changing magnetic field. The problem of thermal hysteresis for efficient materials with a first-order phase transition can be overcome by applying stress as a second stimulus [1].

In this work, we develop Ni-Co-Mn-In and Ni-Co-Mn-Ti Heusler alloys towards using them in a novel multi-stimuli cooling concept. We investigated the influence of different microstructures from chemical variation and different processing routes on the magnetocaloric and elastocaloric performance of these materials [2,3]. The introduction of secondary phases significantly enhances the mechanical stability.

We acknowledge funding by ERC (Adv. Grant Cool Innov, GrantNo. 743116) and by DFG (CRC HoMMage, ID 405553726 *TRR 270)

[1] T. Gottschall et al., Nature Mat. 17, 929*934 (2018)

[2] L. Pfeuffer et al., Acta Materialia 217 1175157 (2021)

[3] A. Taubel et al., Acta Mater. 201, 425-434 (2020)

MA 3.10 Mon 12:00 HSZ 401

Influence of Cu addition and chemical order on the thermomagnetic properties of Ni-Mn-Ga-based films — •LUKAS FINK^{1,2,3}, KORNELIUS NIELSCH^{2,3}, and SEBASTIAN FÄHLER¹ — ¹Helmholtz-Zentrum Dresden-Rossendorf, Institute of Ion Beam Physics and Materials Research, D-01328 Dresden, Germany — ²Leibniz IFW Dresden, Institute for Metallic Materials, D-01171 Dresden, Germany — ³TU Dresden, Institute of Materials Science, D-01062 Dresden, Germany

One way to harvest low-grade waste heat is a microscale thermomagnetic generator (TMG), which uses magnetocaloric films as active material. The high surface-to-volume ratio of thin films enables a fast heat transfer, increasing the cycling frequency and power density compared to bulk devices. Selecting the optimal active material is decisive for the efficiency of a TMG since it will determine the temperature regime and the cycling frequency. Recently Ni-Mn-based Heusler alloys were proposed as they can be prepared by standard thin-film technologies.

Here we use combinatorial growth of Cu alloyed Ni-Mn-Ga films and subsequent heat treatment for systematic optimization of thermomagnetic properties. We examine the key thermomagnetic properties like 1) the working temperature T^* and 2) the performance $\frac{\Delta M}{\Delta T}$ and correlate them with common properties like 3) crystal structure, 4) 1st and 2nd order transition and 5) spontaneous magnetization. Within our research, we can disentangle the effects of valence electron number e/a and chemical order. This work is funded by the DFG (FA453/14).

MA 3.11 Mon 12:15 HSZ 401

Study of the corrosion behaviour of Ni-Co-Mn-In Heusler — •ULYSSE ROCABERT, LUKAS PFEUFFER, and OLIVER GUTFLEISCH — Functional Materials Group, Department of Materials and Earth Sciences, Technische Universität Darmstadt, Alarich-Weiss-Straße 16, 64287 Darmstadt, Germany

Heusler materials are one of the promising material classes that are considered for their very useful magnetocaloric properties at room temperature. While their magnetic and mechanical properties have seen broad investigation, their electrochemical properties especially in aqueous environment remain largely unstudied. This study focuses on the characterization of such properties of Ni-Co-Mn-In alloys in different chemical environments and proposes an assessment on their implementation into refrigeration systems in comparison with LaFeSi-Mn alloys.

MA 4: Spin Transport and Orbitronics, Spin-Hall Effects (joint session MA/TT)

Time: Monday 9:30–13:00

Location: HSZ 403

MA 4.1 Mon 9:30 HSZ 403

Topological information device operating at the Landauer limit — •AHMET MERT BOZKURT^{1,2,3}, ALEXANDER BRINKMAN⁴, and INANC ADAGIDELI^{3,4} — ¹QuTech, Delft University of Technology, 2600 GA Delft, The Netherlands — ²Kavli Institute of Nanoscience, Delft University of Technology, 2600 GA Delft, The Netherlands — ³Faculty of Engineering and Natural Sciences, Sabanci University, Orhanli-Tuzla, Istanbul, Turkey — ⁴MESA+ Institute for Nanotechnology, University of Twente, The Netherlands

We propose and theoretically investigate a novel Maxwell's demon implementation based on the spin-momentum locking property of topological matter. We use nuclear spins as a memory resource which provides the advantage of scalability. We show that this topological information device can ideally operate at the Landauer limit; the heat dissipation required to erase one bit of information stored in the demon's memory approaches $k_B T \ln 2$. Furthermore, we demonstrate that all available energy, $k_B T \ln 2$ per one bit of information, can be ex-

tracted in the form of electrical work. Finally, we find that the current-voltage characteristics of the topological information device satisfy the conditions of an ideal memristor.

MA 4.2 Mon 9:45 HSZ 403

Controlling 3D spin textures by manipulating sign and amplitude of interlayer DMI with electrical current — •FABIAN KAMMERBAUER¹, WON-YOUNG CHOI¹, FREIMUTH FRANK^{1,2}, ROBERT FRÖMTER¹, YURIY MOKROUSOV^{1,2}, and MATHIAS KLÄUI¹ — ¹Institute of Physics, Johannes Gutenberg University, Staudingerweg 7, 55128 Mainz, Germany — ²Peter Grünberg Institut and Institute for Advanced Simulation, Forschungszentrum Jülich and JARA, 52425 Jülich, Germany

The recently discovered interlayer Dzyaloshinskii-Moriya interaction (IL-DMI) in multilayers with perpendicular magnetic anisotropy favors a canting of spins in the in-plane direction [1]. It could thus stabilize exciting spin textures such as

Hopfions. A key requirement for nucleation is to control the IL-DMI and so, we investigate the influence of an electric current on the strength of the IL-DMI, as previously found for FMI. The IL-DMI is quantified using out-of-plane hysteresis loops while applying a static in-plane magnetic field at varied azimuthal angles. We observe a shift in the azimuthal dependence with increasing current, which is concluded to originate from the additional in-plane symmetry breaking introduced by the current flow. Fitting the angular dependence we demonstrate the presence of an additive current-induced term [3]. With this, an easily accessible possibility to manipulate 3D spin textures by current is realized.

- [1] Han et al., Nat. Mater. 18, 703-708 (2019)
 [2] Karnad et al., Phys. Rev. Lett. 121, 147203 (2018)
 [3] Kammerbauer et al., arXiv:2209.01450 (2022)

MA 4.3 Mon 10:00 HSZ 403

Nonequilibrium dynamics in a spin valve with noncollinear magnetization — •RUDOLF SMORKA¹, PAVEL BALÁŽ², MICHAEL THOSS¹, and MARTIN ŽONDA^{3,1} — ¹University of Freiburg, Germany — ²Institute of Physics of the Czech Academy of Sciences Prague, Czech Republic — ³Charles University Prague, Czech Republic

Manipulation of magnetization by electric currents enables novel functions for spin-transfer torque devices. We study the nonequilibrium spin dynamics and spin-transfer torques in noncollinear spin-valve heterojunctions using a mixed quantum-classical Ehrenfest approach.

In an isolated valve for short spacer layers and weak spin-electron couplings, magnetization dynamics of the ferromagnetic layers is in agreement with the macrospin approximation. For large spacer layers, our quantum-classical approach predicts electron-induced spin relaxation. For intermediate electron-spin couplings, a change in the localization character of the electronic eigenstates from metallic-like to insulator-like leads to a reduced indirect exchange interaction between spins mediated by the conduction electrons. In a spin valve coupled to leads, spin relaxation times differ by several orders of magnitude depending on whether the DC bias is introduced by shifting the electrochemical potentials of both leads symmetrically about the equilibrium Fermi level of the spin valve (reminiscent of a gate-tunable junction) or by shifting the chemical potential of only one lead (as realized in a scanning tunneling microscope geometry).

- [1] R. Smorka, P. Baláz, M. Thoss, M. Žonda, Phys. Rev. B 2022, 106, 144435.

MA 4.4 Mon 10:15 HSZ 403

Nonrelativistic spin currents in altermagnets — •RODRIGO JAESCHKE-UBIERGO, JAIRO SINOVA, and LIBOR ŠMEJKA — Institut für Physik, Johannes Gutenberg Universität Mainz, D-55099 Mainz, Germany

Altermagnetism has emerged recently as a third basic collinear magnetic phase [1], in addition to ferromagnets and antiferromagnets. Conventional antiferromagnets exhibit two sublattices with opposite magnetic moment related by translation or inversion. In altermagnets the magnetic sublattices are connected by a rotation or a mirror operation. The particular symmetry causes that altermagnets display time-reversal (T) symmetry breaking and spin split band structure even in absence of spin-orbit coupling [2]. In this work, we study the spin conductivity tensor in altermagnets by using spin group theory formalism [1]. We also use Kubo's linear response to calculate the spin conductivity tensor in all the altermagnetic spin point groups models. Additionally, we identify and sort 200 altermagnetic candidates into spin conductivity tensor classes. We will discuss some spin point groups that allow for a transverse spin current in detail. This is the case of spin splitter current in RuO₂ [3,4], which is a nonrelativistic effect that conserves spin unlike in general magnetic spin Hall effect in noncollinear magnets. Moreover, the spin conductivity tensor is symmetric and T-odd, which makes it different from the conventional spin Hall effect. [1] Šmejkal et al., PRX, 12, 031042 (2022). [2] Šmejkal, et al. Sci. Adv. 2020. [3] Gonzalez- Hernandez, et al. PRL 2021. [4] Šmejkal, et al. PRX 12, 011028 (2022).

MA 4.5 Mon 10:30 HSZ 403

Quantification and modulation of intrinsic spin transport in 5d transition metals — •AKASH BAJAJ, REENA GUPTA, ANDREA DROGHETTI, and STEFANO SANVITO — School of Physics and CRANN, Trinity College Dublin, Dublin 2, Ireland

Spin-Hall effect (SHE) enables charge-to-spin conversion in heavy transition metals, such as Ta and Pt, with strong spin-orbit coupling (SOC) strengths. It has been extensively studied as a viable mechanism for the development of next-generation spintronics-based non-volatile memory devices. Numerous experimental and first-principles approaches have been devised to quantify the charge-to-spin conversion efficiency i.e., the spin-Hall angle (SHA), for the SHE. However, such approaches unavoidably involve interface contributions and, in general, extrinsic effects such as disorder and impurities, which are known to be less dominant than the bandstructure-only intrinsic contribution in such heavy metals. In this work, we use density functional theory combined with a bond-current-based non-equilibrium Green's functions approach to quantify the intrinsic SHAs of bulk elemental and thin-film models of 5d transition metals. We then computationally demonstrate a strategy for modulating the SHA within the same device, using Pt and Au as contrasting examples. Our computational work

not only provides a quantitative estimation of the intrinsic SHAs for these materials, but also enables its theoretical understanding aimed towards the development of higher performance and power-efficient spintronics-based non-volatile memory devices.

MA 4.6 Mon 10:45 HSZ 403

Influence of Disorder at Insulator-Metal Interface on Spin Transport — MAHSA ALSADAT SEYED HEYDARI, WOLFGANG BELZIG, and •NIKLAS ROHLING — Department of Physics, University of Konstanz

Motivated by experimental work showing enhancement of spin transport between yttrium iron garnet and platinum by the thin antiferromagnetic insulator NiO [1] between them, we consider spin transport through the interface of a non-magnetic metal and a ferro- or antiferromagnetically ordered insulator. The spin transport is carried by spin-polarized electrons in the metal and by magnons in the insulator. Spin current can be generated by a spin accumulation in the metal due to the inverse spin Hall effect, a microwave field exciting magnons in the insulator, or by a thermal gradient (spin Seebeck effect). The spin current can be computed using Fermi's Golden Rule [2]. For a perfectly clean interface, the in-plane momentum is conserved for the electron-magnon scattering events which govern the spin transport through the interface. We calculate how disorder-induced broadening of the scattering matrix elements with respect to the in-plane momentum influences the spin current. As a general result, we observe that for many experimental setups, one should expect a rather small effect of interface disorder on the measured spin current.

- [1] Wang et al., Phys. Rev. Lett. 113, 097202 (2014), Phys. Rev. B 91, 220410(R) (2015); Lin et al. Phys. Rev. Lett. 116, 186601 (2016)
 [2] Bender et al., Phys. Rev. Lett. 108, 246601 (2012)

MA 4.7 Mon 11:00 HSZ 403

Long-range orbital-Hall torques in Nb(or Ru)/Ni Heterostructures — ARNAB BOSE¹, FABIAN KAMMERBAUER¹, •RAHUL GUPTA¹, DONGWOOK GO², YURIY MOKROUSOV^{1,2}, GERHARD JAKOB¹, and MATHIAS KLÄUI^{1,3} — ¹Institute of Physics, Johannes Gutenberg University Mainz, Staudingerweg 7, 55128 Mainz, Germany — ²Peter Grünberg Institut and Institute for Advanced Simulation, Forschungszentrum Jülich and JARA, 52425 Jülich, Germany — ³Center for Quantum Spintronics, Department of Physics, Norwegian University of Science and Technology, NO-7491 Trondheim, Norway

We report a large orbital Hall torque (OHT) generated by Nb and Ru via strong dependence of torques on the ferromagnets, Ni, in Nb(Ru)/Ni heterostructures. We found the sign reversal of the damping-like torque in Nb/Ni. Moreover, the long-range orbital transport in the ferromagnet was revealed by the thickness dependences of Ni in Ni/Nb(or Ru) heterostructure, which are markedly different from the regular spin absorption in the ferromagnet that takes place within a few angstroms and thus it uniquely distinguishes OHT from the spin Hall torque. The experimentally measured effective orbital-Hall conductivities are found to be $6.1 \times 10^4 \frac{h}{2e} (\Omega m)^{-1}$ and $5.86 \times 10^4 \frac{h}{2e} (\Omega m)^{-1}$ for Nb and Ru, respectively, which is an order of magnitude higher than their measured spin Hall conductivities, as also confirmed by the density functional theory. This study opens a plethora of possibilities to further engineering the torques, utilizing the orbital degree of freedom.

MA 4.8 Mon 11:15 HSZ 403

Layer-resolved spin-orbit torque assisted magnetization dynamics in Pt/Co heterostructure — •HARSHITA DEVDA¹, ANDRÁS DEÁK², LEANDRO SALEMI³, LEVENTE RÓZSA¹, LÁSZLÓ SZUNYOGH², PETER M. OPPENEER³, and ULRICH NOWAK¹ — ¹Universität Konstanz, Konstanz, Germany — ²Budapest University of Technology and Economics, Budapest, Hungary — ³Uppsala University, Uppsala, Sweden

It is well known that the spin-orbit torque (SOT) mechanism is more reliable for current induced magnetization dynamics than the spin-transfer torque. The key phenomenon behind the SOT in heavy metal/ferromagnet (HM/FM) bilayers is attributed to the spin Hall effect (SHE) and the spin Rashba-Edelstein effect (SREE). However, the exact mechanism is still under debate. So far various works have studied the SOT-driven magnetic behavior in different magnetic systems, but the layer-resolved understanding of the SOT effect in the HM/FM bilayer due to spin-orbit coupling (SOC) in heavy metal is still lacking. We focus on current-induced magnetization dynamics in a Pt/Co bilayer assisted by the SOC in Pt. We use a multiscale model which links ab initio calculations with atomistic spin dynamics simulations. We implement a linear-response formalism to compute the electrically induced magnetic moments, caused by SHE in bulk and SREE at the interface, and utilize these in atomistic spin dynamics simulations. We analyse the layer-resolved behavior of both field-like and damping-like torques in FM and determine how they affect magnetization dynamics in ferromagnets.

MA 4.9 Mon 11:30 HSZ 403

Spin and orbital Edelstein effect in a bi- and trilayer system with Rashba interaction — •SERGIO LEIVA¹, JÜRGEN HENK¹, INGRID MERTIG¹, and ANNIKA JOHANSSON² — ¹Martin Luther University Halle-Wittenberg, Halle, Germany — ²Max Planck Institute of Microstructure Physics, Halle, Germany

The spin Edelstein effect has proved to be a promising phenomenon to generate spin polarization from a charge current in systems without inversion symmetry. In recent years, current-induced orbital magnetization, also called the orbital Edelstein effect, has also been predicted for several systems with broken inversion symmetry [1-6].

In the present work, we calculate the current-induced spin and orbital magnetization for a bilayer and a trilayer system with Rashba interaction for the interface and the free-standing slab configurations. We use the modern theory of orbital magnetization [7] and the Boltzmann transport theory. We found a significantly larger orbital than spin effect, with a strong dependence on the model parameters, such as effective mass and spin-orbit coupling per layer. This dependence allows us to enhance and even revert the sign of the orbital effect.

- [1] T. Yoda *et al.*, *Sci. Rep.*, **5**, 12024 (2015).
- [2] D. Go *et al.*, *Sci. Rep.* **7**, 46742 (2017)
- [3] T. Yoda *et al.*, *Nano Lett.*, **18**, 916 (2018).
- [4] L. Salemi *et al.*, *Nat. Commun.* **10**, 5381 (2019)
- [5] D. Hara *et al.*, *Phys. Rev. B*, **102**, 184404 (2020).
- [6] A. Johansson *et al.*, *Phys. Rev. Research*, **3**, 013275 (2021).
- [7] T. Thonhauser *et al.* *Phys. Rev Lett.* **95**, 137205 (2005).

MA 4.10 Mon 11:45 HSZ 403

Optical detection of the orbital Hall effect in a light metal Ti — •YOUNG-GWAN CHOI^{1,2}, DAEGEUN JO³, KYUNG-HUN KO¹, DONGWOOK GO^{4,5}, KYUNGHAN KIM³, HEE GYUM PARK⁶, CHANGYOUNG KIM^{7,8}, BYOUNG-CHUL MIN⁶, URI VOOL², GYUNG-MIN CHOI^{1,9}, and HYUN-WOO LEE^{3,10} — ¹DOES, SKKU, Suwon, Korea — ²MPI-CPFs, Dresden, Germany — ³Physics, POSTECH, Pohang, Korea — ⁴PGI and IAS, FZJ and JARA, Jülich, Germany — ⁵GSE Mainz, Mainz, Germany — ⁶Center for Spintronics, KIST, Seoul, Korea — ⁷Physics, SNU, Seoul, Korea — ⁸CCES, IBS, Seoul, Korea — ⁹CINAP, IBS, Suwon, Korea — ¹⁰APCTP, Pohang, Korea

Electrical generation of the angular momentum current enables the development of novel memory devices, similar to spin current generation. Recently, it has been theoretically proposed that the orbital angular momentum (OAM) current can be driven by a charge current, called as the orbital Hall effect (OHE). Here we report evidence of the OHE, measured by magneto-optical Kerr effect microscopy. We detect large Kerr signals in one of the 3d transition metals, Ti, in which the high orbital Hall conductivity is predicted. We also find that the large OAM is accumulated by the OHE with a relaxation length ~ 70 nm. Moreover, we present the torque results in Ti/Ni. The high torque efficiency shows that the OAM injection allows for the electrical control of the magnetization. We also propose magnetic imaging using a nitrogen-vacancy scanning probe to measure OAM accumulation directly. Our results can pave the way for a deep understanding and provide techniques for generating and detecting orbital transport.

MA 4.11 Mon 12:00 HSZ 403

Spin and orbital Edelstein effects at oxide interfaces — •ANNIKA JOHANSSON¹, BÖRGE GÖBEL², SARA VAROTTO³, SRIJANI MALLIK³, INGRID MERTIG², and MANUEL BIBES³ — ¹Max Planck Institute of Microstructure Physics, Halle, Germany — ²Martin Luther University Halle-Wittenberg, Halle, Germany — ³Unité Mixte de Physique, CNRS, Thales, Université Paris-Saclay, Palaiseau, France

The spin Edelstein effect (SEE) provides charge-spin interconversion in nonmagnetic systems with broken inversion symmetry [1,2]: An external electric field generates a charge current as well as a homogeneous spin density. Further, a finite current-induced magnetization originating from the electrons' orbital moments can be generated, which is called orbital Edelstein effect (OEE) [3-5]. In this talk, the SEE and OEE at SrTiO₃- and KTaO₃-based two-dimensional electron gases are discussed within a semiclassical Boltzmann approach [6-8]. The OEE is predicted to exceed its spin counterpart by one order of magnitude, which can be understood by a band-resolved analysis of the SEE and OEE. Further, we suggest design rules for Rashba-like systems to enhance spin-charge interconversion efficiencies.

- [1] A. G. Aronov, Y. B. Lyanda-Geller, *JETP Lett.* **50**, 431 (1989) [2] V. M. Edelstein, *Solid State Commun.* **73**, 233 (1990) [3] T. Yoda *et al.*, *Sci. Rep.* **5**, 12024 (2015). [4] T. Yoda *et al.*, *Nano Lett.* **18**, 916 (2018). [5] L. Salemi *et al.*, *Nat. Commun.* **10**, 5381 (2019) [6] D. Vaz *et al.*, *Nat. Materials* **18**, 1187 (2019) [7] A. Johansson *et al.*, *Phys. Rev. Research* **3**, 013275 (2021) [8] S. Varotto *et al.*, *Nat. Commun.* **13**, 6165 (2022)

MA 4.12 Mon 12:15 HSZ 403

Anisotropic anomalous Hall effect in altermagnetic Mn₅Si₃ — •MIINA LEIVISKÄ¹, RAFAEL LOPES SEEGER¹, HELENA REICHOVÁ^{2,3}, ISMAÏLA KOUNTA⁴, LIBOR ŠMEJKAL^{5,3}, JAVIER RIAL¹, SEBASTIAN BECKERT², ANTONÍN BADURA^{6,7}, ISABELLE JOUMARD¹, DOMINIK KRIEGNER^{2,3}, EVA SCHMORANZEROVÁ⁶, JAIRO SINOVA⁵, TOMÁŠ JUNGWIRTH³, SEBASTIAN GOENNENWEIN⁷, LISA MICHEZ⁴, and VINCENT BALTZ¹ — ¹Univ. Grenoble Alpes, CNRS, CEA, Grenoble INP, IRIG-SPINTEC, F-38000 Grenoble — ²Institute of Solid State and Materials Physics, TU Dresden, Dresden, Germany — ³Institute of Physics, Czech Academy of Sciences, Prague, Czechia — ⁴Aix-Marseille University, CNRS, CINaM, Marseille, France — ⁵Institute for Physics, Johannes Gutenberg University Mainz, Mainz, Germany — ⁶Department of Chemical Physics and Optics, Faculty of Mathematics and Physics, Charles University, Prague, Czechia — ⁷Department of Physics, University of Konstanz, Konstanz, Germany

The altermagnetic epitaxial films of Mn₅Si₃ exhibit anomalous Hall effect (AHE) despite the vanishing net magnetization [1]. This can be explained by non-relativistic time-reversal symmetry breaking, which allows for momentum-locked alternating spin-splitting of the bands [2]. Here, we investigate the anisotropy of the AHE by varying both the external field and the current channel orientations. In both cases, we observe unconventional, anisotropic behaviour that deviates from the typical behaviour of ferromagnets.

- [1] H. Reichlova *et al.* *arXiv:2012.15651*, (2020)
- [2] L. Šmejkal *et al.* *Phys Rev X* **12**, 031042 (2022)

MA 4.13 Mon 12:30 HSZ 403

Observation of nonreciprocal magnon Hanle effect — •JANINE GÜCKELHORN^{1,2}, SEBASTIÁN DE-LA-PEÑA³, MATTHIAS GRAMMER^{1,2}, MONIKA SCHEUFLE^{1,2}, MATTHIAS OPEL¹, STEPHAN GEPRÄGS¹, JUAN CARLOS CUEVAS³, RUDOLF GROSS^{1,2,4}, HANS HUEBL^{1,2,4}, AKASHDEEP KAMRA³, and MATTHIAS ALTHAMMER^{1,2} — ¹Walther-Meißner-Institut, BadW, Garching, Germany — ²Physik-Department, School of Natural Sciences, TUM, Garching, Germany — ³IFIMAC and Departamento de Física Teórica de la Materia Condensada, Universidad Autónoma de Madrid, Madrid, Spain — ⁴Munich Center for Quantum Science and Technology, München, Germany

The realization of the magnon Hanle effect, which is based on the precession of magnon pseudospin about the equilibrium pseudofield, via electrically injected and detected spin transport in an antiferromagnetic insulator demonstrates its high potential for devices and as a convenient probe for the underlying spin interactions in antiferromagnets. Here, we observe a nonreciprocity in the magnon Hanle signal measured in hematite (α -Fe₂O₃) using two spatially separated platinum electrodes as spin injector/detector [1]. Interchanging their roles was found to alter the detected magnon spin signal. The recorded difference depends on the applied magnetic field and reverses sign when the signal passes its nominal maximum at the so-called compensation field. We explain these observations in terms of a spin transport direction-dependent pseudofield. The latter leads to a nonreciprocity, which is found to be controllable via the applied magnetic field.

- [1] J. Gückelhorn *et al.*, *arXiv:2209.09040* (2022).

MA 4.14 Mon 12:45 HSZ 403

Spontaneous anomalous Hall effect arising from an unconventional compensated magnetic phase in a semiconductor — •DOMINIK KRIEGNER^{1,2}, RUBEN DARIO GONZALEZ BETANCOURT^{1,2,3,4}, JAN ZUBÁČ^{1,3}, RAFAEL JULIAN GONZALEZ HERNANDEZ⁵, KEVIN GEISHENDORF⁴, GUNTHER SPRINGHOLZ⁶, KAMIL OLEJNÍK¹, JAKUB ŽELEZNY¹, LIBOR ŠMEJKAL⁷, ANDY THOMAS^{2,4}, HELENA REICHOVÁ^{1,2}, SEBASTIAN TOBIAS BENEDIKT GOENNENWEIN⁸, and TOMAS JUNGWIRTH^{1,9} — ¹Institute of Physics, AV ČR, Prague, Czech Republic — ²IFMP, TU Dresden — ³Charles University, Prague — ⁴IFW Dresden — ⁵Universidad del Norte, Barranquilla, Colombia — ⁶JKU Linz, Austria — ⁷JGU, Mainz — ⁸University of Konstanz — ⁹University of Nottingham, United Kingdom

The anomalous Hall effect, commonly observed in metallic magnets, has been established to originate from the time-reversal symmetry breaking by an internal macroscopic magnetization in ferromagnets or by a non-collinear magnetic order. Here we observe a spontaneous anomalous Hall signal in the absence of an external magnetic field in an epitaxial film of MnTe, which is a semiconductor with a collinear antiparallel magnetic ordering of Mn moments and a vanishing net magnetization. The anomalous Hall effect arises from an unconventional phase with strong time-reversal symmetry breaking and alternating spin polarization in real-space crystal structure and momentum-space electronic structure.

- R. D. Gonzalez Betancourt *et al.*, *arXiv:2112.06805*

MA 5: Thin Films: Magnetic Coupling Phenomena / Exchange Bias

Time: Monday 9:30–11:00

Location: POT 6

MA 5.1 Mon 9:30 POT 6

Study of Amorphous CoFeB Film Interfaced with Heavy Metals using Magnetic Circular Dichroism in Hard X-Ray Photoemission — •A. GLOSKOVSKI¹, C. SCHLUETER¹, M. SINGH², S. K. VAYALIL², M. GUPTA³, V. R. REDDY³, and A. GUPTA² — ¹Photon Science, Deutsches Elektronen-Synchrotron DESY, Hamburg, Germany — ²Physics Department, University of Petroleum and Energy Studies, Dehradun, India — ³UGC-DAE Consortium for Scientific Research, Indore, India

Heterostructures consisting of HM/CoFeB/HM (HM=Heavy Metal) are important for the development of low power spintronics, thanks to the phenomena like Interfacial Dzyaloshinskii-Moriya Interaction, spin Hall effect etc. The HM interface layers can significantly affect the magnetic properties as well as thermal stability of the CoFeB layer. In the present work, magnetic circular dichroism in hard X-ray photoemission (MCD-HAXPES) has been used to elucidate the possible difference in the electronic structure of Fe and Co atoms and the effect of interfacing HM layer on the same. Multilayers: Si(substrate)/HM 20nm/Co₄₀Fe₄₃B₁₇ 10nm/HM 3nm/Al 3nm (HM=Mo, W) were deposited using magnetron sputtering. CoFeB layer is amorphous in nature. MCD-HAXPES measurements were done at beamline P22 of PETRA III, Hamburg, using 6 keV X-rays, falling at a grazing angle. The maximum asymmetry is found to be 39% for Fe and 23.6% for Co. Co spectrum has an additional weak shoulder at 4 eV from the main 2p line. This may be an indication of a correlation-induced satellite of majority spin nature in Co.

MA 5.2 Mon 9:45 POT 6

Ferromagnetic springs in exchange biased trilayers — •SAPIDA AKHUNDZADA¹, LUKAS PAETZOLD¹, ARNE VEREIJKEN¹, CHRISTIAN JANZEN¹, THOMAS SAERBECK², and ARNO EHRESMANN¹ — ¹Institute of Physics and Center for Interdisciplinary Nanostructure Science and Technology (CINSAIT), University of Kassel, Kassel, Germany — ²Institut Laue-Langevin, Grenoble, France

Exchange springs or magnetic helices, consisting of multilayered thin film systems, exhibit spiral spin configurations during magnetization reversal [1]. By combining magnetically soft/hard bilayers [2] or exchanged biased ferromagnetic/antiferromagnetic layer systems [3], comparably short domain walls can be engineered, making these systems interesting for fundamental as well as applied research [1]. Here we show how magnetic order can be induced in exchange biased trilayer systems consisting of a single ferromagnetic layer embedded between two antiferromagnetic layers. The exchange coupling between the ferromagnet and one antiferromagnet is modified by light helium ion bombardment [4] leading to a trilayer system in which the exchange bias at the two ferromagnet/antiferromagnet interfaces points in different directions. The trilayer system is characterized by angular-resolved vibrating sample magnetometry revealing the existence of the spiral domain state in the designed layer system.

[1] A.C. Basaran, et al., MRS Bull. 40, 925 (2015).

[2] F. Magnus, et al., Nat. Commun. 7, (2016).

[3] A. Scholl, et al., Phys. Rev. Lett. 92, 18 (2004).

[4] T. Mewes, et al., Appl. Phys. Lett. 76, 1057 (2000).

MA 5.3 Mon 10:00 POT 6

Mesoscale Dzyaloshinskii-Moriya interaction in corrugated ultra-thin asymmetric magnetic layers — •SHAHRUKH SHAKEEL, OLEKSII M. VOLKOV, PAVLO MAKUSHKO, EDUARDO SERGIO OLIVEROS MATA, DENISE ERB, SHENGQIANG ZHOU, JUERGEN FASSBENDER, and DENYS MAKAROV — Helmholtz-Zentrum Dresden-Rossendorf e. V., 01328 Dresden, Germany

Asymmetrically sandwiching thin magnetic layers with perpendicular anisotropy and Dzyaloshinskii-Moriya interaction (DMI) produces chiral non-trivial textures, e.g. skyrmions and chiral domain walls, which exhibit unexplored application potential in logic and memory devices [1]. Conversely, extrinsic DMI is observed by breaking local inversion symmetry appearing in curvilinear structures of conventional materials [2]. Here, employing ion beam irradiation of SiO₂ substrates we fabricate corrugated ultra-thin Cr₂O₃/Co/Pt asymmetric layer stacks with different geometric parameters. By means of magnetometric and transport measurements, we demonstrate the appearance and controllability of mesoscale DMI [3] by tuning geometric and material parameters of the system.

[1] O. M. Volkov et al., Phys. Rev. Appl. 15, 034038 (2021).

[2] O. M. Volkov et al., Phys. Rev. Lett. 123, 077201 (2019).

[3] O. Volkov et al., Sci. Rep. 8, 866 (2018).

MA 5.4 Mon 10:15 POT 6

Polycrystalline exchange-biased bilayers: Magnetically effective versus structural antiferromagnetic grain volume distribution — •MAXIMILIAN MERKEL, MEIKE REGINKA, RICO HUHNSTOCK, and ARNO EHRESMANN — Institute of Physics and Center for Interdisciplinary Nanostructure Science and Technology (CINSAIT), University of Kassel, Heinrich-Plett-Str. 40, D-34132 Kassel

The macroscopic magnetic characteristics of polycrystalline exchange-biased antiferromagnet/ferromagnet bilayers are generally determined by a complex interplay of several parameters that describe the structural and magnetic properties of the material system. [1] We demonstrate the possibility to determine averaged microscopic parameters from macroscopic magnetic quantities measured by vectorial Kerr magnetometry in comparison to an elaborate model. In particular, we estimated the magnetically effective antiferromagnetic grain size distribution, finding that it differs significantly from the structural one. [2] This indicates, that the antiferromagnetic order, being essential for the interface exchange coupling to the ferromagnetic layer, extends only over a part of the grains' structural volumes.

[1] Merkel et al., Phys. Rev. B 102, 144421 (2020)

[2] Merkel et al., Phys. Rev. B 106, 014403 (2022)

MA 5.5 Mon 10:30 POT 6

Spin current generation in ferrimagnetic heterostructures — •FELIX FUHRMANN¹, SVEN BECKER¹, AKASHDEEP AKASHDEEP¹, ZENGYAO REN^{1,2}, MATHIAS WEILER³, GERHARD JAKOB^{1,2}, and MATHIAS KLÄUI^{1,2,4} — ¹Institute of Physics, University of Mainz, Germany — ²Graduate School of Excellence "Materials Science in Mainz" (MAINZ), Germany — ³Fachbereich Physik and Landesforschungszentrum OPTIMAS, Technische Universität Kaiserslautern, Germany — ⁴Center for Quantum Spintronics, Norwegian University of Science and Technology, Trondheim, Norway

With growing demand for more energy-efficient information technology, the utilization of magnons as information carriers entails potential advantages [1]. To successfully develop magnon-based devices, there are several requirements for the applied materials to meet. The insulating ferrimagnet Yttrium Iron Garnet (Y₃Fe₅O₁₂, YIG) and related garnets are good candidates with outstanding low damping and large magnon propagation lengths [1]. Our heterostructures of YIG and Gadolinium Iron Garnet (Gd₃Fe₅O₁₂, GIG) were grown by pulsed laser deposition. We observe a ferromagnetic coupling between the Fe sublattices of the two layers, leading to complex magnetic response to external magnetic fields and a nontrivial temperature dependence [2]. We investigate the spin current generation by means of the spin Seebeck effect and spin pumping at ferromagnetic resonance. SQUID magnetometry and spin Hall magnetoresistance measurements support our observations [2]. [1] A. Chumak et al., Nat. Phys. 11, 453 (2015). [2] S. Becker et al., Phys. Rev. Appl., 16, 014047(2021).

MA 5.6 Mon 10:45 POT 6

In-situ monitoring of the electric-field induced switching process in Fe₃O₄/Nb:STO heterostructures — •YIFAN XU¹, MAI HUSSEIN HAMED^{1,2}, CONNIE BEDNARSKI-MEINKE¹, ASMAA QDEMAT¹, STEFFEN TOBER¹, EMMANUEL KENTZINGER¹, ULRICH RÜCKER¹, OLEG PETRACIC¹, and THOMAS BRÜCKEL¹ — ¹Jülich Centre for Neutron Science (JCNS-2) and Peter Grünberg Institut (PGI-4), JARA-FIT, Forschungszentrum Jülich GmbH, 52425 Jülich, Germany — ²Faculty of Science, Helwan University, 11795 Cairo, Egypt

The ability to tune magnetic oxide phases via redox reactions across their heterointerfaces could lead to useful spintronic and memristive device applications. By applying a small electric field, oxidation/reduction occurs at the heterointerface and leads to a reversible phase transition. In this talk, we present the preparation and characterization of epitaxial (001)Fe₃O₄ thin films grown on TiO₂-terminated (001)Nb:STO via pulsed laser deposition. Using magnetometry, we detect the Verwey transition; a strong indicator of the oxygen content in the Fe₃O₄ films. We observe the disappearance in the Verwey transition temperature with an applied positive electric field. This could be explained by oxygen diffusion through the interface which then leads to a reversible phase transition from Fe₃O₄ (magnetite) to γ-Fe₂O₃ (maghemite). Using ex-situ x-ray diffraction, we observe an additional Fe₃O₄(111) peak in the out-of-plane direction influenced by the applied voltage. Interestingly, by grazing-incidence small-angle X-ray scattering, we observe a change in the magnetite domain size for the sample after applying the electric field.

MA 6: Focus: Dislocations in Ceramics: Mechanics, Structures and Functionality (joint session KFM/MA)

Contrasting the common (mis)belief that ceramics are brittle, a new horizon of dislocation engineering in ceramics is being revealed, where dislocations are used to harness the mechanical and electro-functional properties. This session will bring together researchers who are interested in dislocations in ceramics, covering experiments and simulations, to stimulate new ideas for dislocation-based mechanics, characterization, and functionality in ceramics.

Chair: Dr. Xufei Fang (TU Darmstadt), Dr. Till Frömling (TU Darmstadt)

Time: Monday 14:30–17:05

Location: POT 51

See KFM 2 for details of this session.

MA 7: Computational Magnetism

Time: Monday 15:00–18:00

Location: HSZ 02

MA 7.1 Mon 15:00 HSZ 02

Quantitative theories of magnetic interactions in solids — •ATTILA SZILVA¹, YAROSLAV KVASHNIN¹, EVGENY A. STEPANOV², LARS NORDSTRÖM¹, OLLE ERIKSSON¹, ALEXANDER I. LICHTENSTEIN³, and MIKHAIL I. KATSNELSON⁴ — ¹Uppsala University — ²Institut Polytechnique de Paris — ³Universität Hamburg — ⁴Radboud University

The talk will summarize the review paper Quantitative theories of magnetic interactions in solids, by focusing on the derivation of the LKAG formula and the extension of the formalism for the case of non-collinear magnets. A first version of the paper can be read here: <https://arxiv.org/abs/2206.02415>. The paper reviews the method of explicit calculations of interatomic exchange interactions of magnetic materials. This involves exchange mechanisms normally referred to as Heisenberg exchange, Dzyaloshinskii-Moriya interaction and anisotropic symmetric exchange. The connection between microscopic theories of the electronic structure, such as density functional theory or dynamical mean field theory, and interatomic exchange, is given in detail.

MA 7.2 Mon 15:15 HSZ 02

Magnetic Anisotropy and Ground States of α -RuCl₃ — •SEUNG-JU HONG¹ and CHEOL-HWAN PARK^{1,2,3} — ¹Department of Physics and Astronomy, Seoul National University, Seoul 08826, Korea — ²Center for Correlated Electron Systems, Institute for Basic Science, Seoul 08826, South Korea — ³Center for Theoretical Physics, Seoul National University, Seoul 08826, South Korea

In this talk, I will talk about the magnetic anisotropy of the Kitaev candidate α -RuCl₃. This material gained much attention due to its proximity to Kitaev spin liquid. Thus, there are many kinds of research that computed the anisotropic exchange parameters from first principles.

However, in our work, we conducted an unprecedented number of *ab initio* calculations with constrained density functional theory and total energy fitting. We both examined the monolayer and multilayer systems and computed the intra/inter-layer exchange parameters. Then, from Monte Carlo simulations, we compute the thermodynamical quantities. From these computations, we obtained a non-trivial results.

MA 7.3 Mon 15:30 HSZ 02

Modification of Magnetic Anisotropy at Organic-Inorganic Interfaces — •ANITA HALDER, SUMANTA BHANDARY, DAVID O'REGAN, STEFANO SANVITO, and ANDREA DROGHETTI — School of Physics and CRANN, Trinity College, Dublin 2, Ireland

The adsorption of nonmagnetic organic molecules on ferromagnetic materials offers an opportunity to tune their magnetic properties for promising applications in high-density data storage and spintronic devices. In this work, we report the manipulation of the magnetocrystalline anisotropy (MCA) of Co slabs through the adsorption of small molecules, such as benzene, cot etc. We consider a simple model based on 2nd-order perturbation theory to explain the modification of MCA due to molecular adsorption in a qualitative way. Further, we have used Density Functional Theory and the magnetic force theorem to calculate magnetic anisotropy. The results indicate that molecular adsorption tends to favour perpendicular MCA at surfaces by reducing in-plane MCA of the slab. A detailed analysis of various atom-resolved quantities demonstrates that the underlying physical mechanism is the metal-molecule interfacial hybridization, and, in particular, it is related to the chemical bond between the molecular p_z and the surface d_{z²} orbitals. Generalizing the same argument, we also show that the complex molecules C₆₀ and Alq₃ deposited on fcc-Co induce a similar modification of the in-plane MCA, and we related the results to recent experimental observations.

MA 7.4 Mon 15:45 HSZ 02

Strain dependence of magnetism in transition-metal phosphorus trichalcogenides — •YANG-JUN LEE^{1,2,3}, TAE YUN KIM², and CHEOL-HWAN PARK^{1,2,3} — ¹Department of Physics and Astronomy, Seoul National University, Seoul 08826, Korea — ²Center for Correlated Electron Systems, Institute for Basic Science, Seoul 08826, Korea — ³Center for Theoretical Physics, Seoul National University, Seoul 08826, Korea

Few-layer transition-metal phosphorus trichalcogenides (TMPX₃) are two-dimensional (2D) antiferromagnetic materials, which have recently attracted attention because they can realize interesting 2D magnetic phenomena; they are considered materials whose magnetism can be described by the Heisenberg model, Ising model, or XY model depending on the transition metal ion. In this talk, we present the strain effects on the magnetism of TMPX₃ compounds obtained from first principle calculations. Also, we will talk about the change in the symmetry and the magnetic model due to the strain.

MA 7.5 Mon 16:00 HSZ 02

Microscopic Insights for Beyond Room-Temperature Ferromagnetism in Two-Dimensional Fe₅-xNi_xGeTe₂ — •SUKANYA GHOSH¹, SOHEIL ERSHADRAD², and BIPLAB SANYAL³ — ¹Department of Physics and Astronomy, Uppsala University, Uppsala, Sweden — ²Department of Physics and Astronomy, Uppsala University, Uppsala, Sweden — ³Department of Physics and Astronomy, Uppsala University, Uppsala, Sweden

The Fe_nGeTe₂ (n=3-5) (FGT) systems belong to the class of two-dimensional (2D) van der Waals (vdW) materials, promising candidates to explore magnetism in low-dimension with potential applications in spintronics. These systems are special due to their tunable structural, electronic and magnetic properties. Among the existing members of FGT family, Fe₅GeTe₂ has room temperature ferromagnetism with several intriguing properties. With the inclusion of dynamic electron correlation effect, our DFT+DMFT study shows how the spin moments, exchange interactions and Curie temperature (TC) of 2D Fe₅-xGeTe₂ can be varied significantly by substitutional doping with Ni. More importantly, the highest TC ~400 K is achieved for 20% doping concentration, beyond which the ferromagnetic order gets gradually suppressed. Our DFT+DMFT results are in good agreement with the experimental reports on bulk Fe₅-xNi_xGeTe₂ [1]. Moreover, we investigate the microscopic mechanisms responsible for the observed trend of TC in Fe₅-xNi_xGeTe₂ monolayer as an interplay between specific magnetic exchange interactions.

1. X. Chen et al, Phys. Rev. Lett. 128, 217203 (2022).

MA 7.6 Mon 16:15 HSZ 02

Efficient calculation of exchange interactions in magnetic materials — •TAE YUN KIM^{1,2,3} and CHEOL-HWAN PARK^{1,2,3} — ¹Center for Correlated Electron Systems, Institute for Basic Science, Seoul 08826, Korea — ²Department of Physics and Astronomy, Seoul National University, Seoul 08826, Korea — ³Center for Theoretical Physics, Seoul National University, Seoul 08826, Korea

Accurate description of the total energy of a magnetic system as a function of the local magnetic moments has always been a matter of importance, since it allows one to access the relevant low-energy excitation of the system, i.e. the magnon, which governs the low-temperature thermodynamics and remains important even at temperatures as high as the Curie temperature [1]. In this contribution, I will talk about an efficient way of calculating exchange interactions based on a constrained density functional theory method that captures accurately the magnetic total energy surface. As a concrete example, our *ab-initio* results on a magnetic system with substantial Dzyaloshinskii-Moriya interactions will be presented and be compared with that reported from previous studies to confirm the validity of our scheme.

[1] S. V. Halilov et al., Phys. Rev. B 58, 293 (1998)

MA 7.7 Mon 16:30 HSZ 02

Magnetic phases and stability of MPS4 — •BEATRIZ COSTA GUEDES¹, THOMAS BRUMME², ANDREA LEON³, and THOMAS HEINE² — ¹Helmholtz-Zentrum Dresden-Rossendorf, Dresden, Germany — ²Chair of Theoretical Chemistry, Technische Universität Dresden, Dresden, Germany — ³Physics Faculty, Pontificia Universidad Católica de Chile, Santiago, Chile

The discovery of magnetic van der Waals materials provided a new playground for studying different aspects of magnetic interactions in reduced dimensions. Some interesting materials in this regard are the transition metal phosphorous chalcogenides MPS3 and CrPS4 (M = Mn, Fe, Co, and Ni), which are semiconductors exhibiting novel magnetic properties such as an intriguing dependence of the magnetic ordering on the transition metal (M). CrPS4 is particularly interesting because it exhibits a magnetic transition from antiferromagnetic (AFM) to ferromagnetic (FM) ordering in the monolayer limit, analog to the CrI3 compound, which is, in contrast, not stable in air. In this research, we study the stability and the electronic properties of the whole MPS4 family using density functional theory with a special focus on magnetic properties. Our results reveal a rich magnetic phase diagram with a complex electronic and magnetic dependence on M. They can be semiconductors, metals, or half-metals with AFM, FM, and non-magnetic configurations. We explain this behavior by discussing the interplay among structure, magnetism, and Coulomb interaction. By comparing it with the MPS3 system, we find some keys to understanding the magnetic properties of the MPS4 family.

MA 7.8 Mon 16:45 HSZ 02

Effect of Coulomb interaction on the magnetic properties of orthorhombic monolayer CrSBr — •ALEXANDER RUDENKO — Radboud University, Nijmegen, The Netherlands

Two-dimensional CrSBr is a recently discovered semiconducting spin-3/2 ferromagnet with the Curie temperature around 140 K. Unlike many other known 2D magnets, CrSBr has an orthorhombic lattice, giving rise, for instance, to spatial anisotropy of the magnetic excitations within the 2D plane. Theoretical description of CrSBr within the spin Hamiltonian approach turns out to be essentially nontrivial due to the complex character of the magnetic anisotropy resulting from low crystal symmetry. Here, we employ the Green's function formalism combined with first-principles calculations to systematically study magnetic properties of monolayer CrSBr. We find that the magnetic anisotropy and thermodynamical properties of CrSBr depend strongly on the Coulomb interaction and its external screening. In the free-standing limit, the system is close to an easy-plane magnet, whose long-range ordering is partially suppressed. On the contrary, in the regime of large external screening, monolayer CrSBr behaves like an easy-axis ferromagnet with more stable magnetic ordering. Our findings suggest that 2D CrSBr is an excellent platform for studying the effects of substrate screening on magnetic ordering.

MA 7.9 Mon 17:00 HSZ 02

Cu(VO)2(AsO4)2 with ferromagnetic V-V and antiferromagnetic Cu-V interactions — •VICTORIA GINGA^{1,2}, ALEXANDER TSIRLIN¹, and OLEG SHIDRA² — ¹Universität Leipzig, Felix Bloch Institute for Solid State Physics, Linnestraße 5, 04109 Leipzig — ²St. Petersburg, Russia

Recent years have seen an increased interest in studying the magnetic properties of mineral-like compounds. The Cu(VO)2(AsO4)2 obtained by the CVT reaction method reproducing exhalative conditions has a new type of structure, which is characterized by layers formed by two $[1+4+1]V4+-tOeq-[1+4+1]V4+$ and one $[1+4+1]V4+-vOeq-[1+4+1]V4+$ linkages of V-centered octahedra. Arsenate groups decorate vanadate layers via corner-sharing with the VO6 octahedra, while single CuO6 octahedra are connecting vanadate layers into a framework via edge-sharing. Our ab initio calculations show that the magnetism of Cu(VO)2(AsO4)2 is dominated by the antiferromagnetic Cu-V coupling $J_{Cu-V} = 257$ K and the ferromagnetic V-V coupling $J_{V-V} = -277$ K. This high energy scale is not uncommon in both Cu²⁺ and V⁴⁺ oxide compounds with

the edge-shared octahedral geometry. Our results show the formation of unusual interaction geometries through the mixing of different spin-1/2 ions in the crystal structure. Experimental and computational results of the study of the Cu(VO)2(AsO4)2 with two distinct spin-1/2 magnetic ions will be presented.

MA 7.10 Mon 17:15 HSZ 02

SU(4) magnetism on a triangular moiré superlattice — •LASSE GRESISTA¹, DOMINIK KIESE², MICHAEL SCHERER³ und SIMON TREBST¹ — ¹Institute for Theoretical Physics, University of Cologne, Germany — ²Center for Computational Quantum Physics, Simons Foundation Flatiron Institute, New York, USA — ³Institute for Theoretical Physics III, Ruhr-University Bochum, Germany

The discovery of correlated insulating states in several graphene based moiré heterostructures such as trilayer graphene aligned with hexagonal boron nitride (TG/h-BN) has renewed the interest in strongly coupled electron systems where spin and orbital (or valley) degrees of freedom are intertwined. Considering the strong coupling limit, the localized degrees of freedom in such systems may be described by generators of SU(4) instead of the conventional SU(2) spin operators. Here, we study such an SU(4) 'spin-valley' model on a triangular lattice at a filling of two electrons (or holes) per moiré unit cell, with interactions that strongly break the SU(4) symmetry down to $SU(2)_{\text{spin}} \otimes U(1)_{\text{valley}}$. This is, e.g., relevant for the flat band physics of TG/h-BN within the topologically trivial regime. Using a pseudo-fermion functional renormalization group approach and semi-classical Monte Carlo calculations, we are able to distinguish parameter regimes showing no magnetic order, suggesting a spin-valley liquid or other quantum disordered ground state, and a multitude of classically ordered phases including ferromagnetic, antiferromagnetic, incommensurate and stripe order that manifests in different sectors of the coupled spin-valley space.

MA 7.11 Mon 17:30 HSZ 02

YSrFeCrO₆ as a Robust Ferromagnetic Semiconductor with Large Photovoltaic Efficiency — •AVIJEET RAY, PARESH C. ROUT, and UDO SCHWINGENSCHLÖGL — Physical Sciences and Engineering Division (PSE), King Abdullah University of Science and Technology (KAUST), Thuwal 23955-6900, Saudi Arabia

Semiconducting ferromagnetic transition metal oxides play a key role in spintronics applications. Employing first-principles calculations, we predict the existence of the double perovskite Y₂FeCrO₆ and study its properties. While both rock-salt (RS) and layered (L) structures are found to be dynamically stable, the L structure turns out to be energetically favorable. We determine the magnetic phase diagram under hydrostatic pressure. We find that the RS structure is dynamically stable and energetically favorable over the L structure in the case of YSrFeCrO₆ (hole doping by substitution of Y by Sr). YSrFeCrO₆ realizes a ferromagnetic ordering with a magnetic moment of 7 μ_B per formula unit, which is promising for spintronics applications. In addition, the ferromagnetic ordering is not compromised by hydrostatic pressure from -10 to 16 GPa. While the L structure of Y₂FeCrO₆ is an indirect bandgap semiconductor, the RS structure of YSrFeCrO₆ shows a direct bandgap of 0.90 eV (spin-orbit coupling taken into account in the calculation). We obtain a large spectroscopic limited maximum efficiency of 26% for YSrFeCrO₆, which is suitable for photovoltaic applications.

MA 7.12 Mon 17:45 HSZ 02

Magnetic Anisotropy of α-RuCl₃ — •SEUNG-JU HONG¹, TAE YUN KIM², and CHEOL-HWAN PARK^{1,2,3} — ¹Department of Physics and Astronomy, Seoul National University, Seoul 08826, Korea — ²Center for Correlated Electron Systems, Institute for Basic Science, Seoul 08826, South Korea — ³Center for Theoretical Physics, Seoul National University, Seoul 08826, South Korea

α-RuCl₃ has gained much attention due to its proximity to Kitaev spin liquid. In this talk, we will discuss the magnetic anisotropy of α-RuCl₃. We performed first-principles calculations on the magnetic anisotropy of α-RuCl₃. We will compare the results of our first-principles calculations with available previous experimental and theoretical studies.

MA 8: Ultrafast Magnetization Effects I

Time: Monday 15:00–18:00

Location: HSZ 04

Invited Talk

MA 8.1 Mon 15:00 HSZ 04

Optical control of antiferromagnetism — •CHRISTIAN TZSCHASCHEL — Department of Chemistry and Chemical Biology, Harvard University, USA

Antiferromagnets are a promising class of materials for novel spintronic applications. The absence of a net magnetization not only leads to a robustness of the magnetic state against magnetic fields but may also enable faster and potentially more energy efficient switching dynamics compared to their ferromagnetic counterparts. However, probing and controlling an antiferromagnetic state, in particular on ultrafast timescales, is a major challenge of antiferromagnetic spintronics.

Here, we will exploit magneto-optical and inverse magneto-optical effects to control antiferromagnetism. For example, the inverse Faraday effect, whereby circularly polarized light acts as a magnetic field in a material, allows us to selectively excite specific magnon modes in fully compensated antiferromagnets. The excitation mechanism can be based on a rotation of the antiferromagnetic vector or the generation of a net magnetization in the material. We will show that excitation mechanisms that induce a net magnetization exhibit a significantly higher efficiency. Moreover, we uncover a new inverse magneto-optical effect that allows us to deterministically induce an antiferromagnetic state in a magneto-electric antiferromagnet.

Our results demonstrate a high degree of optical control of antiferromagnetism, where we use light as both a probe and a handle to act on an antiferromagnetic state. We thus move closer to achieving a fundamental requirement for future ultrafast opto-spintronic devices.

MA 8.2 Mon 15:30 HSZ 04

Accelerating write/erase cycles in all-optical magnetization switching — •FELIX STEINBACH¹, NELE STETZUHN¹, DANIEL SCHICK¹, DIETER ENGEL¹, UNAI ATXITIA², CLEMENS VON KORFF SCHMISING¹, and STEFAN EISEBITT^{1,3} — ¹Max Born Institute for Nonlinear Optics and Short Pulse Spectroscopy — ²Dahlem Center for Complex Quantum Systems and Fachbereich Physik — ³Institut für Optik und Atomare Physik, Technische Universität Berlin

All-optical switching of magnetic order presents a promising route toward faster and more energy efficient data storage. However, a realization in future devices is ultimately dependent on the maximum repetition rates of optically induced write/erase cycles. Here, we present two strategies to minimize the temporal separation of two consecutive femtosecond laser pulses to toggle the out-of-plane direction of the magnetization of ferrimagnetic rare-earth transition metal alloys. First, by systematically changing the heat transfer rates using either amorphous glass, crystalline silicon, or polycrystalline diamond substrates, we show that efficient cooling rates of the magnetic system present a prerequisite to accelerate the sequence of double pulse toggle switching. Second, we demonstrate that replacing the transition metal iron by cobalt leads to a significantly faster recovery of the magnetization after optical excitation allowing us to approach terahertz frequency of write/erase cycles with a minimum pulse-to-pulse separation of 7 ps [1].

[1] F. Steinbach et al., Appl. Phys. Lett. 120, 112406 (2022)

MA 8.3 Mon 15:45 HSZ 04

Variation of magnetic model parameters during ultrafast demagnetisation — •S. POLESYA, S. MANKOVSKY, and H. EBERT — Department Chemie, Ludwig Maximilian University, Munich, Germany

Recent developments in time-dependent density functional theory (TD-DFT) paved the way towards investigating the ultrafast demagnetisation caused by a strong laser pulse on an *ab initio* level. However, the relaxation processes after a pump pulse still require to use phenomenological models that allow to account for different types of relaxation mechanisms on the basis of model parameters, that can be calculated from first principles. A stumbling block for such schemes is that the electronic structure is strongly out of equilibrium after the laser pulse and changes with time due to the relaxation. In the present work, we explore whether the parameters which determine the magnetization dynamics in this time regime can indeed be described on a first-principles level. This concerns first of all the exchange coupling, magnetic anisotropy and the Gilbert damping parameters that have been calculated for several transition metals using the spin-polarized relativistic Korringa-Kohn-Rostoker method. To account for the time evolution of the system, the calculations have been performed employing the TD-DFT potentials and occupation numbers generated by the Elk code [http://elk.sourceforge.net] for different time steps during the laser pulse and shortly after it, i.e. in the non-relaxed situation. In all cases a strong modification of the parameters compared to the equilibrium situation is found.

MA 8.4 Mon 16:00 HSZ 04

Temperature- and density-dependent spin-resolved coupling parameters in the μT -model — •CHRISTOPHER SEIBEL, SEBASTIAN T. WEBER, TOBIAS HELD, SANJAY ASHOK, HANS CHRISTIAN SCHNEIDER, and BAERBEL RETHFELD — Department of Physics and Research Center OPTIMAS, RPTU Kaiserslautern-Landau

Since the first ultrafast demagnetization experiment by Beaurepaire *et al.* in 1996, many models have been developed. They reach from complex kinetic descriptions to simpler temperature-based models. The former consider the microscopic interactions between the individual (quasi-)particles involved and allow to extract coupling parameters of the individual interactions. These parameters can enter temperature-based models and depend on the nonequilibrium distribution, (quasi-)temperature, densities and the spin-dependent density of states [1,2,3]. However, these coupling parameters are often assumed to be constant in temperature-based models.

In this work, we investigate the influence of transient coupling parameters, like the electron-phonon coupling parameter, on the magnetization dynamics. The spin-resolved coupling parameter is calculated using complete Boltzmann collision integrals and depends on the transient temperatures and densities of the individual subsystems.

[1] Lin *et al.*, Phys. Rev. B 77, 075139

[2] Mueller and Rethfeld, Phys. Rev. B 87, 035139

[3] Zahn *et al.*, Phys. Rev. Research 3, 023032

MA 8.5 Mon 16:15 HSZ 04

Investigating the interplay of local electron correlations and ultrafast spin dynamics in fcc Ni at the European XFEL — •TOBIAS LOJEWSKI — University of Duisburg-Essen

The interplay between exchange interaction, electron hopping and local Coulomb repulsion is of great interest as it influences the magnetic order in the 3d transition metals. We report the investigation of the electronic structure in fcc Nickel on the time scale of these interactions by combining the femtosecond time-resolved spectroscopic analysis of Nickel X-ray absorption spectra, measured at the SCS instrument of the European XFEL, with *ab initio* TD-DFT. We find a transient broadening and redshift of the $L_{2,3}$ -edge absorption spectra, which we relate to electron repopulation and correlation-induced electronic structure modifications, demonstrating a time-dependent interaction between band formation, exchange interaction and Coulomb repulsion.

[1] T. Lojewski, M. F. Elhanoty, L. Le Guyader, O. Grånäs, N. Agarwal, C. Boeglin, R. Carley, A. Castoldi, C. David, C. Deiter, F. Döring, R. Y. Engel, F. Erdinger, H. Fangohr, C. Fiorini, P. Fischer, N. Gerasimova, R. Gort, F. de Groot, K. Hansen, S. Hauf, D. Hickin, M. Izquierdo, B. E. Van Kuiken, Y. Kvashnin, C. H. Lambert, D. Lomidze, S. Maffessanti, L. Mercadier, G. Mercurio, P. S. Miedema, K. Ollefs, M. Pace, M. Porro, J. Rezvani, B. Rösner, N. Rothenbach, A. Samartsev, A. Scherz, J. Schlappa, C. Stamm, M. Teichmann, P. Thunstrom, M. Turcato, A. Yaroslavtsev, J. Zhu, M. Beye, H. Wende, U. Bovensiepen, O. Eriksson and A. Eschenlohr, arXiv:2210.13162.

MA 8.6 Mon 16:30 HSZ 04

Laser-induced spin polarization on ultrafast time scales — •OLIVER BUSCH, FRANZISKA ZIOLKOWSKI, INGRID MERTIG, and JÜRGEN HENK — Institut für Physik, Martin-Luther-Universität, D-06099 Halle

In ultrafast spin dynamics one focuses often on demagnetization. However, the incident laser pulse should produce spin-polarized excited electrons – an effect ubiquitous in spin- and angle-resolved photoemission [1]. This laser-induced spin polarization certainly affects the ultrafast dynamics.

We study systematically the laser-induced spin polarization and its effect on the electron dynamics in Co/Cu heterostructures, modeled within our theoretical framework *EVOLVE* [2]. The spin polarization depends strongly on polarization and angle of incidence of the femtosecond laser pulse, similar to photoemission [3]. Moreover, we find a significant spatial dependence, which underlines the importance of inhomogeneities in ultrafast spin dynamics.

[1] W. Schatke and M. A. Van Hove (eds.), *Solid-State Photoemission and Related Methods: Theory and Experiment* (Wiley-VCH, Weinheim, 2003)

[2] F. Töpler *et al.*, New J. Phys. 23 033042 (2021)

[3] J. Henk *et al.*, J. Phys.: Condens. Matter 8 47 (1996)

MA 8.7 Mon 16:45 HSZ 04

Finite-size effects in [Fe/MgO] $_n$ heterostructures on ultrafast timescales

— •MOUMITA KUNDU¹, NICO ROTHENBACH², TOBIAS LOJEWSKI², ANDREA ESCHENLOHR², MARKUS GRUNER², KATHARINA OLLEFS², CAROLIN SCHMITZ-ANTONIAK³, KLAUS SOKOLOWSKI-TINTEN², WILLIAM WINDSOR⁴, LAURENZ RETTIG⁴, ROSSITZA PENTCHEVA², HEIKO WENDE², ULRICH NOWAK¹, and UWE BOVENSIEPEN² — ¹University of Konstanz, Konstanz, Germany — ²University of Duisburg-Essen, Duisburg, Germany — ³TH Wildau, Wildau, Germany — ⁴FHI Berlin, Berlin, Germany

The analysis of magnetization dynamics on ultrafast timescales provides insight into microscopic interactions of magnetic moments with the charge and lattice degrees of freedom in solids. Here we analyze the finite size effect of ferromagnets on ultrafast timescales for [Fe/MgO] $_n$ heterostructures. Using femtosecond time-resolved XMCD, measured at the Femtoslicing facility, BESSY II, we observe an increasing laser-induced demagnetization at time delays > 0.5 ps as the Fe layers get thinner, and it can be clearly distinguished from the primary ultrafast demagnetization occurring at < 0.5 ps. Atomistic spin simulations are used to investigate the thickness dependence of the ultrafast magnetization dynamics in iron thin films, modeled using an extended Heisenberg-type Hamiltonian in the stochastic Landau-Lifshitz-Gilbert equation, coupled with the 2-temperature model. Comparing with our measurements, we conclude that finite size effects are the dominating factor for the different demagnetization rates due to a reduced spin-spin coordination at the interfaces.

MA 8.8 Mon 17:00 HSZ 04

A real-space tight-binding approach to ultrafast spin dynamics in inhomogeneous systems — •FRANZISKA ZIOLKOWSKI, OLIVER BUSCH, INGRID MERTIG, and JÜRGEN HENK — Martin Luther University Halle-Wittenberg, Halle, Germany

In laser-induced ultrafast spin dynamics a spin current is generated at a magnetic-nonmagnetic interface, whose origin and properties are still under debate. To better understand the microscopic processes and the role of the interface we are developing the theoretical framework *evolve* [1].

In a real-space tight-binding model the electron system is optically excited by a femtosecond laser pulse and coupled to a bosonic bath. The time evolution of the density operator yields occupation numbers, demagnetization profiles as well as spin- and orbital-resolved occupation flows.

Our simulations confirm the importance of interfaces for ultrafast transport phenomena and demagnetization processes. We identify a reflow from Cu d orbitals across the interface into Co d orbitals as an important contribution to

demagnetization. This refilling manifests itself as a minority-spin current proceeding several layers into the Cu region.

Moreover, we investigate the influence of pulse parameters such as polarization and photon energy.

[1] Töpler *et al* 2021 *New J. Phys.* **23** 033042

MA 8.9 Mon 17:15 HSZ 04

Measuring the spin-flip scattering rates in the demagnetization transient state of ferromagnets — •RÉGIS DECKER¹, ARTUR BORN^{1,2}, KARI RUOTSALAINEN¹, KARL BAUER¹, ROBBY BÜCHNER^{1,2}, ROBERT HAVERKAMP^{1,2}, ANNETTE PIETZSCH¹, and ALEXANDER FÖHLISCH^{1,2} — ¹Institute Methods and Instrumentation for Synchrotron Radiation Research PS-ISRR, Helmholtz-Zentrum Berlin für Materialien und Energie Albert-Einstein-Strasse 15, 12489, Berlin, Germany. — ²Institut für Physik und Astronomie, Universität Potsdam, Karl-Liebknecht-Strasse 24-25, 14476, Potsdam, Germany

In crystalline ferromagnets, one of the main microscopic mechanisms of spin relaxation is the electron-phonon driven (Elliott-Yafet) spin-flip scattering. To deduce the spin-flip scattering rate, we exploit the stringent atomic symmetry selection rules of X-ray Emission Spectroscopy (XES) and observe the quantifiable change in the decay peak intensities in static XES spectra when changing the temperature, *i.e.* the phonon population. We deduce the temperature-dependent spin-flip scattering rate for Ni [1]. In FeNi alloys, we evidence a thresholding the Elliott-Yafet mechanism linked to the intra- and intersublattice exchange energies [2]. In Gd, we show an Elliott-Yafet mechanism for the itinerant 5d electrons and its absence for the localized 4f electrons [3].

[1] R. Decker *et al.*, *Sci. Rep.* **9**, 8977 (2019). [2] A. Born *et al.*, *Sci. Rep.* **11**, 1883 (2021). [3] R. Decker *et al.*, *Appl. Phys. Lett.* **119**, 152403 (2021).

MA 8.10 Mon 17:30 HSZ 04

Electron-magnon interactions and Elliot-Yafet Spin Flips in a Two Band Stoner Model — •FELIX DUSABIRANE, KAI LECKRON, BÄRBEL RETHFELD, and HANS CHRISTIAN SCHNEIDER — Physics Department & Research Center OPTIMAS, RPTU Kaiserslautern, Germany

We study electronic scattering dynamics in ferromagnets due to electron-magnon and electron-electron scattering. We also include an electron-electron

spin-flip process, *i.e.*, an electronic Elliott-Yafet mechanism and study the dynamics due to the interplay of the different scattering processes on the magnetization on ultrafast timescales. For the ferromagnetic band structure, we employ a model system consisting of two Stoner-exchange split bands and electron-magnon interaction, as can be obtained using a Heisenberg model where magnons (and electrons) are treated as bosons (and fermions). Electron-electron and electron-magnon scattering dynamics are studied with Boltzmann scattering integrals. We show that the spin-flip electron-electron scattering together with electron-magnon scattering generates non-equilibrium magnons, leading to a pronounced magnetization change that is mostly due to magnon generation and only to a very limited extent to a change in the spin polarization of the electrons. The effect of electron spin-flips and time dependent spin splitting will also be discussed.

MA 8.11 Mon 17:45 HSZ 04

Nonequilibrium Magnons from Hot Electrons in Antiferromagnetic Systems — MARION BARBEAU¹, MIKHAIL TITOV², MIKHAIL KATSNELSON², and •ALIREZA QAIUMZADEH¹ — ¹Center for Quantum Spintronics, Department of Physics, Norwegian University of Science and Technology, NO-7491 Trondheim, Norway — ²Radboud University, Institute for Molecules and Materials, 6525 AJ Nijmegen, The Netherlands

We describe a *nonthermal* magnon activation mechanism in antiferromagnetic (AFM) systems via locally equilibrated *spin-unpolarized* hot electrons excited by an ultrafast intense laser pulse. We employ a quantum kinetic equation that takes into account a direct electron-magnon scattering channel in either bulk AFM metal or at the interface of the AFM/normal-metal heterostructure. The mechanism is responsible for the nonequilibrium population of AFM magnon modes on a subnanosecond timescale, which are formed shortly after the local thermalization of hot electrons by Coulomb interactions. Nonequilibrium magnon populations can be additionally manipulated by applying an external magnetic field. Our work paves the way toward spin dynamics control in AFM systems via the ultrafast manipulation of out-of-equilibrium magnon excitations [1].

[1] M. M. S. Barbeau, M. Titov, M. I. Katsnelson, A. Qaiumzadeh, arXiv:2209.03469v1

MA 9: Cooperative Phenomena: Spin Structures and Magnetic Phase Transitions

Time: Monday 15:00–17:45

Location: HSZ 401

MA 9.1 Mon 15:00 HSZ 401

Spin functional renormalization group for dimerized quantum spin systems — ANDREAS RÜCKRIEGEL, •JONAS ARNOLD, RAPHAEL GOLL, and PETER KOPITZ — Institut für Theoretische Physik, Universität Frankfurt, Max-von-Laue Straße 1, 60438 Frankfurt, Germany

We investigate dimerized quantum spin systems using the spin functional renormalization group approach proposed by Krieg and Kopietz [*Phys. Rev. B* **99**, 060403(R) (2019)] which directly focuses on the physical spin correlation functions and avoids the representation of the spins in terms of fermionic or bosonic auxiliary operators. Starting from decoupled dimers as initial condition for the renormalization group flow equations, we obtain the spectrum of the triplet excitations as well as the magnetization in the quantum paramagnetic, ferromagnetic, and thermally disordered phases at all temperatures. Moreover, we compute the full phase diagram of a weakly coupled dimerized spin system in three dimensions, including the correct mean field critical exponents at the two quantum critical points.

MA 9.2 Mon 15:15 HSZ 401

Magnetic correlations in the presence of disorder in the Hubbard model — •FABIO PABLO MIGUEL MÉNDEZ-CÓRDOBA^{1,2,3}, JOSEPH TINDALL⁴, DIETER JAKSCH^{2,5}, and FRANK SCHLAWIN^{2,3,6} — ¹Departamento de Física, Universidad de Los Andes, A.A. 4976, Bogotá, Colombia — ²Universität Hamburg, Luruper Chaussee 149, Gebäude 69, D-22761 Hamburg, Germany — ³The Hamburg Centre for Ultrafast Imaging, Luruper Chaussee 149, Hamburg D-22761, Germany — ⁴Center for Computational Quantum Physics, Flatiron Institute, 162 5th Avenue, New York, NY 10010 — ⁵Clarendon Laboratory, University of Oxford, Parks Road, Oxford OX1 3PU, UK — ⁶Max Planck Institute for the Structure and Dynamics of Matter, Luruper Chaussee 149, 22761 Hamburg, Germany

By selectively modifying hopping integrals in the triangular Hubbard model at half filling [1], we show that it is possible to change the ground state's spin angular momentum magnetization. We further demonstrate that this change does not appear in the corresponding effective Heisenberg model. The latter does not predict any magnetic coherence between distant sites [2]. Instead, higher-order interactions are required to anticipate the symmetry breaking that leads to the lifting of the degeneracy present in the Heisenberg model. Our results can be understood as an extension of Lieb's theorem to non-bipartite lattices [3].

[1] J. Tindall, *et al.*, *Phys. Rev. Lett.* **125**, 137001 (2020). [2] J. Strecka, *et al.*, *Phys. Rev. B* **105**, 064420 (2022). [3] E. H. Lieb, *Phys. Rev. Lett.* **62**, 1201 (1989).

MA 9.3 Mon 15:30 HSZ 401

Subsequent Mott transitions and magnetic ground state in NiS₂ — •JONAS A. KRIEGER¹, FABIO ORLANDI², MIKEL I. IÑURRIETA³, IÑIGO ROBREDO³, ZACHER SALMAN⁴, NIELS B. M. SCHRÖTER¹, MAIA GARCIA-VERGNORY³, STUART S. P. PARKIN¹, and LESLIE SCHOOP⁵ — ¹Max Planck Institute of Microstructure Physics, Halle, Germany — ²Rutherford Appleton Laboratory, Didcot, UK — ³Donostia International Physics Center, San Sebastián, Spain — ⁴Paul Scherrer Institute, Villigen, Switzerland — ⁵Princeton University, Princeton, USA

We present muon spin spectroscopy (μ SR) measurements on the antiferromagnetic Mott insulator NiS₂. This compound features two subsequent magnetic phase transitions around 38.9K and 29K associated with the opening of a Mott gap. From the zero field and rotation dependence of transverse field μ SR spectra we confirm the magnetic space group 205.33 in the 38.9K to 29K phase, determined from neutron diffraction [1]. We refine the muon stopping sites by using ab-initio density functional theory (DFT) and show that the resulting 8c and 24d muon sites can fully explain the observed μ SR precession frequencies. A disproportionate temperature evolution of the two frequencies associated with these sites points to the presence of a strong temperature dependence in the muon hyperfine coupling strength due to concomitant changes in the electronic structure. We then use the number of μ SR frequencies in combination with complementary neutron diffraction results to identify the magnetic ground state.

[1] S. Yano, *et al.*, *Phys. Rev. B* **93**, 024409 (2016)

MA 9.4 Mon 15:45 HSZ 401

Magnetocrystalline anisotropies and quantum phase transitions in the cubic chiral magnets Mn_{1-x}Fe_xSi and Mn_{1-x}Co_xSi — •VIVEK KUMAR, ANDREAS BAUER, MARC ANDREAS WILDE, and CHRISTIAN PFLEIDERER — Physik Department, Technische Universität München, D-85748 Garching, Germany

In the archetypical cubic chiral magnet MnSi, an extended regime of topological non-Fermi liquid behavior emerges without quantum criticality as magnetic order is suppressed by means of hydrostatic pressure [1]. Substitutional doping with iron or cobalt also results in the suppression of magnetic order, where quantum critical behavior is masked by the influence of disorder [2]. Recent small-angle neutron scattering studies suggested that in this context magnetocrystalline anisotropies may subtly but decisively influence the magnetic textures, however, no quantitative information was available [3]. Here, we report a study of a series of single crystals of Mn_{1-x}Fe_xSi and Mn_{1-x}Co_xSi by means of

cantilever torque magnetometry. An analytic description that takes into account the tetrahedral point group of the cubic chiral magnets allows us to quantitatively infer anisotropy constants up to sixth-order in spin-orbit coupling and discuss their evolution as a function of temperature, magnetic field, and dopant concentration x .

[1] Pfeleiderer *et al.*, *Science* **316**, 1871 (2007).

[2] Bauer *et al.*, *Phys. Rev. B* **82**, 064409 (2010).

[3] Kindervater *et al.*, *Phys. Rev. B* **101**, 104406 (2020).

15 min. break

MA 9.5 Mon 16:15 HSZ 401

Investigating the CMR Effect in EuCd_2P_2 by Means of Nonlinear Transport and Fluctuation Spectroscopy — •MARVIN KOPP¹, CHARU GARG¹, SARAH KREBBER¹, KRISTIN KLIEMT¹, CORNELIUS KRELLNER¹, SUDHAMAN BALGURI², FAZEL TAFTI², and JENS MÜLLER¹ — ¹Institute of Physics, Goethe-University Frankfurt, Frankfurt (Main), Germany — ²Departments of Physics, Boston College, USA

The colossal magnetoresistance (CMR) effect has inspired extensive studies for decades and is still the subject of intense research due to its central place in the physics of correlated electron systems as well as its potential relevance for applications. Unlike the prototypical CMR compounds based on mixed valence and double exchange in manganites or a structural Jahn-Teller distortion and ferromagnetic ordering, we focus on EuCd_2P_2 , that exhibits a strikingly large ($10^4\%$) negative MR significantly above its antiferromagnetic ordering temperature $T_N = 11$ K. Initial reports suggest that strong magnetic fluctuations within the layered structure could be responsible for the drastic change of resistance in the magnetic field [1]. In this work, we aim to investigate these fluctuations using higher harmonic resistance and resistance fluctuation (noise) spectroscopy. Higher harmonic measurements are sensitive to the small changes in magneto-electric coupling caused by the postulated forming of magnetic clusters (polarons), often hidden in standard resistance measurements. The dynamics of these magnetic clusters is studied using resistance noise spectroscopy as a function of temperature and magnetic field. [1] *Adv. Mat.*, 2021, 33, 2005755.

MA 9.6 Mon 16:30 HSZ 401

Investigating the electronic charge and magnetic spin dynamics in the ferromagnetic semiconductor HgCr_2Se_4 using resistance fluctuation (noise) spectroscopy — •CHARU GARG¹, ZHILIN LI², YOUGUO SHI², and JENS MÜLLER¹ — ¹Institute of Physics, Goethe University, 60438 Frankfurt (M), Germany — ²Beijing National Laboratory for Condensed Matter Physics, Institute of Physics, Chinese Academy of Sciences, Beijing 100190

The n-type HgCr_2Se_4 has been reported to exhibit a pronounced semiconductor-to-metal transition below and a CMR effect at the ferromagnetic transition at $T_C = 107$ K. Our recent study of charge carrier dynamics [*Phys. Rev. B* **105**, 064404 (2022)] suggests isolated magnetic polarons forming at $T > 2T_C$ which coalesce at T_C . In this talk, we discuss new results highlighting the strong correlation between the magnetic and electronic degrees of freedom that can lead to complex exchange pathways. Likely due to competing AF and FM interactions, we observe a distinctly slow decrease in resistance below the CMR transition. The striking dynamics of a distinct two-level fluctuations superimposed on $1/f$ -type noise corroborates a slowing down of charge carrier and/or magnetic dynamics. Further, below 20 K, a strong upturn in resistance and simultaneously in resistance noise down to 500 mK is observed and is speculated to be linked to the emergence of spiral type magnetic order. Our results demonstrate that the presence of pronounced electron-spin correlations plays a key role in the unconventional temperature dependence of resistance and CMR effect in this spinel.

MA 9.7 Mon 16:45 HSZ 401

Field-induced magnetic excitations in phases II and II' of $\text{Ce}_3\text{Pd}_{20}\text{Ge}_6$ — •FEDERICO MAZZA¹, JAKOB LASS², DANIEL MAZZONE², STEWART ROSS³, EUN SANG CHOI⁴, MARTIN NIKOLO⁵, XINLIN YAN¹, ANDREY PROKOFIEV¹, SILKE PASCHEN¹, and DMYTRO S. INOSOV⁶ — ¹TU Wien, Austria — ²PSI, Villigen, Switzerland — ³ISIS, Didcot, UK — ⁴Florida State University, Tallahassee, USA — ⁵St. Louis University, USA — ⁶TU Dresden, Germany

$\text{Ce}_3\text{Pd}_{20}\text{Ge}_6$ is known for its unique quantum phase transitions between anti-ferromagnetic ordering phase III and ferroquadrupolar phases II and II'. Using torque magnetometry at subkelvin temperatures, we were able to map the phase diagram in field and momentum space, here we find the crossover between phases III-II' at 1.5 T and II'-II at 8 T. In addition, with inelastic neutron scattering we investigate dispersive collective excitations with a strong magnetic field dependence for $\mathbf{B} \parallel (110)$, revealing a magnon soft mode (Goldstone mode) at (001) for phase III and (111) for phases II and II'. At 4 meV we discover the presence of two (CEF) excitations exhibiting a weak dispersion best seen in the (HH1) direction. They are degenerate in the absence of magnetic field but split progressively as the field is increased.

MA 9.8 Mon 17:00 HSZ 401

Magnetoelastic coupling in the skyrmion lattice magnet GdRu_2Si_2 — •LUKAS GRIES¹, DANIEL MAYOH², GEORGE WOOD², GEETHA BALAKRISHNAN², and RÜDIGER KLINGELER¹ — ¹Kirchhoff Institute for Physics, Heidelberg University, Germany — ²Department of Physics, University of Warwick, United Kingdom

We present high-resolution thermal expansion and magnetostriction studies on the centrosymmetric skyrmion-hosting tetragonal magnet GdRu_2Si_2 in high magnetic fields up to 15 T. Our data show magnetoelastic coupling associated with the onset of long-range antiferromagnet order in form of pronounced anomalies in thermal expansion and magnetostriction. We extract the uniaxial pressure dependencies of the different phase boundaries and discuss them in terms of spin-lattice coupling. Our data suggest additional phases in magnetic field and allow us to complement the previously published magnetic phase diagram.

MA 9.9 Mon 17:15 HSZ 401

Charge dynamics of heavy fermions near their quantum critical point — •RENJITH MATHEW ROY¹, RUN YANG¹, SOOHEYON SHIN², SEULKI ROH¹, and MARTIN DRESSEL¹ — ¹Physikalisches Institut, Universität stuttgart, Germany — ²Laboratory for Multiscale Materials Experiments, Paul Scherrer Institut, Switzerland

Using infrared spectroscopy, we investigate the evolution of hybridization strength between the localized magnetic moments and itinerant electrons in heavy fermionic compound $\text{CeRh}(\text{In}_{1-x}\text{Sn}_x)_5$, with three different Sn concentrations, Sn 4.4%, Sn 6.9%, and 9.8% respectively. CeRhIn_5 has an antiferromagnetic ground state, which is suppressed with Sn doping revealing a quantum-critical region. From our optical conductivity result, we report an enhancement of hybridization strength with increasing Sn concentration, and the observation of a non-Fermi liquid behaviour near the quantum critical point. The phase characterization was performed by magnetic susceptibility and resistivity measurements, which also support the non-Fermi liquid behavior observed near the quantum critical point.

MA 9.10 Mon 17:30 HSZ 401

Local structure of disordered $\text{Fe}_{60}\text{V}_{40}$ and the impact on its magnetism — •SIMON RAULS¹, BENEDIKT EGGERT¹, SHADAB ANWAR², DAMIAN GÜNZING¹, PHILIPP KLASSEN¹, TOM HELBIG¹, RANTEE BALI², and HEIKO WENDE¹ — ¹Faculty of Physics and CENIDE, University of Duisburg-Essen — ²Helmholtz-Zentrum Dresden-Rossendorf

Control of the structural order and nearest-neighbour interactions can provide a path to modify application relevant magnetic properties, such as the Gilbert damping. The binary alloy $\text{Fe}_{60}\text{V}_{40}$ shows an amorphous to polycrystalline phase transition, which can be triggered by annealing or ion irradiation. This phase transition also is a transition from a paramagnetic phase towards a ferromagnetic phase with very low Gilbert damping of ~ 0.002 [1], which makes the material a promising candidate for the fabrication of embedded magnetic nanostructures in a single irradiation step. We want to highlight the results of our structural and magnetic investigations on $\text{Fe}_{60}\text{V}_{40}$ thin films, using EXAFS, magnetometry and Mössbauer spectroscopy, in order to understand the interconnection between the evolving ferromagnetism and nearest-neighbour interactions along the ion-irradiation induced phase transition.

We acknowledge financial support from the DFG through project no. 322462997 and DESY for beamtime allocation at beamline P65.

[1] S. Anwar *et al.* *ACS Appl. Electron. Mater.* **2022**, *4*, 8 3860-3869

MA 10: Topological Insulators (joint session MA/TT)

Time: Monday 15:00–17:15

Location: HSZ 403

MA 10.1 Mon 15:00 HSZ 403

Benchmark study of symmetry-adapted ML-DFT models for magnetically doped topological insulators — •JOHANNES WASMER¹, RUBEL MOZUMDER¹, PHILIPP RÜSSMANN^{1,2}, IRA ASSENT^{1,3}, and STEFAN BLÜGEL¹ — ¹Forschungszentrum Jülich, Germany — ²University of Würzburg, Germany — ³Aarhus University, Denmark

We present a benchmark study of surrogate models for impurities embedded into crystalline solids. Using the Korrington-Kohn-Rostoker Green Function method [1], we have built databases of several thousand calculations of single impurities (monomers) embedded into different elemental crystals, as well as magnetic transition metal impurity dimers embedded in the topological insulator Bi_2Te_3 . We predict the converged monomer impurity electron potential and the isotropic

exchange interaction of the impurity dimer in the classical Heisenberg model. From these surrogates, we intend to build transferable models for larger systems in the future, which will accelerate the convergence of our DFT codes. The study compares various recent E(3)-equivariant models such as ACE and MACE [2] in terms of performance and reproducible end-to-end workflows.

[1] P. Rüßmann et al., *npj Comput Mater* 7, 13 (2021)

[2] I. Batatia et al., arXiv:2206.07697 (2022)

MA 10.2 Mon 15:15 HSZ 403

High throughput magnetic topological materials search II — •IÑIGO ROBBEDO^{1,2}, YUANFENG XU^{3,4}, ANDREI BERNEVIG^{2,3}, CLAUDIA FELSER¹, NICOLAS REGNAULT^{3,6}, LUIS ELCORO⁵, and MAIA G. VERGNIORY^{1,2} — ¹MPI CPFS Dresden — ²DIPC — ³Princeton University — ⁴Zhejiang University — ⁵Basque Country University — ⁶Sorbonne Université

The development of topological quantum chemistry has proven to be a game changing tool for predicting topological phases in realistic materials, both non-magnetic and magnetic. Building on the work of previous studies, in this work we expand the family of magnetic insulators and semimetals with non-trivial topological properties. We analyzed 408 magnetic structures from the Bilbao Crystallographic Server magnetic database, whose crystal and magnetic structures have been experimentally reported. To take into account the localized nature of magnetic elements, we perform electronic structure calculations and topological diagnosis as a function of the Hubbard U parameter. This results in a topological phase diagram for each material as a function of the Hubbard interaction potential. We provide full details of the materials, which can be readily grown to explore their new topological phenomena.

MA 10.3 Mon 15:30 HSZ 403

Manipulating topological feature of massive Dirac particle with scalar potential — •SUMIT GHOSH^{1,2}, YURIY MOKROSOV^{1,2}, and STEFAN BLÜGEL¹ — ¹PGI-1, Forschungszentrum Jülich, Germany — ²Institute of Physics, Johannes Gutenberg University Mainz, Germany

Topology is one of the central aspect of modern spintronics. Different physical observables as well as transport properties that originates from the nontrivial topology of the system shows significant robustness against different external perturbation. Manipulating the topology of a system on the other hand is a highly non-trivial task since it requires tuning the internal degrees of freedom. In this presentation we are going to present an intrinsic mechanism to manipulate the topological feature and associated transport properties by using scalar potential. We systematically demonstrate how a scalar potential can invert the mass term of a massive Dirac particle which subsequently leads to the change of the topological index. We further demonstrate how this mechanism can be exploited to control the formation of edge states which can control the transport properties. This study thus provides a better understanding of the origin of the topological properties as well as a simple way to manipulate them. [https://arxiv.org/abs/2204.06412]

MA 10.4 Mon 15:45 HSZ 403

Mapping out the topological phase diagram of FeSn — SOUMYA SANKAR¹, RUIZI LIU², XUEJIAN GAO¹, QIFANG LI^{3,4}, JIACHANG ZHENG¹, CAIYUN CHEN¹, CHENGPING ZHANG¹, KUN QIANG², ZI YANG MENG^{3,4}, KAM TUEN LAW¹, QIMING SHAO^{1,2}, and •BERTHOLD JÄCK¹ — ¹HKUST, Clear Water Bay, Kowloon, Hong Kong SAR — ²HKUST, Department of Computer Science and Electrical Engineering, Clear Water Bay, Kowloon, Hong Kong SAR — ³Hong Kong University, Department of Physics, Pokfulam Road, Hong Kong SAR — ⁴University of Tokyo, Department of Physics, Hongo, Bunkyo City, Tokyo

Metallic kagome magnets exhibit a flat band and a Dirac point in their electronic structure and long-range magnetic order. The combination of these properties creates favourable conditions to search for strongly correlated and topological electronic states. The near-ideal kagome band structure of the inter metallic kagome series X1Y1 offers opportunities to study the interplay between strong electronic correlations, topology, and magnetism.

We have used molecular beam epitaxy and electronic transport measurements to study the interplay of magnetism and band topology in thin films of antiferromagnetic FeSn. We will present results from a magnetic field and temperature dependent study of the anomalous Hall effect. Combining these measurements with magnetic Monte-Carlo simulations and theoretical model calculations, we map out the topological phase diagram of FeSn over a large temperature range.

We acknowledge support by the GRC, and the Croucher Foundation.

15 min. break

MA 10.5 Mon 16:15 HSZ 403

Investigation of the magnetic topological insulator family (MnPn2Te4) (Pn=Bi, Sb) by μ SR and NMR — •MANASWINI SAHOO^{1,2}, ANNA ISAEVA¹, BERND BÜCHNER¹, and ROBERTO DE RENZI² — ¹Leibniz IFW Dresden, Dresden, Germany — ²University of Parma, Parma, Italy

Time-reversal symmetry breaking in a topological insulator (TI) opens a surface gap and distinguishes chiral quantum states that could eventually be exploited

in electrically controlled spintronic devices. The recent discovery of layered van der Waals materials opens a new approach to achieve this. (MnBi2Te4) (Bi2Te3) n is one of the first such examples, where the increasing number n of TI layers controls the magnetic dimensionality of the material. These compounds do display the quantum anomalous Hall effect, where spontaneous magnetization and spin-orbit coupling lead to a topologically non-trivial electronic structure. In the case of (MnBi2Te4) (Bi2Te3) n, Zero Field μ SR shows more than one internal field at the muon site with the majority one decreasing in value when n is increased. The muon spin precessions display very fast relaxations of static inhomogeneous nature. Whereas in the sister compound MnSb2Te4, Zero Field μ SR shows a broader distribution of magnetic field at the muon due to larger intermixing between Mn/Sb in the sample. Importantly, the weak Transverse Field shows a sharp magnetic transition at the same Tc, with a clear relaxation peak due to critical fluctuations, taking place in the whole volume of the material. This local information from μ SR together with NMR is crucial to correctly interpret macroscopic magnetization data.

MA 10.6 Mon 16:30 HSZ 403

Magnetic dilution effect and topological phase transitions in antiferromagnet Mn_{1-x}Pb_xBi₂Te₄ — •YUEH-TING YAO¹, TIEMA QIAN², TAY-RONG CHANG^{1,3,4}, and NI NI² — ¹Department of Physics, National Cheng Kung University, Tainan 70101, Taiwan — ²Department of Physics and Astronomy and California NanoSystems Institute, University of California, Los Angeles, California 90095, USA — ³Center for Quantum Frontiers of Research and Technology (QFort), Tainan 701, Taiwan — ⁴Physics Division, National Center for Theoretical Sciences, Taipei 10617, Taiwan

The interplay between magnetism and topology have taken the central stage of modern condensed matter physics in the past three years. The fine control of magnetism and topology in a magnetic topological insulator is crucial for realizing various novel magnetic topological phases, such as axion insulator, magnetic Weyl semimetals, etc. In this work, we investigate the evolution of magnetism and band topology in Mn_{1-x}Pb_xBi₂Te₄ via angle resolved photoemission spectroscopy (ARPES), first-principles calculations, and electronic transports. We present the comprehensive phase diagram by controlling Pb content and magnetism in this alloy system. Moreover, we provide the first topological crystalline insulator with non-trivial glide mirror Chern number in MnBi2Te4-family materials, which is protected by non-symmorphic symmetry arise from antiferromagnetic (AFM) configuration. Our work provides a fruitful platform with continuously tunable magnetism and topology for investigating emergent phenomena and pave a way towards potential new applications of nanoelectronics.

MA 10.7 Mon 16:45 HSZ 403

Thermal Hall Effect of Magnon-Phonon Hybrid Quasiparticles in a Fluctuating Heisenberg-Kitaev Antiferromagnet — •ROBIN R. NEUMANN¹, ALEXANDER MOOK², JÜRGEN HENK¹, and INGRID MERTIG¹ — ¹Martin Luther University Halle-Wittenberg, Halle (Saale), Germany — ²Johannes Gutenberg University, Mainz, Germany

Magnons, the quantized excitations of localized spins, and phonons, the quantized excitations of the lattice, are two types of quasiparticles that are responsible for heat transport in magnetic insulators. However, phonons by themselves do not contribute to the *transverse* heat current induced by a temperature gradient, i.e., the thermal Hall effect (THE). Magnons, on the other hand, may exhibit a Berry curvature, a magnetic field in reciprocal space, that leads to an intrinsic THE.

In this talk, I address the THE in a Heisenberg-Kitaev antiferromagnet subjected to a magnetic field. The applied field drives the system from a zigzag antiferromagnetic to a spin-flop state. The magnon-driven THE indicates the magnetic phase transition by a sign change at the critical field. Furthermore, when the magnetoelastic interaction is considered, the phonon and magnon bands hybridize and additional Berry curvature at the avoided crossings emerge. Depending on the strength of the spin-phonon coupling, this may lead to an overall reversal of the THE while the field-induced sign change at the critical field remains mostly robust. These results showcase that magnon-phonon hybridization can be pivotal for the interpretation of transport experiments.

MA 10.8 Mon 17:00 HSZ 403

Limitations of the Bulk-Boundary Correspondence in Topological Magnon Insulators due to Magnon-Magnon Interactions — •JONAS HABEL¹, JOHANNES KNOLLE¹, ALEXANDER MOOK², and JOSEF WILLSHER¹ — ¹Technical University of Munich, Germany (Theory of Quantum Matter and Nanophysics) — ²Johannes Gutenberg University Mainz, Germany

Magnon excitations in ordered quantum magnets can exhibit topological band structures characterized by non-zero Chern numbers. Such magnonic Chern insulators are widely believed to host protected chiral edge modes due to the bulk-boundary correspondence, in analogy to electronic Chern insulators. However, in contrast to electrons, magnons are bosons and can thus be subject to exotic number-non-conserving many-body interactions, enabling potentially strong spontaneous decays at zero temperature.

To assess their effect on the chiral edge magnons, we study a topological honeycomb-lattice ferromagnet with Dzyaloshinskii-Moriya interactions using many-body perturbation theory. We discover that non-harmonic terms of the spin-wave expansion may lead to severe lifetime reduction of edge modes and their delocalisation into the bulk. For sufficiently strong interactions, the spectral

weight of the chiral edge magnons vanishes entirely. These findings indicate that topological magnon bands within the harmonic framework do not necessarily give rise to protected edge modes in the full spin theory, suggesting limitations of the bulk-boundary correspondence in this case.

MA 11: Non-Skyrmionic Magnetic Textures I

Time: Monday 15:00–16:45

Location: POT 6

MA 11.1 Mon 15:00 POT 6

Topological defects in a multiferroic antiferromagnet — •AUREO FINCO¹, ANGELA HAYKAL¹, STÉPHANE FUSIL², PAWAN KUMAR¹, PAULINE DUFOUR², ANNE FORGET³, DOROTHÉE COLSON³, JEAN-YVES CHAULEAU³, MICHEL VIRET³, NICOLAS JAOUEN⁴, VINCENT GARCIA², and VINCENT JACQUES¹ — ¹Laboratoire Charles Coulomb, Université de Montpellier, CNRS, Montpellier, France — ²Unité Mixte de Physique, CNRS, Thales, Université Paris-Saclay, Palaiseau, France — ³SPEC, CEA, CNRS, Université Paris-Saclay, Gif sur Yvette, France — ⁴Synchrotron SOLEIL, Gif-sur-Yvette, France

We report on the formation of topological defects emerging from the cycloidal order at the surface of bulk BiFeO₃ crystals [1]. Combining reciprocal and real-space magnetic imaging techniques, we first observe, in a single ferroelectric domain, the coexistence of regions in which the antiferromagnetic cycloid propagates along different wave vectors. We then show that the direction of these wave vectors is not strictly locked to the preferred crystallographic axes but rather rotates continuously. At the junctions between the magnetic domains, we observe topological line defects identical to those found in a broad variety of lamellar physical systems with rotational symmetries. Our work establishes the presence of these magnetic objects at room temperature in the multiferroic antiferromagnet BiFeO₃, offering new opportunities in terms of robustness and electrical control towards their use in spintronic devices.

[1] Finco et al, *Phys. Rev. Lett.* 128, 187201 (2022)

MA 11.2 Mon 15:15 POT 6

Domain structures of stressed free-hanging magnetic thin films — DHAVALKUMAR MUNGPARA¹, •ALEXANDER SCHWARZ¹, FEDERICO MASPERO², RICCARDO BERTACCO², NICOLA MANCA³, LEONÉLIO CICHETTO JR.³, and LUCA PELLEGRINO³ — ¹INF, University of Hamburg, Jungiusstr. 11, 20355 Hamburg — ²CNR-IFN, Piazza Leonardo da Vinci 32, 20133 Milano, Italy — ³CNR-SPIN Corso F. M. Perrone 24, 16152 Genova, Italy

This work has been conducted as part of the OXiNEMS project, which aims to realize a miniaturized all-oxide hybrid sensor able to detect magnetic fields in the fT-regime. Our envisaged design encompasses a superconducting pick-up loop with a constriction and a magnetically sensitive resonator placed directly above.

To achieve a high sensitivity, the resonator must have a high Q-value, which is accomplished by a large in-plane stress. To obtain magnetic sensitivity, the resonator itself can be magnetic, or a magnetic thin film element is grown on top of a non-magnetic resonator. Of course, the magnetic sensitivity of the whole device depends on the magnetic properties of the resonator. Therefore, we investigated the domain structure of two promising resonator candidates using magnetic force microscopy: 100 nm thick Co rectangles on non-magnetic silicon nitride trampoline resonators and 100 nm thick magnetic La_{0.7}Sr_{0.3}MnO₃ trampoline resonators.

The OXiNEMS project (www.oxinems.eu) has received funding from the European Union's Horizon 2020 research and innovation program under Grant Agreement No. 828784.

MA 11.3 Mon 15:30 POT 6

Stability and dynamics of SO(3) solitons in magnetically frustrated systems — •RICARDO ZARZUELA — Institut für Physik, Johannes Gutenberg Universität Mainz, D-55099 Mainz, Germany

In recent years frustrated magnets have resurged in condensed matter due to their striking spin transport properties [1,2] and ability to host three-dimensional magnetic solitons, such as Shankar skyrmions [3] or Anderson-Toulouse vortices [4]. The latter emerge in the corresponding SO(3)-order parameter (describing the spin-spin correlation of the system), have potential use in topological computing and high-density memory storage, and coexist with those conventional magnetic solitons encoded in the total magnetization field (e.g., domain walls and baby skyrmions). We discuss the stability of these SO(3) solitons for several phenomenological models for a magnetically frustrated platform and, within a collective variable approach, we also explore their dynamics in the presence of spin-transfer torques and topological defects.

[1] N.L. Nair, E. Maniv, C. John, S. Doyle, J. Orenstein, and J.G. Analytis. *Nat. Mater.* 19, 153 (2020).

[2] R. Zarzuela and J. Sinova, arXiv:2112.06680 (2022).

[3] R. Shankar, *J. Physique* 38, 1405 (1977).

[4] P.W. Anderson and G. Toulouse, *Phys. Rev. Lett.* 38, 508 (1976).

15 min. break

MA 11.4 Mon 16:00 POT 6

Interaction of antiferromagnetic domain walls with crystal defects — •OLEKSANDR V. PYLYPOVSKYI^{1,2}, ARTEM V. TOMILO¹, NATASCHA HEDRICH³, KAI WAGNER³, BRENNAN J. SHIELDS³, TOBIAS KOSUB¹, RENÉ HÜBNER¹, JÜRGEN FASSBENDER¹, DENIS D. SHEKA⁴, PATRICK MALETINSKY³, and DENYS MAKAROV¹ — ¹Helmholtz-Zentrum Dresden-Rossendorf e.V., 01328 Dresden, Germany — ²Kyiv Academic University, 03142 Kyiv, Ukraine — ³University of Basel, Basel CH-4056, Switzerland — ⁴Taras Shevchenko National University of Kyiv, 01601 Kyiv, Ukraine

Understanding behavior of magnetic texture in antiferromagnetic nanostructures and thin films is crucial for the design of novel magnetic data storage and logic devices. Here, we derive the boundary conditions for the Néel vector in a two-sublattice antiferromagnet (AFM) and apply them to describe the shape of the domain walls [1,2] and skyrmions [2] in confined samples. In general, the surface of a 3D domain wall behaves as an elastic ribbon which bends in response on the topographic features of the single crystal Cr₂O₃ [1]. In presence of the Dzyaloshinskii-Moriya interaction, topologically non-trivial AFM textures possess broadening near the surface. In thin films, the sample's granularity becomes crucial. We present a model of a granular AFM and, by comparison with Nitrogen Vacancy magnetometry of 200-nm-thick Cr₂O₃ films, estimate the inter-grain exchange strength. The grain boundaries act as strong pinning sites for the AFM texture. [1] N. Hedrich et al., *Nat. Phys.* 17, 574 (2021); [2] O. Pylypovskiy et al., *Phys. Rev. B* 103, 134413 (2021).

MA 11.5 Mon 16:15 POT 6

Evaluation of phase images obtained by electron holography for three-dimensional spin-textures — •MORITZ WINTEROTT^{1,2} and SAMIR LOUNIS^{1,2} — ¹Peter Grünberg Institut and Institute for Advanced Simulation, Forschungszentrum Jülich & JARA, D-52425 Jülich, Germany — ²Faculty of Physics, University of Duisburg-Essen and CENIDE, 47053 Duisburg, Germany

Three-dimensional (3D) spin-textures, similarly to their 2D counterpart (skyrmions), are attracting widespread interest, especially because of their potential application as magnetic bits for energy-efficient storage devices. Thereby, a major challenge is their identification. Here we focus on electron holography, where phase images are reconstructed in order to recognize 3D spin-textures. The phase image consists of an electronic and a magnetic contribution, with the latter being assumed to emerge from the stray field, and thus should vanish for antiferromagnets, while the former is conjectured to be inert to the magnetic texture. Here we demonstrate that the electronic phase image carries non-trivial magnetic information induced by spin-mixing and spin-orbit mechanisms. We calculate and compare systematically the strength of both electronic and magnetic phase images employing the optimized forward model [1] and a tight-binding scheme combined with multiple-scattering theory. We explore the impact of spin-orbit interaction, exchange splitting and hopping.

[1] J. Caron, Model-Based Reconstruction of Magnetisation Distributions in Nanostructures from Electron Optical Phase Images, PhD thesis, RWTH Aachen Uni. (2017).

MA 11.6 Mon 16:30 POT 6

X-ray holographic imaging of magnetic surface spirals in FeGe lamellae — •LUKE A. TURNBULL¹, MATTHEW T. LITTLEHALES¹, MURRAY N. WILSON¹, MAX T. BIRCH², HORIA POPESCU³, NICOLAS JAOUEN³, JOEL VEREZHAZ⁴, GEETHA BALAKRISHNAN⁴, and PETER D. HATTON¹ — ¹Department of Physics, Durham University, Durham, DH1 3LE, UK — ²Max Planck Institute for Intelligent Systems, 70569 Stuttgart, Germany — ³Synchrotron SOLEIL, Saint Aubin, BP 48 91192 Gif-sur-Yvette, France — ⁴Department of Physics, University of Warwick, Coventry, CV4 7AL, UK

Isotropic helimagnets are known to host a diverse range of chiral magnetic states. In 2016, F.N. Rybakov et al. theorized the presence of a surface-pinned stacked spin spiral phase [F.N. Rybakov et al., 2016 *New J. Phys.* 18 045002], which had yet to be observed experimentally. The phase is characterized by surface spiral periods exceeding the host material's fundamental winding period, L. In this talk we present experimental evidence for the observation of this state in lamellae of FeGe using resonant x-ray holographic imaging data and micromagnetic simulations. We find images of FeGe lamellae, exceeding a critical thickness of 300 nm (4.3L), exhibit contrast modulations with a field-dependent periodicity of

$x < 1.4L$, consistent with theoretical predictions of the stacked spiral state. The identification of this spiral state carries significant implications for the stability

of other coexisting spin textures in chiral helimagnets, and indicates the utility in considering magnetic systems in three-dimensions.

MA 12: Skyrmions II

Time: Tuesday 9:30–11:30

Location: HSZ 02

MA 12.1 Tue 9:30 HSZ 02

Coexistence of distinct skyrmionic spin textures — •BÖRGE GÖBEL¹, JAGANNATH JENA², STUART PARKIN², and INGRID MERTIG¹ — ¹Institut für Physik, Martin-Luther-Universität Halle-Wittenberg — ²Max-Planck-Institut für Mikrostrukturphysik, Halle

The field of skyrmionics has attracted great research interest, as skyrmions – whirl-like nano-objects – are very stable which makes them potential carriers of information in future data storage devices. However, their integer topological charge causes two shortcomings of skyrmion-based racetrack storages: The skyrmions do not move parallel to a current and multiple skyrmions attract and repel each other.

In this talk, I present several alternative nano-objects that go beyond conventional skyrmions [1]. We discuss via simulations, Lorentz transmission electron microscopy measurements [2,3] and Hall transport measurements [4] that skyrmions, antiskyrmion and topologically trivial bubbles [5] can coexist. They can even appear fractionally near the sample's edges [6]. The interplay of Dzyaloshinskii-Moriya and dipolar interactions leads to interesting coexistence and deformation phenomena that may even be utilized for neuromorphic applications.

[1] BG et al. Physics Reports 895, 1-28 (2021), [2] Jena, BG et al. Nat. Com. 11, 1115 (2020), [3] Jena, BG et al. Science Advances 6, eabc0723 (2020), [4] Sivakumar, BG et al. ACS Nano 14, 13463 (2020), [5] BG et al. PRAppl. 15, 064052 (2021), [6] Jena, BG et al. Nat. Com 13, 2348 (2022) [7] Ribeiro de Assis, Mertig, BG arXiv: 2209.11017

MA 12.2 Tue 9:45 HSZ 02

Magnetic Néel Domain Walls and Skyrmions in La_{0.7}Sr_{0.3}Mn_{1-x}Ru_xO₃ Multilayers — •ARSHA THAMPI¹, JÖRG SCHÖPF², DANIEL WOLF¹, IONELA LINDFORS-VREJOIU², and AXEL LUBK^{1,3} — ¹Leibniz Institute for Solid State and Materials Research Dresden, Helmholtzstraße 20, 01069 Dresden, Germany — ²Physics Institute, University of Cologne, 50937 Cologne, Germany — ³Institute of Solid State and Materials Physics, TU Dresden, 01069 Dresden, Germany

Magnetic domain walls (DWs) in ferromagnetic thin films exhibit a rich variety of configurations and corresponding dynamic properties depending on parameters like film thickness, defect density, magnetocrystalline anisotropy, exchange stiffness, and Dzyaloshinskii-Moriya interaction (DMI). Here, we study epitaxial ferromagnetic multilayer devices of La_{0.7}Sr_{0.3}Mn_{1-x}Ru_xO₃, consisting 8 nm thick manganite layers with varying Ru/Mn content, in order to engineer symmetric and antisymmetric exchange interaction and magnetic anisotropy across the multilayer stack. We particularly map the DW states as a function of temperature and external out-of-plane magnetic fields employing high-resolution magnetic imaging in the Transmission Electron Microscopy (TEM). Lorentz TEM and transport of intensity phase reconstruction is used to characterize the magnetic domains and DWs formed as a function of temperature and perpendicular magnetic field strength. High-resolution magnetic field mapping of La_{0.7}Sr_{0.3}Mn_{1-x}Ru_xO₃ multilayer system demonstrates the possibility to engineer chiral Néel domain walls and skyrmions.

MA 12.3 Tue 10:00 HSZ 02

In-situ correlation of the anomalous Hall effect with the occurrence of topological and non-topological magnetic phases in Mn_{1.4}PtSn — •DARIUS POHL¹, ANDY THOMAS², SEBASTIAN SCHNEIDER¹, DOMINIK KRIEGER³, YEJIN LEE², PRAVEEN VIR⁴, CLAUDIA FELSER⁴, MORITZ WINTER^{1,4}, and BERND RELLINGHAUS¹ — ¹Dresden Center for Nanoanalysis (DCN), cfaed, TU Dresden — ²Leibniz Institute for Solid State and Materials Research Dresden — ³Institute of Solid State and Materials Physics, TU Dresden — ⁴Max Planck Institute for Chemical Physics of Solids, Dresden

Topologically protected (anti-)skyrmions are potential future information carriers, since they can be electrically manipulated and detected, e.g., by measuring their Hall signature. Hall measurements are usually conducted on samples with different geometries as compared to those used for Lorentz TEM magnetic imaging. In magnetic phases which are strongly influenced by dipole-dipole interactions, such comparisons are problematic. We devised an experimental setup that bridges this gap and allows for the conduction of in-situ Hall measurements in a TEM. Besides proof-of-principle experiments on thin Ni films, our new setup allows us to follow in detail the field dependence of the Hall voltage while simultaneously monitoring the magnetic phases in Mn_{1.4}PtSn. This provides valuable insights into the existence and nature of an intensely debated electrical signature of skyrmionics structures. Financial support by DFG through SPP 2137 is gratefully acknowledged.

MA 12.4 Tue 10:15 HSZ 02

Room temperature stabilization of skyrmionic spin textures in synthetic antiferromagnets — •MONA BHUKTA, TAKA AKI DOHI, M-A. SYSKAKI, ROBERT FRÖMTER, and MATHIAS KLÄUI — Institut für Physik, Johannes Gutenberg-Universität Mainz, Staudingerweg 7, 55128 Mainz, Germany

Magnetic skyrmions [1] are twisted spin configurations, which show a non-zero skyrmion Hall angle when driven by current due to their topological nature [2], which is detrimental for applications. Skyrmions in synthetic antiferromagnet (SAFs), suppress this effect owing to an overall zero topological charge. Recent observations of skyrmions in SAFs have opened the possibility for using skyrmions as a candidate for logic operations in data storage devices [3]. Here, we investigate different, more exotic spin textures beyond skyrmions in a SAF consisting of CoFeB/Ir/CoFeB multilayers by using scanning electron microscopy with polarization analysis (SEMPA). The surface sensitivity of SEMPA is especially effective on SAFs enabling us to investigate the topological spin textures even in a fully compensated composition. We report merons and antimerons in the SAF that are stable at zero magnetic fields and room temperature. Micromagnetic simulations of the investigated SAF stacks have been carried out to understand the way of stabilization of these exotic spin textures as well as to explore the possible emergence of three-dimensional (3D) spin structures in the SAF multilayer system. [1] K. Everschor-Sitte et al., J. Appl. Phys. 124, 240901 (2018). [2] K. Litzius et al., Nat. Phys. 13, 170 (2017). [3] T. Dohi et al, Nat. Commun. 10, 5153 (2019)

MA 12.5 Tue 10:30 HSZ 02

Evidence for Chiral Soliton Lattice formation in the Antiskyrmion compound Mn_{1.4}PtSn — •M. WINTER^{1,2,3}, M. RAHN⁴, D. WOLF³, S. SCHNEIDER², M. VALVIDARES⁵, C. SHEKAR¹, P. VIR¹, B. ACHINUQ⁶, H. POPESCU⁷, T. HELM⁸, G. VAN DER LAAN⁹, T. HESJEDAL⁶, B. RELLINGHAUS², and C. FELSER¹ — ¹MPI CPFS, Dresden, Germany — ²DCN, TU Dresden, Germany — ³IFW, Dresden, Germany — ⁴IFMP, TU Dresden, Germany — ⁵ALBA Synchrotron, Barcelona, Spain — ⁶Clarendon Laboratory, University of Oxford, UK — ⁷Synchrotron SOLEIL, Saint-Aubin, France — ⁸HZDR, Dresden, Germany — ⁹Diamond Light Source, Didcot, UK

The Antiskyrmion (aSk) compound Mn_{1.4}PtSn has a rich magnetic phase diagram that strongly depends on strength and orientation of an external magnetic field as well as on the history of its application. We conducted combined experiments of resonant elastic x-ray scattering (REXS) and Lorentz transmission electron microscopy (LTEM) on an identical lamella of Mn_{1.4}PtSn. Our complementary approach allows for an unambiguous correlation of the real space magnetic textures in Mn_{1.4}PtSn, i.e., helices, non-topological (NT) bubbles and aSk as determined by LTEM and transitions between them with their corresponding *k* space scattering patterns obtained by REXS. The octupole vector magnet of the REXS setup enabled us to gain extended information on the dependence of the phase diagram of Mn_{1.4}PtSn on the direction of the external field, revealing the interplay of chiral soliton lattices, NT bubbles, the conical phase and aSk. Part of this work is gratefully supported by DFG within SPP 2137.

MA 12.6 Tue 10:45 HSZ 02

Spin dynamics of skyrmion lattices in a chiral magnet resolved by micro-focused Brillouin light scattering — PING CHE¹, •RICCARDO CIOLA², MARKUS GARST², VOLODYMYR KRAVCHUK², ARNAUD MAGREZ¹, HELMUTH BERGER¹, THOMAS SCHÖNENBERGER¹, HENRIK M. RØNNOW¹, and DIRK GRÜNDLER¹ — ¹École Polytechnique Fédérale de Lausanne, Switzerland — ²Karlsruhe Institute of Technology, Germany

Chiral magnets provide an innovative framework to study non-collinear spin textures and their associated magnetization dynamics. They include helical and conical magnetic textures that are spatially modulated with a wavevector k_h as well as the topologically non-trivial skyrmion lattice (SkL) phase. So far, different techniques have been used to probe the magnetization dynamics of the latter SkL phase in the small wavevectors limit, $k \ll k_h$, as well as for $k > k_h$. Here, we show that Brillouin light scattering (BLS) is ideally suited to probe the complementary range of wavevectors $k \leq k_h$. We analysed bulk spin waves in the SkL phase of Cu₂OSeO₃. We provide parameter-free predictions for the BLS cross section and compute both the resonances and their spectral weights. The theoretical results are compared to a BLS experiment in the backscattering geometry that probe magnons with a wavevector $k = 48 \text{ rad}/\mu\text{m} < k_h = 105 \text{ rad}/\mu\text{m}$. The clockwise, counterclockwise and breathing modes are clearly resolved. Due to the finite wavevector of the magnon excitations, finite spectral weight is theoretically predicted also for other resonances. Experimentally, at least one additional resonance is clearly identified.

MA 12.7 Tue 11:00 HSZ 02

Modelling thermal transport in spiral magnets — •MARGHERITA PARODI^{1,2} and SERGEY ARTYUKHIN² — ¹University of Genova, Italy — ²Italian Institute of Technology, Genova, Italy

Magnetic memory and logic devices, including prospective ones based on skyrmions, inevitably produce heat. Thus, controlling heat flow is essential for their performance. Here we study magnon contribution to thermal conductivity in the most basic non-collinear magnet with a spin spiral ground state. Non-collinearity leads to anharmonic terms, resulting in magnon fusion and decay processes. These processes determine the magnon lifetime which can be used to estimate thermal conductivity in single mode approximation. However, by solving the full Boltzmann equation numerically, we find much higher thermal conductivity. This signifies that heat is carried not by individual magnons but by their linear combinations, called relaxons. The thermal conductivity is found to be increasing with the diminishing twist angle, consistent with recent experiments. The results pave the path to understanding magnetic thermal transport in other non-collinear magnets.

MA 12.8 Tue 11:15 HSZ 02

Enhanced Skyrmion Diffusion by Periodic Excitation — •RAPHAEL GRUBER, MAARTEN BREMS, JAN ROTHÖRL, TOBIAS SPARMANN, FABIAN KAMMERBAUER, IRYNA KONONENKO, MARIA-ANDROMACHI SYSKAKI, PETER VIRNAU, and MATHIAS KLÄUI — Institut für Physik, Johannes-Gutenberg Universität Mainz, 55099 Mainz, Germany

Magnetic skyrmions are chiral, quasi-particle spin structures that are considered as promising candidates for data storage, logic and non-conventional computing devices. When thermal excitation of the spins overcomes the variations in the energy landscape of a sample, skyrmions exhibit thermal motion as recently reported [1]. For non-conventional computing, diffusion is essential and its speed is key. Although pinning slows down diffusion, a finite effect of pinning is even required in order to ensure the system's complexity and non-linearity for non-conventional computing [2]. Using magneto-optical Kerr microscopy, we demonstrate that we can drastically increase the diffusion coefficient of micrometer-sized skyrmions in magnetic thin films by excitation with oscillating magnetic fields. The faster motion is traced back to a reduction of the effective pinning since the skyrmion pinning is strongly size-dependent [3]. Our findings thus pave the way to a significant increase of both performance and reliability of skyrmion devices, especially in non-conventional computing.

[1] Zázvorka, et al. Nat. Nanotechnol. 14, 658-661 (2019) [2] Raab et al. Nat Commun 13, 6982 (2022). [3] Gruber et al. Nat Commun 13, 3144 (2022).

MA 13: Focus Session: New Perspectives for Adiabatic Demagnetization Refrigeration in the Kelvin and sub-Kelvin Range (joint session TT/MA)

Efficient cooling into the Kelvin and sub-Kelvin range is a long-standing challenge relevant to both fundamental research and future quantum technologies. The standard cooling cycle based on vapor compression exploits expensive and rare helium. Low-temperature physicists world-wide are presently looking for cheaper and accessible alternatives, not to mention the need of compact cooling technology for desktop quantum technology, or special requirements for applications such as space missions and scanning tunneling microscopes. One of the key candidates is adiabatic demagnetization refrigeration (ADR). ADR is based on magnetic solids with a huge magnetocaloric effect and requires no helium. Even if paramagnetic salts are known and used for ADR applications for almost a century, there is an ongoing quest for materials with better magnetocaloric and mechanical properties, thermal conductivity, and vacuum compatibility. In this symposium, new fundamental ideas and the recent successful design and characterization of quantum materials for improved ADR will be highlighted. These materials exploit collective phenomena in correlated electron systems, such as the concept of geometrically frustrated magnetism to push the entropy to low temperatures, as well as heavy-fermion, and quantum-critical states.

Organizers: Andreas Honecker (CY Cergy Paris Université) and Jürgen Schnack (Universität Bielefeld)

Time: Tuesday 9:30–13:15

Location: HSZ 03

Invited Talk

MA 13.1 Tue 9:30 HSZ 03

Self-cooling molecular spin quantum processors — •MARCO EVANGELISTI¹, FERNANDO LUIS¹, ELIAS PALACIOS¹, DAVID AGUILA², and GUILLEM AROMI² — ¹INMA, CSIC & Universidad de Zaragoza, Spain — ²Dept. Química Inorgánica, Universidad de Barcelona, Spain

Cryogenic refrigeration is crucial for a wide range of emerging applications in the field of quantum technologies. Indeed, thermal energy must be minimized to avoid the excitation of vibrational motions that could disturb quantum operations. Synthetic chemistry provides a sophisticated methodology for the design and synthesis of materials displaying a wide variety of properties. Molecular materials are capable of excellent and unique characteristics that can be exploited either for caloric cooling[1] or spin-based quantum computing[2]. However, these features are not yet being implemented as such to act together within the same material, that is, at the molecular scale. Here, we show that a spin qubit (or qudit) can be brought into proximity with a spin centre that acts as a cooler. To this end, we make use of rare-earth-based asymmetric molecular dimers. A chemically engineered structural asymmetry introduces different coordination environments for each metal ion, operating similarly as for molecular quantum gates reported by some of us[3]. This strategy allows selecting individually both constituent ions, leading to e.g. the direct observation of the cooling of a single Er(III) ion qubit, or a Tm(III) electronuclear spin qudit, driven chiefly by the demagnetization of a single Gd(III) ion located within the same molecule.

[1] Dalton Trans. 39, 4672 (2010)

[2] Nat. Chem. 11, 301 (2019)

[3] Phys. Rev. Lett. 107, 117203 (2011)

Invited Talk

MA 13.2 Tue 10:00 HSZ 03

Triangular rare-earth borates for milli-Kelvin adiabatic demagnetization refrigeration — •PHILIPP GEGENWART — Experimental Physics VI, Center for Electronic Correlations and Magnetism, University of Augsburg

Adiabatic demagnetization refrigeration (ADR) is a classical cooling technique with renewed recent attention as alternative to costly and elaborate ³He/⁴He dilution refrigeration. Established water containing ADR salts suffer from chemical instability which requires delicate treatment to avoid degradation and ensure good thermal contact. Water-free K₂Yb(BO₃)₂ is an excellent alternative with high entropy density that allows ADR to below 20 mK [1]. Sintered pellets with silver powder admixture to ensure good thermal coupling are easy to manufacture, inexpensive and long-term stable even upon heating up to 700°C, enabling also ultra-high vacuum applications. K₂Yb(BO₃)₂ belongs to a family of rare-earth-based borates with triangular arrangement of magnetic moments. We discuss the impact of geometrical frustration and structural randomness on its low-temperature properties and demonstrate the enormous tunability of cooling power and operating temperature by chemical substitution.

[1] Y. Tokiwa, S. Bachus, K. Kavita, A. Jesche, A.A. Tsirlin, and P. Gegenwart, Commun. Mater. 2 (2021) 42.

Invited Talk

MA 13.3 Tue 10:30 HSZ 03

A millikelvin scanning tunnelling microscope in ultra-high vacuum with adiabatic demagnetisation refrigeration — •RUSLAN TEMIROV — Peter Grünberg Institut (PGI-3), Forschungszentrum Jülich, Germany — University of Cologne, Institute of Physics II, Cologne, Germany

Scanning tunnelling microscopes (STMs) operating in ultra-high vacuum (UHV) and low-temperature conditions are used widely for imaging and precise manipulation of surface nanostructures. A growing interest in studies of quantum-coherent phenomena in such nanostructures stimulates the development of STMs that operate at very low millikelvin temperatures. This contribution presents the design of a first-ever UHV STM cooled by adiabatic demagnetisation refrigeration (ADR) to below 30 mK. The use of ADR makes the STM design modular and helps it to reach a remarkable degree of mechanical stability. Tunnelling spectra collected on an atomically clean superconducting Al(100) surface reveal that the electronic temperature of the tunnelling junction is less

than 80 mK. The inelastic electron tunnelling spectroscopy of an individual electron spin performed in magnetic fields of up to 8 Tesla validates the STM capabilities for quantum nanoscience research.

15 min. break

Invited Talk MA 13.4 Tue 11:15 HSZ 03
ADR cryostats in low temperature physics and their applications — •DOREEN WERNICKE — Entropy GmbH, Gmunder Str. 37a, 81379 München

Entropy GmbH is a company founded in 2010 in Munich, Germany, specializing in the development and manufacture of low temperature cryostats. All Entropy cryostats are based on closed-cycle pre-cooling to temperatures below 3K. Further cooling stages such as ADR units, Joule-Thomson stages, and dilution refrigerators including electronics and software are proprietary developments. The modular design of all cryostats offers the possibility of adaptation to many different experiments and applications. One of Entropy's most common products are the ADR cryostats. The presentation will explain the principle of ADR cooling and features such as base temperature and holding time at operating temperature. Applications for low temperature device operation such as various types of superconducting detectors (TES, MKIDs, SQUIDS, SNSPDs) and Qubit characterization will be presented to demonstrate the performance and limitations of adiabatic demagnetization refrigeration.

Invited Talk MA 13.5 Tue 11:45 HSZ 03
Frustrated dipolar materials for low-temperature magnetic refrigeration — •MIKE ZHITOMIRSKY — Institute of Interdisciplinary Research, CEA-Grenoble, France

Low-temperature refrigeration is crucial for emergent quantum-information technologies and other scientific applications that outstretch from space telescopes to medicine. This growing demand fuels an interest in alternative low-temperature techniques including the adiabatic demagnetization refrigeration. The existing ADR technologies for the sub-Kelvin range utilize dilute paramagnetic salts of Cr and Fe magnetic ions, which have limited efficiency at higher temperatures. I shall discuss general directions of the ongoing search of prospective refrigerant materials by exploring collective effects in systems of interacting magnetic moments as opposed to noninteracting moments in paramagnetic salts. Specifically, I focus on geometrically frustrated magnets with a residual ground-state degeneracy as well as on dipolar magnets. I present new experimental and theoretical results obtained recently in Grenoble for two dipolar materials: $\text{Yb}_3\text{Ga}_5\text{O}_{12}$, which is a spin-1/2 dipolar ferromagnet on a hyper-Kagome lattice, and GdLiF_4 , which exhibits a hidden magnetic frustration. The striking properties of the latter material including a fractional magnetization plateau demonstrate importance of new magnetocaloric materials not only for applied but also for basic research in magnetism.

MA 13.6 Tue 12:15 HSZ 03
ADR based sub-Kelvin cryostats for applied quantum technologies — •PAU JORBA¹, FELIX RUCKER¹, STEFFEN SÄUBERT¹, ALEXANDER REGNAT¹, JAN SPALLEK¹, and CHRISTIAN PFLEIDERER² — ¹kiutra GmbH, Flößergasse 2, D-81369 München, Germany — ²Physik-Department, Technische Universität München, D-85748 Garching, Germany

In view of the increasing demand for the cooling of quantum electronic devices, the development of scalable cooling solutions that provide low temperatures independent of rare helium-3 will be mandatory for the adoption and commercial use of next-generation quantum technologies. We present novel ADR based sub-Kelvin cryostats¹ specifically developed for the characterization and operation of quantum devices. We address how known challenges of ADR systems such as limited hold time and magnetic stray fields can be overcome. Specifically, we describe how continuous sub-Kelvin cooling and wide-range temperature control can be achieved by combining multiple ADR units and mechanical thermal switches. We also present a novel sample loader mechanism² that allows taking advantage of the solid-state nature of ADR and to cool samples from room temperature to 100 mK in less than 3 hours.

[1] Regnat et al. (2018) Cryogen-free cooling apparatus (EP 3163222). European Patent Office.

[2] Spallek et al. (2022) System and method for inserting a sample into a chamber (EP 3632560). European Patent Office.

MA 13.7 Tue 12:30 HSZ 03

ADR below the ordering temperature in triangular $\text{KBaGd}(\text{BO}_3)_2$ — •NOAH WINTERHALTER-STOCKER¹, ALEXANDER BELLON¹, FABIAN HIRSCHBERGER¹, SEBASTIAN BACHUS¹, SEBASTIAN ERDMANN¹, ALEXANDER TSIRLIN^{1,2}, YOSHIFUMI TOKIWA^{1,3}, ANTON JESCHE¹, and PHILIPP GEGENWART¹ — ¹Experimental Physics VI, Center for Electronic Correlations and Magnetism, University of Augsburg, D-86159 Augsburg, Germany — ²Felix Bloch Institute for Solid-State Physics, Leipzig University, D-04103 Leipzig, Germany — ³Advanced Science Research Center, Japan Atomic Energy Agency, Tokai, Ibaraki 319-1195, Japan
Compared to the triangular ADR magnet $\text{KBaYb}(\text{BO}_3)_2$ [1] the isostructural sister compound $\text{KBaGd}(\text{BO}_3)_2$ with spin 7/2 moments has a three times enhanced magnetic entropy density of $192 \text{ mJ K}^{-1} \text{ cm}^{-3}$. We report a low-temperature magnetic and thermodynamic investigation of polycrystalline $\text{KBaGd}(\text{BO}_3)_2$ down to 50 mK. Specific heat indicates an antiferromagnetic phase transition at 263 mK, strongly broadened due to randomness and frustration, that becomes suppressed beyond 0.5 T. Further increase of magnetic field shifts the available entropy of $R \log 8$ towards high temperatures. Interestingly, ADR of a pellet utilizing the same setup as used in [1] reveals a minimal temperature if $T_{\min} = 122 \text{ mK}$ that is more than twice below T_N along with a hold time of more than 8 hours. The combination of minimal temperature and entropy density in $\text{KBaGd}(\text{BO}_3)_2$ is outstanding among known ADR materials.

[1] Y. Tokiwa et al., Communications Materials 2.1, 1-6 (2021)

MA 13.8 Tue 12:45 HSZ 03

Magnetocaloric properties of $(\text{RE})_3\text{Ga}_5\text{O}_{12}$ (RE=Tb, Gd, Nd, Dy) — MARKUS KLEINHANS¹, KLAUS EIBENSTEINER^{1,2}, JON LEINER¹, •CHRISTOPH RESCH¹, LUKAS WORCH¹, MARC WILDE¹, JAN SPALLEK^{1,2}, ALEXANDER REGNAT^{1,2}, and CHRISTIAN PFLEIDERER¹ — ¹Physik Department, Technical University Munich, D-85748 Garching, Germany — ²kiutra GmbH, Rupert-Mayer-Str. 44, D-81379 Munich, Germany

We report the characteristic magnetic properties of several members of the rare earth garnet family, $\text{Gd}_3\text{Ga}_5\text{O}_{12}$ (GGG), $\text{Dy}_3\text{Ga}_5\text{O}_{12}$ (DGG), $\text{Tb}_3\text{Ga}_5\text{O}_{12}$ (TGG), and $\text{Nd}_3\text{Ga}_5\text{O}_{12}$ (NGG), and compare their relative potential utility for magnetocaloric cooling, including their minimal adiabatic demagnetization refrigeration (ADR) temperatures and relative cooling parameters. A main objective of this work was to find potential improvements over the magnetocaloric properties of GGG for use in low temperature ADR cryostats. Using Tb^{+3} and Dy^{+3} in the RE-site offers, in principle, a higher saturation magnetization and Nd^{+3} gives a lower de Gennes factor and therefore potentially low transition temperature. Our results show that $\text{Dy}_3\text{Ga}_5\text{O}_{12}$ yields an optimal relative cooling parameter (RCP) at low applied fields and a low transition temperature, which would allow for the design of more efficient ADR cryostats.

[1] M. Kleinhans et al., arXiv/2204.01752; Phys. Rev. Appl. in press (2022).

MA 13.9 Tue 13:00 HSZ 03

Study of the large rotational magnetocaloric effect in $\text{Ni}(\text{en})(\text{H}_2\text{O})_4\text{SO}_4 \cdot 2\text{H}_2\text{O}$ — •RÓBERT TARASENKO, PETRO DANYLCHENKO, ERİK ČIŽMÁR, VLADIMÍR TKÁČ, ALEXANDER FEHER, ALŽBETA ORENDÁČOVÁ, and MARTIN ORENDÁČ — Institute of Physics, Faculty of Science, Pavol Jozef Šafárik University, Park Angelinum 9, 041 54 Košice, Slovakia

The title compound $\text{Ni}(\text{en})(\text{H}_2\text{O})_4\text{SO}_4 \cdot 2\text{H}_2\text{O}$ (*en* = ethylenediamine) has been identified as a spin-1 paramagnet with the nonmagnetic ground state introduced by the easy-plane anisotropy $D/k_B = 11.6 \text{ K}$ with $E/D = 0.1$ and negligible exchange interactions $J \approx 0$. We present an experimental study of the rotational magnetocaloric effect (MCE) in single crystals at temperatures above 2 K, associated with adiabatic crystal rotation between the easy plane and hard axis in magnetic fields up to 7 T. The experimental observations are completed with *ab initio* calculations of the anisotropy parameters. Theoretical simulations of the rotational MCE in the $S = 1$ paramagnet were performed and the simulations were compared with experimental data. A large rotational magnetic entropy change $\approx 16.9 \text{ J kg}^{-1} \text{ K}^{-1}$ has been achieved in 7 T. The adiabatic rotation of the crystal in 7 T starting at the initial temperature of 4.2 K leads to the cooling of the sample down to 0.34 K, which suggests the application of this material in low-temperatures cooling. Our simulations show that $S = 1$ Ni(II)-based systems with easy-plane anisotropy can have better rotational magnetocaloric properties than costly materials containing rare-earth elements.

Supported by project No. APVV-18-0197.

MA 14: Surface Magnetism

Time: Tuesday 9:30–11:45

Location: HSZ 04

Invited Talk MA 14.1 Tue 9:30 HSZ 04
Antiferromagnetism-driven two-dimensional topological nodal-point superconductivity — •ROBERTO LO CONTE¹, MACIEJ BAZARNIK^{1,2}, ERIC MASCOT¹, KRISZTIÁN PALOTÁS³, LEVENTE RÓZSA⁴, LÁSZLÓ SZUNYOGH³, ANDRÉ KUBETZKA¹, DIRK K. MORR⁵, KIRSTEN VON BERGMANN¹, and ROLAND

WIESENDANGER¹ — ¹Department of Physics, University of Hamburg, Germany — ²Institute of Physics, Poznan University of Technology, Poland — ³Department of Theoretical Physics, Budapest University of Technology and Economics, Hungary — ⁴Department of Physics, University of Konstanz, Germany — ⁵Department of Physics, University of Illinois at Chicago, USA

In the recent years, pioneering studies have been carried out on magnet/superconductor hybrid systems[1-4], motivated by their potential to host emergent quantum phases such as topological superconductivity. Here, we present the discovery of a topological nodal-point superconducting phase in antiferromagnetic manganese (Mn) monolayer islands on superconducting niobium (Nb) via low temperature spin-polarized STM[5]. Low-energy edge modes are found to separate the topological phase from the trivial one. The relative spectral weight of the edge modes depends on the edge's atomic configuration, which is a fingerprint of the discovered topological state. [1]S. Nadj Perge et al., Science 346, 602(2014). [2]A. Palacio-Morales et al., Sci. Adv. 5, eaav6600(2019). [3]L. Schneider et al., Nat. Phys. 17, 943(2021). [4]S. Kezilebieke et al., Nature 588, 424(2020). [5]R. Lo Conte et al., PRB 105, L100406(2022). M. Bazarnik et al., arXiv:2208.12018(2022).

MA 14.2 Tue 10:00 HSZ 04

Structure-Property Relationship of Reversible Magnetic Chirality Tuning — •JING QI¹, PAULA M. WEBER¹, TYLMAN KISSLINGER², LUTZ HAMMER², M. ALEXANDER SCHNEIDER², and MATTHIAS BODE¹ — ¹Julius-Maximilians-Universität Würzburg — ²Universität Erlangen-Nürnberg

The Ruderman-Kittel-Kasuya-Yosida (RKKY) interaction mediates collinear magnetic interactions via the conduction electrons of a non-magnetic spacer, resulting in a ferro- or antiferromagnetic magnetization in magnetic multilayers [1]. Recently it has been discovered that heavy non-magnetic spacers are able to mediate an indirect magnetic coupling that is non-collinear and chiral. This Dzyaloshinskii-Moriya-enhanced RKKY (DME-RKKY) interaction causes the emergence of a variety of interesting magnetic structures, such as skyrmions and spin spirals [2]. Here, we show by spin-polarized STM that the interchain coupling between manganese oxide chains on Ir(001) can reproducibly be switched from chiral to collinear antiferromagnetic by increasing the oxidation state of MnO₂ while the reverse process can be induced by thermal reduction. The underlying structure-property relationship is revealed by low-energy electron diffraction intensity (LEED-IV) analysis. Density functional theory calculations suggest that the magnetic transition may be caused by a significant increase of the Heisenberg exchange which overrides the DMI interaction upon oxidation. [1] P. Bruno et al., Phys. Rev. Lett. 67, 1602-1605 (1991). [2] M. Schmitt et al., Nat. Commun. 10, 2610 (2019).

MA 14.3 Tue 10:15 HSZ 04

Lifting the frustration of higher-order exchange interactions in ultrathin films — •FELIX NICKEL¹, SOUMYAJYOTI HALDAR¹, ROLAND WIESENDANGER², STEFAN HEINZE¹, and KIRSTEN VON BERGMANN² — ¹Institute of Theoretical Physics and Astrophysics, University of Kiel — ²Department of Physics, University of Hamburg

The 3Q state – a three-dimensional spin structure on a two-dimensional lattice predicted about 20 years ago [1] – has been observed in a Mn monolayer on Re(0001) using spin-polarized scanning tunneling microscopy (SP-STM) [2]. The 3Q state is a superposition of three symmetry equivalent spin spirals with the same period and can be stabilized by higher-order exchange interactions (HOI) such as the biquadratic or four-spin interactions [1,2]. Recently, it has been suggested based on density functional theory (DFT) calculations that the 3Q state in Mn/Re(0001) is significantly distorted due to topological chiral magnetic interactions [3]. Here, we show using DFT that the competition of biquadratic, four-spin, and topological chiral interactions can be tuned in Mn/Re(0001) by single atomic adlayers of Pd or Rh. Thereby, the frustration of HOI present in Mn/Re(0001) is lifted which results in the occurrence of the ideal 3Q state. SP-STM experiments confirm the predicted 3Q ground state of Pd/Mn/Re(0001) and Rh/Mn/Re(0001) and reveal differences to Mn/Re(0001). [1] Ph. Kurz et al., Phys. Rev. Lett. 86, 1106 (2001) [2] J. Spethmann et al., Phys. Rev. Lett. 124, 227203 (2020) [3] S. Haldar et al., Phys. Rev. B 104, L180404 (2021)

15 min. break

MA 14.4 Tue 10:45 HSZ 04

Conical spin-spirals at a ferromagnet's surface: experimental observations — •PATRICK HAERTL¹, GUSTAV BIHLMAYER², MARKUS LEISEGANG¹, STEFAN BLUEGEL², and MATTHIAS BODE¹ — ¹Universität Würzburg, Germany — ²Forschungszentrum Jülich and JARA, Germany

The spin-orbit-driven Dzyaloshinskii-Moriya interaction (DMI) can lead to chiral spin structures in magnetic systems with broken inversion symmetry [1]. The purely interfacial origin of DMI generally results in a reciprocal scaling with the magnetic layer thickness [2]. Here we report on the observation of a conical spin-spiral state at the surface of epitaxial Gd(0001) films grown on W(110). In a recently performed spin-polarized scanning tunneling microscopy (SP-STM) investigation of the thickness-dependent domain structures of Gd/W(110) we confirmed the existence of a spin reorientation transition (SRT) [3] from in-plane to out-of-plane magnetized films at a critical thickness $\Theta_{\text{crit}} \approx (100 \pm 20)$ AL [4]. In the vicinity of this SRT, we identify striped regions with a periodicity of about 2 nm. The application of an external magnetic field induces a rearrange-

ment of the stripes, thereby unambiguously confirming its magnetic origin. The experimental observations are discussed on the basis of density functional theory (DFT).

- [1] T. Moriya, Phys. Rev. 120, 91-98 (1960).
[2] J. Cho et al., Nature Comm. 6, 7635 (2015).
[3] A. Berger et al., Phys. Rev. B 52, 1078 (1995).
[4] P. Härtl et al., Phys. Rev. B 105, 174431 (2022).

MA 14.5 Tue 11:00 HSZ 04

Conical spin-spirals at a ferromagnet's surface: a theoretical analysis — •GUSTAV BIHLMAYER¹, PATRICK HÄRTL², MARKUS LEISEGANG², MATTHIAS BODE², and STEFAN BLÜGEL¹ — ¹Peter Grünberg Institut and Institute for Advanced Simulation, Forschungszentrum Jülich and JARA, D-52425 Jülich, Germany — ²Universität Würzburg, Germany

The properties of surface layers of a magnetic material can differ substantially from those of the bulk material. A prominent example is the Dzyaloshinskii-Moriya interaction (DMI), resulting from inversion-symmetry breaking at the surface, but also the magnetic anisotropy and the exchange interactions are locally modified. Gd(0001) is here a well-investigated model surface but despite its sensitivity of exchange interactions to the local environment, experimental data indicated that it behaves as homogeneous Heisenberg system [1]. Recent observations of spin-spirals at the surface of epitaxial Gd(0001) with spin-polarized scanning tunneling microscopy let us re-investigate this system. Density functional theory (DFT) calculations show that not only a sizable DMI can be found at the Gd(0001) surface but also the exchange interactions are modified to drive the system locally towards a conical spin-spiral state. Since the magnetic anisotropy and the exchange interactions with the ferromagnetic bulk material disfavor non-collinear magnetic states, only slight modifications of the exchange interactions make these spirals visible. We explore the phase diagram numerically and with the help of atomistic spin-dynamics simulations.

- [1] C. S. Arnold and D. P. Pappas, Phys. Rev. Lett. 85, 5202 (2000)

MA 14.6 Tue 11:15 HSZ 04

Non-collinear spin structure of trilayer Mn films on W(001) — •TIM DREVELOW¹, PAULA M. WEBER², JING QI², MATTHIAS BODE^{2,3}, and STEFAN HEINZE¹ — ¹Institute of Theoretical Physics and Astrophysics, University of Kiel, Leibnizstraße 15, 24098 Kiel, Germany — ²Physikalisches Institut, Experimentelle Physik II, Universität Würzburg, Am Hubland, 97074 Würzburg, Germany — ³Wilhelm Conrad Röntgen-Center for Complex Material Systems (RCCM), Universität Würzburg, Am Hubland, 97074 Würzburg, Germany

The spin structure of Mn films on the W(001) surface depends sensitively on the number of atomic layers. It has been shown that a Mn monolayer exhibits a spin spiral driven by the Dzyaloshinskii-Moriya interaction (DMI) [1] while the Mn double layer possesses an antiferromagnetic checkerboard state and vanishing Mn moments at the interface [2]. Here, we study the Mn trilayer on W(001) with a combination of spin-polarized scanning tunneling microscopy (SP-STM) and density functional theory (DFT) calculations. Experimentally, it is shown that the Mn films grow pseudomorphically and exhibit a $c(4 \times 2)$ magnetic superstructure consistent with a conical spin spiral ground state. Based on our DFT calculations we compare the total energies of different collinear and non-collinear spin structures including the effect of spin-orbit coupling. We find a complex interplay of magnetic interactions and structural relaxations of the Mn trilayer.

- [1] Ferriani et al. Phys. Rev. Lett. 101, 027201 (2008).
[2] Meyer et al. Phys. Rev. Research 2, 012075(R) (2020)

MA 14.7 Tue 11:30 HSZ 04

Structural transitions of magnetic thin films induced by two-dimension materials — •HANGYU ZHOU^{1,2}, MANUEL DOS SANTOS DIAS^{1,3,4}, WEISHENG ZHAO², and SAMIR LOUNIS^{1,3} — ¹Peter Grünberg Institut and Institute for Advanced Simulations, Forschungszentrum Jülich & JARA, 52425 Jülich, Germany — ²School of Integrated Circuit Science and Engineering, MIIT Key Laboratory of Spintronics, Beihang University, Beijing 100191, China — ³Faculty of Physics, University of Duisburg-Essen and CENIDE, 47053 Duisburg, Germany — ⁴Scientific Computing Department, STFC Daresbury Laboratory, Warrington WA4 4AD, United Kingdom

Interfaces of magnetic thin films play a key role in determining magnetic behaviors and implementations of spintronic devices. In the last decade, the increased availability of high-quality two-dimensional (2D) materials has helped to broaden the scope of interfaces, leading to the discovery of novel electronic and magnetic properties. Here, we explore with density functional theory calculations the impact of hexagonal boron nitride (h-BN) on the magnetism and structural properties of magnetic monolayers placed on heavy metal surfaces. We found that h-BN induces various structural transitions, and we investigate how magnetic interactions, such as the Heisenberg exchange interaction and the Dzyaloshinskii-Moriya interaction (DMI), are influenced by these reconstructions. These results contribute to new avenues for stabilizing complex spin-textures.

Work funded by DFG (SPP 2244; LO 1659/7-1) and China Scholarship Council program.

MA 15: INNOMAG e.V. Prizes 2023 (Diplom-/Master and Ph.D. Thesis)

Die Arbeitsgemeinschaft Magnetismus der DPG hat einen Dissertationspreis und einen Diplom-/Masterpreis ausgeschrieben, welche auf der Tagung der DPG 2023 in Dresden vergeben werden. Ziel der Preise ist die Anerkennung herausragender Forschung im Rahmen einer Diplom-/Masterarbeit beziehungsweise einer Promotion und deren exzellente Vermittlung in Wort und Schrift. Im Rahmen dieser Sitzung tragen die besten der für ihre an einer deutschen Hochschule durchgeführten Diplom-/Masterarbeit beziehungsweise Dissertation Nominierten vor. Im direkten Anschluss entscheidet das Preiskomitee über den Gewinner des INNOMAG e.V. Diplom-/Master-Preises und des Dissertationspreises 2023. Talks will be given in English!

Time: Tuesday 9:30–11:50

Location: HSZ 401

MA 15.1 Tue 9:30 HSZ 401

Cubic magneto-optic Kerr effect in Ni(111) thin films — •MAIK GAERNER¹, ROBIN SILBER², TOBIAS PETERS¹, JAROSLAV HAMRLE³, and TIMO KUSCHEL¹ — ¹Bielefeld University, Germany — ²IT4Innovations, VŠB - Technical University of Ostrava — ³Charles University, Prague, Czech Republic

In most studies utilizing the magneto-optic Kerr effect (MOKE), the detected change of polarized light upon reflection from a magnetized sample is supposed to be proportional to the magnetization M . However, MOKE signatures quadratic in M have also been identified and utilized, e.g., to sense the structural order in Heusler compounds, to detect spin-orbit torque or to image antiferromagnetic domains.

In our study, we observe a strong anisotropic MOKE contribution of third order in M in Ni(111) thin films, attributed to a cubic magneto-optic tensor $\propto M^3$ [1]. This cubic MOKE (CMOKE) is responsible for a threefold in-plane angular dependence of the magnetically saturated longitudinal MOKE response. We further show that this angular dependence is affected by the amount of structural domain twinning in the sample. The degree of twinning is determined by off-specular X-ray diffraction. Finally, the dependence of the anisotropic CMOKE on the external magnetic field strength is investigated up to nearly 2 T. Our detailed study on CMOKE for two selected photon energies will open up new opportunities for CMOKE applications with sensitivity to twinning properties of thin films, e.g. CMOKE spectroscopy and microscopy or time-resolved CMOKE.

[1] M. Gaerner et al., arXiv: 2205.08298

MA 15.2 Tue 9:50 HSZ 401

Switching of Sublattice Magnetization in Quantum Antiferromagnets Described by Schwinger Bosons — •KATRIN BOLSMANN — Technische Universität Dortmund

Harvesting magnetic excitations in antiferromagnets for information processing is a promising and fast-growing field in the research of magnetism. One of the main foci is the readout and manipulation of the Néel vector of antiferromagnetic (AFM) materials. We study a theoretical approach to describe the non-equilibrium switching of a two-dimensional AFM magnetization on a square lattice. We recall the use of Schwinger bosons in equilibrium to describe the elementary excitations, of the isotropic and anisotropic AFM square lattice, in mean-field approximation. The Bose-Einstein condensation of Schwinger bosons describes the long-range magnetic order. Then, the Schwinger boson mean-field theory is applied to investigate the switching of the sublattice magnetization on the AFM square lattice via an external magnetic field. In the anisotropic system, there is an increase in energy after switching, which depends on the degree of anisotropy. Furthermore, we find a threshold field, below which switching is no longer possible, and investigate its dependence on the anisotropy. Even for low anisotropy, the threshold for the magnetic field turns out to be too large for standard technical applications. Finally, we discuss possible modifications of the protocol to enable switching of the sublattice magnetization with smaller fields.

MA 15.3 Tue 10:10 HSZ 401

Magneto-optical Investigation of nonreciprocal Phonon-Magnon Interaction — •YANNIK KUNZ¹, MICHAEL SCHNEIDER¹, MORITZ GEILEN¹, MATTHIAS KÜSS², MANFRED ALBRECHT², PHILIPP PIRRO¹, and MATHIAS WEILER¹ — ¹Fachbereich Physik und Landesforschungszentrum OPTIMAS, Rheinland-Pfälzische Technische Universität Kaiserslautern-Landau, 67663 Kaiserslautern, Germany — ²Institut für Physik, Universität Augsburg

The coupling of surface acoustic waves (SAWs) with spin waves (SWs) intrinsically breaks the time-inversion symmetry. The resulting nonreciprocity can be exploited for applications such as miniaturized microwave isolators. SAWs can

be efficiently excited and detected by interdigital transducers. Therefore, in experiments the magnetic field dependent transmission induced by the coupling with SWs is commonly detected via electrical methods [1]. However, for the investigation of magnetoelastic interactions with spatial resolution, magneto-optical measurement methods are needed. We employed microfocused Brillouin light scattering spectroscopy and frequency-resolved magneto-optical Kerr effect spectroscopy [2] to map the spatial dependence of the phonon-magnon-coupling on a LiNbO₃/Co₄₀Fe₄₀B₂₀(10 nm)/SiN(5 nm)-structure. Our experiments provide direct evidence for coherent and nonreciprocal conversion of phonons to magnons along the SAW propagation path.

We acknowledge the funding by DFG via project No. 492421737.

[1] M. Küß et al., Phys. Rev. Lett. 125, 217203 (2020).

[2] L. Liensberger et al, IEEE Magnetics Letters 10, 5503905 (2019).

MA 15.4 Tue 10:30 HSZ 401

The Turn of the Screw and the Slide of the Skyrmion — •NINA DEL SER — Institute for Theoretical Physics, University of Cologne

We explore the non-equilibrium dynamics of chiral magnets driven by oscillating magnetic fields in the GHz regime. Universal activation of the magnets' translational and rotational Goldstone modes invites many exciting applications. Magnetic screws will turn, skyrmions will swim and skyrmion lattices will rotate. The magnetic Archimedean screw opens the door to new transport applications on the nano-scale, and is shown to be a very efficient electron pump even in the presence of disorder. At stronger driving, Floquet spin wave instabilities provoke the formation of a time quasicrystal, where the magnetisation oscillates at new incommensurate spatial and temporal frequencies. We also investigate the role of fractional charge topological charge in magnets. We show that such charges turn up for example in cubic magnets and in the fragments of exploding skyrmions or trapped between symmetry-broken domain walls. We show how their remarkable scattering properties can be used to build a magnon-powered fractional defect engine.

MA 15.5 Tue 10:55 HSZ 401

Imaging vortex pinning and gyration by time-resolved and in-situ Lorentz microscopy — •MARCEL MÖLLER — Max Planck Institute for Multidisciplinary Sciences, Göttingen, Germany — 4th Physical Institute - University of Göttingen, Göttingen, Germany

Nanosopic magnetic textures, including vortices, merons and skyrmions promise future applications three-dimensional memory, logic gates or neuro-morphic computing. Studying the control of such textures employing electric, magnetic or optical fields, demands instruments with sufficient spatial and temporal resolution. Ultrafast transmission electron microscopy allows for the study of optically-driven dynamics in materials. Yet, its potential to probe current- or field-driven dynamics of magnetic textures has remained unexplored.

In this work, ultrafast Lorentz imaging is developed to map the time-resolved gyration of vortices in a magnetic nanostructure driven by radio-frequency currents. The tracking of the vortex core with a localization precision of ± 2 nm and a temporal resolution below 3 ps is demonstrated [1]. Moreover, we find a transient change in the frequency and damping of the core orbit, attributed to structural disorder in the sample. Combining time-resolved Lorentz microscopy with bright-field imaging is used to identify the origin of this disorder, indicating grain boundaries in the polycrystalline film to be a major source of pinning [2].

[1] M. Möller et al., Commun Phys 3, 36 (2020).

[2] M. Möller et al., Phys. Rev. Research 4, 013027 (2022).

30 min. discussion break and bestowal of INNOMAG e.V. Diplom-/Master Prize and Ph.D. Thesis Prize

MA 16: Magnonics

Time: Tuesday 9:30–12:00

Location: HSZ 403

MA 16.1 Tue 9:30 HSZ 403

Resonances in periodically driven magnon systems — •JAN MATHIS GIESEN, CHRISTOPH DAUER, IMKE SCHNEIDER, SEBASTIAN EGGERT, ALEXANDRE ABBASS HAMADEH, and PHILIPP PIRRO — Department of Physics and Research Center Optimas, Technical University of Kaiserslautern, 67663 Kaiserslautern, Germany
Parametric resonances in ferro- and ferri-magnetic systems under a periodic drive are known for quite some while. So called parallel pumping, which is for example used to realize Magnon BECs in materials like YIG, is normally achieved by driving the system with twice the frequency of a certain magnon mode. Much less research has been dedicated to lower lying resonances, which in theory should also be possible and give rise to some interesting behaviours.

We establish a method based on Floquet theory to efficiently determine and examine instabilities of the microscopic magnon system. As a central consequence parametric resonances occur if the driving frequency is an integer multiple of two times the energy of the elementary excitation. In particular we examine regions of resonances for frequencies below the energy spectrum and predict different effects depending on the driving amplitude and frequency, like the vanishing of instabilities at high driving fields. We compare our results with phenomenological approaches to investigate the role damping plays in such systems and perform micromagnetic simulations in order to confirm our results.

MA 16.2 Tue 9:45 HSZ 403

Topological Hybrids of Magnons and Magnon Bound Pairs — ALEXANDER MOOK¹, •RHEA HOYER¹, JELENA KLINOVAJA², and DANIEL LOSS² — ¹Johannes Gutenberg-University, Mainz, Germany — ²University of Basel, Basel, Switzerland

We employ anisotropic and spin-nonconserving Heisenberg models on Bravais lattices to predict the existence of topological quantum spin excitations in ferromagnets. We show that a hybridization of a single magnon and a two-magnon bound state can lead to topological spectral gaps that support quantum-Hall-like edge excitations. Such topological chiral hybrids of magnons and magnon pairs are a quantum phenomenon that vanishes in the classical limit and goes beyond the established theory of magnon topology.

Reference: Mook, Hoyer, Klinovaja, Loss, arXiv:2203.12374.

MA 16.3 Tue 10:00 HSZ 403

Finite-element micromagnetic modeling of spin-wave propagation with the open-source package TetraX — •LUKAS KÖRBER^{1,2}, GWENDOLYN QUASEBARTH^{1,2}, ALEXANDER HEMPEL^{1,2}, ANDREAS OTTO², JÜRGEN FASSBENDER^{1,2}, and ATTILA KÁKAY¹ — ¹Helmholtz-Zentrum Dresden - Rossendorf, Bautzner Landstraße 400, Dresden Germany — ²Fakultät Physik, Technische Universität Dresden

We present a finite-element-method (FEM) dynamic-matrix approach to efficiently calculate the dispersion and spatial mode profiles of spin waves propagating in waveguides with arbitrary cross-section, where the equilibrium magnetization is invariant along the propagation direction. This is achieved by solving a linearized version of the equation of motion of the magnetization numerically only in a single cross-section of the waveguide at hand. To compute the dipolar field, we present an extension of the well-known Fredkin-Koehler method to plane waves. The presented dynamic-matrix approach is implemented within our recently published open-source micromagnetic modeling package TetraX [1], which aims to provide user-friendly and versatile FEM workflows for the magnonics community (not only for the magnonics community but FEM simulations in general), covering several classes of sample geometries and, soon, also antiferromagnets. As a brief introduction, this talk will include a short live demo of TetraX.

[1] <https://gitlab.hzdr.de/micromagnetic-modeling/tetraX>

MA 16.4 Tue 10:15 HSZ 403

Confinement of Bose-Einstein magnon condensates in adjustable complex magnetization landscapes — •MATTHIAS R. SCHWEIZER, ALEXANDER J.E. KREIL, GEORG VON FREYMAN, ALEXANDER A. SERGA, and BURKARD HILLEBRANDS — Fachbereich Physik and Landesforschungszentrum OPTIMAS, RPTU Kaiserslautern-Landau, Germany

We demonstrate the capability to control a room-temperature magnon Bose-Einstein condensate (BEC) by spatial modulation of the saturation magnetization. We use laser heating in combination with a phase-based wavefront modulation technique to create adjustable temperature patterns in an yttrium-iron-garnet film. The increase in temperature leads to a decrease of the local saturation magnetization and in turn to the modification of the corresponding BEC frequency. Over time, a phase accumulation between different BEC-areas arises, leading to phase-driven magnon supercurrents.

The BEC is created by microwave parametric pumping and probed by Brillouin light scattering spectroscopy. We observe a strong magnon accumulation effect caused by magnon supercurrents for several distances between heated

regions. This accumulation effect manifests itself in the confinement of the magnon BEC, which exhibits an enhanced lifetime due to the continuous influx of magnons.

Funded by the Deutsche Forschungsgemeinschaft (DFG, German Research Foundation) – TRR 173 – 268565370 (project B04).

15 min. break

MA 16.5 Tue 10:45 HSZ 403

Time-correlated nonlinear spiking spin waves in Ga:YIG — •DAVID BREITBACH¹, MORITZ BECHBERGER¹, BJÖRN HEINZ¹, JAN MASKILL¹, BERT LÄGEL¹, CARSTEN DUBS², BURKARD HILLEBRANDS¹, and PHILIPP PIRRO¹ — ¹Fachbereich Physik and Landesforschungszentrum OPTIMAS, RPTU Kaiserslautern-Landau, Germany — ²INNOVENT e.V. Technologieentwicklung, Jena, Germany

Nonlinear spin-wave phenomena are key for magnon-based information processing and have led to the realization of numerous building blocks for spin-wave based computing. For coherent spin waves, the nonlinear frequency shift is one of the most robust nonlinear effects. In this study, we utilize this effect to build a spin-wave reservoir with temporal signal correlation. We apply time-resolved BLS microscopy to investigate the coherent excitation of spin waves by a microantenna in an in-plane magnetized, gallium-substituted yttrium iron garnet film. This system exhibits an exchange-dominated dispersion relation and PMA, resulting in a positive nonlinear frequency shift. We observe a strongly power-dependent nonlinear excitation and show that the nonlinear frequency shift creates an effective interaction between successive spin-wave excitations. This effectively serves as a fading memory in the system which can be used to temporally correlate input signals. Our work provides a foundation for future implementations of reservoir and neuromorphic computing in magnonic systems. This research is funded by the DFG - Project No. 271741898 and TRR 173-268565370 (B01) and by the ERC Grant No. 101042439 CoSpin¹.

MA 16.6 Tue 11:00 HSZ 403

Simultaneous multitone microwave emission by DC-driven spintronic nanoelement — •A. HAMADEH¹, D. SLOBODIANUK^{2,3}, R. MOUKHADER⁴, G. MELKOV², V. BORYNSKYI³, M. MOHSEN¹, G. FINOCCHIO⁴, V. LOMAKIN⁵, R. VERBA³, G. DE LOUBENS⁶, P. PIRRO¹, and O. KLEIN⁷ — ¹Fachbereich Physik and Landesforschungszentrum OPTIMAS, Technische Universität Kaiserslautern, Kaiserslautern, Germany — ²Taras Shevchenko National University of Kyiv, Kyiv 01601, Ukraine — ³Institute of Magnetism, Kyiv 03142, Ukraine — ⁴Dept. Mathematical and Computer Sciences, Physical Sciences and Earth Sciences, University of Messina, 98166 Messina, Italy — ⁵Center for Magnetic Recording Research, University of California San Diego, La Jolla, California 92093-0401, USA — ⁶SPEC, CEA, CNRS, Université Paris-Saclay, 91191 Gif-sur-Yvette, France — ⁷Univ. Grenoble Alpes, CEA, CNRS, Grenoble INP, INAC-Spintec, 38054 Grenoble, France

The generation of microwave radiation by DC-driven spintronic elements is generally considered a process that generates only one frequency at a time. In our study however, we can show by means of experimental data, micromagnetic simulations, and an analytical model that several frequencies can be generated simultaneously due to non-linear magnon coupling. This discovery opens the way for entirely new multiplexing techniques and synchronization mechanisms that can be used for communication and neuromorphic computing.

MA 16.7 Tue 11:15 HSZ 403

Sensing magnetic excitations in two-dimensional materials with single NV-centers — •HOSSEIN MOHAMMADZADEH, DOMINIK MAILE, and JOACHIM ANKERHOLD — Institute for Complex Quantum Systems Albert-Einstein-Allee 11 D-89069 Ulm

Magnetism in two-dimensional (2D) van der Waals (vdW) materials has recently emerged as one of the most promising areas in condensed matter research, with a significant potential for applications ranging from topological magnonics to low-power spintronics, quantum computing, and optical communications [1]. In this talk, we theoretically investigate the possibility of sensing magnetic excitations in such materials with nitrogen-vacancy (NV) center in diamond. The NV center in diamond is an excellent platform for noninvasively detecting nanoscale signatures and magnetic domain walls [2]. We present a description of the low-energy magnetic excitations within a Kitaev-Heisenberg model for a honeycomb lattice. Coupling these excitations to the single NV-electronic spin paves the way to use magnetic noise spectroscopy to probe magnons in such a system. Utilizing Fermi's golden rule and quantum linear response theory, we show how the spin relaxation time of the NV alters in the magnetic field induced by magnons in both bulk and topologically protected edge states. The relaxation time of the NV changes by different NV-sample distances and in various strengths of spin-spin interactions inside the material.

- [1] Qing Hua Wang et al., ACS Nano, 16, 5, 6960-7079 (2022)
 [2] Jörg Wrachtrup et al. Nat Commun 12, 1989 (2021)

MA 16.8 Tue 11:30 HSZ 403

Magnetic excitations in the conductive altermagnet RuO₂: ab initio calculations — •ALBERTO MARMODORO¹, SERGIY MANKOVSKY², HUBERT EBERT², ILJA TUREK³, TOMAS JUNGWIRTH¹, and ONDŘEJ ŠÍPŘ^{1,4} — ¹Institute of Physics (FZU) of the Czech Academy of Sciences, Prague, Czech Republic — ²Department of Chemistry, Ludwig-Maximilians- University (LMU), Munich, Germany — ³Institute of Physics of Materials (IPM) of the Czech Academy of Sciences, Brno, Czech Republic — ⁴New Technologies Research Centre, University of West Bohemia, Pilsen, Czech Republic

Altermagnets are materials with zero net magnetization, alike traditional antiferromagnets, as well as a characteristic alternation of spin polarization for the electronic structure in reciprocal space, due to the relative orientation for anisotropic crystal field effects on different magnetic sublattices in direct space. This may have significant implications for possible spintronics and nano-electronics applications [1]. We report about the ab initio study of magnetic excitations in the case of the conducting, colinear antiferromagnetic altermagnet material RuO₂ [2].

- [1] <http://doi.org/10.1103/PhysRevX.12.031042>
 [2] <http://doi.org/10.48550/arXiv.2211.13806>

MA 17: Thin Films: Magnetic Anisotropy

Time: Tuesday 9:30–11:00

MA 17.1 Tue 9:30 POT 6

Micromagnetic parameters and longitudinal relaxation in ultrathin asymmetrically sandwiched magnetic films — •OLEKSII M. VOLKOV¹, IVAN A. YASTREMSKY², OLEKSANDR V. PYLYPOVSKYI^{1,3}, FLORIAN KRONAST⁴, CLAAS ABERT⁵, EDUARDO SERGIO OLIVEROS MATA¹, PAVLO MAKUSHKO¹, MOHAMAD-ASSAAD MAWASS⁴, VOLODYMYR P. KRAVCHUK⁶, DENIS D. SHEKA², BORIS A. IVANOV⁷, JÜRGEN FASSBENDER¹, and DENYS MAKAROV¹ — ¹Helmholtz-Zentrum-Dresden-Rossendorf, Dresden, Germany — ²Taras Shevchenko National University of Kyiv, Kyiv, Ukraine — ³Kyiv Academic University, Kyiv, Ukraine — ⁴Helmholtz-Zentrum Berlin für Materialien und Energie, Berlin, Germany — ⁵University of Vienna, Wien, Austria — ⁶Karlsruher Institut für Tech, Karlsruhe, Germany — ⁷Institute of Magnetism, Nation, Kyiv, Ukraine

Ultrathin asymmetric magnetic films are a prominent material science platform, which combines unique magnetic and electronic properties enabling prospective memory and logic spin-orbitronic devices. Here, we present the quantification mechanism to distinguish all static and dynamic micromagnetic parameters of the layer stack based on magnetometry [1] and quasi-static morphology experiments on domain wall equilibrium tilts [2]. The DW damping is found to be about 0.1 [2] and it is demonstrated to arise from a longitudinal relaxation being dominant among transversal mechanisms for ultrathin films [3].

- [1] I. A. Yastremsky et al., Phys. Rev. Appl. 12, 064038 (2019).
 [2] O. M. Volkov et al., Phys. Rev. Appl. 15, 034038 (2021).
 [3] I. A. Yastremsky et al., Phys. Rev. Appl. 17, L061002 (2022).

MA 17.2 Tue 9:45 POT 6

Control of magnetoelastic coupling in Ni/Fe multilayers using He⁺ ion irradiation — •GIOVANNI MASCIOCCHI^{1,2}, GYAN VAN DER JAGT^{3,4}, MARIA-ANDROMACHI SYSKAKI^{2,5}, ALESSIO LAMPERTI⁶, NIKLAS WOLFF⁷, ANDRIY LOTNYK⁸, JURGEN LANGER⁵, LORENZ KIENLE⁷, GERHARD JAKOB², BENJAMIN BORIE³, ANDREAS KEHLBERGER¹, DAFINE RAVELOSONA³, and MATHIAS KLÄUI² — ¹Sensitec GmbH, Mainz, Germany — ²Johannes Gutenberg University Mainz, Mainz, Germany — ³Spin-Ion Technologies, Palaiseau, France — ⁴Universite Paris-Saclay, Gif-sur-Yvette, France — ⁵Singulus Technologies AG, Kahl am Main, Germany — ⁶CNR-IMM, Agrate Brianza, Italy — ⁷Kiel University, Kiel, Germany — ⁸Institute of Surface Engineering, Leipzig, Germany

The requirements for the magnetoelastic coefficient in thin films are often demanding. For example, magnetic sensors mostly require strain immunity, while actuators require giant strain effects. One way to obtain the desired value of the saturation magnetostriction, is to use the combination of two or more materials with different magnetic and magnetoelastic properties in a multilayer fashion. However, the material choice alone, does not allow for a local control of the magnetostriction. In this study [1], we investigate the effects of He⁺ irradiation on the magneto-elastic properties of a Ni/Fe multi-layered stack. The progressive intermixing caused by He⁺ irradiation at the interfaces of the multilayer, allows us to locally change the magnetoelastic coupling sign with increasing He⁺ fluences.

- [1] Masciocchi, et al. Appl. Phys. Lett. 121.18 182401, 2022

MA 16.9 Tue 11:45 HSZ 403

Investigation of magnon-phonon coupling in two dimensional ferromagnetic Fe₃GeTe₂ — •NAMRATA BANSAL¹, QILI LI¹, PAUL NUFER¹, HUNG-HSIANG YANG¹, LICHUAN ZHANG², DONGWOOK GO², AMIR-ABBAS HAGHIGHIRAD³, YURIY MOKROUSOV^{2,4}, and WULF WULFHEKEL^{1,3} — ¹Physikalisches Institut, Karlsruhe Institute of Technology, 76131 Karlsruhe, Germany — ²Peter Gruenberg Institut (PGI-1) and Institute for Advanced Simulation (IAS-1) Forschungszentrum Juelich GmbH, D-52425 Juelich — ³Institute for Quantum Materials and Technologies, Karlsruhe Institute of Technology, 76131 Karlsruhe, Germany — ⁴Institute of Physics, Johannes Gutenberg-University Mainz, 55099 Mainz, Germany

We use inelastic tunneling spectroscopy (ITS) at 35 mK to investigate phonon-magnon coupling in the ferromagnetic van der Waals crystals Fe₃GeTe₂ (FGT). ITS is a powerful tool for determining the inelastic scattering of hot carriers with magnons or phonons with the second derivative of the tunneling current with respect to the bias voltage being proportional to the density of states of phonons and/or magnons. We observe excitation peaks at low energy which do not correspond to van Hove singularities of the phonon or magnon density of states but to points in their dispersion, where magnon and phonon bands cross, indicative for phonon-magnon coupling.

Location: POT 6

MA 17.3 Tue 10:00 POT 6

Simulating the magnetic structures in twisted double bilayer CrI₃ — •JUNICHI OKAMOTO¹, BOWEN YANG², TARUN PATEL², and ADAM TSEN² — ¹University of Freiburg, Freiburg, Germany — ²University of Waterloo, Waterloo, Canada

After the discovery of superconductivity in twisted bilayer graphene at magic angles, control of material properties by twisting two-dimensional materials has emerged as "twistronics". In this talk, we will discuss the magnetic structures appearing in the Moiré superlattices of twisted double bilayer CrI₃. By using classical spin simulations, we will demonstrate that the subtle competition between the exchange anisotropy and the spatially modulated interlayer coupling is the key to understanding the experimentally observed magnetic transitions. We will further explain how the interlayer charge transport depends on the magnetic structures. The effect of various domain walls and skyrmions will also be scrutinized.

MA 17.4 Tue 10:15 POT 6

Characteristics and origin of a SrRuO₃ exchange spring — •MARTIN M. KOCH, ANTONIA RIECHE, DIANA A. RATA, and KATHRIN DÖRR — Martin-Luther-Universität Halle-Wittenberg

A particular type of strong interface coupling between magnets is the exchange spring which resembles an interface-parallel domain wall formed in one (or both) magnets. Advances in thin film growth and resulting interface quality of magnetic oxides improve chances to observe such strong exchange coupling across interfaces. Nevertheless, known exchange springs in oxides are yet scarce [1], since the unambiguous identification is not straightforward. An intensely studied model system for strong interface coupling is SrRuO₃/La_{0.7}Sr_{0.3}MnO₃ coherently grown on SrTiO₃(001) substrate. We summarize here the characteristics and suggested origin of the Bloch-type exchange spring forming at this interface in bilayers grown by pulsed laser deposition. Strikingly, the spring forms in hard-magnetic SrRuO₃ where magnetic anisotropy is suppressed within few unit cells from the interface. We suggest the transfer of oxygen octahedra rotations / tilts to be responsible, a structural coupling mechanism occurring at many other coherent oxide interfaces. Implications of the noncollinear spin configuration for spintronic functionalities will be addressed.

- [1] A. M. Kane, Phys. Rev. Mater. 3, 014413 (2019)

MA 17.5 Tue 10:30 POT 6

Characterization of buffer-free Sm(Co_{5-x}Cu_x)₅ thin films grown by molecular beam epitaxy — •GEORGIA GKOUZIA¹, DAMIAN GÜNZING², TERESA WESSELS^{2,3}, MARTON MAJOR¹, ALPHA T. N DIAYE⁴, ANDRAS KOVACS³, HEIKO WENDE², KATHARINA OLLEFS², and LAMBERT ALFF¹ — ¹Technical University of Darmstadt, Materials Science, Darmstadt, Germany — ²University of Duisburg-Essen, Faculty of Physics and Center for Nanointegration, Duisburg, Germany — ³Ernst Ruska-Centre for Microscopy and Spectroscopy with Electrons and Peter Gruenberg Institute, Forschungszentrum Juelich, Germany — ⁴Lawrence Berkeley National Laboratory, Berkeley, USA

SmCo₅ permanent magnets were already known in the 60s due to their enormous uniaxial magnetic anisotropy K₁=17.2 MJ/m³ which has made them key materials for many applications. Sm-Co system, in a certain parameter range, undergoes a phase decomposition into a nanocomposite of SmCo₅ and Sm₂Co₁₇

phases. Since it is known that Cu stabilizes the SmCo_5 phase, in this work, buffer-free $\text{Sm}(\text{Co}_{5-x}\text{Cu}_x)_5$ thin films have been grown by molecular beam epitaxy (MBE). The films have been characterized by x-ray diffraction (XRD), superconducting quantum interference device (SQUID), and transition electron microscopy (TEM). High coercivity, 1.67 T has been achieved, among the largest values for buffer-free SmCo_5 films. X-ray magnetic circular dichroism (XMCD) element-specific hysteresis loops show clear evidence of the Sm-Co de-coupled moments due to Cu substitution in the Co-sublattice.

MA 17.6 Tue 10:45 POT 6

Europium oxide: Growth guide for the first monolayers on oxidic substrates — •PAUL ROSENBERGER^{1,2} and MARTINA MÜLLER² — ¹Fakultät Physik, Technische Universität Dortmund, 44221 Dortmund, Germany — ²Fachbereich Physik, Universität Konstanz, 78457 Konstanz, Germany

Interfacial oxygen exchange at oxide interfaces bears huge potential in stabilizing metastable or novel phases of functional oxides down to the monolayer

limit. Consequently, controlling the underlying interfacial processes opens up the possibility to tailor and tune functionalities of oxide interfaces. By taking advantage of active oxygen supply of the substrate material, waiving any external oxygen dosage, high-quality, crystalline ultrathin films of the Heisenberg ferromagnet europium monoxide (EuO) were stabilized on YSZ (001)[1]. This so-called redox-assisted growth mode was monitored end to end by in situ x-ray photoelectron spectroscopy. The evolution of Eu 3d core levels allows us to disentangle the processes of interfacial oxygen diffusion and vacancy formation in stabilizing the very first monolayers of EuO on YSZ (001). An expedient background correction analysis is presented, which allows us to quantify the critical $\text{Eu}^{3+}/\text{Eu}^{2+}$ ratio in the ultrathin film regime. We concluded on the key mechanisms of redox-assisted EuO/YSZ (001) thin film synthesis, merging in a universal three-process growth model that may serve as guideline for redox-assisted synthesis of metastable low-dimensional oxides.

[1] P. Rosenberger and M. Müller, Phys. Rev. Mater. 6, 044404 (2022).

MA 18: Functional Antiferromagnetism I

Time: Tuesday 15:00–17:15

Location: HSZ 02

MA 18.1 Tue 15:00 HSZ 02

Magnetization dynamics in hybrid $\text{Mn}_2\text{Au}/\text{Ni}_{80}\text{Fe}_{20}$ system — •HASSAN AL-HAMDO¹, TOBIAS WAGNER², YARYNA LYTUVYENKO², GUTENBERG KENDZO¹, SONKA REIMERS², MORITZ RUHWEDDEL¹, MISBAH YAQOUB¹, PHILIPP PIRRO¹, OLENA GOMONAY², VITALIY I. VASYUCHKA¹, MATHIAS KLÄUI², MARTIN JOURDAN², and MATHIAS WEILER¹ — ¹Fachbereich Physik and Landesforschungszentrum OPTIMAS, Rheinland-Pfälzische Technische Universität Kaiserslautern-Landau, 67663 Kaiserslautern, Germany — ²Institute of Physics, Johannes Gutenberg-University Mainz, 55099 Mainz, Germany

We study the magnetization dynamics of $\text{Mn}_2\text{Au}/\text{Ni}_{80}\text{Fe}_{20}$ thin film bilayers. This system allows us to control the Mn_2Au Néel vector orientation with moderate external magnetic fields [1]. Furthermore, Mn_2Au enables current pulse induced switching of the Néel vector via Néel spin-orbit torques [2] making this system intriguing for antiferromagnetic spintronics. By varying the thickness of the ferromagnetic layer, we investigated the effect of strongly exchange coupled $\text{Mn}_2\text{Au}/\text{Ni}_{80}\text{Fe}_{20}$ interface on the spin dynamics. Broadband ferromagnetic resonance and Brillouin light scattering experiments reveal that interfacial exchange coupling causes an increase in the resonance frequency of $\text{Ni}_{80}\text{Fe}_{20}$. Our theoretical model based on the modification of the spin-wave wavevector due to interfacial coupling yields good agreement with the experimental observations.

[1] Bommanaboyena et al., Nature Communications 12, 6539 (2021) [2] Y. Lytvynenko et al., arXiv:2208.04048v1 (2022).

MA 18.2 Tue 15:15 HSZ 02

Magnetization dynamics in hybrid ferromagnetic / antiferromagnetic systems — •TOBIAS WAGNER¹, HASSAN AL-HAMDO², MATHIAS WEILER², and OLENA GOMONAY¹ — ¹Institut für Physik, JGU Mainz, Germany — ²Fachbereich Physik and Landesforschungszentrum OPTIMAS, RPTU in Kaiserslautern, Germany

Strong exchange coupling between Mn_2Au and thin layers of Permalloy ($\text{Ni}_{80}\text{Fe}_{20}$) has been shown [1]. As a consequence, the coercive field of $\text{Mn}_2\text{Au}/\text{Ni}_{80}\text{Fe}_{20}$ was reported to be 0.5 T, which is high compared to 0.02 T in CuMnAs/Fe [2]. Due to strong exchange coupling, the AFM Néel vector and the ferromagnetic (FM) magnetisation rotate coherently, when an external field is applied to the FM. Control of the Néel ordered state in Mn_2Au and the $\text{Ni}_{80}\text{Fe}_{20}$ spin dynamics has been studied by varying the $\text{Ni}_{80}\text{Fe}_{20}$ layer thickness [3]. Ferromagnetic resonance spectroscopy revealed two distinct frequencies for the coupled bilayer system, both of which lie above the resonance frequency of Permalloy [3]. We calculate the spectra of the magnons in the coupled FM/AFM system within micromagnetic model. Our model enables us to demonstrate how the interfacial exchange coupling enables tuning of the ferromagnetic resonance frequency by variation of the thickness of the ferromagnetic layer. We estimate the exchange coupling strength to be 5 T [3]. References: [1] Bommanaboyena, S. P. et al., Nat. Comm. 12, 6539 (2021), [2] Wadley, P. et al., Sci. Rep. 7, 11147 (2017), [3] Al-Hamdo, H. et al., unpublished.

MA 18.3 Tue 15:30 HSZ 02

Optically Triggered Néel Vector Manipulation of a Metallic Antiferromagnet Mn_2Au under Strain — VLADIMIR GRIGOREV¹, MARIJA FILIANINA¹, YARYNA LYTUVYENKO¹, SERGEI SOBOLEV¹, AMRIT RAJ POKHAREL¹, •AMON P. LANZ¹, ALEXEY SAPOZHNIK², ARMIN KLEIBERT³, STANISLAV BODNAR⁴, PETR GRIGOREV⁵, YURI SKOURSKI⁶, MATHIAS KLÄUI¹, HANS-JOACHIM ELMERS¹, MARTIN JOURDAN¹, and JURE DEMSAR¹ — ¹JGU, Mainz, Germany — ²École Polytechnique, Lausanne, Switzerland — ³PSI, Villigen, Switzerland — ⁴TUM, Munich, Germany — ⁵Aix-Marseille Université, Marseille, France — ⁶HZDR, Dresden, Germany

The absence of stray fields, their insensitivity to external magnetic fields, and ultrafast dynamics make antiferromagnets promising candidates for active elements in spintronic devices. Here, we demonstrate manipulation of the Néel vector in the metallic collinear antiferromagnet Mn_2Au by combining strain and femtosecond laser excitation. Applying tensile strain along either of the two in-plane easy axes and locally exciting the sample by a train of femtosecond pulses, we align the Néel vector along the direction controlled by the applied strain. The dependence on the laser fluence and strain suggests the alignment is a result of optically triggered depinning of 90° domain walls and their motion in the direction of the free energy gradient, governed by the magneto-elastic coupling. The resulting, switchable state is stable at room temperature and insensitive to magnetic fields. Such an approach may provide ways to realize robust high-density memory device with switching time scales in the picosecond range.

MA 18.4 Tue 15:45 HSZ 02

Long-distance magnon spin transport in Orthoferrites. — •E.F. GALINDEZ-RUALES¹, S. DAS¹, X. X. MA², G. JAKOB¹, S. X. CAO², R. LEBRUN³, and M. KLÄUI¹ — ¹Institute of Physics, Johannes Gutenberg University Mainz, Staudingerweg 7, 55128 Mainz, Germany. — ²Department of Physics, Materials Genome Institute, International Center for Quantum and Molecular Structures, Shanghai University, Shanghai 200444, China. — ³Unité Mixte de Physique CNRS, Thales, Université Paris-Saclay, Palaiseau 91767, France.

Antiferromagnets have advantages over ferromagnets, such as terahertz-range magnetization dynamics and stability against external magnetic fields. The efficient transport of spin waves has until now only been observed in the insulating antiferromagnet hematite [1]. In this work [2], we report long-distance spin transport in the antiferromagnetic orthoferrite $Y\text{FeO}_3$; although the magnetic damping order is in the same range as hematite, the spin transport is different. At zero magnetic field, the magnon modes in $Y\text{FeO}_3$ are linearly polarized, which cannot transport the spin angular momentum. Nevertheless, under an external magnetic field and the presence of DMI, spin information is carried by elliptically polarized modes. We observe a strong anisotropy in the magnon decay lengths that we attributed to the role of the magnon group velocity in the transport of spin waves in antiferromagnets. This unique mode of transport identified in $Y\text{FeO}_3$ opens up all the canted antiferromagnets for long-distance spin transport. [1] Lebrun, R., et al. Nat Commun. 11, 6332 (2020). [2] Das, S., et al. Nat. Commun. 13, 6140 (2022).

15 min. break

MA 18.5 Tue 16:15 HSZ 02

Coexistence of antiferromagnetism and ferrimagnetism in adjacent honeycomb layers — •LILIAN PRODAN^{1,2}, VIOREL FELEA^{1,2,3}, YURI SKOURSKI³, SERGEI ZHERLITSYN³, JOACHIM WOSNITZA³, ALEXANDER TSIRLIN⁴, VLADIMIR TSURKAN^{1,2}, and ISTVAN KEZSMARKI¹ — ¹Experimental Physics V, Institute of Physics, University of Augsburg, D-86159, Augsburg, Germany — ²Institute of Applied Physics, MD 2028, Chisinau, R. Moldova — ³Hochfeld-Magnetlabor Dresden (HLD-EMFL), HZDR, 01328 Dresden, Germany — ⁴Felix Bloch Institute for Solid-State Physics, Leipzig University, 04103 Leipzig, Germany

Recent theoretical and experimental studies of the honeycomb antiferromagnets $\text{A}_2\text{Mo}_3\text{O}_8$ ($\text{A} = \text{Mn}, \text{Fe}, \text{Co}, \text{Ni}, \text{Zn}$) revealed a plethora of fascinating effects, such as strong linear and non-linear magnetoelectric effects, giant magnetoelectricity, hidden ferromagnetism, and topological magnons, being of interest for both fundamental and applied research. Here, we report a sequence of metamagnetic transitions in the polar antiferromagnet $\text{Co}_2\text{Mo}_3\text{O}_8$ based on magnetization, torque and ultrasound measurements in static and pulsed magnetic fields up to 65 T. Our studies reveal a novel spin state that is composed of an alternating

stacking of antiferromagnetic and ferrimagnetic honeycomb layers. The strong intra-layer and the weak inter-layer exchange couplings together with competing anisotropies at octahedral and tetrahedral Co sites are identified as the key ingredients to stabilize antiferromagnetic and ferrimagnetic layers in such a close proximity [1]. [1]. D. Szaller et al., arXiv:2202.04700 (2022).

MA 18.6 Tue 16:30 HSZ 02

Anisotropic effects in antiferromagnetic curvilinear spin chains — •OLEKSANDR V. PYLYPOVSKIY^{1,2}, YELYZAVETA A. BORYSENKO³, DENYS Y. KONONENKO⁴, KOSTIANTYN V. YERSHOV⁴, ULRICH K. ROESSLER⁴, ARTEM V. TOMILO^{1,3}, JEROEN VAN DEN BRINK⁴, JÜRGEN FASSBENDER¹, DENIS D. SHEKA³, and DENYS MAKAROV¹ — ¹Helmholtz-Zentrum Dresden-Rossendorf e.V., Institute of Ion Beam Physics and Materials Research, Dresden — ²Kyiv Academic University, 03142 Kyiv, Ukraine — ³Taras Shevchenko National University of Kyiv, 01601 Kyiv, Ukraine — ⁴IFW Dresden

Curvilinear spin chains are simplest antiferromagnetic systems revealing direct influence of their shape onto magnetic states via geometry-tracking anisotropies stemming from the dipolar interaction [1] or local surrounding [2]. Here, we show that in addition to the strongest effect onto magnetic state from exchange (biaxial anisotropy and chiral energy term) [1], the local break of the translational symmetry in curvilinear anisotropic antiferromagnets leads to (i) the longitudinal Dzyaloshinskii-Moriya energy term stemming from the single-ion anisotropy and (ii) the local weakly ferromagnetic response [2]. Furthermore, non-zero curvature κ can drive the helimagnetic phase transition in the spin-flop phase and enables the intermediate canted state for rings with large enough κ . [1] O. Pylypovskiy, D. Kononenko et al., Nano Lett. 20, 8157 (2020); [2] O. Pylypovskiy et al., Appl. Phys. Lett. 118, 182405 (2021); [3] Y. Borysenko et al., Phys. Rev. B, 106, 174426 (2022).

MA 18.7 Tue 16:45 HSZ 02

Spin-current driven Dzyaloshinskii-Moriya interaction in the multiferroic BiFeO₃ from first-principles — •SEBASTIAN MEYER¹, BIN XU^{2,3}, MATTHIEU J. VERSTRAETE¹, LAURENT BELLAÏCHE³, and BERTRAND DUPÉ^{1,4} — ¹Université de Liège, Belgium — ²Soochow University, China — ³University of Arkansas, USA — ⁴Fonds de la Recherche Scientifique (FRS-FNRS), Belgium

The electrical control of magnons opens up new ways to transport and process information for logic devices. In magnetoelectrical multiferroics, the

Dzyaloshinskii-Moriya (DM) interaction directly allow for such a control and, hence, is of major importance [1]. We determine the origin and strength of the (converse) spin current DM interaction [2,3] in the *R3c* bulk phase of the multiferroic BiFeO₃ based on density functional theory. Our data supports only the existence of one DM interaction contribution originating from the spin current model. By exploring the magnon dispersion in the full Brillouin Zone, we show that the exchange is isotropic, but the DM interaction and anisotropy prefer any propagation and magnetization direction within the full (111) plane. Our work emphasizes the significance of the asymmetric potential induced by the spin current over the structural asymmetry induced by the anionic octahedron in multiferroics such as BiFeO₃.

[1] P. Rovillain, *et. al.*, Nature Materials 9, 975 (2010)

[2] H. Katsura, *et. al.*, Phys. Rev. Lett. 95, 057205 (2005)

[3] D. Rahmedov, *et. al.*, Phys. Rev. Lett. 109, 037207 (2012)

MA 18.8 Tue 17:00 HSZ 02

Decoding Antiferromagnetism via Quadrupolar Far Fields — •MICHAEL PAULSEN¹, MICHAEL FECHNER², JULIAN LINDNER³, RALF FEYERHERM³, JÖRN BEYER¹, BASTIAN KLEMKE³, YUKI LINO⁴, TSUYOSHI KIMURA⁵, KLAUS KIEFER³, and DENNIS MEIER^{6,7} — ¹Physikalisch-Technische Bundesanstalt, Berlin, Germany — ²Max Planck Institute for the Structure and Dynamics of Matter, CFEL, Hamburg, Germany — ³Helmholtz-Zentrum Berlin für Materialien und Energie, Germany — ⁴Division of Materials Physics, Osaka University, Japan — ⁵Department of Advanced Materials Science, University of Tokyo, Japan — ⁶Department of Materials Science and Engineering, Norwegian University of Science and Technology (NTNU), Trondheim, Norway — ⁷Center for Quantum Spintronics, NTNU, Trondheim, Norway

Antiferromagnets possess zero net dipole magnetization, whereas magnetic higher-order contributions are, in principle, allowed by symmetry. Such higher-order contributions are, however, usually extremely weak and hard to detect experimentally. Here, we present low-temperature magnetometry measurements of the higher-order far fields of the antiferromagnetic model systems Cr₂O₃ and TbMnO₃, using a dedicated SQUID setup. Our results reveal exterior quadrupolar magnetic fields specific to the emergent microscopic spin textures, providing new opportunities for the characterization of antiferromagnets and materials with ultra-small remanent magnetization in general.

MA 19: Molecular Magnetism I

Time: Tuesday 15:00–17:00

Location: HSZ 04

MA 19.1 Tue 15:00 HSZ 04

Molecular orientation of Er(III) cyclooctatetraene-based single-molecule magnets on Ag(100) — •VLADYSLAV ROMANKOV¹, NIÉLI DAFFÉ¹, DIANA VACLAVKOVA¹, MARTIN HEINRICH¹, MATTHIAS MUNTWILER¹, BERNARD DELLEY¹, KATIE HARRIMAN², MURALEE MURUGESU², MORITZ BERNHARDT³, MACIEJ KORZYŃSKI³, CHRISTOPHE COPÉRET³, and JAN DREISER¹ — ¹PSI, Switzerland — ²uOttawa, Canada — ³ETH Zurich, Switzerland

Recently, organometallic lanthanide(III)-based single-molecule magnets (SMMs) have shown outstanding magnetic properties up to liquid nitrogen temperature [1]. SMMs with planar ligands, like COT²⁻ (cyclooctatetraene anion) and Cp^{*-} (pentamethylcyclopentadienide), are good candidates to form ordered monolayers, but the packing and the molecule-substrate interaction play a vital role in the properties of such molecules when deposited on metal surfaces [2]. In the present work we show how two similar Er(III) SMMs, K[Er(COT)₂] and Cp^{*}ErCOT, order very differently on Ag(100). In particular, X-ray linear and magnetic circular dichroism measurements show that the easy axis of K[Er(COT)₂] aligns parallel to the surface, while that of Cp^{*}ErCOT SMMs is consistent with a mixed standing-lying phase. Indeed, low-temperature scanning tunneling microscopy reveals that Cp^{*}ErCOT forms alternating rows of standing-up and lying-down molecules, while X-ray photoemission spectroscopy reveals the integrity of both the SMMs and suggests a weak molecule-surface interaction.

References: [1] F. S. Guo et al., Science, 362, 1400, (2018); [2] C. Wäckerlin et al., Advanced Materials, 28, 5142, (2016).

MA 19.2 Tue 15:15 HSZ 04

Machine learning based parameterization of magnetic data of single-molecule magnets — •ZAYAN AHSAN ALI, JULIUS MUTSCHLER, and OLIVER WALDMANN — Physikalisches Institut, Universität Freiburg, D-79104 Freiburg, Germany

Single molecule magnets (SMMs) have attracted a rich volume of research in the last two decades due to their potential applications in magnetic memory and quantum computing. Lanthanide-based SMMs in particular demonstrate promising magnetic retention due to large inherent anisotropies. Their magnetic properties can be parameterized by ligand-field theories involving a set

of 28 parameters. Experimental data such as magnetization and susceptibility curves, however, are typically featureless for these materials. Multiple distinct parameter sets can describe the data to equal accuracy, making it a formidable task to determine the model parameters for a compound. In this work, the over-parameterization is tackled by Machine Learning (ML) applied to data simulated for a single-ion model. For dimensionality reduction, a variational autoencoder is used to determine hidden system parameters of the data, and an invertible neural network is used to relate hidden parameters with the model parameters from ligand-field theory. The effectiveness of this ML model in producing consistent sets of ligand-field parameters for novel experimental data is investigated and presented.

MA 19.3 Tue 15:30 HSZ 04

Temperature-dependent Raman spectroscopy studies of a Fe(II) spin-crossover complex — •LEA SPIEKER¹, STEPHAN SLEZIONA¹, GÉRALD KÄMMERER¹, ANDRÉ MAAS¹, SOMA SALAMON¹, SENTHIL KUMAR KUPPUSAMY², MARIO RUBEN², UWE BOVENSIEPEN¹, PETER KRATZER¹, MARIKA SCHLEBERGER¹, and HEIKO WENDE¹ — ¹Faculty of Physics and Center for Nanointegration Duisburg-Essen (CENIDE), University of Duisburg-Essen — ²Institute of Quantum Materials and Technologies (IQMT), Karlsruhe Institute of Technology

Spin-crossover complexes with a bi-stable spin-state switching in the room temperature regime, influenced by external stimuli such as light, pressure, or temperature, are desirable for future applications, e.g., molecular switches. Combining Raman spectroscopy with optical microscopy, we investigated a Fe(II) complex showing a spin-state switching from a diamagnetic low-spin (S=0) to a paramagnetic high-spin (S=2) state in the room temperature regime ($T_{1/2} = 298$ K) with a broad thermal hysteresis of $\Delta T = 44$ K. Notable molecular bond changes during the temperature-induced spin-state switching are confirmed by Raman spectroscopy measurements combined with density functional theory calculations. In addition, optical microscopy during heating and cooling allowed us to observe the spin-state switching on a macroscopic scale. We gratefully acknowledge the financial support by CRC 1242 Projects A05, B02, and C05 (Project-ID 278162697).

MA 19.4 Tue 15:45 HSZ 04

Spin transition of spin-crossover molecules supported by tridentate ligands deposited on HOPG — •JORGE TORRES¹, JAN GRUNWALD², SASCHA OSSINGER², SANGEETA THAKUR¹, CLARA W. A. TROMMER², MARCEL WALTER¹, IVAR KUMBERG¹, RAHL HOSSEINIFAR¹, EVANGELOS GOLIAS¹, SEBASTIEN HADJAJ¹, JENDRIK GÖRDES¹, PIN-CHI LIU¹, CHEN LUO³, LALMINTHANG KIPGEN¹, TAUQUIR SHINWARI¹, FLORIN RADU³, FELIX TUCZEK², and WOLFGANG KUCH¹ — ¹Freie Universität Berlin, Institut für Experimentalphysik, Berlin, Germany — ²Christian-Albrechts-Universität zu Kiel, Institut für Anorganische Chemie, Kiel, Germany — ³Helmholtz-Zentrum Berlin für Materialien und Energie, Berlin, Germany

In a spin-crossover molecule (SCM) the excitation and relaxation processes can be stimulated by temperature, pressure or light. The latter is known as the light-induced excited spin-state trapping (LIESST) effect. The excitation of the high-spin (HS) and relaxation to low-spin (LS) state can exhibit single- or multi-exponential behavior. Here, we investigate the behavior of different thicknesses of the SCM [Fe{H₂B(pz)(pypz)}₂] [1] and [Fe{pypypyr}₂] deposited on highly oriented pyrolytic graphite (HOPG) by X-ray absorption and differential reflectance spectroscopy. The results show that the amount of molecules in the HS state as a function of temperature at constant illumination presents a sigmoidal behavior. The relaxation rates are discussed in the context of the inverse energy gap law, which is usually invoked to interpret the LIESST behaviour of Fe(II) complexes.

[1] S. Ossinger et al., *Inorg. Chem.*, 2020, 59, 7966-7979

15 min. break

MA 19.5 Tue 16:15 HSZ 04

Observation of exchange interaction in Iron(II) spin crossover molecules in contact with passivated ferromagnetic surface of Co/Au(111) — •HONGYAN CHEN¹, HUNG-HSIANG YANG¹, TIMO FRAUHAMMER¹, HAORAN YOU¹, QING SUN², PETER NAGEL^{3,4}, STEFAN SCHUPPLER^{3,4}, ANA BELÉN GASPÁR⁵, JOSÉ ANTONIO REAL⁵, and WULF WULFHEKEL^{1,3} — ¹Physikalisches Institut, Karlsruhe Institute of Technology (KIT), Germany — ²Laboratory for Electron Microscopy, KIT — ³Institute for Quantum Materials and Technologies, KIT — ⁴Karlsruhe Nano Micro Facility, KIT — ⁵Institut de Ciència Molecular, Universitat de València, Spain

Spin crossover (SCO) complexes sensitively react on changes of the environment by a change in the spin of the central metallic ion making them ideal candidates for molecular spintronics. In particular, the composite of SCO complexes and ferromagnetic (FM) surfaces would allow spin-state switching of the molecules in combination with the magnetic exchange interaction to the magnetic substrate. Unfortunately, when depositing SCO complexes on ferromagnetic surfaces, spin-state switching is blocked by the relatively strong interaction between the adsorbed molecules and the surface. Here, the Fe(II) SCO complex with submonolayer (sub-ML) thickness in contact with a passivated FM film of Co on Au(111) is studied. In this case, the molecules preserve thermal spin crossover and at the same time the high-spin species show a sizable exchange interaction of

more than 0.7 T with the FM Co substrate. These observations provide a feasible design strategy in fabricating SCO-FM hybrid devices.

MA 19.6 Tue 16:30 HSZ 04

Magnetic coupling of guest metallocene molecules with SURMOF-2 host matrix — •ALEXEI NEFEDOV¹, CHUN LI¹, KAI MÜLLER¹, ANEMAR BRUNO KANJ¹, LARS HEINKE¹, CHEN LUO², KAI CHEN², FLORIN RADU², EVANGELOS GOLIAS³, WOLFGANG KUCH³, and CHRISTOF WÖLL¹ — ¹Karlsruhe Institute of Technology, Eggenstein-Leopoldshafen, Germany — ²Helmholtz-Zentrum Berlin für Materialien und Energie, Berlin, Germany — ³Freie Universität Berlin, Berlin, Germany

Metal-organic frameworks (MOFs) are crystalline and porous, molecular solids consisting of metal nodes and organic ligands. In the case of surface-anchored MOF-2 (SURMOF-2) systems the Cu²⁺ ions are connected via carboxylate and OH groups in a zipper-like fashion. This unusual coupling of the spin-1/2 ions within the resulting 1-D chains stabilizes a low-temperature ferromagnetic (FM) phase. In this study, the magnetic properties of SURMOF-2 systems (Cu(bdc) and Cu(bpdc)) were investigated using X-ray magnetic circular dichroism both in the absorption and in the scattering geometry. Taking advantage of the element sensitivity of this technique it was established that the magnetic signal originates from Cu²⁺ ions. After loading of SURMOF-2 with metallocene molecules, the magnetic properties of the SURMOF were found to be substantially changed. In the case of nickelocene loading, a polarization effect was found resulting in ferromagnetic ordering of the guest molecules. However, the polarization effect is not observed in the case of manganocene derivatives, these molecules remained in their paramagnetic state.

MA 19.7 Tue 16:45 HSZ 04

Nickelocene molecule as an STM magnetic sensor — •ANDRES PINAR SOLE¹, OLEKSANDR STETSOVYCH¹, PAVEL JELÍNEK¹, JINDRICH KOLARENC¹, SHAOTANG SONG², JIONG LU², CHRISTIAN WACKERLIN³, and ALES CAHLIK⁴ — ¹Czech Institute of Physics — ²University of Singapore — ³Empa — ⁴University of Zurich

Functionalization of the scanning probe of a scanning tunnelling microscopy (STM) with metallocene molecule allows performing spin-sensitive measurements on magnetic systems. Here, as a magnetic sensor, we used a nickelocene molecule (NiCp2) to probe the magnetism on 1D metallorganic chains and graphene nanoribbons (GNR).

In the first part of the work, we examined two derivatives of 1D metallorganic coordination polymers (2,5-diamino-1,4-benzoquinonediimines) on Au(111) [3] with Co or Cr atoms as metal sites respectively. Nickelocene IETS conductance spectrum deformation was observed when approaching the Nc functionalized tip to the Cr sites while no spectra changes were seen on neither Co sites nor ligand sites of the polymers.

In the second part of the work, the Nc functionalized probe was also used to measure the magnetism emerging from the unpaired electron on the edge of a wave-like graphene nanoribbon (GNR) on Au(111).

To understand the IETS from the magnetic sensor, a many-body Hubbard model was proposed. It describes the electron tunnelling through the STM tip, the nickelocene, the magnetic center, and the metallic substrate.

MA 20: Spintronics (other effects)

Time: Tuesday 15:00–17:45

Location: HSZ 401

MA 20.1 Tue 15:00 HSZ 401

Ab initio studies of chiral crystals for generalized linear response transport and x-ray absorption spectroscopy — •ALBERTO MARMODORO¹, HUBERT EBERT², and ONDREJ ŠÍPŘ^{1,3} — ¹Institute of Physics (FZU) of the Czech Academy of Sciences, Prague, Czech Republic — ²Department of Chemistry, Ludwig-Maximilians-University (LMU), Munich, Germany — ³New Technologies Research Centre, University of West Bohemia, Pilsen, Czech Republic

Materials with a chiral atomic arrangement exhibit specific electronic structure features [1]. The clock-wise or anti-clock-wise winding of sublattices has been associated with a radial spin texture of the Fermi surface in reciprocal space [2]. This provides interesting consequences for the response [3] to e.g. an applied electric field, for instance in terms of Edelstein effect and particularly its dependence on the sign of the perturbation. We report generalized linear response predictions [3] and theoretical x-ray spectroscopy cross-sections [4] for inorganic bulk crystals from first-principles studies performed within the frameworks of a spin-polarized relativistic Korringa, Kohn, Rostoker (SPRKKR) treatment.

[1] <http://dx.doi.org/10.7566/JPSJ.83.061018>

[2] <http://dx.doi.org/10.1103/PhysRevLett.127.126602>, <http://dx.doi.org/10.1038/s42005-021-00564-w>

[3] <http://dx.doi.org/10.1103/PhysRevB.91.165132>

[4] <http://dx.doi.org/10.1107/S090904959801680X>

MA 20.2 Tue 15:15 HSZ 401

Crystallisation behaviour of Yttrium Iron Garnet thin films — •SEBASTIAN SAILLER¹, MICHAELA LAMMEL¹, GREGOR SKOBYJIN¹, HEIKE SCHLÖRB², ANDY THOMAS^{2,3}, and SEBASTIAN T.B. GOENNENWEIN¹ — ¹Fachbereich Physik, Universität Konstanz, 78457 Konstanz, Germany — ²Institute for Integrative Nanosciences, Leibniz Institute of Solid State and Materials Science, 01069 Dresden, Germany — ³Institut für Festkörper- und Materialphysik, Technische Universität Dresden, 01069 Dresden, Germany

Yttrium Iron Garnet (YIG) is a ferrimagnetic insulator commonly used in spin transport and spin dynamics. To obtain highly crystalline thin films we use RF-magnetron sputtering at room temperature to deposit amorphous films and a subsequent annealing step to crystallise them. However, the crystallisation from the amorphous state has not been systematically studied. We therefore analyse the crystallisation behaviour on different substrates utilizing extensive time and temperature series. Structural characterisation using X-ray techniques as well as electron diffraction allow to differentiate between amorphous, polycrystalline and epitaxial films, and to determine the optimal annealing parameters for each substrate. Additionally, we correlate the crystalline state with the resulting magnetic properties inferred from magnetometry and Kerr-microscopy. Our results provide a precise tunability of the structural and magnetic properties of YIG by a rigorous control over the crystallization induced by the subsequent annealing step.

MA 20.3 Tue 15:30 HSZ 401

Excited-state exchange interaction in NiO determined by high-resolution resonant inelastic x-ray scattering at the Ni $M_{2,3}$ edges — •CHUN-YU LIU^{1,2}, KARI RUOTSALAINEN¹, KARL BAUER¹, RÉGIS DECKER¹, ANNETTE PIETZSCH¹, and ALEXANDER FÖHLISCH^{1,2} — ¹Institute for Methods and Instrumentation for Synchrotron Radiation Research (PS-ISRR), Helmholtz-Zentrum Berlin für Materialien und Energie GmbH (HZB), Albert-Einstein-Strasse 15, 12489 Berlin, Germany — ²Institut für Physik und Astronomie, Universität Potsdam, Karl-Liebknecht-Strasse 24-25, 14476 Potsdam, Germany

The electronic and spin excitations of bulk NiO have been determined using the $^3A_{2g}$ to $^3T_{2g}$ crystal-field transition at the Ni $M_{2,3}$ edges with high resolution resonant inelastic x-ray scattering. We extract an effective exchange field of 89 ± 4 meV in the $^3T_{2g}$ excited final state from empirical two-peak spin-flip model, which is further confirmed with crystal-field model calculations using exchange fields of 60-100 meV. The lower exchange parameter in the excited state is discussed in terms of the modification of the orbital occupancy and of the structural dynamics: (A) With pure electronic effects, the lower exchange energy is attributed to the reduction in effective hopping integral. (B) With no electronic effects, we use the $S = 1$ Heisenberg model to derive a second-nearest-neighbor exchange constant $J_2 = 14.8 \pm 0.6$ meV. Based on the linear correlation between J_2 and the lattice parameter from pressure-dependent experiments, an upper limit of 2% local Ni-O bond elongation during the fs scattering duration is derived.

MA 20.4 Tue 15:45 HSZ 401

Strongly coupled magnon-plasmon polaritons in graphene-2D ferromagnet heterostructures — •ANTÓNIO COSTA¹, MIKHAIL VASILEVSKIY^{1,2}, JOAQUÍN FERNÁNDEZ-ROSSIER¹, and NUNO PERES^{1,2} — ¹International Iberian Nanotechnology Laboratory (INL) — ²Department of Physics, Center of Physics, University of Minho

Magnons and plasmons are two very different types of collective modes, acting on the spin and charge degrees of freedom, respectively. At first sight, the formation of hybrid plasmon-magnon polaritons in heterostructures of plasmonic and magnetic systems would face two challenges, the small mutual interaction, via Zeeman coupling of the electromagnetic field of the plasmon with the spins, and the energy mismatch, as in most systems plasmons have energies in the eV range, orders of magnitude larger than magnons. Here we show that graphene plasmons form polaritons with the magnons of two-dimensional ferromagnetic insulators, placed up to half a micron apart, with Rabi couplings in the range of 100 GHz (dramatically larger than cavity QED magnonics). This strong coupling is facilitated both by the small energy of graphene plasmons and the cooperative super-radiant nature of the plasmon-magnon coupling afforded by phase matching. We show that the Rabi coupling can be modulated both electrically and mechanically and we propose an attenuated total internal reflection experiment to implement ferromagnetic resonance experiments on 2D ferromagnets driven by plasmon excitation.

MA 20.5 Tue 16:00 HSZ 401

Doping induced ferromagnetism in EuTiO₃ and STO/ETO/LAO heterostructures by ab-initio calculations — •PAYAL WADHWA and ALESSIO FILIPPETTI — Department of Physics, University of Cagliari, Sardinia, Italy

The emergence of 2DEG at oxide interfaces such as LaAlO₃ (LAO) and SrTiO₃ (STO) raised an immense interest in the community of oxide electronics, because of depicting outstanding properties such as field-effect driven superconductivity, high electron mobility, and magnetoresistance. An old dream of the spintronic community, remained eluded so far, has been to spin-polarize the 2DEG by introducing a magnetic layer at the interface of LAO/STO heterostructure, which may enable it to be a paramount material for spintronics and spin-orbitronic technology. A potential candidate as magnetic interlayer is EuTiO₃ (ETO), having an identical lattice constant to STO. It is reported that ETO possesses G-type AFM ground state below $T_n = 5.3$ K, while becomes FM under tensile strain or doping. We have employed an ab-initio approach to study structural, electronic, and magnetic properties of ETO bulk and the STO/ETO/LAO heterostructure. We found, for increasing electron doping, a progressive enhancement of the FM phase in bulk ETO. Since conduction electrons can also be added to the ETO by creating a heterointerface, so we also compared the n-doped bulk ETO results with the STO/ETO/LAO heterostructure. Overall, our results for n-doped ETO and STO/ETO/LAO heterostructure depict them to be potential candidates for electronic transport and magneto-transport applications.

15 min. break

MA 20.6 Tue 16:30 HSZ 401

Magnetism and proximity-induced Rashba effect at Mn-3d bands of asymmetric BaMnO₃|KTaO₃ heterojunction — •VIVEK KUMAR and NIRMAL GANGULI — Indian Institute of Science Education and Research Bhopal, Bhauri, Bhopal 462066, India

Rashba-like spin-orbit interaction (SOI) at oxide heterostructures emerges as a much sought-after feature in the context of oxide spintronics and spin-orbitronics. KTaO₃ (KTO) is one of the best substrates available for the purpose,

owing to its strong SOI and alternating $+1| - 1$ charged layers along the (001) direction. We visualize the Rashba-like interaction in the KTO (001) surface with the help of spin texture plotted directly from DFT calculations along with the isoenergetic contours, providing a confirmatory test of the presence of only linear Rashba interaction [1]. We use *ab initio* DFT to examine the asymmetric BaMnO₃|KTaO₃ (BMO|KTO) oxide heterostructure where the inequivalent bottom and top interfaces break the inversion symmetry due to their opposite polar discontinuities. We observe Rashba-like splitting for the bands of Mn-3d near the Fermi level of C-type antiferromagnetic (AFM) BMO|KTO owing to the proximity to Ta atoms from the 5d series. We comprehensively analyze Rashba-like SOI with the help of three-dimensional band dispersion and projected spin textures for Rashba-like Mn-3d bands. Our results reveal reasonably strong linear Rashba interaction in the heterostructure. The rigorous analysis of spin textures of the AFM heterostructure presented here may be crucial for spintronics. [1] V. Kumar and N. Ganguli, Phys. Rev. B 106, 125127 (2022).

MA 20.7 Tue 16:45 HSZ 401

Spin-mixing states at finite temperature — •DANNY THONIG^{1,2}, SIMON STREIB², RAMON CARDIAS³, SUMANTA BHANDARY⁴, YAROSLAV KVASHNIN², and OLLE ERIKSSON^{2,1} — ¹Örebro University, Sweden — ²University Uppsala, Sweden — ³KTH Royal Institute of Technology, Sweden — ⁴Trinity College Dublin, The University of Dublin, Ireland

In spintronics, the electron spins are used as information carriers and, thus, the description of spin relaxation is of fundamental relevance. Spin relaxation characterises how rapidly the non-equilibrium spin population decays due to spin mixing [1], which wise versa depends on the magnetic moment length and on the temperature simulated by disorder acting on the magnetic state. But the latter phenomenon is barely understood.

We quantify the presence of spin-mixed states in spin and lattice disordered magnetic 3d transition metals by calculating the Elliot-Yafet spin-mixing parameter b^2 . Here, we are using a self-consistent, relativistic, Slater-Koster parametrized tight-binding electronic structure model.

We, first, compare our results of the collinear order in itinerant magnets with density functional theory calculations and experiment. After, we analyse b^2 at finite temperature, finding a drastic increase by a factor > 10 . This can be understood since both spin orbit coupling and disorder have a similar impact on the electronic potential [2].

[1] D. Steiauf et al., Phys. Rev. B 79 140401 (2009)

[2] L. Nordström et al., Phys. Rev. Lett. 76 4420 (1996)

MA 20.8 Tue 17:00 HSZ 401

Spin-caloritronics using spin-polarized scanning tunneling microscopy — •CODY FRIESEN and ROLAND WIESENDANGER — Department of Physics, University of Hamburg, Hamburg, Germany

The study and control of magneto- and thermoelectric effects have long been of fundamental importance, from the perspectives of both basic condensed matter research and technological development. More recently, driven by the discovery of the spin-Seebeck effect, a growing amount of research is being done at the intersection of these transport channels; a field known as spin-caloritronics [1]. The possible applications of these effects, e.g. the efficient conversion of waste heat into spin or charge currents, or the magnetic control of heat transfer on the atomic scale, have far-reaching implications for future technology.

Using spin-polarized scanning tunneling microscope (SP-STM) we have investigated magneto-Seebeck tunneling, i.e. the spin-dependent tunneling of electrons across a magnetic tunnel junction driven by a temperature gradient [2]. By scanning a (relatively) heated magnetic probe tip in tunneling contact with a magnetic sample, at cryogenic temperatures the spin-resolved thermopower of the junction can be resolved with atomic-scale lateral resolution [3,4].

In this talk I will present the experimental requirements, challenges, and advantages of using SP-STM for studies of spin-caloritronics. Following this, the expansion of this approach to the measurement of thermal spin-transfer torque, as well as further development of SP-STM as a tool for spin-caloritronic studies, will be discussed.

MA 20.9 Tue 17:15 HSZ 401

Fractional Landau-Lifshitz-Gilbert equation — ROBIN C. VERSTRATEN¹, •TIM LUDWIG¹, REMBERT A. DUINE^{1,2}, and CRISTIANE MORAIS SMITH¹ — ¹Institute for Theoretical Physics, Utrecht University, Princetonplein 5, 3584CC Utrecht, The Netherlands — ²Department of Applied Physics, Eindhoven University of Technology, P.O. Box 513, 5600 MB Eindhoven, The Netherlands

Gaining a deeper understanding of magnetization or spin dynamics is of great interest to improve modern technological devices. In particular, a deeper understanding of dissipation could help to improve device efficiency. Magnetization dynamics is often described by the Landau-Lifshitz-Gilbert equation with phenomenological Gilbert damping. Using the Caldeira-Leggett approach, we can re-derive Gilbert damping for a specific type of environment (Ohmic) but, in general, we find fractional Gilbert damping. Fractional Gilbert damping is similar to Gilbert damping but the time derivative is replaced by a fractional time derivative. Finally, we discuss experimental consequences of fractional Gilbert damping with a focus on ferromagnetic resonance experiments.

MA 20.10 Tue 17:30 HSZ 401

Driving a magnetic texture by magnon currents — •MICHAEL VOGEL^{1,2}, BERNHARD ZIMMERMANN¹, JOHANNES WILD¹, FELIX SCHWARZHUBER¹, CLAUDIA MEWES³, TIM MEWES³, JOSEF ZWECK¹, and CHRISTIAN H. BACK^{1,4} — ¹Department of Physics, Regensburg University, Regensburg, Germany — ²Institute for Materials Science, Kiel University, Kiel, Germany — ³Department of Physics and Astronomy, The University of Alabama, Tuscaloosa, USA — ⁴Department of Physics, Technical University Munich, Munich, Germany

Thermally-induced spin dynamics in solids have sparked broad interest in both fundamental physics and spintronic applications. As theoretically proposed, thermally excited magnons created by temperature gradients can be used to ma-

nipulate spin textures such as topological magnetic solitons. However, in practice, the effectiveness of such thermomagnonic torques has remained a problem. Here the dynamics of magnetic vortex cores driven by thermomagnonic torques are explored by high-resolution Lorentz Transmission Electron Microscopy. Large deflections of the magnetic vortex core transverse to the direction of the temperature gradient are observed. The magnitude of the contribution of the associated torques is determined using a generalized Thiele equation model. Our findings pave the path for thermomagnonic currents to manipulate magnetic domains and shed light on the relationship between temperature and spin. The authors gratefully acknowledge financial support from the DFG within SpinCaT (SPP 1538) and the BMBF.

MA 21: Spin-Dependent Phenomena in 2D

Time: Tuesday 15:00–17:15

Location: HSZ 403

MA 21.1 Tue 15:00 HSZ 403

Material design of topological magnetism in 2D heterostructures — •NIHAD ABUAWWAD^{1,2}, MANUEL DOS SANTOS DIAS³, and SAMIR LOUNIS^{1,2} — ¹Peter Grünberg Institut and Institute for Advanced Simulation, Forschungszentrum Jülich & JARA, 52425 Jülich, Germany — ²Faculty of Physics, University of Duisburg-Essen, 47053 Duisburg, Germany — ³Scientific Computing Department, STFC Daresbury Laboratory, Warrington WA4 4AD, United Kingdom

The discovery of two-dimensional (2D) van der Waals magnetic materials and their heterostructures provided an exciting platform for emerging phenomena with intriguing implications in information technology. CrTe₂ is a particular example that hosts complex magnetism strongly intertwined with its crystal structures [1,2]. Here, based on a multiscale modelling approach that combines first-principles calculations and a Heisenberg model, we demonstrate that interfacial this 2D layer with various Te-based layers hosting heavy or light elements enables the control of the Dzyaloshinskii-Moriya interaction and magnetic anisotropy energy of the whole heterostructure, and thereby the emergence of new magnetic phases of matter, which are of topological nature such as skyrmions and merons.

–Work funded by the Palestinian-German Science Bridge (BMBF–01DH16027) and Priority Programme SPP 2244 2D Materials Physics of van der Waals Heterostructures of the DFG (project LO 1659/7-1). [1] AbuAwwad *et al.*, J. Phys.: Condens. Matter **34**, 454001(2022). [2] Xian *et al.*, Nat. Commun. **13**, 257 (2022).

MA 21.2 Tue 15:15 HSZ 403

Tuning the magnetic interactions in van der Waals Fe₃GeTe₂ heterostructures — DONGZHE LI¹, •SOUMYAJYOTI HALDAR², TIM DREVELOW², and STEFAN HEINZE² — ¹CEMES, Université de Toulouse, CNRS, 29 rue Jeanne Marvig, F-31055 Toulouse, France — ²Institute of Theoretical Physics and Astrophysics, University of Kiel, Leibnizstrasse 15, 24098 Kiel, Germany

We investigate the impact of mechanical strain, stacking order, and external electric fields on the magnetic interactions of a Fe₃GeTe₂ monolayer deposited on Germanene using density functional theory [1]. We find that an electric field of $\mathcal{E} = \pm 0.5$ V/Å applied perpendicular to the Fe₃GeTe₂/germanene heterostructure leads to significant changes of the exchange constants. We show that the Dzyaloshinskii-Moriya interaction (DMI) in Fe₃GeTe₂/Germanene is mainly dominated by the nearest neighbors. Furthermore, we demonstrate that the DMI is highly tunable by strain, stacking, and electric field, leading to a large DMI comparable to that of ferromagnetic/heavy metal interfaces. The geometrical change and hybridization effect explain the origin of the high tunability of the DMI at the interface. The magnetocrystalline anisotropy energy (MAE) can also be drastically changed by the application of compressive or tensile strain. The tunability of DMI and MAE by using strain allows the occurrence of nanoscale skyrmions [2].

[1] D. Li, S. Haldar, T. Drevelow, S. Heinze, arXiv:2210.15351.

[2] D. Li, S. Haldar, S. Heinze, Nano Lett. **22**, 7706 (2022).

MA 21.3 Tue 15:30 HSZ 403

Spin-texture of graphene on Co films on heavy metals — •DONYA MAZHJOO^{1,2}, GUSTAV BIHLMAYER¹, and STEFAN BLÜGEL¹ — ¹Peter Grünberg Institut and Institute for Advanced Simulation, Forschungszentrum Jülich and JARA, D-52425 Jülich, Germany — ²Physics Department, RWTH-Aachen University, 52062 Aachen, Germany

Graphene(Gr) covered ferromagnetic films deposited on heavy metals (HM) have been proposed for the exploration of novel spin-orbitronic devices since they possess a perpendicular magnetic anisotropy (MA) as well as a sizable Dzyaloshinskii-Moriya interaction (DMI). By using density functional theory as implemented in the FLEUR-code [1], we investigate the spin-orbit (SO) induced spin-texture of Gr covered Co/Ir(111) heterostructures. We consider SOC in first order perturbation theory to study the DMI and self-consistently for the MA energy. Various thicknesses of Co are investigated and compared to experimental

data. There, for thin Co films, spin- and angular-resolved photoemission spectroscopy found an in-plane spin-polarization of the Gr π bands, consistent with a HM induced Rashba-type SO coupling at the Gr/Co interface [2]. We compare to Pt(111) as HM substrate looking for signatures of the DMI in the (induced) spin-textures.

Support from the FLAG-ERA JTC 2019 grant SOgraphMEM is gratefully acknowledged.

[1] <https://www.flapw.de>

[2] B. Cano *et al.* arXiv:2206.04351

MA 21.4 Tue 15:45 HSZ 403

Magnetism and THz excitations in quasi-2D systems perturbed by external fields — •KAREL CARVA and KRISHNA K. POKHREL — Charles University, Faculty of Mathematics and Physics, DCMP, Ke Karlovu 5, 121 16 Prague 2, Czech Republic

Systems with a very weak exchange coupling between magnetically ordered layers represent an interesting intermediate stage between the well-known isotropic bulk magnets and the recently intensively studied 2D magnets [1]. We perform a complex investigation of lattice and magnetic excitations induced by external perturbations in such quasi-2D system, trihalide VI₃, employing the synergy of DFT calculations, infrared, THz, and Raman spectroscopies [2]. The transition to the long-range ferromagnetic order is accompanied by the observed variations of phonon frequencies indicating strong magnetoelastic coupling. The acoustic magnon mode acquires here unusually high energy reaching to the THz range, but dramatically softens at temperatures where a second lattice distortion has been reported. First-principles calculations also show the strong connection of magnetic ordering and anisotropy to the lattice and its low temperature distortions [3]. These findings suggest the possibility of controlling magnetic anisotropy in this system by selective occupation of specific lattice modes. In this way magnon spectra would be strongly modified as well. We also show changes induced by strong magnetic fields in VI₃ and similar systems.

[1] M. Gibertini *et al.*, Nat. Nanotech. **14**, 408 (2019)

[2] D. Hovančík *et al.*, J. Phys. Chem. Lett. **13**, 11095 (2022)

[3] L. M. Sandratskii, K. Carva, Phys. Rev. B **103**, 214451 (2021)

15 min. break

MA 21.5 Tue 16:15 HSZ 403

Characterisation of the Ising-type 2D magnet FePS₃: A DFT+U study — MOHAMMAD AMIRABBASI and •PETER KRATZER — Faculty of Physics, University Duisburg-Essen, 47057 Duisburg, Germany

Among the 2D magnetic system that can be prepared via exfoliation, iron phosphorus trisulfide (FePS₃) excels due to its unusual Ising-type magnetic order which makes it interesting for applications in spintronic nano-devices. We carried out a computational study of the structural and magnetic properties of single-layer FePS₃ by using Density Functional Theory (DFT+U). Our findings show that the sublattice of the Fe²⁺ ions is not a perfect honeycomb; rather the nearest-neighbor Fe distances vary by 0.14 Å as a result of orbital ordering. These lattice distortions, albeit small, trigger different (ferromagnetic and antiferromagnetic) exchange couplings so that the ground state consists of ferromagnetically aligned zig-zag chains along the long Fe-Fe bonds which couple antiferromagnetically along the shorter Fe-Fe bonds of the distorted honeycomb. Within the DFT+U framework, we parameterize a spin Hamiltonian including Heisenberg, single-ion anisotropy, Dzyaloshinskii-Moriya and biquadratic interactions that allows us to calculate the critical temperature and the magnon spectrum. By comparing to prior results from neutron scattering, we conclude that it is the upper magnon branch in a doubled unit cell that has been observed in these experiments.

MA 21.6 Tue 16:30 HSZ 403

Interaction parameters in magnetic 2D systems from symmetric invariants — •JONATHAN KIPP^{1,2}, YURIY MOKROUSOV^{2,3}, and FABIAN R. LUX³ — ¹Department of Physics, RWTH Aachen University, 52056 Aachen, Germany — ²Institute for Advanced Simulation, Forschungszentrum Jülich Wilhelm-Johnen-Straße, 52428 Jülich — ³Institute of Physics, Johannes Gutenberg University Mainz, 55099 Mainz, Germany

The electronic properties of 2D materials hosting complex magnetic order can have crucial implications for information storage and processing applications. At the heart of the complexity in these materials is the interplay of external fields, fluctuations and electronic structure with the magnetic properties. In this work, we are aiming to uncover the direct implications that changes in the magnetic texture have on the electronic characteristics of the system. We develop an expansion in terms of the textures symmetric invariants and compare to data obtained from Heisenberg Hamiltonians, tight-binding (TB) calculations or possibly even density functional theory (DFT) calculations by employing a machine learning (ML) algorithm for the fitting task. Specifically, this enables us to identify the relevant interaction terms from the expansion to the total energy, since there is a diverse palette of ML fitting algorithms aiming at sparse models with the smallest possible number of coefficients, including regularized and sequential approaches.

MA 21.7 Tue 16:45 HSZ 403

Locally driven quantum phase transition cascades in a strongly correlated molecular monolayer — SOROUSH ARABI^{1,2,3}, TANER ESAT^{2,5}, AIZHAN SABITOVA^{2,5}, YUQI WANG^{2,3}, HOVAN LEE⁷, CEDRIC WEBER⁷, KLAUS KERN^{3,4}, F. STEFAN TAUTZ^{1,2,5}, RUSLAN TEMIROV^{2,6}, and MARKUS TERNES^{1,2,5} — ¹Institute of Physics IIB, RWTH Aachen University, 52074 Aachen, Germany — ²Peter-Grünberg-Institute (PGI 3), Research Center Jülich, 52425 Jülich, Germany — ³Max Planck Institute for Solid State Research, 70569 Stuttgart, Germany — ⁴Institut de Physique, École Polytechnique Fédérale de Lausanne, 1015 Lausanne, Switzerland — ⁵Jülich Aachen Research Alliance, 52425 Jülich, Germany — ⁶Institute of Physics II, University of Cologne, 50937 Cologne, Germany —

⁷King's College London, Theory and Simulation of Condensed Matter, London WC2R 2LS, UK

The molecular monolayer of 1,4,5,6-naphthalene tetracarboxylic acid dianhydride on Ag(111) creates a perfectly ordered lattice of π -conjugated organic molecules. Using a movable atomically sharp electrostatic gate we drive this lattice of strongly correlated electrons through a cascade of quantum phase transitions. Performing spectroscopic imaging with sub-Angstrom resolution, we show that as the gate field is increased, the molecular building blocks change from a Kondo-screened to a paramagnetic phase one by one, enabling us to reconstruct their complex interactions in detail. We anticipate that the supramolecular nature of the system will, in future, allow engineering quantum correlations in arbitrary patterned structures.

MA 21.8 Tue 17:00 HSZ 403

Electrically Tunable Curie Temperature in a 2D Ferromagnetic Semiconductor — •TANIA MUKHERJEE^{1,2} and SOUMYA JYOTI RAY¹ — ¹Department of Physics, Indian Institute of Technology Patna, Bihta 801106, India — ²Institute of Optics and Atomic Physics, Technical University of Berlin, Straße des 17. Juni 135, 10623 Berlin, Germany

Magnetic van der Waal's nanocrystals with intrinsic magnetic anisotropy provide an ideal platform for exploring magnetism in the low-dimensional limit. We investigate the electronic and magnetic properties of a novel 2D material VClBr₂ by using spin polarised density functional theory calculations. We observe complex electronic and magnetic phase transitions, tunable bandgap, and extremely large enhancement of the Curie temperature under the application of strain (η) and electric field (Ez). A Monte Carlo approach to the resolution of the Ising model reveals that the Curie temperature (T_c) can reach up to 340K under the application of an $E_z = 2.5$ V/nm, a colossal enhancement of $\sim 6700\%$ of its base value. The coexistence of high-temperature spin-ordering along with large magnetic anisotropic energy (MAE), high magnetic moment, tunable band gap, and excellent stability make single layer VClBr₂ a promising material for applications in an electric field driven spin gating, room temperature spintronics, and 2D spin circuit design.

MA 22: Terahertz Spintronics

Time: Tuesday 15:00–16:15

Location: POT 6

MA 22.1 Tue 15:00 POT 6

Optimizing spin-based terahertz emission from magnetic heterostructures — •FRANCESCO FOGGETTI, FRANCESCO COSCO, and PETER M. OPPENEER — Uppsala University, Uppsala, Sweden

Terahertz radiation pulses can be generated efficiently through femtosecond laser excitation of a magnetic heterostructure, where an ultrafast laser-induced spin current results in an electromagnetic THz pulse due to the inverse spin Hall effect. It is however still poorly known how the THz emission amplitude and its bandwidth in the frequency regime can be optimized. Here, we perform a systematic analysis of the THz emission from various magnetic heterostructures. The dynamics of the spin current is described by the semiclassical, superdiffusive spin-transport model and, in order to identify the optimal setup for the THz emission, the properties of the wave profile are studied by changing the materials of the heterostructures, their thicknesses, and the laser pulses, allowing us to give optimization guidelines. The energy dependence of spin Hall effect of hot electrons is furthermore taken into account, leading to emission profiles comparable to experiment.

MA 22.2 Tue 15:15 POT 6

Terahertz probing of interfacial Curie temperatures in spintronic thin-film stacks — •OLIVER GUECKSTOCK¹, REZA ROUZEGAR¹, VINCENT BALTZ², GERHARD JAKOB³, MATHIAS KLÄUI³, TOM S. SEIFERT¹, and TOBIAS KAMPFRATH¹ — ¹FU Berlin, Germany — ²SPINTEC, France — ³JGU Mainz, Germany

Transport of spin angular momentum and spin-charge-current interconversion are fundamental operations for future spin-electronic devices. Femtosecond laser pulses are well suited to trigger ultrafast spin transport from a ferromagnetic metal F into an adjacent paramagnetic layer P [1,2]. The inverse spin Hall effect converts the spin current into an in-plane charge current that gives rise to the emission of an electromagnetic pulse with frequencies extending into the terahertz (THz) range. As the ultrafast currents are confined to only ~ 1 nm around the F/P interface, the emitted THz pulse is expected to be a highly sensitive probe of interface properties. Here, we investigate the impact of the F/P interface morphology and sample temperature on the THz-emission signal. We find that the temperature-dependence of the THz emission signal depends critically on the roughness of the F/P interface. We conclude that the Curie temperature of F at the F/P interface is strongly reduced relative to the bulk by the higher degree of disorder at the F/P interface.

[1] T. Seifert et al., Nature Photonics 10, 483 (2016).

[2] R. Rouzegar et al., Physical Review B 106, 144427 (2022).

MA 22.3 Tue 15:30 POT 6

Switching and excitation of THz spin waves in Mn₂Au due to femtosecond spin-transfer torques — •MARKUS WEISSENHOFER^{1,2}, FRANCESCO FOGGETTI¹, and PETER OPPENEER¹ — ¹Department of Physics and Astronomy, Uppsala University — ²Department of Physics, Free University Berlin

In trilayer spin valves consisting of Fe[Cu]Fe, ultrafast laser pulses can generate hot-electron spin currents that exert spin-transfer torques, which excite THz spin waves [1]. Here, we replace the second Fe layer by antiferromagnetic Mn₂Au and demonstrate that spin waves with even higher frequencies can be excited. We compute the temporal evolution of the hot-electron spin currents by means of the superdiffusive transport model and simulate the response of the Mn₂Au layer to the resulting femtosecond spin-transfer torque pulse using atomistic spin dynamics simulations. Our results reveal that - due to the small thickness of the Mn₂Au layer and exchange enhancement - standing spin waves of up to several THz can be excited. Upon increasing the laser fluence, we even find that the excited spin-current pulses are sufficient to induce switching of Mn₂Au layer, faster than the experimentally demonstrated electrically induced switching of Mn₂Au [2].

[1] U. Ritzmann, P. Baláz, P. Maldonado, K. Carva, and P. M. Oppeneer, Phys. Rev. B 101, 174427 (2020).

[2] S. Y. Bodnar, L. Šmejkal, I. Turek, T. Jungwirth, O. Gomonay, J. Sinova, A. A. Sapozhnik, H.-J. Elmers, M. Kläui, and M. Jourdan, Nature Communications 9, 348 (2018).

MA 22.4 Tue 15:45 POT 6

Element-selective and THz study of spin dynamics in Fe/Ru/Ni tri-layer systems — •CHRISTIAN GREB^{1,2}, ROMAN ADAM¹, DANIEL BÜRGLER¹, SARAH HEIDTFELD^{1,2}, MARKUS BÜSCHER^{1,3}, and CLAUD M. SCHNEIDER^{1,2} — ¹Peter Grünberg Institut (PGI-6), Forschungszentrum Jülich, 52425 Jülich, Germany — ²Faculty of Physics, University of Duisburg-Essen, 47048 Duisburg, Germany — ³Institut für Laser- und Plasmaphysik, Heinrich-Heine-Universität Düsseldorf, 40225 Düsseldorf, Germany

Ultrafast spin dynamics induced by femtosecond optical laser pulses in ferromagnetic thin films are of great interest due to their high potential for future information technology. Relevant materials are often multi-element compounds or multilayer stacks. We present an element-selective study of Ni/Ru/Fe/MgO(capping) multilayers in which Ni and Fe layers are coupled either ferromagnetically or antiferromagnetically, depending on the Ru thickness. The spin dynamics in the multilayers can be explained by super-diffusive spin

transport [1,2]. In addition to element-selective T-MOKE measurements using a high harmonic generation source, we measured and analyzed THz transients [3] to gain further insight into the non-equilibrium interlayer spin transport. We show that spin currents can be triggered at lower laser fluences ($<1\text{uJ}/\text{cm}^2$) than previously reported [1]. The THz amplitude as a function of the external magnetic field gives insights into the interlayer exchange coupling. [1] D. Rudolf et al., Nature Commun. 3, 1037 (2012). [2] M. Battiato et al., Phys. Rev. Lett. 105, 027203 (2010). [3] R. Adam et al., Appl. Phys. Lett. 114, 212405 (2019).

MA 22.5 Tue 16:00 POT 6

Impact of the magnetic layer crystal growth optimization on the THz emission from spintronic Fe/Pt emitters — •LAURA SCHEUER¹, AGNE CIUCIULKAITE², ANNA L. RAVENSBURG², MERLIN POHLIT², TOBIAS WARNATZ², GARIK TOROSYAN³, RENÉ BEIGANG¹, GEORG SCHMIDT⁴, EVANGELOS TH. PAPAIOANNOU⁴, and VASSILIOS KAPAKLIS² — ¹Fachbereich Physik and Landes-

forschungszentrum OPTIMAS, Technische Universität Kaiserslautern, Erwin-Schrödinger-Str. 56, 67663, Kaiserslautern, Germany — ²Department of Physics and Astronomy, Uppsala University, Box 516, SE-75120 Uppsala, Sweden — ³Photonic Center Kaiserslautern, 67663, Kaiserslautern, Germany — ⁴Institut für Physik, Martin-Luther-Universität Halle-Wittenberg, Von-Danckelmann-Platz 2, 06120 Halle, Germany

We investigate the THz emission characteristics of ferromagnetic/non-magnetic metallic heterostructures, focusing on thin Fe/Pt bilayers. In particular, we report on the impact of optimized crystal growth of the epitaxial Fe layers on the THz emission amplitude and spectral bandwidth. We demonstrate a 5% enhancement of the emitted intensity related to structural quality of the Fe layer. Our work provides a pathway for optimal spintronic THz emitters devices based on epitaxial Fe. It also highlights how THz emission measurements can be utilized to characterize the changes in out-of-equilibrium spin current dynamics in metallic heterostructures, driven by subtle structural refinement.

MA 23: Poster Magnetism I

Skyrmions (MA 23.1-23.13), Non-Skyrmionic Magnetic Textures (MA 23.14-23.15), Caloric Effects in Ferromagnetic Materials (MA 23.16-23.19), Molecular Magnetism (MA 23.20-23.25), Biomagnetism, Biomedical Applications (MA 23.26-23.28), Electron Theory of Magnetism and Correlations (MA 23.29-23.33), Magnetic Imaging Techniques (MA 23.34-23.43), Neuromorphic Magnetism / Magnetic Logic (MA 23.44), Computational Magnetism (MA 23.45-23.49), Spin Transport and Orbitronics, Spin-Hall Effects (MA 23.50-23.53), Terahertz Spintronics (MA 23.54-23.56), Spin-Dependent Phenomena in 2D (MA 23.57-23.58), Spintronics (other effects) (MA 23.59-23.62), Functional Antiferromagnetism (MA 23.63-23.65), Magnonics (MA 23.66-23.80)

Time: Tuesday 17:00–19:00

Location: P1

MA 23.1 Tue 17:00 P1

Lattice effects of the skyrmion compound SrFeO₃ in high magnetic fields — •MATHIAS DOERR¹, NIKITA ANDRYUSHIN¹, CLARA EBERSBACH¹, SERGEY GRANOVSKY¹, DARREN PEETS¹, YURI SKOURSKI², and DMITRO INOSOV¹ — ¹Institut für Festkörper- und Materialphysik, TU Dresden, Germany — ²Dresden High Magnetic Field Laboratory, Helmholtz-Zentrum Dresden-Rossendorf, Germany

The magnetic properties of the cubic perovskites ABO_3 ($A =$ alkalis, $B =$ transition metal, e.g. Mn, Fe, Co) strongly depend on lattice variations. In particular, the magnetoelastic properties of SrFeO₃, which is characterised by a variation of topological helical spin structures with the formation of skyrmions, were investigated in steady and pulsed magnetic fields up to 50 T. Magnetostriction measurements in longitudinal and transversal geometry confirmed lattice distortions in the order of 10^{-5} only occur in the domain-selection processes, in these cases with an irreversible character. Other magnetic phase transitions are not triggered by lattice effects. Based on the new data, the (H, T) phase diagram could be refined and supplemented. At the same time, the results show fundamental differences to other perovskites containing Mn or Co on the B-site.

MA 23.2 Tue 17:00 P1

Asymmetric skyrmion flow in a periodically modulated channel — •KLAUS RAAB¹, MAARTEN A. BREMS¹, MAURICE SCHMIDT¹, JAN ROTHÖRL¹, FABIAN KAMMERBAUER¹, PETER VIRNAU¹, and MATHIAS KLÄUI^{1,2} — ¹Institut für Physik, Johannes Gutenberg-Universität Mainz, Staudingerweg 7, 55128 Mainz, Germany — ²Graduate School of Excellence Materials Science in Mainz, Staudingerweg 9, 55128 Mainz, Germany

We investigate the non-equilibrium flow behavior of skyrmions driven by spin-torques in complex channel geometries and construct functional building blocks for targeted manipulation of skyrmion flow. Poiseuille-like velocity flow-profiles usually occur due to no-slip boundary conditions, meaning moving particles do interfere with the boundary e.g. the wall of a geometry, reducing the velocity of particles closer to a wall. Skyrmions on the other hand should experience slip at the boundaries due to the repulsive nature of the skyrmion-edge and skyrmion-skyrmion interaction. Adding structured obstacles along the boundary may lead to partial or even no-slip behavior and thus to Poiseuille-like flow profiles while skyrmions are forced through a wire due to spin-torques. Selected edge shapes (sawtooth, triangles, ...) and the periodicity and amplitude of the modulation of the wire width influencing the flow were optimized and tested using simulations. Understanding flow dynamics and velocity profiles of skyrmions, their interaction with each other and their harboring geometry is essential for skyrmionic applications like the racetrack memory.

MA 23.3 Tue 17:00 P1

Time-Multiplexed Reservoir Computing with Skyrmions — •GRISCHA BENEKE¹, THOMAS WINKLER¹, MAARTEN A. BREMS¹, KLAUS RAAB¹, FABIAN KAMMERBAUER¹, JOHAN H. MENTINK², and MATHIAS KLÄUI¹ — ¹Institut für Physik, Johannes Gutenberg-Universität Mainz, Germany — ²Institute for Molecules and Materials, Radboud University, The Netherlands

Reservoir computing (RC) is a key method for significantly reducing the computational effort of complex tasks like pattern recognition [1]. Magnetic skyrmions, topological particle-like spin textures, are very promising candidates for RC systems given their non-linear interactions and a multitude of established mechanisms for skyrmion manipulation. By exploiting the thermally activated diffusive motion of skyrmions [2] and an automatic reset mechanism enabled by the repulsion of skyrmions from the boundaries of the magnetic materials, we have previously realized spatially multiplexed RC using a single skyrmion [3]. Here, we employ time-resolved inputs, exploiting the electrically gated skyrmion motion and use the time-dependent state of our device as an output mechanism [4]. We experimentally demonstrate that already a minimalistic device suffices to perform linearly non-separable logic operations. Increasing the complexity of the device using multiple skyrmions or an interplay of multiple devices, may pave the way for low-power and low-training classification of real-life data. [1] D. Gauthier et al., Nat. Comms. 12, 5564 (2021). [2] J. Zázvorka et al., Nat. Nanotechnol. 14, 658 (2019). [3] K. Raab et al., Nat. Comms. 13, 6982 (2022). [4] G. Beneke et al., in preparation (2022).

MA 23.4 Tue 17:00 P1

Skyrmionic spin structures in layered Fe₅GeTe₂ up to room temperature — •MAURICE SCHMITT¹, THIBAUD DENNEULIN², ANDRÁS KOVÁCS², TOM SAUNDERSON^{1,3}, PHILIPP RÜSSMANN^{3,4}, AGA SHAHEE¹, TANJA SCHOLZ⁵, AMIR TAVABI², MARTIN GRADHAND^{1,6}, PHIVOS MAVROPOULOS⁷, BETTINA LOTSCH^{5,8}, RAFAL DUNIN-BORKOWSKI², YURIY MOKROUSOV^{1,3}, STEFAN BLÜGEL³, and MATHIAS KLÄUI^{1,9} — ¹JGU Mainz — ²Ernst Ruska-Centre, Jülich — ³Peter Grünberg Institut and Institute for Advanced Simulation, Jülich — ⁴University of Würzburg — ⁵Max Planck Institute for Solid State Research, Stuttgart — ⁶University of Bristol — ⁷University of Athens — ⁸LMU, München — ⁹NTNU, Trondheim

The role of the crystal lattice, temperature and magnetic field for the spin structure formation in the 2D van der Waals magnet Fe₅GeTe₂ with magnetic ordering up to room temperature is a key open question. Using Lorentz transmission electron microscopy, we experimentally observe topological spin structures up to room temperature in the metastable pre-cooling and stable post-cooling phase of Fe₅GeTe₂. Over wide temperature and field ranges, skyrmionic magnetic bubbles form without preferred chirality, which is indicative of centrosymmetry. These skyrmions can be observed even in the absence of external fields. To understand the complex magnetic order in Fe₅GeTe₂, we compare macroscopic magnetometry characterization results with microscopic density functional theory and spin-model calculations. Our results show that even up to room temperature, topological spin structures can be stabilized in centrosymmetric van der Waals magnets.

MA 23.5 Tue 17:00 P1

Enhanced diffusion of antiferromagnetically coupled skyrmions — TAKAAKI DOHI¹, MARKUS WEISSENHOFER², NICO KERBER¹, FABIAN KAMMERBAUER¹, •MARIA-ANDROMACHI SYSKAKI¹, GERHARD JAKOB¹, ULRICH NOWAK², and MATHIAS KLÄUI¹ — ¹Institut für Physik, Johannes Gutenberg-Universität

Mainz, Staudingerweg 7, 55128 Mainz, Germany — ²Fachbereich Physik, Universität Konstanz, DE-78457 Konstanz, Germany

Magnetic skyrmions are attractive for the intriguing responses governed by their topology [1]. However, some of the topology-dependent features of magnetic skyrmions are recognized as an obstacle to device applications, e.g. the skyrmion Hall effect [2], which however does not occur in antiferromagnetic skyrmions. Here we demonstrate that a synthetic antiferromagnetic (SyAFM) system [3] with low pinning enables thermally-activated diffusive motion of antiferromagnetically-coupled skyrmions. The systematic investigation varying the compensation ratio of magnetic moments in the magnetic sub-lattices with our analysis accounting for pinning effects allows for disentangling the influence of the topology on the diffusive motion. Our analysis reveals an at least 10 times larger diffusion coefficient for highly compensated antiferromagnetically-coupled skyrmions that is a direct consequence of the reduction of the effective topological charge, which enables energy-efficient unconventional computing. [1] N. Nagaosa and Y. Tokura, Nat. Nanotechnol. 8, 899 (2013). [2] K. Litzius et al., Nat. Phys. 13, 170 (2017). [3] T. Dohi et al., Nat. Commun. 10, 5153 (2019).

MA 23.6 Tue 17:00 P1

Thermal skyrmion diffusion with alternating current excitations — •TOBIAS SPARMANN, RAPHAEL GRUBER, JAN ROTHÖRL, MAARTEN A. BREMS, FABIAN KAMMERBAUER, and MATHIAS KLÄUI — Department of Physics, Johannes-Gutenberg University Mainz

Magnetic skyrmions are considered promising candidates for implementing probabilistic computing devices since they respond strongly nonlinearly to external stimuli and feature multiscale dynamics [1].

The implementation of such probabilistic computing relies on thermal excitation and diffusive movement of the magnetic skyrmions within thin films, which exhibit pinning due to sample defects [2]. Especially the combination of skyrmion diffusion and current-induced motion has been shown to be useful in Brownian reservoir computing devices [3]. As thermal skyrmion diffusion is often slow due to the impact of pinning, a depinning procedure using the already present electric excitation of the skyrmions can be key for applications.

To reach such a regime of very high diffusion, we propose and experimentally demonstrate depinning by applying alternating currents to the sample [4]. In particular, we show that the energy landscape is effectively flattened and diffusion drastically enhanced for sufficient current densities. This can therefore be useful to reduce pinning effects and accelerate non-conventional computing devices.

[1] D. Prychynenko et al., Phys. Rev. Applied, 9, 014034 (2018).

[2] J. Zázvorka et al., Nat. Nanotechnol., 14, 658 (2019).

[3] R. Gruber et al., Nat. Comm., 13, 3144 (2022).

[4] T. Sparrmann et al., in preparation (2022).

MA 23.7 Tue 17:00 P1

Current driven skyrmion movement and their electrical detection in Ta/CoFeB/MgO — •HAUKE LARS HEYEN¹, MALTE RÖMER-STUMM², JAKOB WALOWSKI¹, CHRISTIAN DENKER¹, KORNEL RICHTER², JEFFEY MCCORD², and MARKUS MÜNZENBERG¹ — ¹Institute of Physics, University of Greifswald, Felix-Hausdorff-Straße 6, 17489 Greifswald, Germany — ²Christian-Albrechts-University in Kiel, Institute for Materials Science, Nanoscale Magnetic Materials and Magnetic Domains, 24143 Kiel, Germany

Magnetic skyrmions, the two-dimensional topological protected round spin structures, have a strong potential for implementation into future storage devices as information bits e.g., in the conceptual racetrack memory. For this purpose, the dynamics of skyrmion motion and their detection is an essential tool. Skyrmions can be generated in Ta/CoFeB/MgO layer stacks at room temperature. Using current pulses in the nanosecond range, it is possible to move the skyrmions with current densities of 10^{12} - 10^{13} A/m². The dynamic trajectories hint to the skyrmion-Hall-effect and superdiffusion, requiring special racetrack design. The skyrmion-Hall-effect results from the skyrmion topology and the superdiffusion occurs due to defects on the motion path. Magnetic tunnel junctions (MTJ) are a promising tool to detect small magnetization changes. The selected Ta/CoFeB/MgO material system allows to build MTJs into skyrmion samples. But this integration of MTJs remains challenging, even though they work fine independently.

MA 23.8 Tue 17:00 P1

Design of an rf antenna for fast skyrmion lattice relaxation — •EPHRAIM SPINDLER¹, PHILIPP SCHWENKE¹, ABBASS HAMADEH¹, RAPHAEL GRUBER², VITALIY VASYUCHKA¹, MATHIAS KLÄUI², and MATHIAS WEILER¹ — ¹Fachbereich Physik und Landesforschungszentrum OPTIMAS, Rheinland-Pfälzische Technische Universität Kaiserslautern-Landau, 67663 Kaiserslautern, Germany — ²Institut für Physik, Johannes Gutenberg-Universität Mainz, Mainz, Germany

Understanding skyrmion dynamics is a key requirement for their potential applications in data storage and processing. We designed an omega-type microwave antenna to study the lattice formation dynamics of micrometer-scale skyrmions in thin film materials under rf excitation. We evaluated the antenna performance by measuring its electrical transmission and the magnetic field generated by dc

current flow through the antenna. To quantify the rf performance of the antenna further, we used it for ferromagnetic resonance (FMR) measurements on reference thin-film Y₃Fe₅O₁₂ samples. From our power-dependent FMR measurements we determined the microwave power of the transition to the nonlinear regime. The microwave power thresholds are compared to expectations from micromagnetic simulations considering the inhomogeneous rf field profile of the antenna. These power-dependent measurements and simulations allowed us to quantify the rf fields generated by the antenna. The rf fields generated by the omega antenna can potentially accelerate the skyrmion lattice relaxation through its direct influence on skyrmion size oscillations.

MA 23.9 Tue 17:00 P1

Influence of lattice strain on possible skyrmions in SrRuO₃-based oxide heterostructures — •ROBERT GRUHL, LUDWIG SCHEUCHENPFLUG, and PHILIPP GEGENWART — Experimentalphysik VI, Universität Augsburg, 86159 Augsburg, Germany

Dzyaloshinskii-Moriya interaction can lead to the formation of skyrmions in crystal lattices with a broken inversion symmetry, as it is the case at interfaces of artificial heterostructures. Néel-type skyrmions were proposed to form in bilayers of ferromagnetic SrRuO₃ and paramagnetic SrIrO₃ with strong spin-orbit coupling as indicated by the observation of a topological hall effect [1].

Heterostructures of SrRuO₃ and SrIrO₃ on SrTiO₃ substrates show a rather bad structural compatibility due to the large lattice mismatch of about 1.1% between SrIrO₃ and the substrate. To address this, we reduced the lattice constant of the iridate by doping it with calcium. Superlattices composed of [SrRuO₃]₅/[Ca_xSr_{1-x}IrO₃]₂ with various levels of doping were grown on STO (001) substrates by the means of metal-organic aerosol deposition. The structural properties of the samples were studied by x-ray diffraction, reciprocal space mapping and TEM imaging. Hall measurements were carried out to search for topological contributions as an indication for the formation of skyrmions and compared with the results of [1,2].

[1] J. Matsuno et al., Science Adv. 2 (2016) e1600304.

[2] S. Esser et al., Phys. Rev. B 103 (2021) 214430.

MA 23.10 Tue 17:00 P1

Magnon propagation across Quantum Hall Skyrmion crystals — •NILOTPAL CHAKRABORTY¹, RODERICH MOESSNER¹, and BENOIT DOUCOT^{1,2} — ¹Max Planck Institute for Physics of Complex Systems, Dresden — ²LPTHE, CNRS and Sorbonne Universite,

Skyrmion crystals have a rich collective mode spectrum and are hypothesized to appear in quantum Hall ferromagnets in the lowest Landau level at small dopings away from one filled level. We develop a model of a ferromagnetic-skyrmion crystal-ferromagnet junction, relevant to recent experiments in monolayer graphene, to study the influence of collective modes of skyrmion crystals on the propagation of a ferromagnetic magnon. We show, using an appropriate set of generalized theta functions, how to smoothly interpolate between regions of zero (the ferromagnetic ends) and spatially modulating finite topological charge density (the sandwiched skyrmion crystal). The collective mode equations for such a configuration, from a suitably defined energy functional, map onto the Bogoliubov-De Gennes equation. Using this mapping, along with a slice-wise recursive transfer matrix approach, we calculate the transmission amplitudes of an incoming ferromagnetic magnon. We also show how changing the collective mode spectrum of the skyrmion crystal, by varying the strength of the topological charge density terms in the functional, affects magnon transmission. Our results present unique signatures of Skyrmion crystals due to their characteristic collective mode spectrum, and can be used as evidence for their presence in graphene and possibly in twisted bilayer graphene.

MA 23.11 Tue 17:00 P1

Magnetization dynamics of skyrmions in thin film and bulk materials — •PHILIPP SCHWENKE¹, EPHRAIM SPINDLER¹, RAPHAEL GRUBER², VITALIY VASYUCHKA¹, AISHA AQEEL³, MATHIAS KLÄUI², and MATHIAS WEILER¹ — ¹Fachbereich Physik und Landesforschungszentrum OPTIMAS, Rheinland-Pfälzische Technische Universität Kaiserslautern-Landau, 67663 Kaiserslautern, Germany — ²Institut für Physik, Johannes Gutenberg-Universität Mainz, 55122 Mainz, Germany — ³Physik-Department, Technische Universität München, 85748 Garching, Germany

Magnetic skyrmions are topologically protected chiral spin textures which hold a rich variety of phenomena and that can be stabilized in both bulk materials and thin films. In order to establish efficient means to control skyrmions it is important to understand the magnetization dynamics of these magnetic textures. Therefore, we study the magnetization dynamics of a CoFeB thin film exhibiting μm sized quasi 2D skyrmions [1] and compare these to the dynamics observed in a bulk Cu₂OSeO₃ crystal exhibiting a skyrmion lattice phase [2] by means of broadband ferromagnetic resonance measurements at varying temperatures. Additionally, we investigate the dynamics of μm sized quasi 2D skyrmions in CoFeB-based thin film heterostructures in a Kerr-microscope while applying out-of plane rf fields. We observe a perturbation of the skyrmion lattice due to finite size oscillations which might provide a pathway for the manipulation of skyrmion lattices.

- [1] J. Zázvorka *et al.*, *Adv. Funct. Mater.* **30**, 2004037 (2020)
 [2] A. Aqeel *et al.*, *Phys. Rev. B* **103**, L100410 (2021)

MA 23.12 Tue 17:00 P1

Static and dynamical properties of magnetic (bi-)skyrmions in the absence of Dzyaloshinskii-Moriya interaction — •DAVID EILMSTEINER¹, LEVAN CHOTORLISHVILI², XI-GUANG WANG³, PAWEŁ BUCZEK⁴, and ARTHUR ERNST¹ — ¹Johannes Kepler University Linz, Linz, Austria — ²Rzeszów University of Technology, Rzeszów, Poland — ³Central South University, Changsha, China — ⁴Hamburg University of Applied Sciences, Hamburg, Germany

The interest in topologically non-trivial states in magnetic materials, for instance magnetic skyrmions, arises not only from the fascinating connection between the mathematical concept of topology and phenomena observable in the lab, but also from possible future applications of those configurations in technology. The main obstacle towards a future technological applicability is the limited range of materials in which skyrmions intrinsically occur – for instance, Dzyaloshinskii-Moriya interaction is usually required. However, a sophisticated design of multi-layer systems can help to circumvent this constraint. My poster will discuss two such set-ups. The one demonstrates how a circular nanodot in combination with a switching magnetic field can help to nucleate a magnetic skyrmion. The other studies the motion of a bi-skyrmion bound to a vortex-domain wall. In the latter case, we not only found the, for technological application highly favorable, disappearance of the skyrmion Hall effect, we also observed a chirality dependence of the propagation velocity.

MA 23.13 Tue 17:00 P1

muSR on single crystals of GaV4S8 — •ELAHEH SADROLLAHI^{1,2}, ANDRE BORCHERS², JOCHEN LITTERST^{2,3}, ISVÁN KÉZSMÁRKI⁴, SANDOR BORDACS⁵, VLADIMIR TSURKAN⁴, and ALOIS LOIDL⁴ — ¹Institut für Festkörper- und Materialphysik, Technische Universität Dresden, 01062 Dresden, Germany — ²Institut für Physik der kondensierten Materie, Technische Universität Braunschweig, 38110 Braunschweig, Germany — ³Centro Brasileiro de Pesquisas Físicas, 22290-180, Rio de Janeiro, RJ, Brazil — ⁴Institut für Physik, Universität Augsburg, 86135 Augsburg, Germany — ⁵Department of Physics, Budapest University of Technology and Economics, 1111 Budapest, Hungary

The lacunar thio-spinel GaV4S8 possesses a complex magnetic phase diagram with several magnetic phases in zero and applied field, in part with supposed cycloidal, ferromagnetic, and/or short-range cycloidal spin structures, eventually even including skyrmion structures in the ferromagnetic phase [1,2]. We have performed muon spin rotation and relaxation (muSR) experiments on oriented single crystals. In a zero magnetic field, the spontaneous rotation signals allow us to distinguish between the cycloidal (ca. 8-13 K) and the low temperature 'ferromagnetic' phase, yet with a smooth continuous transition extending over several degrees, which is interpreted with a spin-reorientation. The observed changes at low temperatures and in the applied field indicate that this phase has no simple ferromagnetic character. We will discuss the observed field distribution patterns under various applied fields. [1] I. Kezsmarki *et al.*, *Nature Mater.* **14**, 1116 (2015). [2] S. Widmann *et al.*, unpubl., arXiv 1606.04511 (2016).

MA 23.14 Tue 17:00 P1

Bloch points in helimagnetic nanostrips — •MARTIN LANG^{1,2}, MARIJAN BEG^{1,3}, ONDREJ HOVORKA¹, and HANS FANGOHR^{1,2,4} — ¹University of Southampton, Southampton, United Kingdom — ²Max Planck Institute for the Structure and Dynamics of Matter, Hamburg, Germany — ³Imperial College London, London, United Kingdom — ⁴Center for Free-Electron Laser Science, Hamburg, Germany

Complex magnetic materials hosting topologically non-trivial particle-like objects such as skyrmions are intensely researched. One important class of materials are helimagnetic materials with Dzyaloshinskii-Moriya interaction. Recently, it was demonstrated that nanodisks consisting of two layers with opposite chirality can host a single stable Bloch point (BP) of two different types [1]. The BP represents an interesting topological excitation in a helimagnetic system, which expands the set of well-known magnetic states such as domain walls, vortices, and skyrmions.

In this work [2], we use micromagnetic simulations [3] to show that FeGe nanostrips consisting of two layers with opposite chirality can host multiple co-existing BPs. We demonstrate that the two different BP types can be geometrically arranged in any arbitrary order and these magnetization configurations are meta-stable. We can determine an optimal spacing between BPs within a line of BPs allowing us to predict strip geometries suitable for an arbitrary number of BPs.

[1] M. Beg *et al.*, *Scientific Reports*, **9**, p. 7959 (2019). [2] M. Lang *et al.* arXiv:2203.13689 (2022). [3] M. Beg, M. Lang and H. Fangohr, *IEEE Transactions on Magnetics*, **58**, p. 7300205 (2022).

MA 23.15 Tue 17:00 P1

Magnetic hopfions in frustrated magnets — •SANDRA CHULLIPARAMBIL SHAJU¹, ROSS KNAPMAN¹, RICCARDO HERTEL², and KARIN EVERSCHOR-SITTE¹ — ¹Faculty of Physics and CENIDE, University of Duisburg-Essen, 47057 Duis-

burg, Germany — ²Université de Strasbourg, CNRS, Institut de Physique et Chimie des Matériaux de Strasbourg, F-67000 Strasbourg, France

Research in 3D nanomagnetism, driven by advanced nanofabrication methods [1] and novel experimental 3D magnetization visualization methods [2], has revealed new nanostructures and physics beyond those in 1D and 2D. Magnetic Hopfions are topological magnetic textures that can be considered as closed loops of twisted Skyrmion strings [3]. The number of twists and knots of the Hopfion is characterized by the Hopf index. Both Skyrmions and Hopfions require the interplay of competing interactions to stabilize them. In contrast to Skyrmions, which can be stabilized, for example, by the competition of inversion symmetry-breaking Dzyaloshinskii-Moriya interactions and standard exchange interactions, Hopfions require competing exchange interactions beyond second-order derivatives [3,4]. We consider frustrated magnets that obey the interplay of such competing exchange interactions and want to investigate the physics of three-dimensional topological structures.

- [1] P. Fischer *et al.*, *APL Mater.* **8**, 010701 (2020).
 [2] C. Donnelly *et al.*, *Nature* **547**, 328 (2017).
 [3] P. Sutcliffe, *Phys. Rev. Lett.* **118**, 247203 (2017).
 [4] F. N. Rybakov *et al.*, *APL Mater.* **10**, 111113 (2022).

MA 23.16 Tue 17:00 P1

Suppression of magnetic fluctuations lead to a better reversibility in low-field entropy changes near triple point — •TAPAS SAMANTA¹, CHRIS TAAKE¹, and LUANA CARON^{1,2} — ¹Faculty of Physics, Bielefeld University, PO Box 100131, D-33501 Bielefeld, Germany — ²Helmholtz-Zentrum Berlin für Materialien und Energie, Berlin 12489, Germany

We report the detailed study of the phase transitions in $MnNi_{1-x}Co_xGe_{0.97}Al_{0.03}$ ($x=0.20, 0.25, 0.30, 0.35, 0.37, 0.40$ and 0.45) compounds. In the parent Al-free compound, the structural and magnetic phase transitions are decoupled. Small amounts of Al substitution for Ge can lower the structural phase transition temperature, resulting in a coupled first-order magnetostructural transition (MST) near room temperature for all reported compositions. An antiferromagnetic-type (AFM) to paramagnetic (PM) MST has been observed for lower Co concentrations. At $x=0.37$ the phase transition transforms to a ferromagnetic-type (FM) to PM MST after exhibiting a triple point (where AFM, FM and PM phase transitions coincide) in the close vicinity of $x=0.36$. Interestingly, a relatively large reversible low-field entropy change ($\Delta S=-6.9$ J/kg K for $\Delta H=2$ T) has been observed near the triple point for $x=0.37$, which is rather rare in this class of materials due to the large associated thermal hysteresis. The observed reversible ΔS reaches values of -17.2 and -24.5 J/kg K for $\Delta H=5$ and 7 T, respectively, for $x=0.30$. Our observations further reveal that a sudden decrease of magnetic fluctuation results in larger reversible entropy change near triple point.

MA 23.17 Tue 17:00 P1

Probing the nature of first-order magnetostructural transitions as responsible for magnetocaloric effects: A case study for In-based Heusler alloys — •CHRIS TAAKE¹, TAPAS SAMANTA¹, and LUANA CARON^{1,2} — ¹Faculty of Physics, Bielefeld University, PO Box 100131, D-33501 Bielefeld, Germany — ²Helmholtz-Zentrum Berlin für Materialien und Energie, Berlin 12489, Germany

The subtle nature of magnetostructural transitions (MST) and associated magnetocaloric effects (MCE) in B-substituted In-based Heusler alloys $Ni_{50}Mn_{34.8}In_{15.2-x}B_x$ ($x=1, 2$ and 3) have been studied. Boron substitution acts as a positive chemical pressure and shifts the martensitic phase transition temperature (T_M) towards higher temperature with increasing B concentration. Magnetic field sensitivity of T_M as well as thermal hysteresis decrease with increasing B substitution. Because of the compensation effect between the loss of field sensitivity and decreased thermal hysteresis, a similar reversible MCE can be expected for all studied compositions. However, a much better reversible isothermal entropy change (ΔS) has been observed for $x=1$, which reaches a value of $+20.8$ J/kg K for $\Delta H=5$ T. The observed behavior clearly indicates that the nature of the MST responsible for the MCE is changing with composition. To understand the nature of the MST in depth, the behavior of the local magnetic field exponent, n ($\Delta S \propto H^n$), has been examined for all the compositions. Interestingly, a much larger n^{max} ($=10.35$, where $n > 2$ is the indication of a first-order phase transition) has been detected for $x=1$ when compared to other compositions which are less field sensitive ($n^{max}=3.66$, $x=3$).

MA 23.18 Tue 17:00 P1

Magnetocaloric materials for the liquefaction of hydrogen — •TINO GOTTSCHALL¹, EDUARD BYKOV^{1,2}, MARC STRASSHEIM^{1,2}, TIMO NIEHOFF^{1,2}, CATALINA SALAZAR-MEJIA¹, and J. WOSNITZA^{1,2} — ¹Dresden High Magnetic Field Laboratory (HLD-EMFL), HZDR, Dresden, Germany — ²Institut für Festkörper- und Materialphysik, TU Dresden, Germany

Magnetic cooling is a refrigeration technique that is based on the so-called magnetocaloric effect, the change of temperature caused by a magnetic field. It can be utilized to construct environmentally friendly cooling devices, air conditioners, and heat pumps. Originally, magnetic cooling was used to achieve ultra-low temperatures by adiabatic demagnetization of magnetic salts. Recently, low tem-

peratures have once again become the focus of attention as an area of application for magnetocaloric cooling namely for hydrogen liquefaction. In this work, we would like to discuss our current progress for the creation of a materials library for cryogenic applications. The basis for this is our characterization infrastructure for materials research at the Dresden High Magnetic Field Laboratory in static and pulsed fields. With this, we aim to understand these materials better to further optimize their magnetic cooling performance near the boiling temperature of hydrogen.

MA 23.19 Tue 17:00 P1

Direct measurements of the adiabatic temperature change in heavy rare-earth $R\text{Co}_2$ compounds in high magnetic fields — •E. BYKOV^{1,2}, T. GOTTSCHALL¹, K. SKOKOV³, A. KARPENKOV³, W. LIU³, F. SCHEIBEL³, O. GUTFLEISCH³, and J. WOSNITZA^{1,2} — ¹Hochfeld-Magnetlabor Dresden (HLD-EMFL), HZDR, Dresden, Germany — ²Technische Universität Dresden, Dresden, Germany — ³Technische Universität Darmstadt, Darmstadt, Germany

Rare-earth elements and their intermetallic compounds are interesting candidate materials for magnetic cooling at and below room temperature. Although the group of heavy rare-earth Laves phases RM_2 (R is a rare earth, M a transition metal) is one of the most intensively investigated classes of magnetocaloric materials, data on directly determined adiabatic temperature changes are scarce. Continuing our work with ferromagnetic $R\text{Ni}_2$ and RA_2 compounds, we are now focussed on ferrimagnetic $R\text{Co}_2$. Some of them show complex magnetic behavior, such as metamagnetism at T_C , or an additional spin-reorientation transition and reduction of the Co magnetic moment below this temperature. In this work, we present a comprehensive analysis of the magnetocaloric effect in polycrystalline $R\text{Co}_2$ with $R = \text{Er}, \text{Ho}, \text{Dy}$, and Tb in high magnetic fields up to 20 T.

MA 23.20 Tue 17:00 P1

Single Molecule Magnets based on dimetallofullerenes — •MATHEUS BARBOSA, WEI YANG, FUPIN LIU, and ALEXEY POPOV — Leibniz Institute for Solid State and Materials Research - Dresden, Germany

Dimetallofullerenes are compounds with metal-metal bonds encapsulated in fullerene cages, recognized as good Single Molecule Magnets (SMMs). In the last years, molecules based on Terbium (Tb) and Dysprosium (Dy) have been demonstrating high potential applicability owing to the strong ferromagnetic coupling of 4f-electrons and trapped valence electron of the bond between them. Their static and dynamic properties are under investigation and have showed high blocking temperatures of magnetization, giant coercive fields and complex relaxation processes. Dy-Dy dimer inside the fullerene cage C_{80} ($\text{Dy}_2@C_{80}$) shows different magnetic behavior depending on the chosen stabilizing chemical groups. In comparison, for $\text{Dy}_2@C_{80}(\text{CF}_3)$ the susceptibility χ_m per temperature (ZFC-FC curves) is observed to be double-peak below 21 K, with the shape dependent of the temperature and field sweep rates, in contrast to $\text{Dy}_2@C_{80}(\text{CH}_2\text{C}_6\text{H}_5)$. The estimated energy barrier (613 K for $\{\text{Dy}_2\} - \text{CF}_3$ and 615 K for $\{\text{Dy}_2\} - \text{CH}_2\text{C}_6\text{H}_5$) and the ferromagnetic coupling constant have the similar values. However, at low temperature in zero magnetic field (QTM regime) the relaxation rate is c.a. 10 times faster for $\{\text{Dy}_2\} - \text{CF}_3$ than for the $\{\text{Dy}_2\} - \text{CH}_2\text{C}_6\text{H}_5$. Dilution studies demonstrated that this difference does not depend on the intermolecular interactions and should be ascribed to a different influence of the exohedral group.

MA 23.21 Tue 17:00 P1

Study of magneto-electric (M-E) coupling effect in spin triangle based metal (III) carboxylate $[\text{M}_3\text{O}(\text{O}_2\text{CPh})_6(\text{py})_3]\text{ClO}_4 \cdot \text{py}$ ($\text{M} = \text{Fe}, \text{Ga}$) molecular magnet. — •BALWANT SINGH CHAUHAN¹, RATNAMALA CHATTERJEE¹, AK BOUDALIS², and P TUREK² — ¹Department of Physics, IIT Delhi, Hauz Khas, New Delhi 110016, India — ²Institut de Chimie de Strasbourg (UMR 7177, CNRS-Unistra), Université de Strasbourg, 4 rue Blaise Pascal, CS 90032, Strasbourg, 67081, France

Materials with magneto-electric coupling effect having coupled magnetic and electric properties have potential applications in energy efficient data storage and other multifunctional device technology. In recent literature organic molecules like molecular magnets/molecular ferroelectric materials are being explored for their possible novel magneto-electric characteristics. In this context, a work by French group [1] on Fe spin triangle based metal carboxylates $[\text{F}_3\text{O}(\text{O}_2\text{CPh})_6(\text{py})_3]\text{ClO}_4 \cdot \text{py}$ have attracted a lot of attraction. In this work, we would clearly demonstrate a correlation between dielectric and magnetic properties of the $[\text{F}_3\text{O}(\text{O}_2\text{CPh})_6(\text{py})_3]\text{ClO}_4 \cdot \text{py}$ complex. The highlight of the work is the observation of direct ME coupling coefficient in this molecular magnet complex. A comparison of the same with nonmagnetic Ga(III) complex will be discussed too. References: [1] A. K. Boudalis, J. Robert and P. Turek, Chemistry - A European Journal, 24 (2018) 56

MA 23.22 Tue 17:00 P1

Chiral induced spin selectivity effect at hybrid molecule metal interfaces. — •ASHISH MOHARANA¹, SHUANGLONG WANG², HAO WU², FABIAN KAMMERBAUER¹, MARIA-ANDROMACHI SYSKAKI¹, TOMASZ MARSZALEK², QIU ZIJIE^{2,3}, and ANGELA WITTMANN¹ — ¹Institut für Physik, Johannes-Gutenberg-Universität Mainz, 55128 Mainz, Germany — ²Max Planck Institute for Polymer Research, Ackermannweg 10, 55128, Mainz, Germany — ³Shenzhen Institute of Aggregate Science and Technology, School of Science and Engineering, The Chinese University of Hong Kong, 2001 Longxiang Boulevard, Longgang District, Shenzhen City, Guangdong, 518172, China

The observation of spin-dependent transmission of electrons through chiral molecules has led to the discovery of chiral-induced spin selectivity. The high efficiency of the spin filtering effect in chiral molecules has recently gained significant interest due to the high potential for novel hybrid molecule magnetic spintronics applications. In our work, we explore spintronic phenomena at hybrid chiral molecule magnetic interfaces to elucidate the underlying mechanisms of the chiral-induced spin selectivity effect. For this, we investigate the spin-to-charge conversion efficiency in chiral molecule/ metallic thin film heterostructures. Quantifying the impact of the adsorption as a function of the structure of the chiral molecules will reveal the role of the structural design in the spin filtering effect paving the path towards three dimensional engineering of hybrid interfaces.

MA 23.23 Tue 17:00 P1

Chiral induced spin selectivity effect at hybrid molecule metal interfaces. — •ASHISH MOHARANA¹, SHUANGLONG WANG², HAO WU², FABIAN KAMMERBAUER¹, MARIA-ANDROMACHI SYSKAKI¹, TOMASZ MARSZALEK², QIU ZIJIE^{2,3}, and ANGELA WITTMANN¹ — ¹Institut für Physik, Johannes-Gutenberg-Universität Mainz, 55128 Mainz, Germany — ²Max Planck Institute for Polymer Research, Ackermannweg 10, 55128, Mainz, Germany — ³Shenzhen Institute of Aggregate Science and Technology, School of Science and Engineering, The Chinese University of Hong Kong, 2001 Longxiang Boulevard, Longgang District, Shenzhen City, Guangdong, 518172, China

The observation of spin-dependent transmission of electrons through chiral molecules has led to the discovery of chiral-induced spin selectivity. The high efficiency of the spin filtering effect in chiral molecules has recently gained significant interest due to the high potential for novel hybrid molecule magnetic spintronics applications. In our work, we explore spintronic phenomena at hybrid chiral molecule magnetic interfaces to elucidate the underlying mechanisms of the chiral-induced spin selectivity effect. For this, we investigate the spin-to-charge conversion efficiency in chiral molecule/metallic thin film heterostructures. Quantifying the impact of the adsorption as a function of the structure of the chiral molecules will reveal the role of the structural design in the spin filtering effect paving the path towards three dimensional engineering of hybrid interfaces.

MA 23.24 Tue 17:00 P1

Density-functional studies of Cu-based metallacrowns on metal surfaces — •ABOLFAZL TAVAKOLI¹, BENJAMIN STADTMÜLLER¹, and HANS CHRISTIAN SCHNEIDER^{1,2} — ¹Department of Physics and OPTIMAS Research Center, TU Kaiserslautern — ²Institute of Physics, Johannes Gutenberg University Mainz

Metallacrowns are a promising material system for single-molecule magnets as they exhibit favorable chemical and structural features. Here, we present a first-principles study of the electronic and magnetic properties of Cu₄-Cu metallacrown complexes adsorbed on an Au (111) surface. We benchmark our calculations on the drosophila system CuPc and discuss the changes of the ligand structure and DOS around the metal centers. As an outlook, preliminary results on the Fe₄-Cu metallacrown will also be presented.

MA 23.25 Tue 17:00 P1

Origin of Ferromagnetism in the Copper(II) Triangle $\text{NMe}_4[\text{Cu}_3(\mu_3\text{-F})(\text{TFA})_6(\text{Py})_3]$ — •KEVIN ACKERMANN^{1,2}, CHANGHYUN KOO¹, AHMED ELGHANDOUR¹, RÜDIGER KLINGELER¹, and MAURITS W. HAVERKORT² — ¹Kirchhoff Institute for Physics, Heidelberg, Germany — ²for Theoretical Physics, Heidelberg, Germany

The new copper(II) triangle $\text{NMe}_4[\text{Cu}_3(\mu_3\text{-F})(\text{TFA})_6(\text{Py})_3]$ [1] was studied using magnetic susceptibility and high-field electron paramagnetic resonance (HF-EPR) experiments, as well as numerically by ab-initio methods. The magnetization and susceptibility data reveal dominant ferromagnetic spin-spin exchange as well as the importance of anisotropy in the system. An Anderson Impurity Model based on LDA-DFT calculations elucidates that the ferromagnetic interactions originate from super-exchange via the central fluorine. For the super-exchange interaction, not only the fluorine's 2p shell but also the 2s shell needs to be considered. In the HF-EPR data a substantial curvature of the resonance branches is observed and explained within the model by mixing between excited $S_z \approx 1/2$ and $S_z \approx -1/2$ states. The model also suggests that the spins are not parallel to each other in the ferromagnetic ground state but rather arranged in a chiral manner which is given by the molecular structure.

[1] A. Vassiliev *et al.*, unpublished.

MA 23.26 Tue 17:00 P1

Magnetization of magnetotactic bacteria: influence of additional nitrate during incubation — •NICOLE SANDER, IMKE WELLESEN, and MATHIAS GETZLAFF — Institute of Applied Physics, Heinrich-Heine-Universität Düsseldorf
Magnetotactic bacteria (MTB) have the ability to orient and migrate along a magnetic field. The orientation of those bacteria is based on intracellular magnetic structures called magnetosomes, which are formed from magnetite surrounded by a lipid-biolyer. These magnetic properties of MTB are currently of interest for magnetic hyperthermia as an application for cancer therapy.

Here we report on new findings how additional nitrate during incubation of MTB can prolong cell formation and increase magnetization. With additional nitrate we found, that the storage in an incubator can be extended and magnetosome concentration per bacteria was increased due to higher cell mass. A feeding of MTB after five days of incubation maximized the measured optical density being a measure for the number of bacteria respectively a feeding on the seventh day of incubation maximized magnetization. The data was obtained twenty-four hours after adding nitrate and further incubation. Considering a longer incubation period the data shows, that incubating up to forty-eight hours after feeding bacteria with nitrate apoptosis can be delayed. These findings display an advantage for magnetic hyperthermia because of higher cell mass and magnetosome concentration per cell the specific absorption rate (SAR) will be enlarged. Otherwise for same SAR a smaller concentration of bacteria is needed.

MA 23.27 Tue 17:00 P1

The influence of storage on magnetotactic bacteria — •IMKE WELLESEN, NICOLE SANDER, and MATHIAS GETZLAFF — Heinrich-Heine-Universität, Düsseldorf

Magnetic nanoparticles offer many new possibilities in medical applications e.g. in hyperthermia for cancer therapy. However, their production is largely challenging since it is often very complicated and costly. Therefore, the focus of research has been drawn to special organisms: Magnetotactic bacteria (MTB) naturally synthesize magnetic nanoparticles to orient themselves along the earth's magnetic field. In the future they could be used as nanoparticle producers. A problem is the resulting dependence of the applications on the life cycles of the bacteria. Therefore, optimal storage conditions must be evaluated so that the nanoparticles may still be used effectively at all times.

In this work we investigated the influence of storage at room and low temperatures on the bacteria and nanoparticles. The bacterial growth was examined via the optical density. The progression of the optical density and magnetisation of the organisms was observed over a period of 19 days. The results showed the positive effect of low temperatures on the bacteria. Storage at room temperature resulted in exponentially decreasing optical density and the destruction of the chain structure of the nanoparticles. Optical density and magnetisation of the bacteria at low temperatures on the other hand remained constant. Thus, the experiments showed that storage of magnetotactic bacteria should be realised at lower temperatures.

MA 23.28 Tue 17:00 P1

Biomarker detection using Frequency Mixing Magnetic Detection Technique — •FARANAK EIVAZI and HANS-JOACHIM KRAUSE — Institute of Biological Information Processing (IBI-3), Forschungszentrum Jülich

Superparamagnetic nanoparticles (SPNs) with non-hysteretic magnetization curves have significant potential for biomarker detection. The aim of our study is to probe the binding states of targets to SPNs using the frequency mixing magnetic detection technique (FMMD) [1]. As the SPNs bind to the target, the change in the hydrodynamic radius of the system leads to a longer Brownian relaxation time. The FMMD exposes SPNs bound to their targets to 2 alternating magnetic fields. The low-frequency field f_2 with high amplitude drives the SPNs to saturation, and a high-frequency field f_1 with low amplitude is used to probe the nonlinear magnetization. The response of the particles induces a voltage in the detection coil. The demodulated frequency mixing harmonics $f_1 + n f_2$ are characteristic of particle properties. The hydrodynamic radius of SPNs can be determined by observing a phase shift toward lower frequencies caused by the longer Brownian relaxation of the particles. This method can be used to determine the quantity and size of the target in the sample. [1] S. Achtsnicht, et al., PLoS ONE, 14(7), 2019.

MA 23.29 Tue 17:00 P1

Methods of electron transport in the theory of spin stiffness — •ILJA TUREK¹, JOSEF KUDRNOVSKY², and VACLAV DRCHAL² — ¹Institute of Physics of Materials, Czech Acad. Sci., Brno, Czech Rep. — ²Institute of Physics, Czech Acad. Sci., Prague, Czech Rep.

We present an ab initio theory of the spin-wave stiffness for itinerant ferromagnets [1] with pair exchange interactions derived from the magnetic force theorem [2]. The resulting formula involves one-particle propagators and effective velocity operators appearing in a recent theory of electron transport [3]. Application of this approach to clean crystals allows one to overcome the problem of ill-converging lattice summations, as documented by results for pure metals Fe, Co, and Ni. Application to random alloys within the coherent potential approxi-

mation, illustrated by results for fcc Ni-Fe and bcc Fe-Al systems, enables one to include the disorder-induced vertex corrections, often neglected in evaluation of the exchange interactions.

[1] I. Turek et al., Phys. Rev. B 101 (2020) 134410. [2] A. I. Liechtenstein et al., J. Magn. Magn. Mater. 67 (1987) 65. [3] I. Turek et al., Phys. Rev. B 65 (2002) 125101.

MA 23.30 Tue 17:00 P1

Abelian spin-Berry curvature of the Haldane model and non-Abelian generalisation — •NICOLAS LENZING, SIMON MICHEL, and MICHAEL POTTHOFF — I. Institute of Theoretical Physics, Department of Physics, University of Hamburg
The feedback of the geometrical Berry phase, accumulated in an electron system, on the slow dynamics of classical degrees of freedom is governed by the Berry curvature. Here, we study local magnetic moments, modelled as classical spins, which are locally exchange coupled to the (spinful) Haldane model. In the emergent equations of motion for the slow classical-spin dynamics there is an additional anomalous geometrical spin torque, which originates from the corresponding spin-Berry curvature. Due to the explicitly broken time-reversal symmetry, this is nonzero but usually small in a condensed-matter system. We develop the general theory and compute the spin-Berry curvature, mainly in the limit of weak exchange coupling, in various parameter regimes, particularly close to a topological phase transition. The spatial structure of the spin-Berry curvature tensor, its symmetry properties and the distance dependence of its nonlocal elements are discussed. The investigation has been done in the strict adiabatic limit, where one considers the groundstate only, resulting in an Abelian spin-Berry curvature. It is possible to generalise the formalism for a relaxed adiabatic constraint that takes into account a low-energy subspace. This type of subspace arises, for example, in the case of a degenerate groundstate. The spin-Berry curvature corresponding to the subspace is non-Abelian and does not necessarily vanish for time-reversal symmetric systems.

MA 23.31 Tue 17:00 P1

Nonlocal correlation effects due to virtual spin-flip processes in itinerant electron ferromagnets — •SEBASTIAN PAISCHER¹, MIKHAIL KATSNELSON², GIOVANNI VIGNALE³, ARTHUR ERNST¹, and PAWEŁ BUCZEK⁴ — ¹Johannes Kepler University, Linz, Austria — ²Radboud University, Nijmegen, Netherlands — ³National University of Singapore, Singapore — ⁴Hamburg University of Applied Sciences, Hamburg, Germany

An important type of the many-body effects in itinerant-electron magnets originates from the interaction of electrons with bosonic spin-flip excitations, both coherent (magnons) and incoherent (Stoner particle-hole excitations). While there has been a steady progress in understanding the properties of spin-flip excitations at a model level only little is known about microscopic details of their interactions with the electronic degrees of freedom in specific materials. Over the last few years we developed a first-principles method to account for the electron-magnon interaction in complex solids. While the method is based upon many body perturbation theory, we approximate the complex quantities from perturbation theory with quantities from time dependent density functional theory. This drastically reduces the numerical burden of the calculations and allows to consider complex materials like half-metallic ferromagnets. In this poster session some details of the theory and selected results will be presented.

MA 23.32 Tue 17:00 P1

Exploration of 2D magnetic materials using parallelized HSE functionals in FLEUR — •SABASTIAN GRANBERG CAUCHI^{1,2}, DANIEL WORTMANN¹, GREGOR MICHALICEK¹, and STEFAN BLÜGEL^{1,2} — ¹Peter Grünberg Institute and Institute for Advanced Simulation, Forschungszentrum Jülich and JARA, Germany — ²RWTH Aachen University, Germany

Density functional theory has become a standard of electronic structure calculations, often implemented in the LDA/GGA approximations. Increased accuracy can be achieved in many systems using computationally expensive hybrid functionals, e.g. PBE0 and HSE, which factor in the exact exchange energy. An implementation of hybrid functionals in the all-electron full-potential linearized augmented-plane-wave code FLEUR [1,2,3] has been realized and applied to many materials, e.g. perovskites and rare-earth compounds, in the past. Recently, high-performance techniques have been employed to achieve extreme parallelization scaling of the PBE0 implementation for optimized supercomputer use [4]. In this study, these techniques are extended to the HSE06 functional and applied to 2D magnetic materials.

We acknowledge financial support by MaX CoE funded by the EU through H2020-INFRAEDI-2018 (project: GA 824143).

[1] M. Betzinger et al., Phys. Rev. B 81, 195117 (2010).

[2] M. Schlipf, Phys. Rev. B 84, 125142 (2011).

[3] FLEUR official website, flap.wde

[4] M. Redies, Front. Mater. 9, doi:10.3389/fmats.2022.851458 (2022).

MA 23.33 Tue 17:00 P1

Magnon excitations in two-dimensional doped Antiferromagnets — •PRT BERMES — Department of Physics and Arnold Sommerfeld Center for Theoretical Physics (ASC), Ludwig-Maximilians-Universität München, Theresienstr. 37, München D-80333, Germany — Munich Center for Quantum Science and Technology (MCQST), Schellingstr. 4, D-80799 München, Germany

When a mobile hole is doped into an antiferromagnet, its movement will distort the surrounding magnetic order and yield a magnetic polaron. The resulting complex interplay of spin and charge degrees of freedom gives rise to very rich physics and is widely believed to be at the heart of high-temperature superconductivity in cuprates. Although the parton theory has been successful in describing many properties of these magnetic polarons, it is still unclear how these couple to the collective magnon excitations. In this paper, we derive this effective coupling between the polaron and magnons and their influences on the polaron's properties. We therefore start from a single hole doped into an AFM described in the aforementioned polaron model by a 'geometric string' and will then introduce magnon excitations through a generalized 1/S expansion to arrive at an effective Hamiltonian. After making a Born-Oppenheimer-type approximation, this system will be solved using the self-consistent Born approximation to extract the renormalized polaron properties, like its dispersion relation and the single-particle spectrum.

MA 23.34 Tue 17:00 P1

Self-assembly as a tool to study microscale curvature and strain-dependent magnetic properties — •BALRAM SINGH¹, JORGE. A. OTÁLORA², TONG H. KANG¹, IVAN SOLDATOV¹, DMITRIY D. KARNAUSHENKO³, CHRISTIAN BECKER³, RUDOLF SCHÄFER¹, DANIIL KARNAUSHENKO³, VOLKER NEU¹, and OLIVER G. SCHMIDT³ — ¹Institute for Integrative Nanosciences, Leibniz IFW Dresden, 01069 Dresden, Germany. — ²Departamento de Física, Universidad Católica del Norte, Avenida Angamos 0610, Casilla 1280 Antofagasta, Chile — ³Center for Materials, Architectures and Integration of Nanomembranes (MAIN), Chemnitz University of Technology, 09126 Chemnitz, Germany

The extension of 2D ferromagnetic structures into 3D curved geometry enables tuning its magnetic properties such as magnetic anisotropy. Tuning the anisotropy with strain and curvature has become a promising ingredient in modern magnetoelectronic devices, however, has been limited to extended thin films and to only moderate bending. By applying a self-assembly rolling technique using a polymeric platform, we provide a template that allows homogeneous and controlled bending of a functional layer adhered to it, irrespective of its shape and size. This is an intriguing possibility to tailor the sign and magnitude of the surface strain of integrated, micron-sized devices. In this article, the impact of strain and curvature on the magnetic ground state and anisotropy is quantified for thin-film Permalloy micro-scale structures, fabricated on the surface of the tubular architectures, using solely electrical measurements.

MA 23.35 Tue 17:00 P1

Switchable magnetic probe for scanning probe microscopy — •RACHAPPA RAVISHANKAR, ANIRUDDHA SATHYADHARMA PRASAD, STEFAN BAUNACK, THOMAS MÜHL, VOLKER NEU, RUDOLF SCHÄFER, and BERND BÜCHNER — Leibniz Institute for Solid State and Materials Research (IFW) Dresden

Magnetic force microscopy (MFM) has been demonstrated as a valuable technique for the characterization of magnetic nanomaterials. Conventional MFM is a two-pass method, in which the topography of the surface is first obtained by probing the strong Van der Waals and other short-range interactions between probe and sample. During the second scan, the probe is lifted away from the sample, and it experiences long-range magnetic and electrostatic interactions.

A typical approach to disentangle magnetic from non-magnetic signals is by switching the magnetization of the tip in a global external field by means of physically removing the tip from the MFM setup. In the course of our work, we aim at developing an on-chip solution for switching the magnetization of a magnetic probe. We accomplish this by a local Oersted field from a current carrying planar coil, lithographically patterned on either the tip or sample.

This poster highlights switching tip magnetization by a homogeneous field source from a macroscale electromagnetic coil versus an inhomogeneous field from lithographically patterned micro coils on the sample. We showcase this for: (i) commercial MFM probes, and (ii) commercial MFM probes tailored by focused ion beam milling.

MA 23.36 Tue 17:00 P1

Imaging magnetization dynamics of non-bubble domains in ferromagnetic multilayer systems for quantification of Dzyaloshinskii-Moriya interaction (DMI) — •ARNE VEREIJKEN¹, SAPIDA AKHUNDZADA¹, FLORIAN OTT¹, MAXWELL LI², TIM MEWES³, MICHAEL VOGEL¹, VINCENT SOKALSKI², and ARNO EHRESMANN¹ — ¹Institute of Physics and Center for Interdisciplinary Nanostructure Science and Technology (CINaT), University of Kassel, Kassel, Germany — ²Department of Materials Science and Engineering, Carnegie Mellon University, Pittsburgh, USA — ³Department of Physics and Astronomy, University of Alabama, Tuscaloosa, USA

DMI promotes chiral coupling between spins [1], giving rise to robust, chiral spin textures, e.g., skyrmions with excellent properties for information storage

and processing [2]. Recently it has been demonstrated that the DMI is measurable via imaging of magnetization dynamics of bubble domains, which possesses great potential in becoming an experimental standard method [3]. By enhancing this method with a self-segmentation for growth identification, more complex domain shapes may be accessible. We systematically studied the DMI in a perpendicularly magnetized ferromagnet/heavy metal system with different dendritic domain textures. [1] T. Moriya, New Mechanism of Anisotropic Superexchange Interaction, Phys. Rev. Lett. 4 (1960) [2] C. Back et al., The 2020 Skyrmionics Roadmap, J. Phys. D 53.36 (2020) [3] A. Magni et al., Key Points in the Determination of the Interfacial DMI from Asymmetric Bubble Domain Expansion, (2022)

MA 23.37 Tue 17:00 P1

Kerr microscopy for all-optical helicity-dependent magnetization switching (AOHDS) — •LUCAS VOLLROTH¹, MARCEL KOHLMANN¹, KRISTÝNA HOVOŘÁKOVÁ², EVA SCHMORANZEROVÁ², MARKUS MÜNZENBERG¹, and JAKOB WALOWSKI¹ — ¹Greifswald University, Greifswald, Germany — ²Charles University, Prague, Czech Republic

The demand of data storage capabilities is growing rapidly since the invention of the computer. The development of big data in science and economy intensifies this evolution. To fulfill the demand of storage capabilities there is need of new data storage techniques. One of these new techniques is heat assisted magneto recording (HAMR) where the bit size is drastically decreased by high coercive fields of granular FePt.

Besides the heat assisted writing with a magnet, we are investigating the writing on HAMR media with all-optical helicity-dependent switching (AOHDS) as a novel data storage technology [1]. Wide field Kerr-microscopy is a well-suited method to explore and analyze the outcome of our AOHDS experiments.

We present a build from scratch and cost-efficient Kerr microscope for the observation of magnetic domains and writing with AOHDS on HAMR media simultaneously. It can also be used for the investigation of skyrmions and can be refined to investigate magnetization changed in a pump-probe experiment after the deposition of ultrashort laser pulses on magnetic thin films.

[1] John, R. et al. Magnetisation switching of FePt nanoparticle recording medium by femtosecond laser pulses. Sci Rep 7, 4114 (2017)

MA 23.38 Tue 17:00 P1

Nitrogen Vacancy Center in Diamond - Study of Correlated Electron Systems — •SREHARI JAYARAM and MALIK LINGER — 3rd Physics Institute, University of Stuttgart, Allmandring 13, Stuttgart, Germany

Investigation of emergent nanoscale magnetic properties of materials is a challenging field, which requires both, high sensitivity and spatial resolution. The scanning probe magnetometry based on the nitrogen-vacancy (NV) center in diamond is capable to fulfill these requirements and delivers complete vectorial magnetic field reconstructions. Due to optically detected magnetic resonance (ODMR), the NV center can operate as a quantum sensor from cryogenic temperatures up to room temperature with a frequency range from DC to GHz under high bias field conditions and UHV. In combination with atomic force microscopy, a sensor-sample distance of a few nanometers can be achieved with an NV-containing diamond AFM tip.

This has enabled investigations into the imaging of magnetic domains in single-layer CrBr₃, the coexistence of AFM and FM domains in Moire twisted CrI₃ trilayer, antiskyrmions in Heusler compounds, etc.

Thus, NV magnetometry opens the path to observe static and dynamic magnetic phenomena with nanoscale spatial resolution at a wide temperature range.

MA 23.39 Tue 17:00 P1

Improvement of Magnetic Force Microscopy measurements using magnetics tips grown by Focused Electron Beam Induced Deposition —

•A.T. ESCALANTE-QUICENO¹, V.V. FERNÁNDEZ², A. HIERRO-RODRÍGUEZ^{2,3}, J.I. MARTÍN^{2,3}, C. MAGÉN^{1,4}, and J.M. DE TERESA^{1,4} — ¹Instituto de Nanociencia y Materiales de Aragón (INMA), CSIC-Universidad de Zaragoza, 50009 Zaragoza, Spain — ²Depto. Física, Universidad de Oviedo, 33007 Oviedo, Spain — ³CINN (CSIC-Universidad de Oviedo), 33940 El Entrego, Spain — ⁴Laboratorio de Microscopías Avanzadas (LMA), Universidad de Zaragoza, 50009 Zaragoza, Spain

We report the fabrication of magnetic tips for Magnetic Force Microscopy (MFM) using Focused Electron Beam Induced Deposition (FEBID). Due to their high aspect ratio and metallic content, these magnetic tips present a good magnetic behaviour, providing a number of advantages as lower non-magnetic tip-sample interaction, higher lateral resolution and higher coercivity than commercial magnetic tips when used for simultaneous topographical and magnetic measurements. A sharp tip apex with a diameter of 10 nm enables a high lateral resolution. Depending on the particular needs of the samples, the shape, length and diameter of the tip can be adjusted in a reproducible way. Because of its versatility, FEBID can produce magnetically hard tips customized with specific requirements. Ni₈₀Fe₂₀/NdCo₅ bilayers with perpendicular magnetic anisotropy will be measured with FEBID-grown magnetic tips, where the resolution limit in MFM measurements will be tested.

MA 23.40 Tue 17:00 P1

Spatio-temporal Characterization of 3D Perovskites with Faraday Holography — •JULIA ANTHEA GESSNER, JONATHAN ZERHOCH, SHANGPU LIU, and FELIX DESCHLER — Physikalisch-Chemisches Institut, Im Neuenheimer Feld 229, Heidelberg, Germany

Hybrid metal halide perovskites have shown to be a promising class of semi-conducting materials for a variety of applications ranging from LEDs, solar cells to spintronic devices. Compared to conventional materials, perovskites exhibit some advantageous features as a high quantum efficiency and tunability in the visible range, as well as a strong spin-orbit coupling for an efficient optical spin manipulation.

A preliminary step towards the integration of perovskites in spintronic devices is the time- and space-resolved optical study of their magnetic properties. In the present work, we study the spatio-temporal spin dynamics of Methylammonium Lead Tribromide (MAPbBr₃) by the unique combination of two spectroscopic methods: time-resolved Faraday rotation spectroscopy and off-axis holographic imaging. The Faraday angle, which is a measure for the materials' magnetic moment, is imaged by an Ultrafast Transient Holographic Microscope (UTHC). The UTHC works as an all-optical lock-in amplifier with no upper limitations in the signal repetition rate.

By performing Faraday Holography at different temperatures and fluences, we are hence able to investigate the spatial evolution of optically spin-polarized excitons and identify the dominating spin relaxation mechanisms. This is essential for the optimization of the materials' properties and the future realization of spintronic systems.

MA 23.41 Tue 17:00 P1

Planar scanning probes - A new platform for nanoscale magnetometry with NV centers and nearfield microscopy — •PAUL WEINBRENNER¹, STEFAN ERNST², PATRICIA QUELLMALZ³, CHRISTIAN GIESE³, and FRIEDEMANN REINHARD¹ — ¹Universität Rostock, Rostock, Germany — ²ETH Zürich, Zürich, Switzerland — ³Fraunhofer Institut für Angewandte Festkörper Forschung, Freiburg, Germany

We present the application of a new scanning probe technique to magnetometry with nitrogen-vacancy (NV) centers in diamond. Instead of using sharp tips we use flat mesas (shallow pillars) with a lateral size of 50 micrometers and height of up to 5 micrometers. Due to their geometry these so-called planar scanning probes offer a unique advantage for nanoscale magnetometry and novel optical near-field sensors.

Despite their large lateral size, they can still be scanned at a standoff distance of several nanometers. To achieve this alignment, we use tilt and distance control with optical far- and near-field measurements.

We fabricate planar diamond probes and use NV center quantum sensors for magnetic field measurements. The lateral size of the planar probes enables highly parallel scanning probe magnetometry. Additionally, the fabrication is less complex compared to conventional diamond tips.

With this new approach to scanning probe measurements, we propose the emergence of new material systems as sensors for nanoscale imaging. These next generation sensors include plasmonic nanostructures, defects in 2D materials, and encapsulated, single molecules.

MA 23.42 Tue 17:00 P1

Analysing the Domain Structure of a Thin Film and a GMR Stack with Magnetic Transmission Electron Microscopy — •JUDITH BÜNTE, BJÖRN BÜKER, DANIELA RAMERMANN, INGA ENNEN, and ANDREAS HÜTTEN — Universität Bielefeld, Dünne Schichten und Physik der Nanostrukturen, Universitätsstr. 25, 33615 Bielefeld, Germany

The Transmission Electron Microscope (TEM) can be used to image magnetic domains in magnetic samples. Two prominent techniques for magnetic imaging are Differential Phase Contrast (DPC) and Lorentz Microscopy (LTEM). Both techniques base on the Lorentz force inside the magnetic domain of a specimen which deflects the transmitted electron beam depending on the orientation of the corresponding magnetic field. This deflected beam results in a different intensity distribution in the recorded image which can be analysed.

In this contribution both the DPC and the LTEM technique are used to image the magnetic landscape of two different model systems: One sample consists of pure cobalt, while the other sample is a nanostructured multilayer CoFe/Co/Ru sample. While the domains of the pure cobalt sample are unbound, the nanostructure inside the multilayer sample yields an interesting domain structure, which is constrained to the structure of the sample. Both samples are analysed quantitatively to draw conclusions regarding the characteristics of the samples through the measurements.

MA 23.43 Tue 17:00 P1

Application of high magnetic fields to micron-scale NMR spectroscopy with quantum sensors in diamond — •ROUVEN MAIER, JONAS MEINEL, VADIM VOROBYOV, and JÖRG WRACHTRUP — 3rd Institute of Physics, University of Stuttgart, Germany

Nuclear magnetic resonance (NMR) spectroscopy is widely used in fields ranging from chemical structure analysis to tissue imaging in clinical applications.

The requirement of large sample volumes poses one of the major drawbacks of classical NMR measurements. Micron- and nano-scale NMR spectroscopy using quantum sensors, such as nitrogen-vacancy (NV) centers in diamond, has been a constant field of research over the past years. Recent developments of innovative detection schemes, such as the quantum-heterodyne (qdyne) protocol showed promising results by enabling resolutions independent of the inherent lifetime of the sensor spin. We present the experimental layout for the extension of quantum NMR sensing towards high magnetic fields, to enable chemical resolution at the micron-scale. This approach combines the frequency resolution necessary for chemical characterization with accurate spatial information. Signal sources could include ²H, ¹³C and ¹⁹F from biomolecules and materials attached to the diamond surface.

MA 23.44 Tue 17:00 P1

Modulated spin-wave system for neuromorphic machine learning — •JAN MASKILL, DAVID BREITBACH, MILAN ENDER, BURKARD HILLEBRANDS, and PHILIPP PIRRO — Landesforschungszentrum OPTIMAS und Rheinland Pfälzische Technische Universität

In this work, a prototype physical reservoir based on spin-wave dynamics is developed and investigated numerically by micromagnetic simulations. The system under study is a nanometer-sized magnonic waveguide, on top of which a coplanar waveguide (CPW) antenna is placed for spin-wave excitation, as well as a localized region for spin current injection. The inputs of the reservoir are spin current pulses injected via the spin Hall effect, which modulates the amplitude of a carrier spin-wave created by the CPW. The carrier spin wave is reflected at the end of the waveguide, which allows for an interaction of the subsequent input signals. The resulting spin dynamics are shown to become highly nonlinear under the influence of the spin current. The output of the reservoir is its magnetic state as a function of time, which is calculated as part of numerical simulations. Based on an analysis using the kernel and generalization rank, it is shown that the reservoir exhibits a non linear input-output relation. In the kernel rank analysis, the nonlinearity of the reservoir is extracted with spatial resolution, uncovering regions of interest for possible output definitions. This work contributes to the realization of neuromorphic applications based on spin waves and helps to improve benchmarks for physical reservoirs.

MA 23.45 Tue 17:00 P1

Calculation of the temperature-dependent exchange stiffness from Domain Wall modelling — •FELIX SCHUG^{1,2}, NILS NEUGEBAUER^{2,3}, MICHAEL CZERNER^{1,2}, and CHRISTIAN HEILIGER^{1,2} — ¹Institute for Theoretical Physics, Justus Liebig University Giessen — ²Center for Materials Research (LaMa), Justus Liebig University Giessen — ³Institute of Experimental Physics I, Justus Liebig University Giessen

Understanding the different influences on the macroscopic magnetic properties of a material at finite temperatures is of great interest from a theoretical point of view. As macroscopic magnetic properties, such as anisotropies or the exchange stiffness, are related to the quantum nature of electrons and thus to the most fundamental level of solids, the atomic level, atomistic modelling of magnetic material may promote a more profound understanding of the microscopic processes. Performing the corresponding numerical simulations at various temperatures from 0 K to the Curie-temperature T_C , the temperature dependence of the associated macroscopic properties may be modelled. These modelled material parameters can be used to simulate magnetic properties in large-scale temperature-dependent micromagnetic simulations, leading to the so-called multiscale modelling approach. Here the approach of simulating Bloch walls of a finite cobalt stripe at different temperatures is demonstrated to extract the macroscopic crystalline anisotropy constant K_C and the exchange stiffness parameter A_{ex} .

MA 23.46 Tue 17:00 P1

Calculation of magnetic fields, forces and velocities by means of conductor trace segmentation using the example of the magnetic on-off ratchet. — •TORBEN TAPPE, INGA ENNEN, and ANDREAS HÜTTEN — Bielefeld University, Bielefeld, Germany

For the evaluation of an optimal combination of ratchet geometry and particles, the calculation of the magnetic fields is essential, since in this way the acting forces on the particles and the resulting velocity of these can be determined prior to manufacturing. While the finite element method (FEM) is a standard tool for the calculation of magnetic fields of systems, in this work the trace segmentation is used for the modeling of the magnetic field occurring in the ratchet and is compared to the results of the FEM. Trace segmentation is based on the superposition principle, in which the magnetic field of a trace is approximated by many individual straight conductors whose magnetic fields are known. To evaluate the results of this method, various examples, ranging from just one trace to modeling an entire ratchet, were used and compared to Finite Element Method Magnetics (FEMM) calculations. These comparisons showed that the two methods, with a mean squared error of $2 \cdot 10^{-17}$ T to $3 \cdot 10^{-16}$ T, give the same results. This demonstrated that the trace segmentation is capable of reproducing the results of the standard tool FEM and therefore it is suitable for modeling a magnetic on-off ratchet.

MA 23.47 Tue 17:00 P1

Finite-size scaling for 5D Ising model with free boundary conditions — •YULIAN HONCHAR^{1,2,3}, BERTRAND BERCHE^{1,4}, YURIJ HOLOVATCH^{1,3}, and RALPH KENNA^{1,2} — ¹L⁴ Collaboration & Doctoral College for the Statistical Physics of Complex Systems, Leipzig-Lorraine-Lviv-Coventry, Europe — ²Centre for Fluid and Complex Systems, Coventry University, United Kingdom — ³Institute for Condensed Matter Physics, National Acad. Sci. of Ukraine, Lviv, Ukraine — ⁴Laboratoire de Physique et Chimie Théoriques, Université de Lorraine - CNRS, Nancy, Vandœuvre les Nancy, France

It is widely known that in systems with dimensionality higher than the upper critical, the scaling exponents assume their mean field values. However, in this case, the hyperscaling relation, which contains the dimensionality of space, is violated. In addition, mean-field exponents do not agree with the finite-size scaling. One of the theories that aimed to theoretically describe the behaviour of a finite-sized system is the Gaussian fixed point (so-called G-scaling) at which the interactions in the Landau-Ginsburg action are put to zero. Monte Carlo simulations of hypercubic lattices in the Ising model, where $d_{uc} = 4$, show that for periodic boundary conditions the exponents of the GFP do not correspond to the FSS. Another theory emerges with the introduction of a new exponent q into hyperscaling, which is equal to 1 for the dimensions $d \leq d_{uc}$, and $q = d/d_{uc}$ for higher dimensions. Q-scaling is confirmed for lattices with PBC. In this work, we investigated FSS on $d = 5$ lattices with free boundary conditions and showed that, unlike in systems with PBC, it is closer to G-scaling.

MA 23.48 Tue 17:00 P1

Equivalent Circuit for the Consideration of Frequency-Dependent Effects in Electronics Simulations of Induction Hobs — •LENNART SCHWAN^{1,2}, MICHAEL FEIGE¹, ANDREAS HÜTTEN², and SONJA SCHÖNING¹ — ¹Bielefeld Institute for Applied Materials Research (BifAM), Bielefeld University of Applied Sciences, Department of Engineering Sciences and Mathematics — ²Thin Films & Physics of Nanostructures, Bielefeld University, Department of Physics

Inductive power transfer is a well-established technology, e.g. for inductive heating in industrial applications and household appliances like inductions hobs. An inductive heating system usually consists of a coil (transmitter) which is powered by an alternating current and a ferromagnetic material (receiver), for example a cooking vessel. FEM simulations are a powerful tool for simulating the electromagnetic processes in coil and vessel. For electronics development, FEM simulations of the coil cooking vessel system are too computationally intensive.

In electronics, the coil is an RL element and thus is also represented as such in electronics simulations. This equivalent circuit is sufficient for simple considerations, but neglects that R and L are frequency dependent. Frequency dependent variables can be used in the frequency domain only but not in the important time domain simulations with non-sinusoidal signals. In order to consider the frequency dependence of R and L in time domain simulations for non-sinusoidal signals, we use an improved equivalent circuit based on passive components that includes the frequency dependence.

MA 23.49 Tue 17:00 P1

Demystifying exchange mechanisms in the 2D FenGeTe2 family through Wannierization — •SOHEIL ERSHADRAD, SUKANYA GHOSH, and BIPLAB SANYAL — Uppsala University, Uppsala, Sweden

The FenGeTe2 ($n=3,4,5$) family of 2D ferromagnets features near-room temperature ferromagnetism, making them promising for use in spintronic devices. In these crystals, a metallic film of FenGe is sandwiched between two layers of Te, separated by a van der Waals (vdW) gap. Due to their complex structures, the physics behind their exotic magnetic behavior is not well understood. Using density functional theory, we investigated the magnetic properties of the FenGeTe2 family. Through the projection of Bloch states into Wannier functions, the orbital resolved Heisenberg exchange parameters based on the tight-binding hopping parameters were determined. Based on the extracted hopping parameters, we investigate exchange mechanisms and explain the differences in exchange interactions. Our calculations indicate that the relative position of Ge with respect to Fe atoms has a significant impact on the strength of the exchange, resulting in a strong short-range indirect exchange in the FenGeTe2 structures along with a long-ranged RKKY type of interaction.

MA 23.50 Tue 17:00 P1

Magnon transport in magnetically ordered insulator/platinum nanostructures — •MARIA SIGL^{1,2}, JANINE GÜCKELHORN^{1,2}, MONIKA SCHEUFELE^{1,2}, FRANZ WEIDENHILLER^{1,2}, MATTHIAS OPEL¹, STEPHAN GEPRÄGS¹, HANS HUEBL^{1,2,3}, MATTHIAS ALTHAMMER^{1,2}, and RUDOLF GROSS^{1,2,3} — ¹Walther-Meißner-Institut, Bayerische Akademie der Wissenschaften, Garching, Germany — ²Technical University of Munich, TUM School of Natural Sciences, Physics Department, Garching, Germany — ³Munich Center for Quantum Science and Technology, München, Germany

For energy-efficient information processing, the transport and manipulation of spin waves (magnons) in magnetically ordered insulators (MOIs) offers a promising route. To this end, we investigate the magnon transport in MOI/Pt bilayers by all-electrical means utilizing the spin Hall effect. Here, we focus on

the transport in the ferrimagnet yttrium iron garnet ($Y_3Fe_5O_{12}$, YIG) and the antiferromagnet hematite ($\alpha-Fe_2O_3$) using two- and three-terminal devices. Two electrically isolated Pt strips on top of the MOI, act as spin current injector and detector. An applied charge current to a third strip, the modulator, in between injector and detector allows for electrical control of the diffusive magnon spin transport. We systematically study the distance and magnetic field dependence of the magnon transport in YIG and hematite and compare our results to simultaneous spin Hall magnetoresistance measurements.

MA 23.51 Tue 17:00 P1

Super-Nyquist-sampling MOKE elucidates the role of interfacial exchange coupling when measuring spin Hall effect in the noncollinear antiferromagnet Mn₃Ir — PIET URBAN¹, ROUVEN DREYER¹, JAMES M TAYLOR¹, •SRISHTI DONGARE¹, BINOY K HAZRA², STUART S P PARKIN², and GEORG WOLTERS DORF¹ — ¹Institute of Physics, Martin Luther University Halle-Wittenberg, 06120 Halle, Germany — ²Max Planck Institute for Microstructure Physics, 06120 Halle, Germany

Non-collinear antiferromagnets (AFs) have been found to serve as an efficient source of intrinsic spin Hall effect (SHE). However, the role of their chiral domain structure in this process, and the transmission of the resulting spin current across interfaces with ferromagnets (FMs), remain open questions. Using a combination of electrically-detected spin-torque ferromagnetic resonance (ST-FMR) and optically-detected super-Nyquist-sampling magneto-optical Kerr effect (SNS-MOKE) measurements, we investigate the SHE generated by the non-collinear spin texture of Mn₃Ir in heterostructures with Ni₈₀Fe₂₀. The enhanced damping due to interfacial exchange coupling between the AF and FM complicates extraction of the spin Hall angle (SHA) using ST-FMR. In contrast, spatially-resolved SNS-MOKE studies allow for a local detection of the SHA, and reveal modifications of the coupling-induced anisotropy upon exposure to a combination of DC current and RF power. These findings offer us a path to quantify the SHE generated by an AF more accurately, as well as to control their domain structure in a local manner.

MA 23.52 Tue 17:00 P1

Magneto-optical probing of orbital accumulation in a light metal — •SANAZ ALIKHAH¹, MARCO BERRITTA², PETER M. OPPENEER¹, IGOR LYALIN³, and ROLAND K. KAWAKAMI³ — ¹Uppsala University, Uppsala, Sweden — ²University of Exeter, Exeter, United Kingdom — ³Ohio State University, Ohio, USA

Orbital currents and orbital accumulation are attractive alternatives to the commonly employed spin counterparts, generated typically by the spin Hall effect in heavy metals. However, the detection of orbital currents and accumulation is a challenging task. Here we investigate theoretically the possibility of magneto-optical (MO) detection of current-induced orbital accumulation in the light metal chromium. Using linear-response theory, we compute, first, the spin and orbital accumulation and then predict the expected MO spectrum for pure spin accumulation or pure orbital accumulation. We find that the orbital Hall effect is much larger than the spin Hall effect, and that the orbital MO response is much larger than that due to the spin polarization. This result opens the door for MO detection of current-induced orbital accumulation. Finally, we compare the computed MO responses with recent MO Kerr effect measurements on chromium.

MA 23.53 Tue 17:00 P1

Spin Hall Magnetoresistance in Hybrid Chiral Molecule / Metal / Magnet Systems — •SIMON SOCHIERA¹, ASHISH MOHARANA¹, SHUANGLONG WANG², HAO WU², FABIAN KAMMERBAUER¹, MARIA-ANDROMACHI SYSKAKI³, ZIJIE QIU^{2,3}, TOMASZ MARZALEK², and ANGELA WITTMANN¹ — ¹Institut für Physik, Johannes-Gutenberg-Universität Mainz, 55099 Mainz, Germany — ²Max Planck Institute for Polymer Research, Ackermannweg 10, 55128, Mainz, Germany — ³Shenzhen Institute of Aggregate Science and Technology, School of Science and Engineering, The Chinese University of Hong Kong, 2001 Longxiang Boulevard, Longgang District, Shenzhen City, Guangdong, 518172, China

The high efficiency of spin filtering has propelled chiral molecules to the center of attention in molecular spintronics. In conventional ferromagnet/ heavy-metal heterostructures, the spin Hall magnetoresistance has been established as a highly sensitive probe of the interplay between a charge current and magnetization mediated via spin currents. Here, we investigate the chiral-induced spin selectivity effect by probing the impact of the adsorption of chiral molecules on the spin Hall magnetoresistance of a well-characterized device. The change in the magnetoresistive behavior of the device will give insight into the underlying mechanisms at in hybrid chiral molecule/ metal/ ferromagnet multilayer structures.

MA 23.54 Tue 17:00 P1

2D nearfield imaging of cells with high broadband spintronic THz emitters — •TRISTAN WINKEL, FINN-FREDERIK STIEWE, DOREEN BIEDENWEG, OLIVER OTTO, and MARKUS MÜNZENBERG — Universität Greifswald, Greifswald, Deutschland

Gaining information about cells is very important in many fields of science such as biology and medicine. 2D nearfield imaging of cells with high broadband

spintronic THz emitters provides effective means to gain information about the cells. Since measurements are made with broadband terahertz pulses, the absorption spectrum can also be determined for each spatial measurement point. The spatial resolution can reach $5\mu\text{m}$ with our setup[1]. Among other things, this allows conclusions to be drawn about the water content of the cell. Our technical approach offers great potential for medical applications due to the high gain of information.

[1] Spintronic emitters for super-resolution in THz-spectral imaging Appl. Phys. Lett. 120, 032406 (2022); <https://doi.org/10.1063/5.0076880>

MA 23.55 Tue 17:00 P1

THz emission from Ni/NiO/Pt and Co/CoO/Pt multilayers — •NIKOS KANISTRAS¹, LAURA SCHEUER², DIMITRIOS ANYFANTIS³, PANAGIOTIS POULOPOULOS³, and EVANGELOS TH. PAPAIOANNOU¹ — ¹Institut für Physik, Martin-Luther-Universität Halle-Wittenberg, 06120 Halle, Germany — ²Fachbereich Physik and Landesforschungszentrum OPTIMAS, Technische Universität Kaiserslautern, 67663, Kaiserslautern, Germany — ³Department of Materials Science, School of Natural Sciences University of Patras, Rio, 26504 Patras, Greece

Ultrafast spin-to-charge conversion in heterostructures composed of ferromagnetic (FM)/non-magnetic(NM) thin films can give rise to the emission of THz electromagnetic waves[1]. In this work we investigate the role of an antiferromagnetic oxide interlayer like NiO and CoO in the THz emission. The trilayers are grown with the sputtering technique. The samples exhibit in plane magnetic easy axis as revealed by magneto-optical and Squid magnetometry. The presence of very thin NiO and CoO allows the spin transport from the ferromagnetic to the Pt layer and lead to the THz emission. However, there is a reduction on the signal which is discussed in conjunction of the structural and magnetic properties of the antiferromagnetic layers. [1]E. Papaioannou, R. Beigang Nanophotonics10, 1243*1257 (2021).

MA 23.56 Tue 17:00 P1

Investigating spin dynamics in MoS₂/permalloy bilayers — •RIEKE VON SEGGERN, LINA HANSEN, JONATHAN WEBER, CHRISTOPHER RATHJE, and SASCHA SCHÄFER — Insitute of Physics, University of Oldenburg, Germany

For the successful integration of spin degrees of freedom in information processing devices, spin-injection into semiconductors plays a crucial role. It was recently demonstrated that an optically generated out-of-equilibrium spin population in a ferromagnetic metal can be efficiently transferred into an adjacent MoS₂ layer across its bandgap [1]. Due to the deflection of the spin current the bilayer then emits electromagnetic pulses in the terahertz (THz) domain analogous to the already established metallic spintronic THz emitters (STE) [2].

In this work, we explore the microscale THz emission properties of single-flake MoS₂/permalloy bilayer systems driven by ultrashort optical pulses (780-nm central wavelength, 70-fs pulse duration). We apply electro-optic sampling to measure the emitted THz electric field in the time domain. An optical excitation spot size in the micrometer range allows for a high spatial resolution of the sample's emission features. With this approach a more detailed understanding of the underlying processes in these TMDC-based samples can be achieved.

[1] Cheng et al., Nat. Phys. 15, 347 (2019)

[2] Seifert et al., Nat. Photonics 10, 483 (2016)

MA 23.57 Tue 17:00 P1

Modulation of exchange bias in Fe₃GeTe₂/CrPS₄ van der Waals heterostructures — ARAVIND P. BALAN¹, •ADITYA KUMAR¹, ULRICH NOWAK², and MATHIAS KLÄUT¹ — ¹Institute of Physics, Johannes Gutenberg-University Mainz, Staudingerweg 7, Mainz 55128, Germany — ²Department of Physics, University of Konstanz, Universitätsstraße 10, Konstanz 78464, Germany

Exchange bias (EB) is a well-explored phenomenon in thin film systems. The mechanism of exchange bias in such systems is often associated with defects at the interface. Due to the intrinsic layered structure of the 2D materials, they can be mechanically stacked to form heterostructures with extremely clean and flat interfaces. CrPS₄ is an A-type anti-ferromagnet that is stable in an ambient atmosphere. Its out-of-plane anisotropy and layered spin structure make it an ideal anti-ferromagnet for inducing exchange bias in a ferromagnet (FM)/antiferromagnet (AFM) van-der Waal (vdW) heterostructures.[1] In this work exchange bias in Fe₃GeTe₂ (FGT)/ CrPS₄ (CPS) heterostructure has been studied using anomalous hall effect measurements. For a clean FGT/CPS interface, an EB of magnitude 50 mT was observed at 5 K with a blocking temperature of 20 K. Interestingly, the introduction of oxidized FGT at the interface modulates the EB considerably. EB in this system could be induced even without the conventional field-cooling, but by just applying a small pre-set field. References : [1] R. Wu et al., Phys. Rev. Applied 17, 064038 (2022) [2] T. Zhang et al., Advanced Science 9.11, 2105483 (2022)

MA 23.58 Tue 17:00 P1

Quantum transport through 2D metallic magnets: Effects of defects and stacking sequence — MASOUMEH DAVOUDINIYA and •BIPLAB SANYAL — Department of Physics and Astronomy, Uppsala University, Box 516, 751,20 Uppsala, Sweden

In recent times, two-dimensional van der Waals (vdW) bonded magnetic materials with high Curie temperatures have attracted a lot of attraction due to their high potential in future spintronic nanodevices. In this regard, it is important to understand the properties of these magnetic systems even in the presence of several types of defects and stacking of layers, often controlling the properties. Based on density functional theory calculations, this work aims to theoretically address the quantum transport properties of Fe₄GeTe₂ (FGT) as new 2D vdW layered metallic magnetic materials applicable for the next-generation electronic and magnetic industry. In particular, we investigate the spin-dependent electronic transport through vdW bonded FGT layers connected to Cu electrodes by nonequilibrium Green's function approach. The influence of the inclusion of Fe atoms in the vdW gap and stacking sequence of layers will be discussed too. Moreover, we will present the studies on the magnetoresistance of the system for different magnetic configurations of FGT layers separated by semimetallic and insulating 2D layers.

MA 23.59 Tue 17:00 P1

Dependence of resistance area product and tunnel magnetoresistance on MgO crystalline quality in CoFeB/ MgO/ CoFeB Magnetic Tunnel Junctions — •TOBIAS PETERS and GÜNTER REISS — Center for Spinelectronic Materials and Devices, University of Bielefeld, Germany

We investigated the tunnel magnetoresistance (TMR) and resistance area product (RA) in CoFeB/MgO/CoFeB magnetic tunnel junctions (MTJs) grown via sputtering deposition and investigated the influence of MgO crystalline quality. Therefore, the Ar-pressure was varied from 0.004 mbar to 0.14 mbar during the MgO deposition. X-ray diffraction (XRD) measurements performed on pseudo spin valves with 10nm thick MgO reveal the highest (001) oriented crystallographic texture of MgO for an Ar-pressure of 0.08 mbar. This MgO sputtering conditions transferred to exchange biased MTJs provides the best barrier quality, which resulted in the lowest RA ($17\ \Omega\mu\text{m}^2$) with high TMR ratio (198%) for a MgO thickness of 0.8nm. Additionally we found higher Ar partial pressure (above 0.14 mbar) resulting in amorphous MgO with even lower RA ($5\ \Omega\mu\text{m}^2$), but with significantly reduced TMR ratio (74%).

MA 23.60 Tue 17:00 P1

Atomic Layer Deposition of Yttrium Iron Garnet (YIG) for 3D Spintronics — •MICHAELA LAMMEL^{1,2,3}, DANIEL SCHEFFLER⁴, DARIUS POHL⁵, PETER SWEKIS^{4,6}, SVEN REITZIG², HELENA REICHLLOVA^{3,4}, RICHARD SCHLITZ⁴, KEVIN GEISHENDORF^{1,2}, LUISE SIEGL^{2,4}, BERND RELLINGHAUS⁵, LUKAS M. ENG^{2,7}, KORNELIUS NIELSCH^{1,2,7,8}, SEBASTIAN T. B. GOENNENWEIN^{3,4,7}, and ANDY THOMAS^{1,4} — ¹IFW Dresden — ²Institute of Applied Physics, TU Dresden — ³FB Physik, Universität Konstanz — ⁴Institut für Festkörper- und Materialphysik, TU Dresden — ⁵DCN, cfaed, TU Dresden — ⁶MPI CPFS, Dresden — ⁷ct.qmat, TU Dresden — ⁸Institute of Materials Science, TU Dresden

Three-dimensional (3D) magnetic structures have recently gained increasing interest in the field of spintronics, since going beyond planar films is expected to lead to a variety of new phenomena. Routes for the fabrication of 3D magnetic insulators are of key importance in order to separately study the magnetic and the electronic response of a given 3D structure. Here, we demonstrate the fabrication of thin films of the magnetic insulator yttrium iron garnet (Y₃Fe₅O₁₂, YIG) via atomic layer deposition. To that end we utilize a supercycle approach based on sub-nanometer thin layers of the binary systems Fe₂O₃ and Y₂O₃ with the corresponding atomic ratios. We deposit Y₂O₃/Fe₂O₃ multilayer stacks on Y₃Al₅O₁₂ substrates and use a subsequent annealing step to obtain YIG films with a high crystalline quality and magnetic properties comparable to the ones realized via other deposition techniques.

MA 23.61 Tue 17:00 P1

Coupling Strength Controlling Vortex Trajectories' Oscillations in Coupled Vortices Spintronic Oscillator — •ABBAS HAMADEH¹, ABBAS KOUJOK¹, SALVATORE PERNA², STEFFEN WITTRÖCK³, VITALIY LOMAKIN⁴, GREGOIRE DE LOUBENS⁵, OLIVIER KLEIN⁶, and PHILIPP PIRRO¹ — ¹Fachbereich Physik and Landesforschungszentrum OPTIMAS, Technische Universität Kaiserslautern, Kaiserslautern, Germany — ²University of Naples Federico II, Naples, Italy — ³Max-Born-Institute for Nonlinear Optics & Short Pulse Spectroscopy, Berlin, Germany — ⁴Center for Magnetic Recording Research, Uni. of California San Diego, La Jolla, California 92093-0401, USA — ⁵SPEC, CEA, CNRS, Université Paris-Saclay, 91191 Gif-sur-Yvette, France — ⁶Univ. Grenoble Alpes, CEA, CNRS, Grenoble INP, INAC-Spintec, 38054 Grenoble, France

The magnetic vortex state in nano-magnetic structures is a subject of intensive research since it can be brought into auto-oscillation by spin transfer torque. The coupling of vortices via spin-transfer torque and dipolar fields allows to realize complex non-linear dynamics potentially useful for unconventional computing and data processing. For this purpose, we have studied the auto-oscillating modes of an oscillator based on two coupled vortices in a NiFe/Cu/NiFe nano-patterned stack. The respective system was investigated both experimentally and micro-magnetically for different applied magnetic fields and currents. Experimentally, we observed four qualitatively different configurations of GMR spectra. Our simulations show that these different states can be related to the complex, non-circular motion of the coupled vortices.

MA 23.62 Tue 17:00 P1

Experimental detectability of spin current shot noise — •LUISE SIEGL¹, MICHAELA LAMMEL¹, AKASHDEEP KAMRA², HANS HUEBL^{3,4,5}, WOLFGANG BELZIG¹, and SEBASTIAN T. B. GOENNEWWEIN¹ — ¹Department of Physics, University of Konstanz — ²Condensed Matter Physics Center (IFIMAC) and Departamento de Física Teórica de la Materia Condensada, Universidad Autónoma de Madrid, Spain — ³Walther-Meißner-Institut, Bayerische Akademie der Wissenschaften, Garching — ⁴TUM School of Natural Sciences, Technische Universität München, Garching — ⁵Munich Center for Quantum Science and Technology (MCQST), München

A spin current crossing a ferromagnet-metal interface is accompanied by spin current shot noise. This shot noise is well understood in spin space. However, its experimental detection requires a conversion to an observable quantity. Consideration of the established conversion from a spin current to a charge current enables a quantitative analysis of the entire process. Here, we analyze the challenges of detecting spin current shot noise from an experimental perspective. In detail, we show that in a typical electrically detected spin pumping experiment, the voltage noise originating from the spin current shot noise is orders of magnitude smaller compared to the contribution of the Johnson-Nyquist noise. We quantify the ratio between spin current shot noise and Johnson-Nyquist noise and find that this ratio does not scale favorably with geometry and only depends on intrinsic material parameters. Our results suggest that the detection of spin current shot noise using the spin Hall effect is experimentally at best very challenging.

MA 23.63 Tue 17:00 P1

Strain engineering M, L and P in antiferromagnetic AFeO₃ films (A = La, Bi) — •ANTONIA RIECHE, AURORA DIANA RATA, WOLFGANG HOPPE, and KATHRIN DÖRR — Martin-Luther-Universität Halle-Wittenberg

Magnetization (M), antiferromagnetic order (L) and ferroelectric polarization (P) are ferroic properties which can be probed and potentially also manipulated with light. A major requirement for this is a successful control over the ferroic domain structures in samples, such that a large averaged value of M (L, P) can be reached. Antiferromagnetic ferrites AFeO₃ with weak canted ferromagnetism have revealed fascinating optical properties in bulk (crystal) form, whereas film work is quite limited due to nanoscopic multidomain coexistence in such films. Here, early results of our attempt to optimize such ferrite films for optical experiments are presented. Epitaxial strain controlled by the choice of substrate is employed to direct the structural domain formation in AFeO₃ (A = La or Bi) films in a desirable way regarding the magnitude and orientation of ferroic order parameters. The films are grown using pulsed laser deposition (KrF 248 nm) and characterized by x-ray diffraction, magnetization measurements, magnetooptical Kerr effect (MOKE) and scanning probe microscopies.

MA 23.64 Tue 17:00 P1

Optimizing the growth of Mn₃Sn thin films in order to investigate magneto-optical Kerr effect, anomalous Nernst effect, and spin-orbit torque switching — •ANAGHA MATHEW^{1,2}, SRISHTI DONGARE¹, ATUL PANDEY^{1,2}, JAMES M TAYLOR¹, BINYOY K HAZRA², STUART SP PARKIN², and GEORG WOLTERS DORF^{1,2} — ¹Institute of Physics, Martin Luther University Halle-Wittenberg, 06120 Halle, Germany — ²Max Planck Institute for Microstructure Physics, 06120 Halle, Germany

Mn₃Sn is a promising candidate material for antiferromagnetic spintronic devices, because of its large magneto-transport responses, such as the anomalous Hall effect (AHE), arising from topological band structure features. For future applications, it is important to be able to efficiently reverse the sense of rotation of its noncollinear spin texture on short timescales via spin torques. Achieving this requires a more detailed understanding of such switching mechanisms, in particular the role of chiral domains. To this end, we have optimized the growth of Mn₃Sn films, to show low coercive field and a large fractional change of AHE during spin-orbit torque switching. In addition, these thin films demonstrate significant magneto-optical Kerr effect and anomalous Nernst effect arising from Berry curvature generated by their noncollinear spin texture. We exploit these measurement techniques to map the chiral domain structure of the Mn₃Sn films in an optical and electro-optical manner, respectively.

MA 23.65 Tue 17:00 P1

Dilution of polar antiferromagnet Co₂Mo₃O₈ — •LILLIAN PRODAN^{1,2}, IRINA FILIPPOVA², ALEXANDER TSIRLIN³, VLADIMIR TSURKAN^{1,2}, and ISTVAN KEZSMARKI¹ — ¹Experimental Physics V, Institute of Physics, University of Augsburg, D-86159, Augsburg, Germany — ²Institute of Applied Physics, MD 2028, Chisinau, R. Moldova — ³Felix Bloch Institute for Solid-State Physics, Leipzig University, 04103 Leipzig, Germany

Antiferromagnetic materials hold great promise for design of ultra-fast and energy-efficient spintronic devices. To this end, understanding the robustness of crystal and magnetic structures and their manipulation are of high importance. Here, we report the effects of site-selective substitution of Zn²⁺ for Co²⁺ ions on the crystal structure, magnetic and thermodynamic properties of the hexagonal polar antiferromagnet Co₂Mo₃O₈. In contrast to the transformation from the

antiferromagnetic to a ferrimagnetic state in the isostructural Fe₂Mo₃O₈ upon even a small Zn-doping [1], a robust antiferromagnetic behavior is preserved in Co_{2-x}Zn_xMo₃O₈ up to x = 0.55. We found that in the low doping regime (x < 0.2) the Zn²⁺ ions primarily occupy the octahedrally coordinated sites, although at higher doping levels they show a clear preference for occupying the tetrahedral sites [2]. Due to the multiple inter-layer exchange paths, dependent on the different coordination of the Co²⁺ ions, the site-selective substitution is reflected in the non-monotonic variation of the magnetic parameters.

[1] T. Kurumaji, et al., Phys. Rev. X 5, 031034 (2015).

[2] L. Prodan, et al., Phys. Rev. B 106, 174421 (2022).

MA 23.66 Tue 17:00 P1

Epitaxial Growth of Magnetic Oxides and their magnetic Coupling — •AKASHDEEP AKASHDEEP¹, SVEN BECKER¹, MATHIAS KLÄUI^{1,2}, and GERHARD JAKOB^{1,2} — ¹Institute of Physics, Johannes Gutenberg-University Mainz, Staudingerweg 7, Mainz 55128, Germany — ²Graduate School of Excellence *Materials Science in Mainz* (MAINZ), Staudingerweg 9, Mainz 55128, Germany

Due to its exceptionally low damping, ferrimagnetic Y₃Fe₅O₁₂ Y₃Fe₅O₁₂ (YIG) is the prototypical material for studying magnonic properties. By substituting the non-magnetic yttrium with the temperature-dependent magnetic moment of gadolinium, we can introduce an additional spin degree of freedom in the form of a magnetic compensation point. Here, we grow epitaxial RuO₂ films and Y₃Fe₅O₁₂/Gd₃Fe₅O₁₂ (YIG/GIG) by pulsed laser deposition and study the magnetic coupling in the heterostructures. The XRD patterns show Laue oscillations and a narrow rocking curve, indicating a smooth surface and interface. From bulk-sensitive magnetometry and surface-sensitive spin Hall magnetoresistance measurements, we can control the heterostructures' magnetic properties by tuning the thickness of the individual layers. These bilayer devices could potentially control the magnon transport analogously to electron transport in giant magnetoresistive devices [1]. The RuO₂ is tested for the novel altermagnetism effects[2].

[1] H. Wu et al.; Phys. Rev. Lett. 120, 097205 (2018) [2] L. Šmejkal et al.; Sci. Adv. 6, 23 (2020)

MA 23.67 Tue 17:00 P1

AI-based Recognition of Numerically Generated Multimode Dispersions — •PAUL SCHREIER¹, MILAN ENDER^{1,2}, PASCAL FREY^{1,2}, and PHILIPP PIRRO¹ — ¹Fachbereich Physik und Landesforschungszentrum OPTIMAS, RPTU Kaiserslautern-Landau, Germany — ²Aithericon, Kaiserslautern, Germany

The collective excitation of a magnetic system can lead to the excitation of spin waves. The relation between their wave vector and frequency is described by their dispersion relation. This can be determined by means of micromagnetic simulations. The resulting numerical data give an intensity distribution of all frequency-wave vector combinations. To extract the dispersion relations from these data, peak detection algorithms must be used. Compared to, for example, optical dispersion relations, spin wave dispersion relations are much more complex and non-linear, which makes their extraction from the raw data difficult. For this reason, a Convolutional Neural Network is trained with synthetic data to obtain a robust analysis tool. The network is specialized to classify segments in images. The training data consists of intensity distributions and dispersion relations calculated from micromagnetic simulations. Conventional peak detection algorithms were first applied to simple dispersion relations to generate a base set of training data. Recombination of this data produces a more complex and larger data set that requires very few resources. Compared to conventional peak detection algorithms, the robustness and fault tolerance can be increased by appropriate training. Evaluations based on dispersion relations can thus be automated to a large extent.

MA 23.68 Tue 17:00 P1

Imaging and phase-locking of non-linear spin waves — •ROUVEN DREYER¹, ALEXANDER F. SCHÄFFER¹, HANS G. BAUER², NIKLAS LIEBING¹, JAMAL BERAKDAR¹, and GEORG WOLTERS DORF^{1,3} — ¹Institute of Physics, Martin Luther University Halle-Wittenberg, Von-Danckelmann-Platz 3, 06120 Halle, Germany — ²Jahnstrasse 23, 96050 Bamberg, Germany — ³Max Planck Institute of Microstructure Physics, Weinberg 2, 06120 Halle, Germany

Non-linear processes are a key feature in the emerging field of spin-wave based information processing and allow to convert uniform spin-wave excitations into propagating modes at different frequencies. Recently, the existence of non-linear magnons at half-integer multiples of the driving frequency has been predicted for Ni₈₀Fe₂₀ at low bias fields. However, it is an open question under which conditions such non-linear spin waves emerge coherently and how they may be used in device structures. Usually non-linear processes are explored in the small modulation regime and result in the well known three and four magnon scattering processes. Here we demonstrate and image a class of spin waves oscillating at half-integer harmonics that have only recently been proposed for the strong modulation regime. The direct imaging of these parametrically generated magnons in Ni₈₀Fe₂₀ elements allows to visualize their wave vectors. In addition, we demonstrate the presence of two degenerate phase states that may be selected

by external phase-locking. These results open new possibilities for applications such as spin-wave sources, amplifiers and phase-encoded information processing with magnons.

MA 23.69 Tue 17:00 P1

Magnetoacoustic excitation of spinwaves in yttrium iron garnet / zinc oxide heterostructures — •KEVIN KÜNSTLE¹, FINLAY RYBURN², MICHAEL SCHNEIDER¹, YANNIK KUNZ¹, VITALIY VASYUCHKA¹, CARSTEN DUBS³, JOHN GREGG², and MATHIAS WEILER¹ — ¹Fachbereich Physik and Landesforschungszentrum OPTIMAS, RPTU in Kaiserslautern — ²University of Oxford — ³INNOVENT e.V. Technologieentwicklung, Jena, Germany
Surface Acoustic Waves (SAWs) that operate in the Gighertz regime with wavelengths on the micrometer scale enable the miniaturization of telecommunication microwave devices. In recent years, the coupling of SAWs with spin waves (SWs) in ferromagnetic metals has proven to be a viable option for the realization of applications like acoustic diodes, as the interaction is intrinsically nonreciprocal [1]. However, the coupling of SAWs with SWs in ferrimagnetic insulators is much less explored. We investigated SAWs excited by interdigital transducers made of Ti/Au, which were deposited on a GGG/YIG structure and covered by a piezoelectric ZnO layer. The ferrimagnetic YIG layer serves as a source for SWs to which the SAWs can couple. We used a vector network analyzer and micro-focused Brillouin light scattering spectroscopy to identify the SAW characteristics in the YIG-based heterostructure. The observed magnetoelastic coupling of SAWs with SWs is highly nonreciprocal.

[1] M. Küß et al., Phys. Rev. Lett. 125, 217203 (2020).

MA 23.70 Tue 17:00 P1

Ultrafast magnetization precession in metallic heterostructures driven by different excitation mechanisms — •JASMIN JARECKI¹, MAXIMILIAN MATTERN¹, JAN-ETIENNE PUDELL^{1,2,3}, MICHEL HEHN⁴, FRIED WEBER¹, ALEXANDER VON REPPERT¹, and MATIAS BARGHEER^{1,2} — ¹Institut für Physik und Astronomie, Universität Potsdam, Potsdam, Germany — ²Helmholtz-Zentrum Berlin für Materialien und Energie, Berlin, Germany — ³European X-Ray Free-Electron Laser Facility, Schenefeld, Germany — ⁴Institut Jean Lamour (UMR CNRS 7198), Université Lorraine, Nancy, France

We study the magnetization precession induced by different excitation mechanisms, i.e. ultrafast demagnetization, temperature dependent anisotropy change and magneto-elastic coupling, in 20 nm Ni films within PtCuNi heterostructures. The samples are excited by an ultrashort laser pulse from the Pt side and designed such that light does not excite Ni directly. The indirect excitation of the Ni is tailored in different ways: strain waves, heat waves and/or hot electrons. We combine time-resolved x-ray diffraction (UXRD) and magneto-optical Kerr effect measurements (MOKE) under variation of the external field angle to access the strain dynamics and therefore also the energy transfer within the sample and the out-of-plane component of the Ni magnetization. We observe a distinct angle-dependence of the precession amplitude depending on the predominant excitation mechanism. While temperature related effects cause high amplitudes for nearly out-of-plane external fields, recurring strain pulses amplify the amplitudes resonantly around 50°.

MA 23.71 Tue 17:00 P1

Dynamics of magnon condensates in microscopic temperature landscapes — •FRANZISKA KÜHN¹, MATTHIAS R. SCHWEIZER¹, GEORG VON FREYMAN^{1,2}, ALEXANDER A. SERGA¹, and BURKARD HILLEBRANDS¹ — ¹Fachbereich Physik and Landesforschungszentrum OPTIMAS, RPTU Kaiserslautern-Landau, Germany — ²Fraunhofer Institute for Industrial Mathematics ITWM, Fraunhofer-Platz 1, 67663 Kaiserslautern, Germany

This contribution focuses on the behavior of a magnon-Bose-Einstein condensate (BEC) in artificial magnetization landscapes on the scale of wavelengths of condensed magnons. In our work, the magnon condensate is created by overpopulating a magnon gas using parametric microwave pumping. A heating laser combined with a phase-based wave front modulation technique imprints a complex microscopic temperature pattern onto the yttrium-iron-garnet film sample that can be varied in magnitude and intensity. In this way, the spatial saturation magnetization profile is adjusted and acts as an artificial potential for the BEC, affects its dynamics and drives magnon supercurrents and Bogoliubov waves. Since these micro-sized patterns are small compared to the area of BEC formation, it is possible to investigate the BEC in two-dimensional potential landscapes. In the experiment, we use micro-focused Brillouin light scattering spectroscopy to investigate the anisotropy of the two-dimensional density distribution of a magnon BEC and the possibility of interference effects between Bogoliubov waves. Funded by the Deutsche Forschungsgemeinschaft (DFG, German Research Foundation) - TRR 173-268565370 (project B04)

MA 23.72 Tue 17:00 P1

Nonreciprocal microwave transmission enabled by magnon-phonon conversion — •FLORIAN KRAFT¹, YANNIK KUNZ¹, MICHAEL SCHNEIDER¹, MATTHIAS KÜSS², MANFRED ALBRECHT², and MATHIAS WEILER¹ — ¹Fachbereich Physik and Landesforschungszentrum OPTIMAS, Rheinland-Pfälzische Technische

Universität Kaiserslautern-Landau, 67663 Kaiserslautern, Germany — ²Institut für Physik, Universität Augsburg

The magnetoelastic coupling between surface acoustic waves (SAWs) and spin waves (SWs) may enable applications such as miniaturized microwave isolators. The required nonreciprocity can be induced by symmetry breaking coupling mechanisms between phonons and magnons [1]. Here, we investigate nonreciprocal microwave transmission in a device based on the conversion of SAWs, excited by interdigital transducers (IDTs), to SWs, which are detected by a microwave antenna and vice versa. To this end, we use a sample structure made of LiNbO₃/Ta(3 nm)/Co₄₀Fe₄₀B₂₀(10 nm). We use a setup for combined microwave and optical spectroscopy based on microfocused Brillouin light scattering spectroscopy and vector network analysis. This allows for simultaneous electrical and optical detection of phonon-magnon-interactions. We analyze the nonreciprocal microwave transmission while simultaneously investigating the phonon-magnon-coupling with spatial resolution.

We acknowledge funding by DFG via project No. 492421737.

[1] M. Küß et al., Phys. Rev. Lett. 125, 217203 (2020).

MA 23.73 Tue 17:00 P1

Frequency multiplication by collective nanoscale spin-wave dynamics — •CHRIS KOERNER¹, ROUVEN DREYER¹, MARTIN WAGENER¹, NIKLAS LIEBING¹, HANS G. BAUER², and GEORG WOLTERS DORF^{1,3} — ¹Institute of Physics, Martin Luther University Halle-Wittenberg, Von-Danckelmann-Platz 3, 06120 Halle, Germany — ²Jahnstrasse 23, 96050 Bamberg, Germany. — ³Max Planck Institute of Microstructure Physics, Weinberg 2, 06120 Halle, Germany

Frequency multiplication is a process in modern electronics in which harmonics of the input frequency are generated in nonlinear electronic circuits. Devices based on the propagation and interaction of spin waves are a promising alternative to conventional electronics. The characteristic frequency of these excitations is in the gigahertz (GHz) range and devices are not readily interfaced with conventional electronics. Here, we locally probe the magnetic excitations in a soft magnetic material by optical methods and show that megahertz-range excitation frequencies cause switching effects on the micrometer scale, leading to phase-locked spin-wave emission in the GHz range. Indeed, the frequency multiplication process inside the magnetic medium covers six octaves and opens exciting perspectives for spintronic applications, such as all-magnetic mixers or on-chip GHz sources.

C. Koerner et al., Science 375, 6585 (2022)

MA 23.74 Tue 17:00 P1

Excitation of propagating spin waves in Ga:YIG thin films — •MORITZ BECHBERGER¹, DAVID BREITBACH¹, BJÖRN HEINZ¹, BERT LÄGEL¹, CARSTEN DUBS², BURKARD HILLEBRANDS¹, and PHILIPP PIRRO¹ — ¹Fachbereich Physik and Landesforschungszentrum OPTIMAS, RPTU Kaiserslautern-Landau, Germany — ²INNOVENT e.V. Technologieentwicklung, Jena, Germany

The material parameters of yttrium-iron-garnet (YIG), a well-known material in the research field of magnonics, can be modified by a partial substitution with gallium atoms leading to a lower saturation magnetization. In this study the propagation properties of spin waves in a YIG thin film doped with gallium (Ga:YIG) were investigated and characterized. Direct excitation of coherent spin waves was performed by patterned microantennas and they were detected using TR-BLS microscopy. Our experiments confirm the presence of fast, exchange dominated spin waves, as well as an isotropic spin-wave dispersion relation. In addition, the influence of nonlinear effects on the spin wave excitation was determined. In agreement with the negative effective magnetization of the Ga:YIG film, using high amplitude excitation, we find a positive nonlinear frequency shift for an in-plane magnetization. This results in a significant power-dependent foldover effect, which provides nonlinear power dependencies for the excitation. This study is of high interest for magnonic data processing and reveals novel possibilities for magnonic devices with a tunable nonlinearity. This research is funded by the DFG - Project No. 271741898 and TRR 173-268565370 (B01) and the ERC Grant No. 101042439 ³CoSpin³.

MA 23.75 Tue 17:00 P1

In Situ Inverse Design for Magnonic Logic Devices — •MALTE KOSTER¹, PHILIPP PIRRO¹, and GEORG VON FREYMAN^{1,2} — ¹Physics Department and Research Center OPTIMAS - Technical University of Kaiserslautern, 67663 Kaiserslautern, Germany — ²Fraunhofer Institute for Industrial Mathematics ITWM, 67663 Kaiserslautern, Germany

The need for fast and energy-efficient computing devices is currently a topic of great interest. Magnonic logic devices could offer a promising solution to this need. Due to the intrinsic nonlinearity of spin waves, novel approaches to computation arise in a single logic gate. At the same time, the nonlinear nature makes the design of such devices particularly challenging. We propose a method for inverse design of magnetic logic gates in structured or unstructured yttrium-iron-garnet film samples by using thermal landscapes.

In this design approach, the desired function is specified and the design is modified until it is achieved. The thermal landscapes are created using a laser whose intensity distribution on the sample is arbitrarily modified via a spatial

light modulator. The resulting local heating modifies the magnetization landscape. The function of the device is determined using a vector network analyzer. Compared to inverse design via micromagnetic simulations [1], our approach promises significantly higher speed as well as direct proof of functionality in real applications.

[1] Wang, Q et al. Inverse-design magnonic devices. *Nat Commun.* **12**, 2636 (2021)

MA 23.76 Tue 17:00 P1

Microwave Control of Magnon Transport and Spin Pumping in Nanostructures — •FRANZ WEIDENHILLER^{1,2}, JANINE GÜCKELHORN^{1,2}, MANUEL MÜLLER^{1,2}, KORBINIAN RUBENBAUER^{1,2,3}, HANS HUEBL^{1,2,3}, MATTHIAS ALTHAMMER^{1,2}, and RUDOLF GROSS^{1,2,3} — ¹Walther-Meißner-Institut, Bayerische Akademie der Wissenschaften, Garching, Germany — ²Technical University of Munich, TUM School of Natural Sciences, Physics Department, Garching, Germany — ³Munich Center for Quantum Science and Technology, München, Germany

Magnon transport in magnetically ordered insulators is of great interest for the implementation of magnonic devices. Here we report our results on the diffusive magnon transport in yttrium iron garnet (YIG) and its control by the simultaneous excitation of magnons with electromagnetic microwaves. Using e-beam lithography, we pattern two platinum (Pt) strips on top of the YIG for the injection and detection of magnons. The Pt strips are electrically insulated from an aluminum microwave antenna, which covers both strips and the gap in between. Via the antenna, microwave-driven generation of magnons in the active device area by parallel and perpendicular pumping is possible. Our proposed device geometry allows us to distinguish these two pumping contributions in the acquired signal. We investigate how these microwave injected magnons affect the magnon transport between the two Pt strips. Moreover we study the spin pumping signal at different magnetic fields, microwave frequencies and powers. Finally, we discuss relevant magnon relaxation mechanisms in our experiments.

MA 23.77 Tue 17:00 P1

Elementary magnetic excitations in epitaxial strained Sr₂IrO₄ thin films probed by resonant inelastic X-ray scattering — •HERMAN MUZYCHKO^{1,2}, MONIKA SCHEUFELE^{1,2}, DAN MANNIX^{3,4}, STEPHAN GEPRÄGS¹, and RUDOLF GROSS^{1,2,5} — ¹Walther-Meißner-Institut, Bayerische Akademie der Wissenschaften, Garching, Germany — ²Technical University of Munich, TUM School of Natural Sciences, Physics Department, Garching, Germany — ³European Spallation Source, Lund, Sweden — ⁴Institut Néel, CNRS, Grenoble, France — ⁵Munich Center for Quantum Science and Technology (MCQST), Munich, Germany

The Ruddlesden-Popper series Sr_{n+1}Ir_nO_{3n+1} has attracted considerable scientific attention due to the possibility of generating new physics properties within a strong spin-orbit coupling regime. In the first member of the series, the layered Sr₂IrO₄ (SIO) compound, the large spin-orbit coupling combined with a moderate Coulomb repulsion results in a Mott insulating $J_{\text{eff}} = 1/2$ -ground state, which is similar to the $S = 1/2$ -ground state of high- T_c superconducting Cu oxides. By performing resonant inelastic X-ray scattering (RIXS) experiments, we have investigated the elementary magnetic excitations in epitaxial strained-SIO thin films. The thus obtained spin wave dispersions have been simulated within the linear-spin wave theory by using the program package SpinW. With this, we are able to resolve the effect of epitaxial strain [1] on the elementary magnetic excitations in SIO by comparing our results to bulk SIO spin wave properties.

[1] S. Geprägs *et al.*, *Phys. Rev. B* **102**, 214402 (2020).

MA 23.78 Tue 17:00 P1

Spontaneous emergence of spin-wave frequency combs mediated by vortex gyration — •CHRISTOPHER HEINS^{1,2}, KATRIN SCHULTHEISS¹, LUKAS KÖRBER^{1,2}, ATTILA KÁKAY¹, TOBIAS HULA^{1,3}, MAURICIO BEJARANO^{1,2}, JÜR-

GEN LINDNER¹, JÜRGEN FASSBENDER^{1,2}, and HELMUT SCHULTHEISS^{1,2} — ¹Helmholtz-Zentrum Dresden-Rossendorf, Dresden, Germany — ²Fakultät Physik, Technische Universität Dresden, Dresden, Germany — ³Institut für Physik, Technische Universität Chemnitz, Chemnitz, Germany

We present experimental investigations of spin-wave frequency combs forming in a confined system, a magnetic vortex. The magnetic vortex shows rich spin-wave dynamics with frequencies in the GHz range, which can be harnessed for pattern recognition [1]. Additionally, there is the low frequency gyration of the vortex core itself. The combination of these dynamics on two different time scales inside magnetic vortices, results in the generation of spin-wave frequency combs with their spacing given by the vortex gyration frequency. Using time-resolved Brillouin light scattering microscopy, we show that large amplitude excitations of spin waves purely in the GHz range can induce a gyration of the vortex core and vice versa, which leads to the formation of frequency combs.

The authors acknowledge financial support from the Deutsche Forschungsgemeinschaft within program SCHU 2922/1-1.

[1] L. Körber, et al., arXiv preprint arXiv:2211.02328 (2022).

MA 23.79 Tue 17:00 P1

Manipulation of spin-waves dynamics in two-sublattice antiferromagnet by an electric field — •OLHA BOLIASOVA^{1,2} and VLADIMIR KRIVORUCHKO² — ¹Leibniz Institute for Solid State and Materials Research Dresden, Dresden, Germany — ²Donetsk Institute for Physics and Engineering named after O.O. Galkin, Kyiv, Ukraine

Spin waves are one of the promising candidates for information carriers in future electronic devices. They are applicable in the wide frequency region and reduce energy losses. Now the main challenge is to uncover mechanisms of proper propagation, manipulation, and detection of spin waves. Recent research shows that a magnetic and electric field could manipulate spin dynamics. The last variant opens the possibility to realize different propagation spin-waves in opposite directions, not limited to the magnets with inversion symmetry breaking. It is possible as an external electric field could induce the Dzyaloshinskii-Moriya interaction that changes the spatial distribution of spin waves in the nonchiral magnets. Confirmation of this is already available for ferromagnets, and we provide more in-depth studies of this effect for a two-sublattice antiferromagnet. We use a phenomenological approach based on the Landau-Lifshitz-Gilbert equations to detect spin dynamics. The dependence of spin dynamics on the magnitude of the applied electric field was found.

MA 23.80 Tue 17:00 P1

Unidirectional spin wave propagation mediated by Co₂₅Fe₇₅- and Ni₈₀Fe₂₀-nanogratings — •MONIKA SCHEUFELE^{1,2}, CHRISTIAN MANG^{1,2}, MANUEL MÜLLER^{1,2}, JOHANNES WEBER^{1,2}, VINCENT HAUEISE^{1,2}, HANS HUEBL^{1,2,3}, MATTHIAS ALTHAMMER^{1,2}, STEPHAN GEPRÄGS¹, and RUDOLF GROSS^{1,2,3} — ¹Walther-Meißner-Institut, Bayerische Akademie der Wissenschaften, Garching, Germany — ²Technical University of Munich, TUM School of Natural Sciences, Physics Department, Garching, Germany — ³Munich Center for Quantum Science and Technology (MCQST), Munich, Germany

The unidirectional propagation of spin waves provides novel functionalities for magnonic logic devices. Here, we report the fabrication of Co₂₅Fe₇₅ (CoFe)- and Ni₈₀Fe₂₀ (Py)-nanogratings via electron beam lithography and DC magnetron sputtering on yttrium iron garnet (YIG) and CoFe thin films, respectively. The dipolar magnetic coupling between the nanogratings and the continuous thin films induces a finite nonreciprocity of the spin wave propagation if the magnetization within the gratings and the thin films is collinear [1]. By performing broadband ferromagnetic resonance as well as spin wave spectroscopy, we study the coupled spin wave modes in these magnonic devices. Moreover, we compare the properties of the CoFe/YIG and Py/CoFe platforms and also compare them with micromagnetic simulations.

[1] J. Chen *et al.*, *Phys. Rev. B* **100**, 104427 (2019).

MA 24: Molecular Magnetism II

Time: Wednesday 9:30–11:00

Location: HSZ 02

MA 24.1 Wed 9:30 HSZ 02

Studies of decoherence in strongly anisotropic spin triangles with toroidal or general non-collinear easy axes — KILIAN IRLÄNDER and JÜRGEN SCHNACK — Universität Bielefeld, Bielefeld, Deutschland

Magnetic molecules are investigated with respect to their usability as units in future quantum devices. In view of quantum computing, a necessary prerequisite is a long coherence time of superpositions of low-lying levels. In this article, we investigate by means of numerical simulations whether a toroidal structure of single-ion easy anisotropy axes is advantageous as often conjectured. Our results demonstrate that there is no general advantage of toroidal magnetic molecules, but that arrangements of tilted anisotropy axes perform best in many cases.

MA 24.2 Wed 9:45 HSZ 02

Electrically driven singlet-triplet transition in triangulene spin-1 chains — GABRIEL MARTÍNEZ-CARRACEDO^{1,2}, LÁSZLÓ OROSZLANY^{3,4}, AMADOR GARCÍA-FUENTE^{1,2}, LÁSZLÓ SZUNYOGH^{5,6}, and JAIME FERRER^{1,2} — ¹Universidad de Oviedo, Oviedo, Spain — ²CINN, Universidad de Oviedo-CSIC, El Entrego, Spain — ³Eotvos Lorand University, Budapest, Hungary — ⁴MTA-BME Lendulet Topology and Correlation Research Group, Budapest University of Technology and Economics, Budapest, Hungary — ⁵Budapest University of Technology and Economics, Budapest, Hungary — ⁶ELKH-BME Condensed Matter Research Group, Budapest University of Technology and Economics, Budapest, Hungary

Recently, graphene triangulene chains have been synthesized and their magnetic response has been analyzed by STM methods by Mishra and coworkers (Nature 598, 287 (2021)). Motivated by this study, we determine the exchange bilinear and biquadratic constants of the triangulene chains by calculating two-spin rotations in the spirit of the magnetic force theorem. We then analyze open-ended, odd-numbered chains, whose edge states pair up forming a triplet ground state. We propose three experimental approaches that enable us to trigger and control a singlet-triplet spin transition. Two of these methods are based on applying a mechanical distortion to the chain. We finally show that the transition can be controlled efficiently by the application of an electric field.

MA 24.3 Wed 10:00 HSZ 02

Linear magnets: a structure-property-relation for finding unquenched orbital moments — •ANTON JESCHE — EP VI, Center for Electronic Correlations and Magnetism, Augsburg University, 86135 Augsburg, Germany

The presence of orbital magnetic moments in rare-earth-elements is one of the major differences to transition metal compounds and is at the heart of magnetic anisotropy, stability, and functionality. A large crystal electric field effect acting on an unquenched orbital moment can lead to extremely large anisotropy and coercivity as experimentally verified for iron-doped lithium nitride [1]. In the dilute limit, those iron atoms can be considered as single-atom magnets and are ideal candidates to study the quantum dynamics of anisotropic spins [2,3]. This, together with the strong field dependence of the spin reversal, allows the creation of stable but switchable states that could act as a 'quantum bit' at elevated temperatures of 10 K. A recent Mössbauer study revealed dominant magnetic quantum tunneling at even higher temperatures [4]. The presence of orbital moments in iron-doped lithium nitride is not a coincidence and not a solitary case: based on the proposed structural motif of the 'linear chain', we have identified several other 'linear magnets' with similar physical properties: iron-doped Li_4SrN_2 , $\text{LiSr}_2(\text{CoN}_2)$, and $(\text{Sr}_6\text{N})[\text{FeN}_2][\text{CN}_2]_2$. Implications and limitations of linear coordination are discussed in relation to the electronic structure. [1] M. Fix et al. PRB 97, 064419 (2018) [2] M. Fix et al. PRL 120, 147202 (2018) [3] M. Huzan et al. Chem. Sci. 11, 11801 (2020) [4] S. A. Bräuninger et al. PRB 102, 054426 (2020)

MA 24.4 Wed 10:15 HSZ 02

Modelling of saw-tooth chain molecules composed of 3d and 4f ions — •DENNIS WESTERBECK and JÜRGEN SCHNACK — Universität Bielefeld, D-33501 Bielefeld, Deutschland

Metal- and lanthanide-ion containing systems are of great interest for the investigation of the magnetic properties of molecular systems. Especially the gadolinium containing systems are promising in view of magnetocaloric applications. In addition, saw-tooth like systems are considered as favorable for low-temperature cooling due to their massively degenerate ground-state. Although Fe^{III} and Gd^{III} are mostly considered as isotropic in multi-ion systems, we show that zero-field splittings are inevitable for the proper description of some of these molecules.

Furthermore, these anisotropic saw-tooth systems show a significant isothermal entropy change, which is surprisingly well described by our simulations.

MA 24.5 Wed 10:30 HSZ 02

High-field/high-frequency EPR studies on heterometallic 3d-4f-complexes — •JAN ARNETH¹, CHANGYUN KOO¹, XIANGFENG LI², ANNIE K. POWELL², and RÜDIGER KLINGELER¹ — ¹Kirchhoff Institute for Physics, Heidelberg University, Germany — ²Institute of Inorganic Chemistry, Karlsruhe Institute of Technology, Germany

On the road to the construction of novel efficient single molecular magnets and molecular magnetic refrigerants experimental investigation of the exchange coupling mechanism between 4f and 3d moments is an important, yet still challenging, task. The difficulty in understanding the rich physics underlying this coupling arises from the strong participation of orbital angular momentum leading to large anisotropy and a complex energy spectrum in 4f metal compounds. Here, we present high-field/high-frequency electron paramagnetic resonance (HF-EPR) studies on heterometallic 3d-4f complexes with so-called butterfly motif Fe_2Ln_2 (Ln = Y, Gd, Dy), V_2Ln_2 (Ln = Er, Ho) and in the sawtooth coordination V_4Ln_4 (Ln = La, Gd), which allow us to directly determine not only the exchange coupling constants but also other spin-hamiltonian parameters, such as g-values and anisotropy. Our spectroscopic measurements are further complemented by high-field magnetisation studies.

MA 24.6 Wed 10:45 HSZ 02

AOM-guided Linked Fits for Analysing Inelastic Neutron Scattering and Magnetic Data of 3d-4f Heterometallic M_2Ln_2 Single-Molecule Magnets — •JULIUS MUTSCHLER¹, THOMAS RÜPPERT², YAN PENG², JACQUES OLLIVIER³, QUENTIN BERROD³, JEAN-MARC ZANOTTI³, CHRISTOPHER E. ANSON², ANNIE K. POWELL², and OLIVER WALDMANN¹ — ¹Physikalisches Institut, Universität Freiburg, D-79104 Freiburg, Germany — ²Institut of Inorganic Chemistry, Karlsruhe Institute of Technology (KIT), D-76131 Karlsruhe, Germany — ³Institut Laue-Langevin, F-38042 Grenoble Cedex 9, France

The discovery two decades ago of slow relaxation and quantum tunnelling of the magnetization in the single molecule magnets (SMMs) has inspired a flurry of research into their magnetic properties. This class of molecules has been extended to heterometallic clusters containing ions of transition metals and rare earths. The 4f ions are of interest because of their large angular momentum and magnetic anisotropies, but also present challenges in the analysis of inelastic neutron scattering (INS) and magnetic data. As presented in the previous meeting, excellent INS data were recorded on the time-of-flight disk-chopper spectrometers IN5 and IN6 at ILL on the Mn_2Ln_2 -squares with $\text{Ln} = \text{Y, Tb, Ho, Dy}$, and the M_2Ln_2 -butterflies with $\text{M} = \text{Fe, Al}$ and $\text{Ln} = \text{Dy, Er}$. In this talk, the analysis of the complete set of magnetic data using an AOM-guided linked fit is presented. The resulting ligand field and coupling parameters give crucial hints for the analysis of the rich INS spectra.

MA 25: Focus Session: Startups in Magnetism

This session offers academic researchers an insight into a possible third career path, besides staying in science or going to industry. Building your own company can be very rewarding and fun, big decisions to make decide over success or failure. 5 young entrepreneurs describe their business cases developed out of our magnetism community and will explain challenges, pitfalls, university support and constraints, IP, legal and business issues. After the talks there is a Panel Discussion with all speakers and Q and A with the audience.

Organizers: Manfred Fiebig (ETH Zürich) and Oliver Gutfleisch (TU Darmstadt).

Time: Wednesday 9:30–12:30

Location: HSZ 04

Invited Talk

MA 25.1 Wed 9:30 HSZ 04

MAGNOTHERM – One way to start a deep tech spin-off from research — •MAX FRIES — MagnoTherm Solutions GmbH, Pfungstädter Straße 102, 64297 Darmstadt

Founded as a spin-off from Prof. Oliver Gutfleisch's Functional Materials group at Technische Universität Darmstadt in 2019, MAGNOTHERM holds world-leading expertise in permanent magnets and magnetic cooling.

Our technology, based on solid state materials and water, is capable of revolutionizing the way we provide temperatures: By updating the standard gas compression cycle by our magnetic refrigeration cycle, we can build the next-generation cooling or heating solutions.

What does it mean for scientists to become entrepreneurs? What does it need to transform innovative research into market-ready, valuable products? From initial idea, raising first (venture) capital and sales over to recruiting talents and building a diverse team, I will take you along my professional journey so far. Doing so, I will highlight my personal key learnings along the way, while still providing time for a vivid discussion.

My aim is to motivate and inspire potential founders as well as up and coming Startup-entrepreneurs with a scientific background to implement their ideas by themselves, developing a beneficial impact on the world of today and the future.

Invited Talk

MA 25.2 Wed 10:00 HSZ 04

Spin-Ion Technologies : taking the research from a lab to a start-up company — •DAFINÉ RAVELOSONA — Spin-Ion Technologies, 10 Bd Thomas Gobert, 91120 Palaiseau, FRANCE

At Spin-Ion technologies, we have developed a new manufacturing process based on He ion irradiation to tailor the structural properties of ultra-thin magnetic films and spintronic devices at atomic level and improve their performance. The key feature of the technology is the post-growth control at the atomic scale of structural properties, which enables a precise control of magnetic properties. When realized through a mask this technology enables lateral modulation of magnetic properties without any physical etching. In this talk, I will describe the development of our idea from a research lab to a start-up company and how we envision our development toward the commercialization of our solution.

Invited Talk MA 25.3 Wed 10:30 HSZ 04

MagREESource : the green Rare Earth Magnet company — •SOPHIE RIVOIRARD^{1,2} and ERICK PETIT² — ¹CNRS-UGA/Institut Neel, Grenoble, France — ²MagREESource SAS, Grenoble, France

Nd-Fe-B is the most widely used hard magnetic material in applications including the electronic and automotive sectors, electromobility and wind powder (e.g. motors, turbines, magnetic valves, sensors). Current standard Nd-Fe-B magnets contain up to 30% of rare earth elements, such as Neodymium or Dysprosium, which are on the EU list of critical elements and which are, for more than 95%, mined in the People's Republic of China. This sourcing raises both environmental and geopolitical issues while the present demand for rare earth magnets is increasing by a rate of nearly 9%/year due to an increasing production of green technologies items (electric vehicles, wind turbines*). Therefore, one incentive in the European Union is to develop recycling processes for Nd-Fe-B magnets. MagREESource is a spin off company from CNRS founded in 2020, which benefits from more than 25 years of expertise within CNRS laboratories in Grenoble. MagREESource has licensed the know-how and Intellectual Property developed in Neel Institute at CNRS Grenoble on the recycling of Rare Earth based magnets. MagREESource is currently working on an industrial plant in the Rhone-Alpes region to start high scale production. As a player in the Circular Economy, MagREESource's objective is therefore to promote magnets at the end of their life, by producing new magnets for European manufacturers of motors promoting a loop as short as possible between supply and customer.

Invited Talk MA 25.4 Wed 11:00 HSZ 04

THATec Innovation - we automate your lab — •THOMAS SEBASTIAN — THATec Innovation GmbH, Ludwigshafen, Deutschland

The idea behind THATec Innovation was born in the lab with the major goal to develop hardware and software solutions to overcome the challenges many

scientists face in their daily work. Based on our long-standing experience as experimentalists, our services encompass the following areas: the automation of laboratory devices, optical scanning microscopy, and Brillouin light scattering.

THATec Innovation GmbH was founded in 2016 as a spin-off of the Helmholtz Center Dresden-Rossendorf and supported by the Helmholtz association in the framework of the Helmholtz Enterprise program. Since then, THATec Innovation offers the software framework thaTEC:OS for laboratory automation as well as software and hardware for Brillouin light scattering spectroscopy and microscopy.

In this talk, I am going present the experiences I gathered from the foundation of THATec Innovation as well as from my day-to-day business.

Invited Talk MA 25.5 Wed 11:30 HSZ 04

Kiutra: Magnetic refrigeration for science and technology — •ALEXANDER REGNAT¹, JAN SPALLEK¹, TOMEK SCHULZ¹, and CHRISTIAN PFLEIDERER^{1,2} — ¹kiutra GmbH, D-81369 Munich, Germany — ²Physik-Department, Technische Universität München, D-85748 Garching, Germany

Kiutra was founded in 2018 as a spin-off of the Technical University of Munich. With an interdisciplinary team of more than 30 employees, we innovate cryogenics to provide the best, most scalable and sustainable cooling solutions for basic research, material science and applied quantum technologies. Our products and services are successfully used by academic and industrial customers in Germany, Europe and the USA. Here we report on the scientific roots of our company, as well as the main challenges and successes we experienced developing our business. In addition, we highlight the various financing tools that have helped kiutra grow as a deep-tech hardware manufacturer.

30 min. Panel discussion with all speakers/industry representatives; then Q and A with the audience

MA 26: Non-Skyrmionic Magnetic Textures II

Time: Wednesday 9:30–11:30

Location: HSZ 401

Invited Talk MA 26.1 Wed 9:30 HSZ 401

The self-induced spin glass: the perplexing magnetism of elemental neodymium — •ALEXANDER KHAJETOORIANS — Institute for Molecules and Materials, Radboud University, Nijmegen, The Netherlands

Spin glasses are a class of disordered magnetic materials characterized by a flat multi-well energy landscape that exhibits aging dynamics. Spin glass behavior is often described by two key ingredients: (a) competing spin interactions, and (b) external disorder. It was recently proposed that a special type of spin glass can be realized, solely by competing interactions (1). In 2020 (2), we discovered that the controversial and perplexing magnetic state of elemental Nd(0001) is a self-induced spin glass. Using spin-polarized scanning tunneling microscopy/spectroscopy (SP-STM/STS), we found that the zero-field state shows a multiplicity of favorable short-range ordered Q-states, but in the absence of long-range order. The magnetic state shows aging dynamics, and it stems from frustrated indirect exchange. More recently (3), we showed that with increasing temperature, frustration is broken leading to a long-range ordered multi-Q state. In this talk, I will review the concept of the self-induced spin glass in Nd. Moreover, I will discuss new results concerning the aging dynamics and magnetic phase diagram of the material, as well as perspectives to use such multi-well systems for new memory and computing applications. [1] A. Principi, M.I. Katnelson, PRL, 117, 137201 (2016); [2] U. Kamber et al, Science, 368, 6494 (2020); [3] B. Verlhac, L. Niggli, et al, Nature Physics, 18, 905 (2022)

MA 26.2 Wed 10:00 HSZ 401

Low-temperature properties of single-crystal ErB₂ — •CHRISTOPH RESCH, GEORG BENKA, DARIA NUZHINA, ANH TONG, ANDREAS BAUER, and CHRISTIAN PFLEIDERER — Physik Department E51, Technische Universität München, 85748 Garching, Germany

We present a comprehensive study of single crystals of the hexagonal rare-earth diboride ErB₂ prepared by means of the optical floating-zone approach. Measurements of the specific heat, the ac susceptibility, the magnetisation, and the electrical transport at low temperatures and fields up to 18 T consistently establish magnetic order of the Er³⁺ moments below a second-order phase transition at $T_c = 14$ K with competing ferromagnetic and antiferromagnetic interactions. The magnetocrystalline anisotropies exhibit strong easy-plane characteristics with (001) being the magnetic hard axis.

MA 26.3 Wed 10:15 HSZ 401

Helitronics for unconventional computing — •NICOLAI TIMON BECHLER¹ and JAN MASELL^{1,2} — ¹Karlsruhe Institute of Technology (KIT), Karlsruhe, Germany — ²RIKEN CEMS, Wako, Japan

Non-trivial magnetic structures have been proposed to be a promising route to unconventional computing. The interplay between magnetic stiffness and

Dzyaloshinskii-Moriya interaction can stabilize a helical order of the magnetisation which is often discarded as trivial. However, recent studies have shown that the orientation of these helical magnetisation structures can be manipulated by strong enough magnetic fields [1] and spin currents [2] which revealed their unexpectedly complex dynamics. Using micromagnetic simulations, we investigate novel magnetic memory devices such as MRAM-cells and memristors which use the orientation of the helical phase as an order parameter, dubbed helitronics. We propose a way to read-out said devices using the anisotropic magneto resistance and point out their use for unconventional computing purposes.

[1] A. Bauer, A. Chacon, M. Wagner, M. Halder, R. Georgii, A. Rosch, C. Pfeleiderer, and M. Garst, Phys. Rev. B 95, 024429 (2017). [2] J. Masell, X. Z. Yu, N. Kanazawa, Y. Tokura, and N. Nagaosa, Phys. Rev. B 102, 180402(R) (2020).

15 min. break

MA 26.4 Wed 10:45 HSZ 401

Investigating a stable Bloch point in a magnetic disk comprising layers with two different chiralities — •THOMAS BRIAN WINKLER¹, MARIJAN BEG², MARTIN LANG^{3,4}, MATHIAS KLÄUI¹, and HANS FANGOHR^{3,4} — ¹Institute of Physics, Johannes Gutenberg University Mainz, Germany — ²Department of Earth Science and Engineering, Imperial College London, United Kingdom — ³Faculty of Engineering and Physical Sciences, University of Southampton, United Kingdom — ⁴Max Planck Institute for the Structure and Dynamics of Matter Hamburg, Germany

Bloch points (BPs) are highly confined spin structures, that often occur in transient processes [1]. However, they can also be stabilized in specific systems. Beg et al. showed the existence of a stable Bloch point by stacking two cylindrical nanodisks of FeGe on top of each other, with opposite sign of the DMI vector [2]. In both layers a magnetic vortex is formed, with the same circularity, but opposite polarity, leading to a Bloch point at the interface. In this study we investigate the energetics of the system within the micromagnetic (MM) framework and validate results with atomistic simulations. Further, an in-plane field is applied to shift the BP out of the center of the disk. The dynamics of the system are analysed after the field switch-off. The BP does not show any precessional motion, which is different to a classical magnetic vortex [3]. We also find, that qualitatively, the MM framework produces the same results as atomistic simulation.

[1] T. B. Winkler et al., PRApplied 16, 044014 (2021). [2] M. Beg et al., Sci Rep 9, 7959 (2019). [3] K. Yu. et al., JAP 91, 8037 (2002).

MA 26.5 Wed 11:00 HSZ 401

Stability of Hopfions in Bulk Magnets with Competing Exchange Interactions — •MORITZ SALLERMANN^{1,2,3}, HANNES JÓNSSON³, and STEFAN BLÜGEL¹ — ¹PGI-1 and IAS-1, Forschungszentrum Jülich and JARA, Jülich, Germany — ²Department of Physics, RWTH Aachen, Aachen, Germany — ³Science Institute and Faculty of Physical Sciences, University of Iceland, Reykjavik, Iceland

Magnetic hopfions are three-dimensional topological solitons, characterised by the Hopf number. Based on a micromagnetic model, the existence of free moving hopfions has been predicted in certain magnets with competing exchange interactions [1]. However, physical realisations of free moving hopfions in bulk magnets have so far been elusive. Here, we consider an effective spin lattice Heisenberg model with competing exchange interactions and computationally study the stability of small toroidal hopfions with unity Hopf number by finding first-order saddle points representing the transition state for the decay of hopfions to the ferromagnetic ground state, via the formation of two coupled Bloch points. We show that the energy barriers can reach substantial heights and are largely determined by the size of the hopfions. The saddle point methods are discussed.

We acknowledge funding by DFG through SPP 2137 and SFB 1238, through the Helmholtz-RSF Joint Research Group "TOPOMANN", the ERC under the

EU Horizon 2020 research and innovation programme (no. 856538) and the Icelandic Research Fund (no. 185405-053).

[1] F. N. Rybakov *et al.*, *Apl. Mater.* **10**, 111113 (2022)

MA 26.6 Wed 11:15 HSZ 401

Blowing magnetic smoke rings (hopfions) — •PHILIPP GESSLER¹ and JAN MASELL^{1,2} — ¹Karlsruhe Institute of Technology (KIT), Karlsruhe, Germany — ²RIKEN CEMS, Wako, Japan

Hopfions are three-dimensional topological defects in magnetization, consisting of a closed skyrmion-string loop. Embedded in the field polarized phase, they are reminiscent of smoke rings in the air. In contrast to their two-dimensional counterparts, i.e. skyrmions, hopfions appear anything but ubiquitously in experiments. One reason is the lack of proposals for efficient ways to create these complex magnetic textures. Recently, ideas emerged for the creation of skyrmion-antiskyrmion pairs in two dimensions [1]. We generalize this idea to three dimensions. Using micromagnetic simulations, we show that spin-polarized currents can create hopfions at defects, similar to blowing smoke rings.

[1] K. Everschor-Sitte *et al.*, *New J. Phys.* **19**, 092001 (2017)

MA 27: Electron Theory of Magnetism and Correlations

Time: Wednesday 9:30–11:30

Location: HSZ 403

MA 27.1 Wed 9:30 HSZ 403

Electronic structure of the non-centrosymmetric antiferromagnetic AgCrSe₂ — •SEO-JIN KIM¹, HAIJING ZHANG¹, MARCUS SCHMIDT¹, MICHAEL BAENITZ¹, GESA SIEMANN², CHIARA BIGI², PHIL D. C. KING², VINCENT POLEWCZYK³, GIOVANNI VINAI³, and HELGE ROSNER¹ — ¹MPI CPFS, D-01187 Dresden, Germany — ²IOM-CNR, Laboratorio TASC, Area Science Park, S.S. 14 km 163.5, Trieste I-34149, Italy — ³School of Physics and Astronomy, University of St. Andrews, St. Andrews KY16 9SS, United Kingdom

We present the theoretical studies of the electronic structure and the anomalous Hall effect in AgCrSe₂ based on density functional theory together with experimental results. AgCrSe₂ is a layered triangular lattice system that lacks inversion symmetry. It exhibits a cycloidal coupling in the CrSe₂ layer with a small angle and an antiferromagnetic coupling between adjacent layers with a small canting along *c*-axis. The comparison of the Cr partial DOS determined from the photoemission measurements and the magnetic LDA+U calculations with a value of $U = 0.75$ eV shows a good agreement. This reveals that this compound is rather weakly correlated due to a strong hybridization with the ligands. The Se 4p states are dominating near the Fermi energy, resulting in a sizable band split of the order of 300 meV induced by the SOC. This system shows an unconventional anomalous Hall effect. The anomalous Hall conductivity is calculated based on the Berry curvature using an effective model constructed by the Wannierisation. The calculated σ_{xy} shows a good agreement to the experiments.

MA 27.2 Wed 9:45 HSZ 403

Geometrical dynamics of magnetic moments coupled to a correlated antiferromagnet — •DAVID ALAN KRÜGER, NICOLAS LENZING, and MICHAEL POTTHOFF — Department of Physics, University of Hamburg, Hamburg, Germany

The geometrical spin torque represents an indirect interaction of magnetic moments, which are weakly exchange coupled to a system of itinerant electrons. It originates from a finite spin-Berry curvature, it modifies and adds to the conventional indirect RKKY exchange, and it leads to an anomalous, non-Hamiltonian dynamics of the magnetic moments. We demonstrate that there is an unprecedentedly strong geometrical spin torque in case of an electron system, where correlations cause antiferromagnetic long-range order. The key observation is that the anomalous torque is strongly boosted by low-energy magnon modes emerging in the two-electron spin-excitation spectrum as a necessary consequence of spontaneous spin-rotation symmetry breaking. As long as single-electron excitations are gapped out, the effect is largely universal, i.e., essentially independent of the details of the electronic structure, but decisively dependent on the lattice dimension. Analogous to the reasoning that leads to the Mermin-Wagner theorem, there is a lower critical dimension at and below which the spin-Berry curvature diverges. Our proposal is supported by numerical results obtained by the random-phase approximation and by Holstein-Primakov spin-wave theory for the Hubbard model in the weak- and in the strong-coupling limit, respectively.

MA 27.3 Wed 10:00 HSZ 403

Exploring electron correlation effects in the electronic structure and spin transport properties of transition metal multilayers — •ANDREA DROGHETTI¹, MILOŠ RADONIĆ², DECLAN NELL¹, LIVIU CHIONCEL³, and IVAN RUNGGER⁴ — ¹Trinity College Dublin (Ireland) — ²University of Belgrade (Serbia) — ³University of Augsburg (Germany) — ⁴National Physical Laboratory (UK)

Magnetic thin film heterostructures, which are the material platforms for spintronic devices, are quite correlated systems. However, to date, most theoretical studies dedicated to their electronic and spin transport properties, rely on effective single-particle pictures. To go beyond these limitations, we present a computational approach, which combines Density Functional and Dynamical Mean Field Theory, for layered systems, using a multi-orbital perturbative solver for the many-body problem [1]. Calculations accurately describe the spin splitting of 3d states and the appearance of satellite features at transition metal surfaces and interfaces, where electron correlations can get drastically enhanced [2]. Furthermore, when combined with quantum transport schemes [3], our method allows for the simulation of spintronic devices thus addressing how electron correlations affect the giant and tunnel magnetoresistance [4].

[1] A. Droghetti, M.M. Radonjić, A. Halder, I. Rungger, and L. Chioncel, *Phys. Rev. B* **105**, 115129 (2022). [2] D.M. Janas, A. Droghetti, *et al.*, *Adv. Mater.* **2205698** (2022). [3] A. Droghetti, I Rungger, *Phys. Rev. B* **95**, 085131 (2017). [4] A. Droghetti, M.M. Radonjić, L. Chioncel, I. Rungger, *Phys. Rev. B* **106**, 075156 (2022).

MA 27.4 Wed 10:15 HSZ 403

The role of non-local Coulomb interaction on spin models in the Hubbard limit — •WEJDAN BEIDA, MARKUS HOFFMANN, JUBA BOUAZIZ, and STEFAN BLÜGEL — Peter Grünberg Institut and Institute for Advanced Simulation, Forschungszentrum Jülich and JARA, 52425 Jülich Germany

We extend the derivation of model spin Hamiltonians by including the non-local Coulomb interaction in the multi-band Hubbard model. We use Löwdin partitioning as the downfolding method of the dynamical electronic degrees of freedom described in the extended Hubbard model at half filling into low energy spin corner. The ground state of spin systems has been perturbatively corrected up to fourth order in the hopping parameter of the Hubbard model. The role which the non-local Coulomb interaction plays is strengthening the magnetism of the ground state. More importantly, it increases the importance of higher-order spin interactions beyond Heisenberg; Biquadratic, Four-spin, and Three-spin interactions. Generally speaking, this is confirmed by spin lattices with a site total spin in the range $1/2 * S * 3/2$. For $S = 1/2$, we characteristically investigate the effect of next nearest neighbour hopping and inter-site Coulomb interaction on spin models for square and hexagonal lattice geometries.

15 min. break

MA 27.5 Wed 10:45 HSZ 403

Influence of the temperature on the relation between the magnetic hyperfine field and the magnetic moment — •ONDREJ ŠÍP^{1,2} and HUBERT EBERT³ — ¹Institute of Physics, Czech Academy of Sciences, Praha — ²New Technologies Research Centre, University of West Bohemia, Plzeň — ³Ludwig-Maximilians-Universität München

The magnetic hyperfine field B_{hf} is often used to probe magnetism in alloys, compounds and doped systems in an element-specific way. Accompanying this is the question about the relationship between B_{hf} and the magnetic moment. It was shown before both experimentally and theoretically that the ratio between B_{hf} and the magnetic moment depends on the alloy system and the composition. Here, we apply ab initio calculations to investigate how B_{hf} and its relation to the magnetic moment depend on the temperature.

We find that the contribution of the core electrons to B_{hf} is indeed proportional to the magnetic moment over the whole temperature range, from zero up to the Curie temperature. However, the temperature-dependence of the contribution of the valence electrons is more complicated and as a result of this, the ratio between the total B_{hf} and the magnetic moment significantly varies with the temperature. Based on our theoretical results, we show that probing element-specific magnetism by means of measuring the magnetic hyperfine field and by measuring the x-ray magnetic circular dichroism will lead in general to different pictures.

MA 27.6 Wed 11:00 HSZ 403

Nonlocal correlation effects due to virtual spin-flip processes in itinerant electron ferromagnets — •SEBASTIAN PAISCHER¹, MIKHAIL KATSNELSON², GIOVANNI VIGNALE³, ARTHUR ERNST¹, and PAWEŁ BUCZEK⁴ — ¹Johannes Kepler University, Linz, Austria — ²Radboud University, Nijmegen, Netherlands — ³National University of Singapore, Singapore — ⁴Hamburg University of Applied Sciences, Hamburg, Germany

An important type of the many-body effects in itinerant-electron magnets originates from the interaction of electrons with bosonic spin-flip excitations, both coherent (magnons) and incoherent (Stoner particle-hole excitations). While there has been a steady progress in understanding the properties of spin-flip excitations at a model level only little is known about microscopic details of their interactions with the electronic degrees of freedom in specific materials. Over the last few years we developed a first-principles method to account for the electron-magnon interaction in complex solids. While the method is based upon many-body perturbation theory, we approximate the complex quantities from pertur-

bation theory with quantities from time dependent density functional theory. This drastically reduces the numerical burden of the calculations and allows to consider complex materials like half-metallic ferromagnets. In this talk some of the main results and insights from this method will be presented.

MA 27.7 Wed 11:15 HSZ 403

Data-driven estimation of spin models in undoped cuprates — •DENYS Y. KONONENKO¹, ULRICH K. RÖSSLER¹, JEROEN VAN DEN BRINK^{1,2}, and OLEG JANSON¹ — ¹Institute for Theoretical Solid State Physics, IFW Dresden, Dresden, Germany — ²Institute for Theoretical Physics, TU Dresden, Dresden, Germany

Undoped cuprates host a wide variety of low-dimensional and frustrated spin models. The typically leading antiferromagnetic contribution to a magnetic exchange can be accurately estimated if the respective transfer integral is known. To date, the computational estimation of the transfer integral involves a well-established but cumbersome computational procedure. We demonstrate how the Gaussian Process Regression (GPR) model, trained on the results of the density functional theory calculations, can be employed to predict the transfer integrals using crystal structure as the only input. The GPR model receives descriptors of the local crystal environment of two copper sites as an input. The descriptors are based on the truncated expansion of the site position functions on the basis of the three-dimensional Zernike functions [1]. In this way, information on the spatial configuration and the chemical composition of the local crystal environment is incorporated into the descriptor. The approach facilitates rapid screening of spin models with desirable features among a broad range of known and unknown cuprates.

[1] M. Novotni and R. Klein, Computer Aided Design 36, 1047 (2004)

MA 28: Bulk Materials: Soft and Hard Permanent Magnets

Time: Wednesday 9:30–10:45

Location: POT 6

MA 28.1 Wed 9:30 POT 6

Local stiffness tailoring of magneto-active composites produced by laser powder bed fusion — •KILIAN SCHÄFER¹, MATTHIAS LUTZI¹, MUHAMMAD BILAL KHAN¹, SEBASTIAN BRUNS², CLAAS HARTMANN³, and OLIVER GUTFLEISCH¹ — ¹Functional Materials, Institute of Materials Science, TU Darmstadt, — ²Physical Metallurgy, Institute of Materials Science, TU Darmstadt, — ³Measurement and Sensor Technology Group, TU Darmstadt,

Magnetic actuation of mechanically soft actuators allows fast response, wireless operation and safe interaction with the human body. With additive manufacturing, the production of magneto-active composites in complex and bioinspired shapes is possible. To mimic the properties of biological systems, the fabrication of composites with locally different mechanical properties is needed. Here, we present a method to locally tailor the stiffness of a magneto-active compound, consisting of hard magnetic Nd₂Fe₁₄B particles in a thermoplastic polyurethane (TPU) matrix with laser powder bed fusion. By utilizing different laser parameters at different locations during the process, the mechanical properties of the composite are modified locally. The range in which the mechanical properties can be tailored is investigated with compression and tensile tests of the composite produced with different laser parameters. The stiffness can be increased tenfold when the laser power is increased from low to high values. The stiffness gradient within one sample is verified by line scans of Vickers indentations with a nanoindentation system. Then the actuation performance is evaluated for samples with and without stiffness gradients.

MA 28.2 Wed 9:45 POT 6

Magnetic properties of rare-earth-lean ThMn₁₂-type (Nd,X)Fe₁₁Ti (X: Y and Ce) compounds: A DFT study — •STEPHAN ERDMANN, THORSTEN KLÜNER, and HALIL IBRAHIM SÖZEN — Institute of Chemistry, Carl-von-Ossietzky University of Oldenburg, D-26129 Oldenburg, Germany

Due to the resource criticality of rare-earths (RE), an alternative to the well-known Nd₂Fe₁₄B magnets with a lower amount of critical elements is required. In this work, we performed density functional theory (DFT) calculations to investigate the influence of partial Nd substitution with more abundant elements (X: Y and Ce) in ThMn₁₂-type (Nd,X)Fe₁₁Ti compounds. In order to have a systematic understanding, the intrinsic magnetic properties such as saturation magnetization M_S , Curie temperature T_C and magnetocrystalline anisotropy energy, are screened starting from binaries RFe₁₂ (R: Y, Ce and Nd). Ti is considered for the thermodynamic stabilization and different concentrations of Ti are taken into account for ternaries RFe_{12-y}Ti_y, and quaternaries (Nd,X)Fe_{12-y}Ti_y ($0.5 \leq y \leq 1$). In addition, the effect of nitrogenation is examined for each considered compound. In case of (Nd,Y)Fe₁₁Ti, $|BH|_{\text{max}}$ is found to be 384 kJ/m³ and T_C is calculated to be 595 K. Similarly, $|BH|_{\text{max}}$ and T_C are calculated to be 365 kJ/m³ and 593 K for (Nd,Ce)Fe₁₁Ti magnet, respectively. Both 50 % Nd-lean magnets exhibit higher $|BH|_{\text{max}}$ compared to Sm₂Co₁₇ and T_C than Nd₂Fe₁₄B. For both cases, our theoretical magnetic hardness factor κ is calculated to be 1.20, which qualifies them as good candidates for RE-lean permanent magnets.

MA 28.3 Wed 10:00 POT 6

Ab initio thermodynamic modelling for Ce-based alternative hard magnetic materials — •HALIL IBRAHIM SÖZEN¹, TILMANN HICKEL², and THORSTEN KLÜNER¹ — ¹Institute of Chemistry, Carl-von-Ossietzky University of Oldenburg, D-26129 Oldenburg, Germany — ²BAM Federal Institute for Materials Research and Testing, 12489 Berlin, Germany

The utilization of the RE-lean ThMn₁₂ materials system in combination with the abundant RE element Ce is a promising strategy for modern hard magnet applications. One of the main challenges for the Ce-based hard-magnetic materials is the formation of detrimental Laves phases next to the ThMn₁₂-type compound CeFe₁₁Ti. In this contribution, we present an ab initio-based approach to modify the stability of these phases in the Ce-Fe-Ti system by additions of 3d and 4d-elements. The results are used to provide two fundamental methodological insights. One of them is our recently developed modeling concept of partial decomposition, which considers the enrichment of the added solutes in phases that would at the considered temperature not be stable in a conventionally used full decomposition model. The second conclusion is the dominant impact of 0 K formation enthalpies on the solute-enhances phase stability compared to finite temperature entropy terms. Based on this, a screening approach is developed, considering the substitution of all 3d and 4d-elements. We show that substituted elements with more than a half-filled 3d-shell or with less than a half-filled 4d-shell mainly reduce the formation temperature of the 1:12 phase.

MA 28.4 Wed 10:15 POT 6

Rare earth lean permanent magnets from computational design and the challenge of the 4f electrons — •H. C. HERPER¹, K. P. SKOKOV², S. ENER², P. THUNSTRÖM¹, L. V. B. DIOP³, O. GUTFLEISCH², and O. ERIKSSON^{1,4} — ¹Department of Physics and Astronomy, Uppsala University, Sweden — ²Functional Materials, Department of Material Science, TU Darmstadt, Germany — ³Université de Lorraine, CNRS, IJL, Nancy, France — ⁴School of Science and Technology, Örebro University, Örebro, Sweden

Computational design has been proven to be a powerful tool to tailor properties of functional materials but it becomes challenging in presence of 4f electrons. Here, NdFe₁₁Ti and YFe₁₁Ti serve as prototypes for rare-earth (RE) lean or RE-free magnets with the ThMn₁₂ structure. Though, for Sm (Ce) counterparts a core (valence) treatment was sufficient to describe the magnetic properties, the complex low temperature magnetism of NdFe₁₁Ti could only be reproduced with an intermediate sized LDA+U or a DMFT approach (full potential LMTO). We compare our calculations to experimental values obtained from single crystals. The investigations clearly demonstrate the crucial dependence of the calculated magnetic properties of NdFe₁₁Ti on the treatment of the 4f electrons.[1]

Using Nd_{1-x}Y_xFe_{12-y}Ti_{1+y} as a test case we investigated how far the strong dependence of the magnetic properties on the description of the Nd 4f states influences the prediction of new phases.

[1] H.C. Herper et al., Acta Materialia 242, 118473 (2023)

MA 28.5 Wed 10:30 POT 6

MAELAS: Magneto-ELAStic properties calculation via computational high-throughput approach — PABLO NIEVES¹, SERGIU ARAPAN¹, SHIHAO ZHANG², ANDRZEJ KADZIELAWA¹, RUIFENG ZHANG², and •DOMINIK LEGUT¹ — ¹IT4Innovations, VSB-TU Ostrava, Ostrava, Czech Republic — ²School of Mat. Sci. and Eng., Beihang University, Beijing, China

Magnetostriction is a physical phenomenon in which the process of magnetization induces a change in the shape or dimension of a magnetic material. Nowadays, materials with large magnetostriction are used in many electromagnetic microdevices as actuators and sensors. By contrast, magnetic materials with extremely low magnetostriction are required in applications such as electric trans-

formers. In this work, we present results based on the in-house developed code MAELAS to determine anisotropic magnetostriction coefficients and magnetoelastic constants in an automated way by quantum-mechanical calculations. The behavior of the magnetocrystalline anisotropy energy and magnetostrictive coefficients under a general external magnetic field could be visualized as a relative length change using our MAELASviewer tool. To verify accuracy and our approach in general we present a number of examples of each crystal symmetry class with calculated magnetostriction and magnetoelastic constants and compare them with recorded data. One of our highlights with this novel approach is an ability to separate exchange-contraction (ω_s) from the magnetic part and to avoid the calculation of the paramagnetic state that is still a challenge.

MA 29: Neuromorphic Magnetism / Magnetic Logic

Time: Wednesday 11:30–12:45

Location: HSZ 02

MA 29.1 Wed 11:30 HSZ 02

Brownian Computing Realized Using Skyrmions — •MAARTEN A. BREMS¹, KLAUS RAAB¹, GRISCHA BENEKE¹, JAN ROTHÖRL¹, PETER VIRNAU¹, JOHAN H. MENTIK², and MATHIAS KLÄUI¹ — ¹Institut für Physik, Johannes Gutenberg-Universität Mainz, Staudingerweg 7, 55128 Mainz, Germany — ²Radboud University, Institute for Molecules and Materials, Heyendaalseweg 135, 6525 AJ Nijmegen, The Netherlands

Reservoir computing (RC) has been considered as one of the key computational principles beyond von-Neumann computing. Magnetic skyrmions, topological particle-like spin textures in magnetic films, are particularly promising for implementing RC since they respond strongly nonlinear to external stimuli and feature inherent multiscale dynamics. We propose and experimentally demonstrate a conceptually new approach to skyrmion computing that combines the RC and Brownian computing [1] concepts. By confining the thermal skyrmion motion [2] that can be electrically gated, we find that already a single skyrmion in a confined geometry suffices to realize non-linearly separable functions, which we demonstrate for the XOR gate along with all other Boolean logic gate operations [3]. Our proposed concept ensures low training costs as well as ultra-low power operation and can be readily extended by including more skyrmions in the reservoir, suggesting high potential for scalable and low-energy reservoir computing. [1] M. A. Brems et al., Appl. Phys. Lett. 119, 132405 (2021). [2] J. Závorka et al., Nat. Nanotechnol. 14, 658 (2019). [3] K. Raab, M. A. Brems et al., Nat. Commun. 13, 6982 (2022).

MA 29.2 Wed 11:45 HSZ 02

Superparamagnetic tunnel junctions for neuromorphic computing — •LEO SCHNITZSPAN^{1,2}, GERHARD JAKOB^{1,2}, and MATHIAS KLÄUI^{1,2} — ¹Institut für Physik, Johannes Gutenberg Universität Mainz — ²Max Planck Graduate Center, Mainz

Superparamagnetic tunnel junctions (SMTJ) are promising building blocks in the field of neuromorphic computing. In a SMTJ, the magnetic free layer can switch its magnetic orientation induced by thermal activation, leading to a random two-level resistance fluctuations[1]. We show nanosecond fluctuations with dwell times below 10 ns for our in-plane magnetized SMTJs. Their intrinsic stochastic behaviour and additional tunability by external magnetic fields, Spin Transfer Torques (STT) or Spin Orbit Torques (SOT) are prerequisites for low-energy artificial neurons in neural networks. True random number generation is demonstrated and evaluated by the statistical test suite from NIST. The probability of a P- (=0) or AP- (=1) state depends on the energy landscape and can be affected by STT. However, the average fluctuation speed is strongly dependent on the temperature. We demonstrate that Joule heating, induced by a large applied current, leads to significantly shorter dwell times. From dwell time measurements, the contributions of STT and Joule heating are extracted.

[1] Hayakawa, K. et al., Phys. Rev. Lett. 126, 117202 (2021).

MA 29.3 Wed 12:00 HSZ 02

Impact of DMI on magnonic antiferromagnetic leaky integrate-and-fire neuronal networks — •VERENA BREHM and ALIREZA QAIUMZADEH — QuSpin, NTNU Trondheim, Norway

Two shifts of paradigms promise to revolutionize modern day computation: First, neuromorphic computing aims to mimic the human brain, which is a fundamentally different approach compared to the state-of-the-art von Neuman computing architecture. Second, antiferromagnetic magnonics promises to be faster and more energy-efficient compared to conventional electronics through avoidance of Joule heating and high-frequency eigenexcitations. We combine both fields and study a proof-of-principle antiferromagnetic spiking neural network, more specifically a leaky integrate-and-fire model both analytically and numerically [1,2].

[1] Johannes W. Austefjord, Verena Brehm, Serban Lepadatu and Alireza Qaiumzadeh: 'Non-volatile leaky integrate-and-fire neurons with domain walls in antiferromagnetic insulators'. <http://arxiv.org/abs/2211.16845> (2022).

[2] Even Tønseth, Verena Brehm, Alireza Qaiumzadeh: 'Effects of DMI on spike propagation in neuromorphic systems', to be submitted.

MA 29.4 Wed 12:15 HSZ 02

Light-controlled nanomagnetic logic circuits — •NAËMI LEO^{1,2}, MATTEO MENNITI², PIETER GYPENS², JONATHAN LELIAERT³, and PAOLO VAVASSORI² — ¹CSIC - INMA, Zaragoza, Spain — ²CIC nanoGUNE BRTA, Spain — ³Ghent University, Belgium

Magnetic metamaterials with magnetostatically-coupled elements offer an interesting platform to implement low-power and neuromorphic-inspired data processing, in particular when combined with thermally-driven switching processes. By combining nanomagnetic elements with light-controlled plasmonic heaters, here we demonstrate how to design nanomagnetic Boolean OR or AND gates with nanosecond operation. The reconfigurability logic is achieved either by modifying the field protocol setting the initial state or optically, by changing the polarisation and order of the laser pulses exciting the system. Thermoplasmonic-nanomagnetic metamaterials thus lend themselves for the implementation of future fast (up to GHz), energy-efficient (picojoule), and optically-reconfigurable platform for in-memory computation schemes.

MA 29.5 Wed 12:30 HSZ 02

Antiferromagnet-based neuromorphics using dynamics of topological charges — •SHU ZHANG — Max Planck Institute for the Physics of Complex Systems, Dresden, Germany

We propose a spintronics-based hardware implementation of neuromorphic computing, specifically, the spiking neural network, using topological winding textures in one-dimensional antiferromagnets. The consistency of such a network is emphasized in light of the conservation of topological charges, and the natural spatiotemporal interconversions of magnetic winding. We discuss the realization of the leaky integrate-and-fire behavior of neurons and the spike-timing-dependent plasticity of synapses. Our proposal opens the possibility for an all-spin neuromorphic platform based on antiferromagnetic insulators.

MA 30: PhD Focus Session: Non-equilibrium dynamics in theory and experiment

Non-equilibrium phenomena often occur at the edge of phase transitions, for example, in maintaining the organism and cells, photosynthesis, or other exciting reactions. Nevertheless, many of these phenomena are poorly understood or require various disciplines to come together to understand these phenomena in a significant context. Here, however, there is still a need for communication between theory and experiment. Since today's experiments and ideas often have a large gap, we want to use this focus session to create an environment where young researchers can get an overall picture. In doing so, this Ph.D. focus session should emphasize highlights and show the current front of research, in addition to the character of tutorial lectures, and give a chance to conclude in a lively discussion. This PhD Focus Session is organized by Lea Spieker and Gérald Kämmerer (Faculty of Physics and Center for Nanointegration Duisburg-Essen (CENIDE), University of Duisburg-Essen, Germany).

Time: Wednesday 15:00–18:00

Location: HSZ 02

Invited Talk

MA 30.1 Wed 15:00 HSZ 02

Femto- phono- magnetism — •SANGEETA SHARMA — Max Born Institute for Nonlinear Optics and Short Pulse Spectroscopy, Max-Born-Str. 2A, 12489 Berlin, Germany

From the outset of research into femtomagnetism, the field in which spins are manipulated by light on femtosecond or faster time scales, several questions have arisen and remain highly debated: How does the light interact with spin moments? How is the angular momentum conserved between the nuclei, spin, and angular momentum during this interaction? What causes the ultrafast optical switching of magnetic structures? What is the ultimate time limit on the speed of spin manipulation? What is the impact of nuclear dynamics on the light-spin interaction?

In my talk I will advocate a parameter free ab-initio approach to treating ultrafast light-matter interactions, and discuss how this approach has led both to new answers to these old questions but also to the uncovering of novel and hitherto unsuspected early time spin dynamics phenomena. In particular I will show that selective excitation of phonon modes exert a strong influence on femtosecond demagnetisation. Our finding demonstrates that the nuclear system, typically assumed to play a role of an energy sink aiding remagnetization of the spin system, plays a profound role in controlling femtosecond demagnetization of magnetic materials.

Invited Talk

MA 30.2 Wed 15:30 HSZ 02

Spin-switchable molecules in interaction with their environment. — •CYRILLE BARRETEAU — University Paris-Saclay, CEA, CNRS, SPEC, 91191, Gif-sur-Yvette, France

Molecules that can switch spin-state form a very important class of molecules that offers a formidable test bed for fundamental studies and applied research due to the multiple possible channels to tune their properties. Spin-crossover (SCO) molecules are the most common spin-switchable molecules where the spin-state of the metal complex changes under the application of an external stimulus such as light, temperature, pressure etc.. SCO crystals have been the subject of intense studies however; it is much more recent that these molecules have been deposited on surfaces. In practice, the number of SCO that are robust enough to remain intact on surface and retain their switchability is rather limited. In addition, from the modelling point, these systems are also delicate to describe accurately. In this talk, I will present coupled experimental and theoretical results of various spin-switchable molecules that have successfully been deposited on inorganic surfaces. It will be shown how their properties are affected by their environment, in particular we will investigate the role of molecule-molecule and molecule-substrate interaction or the application of an electric field. This will provide us with the tools to manipulate the properties of such systems and give hint for possible strategies to optimize the magneto-transport properties of materials/devices.

15 min. break

Invited Talk

MA 30.3 Wed 16:15 HSZ 02

Yep, real photodoping. — LUKAS GIERSTER^{1,2} and •JULIA STÄHLER^{1,2} — ¹Humboldt-Universität zu Berlin, Inst. f. Chemie, Berlin, Germany — ²Fritz-Haber-Institut der MPG, Abt. PChem, Berlin, Germany

The advent of photoinduced phase transitions and the investigation of their non-equilibrium dynamics on ultrafast timescales coined various fashionable terms like *hidden phases*, *new phases of matter*, or *photodoping*. They were not always used rigorously and partially developed a life on their own. For instance, a photoexcited solid is not necessarily in a different phase just because it shows different properties than in its ground state - and the pure redistribution of charges after photoexcitation is not equivalent with chemical doping even if the photoexcitation drives a phase transition.

I will discuss these subtle, but important differences using the example of ZnO that undergoes a semiconductor-to-metal transition upon real photodoping at very low excitation densities [1]. Notably, the hidden, metallic phase has no equivalent in the equilibrium phase diagram and shows decay dynamics on ultrafast timescales, but can also be retained and become metastable [2].

[1] Nat. Commun. 12 978 (2021)

[2] Faraday Disc. (2022) DOI:10.1039/D2FD00036A

Invited Talk

MA 30.4 Wed 16:45 HSZ 02

Probing ultrafast magnetization thanks to ultrashort soft X-ray pulses — •EMMANUELLE JAL — Sorbonne Université, CNRS, Laboratoire de Chimie Physique - Matière et Rayonnement, LCPMR, Paris 75005, France

Even after more than 25 years of studies and debates, the mechanisms of ultrafast demagnetization remain disputed. In order to bring new experimental information into this field, and with the advent of femtosecond X-rays sources, new time-resolved XUV and soft X-ray-based pump/probe techniques are performed on magnetic thin films. During this talk, I will give an overview of what can be done with XUV and soft x-ray short pulses to probe electronic, magnetic, and structural dynamics. A special emphasis will be given to (i) simultaneous electronic and magnetism dynamics [1,2] and (ii) simultaneous structural and magnetism dynamics [3, 4,5].

[1] Rösner et al. Struct. Dyn. 7, 054302 (2020)

<https://doi.org/10.1063/4.0000033>

[2] Hennes et al Appl. Sci. 11m 325 (2021)

<https://doi.org/10.3390/app11010325>

[3] Jal et al. Phys. Rev. B 95, 184422 (2017)

<https://doi.org/10.1103/PhysRevB.95.184422>

[4] Chardonnet et al. Struct. Dyn. 8, 034305 (2021)

<https://doi.org/10.1063/4.0000109>

[5] V. Chardonnet, PhD 2022

<https://tel.archives-ouvertes.fr/tel-03864973>

45 min. Panel discussion with all speakers

MA 31: Functional Antiferromagnetism II

Time: Wednesday 15:00–17:15

Location: HSZ 04

MA 31.1 Wed 15:00 HSZ 04

Role of substrate clamping on anisotropy and domain structure in the canted antiferromagnet α -Fe₂O₃ — •ANGELA WITTMANN^{1,2}, O GOMONAY¹, K LITZIUS^{2,3}, A KACZMAREK², A KOSSAK², D WOLF⁴, A LUBK⁴, T N JOHNSON⁵, E TREMSINA², A CHURIKOVA², F BÜTTNER⁶, S WINTZ⁶, M A MAWASS⁶, M WEIGAND⁶, F KRONAST⁶, L SCIPIONI⁷, A SHEPARD⁷, T NEWHOUSE-ILLIGE⁷, J A GREER⁷, G SCHÜTZ³, N O BIRGE^{2,5}, and G S D BEACH² — ¹Johannes Gutenberg Universität Mainz, Germany — ²Massachusetts Institute of Technology, USA — ³Max Planck Institute for Intelligent Systems, Germany — ⁴Leibniz IFW

Dresden, Germany — ⁵Michigan State University, USA — ⁶Helmholtz-Zentrum Berlin, Germany — ⁷PVD Products, USA

Antiferromagnets are at the forefront of research in spintronics. However, many of the underlying phenomena remain to be explored. This work investigates the domain structure in a thin-film canted antiferromagnet α -Fe₂O₃ in an external magnetic field. Using x-ray magnetic linear dichroism (XMLD) and spin Hall magnetoresistance (SMR) measurements, we find that the internal long-range dressing fields driving the formation of domains do not follow the crystal symmetry of α -Fe₂O₃ but fluctuate due to substrate clamping [1]. This leads

to locally varying effective anisotropy in thin films allowing for the stabilization of long-range complex domain structures. The insights gained from our work serve as a foundation for further studies of electrical and optical manipulation of the domain structure of antiferromagnetic thin films. [1] arXiv:2210.16141

MA 31.2 Wed 15:15 HSZ 04

Two-directional electrical switching of insulating antiferromagnetic thin films — •CHRISTIN SCHMITT¹, ADITHYA RAJAN¹, GRISCHA BENEKE¹, ADITYA KUMAR¹, TOBIAS SPARMANN¹, HENDRIK MEER¹, RAFAEL RAMOS², MIGUEL ANGEL NIÑO³, MICHAEL FÖRSTER³, EIJI SAITOH^{2,4}, and MATHIAS KLÄUI¹ — ¹Institute of Physics, Johannes Gutenberg University Mainz, Germany — ²WPI-AIMR, Tohoku University, Japan — ³ALBA Synchrotron Light Facility, Spain — ⁴Department of Applied Physics, The University of Tokyo, Japan

Antiferromagnets (AFMs) have gained increasing interest as active elements in spintronic devices due to intrinsic dynamics in the THz range and the absence of stray fields. However, efficient electrical writing and reading is necessary for applications. For insulating antiferromagnets different switching mechanisms based on spin-orbit torques or thermomagnetoelastic effects have been put forward [1,2]. Here, we focus on CoO/Pt thin films where we observe that electrical pulses along the same trajectory can lead to an increase or decrease of the electrical signal, depending on the current density of the pulse. By photoemission electron microscopy (PEEM) employing the x-ray magnetic linear dichroism (XMLD) effect we shed light on this observation and determine whether this is a sign for two competing switching mechanisms or rather some result of the sensitivity distribution of how the electrical measurement is conducted [3]. [1] T. Moriyama, et al., *Sci. Rep.* 8, 14167 (2018). [2] P. Zhang, et al., *Phys. Rev. Lett.* 123, 247206 (2019). [3] F. Schreiber, et al., *Phys. Rev. Applied* 16, 064023 (2021).

MA 31.3 Wed 15:30 HSZ 04

Control and manipulation of antiferromagnetic domains in NiO — •HENDRIK MEER¹, CHRISTIN SCHMITT¹, OLENA GOMONAY¹, STEPHAN WUST², PAUL HERRGEN², BAERBEL RETHFELD², BENJAMIN STADMÜLLER^{1,2}, MARTIN AESCHLIMANN², JAIRO SINOVA¹, RAFAEL RAMOS^{3,4}, LORENZO BALDRATI¹, EIJI SAITOH^{4,5}, and MATHIAS KLÄUI¹ — ¹Institute of Physics, Johannes Gutenberg University Mainz, Mainz, Germany — ²Department of Physics and Research Center OPTIMAS, Technische Universität Kaiserslautern, Kaiserslautern, Germany — ³CIQUS, Departamento de Química-Física, Universidade de Santiago de Compostela, Santiago de Compostela, Spain — ⁴WPI-Advanced Institute for Materials Research, Tohoku University, Sendai, Japan — ⁵Department of Applied Physics, The University of Tokyo, Tokyo, Japan

Control of the spin structure is key for the development of future antiferromagnetic spintronic devices. We show how the antiferromagnetic domains of NiO/Pt bilayers can be modified by applying electric currents [1], patterning geometric elements [2], and irradiating with laser light [3]. We image the induced changes in the antiferromagnetic order with synchrotron and lab-based magnetic microscopy. We are able to reveal writing mechanisms for the antiferromagnetic order, laying the foundation for an active role of antiferromagnets in future devices.

[1] H. Meer *et al.*, *Nano Lett.* 21, 114 (2021).

[2] H. Meer *et al.*, *Phys. Rev. B* 106, 094430 (2022).

[3] H. Meer *et al.*, arXiv:2210.11009 [cond-mat.mtrl-sci] (2022).

MA 31.4 Wed 15:45 HSZ 04

Gate-tunable anomalous Hall effect in an antiferromagnet — SEO-JIN KIM¹, JIHANG ZHU², MARIO PIVA¹, MARCUS SCHMIDT¹, DORSA FARTAB¹, ANDREW MACKENZIE^{1,3}, MICHAEL BAENITZ¹, MICHAEL NICKLAS¹, HELGE ROSNER¹, ASHLEY COOK^{1,2}, and •HAIJING ZHANG¹ — ¹Max Planck Institute for Chemical Physics of Solids, 01187 Dresden, Germany — ²Max Planck Institute for the Physics of Complex Systems, 01187 Dresden, Germany — ³Scottish Universities Physics Alliance, School of Physics and Astronomy, University of St Andrews, St Andrews KY16 9SS, UK

Probing and engineering the magnetic states is a key goal in contemporary condensed matter physics because it can facilitate the understanding of underlying mechanisms of many fundamental physical phenomena, such as the anomalous Hall effect. Here, we report the observation of an anomalous Hall effect in AgCrSe₂, a layered triangular lattice metal that lacks inversion symmetry, and has a sizeable antiferromagnetic coupling between Cr spin 3/2 moments in adjacent layers. The anomalous Hall resistivity 3 $\mu\Omega$ cm is comparable to the largest magnitude observed in any antiferromagnetic system to date. We further demonstrate that the anomalous Hall response in thin layer devices can be switched on and off by an ionic gate. We also present the results of an illustrative model that suggests the anomalous Hall effect is driven by Berry curvature that correlates closely with the Rashba spin-orbit coupling. The capability of electrically switching the anomalous Hall effect opens up new avenues for potential voltage controlled spintronic devices.

15 min. break

MA 31.5 Wed 16:15 HSZ 04

In plane magnetic field dependence of anomalous Hall effect in a non-collinear antiferromagnet — •ADITHYA RAJAN¹, TOM SAUNDERSON^{1,2}, FABIAN LUX¹, DONGWOOK GO¹, HASAN ABDULLAH³, TETSUYA HAJIRI⁴, HIDEFUMI ASANO⁴, UDO SCHWINGENSCHLOEGL³, YURIY MOKROUSOV^{1,2}, and MATHIAS KLÄUI¹ — ¹Institute of Physics, Johannes Gutenberg University, Staudingerweg 7, 55128 Mainz, Germany — ²Peter Grünberg Institut and Institute for Advanced Simulation, Forschungszentrum Jülich, 52424 Jülich, Germany — ³King Abdullah University of Science and Technology (KAUST), Thuwal 23955-6900, Saudi Arabia — ⁴Department of Materials Physics, Nagoya University, Nagoya 464-8603, Japan

Non-collinear antiferromagnets (NC-AFM) have attracted much attention recently due to the observation of the anomalous Hall effect (AHE) in these materials [1]. Here we study the AHE as a function of magnetic field direction in the Kagome plane of the antiperovskite nitride Mn₃Ni_{0.35}Cu_{0.65}N. We explain the results in the context of irreducible representations of the three-spin unit cell, showing a strong interplay between field dependence of AHE and the octupole moment by fitting to density functional theory calculations. Further, we present non-trivial features in the field dependent AHE loops signifying additional stable spin configurations, and potentially novel transport phenomena. These results open the possibility of a lever through which the spin structure in NC-AFMs can be controlled.

[1] S. Nakatsuji *et al.*, *Nature* 527, 212 (2015).

MA 31.6 Wed 16:30 HSZ 04

Anomalous Hall Effect in Antiperovskite Nitride Thin Films Driven by Structural Disorder — •BERTHOLD H. RIMMLER, BINYOY K. HAZRA, HOLGER L. MEYERHEIM, and STUART S. P. PARKIN — Max Planck Institute of Microstructure Physics, Halle

Antiperovskites display unusual properties such as complex magnetism, superconductivity, negative thermal expansion and distinct magneto-transport effects, which render them interesting for various applications. For instance, Mn-based antiperovskite nitrides, Mn₃ZN (Z = Ni, Ga, Sn), have attracted attention in spintronics, as they can host non-collinear antiferromagnetism and other complex magnetic phases. These give rise to unusual intrinsic magneto-transport effects, such as the anomalous Hall effect in absence of magnetization or the spin Hall effect where spin currents display arbitrary spin polarization directions. Control of the antiferromagnetic domain structure in these materials is essential for using these effects in spintronic devices. Therefore, an imbalance of the otherwise fully compensated non-collinear antiferromagnetic textures is required. Previously, strain-driven tetragonal distortion was assumed to be the mechanism allowing for domain control. In this work we show, by comparison of different Mn-based antiperovskite nitrides and using advanced X-ray diffraction measurements, that domain structure control is, instead, enabled by displacements of Mn atoms out of high symmetry positions that locally break the global crystal and magnetic symmetry. We demonstrate that this effect is a general feature of a number of Mn₃ZN compounds and might, therefore, also have implications for other antiperovskites.

MA 31.7 Wed 16:45 HSZ 04

Flexomagnetism and vertically graded Néel temperature of antiferromagnetic Cr₂O₃ thin films — •PAVLO MAKUSHKO¹, TOBIAS KOSUB¹, OLEKSANDR PLYPOVSKYI¹, NATASCHA HEDRICH¹, JIANG LI¹, ALEXEY PASHKIN¹, STANISLAV AVDOSHENKO³, RENÉ HÜBNER¹, FABIAN GANSS¹, DANIEL WOLF³, AXEL LUBK^{3,4}, MACIEJ OSKAR LIEDKE¹, MAIK BUTTERLING¹, ANDREAS WAGNER¹, KAI WAGNER², BRENDAN SHIELDS², PAUL LEHMANN², IGOR VEREMCHUK¹, JÜRGEN FASSBENDER¹, PATRICK MALETINSKY², and DENYS MAKAROV¹ — ¹HZDR, Dresden, Germany — ²University of Basel, Basel, Switzerland. — ³IFW Dresden, Dresden, Germany — ⁴TU Dresden, Dresden, Germany.

Thin films of antiferromagnetic insulators are a prospective material platform for magnonics, spin superfluidity, THz spintronics, and non-volatile data storage. Here, we explore the presence of flexomagnetic effects in epitaxial Cr₂O₃ [1]. We demonstrate that a gradient of mechanical strain affects the order-disorder magnetic phase transition, resulting in the distribution of the Néel temperature along the thickness of a Cr₂O₃ film. The inhomogeneous reduction of the antiferromagnetic order parameter induces a flexomagnetic coefficient of about 15 $\mu\text{B nm}^{-2}$. The antiferromagnetic ordering in the strained films can persist up to 100°C, rendering Cr₂O₃ as a prospective material for industrial electronics applications.

[1] P. Makushko *et al.*, *Nat Commun* 13, 6745 (2022).

MA 31.8 Wed 17:00 HSZ 04

Ferromagnetism and Ferroelectricity in a Superlattice of Antiferromagnetic Perovskite Oxides Without Ferroelectric Polarization — •AVIJEET RAY, PARESH C. ROUT, and UDO SCHWINGENSCHLOEGL — Physical Sciences and Engineering Division (PSE), King Abdullah University of Science and Technology (KAUST), Thuwal 23955-6900, Saudi Arabia

Using density functional theory with onsite Coulomb interaction, we study the structural, electronic, and magnetic properties of the SrCrO₃/YCrO₃ superlat-

tice and their dependence on epitaxial strain. We discover that the superlattice adopts an A-type antiferromagnetic (A-AFM) ordering in contrast to its constituents (SrCrO₃: C-AFM; YCrO₃: G-AFM) and retains it under compressive strain while becoming ferromagnetic (5 μ_B per formula unit) at +1% strain. The obtained ferroelectric polarization is significantly higher than that of the R₂NiMnO₆/La₂NiMnO₆ (R = Ce to Er) series of superlattices [Nat. Commun. 5, 4021 (2014)] due to a large difference between the antipolar displacements of the Sr and Y cations. The superlattice is a hybrid-improper multiferroic ma-

terial with a spontaneous ferroelectric polarization (13.5 $\mu\text{C}/\text{cm}^2$) approaching that of bulk BaTiO₃ (19 $\mu\text{C}/\text{cm}^2$). In addition, the charge-order-driven p-type semiconducting state of the ferromagnetic phase (despite the metallic nature of SrCrO₃) is a rare property and interesting for spintronics. Monte Carlo simulations demonstrate a magnetic critical temperature of 90 K for the A-AFM phase without strain and of 115 K for the ferromagnetic phase at +5% strain, for example.

MA 32: Magnetic Imaging Techniques I

Time: Wednesday 15:00–16:30

Location: HSZ 401

MA 32.1 Wed 15:00 HSZ 401

Correlating Magnetic Force Microscopy imaging with bulk Magnetometry for ferroelastic Fe7S8 inspection — •SAMUEL SEDDON¹, PETER MILDE¹, MARIN ALEXE², CHARLES HAINES³, MICHAEL CARPENTER³, and LUKAS ENG^{1,4} — ¹TU Dresden, Institute of Applied Physics, Noethnitzer Straße 61, 01187 Dresden, Germany — ²University of Warwick, Coventry, CV4 7AL, England — ³University of Cambridge, Cambridge, CB3 0WA, England — ⁴ct.qmat: Dresden-Wuerzburg Cluster of Excellence-EXC 2147, TU Dresden, 01062 Dresden

Pyrrhotite, Fe₇S₈, is a natural mineral exhibiting a strong magnetoelastic coupling - which is to say that the material's ferroelastic domains directly determine the allowed directions of its magnetic moments. This system provides an interesting environment to explore the role that a material's crystal structure has on its magnetic properties, on a unit-cellular level. Here, magnetic force microscopy (MFM) is used to directly correlate local magnetic switching behaviors with various features observed from the bulk magnetic hysteresis; a magnetic hysteresis as acquired from MFM field dependent measurements is visualized. Local magnetic domains thus can be directly correlated to the expected ferroelastic domain wall pinning, as well as to domains that are responsible for the differences observed in saturation magnetization. Preliminary results pertaining to the application of mechanical strain will also be presented.

MA 32.2 Wed 15:15 HSZ 401

Simultaneous Magnetic Field and Field Gradient Mapping of Hexagonal MnNiGa by Quantitative Magnetic Force Microscopy — NORBERT H. FREITAG¹, CHRISTOPHER F. REICHE², VOLKER NEU¹, PARUL DEV³, ULRICH BURKHARDT³, CLAUDIA FELSER³, DANIEL WOLF¹, AXEL LUBK¹, BERND BÜCHNER¹, and •THOMAS MÜHL¹ — ¹Leibniz Institute for Solid State and Materials Research IFW Dresden, 01069 Dresden, Germany — ²Department of Electrical and Computer Engineering, University of Utah, Salt Lake City, UT-84112, USA — ³Max Planck Institute for Chemical Physics of Solids Dresden, 01187 Dresden, Germany

A quantitative, single-pass magnetic force microscopy (MFM) technique is presented that maps one magnetic stray-field component and its spatial derivative at the same time. This technique uses a special cantilever design and a special high-aspect-ratio magnetic interaction tip that approximates a monopole-like moment. Experimental details, such as the control scheme, the sensor design, which enables simultaneous force and force gradient measurements, as well as the potential and limits of the monopole description of the tip moment are discussed. To demonstrate the merit of this technique for studying complex magnetic samples it is applied to the examination of polycrystalline MnNiGa bulk samples. In these experiments, the focus lies on mapping and analyzing the stray-field distribution of individual bubble-like magnetization patterns in a centrosymmetric [001] MnNiGa phase. The results indicate that the magnetic bubbles have a significant spatial extent in depth and a buried bubble top base.

MA 32.3 Wed 15:30 HSZ 401

Quantum calibration of Magnetic Force Microscopy — •BAHA SAKAR¹, YAN LIU², SIBYLLE SIEVERS¹, FEDOR JELEZKO², and HANS W. SCHUMACHER¹ — ¹Physikalisches Technische Bundesanstalt — ²University of Ulm

Magnetic Force Microscopy (MFM) is a magnetic imaging technique that allows to image magnetic structures with nanometer resolution. However, per se it only delivers qualitative information since the magnetic properties of the tip are not known. The only method of obtaining quantitative information from these qualitative data is through a calibration. In this study we report the quantum calibration of a magnetic force microscope (MFM) by measuring the two-dimensional magnetic stray-field distribution of the MFM tip using a single nitrogen vacancy (NV) center in diamond. From the measured stray-field distribution and the mechanical properties of the cantilever a calibration function is derived allowing to convert MFM images to quantum calibrated stray-field maps. This approach overcomes limitations of prior MFM calibration schemes and allows quantum calibrated nanoscale stray-field measurements in a field range inaccessible to scanning NV magnetometry. Quantum calibrated measurements of a stray-field reference sample allow its use as a transfer standard, opening the road towards fast and easily accessible quantum traceable calibrations of virtually any MFM.

MA 32.4 Wed 15:45 HSZ 401

Controlled surface-modification to revive shallow NV⁻centers — •TONI HACHE^{1,5}, JEFFREY N. NEETHIRAJAN^{1,2,5}, DOMENICO PAONE^{1,2,5}, DINESH PINTO^{1,3}, ANDREJ DENISENKO², RAINER STÖHR², PÉTER UDVARHELYI⁴, ANTON PERSHIN⁴, ÁDÁM GALI⁴, JÖRG WRACHTRUP^{1,2}, KLAUS KERN^{1,3}, and APARAJITA SINGHA¹ — ¹Max Planck Institute for Solid State Research — ²3rd Institute of Physics and Research Center SCoPE, University of Stuttgart — ³Institute de Physique, École Polytechnique Fédérale de Lausanne — ⁴Wigner Research Centre for Physics, Institute for Solid State Physics and Optics, Hungarian Academy of Sciences — ⁵Equal contribution.

Nitrogen-vacancy (NV) centers in diamond have attracted an immense interest for non-invasive magnetic imaging and quantum sensing. All NV based magnetic sensing protocols rely on the negative charge state of this quantum sensor (NV⁻). In this work we demonstrate dramatic charge state conversions within individual NV centers at cryogenic (4.7 K) and $2 \cdot 10^{-10}$ mbar ultra-high-vacuum (UHV) conditions. The NV centers are characterized based on autocorrelation measurements, ODMR contrast and emission spectra. Under these extreme conditions, each of these measurements indicate a significant decrease of the relative occupancy of the NV⁻ charge state. Furthermore, we note a slight recovery of the NV⁻ charge state by dosing water (H₂O) on top of the diamond surface under UHV conditions. These results indicate that controlled surface treatments are essential for implementing NV center based quantum sensing protocols at cryogenic-UHV conditions.

MA 32.5 Wed 16:00 HSZ 401

Deep learning assisted reconstruction of the magnetization from the 2D antiferromagnetic van der Waals material CrSBr — •RICCARDO SILVIOLI, MICHELE BISSOLO, KARTIKAY TEHLAN, MARTIN SCHALK, FERDINAND MENZEL, NATHAN P. WILSON, ANDREAS V. STIER, and JONATHAN J. FINLEY — Walter Schottky Institute and TUM School of Natural Sciences, Technische Universität München

We investigate the layered antiferromagnet (AFM) CrSBr, a material with three phase transitions. Order within the layers ($T_{intra} \sim 160\text{K}$), order between the layers ($T_N \sim 135\text{K}$) and a low T phase close to 40K that is speculated to originate from the ordering of Br vacancies. We use widefield nitrogen vacancy (NV) vector magnetometry to investigate the magnetic phases of this material. We image the 3D magnetic stray field in the plane of the NV centers, located 100nm from the surface of the diamond. Retrieving information on the magnetization (M) from an NV measurement requires reconstruction of M. For out-of-plane M, this is an analytically solvable problem, whereas for in-plane M this problem is ill-posed. We employ a deep learning (DL) approach based on a convolutional neural network (CNN), in order to solve the inverse problem, and determine M from the data. We apply additional constraints to the CNN to follow Maxwell's equations by incorporating micro magnetic simulations in the computation of loss during the training phase. We discuss the advantages of this physics informed CNN training approach and compare it to conventional CNN methods as well as reconstruction efforts.

MA 32.6 Wed 16:15 HSZ 401

Magnetic imaging with spin defects in hexagonal boron nitride — PAWAN KUMAR¹, FLORENTIN FABRE¹, ALRIK DURAND¹, TRISTAN CLUA-PROVOST¹, JIAHAN LI², JAMES H. EDGAR², NICOLAS ROUGEMAILLE³, JOHANN CORAUX³, XAVIER MARIE⁴, PIERRE RENUCCI⁴, CÉDRIC ROBERT⁴, ISABELLE ROBERT-PHILIP¹, BERNARD GIL¹, GUILLAUME CASSABOIS¹, •AURORE FINCO¹, and VINCENT JACQUES¹ — ¹Laboratoire Charles Coulomb, Université de Montpellier, CNRS, Montpellier, France — ²Tim Taylor Department of Chemical Engineering, Kansas State University, Manhattan, Kansas, USA — ³Université Grenoble Alpes, CNRS, Grenoble INP, Institut Néel, Grenoble, France — ⁴Université de Toulouse, INSA-CNRS-UPS, LPCNO, Toulouse, France

Optically-active spin defects hosted in hexagonal boron nitride (hBN) are promising candidates for the development of a two-dimensional quantum sensing unit. Here, we demonstrate quantitative magnetic imaging with hBN flakes doped with negatively-charged boron-vacancy (V_B^-) centers through neutron irradiation [1]. As a proof-of-concept, we image the magnetic field produced by

CrTe₂, a van der Waals ferromagnet with a Curie temperature slightly above 300 K. The advantages of the hBN-based magnetic sensor described in this work are its ease of use, high flexibility and, more importantly, its ability to be placed in

close proximity to a target sample and included in van der Waals heterostructures.

[1] Kumar et al, arXiv 2207.10477 (2022).

MA 33: Frustrated Magnets I

Time: Wednesday 15:00–17:15

Location: HSZ 403

MA 33.1 Wed 15:00 HSZ 403

Frequency-resolved functional renormalization group for quantum magnetic systems — •JANIK POTTEN, TOBIAS MÜLLER, and RONNY THOMALE — Julius-Maximilians-Universität, Würzburg, Deutschland

Strongly correlated materials are one of the most prolific topics of contemporary condensed matter physics. Within this field, the functional renormalization group (FRG) approach for spin models relying on a pseudo-fermionic description has proven to be a very powerful technique in simulating ground state properties of strongly frustrated magnetic lattices. However, the FRG as well as many other theoretical models, suffer from the fact that they are formulated in the imaginary-time Matsubara formalism and thus are only able to predict static correlations directly. Nevertheless, describing the dynamical properties, especially of magnetic systems is one of the fundamental theoretical challenges, as they are the key to bridging the gap to experimental data from neutron scattering experiments. For the pseudo-fermion FRG, we remedy this shortcoming by establishing a methodical approach based on the Keldysh formalism, originally developed to handle non-equilibrium physics. This novel approach allows for calculating the dynamic properties of spin systems on arbitrary lattices. We can identify the correct low-energy behavior of the dynamic spin structure factors for exemplary nearest neighbor Heisenberg systems. These first results are promising and extensions of this work might allow for an easy calculation of dynamic properties even for non-equilibrium magnetic systems in the future.

MA 33.2 Wed 15:15 HSZ 403

Spin functional renormalization group for the $J_1J_2J_3$ quantum Heisenberg model — DMYTRO TARASEVYCH, •ANDREAS RÜCKRIEGEL, SAVIO KEUPERT, VASILIOS MITSIOANNOU, and PETER KOPIETZ — Institut für theoretische Physik, Universität Frankfurt

We use our recently developed functional renormalization group (FRG) approach for quantum spin systems to investigate the phase diagram of the frustrated $J_1J_2J_3$ quantum Heisenberg model on a cubic lattice. From a simple truncation of the hierarchy of FRG flow equations for the irreducible spin-vertices which retains only static spin fluctuations and neglects the flow of the four-spin interaction, we can estimate the critical temperature with a similar accuracy as the numerically more expensive pseudofermion FRG. In the regime where the ground state exhibits either ferromagnetic or antiferromagnetic order, a more sophisticated truncation including the renormalization of the four-spin interaction as well as dynamic spin fluctuations reveals the underlying renormalization group fixed point and yields critical temperatures which deviate from the accepted values by at most 4%.

MA 33.3 Wed 15:30 HSZ 403

Thermal Hall conductivity near field suppressed magnetic order in a Kitaev Heisenberg model — •AMAN KUMAR and VIKRAM TRIPATHI — Tata Institute Of Fundamental Research, Mumbai, India

We investigate thermal Hall conductivity κ_{xy} of a J - K Kitaev-Heisenberg model with a Zeeman field in the (111) direction in the light of the recent debate surrounding the possible re-emergence of Ising topological order (ITO) and half-quantized κ_{xy}/T upon field-suppression of long-range magnetic order in Kitaev materials. We use the purification-based finite temperature Tensor Network approach making no prior assumptions about the nature of the excitations: Majorana, visons or spin waves. For purely Kitaev interactions and fields $h/K \geq 0.02$ sufficient to degrade ITO, the peak κ_{xy}/T monotonously decreases from half-quantization associated with lower fields - a behavior reminiscent of vison fluctuation corrections. In our J - K model (with ferro- K and antiferro- J), in the vicinity of field-suppressed magnetic order, we found κ_{xy}/T to be significant, with peak magnitudes exceeding half-quantization followed by a monotonous decrease with increasing h . We thus conclude that half-quantized thermal Hall effect, if found in our model in the vicinity of field suppressed magnetic order, is a fine-tuning effect and is not associated with a Majorana Hall state with ITO.

MA 33.4 Wed 15:45 HSZ 403

Thermal spin dynamics of Kitaev magnets — •OLIVER FRANKE — Institut für Theoretische Physik, Freie Universität Berlin, Arnimallee 14, 14195 Berlin, Deutschland

The honeycomb magnet α -RuCl₃ is a prime candidate material for realizing the Kitaev quantum spin liquid (QSL), but it shows long-range magnetic order at low temperature. Nevertheless, its broad inelastic neutron scattering (INS) response at finite frequency has been interpreted as that of a 'proximate QSL'. A moder-

ate magnetic field indeed melts the residual zigzag order, giving rise to peculiar intermediate field phases before the high-field polarized state.

Are the scattering continua observed in experiments signatures of quantum fractionalized excitations in a QSL phase? Or are they caused by thermal fluctuations that break the large unit cell intermediate field phases predicted by theory? In this talk, I will present our recent study on the subject, which helps to answer these topical questions and highlights the importance of distinguishing finite temperature fluctuations from genuine quantum fractionalization signatures in frustrated magnets.

15 min. break

MA 33.5 Wed 16:15 HSZ 403

Disorder effects in the Kitaev-Heisenberg model — •AYUSHI SINGHANIA¹, JEROEN VAN DEN BRINK^{1,2}, and SATOSHI NISHIMOTO^{1,2} — ¹Institute for Theoretical Solid State Physics, IFW Dresden, 01069 Dresden, Germany — ²Department of Physics, Technical University Dresden, 01069 Dresden, Germany

We study the interplay of disorder and Heisenberg interactions in Kitaev model on honeycomb lattice. The effect of disorder on the transition between Kitaev spin liquid and magnetic ordered states as well as the stability of magnetic ordering is investigated. Using Lanczos exact diagonalization we discuss the consequences of two types of disorder: random-coupling disorder & singular-coupling disorder. They exhibit qualitatively similar effects in the pure Kitaev-Heisenberg model without long-range interactions. The range of spin liquid phases is reduced and the transition to magnetic ordered phases becomes more crossover-like. Furthermore, the long-range zigzag and stripy orderings in the clean system are replaced by their three domains with different ordering direction. Especially in the crossover range the coexistence of magnetically ordered and Kitaev spin-liquid domains is possible. Surprisingly, in presence of long range interactions, the stability of magnetic ordered state is diminished by singular-coupling disorder, and accordingly, the range of spin-liquid regime is extended. This mechanism may be relevant to materials like α -RuCl₃ and H₃LiIr₂O₆ where the zigzag ground state is stabilized by weak long-range interactions. We also find that the flux gap closes at a critical disorder strength and vortices appears in the flux arrangement.

MA 33.6 Wed 16:30 HSZ 403

ZnCr₂Se₄ as a spiral-spin-liquid approximant — •D. S. INOSOV¹, Y. V. TYMOSHENKO¹, A. AKOPYAN², D. SHUKLA², N. PRASAI², M. DOERR¹, D. GORBUNOV³, S. ZHERLITSYN³, D. J. VONESHEN^{4,5}, M. BOEHM⁶, V. TSURKAN^{7,8}, V. FELEA⁸, A. LOIDL⁷, Y. O. ONYKIENKO¹, J. OLLIVIER⁶, and J. L. COHN² — ¹IFMP, TU Dresden — ²University of Miami, Florida, USA — ³Hochfeld-Magnetlabor Dresden-Rossendorf — ⁴ISIS Facility, RAL, Didcot, UK — ⁵Royal Holloway University of London, UK — ⁶Institut Laue-Langevin, Grenoble, France — ⁷Institute of Physics, University of Augsburg — ⁸Institute of Applied Physics, Chisinau, Moldova

We investigated the cubic spinel helimagnet ZnCr₂Se₄ in its single-domain spin-spiral state by a combination of neutron scattering, thermal conductivity, ultrasound velocity, and dilatometry measurements. In zero magnetic field, the magnon spectrum consists of conventional gapless Goldstone modes and soft pseudo-Goldstone modes with a small energy gap of ~ 0.17 meV. In an applied magnetic field, this gap closes nonmonotonically, so that upon reaching a critical field of 6 T, the gap vanishes over a whole 2D manifold in the reciprocal space. This was recently identified as a prerequisite for a putative spiral-spin-liquid ground state [see S. Gao *et al.*, Phys. Rev. Lett. **129**, 237202]. This highly unusual behavior of the spin gap causes large anomalies in thermal conductivity at subkelvin temperatures — nearly two orders of magnitude below the Néel temperature. Our results apply to a broad class of centrosymmetric Heisenberg helimagnets where discrete lattice symmetry is spontaneously broken by the magnetic order.

MA 33.7 Wed 16:45 HSZ 403

Magneto-elastic coupling and new phases in the Shastry-Sutherland compound NdB₄ discovered by high-resolution dilatometry — •RAHEL OHLENDORF¹, SVEN SPACHMANN¹, LUKAS FISCHER¹, DANIEL BRUNT², JASPER LINNARTZ³, STEFFEN WIEDMANN³, GEETHA BALAKRISHNAN², OLEG PETRENKO², and RÜDIGER KLINGELER¹ — ¹Kirchhoff Institute for Physics, Heidelberg, Germany — ²Department of Physics, University of Warwick, Coventry, UK — ³HFML Nijmegen, Netherlands

We report high-resolution dilatometry studies on single crystals of the Shastry-Sutherland-lattice magnet NdB₄ supported by specific heat and magnetometry data. The evolution of magnetically ordered phases below $T_N = 17.2$ K (commensurate antiferromagnetic phase), $T_{IT} = 6.8$ K (intermediate incommensurate phase), and $T_{LT} = 4.8$ K (low-temperature phase) is associated with pronounced anomalies in the thermal expansion coefficients. The data imply significant magneto-elastic coupling and evidence of a structural phase transition at T_{LT} . Grüneisen analysis of the ratio of thermal expansion coefficient and specific heat enables the derivation of uniaxial as well as hydrostatic pressure dependencies. From the observed anomalies the magnetic phase diagrams for B||c up to 15 T and for B||[110] up to 35 T are constructed. New in-field phases are discovered for both field directions and already known phases are confirmed. In particular, phase boundaries are unambiguously shown by sign changes of observed anomalies and corresponding changes in uniaxial pressure effects.

MA 33.8 Wed 17:00 HSZ 403

Emergent U(1) symmetry due to off-diagonal symmetric exchange interactions — •SAGAR RAMCHANDANI, CIARÁN HICKEY, and SIMON TREBST — Institute for Theoretical Physics, University of Cologne, Germany

Frustrated magnetic systems are a result of competing interactions. These systems are of interest as they can exhibit a large ground state degeneracy, sometimes in the form of an emergent symmetry for the ground state.

Here, we study the effects of off-diagonal symmetric exchange interactions on classical O(3) spins on the Kagome lattice. We find an emergent U(1) symmetry in the ground state. We study the critical properties and the influence of thermal order-by-disorder on this symmetry using a combination of analytical and Monte Carlo methods.

The symmetry can be understood on the level of a single triangle. Using this understanding, we also propose a set of rules to generate a lattice model with these off-diagonal interactions that will exhibit the same emergent U(1) symmetry. The rules combine N triangles exhibiting N*U(1) symmetries into a single U(1) symmetry. These lattices can be generated in 1D, 2D & 3D.

MA 34: Focus Session: Spin-Phonon Coupling

Recent work on ultrafast demagnetization in ferromagnets has demonstrated that angular momentum can be transferred from the spin system to the lattice on ultrashort time scales. These findings demonstrate that a detailed understanding of the mechanisms that transfer angular momentum between the spin system and the lattice are of key importance in spintronics. The goal of this focus session is to give an overview over spin-phonon coupling effects in solids, ranging from the Einstein-de Haas effect on ultrafast time scales to magnon-phonon coupling and acoustic spin pumping at GHz frequencies. Coordinators: Tobias Kampfrath, Freie Universität Berlin and Uli Nowak, Universität Konstanz.

Time: Thursday 9:30–13:00

Location: HSZ 02

Invited Talk

MA 34.1 Thu 9:30 HSZ 02

Polarized phonons carry angular momentum in ultrafast demagnetization —

•PETER BAUM — Universität Konstanz, Germany

Many laser-excited magnetic materials lose their magnetic order almost completely within femtosecond timescales, but where is the missing angular momentum in such a short time? Here we use ultrafast electron diffraction with THz-compressed electron pulses to reveal in nickel an almost instantaneous, long-lasting, non-equilibrium population of anisotropic high-frequency phonons with an anisotropy plane that is perpendicular to the direction of the initial magnetization. We explain these observations by means of circularly polarized phonons that quickly absorb the angular momentum of the spin system before macroscopic sample rotation. The time that is needed for demagnetization is related to the time it takes to accelerate the atoms. These results provide an atomistic picture of the Einstein-de Haas effect and signify the general importance of polarized phonons for non-equilibrium dynamics and phase transitions.

Invited Talk

MA 34.2 Thu 10:00 HSZ 02

Spin-phonon coupling in ordered magnets: origin and consequences —

•AKASHDEEP KAMRA — Universidad Autónoma de Madrid, Madrid, Spain

Interaction between the spin and lattice degrees of freedom in magnets underlies a broad range of phenomena from magnetic damping to the Einstein-de Haas effect. Despite its long history and high importance, an adequate understanding of spin-phonon coupling's origin and potential consequences have eluded us. In this talk, we will discuss the microscopic mechanisms and related symmetry-breaking that underlie the spin-phonon coupling thereby achieving guidance on how to engineer it. In this discussion, we will pay special attention to the rotational invariance or total angular momentum conservation and how to account for it in the simulation of coupled spin and lattice dynamics. Then, we will examine some of the direct consequences of this coupling, focusing on magnon-polaron formation in ferro and antiferromagnets as well as the Einstein-de Haas effect in magnetic nanoparticles. If time permits, we will briefly discuss future directions and challenges.

References:

- [1] M. Weisshofer et al., arXiv:2211.02382.
- [2] H. T. Simensen et al., Phys. Rev. B 99, 064421 (2019).
- [3] A. Kamra et al., Phys. Rev. B 91, 104409 (2015).

Invited Talk

MA 34.3 Thu 10:30 HSZ 02

Magnon-mechanics in high overtone acoustic resonators — •HANS HUEBL — Walther-Meißner-Institut, Bayerische Akademie der Wissenschaften, Garching, Germany — School of Natural Sciences, Technische Universität München, Garching, Germany — 3Munich Center for Quantum Science and Technology (MCQST), Munich, Germany

Magnetoelastic coupling between excitation modes of the spin system (spin waves) and the lattice (phonons) is of interest from a fundamental perspective

and can enable mode hybridization. For quantum sensing and transduction protocols, excitation exchange between the magnetic and elastic systems is of importance, however typically this requires strong coupling between the modes. In this presentation, I will present our current results on coupling the magnetization dynamics of a Kittel mode to a high-overtone bulk acoustic resonator and discuss this hybrid system in the context of sensing and transduction.

15 min. break

Invited Talk

MA 34.4 Thu 11:15 HSZ 02

Cavity Magnomechanics: Harnessing the Magnomechanical Coupling for Applications in the Microwave and Optical Regimes —

•SILVIA VIOLA KUSMINSKIY — Institute for Theoretical Condensed Matter, RWTH Aachen University, 52074 Aachen, Germany — Max Planck Institute for the Science of Light, Staudtstr. 2 91058 Erlangen, Germany

Cavity magnonic systems are ideally suited to explore the range of possibilities opened by tailoring the interactions between photons, phonons, and magnons. In this talk I will discuss the different coupling mechanisms and propose applications ranging from quantum thermometry to wavelength conversion.

Invited Talk

MA 34.5 Thu 11:45 HSZ 02

Coherent spin-wave transport in an antiferromagnet —

•ANDREA CAVIGLIA — Department of Quantum Matter Physics, University of Geneva, 24 Quai Ernest Ansermet, CH-1211 Geneva, Switzerland

Magnonics is a research field complementary to spintronics, in which the quanta of spin waves replace electrons as information carriers, promising lower dissipation. The development of ultrafast, nanoscale magnonic logic circuits calls for new tools and materials to generate coherent spin waves with frequencies as high and wavelengths as short as possible. Antiferromagnets can host spin waves at terahertz frequencies and are therefore seen as a future platform for the fastest and least dissipative transfer of information. However, the generation of short-wavelength coherent propagating magnons in antiferromagnets has so far remained elusive. Here we report the efficient emission and detection of a nanometre-scale wavepacket of coherent propagating magnons in the antiferromagnetic oxide dysprosium orthoferrite using ultrashort pulses of light. The subwavelength confinement of the laser field due to large absorption creates a strongly non-uniform spin excitation profile, enabling the propagation of a broadband continuum of coherent terahertz spin waves. The wavepacket contains magnons with a shortest detected wavelength of 125nm that propagate into the material with supersonic velocities of more than 13kms⁻¹. This source of coherent short-wavelength spin carriers opens up new prospects for terahertz antiferromagnetic magnonics and coherence-mediated logic devices at terahertz frequencies.

MA 34.6 Thu 12:15 HSZ 02

Magnon-phonon coupling in polycrystalline metallic thin films — •MANUEL MÜLLER^{1,2}, JOHANNES WEBER^{1,2}, FABIAN ENGELHARDT^{3,4,5}, VICTOR A. S. V. BITTENCOURT^{3,6}, THOMAS LUSCHMANN^{1,2,7}, SILVIA VIOLA KUSMINSKIY^{5,3}, STEPHAN GEPRÄGS¹, RUDOLF GROSS^{1,2,7}, MATTHIAS ALTHAMMER^{1,2}, and HANS HUEBL^{1,2,7} — ¹Walther-Meißner-Institut, Bayerische Akademie der Wissenschaften, Garching, Germany — ²TUM School of Natural Sciences, Technische Universität München, Garching, Germany — ³Max Planck Institute for the Science of Light, Erlangen, Germany — ⁴Department of Physics, University Erlangen-Nuremberg, Erlangen, Germany — ⁵Institute for Theoretical Solid State Physics, RWTH Aachen University, Aachen, Germany — ⁶ISIS (UMR 7006), Université de Strasbourg, 67000 Strasbourg, France — ⁷Munich Center for Quantum Science and Technology (MCQST), Munich, Germany

Magnetoelastic coupling between wave-like excitations of the spin system (spin waves) and the lattice (elastic waves) can result in a hybridization of both modes. This is of interest for future applications, such as microwave-to-optics transducers and phononic spin valve devices. As a finite magnetoelastic coupling affects the magnetization dynamics of the magnetic layer, it can be characterized with high sensitivity using ferromagnetic resonance spectroscopy. By using broadband ferromagnetic resonance spectroscopy, we have studied the magnetoelastic coupling between silicon and sapphire substrates and ferromagnetic thin films deposited on them via DC sputtering.

MA 34.7 Thu 12:30 HSZ 02

Parametric excitation and instabilities of spin waves driven by surface acoustic waves — •MORITZ GEILEN¹, ROMAN VERBA², ALEXANDRA NICOLOIU³, DANIELE NARDUCCI⁴, ADRIAN DINESCU², MILAN ENDER¹, MORTEZA MOHSENI¹, FLORIN CIUBOTARU⁴, MATHIAS WEILER¹, ALEXANDRU MÜLLER³, BURKARD HILLEBRANDS¹, CHRISTOPH ADELMANN⁴, and PHILIPP PIRRO¹ — ¹Fachbereich Physik und Landesforschungszentrum OPTIMAS, RPTU Kaiserslautern Landau, Germany — ²Institute of Magnetism, Kyiv, Ukraine — ³National Institute for Research and Development in Microtechnologies, Bucharest, Romania — ⁴imec, Leuven, Belgium

We present our experimental results on the parametric excitation of spin waves by coherent surface acoustic waves in metallic magnetic thin film structures.

The involved magnon modes are analyzed with micro-focused Brillouin light scattering spectroscopy and complementary micromagnetic simulations combined with analytical modelling to determine the origin of the spin-wave instabilities. Depending on the experimental conditions, we observe spin-wave instabilities originating from different phonon-magnon and magnon-magnon scattering processes. Our results demonstrate that an efficient excitation of high amplitude, strongly nonlinear magnons in metallic ferromagnets is possible by surface acoustic waves, which opens novel ways to create micro-scaled nonlinear magnonic systems for logic and data processing.

We acknowledge financial support by EU via EU Horizon 2020 (contract no.801055) and ERC Starting Grant No. 101042439.

MA 34.8 Thu 12:45 HSZ 02

Magnetic ordering and spin-lattice interactions in $M\text{CrO}_2$ and $M\text{CrS}_2$ (with $M = \text{Li, Na, K, Cu, Ag, Au}$) — •S. MANKOVSKY, H. LANGE, S. POLESYA, and H. EBERT — Department Chemie, Ludwig Maximilian University, Munich, Germany

The triangular lattice antiferromagnets (TLA) are discussed in the literature as materials exhibiting a variety of magneto-elastic and magneto-electric properties determined by a complex magnetic structure driven by magnetic frustrations. In the present work we have investigated two groups of TLA compounds, $M\text{CrO}_2$ and $M\text{CrS}_2$, with $M = \text{Li, Na, K, Cu, Ag, Au}$. Their properties are discussed on the basis of first-principles calculations of their electronic structure as well as exchange coupling and spin-lattice coupling (SLC) parameters. The properties of these two groups are expected to be quite different, among others, because of a different distance dependency of the Cr-Cr exchange interactions. In particular one finds that the Cr layers in $M\text{CrS}_2$ cannot be treated as independent, in contrast to $M\text{CrSO}_2$ with quasi-2D frustrated AFM Cr layers. We discuss different contributions to the magnon-phonon interaction responsible for a modification of the phonon spectra in these materials, as well as a transition to the AFM state in some of them, accompanied by a lattice distortion as observed by experiment. In addition, a contribution of the inverse Dzyaloshinskii-Moriya (DM) interaction mechanism [PRL **95**, 057205 (2005)] to the ferroelectric properties driven by the magnetic ordering is discussed on the basis of the calculated DM-SLC parameters.

MA 35: Skyrmions III

Time: Thursday 9:30–12:00

Location: HSZ 04

MA 35.1 Thu 9:30 HSZ 04

Skyrmion dynamics and applications — •ISMAEL RIBEIRO DE ASSIS, INGRID MERTIG, and BÖRGE GÖBEL — Martin-Luther-Universität Halle-Wittenberg, Halle, Germany

Skyrmionics and neuromorphics are among the most promising fields of physics with the perspective of creating future devices and technologies. Magnetic skyrmions are nanoscale magnetic whirls that are topologically protected and can be moved by currents, leading to the prediction of several applications. Its topological charge leads to high stability; however, it also leads to the skyrmion Hall effect. From memory storage devices, like the racetrack memory [1], to computing devices, like artificial neurons[2,3], this shortcoming is one of the primary reasons why skyrmion-based spintronic devices have yet to be achieved. Here, we study the motion of skyrmions with different topological charges and helicities. Using an effective center-of-mass description of these magnetic quasiparticles, namely, the Thiele equation, we analyze their dynamics under different gradient landscapes and interactions aiming to suppress or take advantage of the skyrmion Hall effect. Additionally, we discuss possible applications in neuromorphic computing. [1] A. Fert et al., Nature Nanotechnology **8**, 152-156(2013) [2] S. Li et al., Nanotechnology **28**, 31LT01 (2017) [3] I.R. de Assis et al., arXiv preprint arXiv:2209.11017 (2022).

MA 35.2 Thu 9:45 HSZ 04

Moving Antiferromagnetic Skyrmions with Spin Waves — •MICHAEL LAU^{1,2}, WOLFGANG HÄUSLER³, and MICHAEL THORWART^{1,2} — ¹I. Institut für Theoretische Physik, Universität Hamburg — ²The Hamburg Centre for Ultrafast Imaging, Universität Hamburg — ³Institute of Physics, University of Augsburg

The possibility to move magnetic Skyrmions opens the pathway of technical applications in the form of nanoscale information carriers. While it is well-studied for ferromagnetic materials that spin waves are able to move Skyrmions, driving antiferromagnetic Skyrmions with spin waves is a relatively new topic. We present simulations on a two-dimensional lattice, with classical magnetic moments on each site, which reveal that antiferromagnetic Skyrmions can be accelerated by spin waves injected at one edge of the lattice. We consider in detail various forms of spin waves and draw connections between Skyrmion behavior and the spin wave attributes. To this end we analytically and numerically investigate classical antiferromagnetic spin waves at first. We derive a consistent analytical description of circularly- and linearly polarized spin waves and the two

modes of each polarization. Using this knowledge we investigate their impact on the Skyrmion and show that the symmetries of the spin wave modes is reflected in the resulting Skyrmion motion. One example is the non-vanishing Skyrmion Hall effect for circularly polarized spin waves. It turns out that also frequency and amplitude of the spin waves significantly influence the Skyrmion motion.

MA 35.3 Thu 10:00 HSZ 04

Geometry-induced motion of magnetic skyrmions in curved ferro- and antiferromagnetic films — •KOSTIANTYN V. YERSHOV^{1,2}, ATTILA KÁKAY³, and VOLODYMYR P. KRAVCHUK^{2,4} — ¹Leibniz Institute for Solid State and Materials Research, Dresden, Germany — ²Bogolyubov Institute for Theoretical Physics, Kyiv, Ukraine — ³Helmholtz-Zentrum Dresden-Rossendorf e.V., Institute of Ion Beam Physics and Materials Research, Germany — ⁴Institut für Theoretische Festkörperphysik, Karlsruher Institut für Technologie, Germany

Here, we present the effect of the spontaneous drift of a magnetic skyrmion in curved films under the action of the curvature gradients without any external stimuli [1]. The strength of the curvature-induced driving is determined by the type of the intrinsic Dzyaloshinskii-Moriya interaction, while the trajectory is determined by the type of magnetic ordering: ferro- or antiferromagnetic. Using rigid particle approximation, we show that for the case of Néel skyrmion the driving force is linear with respect to the gradient of the curvature, while for Bloch skyrmion the driving is proportional to the product of mean curvature and its gradient. During the motion along the surface, skyrmion experiences deformation which depends on the skyrmion type. Equations of motion for Néel and Bloch magnetic skyrmions in curved ferromagnetic and antiferromagnetic materials are obtained in terms of collective variables. [1] K. Yershov et al, PRB **105** (2022), 054425.

MA 35.4 Thu 10:15 HSZ 04

Non-equilibrium dynamics of quantum skyrmion upon projective measurements — •FABIO SALVATI, ANDREY BAGROV, TOM WESTERTHOUT, and MIKHAIL I. KATSNELSON — Institute for Molecules and Materials, Radboud University, Heijendaalseweg 135, 6525 AJ Nijmegen, The Netherlands

Magnetic skyrmions are particle-like spin structures characterized by nanometer size and long lifetime. These remarkable properties make them a promising candidate for the role of information carriers in magnetic information storage and processing devices.

Although considerable progress has been made in studying skyrmions in classical systems, little is known about skyrmions in quantum systems, since the quantum skyrmion state cannot be directly observed probing the local magnetization of the system. A characterization is possible using the scalar chirality - a particular local three-spin correlation function defined on neighboring lattice sites - as a quantum analog of the skyrmionic topological index.

In our work, we use the scalar chirality to investigate the local dynamics of a quantum skyrmion on a triangular lattice, following a projective measurement. Findings reveal the robustness of the quantum skyrmion state supported by spin waves. Besides we identify a feature to detect experimentally quantum skyrmions, performing the analysis of the Fourier transform of the spin-spin correlation function.

MA 35.5 Thu 10:30 HSZ 04

Nonlinear dynamics of skyrmion strings — •VOLODYMYR KRAVCHUK^{1,2} and MARKUS GARST¹ — ¹Institut für Theoretische Festkörperphysik, Karlsruher Institut für Technologie, 76131 Karlsruhe, Germany — ²Bogolyubov Institute for Theoretical Physics of the National Academy of Sciences of Ukraine, 03143 Kyiv, Ukraine

A skyrmion core, percolating the magnet volume, forms a skyrmion string – the topological Dirac string-like object. Here we analyze the nonlinear dynamics of a skyrmion string in a low-energy regime by means of the collective variables approach generalized for the case of strings. Using the perturbative method of multiple scales (both in space and time), we show that the weakly nonlinear dynamics of the translational mode propagating along the string is captured by the Nonlinear Schrödinger equation of the focusing type. As a result, the fundamental helix-shaped “planar-wave” solution experiences modulational instability, which leads to the formation of cnoidal waves. Both types of cnoidal waves, dn- and cn-waves, as well as the separatrix soliton solution [1], are confirmed by the micromagnetic simulations. Beyond the class of the traveling-wave solutions, we found Ma-breather propagating along the string. Finally, we proposed a generalized approach, which enables one to describe nonlinear dynamics of the modes of different symmetries, radially symmetrical, elliptical, etc.

[1] V.P. Kravchuk, U.K. Rößler, J. van den Brink, M. Garst, Phys. Rev. B 102, 220408(R) (2020).

15 min. break

MA 35.6 Thu 11:00 HSZ 04

Manipulation of Skyrmion Helicity in Frustrated Magnets — •ROSS KNAPMAN^{1,2}, TIMON TAUSENDPFUND¹, SEBASTIÁN A. DÍAZ², and KARIN EVERSCHOR-SITTE^{2,3} — ¹Institute of Physics, Johannes Gutenberg University Mainz, 55128 Mainz, Germany — ²Faculty of Physics, University of Duisburg-Essen, 47057 Duisburg, Germany — ³Center for Nanointegration Duisburg-Essen (CENIDE), University of Duisburg-Essen, 47057 Duisburg, Germany

Aside from the well-studied mechanisms of the stabilisation of magnetic skyrmions via the Dzyaloshinskii-Moriya interaction, skyrmions can be stabilised with magnetic frustration. [1] In such a system, the helicity becomes a degree of freedom which can be manipulated using externally-applied electric and magnetic fields. [2,3] In our work, we use a Ginzburg-Landau description of the system [4] to model the dynamics of the skyrmion using analytical and numerical approaches. In tuning in the time dependences of the electric and magnetic fields, we can manipulate the energy landscape to induce interesting phenomena, including helicity rotations.

[1] Okubo, T., Chung, S., Kawamura, H., Phys. Rev. Lett. **108**, 017206 (2012)

[2] Y., X., Chen, J., Dong, S., New J. Phys. **22**, 083032 (2020)

[3] Psaroudaki, C., Panagopoulos, C., Phys. Rev. Lett. **127**, 067201 (2021)

[4] Lin, S. Z., Hayami, S., Phys. Rev. B **93**, 064430 (2016)

MA 35.7 Thu 11:15 HSZ 04

Non-synthetic antiferromagnetic multi-meronic Néel spin-textures in thin films — •AMAL ALDARAWSEH^{1,2}, MORITZ SALLERMANN^{1,3,4}, MUAYAD ABUSAA⁵, and SAMIR LOUNIS^{1,2} — ¹Peter Grünberg Institute and Institute for Advanced Simulation, Forschungszentrum Jülich and JARA, D-52425 Jülich,

Germany — ²Faculty of Physics, University of Duisburg-Essen and CENIDE, 47053 Duisburg, Germany — ³RWTH Aachen University, 52056 Aachen, Germany — ⁴Science Institute and Faculty of Physical Sciences, University of Iceland, VR-III, 107 Reykjavík, Iceland — ⁵Arab American University, Jenin, Palestine

The realization of topological antiferromagnetic (AFM) solitons in real materials is a major goal towards their use in information technology. In contrast to their ferromagnetic version, they are expected to be insensitive to the Hall effect and dipolar interactions. Here, based on density functional theory in conjunction with atomistic spin dynamics, we predict the emergence in a triangular lattice of complex Néel AFM vortex-antivortex structures in transition metallic thin films interfaced with Ir and Pd layers. These topological structures are intrinsic, i.e. they form in a single AFM material, but are different from the recently predicted intrinsic AFM skyrmions [1]. They can carry various topological charges and can combine in hexameronic or dodecameronic textures, which can show enhanced stability with respect to external magnetic field depending on the electronic nature of the interfaces. [1] A. Aldarawsheh et al., ArXiv:2202.12090 (2022). Work funded by the PGSB (BMBF-01DH16027) and DFG (SPP 2137; LO 1659/8-1).

MA 35.8 Thu 11:30 HSZ 04

Investigation of the stability of exchange-stabilized skyrmions — •SARINA LEBS¹, MARKUS HOFFMANN¹, MORITZ SALLERMANN^{1,2}, and STEFAN BLÜGEL¹ — ¹Peter Grünberg Institut & Institute for Advanced Simulation, Forschungszentrum Jülich & JARA, Jülich, Germany — ²Science Institute of the University of Iceland, VR-III, Reykjavík, Iceland

To utilize magnetic skyrmions, localized topologically nontrivial textures, in technological applications, a long lifetime at room temperature is required. Therefore, a major focus of magnetism research is the analysis of the stability of such skyrmions. The main focus in the past was on DMI-stabilized skyrmions, little is known about exchange stabilized ones.

In this presentation, we discuss the significance of the different stabilization mechanisms for the skyrmion lifetimes. Using the Spirit code [1], we perform LLG, GNEB, as well as HTST simulations to calculate skyrmion profiles, transition paths, and lifetimes for both DMI- as well as exchange-stabilized skyrmions. We discuss similarities as well as differences between the stabilization mechanisms for the lifetime.

We acknowledge funding by the European Research Council (ERC) under the European Union's Horizon 2020 research and innovation programme (Grant No. 856538, project 3D MAGiC).

[1] Spirit - spin simulation framework, <https://spirit-code.github.io>

MA 35.9 Thu 11:45 HSZ 04

Lifetime of coexisting sub-10 nm zero-field skyrmions and antiskyrmions — •MORITZ A. GOERZEN¹, STEPHAN VON MALOTTKI^{1,2,3}, SEBASTIAN MEYER^{1,4}, PAVEL F. BESSARAB^{2,5}, and STEFAN HEINZE¹ — ¹ITAP, University of Kiel, Germany — ²Science Institute of the University of Iceland, Iceland — ³Thayer School of Engineering, Dartmouth College, USA — ⁴Nanomaterials/CESAM Université de Liège, Belgium — ⁵Department of Physics and Electrical Engineering, Linnaeus University, Sweden

Localized spin structures such as magnetic skyrmions have raised high hopes for future spintronic devices. For many applications it can be of great advantage to have more than one particle-like texture available. The coexistence of skyrmions and antiskyrmions has been proposed in inversion symmetric magnets with exchange frustration. However, so far only model systems have been discussed and the interplay with the Dzyaloshinskii-Moriya interaction (DMI) has not been studied. Here, we predict that skyrmions and antiskyrmions with diameters below 10 nm can coexist at zero magnetic field in a Rh/Co bilayer on the Ir(111) surface. Based on an atomistic spin model parameterized from density functional theory, we show that the lifetimes of metastable skyrmions and antiskyrmions in the ferromagnetic ground state are above one hour for temperatures up to 75 K and 48 K, respectively. The entropic contribution to nucleation and annihilation rates is different for skyrmions and antiskyrmions. This opens the route to thermal control of coexisting skyrmions and antiskyrmions in frustrated magnets with DMI.

MA 36: Magnetic Particles / Clusters

Time: Thursday 9:30–11:00

Location: HSZ 401

MA 36.1 Thu 9:30 HSZ 401

Magnetic properties of metastable single-crystalline cobalt iron oxide nanoflakes investigated by Mössbauer spectroscopy — SOMA IRALAMON¹, JOACHIM LANDERS¹, •ANNA RABE^{1,2}, FRANZ-PHILIPP SCHMIDT³, THOMAS LUNKENBEIN³, MALTE BEHRENS², and HEIKO WENDE¹ — ¹Faculty of Physics and CENIDE, University of Duisburg-Essen — ²Institute of Inorganic Chemistry, Kiel University — ³Department of Inorganic Chemistry, Fritz Haber Institute of the Max Planck Society

Spinel-type transition metal oxides are of high interest for a variety of applications, including heterogeneous catalysis, energy conversion and magnetic materials with fine-tuned properties. The compound Co_2FeO_4 is of particular interest, but its phase diagram contains a large immiscibility. Using Mössbauer spectra recorded at low temperatures (4.3 K) and high magnetic fields (10 T), we were able to precisely determine the distribution of Fe ions across tetrahedral and octahedral sites. This enabled us to characterize the influence of different calcination temperatures from 400 °C up to 900 °C on the phase composition and

miscibility, while also providing valuable insights on the temperature dependent evolution of the spectral hyperfine structure. These findings were successfully correlated with results from magnetometry, showing clear signs of a change in magnetic properties based on different degrees of intermixing, interface area, and phase separation, as also supported by TEM and EDX measurements. Financial support by the German Research Foundation (DFG) via the CRC/TRR 247 (Project-ID 388390466, sub-project B02) is gratefully acknowledged.

MA 36.2 Thu 9:45 HSZ 401

Mössbauer spectroscopy study of anisotropic barium ferrite hybrid systems — •JURI KOPP¹, JOACHIM LANDERS¹, SOMA SALAMON¹, BENOÎT RHEIN³, HAJNALKA NÁDASI², DARJA LISJAK⁴, PATRICIJA HRIBAR BOŠTJANČIČ⁴, ALENKA MERTELJ⁴, ALEXEY EREMIN², ANNETTE SCHMIDT³, and HEIKO WENDE¹ — ¹Faculty of Physics and Center for Nanointegration Duisburg-Essen (CENIDE), University of Duisburg-Essen — ²Department of Nonlinear Phenomena, Institute for Experimental Physics, Otto von Guericke University Magdeburg — ³Department of Chemistry, Physical Chemistry, University of Cologne — ⁴Department of Complex Matter, Jožef Stefan Institute

Using anisotropic barium ferrite nanoplatelets in liquid or liquid crystalline (LC) environments, we obtain ferrofluids with anisotropic properties such as nematic formation of the platelets or a magneto-responsive LC system. The aim of this work is to study magnetic hybrid systems with temperature- and field-dependent Mössbauer spectroscopy, which gives us access to the diffusion processes of the particles via line broadening, and to the magnetic orientation behavior based on relative line intensity ratios. As barium ferrite exhibits a rather complex crystal structure, we use reference data of powder samples in order to investigate each individual iron sublattice position of this system. In an approach to analyze anisotropic diffusion and alignment processes more efficiently, spectra are recorded with gamma incidence direction perpendicular and parallel relative to the applied magnetic field. This work is supported by the DFG (LA5175/1-1).

MA 36.3 Thu 10:00 HSZ 401

High throughput analysis of surface-functionalized superparamagnetic particles in dynamic magnetic field landscapes — •YAHYA SHUBBAK^{1,2}, RICO HUHNSTOCK^{1,2}, KRISTINA DINGEL^{2,3}, BERNHARD SICK^{2,3}, and ARNO EHRESMANN^{1,2} — ¹Institute of Physics & Center for Interdisciplinary Nanostructure Science and Technology (CINSA-T), University of Kassel, D-34132 Kassel — ²AIM-ED - Joint Lab Helmholtzzentrum für Materialien & Energie, D-14109 Berlin — ³Intelligent Embedded Systems, University of Kassel, D-34121 Kassel

The precise manipulation of magnetic micro- and nano-particles in microfluidic environments opens new avenues for investigations of biomolecular analyte detection and interactions.[1] Motion control schemes based on a combination of static magnetic field landscapes superposed with external magnetic field pulses enable translatory motion control of magnetic particles at the nanoscale over macroscopic distances.[3] Here we demonstrate a novel method harnessing AI-enhanced fully-automated optical recognition algorithms [4] to analyze changes in the motion behaviour of such particles due to liquid mediated surface to surface (particle to substrate) interaction.

[1] Lim, B., Vavassori, P., Sooryakumar, R. & Kim, C. Nano/microscale magnetophoretic devices for biomedical applications. *J. Phys. D: Appl. Phys.* 50, 33002 (2017) [2] Lin, G., Makarov, D. & Schmidt, O. G. Magnetic sensing platform technologies for biomedical applications. *Lab on a chip* 17, 1884-1912 (2017) [3] Issadore, D. et al. Magnetic sensing technology for molecular analyses. *Lab on a chip* 14, 2385-2397

MA 36.4 Thu 10:15 HSZ 401

Reversible on-chip focusing and clustering of superparamagnetic beads using engineered magnetic domain patterns — •RICO HUHNSTOCK¹, LUKAS PAETZOLD¹, MAXIMILIAN MERKEL¹, PIOTR KUŚWIK², and ARNO EHRESMANN¹ — ¹Institute of Physics and Center for Interdisciplinary Nanostructure Science and Technology (CINSA-T), University of Kassel, Heinrich-Plett-Str. 40, D-34132 Kassel — ²Institute of Molecular Physics, Polish Academy of Sciences, M. Smoluchowskiego 17, Poznań 60-179, Poland

To realize fast and reliable point-of-care medical diagnostics, incorporating magnetic particles into a Lab-on-a-chip technology platform is considered promising. For sensitive detection, binding of the analyte species to surface-functionalized particles and subsequent formation of particle aggregates with the analyte acting as molecular bridges is a possible route [1]. As close proximity between particles is required for this scheme, we demonstrate in this work a locally defined focusing of superparamagnetic microparticles within an aqueous medium above a magnetically patterned flat substrate. Combining the magnetic stray field landscape that originates from periodic magnetic stripe domains of gradually decreasing/increasing length with external magnetic field pulses, converging and diverging motion trajectories were induced for the particles. Ultimately, this led to a controlled formation and decomposition of closely packed particle clusters. We will discuss how the observed behavior is determined by the acting forces and how it is influenced by the duration of the external field pulses.

[1] Rampini *et al.* (2021), *Scientific Reports*, 11(1):5302.

MA 36.5 Thu 10:30 HSZ 401

Distance- and size-dependence of the interactions within highly ordered magnetic nanoparticle mesocrystals — •NILS NEUGEBAUER^{1,2}, YI WANG³, MATTHIAS ELM^{1,2}, XINGCHEN YE³, CHRISTIAN HEILIGER^{1,4}, and PETER KLAR^{1,2} — ¹Institute of Experimental Physics I, Justus Liebig University Giessen, Heinrich-Buff-Ring 16, 35392 Giessen, Germany — ²Center for Materials Research (LaMa), Justus Liebig University Giessen, Heinrich-Buff-Ring 16, 35392 Giessen, Germany — ³Department of Chemistry, Indiana University, Bloomington, Indiana 47405, United States — ⁴Institute for Theoretical Physics, Justus Liebig University Giessen, Heinrich-Buff-Ring 16, 35392 Giessen, Germany

Ferromagnetic resonance (FMR) experiments in combination with micromagnetic simulations are employed to investigate and characterize dipolar interactions between magnetic nanoparticles (MNPs) within such mesocrystals. The MNPs investigated in this work consist of iron oxide (magnetite - Fe₃O₄) and are coated with non-magnetic polymers, forming highly ordered hexagonal monolayer crystals. The magnetic response of the regularly arranged hexagonal mesocrystals can be tuned in a controlled way by varying the thickness of the non-magnetic polymer coating of the MNPs and thus the lattice constant of the mesocrystal.

The spectral features show distinct dipolar coupling phenomena within the mesocrystal and reveal that the material parameters of the MNPs such as the magnetization and the magnetocrystalline anisotropy are reduced with respect to their bulk counterpart.

MA 36.6 Thu 10:45 HSZ 401

Monte Carlo simulation of the aggregation of confined superparamagnetic colloids — •JAVIER VALENZUELA^{1,2}, FRANCISCO GÁMEZ², and PERLA VIVEROS-MÉNDEZ³ — ¹Fritz Haber Institute of the Max Planck Society, Berlin, Germany — ²Complutense University of Madrid, Madrid, Spain — ³Autonomous University of Zacatecas, Zacatecas, Mexico

The properties of colloidal suspensions of superparamagnetic nanoparticles confined within inorganic and organic cavities have led to a number of interesting applications in areas such as nanomedicine, microfluidics, and nanorobotics. Therefore, predicting the morphology of the structures formed during the aggregation process of these particles under different scenarios is of key scientific interest.

In this work, the Monte Carlo and cluster-moving Monte Carlo methods have been employed to study the aggregated structures formed by magnetic particles confined in spherical (3D) and circular (2D) cavities. The impact of the number of particles, their initial configuration and the pair-potential model between the particles and between the particles and the cavity surface on the aggregated structure is assessed. Moreover, we present an improvement of the cluster-moving Monte Carlo method to increase the computational performance under curved confinement situations. This work provides insights that might prove useful for the development of more efficient simulation strategies that could play a crucial role in the design and prediction of new applications of this relevant type of colloidal systems.

MA 37: Magnetic Heuslers

Time: Thursday 9:30–11:00

Location: HSZ 403

MA 37.1 Thu 9:30 HSZ 403

Enhanced magnetism of antiphase boundaries in Fe₂CoAl compound — MARTIN FRIÁK¹, JOSEF GRACIAS², JANA PAVLŮ², and •MOJMIŘ ŠOB^{2,1} — ¹Inst. Phys. Mat., Czech Acad. Sci., Brno, Czech Rep. — ²Dept. Chem., Fac. Sci., Masaryk Univ., Brno, Czech Rep.

We performed a quantum mechanical examination of thermodynamic, structural, elastic, and magnetic properties of single-phase ferromagnetic Fe₂CoAl with a chemically disordered B2-type lattice with and without antiphase bound-

aries (APBs) with (001) crystallographic orientation. Fe₂CoAl was modeled using two different 54-atom supercells with atoms on the two B2 sublattices distributed according to the special quasi-random structure (SQS) concept. Both computational models used exhibited very similar formation energies (−0.243 and −0.244 eV/atom), B2-structure lattice parameters (2.849 and 2.850 Å), magnetic moments (1.266 and 1.274 μ_B/atom), practically identical single-crystal elastic constants (C₁₁ = 245 GPa, C₁₂ = 141 GPa, and C₄₄ = 132 GPa) and auxetic properties (the lowest Poisson ratio close to -0.1). In contrast to these similari-

ties, the averaged APB interface energies were observed to be 199 and 310 mJ/m² for the two models. The studied APBs increased the total magnetic moment by 6 and 8 % due to a volumetric increase as well as local changes in the coordination of Fe atoms (their magnetic moments are reduced for increasing number of Al neighbors but increased by the presence of Co). The APBs also enhanced the auxetic properties.

MA 37.2 Thu 9:45 HSZ 403

VTaNbAl: A new class of spin gapless semiconductor with topological non-trivial features — •DEEPIKA RANI¹, P. C. SREEPARVATHY², K. GOPI SURESH², RATNAMALA CHATTERJEE¹, and AFTAB ALAM² — ¹Department of Physics, Indian Institute of Technology Delhi, Hauz Khas, New Delhi 110016, India — ²Department of Physics, Indian Institute of Technology Bombay, Mumbai 400076, Maharashtra, India

We report the theoretical prediction of a new class of spin gapless semiconductor (SGS) hosting topological non-trivial features along with a fully compensated ferrimagnetic state in VTaNbAl, a quaternary Heusler alloy. Unlike conventional SGS, this new class of compound acquires a unique band structure with opposite spin characters in the valance and conduction band edges making them potential candidates for spin valves and large anomalous Nernst effect. Interestingly, despite of a compensated ferrimagnetic (CF) behavior, VTaNbAl shows a reasonably large anomalous Hall effect possibly arising from the intrinsic non-vanishing Berry curvature. The CF state breaks the time-reversal symmetry and hence opens the possibility of Weyl nodes. We found four pairs of Weyl nodes located near the Fermi level leading to the non-zero Berry curvature, and hence a large anomalous Hall conductivity (~ 100 S/cm). Our experimental synthesis confirms NbVTaAl to crystallize in a cubic Heusler structure with an A2-type disorder. Magnetization measurement shows a very small saturation moment, which agrees fairly well with our theoretical findings of fully compensated ferrimagnetism in the alloy.

MA 37.3 Thu 10:00 HSZ 403

Long range ordering in NiCoMnAl magnetic shape memory thin films with martensitic intercalations — •INGA ENNEN, DARIO STIERL, LAILA BONDIJO, and ANDREAS HÜTTEN — Thin Films and Physics of Nanostructures, Physics Department, Bielefeld University, 33615 Bielefeld, Germany

Magnetic shape memory Heusler alloys, like NiMnX (X=Al,Ga,Sn,In), are considered as promising materials for magnetocaloric cooling applications due to their magnetoelastic coupling near room temperature. In order to reduce the thermal hysteresis in NiCoMnAl thin films, the usage of alternating active transforming austenitic and martensitic intercalation layers are beneficial. Therefore, the stoichiometry of these two layers is chosen in such a way that their thermal hysteresis does not overlap. If the austenite active layers have a similar thickness compared to the martensite intercalations a 3D check board pattern becomes visible in HRTEM cross section images. The contrast is due to alternating martensite/austenite domains.

In this contribution we aim for an improved understanding of the 3D check board pattern formation. Therefore, the number of the alternating layers as well as the ratio between the thicknesses of the two different layers have been varied. The phase transition has been characterized by temperature dependent XRD and TEM analysis. Furthermore, freestanding Heusler films have been prepared and analyzed in comparison to the substrate-bounded systems.

MA 37.4 Thu 10:15 HSZ 403

Anomalous Hall effect in epitaxial thin films of the hexagonal Heusler MnPtGa noncollinear hard magnet — •EDOUARD LESNE¹, REBECA IBARRA^{1,2}, BUSHRA SABIR³, BACHIR OULADDIAF⁴, KETTY BEAUVOIS⁴, ALEXANDR SUKHANOV², RAFAL WAWRZYNCZAK¹, WALTER SCHNELLE¹, ANTON DEVISHVILI⁴, DMYTRO INOSOV², JACOB GAYLES³, CLAUDIA FELSER¹, and ANASTASIOS MARKOU¹ — ¹Max Planck Institute for Chemical Physics of Solids, Dresden, Germany — ²Technische Universität Dresden, Dresden, Germany — ³University of South Florida, Tampa, United States of America — ⁴Institut Laue-Langevin, Grenoble, France

Centrosymmetric MnPtGa Heusler films grown by magnetron sputtering on (0001)-Al₂O₃ crystallize with an out-of-plane *c*-axis crystal orientation, along which they exhibit perpendicular magnetic anisotropy below their Curie temperature (*T*_C = 263 K). Further, below a thermally induced spin reorientation transition at 160 K, the magnetic groundstate, determined by single-crystal neutron diffraction, is found to be a noncollinear spin-canted state where the Mn moments tilt 20° away from the *c*-axis [*Appl. Phys. Lett.* 120, 172403 (2022)].

Furthermore, the anomalous Hall conductivity (AHC) of 20–60 nm thick MnPtGa epitaxial films is found to exhibit a strongly nonmonotonic behaviour as a function of longitudinal conductivity and temperature, whereby the AHC changes sign at *T** = 110 K. Our findings, supported by first-principle calculations, hint at an anomalous Hall effect of intrinsic origin driven by a momentum-space Berry curvature mechanism [*Adv. Mater. Interfaces* 9, 2201562 (2022)].

MA 37.5 Thu 10:30 HSZ 403

Effect of increasing Mn content on twin mobility in Mn-excess Ni-Mn-Ga alloys — •MARTIN HE CZKO¹, PETR ŠESTÁK², and MARTIN ZELENÝ¹ — ¹Institute of Materials Science and Engineering, Faculty of Mechanical Engineering, Brno University of Technology, Brno, Czech Republic — ²Institute of Physical Engineering, Faculty of Mechanical Engineering, Brno University of Technology, Brno, Czech Republic

Martensitic phases of Ni-Mn-Ga ferromagnetic shape memory alloy are considered to be useful in various advanced engineering applications due to reported giant magnetic field induced strain (MFIS). The MFIS originates in the high mobility of twin boundaries combined with large magneto-crystalline anisotropy. We calculated the generalized planar fault energy (GPFE) curves using the spin-polarized DFT method implemented in the Vienna Ab Initio Simulation Package (VASP) to reveal the effect of increasing concentration of excess Mn and its magnetic ordering on formation and propagation of twin boundaries. Effects of local arrangement of excess Mn atoms in Ga sublattice has been considered as well.

Our results show that the barriers for nucleation and grow of a twin rise with increasing content of Mn. It results in more difficult twin formation and propagation in compositions far from stoichiometry. This effect is even more enhanced if excess Mn atom in Ga sublattice is located exactly in the planar fault, and when they are ordered antiferromagnetically.

MA 37.6 Thu 10:45 HSZ 403

The impact of disorder on the 40-martensite of Ni-Mn-Sn Heusler alloy — •MARTIN FRIÁK¹, MARTIN ZELENÝ^{2,3}, JIŘÍ KAŠTIL⁴, JIŘÍ KAMARÁD⁴, MARTIN MÍŠEK⁴, ZDENĚK ARNOLD⁴, ILJA TUREK¹, OLDŘICH SCHNEEWEISS¹, and MOJMIŘ ŠOB^{5,1} — ¹Institute of Physics of Materials, Czech Academy of Science, Brno, CZ — ²Institute of Materials Science and Engineering, Faculty of Mechanical Engineering, Brno University of Technology, Brno, CZ — ³Faculty of Mathematics and Physics, Charles University, Prague, CZ — ⁴Institute of Physics, Czech Academy of Sciences, Prague, CZ — ⁵Department of Chemistry, Faculty of Science, Masaryk University, Brno, CZ

We have performed a quantum-mechanical study of thermodynamic, elastic, magnetic and structural properties of four different ferrimagnetic states in Ni_{1.9375}Mn_{1.5625}Sn_{0.5} martensite. They are modeled by the four-layer modulated 4O structures with Mn-excess atoms randomly distributed in Ni and Sn sublattices. The Mn atoms at the Ni sublattice turn out to play a key role in the system. A reversal of the orientation of their local magnetic moments has a huge impact on the properties of the whole system. The lowest-energy configuration exhibits anti-parallel local magnetic moments of these Mn atoms with respect to the orientation of the total magnetic moment. By testing both elasticity and phonons we conclude that the lowest-energy state is mechanically stable. Vibrational properties of individual atoms are found to be very sensitive to the chemical disorder. For details see *Intermetallics* 151 (2022) 107708, DOI:10.1016/j.intermet.2022.107708.

MA 38: Micro- and Nanostructured Magnetic Materials

Time: Thursday 11:30–12:45

Location: HSZ 401

MA 38.1 Thu 11:30 HSZ 401

Chemically modulated Fe-Ni cylindrical nanowires with asymmetric magnetic response — •CLAUDIA FERNANDEZ^{1,2}, ALBA BERJA^{2,3}, LUCIA ABALLE⁴, LAURA ALVARO¹, CAROLINA MARTIN⁵, MICHAEL FOERSTER⁴, RUY SANZ⁵, ARANTZAZU MASCARAQUE², LUCAS PEREZ^{1,2}, and SANDRA RUIZ⁶ — ¹IMDEA Nanoscience, 28049, Spain — ²Materials Physics Department, UCM, 28040, Spain — ³Institute of Ceramics and Glass (CSIC), 28040, Spain — ⁴ALBA Synchrotron, 08290, Spain — ⁵National Institute of Aerospace Technology, 28850, Spain — ⁶MPI for Chemical Physics of Solids, 01187, Germany

The control of the magnetic domain walls (DWs) movement along cylindrical nanowires (NWs) by means of magnetic fields or electric currents is a key aspect in the design of novel spintronic devices. In recent studies, we have demonstrated that local changes in composition along the axis of Fe₂₀Ni₈₀ nanowires can pin the DWs and that the DWs can be moved under the application of magnetic field. Expanding this concept, in this work we propose a gradual change in Fe/Ni ratio along the axial direction of the nanowires in order to create an asymmetric energy landscape with the aim to induce asymmetric domain wall motion. Combining X-ray imaging techniques (XAS and XMCD) we have cor-

related the chemical structure of single nanowires with their magnetic configuration. In First Order Reversal Curves (FORC) diagrams we have observed that an asymmetry arises evidencing the emerging of asymmetrical magnetization processes in the array.

MA 38.2 Thu 11:45 HSZ 401

Chirality coupling in curvilinear nanoarchitectures — •OLEKSII M. VOLKOV¹, DANIEL WOLF², OLEKSANDR V. PYLYPOVSKYI^{1,3}, ATTILA KÁKAY¹, DENIS D. SHEKA⁴, BERND BÜCHNER^{2,5}, JÜRGEN FASSBENDER¹, AXEL LUBK^{2,5}, and DENYS MAKAROV¹ — ¹Helmholtz-Zentrum-Dresden-Rossendorf, Dresden, Germany — ²Institute for Solid State Research, IFW Dresden Dresden, Germany — ³Kyiv Academic University, Kyiv, Ukraine — ⁴Taras Shevchenko National University of Kyiv, Kyiv, Ukraine — ⁵Institute of Solid State and Materials Physics, TU Dresden, Dresden, Germany

Symmetry effects are key building blocks of condensed matter physics as they define not only interactions but also resulting responses for the intrinsic order parameter. Namely, in magnetism geometric curvature governs the appearance of chiral and anisotropic responses [1], that introduce a new toolbox to create artificial chiral nanostructures from achiral magnetic materials [2,3]. Here, we demonstrate both theoretically and experimentally the existence of non-local chiral effects in geometrically curved asymmetric permalloy caps with the vortex texture. We find that the equilibrium vortex core obtain bend and curling deformation, that are dependent on the geometric symmetries and magnetic texture parameters.

[1] D. D. Sheka et al., *Comm. Phys.* **3**, 128 (2020).

[2] O. M. Volkov et al., *Phys. Rev. Lett.* **123**, 077201 (2019).

[3] D. Makarov et al., *Adv. Mater.* **34**, 2101758 (2022).

MA 38.3 Thu 12:00 HSZ 401

Towards magnetic MXenes via thermal activation of $Ti_3C_2T_x$ and Fe intercalation — •TIM SALZMANN¹, HANNA PAZNAK², IVAN TARASOV¹, MICHAEL FARLE¹, and ULF WIEDWALD¹ — ¹University of Duisburg-Essen and Center for Nanointegration Duisburg-Essen, Germany — ²Université Grenoble Alpes, CNRS, Grenoble INP, LMGP, France

MXenes are 2D materials obtained from a MAX phase precursor. The $Ti_3C_2T_x$ MXene surface is stabilized by a T_x termination in the form of $-F$, $-Cl$, $-O$, $-OH$ [1]. $Ti_3C_2T_x$ MXenes deposited on Si(100)/SiO₂ are annealed at $T=1023$ K in ultrahigh vacuum removing $-F$, $-Cl$ and $-OH$ confirmed by in situ mass spectroscopy, and Auger electron spectroscopy (AES). Additionally, we find a reduction of interplanar spacing between MXene sheets ($d_{ini} - d_{ann} = 0.30 \pm 0.04$ nm) by X-ray diffraction (XRD). Subsequently, a 6 nm thick Fe film is deposited and annealed between 550 K and 1000 K. AES displays a linear decrease of the Fe concentration at the surface from 85% to 15% as a function of annealing temperature. The intercalation of Fe is confirmed by XRD measurements showing an increase of the interplanar spacing between MXene sheets ($d_{int} - d_{ann} = 0.16 \pm 0.02$ nm). In plane vibrating sample magnetometry reveals a saturation magnetization of 1728 ± 150 kA/m for the 6 nm Fe film on top of MXenes confirming bulk metallic Fe. After annealing up to 800 K, the

magnetization decreases to 660 ± 80 kA/m and the Curie temperature to 485 K. Funded by DFG-Project-ID 405553726-TRR 270.

[1] James L. Hart et al., *ACS Nanoscience Au* 2022 2, 433-439

MA 38.4 Thu 12:15 HSZ 401

Magneto-optical investigation of 3D-curved toroidal ferromagnetic thin films — •CHRISTIAN JANZEN¹, SAPIDA AKHUNDZADA¹, BHAVADIP BHARATBHAI RAKHOLIYA¹, ARNE VEREIJKEN¹, CLAUDIO BECK¹, PIOTR KUŚWIK², MICHAŁ MATCZAK^{2,3}, MICHAEL VOGEL^{1,4}, and ARNO EHRESMANN¹ — ¹Institute of Physics and Center for Interdisciplinary Nanostructure Science and Technology (CINaT), University of Kassel, Germany — ²Institute of Molecular Physics, Polish Academy of Science, Poznań, Poland — ³Faculty of Physics, University of Białystok, Poland — ⁴Department of Materials Science, University of Kiel, Germany

Magnetic thin films, typically examined as flat two-dimensional systems, may be extended to the third dimension by deposition of the magnetic material on curved substrates. To experimentally investigate physical effects induced by the geometry and curvature of a thin film magnet, micron-sized curved structures with minimal surface roughness were prepared by optimized two-photon polymerization lithography processes. These structures are deliberately placed with well-defined lateral as well as axial spacing, leading to periodic arrays where, e.g., the influence of varying magnetostatic interactions between the individual objects can be investigated. In this work, the magnetization reversal of periodic arrays of hemispherical tori with varying lattice geometry of the periodic array will be investigated by magneto-optical Kerr magnetometry/microscopy. The experimental results are further compared with micromagnetic simulations.

MA 38.5 Thu 12:30 HSZ 401

Sprayed Nanometer-Thick Hard Magnetic Coatings with Strong Perpendicular Anisotropy for Data-Storage Applications — •ANDREI CHUMAKOV¹, CALVIN J. BRETT^{1,2}, KORNELIYA GORDEYEVA², DIRK MENZEL³, LEWIS O. O. AKINSINDE⁴, MARC GENSCH¹, MATTHIAS SCHWARTZKOPF¹, WEI CAO⁵, SHANSHAN YIN⁵, MANUEL A. REUS⁵, MICHAEL A. RÜBHAUSEN⁴, PETER MÜLLER-BUSCHBAUM^{5,6}, DANIEL SÖDERBERG², and STEPHAN V. ROTH^{1,2} — ¹Deutsches Elektronen-Synchrotron DESY, Hamburg, Germany — ²DE 118714904 — ³Notkestraße 85, DESY — ⁴Universität Hamburg, Hamburg, Germany — ⁵Technische Universität München, Garching, Germany — ⁶Heinz Maier-Leibnitz Zentrum, Garching, Germany

We present a study of a facile technology for establishing mono- and multi-layer surfaces from various single-domain flat magnetic nanoparticles that exhibit a strong perpendicular-oriented magnetic moment on solid and flexible substrates. Surfactant-free, hard ferromagnetic and single-domain anisotropic strontium hexaferrite nanoparticles with perpendicular magnetic moment orientation and two different aspect ratios are self-ordered into magnetic thin nanofilms exploiting the templating effect of cellulose nanofibrils and magnetic fields. Uniform magnetic coatings obtained by scalable layer-by-layer spray deposition from a monolayer coverage up to thicknesses of a few tens of nanometers show preferred in-plane orientation of the hard-magnetic nanoparticles.

MA 39: Weyl Semimetals

Time: Thursday 11:30–12:45

Location: HSZ 403

MA 39.1 Thu 11:30 HSZ 403

Topological spin textures stabilised by Weyl fermions — •JUBA BOUAZIZ¹, GUSTAV BIHLMAYER¹, JULIE B. STAUNTON², and STEFFAN BLÜGEL¹ — ¹Peter Grünberg Institut Forschungszentrum Jülich — ²The university of Warwick

Rare-earth intermetallic (REI) constitute a playground for the realization of topological spin textures relying on Ruderman-Kittel-Kasuya-Yosida (RKKY) interactions between the localized 4f-moments [1]. In non-centrosymmetric REI, namely REAlGe (Si), the breaking of inversion symmetry generates Weyl nodes which display interesting topological properties. The Weyl fermions mediate highly anisotropic RKKY interactions leading to the emergence of Kitaev (KT) and Dzyaloshinskii-Moriya (DM) interactions. The incommensurate magnetic order present in these systems can be tied to the nesting of topological Fermi pockets [2]. We perform a systematic first-principles analysis in the framework of the DFT+U for REAlGe (RE=Ce-Gd) and investigate the contributions of the different exchange interactions (isotropic, DM, and KT) to incommensurate order. The local crystal field coefficients are computed from first-principles as well and are used to evaluate the magneto-crystalline anisotropy. Finally, we employ atomistic spin-dynamic simulations and identify the magnetic phases that are stabilized in presence of an external magnetic field. Our analysis aims at drawing a direct connection between the topology of the electronic band structure and the topology of the spin structures in real space. [1] J. Bouaziz et al. *PRL* **128**, 157206 (2022) [2] J. Gaudet et al. *Nat Mat* **20**, 1650 (2021)

MA 39.2 Thu 11:45 HSZ 403

Pressure induced ferromagnetic collapse and valence instability in EuB₆ — •LEONARDO KUTELAK¹, RAIMUNDA SEREIKA², GILBERTO FABBRIS³, GUSTAVO LOMBARDI¹, DANIEL HASKEL³, NARCIZO SOUZA NETO¹, PRISCILA ROSA⁴, WENLI BR², and RICARDO REIS¹ — ¹Brazilian Synchrotron Light Laboratory (LNLS), Brazilian Center for Research in Energy and Materials (CN-PEM), Campinas, Sao Paulo, Brazil — ²University of Alabama at Birmingham - Birmingham, AL 87545, USA — ³Advanced Photon Source, Argonne National Laboratory, Argonne, Illinois 60439, USA — ⁴Los Alamos National Laboratory - Los Alamos, NM 87545, USA

The only ferromagnetic rare earth hexaboride, EuB₆, presents previously reported interesting behavior such as a two-step magnetic transition below 15 K¹ and magnetic polarons up to 40 K¹. Most recently, it was proposed that EuB₆ may host non-trivial electronic behavior near Fermi surface presenting either Weyl Points or nodal lines depending upon magnetization ordering and direction. We show evidences for EuB₆ ferromagnetic collapse above 20 GPa with mean valency increase by X-ray spectroscopy techniques. No signs for structural phase transitions were observed in high pressure X-ray diffraction. This opens up new possibilities for fine tuning topological properties utilizing pressure in rare earth hexaborides.

¹Süllow, Structure, et al. *Physical Review B* **57**.10 (1998): 5860. ²Pohlitz, Merlin, et al *Physical review letters* **120**.25 (2018): 257201. ³Nie, Simin, et al. *Physical Review Letters* **124**.7 (2020): 076403.

MA 39.3 Thu 12:00 HSZ 403

High pressure studies of the topological Hall effect on CeAlGe — •MARIO M. PIVA¹, JEAN C. SOUZA², GUSTAVO A. LOMBARDI^{3,1}, KEVIN R. PAKUSZEWSKI⁴, CRIS ADRIANO⁴, PASCOAL G. PAGLIUSO^{4,5}, and MICHAEL NICKLAS¹ — ¹Max Planck Institute for Chemical Physics of Solids, Dresden, Germany — ²The Weizmann Institute of Science, Rehovot, Israel — ³Brazilian Synchrotron Light Laboratory (LNLS), Campinas, Brazil — ⁴“Gleb Wataghin” Institute of Physics, Campinas, Brazil — ⁵Los Alamos National Laboratory, Los Alamos, USA

The Weyl semimetal CeAlGe is an excellent playground to investigate non-trivial topologies in real and momentum space due to the presence of a topological magnetic phase [1]. Our findings show that, the THE in CeAlGe is sensitive to slight stoichiometric variations, similar to its magnetism [2]. The observed change of a single THE region to two distinct regions upon application of external pressure is in agreement with previous reports [3]. Remarkably, we find that application of high pressures leads to the appearance of a THE even in samples where it was absent at ambient pressures.

This project has received funding from the European Unions Horizon 2020 research and innovation programme under the Marie Skłodowska-Curie grant agreement No 101019024.

[1] P. Puphal, *et al.*, Phys. Rev. Lett. **124** 017202 (2020); [2] P. Puphal, *et al.*, Phys. Rev. Mat. **3** 024204 (2019); [3] X. He, *et al.*, arXiv:2207.08442.

MA 39.4 Thu 12:15 HSZ 403

Magnetic and Electronic Structure of Eu(Cd,Zn)₂P₂ — •SARAH KREBBER¹, KRISTIN KLIEMT¹, MARVIN KOPP¹, CHARU GARG¹, JENS MÜLLER¹, KURT KUMMER², DENIS VYALIKH³, and CORNELIUS KRELLNER¹ — ¹Institute of Physics, Goethe-University, Frankfurt (Main), Germany — ²ESRF, Grenoble, France — ³DIPC, Donostia-San Sebastián, Spain

The interplay of topology and magnetism has been of great interest in the last few years. The coexistence of both phenomena can be realized in europium based compounds with the 122 stoichiometry and a trigonal crystal structure (P3m1). Recently, a spin fluctuation induced Weyl semimetal state in the paramagnetic phase of EuCd₂As₂ [1,2] and its tunability by pressure [3] was discovered. Fur-

thermore, EuCd₂P₂ has been explored due to its colossal magnetoresistance [4], where the origin of the effect was explained by the formation of ferromagnetic clusters [5].

With the aim of studying the magnetic and electronic properties of EuCd₂P₂ compound in detail and finding similar effects in EuZn₂P₂ both systems were studied. Here, we present the successful crystal growth and characterization via magnetization, electrical transport, heat capacity and spectroscopy.

[1] Ma et al., Science Adv. **5**, eaaw4718 (2019). [2] Jo et al., Phys. Rev. B **101**, 140402(R) (2020). [3] Gati et al., Phys. Rev. B **104**, 155124 (2021). [4] Wang et al., Adv.Mater., **33**, 2005755 (2021). [5] Sunko et al., arXiv:2208.05499, (2022).

MA 39.5 Thu 12:30 HSZ 403

Novel thermo-electric transport channel in the conformal limit of tilted Weyl semimetals — THORVALD BALLESTAD¹, ALBERTO CORTIJO², MARÍA VOZMEDIANO³, and •ALIREZA QAIUMZADEH¹ — ¹Center for Quantum Spintronics, Norwegian University of Science and Technology, Trondheim, Norway — ²Universidad Autonoma de Madrid, Madrid, Spain — ³Instituto de Ciencia de Materiales de Madrid, CSIC, Madrid, Spain

Recently, a new contribution to the Nernst current was proposed in 3D Dirac and Weyl semimetals, originated from quantum conformal anomaly [1,2]. In the present study, we analyze the effect of the tilt on the transverse thermo-electric coefficient of Weyl semimetals in the conformal limit, i.e., zero temperature and zero chemical potential. Using the Kubo formalism, we find a non-monotonic behavior of the thermoelectric conductivity as a function of the tilt perpendicular to the magnetic field, and a linear behavior when the tilt is aligned to the magnetic field. An “axial Nernst” current is generated in inversion symmetric materials when the tilt vector has a projection in the direction of the magnetic field. This analysis will help in the design and interpretation of thermo-electric transport experiments in recently discovered topological quantum materials [3].

[1] M. N. Chernodub et al, Phys. Rev. Lett. **120**, 206601 (2018). [2] V. Arjona et al, Phys. Rev. B **99**, 235123 (2019). [3] T. M Ballestad, A. Cortijo, M. A. H. Vozmediano, A. Qaiumzadeh, arXiv:2209.14331 (2022).

MA 40: Poster Magnetism II

Magnetic Domain Walls (non-skyrmionic) (MA 40.1-40.5), Ultrafast Magnetization Effects (MA 40.6-40.12), Magnetic Relaxation and Gilbert Damping (MA 40.13), Magnetic Semiconductors (MA 40.14-40.15), Complex magnetic oxides (MA 40.16-40.20), Frustrated Magnets (MA 40.21-40.27), Thin Films: Magnetic Coupling Phenomena / Exchange Bias (MA 40.28-40.32), Thin Films: Magnetic Anisotropy (MA 40.33-40.34), Magnetic Instrumentation and Characterization (MA 40.35-40.42), Magnetic Particles / Clusters (MA 40.43-40.44), Magnetic Information Technology, Recording, Sensing (MA 40.45-40.48), Micro- and Nanostructured Magnetic Materials (MA 40.49-40.50), Multiferroics and Magnetoelectric Coupling (MA 40.51), Surface Magnetism (MA 40.52-40.55), Cooperative Phenomena: Spin Structures and Magnetic Phase Transitions (MA 40.56-40.58), Topological Insulators (MA 40.59), Topological Insulators (MA 40.60-40.61), Disordered Magnetic Materials (MA 40.62), Focus Session: Altermagnetism: Transport, Optics, Excitations (MA 40.63-40.64), Spin-Phonon Coupling (MA 40.65-40.66)

Time: Thursday 14:00–16:00

Location: P2/EG

MA 40.1 Thu 14:00 P2/EG

The spectrum of localized excitations of spin nanoclusters and their stability in a magnetic field — •OKSANA CHARKINA^{1,2}, MIKHAIL BOGDAN², and IGOR POLTAVSKY¹ — ¹University of Luxembourg, L-1511 Luxembourg City, Luxembourg — ²B. Verkin ILTPE of NASU, Kharkiv, 61103, Ukraine

Engineering novel materials with predefined spectral and dynamical properties from recently synthesized giant magnetic molecules, permitting well-controlled exchange interaction, is essential for creating memory elements in modern computer technologies. To provide the necessary theoretical basis, we studied the structure and internal dynamics of spin nanoclusters limited by discrete domain walls in ferromagnetic chains placed in a magnetic field. The spin nanoclusters and their spectra of localized excitations are described analytically within the framework of the discrete Takeno-Homma equation [1], which fully accounts for the exchange interaction between spins. Explicit expressions for the internal mode oscillations were found, and the frequency dependences on the parameters of the exchange and the magnetic field were calculated. In addition, a stripe-like stability diagram and the Peierls energy barrier for the noncollinear discrete domain walls were established. We found that the magnetic field can effectively control the localization of information and energy on spin clusters. Our results can be used in developing spin-cluster resonance methods for investigating magneto-optical properties of a new class of low-dimensional metamaterials.

1. Takeno S. and Homma S., J.Phys.Soc.Jpn. **55**, 2547 (1986).

MA 40.2 Thu 14:00 P2/EG

Curvature-induced effects in dynamics of domain walls in chiral biaxial nanotubes — •KOSTIANTYN V. YERSHOV^{1,2} and DENIS D. SHEKA³ — ¹Leibniz Institute for Solid State and Materials Research, Dresden, Germany — ²Bogolyubov Institute for Theoretical Physics, Kyiv, Ukraine — ³Taras Shevchenko National University of Kyiv, Ukraine

Tubular geometry is paradigmatic example for studying numerous chiral effect. The competition between intrinsic Dzyaloshinskii-Moriya interactions (DMI) and geometry-governed DMI become the source of emergent magnetochiral effects leading to essential modification of critical DMI strength, appearance of new type of domain walls (DWs) [1]. Here, we present a detailed study of static and dynamic properties of DWs in chiral biaxial nanotubes. The easy and hard axes are oriented in azimuthal and radial directions, respectively. (i) First, we considered the static properties of magnetic DWs in nanotubes with different symmetries of DMI. We found that the presence the chiral interaction results in the deformation of the DW profile: for interfacial type of DMI the DW phase has an asymmetrical slope; for bulk type of DMI the DW phase has a linear shift. In both cases deformation is proportional to the strength of DMI (ii) Dynamics of DWs with interfacial DMI results in the linear shift of the Walker field. While, for the case of the a bulk type of DMI we show that the presence of chiral interaction results in the emergent magnetochiral effect, i.e. the polarity-helicity coupling. [1] K. Yershov et al, SciPost Phys. **9** (2020), 043.

MA 40.3 Thu 14:00 P2/EG

Dynamics of bound domain walls in the 3D magnetic double helix — •IMELDA PAMELA MORALES FERNANDEZ¹, SANDRA RUIZ-GÓMEZ¹, AURELIO HIERRO-RODRÍGUEZ², SIMONE FINIZIO³, SEBASTIAN WINTZ⁴, NÁEMI LEO⁵, MARKUS KÖNIG¹, CLAAS ABERT⁶, DIETER SÜSS⁶, AMALIO FERNANDEZ-PACHECO⁵, and CLAIRE DONNELLY¹ — ¹Max Planck Institute for Chemical Physics of Solids — ²University of Oviedo — ³Paul Scherrer Institute — ⁴Helmholtz Center Berlin — ⁵Institute of Nanoscience and Materials of Aragon — ⁶University of Vienna

Magnetic domain walls are stable magnetic textures that promise exciting opportunities for advances in technological applications in a wide range of fields. In contrast with their 2D counterparts, DWs in 3D nanosystems can exhibit more complex configurations, with prospects for exotic dynamic behavior. In this framework, double helix nanostructures combine geometrical effects of curvature and chirality with intrinsic exchange and magnetostatic coupling giving rise to a new state consisting of a highly coupled pair of domain walls (head-to-head and tail-to-tail) within the neighboring helices. The cobalt double helix fabricated by the FEBID technique is an ideal platform to experimentally investigate the static and dynamic properties of the coupled domain walls: it is a trustworthy platform to induce the vortex and antivortex textures in the magnetic field of the coupled domain wall state and on the other hand it is a promising system to achieve robust DW motion and synchronous dynamics with ultra-high DW mobilities overcoming the Walker breakdown.

MA 40.4 Thu 14:00 P2/EG

Current-induced creation of domain walls in synthetic antiferromagnets — ROBIN MSISKA¹, •OMER FETAI¹, RAPHAEL KROMIN², DAVI RODRIGUES³, and KARIN EVERSCHOR-SITTE^{1,4} — ¹TWIST group, University of Duisburg-Essen, Germany — ²Institute of Physics, Johannes Gutenberg University Mainz, Germany — ³Politecnico di Bari, Italy — ⁴Center for Nanointegration Duisburg - Essen (CENIDE)

Improvements in the storage capacity of modern-day memory devices are slowing down and new concepts for storing data are required. A suggestion for a three-dimensional data storage is the racetrack memory which stores information in terms of magnetic domains. The use of synthetic antiferromagnets (SAF), i.e., antiferromagnetically coupled ferromagnetic bilayer systems, accelerates the information access time because the domain walls can be moved up to ten times faster [1]. To obtain a market-ready device, many challenges must be overcome, one of which is integrating a controlled domain wall write process into SAFs. We study the controlled creation of domain walls in SAFs by electrical means. In the case of spin-transfer torques, we find a critical current strength above which antiferromagnetic domain walls are created from an inhomogeneity. In contrast to the ferromagnetic case [2] we show that the critical current density is an order of magnitude higher.

- [1] Stuart S. P. Parkin and et. al. *Nat.Nanotechnol.* 10 (2015)
 [2] M. Sitte et al. *Phys. Rev. B* 94, 064422 (2016)

MA 40.5 Thu 14:00 P2/EG

Imaging the antiferromagnetic domain structure of α -Fe₂O₃ and its magnetic field dependence — •JULIAN SKOLAUT¹, KAI LITZIUS^{2,3}, MARKUS WEIGAND⁴, OLENA GOMONAY¹, ELIZAVETA TREMSINA⁵, SEBASTIAN WINTZ^{3,4}, NORMAN BIRGE⁶, GEOFFREY BEACH⁵, and ANGELA WITTMANN¹ — ¹Johannes Gutenberg University, Mainz — ²University Augsburg — ³MPI Intelligent Systems, Stuttgart — ⁴HZB, Berlin — ⁵MIT, Cambridge, USA — ⁶Michigan State University, East Lansing, USA

In recent years, antiferromagnets have gained increasing attention for spintronics applications due to their favorable properties such as vanishing stray fields. Moreover, the domain structure formation mechanism is different from ferromagnets. Here, we study the canted antiferromagnet hematite α -Fe₂O₃. The canting of the spins yields a small in-plane magnetization, lifting the degeneracy of the Néel vector orientation w.r.t. an external magnetic field. Our measurements investigate the magnetic domain structure of hematite, specifically the movement of domain walls by application of an external magnetic field. For this, we have imaged the domain structure of α -Fe₂O₃ by taking x-ray magnetic linear dichroism (XMLD) contrast images of the domain structure of α -Fe₂O₃ by total electron yield using a scanning x-ray microscope. This method allows imaging of the domain structure within an applied magnetic field and studying the domain structure, as well as the displacement of domain walls as a function of the magnetic field. A thorough analysis of the changes in domain structure will elucidate the underlying mechanisms for the formation of magnetic domains.

MA 40.6 Thu 14:00 P2/EG

Tuning all-optical magnetization switching efficiency by laser pulse wavelength variation — •MARCEL KOHLMANN¹, LUCAS VOLLROTH¹, KRISTÝNA HOVOVŘÁKOVÁ², EVA SCHMORANZEROVÁ², ROBIN JOHN¹, DENISE HINZKE⁴, PETER OPPENEER³, ULRICH NOWAK⁴, MARKUS MÜNZENBERG¹, and JAKOB WALOWSKI¹ — ¹Greifswald University, Greifswald, Germany — ²Charles University, Prague, Czech Republic — ³Uppsala University, Uppsala, Sweden — ⁴Konstanz University, Konstanz, Germany

The relevance of heat-assisted magnetic recording (HAMR) motivates ongoing research and development in magnetization manipulation. We study all-optical helicity-dependent switching (AOHDS) of FePt granular media as a viable alternative method for magnetic writing of HAMR media. The interplay of magnetic dichroism and inverse Faraday effect is currently understood as driving process behind the magnetization reversal. Ab-initio calculations of magnetic dichroism and inverse Faraday effect for the switching rates of single FePt nanoparticles provided us with a stochastic model for the switching process. We now present data for the wavelength dependent efficiency of the writing process from 800 nm - 1550 nm. We greatly acknowledge the DFG funding within the project "Fundamental aspects of all-optical single pulse switching in nanometer-sized magnetic storage media.

MA 40.7 Thu 14:00 P2/EG

Coherent excitation of spin waves in thin nickel films during ultrafast remagnetization — •AKIRA LENTFERT¹, ANULEKHA DE¹, LAURA SCHEUER¹, BENJAMIN STADTMÜLLER^{1,2}, BURKARD HILLEBRANDS¹, GEORG VON FREYMAN^{1,3}, MARTIN AESCHLIMANN¹, and PHILIPP PIRRO¹ — ¹Department of Physics and Research Center OPTIMAS, RPTU Kaiserslautern-Landau, Germany — ²Institute of Physics, Johannes Gutenberg University Mainz, Germany — ³Fraunhofer Institute for Industrial Mathematics ITWM, Germany

The remagnetization process after ultrafast demagnetization can be described by relaxation mechanisms between the spin, electron, and lattice reservoirs. The angular momentum transfer between them is the subject of current research, especially the role of collective spin excitations remains comparably unexplored. In our work, we study the pump fluence-dependent excitation of coherent spin waves in thin nickel films. Using the all-optical, time-resolved magneto-optical Kerr-effect (tr-MOKE) technique, we investigate the role of coherent spin waves after the laser-induced demagnetization. We show that the largest spin-wave amplitude is observed close to the fully demagnetized state. Furthermore, the coherence of the system appears to be conserved during de- and remagnetization, even when the magnetization is quenched by up to 90%. Interestingly, the phase of the coherent oscillations relative to the initial laser pulse is strongly dependent on the laser fluence which indicates that the coherent precession is influenced by the demagnetization itself. This research was supported by the DFG through No. TRR 173-268565370 (project B11).

MA 40.8 Thu 14:00 P2/EG

Laser-induced ultrafast magnetization dynamics in Ni|Au heterostructures — •STEPHANIE RODEN¹, CHRISTOPHER SEIBEL¹, MARIUS WEBER¹, MARTIN STIEHL¹, SEBASTIAN T. WEBER¹, MARTIN AESCHLIMANN¹, BENJAMIN STADTMÜLLER^{1,2}, HANS CHRISTIAN SCHNEIDER¹, and BÄRBEL RETHFELD¹ — ¹Department of Physics and Research Center OPTIMAS, RPTU, Kaiserslautern, Germany — ²Institute of Physics, Johannes Gutenberg University Mainz, Germany

Studying the optically induced magnetization dynamics of heterostructures has provided clear insights into the particle and energy transport effects on ultrafast timescales. This understanding leads to new concepts to control the magnetization dynamics by tuning the wavelength of optical excitation [1, 2, 3].

In this contribution we demonstrate how the magnetization dynamics of Ni|Au heterostructures can also be controlled by the thickness of the non-magnetic gold layer. Our conclusions are based on an extended temperature-based μ T-model which includes the thickness-dependent absorption profile. We find that thin gold films slow down the demagnetization process of nickel while the demagnetization times decrease again for larger gold film thicknesses. Furthermore we consider transport effects within the gold layer and demonstrate the dependence of the induced spin polarization into the substrate on the considered depth in the substrate.

- [1] V. Cardin *et al.*, *Phys. Rev. B* 101, 054430 (2020)
 [2] M. Stiehl *et al.*, *Appl. Phys. Lett.* 120, 062410 (2022)
 [3] C. Seibel *et al.*, *Phys. Rev. B* 106, L140405 (2022)

MA 40.9 Thu 14:00 P2/EG

Optical manipulation of magnetic order parameter in magnetic insulators by ultrashort laser pulses — •PAUL HERRGEN¹, BENJAMIN STADTMÜLLER^{1,2}, and MARTIN AESCHLIMANN¹ — ¹Department of Physics and Research Center OPTIMAS, Technische Universität Kaiserslautern, 67663 Kaiserslautern, Germany — ²Institute of Physics, Johannes Gutenberg-Universität Mainz, 55128 Mainz, Germany

Magnetic insulators are highly intriguing materials for high performance and sustainable magnetic storage technology. However, the existence of a band gap of several eV makes it rather challenging to optically manipulate these materials on an ultrafast, fs timescale.

Here, we used strong fs laser pulses with high photon energies to optically overcome this bandgap. Using a second ultrashort laser pulse, we were able to measure the dynamics of the magnetic order parameter of this insulator in a time-resolved manner. We find that the optical excitation leads to a fast reduction of the magnetic order on a subpicosecond time scale. In addition, the remagnetization process takes more than 100ps to fully return to the initial magnetic ground state.

MA 40.10 Thu 14:00 P2/EG

Laser-induced metamagnetic phase transition of FeRh studied by combined UXRD and MOKE experiments — •MAXIMILIAN MATTERN¹, JASMIN JARECKI¹, VOJTECH UHLIR², JON ANDER ARREGI², and MATIAS BARGHEER^{1,3} — ¹Institut für Physik und Astronomie, Universität Potsdam, Germany — ²CEITEC BUT, Brno University of Technology, Czech Republic — ³Helmholtz-Zentrum Berlin, Germany

We use time-resolved x-ray diffraction (UXRD) and the time-resolved polar magneto-optical Kerr effect (MOKE) to study the laser-induced metamagnetic phase transition in FeRh. The first-order phase transition from an antiferromagnetic (AFM) to a ferromagnetic (FM) phase is accompanied by a gigantic expansion ($\approx 0.6\%$) of the unit cell. While UXRD access the transient FM volume fraction independent of the orientation of the magnetic moment probing the enhanced lattice constant, MOKE is sensitive on the orientation of the magnetization probing the net out-of-plane magnetization.

Our combined UXRD and MOKE experiments access the nucleation, growth and coalescence of the arising FM domains and disentangle their in- and out-of-plane expansion by comparing two samples, with a thickness below and above the optical penetration depth. The thin FeRh film displays a fluence-independent rise time of the FM phase of 8 ps and a much slower rise of the net magnetization within 150 ps starting 10 ps after excitation. For the inhomogeneously excited film, we observe a strong fluence dependence of these rise times originating from an out-of-plane growth of the FM domains by heat transport.

MA 40.11 Thu 14:00 P2/EG

Consequences of Orbital Angular Momentum of Light for Electronic Dynamics — •MARVIN GORONCZY and HANS CHRISTIAN SCHNEIDER — Physics Department, RPTU Kaiserslautern, 67653 Kaiserslautern

Recent experiments show that the orbital angular momentum (OAM) of laser pulses affects the demagnetization dynamics in ferromagnets by slowing it down or speeding it up depending on the direction of the orbital angular momentum. [1] Motivated by these experiments, we consider here the basic problem of the interaction of OAM-light with electrons in a generic band structure in order to study the effect of OAM-light on the electronic system, without attempting to include demagnetization dynamics yet. We derive the dynamical equations for the reduced electronic density matrix and its Wigner transform. We discuss the role played by different contributions, such as multipole transitions and the inhomogeneities introduced by the beam profile. Finally, we compare our results with earlier approaches to this problem.[2]

[1] E. Prinz, B. Stadtmüller, M. Aeschlimann, arXiv.2206.07502 [2] G. F. Quinteiro, P. I. Tamborenea, EPL 85/47001

MA 40.12 Thu 14:00 P2/EG

Magnetization dynamics in magnetic trilayers with a wedged antiferromagnetic spacer layer at ultrafast timescales — •JENDRIK GÖRDES¹, IVAR KUMBERG¹, CHOWDHURY AWSAF¹, RAHIL HOSSEINFAR¹, MARCEL WALTER¹, TAUQIR SHINWARI¹, SANGEETA THAKUR¹, CHRISTIAN SCHÜSSLER-LANGEHEINE², NIKO PONTIUS², and WOLFGANG KUCH¹ — ¹Institut für Experimentalphysik, Freie Universität Berlin, Arnimallee 14, 14195 Berlin — ²Helmholtz-Zentrum Berlin für Materialien und Energie, Albert-Einstein-Straße 15, 12489 Berlin

We studied the time-resolved magnetization dynamics of an epitaxially grown heterostructure comprised of an antiferromagnetic (AFM) Mn wedge sandwiched between two ferromagnetic (FM) Co layers on Cu(001). The two FM layers were coupled indirectly by the Ruderman-Kittel-Kasuya-Yosida (RKKY) interaction and directly exchange coupled through the AFM spin structure, leading to parallel or antiparallel alignment of the FM layers, depending on the Mn thickness [1]. Deposition of Mn in a wedge allowed for access to different coupling regimes on the same sample. Magnetization dynamics were observed after excitation with 800 nm laser pulses by X-ray magnetic circular dichroism (XMCD) in resonant soft X-ray reflectivity. We point out the effect an antiferromagnetic spacer layer has on the magnetization dynamics of the FM layers.

[1] Bin Zhang et al., J. Appl. Phys. 115, 233915 (2014)

MA 40.13 Thu 14:00 P2/EG

Anomalous relaxation dynamics of different types of impurity models — •MICHAEL ELBRACHT and MICHAEL POTTHOFF — I. Institute of Theoretical Physics, University of Hamburg, Germany

The real-time relaxation dynamics of different types of one-dimensional lattice models with two additional impurities is investigated numerically. We study purely classical, purely quantum mechanical as well as semiclassical systems: (i) a model with two classical spins exchanged coupled to the classical Heisenberg model, (ii) two classical spins exchanged coupled to a tight-binding model of independent electrons, and (iii) a model with the spins replaced by two additional orbitals locally hybridizing with the tight-binding chain.

After an initial local excitation of the impurities, we trace the real-time dynamics by solving the respective fundamental equations of motion. Depending on the exact position of the impurities, the system does or does not fully relax to its local ground state. In all cases, one observes for an even distance between

the impurities and after a preresolution to a low-energy state, that the system is trapped in a stationary oscillatory mode. Various mechanisms for this incomplete relaxation are considered, including the dynamical emergence of conserved local quantities.

MA 40.14 Thu 14:00 P2/EG

Spin reduction in the covalent chain antiferromagnets RbFeSe₂ and KFeS₂ — •Z. SEIDOV¹, H.-A. KRUG VON NIDDA¹, A. KHAMOV², M. KUZNETSOV², V. TSURKAN^{2,3}, I. FILIPPOVA³, D. CROITORI³, F. MAYR¹, S. WIDMANN¹, F. VAGIZOV², D. TAYURSKI², and L. TAGIROV² — ¹EPV, EKM, Institute of Physics, University of Augsburg, D-86135 Augsburg, Germany — ²Kazan, Russia — ³Institute of Applied Physics, MD-20208 Chisinau, Moldova

SQUID susceptibility, Mössbauer and specific-heat measurements show that RbFeSe₂ and KFeS₂ exhibit antiferromagnetic order below $T_N = 248$ K and $T_N = 251$ K, respectively. The magnetic specific heat and the spin state of the Fe³⁺ ions in the compounds have been analyzed. Phonon dispersion and phonon density of states (PDOS), were evaluated from first-principles calculations. Analysis of our Mössbauer data, utilizing the calculated Fe PDOS, as well as our optical absorption measurements have shown full agreement with the location of the high-frequency optical-type lattice vibrations within the FeX₄ (X = S, Se) tetrahedra. The phonon contribution to the heat capacity has been calculated from the PDOS and subtracted from the experimental data to extract the magnetic specific heat of the quasi 1D antiferromagnetically correlated Fe³⁺ ion chains. The corresponding magnetic entropy suggests a reduced spin value for the Fe³⁺ ions in both compounds, which seems to be close to an intermediate spin state $S = 3/2$ in RbFeSe₂ and to a low-spin state $S = 1/2$ in KFeS₂.

MA 40.15 Thu 14:00 P2/EG

Growth optimization and magnetotransport properties of ferromagnetic gadolinium nitride (GdN) thin films — •RAPHAEL HOEPLF^{1,2}, MANUEL MÜLLER^{1,2}, JOHANNES WEBER^{1,2}, MATTHIAS OPEL¹, STEPHAN GEPRÄGS¹, HANS HUEBL^{1,2,3}, RUDOLF GROSS^{1,2,3}, and MATTHIAS ALTHAMMER^{1,2} — ¹Walther-Meißner-Institut, Bayerische Akademie der Wissenschaften, Garching, Germany — ²Technical University of Munich, TUM School of Natural Sciences, Physics Department, Garching, Germany — ³Munich Center for Quantum Science and Technology (MCQST), München, Germany

Ferromagnetic (FM) semiconductors are of great interest for spintronic devices. Gadolinium nitride (GdN) is one candidate for a FM semiconductor with a Curie temperature $T_C = 65-70$ K [1]. By performing SQUID magnetometry and magnetotransport experiments in a cryogenic environment, we investigate the static magnetic and magnetoresistive properties of GdN thin film heterostructures. Tantalum nitride (TaN)/GdN/TaN trilayers are grown on the thermal oxide of Si substrates using DC magnetron sputtering, where the TaN is used as an electrically conductive seed and top layer. We study the impact of the various deposition parameters, such as deposition pressure, substrate temperature, growth rate and reactive N₂ gas flow on the static magnetic properties of GdN such as T_C and saturation magnetization M_S . For GdN layer stacks grown with our optimized recipe, we perform magnetotransport experiments and identify the origin of magnetoresistance in our heterostructures.

[1] W. B. Mi et al., Appl. Phys. Lett. 102, 222411 (2013).

MA 40.16 Thu 14:00 P2/EG

Tuning the physical properties of La_{0.7}Sr_{0.3}MnO_{3- δ} via oxygen off-stoichiometry using thermal annealing — •CHENYANG YIN¹, LEI CAO¹, SUQIN HE², TOMAS DUCHON³, YUNXIA ZHOU⁴, OLEG PETRACIC¹, and THOMAS BRÜCKEL¹ — ¹Jülich Centre for Neutron Science (JCNS-2) and Peter Grünberg Institut (PGI-4), JARA-FIT, Forschungszentrum Jülich GmbH, Jülich, Germany — ²Peter Grünberg Institut (PGI-7), JARA-FIT, Forschungszentrum Jülich GmbH, Jülich, Germany — ³Peter Grünberg Institut (PGI-6), JARA-FIT, Forschungszentrum Jülich GmbH, Jülich, Germany — ⁴Helmholtz-Zentrum Dresden-Rossendorf (HZDR), Dresden, Germany

The oxygen off-stoichiometry in La_{0.7}Sr_{0.3}MnO_{3- δ} (LSMO) thin films on SrTiO₃ (STO) substrates has been investigated employing Al-assisted vacuum annealing. The gradual deoxygenation during annealing induces a topotactic phase transition from the as-prepared Perovskite (PV, ABO₃) phase to a layered oxygen-vacancy-ordered Brownmillerite (BM, ABO_{2.5}) phase. The structural change is monitored by XRD. A metal-to-insulator and simultaneously a ferromagnetic (FM)-to-antiferromagnetic (AF) transition is found. The variation of the manganese oxidation state is characterized using XAS. The BM phase shows in magnetization vs. temperature curves a peculiar peak above room temperature which cannot be explained within the usual AF ordering at low temperatures. Moreover, to elucidate the role of the strain to the substrate, bulk-like LSMO powder samples were prepared and annealed at similar conditions as the film samples. Also here the PV-BM phase transition is achieved.

MA 40.17 Thu 14:00 P2/EG

Growth and characterization of $\text{Ca}_x\text{Sr}_{1-x}\text{RuO}_3$ ($x = 0, 0.3, 0.5, 0.7$) and $\text{Sr}_4\text{Ru}_3\text{O}_{10}$ single crystals — •ZAHRASADAT GHAZINEZHAD¹, AKSHAY TEWARI¹, AGUSTINUS AGUNG NUGROHO², KEVIN JENNI¹, and MARKUS BRADEN¹ — ¹II. Physikalisches Institut, Universität zu Köln, Zùlpicher Straße 77, D-50937 Köln, Germany — ²Faculty of Mathematics and Natural Sciences, Institut Teknologi Bandung, Jl. Ganesha 10, Bandung 40132, Indonesia

The Ruddlesden-Popper (RP) series of strontium ruthenates $\text{Sr}_{n+1}\text{Ru}_n\text{O}_{3n+1}$ manifests an interesting variety of phenomena. Here we focus on the crystal growth and on the detailed characterization of the ferromagnetic SrRuO_3 ($n=\infty, 1-1-3$) and $\text{Sr}_4\text{Ru}_3\text{O}_{10}$ ($n=3, 4-3-10$) systems. A peculiar property of the mixed 1-1-3 materials $\text{Ca}_x\text{Sr}_{1-x}\text{RuO}_3$ with $x = 0, 0.3, 0.5, 0.7$ concerns the tuning of electronic and magnetic features by substitution of smaller Ca^{2+} ions into the Sr^{2+} sites while not changing the electronic configuration [1]. The triple-layer ruthenate compound $\text{Sr}_4\text{Ru}_3\text{O}_{10}$ exhibits a ferromagnetic transition at $T_C = 105\text{K}$ followed by an additional magnetic transition at $T_M = 50\text{K}$ which remains matter of controversy. This layered material also shows strong anisotropy concerning the application of magnetic fields [2]. Large single-crystals of $\text{Sr}_4\text{Ru}_3\text{O}_{10}$ could be grown by the floating-zone technique and were characterized by structural and magnetization measurements.

[1] K. Yoshimura, et al. Phys. Rev. Lett. **83**, 4397 (1999).

[2] M. Zhu, et al. Scientific reports **8**, 1 (2018).

MA 40.18 Thu 14:00 P2/EG

Analysis of Exchange Bias training effect in Exchange coupled LaFeO₃/NiO nanocomposite — •PRIYANKA SHARMA¹ and RATNAMALA CHATTERJEE² — ¹Indian Institute of Technology Delhi, New Delhi 110016, India — ²Indian Institute of Technology Delhi, New Delhi 110016, India

Existence of exchange bias (EB) resulting from antiferromagnetic/ferromagnetic interface is well known in the literature. EB phenomenon is characterized by the horizontal shift of the magnetic hysteresis loop as the system is cooled through Neel's temperature in presence of an external magnetic field. EB is the backbone of designing magnetic storage devices and is among the modern approaches to spintronics. One of the interesting characteristics of EB is the training effect [1]. In this work, we investigate the EB training effect (TE) in LaFeO₃/NiO nanocomposite synthesized by a chemical route. The consecutive measurement of field cooled (60 kOe) magnetic hysteresis loops at 5 K show that the exchange bias field (HE) decreases with the increasing number of cycles of M-H loops (n) confirming the presence of the TE effect in our sample. The experimentally observed trend between HE and n was fitted using the power law and Binek's recursive relation. From the Binek's recursive relation, the obtained value of HE infinity (EB field in the limit of infinite loops) and γ (sample dependent constant) is 1118 Oe & 6.9×10^{-7} (Oe)⁻², respectively. Both, the power law and Binek's recursive relation points coincide well with the experimental observations.

[1] C. Binek, Physical Review B **70** (1), 014421 (2004).

MA 40.19 Thu 14:00 P2/EG

Impact of Currents on SDW Order in Sr_2RuO_4 — •FELIX WIRTH, THOMAS LORENZ, and MARKUS BRADEN — II. Physikalisches Institut, Köln, Germany

Unconventional superconductivity and magnetic correlations are expected to be closely coupled in Sr_2RuO_4 . Ca- and Ti-doped Sr_2RuO_4 exhibit incommensurate (IC) spin density wave (SDW) order below about 20 K appearing at the same wave vector where IC antiferromagnetic spin fluctuations exist in the pure compound. A recent attempt to explain the magnetic order induced by Ti-doping, proposed a potential enhancement of the SDW order by applying an external charge current [1]. To prove this idea Sr_2RuO_4 single crystals doped with 25 % Ca or with 9 % Ti were grown by the optical floating zone technique. The crystal quality was greatly improved during the iterative process of crystal growth. For the investigations of the impact of currents on the SDW order, the MPMS SQUID magnetometer was adapted. No influence of currents on the SDW state was observed that could not be attributed to sample heating issues. Recorded I-U characteristics did not reveal correlations between the SDW and the electronic properties of the system. Thermal expansion shows significant differences for both cases. The thermal expansion of the Ca-doped crystal qualitatively agrees with results for higher Ca concentrations but does not indicate connections to the SDW state. A negative thermal expansion at low temperatures in the Ti-doped crystal may point to a weak correlation to the SDW state but it also resembles the behaviour in pure Sr_2RuO_4 .

[1] B. Zinkl, et al. Phys. Rev. Res. **3** (2021).

MA 40.20 Thu 14:00 P2/EG

Magnetic phases in the perovskite vanadate ErVO₃ — •ELAHEH SADROLLAHI¹, JOCHEN LITTERST², TOBIAS RITSCHHEL¹, and JOCHEN GECK¹ — ¹Institut für Festkörper- und Materialphysik, Technische Universität Dresden, 01069 Dresden, Germany — ²Institut für Physik der Kondensierten Materie, Technische Universität Braunschweig, 38106 Braunschweig, Germany

The perovskite-type vanadium oxide, ErVO₃, with Jahn-Teller active t_{2g} electrons at the V site, is a prototypical correlated electron system with orbital degrees of freedom [1-3]. It features an intimate interplay between spin, orbital, and

lattice interactions leading to several magnetic transitions. We have performed μSR on the perovskite vanadate ErVO₃. Magnetic susceptibility, specific heat, and neutron diffraction measurements on single crystals reveal orbital ordering and orbital-flipping transitions, as well as spin ordering/spin reorientation transitions. Our μSR survey picks up these magnetic transitions and spin freezing of about 20% of the sample volume below 3 K. [1] P. Telang et al, Journal of Crystal Growth **507**, 406-412 (2019) [2] P. Bordet et al. J.Solid State Chem. **106**, 253 (1993) [3] M. Reehuis et al. Phys. Rev. B **73**, 094440 (2006)

MA 40.21 Thu 14:00 P2/EG

Theoretical investigation of magnetic order in crystals with space group $I4_1md$ — •MAURICE COLLING¹ and JAN MASELL^{1,2} — ¹Karlsruhe Institute of Technology (KIT), Karlsruhe, Germany — ²RIKEN CEMS, Wako, Japan

Non-collinear magnetic textures with short ranged modulation in the magnetization exhibit novel transport behavior. Such textures have been proposed to be useful in next generation magnetic memory devices. [1] Materials in the space group $I4_1md$ (#109), such as the Weyl semimetal GdAlSi, are interesting candidates for investigations in this direction because of the many potentially competing interactions. Long-ranged RKKY interaction might stabilize atomic scale spin spirals. Broken inversion symmetry generates an interfacial Dzyaloshinskii-Moriya interaction which favors Néel type spirals. Dipolar interactions, in turn, favor Bloch type helices. We derive a phenomenological Hamiltonian based on symmetry analysis and present the rich phase diagram.

[1] J. Masell, X. Z. Yu, N. Kanazawa, Y. Tokura, and N. Nagaosa, Phys. Rev. B **102**, 180402 (2020).

MA 40.22 Thu 14:00 P2/EG

Crystal structural investigations of frustrated 3D spin- $\frac{1}{2}$ system $\text{CuSn}(\text{OH})_6$

— •KAUSHAL PARUI¹, ANTON KULBAKOV¹, ELLEN HÄUSSLER², THOMAS DOERT², VLADIMIR POMJAKUSHIN³, DMYTRO INOSOV¹, and DARREN PEETS¹ — ¹IFMP, TU Dresden, Germany — ²Professor f. Anorganische Chemie II, TU Dresden, Germany — ³LNS, Paul Scherrer Institut, Switzerland

Copper tin hydroxide, $\text{CuSn}(\text{OH})_6$ is an A-site-vacant double perovskite with the general stoichiometry $\square_2(BB')(\text{OH})_6$, where B and B' are transition metals. Here, the magnetic Cu^{2+} ions sit on a face-centred sublattice, which makes the system frustrated and is expected to exhibit exotic quantum magnetism. Room-temperature x-ray diffraction performed on polycrystalline samples reveals tetragonal $P4_2/n$ symmetry, possibly with a minor monoclinic distortion. The structure is characterized by the presence of alternating corner-sharing $[\text{Cu}^{2+}(\text{OH})_6]$ and $[\text{Sn}^{4+}(\text{OH})_6]$ at 4d and 4c sites, respectively. Low-temperature neutron diffraction performed on deuterated powder samples accurately determined hydrogen positions. The positions of other atoms differ significantly from the previously published structure. Our proposed crystal structure of $\text{CuSn}(\text{OH})_6$ is consistent with the tilt system $a^+a^+c^-$, as compared to the earlier proposed $a^+b^+b^+$. Magnetization measurements reveal a weak anomaly at 4.1 K suggesting a possible magnetic transition. Surprisingly, magnetic neutron diffraction revealed no long-range order down to 1.6 K. The Curie-Weiss temperature of $-7.1(3)$ K, indicating antiferromagnetic interactions, and a paramagnetic moment of $\approx 2.2\mu_B$ were also determined.

MA 40.23 Thu 14:00 P2/EG

Magnetoelastic Coupling, Grüneisen Scaling and Magnetic Phase Diagram of the Kitaev Material $\text{Na}_2\text{Co}_2\text{TeO}_6$ — •MARIUS SÄUBERT¹, JAN ARNETH¹, KWANG-YONG CHOI², and RÜDIGER KLINGELER¹ — ¹Kirchhoff Institute for Physics, Heidelberg University, Germany — ²Department of Physics, Sungkyunkwan University, Republic of Korea

We report high-resolution thermal expansion and magnetostriction measurements on the Kitaev candidate material $\text{Na}_2\text{Co}_2\text{TeO}_6$ down to low temperatures and up to high magnetic fields. Our data enable us to quantify magnetoelastic coupling and identify dominant energy scales by means of Grüneisen analysis. Combined magnetisation and magnetostriction studies reveal a hitherto unreported, field-induced crossover for $B||c$ accompanied by a sign change of $\partial T_N/\partial B$. For magnetic fields applied parallel to the honeycomb planes, magnetostriction shows that the anomaly in magnetisation at $B_C \approx 6\text{T}$, which has recently been speculated to mark the onset of magnetic disorder, is connected to discontinuous lattice changes. Finally, our dilatometric studies allow us to construct the magnetic phase diagram of $\text{Na}_2\text{Co}_2\text{TeO}_6$ which displays strong hysteresis at low temperatures.

MA 40.24 Thu 14:00 P2/EG

Non-Coplanar Magnetic Orders in Classical Square-Kagome Antiferromagnets — •MARTIN GEMBE¹, HEINZ-JÜRGEN SCHMIDT², CIARÁN HICKEY¹, JOHANNES RICHTER^{3,4}, YASIR IQBAL⁵, and SIMON TREBST¹ — ¹Institute for Theoretical Physics, University of Cologne, Germany — ²Fachbereich Physik, Universität Osnabrück, Germany — ³Institut für Physik, Otto-von-Guericke-Universität Magdeburg, Germany — ⁴Max-Planck-Institut für Physik Komplexer Systeme, Dresden, Germany — ⁵Department of Physics and Quantum Centers in Diamond and Emerging Materials (QuCenDiEM) group, Indian Institute of Technology Madras, India

Motivated by the recent synthesis of $\text{KCu}_6\text{AlBiO}_4(\text{SO}_4)_5\text{Cl}$, we study the classical Heisenberg model on the square-kagome lattice – also called the squagome or shuriken lattice. This cousin of the kagome lattice exhibits, already on the classical level, a rich phenomenology of frustrated magnetism including residual entropy, order-by-disorder, and non-coplanar ordering tendencies. Having in mind that upon introducing quantum fluctuations, non-coplanar order melts into chiral spin liquids, we explore the multitude of non-coplanar orders including some which break rotational symmetry (possibly leading to nematic quantum orders), for an elementary, classical Heisenberg model on the squagome lattice supplemented by cross-plaquette interactions.

MA 40.25 Thu 14:00 P2/EG

Frustrated Low-dimensional Copper Compounds Bluebellite and Rouaite. — •ASWATHI MANNATHANATH CHAKKINGAL¹, FALK PABST², VLADIMIR POMJAKUSHIN³, MAXIM AVDEEV⁴, ROMAN GUMENIUK⁵, DARREN PEETS¹, and DMYTRO INOSOV¹ — ¹IFMP, TU Dresden, Germany — ²Professur f. Anorganische Chemie II, TU Dresden, Germany — ³PSI, Switzerland — ⁴ANSTO, Australia — ⁵Institut für Experimentelle Physik, TU Bergakademie Freiberg, Germany

The hydrothermal technique is an efficient strategy to synthesize mineralogically inspired structures, including natural and synthetic cuprate minerals with a variety of exciting frustrated magnetic lattices. We report the hydrothermal synthesis of bluebellite ($\text{Cu}_6[(\text{IO}_3)(\text{OH})_3](\text{OH})_7\text{Cl}$) and rouaite ($\text{Cu}_2(\text{NO}_3)(\text{OH})_3$). Neutron diffraction studies were performed to determine both compound's crystal structure and magnetic structure. $\text{Cu}_2(\text{NO}_3)(\text{OH})_3$ crystallizes in a monoclinic structure consisting of a ferromagnetic chain and an antiferromagnetic chain of Cu^{2+} . This is similar to the botallackite ($\text{Cu}(\text{OH})_3\text{Br}$) in which spinon-magnon mixing was recently reported. $\text{Cu}_6[(\text{IO}_3)(\text{OH})_3](\text{OH})_7\text{Cl}$ crystallizes in a trigonal structure, and the magnetic Cu^{2+} forms a distorted maple-leaf lattice. Frustration effects and quantum fluctuations in spin-1/2 maple-leaf lattice antiferromagnets may give rise to interesting phenomena. We report details of the crystal structure, magnetic structure, and the low-temperature magnetic and thermal properties.

MA 40.26 Thu 14:00 P2/EG

Variational iPEPS — •ERIK WEERDA¹, JAN NAUMANN², MATTEO RIZZI², JENS EISERT¹, and PHILIPP SCHMOLL¹ — ¹Institute for Theoretical Physics, University of Cologne, D-50937 Köln, Germany — ²Dahlem Center for Complex Quantum Systems and Institute for Theoretical Physics, Freie Universität Berlin, 14195 Berlin, Germany

Tensor networks capture large classes of ground states of phases of quantum matter faithfully and efficiently. Their manipulation and contraction has remained a challenge over the years, however. For most of the history of projected entangled pair states, ground state simulations of two-dimensional quantum lattice systems using (infinite) projected entangled pair states have relied on what is called a time-evolving block decimation. In recent years, multiple proposals for the variational optimization of the quantum state have been put forward, overcoming accuracy and convergence problems of previously known methods. The incorporation of automatic differentiation in tensor networks algorithms has ultimately enabled a new, flexible way for variational simulation of ground states and excited states. In this work, we present and explain the functioning of an efficient, comprehensive and general tensor network library for the simulation of infinite two-dimensional systems using iPEPS, with support of different lattice geometries, flexible unit cells, the use of symmetries and GPU calculations.

MA 40.27 Thu 14:00 P2/EG

Charge dynamics in doped frustrated magnets and quantum spin liquids — •LUKE STASZEWSKI and ALEXANDER WIETEK — Max Planck Institute for the Physics of Complex Systems, 01187 Dresden, Germany

The advent of recent developments in algorithms, namely finite temperature tensor network related algorithms, has opened the doors to a serious numerical testbed for investigating the plethora of interesting phenomenology in strongly interacting electron systems. This testbed is taking us a step closer to understanding an array of systems displaying unconventional superconductivity as well as helping answer questions about the delicate interplay between magnetic correlations and the onset of superconductivity in such materials. This work looks at how the mobility of holes is affected by various magnetic environments and vice versa in the hope to shed some more light on the nature of the mechanisms at play in the resulting phases that have recently been demonstrated both numerically and experimentally. We focus on the role geometric magnetic frustration plays in leading to both unconventional superconductivity, and exotic magnetic order, such as quantum spin liquids.

MA 40.28 Thu 14:00 P2/EG

Micromagnetic simulation of magnetic reversal processes in exchange biased thin film geometries — •LUKAS PAETZOLD, SAPIDA AKHUNDZADA, CHRISTIAN JANZEN, and ARNO EHRESMANN — Institute of Physics and Center for Interdisciplinary Nanostructure Science and Technology (CINaT), University of Kassel, Heinrich-Plett-Strasse 40, 34132 Kassel, Germany

As first observed by Meiklejohn and Bean [1] and described as a unidirectional anisotropy, the exchange bias is a well-known interface effect between antiferromagnetic and ferromagnetic thin films. Initiated by field cooling [1], sputter deposition [2], or light-ion bombardment [3] the effect appears as a shift of the hysteresis loop and increased coercive fields [4]. Micromagnetic simulations [5,6] are presented for investigating the magnetic reversal processes in exchange biased thin film systems with a polycrystalline uncompensated antiferromagnetic layer. Different geometries like stripes, squares and discs in the micrometer range are simulated and the influence of modified magnetic parameters in the edges is investigated.

- [1] W. H. Meiklejohn et al., Phys. Rev. 105, 904 (1956)
 [2] A. E. Berkowitz et al., J. Magn. Magn. Mater. 200, 552-570 (1999)
 [3] D. Engel et al., J. Magn. Magn. Mater. 293, 849-853 (2005)
 [4] J. Nogués et al., J. Magn. Magn. Mater. 192(2), 203-232 (1999)
 [5] A. Vansteenkiste et al., AIP Advances 4, 107133 (2014)
 [6] J. De Clercq et al., J. Phys. D: Appl. Phys. 49, 435001 (2016)

MA 40.29 Thu 14:00 P2/EG

Magneto-ionic control of magnetic properties in perpendicular magnetized synthetic antiferromagnet stacks — •MARIA-ANDROMACHI SYSKAKI¹, TAKA AKI DOHI^{2,3}, MONA BHUKTA², JÜRGEN LANGER¹, MATHIAS KLÄUI², and GERHARD JAKOB² — ¹Singulus Technologies AG, 63796 Kahl am Main, Germany — ²Institut für Physik, Johannes Gutenberg-Universität Mainz, Staudingerweg 7, 55128 Mainz, Germany — ³Laboratory for Nanoelectronics and Spintronics, Research Institute of Electrical Communication, Tohoku University, Sendai, Japan

Voltage-controlled spintronic devices are the key to a more energy-efficient way for future storage applications [1]. Electric field effect experiments in this direction reported that the application of a low-power ionic liquid gating technique [2] to nearly compensated synthetic antiferromagnet (SAF) stacks gives rise to high domain wall velocities [3]. In our work, we have grown a SAF stack by magnetron sputtering consisting of two ferromagnetic layers coupled by a non-magnetic spacer layer. The coupling strength is modified by tuning the thickness of the spacer layer to investigate the electric field modulation. With room temperature voltage-controlled magneto-ionic effects, we focus on the modulation of the magnetic properties in this system, i.e., the control of the compensation ratio, the perpendicular magnetic anisotropy, and the antiferromagnetic RKKY coupling strength. [1] T. Nozaki et al., Micromachines 10(5), 327 (2019). [2] C. Leighton et al., Nature Mater 18, 13 (2019). [3] Y. Guan et al., Nat. Commun. 12, 5002 (2021).

MA 40.30 Thu 14:00 P2/EG

Exchange bias in PtMn/Co: New insights into its origin and possibilities for manipulation — •BEATRICE BEDNARZ¹, MARIA-ANDROMACHI SYSKAKI², ROHIT PACHAT³, LIZA HERRERA-DIEZ³, ARMIN KLEIBERT⁴, MATHIAS KLÄUI¹, and GERHARD JAKOB¹ — ¹Johannes Gutenberg-University, Mainz, Germany — ²Singulus Technology AG, Kahl, Germany — ³Université Paris-Saclay, Palaiseau, France — ⁴Paul Scherrer Institute, Villigen PSI, Switzerland

Exchange bias is fundamental for many spintronic devices as a means of pinning the direction of the ferromagnetic layer [1,2] and for exerting an intrinsic magnetic field for field-free switching [3]. One of the most commonly used antiferromagnets for this purpose is PtMn [4]. It has a CuAu-I type structure with a high bulk Néel temperature of 975 K and high thermal stability [4]. In this study, we report on new insights into its magnetic structure and the effect on the exchange bias. The magnetic domains were imaged for crystalline as well as polycrystalline PtMn by x-ray magnetic linear dichroism (XMLD) photo-emission electron microscopy (PEEM). We found that the drastic difference in the exchange bias is not caused by a difference in the domain size but only by differences in the domain orientations. Furthermore, we show that the magnetic properties of the exchange biased system can be reversibly controlled by ionic liquid gating.

- [1] A.V. Khvalkovskiy et al., J. Phys. D: Appl. Phys. 46, 074001 (2013). [2] S.S.P. Parkin et al., J. Appl. Phys. 85, 5828 (1999). [3] A. van den Brink et al., Nat. Commun. 7, 10854 (2016). [4] G.W. Anderson et al., J. Appl. Phys. 87, 5726 (2000).

MA 40.31 Thu 14:00 P2/EG

Relaxation behavior of antiferromagnetic grains in polycrystalline exchange-biased bilayers — •MAXIMILIAN MERKEL, RICO HUHNSTOCK, MEIKE REGINKA, and ARNO EHRESMANN — Institute of Physics and Center for Interdisciplinary Nanostructure Science and Technology (CINaT), University of Kassel, Heinrich-Plett-Str. 40, D-34132 Kassel

Measuring first-order reversal curves, a prototypical polycrystalline exchange-biased bilayer was found to exhibit a viscous decrease of the ferromagnetic in-plane magnetization upon increasing the external magnetic field. [1] The observed phenomenon is mediated by a rotatable magnetic anisotropy arising from thermally unstable antiferromagnetic grains coupled to the probed ferromagnet. The investigations, performed with the help of angular-resolved vectorial Kerr magnetometry and Kerr microscopy, are further in agreement with a generalized description of polycrystalline exchange-bias systems. The study emphasizes

the relevance of understanding minor loop behavior addressing non-saturated magnetic states for systems susceptible to dynamic changes on the hysteresis loop timescale.

[1] Merkel et al., Phys. Rev. B 104, 214406 (2021)

MA 40.32 Thu 14:00 P2/EG

Tailoring the electronic and magnetic properties of the layered antiferromagnet CrCl₂ — •DIANA VACLAVKOVA, VLADYSLAV ROMANKOV, NIÉLI DAFÉ, and JAN DREISER — Swiss Light Source (SLS), Paul Scherrer Institut (PSI), CH-5232 Villigen PSI, Switzerland

The electronic and magnetic properties of two-dimensional van der Waals (vdW) materials differ greatly when comparing mono- and few-layered flakes to their bulk counterparts. In the case of atomically thin single layers the substrate has a profound influence on their properties. CrCl₂, belonging to the family of vdW materials, is expected to show a geometrical frustration in the monolayer limit given antiferromagnetic interactions are present [1]. Our preliminary studies involve X-ray magnetic circular dichroism measurements of mono- and few-layered CrCl₂ deposited on different materials. Based on the initial interpretation of the experimental data, methods for tailoring the magnetic properties by careful choice of the substrate material will be discussed.

[1] McGuire, M. A. (2017). Crystal and magnetic structures in layered, transition metal dihalides and trihalides. Crystals, 7(5), 121.

MA 40.33 Thu 14:00 P2/EG

Angle dependent FMR studies on YIG films — •TIM VOGEL¹, DAVID BREITBACH¹, CARSTEN DUBS², BURKARD HILLEBRANDS¹, and PHILIPP PIRRO¹ — ¹Fachbereich Physik and Landesforschungszentrum OPTIMAS, RPTU Kaiserslautern-Landau, Germany — ²INNOVENT e.V. Technologieentwicklung, Jena, Germany

Yttrium iron garnet (YIG) is a commonly used material in magnonics due to its low spin-wave damping. Previous ferromagnetic resonance spectroscopy (FMR) studies on (111) grown YIG thin films suggested a deviation from the expected sixfold symmetry of the magnetocrystalline anisotropy for large external fields. For more in-depth investigations, we developed a fully automated setup for angle dependent vector-network-analyzer-FMR studies of in-plane magnetized YIG films. We apply this setup to investigate a (111) grown, d=55nm thick LPE YIG film. Our results confirm the expected sixfold symmetry even for high external field values. Further, we apply the setup to quantify the effect of the present anisotropy field. This study contributes to the understanding of YIG thin films and the impact of magnetocrystalline anisotropy for magnonic applications.

This research is funded by the DFG - Project No. 271741898 and TRR 173-26856370 (B01) and the ERC Grant No. 101042439 'CoSpin'.

MA 40.34 Thu 14:00 P2/EG

Quantification of anisotropic and magneto-elastic contributions to the SSW excitation in Bi:YIG films via UXRD — •STEFFEN PEER ZEUSCHNER¹, XI-GUANG WANG^{3,4}, MARWAN DEB¹, ELENA POPOVA⁵, GREGORY MALINOWSKI⁶, MICHEL HEHN⁶, ALEXANDER VON REPPERT¹, NILS KELLER⁵, JAMAL BERAKDAR⁴, and MATIAS BARGHEER^{1,2} — ¹Universität Potsdam, 14476 Potsdam, Germany — ²Helmholtz-Zentrum Berlin, 12489 Berlin, Germany — ³Central South University, Changsha 410083, China — ⁴Martin-Luther Universität, 06099 Halle/Saale, Germany — ⁵Institut de Physique de Rennes (IPR, CNRS) UMR6251 Université Rennes, 35000 Rennes, France — ⁶Institut Jean Lamour (IJL, CNRS) UMR 7198, Université de Lorraine, 54506 Vandœuvre-lès-Nancy, France

The photoexcited standing spin waves (SSWs) in the ferromagnetic insulator Bi:YIG are generated by the ultrafast change of the magnetocrystalline anisotropy and the picosecond strain dynamics via magneto-elasticity. Ultrafast X-ray diffraction (UXRD) quantifies the strain and temperature spatiotemporally which is used as input to a numerical micromagnetic model to fit the ultrafast time-resolved magneto-optical Kerr-effect (tr-MOKE) data of the thin film which exhibits SSWs. With this, we prove that both mechanisms drive the fundamental mode with opposite phase. Both mechanisms are also substantially active as the relative amplitude of the higher order modes indicates. This is a prime example for the exceptional assistance UXRD offers in the understanding and modelling of ultrafast magnetic phenomena.

MA 40.35 Thu 14:00 P2/EG

Generating small magnetic fields inside an open-end magnetic shielding with a superconducting solenoid magnet — •LUKAS VOGL^{1,2}, ANA STRINC^{1,2,3}, FRANZ HASLBECK¹, RUDOLF GROSS^{1,2,3}, and NADEZHDA KUKHARCHYK^{1,2,3} — ¹Walther-Meißner-Institut, Bayerische Akademie der Wissenschaften, Garching, Germany — ²Physik-Department, Technische Universität München, Garching, Germany — ³Munich Center for Quantum Science and Technologies, München, Germany

Quantum memory is an essential part for the development of quantum computers. One of the most promising realisation of quantum memories has been realised for storage of optical photons in rare-earth-doped crystals, reaching a storage time of 6 hours. The long storage time has been achieved due to working

at the zero first-order Zeeman shift point (ZEFOZ). At this point, the phase-sensitivity of a spin system to the magnetic field fluctuations is strongly reduced, and thus longer coherence times can be achieved. Such ZEFOZ transitions are present in the hyperfine states of rare earth ions close to zero magnetic fields, which enables the design of quantum memories compatible with the zero-field environments required for superconducting quantum computing circuits. Here, we present a setup for a highly controllable homogeneous magnetic environment with additional shielding from external background magnetic fields. This environment will allow for precise control of the magnetic field at the sample position, fine tuning to the ZEFOZ transitions, and additional protection of the superconducting quantum circuits from the fields applied to the rare earth spins.

MA 40.36 Thu 14:00 P2/EG

Design and set-up of an optomechanical readout apparatus to characterize magnetic field sensors encompassing high-Q resonators down to 4 K — TORBEN HÄNKE, •DHAVALKUMAR MUNGPARA, and ALEXANDER SCHWARZ — Institute of Nanostructure and Solid State Physics, University of Hamburg, Jungiusstr. 11, 20355 Hamburg

This work has been conducted as part of the OXiNEMS project that aims to realize a miniaturized all-oxide hybrid sensor able to detect magnetic fields in the fT-regime. Our envisaged design encompasses a superconducting pick-up loop with a constriction and a magnetically sensitive high-Q resonator placed directly above it.

Here, we present a set-up to characterize the mechanical properties of potential resonators alone or already integrated into the hybrid sensor. To do so, the resonator motion is detected using an all-fiber interferometer inside a dip stick, which can be pumped to pressures below 10⁻⁶ mbar and cooled down to 4 K. Alignment between fiber and resonator in x-, y- and z-directions is done with remotely operated precision piezomotors. The resonator can be excited using an integrated shaker piezo to record amplitude and phase response curves. Without external excitation the power spectral density can be recorded and to test the performance of the complete hybrid sensor in operation, the frequency change of the resonator can be monitored.

The OXiNEMS project (www.oxinems.eu) has received funding from the European Union's Horizon 2020 research and innovation program under Grant Agreement No. 828784.

MA 40.37 Thu 14:00 P2/EG

Micro-Hall magnetometry for multiscale magnetic measurements — •BEREKET GHEBRETINSAE¹, CHARU GARG¹, MARTIN LONSKY¹, MOHANAD AL MAMOORI¹, MICHAEL HUTH¹, CHRISTIAN SCHRÖDER², PRISCILA ROSA³, and JENS MÜLLER¹ — ¹Institute of Physics, Goethe University, 60438 Frankfurt (M), Germany — ²Institute for Applied Materials Research, University of Applied Sciences Bielefeld, Bielefeld 33619, Germany — ³Los Alamos National Laboratory, Los Alamos, New Mexico 87545, USA

Micro-Hall magnetometry is a technique that allows for ultra-sensitive magnetic stray field measurements on macro- to micro- to nanoscaled samples. The magnetometer is a Hall sensor that utilizes the very high electron mobility of a two-dimensional electron gas inside a GaAs/AlGaAs heterostructure to resolve even smallest changes in the sample's stray field almost instantaneously. The technique is unique especially in its versatility. Firstly, the Hall sensor itself can serve as a substrate for the growth of nanoscaled magnetic samples with complex geometries. Secondly, microscopic and even macroscopic samples can be placed directly on top of the sensor surface such that the stray field emanating from the surface of the sample is captured by the Hall sensor. Here we demonstrate the utility of this technique using (i) 3D ferromagnetic FeCo nanostructures and (ii) single crystalline micro-sized Eu₅In₂Sb₆ with two antiferromagnetic transitions. We present magnetic field- and temperature dependent micro-Hall measurements to explain the details of the technique and prove its usefulness as a tool for the study of multiscale magnetic phenomena.

MA 40.38 Thu 14:00 P2/EG

PUMA: Thermal neutron three axes spectrometer — •ALSU GAZIZULINA¹, AVISHEK MAITY², JITAEE PARK², and FRANK WEBER¹ — ¹Institute of Quantum Materials and Technologies, Karlsruhe Institute of Technology, Eggenstein-Leopoldshafen, Germany — ²Heinz Maier-Leibnitz Zentrum, Technical University of Munich, Garching, Germany

Thermal neutron three axes spectrometer PUMA is characterized by a very high neutron flux as a result of the efficient use of focusing techniques. An innovative option of the spectrometer is the multianalyzer/detector system, which allows a unique and flexible type of multiplexing. Using this option, a scattering angle range of 16° can be measured simultaneously and flexible Q - ω paths can be realized without repositioning the instrument. The typical scientific applications of PUMA are studies of phonons and magnons. Furthermore, a unique feature of the instrument is the possibility to perform stroboscopic, time resolved measurements of both elastic and inelastic signals on time scales down to the microsecond regime. Using this technique, the sample is periodically perturbed by an external variable such as temperature, electric field, etc. The signal is then recorded not only as a function of momentum and energy transfer, but also given

a time stamp, relative to the periodic perturbation. Since 2021, the Neutron Scattering Group of the Institute of Quantum Materials and Technologies (IQMT) of the Karlsruhe Institute of Technology (KIT) has been jointly operating the PUMA three-axes spectrometer at MLZ within the framework of a collaboration contract.

MA 40.39 Thu 14:00 P2/EG

Pulse-triggered detection of resonant magnetic small-angle scattering at a laser-driven X-ray source — •LEONID LUNIN¹, MARTIN BORCHERT¹, DANIEL SCHICK¹, BASTIAN PFAU¹, and STEFAN EISEBITT^{1,2} — ¹Max-Born-Institut, Berlin, Germany — ²Technische Universität, Berlin, Germany

Resonant soft-x-ray scattering methods provide unique possibilities to study nanometer-scale magnetization dynamics on ultrashort timescales. Typically, these experiments are performed at synchrotron-radiation (SR) sources or x-ray free-electron lasers (XFELs) due to the required tunability and intensity of the radiation. While XFELs still offer only limited access, the available time resolution at SR sources on the order of 100 ps is insufficient for many phenomena in ultrafast magnetism. We developed an instrument based on a laser-driven plasma x-ray source to perform resonant x-ray scattering in the wavelength regime between 50 eV and 1500 eV with pulses of 10 ps duration. Specifically, we here present the first resonant small-angle x-ray scattering experiment on a laboratory scale with photon energies in the range of the transition-metal L edges and the rare-earth-metal M edges. In our pilot experiment, we detect scattering from domains forming in a ferrimagnetic Fe/Gd multilayer using an electronically triggered hybrid detector with single-photon sensitivity. Such laboratory-based measurements will allow studying magnetization dynamics with high spatio-temporal resolution in a much more efficient and flexible way than possible today.

MA 40.40 Thu 14:00 P2/EG

Quantitative high sensitivity Magnetic Force Microscopy in vacuum — •CHRISTOPHER HABENSCHADEN¹, SIBYLLE SIEVERS¹, and ANDREA CERRETA² — ¹Physikalisch-Technische Bundesanstalt, Braunschweig, Germany — ²Park Systems Europe GmbH, Mannheim, Germany

Magnetic Force Microscopy (MFM) allows the imaging of magnetic samples with spatial resolution of tens of nm and stray field resolution down to the mT range. However, it lacks comparability between measurements, which can be overcome by calibrating the tip, using a magnetic reference sample. This enables the calculation of sample stray fields in A/m, allowing quantitative MFM measurements.

Spatial resolution and field sensitivity can be pushed to several nm and the hundred μT range by measuring in vacuum conditions. This is due to the higher cantilever quality factors Q , that can be achieved in vacuum, directly leading to an increase in measurement signal. However, with increasing signal amplitude, non-linear behavior must be considered. Additionally, advanced feedback techniques are required for stable operation in vacuum.

Here we present an implementation by using phase-locked loops into a commercial Atomic Force Microscope (Park NX Hivac AFM), overcoming nonlinearities in measurement signal. This allows stable, transfer function based, quantitative MFM also in vacuum. Advances in resolution and sensitivity are discussed and measurements on samples like skyrmion hosting multilayer stacks are shown and analyzed to demonstrate the feasibility of our measurement approach.

MA 40.41 Thu 14:00 P2/EG

Development of an AC susceptometer for magnetic thin film systems — •MATTHIAS ZETZL, GRACE CAUSER, and CHRISTIAN PFLEIDERER — Physik-Department, Technical University of Munich, D-85748 Garching, Germany

An ongoing challenge in thin film magnetism concerns the need for easy-to-use characterization tools exploiting the response to alternating magnetic fields. We report the development of a bespoke ac-susceptometer comprising a primary and a balanced pair of secondaries specifically tailored for thin film systems. To gauge the performance of the susceptometer we have revisited the properties of epitaxial layers of MnSi in the thick film limit, in which high-resolution measurements of the temperature and field history of the magnetization, complemented by neutron scattering and neutron reflectometry, have recently identified the formation of a cascade of solitonic layers.

MA 40.42 Thu 14:00 P2/EG

Comparison of continuous and pulsed neutron sources for MIEZE witz McStas. — •KORBINIAN FELLNER¹, JOHANNA K. JOCHUM¹, LUKAS VOGL¹, LUKAS BEDDRICH¹, JONATHAN LEINER¹, CHRISTIAN FRANZ², and CHRISTIAN PFLEIDERER³ — ¹Heinz Maier-Leibnitz Zentrum (MLZ), Technische Universität München, Garching, Germany — ²Jülich Centre for Neutron Science JCNS-MLZ, Germany — ³Physik-Department, Technische Universität München, Germany

The MIEZE method is a type of the neutron spin-echo technique that uses oscillating neutron intensities to record changes to the energy of a scattered neutron. This allows MIEZE, which is implemented at the spectrometer RESEDA

to study magnetic dynamics, quantum phenomena, and molecular diffusion in soft matter, to achieve an energy resolution of neV, taking advantage of a broad wavelength band of $\Delta\lambda/\lambda=11.6\%$. Nonetheless, a significant portion of the neutron beam is discarded by the velocity selector, making MIEZE at pulsed neutron sources increasingly attractive. We have implemented the polarization shaping components of RESEDA in the McStas framework to investigate the feasibility and data reduction of a MIEZE spectrometer at a pulsed neutron source (PNS). The large wavelength spread of a PNS allows for the measurement of the intermediate scattering function over many points in Fourier time, similar to a multi-detector option at a triple-axis spectrometer. Simulations of a quasielastic sample enable a comparison of the performance between a reactor source and a PNS. Additionally, tests of crucial data reduction algorithms that have not been addressed in previous instrument proposals, are discussed.

MA 40.43 Thu 14:00 P2/EG

Characterizing the defocusing behaviour of magnetic microparticles for the application in three-dimensional trajectory tracking — •NIKOLAI WEIDT, RICO HUHNSTOCK, YAHYA SHUBBAK, and ARNO EHRESMANN — Institute of Physics and Center for Interdisciplinary Nanostructure Science and Technology (CINSaT), University of Kassel, Heinrich-Plett-Str. 40, D-34132 Kassel

For the implementation in Lab-on-a-chip systems, superparamagnetic particles can be surface-functionalized to bind to specific analytes [1]. Making use of the transport of particles above magnetically stripe-patterned exchange bias layer systems is a promising approach to achieve a remote-controlled and directed transport of these particles [2]. The trajectories of particles during transport can be evaluated for detection of analyte binding events. To get access to the third dimension in optical microscopy, the image characteristics of particles moving out of the focal plane during transport steps are analyzed [3]. In this work quantization of defocusing is achieved by determining the Tenenbaum gradient of single particle images. Correlation between Tenenbaum gradient and the particle's vertical position is established by moving the particles in z-direction through the focal plane of the microscope defined steps. Here we show Tenenbaum gradient curves for differently composed particles and changing illumination conditions. [1] Rampini et al. (2016) Lab on a Chip, 16(19), pp. 3645-3663. [2] Holzinger et al. (2015) ACS Nano, 9(7), pp. 7323-7331. [3] Tasadduq et al. (2015) Flow Measurement and Instrumentation, 45, pp. 218-224.

MA 40.44 Thu 14:00 P2/EG

Simulation of Interaction and Self-assembly of Magnetically Decorated Particles — SIBYLLE GEMMING, •MAXIMILIAN NEUMANN, and AARON STEINHÄUSSER — TU Chemnitz, Chemnitz, Germany

Magnetic particles with the ability to self-assemble allow for the creation of complex structures from simple parts while retaining malleability, enabling easy manipulation through external influences (e.g. magnetic fields). By arranging permanent magnets along the edges of particles in specific patterns we can assign (multiple) unique patterns to different species of particles without introducing additional geometric limitations. This kind of magnetic assembly schemes improves the selectivity between different types of particles and promotes fixed orientations between those on assembly. Our work shows different simulations of assembly schemes with a focus on finding optimal parameters to maximize interaction and selectivity.

MA 40.45 Thu 14:00 P2/EG

Giant Magnetic Resistance sensor array directly on board — •LAILA BONDZIO, TORBEN TAPPE, and ANDREAS HÜTTEN — Bielefeld University, Germany

GMR multilayer systems of Py/Cu-bilayers exhibit nearly triangular shaped GMR curves with a high sensitivity, which is desirable for sensor applications. With a grid of multiple sensor elements a two dimensional magnetic landscapes can be mapped as changes in a magnetic field. To organize and contact a large number of sensor elements on a wide spread area of few centimeters it might be useful to sputter the structure directly onto contacts on a circuit board. Although the circuit board is not an ideal substrate, it has been shown that such application is feasible.

MA 40.46 Thu 14:00 P2/EG

Multifunctional Magneto-Optical Sensing of Temperature and Magnetic Field — •MICHAEL P. PATH, FINN KLINGBEIL, and JEFFREY MCCORD — Institute of Materials Science, Kiel University, Germany

Measurements of temperature and magnetic field are vital in laboratory and industry settings. We demonstrate multi-functional magneto-optical measurement schemes to relate magnetic and micromagnetic features to temperature and magnetic field using magneto-optical active iron garnet films. The focus lies upon a dual quadrature polarimetric measurement scheme. A calibration free temperature measurement using the relation of the first and third harmonic of the obtained signal during a magnetic sinusoidal excitation of the garnets is presented. Using the domain wall susceptibility a limit of detection of the magnetic field below $14 \text{ nT}/\sqrt{\text{Hz}}$ is reached. Indirect measurements of current in integrated circuits is demonstrated using spatially resolved magnetic field sensitivity utilizing a direct magneto-optical imaging setup. A connection of field

and temperature measurements in magneto-optical imaging is discussed.

We acknowledge the DFG for funding through grant MC 9/20-2.

F. Klingbeil, S.D. Stöling, J. McCord, APL 118, 092403 (2021)

MA 40.47 Thu 14:00 P2/EG

Supervised folding of magnetic origami actuators using highly compliant magnetic field sensors — •EDUARDO SERGIO OLIVEROS-MATA¹, MINJEONG HA^{1,2}, GILBERT SANTIAGO CAÑÓN BERMÚDEZ¹, JESSICA A.-C. LIU³, BENJAMIN A. EVANS⁴, JOSEPH B. TRACY³, and DENYS MAKAROV¹ — ¹Helmholtz-Zentrum Dresden-Rossendorf, Dresden, Germany — ²Gwangju Institute of Science and Technology, Gwangju, South Korea — ³North Carolina State University, Raleigh, NC, United States — ⁴Elon University, Elon, NC, United States

Soft actuators are mechanically active functional systems. Magnetic polymeric composites have been used as grippers, rollers, and walkers responding to applied magnetic fields. Flexible, light and conformal sensory systems are still under research to have on-board control of the actuation of soft systems. Here, we show electronic skins with magnetic field sensors that provide awareness of the folding state of origami-like magnetic foils.

[1] M. Ha, E.S. Oliveros Mata, et al. Adv. Mater. 33, 2008751 (2021)

MA 40.48 Thu 14:00 P2/EG

Single magnetic domain magnetoelectric composites for picotesla field sensing — •DENNIS SEIDLER, PATRICK HAYES, LARS THORMÄHLEN, DIRK MEYERS, ECKHARD QUANDT, and JEFFREY MCCORD — Kiel University, Institute for Materials Science, Kaiserstraße 2, 24143 Kiel, Germany

The contactless measurement of biomagnetic signals i.e., magnetocardiography or magnetoencephalography at ambient conditions has gained high interest for medical applications. Magnetoelectric (ME) cantilever-based field sensors have shown promising results in that regard [1]. To achieve the necessary limit of detection (LOD) a minimization of all noise sources has to be performed. Magnetic noise mainly results from magnetic domain wall activity during sensor operation. We demonstrate a single-domain thick magnetic multilayer stack, to minimize the magnetic noise in the ME sensors. The multilayer is prepared via sputter deposition in an applied magnetic field. We utilize a scalable approach based on magneto-statically coupled $(\text{Fe}_{90}\text{Co}_{10})_{78}\text{Si}_{12}\text{B}_{10}$ layers, with the magnetic sensitive layer showing single domain behavior while still achieving high field sensitivity. Integrated in converse ME composite sensors, we obtain a LOD of $40 \text{ pT}\cdot\text{Hz}^{-0.5}$ at 10 Hz.

This work was funded by the German Research Foundation (DFG) through the Collaborative Research Centre CRC 1261.

[1] P. Hayes, M. Jovičević Klug, S. Toxværd, P. Durdaut, V. Schell, A. Teplyuk, D. Burdin, A. Winkler, R. Weser, Y. Fetisov, M. Höft, R. Knöchel, J. McCord, and E. Quandt, Sci Rep. 9, 16355 (2019)

MA 40.49 Thu 14:00 P2/EG

Spin-transfer torque ferromagnetic resonance in vortex magnetic tunnel junctions — •JOHANNES DEMIR, KARSTEN ROTT, and GÜNTER REISS — Bielefeld University, Germany

We investigate the gyrotropic mode resonance frequency of the vortex as the free layer of a magnetic tunnel junction (MTJ) by means of spin-transfer torque ferromagnetic resonance (STT-FMR) using a two-port vector network analyzer (VNA). In order to obtain a proper resistance-area (RA) product the capping layer of a commercial wafer was mostly etched down to sputter 8.5 nm permalloy as the vortex layer on top of it afterwards. Subsequently, nanopillars of 300 and 600 nm diameter were fabricated using electron-beam lithography. Using a coplanar-waveguide to feed the GHz-range current through the nanopillar the transmission scattering-parameter S_{21} was determined. Resonance frequencies of around 240 and 150 MHz for the 300 and 600 nm diameter samples, respectively, were measured in accordance with literature [1]. We recognize a shift of the frequency with increasing the bias voltage indicating a DC-STT contribution.

[1] V. Novosad et al., Phys. Rev. B 72, 024455 (2005)

MA 40.50 Thu 14:00 P2/EG

Growth and magnetic properties of Fe/Pt heterostructures with L10-FePt alloyed interface — LAURA SCHEUER¹ and •EVANGELOS TH. PAPAIOANNOU² — ¹Fachbereich Physik und Landesforschungszentrum OPTIMAS, Technische Universität Kaiserslautern, Erwin-Schrödinger-Str. 56, 67663, Kaiserslautern, Germany — ²Institut für Physik, Martin-Luther-Universität Halle-Wittenberg, Von-Danckelmann-Platz 3, 06120 Halle, Germany

The growth of Fe/L10FePt/Pt trilayers was achieved by means of electron beam evaporation technique and appropriate annealing. We show the formation of the L10 alloy for the case of Fe(12nm)/Pt (6nm) [1] and we investigate the formation of L10 phase for Fe,Pt thicknesses smaller than 3 nm. Magneto-optical and Squid magnetometry reveal the strong change in the magnetization reversal when the L10 phase appears. Furthermore, ferromagnetic resonance studies show a large enhancement of the gilbert damping parameter for the alloyed interface. Mumax simulations are implemented in order to understand the role of the L10 in the magnetic properties of the heterostructures.

[1] L.Scheuer et al., iScience25, 104319, (2022)

MA 40.51 Thu 14:00 P2/EG

Light-poling of antiferromagnetic domains in a magnetoelectric LiCoPO₄ — •JAKUB VIT^{1,2}, OLEKSIY PASHKIN³, VILMOS KOCSIS⁴, YASUJIRO TAGUCHI⁵, ISTVAN KEZSMARKI⁶, and SANDOR BORDACS¹ — ¹Budapest University of Technology and Economics, Hungary — ²Institute of Physics, Czech Academy of Sciences, Czechia — ³Helmholtz-Zentrum Dresden-Rossendorf, Germany — ⁴Institut für Festkörperforschung, Leibniz IFW-Dresden, Germany — ⁵RIKEN Center for Emergent Matter Science (CEMS), Japan — ⁶University of Augsburg, Germany

We selected antiferromagnetic domains in a magnetoelectric LiCoPO₄ single crystal by illuminating the sample by light while cooling through the Néel temperature. The experimental results and symmetry analysis indicate that the thermal gradient and resulting heat flow are responsible for such a novel effect: Propagation of thermally-activated quasi-particles is nonequivalent in different antiferromagnetic domains. The microscopic mechanism behind the observed effect is not clear at the moment, calling for future theoretical modeling.

MA 40.52 Thu 14:00 P2/EG

Spontaneous nanoscale square vs. hexagonal skyrmion lattices in Fe/Ir(111) — •MARA GUTZEIT, SOUMYAJYOTI HALDAR, TIM DREVELOW, MORITZ A. GOERZEN, and STEFAN HEINZE — Institute of Theoretical Physics and Astrophysics, University of Kiel, Leibnizstraße 15, 24098 Kiel, Germany

We investigate the occurrence of spontaneous skyrmion lattices in an Fe monolayer in both fcc and hcp stacking on the Ir(111) surface employing first-principles calculations based on density functional theory (DFT). For fcc-Fe the well-known non-collinear square nanoskyrmion lattice is confirmed as the magnetic ground state [1]. Surprisingly, for hcp-Fe a nearly collinear hexagonal multi-Q state turns out energetically more favourable than the hexagonal skyrmion lattice proposed based on spin-polarized scanning tunneling microscopy experiments [2]. By mapping total DFT energies of a variety of complex magnetic structures to an atomistic spin model we reveal the interplay of pairwise Heisenberg exchange, Dzyaloshinskii-Moriya interaction and higher-order exchange interactions to be responsible for the symmetry and the degree of collinearity of the respective spin lattice.

[1] Heinze et al. Nat. Phys. 7, 713 (2011)

[2] von Bergmann et al. Nano Lett. 15, 3280 (2015)

MA 40.53 Thu 14:00 P2/EG

Temperature dependent μ -ARPES of the exfoliated zigzag-type intralayer antiferromagnet FePS₃ — •B. PESTKA¹, J. STRASDAS¹, A. K. BUDNIAK², D. BARANOWSKI³, N. LEUTH¹, H. BOBAN³, M. LIEBMANN¹, V. FEYER³, L. PULCINSKI³, E. LIFSHITZ², and M. MORGENSTERN¹ — ¹II Institute of Physics B and JARA-FIT, RWTH Aachen University, Germany — ²Schulich Faculty of Chemistry, Solid State Institute of Technology, Haifa 3200003, Israel — ³Forschungszentrum Jülich, Peter Grünberg Institute (PGI-6), Germany

The exfoliable intralayer antiferromagnets MPX₃ (M: transition metal, P: phosphorus, X: chalcogenide) provide a multitude of spin arrangements such as Néel-, stripe- and zigzag-type. However, the electronic band structure of these semiconductors has barely been probed. Here, we provide micro-scale angle-resolved photoelectron spectroscopy (μ -ARPES) of the exfoliated intralayer antiferromagnet FePS₃ above and below the Néel temperature TN. The material exhibits the zig-zag-type spin arrangement consisting of ferromagnetic zig-zag lines that are mutually coupled antiferromagnetically. We find changes of some of the probed bands across TN. Additionally, the changing bands differ in the different Gamma-K directions, if probed below TN, which is likely related to the selected orientation of the ferromagnetic zig-zag stripes. First low-temperature scanning tunneling spectroscopy results obtained with a Cr tip are also presented. The novel access to the electronic band structure will contribute to a detailed understanding of 2D antiferromagnets.

MA 40.54 Thu 14:00 P2/EG

Optimised mechanical exfoliation of antiferromagnetic MnPS₃ — •NIKLAS LEUTH — II. Institute of Physics B, RWTH Aachen University, Aachen, Germany

An optimized mechanical exfoliation technique was developed to exfoliate large-area few-layer flakes of the antiferromagnetic van-der-Waals material MnPS₃. This was achieved by utilizing the process of oxygen plasma ashing on gold surfaces and making use of the good bonding strength between the gold surface and the sulfur atoms which terminate the individual layers of MnPS₃. Furthermore, there is evidence that the gold surface of the substrate gets oxidised by the oxygen plasma. With the optimised technique, it was possible to exfoliate ~ 100 μm^2 -large mono- and bilayer flakes. Furthermore, a method was developed which characterises the layer thickness of the exfoliated flakes quantitatively based on the optical Michelson contrast.

MA 40.55 Thu 14:00 P2/EG

Dual-pulse-excitation all-optical switching of a Gd₂₆Fe₇₄ ferrimagnet — •RAHIL HOSSEINIFAR¹, IVAR KUMBERG¹, SANGEETA THAKUR¹, SEBASTIEN HADJADJ¹, JENDRIK GORDES¹, CHOWDHURY AWSAF¹, MRIO FIX³, FLORIAN KRONAST², MANFRED ALBRECHT³, and WOLFGANG KUCH¹ — ¹Institut für Ex-

perimentalphysik, Freie Universität Berlin, Berlin, Germany — ²Helmholtz-Zentrum Berlin, Albert-Einstein-Straße 15, 12489 Berlin, Germany — ³Institut für Physik, Universität Augsburg, Universitätsstraße 1, Augsburg, Germany

Individual linearly *p*-polarized laser pulses of 800 nm wavelength above a specific threshold fluence can reverse the magnetization of ferrimagnetic samples. We study this all-optical toggle switching in Gd₂₆Fe₇₄ ferrimagnetic alloys with out-of-plane easy axis of magnetization after dual-pulse excitation by x-ray magnetic circular dichroism photoelectron emission microscopy. The time between the two spatially overlapped pulses is varied. The experiment is done at room temperature and at 70 K, above and below the magnetic compensation temperature of the sample. In both cases, when the time delay is less than 1 ps, the threshold for toggle switching decreases. At *T* = 70 K, all the region in the footprint of the laser pulse above a certain fluence switches deterministically. However, at room temperature, in addition to a region of deterministic switching, another region appears at higher fluences where multi-domain nucleation is observed.

MA 40.56 Thu 14:00 P2/EG

Magnetoelastic coupling and magnetic anisotropy in LiMnPO₄ — •TIMO KLEINBEK¹, SVEN SPACHMANN¹, MARTIN JONAK¹, MAHMOUD ABDEL-HAFIEZ², and RÜDIGER KLINGELER¹ — ¹Kirchhoff Institute for Physics, Heidelberg University, Germany — ²Department of Physics and Astronomy, Uppsala University, Sweden

We report high-resolution capacitance dilatometry, magnetisation, and high-frequency electron-spin-resonance studies on LiMnPO₄ single crystals. Our findings imply sizeable magnetoelastic coupling as demonstrated by large anomalies in the thermal expansion coefficients associated with the evolution of long-range magnetic order at *T_N* = 33 K. We extract the uniaxial pressure dependencies. Existence of short-range magnetic order above *T_N* is indicated by magnetic entropy changes up to around 70 K. A spin flip for *B*||*b*-axis is indicative of a Dzyaloshinskii-Moriya-interaction-caused spin-canting in the ground state. The magnetic phase diagrams are constructed for the three crystallographic directions. The field dependence of the magnon branches implies a two-sublattice model of antiferromagnetic resonance with orthorhombic anisotropy. An anomalous magnon branch detected above the spin-flop field is shown to be accountable-for by a rotation of the easy anisotropy axis at the spin-flop field by 6.5° away from the *a*-axis towards the hard *b*-axis. With increasing temperature, the two zero-field excitation gaps remain distinct, implying the preservation of the orthorhombic anisotropy.

MA 40.57 Thu 14:00 P2/EG

Magnetoelastic coupling and uniaxial pressure dependencies of AFM ordering in 2D vdW M₂P₂S₆ (M=Ni & Fe) — •KRANTHI KUMAR BESTHA^{1,2}, LAURA TERESA CORREDOR BOHORQUEZ¹, VILMOS KOCSIS¹, SEBASTIAN SELTER¹, SAICHARAN ASWARTHAM¹, BERND BUECHNER^{1,2}, and ANJA U. B. WOLTER¹ — ¹Institute for Solid State Research, Leibniz IFW Dresden, 01069, Dresden, Germany — ²Institute of Solid State and Materials Physics and Wuerzburg-Dresden Cluster of Excellence ct.qmat, Technical University Dresden, 01062 Dresden, Germany

Two-dimensional van der Waals(vdW) magnets research has been intensified recently due to their myriad of applications. For these applications, an understanding of coupling of the mechanical degrees of freedom to electronic and magnetic order is crucial. In this work, we employed thermodynamic methods to study the magnetoelastic coupling in 2D vdW Fe₂P₂S₆ and Ni₂P₂S₆. These materials belong to the class of transition metal chalcogenophosphates(M₂P₂S₆), with XXZ- and Ising type antiferromagnetic order respectively. *M*(*T*) and *C_p*(*T*) on single crystals confirm AFM ordering in both Fe₂P₂S₆(*T_N*=118 K) and Ni₂P₂S₆(*T_N*=158 K). Our thermal expansion studies demonstrate positive thermal expansion coefficient along the crystallographic stacking axis, with signatures of magnetoelastic coupling by the onset of magnetic order for both Fe₂P₂S₆ and Ni₂P₂S₆ single crystals. We estimated the uniaxial pressure dependence of antiferromagnetic ordering temperature from heat capacity and thermal expansion.

MA 40.58 Thu 14:00 P2/EG

Unconventional Spin State Driven Spontaneous Magnetization in RE₃Fe₃Sb₇ — •S. PALAZZESE^{1,2}, F. PABST³, S. CHATTOPADHAY¹, SH. YAMAMOTO¹, T. HERRMANNDOERFER¹, D. GORBUNOV¹, E. WESCHKE⁴, O. PROKHENKO⁴, H. NOJIRI⁵, T. DOERT³, B. LAKE^{4,6}, J. WOSNITZA^{1,2}, and M. RUCK³ — ¹Hochfeld-Magnetlabor Dresden (HLD-EMFL), HZDR, Dresden, Germany — ²Institut für Festkörper und Materialphysik, Technische Universität Dresden (TUD), Germany — ³Fakultät für Chemie und Lebensmittelchemie, TUD, Germany — ⁴Helmholtz-Zentrum Berlin für Materialien und Energie (HZB), Berlin, Germany — ⁵Institute for Materials Research, Tohoku University, Sendai, Japan — ⁶Institut für Festkörperphysik, Technische Universität Berlin, Germany

Consolidating a microscopic understanding of magnetic properties is crucial for a rational design of magnetic materials with tailored characteristics. The interplay of 3*d* and 4*f* magnetism in rare-earth transition metal antimonides is an ideal platform to search for such complex behavior. Here we present a detailed magnetization and electrical-transport study of novel RE₃Fe₃Sb₇ compounds. RE₃Fe₃Sb₇ shows an emergent spontaneous magnetization in zero applied

field and a kink in the temperature-dependent resistivity, indicating a symmetry breaking at the spin-reorientation transition (SRT). Our XMCD and additional neutron scattering results reveal an unusual antiparallel alignment of Pr and Fe magnetic moments.

MA 40.59 Thu 14:00 P2/EG

2D van-der Waals Heterostructures — •BURAK ÖZER¹, ARTHUR VEYRAT¹, SEBASTIAN SELTER¹, SAICHARAN ASWARTHAM¹, RUDOLF SCHÄFER², IVAN SOLDATOV², BERND BÜCHNER^{1,3}, and BURAK ÖZER¹ — ¹Leibniz IFW Dresden, Institute for Solid State Research, 01069 Dresden, Germany — ²Helmholtzstr 20 — ³Technische Universität Dresden, Faculty of Physics, 01062 Dresden, Germany

2D materials and their properties are being investigated since 2004 when researchers obtained the monolayer graphene and investigated its excellent electrical properties. To produce down-to-monolayer materials the mechanical exfoliation technique has been used since the very beginning. In 2013, researchers found a technique that allows to build a 3D structure from exfoliated 2D materials like LEGO blocks and control their physical properties, called van-der-Waals (vdW) stacking. Combining 2D materials for the discovery and characterization of new topological phases could pave the way for many opportunities for new and interesting fundamental aspects of physics, also for potential applications. This work shows how to exfoliate and encapsulate different materials, including graphene, hBN and Cr₂Ge₂Te₆ (*T_c* ~62 K) crystal, which is a paramagnetic at bulk; but recently researchers have found out at down-to-monolayer thicknesses, it showed ferromagnetic behavior. The magnetism of Cr₂Ge₂Te₆ has investigated at several thicknesses to observe their hysteresis curves by MOKE; to compare the difference between encapsulated with hBN and free-standing CGT behavior, we conducted the magnetic measurement for two different flakes.

MA 40.60 Thu 14:00 P2/EG

Strain control on band topology and surface states in antiferromagnetic EuCd₂As₂ — •NAYRA ALVAREZ¹, VENKATA BHARADWAJ¹, BENNET KARETTA¹, RODRIGO JAESCHKE¹, ADRIAN VALADKHANI², LIBOR SMEJKAL¹, and JAIRO SINOVA¹ — ¹Institut für Physik, Johannes Gutenberg Universität, Mainz, Germany — ²Institut für Theoretische Physik, Goethe-Universität, Frankfurt am Main, Germany

We study the effect of strain on EuCd₂As₂ and the effect on its topological features in different interlayer antiferromagnetic configurations [1]. Magnetic Anisotropy calculations indicate that the modulation of the lattice structure with strain can lead to a change in the direction of the magnetic moment changing the topology of the system [2,3]. We performed band structure calculations for the different strained configurations, applying three different kinds of stress along the x-y plane: volumetric, longitudinal, and shear. In addition, we analyse the surface states at different cleavage surfaces.

[1] J. Ma, H. Wang, S. Nie, et al., "Emergence of nontrivial low-energy Dirac fermions in antiferromagnetic EuCd₂As₂", *Advanced Materials*.

[2] G. Hua, S. Nie, et al., "Dirac semimetal in type-IV magnetic space groups", *Physical Review B*.

[3] E. Gati, S. L. Budko, et al., "Pressure-induced ferromagnetism in the topological semimetal EuCd₂As₂", *Physical Review B*.

MA 40.61 Thu 14:00 P2/EG

Strain control of band topology and surface states in antiferromagnetic EuCd₂As₂ — •NAYRA ALVAREZ¹, VENKATA BHARADWAJ¹, BENNET KARETTA¹, RODRIGO JAESCHKE¹, ADRIAN VALADKHANI², LIBOR SMEJKAL¹, JAIRO SINOVA¹, and ROSER VALENTI² — ¹Institut für Physik, Johannes Gutenberg Universität, Mainz, Germany — ²Institut für Theoretische Physik, Goethe-Universität, Frankfurt am Main, Germany

We study the effect of strain on EuCd₂As₂ and the effect on its topological features in different interlayer antiferromagnetic configurations [1]. Magnetic anisotropy calculations indicate that the modulation of the lattice structure with strain can lead to a change in the direction of the magnetic moment changing the topology of the system [2,3]. We performed band structure calculations for the different strained configurations. We consider three different kinds of stress along the x-y plane: volumetric, longitudinal, and shear. In addition, we analyse the surface states at different cleavage surfaces.

[1] J. Ma, H. Wang, S. Nie, et al., "Emergence of nontrivial low-energy Dirac fermions in antiferromagnetic EuCd₂As₂", *Advanced Materials*.

[2] G. Hua, S. Nie, et al., "Dirac semimetal in type-IV magnetic space groups", *Physical Review B*.

[3] E. Gati, S. L. Budko, et al., "Pressure-induced ferromagnetism in the topological semimetal EuCd₂As₂", *Physical Review B*.

MA 40.62 Thu 14:00 P2/EG

Influence of disorder and multi-magnon processes on the magnonic properties of ultrathin metallic ferromagnets — •SEBASTIAN PAISCHER¹, ARTHUR ERNST¹, IGOR MAZNICHENKO², DAVID EILMSTEINER¹, KHALIL ZAKERI³, and PAWEŁ BUCZEK⁴ — ¹Johannes Kepler University, Linz, Austria — ²Martin-Luther-Universität Halle-Wittenberg, Halle, Germany — ³Karlsruhe Institute of

Technology, Karlsruhe, Germany — ⁴Hamburg University of Applied Sciences, Hamburg, Germany

Understanding the processes behind the excitation and relaxation of spin excitations in low-dimensional magnetic structures is one of the most intriguing research directions in solid-state physics. A detailed knowledge of the fundamental mechanisms involved in such processes is the key to understanding many different phenomena like ultrafast magnetization reversal. In this poster session we compare different magnon damping mechanisms in ultrathin metallic films. While the Landau-damping is the most dominant channel, we show that a significant contribution of the damping originates from substitutional disorder. Also the influence of multi-magnon processes on the magnonic properties of these materials will be discussed.

MA 40.63 Thu 14:00 P2/EG

Transverse magnetotransport in unconventional antiferromagnet Mn_5Si_3 — •SEBASTIAN BECKERT¹, ANTONIN BAD'URA², MIINA LEIVISKÄ³, EVA SCHMORANZEROVÁ⁴, ISMAILA KOUNTA⁵, DOMINIK KRIEGNER², ANDY THOMAS^{1,6}, LIBOR ŠMEJKAL⁷, JAIRO SINOVA⁷, TOMÁŠ JUNGWIRTH², LISA MICHÉZ⁵, SEBASTIAN T. B. GOENNENWEIN⁸, VINCENT BALTZ³, and HELENA REICHLÓVÁ^{1,2} — ¹TU Dresden — ²IOF ASCR Prague — ³Spintec Grenoble — ⁴Charles University Prague — ⁵CINaM Marseille — ⁶IFW Dresden — ⁷JGU Mainz — ⁸University of Konstanz

Traditional collinear antiferromagnets do not exhibit a spin polarization in the band structure. Therefore, the anomalous Hall and Nernst effect are forbidden in these materials. Recent theory developments predict a new class of magnetically ordered compensated materials with particular crystal and spin symmetries that break the time inversion symmetry in the reciprocal space [1,2]. One experimental demonstration are epitaxially grown Mn_5Si_3 films. In these samples with a (0001) film normal, we observe a robust anomalous Hall effect despite vanishing magnetization [3]. On this poster, we will discuss the magneto-thermal transport properties of this compound in more detail and the symmetry of measured signals.

[1] L. Šmejkal et al., *Sci. Adv.* **6**, aaz8809 (2020).

[2] L. Šmejkal et al., *Phys. Rev. X* **12**, 031042 (2022).

[3] H. Reichlova et al., arXiv preprint arXiv:2012.15651 (2020).

MA 40.64 Thu 14:00 P2/EG

Magneto-transport measurements in altermagnetic RuO_2 and $MnTe$ — •RUBEN DARIO GONZALEZ BETANCOURT^{1,2,3,4}, JAN ZUBÁČ^{3,4}, RAFAEL JULIAN GONZALEZ HERNANDEZ⁵, KEVIN GEISHENDORF³, ZBYNEK ŠOBÁN³, GUNTHER SPRINGHOLZ⁶, KAMIL OLEJNÍK³, JAKUB ŽELEZNY³, PHILIPP RITZINGER³, JOSEPH DUFOULEUR², LOUIS VEYRAT², TERESA TSCHIRNER², SIMON MOSER⁷, LIBOR ŠMEJKAL⁸, TOMAS JUNGWIRTH^{3,9}, SEBASTIAN TOBIAS BENEDIKT GOENNENWEIN^{1,10}, ANDY THOMAS^{1,2}, DOMINIK KRIEGNER³, and HELENA REICHLÓVÁ^{1,3} — ¹IFMP, TU Dresden — ²IFW Dresden — ³Institute of Physics, AV ČR, Prague — ⁴Charles University, Prague — ⁵Universidad del Norte, Barranquilla — ⁶JKU Linz — ⁷University of Wuerzburg — ⁸JGU, Mainz — ⁹University of Nottingham — ¹⁰University of Konstanz

In altermagnets [1], spin polarization in both crystal-structure real space and electronic-structure momentum space alternates and, consequently, it enables effects that were believed to be exclusive to ferromagnets. Many of the predicted

altermagnetic phenomena [2] await their experimental confirmation. Here, we present a magneto-transport characterization of two altermagnetic materials - semiconducting $MnTe$ [3] and metallic RuO_2 . We discuss which contributions to the measured transversal and longitudinal signals can be signatures of the unconventional altermagnetic phase.

[1] L. Šmejkal et al., *Phys. Rev. X* **12**, 031042 (2022) [2] L. Šmejkal et al., *Phys. Rev. X* **12**, 011028 (2022) [3] R. D. Gonzalez Betancourt et al., (2021) arXiv:2112.06805

MA 40.65 Thu 14:00 P2/EG

Tuning of magnetoelastic coupling with acoustic impedance matching techniques — •JOHANNES WEBER^{1,2}, MANUEL MÜLLER^{1,2}, STEPHAN GEPRÄGS¹, RUDOLF GROSS^{1,2,3}, HANS HUEBL^{1,2,3}, and MATTHIAS ALTHAMMER^{1,2} — ¹Walther-Meißner-Institut, Bayerische Akademie der Wissenschaften, Garching, Germany — ²TUM School of Natural Sciences, Technische Universität München, Garching, Germany — ³Munich Center for Quantum Science and Technology (MCQST), Munich, Germany

Magnetoelastic coupling and the coherent emission of phonon modes generated by magnon Kittel modes have regained interest because of their potential applications in quantum devices [1]. So far primarily the ferrimagnetic insulator yttrium iron garnet (YIG) grown on single crystal substrates of the paramagnetic insulator gadolinium gallium garnet (GGG) has been used in experiments. However, as YIG requires epitaxial growth, the choice of material combinations is limited. Therefore we studied magnon-phonon coupling in acoustic resonators consisting of polycrystalline magnetic thin-films grown on silicon substrates, as this material platform would allow for the implementation of magnetoelastic coupling effects in existing CMOS-technology. In particular, we investigate whether a tuning of the magnetoelastic coupling between magnetic metal thin films and silicon substrate can be achieved by inserting an interdigitated metallic layer, allowing for better acoustic impedance matching [2].

[1] K. An et al., *Phys. Rev. X* **12**, 011060, (2022).

[2] V. Rathod, *Sensors*, **20**, 4051, (2020).

MA 40.66 Thu 14:00 P2/EG

Towards shaping picosecond strain pulses via magnetostrictive transducers — MAXIMILIAN MATTERN¹, JAN-ETIENNE PUDELL^{1,2,3}, KARINE DUMESNIL⁴, •ALEXANDER VON REPERT¹, and MATIAS BARGHEER^{1,2} — ¹Institut für Physik und Astronomie, Universität 14476 Potsdam, Potsdam, Germany — ²Helmholtz-Zentrum Berlin, 12489 Berlin, Germany — ³European XFEL, 22869 Schenefeld, Germany — ⁴Institut Jean Lamour (UMR CNRS 7198), Université Lorraine, 54000 Nancy, France

Using time-resolved x-ray diffraction, we demonstrate the manipulation of the picosecond strain response of a metallic heterostructure consisting of a dysprosium (Dy) transducer and a niobium (Nb) detection layer by an external magnetic field. We utilize the first-order ferromagnetic-antiferromagnetic phase transition of the Dy layer, which provides an additional large contractive stress upon laser excitation compared to its zero-field response. This enhances the laser-induced contraction of the transducer and changes the shape of the picosecond strain pulses driven in Dy and detected within the buried Nb layer. Based on our experiment with rare-earth metals we discuss required properties for functional transducers, which may allow for novel field-control of the emitted picosecond strain pulses.

MA 41: Focus Session: Altermagnetism: Transport, Optics, Excitations

While antiferromagnetic spintronics is an established research field, key spintronic functionalities such as giant/tunneling magnetoresistance (GMR/TMR), have remained elusive in compensated magnetic systems. This paradigm could change in the light of the recent theoretical discovery of a new class of magnetic materials so called altermagnets which feature alternating spin polarizations in both crystal-structure real space and electronic-structure momentum space. Despite the vanishing net magnetization and antiparallel spin arrangement, altermagnets were predicted to exhibit a robust anomalous Hall effect and GMR and spin transfer torque phenomena. The predictions have been already supported by initial experiments. The goal of this focus session is to introduce the concept of altermagnetism to the broad research community, to present the first experimental works and stimulate future research directions. Here, altermagnets are predicted to have a broad impact beyond spin-electronics in fields ranging from magneto-transport, ultra-fast photo-magnetism to superconductivity and magnetic topological matter. The Focus Session is organized by Dr. Matthias Althammer (Walther-Meißner-Institut, Garching), Prof. Sebastian Goennenwein (Uni Konstanz) and Dr. Andy Thomas (IFW Dresden).

Time: Thursday 15:00–18:00

Location: HSZ 02

Invited Talk

MA 41.1 Thu 15:00 HSZ 02

Altermagnetism and spin symmetries — •LIBOR ŠMEJKAL — Johannes Gutenberg Universität Mainz, Germany — Institute of Physics, Czech Academy of Sciences, Prague, Czech Republic

Different phases of matter can be distinguished by symmetries and order parameters. In this talk, we will discuss the classification of magnetically ordered crystals according to recently studied spin symmetries [1]. Spin symmetries consider pairs of operations in spin and crystal space and remarkably reveal an un-

conventional magnetic class. This unconventional class, called altermagnetism, is sharply distinct from ferromagnets and antiferromagnets. It is characterized by an unconventional alternating spin order in electronic momentum space that breaks time-reversal symmetry and is spin compensated and anisotropic [1,2]. We show that these properties can arise from ordered and anisotropic spin densities and crystal fields, as described for a typical Ruthenium Dioxide altermagnet [1-4]. Finally, we show that altermagnetism provides a unifying explanation for the recently predicted and experimentally observed unconventional anomalous Hall effects in collinear systems without magnetisation [2,3,5 and references therein].

[1] Šmejkal, L., Sinova, J., and Jungwirth, T., Phys. Rev. X 12, 031042 (2022), [2] Šmejkal, L. et al., Science Advances 6, eaaz8809 (2020) [3] Feng, Z., et al. Nature Electron. 5, 735-743 (2022) [4] Šmejkal, L. et al., Phys. Rev. X 12, 011028 (2022) [5] Mazin, I.I et al., PNAS 118 (42) e2108924118 (2021)

Invited Talk

MA 41.2 Thu 15:30 HSZ 02

Spontaneous Hall effect in Mn₅Si₃ altermagnet — •H. REICHLVA^{1,2}, R. LOPES SEEGER³, R. GONZÁLEZ-HERNÁNDEZ⁴, I. KOUTA⁶, R. SCHLITZ¹, D. KRIEGNER², P. RITZINGER², M. LAMMEL⁹, M. LEIVISKA³, V. PETRICEK², E. SCHMORANZEROVA⁷, A. BADURA², A. THOMAS^{1,8}, V. BALTZ³, L. MICHEZ⁶, J. SINOVA^{5,2}, S.T.B. GOENNENWEIN⁹, T. JUNGWIRTH^{2,10}, and L. SMEJKAL^{5,2} — ¹IFMP, Technische Universität Dresden — ²Institute of Physics CAS, Czech Republic — ³CNRS, CEA, Grenoble, France — ⁴Universidad del Norte, Barranquilla, Colombia — ⁵Johannes Gutenberg Universität Mainz — ⁶CINAM, Marseille, France — ⁷MFF Charles University, Praha, Czech Republic — ⁸IFW Dresden — ⁹Universität Konstanz — ¹⁰University of Nottingham, United Kingdom
The family of materials that can exhibit spontaneous Hall effect has been significantly expanded by discovery of altermagnets with opposite spin sublattices coupled by crystallographic rotations [1]

I present our observations of the spontaneous Hall effect in an altermagnetic candidate - Mn₅Si₃ epilayers [2]. Epitaxial constraints stabilize a hexagonal unit cell in the magnetic state distinct from previously described phases in bulk crystals and we observe a sizable spontaneous Hall conductivity. The signal can be explained by an unprecedented altermagnetic band structure with time-reversal symmetry breaking spin-polarized valleys.

[1] Smejkal et al. Science Advances 6, 23 (2020) [2] Reichlova H. et al., arXiv:2012.15651

MA 41.3 Thu 16:00 HSZ 02

Spin-split collinear antiferromagnets: a large-scale ab-initio study — •YAQIAN GUO¹, HUI LIU^{1,2}, OLEG JANSON¹, ION COSMA FULGA^{1,2}, JEROEN VAN DEN BRINK^{1,2}, and JORGE I. FACIO^{1,3,4} — ¹Leibniz Institute for Solid State and Materials Research, Germany — ²Würzburg-Dresden Cluster of Excellence ct.qmat, Technische Universität Dresden, Germany — ³Centro Atómico Bariloche and Instituto Balseiro, Argentina — ⁴Instituto de Nanociencia y Nanotecnología CNEA-CONICET, Argentina

It was recently discovered that, depending on their symmetries, collinear antiferromagnets can break the spin degeneracy in momentum space, even in the absence of spin-orbit coupling. Such systems are signalled by the emergence of a spin-momentum texture set mainly by the crystal and magnetic structure, relativistic effects playing a secondary role. Here we consider all collinear $q=0$ antiferromagnetic compounds in the MAGNDATA database allowing for spin-split bands. Based on density-functional calculations for the experimentally reported crystal and magnetic structures, we study more than sixty compounds and introduce numerical measures for the average momentum-space spin splitting. We highlight some compounds that are of particular interest, either due to a relatively large spin splitting, such as CoF₂ and FeSO₄F, or because of their low-energy electronic structure. The latter include LiFe₂F₆, which hosts nearly flat spin-split bands next to the Fermi energy, as well as RuO₂, CrNb₄S₈, and CrSb, which are metals.

MA 41.4 Thu 16:15 HSZ 02

Giant magnetoresistance effects in altermagnets — •ANNA BIRK HELLENES¹, RAFAEL GONZÁLEZ-HERNÁNDEZ², JAIRO SINOVA^{1,3}, TOMAS JUNGWIRTH^{3,4}, and LIBOR ŠMEJKAL^{1,3} — ¹Johannes Gutenberg Universität Mainz, Germany — ²Universidad del Norte, Barranquilla, Colombia — ³Czech Academy of Sciences, Prague, Czech Republic — ⁴University of Nottingham, United Kingdom

Commercial spintronics devices using magnetoresistance effects rely on spin currents in ferromagnets, generated by a time-reversal symmetry broken band structure. To realise a counterpart effect with all-antiferromagnetic electrodes has remained experimentally elusive, as the combined time-reversal symmetry with translation or inversion in antiferromagnets prohibits nonrelativistic spin polarisation. Recently, a third fundamental magnetic order was discovered,

which exhibits exclusively different spin symmetries from ferromagnets and antiferromagnets[1]. In these altermagnets, the spin polarisation forms d.g. or α -wave compensated spin order in momentum space which breaks time-reversal symmetry. Hence, altermagnetism provides a unifying explanation for our recently predicted giant TMR and GMR effects[2,3]. In the present contribution, we describe the symmetry requirements that lead to distinct spin polarisations such as the d-wave type, and illustrate the GMR and TMR mechanism with tight-binding models and in the candidate materials RuO₂ and Mn₅Si₃. [1] L. Šmejkal et al., Phys. Rev. X 12, 031042, 2022. [2] L. Šmejkal, A. B. Hellenes et al., Phys. Rev. X 12, 011028, 2022. [3] H. Reichlova et al., arXiv:2012.15651v2.

Invited Talk

MA 41.5 Thu 16:30 HSZ 02

Generation of tilted spin-current by the collinear antiferromagnet RuO₂ — •ARNAB BOSE — Johannes Gutenberg Universität, Mainz, Germany

Recently a new type of magnetic material is theoretically proposed, referred to as *altermagnet* which is a collinear antiferromagnet in real space although hosting the spin-split bands in the momentum space that allows it to exhibit the properties of ferromagnet depending upon the direction of the current flow with respect to the crystal axis [1,2]. We report the first experimental evidence of strongly crystal axis-dependent unconventional transverse spin-current generation by the altermagnet RuO₂ [3] arising from the novel spin-split bands as theoretically predicted [1]. This unconventional tilted spin-current is the key to the implementation of high-density nonvolatile magnetic memories.

[1] R. González-Hernández et. al. Phys. Rev. Lett. 126, 127701 (2021) [2] L. Šmejkal et. al. arXiv: 2204.10844 (2022) [3] A. Bose et. al. Nature Electronics 5, 267 (2022).

Invited Talk

MA 41.6 Thu 17:00 HSZ 02

First-principles studies on the anomalous transport properties of ferromagnets, antiferromagnets, and altermagnets — •WANXIANG FENG — School of Physics, Beijing Institute of Technology, Beijing 100081, China

Magnetic topological semimetals bring new vitality to the ideas evolving around the next generation of dissipationless spintronic devices benefiting from their exotic anomalous and spin transport properties. I shall first show that ferromagnetic MF₃ ($M = \text{Pd, Mn}$) are high-quality nodal chain spin-gapless topological semimetals with 100% spin-polarized transport properties. The dominant intrinsic origin is found to originate entirely from the gapped nodal chains without the entanglement of any other trivial bands. The side-jump mechanism is predicted to be negligibly small, but the skew scattering enhances the intrinsic Hall and Nernst signals significantly. Second, I shall present the spin-chirality-dependent anomalous Hall and Nernst effects in coplanar noncollinear antiferromagnets Mn₃XN ($X = \text{Ga, Zn, Ag, and Ni}$) as well as the topological magneto-optical effects and their quantization in noncoplanar antiferromagnets $\gamma\text{-Fe}_x\text{Mn}_{1-x}$ and K_{0.5}RhO₂. Beyond ferromagnetism and antiferromagnetism, altermagnetism is recently discovered to be the third essential magnetic phase. Room-temperature metallic RuO₂ is a typical altermagnet, in which the rearrangement of nonmagnetic atoms induces crystal chirality playing a critical role in anomalous transport properties. Finally, I will discuss the crystal-chirality-dependent anomalous Nernst, anomalous thermal Hall, and magneto-optical effects in RuO₂.

Invited Talk

MA 41.7 Thu 17:30 HSZ 02

Insight into chemical and magnetotransport properties of epitaxial $\alpha\text{-Fe}_2\text{O}_3/\text{Pt}$ bilayers — •ANNA KOZIOŁ-RACHWAŁ¹, NATALIA KWIATEK², WITOLD SKOWROŃSKI³, KRZYSZTOF GROCHOT³, JAROSŁAW KANAK³, EWA MADEJ², KINGA FREINDL², JÓZEF KORECKI², and NIKA SPIRIDIS² — ¹Faculty of Physics and Applied Computer Science, AGH University of Science and Technology, Mickiewiczza 30, 30-059 Kraków, Poland — ²Jerzy Haber Institute of Catalysis and Surface Chemistry, Polish Academy of Sciences, 30-239 Kraków, Poland — ³Institute of Electronics, AGH University of Science and Technology, Mickiewiczza 30, 30-059 Kraków, Poland

Recently a spin Hall magnetoresistance (SMR) was presented for Pt/ $\alpha\text{-Fe}_2\text{O}_3$ (hematite) bilayer.[1],[2] In our studies we investigated the chemical structure and SMR in epitaxial $\alpha\text{-Fe}_2\text{O}_3(0001)/\text{Pt}(111)$ bilayers with hematite layers grown by molecular beam epitaxy on a MgO(111) substrate.[3] We observed a sign change of the SMR from positive to negative when the thickness of the hematite increased from 6 to 15 nm. For $\alpha\text{-Fe}_2\text{O}_3(15\text{ nm})/\text{Pt}$, we demonstrated room-temperature switching of the Néel order with rectangular, nondecaying switching characteristics. Such structures open the way to extending magnetotransport studies to more complex systems with double asymmetric metal/hematite/Pt interfaces. [1] J. Fischer et al. Phys. Rev. Applied 13, 014019 (2020). [2] Y. Cheng et al. Phys. Rev. Lett. 124, 027202 (2020). [3] A. Kozioł-Rachwał et al., Phys. Rev. B 106, 104419 (2022).

MA 42: Caloric Effects in Ferromagnetic Materials

Time: Thursday 15:00–17:45

Location: HSZ 04

MA 42.1 Thu 15:00 HSZ 04

Exploring rare earth Laves phases for magnetocaloric hydrogen liquefaction — •BRUNO WEISE¹, MARVIN HOFMANN^{1,2}, LUKAS BEYER^{1,3}, and TINO GOTTSCHALL⁴ — ¹Leibniz IFW, Dresden, Germany — ²TU Dresden, Dresden, Germany — ³TU Bergakademie Freiberg, Freiberg, Germany — ⁴Helmholtz-Zentrum Dresden-Rossendorf, Dresden, Germany

The replacement of fossil fuels with renewable energies is an integral part of fighting the global climate crisis. Green hydrogen, produced with renewable energies, is one of the most promising energy sources. The unsurpassed high storage density of liquid hydrogen offers great advantages, especially on long transport routes. By magnetocaloric cooling the efficiency of the energy-intensive liquefaction of hydrogen will be increased. RE-X₂ Laves phases, are ideal for low temperature hydrogen liquefaction in the temperature range between 77 and 20 K.

By substitution of individual elements in the RE-X₂ Laves phases the transition temperature can be manipulated, while maintaining the magnetocaloric performance. A substitution series of DyNi_{2-x}Al_x was prepared by arc melting and studied by structural, magnetic and thermodynamic characterization methods. The investigated alloy series DyNi_{2-x}Al_x shows a nonlinear substitution dependency of the Curie Temperature and adiabatic temperature change. In pulsed field measurements a temperature of up to 17 K for 10 T magnetic field pulse was measured. In the present contribution we will evaluate the suitability of the DyNi_{2-x}Al_x rare earth Laves phases for magnetocaloric hydrogen liquefaction.

MA 42.2 Thu 15:15 HSZ 04

Lattice contribution to entropy change at first-order phase transition in Laves phase DyCo₂ — •JOHANNA LILL¹, BENEDIKT EGGERT¹, JIYONG ZHAO², BENEDIKT BECKMANN³, BARBARA LAVINA², MICHAEL HU², KONSTANTIN SKOKOV³, TOM TOELLNER², ESEN E. ALP², KATHARINA OLLEFS¹, OLIVER GUTFLEISCH³, and HEIKO WENDE¹ — ¹Faculty of Physics and CENIDE, University of Duisburg-Essen, Duisburg, Germany — ²APS, Lemont, Illinois - US — ³TU Darmstadt, Darmstadt, Germany

Laves phases are promising candidates for facilitating liquefaction, applying the magnetocaloric effect. The Laves phase of DyCo₂ undergoes a first-order phase transition around 140 K from a ferromagnetic (at low temperatures) to a disordered magnetic phase (at higher temperatures). The magnetic phase transition accompanies a structural change from cubic to tetragonal symmetry also resulting in a volume discontinuity. The magnetocaloric effect is a change in entropy along a phase transition, which in an adiabatically performed cooling cycle can lead to the desired cooling effect. This effect can be characterized by the amount of entropy change at the first-order phase transition. For magnetocaloric applications and improvement of reversible magnetocaloric effect it is therefore essential to understand the contributions of different subsystems to the overall entropy change. In this presentation, we show experimental data that resolves the Dy-partial lattice entropy of the DyCo₂ Laves phase along the first-order phase transition utilizing nuclear resonant inelastic x-ray scattering. We acknowledge financial support from DFG through TRR270 HoMMage.

MA 42.3 Thu 15:30 HSZ 04

Designing a light rare-earth-based material system for magnetocaloric hydrogen liquefaction — •WEI LIU¹, FRANZISKA SCHEIBEL¹, TINO GOTTSCHALL², EDUARD BYKOV², KONSTANTIN SKOKOV¹, and OLIVER GUTFLEISCH¹ — ¹TU Darmstadt — ²Hochfeld- Magnetlabor Dresden, Helmholtz-Zentrum Dresden-Rossendorf, Germany

Hydrogen will play a key role in building a climate-neutral society, where renewables are the major energy sources [1]. Liquid hydrogen is essential for efficient storage and transport of hydrogen, but expensive due to the low efficiency of traditional gas-compression refrigeration [2]. As an emerging and energy-saving technology, magnetocaloric gas liquefaction can be a "game-changer". However, the high criticalities of the heavy rare-earth elements put a question on the usage of the heavy rare-earth-based magnetocaloric materials in industrial scales, although they show large magnetic entropy and adiabatic temperature changes.[3] On the other hand, the relatively high abundances of light rare-earth elements make their alloys appealing for industrial-scale applications. In this work, based on the analysis of mean-field theory, we propose a method of designing a light rare-earth-based magnetocaloric material system with Ce, Pr, and Nd for hydrogen liquefaction.

MA 42.4 Thu 15:45 HSZ 04

Multicaloric effect and exploited hysteresis in the Heusler alloy Ni-Mn-Sn-Fe-Co — •T. NIEHOFF^{1,2}, T. GOTTSCHALL¹, C. SALAZAR MEJIA¹, and J. WOSNITZA^{1,2} — ¹Hochfeld-Magnetlabor Dresden (HLD-EMFL), HZDR, Dresden, Germany — ²Institut für Festkörper- und Materialphysik TUD, Dresden, Germany

Today's research on commercial magnetocaloric cooling focuses on reducing the hysteresis of materials with first-order phase transitions. In contrast, this work exploits the width of hysteresis to achieve more effective cooling performance with a combination of multiple caloric effects and investigates the coupling between the magnetocaloric and elastocaloric effects. The hysteresis is finetuned by substituting the proper amount of Fe and Co in the Heusler alloy Ni-Sn. To study the material, simultaneous magnetization, strain, and adiabatic temperature changes are compared at a range of different initial temperatures and various uniaxial loads in pulsed magnetic fields up to 50 T.

MA 42.5 Thu 16:00 HSZ 04

Effect of Pt substitution on the reversibility of the magnetocaloric effect in Ni-Pt-Mn-In Heusler alloys — •PARUL DEVI¹, C. SALAZAR-MEJIA¹, S. SINGH², and J. WOSNITZA^{1,3} — ¹High Magnetic Field Laboratory (HLD-EMFL), Helmholtz-Zentrum Dresden-Rossendorf, Germany — ²School of Materials Science and Technology, Indian Institute of Technology (BHU), Varanasi, India — ³Institut für Festkörper –und Materialphysik, TU Dresden, Germany

Among different magnetic shape memory Heusler alloys, Ni₂Mn_{1.4}In_{0.6} is one of the most studied system for multiple caloric effects. However, obstacles such as the low-temperature martensitic transition and large thermal hysteresis hinder its technological applications motivating the search for novel materials showing better mechanical properties as well as higher martensitic transition temperature [1 and references within]. Here, we will present the experimental results such as the crystal structure determined by x-ray diffraction, magnetization in static magnetic fields, and the adiabatic temperature change in pulsed magnetic field of quaternary Ni_{2-x}Pt_xMn_{1.4}In_{0.6} (0 ≤ x ≤ 0.2) shape memory alloys. The substitution of Pt affects the geometric compatibility condition without changing the space group symmetry of the austenite and the martensite phase. Around the martensitic transition temperature, a large value of ΔT_{ad} was found in pulsed magnetic fields due to the compatibility of austenite and martensite phase.

[1] K. K. Dubey et al., J. Magn. Magn. Mat. **507**, 166818 (2020).

15 min. break

MA 42.6 Thu 16:30 HSZ 04

Simultaneous measurements of adiabatic temperature change and magnetization in Fe-Ni-Rh. — •CATALINA SALAZAR-MEJIA¹, ALISA M. CHIRKOVA², SHINGO YAMAMOTO¹, JOCHEN WOSNITZA^{1,3}, and TINO GOTTSCHALL¹ — ¹High Magnetic Field Laboratory (HLD-EMFL), Helmholtz-Zentrum Dresden-Rossendorf, Germany — ²FH Bielefeld, University of Applied Sciences, Germany — ³Institut für Festkörper- und Materialphysik, TU Dresden, Germany

We have performed simultaneous measurements of the magnetization and the adiabatic temperature change in an Fe₄₉Ni₁Rh₅₀ alloy. The material exhibits an antiferromagnetic (AFM) to ferromagnetic (FM) transition at T_{tr} ≈ 326 K. Specifically, we have studied the field-induced metamagnetic AFM-FM transition at temperatures well below T_{tr} in high pulsed magnetic fields. Due to the large magnetocaloric effect (MCE) of the material, magnetization measurements in pulsed magnetic fields are not isothermal. Recording the temperature of the sample during the measurement allows not only to characterized the MCE of the material, but to precisely determine the magnetic phase diagram.

MA 42.7 Thu 16:45 HSZ 04

The local magnetic and geometric structure in Mn-doped La(Fe,Si)₁₃ — •BENEDIKT EGGERT¹, JOHANNA LILL¹, KONSTANTIN SKOKOV², CYNTHIA PILLICH¹, ALEXANDRA TERWEY¹, FABRICE WILHELM³, MAURO ROVEZZI³, ANDREI ROGALEV³, KATHARINA OLLEFS¹, MARKUS E. GRUNER¹, OLIVER GUTFLEISCH², and HEIKO WENDE¹ — ¹Faculty of Physics and CENIDE, University of Duisburg-Essen — ²Functional Materials, TU Darmstadt — ³European Synchrotron Radiation Facility

Magnetic cooling has the potential to replace conventional gas compression refrigeration. Materials such as La(Fe,Si)₁₃ exhibit a sizeable first-order magnetocaloric effect. For Mn-H doped La(Fe,Si)₁₃, it is possible to tailor the phase transition towards room temperature while maintaining first-order character. In this contribution, we discuss the effects of Mn-doping in La(Fe,Si)₁₃ on the magnetic moments and the local environment by means of X-ray magnetic circular dichroism and extended X-ray absorption spectroscopy in the hard X-ray regime. Spectroscopic results indicate a reduction of the Fe magnetic moment and an increased structural disorder around the La site, which is not identified for the Fe sites. Furthermore, first-principles calculations reveal energetically unfavourable Mn-Si bonds that lead to a broad distribution of La-Si bond lengths that explain the experimentally observed structural disorder. We acknowledge the financial support through the Deutsche Forschungsgemeinschaft within the framework of the CRC/TRR 270 HoMMage and thank the ESRF for allocating beamtimes at ID12 and BM30.

MA 42.8 Thu 17:00 HSZ 04

Magnetocaloric effect in (La,Ce)(Fe,Si,Mn)₁₃ with tunable, low transition temperature — •M. STRASSHEIM^{1,2}, C. SALAZAR MEJIA¹, J. WOSNITZA^{1,2}, and T. GOTTSCHALL¹ — ¹Hochfeld-Magnetlabor Dresden (HLD-EMFL), HZDR, Dresden, Germany — ²Institut für Festkörper- und Materialphysik Technische Universität Dresden, Dresden, Germany

The La(Fe,Si)₁₃ family is a very promising group of magnetocaloric materials due to their overall good cost-benefit ratio in comparison to alloys based on scarce rare earths such as Gd or Ho. By partly substituting La with Ce and Fe with Mn, the metamagnetic transition can be tuned down to at least 40 K, while maintaining a rather sharp transition to enable a notable magnetocaloric effect. Tuning the magnetocaloric effect down to these temperatures opens up large-scale applications such as the magnetic liquefaction of hydrogen. In this work, we synthesized (La_{1-z}Ce_z)(Fe_{0.88-y}Mn_ySi_{0.12})₁₃ with $z = 0 \dots 0.4$, $y = 0 \dots 0.04$ and determined the adiabatic temperature change in pulsed magnetic fields. For selected samples, we calculated the magnetic entropy change using isothermal magnetization measurements.

MA 42.9 Thu 17:15 HSZ 04

Rapid bulk sintering and magnetocaloric performance of polycrystalline Fe₂Al_{1.15-x}B₂Ge_xGa_x (x=0, 0.05) MAB phases — •BENEDIKT BECKMANN¹, TAREK EL-MELEGY², DAVID KOCH¹, ULF WIEDWALD³, MICHAEL FARLE³, FERNANDO MACCARI¹, JOSHUA SNYDER², KONSTANTIN SKOKOV¹, MICHEL BARSOUM², and OLIVER GUTFLEISCH¹ — ¹TU Darmstadt, Institute of Materials Science, Darmstadt, Germany — ²Drexel University, Department of Materials Science & Engineering, Philadelphia, PA, USA — ³University of Duisburg Essen, CENIDE, Duisburg, Germany

Reactive single-step hot-pressing at 1473 K and 36 MPa for 4 h produces dense, bulk, near single-phase, low-cost and low-criticality Fe₂Al_{1.15}B₂ and Fe₂Al_{1.1}B₂Ge_{0.05}Ga_{0.05} MAB samples, showing a second-order magnetic phase transition with favorable magnetocaloric properties at room temperature. The

maximum isothermal entropy change Δs_T of hot-pressed Fe₂Al_{1.15}B₂ in magnetic field changes of 2 and 5 T amounts to 2.5 and 5 J/(kgK)⁻¹ at 287.5 K and increases by Ge and Ga addition to 3.1 and 6.2 J/(kgK)⁻¹ at 306.5 K, respectively. The directly measured maximum adiabatic temperature change ΔT_{ad} in magnetic field changes of 1.93 T is improved by the alloy design from 0.9 to 1.1 K. Our criticality assessment shows that hot-pressed Fe-based MAB phases provide a promising compromise between material and processing cost, criticality and magnetocaloric performance around room temperature.

We acknowledge financial support from DFG (CRC/TRR 270, Project-ID 40553726).

MA 42.10 Thu 17:30 HSZ 04

Effect of Pt substitution on the reversibility of the magnetocaloric effect in Ni-Pt-Mn-In Heusler alloys — •PARUL DEVI¹, C. SALAZAR-MEJIA¹, S. SINGH², and J. WOSNITZA^{1,3} — ¹High Magnetic Field Laboratory (HLD-EMFL), Helmholtz-Zentrum Dresden-Rossendorf, Germany — ²School of Materials Science and Technology, Indian Institute of Technology (BHU), Varanasi, India — ³Institut für Festkörper- und Materialphysik, TU Dresden, Germany

Among different magnetic shape memory Heusler alloys, Ni₂Mn_{1.4}In_{0.6} is one of the most studied system for multiple caloric effects. However, obstacles such as the low-temperature martensitic transition and large thermal hysteresis hinder its technological applications motivating the search for novel materials showing better mechanical properties as well as higher martensitic transition temperature [1 and references within]. Here, we will present the experimental results such as the crystal structure determined by x-ray diffraction, magnetization in static magnetic fields, and the adiabatic temperature change in pulsed magnetic field of quaternary Ni_{2-x}Pt_xMn_{1.4}In_{0.6} ($0 \leq x \leq 0.2$) shape memory alloys. The substitution of Pt affects the geometric compatibility condition without changing the space group symmetry of the austenite and the martensite phase. Around the martensitic transition temperature, a large value of ΔT_{ad} was found in pulsed magnetic fields due to the compatibility of austenite and martensite phase.

[1] K. K. Dubey et al., J. Magn. Magn. Mater. **507**, 166818 (2020).

MA 43: Magnetic Imaging Techniques II

Time: Thursday 15:00–16:45

Location: HSZ 401

MA 43.1 Thu 15:00 HSZ 401

Three-dimensional tomographic imaging of the magnetization vector field using Fourier transform holography — •MARISEL DI PIETRO MARTÍNEZ^{1,2}, ALEXIS WARTELE^{1,3}, CARLOS HERRERO MARTÍNEZ¹, FARID FETTAR⁴, JEAN-FRANÇOIS MOTTE⁴, CLAIRE DONNELLY², LUKE TURNBULL⁵, FEODOR OGRIN⁵, GERRIT VAN DER LAAN⁶, HORIA POPESCU⁷, NICOLAS JAOUEN⁷, FLORA YAKHOU-HARRIS³, and GUILLAUME BEUTIER¹ — ¹UGA, CNRS, G-INP, SIMaP, Grenoble, France — ²MPI-CPFS, Dresden, German — ³ESRF, Grenoble, France — ⁴UGA, CNRS, G-INP, Institut Néel, Grenoble, France — ⁵School of Phys. and Engineering, University of Exeter, Exeter, UK — ⁶Diamond Light Source, Didcot OX11 0DE, UK — ⁷Synchrotron SOLEIL, Gif-sur-Yvette, France

Three-dimensional magnetic textures have recently attracted increasing interest both from a fundamental and a technological point of view. This emergent field of research comes with the need of new characterization techniques, specifically tomographic imaging. Here, we present a new tomographic technique based on Fourier transform holography, a lensless imaging technique that uses a known reference in the sample to retrieve the object of interest from its diffraction pattern in one single step of calculation. We obtain a 3D vectorial image of a 850nm-thick extended Fe/Gd multilayer in a 5000nm-diameter field of view with a resolution of 100nm, that reveals worm-like domains with magnetization pointing mostly out of plane near the surface of the sample but that falls in-plane near the substrate. As an outlook, this technique will enable a 3D study on the response to an external magnetic field.

MA 43.2 Thu 15:15 HSZ 401

Soft X-ray Ptychography of micrometer thick samples — •JEFFREY N. NEETHIRAJAN¹, BENEDIKT DAURER², ALES HRABEC^{3,4}, MAJID KAZEMIAN², MARISEL DI PIETRO MARTÍNEZ¹, BURKHARD KAULICH², and CLAIRE DONNELLY¹ — ¹Max Planck Institute for Chemical Physics of Solids, Dresden, Germany — ²Diamond Light Source, Harwell Science and Innovation Campus, Didcot, United Kingdom — ³Laboratory for Mesoscopic Systems, Department of Materials, ETH Zurich, Zurich, Switzerland — ⁴Laboratory for Multiscale Materials Experiments, Paul Scherrer Institute, Switzerland

Magnetism at the nanoscale offers a playground to study topology in real space. Although topological spin textures have so far been mainly studied in 2D, there is a growing interest in 3D topological spin textures. Recently, 3D imaging of extended systems with hard X-rays has revealed topological singularities called Bloch points and spin structures called vortex rings with nanoscale spatial resolution. However, the imaging of extended systems with hard X-rays is limited by the weak XMCD signals observed in this regime and restricted currently to a few

rare-earths. In contrast, soft X-rays offer a stronger XMCD signal but limited to imaging samples that are 200-300 nm thick. Here we demonstrate the imaging of micrometer thick samples using soft X-ray ptychography - accessing a thickness regime previously impractical with conventional soft X-ray imaging techniques. This result is a step forward in realizing 3D imaging of extended systems with soft X-rays which offers a strong XMCD signal and the possibility to image exotic systems hosting topological textures.

MA 43.3 Thu 15:30 HSZ 401

Soft X-ray Ptychography of Bismuth Ferrite Nanoplates — •TIM A. BUTCHER¹, MANUEL LANGER¹, SIMONE FINIZIO¹, LARS HELLER¹, MIRKO HOLLER¹, MICHAL JAMBOR², ELISABETH MÜLLER³, ASHNA BAJPAI^{4,5}, CARLOS A. F. VAZ¹, ARMIN KLEIBERT¹, and JÖRG RAABE¹ — ¹Swiss Light Source, Paul Scherrer Institut, 5232 Villigen PSI, Switzerland — ²Institute of Physics of Materials, Czech Academy of Sciences, Žitkova 22, 61600 Brno, Czech Republic — ³Electron Microscopy Facility, Paul Scherrer Institut, 5232 Villigen PSI, Switzerland — ⁴Department of Physics, Indian Institute of Science Education and Research, Pune 411008, India — ⁵Centre for Energy Science, Indian Institute of Science Education and Research, Pune 411008, India

Soft x-ray ptychography is a scanning coherent diffractive imaging technique with spatial resolutions in the order of 10 nm, which relies on collecting diffraction patterns from overlapping illumination spots of the sample. The magnetic and ferroelectric structure of multiferroic bismuth ferrite nanoplates was studied with a new soft x-ray ptychography endstation at the Swiss Light Source. In particular, we demonstrate that the technique is able to resolve the antiferromagnetic spin cycloid and can yield the chirality in bismuth ferrite.

MA 43.4 Thu 15:45 HSZ 401

Direct imaging of nanoscale field-driven domain wall oscillations in Landau structures — •BALRAM SINGH¹, RACHAPPA RAVISHANKAR¹, JORGE A. OTÁLORA², IVAN SOLDATOV¹, RUDOLF SCHÄFER¹, DANIIL KARNAUSHENKO³, VOLKER NEU¹, and OLIVER G. SCHMIDT³ — ¹Institute for Integrative Nanosciences, Leibniz IFW Dresden, 01069 Dresden, Germany — ²Departamento de Física, Universidad Católica del Norte, Avenida Angamos 0610, Casilla 1280, Antofagasta, Chile — ³Center for Materials, Architectures and Integration of Nanomembranes (MAIN), Chemnitz University of Technology, 09126 Chemnitz, Germany.

Linear oscillatory motion of domain walls (DWs) in the kHz and MHz regime is crucial when realizing precise magnetic field sensors such as giant magnetoimpedance devices. Here, we report an imaging approach to investigate such

DW dynamics with nanoscale spatial resolution employing conventional tabletop microscopy techniques. Time-averaged magnetic force microscopy and Kerr imaging methods are applied to quantify the DW oscillations in Permalloy rectangular structures with Landau domain configuration and are complemented by numeric micromagnetic simulations. We study the oscillation amplitude as a function of external magnetic field strength, frequency, magnetic structure size, thickness, and anisotropy and understand the excited DW behavior as a forced damped harmonic oscillator with restoring force being influenced by the geometry, thickness, and anisotropy of the Permalloy structure.

MA 43.5 Thu 16:00 HSZ 401

Tailoring magnetic switching via topology in nanoimprinted networks of Pt/Co/Pt caps on flexible membranes — •JOSE A. FERNANDEZ-ROLDAN¹, RUI XU¹, OLEKSI VOLKOV¹, OLEKSANDR PYLYPOVSKYI¹, IVAN SOLDATOV², ANDREAS WORBS¹, RENE HÜBNER¹, RUDOLF SCHÄFER², JÜRGEN FASSBENDER¹, and DENYS MAKAROV¹ — ¹Helmholtz-Zentrum Dresden-Rossendorf, Dresden, Germany — ²Leibniz IFW, Dresden, Germany

Perpendicular magnetic bit media consist of regular rigid nanostructured networks where data is stored in decoupled nanostructures. Flexible magnetic nanoelectronic devices rely on curvature-induced effects that introduce topological patterning [1]. We prepared arrays of magnetic bits with a size of 400 nm arranged in close-packed square and hexagonal arrays of Pt/Co/Pt cap-like structures on PDMS elastic membranes by means of nanoprinting and Al anodization. The magnetization reversal process indicates a magnetically decoupled switching process in the individual caps of the square array in contrast to the hexagonal array. Here we propose a method to evaluate this coupling by means of analysis of a series of field-dependent MOKE images. The results indicate that the magnetic coupling between the caps can be quantitatively characterized in terms of a fractal dimension. Overall, these results suggest that the magnetization switching in densely-packed networks can be tailored via topology.

References: [1] D. Makarov et al., Adv. Mater. 34, 2101758 (2022)

MA 43.6 Thu 16:15 HSZ 401

Coherent Correlation Imaging for resolving fluctuating states of matter — •CHRISTOPHER KLOSE¹, FELIX BUETTNER^{2,3,4}, WEN HU³, CLAUDIO MAZZOLI¹, KAI LITZIUS², RICCARDO BATTISTELLI⁴, IVAN LEMESH², JASON M. BARTELL², MANTAO HUANG², CHRISTIAN M. GUENTHER⁵, MICHAEL SCHNEIDER¹, ANDI BARBOUR³, STUART B. WILKINS³, GEOFFREY S.D. BEACH², STEFAN EISEBITT^{1,5},

and BASTIAN PFAU¹ — ¹Max Born Institute, Berlin — ²Massachusetts Institute of Technology, Cambridge, MA, USA — ³National Synchrotron Light Source II, Upton, NY, USA — ⁴Helmholtz-Zentrum Berlin — ⁵Technische Universität Berlin

Fluctuations and stochastic transitions are ubiquitous in nanometer-scale systems, especially in the presence of disorder. However, their direct observation has so far been impeded by a seemingly fundamental, signal-limited compromise between spatial and temporal resolution.

Here, we develop coherent correlation imaging (CCI) — a high-resolution, full-field imaging technique that realizes multi-shot, time-resolved imaging of stochastic processes. The key of CCI is the classification of camera frames that correspond to the same physical state by combining a correlation-based similarity metric with powerful classification algorithm developed for genome research.

We apply CCI to study previously inaccessible magnetic fluctuations in a highly degenerate magnetic stripe domain state with nanometer-scale resolution. The spatiotemporal imaging reveals the transition network between the states and details of the magnetic pinning landscape which have been inaccessible so far.

MA 43.7 Thu 16:30 HSZ 401

Origin of helicity-dependent photoconductivity in magnetic and nonmagnetic wires — •ATUL PANDEY^{1,2}, ROUVEN DREYER¹, PALVAN SEYIDOV¹, CHRIS KOERNER¹, SABAN TIRPANC¹, BINOY K. HAZRA², STUART PARKIN², and GEORG WOLTERSDOERF^{1,2} — ¹Institute of Physics, Martin Luther University Halle-Wittenberg, Von-Danckelmann-Platz 3, 06120 Halle, Germany — ²Max Planck Institute of Microstructure Physics, Weinberg 2, 06120 Halle, Germany

We study the opto-electric response in metallic wire structures. The aim is to understand the origin of helicity-dependent photoconductivity. For nonmagnetic metals this effect is generally believed to probe spin polarization. Using magnetic wires we show that this method enables background free imaging of spin textures. Analyzing the physical origin we find that the circular dichroism slightly modulates the absorption. The corresponding thermal modulation explains the measured electrical signals. We apply this result to examine the spin Hall effect induced spin accumulation in heavy metals. Here, we show that previously reported results in nonmagnetic wires are well reproducible, but not related to the spin polarization.

A. Pandey et al., Phys. Rev. B 106, 174420 (2022)

MA 44: Frustrated Magnets II

Time: Thursday 15:00–17:30

Location: HSZ 403

MA 44.1 Thu 15:00 HSZ 403

Magnetic Force Microscopy Investigations of the Kagome Spin Ice Host HoAgGe — •TSUEI-SHIN WU¹, SUBHAJIT ROYCHOWDHURY², SAMUEL D. SEDDON¹, PETER MILDE¹, CLAUDIA FELSER², and LUKAS M. ENG^{1,3} — ¹Institute of Applied Physics, Technische Universität Dresden, Dresden, Germany — ²Max-Planck-Institute for Chemical Physics of Solids, Dresden, Germany — ³Dresden-Würzburg Cluster of Excellence * Complexity and Topology in Quantum Matter (ct.qmat), TU Dresden, 01062 Dresden, Germany

The recent discovery of the quasi-2D spin ice on a Kagome lattice in HoAgGe [1] has highlighted this material system as the perfect environment in order to explore emerging questions and to clarify ongoing discussions regarding 2D spin ices within the scientific community. The presence of several high-order magnetization plateaus implies the possible existence of quantum magnetic states and/or non-collinear spin textures that may originate from quantum or thermal fluctuations [2]. Peaks in the topological Hall effect, which correlate with these magnetization plateaus, also potentially imply the presence of exotic spin textures - or at the very least non-collinear spin textures, which low-temperature (LT) Magnetic Force Microscopy (MFM) is perfectly placed to uncover. Here we present LT-MFM results when investigating the magnetic textures and their behaviors in HoAgGe samples under magnetic fields applied along the relevant crystallographic Kagome lattice directions.

Reference [1] Zhao et al., Science 367, 1218 (2020). [2] Baran et al., Journal of Alloys and Compounds 281, 92 (1998).

MA 44.2 Thu 15:15 HSZ 403

Coexistence of antiferromagnetism and ferrimagnetism in adjacent honeycomb layers — •DÁVID SZALLER¹, LILIAN PRODAN^{2,3}, KORBINIAN GEIRHOS², VIÖREL FELEA^{2,3,4}, YURII SKOURSKI⁴, DENIS GORBUNOV⁴, TOBIAS FÖRSTER⁴, TONI HELM⁴, TOSHIHIRO NOMURA^{4,5}, ATSUHIKO MIYATA⁴, SERGEI ZHERLITSYN⁴, JOCHEN WOSNITZA^{4,6}, ALEXANDER A. TSIRLIN², VLADIMIR TSURKAN^{2,3}, and ISTVAN KEZSMARKI² — ¹TU Wien — ²University of Augsburg — ³Institute of Applied Physics, R. Moldova — ⁴Hochfeld-Magnetlabor Dresden — ⁵University of Tokyo, Kashiwa — ⁶TU Dresden

Ferro/ferri- and antiferromagnetic orders are typically exclusive in nature, thus, their co-existence in atomic-scale proximity is expected only in heterostructures. Breaking this paradigm we report the observation of a new, atomic-scale hybrid spin state. This ordering is stabilized in three-dimensional crystals of the polar antiferromagnet $\text{Co}_2\text{Mo}_3\text{O}_8$ by magnetic fields applied perpendicular to the Co honeycomb layers and possesses a spontaneous in-plane ferromagnetic moment. Our microscopic spin model, capturing the observed field dependence of the longitudinal and transverse magnetization as well as the magnetoelectric/elastic properties, reveals that this novel spin state is composed of an alternating stacking of antiferromagnetic and ferrimagnetic honeycomb layers. We show that the proper balance of magnetic interactions can extend the stability range of this hybrid phase down to zero magnetic field. The layer-by-layer stacking of distinct spin orders via suitable combinations of microscopic interactions opens a new dimension toward the nanoscale engineering of magnetic states.

MA 44.3 Thu 15:30 HSZ 403

Coupled frustrated ferromagnetic and antiferromagnetic quantum spin chains in the quasi-one-dimensional mineral antlerite, $\text{Cu}_3\text{SO}_4(\text{OH})_4$ — A.A. KULBAKOV¹, D.Y. KONONENKO², S. NISHIMOTO^{2,3}, Q. STAHL¹, A. MAN-NATHANATH CHAKKINGAL¹, M. FEIG⁴, R. GUMENIUK⁴, Y. SKOURSKI⁵, L. BHASKARAN⁵, S.A. ZVYAGIN⁵, J.P. EMBS⁶, I. PUENTE-ORENCH^{7,8}, A. WILDES⁸, J. GECK^{1,9}, O. JANSON², D.S. INOSOV^{1,9}, and •D.C. PEETS¹ — ¹IFMP, TU Dresden — ²Leibniz IFW-Dresden — ³ITP, TU Dresden — ⁴IEP, TU Bergakademie Freiberg — ⁵HLD-EMFL, HZRD Dresden — ⁶PSI, Villigen, Schweiz — ⁷INMA, CSIC-U. Zaragoza, Spain — ⁸ILL, Grenoble, France — ⁹ct.qmat

Magnetic frustration, the competition among exchange interactions, often leads to novel magnetic ground states with unique physical properties which can hinge on details of interactions that are otherwise difficult to observe. Such states are particularly interesting when it is possible to tune the balance among the interactions to access multiple types of magnetic order. We present antlerite, $\text{Cu}_3\text{SO}_4(\text{OH})_4$, as a potential platform for tuning frustration. Contrary to previous reports, the low-temperature magnetic state of its three-leg zigzag ladders is a quasi-one-dimensional analogue of the magnetic state recently proposed to

exhibit spinon-magnon mixing in botallackite. Density-functional-theory calculations indicate that antlerite's magnetic ground state is exquisitely sensitive to fine details of the atomic positions, with each chain independently on the cusp of a phase transition, indicating an excellent potential for tunability.

MA 44.4 Thu 15:45 HSZ 403

High-Frequency Electron Spin Resonance Studies on the Quasi One-Dimensional Spin-1/2 Quantum Magnet $\text{PbCuSeO}_4(\text{OH})_2$ — •RAHEL OHLENDORF, DANIEL KNAUER, CHANGHYUN KOO, and RÜDIGER KLINGELER — Kirchhoff Institute for Physics, Heidelberg, Germany

We report high-frequency ESR studies on a polycrystalline sample of the frustrated quasi-1D spin-1/2 quantum material $\text{PbCuSeO}_4(\text{OH})_2$, isostructural to the well-studied natural mineral linarite ($\text{PbCuSO}_4(\text{OH})_2$). Magnetisation data show the evolution of a magnetically ordered phase below $T_N = 4.8$ K and a spin-flop transition at $B_{\text{SF}} = 2.8$ T. A complex magnetic phase diagram is constructed from the data. ESR measurements on a loose powder evidence a gapless linear excitation mode within the ground state, which can be traced across the spin-flop transition, as well as two linear excitation modes within the in-field phase with a zero field gap of -31 ± 9 GHz and 32.9 ± 1.4 GHz, respectively. Measurements on fixed powder reveal a gapped magnon mode in the ground state with a zero field splitting of 70 ± 20 GHz. This mode might be accounted for by assuming an excitation of a spiral spin order in the ground state. Tracing the resonance positions with temperature suggests an easy-axis-type anisotropy with the paramagnetic g -factors 2.3 and 2.07. Changes in resonance position evidence the onset of short range fluctuations at around 70 K corresponding to $14 \times T_N$.

15 min. break

MA 44.5 Thu 16:15 HSZ 403

K_2ReCl_6 : an unconventional Jahn-Teller system? — •ALEXANDRE BERTIN¹, TUSHARKANTI DEY¹, DANIEL BRÜNING¹, DMITRY GORKOV^{1,2}, KEVIN JENNI¹, ASTIN KRAUSE¹, PETRA BECKER³, LADISLAV BOHATÝ³, DANIEL KHOMSKII¹, THOMAS LORENZ¹, and MARKUS BRADEN¹ — ¹II. Physikalisches Institut, Universität zu Köln — ²Heinz Maier-Leibnitz Zentrum (MLZ), Technische Universität München — ³Abteilung Kristallographie, Institut für Geologie und Mineralogie, Universität zu Köln

Antifluorite compounds of chemical formula K_2MX_6 (where M is a transition metal and $X=\text{Cl,Br}$) can exhibit various crystallographic phase transitions, often understood by the softening of rotary phonon modes of the ligand octahedra surrounding the central transition metal. Among this family, K_2ReCl_6 exhibits on cooling four distinct structural phases and may constitute a playground to investigate the interplay between spin-orbit coupling (SOC) and Jahn-Teller (JT) effect. The question whether one of the crystallographic phase transitions is JT driven will be tackled by presenting a detailed temperature dependent structural study of K_2ReCl_6 and of its non magnetic counterpart K_2SnCl_6 by means of powder and single crystal XRD. With neutron diffraction experiments and by taking the low temperature monoclinic symmetry into account, the magnetic structure was solved. Frustration is only partially lifted by the structural distortions and the magnetic order causes further symmetry reduction. Finally, the strong magneto-elastic effect seen in thermal expansion measurements will be discussed in terms of domain re-orientation and weak ferromagnetism.

MA 44.6 Thu 16:30 HSZ 403

Non-collinear magnetism and Fe-R interaction in $\text{R}_3\text{Fe}_3\text{Sb}_7$ — •FELIX SEEWALD¹, FALK PABST^{2,5}, SABRINA PALAZZESE^{1,3,5}, VADIM GRINENKOV^{1,6}, HUBERTUS LUETKENS⁷, THOMAS HERRMANNSDÖRFER³, SHINGO YAMAMOTO^{3,5}, DENIS GORBUNOV^{3,5}, SUMANTA CHATTOPADHYAY^{3,5}, CLEMENS RITTER⁴, KATI FINZEL², THOMAS DOERT^{2,5}, MICHAEL RUCK^{2,5}, JOCHEN WOSNITZA^{1,3,5}, and HANS-HENNING KLAUSS¹ — ¹IFMP, TU Dresden, Germany — ²Fakultät für Chemie und Lebensmittelchemie, TU Dresden, Germany — ³HLD-EMFL, Helmholtz-Zentrum Dresden-Rossendorf, Germany — ⁴Institute Laue-Langevin Grenoble, France — ⁵Würzburg-Dresden Cluster of Excellence ct.qmat — ⁶Tsung-Dao Lee Institute, Shanghai, China — ⁷PSI, Villigen, Switzerland

In $\text{R}_3\text{Fe}_3\text{Sb}_7$ ($R = \text{Pr, Nd}$) Fe and R atoms form columns of stacked triangles separated by Sb. Fe exhibits non-collinear ferromagnetic order below $T_c \approx 380$ K. On cooling at the onset of R order a spin reorientation ($T_{\text{SRT,Pr}} \approx 40$ K, $T_{\text{SRT,Nd}} \approx 50$ K) and magnetization reversal is observed [1].

Mössbauer spectra show two distinct magnetic Fe sites between T_c and T_{SRT} , both collapsing into one new site below T_{SRT} , reaching a static magnetic hyperfine-field of $B_{\text{hyp}} = 20.59(21)$ T at 4.2 K. The data is the same for Nd and Pr except for the value of T_{SRT} . The local field obtained from μSR investigations is consistent with Mössbauer hyperfine-field at high temperatures. We will discuss

the implications of our findings on the magnetic structure of the system.

[1] Falk Pabst, Sabrina Palazzese et. al., Advanced materials, accepted

MA 44.7 Thu 16:45 HSZ 403

Reentrant topological magnetic order and a spin-cholesteric phase in the $\text{Sr}_3\text{Fe}_2\text{O}_7$ perovskite — •NIKITA ANDRIUSHIN¹, NIKOLAI PAVLOVSKII¹, YULIYA TYMOSHENKO¹, DARREN C. PEETS¹, ALEXANDRE IVANOV², JACQUES OLLIVIER², BERNHARD KEIMER³, OKSANA ZAHARKO⁴, and DMYTRO INOSOV¹ — ¹TU Dresden, Germany — ²ILL, Grenoble, France — ³MPI for Solid State Research, Stuttgart, Germany — ⁴PSI, Villigen, Switzerland

Topologically nontrivial magnetic structures, e.g., skyrmion lattices and magnetic vortex crystals, are well known in noncentrosymmetric materials, so that antisymmetric exchange interactions are allowed. Only recently, topological multi- \mathbf{q} magnetic textures that spontaneously break the chiral symmetry, for example three-dimensional hedgehog lattices, were discovered in centrosymmetric compounds, where they are instead driven by frustrated interactions. Here we show that the bilayer perovskite $\text{Sr}_3\text{Fe}_2\text{O}_7$, previously believed to adopt a simple single- \mathbf{q} spin-spiral order, hosts two distinct types of multi- \mathbf{q} topological spin textures. Its ground state represents an unusual multi- \mathbf{q} spin texture with unequally intense helical spin modulations at the two ordering vectors. It is followed in temperature by a new "spin cholesteric" phase, in which the chiral symmetry is spontaneously broken along one of the crystal directions, but the weaker modulation along the orthogonal direction melts, giving rise to intense short-range dynamical fluctuations. Shortly before the transition to the paramagnetic state, a more conventional skyrmion-lattice order spanned by two equivalent \mathbf{q} vectors emerges.

MA 44.8 Thu 17:00 HSZ 403

Incommensurate and multiple- q magnetic misfit order in $\text{Cu}_3\text{SO}_4(\text{OH})_4$ — •ANTON KULBAKOV¹, ELAHEH SADROLLAHI¹, FLORIAN RASCH¹, MAXIM AVDEEV^{2,3}, SEBASTIAN GASS⁴, LAURA BOHORQUEZ⁴, ANJA WOLTER^{4,5}, MANUEL FEIG⁶, ROMAN GUMENIUK⁶, HAGEN PODDIG⁷, MARKUS STÖTZER⁸, JOCHEN LITTERST⁹, INES PUENTE-ORENCH^{10,11}, ANDREW WILDES¹¹, EUGEN WESCHKE¹², JOCHEN GECK^{1,5}, DMYTRO INOSOV^{1,5}, and DARREN PEETS¹ — ¹IFMP, TU Dresden, Germany — ²ANSTO, Australia — ³USYD, Australia — ⁴IFW Dresden, Germany — ⁵ct.qmat, TU Dresden, Germany — ⁶TUBA Freiberg, Germany — ⁷ACII, TU Dresden, Germany — ⁸ACI, TU Dresden, Germany — ⁹IPKM, TU Braunschweig, Germany — ¹⁰INMA, Spain — ¹¹ILL, Grenoble, France — ¹²HZB, Berlin, Germany

In antlerite, $\text{Cu}_3\text{SO}_4(\text{OH})_4$, Cu^{2+} ($S = \frac{1}{2}$) quantum spins populate three-leg zigzag ladders in a highly frustrated quasi-one-dimensional structural motif. We demonstrate that at zero applied field, in addition to its recently reported low-temperature phase of coupled ferromagnetic and antiferromagnetic spin chains, this mineral hosts an incommensurate helical+cycloidal state, an idle-spin state, and a multiple- q phase which is the magnetic analog of misfit crystal structures. The antiferromagnetic order on the central leg is reentrant. The high tunability of the magnetism in antlerite makes it a particularly promising platform for pursuing exotic magnetic order.

MA 44.9 Thu 17:15 HSZ 403

Spin-liquid and Spin-glass states in Frustrated Tetragonal Pyrochlore $\text{Zn}_{0.8}\text{Cu}_{0.2}\text{FeMnO}_4$ — •SUCHIT KUMAR JENA¹, MANFRED REEHUIS², and SUBHASH THOTA¹ — ¹Department of Physics, Indian Institute of Technology Guwahati, Assam-781039, India — ²Helmholtz-Zentrum Berlin für Materialien und Energie, Hahn-Meitner-Platz 1, D-14109 Berlin, Germany

Spinel (AB_2O_4) Pyrochlore lattices are capable of generating high degree of magnetic frustration owing to tunable competing exchange interactions achieved via suitable magnetic elements on B site together with non-magnetic A site, which leads to quantum spin-liquid/Ice state [1]. One such compound is cubic ZnFe_2O_4 , which manifests high magnetic frustration index ($f \approx 12$) with antiferromagnetic Néel temperature, $T_N \sim 10$ K [2]. Our results based on the neutron powder diffraction analysis shows that polycrystalline tetragonal $\text{Zn}_{0.8}\text{Cu}_{0.2}\text{FeMnO}_4$ (ZCFMO) lacks presence of long-range magnetic ordering. The dynamic ac magnetic susceptibility (χ' and χ'') measurements show multiple anomalies across 9K, 47K and 79K. Frequency dispersion in the loss spectrum ($\chi''(f, T)$) analyzed by employing empirical scaling-laws such as Vogel-Fulcher law and Power Law: $\tau = \tau_0 [(T - T_{\text{SG}})/T_{\text{SG}}]^{-z\nu}$, yields cluster spin-glass state in ZCFMO with the spin freezing temperature (T_{SG}) at 41.8K and critical exponent $z\nu \approx 8.9$, below the ferrimagnetic Néel temperature $T_{\text{FM}} \approx 79$ K. These results are further supported by the heat capacity ($C_p(T)$) studies. Below 9K, $C_p \sim T^2$, indicates co-existence of spin-glass and spin-liquid states in ZCFMO. [1] *Phys. Rev. B* **28**, 1 (1983). [2] *Phys. Rev. B* **66**, 064401 (2002).

MA 45: Members' Assembly

Time: Thursday 18:00–19:00

All members of the Magnetism Division are invited to participate.

Location: HSZ 04

MA 46: Ultrafast Magnetization Effects II

Time: Friday 9:30–12:45

Location: HSZ 02

MA 46.1 Fri 9:30 HSZ 02

Spin noise in magnetically ordered models — •JULIUS SCHLEGEL, MARTIN EVERS, and ULRICH NOWAK — Department of Physics, University of Konstanz

Spin noise spectroscopy has emerged in the last years as a new tool to investigate magnetic material properties [1].

On the basis of a classical HEISENBERG model and the stochastic LANDAU-LIFSHITZ-GILBERT equation of motion we numerically compute the time evolution of magnetically ordered structures on a time scale of several hundreds of picoseconds. By analyzing the spectral noise power density and the autocovariance of the magnetization in both ferro- and antiferromagnetic models, we find that the magnetic noise in thermal equilibrium comprises several features of the system. Resonances in the noise spectra are observed, which can be assigned to the eigenmodes of the magnetic structure. Moreover, the noise can mark phase transitions like the transition to the paramagnetic state or a spin-flop transition.

We thus conclude that by means of investigating the noise of the magnetization, the magnetic order of a system can be extracted even in cases where the mean equilibrium magnetization does not reflect the transition at all.

[1] Valerii S. Zapasskii, "Spin-noise spectroscopy: from proof of principle to applications", *Adv. Opt. Photon.* 5, 131-168 (2013)

MA 46.2 Fri 9:45 HSZ 02

Spin and momentum resolved ultrafast carrier dynamics in antiferromagnetic Dirac semimetal models — •MARIUS WEBER¹, KAI LECKRON¹, BAERBEL RETHFELD¹, LIBOR ŠMEJKAL², JAIRO SINOVA², and HANS CHRISTIAN SCHNEIDER¹ — ¹Department of Physics and Research Center OPTIMAS, RPTU Kaiserslautern-Landau, Germany — ²Institute of Physics, Johannes Gutenberg University Mainz, Germany

Systems with antiferromagnetic ordering in real space often exhibit topological features in momentum space that only recently have been investigated in a comprehensive fashion [1]. For instance, depending on the magnetic ordering, they may have band structures with a pronounced anisotropy in band energies and in the spin structure of their single-particle states due to Dirac fermions. We present numerical calculations of the electron dynamics due to electron-phonon interactions [2,3] in model systems with two-dimensional k-space that capture key properties of antiferromagnetic Dirac materials in momentum space. After an instantaneous heating of the electronic system we obtain a transient carrier distributions, which reflect the momentum-space features. Surprisingly, completely anisotropic carrier distribution may evolve, even from excited carrier distributions that are isotropic in energy, i.e., $f(E(k)) = f(E)$.

[1] L. Šmejkal et al.; *Phys. Rev. Lett.* 118, 106402 (2017).

[2] K. Leckron et al.; *Phys. Rev. B* 96, 140408 (2017).

[3] S. Essert et al.; *Phys. Rev. B* 84, 224405 (2011).

MA 46.3 Fri 10:00 HSZ 02

Inertial spin dynamics in ferromagnets and antiferromagnets — RITWIK MONDAL¹, LUCAS WINTER², SEBASTIAN GROSSENBACH², ULRICH NOWAK², and •LEVENTE RÓZSA^{2,3} — ¹Indian Institute of Technology (ISM) Dhanbad, Dhanbad, India — ²University of Konstanz, Konstanz, Germany — ³Wigner Research Centre for Physics, Budapest, Hungary

Inertial spin dynamics emerges in magnetic materials at very short time scales where the directions of the atomic magnetic moment and angular momentum become separated, and nutation can be observed. The inertia gives rise to additional high-frequency or nutational excitations recently detected in ferromagnetic resonance experiments [1].

Here the signatures of inertial spin dynamics are discussed theoretically in ferromagnets (FMs) and antiferromagnets (AFMs). The nutational spin-wave bands are shifted by a constant frequency compared to the low-frequency bands in FMs, while in AFMs the nutational bands have a maximum in the center of the Brillouin zone [2]. It is demonstrated that a resonant excitation of the nutation may be utilised for switching the order parameter [3]. The switching is found to proceed faster in AFMs than in FMs, and in AFMs tuning the excitation frequency can be used to control the direction of the switching.

[1] K. Neeraj et al., *Nat. Phys.* 17, 245 (2021).

[2] R. Mondal et al., *Phys. Rev. B* 106, 134422 (2022).

[3] L. Winter et al., arXiv:2207.08566.

MA 46.4 Fri 10:15 HSZ 02

Magnetic field-dependent ultrafast control of an antiferromagnet — •ABEER ARORA^{1,6}, YOAV WILL WINDSOR², SANG-EUN LEE¹, JIT SARKAR¹, KRISTIN KLIEMT³, CH. SCHÜSSLER-LANGEHEINE⁴, NIKO PONTIUS⁴, CORNELIUS KRELLNER³, DENIS V. VYALIKH⁵, and LAURENZ RETTIG¹ — ¹FHI der MPG, Berlin — ²IOAP, TU Berlin — ³Phy. Inst., Goethe-Uni., Frankfurt am Main — ⁴HZB für Materialien und Energie GmbH, Berlin — ⁵DIPC, Basque, Spain — ⁶Fachbereich Physik, FU Berlin

Antiferromagnetic (AF) materials offer faster manipulation of spins, while making control of magnetic order challenging. A promising approach is utilizing the magnetic anisotropy (MA) to manipulate the spin arrangement on femtosecond timescales [1]. In addition, external magnetic fields can induce a spin flop (SF), providing an additional control knob for AF order. Understanding the interplay of these effects is of strong interest. Here, we present time-resolved resonant soft X-ray diffraction (RSXRD) experiments on the prototypical A-type antiferromagnet GdRh₂Si₂. We observe a coherent rotation of the AF arrangement followed by oscillations of the AF order due to light-induced change in the MA potential. Remarkably, upon increasing magnetic field, the frequency of the oscillations increases while the amplitude of reorientation upon photoexcitation decreases. These observations demonstrate the interplay of the MA potential and the SF field, and offer new ways towards deterministic control of AF spin order. [1] Windsor et al. *Commun Phys* 3, 139 (2020)

MA 46.5 Fri 10:30 HSZ 02

Dynamics of the Morin transition in hematite — •MAIK KERSTINGSKÖTTER¹, TOBIAS DANNEGGER¹, ANDRÁS DEÁK², LÁSZLÓ SZUNYOGH^{2,3}, and ULRICH NOWAK¹ — ¹Department of Physics, University of Konstanz — ²Department of Theoretical Physics, Budapest University of Technology and Economics — ³ELKH-BME Condensed Matter Research Group, Budapest University of Technology and Economics

Below a critical temperature T_M of about 264 K, hematite is a perfect antiferromagnet with zero net magnetization due to the fact that the spins of the four sublattices are antiparallel and aligned with the c -axis. If the temperature exceeds this critical point, the spins reorient into the basal plane and assume a small canting angle that results in a finite net magnetization. This first-order phase transition from the antiferromagnet to the weak ferromagnetic phase is the Morin transition. While the equilibrium properties are well known, we want to investigate the nonequilibrium dynamics of the transition. Here we use atomistic spin dynamics simulations on the basis of an ab initio model to study the system's response to an instantaneous temperature increase from $T < T_M$ to $T > T_M$. In the model used, we indeed observe this Morin transition, which takes place in the range of five to a few hundred picoseconds, depending on the size of the Gilbert damping used.

MA 46.6 Fri 10:45 HSZ 02

Non-collinear spin reorientation in FeRh from first principles: Ultrafast laser quenching vs. coherent rotation of Fe moments — •MIKE JOS BRUCKHOFF, MARKUS ERNST GRUNER, and ROSSITZA PENTCHEVA — Faculty of Physics and Center for Nanointegration (CENIDE), University of Duisburg - Essen

The binary alloy FeRh exhibits a metamagnetic first-order phase transition from antiferromagnetic (AFM) to ferromagnetic (FM) order, which can be driven by an external magnetic field or laser excitation. Here, we present a comprehensive non-collinear density functional theory study, where we investigate the multi-dimensional energy landscape $E(M, V)$, by constraining the total spin moment in order to compare different kinds of spin reorientation pathways. The absence of significant energy barriers suggests that the coherent in-plane rotation of the Fe moments is a likely scenario for the magnetic phase transition in an external magnetic field. In contrast to this, FeRh exhibits an laser-induced ultrafast demagnetization, which is initiated by optical inter-site spin transfer (OISTR) and a net Rh-to-Fe charge transfer at early times after excitation. We study extensively the response of FeRh to laser pulses with different laser parameters in both magnetic phases, simulated by means of real-time time-dependent DFT (RT-TDDFT). We find that the magnitude of the response strongly depends on the incident laser pulse, as well as the magnetic state of FeRh. We conclude that laser excitations and applied magnetic fields initiate distinct transition pathways, which may be exploited to control the phase transition by the external stimuli.

MA 46.7 Fri 11:00 HSZ 02

Signature of spatial gradients in ultrafast demagnetization observed with angle-resolved complex magneto-optical Kerr-effect (CMOKE) — •SANJAY ASHOK¹, JONAS HOEFER¹, MARTIN STIEHL¹, MARTIN AESCHLIMANN¹, HANS CHRISTIAN SCHNEIDER¹, BÄRBEL RETHFELD¹, and BENJAMIN STADTMÜLLER^{1,2} — ¹Department of Physics and Research Center OPTIMAS, RPTU Kaiserslautern-Landau, Germany — ²Institute of Physics, Johannes Gutenberg-University Mainz, Germany

Understanding the laser-induced ultrafast magnetization dynamics of thick metallic films is even in simple materials still challenging due to different transport mechanisms contributing to the magnetization dynamics. While heat- and particle diffusion are slow processes, ballistic and superdiffusive transport lead to an ultrafast equilibration of spatial inhomogeneities. However, quantifying experimentally their impact on ultrafast demagnetization of bulk material is difficult, since surface-sensitive experimental techniques integrate the response of the material over a certain depth.

Our theoretical calculations reveal that the Kerr-rotation dynamics is nearly insensitive to gradients in magnetization. In contrast, we find a strong influence for the angle-resolved ellipticity dynamics. These findings are confirmed by CMOKE experiments on Nickel films of varying thicknesses. The probe-angle resolved CMOKE technique thus provides a method to study the presence of transient gradients in magnetization at ultrafast timescales.

MA 46.8 Fri 11:15 HSZ 02

Dynamic versus Static Spectral Weight Transfer in LPCMO Thin Films — •KAREN P. STROH, TIM TITZE, PIA HENNING, DANIEL STEIL, STEFAN MATHIAS, and VASILY MOSHNYAGA — I. Physikalisches Institut, Georg-August-Universität Göttingen, DE

$(\text{La}_{1-y}\text{Pr}_y)_{1-x}\text{Ca}_x\text{MnO}_3$ (LPCMO) is a prototypical bandwidth-controlled magnetite with strong electron-phonon coupling and colossal magnetoresistance (CMR), originating from a nm-scale phase separation with ferromagnetic nanodomains antiferromagnetically coupled by correlated Jahn-Teller polarons (CPs).

The present study made use of strain-engineered LPCMO thin films prepared by a metalorganic aerosol deposition technique on LAO-buffered STO(100) substrates. Temperature-dependent static reflectivity spectra, showing the phase-transition-mediated spectral weight transfer (SWT), served as reference for identifying thermally driven behaviour. Further, pump-probe reflectivity (PPR) and time-resolved magneto-optical-Kerr effect (MOKE) data at different temperatures and probe wavelengths provided insights into the role of CPs in ultrafast electron and magnetization dynamics on femto- to nanosecond timescales.

As a main result, we observed a long-lived non-thermal state with increased optical conductivity in the polaron hopping regime at a probe energy of 0.7eV, indicating the destruction of polarons or a loss of their correlation upon laser excitation.

Financial support by the German Research Foundation DFG (project 399572199 and CRC 1073/A02) is acknowledged.

MA 46.9 Fri 11:30 HSZ 02

Experimental exploration of criticality in dynamic magnetic phase transitions — •MIKEL QUINTANA and ANDREAS BERGER — CIC nanoGUNE BRTA, E-20018 Donostia-San Sebastián, Spain.

The dynamic phase transition (DPT) of ferromagnets is a well-known phenomenon describing an abrupt change in the time-evolution behavior of magnetization in the presence of a time-dependent magnetic field. Its similarities with the conventional thermodynamic phase transition (TPT), particularly in terms of scaling behavior close to their respective critical points, are of utmost importance to understand collective behaviors in systems out-of-equilibrium [1]. However, a lack of experimental verification of these theoretical predictions has impeded further progress in the field up to now. Here, we experimentally explore for the first time the scaling behavior and critical exponents of the DPT in ultrathin Co films by means of real-time magneto-optical Kerr effect measurements in the relevant dynamic phase space. Surprisingly, we observe that the DPT and TPT critical exponents correspond to different dimensionalities for the same film. Our results seem to indicate different dimensional crossover length-scales for the TPT and DPT, a fact that has not been explored to date. [1] P. Riego et. al., *Physica B* 549, 13-23 (2018).

MA 46.10 Fri 11:45 HSZ 02

Slow dynamics from ultrafast phononic driving in CuGeO_3 — •LEONIE SPITZ¹, EUGENIO PARIS¹, FLAVIO GIORGIANNI¹, BRUCE NORMAND¹, THORSTEN SCHMITT¹, and CHRISTIAN RÜEGG^{1,2,3,4} — ¹Paul Scherrer Institute, CH-5232 Villigen-PSI, Switzerland — ²Department of Quantum Matter Physics, University of Geneva, CH-1211 Geneva, Switzerland — ³Institute of Physics, Ecole Polytechnique Fédérale de Lausanne (EPFL), CH-1015 Lausanne, Switzerland — ⁴Institute of Quantum Electronics, ETH Zürich, CH-8093 Höggerberg, Switzerland

The coherent manipulation of magnetism by optically driven phonons is a rapidly growing field [1-4]. However, experimental studies of quantum spin systems by ultrafast pump-probe schemes remain rare, because the most common optical techniques to probe magnetic phenomena fail in the absence of magnetic

order. We present a multi-method study of the spin-chain material CuGeO_3 , in which the magnetic correlations are associated with a lattice instability, also called the spin-Peierls (SP) transition, that drives the system into a collective singlet ground state of spin dimers [5]. By the coherent driving of phonons we observe low-frequency dynamics of the optical response which may offer new insight into the mechanism driving the SP transition in CuGeO_3 , a problem that has remained unsolved for almost 3 decades.

[1] T. F. Nova et al., *Nat. Phys.* 13, 132-136 (2017). [2] A. S. Disa et al., *Nat. Phys.* 16, 937-941 (2020). [3] D. Afansiev et al., *Nat. Mater.* 20, 607-611 (2021). [4] F. Giorgianni et al., arXiv:2101.01189 (2021). [5] M. Hase et al., *Phys. Rev. Lett.* 70, 3651 (1993).

MA 46.11 Fri 12:00 HSZ 02

Spin-lattice coupling in a Van der Waals ferromagnet on ultrafast time scales — •HYEIN JUNG^{1,2}, VICTORIA C. A. TAYLOR², YOAV WILLIAM WINDSOR^{1,2}, and RALPH ERNSTORFER^{1,2} — ¹Technische Universität Berlin, Berlin, Germany — ²Fritz Haber Institute der MPG, Berlin, Germany

Two-dimensional (2D) van der Waals (vdW) magnetic materials hold great potential for spintronic applications. $\text{Cr}_2\text{Ge}_2\text{Te}_6$ (CGT) is one such material which exhibits ferromagnetism even at the monolayer limit. With functionality in mind, investigation of dynamic processes on their fundamental time scales is of great importance, in particular energy flow and coupling between subsystems (carriers, spins, lattice). Furthermore, we have recently shown that understanding lattice dynamics in ferromagnets is essential for a complete understanding of ultrafast spin dynamics. Here we use femtosecond electron diffraction (FED) to study lattice dynamics in CGT and other 2D magnets. We discuss the interaction between magnetic order and the lattice, and the influence of studying such effects at the monolayer limit.

MA 46.12 Fri 12:15 HSZ 02

Modelling spin-lattice coupling in computer simulation — •MICHAEL SAUR¹, MARKUS WEISSENHOFER¹, HANNAH LANGE², AKASHDEEP KAMRA³, SERGIY MANKOVSKY², SVITLANA POLESYA², HUBERT HUBERT², and ULRICH NOWAK¹ — ¹University of Konstanz, Germany — ²LMU Munich, Germany — ³Universidad Autónoma de Madrid, Spain

We develop a multiscale framework for the description of spin-lattice coupling in computer simulations [1]. The derived Hamiltonian describes a closed system of spin and lattice degrees of freedom and explicitly conserves the total momentum, angular momentum and energy. Using a new numerical implementation that corrects earlier Suzuki-Trotter decompositions we perform simulations on the basis of the resulting equations of motion to investigate the combined magnetic and mechanical motion of a ferromagnetic nanoparticle. The framework developed herein will enable the use of multi-scale modeling for investigating and understanding a broad range of spin-phonon-mediated phenomena from slow to ultrafast time scales.

[1] M. Weißenhofer, H. Lange, A. Kamra, S. Mankovsky, S. Polesya, H. Ebert, U. Nowak, doi 10.48550/ARXIV.2211.02382

MA 46.13 Fri 12:30 HSZ 02

Ultrafast energy flow in the van der Waals ferromagnet Fe_3GeTe_2 (FGT) — •YOAV WILLIAM WINDSOR^{1,2}, DANIELA ZAHN², VICTORIA C. A. TAYLOR², THEODOR GRIEPE⁴, TOMMASO PINCELLI², HYEIN JUNG², SANG-EUN LEE², CHRISTIAN SCHÜSSLER-LANGEHEINE³, NIKO PONTIUS³, UNAI ATXITIA⁴, RALPH ERNSTORFER^{1,2}, and LAURENZ RETTIG² — ¹TU Berlin — ²Fritz Haber Inst. — ³Helmholtz Zentrum Berlin — ⁴CSIC Madrid

Van der Waals bonded magnetic materials expand the technological promise of 2D materials (TMDCs, Graphene) into the field of spintronics. To this end, understanding their nonequilibrium behavior is essential. Here we experimentally probed the response of FGT to photoexcitation using three probes: time-resolved ARPES (probes the carriers), time-resolved XMCD (probes the spins), and femtosecond electron diffraction (FED; probes the lattice). We resolve sub-picosecond responses in all three sub-systems, and find that the conventional M3TM model must be modified to reliably reproduce the combined response of all three sub-systems together.

MA 47: Skyrmions IV

Time: Friday 9:30–12:30

Location: HSZ 04

MA 47.1 Fri 9:30 HSZ 04

Systematic parameter study of magnetic skyrmions and antiskyrmions stabilised by exchange interactions — •STEPHAN VON MALOTTKI and GEOFFROY HAUTIER — Thayer School of Engineering at Dartmouth College, Hanover, NH, USA

It is a major ongoing task to optimize the thermal stability of magnetic skyrmions (Sk) and antiskyrmions (ASk), which is in particular limited for sub-10 nm

Sk and ASk in 2D magnetic materials. We focus on a stabilisation of Sk and ASk by exchange frustration [1] and higher order exchange interactions (HOI) [2]. We explore the large interaction parameter space of the atomistic Heisenberg model, consisting of exchange interaction beyond nearest neighbours, DMI, magnetocrystalline anisotropy and HOI by means of highly automatized energetic optimisation and geodesic nudged elastic band method (GNEB) simulations. Here we present the resulting sizes and energy barriers for SK and ASK

in ferromagnetic and antiferromagnetic lattices with hexagonal and square geometry. This enables us to identify systematically the areas of parameters space in which metastable Sk and ASk can exist and how much their energy barriers can be enhanced in the framework of the atomistic extended Heisenberg model beyond nearest neighbours.

[1] S. von Malottki et al., *Sci. Rep.* 7, 12299 (2017)

[2] S. Paul et al., *Nat. Commun.* 11, 4756 (2020)

MA 47.2 Fri 9:45 HSZ 04

Coarse-graining skyrmion ensemble analysis — •THOMAS BRIAN WINKLER¹, JAN ROTHÖRL¹, MAARTEN A. BREMS¹, HANS FANGOHR^{2,3}, and MATHIAS KLÄUI¹ — ¹Institute of Physics, Johannes Gutenberg University Mainz, Germany — ²Faculty of Engineering and Physical Sciences, University of Southampton, United Kingdom — ³Max Planck Institute for the Structure and Dynamics of Matter Hamburg, Hamburg

Magnetic skyrmion are heavily investigated due to their interesting physics and their potential for unconventional computing schemes [1,2]. In confined geometries the thermal diffusion of skyrmions depends heavily on the ability of the skyrmion ensemble to arrange with respect to the confinement in a commensurate manner [3,4]. If external forces like spin-orbit torques are applied to such systems, the steady states of the system might change. We use a coarse-graining to analyse the system with methods from statistical physics [5] to ascertain the relevant states that the collective system is entering. We find in a simulational case study of four skyrmions in a triangular geometry that the steady states of a system are changing when external forces are applied. Such analysis is useful to optimise geometries or read-out positions of magnetic tunnel junctions for skyrmion-based devices. [1] K. Everschor-Sitte et al., *Journal of Applied Physics* 124, 240901 (2018). [2] K. Raab et al., *Nat. Comm.* 13, 6982 (2022). [3] C. Song et al., *Adv. Funct. Mater.* 31, 2010739 (2021). [4] A. F. Schäffer et al., *Commun Phys* 2, 72 (2019). [5] B. Reuter et al., *J Chem. Theory Comput.* 14, 3579 (2018).

MA 47.3 Fri 10:00 HSZ 04

Dzyaloshinskii-Moriya interactions in skyrmionic lacunar spinel GaV₄S₈ — •VLADISLAV BORISOV¹, PATRIK THUNSTRÖM¹, ANNA DELIN^{2,3}, and OLLE ERIKSSON^{1,4} — ¹Department of Physics and Astronomy, Uppsala University, Sweden — ²Department of Applied Physics, School of Engineering Sciences, KTH Royal Institute of Technology, Stockholm, Sweden — ³SeRC (Swedish e-Science Research Center), KTH Royal Institute of Technology, Stockholm, Sweden — ⁴Örebro University, Örebro, Sweden

Using the first-principles full-potential linear muffin-tin orbital method and magnetic force theorem we study the Heisenberg and Dzyaloshinskii-Moriya interactions in the lacunar spinel GaV₄S₈. This material hosts magnetic Néel skyrmions, in contrast to most other bulk magnets. The symmetry of the calculated DM vectors agrees with the C_{3v} structural symmetry and supports the stability of Néel skyrmions. The sizes of the magnetic interactions show some variations as a function of electronic correlations. These changes are also reflected in the estimated wavelength of the helical magnetic state. Our theoretical results indicate that the electronic and magnetic properties depend strongly on the spin configuration of the V₄ clusters, on which there is no clear consensus in the literature, and we make a suggestion for the configuration that fits better to the known measurements.

MA 47.4 Fri 10:15 HSZ 04

On the correlation between spin, orbital and chiral magnetizations of skyrmions — IMARA LIMA FERNANDES¹ and •SAMIR LOUNIS^{1,2} — ¹Peter Grünberg Institut and Institute for Advanced Simulation, Forschungszentrum Jülich & JARA, 52425 Jülich, Germany — ²Faculty of Physics, University of Duisburg-Essen & CENIDE, 47053 Duisburg, Germany

Skyrmions are spin-swirling textures hosting wonderful properties with potential implications in information technology. The magnetization carried by such objects is prospected as a mean of encoding magnetic bits while their topological nature gives rise to a plethora of exquisite features such as topological protection, the skyrmion Hall effect, topological Hall effect and topological orbital moment [1]. Here, the emergent magnetic field, which is directly proportional to the three-spin scalar chirality χ , plays a key role. We explore from ab-initio the rich set of magnetizations carried by single small magnetic skyrmions generated in PdFe bilayer on Ir(111) surface and focus on the correlation between spin, orbital, chiral magnetizations and χ after being excited by single atomic defects [2]. We identify a universal pattern that can guide the design of storage devices by engineering the magnitude of the magnetization carried by skyrmions via controlled implantation of defects.

–Work funded by the Priority Programmes SPP 2137 “Skyrmionics” and SPP 2244 “2D Materials” of the DFG (Projects LO 1659/8-1 and LO 1659/7-1). [1] dos Santos Dias et al. *Nat. Commun.* 7, 13613 (2016); [2] Lima Fernandes et al. *Nat. Commun.* 9, 4395 (2018).

MA 47.5 Fri 10:30 HSZ 04

Nature of magnetic Exchange interactions in Centrosymmetric Hexagonal NiMnGa — •SUNIL WILFRED DSOUZA¹, SANJAY SINGH², and JAN MINÁR¹ — ¹New Technologies Research Centre, University of West Bohemia, Univerzity 8, CZ-306 14 Pilsen, Czech Republic. — ²School of Materials Science and Technology, Indian Institute of Technology (Banaras Hindu University) Varanasi-221005, India.

Hexagonal NiMnGa hosts Novel magnetic biskyrmion state in which vortex-like nanometric spin textures are stable over a wide temperature range extending upto the Curie temperature making it a contender for potential applications in future high-performance spintronic devices. We present, The Heisenberg exchange couplings determined from the paramagnetic phase using the disordered local moment theory which is found to give a significantly more realistic description in comparison with the treatment of the material as a ferromagnet. Frustration caused by competing ferromagnetic and antiferromagnetic exchange couplings at the nearest-neighbor Mn-Mn interactions has been noticed in NiMnGa which is known to lead to non-collinear magnetic ordering. Total energy calculations establishes a non-collinear spin-structure which is stable at a specific Mn spin canting angle in c-plane which is resulting from the magnetocrystalline anisotropy. The Mean-Field Curie temperature determined from the exchange interactions is in good agreement with experiment.

MA 47.6 Fri 10:45 HSZ 04

Skyrmions in 4d- and 5d-doped B20 compounds — •VLADISLAV BORISOV¹, QICHEN XU^{2,3}, NIKOLAOS NTALLIS¹, REBECCA CLULOW⁴, VITALII SHTENDER⁴, JOHAN CEDERVAL⁵, MARTIN SAHLBERG⁴, KJARTAN THOR WIKFELDT⁶, DANNY THONIG^{7,1}, MANUEL PEREIRO¹, ANDERS BERGMAN¹, ANNA DELIN^{2,3}, and OLLE ERIKSSON^{1,7} — ¹Department of Physics and Astronomy, Uppsala University, Sweden — ²Department of Applied Physics, School of Engineering Sciences, KTH Royal Institute of Technology, Stockholm, Sweden — ³SeRC (Swedish e-Science Research Center), KTH Royal Institute of Technology, Stockholm, Sweden — ⁴Department of Chemistry, Uppsala University, Sweden — ⁵Department of Materials and Environmental Chemistry, Stockholm University, Sweden — ⁶PDC Center for High Performance Computing, KTH Royal Institute of Technology, Stockholm, Sweden — ⁷Örebro University, Örebro, Sweden

Based on theoretical calculations, we predict that 4d- and 5d-doped FeSi and CoSi compounds host skyrmions with a size between 50 nm for (Co,Os)Si and 148 nm for (Fe,Co)Si. Calculations are done using the full-potential linear muffin-tin orbital method and magnetic force theorem which allow to address the Heisenberg and Dzyaloshinskii-Moriya (DM) interactions, and the skyrmionic properties were determined using micromagnetic simulations. We find that the 5d doping (by Ir or Os) is particularly efficient in terms of enhancing the DM interaction. Convex-hull analysis suggests that the doped compounds are structurally stable, and we have managed to synthesize and characterize Co_{1-x}Ru_xSi systems both in powder and single-crystal forms.

15 min. break

MA 47.7 Fri 11:15 HSZ 04

Bloch points in the ground state of chiral magnet nanocylinder — •ANDRII SAVCHENKO¹, FENGSHAN ZHENG^{2,3}, NIKOLAI KISELEV¹, LUYAN YANG^{1,2}, QIANQIAN LAN^{1,2}, FILIPP RYBAKOV⁴, STEFAN BLÜGEL¹, and RAFAL DUNIN-BORKOWSKI^{1,2} — ¹Peter Grünberg Institute, Forschungszentrum Jülich, 52425 Jülich, Germany — ²Ernst Ruska-Centre for Microscopy and Spectroscopy with Electrons, Forschungszentrum Jülich, 52425 Jülich, Germany — ³Spin-X Institute, South China University of Technology, Guangzhou 511442, China — ⁴Department of Physics and Astronomy, Uppsala University, SE-75120 Uppsala, Sweden

Experimental observation of Bloch points (BPs) is challenging since these topological defects represent energetically unfavorable configurations and usually appear only as a metastable state. The present study aims to find the systems where due to the competition between short-range and long-range interactions the BPs can emerge in the ground state of the system. A nanocylinder of an isotropic chiral magnet might be a good candidate for such a system. We found that the dipole string - the configuration containing two coupled BPs of opposite topological charge, at some geometrical parameters corresponds to the lowest energy state in such nanocylinder. Our micromagnetic simulations with realistic parameters agree well with the results of the transmission electron microscopy experiment on the FeGe sample.

MA 47.8 Fri 11:30 HSZ 04

Quantum correlation functions of magnetic skyrmions in chiral magnets — •SOPHEAK SORN¹ and MARKUS GARST^{1,2} — ¹Institute of Quantum Materials and Technologies, Karlsruhe Institute of Technology, 76021 Karlsruhe, Germany — ²Institute of Theoretical Solid State Physics, Karlsruhe Institute of Technology, 76131 Karlsruhe, Germany

Recent research activities have turned to studying quantum effects in skyrmion-hosting ordered phases within the context of numerical diagonalization of quantum spin Hamiltonians as well as semiclassical magnonic theories. In the later,

one can expand various operators in magnon fields around a classical spin-texture background. In this talk, I will present results from such a semiclassical theory for chiral magnets, focusing on various correlation functions involving the topological charge and the energy-momentum tensor at zero and nonzero temperature. I will also discuss how these correlation functions are related to linear responses of skyrmions to external perturbation.

MA 47.9 Fri 11:45 HSZ 04

Modeling stray fields using Bi-axial anisotropy in in-plane magnets — •VENKATA KRISHNA BHARADWAJ¹, KARIN EVERSCHOR-SITTE², JAIRO SINOVA^{1,3}, and RICARDO ZARZUELA¹ — ¹Johannes Gutenberg-University, Mainz — ²Faculty of Physics, University of Duisburg-Essen, D-47057 Duisburg, Germany — ³Institute of Physics Academy of Sciences of the Czech Republic, Cukrovarnická 10, 162 00 Praha 6, Czech Republic

Recently [1,2], magnetic bimerons, skyrmion analogs in in-plane magnetized films have gained interest due to their stark difference in current-driven dynamics with respect to Neel skyrmions showing uni-directional motion with SOT-driven torques. The other technological advantage is that they can be densely stacked without worrying about stray fields between the layers. However, the stray fields need to be handled carefully as they are not trivial as in out-of-plane films. In this work, we study the bi-axial anisotropy to model the stray field in in-plane magnetized films. We provide the phase diagram and look at the deformations of spin spiral phases and the presence of tilted fields. Finally, we study the shape deformation of skyrmions due to stray fields and the effects in current-driven dynamics. [1] R. Zarzuela et al., Physical Review B 101, 054405 (2020), [2] B. Göbel, et al., Phys. Rev. B 99, 060407(R) (2019).

MA 47.10 Fri 12:00 HSZ 04

Magnetolectric Cavity Magnonics in Skyrmion Crystals — TOMOKI HIROSAWA^{1,2}, •ALEXANDER MOOK^{1,3,4}, JELENA KLINOVAJA¹, and DANIEL LOSS¹ — ¹University of Basel, Basel, Switzerland — ²Aoyama Gakuin University, Sagami-hara, Kanagawa, Japan — ³Technical University of Munich, Garching, Germany — ⁴Johannes Gutenberg University, Mainz, Germany

We present a theory of magnetolectric magnon-photon coupling in cavities hosting noncentrosymmetric magnets. Analogously to nonreciprocal phenomena in multiferroics, the magnetolectric coupling is time-reversal and inversion asymmetric. This asymmetry establishes a means for exceptional tunability of magnon-photon coupling, which can be switched on and off by reversing the

magnetization direction. Taking the multiferroic skyrmion host Cu_2OSeO_3 with ultralow magnetic damping as an example, we reveal the electrical activity of skyrmion eigenmodes and propose it for magnon-photon splitting of “magnetically dark” elliptical modes. Furthermore, we predict a cavity-induced magnon-magnon coupling between magnetoelectrically active skyrmion excitations. We discuss applications in quantum information processing by proposing protocols for all-electrical magnon-mediated photon quantum gates, and a photon-mediated split operation of magnons. Our study highlights magnetoelectric cavity magnonics as a novel platform for realizing coherent transduction between photons and magnons.

Reference: Tomoki Hiroswawa*, Alexander Mook*, Jelena Klinovaja, and Daniel Loss, PRX Quantum 3, 040321 (2022)

MA 47.11 Fri 12:15 HSZ 04

Artificial surface conductivity on metallic metamaterials and its effect on localized plasmon skyrmions — •AMIN KHAVASI¹ and KARIN EVERSCHOR-SITTE^{1,2} — ¹Faculty of Physics, University of Duisburg-Essen, 47057 Duisburg, Germany — ²Center for Nanointegration Duisburg-Essen (CENIDE), Duisburg, Germany

Metallic metamaterials have been widely investigated for realizing different peculiar effects such as spoof surface plasmons [1] and extraordinary transmission of light [2]. Recently, topologically robust localized plasmonic skyrmions have been realized by spiral metallic meta-structures [3, 4].

For metal films with a periodic arrangement of cut-through slits, Khavasi and others have shown that the structure can be modeled by an anisotropic medium with an artificial surface conductivity [5]. In the subwavelength regime, the surface conductivity is imaginary considering lossless systems representing non-specular higher diffracted orders. We investigate the consequences of such artificial surface conductivities for the skyrmionic modes of the spiral meta-structures to obtain more insight on the behavior of the localized plasmonic skyrmions.

References:

- [1] Pendry, J. B., et al., science 305, (2004): 847-848.
- [2] Porto, J. A., et al., Physical review letters 83,(1999): 2845.
- [3] Davis, T. J., et al. Science 368, (2020): eaba6415.
- [4] Deng, Z., et al., Nature Communications 13, (2022): 1-7.
- [5] Edalatipour, M., et al., Journal of lightwave technology 30, (2012): 1789-1794.

MA 48: Magnetic Instrumentation and Characterization

Time: Friday 9:30–11:45

Location: HSZ 401

MA 48.1 Fri 9:30 HSZ 401

Portable devices for adding Spatial-Intensity-Modulation-mode capabilities to polarized neutron beams — •DENIS METTUS¹, JONATHAN LEINER¹, JOHANNA JOCHUM², and CHRISTIAN PFLEIDERER¹ — ¹Physik-Department, Technische Universität München, D-85748 Garching, Germany — ²Heinz Maier-Leibnitz Zentrum (MLZ), Technische Universität München, Garching, Germany

The MIEZE (Modulated Intensity with Zero Effort) resonant spin-echo technique at the RESEDA instrument at FRM II has its optimum resolution at small scattering angles, i.e. SANS type geometries. It is possible to extend the MIEZE application to wide angles by incorporating magnetic Wollaston prisms (MWPs) into the beamline. MWPs can produce controlled spatially intensity modulations in addition to the intensity modulations in time inherent to MIEZE. This would allow correcting to the neutron time of flight differences, extending the MIEZE resolution function to any desired scattering angle.

Additionally, MWPs will be useful in the context of intra-particle mode-entangled neutron beams for potential use in probing many-body quantum entanglement in materials. Finally, the compact and modular nature of the MWPs will allow them to be used to measure diffraction peaks with enhanced resolution at several polarized beam instruments such as KOMPASS, LaDiff, and in general at small angle neutron scattering instruments. We present the plans for the construction of these superconducting MWPs for use at FRM II, and describe the details of their operation and the various possibilities they offer.

MA 48.2 Fri 9:45 HSZ 401

A signal-integrating approach to second harmonic generation imaging and spectroscopy — LEA FORSTER¹, •JAN GERRIT HORSTMANN¹, JANNIS LEHMANN^{1,2}, THOMAS LOTTERMOSER¹, and MANFRED FIEBIG¹ — ¹Dept. of Materials, ETH Zurich, Switzerland — ²RIKEN Center for Emergent Matter Science (CEMS), Japan

We investigate the impact of different data normalization procedures on the signal-to-noise ratio in second harmonic generation (SHG) imaging and spectroscopy. Using both nanosecond and femtosecond laser systems in combination with standard detection schemes for SHG, we find that uncorrelated noise in the detection electronics often dominates over the contributions of pulse-to-

pulse fluctuations of the laser system, long-term power drifts, or time-dependent changes of the beam profile. Consequently, normalization of SHG signals averaged over thousands of pulses can yield similar signal-to-noise ratios comparable with pulse-to-pulse-normalized data. Based on these results, we demonstrate that state-of-the-art CCD or sCMOS cameras can, in many cases, replace photomultiplier tubes as detectors in pump-probe SHG measurements, enabling ultrafast high-resolution SHG imaging of nonequilibrium dynamics in solids.

MA 48.3 Fri 10:00 HSZ 401

New versatile instruments for magnetism research at ID12 of the ESRF — •A. AUBERT¹, K. SKOKOV¹, G. GOMEZ^{2,3}, F. WILHELM³, A. ROGALEV³, H. WENDE², O. GUTFLEISCH¹, and K. OLLEFS² — ¹Functional Materials, TU Darmstadt (Germany) — ²Fac. of Phys., Uni. Duisburg-Essen (Germany) — ³ESRF, Grenoble (France)

I will introduce two new instruments which have been implemented at the beamline ID12 of the European Synchrotron Radiation Facility (ESRF), in the framework of the ULMAG project funded by BMBF (grant 05K2019). These instruments offer the ESRF users a unique possibility to measure under strictly the same experimental conditions the element-specific X-ray absorption spectroscopy (XAS)/X-ray magnetic circular dichroism (XMCD), XRD simultaneously with the measurement of various macroscopic properties (magnetization, magnetostriction, magnetocaloric, magnetoresistance), as a function of magnetic field (up to 17 T) and temperature (5-325 K) [1].

To demonstrate the potential and features of these scientific instruments, I will present two case studies: (1) FeRh, which has a first-order anti-ferromagnetic to ferromagnetic transition around room temperature (2) HoCo2, which exhibits a first-order ferrimagnetic to paramagnetic transition. These two cases demonstrate new horizons for studying the physics of magnetic materials, where the interplay between the magnetic, structural, and electronic subsystems of the solid is essential.

[1] A. Aubert et al. IEEE Instr. Meas. (2022) 10.1109/TIM.2022.3157001

MA 48.4 Fri 10:15 HSZ 401

XMCD in fluorescence-yield mode can measure the spin-orbit torque switching of both rare-earth and transition-metal sublattices in mesoscale devices of GdFe₃ thin films — •JAMES M TAYLOR^{1,2}, CHEN LUO^{1,2}, VICTOR UKLEEV¹, CHRISTIAN H BACK², and FLORIN RADU¹ — ¹Helmholtz-Zentrum Berlin for Materials and Energy, 12489 Berlin, Germany — ²Department of Physics, Technical University of Munich, 85748 Garching, Germany

Ferrimagnets containing one rare-earth and one transition-metal sublattice are of interest both for future spintronic devices and as sandbox materials for exploring ultrafast magnetism. In regard to the latter, ferrimagnetic Gd+Fe has been widely studied, due to its demonstration of all-optical switching (AOS). On the other hand, more interesting for technological applications is current-induced magnetization reversal driven by spin-orbit torques (SOTs). To fully understand SOT switching in ferrimagnets, it is important, as with AOS, to look at the respective behaviour of both sublattices. In this work, we take a step towards making such measurements more readily available: by using conventional, static x-ray magnetic circular dichroism (XMCD) operated in fluorescence-yield mode to measure the relative responses of the Gd and Fe sublattices during an SOT switching process. This was performed using sub-ms current pulses in μm -sized devices fabricated from GdFe₃ heterostructures down to 10 nm thick, in-situ in the VEKMAG beamline at the BESSY II synchrotron. We compare this with electrical detection of the switching using simultaneous anomalous Hall effect measurements, which follow the Fe sublattice, as expected.

15 min. break

MA 48.5 Fri 10:45 HSZ 401

Periodogram-based detection of unknown frequencies in time-resolved scanning transmission X-ray microscopy — •SIMONE FINIZIO¹, JOE BAILEY^{1,2}, BART OLSTHOORN³, and JÖRG RAABE¹ — ¹Paul Scherrer Institut, Villigen PSI, Switzerland — ²EPFL, Lausanne, Switzerland — ³Nordita, KTH Royal Institute of Technology and Stockholm University, Stockholm, Sweden

Pump-probe time-resolved imaging is a powerful technique that enables the investigation of dynamical processes. Signal-to-noise and sampling rate restrictions normally require that cycles of an excitation are repeated many times with the final signal reconstructed using a reference. However, this approach imposes restrictions on the types of dynamical processes that can be measured, namely that they are phase locked to a known external signal (e.g. a driven oscillation or impulse). This rules out many interesting processes such as auto-oscillations and spontaneously forming populations e.g. condensates. In this work we present a method for time-resolved imaging, based on the Schuster periodogram, that allows for the reconstruction of dynamical processes where the intrinsic frequency is not known. In our case we use time of arrival detection of x-ray photons to reconstruct magnetic dynamics without using *a-priori* information on the dynamical frequency. This proof of principle demonstration will allow for the extension of pump-probe time-resolved imaging to the important class of processes where the dynamics are not locked to a known external signal and in its presented formulation can be readily adopted for x-ray imaging and also adapted for wider use.

MA 48.6 Fri 11:00 HSZ 401

Towards switchable probes for advanced Magnetic Force Microscopy — •ANIRUDDHA SATHYADHARMA PRASAD, RACHAPPA RAVISHANKAR, RUDOLF SCHÄFER, VOLKER NEU, BERND BÜCHNER, and THOMAS MÜHL — IFW Dresden, Helmholtzstraße 20, 01069 Dresden

In magnetic force microscopy (MFM) on samples consisting of non-homogeneous materials and challenging topography, the "magnetic" contrast is often overwhelmed by additional non-magnetic forces arising from differing contact potentials and from changes in the capacitive coupling due to topographical features. The elimination of such interfering signals can be done by a differ-

ential imaging process with inverted tip magnetization. Earlier implementations either require precise repositioning of the probe after external switching of the magnetization or application of global magnetic fields which can cause changes in the sample. In our work, we overcome these difficulties by switching the magnetization externally, and using feature matching in the post processing step to eliminate the need for precise repositioning. We also showcase first steps towards an in-situ switching of MFM probes for developing a high-speed differential process within the MFM instrument. This involves the design and fabrication of planar micro-coils capable of providing sufficient magnetic field to switch high quality Iron filled Carbon Nanotube (FeCNT) MFM probes. The switching was verified by applying the inhomogeneous field distributions of planar micro-coils in micromagnetic simulation studies on a FeCNT. Preliminary MFM results from an FeCNT probe interacting with such a coil are also presented.

MA 48.7 Fri 11:15 HSZ 401

Measuring Antiferromagnets at Room Temperature in a Magnetically Shielded Environment — •MICHAEL PAULSEN¹, SILVIA KNAPPE-GRÜNEBERG¹, JENS VOIGT¹, ALLARD SCHNABEL¹, RAINER KÖRBER¹, MICHAEL FECHNER², and DENNIS MEIER³ — ¹Physikalisch-Technische Bundesanstalt, Berlin, Germany — ²Max Planck Institute for the Structure and Dynamics of Matter, CFEL, Hamburg, Germany — ³NTNU Norwegian University of Science and Technology, Trondheim, Norway

Antiferromagnetic materials possess zero net dipole magnetization. However, higher-order magnetizations, such as quadrupolar magnetic field contributions, have been predicted for non-centrosymmetric antiferromagnets. Classical low-temperature measurements on Cr₂O₃ [1] indeed indicated an external quadrupole field at 4.2 K [2, 3], but the validity of the results was put into question due to the limited sensitivity of the applied experiment. Here, we present magnetization measurements gained at room temperature in an ultra-low magnetic field environment (< 1 nT). A multi-channel setup with Superconducting Quantum Interference Devices (SQUIDs) and Optically Pumped Magnetometers (OPMs) are used as magnetic field detectors. The results corroborate the emergence of a quadrupolar far-field in Cr₂O₃, providing new opportunities for the characterization of antiferromagnets and materials with ultra-small remanent magnetization in general.

[1] I. Dzyaloshinskii, Sol. Stat. Comm. 82:7, 579-580, 1992.

[2] D. N. Astrov and N. B. Ermakov, JETP, 59:4, 274-277, 1994.

[3] D. N. Astrov et al, JETP Letters, 63:9, 745-751, 1996.

MA 48.8 Fri 11:30 HSZ 401

Improving the magnetic adhesion of a metal-pipe crawling robot using elastomeric toes — •MUHAMMAD KHAN, KILIAN SCHÄFER, and OLIVER GUTFLEISCH — Functional Materials, Institute of Materials Science, Technical University Darmstadt, D-64287 Darmstadt, Germany

To assist human inspectors who examine thousands of kilometres spread oil and gas pipelines, robots are being utilized. A key challenge in robotic pipeline inspection is to ensure that a robot does not fall off a metal pipe. In this work, we show that a two-legged robot crawls on metal pipes using its electromagnetism. The robot slip was fixed by introducing an elastomeric toe, implanted under the robot feet. It was shown that the soft toe increased the magnetic adhesion of the feet by enabling the stable stance of the robot feet. The behaviour of the foot-toe was further characterized by conducting surface adaptability test (measurement of toe deformation), calculating its coefficient of friction on different metal pipes, and real-world robot pipe-crawling experiments. Furthermore, use of a magneto-active compound consisting of hard magnetic Nd₂Fe₁₄B particles in a thermoplastic polyurethane (TPU) matrix, fabricated to form the fin-ray structure will be also discussed as a potential replacement of the electromagnet. However, such a fin-ray structure would require a large and continuously available activation field which is obviously highly challenging. Here, a concept demonstration at the miniature level can be shown by modifying the robot's shape and size, matching the miniature setup.

MA 49: Magnetic Information Technology, Recording, Sensing

Time: Friday 9:30–11:45

Location: HSZ 403

MA 49.1 Fri 9:30 HSZ 403

Spin revolution breaks time reversal symmetry of rolling magnets — •ELENA VEDMEDENKO and ROLAND WIESENDANGER — University of Hamburg
The classical laws of physics are usually invariant under time reversal. Here, we reveal a novel class of magnetomechanical effects rigorously breaking time-reversal symmetry. These effects are based on the mechanical rotation of a hard magnet around its magnetization axis in the presence of friction and an external magnetic field, which we call spin revolution. The spin revolution leads to a variety of symmetry breaking phenomena including upward propulsion on vertical surfaces defying gravity as well as magnetic gyroscopic motion that is perpendicular to the applied force. The angular momentum of spin revolution differs

from those of the magnetic field, the magnetic torque, the rolling axis, and the net torque about the rolling axis. The spin revolution emerges spontaneously, without external rotations, and offers various applications in areas such as magnetism, robotics and energy harvesting.

E. Y. Vedmedenko and R. Wiesendanger, Spin revolution breaks time reversal symmetry of rolling magnets, Sci. Rep. 12, 13608 (2022).

MA 49.2 Fri 9:45 HSZ 403

Improved Planar Hall Effect sensors for fluid measurement techniques — •JAN SCHMIDTPETER, THOMAS WONDRAK, DENYS MAKAROV, and YEVHEN ZABILA — Helmholtz-Zentrum Dresden-Rossendorf (HZDR), Dresden Germany

Inductive flow measurement techniques such as the Contactless Inductive Flow Tomography require sensors that provide a magnetic field resolution of 1 nT while operating in magnetic fields of several mT. With advancements in state-of-the-art magnetoresistive thin-film sensors the required behavior regarding sensitivity, precision and hysteresis can be achieved [1]. Planar Hall Effect sensor have been shown to be one of the leading sensor types in this area. Therefore we present a detailed study on the effect of different sensor layouts, geometries, magnetic flux concentrators and other parameters on the characteristics of single layer Permalloy Planar Hall Effect sensors.

[1] Granell, Pablo Nicolás, et al. *npi Flexible Electronics* 3.1 (2019): 1-6.

MA 49.3 Fri 10:00 HSZ 403

Towards nanomechanical detection of fT magnetic fields — DHAVALKUMAR MUNGPARA, TORBEN HÄNKE, and ALEXANDER SCHWARZ — Institute of Nanotechnology and Solid State Physics, University of Hamburg, Jungiusstr. 11, 20355 Hamburg

This work has been conducted in the framework of the OXiNEMS project that aims to establish etching protocols for oxides similar to those nowadays available for silicon and to develop a novel all-oxide nano-mechanical sensor to detect bio-magnetic field in the fT-regime required for magnetoencephalography (MEG).

Our envisaged hybrid sensor consists of a superconducting loop with a constriction that functions as field-to-gradient converter and a magnetically sensitive mechanical resonator that detects the Oersted field above the constriction. To increase the signal above the thermal noise limit we present an optimized constriction-resonator arrangement that encompasses a spiral geometry instead of a single constriction. This optimized geometry, can be fabricated using up-to date technology and should be able reach a sensitivity of $10 \text{ fT}/\sqrt{\text{Hz}}$ at 77 K.

The OXiNEMS project (www.oxinems.eu) has received funding from the European Union's Horizon 2020 research and innovation program under Grant Agreement No. 828784. The author gratefully acknowledges the fruitful discussions with all members of the consortium, particularly Luca Pellegrino, Stefania Della Penna, Alexei Kalaboukhov, Federico Maspero, Nicola Manca, Simone Cuccurullo, Warner Venstra, Daniele Marré and Riccardo Bertacco.

MA 49.4 Fri 10:15 HSZ 403

Magnetic noise theory of magnetoelastic magnetic field sensors — ELIZAVETA SPETZLER¹, BENJAMIN SPETZLER², and JEFFREY MCCORD¹ — ¹Institute for Materials Science, Kiel University, Kiel, Germany — ²Department of electrical engineering and information technology, Technical University Ilmenau, Ilmenau, Germany

Intrinsic magnetic noise currently limits the performance of many magnetoelastic magnetic field sensors. Therefore, understanding and estimating the magnetic noise level is crucial for further sensor improvement. This work reviews the theory of thermal-magnetic noise in general and discusses additional magnetic noise sources relevant to magnetoelastic magnetic field sensors. We highlight the limitations and assumptions of previous approaches and develop important model extensions. We demonstrate and quantify the strong connection between magnetic sensitivity, loss, and noise by implementing the magnetic noise description in a multilevel model of a magnetoelastic magnetic field sensor based on the ΔE effect. The excellent match of simulations and measurements reveals a significant influence of the fundamental nonlinearity of the ΔE effect on the sensor performance. While the model is applied to ΔE effect sensors, many of the results are also valid for other magnetic field sensors and magnetoelastic modulated devices.

This work was funded by the German Research Foundation (DFG) through the Collaborative Research Centre CRC 1261 "Magnetolectric Sensors - From Composite Materials to Biomagnetic Diagnostics" and the Carl-Zeiss Foundation via the Project MemWerk.

15 min. break

MA 49.5 Fri 10:45 HSZ 403

Transfer printing of GMR sensing elements for curved electronics — BEZSMERTNA OLHA¹, RUI XU¹, EDUARDO SERGIO OLIVEROS-MATA¹, CLEMENS VOIGT², SINDY MOSCH², JÜRGEN FASSBENDER¹, MYKOLA VINNICHENKO², and DENYS MAKAROV¹ — ¹Helmholtz-Zentrum Dresden-Rossendorf e.V., 01328 Dresden, Germany — ²Fraunhofer Institute for Ceramic Technologies and Systems IKTS, 01277 Dresden, Germany

In the post-covid era, touchless interaction between human beings and environments is attracting more and more attentions. Sensors based on giant magnetoresistance (GMR) effect are widely considered as a workhorse to address this demand. However, the fabrication of GMR multi-layer elements face many limitations (e.g., inappropriate to substrates with curved and/or rough surfaces) due to the layer thickness dependence of performance. Here, we propose a transfer technique to overcome the aforementioned limitations. With the assistance of two sacrificial layers, a large scale and wrinkle-free coverage is realized on various substrates (of different materials, roughness, and curvatures) with little loss of GMR performance. Notably, such technique is easy processing, without the need of any substrate deformation, temporary carriers or high-temperature processing. The transferred sensors are integrated into skin-mountable electronics, successfully functioning as a human-machine interface.

MA 49.6 Fri 11:00 HSZ 403

Printed Giant Magnetoresistive Sensors — YEVHEN ZABILA, EDUARDO SERGIO OLIVEROS MATA, MINJEONG HA, GILBERT SANTIAGO CAÑÓN BERMÚDEZ, RICO ILLING, INGOLF MÖNCH, JÜRGEN FASSBENDER, and DENYS MAKAROV — Helmholtz-Zentrum Dresden-Rossendorf, Dresden, Germany

Printing is an affordable and high-throughput method to process electronics in soft substrates. Printable magnetoresistive pastes have been developed as an alternative single-step fabrication method to obtain magnetic field sensors. Until now, there were no examples of magnetic printed sensors that deliver steady sensing behavior upon mechanical stretching. Here, we will present low-noise printable magnetic field sensors sensitive down to sub-mT, which are mechanically stretchable after printing. The pastes are composites of poly(styrene-butadiene-styrene) copolymer (SBS) with embedded magnetoresistive microflakes. Our printed sensors were demonstrated to be used as electronic skin interfaces.[1]

[1] M. Ha, Y. Zabila, et. al. *Adv. Mater.* 33 (12), 2005521 (2021)

MA 49.7 Fri 11:15 HSZ 403

Printed magnetic field sensors based on bismuth showing large non-saturating magnetoresistance — EDUARDO SERGIO OLIVEROS-MATA¹, CLEMENS VOIGT², GILBERT SANTIAGO CAÑÓN BERMÚDEZ¹, ZEVHEN ZABILA¹, RICO ILLING¹, MARCO FRITSCH², SINDY MOSCH², MIHAILS KUSNEZOFF¹, JÜRGEN FASSBENDER¹, MYKOLA VINNICHENKO², and DENYS MAKAROV¹ — ¹Helmholtz-Zentrum Dresden-Rossendorf, Dresden, Germany — ²Fraunhofer-Institut für Keramische Technologien und Systeme, Dresden, Germany

The development of functional inks allows to create novel printed electronics with unconventional form factors. Here, we show the fabrication of printed magnetic field sensors based on bismuth microparticles. Sensors showed non-saturating large magnetoresistance (146%, 5T, at room temperature), and resilience to mechanical bending (2000 cycles). We demonstrated large area magnetically sensitive interfaces such as smart locks and interactive wallpapers.[1]

[1] E.S. Oliveros-Mata, C. Voigt, et al. *Adv. Mater. Technol.* 2200227 (2022)

MA 49.8 Fri 11:30 HSZ 403

Self-healable printed magnetic field sensors using alternating magnetic fields — RUI XU¹, GILBERT SANTIAGO CAÑÓN BERMÚDEZ¹, OLEKSANDR V. PLYPOVSKYI¹, OLEKSII M. VOLKOV¹, EDUARDO SERGIO OLIVEROS MATA¹, YEVHEN ZABILA¹, RICO ILLING¹, PAVLO MAKUSHKO¹, PAVEL MILKIN², LEONID IONOV², JÜRGEN FASSBENDER¹, and DENYS MAKAROV¹ — ¹Helmholtz-Zentrum Dresden-Rossendorf, Dresden, Germany — ²University of Bayreuth, Ludwig Thoma Str 36a, 95447 Bayreuth, Germany

Percolation network of fillers plays a critical role in rendering printable electronics functionality and durability. We employ alternating magnetic fields (AMF) to drive magnetic fillers actively and guide the formation and self-healing of percolation networks. Relying on AMF, we fabricate printable magnetoresistive sensors revealing an enhancement in sensitivity and figure of merit of more than one and two orders of magnitude relative to previous reports. These sensors display low noise, high resolution, and are readily processable using various printing techniques that can be applied to different substrates. The AMF-mediated self-healing has six characteristics: 100% performance recovery; repeatable healing over multiple cycles; room-temperature operation; healing in seconds; no need for manual reassembly; humidity insensitivity. By virtue of these advantages, the AMF-mediated sensors are used in safety application, medical therapy, and human-machine interfaces for augmented reality. *1 Nat. Electron.* 2, 144-150 (2019); *2 Nat. Commun.* 13, 6587 (2022).

MA 50: Magnetic Domain Walls (non-skyrmionic)

Time: Friday 9:30–11:15

Location: POT 6

MA 50.1 Fri 9:30 POT 6

Geometrically controlled domain wall dynamics in curved 3D nanostructures — SANDRA RUIZ-GOMEZ¹, PAMELA MORALES¹, CLAUDIA FERNANDEZ-GONZALEZ¹, AURELIO RODRIGUEZ-HIERRO², MICHAEL FOERSTER³, MIGUEL

ANGEL NINO³, EWA MADEJ⁴, DOROTA WILGOCKA-SLEZAK⁴, ANNA MANDZIAK⁴, AMALIO FERNANDEZ-PACHECO⁵, and CLAIRE DONNELLY¹ — ¹MPI-CPfS, Dresden, Germany — ²Nothnitzer strasse 40 — ³Alba Synchrotron, Barcelona, Spain — ⁴Solaris synchrotron, Krakow, Poland — ⁵INMA, Zaragoza, Spain

Three dimensional nanomagnetic systems, with novel and unconventional spin textures, represent an exciting platform to explore new magnetic phenomena for the development of more efficient, capable and multifunctional technologies. In particular, the 3D geometry is predicted to have a significant influence on the dynamics of magnetic domain walls through the introduction of curvature and torsion, where new physics and functionalities can be realised.

Here, we experimentally explore the influence of 3D geometry on the energetics of domain walls by introducing curvature using focused electron beam induced deposition. We probe the behaviour of DWs within 3D curved systems with soft x-ray magnetic microscopy, that allows us to directly observe the magnetic state and the domain walls, and determine their response to the application of magnetic fields. This insight into the control that can be obtained via complex geometries will help pave the way to the next generation of 3D spintronic devices.

MA 50.2 Fri 9:45 POT 6

Geometry-induced effects in domain wall dynamics in stripes with spatially varying cross section — •KOSTIANTYN V. YERSHOV^{1,2} and DENIS D. SHEKA³ — ¹Leibniz Institute for Solid State and Materials Research, Dresden, Germany — ²Bogolyubov Institute for Theoretical Physics, Kyiv, Ukraine — ³Taras Shevchenko National University of Kyiv, Ukraine

Here we study both analytically and numerically the influence of curvature and cross section deformation effects on the motion of a domain wall in curved stripes which corresponds to geometry of recent experiments [1]. We base our study on a phenomenological Landau-Lifshitz-Gilbert equations using collective variable approach based on a $q - \Phi$ model. We show that (i) curvature and nonzero gradient of cross-section deformation result in a modification of a ground state and can be interpreted as an effective magnetic field. (ii) The presence of a nonzero gradient of cross section deformation also results in a pinning potential for domain walls in addition to the curvature-induced potential [2]. In effective equations of motions the spatially varying cross section and curvature appear as a driving forces which can suppress or reinforce the action of each other. The eigenfrequency oscillations of domain wall in vicinity of the pinning potential is obtained as a function of curvature and cross section deformation and their gradients. All analytical predictions are well confirmed by full scale micromagnetic simulations. [1] L. Skoric et al, ACS Nano **16**, 8860 (2022); [2] K. V. Yerшов et al, PRB **92**, 104412 (2015).

MA 50.3 Fri 10:00 POT 6

Domain wall tilt in thin CrOx/Co/Pt corrugated stripes — •JOSE A. FERNANDEZ-ROLDAN¹, MIKEL QUINTANA^{1,2}, SHAHRUKH SHAKEEL¹, OLEKSII VOLKOV¹, OLEKSANDR PYLYPOVSKYI¹, EDUARDO SERGIO OLIVEROS-MATA¹, FLORIAN KRONAST³, MOHAMAD-ASSAAD MAWASS³, CLAAS ABERT⁴, DIETER SUESS⁴, DENISE ERB¹, JÜRGEN FASSBENDER¹, and DENYS MAKAROV¹ — ¹Helmholtz-Zentrum Dresden-Rossendorf, Dresden, Germany — ²CIC nanoGUNE BRTA, Donostia-San Sebastian, Spain — ³Helmholtz-Zentrum Berlin für Materialien und Energie, Berlin, Germany — ⁴Physics of Functional Materials, University of Vienna, Vienna, Austria

Curvilinear magnetism is a flourishing field of interest for applications in flexible magnetoelectric devices, microrobots, sensors and nanoelectronics [1-2]. Curvilinear phenomena often result in magnetization patterning, symmetry breaks and Domain Wall (DW) pinning. However, these phenomena have remained so far unexplored in stripes. Here, spin-orbit torques allow the manipulation of DWs [3] with a low power consumption. A recent approach permits the estimation of Dzyaloshinskii-Moriya interaction from DW tilt in thin stripes [4]. Here we provide first results on 100 nm wide 2 nm thin corrugated CrOx/Co/Pt stripes with a mean curvature of 0.06 nm^{-1} . Our results open a perspective for the design of curvature-induced effects with application prospects in current challenges of nanoelectronics. [1] D. Makarov et al., Adv.Mater. **34**(3), 2101758 (2022); [2] D. Sheka et al., Small **18**, 2105219 (2022); [3] O. Pylypovskiy et al. Sci.Rep. **6**, 23316 (2016); [4] O. M. Volkov et al., Phys.Rev.Appl. **15**, 034038 (2021).

MA 50.4 Fri 10:15 POT 6

Get in Shape - Closed Magnetoelastic Domain Wall Loops in Antiferromagnets — •BENNET KARETTA and OLENA GOMONAY — Johannes-Gutenberg Universität Mainz

Antiferromagnets are new candidates to be used as active spintronics elements as they are faster and more stable than the ferromagnets in current devices. However, their lack of a net magnetization introduces the challenge to manipulate the magnetic state. Recent studies suggested that the magnetoelastic coupling can be used for this task. Thus, understanding the interaction between strain and Néel vector is of high priority. We study the orientation in different antiferromagnetic domain walls which is influenced by magnetostriction. We show how the energy of the domain wall depends on its orientation on the antiferromagnet. Further, we apply the results to a system of a closed domain wall loops. The anisotropy of the energy significantly changes the shape of the closed loop to an anisotropic

form. The exact shape is given by the type of domain wall and magnetoelastic coupling strength. For its determination we finally present a method to quantify the change of the domain wall shape from the zero magnetoelastic coupling case.

MA 50.5 Fri 10:30 POT 6

Magneto-Optic Effects and Domain Imaging in EuO film and EuO/Co Heterostructure — •SEEMA SEEMA¹, HENRIK JENTGENS¹, PAUL ROSENBERGER^{1,2}, and MARTINA MÜLLER¹ — ¹Fachbereich Physik, Universität Konstanz, 78457 Konstanz, Germany — ²Fakultät Physik, Technische Universität Dortmund, 44221 Dortmund, Germany

Ferromagnetic semiconductors and stable half-metallic ferromagnets with Curie temperatures (T_c) equal to or more than room temperature have been sought for their applications in novel spintronic devices. Europium oxide (EuO) is one of the potential candidates as it possesses strong ferromagnetism (FM) of $7 \mu\text{B}$ with a T_c of 69 K. The present work focuses on the magnetization reversal mechanisms and domain images in EuO probed using magneto-optic Kerr microscopy. We aimed to visualize magnetic proximity effect induced changes in the coercivity of hysteresis loops as well as magnetic domains in EuO film and in a EuO/3d-FM heterostructure. We synthesized EuO/Co heterostructure sample using molecular beam epitaxy on Nb:STO and observed the differences in the domain saturation behavior as well as the Kerr rotation below T_c . This had been performed by magnetic hysteresis measurement along with simultaneous domain imaging using a Kerr microscope. To explore the temperature-dependent magneto-optic effects in EuO in the proximity of Co, we measured hysteresis at various temperatures below and above T_c . This study of proximity effect-induced changes in magnetic domains in EuO due to Co can provide insights into achieving room-temperature FM in EuO.

MA 50.6 Fri 10:45 POT 6

Electric field induced magnetic switching in spin-spiral multiferroics — FRANCESCO FOGGETTI^{1,2} and •SERGEY ARTYUKHIN¹ — ¹Italian Institute of Technology, Genova, Italy — ²Uppsala University, Sweden

Switching in magnetic materials gives rise to rich physical phenomena and lies at the heart of their technological applications. Although domain wall motion in ferro- and antiferromagnets has been studied, in spiral magnets it is still poorly understood despite 20 years of active research since the discovery of spiral multiferroics. The problem of the domain wall motion in a spiral magnet is a compelling one, the more so the magnetic domain walls in cycloidal spiral phase are also ferroelectric, thus enabling electric control of magnetism, i.e. domain wall motion under the action of an external electric field. Phase transition to a spiral phase leads to a formation of chiral domains with opposite spin rotation senses, that are separated by chiral domain walls. Spiral order breaks inversion symmetry and induces a ferroelectric polarization, whose sign is determined by the chirality of the domain. Thus the spiral order allows for the manipulation of spins via an external electric field. Here we study domain wall motion in magnets with spiral ground state, that are the most basic non-collinear magnets. We formulate a simplified variational model and derive the equation of motion for the domain wall driven by an external electric field. The results are corroborated with atomistic spin dynamics simulations. The results suggest a linear dependence of the wall speed on the external electric field, and a peculiar dependence on the system geometry and domain structure.

MA 50.7 Fri 11:00 POT 6

Visualisation of an 4f-antiferromagnetic domain pattern in multiferroic $\text{Dy}_{0.7}\text{Tb}_{0.3}\text{FeO}_3$ — •YANNIK ZEMP¹, MADS C. WEBER^{1,2}, EHSAN HASSANPOUR^{1,3}, THOMAS LOTTERMOSER¹, YUSUKE TOKUNAGA⁴, YASUJIRO TAGUCHI⁵, YOSHINORI TOKURA^{5,6}, and MANFRED FIEBIG¹ — ¹Department of Materials, ETH Zurich — ²IMMM, Le Mans Université — ³UDEM Inselspital, University of Bern — ⁴Department of Advanced Materials Science, University of Tokyo — ⁵RIKEN CEMS, Japan — ⁶Department of Applied Physics, University of Tokyo

We visualize the antiferromagnetic (AFM) domain pattern of the 4f-rare-earth subsystem in $\text{Dy}_{0.7}\text{Tb}_{0.3}\text{FeO}_3$. To do so, we exploit the unique order-parameter interaction in the multiferroic phase of this material, where the magnetic rare-earth- and iron subsystems induce ferroelectricity. By magnetic-field cooling into the multiferroic phase, we force the 4f-rare-earth- and ferroelectric domain pattern to be identical. We can then access the former by imaging the latter using optical second harmonic generation, which is very sensitive to a breaking of inversion symmetry. The 4f-AFM domains form stripes with a thickness of several $10 \mu\text{m}$ along the antiferromagnetic easy axis. As a consequence, the ferroelectric domains are forced to form energetically unfavourable head-to-head and tail-to-tail domain walls. Also, the domain pattern is very dissimilar to the weakly ferromagnetic bubble-domain structure of the iron sublattice that is present at higher temperatures. These observations show that the rare-earth system orders independently from the other magnetic- and electric influences.

Metal and Material Physics Division Fachverband Metall- und Materialphysik (MM)

Astrid Pundt
Institut für Angewandte Materialien-Werkstoffkunde (IAM-WK)
Karlsruher Institut für Technologie (KIT)
Kaiserstraße 12
76131 Karlsruhe
astrid.pundt@kit.edu

Overview of Invited Talks and Sessions

(Lecture halls SCH A 118, SCH A 215, SCH A 216, and SCH A 251; Poster P2/OG1+2)

Invited Talks

MM 2.1	Mon	9:30–10:00	SCH A 251	Function follows form: on tailoring functional materials via microstructural design — •ERICA LILLEODDEN
MM 7.1	Mon	15:00–15:30	SCH A 251	Molecular dynamics simulations of shock waves in alloys: Interplay of defects and phase transition — •NINA MERKERT
MM 13.1	Tue	9:30–10:00	SCH A 251	Exploring the Slow Dynamics of Interfaces and Glasses via Markov State Models — SIAVASH SOLTANI, JOERG ROTTNER, •CHAD SINCLAIR
MM 24.1	Wed	9:30–10:00	SCH A 251	Characterization of hydrogen effect on mechanical properties of metals at different length scales — •AFROOZ BARNOUSH, PRINCE BARANWAL, HANAN FARHAT
MM 30.1	Wed	15:00–15:30	SCH A 251	Direct observations of grain boundary phase transformations in metallic alloys — •CHRISTIAN LIEBSCHER

Invited Talks of the joint Symposium SKM Dissertation Prize 2023 (SYSD)

See SYSD for the full program of the symposium.

SYSD 1.1	Mon	9:30–10:00	HSZ 04	Diffusion of antibodies in solution: from individual proteins to phase separation domains — •ANITA GIRELLI
SYSD 1.2	Mon	10:00–10:30	HSZ 04	Intermediate Filament Mechanics Across Scales — •ANNA V. SCHEPERS
SYSD 1.3	Mon	10:30–11:00	HSZ 04	Ultrafast Probing and Coherent Vibrational Control of a Surface Structural Phase Transition — •JAN GERRIT HORSTMANN
SYSD 1.4	Mon	11:00–11:30	HSZ 04	Electro-active metasurfaces employing metal-to-insulator phase transitions — •JULIAN KARST
SYSD 1.5	Mon	11:30–12:00	HSZ 04	The role of unconventional symmetries in the dynamics of many-body systems — •PABLO SALA

Invited Talks of the joint Symposium Green Magnets for Efficient Energy Conversion (SYGM)

See SYGM for the full program of the symposium.

SYGM 1.1	Mon	15:00–15:30	HSZ 01	Data mining protocols for functional magnetic materials — •OLLE ERIKSSON
SYGM 1.2	Mon	15:30–16:00	HSZ 01	High performance permanent magnets; elements criticality, new demands, and extrinsic magnetic properties — •HOSSEIN SEPEHRI-AMIN, XIN TANG, TADAKATSU OHKUBO, KAZUHIRO HONO
SYGM 1.3	Mon	16:00–16:30	HSZ 01	Magnetic shape memory Heuslers: microstructure-related effects on the martensitic transformation — •FRANCA ALBERTINI
SYGM 1.4	Mon	16:45–17:15	HSZ 01	Thin film combinatorial studies of hard magnetic materials — •NORA DEMPSEY
SYGM 1.5	Mon	17:15–17:45	HSZ 01	Magnetocaloric materials for energy-efficient thermal control systems — •VICTORINO FRANCO, AUN N. KHAN, JORGE REVUELTA-LOSADA, ÁLVARO DÍAZ-GARCÍA, LUIS M. MORENO-RAMÍREZ, JIA YAN LAW

Invited Talks of the joint Symposium Topological Superconductor-Magnet Heterostructures (SYTS)

See SYTS for the full program of the symposium.

SYTS 1.1	Thu	15:00–15:30	HSZ 01	Blending of superconductivity and magnetism via topological solitons — •CHRISTOS PANAGOPOULOS
SYTS 1.2	Thu	15:30–16:00	HSZ 01	Topological landscaping in magnet-superconductor heterostructures — •SEBASTIÁN A. DÍAZ
SYTS 1.3	Thu	16:00–16:30	HSZ 01	Experimental study of minigaps and end states in bottom-up designed multi-orbital Shiba chains — •JENS WIEBE
SYTS 1.4	Thu	16:45–17:15	HSZ 01	Quantum spins and hybridization in artificially-constructed chains of magnetic adatoms on superconducting 2H-NbSe₂ — •KATHARINA J. FRANKE
SYTS 1.5	Thu	17:15–17:45	HSZ 01	Braiding of Majorana zero modes — •STEPHAN RACHEL

Sessions

MM 1.1–1.1	Sun	16:00–18:00	HSZ 03	Hands-on Tutorial on Workflows for Materials Science Simulation (joint session MM/TUT)
MM 2.1–2.1	Mon	9:30–10:00	SCH A 251	Invited Talk: Lilleodden
MM 3.1–3.10	Mon	10:15–13:00	SCH A 251	Development of Computational Methods: Evaporation, Growth and Oxidation – Density Functional, Tight Binding
MM 4.1–4.7	Mon	10:15–13:00	SCH A 216	Topical Session: Fundamentals of Fracture – Micromechanical Fracture Experiments
MM 5.1–5.10	Mon	10:15–13:00	SCH A 215	Materials in Energy Conversion: Mechanical Properties and Solid State Batteries
MM 6.1–6.10	Mon	10:15–13:00	SCH A 118	Transport in Materials: Ion, Charge and Heat Transport
MM 7.1–7.1	Mon	15:00–15:30	SCH A 251	Invited Talk: Merkert
MM 8.1–8.7	Mon	15:45–17:45	SCH A 251	Development of Computational Methods: Diverse Topics and Machine Learning
MM 9.1–9.7	Mon	15:45–18:00	SCH A 216	Topical Session: Fundamentals of Fracture – Interface Fracture
MM 10.1–10.4	Mon	15:45–16:45	SCH A 215	Materials for Storage and Conversion of Energy: New Storage Materials
MM 11.1–11.5	Mon	17:00–18:15	SCH A 215	Functional Materials: Performance, Reliability and Degradation
MM 12.1–12.37	Mon	18:15–20:00	P2/OG1+2	Poster I
MM 13.1–13.1	Tue	9:30–10:00	SCH A 251	Invited Talk: Sinclair
MM 14.1–14.10	Tue	10:15–13:00	SCH A 251	Development of Computational Methods: Thermodynamics and Local Chemistry, Electronic Structure
MM 15.1–15.9	Tue	10:15–13:00	SCH A 216	Topical Session: Fundamentals of Fracture – Atomistic Studies of Fracture
MM 16.1–16.10	Tue	10:15–13:00	SCH A 215	Energy Conversion
MM 17.1–17.4	Tue	10:15–11:15	SCH A 118	Phase Transformations: Microstructural Transformations
MM 18.1–18.6	Tue	11:30–13:00	SCH A 118	Transport in Materials: Metals, Alloys and Oxides
MM 19.1–19.5	Tue	14:15–15:30	SCH A 251	Development of Computational Methods: Simulation Methods – Theory
MM 20.1–20.5	Tue	14:15–15:30	SCH A 216	Topical Session: Fundamentals of Fracture – Microstructure Impact on Fracture (Experiments)
MM 21.1–21.5	Tue	14:15–15:30	SCH A 215	Materials for Storage and Conversion of Energy: Energy Conversion
MM 22.1–22.6	Tue	14:15–15:45	SCH A 118	Mechanical Properties and Alloy Design: Porous and Nanostructured Materials
MM 23.1–23.35	Tue	18:15–20:00	P2/OG1+2	Poster II
MM 24.1–24.1	Wed	9:30–10:00	SCH A 251	Invited Talk: Barnoush
MM 25.1–25.5	Wed	10:15–11:30	SCH A 251	Development of Computational Methods: Crystal Structure and Properties
MM 26.1–26.10	Wed	10:15–13:00	SCH A 216	Interface Controlled Properties and Nanomaterials: Grain Boundaries and Stability, Spectroscopy and Interatomic Potentials
MM 27.1–27.10	Wed	10:15–13:00	SCH A 215	Hydrogen in Materials
MM 28.1–28.9	Wed	10:15–12:45	SCH A 118	Liquid and Amorphous Metals
MM 29.1–29.5	Wed	11:45–13:00	SCH A 251	Data Driven Materials Science: Big Data and Work Flows – Electronic Structure
MM 30.1–30.1	Wed	15:00–15:30	SCH A 251	Invited Talk: Liebscher
MM 31.1–31.10	Wed	15:45–18:30	SCH A 251	Data Driven Materials Science: Big Data and Work Flows – Machine Learning
MM 32.1–32.8	Wed	15:45–18:30	SCH A 216	Topical Session: Defect Phases I
MM 33.1–33.8	Wed	15:45–18:00	SCH A 215	Topical Session: Fundamentals of Fracture – Amorphous Metals
MM 34	Wed	18:45–19:45	SCH A 251	Members' Assembly

MM 35.1–35.1	Thu	9:30–10:00	SCH A 251	Invited Talk: Champion
MM 36.1–36.11	Thu	10:15–13:15	SCH A 251	Data Driven Materials Science: Big Data and Work Flows – Microstructure-Property-Relationships (joint session MM/CPP)
MM 37.1–37.8	Thu	10:15–13:00	SCH A 216	Topical Session: Defect Phases II
MM 38.1–38.3	Thu	10:15–11:15	SCH A 215	Topical Session: Fundamentals of Fracture – Fracture Experiments
MM 39.1–39.6	Thu	11:45–13:15	SCH A 215	Phase Transformations: Simulation and Machine Learning
MM 40.1–40.10	Thu	15:45–18:30	SCH A 251	Mechanical Properties and Alloy Design
MM 41.1–41.7	Thu	15:45–18:00	SCH A 216	Topical Session: Defect Phases III
MM 42.1–42.10	Thu	15:45–18:30	SCH A 215	Interface Controlled Properties and Nanomaterials: Nanoporous Materials and Nanolaminates

Members' Assembly of the Metal and Material Physics Division

Wednesday 18:45–19:45 SCH A 251

Sessions

– Invited Talks, Topical Talks, Tutorials, Contributed Talks, and Posters –

MM 1: Hands-on Tutorial on Workflows for Materials Science Simulation (joint session MM/TUT)

Time: Sunday 16:00–18:00

Location: HSZ 03

Tutorial

MM 1.1 Sun 16:00 HSZ 03

Hands-on tutorial on workflows for materials science simulations — •JÖRG NEUGEBAUER¹, TILMANN HICKEL¹, and RALF DRAUTZ² — ¹Max-Planck-Institut für Eisenforschung, Düsseldorf — ²ICAMS, Ruhr-Universität Bochum

Advanced computational simulations in materials science have reached a maturity that allows one to accurately describe and predict materials properties and processes. The underlying simulation tasks often involve several different models and software that requires expert knowledge to set up a project and to vary input parameters. The accompanying increasing complexity of simulation protocols means that the workflow along the simulation chain becomes an integral part

of research. Effective workflow management therefore is important for efficient research and transparent and reproducible results.

In this hands-on tutorial we will provide an interactive hands-on introduction into managing workflows with pyiron (www.pyiron.org). Pyiron is an integrated development environment for materials science built on python and Jupyter notebooks that may be used for a wide variety of simulation tasks, from rapid prototyping to high performance computing. The tutorial will first give a general introduction to using pyiron, with a focus on atomistic simulation tasks. In the second part of the tutorial, the training and validation of machine learning potentials from reference density functional calculations will provide a real-life application example.

MM 2: Invited Talk: Lilleodden

Time: Monday 9:30–10:00

Location: SCH A 251

Invited Talk

MM 2.1 Mon 9:30 SCH A 251

Function follows form: on tailoring functional materials via microstructural design — •ERICA LILLEODDEN — Fraunhofer-IMWS

While the Bauhaus adage says that form follows function, materials scientists understand that function follows form; we aim to exploit structuring of materials to achieve targeted function; the inherent interplay between processing, structure and properties is indeed the cornerstone of materials science. In this talk, I will

present two examples in which various structural elements can be used to tune the functional response of materials in ways that may be unexpected: exploiting structural geometry to tailor strength to stiffness ratios; and how alloying and thermal treatments can lead to a simultaneous increase in both strength and hardening. These examples will be placed in the context of how we view classical laws governing structure-property relations, with an outlook on new approaches to materials design going forward.

MM 3: Development of Computational Methods: Evaporation, Growth and Oxidation – Density Functional, Tight Binding

Time: Monday 10:15–13:00

Location: SCH A 251

MM 3.1 Mon 10:15 SCH A 251

Towards machine learning potentials for field evaporation — •SHYAM KATNAGALLU, JOERG NEUGEBAUER, and CHRISTOPH FREYSOLDT — Department of computational materials design, Max Planck Institut für Eisenforschung GmbH, Düsseldorf, Germany.

Field evaporation, an electrostatic field-induced ionization and subsequent evaporation of surface atoms, is the underlying principle of atom probe tomography. Ab initio simulations including 1-10 V/Å fields on metallic slabs have recently shed light [1] on the intricacies of the field evaporation process. These simulations underscore the importance of knowing the path of the evaporating atom prior to complete ionization to improve the spatial resolution of the technique. However, to properly sample the extremely shallow potential energy surface due to the electrostatic field extensive simulations with computationally expensive ab initio accuracy are needed. We, therefore, combine machine learning interatomic potentials with a charge equilibration scheme. To demonstrate the performance and accuracy of our scheme, we validate the Rappe et al charge equilibration model [2] using Hirshfeld decomposed DFT reference charges acquired from (13,5,7) Pt slab under electric fields ranging from (1-4.5 V/Å) and develop potentials for field evaporation in Al. [1]*M. Ashton, A. Mishra, J. Neugebauer, and C. Freysoldt, Ab Initio Description of Bond Breaking in Large Electric Fields, Phys. Rev. Lett. 124, (2020). [2]*A. K. Rappe and W. A. G. III, Charge Equilibration for Molecular Dynamics Simulations, J. Phys. Chem 95, 3358 (1991).

MM 3.2 Mon 10:30 SCH A 251

High temperature chlorine corrosion in waste-to-energy-plants: sulphation of chloride particles as source of released chlorine — •SEBASTIAN PENTZ, MATTHIAS KROH, and FERDINAND HAIDER — University of Augsburg, Chair for Experimental Physics I, Universitätsstr. 1, 86159 Augsburg

Chlorine induced high temperature corrosion leads to massive problems especially in waste-to-energy-plants. During the combustion process chloride containing particles are released and deposited on heat exchanger surfaces. These chlorides get converted into sulphates with a release of chlorine species which then lead to severe corrosion. For chloride particle sampling from a plant a tempered probe was developed, allowing time series of deposit built-up at defined

temperatures. From this online particle sampling during plant operation we collect information about sticking probability, size distribution of deposited particles and the chemical composition of the deposit built up. Especially the relation between detected chlorine to sulphur is of high interest, leading to the degree of conversion of deposited chlorides, which equals the amount of released chlorine. In further laboratory experiments the sulphation process of synthetic chloride particles can be systematically studied. From this we get the sulphation kinetics under various conditions like temperature, particle size or gas composition, which lead to an estimation of the time required for full chloride conversion. By combining the results gained from laboratory experiments, online particle sampling and offline deposit analysis, we try to model the ongoing sulphation process.

MM 3.3 Mon 10:45 SCH A 251

How to teach my deep generative model to create new RuO₂ surface structures? — •PATRICIA KÖNIG, HANNA TÜRK, YONGHYUK LEE, CHIARA PANOSSETTI, CHRISTOPH SCHEURER, and KARSTEN REUTER — Fritz-Haber Institute, Max-Planck-Society, Faradayweg 4-6, 14195 Berlin, Germany

Data-driven approaches to inversely design novel materials with desired properties constitute an emerging pillar in the exploration of energy conversion materials. In recent works, artificial neural networks were successfully used to create crystalline porous materials. Here, we present a related approach to tackle the problem of structure generation for nano-porous to partially amorphous surfaces. As a model system, we use the well-studied RuO₂ catalyst for oxidative conversion of CO to CO₂. To explore the chemical space of RuO₂ surface structures, we trained a Generative Adversarial Network (GAN) that is capable of cheaply generating diverse structural guesses for novel surface structures. For the training set, 28,903 RuO₂ surface terminations were created with a grand-canonical basin hopping method using ML potential energetics. The atomic positions of these structures were mapped to Gaussian densities on a three-dimensional grid to generate the GAN input. We demonstrate how realistic three-dimensional surface models with inferred lattice lengths and energy conditioning can be created and how these generated densities can be mapped back to atomistic structures as a basis for property calculations.

MM 3.4 Mon 11:00 SCH A 251

Liquid-Diffusion-Limited Growth of Vanadium Dioxide Single-Crystals — •NICO SPRINKART, DANIEL KAZENWADEL, ROMAN HARTMANN, and PETER BAUM — Department of Physics, University of Konstanz
Vanadium dioxide (VO₂) is a strongly correlated material with an ultrafast first-order phase transition between rutile/insulator and monoclinic/metallic close to room temperature. The unusual and complex properties of this transition make VO₂ one of the most heavily investigated materials in modern condensed matter physics. Consequently, high-quality single-crystals are in large demand.

Here we present a method for the growth of mm-sized stoichiometric VO₂ crystals by thermal decomposition of liquid V₂O₅. Time-resolved measurements of the oxygen release reveal that the crystal growth rate is limited by liquid-phase diffusion; the properties of the gaseous environment, which were previously assumed to be decisive, are almost insignificant.

Our results signify the role of gas-liquid diffusion in crystal growth and will simplify future research on VO₂ and its subsequent application in ultrafast electronics and thermal energy management.

MM 3.5 Mon 11:15 SCH A 251

Dynamic restructuring of oxidation states in magnetite — •EMRE GÜRSOY¹, GREGOR B. VONBUN-FELDBAUER², and ROBERT H. MEISSNER^{1,3} — ¹Institute of Polymer and Composites, Hamburg University of Technology, Hamburg, Germany — ²Institute of Advanced Ceramics, Hamburg University of Technology, Hamburg, Germany — ³Institute of Surface Science, Helmholtz-Zentrum Hereon, Geesthacht, Germany

Magnetite is a mineral that undergoes a metal-insulator transition called the Verwey transition at 125 K (T_V). Its conducting behaviour above T_V is linked to electron hops between Fe²⁺ and Fe³⁺ on octahedral sites and complex oxidation state patterns emerge as a direct consequence. Oxidation states are frequently assessed using quantum mechanical methods, but these computationally expensive methods are not scalable to relevant systems with several thousand atoms. Therefore, a computationally inexpensive method that provides a detailed atomistic description of magnetite would be beneficial. We present a hybrid Monte Carlo/Molecular Dynamics (MC/MD) approach for atomistic modeling of magnetite, magnetite surfaces, and nanoparticles that can capture many aspects of this oxidation state patterning. It is based on swapping the oxidation states of Fe ions using MC either in simulated annealing, or in a hybrid combination with MD. We confirmed the accuracy of our model by comparison with oxidation states determined from density functional theory. This simple yet efficient approach paves the way to elucidate aspects of oxidation state ordering and electron hopping in inverse spinel structures in general.

15 min. break

MM 3.6 Mon 11:45 SCH A 251

Role of an adsorbed gas layer in field ion microscopy contrast — •SHALINI BHATT, FELIPE F. MORGADO, SHYAM KATNAGALLU, CHRISTOPH FREYSOLDT, and JÖRG NEUGEBAUER — Max Planck Institut für Eisenforschung GmbH Düsseldorf Germany

The imaging contrast in field ion microscopy (FIM) is associated with the ionization probability of gas atoms near a surface under 10-100 V/nm electric fields. To better understand contrast variations among atoms observed in FIM, we employ density functional theory (DFT) in combination with the Tersoff-Hamann approximation that links electron tunneling from the gas atom to the surface with the surface's local density of states at the position of the gas atom 3-6 Å away from the surface. Based on our new EXTRA approach (extrapolated tail via reverse algorithm) that eliminates numerical noise in the tails of the wavefunctions, we demonstrate a chemical brightness contrast for Ta in Ni (012) surface. However, we find that the simulated imaging contrast for Ni alone is much lower than in experiment. We therefore explore the role of an adsorbed gas layer as an essential ingredient to explain FIM's unexpectedly large spatial resolution.

MM 3.7 Mon 12:00 SCH A 251

A Workflow for Obtaining Robust Density Functional Tight Binding Parameters Across the Periodic Table — •MENGAN CUI, JOHANNES T. MARGRAF, and KARSTEN REUTER — Fritz-Haber-Institut der MPG, Berlin, Germany
The Density Functional Tight Binding (DFTB) approach allows electronic structure based simulations at length and time scales far beyond what is possible with first-principles methods. This is achieved by using minimal basis-sets and empirical approximations. Unfortunately, the sparse availability of parameters across the periodic table is a significant barrier to the use of DFTB in many cases.

In this contribution, we therefore propose a workflow which allows the robust

and consistent parameterization of DFTB across the periodic table. Importantly, the approach requires no element-pairwise parameters and can thus easily be extended to new elements. Specifically, the parameters defining the band energy and repulsive potential are obtained via Bayesian Optimization on a set of elemental solids. In this way, robust baseline parameters can be obtained for arbitrary element combinations. The transferability of the parameters and applications in hybrid DFTB/Machine Learning models will be discussed.

MM 3.8 Mon 12:15 SCH A 251

Coupling Many Body Perturbation Theory (MBPT) with Polarizable Continuum Models (PCM) — •PINO D'AMICO¹, DARIO A. LEON VALIDO², MARGHERITA MARSILI³, DANIELE VARSANO¹, STEFANO CORNI⁴, and ANDREA FERRETTI¹ — ¹S3 Center, Istituto Nanoscienze CNR, Modena, Italy — ²Dpt. REALTEK, Norw. Univ of Life Sci., Ås, Norway — ³Dpt. di Fisica e Astronomia, Univ. di Bologna, Italy — ⁴Dpt. di Scienze Chimiche, Univ. di Padova, Italy

The theoretical description of quantum systems embedded in external environments represents a challenge for the application of MBPT approaches to the study of the electronic excitations. Different level of accuracy can be used to treat the actual system, for which a quantum mechanical description is employed, and its surrounding environment, that can be approximated through a simplified quantum model, a molecular mechanical approach, or a continuum model. We will present a theoretical framework in which a MBPT treatment of the quantum system (eg at the level of GW and BSE) is coupled to a PCM description of its surrounding environment. The formalism has been implemented within the YAMBO code[1], based on plane-waves and pseudopotentials, by exploiting the ENVIRON package[2] coupled to the Quantum ESPRESSO suite[3]. Preliminary results of the newly developed methodology will be presented, focusing on selected molecules and two-dimensional materials in water. [1] D. Sangalli et al., J.of Phys.:Cond.Mat. 31, 325902 (19).[2] O. Andreussi et al., J.Chem.Phys. 136, 064102 (12).[3] P. Giannozzi et al., J.Phys.:Cond.Mat. 29, 465901 (17).

MM 3.9 Mon 12:30 SCH A 251

A DFTB-based approach to calculating electron-phonon couplings — •ALEXANDER CROY¹, ELIF UNSAL², GIANAURELIO CUNIBERTI², and ALESSANDRO PECCHIA³ — ¹Institute of Physical Chemistry, FSU Jena, Germany — ²Institute of Materials Science, TU Dresden, Germany — ³Institute of Nanostructured Materials, CNR, Italy

The calculation of electron-phonon couplings from first principles is computationally very challenging and remains mostly out of reach for systems with a large number of atoms. Resorting to semi-empirical methods, like density-functional based tight-binding (DFTB), has been shown to be a viable approach for obtaining quantitative results at moderate computational costs. In this contribution, we present a method for calculating the electron-phonon coupling matrix within the DFTB approach and demonstrate its implementation which is based on dftb+ and phonopy. It further allows the calculation of relaxation times and interfaces with BoltzTrap2 to compute transport properties. Exemplarily, we show results for γ -graphyne which was recently synthesized. Consistent with earlier predictions we obtain mobilities on the order of $10^4 \text{ cm}^2 \text{ V}^{-1} \text{ s}^{-1}$ at room temperature.

MM 3.10 Mon 12:45 SCH A 251

Toward Coarse-Grained Elasticity of Single-Layer Covalent Organic Frameworks — •DAVID BODESHEIM¹, ANTONIOS RAPTAKIS¹, AREZOO DIANAT¹, ALEXANDER CROY², and GIANAURELIO CUNIBERTI¹ — ¹TU Dresden, Dresden, Germany — ²FSU Jena, Jena, Germany

Covalent Organic Frameworks (COFs) are crystalline porous materials that are based on organic monomeric units, so called building blocks. As a multitude of different building blocks can be combined in reticular chemistry, manifold different porous structures with tailored properties have been synthesized in recent years. Through current experimental progress, monolayer COF materials have been synthesized, providing a new class of 2D materials.[1,2] However, these materials have defects and grain boundaries which make it challenging to describe properties of realistic materials computationally. To approach this issue, we show in this work how to use a surrogate model to calculate elastic properties of 2D COFs based on density functional based tight binding (DFTB) calculations.[3] This allows us to model defective systems at low computational cost and paves the way for multiscale modeling. Furthermore, this approach enables us to predict elastic properties from the properties of the monomeric building blocks.

[1] A. Ortega-Guerrero, et al. ACS Appl. Mater. Interfaces, 13, 22, 26411-26420 (2021).

[2] Z. Wang, et al., Nat. Synth., 1, 69-76 (2022).

[3] A. Croy, et al. J. Phys. Chem. C, 126, 44, 18943-18951 (2022).

MM 4: Topical Session: Fundamentals of Fracture – Micromechanical Fracture Experiments

Time: Monday 10:15–13:00

Location: SCH A 216

Topical Talk

MM 4.1 Mon 10:15 SCH A 216

Crack and dislocations interactions: coupling DDD and XFEM — ELENA JOVER-CARRASCO¹, ERIK BITZEK², and MARC FIVEL¹ — ¹CNRS/SiMaP, Univ. Grenoble Alpes, Grenoble, France — ²MPIE, Computational Materials Design, Dusseldorf, Germany

The objective of this study is to build a numerical tool which could handle both cracks and dislocations in a dynamic manner. To do so, a 3D Discrete Dislocation Dynamics (DDD) code has been combined to the Extended Finite Element Method (X-FEM) via a strong coupling with the Finite Element software CAST3M. In the original FEM code, the crack advance is computed from the G- θ method which gives access to the stress intensity factors K. In this formalism, θ is the kinematically admissible virtual displacement of the crack and G is the energy release rate at the crack tip. When dislocations are present in the simulated box, they modify the evaluations of the energy and consequently the values of the derived stress intensity factors. These modifications are computed locally all along the crack front which is defined using level set functions. The crack front may locally change its direction of motion depending on the relative values of the stress intensity factors, especially KII. This will then lead to blunting effect of the crack tip.

In this presentation, full details of the coupling will be given. Test cases will then be presented where the behavior of a single dislocation in vicinity of a crack will be compared to atomistic simulations. Finally, large scale simulations of a mode I opening crack will be performed.

Topical Talk

MM 4.2 Mon 10:45 SCH A 216

multiscale studies on the fracture behaviors of body centered cubic metal — YINAN CUI, ZHIJIE LI, and ZHANGTAO LI — Applied Mechanics Lab., School of Aerospace Engineering, Tsinghua University, Beijing 100084, PR China

How the plasticity features influence the fracture behaviors of material is a critical question but remains far from well understood. To disclose this mystery, a multiscale plasticity-fracture coupled model is developed, which considers the atomistic-scale dislocation motion mechanism, the mesoscopic scales of discrete crack-dislocation interactions, and the continuum scale of crystalline plastic-fracture response. Body center cubic (bcc) material is chosen as an example to demonstrate the effectiveness of the developed model due to their wide applications and their special plasticity features, such as strong temperature dependence and non-Schmid effect. Several new insights about the fracture behavior of bcc material are gained.

MM 4.3 Mon 11:15 SCH A 216

Micro-cantilever experiments to study the influence of pre-deformation and He irradiation on the fracture toughness of W single crystals — STEFAN GABEL¹, MANUEL KÖBRICH¹, JAN VOLLHÜTER¹, BENEDIKT EGGLE-SIEVERS¹, BENOIT MERLE², ERIK BITZEK³, and MATHIAS GÖKEN¹ — ¹Friedrich-Alexander-University Erlangen-Nürnberg (FAU) — ²University Kassel — ³Max-Planck-Institut für Eisenforschung, Düsseldorf

Micro-cantilever fracture testing has been proven to be a very reliable method to determine the fracture toughness at the very small scale. In the work by Ast et al.[1] the influence of the specimen size on the fracture behavior of single and polycrystalline tungsten has been investigated in detail from which it can be concluded that the fracture toughness as analysed with the J-integral approach slightly increases with the specimen size. Here we focus on the brittle-to-ductile transition and the influence of pre-deformation and He irradiation on w single crystals. The fracture toughness is analysed in a temperature regime from 233 K up to 353 K with a FemtoTools in-situ nanoindentation system. Pre-deformation by compression in the <110>direction led to a population of specific glide systems. The results show depending on the sample orientation an increase of the hardness and a slightly higher fracture toughness at low temperatures. Irradiation by He+ ions clearly lead to a decrease of the fracture toughness although the hardness increases. The experimental results will be discussed in comparison with modelling results. [1] *J. Ast, M. Göken, K. Durst, Acta Materialia 138 (2017) 198-211

15 min. break

Topical Talk

MM 4.4 Mon 11:45 SCH A 216

Capturing Micromechanical Crack Tip Stress States and Toughening Plasticity in 2D and 3D — THOMAS E. J. EDWARDS¹, JOHANNES AST^{1,2}, SZILVIA KALÁCSKA^{1,3}, XAVIER MAEDER¹, JON WRIGHT⁴, and JOHANN MICHLER¹ — ¹Empa, Feuerwerkerstrasse 39, 3602 Thun, Switzerland — ²CEA, 17 rue des Martyrs, 38054 Grenoble, France — ³Mines Saint-Etienne, Univ Lyon, CNRS, UMR 5307 LGF, France — ⁴ESRF, 38000, Grenoble, France

Crack tip toughening mechanisms in metals require plasticity, i.e. slip; the present study sheds predictive light on what local stress states lead to an increased dissipation of mechanical energy through plasticity. It also confirms the notion

that the plastic performance of a material cannot be solely interpreted from elastic strain measurements, even if undertaken in-situ, or from post-mortem TEM imaging of dislocation structures. Pre-notched single crystal W microcantilevers were deformed in situ, whilst elastic and total strains at the notch tip were captured correlatively by DIC and HR-EBSD with sub-100 nm resolution. From the basic elastic and total strains and rotations hence measured, as well as post-mortem TEM, the following could be extracted: maps of shear stresses resolved onto individual slip systems, pure plastic strain resolved onto slip axes and GND density - all throughout loading, as well as the total dislocation density of the near-surface layer post-mortem. Further, we demonstrate a novel method to extract the full stress tensor, point-wise in 3D, again with ~100 nm resolution, on micromechanical testpieces under load: nano-beam 3D-XRD computed tomography at ESRF ID11.

MM 4.5 Mon 12:15 SCH A 216

Size effect in fracture mechanics: a detailed investigation regarding crack initiation and growth on the micro- and mesoscale — JUTTA LUKSCH¹, ALOSHIOUS LAMBAI², GAURAV MOHANTY², FLORIAN SCHAEFER¹, and CHRISTIAN MOTZ¹ — ¹Materials Science and Methods, Saarland University, 66123 Saarbruecken, Germany — ²Materials Science and Environmental Engineering, Tampere University, 33014 Tampere, Finland

Fracture mechanics are strictly regulated by standards. This includes limitations of specimen size as a function of the plastic zone size that mainly depends on the material itself. Hence, established test procedures are not easily downscalable to nanomechanic testing. With progress in specimen preparation by FIB and test design e.g. in-situ testing in SEM, there are now ways to investigate a size effect systematically according crack initiation and growth. In the present study nanocrystalline nickel with a grain size of 40-50 nm is used as material to ensure a polycrystalline, quasi-homogeneous microstructure even for small samples. Micro bending beams of different dimensions are made using a FIB in order to study the fatigue size effect. Special attention was layed to introduce a fatigue pre-crack into the sample by cyclic loading with R<0 in a SEM with a nanoindenter. A study of crack initiation stress and number of needed cycles was made. The focus was given on microstructural changes. This pre-crack is then subjected to fatigue (R>0) and crack growth is quantified by the compliance method. In addition, the stress intensity factor is evaluated and related to the crack growth.

MM 4.6 Mon 12:30 SCH A 216

Quantitative measurement of fracture toughness from the bridge notch failure in microcantilever — YINXIA ZHANG¹, MATTHIAS BARTOSIK², STEFFEN BRINCKMANN³, SUBIN LEE¹, and CHRISTOPH KIRCHLECHNER¹ — ¹Institute for Applied Materials, Karlsruhe Institute of Technology, Eggenstein-Leopoldshafen, 76344, Germany — ²Department of Materials Science, Montanuniversität Leoben, Leoben, 8700, Austria — ³Microstructure and Properties of Materials (IEK-2), Forschungszentrum Jülich, 52425, Jülich, Germany

Focused ion beam (FIB) milling has been widely used to prepare micron-sized specimens for micromechanical testing, but there are different types of artefacts originated from FIB. One is the imperfections in through-thickness notch geometries of microcantilevers. Bridge notches can overcome some of the problems by, upon loading, thin bridges fail first, creating atomically sharp natural cracks. Even though this bridge failure is widely assumed and predicted by FEM simulations, it has never been observed and quantified experimentally. This study presents the first experimental observation of cracking at the bridge notch and crack arrest before the entire through-thickness notch fails. This is possible by designing very thin bridges and using a very stiff loading rig with superior load resolution. Consequently, we obtained multiple fracture toughness values from one test. Using reported geometry correction factors calculated by FEM simulations, the fracture toughness estimated from the bridge failure was corrected and compared with the one from the failure of the through-thickness notch. The two approaches show consistent results.

MM 4.7 Mon 12:45 SCH A 216

Stable fracture of ceramics in the TEM — ORIO GALVALDA-DIAZ^{1,2}, SHELLY CONROY¹, EDUARDO SAIZ¹, and FINN GIULIANI¹ — ¹Department of Materials, Imperial College London, UK — ²Department of Mechanical, Manufacturing and Materials Engineering, University of Nottingham, UK

Small scale fracture tests have allowed many elements of a microstructure to be tested in isolation such as phase or grain boundaries. In our previous work we have shown that stable fracture tests in the SEM can accurately measure surface energies and the energy of individual grain boundaries. Furthermore, these tests allow the crack path and the effect of crack-defect interactions to be studied. However, tests in the SEM struggle to give in-depth information around the crack tip. Therefore, in this work we will demonstrate how it is possible to carry out stable fracture experiments in the TEM via a double cantilever geometry. This will be demonstrated on both silicon carbide and zirconia samples where

the different mechanisms of energy dissipation will be discussed. Furthermore, a stable geometry allows additional analysis to be carried out during the test, here

we will discuss the possibility of using 4D STEM to map the strain field around the crack tip.

MM 5: Materials in Energy Conversion: Mechanical Properties and Solid State Batteries

Time: Monday 10:15–13:00

Location: SCH A 215

MM 5.1 Mon 10:15 SCH A 215

Interplay between mechanics and electrochemistry in Li-Si anodes by atomistic simulation — •DANIEL MUTTER¹, MANISHA POUDEL^{1,2}, DANIEL PFALZGRAF¹, and LEONHARD MAYRHOFER¹ — ¹Fraunhofer IWM, 79108 Freiburg — ²Institute of Physics, University of Freiburg, 79104 Freiburg
Silicon is a promising anode material for Li-ion batteries due to its high capacity, which considerably exceeds that of commonly used graphite. Its direct applicability however is hampered by the huge volume change the material undergoes during loading and unloading with Li, concomitant with mechanical stresses arising in the microstructure. In this work, we provide a deeper understanding on the interplay of mechanics and electrochemistry by analyzing the effect of deformation on the electrochemical potential. Using atomistic first principles calculations, we studied crystalline as well as amorphous Li-Si phases with different Li concentrations. We present results of elastic moduli, and the change of voltage during charging and discharging cycles under various characteristic mechanical loading scenarios. The results are essential input for continuum models acting on the nanoparticle scale to correctly describe the microstructural evolution.

MM 5.2 Mon 10:30 SCH A 215

Design of zero strain cathode materials based on colquiriite-type $\text{Li}_x\text{Ca}(\text{M},\text{M}')\text{F}_6$ — •ALJOSCHA FELIX BAUMANN^{1,2}, DANIEL MUTTER², DANIEL URBAN^{1,2}, and CHRISTIAN ELSÄSSER^{1,2} — ¹Freiburger Materialforschungszentrum, Stefan-Meier-Straße 21, 79104 Freiburg im Breisgau — ²Fraunhofer-Institut für Werkstoffmechanik IWM, Wöhlerstr. 11, 79108 Freiburg
The long-term stability of Li ion batteries can be negatively affected by mechanical stresses in the microstructure of the cathode material during charge/discharge cycles. Therefore, materials are of great interest which show a zero-strain (ZS) behavior, i.e. a negligible volume change during insertion or extraction of Li ions. For specific compounds of the material class of colquiriites, $\text{Li}_x\text{A}^{\text{II}}\text{M}^{\text{III}}\text{F}_6$, ZS behavior was predicted theoretically and measured experimentally for different Li concentration ranges. In this work we investigate the effect of the electrochemically active cation M^{III} (M = Ti, V, Cr, Mn, Fe, Co, Ni) on the volume change during (de-)lithiation. Using density-functional theory we calculated the equilibrium volumes at different Li concentrations. The analysis of the electronic and magnetic structures and the calculation of local structural parameters indicate that the total volume change depends mainly on the counteracting effects of expanding fluorine octahedra around the M ions due to the changing oxidation state, and a decrease of repulsion between fluorine anions due to the inserted Li ions. The trends in the properties along the period of the 3d transition metals provide a guideline for a design of new ZS cathode materials in solid solutions of type $\text{Li}_x\text{Ca}(\text{M},\text{M}')\text{F}_6$.

MM 5.3 Mon 10:45 SCH A 215

Planar gliding and vacancy condensation: The role of dislocations in the chemomechanical degradation of layered transition metal oxides — •MARCEL SADOWSKI¹, KARSTEN ALBE¹, and SABRINA SICOLO² — ¹Technical University of Darmstadt, Darmstadt, Germany — ²BASF SE, Ludwigshafen, Germany
Stacking faults driven by dislocations have been observed in layered transition metal oxides cathodes both in cycled and uncycled materials. The reversibility of stacking-sequence changes directly impacts the material performance. Irreversible glide due to lattice invariance or local compositional changes can initiate a catastrophic sequence of degradation mechanisms. In this study we compare the chemomechanical properties of LiCoO_2 and LiNiO_2 by combining density functional theory (DFT) and anisotropic linear elasticity theory. We calculate stacking fault energies as a function of Li content and quantify the “pillar effect” of excess Ni in hindering stacking-sequence changes. We then characterize screw dislocations, which mediate stacking-sequence changes, and find a peculiarly compliant behavior of LiNiO_2 due to the interaction of Jahn-Teller distortions with the dislocation strain field. Finally, we analyze the tendency of vacancies to segregate along dislocation lines. This study represents the first instance of explicit ab-initio atomistic dislocation models in layered oxides and paves the way for the understanding and optimization of the chemomechanical behavior of cathode active materials during battery operation.

MM 5.4 Mon 11:00 SCH A 215

Modification of iron-based oxide anodes for potassium ion storage — •ZIDONG WANG, HUAPING ZHAO, and YONG LEI — Fachgebiet Angewandte Nanophysik, Institut für Physik & IMN MacroNano, Technische Universität Ilmenau, 98693 Ilmenau, Germany
Due to the abundance of potassium and its easy accessibility, potassium-based electrochemical energy storage technology has attracted extensive research in-

terests and significant progress of it has been made in recent years. Among different anode materials for anodes of potassium-ion storage devices, transition metal oxides especially of iron-based oxides have high potential due to their high capacity and low cost. However, their poor electrical conductivity and weak structure impede their development. In this work, adjustment of the anionic and cationic composition of iron oxides is achieved. This adjustment can effectively result in a high-performance anode for potassium ion storage. In brief, the synergistic effect of multivalent metal cations will result in excellent potassium storage properties. And the conductivity can be further improved by the replacement of anions. Our results indicate that the adjusted iron-based compound can be used as a promising high-performance anode material for potassium ion storage devices.

MM 5.5 Mon 11:15 SCH A 215

Construction of V5S8/Sb2S3@C Heterostructures as High-Performance Anode Materials for Potassium-ion Batteries — •VINCENT HARTMANN, YULIAN DONG, HUAPING ZHAO, and YONG LEI — Fachgebiet Angewandte Nanophysik, Institut für Physik & IMN MacroNano, Technische Universität Ilmenau
Transition metal sulfides (TMSs) have been studied widely and deeply as anode materials for potassium ion batteries (PIBs) owing to their relatively high theoretical capacities. However, poor electrical conductivity, large volume expansion, and slow diffusion kinetics hinder their further applications. Herein, a unique hierarchical structure of V5S8/Sb2S3@C is fabricated by a concise solvothermal method and subsequently annealing. Such a well-designed architecture affords fast K⁺ diffusion kinetics and improved charge transfer at the heterointerfaces due to the metallicity of the internal V5S8. In addition, the synergistic coupling interaction among the interior V5S8, interlayer Sb2S3, and external C layer generates a stable nanostructure, which extremely accelerates the electronic/ion transport and effectively alleviates the volume expansion upon long cyclic performance. As a result, it exhibits a high initial capacity of 525.19 mAh/g at 100 mA/g and excellent cyclic stability with 95% capacity retention after 500 cycles at 1 A/g. Our results reveal that the combination of heterostructures construction and interfacial interaction enables optimizing electronic structures and macroscopic mechanical properties of TMSs, thus achieving high-performance anodes for PIBs with high energy density.

15 min. break

MM 5.6 Mon 11:45 SCH A 215

Influence of interstitial Li on the electronic properties of $\text{Li}_x\text{CsPbI}_3$ for photovoltaic and battery applications — •WEI WEI^{1,2}, JULIAN GEBHARDT^{1,2}, DANIEL URBAN^{2,3}, and CHRISTIAN ELSÄSSER^{1,2,3} — ¹Cluster of Excellence liv-MatS, University of Freiburg, Germany — ²Fraunhofer Institute for Mechanics of Materials IWM, Freiburg, Germany — ³Freiburg Materials Research Center (FMF), University of Freiburg, Germany
The stability of crystalline CsPbI_3 with interstitial Li ions is investigated together with the effect that Li has on the electronic structure of the resulting compound $\text{Li}_x\text{CsPbI}_3$. We analyze this by two structural models for CsPbI_3 at room temperature, the cubic α phase and a distorted structure analogous to the γ phase (γ' structure). The hypothetical α phase does thermodynamically not allow Li uptake and is likely to be structurally unstable for $x > 1/4$, while adding Li up to $x=1$ in the γ' structure is possible. In all cases, Li promotes structural distortions, namely tilting of bond angles $\Delta_{\text{pb-i-pb}}$ and Cs off-center displacements Δ_{rCs} , which are increasing with the Li concentration.
Interstitial Li has the following effects on the electronic structure of CsPbI_3 : i) the induced structural distortion leads to a significant increase of the band gap; ii) the screening of additional electrons in the conduction band leads to a small increase of the band gap; iii) the effect of Li 2s states on the band edges and band gap is negligible. Altogether, the change of the band gap is dominated by the tilting of $\Delta_{\text{pb-i-pb}}$ angles: stronger distortion caused by increasing Li content is accompanied by an increased band gap.

MM 5.7 Mon 12:00 SCH A 215

Design for Dual-Functional Electrode Promoting Dendrite-free and CO₂ Utilization Enabled High-Reversible Symmetrical Na-CO₂ batteries — •CHANGFAN XU, HUAPING ZHAO, and YONG LEI — Fachgebiet Angewandte Nanophysik, Institut für Physik & IMN MacroNano, Technische Universität Ilmenau, 98693 Ilmenau, Germany
A one stone two-birds strategy is presented by using carbon paper embedded with Ru nanoparticles (RuCP) as dual-functional electrodes for both the Na anode and CO₂ cathode. As an anode host, the RuCP with remarkable sodiophilic-

ity can dominate Na nucleation behavior and achieve a uniform Na ion flux for the inhibition of dendrite formation, meanwhile, the RuCP affords high catalytic activity for catalyzing the formation/decomposition of Na₂CO₃ in CO₂ cathode. As a result, the Na was homogeneously deposited on the RuCP anode without Na dendrite formation, showing a high Coulombic efficiency of over 99% and a long cycle lifetime, and the RuCP cathode demonstrates low overpotentials and excellent cycling stability (>300 cycles). Implementation of the RuCP@Na anode and RuCP cathode allows for the construction of a symmetrical Na-CO₂ battery with long-duration cyclability because of the dendrite-free sodium morphology and numerous Ru catalytic sites. Such electrodes and battery designs offer an effective method for the tailoring and optimization of sodium metal batteries with high energy density.

MM 5.8 Mon 12:15 SCH A 215

Dynamic stability and *ab initio* free energy calculations of argyrodite Li₆PS₅Cl solid electrolyte — •YONGLIANG OU, YUJI IKEDA, PRASHANTH SRINIVASAN, and BLAZEJ GRABOWSKI — Institute for Materials Science, University of Stuttgart, 70569 Stuttgart, Germany

High ionic conductivity of argyrodite Li₆PS₅Cl, which was shown in both experiments and simulations, renders it a promising candidate for the solid electrolyte in all-solid-state lithium-ion batteries. Although the diffusion mechanism has been intensively investigated in previous studies, the dynamic and thermodynamic stability of Li₆PS₅Cl have not yet been fully understood. To address this issue, systematic investigations are carried out under the *ab initio* framework in this study. At 0 K, the dynamic instability of the ideal structure is revealed by the calculated imaginary phonon modes. Molecular dynamics simulations accelerated by machine-learning interatomic potentials show dynamic stabilization via vibrational entropy at finite temperatures. Further, *ab initio* free energy calculations are performed in wide temperature and pressure ranges utilizing a multistage thermodynamic integration technique. The calculated free energies provide important information for subsequent studies focusing on the energetic aspects, e.g., defect or grain boundary formation energy, of Li₆PS₅Cl. It can be expected that the present results benefit the research and application of all-solid-state lithium-ion batteries.

MM 5.9 Mon 12:30 SCH A 215

Exploration of cathode-stable layered solid-state electrolytes — •SINA ZIEGLER, CHRISTOPH SCHEURER, and KARSTEN REUTER — Fritz-Haber-Institut der MPG, Berlin, Germany

Promising higher safety and capacity, all-solid-state lithium batteries are envisioned to replace standard lithium-ion batteries in the future. Lithium thio-

phosphates achieve the highest Li ion conductivities of all solid-state electrolytes (SSE) known to date but their instability towards high-performance electrodes remains a critical challenge. To address this issue, we investigate the concept of rare earth lithium halides as a material-efficient, nanometer thick cathode coating in contact with thiophosphate electrolytes. Halides provide wide electrochemical stability windows as well as good chemical and thermodynamic stability [1,2].

To determine a suitable halide/thiophosphate combination, an energetically feasible reaction pathway in the multidimensional phase diagram between the two materials needs to be identified. Consequently, the thermodynamic stabilities of the emerging SSE / halide interfaces are examined by *ab initio* thermodynamics to screen reaction free enthalpies of possible interface reactions. Next, an end member analysis is performed to analyze possible compositions of interface products and possible secondary phases.

[1] J. Liang et al., Acc. Chem. Res. 2021, 54, 1023-1033 [2] K. Kim et al., Chem. Mater. 2021, 33, 10, 3669-3677

MM 5.10 Mon 12:45 SCH A 215

Active Site Deactivation of the Air Electrode in High-Temperature Solid Oxide Cells — •HANNA TÜRK, THOMAS GÖTSCH, FRANZ-PHILIPP SCHMIDT, AXEL KNOP-GERICKE, ROBERT SCHLÖGL, THOMAS LUNKENBEIN, KARSTEN REUTER, and CHRISTOPH SCHEURER — Fritz-Haber-Institut der MPG, Berlin, Germany
Degradation of the air electrode in electrolysis mode severely limits the commercial adoption of solid oxide cells (SOCs). This degradation goes hand in hand with the oxygen evolution reaction (OER) taking place at the triple-phase boundary (TPB) between the anode, the solid electrolyte, and the gas phase. Up to now, the atomistic structure of this active catalyst region is essentially unknown, though, which prevents a detailed analysis of the actual degradation mechanisms.

Recently, we took the first step in elucidating the TPB structure by revealing a complexation at the underlying solid/solid interface of the sintered anode[1], featuring partial amorphization and varying elemental distributions deviating from the confining bulk phases. Based on this finding, we now expand our force field based Monte-Carlo simulations to the OER active site. Our experimentally validated results show unexpected compositional changes with respect to the thermodynamic equilibrium, that combined with a spatially resolved diffusion study indicate a hitherto unknown mechanism underlying the deactivation of the anode[2].

[1] H. Türk et al., Adv. Mater. Interfaces 8, 2100967 (2021).

[2] H. Türk et al., ChemCatChem 14, e202200300 (2022).

MM 6: Transport in Materials: Ion, Charge and Heat Transport

Time: Monday 10:15–13:00

Location: SCH A 118

MM 6.1 Mon 10:15 SCH A 118

Large-scale Atomistic and Quantum Mechanical Study of the Na⁺ Transport Mechanism in Sodium-ion Battery Electrolytes — •AMAL KANTA GIRI¹ and HARALD OBERHOFER^{1,2} — ¹University of Bayreuth — ²TU Munich

A steady increase of the greener and safer energy sources have led to a rise in the need for energy storage technologies. In the last three decades, the lithium ion batteries (LIBs) dominated the global market from small to large scale storage of the energy. Yet, the shortage of the lithium and its localized geographical distribution raises concerns. New charge carriers for batteries beyond the lithium such as Na, is viable alternative for safe and large-scale energy storage, mainly due to its large abundance and high electrochemical potential.

Here, to improve our understanding of the Na⁺ transport mechanism, aggregation, and electrolyte performance in sodium ion batteries, we perform a theoretical investigation using a combination of all-atoms molecular dynamics (MD) simulations based on the OPLS forcefield and density functional theory calculations (DFT). In this regard, we simulate NaPF₆ salt in various organic electrolytes including ethylene carbonate (EC), propylene carbonate (PC), dimethoxyethane (DME), and dimethyl carbonate (DMC), and their binary mixtures at 320 K. Specifically, we focus on the conductivity, diffusivity and solvation of Na⁺ in the liquid electrolyte mediums. Furthermore, the solvation structure and the binding energy of ions in the electrolytes are thoroughly analyzed. We find the diffusivity of Na⁺ ions in the order DMC>DME>EC>PC, which follow the viscosity of the electrolytes.

MM 6.2 Mon 10:30 SCH A 118

Fast ion conduction in glassy and crystalline phases of Na₃PS₄: Insight from a machine-learning potential molecular dynamics study — •YU-TAO LI, TABEA HUSS, CARSTEN STAACKE, KARSTEN REUTER, and CHRISTOPH SCHEURER — Fritz-Haber-Institute of the Max-Planck-Society

Its earth-abundance and chemical similarity makes sodium a promising substitute for lithium in future, sustainable solid-state batteries. In that respect the

sodium thiophosphate (NaPS) material class has proven to provide electrolytes with high ionic conductivities [1]. Similar to the lithium thiophosphate (LiPS) material class, the NaPS class is characterized by a high degree of structural variety. It limits the transferability of *ab initio* studies, which are restricted to small model systems or short time scales for more complex models. Machine learning force-fields (ML-FF) provide a computationally cheaper yet sufficiently accurate alternative.

We have previously reported on a universal ML-FF for the whole LiPS material class [2]. In this work, we now develop a related ML-FF for glassy and crystalline phases of Na₃PS₄. Using the obtained ML-FF, we probe sodium ion conductivity in the glassy and crystalline phases. We systematically compare ion conductivity in LiPS vs. NaPS, and disentangle cation and anion dynamics in both material classes. Our aim is to understand the influence of stoichiometry and thiophosphate microchemistry on phase stability and ion conductivity.

[1] A. Hayashi et al., J. Power Sources 258, 420 (2014).

[2] C.G. Staacke et al., Nanomaterials 12, 2950 (2022).

MM 6.3 Mon 10:45 SCH A 118

Accelerating structure prediction of solid-solid interfaces in solid electrolytes using Machine Learning Potentials — •TABEA HUSS, CARSTEN STAACKE, KARSTEN REUTER, and CHRISTOPH SCHEURER — Fritz-Haber-Institut der MPG

The lithium thiophosphate (LPS) material class provides promising candidates for solid-state electrolytes (SSE) in lithium ion batteries due to high lithium ion conductivities, non-critical elements, and low material cost. LPS materials are characterized by structural disorder and occur in a multitude of glassy and crystalline phases, depending on their stoichiometry. The most performant glass-ceramic SSEs from the LPS class are characterized by omnipresent two-dimensional interfaces between crystalline and glassy domains, which can dominate the materials performance and cycle stability. To address this complexity we present a protocol for the construction of polycrystalline solid-solid interfaces in the LPS system. Within our protocol, expensive *ab-initio* random structure

search (AIRSS) calculations are replaced by a Machine Learning surrogate accelerated approach. We present a pathway towards a full assessment of partially amorphous interfaces in the LPS material class.

MM 6.4 Mon 11:00 SCH A 118

Understanding Oxide Ion Transport In Yttria Stabilized Zirconia: Fresh Insights from Molecular Dynamics Simulations — •SUDESHNA MADHUAL, KRISHNANJAN PRAMANIK, and PADMA KUMAR PADMANABHAN — Indian Institute of Technology Guwahati, Guwahati, Assam, India, 781039

A comprehensive molecular dynamics investigation of yttria stabilized zirconia, $Y_x Zr_{1-x} O_{2x/2}$, is carried out for a wide range of compositions, $x = 4$ to 40 mol%, and over temperatures spanning 800 - 2200 K. The lattice parameter of the fluorite cell shows a monotonic increase with concentration, while the self-diffusivity of oxide ion as well as the resulting ionic conductivity, shows an optimum value around $x = 10$ mol%. These gross structural and transport properties of the system from the present study is in good agreement with previous experimental and theoretical investigations. It is noted that the oxygen migration occurs along straight channels parallel to the crystallographic axes, connecting the tetrahedral holes of the fluorite lattice occupied by them. A microscopic investigation of distinct oxygen environments, variably coordinated to Y^{3+} and Zr^{4+} cations, and of the channels connecting them is carried out. Analysis of these local channels for their energetics and their contribution to overall oxygen transport, resolved in terms of the cationic edges connecting them, provides fresh insights on the oxygen migration mechanism in the system.

MM 6.5 Mon 11:15 SCH A 118

Modelling accelerated ion transport in porous metal organic frameworks — •THOMAS BERGLER^{1,2} and HARALD OBERHOFER^{1,2} — ¹University of Bayreuth — ²Bavarian Center for Battery Technologies

To date, metal organic frameworks (MOFs) have found a number of successful applications, for example in gas storage or as a filter for gas mixtures. So far, these mostly incorporated them as passive materials, but recent research points the way towards a more active role, possibly through the external manipulation of the materials's internal properties. One recent example for such a property is the susceptibility of the lattice parameters of multiple specific MOFs towards electric fields, which have been shown to distort on application of the fields. The aim of this project is to further investigate this behaviour from a theoretical point of view and gain insight into it through the use of molecular dynamics (MD) and meta-dynamics (MTD) simulations. These simulations are based on density functional theory (DFT) with the Perdew-Burke-Ernzerhof (PBE) functional but also on extended tight-binding (xTB) models and MOF-specialized force-fields. After confirmation that xTB-DFT and force-field MDs yield similar results to PBE-DFT MDs, MTDs have been performed with xTB-DFT to gain information on the energy-barriers for linker rotations inside some MOFs. Afterwards, MDs of multiple ps-length and an applied external E-field were performed with these force-fields to find the minimum strength of the E-field required to have an influence on the linker's rotation statistics.

15 min. break

MM 6.6 Mon 11:45 SCH A 118

Opposite in-plane anisotropy in thermal diffusivity and resistivity — •FEI SUN¹, SIMLI MISHRA¹, PHILIPPA MCGUINNESS¹, ZUZANNA FILIPIAK¹, IGOR MARKOVIC¹, DMITRY SOKOLOV¹, SEAN HARTNOLL², ANDREW MACKENZIE^{1,3}, and VERONIKA SUNKO⁴ — ¹MPI, CPFS, Dresden, Germany — ²Univ. of Cambridge, Cambridge, UK — ³Univ. of St Andrews, St Andrews, UK — ⁴UC Berkeley, California, USA

We report the temperature dependence of the anisotropic thermal and electrical transport in the orthorhombic bilayer ruthenate $Ca_3Ru_2O_7$. Measurements are performed using two bespoke experimental techniques: optical measurement of thermal diffusivity, and resistivity measurements on devices micro-structured using Focused Ion Beam (FIB) sculpting. Intriguingly, we find that the electrical conductivity is higher along the direction where thermal conductivity is lower at all temperatures. The mechanism underlying this unusual behavior will be discussed in this talk.

MM 6.7 Mon 12:00 SCH A 118

Non-local microwave electrostatics in ultra-pure $PdCoO_2$ — •GRAHAM BAKER¹, TIMOTHY W BRANCH¹, JAKE BOBOWSKI¹, JAMES DAY¹, DAVIDE VALENTINIS², MOHAMED OUDAH¹, PHILIPPA MCGUINNESS³, SEUNGHYUN KHIM³, PIOTR SURÓWKA⁴, YOSHITERU MAENO⁵, RODERICH MOESSNER⁶, JÖRG SCHMALIAN², ANDREW MACKENZIE³, and DOUG BONN¹ — ¹University of British Columbia — ²Karlsruhe Institute of Technology — ³Max Planck Institute for Chemical Physics of Solids — ⁴Wrocław University of Science and Technology — ⁵Kyoto University — ⁶Max Planck Institute for the Physics of Complex Systems

There has been significant recent interest in unconventional electronic transport regimes in which a local, Ohmic relationship between electric current and field breaks down. To date, the vast majority of experimental work has been done in the DC limit. Here we introduce a novel approach via AC measurements with a bespoke microwave spectrometer, using the skin effect rather than sample dimensions to induce non-local transport. Through measurements on Sr_2RuO_4 and Sn, we verify the predictions for the magnitude and frequency dependence of the surface resistance for the classical and anomalous skin effects. Data from $PdCoO_2$, in contrast, deviate from any previous prediction of frequency-dependent surface resistance. Analysis of such data required the construction of a more complete electrodynamic theory of metals than previously existed, and allows us to conclude that the $PdCoO_2$ data are due to the combination of a highly anisotropic Fermi surface and a contribution from momentum-conserving scattering.

MM 6.8 Mon 12:15 SCH A 118

Spin Hall effect in tungsten and tantalum via first-principles calculations — •REENA GUPTA, STEFANO SANVITO, and ANDREA DROGHETTI — School of Physics and CRANN, Trinity College, 2, Dublin, Ireland

We study theoretically the spin Hall effect (SHE), a phenomenon where a longitudinal charge current in a material sample gets converted into a transverse spin current and leads to spin accumulation on the sample boundaries. The common theoretical methods to calculate the intrinsic SHE conversion efficiency (i.e., the "spin Hall angle") are semi-classical or rely on the relaxation time approximation. To go beyond these limitations, we combine the non-equilibrium Green's function approach with Density Functional Theory. We study the SHE in bulk as well as slab geometries for different phases of tungsten and tantalum. We find values for the spin Hall angles, which are comparable to the most recent experimental results. Furthermore, in the slab geometries, we find that the spin Hall effect is accompanied by current-induced spin polarization (CISP). We then discuss the relative magnitude of the SHE and of CISP suggesting how the two effects can be distinguished in experiments.

MM 6.9 Mon 12:30 SCH A 118

Transport properties of Dirac materials: the role of plasmons — •KITINAN PONGSANGANGAN — TU Dresden, Dresden, Germany

We study the thermoelectric transport of Coulomb interacting Dirac electrons with Keldysh quantum field theory. We study it from a weak-coupling and a strong-coupling perspective. We demonstrate that long-range Coulomb interactions play two independent roles: (i) they provide the inelastic and momentum-conserving scattering mechanism that leads to fast local equilibration; (ii) they facilitate the emergence of collective excitations, for instance plasmons, that contribute to transport properties on equal footing with electrons. Our approach is based on an effective field theory of the collective field coupled to electrons. Within a conserving approximation for the coupled system we derive a set of coupled quantum-kinetic equations. This builds the foundation of the derivation of the Boltzmann equations for the interacting system of electrons and plasmons. From this, we explicitly derive all the conservation laws and identify the extra contributions of energy density and pressure from the plasmons. We demonstrate that plasmons show up in thermo-electric transport properties as well as in quantities that enter the energy-momentum tensor, such as the viscosity.

MM 6.10 Mon 12:45 SCH A 118

Dragging effect of the Berry curvature in ferromagnetic Weyl semimetals $NiMnSb$ and $PtMnSb$ — SUKRITI SINGH¹, •ANA GARCÍA-PAGE¹, JONATHAN NOKY¹, SUBHAJIT ROYCHOWDHURY¹, MAIA G. VERGNIORY^{1,2}, HORST BORRMANN¹, HANS-HENNING KLAUSS³, CLAUDIA FELSER¹, and CHANDRA SHEKHAR¹ — ¹Max-Planck-Institute for Chemical Physics of Solids, Dresden 01187, Germany — ²Donostia International Physics Center, Donostia-San Sebastián 20018, Spain — ³Institute for Solid State and Materials Physics, Technische Universität Dresden, Dresden 01069, Germany

The Anomalous Hall effect is a transport phenomenon in ferromagnets, which exhibit currents even in the absence of a magnetic field. Their inner magnetization breaks Time Reversal Symmetry, allowing the Berry Curvature (BC) to be finite. As a result, topological features close to the Fermi energy have a deep impact in the transport properties, leading to huge Anomalous Hall Conductivities (AHC). This has been a well-established paradigm for the last years for the linear AHC.

However, recent experimental results in the Weyl semimetals $NiMnSb$ and $PtMnSb$ might be pointing to something beyond it. By combining ab-initio calculations with a toy-model, we show that the steep slope-bands both compounds exhibit are capable of dragging the BC originated in Weyl nodes far away from the Fermi level, leading to a huge AHC in these compounds. We propose that this dragging effect of the BC can be generalized to the other materials exhibiting this band structure behaviour, which enriches the paradigm described above. Further research in this direction is currently being done.

MM 7: Invited Talk: Merkert

Time: Monday 15:00–15:30

Location: SCH A 251

Invited Talk

MM 7.1 Mon 15:00 SCH A 251

Molecular dynamics simulations of shock waves in alloys: Interplay of defects and phase transition — •NINA MERKERT — TU Clausthal, Germany

The study of materials under high-pressure conditions is essential not only for industrial activities but also for geological and astronomical applications. We consider iron and iron-carbon alloys showing a pressure induced phase transformation from the bcc to the hexagonal close-packed phase at around 13 GPa depending on the carbon content. We study compression waves in polycrystalline Fe and Fe-C using interatomic potentials that faithfully incorporate this phase transition at the desired equilibrium pressure.

Our simulations show that the phase transformation is preceded by plastic activity, leading to the so-called 3-wave structure: An elastic compression wave is followed by a plastic wave, which then leads to a phase-transformation front. We investigate the interplay of defects in bcc with the transformation process. These defects also influence the fracture (spallation) of the shocked iron samples.

Recently, we extended our results to high-entropy alloys (HEAs) that consist of equiatomic mixtures of five or more elements and are attracting increasing interest due to their promising material properties. We studied shock-induced spallation in HEAs and found exceptionally high spall strengths that are beneficial for high strain-rate applications.

MM 8: Development of Computational Methods: Diverse Topics and Machine Learning

Time: Monday 15:45–17:45

Location: SCH A 251

MM 8.1 Mon 15:45 SCH A 251

Adaptively Compressed Exchange in LAPW — •DAVIS ZAVICKIS, KRISTIAN KACARS, JANIS CIMURS, and ANDRIS GULANS — Electronic Structure Group, University of Latvia, Jelgavas st. 3, LV-1004, Riga, Latvia

We address precision and reproducibility issues in DFT calculations with hybrid functionals. Linearized augmented plane waves (LAPW) method currently serves as the de facto reference tool within the electronic structure community. In the current implementation of the Fock exchange in LAPW, the total and band energies depend on the number of orbitals used. We overcome these issues by implementing the adaptively compressed exchange (ACE) method [Lin Lin, J. Chem. Comput., 2016, 12, 5] in `exciting` code that introduces a low rank approximation and apply it to light atoms, molecules and solids [D. Zavickis et al., Phys. Rev. B., 2022, 106, 165101]. In case of atoms and molecules, we show that ACE leads to highly precise total energies which are within a few microhartrees off the results obtained by multi-resolution analysis method. In solids we calculate band structures that are compared with other all-electron hybrid implementations. Lastly, we apply optimizations and fine tuning to ACE, analyze its complexity and computational performance by comparing it to the previous Fock-exchange implementation in the `exciting` code.

MM 8.2 Mon 16:00 SCH A 251

How much laser power can two-photon 3D printed microoptics withstand? — •SEBASTIAN KLEIN, PAVEL RUCHKA, TOBIAS STEINLE, and HARALD GIESSEN — 4th Physics Institute and Research Center SCoPE, University of Stuttgart, Germany

In recent years, the manufacturing of small 3D printed microoptics has seen a rise in importance. 3D printed lenses are used for applications where space is of big concern. Tailored free form optics are ideally suited to improve the performance for specific use cases. New applications also include printing these optics onto optical fibers, for example for endoscopes in the biomedical field or for focusing a laser beam inside a compact fiber laser. In the latter case, the sustainability of high intensities of the pump laser is important. This is directly dependent on the maximum power the material of the lens can withstand.

In this work, we obtain a first insight into laser damage thresholds of the 2PP photoresist IP-S in the near-IR spectral range. We determine damage thresholds with femtosecond laser pulses for wavelengths in the range of 1550–2000 nm. We conduct these experiments on cube samples printed from IP-S and evaluate the damage of the exposed samples visually under a microscope, employing also differential interference contrast. The observed damage is mostly of thermal nature. Knowledge of damage thresholds of 3D printed micro-optics further pushes the applications to these limits, enabling high-power applications at safe operating intensities.

MM 8.3 Mon 16:15 SCH A 251

Molecular Dynamics Simulation of Selective Laser Melting — FABIO OELSCHLÄGER¹, AZAD GORGIS¹, DOMINIC KLEIN¹, SARAH MÜLLER², and •JOHANNES ROTH¹ — ¹FMQ, Universität Stuttgart, Germany — ²GSaME, Universität Stuttgart, Germany

Traditionally, manufacturing has been subtractive which means removing material from a workpiece. Additive manufacturing on the other hand is defined by successive addition of material and fusion with the help of heat for example. Here we report atomistic simulations of selective laser melting (SLM) used to produce additive manufactured objects. After a short introduction into the subject we present challenges to SLM. Next, modifications to basic molecular dynamics simulation are described which are required to simulate the annealing process. Although the sample sizes studied are already impressively large, scaling of system parameters are required to relate simulation and experiment. First

results from the study of single and rows of spheres will be reported and further developments and improvements will be addressed.

MM 8.4 Mon 16:30 SCH A 251

Exploring Enhanced Sampling Concepts based on Boltzmann Generators — •DAVID GRETEN, KARSTEN REUTER, and JOHANNES T. MARGRAF — FHI Theory Department, Berlin, DE

Computational surface science and catalysis research is still mainly conducted with static density functional theory (DFT) calculations. This approach is computationally convenient, but misses important aspects of surface chemistry, such as anharmonic free energy contributions. In principle, DFT-based molecular dynamics (MD) simulations (ideally combined with enhanced sampling algorithms) would allow a much more accurate description of these processes. Unfortunately, these are far too expensive to be routinely applied to complex surface/adsorbate systems. This is due to the fact that configurations in MD are generated sequentially. As a consequence, MD configurations are not statistically independent so that a very large number of samples is required to obtain converged ensemble properties. To overcome this limitation, Noé and co-workers recently proposed a generative machine learning model called the Boltzmann Generator, which was used to generate independent configurations of biomolecules. In this contribution, we explore how we can expand ML based sampling concepts utilizing Boltzmann Generators. In particular, training protocols and validation metrics will be discussed.

15 min. break

MM 8.5 Mon 17:00 SCH A 251

When does the Tamura model of phonon-isotope scattering break down? — •NAKIB PROTIK and CLAUDIA DRAXL — Institut für Physik and IRIS Adlershof, Humboldt-Universität zu Berlin, Berlin, Germany

A standard approach to the phonon-isotope scattering problem is the Tamura model [1]. This non-self-consistent 1st Born approximation of the scattering T-matrix expansion is exact for the low energy phonons, and higher order perturbative corrections for the higher energy, dispersive acoustic phonons have been argued to be small [1]. To our knowledge, the validity of this approach for the optic phonons has not yet been demonstrated. In this talk, we compare the Tamura model to the ab initio computed non-perturbative phonon-isotope scattering T-matrix for a set of well-studied materials. We show under what conditions the Tamura model breaks down.

[1] Tamura, S. I. (1983). Isotope scattering of dispersive phonons in Ge. Physical Review B, 27(2), 858.

MM 8.6 Mon 17:15 SCH A 251

Physics-inspired Machine Learning for Predicting Ionization Energies of Electronically Localized Systems — •KE CHEN^{1,2,3}, CHRISTIAN KUNKEL¹, BINGQING CHENG³, KARSTEN REUTER¹, and JOHANNES T. MARGRAF¹ — ¹Fritz-Haber-Institut der MPG, Berlin, Germany — ²Technische Universität München, Garching, Germany — ³Institute of Science and Technology, Klosterneuburg, Austria

Machine learning (ML) has been successfully applied to predict many chemical properties, most prominently energies and forces in molecules and materials. The strong interest in predicting energies in particular has led to a 'local energy'-based paradigm for modern chemical ML models, which ensures size extensivity and linear scaling of computational cost. However, some electronic properties (such as excitation energies or ionization potentials) are not size-extensive and may even be spatially localized. Using extensive models in these cases can lead to large errors. In this work, we explore different strategies for predicting intensive and localized properties, using ionization energies

in organic molecules as a test case. In particular, we compare size-intensive aggregation functions and effective, machine-learned Hamiltonians. The physical interpretability and cost/benefit ratios of the approaches will be discussed.

MM 8.7 Mon 17:30 SCH A 251

Kernel Charge Equilibration: Machine Learned Interatomic Potentials With Full Long-Range Electrostatics — •MARTIN VONDRAK, JOHANNES T. MARGRAF, and KARSTEN REUTER — Fritz Haber Institute of the Max Planck Society, Berlin, Germany

Machine learning (ML) techniques have recently been shown to bridge the gap between accurate first-principles methods and computationally cheap empirical potentials. This is achieved by learning a mapping between a systems structure its

physical properties. State-of-the-art models typically represent chemical structures in terms of local atomic environments to this end. This inevitably leads to the neglect of long-range interactions (most prominently electrostatics) and non-local phenomena (e.g. charge transfer), resulting in significant errors in the description of polar molecules and materials (particularly in non-isotropic environments). To overcome these issues, we recently proposed a ML framework for predicting charge distributions in molecules termed Kernel Charge Equilibration (kQEq). Here, atomic charges are derived from a physical model using environment-dependent atomic electronegativities. In this contributions, strategies for creating kQEq interatomic potentials are discussed, including the combination of short-ranged Gaussian Approximation Potentials with kQEq.

MM 9: Topical Session: Fundamentals of Fracture – Interface Fracture

Time: Monday 15:45–18:00

Location: SCH A 216

Topical Talk

MM 9.1 Mon 15:45 SCH A 216

Modeling of grain boundary embrittlement phenomena in metallic materials — •LORENZ ROMANER¹, ALEXANDER REICHMANN¹, CHRISTOPH DÖSINGER¹, TOBIAS SPITALER¹, DANIEL SCHEIBER², OLEG PEIL², MARKUS ALFREIDER¹, MICHAEL WURMSHUBER¹, and DANIEL KIENER¹ — ¹Department of Materials Science, Montanuniversität Leoben, 8700 Leoben, Austria. — ²Materials Center Leoben Forschung GmbH, 8700 Leoben Austria.

Intergranular embrittlement phenomena are of strong relevance for many technological materials including steels, nickel-based alloys, coinage metals or refractory metals. The decisive process is grain boundary segregation where solutes diffuse and enrich at grain boundaries thereby modifying their cohesive properties which can favor or impede crack propagation. We present a multi-scale simulation framework for grain boundary segregation employing atomistic, thermokinetic and data-driven computational methods and show how chemistry and propensity against crack propagation can be modeled from basic knowledge of composition and processing parameters. Validation examples with several experimental methods including atom probe tomography, high resolution transmission electron microscopy and micromechanical testing are presented. Furthermore, we discuss the potential of statistical learning methods to replace density functional theory simulations in future, in particular to address advanced phenomena such as concentration dependence and co-segregation.

MM 9.2 Mon 16:15 SCH A 216

Atomistic study of impurity-induced intergranular embrittlement in tungsten — •PÅR A. T. OLSSON^{1,2}, PRAVEENKUMAR HIREMATH², and SOLVEIG MELIN² — ¹Materials Science and Applied Mathematics, Malmö University, SE-205 06 Malmö, Sweden — ²Division of Mechanics, Materials & Components, Lund University, Box 118, SE-221 00 Lund, Sweden

In the present work we study the impact of phosphorus (P) impurities on the grain boundary strength of tungsten (W) by means of classical atomistic modelling to explore the role of impurities on the grain boundary (GB) embrittlement of W. To this end, we have fitted a new binary 2NN-MEAM potential for the W-P system that is designed to capture the embrittling potency of P in W GBs as predicted by means of density functional theory (DFT) modelling. Analysis of the GB work of separation and generalized stacking fault energy data derived from DFT and the 2NN-MEAM potential show that substitutional P-impurities reduce the resistance to both cleavage and slip. Mode I tensile and crack simulations reveal that the most dominant mode of GB failure is cleavage and that pristine GBs, which are initially ductile, on most accounts change to brittle upon introduction of impurities. Such tendencies are in line with experimentally observed correlations between P-impurity content and reduced ductility.

MM 9.3 Mon 16:30 SCH A 216

Characterization of the stability of metal/metal interfaces by atomistic simulations — •DANIEL F. URBAN, REYHANEH GHASSEMIZADEH, and CHRISTIAN ELSÄSSER — Fraunhofer Institute for Mechanics of Materials IWM, Freiburg, Germany

The reliable prediction of the adhesion and mechanical stability of interfaces between two metal phases from density functional theory (DFT) calculations remains a challenge. One possible approach to systematically address this issue is an idealized cleavage simulation analysed in terms of the Rose-Ferrante-Smith universal binding energy relationship (UBER) which results in a measure for the ideal work of separation and the maximum tolerable normal strain. Another approach is the study of the gamma surface, i.e. the generalized stacking fault energy, as function of lateral displacement, which yields information on the critical resolved shear stress of dislocation motion. Here we systematically study coherent [111]-oriented interfaces between fcc metals in terms of the above mentioned methods. We analyze the interface energy in terms of coupled tensile and shear displacements which include the effect of the tension softening of the interface. Furthermore, the influence of an additional lateral mechanical strain on the two phases, as often present in experimentally grown thin layers, is examined.

15 min. break

MM 9.4 Mon 17:00 SCH A 216

The heterogeneous nature of grain boundary segregation and embrittlement — •REMI DINGREVILLE — Sandia National Laboratories, Albuquerque NM, USA
Nanostructured materials are inherently unstable due to the high density of non-equilibrium defects that provide a substantial driving force for exaggerated or unexpected evolution. Departing from most mesoscale models for grain boundaries (GB), there is a clear recognition that GB properties, especially GB embrittlement and GB fracture, are not single-valued for a given material, but widely disparate depending on the configuration of the particular boundary and its neighboring grain. Taking this one step further, both GB character and GB defects control the GB embrittlement and fracture in response to mechanical, thermal, and irradiation stimuli. Each different type of stimuli perturb the GB character in distinctly different processes: e.g. stress causes elastic mismatch that tilts the energy barrier whereas strain drives specific dislocation content into the GB; non-implanting irradiation on the other hand creates local thermal spikes and atomic shuffling. In this presentation, I will discuss these effects on GB segregation and GB fracture properties from both a theoretical and atomistic perspectives.

Sandia National Laboratories is a multi-mission laboratory managed and operated by National Technology and Engineering Solutions of Sandia, LLC., a wholly owned subsidiary of Honeywell International, Inc., for the U.S. Department of Energy National Nuclear Security Administration under contract DE-NA0003525.

MM 9.5 Mon 17:15 SCH A 216

Modelling the grain boundary segregation of phosphorus in iron using thermodynamical approaches and Bayesian inference — •ALEXANDER REICHMANN¹, CHRISTOPH DÖSINGER¹, DANIEL SCHEIBER², OLEG PEIL², VSEVOLOD RAZUMOVSKIY², and LORENZ ROMANER¹ — ¹Department of Materials Science, Montanuniversität Leoben, Austria — ²Materials Center Leoben Forschung GmbH, Leoben, Austria

The chemistry and structure of grain boundaries (GBs) play a key role for understanding fracture in metallic alloys. Atomistic simulations provide a direct access to one of the key fundamental GB characteristics, the GB solute segregation energy. Experimentally, the solute segregation can be evaluated by measuring the GB solute concentration using a variety of techniques, one of which is the Auger electron spectroscopy. However, a direct comparison of experimentally measured GB solute excess and calculated GB segregation energy requires an additional step of conversion, which is a non-trivial task in many cases. As a result, calculated and measured data are not always found in good agreement with each other and often require an in-depth investigation. In this talk, we will present an approach for getting a consistent comparison between the calculated and experimentally measured data based on the Bayesian inference framework, which we use in combination with Markov chain Monte Carlo simulations for uncertainty quantification and model evaluation. We apply this framework to analyze phosphorus segregation in iron and evaluate theoretical and experimental data on GB excess.

MM 9.6 Mon 17:30 SCH A 216

Characterizing interface toughness in functional materials — •ELOHO OKOTETE¹, SUBIN LEE¹, STEFFEN BRINCKMANN², and CHRISTOPH KIRCHLECHNER¹ — ¹Institute for Applied Materials, Karlsruhe Institute of Technology, 76344 Eggenstein-Leopoldshafen, Germany — ²Structure and Function of Materials (IEK-2), Forschungszentrum Jülich, 52425 Jülich, Germany

Interfaces are the backbones of functionality in emerging material systems for this new age. However, mechanical failure usually occurs in these interfaces leading to degradation of functional properties. Experimental methods to investigate the interface strength and its failure mechanisms include peel test, super layer test, or indentation test. These methods output qualitative data with

huge experimental scatter and a lack of in-depth understanding of underlying mechanisms of failure. Small-scale mechanical testing using single and double cantilever beams makes it possible to extract quantitative data for interface properties of micro/ nanometer-sized films. However, these methods are prone to unstable crack growth, finite notch root radius, and other problems arising from testing geometries. In this talk, we propose a new micro cantilever design that provides reliable quantitative interface toughness. Our initial finite element calculations showed the optimized geometry could propagate a pre-notch in a stable manner, which is essential to generate a natural crack front without FIB-induced damage/artifacts. This observation is validated with in situ experiments on the interface between a hard coating and silicon substrate.

MM 9.7 Mon 17:45 SCH A 216

Abnormal internal oxidation of grain boundary and its cracking behavior under mechanical stress in an FeCr alloy — •KUAN DING¹, XIAO SHEN², SIYUAN ZHANG³, JIEJIE LI⁴, ENRICO BRUDER¹, JIANJUN LI⁴, WENWEN SONG², KARSTEN DURST¹, JAMES P. BEST³, and XUFEI FANG¹ — ¹Department of Materials and Earth Sciences, TU Darmstadt, 64287 Darmstadt, Germany — ²Steel Institute

(IEHK), RWTH Aachen University, 52072 Aachen, Germany — ³Max-Planck-Institut für Eisenforschung GmbH, 40237 Düsseldorf, Germany — ⁴School of Mechanical and Electrical Engineering, Central South University, 410083 Changsha, China

FeCr-based Ferritic stainless steels display great potential for applications as interconnects of solid oxide fuel cells at temperatures below 800 °C. Cr provides good oxidation resistance by forming a protective oxide layer to prevent the substrate from exposing to corrosive environment. However, grain boundaries (GBs) act as fast diffusion paths, and internal oxidation along the GB can form brittle oxide, which is prone to cracking under mechanical stresses. In this work, we investigated the abnormal growth of GB oxide at 600 °C in air and its impact on GB cracking in Fe-15wt.%Cr alloy. The microstructure and chemical characterization of the abnormal GB oxide revealed a layer of chromium oxide forming with a large penetration depth. To study the mechanical response, we conducted both ex-situ and in-situ micromechanical tests and simulation and observed the cracking behavior of the abnormal GB oxide. Our finding provides insights into improving the oxidation and fracture resistance through material design.

MM 10: Materials for Storage and Conversion of Energy: New Storage Materials

Time: Monday 15:45–16:45

Location: SCH A 215

MM 10.1 Mon 15:45 SCH A 215

Improving the cleanliness of TEM investigation of catalyst samples — •JULIA MENTEN¹, ROBERT SCHLÖGL^{1,2}, and WALID HETABA¹ — ¹Max Planck Institute for Chemical Energy Conversion, Mülheim an der Ruhr, Germany — ²Fritz Haber Institute of the Max Planck Society, Berlin, Germany

Transmission electron microscopy (TEM) offers a powerful tool for the analysis of specimens down to an atomic scale. In order to achieve high quality data, sample preparation is a crucial step. Many samples contain a high carbon content, e.g. as organic ligands or solvents. Electron beam exposure can lead to the deposition of carbon on the specimen surface and limit the image resolution and quality of obtained spectroscopic data. Different mitigation strategies can be applied in order to reduce contamination, though these methods can easily harm the specimens or lead to accumulation of carbonaceous molecules in the microscope environment [1].

In our work we focus on the removal of undesirable carbon species before the sample is inserted into the microscope. Our sample cleaning setup allows to investigate the influence of different preparation parameters, e.g. drying time or temperature, on how long solvents remain in the vacuum system and therefore can have an impact on the TEM analysis. Evaluation of the decrease in pressure while pumping our setup with a TEM sample gives insight in necessary drying times. The impact of our sample treatment can be investigated in the TEM by evaluating contrast and thickness measurements.

[1] Mitchell, *Micron* 73 (2015) 36-46

MM 10.2 Mon 16:00 SCH A 215

Ultrafast Electron Transfer in Photoexcited Fullerene-Derivatives — •MOHAMED E. MADJET, ADRIAN DOMINGUEZ-CASTRO, FULU ZHENG, and THOMAS FRAUENHEIM — Bremen Center for Computational Materials Science, University of Bremen, Bremen, Germany

Fullerene derivatives continue to attract a lot of interest both experimentally and theoretically. They have been known to be excellent electron acceptors due to their interesting ground and excited state properties. The chemical functionalization of fullerenes makes possible to synthesize and develop new compounds. These derivatives are used as building blocks for molecular complexes and devices with potential applications in solar cells, sensing and in biomedical applications. Using non-adiabatic molecular dynamics simulations combined with time-dependent density functional theory [1-3], we study the photoinduced electron dynamics and charge transfer processes in some fullerene derivatives upon a selective and localized excitation on the donor molecule. Results on hot electron dynamics, charge transfer and nonradiative recombination processes will be presented, discussed, and compared to the experimental results in [4].

[1] Madjet et al, *PRL* 126, 183002(2021) [2] Smith, Shakiba and Akimov,

J.Chem. Theory Comp. 17, 678 (2021). [3] Shakiba, Stippel and Akimov, *J. Chem. Theory Comp.*, in print (2022) [4] Julio R. Pinzo et al, *J. Am. Chem. Soc.* 131, 7727 (2009)

MM 10.3 Mon 16:15 SCH A 215

Carrier Multiplication in Transition Metal Dichalcogenides Beyond Threshold Limit — •YUXIANG LIU¹, THOMAS FRAUENHEIM¹, and CHIYUNG YAM² — ¹Bremen Center for Computational Materials Science, University of Bremen, Am Fallturm 1, 28359 Bremen, Germany — ²Shenzhen Institute for Advanced Study, University of Electronic Science and Technology of China, Shenzhen, 518000, China

Carrier multiplication (CM), multiexciton generation by absorbing a single photon. Beard et al. predicted that CM could overcome the Schokley-Queisser limit and raise solar cell efficiency to ~46%[1]. The current state-of-the-art nanomaterials including quantum dots and carbon nanotubes have demonstrated CM phenomenon, but not satisfactory owing to high threshold energy and inherent difficulties with carrier extraction. We found a below threshold limit CM in monolayer transition metal dichalcogenides (TMDCs) MX₂ (M = Mo, W; X = S, Se, Te). Surprisingly, the threshold energy of CM in monolayer TMDCs can be substantially reduced due to lattice vibrations. Electron-phonon couplings (EPC) could cause significant changes in electronic structures, even trigger semiconductor-metal transition, and eventually decrease the threshold energy of CM to less than twice bandgap[2]. Our results identify TMDCs as attractive candidate materials for efficient optoelectronic devices with the advantages of high photoconductivity and phonon-assisted tunable CM characteristics.

Reference [1] Beard, M. C., et al., *Acc. Chem. Res.*, 46, 1252–1260(2013). [2] Yuxiang L., et al., *Adv. Sci.*, 9, 2203400 (2022).

MM 10.4 Mon 16:30 SCH A 215

Vibronic quantum coherences in orthorhombic lead halide perovskite — •AJAY JHA^{1,2}, ZIHUI LIU⁵, VANDANA TIWARI², PABITRA NAYAK³, HENRY SNAITH³, XIAN-TING LIANG⁵, R. J. DWAYNE MILLER⁴, and HONG-GUANG DUAN⁵ — ¹Rosalind Franklin Institute, Didcot, UK — ²MPI-Structure and Dynamics of Matter, Hamburg, Germany — ³University of Oxford, Oxford, UK — ⁴University of Toronto, Toronto, Canada — ⁵Ningbo University, Ningbo, China

To unravel the quantum coherent dynamics in orthorhombic perovskite, we employ the ultrafast two-dimensional coherent spectroscopy in methylammonium lead iodide perovskite at 15 K. The data clearly resolve the exciton and carrier band in perovskite along with the interaction between exciton and carriers by observation of cross peaks. The ultrafast population transfer from charge carriers to exciton in perovskite is associated with the vibrational coherences. The nature and role of these coherences will be discussed in detail.

MM 11: Functional Materials: Performance, Reliability and Degradation

Time: Monday 17:00–18:15

Location: SCH A 215

MM 11.1 Mon 17:00 SCH A 215

Stability and electronic structure of NV centers at dislocation cores in diamond — •REYHANEH GHASSEMIZADEH, WOLFGANG KÖRNER, DANIEL F. URBAN, and CHRISTIAN ELSÄSSER — Fraunhofer Institute for Mechanics of Materials IWM, Freiburg, Germany

Due to its outstanding coherence properties, the negatively charged nitrogen-vacancy defect (NV center) in diamond is a promising system for quantum magnetometry and solid-state based quantum computing. However, its performance can be limited by the presence of crystal defects. We study the influence of dislocations on the stability and physical properties of the NV center within a density

functional theory analysis [1]. We model the most common dislocations in diamond, namely the 30° and 90° partial glide, and calculate the defect formation energy, structural geometry, electronic defect levels and zero-field splitting (ZFS) parameters. Our simulations reveal that dislocations potentially trap NV defects with an energy release of up to 3 eV. In general, the properties of NV centers at dislocations show strong deviations with respect to their bulk values. However, the lowest energy configuration of a NV center at the core of a 30° dislocation shows very bulk-like properties. Its electronic level spectrum is only slightly modified and ZFS values deviate less than 5% from their bulk values. These results open the perspective to align multiple NV centers along this dislocation type with a linear-chain arrangement whose collective behavior may become advantageous for quantum technology applications. [1] R. Ghassemizadeh et al., Phys. Rev. B 106, 174111 (2022)

MM 11.2 Mon 17:15 SCH A 215

First-principles calculation of electroacoustic properties of wurtzite (Al,Sc)N — •DANIEL F. URBAN¹, OLIVER AMBACHER², and CHRISTIAN ELSÄSSER¹ — ¹Fraunhofer Institute for Mechanics of Materials IWM, Freiburg, Germany — ²INATECH—Department of Sustainable Systems Engineering, University Freiburg, Germany

We study the electroacoustic properties of aluminum scandium nitride crystals Al_{1-x}Sc_xN with the metastable wurtzite structure by means of first-principles calculations based on density functional theory [1]. We extract the material property data relevant for electroacoustic device design, namely the full tensors of elastic and piezoelectric constants. Atomistic models were constructed and analyzed for a variety of Sc concentrations 0 ≤ x ≤ 50%. The functional dependence of the material properties on the scandium concentration was extracted by fitting the data obtained from an averaging procedure for different disordered atomic configurations. We give an explanation of the observed elastic softening and the extraordinary increase in piezoelectric response as a function of Sc content in terms of an element specific analysis of bond lengths and bond angles.

[1] D. F. Urban, O. Ambacher, and C. Elsässer, Phys. Rev. B 103, 115204 (2021)

MM 11.3 Mon 17:30 SCH A 215

Template-mediated well-defined nanostructure arrays for optical, electrical, and magnetic applications — •RUI XU¹, DENYS MAKAROV¹, and YONG LEI² — ¹Helmholtz-Zentrum Dresden-Rossendorf, Dresden, Germany — ²Ilmenau University of Technology, Ilmenau, Germany.

Advanced devices play a critical role for sustaining the ever-growing demands of our society for energy, information, health care, etc. To achieve high performance, devices with nanoscaled features are attracting more and more attentions by virtue of their unique and promising effects emerging at nanoscale. Structural design and engineering of materials provides a versatile platform to optimize the device performance and improve the commercial competitiveness. Regarding the structural engineering, controlling the geometrical parameters (i.e., size, shape, hetero-architecture, and spatial arrangement) of nanostructures have been the central aspects of investigations and practical applications. By using anodic aluminum oxide template, we realized well-defined controlling of nanostructures over the size, in-plane/out-of-plane shape, hetero-architecture, and spatial ar-

angement. With such well-defined nanostructures, the optical, electrical, and magnetic performance of nanodevices can be obviously enhanced.

MM 11.4 Mon 17:45 SCH A 215

Advantages of oxygen-free wire-arc sprayed titanium coatings — •MAIK SZAFARSKA¹, MANUEL RODRIGUEZ DIAZ², CORNELIUS BOEKHOFF¹, RENÉ GUSTUS¹, KAI MÖHWALD², HANS JÜRGEN MAIER², and WOLFGANG MAUS-FRIEDRICHS¹ — ¹TU Clausthal, Clausthal Centre of Material Technology — ²Leibniz Universität Hannover, Institut für Werkstoffkunde

Typically, thermal spraying is carried out in air, with compressed air acting as the cooling agent. However, the application of oxygen-affinitive materials like titanium is heavily influenced by the oxygen content in the atmosphere. Besides the impact on chemical composition, it can negatively influence the wetting behavior of the surface, the residual stress inside the coating and the formation of cracks and defects. Alternatives like cold gas spraying and vacuum plasma spraying grant only slight improvements coupled with an increased difficulty or cost for industrial use. Using silane-doped argon, it is possible to reduce the oxygen partial pressure to extremely low levels well below 10E-23 mbar. This makes application of wire-arc spraying possible for oxygen-affinitive materials like titanium. The titanium coatings feature a significantly reduced porosity caused by improved wetting behavior of titanium particles during the spraying process. Additionally, the coatings show extremely high adhesive tensile strengths compared to coatings formed in air. Discussed topics include particle formation, surface morphology and chemical composition, splat profiles, coating cross sections and interfacial diffusion between titanium coatings with iron-substrates.

MM 11.5 Mon 18:00 SCH A 215

Simulative study on crocheted fabrics via finite element method — •JAN LUKAS STORCK¹, DENNIS GERBER¹, LISKA STEENBOCK¹, and YORDAN KYOSEV² — ¹Bielefeld University of Applied Sciences, Bielefeld, Germany — ²Technische Universität Dresden, Dresden, Germany

Crochet is a rarely studied but very versatile textile technology. Industrial production of crochet does not yet exist but approaches to automation have recently emerged. In order to research the properties of crocheted fabrics by simulation, the finite element method (FEM) is well suited as a numerical approach due to the high complexity of the crochet structure. To the best of our knowledge, the FEM study presented here is the first one on the basic mechanical properties of crocheted fabrics [1]. A topology based key point model of an exemplary crocheted fabric at the meso scale was developed and studied with LS-DYNA (Livermore Software Technology Corporation). Displacements in the two textile directions (course and wale) revealed an even distribution of stresses in the fabric, whereby the stresses in course direction propagated faster. This and the differing stitch deformations show anisotropic properties. Such fast-calculating FEM simulations in combination with the developed flexible modelling can also be used in the future for engineering crocheted textiles for technical applications.

Reference [1]: J. L. Storck, D. Gerber, L. Steenbock, Y. Kyosev. Topology based modelling of crochet structures. Journal of Industrial Textiles, 2022, accepted, doi: 10.1177/15280837221139250.

MM 12: Poster I

Time: Monday 18:15–20:00

Location: P2/OG1+2

MM 12.1 Mon 18:15 P2/OG1+2

Time-of-Flight X-ray Photoelectron Microscopy (ToF-X-PEEM) — •G. SCHÖNHENSE¹, O. TKACH^{1,2}, O. FEDCHENKO¹, Y. LYTUVYENKO¹, D. VASILYEV¹, Q.L. NGUYEN³, T.R.F. PEIXOTO⁴, A. GŁOSKOVSKII⁴, S. CHERNOV⁴, M. HOESCH⁴, N. WIND^{4,5}, M. HEBER⁴, C. SCHLUETER⁴, C. SHARMA⁵, K. ROSSNAGEL^{4,5}, M. SCHOLZ⁴, and H.-J. ELMERS¹ — ¹Mainz Univ. — ²Sumy State Univ. — ³SLAC Nat. Accel. Lab., USA — ⁴DESY Hamburg — ⁵Kiel Univ.

The classical solution for photoelectron imaging in the X-ray range (X-PEEM) employs a hemispherical analyzer, as first described by Tonnerl. X-PEEM shows reduced spatial and energy resolution and notoriously low transmission, a consequence of the slits and small angular acceptance of the hemisphere. ToF-X-PEEM combines time-of-flight energy recording with a new lens optics minimizing spherical aberration. Systematic ray tracings predict a resolution in the (sub-) micron range, when a k-confining aperture array is placed in the second reciprocal plane, where the k-magnification can be zoomed in a large range. The new optics has been recently commissioned at PETRA-III (soft X-rays), studying ultrathin flakes and Moiré sandwich patterns of various transition-metal dichalcogenides. We demonstrate the high quality of deposited flakes by systematic ToF-X-PEEM characterization. Imaging large field of view >3mm with widened X-ray beam profile enables rapid chemical mapping with frame rates up to 1/s for strong core levels. Contracting the beam spot to <20mu and placing it on the desired flake allows small-area SX-ARPES employing the momentum-microscopy mode. [1] B.Tonner, NIMS A291, 60(1990)

MM 12.2 Mon 18:15 P2/OG1+2

Chlorine Corrosion of Superheater Steels — •MATTHIAS KROH, SEBASTIAN PENTZ, FERDINAND HAIDER, and GEORG KRUPKOV — Univ. Augsburg, Inst. f. Physik, 86159 Augsburg

During combustion in waste-incineration-plants a variety of chemical substances are released into the gas stream. Especially under the environment present in an incineration plant the active Chlorine-catalysed high temperature corrosion caused by released Cl₂ and HCl proves detrimental to the lifetime of heat exchanger tubes, which are essential for the power production. According to literature, Cl₂ is far more corrosive than HCl, but these studies were rather qualitative and do not reflect conditions like e.g. in a real power plant To simulate this process in a laboratory environment with realistic Cl-concentrations, a Chlorine generator was designed, which produces Cl₂ from a reaction of liquid NaOCl and H₂SO₄. The formed Chlorine concentrations were quantified via GCMS and UV VIS spectrometry to produce Cl₂ concentrations akin to those in real plants. In these experiments the corrosional attack of Cl₂ and of HCl on samples of a typical superheater steel was determined for various temperatures and defined gas atmospheres. Especially the influence of water and sulfur dioxide in the gas atmosphere were studied. The experimental setup is based on a horizontal furnace, containing the samples in a quartz tube, exposed to a flow of the desired gas atmosphere, and a subsequent gas analysis. Weight loss of the samples after removing reaction products as well as the morphology of the reaction zone are determined after various exposure times.

MM 12.3 Mon 18:15 P2/OG1+2

Nanoscale heat transport in heterostructures measured with UXRD at European XFEL — •JAN-ÉTIENNE PUDELL^{1,2,3}, MARC HERZOG², MAX MATTERN², JASMIN JARECKI², ALEXANDER VON REPPERT², ULRIKE BOESENBERG¹, ANGEL RODRIGUEZ-FERNANDEZ¹, WONHIUK JO¹, ROMAN SHAYDUK¹, WEI LU¹, GREGORY MALINOWSKI⁴, MICHEL HEHN⁴, MATIAS BARGHEER^{2,3}, and ANDERS MADSEN¹ — ¹European XFEL, Germany — ²Institut für Physik und Astronomie, Universität Potsdam, Germany — ³Helmholtz-Zentrum Berlin, Germany — ⁴Institut Jean Lamour, Université Lorraine, France

The transport of heat (or energy in general) in nanoscopic heterostructures is of great interest on a fundamental as well as a technological level, e.g. in the context of thermal management in devices or heat-assisted magnetic recording. In metal heterostructures, heat can be conducted by electrons that are in or out of equilibrium with lattice vibrations. Using ultrafast x-ray diffraction (UXRD), we investigate the influence of thin layers with high electron-phonon coupling on the thermal transport through a 100 nm Cu/Au layer sandwiched by thin Pt and Ni films on picosecond time scales after femtosecond laser excitation. The MID end-station at European XFEL is able to perform these time-resolved laser-pump x-ray-probe measurements to track the time dependence of the heat transport.

A time-dependent diffusive two temperature transport model reproduces our experimental data and thus verifies the efficient transport channel from the laser excited Pt-layer to the Ni-layer via hot electrons.

MM 12.4 Mon 18:15 P2/OG1+2

Structural evolution and atomic transport in severely deformed bi-metallic samples — •SHRADDHA V. SEVLIKAR, GERHARD WILDE, and SERGIY V. DIVINSKIY — Westfälische Wilhelms-Universität Münster, Institut für Materialphysik, Münster, Germany

Mechanical mixing, deformation-induced transport, and chemically-driven diffusion in layered bi-metallic Ni/Cr, Ni/Cu, Cu/Ag, and Cu/Au systems are investigated using scanning- and transmission electron microscopy, electron probe microanalysis and secondary ion mass spectroscopy. Alternatively, stacked Ni/Cr, Ni/Cu, Cu/Ag, and Cu/Au layers were subjected to room temperature high pressure torsion (HPT) using 10 and more revolutions. Atomic mixing is observed and discussed in terms of a high dislocation density, high concentration of non-equilibrium vacancies, and an impact of grain boundaries. The role of creep deformation is addressed by performing shear compression tests at selected temperatures on specially designed Ni or Cu samples with layers of Cr/Cu or Ag/Au deposited on the gauge sections. Mechanical mixing-induced recrystallization in the Cu-Au and Cu-Ag systems is observed and is discussed.

MM 12.5 Mon 18:15 P2/OG1+2

Study of Electron Transport in a DNA model — •JORGE CARDENAS-GAMBOA¹, JOSÉ GARCÍA², and SOLMAR VARELA^{1,3} — ¹Yachay Tech University, School of Chemical Sciences & Engineering, 100119-Urcuquí, Ecuador — ²Institut Català de Nanociència i Nanotecnologia (ICN2), 08193-Barcelona, España — ³Institute for Materials Science and Nanotechnology, Technische Universität Dresden, Dresden 01062, Germany

In this work, we use the Landauer-Buttiker formula as implemented in the package KWANT (Python library) for studying quantum transport in a DNA molecule based in an analytical tight-binding Hamiltonian recently developed. In our simulation, we used a Hamiltonian considering a kinetic term, a term for intrinsic Spin-Orbit (SO) interaction related to the atomic SO coupling, and a Rashba interaction due to the electric dipoles associated with hydrogen bonds between the bases of the double strand of DNA and we tested the effect of magnetic and no-magnetic leads in the spin-selectivity of the molecule. We obtained that in our model, the spin-orbit coupling associated with the molecule can not be enough to explain the spin selectivity, however, in a system with presence of ferromagnetic leads, enhance the spin selectivity when it is included, which could explain the selectivity observed in similar experiments.

MM 12.6 Mon 18:15 P2/OG1+2

Investigations on thermal contact conductance between filled polymer composites and solids using micro thermography — •OLIVER ROSER^{1,2}, ANDREAS GRIESINGER³, and OTHMAR MARTI² — ¹Center for Heat Management (ZFW), Stuttgart — ²Institute of Experimental Physics, Ulm University — ³Baden-Wuerttemberg Cooperative State University (DHBW) Stuttgart

When optimizing cooling paths in electronic devices, thermal interface materials (TIMs) are used to optimize the thermal transfer between two solid surfaces. TIMs are thermally conductive filled polymer composites with a complex microstructure. We investigated the intrinsic thermal conductivity of TIMs and the thermal contact conductance between TIMs and solid substrate surfaces using micro thermography. The physical principles of thermal transport when considering this kind of contact have not yet been investigated in detail and just a few experimental results are available. Most common measurement techniques determine a macroscopic conductance. Random surface and filler structures however, cause several variations and some specific effects on contact conductance, which need to be investigated on a microscale. With the utilized IR camera system, we can take pictures with a resolution of down to 14 microns per pixel. The

new method allows us to analyze the microscopic heat paths on the particle scale and to understand the physical principles of heat transport in contact zones of TIMs. The main parameters which affect the contact conductance were identified and will be presented in addition to comparisons to other measurement methods, and a microscale simulation approach.

MM 12.7 Mon 18:15 P2/OG1+2

Hydrogen Diffusion in High-Pressure Torsion (HPT) deformed Magnesium and Magnesium-alloys — •GEORGIA GUARDI¹, SABINE SCHLABACH^{1,2,3}, JULIA IVANISENKO^{2,3}, STEFAN WAGNER¹, and ASTRID PUNDT¹ — ¹Karlsruhe Institute of Technology, Institute for Applied Materials, Karlsruhe, Germany — ²Karlsruhe Institute of Technology, Institute of Nanotechnology, Karlsruhe, Germany — ³Karlsruhe Institute of Technology, Karlsruhe Nano Micro Facility, Karlsruhe, Germany

Magnesium is considered a promising material for solid-state Hydrogen storage due to the high achievable gravimetric density of 7.6 wt.% upon Magnesium Hydride (MgH_2) formation. There are however limitations to its practical application, mainly due to the low diffusion rate of Hydrogen in the Magnesium hydride phase, which leads to slow absorption kinetics. A possible way to improve hydrogen kinetics in Magnesium hydride is by increasing the volume fraction of grain boundaries, which can act as fast-diffusion pathways; this can be achieved in bulk samples by severe plastic deformation. In this work we use High-Pressure Torsion (HPT) to increase the grain boundaries concentration in bulk Mg and Mg-Zn-Zr alloys (ZK30 and ZK60) and we investigate how this affects hydrogen diffusion. The diffusivity of hydrogen in Magnesium is evaluated by gas volumetry at room temperature.

MM 12.8 Mon 18:15 P2/OG1+2

A systematic investigation of metastable phases in Niobium using density-functional theory — •SUSANNE KUNZMANN¹, GABI SCHIERNING¹, and ANNA GRÜNEBOHM² — ¹Universität Bielefeld, Germany — ²Ruhr-Universität Bochum

Although Niobium is a well studied transition metal, it exhibits anomalies such as type II superconductivity, unusual instabilities under pressure. Furthermore a martensitic phase transition has been reported, which is still under debate and raises questions concerning the source.

The present work attempts to approach these previously unexplained observations in a multifaceted manner. Using density functional theory we investigate low energy metastable phases, their instability against deformation and potential transition paths to bcc ground state for selected phases and the influence of Tantalum contamination. We find both A15 and Pnma phases to be potential candidates for distorted Niobium, as they are low in energy and we discuss a simple transition path with a low energy barrier for the latter.

MM 12.9 Mon 18:15 P2/OG1+2

Computational local point-based boundary conditions method for eigenfrequencies in microwave eccentric spherical cavities — •ZOYA EREMENKO¹, IGOR VOLOVICHEV¹, OLEKSIY BRESLAVETS¹, and GRIGORIOS ZOUROS² — ¹O. Ya. Usikov Inst. for Rad. & Electr. Nat. Acad. of Sci. of Ukraine Kharkiv, Ukraine — ²School of Electrical & Comp. Eng. Nat. Tech. Univ. of Athens, Athens, Greece

We have elaborated a new method for solving the electrodynamic problem for a resonant structure like a spherical cavity with a spherical dielectric inhomogeneity is randomly located without any limitations. The main feature of the method is the ability to satisfy the boundary conditions at the interface between two dielectric media at individual points located on these boundaries. There is no need to integrate and formulate boundary conditions for each basic mode, as it is usually done by classical methods for solving electrodynamic problems in the frequency domain. We carry out a numerical study to compute the eigenfrequencies in such eccentric configurations. We validate the results and compare the computational efficiency of our method with HFSS commercial software.

MM 12.10 Mon 18:15 P2/OG1+2

Machine learning force fields in VASP — •FERENC KARSAI¹, ANDREAS SINGRABER¹, JONATHAN LAHNSTEINER¹, RYOSUKE JINNOUCHI², and GEORG KRESSE² — ¹VASP Software GmbH, Sensengasse 8, Vienna, Austria — ²University of Vienna, Department of Physics, Kolingasse 14-16, Vienna, Austria

An efficient and robust method for on-the-fly machine learning force fields implemented into the Vienna Ab-initio Simulation Package (VASP) is presented. This method realizes the automatic generation of machine learning force fields on the basis of Bayesian inference during molecular-dynamics simulations, where the first-principles calculations are only executed when new configurations out of already sampled data sets appear. The power of the method is demonstrated in several applications such as e.g. melting points of ionic and covalent compounds, thermal transport in Zirconia, delta-learning of Carbon monoxide adsorbed on transition-metal surfaces and solid-solid phase transitions in perovskites. The applications show that during learning 99% of the ab-initio calculations are skipped. The implementation of our on-the-fly learning scheme is fully automatized and is mainly controlled by a few parameters. Hence one can optimally sample through a large phase space and the amount of human intervention for the usually laborious task of training is drastically reduced. Finally,

the calculations are accelerated by more than 4 orders of magnitude compared to ab initio, while the accuracy remains the same.

MM 12.11 Mon 18:15 P2/OG1+2

Structure prediction of iron hydrides at high pressures by machine-learned interatomic potentials — •HOSSEIN TAHMASBI¹, KUSHAL RAMAKRISHNA¹, MANI LOKAMANI¹, MANDY BETHKENHAGEN², and ATTILA CANGI¹ — ¹Center for Advanced Systems Understanding (CASUS), HZDR, Görlitz, Germany — ²CNRS, ENS de Lyon, Laboratoire de Géologie, Lyon, France

The structure and properties of iron hydrides under pressure have been of interest to geoscientists. At ambient conditions, there are no stable solid iron hydrides. Previous theoretical and experimental studies suggest that the double hcp phase of FeH is stable at low pressures with phase transitions to the hcp and fcc phases up to 80 and 140 GPa, respectively. Here, we present a theoretical investigation of the potential energy surfaces of FeH at high pressure. We construct a highly transferable machine-learned interatomic potential with a hierarchical approach using the PyFLAME code. Then, using this fast and accurate neural network potential, we systematically explore the potential energy surfaces of bulk structures of FeH by global sampling using the minima hopping method, to predict stable and metastable iron hydrides up to 200 GPa. We have carried out density functional theory calculations to refine the predicted structures and to evaluate the dynamical stability of selected structures as well. In an automated and systematic approach, we are going to show how a transferable machine-learned interatomic potential can be trained and validated using global optimization and analyze the phase diagram of the stoichiometric Fe-H system under pressure.

MM 12.12 Mon 18:15 P2/OG1+2

Machine Learning Interatomic Potentials for amorphous mesoporous metallosilicates — •JULIAN GREIF, KONSTANTIN GUBAEV, and BLAZEJ GRABOWSKI — Universität Stuttgart, D-70049, Stuttgart, Germany

Improving the efficiency of catalysis continues to be an important topic in modern chemistry. A promising approach currently under investigation is to utilize molecular catalysts in confined geometries. In the present project, we aim to model porous amorphous silica containing metal atoms on the pore surfaces that can act as co-catalysts. We conduct atomistic simulations using ab initio-trained machine learning potentials to obtain insights into the location of the metal atoms and the chemical configuration of hydrogen saturated surfaces in the silica structure. To that end, a potential capable of simulating the remelting of SiO₂ + Al was trained and checked on the bulk amorphous SiO₂-system against experimental data in terms of realistic densities, bond lengths and bond angles. Using this potential, new structures are then created by melting and quenching and a new potential is trained for simulations of mesoscale cells.

MM 12.13 Mon 18:15 P2/OG1+2

Deep learning for generation of optimal reaction environments — •RHYAN BARRETT¹ and JULIA WESTERMAYER² — ¹Leipzig University — ²Leipzig University

The design of reaction environments to reduce activation energies holds enormous potential for advancing many areas of chemical engineering but remains a difficult task due to the high combinatorial complexity of different conditions that influence a reaction. Herein, we use a cutting-edge deep learning model to enable the optimization of reactions. Initially we use a model to generate an abstract electrostatic field that reduces the activation barrier of a given reaction. We then look to optimize the ratio of continuum solvents to match the influence of the optimal electrostatic field generated by the model. The advantage of our method is that it is not limited to the initial solvent selection since any designed mixture will be compared with the global optimum electrostatic field produced by our model. The potential of the method will be demonstrated by optimization of the Claisen rearrangement reaction of allyl-p-tolyl ether and construction of an optimal environment but is generally applicable to any organic reaction.

MM 12.14 Mon 18:15 P2/OG1+2

Efficient graph neural networks for accurate interatomic potentials between surfaces and adsorbed atoms — •NIAN WU¹, FABIO PRIANTE¹, ERIC KRAMER ROSADO¹, and ADAM S FOSTER^{1,2} — ¹Department of Applied Physics, Aalto University, 00076, Espoo, Finland — ²WPI Nano Life Science Institute (WPI-NanoLSI), Kanazawa University, Kakuma-machi, Kanazawa 920-1192, Japan
Various advanced microscopy techniques have been developed to resolve molecular systems on surfaces with increasing resolution. However, 2D images representing 3D structures generally lead to missing information, making the interpretation of images challenging. Density functional theory (DFT) with explicit 3D structures offer a route to understanding through analyzing multiple molecular conformations, but the DFT is extremely computationally demanding. To address this issue, in this work we train a neural network potential to predict the interatomic interactions between adsorbates and surfaces as an efficient substitute for DFT calculations with decent accuracy. Firstly, we established a dataset of 2000 organic molecules adsorbed on the Cu(111) surface either in equilibrium or distorted, which includes total energy, atomic force, electrostatic potential,

and charge obtained by DFT calculations. And then, based on the small training dataset, we further developed a model on a basis of the NequIP framework, to predict forces. With the auxiliary information from charge and electrostatic potential, our modified model could reach state-of-the-art performance with forces mean absolute errors of ~1.0 meV/atom, comparable to DFT accuracy.

MM 12.15 Mon 18:15 P2/OG1+2

Investigation of bonding mechanism between early transition metals and antimony — •CAROLIN PETERSEN, CHRISTIAN STENZ, and MATTHIAS WUTTIG — I. Institute of Physics (IA), RWTH Aachen University

Using density functional theory (DFT) one can calculate the number of electron transferred (ET) and electron shared (ES) for crystalline materials. By plotting ET and ES for different materials on the x- and y- axes, the so-called bonding map is created. It can categorize the different bonding mechanisms, like covalent, ionic, metallic or metavalent and can predict properties such as the band gap, effective coordination number, electrical conductivity, or Born effective charge.

This algorithm works especially for crystalline s- and p-bonded materials. Due to the complexity of d-orbitals in early transition metals, it is unclear how to reasonably normalize ET in that case. The question is where such systems with bonding between d- and p-electrons are located in the bonding map. By examining the properties of such a material, the region in the bonding map can be identified reversely.

Therefore, TiSb is produced by co-sputter deposition and the amorphous phase is investigated by means of electrical transport, e.g. by Hall- and magneto-resistance measurements down to 2K. It is assumed that TiSb is an exotic metal and shows unconventional transport properties.

MM 12.16 Mon 18:15 P2/OG1+2

DFT structural characterization of β - and δ - intermetallic Al-Fe-Si phases — •NEBAHAT BULUT¹, HANKA BECKER², ANDREAS LEINWEBER², and JENS KORTUS¹ — ¹TU Bergakademie Freiberg, Institute of Theoretical Physics, Germany — ²TU Bergakademie Freiberg, Institute of Materials Science, Germany

The β -Al_{4.5}FeSi and δ -Al₃FeSi₂ phases are known stable phases of Fe-containing hypoeutectic Al-Si alloys. Despite the known stoichiometry of the β - and δ -phase the positions of the Al and Si atoms in these Al-Fe-Si intermetallic phases could not be uniquely determined experimentally. Therefore possible positions of Si atoms in these intermetallic phases were investigated using the density functional theory (DFT) code Quantum Espresso, which is based on plane waves and pseudopotentials [2]. For both β - and δ - phase different arrangements of Si atoms in the Al-Fe-Si intermetallics were considered. We compare the energies of these arrangements (1) relaxing the atomic positions keeping the unit cell volume constant and (2) fully relaxing atomic positions and unit cell shape and volume. As result we find that arrangements where the Si atoms are not nearest neighbours are energetically favored [2]. Further, we analyze the electronic structure and investigate the bonding.

[1] P. Giannozzi et al., J.Phys.Condens.Matter 21, 395502 (2009)

[2] Becker et al. J. Alloys and Comp. 911 (2022) 165015

MM 12.17 Mon 18:15 P2/OG1+2

A method for charge-sloshing free precise linear-scaling density-functional calculations — •RUDOLF ZELLER — Forschungszentrum Jülich and JARA, D-52425 Jülich, Germany

A fundamental problem for large-scale density-functional calculations is charge sloshing caused by the long-ranged Coulomb potential which necessitates that the number of self-consistency steps increases proportionally to the square of system length. To overcome this problem, Manninen et al. (1975) used a screened Coulomb potential to devise a real-space potential-mixing scheme which in reciprocal space is well-known as Kerker mixing.

It will be described how (1) this scheme works in the linear-scaling real-space code KKRnano which is part of the JuKKR code family developed at the research center Jülich, how (2) it can be turned into a real-space preconditioning method for potential mixing and how (3) it can be refined for excellent numerical performance.

Benchmark calculations will be presented for spin-orbit induced noncollinear magnetism in B20 MnGe and for a vacancy in Cu. It will be shown that the computing effort is drastically reduced, that the number of self-consistency steps does not increase with system size and that precise total-energy differences can be obtained even for supercells with more than 100000 atoms.

It should be noted that the method presented does not rely on using linear response or properties of the static dielectric matrix.

MM 12.18 Mon 18:15 P2/OG1+2

How to Train a Neural Network Potential — •ALEA MIAKO TOKITA^{1,2} and JÖRG BEHLER^{1,2} — ¹Lehrstuhl für Theoretische Chemie II, Ruhr-Universität Bochum, 44780 Bochum, Germany — ²Research Center Chemical Sciences and Sustainability, Research Alliance Ruhr, 44780 Bochum, Germany

High-Dimensional Neural Network Potentials (HDNNPs) provide potential energy surfaces (PESs) with the accuracy of electronic structure calculations at strongly reduced computational costs, which enables extended molecular dy-

namics simulations of large systems. They are trained on reference energy and force data to learn an approximate but accurate functional relation between the atomic structure and the PES. However, due to the non-physical functional form, which is shared with many other types of machine learning potentials, this training and the validation of the potential have to be done with great care. In this contribution the construction of HDNNPs will be explained step by step including a discussion of possible pitfalls and tricks of the trade.

MM 12.19 Mon 18:15 P2/OG1+2

PyRamanGUI: An open-source multi-purpose tool to analyze Raman spectra — •SIMON BREHM, CAMELIU HIMCINSCHI, JAKOB KRAUS, and JENS KORTUS — TU Bergakademie Freiberg, Germany

PyRamanGUI is a software tool which was developed to process and analyze Raman spectra. Available functionalities include smoothing, baseline correction, cosmic spikes removal, peak fitting, and multivariate statistical methods. Furthermore, it is possible to create workflows, which can be personalized and adapted. The application is designed as a graphical user interface (GUI), so no prior knowledge in programming is needed. The program is completely written in python and thus usable across different platforms. The source code is freely available on GitLab (<https://gitlab.com/brehmsi/PyRamanGUI>).

MM 12.20 Mon 18:15 P2/OG1+2

Non-contact friction on various material systems — •KIM LAMBERT¹, NIKLAS WEBER¹, MATTHIAS KRÜGER², and CYNTHIA VOKERT¹ — ¹Institut für Materialphysik, Friedrich-Hund-Platz 1, 37077 Göttingen — ²Institut für Theoretische Physik, Friedrich-Hund-Platz 1, 37077 Göttingen

To gain a deeper understanding of the origins of frictional losses and of how these connect to internal damping in the material, we investigate non-contact friction in various material systems, including graphene flakes and spinodal decomposed systems using AFM-based methods. A main goal of this work is to understand the degrees of freedom that contribute to energy dissipation and to identify the mechanisms contributing to non-contact friction.

For this purpose, we perform friction measurements on these systems under UHV and ambient conditions as well as with different dynamic AFM-based methods. Furthermore, we conduct experiments in contact mode to understand how the damping measured in non-contact is correlated with the energy dissipation measured in contact mode. These insights will be compared to the results of previous studies on [LaMnO₃]/[SrMnO₃]_n superlattices [1] as well as to theoretical studies on frictional damping via a theory of viscoelasticity [2].

[1] N. A. Weber et al., arXiv:2210.09677 [2] M. Lee et al., arXiv:2205.01151

MM 12.21 Mon 18:15 P2/OG1+2

Thermodynamical Stability Analysis of a Model Quasicrystal — •MORITZ HOLZWARTH, JOHANNES ROTH, and HANS-RAINER TREBIN — FMQ, Uni Stuttgart, Germany

The random tiling hypothesis, first proposed by Henley in 1991, states that quasicrystals are entropy-stabilized and, hence, are high temperature phases. We confirm the hypothesis for a two-dimensional Tübingen triangle tiling which arises in molecular dynamics simulations with a Lennard-Jones-Gauß potential, by investigating the temperature dependence of its two phason elastic constants λ_6 and λ_8 . These are the second derivatives of the free energy $F(\chi_6, \chi_8, T)$ with respect to the symmetrized phason strain modes χ_6 and χ_8 . At $T = 0$, F has a saddle point by descending along the χ_8 direction. Therefore, $\lambda_8 < 0$ characterizes the quasicrystal's initial instability. The configurational entropy due to phason flips turns F upwards at higher temperatures, reverses the sign of λ_8 and leads to a stable quasicrystal. We obtain this result by applying exclusively geometric methods in the form of the polar calculus, where the atomic domain (AD) is divided into sections for each vertex environment. We extend the calculus to a dynamic one by separating the AD into areas that characterize the different kinds of phason flips. By phasonic deformation of the AD, we can determine the types of flips and their frequency in dependence of phason strain, can perform energy relaxations by flips and compute the configurational entropy. We find that an important mechanism supporting the quasicrystal stability is the symmetric nearest neighbour coupling of phasonic flips.

MM 12.22 Mon 18:15 P2/OG1+2

Excitation-induced non-thermal effects in silicon — •SIMON KÜMMEL, DOMINIC KLEIN, and JOHANNES ROTH — FMQ University of Stuttgart, Germany
Ultra-fast laser excitation of silicon leads to highly non-linear, non-equilibrium effects in covalent materials. Especially the non-thermal melting in covalent materials like silicon has been observed in experiments. A rigorous explanation in the context of the induced macroscopic material dynamics during laser ablation is still missing. Here, we present novel results from laser ablation simulations taking this effect into account via an electron temperature-dependent interaction potential. We report non-thermal surface evaporation and pre-shockwave melting comparable to experimental investigations. Furthermore, we give more insight into non-thermal melting from electron temperature-dependent phase diagrams obtained from thermodynamic integration of the same electron temperature-dependent interaction potential.

MM 12.23 Mon 18:15 P2/OG1+2

Towards understanding the chemical bonding of unconventional metals — •CHRISTIAN STENZ, JOHANNES HOLTERS, and MATTHIAS WUTTIG — Institute of Physics IA, RWTH Aachen University, 52074 Aachen, Germany.

Solids can be distinguished based on their properties such as the band gap, effective coordination number, electrical conductivity, Born effective charge and so on. Based on these properties a classification into metallic, covalent, ionic and metavalent bonding seems appropriate. Metavalent bonding is a distinct bonding mechanism characterized by a competition between electron localization and electron delocalization. Chalcogenides like GeTe and Sb₂Te₃ and pnictides like Sb employ this bonding mechanism and can be characterized as 'incipient metals'. This raises the question if there are related metals, which are characterized by the same competition between electron localization and electron delocalization. We thus have been looking for such unconventional metals and focus on compounds of Te with transition metals. The overlap between Te p- and transition metal d- orbitals gives rise to a configuration which resembles the p-p σ -bond in incipient metals. Hence we are looking for related fingerprints such as soft, anharmonic bonds, an unconventional bond rupture and other characteristics which are found for incipient metals.

MM 12.24 Mon 18:15 P2/OG1+2

An efficiently automated method to sample the energies of grain boundaries — •TIMO SCHMALOFSKI¹, MARTIN KROLL^{2,3}, REBECCA JANISCH¹, and HOLGER DETTE³ — ¹ICAMS, Ruhr-University Bochum — ²Department of Mathematics, Physics, and Computer Science, University of Bayreuth — ³Department of Mathematics, Ruhr-University Bochum

Grain growth and microstructure evolution depend on the anisotropy of the energy of grain boundaries, which is a function of the five geometric degrees of freedom (DOF) of the grain boundaries. To access this parameter space in an efficient way and discover energy cusps in unexplored regions, a method was established, which combines atomistic simulations with statistical methods [1]. It has been successfully applied to sample the 2D subspace of GB plain inclinations for fixed misorientations. The poster explains the main features of the algorithm: Initial design, sequential design, the stopping criterion and the final interpolation of the energy. The algorithm draws its strengths from two aspects, the choice of the next point, which balances a homogeneous distribution of points with a precise sampling of the cusps, and the stopping criterion, which monitors the error of the prediction as well as the number of cusps which have been found. With these features, the method is able to outperform a regular high-throughput sampling.

MM 12.25 Mon 18:15 P2/OG1+2

Cubic scaling GW in the exciting code — •MANOAR HOSSAIN¹, ALEXANDER BUCCHERI¹, ANDRIS GULANS², and CLAUDIA DRAXL¹ — ¹Physics Department and IRIS Adlershof, Humboldt-Universität zu Berlin, Berlin Germany — ²Department of Physics, University of Latvia, Riga, Latvia

The GW approximation is the state-of-the-art method to incorporate many-body effects through the self-energy correction to the Kohn-Sham single-particle states. A serious drawback is that it becomes often computationally prohibitive due to its typical quartic dependence on system size. This restricts its use to systems with a few tens of atoms, highlighting the need to develop computationally efficient algorithms to extend the computation of the quasi-particle electronic structure to materials consisting of hundreds of atoms. In this work, we present a cubic-scaling algorithm implementation of the GW approximation in the exciting[1] code which is based on the linearized augmented plane-wave method. Our implementation employs the real-space imaginary-time formalism[2, 3] and relies heavily on Fast Fourier Transforms and efficient linear-algebra operations. To this extent we develop and make use of high-performance libraries, within the NOMAD CoE[4] with the aim to bring GW to exascale performance.

[1] A. Gulans, et al. J. Phys.: Condens. Matter 26, 363202 (2014).

[2] P. Liu, et al. Phys. Rev. B 94, 165109 (2016).

[3] A. L. Kutepov, et al. Comp. Phys. Commun. 219, 407 (2017).

[4] <https://nomad-coe.eu>

MM 12.26 Mon 18:15 P2/OG1+2

Physics Informed Neural Networks based Solvers for the Time-Dependent Schrödinger Equation — •KARAN SHAH and ATTILA CANGI — Center for Advanced Systems Understanding, Helmholtz-Zentrum Dresden-Rossendorf, Görlitz, Germany

We demonstrate the utility of Physics Informed Neural Network based solvers for the solution of the Time-Dependent Schrödinger Equation. We study the performance and generalisability of PINN solvers on a simple quantum system. The method developed here can be potentially extended as a surrogate model for Time-Dependent Density Functional Theory, enabling the simulation of large-scale calculations of electron dynamics in matter exposed to strong electromagnetic fields, high temperatures, and pressures.

MM 12.27 Mon 18:15 P2/OG1+2

High-throughput calculations for property maps of solids — •DANIELA IVANOVA¹, DANIEL WORTMANN¹, STEFAN BLÜGEL¹, MATTHIAS WUTTIG², and CARL-FRIEDRICH SCHÖN² — ¹Peter Grünberg Institute and Institute for Advanced Simulation, Forschungszentrum Jülich, Germany — ²Department of Physics, RWTH Aachen University, Aachen, Germany

Over the last two decades, high-throughput computations have become a vital pillar of the scientific research and development process in the field of computational science. In order to forecast material properties for larger sets of atomic configurations, Density Functional Theory (DFT) has been employed as an automated, robust, and highly-predictive first-principles approach. In this work, the DFT code Quantum ESPRESSO is deployed through the open source Automated Inter-active Infrastructure and Database for Computational Science AiDA framework. Aside from the existence of (1) covalent, (2) metallic, and (3) ionic bonding, as well as the two weaker forms of (4) hydrogen and (5) van der Waals bonding, compelling evidence has recently been found for another bonding mechanism in solids such as crystalline chalcogenides, termed as (6) 'metavalent bonding'. Effective mass calculations promise essential data for mapping distinctions between the bonding mechanisms along the materials data set chosen for high-throughput computing.

MM 12.28 Mon 18:15 P2/OG1+2

A high-level workflow-based approach towards the exploration of magnetocaloric Heusler alloys by automated high-throughput simulations — •SIMON BEKEMEIER¹, ALISA CHIRKOVA¹, and CHRISTIAN SCHRÖDER^{1,2} — ¹Bielefeld Institute for Applied Materials Research, FH Bielefeld — ²Faculty of Physics, Bielefeld University

Digitalization poses a huge chance to accelerate knowledge generation and materials discovery. Due to increasing computational capacities ever more materials data and simulations can be processed. Still the underlying processing and simulations often must be run by scientists manually, slowing down the digital process and hindering the useage of its full potential. One major issue is the translation between tools, to concatenate the tools required to transform given input data via several steps into the wanted output. We present one 'workflow' to calculate entropy change induced by the magnetocaloric effect starting from a description of the material under consideration. It consists of several simulation steps using different methods: from DFT, via spin dynamics simulation, to calculating the entropy change. It allows our group to perform high-throughput simulations but also enables exchange of simulation tools with other scientists, who otherwise need to develop and handle those tools themselves. Especially, experimentalists are enabled to use simulations to further enhance their knowledge generation process by extending their work with theoretical simulations on their own. Furthermore such a workflow opens doors to use AI methods to reveal relations, that were unknown before.

MM 12.29 Mon 18:15 P2/OG1+2

Ontology-Template-Based Description of Anisotropic Conductivity Measurements — •LENNART SCHWAN^{1,2}, MICHAEL FEIGE², MORITZ BLUHM³, BASIL ELL³, ANDREAS HÜTTEN², and SONJA SCHÖNING¹ — ¹Bielefeld Institute for Applied Materials Research (BIFAM), Bielefeld University of Applied Sciences, Department of Engineering Sciences — ²Thin Films & Physics of Nanostructures, Bielefeld University, Department of Physics — ³Semantic Computing Group, Bielefeld University, Faculty of Technology

Digitalization in materials science is an emerging field of research that opens up many new opportunities, e.g. in materials engineering. In particular, if large data sets of many experiments can be evaluated with the help of artificial intelligence. The more information about production, characterization, etc. can be recorded and processed in a machine-readable form, the greater the additional benefit.

A particular challenge is to transfer information that would be recorded in the classic lab book with a simple sketch into a machine-readable form, like the exact position of a measurement. However, this data is important for the evaluation of the experiment.

The application considered is the 3D printing of conductive nanosilver and the determination of the anisotropic electrical conductivity. We semantically describe printing process, environment parameters and characterization in an ontology to investigate dependencies of the conductivity. Therefore, we developed a template-based ontology engineering approach with OTTR templates, to add an abstraction layer to the common but very technical ontology engineering processes.

MM 12.30 Mon 18:15 P2/OG1+2

An Ontology of Magnetocaloric Materials Research — SIMON BEKEMEIER¹, MORITZ BLUM², LUANA CARON³, PHILIPP CIMIANO², BASIL ELL², INGA ENNEN³, MICHAEL FEIGE¹, THOMAS HILBIG¹, ANDREAS HÜTTEN³, GÜNTER REISS³, TAPAS SAMANTA³, SONJA SCHÖNING¹, CHRISTIAN SCHRÖDER^{1,3}, LENNART SCHWAN^{1,3}, and •MARTIN WORTMANN³ — ¹Bielefeld Institute for Applied Materials Research, University of Applied Sciences Bielefeld, Interaktion 1, Bielefeld, Germany — ²Faculty of Technology and CITEC, Inspiration 1, Bielefeld, Germany — ³Faculty of Physics, Bielefeld University, Germany

Magnetic refrigeration based on the magnetocaloric effect is an energy-saving and environmentally friendly alternative to compression based cooling. The cooling effect is based on the heat release or uptake during a magnetic phase-transitions of a magnetocaloric material that can be controlled by a magnetic field. The decades-long search for an alloy suitable for mass application could be made much more efficient by digitizing the scientific process chain. The research project DiProMag thus seeks to digitize the entire research procedure from the production and characterization of magnetocaloric materials to their theoretical description and prototypical application. For this purpose, an ontology - that is a structured representation of knowledge - was developed using a hierarchical template-based approach for the acquisition, semantic representation and abstraction of raw ontological data. The focus of the project is on the advancement of Heusler alloys, with Co₂CrAl serving as the first promising model system.

MM 12.31 Mon 18:15 P2/OG1+2

Laser processing of metal materials created by additive technologies. Optimization of structure and mechanical properties — •IRYNA GALSTIAN¹, EVGEN LEN¹, TOBIAS GUSTMANN², and NICOLE GEISSLER² — ¹G. V. Kurdyumov Institute for Metal Physics of the N.A.S.U. Kyiv, Ukraine — ²IFW Institute for Complex Materials. Dresden, Germany

In this work, the authors investigated the physical regularities of the structural-phase and chemical state formation in the volume of 3D printed titanium products consisting of several layers (surface layers of 3D printed alloys in the original and modified state and transition zones surface layers of 3D printed alloys in the original and modified state and transition zones) depending on the applied methods and regimes of obtaining and high-energy processing. The authors of the method provided a physical justification of the effectiveness of the combination of electron beam 3D printing with surface treatment by means of precision gas dynamic 3D printing and laser treatment. It has been established that this approach makes it possible to eliminate the main disadvantages of 3D-printed alloys, which are their structural imperfection, which causes low plasticity, fatigue strength and corrosion resistance. From a fundamental point of view, it allows to give a complete physical picture of the process of forming the structure and physical and mechanical properties of metal materials during 3D printing and to find ways of managing this process.

MM 12.32 Mon 18:15 P2/OG1+2

MD Simulation of 3D Laser Printing — •JONAS SCHMID, KEVIN VIETZ, DOMINIC KLEIN, and JOHANNES ROTH — FMQ University of Stuttgart, Stuttgart, Germany

While most people associate the manufacturing of metal parts with a CNC milling machine, the Fraunhofer Society developed an additive manufacturing process in 1995 which is based on laser melting of a metal powder. In this process, metal components are printed layer by layer, while the metal powder is fused onto the previous layer.

Our research focuses on developing molecular dynamics (MD) simulations of 3D laser printing in order to study defects such as gas pockets, cracks or structural irregularities caused by the manufacturing process. In contrast to finite element method calculations, MD simulations describe the highly non-equilibrium dynamics on an atomistic scale. This allows for a more physical interpretation while making less assumptions on the system.

In particular, our simulated system contains a three-dimensional multi-layer powder structure on a fixed ground surrounded by a protective gas. The simulation features laser absorption depending on atom density and atom type, as well as active cooling by using a different thermostat integrator for the ground layer. The overall goal of our research is to optimize the laser and powder properties to reduce defects and increase the stress resistance of the sample.

MM 12.33 Mon 18:15 P2/OG1+2

Molecular dynamics simulation of additive manufacturing: A highly non-equilibrated business — •KEVIN VIETZ, AZAD GORGIS, DOMINIC KLEIN, and JOHANNES ROTH — FMQ University of Stuttgart, Germany

Powder-bed additive manufacturing is a process that melts the powder with a laser beam, layer upon layer. By performing this melting-solidification process several times, one can build three-dimensional samples. This process is known as 3D printing. Up to now, most simulation studies on additive manufacturing rely on pure metals in vacuum. To fill this gap, we investigate the influence of argon gas on pure metals and explore the suitability of binary alloys for various initial cluster structures, such as core-shell-clusters. We perform large-scale molecular dynamics simulations to depict the highly non-equilibrium material dynamics and evaluate our results by analyzing defects and properties on microscopic and macroscopic scales. Results show that the argon gas stabilizes the system and new material compositions could enhance the variety of applicable materials for additive manufacturing.

MM 12.34 Mon 18:15 P2/OG1+2

Atomistic simulations of crack-tip interface interactions in lamellar TiAl microstructures — •ONUR CAN SEN and REBECCA JANISCH — ICAMS, Ruhr-University Bochum, Germany

Molecular dynamics simulations are an excellent tool for understanding crack-tip interactions in interface-dominated microstructures, but the simulation setup can affect the predicted behavior as there are many degrees of freedom. To shed light on this and at the same time to understand the impact of the specific interface structure, a systematic study of crack-tip interface interactions in nanolamellar two-phase TiAl was carried out. To separate microstructure and crack geometry influences, the type of interface, crack configuration, and loading direction were varied in these simulations. Results show that the semi-coherent γ -pseudo twin interface is the strongest barrier for the crack propagation while the coherent true twin interface is the weakest. The analysis of the contributing factors shows, that the crack orientation has more influence on the crack evolution than the crack aspect ratio. The effect of the individual interfaces can be quantified by calculating their shielding effects, but as it turns out this effect is strongly dependent on the crack configuration. However, regardless of the crack configurations, the coherent γ -true twin interface appears to be the most effective interface in terms of shielding.

MM 12.35 Mon 18:15 P2/OG1+2

Overview of Crack-Heterogeneity Interactions at the Atomic Scale — •LEON PYKA¹, TARAKESHWAR LAKSHMIPATHY², and ERIK BITZEK² — ¹Friedrich-Alexander-Universität Erlangen-Nürnberg, Germany — ²Department Computational Materials Design, Max-Planck-Institut für Eisenforschung GmbH, Düsseldorf, Germany

The study of nano- and microstructure is crucially important for creating materials with more favorable mechanical properties. Specifically in the design of fracture resistant materials, the interaction of cracks with other heterogeneities plays a vital role. In this regard classical atomistic simulations are beneficial. They allow us to gain information on crack-heterogeneity interactions, some of which require sample sizes too large for more accurate electronic structure methods. This information can then be used to improve meso- and continuum-scale models.

We provide an overview of a variety of crack-heterogeneity interactions studied at the atomic scale and their relation to established models. Some simulations of cracks interacting with heterogeneities are also performed using a nearest neighbour "snapping-spring" harmonic potential. In addition to providing material-generic insights, due to the linear interatomic force interactions such potentials allow for direct comparisons with continuum models based on linear elasticity.

MM 12.36 Mon 18:15 P2/OG1+2
Fracture surface energy of glasses obtained from crystalline structure and bond energy data — •MARCO HOLZER¹, TINA WAURISCHK¹, JANINE GEORGE^{1,2}, ROBERT MAASS^{1,3}, and RALF MÜLLER¹ — ¹Bundesanstalt für Materialforschung und -prüfung (BAM), Berlin, Germany — ²Institute of Condensed Matter Theory and Solid-State Optics at Friedrich Schiller University, Jena, Germany — ³Department of Materials Science and Engineering at University of Illinois, Urbana-Champaign, USA

Extending our earlier work on nucleation and surface energies [1], we present a simple approach for predicting the fracture surface energy (γ) of oxide glasses using readily available crystallographic structure data and diatomic bond energies. The proposed method assumes that (γ) of a glass equals the surface fracture energy of the weakest fracture (cleavage) plane of the isochemical crystal. For non-isochemically crystallizing glasses, an average (γ) is calculated from the weighed fracture energy data of the constitutional crystal phases according to Conrad [2]. Our predictions yield good agreement with the glass density- and chemical bond energy-based prediction model of Rouxel [3] and with experimentally obtained (γ) values known at present. [1] C. Tieleman, S. Reinsch, R. Maass, J. Deubener, R. Müller, J. Non-Cryst. Solids 2022, 14, 100093 [2] R. Conrad, J. Non-Cryst. Solids 2004, 345-346, 16 [3] R., Tanguy, Scripta Materialia 2017, 109-13, 137

MM 12.37 Mon 18:15 P2/OG1+2

An in situ crack detection approach in additive manufacturing based on acoustic emission and machine learning — •VIKTORIA NIKONOVA¹, DENYS KONONENKO¹, DMITRY CHERNYAVSKY¹, MIKHAIL SELEZNEV², and JEROEN VAN DEN BRINK^{1,3} — ¹Institute for Theoretical Solid State Physics, IFW Dresden, 01069 Dresden, Germany — ²Institute of Materials Engineering, Technische Universität Bergakademie Freiberg, Gustav-Zeuner-Straße 5, D-09599, Freiberg, Germany — ³Institute for Theoretical Physics, TU Dresden, 01069 Dresden, Germany

Laser Powder Bed Fusion (LPBF) is a state-of-the-art solution for producing metal elements with complex shapes in various industries, from automotive to aerospace. One of the crucial practical drawbacks of LPBF is the presence of structural defects in the printed part, especially cracks. Here we propose an in situ monitoring system of cracks formation during the LPBF process utilizing acoustic emission and machine learning. We demonstrate that the representation of acoustic emission events in the space of principal components (PC) of the spectra yields a robust differentiation of crack events from the noise bursts. The ML classification algorithms achieve high accuracy of ~99 % for the PC-based descriptors. The presented approach advances the method of in situ quality control systems and brings it closer to practical implementations.

MM 13: Invited Talk: Sinclair

Time: Tuesday 9:30–10:00

Location: SCH A 251

Invited Talk MM 13.1 Tue 9:30 SCH A 251
Exploring the Slow Dynamics of Interfaces and Glasses via Markov State Models — SIAVASH SOLTANI¹, JOERG RÖTTLER^{2,3}, and •CHAD SINCLAIR¹ — ¹Department of Materials Engineering, The University of British Columbia, Vancouver, BC, Canada V6T 1Z4 — ²Department of Physics and Astronomy, The University of British Columbia, Vancouver, BC, Canada V6T 1Z1 — ³Stewart Blusson Quantum Matter Institute, The University of British Columbia, Vancouver, BC, Canada V6T 1Z4

A persistent challenge for molecular simulations is to assess slow processes efficiently from short trajectories. Important examples of slow phenomena in materials are the motion of interfaces in alloy crystals or the structural relaxation

in glass forming liquids. Markov State Models (MSM) are an attractive tool to unveil the slowest processes of a complex atomistic system in a low dimensional space of feature variables. This talk describes the predictions and insights gained from such MSMs constructed using machine learning techniques. For grain boundaries, the model learns a hierarchy of timescales associated with transformations between geometrically distinct motifs. When applied to a binary glass former, our model finds a transition timescale between states that is larger than the conventional structural α -relaxation time. In both systems, the MSMs are able to access kinetics at temperatures where brute force calculations become computationally expensive or impossible.

MM 14: Development of Computational Methods: Thermodynamics and Local Chemistry, Electronic Structure

Time: Tuesday 10:15–13:00

Location: SCH A 251

MM 14.1 Tue 10:15 SCH A 251
Performance of pseudopotentials in chemically diverse materials — •ANDRIS GULANS¹ and STEFAN GOEDECKER² — ¹University of Latvia, Riga, Latvia — ²University of Basel, Switzerland

We present a novel framework for assessing quality of pseudopotentials. It comprises a database of atomization energies and new highly precise norm-conserving pseudopotentials. The database covers more than 700 molecules with 65 elements from six rows of the periodic table. It accounts for chemical diversity by considering every atom in a variety of oxidation states. For each molecule, we provide highly precise scalar-relativistic atomization energies obtained with lin-

earized augmented plane waves obtained using PBE exchange-correlation functionals. The new pseudopotentials reproduce the reference data within the chemical accuracy limit of 1 kcal/mol. They are crucial for assessing other pseudopotentials, as we use them for decomposing the total error in atomization energies into individual atomic contributions. Our calculations reveal that even state-of-the-art pseudopotential families are still not fully compliant with chemical accuracy, and the largest errors arise in molecules with atoms in high oxidation states.

MM 14.2 Tue 10:30 SCH A 251

Pushing to the limits of machine-learning potentials for high-entropy alloys — •KONSTANTIN GUBAEV, VICTOR ZAVERKIN, PRASHANTH SRINIVASAN, and BLAZEJ GRABOWSKI — University Stuttgart

Chemically complex multicomponent alloys have garnered widespread interest owing to their exceptional properties coming from a sheer inexhaustible compositional space. The complexity poses severe challenges for atomistic modelling and interatomic potential development. Here, we explore the limits of two complementary state-of-the-art machine-learned potentials—the moment tensor potential (MTP) and the Gaussian moment neural network (GM-NN)—in simultaneously describing both the configurational *and* vibrational degrees of freedom in the prototype Ta-V-Cr-W alloy family. Both models are equally accurate with exceptional performance in comparison to classical potentials. A single potential is able to achieve root-mean-square-errors of 1.37-4.35 meV/atom and 0.023-0.057 eV/Å in 0 K energies and forces, respectively, across all subsystems of the alloy family, and 0.156-0.179 eV/Å in high-temperature molecular dynamics forces for the disordered quaternary. MTPs achieve faster convergence with the training size than the GM-NNs, whereas GM-NNs are faster in execution. Active learning is partially beneficial and has to be complemented with a conventional human-based training set generation.

MM 14.3 Tue 10:45 SCH A 251

Extracting free energies from local composition fluctuations in solids: Theoretical background and atomistic simulations — DANIEL BITTER¹, MARVIN POUL², GUIDO SCHMITZ¹, and •SEBASTIAN EICH¹ — ¹Institute of Materials Science, University of Stuttgart, Heisenbergstraße 3, D-70569 Stuttgart, Germany — ²Max-Planck-Institut für Eisenforschung GmbH, Max-Planck-Straße 1, D-40237 Düsseldorf, Germany

While thermodynamic fluctuation theory has been applied to liquids for decades in order to obtain direct thermodynamic information, i.e. Gibbs free energies, from local composition fluctuations, the present work offers an extension for the application in solids. It is demonstrated that composition fluctuations are affected by an additional elastic work term which arises only in solids, thus covering liquids as a special case. The extended fluctuation model is verified through atomistic simulations in an exemplary Cu-Ni embedded-atom system for which Monte Carlo simulations have been carried out in the semi-grandcanonical ensemble at fixed temperature over the entire composition range. Composition fluctuations were monitored in a subvolume over time and statistically evaluated in terms of the variance, demonstrating perfect agreement with the prediction from the extended model. This method has been developed primarily for the application to experimental atom probe data, where three-dimensional chemical information is available with sub-nanometer accuracy, allowing a direct measurement of local composition fluctuations to extract thermodynamic information.

MM 14.4 Tue 11:00 SCH A 251

Extracting free energies from local composition fluctuations in solids: Application on the atom probe data obtained from TAPSim simulations — •JIANSHU ZHENG¹, MARVIN POUL², and SEBASTIAN EICH¹ — ¹Institute of Materials Science, University of Stuttgart, Heisenbergstr. 3, D-70569 Stuttgart, Germany — ²Max-Planck-Institute für Eisenforschung GmbH, Max-Planck-Straße 1, D-40237 Düsseldorf, Germany

This work proposes a novel methodology to extract direct thermodynamic information, i.e. Gibbs free energies, from local composition fluctuations found in atom probe data based on statistical mechanics. The proof-of-concept is demonstrated with an exemplary simulated Cu-Ni alloy, which has first been equilibrated using Monte Carlo techniques with an embedded-atom potential and subsequently field evaporated by TAPSim[1]. It is shown that the variance of the local composition on the reconstructed data reveals a significant dependence on the size of the chosen (sub-) volume used for the evaluation, but nevertheless the extrapolation to an infinitely large volume unveils a remarkable link to the curvature of the Gibbs free energy. Given the composition range is explored at several points, the Gibbs excess free energy of mixing could be recovered in a CALPHAD-style parametrization. This methodology promises to improve the accuracy of thermodynamic information from direct atom probe measurements. [1] C. Oberdorfer, S.M. Eich, G. Schmitz. *Ultramicroscopy* 128, (2013), 55.

MM 14.5 Tue 11:15 SCH A 251

A general-purpose framework for kinetic Monte-Carlo simulations — •ROYA EBRAHIMI VIAND and SEBASTIAN MATERA — Fritz Haber Institute of the Max Planck Society, Berlin, Germany

The kinetic Monte Carlo (kMC) method has gained popularity in the last years for the simulation of problems whose dynamics are controlled by rare events. Applications range from atomic-scale models for heterogeneous catalysis or charge transport to disease modeling, and a number of specialized codes have been developed for different classes of models. However, specialization is often the bottleneck when trying to extend the codes to a more general setting or to implement new algorithms. We present our first steps towards a flexible general-purpose framework for implementing kMC models to overcome these limita-

tions. This assumes nothing more than that the model can be regarded as a continuous time, discrete state Markov process, which is common among all kMC models. The specific physical model must be provided by the user in terms of update functions for the transition rates of the different possible elementary processes. Besides illustrating the usage on simple and well investigated models, we demonstrate how the tool can be used to implement models with long range interactions, e.g., for the simulation of charge transport in solid materials.

15 min. break

MM 14.6 Tue 11:45 SCH A 251

Pressure-driven tunable properties of the small-gap chalcopyrite topological quantum material ZnGeSb₂: A first-principles study — •SURASREE SADHUKHAN¹, BANASREE SADHUKHAN², and SUDIPTA KANUNGO¹ — ¹Indian Institute of Technology Goa, 403401 Ponda, India — ²KTH Royal Institute of Technology, Stockholm

Search for new topological quantum materials is the demand to achieve substantial growth topological phase of matter. In this search process, theoretical prediction is crucial besides the obvious experimental verification. The divination of topological properties in already well-known narrow gap semiconductors is flourishing in quantum material science. We revisited the semiconductor compound in the chalcopyrite series, some of which were potential topological materials. Using this density functional theory-based first-principles calculations, we report a strong topologically nontrivial phase in chalcopyrite ZnGeSb₂, which can act as a model system of strained HgTe. The estimates reveal the non-zero topological invariant (Z_2), Dirac cone crossing in the surface spectral functions with spin-momentum locked spin texture. We also report the tunable topological properties from nontrivial to trivial phases under moderate hydrostatic pressure within *7 GPa. A minor modification of a lattice parameter is enough to achieve this topological phase transition easily accomplished in an experimental lab. We have incorporated the discontinuity in the tetragonal distortion of non-centrosymmetric ZnGeSb₂ to drive the topological quantum phase transition.

MM 14.7 Tue 12:00 SCH A 251

electronic structure of a non-symmorphic kondo lattice system CeAgSb₂ — •SAWANI DATTA¹, KHADIZA ALI², RAHUL VERMA¹, SAROJ P. DASH², BAHADUR SINGH¹, ARUMUGAM THAMIZHAVEL¹, and KALOBARAN MAITI¹ — ¹Tata institute of fundamental research, Mumbai, India — ²Chalmers university of technology, Goteborg, Sweden

Topological Dirac semimetal with non-symmorphic symmetry (NSS) is one of the most recent discoveries in the field of novel topological quantum materials [1]. The uniqueness of this system is the presence of robust (including spin-orbit coupling) Dirac line nodes with NSS protection. CeAgSb₂, a Kondo system, exhibits a large anisotropic resistivity and a complex magnetic ground state at a lower temperature [2]. Employing angle-resolved photoemission spectroscopy (ARPES), we find that CeAgSb₂ possesses several non-trivial crossings near the Fermi level protected by the NSS. The ARPES data collected at different photon energies suggest a quasi-2-D behavior which is consistent with the transport results. In addition, we observe energy bands of the surface states in the near-Fermi-level region along with the non-trivial bulk bands that make the electronic structure complex. Our study shows the CeAgSb₂ family of materials as a new platform to study the robust non-symmorphic symmetry-protected Dirac semimetallic systems with high spin-orbit coupling.

[1] L. M. Schoop et. al., *Nat. Commun.* 7, 11696 (2016). [2] Y. Inada et. al., *Philos. Mag. B*, 82, 1867 (2002).

MM 14.8 Tue 12:15 SCH A 251

An amplitude expansion of magnetic phase field crystal: A continuum model for magnetically driven dislocation networks — •RAINER BACKOFEN, MARCO SALVALAGLIO, and AXEL VOIGT — Institute of Scientific Computing, TU Dresden

The amplitude expansion of the phase-field-crystal (APFC) model enables a convenient coarse-grained description of crystalline structures. It allows the description of length scales that are orders of magnitude larger than the lattice spacing while retaining microscopic features, such as dislocations. Adaptive finite elements are used to treat the different involved length scales efficiently [1].

Here, an APFC model is presented that captures the basic physics of magnetostructural interactions: magnetostriction and magnetic anisotropy. The free energy of APFC is combined with a continuum field representing local magnetization [2]. The proposed coupling does not increase the partial differential equation to solve compared with the basic APFC model. Still, it is flexible enough to adapt the magnetic anisotropy of the model to basic ferromagnetic materials such as Fe and Ni. Exploiting this model, the influence of external magnetic fields on the evolution of defects and grain boundaries is discussed.

[1] Salvalaglio, Backofen, Voigt (2018) *PRMat*, 2(5), 053804. [2] Backofen, Salvalaglio, Voigt (2022) *Model Simul Mat Sci Eng*

MM 14.9 Tue 12:30 SCH A 251

Multi-orbital models within the ghost Gutzwiller approximation — •CARLOS MEJUTO-ZAERA and MICHELE FABRIZIO — SISSA, Trieste, Italy

In the pursuit towards targeted material design leveraging strong electronic correlation, computationally inexpensive yet qualitatively reliable methods play a fundamental role. These approaches should allow for a rapid mapping of phase space, unveiling a first impression of possible phases of matter, which can then be explored in selected regions of parameter space with more accurate yet involved techniques. Recently, the ghost Gutzwiller Approximation (gGA) has been shown to be an interesting candidate for this kind of phenomenological search. Based on a self-consistency condition for the simple one-body reduced density matrix of a discretized impurity model, this method can capture spectral features of both coherent and incoherent nature in the one-body Green's function. In this work we extend its applicability to the multi-orbital regime employing a truncated solver based on selected configuration interaction. This allows for increasing the number of correlated orbitals while keeping the size ratio of bath to impurity constant. We explore the reliability of the gGA for describing the phase diagram of multi-band models, comparing to more sophisticated embedding methods. We shall assess the potential of gGA for modelling of complex materials, possibly in combination with ab-initio methods.

MM 14.10 Tue 12:45 SCH A 251

Understanding the success of mGGAs for band gaps. Is it the orbital dependence? — •PÉTER KOVÁCS, PETER BLAHA, and GEORG K. H. MADSEN — Institute of Materials Chemistry, Technical University of Vienna

Density functional theory has shown remarkable success in predicting various properties of solids, such as lattice parameters and cohesive energies, yet with most functionals it is known to heavily underestimate band gaps. mGGA functionals tend to result in better band gap predictions than LDA or GGAs, but the best results are still achieved at the cost of accuracy for the other properties. Recently using a systematic search in the space of mGGA functionals we were able to find functionals, where this tradeoff is small. [Péter Kovács et al., J. Chem. Phys. 157, 094110 (2022)]

While the failure of LDA and GGA functionals for gaps are often attributed to their lack of the derivative discontinuity, the success of mGGAs can not be explained solely based on their ability to exhibit discontinuous behaviour. On a database of 440 solids, we analyze how two specialized functionals, TASK and our own mGGA23, are able to better predict gaps. We aim to understand what parts of the functional shape is responsible for their success and how these affect their prediction of structural properties, such as lattice parameter. These findings can be used in functional design and also to understand failure cases of already existing functionals.

MM 15: Topical Session: Fundamentals of Fracture – Atomistic Studies of Fracture

Time: Tuesday 10:15–13:00

Location: SCH A 216

Topical Talk

MM 15.1 Tue 10:15 SCH A 216

Multiscale Quantum-Atomistic and Atomistic-Continuum Modelling of Crack Propagation — •JAMES KERMODE — Warwick Centre for Predictive Modelling, School of Engineering, University of Warwick, Coventry, United Kingdom

I will review recent progress on the development and application of advanced algorithms to simulate chemomechanical systems where local chemistry and long-range stress are tightly coupled, e.g. at the tip of a propagating crack or the core of a dislocation. I will discuss two general approaches (i): hybrid quantum/classical approaches where bond-breaking is treated at the DFT level embedded within a large-scale classical atomistic model to capture elastic relaxation, including recent applications to tungsten [1] and diamond [2]; (ii) atomistic-to-continuum modelling for crack propagation, either through extracting effective continuum models from large-scale atomistic simulations of fracture [3], or by flexibly embedding an atomistic domain within a continuum model, using a new algorithm to compute bifurcation diagrams for fracture systems [4].

[1] P. Grigorev et al., arXiv:2111.11262 (2022); [2] J. Brixey, T. Cowie, A. Jardine and J. R. Kermode, In Prep (2022); [3] S. M. Khosrownejad, J. R. Kermode, and L. Pastewka, Phys. Rev. Materials 5, 023602 (2021); [4] M. Buze and J. R. Kermode, Phys. Rev. E 103, 033002 (2021)

MM 15.2 Tue 10:45 SCH A 216

Modelling Fracture in α -Iron via a Numerical-Continuation Scheme — •LAKSHMI SHENOY¹, ALBERT BARTOK-PARTAY², and JAMES KERMODE¹ — ¹Warwick Centre for Predictive Modelling, School of Engineering, University of Warwick, Coventry CV4 7AL, United Kingdom — ²Department of Physics, University of Warwick, Coventry CV4 7AL, United Kingdom

I will present results for the stability range of fracture in α -iron mapped using the numerical-continuation flexible boundary scheme (NCFlex) proposed by Buze et al. [1]. The predictions by two new machine learning interatomic potentials for α -iron [2] - Gaussian approximation potential and atomic cluster expansion - will be compared with those by the classical embedded atom model [3]. From the bifurcation plots produced by NCFlex, the 0K energy barriers to brittle fracture propagation along different crystallographic planes in α -iron will be computed. Using these, a model for the temperature dependence of the brittle-to-ductile transition temperature of α -iron will be proposed, and validated against experimental results. Methods for extending this scheme to finite temperature energy barriers and interaction of the crack tip with point defects will also be discussed.

[1] M. Buze and J. R. Kermode, Phys. Rev. E 103, 033002 (2021); [2] Zhang, Lei, et al. arXiv:2208.05912 (2022); [3] Mendeleev, M. I., et al. Phil. Mag. 83.35 (2003)

MM 15.3 Tue 11:00 SCH A 216

Revealing Atomistic Fracture in BCC Iron by Active Learning — LEI ZHANG¹, GABOR CSANYI², ERIK VAN DER GIESSEN¹, and •FRANCESCO MARESCA¹ — ¹University of Groningen, Netherlands — ²University of Cambridge, UK

Fracture is multi-scale process that originates from atomic-scale bond rupture and dislocation activity. A clear understanding of these processes is often lacking, because classical interatomic potentials (IAPs) for Molecular Dynamics simulations yield contradicting results that agree only partially with experiments. This is also due to the limited flexibility of their functional form, which is inadequate

to describe the complex potential energy surface associated with fracture processes. Emerging machine learning (ML) IAPs allow near-quantum accuracy, based on density functional theory (DFT), but are orders of magnitude faster than DFT. In this work, we develop an active learning algorithm that enables the prediction of atomistic fracture mechanisms via the Gaussian Approximation Potential (GAP) approach. An existing DFT database for ferromagnetic bcc iron is first enriched with configurations that are relevant for the fracture process. Next, the active learning approach is applied to four crack systems, in which the maximum predicted per-atom error is reduced to 10 meV. The predicted critical stress intensity factors are compared with theory estimates, and the learning efficiency of the approach is analysed. Our work provides an active learning strategy for improving ML-IAPs for fracture, while revealing for the first time the atomic scale mechanisms that initiate fracture in iron with quantum accuracy.

MM 15.4 Tue 11:15 SCH A 216

Benchmarking of Tungsten Potentials using Blunted Cracks — •TARAKESHWAR LAKSHMIPATHY and ERIK BITZEK — Department Computational Materials Design, Max-Planck-Institut für Eisenforschung GmbH

Blunted cracks can have radically different fracture behavior compared to their atomically sharp counterparts due to the additional degrees of freedom available to atoms at the crack tip surface. Simulating realistic notch or crack tip radii requires computationally inexpensive atomic interaction potentials. However, empirical potentials are known to show artefacts like the formation of planar faults at the crack tip due to unrealistic minima in their generalized stacking fault energies or fail to reproduce surface reconstructions. Such drawbacks could play an even larger role in blunted crack simulations than in typically studied sharp cracks due to additional surfaces at the crack tip. In this work, the fracture behavior and fracture toughness of some commonly used EAM potentials are benchmarked against density functional theory (DFT) simulations of blunted cracks in tungsten and compared to recently developed modified-EAM (MEAM), atomic cluster expansion (ACE) and bond order potentials (BOP).

15 min. break

MM 15.5 Tue 11:45 SCH A 216

Development of machine learning interatomic potentials for far-from-equilibrium states: a case study of deformation mechanisms in ceramics — •SHUYAO LIN¹, DAVIDE SANGIOVANNI², LARS HULTMAN², and NIKOLA KOUTNA¹ — ¹Technical University of Vienna, Institute of Materials Science and Technology, A-1060, Vienna, Austria — ²Linköping University, Department of Physics, SE-58183, Linköping, Sweden

Besides the high chemical stability, the applications of ceramic-based materials into the coating technology require not only high strength but also ductility, a combination of properties necessary for material's resistance to crack growth. The mechanical properties of ceramic materials are dominated by both their movement and interactions. In this talk, we study mechanical response of selected ceramics, including transition metal diborides and nitrides. First, ab initio molecular dynamics simulations (AIMD) are employed to model tensile deformation along main crystallographic directions and under extreme high temperatures with fluid status. Then we develop machine learning interatomic potentials within the moment tensor potential (MTP) framework. The potentials are thor-

oroughly tested and validated against AIMD stress-strain curves. With the aid of newly developed potentials, we carry out large-scale simulations during which the ceramics are continuously loaded and can shrink due to Poisson contractions. The observed deformation mechanisms are described and compared to those present in the small-scale training data.

MM 15.6 Tue 12:00 SCH A 216

Atomistic studies of crack tip twin-boundary interactions in lamellar TiAl alloys: Effect of misfit, misorientation and lamella spacing — ANUPAM NEOGI^{1,2} and REBECCA JANISCH¹ — ¹ICAMS, Ruhr-University Bochum, Germany — ²ANSYS Inc., Pune, India

Nano-scale coherent twin boundaries can be an effective way in overcoming the strength-ductility trade-off of metals and their alloys. In this sense also twin boundaries in nano-lamellar lightweight Ti-Al alloys promise a great potential. Furthermore, the existence of three types of these twin boundaries with different misorientation and coherency state at the interface provide an excellent opportunity to study the effect of exactly these parameters in a realistic model system. To this end, we carried out molecular statics simulations to characterize the crack advancement at and across internal true-twins (TTs), rotational boundaries (RBs), and pseudo-twins (PTs) in lamellar γ -TiAl alloys, as well as crack propagation in fully lamellar structures.

It was confirmed that both interface type and spacing affect the fracture toughness and crack growth resistance. Furthermore, the crack tip mechanisms exhibit prominent sensitivity to the crack system and crystallographic directions. For trans-lamellar cracks the tip shows plastic deformation and toughening at all interfaces. The overall fracture initiation toughness in a microstructure of TTs exhibits an increasing trend with decreasing lamellar size down to a critical thickness, below which the fracture toughness drops again. These and more phenomena and their origins will be discussed in the presentation.

MM 15.7 Tue 12:15 SCH A 216

Crack Dislocation Interactions in Tungsten — BENEDIKT EGGLE-SIEVERS and ERIK BITZEK — Max-Planck-Institut für Eisenforschung GmbH, Max-Planck-Straße 1, 40237 Düsseldorf

The fracture toughness of Tungsten at low temperature is critically influenced by its microstructure. Understanding the underlying crack-microstructure interactions is therefore necessary to model and predict failure. In order to gain insight into the interactions of dislocations with the crack-tip, large scale atomistic simulations are carried out. Dislocations of different character and Burgers vector are placed in the vicinity of a strain controlled crack geometry, resulting either in an attraction or repulsion of the dislocation. In the former case interactions can be observed in the course of the simulation, e.g. cross-slipping of screw parts, changes in crack front or crack plane as well as subsequent dislocation emission.

Dependencies on the stress state, the crack system, dislocation type and distance between dislocation and the crack are investigated. The results are discussed with respect to mesoscale and continuum models for crack tip plasticity and fracture toughness.

MM 15.8 Tue 12:30 SCH A 216

Atomistic study of fracture in Laves phases — ALIREZA GHAFAROLLAHI and ERIK BITZEK — Max-Planck-Institut für Eisenforschung GmbH, Max-Planck-Straße 1, Düsseldorf 40237, Germany

Laves phases are intermetallic phases with complex structures that exist in many alloys and have a pronounced impact on their mechanical properties. Although these materials often exhibit superior mechanical properties at high temperatures, their applications as structural materials are limited due to their intrinsic brittleness at ambient temperature. Therefore, understanding the fundamental fracture mechanisms in Laves phases is crucial for tailoring their mechanical properties. Here, with the aid of atomistic simulations, the fracture behavior in C14 and C15 Laves phases is explored using NbCr₂ and MgZn₂ as model systems. In particular, different crack systems are analyzed and the corresponding fracture toughnesses are computed and compared with the Griffith theory.

MM 15.9 Tue 12:45 SCH A 216

Tailoring negative pressure by crystal defects: Crack induced hydride formation in Al alloys — ALI TEHRANCHI¹, POULAMI CHARABORTY¹, MARTI LOPEZ FREIXES¹, EUNAN MCENIRY¹, BAPTISTE GAULT^{1,2}, TILMANN HICKEL^{1,3}, and JÖRG NEUGEBAUER¹ — ¹Max-Planck-Institut für Eisenforschung GmbH, D-40237 Düsseldorf, Germany — ²Department of Materials, Imperial College, South Kensington, London, SW7 2AZ, UK — ³Bundesanstalt für Materialforschung und -prüfung (BAM)

Climate change motivates the search for non-carbon-emitting energy generation and storage solutions. Metal hydrides show promising characteristics for this purpose. To enhance the formation and stability of such often highly volatile hydrides we have consider a novel concept: tailoring and employing the negative pressure of microstructural and structural defects to enhance H solubility and thus hydride formation. Using systematic ab initio and atomistic simulations, we demonstrate that an enhancement in the formation of hydrides at the negatively pressurized crack tip region is feasible by increasing the mechanical tensile load on the specimen. The theoretical predictions have been used to re-assess and interpret atom probe tomography experiments for a high-strength 7XXX-aluminium alloy that show a substantial enhancement of hydrogen concentration at structural defects near a stress-corrosion crack tip. Based on these insights we derive strategies for enhancing the capability of metals as H-storage materials.

MM 16: Energy Conversion

Time: Tuesday 10:15–13:00

Location: SCH A 215

MM 16.1 Tue 10:15 SCH A 215

Spins at Work: Probing Charging and Discharging of Organic Radical Batteries by Electron Paramagnetic Resonance Spectroscopy — ILIA KULIKOV¹, NAITIK PANJWANI¹, ANATOLIY VERESHCHAGIN², DOMENIK SPALLEK¹, DANIIL LUKIANOV², ELENA ALEXEEVA², OLEG LEVIN¹, and JAN BEHREND¹ — ¹Berlin Joint EPR Lab, Freie Universität Berlin, Arnimallee 14, D-14195 Berlin — ²St. Petersburg, 199034, Russian Federation

We report on the development of an operando setup for spectroelectrochemical Electron Paramagnetic Resonance (EPR) measurements on redox conductive polymers for organic radical batteries. [1]

Quantitative EPR experiments performed on electrochemical cells with a TEMPO containing polymer cathode demonstrate a strong decrease in the number of paramagnetic centres upon oxidation. [2] The distinct EPR signatures of the polymer are used to study its degradation upon repeated cycling. A comparison between the EPR and electrochemical data is used to monitor the degradation process.

Low-temperature ex-situ pulse EPR measurements on an oxidized cathode film reveal a spectrum of dilute nitroxide species, which indicates formation of electrochemically inactive islands. These experiments pave the way for studying organic radical battery materials by advanced EPR techniques.

[1] I. Kulikov et al., Energy and Environmental Science, 2022, 15, 3275.

[2] A. A. Vereshchagin et al., Batteries & Supercaps 2021, 4, 336.

MM 16.2 Tue 10:30 SCH A 215

Revisiting the storage capacity limit of graphite battery anodes: spontaneous lithium overintercalation at ambient pressure — CRISTINA GROSU^{1,2}, CHIARA PANOSSETTI¹, STEFFEN MERZ², PETER JAKES², SEBASTIAN MATERA¹, RÜDIGER-A. EICHEL², JOSEF GRANWEHR², and CHRISTOPH SCHEURER^{1,2} — ¹Fritz-Haber-Institut der MPG, Berlin, Germany — ²IEK-9, FZ Jülich, Germany

The market quest for fast-charging, long-lasting, safe batteries drives the exploration of new energy storage materials, but also promotes fundamental studies of those already widely used—primarily graphite anodes for Li-ion batteries. We focus on the upper intercalation limit in the morphologically quasi-ideal highly oriented pyrolytic graphite, with a LiC₆ stoichiometry corresponding to 100% state of charge. A sample prepared by immersion in liquid Li at ambient pressure, investigated by ⁷Li nuclear magnetic resonance (NMR), shows unexpected signatures of superdense intercalation compounds, LiC_{6-x}. These were ruled out for decades, as the highest geometrically accessible composition, LiC_{2,2}, can only be prepared under high pressure. We monitored the sample upon calendaric aging and employed DFT calculations to rationalise NMR findings. Computed free energies reveal that non-negligible overintercalation proceeds spontaneously beyond the currently accepted capacity limit. Challenging the widespread notion that any additional intercalation beyond LiC₆ is not possible under ambient conditions, we highlight the implications on performance-crucial phenomena and critically discuss possible quantitative characterization routes[1].

[1] C. Grosu et al., arXiv:2107.11137 (2021)

MM 16.3 Tue 10:45 SCH A 215

Computational investigation of carbon based anode materials for Li- and post-Li ion batteries — JAFAR AZIZI¹, HOLGER EUCHNER², and AXEL GROSS¹ — ¹Institute of Theoretical Chemistry, Ulm University, 89069 Ulm, Germany — ²Institute of Physical and Theoretical Chemistry, University of Tübingen, 1572076 Tübingen, Germany

With respect to sodium ion batteries, traditional graphite anodes exhibit a severe limitation due to their inability to intercalate sodium atoms. Hard carbon materials, on the other hand, provide a promising alternative for Na-ion and K-ion batteries with high theoretical capacities and low reaction potentials. The presence of the particular nanostructure of these functionalized carbon-based

materials have been shown to be responsible for these features. The major obstacle for a continued development and improvement is a lack of a functional understanding of the role of these structural features with regard to the intercalation and storage mechanism. To overcome these problems, the intercalation of Li, Na, and K in the presence of distinct defects have been investigated by density functional theory (DFT) calculations. It will be shown how the combination of phonon simulations with electronic band structure calculations allows for a validation of the so-called modified card house model for the alkali metal storage in hard carbon.

MM 16.4 Tue 11:00 SCH A 215

Detailed structural and electrochemical comparison between high potential layered P2-NaMnNi- and doped P2-NaMnNiMg-oxides — •MANUEL DILLENZ¹, CORNELIUS GAUCKLER², MOHSEN SOTOUDEH¹, HOLGER EUCHNER³, MARIO MARINARO², and AXEL GROSS^{1,4} — ¹Institute of Theoretical Chemistry, Ulm University, Mez-Starck-Haus, Oberberghof 7, 89081 Ulm — ²ZSW-Zentrum für Sonnenenergie und Wasserstoff-Forschung, Helmholtzstrasse 8, 89081, Ulm, Germany — ³Institute of Physical and Theoretical Chemistry, Universität Tübingen, Auf der Morgenstelle 15, 72076 Tübingen, Germany — ⁴Helmholtz Institute Ulm (HIU) for Electrochemical Energy Storage, Helmholtzstraße 11, 89069 Ulm, Germany

Manganese-based transition metal oxides with a P2 structure are promising cathode materials for sodium ion batteries. Although these materials exhibit high working potential vs Na⁺/Na and high capacity, they are affected by Na⁺ ion/vacancy ordering transitions and phase transformations at high voltages, resulting in poor reversibility. Here we present a combined experimental/theoretical approach to investigate the effect of magnesium doping on the layered P2-Na_{0.67}Mn_{0.75}Ni_{0.25}O₂ cathode material. The Mg-doped material showed stabilization of the high potential plateau and improved cycle life. Based on our experimental data and periodic density functional theory (DFT) calculations, phase stabilities of the O2, P2, and OP4 phases for the pristine and Mg-doped systems were investigated to elucidate the origin of the "Z"-phase formation in the Mg-doped systems.

MM 16.5 Tue 11:15 SCH A 215

Coarse-Grained Simulation of Dendrite Growth in Lithium Metal Batteries — •LEN KIMMS, DIDDO DIDDENS, and ANDREAS HEUER — Institut für physikalische Chemie, Westfälische Wilhelms-Universität Münster, Corrensstraße 28/30, 48149 Münster

In this talk, we will present a simulation study that investigates the formation and growth of dendrites. Due to the increasing demand for portable high-capacity energy storage, there is a renewed interest in Lithium metal batteries (LMBs). In LMBs one electrode is replaced by lithium metal anchored on a current collector. Lithium metal is electrochemically plated on the anode side when charging the battery. Depositing the metal uniformly is a hugely challenging undertaking. The intrinsically high reactivity of lithium metal, electric field effects, and spatial variations of the local composition in the electrolyte all drive dendritic deposition. We employ a versatile coarse-grained model to understand the influence of various electrochemical conditions on the dendrite morphology. The model allows not only the investigation of fundamental driving forces like the electric field and the cation concentration but also the evaluation of more intricate procedures e.g. pulse charging. Different particle types with varying reactivity are implemented, which allows the representation of local passivation. Also, a solid electrolyte interface (SEI) layer can be incorporated either explicitly with a particle layer on the surface or implicitly by modifying the cationic diffusion locally. Here we report results on how to suppress non-uniform deposition by employing charging, microstructured electrode surfaces, and SEI effects.

15 min. break

MM 16.6 Tue 11:45 SCH A 215

Modelling Hard Carbon with High-Dimensional Neural Network Potentials — •ALEXANDER L. M. KNOLL^{1,2}, JAFAR AZIZI³, HOLGER EUCHNER⁴, AXEL GROSS³, and JÖRG BEHLER^{1,2} — ¹Lehrstuhl für Theoretische Chemie II, Ruhr-Universität Bochum, 44780 Bochum, Germany — ²Research Center Chemical Sciences and Sustainability, Research Alliance Ruhr, 44780 Bochum, Germany — ³Institut für Theoretische Chemie, Universität Ulm, 89081 Ulm, Germany — ⁴Institut für Physikalische und Theoretische Chemie, Eberhard Karls Universität Tübingen, 72076 Tübingen, Germany

Hard carbon (HC) is widely regarded as a promising anode material for lithium and sodium ion batteries. However, this material is notoriously difficult to characterize experimentally, as its properties strongly depend on the carbon precursor and the conditions of preparation. *Ab initio* investigations could help to illuminate its structure, but are severely hampered by its complexity involving large graphitic domains as well as amorphous motifs. To bypass these challenges, we present a high-dimensional neural network potential (HDNNP) for HC that accurately reproduces short-range and dispersion interactions in the system. We show that elaborate structural models can be constructed with this potential using various simulation protocols and demonstrate their validity through comparison to experimental data.

MM 16.7 Tue 12:00 SCH A 215

Computational Studies on the Electrochemical Performance of Doped and Substituted Ti₃C₂T_x (T = O, OH) MXene — •MANDIRA DAS¹ and SUBHRADIP GHOSH² — ¹Indian Institute of Technology Guwahati, Guwahati, Assam, India — ²Indian Institute of Technology Guwahati, Guwahati, Assam, India

Using Density functional theory (DFT) in conjunction with a solvation model, we have investigated the phenomenon of electrode-electrolyte interaction at the electrode surface and its consequences on the electrochemical properties like the charge storage and total capacitance of doped and substituted functionalized Ti₃C₂T_x (T = O, OH) supercapacitor electrode. We have studied nitrogen-doped, nitrogen substituted, and molybdenum substituted MXenes in acidic electrolyte H₂SO₄ solution. By considering nitrogen doping at different sites, we found that the greatest capacitance is obtained for doping at functional sites. Our results agree well with the available experiment. We also found that the enhancement in capacitances due to nitrogen doping is due to amplifications in the pseudo-capacitance. We propose that the primary mechanism leading to the enhanced value of the capacitances due to nitrogen doping is surface redox activity. The performances of substituted systems, on the other hand, are degraded compared to the pristine ones. This suggests that better storage capacities in Ti₃C₂T_x electrode can be obtained by doping only. We provide insights into the reasons behind contrasting behavior in doped and substituted systems and suggest ways to further improve the capacitances in the doped system.

MM 16.8 Tue 12:15 SCH A 215

Structure-property relationships in functionalized metal organic framework from first-principles high-throughput screening — •JOSHUA EDZARDS¹, HOLGER-DIETRICH SASSNICK¹ und CATERINA COCCHI^{1,2} — ¹Institut für Physik, Carl von Ossietzky Universität Oldenburg, 26129 Oldenburg — ²Institut für Physik and IRIS Adlershof, Humboldt-Universität zu Berlin, 12489 Berlin

Metal organic frameworks (MOFs) are novel materials with high potential in many fields of application, ranging from gas storage and catalysis to optoelectronics. MOFs are constituted by metal atoms bound together by linker molecules which can be modified by functional groups. This leads to an enormous variety of MOFs with different structural properties, which can in turn affect their band structures, projected density of states, charge density distribution, etc. In this project, we perform high-throughput first-principles calculations on MOF-5 a well-known member of the MOF family. We scan all possible structures that arise by exchanging the metal ion Zn with alkaline-earth metals, and by functionalizing the linker molecule (1,4-benzodicycarboxylate) with Br, CH₃, Cl, COOH, NO₂, and OH. We investigate the electronic properties of the stable structures and assess how they are influenced by the choice of the metal ion and by the functionalization of the linkers.

MM 16.9 Tue 12:30 SCH A 215

Lithium diffusion visualized in Li₄+xTi₅O₁₂ using optical microscopy (revealing slow-moving phase boundary) — •YUG JOSHI, ROBERT LAWITZKI, and GUIDO SCHMITZ — Chair of Materials Physics, Institute of Materials Science, University of Stuttgart, Stuttgart, Germany

Lithium titanate (Li₄Ti₅O₁₂) undergoes a phase transformation from spinel structured (Li₄Ti₅O₁₂) to rock-salt (Li₇Ti₅O₁₂). The material has been reported to show sluggish mobility of lithium in fully lithiated and delithiated phases. This challenges the high-rate performance observed in this material. To elucidate this behavior, optical microscopy and the electrochromic character of the material have been used to visualize the phase transformation. The kinetics of lithium transport is observed in a constrained region of sputter-deposited thin-film samples. This enables a study of the lateral transport on the length scales of tens of micrometers. Furthermore, with a thermostatically controlled cell, the Arrhenius-like temperature dependence of lithium diffusivity is revealed. Our quantitative findings demonstrate that indeed the end phases have poor diffusivity. Surprisingly, the phase boundary moves slowly upon lithiation, which has been refuted in prior reports, however, it is confirmed here by the linear growth kinetics of the Li-rich phase in the initial stages of the lithium transport. Interestingly, the partial solubility of lithium in the spinel structured Li_{4/3+δ}Ti₅/3O₄ phase increases the diffusivity of lithium drastically. This increase in diffusivity along with the reduction in size of the electrode seems to be compensating the kinetic hindrance induced by the phase boundary.

MM 16.10 Tue 12:45 SCH A 215

Photocatalytic water splitting from Koopmans spectral functionals: The case of TiO₂ polymorphs — •MARIJA STOJKOVIC¹, EDWARD LINSKOTT¹, and NICOLA MARZARI^{1,2} — ¹Theory and Simulations of Materials (THEOS), and National Centre for Computational Design and Discovery of Novel Materials (MARVEL), École Polytechnique Fédérale de Lausanne, 1015 Lausanne, Switzerland — ²Laboratory for Materials Simulations, Paul Scherrer Institut, 5232 Villigen PSI, Switzerland

Photocatalytic water splitting has drawn considerable attention for renewable energy production. Since the first reported photocatalytic water splitting by titanium dioxide, this material remains one of the most promising photocatalysts,

due to its suitable band gap and band-edge positions. However, estimating both of these properties is a challenging task for standard DFT functionals. Here we show how Koopmans spectral functionals can accurately predict the band

structure and level alignment of rutile, anatase and brookite, demonstrating the advantage of orbital-density dependent functionals for predicting the spectral properties of materials.

MM 17: Phase Transformations: Microstructural Transformations

Time: Tuesday 10:15–11:15

Location: SCH A 118

MM 17.1 Tue 10:15 SCH A 118

About the transformation speed of martensitic transformations — •SEBASTIAN FÄHLER¹, STEFAN SCHWABE², KLARA LÜNSER¹, DANIEL SCHMIDT³, KORNELIUS NIELSCH³, and PETER GAAL³ — ¹Helmholtz-Zentrum Dresden-Rossendorf, Dresden, Germany — ²Leibniz IFW Dresden, Dresden, Germany — ³Leibniz-Institut für Kristallzüchtung (IKZ), Berlin, Germany

Structural martensitic transformations enable various applications, which range from high stroke actuation and sensing to energy efficient magnetocaloric refrigeration and thermomagnetic energy harvesting. All these emerging applications benefit from a fast transformation, but up to now the speed limit of martensitic transformations has not been explored. Here, we demonstrate that a martensite to austenite transformation can be completed in under ten nanoseconds. We heat an epitaxial Ni-Mn-Ga film with a laser pulse and use synchrotron diffraction to probe the influence of initial sample temperature and overheating on transformation rate and ratio. We demonstrate that an increase of thermal energy drives this transformation faster. Though the observed speed limit of 2.5×10^{27} (Js)⁻¹ per unit cell leaves plenty of room for a further acceleration of applications, our analysis reveals that the practical limit will be the energy required for switching. Our experiments unveil that martensitic transformations obey similar speed limits as in microelectronics, which are expressed by the Margolus-Levitin theorem. [1] S. Schwabe, K. Lünser, D. Schmidt, K. Nielsch, P. Gaal and S. Fähler, *Science and Technology of Advanced Materials*, 23 (2022) 633

MM 17.2 Tue 10:30 SCH A 118

Solving the 3D puzzle of the martensitic microstructure in epitaxial NiTi films — •KLARA LÜNSER^{1,2,3}, ANDREAS UNDISZ^{4,5}, KORNELIUS NIELSCH^{2,3}, and SEBASTIAN FÄHLER¹ — ¹Helmholtz-Zentrum Dresden-Rossendorf, Dresden, Germany — ²Leibniz IFW Dresden, Dresden, Germany — ³TU Dresden, Dresden, Germany — ⁴TU Chemnitz, Chemnitz, Germany — ⁵Friedrich-Schiller-Universität Jena, Jena, Germany.

The shape memory effect in the most frequently used shape memory alloy NiTi is driven by a martensitic transformation, resulting in a complex martensitic microstructure with a variety of interfaces. As shape memory properties depend on the microstructure, a detailed understanding is crucial. However, the martensitic microstructure is still puzzling, especially how it is built up in 3 dimensions. The analysis of this puzzle is complicated by grain boundaries present in polycrystalline NiTi. Here, we eliminate the influence of grain boundaries by using epitaxial NiTi films in (111)-orientation as a model system. We analyze the films with electron microscopy to identify clusters and interfaces and compare results to the phenomenological theory of martensite. With this approach, we generate a scale-bridging understanding of the martensitic microstructure. Three kinds of twin boundaries on different length scales are required for the complete, hierarchical microstructure. Integral X-ray measurements confirmed our microstructure model. The results are transferable to NiTi bulk and polycrystalline films,

showing that NiTi epitaxial films are important to extend our understanding of the martensitic microstructure.

MM 17.3 Tue 10:45 SCH A 118

Elucidating the nucleation and growth mechanism of {11-22} twin in titanium — ANDRIY OSTAPOVETS¹, •RITU VERMA^{1,2}, and ANNA SERRA³ — ¹Institute of Physics of Materials, Czech Academy of Sciences, 616 00 Brno, Žitkova 513/22 Czech Republic — ²Central European Institute of Technology, Brno University of Technology, Purkyňova 656/123 612 00 Brno, Czech Republic — ³Universitat Politècnica de Catalunya, Campus Nord, C-2, Jordi Girona, 1-3, 08034 Barcelona, Spain

{11-22} Twin is the predominant twinning mode in hcp metals such as Ti, Zr and Mg under <c> axis compression. We analyze the {11-22} twin nucleation in Ti by reverse α - ω - α phase transformation. The twin nucleated by this mechanism can grow by the migration of the {11-22} twin boundary. This migration is mediated by the gliding of line defects with step and dislocation character, i.e. b3/3 disconnection, along with {11-22} twin boundary. Their structure can be interpreted as a pair of disconnections (bt and bt*) i.e. dissociated core of b3/3 disconnection, which contains ω -phase structure inside. These studies reveal the role of ω - phase in the connection with nucleation and growth mechanism of {11-22} twin boundary. These results clarify the uncertainties with the growth of the {11-22} twins.

MM 17.4 Tue 11:00 SCH A 118

Bicontinuous microstructure formation through peritectic melting — •ZHONGYANG LI¹, NINA PETERSEN¹, LUKAS LÜHRS¹, and JÖRG WEISSMÜLLER^{1,2} — ¹Institute of Materials Physics and Technology, Hamburg University of Technology, Hamburg — ²Institute of Materials Mechanics, Helmholtz-Zentrum Hereon, Geesthacht

Recent research has found that when heated above the peritectic line, the intermetallic compound TiAg decomposes into a separated solid Ti phase and a liquid Ag phase, thereby forming a bicontinuous microstructure. This shows that monolithic networks such as porous Titanium, which has potential application in the field of biomedicine, can be produced with simple heat treatment followed by selective removal of other phases. As a novel dealloying method for bulk materials, the underlying mechanism is still not completely understood. It is also unclear if this method could be used in different alloy systems.

In our research we find a similar microstructural phenomenon for CuSn alloys. With the help of electron microscopy and X-Ray diffraction, formation and evolution processes of the bicontinuous structure of both TiAg and CuSn systems are studied. Research on microstructure evolution can help both, setting up the criteria for searching new alloy systems and optimizing thermal treatment parameters. This enables us to further develop this method for porous metal preparation, and also broaden the application of this method from peritectic dealloying to dealloying at crystal-melt coexistence.

MM 18: Transport in Materials: Metals, Alloys and Oxides

Time: Tuesday 11:30–13:00

Location: SCH A 118

MM 18.1 Tue 11:30 SCH A 118

Understanding diffusion in high entropy alloys from an experiment-ab initio approach — •XI ZHANG¹, SERGIY DIVINSKI², and BLAZEJ GRABOWSKI¹ — ¹Institute for Materials Science, University of Stuttgart, D-70569 Stuttgart, Germany — ²Institute of Materials Physics, University of Münster, 48149 Münster, Germany

Diffusion in high entropy alloys (HEAs), due to the significant chemical complexity and the severe lattice distortion, has many fundamental features that are extremely important for both basic research and industrial development. The most accurate and direct method to study diffusion is the radiotracer technique whereby a number of intriguing phenomena, e.g., ultra-fast, non-/anti-sluggish diffusion, have been observed. To advance the current understanding of the observed phenomena, accurate theoretical analysis is highly required. The key point of the present approach is the combined measurement of diffusivities and interdiffusion profiles on the one hand and a highly accurate DFT-informed assessment of the diffusion mechanisms on the other. In this way, the long-standing mysteries in HEA diffusion, e.g., "sluggish" diffusion, can be compre-

hensively examined and understood. Remarkably, we show by investigating an HCP AlScHfTiZr HEA system that the increasing chemical complexity results in a considerably broadened distribution of the defect formation and migration energies which may enhance the mobility of the defects and thus the diffusion rates. The observed "anti-sluggish" diffusion can be traced back to the lattice distortion as revealed by the DFT calculations.

MM 18.2 Tue 11:45 SCH A 118

Composition dependent thermodynamic factor, Manning factor, and impurity diffusion coefficients estimated by a tracer-interdiffusion couple technique — •ESAKKIRAJA NEELAMEGAN¹, DANIEL GAERTNER¹, JASPER BERNDT², STEPHAN KLEMM², ALOKE PAUL³, GERHARD WILDE¹, and SERGIY V DIVINSKI¹ — ¹Institute of Materials Physics, University of Münster, Münster, Germany — ²Institut für Mineralogie, University of Münster, Münster, Germany — ³Department of Materials Engineering, Indian Institute of Science, Bangalore, India

The thermodynamic driving force for the diffusion was never validated experimentally. The newly proposed augmented tracer-interdiffusion couple method

could be adapted to validate the thermodynamic factor. The approach is demonstrated for a model Ni-Fe binary system, especially for the Ni-rich corner. Pure Ni is diffusion-coupled with a Ni-10 at. % Fe diluted alloy at 1000 C for 24h. The interdiffusion coefficients are estimated from the composition profile measured by an Electron Microprobe Analyser. The composition-dependent tracer diffusion coefficients are estimated following the Belova-Murch approach. Diffusion of the Fe55 and Ni63 isotopes under a chemical gradient is followed. The Fe tracer diffusion coefficients are found to be faster than those of Ni in this composition region. Utilizing the Darken-Manning relation, the thermodynamic factor is estimated and compared with that provided by a ThermoCalc software database. As a result, the composition-dependent impurity diffusion coefficients of Co, Cr, and Mn in these alloys are analysed in detail.

MM 18.3 Tue 12:00 SCH A 118

Control of microstructure in binary alloy thin films by means of electromigration — •THOMAS BREDE, REINER KIRCHHEIM, and CYNTHIA A. VOLKERT — Universität Göttingen, Insitut für Materialphysik, Göttingen, Deutschland
Magnetic and electric fields and currents open new and efficient materials processing paths for microstructure optimization than were previously available. For example, it has recently been shown that high DC electric currents can be used to create anisotropic microstructures with elongated ferrite grains in iron-carbon thin films [1]. The elongated grains form in the wake of carbides that migrate due to electromigration induced carbon flux divergences. The underlying mechanisms controlling the microstructural evolution will be presented and will be used to discuss other materials systems that might show this effect and how they could be implemented to achieve precise microstructure control.

[1] Brede, T., Kirchheim, R., & Volkert, C. A. (2020). Anisotropic grain growth in iron-carbon films at high electric current densities. *Scripta Materialia*, 178, 18-23.

MM 18.4 Tue 12:15 SCH A 118

GP-zone formation and growth in rapidly quenched Al-Cu alloys — •DAVID STEIN, JOHANNES BERLIN, TOBIAS STEGMÜLLER, and FERDINAND HAIDER — Universität Augsburg, Institut für Physik, 86159 Augsburg, Germany
Natural aging by the formation of Guinier Preston zones in Al-Cu alloys is only possible in the presence of excess vacancies, quenched in from high temperatures. In collision welded samples of Al and Cu, an unexpected high density of GPII-zones was observed in the TEM. In order to obtain similarly high quenching rates of about 104 K/s, meltspinning was used for alloys with a Cu content from 2-5 wt%. After the quenching process, the samples were analyzed after different natural aging times using Differential Scanning Calometry (DSC), hardness measurements, resistometry and STEM to obtain information about the unmixing kinetics. Additionally EDX and EBSD were used to characterize the microstructure and chemical homogeneity of the samples.

MM 19: Development of Computational Methods: Simulation Methods – Theory

Time: Tuesday 14:15–15:30

Location: SCH A 251

MM 19.1 Tue 14:15 SCH A 251

Multi-methodological study of temperature trends in Mössbauer effect in beta-Sn — •MARTIN FRIÁK¹, NIKOLAS MASNIČÁK¹, OLDŘICH SCHNEWEISS¹, PAVLA ROUPCOVÁ¹, ALENA MICHALCOVÁ², ŠÁRKA MSALLAMOVIČOVÁ², and MOJMÍR ŠOBER^{3,1} — ¹Institute of Physics of Materials, Czech Academy of Science, Brno, CZ — ²Department of Metals and Corrosion Engineering, University of Chemistry and Technology in Prague, Prague, CZ — ³Department of Chemistry, Faculty of Science, Masaryk University, Brno, CZ

We have performed a multi-methodological theoretical study of impact of thermal vibrations on the Mössbauer effect in the tetragonal beta-phase of tin. We have seamlessly combined (i) atomic-scale numerical data in the form of mean square displacements of Sn atoms determined by quantum-mechanical calculations, (ii) continuum-level thermodynamic modeling based on the quasi-harmonic approximation and (iii) theoretical analysis of Mössbauer effect resulting in the prediction of temperature dependence of Mössbauer factor. The computed results were compared with our Mössbauer and X-ray experimental data. We show that classical theoretical approaches based on simplistic Debye model of thermal vibrations of solids can be nowadays replaced by exact ab initio calculations of individual thermal vibrations. For details see M. Friák et al., *Computational Materials Science* 215 (2022) 111780, doi:10.1016/j.commatsci.2022.111780.

MM 19.2 Tue 14:30 SCH A 251

Increasing the Diversity of One-Sided Transition State Searches with Biasing Potentials — •NILS GÖNNHEIMER, KING CHUN LAI, KARSTEN REUTER, and JOHANNES T. MARGRAF — Fritz-Haber-Institut der Max-Planck-Gesellschaft, Berlin, Germany

MM 18.5 Tue 12:30 SCH A 118

Theoretical studies on the oxygen migration through crystalline strontium titanate — •CARMEN FUCHS¹ and TIMO JACOB^{1,2,3} — ¹Ulm University, Institute of Electrochemistry, D-89069 Ulm — ²Helmholtz-Institute-Ulm (HIU), D-89081 Ulm — ³Karlsruhe Institute of Technology (KIT), D-76131 Karlsruhe

Transition metal oxides with perovskite structure (ABO₃) display a range of complex physical phenomena of condensed matter physics, including superconductivity, ferroelectricity, and magnetism. Strontium titanate, SrTiO₃ (STO), is the archetypical and most frequently studied representative of perovskite materials. By changing the stoichiometry, major changes in several important properties can be induced including blue light emission,[1] local conductivity,[2] and electron doping.[3] The relationship between the structure and the diffusion behavior of defects in SrTiO₃ is studied via DFT calculations using the plane-augmented wave method and the PBE exchange-correlation functional with and without Hubbard U correction. The obtained defect formation energy and activation barriers for oxygen migration through Frenkel- and Schottky-like defects within the crystalline STO structure are discussed and summarized.

[1] D. Kan et al, *Nat. Mater.* 4 (2005), 816-819.

[2] K. Szot, W. Speier, G. Bihlmayer, R. Waser, *Nat. Mater.* 5 (2006), 312-320.

[3] A.F. Santander-Syro et al, *Nature* 469 (2011), 189-193.

MM 18.6 Tue 12:45 SCH A 118

Impact of alloying elements on point defects and diffusion in B2 alloys: an ab initio study — •ADITYA VISHWAKARMA¹, OSAMU WASEDA¹, TILMANN HICKEL¹, NEELAMEGAN ESAKKIRAJA², SERGIY DIVINSKI², and ALOKE PAUL³ — ¹Max-Planck-Institut für Eisenforschung GmbH, Düsseldorf, Germany — ²Institute of Materials Physics, University of Münster, Germany — ³Department of Materials Engineering, IISc Bangalore, India

Turbine blades in jet engines are vulnerable to many problems due to the harsh application environments. To prevent oxidation and surface degradation, bond coats of B2 NiAl are most widely used. During the operation at high temperatures, however, the Al content in the bond coat is lost by the formation of an Inter Diffusion Zone (IDZ) between the superalloy (turbine blade) and the bond coat. In this report, ab-initio based studies of point defect formation and kinetics are performed, in order to investigate the diffusion mechanisms and the impact of alloying elements on diffusion in B2 NiAl phase. Our results show that isoelectronic substitutions by Pt and Pd decreases the triple defect migration barriers and increases the Ni vacancy concentration in comparison to pure B2 NiAl. Accordingly, the contribution of the triple defect mechanism increases down the periodic table. These results explain the experimentally observed increase of the thickness of IDZ compared to binary B2 NiAl and have, therewith, an impact on the future design of turbine blades.

Chemical processes on catalytic surfaces are commonly described in terms of complex networks of chemical reactions. One-sided transition state (TS) searches are a powerful tool for exploring these networks, when not all reactants, products and intermediates are known. To this end, the dimer method is commonly used, since it avoids the computationally demanding calculation of second derivatives. However, a prominent disadvantage of the dimer method is the convergence to the same few TSs even with differently initialised simulations, which raises the possibility of overlooking reaction pathways. Here, we propose a method to overcome this limitation. Specifically, we use a biasing potential to modify the potential energy surface (PES) based on information gathered from previous calculations. This biasing potential is adaptively generated in a series of dimer searches to drive the searching algorithm away from already known TSs. Intuitively, such potentials can be built within the Cartesian space by placing an energy bias at the atomic positions of a found TS. Alternatively, a similarity kernel between the structure and the known TS based on a local environment descriptor can be employed. This ensures that the biasing potential is invariant to permutations between identical atoms, as well as rotations and translations. The performance of both approaches is discussed for adatom diffusion and island formation on the Pd(100) surface.

MM 19.3 Tue 14:45 SCH A 251

How to Speed up First-Principles Based Geometry Optimization with Small Numerical Basis Sets — •ELISABETH KELLER, JOHANNES T. MARGRAF, and KARSTEN REUTER — Fritz-Haber-Institut der Max-Planck-Gesellschaft, Berlin, Germany

First-principles based geometry optimizations are often the most expensive part of high-throughput virtual screening studies for functional materials. This is particularly true for large systems, i.e. when studying complex surface reconstruc-

tions or nanoparticles. Here, the computational cost is strongly influenced by the size of the basis set. Large, converged basis sets result in precise equilibrium geometries, yet demand high computational cost and thus limit the simulation scale. Semiempirical methods using minimal basis sets offer a much lower computational cost, but may yield unacceptably large and uncontrolled errors. Furthermore, the availability of adequate parameterizations is rather sparse across the periodic table.

In this presentation, we will discuss the potential of using near-minimal basis sets for accelerating and enabling large-scale geometry optimizations at the DFT level. For this purpose, we studied how the size of the numeric atom-centered orbital (NAO) basis set in FHI-aims impacts the accuracy of bulk geometries. We recover equilibrium geometries at a nearly converged level with a highly compact basis by employing a simple short-ranged pair-potential correction. We show the scheme's ability to treat different systems across the periodic table ranging from small molecules and clusters to large-scale bulk and surface structures.

MM 19.4 Tue 15:00 SCH A 251

Automated Wannierizations — •JUNFENG QIAO^{1,2}, GIOVANNI PIZZI^{1,2,3}, and NICOLA MARZARI^{1,2,3} — ¹THEOS, EPFL — ²NCCR MARVEL — ³LMS, Paul Scherrer Institut

Maximally localized Wannier functions (MLWFs) are widely used in computational condensed matter physics. The standard approach to construct MLWFs often requires initial guesses which are based on chemical intuition and some measure of trial and error. Here, we first introduce an algorithm based on "projectability disentanglement" that provides reliably and automatically atom-

centered Wannier functions describing both occupied and empty states. Then, we show how to mix these again into target subspaces; e.g., to describe valence and conduction bands separately. We test these algorithms on 200 representative materials (77 insulators), showing that the final MLWFs are very well localized and can accurately interpolate band structures at the meV scale. Such approaches enable automated Wannierizations for both metals and insulators, promoting further applications of MLWFs in physical applications and high-throughput calculations.

MM 19.5 Tue 15:15 SCH A 251

Higher-order finite difference method for accurate calculation of Wannier centers and position matrix elements — •MINSU GHIM^{1,2,3}, JAE-MO LIHM^{1,2,3}, and CHEOL-HWAN PARK^{1,2,3} — ¹Department of Physics and Astronomy, Seoul National University, Seoul 08826, Korea — ²Center for Correlated Electron Systems, Institute for Basic Science, Seoul 08826, Korea — ³Center for Theoretical Physics, Seoul National University, Seoul 08826, Korea

An accurate calculation of Wannier function centers and position matrix elements is crucial for calculating many physical quantities such as the electric polarization and optical responses from first-principles Wannier interpolation. Since the Fourier transform of the position operator is the gradient in momentum space, a finite difference technique is used to calculate the position matrix elements for Wannier functions. However, so far, only the first-order finite difference has been considered therein. We present a higher-order finite difference method and demonstrate the advantage of our method over the conventional first-order finite difference method.

MM 20: Topical Session: Fundamentals of Fracture – Microstructure Impact on Fracture (Experiments)

Time: Tuesday 14:15–15:30

Location: SCH A 216

MM 20.1 Tue 14:15 SCH A 216

Fatigue damage prediction using graph neural networks on microstructure representations — •ALI RIZA DURMAZ^{1,2,3}, AKHIL THOMAS^{1,2}, CHRIS EBERL^{1,2}, and PETER GUMBSCH^{1,3} — ¹Fraunhofer Institute for Mechanics of Materials IWM, Freiburg im Breisgau, Germany — ²University of Freiburg, Freiburg im Breisgau, Germany — ³Karlsruhe Institute of Technology, Karlsruhe, Germany

Crack initiation governs high-cycle fatigue (HCF) life and makes HCF very susceptible to microstructural details. Predicting microscopic cyclic plasticity in polycrystals requires thorough microstructure representations.

In this work, we compare phenomenological crystal plasticity models with graph machine learning models on the task of predicting local cyclic plasticity in ferritic steel (EN1.4003). A workflow is presented which consists of a combined experimental and data post-processing pipeline to establish fatigue damage/crack initiation and short crack propagation data sets efficiently. It evolves around fatigue testing of mesoscale specimens to increase damage detection sensitivity, data fusion through multi-modal registration to address data heterogeneity, and image-based data-driven damage localization. The resulting data feeds both crystal plasticity and graph machine learning efforts. For the latter, the pixel data is transcribed into graph representations of the microstructure before being fed to different graph neural network variants. Interpretability techniques are applied to the machine learning models to learn about driving forces for the formation of extrusions and protrusions in individual grains.

MM 20.2 Tue 14:30 SCH A 216

analysis of plasticity in cyclic compression precracking — •MOHAMED AMINE FAHAM, NATHALIE LIMODIN, JEAN FRANÇOIS WITZ, and JÉRÔME HOSDEZ — Univ. Lille, CNRS, Centrale Lille, UMR 9013 - LaMcube - Laboratoire de Mécanique, Multiphysique, Multiéchelle, F-59000 Lille, France

Determining whether a defect will grow or not is of outmost importance particularly for railway axles. In this context, compressive precracking is an interesting procedure to get fatigue crack growth threshold. Using this method, specimens are precracked with both maximum and minimum compressive loads. This study uses fracture mechanics analysis, digital image correlation (DIC) and finite element method (FEM) to assess compressive plastic zone and precrack length ahead of a SENT specimen notch.

The DIC strain field in the direction of loading shows the evolution of the monotonic compressive zone ahead of the notch with increasing load. Other techniques were used to assess the plasticity ahead of the notch and to verify DIC vertical strain field results. One technique consists of projecting (in the least squares sense) the measured DIC displacement fields on Williams' basis. The difference between the DIC vertical displacement field and the analytical one highlights the plasticity in the notch region. A coupled DIC-FEM simulation with boundary conditions issued from DIC displacement fields applied on a numerical model of the specimen with inelastic material behavior was done in order to verify the extent of the compressive plastic zone and to estimate the compressive precrack length.

MM 20.3 Tue 14:45 SCH A 216

Microstructural damage analysis in a DP800 steel subjected to complex strain paths — •MAXIMILIAN A. WOLLENWEBER, LUIZ R. GUIMARÃES, NICOLE LOHREY, SETAREH MEDGHALCHI, TALAL AL-SAMMAN, and SANDRA KORTE-KERZEL — RWTH Aachen, Aachen, Germany

During forming processes, initiation and evolution of microstructural damage sites have a strong negative influence on the mechanical properties of the finished product. It is therefore important to investigate the damage behavior during deformation and unravel its relationship with the strain path. The current work investigates the microscopic damage evolution in a dual-phase steel DP800 subjected to different loading scenarios in tension and bending. The aim is to elucidate how the strain path influences the initiation and growth of microstructural damage in order to design more damage-tolerant industrial forming processes. The methods used comprise machine-learning algorithms and in-situ testing in a scanning electron microscope to observe and classify damage sites in the deformed samples. The results show that strain hardening inhibits damage formation, while pre-existing damage sites tend to facilitate further damage formation.

MM 20.4 Tue 15:00 SCH A 216

Three-dimensional characterization of damage sites and strain dependence in dual phase steel — •SETAREH MEDGHALCHI¹, BINBIN LIN², JOSCHA KORTMANN¹, BAI-XIANG XU², ULRICH KERZEL³, and SANDRA KORTE-KERZEL¹ — ¹Institute for Physical Metallurgy and Materials Physics, RWTH Aachen University, Aachen, Germany — ²Mechanics of Functional Materials Division, Institute of Materials Science, Technische Universität Darmstadt, Darmstadt, Germany — ³Fakultät für Georesourcen und Materialtechnik, RWTH Aachen University, Aachen, Germany

High performance materials like dual phase steels possess a heterogeneous microstructure resulting in the unique interplay between the two phases. High resolution scanning electron microscopy serves as a tool to unravel many of the microscale properties related to the deformation and mechanical properties of these materials. Damage sites in the microstructure serve as the main controlling feature during deformation. There are two fronts to tackle for a deeper understanding of the global damage accumulation: First, bringing high resolution analysis to large scales, and second, moving from two dimensional to three-dimensional characterization. We approach this challenge by employing slice-and-view SEM sectioning in combination with automated convolutional neural networks. With the knowledge of the damage occurring in different positions with various local conditions, we combine some related parameters to capture not only the trajectory of the damage sites inside the volume of the sample, but also the relative local stress-strain distribution condition.

MM 20.5 Tue 15:15 SCH A 216

Experimental and computational crack growth analysis under in-phase and out-of-phase thermo-mechanical fatigue — •VALERY SHLYANNIKOV, ALEXSANDR SULAMANIDZE, and DMITRY KOSOV — Kazan, Russia

This study presents interpretation and evaluation of non-isothermal experimental crack growth data generated by tests carrying out by stress-controlled in-phase (IP) and out-of-phase (OOP) thermo-mechanical fatigue (TMF) conditions. A crack growth testing method has been developed utilizing inductive heating and direct the crack tip opening displacement (CTOD) techniques for polycrystalline XH73M nickel-based alloy. The crack growth experimental results interpretation is based on finite element analyses of the mechanical stress-strain rate fields at the crack tip and new fracture resistance parameters. To this

end, an algorithm for multi-physics numerical calculations was developed and implemented by incorporating Maxwell 3D, Fluent, and the transient structural modules of ANSYS 2021R1, to understand the mechanics of crack tip deformation under thermo-mechanical loading conditions. Fatigue fracture diagrams build in terms of new crack growth parameters have shown that in-phase testing produces accelerated crack growth rates compared with out-of-phase due to increased temperature at peak stress and therefore increased time dependent crack growth.

MM 21: Materials for Storage and Conversion of Energy: Energy Conversion

Time: Tuesday 14:15–15:30

Location: SCH A 215

MM 21.1 Tue 14:15 SCH A 215

Harvesting of low-grade waste heat with shape memory alloys — •BRUNO NEUMANN^{1,2} and SEBASTIAN FÄHLER¹ — ¹Helmholtz-Zentrum Dresden-Rossendorf — ²Technische Universität Dresden

More than half of all energy converted by humankind is lost in the form of waste heat. Not only does that strongly contribute to the acceleration of global warming, it also leaves an enormous economic potential untouched. However, suitable technologies are limited, since most of this heat is of low temperature (< 100 °C). In the last years, materials and technologies for thermoelectric harvesting and thermomagnetic harvesting have been explored, but a high efficiency of those systems remain a challenge. With our work, we present a thermoelastic harvesting approach for converting the waste heat of a fluid into electricity, utilizing shape memory alloy wires. These wires bring the inherit advantage that their transformation temperatures can be adapted to the required temperature range of the waste heat. Moreover, they provide a very high actuation energy density and are commercially available. In our set-up, we use two mechanically connected arrays of wires to reach a high power density of the system. Our simulation data predicts a thermodynamic efficiency in respect to the Carnot efficiency of 22.7 %, which exceeds current efficiency benchmarks set by thermoelectric materials.

MM 21.2 Tue 14:30 SCH A 215

Atomistic simulations of the Seebeck effect in electrolytes — •OLE NICKEL¹, MATHIJS JANSSEN², and ROBERT MEISSNER¹ — ¹Hamburg University of Technology, Hamburg, Germany — ²University of Oslo, Oslo, Norway

The Seebeck effect allows electrical energy to be obtained directly from thermal gradients. In electrolytes it is based on an different heat of transport of the ions.

We perform molecular dynamic simulations with different electrolytes between graphene electrodes. We apply an external resistance between the electrodes via a thermopotentiostat, where the thermal fluctuation term is deactivated, effectively resembling an RC-circuit with a time constant of $\tau=RC$.

With this method it is possible to simulate a complete electrochemical cell in open circuit conditions which is charged with a thermal gradient and then discharged at constant temperature. The Seebeck energy is the energy that is dissipated across the external resistance. The goal is to investigate optimal electrolyte parameters to maximize this energy.

MM 21.3 Tue 14:45 SCH A 215

Non-Local DFT calculations towards the discovery of stable water-splitting catalysts — •AKHIL S. NAIR, LUCAS FOPPA, EVGENY MOERMAN, and MATTHIAS SCHEFFLER — The NOMAD Laboratory at the FHI of the Max-Planck-Gesellschaft and IRIS-Adlershof of the Humboldt-Universität zu Berlin, Germany

Efficient prediction of the thermodynamic and aqueous stability of materials is essential for leveraging the catalyst discovery for the water splitting reaction. In particular, the oxygen evolution half-reaction is usually carried out using oxide catalysts under harsh potential and pH conditions.[1] This necessitates the

application of DFT methods which can predict the oxide stability under experimentally relevant conditions without any *ad hoc* corrections.[2] In this regard, herein, we employ a non-local DFT method using the hybrid HSE functional for calculating the stability of oxide catalysts. Crucially, we scrutinize the effect of the HSE mixing parameter on the formation energies and aqueous stability of oxides and compare to higher-level calculations using coupled-cluster theory for reference systems. Through this approach, we attempt to standardize the application of HSE method for accurate oxide stability prediction which could augment the large-scale catalyst discovery.

[1] Z.Wang, *et al.*, *npj Comput. Mater.* **6**, 160 (2020).

[2] L.-F. Huang, J. M. Rondinelli, *npj Mater. Degrad.* **3**, 26 (2019).

MM 21.4 Tue 15:00 SCH A 215

Photocatalytic water splitting from Koopmans spectral functionals: The case of TiO₂ polymorphs — •MARIJA STOJKOVIC¹, EDWARD LINSKOTT¹, and NICOLA MARZARI^{1,2} — ¹Theory and Simulations of Materials (THEOS), and National Centre for Computational Design and Discovery of Novel Materials (MARVEL), École Polytechnique Fédérale de Lausanne, 1015 Lausanne, Switzerland — ²Laboratory for Materials Simulations, Paul Scherrer Institut, 5232 Villigen PSI, Switzerland

Photocatalytic water splitting has drawn considerable attention for renewable energy production. Since the first reported photocatalytic water splitting by titanium dioxide, this material remains one of the most promising photocatalysts, due to its suitable band gap and band-edge positions. However, estimating both of these properties is a challenging task for standard DFT functionals. Here we show how Koopmans spectral functionals can accurately predict the band structure and level alignment of rutile, anatase and brookite, demonstrating the advantage of orbital-density dependent functionals for predicting the spectral properties of materials.

MM 21.5 Tue 15:15 SCH A 215

DFTB Description of the Ground and Excited States Properties of Thiolate Protected Gold Nanoclusters — •CARLOS R. LIEN-MEDRANO¹, ARNAUD FIHEY², and THOMAS FRAUENHEIM¹ — ¹University of Bremen, Bremen, Germany — ²University of Rennes, Rennes, France

Gold nanoclusters stand as promising building blocks for solar energy harvesting applications, luminescent materials and catalytic devices. At the frontier between molecular and metallic structures, their large number of electrons prevent the use of *ab initio* quantum mechanic method to rationalize and predict their structure-property relationships, especially when fully coated with organic ligands. Using a semi-empirical DFT-based scheme, namely Tight-Binding Density Functional (DFTB), we demonstrate that is possible to rapidly access the ground (geometry and electronic structure) and excited state (UV-Visible absorption) properties of these nano-objects without sacrificing the qualitative accuracy of its parent DFT, paving the way towards a quantum material design of gold-organic nano-devices.

MM 22: Mechanical Properties and Alloy Design: Porous and Nanostructured Materials

Time: Tuesday 14:15–15:45

Location: SCH A 118

MM 22.1 Tue 14:15 SCH A 118

tailoring mechanical properties of lightweight 1D Nanostructures — SAMUEL BALTAZAR^{1,2}, JAVIER ROJAS^{1,2}, •FELIPE VALENCIA^{2,3}, SEBASTIAN ALLENDE^{1,2}, RAFAEL GONZALEZ^{2,4}, EDUARDO BRINGA⁵, and PIERRE COCCO-MAGNARD² — ¹Physics Department, Universidad de Santiago de Chile, Chile — ²Center for the development of Nanoscience and Nanotechnology, Universidad de Santiago de Chile, Chile — ³Engineering Faculty, Universidad Católica del Maule, Chile — ⁴Centro de Nanotecnología Aplicada, Universidad Mayor, Chile — ⁵CONICET & Facultad de Ingeniería, Universidad de Mendoza, Argentina

1D Nanostructures such as nanowires (NW) and nanotubes (NT) have gained

a lot of attention due to their mechanical and electronic properties. The deformation of NT and NW has been previously studied, finding different fracture mechanisms. Tension and compression deformations show elastic regimes until a sudden stress drop due to the fast generation of dislocations. Synthesis of polycrystalline NW allows the reinforcement of the material's response. We report the mechanical properties are studied for mono and bimetallic systems by means of molecular dynamics simulations. Interatomic potentials were used to model Ni, Fe, and bimetallic NTs and NWs with dimensions similar to the experimental setup. Ni NT shows an asymmetry in the stress response under tension and compression, mediated by twins and stacking-faults dislocations, with no signif-

icant degradation of mechanical properties up to 60% mass reduction than NW, opening the generation of new lightweight and resistant materials.

MM 22.2 Tue 14:30 SCH A 118

Comparing structural response of filled and porous 3D Titanium network structures by application of nanotomography and graph theory — •STEFAN A. BERGER¹, MARKUS ZIEHMER¹, and JÜRGEN MARKMANN^{1,2} — ¹Helmholtz Zentrum Hereon — ²Technische Unoversität Hamburg

Recently, refinements of the classical Gibson-Ashby relation have been invoked to extend its applicability to the description of the mechanical properties of bi-continuous, nanoporous metals. In particular, the network connectivity has been identified as a crucial parameter that needs to be taken under consideration. So far, global parameters like connectivity or genus (density) have been employed. However, these do not uniquely identify the underlying microstructure. This can be achieved by making use of graph theoretical aspects, as demonstrated in Ziehmer et al[1]. In this work, we have investigated the changes in the network structures of porous Titanium and Ti-Mg composites, fabricated by Liquid Metal Dealloying, during compression tests in a x-ray nanotomograph. The reconstructed sample volumes were simplified by skeletonization, the resulting skeletons transferred into a weighted graph representation, and further decomposed into the constituent rings that built the network. This approach allowed for a statistical description of the behavior of the ring elements under load. One major result is that the essential part of deformation is carried by larger rings. [1] M. Ziehmer, E. T. Lilleodden, Acta Materialia 199 (2020).

MM 22.3 Tue 14:45 SCH A 118

Hierarchical-structural effects on mechanical behavior of nanoporous gold in electrochemical environment — •HANSOL JEON¹, SHAN SHI^{3,1}, and JÜRGEN MARKMANN^{1,2} — ¹Institute of Materials Mechanics, Helmholtz-Zentrum Hereon, 21502 Geesthacht, Germany — ²Institute of Materials Physics and Technology, Hamburg University of Technology, 21073 Hamburg, Germany — ³Research Group of Integrated Metallic Nanomaterials Systems, Hamburg University of Technology, 21073 Hamburg, Germany

Recently, hierarchical nanoporous gold (HNPG) has been emerged with having multiple-level structures. HNPG is more active because of higher surface area than nanoporous gold (NPG) since Au ligaments are supposed to be converted into another porous structure with smaller ligaments and pores. Regarding mechanical behavior, especially with the same solid fraction for both, it has been not directly compared yet whether HNPG would have better mechanical properties. Here, we investigated the mechanical properties of NPG and HNPG with the same solid fraction by conducting compressive tests at the micro-scale. The NPG and HNPG were prepared from the same precursor alloy Ag₈₅Au₁₅ by dealloying. The pillars were milled by a focused ion beam (FIB), and compressive tests were performed by a nanoindenter with a flat-punch tip. We discussed the difference of dislocation activities and connectivity for NPG and HNPG. Finally, by conducting additional compressive tests in an electrochemical environment, we explored the role of surface state on the mechanical behavior of NPG and HNPG by imposing electrode potential.

MM 22.4 Tue 15:00 SCH A 118

Mechanical properties and oxidation performance of nanostructured self-passivating WCrY material — •JIE CHEN¹, ANDREY LITNOVSKY¹, JESUS GONZALEZ-JULIAN^{1,2}, JAN WILLEM COENEN¹, and CHRISTIAN LINSMEIER¹ — ¹Forschungszentrum Jülich GmbH, Institut für Energie- und Klimaforschung - Plasmaphysik, 52425 Jülich, Germany — ²Institute of Mineral Engineering, RWTH Aachen University, 52074 Aachen, Germany

Self-passivating W-11.4wt%-0.6wt%Y alloy have been considered as a promising plasma-facing material in fusion power plants. In the present work, bulk material are fabricated via holding at 1300C for 2 minutes in field-assisted sintering. As a result, an average matrix's grain size of 98.9nm and 6.7% surface

area of Cr-rich phase was obtained. Cr-rich phase is formed on the surface of particles during sintering and over 70 at% of Cr is detected by EDX. A hardness HV0.5 of 1287.6 is obtained as a result of small grains while a fraction of Cr-rich phase in the microstructure softens material to some extent. Three point bending tests at temperature up to 1000C are performed to measure fracture toughness and ductile brittle transition temperature. This is done combining with fractography study to investigate the effect of grain size as well as Cr-rich phase on the thermo-mechanical properties. Reduction in grain size down to the order of sub-micrometer range is proven to improve material's anti-oxidation performance in previous study. Oxidation test was performed at 1000C to investigate performance of the microstructure developed. Details of the work are presented in this contribution.

MM 22.5 Tue 15:15 SCH A 118

Study of the oxidation mechanism of Cr₂AlC MAX phase through nanoscale analysis of alumina scale formation — •ANICHA REUBAN^{1,2}, JESUS GONZALEZ-JULIAN^{1,2}, IVAN POVSTUGAR¹, ANDREY LITNOVSKY¹, and CHRISTIAN LINSMEIER¹ — ¹Forschungszentrum Jülich GmbH, 52425 Jülich, Germany — ²Institute of Mineral Engineering, RWTH Aachen University, 52074 Aachen, Germany

In a Concentrated Solar Power (CSP) plant, the receiver must withstand temperatures >800 °C, be resistant to oxidation by air and/or corrosion by molten salts and maintain its properties over time. MAX phases, which are ternary carbides and nitrides with a unique combination of ceramic and metallic properties, are candidate materials for the receiver. In this work, the oxidation mechanism of the alumina-forming MAX phase Chromium Aluminium Carbide (Cr₂AlC) is studied. The samples are oxidized in a thermogravimetric analyzer (TGA) at 1000 °C and 1200 °C in humid air. The oxide scale is characterized using XRD, FIB-SEM, EDX and STEM. The alpha alumina layer formed consists of needle-like grains on top, with larger grains at the bottom, below which is a layer of chromium carbide. The elemental distribution across grain boundaries and interfaces of various regions of the oxide scale, carbide and bulk material are being analyzed with Atom Probe Tomography (APT), since these are possible pathways for the diffusion of aluminium and oxygen ions to form the oxide layer. The effect of dissolved chromium in the oxide scale and the segregation of impurities such as iron and silicon to interfaces is examined.

MM 22.6 Tue 15:30 SCH A 118

Phase stability of iron and its alloys from first principles dynamical simulations and thermodynamic integration — •DAVIDE GAMBINO and BJÖRN ALLING — Linköping University, Linköping, Sweden

In recent years, thermodynamic integration (TI) based on first principles simulations has been shown to accurately reproduce phase diagrams and is now able to guide the design of functional materials and alloys. For what concerns iron and steels, this methodology is complicated by the presence of magnetic degrees of freedom (DOF) and their interplay with electronic and vibrational DOFs. Here I will show how the phase stability of iron and its alloys can be obtained from first principles employing atomistic spin dynamics - ab initio molecular dynamics (ASD-AIMD) simulations and TI accounting for all DOFs [1].

The free energy difference between bcc and fcc Fe was calculated close to the melting point in the magnetically disordered state, carrying out TI over stress-strain variables along the Bain path, and then propagating it to low temperatures with TI over temperature employing the ASD-AIMD energies. The method captures the $\alpha \rightarrow \gamma \rightarrow \delta$ transitions, with the latter transition temperature reproduced within 50 K from experiments, and the calculated Gibbs free energy difference being within 5 meV/atom from the CALPHAD estimate over the whole temperature range. The method is then applied to Fe_{1-x}Mn_x alloys for concentrations of $x = 0.05, 0.10$ and for temperatures $T \geq 1400$ K and results are compared with the experimental phase diagram.

[1] Gambino et al., arXiv:2210.14718 [cond-mat.mtrl-sci]

MM 23: Poster II

Time: Tuesday 18:15–20:00

Location: P2/OG1+2

MM 23.1 Tue 18:15 P2/OG1+2

(ZnO) 42 Nanocluster: A Novel Visibly Active Magic Quantum Dot under First Principle Investigation — •BIJAL MEHTA and DEBESH ROY — Materials and Biophysics Group, Department of Physics, Sardar Vallabhbhai National Institute of Technology, Surat 395007, India.

A systematic density functional investigation on the structural, electronic and optical properties of the growth of (ZnO) 6 cluster unit in the series of (ZnO) 6n for n=1*9 is performed in this report. Different electronic properties of (ZnO) 6n nanoclusters are analyzed in terms of HOMO-LUMO gap (HLG), ionization potential (IP), electron affinity (EA), chemical hardness (η), and electrophilicity index (ω) which all shows a zigzag behavior as the size of (ZnO) 6n clusters increases. The clusters' electronic energy gain (*E) identified an exceptionally sta-

ble *magic* nanocluster, viz. (ZnO) 42. Frontier orbitals analysis results indicate easy electron transfer in (ZnO) 42 nanocluster system. The optical absorption spectra confirm that the magic (ZnO) 42 nanocluster is active in electromagnetic radiation's visible range ($\lambda=406.8$ Å). Interestingly, similar optical switching towards the growth of (ZnO) 6 unit is also observed like zig-zag electronic properties. The simulation results of electronic properties as well as the infrared spectra of magic (ZnO) 42 cluster will open up a vista to the experimentalists for its possible synthesis, which in turn will help in the development of the visibly active magic (ZnO) 42 nanocluster with novel applications in the fields of quantum dots or assembled materials.

MM 23.2 Tue 18:15 P2/OG1+2

Investigation of the stability for AlB_2 -type transition metal diborides from electronic structure — •NEBAHAT BULUT and JENS KORTUS — TU Bergakademie Freiberg, Institute of Theoretical Physics, Germany

Boron has huge chemical bonding diversity (metallic, ionic, and covalent bonds) because it provides fewer valence electrons compared to the number of orbitals it can form. Not surprisingly, intermetallic borides can crystallize in many different crystal symmetries, for example cubic, hexagonal or orthorhombic. The unit cell of the hexagonal AlB_2 -type has two trigonal prisms in which borons are in the center surrounded by six metal atoms. Interestingly, not all twenty eight transition metals form the AlB_2 -type crystal structure. The goal of the study is to understand the chemical bonding nature in detail in order to answer why some of these compounds are stable in AlB_2 -type structure while others are not. We investigate the impact of the d -orbitals of the transition metals on the stability in order to provide a guideline to possible new transition metal diborides. The chemical bonding and charge transfer in these transition metal diborides is investigated by electronic structure calculations based on density functional theory as implemented in Quantum Espresso [1]. The study is focused on the analysis of the electron density together with the electron localization function (ELF) and provide thermodynamic information e.g. formation enthalpies, and mechanical properties.

[1] P. Giannozzi et al., J. Chem. Phys. 152 154105 (2020)

MM 23.3 Tue 18:15 P2/OG1+2

Trapping and detrapping of excess vacancies during natural ageing in Al-Cu — •TOBIAS STEGMÜLLER, JOHANNES BERLIN, ANDREAS SCHUSS, and FERDINAND HAIDER — University of Augsburg, Chair for Experimental Physics I, Universitätsstr. 1, 86159 Augsburg

A special feature of Al-Cu alloys is the occurrence of decomposition in supersaturated solid solutions by the formation of Guinier-Preston zones (GPZ) even at ambient temperature, where the equilibrium diffusion coefficient is far too low for any unmixing. A condition for this natural ageing is the existence of excess vacancies which remain in the material after quenching from the homogenisation temperature. As the ageing process proceeds for surprisingly long times (hours or days), the vacancies seem to be stabilised in the material and do not decay to the equilibrium value, which would stop the ageing.

Although there exist theories on the stabilisation of excess vacancies, there is no established and verified model to explain the effect. To illuminate the mechanisms behind the long term formation of GPZ we combine results from TEM and DSC measurements as well as Monte Carlo, molecular static and DFT simulations, which reveal that the GPZ themselves may act as temporal vacancy traps. Values for the trapping energy for vacancies in GPZ and on dislocations are estimated from simulations.

MM 23.4 Tue 18:15 P2/OG1+2

Proof of concept for micro pulling down growth of phase change materials in the example system of NiTi — •LAURITZ SCHNATMANN, TIMON SEWEKE, and GABI SCHIERNING — University of Bielefeld

The micro pulling down growth method (mPD) is a common approach to synthesize small crystals for material screening in e.g. high-entropy oxides. Another interesting group of materials are phase change materials namely showing unique structural transitions interplaying with electronic and magnetic contributions. However, the interplay between the different contributions is strongly dependent on the composition of materials. We built up a micro pulling down set up for fast material screening of phase changing materials. We grew a NiTi-shape memory alloy to show the possibility of comparable easy growth of crystals by mPD. Hereby, we verified mPD as a powerful tool for the versatile fabrication of small crystals in the field of phase change materials.

MM 23.5 Tue 18:15 P2/OG1+2

The role of electrons during the martensitic phase transformation in NiTi-based shape memory alloys — •ALEXANDER KUNZMANN¹, JAN FRENZEL², ULRIKE WOLFF³, JEONG WOO HAN⁴, LARS GIEBELER³, DAVID PIORUNEK², MARTIN MITTENDORF⁴, JULIANE SCHEITER³, HEIKO REITH³, NICOLAS PEREZ³, KORNELIUS NIELSCH^{3,5}, GUNTHER EGGELER², and GABI SCHIERNING¹ — ¹Bielefeld University — ²Ruhr University Bochum — ³IFW-Dresden — ⁴University of Duisburg-Essen — ⁵TU Dresden

The present work provides an experimental contribution to the investigation of the role of conduction electrons in the martensitic phase transition of Nickel-Titanium. This material, which is structurally very well studied due to its shape memory effect, still offers room for further knowledge more than 60 years after its discovery. For this purpose, a series of alloys within the equiatomic NiTi phase was characterized by temperature-resolved transport experiments, thermodynamic characterizations and structural investigations. In addition to the well-known resistivity anomaly, a reduction of the charge carrier density by 90% was measured, which has not been described before for this class of materials. Using a novel approach for structural materials, conclusions could be drawn about the entropy of the electronic system and a correlation with the phase transition temperature could be demonstrated. The obtained data allow an interpretation as the

formation of a charge carrier density wave phase, which explains both the drastic reduction of charge carriers and the large electronic entropy contribution.

MM 23.6 Tue 18:15 P2/OG1+2

developing high-hardness, high-electrical conductivity and gradient structure of bulk Al-2.5Fe alloy by a new severe plastic deformation: high pressure torsion extrusion — •RUI XU — Institute of Nanotechnology, Karlsruhe Institute of Technology, Germany

The effect of High Pressure Torsion Extrusion (HPTE) on microstructure, hardness and electrical conductivity has been investigated in the bulk Al-2.5Fe alloy. The equivalent strain accumulated in the samples after one pass of HPTE varied in a wide range between 0.9 and 24.8, depending on the processing parameters. HPTE led to the formation of a gradient microstructure in which the grain and Al₆Fe intermetallic size decreased by increasing the distance from the central axis of the samples. With increasing the equivalent strain, which is below 5.7, the microhardness and the electrical conductivity simultaneously increased, from 53.7 HV to 87 HV, from 38% IACS to 47% IACS respectively. This can be attributed to the grain size and Al₆Fe intermetallic size decreased. When the equivalent strain gradually increased to 24.8, the microhardness continuously increased from 87 Hv to 126 Hv, the electrical conductivity decreased from 47% IACS to 43% IACS. This is contributed to the grain and Al₆Fe intermetallic transformed into nanometer size, which significantly increased the microhardness, and some Fe atoms into Al matrix, which decreased the electrical conductivity. The High Pressure Torsion Extrusion process can lead to gradient microstructure and simultaneously increase the microhardness and the electrical conductivity of bulk Al-2.5Fe alloy.

MM 23.7 Tue 18:15 P2/OG1+2

In situ XRD measurements of a Si Li half battery cell — •LEONARD AUE, FREDERIK STENDER, THOMAS BREDE, and CYNTHIA VOLKERT — Georg-August-Universität Göttingen, Deutschland

Li-ion batteries have become an indispensable part of modern life. They enable the repeated storage of energy on a medium and small scale, for example in electric vehicles or mobile devices.

In addition to the commonly used graphite, silicon is gaining increasing attention as a suitable anode material due to its higher capacity. However, this capacity decreases rapidly in application and a significant increase of the internal resistance occurs. Both are mainly caused by the large volume changes during lithium uptake and release.

In this work, we investigate the amorphization process that first starts during loading in in-situ XRD measurements of Si-Li composite materials in a half-battery setup. This will give us insight into Si phase changes under direct control of critical parameters such as charge or discharge rates. This knowledge could help to understand and control the phase transformations and thereby improve Si anode performance.

MM 23.8 Tue 18:15 P2/OG1+2

High capacity thin film battery electrodes from lithium titanate — YIJIE TAO, •YUG JOSHI, and GUIDO SCHMITZ — Chair of Materials Physics, Institute of Materials Science, University of Stuttgart, 70569 Stuttgart, Germany

Lithium titanium oxide is becoming an increasingly popular anode material for high-power Li-ion batteries due to their safe operating voltages and high cycle lifetime. The motivation to enhance the specific capacity of Li₄Ti₅O₁₂ (LTO) is of practical significance. In this work, reactive ion beam sputtering is used to deposit the titanium-based metal oxide thin films. A Li₂CO₃ modification is introduced by mixing it with LTO and using the composite as a target material. The deposition conditions (i.e., reactive oxygen) and annealing treatment (i.e., under air or vacuum at varying temperatures) are explored to optimize the thin films for the best possible capacity. X-ray diffraction (XRD), X-ray photoelectron (XPS) and electron diffraction (TEM) are used to unravel the chemical and structural nature of the thin films. The films were electrochemically characterized using cyclic voltammetry with a broad potential window, much wider than conventional LTO (i.e., 2.5V to 0.1 V vs Li/Li+), whereas conventional electrode is generally limited to a lower voltage of 1V). The optimized film shows good cyclic stability at a relatively high rate of 1 mV/s and show an astounding maximum capacity of 101.4 $\mu\text{Ah}\cdot\text{cm}^{-2}\cdot\mu\text{m}^{-1}$ after 50 cycles. To put this in context, conventional LTO shows theoretically 60.8 $\mu\text{Ah}\cdot\text{cm}^{-2}\cdot\mu\text{m}^{-1}$ and 91 $\mu\text{Ah}\cdot\text{cm}^{-2}\cdot\mu\text{m}^{-1}$ when cycled down to 1 V and 0.1 V vs Li/Li+, respectively.

MM 23.9 Tue 18:15 P2/OG1+2

high-rate and long-duration Sodium Storage Enabled by Sodiation-Driven Reconfiguration — •YULIAN DONG, HUAPING ZHAO, and YONG LEI — Fachgebiet Angewandte Nanophysik, Institut für Physik & IMN MacroNano, Technische Universität Ilmenau, 98693 Ilmenau, Germany

Vanadium sulfides, with various crystal structures, such as VS₂, V₂S₃, V₃S₄, V₅S₈, and VS₄ have attracted increasing attention because they could provide high theoretical specific capacity. Nevertheless, such vanadium-based sulfides frequently suffer significant mechanical pulverization during long-term cycling as a result of volume expansion caused by sodiation/desodiation, which result

in severe irreversible capacity degradation, poor initial coulombic efficiency, reduced rate capability, and inappreciable cycling stability. Here, we demonstrate a carbon-free 3D micro-nano flower-like VSx heterostructure electrode material that is synthesized by a facile hydrothermal process for SIB applications. The 3D micro-nano flower-like structure can well prevent the accumulation of nanosheets during electrochemical cycles and ensure full contact between the active material and the electrolyte. Therefore, 3D micro-nano flower-like VSx electrode that finally achieves an ultrahigh-rate capacity (613.8 mAh/g at 10 A/g) and an ultra-long cyclability (more than 1500 cycles) by sodiation-driven reconfiguration for sodium ions batteries. This work presents a general approach for preparing super-high specific capacity and rate capacity electrode materials for further improving the SIBs performance.

MM 23.10 Tue 18:15 P2/OG1+2

Detection of Lithium in potential electrode materials — •PATRICK KIRSCHT and HANS HOFSSÄSS — II Physikalisches Institut, Georg August Universität, Göttingen, Deutschland

Nuclear reaction analysis is used to quantify light elements such as lithium in a sample. The advantage of NRA is the isotope specific measurement of elements in a sample. In the current investigations we demonstrate the detection limits and sensitivity of a new setup for the detection of lithium via its nuclear reaction with protons $p(7\text{-Li},\alpha)\alpha$ with $Q=17\text{MeV}$. For this purpose an external proton beam with 2.5MeV is used. To determine the detection limit, lithium was implanted into silicon and ta-C near the surface by ultra-low energy ion implantation at 100eV. Furthermore, the depth profile and penetration depth were simulated using Imintdyn and SRIM and were compared with the measurements. For the measurement of diffusivity of lithium, the samples were baked at different temperatures. For comparison, MD simulation was performed using LAMMPS. These investigations are the starting point of measurements on graphene and biological materials like wood, which are considered for possible applications as electrode materials in batteries.

MM 23.11 Tue 18:15 P2/OG1+2

High-resolution measurement of displacement field from gold nanoparticles tracking — •ANTOINE OLLIVIER, NICHOLAS BLANCHARD, ANTONIO PEREIRA, LOÏC VANEL, and DÔME TANGUY — Institut Lumière Matière-UMR 5306, Université Claude Bernard Lyon 1, 6 rue Ada Byron, 69622 Villeurbanne cedex

A new method has been developed to measure displacement field during a tensile test with both high resolution (~ 50 nm) and good precision (~ 1 nm). This method has been applied on the reduced activation ferrite-martensitic steel Eurofer97. Gold nanoparticles are created by pulsed-laser induced dewetting of a nanofilm. This technique does not modify the structure of the steel below. Nanoparticles are then observed with a scanning electron microscope during tensile test. Their tracking allows to see displacement field *in situ*. This method is particularly adapted for locating heterogeneities in the displacement field and it could be very useful to understand how fracture appears.

MM 23.12 Tue 18:15 P2/OG1+2

Electronic Properties of Self-assembled 1D Gold Nanoparticle Chains — •STEFAN M. SCHUPP¹, DAVID J. SCHUPP², EMIL SCHWARZ², REBECCA KÖSER², HELMUT CÖLFEN², and LUKAS SCHMIDT-MENDE¹ — ¹Department of Physics, University of Konstanz, Germany — ²Department of Chemistry, University of Konstanz, Germany

1D nanoparticle (NP) assemblies exhibit unique electronic properties due to their directional charge transport. In addition, the usage of stabilizing ligands enables a further possibility to add new functionalities and tune their conductivities. However, the assembly and characterization of 1D NP chains remains a challenge to this day. Here, we present a study on thiol-induced dipoles on gold (Au) nanoparticle surfaces which result in chain-like assemblies in solution under ambient conditions. Thereby, 1D assemblies of 40 nm Au-NPs with different shapes and thiolated ligands could be achieved. Afterwards, a developed transfer technique allows the electrical characterization of individual 1D NP chains through prefabricated gold electrodes. In this configuration, the temperature-dependent resistance of different NP assemblies is investigated to understand the underlying conduction mechanisms. With the gained knowledge it should be possible to generate 1D Au NP chains with controllable electronic conductivities for future applications.

MM 23.13 Tue 18:15 P2/OG1+2

Local hydrogen absorption in Pd nanoparticles observed with in-situ TEM — •SVETLANA KORNEYCHUK¹, STEFAN WAGNER¹, GEORGIAN MELINTE², DARIUS ROHLER³, PHILLIPP VANA³, and ASTRID PUNDT¹ — ¹Karlsruhe Institute of Technology, Karlsruhe, Germany — ²King Abdullah University of Science and Technology, Saudi Arabia — ³Institute of Physical Chemistry Georg-August-University Göttingen, Göttingen, Germany

The mechanism of the hydrogen absorption in metals is of a high interest for many areas of hydrogen technology, such as hydrogen storage, hydrogen detection and catalysis. Palladium is an ideal model system to study hydrogen absorp-

tion in metals due to its extreme affinity to hydrogen. Nanoscale systems, such as nanoparticles and thin films, are of the high interest to hydrogen technology due to their faster interaction with hydrogen. In this work, we investigate the behavior of a model system, Pd nanoparticles, in real time with in-situ H₂-gas TEM. With the special gas holder from Protochips it is possible to reach pressures up to 1 atmosphere and study the particles at elevated temperatures within the stability limit of the nanoparticles up to 200°C. We can observe initial stages of hydrogen absorption in Pd nanoparticles and local formation of PdH_x at different temperatures and pressures by using EELS. We support our observations with the in-situ strain measurements carried out with nanobeam electron diffraction. Finally, we propose a mechanism of hydrogen absorption in metallic nanoparticles based on the local PdH_x formation and strain measures at different loading conditions.

MM 23.14 Tue 18:15 P2/OG1+2

Investigation of the MoS₂ crystallization process in thin films — •ANNIKA KORN, THOMAS BREDE, and CYNTHIA A. VOLKERT — Institut für Materialphysik, Göttingen, Germany

Crystalline transition metal dichalcogenide thin films show interesting potential in various application areas (e.g. optoelectronics and data storage). Crystallization of amorphous sputtered thin films is one way to produce large crystalline regions suitable for the application [1]. The aim of this work is to follow the structure of the thin films over the course of crystallization and to characterize them in different intermediate states. In this way, the process and properties of the transition can be studied and better understood. Specifically, various methods (XRD, SEM, EDX, XPS, AFM, TEM) will be used to analyze the microstructures and compositions of the samples. In addition, DSC and TGA will be used to directly measure the crystallization and possible decomposition processes.

[1] Krbal, Milos, et al.: Amorphous-to-Crystal Transition in Quasi-Two-Dimensional MoS₂: Implications for 2D Electronic Devices. In: ACS Applied Nano Materials 2021 4 (9), 8834-8844. DOI: 10.1021/acsnm.1c01504

MM 23.15 Tue 18:15 P2/OG1+2

Towards measuring fatigue-generated vacancies in thin copper films using nanoindenter creep tests — •MY NGUYEN, THOMAS BREDE, JAN VERHOEVEN, and CYNTHIA VOLKERT — Institute for Materials Physics, Georg-August University of Göttingen

Vacancies can be created in metals during cyclic loading, however, they have been only rarely directly detected. In this study, we develop an experimental set-up to detect fatigue generated vacancies by measuring their contribution to creep deformation. Our methodology involves performing nanoindenter creep tests on thin metal films while they are being fatigued by cyclic loading. The fatigue is realized using delay line structures, with thin copper films on top, on which standing surface acoustic waves are generated. Contributions from thermal drift during the creep tests have been minimized using a continuous stiffness measurement method.

MM 23.16 Tue 18:15 P2/OG1+2

Optical Modulation and Phase Distribution in LiCoO₂ upon Li-ion De/Intercalation — SANAZ BANIFARSI, •YUG JOSHI, ROBERT LAWITZKI, GÁBOR CSISZÁR, and GUIDO SCHMITZ — Chair of Materials Physics, Institute of Materials Science, University of Stuttgart, 70569 Stuttgart, Germany

The optical modulation of sputter deposited thin-films of LiCoO₂ upon de-/lithiation is probed in reflectance geometry. The thin-films of LiCoO₂ (LCO) are sputter-coated using ion-beam sputtering, onto mirror-like platinum current collectors. A reversible electrochemical and electrochromic behavior is obtained from the in-operando electrochemical and optical measurements. The optical constants (using ex-situ optical spectroscopy) are obtained by modelling the obtained spectra using Clausius-Mossotti relation. The model parameters reveal a dominant resonant wavelength at 646 nm for the fully intercalated LCO. For the delithiated state, Li_{0.5}CoO₂, a much broader and more intense absorption peak is obtained. This broad and intense peak is correlated to the conducting nature of the delithiated state. The obtained complex refractive index (CRI) are justified by prior reported calculations of the density of states. With the evolving CRI, the variation in the imaginary and real part of the dielectric constant is understood by a layered phase propagation. This is due to (i) the faster diffusion between the layers of CoO₆ octahedra of the layered structured LCO and, (ii) the alignment of these octahedral planes almost perpendicular to surface of the electrode as a result of the identified growth texture (due to the deposition and the subsequent annealing).

MM 23.17 Tue 18:15 P2/OG1+2

Simulations of two-dimensional amorphous materials based on force fields and ab initio calculations — •EMEL GURBUZ and BIPLAB SANYAL — Uppsala University, Uppsala, Sweden

In recent times, low dimensional crystalline structures and van der Waals (vdW) solids have attracted a lot of attention for their huge potential in device applications. However, the exploration of two-dimensional (2D) amorphous forms is less explored. Here, we present a detailed study of structural, electronic and thermal properties of 2D amorphous graphene (A-Gra), silicene (A-Si) and sil-

icon carbide(A-SiC) by Classical Molecular Dynamics (CMD) simulations for structure generation, stability tests, thermal conductivity and vibrational analysis along with density functional theory (DFT) calculations for the electronic structure. We find that A-Gra is planar and metallic with a thermal conductivity around 55.30 W/Km whereas the monolayer A-Si has a much lower thermal conductivity (2.68 W/Km). Among our studied materials, A-SiC's thermal conductivity is found to be the highest (70.29 W/Km). Vibrational analysis shows that the heat carriers in A-Si and A-SiC are extendons, especially diffusions in the absence of localized vibrational modes. Bilayer and trilayer structures of amorphous structures resulted respectively, in vdW bonding of A-Gra layers; covalent bonding of A-Si layers and weak bonding of SiC layers through only Si atoms. Finally, the observed uneven charge distributions can lead to the designing future electronic devices by tuning the local functionalities of 2D-amorphous structures.

MM 23.18 Tue 18:15 P2/OG1+2

Effect of micro-alloying and structural relaxation on the nanoindentation behavior of Pd-based metallic glasses — •RICHARD VON DESTINON, MARTIN PETERLECHNER, and GERHARD WILDE — Institut für Materialphysik, Westfälische Wilhelms-Universität Münster, Münster, Germany

Two methods rising in interest to modify the mechanical properties of metallic glasses consist of micro-alloying as well as relaxation. We study the influence of structural relaxation and 1 at.% additions of Fe or Co on the well-researched metallic glass Pd₄₀Ni₄₀P₂₀. The relaxation states are created by quenching from temperatures above T_g with different cooling rates. The samples are analyzed using nanoindentation with force ranges up to 1 mN. Correlations between the change in mechanical properties, such as hardness and young's modulus, and the shear deformation behavior through the pop-in distribution are investigated in detail. The results indicate that both, micro-alloying and relaxation increase the hardness of the material significantly, while the pop-in frequency remains insensitive to either.

MM 23.19 Tue 18:15 P2/OG1+2

Orientation-tunable Rod-shaped Liquid Crystal Under Surface Acoustic Wave — •ZHUOQING LI¹, PAI ZHAO¹, PATRICK HUBER², and ROBERT BLICK² — ¹TU Hamburg Institut für Material- und Röntgenphysik, Hamburg, Germany — ²Center for Hybrid Nanostructures, University of Hamburg, Hamburg, Germany

Surface acoustic waves (SAW) are widely used in both industry and science, while liquid crystals are unique fluids exhibiting long-rang order and self-organization. In this work, a combination of SAW and rod-shaped nematic liquid crystals will be studied to explore the tunability of liquid crystal orientations under SAW. Surface acoustic waves are introduced into miniaturized solid-state devices on piezoelectric LiNbO₃ substrates by interlocking metallic gates called interdigitated transducers (IDT). When a high-frequency sinusoidal signal is applied to the IDT, a mechanical deformation wave will propagate along the surface of the substrate and the induced shear strain will influence the orientation of the nematic liquid crystals on the surface of the substrate. A feature of the nematic phase is that the anisotropic rod-shaped molecules are collectively orientated in preferred directions. Considering the optical anisotropy of rod-shaped liquid crystals, the collective orientation change of liquid crystal molecules under SAW can be analyzed through birefringence measurements. By studying the tunability of the liquid crystal orientation under SAW induced shear component of the wave, we will be able to develop a novel wireless LC-based optical modulator controllable by acoustic stimuli.

MM 23.20 Tue 18:15 P2/OG1+2

Strain-coupled polar textures in ferroelectric nanocylinders — •SVITLANA KONDOVYCH¹ and IGOR LUKYANCHUK² — ¹Institute for Theoretical Solid State Physics, IFW Dresden, 01069 Dresden, Germany — ²Laboratory of Condensed Matter Physics, University of Picardie, 80039 Amiens, France

We consider ferroelectric PbTiO₃ nanocylinders of various size hosting strain-coupled polarization vortices. Depending on the cylinder height and radius, the polarization either swirls around the *c*-oriented cylinder axis (*c*-vortex) or falls into the state with the *a*- or *b*-oriented vortex core (*a*-vortex). The emergence of vortices occurs due to the competition of elastic and electrostatic interactions and complies with the Arnold theorem for divergenceless vector fields, which exist as two types of topological excitations, either vortices or Hopfions [2]. In PbTiO₃ cylinders, we observe the geometry- and temperature-induced vortex axis rotation and corresponding transition between the *c*- and *a*-vortex states. The resulting phase diagram, obtained by phase-field modeling in line with analytical calculations, illustrates the variety of polar textures in nanocylinders, applicable for the efficient design of ferroelectric-based device components.

S.K. acknowledges the support from the Alexander von Humboldt Foundation.

[1] S. Kondovych, et al., arXiv:2112.10129v3 (2022).

[2] I. Luk'yanchuk, et al., Nat. Commun. 11, 2433 (2020).

MM 23.21 Tue 18:15 P2/OG1+2

Tuning porous silicon's pore geometry and its influence on laser-excited guided waves — •MARC THELEN¹, NICOLAS BOCHUD², MANUEL BRINKER¹, CLAIRE PRADA³, and PATRICK HUBER^{1,4,5} — ¹MXP, TUHH, Hamburg, Germany — ²MSME, UPEC, Creteil, France — ³Institut Langevin, ESPCI Paris, Université PSL, CNRS, Paris, France — ⁴CXNS, DESY, Hamburg, Germany — ⁵CHyN, UHH, Hamburg, Germany

Nanoporosity in silicon leads to entirely new functionalities of this mainstream semiconductor with a wide range of applications. In a recent study, we investigated the complex mechanics and the influence of the pores' conicity [1]. This provided the basis for predictable applications in robust on-chip devices and evidence that recent breakthroughs in laser ultrasound technology open up entirely new possibilities for non-destructive in-situ mechanical characterization of dry and liquid-functionalized porous materials. The pores' conicity, which is unintentionally generated during the electrochemical synthesis of porous silicon, can be actively influenced by the process parameters and, within certain limits, arbitrary pore profiles can be generated. This is used, for example, in the production of Bragg mirrors. By tuning the pore shape, we are now investigating its influence on guided waves further, with the goal of developing a phononic material.

[1] Thelen, M., Bochud, N. et al., Nat Commun., 12, 3597 (2021)

MM 23.22 Tue 18:15 P2/OG1+2

Unraveling Fluid Phase Behavior in Geometrically Disordered Nanoporous Materials — •HENRY R. N. B. ENNINFUL and RUSTEM VALIULLIN — Faculty of Physics and Earth Sciences, Felix Bloch Institute for Solid State Physics, Leipzig University, Linnéstraße 5, 04103, Leipzig, Germany.

Mesoporous solids exhibit structural disorder which strongly influence confined fluid properties. This renders quantification of structural disorder and its correlation with physical properties of confined matter a necessary step towards their optimization in practical applications.

In this work, we present advances made in the understanding of correlations between the phase state and geometric disorder in a series of nanoporous solids with variable morphologies. We overview the recently developed statistical theory for phase transitions in a minimalistic model of disordered pore networks represented by the linear chains of pores with statistical disorder. Furthermore, we show that correlating its predictions with various experimental observations, the model gives notable insights into collective phenomena in phase-transition processes in disordered materials and is capable of explaining self-consistently the majority of the experimental results obtained for gas*liquid and solid*liquid equilibria in mesoporous solids. We also show how a newly-introduced interconnectivity parameter of the pore network can be assessed to describe the morphology of porous solids.

MM 23.23 Tue 18:15 P2/OG1+2

Negative Poisson's Ratio in Hierarchical Nanoporous Gold — •HAONAN SUN^{1,2}, LUKAS LÜHRS², and SHAN SHI^{1,3} — ¹Research Group of Integrated Metallic Nanomaterials Systems, Hamburg University of Technology, 21073 Hamburg, Germany — ²Institute of Materials Physics and Technology, Hamburg University of Technology, 21073 Hamburg, Germany — ³Institute of Materials Mechanics, Helmholtz-Zentrum Hereon, 21502 Geesthacht, Germany

The recent fabrication of crack-free monolithic hierarchical nested network nanoporous gold enables the investigation on the benefits of hierarchy in the aspect of mechanical properties [1]. It has been demonstrated that hierarchical nanoporous gold (HNPG) can achieve a substantially reduced solid fraction and enhanced specific stiffness and strength compared with non-hierarchical nanoporous gold. However, the role of the hierarchical structure on Poisson's ratio is not explored yet. In this work, we synthesize mm-sized HNPG samples out of a Ag₉₃Au₇ master alloy with a dealloying-coarsening-dealloying method. We then explore the elastic and plastic Poisson's ratios of HNPG by using digital image correlation during compression testing. Remarkably, we find Poisson's ratio of HNPG is negative for a given strain regime, which suggests their potential application as auxetic materials. Furthermore, the effect of ligament size at both hierarchy levels on Poisson's ratio is also investigated. [1] S. Shi, Y. Li, B.-N. Ngo-Dinh, J. Markmann and J. Weissmüller, Scaling behavior of stiffness and strength of hierarchical network nanomaterials, Science 371 (6533), 2021.

MM 23.24 Tue 18:15 P2/OG1+2

Mechanical actuation of nanoporous metal driven by electroactive self-assembled monolayers — •MATTIS OLGA and MAMEKA NADIIA — Helmholtz-Zentrum Hereon, Geesthacht, Germany

Nanoporous (np) metals fabricated by alloy corrosion are emerging as promising functional materials for (bio-)chemical sensing and actuation. The actuation with np metals exploits the electrocapillary phenomena of metal surfaces, in which surface stress responses to changes of the surface state (e.g. due to adsorption). As the surface stress is coupled with stresses of opposite sign in the metal bulk [1], its variations manifest themselves through macroscopic movements of the entire solid [2].

Due to high surface area, surface-functionalized np metals offer an ideal platform for highly sensitive sensing and actuation technologies. Here, we report

reversible electroactuation of unimodal and hierarchical np-Au modified with an electroactive ferrocene-terminated self-assembled monolayer (SAM). In our experiment utilizing in situ dilatometry in electrolyte, an electrode potential is imposed on np-Au modulates redox transformations of SAM by oxidation and reduction of the ferrocene moiety. We find pronounced actuation strain variations that accompany the monolayer structural transformations triggered by potential. We discuss an origin of the phenomena in view of surface stress change of gold surfaces functionalized with the redox-active SAM. [1] Weissmüller, Cahn. *Acta Mater.* 45(5) 1899 (1997). [2] Kramer, et al. *Nano Lett.* 4(5) 793 (2004).

MM 23.25 Tue 18:15 P2/OG1+2

Importance of symmetry for the collapse of nanowire arrays — •MALTE GRUNERT, CHENGZHANG YHANG, HUAPING ZHAO, and YONG LEI — Technische Universität Ilmenau

We present numerical results highlighting the importance of symmetry considerations in the capillary collapse of nanowire arrays. For many of the envisaged applications of nanowire arrays, for example as a novel electrode material in lithium-ion batteries [1], maximizing the aspect ratio of the individual nanowires is one of the main goals. However, collapse occurs for wet-chemical fabrication processes after a critical aspect ratio is exceeded. As the length of the nanowires is increased, the torque resulting from surface tension during the drying step is increased as well, leading to collapse. In literature, only systems consisting of few nanowires are considered [2]. We show using multiphysics FEM simulations that a perfectly symmetric periodic nanowire array does not collapse, as the forces acting on the nanowires exactly cancel out. However, we also show that even slight length variations below the currently achievable experimental precision suffice to break the symmetry enough to load to the collapse of the entire array.

[1] L. Liang, Y. Xu, C. Wang, L. Wen, Y. Fang, Y. Mi, M. Zhou, H. Zhao, and Y. Lei, Large-scale highly ordered Sb nanorod array anodes with high capacity and rate capability for sodium-ion batteries, *Energy & Environmental Science*, 8, (2015).

[2] D. Chandra and S. Yang, Stability of high-aspect-ratio micropillar arrays against adhesive and capillary forces, *Accounts of Chemical Research*, 43, (2010)

MM 23.26 Tue 18:15 P2/OG1+2

Architecting Nanoscaffolds to Ward Off Agglomeration of Nanowire arrays: Achieving Reliable Length Retention — •CHENGZHAN YAN, HUAPING ZHAO, and YONG LEI — Fachgebiet Angewandte Nanophysik, Institut für Physik & IMN MacroNano, Technische Universität Ilmenau, 98693 Ilmenau, Germany.

Nanowire arrays with well-defined arrangements and high aspect ratios are of particular interest for energy storage systems. To this end, one prevailing strategy is to combine ordered porous templates with wet chemical techniques. However, nanowires with high aspect ratios have a more severe tendency to self-agglomerate because of uneven capillary forces, which leads to poor arrangement reliability and degrades the electrochemical performance. Herein, an ultra-thin honeycomb alumina nanoscaffold (HAN) is constructed to ensure the structural stability of nanowire arrays, achieving a four-fold increase in the aspect ratio over the restriction. Within the integrated architecture, each nickel nanowire is individually separated by HAN so that the capillary forces around the nanowire cancel each other out during drying. Moreover, MnO₂ and polypyrrole are further electrodeposited on these free-standing nanowires to form a vertically aligned core-shell 1D nanostructure arrays as cathodes and anodes for assembling micro-supercapacitors (MSCs). Attributed to the high specific surface area and low charge diffusion resistance, the assembled MSCs attain remarkably improved energy density, rate performance and lifespan.

MM 23.27 Tue 18:15 P2/OG1+2

Porous alumina membranes: how close to perfection? — •MARINE BOSSERT¹, PANAYOTIS SPATHIS², PIERRE-ÉTIENNE WOLF², LAURENT CAGNON², ISABELLE TRIMAILLE³, and ÉTIENNE ROLLEY⁴ — ¹Institut of Materials Physics and Technology, Hamburg University of Technology, Germany — ²Institut Néel, Grenoble, France — ³Institut des NanoSciences de Paris, Paris, France — ⁴Laboratoire de Physique de l'École Normale Supérieure, Paris, France

Alumina, and to a lesser extent, silicon porous membranes are considered often as model systems made of straight and independent pores, and, as such, porous alumina is used as templates for the synthesis of magnetic or thermoelectric materials [1].

In order to assess to which extent this ideal picture is valid, we have carried out extensive sorption measurements on membranes of different thicknesses, either native or with a pore aperture reduced by Atomic Layer Deposition. For porous silicon membranes, we find constrictions along the pore axis for all samples and interconnections between neighbouring pores when the latter are longer than 2 microns [2]. For alumina membranes, the pores are independent, but conical in shape rather than cylindrical, and rough rather than smooth. Moreover, their average diameter (along their length) is distributed from pore to pore.

We present quantitative estimates of these deviations to ideality, and discuss how to minimize them. [1] Lee and Park *Chemical Reviews* 2014 114 (15), 7487-7556 [2] Bossert et al, *Langmuir* 2021 37 (49), 14419-14428

MM 23.28 Tue 18:15 P2/OG1+2

Freezing of water in 3 nm silica nanopores: A molecular dynamics study — •LARS DAMMANN^{1,2}, ROBERT HORST MEISSNER^{2,3}, and PATRICK HUBER^{1,2} — ¹Deutsches Elektronen-Synchrotron DESY, Notkestr. 85, Hamburg 22607, Germany — ²Hamburg University of Technology, Am Schwarzenberg-Campus 1, Hamburg 21073, Germany — ³Institute of Surface Science, Helmholtz-Zentrum Hereon, Max-Planck-Str. 1, Geesthacht 21502, Germany

The crystallization of water in extreme spatial confinement of nanoporous media plays a pivotal role in many natural and technological processes, ranging from frost heave to modern materials processing. However, the induced interfacial stresses in the porous medium during crystallization, the crystalline structures of nanoconfined water and the lower bounds of pore sizes that still permit phase transitions are subject of scientific discussions. Molecular dynamics simulations might support the investigation of open questions about the phase transitions of water in nanoporous systems. However, liquid to solid phase transitions of bulk water are difficult to simulate since the nucleation process is energetically hindered. In strong confinement the phase transition of water is further frustrated which makes a brute force approach computationally unfeasible. Additionally it is difficult to find collective variables for enhanced sampling techniques without knowledge about the target structure. We present our ongoing investigation on if and how MD simulations about the freezing of water in nanoporous media can be conducted with an exemplary silica nanopore structure of 3 nm pore diameter.

MM 23.29 Tue 18:15 P2/OG1+2

Mechanical properties of bicontinuous Ti networks formed via peritectic melting — •NINA PETERSEN¹, ZHONGYANG LI¹, LUKAS LÜHRS¹, and JÖRG WEISSMÜLLER^{1,2} — ¹Institute of Materials Physics and Technology, Hamburg University of Technology, Hamburg — ²Institute of Materials Mechanics, Helmholtz-Zentrum hereon, Geesthacht

Recent work has shown, that bicontinuous networks can be obtained from TiAg alloys by peritectic melting. These microstructures can then be transformed to open porous networks by selective etching of the Ti or Ag phase. For open porous Ti networks, the ligament size as well as the morphology can be influenced by variation of the melting parameters like temperature and duration of the heat treatment.

In this work, the microstructure of open porous Ti samples was analysed by scanning electron microscopy. The samples were then mechanically tested using continuous compressive loading as well as loading-unloading protocols. The strain was analysed with digital image correlation. The samples exhibit strength values of over 150 MPa that increase with the duration of the heat treatment. This research links the mechanical performance of these Ti networks to the morphological evolution of the microstructures during heat treatment.

MM 23.30 Tue 18:15 P2/OG1+2

Time-resolved EBSD investigation of abnormal grain growth in the aluminum alloy AA5252 — •KAROLÍNA HOLÍKOVÁ¹, JULES M. DAKE¹, MADLEN ATZEN¹, THOMAS WILHELM², LUKAS PETRICH², ORKUN FURAT², VOLKER SCHMIDT², BAPTISTE FLIPON³, MARC BERNACKI³, and CARL E. KRILL III¹ — ¹Institute of Functional Nanosystems, Ulm University, Germany — ²Institute of Stochastics, Ulm University, Germany — ³MINES ParisTech, PSL University, France

Heat treatment causes changes in the microstructure of polycrystalline materials, with growth of the average grain size being a prominent example. The driving force is the reduction in free energy of the system. When the average grain size increases monotonically with time but the grain size distribution remains self-similar, the process is called normal grain growth (NGG). In contrast, abnormal grain growth (AGG) is characterized by the much faster growth of a few grains at the expense of neighbors, resulting in a bimodal size distribution. Analytic models and computer simulations do a good job of describing NGG, but they generally fail at predicting AGG in real systems—owing to insufficient knowledge of the underlying mechanism(s). If one could observe sequential microstructural changes during AGG, then one might gain a deeper understanding of the phenomenon. To that end, we have investigated grain growth in the aluminum alloy AA5252, which is known to manifest AGG. Time-resolved electron backscatter diffraction (EBSD) measurements reveal abnormal microstructural evolution in 2D, from which we extract clues regarding the underlying mechanism for AGG.

MM 23.31 Tue 18:15 P2/OG1+2

Resistometric and dilatometric determination of GP-zone formation and growth — •FABIAN MILLER, NIKOLAI RIEDMILLER, JOHANNES BERLIN, TOBIAS STEGMÜLLER, and FERDINAND HAIDER — Universität Augsburg, Institut für Physik, 86135 Augsburg

Aluminium alloys are of crucial importance in today's economy, therefore the deeper understanding of their mechanical and electrical properties is important. These properties can be influenced by precipitate formation. Both resistometry and dilatometry are simple online methods to monitor changes in the microstructure of a metallic alloy. In this work we focused on natural and artificial aging of Al-Cu system with samples containing 2 - 4 wt.% of Cu. Natural

aging depends on quenched in vacancies, so on the quenching conditions. Samples were homogenized at various temperatures and rapidly quenched to ambient temperature. Afterwards measurements with both techniques were conducted during natural and artificial aging. Due to formation of Guinier Preston zones, the resistivity first increases, then slowly decreases, allowing to monitor the unmixing for different temperatures and for different quenching conditions for samples with ternary trace alloying metals than Cu. Dilatometry shows a clear contraction of the samples during GP-zone formation and an expansion, if θ' phase forms.

MM 23.32 Tue 18:15 P2/OG1+2

Circularity: a microstructural clue to the origin of extreme abnormal grain growth in nanocrystalline Pd-Au — •FABIAN ANDORFER¹, JULES M. DAKE¹, JOHANNES WILD², TORBEN BOLL², DOROTHÉE VINGA SZABÓ², STEFAN WAGNER², ASTRID PUNDT², and CARL E. KRILL III¹ — ¹Institute of Functional Nanosystems, Ulm University — ²Karlsruhe Institute of Technology KIT

Heat treatment causes polycrystalline materials to manifest either normal or abnormal grain growth. During normal growth, the average grain size increases monotonically, but the grain size distribution remains unimodal. In contrast, when abnormal grain growth occurs, some grains acquire a significant growth advantage compared to the remaining matrix grains, resulting in a bimodal distribution of grain sizes. Inert-gas condensed nanocrystalline Pd-Au alloys undergo an extreme form of such abnormal grain growth: While the grain boundaries separating the abnormal and matrix grains in conventional samples tend to be rather smooth, in nanocrystalline Pd-Au the same boundaries take on rough and highly convoluted shapes - similar to a jagged coastline! In such cases, the measurement and calculation of grain circularity has proven to be a promising tool for classifying the nature of a given grain's abnormality. We have determined the circularity of abnormal grains emerging in nanocrystalline Pd-Au samples, and we have compared the results to values reported in the literature or obtained from simulations. From this information, we hope to gain a deeper understanding of the mechanism(s) responsible for the extreme growth mode observed in nanocrystalline Pd-Au.

MM 23.33 Tue 18:15 P2/OG1+2

Manipulating microstructures by means of magnetic fields — •THOMAS BREDE¹, FERNANDO MACCARI², and RAINER BACKOFEN³ — ¹Institut für Materialphysik, Universität Göttingen, Deutschland — ²Institut für Materialwissenschaften, Technische Universität Darmstadt, Darmstadt — ³Institut für wissenschaftliches Rechnen, Technische Universität Dresden, Dresden

In this project, the isolated influence of strong magnetic fields on the development of the microstructure of ferromagnetic thin films during annealing processes is investigated. For this purpose, thin films out of Iron, Nickel and Cobalt are prepared and characterized, then heat treated in the same heater with and without magnetic field and subsequently characterized. The experiments are accompanied by phase field crystal modeling to separate the different possible influences on the microstructure.

Through the parallel approach of experimental and modeling work, the effect of external magnetic fields on the development of microstructure and grain orientation will be investigated to understand the direct effect of the magnetic field.

Through a deeper understanding of the isolated influence of a magnetic field, additional conclusions should be possible about the influence of induced magnetic fields in the case of sample treatment with high currents.

MM 23.34 Tue 18:15 P2/OG1+2

Anharmonicity of the antiferrodistortive soft mode in barium zirconate BaZrO₃ — •PETER ROSANDER¹, ERIK FRANSSON¹, COSME MILESI-BRAULT^{2,3,4}, CONSTANCE TOULOUSE², FRÉDÉRIC BOURDAROT⁵, ANDREA PIOVANO⁵, ALEXEI BOSSAK⁶, MAEL GUENNOU², and GÖRAN WAHNSTRÖM¹ — ¹Chalmers University of Technology, Göteborg, Sweden — ²University of Luxembourg, Belvaux, Luxembourg — ³Luxembourg Institute of Science and Technology, Belvaux, Luxembourg — ⁴Institute of Physics of the Czech Academy of Sciences, Prague, Czech Republic — ⁵Institut Laue-Langevin, Grenoble, France — ⁶European Synchrotron Radiation Facility, Grenoble, France

Few perovskites adopt the ideal cubic phase at low temperatures. However, a promising candidate to, on average, remain cubic, even at 0K, is barium zirconate. The competing phase is a structure with sequentially tilted oxygen octahedra. This distortion is driven by the soft tilt mode at the R-point of the cubic Brillouin zone.

We report data from inelastic neutron scattering (INS) on a single crystal of barium zirconate. This reveals that the tilt mode softens substantially from 9.4 meV at room temperature to 5.6 meV at 2K. Additionally, the INS measurement unveils that the acoustic phonon mode at the same point in the Brillouin zone is almost temperature independent, which is in stark contrast to the tilt mode. The theoretical calculations show that it is critical to account for quantum fluctuations in order to correctly reproduce the experimental temperature dependence.

MM 23.35 Tue 18:15 P2/OG1+2

Terahertz third harmonic generation from a correlated metal — •GULLOO LAL PRAJAPATI¹, SERGEY KOVALEV¹, JAN-CHRISTOPH DEINERT¹, ALEXEY PONOMARYOV¹, ATIQA ARSHAD¹, GAURAV DUBEY², and DHANVIR SINGH RANA² — ¹Helmholtz-Zentrum Dresden-Rossendorf, Dresden, Germany — ²Department of Physics, Indian Institute of Science Education and Research Bhopal, Bhopal, India

High harmonic generation, a result of intense nonlinear light-matter interaction, has exciting prospects for probing fundamental ultrafast dynamics in matter and it is the basis for attosecond photonics [1, 2]. Here, we present an experimental study on terahertz (THz) third harmonic generation (THG) on a correlated metal, LaNiO₃ which exhibits non-Fermi liquid type of metallic state [3]. We observe an intense THG signal, which is usually not expected in metals, upon pumping it by 0.3 THz pulses with peak fields of about 100 kV/cm. Decreasing temperature or increasing fluence increases the intensity of this THG signal. We speculate the origin of such THG emission could be due to the anharmonic nature of LaNiO₃ conduction band caused by electronic correlation or directional nature of Ni-3d orbitals. Further investigations are under way to pinpoint the exact mechanism of the observed THG. Our study paves the way for THz THG emission from strongly correlated systems, and enables tracking of their properties on ultrafast timescales. References: 1. Nature Photon 12, 266, 270 (2018). 2. Nature 561, 507, 511 (2018). 3. Annu. Rev. Mater. Res. 46, 305-34 (2016).

MM 24: Invited Talk: Barnoush

Time: Wednesday 9:30–10:00

Location: SCH A 251

Invited Talk

MM 24.1 Wed 9:30 SCH A 251

Characterization of hydrogen effect on mechanical properties of metals at different length scales — •AFROOZ BARNOUSH, PRINCE BARANWAL, and HANAN FARHAT — Qatar Environment and Energy Research Institute (QEERI), Hamad Bin Khalifa University (HBKU), P.O. Box 34110, Doha, Qatar

Conventional macroscopic mechanical tests cannot resolve the spatiotemporally distributed hydrogen interaction with the metal microstructure under stress and give us enough information to develop predictive models for the hydrogen ef-

fect on mechanical properties. They typically measure an integration of these incidents over time, which manifests in loss of ductility, hence hydrogen embrittlement. Therefore, it is necessary to isolate these incidents and study them separately. To realize it, we develop mechanical testing approaches at different length scales to look at the interaction of hydrogen with different types of defects and how they behave in the presence of hydrogen. This talk will give an overview of the work that has been done in the past 20 years to get an insight into the hydrogen effect on mechanical properties at different length scales.

MM 25: Development of Computational Methods: Crystal Structure and Properties

Time: Wednesday 10:15–11:30

Location: SCH A 251

MM 25.1 Wed 10:15 SCH A 251

A hybrid multiscale phase-field crystal, amplitude phase-field crystal approach - elastic properties and numerical studies — •MATK PUNKE and MARCO SALVALAGLIO — Technische Universität Dresden, Institut für Wissenschaftliches Rechnen, Bürogebäude Z21, Zellescher Weg 25, 01217 Dresden

The modeling of crystalline materials requires the resolution of microscopic details on large length and time scales to guarantee the description of lattice-

dependent features as well as the dynamics of solidification. The so-called phase-field crystal (PFC) model emerged as a prominent framework to model crystalline systems. Indeed, it describes crystalline materials through a continuous order parameter related to the atomic number density and its dynamic at relatively large (diffusive) time scales. The amplitude expansion of the PFC model (APFC) was developed to further overcome the length scale limitations in the PFC framework. Herein, the continuous density in PFC models is replaced by

the amplitudes of the minimum set of Fourier modes (wave vectors) for a given crystal symmetry.

We propose a multiscale model with local PFC accuracy and APFC length scale limitations. In our hybrid multiscale approach, the PFC and APFC models are coupled through Dirichlet conditions by penalty terms within the spectral framework. We showcase the model capabilities via selected numerical investigations which focus on the energetic and elastic properties of two-dimensional crystals. Furthermore, runtime and accuracy comparisons with the standard PFC and APFC models are made.

MM 25.2 Wed 10:30 SCH A 251

Corrosion evolution in Mg-based alloys: the role of precipitates studied by synchrotron X-ray nanotomography — •TATIANA AKHMETSHINA¹, ROBIN E. SCHÄUBLIN¹, ANDREA M. RICH¹, NICHOLAS W. PHILLIPS², and JÖRG F. LÖFFLER¹ — ¹Laboratory of Metal Physics and Technology, Department of Materials, ETH Zurich, Switzerland — ²Paul Scherrer Institute, 5232 Villigen PSI, Switzerland

Magnesium alloys are very promising candidates for light-weight and bioresorbable medical applications. However, being an active metal, magnesium is susceptible to localized corrosion caused by precipitates or solute elements. In this work, we compare the corrosion behaviour of lean Mg-Ca (X0), developed in our laboratory, with the well-known Mg-Y-Nd-Zr (WE43) alloy that is currently deployed as biomedical material. X0 alloys (0.2-0.6 wt.% Ca) offer a combination of high strength and high ductility and can be considered a safe substitute for WE43 in bioresorbable implants. Using the 3D ptychography technique at the cSAXS beamline of the Swiss Light Source, we monitored the corrosion evolution in X0 and WE43. Both exhibit very different precipitates, which can be distinguished by their electron density in X-ray imaging. We found that the rare-earth-rich precipitates in WE43 tend to remain in the corrosion layer, whereas the Ca-rich ones in X0 predominantly dissolve without any pitting effect. The appearance of the corrosion product and the related chemical composition were also quite different. These findings of in-vitro corrosion can help to better understand the in-vivo degradation of Mg-based biomedical devices.

MM 25.3 Wed 10:45 SCH A 251

Amplitude expansion of the phase-field crystal model for complex crystal structures — •MARCELLO DE DONNO¹ and MARCO SALVALAGLIO^{1,2} — ¹Institute of Scientific Computing, Technische Universität Dresden, 01062 Dresden, Germany — ²Dresden Center for Computational Materials Science (DCMS), TU Dresden, 01062 Dresden, Germany

The phase field crystal model allows for studying phenomena on atomic length and diffusive time scales. It accounts for elastic and plastic deformation in crystals, including several processes such as crystal growth, dislocation dynamics, and microstructure evolution. The amplitude expansion of the phase field crystal model describes the atomic density by a small set of slowly-oscillating Fourier modes, making it possible to tackle large three-dimensional systems. However, only basic crystal symmetries have been studied so far. We present a general treatment of virtually any lattice symmetry using the amplitude phase field crystal model, incorporating approaches originally proposed for the phase field crystal model which enable the treatment of non-trivial lattices. We discuss the sta-

bility of selected crystal structures, focusing on non-Bravais lattices. As pivotal examples, we show that the proposed approach allows a coarse-grained description of the kagome lattice, exotic square arrangements, and the diamond lattice, hosting dislocations.

MM 25.4 Wed 11:00 SCH A 251

Efficient molecular dynamics simulations using fourth-generation neural network potentials — •EMIR KOČER^{1,2}, ANDREAS SINGRABER³, TSZ WAI KO^{1,2}, JONAS FINKLER⁴, PHILIPP MISOF³, CHRISTOPH DELLAGO³, and JÖRG BEHLER^{1,2} — ¹Lehrstuhl für Theoretische Chemie II, Ruhr-Universität Bochum, Bochum, Germany — ²Research Center Chemical Sciences and Sustainability, Research Alliance Ruhr, Bochum, Germany — ³Institut für Experimentalphysik, Universität Wien, Wien, Austria — ⁴Departement Physik, Universität Basel, Basel, Switzerland

Machine learning potentials (MLP) have become a common tool in materials modelling due to their ability to bridge the gap between ab initio and classical molecular dynamics. A limitation of most MLPs, however, is the locality approximation in that only interactions within a cutoff range are considered. This could lead to inaccurate dynamics in systems with relevant long-range interactions. Recently, a fourth-generation of MLPs has emerged that can take also global phenomena like non-local charge transfer into account. An example is the fourth-generation high-dimensional neural network potential (4G-HDNNP), which utilizes a global charge equilibration. In this study, a modified version of 4G-HDNNPs with enhanced efficiency will be presented. The new algorithm has been implemented in the LAMMPS software and tested in large-scale molecular dynamics simulations.

MM 25.5 Wed 11:15 SCH A 251

Sampling-free determination of accurate free energies: A bond lattice mean-field model for central potentials — •RAYNOL DSOUZA¹, THOMAS SWINBURNE², LIAM HUBER³, and JÖRG NEUGEBAUER¹ — ¹Max-Planck-Institut für Eisenforschung GmbH, 40237 Düsseldorf, Germany — ²CINaM, Campus de Luminy, 13288 Marseille, France — ³Grey Haven Solutions, Victoria, Canada

The computation of accurate anharmonic free energies at finite temperatures commonly involves the sampling of a large number of configurations. The commonly used (quasi)-harmonic approximation sacrifices physical fidelity by only sampling very few of these configurations. A recent study by the co-authors showed that a mean-field of a lattice of uncorrelated anharmonic first nearest-neighbour bonds can be used to approximate anharmonic free energies of fcc crystals with meV/atom accuracy when paired with a polarized bonding potential [1], thus recapturing an approximation of the anharmonic contributions with minimal computational expense. We extend this approach to central potentials, while maintaining the original constraints of material compatibility and thermodynamic self-consistency of the model. Using a parameterized bonding potential generated from a few T=0 K ab initio calculations [2] for fcc aluminium, we show that the model yields free energies close to meV/atom of those calculated from ab initio thermodynamic integration for a fraction of the computational effort. [1] Swinburne et al., Phys. Rev. B 102, 100101(R) (2020) [2] Glensk et al., Phys. Rev. Lett. 114, 195901 (2015)

MM 26: Interface Controlled Properties and Nanomaterials: Grain Boundaries and Stability, Spectroscopy and Interatomic Potentials

Time: Wednesday 10:15–13:00

Location: SCH A 216

MM 26.1 Wed 10:15 SCH A 216

Grain-boundary segregation effects on bicrystal Cu pillar compression — •TOBIAS BRINK, MOHAMMED KAMRAN BHAT, JAMES BEST, and GERHARD DEHM — Max-Planck-Institut für Eisenforschung GmbH, Max-Planck-Straße 1, 40237 Düsseldorf

It is well known that segregation to grain boundaries (GBs) can modify the mechanical properties of metals, leading for example to improved strength, but also to detrimental effects like embrittlement. Despite this, the nanoscale mechanisms of these changes are currently not fully understood. Here, we present the results of atomistic computer simulations of bicrystalline Cu pillar compression and corresponding micromechanics experiments. The experiments show that Ag segregation to the GB increases the yield stress of the pillars, but only slip traces observed post mortem hint towards the mechanisms. We prepared segregated GB structures with combined molecular dynamics/Monte-Carlo simulations by matching the resulting excess Ag concentration to atom probe tomography results. The virtual nanopillars were cut from this material and varying amounts of dislocation loops were inserted in order to model the pre-existing dislocation networks in the experiment. Switching the atomic types of the segregants between Ag and Cu allowed us to model the exact same pillar and dislocation network with and without segregation, thereby enabling an investigation of the mechanisms underlying the experimentally observed strengthening.

Acknowledgment: This result is part of a project that has received funding from the ERC under the European Union's Horizon 2020 research and innovation programme (Grant agreement No. 787446).

MM 26.2 Wed 10:30 SCH A 216

When grains go wild! Tracing microstructural outcomes back to possible mechanisms for abnormal grain growth — •CARL E. KRILL III¹, ELIZABETH A. HOLM², JULES M. DAKE¹, RYAN COHN², KAROLÍNA HOLÍKOVÁ¹, and FABIAN ANDORFER¹ — ¹Ulm University, Ulm, Germany — ²Carnegie Mellon University, Pittsburgh, PA, USA

Usually, the coarsening of a polycrystalline material is a civilized affair, with adjacent grains swiping atoms so surreptitiously that relative growth rates remain moderate, and the mutual boundary stays smooth. In some cases, however, certain participants in this competition give free rein to an innate hunger for growth! The result is a subpopulation of large, "abnormal" crystallites embedded in a matrix of much smaller grains, whereby the abnormal/matrix interface can be anywhere from perfectly flat to fractally convoluted. The formation of such a microstructure is the telltale signature of abnormal grain growth (AGG). Although the most prominent feature of AGG is the shape of the abnormal grains, simulations indicate that the mechanism of AGG is encoded to a greater extent in the morphology of the interfaces between abnormal and matrix grains. Based on

this finding, we propose a scheme for inferring the possible mechanism(s) underlying any experimentally observed case of (sufficiently extreme) AGG, and we illustrate our phenomenological method with experimental examples taken from the literature. Surprisingly, in the most clear-cut cases of AGG we have encountered, microstructural outcomes point to boundary-to-boundary mobility variation as the sole governing factor.

MM 26.3 Wed 10:45 SCH A 216

Influence of precipitates during anodization of aluminum alloys studied by TEM at cryogenic temperatures — •LYDIA DAUM, STEFAN OSTENDORP, MARTIN PETERLECHNER, and GERHARD WILDE — Westfälische-Wilhelms-Universität, Münster, Germany

Aluminum alloys with predefined alloying elements are chosen regarding their performance in certain areas of industrial applications due to their hardness, strength and corrosion resistance. Precipitates such as Mg₂Si and dispersoids, e.g. enrichments of Mn in EN * AW6xxx alloys hinders the formation of ordered anodic aluminum oxides (AAOs) as achievable using high-purity aluminum samples.

The focus of this work is on correlating the structural and chemical properties of precipitates within AAOs and at the interface to the alloy. Due to geometry and size of the precipitates, transmission electron microscopy (TEM) is performed at selected areas. Measuring the same properties inside an Al 6xxx alloy close to the interface provides information about the contribution of the segregations during anodization. Previous scanning transmission electron microscopy (STEM) studies have shown that cryogenic temperatures can partially reduce the beam damage in electron beam sensitive materials as organics or AAOs [1]. In this study, the sample is also characterized by nanobeam diffraction pattern analysis and electron dispersive X-ray spectroscopy at cryogenic temperatures.

[1] A. M. Jasim, X. He, Y. Xing, T. A. White, and M. J. Young. ACS Omega 6.13 (2021), 8986-9000.

MM 26.4 Wed 11:00 SCH A 216

Disconnection-mediated migration of interfaces: continuum modeling and applications — •MARCO SALVALAGLIO¹, CAIHUA QUI², JIAN HAN², and DAVID J. SROLOVITZ³ — ¹Institute of Scientific Computing, TU Dresden, 01062 Dresden, Germany — ²Department of Materials Science and Engineering, City University of Hong Kong, Hong Kong SAR, China — ³Department of Mechanical Engineering, The University of Hong Kong, Pokfulam Road, Hong Kong SAR, China

We present a model for the motion of arbitrarily curved interfaces that respects the underlying crystallography of two phases/domains meeting at an interface and is consistent with microscopic mechanisms of interface motion, i.e., migration of disconnection (line defects in the interface with step and dislocation character) [1]. The equation of motion for interface migration under the influence of a wide range of driving forces is discussed with the aid of numerical simulations [1,2]. A diffuse interface framework is also used to handle complex morphology and deliver proof of concept for microstructure evolution [2]. Recent results achieved with this model, concerning grain boundary morphologies, the competition among thermodynamic and kinetic effects, and grain rotation will be illustrated. [1] J. Han et al. Acta Materialia 227, 117178, (2022). [2] M. Salvalaglio et al. Acta Materialia 227, 117463, (2022).

MM 26.5 Wed 11:15 SCH A 216

Simulated mechanical deformations on graphene oxide — •JAVIER ROJAS-NUNEZ¹, SAMUEL BALTAZAR¹, EDUARDO BRINGA², and ALEJANDRA GARCIA³ — ¹Physics Department and CEDENNA, Universidad de Santiago de Chile (USACH), Santiago, Chile — ²Laboratorio de síntesis y modificación de nanoestructuras y materiales bidimensionales, Centro de Investigación en Materiales Avanzados, Nuevo León, México — ³CONICET & Facultad de Ingeniería, Universidad de Mendoza, Mendoza, Argentina

The better understanding of nanomaterial properties will be a key factor to tailor and enhance properties of new materials. Graphene oxide in particular can be synthesized with different oxidation levels in order so gain similar properties to its deoxidized counterpart, graphene. Through the molecular dynamic simulations, the atomistic behavior of a tri-layer graphene membrane under mechanical indentation will be studied in this work.

This work will study a highly oxidized graphene oxide tri-layer that will be indented with a repulsive spherical indenter. The modeling of the membrane will generate single layer graphene oxide candidates to pick the lowest energy configuration and later stack this layer over itself. The final tri-layer was used for the indentation simulation, where the young modulus was reproduced with decent similarity to experimental results.

The atomistic analysis of the indentation process suggest an important role of epoxide groups in the mechanical deformation of the membrane.

15 min. break

MM 26.6 Wed 11:45 SCH A 216

Atomic cluster expansion for Ag-Pd — •YANYAN LIANG, MATOUŠ MROVEC, YURY LYSOGORSKIY, and RALF DRAUTZ — ICAMS, Ruhr-Universität Bochum, Germany

Binary alloys of silver and palladium have recently attracted attention due to their importance in catalysis and nanotechnology. However, the binary Ag-Pd system lacks reliable and efficient interatomic potentials that provide an accurate description of structural and thermodynamic properties, in particular for atomistic simulations of nanoparticles. In this work, we present an atomic cluster expansion (ACE) parametrized for binary Ag-Pd. We show that the Ag-Pd ACE potential provides an ab-initio accurate description of elastic, structural and thermodynamic properties of both, elements as well as their compounds. We demonstrate the computational efficiency and the applicability of our ACE for atomistic investigations of complex phenomena in Ag-Pd nanoparticles.

MM 26.7 Wed 12:00 SCH A 216

Spin-orbit interactions in plasmonic crystals probed by site-selective cathodoluminescence spectroscopy — MASOUD TALEB¹, •MOHSEN SAMADI¹, FATEMEH DAVOODI¹, MAXIMILIAN BLACK¹, JANEK BUHL², HANNES LÜDER², MARTINA GERKEN², and NAHID TALEBI^{1,3} — ¹Institute of Experimental and Applied Physics, Kiel University, Germany — ²Integrated Systems and Photonics, Faculty of Engineering, Kiel University, Germany — ³Kiel, Nano, Surface, and Interface Science, Kiel University, Germany

The study of spin-orbit coupling (SOC) of light is crucial to explore the light-matter interactions in sub-wavelength nanostructures with broken symmetries. Herein, we explore the SOC in a plasmonic crystal, both theoretically and experimentally. Cathodoluminescence (CL) spectroscopy combined with the numerically calculated photonic band structure reveals an energy band splitting that is ascribed to the behavior of light in the plasmonic crystal where the inversion symmetry is locally broken. By shifting the impact position of the electron beam throughout a unit cell of the plasmonic crystal, we show that the emergence of the energy band splitting strongly depends on the excitation position of the surface plasmon (SP) waves on the crystal. Moreover, we exploit angle-resolved CL and dark-field polarimetry to demonstrate polarization-dependent scattering of SP waves interacting with the plasmonic crystal. Our study gives insight into the design of novel plasmonic devices with polarization-dependent directionality of the Bloch plasmons.

MM 26.8 Wed 12:15 SCH A 216

Soft and Hard X-ray Circular Dichroism in Valence-Band and Core-Level Momentum Microscopy — •O. TKACH^{1,2}, O. FEDCHENKO¹, K. MEDJANIK¹, Y. LYTUVYENKO¹, S. BABENKOV¹, D. VASILYEV¹, Q.L. NGUYEN³, T.P. VO⁴, T.R.F. PEIXOTO⁵, A. GLOSKOVSKIY⁵, C. SCHLUETER⁵, M. HOESCH⁵, D. KUTNYAKHOV⁵, M. SCHOLZ⁵, L. WENTHAUS⁵, N. WIND^{5,6}, S. MAROTZKE⁵, A. WINKELMANN⁷, J. MINAR⁴, K. ROSSNAGEL^{5,8}, H.-J. ELMERS¹, and G. SCHÖNHENSE¹ — ¹Univ. Mainz — ²SSU, Ukraine — ³SLAC Nat. Accel. Lab., USA — ⁴Univ. West Bohemia, Czech — ⁵DESY Hamburg — ⁶Univ. Hamburg — ⁷AGH Univ., Poland — ⁸Univ. Kiel

We introduce full-field mapping of the circular dichroism texture in X-ray momentum microscopy. I(EB,k) energy-momentum space tomography with both soft and hard X-rays at PETRA-III yields CDAD patterns. Kinetic energies of up to >7 keV and a large k-field-of-view enable capturing of structural information via XPD Kikuchi patterns, which show pronounced asymmetries. Patterns at different azimuthal angles exhibit sharp zero lines, when the helicity vector lies in a mirror plane. Similar zero lines also appear in the XPD patterns of core levels, as exemplified for Ge 3p, Si 2p and various W core levels at hv = 6 keV. Calculations using Bloch-wave approach and one-step photoemission show good agreement with experiment. In order to disentangle the contributions of the photoexcitation (intrinsic part) from the Kikuchi process (extrinsic), XPD has been implemented in the Munich SPRKKR package, unifying one-step model of photoemission and multiple scattering theory.

MM 26.9 Wed 12:30 SCH A 216

Direct writing of three-dimensional nano-superconductors — •ELINA ZHAKINA¹, MARKUS KÖNIG¹, SEBASTIAN SEIFERT¹, AMALIO FERNÁNDEZ-PACHECO², PAUL SIMON¹, WILDER CARRILLO-CABRERA¹, and CLAIRE DONNELLY¹ — ¹Max-Planck-Institut für Chemische Physik fester Stoffe, Dresden, Germany — ²Institute of Nanoscience & Materials of Aragón CSIC-University of Zaragoza, Zaragoza, Spain

In recent years, superconductivity and vortex matter in curved 3D nanoarchitectures have become a vibrant research avenue because of the rich physics of the emerging geometry- and topology-induced phenomena [1]. However, the fabrication of such architectures is still challenging. Currently, fabrication techniques of innovative three-dimensional (3D) nano-objects are being developed [2].

Here, we present a new route to fabricating superconducting 3D nanoarchitectures by focused electron-beam-induced-deposition [3] of tungsten, allowing for the realisation of complex 3D superconducting geometries with a critical temperature on the order of 5 K. We observe a geometrical effect of the 3D nanoarchitecture, namely, the angular dependence of the upper-critical magnetic field

that is not possible in bulk superconductors. This method unveils a wide perspective in experimental studies of the dynamics of topological defects in curved 3D nanoarchitectures.

[1] V. M. Fomin et al, Appl. Phys. Lett. 120, (2022) [2] R. Corboda et al, Beilstein J. Nanotechnol, 11, (2020) [3] L. Skoric et al, Nano Letters 20 (2020)

MM 26.10 Wed 12:45 SCH A 216

Influence of a p-n Heterojunction on the Diffusive Transport in Tungsten Trioxide Thin Films — •JAN L. DORNSEIFER^{1,2}, MARKUS S. FRIEDRICH^{1,2}, and PETER J. KLAR^{1,2} — ¹Institute of Experimental Physics I, Justus-Liebig-University, Giessen, Germany — ²Center for Materials Research (ZfM), Justus-Liebig-University, Giessen, Germany

Tungsten trioxide (WO₃) is (typically) an n-type semiconductor and a prominent electrochromic material. It changes its optical properties when charge carriers are inserted. Due to its excellent electrochromic properties, WO₃ is the

most commonly used functional material in so called "smart" windows which are a promising technology for significantly lowering the energy consumption for building climatization. Industrially manufactured polycrystalline WO₃ thin films were coated with p-type nickel monoxide (NiO_x) thin films by ion beam sputter deposition. In order to investigate the diffusive transport of hydrogen in WO₃ thin films influenced by a p-n heterojunction, spatially and temporally resolved optical transmission measurements are conducted on NiO_x/WO₃-heterostructures during the potentiostatic coloration of the WO₃ thin films. Spatial and temporal diffusion profiles determined by analyzing these measurements indicate that the lateral propagation of hydrogen in NiO_x coated WO₃ films is accelerated. In addition, an increased transmittance is observed in the colored state. To describe these findings, a model is set up based on an increase in hydrogen concentration inside the WO₃ layer outside the space-charge region formed at the NiO_x/WO₃ interface.

MM 27: Hydrogen in Materials

Time: Wednesday 10:15–13:00

Location: SCH A 215

MM 27.1 Wed 10:15 SCH A 215

Strain-induced twins and martensite: Effects on hydrogen embrittlement of additive manufactured (AM) 316L — •STEFAN WAGNER¹, YUANJIAN HONG², CHENGSHUANG ZHOU², SABINE SCHLABACH^{1,3}, ASTRID PUNDT¹, LIN ZHANG⁴, and JINYANG ZHENG⁴ — ¹Karlsruhe Institute of Technology (KIT), Institute for Applied Materials - Materials Science and Engineering (IAM-WK), Karlsruhe, Germany — ²Institute of Material Forming and Control Engineering, Zhejiang University of Technology, Hangzhou, China — ³Karlsruhe Nano Micro Facility (KNMFi), KIT-Campus North, Eggenstein-Leopoldshafen, Germany — ⁴Institute of Process Equipment, Zhejiang University, Hangzhou, China

Extending the use of hydrogen as a renewable energy carrier 316L is one of the most important structural materials. Additive manufacturing significantly enhances the steels' strength, allowing for weight reduction of construction parts. In this contribution [1] we investigate effects of strain-induced twins and martensite on hydrogen embrittlement of AM316L under tension in the temperature range from 80 K to 300 K. It is revealed that quasi-cleavage of twin boundaries is the major path of material failure. Strain-induced martensite has low impact on the H-embrittlement of AM316L, since it emerges only late in the deformation process.

[1]: Yuanjian Hong et al., 2022. Corrosion Science, 208; 110669-1-16.

MM 27.2 Wed 10:30 SCH A 215

Ab-initio insights into hydrogen-carbide interaction in bcc Fe — SAURABH SAGAR and •POULUMI DEY — Delft University of Technology, Delft, The Netherlands

Development of advanced high-strength steels is in high demand owing to its wide scale applications. The excellent mechanical properties of these steel grades are attributed to the underlying microstructure which comprises of finely dispersed nano-precipitates. However, one major factor restricting their application is their susceptibility to Hydrogen Embrittlement (HE). Experimental and theoretical work have been carried out to understand if the nano-sized carbides can aid in reducing the susceptibility to HE along with providing strengthening. Within this study, we investigated the effectiveness of finely dispersed nanocarbitides (i.e., TiC, NbC and VC) to limit the diffusible hydrogen content in bcc Fe. Our study revealed that the interplay between hydrogen and carbon vacancies, local atomic environment at interface as well as interface geometry can lead to significantly increased hydrogen solubilities. Thus, the trapping at these sites leads to a reduction in concentration of diffusible hydrogen. However, the question remains whether hydrogen can populate the deepest traps (i.e., the carbon vacancies) in the bulk of these carbides. We, thus, extended our study to compute migration barriers of hydrogen across the coherent interface between bcc Fe and TiC, NbC and VC using climbing-image Nudged Elastic Band method. Furthermore, we evaluated whether a chain of interconnected carbon vacancies from the interface to the bulk of the carbides leads to a reduction in the migration barrier of hydrogen.

MM 27.3 Wed 10:45 SCH A 215

Role of diffusible hydrogen on the mechanical behavior of bcc alloys by in situ micromechanics during hydrogen charging — •MARIA JAZMIN DUARTE CORREA, JING RAO, and GERHARD DEHM — Max-Planck-Institut für Eisenforschung, Düsseldorf, Germany

Hydrogen embrittlement represents a major challenge for the use of hydrogen (H) as energy carrier. Understanding individual hydrogen-microstructure interactions by targeting analyses at the nano-/microscale during H exposure is essential to prevent material degradation. We will present nanoindentation and micropillar compression tests during H charging of Fe-Cr alloys (8-20 wt.%Cr) using our novel "back-side" electrochemical H charging approach for nanoin-

dentation related techniques. An enhanced dislocation nucleation is shown consistent with the defactant theory, and a hardening effect while increasing the Cr content and the H entry. The mechanical data is as well analyzed in terms of the diffusion behavior and used to develop a nanohardness-based H diffusion coefficient approach. On the other hand, our unique method allows differentiating between the effects of trapped and mobile H, and performing well controlled measurements with different H levels monitored over time to consider H absorption, diffusion and release through the metal which will be shown using the example of the model alloys mentioned above.

MM 27.4 Wed 11:00 SCH A 215

Hydrogen interstitials in iron oxides using ab-initio calculations — •AHMED ABDELKAWY, MIRA TODOROVA, and JÖRG NEUGEBAUER — Max-Planck-Institut für Eisenforschung, Max-Planck-Str.1, 40470 Düsseldorf

The steel making industry is responsible for more than 6% of CO₂ emissions. These emissions come from the dependency on carbon and carbon monoxide as reducing agents. Hydrogen, on the other hand, can reduce iron oxides with water released instead. The reduction route from Magnetite to Hematite, then Wüstite, and finally to pure iron requires hydrogen to diffuse into and react with the different solid structures as well as with the multiple solid-solid interfaces. To optimize the reduction process, the mechanistic details of this process requires understanding to the role of hydrogen interstitials in the bulk iron oxides. We therefore computed the diffusion paths of hydrogen through the different iron oxide phases employing density functional theory (DFT) calculations for all three iron oxides - Magnetite, Hematite, and Wüstite. Analyzing the electronic structure of the studied oxides, we examine the reliability of the used exchange correlation functionals and how the electronic structure is affected by the inclusion of hydrogen, both as a neutral and a charged point defect. Finally, we utilize symmetrized plane waves to map the full 3D potential energy surfaces (PESs) for hydrogen interstitials within these iron oxides using a modest number of DFT calculations. Based on these calculations we identify the hydrogen preferential interstitial sites, diffusion barriers, and diffusion paths.

MM 27.5 Wed 11:15 SCH A 215

Influence of impurity atoms on the hydrogen diffusion into ruthenium — •JULIAN GEBHARDT and DANIEL URBAN — Fraunhofer IWM, 79108 Freiburg

Ruthenium is considered as a promising protection layer to prevent the penetration of small atoms such as hydrogen into the underlying material. However, hydrogen is known to be able to penetrate ruthenium films under certain conditions and it has been hypothesized that impurity atoms, such as Sn, could play a major role in this process, decreasing the barrier of diffusion into the material for incoming hydrogen. We demonstrate that this is not the case for low to medium coverages, i.e., as long as the adsorbed species can be treated individually without significant adsorbate-adsorbate interactions. Within this coverage regime, the hydrogenation is destabilized in the vicinity of impurity atoms, such as X=Mg, P, S, Si, or Zn, due to the strong bonding of the adsorbates with the free ruthenium surface. As a result, the diffusion barriers are not significantly reduced in the vicinity of any of the tested impurity atoms. The most likely and energetically favorable process occurs at a sufficiently large distance to the impurity, with an energy barrier that is almost identical to that of the free surface. Due to the chemical variety of the considered impurity atoms, this finding appears to be general. This means that impurities can be ruled out to enhance hydrogen uptake of ruthenium layers for the considered coverages and other structural properties such as grain boundaries and dislocations should be considered as pathway for the hydrogen penetration.

15 min. break

MM 27.6 Wed 11:45 SCH A 215

Metal Hydride Materials for Solid-State Hydrogen Storage Applications: Utilizing the Synergy of Experiment & Theory for Future Materials Design Challenges — PAUL JERABEK¹, BRANDON WOOD², TAE WOOK HEO², and CLAUDIO PISTIDDA¹ — ¹Institute of Hydrogen Technology, Helmholtz-Zentrum Hereon, Geesthacht, Germany — ²Materials Science Division, Lawrence Livermore National Laboratory (LLNL), Livermore, USA

Metal hydride materials present a safe, efficient and long-term storage option for hydrogen under mild conditions for many stationary and mobile applications and will play an important role in the transition towards an emission-free energy economy.

Deep understanding of (de)hydrogenation thermodynamics and kinetics of such materials is essential to enable targeted design of novel storage materials and optimization of existing compositions tailor-made for specific applications. To obtain the necessary insights, computation and experiment need to work closely together to fully leverage theory-experiment feedback loops.

In this talk, an overview will be given of how experimental activities can be connected with computational multi-scale methodology (from atomistic to mesoscale), as currently performed in the joint efforts by the metal hydride materials research groups at Hereon and LLNL, with the goal being to develop virtual workflows linking Density Functional Theory methods, thermodynamic modeling and phase-field simulations together with experimental investigations for an integrated description of metal hydride (de)hydrogenation processes.

MM 27.7 Wed 12:00 SCH A 215

Ab Initio Simulations of Laves-phase high-entropy alloys for hydrogen storage — YUJI IKEDA¹, KAVEH EDALATI², and BLAZEJ GRABOWSKI¹ — ¹University of Stuttgart, Stuttgart, Germany — ²Kyushu University, Fukuoka, Japan

High-entropy alloys (HEAs), particularly those in the Laves phases, are promising candidates for hydrogen-storage alloys. Recent experiments have indeed revealed that the equiatomic TiZrCrMnFeNi Laves-phase HEA can work as a hydrogen-storage alloy at room temperature (i.e., without heating) under nearly atmospheric pressure [1,2]. Tuning the compositions of such Laves-phase HEAs should be possible to design hydrogen-storage alloys with more desirable properties. We have demonstrated that ab initio H adsorption energies in $Ti_xZr_{2-x}CrMnFeNi$ become more negative (thus energetically more favorable) on average with increasing the Ti content, consistent with experiments [3]. We will also show how the H adsorption energy depends on the local chemical environment in the Laves-phase HEAs.

[1] P. Edalati, A. Mohammadi, Y. Li, H.-W. Li, R. Floriano, M. Fuji, and K. Edalati, *Scr. Mater.* 209, 114387 (2022).

[2] P. Edalati, R. Floriano, A. Mohammadi, Y. Li, G. Zepon, H.-W. Li, and K. Edalati, *Scr. Mater.* 178, 387 (2020).

[3] A. Mohammadi, Y. Ikeda, P. Edalati, M. Mito, B. Grabowski, H.-W. Li, and K. Edalati, *Acta Mater.* 236, 118117 (2022).

MM 27.8 Wed 12:15 SCH A 215

Visualizing radiation-induced damage by Hydrogen/Deuterium — APARNA SAKSENA, BINHAN SUN, HEENA KHANCHANDANI, and BAPTISTE GAULT — Max-Planck-Institut für Eisenforschung GmbH, Max-Planck-Straße 1, Düsseldorf 40237, Germany

Atom probe tomography (APT) is now extensively used to measure the local chemistry of materials. APT proceeds by field evaporating a sharp, needle-shaped specimen with a radius ≈ 50 nm, often prepared by focused ion beam

(FIB) milling. The interaction of the ion beam at high currents is known to amorphize crystalline materials by changing the lattice and creating vacancies. Therefore, a platinum protective layer and a low-energy ion shower are routinely used to avoid or remove the damaged layer from the specimen. Additionally, for investigating the local chemistry of defects such as interfaces via APT, transmission Kikuchi diffraction (TKD) can be performed during milling steps. The damage resulting from these techniques is considered negligible. Here, we use deuterium charging to probe the damage associated with specimen preparation as vacancies are known to be strong trapping sites for hydrogen/deuterium. We analyzed a medium Mn steel containing austenite (fcc) and ferrite (bcc). APT specimens were charged in a deuterium gas atmosphere, and the distribution of deuterium shows clusters of point defects after Pt deposition, conventional Ga-FIB preparation, and TKD. These deuterium-rich clusters are sequentially minimized by systematically eliminating these preparation-induced damages.

MM 27.9 Wed 12:30 SCH A 215

Mechanism-based Lifetime Assessment under the Influence of Hydrogen — FABIE EBLING^{1,2}, HEINER OESTERLIN², ASTRID PUNDT¹, and KEN WACKERMANN² — ¹Karlsruhe Institute of Technology (KIT) Institute for Applied Materials - Materials Science and Engineering (IAM-WK), Karlsruhe, Germany — ²Fraunhofer Institute for Mechanics of Materials IWM, Freiburg, Germany

Components see a variety of mechanical and thermal loads during service. Increased damage can occur when used in a hydrogen atmosphere. The experimental investigation of all states is very time-consuming and expensive, especially for testing under hydrogen influence. Mechanism-based lifetime assessments can be used to model crack growth and predict service life. This can significantly reduce the need of experimental investigations for a safe design of components. This work discusses different approaches of modeling hydrogen assisted cracking and presents an adaptation of the ZD parameter according to Heitmann (1983) for the influence of hydrogen at different temperatures.

MM 27.10 Wed 12:45 SCH A 215

Validation of continuum simulations of materials at the mesoscopic level with X-ray and neutron diffraction with a focus on hydrogen storage materials —

ARNAB MAJUMDAR¹, MARTIN MÜLLER², and SEBASTIAN BUSCH¹ — ¹GEMS at MLZ, Helmholtz-Zentrum hereon GmbH, Lichtenbergstr. 1, 85748 Garching, Germany — ²Institute of Materials Physics, Helmholtz-Zentrum hereon GmbH, Max-Planck-Str. 1, 21502 Geesthacht, Germany

With the advent of new technologies, it has been possible to design new materials through theoretical analysis and simulation. However, these simulations have to be validated by experiments. In this work, we develop a method to validate the structural features in continuum simulations directly on the mesoscopic level with X-ray and neutron scattering experiments. The workflow to compare atomistic computer simulations to scattering patterns is well established: the scattering amplitude of individual atoms is summed, whose positions are obtained from the simulation. This approach fails for larger mesoscopic structures due to the unrealistic computation time required to generate the simulations and scattering pattern on a mesoscopic scale with atomic resolution. We developed a methodology that calculates scattering patterns from a continuum simulation like phase-field modeling, where the material description is continuous instead of a collection of atoms. The approach is validated with simple structures and gradually applied to more complex structures. The long term goal is to use this technique for the simulation of hydrogen storage materials and validation of the simulations with scattering data.

MM 28: Liquid and Amorphous Metals

Time: Wednesday 10:15–12:45

Location: SCH A 118

MM 28.1 Wed 10:15 SCH A 118

Relation between decoupled α and β relaxation processes and medium-range ordering in $Pd_{40}Ni_{40}P_{20}$ bulk metallic glasses — MANOEL WILKER DA SILVA PINTO, MARK STRINGE, DRAŽEN RADIĆ, HARALD RÖSNER, and GERHARD WILDE — Institut für Materialphysik, Westfälische Wilhelms-Universität Münster, Wilhelm-Klemm-Str. 10, 48149 Münster, Germany

Individual annealing treatments at $0.8T_g$ and $0.9T_g$ on $Pd_{40}Ni_{40}P_{20}$ bulk metallic glass samples were performed in a differential scanning calorimeter to either activate mainly β or both α and β relaxation processes. Prior to and after these measurements the samples were heated into the supercooled liquid in order to establish a comparable reference relaxation state.

The medium-range order of the different stages of the amorphous structures were investigated by fluctuation electron microscopy and compared with that of the as-cast state. The results indicate that first, a defined structural reset was achieved when heating into the supercooled liquid; however, with increased strain due reduction of excess volume. Second, the annealing treatment at $0.8T_g$

increases the volume fraction of medium-range order again with annealing time and third, a depletion of the volume fraction is observed after annealing at $0.9T_g$.

MM 28.2 Wed 10:30 SCH A 118

Analysis of the relaxational behavior of PdNiS — MAXIMILIAN DEMMING¹, NICO NEUBER², MARTIN PETERLECHNER¹, RALF BUSCH², and GERHARD WILDE¹ — ¹University of Münster, Münster, Germany — ²Saarland University, Saarbrücken, Germany

In this work we examine a sulfur-containing bulk metallic glass, PdNiS. The impact of sulfur is investigated with a focus on the thermodynamic behavior and the comparison with the well-known PdNiP bulk metallic glass. Several samples from the same initial state were annealed at a certain temperature below T_g for different annealing times in order to adjust distinct relaxation states. After isothermal annealing in a differential scanning calorimeter (DSC), a calorimetric study was carried out to examine the relaxation behavior. Especially the so-called overshoot during heating the samples through the glass transition was

evaluated, since it is one of the most prominent signals which depends on the thermal history of a metallic glass. Additionally, low temperature heat capacity measurements were performed to quantify the so-called boson peak. The boson peak can be related to soft vibrational modes, and thus it is characteristic to the relaxational state of a metallic glass and it is affected by the thermal history of a glass. All methods combined deliver a picture of the relaxational behavior under pre-Tg annealing of this Sulphur-containing metallic glasses.

MM 28.3 Wed 10:45 SCH A 118

Unravelling the origin of the anomalous thermal expansion in Fe-based bulk metallic glasses — •ALEXANDER FIRLUS¹, MIHAI STOICA¹, GAVIN VAUGHAN², STEFAN MICHALIK³, ROBIN E. SCHÄUBLIN¹, and JÖRG F. LÖFFLER¹ — ¹Laboratory of Metal Physics and Technology, ETH Zurich, 8093 Zurich, Switzerland — ²European Synchrotron Radiation Facility (ESRF), Grenoble, France — ³Diamond Light Source Ltd., Didcot, UK

Fe-based bulk metallic glasses (BMGs) are known for their soft-magnetic properties but their magnetic interactions also give rise to an anomalous thermal expansion, called the Invar effect. In the ferromagnetic state, their coefficient of thermal expansion is reduced by a factor of four. This phenomenon has been observed in all ferromagnetic Fe-based BMGs at the macroscopic scale, but due to the lack of long-range order the physics of this effect needs to be described at the atomic scale. Although it is now widely accepted to be of magnetic origin, the contributions of the different atomic species to the Invar effect have been unknown. We studied the atomic-scale thermal expansion of multiple quaternary BMGs by in situ X-ray diffraction. The anomalous thermal expansion is visible in all diffraction patterns and can clearly be associated with the disordered Fe network. Through variations of the minor alloying elements, we elucidated the effect of different atomic species and provide a framework in which their respective influence on the Invar effect can be understood.

MM 28.4 Wed 11:00 SCH A 118

Rejuvenation engineering in metallic glasses by complementary stress and structure modulation — •DANIEL ŠOPU^{1,2}, FLORIAN SPIECKERMANN³, SIMON FELLNER¹, CHRISTOPH GAMMER¹, and JÜRGEN ECKERT^{1,3} — ¹Erich Schmid Institute of Materials Science, Austrian Academy of Sciences, Leoben, Austria — ²Institut für Materialwissenschaft, Technische Universität Darmstadt, Germany — ³Department of Materials Science, Chair of Material Physics, Montanuniversität Leoben, Austria

Residual stress engineering is very widely used in the design of new advanced lightweight materials. For metallic glasses the attention has been on structural changes and rejuvenation processes. Here, based on high energy scanning X-ray diffraction strain mapping, transmission electron microscopy (TEM) and microindentation we distinguish between structural and elastic fluctuations, the two key factors for the observed extreme rejuvenation in triaxial compression. TEM characterization shows that structural rejuvenation under room temperature deformation relates to shear-induced softening and dilatation (large volumetric strain). High energy scanning X-ray diffraction strain mapping reveals large elastic fluctuations in metallic glasses after deformation under triaxial compression. Microindentation hardness mapping hints to a competing hardening-softening mechanism after compression and further reveals the complementary effects of stress and structure modulation. Molecular dynamics simulations provide an atomistic understanding of the complex shear band activity in notched metallic glasses and the related fluctuations in the strain/stress heterogeneity.

MM 28.5 Wed 11:15 SCH A 118

Enhancing mechanical properties by introducing surface grooves in metallic glasses — •XUDONG YUAN¹, DANIEL ŠOPU^{1,2}, KAIKAI SONG³, and JÜRGEN ECKERT^{1,4} — ¹Erich Schmid Institute of Materials Science, Austrian Academy of Sciences, Jahnstraße 12, Leoben A-8700, Austria — ²Institut für Materialwissenschaft, Fachgebiet Materialmodellierung, Technische Universität Darmstadt, Otto-Berndt-Str.3, Darmstadt D-64287, Germany — ³School of Mechanical, Electrical and Information Engineering, Shandong University (Weihai), Weihai 264209, China — ⁴Department of Materials Science, Chair of Materials Physics, Montanuniversität Leoben, Jahnstraße 12, Leoben A-8700, Austria

The correlation between the mechanical properties and surface defects in metallic glasses (MGs) is investigated by surface ultrasonic bonding experiments and molecular dynamics simulations. The strength together with the compression ductility of Zr₆₅Cu₁₅Ni₁₀Al₁₀ MG can be enhanced by introducing surface grooves. Induced grooves and pre-shear bands (SBs) lead to the formation and interaction of multiple SBs during compression, which consequently enhances ductility. Additionally, the thermal-induced nanocrystallization, together with generated free volume and residual stresses around the grooves contribute to the emergence of hierarchical structure and stress heterogeneity, which delays the propagation of dominant SB and enables the improvement of strength and plasticity of MG.

15 min. break

MM 28.6 Wed 11:45 SCH A 118

Atomic transport in heavy ion irradiated amorphous PdNiP near the glass transition temperature — •SABA KHADEMOREZAIAN¹, MARILENA TOMUT^{1,2}, MAXIMILIAN DEMMING¹, SERGIY DIVINSKI¹, and GERHARD WILDE¹ — ¹Institute of Materials Physics, University of Münster, Wilhelm-Klemm-Str. 10, 48149 Münster — ²GSF Helmholtzzentrum für Schwerionenforschung, 64291 Darmstadt, Germany

The influence of ion irradiation on Ag diffusion in Pd₄₀Ni₄₀P₂₀ bulk metallic glass was investigated by the tracer diffusion technique at temperatures below the glass transition. Bulk samples of Pd₄₀Ni₄₀P₂₀ relaxed states were irradiated with 4.8 MeV/u Au, U, and Ca ions at the UNILAC accelerator at GSI Darmstadt. The achieved fluences were in the range of 5e10 to 1e13 ions/cm². The diffusion rates of ^{110m}Ag isotopes after irradiation with heavy ions, Au and U, were found to be monotonously increasing with increasing total fluence. For the light ions, Ca, the diffusion enhancement shows an unexpected non-monotonous, cross-over behavior. The results are discussed relating the impacts of irradiation with swift heavy ions on structure modifications and the atomic kinetics in a bulk metallic glass.

MM 28.7 Wed 12:00 SCH A 118

Nanostructural investigations on thin film nanoglasses using different TEM techniques — •HENDRIK VOIGT¹, EVGENIY BOLTYNJUK², AARON RIGONI¹, HORST HAHN², HARALD RÖSNER¹, and GERHARD WILDE¹ — ¹University of Münster, Institute of Materials Physics, Wilhelm-Klemm-Str. 10, 48149 Münster, Germany — ²Karlsruhe Institute of Technology, Institute of Nanotechnology, Hermann-von-Helmholtz-Platz 1, 76344 Eggenstein-Leopoldshafen, Germany

Nanoglasses as a relatively new family of amorphous alloys present an attempt to tailor the structure of glasses to improve their properties. The concept of nanoglasses is based on the introduction of glass-glass interfaces into the amorphous material, mimicking the effect that defects have in crystalline matter. Different transmission electron microscopy (TEM) techniques were used to investigate the microstructure of Cu₆₀Zr₄₀ columnar thin film nanoglasses. Nanobeam diffraction pattern (NBDP) analysis and energy dispersive X-ray spectroscopy (EDX) were employed to investigate differences in the excess free volume and chemical composition. NBDP acquired over an extended region of interest were used to perform an angular correlation analysis revealing different symmetry motives compared to a compositionally equivalent homogenous glass. Additionally, time-of-flight secondary ion mass spectroscopy (ToF SIMS) measurements discovered an increase in diffusivity in the nanoglasses. All the results shown here provide clear evidence for the existence of glass-glass interfaces with two structurally different phases present in the nanoglass.

MM 28.8 Wed 12:15 SCH A 118

Properties of Sodium Borosilicate Glasses via Dynamics Simulations with Ultra-Fast Machine-Learning Potentials — •HENDRIK KRASS¹, BENEDIKT ZIEBARTH², WOLFGANG MANNSTADT², and MATTHIAS RUPP³ — ¹University of Konstanz, Konstanz, Germany — ²Schott AG, Mainz, Germany — ³Luxembourg Institute of Science and Technology (LIST), Belvaux, Luxembourg

Glasses are of scientific interest and have many industrial applications. However, their investigation and development are limited by the duration and costs of experiments. The computational study of glasses can in principle overcome these limits, but current atomistic glass models are either fast but not accurate enough (classical empirical potentials) or accurate but too slow (ab initio potentials). Machine-learning potentials (MLPs) trained on ab initio reference calculations promise to be both fast and accurate enough.

We investigate the suitability of “ultra-fast potentials” (UFPs) [1]—a class of MLPs that are data-efficient, physically interpretable, sufficiently accurate for applications, can be parametrized automatically, and are as fast as the fastest traditional empirical potentials—to study glasses. For this, we compute structure and properties of interest via dynamics simulations with UFPs and compare them against state-of-the-art models and experimental values for sodium borosilicate glasses, a prototypical glass system.

[1] Stephen R. Xie, Matthias Rupp, Richard G. Hennig: Ultra-Fast Interpretable Machine-Learning Potentials, arXiv 2110.00624, 2021.

MM 28.9 Wed 12:30 SCH A 118

An atomic scale inspired phase-field approach to model fracture in amorphous silica — •GERGELY MOLNAR¹, GAYLORD GUILLONNEAU², GUILLAUME KERMOUCHE³, and ETIENNE BARTHEL⁴ — ¹Univ Lyon, CNRS, INSA Lyon, LaM-CoS, UMR5259, 69621 Villeurbanne, France — ²Univ Lyon, Ecole Centrale de Lyon, CNRS, LTDS, UMR CNRS 5513, 69134 Ecully, France — ³Mines Saint-Etienne, CNRS, UMR 5307 LGE, Centre SMS, 42023 Saint Etienne, France — ⁴ESPCI, CNRS, SIMM, UMR7615, 75231 Paris, France

In the last decade, phase-field models have gained great popularity in fracture simulation. These models regularize the sharp crack using an internal length-scale by diffusing the damage into the material. This work was set out to investigate the competition between homogeneous plastic deformation, shear banding, and brittle failure in amorphous silica. The molecular dynamics inspired finite

element model uses the phase-field approach to model fracture, while a pressure-dependent yield criterion accounts for densification and shear plasticity. The talk

presents a proof of concept to model plasticity and crack propagation in micrometer size silica samples.

MM 29: Data Driven Materials Science: Big Data and Work Flows – Electronic Structure

Time: Wednesday 11:45–13:00

Location: SCH A 251

MM 29.1 Wed 11:45 SCH A 251

Band Gap and Formation Energy Inference of Solids using Message Passing Neural Networks — •TIM BECHTEL, DANIEL SPECKHARD, and CLAUDIA DRAXL — Humboldt-Universität zu Berlin, Physics Department and IRIS Adlershof, Berlin, Germany

Graph-based neural networks and, specifically, message-passing neural networks have shown great promise in predicting physical properties of solids. Here, we target three tasks, formation energy regression, metal- non-metal classification, and band gap regression, using data from the AFLOW materials database [1]. In order to find optimal hyperparameters and model architecture, we perform a neural architecture search on the band gap regression task, using a random search algorithm. The model is based on a message passing neural network with edge updates [2], and provides users with uncertainty estimates via Monte-Carlo dropout. We analyze the domain of applicability of the model, for different space group symmetries, atomic species, and corrections applied to the underlying calculation. While we obtain overall excellent results, the model struggles to accurately predict oxide materials. We find that the uncertainty in different domains reflects the model's predictive performance.

[1] S. Curtarolo et al., *Comput. Mater. Sci.*, 58 (2012), pp. 227-235.

[2] P.B. Jørgensen et al., Preprint at arXiv:1806.03146 (2018).

MM 29.2 Wed 12:00 SCH A 251

Predicting electron density using a convolutional neural network — •JAE-MO LIHM^{1,2,3}, WANHEE LEE⁴, and CHEOL-HWAN PARK^{1,2,3} — ¹Department of Physics and Astronomy, Seoul National University, Seoul, Korea — ²Center for Correlated Electron Systems, Institute for Basic Science, Seoul, Korea — ³Center for Theoretical Physics, Seoul National University, Seoul, Korea — ⁴Department of Applied Physics, Stanford University, California, USA

Machine-learning methods are being widely applied to computational materials science. Most applications of machine learning in electronic structure calculations focus on learning the total energy and forces, while few works study the prediction of electronic properties. In this work, we develop a machine-learning model for predicting electron density using the convolutional neural network, a standard machine-learning method for image processing. We train the neural network using the electron density calculated from density functional theory. We show that the trained neural network can successfully predict the electron density of systems that were not included in the training set, bypassing the need for the self-consistent density functional theory calculation.

MM 29.3 Wed 12:15 SCH A 251

Chemical ordering and magnetism in CrCoNi Medium Entropy Alloy — •SHEULY GHOSH¹, VADIM SOTSKOV², ALEXANDER SHAPEEV², JÖRG NEUGEBAUER¹, and FRITZ KÖRMANN^{1,3} — ¹Max-Planck-Institut für Eisenforschung GmbH — ²Skolkovo Institute of Science and Technology — ³Delft University of Technology

The equiatomic CrCoNi medium entropy alloy is a prototypical multiple-principal element alloy (MPEA), exhibiting many superior mechanical properties. Short-range order (SRO) is known to affect the thermodynamic phase stability as well as mechanical and magnetic properties of MPEA alloys. In CrCoNi also, the presence of SRO and its impact on different aspects has been intensively discussed in various studies. In our recent study, we identified the ground-state ordered structure for this alloy combining *ab initio* calculations and on-lattice

machine-learning interatomic potentials. Based on these studies, an ordered Cr(Ni,Co)₂ phase (MoPt₂-type) was found. In present work, we further discuss the stability of the newly identified ordered structure and compare them with the previously suggested ones, particularly with respect to magnetism, local atomic relaxation energies as well as volume fluctuations.

MM 29.4 Wed 12:30 SCH A 251

Charge-dependent Atomic Cluster Expansion — •MATTEO RINALDI, ANTON BOCHKAREV, YURY LYSOGORSKIY, MATOUS MROVEC, and RALF DRAUTZ — Interdisciplinary Centre for Advanced Materials Simulation, Bochum, Germany

The atomic cluster expansion (ACE) [1,2,3] has proven to be a valuable tool to parametrize complex energy landscapes of pure elements and alloys outperforming popular approaches based on limited body-order descriptions. However, due to the local nature of the many body basis, it is inherently near-sighted. Therefore, long range interactions, such as electrostatics, are ignored in the description. Here, we introduce charge-dependent ACE to be able to tackle the missing electrostatic contributions. This formalism is based on the QEQ charge equilibration scheme from Rappe et al.^[4], where partial charges are obtained by equalizing atomic electronegativities and imposing charge conservation. Moreover, atomic electronegativities and hardness are considered as dependent on the local atomic environment. We demonstrate that our approach yields atomic charges in agreement with those obtained from popular partitioning schemes, such as Mulliken and Hirshfeld, including periodic and non-periodic systems, together with an accurate reproduction of the potential energy landscape. This work opens the possibility to model charge transfer and dielectric response within the increasingly popular ACE framework.

[1] R. Drautz, *Phys. Rev. B* 99, 014104 [2] Y. Lysogorskiy et al., *npj Comput Mater* 7, 97 (2021) [3] R. Drautz, *Phys. Rev. B* 102, 024104 [4] Rappe, *J. Phys. Chem.* 1991, 95, 8, 3358*3363

MM 29.5 Wed 12:45 SCH A 251

A machine-learned interatomic potential for silica and mixed silica-silicon systems — •LINUS C. ERHARD¹, JOCHEN ROHRER¹, KARSTEN ALBE¹, and VOLKER L. DERINGER² — ¹Institute of Materials Science, TU Darmstadt, Darmstadt, Germany — ²Department of Chemistry, Inorganic Chemistry Laboratory, University of Oxford, Oxford, United Kingdom

The interface between silica and silicon has enormous relevance in various applications, including semiconductors and novel battery materials. However, atomistic modeling of this interface is a challenge due to the different charge states of silicon and the limitations of classical interatomic potentials. To overcome these limitations, we introduce a machine-learning-based interatomic potential based on the non-linear atomic cluster expansion (ACE) for various Si-O phases. This model is based on the previously developed database for silica [1], which was substantially extended by active learning. The new model shows improved performance for high-pressure silica and is also able to describe silica surfaces. Moreover, the use of the ACE formalism enables us to reach more than 100 times longer time or larger length scales compared to the Gaussian approximation potential (GAP). Finally, the potential is able to describe off-stoichiometric mixtures of Si and SiO₂. This capability is used to investigate the nanostructure of silicon monoxide.

[1] Erhard et al. A machine-learned interatomic potential for silica and its relation to empirical models. *npj Comput Mater* 8, 90 (2022)

MM 30: Invited Talk: Liebscher

Time: Wednesday 15:00–15:30

Location: SCH A 251

Invited Talk

MM 30.1 Wed 15:00 SCH A 251

Direct observations of grain boundary phase transformations in metallic alloys — •CHRISTIAN LIEBSCHER — Max-Planck-Institut für Eisenforschung, 40237 Düsseldorf, Germany

Grain boundaries (GBs) play a pivotal role in determining the properties of metallic materials. In most considerations, GBs are seen as a simple 2D defect. However, thermodynamic concepts already proposed 60 years ago showed that GBs can undergo phase transformations, but the search for them has been in vain due to their confined nanoscale nature.

We show that GB phases exist in elemental copper. Atomic resolution scanning transmission electron microscopy is used to unravel multiple coexisting GB

structures in the same GB. The intrinsic character and thermodynamic properties of the GB phases and their transitions is investigated by atomistic simulations. We find that the GB phase junction, a line defect that separates different GB phases, is kinetically limiting the transformation and plays a decisive role in the nucleation and arrangement of GB phases within the interface. By heating GBs inside of the electron microscope, we are able to directly observe how GB phases evolve at elevated temperatures with atomic resolution. In the remainder of the talk, we will also discuss the impact of solute segregation on GB transitions in copper and titanium alloys by exploring the local atomic arrangement of solutes within the GB.

MM 31: Data Driven Materials Science: Big Data and Work Flows – Machine Learning

Time: Wednesday 15:45–18:30

Location: SCH A 251

MM 31.1 Wed 15:45 SCH A 251

Neural networks trained on synthetically generated crystals can classify space groups of ICSD powder X-ray diffractograms — •HENRIK SCHOPMANS, PATRICK REISER, and PASCAL FRIEDERICH — Institute of Theoretical Informatics, KIT, Karlsruhe, Germany

Machine learning techniques have successfully been used to extract structural information such as the crystal space group from powder X-ray diffraction (XRD) patterns. However, training directly on simulated patterns from databases like the ICSD is problematic due to its limited size, class-inhomogeneity, and bias toward certain structure types. We propose an alternative approach of generating random crystals with random coordinates by using the symmetry operations of each space group. Based on this approach, we present a high-performance distributed python framework to simultaneously generate structures, simulate patterns, and perform online learning. This allows training on millions of unique patterns per hour. For our chosen task of space group classification, we achieve a test accuracy of 77.4% on new ICSD structure types not included in the statistics dataset guiding the random generation. Instead of space group classification, the developed framework can also be used for other common tasks, such as augmentation and mixing of patterns for phase fraction determination. Our results demonstrate, using the domain of X-ray diffraction, how state-of-the-art models trained on large, fully synthetic datasets can be used to guide the analysis of physical experiments.

MM 31.2 Wed 16:00 SCH A 251

Critical Assessment of Uncertainty Estimates of Machine-Learning Potentials — •SHUAIHUA LU^{1,2}, LUCA M. GHIRINGHELLI¹, CHRISTIAN CARBOGNO¹, and MATTHIAS SCHEFFLER¹ — ¹Novel Materials Discovery at the FHI of the Max-Planck-Gesellschaft and IRIS-Adlershof of the Humboldt-Universität zu Berlin, Berlin, Germany — ²School of Physics, Southeast University, Nanjing, China

Machine-learning potentials (MLP) trained on first-principles datasets are becoming increasingly popular since they enable the treatment of larger system sizes and longer time scales compared to straight ab initio techniques. A key aspect for the use of these MLPs is to reliably assess the accuracy viz. uncertainty of the predictions, e.g., by training an ensemble of models. Here, we critically examine the robustness of such uncertainty predictions using equivariant message-passing neural networks as an example [1]. We train an ensemble of models on liquid silicon simulated at the gradient-corrected density-functional-theory level and compare the predicted uncertainties with actual errors for various test sets, including liquid silicon at different temperatures and out-of-training-domain data such as solid phases with and without point defects as well as surfaces. These studies reveal that the predicted uncertainties are often overconfident. This is ascribed to the insufficient diversity in the members of the ensemble, as measured via error correlations. [1] S. Batzner et al., Nat. Commun. 13, 2453 (2022).

MM 31.3 Wed 16:15 SCH A 251

Learning to Spell Materials - Coordinate-free Discovery with Natural Language Processing — •KONSTANTIN JAKOB, KARSTEN REUTER, and JOHANNES T. MARGRAF — Fritz Haber Institute, Berlin, Germany

Over the last decade, computational screening with structure-based machine learning models has led to some advances in the discovery of novel inorganic materials. Unfortunately, the overwhelmingly large space of possible compositions and atomic configurations together with the exceeding rarity of well-suited candidates ultimately poses a limit to the applicability of this approach. In contrast, purely composition-based representations neglect differences in the chemical properties of different crystal polymorphs and thus lack accuracy. A middle ground between full structural and simple compositional representations has been established for organic molecules using string representation such as SMILES. While these have proven highly advantageous for molecular discovery when combined with natural language processing models, analogous representations for the more complex class of inorganic materials are still missing. Bridging this gap, we investigate the performance of recurrent neural networks (RNNs) in predicting crystallographic properties by reading a materials composition element by element. Their striking accuracy suggests that symmetry- or prototype-based string representations could be generated with little computational effort at a large scale. The invertibility of these intermediate representations via restricted structure searches is investigated, paving the way to their application for conditional generative models.

MM 31.4 Wed 16:30 SCH A 251

Exploring materials dataspace by combining supervised and unsupervised machine learning — •ANDREAS LEITHERER¹, ANGELO ZILETTI¹, CHRISTIAN H. LIEBSCHER², TIMOFEY FROLOV³, and LUCA M. GHIRINGHELLI^{1,4} — ¹NOMAD Laboratory at the FHI of the Max-Planck-Gesellschaft and IRIS-Adlershof of the Humboldt-Universität (HU) zu Berlin — ²Max-Planck-Institut für Eisen-

forschung — ³Lawrence Livermore National Laboratory — ⁴Physics Department and IRIS-Adlershof of HU zu Berlin

To enable meaningful applications of AI to materials science, much of current efforts is concentrated on the creation of characterized datasets. In this talk, we discuss a rarely addressed topic - the development of automatic tools to explore available materials-science data. In particular, we go beyond purely supervised learning by combining unsupervised analysis with a recently developed crystal-structure recognition method [1]. This neural-network (NN) model automatically learns data representations that contain information on structurally diverse geometries. Using clustering, physically meaningful subgroups can be identified in the NN latent space, which are shown, e.g., to correspond to distinct, experimentally verified grain-boundary phases [2]. Moreover, dimension-reduction analysis allows us to create low-dimensional, interpretable materials charts that visualize complex structural data from both theoretical and experimental origin.

[1] A. Leitherer, A. Ziletti and L. M. Ghiringhelli. Nat. Commun. 12, 6234 (2021)

[2] T. Meiners et al. Nature 579, 375-378 (2020)

MM 31.5 Wed 16:45 SCH A 251

Minimizing data requirements by transfer learning for structure search on organic/inorganic interfaces — •ELIAS FÖSLEITNER, JOHANNES CARTUS, LUKAS HÖRMANN, and OLIVER T. HOFMANN — Institute of Solid State Physics, Graz University of Technology, Graz, Austria

Performing structure search of organic molecules on metallic surfaces requires finding the structure with the lowest energy. However, calculating energies using conventional DFT codes proves to be a time-consuming task since single calculations are expensive and the number of configurations is large. To avoid the calculation of all possible structures, machine learning techniques such as Gaussian process regression have shown to be a useful tool in order to reduce the amount of DFT data needed. In our work we try to further reduce the amount of necessary data by using transfer learning from one substrate to another. To do this we include DFT data from structures of more than one substrate in our training set. In order to calculate the similarities between structures on different substrates we use the SOAP descriptor combined with an alchemical kernel which provides couplings between the different substrate elements. By optimizing these couplings, although molecule-substrate interactions differ notably (e.g. the interfacial charge transfer) between different substrates, we can save up to 50 % of the training data for one substrate A by also using the data of another substrate B. This serves as a stepping stone for the investigation of structures on computationally costly substrates.

15 min. break

MM 31.6 Wed 17:15 SCH A 251

Accelerating the Search for High-Performance, Novel Materials with Active Learning — •THOMAS A. R. PURCELL¹, MATTHIAS SCHEFFLER^{1,2}, LUCA M. GHIRINGHELLI^{1,2}, and CHRISTIAN CARBOGNO¹ — ¹The NOMAD Laboratory at the FHI of the Max-Planck-Gesellschaft and IRIS-Adlershof of the Humboldt-Universität zu Berlin — ²Physics Department and IRIS-Adlershof at Humboldt Universität zu Berlin, Berlin, Germany.

Active-learning frameworks have the potential to greatly accelerate the search for new materials. By balancing exploitation and exploration, these approaches can efficiently search through materials space and find the regions that are most likely to contain promising candidate materials [1]. Here we present an active learning framework, that uses an ensemble of expressions found by the sure-independence screening and sparsifying operator (SISSO) approach [2,3], and we demonstrate it for the example of discovering new thermal insulators. We statistically process the predictions of independent SISSO models to automatically select the most promising material candidates and then calculate their thermal conductivity κ_L using the *ab initio* Green Kubo method [4]. Using this approach we are able to find multiple new thermal insulators and gain insights into what is driving down their κ_L .

[1] A. G. Kusne, et al. Nat. Comm. 11, 5966 (2020)

[2] R. Ouyang, et al. Phys. Rev. Mater. 2, 083802 (2018)

[3] T. A. R. Purcell, et al. J. Open Source. Softw. 7, 3960 (2022)

[4] F. Knoop, et al. arXiv:2209.12720

MM 31.7 Wed 17:30 SCH A 251

Machine learning discovery of new materials — •JONATHAN SCHMIDT^{1,2}, HAICHEN WANG², NOAH HOFFMAN², TIAGO CERQUEIRA³, PEDRO BORLIDO³, PEDRO CARRICO³, LOVE PETERSSON⁴, CLAUDIO VERDOZZI⁴, SILVANA BOTTI¹, and MIGUEL MARQUES² — ¹Friedrich-Schiller-University Jena, Germany — ²Martin-Luther-University Halle-Wittenberg, Germany — ³University of Coimbra, Portugal — ⁴Lund University, Sweden

Graph neural networks for crystal structures typically use the atomic species and atomic positions as input. We construct crystal-graph attention networks replacing these precise bond distances with embeddings of graph distances. This allows us to perform high-throughput studies based on both compositions and crystal structure prototypes. Combining a newly curated dataset of 3M materials and the networks we have already scanned more than two thousand prototypes spanning a space of more than 5 billion materials and identified tens of thousands of theoretically stable compounds. We also demonstrate the effectiveness of transfer learning to adapt the networks to new domains such as of two dimensional structures.

Schmidt et al. Crystal graph attention networks for the prediction of stable materials, *Sci. Adv.* 7.49 (2021)

Schmidt et al., Large-scale machine-learning-assisted exploration of the whole materials space, arXiv:2210.00579 (2022)

Wang et al., Symmetry-based computational search for novel binary and ternary 2D materials, submitted (2022)

MM 31.8 Wed 17:45 SCH A 251

Data-driven magneto-elastic interatomic potentials for discovering novel phases of transition metal alloys — •MANI LOKAMANI¹, KUSHAL RAMAKRISHNA⁴, JULIAN TRANCHIDA³, SVETOSLAV NIKOLOV², HOSSEIN TAHMASBI⁴, MICHAEL WOOD², and ATTILA CANGI⁴ — ¹HZDR Dresden, Germany — ²SNL New Mexico, USA — ³CEA Cadarache, France — ⁴CASUS Görlitz, Germany

Structural prediction methods are used for identifying stable and metastable structures in a broad spectrum of materials. The presence of the electron spin degree of freedom in magnetic materials increases the complexity of finding such structures, constraining the analysis to the thermodynamically most relevant structures in a narrow range of temperatures and pressures. We achieve a search over much wider temperature and pressure conditions by utilizing machine-learning interatomic potentials based on the spectral neighbor analysis method within the coupled spin-molecular dynamics framework implemented in LAMMPS. This data-driven methodology enables predicting the properties of magnetic materials on much larger spatial, spin, and temporal domains and is parametrized by first-principles data. Leveraging this methodology, we predict the formation of metastable crystalline structures in transition metal alloys (FeNi, FeMn, FeCr, FeCo, FeGd) at high temperature-pressure conditions and assess their magnetic properties. This enables studying long-range spin structures in novel phases of transition metal alloys and complements the quest for permanent magnets for renewable energy applications that do not depend on rare-earth elements.

MM 31.9 Wed 18:00 SCH A 251

FAIR Modelling Recipes for High-Throughput Screening of Metal Hydrides — •KAI SELLSCHOPP¹, PHILIPP ZSCHUMME², MICHAEL SELZER², CLAUDIO PISTIDDA¹, and PAUL JERABEK¹ — ¹Institute for Hydrogen Technology,

Helmholtz-Zentrum Hereon, Geesthacht, Germany — ²IAM - Microstructure Modelling and Simulation, Karlsruhe Institute of Technology, Karlsruhe, Germany

A simple modelling recipe for calculating the hydrogenation enthalpy of metal hydrides with ab-initio methods is presented. It consists of the everyday tasks of a computational materials scientist: relaxing a structure, optimising its volume, and calculating vibrational energies. The corresponding workflow is implemented in the framework of KadiStudio^[1], where the scientific process is broken down into simple input-processing-output (IPO) tasks. The approach allows to track the inputs and outputs, to easily re-use the modular tasks in other workflows, and to share the workflow as a simple bash or python script. Therefore, not only the generated research data, but also the workflow itself fully comply with the FAIR data principles. As a first application, the recipe is employed to test how the different ingredients of an ab-initio calculation (e.g. xc-functional) affect the accuracy of predicting hydrogenation enthalpies. This helps to make better choices for studying this class of materials in the future and to judge the uncertainty in existing data. Furthermore, the standardized workflow enables a reliable high-throughput screening of new candidate materials for high-density hydrogen storage at near ambient conditions.

[1] L. Griem, *et al.*, *Data Science Journal* 21, 16 (2022)

MM 31.10 Wed 18:15 SCH A 251

Take Two: Δ -Machine Learning for Molecular Co-Crystals — •SIMON WENGER¹, GÁBOR CSÁNYI², KARSTEN REUTER¹, and JOHANNES THEO MARGRAF¹ — ¹Fritz-Haber Institute, Berlin, Germany — ²University of Cambridge, Cambridge, United Kingdom

Co-crystals are a highly interesting material class, as varying their components and stoichiometry in principle allows tuning supramolecular assemblies towards desired physical properties. The *in silico* prediction of co-crystal structures represents a daunting task, however, as they span a vast search space and usually feature large unit-cells. This requires theoretical models that are accurate and fast to evaluate, a combination that can in principle be accomplished by modern machine-learned (ML) potentials trained on first-principles data. Crucially, these ML potentials need to account for the description of long-range interactions, which are essential for the stability and structure of molecular crystals. In this contribution, we present a strategy for developing Δ -ML potentials for co-crystals, which use a physical baseline model to describe long-range interactions. The applicability of this approach is demonstrated for co-crystals of variable composition consisting of an active pharmaceutical ingredient and various co-formers. We find that the Δ -ML approach offers a strong and consistent improvement over the density-functional tight binding baseline. Importantly, this even holds true when extrapolating beyond the scope of the training set as demonstrated via molecular dynamics simulations at ambient conditions.

MM 32: Topical Session: Defect Phases I

Time: Wednesday 15:45–18:30

Location: SCH A 216

Topical Talk

MM 32.1 Wed 15:45 SCH A 216

Defect phase diagrams: Concepts, computational approaches and applications — MARVIN POUL, PRINCE MATHEWS, ALI TEHRANCI, JING YANG, MIRA TODOROVA, TILMANN HICKEL, and •JÖRG NEUGEBAUER — Max-Planck-Institut für Eisenforschung GmbH, Düsseldorf, Germany

Extending the well-known concept of bulk phase diagrams to defects allows to predict the thermodynamically stable defect states at any given temperature and bulk composition. Similar to bulk phase diagrams such diagrams allow to identify processing conditions where defect states with particularly desirable stoichiometries, structures and properties form. These diagrams thus provide an exciting new approach in designing materials. Modern atomistic tools based on density functional theory or machine learning potentials can provide all the necessary information to construct such phase diagrams but face severe conceptual and computational challenges: The description of such defects requires thermodynamically open boundary conditions as well as the inclusion of a large number of structural, chemical and electronic degrees of freedom. In the presentation, key concepts of efficiently sampling the large configuration spaces associated with computing defect states and phase diagrams will be discussed. Examples of how this insight can be used to understand and control grain boundary formation, morphology or improved corrosion resistance will be given.

MM 32.2 Wed 16:15 SCH A 216

Fully Automated Calculation of Defect Phase Diagrams — •MARVIN POUL, ERIK BITZEK, and JOERG NEUGEBAUER — Max-Planck-Institut fuer Eisenforschung, Duesseldorf, Deutschland

Understanding the thermodynamics of segregation at crystal defects is an important part of successful materials engineering.[1] We present an efficient method that constructs finite temperature Defect Phase Diagrams (DPDs) for binary alloys from fully relaxed molecular calculations using machine learning interatomic potentials (MLIP) without user intervention and implemented it as a pyiron[2] workflow. A major challenge that we had to address is the combinatorially growing number of different segregation configurations at any extended defect. The proposed method is able to efficiently tackle hundreds of thousands to millions of configurations and is based on a fast proxy model. This model is based on the ACE descriptors and avoids having to evaluate a full MLIP. This proxy model together with the MAXVOL active learning algorithm allows to pre-screen which configurations to calculate with the underlying MLIP. We apply the workflow on the example of Al and Ca segregation to Mg grain boundaries.

[1]: Korte-Kerzel, S. et al. (2022) Defect phases: thermodynamics and impact on material properties, *International Materials Reviews*, 67:1, 89-117

[2]: Janssen, J, et al. "pyiron: An integrated development environment for computational materials science." *Computational Materials Science* 163 (2019): 24-36.

MM 32.3 Wed 16:30 SCH A 216

Effect of chemical changes on the defect structures in lean rare-earth free ternary Mg alloys — •WASSILIOS DELIS¹, DEBORAH NEUSS², MARCUS HANS², DIERK RAABE³, SANDRA KORTE-KERZEL¹, and STEFANIE SANDLÖBES-HAUT¹ — ¹Institute for Physical Metallurgy and Materials Physics, RWTH Aachen University, Germany — ²Materials Chemistry, RWTH Aachen University, Germany — ³Max-Planck Institut für Eisenforschung, Max-Planck-Straße 1, 40237 Düsseldorf, Germany

Mg is a lightweight structural material with a good specific strength. Unfortunately, it lacks sufficient room temperature formability and therefore a wider commercial use of Mg is hindered. The preferred basal slip and strong basal-type texture were found to be the main reasons for the poor room temperature formability. Alloys containing low amounts of Al and Ca showed a highly increased room temperature ductility. Here, TEM and APT measurements and ab initio calculations showed an increased activity of $c+a$ dislocation slip. The effects of the alloying elements are yet not fully understood. Further research has been performed to investigate how the changes in chemistry affect the structure of defects such as boundaries and dislocations.

MM 32.4 Wed 16:45 SCH A 216

High-throughput generation of defect phase diagrams: A case study in grain boundary solute segregation analysis in Ni base alloys — •HAN LIN MAI, TILMANN HICKEL, and JÖRG NEUGEBAUER — Max-Planck-Institut für Eisenforschung GmbH, Max-Planck-Straße 1, 40237 Düsseldorf, Germany

Understanding segregation to grain boundaries, and eventually their defect phase diagrams, is critical to enable rational grain boundary engineering for alloys design. Here, we discuss the progress and challenges one may face when generating such a database of defect-solute interactions, in the context of studying of grain boundary segregation of solutes and impurities in Ni GBs. To compute the large number of relevant defect-solute interactions we have performed high-throughput ab initio calculations using efficient and highly automated workflows using pyiron. The study has been performed across a representative set of coincident-site-lattice (CSL) type tilt GBs. Based on the large ab-initio datasets, we extract and analyse the chemical and structural trends observed in the solute segregation behaviour across the periodic table. The features which are most important in evaluating site segregation are presented and discussed.

15 min. break

MM 32.5 Wed 17:15 SCH A 216

Planar defects in intermetallic $Mg_xAl_{2-x}Ca$ Laves phases — •ALI TEHRANCHI¹, TILMANN HICKEL^{1,2}, and JÖRG NEUGEBAUER¹ — ¹Max-Planck-Institut für Eisenforschung GmbH, D-40237 Düsseldorf, Germany — ²Bundesanstalt für Materialforschung und -prüfung (BAM)

The intermetallic Laves phases that are present in Mg-based alloys when adding Ca and Al beyond the solubility limit have a beneficial impact on the mechanical properties of these alloys. For example, Laves phases have been observed to enhance the alloy's creep resistance and to extend their application to higher-temperature domains. However, the mechanism of deformation of these phases and their effect on the surrounding matrix is not fully understood. Laves phases not only contain planar defects but also their motifs are observed in planar defects in Mg. In this work, using the concept of defect phase diagrams, we study hcp-like planar defects in the C36 phase and the thermodynamically stable Laves-type planar defects in Mg-based alloys. We show, that while conventional bulk thermodynamic phase diagrams fail to predict the experimentally observed phases the predictions obtained by the defect phase diagrams match well with the experiments. Defect phase diagrams thus provide a powerful tool to predict and interpret the formation of chemically and structurally complex motifs at defects as function of experimentally accessible and controllable parameters such as temperature or alloy composition.

MM 32.6 Wed 17:30 SCH A 216

Oxygen vacancy formation energies at grain boundaries in perovskite-type electro-ceramics — •CONG TAO¹, DANIEL MUTTER¹, DANIEL F. URBAN^{1,2}, and CHRISTIAN ELSÄSSER^{1,2} — ¹Fraunhofer IWM, 79108 Freiburg — ²Freiburg Materials Research Center (FMF), University of Freiburg, 79104 Freiburg

Oxygen vacancy concentrations are assumed to play a major role in the electric-field assisted grain growth of technologically relevant single crystal perovskite phases. The underlying effect on the atomic scale is the redistribution of cationic and anionic point defects between grain boundaries and bulk phases due to different defect formation energies in the structurally different regions, accompanied by the formation of space charge zones. In this study, we present results of classical atomistic calculations of oxygen vacancy formation energy profiles across supercells containing the symmetric tilt grain boundaries $\Sigma 5$ (210) [001], $\Sigma 5$ (310) [001], and the asymmetric tilt grain boundary (430) || (100). The electro-ceramic perovskite materials SrTiO₃, BaTiO₃, and BaZrO₃ were systematically analyzed. We discuss the dependence of formation energies and resulting concentration profiles on composition and grain boundary type.

MM 32.7 Wed 17:45 SCH A 216

Temperature-dependent impact of antiphase boundaries on properties of Fe₃Al — •MARTIN FRIÁŘ^{1,2}, MIROSLAV ČERNÝ^{2,3}, and MOJMÍR ŠOB^{4,1} — ¹Institute of Physics of Materials, Czech Academy of Science, Brno, CZ — ²Central European Institute of Technology (CEITEC), Brno University of Technology, Brno, CZ — ³Faculty of Mechanical Engineering, Brno University of Technology, Brno, Czech Republic — ⁴Department of Chemistry, Faculty of Science, Masaryk University, Brno, CZ

We have performed a quantum-mechanical study of the influence of antiphase boundaries (APBs) on the temperature dependence of selected materials properties of Fe₃Al. We show that the studied APBs very strongly affect thermal vibrations of Fe₃Al and reduce the width of the band gap in phonon frequencies. Our results also show that the Fe₃Al with APBs exhibits higher volumetric thermal expansion than the defect-free Fe₃Al. The computed free energy of APBs is found to be strongly temperature-dependent. It is lower than the static-lattice temperature-independent APB energy and the reduction is enhanced by increasing temperature (to 76% at T = 700 K). We have also addressed the discrepancy between the experimental bulk modulus and previous theoretical results obtained for the defect-free Fe₃Al. Due to the presence of APBs, the bulk modulus is reduced from the value of 173 GPa, that corresponds to the defect-free Fe₃Al, to 153 GPa, i.e. very close to the experimental value of 147 GPa (at T = 0 K). For details see *Intermetallics* 151 (2022) 107746, DOI:10.1016/j.intermet.2022.107746.

Topical Talk

MM 32.8 Wed 18:00 SCH A 216

Towards a Rigorous Theory of Grain Boundary Segregation in Polycrystals — •CHRISTOPHER SCHUH — MIT, Department of Materials Science and Engineering, Cambridge, MA USA

Although grain boundary segregation is pervasive across metals and materials, the models used to describe it generally fall short in one of two ways. One class of models is too approximate, using, e.g., a scalar 'average' segregation energy; the other is too detailed, focusing on specific atomic sites in select boundaries. Both approaches fail to capture the complex range of sites in the grain boundary network of polycrystals. This talk will overview a project in our group at MIT that aims to develop a new type of grain boundary segregation theory that bridges this gap: it is designed to be quantitatively accurate at the level of specific grain boundary sites, but simple enough to admit solution with an isotherm that can be analytically represented. The approach is based on the parameterization of segregation spectra: distribution functions of all the key thermodynamic quantities necessary to capture the full physics of segregation in polycrystals. We address the spectra of: segregation sites and their enthalpies, interaction parameters amongst solutes, and vibrational contributions to the segregation free energy. After describing computational methods to determine these spectra, we then address the problem of high-throughput computation of them for many alloy systems using tools of data science.

MM 33: Topical Session: Fundamentals of Fracture – Amorphous Metals

Time: Wednesday 15:45–18:00

Location: SCH A 215

MM 33.1 Wed 15:45 SCH A 215

In situ measurement of plasticity accompanying Hydrogen induced cracking — LEONEL STERMANN, LOÏC VANEL, and •DÔME TANGUY — Institut Lumière Matière, UMR5306 Université Lyon 1 - CNRS, Université de Lyon 69622 Villeurbanne cedex, France

Single crack propagation is studied in a Hydrogen embrittled aluminum alloy. Hydrogen is introduced in the system by electrochemical reactions in an acid aqueous medium. After Hydrogen charging, tensile tests are performed in air, on notched samples, with a micro-tensile machine. An optical microscope is used to follow single crack initiation and propagation at a high magnification. Digital Image Correlation gives the displacement field on the surface with a spatial resolution of about 1 micron. It enables the determination of the position of the crack tip and the local velocity at a sub-grain scale. The equivalent Von Mises strain is calculated and gives a precise measure of the local plastic field which

accompanies crack propagation. In addition to the primary plasticity which is emitted from the crack tip or its immediate neighborhood in the form of two intense slip bands, it is systematically found a secondary plastic zone which spreads over several microns ahead of the tip. The characteristics of the plastic zone are measured, together with the velocity and the applied stress intensity factor. In addition, different fracture mechanisms are found on the fracture surface. In particular there are transitions in the fracture mode from intergranular smooth to transgranular parallel to the grain boundary plane. The local fracture mechanisms, in the vicinity of the surface, are linked to the local velocities and plastic deformations.

MM 33.2 Wed 16:00 SCH A 215

Liquid metal induced fracture : modelling and supporting experiments — THIERRY AUGER¹, ANTOINE CLEMENT¹, MARCO EZEQUIEL², EVA HÉRIPRÉ¹, INGRID SERRE², ZEHOUA HAMOUCHE¹, JULIE BOURGON³, ERIC LEROY³, and MAXIME VALLET⁴ — ¹PIMM/Arts et Métiers Technology Institute, CNRS, CNAM, 151 Bd de l'hôpital 75013 Paris, France — ²Univ. Lille, CNRS, INRAE, Centrale Lille, UMR 8207 - UMET - Unité Matériaux et Transformations, F-59000 Lille, France — ³ICMPE - UMR 7182 2/8, rue Henri Dunant 94320 Thiais, France — ⁴MSSMAT, CentraleSupélec, University Paris-Saclay, France

Liquid metal embrittlement of an otherwise ductile material is an environmentally induced fracture phenomenon characterized by potentially high brittle crack propagation rate and deleterious effects on mechanical properties. Its phenomenology is still not well understood, in particular in terms of prediction of sensible couples and about the detailed intergranular fracture mechanisms. Here we will report on the study in the copper systems via both an energetic and QM/MM approaches at the atomic level to predict the sensitivity of model materials to liquid metal embrittlement. The main goal is to try to link micro-testing (flexion in FIB prepared samples or by in-situ TEM) to a sound modelling at the atomistic scale via fracture mechanics type sollicitations. The progress towards predictability of liquid metal embrittlement systems and understanding of fracture mechanisms will be presented along with a vision about their experimental validation.

MM 33.3 Wed 16:15 SCH A 215

Microscale fracture behavior of Laves phases in the Mg-Ca-Al ternary alloy system — ANWESHA KANJILAL, UZAIR REHMAN, JAMES P. BEST, and GERHARD DEHM — Max-Planck-Institut für Eisenforschung GmbH, Düsseldorf, Germany

Brittle intermetallic Laves phases often act as preferential sites for defects such as cracks in the Mg-Ca-Al alloys. This study investigates the nano- and microscale fracture behavior of C15 Al₂Ca and C14 Mg₂Ca Laves phases prepared as single-phase specimens. Spherical nanoindentation was performed at room temperature in grains of varying surface orientation to identify cleavage planes and orientation effects. Post mortem microscopic examination using electron channeling contrast imaging revealed cracks around indents in both Laves phases, and together with electron backscatter diffraction low index crack planes were identified using trace analyses. For C15 phase, further microcantilever bending and micropillar splitting geometries were fabricated using focused ion beam methodology, wherein fracture toughness $K_{IC} \sim 1-2 \text{ MPam}^{0.5}$ was obtained from in-situ testing. Fast screening methodology based on in-situ scratch and nanoindentation at temperatures from 25 to 500 °C was employed to determine brittle-to-ductile transitions in the Laves phases. The morphology of slip lines and cracks, and decrease in hardness during nanoindentation suggests probable transition $\sim 0.5T_m$ for C15 phase, while studies on C14 are ongoing.

The authors gratefully acknowledge the financial support of Deutsche Forschungsgemeinschaft (DFG) within project B06 of Collaborative Research Center (SFB) 1394, project number 409476157.

MM 33.4 Wed 16:30 SCH A 215

Fracture mechanics concepts in application to functionally graded coatings (FGCs) and FGC structures — VERA PETROVA and SIEGFRIED SCHMAUDER — IMWF, University of Stuttgart, Pfaffenwaldring 32, 70569 Stuttgart, Germany

The problem of thermal fracture of functionally graded thermal barrier coatings on a homogeneous substrate under the influence of thermo-mechanical loadings is analyzed. It is assumed that FGCs contain a pre-existing system of multiple cracks, edge and/or internal. The thermal and mechanical properties, as well as the fracture toughness of the FGC, are modeled by functions based on the rule of mixtures with a power-law coefficient as the gradation parameter. The problem is formulated using the method of singular integral equation, which are solved numerically. The following fracture characteristics are calculated: stress intensity factors, energy release rates, critical stresses and fracture angles. A series of computational experiments is carried out for FGC/homogeneous structures with typical systems of multiple cracks in the FGC at different gradation parameters and for different material combinations. It is known that the fracture resistance of a TBC can be increased by introducing dense vertical cracks in ceramic coatings; this mechanism is due to the shielding effect in these crack systems. These crack systems are studied and discussed. The goal of this study and the investigation based on the model is to find ways to improve the fracture resistance of FGC/homogeneous structures by avoiding certain critical crack systems.

MM 33.5 Wed 16:45 SCH A 215

Nonlinear elastic effect on interacting crack paths in PDMS films — LOIC VANEL¹, OSVANNY RAMOS¹, THIERRY BIBEN¹, STÉPHANE SANTUCCI², and ANTHONY GRAVOUIL³ — ¹ILM - UCBL, Villeurbanne, France — ²LPENS - ENS Lyon, France — ³LAMCOS, INSA Lyon, France

The observed repulsive behaviour of two initially collinear cracks growing towards each other and leading to a hook-shaped path questioned recently the validity of the Principle of Local Symmetry within Linear Elastic Fracture Mechan-

ics theory [1]. Theoretical and numerical work has solved this dilemma, providing the precise geometric conditions for the existence of the repulsive phase and revealing a multi-scale behaviour of the repulsive/attractive transition [2].

Nonlinear elastic materials such as elastomers depart from the prediction of linear elasticity for interacting cracks. We performed experiments on PDMS film that indeed show a maximum angle of repulsion not only significantly smaller than the one of linear elasticity, but also smaller than the one observed in polymer films with a plastic process zone. Our FEM simulations on a Mooney-Rivlin material confirm that the nonlinear elastic response of PDMS modifies the crack path, reducing the repulsive strength between the two interacting cracks.

[1] Dalbe, M.-J.; Koivisto, J.; Vanel, L.; Miksic, A.; Ramos, O.; Alava, M.; Santucci, S.; Phys. Rev. Lett. 2015 114, 205501

[2] Schwaab, M.-E.; Santucci, S.; Biben, T.; Gravouil, A.; Vanel, L.; Phys. Rev. Lett. 2018 120, 255501.

15 min. break

MM 33.6 Wed 17:15 SCH A 215

Modelling mechanochemical reactions in epoxy resins under tensile load using hybrid QM/MM/MD approaches — CHRISTIAN R. WICK¹, MATTIA LIVRAGHI¹, SAMPANNAH PAHI¹, BARISCAN ARICAN¹, DAVID M. SMITH², and ANA-SUNČANA SMITH¹ — ¹FAU Erlangen-Nürnberg, PULS Group, Institute for theoretical physics, Erlangen, Germany — ²Division of Physical Chemistry, IRB, Zagreb, Croatia

Epoxy resins are important thermosetting polymers in our everyday life with a large variety of applications, e.g. as structural materials in airplanes, as coatings, flooring materials or adhesives. With the aim to understand these complex materials at the molecular scale, we investigate the formation and the mechanochemical response of epoxy resins, including the reactions taking place during curing and under tensile load, by means of quantum chemistry and hybrid Molecular Dynamics (MD) simulations. We present a block chemistry based AMBER force field, [1,2] which allows generation of fragment partial charges covering all states of curing and fracture, due to cleavage of molecular bonds. Further, we develop an on-the-fly hybrid QM/MM/MD Ansatz to identify bond rupture events in bulk epoxies to improve our understanding of the mechanochemical behavior of these materials.

[1] M. Livraghi, S. Pahi, P. Nowakowski, D.M. Smith, C.R. Wick, A.-S. Smith, Block Chemistry for Accurate Modeling of Epoxy Resins, chemrxiv, 2022

[2] M. Livraghi, K. Höllring, C.R. Wick, D.M. Smith, A.-S. Smith, J. Chem. Theory Comput. 17 (2021) 6449

MM 33.7 Wed 17:30 SCH A 215

Machine Learning of fracture in glasses — FRANCESC FONT-CLOS¹, MARCO ZANCHI¹, STEFAN HIEMER², SILVIA BONFANTI³, ROBERTO GUERRA¹, MICHAEL ZAISER², and STEFANO ZAPPERI^{1,4} — ¹Center for Complexity and Biosystems, Department of Physics, University of Milan, via Celoria 16, 20133 Milan, Italy. — ²Institute of Materials Simulation, Department of Materials Science and Engineering, Friedrich-Alexander-University Erlangen-Nuremberg, Dr.-Mack-Str. 77, 90762 Fürth, Germany — ³NOMATEN Centre of Excellence, National Center for Nuclear Research, ul. A. Sołtana 7, 05-400 Swierk/Otwock, Poland — ⁴CNR Consiglio Nazionale delle Ricerche, Istituto di Chimica della Materia Condensata e di Tecnologie per l'Energia Via R. Cozzi 53, 20125 Milan, Italy.

Being able to predict the failure of materials based on structural information is a fundamental issue with enormous practical and industrial relevance for the monitoring of devices and components. Thanks to recent advances in deep learning, accurate fracture predictions are becoming possible even for strongly disordered solids, but the sheer number of parameters used in the process renders a physical interpretation of the results impossible. Here we address this issue and use machine learning methods to predict the failure of simulated two-dimensional silica glasses from their initial undeformed structure. We show that our predictions can be transferred to samples with different shapes or sizes than those used in training, as well as to experimental images.

MM 33.8 Wed 17:45 SCH A 215

Using deep neural networks to bridge the gap between statistical fractographic analysis and fracture toughness prediction for polymers —

•GUILLAUME DE LUCA^{1,2}, MOHAMMED IDRİ², and LAURENT PONSON^{1,2} — ¹Institut Jean le Rond d'Alembert, Sorbonne Université, CNRS, 4 place Jussieu 75006 Paris, France — ²Tortoise, 231 rue Saint-Honoré, 75001 Paris, France

We propose to deploy DNNs to bridge the gap between statistical fractography and the toughness K_{IC} prediction for polymers as well as shed light on the role played by the different structures on their fracture surfaces. We generate the fracture surfaces in laboratory through tensile fracture tests while using DIC (Digital Image Correlation) to locally measure and compute the sought mechanical properties along the crack. An interferometric profilometer extracts the topography from the fracture surfaces, and the resulting height fields are post-treated with tools from statistical fractography to be used as input, while the experimental data are used as labels for the regression problem.

By doing so, we can estimate from a scanned fracture surface a material toughness value $K_{Ic}(x)$ along the crack propagation direction. Furthermore, the advancements in explainable neural networks allow us to go one step further by

making assumptions about what roughness elements present on the fracture surface influence the most the results coming out of the pipeline.

MM 34: Members' Assembly

Welcome to this general meeting of the DPG-SKM division MM! All of you, presenters of MM talks or posters and other interested participants of this conference, are cordially invited to this meeting. The poster prizes will be presented, here. We will come together in a relaxed atmosphere and exchange information regarding MM. The current conference will be discussed and your feedback will be welcome. We will ask for your suggestions for topics for symposia or speakers to be invited for the next conference. Pretzels and drinks will be provided for free. Take this opportunity to tell us your ideas for MM at the next spring meeting and come to this general meeting of MM.

Time: Wednesday 18:45–19:45

Location: SCH A 251

All members of the Metal and Material Physics Division are invited to participate.

MM 35: Invited Talk: Champion

Time: Thursday 9:30–10:00

Location: SCH A 251

Topical Talk

MM 35.1 Thu 9:30 SCH A 251

Configuration entropy and sample size effect on glass transition temperature — •YANNICK CHAMPION — Univ. Grenoble Alpes, CNRS, Grenoble-INP, SIMaP, 38000 Grenoble, France.

Amorphous materials show an intriguing transition at room temperature between localized and homogeneous deformation. This effect is observed for sample sizes in the micron range for silica glass, tens to hundreds of nm for metallic glasses and less than 20 nm for polymers. It is interpreted as a dependence of the glass transition temperature (T_g) with the sample size. Besides, this has been observed for polymer films and described by an empirical law proposed by Ked-

die and collaborators (Keddie et al, Europhys. Lett 1994). A demonstration of this law is proposed from a statistical physics approach and using the potential energy landscape (PEL) description. The work is performed on a Mg-based metallic glass. A configuration entropy is derived from the size distribution of local areas in the PEL favorable to rearrangement. These zones are probed by nano-indentation and assumed to be related to the serrations observed in the deformation curves. The size of the serrations follows a Poisson distribution, indicating that their formation is a rare event. In addition to understanding the effect of size on T_g , the analysis allows the identification of statistical parameters describing the glass structure.

MM 36: Data Driven Materials Science: Big Data and Work Flows – Microstructure-Property-Relationships (joint session MM/CPP)

Time: Thursday 10:15–13:15

Location: SCH A 251

MM 36.1 Thu 10:15 SCH A 251

Orisodata: A methodology for grain segmentation in atomistic simulations using orientation based iterative self-organizing data analysis — •ARUN PRAKASH — Micro-Mechanics and Multiscale Materials Modeling (M5), TU Bergakademie Freiberg

Atomistic simulations of the molecular statics/dynamics kind have established themselves as a cornerstone in the field of computational materials science. Large scale simulations with tens to hundreds of millions of atoms are regularly used to study the behavior of nano-(poly)crystalline materials. Identifying grains a posteriori in such simulations is a challenging task, particularly for simulations at high temperatures or at large strains. In this work, we propose a methodology for grain segmentation of atomistic configurations using unsupervised machine learning [1]. The proposed algorithm, called OrISODATA, is based on the iterative self-organizing data analysis technique and is modified to work in the orientation space. The algorithm is demonstrated on a 122 grain nanocrystalline thin film sample in both undeformed and deformed states. The Orisodata algorithm is also compared with two other grain segmentation algorithms available in open-source visualization tool Ovito. The results show that the Orisodata algorithm is able to correctly identify deformation twins as well as regions separated by low angle grain boundaries. The intuitive model parameters relate to similar thresholds in experiments, which helps obtain optimal values and facilitates easy interpretation of results.

References: [1]: M. Vimal, S. Sandfeld and A. Prakash [2022]: *Materialia*, 21, 101314

MM 36.2 Thu 10:30 SCH A 251

Comparison of atomic environment descriptors with domain knowledge of the interatomic bond — •MARIANO FORTI, RALF DRAUTZ, and THOMAS HAMMERSCHMIDT — ICAMS, Ruhr Universität Bochum, Universität Straße 150, 44801 Bochum

The study of the relative stability of multicomponent materials and the search for new materials for high performance applications requires extensive samplings of the composition space. This is a demanding task due to the computational effort that is required for the electronic structure calculations. In this work we propose a machine learning approach with descriptors of the local atomic envi-

ronment using different chemistry heuristics based on smooth overlap of atomic positions, recursive solutions of tight-binding Hamiltonians and atomic cluster expansions. We demonstrate that these descriptors, which retain different levels of domain knowledge of structural and electronic properties of the chemical compounds, can be used to predict formation energies with high accuracy even with simple regression algorithms. We apply the methodology to complex crystal structures in binary and ternary intermetallic systems.

MM 36.3 Thu 10:45 SCH A 251

A Machine-Learning Framework to Identify Equivalent Atoms at Real Crystalline Surfaces — •KING CHUN LAI, SEBASTIAN MATERA, CHRISTOPH SCHEURER, and KARSTEN REUTER — Fritz Haber Institute of the Max Planck Society, Berlin, Germany

Functional surfaces and interfaces even of crystalline materials are characterized by breaks of symmetry and long-range order. Yet, even though such a crystalline surface may for instance exhibit numerous vacancies, adatoms, steps, kinks or islands, there are generally still many equivalent atoms, where equivalence refers to an identical or near-identical local environment. There are many equivalent terrace atoms, adatoms, step or kink atoms. In atomic-scale modeling and simulation, identifying these groups of equivalent atoms is a routine task, not least because one would e.g. restrict demanding first-principles calculations like the determination of an adsorption configuration and concomitant adsorption energy to only one site of each equivalence group. Aiming to automatize this routine task, we here present a machine-learning framework to identify all groups of equivalent atoms for any surface or nanoparticle geometry. The initial classification rests on the representation of the local atomic environment through a high-dimensional smooth overlap of atomic positions (SOAP) vector. We then achieve a fuzzy classification by mean-shift clustering within a low-dimensional embedded representation of the SOAP points as obtained by multidimensional scaling (MDS). The performance of this classification framework will be demonstrated with examples of Pd surfaces.

MM 36.4 Thu 11:00 SCH A 251

Identifying ordered domains in atom probe tomography using machine learning — •ALAUKE SAXENA, NAVYANTH KUSAMPUDI, SHYAM KATNAGALLU, BAPTISTE GAULT, DIERK RAABE, and CHRISTOPH FREYSOLDT — Max-Planck-Institut für Eisenforschung GmbH, Düsseldorf 40237, Germany

Atom probe tomography (APT) is a unique technique that provides 3D elemental distribution with near-atomic resolution for a given material. The spatial resolution of APT is $\sim 1\text{-}3$ Å in depth and $\sim 3\text{-}5$ Å in the lateral direction, respectively. Due to the limited spatial resolution, most of the APT data analysis focuses on composition to extract various microstructural features. Here, we aim at identifying additional on-lattice short-range order within an Al-Mg-Li alloy even though the underlying FCC lattice itself is not resolved. We propose a machine learning (ML) methodology to distinguish disordered solid solutions from ordered L12 domains. To encapsulate the local chemistry and noisy structure in APT independent of orientation, we use Smooth Overlap of Atomic Positions (SOAP). To find suitable hyperparameters of the high-dimensional SOAP features, we visualize the data distribution within the latent space of an auto-encoder neural network trained on experimental data with a preliminary classification. After the optimization, synthetic data corresponding to FCC and L12 structures is created with APT level spatial noise and then used for training from scratch a dense neural network for order/disorder classification. The trained model is then able to distinguish between ordered and disordered structures in experimental data.

MM 36.5 Thu 11:15 SCH A 251

Atomic cluster expansion: training a transferable water interatomic potential from the local atomic environments of ice — •ESLAM IBRAHIM, YURY LYSOGORSKIY, MATOUS MROVEC, and RALF DRAUTZ — ICAMS, Ruhr Universität Bochum, 44780 Bochum, Germany

We show the predictive power of the atomic cluster expansion (ACE) for modeling challenging systems such as water. We trained ACE on data from ab-initio molecular dynamics simulations (AIMD) of water at 300 K. ACE displays excellent agreement to the first-principles reference data in predicting radial distribution functions and covalent and hydrogen bonding characteristics. However, our investigation confirms that describing properties that require sampling a larger fraction of phase space, for example, self-diffusion or the free energies, requires longer AIMD simulation times at different pressures/densities and temperatures. We then show that ice structures provide a more efficient means of sampling the phase space of water: training ACE to diverse ice phases only describes liquid water in quantitative and qualitative agreement with first principles reference data. This reveals a powerful and efficient strategy for building transferable water interatomic potentials without running expensive AIMD.

15 min. break

MM 36.6 Thu 11:45 SCH A 251

Enhancing molecular dynamics simulations of water in comparison to neutron scattering data with algorithms — •VERONIKA REICH¹, LUIS CARLOS PARDO², MARTIN MÜLLER³, and SEBASTIAN BUSCH¹ — ¹GEMS at Maier-Leibnitz Zentrum, Helmholtz-Zentrum hereon, 85748 Garching, Germany — ²Departament de Física Escola d'Enginyeria de Barcelona Est Universitat Politècnica de Catalunya, 08019 Barcelona, Spain — ³Helmholtz-Zentrum hereon, 21502 Geesthacht, Germany

The structure and dynamics of materials can be studied on the atomic level with neutron and X-ray scattering experiments as well as molecular dynamics (MD) simulations. We connect experimental data with MD simulations to further enhance the simulations and obtain forcefields that are able to reproduce the measured structure and dynamics.

On the example of water, we established a workflow of running MD simulations in the program LAMMPS, calculating X-ray and neutron scattering data with the program Sassena, and comparing the diffractograms and incoherent intermediate scattering functions to already published experimental data.

The agreement between computed scattering curves and experimental data was optimized with algorithms to obtain a set of parameters that can simultaneously reproduce the real nanoscopic structure and dynamics of water probed by the neutron and X-ray scattering experiments.

This scheme is highly adaptable to different MD simulations of various models.

MM 36.7 Thu 12:00 SCH A 251

Stress and Heat Flux via Automatic Differentiation — •MARCEL F. LANGER^{1,2,3}, FLORIAN KNOOP^{3,4}, J. THORBEN FRANK^{1,2}, CHRISTIAN CARBOGNO³, MATTHIAS SCHEFFLER³, and MATTHIAS RUPP^{3,5} — ¹BIFOLD – Berlin Institute for the Foundations of Learning and Data, Berlin, Germany — ²Machine Learning Group, Technische Universität Berlin, Germany — ³The NOMAD Laboratory at the Fritz Haber Institute of the Max Planck Society and Humboldt University, Berlin, Germany — ⁴Theoretical Physics Division, Department of Physics, Chemistry and Biology (IFM), Linköping University,

Sweden — ⁵Materials Research and Technology Department, Luxembourg Institute of Science and Technology (LIST), Luxembourg

Computationally efficient approximations of the Born-Oppenheimer potential energy surface can be obtained by parametrising an analytical force field based on a set of reference calculations. Inspired by recent developments in machine learning, such potentials can include equivariant semi-local interactions through message-passing mechanisms and rely on automatic differentiation (AD), overcoming the need for manual derivative implementations or finite-difference schemes. We provide a unified framework for using AD in such state-of-the-art potentials, and discuss how AD can be used to efficiently and simply compute the stress tensor and the heat flux. We validate the framework by predicting thermal conductivity for selected semiconductors and insulators with an equivariant machine learning potential [1].

[1]: J.T. Frank, O.T. Unke, K.-R. Müller, arXiv 2205.14276 (2022).

MM 36.8 Thu 12:15 SCH A 251

Accurate thermodynamic properties of bcc refractories through Direct Upsampling — •AXEL FORSLUND, JONG HYUN JUNG, PRASHANTH SRINIVASAN, and BLAZEJ GRABOWSKI — Institute for Materials Science, University of Stuttgart, Pfaffenwaldring 55, 70569 Stuttgart

The outstanding high-temperature properties of the bcc refractory elements make them important in many industrial and scientific applications. Accurate thermodynamic data of unary bcc refractories are a requisite, for example, when used as end members for phase diagrams of high entropy alloys. In this work, we have calculated thermodynamic properties of the four bcc refractory elements V, Ta, Mo and W up to the melting point with full DFT accuracy with the newly developed Direct Upsampling method. We present highly converged Gibbs energy surfaces, from which accurate temperature dependence of heat capacity, thermal expansion coefficient and bulk modulus can be derived. We show their convergence with respect to fitting polynomial order and volume-temperature-grid density. Some group trends are observed, related to the electronic densities of states. In our analysis, we also estimate the contribution from thermal vacancies based on a single high-temperature calculation of the vacancy formation free energy. Further, our results are analysed in terms of homologous temperature for the elements of which a theoretical melting point (connected to the specific exchange correlation functional used) is known. The homologous temperature dependence of the calculated properties show a remarkable agreement with experiments.

MM 36.9 Thu 12:30 SCH A 251

Efficient workflow for treating thermal and zero-point contributions to the formation enthalpies of ionic materials — •RICO FRIEDRICH^{1,2,3}, MARCO ESTERS¹, COREY OSES¹, STUART KI¹, MAXWELL J. BRENNER¹, DAVID HICKS¹, MICHAEL J. MEHL¹, CORMAC TOHER¹, and STEFANO CURTAROLO¹ — ¹Duke University, USA — ²TU Dresden — ³Helmholtz-Zentrum Dresden-Rossendorf

The formation enthalpy, quantifying the enthalpy of a compound with respect to its elemental references, is a key parameter for predicting the thermodynamic stability of materials thus enabling data-driven materials design. Although for instance zero-point vibrational and thermal contributions to the formation enthalpy can be quite substantial reaching absolute values of up to ~ 50 meV/atom for ionic systems such as oxides, they are often neglected in *ab initio* workflows.

Here, we first calculate the thermal and zero-point contributions accurately from a quasi-harmonic Debye model. At room temperature, they largely cancel each other due to the different bond stiffness of compound and references reducing the total vibrational contribution to maximally ~ 20 meV/atom [1]. Moreover, the vibrational contributions can be parametrized within the coordination corrected enthalpies (CCE) method completely eliminating the need to compute these terms explicitly. On this basis, using only 0 K *ab initio* data as input, a workflow can be designed providing access to formation enthalpies at different temperatures from the AFLOW-CCE tool [2].

[1] R. Friedrich *et al.*, npj Comput. Mater. 5, 59 (2019).

[2] R. Friedrich *et al.*, Phys. Rev. Mater. 5, 043803 (2021).

MM 36.10 Thu 12:45 SCH A 251

Microstructure-Property Linkages for Effective Elasticity Tensors by Deep Learning — •BERNHARD EIDEL — TU Freiberg, M5-Micro Mechanics & Multi-scale Materials Modeling, Lampadiusstraße 4, 09599 Freiberg

The objective of the present work is to link random heterogeneous, multiphase materials to their elastic macroscale stiffness by 3D convolutional neural networks (CNNs). In an approach of supervised learning the effective elasticity tensors stem from homogenization simulations.

The proposed CNN model is a universal predictor for its extended generalization abilities overcoming bottlenecks in existing studies. It accounts for a large variety of microstructures, for arbitrary phase fractions, for almost arbitrary elastic moduli of the constituent phases, and it predicts the stiffness for periodic boundary conditions (BCs) along with sharp upper and lower bounds for the case of non-periodic matter. The proposed universal CNN model achieves high accuracy in its predictions. For a real, two-phase diamond/SiC coating material the universal CNN is almost as accurate as a CNN exclusively trained for

fixed elastic phase properties of that material. The speedup compared to finite element computations for homogenization is above factor 20 500. The proposed CNN model hence enables fast and accurate stiffness predictions in universal analyses of heterogeneous materials in their linear elastic regime, for details see [1].

[1] B. Eidel: Deep CNNs as universal predictors of elasticity tensors in homogenization, *Comput. Methods Appl. Mech. Eng.* (2023).

MM 36.11 Thu 13:00 SCH A 251

Influence of doping atoms on twinning in Ni-Mn-Ga alloy: an ab initio study — •PETR ŠESTÁK, MARTIN HEZCKO, and MARTIN ZELENÝ — Brno University of Technology, Brno, Czechia

Magnetic shape memory alloys (MSMAs) are multifunctional materials which - owing to the tight coupling between their magnetic and ferroelastic order - exhibit interesting phenomena, such as giant magnetoresistance, mag-

netocaloric and elastocaloric effects, and magnetically-induced reorientation (MIR) of martensite. The prototype MSMAs are the Heusler Ni-Mn-Ga based alloys. By combining the large strain and fast response, they may fill the application gap between the shape memory actuators (large strain, slow response) and magnetostrictive/piezo actuators (small strain, fast response). The MSMAs strongly depends on the twinning structure and especially on the twinning stress that is highly dependent on exact alloy composition, as it significantly decreases with increasing content of Mn, which hinders the MIR in Mn-excess alloy.

The recent development in atomistic simulations allows to determine the twinning stress not only from experimental methods but also from theoretical simulations. For example, generalized-planar-fault-energy (GPFE) curves describe the energy pathways associated with twinning as a function of shearing vector. Here, we present results of our calculations to reveal, how doping elements Co, Cu and Fe affects the GPFE curves, and consequently formation and propagation of twins.

MM 37: Topical Session: Defect Phases II

Time: Thursday 10:15–13:00

Location: SCH A 216

Topical Talk

MM 37.1 Thu 10:15 SCH A 216

Structural and chemical atomic complexity of lattice defects – From defect phase diagrams to properties of intermetallics — MARTINA FREUND, XIE ZHUOCHENG, LUKAS BERNERS, PEI LING SUN, STEFANIE SANDLÖBES-HAUT, and •SANDRA KORTE-KERZEL — Institut für Metallkunde und Materialphysik, RWTH Aachen University

Two approaches in materials physics have proven immensely successful in alloy design: First, thermodynamic and kinetic descriptions for tailoring and processing alloys to achieve a desired microstructure. Second, crystal defect manipulation to control strength, formability and corrosion resistance. However, to date, the two concepts remain essentially decoupled. A bridge is needed between these powerful approaches to achieve a single conceptual framework. Considering defects and their thermodynamic state holistically as defect phases, provides a future materials design strategy by jointly treating the thermodynamic stability of both, the local crystalline structure and the distribution of elements at defects.

Here, we will report our work on intermetallics, which are complex already in their underlying crystal structure, to reveal active deformation mechanisms and their dependence on both structure and chemical composition.

MM 37.2 Thu 10:45 SCH A 216

The synthesis and studies of unique oxygen structure on silica-aluminate catalysts — •LINFENG SU¹, XU CHEN², HUAPING ZHAO¹, ZHIYI LU², and YONG LEI¹ — ¹Fachgebiet Angewandte Nanophysik, Institut für Physik & IMN MacroNano, Technische Universität Ilmenau, 98693 Ilmenau, Germany — ²Key Laboratory of Advanced Fuel Cells and Electrolyzers Technology of Zhejiang Province, Ningbo Institute of Materials Technology and Engineering, CAS, Zhejiang, 315201, PR China

To promote the application of silica-aluminate catalysts in catalytic reactions, the unique active oxygen structures on the surface of silica-aluminate were investigated. 4A molecular sieves were prepared with oxygen-rich vacancies of various contents and different chemical environments. Three different types of oxygen vacancies (due to the covalent and coordination bonds of O) on the surface have different mechanisms in catalytic reactions, and the specific structures exhibit the best catalytic activity (87.5% removal rate of pollutants within 6 min in catalytic ozonation). Moreover, silica-aluminate mullite containing abundant neo-oxygen structure (unique bridging oxygen) was successfully prepared at a low preparation temperature. The abundant oxygen structure in silica-aluminate leads to abundant unique bridging oxygen structures with high catalytic activities (81.2% removal rate of pollutants within 15 min under low ozone concentration). The research on the unique oxygen structure of silicate-aluminate provides theoretical guidance for the design and synthesis of catalysts with high catalytic activities for future industrial applications.

MM 37.3 Thu 11:00 SCH A 216

Understanding corrosion phenomena based on surface phase diagrams for Mg alloys in contact with water — •JING YANG, MIRA TODOROVA, and JÖRG NEUGEBAUER — Max-Planck-Institut für Eisenforschung GmbH, Max-Planck-Strasse 1, D-40237 Düsseldorf, Germany

Defect phases formed at alloy surfaces and interfaces govern their chemical and mechanical behavior. Constructing phase diagrams from ab initio modeling provides valuable information for understanding the microscopic mechanisms of surface and interface processes. In this work, we apply this approach to study the aqueous corrosion of magnesium alloyed with Al and Ca, an important structural material for the automotive and aerospace industries. Constructing defect phase diagrams for the passive film formed on the magnesium surface, we analyze how the Al and Ca alloying atoms evolve during the corrosion process and how they impact the corrosion resistance of the magnesium alloy. In particular,

we resolve the cause of Al enrichment in the passive film, which has been recently observed in experiment. Based on these examples we discuss how defect phase diagrams can help us to better understand microscopic chemical processes under realistic conditions.

MM 37.4 Thu 11:15 SCH A 216

Ab-initio informed CALPHAD modelling of grain boundaries — •TOBIAS SPITALER¹, RISHI BODLOS², DANIEL SCHEIBER², and LORENZ ROMANER¹ — ¹Montanuniversität Leoben, Department Werkstoffwissenschaft, Leoben, Österreich — ²Materials Center Leoben Forschung GmbH, Leoben, Österreich

The CALPHAD method is an important tool in material science to calculate phase diagrams and to predict phase stabilities of complex systems. Based on a model of the Gibbs Free energy of the bulk phases as function of composition, pressure and temperature the thermodynamic equilibrium quantities can be calculated with computer programs. In materials grain boundaries play an important role for mechanical properties and grain growth. Alloying elements often tend to segregate from or to the grain boundary, changing the properties of the grain boundary for example by weakening or strengthening the cohesion or by preventing grain boundary movement, which can lead to stabilisation of a nano-crystalline structure.

We therefore devise a formulation of the grain boundary Gibbs Free energy within the compound energy formalism with the goal to obtain the grain boundary state parameters such as composition and grain boundary area. We use DFT calculations to explore energy configurations of grain boundaries and couple them to thermodynamic models to investigate solute segregation and its impact on the grain boundary energy. With these results we can provide grain boundary phase diagrams and address thermodynamic nanocrystalline stability in metallic alloys.

15 min. break

Topical Talk

MM 37.5 Thu 11:45 SCH A 216

Density-based Grain Boundary Phase Diagrams — •REZA DARVISHI KAMACHALI — Federal Institute for Materials Research and Testing (BAM)

Phase diagrams are the roadmaps of material design yet primarily developed and discussed for defect-free bulk phases. Real microstructures, however, also contain large populations of defects, such as grain boundaries, which show their own distinct phase behavior. Recently, CALPHAD-integrated density-based phase diagrams were proposed for studying segregation and phase evolution in grain boundaries. In this method, the connection to available bulk thermodynamic data allows rapid assessment of grain boundary phase behavior. In this talk, density-based phase diagrams of several binary and ternary alloy systems will be discussed, with direct implications for alloy and microstructure design. The significance and integration of elastic energies to the density-based model will be presented. It will be shown that Cu segregation and segregation transition in Al-Cu and Al-Cu-Mg systems can be explained by the presence of solutes' elastic interactions with grain boundaries.

MM 37.6 Thu 12:15 SCH A 216

Learning chemistry dependence of grain boundary segregation energies — •CHRISTOPH DÖSINGER¹, DANIEL SCHEIBER², OLEG PEIL², VSEVOLOD RAZUMOVSKIY², and LORENZ ROMANER¹ — ¹Montanuniversität Leoben, Department of Materials Science, Leoben, Austria — ²Materials Center Leoben Forschung GmbH, Leoben, Austria

The grain-boundary segregation energy (E_{seg}) is the central quantity for describing the process of grain-boundary segregation which influences fracture. Usually, to obtain highly accurate values for E_{seg} , density functional theory is

employed, which incurs high computational costs. This makes it impractical to do a thorough study of segregation to multiple grain-boundaries for a range of solutes. To reduce the number of calculations needed for such a complete description, we apply machine learning methods to density functional theory data. By using separate sets of descriptors for the local atomic environment and the solute types, we fit a model based on gaussian process regression. This approach is evaluated on a comprehensive data-set for E_{seg} in tungsten. The tests indicate that the model has the ability to extrapolate to solutes which are not contained in the training data.

MM 37.7 Thu 12:30 SCH A 216

Rationalising the impact of experimental preparation routes on impurity content in Pd nano-aerogels using ab-initio phase diagrams — •MIRA TODOROVA, SU-HYUN YOO, POULAMI CHAKRABORTY, TILMANN HICKEL, SE-HO KIM, BAPTISTE GAULT, and JÖRG NEUGEBAUER — Max-Planck-Institut für Eisenforschung, Düsseldorf

Recent advances of experimental techniques with atomic resolution enable us to analyze the structure and composition of samples at the sub-nanometer scale, providing information about contamination with impurities and their distribution. Understanding the factors which govern the ingress, amount and distribution of contaminating elements, opens routes to both improving the sample quality and their utilization in targeted design to achieve a desired functionality. Using an ab-initio based thermodynamic approach and surface phase diagrams we unravel the impact of preparation conditions on experimental observations and materials properties. The power and the performance of these ab-initio based thermodynamic concepts will be highlighted using the example of impurity incorporation during wet-synthesis of nano-aerogels, specifically Na

and K incorporation into grain boundaries [JACS 144, 987 (2022)] and B into the bulk [Adv. Mater. 2203030 (2022)] of Pd nano-aerogels.

MM 37.8 Thu 12:45 SCH A 216

Influence of stoichiometric change on plasticity in the Ca(Al₂Mg)₂C15-Laves Phase — •MARTINA FREUND¹, PEI-LING SUN¹, CARSTEN THOMAS², DEBORAH NEUSS³, MICHAEL FEUERBACHER², MARCUS HANS³, and SANDRA KORTEKERZEL¹ — ¹Institut für Metallkunde und Materialphysik, RWTH Aachen University — ²Ernst Ruska-Centrum für Mikroskopie und Spektroskopie mit Elektronen und Peter-Grünberg Institut Forschungszentrum Jülich GmbH — ³Materials Chemistry, RWTH Aachen University

Magnesium is a promising material for light weight applications but is strongly limited because of its low room temperature ductility and low creep resistance. By alloying with Al and Ca different Laves phases form, which improve creep strength properties. We did investigations of the stoichiometric C15 Laves phase, finding slip on {111} and {112} planes with the same activation frequency and approximately same CRSS values. The influence of the stoichiometry regarding the plasticity was analysed using a sample with 6at.-% Mg, by nanoindentation tests, APT and TEM. Hardness and indentation modulus values were in the same range for all indented orientations. Comparing this to the stoichiometric one, the hardness has shown a slight increase around 1 GPa. Changes of plasticity were seen by analysing resulting slip lines. Most activated slip planes were the {112} planes, followed by the {110}. APT was done for both, the stoichiometric and the off-stoichiometric, to evaluate the local chemistry on {112} slip planes. Ultimately, we aim to reveal the connection between the local chemical potential and motion of dislocations on different slip planes.

MM 38: Topical Session: Fundamentals of Fracture – Fracture Experiments

Time: Thursday 10:15–11:15

Location: SCH A 215

Topical Talk

MM 38.1 Thu 10:15 SCH A 215

The Fundamental physics of the onset of frictional motion: How does friction start? — •JAY FINEBERG — The Racah Institute of Physics, The Hebrew University, Jerusalem Israel

Recent experiments have demonstrated that rapid rupture fronts, akin to earthquakes, mediate the transition to frictional motion. Moreover, once these dynamic rupture fronts ("laboratory earthquakes") are created, their singular form, dynamics and arrest are well-described by fracture mechanics. Ruptures, however, need to be created within initially rough frictional interfaces, before they are able to propagate. This is the reason that "static friction coefficients" are not well-defined; frictional ruptures can nucleate for a wide range of applied forces. A critical open question is, therefore, how the nucleation of rupture fronts actually takes place. We experimentally demonstrate that rupture front nucleation is prefaced by slow nucleation fronts. These nucleation fronts, which are self-similar, are not described by our current understanding of fracture mechanics. The nucleation fronts emerge from initially rough frictional interfaces at well-defined stress thresholds, evolve at characteristic velocity and time scales governed by stress levels, and propagate within a frictional interface to form the initial rupture from which fracture mechanics take over. These results are of fundamental importance to questions ranging from earthquake nucleation and prediction to processes governing material failure.

MM 38.2 Thu 10:45 SCH A 215

Macro to micro in fracture - shorter is tougher — •DOV SHERMAN — School of Mechanical Engineering, Tel-Aviv University, Tel-Aviv, Israel

Fracture of brittle solids is ultimately executed by atomistic-scale, discrete, and ultrafast bond-breaking mechanisms along the crack path. Here, we show new fracture behavior and properties of brittle materials not previously explored. It is based on macroscopic fracture cleavage experiments of brittle single-crystal silicon specimens, including cracks energy-speed relationships, and an atomistic-scale semi-empirical model for bond-breaking mechanisms in form of planer kinks along the (curved) crack front. As a result, we identified that the cleavage

energy is not a constant but bounded by the Griffith Barrier and lattice-trapping barrier. Hence, a brittle material can be envisaged as having a pseudo-R-Curve behavior typical of metallic materials. A new and essential fracture mechanism was identified, which we termed "quasi-propagation", occurring between initiation and propagation. During this mechanism, the sequence of the bond-breaking mechanisms is varying, causing an increase in the macroscale cleavage energy. The range of these changes is dictated by the energy release rate and its first derivative following initiation. The evaluated cleavage energy shows that "shorter is tougher" and hence the material is stronger than that predicted by the Griffith theory.

MM 38.3 Thu 11:00 SCH A 215

How hidden 3D structure within crack fronts reveals energy balance — •MENG WANG and JAY FINEBERG — The Racah Institute of Physics, The Hebrew University of Jerusalem, Jerusalem, 91904, Israel

Griffith's energetic criterion, has been pervasively used to measure material resistance to failure and describe the propagation dynamics of simple cracks. When cracks contain secondary structure, full crack fronts must be considered. Secondary structure within a crack front will increase energy dissipation, and it is not, a priori, clear how its presence affects the crack dynamics and contributes to the fracture energy. Here, we study low-speed crack propagation in hydrogels under tensile loading conditions. Such slow cracks are shown to be bistable; either simple or faceted crack states can be generated under identical loading conditions. The selection of either crack state is determined by the form of the initial seed crack. We find that seed cracks containing a small local mode III component generally leads to a single step that propagates along a crack front. In contrast to simple cracks, faceted cracks can no longer be considered as existing in a quasi-2D system. For both simple and faceted cracks, we simultaneously measure the energy flux and local fracture toughness along the crack fronts over velocities. We find that the concept of energy balance must be generalized for 3D systems; faceted cracks obey energy balance, only when we account for the local dynamic dissipation at each point along the crack front. If the local structure is not properly accounted for, energy balance will appear to fail.

MM 39: Phase Transformations: Simulation and Machine Learning

Time: Thursday 11:45–13:15

Location: SCH A 215

MM 39.1 Thu 11:45 SCH A 215

Simultaneous structural and thermal characterisation of Zr-based bulk metallic glasses via synchrotron X-ray diffraction and fast differential scanning calorimetry — •STEFAN T. STANKO¹, JÜRGEN E.K. SCHAWÉ^{1,2}, and JÖRG F. LÖFFLER¹ — ¹Laboratory of Metal Physics and Technology, Department of

Materials, ETH Zurich, 8093 Zurich, Switzerland — ²Mettler-Toledo GmbH, Analytical, 8606 Nänikon, Switzerland

Fast differential scanning calorimetry (FDSC) experiments were performed to measure time-temperature-transformation (TTT) diagrams of Zr-based bulk metallic glasses used for additive manufacturing. The alloys were measured in

powder and bulk form, and multiple crystallisation events upon cooling were observed in both cases. The fast differential scanning calorimeter was modified to allow its integration into a synchrotron X-ray beamline and thus to characterise *in situ* metastable phase transformations. With the *in situ* setup it was possible to simultaneously investigate the structure of the phases involved and their transformation kinetics. The results were correlated with the oxygen content of the alloys, with the aim of optimising the additive manufacturing process of metallic parts.

MM 39.2 Thu 12:00 SCH A 215

Measurement and simulation of cooling times in pump-probe experiments of phase transitions with latent heat — •DANIEL KAZENWADEL, NOEL NEATHERY, and PETER BAUM — Universität Konstanz, Konstanz, Germany

Ultrafast pump-probe experiments are often limited by the need to wait for a sample's back reaction to take place between adjacent laser pulses. Here we investigate by experiments and simulations how the sample geometry influences the cooling rate of VO₂, a strongly correlated phase-transition material with substantial latent heat. We measure back reaction times of milliseconds, microseconds and nanoseconds in free-standing thin-films, coated substrates and bulk crystals, respectively. A simple latent heat model reproduces the behavior of all geometries and can therefore be used to predict the speed of the back reaction in other phase-change materials as well.

MM 39.3 Thu 12:15 SCH A 215

Ab initio thermodynamics and atomistic modeling of NiTi SMA with machine learning interatomic potentials — •PRASHANTH SRINIVASAN and BLAZEJ GRABOWSKI — Institute for Materials Science, University of Stuttgart, Germany
Equiatomic Nickel-Titanium (NiTi) possesses interesting properties such as pseudoelasticity and shape memory effect that arise from a reversible transformation between the austenite (B2) and the martensite phase (B19'). Other competing phases (B19 and B33) make modeling of NiTi challenging. *Ab initio* molecular dynamics (AIMD) calculations have shown that B19' and B2 phases are entropically stabilized (Haskins et. al., 2016), but the calculations were restricted to a single DFT exchange correlational functional (XC). Studying the kinetics of phase transformation using only DFT is also severely expensive.

In this work, we address both challenges. Using a recently developed thermodynamic integration technique (Jung et. al., 2022) aided with machine-learning based moment tensor potentials (MTPs, Shapeev 2016), it is possible to efficiently compute high-temperature thermodynamic phase stability to DFT accuracy. We perform such calculations to analyze three different XCs (GGA, LDA and SCAN). We also perform large-scale molecular dynamics (MD) simulations using the MTPs to study the kinetically-driven phase transformation behavior in each of these cases. Preliminary results show the necessity of having a high *k*-point density in the underlying DFT calculations. When fitted to such a training set, the MTPs predict highly accurate thermodynamic properties and phase transformation behavior.

MM 39.4 Thu 12:30 SCH A 215

Prediction of quantum paraelectricity and quantum phase transitions using ab initio self-consistent lattice dynamics and machine learning — •QUINTIN MEIER¹, AMBROISE VAN ROEKEGHEM², and NATALIO MINGO² — ¹Université Grenoble Alpes, CNRS, Institut Neel, 25 Av. des Martyrs, 38042 Grenoble — ²Université Grenoble Alpes, CEA, LITEN, 17 Rue des Martyrs, 38054 Grenoble, France

Anharmonic interactions of the lattice are essential for understanding the temperature- dependent behavior of many materials. Here we present a method combining DFT and the active learning of interatomic potentials to obtain the necessary sets of forces to calculate the temperature dependent force constants using the quantum self-consistent lattice dynamics formalism [1]. A particularly strong anharmonicity has been shown in incipient ferroelectrics like KTaO₃. We show that we are method can be used to accurately and efficiently compute the strongly anharmonic low temperature behaviour of the soft mode in quantum paraelectric KTaO₃, and we study its stability range under pressure and uniaxial strain.

[1] Van Roekeghem, A et al, Comp. Phys. Commun, Vol 263 (2021)

MM 39.5 Thu 12:45 SCH A 215

Atomic cluster expansion for modelling of transition metal carbide systems — •MINAAM QAMAR — ICAMS, Ruhr University Bochum, Bochum, Germany

Atomic cluster expansion (ACE) provides an alternative to classical and machine learning potentials by modelling the local environment of an atom with a mathematically complete descriptor. We present an ACE potential for the Mo-C system, which is parametrized over an exhaustive dataset of important phases and defect structures. The resulting ACE is shown to be accurate with respect to the DFT reference data and computationally efficient which allows us to perform large scale finite temperature applications.

MM 39.6 Thu 13:00 SCH A 215

Structure-mapping workflow for the investigation of solid-solid phase transitions — •ARTEM SAMTSEVICH, CHRISTOPH SCHEURER, and KARSTEN REUTER — Fritz Haber Institute of the Max Planck Society, Berlin, Germany

Solid-solid transformations are common in nature and in the aging of functional materials. It is thus crucial to understand the origin of these complex phenomena at the atomistic level. The involved activated processes can be modeled as transitions between basins on a high-dimensional free energy landscape (FES). Using the harmonic approximation to transition state theory (hTST), one can estimate reaction rate constants from the location of saddle points on the FES. The chain-of-states method optimizes presumed pathways between two structural endpoints towards the minimum energy pathway (MEP), yielding transition state estimates. The generation of the initial pathway requires the mapping of atomic structures onto each other, which can be achieved either by purely geometrical methods (mapping of atomic positions and cells) or by the topology-based method, which maps the graphs of interatomic bonds. Both approaches are complementary to each other and generate a diverse set of mappings.

The combination of mapping algorithms with the chain-of-state method has recently been merged into a generalized workflow. We will present applications to phase transitions in high-energy-density and superhard materials [1,2] as well as catalyst aging.

[1] Wang, Y., Bykov, M., et al., Nat. Chem. 14, (2022).

[2] Kvashnin, A. G., Samtsevich A.I., JETP Lett. 111, (2020).

MM 40: Mechanical Properties and Alloy Design

Time: Thursday 15:45–18:30

Location: SCH A 251

MM 40.1 Thu 15:45 SCH A 251

First principles validation of barriers in Ni₃Al — •ADAM FISHER¹, THOMAS HUDSON¹, HUAN WU², TYLER LONDON², and PETER BROMMER¹ — ¹University of Warwick, Coventry, UK — ²TWI Ltd, Cambridge, UK

Precipitates in Nickel-based superalloys form during heat treatment on a time scale inaccessible to direct Molecular Dynamics simulation, but can be studied using kinetic Monte Carlo (KMC). This requires reliable values for the barrier energies separating distinct configurations over the trajectory of the system. In this study, we validate barriers found with the activation relaxation technique nouveau (ARTn) method in a Ni₃Al using a published potential for the atomic interactions against first-principles methods. In a first step, we confirmed that the ARTn barrier energies agree with those determined with the nudged elastic band (NEB) method. As the number of atoms used in those calculations is too great for direct *ab initio* calculations, we then cut the cell size to 255 atoms, thus controlling finite size effects. We then use the plane-wave density functional theory (DFT) code CASTEP and its inbuilt NEB method in the smaller cells. This provides us with a continuous validation chain from first principles to large-scale KMC and allows us to quantify the errors incurred in simulations of precipitate formation and evolution.

MM 40.2 Thu 16:00 SCH A 251

Ab-initio study of partitioning of transition-metal elements in the γ/γ' microstructure of single-crystal superalloys — •ISABEL PIETKA¹, ANDREAS FÖRNER², MANUEL KÖBRICH², STEFFEN NEUMEIER², RALF DRAUTZ¹, and THOMAS HAMMERSCHMIDT¹ — ¹Ruhr-Universität Bochum, Interdisciplinary Centre for Advanced Materials Simulation (ICAMS) — ²Friedrich-Alexander-Universität Erlangen-Nürnberg, Department of Materials Science & Engineering

The outstanding mechanical properties at high temperatures of Ni- and Co-base superalloys are closely tied to the underlying γ/γ' microstructure. Understanding the preferences of alloying elements for the γ matrix or γ' precipitates helps to develop new alloy compositions. In this work, we investigate the partitioning of the 3d, 4d, and 5d transition metals (TMs) in Ni₃Al and Co₃(Al,W) superalloys. In particular, we determine the preference of the TM elements for the γ or γ' phase by density functional theory calculations. We find clear trends of partitioning across the TM series that are in good agreement with experimental data. Our findings can be rationalized in terms of band filling and atomic size differences by moments analysis from bond order potential theory.

MM 40.3 Thu 16:15 SCH A 251

Towards understanding the yield stress anomaly of Ni₃Al from the energetics of planar defects — •XIANG XU^{1,2}, XI ZHANG², ANDREI RUBAN^{3,4}, SIEGFRIED SCHMAUDER¹, and BLAZEJ GRABOWSKI² — ¹Institute for Materials Testing, Materials Science and Strength of Materials, University of Stuttgart, Germany — ²Institute for Materials Science, University of Stuttgart, Germany — ³KTH Royal Institute of Technology, Stockholm, Sweden — ⁴Materials Center Leoben Forschung GmbH, Leoben, Austria

The yield stress anomaly of L1₂ intermetallic compounds, especially Ni₃Al, has been investigated for several decades. It is believed that planar defects, e.g., the complex stacking fault and the antiphase boundaries, play an essential role in the dislocation activities during plastic deformation. However, a thorough temperature dependence of the formation energy of these planar defects is still elusive. Facilitated by the state-of-the-art methodology which acquires different thermal mechanisms, especially the magnetic excitations and the full vibrations, the Gibbs energies of the complex stacking fault and the antiphase boundaries of Ni₃Al were calculated within the ab-initio framework up to the melting temperature. The accurate results obtained here are helpful to scrutinize the available experimentally measured data and provide fruitful insights to understand the mechanism behind the yield stress anomaly as well.

MM 40.4 Thu 16:30 SCH A 251

Observation of in-plane oriented Guinier-Preston zones in Al-Cu — •JOHANNES BERLIN, TOBIAS STEGMÜLLER, and FERDINAND HAIDER — Universität Augsburg, Deutschland

Known for a long time, the first metastable precipitates forming in Al-Cu alloys during natural ageing are the so-called Guinier-Preston zones (GPZ), platelets of Cu on {100} planes of only one atomic layer thickness. With the development of aberration corrected (S)TEMs, direct observation and imaging of these platelets was possible, but with the restriction, that only edge view was possible. Using a Cs-probe corrected scanning transmission electron microscopy with HAADF detector (DF-STEM), a single Cu atom in a Al column results in sufficient contrast to the neighbouring columns. In sufficiently thin samples, planar zones then lead to theoretically forbidden reflections of type {110} in the fourier transformed image, since only half of the columns in the GP zone contain a Cu atom. Thus, fourier filtering of such an image with only these forbidden reflections allows to observe GP Zones in a plan-view. The average size, shape and density of the GP-zones was determined for different aging times, and STEM image simulations using the software package DrProbe support this interpretation.

MM 40.5 Thu 16:45 SCH A 251

Dynamic and structural properties of undercooled Cu-Ti melts — •LUCAS KREUZER^{1,2}, FAN YANG², THOMAS HANSEN³, ANDREAS MEYER^{2,3}, and WINFRIED PETRY¹ — ¹Heinz Maier-Leibnitz Zentrum (MLZ), Garching, Germany — ²Institute for Material Physics in Space, German Aerospace Center (DLR), Cologne, Germany — ³Institute Laue-Langevin (ILL), Grenoble, France

Cu-Ti alloys feature a large, undercooled liquid region and a high glass-forming ability (GFA) and thus, provide the possibility to obtain two component bulk metallic glasses (BMGs). This unusual behavior could be due to the special properties of the liquid Cu-Ti system: a positive excess volume and a negative enthalpy of mixing. However, the relevant atomic mechanisms responsible for such good GFA are still to be explored. Here we discuss the temperature-dependent dynamical and structural properties of Cu-Ti melts, within a compositional range of 24 to 69 at% Ti. Accurate data about viscosity, density, and atomic structure, the Cu-Ti samples was obtained by using have been processed without any container using the electrostatic levitation technique. We found a non-monotonous trend of the viscosity, with the highest values at intermediate Ti contents. Surprisingly, this dynamical trend is not reflected by the macroscopic packing fraction, meaning a high viscosity does not necessarily correlate with a dense packing. However, on the atomic scale, x-ray and neutron diffraction reveal a denser, local packing and a pronounced chemical short-range order. These short-range interactions can explain the high viscosity, while the macroscopic packing fraction is rather governed by long-range interactions.

15 min. break

MM 40.6 Thu 17:15 SCH A 251

Can we measure twinning stress of a high entropy alloy with micromechanics? — •CAMILA AGUIAR TEIXEIRA, SUBIN LEE, and CHRISTOPH KIRCHLECHNER — Institute for Applied Materials, Karlsruhe Institute of Technology, Eggenstein-Leopoldshafen, Germany

CoCrFeMnNi and CoCrNi high entropy alloys (HEAs) have attracted attention due to their mechanical properties. Extensive mechanical twinning is mainly responsible for their outstanding mechanical response under cryogenic temperatures, e.g. increase in ductility and tensile strength. However, at room temperature dislocation slip is dominant and twinning only observed in highly deformed samples. Although both HEAs have been broadly studied, there is still a lack of in-depth understanding of twinning mechanism and stresses required for its activation, which is crucial for advanced HEAs design. In this work, we aim to

develop protocols to assess the critical resolved shear stress required for twinning by applying in situ micromechanics. Therefore, two points were addressed within the scope of this work: (i) study the transition from full to partial slip using micropillar compression and (ii) observe deformation twinning by shear stress using micro-shear test. Specific grain orientations were chosen through EBSD analyses, for the micropillar single slip orientation with higher Schmid factor for partial slip and for micro-shear [1 1 2] ND and [-1 1 1] TD orientation. Samples were then micromachined by FIB and tested in situ. Post-mortem analysis included SEM imaging, EBSD and (S)TEM to verify if twinning could be observed. The results provided quantitative insights essential for further understanding of the twinning mechanisms.

MM 40.7 Thu 17:30 SCH A 251

Influence of crystal structure on helium-induced tndril formation in an FeCoCrNiV high-entropy alloy — •SVENJA LOHMANN¹, RUSSELL GOODALL², GREGOR HLAWACEK¹, RENÉ HÜBNER¹, LE MA², and AMY S. GANDY² — ¹Helmholtz-Zentrum Dresden-Rossendorf, Germany — ²University of Sheffield, UK

High-entropy alloys (HEAs) are a relatively new class of metal alloys composed of several principal elements, usually at (near) equiatomic ratios. Our goal is to understand how such a multicomponent alloy behaves under irradiation. The FeCoCrNiV HEA exhibits both a face-centred cubic (fcc) and a body-centred tetragonal (bct) phase, thus allowing us to specifically study the influence of crystalline structure at very similar chemical composition. We irradiated both phases with a focussed He beam provided by a helium ion microscope (HIM) at temperatures between room temperature and 500°C. The irradiation fluence was varied between 6×10^{17} ions/cm² and 1×10^{20} ions/cm². High-resolution images of the irradiated areas were taken with the same HIM. Selected irradiated areas were additionally studied by TEM in combination with EDXS. Under irradiation, pores start to be generated in the material with pore sizes differing significantly between the two phases. At higher fluences and above a critical temperature, a tndril structure forms in both phases. We found that the critical temperature depends on the phase and is lower for fcc. TEM images reveal that the tndrils span the whole depth of the irradiated area, and are accompanied by bubbles of various sizes. Scanning TEM-based EDXS of these structures indicates a He-induced change in composition.

MM 40.8 Thu 17:45 SCH A 251

Diffusion and phase stability in a HCP HfScTiZr multicomponent alloy — •MOHAN MURALIKRISHNA GARLAPATI¹, SANDIPAN SEN¹, XI ZHANG², SANKARAN S³, JULIANA SCHELI^{4,5}, LUKASZ ROGAL⁶, GERHARD WILDE¹, GRABOWSKI B², and SERGIY V. DIVINSKI¹ — ¹Institute of Materials Physics, University of Muenster, Muenster, Germany — ²Institute of Materials Science, University of Stuttgart, Stuttgart, Germany — ³Department of Metallurgical and Materials Engineering, Indian Institute of Technology, Madras, Chennai, India — ⁴European Organization for Nuclear Research (CERN), CH-1211 Geneva, Switzerland — ⁵Institute for Materials Science and Center for Nanointegration Duisburg-Essen (CENIDE), University of Duisburg-Essen, Essen, Germany — ⁶Institute of metallurgy and Materials Science, Polish Academy of Sciences, Krakow, Poland

Phase stability and tracer diffusion in a hexagonal close-packed (HCP) HfScTiZr multicomponent alloy are investigated. The microstructure stability is examined by an in-depth electron microscopy characterization of samples subjected to prolonged heat treatments. It is found that the alloy decomposes into two HCP phases with similar lattice constants. The DFT calculations confirm the possibility of the phase decomposition. The minor and major phases are observed to be enriched with Ti and Sc, respectively. Self-diffusion is measured using the 44Ti, 46Sc, and 89Zr radioactive isotopes. The phase decomposition is found to influence marginally Zr, but significantly Ti and Sc diffusion. The diffusion properties are analyzed in correlation to the microstructure stability and thermodynamic properties of the alloy.

MM 40.9 Thu 18:00 SCH A 251

Solid solution strengthening in single-phase HEAs based on Au-Cu-Ni-Pd-Pt — •SOPHIE DRESCHER¹, JENS FREUDENBERGER¹, SASCHA SEILS², ALEXANDER KAUFFMANN², and MARTIN HEILMAIER² — ¹Leibniz-IFW Dresden, Helmholtzstr. 20, 01099 Dresden, Germany — ²Karlsruhe Institute of Technology, Institute for Applied Materials, Engelbert-Arnold-Str. 4, 76131 Karlsruhe, Germany

Solid solution strengthening (SSS) is the dominant strengthening mechanism in High entropy alloys (HEAs). In contrast to dilute alloys, SSS of HEAs is yet not well understood. Therefore, it is necessary to develop reliable models to predict their mechanical properties. To verify such models experimental work is needed that illustrates the concentration-dependent solid solution strengthening of different alloys over a large composition range.

The high entropy alloy system Au-Cu-Ni-Pd-Pt is unique as it crystallizes in face-centered cubic crystal structure and is single-phase presumably within the entire concentration range. Hence, it serves a suitable benchmark system to investigate composition-dependent effects on the strength. In this study, it has

been examined whether the model of Varvenne [1] is suitable to predict the SSS in this alloy system. The concentrations of individual elements were varied and the strength and hardness were evaluated. The model of Varvenne is misleading the development of the strength in a large compositional range. However, the results give insights into the impact of different elements on the strength and can help to further enhance the model.

[1] C. Varvenne, et al., *Acta Mater.* 118 (2016) 164.

MM 40.10 Thu 18:15 SCH A 251

Magnetism in nanocrystalline CoMnFeNiGa high entropy alloys: "from micro and bulk to nano" — •NATALIA SHKODICH^{1,2}, VARATHARAJA NALLATHAMBI^{1,2}, TATYANA SMOLYAROVA¹, SVEN REICHENBERGER¹, and MICHAEL FARLE¹ — ¹Faculty of Physics and Center of Nanointegration (CENIDE), University of Duisburg-Essen, Duisburg, 47057 Germany — ²Max-Planck-Institut für Eisenforschung Max-Planck-Straße 1, 40237 Düsseldorf, Germany

We report the successful fabrication of three types of CoMnFeNiGa high entropy alloys: a) nanoparticles, b) nanocrystalline micron-sized powder, and c) nanocrystalline metallic bulk. Homogeneous micron-sized CoMnFeNiGa HEA powders with a nanocrystalline structure and compositional homogeneity were produced by high energy ball milling (HEBM) for 190 min in Ar at 900/1800 rpm. From these powders we synthesized (a) homogeneous nanocrystalline bulk HEAs by spark plasma sintering (SPS) and (b) HEA nanoparticles - by laser fragmentation in liquids (LFL). The XRD, SEM/EDX, and HR TEM results showed that single fcc phase nanosized grains (~10 nm) are obtained after 190 min of HEBM. These partially transform into a bcc one after SPS at 1073K, while the LFL leads to the formation of nanoparticles with two morphologies, that is spheres and platelets with fcc, bcc and hexagonal structures. Fast annealing up to 1000K of HEBM and LFL HEA particles leads to significant structural and composition changes and increases the saturation magnetization M_s (300K) from 35.4 to 96.1 Am²/kg, and from 37.3 to 49.7 Am²/kg, respectively. We acknowledge financial support from DFG (CRC/TRR 270, project S01).

MM 41: Topical Session: Defect Phases III

Time: Thursday 15:45–18:00

Location: SCH A 216

Topical Talk MM 41.1 Thu 15:45 SCH A 216

Entropy in grain boundary segregation — •PAVEL LEJCEK — CEITEC, BUT, Brno, Czechia — Institute of Physics, AS CR, Prague Czechia

Experimentally, a linear dependence between the standard entropy and the standard enthalpy of solute segregation at grain boundaries was established which is called *enthalpy-entropy compensation effect*. In this dependence, there exists a region in which the product of temperature and segregation entropy (entropy term) is larger than the absolute value of the segregation enthalpy, so that the controlling parameter, the Gibbs energy of segregation, is negative. Under this condition the grain boundary segregation is dominated by the entropy, i.e., the phenomenon of the entropy-dominated grain boundary segregation occurs. We show numerous examples of the grain boundaries and solutes in bcc-iron-based alloys exhibiting this phenomenon. In addition, we formulate the idea that a solute can also segregate at the grain boundary (site) that exhibits positive segregation energy/enthalpy (so called *anti-segregation site*) if the entropy term is larger than the segregation enthalpy, so that the Gibbs energy of segregation is negative. In this way, the solute segregation is completely controlled by the entropy term and an entropy-driven grain boundary segregation will exist. We suggest the entropy-driven grain boundary segregation for several model examples in iron-based systems thus serving as indirect evidence of the phenomenon. Finally, the grain boundary configurational entropy is discussed in relation to its volume counterpart and to the segregation variables.

MM 41.2 Thu 16:15 SCH A 216

Impact of precipitation on grain boundary diffusion in microstructure-engineered Ni-Cr-Fe alloy — •BAIXUE BIAN, MOHAN MURALIKRISHNA GARLAPATI, SHABNAM TAHERINIYA, SANDIPAN SEN, GERHARD WILDE, and SERGIY V. DIVINSKI — Institute of Materials Physics, University of Münster, Wilhelm-Klemm-Str. 10, 48149 Münster, Germany

Grain boundary structure-property relationship is studied in a Ni-based Inconel 602CA coarse-grained alloy using a novel correlative tracer diffusion-analytical microscopy approach. Homogenized and intermediate-annealed states are used to engineer the alloy microstructure. Grain boundary diffusion of Ni and Cr is measured in both C- and B-type kinetic regimes. A co-existence of several short-circuit contributions to tracer diffusion is distinguished and correlated to distinct grain boundary precipitation and segregation as revealed by HAADF-STEM combined with EDX measurements. The homogenized state reveals precipitation of Ni-based L12 and Cr₂₃C₆ phases which influence significantly diffusion properties. The intermediate annealing promotes a uniform formation of Cr carbides with a minimal/negligible fraction of the L12 phase. The present study demonstrates the correlated structure-kinetic property measurements provide a unique tool to probe the grain boundary precipitation in these industrially used Inconel alloys.

MM 41.3 Thu 16:30 SCH A 216

Orientation relationship and interface inclination in dependence of heat treatment time between Al₂Ca and Mg Matrix — •LUKAS BERNERS¹, ZHUOCHENG XIE¹, MATTIS SEEHAUS¹, SIYUAN ZHANG², and KORTE-KERZEL SANDRA¹ — ¹IMM, RWTH Aachen — ²MPIE, Düsseldorf

Mechanical properties of two phase-alloys are highly dependent on the morphology of the second phase as well as the interface character. Analysis of the orientation-relationship between the magnesium matrix and C15 (Al₂Ca) Laves phase precipitate is up to now mainly conducted via TEM analysis. However, where defect phases as thermodynamically stable interface configurations are to be identified, a more statistically significant approach is needed. To this end, we use large scale EBSD to reveal prevalent orientation relationships as well as in-

terface character during the transition from hexagonal C36 phase to cubic C15 phase during heat treatment at 500 °C and thus unravelling a pathway to the thermodynamically stable interface configuration.

MM 41.4 Thu 16:45 SCH A 216

Non-Arrhenius temperature dependence of grain boundary diffusion in additively manufactured high-entropy CoCrFeMnNi alloy — •NURI CHOI¹, MA-NOEL W. DA SILVA PINTO¹, SABA KHADEMOREZAIAN¹, SANGSUN YANG², JI HUN YU², JAI SUNG LEE³, GERHARD WILDE¹, and SERGIY V. DIVINSKI¹ — ¹Institute of Material Physics, University of Münster, Münster, Germany — ²Center for 3D Printing Materials Research, Korea Institute of Materials Science, Changwon, South Korea — ³Dep. of Mat. Sci. & Chem. Eng., Hanyang University, Ansan, South Korea

Additive manufacturing process induces numerous crystalline defects such as vacancies, dislocations and dislocation networks, non-equilibrium segregation which affect mechanical, kinetic and structural properties of the fabricated materials. Moreover, a non-equilibrium state of grain boundaries has been discovered, too, which is characterized by enhanced rates of grain boundary diffusion at relatively low temperatures [1]. In the present study, grain boundary diffusion of Ni in additively manufactured CoCrFeMnNi high-entropy alloys is measured in an extended temperature interval. A non-monotonous temperature dependence is observed and interpreted in terms of a thermally-activated relaxation of the non-equilibrium state. The grain boundary energy is evaluated from the grain boundary diffusivity data for various heat-treatment conditions and compared to the total energy released during annealing by differential scanning calorimetry. The evolution of microstructure and mechanical properties is discussed, too.

15 min. break

MM 41.5 Thu 17:15 SCH A 216

Unveiling the mechanisms of motion of synchro-Shockley dislocations in Laves phases — •ZHUOCHENG XIE¹, DIMITRI CHAURAUD², ACHRAF ATILA^{2,3}, ERIK BITZEK^{2,3}, SANDRA KORTE-KERZEL¹, and JULIEN GUÉNOLÉ^{4,5} — ¹Institute of Physical Metallurgy and Materials Physics, RWTH Aachen University, 52056 Aachen, Germany — ²Max-Planck-Institut für Eisenforschung GmbH, Max-Planck-Str. 1, 40237 Düsseldorf, Germany — ³Department of Materials Science and Engineering, Institute I: General Materials Properties, Friedrich-Alexander-Universität Erlangen-Nürnberg, 91058 Erlangen, Germany — ⁴Université de Lorraine, CNRS, Arts et Métiers ParisTech, LEM3, 57070 Metz, France — ⁵Labex Damas, Université de Lorraine, 57070 Metz, France

Synchroshear as the dominant basal slip mechanism in Laves phases is accomplished by the glide of synchro-Shockley dislocations. However, the mechanism of synchro-Shockley dislocation motion is still not well understood. In this work, we demonstrate kink propagation as the energetically favorable mechanism for the motion of synchro-Shockley dislocation using atomistic simulations. Vacancy hopping and interstitial shuffling are identified as two key mechanisms of kink propagation. The assistance of vacancy and antisite defects on kink nucleation and propagation are investigated and shown crucial for kink mobility. These findings provide insights into the dependency on temperature and chemical composition of plastic deformation of topologically close-packed phases.

MM 41.6 Thu 17:30 SCH A 216

Defect bulk-boundary correspondence of topological skyrmion phases of matter — •SHUWEI LIU^{1,2}, LIKUN SHI¹, and ASHLEY M. COOK^{1,2} — ¹Max Planck Institute for the Physics of Complex Systems, — ²Max Planck Institute for Chemical Physics of Solids

Unpaired Majorana zero-modes are central to topological quantum computation schemes as building blocks of topological qubits, and are therefore under intense experimental and theoretical investigation. Their generalizations to parafermions and Fibonacci anyons are also of great interest, in particular for universal quantum computation schemes. In this work, we find a different generalization of Majorana zero-modes in effectively non-interacting systems, which are zero-energy bound states that exhibit a cross structure, two straight and perpendicular lines in the complex plane, composed of the complex number entries of the zero-mode wavefunction on a lattice, rather than a single straight line formed by complex number entries of the wavefunction on a lattice as in the case of an unpaired Majorana zero-mode. These *cross* zero-modes are realized for topological skyrmion phases under certain open boundary conditions when their characteristic momentum-space spin textures trap topological defects. In the process of characterizing this defect bulk-boundary correspondence, we develop recipes for constructing physically-relevant model Hamiltonians for topological skyrmion phases, efficient methods for computing the skyrmion number, and introduce three-dimensional topological skyrmion phases into the literature.

MM 41.7 Thu 17:45 SCH A 216

Ga Induced Defect Phase Transformations in the $\Sigma 7$ Mg Grain Boundary — •PRINCE MATHEWS¹, SIYUAN ZHANG¹, CHRISTINA SCHEU¹, TILMANN HICKEL^{1,2}, and JÖRG NEUGEBAUER¹ — ¹Max-Planck-Institut für Eisenforschung, D-40237 Düsseldorf — ²Federal Institute for Materials Research and Testing (BAM), D-12489 Berlin, Germany

MM 42: Interface Controlled Properties and Nanomaterials: Nanoporous Materials and Nanolaminates

Time: Thursday 15:45–18:30

Location: SCH A 215

MM 42.1 Thu 15:45 SCH A 215

Nanoporous high entropy alloys – functional nanoscale networks — •LUKAS LÜHRS¹, FRIEDERIKE IHLE¹, and JÖRG WEISSMÜLLER^{1,2} — ¹Institute of Materials Physics and Technology, Hamburg University of Technology — ²Institute of Materials Mechanics, Hybrid Materials Systems, Helmholtz-Zentrum hereon

Both, high entropy alloys as well as nanoporous metals have been the subject of considerable interest in recent years. The former topic explores alloys that are composed of multiple major alloying elements yielding countless opportunities for tailor-made material properties, such as outstanding mechanical performance. The latter investigates self-assembled network structures entirely composed of nanoscale elements. Owing to their large surface area to volume ratio, interfaces of nanoporous metals can be manipulated to obtain functional materials that can be used, e.g. as actuators, sensor or structural material with tunable mechanical properties.

In this work we combine both research topics to make monolithic bodies of a nanoporous high entropy alloy (np-HEA) by dealloying, a selective corrosion method, in aqueous media. Structural investigation finds a uniform, bicontinuous network with feature sizes in the range of a few tens of nanometer. Moreover, samples of np-HEA exhibit a single phase microstructure with homogeneous elemental distribution. Compression tests on macroscopic samples reveal considerable mechanical strength. In electrolyte, functionality is introduced by electrochemical modulation of the electrode potential which enables the generation of significant actuation strains.

MM 42.2 Thu 16:00 SCH A 215

Microstructure and mechanical behavior of hierarchical nanoporous gold-polypyrrole electrochemical actuators — •OLGA MATTS and NADIA MAMEKA — Helmholtz-Zentrum Hereon, Geesthacht, Germany

Dealloyed nanoporous (np) metals have emerged as promising (electro-)chemical actuators that can compete with conventional actuator materials in terms of large actuation stroke, high strain energy density and low operating voltage [1]. Combining np metals with a conducting polymer polypyrrole (PPy) has been found as an effective way to enhance the actuation strain, mechanical strength and stiffness of np metals [2, 3]. Due to the synergistic effect of the two individual components at the nanoscale, such hybrid structures demonstrate enlarged actuation and tunable elastic modulus amplitudes as well as afford fast response times as compared to PPy alone [1].

In this work, we investigate an effect of structural hierarchy on actuation and elastic properties of *hierarchical* (hc) np-Au/PPy hybrids. We study the behavior in aqueous electrolyte under potential control, exploiting the ability of PPy to change its volume under reversible redox reactions. We reveal pronounced variations in the macroscopic length and Young's modulus in response to the voltage-induced volume changes of PPy. We correlate this behavior with PPy fractions in pores and discuss the underlying mechanisms of the observations.

[1] Wittstock et al. (ed.), RCS (2012). [2] Roschning et al., Adv. Mater. Interfaces (2020). [3] Li et al., Acta Mater., 212 (2021).

The design of tailored materials requires to understand not only bulk phases but also the stability of various defect phases. Grain boundaries (GBs) form one class of defects that directly influence the properties of the material. Therefore, GB phase transformations introduced by alloying can alter mechanical performance. In this work, the $\Sigma 7$ [0001] | 21.78° (sym. plane 12-30) GB in hcp Mg is investigated, for which an A- and a T-type is known. Ab-initio simulations as a function of stress and temperature (using quasi-harmonic approximation) are performed, and show the presence of a phase transformation. Based on the computed Gibbs energies, the defect phase diagram as a function of the Ga chemical potential is determined. To this end, a complete set of Ga configurations at the GB is first screened with an empirical potential, before accurate ab initio calculations are performed for the low-energy configurations. Ga is not only found to trigger a transformation between T and A type, but a systematic transition of the preferred segregation sites is also seen with an increasing number of Ga atoms at the GB. The results qualitatively agree well with experimental results from high-resolution transition electron microscopy (HR-TEM). Physical mechanisms are provided to explain remaining discrepancies.

MM 42.3 Thu 16:15 SCH A 215

Electrosorption-Induced Actuation in Nanoporous Silicon — •MANUEL BRINKER and PATRICK HUBER — Institut für Material- und Röntgenphysik, Technische Universität Hamburg, Denickestraße 15, 21073 Hamburg, Deutschland

Porous silicon provides a scaffold structure to study the confinement related effects of soft matter. We investigate the electro-sorption of electrolyte anions and the electrochemical behaviour of nanoporous silicon in acidic electrolytes. The silicon-electrolyte interface acts as a capacitor which allows the accumulation of electrolyte anions in a chemical double layer by an applied voltage, whose characteristics can be measured by cyclic voltammetry. The surface stresses that are caused to the monolithic porous silicon membrane by such an accumulation lead to a macroscopic strain which can be determined in-situ with a laser beam-bending setup. Comparing nanoporous silicon with a planar silicon surface yields insights on the observed electrocapillarity – in particular with respect to the importance of oxide formation and wall roughness on the single-nanopore scale.[1]

[1] Brinker, M., & Huber, P. (2021). Wafer-Scale Electroactive Nanoporous Silicon: Large and Fully Reversible Electrochemo-Mechanical Actuation in Aqueous Electrolytes. *Advanced Materials*, 2105923.

MM 42.4 Thu 16:30 SCH A 215

Structural analysis of hierarchical nanoporous gold — •LUKAS RIEDEL¹, JÜRGEN MARKMANN^{1,2}, JÖRG WEISSMÜLLER^{2,1}, and SHAN SHI^{3,1} — ¹Institute of Materials Mechanics, Helmholtz-Zentrum Hereon, Geesthacht, Germany — ²Institute of Materials Physics and Technology, Hamburg University of Technology, Hamburg, Germany — ³Research Group of Integrated Metallic Nanomaterials Systems, Hamburg University of Technology, Hamburg, Germany

Hierarchical nanoporous metals offer the possibility to produce mechanically stable materials with a reduced solid fraction [1], which therefore qualify for lightweight application. Here, hierarchical nanoporous gold is produced from Ag90Au10, following a three-step procedure which consists of first dealloying, coarsening and second dealloying. The ligament size on the upper and the lower hierarchy level can be tuned independently. In addition to scanning electron microscopy (SEM), small- and ultra-small-angle X-ray scattering (SAXS/USAXS) are applied for structural analysis and show consistent results. Descriptive parameters including length scale, specific surface area and pore volume fraction are obtained. From a comparison of the length scale parameters, ligament diameter and mean ligament distance, a conversion factor is yielded. Ultra-small-angle X-ray scattering was found to be suitable for the analysis of structures with a ligament size range of several hundreds of nanometers.

[1] S. Shi, Y. Li, B.-N. Ngo-Dinh, J. Markmann and J. Weissmüller, Scaling behavior of stiffness and strength of hierarchical network nanomaterials, *Science* 371 (6533), 2021.

MM 42.5 Thu 16:45 SCH A 215

Self-detachment of nanoporous thin films — •GIDEON HENKELMANN¹, DIANA WALDOW¹, MAOWEN LIU^{1,2}, LUKAS LÜHRS¹, YONG LI^{1,2}, and JÖRG WEISSMÜLLER^{1,2} — ¹Institute of Materials Physics and Technology, Hamburg University of Technology, Hamburg, Germany — ²Institute of Materials Research, Materials Mechanics, Helmholtz-Zentrum Geesthacht, Geesthacht, Germany

Experiment shows thin films of dealloyed nanoporous gold (NPG) spontaneously detaching from massive gold base layers. NPG can also densify near its external surface. This is naturally reproduced by kinetic Monte Carlo (KMC) simulations of dealloying and coarsening and so appears generic for nanoscale network materials evolving by surface diffusion. This talk focuses on how the KMC simulation manages to predict intricate physical phenomena with few and simple assumptions to the kinetics. This contrasts with contemporary popular efforts to fit a multitude of independent energy barriers to quantum mechanical calculations. Simplified kinetics significantly speed up computation, provide clearer understanding of the underlying processes, while still reproducing relevant phenomena. The KMC simulation model is further motivated by thermodynamic principles.

15 min. break

MM 42.6 Thu 17:15 SCH A 215

Wetting and Drying Dynamics in Hierarchically Porous Silicon: An In-Situ X-Ray Microscopy Study — •STELLA GRIES^{1,2,3}, LAURA GALLARDO DOMÍNGUEZ^{1,2,3}, MARK BUSCH^{1,2,3}, MARIIA LISEANSKAIA^{1,2,3}, JUAN SÁNCHEZ CALZADO^{1,2,3}, MATHIS BODERUS^{1,2,3}, SILJA FLENNER⁴, IMKE GREVING⁴, and PATRICK HUBER^{1,2,3} — ¹Institute for Materials and X-Ray Physics, Hamburg University of Technology, Hamburg, Germany — ²Deutsches Elektronen-Synchrotron DESY, Hamburg, Germany — ³Center for Hybrid Nanostructures CHyN, University of Hamburg, Hamburg, Germany — ⁴Institute of Materials Physics, Helmholtz Zentrum Hereon, Geesthacht, Germany

Hierarchical porosities consist of small, often nano-scaled pores as well as large, macroscopic pores to simultaneously achieve large inner surfaces in combination with optimized mass transport. The investigation of capillary dynamics within optically opaque hierarchically porous membranes necessitates sophisticated microscopy techniques. First hints to unveil the dynamics are obtained from lab-scale experiments, e.g. mass-uptake as a function of time or the mechanical response depending upon wetting and drying in dilatometry. However, these techniques do not spatially resolve on the rising liquid front, which is achieved with transmission X-ray microscopy (TXM). The samples are scanned in radiography (2D) and tomography (3D) to resolve both the static structure and the capillary dynamics. These findings can help to tailor hierarchical porous materials for their designated application and to tune the dynamics depending on the needs.

MM 42.7 Thu 17:30 SCH A 215

Scaling between elasticity and topological genus of nanoporous metals — •SEYUN SOHN^{1,2}, CLAUDIA RICHERT¹, SHAN SHI^{3,1}, JÜRGEN MARKMANN^{1,2}, NORBERT HUBER^{1,2}, and JÖRG WEISSMÜLLER^{2,1} — ¹Institute of Materials Mechanics, Helmholtz-Zentrum Hereon, Geesthacht, Germany — ²Institute of Materials Physics and Technology, Hamburg University of Technology, Hamburg, Germany — ³Research Group of Integrated Metallic Nanomaterials Systems, Hamburg University of Technology, Hamburg, Germany

Nanoporous gold (NPG) made by dealloying has emerged as a model material for random networks and specifically for studies of their mechanics. The mechanical behavior of such open-cell foam structures has been expressed by classical Gibson-Ashby relations. They highlight the solid volume fraction as the most obvious descriptor of strength and stiffness. Yet, recent research acknowledges that Young's modulus, Y , of NPG may significantly depend on additional microstructural descriptors, specifically on the scaled topological genus, g , as a measure of the network's connectivity. It represents the number of connections within a representative volume element of the microstructure. Here, we explore the nature of the dependency of Y on g , and we condense the observations into a scaling law that explicitly involves the scaled genus. Our study inspects and assesses the implications of the existing database, from experiment and simulation, and it adds simulation data for random networks with various

scaled genera. The results suggest a common scaling that is broadly comparable to experimental observations.

MM 42.8 Thu 17:45 SCH A 215

An Improved Kernel-Based NMR Cryoporometry Characterization of Mesoporous Solids — •HENRY R. N. B. ENNINFUL and RUSTEM VALIULLIN — Faculty of Physics and Earth Sciences, Felix Bloch Institute for Solid State Physics, Leipzig University, Linnéstraße 5, 04103, Leipzig, Germany.

NMR cryoporometry is a pore space characterization technique for industrial and natural materials such as catalysts, gas storage materials, cartilage, bones, rocks and many more. While gaining wide use, the fundamental phenomena underlying solid-liquid phase transitions in geometrically disordered porous materials is still not fully understood. This may lead to inaccurate pore size distributions from the NMR cryoporometry technique.

In this work, we have developed a new approach to NMR cryoporometry. Herein, it takes account of cooperativity effects in pores, the existence of a variable non-frozen layer (NFL) thickness between the frozen core and pore wall and the effect of curvature on thermal fluctuations in pores which hitherto are missing in the current approach. In the first place, we compile a family of transition curves characterizing the phase state in pores with different pore sizes, so called kernels. Thereafter, we apply a general framework for predicting phase equilibria in collection of pores. We demonstrate the new approach by first applying it to ordered porous materials such as MCM-41 and SBA-15. Further more, the technique is used to characterize a highly disordered random porous material where we reproduce all states seen in the material. A more accurate pore size distribution (PSD) is, thus, obtained.

MM 42.9 Thu 18:00 SCH A 215

Interface-related defect annihilation in high entropy amorphous/crystalline nanolaminates under ion irradiation — •QI XU¹, DANIEL SOPU¹, XUDONG YUAN¹, and JÜRGEN ECKERT^{1,2} — ¹Erich Schmid Institute of Materials Science, Austrian Academy of Sciences, Jahnstraße 12, Leoben A-8700, Austria — ²Department of Materials Science, Chair of Materials Physics, Montanuniversität Leoben, Jahnstraße 12, Leoben A-8700, Austria

The main challenge of designing nuclear materials that possess a high irradiation resistance is accumulation of point defects-induced structural damage. The interfaces and grain boundaries play a critical role on the defect generation and annihilation in nanostructured materials. In this work, the irradiation-induced microstructure evolution as well as defect production and recovery in metallic glass (MG) / high entropy alloy (HEA) nanolaminates were investigated by molecular dynamics (MD) simulations. The displacement cascades were simulated for the energies of primary knock-on atoms (PKA) at 5, 10 keV and 15 keV. It was found that, there are more displaced atoms in the thermal spike phase for MG/HEA laminate compared with free-standing MG and HEA. In addition, the interface acts as defect sink and accelerates the recombination and annihilation of interstitial in HEA plate, which leads to more residual vacancies in crystalline plate. Moreover, the residual vacancies diffusion induces the generation of dislocation loops in the HEA plate. Furthermore, the interface acts as a transfer medium that accelerates the crystallization of MG plate during irradiation.

MM 42.10 Thu 18:15 SCH A 215

Anode engineering via ultrathin alumina membrane for next-generation stable sodium metal batteries — •JIAJIA QIU, CHANGFAN XU, HUAPING ZHAO, and YONG LEI — Fachgebiet Angewandte Nanophysik, Institut für Physik & IMN MacroNano, Technische Universität Ilmenau, 98693 Ilmenau, Germany

Sodium metal batteries are recognized as one of the most promising candidates for next-generation batteries, owing to their high theoretical specific capacity and energy density. However, a major bottleneck is the mossy or dendritic growth of Na in the repetitive stripping/plating process with an unstable solid electrolyte interphase (SEI), which limits the Coulombic efficiency and even leads to short circuit risks. In this work, ultrathin alumina membrane (UTAM) is first validated as a functional layer to effectively protect the Na anode for Na-metal batteries. By protecting Na metal with UTAM, the mossy or dendritic growth of Na has been suppressed, resulting in uniform electrodeposition. This highly ordered alumina oxide nanostructure improved electrochemical performance significantly and has the potential to be applied to other metal anodes. The novel design of UTAM protected metal Na anode may bring in new opportunities for next-generation high performance Na metal batteries.

Surface Science Division Fachverband Oberflächenphysik (O)

Ulrich Höfer
Philipps-Universität Marburg
Renthof 5
35032 Marburg
hoefer@physik.uni-marburg.de

Overview of Invited Talks and Sessions

(Lecture halls CHE 89, CHE 91, GER 37, GER 38, GER 39, WIL A 213,
REC C 213, TRE Phy, TRE Ma, HSZ 01 and HSZ 02; Poster P2/EG)

Plenary Talk

PLV V Wed 8:30– 9:15 HSZ 01 **Advances in Ultrafast Electron Microscopy** — •CLAUS ROPERS

Laureate of the Gaede Prize 2023

PRV II Wed 13:15–13:45 HSZ 01 **Towards chemical and optical band structure engineering in molecular-based heterostructures** — •BENJAMIN STADTMUELLER

Overview Talks

O 1.1 Mon 9:30–10:15 TRE Phy **From surface structure to exciton evolution: a many-body theoretical perspective** — •SIVAN REFAELY-ABRAMSON

O 27.1 Tue 9:30–10:15 TRE Phy **Dive right in! Molecular insights into electrochemical surface science** — •KATRIN F. DOMKE

O 44.1 Wed 9:30–10:15 TRE Phy **Spins on Surfaces: A Gateway to the Quantum World** — •CHRISTIAN R. AST

O 71.1 Thu 9:30–10:15 TRE Phy **Surface dynamics under reaction conditions** — •EDVIN LUNDGREN

O 90.1 Fri 9:30–10:15 TRE Phy **Molecular Surfaces With a Twist: Magneto-chiral Asymmetries and Topological Self-Assembly** — •KARL-HEINZ ERNST

O 98.1 Fri 13:15–14:00 HSZ 03 **Surfaces go topological – third generation 2D quantum materials** — •RALPH CLAESSEN

Invited Talks of the joint Symposium Ultrafast Excitation Pathways of Quantum Materials (SYUE)

See SYUE for the full program of the symposium.

SYUE 1.1 Wed 9:30–10:00 HSZ 01 **Dynamics and control in quantum materials using multi-terahertz spectroscopy** — •RICHARD AVERITT

SYUE 1.2 Wed 10:00–10:30 HSZ 01 **Accessing the nonthermal phonon populations in 2D materials with femtosecond electron diffuse scattering** — •HÉLÈNE SEILER, MARIOS ZACHARIAS, DANIELA ZAHN, PATRICK-NIGEL HILDEBRANDT, THOMAS VASILEIADIS, YOAV WILLIAM WINDSOR, YINGPENG QI, CHRISTIAN CARBOGNO, CLAUDIA DRAXL, RALPH ERNSTORFER, FABIO CARUSO

SYUE 1.3 Wed 10:30–11:00 HSZ 01 **Exciting potentials – Exploring the realms of ultrafast phase transitions** — •LAURENZ RETTIG

SYUE 1.4 Wed 11:15–11:45 HSZ 01 **Sub-cycle multidimensional spectroscopy of strongly correlated materials** — VIKTOR VALMISPILD, EVGENY GORELOV, MARTIN ECKSTEIN, ALEXANDER LICHTENSTEIN, HIDEO AOKI, MIKHAIL KATSNELSON, MISHA IVANOV, •OLGA SMIRNOVA

SYUE 1.5 Wed 11:45–12:15 HSZ 01 **Witnessing many-body entanglement in light-driven quantum materials** — •MATTEO MITRANO, DENITSA BAYKUSHEVA, MONA KALTHOFF, DAMIAN HOFMANN, MARTIN CLAESSEN, DANTE KENNES, MICHAEL SENTEF

SYUE 1.6 Wed 12:15–12:45 HSZ 01 **Optical responses of photoexcited materials: from parametric amplification to photoinduced superconductivity** — •EUGENE DEMLER

Invited Talks of the joint Symposium Physics of van der Waals 2D Heterostructures (SYHS)

See SYHS for the full program of the symposium.

SYHS 1.1	Fri	9:30–10:00	HSZ 01	Novel moiré excitons and ultrafast optical dynamics in van der Waals 2D heterostructures — •STEVEN G. LOUIE
SYHS 1.2	Fri	10:00–10:30	HSZ 01	Interaction induced magnetism in 2D semiconductor moiré superlattices — •XIAODONG XU
SYHS 1.3	Fri	10:30–11:00	HSZ 01	Ions in tight places: intercalation and transport of ions in van der Waals heterostructures — •IRINA GRIGORIEVA
SYHS 1.4	Fri	11:15–11:45	HSZ 01	Spin-orbit proximity in van der Waals heterostructures — •FELIX CASANOVA
SYHS 1.5	Fri	11:45–12:15	HSZ 01	Plethora of many-body ground states in magic angle twisted bilayer graphene — •DMITRI EFETOV

Topical Talks of the Focus Session "Frontiers of Electronic-Structure Theory" (joint Session O/HL)

O 9.3	Mon	11:00–11:30	TRE Ma	Large-scale machine-learning assisted discovery and characterization of materials — •MIGUEL ALEXANDRE LOPES MARQUES
O 17.1	Mon	15:00–15:30	TRE Ma	Coupled-cluster theory for complex solids made ready — •ANDREAS GRÜNEIS
O 35.4	Tue	11:15–11:45	TRE Ma	Towards low-scaling GW calculations for 2D materials — •JAN WILHELM
O 53.2	Wed	10:45–11:15	TRE Ma	TREX: an integrated HPC software platform for quantum Monte Carlo calculations — •CLAUDIA FILIPPI
O 61.5	Wed	16:15–16:45	TRE Ma	Challenges in modelling correlated electronic matter — •ROSER VALENTI
O 79.3	Thu	11:00–11:30	TRE Ma	New Opportunities for First Principles Simulations of Thousands of Atoms Using Linear Scaling Density Functional Theory — •LAURA RATCLIFF

Topical Talks of the Focus Session "Ion Beam Interaction with Surfaces and 2D Materials"

O 5.1	Mon	10:30–11:00	GER 38	Highly charged, slow and swift ions interacting with surfaces and 2D materials — •MARIKA SCHLEBERGER
O 5.4	Mon	11:30–12:00	GER 38	A contactless single-step process for simultaneous nanoscale patterning and cleaning of large-area graphene — •TUAN TRAN
O 13.1	Mon	15:00–15:30	GER 38	Space weathering of planetary surfaces — •PETER WURZ
O 31.1	Tue	10:30–11:00	GER 38	Ultra-low energy ion implantation of two-dimensional materials — •HANS HOFSSÄSS

Topical Talks of the Focus Session "Scanning Probe Microscopy with Quartz Sensors"

O 45.2	Wed	10:45–11:15	CHE 89	Single-molecule reactions performed and characterized using atomic force microscopy — •LEO GROSS
O 54.1	Wed	15:00–15:30	CHE 89	Peering into interfacial water by qPlus-based atomic force microscopy — •YING JIANG
O 54.5	Wed	16:15–16:45	CHE 89	AFM with the qPlus sensor: An ideal tool for oxide surface science — •ULRIKE DIEBOLD
O 87.1	Thu	15:00–15:30	TRE Ma	Quartz-sensor detection for single-electron tunneling spectroscopy — •JASCHA REPP
O 87.5	Thu	16:15–16:45	TRE Ma	Application of atomic force microscopy with quartz sensors to quantum states in graphene and related twisted heterostructures — •JOSEPH STROSCIO
O 97.4	Fri	11:15–11:45	TRE Ma	Heteroatom-substituted and three-dimensional nanocarbon materials studied with low temperature STM and qPlus AFM — •SHIGEKI KAWAI

Topical Talks of the Focus Session "Semiconductor Surface Chemistry - from Reaction Mechanisms to Well-Ordered Interfaces"

O 48.1	Wed	10:30–11:00	GER 38	Surface functionalization of semiconductors: Introducing spectroscopic labels, monolayer control for ultra-shallow doping, and providing surface passivation for atomically-precise processes — •ANDREW TEPLYAKOV
O 48.3	Wed	11:15–11:45	GER 38	Growth of organic monolayers on Si(111) — •MARTIN FRANZ
O 57.1	Wed	15:00–15:30	GER 38	Incorporation of arsenic into silicon (001) and germanium (001) for atomic-scale device fabrication. — •STEVEN R. SCHOFIELD
O 57.3	Wed	15:45–16:15	GER 38	Semiconductor surface chemistry towards hybrid interfaces with ab initio approaches — •RALF TONNER-ZECH

Topical Talks of the Focus Session "Ultrafast Dynamics in Nanostructures"

O 75.1	Thu	10:30–11:00	GER 38	Ultrafast nano-imaging: probing quantum dynamics in space and time — •MARKUS RASCHKE
O 75.5	Thu	11:45–12:15	GER 38	Lightwave-driven scanning tunneling microscopy and spectroscopy at the atomic scale — •VEDRAN JELIC
O 83.1	Thu	15:00–15:30	GER 38	Imaging ultrafast electron dynamics in isolated nanoparticles — •DANIELA RUPP
O 83.5	Thu	16:15–16:45	GER 38	Ultrafast coherent manipulation of free electrons via quantum interaction with shaped optical fields — •GIOVANNI MARIA VANACORE

General Invited Topical Talks

O 7.1	Mon	10:30–11:00	REC C 213	Superconductivity in atom-by-atom crafted quantum corrals — •LUCAS SCHNEIDER
O 10.1	Mon	15:00–15:30	CHE 89	Photoemission Orbital Tomography: Imaging Molecular Wave Functions in Reciprocal and Real Space — •F. S. TAUTZ
O 16.4	Mon	15:45–16:15	TRE Phy	Microscopic insight into non-equilibrium dynamics through time-resolved x-ray absorption spectroscopy — •ANDREA ESCHENLOHR
O 33.1	Tue	10:30–11:00	REC C 213	Fermi liquids, Luttinger integrals, topological invariants ... and magnetic molecules — •ROK ZITKO
O 34.6	Tue	11:45–12:15	TRE Phy	Photoemission orbital tomography for excitons — •PETER PUSCHNIG
O 52.4	Wed	11:15–11:45	TRE Phy	Modeling and Design of Single-Atom Alloy Catalysts — •MIE ANDERSEN
O 59.1	Wed	15:00–15:30	REC C 213	Interplay of Inversion Symmetry Breaking and Spin-Orbit Coupling — •MAXIMILIAN ÜNZELMANN
O 58.3	Wed	15:30–16:00	WIL A317	Phase-locked photon-electron interaction without a laser — •NAHID TALEBI
O 55.6	Wed	16:15–16:45	CHE 91	Towards Understanding and Controlling On-Surface Reactions and Self-Assembly Mechanisms — •DANIEL EBELING
O 80.3	Thu	15:30–16:00	CHE 89	Topological Plasmonics and Plasmonic Twistronics: Skyrmions, Merons, Quasicrystals, and Skyrmion Bags — •HARALD GIESSEN
O 86.3	Thu	15:30–16:00	TRE Phy	Novel concepts to simulate electrified liquid/solid interfaces from first principles — •STEFAN WIPPERMANN

Sessions

O 1.1–1.1	Mon	9:30–10:15	TRE Phy	Overview Talk Sivan Refaely-Abramson
O 2.1–2.10	Mon	10:30–13:00	CHE 89	Organic Molecules on Inorganic Substrates I: Electronic, Optical and Other Properties I
O 3.1–3.7	Mon	10:30–12:15	CHE 91	Metal Substrates: Adsorption and Reaction of Small Molecules I
O 4.1–4.8	Mon	10:30–12:30	GER 37	Tribology: Surfaces and Nanostructures
O 5.1–5.8	Mon	10:30–13:00	GER 38	Focus Session: Ion Beam Interaction with Surfaces and 2D Materials I
O 6.1–6.10	Mon	10:30–13:00	GER 39	New Methods: Experiments and Theory
O 7.1–7.9	Mon	10:30–13:00	REC C 213	Spins on Surfaces at the Atomic Scale I
O 8.1–8.9	Mon	10:30–12:45	TRE Phy	Ultrafast Electron Dynamics at Surface and Interfaces I
O 9.1–9.8	Mon	10:30–13:00	TRE Ma	Focus Session: Frontiers of Electronic-Structure Theory I (joint session O/HL)
O 10.1–10.9	Mon	15:00–17:30	CHE 89	Organic Molecules on Inorganic Substrates II: Electronic, Optical and Other Properties II
O 11.1–11.9	Mon	15:00–17:15	CHE 91	Surface Reactions
O 12.1–12.8	Mon	15:00–17:00	GER 37	Scanning Probe Techniques: Method Development I
O 13.1–13.8	Mon	15:00–17:15	GER 38	Focus Session: Ion Beam Interaction with Surfaces and 2D Materials II
O 14.1–14.11	Mon	15:00–17:45	GER 39	Nanostructures at Surfaces (joint session O/PPP)
O 15.1–15.12	Mon	15:00–18:00	REC C 213	Spins on Surfaces at the Atomic Scale II
O 16.1–16.9	Mon	15:00–17:30	TRE Phy	Ultrafast Electron Dynamics at Surface and Interfaces II
O 17.1–17.7	Mon	15:00–17:15	TRE Ma	Focus Session: Frontiers of Electronic-Structure Theory II (joint session O/HL)
O 18.1–18.9	Mon	18:00–20:00	P2/EG	Poster: 2D Materials I
O 19.1–19.9	Mon	18:00–20:00	P2/EG	Poster: Ultrafast Electron Dynamics at Surface and Interfaces I
O 20.1–20.11	Mon	18:00–20:00	P2/EG	Poster: Spins and Magnetism at Surfaces
O 21.1–21.7	Mon	18:00–20:00	P2/EG	Poster: Scanning Probe Techniques
O 22.1–22.9	Mon	18:00–20:00	P2/EG	Poster Session: Organic Molecules on Inorganic Substrates I
O 23.1–23.6	Mon	18:00–20:00	P2/EG	Poster: Surface Reactions
O 24.1–24.5	Mon	18:00–20:00	P2/EG	Poster: Ion Beam Interaction with Surfaces and Interfaces

O 25.1–25.5	Mon	18:00–20:00	P2/EG	Poster: Metal Substrates
O 26.1–26.8	Mon	18:00–20:00	P2/EG	Poster: New Methods
O 27.1–27.1	Tue	9:30–10:15	TRE Phy	Overview Talk Katrin Domke
O 28.1–28.10	Tue	10:30–13:00	CHE 89	Organic Molecules on Inorganic Substrates III: Adsorption and Growth I
O 29.1–29.10	Tue	10:30–13:00	CHE 91	Supported Nanoclusters: Structure, Reactions and Catalysis
O 30.1–30.11	Tue	10:30–13:15	GER 37	2D Materials I: Electronic Structure
O 31.1–31.8	Tue	10:30–12:45	GER 38	Focus Session: Ion Beam Interaction with Surfaces and 2D Materials III
O 32.1–32.9	Tue	10:30–12:45	GER 39	Semiconductor Substrates
O 33.1–33.9	Tue	10:30–13:00	REC C 213	Spins on Surfaces at the Atomic Scale III
O 34.1–34.10	Tue	10:30–13:15	TRE Phy	Ultrafast Electron Dynamics at Surface and Interfaces III
O 35.1–35.7	Tue	10:30–12:45	TRE Ma	Focus Session: Frontiers of Electronic-Structure Theory III (joint session O/HL)
O 36.1–36.12	Tue	18:00–20:00	P2/EG	Poster: 2D Materials II
O 37.1–37.13	Tue	18:00–20:00	P2/EG	Poster: Ultrafast Electron Dynamics at Surface and Interfaces II
O 38.1–38.7	Tue	18:00–20:00	P2/EG	Poster: Organic Molecules on Inorganic Substrates II
O 39.1–39.6	Tue	18:00–20:00	P2/EG	Poster Session: Heterogeneous Catalysis and Surface Dynamics
O 40.1–40.4	Tue	18:00–20:00	P2/EG	Poster: Semiconductor Substrates
O 41.1–41.4	Tue	18:00–20:00	P2/EG	Poster: Supported Nanoclusters
O 42.1–42.12	Tue	18:00–20:00	P2/EG	Poster: Nanostructures at Surfaces
O 43.1–43.8	Tue	18:00–20:00	P2/EG	Poster: Plasmonics and Nanooptics I
O 44.1–44.1	Wed	9:30–10:15	TRE Phy	Overview Talk Christian Ast
O 45.1–45.7	Wed	10:30–12:30	CHE 89	Focus Session: Scanning Probe Microscopy with Quartz Sensors I
O 46.1–46.7	Wed	10:30–12:15	CHE 91	Electron-Driven Processes at Surfaces and Interfaces
O 47.1–47.10	Wed	10:30–13:00	GER 37	2D Materials II: Growth, Structure and Substrate Interaction I
O 48.1–48.5	Wed	10:30–12:15	GER 38	Focus Session: Semiconductor Surface Chemistry – from Reaction Mechanisms to Well-Ordered Interfaces I
O 49.1–49.9	Wed	10:30–12:45	WIL A317	Plasmonics and Nanooptics I: Fabrication and Application
O 50.1–50.4	Wed	10:30–11:30	REC C 213	Spins on Surfaces at the Atomic Scale IV
O 51.1–51.6	Wed	11:30–13:00	REC C 213	Surface Magnetism
O 52.1–52.8	Wed	10:30–12:45	TRE Phy	Heterogeneous Catalysis and Surface Dynamics I
O 53.1–53.8	Wed	10:30–13:00	TRE Ma	Focus Session: Frontiers of Electronic-Structure Theory IV (joint session O/HL)
O 54.1–54.8	Wed	15:00–17:30	CHE 89	Focus Session: Scanning Probe Microscopy with Quartz Sensors II
O 55.1–55.10	Wed	15:00–17:45	CHE 91	Organic Molecules on Inorganic Substrates IV: Adsorption and Growth II
O 56.1–56.10	Wed	15:00–17:30	GER 37	2D Materials III: Growth, Structure and Substrate Interaction II (joint session O/PPP)
O 57.1–57.6	Wed	15:00–17:00	GER 38	Focus Session: Semiconductor Surface Chemistry – from Reaction Mechanisms to Well-Ordered Interfaces II
O 58.1–58.9	Wed	15:00–17:30	WIL A317	Plasmonics and Nanooptics II: Light-Matter Interaction and Spectroscopy I
O 59.1–59.10	Wed	15:00–17:45	REC C 213	Electronic Structure of Surfaces I
O 60.1–60.12	Wed	15:00–18:00	TRE Phy	Solid-Liquid Interfaces I: Structure and Spectroscopy
O 61.1–61.8	Wed	15:00–17:30	TRE Ma	Focus Session: Frontiers of Electronic-Structure Theory V (joint session O/HL)
O 62.1–62.8	Wed	15:00–18:30	POT 81	Focus Session: Wissenschaftskommunikation / Outreach (joint session HL/O/TT)
O 63.1–63.2	Wed	18:00–20:00	P2/EG	Poster: Data Management
O 64.1–64.12	Wed	18:00–20:00	P2/EG	Poster: Graphene
O 65.1–65.6	Wed	18:00–20:00	P2/EG	Poster: Topology and Symmetry-Protected Materials
O 66.1–66.11	Wed	18:00–20:00	P2/EG	Poster: Scanning Probe Microscopy with Quartz Sensors
O 67.1–67.10	Wed	18:00–20:00	P2/EG	Poster: Electronic Structure of Surfaces
O 68.1–68.5	Wed	18:00–20:00	P2/EG	Poster: Oxide and Insulator Surfaces
O 69.1–69.14	Wed	18:00–20:00	P2/EG	Poster: Solid-Liquid Interfaces
O 70.1–70.10	Wed	18:00–20:00	P2/EG	Poster: Plasmonics and Nanooptics II
O 71.1–71.1	Thu	9:30–10:15	TRE Phy	Overview Talk Edvin Lundgren
O 72.1–72.5	Thu	10:30–13:00	CHE 89	Gerhard Ertl Young Investigator Award Competition
O 73.1–73.8	Thu	10:30–12:30	CHE 91	Metal Substrates: Adsorption and Reaction of Small Molecules II
O 74.1–74.9	Thu	10:30–12:45	GER 37	2D Materials IV: Heterostructures (joint session O/PPP)
O 75.1–75.9	Thu	10:30–13:15	GER 38	Focus Session: Ultrafast Dynamics in Nanostructures I
O 76.1–76.9	Thu	10:30–12:45	WIL A317	Plasmonics and Nanooptics III: Light-Matter Interaction and Spectroscopy II
O 77.1–77.9	Thu	10:30–12:45	REC C 213	Scanning Probe Techniques: Method Development II
O 78.1–78.9	Thu	10:30–12:45	TRE Phy	Heterogeneous Catalysis and Surface Dynamics II

O 79.1–79.7	Thu	10:30–12:45	TRE Ma	Focus Session: Frontiers of Electronic-Structure Theory VI (joint session O/HL)
O 80.1–80.8	Thu	15:00–17:15	CHE 89	Plasmonics and Nanooptics IV: Light-Matter Interaction and Spectroscopy III
O 81.1–81.12	Thu	15:00–18:00	CHE 91	Oxide and Insulator Surfaces I: Adsorption and Reaction of Small Molecules
O 82.1–82.9	Thu	15:00–17:15	GER 37	Graphene I: Adsorption, Intercalation and Doping
O 83.1–83.8	Thu	15:00–17:30	GER 38	Focus Session: Ultrafast Dynamics in Nanostructures II
O 84.1–84.11	Thu	15:00–18:30	WIL A317	Focus Session: Making Experimental Data F.A.I.R. – New Concepts for Research Data Management I (joint session O/TT)
O 85.1–85.11	Thu	15:00–17:45	REC C 213	Electronic Structure of Surfaces II
O 86.1–86.10	Thu	15:00–17:45	TRE Phy	Solid-Liquid Interfaces II: Reactions and Electrochemistry I
O 87.1–87.8	Thu	15:00–17:30	TRE Ma	Focus Session: Scanning Probe Microscopy with Quartz Sensors III
O 88	Thu	19:00–19:30	HSZ 01	Members' Assembly
O 89	Thu	19:30–20:30	HSZ 01	Post-Deadline Session
O 90.1–90.1	Fri	9:30–10:15	TRE Phy	Overview Talk Karl-Heinz Ernst
O 91.1–91.9	Fri	10:30–12:45	CHE 89	Plasmonics and Nanooptics V: Waveguides and Antennas
O 92.1–92.10	Fri	10:30–13:00	CHE 91	Oxide and Insulator Surfaces II: Structure, Epitaxy and Growth
O 93.1–93.8	Fri	10:30–12:30	GER 37	Graphene II: Electronic Structure and Growth
O 94.1–94.10	Fri	10:30–13:00	GER 38	Topology and Symmetry-Protected Materials
O 95.1–95.11	Fri	9:30–12:45	WIL A317	Focus Session: Making Experimental Data F.A.I.R. – New Concepts for Research Data Management II (joint session O/TT)
O 96.1–96.10	Fri	10:30–13:00	TRE Phy	Solid-Liquid Interfaces III: Reactions and Electrochemistry II
O 97.1–97.8	Fri	10:30–12:45	TRE Ma	Focus Session: Scanning Probe Microscopy with Quartz Sensors IV
O 98.1–98.1	Fri	13:15–14:00	HSZ 03	Overview Talk Ralph Claessen

Members' Assembly of the Surface Science Division

Thursday 19:00–19:30 HSZ 01

- Report of the Chairman
- Presentation of the Gerhard Ertl Young Investigator Award
- Miscellaneous

Sessions

– Invited Talks, Topical Talks, Contributed Talks, and Posters –

O 1: Overview Talk Sivan Refaely-Abramson

Time: Monday 9:30–10:15

Location: TRE Phy

Invited Talk

O 1.1 Mon 9:30 TRE Phy

From surface structure to exciton evolution: a many-body theoretical perspective — •SIVAN REFAELY-ABRAMSON — Weizmann Institute of Science, Rehovot, Israel

Excited-state processes involving Coulomb-bound electron-hole pairs in functional materials are essential for emerging applications, from energy conversion to quantum information science. The associated exciton creation and relaxation mechanisms are often coupled to optical selection rules, stemming from the underlying material structure. In this talk, I will discuss the relation between exciton evolution and structural modifications in monolayer semiconductors. Two broadly explored examples of such modifications are the introduction of atomic

defects and the composition of layered heterostructures. Both offer controllable design pathways to induce long-lived, low-lying excitons with tunable spatial localization and spin polarization. These structure-sensitive exciton properties can be detected in a variety of experimental scenarios from absorption and luminescence under electric and magnetic fields to angle-resolved photoemission spectroscopy, allowing for a close inspection of the microscopic interaction mechanisms. I will present an overview of a many-body ab initio theoretical approach to capture and predict the involved excitonic phenomena and discuss our recent theory-experiment collaborations to explore these effects and their tunability through defect engineering and interlayer twisting.

O 2: Organic Molecules on Inorganic Substrates I: Electronic, Optical and Other Properties I

Time: Monday 10:30–13:00

Location: CHE 89

O 2.1 Mon 10:30 CHE 89

Hooke's law in a molecular spring: An nc-AFM and STM study of nonahelicene on Ag(110) — •MAX HALBAUER¹, TAKASHI KUMAGAI², MARTIN WOLF¹, and AKITOSHI SHIOTARI¹ — ¹Fritz-Haber-Institute of the Max-Planck-Society, Faradayweg 4-6, 14195 Berlin, Germany — ²Institute for Molecular Science, 38 Nishigo-Naka, Myodaiji, 444-8585 Okazaki, Japan

Helicenes are a class of conjugated aromatic molecules representing macroscopic springs on the molecular scale. However, experimental insights on their mechanical properties remain scarce. This contribution employs scanning tunneling microscopy (STM) and noncontact atomic force microscopy (nc-AFM) measurements (UHV, liq. He) in order to address this issue. Frequency shift-distance traces were acquired on individual nonahelicene molecules and a planar reference molecule (coronene) and converted subsequently to force-distance curves. Model-functions accounting for the elasticity of the molecule were fitted to the data, which yielded the spring-constant k for elongation of nonahelicene. This work shows therefore that Hooke's law can be verified on the single-molecule scale by nc-AFM.

O 2.2 Mon 10:45 CHE 89

Complex rotational behavior of ground and excited molecular states — •ANDREAS CHRIST, MARKUS LEISEGANG, PATRICK HÄRTL, and MATTHIAS BODE — Physikalisches Institut, Experimentelle Physik II, Universität Würzburg, Am Hubland, D-97074 Würzburg, Germany

The high sensitivity of molecular rotors to the intricate molecule–substrate interaction leads to a large variety of their rotational behavior [1]. In some cases this interaction can even change for different rotational positions on a molecule's rotation path. We have studied these dependencies for copper-phthalocyanine (CuPc) on Cu(111) by means of low-temperature scanning tunneling microscopy. In agreement with previous results [2,3], we find one ground state oriented along the high-symmetry axes of the substrate and two excited states tilted by $\approx \pm 7^\circ$. A more detailed analysis reveals an exceptionally low threshold of ≈ 20 meV for rotations between these three stable states. Interestingly, the interaction of the molecule with the substrate and therefore the rotation rate varies significantly between the ground and the excited states due to their different molecular bending. Additionally, we find two adsorption positions, which slightly lift the degeneracy between the two excited states.

[1] D. Lensen *et al.*, *Soft Matter* **8**, 9053 (2012)[2] J. Schaffert *et al.*, *Phys. Rev. B* **88**, 075410 (2013)[3] S. Freym-Koch *et al.*, *Phys. Rev. B* **100**, 155427 (2019)

O 2.3 Mon 11:00 CHE 89

Current Driven Unidirectional Rotation of Geländer Molecule — •ŠTĚPÁN MAREK¹, JAN WILHELM², RICHARD KORYTÁR¹, and FERDINAND EVERS² — ¹Department of Condensed Matter Physics, Faculty of Mathematics and Physics, Charles University, Czech Republic — ²Condensed Matter Theory Group, Institute of Physics, Faculty of Theoretical Physics, University of Regensburg, Bavaria, Germany

Rotations of molecules driven by current are possible basis for construction of molecular motors. In "Geländer" molecules, the chiral structure was thought to drive the momentum transfer from travelling electrons to the molecule. We construct a simple model, motivated by our DFT based study, to explore the

structure of the current density in such a molecule and identify the regions of the molecule that contribute majority of the angular momentum of the electron current. We also discuss the particularities of our results, especially the conservation of rotation direction under the exchange of electric bias direction. The results are compared with experimental observations.

O 2.4 Mon 11:15 CHE 89

SPM Tip-induced Cleavage of Bridging Groups to Generate Carbon Nanomaterials — •ZILIN RUAN¹, TIM NAUMANN¹, JOHN B. BAUER², LUKAS HEUPLICK¹, HOLGER F. BETTINGER², and J. MICHAEL GOTTFRIED¹ — ¹Department of Chemistry, Philipps University Marburg, Hans-Meerwein-Straße 4, 35037 Marburg (Germany) — ²Institut für Organische Chemie, Auf der Morgenstelle 18, 72076 Tübingen (Germany)

The on-surface synthesis of carbon nanomaterials is usually carried out on a metal surface by thermal activation, wherein the reaction selectivity and outcome are influenced by various factors. By contrast, manipulations with a scanning probe microscope (SPM) avoid these obstacles by electrically triggering the chemical transformation of individual molecules via the SPM tip due to electronic excitation or inelastic energy transfer. Here, using tip manipulation, we explore the suitability of the removal of etheno- and diastereomeric 1,2-diol moieties to generate acenes. Compared to other previously used leaving groups such as monoketone, diketone and oxo bridges, the here used bridges have certain advantages in the precursor synthesis, but are more challenging regarding their on-surface removal. Investigation of the various main and side reactions offer a deeper understanding of complex elimination and rearrangement reactions induced by SPM manipulation.

O 2.5 Mon 11:30 CHE 89

Illuminating an individual non-fluorescent molecule — •TZU-CHAO HUNG^{1,2}, YOKARI GODINEZ LOYOLA³, MANUEL STEINBRECHER¹, BRIAN KIRALY¹, ALEXANDER A. KHAJETOORIAN¹, NIKOS L. DOLTSINIS³, CRISTIAN A. STRASSERT³, and DANIEL WEGNER¹ — ¹Institute for Molecules and Materials, Radboud University, 6525 AJ Nijmegen, The Netherlands — ²Department of Physics, University of Regensburg, Regensburg, 93040, Germany — ³Physikalisches Institut and Center for Nanotechnology (CeNTech), Westfälische Wilhelms-Universität Münster, 48149 Münster, Germany

Combining scanning tunneling microscopy, spectroscopy and STM-induced luminescence (STML) allows us to study the optoelectronic properties down to the atomic scale. Generalizing the atomic control and imaging capabilities of STML to phosphorescent or even non-fluorescent molecules can provide a new route to fundamentally understand the photophysical properties of an individual molecule. Nickel phthalocyanine (NiPc) is a non-fluorescent molecule. Light emission from the ligand-centered excited state known as Q-band is quenched due to fast relaxation into the nonradiative metal-centered excited state. Hence, the transition energy of the Q-band can only be determined by absorption spectroscopy. Here, we propose an alternative approach to activate radiative decay of the Q-band of NiPc by utilizing STML in combination with control of the local environment and discuss the involved excitation and relaxation pathways. We compare our results with optical spectroscopy and ab initio calculations and discuss the involved excitation and relaxation pathways.

O 2.6 Mon 11:45 CHE 89

STM-induced luminescence from single graphene nanoribbons — •SONG JIANG¹, TOMÁŠ NEUMAN^{1,2}, ALEX BOEGLIN¹, FABRICE SCHEURER¹, and GUILAUME SCHULL¹ — ¹Université de Strasbourg, CNRS, IPCMS, UMR 7504, F-67000 Strasbourg, France — ²Institut des Sciences Moléculaires d'Orsay (ISMO), UMR 8214, CNRS, Université Paris-Saclay, 91405 Orsay Cedex, France

Graphene nanoribbons (GNRs) have emerged as promising candidates for high-performance nanoelectronic devices due to their tunable energy band gaps resulting from lateral quantum confinement and edge effects. The recent development of on-surface synthesis has achieved various types of atomically precise GNRs, revealing fascinating electronic, magnetic, and mechanical properties. Their optical properties, on the other hand, remain largely unexplored. The intrinsic luminescence properties of atomically precise GNR remain to be addressed at single molecule level. Here, excitonic emission from atomically precise GNRs synthesized on a metal surface is probed using a scanning tunneling microscopy (STM) approach. A STM-based strategy to transfer the GNRs to a partially insulating substrate is used to prevent light emission quenching of the ribbons by the metal substrate. Sub-nanometer resolved STM-induced fluorescence spectra reveal emission from localized dark excitons build upon the topological end states of the GNRs accompanying with a series of vibronic peaks. Our study provides a novel path to investigate the interplay between excitons, vibrons and topology in atomically precise graphene nanostructures.

O 2.7 Mon 12:00 CHE 89

Substrate induced magnetic alignment and magnetization dynamics of dimetallofullerene single-molecule magnets — •TOBIAS BIRK¹, FABIAN PASCHKE², VIVIEN ENENKEL¹, FUPIN LIU³, JAN DREISER⁴, VLADYSLAV ROMANKOV⁴, STANISLAV M. AVDOSHENKO³, ALEXEY A. POPOV³, and MIKHAIL FONIN¹ — ¹Department of physics, University of Konstanz, 78457 Konstanz, Germany — ²IBM Research Europe, 8803 Rüschlikon, Switzerland — ³IFW Dresden, 01069 Dresden, Germany — ⁴SLS, PSI, 5232 Villigen, Switzerland

Since several years, lanthanide based single-molecule magnets (SMMs) are in focus of a broad research community due to their record high blocking temperatures above 77 K [1]. However, surface supported SMMs lag behind in terms of blocking temperatures and relaxation times due to molecule-substrate interactions. Yet, for the surface-supported lanthanide dimetallofullerene SMMs blocking temperatures of up to 28 K and long relaxation times were reported [2]. Here, we study the effect of coupling to a metallic substrate on the electronic and magnetic properties of Dy₂@C₈₀CH₂Ph and compare those to our results for the graphene substrate [3, 4]. A combination of scanning tunneling microscopy, -spectroscopy and X-ray absorption spectroscopy provides a detailed insight into the local electronic properties as well as magnetization dynamics of the studied SMMs.

[1] F.S. Guo *et al.* Science 362, 6421. [2] F. Liu *et al.* Nat. Comm. 10, 571 (2019). [3] F. Paschke *et al.* Adv. Mater. 2102844 (2021). [4] F. Paschke *et al.* Small 2105667 (2022)

O 2.8 Mon 12:15 CHE 89

Enantiospecific adsorption on a ferromagnetic surface at the single-molecule scale — •M.R. SAFARI¹, F. MATTHES¹, K-H. ERNST², D.E. BÜRGLER¹, and C.M. SCHNEIDER¹ — ¹Peter Grünberg Institut (PGI-6), Forschungszentrum Jülich, 52425 Jülich, Germany — ²Molecular Surface Science Group, Empa, Swiss Federal Laboratories for Materials Science and Technology, 8600, Dübendorf, Switzerland

The recently discovered effect of chirality-induced spin selectivity (CISS) not only enables spin-selective electron transport in organic molecules [1], but also offers a novel approach to chiral separation by exploiting the CISS-induced enantiospecific interaction of chiral molecules with perpendicularly magnetized substrates [2]. Using low-temperature spin-polarized scanning tunneling microscopy, we have investigated the enantiospecific adsorption of heptahelicene molecules on ferromagnetic Co bilayer islands [3,4]. High-resolution and spin-polarized STM images enable direct determination of the enantiomeric adsorption ratio R on oppositely magnetized Co islands. Statistical analysis of 748 molecules on 110 islands yields $R = 0.69 \pm 0.05$, which we attribute to different enantiospecific adsorption energies. The well-defined structural, electronic, and magnetic properties of the molecule-substrate systems make our results readily amenable to theoretical modeling that will hopefully shed light on the microscopic origin of enantiospecific adsorption on ferromagnetic surfaces. [1] R. Naaman *et al.*, J. Phys. Chem. Lett. 3, 2178 (2012); [2] K. Banerjee-Ghosh *et al.*, Science 360, 1331 (2018); [3] M.R. Safari *et al.*, Nanomaterials 12, 3281 (2022); [4] M.R. Safari *et al.*, arXiv:2211.12976 (2022)

O 2.9 Mon 12:30 CHE 89

Clars goblet based J1 & J2 alternative heisenberg spin half chain — •LIN YANG — TU Dresden, Dresden, Germany

Spin-1/2 alternating-exchange Heisenberg chain has been intensively pursued for decades not only for understanding its underlying many-body physics but also for its great potential of realizing quantum computing and information. The existing candidates are limited in effective spin arrays embedded in three dimensional crystals, where the quasi-one dimensional spin system is inevitably affected by the cross talk between arrays and the spin-phonon coupling. Here, paradigmatic alternating-exchanging Heisenberg chains with spin-1/2 are realized in a designer graphene system using on-surface synthesis. The couplings: $J_1 = 38$ meV, $J_2 = 23$ meV are determined by inelastic tunneling spectra, which is strong enough to support practical quantum operation.

O 2.10 Mon 12:45 CHE 89

CoPc on Ag(100): getting the most out of PEEM images — •THORSTEN WAGNER¹, GRAZYNA ANTCHAK², MICHAEL GYÖRÖK¹, ANNA VOLOKITINA¹, FELIX MARSCHNER¹, AGATA SABIK², FRANCISZEK GOŁEK², and PETER ZEPPEFELD¹ — ¹Johannes Kepler University, Institute of Experimental Physics, Surface Science Division, 4040 Linz, Austria — ²University of Wrocław, Institute of Experimental Physics, 50-204 Wrocław, Poland

We use photoelectron emission microscopy (PEEM) and the Anderson method to study in situ the thin-film growth of cobalt-phthalocyanine (CoPc) on Ag(100) surfaces. Based on the Fowler-DuBridge theory, we were able to correlate the evolution of the mean electron yield acquired with PEEM for coverages up to two molecular layers of CoPc to the global work function changes measured with the Anderson method. For coverages above two monolayers, the transients measured with the Anderson method and those obtained with PEEM show different trends allowing us to determine the inelastic mean free path of the low-energy electrons while passing through the third layer of CoPc. [1] Already before (and during) the condensation of solid phases (2D islands or 3D crystallites), there is a dilute 2D gas phase consisting of individual molecules diffusing across the surface or clusters, which can not be resolved with PEEM. Therefore, we discuss, how image features below and above the resolution limit of a PEEM affect the mean electron yield and the (normalized) standard deviation. [2]

[1] Th. Wagner *et al.*, ACS Appl. Mater. Interfaces 12 (2022), 23983–23989 [2] Th. Wagner *et al.*, Ultramicroscopy 233 (2022), 113427

O 3: Metal Substrates: Adsorption and Reaction of Small Molecules I

Time: Monday 10:30–12:15

Location: CHE 91

O 3.1 Mon 10:30 CHE 91

A Nanocar and rotor in a molecule — •KWAN HO AU-YEUNG¹, SUCHETANA SARKAR¹, TIM KÜHNE¹, OUMAIMA AIBOUDI², DMITRY A. RYNDYK^{3,4}, ROBERTO ROBLES^{5,6}, NICOLAS LORENTE^{5,6}, FRANZISKA LISSEL², CHRISTIAN JOACHIM⁷, and FRANCESCA MORESCO¹ — ¹Center for Advancing Electronics Dresden, TU Dresden, 01062 Dresden, Germany — ²Leibniz-Institut für Polymerforschung Dresden e.V., 01069 Dresden, Germany, and Faculty of Chemistry and Food Chemistry, TU Dresden, 01062 Dresden, Germany — ³Institute for Materials Science, TU Dresden, 01062 Dresden, Germany — ⁴Theoretical Chemistry, TU Dresden, 01062 Dresden, Germany — ⁵Centro de Física de Materiales CFM/MPC (CSIC-UPV/EHU), 20018 Donostia-San Sebastián, Spain — ⁶Donostia international physics center, 20018 Donostia-San Sebastián, Spain — ⁷GNS & MANA Satellite, CEMES, CNRS, 29 rue J. Marvig, 31055 Toulouse, France

Depending on its adsorption conformation on the Au(111) surface, a zwitterionic single molecule machine works in two different ways under STM voltage pulses: It is a unidirectional single molecule-rotor while anchoring on the sur-

face; It is a fast-drivable molecule-vehicle (nanocar) while physisorbed. By tuning the molecular coverage, the conformation of the molecule can be selected as a rotor or a nanocar. The movement triggered by inelastic tunneling excitation is investigated under the same experimental conditions for the unidirectional rotation of the rotor and the directed movement of the nanocar.

O 3.2 Mon 10:45 CHE 91

Controlling the Switching of Azobenzene Derivatives on Graphite-Air Interface — •THIRUVANCHERIL G. GOPAKUMAR¹, KHUSHBOO YADAV¹, HARIOM BIRLA¹, SHOWKAT H. MIR², THOMAS HALBRITTER³, ALEXANDER HECKEL³, and JAYANT K. SINGH² — ¹Department of Chemistry, Indian Institute of Technology Kanpur, Kanpur 208016, India — ²Department of Chemical Engineering, Indian Institute of Technology Kanpur, Kanpur 208016, India — ³Institute for Organic Chemistry and Chemical Biology, Goethe-University Frankfurt, Max-von-Laue-Str. 9, 60438 Frankfurt, Germany

The trans isomer of azobenzene (AB) and its derivatives is the most abundant under equilibrium-thermodynamical conditions and is known to switch between

its trans and cis states when triggered by light and electrons/holes on graphite.[1] In this work, we show that AB derivatives are switching between two cis states (cis, cis') when electrons/holes induced switching is performed on a cis dominant non-equilibrium initial condition at HOPG-air interface. The switching efficiency in the cis adlayer is several folds higher than that in the trans adlayer. This is related to the low switching barrier for cis-cis' switching compared to that of trans-cis switching as revealed by density functional theory (DFT) calculations.[2]

1) K. Yadav, S. Mahapatra, T. Halbritter, A. Heckel, T. G. Gopakumar, J. Phys. Chem. Lett., 2018, 9, 6326-6333. 2) K. Yadav, H. Birla, S. H. Mir, T. Halbritter, A. Heckel, J. K. Singh, T. G. Gopakumar, Appl. Surf. Sci. 2023, 612, 155747

O 3.3 Mon 11:00 CHE 91

STM-induced ring closure of vinylheptafulvene molecular dipole switches on Au(111) — •SUCHETANA SARKAR¹, KWAN HO AU-YEUNG¹, TIM KUEHNE¹, OUMAIMA AIBOUDI², DMITRY A. RYNDYK^{3,4}, THOMAS HEINE⁴, FRANZISKA LISSEL^{2,4}, and FRANCESCA MORESCO¹ — ¹Center for Advancing Electronics Dresden, TU Dresden, 01062 Dresden, Germany — ²Leibniz Institute of Polymer Research, 01069 Dresden, Germany — ³Institute for Materials Science, TU Dresden, 01062 Dresden, Germany — ⁴Faculty of Chemistry and Food Chemistry, TU Dresden, 01062 Dresden Germany

Dihydroazulene/vinylheptafulvene pairs are known as molecular dipole switches that undergo a ringopening/- closure reaction by UV irradiation or thermal excitation. We show that the ring-closure reaction of a single vinylheptafulvene adsorbed on the Au(111) surface can be induced by voltage pulses from the tip of a scanning tunneling microscope. This cyclization is accompanied by the elimination of HCN, as confirmed by simulations. Post the ring closure reaction, lateral movement induced via voltage pulses from the STM tip shows a different response. This behaviour is discussed by comparing the dipole moment and the charge distribution of the open and closed forms on the surface.

O 3.4 Mon 11:15 CHE 91

Surface segregation of PdAu(111) in reactive gas environments from ab initio thermodynamics — •OLGA V VINOGRADOVA, VANESSA J BUKAS, and KARSTEN REUTER — Fritz Haber Institute of the Max Planck Society, Berlin, Germany
Catalytic properties of alloys are largely determined by the specific chemical composition at the surface. Differences in composition between surface and bulk regions depend intricately on both the parent metals and surrounding gas-phase environment. While a non-reactive environment is expected to induce surface segregation of the more noble alloy component, a reactive environment such as oxygen often favors the more active component at the surface. Using ab initio thermodynamics, here we explore the structure and composition of the PdAu(111) alloy surface in oxygen, nitrogen, and carbon containing environments. An exhaustive, yet systematic, search of the available phase-space shows the segregation profile in an oxygen atmosphere to follow the anticipated picture described above. Unlike oxygen, however, carbon at low coverages burrows deeper into the alloy substrate without first the adsorbate-induced segregation of Pd at the surface. A nitrogen environment induces an intermediate behavior to oxygen and carbon where the nitrogen atoms first favor either surface or subsurface sites depending on the detailed metallic composition profile.

O 3.5 Mon 11:30 CHE 91

Atomistic investigations on the effect of vibrational excitation on O₂ adsorption on Pt surfaces — •SIMON HOMANN, BJÖRN KIRCHHOFF, and TIMO JACOB — Institute of Electrochemistry, Ulm University, D-89081 Ulm

Platinum is considered an excellent model system for surface studies and is also an important heterogeneous catalyst. Combined with non-thermal plasmas,

many studies found an improvement in turn-over frequency compared to thermal catalysis with the non-excited gas phase. One possible contender towards an explanation of this is the interaction of the vibrationally excited molecules in the plasma with the metal surface. As a first proof of concept, we present in this study Born-Oppenheimer molecular dynamics simulations of vibrationally excited Oxygen on low-indexed Platinum surfaces using a reactive force field (ReaxFF). The vibrational density of states simulated this way is in agreement with typical results obtained, e.g. from kinetic modeling of the plasma afterglow. The higher vibrational energy leads to an altered adsorption behavior in terms of dissociation and preferred adsorption positions, as well as changes in surface morphology.

O 3.6 Mon 11:45 CHE 91

Fluctuating nature of CO adlayer structures on metal surfaces — •SUNG SAKONG and AXEL GROSS — Ulm University, Ulm, Germany

The dynamics of atomic and molecular adlayers on surfaces is an critical issue in heterogeneous catalysis and electrocatalysis as it determines how reaction partners can meet on the catalyst surfaces. The adlayer formation influences the performance of catalysts and the structure of the electric double layer. Recently, video scanning tunneling microscope (V-STM) experiments have demonstrated the influence of the CO adlayer dynamics on oxygen diffusion on Ru(0001) [1,2] and the dynamical nature of a CO monolayer on Pt(111) [3]. We will present microscopic pictures of CO adlayer fluctuations on Ru(0001) and Pt(111) based on density functional theory (DFT) calculations and kinetic Monte Carlo (kMC) simulations. The calculations demonstrate how local disorder can lower the adsorption energy of a CO adlayer. We will particularly demonstrate the importance of the so-called door opening mechanism for oxygen diffusion on a CO-covered surface [1,2] and the dynamical nature of CO adlayers [3] by comparing DFT-based simulations with V-STM experiments.

[1] A. Henß *et al.*, Science **363**, 715 (2019).

[2] S. Sakong *et al.*, J. Phys. Chem. C **124**, 15216 (2020).

[3] J. Wei *et al.*, Angew. Chemie. Int. Ed. **59**, 6182 (2020).

O 3.7 Mon 12:00 CHE 91

Self-assembly and dehydrogenation reactions of borazine on Ag(111) —

•TOBIAS WEISS¹, ALEKSANDR BAKLANOV¹, GEORG S. MICHELITSCH², MARTIN SCHWARZ¹, MANUELA GARNICA¹, KARSTEN REUTER³, and WILLI AUWÄRTER¹ — ¹Physics Department E20, Technical University of Munich, Germany — ²Laboratoire des Solides Irradiés, École Polytechnique, France — ³Chair of Theoretical Chemistry, Technical University of Munich, Germany

Borazine (B₃N₃H₆), is a prominent precursor for the growth of hexagonal boron nitride (hBN) on metal supports [1]. With monolayer hBN playing an important role in the field of 2D-materials, borazine adsorption, assembly and decomposition on surfaces is a topic of interest. Space-averaging studies revealed flat or tilted adsorption geometries on different substrates depending on their catalytic activity [2,3].

Here, we provide unprecedented real-space insight into adsorbed borazine molecules and their on-surface chemistry in ultra-high vacuum. This scanning tunneling microscopy investigation of the self-assembly of borazine on Ag(111) reveals a highly regular, porous hexagonal phase or a dense packed structure, depending on exposure. Furthermore, tip-induced dehydrogenation reactions of single molecules result in a tilted adsorption geometry. Complementary density functional theory calculations were performed to comprehensively characterize potential reaction products and adsorption configurations.

[1] W. Auwärter, Surf. Sci. Rep., 2019, 74, 1-95

[2] R. Simonson, Surf. Sci., 1991, 254, 29-44

[3] L. Haug, Phys. Chem. Chem. Phys., 2020, 22, 11704

O 4: Tribology: Surfaces and Nanostructures

Time: Monday 10:30–12:30

Location: GER 37

O 4.1 Mon 10:30 GER 37

High throughput first-principle prediction of interfacial adhesion energies in metal-on-metal contacts — PAOLO RESTUCCIA, •MARGHERITA MARSILI, and MARIA CLELIA RIGHI — Department of Physics and Astronomy, University of Bologna, 40127 Bologna, Italy

Adhesion energy ultimately dictates the mechanical behavior and failure of interfaces. As natural and artificial solid interfaces are ubiquitous, it represents a key quantity in a variety of fields, from geology to nanotechnology. An *ab-initio* determination of adhesion energies is crucial because the specific atomistic details of the interface primarily determine the strength of adhesion, but, especially for heterogeneous interface is challenging, as computations can be very expensive. We performed the high-throughput DFT determination of the adhesion energy of around a hundred metallic heterostructures, ranging from transition to noble metals [1]. We identified general trends confirming that adhesion energies can be reasonably well inferred from the knowledge of the surface energies of the

two interface constituents. Finally, by using a machine learning approach, we obtained a simple analytical expression for predicting the adhesion energy from the intrinsic properties of the two heterostructure constituents alone, which can prove useful for avoiding expensive supercell calculations. These results are part of the SLIDE project funded by the European Research Council under the Horizon 2020 research and innovation program (Grant agreement No. 865633). [1] P. Restuccia *et al.* *High throughput accurate prediction of interfacial adhesion energies in metal-on-metal contacts* submitted to npj Computational Materials (2022)

O 4.2 Mon 10:45 GER 37

Nanoscale Friction across the First Order Charge Density Wave Phase Transition of 1T-TaS₂ — WEN WANG¹, •DIRK DIETZEL², and ANDRÉ SCHIRMEISEN² — ¹School of Mechanical Engineering, Southwest Jiaotong University, Chengdu, China — ²Institute of Applied Physics, Justus Liebig University Giessen, Giessen, Germany

In material science, analyzing phase transitions is a fundamental way to understand material properties and their changes on the atomic level. At the same time, phase transition materials are intriguing model systems for nanotribology, where well-defined transformations can occur if a specific control parameter, like e. g. temperature, changes. On one hand, varying friction between tip and sample can be linked to the specific properties of different phases. On the other hand, during the phase transition localized mechanical probing of the surface can allow for a direct coupling to the reorganization of the material as was recently demonstrated for the case of 1T-TaS₂ [1]. However, previous experiments did not allow for an in-depth analysis of the influence of crucial parameters like sliding velocity and normal force on the process of local nucleation. This was now done by friction force microscopy on 1T-TaS₂ for different stationary temperatures across the charge density wave phase transitions. Our results corroborate an anticipated mechanism, where the AFM-tip gradually induces local transformations of the material close to the spinodal point in a thermally activated and shear assisted process until the surface is fully 'harvested'.

[1] Panizon et al., New Journal of Physics 20, 023033 (2018).

O 4.3 Mon 11:00 GER 37

Kinetic nanoscale friction on van der Waals heterostructures — •BARTOSZ SZCZEFANOWICZ¹, ZHAO LIU¹, JOAO MARCELO J. LOPES², ANTONY GEORGE³, ZIYANG GAN³, ANDREY TURCHANIN³, ALEXANDER ROTHSTEIN⁴, CHRISTOPH STAMPFER⁴, and ROLAND BENNEWITZ¹ — ¹INM - Leibniz Institute for New Materials, Saarbrücken, Germany — ²Paul-Drude-Institut für Festkörperelektronik, Leibniz-Institut im Forschungsverbund Berlin e.V., Berlin, Germany — ³Friedrich Schiller University Jena, Institute of Physical Chemistry, Jena, Germany — ⁴JARA-FIT and 2nd Institute of Physics A, RWTH Aachen University, 52074 Aachen, Germany

2D materials exhibit exceptional tribological properties due to their weak normal-to-plane interactions. Friction Force Microscopy (FFM) demonstrated that the microscopic processes underlying friction can be tuned by application of high contact pressure [1] or by combining different 2D materials into van der Waals heterostructures [2].

Samples of MoSe₂/hBN and graphene/hBN were prepared by the exfoliation technique. Sample of MoS₂/graphene was produced by thermal decomposition of SiC(0001), followed by direct growth of MoS₂ by Chemical Vapor Deposition (CVD). Friction forces were measured on those heterostructures in FFM experiments in ultrahigh vacuum as function of normal load and electric bias. We will discuss the results in terms of atomic potential corrugation, bending rigidity of 2D heterostructures, and bias-induced electrostatic attraction.

[1] T. Filleter, and R. Bennewitz, Phys. Rev. B, 81, 2010, 155412

[2] M. R. Vazirisereshk, et al., Nano Lett., 19, 2019, 5496-5505

O 4.4 Mon 11:15 GER 37

Temperature Dependent Wear Effects on the Nanometer Scale — •JENNIFER KONRAD, DIRK DIETZEL, and ANDRE SCHIRMEISEN — Institute of Applied Physics, Justus-Liebig University Giessen, 35392 Giessen, Germany

On the nanoscale, the temperature dependence of friction as observed by friction force microscopy is a well-known phenomenon that can often be described by the thermally activated Prandtl Tomlinson Model. Similarly, nanoscale wear is also often anticipated as a thermally activated and shear assisted process, which results in a temperature dependence, where the overall wear rate increases with temperature [1]. However, this behavior can change when the effects of interfacial bond formation and breaking have to be taken into consideration. Surprisingly, lower temperatures can then result in higher wear rates as will be demonstrated by temperature dependent wear experiments performed for different interfaces involving silica and diamond surfaces. This behavior can phenomenologically be explained by considering shear assisted bond formation, which leads to a higher number of interfacial bonds formed at lower temperatures [2]. By straining this larger number of bonds during scanning an increased wear rate at low temperatures is then caused, even if the energy barrier for bond breaking is lower than for the removal of adjacent surface atoms.

[1] W. Wang, D. Dietzel, and A. Schirmeisen, Phys. Rev. Lett. 126, 196101 (2021).

[2] M. Vorholzer et al., Physical Review X 9, 041045 (2019).

O 4.5 Mon 11:30 GER 37

Rewritable friction on Nitrogen-doped graphene moiré superstructures — •SHUYU HUANG^{1,2}, ANTOINE HINAUT², YIMING SONG², SEBASTIAN SCHERB², GEMA GNAVARRO², THILO GLATZEL², YUNFEI CHEN¹, and ERNST MEYER² — ¹Jiangsu Key Laboratory for Design and Manufacture of Micro-Nano Biomedical Instruments, School of Mechanical Engineering, Southeast University, Nanjing 211189, China — ²Department of Physics, University of Basel, Klingelbergstrasse 82, 4056 Basel, Switzerland

Graphene, as typical atomically-thin solid lubricant with potential applications in micro- and nano-electromechanical systems (MEMS/NEMS), has been ex-

tensively investigated on its nanotribological properties. In the present work, we compare the frictional properties between pristine graphene and modified graphene, showing that atomic-scale friction can be significantly altered by Nitrogen doping-induced modification, then it can be recovered after tip rubbing. Specifically, C60 nano-flakes are deposited as a mask on graphene/Ir (111) surface by thermal evaporation. The sample is then exposed to a nitrogen radical flux produced by a remote RF plasma source. After thermal annealing, to desorb C60 molecules, both nano-patterned modified graphene and pristine graphene, located below former C60 islands, surface is obtained simultaneously. By the means of high-resolution ultrahigh vacuum atomic force microscopy, the topography of surface with two different regions are characterized and discussed in non-contact mode and friction force variation is measured in contact mode.

O 4.6 Mon 11:45 GER 37

Atomic friction over bonds: Impact of the chemical neighbourhood — •LUKAS HÖRMANN¹, JOHANNES J. CARTUS¹, ALFRED J. WEYMOUTH², and OLIVER T. HOFMANN¹ — ¹Institute of Solid State Physics, Graz University of Technology, Graz, Austria — ²Universität Regensburg, Regensburg, Germany

Friction causes a significant amount of energy loss in any moving mechanical device. Given the trend toward the miniaturisation of devices, studies of the fundamental mechanisms governing friction at the atomic scale become ever more important. At this scale, friction is governed by electronic and phononic excitations as well as by the potential energy surface (PES) at the interface.

We computationally investigate these mechanisms on the example of a CO-tip of a lateral force microscope oscillating above a PTCDA monolayer on Cu(111). Our investigation combines ab-initio electronic structure methods with machine-learning algorithms to predict highly accurate PESs and to estimate frictional energy dissipation. We gauge the dependence of frictional energy dissipation on the local chemical environment, i.e. the location of the CO-tip above the surface during the friction measurement. Moreover, we investigate how the oscillation direction and the stiffness of the CO-tip affect friction. Hereby we study the role of quantum-mechanical interactions by comparing our results to friction estimates based on a Lennard-Jones potential as well as experimental measurements. Finally, we investigate frictional energy dissipation channels by studying how the movement of the CO-tip may be damped as a result of electronic friction.

O 4.7 Mon 12:00 GER 37

Quantum-mechanically enhanced water flow in sub-nanometer carbon nanotubes — •ALBERTO AMBROSETTI, GIORGIO PALERMO, and PIER LUIGI SILVESTRELLI — Dipartimento di Fisica e Astronomia, Università degli Studi di Padova, via Marzolo 8, 35131, Padova, Italy

Water-flow in carbon nanotubes (CNT's) starkly contradicts classical fluid mechanics, with permeabilities that can exceed no-slip Haagen-Poiseuille predictions by two to five orders of magnitude. Semi-classical molecular dynamics accounts for enhanced flow-rates, that are attributed to curvature-dependent lattice mismatch. However, the steeper permeability-enhancement observed experimentally at nm-size radii remains poorly understood, and suggests emergence of puzzling non-classical mechanisms. Here we address water-CNT friction from a quantum-mechanical perspective, in terms of water-energy loss upon phonon excitation. We find that combined weak water-phonon coupling and selection rules hinder water-CNT scattering, providing effective protection to water super flow, whereas comparison with a semiclassical theory evidences a friction increase that can exceed the quantum-mechanical prediction by more than two orders of magnitude. Quasi-frictionless flow up to sub-nm CNT's opens new pathways towards minimally-invasive trans-membrane cellular injections, single-water fluidics and efficient water filtration.

O 4.8 Mon 12:15 GER 37

Screw-like beetle joints and their tribological features — •CORNELIA F. PICHLER¹, RICHARD THELEN¹, THOMAS VAN DE KAMP², and HENDRIK HÖLSCHER¹ — ¹Institute of Microstructure Technology (IMT), Karlsruhe Institute of Technology, Karlsruhe, Germany — ²Institute for Photon Science and Synchrotron Radiation (IPS), Karlsruhe Institute of Technology, Karlsruhe, Germany

Understanding and finally mimicking lubricants in the joints of various insects promises environmentally friendly alternatives for mineral-oil-based lubricants. The compactness of the insect joints and the tiny quantities of their respective lubricants make it challenging to analyze their frictional properties. In my work, I characterize lubricants directly in dissected screw-like beetle joints by lateral force measurements with the atomic force microscope (AFM). This approach gives insight into the frictional properties of the lubricant in its natural form as well as the functional structure found in the joints. In addition to lubricant films, we also observe microstructures which suggest that beetles advance frictional properties of their joints by a sophisticated combination of surface structure and lubrication.

O 5: Focus Session: Ion Beam Interaction with Surfaces and 2D Materials I

Ion beam techniques are an important tool in surface science and nanotechnology in terms of surface composition analysis as well as tailoring of surface properties. Recent important developments took place using ultra-low energy ion implantation to introduce foreign atoms into 2D material lattices or triggering self-organization mechanisms to form large-scale ordered crystalline surface structures. This focus session brings international specialists in the connecting fields of ion physics and surface science together to discuss recent progress to our fundamental understanding of ion-surface interactions as well as pathways towards new applications for emerging material classes.

Organizer: Richard Arthur Wilhelm (TU Wien)

Time: Monday 10:30–13:00

Location: GER 38

Topical Talk

O 5.1 Mon 10:30 GER 38

Highly charged, slow and swift ions interacting with surfaces and 2D materials — •MARIKA SCHLEBERGER — Fakultät für Physik, Universität Duisburg-Essen and CENIDE

Ion beams are a proven, versatile, and efficient tool for material modification and in particular for defect engineering. An ion stores its energy in the form of kinetic (E_{kin}) and so-called potential energy (E_{pot}), the latter corresponding to the energy required to create its respective charge state. At low velocities, the energy deposition is based on elastic collisions leading to linear sputtering cascades or collision peaks in the volume of the material, and ultimately to the emission of atoms. At higher kinetic energy, electronic excitations and ionizations are dominant. The release of potential energy again occurs via electronic processes that can also lead to the emission of atoms from the target material. By adjusting these two parameters, E_{pot} and E_{kin} , one can in principle fine-tune the nature of the interaction and thus the corresponding material changes. However, the basic mechanisms of defect formation through electronic excitation have not yet been clarified. We have introduced 2D materials as target material for the study of ion-solid-interactions. Due to their well-defined thickness, the flexible preparation and last but not least the wide range of available materials, they are an ideal target material for our task. We have studied the interaction of ions of different types with surfaces and 2D materials and I will present key results.

O 5.2 Mon 11:00 GER 38

Model for Nanopore Formation in Two-Dimensional Materials by Impact of Highly Charged Ions — •A. S. GROSEK, A. NIGGAS, R. A. WILHELM, F. AUMAYR, and C. LEMELL — TU Wien

Experiments of highly charged ions (HCI) on 2D-materials have shown that HCIs extract numerous electrons from the 2D target. This interaction has shown to lead to nanopore formation in materials such as monolayer MoS₂ while single layer graphene remains structurally intact. One hypothesis proposed for the cause of nanostructuring of these materials is charge build up by hole charges in the target, which -depending on material charge conductivity- may sustain sufficiently long in order to lead to structural damage of the target atoms. We study this hypothesis of nanostructuring by HCI impact on 2D-materials via molecular dynamics simulations. The charge transfer from target to HCI is well described by the classical-over-the-barrier model, of which a simplified version is implemented into the simulation. Charge conduction in the target is modelled by charge hopping with a hopping time t_h between lattice sites. Our 2D lattice is simulated by a Stillinger-Weber potential with parameters fitted to reproduce graphene. We study different materials by respectively adjusting the hopping time t_h (conductivity) of the graphene lattice in the simulation. After the simulation kinetic and potential energies of the individual target atoms are evaluated to determine if a pore has formed. Our simulation is able to qualitatively reproduce experimental results showing pore formation efficiencies and pore sizes to be dependent on initial HCI charge state and conductivity of the material.

O 5.3 Mon 11:15 GER 38

Charge-state-enhanced ion sputtering of metallic gold nano islands — •GABRIEL L. SZABO¹, BENEDYKT R. JANY², HELMUT MUCKENHUBER¹, ANNA NIGGAS¹, MARKUS LEHNER¹, ARKADIUSZ JANAS², PAUL S. SZABO³, ANTONY GEORGE⁴, ZIYANG GAN⁴, ANDREY TURCHANIN⁴, FRANCISZEK KROK², and RICHARD A. WILHELM¹ — ¹TU Wien, Institute of Applied Physics, 1040 Vienna, Austria, EU — ²Jagiellonian University, Institute of Physics, 30-348 Kraków, Poland, EU — ³University of California, Space Sciences Laboratory, Berkeley 94720, USA — ⁴Friedrich Schiller University Jena, Institute of Physical Chemistry, 07743 Jena, Germany, EU

Irradiation of certain targets with slow highly charged ions (HCIs) can trigger phase transitions or nano-structure formation. The main driving force for these processes is the electronic excitation of the target's electronic sub-system in close proximity of the impact triggered by the ion neutralization. Subsequent electron-phonon coupling mediates lattice heating of the target. So far charge state dependent erosion of metallic surfaces was not unambiguously shown. The potential energy stored in the HCI dissipates quickly before a transfer to the target's atomic lattice can take place. By reducing the size of the target down to the nanometer regime, geometric confinement might prevent free electrons of the target to dis-

sipate the electronic excitations on the fs time-scale. In this work we irradiated gold nano islands with Xe⁹⁺ (q=1,18,25,32,40) with a constant kinetic energy of 180 keV, which results in an erosion of the islands that is strongly enhanced by the potential energy deposition.

Topical Talk

O 5.4 Mon 11:30 GER 38

A contactless single-step process for simultaneous nanoscale patterning and cleaning of large-area graphene — •TUAN TRAN — Department of Physics and Astronomy, Uppsala University, Sweden

In this talk, we will present a contactless single-step process for structuring self-supporting graphene with customizable patterns and over large areas. Using energetic ions passing through a suspended mask with through-hole nanopatterns, we can deterministically structure the graphene with a minimum feature size down to 15 nm, comparable to what can be achieved with focused ion beam techniques. Our process, however, instead uses a broad parallel beam with no stringent requirement on the beam focusing, and hence enables a contactless approach. Neither, any chemicals and coating layers are necessary, substantially reducing the amount of contamination which might otherwise occur using other lithographic methods. In addition to the structuring capability, we found that the method can simultaneously render the graphene cleaner. The areas surrounding the direct ion impacts are significantly cleaned from the initial contamination which commonly are remnants from the transferring process of the graphene. We will explain the mechanism leading to such cleaning effect. Finally, selective area electron diffraction were used for detailed characterization of the graphene lattice after ion irradiation with and without the mask at different doses and temperatures. These diffraction data are necessary for understanding the creation and annihilation of defects and the possible role of the contamination on self-healing and stabilization of the graphene lattice.

O 5.5 Mon 12:00 GER 38

chemical etching of 2D materials — •MITISHA JAIN, SILVAN KRETSCHMER, and ARKADY KRASHENINNIKOV — Institute of Ion Beam Physics and Materials Research, Helmholtz-Zentrum Dresden-Rossendorf, Bautzner Landstraße 400, 01328 Dresden, Germany

Transmission electron microscopes are used for imaging 2D materials to the resolution of single atoms. On the other hand, the imaged material gets damaged (modified by the beam) quite easily. Hence, the information about the damage done by the beam are important for proper imaging. Different channels of damage construction such as knock-on, ionization (excitation), chemical etching (e.g. adatoms) have been determined. In this study, the knock-on threshold energies for graphene (C), h-BN (B and N) and MoS₂ (S) materials in the presence of adsorbed adatoms (H, C, N, O) on the surface are calculated in the framework of spin-polarized density functional theory. From the preliminary results, we found that when an adatom is adsorbed, the threshold energies are reduced by 2-3 eV compared to pristine systems. Further, we consider the additional effect of electronic excitation on the threshold energies in combination with adsorbed adatoms. The displacement cross-section under the electron beam are assessed employing the McKinley-Feshbach formalism allowing to compare different channels of damage creation.

O 5.6 Mon 12:15 GER 38

Influence of the swift heavy ions' charge state on pore creation in single-layer MoS₂ — •YOSSARIAN LIEBSCH¹, LUKAS MADAUSS¹, HENNING LEBIUS², ABDE-NACER BENYAGOUB², CLARA GRYGIEL², RADIA RAHALI², RAJENDRA SINGH³, JANI KOTAKOSKI³, and MARIKA SCHLEBERGER¹ — ¹University Duisburg-Essen, Duisburg, Germany — ²CIMAP/GANIL, Caen, France — ³University Vienna, Vienna, Austria

The initial charge state of a swift heavy ion is usually of no special interest when discussing the interaction of the ion with a bulk target. This is due to the potential energy being small in comparison to the kinetic energy of the ion and due to the equilibrium charge the ion accumulates within a few nanometers after it enters the material. However, in single-layer materials the travelling distance is less than the typical distance needed to establish the equilibrium charge state. Hence, we try to investigate the influence of the charge state of the ions on the defect formation in MoS₂. This is done by irradiating single-layers with swift

heavy ions of different charge states. For this experiment we chose 6.6 MeV/u Xe ions with charge states ranging from +41 to +48. Evaluation of the effect on the material is done by analyzing the pore radii and creation efficiencies with STEM-HAADF. With this experiment we aim to shed light onto the fundamental processes and interactions between ultra thin materials and swift heavy ions as well as quantifying the influence of the charge state on the stopping power in single-layered materials.

O 5.7 Mon 12:30 GER 38

Spectroscopic and microscopic analysis of ion-induced modifications in 2D materials — •CAROLIN FRANK¹, LUCIA SKOPINSKI¹, LARS BREUER¹, JENNIFER SCHMEINK¹, LUKAS KALKHOFF¹, STEPHAN SLEZIONA¹, ULRICH HAGEMANN², and MARIKA SCHLEBERGER¹ — ¹University of Duisburg-Essen, Faculty of Physics and CENIDE, 47057 Duisburg, Germany — ²University of Duisburg-Essen, CENIDE, ICAN, 47057 Duisburg, Germany

In this contribution we present results concerning modifications induced by xenon- and gold-ions in two-dimensional molybdenum disulfide exfoliated on gold including Raman spectroscopy, X-ray photoelectron spectroscopy and friction force microscopy. Irradiations at the target station HICS, located at the University of Duisburg-Essen, as well as at the target stations MSS@CRYRING and MI-Branch, both located at the GSI Helmholtzzentrum für Schwerionenforschung, were implemented with slow, highly charged ions as well as with swift heavy ions, which differ from each other regarding their charge state and their kinetic energy.

A focus will be given to the impact of both the kinetic and potential energy of the ions on modifications of the molybdenum disulfide and also on the size of ion-induced defects. Based on the results of friction force microscopy it is shown for the first time that the impact of the potential energy of the swift ions

regarding generation of defects in 2D materials is significantly larger than the impact of the kinetic energy. Additionally, results regarding interaction between the gold substrate and the molybdenum disulfide will be discussed.

O 5.8 Mon 12:45 GER 38

Manipulation of the electrical and memory properties of MoS₂ field-effect transistors by highly charged ion irradiation — •STEPHAN SLEZIONA¹, ANIELLO PELELLA², ENVER FAELLA², OSAMAH KHARSAH¹, LUCIA SKOPINSKI¹, ANDRÉ MAAS¹, YOSSARIAN LIEBSCH¹, ANTONIO DI BARTOLOMEO², and MARIKA SCHLEBERGER¹ — ¹Fakultät für Physik und Cenide, Universität Duisburg-Essen, Lotharstraße 1, 47057 Duisburg — ²Physics Department, University of Salerno, 84084 Fisciano, Salerno, Italy

Molybdenum disulfide (MoS₂) is a semiconductor that develops a direct bandgap of 1.8 eV when its thickness is reduced to the monolayer limit and is therefore a suitable 2D material for applications in opto-electronic devices. MoS₂ field-effect transistors (FET) in particular exhibit a hysteresis in their transfer characteristics, which can be utilized to realize a 2D memory device. This hysteresis is generally attributed to adsorbates or defects either in the MoS₂ lattice or in the underlying substrate. We fabricated MoS₂ FETs on SiO₂/Si substrates and irradiated these devices with Xe²⁸⁺ ions at a kinetic energy of 180 keV to deliberately introduce defects and modify their electrical and hysteretic properties. We evaluate different electrical properties before and after the irradiation and find clear influences of the irradiation e.g., on the conductivity and charge carrier mobility of the devices. Significantly reduced n-doping and a well-developed hysteresis can be measured after irradiation. We utilize this hysteresis to demonstrate the use of the MoS₂ FET as a memory device, which has remarkably longer relaxation times (≈ minutes) compared to previous works.

O 6: New Methods: Experiments and Theory

Time: Monday 10:30–13:00

Location: GER 39

O 6.1 Mon 10:30 GER 39

A Newly Developed IRAS System to Investigate Adsorbates on Metal-Oxide Single Crystal Surfaces — •DAVID RATH, JIRI PAVELEC, ULRIKE DIEBOLD, MICHAEL SCHMID, and GARETH S. PARKINSON — Institute of Applied Physics, TU Wien, Austria

The IRAS system GRISU (GRazing incident Infrared absorption Spectroscopy Unit) was developed to investigate adsorbates on metal oxide single crystals in the research field of single-atom catalysis [1]. It combines the commercially available FTIR spectrometer Bruker Vertex 80v with an UHV chamber [2]. The compact design requires only one CF150 port for the main optical components, features five mirrors for beam guidance placed in HV and UHV environment and optimises the system's performance, flexibility, and usability. The result is a small controllable focal-spot diameter (max. 3 mm) on the sample, motorised optical components, and an aperture limiting the incidence angle range (variable, 49° to 85°) on the sample. Based on ray tracing results and preliminary intensity measurements, the system shows up to 10× higher intensities compared to a commercial system with two parabolic mirrors with a focal length of 250 mm. First IR spectra measured with the recently installed IRAS measurement system will be shown.

[1] G. S. Parkinson, Catal. Lett. 149, 1137 (2019)

[2] J. Pavelec, et al., J. Chem. Phys. 146, 014701 (2017).

O 6.2 Mon 10:45 GER 39

Insights on the Liquid/vacuum interface of ionic liquids by ARXPS and UHV Pendant Drop — ULRIKE PAAP, •AFRA GEZMIS, FLORIAN MAIER, and HANS-PETER STEINRÜCK — Friedrich-Alexander Universität, Erlangen, Germany

Ionic liquids (ILs) are characterized by a low melting point and a low vapor pressure. Many ILs exhibit high gas solubility along a high chemical and thermal stability. Such properties are beneficial in many areas such as gas absorbents, refrigerants, lubricants, antistatics and surfactants. The low vapor pressure of ILs opens the possibility to investigate them under ultra-high vacuum (UHV) conditions. In this context, angle-resolved X-ray photoelectron spectroscopy (ARXPS) has already proven to be a particularly powerful tool. We now combine information on the surface composition derived from ARXPS and measurements of the surface tension performed under ultraclean conditions with our new pendant drop setup, which operates in UHV. Our results allow for a deeper understanding of enrichment and molecular orientation processes at the outermost surface of these systems on the microscopic and the macroscopic scale. This work was supported by the Collaborative Research Center (CRC) 1452: Catalysis at Liquid Interfaces.

O 6.3 Mon 11:00 GER 39

Kintetic In Situ Synthesis (KISS) technique of large-area 2D materials exfoliation — •ANTONIJA GRUBISIC-CABO^{1,2}, MATTEO MICHARDI³, CHARLOTTE E. SANDERS⁴, MARCO BIANCHI⁵, DAVIDE CURCIO⁵, DIBYA PHYUAL², MAGNUS H. BERNTSEN², QINDA GUO², and MACIEJ DENDZIK² — ¹University of Groningen, Netherlands — ²KTH, Sweden — ³University of British Columbia, Canada — ⁴Central Laser Facility, UK — ⁵Aarhus University, Denmark

Two-dimensional (2D) materials provide an extremely rich platform to investigate novel quantum phenomena and to design nanostructures with desired functionalities. Some of the key techniques employed in studies of 2D materials, such as photoemission spectroscopy, have stringent requirements for the quality, sample size and cleanliness of the surface. Fulfilling these conditions using a standard mechanical exfoliation in a glove box is often problematic. Here, we present a novel method for in situ exfoliation of 2D materials performed directly in ultra-high vacuum, which yields large flakes of excellent crystallinity and purity. In our experiments, multiple semiconducting and metallic transition metal dichalcogenides were exfoliated onto Au, Ag and Ge substrates, showing the versatility of the technique, and characterised by angle resolved photoemission spectroscopy. Importantly, the proposed method is straightforward, simple, and does not require any specialised equipment. This technique is ideally suited for the electronic structure research of air-sensitive 2D materials since the sample preparation process happens entirely in ultra-high vacuum.

O 6.4 Mon 11:15 GER 39

Two new methods for the analysis of TPD data — •MICHAEL SCHMID, GARETH S. PARKINSON, and ULRIKE DIEBOLD — Institute of Applied Physics, TU Wien, Austria

Temperature programmed desorption (TPD) is the most common experimental technique for obtaining the binding energies of adsorbates. TPD data are usually analyzed using the Polanyi–Wigner equation; this is far from straightforward. We present two new methods, based on equilibrium thermodynamics, bypassing the use of the Polanyi–Wigner equation or transition state theory: In the case of all adsorption sites being equivalent, the adsorption energy can be directly calculated from the desorption temperature, the width of the TPD peak, the sticking probability (at the desorption temperature), and thermodynamic data [1]. This “magic formula” is remarkably robust; in many cases even wrong assumptions about the desorption order or the presence of a distribution of adsorption energies lead to negligible errors. In more complex cases, with a distribution of adsorption energies, we show that TPD spectra are approximately given by a convolution integral. We present a method (and computer program) for TPD inversion, i.e. the determination of the energy distribution from a single TPD spectrum at saturation coverage [1]. Although this method is derived for the case of non-interacting adsorbates, we argue that it is a good approximation in cases of short-range repulsion and it can also reveal (though not quantitatively

analyze) the presence of attractive interactions between adsorbates.

[1] M. Schmid et al., doi:10.1021/acspyschemau.2c00031 (2022)

O 6.5 Mon 11:30 GER 39

Surface-Sensitive Spectroscopy from First Principles — •YAIR LITMAN^{1,2}, JINGGANG LAN³, KUO-YANG CHIANG², VENKAT KAPIL¹, YUKI NAGATA², and DAVID WILKINS⁴ — ¹University of Cambridge, Cambridge, United Kingdom — ²MPI for Polymer Research, Mainz, Germany — ³Ecole Polytechnique Fédérale de Lausanne, Lausanne, Switzerland — ⁴Queen's University Belfast, Belfast, United Kingdom

Our current understanding of the structure and dynamics of aqueous interfaces at the molecular level has grown substantially in the last decades due to an increasing synergy between experimental measurements and atomistic simulations. However, the latter are either based on empirical force field models, which are neither suitable to describe bond breaking and formation nor systems with complex electronic structure, or on *ab initio* calculations which due to their computational cost cannot be statistically converged. In this work, we overcome all these limitations by combining high-dimensional neural network potentials with symmetry-adapted Gaussian process regression [1] to simulate the sum-frequency generation (SFG)[2] spectra of the water-air interface with *ab initio* accuracy. We obtain a good agreement with last-generation experiments and show how these models can in principle be improved systematically towards exact results. Overall, the machinery presented in this work paves the way for the modelling of surface-sensitive spectroscopy of complex interfaces. [1] V. Deringer, *et al.*, Chem. Rev. **16**, 121 (2021) [2] A. Morita, J. Hynes, J. Phys. Chem. B **106**, 673 (2002).

O 6.6 Mon 11:45 GER 39

Artificial Neural Network based Interatomic Potentials to Describe Laser-Excited Materials — •BERND BAUERHENNE, PASCAL PLETTENBERG, and MARTIN E. GARCIA — Universität Kassel, Heinrich-Plett-Straße 40, 34132 Kassel, Germany

Femtosecond laser pulses create a transient state with hot electrons at temperature T_e and cold ions, in which ultrafast nonthermal effects occur. Later, the decay of this state due to electron-phonon interactions gives rise to ultrafast effects of more thermal character. Quantum mechanical methods like T_e -dependent density functional theory (DFT) allow a precise description of the non-thermal state with hot electrons. However, simulations of laser material interactions at surfaces on experimentally relevant sizes require to take a huge amount of atoms into account, which is only possible by the usage of interatomic potentials. Most known interatomic potentials are determined assuming that electrons are in their ground state and cannot describe nonthermal effects initiated by bond-softening or hardening. In order to take ultrafast thermal and non-thermal effects on the same theoretical level, T_e -dependent interatomic potentials are needed. Here, we present an T_e -dependent interatomic potential based, for the first time, on an artificial neural network. We studied silicon and show that the phonon band structure, the cohesive energy curves for several crystal structures, the electronic specific heat, atomic forces and cohesive energies are described in excellent agreement with DFT calculations for a wide range of T_e . In addition, we simulated the laser-induced annealing of surface defects on a thin silicon film.

O 6.7 Mon 12:00 GER 39

Real-time TD-DFTB full periodic implementation for solids and low-dimensional materials — •CARLOS R. LIEN-MEDRANO¹, FRANCO P. BONAFÉ², CRISTIÁN G. SÁNCHEZ³, and THOMAS FRAEUNHEIM¹ — ¹University of Bremen, Bremen, Germany — ²MPSD, Hamburg, Germany — ³University of Cuyo, Mendoza, Argentina

The current implementation of the real-time TD-DFTB dynamics for molecules and finite systems in the DFTB+ package[1] is based on the length gauge of the electric field. Here we show a proof-of-concept implementation of the vector potential in the velocity gauge of the electric field that in principle would allow us to extend the real-time dynamics to any periodic direction, making the new implementation suitable for the study of photo-induced dynamics processes in bulk, low-dimensional materials and surfaces. Instead of the dipole moment, the observable of choice is the frequency dependent conductivity which can be obtained from the Fourier transform of the autocorrelation function of the electric current density averaged over a unit cell. The conductivity provides access to the dielectric constant of the system allowing the calculation of optical properties.

[1] Hourahine, B., et al. (2020). DFTB+, a software package for efficient ap-

proximate density functional theory based atomistic simulations. The Journal of Chemical Physics, 152(12), 124101.

O 6.8 Mon 12:15 GER 39

Structure discovery in AFM imaging of ice — •FABIO PRIANTE¹, YE TIAN², DONG GUAN², CHEN XU¹, SHUNING CAI¹, NIKO OINONEN¹, PETER LILJEROTH¹, YING JIANG², and ADAM FOSTER^{1,3} — ¹Department of Applied Physics, Aalto University, Helsinki FI-00076, Finland — ²International Center for Quantum Materials, Peking University, Beijing, 100871, China — ³WPI Nano Life Science Institute (WPI-Nano LSI), Kanazawa University

The interaction of water with surfaces is crucially important in a wide range of natural and technological settings. Using high-resolution AFM and STM, several studies have demonstrated the presence of water pentamers, hexamers, heptamers (and of their combinations) on a variety of metallic surfaces. However, in all these situations, the observed structures were completely flat, providing a relatively straightforward path to interpretation. To address more complex cases, while simultaneously alleviating the interpretation effort, we develop an automated workflow centered around a convolutional neural network (to extract atomic positions) and a neural network potential (to rapidly sort candidate structures with high accuracy). We test our workflow on several high-resolution AFM measurements of water clusters on Cu(111), whose understanding is challenging due to both their highly 3D configuration and to their large size. For each of them, we propose an underlying atomic structure, finally comparing the experimental images with simulated AFM from Density Functional Theory. These results provide new insights into the early phases of ice formation, which is a ubiquitous phenomenon ranging from biology to astrophysics.

O 6.9 Mon 12:30 GER 39

Designing Covalent Organic Frameworks Through Active Machine Learning — •YUXUAN YAO^{1,2}, CHRISTIAN KUNKEL³, KARSTEN REUTER³, and HARALD OBERHOFER² — ¹Chair for Theoretical Chemistry, Technische Universität München — ²Chair for Theoretical Physics VII, University of Bayreuth — ³Fritz-Haber-Institut der Max-Planck-Gesellschaft

Covalent organic frameworks (COFs) are a class of materials, that are formed by molecular building blocks (BBs) connected with covalent bonds. They have found application in many fields such as catalysis, or optoelectronics. It is well known that their design space is far too large to sample one by one because numerous available BBs. We modify an earlier active machine learning (AML) approach that explores the massive available BBs space through the use of surrogate models for charge injection and transport descriptors. In this method, the Gaussian Process Regression (GPR) and AML are combined to train the molecular space. This way we ensure that only promising molecules that are very different from already explored ones have their descriptors evaluated by Density Functional based Tight Binding (DFTB) calculations. Specifically, we modify molecular generation rules in order to produce three-fold rotationally symmetric candidates molecules for use in hexagonal COFs. In the future this approach can be generalized for any other symmetries, to potentially even allow for 3-dimensional network generation. We gauge the performance of our AML by evaluating the success ratio, which is the ratio of promising candidates to all generated molecules.

O 6.10 Mon 12:45 GER 39

Machine-learning-backed evolutionary search for SrTiO₃(110) surface reconstructions — •RALF WANZENBÖCK, FLORIAN BUCHNER, JESÚS CARRETE, and GEORG K. H. MADSEN — Institute of Materials Chemistry, TU Wien, Vienna, Austria

To determine the atomic structure of surface reconstructions, structural models derived from domain knowledge and intuition have historically been essential. Evolutionary algorithms combined with density functional theory have proven to be powerful tools for such structure searches if one accepts the prohibitive cost that comes with a thorough exploration of a potential energy surface. We train a neural-network force field (NNFF) as a surrogate model to drive the exploration of the rich phase diagram of TiO_x overlayers on SrTiO₃(110) utilizing the covariance matrix adaptation evolution strategy (CMA-ES). We verify the transferability of the NNFF by performing CMA-ES runs on SrTiO₃(110) 3×1, 4×1 and 5×1 with a model trained solely on 4×1 data. With the speedup afforded by the surrogate model we were able to perform exhaustive sets of exploratory runs to identify known and new low-energy reconstructions and match different symmetries found in experimental data. [R. Wanzenböck et al., Digital Discovery, 2022, 1, 703-710.]

O 7: Spins on Surfaces at the Atomic Scale I

Time: Monday 10:30–13:00

Location: REC C 213

Topical Talk

O 7.1 Mon 10:30 REC C 213

Superconductivity in atom-by-atom crafted quantum corrals — •LUCAS SCHNEIDER¹, KHAI THAT TON¹, IOANNIS IOANNIDIS^{2,3}, JANNIS NEUHAUS-STEINMETZ¹, THORE POSSKE^{2,3}, ROLAND WIESENDANGER¹, and JENS WIEBE¹ — ¹Department of Physics, University of Hamburg, D-20355 Hamburg, Germany — ²I. Institute for Theoretical Physics, University of Hamburg, D-20355 Hamburg, Germany — ³Centre for Ultrafast Imaging, Luruper Chaussee 149, D-22761 Hamburg, Germany

Gapless materials in electronic contact with superconductors acquire proximity-induced superconductivity in a region near the interface. Here, we investigate the most miniature example of this so-called proximity effect on only a single quantum level of a surface state confined in a quantum corral on a superconducting substrate, built atom-by-atom using a scanning tunneling microscope. Whenever an eigenmode of the corral is pitched close to the Fermi energy by adjusting the corral's size, a pair of particle-hole symmetric states is found to enter the superconductor's gap. By comparison to a resonant level model of a spin-degenerate localized state coupled to a superconducting bath, we identify the in-gap states as scattering resonances theoretically predicted 50 years ago by K. Machida and F. Shibata, which had so far eluded detection. We further show that the observed anticrossings of the in-gap states indicate proximity-induced pairing in the quantum corral's eigenmodes. In a final step, we study how individual magnetic adatoms interact with the corral's eigenmodes.

O 7.2 Mon 11:00 REC C 213

Tailoring Yu-Shiba-Rusinov bands in a Kagome lattice by molecular self-assembly — •LAETITIA FARINACCI, GAEL REECHT, NILS BOGDANOFF, BENJAMIN W. HEINRICH, FELIX VON OPPEN, and KATHARINA J. FRANKE — Freie Universitaet Berlin, Germany

Coupling of magnetic bound states in superconductors (so-called Yu-Shiba-Rusinov or YSR states) leads to fascinating phenomena; such as the formation of topological states. Bottom up approaches allow for a precise characterization of the coupling parameters, shedding light onto the formation of YSR bands and their properties. Most studies so far rely on atom manipulation, which is time demanding and typically limits the size of the systems to below a hundred sites.

Here, we show that self-assembly of Fe-porphine-chloride (FePCL) molecules on Pb(111) can be controlled by varying the sample temperature during and after molecular deposition. In particular, we show that we can obtain islands in which the FeP molecules arrange in a Kagome lattice or in its precursors. This way, we can, on the one hand, characterize the YSR hybridization with molecular precision and, on the other hand, study the long-range band formation across 2D islands.

O 7.3 Mon 11:15 REC C 213

Atom-by-Atom Study of Spin Lattices on a Superconducting Rashba Material — •KHAI THAT TON, LUCAS SCHNEIDER, JENS WIEBE, and ROLAND WIESENDANGER — Department of Physics - University of Hamburg, Hamburg, Germany
In the research field of topological superconductivity, Rashba-spin-orbit-coupling is believed to be a stabilizing parameter for topological phases, increasing the size of the topological gap.

One well-known category of materials with large spin-orbit coupling are Bismuth-based surface alloys, which have been extensively studied by surface-sensitive methods like angle-resolved photoemission and scanning tunneling spectroscopy [1,2,3,4]. However, studies of such materials proximitized by superconducting substrates are lacking so far. In this work, we grew Bismuth-based surface alloys on thin films proximitized by elementary superconducting substrates, adsorbed transition metal atoms, and then built dimers, chains and small two-dimensional lattices of these atoms via STM-tip based atom manipulation. We will present a scanning tunneling spectroscopy investigation of the low-energy electronic structure of these different spin lattices.

[1] C. R. Ast et al. Phys. Rev. Lett. 98, 186807 (2007).

[2] C. R. Ast et al., Phys. Rev. B 75, 201401(R) (2007).

[3] M. Steinbrecher et al., Phys. Rev. B 87, 245436 (2013).

[4] W. Jolie et al., ACS Nano 16, 4876*4883 (2022).

O 7.4 Mon 11:30 REC C 213

Symmetry-dependent coupling in Yu-Shiba-Rusinov dimers — •LISA RÜTTEN¹, EVA LIEBHABER¹, HARALD SCHMID¹, GAËL REECHT¹, KAI ROSSNAGEL^{2,3}, FELIX VON OPPEN¹, and KATHARINA FRANKE¹ — ¹Fachbereich Physik, Freie Universität Berlin, 14195 Berlin, Germany — ²Institut für Experimentelle und Angewandte Physik, Christian-Albrechts-Universität zu Kiel, 24118 Kiel, Germany — ³Ruprecht Haensel Laboratory, Deutsches Elektronen-Synchrotron DESY, 22607 Hamburg, Germany

Unpaired adatom spins on superconductors interact with the Cooper pairs of the substrate and cause Yu-Shiba-Rusinov (YSR) states inside the superconducting gap. These can be probed by scanning tunneling spectroscopy at the single-

atom scale. On superconducting van der Waals materials, the YSR wave functions of magnetic impurities can extend over several nanometers. This provides a wide range of adatom spacings over which their interaction is sufficiently strong to be potentially observed as a splitting in the tunneling spectra. Additionally, the YSR wave functions inherit their symmetry from the substrate. Depending on the symmetry and spacing in YSR dimers, the spins may interact differently via RKKY and Dzyaloshinskii-Moriya interactions. This manifests in splittings and/or shifts of the YSR states.

Here, we manipulate Fe atoms on superconducting 2H-NbSe₂ using the tip of a scanning tunneling microscope and build dimers with different symmetries. Depending on the orientation of the dimers with respect to the crystal symmetry of the substrate we find YSR hybridization but also more complex effects caused by spin interactions.

O 7.5 Mon 11:45 REC C 213

Magnetic impurity states proposed as thermometer for superconducting quasiparticle temperatures — •CIPRIAN PADURARIU¹, SUJOY KARAN², HAONAN HUANG², BJÖRN KUBALA^{1,3}, CHRISTIAN R. AST², and JOACHIM ANKERHOLD¹ — ¹Institute for Complex Quantum Systems and IQST, Ulm University, Ulm, Germany — ²Max-Planck-Institut für Festkörperforschung, Stuttgart, Germany — ³Institute of Quantum Technologies, German Aerospace Center (DLR), Ulm, Germany

The occupation of the quasiparticle continuum in a superconductor is of critical importance for the functionality of Josephson junction-based quantum devices. While significant progress has been made recently, the detection and trapping of quasiparticles remains a significant challenge. This talk will describe the design of a thermometer that detects the presence and effective temperature of superconducting quasiparticles. The device consists of a mK-STM functionalized with a single Yu-Shiba-Rusinov (YSR) state inside the gap. Transport between the tip and a clean superconducting substrate shows Zeeman-split peaks in the differential conductance associated to the YSR state [1]. The current is sensitive to quasiparticles above the gap. We show, based on a simple rate equation model, how the control of the magnetic field, as well as the voltage bias, allows the operation of the junction as a thermometer for the effective temperature of quasiparticles.

[1] W.-V. van Gerven Oei, *et al.*, "Magnetic impurities in spin-split superconductors", Phys. Rev. B 95, 085115 (2017).

O 7.6 Mon 12:00 REC C 213

Magnetic phase diagram of a YSR-molecule — •NIELS P.E. VAN MULLEKOM¹, BENJAMIN VERLHAC¹, WERNER M.J. VAN WEERDENBURG¹, HERMANN OSTERHAGE¹, MANUEL STEINBRECHER¹, KATHARINA J. FRANKE², and ALEXANDER A. KHAJETOORIANS¹ — ¹Institute for Molecules and Materials, Radboud University Nijmegen, the Netherlands — ²Fachbereich Physik, Freie Universität Berlin, Germany

Yu-Shiba-Rusinov (YSR) states arise from the exchange coupling between a local spin and a superconductor, and are strongly linked to Kondo screening. Understanding the interplay of this exchange interaction with other energy scales, as well as the role of higher spin degrees of freedom, requires magnetic field dependent characterization. To date, most studies of YSR states have been limited to bulk superconductors, which easily quench in the presence of modest magnetic fields.

Here, using high resolution milliKelvin scanning tunneling microscopy and spectroscopy, we characterize the magnetic phase diagram of a molecule on the surface of a thin film superconductor. We see nontrivial changes in the YSR excitations, that go beyond the trends that are expected in a spin 1/2 picture. We relate these changes to the various properties of the molecule, including the role of multiple channels and magnetic anisotropy. We additionally propose a model to understand the various changes in the excitation. These results provide an in-depth and detailed approach to understand the role of high spin systems in the presence of Kondo and YSR states.

O 7.7 Mon 12:15 REC C 213

Spin currents in helical molecular wires — •RICHARD KORYTÁR¹, JAN VAN RUITENBEEK², and FERDINAND EVERS³ — ¹Univerzita Karlova, Prague, Czech Republic — ²Leiden University — ³University of Regensburg

Various spin-selective phenomena have been recently reported for helical molecular wires. The explanation of these phenomena is still lacking [1]. I will present a theoretical analysis of spin currents in non-magnetic molecular junctions. First, constraints based on time-reversal invariance will be summarized. Second, I will present results based on Landauer formalism and a simple model Hamiltonian. Possible experimental detection setups will be discussed.

[1] Evers et al., Adv. Mater. 2022, 34, 2106629

O 7.8 Mon 12:30 REC C 213

Controlling the Spin States of iron porphyrin on Au(111) — •XIANGZHI MENG¹, JENNY MÖLLER², MASOUD MANSOURI^{3,4}, DANIEL SÁNCHEZ-PORTAL^{3,4}, ARAN GARCIA-LEKUE^{3,5}, ALEXANDER WEISMANN¹, CHAO LI¹, RAINER HERGES², and RICHARD BERNDT¹ — ¹Institut für Experimentelle und Angewandte Physik, Christian-Albrechts-Universität, 24098 Kiel, Germany — ²Otto-Diels-Institut für Organische Chemie, Christian-Albrechts-Universität, 24098 Kiel, Germany — ³Donostia International Physics Center (DIPC), 20018 Donostia-San Sebastián, Spain — ⁴Centro de Física de Materiales CSIC-UPV/EHU, 20018 Donostia-San Sebastián, Spain; — ⁵Ikerbasque, Basque Foundation for Science, 48013 Bilbao, Spain

Spin-flip excitations of FeTBrPP molecules on Au(111) are investigated with a low-temperature scanning tunnelling microscope under ultrahigh vacuum condition. The molecules show two distinct adsorption configurations that exhibit different magnetic anisotropy energies. Density functional theory calculations show that the different structures and excitation energies reflect unlike occupations of the Fe 3d levels. We demonstrate that the magnetic anisotropy energy can be well controlled by adjusting the adsorption site, the orientation, or the tip-molecule distance.

O 7.9 Mon 12:45 REC C 213

Mapping magnetism with a molecule — •ALEX FÉTIDA¹, MICHELANGELO ROMEO¹, OLIVIER BENGONE¹, MARIE-LAURE BOCQUET², NICOLAS LORENTE³, and LAURENT LIMOT¹ — ¹Université de Strasbourg, CNRS, IPCMS, UMR 7504, 67000 Strasbourg, France — ²PASTEUR, Ecole Normale Supérieure, PSL University, Sorbonne Université, CNRS, 24 Rue Lhomond, 75005 Paris, France — ³Centro de Física de Materiales (CFM MPC) CSIC-EHU, 20018 San Sebastián, Spain

The decoration of metal probe-tips by a molecule intentionally picked up from a surface has proven to be a powerful method to improve the measurement capabilities of a scanning tunneling microscope (STM). The success of this approach opens the prospect of introducing spin sensitivity through the tip functionalization by a magnetic molecule. We show here that a metallocene-terminated tip can probe surface magnetism through the inelastic component of the tunneling current, which provides an electrical access to the metallocene spin states. When the tip is 100 picometers away from point contact, the exchange interaction between the tip and a magnetic sample changes the metallocene spin states. This detection scheme can then be used to independently measure the sample exchange field and spin polarization with atomic-scale resolution with knowledge of spin orientation as we show on ultra-thin cobalt layers.

O 8: Ultrafast Electron Dynamics at Surface and Interfaces I

Time: Monday 10:30–12:45

Location: TRE Phy

O 8.1 Mon 10:30 TRE Phy

Coulomb-correlated few-electron states from a laser-driven Schottky emitter — •RUDOLF HAINDL^{1,2}, ARMIN FEIST^{1,2}, TILL DOMRÖSE^{1,2}, MARCEL MÖLLER^{1,2}, SERGEY V. YALUNIN^{1,2}, and CLAU ROPERS^{1,2} — ¹Max Planck Institute for Multidisciplinary Sciences, Göttingen — ²4th Physical Institute, University of Göttingen

Observing correlation phenomena for free electrons requires a highly confined emission source, readily available by femtosecond photoemission from nanotips [1,2], and can in principle be studied using the supreme beam control provided by electron microscopes [3]. However, ensemble-averaged detection usually prevents studying multi-particle correlations in free-electron beams.

In this work, we use event-based electron microscopy to characterize laser-triggered few-electron pulses generated at a Schottky field emitter [4]. We find surprisingly strong energy correlations of about 2 eV in the two- and three-electron states hinting at a correlated emission process. Furthermore, state-sorted beam caustics show characteristic transverse pair distributions, as well as an increase and a longitudinal shift of the source.

Inducing strong few-electron Coulomb correlations facilitates non-Poissonian electron pulse statistics, promising applications in free-electron quantum optics.

[1] P. Hommelhoff, et al., *Phys. Rev. Lett.* **96**, 077401 (2006).

[2] C. Ropers, et al., *Phys. Rev. Lett.* **98**, 043907 (2007).

[3] A. Feist, et al., *Ultramicroscopy* **176**, 63-73 (2017).

[4] R. Haindl, et al., arXiv:2209.12300 (2022).

O 8.2 Mon 10:45 TRE Phy

Impact of layer thickness on the anisotropic carrier dynamics of a laser-excited Fe_n/(MgO)_m(001) heterostructure from real-time TDDFT — •ELAHEH SHOMALI, MARKUS ERNST GRUNER, and ROSSITZA PENTCHEVA — Department of Physics and Center for Nanointegration, CENIDE, University of Duisburg-Essen, Germany

The carrier dynamics of Fe_n/(MgO)_m(001) metal/insulator heterostructures has been investigated from first-principles as a function of the Fe and MgO layer thickness ($n=1,3,5$ and $m=3,5,7$), excitation energy and polarization direction. The imaginary part of the dielectric tensor calculated within the random phase approximation (RPA) shows for all structures a similar metallic-like behavior in the in-plane component, $\epsilon_{xx}(\omega)$, whereas for $\epsilon_{zz}(\omega)$ the initially low response below the MgO band gap for Fe₁/(MgO)₃(001) increases substantially with the number of Fe layers. Electronic excitations calculated in the framework of RT-TDDFT confirm the concerted excitation mechanism previously proposed for Fe₁/(MgO)₃(001) also for the larger systems, which involves two simultaneous excitations via interface states [1]: one from occupied states of the metal to the conduction band of the insulator and simultaneously, another from the valence band of MgO into Fe states above the Fermi level. This mechanism allows for an effective bidirectional relocation of excitations between the metallic and insulating subsystems even for photon energies below the MgO gap. Funding by DFG via SFB 1242, project C02 is gratefully acknowledged. [1] E. Shomali, M. E. Gruner, and R. Pentcheva, *Phys. Rev. B* **105**, 245103 (2022).

O 8.3 Mon 11:00 TRE Phy

Relaxation and transport dynamics of laser-excited electrons — •MARKUS HECKSCHEN¹, YASIN BEYAZIT¹, FLORIAN KÜHNE¹, ELAHEH SHOMALI¹, MARKUS GRUNER¹, ROSSITZA PENTCHEVA¹, PING ZHOU¹, DETLEF DIESING², AXEL

LORKE¹, UWE BOVENSIEPEN¹, and BJÖRN SOTHMANN¹ — ¹Faculty of Physics and Center for Nanointegration (CENIDE), University of Duisburg-Essen, Lotharstraße 1, 47057 Duisburg, Germany — ²Faculty of Chemistry, University of Duisburg-Essen, Universitätsstraße 5, 45141 Essen, Germany

Scattering of electronic excitations after laser excitation is of key importance to understand transport and relaxation effects. A recent back-pump front-probe two-photon-photoemission experiment in Fe/Au samples measured the electron distribution as a function time and energy [1]. The time at which the maxima of the electron distribution occur as a function of Au-layer thickness provides information on velocity, transport regime and relaxation processes. Here, we present a trajectory-based simulation approach to describe the energy relaxation and the transport through the sample in the ballistic regime. Our results agree qualitatively with the experiment and provide new insight into ultrafast electron dynamics.

[1] Beyazit et al., *PRL* **125**, 076803(2020)

O 8.4 Mon 11:15 TRE Phy

Capturing non-thermal electrons: To what extent can a temperature-based model compete with a kinetic description? — •MARKUS UEHLEIN, SEBASTIAN T. WEBER, and BAERBEL RETHFELD — Department of Physics and Research Center OPTIMAS, RPTU, Kaiserslautern, Germany

The development and usage of laser systems in research allows to study the dynamics of laser-excited electrons in metals on sub-picosecond timescales. Kinetic models can trace non-equilibrium distributions in great detail for instance by using full Boltzmann collision integrals [1]. Due to the excitation of non-thermal electrons, this dynamics cannot be described with purely temperature-based models. However, there are a number of extensions of the well known two-temperature model to trace the non-thermal electrons in a numerically simplified way.

We aim to clarify, whether an extended TTM (first published in Refs. [2, 3], improved in Ref. [4]) can describe this electronic non-equilibrium dynamics by comparing it to the kinetic description. In particular, we compare the spectral particle dynamics to a time-resolved two-photon photoemission measurement [5].

[1] B. Y. Mueller and B. Rethfeld; *Phys. Rev. B* **87**, 035139 (2013)

[2] E. Carpene; *Phys. Rev. B* **74**, 024301 (2006)

[3] G. D. Tsibidis; *Appl. Phys. A* **124**, 311 (2018)

[4] M. Uehlein, S. T. Weber and B. Rethfeld; *Nanomaterials* **12**, 1655 (2022)

[5] Y. Beyazit et al.; *Phys. Rev. Lett.* **125**, 076803 (2020)

O 8.5 Mon 11:30 TRE Phy

Radio-frequency controlled electron pulses for time-resolved LEED — •DENNIS EPP¹, BENJAMIN SCHRÖDER¹, MARCEL MÖLLER¹, and CLAU ROPERS^{1,2} — ¹Max-Planck-Institut für Multidisziplinäre Naturwissenschaften — ²Georg-August-Universität Göttingen

In this contribution, we demonstrate temporal compression of low-energy electron pulses using rf-fields. Specifically, we combine a millimetre-sized electron gun [1] with a rf-cavity driven by a sinusoidal wave. A phase-locked loop synthesizer controls the timing between the incident electron pulses and the sinusoidal signal. By electron energy filtering, we measured an initial energy spread of $\Delta E \sim 1.5$ eV for the uncompressed pulses with mean kinetic energies in the range of 50 eV to 100 eV [2]. In perspective, ULEED with sub-ps resolution

will allow for the observation of the impact of electron-phonon coupling and coherent vibrational motion on the efficiencies of surface phase transitions and the resulting changes in materials functionality. [1] Vogelgesang, et al., *Nature Physics* 14,184-190 (2018). [2] Epp et al., in preparation

O 8.6 Mon 11:45 TRE Phy

High-harmonic generation in topological insulator surface states using wave-packet approaches — •VANESSA JUNK¹, WOLFGANG HOGGER¹, ALEXANDER RIEDEL¹, COSIMO GORINI², and KLAUS RICHTER¹ — ¹Institute for theoretical physics, University of Regensburg, Germany — ²Université Paris-Saclay, CEA, CNRS, SPEC, 91191, Gif-sur-Yvette, France

The interaction of matter with strong-field light gives rise to highly non-linear electron dynamics within the material. The electric field of the light accelerates electrons through the band structure and drives non-perturbative transitions, leading to strongly anharmonic electron velocities and the emission of high-order harmonics.

Here, we want to study these electron dynamics for the surface states of topological insulators by solving the time-dependent Schrödinger equation for wave packets. That the separation of bulk and surface high harmonics is experimentally possible has been demonstrated recently [1]. Furthermore, an alternating polarization rotation between odd and even order harmonics was found and attributed to the hexagonal warping present in Bi₂Te₃ surface states. Using effective Dirac models and taking into account effects of the Fermi sea, we can reproduce these experimental features with our wave-packet approach.

[1] C. Schmid, L. Weigl, P. Grössing, V. Junk, C. Gorini, S. Schlauderer, S. Ito, M. Meierhofer, N. Hofmann, D. Afanasiev, J. Crewse, K. Kokh, O. Tereshchenko, J. Güdde, F. Evers, J. Wilhelm, K. Richter, U. Höfer and R. Huber, *Tunable non-integer high-harmonic generation in a topological insulator*, *Nature* **593**, 385-390 (2021)

O 8.7 Mon 12:00 TRE Phy

Subcycle surface-bulk coupling in a topological insulator — •SUGURU ITO¹, MICHAEL SCHÜLER², MANUEL MEIERHOFER³, JOSEF FREUDENSTEIN³, DMYTRO AFANASIEV³, JENS GÜDDE¹, MICHAEL SENTEF⁴, RUPERT HUBER³, and ULRICH HÖFER¹ — ¹Philipps-Universität Marburg, Germany — ²Paul Scherrer Institute, Switzerland — ³Universität Regensburg, Germany — ⁴Max Planck Institute for the Structure and Dynamics of Matter, Germany

Intense lightwaves at terahertz frequencies can drive currents in electronic bands as well as non-perturbative excitations across the band gap, whose interplay leads to strong-field phenomena such as high-harmonic generation. Angle-resolved photoemission spectroscopy (ARPES) with subcycle time resolution allows us to observe such lightwave-driven processes in momentum space.

Here, we will present our investigation of subcycle coupling between the topological surface state (TSS) and the bulk conduction band (BCB) in Bi₂Te₃, where the TSS is well separated from the bulk along the $\bar{\Gamma}$ - \bar{K} direction. Under exposure of a strong 25-THz lightwave, however, transient replicas of the equilibrium TSS, Floquet-Bloch states, are formed. Their hybridization with the BCB enables an efficient population transfer into the BCB. In contrast, TSS and BCB are less separated along $\bar{\Gamma}$ - \bar{M} , where already an intraband current can induce an efficient subcycle population transfer. Both distinct mechanisms are readily seen in our

experiment. The dynamical Floquet-bulk coupling is confirmed by our full quantum calculations and provides a momentum-resolved view of non-perturbative interband excitations.

O 8.8 Mon 12:15 TRE Phy

Ultrafast electron dynamics in a topological crystalline insulator — •MAGNUS BERTSEN¹, YUZHU FAN¹, ANTONIJA GRUBISIC-CABO^{1,2}, MACIEJ DENDZIK¹, QINDA GUO¹, CONG LI¹, YANG WANG¹, WANYU CHEN¹, DIBYA PHUYAL¹, JONAS WEISSENRIEDER¹, and OSCAR TJERNBERG¹ — ¹Department of Applied Physics, KTH Royal Institute of Technology, Sweden — ²University of Groningen, Nether- lands

Topological crystalline insulators is a class of materials that possesses helical Dirac-like electronic surface states whose existence is protected by crystal symmetries. This intricate coupling of topology and crystal structure makes it particularly interesting to study the transient electronic structure in these materials induced by an optical excitation since an accompanying symmetry-breaking lattice deformation could lead to a break-down of the topological phase on an ultrafast time scale. Here, we have studied the ultrafast electron dynamics in the archetypal topological crystalline insulator (Pb,Sn)Se by time- and angle-resolved photoemission spectroscopy. The electronic excitation occurs mainly along a preferential direction in momentum space determined by the polarization of the pump pulse and the excitation spectrum displays multiple time scales suggestive of the existence of multiple relaxation channels. Supported by time-resolved diffraction data acquired by ultrafast electron microscopy, we discuss our findings both in the light of the specific electronic structure of the surface states as well as the potential influence of lattice dynamics on the decay of the electronic excitation.

O 8.9 Mon 12:30 TRE Phy

Field-induced ultrafast modulation of Rashba coupling in ferroelectric α -GeTe(111) — GEOFFROY KREMER^{1,2}, JULIAN MAKLAR³, LAURENT NICOLAÏ⁴, •CHRIS W. NICHOLSON^{1,3,5}, CHANGMING YUE¹, CAIO SILVA³, PHILIPP WERNER¹, J. HUGO DIL^{6,7}, JURAJ KREMPASKÝ⁶, GUNTHER SPRINGHOLZ⁸, RALPH ERNSTORFER^{3,9}, JAN MINÁR⁴, LAURENZ RETTIG⁶, and CLAUDE MONNEY¹ — ¹Université de Fribourg, Switzerland — ²Université de Lorraine, France — ³Fritz Haber Institute of the Max Planck Society, Germany — ⁴University of West Bohemia, Czech Republic — ⁵SPECS Surface Nano Analysis GmbH, Germany — ⁶Paul Scherrer Institut, Switzerland — ⁷EPFL, Lausanne, Switzerland — ⁸Johannes Kepler Universität, Austria — ⁹TU Berlin, Germany

Rashba materials provide an ideal playground for spin-to-charge conversion in prototype devices. I will present our recent time- and angle-resolved photoemission spectroscopy and momentum microscopy results on α -GeTe(111). This is a non-centrosymmetric ferroelectric (FE) semiconductor displaying a giant FE distortion below 700 K, which hosts spin-polarized states that are promising for a new type of highly efficient non-volatile memory device based on switchable polarization. We find a transient modification of the bulk Rashba splitting corresponding to an enhancement of the FE lattice distortion. This enhanced response results from a transient surface photovoltage which induces a delayed dispersive excitation of a phonon along the FE distortion direction [1].

[1] Kremer et al, *Nature Communications* 13, 6396 (2022)

O 9: Focus Session: Frontiers of Electronic-Structure Theory I (joint session O/HL)

Electronic-structure calculations, based on density-functional theory (DFT) and methodology beyond, are getting increasingly involved as they face the following challenges: First, investigations of modern materials typically require large unit cells, owing to complex crystal structures, mixed compositions, internal interfaces, etc. Second, at the same time, they often require advanced methods, including hybrid functionals of DFT, Green-function techniques from many-body perturbation theory (MBPT), high-level wavefunction-based methods like coupled-cluster (CC) theory, or quantum Monte-Carlo simulations. All these methods should ideally be implemented in scientific software that is running efficiently on modern supercomputers. With both methodology and computer architectures exhibiting increasing complexity, collaborative development and shared tools, including ready-to-use libraries and codes, are becoming indispensable. This interdisciplinary symposium covers recent progress in the broad area of electron-structure methods and highly-sophisticated tools that enable the entire community to explore most exciting materials from different perspectives to either predict peculiar features or get insight into measured counterparts.

Organizers: Claudia Draxl (HU Berlin), Dorothea Golze (TU Dresden), Xavier Gonze (U Louvain), and Andris Gulans (U Latvia)

Time: Monday 10:30–13:00

Location: TRE Ma

O 9.1 Mon 10:30 TRE Ma

Testing the hell out of DFT codes with virtual oxides — EMANUELE BOSONI¹, •STEEFAAN COTTENIER², and GIOVANNI PIZZI³ — ¹ICMAB-CSIC, Spain — ²Ghent University, Belgium — ³EPFL, Switzerland

If you use DFT to predict a property of a crystal, how confident can you be that the prediction is computed in a bug-free way? And if your DFT-code uses pseudopotentials, can you trust that the pseudopotential does not modify your predictions? Answering such questions has been the goal of a study a few years ago,

in which 71 unary crystals were examined in exactly the same way by 40 different DFT methods and codes [DOI 10.1126/science.aad3000]. In a next step, a consortium of 41 scientists (*) has done a similar exercise for a much larger pool of crystals: all elements of the periodic table up to Z=96, each in 10 different crystal structures, 6 of them being (virtual) oxides that sample a range of chemical bond types and 4 being unary crystals that sample low to high coordination environments. In this presentation, we will discuss the reasons to choose these crystals, the different quality criteria by which results can be compared, we will demonstrate how this exercise leads to more precise and more trustworthy pseudopotential libraries, and we will show how this data set is shared with the community in order to foster better-tested codes and pseudopotentials for all.

(*) Unfortunately the size of this abstract does not allow to mention them all.

O 9.2 Mon 10:45 TRE Ma

High-throughput absorption spectra obtained by beyond-DFT workflows — •FABIAN PESCHEL, ALEXANDER BUCCHERI, and CLAUDIA DRAXL — Institut für Physik and IRIS Adlershof, Humboldt-Universität zu Berlin, Berlin, Germany Fully converging *ab initio* calculations can be a challenging task, in particular when it comes to excited states, which require multiple ground-state calculations for different physical quantities. In this work, we aim at computing highly precise absorption spectra by employing the Bethe-Salpeter equation of many-body perturbation theory, as implemented in the all-electron full-potential package `exciting` [1,2]. To obtain benchmark data for a wide range of material classes, we have developed workflows where Python tools automatically create input files, start calculations, and evaluate results. For each material, all relevant input parameters, such as the number of k-points for the Brillouin-zone sampling, basis-set cutoff and the number of unoccupied states, are varied until the targeted convergence criteria are reached. With the help of a workflow manager, the calculations can be executed in a high-throughput fashion on a high-performance computing cluster. We demonstrate our approach with core-level spectra of elemental and binary solids, and provide an in-depth analysis of the obtained data. This work is carried out in the framework of the NOMAD Center of Excellence [3] and the CRC FONDA [4].

[1] A. Gulans et al., *J. Phys. Condens. Matter* **26**, 363202 (2014). [2] C. Vorwerk, B. Aurich, C. Cocchi, and C. Draxl, *Electron. Struct.* **1**, 037001 (2019). [3] <https://nomad-coe.eu> [4] <https://fonda.hu-berlin.de>

Topical Talk

O 9.3 Mon 11:00 TRE Ma

Large-scale machine-learning assisted discovery and characterization of materials — •MIGUEL ALEXANDRE LOPES MARQUES — Institut für Physik Martin-Luther-Universität Halle-Wittenberg, Halle (Saale), Germany

In this talk we discuss our recent attempts to discover, characterize, and understand inorganic compounds using *ab initio* approaches accelerated by machine learning. We start by motivating why the search for new materials is nowadays one of the most pressing technological problems. Then we summarize our recent work in using crystal-graph attention neural networks for the prediction of materials properties. To train these networks, we curated a dataset of over 2 million density-functional calculations with consistent calculation parameters. Combining the data and the newly developed networks we have already scanned more than two thousand prototypes spanning a space of more than one billion materials and identified tens of thousands of theoretically stable compounds. We then discuss how simple, interpretable machine learning approaches can be used to understand complex material properties, such as the transition temperature of superconductors. Finally, we speculate which role machine learning will have in the future of materials science.

15 min. break

O 9.4 Mon 11:45 TRE Ma

Predicting the electronic structure at any length scale with machine learning — •ATTILA CANGI — Helmholtz-Zentrum Dresden-Rossendorf, Görlitz, Germany

The properties of electrons in matter are of fundamental importance. They give rise to virtually all molecular and material properties and determine the physics at play in objects ranging from semiconductor devices to the interior of giant gas planets. Calculations rely primarily on density functional theory (DFT), which has become the principal method for predicting the electronic structure of matter. While DFT calculations have proven to be very useful, their computational scaling limits them to small systems. We have developed a scalable machine learning framework for predicting the electronic structure on any length scale [1,2,3]. It shows up to three orders of magnitude speedup on systems where DFT is tractable and, more importantly, enables predictions on scales where DFT calculations are infeasible. Our work demonstrates how machine learning circumvents a long-standing computational bottleneck and advances science to frontiers intractable with any current solutions.

[1] J. A. Ellis, L. Fiedler, G. A. Popoola, N. A. Modine, J. A. Stephens, A. P. Thompson, A. Cangi, S. Rajamanickam, *Phys. Rev. B* **104**, 035120 (2021). [2] L. Fiedler, N. Hoffmann, P. Mohammed, G. A. Popoola, T. Yovell, V. Oles, J. A. Ellis, S. Rajamanickam, A. Cangi, *Mach. Learn.: Sci. Technol.* **3** 045008 (2022). [3] L.

Fiedler, N. A. Modine, S. Schmerler, D. J. Vogel, G. A. Popoola, A. P. Thompson, S. Rajamanickam, A. Cangi, arXiv:2210.11343 (2022).

O 9.5 Mon 12:00 TRE Ma

Demonstrating temperature transferability of neural network models replacing modern density functional theory — •LENZ FIEDLER and ATTILA CANGI — Helmholtz-Zentrum Dresden-Rossendorf / CASUS

Due to its balance between accuracy and computational cost, Density Functional Theory (DFT) is one of the most important computational methods within materials science and chemistry. However, current research efforts such as the modeling of matter under extreme conditions demand the application of DFT to larger length scales as well as higher temperatures. Such investigations are currently prohibited due to the computational scaling of DFT.

We have recently introduced a machine-learning workflow that replaces modern DFT calculations [1,2,3]. This workflow uses neural networks to predict the electronic structure locally. We show that by employing such an approach, models can be trained to predict the electronic structure of matter across temperature ranges. This paves the way for large-scale simulations of thermodynamically sampled observables relevant to modeling technologically important phenomena such as radiation damage in fusion reactor walls.

- [1] J. A. Ellis et al., *Phys. Rev. B* **104**, 035120
- [2] L. Fiedler et al., *Mach. Learn.: Sci. Technol.*, **3** 045008
- [3] L. Fiedler et al., arXiv:2210.11343

O 9.6 Mon 12:15 TRE Ma

Pure non-local machine-learned density functional theory for electron correlation — •JOHANNES T. MARGRAF — Fritz-Haber-Institut der MPG, Berlin, Germany

Density-functional theory (DFT) is a rigorous and (in principle) exact framework for the description of the ground state properties of atoms, molecules and solids based on their electron density. While computationally efficient density-functional approximations (DFAs) have become essential tools in computational chemistry, their (semi-)local treatment of electron correlation has a number of well-known pathologies, e.g. related to electron self-interaction. Here, we present a type of machine-learning (ML) based DFA (termed Kernel Density Functional Approximation, KDFA) that is pure, non-local and transferable, and can be efficiently trained with fully quantitative reference methods. The functionals retain the mean-field computational cost of common DFAs and are shown to be applicable to non-covalent, ionic and covalent interactions, as well as across different system sizes.

O 9.7 Mon 12:30 TRE Ma

Predicting the response of the electron density to electric field using machine learning — •ALAN LEWIS and MARIANA ROSSI — MPI for Structure and Dynamics of Materials, Hamburg, Germany

The response of the electron density of a molecule or material to a homogeneous electric field defines its dielectric constant, along with its Raman and sum-frequency spectrum. We present a local and transferable machine learning approach capable of predicting the density response of molecules and periodic system on the same footing. This uses a very similar framework to that of the SALTED method recently introduced by these authors,[1,2] requiring only a small modification to the λ -SOAP descriptors used to represent the atomic environments. This allows us to predict the density response of liquid water to a field applied in each Cartesian direction from a single machine learning model. The tensorial dielectric constant can then be derived from this predicted density response, dramatically reducing the computational cost of calculating these properties relative to the standard approach of using density functional perturbation theory. We discuss the transferability of the model to different phases, and demonstrate the extrapolative power of this approach.

- [1] Lewis, Grisafi, Ceriotti, Rossi, *JCTC* **17**, 11, 7203 (2021)
- [2] Grisafi, Lewis, Rossi, Ceriotti, accepted *JCTC* (2022)

O 9.8 Mon 12:45 TRE Ma

Analysis of Batching Methods in Graph Neural Network Models for Materials Science — •DANIEL SPECKHARD, TIM BECHTEL, JONATHAN GODWIN, and CLAUDIA DRAXL — Humboldt-Universität zu Berlin, Physics Department and IRIS Adlershof, Berlin, Germany

Graph neural network (GNN) based models have shown promising results for materials science [1]. These models often contain millions of parameters, and like other big-data based models, require only a portion of the entire training dataset to be fed as a mini-batch to update model parameters. The effect of batching on the computational requirements of training and model performance has been thoroughly explored for neural networks [2] but not yet for GNNs. We explore two different types of mini-batching methods for graph based models, static batching and dynamic batching. We use the Jraph library built on JAX to perform our experiments where we compare the two batching processes for two data-sets, the QM9 dataset of small molecules and the AFLOW materials database [3]. We show that dynamic batching offers significant improvements in terms of computational requirements for training. We also present results on

the effect of the batch size and batching method on model performance.
 [1] T. Xie *et al.*, Physical Review Letters, 120, 14 (2018).

[2] M. Li *et al.*, Proceedings of the 20th ACM SIGKDD (2014).
 [3] S. Curtarolo *et al.*, Comp. Mat. Science, 58, 227-235 (2012).

O 10: Organic Molecules on Inorganic Substrates II: Electronic, Optical and Other Properties II

Time: Monday 15:00–17:30

Location: CHE 89

Topical Talk

O 10.1 Mon 15:00 CHE 89

Photoemission Orbital Tomography: Imaging Molecular Wave Functions in Reciprocal and Real Space — •F. S. TAUTZ — Quantum Nanoscience, Peter Grünberg Institute (PGI-3), Forschungszentrum Jülich, Germany

The photoemission orbital tomography (POT) technique, a variant of angle-resolved photoemission spectroscopy, has been very useful in the characterization of the electronic properties of molecular films. It is a combined experimental and theoretical approach that is based on the interpretation of the photoelectron angular distribution in terms of a one-electron initial state. This includes the unambiguous assignment of emissions to specific molecular orbitals, their reconstruction to real space orbitals in two and three dimensions, the deconvolution of complex spectra into individual orbital contributions beyond the limits of energy resolution, the extraction of detailed geometric information such as molecular orientations, twists and bends, the precise description of the charge balance and transfer at interface, and the detection of momentum-selective hybridization with the substrate, to name only a few examples. In its simplest form, POT relies on the plane-wave approximation for the final state. While this works surprisingly well in many cases, this approximation does have its limitations, most notably for small molecules and with respect to the photon-energy dependence of the photoemission intensity. Regarding the latter, a straightforward extension of the plane wave final state leads to a much-improved description while preserving the simple and intuitive connection between the photoelectron distribution and the initial state.

O 10.2 Mon 15:30 CHE 89

Structural Reorientation of Organic Molecules on Surfaces by Alkali Metal Doping — •RALF HEMM¹, KA-MAN YU¹, STEFFEN-RAMBERT ROTHENBERG¹, SERGEY SOUBATCH², CHRISTIAN KUMPF², MARTIN AESCHLIMANN¹, and BENJAMIN STADTMÜLLER^{1,3} — ¹RPTU Kaiserslautern-Landau, Erwin-Schrödinger-Str. 46, 67663 Kaiserslautern, Germany — ²Peter Grünberg Institut, Forschungszentrum Jülich, 52425 Jülich, Germany — ³Johannes-Gutenberg-Universität Mainz, Staudingerweg 7, 55128 Mainz, Germany

Organic semiconductors are promising materials for the fabrication of next-generation organic-based electronic devices. The electron properties of the organic thin film can be tuned by alkali metal doping and the consequent charge transfer. Here, we study the influence of Cs doping on the structural and electronic properties of the model system PTCDA/Ag(111). Using momentum microscopy, we can simultaneously access changes in occupation of the molecular orbitals and determine modifications of the azimuthal orientation of the PTCDA molecules upon Cs doping. We can identify two structural Cs-PTCDA phases depending on the Cs concentration with either one or two Cs atoms per PTCDA. With increasing Cs concentration, we observe a gradual structural reorientation of the molecules that is accompanied by a modification of the population of the molecular states. Both cases are different from the pristine case. The structural reorientation of the PTCDA molecules can be attributed to the electrostatic interactions between the partially ionized Cs atoms and the negatively polarized oxygen end groups of PTCDA.

O 10.3 Mon 15:45 CHE 89

Tip-enhanced Raman Spectroscopy of a charged molecule — •RODRIGO CEZAR DE CAMPOS FERREIRA¹, JIŘÍ DOLEŽAL^{1,2}, AMANDEEP SAGWAL^{1,2}, SOFIA CANOLA¹, and MARTIN ŠVEC^{1,3} — ¹Institute of Physics, Czech Academy of Sciences; Czech Republic — ²Faculty of Mathematics and Physics, Charles University; Czech Republic — ³Institute of Organic and Inorganic Chemistry, Czech Academy of Sciences; Czech Republic

The Tip-enhanced Raman spectroscopy (TERS) technique has been proven to unveil fundamental features of single molecules at the nanoscale level via near-field spectroscopy [1,2]. The confined light in the STM junction can be used as a probe to obtain an essential understanding of molecular structure and electronic properties. Here, the LT-STM-controlled TERS technique was performed and verified for the perylene tetracarboxylic dianhydride (PTCDA), which was measured the Raman fingerprint for a single molecule on Ag(111) and on insulating NaCl/Ag(111) from different excitation sources. Moreover, the precise control of geometry and charge state of the molecule in the system [3] can be observed together with the Raman fingerprint and revealed an abrupt change in the spectra. We correlate them to the presence of Kondo signature and discuss the implication for other systems.

[1] R. Zhang *et al.*, Nature. 2013, 498, 82-86 [2] J. Lee *et al.*, Nature. 2019, 568, 78-82 [4] M. Žonda *et al.*, J.Phys.Chem.Lett. 2021, 12, 6320

O 10.4 Mon 16:00 CHE 89

Charge-induced symmetry breaking in the adsorption configuration of C60 layers on h-BN/Ni(111) — •MAX BOMMERT, ROLAND WIDMER, NÉSTOR DIEZ, BRUNO SCHULER, and OLIVER GRÖNING — Empa * Swiss Federal Laboratories for Materials Science and Technology, 8600 Dübendorf, Switzerland

Hexagonal Boron Nitride (h-BN) and Nickel's (111) surface share a nearly perfectly matching lattice constant. Consequently, monolayer h-BN can be grown commensurately on Ni(111) without exhibiting a Moiré superstructure like on many other h-BN/transition metal systems. Nevertheless, upon adsorption at room temperature and scanning tunneling microscopy (STM) imaging at 5K, we observe a complex, geometrically frustrated adsorption pattern for sub-monolayer C60 coverages. The fullerenes form large molecular islands with a distinct striped pattern that we can identify as C60 adsorbed in different orientations. We use scanning tunneling spectroscopy (STS) to resolve the lowest unoccupied molecular orbitals (LUMO) of the C60. Tip-induced manipulation of single molecules affects the LUMO energy of neighboring molecules. Based on our STS investigations, we propose a significant charge transfer from the substrate to specific C60 and the associated electrostatic repulsion to be a driving force in forming the stripe pattern. We rationalize the latter by Monte Carlo simulations of the C60 lattice, considering the various contributions to the intermolecular and molecule-substrate interactions. Our results deepen the understanding of molecular adsorption and charge transfer processes, which are crucial for developing organic-inorganic hybrid devices.

O 10.5 Mon 16:15 CHE 89

Nickel(II) Porphyrins versus Nickel(II) Corroles on Different Metal Surfaces: Oxidation-State Tuning of Nickel Tetrapyrrole Complexes — •JAN HERRITSCH¹, JAN-NICLAS LUY^{1,2}, RALF TONNER-ZECH^{1,2}, and J. MICHAEL GOTTFRIED¹ — ¹Fachbereich Chemie, Philipps-Universität Marburg, Germany — ²Wilhelm-Ostwald-Institut, Leipzig, Germany

Using the example of Ni tetrapyrrole complexes, we demonstrate how the oxidation state of the central atom and the molecule-substrate interaction can be influenced by a modification of the ligand. In particular, the effect of the ring size is addressed by comparing porphyrins with corroles. The latter represent a smaller macrocycle and provide a tighter coordination environment for the metal center. In addition, Ni(II) corroles have an unusual electronic structure with an unpaired electron located at the π -electron system of the ligand. Here, we focus on the interactions of Ni(II) porphyrins and corroles with different metal surfaces (Au(111), Ag(111), Cu(111)). Depending on the used substrate, the Ni(II) porphyrin is subject to an interfacial charge transfer resulting in the reduction of the Ni atom as was shown by XPS. However, due to its unique properties Ni(II) corroles exhibit a different behavior at the metal/organic interface. While the corrole's Ni(II) state remains unchanged even on the reactive Cu(111) surface, the ligand is subject to a charge transfer by accepting electron density from the substrate. This charge transfer could be traced with experimental valence spectra (UPS), which were evaluated with the help of quantum chemical calculations (DFT).

O 10.6 Mon 16:30 CHE 89

Electronic Properties of N-Heterotriangulene Derivatives adsorbed on Au(111) — •JAKOB STEIDEL¹, INA MICHALSKY², MILAN KIVALA², and PETRA TEGEDER¹ — ¹Institute of Physical Chemistry, Heidelberg University, Im Neuenheimer Feld 253, 69120 Heidelberg — ²Institute of Organic Chemistry, Heidelberg University, Im Neuenheimer Feld 270, 69120 Heidelberg

A large number of opto-electronic devices based on organic compounds utilize donor-acceptor-systems (D-A-systems), for example as the emitting layer in organic light emitting diodes or for charge separation in organic photovoltaics. Triphenylamine and its derivatives are a class of donors in D-A-systems with a high potential for applications in devices.

Introducing an etheno-bridge in the planar triphenylamine derivative indolo[3,2,1-jk]carbazole (N-heterotriangulene-550, N-HTA-550) closes an antiaromatic ring with seven members in the resulting N-heterotriangulene-557 (N-HTA-557). This significantly changes the electronic structure while retaining the molecular geometry as well as the steric demands. By oxidation of N-HTA-557 and a subsequent condensation reaction with quinoxaline-2,3-diamine an intramolecular D-A-system is created.

In the present contribution we study the electronic properties of N-HTA-550 and its derivatives on a Au(111) surface using two-photon photoemission spectroscopy.

O 10.7 Mon 16:45 CHE 89

Influence of N-introduction in pentacene on the electronic structure — •MOHSEN AJDARI¹, MARVIN HOFFMANN², FELIX LANDWEHR¹, OLENA TVERSKOY³, UWE H. F. BUNZ³, ANDREAS DREUW², and PETRA TEGEDER¹ — ¹Physikalisch-Chemisches Institut — ²Interdisziplinäres Zentrum für Wissenschaftliches Rechnen — ³Organisch-Chemisches Institut, Universität Heidelberg

Organic electron-transporting (n-channel) semiconductors such as N-heteropolycyclic aromatic compounds are of great interest for use in a variety of (opto)electronic applications.

In this study, vibrational and electronic high-resolution electron energy loss spectroscopy (HREELS) in combination with quantum-chemical calculations are utilized to investigate the influence of N- introduction on the adsorption geometry and electronic structure of two pentacene derivatives, namely 6,13-diazapentacene (DAP) and 6,7,12,13-tetraazapentacene (TAP) on Au(111).

Our findings indicate that in comparison to parent pentacene (PEN), introduction of nitrogen atoms in the aromatic backbone of its aza derivatives leads to a narrowing of the optical gap ($S_0 \rightarrow S_1$ transition) from 2.1 eV for PEN to 2.0 eV for DAP and to 1.6 eV for TAP as well as an increase in the first triplet state energy from 0.9 eV for PEN and DAP to 1.2 eV in TAP. Additionally, in the series PEN, DAP, and TAP, the α -band ($S_0 \rightarrow S_2$ transition) gains significantly in intensity due to individual effects of the introduced nitrogen atoms on the orbital energies.

O 10.8 Mon 17:00 CHE 89

Electrostatic design of the internal surfaces of porous organic materials — •EGBERT ZOJER — Institute of Solid State Physics, NAWI Graz, Graz University of Technology, Austria

Collective electrostatic effects are ubiquitous at surfaces and interfaces involving organic materials. [1] Thus, they, for example, allow tuning the electronic properties of interfaces employing monolayers of molecules with embedded dipoles [2]. This raises the question, whether controlled assemblies of dipoles couldn't also be used to control the properties of the inner surfaces of porous structures. This question is addressed for the prototypical case of layered covalent organic

frameworks that are stacked in a way that 1D channels are formed. Employing state-of-the-art quantum-mechanical simulations, it is shown that by changing the polarity of the functional groups covering the surfaces of these pores, the electrostatic energy in the pores can be changed by more than one eV in a comparably straightforward manner. As this energy crucially determines the interaction between the host material and adsorbates within the pores, the proposed strategy holds the promise of revolutionizing various fields of application of such materials, e.g., as battery electrodes, in catalysis, and in excited-state charge separation processes.

[1] E. Zojer, T. C. Taucher, and O. T. Hofmann, *Adv. Mater. Interf. (Hall of Fame Review)*, 1900581 (2019);

[2] E. Zojer, A. Terfort, and M. Zharnikov, *Acc. Chem. Res.* 55, 1857 (2022)

O 10.9 Mon 17:15 CHE 89

Screening Non-alternant π -Electron Systems for Metal-Organic Interfaces: Interplay between Topology, Aromaticity, and Adsorption Behavior — •JAKOB SCHRAMM and RALF TONNER-ZECH — Universität Leipzig, Deutschland

Metal-organic interfaces play an important role in organic electronics. Topology, aromaticity, and interface properties are closely connected here as previously shown by experimental and theoretical studies of isomer pairs of alternant and non-alternant adsorbates. While non-alternant azulene and azupylene chemisorb on Cu(111), the alternant isomers naphthalene and pyrene physisorb.[1,2] This promises to be a general trend and can be exploited for interface design.

Here, we report data based on periodic DFT calculations for a set of 11 non-alternant molecules in comparison to analogous alternant molecules. Influence of topology on atomic and electronic structure, especially aromaticity, was analyzed based on molecular gas phase calculations. Interface properties were then derived using slab approaches at the example of Cu(111). We report on the interplay of topology and adsorption structure, adsorption energy, and charge transfer.

[1] B. P. Klein, R. Maurer, R. Tonner, C. Kumpf, I. Swart, J. M. Gottfried et al., *Phys. Rev. X.* 2019, 9, 011030;

[2] B. P. Klein, R. Maurer, G. Hilt, R. Tonner-Zech, A. Schirmeisen, J. M. Gottfried et al., *ACS Nano* 2022, 16, 11979-11987.

O 11: Surface Reactions

Time: Monday 15:00–17:15

Location: CHE 91

O 11.1 Mon 15:00 CHE 91

Machine-Learning Driven Global Optimization of Surface Adsorbate Geometries — •HYUNWOOK JUNG, LENA SAUERLAND, SINA STOCKER, KARSTEN REUTER, and JOHANNES T. MARGRAF — Fritz-Haber-Institut der Max-Planck-Gesellschaft, Berlin, Germany

The adsorption energies of molecular adsorbates on catalyst surfaces are key descriptors in computational catalysis research. For the relatively large reaction intermediates frequently encountered, e.g., in syngas conversion, a multitude of possible binding motifs leads to complex potential energy surfaces (PES), however. This implies that finding the optimal structure is a difficult global optimization problem, which leads to significant uncertainty about the stability of many intermediates. To tackle this issue, we present a global optimization protocol for surface adsorbate geometries which trains a surrogate machine learning potential on-the-fly. The approach is applicable to arbitrary surface models and adsorbates and minimizes both human intervention and the number of required DFT calculations by iteratively updating the training set with configurations explored by the algorithm. We demonstrate the efficiency of this approach for a diverse set of adsorbates on the Rh(111) and (211) surfaces.

O 11.2 Mon 15:15 CHE 91

The effect of ultrathin ionic liquid films on the adsorption dynamics of 1,3-butadiene and 1-butene on Pt(111) studied by molecular beam techniques — •LEONHARD WINTER, CYNTHIA CAROLINA FERNÁNDEZ, AFRA GEZMIS, TIMO TALWAR, STEPHEN MASSICOT, FLORIAN MAIER, and HANS-PETER STEINRÜCK — Lehrstuhl für Physikalische Chemie II, Friedrich-Alexander-Universität Erlangen-Nürnberg, Egerlandstr. 3, 91058 Erlangen

Ionic Liquids (ILs) are low temperature melting salts. In "Solid Catalyst with Ionic Liquid Layer (SCILL)" systems, IL thin films are used to coat the catalytically active metal and thereby enhance the selectivity of the catalyst; this approach is beneficial, e.g., in the industrially important hydrogenation of 1,3-butadiene to butenes, since further hydrogenation to *n*-butane must be suppressed. We used a supersonic molecular beam to investigate the adsorption dynamics of this reaction in a UHV SCILL model system. Along the method of King and Wells we measured sticking coefficients of 1,3-butadiene and 1-butene on Pt(111) coated with ultrathin layers of the IL 1,3-dimethylimidazolium bis((trifluoromethyl)sulfonyl)imide ($[C_1C_1Im][Tf_2N]$). At 180 K, the sticking coefficients decrease non-linearly with increasing IL coverage. We explain the

deviation from a simple site-blocking model with trapping into a mobile precursor state of the hydrocarbon molecules that arrive on top of IL islands. This deviation is less pronounced for films prepared at 250 K, which we attribute to larger IL island sizes.

Supported by the DFG through SFB 1452 CLINT.

O 11.3 Mon 15:30 CHE 91

On-surface synthesis of porphyrinoid monomers and dimers — •HONGXIANG XU¹, RITAM CHAKRABORTY², BIAO YANG¹, JOACHIM REICHERT¹, ABHISHEK K. ADAK², SHOBHANA NARASIMHAN², JOHANNES V. BARTH¹, and ANTHOULA C. PAPAGEORGIOU^{1,3} — ¹Technical University of Munich, Germany — ²Jawaharlal Nehru Centre for Advanced Scientific Research, India — ³National and Kapodistrian University of Athens, Greece

Porphyrinoid molecules can incorporate a wide array of the elements of the periodic table in a chemical pocket. By engineering their coordination pocket one can tune the functional properties for catalysis, spintronics, electronics and sensors. Here we use a common natural pigment, indigo, with Fe atoms on Au(111). By a series of thermally activated reaction steps including selective C-H activation, we obtain a novel metallated porphyrinoid species with high yield. By McMurry-type coupling on the same surface, this porphyrinoid species fuses into dimers. The reaction products are identified by a combination of scanning tunnelling microscopy, bond resolving atomic force microscopy and density functional theory investigations. Our studies expand the available chemistry for on-surface synthesis of macrocyclic tetrapyrroles [1] and contribute to versatile metal-organic nanostructures with smaller coordination pockets, which are challenging to obtain via solution chemistry.

[1] E. Nardi, et al. *J. Phys. Chem. C* 2014, 118, 27549; Q. Fan, et al. *Nat. Commun.* 2019 10, 5049.

O 11.4 Mon 15:45 CHE 91

Fischer-Tropsch synthesis on magnetite (111) surface — •HESHMAT NOEI¹, ROBERT GLEISSNER¹, MICHAEL WAGSTAFFE¹, CHRISTOPHER GOODWIN², MARKUS SOLDEMO², MIKHAIL SHIPILIN², PATRICK LÖMKER², CHRISTOPH SCHLUETER³, PETER AMANN², and ANDREAS STIERLE¹ — ¹Centre for X-ray and Nano Science CXNS, Deutsches Elektronen-Synchrotron DESY, Notkestraße 85, 22607 Hamburg, Germany — ²Stockholm University, Department of Physics, Roslagstullsbacken 21, 10691 Stockholm, Sweden — ³Deutsches Elektronen-Synchrotron DESY, Notkestraße 85, 22607 Hamburg, Germany

Magnetite (Fe_3O_4) is an important and diverse transition metal oxide with applications in catalysis, data storage and biomedical imaging. In this contribution, we demonstrate an operando Fischer-Tropsch synthesis with a focus on product detection on the magnetite (111) surface and clarify the reaction mechanism and intermediates applying state of the art ambient pressure XPS with ability to measure photoemission spectra 76 at above 1 bar using hard X-ray at PETRA III beamline at DESY in Hamburg and clarify the mechanism of FT synthesis by monitoring reaction products operando on single crystal Fe_3O_4 . We show then the dominant product from FT synthesis is a methoxy species and short chain alkanes under our reaction conditions (500 mbar, 400 °C) and that no aldehydes and ketones are formed during reaction.

O 11.5 Mon 16:00 CHE 91

On-Surface CO_2 Capturing by Electron-Rich Phosphines: Comparison of the Assembly on Ag(100) and on the NaBr(100) Double Layer — •VLADIMIR LYKOV¹, FLORENZ BUSS², FABIAN DIELMANN³, and KARINA MORGENSTERN¹ — ¹Ruhr-Universität Bochum, Germany — ²Institut für Anorganische und Analytische Chemie, Westfälische Wilhelms-Universität Münster, Germany — ³Institute of General, Inorganic and Theoretical Chemistry, University of Innsbruck, Center for Chemistry and Biomedicine, Innsbruck, Austria

Electron-rich phosphines exhibit exceptional electron donor properties and form zwitterionic Lewis base adducts with small inert molecules, for instance, carbon dioxide (CO_2) and sulfur dioxide (SO_2) [1]. The main focus of this project is understanding the influence of geometrical confinement on the capturing of CO_2 by electron-rich phosphines. The effect of geometrical confinement is studied with a surface science approach. For this purpose, we use a low-temperature (7 K) scanning tunneling microscope (STM). To understand the influence of the metal surface on carbon dioxide capture, we compare the molecules adsorbed on Ag(100) to those on NaBr(100) double layer, supported by Ag(100). The subsequent deposition of carbon dioxide and electron-rich phosphines confirmed the affinity of CO_2 to these phosphines. The influence of the two surfaces on the product assembly will be discussed in this presentation.

[1] F. Buß, et al. Chem. Eur. J. 2022, 28, e2021040.

O 11.6 Mon 16:15 CHE 91

On-surface synthesis of enetriynes — NAN CAO^{1,2}, •BIAO YANG¹, ALEXANDER RISS¹, JOHANNA ROSEN², JONAS BJÖRK², and JOHANNES V. BARTH¹ — ¹Physics Department E20, Technical University of Munich, Garching, Germany — ²Department of Physics, Chemistry and Biology, IFM, Linköping University, Linköping, Sweden

Belonging to the enyne family, enetriynes comprise a distinct electron-rich all-carbon bonding scheme. However, the lack of convenient synthesis protocols limits the associated application potential within, e.g., biochemistry and materials science. Herein we introduce a pathway for highly selective enetriyne formation via tetramerization of terminal alkynes on a Ag(100) surface. Taking advantage of a directing hydroxyl group, we steer molecular assembly and reaction processes. Induced by O_2 exposure the terminal alkyne moieties deprotonate and organometallic bis-acetylide dimer arrays evolve. Upon subsequent thermal annealing tetrameric enetriyne-bridged compounds are generated in high yield, readily self-assembling into regular networks. We combine high-resolution scanning probe microscopy, X-ray photoelectron spectroscopy and density functional theory calculations to examine the structural features, bonding characteristics and the underlying reaction mechanism. Our study provides an integrated strategy to precisely fabricated functional enetriyne species, providing access to a distinct class of highly conjugated π -system compounds.

O 11.7 Mon 16:30 CHE 91

Cold plasma deoxidation of copper and iron surfaces — •VIKTOR UDACHIN¹, SEBASTIAN DAHLE², and WOLFGANG MAUS-FRIEDRICHS¹ — ¹Clausthal University of Technology, Clausthal-Zellerfeld, Germany — ²University of Ljubljana, Ljubljana, Slovenia

The removal of native oxides, which are present on metals in ambient atmosphere, is an important step in many industrial applications. Cold plasma meth-

ods, like dielectric barrier discharge (DBD) plasmas, have gained attention due to the high deoxidation efficiencies and relative simplicity of the setups. Several groups have indicated a reduction of copper oxygen layers using DBD hydrogen-containing plasmas, but no detailed information about reduction kinetics and limitations on different metal systems is available. In this study, we investigated the deoxidation effect of a DBD plasma in Ar/H_2 and Ar/SiH_4 atmospheres on natively oxidized Cu and Fe surfaces at 1000 hPa. We observed deoxidation effect on Cu already at 25 °C in both atmospheres. In contrast, reduction of iron oxide was obtained only at the surface temperature of 200 °C, showing an increase in the efficiency of the plasma-induced thermal treatment in comparison to thermal one. The chemical state of the samples and the kinetics of the reduction of oxides were studied via X-ray photoelectron spectroscopy (XPS). The morphology was characterized with the atomic force microscopy (AFM). By using optical emission spectroscopy (OES), the reactive species within the implemented DBD plasmas were described. Funded by the Deutsche Forschungsgemeinschaft (DFG, German Research Foundation) - Project-ID 394563137 - SFB 1368

O 11.8 Mon 16:45 CHE 91

Multiscale modeling and simulation of texture effects on the corrosion of stainless steel in aqueous media — •VAHID JAMEBOZORGI^{1,2}, KARSTEN RASIM³, and CHRISTIAN SCHRÖDER^{1,2} — ¹Bielefeld Institute for Applied Materials Research, Bielefeld University of Applied Sciences, 33619 Bielefeld, Germany — ²Faculty of Physics, Bielefeld University, 33615 Bielefeld, Germany — ³Miele & Cie. KG, Center for Materials (CFM), Carl-Miele-Straße 29, 33332 Gütersloh

Texture plays a crucial role in physical processes and properties of condensed matter as it is broadly highlighted in the literature. In this work we describe a robust methodology to investigate texture effects which does not suffer from common limitations of quantum based computational approaches in time and space but also can provide the same accuracy as atomistic calculations with orders of magnitude less computational costs. Our methodology is based on the finite element method (FEM) and utilizes 3D digital representations of multi grain microstructures. We demonstrate the efficiency of our approach by studying pitting corrosion in stainless steel. As reflected in literature the irregular geometry of pit expansion through pitting corrosion is mostly caused by texture. We found that the texture significantly affects the pitting corrosion rate and consequently causes various irregular pit growth patterns in granular microstructures. These results are consistent with our DFT and reactive force field molecular dynamics simulations which validates our suggested approach.

O 11.9 Mon 17:00 CHE 91

The role of aromaticity in the cyclization and polymerization of alkyne-substituted porphyrins on Au(111) — •NAN CAO¹, JONAS BJÖRK², EDUARDO CORRAL-RASCON¹, ZHI CHEN^{3,4}, MARIO RUBEN³, MATHIAS O. SENGE⁵, JOHANNES V. BARTH¹, and ALEXANDER RISS¹ — ¹Technical University of Munich, Germany — ²Linköping University, Sweden — ³Karlsruhe Institute of Technology, Germany — ⁴Shenzhen University, China — ⁵Institute for Advanced Study, TUM, Germany

Aromaticity is one of the most practical and versatile concepts for the assessment of the reactivity of organic molecules. However, in on-surface chemistry - where the interaction with the substrate can significantly alter the electronic and geometric structure of the adsorbates - the role of aromaticity is not understood. Here we investigate how aromaticity affects the reactivity of alkyne-substituted porphyrin molecules in cyclization and coupling reactions on a Au(111) surface. [1] We examine and quantify the regioselectivity of the reactions by scanning tunneling microscopy and bond-resolved atomic force microscopy at the single-molecule level. Our experiments show a substantially lower reactivity of carbon atoms that are stabilized by the aromatic diaza[18]annulene pathway of free-base porphyrins. The results are corroborated by density functional theory calculations, revealing a direct correlation between aromaticity and thermodynamic stability of the reaction products. These insights will help to design and understand reactions in on-surface chemistry and heterogeneous catalysis. 1. <https://doi.org/10.21203/rs.3.rs-1271465/v1>

O 12: Scanning Probe Techniques: Method Development I

Time: Monday 15:00–17:00

Location: GER 37

O 12.1 Mon 15:00 GER 37

Performance boundaries of piezoelectric friction-inertia walkers due to the choice of contact materials — •FELIX HUBER, SUSANNE BAUMANN, and SEBASTIAN LOTH — University of Stuttgart, Institute for Functional Matter and Quantum Technologies, Stuttgart, Germany

High precision positioners are an important tool to realize and automate cutting edge experiments. Piezoelectric friction-inertia walkers enable high accuracy movement on the millimeter scale with nanometer resolution, which makes them essential to realize scanning probe microscopes. The working principle of

these nanopositioners makes use of the friction-inertia principle [1]. Therefore, the choice of materials for the contact surfaces defines the performance limits and the reproducibility of stepwise motion. We use optical interferometry to determine the key performance parameters of a linear piezoelectric friction-inertia walker and test combinations of metallic and ceramic contact surface materials to improve the capabilities and reliability of high precision positioner devices.

[1] Z.M. Zhang et al. (2012) Int J Adv Manuf Technol 62, 669-685

O 12.2 Mon 15:15 GER 37

Surface tension measurement of microdroplets using AFM — •PRANAV SUDERSAN¹, MOHAMMAD HORMOZI², MAREN MÜLLER¹, SHUAI LI¹, HANS-JÜRGEN BUTT¹, and MICHAEL KAPPL¹ — ¹Max Planck Institute for Polymer Research, Mainz, Germany — ²Technical University of Darmstadt, Darmstadt, Germany

Surface tension is a physical property which is central to our understanding of wetting phenomena. One could easily measure liquid surface tension using commercially available tensiometers. However, these tensiometers are designed for bulk liquid volumes of the order of millilitres. In order to perform similar measurements on extremely small sample volumes in the range of femtoliters, Atomic Force Microscopy (AFM) is a promising tool. It was previously reported that by fabricating a special 'nanoneedle' shaped cantilever probe, a Wilhelmy-like experiment can be performed with an AFM. In our study, we carried out measurements on microscopic droplets with the AFM, but instead using standard pyramidal cantilever tips. The AFM tips were coated with a hydrophilic polymer brush, which reduced its contact angle hysteresis. Numerical simulations of a liquid drop interacting with a pyramidal geometry were used to calculate surface tension from the experimentally measured force. Our method eliminates the need for specially fabricated 'nanoneedle' tips, thus reducing complexity and cost of measurement, making it more suitable for widespread application.

O 12.3 Mon 15:30 GER 37

Modification of Fluid-FM Cantilevers for Studying Local Electrochemistry at Solid | Liquid Interfaces — •MATIN KARIMNIA¹ and TIMO JACOB^{1,2,3} — ¹Institute of Electrochemistry, Ulm University, Ulm, Germany — ²Helmholtz-Institute-Ulm (HIU), Ulm, Germany — ³Karlsruhe Institute of Technology (KIT), Karlsruhe, Germany

Local electrochemical measurements at the solid | liquid interface are of particular interest to gain deeper insights into the structure-activity relationship for electrochemical systems. Atomic force microscopy (AFM), can be effectively used for *in situ* monitoring of electrochemical processes, including adsorption, and metal deposition¹⁻⁴. For a better resolution of local phenomena, in this work, we present the use of Fluid-FM. Here the cantilever has a hollow microfluidic channel, allowing for probing electrochemical processes in the vicinity of the tip. This can be achieved by modifying the Fluid-FM cantilever to serve as a counter electrode in the electrochemical cell formed by the tip and the investigated substrate. The feasibility of the approach is demonstrated using a Au surface in contact with a diluted H₂SO₄ electrolyte. The influence of parameters such as the ratio between the surface area of the working electrode and counter electrode, as well as the volume of the electrolyte on the electrochemical performance is discussed.

[1] Seo, Yongho, *et al. Rep. Prog. Phys.* 71 (2007): 016101. [2] Oorschot, Ralph, *et al. Techn. Instrum.* 2 (2015): 1-11. [3] Zampardi, Giorgia, *et al. RSC Adv.* 5 (2015): 31166-31171. [4] Ossola, Dario, *et al. Phys. Rev. Lett.* 115 (2015): 238103.

O 12.4 Mon 15:45 GER 37

Analysis of DNA-origami-based calibration standard for AFM using artificial intelligence — •ZIBA AKBARIAN^{1,2}, TIM JOHANNES SEIFERT¹, BIRKA LALKENS², INGO BUSCH³, HARALD BOSSE³, and UTA SCHLICKUM^{1,2} — ¹Technische Universität Braunschweig, Braunschweig, Germany — ²Laboratory for Emerging Nanometrology (LENA), Braunschweig, Germany — ³Physikalisch Technische Bundesanstalt, Braunschweig, Germany

In this investigation, we focus on a nanoscale-standard reference system for calibrating atomic force microscopes utilizing DNA origami. To introduce measurable protrusions on the DNA origami nanostructure, markers at well-defined positions have been attached. To analyze the nanostructures as accurately as possible, we propose the use of artificial intelligence (AI) based image analysis techniques. Commonly, evaluation of the obtained data from atomic force microscopes is performed manually and includes preparatory steps to visualize images before analysis. As a result, the data analysis process requires a lot of time and always introduces not-avoidable errors. We present an AI-based measurement procedure using the YOLOv5 object detection and a semantic segmentation network trained on synthetic data to crop origami structures and pixelwise locate markers, respectively. This way, we can achieve a relative calibration accuracy in the range of 1% with an automatic data evaluation tool.

O 12.5 Mon 16:00 GER 37

Interplay between magnetic and electrostatic forces when imaging complex current carrying stripline geometries with Magnetic Force Microscopy — DENIS GOMAN, DHAVALKUMAR MUNGPARA, and •ALEXANDER SCHWARZ — Institute of Nanostructure and Solid State Physics, University of Hamburg, Jungiusstr. 11, 20355 Hamburg

Current carrying strip-lines have been oftentimes used to calibrate the sensitivity of magnetic tips to perform quantitative magnetic force microscopy, because for this system the Oersted field can be calculated analytically. In these investigations possible electrostatic contribution to the measured signal have been usually ignored.

Our research focuses on more complex strip-line arrangements with meander and spiral geometries, which are part of a magnetometer. Current dependent magnetic force microscopy (MFM) images clearly show that the measured signal possesses a large electrostatic contribution, which, in a peculiar fashion, depends on the tip location. We find that electrostatic contributions stem from three sources: (i) the contact potential difference between strip-line and substrate material, (ii) the potential drop along the strip-line and (iii) an edge effect related to the finite size of the tip apex. This knowledge helps to disentangle magnetostatic and electrostatic contributions even for rather complex strip-line geometries.

This work has been conducted as part of the OXiNEMS project, which has received funding from the European Union's Horizon 2020 research and innovation program under Grant Agreement No. 828784.

O 12.6 Mon 16:15 GER 37

Influence of Surfaces Charges and Trap States in KPFM Measurements of Doping Concentration — •THILO GLATZEL, URS GYSIN, and ERNST MEYER — University of Basel, Department of Physics, Klingelbergstr. 82, 4056 Basel, Switzerland

Kelvin Probe Force Microscopy is a scanning probe method for imaging the surface potential by atomic force microscopy. The surface potential is one of the most important surface properties and is correlated to e.g. the work function, surface dipoles, localized surface charges, and structural properties. It gives detailed information on the electrical properties and can be combined with optical and electrical excitation mechanisms providing additional properties like surface band bending and charge carrier mobilities. We will introduce the main concept and will briefly describe the major methods of operation. Based on the analysis of a Si super-junction device structures dopant profiling and the concept of surface photovoltage measurements will be introduced. The influence of local charge accumulation and trap states on these devices will be presented and the effect on the measured contact potential values will be discussed.

O 12.7 Mon 16:30 GER 37

Development of SNOM combining plasmonic picocavities with noncontact AFM — •AKITOSHI SHIOTARI¹, JUN NISHIDA², ADNAN HAMMUD¹, MARTIN WOLFF¹, TAKASHI KUMAGAI², and MELANIE MÜLLER¹ — ¹Fritz-Haber Institute of the Max-Planck Society, Berlin, Germany — ²Institute for Molecular Science, Okazaki, Japan

Scattering-type scanning near-field optical microscopy (s-SNOM) is a powerful tool to visualize the nanoscale optical response of sample surfaces. However, the resolution of conventional s-SNOM is usually limited by thermal instabilities of the tip-apex structure and the weak light intensities scattered from small volumes. On the other hand, it has been shown recently that light can be confined to the atomic scale using plasmonic picocavities. Here we demonstrate the development of plasmonic s-SNOM based on noncontact atomic force microscopy (nc-AFM) under the low-temperature and ultrahigh-vacuum conditions. A quartz tuning fork sensor with a Ag tip sharpened by focused ion beam milling enables precise control of the subnanometer tip-sample gap under illumination with visible laser light. The extremely high field enhancement and localization of light in the picocavity enhances the scattered light intensity and allows to image the optical response of samples at 1 nm resolution. The combination of ncAFM with plasmonic picocavities has high potential for atomic resolution optical imaging of various materials, including insulators.

O 12.8 Mon 16:45 GER 37

Polarization-sensitive scanning near-field optical microscopy — •FELIX G. KAPS^{1,2}, SUSANNE C. KEHR^{1,2}, and LUKAS M. ENG^{1,2} — ¹Technische Universität Dresden, Germany — ²Würzburg-Dresden Cluster of Excellence - EXE 2147 (ct.qmat), Dresden, Germany

Scanning near-field optical microscopy (SNOM) enables nanoscopic optical surface characterization at visible, infrared, and THz wavelengths [1], with applications to various research fields e.g. 2D materials, semiconductors, and in biology [2]. Here, typically the pure out-of-plane field components are considered. For resonant samples however, near-field excitation of all vectorial components becomes possible [3], enabling the full polarization analysis at the nanometer length scale.

In the work presented here, we examine the polarization-dependent near-field response of both non-resonantly (Au) and resonantly (SiC) excited samples at around 10.6 μm . By varying the incident linear polarization direction from s- to p-polarization, we are able to capture differently scattered near-field contributions, showing up in characteristic lobe-shaped polarization signatures. These results are confirmed by theoretical simulations, where we combine the analytic dipole model [5] and the Jones matrix formalism. Comparing the experiment with our simulations, we are able to disentangle the near-field's vectorial contributions via spectral and polarization analysis.

[1] T. Nörenberg *et al.*, *ACS Nano*, **article ASAP** (2022)

[2] T.V.A.G. de Olivera *et al.*, *Adv. Mater.* **33**, 2005777 (2021).

[3] H. Aminpour *et al.*, *Opt. Express* **28**, 32316 (2020)

O 13: Focus Session: Ion Beam Interaction with Surfaces and 2D Materials II

Time: Monday 15:00–17:15

Location: GER 38

Topical Talk

O 13.1 Mon 15:00 GER 38

Space weathering of planetary surfaces — •PETER WURZ — Physics Institute, University of Bern, Bern, Switzerland

The surfaces of planetary objects in interplanetary space are subjected to external agents modifying their chemical and mineralogical composition and causing removal of material from these surfaces into interplanetary space. These external agents are the flow of ions and electrons from the Sun (the solar wind), currents of magnetospheric systems, energetic particles from outer space, impacting micro-meteorites, and photons from the Sun. In particular, the ion precipitation on these surfaces is of high interest. The removal of surface material, e.g., the ion-induced sputtering, contributes atoms to the interplanetary particle population, which eventually end up as ions in the interplanetary plasma flow. The changes in composition of the surface are also of interest because they affect the spectroscopic appearance of these surfaces. Since most of the planetary objects are only studied via telescopic observations, relating the spectroscopic appearance of the space-weathered surface to the underlying material is of high importance.

O 13.2 Mon 15:30 GER 38

Quantifying the erosion of the lunar surface due to solar wind sputtering — •JOHANNES BRÖTZNER¹, HERBERT BIBER¹, NOAH JÄGGI², PAUL STEFAN SZABO³, DANIEL PRIMETZHOFFER⁴, ANDRÉ GALLI², PETER WURZ², and FRIEDRICH AUMAYR¹ — ¹TU Wien, Institute of Applied Physics, Vienna, Austria — ²University of Bern, Physics Institute, Bern, Switzerland — ³University of California, Space Sciences Laboratory, Berkeley, USA — ⁴Uppsala University, Department of Physics and Astronomy, Uppsala, Sweden

Without a protective atmosphere nor its own magnetic field, the lunar surface is subjected to bombardment by the solar wind, a stream of mostly H⁺ and He²⁺ ions originating from the Sun. Combined with other effects, this leads to the ejection of material and subsequently the formation of a tenuous gas layer around the Moon, the exosphere. Understanding its formation and coupling to surface properties could potentially enhance our knowledge of not only the Moon, but also other rocky bodies in the solar system.

Previous attempts at modelling the creation of an exosphere used sputter yield values of limited validity for the sputtering contribution to this process – data for relevant minerals were simply not available. While in the past few years, investigations using adequate analogue materials have progressed, we present both experimental and numerical results for the irradiation of H⁺ and He⁺ ions on samples prepared from actual lunar material, gathered during the Apollo 16 mission in 1972.

O 13.3 Mon 15:45 GER 38

Sputtering from Sinusoidal Surfaces: Monte Carlo Simulations and Comparison to Analytical Results — •GERHARD HOBLER¹ and R MARK BRADLEY² — ¹Institute of Solid-State Electronics, TU Wien, AUSTRIA — ²Departments of Physics and Mathematics, Colorado State University, Fort Collins, CO 80523, USA

Sputtered surfaces are virtually never planar at the nanoscale, and so there has been longstanding interest in the spatially averaged sputter yield \bar{Y} that results when a broad ion beam is incident on a surface with a nontrivial morphology. Considering the simple case of sinusoidal surfaces, the aim of the present study is (i) to investigate the contributions of redeposition and secondary sputtering to \bar{Y} , and (ii) to test a recently developed theory [1] that predicts \bar{Y} for small amplitudes from the angular dependent sputter yield of a flat surface. For the simulations we use the Monte Carlo binary collision code IMSIL [2]. Apart from expected results on redeposition and sputtering by reflected ions, we also find that sputtering by recoils that are sputtered and then strike the surface may compensate for a sizable amount of redeposition. The simulations confirm the theory's prediction that \bar{Y} may either increase or decrease with amplitude depending on the incidence angle. They also confirm the theory's prediction that redeposition scales with the square of the amplitude over the wavelength, and are generally in excellent quantitative agreement with theory.

[1] R.M. Bradley, G. Hobler, submitted for publication.

[2] G. Hobler, Nucl. Instrum. Meth. B 96 (1995) 155.

O 13.4 Mon 16:00 GER 38

MeV-SIMS: mass spectrometry with ultra-fast projectiles — •LARS BREUER¹, TOBIAS HECKHOFF¹, DAVID THEUNER¹, FRIEDER KOCH², and ANDREAS WUCHER¹ — ¹Universität Duisburg-Essen — ²GSI Helmholtzzentrum für Schwerionenforschung

While secondary ion mass spectrometry has become a standard tool in surface analysis, it still offers multiple challenges. While ionization probabilities are usually fairly low and may be altered by the chemical environment of the target surface, fragmentation of molecules introduces even more experimental challenges. Therefore, better understanding of the underlying processes and methodology improvement is an ongoing topic of research. Here, we present strategies devel-

oped to shed light on the fundamental processes in sputtering of different materials from metals and insulators to organic samples by tuning the contribution of nuclear and electronic sputtering. For that purpose, a time-of-flight spectrometer has been coupled to the M-Branch of the UNILAC at GSI in Darmstadt, using swift heavy ions as projectiles. By laser post-ionization not only secondary ions are accessible but their neutral counterparts as well to enable us to gain insight into sputtering and ionization under extreme conditions.

O 13.5 Mon 16:15 GER 38

A new material science target station for swift and highly charged ions at CRYRING@ESR — •KEVIN VOMSCHEE¹, MICHAEL WAGNER², NILS ULRICH^{2,3}, FRIEDER KOCH², SADRA KOUR¹, ANDRÉ MAAS¹, CHRISTINA TRAUTMANN^{2,3}, MARIKA SCHLEBERGER¹, and LARS BREUER¹ — ¹Univ. Duisburg-Essen — ²GSI Helmholtzzentrum für Schwerionenforschung — ³Technische Univ. Darmstadt

This contribution describes the new target station MSS@CRYRING ("Material Science Station at CRYRING") operated at GSI. The new setup at the storage ring CRYRING allows the irradiation of samples with highly charged ions up to completely stripped uranium (U⁹²⁺) with full control over the kinetic energy of the projectile between keV and GeV. This allows the investigation of the specific effect of the kinetic and potential energy. The latter is dissipated in a very shallow volume upon impact while at high kinetic energies the entire bulk material is irradiated.

We report on results from the first beam times using the extracted beam at the new target station. For testing the setup, polymer films were irradiated with ¹⁰⁷Ag⁴⁷⁺ at a kinetic energy of 5.9 MeV/u. Applying track etching techniques the number of ions per cm² was analyzed using scanning electron microscopy. Comparing these results with the number of ions extracted from the storage ring as deduced from a DC-transformer and a Schottky detector gives an ion transmission of 53.7 % and a maximum flux of 3 · 10⁷ cm⁻² per pulse.

O 13.6 Mon 16:30 GER 38

Compact Electron Beam Ion Source — •DANIEL THIMA¹, MATTHIAS WERL¹, GABRIEL LUKAS SZABO¹, PAUL-FRIEDMAR LAUX², MIKE SCHMIDT², GÜNTER ZSCHORNACK², and RICHARD ARTHUR WILHELM¹ — ¹TU Wien, Institute of Applied Physics, Vienna, Austria — ²D.I.S Germany GmbH, Dresden, Germany

In many modern fields of research, such as plasma and atomic physics, material science or astrophysics, highly charged ions play an important role. Research with highly charged ions relies strongly on stable ion sources, providing long-term operation with the low output currents in standard devices. Typically, these devices are heavy, stationary machines such as electron cyclotron resonance ion sources or electron beam ion sources (EBIS), sometimes even relying on cryogenic magnetic systems.

Gaining portability by downsizing an EBIS has been pursued recently by a commercial supplier. With only 30 cm in length and using in-vacuum mounted magnets, the resulting prototype EBIS fits onto almost any ultra high vacuum chamber, needing only a single CF40 port. An included Wien filter allows separation of produced ions based on their charge state and mass.

We are currently characterising this compact EBIS in our laboratory, focusing on ion output current. Here, we present our setup and the results of first measurements.

O 13.7 Mon 16:45 GER 38

On the path to ion based pump-probe experiment: generating picosecond keV Ne⁺ ion pulses from a cooled supersonic gas beam — •LUKAS KALKHOFF, MARIKA SCHLEBERGER, KLAUS SOKOLOWSKI-TINTEN, ANDREAS WUCHER, ALEXANDER GOLOBEK, and LARS BREUER — University Duisburg-Essen, Duisburg, Germany

The dynamics triggered by the impact of an ion onto a solid surface has been explored mainly by theoretical modeling or computer simulation to date. Results indicate that the microscopic non-equilibrium relaxation processes triggered by the interaction of the ion with the solid occur on a (sub-)picosecond time scale. A suitable experimental approach to these dynamics therefore requires a pump-probe method with an appropriate time resolution. Our experiments have successfully used laser photoionization of a supersonic beam of cooled noble gas atoms at $T_{atoms} \approx 4$ K in combination with a Wiley-MacLaren ion buncher. The measured distribution of the arrival time of individual Ne⁺ ions impinging on the surface of a fast microchannel plate with a kinetic energy of 4 keV gives a full width at half maximum of the ion pulse of $t_{ion} = 130$ ps. A more detailed analysis shows that this pulse width is only an upper limit related to the detection limit of the electronics. The true pulse width results from extrapolation of our data and is $t_{ion} = 18 \pm 4$ ps. This opens the door to pump-probe experiments with keV ions with a time-resolution in the picosecond range.

O 13.8 Mon 17:00 GER 38

Generation of pulsed ions using ultrafast electrons — MARIUS CONSTANTIN CHIRITA MIHAILA, GABRIEL LUKAS SZABO, ALEXANDER SAGAR GROSSEK, and RICHARD ARTHUR WILHELM — TU Wien, Institute of Applied Physics, 1040 Vienna, Austria

Ultrafast physics is a very active research field where high temporal and spatial resolution provides unprecedented structural information in material science.

Here, we describe the development of a new technique that allows the creation of pulsed ions using ultrafast electrons. The general technique of using picosecond ion pulses to study novel time-resolved processes in materials will be hugely

impactful and aims at investigating ultrafast phenomena that are intractable with pump-probe measurements using pulsed electrons and lasers. However, the use of pulsed ions has been limited by the complexity of achieving short pulse lengths at the sample plane.

The experimental setup features a Ti: Sapphire laser that triggers femtosecond electron pulses from a low-workfunction cathode. The pulsed electrons then propagate through a miniaturized ion source and generate pulsed ions. Current challenges of preserving a short ion pulse length upon transport to the sample plane and prospects of pump-probe measurements with ultrafast ions are discussed.

O 14: Nanostructures at Surfaces (joint session O/CPP)

Time: Monday 15:00–17:45

Location: GER 39

O 14.1 Mon 15:00 GER 39

Tailoring Stone-Wales transitions in Ti_2O_3 honeycombs with alkaline earth metals — MARTIN HALLER, STEFAN FÖRSTER, and WOLF WIDDRA — Martin-Luther-Universität Halle-Wittenberg, Institute of Physics, Von-Danckelmann-Platz 3, 06120 Halle, Germany

In 2013 the first 2D oxide quasicrystal (OQC) has been discovered in thin Ba-Ti-O films [1]. It shows a twelvefold diffraction pattern that is incompatible with lattice periodicity. In real space it can be described by squares, triangles and rhombus tiles. Just recently, the atomic structure has been solved [2,3]. The essence are Ti_nO_n ring structures with $n = 4, 7$ and 10 . These evolve by Stone-Wales transitions from a pure honeycomb network [4]. The transformations are stabilized by alkaline earth metal ions and their associated dipole and can be controlled by the alkaline earth metal coverage. Here we investigate the basic steps of individual Stone-Wales transformations with LEED and STM for ultra-low coverages deposited onto a Ti_2O_3 honeycomb on a close-packed metal surface. The transformations to ring structures with $n = 4, 5$ and 7 are monitored and related to the formation of square and triangle tilings.

[1] S. Förster et al., *Nature* 502, 215 (2013)[2] S. Schenk et al., *Nat. Comm.*, accepted, (2022)[3] E. Cockayne et al., *Phys. Rev. B* 93, 020101 (2016)[4] S. Wang et al., *Nanoscale* 11, 2412 (2019)

O 14.2 Mon 15:15 GER 39

Formation of an extended quantum dot array driven and auto protected by an atom thick h-BN layer — JOEL DEYERLING¹, IGNACIO PIQUERO-ZULAICA¹, MUSTAFA A. ASHOUSH², KNUD SEUFERT¹, MOHAMMAD A. KHER-ELDEN², ZAKARIA M. ABD EL-FATTAH², and WILLI AUWÄRTER¹ — ¹Physics Department E20, Technical University of Munich, James-Frank-Straße 1, D-85748 Garching, Germany — ²Physics Department, Faculty of Science, Al-Azhar University, Nasr City, Cairo E-11884, Egypt

Fabricating nanoarchitectures to confine two dimensional nearly free electrons on crystalline surfaces by tip manipulation with a scanning tunneling microscope (STM) or by applying supramolecular chemistry principles yields diverse artificial electronic structures. These electronic states are prone to scattering by adsorbates making them extremely susceptible to the environment. Nonetheless, little attention has been given to their protection, e.g., by an inert overlayer.

Here, we show that a quasi-hexagonal CuS nanoporous network can be formed at the h-BN/Cu(111) interface by thermally-induced sulfur segregation from the Cu(111) bulk. The growth and structure is characterized by STM and X-ray photoemission spectroscopy. We demonstrate by employing STM and scanning tunneling spectroscopy that within the pores of the network the surface state of Cu(111) as well as the image potential states of h-BN/Cu(111) are confined, effectively creating arrays of quantum dots with well-defined sizes that are covered by an inert h-BN overlayer.

O 14.3 Mon 15:30 GER 39

First-principles investigation of doped borophene quantum dots as donor materials for solar cell applications — RACHANA YOGI, VAISHALI ROONDHE, and ALOK SHUKLA — Department of Physics, Indian Institute of Technology Bombay, Mumbai 400076, India

Because of fast-depleting fossil fuel reserves, there is an urgent need for harvesting alternative sources of energy. We present a first-principles atomistic study of borophene quantum dots (BQDs) B35 and B36 for their possible utilization in solar-cells. The pristine-BQDs are doped by C, N, and O atoms, and find that they have bowl-like structures in the ground state. The electronic and optical properties of pristine-BQDs, and doped-BQDs are investigated. The chemical potentials of several of these BQDs are slightly higher than that of popular solar-cell acceptor system PC71BM, they will act as electron donors in a PC71BM-based solar-cell. The calculated values of the open-circuit voltage corresponding to PC71BM and BQD-based device indicate efficient electron injection from the BQDs to PC71BM. O-doped B36-QD and B35-QD have the highest value of short-circuit current density attributed to their reduced HOMO-LUMO gap and

high HOMO energy levels as compared to all other considered doped systems further enhancing the photoelectric properties. The power conversion efficiency of doped-BQDs exhibits significant improvement. The efficiency of O-doped B36-QD is maximum due to its high electron injection rate in PC71BM. Present calculations show that adding a foreign atom in BQD makes it a suitable candidate for high-performance solar-cells.

O 14.4 Mon 15:45 GER 39

Electrospray Depositions of a Spin-Crossover Active Iron(II) [2×2] Grid Complex on Ag(111) with Different Landing Energies — DENNIS MEIER¹, BENEDIKT SCHOOF¹, JOACHIM REICHERT¹, NITHIN SURAYADEVARA², ANDREAS WALZ¹, ANNETTE HUETTIG¹, HARTMUT SCHLICHTING¹, MARIO RUBEN², ANTHOULA C. PAPAGEORGIOU^{1,3}, and JOHANNES V. BARTH¹ — ¹Technical University of Munich, Germany — ²Karlsruhe Institute of Technology, Germany — ³National and Kapodistrian University of Athens, Greece

Chiral spin-crossover (SCO) complexes are intriguing building blocks for innovative magneto-optical nanoarchitectures.¹ Such an Fe(II) [2×2] grid complex was deposited in ultra-high vacuum with electrospray controlled ion beam deposition (ES-CIBD)² on Ag(111) and investigated by scanning tunnelling microscopy. Low landing energy (< 3 eV/z) resulted in clusters and single molecules. Higher landing energies (> 3 eV/z) led to coordination bond cleavage and a rich variety of self-assembled surface networks forming from the grid fragments. Applying established on-surface synthesis methodology employing the possible constituents of these networks (ligands and Fe atoms) reproduced only a part of them. It is thus proposed that ES-CIBD provides an unexpected route to novel on-surface coordination network synthesis.

[1] N. Suryadevara et al. *Chem. Eur. J.* 2021, 27, 15172.[2] A. Walz, K. Stoiber, A. Huettig, H. Schlichting, J. V. Barth, *Anal. Chem.* 2022, 94, 7767.

O 14.5 Mon 16:00 GER 39

Giant confinement of surface electrons in a two-dimensional metal-organic porous network — LU LYU¹, TOBIAS EUL¹, WEI YAO¹, ZAKARIA M. ABD EL-FATTAH², MOSTAFA ASHOUSH², IGNACIO PIQUERO-ZULAICA³, JOHANNES V. BARTH³, MARTIN AESCHLIMANN¹, and BENJAMIN STADTMÜLLER^{1,4} — ¹Department of Physics, University of Kaiserslautern, Germany. — ²Physics Department, Faculty of Science, Al-Azhar University, Egypt. — ³Physics Department E20, Technical University of Munich, Germany — ⁴Institute of Physics, Johannes Gutenberg University Mainz, Germany.

Two-dimensional metal-organic porous networks (2D-MOPNs) are highly flexible nano-architectures for exploring the quantum confinement of surface electrons on noble metals. So far, 2D-MOPNs have been predominantly studied for the confinement of occupied Shockley-type surface states (SS). In contrast, the confinement of excited surface states, such as image potential states (IPSS), remains elusive. In this work, we apply two-photon photoemission to investigate the band dispersion of the first image-potential state ($n = 1$ IPS) in a Cu-T4PT nanoporous network on Cu(111). We find the formation of a Bloch-like band structure with a substantially increased effective band mass of the IPS ($> 150\%$). In contrast, the effective band mass of the SS remains almost unchanged ($< 3\%$). This band renormalization of the IPS can be attributed to the spatial distribution of its charge density perpendicular to the surface, which reveals the highest density at the vertical adsorption position of the T4PT backbone. This coincidence is responsible for the giant confinement.

O 14.6 Mon 16:15 GER 39

Modification of Single-Layer Organometallic Networks: from Ag-Bridged to Cu-Bridged Alkynyl Metal-Alkynyl Linkages on Ag(111) Surfaces — WENCHAO ZHAO, FELIX HAAG, IGNACIO PIQUERO-ZULAICA, YI-QI ZHANG, FRANCESCO ALLEGRETTI, BIAO YANG, and JOHANNES V BARTH — Physics Department E20, Technical University of Munich, 85748 Garching, Germany

The metal-exchange reaction, is of importance for the advanced preparation of functional metal-organic frameworks for various applications[1]. Notably,

building two-dimensional organometallic networks (OMNs), can provide versatile nanoarchitectures for potential application in nanodevice[2,3]. Although various OMNs have been constructed with molecular building blocks by abstracting surface metal atoms, the degree of success is often individual and substrate-dependent. Thus metal-exchange reactions hold promise for multiple production by modification and functionalization of OMN templates. Here, we demonstrate the modification of a single-layer OMN by metal-exchange reaction. By introducing external Cu atoms into the alkynyl-Ag OMN[3], we successfully synthesized in situ a highly ordered alkynyl-Cu OMN on a Ag(111) surface. While maintaining a similar lattice periodicity and pore morphology, it possesses higher thermal stability, guaranteeing higher robustness for possible applications. Reference. 1. M.-M. Xu et al., *Coord. Chem. Rev.* 2020, 421, 213421. 2. D. Ecija et al., *Acc. Chem. Res.* 2018, 51, 365-375. 3. Y.-Q. Zhang et al., *J. Am. Chem. Soc.* 2019, 141, 5087-5091

O 14.7 Mon 16:30 GER 39

Structure Formation in Ceramic Thin Films with Hybrid Molecular Dynamics — •NYDIA ROXANA VARELA ROSALES and MICHAEL ENGEL — Institute for Multiscale Simulation, University of Erlangen-Nürnberg, Cauerstraße 3, 91058 Erlangen, Germany

How can we model and predict ceramic thin films? Highest accuracy is achieved with ab-initio quantum mechanical methods. But these methods are not suitable for large systems including their phase transformations. Atomistic modeling with molecular dynamics and Monte Carlo simulations reaches large system sizes but require sophisticated tailored interaction potentials. Here, we develop and apply a coarse-grained simulation method for structure formation in thin films. Our method considers the chemical bond network of the ceramics explicitly to simplify the complexity of the simulation and to reach high simulation speeds and large system sizes. Of particular interest are (quasi-)crystalline ceramic thin films recently discovered in experiments of (Ba/Sr)-Ti-O perovskites. Solely by considering the extrinsic topology of the tiles and utilizing a harmonic interaction potential, we reproduce the appearance of approximants of the dodecagonal quasicrystals, which was also predicted by ab-initio simulations. Our work highlights the role of bond network topology in understanding complex thin film structures without a need for reliance on quantum simulation methods.

O 14.8 Mon 16:45 GER 39

A Holistic Characterisation of Bi Thin Films on Au(111) — •PABLO VEZ-ZONI VICENTE¹, TOBIAS WEISS¹, MARC GONZALEZ-CUIXART⁴, DENNIS MEIER¹, BENEDIKT KLEIN², DAVID DUNCAN², EZEQUIEL TOSI³, PAOLO LACOVIG³, SILVANO LIZZIT³, JOHANNES BARTH¹, PETER FEULNER¹, and FRANCESCO ALLEGRETTI¹ — ¹Physics Department E20, Technische Universität München, Germany — ²I09 beamline, Diamond Light Source, United Kingdom — ³SuperESCA beamline, Elettra Synchrotron, Italy — ⁴IMDEA Nanociencia, Spain

We present a comprehensive analysis of the long-range ordered, coverage-dependent phases of Bi epitaxially grown on a Au(111) surface in UHV, from the sub-monolayer ($\sqrt{37} \times \sqrt{37}$)R25.3° Kagome lattice up to few-layer Bi(110) thin films. Particular focus is devoted to the sub-monolayer, high-coverage ($p \times \sqrt{3}$) phase, paving the way to its use as a buffer layer for epitaxial growth with tunable geometry and low electronic interaction.

Our work clarifies and expands the current literature reports, specifically on the complex ($p \times \sqrt{3}$) phase. The wide range of analysis techniques used, including Low-Energy Electron Diffraction (LEED), Photo-Electron Spectroscopy (XPS, UPS), Temperature Programmed Desorption (TPD), Scanning Tunneling Microscopy and Spectroscopy (STM, STS), and X-ray Standing Waves (XSW), yields an unprecedented understanding of the system's structural and electronic properties.

O 14.9 Mon 17:00 GER 39

Analytical electron microscopy of nanostructured vanadium dioxide — •VLASTIMIL KRÁPEK¹, JAN KRPEŇSKÝ^{1,2}, MICHAL HORÁK¹, KATARÍNA ROVENSKÁ¹, PETER KEPIČ¹, TOMÁŠ ŠIKOLA¹, FILIP LIGMAJER¹, and ANDREA KONEČNÁ¹ — ¹Brno University of Technology, Czechia — ²CIC nanoGUNE, San Sebastián, Spain

Vanadium dioxide (VO₂) is a phase-changing material exhibiting temperature-induced metal-insulator transition (MIT) around 340 K. A rather low transition temperature makes VO₂ a suitable material for active nanophotonics, e.g., switchable optical metasurfaces. Such applications require nanostructuring of VO₂ thin films. Here we study the possibility to employ focused ion beam (FIB) milling for the nanofabrication and its impact on the properties of resulting nanostructures.

Taking the VO₂ thin film with experimentally verified MIT, we utilized FIB milling with Ga ions to fabricate V-shaped lamella of the thickness between 0 and 250 nm, which was subsequently transferred onto a heating chip for transmission electron microscopy and analyzed with analytical electron microscopy: high-resolution imaging, energy-dispersive X-ray spectroscopy, and temperature-dependent electron energy loss spectroscopy. We observed a porous character of the pristine material, a coexistence of several crystal structures, negligible contamination with Ga ions, and a variation of stoichiometry with the thickness of the lamella, with the thinnest parts composed of VO and V₂O₃.

O 14.10 Mon 17:15 GER 39

Tuning Nanoporous Au Film Formation via High Voltage Electrolysis — •EVELYN ARTMANN¹, LUKAS FORSCHNER¹, KONSTANTIN M. SCHÜTTLER², MOHAMMAD AL-SHAKRAN¹, TIMO JACOB¹, and ALBERT K. ENGSTFELD¹ — ¹Institute of Electrochemistry, University of Ulm, Germany — ²Institute of Surface Chemistry and Catalysis, University of Ulm, Germany

Nanoporous Au (NPG) films have different properties compared to the bulk material, which opens up new areas of application, such as (electro)catalysis. Usually, NPG films are prepared by dealloying. One disadvantage of this method is that residues of the precursor alloy guest metal can remain in the resulting NPG film, which can have a decisive influence on the electrocatalytic activity of the NPG film.

In this work we report on the preparation of NPG films by high voltage electrolysis (*Chem. Phys. Chem.*, 22 (2021) 2429). In this process, a Au oxide film is first formed on the Au substrate by applying a high positive voltage (between 100 and 540 V), which can subsequently be reduced to NPG. The Au oxide as well as NPG films were characterized by electrochemical methods, as well as (cross-section) SEM and XPS measurements.

Possibilities to selectively modify the resulting NPG films by tuning experimental parameters such as the applied voltage, and electrolyte temperature during HV electrolysis, or the electrolysis time, were systematically investigated. The influence of the reduction method (electrochemical or by H₂O₂) on the final film structure is discussed.

O 14.11 Mon 17:30 GER 39

Evolution of the Si-Au alloy: from the gold (110) substrate to silicon nanoribbons — •EKATERINA TIKHODEVA¹, MARÍA E DÁVILA², PAOLA DE PADOVA³, GAY LE LAY⁴, MARINA BAIDAKOVA⁵, EVGENIYA LOBANOVA⁵, JAIME SANCHEZ-BARRIGA⁶, DMITRII SMIRNOV⁶, and MANUEL IZQUIERDO¹ — ¹European XFEL, Schenefeld, Germany — ²CSIC, Madrid, Spain — ³Consiglio Nazionale delle Ricerche, Rome, Italy — ⁴Aix-Marseille Université, Marseille, France — ⁵Saint Petersburg, Russia — ⁶Helmholtz-Zentrum Berlin, Berlin, Germany

The development of the Si-Au alloy was investigated on the path from the gold single crystal surface to silicon nanoribbons (SiNR). Si sub-monolayers were deposited on the missing row reconstructed Au(110) substrate. At various stages of evaporation, low-energy electron diffraction (LEED) patterns were recorded to refine the surface geometry. The arrangement of the Si atoms has been correlated with the missing row orientation. The recovery of the Au(1x1) reconstruction, as well as the gradual transition from surface alloy to SiNRs were explored. In parallel with LEED, photoelectron spectroscopy was used to clarify the atom distribution. The profiles of the Au 4f and Si 2p core levels were deconvoluted and analyzed at all stages of Si deposition. The appearance of a new low kinetic energy component was noticed in the Au 4f spectra. It is related to the Si-Au bond and indicates a strong interaction between them. The Si core levels exhibit up to three components corresponding to the different chemical environments.

O 15: Spins on Surfaces at the Atomic Scale II

Time: Monday 15:00–18:00

Location: REC C 213

O 15.1 Mon 15:00 REC C 213

Electron-spin resonance atomic force microscopy — •LISANNE SELLIES, RAFFAEL SPACHTHOLZ, PHILIPP SCHEUERER, and JASCHA REPP — University of Regensburg, Regensburg, Germany

Recently, we combined the high energy resolution of electron spin resonance (ESR) with the spatial resolution offered by atomic force microscopy (AFM). This ESR-AFM technique relies on driving electron spin transitions between the

non-equilibrium triplet state levels of a single molecule. Since these triplet states typically have different lifetimes, driving such transitions modifies the overall triplet lifetime [1,2], which can be detected by an electronic pump-probe scheme [3].

ESR-AFM allows to measure ESR signals with a sub-nanoelectronvolt energy resolution, as we demonstrated for pentacene on thick NaCl films. Thereby, molecules only differing in their isotopic configuration can be distinguished.

Moreover, due to the minimally invasive nature of the ESR-AFM technique, the electron spins of pentacene can be coherently manipulated over tens of microseconds. After introducing ESR-AFM, recent results obtained by this technique will be presented.

References: [1] Köhler et al. (1993). *Nature*, 363(6426), 242-244. [2] Wrachtrup et al. (1993). *Nature*, 363(6426), 244-245. [3] Peng et al. (2021). *Science*, 373(6553), 452-456.

O 15.2 Mon 15:15 REC C 213

Coherent spin dynamics in a single atom hyperfine system — •LUKAS VELD-MAN, LAËTITIA FARINACCI, EVERT STOLTE, MARK CANAVAN, and SANDER OTTE — TU Delft, Delft, The Netherlands

The combination of electron spin resonance (ESR) with scanning tunneling microscopy (STM) has opened up the possibility to investigate the interaction between electrons and nuclei in individual atoms on a surface [1]. Recently, we showed that for TiH atoms on MgO the hyperfine interaction is highly anisotropic and contains information on the groundstate orbital of the atom [2]. In this work, we go to the low field regime where electron and nuclear states hybridize. We use DC voltage pulses [3] to spin pump both the electron and the nuclear spin [4]. We measure the coherent oscillations of the electron spin driven by the hyperfine interaction. These measurements open the door to controlled spin manipulation of nuclear spins in single atoms.

[1] Willke et al. *Science* 362 (2018)

[2] Farinacci et al. *Nano Letters* (2022)

[3] Veldman et al. *Science* 372 (2021)

[4] Yang et al. *Nature Nanotechnology* 13 (2018)

O 15.3 Mon 15:30 REC C 213

Quantum coherence of single atomic $S = 1/2$ spins on ultra-thin insulating layers — HONG BUI^{1,2}, WE-HYO SEO^{1,2}, YU WANG^{1,2}, ANDREAS HEINRICH^{1,2}, and •SOO-HYON PHARK^{1,2} — ¹Center for Quantum Nanoscience, Institute for Basic Science, Seoul 03760, Korea — ²Department of Physics, Ewha Womans University, Seoul 03760, Korea

A scanning tunneling microscope (STM), when combined with electron spin resonance (ESR), provides a solid-state platform of atomic scale spin qubit. However, its quantum coherence is considerably limited by couplings with metallic substrate and tunneling electrons. Here we report a study on the quantum coherence of single Ti atomic spins ($S = 1/2$) on two- (2ML) and three- (3ML) monolayer-thick MgO on Ag(100) using pulsed-ESR equipped in a STM at 0.4 K. We were able to drive the coherent rotations of the spin on the 3ML-MgO with a Rabi rate (Ω) up to 100 MHz, which is an order faster than that on the 2ML-MgO. Coherence time (T_2) from Hahn-echo measurement revealed the role of the tunneling electrons, resetting the state of a Ti spin with a probability of 0.15/electron, which is the same for Ti spins on both 2ML- and 3ML-MgO. Of more interesting is the zero current T_2 of 2 microsec on 3ML-MgO, about 5 times longer than that on 2ML-MgO, emphasizing the importance of decoupling the spin from the metallic substrate as well as tunneling electrons. Such considerable improvements in Ω and T_2 are promising for high fidelity quantum gate operations to a Ti spin qubit, further brightening a way to raise the on-surface spin qubits on a stage of the quantum-coherent applications.

O 15.4 Mon 15:45 REC C 213

Certifying entanglement of spins on surfaces using ESR-STM — •YELKO DEL CASTILLO^{1,2} and JOAQUÍN FERNÁNDEZ-ROSSIER¹ — ¹International Iberian Nanotechnology Laboratory (INL), Av. Mestre José Veiga, 4715-330 Braga, Portugal — ²Centro de Física das Universidades do Minho e do Porto, Universidade do Minho, Campus de Gualtar, 4710-057 Braga, Portugal

We propose a protocol to certify the presence of entanglement in artificial on-surface atomic and molecular spin arrays using electron spin resonance carried by scanning tunnel microscopes (ESR-STM). We first generalize the theorem that relates global spin susceptibility as an entanglement witness to the case of anisotropic Zeeman interactions, relevant for surfaces. We then propose a method to measure the spin susceptibilities of surface-spin arrays combining ESR-STM with atomic manipulation. Our calculations show that entanglement can be certified in antiferromagnetically coupled spin chains using state of the art spectral resolution of ESR-STM magnetometry.

O 15.5 Mon 16:00 REC C 213

Ultrafast dynamics of magnetic adatoms on MgO — •LUKAS ARNHOLD¹, DARIA SOSTINA², NICOLAJ BETZ¹, SUSANNE BAUMANN¹, PHILIP WILLEKE², and SEBASTIAN LOTH¹ — ¹University of Stuttgart, Institute for Functional Matter and Quantum Technologies, Stuttgart, Germany — ²Karlsruhe Institute of Technologies, Physikalisches Institut, Karlsruhe, Germany

The utilization of single magnetic atoms as qubits requires detailed understanding of their energy levels and the associated time-scales, ideally also those of excited states. Ever since coherent driving of a single spin in the junction of a scanning tunneling microscope has been shown [1], the technique of ESR-STM has been established and used for example to perform qubit operations, as well as, to address multiple qubits [2]. Besides the technique of electron spin resonance, quantum stochastic resonance measurements offer new insights into a system's

energy transition cycles, or in other words, it's associated time-scales [3]. Applying this measurement scheme onto ESR active adatoms on a MgO substrate, gives access to additional manipulation pathways and allows for further understanding and mastery of coherent spin manipulation.

[1] Baumann, Susanne et al. 'Electron paramagnetic resonance of individual atoms on a surface.' *Science* 350 (2015): 417 - 420.

[2] Phark, Soo-Hyon et al. 'Double Electron Spin Resonance of Engineered Atomic Structures on a Surface.' arXiv:2108.09880, 2021.

[3] Haenze, Max et al. 'Quantum Stochastic Resonance of individual Fe atoms.' *Sci. Adv.* Vol 7, Issue 33 (2021).

O 15.6 Mon 16:15 REC C 213

All-electrical driving and probing dressed states of a single spin on surface — •HONG BUI THI^{1,2}, CHRISTOPH WOLF^{1,3}, YU WANG^{1,3}, MASAHIRO HAZE^{1,4}, YI CHEN^{1,3}, YUJEONG BAE^{1,2}, ANDREAS HEINRICH^{1,2}, and SOO-HYON PHARK^{1,3} — ¹Center for Quantum Nanoscience, Institute for Basic Science (IBS), Seoul 03760, Korea — ²Department of Physics, Ewha Womans University, Seoul 03760, Korea — ³Ewha Womans University, Seoul 03760, Korea — ⁴The Institute for Solid State Physics, University of Tokyo, Kashiwa 277-8581, Japan

We demonstrate the creation of dressed states of a single electron spin localized on a surface by using a resonant radio-frequency field in a scanning tunneling microscope. Owing to the unique sub-nm probe-sample geometry field strengths as high as 1 GV/m can be achieved at a bias of the radio-frequency field below 100 mV. Magnetic resonance of a single spin in such a cavity is a direct consequence of coupling between the atomic dipole moment and driving electric field, resulting in the dressing of the atomic states. The read-out of these dressed states is facilitated in an all-electrical fashion by a weakly coupled probe spin. Our work highlights the strength of the atomic-scale geometry inherent to the scanning tunneling microscope in terms of the creation and control of dressed states, which are known to provide decoherence-free subspaces critical to the creation of long-lived quantum states.

O 15.7 Mon 16:30 REC C 213

Surface spins as quantum bits - a simulation perspective — JOSE REINA GÁLVEZ¹, NICOLAS LORENTE², and •CHRISTOPH WOLF¹ — ¹Center for Quantum Nanoscience, Institute for Basic Science, Seoul, South Korea — ²Materials Physics Center, San Sebastian, Spain

Spins localized at or close to a clean surface have emerged as systems of interest in quantum nanoscience. They can be tailored to a desired spin state, manipulated to form structures with designed interactions and as of recent have been used to implement basic quantum logic operations - a control-NOT gate - in a scanning tunneling microscope (STM). In this work we want to explore quantum coherent phenomena of surface spins from a computational perspective. Since surface spins interact rather strongly with the environment, we performed open quantum systems calculations. First, we will show how electron-electron double resonance can be understood by solving the time-dependent Schrodinger equation under continuous and pulsed radio-frequency driving. Using the same prototypical system of two coupled electron spins we also show how the AC Stark effect manifests itself as Autler-Townes doublets and Mollow triplets. To go one step further, we use our recently developed approach to explicitly calculate the current present in the STM experiment using the non-equilibrium Green's functions formalism. These simulations show how the current plays a dual role in these systems by driving quantum transitions but also limiting quantum coherence. Our simulations outline realistic expectations for quantum coherent surface spin systems and their prospective applications.

O 15.8 Mon 16:45 REC C 213

A non equilibrium Green's Function formalism applied to STM/ESR experiments — •JOSE REINA-GÁLVEZ¹, NICOLAS LORENTE², and CHRISTOPH WOLF¹ — ¹Center for Quantum nanoscience, Seoul, South Korea — ²Centro de Física de Materiales, San Sebastian, Spain

The demonstration of reproducible single-atom and single-molecule electron spin resonance (ESR) in a STM junction opened new possibilities in the analysis of surface science at the atomic scale. Recent experiments have demonstrated quantum-coherent Rabi oscillations and even the implementation of a quantum logic operation: a CNOT gate.

Here, we want to focus on the theory we developed to reproduce some relevant results in the field. Our theoretical framework uses open quantum systems formalism in combination with non equilibrium Green's Function technique. It consists of a quantum impurity connected to a polarized STM tip and an isolated surface, both considered as fermionic baths. The time dependent bias voltage used in the experiments is introduced in the hopping terms. These hoppings are driving the electron transitions from the baths to the quantum impurity which uses a modified Anderson impurity model with localized electronic states, a Coulomb repulsion term and a Zeeman term.

Our model is general, allowing to connect an arbitrary number of localized spins with the transport spin. We will demonstrate how driving the system on resonance modifies the population and the calculated true current through the many-body impurity which can be directly compared to the experiment.

O 15.9 Mon 17:00 REC C 213

Microscopic theory of spin-relaxation of a single Fe adatom coupled to substrate vibrations — •HARITZ GARAI-MARIN^{1,2}, MANUEL DOS SANTOS DIAS^{3,4,5}, SAMIR LOUNIS^{3,4}, JULEN IBAÑEZ-AZPIROZ^{6,7}, and ASIER EIGUREN^{1,2,8} — ¹Physics Department, University of the Basque Country UPV/EHU, Bilbao, Spain — ²Donostia International Physics Center, Donostia, Spain — ³Peter Grünberg Institut and Institute for Advanced Simulation, Forschungszentrum Jülich & JARA, Jülich, Germany — ⁴Faculty of Physics, University of Duisburg-Essen & CENIDE, Duisburg, Germany — ⁵Scientific Computing Department, STFC Daresbury Laboratory, Warrington, United Kingdom — ⁶Centro de Física de Materiales CSIC-UPV/EHU, Donostia, Spain — ⁷IKERBASQUE Basque Foundation for Science, Bilbao, Spain — ⁸EHU Quantum Center, University of the Basque Country UPV/EHU

Understanding the spin-relaxation mechanism of single adatoms is an essential step towards creating atomic magnetic memory bits or quantum bits. Here we present a theory to study the role of electron-phonon coupling by combining *ab-initio* electronic and vibrational properties with the multiplet many-body nature of atomic states. Our calculations reproduce the millisecond spin lifetime measured on Fe adatoms on MgO/Ag(100), which demonstrates that the essential features of the spin-phonon coupling are successfully captured. We show a clear fingerprint for experimentally detecting a localized spin-phonon excitation and we show how the atomic interaction with the environment should be tuned in order to enhance the magnetic stability.

O 15.10 Mon 17:15 REC C 213

Electron spin resonance of individual magnetic molecules on surfaces — •WANTONG HUANG¹, MÁTÉ STARK¹, PAUL GREULE¹, DARIA SOSTINA², DAVID COLLOMB¹, CHRISTOPH SÜRGER¹, WOLFGANG WERNSDORFER¹, and PHILIP WILKE¹ — ¹Physikalisches Institut (PHI), Karlsruhe Institute of Technology (IKMT), Karlsruhe, Germany — ²Institute of Quantum Materials and Technologies (IQMT), Karlsruhe Institute of Technology, Karlsruhe, Germany

Single molecular magnets which consist of one central metal ion surrounded by ligands are promising building blocks for nanoscale spintronics and future quantum devices. The recent development of scanning tunnelling microscopy (STM) combined with electron spin resonance (ESR) constitutes here a powerful technique to image and coherently control individual molecular spins on surfaces [Zhang et. al, Nat. Chem. 14, 59 (2022); Willke, ACS Nano, 15, 11, 17959 (2021)]. Here, we explore the magnetic properties and spin dynamics of iron phthalocyanine (FePc) molecules adsorbed on magnesium oxide (MgO) grown on Ag(100). We investigate the magnetic properties of different FePc by scanning tunneling spectroscopy and ESR-STM. Such molecular magnetic structures provide a versatile platform to study complex magnetic interactions and atomic-scale spin dynamics.

O 15.11 Mon 17:30 REC C 213

Orbital and spin excitations of hydrogenated titanium modulated by electric field — •DARIA SOSTINA¹, LUKAS ARNHOLD², NICOLAJ BETZ², SUSANNE BAUMANN², PHILIP WILKE³, WOLFGANG WERNSDORFER³, and SEBASTIAN LOTH² — ¹Institute of Quantum Materials and Technologies (IQMT), Karlsruhe Institute of Technology, Karlsruhe, Germany — ²University of Stuttgart, Institute for Functional Matter and Quantum Technologies, Stuttgart, Germany — ³Physikalisches Institut (PHI), Karlsruhe Institute of Technology, Karlsruhe, Germany

The goal for coherent control of individual spins on surfaces has prompted the development of new local probe techniques such as a combination of electron spin resonance (ESR) with scanning tunneling spectroscopy (STM). Yet, the excitation mechanism of ESR in STM is not conclusively determined. [Baumann et.al, Science 350, 6259, 2015, Ferron et. al, Phys. Rev. Research 1, 033185 (2019)]. Here we study a higher order orbital excitation of hydrogenated titanium complexes positioned on the oxygen site of the MgO surface. We observe a strong dependence of its excitation energy on the electric field generated by the STM tip. At the same time an ESR transition on that TiH exhibits a shift with the DC bias voltage applied to the junction which was attributed to a change in g-factor of the complex [Kot et. al, arXiv 2209.10969, 2022]. The ability to tune orbital and spin excitations by means of electric fields gives further insight on new pathways for electrical control of single spins centers on surfaces.

O 15.12 Mon 17:45 REC C 213

Lanthanide atoms on MgO(100)/Ag(100) as Candidate for Single-Atom-Qubits — STEFANO REALE^{1,2,3}, APARAJITA SINGHA^{1,2,4}, SAFA L. AHMED^{1,2}, DENIS KRYLOV^{1,2}, LUCIANO COLAZZO^{1,2}, CHRISTOPH WOLF^{1,2}, CARLO S. CASARI³, ALESSANDRO BARLA⁵, EDGAR FERNANDEZ⁶, FRANCOIS PATTHERY⁶, MARINA PIVETTA⁶, STEFANO RUSPONI⁶, HARALD BRUNE⁶, and •FABIO DONATI^{1,2} — ¹Center for Quantum Nanoscience (QNS), Institute for Basic Science (IBS), Republic of Korea — ²Department of Physics, Ewha Womans University, Republic of Korea — ³Department of Energy, Politecnico di Milano, Italy — ⁴Max Planck Institute for Solid State Research, Germany — ⁵Istituto di Struttura della Materia (ISM), Consiglio Nazionale delle Ricerche (CNR), Italy — ⁶Institute of Physics, Ecole Polytechnique Federale de Lausanne, Switzerland

Lanthanide atoms on surfaces are an exceptional platform for atomic-scale magnetic information storage [Science 352, 318 (2016)]. However, their potential as qubits is yet unexplored. Here we combine x-ray absorption spectroscopy and scanning tunneling microscopy (STM) with density functional theory and multiplet calculations to estimate the performance of Er and Tm on MgO(100)/Ag(100) as spin qubit candidates. For both atoms, we infer a magnetic ground state that is suitable for quantum coherent operations. By adapting the piezoelectric model of electron spin resonance (ESR)-STM [Science Advances 6, eabc5511 (2020)] to the case of lanthanide atoms, we predict a detectable signal and a higher Rabi rate compared to the systems studied up to date [S. Reale et al., accepted in Phys. Rev. B].

O 16: Ultrafast Electron Dynamics at Surface and Interfaces II

Time: Monday 15:00–17:30

Location: TRE Phy

O 16.1 Mon 15:00 TRE Phy

Time Resolved Photoemission Study of the Charge Transfer Dynamics in Rutile TiO₂(110) for CO Photooxidation to CO₂ — •HELENA GLEISSNER^{1,2,3}, MICHAEL WAGSTAFFE², LUKAS WENTHAUS⁴, SIMON CHUNG², STEFFEN PALUTKE⁴, SIARHEI DZIARZHYTSKI⁴, DMYTRO KUTNYAKHOV⁴, MICHAEL HEBER⁴, GÜNTER BRENNER⁴, HARALD REDLIN⁴, HESHMAT NOEI^{1,2}, and ANDREAS STIERLE^{1,2,3} — ¹The Hamburg Centre for Ultrafast Imaging, Hamburg, Germany — ²Center for X-ray and Nano Science (CXNS), Deutsches Elektronen-Synchrotron (DESY), Hamburg, Germany — ³Fachbereich Physik Universität Hamburg, Hamburg, Germany — ⁴Deutsches Elektronen-Synchrotron (DESY), Hamburg, Germany

In a pump-probe experiment at the free electron laser in Hamburg (FLASH) we gained insight into the ultrafast charge transfer on rutile TiO₂(110) during CO oxidation to CO₂. Pumped with a 770 nm optical laser and probed with 643 eV FEL soft x-rays we monitored the changes in the O 1s and Ti 2p core levels on a picosecond timescale using time-resolved photoemission spectroscopy.

We find that oxygen gets activated and reacts with CO to CO₂ in 0.2 ps up to 1 ps after the laser excitation. A complementary study found that the CO oxidation on anatase TiO₂(101) takes place between 1.2 and 2.8 ps after irradiation with an ultrashort laser pulse.[1]

[1] Wagstaffe, M. et al. ACS Catal. 10, 13650-13658 (2020).

O 16.2 Mon 15:15 TRE Phy

Transient Absorption Spectroscopy of NiO — •MAHENDRA KABBINAHITHLU¹, TOBIAS LOJEWSKI¹, SERGEY KOVALENKO², HEIKO WENDE¹, UWE BOVENSIEPEN¹, JULIA STÄHLER², and ANDREA ESCHENLOHR¹ — ¹Universität Duisburg-Essen, Fakultät für Physik und Center for Nanointegration (CENIDE), Lotharstraße 1, 47057 Duisburg, Germany — ²Humboldt-Universität zu Berlin, Institut für Chemie, Brook-Taylor-Straße 2, 12489 Berlin, Germany

In nickel oxide (NiO), a correlated transition-metal oxide, the strong electron-electron repulsion splits the d-bands into an occupied lower Hubbard band (LHB) and an unoccupied upper Hubbard band (UHB). The presence of additional oxygen p-bands at the adjacent sites and their interaction with the Hubbard bands leads to complex properties governed by the Hubbard potential (U) and the charge transfer ($p \leftrightarrow$ LHB) gap Δ . NiO is a charge-transfer insulator with the p-bands located between the LHB and the UHB ($\Delta < U$). We present excited state dynamics in NiO thin films via time-resolved optical spectroscopy. NiO is pumped above the band gap with 4.8 eV photons and the transient absorption spectrum is probed using a time-delayed supercontinuum. The time-resolved absorption spectrum, shows within the first 500 fs positive pump-induced changes at 2.2 eV and 3.2 eV which are separated from substrate contributions. We also see a strong negative change around 4.3 eV. The positive changes from in-gap states decay on a time scale of 100 fs, while the negative change represents the bleached ground state which recovers within 6 ps, potentially by interaction with phonons.

O 16.3 Mon 15:30 TRE Phy

Photoinduced dynamics of flat bands in the kagome metal CoSn by TR-ARPES — •DENNY PUNTEL¹, WIBEKE BRONSCHE², MANUEL TUNIZ¹, MINGU KANG³, PAUL NEVES³, SHIANG FANG³, EFTHIMIOS KAXIRAS^{4,5}, JOSEPH G. CHECKELSKY³, RICCARDO COMIN³, FULVIO PARMIGIANI^{1,2}, and FEDERICO CILENTO² — ¹Dipartimento di Fisica, Università degli Studi di Trieste, Trieste (Italy) — ²Electra - Sincrotrone Trieste S.C.p.A., Trieste (Italy) — ³Department of Physics, Massachusetts Institute of Technology, Cambridge, MA, USA — ⁴Department of Physics, Harvard University, Cambridge, MA, USA — ⁵John A. Paulson School of Engineering and Applied Sciences, Harvard University, Cambridge, MA, USA

In kagome systems, the geometry of the lattice localises the electrons in real space, enhancing the correlations and giving rise to flat bands. In CoSn two flat bands with nontrivial topological character lie below the Fermi level [1]. In order to study the response of the localisation mechanism to impulsive excitation, we performed the first time- and angle-resolved photoelectron spectroscopy study on CoSn. At temporal overlap we observe an increase in the electronic temperature, along with a shift and broadening of the flat bands by few meV. A smaller broadening of the flat band persists for the whole duration of the investigated time delay range (about 6 ps). A possible explanation for this broadening is the partial disruption of the real-space electron localisation, because of the increased mobility of the carriers due to the energy injected by the infrared pump pulse.

[1] M. Kang et al., Nat. Commun. 11, 4004 (2020)

Topical Talk

O 16.4 Mon 15:45 TRE Phy

Microscopic insight into non-equilibrium dynamics through time-resolved x-ray absorption spectroscopy — •ANDREA ESCHENLOHR — Faculty of Physics and CENIDE, University Duisburg-Essen, Lotharstr. 1, 47057 Duisburg, Germany

Time-resolved x-ray absorption spectroscopy provides access to element- and chemically sensitive information on the femto- to picosecond timescales of the elementary microscopic processes involving charge, spin and lattice dynamics in solids via optical pump, x-ray probe experiments. Recently implemented specialized x-ray optics at the SCS instrument of European XFEL allow for a simultaneous acquisition of the ground state and optically excited x-ray spectra as well as a reference signal for normalization of the data to the incident x-ray intensity, and thus provide excellent data quality in combination with kHz repetition rates [1]. We employ this scheme to analyze the temporal evolution of the electronic structure of ferromagnetic Ni after optical excitation and distinguish transient broadening and energy shifts in the absorption spectra, which we show to be caused by electron repopulation and correlation-induced modifications of the electronic structure, respectively. Crucially, an ab initio theoretical description requires taking the local Coulomb interaction into account, revealing the temporal interplay between electron correlations and ultrafast spin-dependent charge dynamics [2].

[1] L. Le Guyader et al., arxiv.org/abs/2211.04265

[2] T. Lojewski et al., arxiv.org/abs/2210.13162

O 16.5 Mon 16:15 TRE Phy

Direct observation of light-induced ultrafast currents in black phosphorus — •MACIEJ DENDZIK^{1,2}, ANDREA MARINI³, SAMUEL BEAULIEU², SHUO DONG², TOMMASO PINCELLI², JULIAN MAKLAR², R. PATRICK XIAN², ENRICO PERFETTO^{3,4}, MARTIN WOLF², GIANLUCA STEFANUCCI^{4,5}, RALPH ERNSTORFER², and LAURENZ RETTIG² — ¹KTH Royal Institute of Technology, Stockholm, Sweden — ²Fritz Haber Institute of the Max Planck Society, Berlin, Germany — ³CNR-ISM, Rome, Italy — ⁴Tor Vergata University of Rome, Rome, Italy — ⁵INFN, Rome, Italy

Understanding intricate details of light-matter interaction on the femtosecond timescale is at the heart of modern photonics and optoelectronics. However, fundamental coupling between charge carriers response and corresponding induced electromagnetic fields upon an ultrafast optical excitation remain largely unexplored in many quantum materials. Here, we present an experimental time- and momentum-resolved photoemission study of black phosphorus (BP) combined with state-of-the-art simulations of ultrafast carrier dynamics and induced fields. We find dramatically different electron dynamics following excitation by light polarized along the zigzag and armchair directions which we associate with a difference in initial population momentum distributions. Remarkably, we observe a sub-picosecond population imbalance of excited carriers with opposite momenta, which correspond to the generation of transient in-plane currents. The results provide a comprehensive picture of the ultrafast carrier dynamics in BP and pave the way for novel applications in optoelectronics or quantum computing.

O 16.6 Mon 16:30 TRE Phy

Band-resolved relaxation of laser-excited gold. — •TOBIAS HELD¹, PASCAL D. NDIONE¹, SEBASTIAN T. WEBER¹, DIRK O. GERICKE², and BAERBEL RETHFELD¹ — ¹RPTU, Kaiserslautern, Germany — ²CFSa, University of Warwick, Coventry, UK

Irradiation of gold with visible light may excite d-band electrons into the free sp-electron states. This process increases the energy content of the electron system and induces an occupational nonequilibrium. Since the particle exchange is significantly slower than the energy transfer between the electron subsystems, the nonequilibrium band occupation persists long after a temperature can be well defined. Subsequently, density equilibration and the electron-phonon relaxation need to be considered consistently. In Ref. [1], we have simulated the non-equilibrium band occupation with electron density-resolved rate equations and coupled them with a two-temperature model to include the energy transfer from the electrons to the lattice. The results are sensitive to the electron-phonon coupling parameter applied.

Here, we investigate the electron-phonon coupling strength in more detail. We describe the interaction of the d- and sp-electrons with the lattice by complete Boltzmann collision integrals and show that the extracted electron-phonon coupling parameters strongly depend on the band occupation. Consequently, we incorporate this aspect into the simulation by assigning different temperatures to these bands and couple them separately to the phonons.

[1] Ndione, Weber, Gericke, and Rethfeld. Sci Rep, 12(1), 2022

O 16.7 Mon 16:45 TRE Phy

Multi-directional energy transfer across hybrid plasmonic-excitonic interface — •TOMMASO PINCELLI¹, THOMAS VASILEIADIS¹, SHUO DONG¹, SAMUEL BEAULIEU¹, MACIEJ DENDZIK¹, DANIELA ZAHN¹, SANG-EUN LEE¹, HÉLÈNE SEILER¹, YINPENG QI¹, RUI PATRICK XIAN¹, JULIAN MAKLAR¹, EMERSON COY², NICLAS S. MUELLER³, YU OKAMURA³, STEPHANIE REICH³, MARTIN WOLF¹, LAURENZ RETTIG¹, and RALPH ERNSTORFER¹ — ¹Fritz-Haber-Institut der MPG, Berlin, Germany — ²NanoBioMedical Centre, Adam Mickiewicz University, Poznan, Poland — ³Freie Universität Berlin, Berlin, Germany

Hybrid plasmonic devices involve a nanostructured metal supporting localized surface plasmons to amplify light-matter interaction, and a non-plasmonic material to functionalize charge excitations. We combine the use of time and angle-resolved photoemission spectroscopy and femtosecond electron diffraction to investigate charge carrier and phonon dynamics in such a system: epitaxial Au nanoislands on bulk WSe₂. The Au nanostructures show delayed electronic temperature increase and cause a shortening of the Σ -exciton lifetime. Lattice heating is accelerated in WSe₂ and delayed in Au. Our results resolve a multi-directional energy exchange on timescales shorter than the electronic thermalization of the nanometal, driven by a non-linear plasmon-exciton interaction. Non-radiative exciton recombination, electron-phonon coupling, and diffusive charge-transfer determine the subsequent energy backflow.

O 16.8 Mon 17:00 TRE Phy

Electronic hybridization and ultrafast dynamics in Terrylene/WS₂ heterostructure. — •SAMUEL PALATO¹, BOUBACAR TANDA BONKANO¹, SERGEY KOVALENKO¹, MICHELE GUERRINI², CATERINA COCCI², and JULIA STÄHLER¹ — ¹Humboldt Universität zu Berlin, DE — ²Carl von Ossietzky Universität Oldenburg, DE

Hybrid organic-inorganic heterostructures offer the possibility of optoelectronic materials with tailored properties. We report on electronic coupling and charge carrier injection in heterostructures formed of terrylene (T) and monolayer WS₂ investigated using steady-state and femtosecond optical spectroscopy.

Terrylene molecules in solution show a typical Frank-Condon transition to a singlet state with a lifetime of 3.7 ns. TD-DFT calculations indicate a transition dipole moment along the long axis of the molecule. In contrast, the spectrum of the T film is complex and implies strong H-aggregation. We assign the dynamics to thermal reorganization of the molecules in the film, giving rise to changes in the magnitude and sign of charge-transfer coupling.

The response of the T/WS₂ hybrid indicates direct hybridization of higher-lying exciton states. Upon excitation of T/WS₂, the transient response is similar to that of WS₂; it suggests direct injection of charge carriers from the organic to the inorganic layer.

The presence of hybrid states and the evidence of direct injection underlines the potential of hybrid organic-inorganic materials with tailored optoelectronic properties.

O 16.9 Mon 17:15 TRE Phy

Ultrafast electron dynamics at D₂O/Na⁺/Cu(111) interfaces — •FLORIAN KÜHNE¹, JAYITA PATWARI^{1,2}, PING ZHOU¹, KARINA MORGENSTERN², and UWE BOVENSIEPEN¹ — ¹Faculty of Physics and Center for Nanointegration (CENIDE), University of Duisburg-Essen — ²Department of Chemistry and Biochemistry, Ruhr-University Bochum

Ion-solvent interactions and electron transfer across the ion-metal hybrid interfaces are of fundamental interest because of their widespread application in energy storage and energy conversion. We aim to understand the effect of solvation on the elementary processes involved in electrochemical applications by developing a microscopic insight into the hybrid interfaces in presence of a solvent. Electron transfer across such interfaces and the consequent relaxation dynamics are the key microscopic steps behind all these applications which occur on femtosecond time scales. Thus, to experimentally analyze the underlying

ing elementary dynamics, we use femtosecond time-resolved two-photon photoelectron spectroscopy (*tr*-2PPE). We discuss the influence of the solvent at the $D_2O/Na^+/Cu(111)$ interface. We conclude on the local structure - dynamics relation as a function of D_2O coverage from the measured energy transfer rate determined by the transient energy shift of the Na 3s resonance on Cu(111). We

analyze furthermore the screening of the excited electron in this resonance by the solvent based on the relaxation time variation with D_2O coverage.

Funding by the DFG through Project No. 278162697 - SFB1242 and EXC 2033 - 390677874 - RESOLV are gratefully acknowledged.

O 17: Focus Session: Frontiers of Electronic-Structure Theory II (joint session O/HL)

Time: Monday 15:00–17:15

Location: TRE Ma

Topical Talk

O 17.1 Mon 15:00 TRE Ma

Coupled-cluster theory for complex solids made ready — •ANDREAS GRÜNEIS — TU Wien, Institute for Theoretical Physics, Wiedner Hauptstraße 8-10/136, 1040 Vienna, Austria

This talk will review recent progress in applying periodic coupled-cluster theory, which has the potential to achieve a systematically improvable level of accuracy, to solids and surfaces. We will discuss novel techniques that reduce the computational cost by accelerating the convergence of calculated properties towards the complete basis set as well as the thermodynamic limit. The newly developed techniques have been implemented in the free and open source simulation software Cc4s that is interfaced to a growing number of widely-used electronic structure theory codes. These developments have enabled an increasing number of ab initio studies and allowed for assessing the level of accuracy of coupled-cluster theory by comparing to experimental findings as well as quantum Monte Carlo results. The presented applications will cover a wide range of materials science problems including the study of phase diagrams, molecule-surface interactions and properties of defects.

O 17.2 Mon 15:30 TRE Ma

Speedup of structural optimisations using hybrid functionals: Case studies for energy materials — •DANIEL FRITSCH — Weierstrass Institute for Applied Analysis and Stochastics, Mohrenstr. 39, 10117 Berlin, Germany — Helmholtz-Zentrum Berlin für Materialien und Energie, Hahn-Meitner-Platz 1, Berlin, 14109, Germany

First-principles calculations based on density functional theory have been established as de facto standard for computational materials investigations. Depending on the size of the unit cell, for every material of interest a suitable choice for the unknown exchange and correlation functional has to be made; taking not only into account the desired accuracy, but also the available computational resources.

In recent years, a promising combination of two approaches emerged, starting from a structural relaxation based on a simpler (semi)local functional, supplemented by a single shot hybrid functional calculation. Here, we propose a new method for combining different levels of exchange and correlation functional for structural relaxations.

In a first benchmarking step, this new method will be applied to various sets of promising energy materials, where full hybrid functional calculations are available, with a main focus on the performance of this new approach on the structural properties and the required computational resources. In a second step, this new approach will be applied to materials, which up-to-now have not been accessible to hybrid functional calculations due to the required computational resources. All the presented results on the structural, electronic, and optical properties will be critically discussed alongside experimental findings.

O 17.3 Mon 15:45 TRE Ma

All-Electron Large-Scale Hybrid Density Functional Simulations — FLORIAN MERZ¹, ANDREAS MAREK², •SEBASTIAN KOKOTT³, CHRISTIAN CARBOGNO³, YI YAO³, MARIANA ROSSI⁴, MARKUS RAMPP², MATTHIAS SCHEFFLER³, and VOLKER BLUM⁵ — ¹Lenovo HPC Innovation Center, Stuttgart — ²Max Planck Computing and Data Facility, Garching — ³The NOMAD Laboratory at the FHI-MPG and IRIS-Adlershof HU, Berlin — ⁴MPI for the Structure and Dynamics of Matter, Hamburg — ⁵Duke University, North Carolina, USA

The localized resolution-of-identity approach [1] enables $O(N)$ hybrid density functional simulations and, thus, the computation of accurate electronic properties of large scale atomistic models in the range of ten thousands of atoms in *FHI-aims* [2]. In this range, parallelization and memory requirements of the exact exchange part, and the evaluation of the Hartree potential remain challenging. The solution of the generalized eigenvalue problem with direct eigensolvers like ELPA [3] naturally becomes a bottleneck due to $O(N^3)$ scaling. In this work, we present recent algorithmic advances for the exact exchange part and the evaluation of the Hartree potential, as well as optimizations of the ELPA library. We systematically perform benchmark tests on CPU and GPU-accelerated architectures covering inorganic solids, large molecules, and organic crystals with up to 50,000 atoms.

[1] Ihrig *et al.*, *New J. Phys.* **17**, (2015).

[2] Levchenko *et al.*, *Comp. Phys. Commun.* **192**, (2015).

[3] Marek *et al.*, *J. Phys. Condens. Matter* **26**, (2014).

15 min. break

O 17.4 Mon 16:15 TRE Ma

A Koopman's compliant exchange correlation potential for semiconductors — •MICHAEL LORKE¹, PETER DEAK², and THOMAS FRAUENHEIM² — ¹Institute for Theoretical Physics, University of Bremen, Otto-Hahn-Allee 1, Bremen, 28359, Germany — ²BCCMS, University of Bremen, Germany

Density functional theory is the workhorse of theoretical materials investigations. Due to the shortcoming of (semi-)local exchange correlation potentials, hybrid functionals have been established for practical calculations to describe surfaces, molecular adsorption, and defects. These functionals operate by mixing between semi-local and Hartree-Fock exchange semi-empirically. However, their parameters have to be optimized for every material separately. To treat materials with a more physics driven approach and without the need of parameter optimization is possible with many-body approaches like GW, but at an immense increase in computational costs and without the access to total energies and hence geometry optimization. We propose a novel exchange correlation potential[1] for semiconductor materials, that is based on physical properties of the underlying microscopic screening. We demonstrate that it reproduces the low temperature band gap of several materials. Moreover it respects the required linearity condition of the total energy with the fractional occupation number, as expressed by the generalized Koopman's theorem. We also show that this novel functional can be used as a kernel in linear response TDDFT to reproduce excitonic effects in optical spectra [1] *Physical Review B* **102** (23), 235168 (2020)

O 17.5 Mon 16:30 TRE Ma

Accurate and efficient treatment of spin-orbit coupling via second variation employing local orbital basis functions — •HANNAH KLEINE¹, ANDRIS GULANS², SVEN LUBECK¹, CECILIA VONA¹, and CLAUDIA DRAXL¹ — ¹Institut für Physik and IRIS Adlershof, Humboldt-Universität zu Berlin — ²Department of Physics, University of Latvia

Spin-orbit-coupling (SOC) effects can significantly change the properties of materials containing heavy elements, mostly by introducing shifts and splittings in the band structure. Including SOC effects in density-functional-theory (DFT) calculations can be challenging. In the linearized augmented planewaves plus local orbitals (LAPW+LO) method, SOC is treated as a perturbation and solved by a second variational (SV) scheme where eigenvectors of the scalar-relativistic Kohn-Sham Hamiltonian are used as basis functions for the SO-coupled problem. For certain materials, especially those with strong SOC effects, many SV basis functions are required which leads to high computational costs. By adding LOs to the SV basis, we are able to drastically reduce the basis-set size and thus the computational cost. We implement this approach in the all-electron full-potential computer package exciting [1] and combine it with the use of relativistic LOs to achieve high accuracy results for a variety of different materials.

[1] A. Gulans *et al.*, *J. Phys. Condens. Matter* **26**, 363202 (2014).

O 17.6 Mon 16:45 TRE Ma

Exact sum-rule approach to polarizability and asymptotic van der Waals functionals - derivation of exact benchmarks — •ALBERTO AMBROSETTI¹, JOHN DOBSON², MATTEO RICCI¹, and PIER LUIGI SILVESTRELLI¹ — ¹Dipartimento di Fisica e Astronomia, Università degli Studi di Padova, via Marzolo 8, 35131, Padova, Italy — ²Nanoscale Science and Technology Centre, Griffith University, Nathan, Queensland 4111, Australia

Using a sum-rule approach we develop an exact theoretical framework for polarizability and asymptotic van der Waals correlation energy functionals of isolated objects[1]. The functionals require only monomer groundstate properties as input. Functional evaluation proceeds via solution of a single position-space differential equation, without the usual summations over excited states or frequency integrations. Explicit functional forms are reported for reference physical systems, including atomic hydrogen and single electrons subject to harmonic confinement, and immersed in a spherical-well potential. Direct comparison with the popular Vydrov-van Voorhis density functional shows that this performs best when density decay occurs at atomic scales. The adopted sum-rule approach implies general validity of our theory, enabling exact benchmarking of van der Waals density functionals, and direct inspection of the subtle long-range correlation effects that constitute a major challenge for approximate (semi-)local density functionals.

[1] M Ricci, PL Silvestrelli, JF Dobson, A Ambrosetti J. Phys. Chem. Lett. 13, 8298-8304

O 17.7 Mon 17:00 TRE Ma

Interacting electrons and bosons in the doubly screened $G\bar{W}$ approximation — •YAROSLAV PAVLYUKH — Department of Theoretical Physics, Wrocław University of Science and Technology

In Ref. [1] we built on the Generalized Kadanoff-Baym Ansatz for electrons and bosons to map a broad class of nonequilibrium Green's function theories onto a coupled system of ordinary differential equations with linear time-scaling. Available methods to treat e - e correlations include GW [2], T -matrix and Faddeev, while e - b correlations are described by Ehrenfest and second-order diagrams in the e - b coupling [3].

In this work we present a substantial advance in the treatment of correlations, requiring no extra computational cost and preserving all conserving properties. Specifically, we include the effects of dynamical screening due to *both* e - e and e - b interactions ($G\bar{W}$ approximation). The $G\bar{W}$ extension opens the door to a wealth of phenomena ranging from carrier relaxation and exciton recombination to molecular charge migration and transfer in optical or plasmonic cavities.

[1] Y. Pavlyukh, E. Perfetto, D. Karlsson, R. van Leeuwen, and G. Stefanucci, Phys. Rev. B **105**, 125134 (2022).

[2] E. Perfetto, Y. Pavlyukh, and G. Stefanucci, Phys. Rev. Lett. **128**, 016801 (2022).

[3] D. Karlsson, R. van Leeuwen, Y. Pavlyukh, E. Perfetto, and G. Stefanucci, Phys. Rev. Lett. **127**, 036402 (2021).

O 18: Poster: 2D Materials I

Time: Monday 18:00–20:00

Location: P2/EG

O 18.1 Mon 18:00 P2/EG

CVD growth of 2D transition metal dichalcogenides for electronics and optoelectronics — •SEUNG HEON HAN¹, ZIYANG GAN¹, EMAD NAJAFIDEHAGHANI¹, JULIAN PICKER¹, CHRISTOF NEUMANN¹, UWE HÜBNER², ANTONY GEORGE¹, and ANDREY TURCHANIN¹ — ¹Institute of Physical Chemistry, Friedrich Schiller University Jena, Jena, Germany — ²Leibniz Institute of Photonic Technology (IPHT), Jena, Germany

Two-dimensional (2D) transition metal dichalcogenides (TMDs) are of great interest for fundamental science and technology due to their exceptional electronic and photonic properties. Chemical vapor deposition (CVD) is a viable method for scalable growth of high-quality monolayer TMDs on various substrates and with tailored properties. Here, we present some of our recent research results on the CVD growth of 2D TMDs including monolayer single-crystal TMDs, atomically sharp TMD1-TMD2 lateral heterostructure, and TMD1-TMD2 lateral heterostructure alloys. Moreover, we demonstrate various exciting applications of these monolayers in field-effect transistors, high-performance photodetectors and memtransistors.

O 18.2 Mon 18:00 P2/EG

Assembly of van der Waals heterostructures with ultra-clean surfaces for surface science techniques — KEDA JIN¹, TOBIAS WICHMANN¹, FELIX LÜPKE¹, TOMÁŠ SAMUELY², OLEKSANDER ONUFRIENKO², F. STEFAN TAUTZ¹, MARKUS TERNES¹, and •JOSE MARTINEZ-CASTRO¹ — ¹Peter Grünberg Institut (PGI-3), Forschungszentrum Jülich, 52425 Jülich, Germany — ²Centre of Low Temperature Physics, Faculty of Science, P. J. Safarik University & Institute of Experimental Physics, Slovak Academy of Sciences, Kosice, Slovakia

Van der Waals heterostructures have become an excellent platform to study emerging physical phenomena that are the result of synergistic proximity effects. Until recently, surface science techniques such as ARPES or STM have been excluded from the study of such heterostructures because of their high sensitivity to surface contamination and the fact that they are sensitive to the top-most layer and thus, not being able to use, boron nitride as the encapsulating layer. Here, we report a novel technique for the assembly of van der Waals heterostructures that do not require encapsulation nor melting of polymers, allowing the study of air-sensitive materials surface. By performing low temperature STM, we demonstrate no surface degradation, achieving atomic resolution as well as detecting a perfectly formed superconducting gap in NbSe₂.

O 18.3 Mon 18:00 P2/EG

Chemical vapor deposition of MoSe₂-WSe₂ lateral heterostructures with atomically sharp one-dimensional interfaces — •ZIYANG GAN¹, DORIAN BERET², IOANNIS PARADISANOS², HASSAN LAMSAADI², EMAD NAJAFIDEHAGHANI¹, CHRISTOF NEUMANN¹, TIBOR LEHNER⁴, JOHANNES BISKUPEK⁴, UTE KAISER⁴, LAURENT LOMBEZ², JEAN-MARIE POUMIROL³, BERNHARD URBASZEK^{2,5}, ANTONY GEORGE¹, and ANDREY TURCHANIN¹ — ¹Friedrich Schiller University Jena, Institute of Physical Chemistry, Jena, Germany — ²Université de Toulouse, INSA-CNRS, Toulouse, France — ³Université de Toulouse, CEMES-CNRS, Toulouse, France — ⁴Ulm University, Central Facility of Electron Microscopy, Ulm, Germany — ⁵Technische Universität Darmstadt, IPKM, Darmstadt, Germany

Chemical vapor deposition (CVD) enables the epitaxial growth of transition metal dichalcogenide (TMD) lateral heterostructures with one-dimensional interfaces. The growth is achieved by in situ controlling the precursor partial pressures by a two-step heating protocol. Here we characterize the lateral heterostructures of MoSe₂-WSe₂ by optical microscopy, Raman spectroscopy, and photoluminescence spectroscopy. Scanning transmission electron microscopy (STEM) demonstrates the high-quality 1D boundary between MoSe₂ and WSe₂ with a width of around 3nm. Furthermore, tip-enhanced photoluminescence (TEPL) enables to demonstrate that the heterojunction acts as an excitonic diode

resulting in unidirectional exciton transfer from WSe₂ to MoSe₂. npj 2D Mater. Appl. 6 (2022) 84

O 18.4 Mon 18:00 P2/EG

Growth and characterization of transition metal dichalcogenides on Au(111) grown by chemical vapor deposition — •JULIAN PICKER¹, FELIX OTTO², ZIYANG GAN¹, MAXIMILIAN SCHAAL², MARCO GRUENEWALD², CHRISTOF NEUMANN¹, ANTONY GEORGE¹, ROMAN FORKER², TORSTEN FRITZ², and ANDREY TURCHANIN¹ — ¹Institute of Physical Chemistry, Friedrich Schiller University Jena, Lessingstraße 10, 07743 Jena, Germany — ²Institute of Solid State Physics, Friedrich Schiller University Jena, Helmholtzweg 5, 07743 Jena, Germany

Transition metal dichalcogenides (TMDs) are layered two-dimensional (2D) materials which have attracted significant attention in recent years. Especially, the exciting properties of their monolayers such as the strong, direct bandgap photoluminescence make them promising for novel electronic and optoelectronic applications. Here, we demonstrate the *ex-vacuo* growth of different TMD monolayers on Au(111) by chemical vapor deposition (CVD). Afterwards, the samples were analyzed in ultra-high vacuum (UHV) with the help of surface sensitive methods, including (low-temperature) scanning tunneling microscopy and spectroscopy (STM/STS), low-energy electron diffraction (LEED), as well as X-ray and angle-resolved ultraviolet photoelectron spectroscopy (XPS/ARPES). While we confirm the formation of high-quality TMDs, we also accessed the structural and electronic properties of these samples down to the atomic scale. In particular, the focus is on the interaction of the TMDs and Au(111) as Au is the most widely used electrical contact material for TMD devices.

O 18.5 Mon 18:00 P2/EG

Unoccupied electronic states of the CDW material 1T-TiSe₂ — •PATRICK GEERS, MARCEL HOLTSMANN, and MARKUS DONATH — Universität Münster, Wilhelm-Klemm-Str. 10, 48149 Münster

We present angle-resolved inverse-photoemission (IPE) measurements of the unoccupied electronic structure of the transition metal dichalcogenide 1T-TiSe₂. The spectra along the $\bar{\Gamma}\bar{M}$ and $\bar{\Gamma}\bar{K}$ high symmetry directions are dominated by the Ti-3d bands with rather flat $E(\mathbf{k}_{\parallel})$ dispersion. The two energetically separated subgroups e_g and t_{2g} are clearly resolved in the spectra. We observe two e_g bands as expected, while the spectral features of the t_{2g} group are too broad to identify the three predicted states individually. In addition, an image-potential surface state with its free-electron-like dispersion is observed below the vacuum energy. We compare our experimental $E(\mathbf{k}_{\parallel})$ results with a theoretical 3D band-structure by estimating the k_{\perp} -component of the electron wavevector within the nearly-free-electron approximation. Furthermore, we observe temperature-dependent changes in our IPE data that are attributed to the charge density wave phase transition. Interestingly, only bands of t_{2g} symmetry show energy shifts, proving the orbital selectivity of bands involved in the phase transition [1].

[1] Watson *et al.*, Phys. Rev. Lett. **122**, 076404 (2019).

O 18.6 Mon 18:00 P2/EG

Electronic structure of benzene on MoS₂ — •JAN-PHILLIP TOPMÖLLER and MICHAEL ROHLFING — Institute of solid state theory, Münster, Germany

TMDs show great potential in terms of their applicability in optical electronics. Due to their large surface, molecules can easily bind to the TMDC, which might affect its electronic properties. We investigate benzene as such a molecule because it is a small, prototypical one.

We use DFT (LDA, GGA) and DFT-D3 to determine the most stable adsorption position of benzene on MoS₂. Subsequently, we use many body perturbation theory to calculate the electronic structure of the adsorbate system and its individual components (MoS₂ and the benzene molecule). For example, we find that the HOMO-LUMO of the benzene molecule decreases from 10.5eV by 2.07eV when considering the screening of the monolayer.

O 18.7 Mon 18:00 P2/EG

Evolution of Band structure in 2D transition metal dichalcogenides alloy $Mo_xW_{1-x}Se_2$ — •SARATH SASI¹, LAURENT NICOLAÏ¹, LUCIE NEDVĚDOVÁ¹, ROS-TISLAV MEDLÍN¹, MICHAL PROCHÁZKA¹, MARIE NETRVALOVÁ¹, SUNIL WIL-FRED DSOUZA¹, CHRISTINE RICHTER^{2,3}, KAROL HRICOVIN^{2,3}, and JÁN MINÁR¹ — ¹New Technologies Research Centre, University of West Bohemia, Pilsen, Czech Republic — ²LPMS, CY Cergy Paris Université, Neuville-sur-Oise, France — ³Université Paris-Saclay, CEA, CNRS, LIDYL, Gif-sur-Yvette, France

Among two-dimensional (2D) materials that emerged in the research scenario after the discovery of graphene, transition metal dichalcogenides (TMDCs) with the general formula MX_2 ($M=Mo, W$; $X=S, Se, Te$) attract huge interest as a potential candidate for electronic and optoelectronic applications. There are many artificial methods to engineer the bandgap and spin-polarized bands, such as chemical doping, external electric field etc. Here we are studying the band structure of $Mo_xW_{1-x}Se_2$ single crystals alloy with various stoichiometric ratio x in comparison with WSe_2 . The structural characterisation of samples was analysed using Low energy electron diffraction, Raman Spectroscopy and Scanning Electron Microscopy with Energy Dispersive X-Ray Analysis, X-ray photoemission spectroscopy (XPS). Angle-Resolved Photoemission Spectroscopy (ARPES) was used to investigate the electronic band structure of the samples. We evaluated the band dispersion and observed the bands' splitting at the K point. Thus we are evaluating a potential way for band engineering in TMDCs.

O 18.8 Mon 18:00 P2/EG

Tuning the electronic structure of MoS₂: how self-intercalation affects screening, interactions and strain — •BORNA PIELIC^{1,2}, MATKO MUZEVIC³, DINO NOVKO², JIAQI CAI¹, ALICE BREMERICH¹, ROBIN OHMANN¹, MARKO KRALJ², IVA SRUT RAKIC², and CARSTEN BUSSE¹ — ¹Department Physik, Universität Siegen, Siegen, Germany — ²Institute of Physics, Zagreb, Croatia — ³Department of Physics, Josip Juraj Strossmayer University of Osijek, Osijek, Croatia

Growth of quasi-freestanding 2D materials on van der Waals (vdW) typed substrates can be accompanied by intercalation in order to modify their intrinsic

properties. In this work, we epitaxially grow MoS₂ monolayer islands on graphene on Ir(111) using two different procedures: (i) two-step molecular beam epitaxy (MBE) growth which results in S intercalation between graphene and Ir(111), and (ii) single-step MBE growth resulting in Mo intercalation. Scanning tunneling microscopy (STM) measurements reveal significant difference in MoS₂ islands morphology, and suggests that S intercalation weakens the interaction in the MoS₂/graphene stack, while Mo intercalation strengthens it. More importantly, our scanning tunneling spectroscopy (STS) measurements show notable non-rigid shifts of electronic states. The numerical calculations reveal a strong correlation between substrate screening, strain and binding energy, that are in line with experiment. We suggest that this elegant and non-invasive technique could in general be used for altering vdW, electron-electron and electron-phonon interactions in 2D materials.

O 18.9 Mon 18:00 P2/EG

Designing a symmetry-correct minimal model for 2H-WSe₂ — •MAX XYLANDER^{1,2}, PHILIPP ECK^{1,2}, SIMON MOSER^{2,3}, LUKASZ PLUCINSKI⁴, and GIORGIO SANGIOVANNI^{1,2} — ¹ITPA, Universität Würzburg, Germany — ²Würzburg-Dresden Cluster of Excellence, ct.qmat — ³EP4, Universität Würzburg, Germany — ⁴PGI-6, Peter Grünberg Institut Jülich, Germany

Transition metal dichalcogenides (TMDCs) have been studied for their structure-dependent valley physics. Due to inversion symmetry breaking in combination with strong SOC originating from the transition metal d -shell, these materials possess momentum-dependent spin splitting. Recently, the interest in TMDCs has been further stimulated by twisted moiré lattices, where the emerging flat bands have been associated to chiral representations in twisted bilayer graphene.

Here we present a study on the chiral wavefunctions in 2H-WSe₂ based on *ab initio* calculations and minimal modeling. Especially, we will focus on an analysis of the irreducible representations, which allow us to design a minimal d -orbital tight-binding Hamiltonian with SOC and inversion symmetry breaking terms. For the validation of the model, we plan further experimental studies with circularly polarized light angle-resolved photoemission.

O 19: Poster: Ultrafast Electron Dynamics at Surface and Interfaces I

Time: Monday 18:00–20:00

Location: P2/EG

O 19.1 Mon 18:00 P2/EG

Ultrafast transport and energy relaxation of hot electrons on tmdc/au/fe/mgo(001) investigated by time resolved photoelectron spectroscopy — •FLORIAN KÜHNE¹, JESUMONY JAYABALAN¹, PING ZHOU¹, DETLEF DIESING², STEPHAN SLEZIONA¹, MARIKA SCHLEBERGER¹, and UWE BOVENSIEPEN¹ — ¹Faculty of Physics and Center for Nanointegration, University of Duisburg-Essen — ²Faculty of Chemistry, University of Duisburg-Essen

Optically excited electrons are of particular interest in solid state physics because analysis of their dynamics allows an understanding of the microscopic interactions. Excited charge carriers in metals and semiconductors relax on a femto- to picosecond timescale due to electron-electron and electron-phonon scattering. Using a back-side pump geometry in time-resolved photoelectron spectroscopy (PES), see Kühne *et al.*, PRR 4, 033239(2022), and Beyazit *et al.*, PRL 125, 076803(2020), we demonstrated the analysis of hot electron transport through metallic heterostructures Au/Fe/MgO(001). By pumping the Fe side by femtosecond laser pulses, hot electrons are excited in the Fe layer and injected into the Au layer. They subsequently propagate to the surface, where they are probed by PES. This work aims to employ these heterostructures as electrodes for photo-excited electrons which are injected into transition metal dichalcogenides. Thereby we aim at an analysis of scattering and propagation of electrons through 2D material layers discerning local and non-local effects. Funding by the DFG through Project No. 278162697 - SFB1242 is gratefully acknowledged.

O 19.2 Mon 18:00 P2/EG

T-ReX: a facility for time-resolved optical and angle-resolved photoemission spectroscopies — •WIBKE BRONCH¹, DENNY PUNTEL², MANUEL TUNIZ², FULVIO PARMIGIANI^{1,2}, and FEDERICO CILENTO¹ — ¹Elettra-Sincrotrone Trieste, Trieste, Italy — ²Università degli Studi di Trieste, Trieste, Italy

The T-ReX laboratory at FERMI, Elettra-Sincrotrone Trieste, is a user facility for ultrafast table-top time-resolved spectroscopies [1-3]. Our facility comprises a number of time-resolved optical spectroscopy (TR-OS) setups and an endstation for time- and angle-resolved photoemission spectroscopy (tr-ARPES). The latter is connected to diverse table-top laser sources, allowing for probe energies ranging from 6 to 30 eV. In order to show how the complementarity of these setups can be beneficial for gaining more comprehensive insights on a sample system, we will present our recent experiments on the charge-density-wave materials VTe₂ and VSe₂, shedding light on phonon dynamics and electronic structures of the samples under investigation.

[1] S. Peli *et al.*, J. Electron Spectrosc. Relat. Phenomena 243, 146978 (2020).

[2] R. Cucini *et al.*, Structural Dynamics 7, 014303 (2020).

[3] M. Perlangeli *et al.*, Optics Express 28, 8819 (2020).

O 19.3 Mon 18:00 P2/EG

Excited state photoemission momentum maps from time-dependent density functional theory — •MELVIN HODŽIĆ, CHRISTIAN S. KERN, ANDREAS WINDSCHBACHER, and PETER PUSCHNIG — Institute of Physics, NAWI Graz, University of Graz, Austria

Angle-resolved photoemission spectroscopy is a powerful experimental technique to reveal the electronic structure of thin films and interfaces. In particular, constant binding energy angular distributions, so called momentum maps, have been shown to be related to the Fourier transform of the electron-emitting initial state molecular orbital, thereby bridging experiment and theory in photoemission orbital tomography (POT). The extension of POT to optically excited states has, of late, been demonstrated via a femtosecond pump-probe setup, paving the way for tracing the momentum distribution of electrons on ultrafast time scales. However, linking the measured momentum maps to the spatial structure of the exciton wave functions has yet to be achieved. We propose a simple procedure which involves a coherent sum of the ground-state Kohn-Sham orbitals that construct the exciton wave function. Here, we validate this approach by solving Casida's equation for a series of organic molecules in the gas phase leading to optical absorption spectra and exciton compositions. With the gained information, momentum maps obtained via linear-response TDDFT are cross-checked by directly simulating angle-resolved photoemission spectra within the framework of real-time TDDFT. To this end, we record the flux of the emitted electrons through a detector surface.

O 19.4 Mon 18:00 P2/EG

Ultrafast all-optical manipulation of the charge-density-wave in VTe₂ — •MANUEL TUNIZ¹, WIBKE BRONCH², DENNY PUNTEL¹, DAVIDE SORANZIO³, DAVIDE BIDOGGIA¹, STEVEN JOHNSON³, MARIA PERESSI¹, FULVIO PARMIGIANI^{1,2}, and FEDERICO CILENTO² — ¹Dipartimento di Fisica, Università degli Studi di Trieste, Italy — ²Elettra - Sincrotrone Trieste S.C.p.A., Italy — ³Institute for Quantum Electronics, ETH Zurich, 8093 Zurich, Switzerland

By means of broadband time-resolved optical spectroscopy (TR-OS) we investigated the ultrafast reflectivity changes caused by collective and single particle excitations in the charge-density wave (CDW) system VTe₂. This material has been recently subject of investigation since the modifications in its electronic structure triggered by the CDW formation are strongly orbital-dependent and

may give rise to a topological change in specific bands [1]. In our contribution, we show by means of TR-OS measurements the possibility to optically excite the amplitude mode (AM) of the CDW phase and therefore couple to the CDW condensate [2]. Moreover, through double pump experiments, we show the possibility to control the intensity and the phase of the amplitude mode of the system.

References

- [1] Mitsuishi, N. et al. *Nat. Commun.* 11, 2466 (2020).
 [2] Schaefer, H. et al. *Phys. Rev. B* 89, 045106 (2014).

O 19.5 Mon 18:00 P2/EG

Modification of the ultrafast charge carrier dynamics in a molecule/TMDC heterostructure — •SEBASTIAN HEDWIG¹, MATTHIAS RÜB¹, BENITO ARNOLDI¹, KAI ROSSNAGEL^{3,4}, BENJAMIN STADTMÜLLER^{1,2}, and MARTIN AESCHLIMANN¹ — ¹Department of Physics, University of Kaiserslautern and Research Center OPTIMAS, 67663 Kaiserslautern, Germany — ²Institute of Physics, Johannes Gutenberg University Mainz, 55128 Mainz, Germany — ³Institut für Experimentelle und Angewandte Physik, Christian-Albrechts-Universität zu Kiel, 24118 Kiel, Germany — ⁴Ruprecht Haensel Laboratory, Deutsches Elektronen-Synchrotron DESY, 22607 Hamburg, Germany

Tailoring the properties of layered van der Waals materials is one of the most intriguing challenges in the field of 2D materials. While for transition metal dichalcogenides (TMDCs) this is mainly achieved by the formation of heterostructures with other 2D materials, our approach is to functionalize the properties of TMDCs by the adsorption of molecular films. Here we present our recent fs-time-resolved optical-pump XUV-probe ARPES experiments on a $C_{60}/TiSe_2$ heterostructure. $TiSe_2$ was selected since it can host a charge density wave phase at low sample temperature that can be melted by fs pulses [1]. We find a clear modification of the optically induced phase transition dynamics from the CDW into the semi-metallic phase. This observation is discussed in the light of interactions and the interfacial charge carrier dynamics at the $C_{60}/TiSe_2$ interface.

- [1] Rohwer T., et al.; *Nature*, 471, 490, (2011)

O 19.6 Mon 18:00 P2/EG

Analysis of Nonlocal Correlations in 1T-TaS₂ Driven Out of Equilibrium — •JESUMONY JAYABALAN¹, FLORIAN K. DIEKMANN², PING ZHOU¹, KAI ROSSNAGEL², and UWE BOVENSIEPEN¹ — ¹Fakultät für Physik, Universität Duisburg-Essen, Germany — ²Institut für Experimentelle und Angewandte Physik, Christian-Albrechts-Universität zu Kiel, Germany

Driving correlated materials out of equilibrium on ultrafast time scales can provide information about the correlation phenomena and their complex free energy landscapes. Time- and angle-resolved photoemission spectroscopy provided access to the ultrafast dynamics of Doublons [Ligges et al., *PRL* 120, 166401 (2018)] and concluded on presence of empty and doubly occupied sites at few tens of femtosecond timescales which match calculated spectra with 5% static hole doping. Thus the doublon decay was concluded to be mediated in 1T-TaS₂ by the presence of holes. We propose experiments aimed at a doping dependent relaxation dynamics measurements that would reveal the role of screening and charge excitations on such photo-induced states. Two different approaches will be used for doping: 1) 1T-TaS₂ crystals are grown by Ta substitution to induce a less than half filled band and hole doping and 2) surface doping by adsorption of alkali adsorbates on the cleaved 1T-TaS₂ surface. Such doping depending studies at the timescale of the charge density wave amplitude mode potentially allow to examine the role of strong correlations in the coupled electron-lattice dynamics of 1T-TaS₂ as well as possibilities to control two-dimensional correlated surfaces via photo excitation of the substrate.

O 19.7 Mon 18:00 P2/EG

Disentangling HOMO and LUMO excitation in momentum space by means of time-resolved photoemission orbital tomography — ALEXA ADAMKIEWICZ¹, MIRIAM RATHS², •MARCEL THEILEN¹, MONJA STETTNER²,

SABINE WENZEL², MARK HUTTER², SERGEY SOUBATCH², CHRISTIAN KUMPF², FRANCOIS C. BOCQUET², ROBERT WALLAUER¹, F. STEFAN TAUTZ², and ULRICH HÖFER¹ — ¹Philipps-University Marburg, Germany — ²Peter Grünberg Institute (PGI-3), Jülich Research Centre, Germany

Time-resolved photoemission orbital tomography allows to trace electron dynamics in momentum space by measuring the angle-resolved photoemission intensity on an ultrafast timescale. For molecule-metal interfaces it proved to be a powerful technique to investigate the population dynamics of molecular states [1]. Here, we find for a well-ordered monolayer of CuPc on Cu(001)-2O a delay-dependent change in the momentum pattern of the molecular LUMO. In addition, we show how the temporal evolution of the momentum distribution can be systematically disentangled from contributions of the projected HOMO by varying the pump photon energy and polarization. By aligning the polarization of the pump pulse along the molecular axis of CuPc molecules, we are able to selectively excite molecules of a specific orientation. The temporal evolution of the excitation and decay from the LUMO can be well described by solving the optical Bloch equations for a three-level system.

- [1] R. Wallauer et al., *Science* 371, 1056-1059 (2021).

O 19.8 Mon 18:00 P2/EG

Spin- and valley-dependent charge carrier dynamics in a WSe₂ bulk crystal — •GREGOR ZINKE¹, SEBASTIAN HEDWIG¹, BENITO ARNOLDI¹, MARTIN AESCHLIMANN¹, and BENJAMIN STADTMÜLLER^{1,2} — ¹Department of Physics and Research Center OPTIMAS, TU Kaiserslautern, 67663 Kaiserslautern, Germany — ²Institute of Physics, Johannes Gutenberg University Mainz, 55128 Mainz, Germany

The intriguing spin functionalities of transition metal dichalcogenides such as WSe₂ are rooted in the spin- and valley-degrees of freedom. These are responsible for the particular spin-texture of TMDCs as well as the helicity- and valley-dependent light absorption. However, despite the clear understanding of the initial spin- and valley-dependent light-matter interaction, a clear picture of the spin-dependent intra- and intervalley scattering of electrons and holes is still elusive. Here, we focus on the ultrafast carrier dynamics in a bulk crystal of WSe₂. Using spin-, time- and angle-resolved photoemission with XUV-radiation, we simultaneously image the temporal evolution of the excited carriers in the conduction band as well as the corresponding hole dynamics within the valence band on a fs timescale. The spin-polarization of the initially excited carriers is controlled by the helicity of the optical excitation. We will show clear changes of the spin-polarization of the excited electrons after intra-band scattering from the K- to the Σ -point, and discuss these results in regards to the influence of electron-electron and electron-phonon scattering for the spin-polarized electron population in the conduction band.

O 19.9 Mon 18:00 P2/EG

Ultrafast dynamics of CT excitons in 2d heterostructures investigated with SHG imaging microscopy — •MARLEEN AXT, JONAS E. ZIMMERMANN, GERSON METTE, and ULRICH HÖFER — Fachbereich Physik, Philipps-Universität Marburg, Germany

The exciton dynamics in vertically stacked TMDC heterostructures can be modified by variation of the twist angle between the two layers. Using time-resolved second harmonic (SH) imaging microscopy we observe the ultrafast formation of charge transfer (CT) excitons in micrometer-sized MoS₂/WSe₂ heterostructures with different stacking angles. We make use of the strong anisotropy of the nonlinear SH response to selectively probe the carrier dynamics in individual layers of the system. For misaligned layers with a stacking angle of 16° the formation of CT excitons takes place within 85 fs after resonant excitation of the WSe₂ A excitation. In contrast, an alignment close to 2H stacking (52°) leads to an enhanced electronic coupling between the layers resulting in a much faster CT exciton formation time of only 12 fs. Moreover, different formation and relaxation pathways are identified depending on the pump-photon energy.

O 20: Poster: Spins and Magnetism at Surfaces

Time: Monday 18:00–20:00

Location: P2/EG

O 20.1 Mon 18:00 P2/EG

Aging behavior in a self-induced spin glass — LORENA NIGGLI, •JULIAN H. STRIK, ANAND KAMLAPURE, MIKHAIL I. KATSNELSON, DANIEL WEGNER, and ALEXANDER A. KHAJETOORIANS — Institute for Molecules and Materials, Radboud University, Nijmegen, The Netherlands

Elemental neodymium has been shown to be a so-called self-induced spin glass, which, unlike conventional spin glasses, shows glassy behavior solely from frustrated magnetic interactions and in the absence of disorder [1]. Additionally, in contrast to most conventional spin glasses, neodymium has a disorder to order transition. As the temperature increases it goes from the self-induced spin glass phase to a multi-Q long range ordered phase resulting from competing long-

range interactions on different length scales [2]. This disorder to order transition might have profound effects on the metastable states and aging dynamics in the low temperature phase. In this study, we use spin-polarized scanning tunneling microscopy combined with varying external magnetic fields to investigate the aging dynamics in the spin glass phase, and quantify this in terms of the various local spin-spin correlations (Q-states) observed. These observations may have interesting implications on the aging behavior in self-induced spin glasses, which might differ from conventional spin glasses.

- [1] U. Kamber et al., *Science* 368 (2020).
 [2] B. Verlhac et al., *Nat. Phys.* 18 (2022).

O 20.2 Mon 18:00 P2/EG

Tuning the frequency response of stochastically switching orbital states of Fe and Co atoms on black phosphorus — •KIRA JUNGHANS, HERMANN OSTERHAGE, WERNER M. J. VAN WEERDENBURG, NIELS P. E. VAN MULLEKOM, RUBEN CHRISTIANEN, EDUARDO J. DOMÍNGUEZ VÁZQUEZ, HILBERT J. KAPPEN, and ALEXANDER A. KHAJETOORIANS — Radboud University, Nijmegen, The Netherlands

The concept of the atomic Boltzmann machine (BM) is based on the recently discovered idea of orbital memory [1,2]. Orbital memory is characterised by two stable valency configurations [2,3]. By applying a bias voltage to a scanning tunneling microscopy (STM) tip above a threshold, stochastic switching between the states can be induced. The favorability of the individual states depends strongly on the applied bias voltage.

Unlike coupled spins under exchange, leading to bistability, coupled atoms that exhibit orbital memory show multi-stability in their stochastic dynamics. This multi-well energy landscape serves as a basis for the BM and realizing multiple time scales.

Here, we show that single Fe and Co atoms respond frequency and amplitude dependent to an AC component of the applied bias. In addition, we present how the stochastic behavior of coupled atoms in the multi-well regime respond to a harmonic drive voltage.

[1] B. Kiraly et al., Nat. Nanotechnol. 16, 414 (2021).

[2] B. Kiraly et al., Nat. Commun. 9, 3904 (2018).

[3] B. Kiraly et al., Phys. Rev. Research 4, 33047 (2022).

O 20.3 Mon 18:00 P2/EG

Development of a gate-tunable graphene substrate for spins on surfaces — •PAUL GREULE¹, MÁTÉ STARK¹, WANTONG HUANG¹, DAVID COLLOMB¹, DARIA SOSTINA², CHRISTOPH SÜRGER¹, WOLFGANG WERNSDORFER¹, and PHILIP WILLKE¹ — ¹Physikalisches Institut (PHI), Karlsruhe Institute of Technology, Karlsruhe, Germany — ²Institute of Quantum Materials and Technologies (IQMT), Karlsruhe Institute of Technology, Karlsruhe, Germany

Single spins on surfaces constitute a promising architecture for future quantum technologies as quantum sensors and possible qubits for quantum information processing. The recent combination of electron spin resonance (ESR) and scanning tunneling microscopy (STM) emerges as a new technique to coherently manipulate spin states on a single atom level [Y. Chen et al., Adv. Mater. 2022, 2107534]. Nevertheless, this architecture does not provide yet any method to continuously tune the coupling between single electron spins. Here, we want to introduce graphene field-effect transistors as a new substrate for ESR-STM on single molecules. Gated graphene devices enable tuning of the charge carrier density of the substrate as already shown by means of scanning tunneling spectroscopy (STS) [Y. Zhang et al., Nature Phys. 5, 722-726 (2009)]. This constitutes a promising way to manipulate the substrate-mediated exchange coupling between single spin centers. We present the development of gated graphene devices for STM using single layer graphene. Moreover, we characterize the samples with in-situ transport measurements and show first topographic and spectroscopic STM measurements.

O 20.4 Mon 18:00 P2/EG

Magnetic phase diagram of a YSR-molecule — •BENJAMIN A. VERLHAC¹, NIELS VAN MULLEKOM¹, WERNER M.J. VAN WEERDENBURG¹, HERMANN OSTERHAGE¹, MANUEL STEINBRECHER¹, KATHARINA J. FRANKE², and ALEXANDER A. KHAJETOORIANS¹ — ¹Institute for Molecules and Materials, Radboud University, Nijmegen, The Netherlands — ²Fachbereich Physik, Freie Universität Berlin, Germany

Yu-Shiba-Rusinov (YSR) states arise from the exchange coupling between a local spin and a superconductor. However, characterizing this exchange interaction, related to Kondo screening, requires a study in magnetic field to understand its interplay with other energy scales, as well as the role of higher spin degrees of freedom. To date, most studies of YSR states have been limited to bulk superconductors, which easily quench in the presence of modest magnetic fields. Here, using high resolution milliKelvin scanning tunneling microscopy and spectroscopy, we characterize the magnetic phase diagram of a molecule on the surface of a thin film superconductor. We observe non-trivial changes in the YSR excitations in applied magnetic field, that cannot be described by the prototypical spin 1/2 model. These variations occur while the superconducting gap remains robust. We relate the changes to the various properties of the molecule, including the role of multiple channels and magnetic anisotropy. We additionally propose a model to understand the various behaviors in the excitation. These results provide an in-depth and detailed approach to understand the role of high spin systems in the presence of Kondo and YSR states.

O 20.5 Mon 18:00 P2/EG

Electronic Structure of Chromium(II)-Bromide Islands on Niobium Diselenide — •XIANZHE ZENG¹, HAONAN HUANG¹, SUJOY KARAN¹, KLAUS KERN^{1,2}, and CHRISTIAN AST¹ — ¹Max-Planck-Institut für Festkörperforschung, Heisenbergstraße 1, 70569 Stuttgart, Germany — ²Institut de Physique, Ecole Polytechnique Fédérale de Lausanne, 1015 Lausanne, Switzerland

Chromium(II) bromide is an inorganic two-dimensional (2D) van der Waals material. With molecular-beam epitaxy (MBE), superconducting islands can be formed after evaporating chromium(II) bromide onto a niobium diselenide substrate. Measurements have been conducted on the islands and at the edge of the islands with low-temperature scanning tunneling microscopy and spectroscopy. At the edge of the islands, a subgap peak could be identified from the dI/dV spectrum, suggesting the existence of an in-gap state. Our discovery is the first observation in the chromium(II) bromide-niobium diselenide heterostructure system, providing an interesting comparison with the reported Majorana zero energy mode at the edge of chromium(III) bromide islands growing on the same substrate.

O 20.6 Mon 18:00 P2/EG

Josephson diode effect due to single magnetic atoms — MARTINA TRAHMS¹, LARISSA MELISCHEK², JACOB F. STEINER², •BHARTI MAHENDRU¹, IDAN TAMIR¹, NILS BOGDANOFF¹, OLOF PETERS¹, GAËL REECHT¹, CLEMENS B. WINKELMANN³, FELIX VON OPPEN², and KATHARINA J. FRANKE¹ — ¹Fachbereich Physik, Freie Universität Berlin, Arnimallee 14, 14195 Berlin, Germany — ²Dahlem Center for Complex Quantum Systems and Fachbereich Physik, Freie Universität Berlin, 14195 Berlin, Germany — ³Université Grenoble Alpes, CNRS, Institut Néel, 25 Avenue des Martyrs, 38042 Grenoble, France

Properties of Cooper-pair tunneling through a Josephson junction can be described by the phase difference between two superconductors. In a current-biased Josephson junction, the phase dynamics can be accessed via switching and retrapping currents. Here, we investigate Josephson junctions formed by a superconducting Pb tip and a Pb surface in a scanning tunneling microscope. While pristine Pb-Pb junctions are hysteretic but symmetric in the biasing direction, we observe asymmetric retrapping currents in the presence of single magnetic atoms placed in the junction. The behavior thus mimics diode properties in the retrapping current. We model the phase dynamics of these junctions by an extended resistively and capacitively shunted Josephson junction (RCSJ). We find the asymmetric retrapping current originates in a non-ohmic dissipative channel due to the particle-hole-symmetry-broken Yu-Shiba-Rusinov (YSR) states. By investigating different magnetic adatoms on different Pb surfaces, we carve out a general relation of asymmetric YSR states and asymmetric retrapping currents.

O 20.7 Mon 18:00 P2/EG

Organometallic sandwich complexes as model spin 1/2 impurities on superconductors — •ADITHYA SADANANDAN¹, LUKAS ARNHOLD¹, NICOLAJ BETZ¹, ANDREA L. SORRENTINO², GIULIA SERRANO², ROBERTA SESSOLI², SUSANNE BAUMANN¹, and SEBASTIAN LOTH¹ — ¹University of Stuttgart, Institute for Functional Matter and Quantum Technologies, Stuttgart, Germany — ²University of Florence, Department of Chemistry 'Ugo Schiff', INSTM Research Unit, Florence, Italy

Self-assembled layers of organometallic sandwich complexes containing transition metal atoms enable selective control of the spin delocalization and hybridization of the molecules with the electron bath of surfaces [1,2]. We study small self-assembled rafts of [CpTi(cot)] sandwich complexes on epitaxial Pb islands on Si(111). [CpTi(cot)] features a single electron in the d orbitals and long coherence times in solution [2] making it an interesting candidate for molecular qubits and a well-defined spin 1/2 system. Using low temperature scanning tunneling microscopy (STM) we find weakly bound Yu-Shiba-Rusinov states (YSR) in the superconducting gap and a crossover between Kondo screening and spin excitations when superconductivity is quenched by a magnetic field. The simple level structure of [CpTi(cot)] makes it possible to model this system with an Anderson impurity model [3] and deduce the dynamics of the YSR states.

[1] M. Briganti et al., Nano Lett. 22 8626 (2022).

[2] L. C. Camargo et al., Angew. Chem. Int. Ed. 60 2588 (2021).

[3] H. Huang et al., Commun Phys. 3 199 (2020).

O 20.8 Mon 18:00 P2/EG

Electrospray deposition for STM sample preparation in UHV — •CAROLINE HOMMEL, LUKAS SPREE, DASOM CHOI, LUCIANO COLAZZO, and ANDREAS HEINRICH — Center for Quantum Nanoscience, 52 Ewhayeodae-gil, Daehyeon-dong, 03760 Seoul, South Korea

Lanthanide single molecule magnets are promising materials for future spintronics applications, such as ultrahigh density memory devices. Using several methods, we have succeeded in synthesizing different double-decker phthalocyanine complexes (M-Pc₂; M = Y, Er, Tb) and depositing them on a metal substrate in ultra-high vacuum (UHV) for scanning tunneling microscopy (STM) analysis. Due to their flat geometry they are very well suited for surface deposition. Based on the very well-known chemical properties of the phthalocyanine ligands, it is possible to functionalize them for various purposes. M-Pc₂ form ordered structures on the surface, which could be further enhanced by long chain alkane groups on the phthalocyanine ligands. However, such large organic molecules cannot be sublimated without fragmentation. Using electro spray deposition (ESD), thin films of thermally unstable molecules can be deposited directly in UHV. Various parameters, such as pressure, time, and solvent

play a role in this process. The influence of the parameters on the deposition will be investigated for M-PC₂ molecules and their chemical derivatives.

O 20.9 Mon 18:00 P2/EG

Scanning tunneling spectroscopy of a spin-crossover complex on a superconductor — •MARTEN TREICHEL¹, FLORIAN GUTZEIT², JAN HOMBERG¹, RAINER HERGES², RICHARD BERNDT¹, and ALEXANDER WEISMANN¹ — ¹Institut für Experimentelle und Angewandte Physik, Christian-Albrechts-Universität zu Kiel, Kiel, Germany — ²Otto-Diels-Institut für Organische Chemie, Christian-Albrechts-Universität zu Kiel, Kiel, Germany

A spin-crossover complex based on Ni-porphyrin is studied on superconducting Pb(100) using scanning tunneling spectroscopy at 0.3 K. A pronounced molecule-induced surface faceting is found with molecular chains located at multiple substrate steps. The step orientations deviate from the high-symmetry directions of the substrate and appear to be imposed by molecular interactions. Monatomic substrate steps remain undecorated. Conductance spectra reveal spin-flip excitations with clear spatial variations. The data suggest that neighbor molecules are rotated by 90° with respect to each other. We find that an $S = 1$ quantum spin model with the hard axis tilted away from the surface normal reproduces spectra measured in magnetic fields up to 9 T.

O 20.10 Mon 18:00 P2/EG

Strong exchange interaction between open-shell nanographenes and TbAu2 — •NICOLÒ BASSI¹, FEIFEI XIANG¹, JAN WILHELM², ROMAN FASEL¹, and PAS-CAL RUFFIEUX¹ — ¹Empa-Swiss Federal Laboratories for Materials Science and Technology, Dübendorf, Switzerland — ²Institute of Theoretical Physics, University of Regensburg, Regensburg, Germany

Rare-earth intermetallic compounds belong to a family of novel substrates, which is becoming a promising platform to control properties of nanomaterials via specific surface-adsorbates interactions. Different combinations, including GdAu₂(1), LaAu₂(2) and TbAu₂(3), have been so far studied. They are all characterized by a ordered hexagonal superstructure with similar lattice constants. Here, we investigate various open-shell nanographenes on TbAu₂ alloy by means

of STM and STS combined supported by ab initio simulation. For on surface synthesized 7-AGNRs, we find that the predicted spin properties of the end states are indeed conserved on TbAu₂. Here, 7-AGNRs are uncharged and the occupied and unoccupied end states have a spin polarization-induced energy splitting of 1.4 eV. In addition, we investigated phenalenyl, the smallest open-shell molecule with spin $S = 1/2$, at monolayer coverage. Low bias spectroscopy reveals a splitting of the peak of more than 20 mV, which we assign to the exchange interaction between the molecular spin and Tb atoms of the surface layer. These results open new perspectives for studying different open-shell molecules on a magnetic substrate. 1 ACS Nano 4, (2010). 2 Phys. Rev. B 88, 125405 (2013). 3 J. Phys. Chem. Lett. 11, (2020).

O 20.11 Mon 18:00 P2/EG

Observation of in-gap states on 4f-shell magnet-superconductor hybrid system — •YU WANG, FELIX FRIEDRICH, ARTEM ODOBESKO, and MATTHIAS BODE — Physikalisches Institut, Experimentelle Physik II, Universität Würzburg, Am Hubland, D-97074 Würzburg, Germany

Magnetic impurities assembled on s-wave superconductor are the prototypical system for the realization of MZMs at the chain ends. Particularly the magnet-superconductor hybrid system of one-dimensional magnetic chains on superconductors has been well demonstrated theoretically and experimentally. Nowadays, various 3d-shell transition metals (Cr, Mn, Fe, Co, Ni) on clean Nb (110) have been studied [1-3]. Among them, only Mn and Fe chains exhibits benchmarks of topological superconductivity with MZMs at the chain ends. In addition to 3d-shell metals as magnetic impurities, 4f-shell magnetic metals could be another option. Among them, Gd shows the highest potential because it has the highest magnetic moment ($s = 7/2$) in 4f-shell. In this study, we will show that Gd dimers on Nb (110) behave similar as Fe/Mn with two pairs of in-gap states. It could be possible to realize MZMs on Gd chain ends in the future.

[1] D. Crawford and E. Mascot, arXiv: 2109.06894v1 [cond-mat.super-con], (2021)

[2] L. Schneider *et al.*, Nature Physics 17, 943 (2021)

[3] A. Odobesko *et al.*, Physical Review B 11, 99 (2019)

O 21: Poster: Scanning Probe Techniques

Time: Monday 18:00–20:00

Location: P2/EG

O 21.1 Mon 18:00 P2/EG

Shot-noise measurements of single-atom junctions using a scanning tunneling microscope — •VERENA CASPARI, IDAN TAMIR, DANIELA ROLF, CHRISTIAN LOTZE, and KATHARINA J. FRANKE — Fachbereich Physik, Freie Universität Berlin, Arnimallee 14, 14195 Berlin, Germany

Current passing through small constrictions fluctuates due to the discreteness of charge. Measuring this so-called shot noise in atomic-scale superconducting junctions can provide valuable information, from the quanta of charge transferred in the tunneling process to the correlations of the involved tunneling channels. Here, we use a scanning tunneling microscope equipped with a high-frequency, low-temperature amplifier to measure simultaneously the noise characteristics and the differential conductance of two types of Pb-Pb-junctions having different geometries. The first type is created by deposition and approaching single Pb adatoms, while the second type is established by a break-junction technique. We observe a correlation between the noise pattern and the strength of the Josephson current, independent on the method of junction preparation.

O 21.2 Mon 18:00 P2/EG

A second generation millikelvin scanning tunneling microscope with adiabatic demagnetization refrigeration — TANER ESAT^{1,2}, •DENIS KRYLOV¹, PETER BORGES^{1,3,7}, XIAOSHENG YANG^{1,3}, PETER COENEN^{1,4}, VASILY CHEREPANOV^{1,4}, ANDREA RACCANELLI^{5,7}, F. STEFAN TAUTZ^{1,2,3}, and RUSLAN TEMIROV^{1,6} — ¹Peter Grünberg Institute (PGI-3), Forschungszentrum Jülich, 52425 Jülich, Germany — ²Jülich Aachen Research Alliance, Fundamentals of Future Information Technology, 52425 Jülich, Germany — ³Experimentalphysik IV A, RWTH Aachen University, 52074 Aachen, Germany — ⁴mProbes GmbH, 52428 Jülich, Germany — ⁵Cryovac GmbH & Co KG, 53842 Troisdorf, Germany — ⁶Faculty of Mathematics and Natural Sciences, Institute of Physics II, University of Cologne, 50937 — ⁷Current address: Peter Grünberg Institute (Cryo-Lab), Forschungszentrum Jülich, 52425 Jülich, Germany

We present the design of a second generation ultra-high vacuum scanning tunneling microscope (STM) that uses adiabatic demagnetization of electron magnetic moments for controlling its operating temperature down to 30 mK. A high degree of vibrational decoupling promises an outstanding mechanical stability, demonstrated by the first generation of this instrument. Additionally, high frequency cables were implemented in the design in order to enable electron spin resonance experiments.

[1] T. Esat, P. Borgens, X. Yang, P. Coenen, V. Cherepanov, A. Raccanelli, F. S. Tautz, and R. Temirov, Review of Scientific Instruments 92, 063701 (2021).

O 21.3 Mon 18:00 P2/EG

atomic friction on TaS₂ over a phase transition — •YIMING SONG¹, DIRK DIETZEL^{1,2}, and ANDRE SCHIRMEISEN^{1,2} — ¹Institute of Applied Physics (IAP), Justus-Liebig-Universität Gießen, 35392 Gießen, Germany — ²Center for Materials Research, Justus-Liebig-Universität Gießen, 35392 Gießen, Germany

Friction force microscopy experiments were performed on tantalum disulfide (TaS₂) surfaces as a function of temperature over the phase transition from nearly commensurate charge density wave (NCCDW) phase to commensurate CDW phase. A giant frictional peak at the temperature of 187 K which separates CCDW and NCCDW phases when the sample is cooled down is observed. This behavior was investigated in detail by comparing atomic stick-slip motion of the single asperity AFM tip over phase transition. The hysteresis of the first order structural transformation is revealed in stick-slip behaviors during the heating up procedure as well. Besides, the load and velocity dependence of friction on TaS₂ surface in CCDW and NCCDW phases have been revealed.

O 21.4 Mon 18:00 P2/EG

Design of a compact dilution refrigerator integrated in a dry mK UHV STM — •MICHAEL TEMMEN, SIMON GERBER, MICHAEL MEYER, and WULF WULFHEKEL — Physikalisches Institut, Karlsruher Institut für Technologie, Karlsruhe, Deutschland

As energy and helium prices are rising we decided to design a new dry, low temperature Scanning Tunneling Microscope with a compact, low ³He volume dilution refrigerator as the main innovation. Special focus was set on the heat exchanger between the still and the mixing chamber as one of the most crucial parts of the system. Next to the standard solution of a tube-in-tube heat exchanger, a new concept of a heat exchanger consisting of two laser cut metal sheets with deep drawn profiles acting as the channels for the Helium and a plain sheet in the middle as a divider is developed. In order to improve heat transfer while keeping the volume minimal, the surface area is increased by electrodeposition of three dimensional porous silver foam. Comparing this concept with the standard solution, an increase in surface area by a factor of 10 could be achieved with a reduction in ³He volume in the exchanger by a factor of 10. The dilution refrigerator is integrated in a small scale cryostat with a closed helium cycle cooled by a pulse tube with a cooling capacity of 400 mW. The complete dilution refrigerator, cryostat and the STM are home-built.

O 21.5 Mon 18:00 P2/EG

Electromagnetic Field Mapping in Plasmonic Nanostructures using Momentum-Resolved Electron Energy-loss Spectroscopy — •JOHANNES SCHULTZ¹, JONAS KREHL¹, GIULIO GUZZINATI², and AXEL LUBK^{1,3} — ¹Leibniz-Institut für Festkörper- und Werkstofforschung Dresden e. V., Helmholtzstraße 20, 01069 Dresden — ²EMAT, University of Antwerp, Groenenborgerlaan 171, 2020 Antwerp — ³Institute of Solid State and Materials Physics, Haeckelstraße 3, 01069 Dresden

Localized surface plasmons (LSPs) are collective oscillations of charge carriers arising at interfaces between media of opposite sign of the dielectric functions. Here, spatial confinement of the LSPs, e.g. in nanoparticles (NPs), may lead to enhanced electromagnetic (e.m.) fields of the LSPs due to resonance. This effect is exploited in several application, e.g., surface enhanced Raman spectroscopy. To characterize the e.m. fields scanning transmission electron microscopy in combination with electron energy loss spectroscopy is a frequently used technique due to its high spectral and spatial resolution. Here, the energy loss of the beam electrons (caused by the electric field component of the LSPs parallel to the beam) is measured at different probe positions. This technique has been generalized to additionally probe in-plane field components by measuring the deflection of the beam electrons from their initial trajectory. To that end spectrally resolved deflection maps (so-called $\omega - q$ maps) are recorded at different probe positions which opens up new capabilities to e.g., probe magnetic field contributions of the LSPs at highest spectral and spatial resolution.

O 21.6 Mon 18:00 P2/EG

SpmImage Tycoon: Organize scanning probe microscopy data — •ALEXANDER RISS — Physics Department E20, Technical University of Munich, D-85748 Garching, Germany

The evolution of the field of scanning probe microscopy (SPM) has been associated with development of instrumental capabilities and methods for data acquisition and analysis. However, much less emphasis has been placed on improving the management and organization of the measured datasets. And while datasets

can consist of thousands of images and spectra per project, it is not uncommon for researchers to go through each image or spectrum and manually select the channels of interest for each one — only to repeat the same procedure every time they want to analyze their data again.

Here we present a cross-platform application that is designed for fast and effortless organization and basic editing of scanning probe microscopy images and spectra [1]. The application is released under an open-source license and supports automatic channel-of-interest detection, image editing (such as background corrections and contrast adjustment), keywording, star-ratings, powerful search and filtering (e.g., by keywords, data type, location, scan size), as well as export of the data into a PowerPoint-compatible presentation format.

Such easy-to-use tools can lower the entry barrier for aspiring scientists, boost the efficiency of experienced researchers, and help to create and leverage large SPM datasets for machine learning and artificial intelligence applications.

[1] A. Riss. JOSS 7, 4644 (2022)

O 21.7 Mon 18:00 P2/EG

Electric field control of spin transitions in a dimer system using ESR-STM — •MANEESHA ISMAIL¹, PIOTR KOT², JANIS SIEBRECHT¹, HAONAN HUANG¹, and CHRISTAN R. AST¹ — ¹Max-Planck-Institute for Solid State Research, Heisenbergstr. 1, 70569 Stuttgart, Germany — ²Center for Quantum Nanoscience, Institute for Basic Science, Seoul 03760, Republic of Korea

Since the demonstration of the control of spins on the atomic scale, the technique of ESR-STM has been used extensively to explore the field of spintronics. Here, we present a new approach to ESR-STM which uses the bias voltage as a parameter to tune the energy of the Zeeman transition. We demonstrate electronic control of spin resonance transitions in a single molecule. We could observe a strong dependency of the g -factor and tip-field shift on the electric field. Finally, we demonstrate an avoided crossing in the energy levels of a dimer as a function of bias voltage, which corresponds to an entangled state. This could be an important step towards quantum computations as they rely on entanglement opening a more coherent and easier method of electronic spin control.

O 22: Poster Session: Organic Molecules on Inorganic Substrates I

Time: Monday 18:00–20:00

Location: P2/EG

O 22.1 Mon 18:00 P2/EG

Charge-state lifetimes of single molecules on ultrathin insulating films — •KATHARINA KAISER^{1,3}, LEONARD-ALEXANDER LIESKE¹, JASCHA REPP², and LEO GROSS¹ — ¹IBM Research - Zurich, Säumerstrasse 4, 8803 Rüschlikon, Switzerland — ²Department of Physics, University of Regensburg, Universitätsstraße 31, 93053 Regensburg, Germany — ³Present address: Institut de Physique et de Chimie des Matériaux de Strasbourg, Département Surfaces et Interfaces, 23 Rue du Loess, BP 43, 67034 Strasbourg, France

In scanning tunneling microscopy (STM) experiments of molecules on insulating films, tunneling through molecular resonances goes along with transiently charging the molecule. The transition back to its charge ground state by tunneling through the insulating film crucially determines the charging dynamics of the system and with this is essential for understanding, e.g., excited state formation and luminescence quenching in electroluminescence experiments. The two quantities describing these processes are the average charging and discharging time, the latter being the lifetime of the charged state, and they are accessible in STM: By approaching the tip to the molecule at resonant tunnel conditions up to a regime where charge transport is limited by tunneling through the NaCl film the saturation of the tunnel current, which is a direct measure of the molecule's charge state lifetime and thus provides a means to study charge and exciton dynamics, can be measured. We report on the charge state lifetimes of individual molecules adsorbed on NaCl films of different thicknesses on Cu(111) and Au(111), and provide insights into the role of the substrate and the spacer layer.

O 22.2 Mon 18:00 P2/EG

Theoretical Investigation of Tetracene-Adsorption on Cu(111)-Substrate — •FLORIAN ALEXANDER PFEIFFER, JOHANNES BLK, and SIMONE SANNA — Institut für Theoretical Physics, Justus-Liebig-University Gießen, Heinrich-Buff-Ring 16, Gießen, 35392, Hesse, Germany

Due to possible catalytic effects of a substrate, chemical reactions can occur within much smaller timescales on metal surfaces than in solutions. Ullmann-coupling of Br-substituents to organic molecules, important to biology, chemistry and medicine, might profit of such catalytic effects. Little is known about this reaction on metallic substrates. Theoretical modelling is crucial for understanding the underlying processes. A first step towards such investigation is the first-principle modelling of tetracene-adsorption on Cu(111). Calculation of adsorption geometry and energy as well as charge transfer between molecule and surface is done utilizing density functional theory (DFT). Our calculations show that dispersion forces (van der Waals corrections) need to be taken into account for adsorption modelling. Adsorption energy and geometry as well as charge

transfer suggest physisorption of tetracene at Cu(111). The Tersoff-Hamann-approximation allows for simulating STM-images using the DFT-calculated charge density. The STM-images show p_z orbitals of the benzene rings.

O 22.3 Mon 18:00 P2/EG

Effects of oxygen functionalization on the molecule-substrate coupling — •JONAS BRANDHOFF, FELIX OTTO, MAXIMILIAN SCHAAL, ROMAN FORKER, and TORSTEN FRITZ — Institute of Solid State Physics, Friedrich Schiller University Jena, Helmholtzweg 5, 07743 Jena, Germany

5,7,12,14-Pentacenetetrone (P4O) is a polycyclic aromatic hydrocarbon which shows promising electronic properties for batteries. Unlike pentacene the π -system is not delocalized over the entire molecule. P4O shows a strong interaction with metal substrates up to a point where the π -system delocalization reemerges partially over the entire molecule. To understand this phenomenon of metallic organic bonding and charge-transfer, as well as the needed interaction strength for enabling a delocalized π -system over the entire molecule, different substrate-P4O systems were investigated. On the one hand, Cu(111) was chosen as a metallic substrate which shows a strong interaction and charge-transfer. On the other hand, the semi-metallic substrate of epitaxial graphene (EG) on SiC(0001) was selected, showing no charge transfer. As an intermediate system, Pt(111) as a noble metal was investigated. Furthermore hexagonal boron-nitride (h-BN) was used to decouple P4O from the Pt(111) substrate. The change in the structure of the adsorbate film was analyzed using STM and LEED. XPS and UPS measurements gain further insights into the electronic properties. Photoemission orbital tomography (POT) was used to characterize the energetic positions of the frontier orbitals.

O 22.4 Mon 18:00 P2/EG

Vectorial Electron Spin Filtering by an All-Chiral Metal-Molecule Heterostructure — •CHETANA BADALA VISWANATHA¹, JOHANNES STÖCKL¹, BENITO ARNOLDI¹, SEBASTIAN BECKER^{1,2}, MARTIN AESCHLIMANN¹, and BENJAMIN STADTMÜLLER^{1,3} — ¹Department of Physics and Research Center OPTIMAS, University of Kaiserslautern, Erwin-Schrödinger-Straße 46, 67663 Kaiserslautern, Germany — ²Department of Chemistry, University of Kaiserslautern, Erwin-Schrödinger-Straße 52, 67663 Kaiserslautern, Germany — ³Institute of Physics, Johannes Gutenberg University Mainz, Staudingerweg 7, 55128 Mainz, Germany

Chiral-induced spin selective transmission (CISS) has predominantly been explored in structurally helical molecules on surfaces, where the spin selectivity only affects the spin polarization of the electrons along their direction of prop-

agation. Here, we demonstrate[1] a spin-selective electron transmission for a point-chiral molecule 3-Methylcyclohexanone (3-MCHO) adsorbed on the chiral Cu(643) surface. Using spin- and momentum-resolved photoelectron spectroscopy, we detect a spin-dependent electron transmission through a single layer of 3-MCHO molecules that depends on all three components of the electrons' spin. The findings are attributed to the enantiomer-specific adsorption configuration on the surface. This opens the intriguing opportunity to selectively tune CISS by the enantiospecific molecule-surface interaction in all-chiral heterostructures.

[1] J. Phys. Chem. Lett. 2022, 13, 26, 6244-6249.

O 22.5 Mon 18:00 P2/EG

Electronic properties of bi- and peri-tetracene on Cu(111) studied by density functional theory — •NINA KAINBACHER¹, MAREN KLEIN^{2,3}, JOHN B. BAUER³, HOLGER BETTINGER³, HEIKO PEISERT², and PETER PUSCHNIG¹ — ¹Institute of Physics, NAWI Graz, University of Graz, Austria — ²Institute of Physical and Theoretical Chemistry, University of Tübingen, Germany — ³Institute of Organic Chemistry, University of Tübingen, Germany

Zigzag edged nanographenes with two rows of fused linear acenes, called n-periacenes, have gained increasing attention in the area of organic electronics due to their interesting electronic properties. However, the synthesis is challenging because of their chemical instability. Here we show that a well-ordered monolayer of peritetracene, an n-periacene with four benzene rings in a row, can be produced by depositing the precursor 1,1'-bitetracene on Cu(111) and a subsequent heat treatment. The as-deposited and the annealed films are investigated by STM and UPS and by electronic structure calculations within DFT using a repeated slab approach. We determine the optimal adsorption sites by using damped molecular dynamics and empirical dispersion corrections according to Grimme. We then analyze the electronic structure of the organic/metal interfaces, in particular we focus on the (local) density of states and charge rearrangements upon interface formation which is decisive for the energy level alignment and work function changes. Our results clarify that the interaction of peritetracene with the Cu(111) substrate leads to a charge transfer into the LUMO which is consistent with the experimental observations.

O 22.6 Mon 18:00 P2/EG

Decoupling of vanadyl-naphthalocyanine from a metal substrate by monolayer MoS₂ — •J. RIKA SIMON, GAËL REECHT, CHRISTIAN LOTZE, and KATHARINA J. FRANKE — Fachbereich Physik, Freie Universität Berlin, Germany

Phthalocyanines with metal centres are well known for their relative stability on surfaces and are of interest because of the spin they can carry in their metal centres. On metal surfaces, the molecular electronic states are often hybridised with the metal underneath, making it difficult to observe fine details in the electronic structure and inelastic excitations. Using monolayers of semiconducting transition-metal dichalcogenides (TMDCs) as a decoupling layer on top of metal surfaces is a well-established way to allow access to highly resolved dI/dV spectra. Here, we use scanning tunnelling microscopy (STM) to probe the properties of vanadyl-naphthalocyanine (VONc) on MoS₂/Au(111). We observe VONc with molecular centres appearing with different apparent heights, which can be interpreted as different configurations of the central oxygen atom sitting on top or below the molecular macrocycle, as observed previously on the closely related molecule vanadyl-phthalocyanine (VOPc) [1,2]. Additionally, we see sharp molecular states in the semiconducting band gap, which are affected by the perturbation potential of the tip [3], causing them to shift in energy across the VONc molecules.

[1] L. Malavolti et al., Nano Lett. 18, 7955 – 7961 (2018)

[2] K. Kaiser et al., ACS Nano 13, 6947 – 6954 (2019)

[3] N. Krane et al., PRB 100, 035410 (2019)

O 22.7 Mon 18:00 P2/EG

Electronic properties of organic/transition metal dichalcogenide heterostructures — •HIBIKI ORIO^{1,2}, MAXIMILIAN ÜNZELMANN^{1,2}, KIANA BAUMGÄRTNER^{1,2}, CHRISTIAN METZGER^{1,2}, MARKUS SCHOLZ³, KAI ROSSNAGEL^{3,4}, and FRIEDRICH REINERT^{1,2} — ¹Experimentelle Physik VII, Universität Würzburg, Germany — ²Würzburg-Dresden Cluster of Excellence ct.qmat, Würzburg Dresden, Germany — ³Deutsches Elektronen-Synchrotron DESY, Hamburg, Germany — ⁴KiNSIS, Universität Kiel, Germany

Adsorption of organic molecules on transition metal dichalcogenides (TMDCs) can modify the electronic properties of both the organic layer as well as the substrate [1]. Here, we investigate the electronic structure of copper phthalocyanine (CuPc) grown on the TMDC TiSe₂ using angle-resolved and X-ray photoelectron spectroscopy. We find that the binding energy of the highest occupied molecular orbital increases gradually from 310 to 430 meV upon 4 hours of X-ray radiation. On this poster, we will discuss the origin of this phenomenon.

[1] Y. L. Huang et al., Chem. Soc. Rev., 2018, 47, 3241

O 22.8 Mon 18:00 P2/EG

Ligand Size Controls Surface Chemical Bond: Cobalt Porphyrin versus Cobalt Corrole on the Ag(111) Surface — •CONG GUO, GRIGORI PASKO, JAN HERRITSCH, and J. MICHAEL GOTTFRIED — Fachbereich Chemie, Philipps-Universität Marburg

The development of novel functional materials based on biologically relevant molecules such as cobalamins, also referred to as vitamin B₁₂, is an important research topic. In particular, cobalt tetrapyrrole complexes which are related to cobalamins are often-used and well-understood model systems. Due to the structural complexity of the ligands, their interaction and bonding at interfaces is still poorly understood. Using XPS, we compare here a cobalt(II) porphyrin with a related cobalt(III) corrole. The latter exhibits a smaller ring size and acts as a trianionic ligand. In the multilayer, the Co 2p signal of the porphyrin shows the typical appearance of a paramagnetic Co²⁺ center. The corresponding Co 2p signal of the corrole has a similar shape indicating the presence of unpaired electrons in the Co 3d subshell. In the monolayer on Ag(111), both complexes are subject to an interfacial charge transfer from the substrate, as can be seen by the Co 2p signals. Thus, the singly occupied orbitals at the cobalt center are accepting electron density from the substrate. However, the N 1s signal and the valence photoemission spectra indicate that the corrole interacts much stronger with the substrate which is confirmed by periodic DFT calculations. Our study reveals that the two adsorbed complexes differ substantially in their overall interaction with the Ag surface, even though cobalt has a similar electronic state in both cases.

O 22.9 Mon 18:00 P2/EG

Charge Transfer on a 2D Insulator: Influence of the Molecular Functionalization — •MAXIMILIAN SCHAAL, JONAS BRANDHOFF, FELIX OTTO, ROMAN FORKER, and TORSTEN FRITZ — Institute of Solid State Physics, Friedrich Schiller University Jena, Helmholtzweg 5, 07743 Jena, Germany

2D materials like hexagonal boron nitride (h-BN) are widely used as interlayer to decouple organic molecules from metallic surfaces. Despite the large band gap of 2D h-BN of ≈ 6 eV, there are also indications for a possible charge transfer into organic molecules. This raises the question: What is the reason for the charge transfer on this 2D insulator?

To address this question, we systematically studied the influence of the molecular functionalization on the lateral structure as well as on the charge transfer on 2D h-BN grown by chemical vapor deposition on Ni(111). Therefore, we compare the structural and electronic properties of pentacene (Pen) monolayers with the oxo-derivatives 6,13-pentacenequinone (P2O) and 5,7,12,14-pentacenetetrone (P4O) by using low energy electron diffraction (LEED), differential reflectance spectroscopy (DRS), X-ray and ultraviolet photoelectron spectroscopy (XPS and UPS) as well as photoemission orbital tomography (POT). For P4O on h-BN/Ni(111) we observed a charge transfer while Pen and P2O remain neutral. This will be discussed in terms of energy-level alignment in these 2D organic/inorganic heterostructures.

O 23: Poster: Surface Reactions

Time: Monday 18:00–20:00

Location: P2/EG

O 23.1 Mon 18:00 P2/EG

XPS Studies of 2-Carboxy-3-Phenyl-NBD/QC as MOST Energy Storage System — •FELIX HEMAUER¹, VALENTIN SCHWAAB¹, EVA MARIE FREIBERGER¹, NATALIE J. WALESKA¹, ANDREAS LENG¹, HANS-PETER STEINRÜCK¹, and CHRISTIAN PAPP^{1,2} — ¹Friedrich-Alexander-Universität Erlangen-Nürnberg, Germany — ²Freie Universität Berlin, Germany

Molecular solar thermal (MOST) systems are a candidate for storing solar energy in a chemical manner. The energy-lean norbornadiene (NBD) is converted to its energy-rich valence isomer quadricyclane (QC) in a photoconversion reac-

tion, whereby the energy is stored as strain. Molecular design leads to advantageous light-harvesting properties. In a model catalytic approach, we investigated the surface chemistry of the molecule pair 2-carboxy-3-phenyl-NBD/QC on Pt(111), Ni(111) and gold by synchrotron radiation-based XPS. Next to in situ observation of the adsorption, temperature-programmed experiments give insights into thermally induced reactions. Hereby, information on the adsorption behavior, the feasibility of the backward reaction of the QC to the NBD derivative, and the respective stability boundaries on the catalyst surfaces is obtained. On Pt(111), the energy release reaction is found to occur between 140 and 230

K. For Ni(111), the back conversion cannot be triggered thermally; instead, individual decomposition routes are monitored. The gold surface shows the highest catalytic activity with an instantaneous reaction upon adsorption at 110 K. The DFG (Project No. 392607742) supported this work. We thank HZB for allocation of synchrotron radiation beamtime.

O 23.2 Mon 18:00 P2/EG

Multiscale modeling and simulation of texture effects on the corrosion of stainless steel in aqueous media — •VAHID JAMEBOZORGI^{1,2}, KARSTEN RASIM³, and CHRISTIAN SCHRÖDER^{1,2} — ¹Bielefeld Institute for Applied Materials Research, Bielefeld University of Applied Sciences, 33619 Bielefeld, Germany — ²Faculty of Physics, Bielefeld University, 33615 Bielefeld, Germany — ³Miele & Cie. KG, Center for Materials (CFM), Carl-Miele-Strasse 29, 33332 Gütersloh

Texture plays a crucial role in physical processes and properties of condensed matter as it is broadly highlighted in the literature. In this work we describe a robust methodology to investigate texture effects which does not suffer from common limitations of quantum based computational approaches in time and space but also can provide the same accuracy as atomistic calculations with orders of magnitude less computational costs. Our methodology is based on the finite element method (FEM) and utilizes 3D digital representations of multi grain microstructures. We demonstrate the efficiency of our approach by studying pitting corrosion in stainless steel. As reflected in literature the irregular geometry of pit expansion through pitting corrosion is mostly caused by texture. We found that the texture significantly affects the pitting corrosion rate and consequently causes various irregular pit growth patterns in granular microstructures. These results are consistent with our DFT and reactive force field molecular dynamics simulations which validate our suggested approach.

O 23.3 Mon 18:00 P2/EG

Model Catalytic Studies on the Thermal Dehydrogenation of 1-Cyclohexylethanol on Pt(111) — •VALENTIN SCHWAAB¹, FELIX HEMAUER¹, EVA MARIE FREIBERGER¹, NATALIE J. WALESKA¹, HANS-PETER STEINRÜCK¹, and CHRISTIAN PAPP^{1,2} — ¹Friedrich-Alexander-Universität Erlangen-Nürnberg, Germany — ²Freie Universität Berlin, Germany

The transition to a sustainable, renewable-based energy system requires novel energy storage technologies. So-called liquid organic hydrogen carriers (LOHCs) enable the safe storage of green hydrogen at high volumetric energy densities through the reversible hydrogenation of organic compounds. Particularly interesting systems are secondary alcohols as they often exhibit exceptionally low dehydrogenation temperatures in their reaction to the respective ketone.

Herein, we investigated the thermal dehydrogenation of the LOHC-pair of 1-cyclohexylethanol and acetophenone on a Pt(111) model catalyst. To gain fundamental insight into the reaction behavior and thermal stability limits of the two compounds, temperature-programmed X-ray photoelectron spectroscopy (TP-XPS) experiments were carried out. Based on the obtained C 1s and O 1s data, the dehydrogenation of the alcohol and the formation of potential catalyst poisoning decomposition products are discussed.

We acknowledge financial support by the Bavarian Ministry of Economic Affairs, Regional Development and Energy, and by the DFG (Project No. 419654270). We thank HZB for the allocation of synchrotron radiation beamtime.

O 23.4 Mon 18:00 P2/EG

On-Surface Collision Reactions — MATTHEW JAMES TIMM¹, •STEFAN HECHT², and LEONHARD GRILL¹ — ¹Institute of Chemistry, University of Graz, Heinrichstraße 28, 8010 Graz, Austria — ²Department of Chemistry & IRIS Adlershof, Humboldt-Universität zu Berlin, Brook-Taylor-Str. 2, 12489 Berlin, Germany

Collisions between atoms and molecules are required to form chemical bonds, and thus lie at the heart of chemistry. Their outcome depends on several parameters: the collision energy, the miss-distance between the centers of the colliding species (the impact parameter), and on the relative alignment of reagents. Studying such reactions on a surface provides a 2D confinement and allows single-molecule imaging by scanning probe microscopy. For surface reactions, it has been demonstrated that the impact parameter can be selected using a 'surface-molecular-beam' of energetic CF₂ 'projectiles' on a Cu(110) surface [1-2]. The inherent corrugation of Cu(110) collimates the projectiles, allowing them to be aimed at nearby molecular 'targets' at chosen impact parameters. However, the relative alignment of reagents could not be varied until now, due to the singular possible adsorption configurations of the studied targets. Here, a singly-debrominated molecular target has been chosen as it can adopt multiple adsorption alignments relative to the incoming CF₂ projectile, thus providing the missing element required for a more general selection of collision geometry. [1] Anggara, K.; Leung, L.; Timm, M. J.; Hu, Z.; Polanyi, J. C.; *Sci Adv.*, 2018, 4, eaau2821. [2] Anggara, K.; Leung, L.; Timm, M. J.; Hu, Z.; Polanyi, J. C.; *Faraday Discuss.*, 2019, 214, 89-103.

O 23.5 Mon 18:00 P2/EG

On-Surface Reaction of Tetrphenylporphyrin with Caesium — •LEONARD NEUHAUS, FLORIAN MÜNSTER, KASSANDRA ZOLTNER, MARIE IRENE ALBUS, JAN HERRITSCH, and J. MICHAEL GOTTFRIED — Fachbereich Chemie, Philipps-Universität Marburg, Germany

Tetrapyrroles such as porphyrins and their metal complexes play important roles in living organisms and for various modern technologies. While the surface chemistry of their transition metal complexes has been well studied in the last decades, the complexes of alkali metals are almost completely unknown. Here, we have studied the reaction of tetrphenylporphyrin (H₂TPP) with caesium in the multilayer and monolayer on Ag (111). N 1s X-ray photoelectron spectroscopy (XPS) data indicate complete metalation of the porphyrin in both cases. In complementary temperature-programmed reaction (TPR) experiments performed for the multilayer, the desorbing species were clearly identified by mass spectrometry as Cs₂TPP. DFT calculations indicate that this stable complex has a bipyramidal structure with Cs ions on both sides of the molecular plane.

O 23.6 Mon 18:00 P2/EG

Chemicurrent measurements during oxidation of Mg films with varying impact energy — •TOBIAS PROST and HERMANN NIENHAUS — Fakultät für Physik, Universität Duisburg-Essen, Germany

The chemicurrent originating from the oxidation of super thin magnesium films in correlation with the kinetic energies of the impinging particles is investigated. The magnesium layer thickness is kept well below the mean free path in Magnesium (Mg) to reduce the influence of the carrier recombination in the metal film. The I-V characteristics of such Schottky-Diodes show a homogeneous Schottky barrier of 0.68 eV. The reverse current is below 100 pA. Based on the X-Ray photoelectron spectroscopy (XPS) spectra recorded, it can be demonstrated that the magnesium films are not pre-oxidized. A particular focus lays on the determination of the influence of hyperthermic oxygen on the kinetics of the oxidation process. The kinetic energy of the oxygen molecules could be varied between 25 and 300 meV by adding helium. The chemical current measurements with constant kinetic energy confirms the nucleation and growth model. Measurements with different oxygen velocities demonstrate that the reaction efficiency increases with kinetic energy of the molecules.

O 24: Poster: Ion Beam Interaction with Surfaces and Interfaces

Time: Monday 18:00–20:00

Location: P2/EG

O 24.1 Mon 18:00 P2/EG

Defect Engineering of Graphene using Ultra-low energy Ion Implantation — •FELIX JUNGE¹, MANUEL AUGE¹, ZVIADI ZARKUA², LINO M.C. PEREIRA², and HANS HOFSSÄSS¹ — ¹II. Physikalisches Institut, Georg-August-Universität Göttingen — ²Quantum Solid State Physics, KU Leuven

Doping and defect engineering of graphene and TMD's to change the electrical properties is highly desirable. To achieve this, we use a unique mass-selected ion beam deposition system, which makes it possible to work in an energy range of $10 < E < 600$ eV for implantation and thus to implant into a 2D-lattice. We use electrostatical masking to control the region which get irradiated. Graphene was doped with Boron and subsequently examined by means of Kelvin probe measurements (SKPM). Furthermore, Helium was implanted into graphene using an electrostatic gradient for deceleration of the ions, to implant the sample with different energies at the same time, which was then analysed with Raman spectroscopy. With these experiments we can see the change of the surface po-

tential of the graphene between a doped and undoped surface region on the one hand and the increasing defect density with increasing implantation energy on the other hand. These results are compared by IMINTDYN (a SDTrimSP based Monte Carlo program for ion implantations) simulations.

Financial support by the DFG and the Volkswagen Foundation is gratefully acknowledged.

O 24.2 Mon 18:00 P2/EG

Sputtering of structured tungsten model surfaces — •MARTINA FELLINGER¹, CHRISTOPHER HAHN¹, CHRISTIAN CUPAK¹, GABRIELE ALBERTI², DAVID DELLASEGA^{2,3}, MATTEO PASSONI^{2,3}, MATTEO PEDRONI³, ANDREA UCCELLO³, ESPEDITO VASSALLO³, and FRIEDRICH AUMAYR¹ — ¹TU Wien, Institute of Applied Physics, Vienna, Austria — ²Politecnico di Milano, Department of Energy, Milan, Italy — ³Istituto per la Scienza e Tecnologia dei Plasmi, Consiglio Nazionale delle Ricerche, Milan, Italy

Erosion of first wall materials in nuclear fusion devices limits the lifetime of plasma-facing materials. In the search for materials with low sputtering yields we have investigated not only the sputtering properties of randomly rough [1] but also of oriented and nano-structured tungsten surfaces. Since oriented tungsten nano-columns have shown a favourable reduction in sputtering yield [2], we have now started also to investigate nano-pyramids. These were obtained depositing a tungsten coating on top of chemically etched silicon substrates. The pyramidal surfaces were then exposed to ion irradiation and the subsequent sputtering process was investigated in situ by using a quartz crystal microbalance measurement setup [3]. We will present the experimental results and compare them to state of the art simulations.

[1] C. Cupak et al., Appl Surf Sci 570 (2021)

[2] A. Lopez-Cazalilla et al., Phys Rev Mat 6 (2022)

[3] B. M. Berger et al., Nucl Instrum Methods Phys Res B 406 (2017)

O 24.3 Mon 18:00 P2/EG

In situ GISAXS observation of ion-induced nanoscale pattern formation on crystalline Ge(001) in the reverse epitaxy regime — •DENISE ERB¹, PECO MYINT^{2,3}, KENNETH EVANS-LUTHERODT⁴, KARL LUDWIG^{4,5}, and STEFAN FACSKO¹ — ¹Institute of Ion Beam Physics and Materials Research, Helmholtz-Zentrum Dresden-Rossendorf, Germany — ²Division of Materials Science and Engineering, Boston University, USA — ³X-ray Science Division, Argonne National Laboratory, USA — ⁴National Synchrotron Light Source II, Brookhaven National Laboratory, USA — ⁵Department of Physics, Boston University, USA

The ion-induced nanoscale pattern formation on a crystalline Ge(001) surface is observed in situ by means of grazing incidence small angle x-ray scattering (GISAXS). Analysis of the GISAXS intensity maps yields the temporal development of geometric parameters characterizing the changing pattern morphology. In comparison with theoretical predictions and with simulations of the patterning process based on a continuum equation we find good agreement for the temporal evolution of the polar facet angle, characteristic length, and surface roughness in the nonlinear regime. To achieve this agreement, we included an additional term in the continuum equation which adjusts the pattern anisotropy.

O 24.4 Mon 18:00 P2/EG

Non-ambient Raman spectroscopy combined with ion bombardment — •ANDRÉ MAAS, LUCIA SKOPINSKI, STEPHAN SLEZIONA, MARIKA SCHLEBERGER, and LARS BREUER — Universität Duisburg-Essen, Fakultät für Physik and CENIDE, Germany

Spectroscopic and electronic characterization of materials under non-ambient condition is an ongoing challenge. Irradiation-induced defects under ambient conditions are usually saturated with adsorbates. The direct analysis of the effects caused by unsaturated defects on the crystal structure and its electronic and optoelectronic properties is however essential to gain a deeper understanding of defect generation, defect saturation and the corresponding relaxations of the lattice due to adsorbates.

A novel experimental setup is presented that allows ion bombardment with two different ion sources and subsequent characterization of samples by a mobile Raman spectrometer in ultra high vacuum. The interaction of highly charged ions (Xe^{17+} - Xe^{40+} at around $E_{kin} = 200$ keV) from an electron beam ion source (EBIS) can be studied at the University of Duisburg-Essen. A second experimental setup utilizes the swift heavy ions (up to 14.8 MeV/u for $^{238}\text{U}^{92+}$) from the CRYRING@ESR at the GSI Helmholtzzentrum für Schwerionenforschung in Darmstadt for defect generation.

Another experiment uses a custom-built cell that allows for electrical and optical characterization of samples under high vacuum and at low temperatures (≈ 77 K).

O 24.5 Mon 18:00 P2/EG

Ion induced defects in two-dimensional tungsten diselenide boron nitride heterostructure — •LEON DANIEL, STEPHAN SLEZIONA, LUCIA SKOPINSKI, ANKE HIERZENBERGER, JENNIFER SCHMEINK, and MARIKA SCHLEBERGER — Universität Duisburg-Essen, Germany

Monolayer transition metal dichalcogenides (TMDCs) like tungsten diselenide (WSe_2) are highly interesting materials for optoelectronic and valleytronic applications. We used Xe^{q+} ions with $E_{kin}=180$ keV to deliberately introduce defects into the WSe_2 lattice and compared its optoelectronic properties before and after irradiation with photoluminescence spectroscopy. Encapsulation in hexagonal boron nitride (hBN) isolates the WSe_2 from environmental influences like adsorbates and detrimental interactions with the widely used Si/SiO_2 substrates. We find differences in the photoluminescence response for encapsulated and non-encapsulated WSe_2 , which can be explained by the encapsulation preventing saturation of the created vacancies by adsorbates. In particular, there are various localized excitonic states in our different sample systems, and we explain this observation with differing ion interactions with encapsulated and non-encapsulated WSe_2 . Furthermore, we observe overall highly increased exciton lifetimes after the irradiation, likely caused by the longer lifetime of the localized excitons.

O 25: Poster: Metal Substrates

Time: Monday 18:00–20:00

Location: P2/EG

O 25.1 Mon 18:00 P2/EG

Ab initio design of Pt-Ir based novel bifunctional electrocatalysts for fuel cell applications — •HALIL IBRAHIM SÖZEN¹, MEHTAP OEZASLAN², and THORSTEN KLÜNER¹ — ¹Institute of Chemistry, Carl-von-Ossietzky University of Oldenburg, D-26129 Oldenburg, Germany — ²Technische Universität Braunschweig, Braunschweig 38106, Germany

Electric vehicles powered by polymer electrolyte membrane fuel cells (PEMFC) have a great potential to reduce a large portion of CO_2 emissions from the transportation sector and facilitate the advent of the hydrogen economy worldwide. However, highly dynamic conditions during the operation of PEMFC in the heavy-duty sector cause hydrogen starvation at the anode electrode, resulting in cell reversal events (< -1.5 V) and therefore carbon oxidation reaction (COR). In this work, we aimed to develop novel bifunctional electrocatalysts for the anode electrode based on Pt-Ir alloys. Our innovative approach involves unifying two functionalities, the hydrogen oxidation reaction (HOR) and oxygen evolution reaction (OER), as an alternative reaction for proton and electron formation to the COR in only one nanoparticle on the same support material. Density functional theory (DFT) based chemisorption energies of H^* , O^* , OH^* , H_2O^* and OOH^* are reported with the effect of hydroxyl species presence and the effect of pH. Calculated chemisorption energies are implemented to model HOR and OER and plot Gibbs free energy diagrams. Various surfaces such as Pt(111), $\text{Pt}_3\text{Ir}(111)$, $\text{PtIr}(111)$ and $\text{Ir}(111)$ have been considered for electrocatalytic reactions and their relative performance is compared.

O 25.2 Mon 18:00 P2/EG

2D Lattice Gas Order-Disorder Transition Observed by LEED and Vibrational Sum Frequency Generation Spectroscopy — •ZHIPENG HUANG, TOBIAS ROOS, YUJIN TONG, and R. KRAMER CAMPEN — Faculty of Physics, University of Duisburg-Essen

Order-disorder phase transition of monoatomic superstructures on single crystal surfaces is commonly described by Ising or lattice-gas model. The molecular orientation needs to be considered for modeling the order-disorder transition

of diatomic superstructures on single crystal surfaces, but it is challenge to be accessed by experiments.

Here we present our studies on CO ordered overlayers on Pt(111) surface by the surface sensitive thermal desorption spectroscopy (TDS), low-energy electron diffraction (LEED) and polarization dependent sum-frequency generation spectroscopy (SFG). An order-disorder phase transition of CO overlayer is observed by LEED under in-situ heating. The CO stretch vibrational frequency shifts suddenly when the transition happens. Combining LEED superstructure patterns and polarization dependent sum-frequency generation spectroscopy results, we reveal the changes of CO molecular orientation on Pt(111) surface during the order-disorder phase transition. We model the sudden CO stretch frequency shift caused by phase transition and the systematic shift as a function of coverage. These results demonstrate how the CO intermolecular interactions influence the molecular orientation and the stretch vibrational frequency. They provide insights on the change of microscopic potential energy level during the order-disorder phase transition.

O 25.3 Mon 18:00 P2/EG

Formation of solid electrolyte interface from polycaprolactone — •KAZEM ZHOUB¹, ANDREAS HEUER¹, and DIDDO DIDDENS² — ¹WWU Münster, Münster, Germany — ²Institute Münster (IEK-12) Forschungszentrum Jülich GmbH, Münster, Germany

As for liquid electrolytes, studying the formation of the solid-electrolyte interface and its implications is one of the most important topics in solid-state batteries. In this study, DFT and AIMD calculations were performed to study the decompositions of polycaprolactone, one main constituent of the electrolytes, and its ending groups at the interface. Additionally, the computational lithium electrode method was applied to study the formation of the SEI under external voltage. The AIMD results suggest that the fragments are highly reactive on the Lithium slab where the fragmentation can be observed in less than 1 ps. The decomposition was triggered by the electrons transferred from the slab to the fragments. The electrochemical mechanism shows only slightly weaker energet-

ics with respect to the non-electrochemical one, showing that Li anode readily reacts with the polymer. After the formation of passivation layers (Li₂O, LiF or Li₂CO₃) on top of the anode, the calculations show that only one monolayer protects the molecules from being decomposed at the interface at short interval of time, where the LiF layer seems to have the most robust protection as compared to the other layers. The electrochemical window and the decomposition of the polymer fragments in the presence of a Li cation, TFSI anion, or LiTFSI ion pair without explicit interface have also been investigated.

O 25.4 Mon 18:00 P2/EG

Single-molecule study of Heck coupling on a Cu(111) surface — •DONATO CIVITA¹, FRIEDRICH ESCH², and LEONHARD GRILL¹ — ¹Department of Physical Chemistry, University of Graz, Austria — ²Faculty of Chemistry, TU München, Germany

The interaction of organic molecules with metallic structures is particularly important in heterogeneous catalysis where metallic particles or surfaces help to overcome energy barriers of chemical reactions. This concept is specifically important for Heck cross-coupling, which relies on a palladium catalyst to form a carbon-carbon bond between two different reagents. Model heterogeneous catalysis reactions can be investigated by scanning tunneling microscopy (STM) on metal single crystals. The role of active sites could be determined [1,2], and Heck coupling could be induced thermally [3].

We studied the cross coupling between vinyl-naphthalene (VN) and different halogenated molecules on a Cu(111) surface by STM at low temperatures (7 K). We investigated the bond of the de-halogenated molecules to different atomic structures of the copper surface as well as the thermally induced cross coupling reaction. By the statistical analysis of the products, and STM manipulation of a

single metal-organic intermediate we obtain insight into the catalytic activity of the copper surface, and the dependence on the surface morphology.

- [1] Hla, S.-W., et al., Phys. Rev. Lett., 85(13) (2000)
- [2] Zambelli, T., et al., Science, 273 (1996)
- [3] Shi, K.-J., et al., Organic Letters, 19(11) (2017)

O 25.5 Mon 18:00 P2/EG

Cobalt Island Growth on Metallic Surfaces — •BENSU GÜNAY, CHRISTOPHE NACCI, and LEONHARD GRILL — University of Graz, Graz, Austria

Molecular-beam epitaxy is an important technique for the fabrication of epitaxial films with reduced dimensionality in the low coverage regime under ultra-high vacuum conditions [1]. Various parameters are important for the morphology of the nanostructures: the flux of the incident atoms, the surface temperature, the source/substrate geometry, and diffusion of the atoms on the surface [2]. In this study, we investigated the growth of cobalt islands on Cu(111) and Au(111) surfaces using different (K-cell and e-beam evaporator) evaporators. The resulting surfaces were then studied by complementary methods: x-ray photoemission spectroscopy (XPS) to analyze the chemical composition of the surface and scanning tunneling microscopy (STM) to investigate the morphology of the islands. The results show how different deposition conditions change the Co growth on the surface.

[1] Prieto, J. E., de La Figuera, J., & Miranda, R. (2000). Surface energetics in a heteroepitaxial model system: Co/Cu (111). Physical Review B, 62(3), 2126. [2] Negulyaev, N. N., Stepanyuk, V. S., Bruno, P., Diekhöner, L., Wahl, P., & Kern, K. (2008). Bilayer growth of nanoscale Co islands on Cu (111). Physical Review B, 77(12), 125437.

O 26: Poster: New Methods

Time: Monday 18:00–20:00

Location: P2/EG

O 26.1 Mon 18:00 P2/EG

Instrumentation for high-resolution biomolecule imaging enabled by electrospray ion beam deposition (ES-IBD) — •LUKAS ERIKSSON, TIM ESSER, MÁRKÓ GRABARICS, PAUL FREMDLING, and STEPHAN RAUSCHENBACH — University of Oxford, Department of Chemistry, United Kingdom

Elucidating the structure of biomolecules is essential to understanding their function. Direct imaging with cryogenic electron microscopy (cryo-EM) or scanning probe microscopy (SPM) is a powerful approach for finding molecular structure. However, sample preparation can be a major challenge: either very time- and resource-intensive or incompatible with the vacuum environment required by the imaging method.

Here, we explore preparative mass spectrometry as an alternative workflow towards structural elucidation of biomolecules. A novel, custom-built deposition stage extending a commercial mass spectrometer allows for the mass-filtered, soft-landed deposition of a wide mass range of target molecules ($m = 100 - 10^6$ amu) onto various surfaces, including cryo-EM grids and metal crystals for SPM.[1] This requires extensive control over conditions such as pressure, temperature, ion trajectories, sample surfaces, and sample transfer to obtain clean, chemically pure samples of the desired species in the right (i.e. native) configuration.

[1] Paul Fremdling, Tim K. Esser, Bodhisattwa Saha, Alexander A. Makarov, Kyle L. Fort, Maria Reinhardt-Szyba, Joseph Gault, and Stephan Rauschenbach: *A Preparative Mass Spectrometer to Deposit Intact Large Native Protein Complexes*. ACS nano 16 (2022)

O 26.2 Mon 18:00 P2/EG

Spectral characterization of battery components from Li-ion battery recycling processes — •JULIA RICHTER^{1,2}, SANDRA LORENZ², CHRISTIAN RÖDER¹, ROMAN TSCHAGAUEW¹, YULEIKA CAROLINA MADRIZ DIAZ², ERIK HERRMANN², RICHARD GLOAGUEN², and JOHANNES HEITMANN¹ — ¹TU Bergakademie Freiberg, Institute of Applied Physics, Leipziger Str. 23, D-09599 Freiberg (Germany) — ²Helmholtz-Zentrum Dresden-Rossendorf, Helmholtz Institut Freiberg for Resource Technology, Chemnitz Str. 40, D-09599 Freiberg (Germany)

The rapid identification of critical compounds in recycling material streams is crucial for an adequate sorting. Recently, the development of adapted multi-sensor systems as well as advanced multi-source data fusion for real-time data integration is in the scope of several research activities. This work deals with the digitalisation of mechanical separation processes in recycling of Li-ion batteries using data which were acquired by hyperspectral sensors. In order to establish a reference data set of the valuable components Al and Cu, in this study a sample set of Al and Cu foils was examined by reflectance spectroscopy in the range (350 * 2500) nm. Based on point measurements and statistical data from imaging sensors, optical material characteristics of the samples were analysed. Proposals for optical sorting steps and possible challenges will be outlined and

discussed. This work is financially supported by the Federal Ministry of Education and Research (BMBF) in the framework of the greenBatt cluster within the project DIGISORT.[1] [1] www.greenbatt-cluster.de/de/projekte/digisort/

O 26.3 Mon 18:00 P2/EG

Dynamics of contact electrification — •ANDRE MÖLLEKEN, HERMANN NIENHAUS, and ROLF MÖLLER — Fakultät für Physik, Universität Duisburg-Essen, Germany

Although the electrical charging of objects brought into contact has been observed for centuries, the details of the underlying mechanism are still not yet fully understood. We have developed an experimental method to follow the charge of a small sphere bouncing on a grounded planar electrode on a time scale down to 1 μ s. In case of a contact between two metals, it reveals that the sphere is discharged in the moment of contact, which lasts about 6 to 8 μ s. However, at the very moment of disruption of the electrical contact, it regains charge far beyond the expectation according to the contact potential difference. The excess charge rises with increasing contact area.

[1] M. Kaponig, A. Mölleken, H. Nienhaus, R. Möller, Dynamics of contact electrification, Sci. Adv. 2021, 7 (22), eabg7595.

O 26.4 Mon 18:00 P2/EG

Surface tension measurement of pure water in vacuum — •PAUL T. P. RYAN, JIRI PAVELEC, JAN BALAJKA, MICHAEL SCHMID, and ULRIKE DIEBOLD — Institute of Applied Physics, TU Wien, Austria

Very little is known about the surface tension of pure liquids in contact with their pure gaseous phases, i.e. without the presence of other gases or liquid phase contaminants. This is surprising given that contaminants are known to greatly affect surface tensions values[1]. Recently we have developed a method to dose liquid water onto pristine surfaces in UHV using a small cryostat[2]. We combine this approach with the pendant drop method[3] to measure the surface tension of ultra-clean liquids in contact with their pure gaseous phases. In the design, the ultra-clean liquid is condensed onto a small cryostat placed in a vacuum chamber. A pendant drop is formed and carefully photographed allowing the surface tension of the ultra-clean liquid to be directly determined. For these types of measurements accurate knowledge and control of the temperature, pressure and the optics of system is of paramount importance. How these parameters are precisely controlled in the instrument design will be discussed along with initial measurements of ultra-pure water. [1] Yuki Uematsu, et. al., Current Opinion in Electrochemistry, Volume 13, (2019) [2] Jan Balajka, et. al., Science, 361, (2018) [3] Berry, J. D. et. al., J. Coll. Interface Sci. 454, (2015).

O 26.5 Mon 18:00 P2/EG

High-Resolution Imaging of Protein Complexes Enabled by Electro Spray Ion-Beam Deposition Sample Preparation — •ASHA THOMPSON, TIM ESSEER, MARKÓ GRABARICS, ISABELLE LEGGE, and STEPHAN RAUSCHENBACH — University of Oxford, Department of Chemistry, United Kingdom

Structural characterisation of biological molecules such as proteins is essential for insight into their processes and interactions within cells. Samples of mass-filtered molecules adsorbed onto surfaces can be obtained using preparative mass spectrometry techniques such as electro spray ion-beam deposition (ES-IBD). ES-IBD generates intense beams of native proteins which are soft-landed onto surfaces. This produces uncontaminated samples which can be further characterised by transmission electron microscopy (EM) or scanning probe microscopy (SPM).

Here we present the application of this approach for the imaging of proteins showing examples of soluble and of membrane proteins, such as Human C Reactive protein, ferritin, Beta-galactosidase and Aquaporin-Z. We can show that the shape of the protein, its subunit conformation, and stoichiometry are retained, which points to intact secondary structure. [1] We intend to extend this approach to map the interactions of antibodies and their targets in order to provide information about the binding site, useful for pharmacology.

[1] T. K. Esser, et al, Mass selective and ion-free electron cryomicroscopy protein sample preparation, PNAS nexus, Volume 1, issue 4, 2022

O 26.6 Mon 18:00 P2/EG

RuNNer 2.0: An efficient and modular program for training and evaluating high-dimensional neural network potentials — •ALEXANDER L. M. KNOLL^{1,2}, MARCO ECKHOFF³, JONAS A. FINKLER⁴, TSZ WAI KO⁵, EMIR KOCER^{1,2}, K. NIKOLAS LAUSCH^{1,2}, MORITZ R. SCHÄFER^{1,2}, GUNNAR SCHMITZ^{1,2}, ALEA MIKO TOKITA^{1,2}, and JÖRG BEHLER^{1,2} — ¹Lehrstuhl für Theoretische Chemie II, Ruhr-Universität Bochum, 44780 Bochum, Germany — ²Research Center Chemical Sciences and Sustainability, Research Alliance Ruhr, 44780 Bochum, Germany — ³ETH Zürich, Laboratorium für Physikalische Chemie, 8093 Zürich, Switzerland — ⁴Department of Physics, Universität Basel, 4056 Basel, Switzerland — ⁵Department of NanoEngineering, University of California, San Diego, CA, USA

Machine learning potentials (MLPs) have become a popular tool for large-scale atomistic simulations in chemistry and materials science. They provide efficient access to highly accurate potential energy surfaces (PES) generated from *ab initio* reference calculations. As methods in this field are becoming increasingly complex and reach maturity, the development of efficient and user-friendly tools is also gaining importance. We present the second major release version of RuNNer, an open source, stand alone software package for the construction and eval-

uation of second, third, and fourth generation high-dimensional neural network potentials (HDNNPs). RuNNer 2.0 unifies an entire workflow in a fully MPI-parallel program: from the generation of atomistic descriptors, over the training of a specific machine learning model, to its final application in molecular dynamics codes.

O 26.7 Mon 18:00 P2/EG

Optical Near-field Electron Microscopy — •ILIA ZYKOV¹, HANIEH JAFARIAN¹, BARBARA PLATZER¹, THOMAS JUFFMANN¹, AMIN MORADI², GUIDO STAM², SENSE JAN VAN DER MOLEN², RUUD TROMP², NESTOR FABIAN LOPEZ MORA³, MARIANA MANUELA AMARO³, MARTIN KALBAC³, MARTIN HOF³, and RADEK ŠACHL³ — ¹University of Vienna, Austria — ²Leiden University, the Netherlands — ³J. Heyrovsky Institute of Physical Chemistry, the Czech Republic

Label- and damage-free imaging of the surface processes on the nanometer scales and over extended periods is required in different fields. Various electron microscopy techniques are applied to meet these requirements. However, the use of electrons in probing the sample may affect some specimens. The novel Optical Near-field Electron Microscopy (ONEM) technique [1] is being developed to overcome this drawback. In the ONEM light nondestructively interacts with a sample. The scattered light from the sample is then transformed into electrons by a nm-thick photocathode layer placed in the near-field region of the sample. The nm resolution images are then achieved through an electron readout using the Low Energy Electron Microscope.

The potential application of ONEM in biochemistry can be to follow the protein dynamics in lipid membranes at single protein resolution. In electrochemistry ONEM will be applied to study the nucleation and growth of nanoscale copper clusters without any electron beam effect.

[1] R. Marchand et al, Phys. Rev. Applied 16, 014008 (2021)

O 26.8 Mon 18:00 P2/EG

Development of a reflektometer for polarised surface sensitive X-ray Absorption Spectroscopy — •LUKAS VOSS, FREDERIC BRAUN, FRANZ ECKELT und DIRK LÜTZENKIRCHEN-HECHT — Bergische Universität Wuppertal, Wuppertal, Deutschland

RefLEXAFS measurements represent a powerful tool for surface-sensitive structure investigations. With the help of high-intensity synchrotron radiation on synchrotron beamlines of the third generation, this measurement method can also be used in a time-resolved mode. In order to keep the construction and adjustment time as short as possible, a simple, compact and transportable reflectometer is to be built in order to give other users easy access to this measurement technology. Here we would like to present the current status of the project with the first measurements.

O 27: Overview Talk Katrin Domke

Time: Tuesday 9:30–10:15

Location: TRE Phy

Invited Talk

O 27.1 Tue 9:30 TRE Phy

Dive right in! Molecular insights into electrochemical surface science — •KATRIN F. DOMKE — Universität Duisburg-Essen, Germany

Surface scientists have become increasingly aware of the importance of expanding the research focus from classical UHV systems to electrochemical settings that adequately represent realistic working conditions of applications based on solid/liquid reactive interfaces, such as (electro)catalysis or energy conversion schemes. Gathering atomistic understanding about the complex interrelation between charge transfer, chemical conversion and interfacial potential in the

present of a solvent is one of the most imminent challenges that surface scientists working with solid/liquid interfaces are facing.

Great efforts are being devoted to the development of novel methodologies to elucidate interfacial electrochemistry mechanisms on the molecular scale. In my talk, I will highlight our advances to achieve simultaneous operando plasmon-supported Raman nanoscopy and break-junction experiments. These approaches allow us to gain unprecedented insights into the correlation of chemical, topographic and electronic properties of individual reactive sites at solid/liquid interfaces, such as catalyst structure or (bio)molecular switches in electrolyte under potential control.

O 28: Organic Molecules on Inorganic Substrates III: Adsorption and Growth I

Time: Tuesday 10:30–13:00

Location: CHE 89

O 28.1 Tue 10:30 CHE 89

Tuning interfaces properties via deposition conditions: thermodynamic's deed and kinetic's contribution — ANNA WERKOVITS, JOHANNES J. CARTUS, LUKAS HÖRMANN, and •OLIVER T. HOFMANN — Institute of Solid State Physics, Tu Graz

The interface dipole of an inorganic-organic interface depends strongly on the structure, i.e. the polymorph, the organic molecules assume. This is not a subtle effect: In the past years, studies reported work functions differing between up to 3 eV between different polymorphs, illustrating how important it is to control the growth of these interfaces.

In this work, we discuss on the basis of first-principle calculations how the molecule-substrate, the intermolecular interaction and the size of the molecule affect the relative thermodynamic stability of different phases for different deposition conditions, and how this directly relates to observed work function

changes. Based on this, we discuss two ways strategies to tune interface properties. Either, the relative stability can be modified, e.g. by growing the interface in an electric field. Alternatively, it is also possible to exploit kinetic effects during the growth and trap desired phases. Based on the example of TCNE on Cu(111) we discuss how a given phase can be kinetically trapped, and under which circumstances we expect thermodynamic equilibrium to prevail.

O 28.2 Tue 10:45 CHE 89

Homo- and Heterochiral Phases of Quinacridone Monolayers on Ag(110) and Ag(111) — •RAVI PRIYA, WEISHAN WU, KEDA JIN, and PETER JAKOB — Fachbereich Physik, Philipps-Universität Marburg, Germany

When adsorbed on a surface, parallel-oriented quinacridone (QA) transforms into a chiral species and lateral interaction between neighboring molecules will depend on the types of enantiomers facing each other. On Ag(111) a homochi-

ral phase comprising rows of (identical) QA has been reported that, upon thermal annealing, converts to a heterochiral phase consisting of alternating pairs (dimers) of the two enantiomers [1]. In our study, we have refined the structural analysis of QA/Ag(111) phases and have extended the available database to QA on Ag(110). Besides SPA-LEED, IR-spectroscopy and TDS were employed to characterize the various phases and associated phase transformations in detail. From IRAS and TDS a stronger molecule-substrate interaction is deduced for Ag(110) as compared to Ag(111). In parallel, interfacial dynamical charge transfer (IDCT) is considerably enhanced for QA/Ag(110) which is ascribed to an extra downshift of the QA-LUMO, increasing its DOS at the fermi energy. Interestingly, IDCT vanishes completely upon the transition of the homochiral to the heterochiral arrangement, both on Ag(111) and Ag(110). This could be explained by a completely empty, or a fully occupied LUMO [2]. As this transition is accompanied by a notable increase in the work function, we conclude that the latter applies.

[1] <https://doi.org/10.1021/jp502148x>

[2] <https://doi.org/10.1103/PhysRevLett.126.116801>

O 28.3 Tue 11:00 CHE 89

Morphology and luminescence of rubrene nanocrystals: a road to tailor nanoplatelets — •MOHA NAEIMI, KATHARINA ENGSTER, CHRISTIAN VÖLKNER, REGINA LANGE, SYLVIA SPELLER, and INGO BARKE — University of Rostock, Institute of physics, Rostock, Germany

Rubrene ($C_{42}H_{28}$ 5,6,11,12-tetraphenyltetracene) single crystals with a few monolayers had been reported to have high charge mobility of $43 \text{ cm}^2/\text{Vs}$ [1] and singlet-fission dynamics [2] which are promising properties for the application of excitons for energy transfer or information processing. We aim for the investigation of the spatial distribution of excitons in molecular assemblies on surfaces, requiring thin films or flat nanocrystals. In the present work, we report on the preparation of rubrene platelets by various methods from simple spin-coating to thermal evaporation and broad growth conditions, followed by a high-rate post-annealing temperature treatment on different types of substrates [3]. Ranging from 10 nm to 150 nm, we show that the thickness of rubrene platelets is widely dependent on the rate and time of temperature treatment as well as on the rubrene coverage on the surface. Moreover, we discuss thermal stability and photo-degradation for different morphologies.

[1] A. Saeki. et al., *Adv. Mater.* 20, 2008, 920-923

[2] Lin Ma. et al., *Phys. Chem. Chem. Phys.* 14, 2012, 8307-8312

[3] Hyeok Moo Lee. et al., *Org. Electron.* 12, 2011, 1446-1453

O 28.4 Tue 11:15 CHE 89

Photoelectron Spectroscopy of N-heterocyclic carbenes on Si(111)($\sqrt{3} \times \sqrt{3}$)R30°-B surface — •MIKE THOMAS NEHRING¹, ROBERT ZIELINSKI¹, MOWPRIYA DAS², HAZEM ALDAHAK³, CONOR HOGAN⁵, UWE GERSTMANN³, WOLF GERO SCHMIDT³, MARIO DÄHNE¹, MARTIN FRANZ¹, FRANK GLORIUS², and NORBERT ESSER⁴ — ¹Institut für Festkörperphysik, Technische Universität Berlin, Berlin, Deutschland — ²Westfälische Wilhelms-Universität Münster, Organisch-Chemisches Institut, Münster, Deutschland — ³Institut für Theoretische Materialphysik, Universität Paderborn, Paderborn, Deutschland — ⁴Leibniz-Institut für Analytische Wissenschaften - ISAS e.V., Berlin, — ⁵Institute for Structure of Matter (ISM-CNR), Rome, Italy

Silicon is the most commonly used element in the industry for manufacturing semiconductor-based components. Semiconductor devices today represent a cornerstone of modern technology, with a multitude of possible applications in research and development. A relatively new area of research is the growth of organic films on modified silicon surfaces. In this work we investigate the adsorption behaviour of various N-heterocyclic carbenes (NHCs) on the Si(111)($\sqrt{3} \times \sqrt{3}$)R30°-B surface. This research is conducted using X-ray photoelectron spectroscopy (XPS). By comparison of the experimental spectra with theoretical calculations it is found that all investigated NHCs bind to the Si adatoms of the Si(111)-B surface in an upright adsorption geometry. In addition, the monolayers show a high thermal stability and large work function reductions.

O 28.5 Tue 11:30 CHE 89

Adsorption and thermal stability of phenyl phosphonic acid on cerium oxide: effect of surface morphology, stoichiometry and composition. — •VIACHESLAV KALINOVYCH¹, LESIA PLIAT¹, YULIYA KOSTO¹, SASCHA L. MEHL², TOMÁŠ SKÁLA¹, IVA MATOLINOVÁ¹, VLADIMÍR MATOLÍN¹, KEVIN C. PRINCE², and NATALIYA TSUD¹ — ¹Charles University, Faculty of Mathematics and Physics, Department of Surface and Plasma Science, V Holešovičkách 2, Prague, 18000, Czech Republic — ²Elettra-Sincrotrone Trieste S.C.p.A., in Area Science Park, Strada Statale 14, km 163.5, Basovizza (Trieste), 34149, Italy

In the present work, the binding properties and thermal stability of the phosphonate group to several well-ordered cerium oxide systems: stoichiometric CeO₂(111), fully reduced Ce₂O₃(111), Ce₆WO₁₂(100) and polycrystalline RF CeO₂ were studied. Phenyl phosphonic acid (PPA) has been chosen as a molecule consisting of a phosphonate group and a benzene ring. PPA deposition was performed in UHV conditions. The binding properties and thermal

stability has been investigated in the range of 25-450 °C by synchrotron radiation photoelectron spectroscopy, resonant photoelectron spectroscopy and near-edge X-ray absorption fine structure spectroscopy. This work comprehensively describes the phosphonate group binding to cerium oxide as a function of substrate morphology, stoichiometry, composition and temperature.

O 28.6 Tue 11:45 CHE 89

Adsorption of a Cyclic (Alkyl)(Amino)Carbene on Si(111)($\sqrt{3} \times \sqrt{3}$)R30°-B: Influence of the Defect Density — •ROBERT ZIELINSKI¹, MOWPRIYA DAS², CANAN KOSBAB¹, MIKE THOMAS NEHRING¹, MARIO DÄHNE¹, NORBERT ESSER^{1,3}, MARTIN FRANZ¹, and FRANK GLORIUS² — ¹Institut für Festkörperphysik, Technische Universität Berlin, Berlin, Deutschland — ²Westfälische Wilhelms-Universität Münster, Organisch-Chemisches Institut, Münster, Deutschland — ³Leibniz-Institut für Analytische Wissenschaften - ISAS e.V., Berlin, Germany

N-Heterocyclic carbenes (NHCs) have been shown to be excellent modifiers and anchors for the functionalization of surfaces, but so far mostly on metals. Thus a controlled functionalization of semiconductor surfaces by ordered NHC layers is of great interest. In the present work we investigate the adsorption behavior of cyclohexyl cyclic (alkyl)(amino)carbene (cyCAAC) molecules on the Si(111)($\sqrt{3} \times \sqrt{3}$)R30°-B surface using scanning tunneling microscopy and X-ray photoelectron spectroscopy. We find a self-limited, well-ordered growth of a stable monolayer with large domains characterized by a 3x3 periodicity and an upright adsorption geometry of the molecules. A strong correlation between the domain size and the substrate defect density is found, revealing that the initial molecular adsorption preferentially takes place on a particular type of surface defect. Work function measurements of the cyCAAC monolayer reveal a large reduction of work function.

O 28.7 Tue 12:00 CHE 89

Electronic properties of radical helicene molecules on metallic substrates — •ALEŠ CAHLÍK¹, DANYANG LIU¹, CAROLINA A. MARQUES¹, YA-CHU HSIEH², YAO-TING WU², KARL-HEINZ ERNST³, and FABIAN D. NATTERER¹ — ¹Department of Physics, UZH, Zurich, Switzerland — ²Department of Chemistry, National Cheng Kung University, Tainan, Taiwan — ³Molecular Surface Science Group, EMPA, Zurich, Switzerland

Helicenes are π -conjugated aromatic compounds with helical shape arising from angularly fused aromatic rings. Radical helicenes combine unpaired electron spins with structural chirality and a π -conjugated framework that can offer intriguing prospects to study the synergy of electronic transport, magnetism and photoactivity. In our work, we employ STM and nc-AFM to investigate an open-shell biradical helicene that we adsorb onto metallic substrates, including magnetic nanoislands. Notably, we observe a Kondo resonance pointing towards the preservation of the open-shell character upon deposition onto Au(111).

O 28.8 Tue 12:15 CHE 89

STM growth studies of 5,14-ol-5,14-diborapentacyclo on low-index coinage metal surfaces — •WUN-CHANG PAN¹, JING QI¹, CARINA MÜTZEL², PAULA WEBER¹, FRANK WÜRTHNER², and MATTHIAS BODE¹ — ¹Physikalisches Institut, Experimentelle Physik II, Universität Würzburg, Am Hubland, D-97074 Würzburg, Germany — ²Institut für Organische Chemie & Center for Nanosystems Chemistry (CNC), Universität Würzburg, Am Hubland, D-97074 Würzburg, Germany

In recent studies [1, 2], heteroatoms-doped precursors have frequently been used to polymerize graphene nanoribbons with a large variety of structures or dopant heteroatoms. Using cryogenic scanning tunneling microscopy, we investigated the structure of self-assembled 5,14-ol-5,14-diborapentacyclo (CM218) on low-index coinage metal surfaces. The main focus of our study is on CM218 on Ag(111), where we find that molecular clusters and chains coexist with molecular islands. At low annealing temperature $T_{\text{ann}} < 100^\circ\text{C}$, the islands exhibit a rail track-like structure with a rhomboid-shaped unit cell. Besides, we find irregular clusters and molecular chains. At higher $T_{\text{ann}} \geq 180^\circ\text{C}$, islands with a honeycomb (HC) structure are observed. Topographic images of these HCs display a pronounced bias dependence. Molecule-functionalized tips allow for high-resolution images of these structures for which we suggest structural models.

[1] L. Grill and S. Hecht, *Nature Chemistry* 12, 115 (2020)

[2] Q. Zhong *et al.*, *Nature Chemistry* 13, 1133 (2021)

O 28.9 Tue 12:30 CHE 89

Variable Temperature Scanning Tunneling Microscopy Investigation on Pyrene Monolayers — •PATRICK PENNER, XIANGHUI ZHANG, BERTHOLD VÖLKEL, and ARMIN GÖLZHÄUSER — Physik Supramolekularer Systeme und Oberflächen, Universität Bielefeld, Bielefeld, Germany

Pyrene (C₁₆H₁₀) monolayers were prepared by physical vapor deposition on Au(111). Afterwards they were investigated with a variable temperature scanning tunneling microscope with the capability to cool the surface down to -80 °C. Without prior cooling, it was impossible to image any molecules at room temperature. After reaching a temperature of 10 °C first images could be made. In-

dependent of the temperature the molecules seem to be lying flat on the sample, with a next-neighbor distance of 1.05 nm. After cooling down it was possible to scan at room-temperature small domains of pyrenes near edges of gold terraces, as well as single mobile pyrene molecules.

O 28.10 Tue 12:45 CHE 89

Predicting optimal growth conditions for metastable interface structures — •SIMON HOLLWEGGER, ANNA WERKOVITS, RICHARD K. BERGER, LUKAS HÖRMANN, JOHANNES CARTUS, and OLIVER T. HOFMANN — Institute of Solid State Physics, University of Technology Graz, Austria

For tailoring organic-inorganic interfaces of organic electronic devices controlling the structure that forms during growth is of high importance. Indeed, interface properties often strongly vary for different interface structures. But growing

the structure that has the optimal properties for a certain technical application is nothing but trivial, due to the subtle interplay of thermodynamics and kinetics that strongly depend on the growth conditions like temperature and pressure. Therefore, we study how to change temperature and pressure over time in an optimal way to maximize the concentration of a specific high-performance polymorph. The target structure must then be one that is either thermodynamically or kinetically accessible. Finding optimal processing parameters experimentally is a tedious trial and error task, which can be greatly simplified with theoretical guidance. Using the framework of Optimal Control theory, such optimal temperature and pressure protocols can be obtained. In this talk we will demonstrate how this method can be technically implemented, discuss first applications, and point out its possible pitfalls and limitations for the case of designing organic-inorganic interfaces.

O 29: Supported Nanoclusters: Structure, Reactions and Catalysis

Time: Tuesday 10:30–13:00

Location: CHE 91

O 29.1 Tue 10:30 CHE 91

There is life after coking for Ir nanocatalyst superlattices — •ANTONIO J MARTÍNEZ-GALERA^{1,2}, HAOJIE GUO³, MARIANO D JIMÉNEZ-SÁNCHEZ³, STEFANO FRANCHI⁴, KEVIN C PRINCE⁴, and JOSÉ M GÓMEZ-RODRÍGUEZ^{2,3,5} — ¹Departamento de Física de Materiales, Universidad Autónoma de Madrid, E-28049 Madrid, Spain — ²Instituto Nicolás Cabrera, Universidad Autónoma de Madrid, E-28049 Madrid, Spain — ³Departamento de Física de la Materia Condensada, Universidad Autónoma de Madrid, E-28049 Madrid, Spain — ⁴Elettra-Sincrotrone Trieste S.C.p.A., in Area Science Park, 34149 Basovizza (Trieste), Italy — ⁵Condensed Matter Physics Center (IFIMAC), Universidad Autónoma de Madrid, E-28049 Madrid, Spain

Achieving superior performance of nanoparticle systems is a major challenge in catalysis. Two main phenomena, occurring during the reactions, hinder the development of the full potential of nanoparticle catalysts: sintering and contamination with carbon containing species, sometimes called coking. Here, we show that Ir nanocrystals, periodically arranged on h-BN supports, can be restored without sintering after contamination by persistent carbon. This restoration yields the complete removal of carbon from the nanocrystals, which keep their crystalline structure, allowing operation without degradation. These findings, together with the possibility of fine tuning the nanocrystals size, confer this nanoparticle system a great potential as a testbed to extract key information about catalysis-mediated oxidation reactions. For the case of the CO oxidation by O₂, the existence of chemical processes not observed before in other nanoparticle systems is proven.

O 29.2 Tue 10:45 CHE 91

Formation of the Pd/Co₃O₄ interface — •YAROSLAVA LYKHACH¹, MAXIMILIAN KASTENMEIER¹, LUKÁŠ FUSEK^{1,2}, MATTEO FARNESI CAMELLONE³, TOMÁŠ SKÁLA², NATALIYA TSUD², VIKTOR JOHÁNEK², SASCHA MEHL⁴, JOSEF MYSLIVEČEK², SIMONE PICCININ³, OLAF BRUMMEL¹, STEFANO FABRIS³, and JÖRG LIBUDA¹ — ¹Friedrich-Alexander-Universität Erlangen-Nürnberg, Erlangen, Germany — ²Charles University, Prague, Czech Republic — ³Istituto Officina dei Materiali, CNR-IOM, Trieste, Italy — ⁴Elettra-Sincrotrone Trieste SCpA, Basovizza-Trieste, Italy

Metal-oxide interfaces play a major role in the design of advanced functional materials for applications in catalysis, energy storage, and nanoelectronics. We investigated the formation of the metal/oxide interface during deposition of Pd nanoparticles onto a well-ordered Co₃O₄(111) substrate by means of synchrotron radiation photoelectron spectroscopy (SRPES), density functional theory (DFT), and scanning tunnelling microscopy (STM). DFT predicted strong interaction between Pd and Co₃O₄(111) which resulted in the growth of two-dimensional Pd islands densely covering the substrate. We observed a charge transfer across the metal/oxide interface resulting in partial oxidation of Pd deposits and partial reduction of Co₃O₄(111). Based on the analysis of the degree of the reduction of Co₃O₄(111), we found that the charge transfer at the Pd/Co₃O₄(111) is confined to the near-surface region of Co₃O₄(111).

O 29.3 Tue 11:00 CHE 91

Structure of PdPt/CeO₂/YSZ model systems in operando methane oxidation — •JAN-CHRISTIAN SCHÖBER^{1,2}, SILVAN DOLLING^{1,2}, THOMAS F. KELLER¹, and ANDREAS STIERLE^{1,2} — ¹DESY, Centre for X-ray and Nanoscience CXNS, Hamburg, Germany — ²Universität Hamburg, Germany

Due to the high ecological impact of gasoline and diesel fuels, natural gas and biofuel alternatives become more important than ever. Methane is a major component of natural gas and many bio fuels and has a much higher environmental impact than carbon dioxide. Thus, it is vital to ensure the elimination of methane in exhaust gas treatment systems. Pd and PdPt alloy NPs supported by ceria, are among the most active catalysts for the oxidation of methane. Yet, many questions about the interplay of the noble metals with the support, the involvement

of palladium oxide species, the role of Pt, and the exact reaction mechanism in the low-temperature regime remain [1,3].

In order to track the active sites and elucidate structure function relationships on an atomistic level we prepare fully epitaxial model systems of PdPt alloy NPs supported by ceria thin films on YSZ single crystals. Using grazing incidence X-ray diffraction techniques in conjunction with our operando catalysis environments we were able to track activity by in-line mass spectrometry and structure of the model catalysts by following the ceria CTRs, as well as Pd, Pt, and their respective oxide Bragg peaks under operando conditions.

[1] J. Dong et al., ACS Catal. 10 (23), pp. 14304-14314.

[2] T. Adriana et al. Surface Science 616, pp. 206-213.

O 29.4 Tue 11:15 CHE 91

Methane activation towards H₂ evolution with sub-nanometer Ta clusters supported on Pt(111) — •TOBIAS HINKE, KEVIN BERTRANG, MATTHIAS KNECHTGES, SEBASTIAN KAISER, and UELI HEIZ — TU Munich, School of Natural Sciences & CRC, Physical Chemistry

The tremendous global energy demand leads to resource shortages as well as environmental consequences. Employing H₂ as an alternative energy carrier from abundant feedstocks such as natural gas is one strategy to tackle these issues. However, efficient hydrogen evolution demands for a fundamental understanding to increase H₂ availability. For this, model systems can be used to elucidate basic principles in chemical reactions, facilitating the design of tailored catalytic systems. Studies of small cationic Ta-clusters and their oxides in the gas phase exhibit high activity towards the activation of highly inert CH₄, yielding Hydrogen, whereas the cluster charge was identified as a key parameter.

These studies are now extended to their supported analogues to approach common catalytic structures. Therefore, Ta_n-clusters (n < 30) supported on metal single crystal substrates are investigated under mild conditions in UHV, with regards to their activity towards H₂ evolution from CH₄ via TPD. Characterization was performed via XPS and STM. Supported Ta₈ clusters exhibit size dispersive stability at room temperature and are active towards H₂ evolution from CH₄.

[1] N. Levin et al. *J. Am. Chem. Soc.* **2020**, 142, 12, 5862-5869

O 29.5 Tue 11:30 CHE 91

Ta atoms & clusters on Pt(111) - an XPS study — •KEVIN BERTRANG, TOBIAS HINKE, MATTHIAS KNECHTGES, FEDERICO LOI, ALESSANDRO BARALDI, SEBASTIAN KAISER, and UELI HEIZ — Physical Chemistry, School of Natural Sciences, & Catalysis Research Center, Technical University of Munich

Thin films comprising Ta/Ta_xO_y have been extensively studied on Pt surfaces. There is still a lack of profound understanding concerning the chemical interaction in the Ta/Pt interface and how it is affected during film growth and oxidation. In particular, an unambiguous attribution of the oxidation state of Ta is lacking which is largely complicated due to the numerous oxides and sub-oxides it can form.

In a bottom up approach we deposited low coverage of Ta atoms & clusters on a Pt(111) surface and probed the system by means of XPS using synchrotron radiation. Oxidation was studied using both atomic and molecular O₂. Stability and surface mobility was studied. At liquid He a high variety of features are observed. In contrast at liquid N₂ most Ta species are mobile and agglomerate to form structures stable up to high temperatures.

O 29.6 Tue 11:45 CHE 91

Cu Nanoparticles on Vicinal and Basal ZnO as Model Catalysts for Methanol Synthesis — •ROBERT GLEISSNER^{1,2}, SIMON CHUNG¹, ESKO ERIK BECK^{1,2}, GUILHERME D. L. SEMIONE^{1,2}, MICHAEL WAGSTAFFE¹, LEON JACOBSE¹, STEFFEN TOBER^{1,2}, GÖKHAN GIZER⁴, CHRISTOPHER GOODWIN³, MARCUS SOLDEMO^{3,6}, MIKHAIL SHIPILIN^{1,3}, PATRICK LÖMKER^{1,3}, CHRISTOPH SCHLUETER¹, PETER AMANN³, OLOF GUTOWSKI¹, ANN-CHRISTIN DIPPPEL¹,

MATTHIAS MUNTWILER⁵, VEDRAN VONK¹, HESHMAT NOEI¹, and ANDREAS STIERLE^{1,2} — ¹Deutsches Elektronen-Synchrotron DESY, Hamburg, Germany — ²Universität Hamburg, Germany — ³University of Stockholm, Sweden — ⁴Helmholtz-Zentrum hereon, Gesthaacht, Germany — ⁵Paul-Scherrer Institut, Villingen, Switzerland — ⁶Stanford University, Stanford, USA

Over recent years, the vicinal ZnO(10-14) surface garnered increased scientific interest, as it combines a high density of surface steps with high stability. However, the role of vicinal ZnO in Cu/ZnO catalysts remained to be investigated. In this study, Cu nanoparticles were grown on vicinal and basal ZnO and studied by STM, LEED, SEM, and ambient pressure XPS, GIXRD, and XRR. On vicinal ZnO, the Cu nanoparticles show a high prevalence of stepped Cu facets, which are interesting for catalytic reactions. Our study elucidates the morphology of the Cu nanoparticles, their interplay with the ZnO support, their stability under oxidation/reduction conditions, and the prospects for improving the activity of Cu/ZnO-based catalysts for methanol synthesis.

O 29.7 Tue 12:00 CHE 91

A hybrid QM/MM framework to study single metal atom adsorption on doped diamond surfaces — •SHAYANTAN CHAUDHURI¹, ANDREW J. LOGSDAIL², and REINHARD J. MAURER¹ — ¹University of Warwick, Coventry, UK — ²Cardiff University, Cardiff, UK

Polycrystalline boron-doped diamond is widely used as a working electrode material in electrochemistry, and its properties such as a high stability make it an appealing support material for nanostructures for (electro)catalytic applications. Experiments have shown that electrodeposition can lead to the creation of stable small nanoclusters and even single metal adatoms on diamond. We investigate the structural stability and reactivity of single atoms on diamond as predicted by density functional theory. As hybrid functionals are computationally intractable for large-scale periodic surface structures, we use the quantum mechanics/molecular mechanics (QM/MM) methodology to compare different density-functional approximations on equal footing. We investigate the adsorption energy and kinetic stability of metal single atoms on an oxygen-terminated diamond (110) surface and explore the role of structural defects such as vacancies and dopants on metal atom adsorption. Our work forms the foundations for the study of metal nanocluster formation on diamond.

O 29.8 Tue 12:15 CHE 91

Reaction Pathways in Heterogeneous Photoreforming of Tertiary Alcohols — •MARTIN TSCHURL, CLARA ALETSEE, PAULA NEUMANN, PHILIP PETZOLDT, CARLA COURTOIS, MORITZ EDER, and UELI HEIZ — Chair of Physical Chemistry, School of Natural Sciences & Catalysis Research Center, Technische Universität München, Lichtenbergstr. 4, 85748 Garching, Germany

While the oxidation of tertiary alcohols remains a challenge in organic chemistry, heterogeneous photocatalysis opens up new pathways for their conversion. In this contribution, we discuss the selective oxidation of those alcohols under illumination on titania model photocatalysts. We reveal the processes occurring on the surface of a rutile single crystal in studies under ultra-high vacuum conditions and address the role of the pressure gap by comparing those results with

reactions of titania powders at ambient pressure. Furthermore, we demonstrate the impact of co-catalyst loading on the selectivity of the reaction and explain the underlying reaction mechanisms.

O 29.9 Tue 12:30 CHE 91

Bottom-up synthesis and transfer of free-standing nanocluster arrays supported by carbon — •TOBIAS HARTL¹, STEFAN SCHULTE¹, MORITZ WILL¹, PANTELIS BAMPOULIS^{1,2}, RAJENDRA SINGH³, JANI KOTAKOSKI³, JAN KNUDSEN⁴, and THOMAS MICHELY¹ — ¹Universität zu Köln — ²MESA+ Institute for Nanotechnology — ³Universität Wien — ⁴MAX IV Laboratory

Cluster superlattices exhibit unique properties stemming from their small size and dimensionality. However, their use in applications is hampered by their low stability when exposed to application relevant conditions, e.g. ambient pressure or high temperature. We succeeded in synthesizing free-standing cluster superlattice membranes (CSLM) which are stable at these conditions. CSLMs consist of a 2D lattice of similar-sized nanoclusters sandwiched between graphene (Gr) and an amorphous carbon (a-C) matrix. In order to make the membrane useful for experiments in nanocatalysis, it needs to be lifted off from the Ir(111) substrate and flipped over, to expose its Gr bottom side. This enables the removal of the covering Gr sheet and provides access to the clusters in the a-C matrix. Turning the membrane around requires a double transfer process, which is preceded by water and gas intercalation below the membrane. The transfer process consists of a first pick-up with a PDMS stamp, then a second pick-up from the PDMS stamp onto a polycarbonate stamp and finally the transfer to a new substrate. We present the fabrication and transfer processes of the membranes and explore the thermal stability and the physicochemical properties of this novel nanomaterial via XPS, TEM and STM.

O 29.10 Tue 12:45 CHE 91

Changing surface morphology and chemistry by scalable atmospheric pressure plasma treatment — •TIMO WAGNER¹, NICOLAS WÖHRL¹, VINEETHA VINAYAKUMAR², DORIS SEGETS², and AXEL LORKE¹ — ¹Faculty of Physics and CENIDE, University Duisburg-Essen, Germany — ²Particle Science and Technology (IVG-PST) and CENIDE, University of Duisburg-Essen

Nickel foams provide a large specific surface area. Yet, compared to bulk nickel plates, they are less desirable for industrial applications due to their higher cost and more difficult handling. As part of H2Giga, the hydrogen flagship project by the German Federal Ministry of Education and Research (BMBWF), we developed a plasma treatment for industry relevant nickel plates and catalyst particles. In a common manufacturing process for electrolyzers, nickel plates or meshes are first coated with a suspension of catalyst particles. Afterwards the solvents get thermally evaporated, yielding the finished electrode. With our process, the blank nickel surface can be roughened up by exposing it to a nitrogen plasma as a form of pre treatment. Also after coating, an exposure to a nitrogen plasma shows significant morphological changes. The individual particles coalesce to bulbs, that are again interspersed by a sponge-like porous structure. These structures have shown to notably improve the electrochemical performance of the electrodes, decreasing the overpotential by ca. 100mV.

O 30: 2D Materials I: Electronic Structure

Time: Tuesday 10:30–13:15

Location: GER 37

O 30.1 Tue 10:30 GER 37

Controlling the charge density wave transition in single-layer TiTe_{2-x}Se_{2(1-x)} alloys by band gap engineering — •TOMMASO ANTONELLI, ANDELA ZIVANOVIC, CHIARA BIGI, BRENDAN EDWARDS, AKHIL RAJAN, and PHIL KING — University of St. Andrews

The narrow gap semiconductor monolayer (ML) TiSe₂ undergoes a controversial charge density wave transition [1, 2] whose nature is still poorly understood. Recently, a similar instability has been observed in the sister semimetallic compound ML-TiTe₂ showing a weaker CDW coupling as compared to the selenide compound [3, 4]. Using molecular beam epitaxy, we grow ML-TiTe_{2-x}Se_{2(1-x)} alloys to engineer the band gap in the normal phase and tune the CDW coupling in the system. Performing angle-resolved photoemission spectroscopy on the alloy films, we demonstrate the effective semiconductor to semimetal transition in the high-temperature phase band structure and observe the consequent modulation of the CDW critical temperature. Our experimental results are rationalised using a simple theoretical model bringing new insight on how to manipulate this collective phase at the 2D limit.

[1] P. Chen *et al.*, Nat. Commun. 6, 8943 (2015) [2] M. D. Watson *et al.*, 2D Materials 8, 015004, (2021) [3] P. Chen *et al.*, Nat. Commun., 8, 516 (2017) [4] T. Antonelli *et al.*, npj Quantum Mater. 7, 98 (2022)

O 30.2 Tue 10:45 GER 37

Charge density wave in 2H-NbSe₂ studied by combined STM/nc-AFM — •NIKHIL SEEJA SIVAKUMAR¹, MARION VAN MIDDEN MAVRIC¹, NORA HUIJGEN¹, UMUT KAMBER², DANIEL WEGNER¹, ALEXANDER AKO KHAJETOORIANS¹, and NADINE HAUPTMANN¹ — ¹Institute for Molecules and Materials, Radboud University, Nijmegen, The Netherlands — ²Department of Physics, Princeton University, USA

Van der Waals materials exhibit interesting quantum phases such as charge density waves (CDW) which originate from an electronic instability along with structural rearrangements. One example is 2H-NbSe₂ which exhibits an incommensurate CDW below 33 K. The origin of the CDW in 2H-NbSe₂ is currently understood to be driven by electron-phonon coupling [1]. To characterize the CDW with atomic scale resolution, Scanning Tunneling Microscopy (STM) is frequently used which is sensitive to the convolution of the geometric structure and the local density of states.

Here, we utilize combined low-temperature STM and non-contact Atomic Force Microscopy (STM/nc-AFM) based on the qPlus design to study the CDW at the surface of 2H-NbSe₂. We detail the distancedependent contrast of the atomic lattice and the CDW in current and frequency shift images. We further compare force spectroscopy data at selected positions of the CDW unit cell and analyze different force contributions.

[1] Flicker, F., van Wezel, J. Nat. Commun. 6, 7034 (2015).

O 30.3 Tue 11:00 GER 37

Circular dichroism in valence band photoemission from CrGeTe₃ — •HONEY BOBAN¹, MOHAMMED QAHOSEH¹, XIAO HOU¹, MAGDALENA SZCZEPANIK², EWA PARTYKA-JANKOWSKA², TOMASZ SOBOL², TOM G SAUNDERSON^{3,4}, YURIY MOKROUSOV^{3,4}, MATHIAS KLÄUI³, CLAUS MICHAEL SCHNEIDER¹, and LUKASZ PLUCINSKI¹ — ¹PGI-6, FZ Jülich, Germany — ²NSRC SOLARIS, Poland — ³University of Mainz, Germany — ⁴PGI-1, FZ Jülich, Germany

CrGeTe₃(CGT) is a layered ferromagnetic semiconductor with a bulk Curie temperature (T_c) of 63K[1] and an indirect bandgap of 0.4eV[2]. A previous band structure mapping study of CGT[1] revealed band renormalizations below and above T_c and resonance enhancements at the Cr 3p absorption edge. CGT contains large Te atoms ($Z=52$), therefore spin-momentum locked splittings, Weyl nodes, and anticrossings are expected due to a combination of ferromagnetism and spin-orbit coupling, as well as the related Berry curvature physics. We performed light-polarization-dependent and temperature-dependent angle-resolved photoemission (ARPES) measurements on surfaces of bulk CGT. We have observed renormalizations in the dichroic ARPES maps below and above T_c , which could be indirectly related to magnetic ordering, even though our technique most likely averages spin-up and spin-down domains. Circular dichroic ARPES maps contain an intrinsic contribution due to the orbital angular momentum through dipole selection rules and an extrinsic contribution due to the experimental geometry. Our current work focuses on disentangling the two effects. Ref: [1] PRB **101**, 205125(2020), [2] PRB **98**, 125127(2018)

O 30.4 Tue 11:15 GER 37

Investigation of phase-transitions in MoTe₂ using ToF-MM — •O. FEDCHENKO¹, F. DIEKMANN², K. MEDJANIK¹, M. KALLMAYER³, S. BABENKOV¹, D. VASILYEV¹, O. TKACH¹, M. SOULIOU⁴, M. FRACHET⁴, M. LE TACON⁴, K. ROSSNAGEL², A. WINKELMANN⁵, G. SCHÖNHENSE¹, and H.-J. ELMERS¹ — ¹JGU, Institut für Physik, Mainz, Germany — ²Institut für Experimentelle und Angewandte Physik, CAU Kiel, Germany — ³Surface Concept GmbH, Mainz — ⁴KIT, IQMT, Karlsruhe, Germany — ⁵ACMN, AGH University of Science and Technology, Krakow, Poland

MoTe₂ is unique among transition metal dichalcogenides (TMDCs) because it can be grown in both the semiconducting (2H) and semimetallic (1T') phase. The transitions between these phases can be controlled with temperature and doping concentration. Using time-of-flight momentum microscopy (ToF-MM), the thermally-induced inversion symmetry breaking in doped Mo_{1-x}W_xTe₂ is investigated. Pristine MoTe₂ and Mo_{0.98}W_{0.02}Te₂ take the 2H phase, which does not show any thermal induced phase transition. For increased W doping concentration we obtain the metastable monoclinic 1T' phase at 300K (RT), which then can be transformed to the orthorhombic T_d phase at T<170 K (LT). Raman and XRD measurements confirm the structural transitions. The T_d-phase exhibits topological states identified by Fermi arcs, up to binding energy of E_B = 75 meV.

O 30.5 Tue 11:30 GER 37

Geometry-induced spin-filtering in photoemission maps from WTe₂ surface states — TRISTAN HEIDER¹, GUSTAV BIHLMAYER², JAKUB SCHUSSER^{3,4}, FRIEDRICH REINERT⁴, JAN MINAR³, STEFAN BLÜGEL², CLAUS M. SCHNEIDER¹, and •LUKASZ PLUCINSKI¹ — ¹PGI-6 Forschungszentrum Jülich — ²PGI-1 Forschungszentrum Jülich — ³University of West Bohemia, Pilsen, Czech Republic — ⁴Experimentelle Physik VII, Universität Würzburg

WTe₂ is a semi-metallic quantum material that exhibits non-saturating magnetoresistance and potentially hosts Weyl type-II nodes [1]. Through laser-driven spin-polarized ARPES Fermi surface mapping, we demonstrate highly asymmetric spin textures of electrons photoemitted from the surface states of WTe₂ [2]. Such asymmetries are not present in the initial state spin textures, which are bound by time-reversal and crystal lattice mirror plane symmetries. The findings are reproduced qualitatively by theoretical modeling within the one-step model photoemission formalism, and a simple toy-model suggests that a similar effect shall be observed in other materials with low symmetry. Our spin-polarized maps, with detail comparable to the previous spin-integrated maps [3], have been measured using the newly developed high-resolution instrument at PGI-6 in Jülich that is based on a hemispherical analyzer with the scanning lens, an exchange-scattering spin detector, and a cw 6 eV laser.

[1] P. K. Das et. al. Electron. Struct. **1**, 014003 (2019) and refs. therein. [2] T. Heider et al., arXiv:2210.10870 (2022). [3] F. Y. Bruno et al., Phys. Rev. B **94**, 121112 (2016).

O 30.6 Tue 11:45 GER 37

Observing Duffing oscillations in 2D materials by ultrafast electron imaging — •ALEXANDER SCHRÖDER, LINA HANSEN, and SASCHA SCHÄFER — Institute of Physics, University of Oldenburg, Germany

Two-dimensional materials are an ideal test bed for probing non-linear mechanical resonances. With sample thicknesses down to the atomic scale, the nonlinear regime of mechanical resonances can be observed even for small actuation forces. Previously, the response of such nano- and micromechanical systems was probed by optical or electronic means, leaving details of the mechanical mode

structures and their connection to atomic defects unresolved. Here, we present the nanoscale probing of nonlinear Duffing resonances in free-standing graphite membranes using large-angle convergent-beam diffraction in an ultrafast transmission electron microscope equipped with an event-based electron detector with nanosecond temporal resolution. The vibrational membrane modes are excited by a diode laser beam with a tunable modulation rate and a series of resonances are observed in the MHz frequency range with high quality factors (up to 10⁴). As expected for prototypical Duffing resonances, increasing the optical excitation strength yields a strong nonlinear hardening of the oscillator, with an increase in vibrational amplitude, an asymmetric broadening of the resonance line shape, bistable behavior, and a characteristic frequency-dependent phase shift. The novel detection scheme as proposed here is ideally suited for characterizing the behavior of ultra-small resonators difficult to address with other techniques.

O 30.7 Tue 12:00 GER 37

Limitations of supercell extrapolation for charged defects at surfaces & 2D materials — •CHRISTOPH FREYSOLDT¹, ANNE MARIE Z. TAN^{2,3}, RICHARD G. HENNIG², and JÖRG NEUGEBAUER¹ — ¹Max-Planck-Institut für Eisenforschung, Max-Planck-Straße 1, 40237 Düsseldorf, Germany — ²Department of Materials Science and Engineering, University of Florida, Gainesville, Florida 32611, USA — ³School of Mechanical and Aerospace Engineering, Nanyang Technological University, Singapore 639798, Singapore

Ab initio calculations of defects often employ the repeated slab approach for its simplicity. Unfortunately, spurious interactions between the defect and its periodic images make it sometimes challenging to estimate the dilute limit, that is relevant for comparison to experiment, from computationally affordable system sizes. A simple and seemingly straightforward approach is to extrapolate from a series of finite supercell sizes to the infinite-size limit, assuming a smooth, polynomial dependence of the energy on inverse supercell size. By means of explicit density-functional theory supercell calculations and simplified electrostatic models we demonstrate that the dependence of the formation energy on supercell size can be more complex than is commonly assumed. We show that this complexity cannot be captured by the simple extrapolation approaches. In contrast, suitable correction schemes are shown to provide rapidly converging results even for 2D materials.

[1] C. Freysoldt, J. Neugebauer, A. M. Z. Tan, R. G. Hennig, Phys. Rev. B **105**, 014103 (2022).

O 30.8 Tue 12:15 GER 37

Excited state geometry relaxation of point defects in hexagonal boron nitride — •ALEXANDER KIRCHHOFF, THORSTEN DEILMANN, and MICHAEL ROHLFING — Westfälische Wilhelms-Universität Münster, Institut für Festkörpertheorie, Wilhelm-Klemm-Straße 10, 48149 Münster

The optical gap of pristine hexagonal boron nitride is above 5 eV and therefore in the deep UV range. Emitters in the optical regime can act as single photon sources and gained attraction due to their possible room temperature stability. However, their atomic composition is still elusive. Experiments combining spectroscopic methods to probe ground as well as excited state of defects in hBN have revealed the relevance of the dependence of optoelectronic properties on the nuclear geometry.

In our work, this dependence is studied within the framework of density functional theory and the GW/BSE approximation. We focus on carbon based defects in hBN and present a detailed analysis of their excitonic spectrum [1]. C_BO_N for example has a defect bound exciton at 1.5 eV. We obtain a Stokes shift of about 1 eV by calculating the energy surfaces of ground and excited state.

[1] Kirchhoff, Deilmann, Krüger and Rohlfing, Phys. Rev. B **106**, 045118 (2022)

O 30.9 Tue 12:30 GER 37

Semiclassical theory of plasmons in inhomogeneous two-dimensional systems — •TJACCO KOSKAMP, KOEN REIJNDERS, and MIKHAIL KATSNELSON — Radboud University, Nijmegen, The Netherlands

We consider plasmons, collective oscillations of conduction electrons, in inhomogeneous two-dimensional systems with parabolic dispersion. In recent years, the quantum regime for plasmons has become experimentally accessible. Although these systems can be studied numerically, this approach is limited to relatively small systems. Recently, a comprehensive analytical theory for plasmons based on the semiclassical (WKB) approximation was proposed [1]. It describes plasmons in inhomogeneous three-dimensional systems, and is applicable when the inhomogeneity, in e.g. the electron density, varies smoothly.

In this talk, we extend this theory to plasmons in inhomogeneous two-dimensional systems. We consider the equation of motion for the density matrix and take the electron-electron interaction into account through the RPA. We solve this system of equations self-consistently, carefully separating the in-plane and out-of-plane degrees of freedom. In this way, the effective classical Hamiltonian for plasmons is obtained. Subsequently, we apply this theory to a scattering experiment. We first construct the classical trajectories and then use the semiclassical phase shift to compute the differential scattering cross section.

[1] K.J.A. Reijnders, T. Tudorovskiy, M.I. Katsnelson, Ann. Phys. **446**, 169116 (2022)

O 30.10 Tue 12:45 GER 37

Hot electron driven charge carrier dynamics at the MoS₂/gold interface: a sum frequency generation study — •TAO YANG, ERIK POLLMANN, STEPHAN SLEZIONA, PETER KRATZER, MARIKA SCHLEBERGER, RICHARD KRAMER CAMPEN, and YUJIN TONG — Fakultät für Physik, Universität Duisburg-Essen, 47057 Duisburg, Germany

Monolayer transition metal dichalcogenides (TMDCs) have potential applications as optoelectronics and (photo)electrocatalysts due to their fascinating electronic and optical properties. Applying these extraordinary properties to build devices and catalysts, it is often necessary to bring TMDCs into contact with a metallic surface. However, the charge transfer process across the semiconductor-metal interface is still not clear. While the quench of photoluminescence spectra has been reported for monolayer TMDCs on gold, which was understood to be a charge transfer of excited electrons from TMDC monolayer into the metal, it's interesting to ask what happens when the charge carrier is excited from the metal side. Here we use an azimuthal-dependent sum frequency generation combined with a pump-probe scheme to study the effect of the selectively excited hot electrons by 800 nm pump laser on the behavior of excitons of monolayer MoS₂. Our results show that the hot electrons from the gold substrate can significantly suppress the formation of excitons.

O 30.11 Tue 13:00 GER 37

Structure and electronic-optical properties of polymeric carbon nitride — •CHANGBIN IM, BJÖRN KIRCHHOFF, and TIMO JACOB — Ulm University, Institute of Electrochemistry, Ulm, Germany

Understanding of the electronic structure and optical properties of polymeric carbon nitrides (PCNs) is of key interest in order to exploit their photo-physical and photo-electrocatalytic capabilities. The numerous defects of typical PCNs, however, present a limitation to computational studies that aim to improve our fundamental understanding of this material class. Here, we demonstrate a systematic thermodynamic study and structural characterization of various heptazine based-PCN models from the viewpoint of electronic and optical properties obtained with hybrid density functional theory (DFT). Our calculations reveal the key structural factors (degree of condensation, interlayer distance, corrugation) that govern the formation of various PCN motifs and their optical properties.[1] We discuss how each of the key factors influences the electronic structure of PCNs. We also suggest the concept of exciton binding energy in PCNs and discuss the polaronic interactions between heptazine units due to the localized exciton nature. Furthermore, we disclose a failure of GGA in the description of correlated electrons that underestimates the energy of the conjugated electrons comparing hybrid DFT. From the results, we could not only deduce a more complete model for the diverse PCN motifs but could additionally derive fundamental trends for future material optimization.

[1] Im, C. et al. (2022). <http://arxiv.org/abs/2208.02582> submitted.

O 31: Focus Session: Ion Beam Interaction with Surfaces and 2D Materials III

Time: Tuesday 10:30–12:45

Location: GER 38

Topical Talk

O 31.1 Tue 10:30 GER 38

Ultra-low energy ion implantation of two-dimensional materials — •HANS HOFSSÄSS¹, FELIX JUNGE¹, MANUEL AUGÉ¹, BEATA KARDYNAL², URSEL BANGERT³, MARTIN WENDEROTH⁴, and LINO PEREIRA⁵ — ¹2nd Institute of Physics, University of Göttingen, Germany — ²Peter Grünberg Institute, Forschungszentrum Jülich, Germany — ³Department of Physics, University of Limerick, Ireland — ⁴4th Institute of Physics, University of Göttingen, Germany — ⁵Department of Physics, KU Leuven, 3001 Leuven, Belgium

Doping of two-dimensional (2D) materials by ion implantation requires unique requirements regarding ion energy, ion beam optics and sample preparation. Efficient substitutional incorporation of low energy ions into the 2D lattice requires energies around 20 eV. We use a low energy mass selected ion beam system with UHV implantation chamber. A 30 keV mass selected ion beam is guided through differential pumping stages and homogenized using a beam sweep. An area of about 1-2 cm² can be uniformly irradiated with these ultra-low-energy (ULE) ions with a beam current up to several microAmp. Results for doping of monolayer graphene with B⁺, N⁺ and P⁺ ions and doping of 2D MoS₂ with Se⁺ and Cr⁺ ions will be presented. We discuss challenges for ULE ion implantation, such as non-flat substrates, ion sources and lateral selective doping. Results for analyses of the implantation efficiency and lateral doping are presented. The simulation of ULE ion implantation using novel Monte Carlo Binary Collision Approximation programs is also discussed.

O 31.2 Tue 11:00 GER 38

Low-Energy Ion Implantation with an electron beam evaporator — •TOM WEINERT, DENISE JENNIFER ERB, STEFAN FACSKO, RENÉ HELLER, and ULRICH KENTSCH — Helmholtz-Zentrum Dresden-Rossendorf, Dresden, Deutschland

For ion implantation of thin films and in particular of two-dimensional materials, it is necessary to reduce the ion energy down to 10eV. For this purpose, we develop a simple and robust setup via a new approach. We use an electron beam evaporator to generate the desired ions. This has the advantage of a relatively small energy distribution of the ions, and in addition numerous different metal ions can be generated. An electrostatic analyzer is used to filter out the neutral atoms and to improve the energy distribution of the ion beam to below 5eV. The used ion energy is below 1keV and is suitable for the implantation of very thin surface layers or, after further energy reduction, for implantation in two-dimensional materials. Ion implantation can change the properties of two-dimensional materials, enabling, for example, new electrical, magnetic or catalytic applications.

O 31.3 Tue 11:15 GER 38

Fabrication of 2D magnets by ion implantation of phyllosilicates — MUHAMMAD ZUBAIR KHAN¹, NICO KLINGNER², GREGOR HLAWEK², ALEKSANDAR MATKOVIĆ¹, and •CHRISTIAN TEICHERT¹ — ¹Institute of Physics, Montanuniversität Leoben, 8700 Leoben, Austria — ²Helmholtz-Zentrum Dresden-Rossendorf e.V., 01328 Dresden, Germany

Since the first reports on intrinsically magnetic two-dimensional (2D) materials in 2017 [1,2], the price-to-pay for accessing their monolayers is still the lack of ambient stability. Recently, we demonstrated weak ferromagnetism in 2D Fe:tal

at room temperature and proposed iron-rich phyllosilicates as a promising platform for air-stable magnetic monolayers [3]. Since these minerals are rather rare and since phyllosilicates are hard to synthesize, we suggest here as an alternative ion implantation to tailor the magnetic properties of the phyllosilicates. Nonmagnetic, single-crystalline bulk talc crystals [4] were implanted with 50 keV iron and cobalt ion beams at different substrate temperatures. In all cases, ultra-thin layers could be exfoliated indicating that the layered crystal structure is maintained after ion irradiation. For both ion species, the Mg-OH Raman peak showed a triplet formation implying a successful substitution of Mg by Fe or Co in the talc layers. [1] Gong, C., et al., Nature 546, 265 (2017). [2] Huang, B., et al., Nature 546, 270 (2017). [3] A. Matković, et al., npj 2D Mat. Appl. 5, 94 (2021). [4] B. Vasić, et al., Nanotechnology 32, 265701 (2021).

O 31.4 Tue 11:30 GER 38

Charge exchange of highly charged ions scattered under grazing incidence — •MATTHIAS WERL, ANNA NIGGAS, FRIEDRICH AUMAYR, and RICHARD A. WILHELM — TU Wien, Institute of Applied Physics, Vienna, Austria

When a highly charged ion approaches a surface, electrons are resonantly captured from the material, starting at distances of $\approx 10 - 25 \text{ \AA}$ above the surface. The electrons are captured into shells with $n \approx q_{in}$ (q_{in} : incident charge state), forming a hollow atom (*HA*) - a state where (mostly) high- n shells are populated. In the free case, these excited *HAs* would then decay via a combination of auto-ionization and radiative pathways, recharging the projectile in the process. At very close distances from a surface ($d_I \leq 3 \text{ \AA}$), another process, known as Interatomic Coulombic Decay (*ICD*), can take place. Here, the *HA* quickly decays to its ground state due to electron-electron scattering with electrons from the material.

To study the *HAs* and their free decay, neutralization via *ICD* is to be prevented. This can be achieved if the distance of closest approach is larger than d_I , which happens at very grazing angles. Previous experiments showed that only a minor fraction of charged particles survive up to the detector under an incident angle of $\alpha_{inc} = 1.6^\circ$. Decreasing the incident angle even further ($0.1^\circ \leq \alpha_{inc} \leq 1.0^\circ$), more charged particles are expected to arrive at the detector.

Here, we present our setup to achieve these small incident angles with an accuracy of $\approx \pm 0.2^\circ$ as well as first experimental results for the charge state distribution of the scattered projectiles.

O 31.5 Tue 11:45 GER 38

Green functions simulation of the energy and charge transfer between highly charged ions and 2D materials — •MICHAEL BONITZ¹, KARSTEN BALZER², HANNES OHLDA¹, JAN-PHILIP JOOST¹, ANNA NIGGAS³, and RICHARD ARTHUR WILHELM³ — ¹CAU Kiel, Institute for Theoretical Physics and Astrophysics — ²CAU Kiel, Computing Center — ³TU Wien, Institute of Applied Physics, Vienna, Austria

We have developed Nonequilibrium Greenfunctions (NEGF) - Ehrenfest dynamics simulations for the energy loss of ions that impact correlated 2D materials. An interesting prediction was an ion-induced increase of the doublon number [1]. Recently, these simulations were extended to highly charged ions and to the associated charge transfer and electron emission. We find reasonable

agreement with the experimental predictions [2]. Here we discuss how these simulations can be extended to longer times and improved selfenergies via our G1-G2 scheme [3], combined with an embedding selfenergy approach [4].

[1] K. Balzer et al., Phys. Rev. Lett. 121, 267602 (2018); [2] A. Niggas et al., Phys. Rev. Lett. 129, 086802 (2022); [3] N. Schluenzen et al., Phys. Rev. Lett. 124, 076601 (2020); [4] N. Schluenzen et al., submitted for publication, arXiv:2211.09615

O 31.6 Tue 12:00 GER 38

Particle emission from 2d materials induced by highly charged ion impact — •LUCIA SKOPINSKI¹, LARS BREUER¹, SILVAN KRETSCHMER², ARKADY V. KRASHENINNIKOV², and MARIKA SCHLEBERGER¹ — ¹Universität Duisburg-Essen, Duisburg, Germany — ²Helmholtz-Zentrum Dresden-Rossendorf, Dresden, Germany

Two-dimensional (2d) materials such as graphene or transition metal dichalcogenides are expected to be key materials for novel applications. Defect engineering by highly charged ion (HCI) beams could be a way to modify their unique properties even further. An ion carries energy in the form of kinetic energy E_{kin} and potential energy E_{pot} , the latter corresponding to the energy required to create its respective charge state. Once the ion impinges on the surface, its energy is deposited into the solid and can lead to modifications and sputtering. However, the fundamental mechanisms of defect formation due to HCI-surface interaction are still under investigation.

Here, we discuss the emission of secondary ions and atoms as well as their velocity distribution from a substrate supported 2d material under HCI irradiation. The measured distributions allow a distinction between sputtering driven by the potential and the kinetic energy of the primary ion. The potential sputtering yield of MoS₂ has a similar dependence on the potential energy as the pore formation found in freestanding MoS₂ after irradiation with HCIs. The low velocities of the emitted particles indicate an interaction mechanism connected to electron-phonon coupling.

O 31.7 Tue 12:15 GER 38

Highly charged ion-induced electron emission from atomically thin materials — •ANNA NIGGAS¹, KARSTEN BALZER², MATTHIAS WERL¹, FRIEDRICH AUMAYR¹, MICHAEL BONITZ³, and RICHARD ARTHUR WILHELM¹ — ¹TU Wien, Institute of Applied Physics, Vienna, Austria — ²Computing Center of Kiel University, Kiel, Germany — ³Kiel University, Institute for Theoretical Physics and Astrophysics, Kiel, Germany

When a highly charged ion impacts on a material surface, its potential energy, i.e., the sum of the binding energies of all missing electrons, is deposited within the very first surface layers. This, in turn, triggers many processes such as the emission of electrons. While both the electron yield and energy distribution of bulk samples have been extensively studied in the past, data for 2D materials is rather scarce. This is due to the challenging task of separating signals of the 2D material itself from its support structure. Therefore, we developed a coincidence setup correlating ions after transmission with electrons emitted from the material. This allows us to discriminate signals from the support via the ion energy loss in the sample and, consequently, to access the emission from the 2D material alone.

In this contribution we will present our recent studies on the electron emission induced by highly charged ion impact on monolayers of graphene and MoS₂ and their 3D counterparts. We find a 6-fold higher emission yield for graphene compared to MoS₂ and a vanishing contribution of < 10 eV electrons for MoS₂. These findings are supported by simulations of the ion-induced surface charge dynamics.

O 31.8 Tue 12:30 GER 38

Light ion transmission through atomically thin material: insights from non-adiabatic first-principles simulations — •SILVAN KRETSCHMER¹, ARKADY V. KRASHENINNIKOV¹, ANNA NIGGAS², LUKAS FISCHER², and RICHARD A. WILHELM² — ¹Helmholtz-Zentrum Dresden-Rossendorf, Institute of Ion Beam Physics and Materials Research, Dresden, Germany — ²TU Wien, Institute of Applied Physics, Vienna, Austria

Two-dimensional materials, as surface-only targets, are ideally suited to study the neutralization and deexcitation of charged particles. Using atomistic Ehrenfest dynamics simulations we rationalize the experimental findings obtained for transmission of H⁺ and He⁺ through graphene and 2D-MoS₂. Here semi-metal and semi-conductor are chosen exemplary to explore potentially different neutralization behaviour. Changes in the electronic structure are calculated along with the energy loss and the charge transfer from the target to the projectile during the transmission and compared to the experiment. Furthermore, low-charge state ions represent a suitable model system to validate the framework of Ehrenfest dynamics to be extended to their highly charged counter parts.

O 32: Semiconductor Substrates

Time: Tuesday 10:30–12:45

Location: GER 39

O 32.1 Tue 10:30 GER 39

Progress in local growth of III/V-semiconductor structures — •CHRISTIAN BRUCKMANN, JÜRGEN BLÄSING, ARMIN DADGAR, and ANDRÉ STRITTMATTER — Otto-von-Guericke-Universität Magdeburg, PF4120 Magdeburg, Germany

We recently developed a laser-assisted metalorganic vapor phase epitaxy (LA-MOVPE) for local growth of III/V-semiconductors¹. The principle is based on local heating of a selected growth area by high-power laser radiation. Metalorganic precursors are fed into the reactor to the locally heated area so that the chemical reactions leading to island growth are confined within the heated area. Thereby, selective area growth can be done without full wafer heating which is advantageous for heteroepitaxy of crystalline materials and monolithic III/V device integration on Si. We report on optimum conditions for homoepitaxial GaAs growth, n- and p-type doping as well as AlGaAs/GaAs heterostructures. We discuss the proper choice of precursors and lateral homogeneity of ternary layers.

¹M. Trippel et al., "Laser-assisted local metal-organic vapor phase epitaxy", Rev. Sci. Instrum. 93, 113904 (2022)

O 32.2 Tue 10:45 GER 39

Post-synthesis of copper nitride monolayers from copper oxide films — •MOHAMMADREZA ROSTAMI¹, BIAO YANG¹, FRANCESCO ALLEGRETTI¹, LIFENG CHI², and JOHANNES V. BARTH¹ — ¹Physics Department E20, Technical University of Munich, Garching, 85748, Germany — ²Institute of Functional Nano & Soft Materials, Collaborative Innovation Center of Suzhou Nano Science and Technology, Soochow University, Suzhou 215123, P. R. China

Copper nitride (CuN) thin films represent insulating layers bearing promise for decoupling functional structures from a metallic copper substrate. [1] Although the nitrogen ion bombardment method was successfully applied for the in-situ preparation of CuN monolayers on Cu surfaces, the reduced domain size limits their application potential. [2] In this work, we have grown extended monolayer CuN films on Cu (111) surfaces by ammonia-mediated post-annealing of copper oxide (CuO) thin films. Structures and properties of CuN and CuO monolayers were characterized by scanning tunneling microscopy and low-energy electron diffraction. The element exchange of nitrogen with oxygen in the respective CuN

and CuO layers on Cu (111) surfaces was evidenced by X-ray photoelectron spectroscopy. This oxidation-reduction two-step strategy provides a new approach to fabricate CuN buffer layers. [1] Z. Zhao et al, Adv. Electron. Mater. 2018, 4, 1700367 [2] H. Baek et al, Appl. Phys. Lett. 91, 253106 (2007)

O 32.3 Tue 11:00 GER 39

The role of mechanical strain in rare-earth silicide monolayers on Si(111) — •KRIS HOLTGREWE and SIMONE SANNA — Justus-Liebig-Universität, Gießen, Deutschland

Rare-earth silicide (RESi₂) nanostructures on silicon surfaces provide a very heterogeneous class of lower-dimensional metallic systems supported by a semiconducting substrate. The RESi₂ monolayer is a two-dimensional semimetal, which grows on Si(111) by self-organisation. While it has intensively been studied by experimental and theoretical works, there are major misunderstandings about the mechanisms which determine the morphological details of the monolayer. In particular, many previous studies state that mechanical strain is responsible for the structural differences between the RESi₂ monolayer on Si(111) (buckled Si honeycomb, vacancy-free), the RESi_{2-x} bulk phase (flat Si honeycomb, vacancy-rich) and the AlB₂ structure (flat Si honeycomb, vacancy-free). This DFT work sheds light on the stability of the established structure model of the monolayer by a combined analysis of the structural details and the electronic band structure. It proves that the buckling of the covering Si honeycomb and the lack of Si vacancies are not due to mechanical strain, but due to charge balance. In this context, the monolayer is structurally more similar to the unstrained CaSi₂ structure than to the strained AlB₂ structure, which explains its stability. It is very likely that the misinterpreted role of mechanical strain is transferable to all RESi₂ nanostructures.

O 32.4 Tue 11:15 GER 39

Electronic and magnetic properties of ultrathin FeBr₂ films grown on Bi/Si(111) — •SHIGEMI TERAKAWA¹, JIABAO YANG¹, SHINICHIRO HATTA², HIROSHI OKUYAMA², TETSUYA ARUGA², NIELS SCHRÖTER¹, and STUART PARKIN¹ — ¹Max Planck Institute of Microstructure Physics, Halle, Germany — ²Graduate School of Science, Kyoto University, Kyoto, Japan

Mono and a few layers of van der Waals (vdW) magnets are promising two-dimensional (2D) materials to fabricate heterostructures with topological materials to realize novel topological phases via proximity effects, such as the quantum anomalous Hall effect. FeBr_2 is a layered Ising antiferromagnet, where the magnetic moments are coupled ferromagnetically in a layer and antiferromagnetically between adjacent layers. We succeeded in the epitaxial growth of ultrathin FeBr_2 films using molecular-beam epitaxy on Bi/Si(111) substrate. We observed insulating band structures using angle-resolved photoelectron spectroscopy (ARPES). The valence band top is located at a flat band with a binding energy of 2 eV, which is ascribed to Fe 3d orbitals. At monolayer coverage, the Fe 3d flat band does not change but dispersive bands of Br 4p at 7–8 eV are largely altered due to the disappearance of inter-layer Br-Br coupling in the monolayer film. The monolayer film shows a strong moiré pattern in low-energy electron diffraction (LEED), suggesting a strong coupling between the FeBr_2 and Bi films. We plan to discuss the magnetic properties of the FeBr_2 films from the results of XMCD experiments.

O 32.5 Tue 11:30 GER 39

In situ XPS Study on ultrathin Fe_xO_y Films on SrTiO_3 — •PIA MARIA DÜRING, TIMO KRIEG, and MARTINA MÜLLER — Fachbereich Physik, Universität Konstanz, 78457 Konstanz, Germany

Oxide interfaces are emerging as one of the most interesting systems in condensed matter physics as they exhibit a multitude of physical phenomena such as 2D electron/hole gas, superconductivity, or the Spin Hall effect. One of the main processes that controls the physical properties is the oxygen exchange between the film and the substrate. The tunability of the oxygen transfer using different growth parameters opens up the possibility to unravel unexplored properties.

Using our UHV-MBE system, we grow high-quality ultrathin Fe-oxide films on SrTiO_3 substrates by systematically varying certain growth parameters. Performing in situ X-ray Photoelectron Spectroscopy and Low Energy Electron Diffraction enables the analysis of the electronic properties and crystalline structure of ultrathin Fe_xO_y films directly after the growth without any atmospheric contamination.

The present work discusses the effect of different growth temperatures, substrate annealing procedures, and film thicknesses of the Fe_xO_y films on the interfacial properties like oxygen vacancies. The results open up the possibility for the emergence of 2D electronic states at the interface by tuning such growth parameters.

O 32.6 Tue 11:45 GER 39

MOVPE of Stacked Quantum Dots Layers at 1250 nm Wavelength — •EGE ÖZMEN, ARMIN DADGAR, and ANDRÉ STRITTMATTER — Otto von Guericke University, Magdeburg, Germany

LIDAR, light detection and ranging, is the technology to produce a 3D model of surroundings using semiconductor laser technology. In LIDAR, the return of laser pulses reflected from an object's surface is recorded in time. For optimum control of laser direction, a tightly bundled laser radiation is required. Since the light output from traditional semiconductor edge-emitting lasers is highly divergent, especially along the vertical axis, novel concepts for optical waveguides in laser diodes with lower output divergence have to be considered. Besides, as LIDAR operates in free space, a proper choice for laser wavelength has to be made. The current choice is around 905 nm wavelength which raises concerns about eye safety. Much better eye safety and therefore higher output powers could be realized if high-brilliance lasers operating at 1250 nm wavelength could be used. Here, we report on an optimization of MOVPE growth conditions to obtain up to 10-fold stacks of InGaAs quantum dots on a GaAs(001) substrate. We compare laser structures with 5–10 QD layers for static output characteristics.

O 32.7 Tue 12:00 GER 39

About the excitation of island growth orthogonal to the surface in the substrate $\text{Pb/Si(111)-(7\times7)}$ — •PAUL PHILIP SCHMIDT, LEA FABER, and REGINA HOFFMANN-VOGEL — Institute of Physics and Astronomy, University of Potsdam, 14476 Potsdam-Golm, Germany

With the increasing miniaturization of systems, the phenomena of surface diffusion is becoming more and more relevant. Pb shows anomalously fast mass transport on $\text{Si(111)-(7\times7)}$ [1,2]. For this system island growth and the behaviour of the wetting layer must be taken into account in order to understand the physical processes at the surface. We investigate the growth of the islands. Si was cleaned by rapid heating to 1200°C. Pb was deposited on the sample by evaporation at room temperature or liquid nitrogen temperature (120K). We create local imbalances of Pb to draw conclusions about diffusion and selectively trigger island growth at individual islands. While we measure the topography with non-contact atomic force microscopy, we simultaneously determine the local work function difference with Kelvin probe force microscopy. Our experiments show an energy barrier before ring growth occurs. Once atoms have reached an existing island, ring growth around occurs quickly. In experiments where we do not force this the islands hardly show any growth perpendicular to the surface. Part of the Pb comes from the restructuring of the island, which initially shrinks in the xy-direction.

[1] M. Hupalo et al. Phys. Rev. B, 23, 235443 (2007)

[2] K. L. Man et al. Phys. Rev. Lett., 101 226102 (2008)

O 32.8 Tue 12:15 GER 39

Solution-Synthesized Extended Graphene Nanoribbons Deposited by High-Vacuum Electrodeposition — •SEBASTIAN SCHERB¹, ANTOINE HINAUT¹, XUELIN YAO², ALICIA GÖTZ^{2,3}, SAMIR H. AL-HILFI², XIAO-YE WANG², YUNBIN HU², ZIJIE QIU², YIMING SONG¹, KLAUS MÜLLEN^{2,3}, THILO GLATZEL¹, AKIMITSU NARITA², and ERNST MEYER¹ — ¹Department of Physics, University of Basel, Basel, Switzerland — ²Max Plank Institute for Polymer Research, Mainz, Germany — ³Department of Chemistry, Johannes Gutenberg University Mainz, Mainz, Germany

Solution-synthesized graphene nanoribbons (GNRs) can facilitate various interesting structures or functionalities, like non-planarity and thermo-labile functional groups, which can be difficult to access via on-surface synthesis [1,2]. However, their deposition and thus study on surfaces remains challenging.

Here, we show high-vacuum electrodeposition (HVESD) of well-elongated solution-synthesized GNRs on metallic and non-metallic surfaces in UHV. Thereby, we compare three distinct GNRs, exhibiting different average lengths, functional groups, and edge structures. nc-AFM studies at room temperature combined with Raman spectroscopy allow the characterization of individual GNRs and confirm their chemical integrity [3].

[1] Narita et al. Nature Chemistry 6 (2014).

[2] Narita et al. Chemical Science 10 (2019).

[3] Scherb et al. accepted in ACS Nano.

O 32.9 Tue 12:30 GER 39

Ultra-thin Noble Metal Films on Superconductors — •CHRISTIAN VON BREDDOW, PHILIP BECK, LUCAS SCHNEIDER, JENS WIEBE, and ROLAND WIESENDANGER — Department of Physics - University of Hamburg, Hamburg, Germany

Magnet-superconductor hybrid systems involving Rashba-split surface states proximitized by a superconducting substrate are promising platforms for the realization of topological superconductivity [1,2,3]. To that end, a large gap of the superconductor, strong spin-orbit coupling, and a high surface quality that allows for the manipulation of individual magnetic atoms using the tip of a scanning tunneling microscope are strongly desired. In order to engineer a system with the desired properties we investigate the growth and surface-state dispersion of thin noble metal films on the (110)-surface of the elemental superconductor with the highest critical temperature, niobium. Starting from a few monolayer thickness, we observe the well known quasiparticle interference of the Shockley (111) surface state. Bias-dependent data is used to extract the layer-thickness dependence of the band bottom and the effective electron mass.

[1] A. C. Potter et al., Phys. Rev. B 85, 094516 (2012).

[2] A. Palacio-Morales et al., Science Advances 5 eaav6600 (2019)

[3] T. Tomanic et al., Phys. Rev. B 94, 220503 (2016).

O 33: Spins on Surfaces at the Atomic Scale III

Time: Tuesday 10:30–13:00

Location: REC C 213

Topical Talk

O 33.1 Tue 10:30 REC C 213

Fermi liquids, Luttinger integrals, topological invariants ... and magnetic molecules — •ROK ŽITKO^{1,2}, GERMAN G. BLESIO^{1,3}, LUIS O. MANUEL³, and ARMANDO A. ALIGIA⁴ — ¹Jozef Stefan Institute, Ljubljana, Slovenia — ²Faculty of Mathematics and Physics, University of Ljubljana, Slovenia — ³Instituto de Física Rosario (CONICET) and Universidad Nacional de Rosario, Argentina — ⁴INN CNEA-CONICET, Centro Atomico Bariloche and Instituto Balseiro, Bariloche, Argentina

The ground state of a system of interacting fermions is often a Fermi liquid with elementary excitations that are in a one-to-one correspondence with those of a

non-interacting Fermi gas. A key idea in Landau's theory is the adiabatic connection between the interacting and the non-interacting system. The adiabatic connection does not, however, always exist and there are several impurity problems where the ground state is known to be a Fermi liquid that is not of the Landau type. I will present the case of the two-channel $S=1$ Kondo model with single-ion magnetic anisotropy which has a topological quantum phase transition separating two different Fermi-liquid phases. I will discuss how the conservation laws constrain the Luttinger integrals so that their linear combinations become topological invariants, and how the modified Friedel sum rules lead to a peculiar variation of the impurity spectral function. I will then show that the

tunneling spectra of iron phthalocyanine molecules on Au(111) surface and of nickelocene molecules on Cu(100) surface can be consistently interpreted in the framework of non-Landau Fermi liquid theory.

O 33.2 Tue 11:00 REC C 213

Locally driven quantum phase transition cascades in a strongly correlated molecular monolayer — SOROUSH ARABI^{1,2,3}, TANER ESAT^{2,5}, AIZHAN SABITOVA^{2,5}, YUQI WANG^{2,3}, HOVAN LEE⁶, CEDRIC WEBER⁶, KERN KLAUS^{3,4}, F. STEFAN TAUTZ^{1,2,5}, RUSLAN TEMIROV^{2,7}, and •MARKUS TERNES^{1,2,5} — ¹Institute of Physics IIB, RWTH Aachen University, 52074 Aachen, Germany — ²Peter-Grünberg-Institute (PGI 3), Research Center Jülich, 52425 Jülich, Germany — ³Max Planck Institute for Solid State Research, 70569 Stuttgart, Germany — ⁴Institut de Physique, École Polytechnique Fédérale de Lausanne, 1015 Lausanne, Switzerland — ⁵Jülich Aachen Research Alliance, 52425 Jülich, Germany — ⁶King's College London, Theory and Simulation of Condensed Matter, London WC2R 2LS, UK — ⁷Institute of Physics II, University of Cologne, 50937 Cologne, Germany

The molecular monolayer of 1,4,5,6-naphthalene tetracarboxylic acid dianhydride on Ag(111) creates a perfectly ordered lattice of π -conjugated organic molecules. Using a movable atomically sharp electrostatic gate we drive this lattice of strongly correlated electrons through a cascade of quantum phase transitions. Performing spectroscopic imaging with sub-Angstrom resolution, we show that as the gate field is increased, the molecular building blocks change from a Kondo-screened to a paramagnetic phase one by one, enabling us to reconstruct their complex interactions in detail. We anticipate that the supramolecular nature of the system will, in future, allow engineering quantum correlations in arbitrary patterned structures.

O 33.3 Tue 11:15 REC C 213

Engineering antiferromagnetic spin coupling in carbon based nanostructures — •ELIA TURCO¹, NILS KRANE¹, FUPENG WU², MICHAL JURICEK³, XINLIANG FENG², PASCAL RUFFIEUX¹, and ROMAN FASEL¹ — ¹Empa Swiss Federal Laboratories for Materials Science and Technology, Dübendorf, Switzerland — ²Faculty of Chemistry and Food Chemistry, and Center for Advancing Electronics Dresden, Technical University of Dresden, Germany — ³Department of Chemistry, University of Zurich, Switzerland

On-surface synthesis offers the possibility to engineer atomically precise nanographenes (NGs) with intrinsic magnetic ground states. Unlike atomic magnets, unpaired π -electrons are highly delocalized and prone to hybridize forming entangled quantum states, which are the main requisite for the emerging quantum technologies. Zigzag-edged triangular NGs are regarded as prototypical magnetic building blocks, hosting a total spin S that scales with molecular size [1]. In this contribution, we will present the on-surface synthesis and scanning probe microscopy & spectroscopy of the two smallest $S = 1/2$ and $S = 1$ triangulenes on a Au(111) surface, where the Kondo screening of the unpaired spins is a direct evidence of their magnetic ground state. Connecting the two $S = 1/2$ and $S = 1$ building blocks into homo- and hetero-dimers and trimers, we realize multilevel quantum systems with increasing complexity, characterized by multiple inelastic spin excitations. The significant hybridization of the unpaired π -electrons results in strong quantum correlations, which have never been achieved for equivalent atomic systems. [1] J.Su et al. *Angew. Chem.* 132 (2020)

O 33.4 Tue 11:30 REC C 213

Moiré tuning of spin excitations: individual Fe atoms on MoS₂/Au(111) — •CHRISTIAN LOTZE¹, SERGEY TRISHIN¹, NILS BOGDANOFF¹, FELIX VON OPPEN², and KATHARINA J. FRANKE¹ — ¹Fachbereich Physik, Freie Universität Berlin, Germany — ²Dahlem Center for Complex Quantum Systems and Fachbereich Physik, Freie Universität Berlin, Germany

Magnetic adatoms on properly designed surfaces constitute exquisite systems for addressing, controlling, and manipulating single quantum spins. Here, we show that monolayers of MoS₂ on a Au(111) surface provide a versatile platform for controllably tuning the coupling between adatom spins and substrate electrons. Even for equivalent adsorption sites with respect to the atomic MoS₂ lattice, we observe that Fe adatoms exhibit behaviors ranging from pure spin excitations, characteristic of negligible exchange and dominant single-ion anisotropy, to a fully developed Kondo resonance, indicating strong exchange and negligible single-ion anisotropy. This tunability emerges from a moiré structure of MoS₂ on Au(111) in conjunction with pronounced many-body renormalizations. We also find striking spectral variations in the immediate vicinity of the Fe atoms, which we explain by quantum interference reflecting the formation of Fe-S hybrid states despite the nominally inert nature of the substrate. Our work establishes monolayer MoS₂ as a tuning layer for adjusting the quantum spin properties over an extraordinarily broad parameter range. The considerable variability can be exploited for quantum spin manipulations.

O 33.5 Tue 11:45 REC C 213

Absence of the Kondo effect for Co on Cu(111) — NEDA NOEI¹, ROBERTO MOZARA², ANA M. MONTERO³, SASCHA BRINKER³, NIKLAS IDE¹, FILIPE S. M. GUIMARAES³, ALEXANDER I. LICHTENSTEIN², RICHARD BERNDT¹, SAMIR LOUNIS³, and •ALEXANDER WEISMANN¹ — ¹Institut für Experimentelle und Angewandte Physik, Christian-Albrechts-Universität zu Kiel, D-24098 Kiel, Germany — ²Institut für Theoretische Physik, Universität Hamburg, D-20355 Hamburg, Germany — ³Peter Grünberg Institut and Institute for Advanced Simulation, Forschungszentrum Jülich, 52425 Jülich, Germany

The zero-bias anomaly in conductance spectra of single Co atoms on Cu(111) observed at ≈ 4 K, which has been interpreted as being due to a Kondo resonance, is strongly modified when the Co atoms are attached to monatomic Cu chains. Scanning tunneling spectra measured at 340 mK in magnetic fields exhibit all characteristics of spin-flip excitations. Their dependence on the magnetic field reveals a magnetic anisotropy and suggests a non-collinear spin state indicating that spin-orbit coupling (SOC), which has so far been neglected in theoretical studies of Co/Cu(111), has to be taken into account. According to our density functional theory and multi-orbital quantum Monte Carlo calculations SOC suppresses the Kondo effect for all studied geometries. The interpretation of the zero-bias anomaly in terms of a Kondo resonance is apparently incorrect.

O 33.6 Tue 12:00 REC C 213

Are excitations of the 4f magnetic moment visible to the scanning tunneling spectroscopy? — DARIA KYVALA and •JINDRICH KOLORENC — Institute of Physics (FZU), Czech Academy of Sciences, Praha, Czech Republic

The inelastic electron tunneling spectroscopy (IETS) has repeatedly proved useful for investigation of spin excitations in transition-metal atoms on surfaces [1,2]. Analogous observations of magnetic excitations in rare-earth atoms remained elusive, the reasoning behind it being that the 4f states that carry the magnetic moment are compact, buried in the atomic core, and the tunneling through a rare-earth atom proceeds via outer, more diffuse orbitals like 5d or 6s. Recently, the exchange coupling between the spin in these outer orbitals and the 4f magnetic moment was observed in IETS as an excitation in the 50–200 meV range [3]. In the same time, some excitations at lower energies were also seen. Employing a variant of the cotunneling theory [4,5] we demonstrate these excitations to be the elusive crystal-field excitations of the 4f magnetic moment. The selection rules prevent the IETS from detecting enough transitions to fully determine the crystal field by itself, but the visible transitions can be used in conjunction with the x-ray absorption spectra [6] to refine the existing estimates of the crystal field. — [1] A. J. Heinrich *et al.*, *Science* **306**, 466 (2004); [2] C. F. Hirjibehedin *et al.*, *Science* **317**, 1199 (2007); [3] M. Pivetta *et al.*, *PRX* **10**, 031054 (2020); [4] F. Delgado and J. Fernández-Rossier, *PRB* **84**, 045439 (2011); [5] C. Wäckerlin *et al.*, *ACS Nano* **16**, 16402 (2022); [6] R. Baltic *et al.*, *PRB* **98**, 024412 (2018).

O 33.7 Tue 12:15 REC C 213

Tuning the magnetic anisotropy of two coupled spins in a dinuclear Co(II) complex — CHAO LI¹, ROBERTO ROBLES², NICOLAS LORENTE³, ALEXANDER WEISMANN¹, RICHARD BERNDT¹, and •MANUEL GRUBER⁴ — ¹Institut für Experimentelle und Angewandte Physik, Christian-Albrechts-Universität zu Kiel, 24098 Kiel, Germany — ²Centro de Física de Materiales CFM/MPC (CSIC-UPV/EHU), 20018 Donostia-San Sebastián, Spain — ³Donostia International Physics Center (DIPC), 20018 Donostia-San Sebastian, Spain — ⁴Faculty of Physics and CENIDE, University of Duisburg-Essen, 47057 Duisburg, Germany

The magnetic properties of transition-metal ions are often described using a phenomenological spin Hamiltonian, which suggests that $S = 1/2$ metal ions are isotropic. We investigated a di-nuclear Co(II) complex on Au(111) with low-temperature scanning tunneling microscopy, X-ray magnetic circular dichroism, and density functional theory. The antiferromagnetically coupled Co spins preferentially align along the axis connecting the two Co(II) ions. The magnetic anisotropy is sizable and may be tuned by varying the electronic coupling of the Co(II) ions with the metal electrodes through manipulation of peripheral groups and by approaching the tip toward the complex. These findings may help better describing the magnetic properties of adsorbed molecules, in particular $S = 1/2$ ions, which are viewed as prototypical systems for quantum operations. Funding from the CRC 1242 is acknowledged.

O 33.8 Tue 12:30 REC C 213

Moiré - induced renormalization of singlet-triplet excitations in antiferromagnetically coupled Mn atoms on MoS₂/Au(111) — •SERGEY TRISHIN¹, CHRISTIAN LOTZE¹, FRIEDEMANN LOHSS¹, GIADA FRANCESCHI¹, LEONID I. GLAZMAN², FELIX VON OPPEN³, and KATHARINA J. FRANKE¹ — ¹Fachbereich Physik, Freie Universität Berlin, 14195 Berlin, Germany — ²Department of Physics, Yale University, New Haven, Connecticut 06520, USA — ³Dahlem Center for Complex Quantum Systems and Fachbereich Physik, Freie Universität Berlin, 14195 Berlin, Germany

The properties of single magnetic atoms can change drastically upon adsorption on a surface, for example due to Kondo-like exchange coupling. The magnitude of these interactions can be tuned by a moiré patterned surface [1]. Here,

we investigate single Mn atoms and dimers on single-layer molybdenum disulfide grown on a Au(111) substrate. The resulting moiré structure enables variations of the Kondo exchange coupling strength. By additionally varying the spacing between single atoms, we can investigate their properties in the direct and indirect exchange coupling regime. We find that at sufficiently close spacings, the Mn atoms form a non-magnetic singlet ground state. However, the singlet-triplet excitation energies vary strongly depending on the dimer location on the moiré structure. We ascribe these variations to a renormalization of the anti-ferromagnetic exchange coupling strength.

[1] S. Trishin and C. Lotze and N. Bogdanoff and F. von Oppen and K.J. Franken, Phys. Rev. Lett. **127**, 236801 (2021)

O 33.9 Tue 12:45 REC C 213

Stochastic dynamics of individual and coupled orbital memory on black phosphorus — •HERMANN OSTERHAGE, WERNER M. J. VAN WEERDENBURG, NIELS P. E. VAN MULLEKOM, RUBEN CHRISTIANEN, KIRA JUNGHANS, EDUARDO J. DOMÍNGUEZ VÁZQUEZ, HILBERT J. KAPPEN, and ALEXANDER A. KHAJETOORIAN — Radboud University, Nijmegen, The Netherlands

Recently, the dynamics of Co atoms adsorbed on a black phosphorus (BP) surface were shown to emulate a Boltzmann machine (BM) [1]. The BM relies on a tunable multi-well energy landscape, realized in the stochastic switching of coupled atoms which exhibit orbital memory [2]. Stochastic switching between orbital memory states can be induced using scanning tunneling microscopy (STM). The system response depends on interatomic distances and is adaptable to the position of the STM tip and to the applied DC bias [2].

Here, we present the response of individual and coupled Fe and Co atoms on BP to AC input voltages (i.e. frequency and amplitude response), measured using STM down to millikelvin temperatures. We find a frequency response of the orbital memory of single atoms. The changes in orbital state population with varying AC frequency can be derived from the switching dynamics in the DC case. The interatomic coupling is discussed based on changes in switching rates conditioned on the state of a second atom. Also the AC stochastic response in the multi-well limit will be discussed.

[1] B. Kiraly et al., Nat. Nanotechnol. **16**, 414 (2021).

[2] B. Kiraly et al., Nat. Commun. **9**, 3904 (2018).

O 34: Ultrafast Electron Dynamics at Surface and Interfaces III

Time: Tuesday 10:30–13:15

Location: TRE Phy

O 34.1 Tue 10:30 TRE Phy

Resolving Intervalley Exciton Couplings in Atomically Thin Semiconductors with Multidimensional Spectroscopy — •LAWSON LLOYD^{1,2}, RYAN WOOD², FAUZIA MUJID², SIDDHARTHA SOHONI², KAREN JI², PO-CHIEH TING², JACOB HIGGINS², JIWOONG PARK², and GREGORY ENGEL² — ¹Fritz-Haber-Institut, Berlin, Germany — ²The University of Chicago, Chicago, IL, USA

Atomically thin transition metal dichalcogenides (TMDs) have emerged as promising candidates for next-generation optoelectronic applications. In particular, an optically addressable “valley” degree of freedom at the K/K’ points can be used to store and readout information by exploiting the valley-dependent chiral optical selection rules. However, intervalley coupling after optical excitation leads to a loss of the valley polarization on ultrafast timescales. Identifying the microscopic mechanisms driving valley depolarization is therefore critical to advancing useful applications.

Here, leveraging multidimensional electronic spectroscopy, we track the exciton dynamics and couplings in large-area monolayer MoS₂ with femtosecond and valley resolution. We show that intervalley coupling between exciton states occurs both on the timescale of excitation (~10 fs) and with minimal dependence on the excitation fluence, temperature, or sample grain size. These results shed light on the strong many-body interactions governing the femtosecond exciton dynamics in TMDs and the factors limiting the realization of novel technologies built around the valley degree of freedom.

O 34.2 Tue 10:45 TRE Phy

Electron dynamics after a spin- and valley-polarized electronic excitation in WS₂ — •LASSE MÜNSTER¹, SARAH ZAJUSCH¹, RAUL PEREA-CAUSIN¹, SAMUEL BREM¹, KATSUMI TANIMURA¹, JENS GÜDDE¹, YAROSLAV GERASIMENKO², RUPERT HUBER², ERMIN MALIC¹, ULRICH HÖFER¹, and ROBERT WALLAUER¹ — ¹Fachbereich Physik, Philipps-Universität Marburg, Germany — ²Fachbereich Physik, Universität Regensburg, Germany

The excitonic landscape of monolayer transition metal dichalcogenides (TMDs) comprises optically accessible bright excitons as well as spin- and momentum-forbidden dark excitonic states. We image the formation process of these states after optical excitation on an ultrashort timescale with time-resolved momentum microscopy.

We excite monolayer WS₂ resonantly to the A 1s exciton with circular polarized light. This excitation leads to a population, which is located purely within the K valley for one helicity and in the K’ valley for the other helicity. In the case of an excitation at K, electron scatter to K’ and Σ by spin-conserving processes within a few tens of femtoseconds. Furthermore, we observe the formation of spin-forbidden excitons in the K valley and electron scattering towards Σ’. Both of these processes involve a spin-flip and are significantly slower (50 - 100 fs).

O 34.3 Tue 11:00 TRE Phy

Influence of the substrate dielectric permittivity on ultrafast quasiparticle dynamics in WS₂ monolayers — •SUBHADRA MOHAPATRA^{1,2}, LUKAS GIERSTER^{1,2}, STEFANO CALATI^{1,2}, NICHOLAS MICHAEL OLSEN³, QUIYANG LI³, XIAOYANG ZHU³, and JULIA STÄHLER^{1,2} — ¹Humboldt-Universität zu Berlin, Institut für Chemie — ²Fritz-Haber-Institut der Max-Planck-Gesellschaft, Abt. Physikalische Chemie, Berlin, Germany — ³Columbia University

In our recent fluence- and photon energy-dependent studies [1,2] of quasiparticle dynamics in WS₂ monolayers on fused silica (FS) and Si-SiO₂ substrates, we observed that excitonic screening reduces the binding energy of the excitons, however the role of screening due to substrates and the quantitative nature of

dynamic screening due to excitons remained inconclusive. On further investigation of such fluence-dependent quasiparticle dynamics studies using a higher dielectric permittivity of a sapphire substrate, we found that scattering rates, relaxation time constants, and band gap renormalization are not influenced by the dielectric permittivity. On the contrary, the dynamic screening parameter of the excitons is approximately two times higher in FS than Sapphire and Bohr radius is approximately 2.5 % higher in sapphire than for FS, which must be a direct consequence of the increased dielectric permittivity likely leading to more delocalized excitons.

[1] Calati et al. PCCP **23**(39) (2021).

[2] Calati et al. arXiv:2204.02125 (2022).

O 34.4 Tue 11:15 TRE Phy

Probing the ultrafast hole-transfer mechanism in a twisted TMD heterostructure — •MARCEL REUTZEL¹, JAN PHILIPP BANGE¹, DAVID SCHMITT¹, WIEBKE BENNECKE¹, GIUSEPPE MENEHINI², ABDULAZIZ ALMUTAIRI³, DANIEL STEIL¹, SABINE STEIL¹, R. THOMAS WEITZ¹, SAMUEL BREM², G. S. MATHIJS JANSEN¹, STEPHAN HOFMANN³, ERMIN MALIC², and STEFAN MATHIAS¹ — ¹I. Physikalisches Institut, Georg-August-Universität Göttingen, Göttingen, Germany — ²Fachbereich Physik, Philipps-Universität, 35032 Marburg, Germany — ³Department of Engineering, University of Cambridge, Cambridge CB3 0FA, U.K.

In type-II band aligned TMD heterostructures, long-lived interlayer excitons (ILX) can be formed via two different processes: Optically excited intralayer excitons either transfer the exciton’s electron or hole component across the interface. Using momentum microscopy [Rev. Sci. Ins. **91**, 063905 (2020)], we have shown that the transfer of the exciton’s electron proceeds via exciton-phonon scattering and layer hybridized Σ-excitons [Schmitt *et al.*, Nature **608**, 499 (2022)].

In this contribution, we show that the Coulomb correlation between the exciton’s hole and electron can be used to probe the hole-transfer dynamics: The intralayer exciton’s hole transfers from the VBM of MoS₂ into the VBM of WSe₂, which is imprinted onto the photoemission signal as an apparent upshift of the mean photoelectron energy. Our analysis provides new insights on the ultrafast hole-transfer mechanism in the WSe₂/MoS₂ heterostructure, and, more generally, on the photoemission signature of Coulomb correlated electron-hole pairs.

O 34.5 Tue 11:30 TRE Phy

Resolving momentum-dependent phonon buildup at a 1T-TiSe₂ surface using diffuse scattering in ultrafast LEED — •FELIX KURTZ¹, TIM DAUWE¹, SERGEY YALUNIN¹, GERO STORECK², JAN GERRIT HORSTMANN¹, HANNES BÖCKMANN-CLEMENS¹, and CLAUD ROPERS^{1,2} — ¹Max Planck Institute for Multidisciplinary Sciences, Am Fassberg 11, D-37077 Göttingen — ²4th Physical Institute, University of Göttingen, Friedrich-Hund-Platz 1, D-37077 Göttingen

Electron-phonon and phonon-phonon couplings govern the energy flow into and within the lattice following femtosecond laser excitation. The resulting transient phonon population can be directly deduced from momentum-resolved maps in ultrafast electron diffuse scattering [1]. Here, we employ ultrafast low-energy electron diffraction (ULEED) [2] to investigate structural dynamics and pathways for energy relaxation in the optically-excited charge-density-wave phase of 1T-TiSe₂. By analyzing the diffuse scattering background, we track the nonequilibrium evolution of the phonon population and observe strongly momentum-dependent rise times. Specifically, we find a rapid buildup of zone-boundary phonons within few picoseconds, followed by a substantially slower generation of low-energy zone-center acoustic phonons. Our findings are cor-

roborated by *ab-initio* DFT calculations of phonon-phonon scattering rates. We believe that the presented approach is generally applicable to a variety of systems and provides fundamental insights into surface phonon dynamics and relaxation pathways.

[1] L. P. René de Cotret, *et al.*, Phys. Rev. B 100, 214115 (2019)

[2] G. Storeck, *et al.*, Structural Dynamics 7, 034304 (2020)

Topical Talk

O 34.6 Tue 11:45 TRE Phy

Photoemission orbital tomography for excitons — •PETER PUSCHNIG, ANDREAS WINDISCHBACHER, MELVIN HODŽIĆ, and CHRISTIAN S. KERN — Institute of Physics, NAWI Graz, University of Graz, Austria

In photoemission orbital tomography (POT), the photoemission angular distribution (PAD) of oriented molecular layers is interpreted in terms of the Fourier transform of the initial molecular orbital from which the electron is emitted. Recently, it has been demonstrated that POT can in principle also be applied to optically excited states using a femtosecond pump-probe setup, which images the excited electron-hole pairs of a system, the excitons, on ultrafast time scales [1]. However, a rigorous and generally applicable connection between the measured PAD and the spatial structure of the excitons is lacking. By considering the expansion of the exciton wave function in the product basis of valence and conduction state orbitals, as typically done when solving the electron-hole Bethe-Salpeter equation or Casida's equations in the framework of TDDFT, we demonstrate in this contribution that the PAD is given by the Fourier transform of a coherent sum of the electronic part of the exciton wave function. This relation, which is based on a plane wave final state, as well as the unexpected consequences of the hole for the measured kinetic energy spectrum an exciton is illustrated for a series of organic molecules in the gas phase for which the PAD is also simulated explicitly, and without resorting to a plane-wave final state, by means of a real-time, real-space TDDFT approach.

[1] Wallauer *et al.*, Science 371, 1056-1059 (2021).

O 34.7 Tue 12:15 TRE Phy

Ultrafast lattice dynamics of Niobium diselenide (2H-NbSe₂) — •VICTORIA C. A. TAYLOR¹, YOAV WILLIAM WINDSOR^{1,2}, HYEIN JUNG¹, and RALPH ERNSTORFER^{1,2} — ¹Fritz Haber Institute — ²TU Berlin

Within the transition metal dichalcogenide family, 2H-NbSe₂ is unusual as it exhibits metallic, charge density wave (CDW), and superconducting phases, evidencing strong electron-lattice interactions. Ultrafast techniques enable investigation of such interactions on femtosecond timescales, and several studies have investigated the ultrafast electronic response of 2H-NbSe₂. However, none have directly probed the ultrafast response of the lattice. We present a femtosecond electron diffraction (FED) study on 2H-NbSe₂ in its metallic phase, probing both coherent and incoherent phononic responses that result from electron-phonon and phonon-phonon scattering. From these data we explore these processes and the associated timescales.

O 34.8 Tue 12:30 TRE Phy

Non-equilibrium dynamics of bulk VSe₂ — •WIBKE BRONSCHE¹, MANUEL TUNIZ², DENNY PUNTEL², ALESSANDRO GIAMMARINO², FULVIO PARMIGIANI^{1,2}, and FEDERICO CILENTO¹ — ¹Elettra-Sincrotrone Trieste, Trieste, Italy — ²Università degli Studi di Trieste, Trieste, Italy

By means of time- and angle-resolved photoemission spectroscopy (tr-ARPES), we investigate the effect of optical excitation on the electronic properties of the transition metal dichalcogenide VSe₂. The electronic band structure of VSe₂ has recently been subject of investigation ranging from the bulk to the mono-

layer regime, in search for the manifestation of the opening of a band gap in its CDW phase [1,2]. However, at present, only a few studies on the effect of an ultrafast optical excitation are available [1,3]. In our contribution we present a study on the bulk material. By selecting the polarization of the probe pulses, tr-ARPES allows us to disentangle states with different orbital character, originating from the V and Se valence bands. Our tr-ARPES data show indication for a novel photoinduced state near the Fermi level, lasting for several picoseconds after photoexcitation.

[1] Biswas *et al.*, Nano Letters 21, 1968-1975 (2021).

[2] Umemoto *et al.*, Nano Research 12, 165-169 (2019).

[3] P. Majchrzak *et al.*, Phys. Rev. B 103, L241108 (2021).

O 34.9 Tue 12:45 TRE Phy

Ultrafast charge separation and charge density wave suppression in monolayer TiSe₂ on graphite — •SEBASTIAN BUCHBERGER^{1,2}, CHARLOTTE SANDERS³, YU ZHANG³, EMMA SPRINGATE³, PAULINA MAJCHRZAK⁴, JILL MIWA⁴, PHILIP HOFMANN⁴, SØREN ULSTRUP⁴, and PHIL D. C. KING¹ — ¹University of St Andrews, UK — ²MPI for Chemical Physics of Solids, Dresden, Germany — ³Central Laser Facility, UK — ⁴Aarhus University, Denmark

The properties of two-dimensional materials and their heterostructures are often governed by the interplay of several coexisting interactions which can be difficult to disentangle in equilibrium. Time and angle resolved photoelectron spectroscopy (trARPES) is emerging as a powerful method to investigate such systems, allowing the observation of ultrafast processes such as the buildup of charge screening¹, optically induced bandgap renormalisation² and interlayer charge separation³. Here we present a trARPES study on monolayer TiSe₂ grown epitaxially on graphite. Monolayer TiSe₂ is a small indirect bandgap semiconductor that exhibits an unconventional charge density wave (CDW) in its ground state, whose origin and nature are still not fully established⁴. We study how the electronic structure evolves upon photoexcitation, tracking band shifts and spectral weight variations to disentangle charge separation, screening, and dynamical suppression of the CDW.

¹T. Rohwer *et al.*, Nature 471, 490-493 (2011), ²S. Ulstrup *et al.*, ACS Nano 10, 6315-6322 (2016), ³S. Aeschlimann, Sci. Adv. 6, eaay0761 (2020), ⁴P. Chen *et al.*, Nat. Commun. 6:8943 (2015)

O 34.10 Tue 13:00 TRE Phy

Manipulation of the charge-density-wave in VTe₂ by femtosecond light pulses — •MANUEL TUNIZ¹, WIBKE BRONSCHE², DENNY PUNTEL¹, GIOVANNI DI SANTO², LUCA PETACCIA², DAVIDE SORANZIO³, DAVIDE BIDOGGIA¹, MARIA PERESSI¹, FULVIO PARMIGIANI^{1,2}, and FEDERICO CILENTO² — ¹Dipartimento di Fisica, Università degli Studi di Trieste, Italy — ²Elettra - Sincrotrone Trieste S.C.p.A., Italy — ³Institute for Quantum Electronics, ETH Zurich, 8093 Zurich, Switzerland

Comparing equilibrium and out-of-equilibrium angle-resolved photoemission spectroscopy (ARPES and tr-ARPES), we investigate the effect of an optical excitation on the electronic properties of the charge-density wave (CDW) system VTe₂. Recently, the modification of the material's electronic structure triggered by CDW formation has been discussed because the strongly orbital-dependent changes may give rise to a topological change in specific bands [1]. In our contribution we show clear modifications to the electronic band structure of VTe₂ induced by the emergence of the CDW phase. Moreover, our tr-ARPES experiments open the possibility to perturb the CDW phase and study the relaxation dynamics of this non-equilibrium state to the ground state of the system.

[1] Mitsuishi, N. *et al.* Nat Commun 11, 2466 (2020)

O 35: Focus Session: Frontiers of Electronic-Structure Theory III (joint session O/HL)

Time: Tuesday 10:30-12:45

Location: TRE Ma

O 35.1 Tue 10:30 TRE Ma

Two-component GW implementation for molecular valence excitations — •QINGLONG LIU, RAMÓN L. PANADÉS-BARRUETA, and DOROTHEA GOLZE — Chair of Theoretical Chemistry, Technische Universität Dresden, 01062 Dresden, Germany

We present an all-electron GW implementation for the computation of charged molecular excitations, that includes scalar relativistic effects and spin-orbit coupling (SOC). Our method is based on a two-component (2c) approach, which can process 2c spinors and their corresponding eigenvalues from different levels of theory. The relativistic input for our 2c GW calculation is obtained in two ways: One approach is a non-self-consistent second variation SOC scheme, i.e. a scalar relativistic (SR) calculation is performed followed by an expansion of the spinors on top of the SR eigenvectors [1]. Another approach is the spinors and their eigenvalues are obtained by running a self-consistent relativistic DFT calculation with the X2C method [2]. Our algorithm has been implemented in the FHI-aims program package, which is based on numeric atom-centered orbitals (NAOs). In our 2c GW algorithm we combine the all-electron NAO scheme with

the resolution of the identity technique based on the Coulomb metric (RI-V) and use the analytical continuation to evaluate the G_0W_0 self energy. We present results for the numerical validation of our implementation and for the influence of the relativistic input (second variation SOC vs X2C) on the valence excitations of small heavy molecules.

[1] W. Huhn and V. Blum, Phys. Rev. Materials 1, 033803 (2017)

[2] M. Iliaš and T. Saue, J. Chem. Phys. 126, 064102 (2007)

O 35.2 Tue 10:45 TRE Ma

Screened potential in two-dimensional GW calculations within the LAPW framework — •BEN ALEX, SVEN LUBECK, and CLAUDIA DRAXL — Physics Department and IRIS Adlershof, Humboldt-Universität zu Berlin, Berlin, Germany

To calculate two-dimensional (2D) materials in a three-dimensional periodic code, one has to consider periodically repeated layers. The calculation of quasi-particle energies for 2D materials within the GW approximation requires the introduction of a 2D cutoff for the Coulomb potential as the layers would otherwise interact with each other. This cutoff leads to a stronger q dependence of the

dielectric function around $q = 0$ which requires much denser sampling of the first Brillouin zone. In order to address this issue, an analytic expression for the dielectric function was previously derived for a plane-wave basis [1]. This expression is then integrated numerically in a small region around $q = 0$. The goal of this work is to adapt this technique to the linearized augmented planewave + local-orbital (LAPW+lo) basis as implemented in the full-potential all-electron code `exciting`. We show that also in our case, we obtain a significant computational speedup. Furthermore, this approach is combined with an approach where the dielectric function is interpolated to a denser q -grid.

[1] F. A. Rasmussen et al., *Phys Rev B* 94, 155406 (2016).

O 35.3 Tue 11:00 TRE Ma

GW multipole approach for the frequency description of the dielectric screening — •CLAUDIA CARDOSO¹, DARIO A. LEON², ANDREA FERRETTI¹, DANIELE VARSANO¹, and ELISA MOLINARI¹ — ¹S3 Centre, Istituto Nanoscienze, CNR, 41125, Modena (Italy) — ²Department of Mechanical Engineering and Technology Management, Norwegian University of Life Sciences, 1430, Ås (Norway)

In the present work, we discuss a numerical approach for GW calculations that takes into account the frequency dependence of the screening via a multipole approximation (MPA), an accurate and efficient alternative to current full-frequency methods, that overcomes several limitations of the plasmon pole approximation (PPA).

MPA was recently developed and validated for semiconductors[1]. We now extend the use of MPA to metallic systems by optimizing the frequency sampling for these class of materials and propose a simple method to include the zero q limit of the intra-band contributions. The good agreement between MPA and full frequency results for the calculations of quasi-particle energies, polarizability, self-energy and spectral functions in different metallic systems confirms the accuracy and computational efficiency of the method. Finally, we discuss the physical interpretation of the MPA poles through a comparison with experimental electron energy loss spectra for Cu.

[1] D. A. Leon, C. Cardoso, T. Chiarotti, D. Varsano, E. Molinari, A. Ferretti, *Phys. Rev. B* 104, 115157

Topical Talk

O 35.4 Tue 11:15 TRE Ma

Towards low-scaling GW calculations for 2D materials — •JAN WILHELM — Institute of Theoretical Physics, University of Regensburg

Semiconducting two-dimensional materials are an ideal platform to study excitons thanks to the strong exciton binding energy and good experimental accessibility of the excitons. The GW+Bethe-Salpeter approach (GW+BSE) has been successful in analyzing excitons in single-layer 2D materials [1], but the application of GW+BSE is challenging for 2D double layers and moiré structures [2]. This is because the large unit cells in these structures contain hundreds to thousands of atoms, resulting in a high computational cost for GW+BSE calculations. In this talk, I will present a low-scaling GW algorithm for 2D materials that potentially allows for the inclusion of more than a thousand atoms in the simulation [3]. This algorithm is based on localized basis functions and can handle periodic boundary conditions and the divergence of Coulomb interactions in the Brillouin zone. I will present first benchmark calculations.

[1] D. Y. Qiu, F. H. da Jornada, S. G. Louie, *PRL* 111, 216805 (2013). [2] *Nat. Phys.* 17, 720 (2021), *Nature* 608, 499 (2022), *Science* 376, 406 (2022), *Nature* 603, 247 (2022). [3] J. Wilhelm, D. Golze, L. Talirz, J. Hutter, C. Pignedoli, *JPCL* 9, 306 (2018), J. Wilhelm, P. Seewald, D. Golze, *JCTC* 17, 1662 (2021).

15 min. break

O 35.5 Tue 12:00 TRE Ma

Accelerating core-level GW calculations by combining the contour deformation with the analytic continuation of W — •RAMÓN L. PANADÉS BARRUETA and DOROTHEA GOLZE — Theoretische Chemie, Technische Universität Dresden, Bergstr. 66c, 01062 Dresden, Deutschland

Many-body methods, like the GW approximation, have recently proven to be a highly effective tool for computing core-level excitations [1]. In particular, the contour deformation (CD) is an efficient, scalable and numerically stable approach that has enabled core-level calculations on systems up to 100 atoms [2]. In this work, we reduce the scaling of CD applied to core-levels from $O(N^3)$ to $O(N^4)$, using an analytic continuation of the screened Coulomb interaction W [3]. The new method (CD-WAC) has been implemented in FHI-aims. CD-WAC has been extensively tested on well established benchmark sets like the GW100 and the CORE65, reporting MAEs of less than 5 meV with respect to CD. The theoretical scaling has been confirmed by performing scaling experiments on large acene chains and amorphous carbon. Speedups of 5 times have been attained with CD-WAC for the largest systems.

[1] D. Golze, M. Dvorak, and P. Rinke. *Front. Chem.*, 7:377, 2019.

[2] D. Golze, J. Wilhelm, M.J. Van Setten, and P. Rinke. *J. Chem. Theory Comput.*, 14(9):4856-4869, 2018.

[3] I. Duchemin and X. Blase. *J. Chem. Theory Comput.*, 16(3):1742-1756, 2020.

O 35.6 Tue 12:15 TRE Ma

Many-Body Effects of Metals Investigated by Means of the GW Method — •ZIMO ZHOU, NAKIB PROTIK, and CLAUDIA DRAXL — Institut für Physik and IRIS Adlershof, Humboldt-Universität zu Berlin, Berlin, Germany

Even if semilocal exchange-correlation functionals of density-functional theory (DFT) can capture the overall band structure of many metals well, they fail to obtain the correct position of the d-bands. This leads, for instance, to the underestimation of the interband absorption onset in the corresponding optical spectra as shown for a set of elemental metals [1]. In this work, we provide a systematic investigation of the quasi-particle band structure and the optical properties of this set of materials. To this extent, the self-energy corrections to the DFT results are computed by the GW approach of many-body perturbation theory as implemented in the full-potential all-electron code `exciting` [2,3]. We show that the optical absorption spectra based on these quasi-particle bands remedy the shortcomings of semi-local DFT, accurately reproducing the experimental counterparts.

[1] W. S. M. Werner, K. Glantschnig, and C. Ambrosch-Draxl, *J. Phys. Chem. Ref. Data* 38, 1013 (2009). [2] A. Gulans, S. Kontur, C. Meisenbichler, D. Nabok, P. Pavone, S. Rigamonti, S. Sagmeister, U. Werner, and C. Draxl, *J. Phys: Condens. Matter* 26, 363202 (2014). [3] D. Nabok, A. Gulans, and C. Draxl, *Phys. Rev. B* 94, 035418 (2016).

O 35.7 Tue 12:30 TRE Ma

Separable Resolution-of-Identity in an all-electron numeric atom-centered basis set framework — •FRANCISCO DELESMA¹, DOROTHEA GOLZE², and PATRICK RINKE¹ — ¹Department of Applied Physics, Aalto University, Espoo, Finland — ²Faculty of Chemistry and Food Chemistry, Technische Universität Dresden, Dresden, Germany

The resolution-of-identity (RI) is a common way in quantum chemistry and computational materials science to reduce the computational cost of two-electron Coulomb integrals, another central entity in computational quantum mechanics. In 2019, Duchemin and Blase proposed the separable-RI approach [1], which preserves the accuracy of the standard, global RI method with the Coulomb metric (RI-V) and permits the formulation of cubic-scaling random-phase approximation (RPA) and Green's function based GW approaches.

In this work, we present the first implementation of the separable-RI in an all-electron numeric atom-centered orbital framework. Separable-RI is implemented in the FHI-aims code [2] and optimized for massively parallel execution. We extend the separable-RI framework beyond the original Hartree-Fock (HF) and GW implementations of Duchemin and Blase to MP2 and RPA, SOSEX and CCSD. Our separable-RI total energies and GW quasiparticle energies for the Thiel test set of small organic molecules reproduce the exact two-electron Coulomb integral calculations within 1 meV or better.

[1] I. Duchemin and X. Blase, *J. Chem. Phys.* 150, 174120 (2019)

[2] V. Blum, et al, *Comput. Phys. Commun.* 180, 2175, (2009)

O 36: Poster: 2D Materials II

Time: Tuesday 18:00–20:00

Location: P2/EG

O 36.1 Tue 18:00 P2/EG

Simulation of proximity effects in epitaxial graphene systems — •ANDRES DAVID PEÑA UNIGARRO¹, FLORIAN STEFFEN GÜNTHER^{2,3}, and SYBILLE GEMMING¹ — ¹Institute of Physics, TU Chemnitz, Chemnitz, Germany — ²IFSC, University of São Paulo, Brazil — ³UNESP, Brazil

Two-dimensional materials such as graphene are fascinating because they combine mechanical flexibility with unique electronic properties. The next level of complexity, however, comprises the assembly of various 2D materials to generate structures with enhanced characteristics. Using proximity effects, changes in the electronic, optical and transport properties of epitaxial graphene have been pro-

duced while preserving the regular honeycomb structure that can be grown on silicon carbide, SiC. Such modifications can, for instance, be achieved by proximity effects in hetero stacks with intercalate and adsorbate layers with other 2D materials or by the presence of a functional integration environment. In the past years, many elements were intercalated below the graphene sheet, forming partly well-defined hetero bilayer systems with different functionalities. As suggested by density functional theory (DFT) studies, elements of the IV group can be used for this purpose. In this case, intercalation of heavy atoms like Pb are expected to introduce additional effects such as spin-orbit coupling to the electron gas of graphene. In this contribution, we present preliminary results obtained with

DFT focusing on the study of modifications of the electronic structure of epitaxial graphene due to proximity effects generated by the intercalation of Pb on buffer layers on SiC.

O 36.2 Tue 18:00 P2/EG

Structural Characterization of a Novel Two-Dimensional Material: Cobalt Sulfide Sheets on Au(111) — •MARCEL ROST¹, MAHESH PRABHU², DAJO BODEN², JÖRG MEYER², and IRENE GROOT² — ¹Huygens-Kamerlingh Onnes Laboratory, Leiden Institute of Physics, Leiden University, 2300 RA Leiden, The Netherlands — ²Leiden Institute of Chemistry, Leiden University, P.O. Box 9502, 2300 RA Leiden, The Netherlands

Transition metal dichalcogenides (TMDCs) are a type of two-dimensional (2D) material that has been widely investigated by both experimentalists and theoreticians because of their unique properties. In the case of cobalt sulfide, density functional theory (DFT) calculations on free-standing S-Co-S sheets suggest there are no stable 2D cobalt sulfide polymorphs, whereas experimental observations clearly show TMDC-like structures on Au(111). In this study, we resolve this disagreement by using a combination of experimental techniques and DFT calculations, considering the substrate explicitly. We find a 2D CoS(0001)-like sheet on Au(111) that delivers excellent agreement between theory and experiment. Uniquely this sheet exhibits a metallic character, contrary to most TMDCs, and exists due to the stabilizing interactions with the Au(111) substrate.

O 36.3 Tue 18:00 P2/EG

Carbon Nanomembranes Fabricated from Amorphous Molecular Layers — •ZHEN YAO¹, NIKOLAUS MEYERBRÖCKER², YUBO QI¹, MICHAEL WESTPHAL¹, YANG YANG¹, and ARMIN GÖLZHÄUSER¹ — ¹Bielefeld University, Bielefeld, Germany — ²CNM Technologies, Bielefeld, Germany

Ultrathin carbon nanomembranes (CNMs), fabricated from crosslinking self-assemblies of molecular precursors, are 2D membranes that possess well-defined physical and chemical properties. With a simple transfer procedure, CNMs can be placed on various supports, enabling versatile applications. Combining high water flux and precise ion selectivity, CNMs are ideal materials for molecular separation and water desalination. However, their practical realization is hindered by the availability of epitaxial metal substrates. Here, we report a new type of CNM fabricated from poly(4-vinylbiphenyl) (PVBP) spin-coated on SiO₂/Si substrate. The electron-induced crosslinking results in the formation of a continuous membrane with a thickness of 15 nm. The nanoporous nature of the PBVP-CNM is revealed by water and ion permeation measurements. The membrane possesses a high density of pores, which allows water flux as high as 530 L m⁻² h⁻¹ bar⁻¹. It also exhibits the rejection of ions and molecules with sizes >1 nm. A further introduction of a reinforcement porous block copolymer layer simplifies the transfer procedure, resulting in a centimetre-scale CNM-composite that works efficiently for dye rejection. These results suggest a feasible route for large-scale nanoporous membrane fabrication.

O 36.4 Tue 18:00 P2/EG

A New Group of Two-Dimensional Non-van der Waals Materials with Ultra Low Exfoliation Energies — •TOM BARNOWSKY^{1,2}, ARKADY V. KRASHENINNIKOV^{1,3}, and RICO FRIEDRICH^{1,2} — ¹Helmholtz-Zentrum Dresden-Rossendorf, 01328 Dresden, Germany — ²Theoretical Chemistry, Technische Universität Dresden, 01062 Dresden, Germany — ³Aalto University, Aalto 00076, Finland

The exfoliation energy, *i.e.* the energy required to separate a single two-dimensional (2D) sheet from a bulk material, is a key factor in whether such 2D systems can be made. Recently, non-van der Waals 2D compounds – materials derived from non-layered bulk counterparts – were outlined as a rich new class of nanoscale materials [1].

In our work, using data-filtering and ab-initio calculations, we propose a group of eight novel non-van der Waals 2D systems [2]. The compounds exhibit ultra-low exfoliation energies close to those of traditional van der Waals bound 2D materials. Especially for the considered sulfides, strong surface relaxations play a key role in the energy gain enabling exfoliation, while the effects of long-range dispersive interactions are minor. The candidates with the smallest exfoliation energies, 2D SbTlO₃ and MnNaCl₃, exhibit appealing electronic, potential topological, and magnetic features as evident from the calculated band structures.

[1] R. Friedrich *et al.*, Nano Lett. **22**, 989 (2022).

[2] T. Barnowsky *et al.*, submitted (2022).

O 36.5 Tue 18:00 P2/EG

Magnetic properties of transition metal dihalides measured by x-ray magnetic circular dichroism (XMCD) — •SEBASTIEN ELIE HADJADI¹, SAMUEL KERSCHBAUMER², ANDREA AGUIRRE BANOS³, DANILO LONGO³, FADI CHOUËKANI⁴, CELIA ROGERO², JOSE IGNACIO PASCUAL³, WOLFGANG KUCH¹, and MAXIM ILYN² — ¹Institut für Experimentalphysik, Freie Universität Berlin, 14195 Berlin, Germany — ²Centro de Física de Materiales (CSIC/UPV-EHU), 20018 Donostia-San Sebastian, Spain — ³CIC nanoGUNE-BRTA, 20018 Donostia-San Sebastian, Spain — ⁴Synchrotron SOLEIL, 91190 Saint-Aubin, France

During the last couple of years, there has been a rising interest in novel two-dimensional magnetic materials. Most recently, several groups have shown that magnetic order in two-dimensional materials can be stable [1]. Here we report the single phase epitaxial growth of ML to multilayer CoBr₂ and CoCl₂ Au(111) as well as on NbSe₂. The samples were characterized via LEED, XPS, XAS, XMCD and LT-STM. Both Co-compounds show a strong in-plane anisotropy and ferromagnetic order up to temperatures of around 20 K.

[1] Djuro Bikaljevic *et al.*, ACS Nano, **15**, 14985 (2021)

O 36.6 Tue 18:00 P2/EG

Silicene's pervasive surface alloy on Ag(111) — JOHANNES T KÜCHLE^{1,2}, ALEXANDR BAKLANOV¹, ARI P SEITSONEN^{3,4}, PAUL TP RYAN^{2,5}, PETER FEULNER¹, PRASHANTH PENDEM¹, TIEN-LIN LEE², MATTHIAS MUNTWILER⁶, MARTIN SCHWARZ¹, FELIX HAAG¹, JOHANNES V BARTH¹, WILLI AUWÄRTER¹, •DAVID A DUNCAN^{1,2}, and FRANCESCO ALLEGRETTI¹ — ¹Physics Department E20, Technische Universität München, Deutschland — ²Diamond Light Source, Oxfordshire, UK — ³Département de Chimie, École Normale Supérieure, Paris, France — ⁴Université Paris Sciences et Lettres, Sorbonne Université, Paris, France — ⁵Imperial College London, UK — ⁶Paul Scherrer Institut, Villigen, Switzerland

Silicene is the two-dimensional (2D) allotrope of silicon. So far, the most direct synthesis strategy has been to grow it epitaxially on metal surfaces; however, the effect of the strong silicon-metal interaction on the structure and electronic properties of the metal-supported silicene is generally poorly understood. Here, we consider the (4 × 4)-silicene monolayer (ML) grown on Ag(111), and show that our experimental results refute the common interpretation of this system as a simple buckled, honeycomb ML with a sharp interface to the Ag substrate. Instead, we demonstrate the pervasive presence of a second silicon species, concluded to be a Si/Ag alloy stacked between the 2D silicene and the silver substrate. These findings question the current structural understanding of the silicene/Ag(111) interface and may raise expectations of analogous alloy systems in the stabilization of other 2D materials grown epitaxially on metal surfaces.

O 36.7 Tue 18:00 P2/EG

Pb-induced proximity effects in epitaxial graphene — ANDRES DAVID PENA UNIGARRO, CHITRAN GHOSAL, •CHRISTOPH TEGENKAMP, and SIBYLLE GEMMING — Institut für Physik, TU Chemnitz, Reichenhainer Str. 70, Chemnitz

A current topic in material science deals with the controlled assembly of various 2D materials to generate structures with new quantum characteristics. Such modifications can be achieved by proximity effects, *e.g.*, by intercalation and adsorption. One promising route is to use epitaxial buffer layer structures on SiC(0001) surfaces, which transforms into a quasi free monolayer graphene with new 2D interface structures upon intercalation. As suggested by density functional theory (DFT) studies, elements of the IV group such as Pb can be used for this purpose. In this case, intercalation of heavy atoms like Pb are expected to introduce additional effects such as spin-orbit coupling to the electron gas of graphene. In this contribution, we investigated the intercalation of Pb on buffer layers on SiC(0001). Suspended and charge neutral graphene emerged, and the intercalated Pb formed plumbene honeycomb lattices, which are rotated by 7.5° with respect to graphene. Along with this twist, a proximity-induced modulation of the hopping parameter in graphene opens a band gap of around 30 meV at the Fermi energy, giving rise to a metal-insulator transition. We present first results obtained with DFT focusing on the modifications of graphene's electronic structure in the presence of twisted Pb layers.

O 36.8 Tue 18:00 P2/EG

Local spectroscopy of acoustic phonons in low-dimensional materials — •YI ZHANG¹, SHAOXIANG SHENG^{1,2}, SUSANNE BAUMANN¹, and SEBASTIAN LOTH^{1,2} — ¹University of Stuttgart, Institute for Functional Matter and Quantum Technologies, Stuttgart, Germany — ²Max Planck Institute for Solid State Research, Stuttgart, Germany

Coherent acoustic phonons (CAPs) enable ultrafast control of solids and have been exploited for applications in various acoustic devices. THz-induced ultrafast Coulomb forces in a scanning tunnelling microscope (STM) junction can locally generate CAP wave packets that propagate with low losses and form longitudinal acoustic standing waves in a thin Au film on mica [1,2]. Here we develop a discrete lattice model to simulate acoustic phonon propagation in well-defined nanostructures. We predict that transverse acoustic phonons can be detected in 1D chains or in 2D thin films by THz-STM. This enables investigation of mechanical properties and electron-phonon interaction in nano-materials at the atomic scale. [1] S. Sheng, *et al.* Physical Review Letters **129**, 043001 (2022). [2] M. Abdo, *et al.* ACS Photonics **8**, 702-708 (2021).

O 36.9 Tue 18:00 P2/EG

Structure and electronic properties of antimonene on Ag(111) — •FRIEDRICH WANIERKE, FELIX OTTO, MAXIMILIAN SCHAAL, MARCO GRÜNWARD, LORENZ BRILL, and TORSTEN FRITZ — Institute of Solid State Physics, Friedrich Schiller University Jena, Helmholtzweg 5, 07743 Jena

The synthesis of new two-dimensional (2D) materials is of great interest for the development of new designs of electronic devices. In this study, we payed spe-

cial emphasis on the growth of the elemental 2D semiconductor antimonene on Ag(111) by molecular beam epitaxy. To characterize and evaluate the deposited films, we used various methods of surface science. On the one hand, we performed in situ reflection high energy electron diffraction (RHEED), low energy electron diffraction (LEED) and low-temperature scanning tunneling microscopy (STM) for structural investigations. On the other hand, photoelectron spectroscopy as well as STM were used to reveal the electronic properties of the ultra-thin films. The alloy Ag_2Sb , as well as β - and α -antimonene, with respect to the amount of deposited antimon, are discussed.

O 36.10 Tue 18:00 P2/EG

Impact of screening and relaxation on weakly coupled 2D heterostructures: implications for molecular spin-coupling — EVA RAULS¹, T.T. NHUNG NGUYEN², CHRISTOPH TEGENKAMP², and UWE GERSTMANN³ — ¹University of Stavanger, Norway — ²Technische Universität Chemnitz, Germany — ³Universität Paderborn, Germany

Phthalocyanines (Pc) at surfaces are prototype molecules which can host magnetic ions in a well-defined surface environment. The precise external control of individual spins, however, require a detailed knowledge of the influence of the substrate. In this combined experimental and theoretical study, we have investigated the influence of different graphene-related substrates onto the structural, electronic and magnetic properties of adsorbed Pb and Mn-phthalocyanines. Formation of almost identical densely packed PbPc molecular layers with strongly tilted molecules were found on *n*-type and *p*-type doped 2D templates. On graphite (HOPG), the dispersing molecular states of the less deformed molecular adsorbate stress the importance of substrate mediated interaction and proximity coupling [1]. After substituting Pb by magnetic Mn, the interaction with the substrate is clearly increased. On epitaxial monolayer graphene (MLG) the MnPc experience even the underlying SiC substrate, resulting in a 4×2 reconstructed molecular layer with very specific substrate mediated magnetic coupling.

[1] T.T. Nhung Nguyen, T. Sollfrank, C. Tegenkamp, E. Rauls, U. Gerstmann, Phys. Rev. B 103, L201408 (2021).

O 36.11 Tue 18:00 P2/EG

Honeycomb structure of alkali metal atoms — JIAQI CAI^{1,2,3}, ROBIN OHMANN¹, NICOLAE ATODIRESEI⁴, HAI CHAU NGUYEN¹, DAVID DUNCAN⁵, CAIO SILVA², CHRISTOPH SCHLUETER⁵, KAI MEHLICH¹, THAIS CHAGAS¹,

VASILE CACIUC⁴, WOUTER JOLIE³, STEFAN BLÜGEL⁴, TIEN-LIN LEE⁵, THOMAS MICHELY³, and CARSTEN BUSSE^{1,2,3} — ¹Department Physik, Universität Siegen, Siegen, Germany — ²Institut für Materialphysik, Westfälische Wilhelms-Universität Münster, Münster, Germany — ³II. Physikalisches Institut, Universität zu Köln, Köln, Germany — ⁴Peter Grünberg Institut (PGI-1) and Institute for Advanced Simulation (IAS-1), Forschungszentrum Jülich and JARA, Jülich, Germany — ⁵Diamond Light Source, Didcot, Oxfordshire, United Kingdom

The formation of honeycomb structures, similar to graphene, is of great scientific and technological interest. Here, we show that the adsorption of Cs on monolayer hexagonal boron nitride (hBN) on Ir(111) substrate kept at elevated temperatures forms a honeycomb lattice. The structure is investigated by scanning tunneling microscopy (STM), X-ray photoelectron spectroscopy (XPS) and X-ray standing waves (XSW) revealing that the Cs atoms are in registry with the moiré pattern of the substrate with a lattice constant of about 30 Å, are partially positively charged and have an adsorption height of 2.9 Å above the hBN layer. The formation is explained via the templating effect of the substrate. Our density functional theory (DFT) results confirm stable binding on the two hill regions of the moiré unit cell and predict a graphene like band structure with a band width of about 1 meV.

O 36.12 Tue 18:00 P2/EG

Unstrained Sb Bilayers on InSb(111)A — BING LIU^{1,2}, STEFAN ENZNER^{1,3}, TIM WAGNER^{1,2}, PHILIPP ECK^{1,3}, MARTIN KAMP², GIORGIO SANGIOVANNI^{1,3}, and RALPH CLAESSEN^{1,2} — ¹Würzburg-Dresden Cluster of Excellence ct.qmat, Universität Würzburg, D-97074 Würzburg, Germany — ²Physikalisches Institut, Universität Würzburg, D-97074 Würzburg, Germany — ³Institut für Theoretische Physik und Astrophysik, Universität Würzburg, D-97074 Würzburg, Germany

Antimonene, a hexagonal arrangement of staggered Sb, is a promising topological material, which has been widely investigated on various substrates. Recently, it has been grown strain-free on InSb(111)A by forming a moiré structure, despite exhibiting covalent interface bonds.

The moiré supercell is theoretically approximated with varying interface stackings of primitive cells by means of ab initio DFT calculations. This approach reproduces the main structural and electronic observations. The agreement allowed us, to investigate the competition of intra-layer and interface interactions and explain the reconstruction-free growth.

O 37: Poster: Ultrafast Electron Dynamics at Surface and Interfaces II

Time: Tuesday 18:00–20:00

Location: P2/EG

O 37.1 Tue 18:00 P2/EG

Probing alternative pathways for electron transfer across a monomolecular film — SAUNAK DAS¹, ZHIYONG ZHAO¹, TAKANORI FUKUSHIMA², ANDREAS TERFORT³, and MICHAEL ZHARNIKOV¹ — ¹Angewandte Physikalische Chemie, Universität Heidelberg, 69120 Heidelberg, Germany — ²Laboratory for Chemistry and Life Science, Institute of Innovative Research, Tokyo Institute of Technology, Yokohama 226-8503, Japan — ³Institut für Anorganische und Analytische Chemie, Johann Wolfgang-Goethe-Universität Frankfurt, 60438 Frankfurt am Main, Germany

Charge transport (CT) across a two-dimensional molecular assembly can involve alternative pathways. Using specifically designed monomolecular films we probe (i) competition of intramolecular and intermolecular pathways in a molecular assembly and (ii) competition of different intramolecular pathways within a single molecule. For this purpose, we apply so-called core-hole-clock approach in the framework of resonant Auger electron spectroscopy, allowing the measurement of the characteristic CT time from the terminal tail group of the assembled molecules to the substrate. We show that the intramolecular CT is generally preferable and so-called matrix effects play a negligible role for CT, strongly favoring the through-bond CT model. In the case of availability of several alternative pathways within an individual molecule, a pathway with the highest conductance becomes highly dominant, while other pathways contribute minorly to the entire CT.

O 37.2 Tue 18:00 P2/EG

Pump-probe second harmonic spectroscopy of molecule/metal interfaces — JINGHAO CHEN¹, RUI SHI², PING ZHOU¹, UWE BOVENSIEPEN¹, WOLFGANG HÜBNER², GEORG LEFKIDIS², and ANDREA ESCHENLOHR¹ — ¹Faculty of Physics and CENIDE, Uni Duisburg-Essen, Lotharstr. 1, 47057 Duisburg, Germany — ²Department of Physics, TU Kaiserslautern, Box 3049, 67653 Kaiserslautern, Germany

Achieving a microscopic understanding of charge transfer dynamics and the relaxation of optically excited electrons and holes at molecule/metal interfaces requires an interface-sensitive analysis on the respective femtosecond timescales. Second harmonic spectroscopy (SHS) is such an interface-sensitive probe in cen-

trosymmetric materials. We perform pump-probe SHS in the visible wavelength range (1.9-2.5 eV) with <20 fs pulse duration. A prototypical molecule/metal interface is prepared by adsorption of iron octaethylporphyrin (FeOEP) molecules on Cu(001) and analyzed *in situ* in ultrahigh vacuum. By comparison with first principles theory, we identify a molecule-induced resonance at about 2.2 eV fundamental photon energy in the SHS of one monolayer of FeOEP/Cu(001). At this resonance, we observe a markedly slower relaxation time of the pump-induced changes in SHS compared to the bare Cu(001) surface, which indicates an increased lifetime of the electronic molecular state.

We thank H. Wende, J. Güdde and E. Riedle for valuable experimental advice, and the German Research Foundation for funding via SPP 1840 QUTIF and Sfb 1242.

O 37.3 Tue 18:00 P2/EG

Second harmonic spectroscopy of Cu(001) surfaces — NEWSHA VESAL-IMAHMOUD, JINGHAO CHEN, MAHENDRA KABBINAHITHLU, PING ZHOU, UWE BOVENSIEPEN, and ANDREA ESCHENLOHR — University of Duisburg-Essen, Faculty of Physics and CENIDE, Lotharstr. 1, 47057 Duisburg, Germany

The nonlinear optical technique of second harmonic generation (SHG) is a surface- and interface-sensitive tool in centrosymmetric materials, which is used to study electron dynamics at metal surfaces. We characterize the polarization and wavelength dependent SHG on a Cu(001) surface using a fundamental beam in the wavelength range of 500 - 700 nm. Polarization dependent measurements show the p-P SHG yield is almost a factor of 1.5 larger than s-P SHG, because more non-zero susceptibility tensor elements are involved in the former and the intrinsic absolute value of $|\chi_{zzz}^{(2)}|$ is much larger than the only relevant component $|\chi_{zxx}^{(2)}|$ in the latter. We also measure the spectral dependence of the SHG intensity, which shows an increase up to a maximum at 2.33 eV. Since the 3d band peak of copper lies about 2.3 eV below Fermi level, a fundamental beam at this photon energy can resonantly excite 3d electrons to the Fermi level, which largely increases the overall probability of SHG processes. Moreover, we discuss electron dynamics analyzed through pump-probe SHG at on and off-resonant photon energies.

O 37.4 Tue 18:00 P2/EG

Formation mechanism of defect levels in rutile TiO₂ (110) — •XIANG ZHANG, LUKAS GIERSTER, and JULIA STÄHLER — Humboldt-Universität zu Berlin, Institut für Chemie

The electron dynamics at TiO₂ surfaces have been widely studied as TiO₂ is a prototypical photocatalyst. Recent studies have specifically addressed the Band Gap State (BGS) at 0.8 eV below the Fermi level and have revealed its role as a trapping center for electrons in the conduction band of rutile TiO₂(110) (with a trapping time of around 45 fs) [1]. However, the origin of the BGS itself remains debated. Using time-resolved photoelectron spectroscopy, we show here that the BGS must be - at least partially - due to long-lived (>5 μs) photoexcited charge carriers which form a photostationary state in pump-probe experiments. The potential formation mechanism of the BGS and implications of this state for previous time-resolved experiments are discussed.

[1] Zhang et al. J. Phys. Chem. Lett. 10(52) (2019).

O 37.5 Tue 18:00 P2/EG

Investigation of low-temperature electron emission properties from sharp needle tips — •MANUEL KNAUFT, STEFAN MEIER, NORBERT SCHÖNENBERGER, and PETER HOMMELHOFF — Department Physik, Friedrich-Alexander-Universität Erlangen-Nürnberg (FAU), 91058 Erlangen

Spectroscopic and microscopic techniques benefit from the small linewidth of coherent electron sources with high brightness. Reducing the operating temperature of the emitter is known to positively influence coherence of field emitted electron beams. This is especially true for superconducting needle tips as shown for niobium [1].

We present an experimental setup capable of cooling electron emitters to liquid helium temperature in ultra-high vacuum. Irradiation of samples with ultrashort laser pulses is possible through optical access to the chamber. Detection of charged particles is realized by a multi-channel plate. First results for sharp needle tips of various materials are shown. In particular, we investigate the emission characteristics and compare them for field emission and laser triggered emission as a function of temperature.

[1] Nagaoka *et al.*, Nature **396**, 557 (1998)

O 37.6 Tue 18:00 P2/EG

Magnetic field effects on ultrafast driven electrons in topological insulator surface states — •ALEXANDER RIEDEL¹, VANESSA JUNK¹, WOLFGANG HOGGER¹, COSIMO GORINI², and KLAUS RICHTER¹ — ¹Institut für Theoretische Physik, Universität Regensburg, Germany — ²Universite Paris-Saclay, CEA, CNRS, SPEC, 91191, Gif-sur-Yvette, France

When strong-field light pulses of various durations and shapes interact with a solid, their electric field component acts as an a.c. bias accelerating electrons through the bandstructure and driving non perturbative transitions. These processes can lead to high-order harmonic emission of radiation which encodes characteristic properties of the underlying material.

However, in the vast majority of cases the magnetic field component of the pulse is completely neglected in theoretical descriptions. In this contribution we incorporate a magnetic field into the description by adding a Zeeman term into an effective minimal model Hamiltonian describing the surface states of the topological insulator material bismuth telluride. We present how magnetic field components influence the Berry curvature and the transitions induced by the pulse. The resulting currents and higher harmonic spectra are discussed and compared to those in the absence of magnetic field effects. All statements rely on both a semiclassical analysis and full quantum mechanical simulations.

O 37.7 Tue 18:00 P2/EG

Use cases for Picosecond Ultrasonics with X-rays (PUX) — •ALEXANDER VON REPERT¹, MAXIMILIAN MATTERN¹, STEFFEN ZEUSCHNER^{1,2}, JAN-ETIENNE PUDELL^{1,2,3}, MARC HERZOG¹, and MATIAS BARGHEER^{1,2} — ¹Institut für Physik und Astronomie, Universität 14476 Potsdam, Potsdam, Germany — ²Helmholtz-Zentrum Berlin, 12489 Berlin, Germany — ³European XFEL, 22869 Schenefeld, Germany

Most studies of picosecond ultrasound have been and will be conducted with flexible all-optical setups, but here we discuss scenarios where ultrashort hard x-ray probe pulses excel. We focus on the extraction of the strain response from Bragg peak shifts in the symmetric diffraction condition for layered, nanoscopic structures upon excitation of metallic transducers with femtosecond laser pulses. This type of experiment can yield direct, layer-specific and quantitative information on the shape and amplitude of picosecond strain pulses and the quasi-static strain. The strain response may serve as a proxy for the local energy-density and temperature rise. The presented use-cases encompass ultrathin as well as opaque metal-heterostructures, nanostructures and negative thermal expansion materials, that each pose a challenge to established all-optical techniques.

O 37.8 Tue 18:00 P2/EG

Photocatalysis on anataseTiO₂(101) in real-time — •HESHMAT NOEI^{1,2}, MICHAEL WAGSTAFFE¹, ADRIAN DOMINGUEZ-CASTRO³, LUKAS WENTHAUS¹, STEFFEN PALUTKE¹, DMYTRO KUTNYAKHOV¹, MICHAEL HEBER¹, FEDERICO PRESSACCO¹, SIRHEI DZIARZHYTSKI¹, HELENA GLEISSNER¹, VERENA KRISTIN

GUPTA¹, ADRIEL DOMINGUEZ¹, THOMAS FRAUENHEIM³, ANGEL RUBIO⁴, and ANDREAS STIERLE¹ — ¹Deutsches Elektronen-Synchrotron (DESY), Hamburg, Germany — ²The Hamburg Centre for Ultrafast Imaging, Hamburg, Germany — ³Bremen Center for Computational Material Science (BCCMS), D-28359, Bremen, Germany — ⁴Max Planck Institute for the Structure and Dynamics of Matter, D-22761, Hamburg, Germany

Obtaining mechanistic insight surrounding interfacial charge transfer and the role of intermediate species during photocatalysis on metal oxide surfaces is challenging due to their ultrafast nature. By applying ultra-fast optical pump-soft X-ray probe experiments at FLASH in DESY, we have obtained first insight into the activation mechanism of CO photooxidation to CO₂ on rutile and anatase TiO₂ surfaces and charge transfer at the interface of water and TiO₂(101). By using an optical laser of 800 nm and a FEL energy of 647.8 eV, the changes in the Ti 2p, O 1s and C 1s core levels have been monitored on a picosecond timescale.

O 37.9 Tue 18:00 P2/EG

Ultrafast UV pulse generation at the SXP instrument of the European XFEL — •EKATERINA TIKHODEEVA¹, PATRIK GRZYCHTOL¹, MARCUS SEIDEL², CHRISTOPH M. HEYL², VAHAGN VARDANYAN¹, DAVID DOBLAS-JIMENEZ¹, and MANUEL IZQUIERDO¹ — ¹European XFEL, Schenefeld, Germany — ²DESY, Hamburg, Germany

At the European XFEL a new instrument, the Soft X-ray Port (SXP), is currently under commissioning. Located downstream of the SASE 3 soft X-ray undulator system, it will provide femtosecond photon pulses with variable polarization in the energy range between 260 eV and 3000 eV at MHz repetition rates. Up to 10¹² photons per pulse will be focus at the interaction region in a micrometer spot size resulting in an intensity of more than 10¹⁸ W/cm². The energy range will enable the complete electronical, chemical and atomic characterization of solids, surfaces and interfaces using femtosecond time-resolved soft X-ray photo-electron spectroscopy. Moreover, two powerful pump lasers operating in a broad spectral range from the mid-infrared to the ultraviolet region will be available. Herriott multi-pass cells (HMPC) will be used to compress their pulses into the few femtosecond range paving the way for ultrafast pump-probe investigations at the SXP instrument combining intense and tunable soft X-rays with the versatile optical lasers. In this contribution, the development of the HMCP and the optical laser system will be presented.

O 37.10 Tue 18:00 P2/EG

Transferring photonic orbital angular momentum to metals — •JANNIS LESSMEISTER¹, TOBIAS EUL¹, EVA PRINZ¹, SEBASTIAN HEDWIG¹, MARTIN AESCHLIMANN¹, and BENJAMIN STADTMÜLLER^{1,2} — ¹Department of Physics and Research Center OPTIMAS, TU Kaiserslautern, Germany — ²Institute of Physics, Johannes Gutenberg University Mainz, Germany

Optical fields can carry an orbital angular momentum (OAM) in helical beams with an azimuthal phase dependence. Since the discovery of this phenomenon in 1992 [1], the interaction of photonic OAM with matter has become a steadily growing field of research. After an initial focus on atoms and molecules, in the last years, scientists also began investigating solids [2]. For example, recent studies revealed that the so-called twisted light can drive photocurrents [3] and affects ultrafast demagnetization dynamics [4].

In our research, we apply time- and angle-resolved photoelectron spectroscopy (TR-ARPES) to gain new insight into the influence of photonic OAM on the hot carrier dynamics in metals. Specifically, we investigated the influence of the added orbital angular momentum on the optical excitation efficiency of photoelectrons from the spin-split band structure of Rashba surface states and the hot carrier dynamics of spin-dependent carriers in the ferromagnet Ni.

[1] Allen et al., Phys. Rev. A **45** (1992)

[2] Quinteiro Rosen et al., Rev. Mod. Phys. **94** (2022)

[3] Ji et al., Science **368** (2020)

[4] Prinz et al., arXiv:2206.070502 (2022)

O 37.11 Tue 18:00 P2/EG

Combining THz-ARPES and THz-HHG to study electrical currents at buried interfaces of topological insulators — •TIM BERGMIEIER, SUGURU ITO, JENS GÜNDE, and ULRICH HÖFER — Fachbereich Physik, Philipps-Universität Marburg, Germany

Angle-resolved photoemission spectroscopy (ARPES) combined with terahertz (THz) excitation has shown to provide a subcycle-resolved momentum space view of lightwave-driven Dirac currents in the surface band of topological insulators [1]. At high electric field strength, these currents have shown to give rise to a unique type of efficient high-harmonic generation (HHG) that reflects the unusual transport properties of the Dirac electrons [2]. As a pure optical technique, THz-HHG is able to access also deeply buried interfaces, but lacks band structure information.

Here, we present an experimental setup which combines both techniques in order to study first the impact of thin protection layers on the current transport in a topologically protected band. The correlation of the time-resolved band structure information provided by THz-ARPES with the properties of THz-HHG will

then allow us to apply the latter for thick layers as will be required for device applications. The setup includes the generation of THz-pulses with field strengths up to 10 MV/cm over a frequency range of 12-80 THz, and of ultrashort 400-nm probe pulses for two-photon photoemission with subcycle time resolution at a repetition rate of 200 kHz.

[1] J. Reimann *et al.*, Nature 562, 396 (2018).

[2] C. P. Schmid *et al.*, Nature 593, 385 (2021).

O 37.12 Tue 18:00 P2/EG

A narrow bandwidth extreme ultra-violet light source for time- and angle-resolved photoemission spectroscopy — QINDA GUO¹, MACIEJ DENDZIK¹, ANTONIJA GRUBIŠIĆ-ČABO¹, MAGNUS H. BERNTSEN¹, CONG LI¹, WANYU CHEN¹, BHARTI MATTA², ULRICH STARKE², BJÖRN HESSMO¹, JONAS WEISSENRIEDER¹, and OSCAR TJERNBERG¹ — ¹Department of Applied Physics, KTH Royal Institute of Technology, Hannes Alfvéns väg 12, 114 19 Stockholm, Sweden — ²Max Planck Institute for Solid State Research, Heisenbergstraße 1, 70569 Stuttgart, Germany

Here, we present a high repetition rate, narrow bandwidth, extreme ultraviolet photon source for time- and angle-resolved photoemission spectroscopy. The narrow bandwidth pulses $\Delta E = 9, 14,$ and 18 meV for photon energies $h\nu = 10.8, 18.1,$ and 25.3 eV are generated through high harmonic generation using ultraviolet drive pulses with relatively long pulse lengths (461 fs). The high harmonic generation setup employs an annular drive beam in tight focusing geometry at a repetition rate of 250 kHz. Photon energy selection is achieved by a spherical focusing grating, which provides high efficiency photon flux with only a small amount of focus size increase ($\sim 30\%$) and temporal broadening (6.8%). A two

stage optical-parametric amplifier provides < 100 fs tunable pump pulses from $0.65 \mu\text{m}$ to $9 \mu\text{m}$. Combined with a time-of-flight electron analyzer, the setup enables for high-resolution studies of ultrafast dynamics over the whole surface Brillouin zone in most quantum materials.

O 37.13 Tue 18:00 P2/EG

Time Resolved Photoelectron Spectroscopy of Thiophen based Conjugated Donor Acceptor Polymers for Organic Photovoltaic — TOBIAS REIKER¹, PRADNY PHANSE¹, NILS FABIAN KLEIMEIER¹, ZITONG LIU², ADRIAN URBAN¹, DEQING ZHANG², and HELMUT ZACHARIAS¹ — ¹Center for Soft Nanoscience, University of Münster, Germany — ²Institute of Chemistry, Chinese Academy of Science, Beijing, China

Thiophene-based polymers are promising candidates for solar cell, OLED or transistor applications. An internal donor - acceptor system is formed by coupling thiophene polymers with pyrrole chains. We report results of temporally resolved photoemission studies on thiophene polymers on silicon substrates. The charge transport behaviour can be tuned by different alkyl side chains since they influence the electronic structure and aggregation. A direct assessment of the intramolecular and intermolecular dynamics may guide synthesis routes. With pF8T2, pDPP4T, pDPP4T-1 and pDPTTT we investigated the electronic dynamics of high hole-mobility organic semiconductors. Either the backbone or the side chains were modified. With the blend of pDPP4T-1 and a Fullerene we compare the excitation dynamics of single component and blended OPV. These different molecular configurations are intended to provide insights into the change in electron configuration due to both backbone modification and intermolecular packing.

O 38: Poster: Organic Molecules on Inorganic Substrates II

Time: Tuesday 18:00–20:00

Location: P2/EG

O 38.1 Tue 18:00 P2/EG

Engineering two-dimensional metal-organic networks on ferromagnetic surfaces — MARTIN ANSTETT¹, LU LYU¹, KA MAN YU¹, MARTIN AESCHLIMANN¹, and BENJAMIN STADTMÜLLER^{1,2} — ¹Department of Physics and Research Center OPTIMAS, University of Kaiserslautern, 67663 Kaiserslautern, Germany — ²Institute of Physics, Johannes Gutenberg University Mainz, Germany

Two-dimensional metal-organic networks (MONs) on noble-metal surfaces have been identified as versatile nanoarchitecture to manipulate electronic and magnetic properties at surfaces. In this contribution, we discuss the growth and the structure formation of a Co-T4PT network on epitaxial Co films grown on an Au(111) single crystal. Using scanning tunnelling microscopy, we will show that the T4PT molecules can coordinate with native Co adatoms forming a long-range ordered two-dimensional porous network structure. This network can further act as a decoupling and templating layer for the subsequent growth of C60 guest molecules. For a C60 sub-monolayer, we find that the periodicity of the network structure mainly determines the adsorption configurations of isolated C60 molecules while the structural properties of ordered C60 islands on the Co-T4PT network are substantially influenced by the intermolecular interaction between the C60 molecules. The findings show that the MON system can be a very flexible template to tailor the interfacial properties of molecular assemblies for molecular-based spintronics and electronics.

O 38.2 Tue 18:00 P2/EG

Film growth and stability of the Ionic Liquid [C₁C₁Im][Tf₂N] on Pt(111) — TIMO TALWAR, STEPHEN MASSICOT, AFRA GEZMIS, CYNTHIA FERNÁNDEZ, LEONHARD WINTER, FLORIAN MAIER, and HANS-PETER STEINRÜCK — Lehrstuhl für Physikalische Chemie 2, Friedrich-Alexander-Universität Erlangen-Nürnberg, Egerlandstr. 3, 91058 Erlangen

Solid catalyst with Ionic Liquid Layer (SCILL) is a new catalytic concept using the advantageous properties of Ionic Liquids (ILs) to improve the catalytic performance such as selectivity and long-term stability of a solid catalyst by the coated IL. In this context, extensive knowledge about the IL-metal interface properties is highly desired.

In this study, the growth and thermal behavior of ultrathin films of 1,3-dimethylimidazolium bis[(trifluoromethyl)sulfonyl]imide [C₁C₁Im][Tf₂N] on Pt(111) are investigated under UHV conditions. The films are prepared in vacuum by physical vapor deposition and measured by angle-resolved and temperature-programmed X-ray photoelectron spectroscopy. Complementary information is gained by Scanning Tunneling Microscopy. At 200 K, an intact closed wetting layer can be deposited on Pt(111). The underlying growth mode is 2D up to 0.5 ML (a closed wetting layer) and moderate 3D for higher coverages. At higher temperatures up to 360 K, the IL continuously decomposes leading to desorption of volatile decomposition products. We will compare this behavior to previous results for this IL on the less-reactive Cu(111) and on the non-reactive Au(111) surface.

We acknowledge support by the DFG (SFB 1452 CLINT).

O 38.3 Tue 18:00 P2/EG

Thiahelicene non-covalent molecular wires on Cu(111) — GEMA NAVARRO¹, ANTOINE HINAUT¹, SHUYU HUANG¹, THILO GLATZEL¹, AKIMITSU NARITA², and ERNST MEYER¹ — ¹Department of Physics, University of Basel, Klingelbergstrasse 82, 4056 Basel, Switzerland. — ²Okinawa Institute of Science and Technology Graduate University, Okinawa 904-0495, Japan

In recent years molecular nanowires have attained a paramount interest due to their potential application in the next generation of nanodevice. Therefore, researchers have been focused in the development of novel synthetic routes to achieve stable nanowires, also in the influence of heteroatoms doping to control optical or electronic properties [1]. Usually, the on-surface synthesis approach is adopted due to the robustness and versatile chemistry reactions available [2].

In the present study, we explore the deposition of thiahelicene molecules on Cu(111) as possible candidates for nanowires formation. Sample preparation and measurements were carried out at room temperature in an UHV system and the images were acquired by a non-contact AFM microscope. AFM-micrographic images illustrated the formation of molecular wires along the monocrystalline terraces. The growth process of the molecular wires retains the three-fold symmetry of the substrate, although, some defect points can be distinguished in their structure. In addition, the high mobility of the molecules indicates a weakly interaction with the copper surface.

[1] B. Mallada *et al.*, ACS Appl. Mater. Interfaces 13, 32393 (2021).

[2] D.Y. Li *et al.*, J. Am. Chem. Soc. 143, 12955 (2021).

O 38.4 Tue 18:00 P2/EG

Fabrication of Kondo Lattice via On-surface Reactions — JUNG-CHING LIU¹, RÉMY PAWLAK¹, XING WANG², CHAO LI¹, OUTHMANE CHAHIB¹, PING ZHOU², ROBERT HÄNER², SILVIO DECURTINS², ULRICH ASCHAUER², SHI-XIA LIU², and ERNST MEYER¹ — ¹Department of Physics, University of Basel, Klingelbergstrasse 82, CH-4056 Basel — ²Department of Chemistry and Biochemistry, University of Bern, Freiestrasse 3, CH-3012 Bern

Magnetic atoms assembled in different lattices can exhibit various characteristics, such as spin frustration, heavy fermion, or spin textures via RKKY interaction [1]. Different from scanning probe tip manipulation [2] or e-beam evaporation [3], we perform on-surface reaction to realize magnetic lattice using pyrene-4,5,9,10-tetraone (PTO) and Fe on Ag(111) [4]. The STM and AFM structural investigation at 4K shows 1:1 coordination of PTO and Fe, resulting in 1D chains which further self-assemble into the close-packed pattern. Tunneling spectra measured at 1K confirm Kondo resonance localized on Fe atoms, with moderate dispersion on PTO. The dip lineshape of the Kondo resonance could indicate the spin-1 state on Fe [5]. The successful synthesis of magnetic organometallic structures demonstrates the tunability of Kondo lattice structure by changing molecule species. We believe our work enables fundamental studies of spin-spin and spin-substrate interactions with different spin lattices. [1] Moro-Lagares *et al.* Nat. Comm. 10, 2211 (2019) [2] Nadj-Perge *et al.* Science 346 [3] Palacio-Morales *et al.* Sci. Adv. 5, eaav6600 (2019) [4] Pia *et al.* Chem. Eur. J. 22, 8105-8112 (2016) [5] Li *et al.* Chem. Commun. 54, 9135-9138 (2018)

O 38.5 Tue 18:00 P2/EG

Growth and structure of *p*-6P thin films as templates for organic heterosystems - a LEEM/PEEM study — •FRANZ NIKLAS KNOOP, WINFRIED DAUM, and KLAUS STALLBERG — Institute of Energy Research and Physical Technologies, TU Clausthal, Germany

The charge carrier dynamics at the contact of two organic semiconductors are strongly influenced by the molecular and mesoscopic structure of the interface. A systematic study of such structure-related effects on the carrier dynamics requires well defined and controllable model systems. Single-crystalline metals are suitable substrates for the epitaxial growth of well-ordered organic layers, but the carrier dynamics are strongly modified by the presence of a conductive surface. Therefore, we explore a different approach for the formation of organic/organic model systems: rod-like molecules such as para-sexiphenyl (*p*-6P) are known to form highly ordered layers on weakly interacting amorphous substrates like SiO₂. These layers are suitable templates for the consecutive epitaxial growth of organic heterostructures. By thermal evaporation under ultrahigh vacuum conditions we deposit *p*-6P films with nominal mono- and bilayer thicknesses on natively oxidized silicon. Characterization with low-energy electron microscopy (LEEM) and atomic force microscopy (AFM) reveals coherent films which comprise single crystalline domains of upright-standing molecules. We discuss the influence of different growth parameters on the film structure and present results from two-photon photoemission electron microscopy (2P-PEEM). Moreover, first results from experiments with organic/organic heterosystems are also presented.

O 38.6 Tue 18:00 P2/EG

Understanding the role of adsorbed CTAB in anisotropic nanostructure growth — •ESMÉE BERGER¹, NARJES KHOSRAVIAN¹, JOAKIM LÖFGREN², and PAUL ERHART¹ — ¹Department of Physics, Chalmers University of Technology, Gothenburg, Sweden — ²Department of Applied Physics, Aalto University, Espoo, Finland

A crucial step towards improved control over the shapes and sizes of wet-chemically synthesized nanostructures is a detailed theoretical understanding of the growth mechanism's different aspects. One of these aspects is the adsorption of surfactants, for example cetyltrimethylammonium bromide (CTAB), which is commonly used for structural tuning and increased stability. In water, CTAB exhibits a complex phase diagram, with a number of different liquid crystal-like phases. The complexity of the system is further increased during nanostructure growth, due to the presence of surfaces. Recent studies have indicated that the micellar phase of CTAB is the primary mechanism for anisotropic growth of silica and gold nanoparticles. These results were, however, based on a single value of the CTAB surface density. To properly understand the role of CTAB during anisotropic growth of nanostructures, a surface phase diagram must be established. In this work, we develop an understanding of the surface phase diagram from a modeling perspective, by means of molecular dynamics simulations.

O 38.7 Tue 18:00 P2/EG

Implementation of a silicon wafer into an UHV STM system for low temperature molecular depositions — •KEN KOLAR, GRANT SIMPSON, CHRISTOPHE NACCI, and LEONHARD GRILL — Uni Graz, Graz, Austria

Sublimation temperatures of organic molecules typically rise as the number of constituting atoms is increased. This can lead to fragmentation and other experimental difficulties during molecular deposition if a standard sublimation Knudsen cell is used. One of the possibilities to overcome this problem is the deposition of molecules using the "energy sudden" sublimation from a silicon wafer. We have installed such a system in our ultrahigh vacuum chamber and used it for depositions onto the sample that is kept at cryogenic temperatures during the preparation. Here, we present how such a device was implemented in our setup, together with first scanning tunneling microscopy (STM) images of the test depositions.

O 39: Poster Session: Heterogeneous Catalysis and Surface Dynamics

Time: Tuesday 18:00–20:00

Location: P2/EG

O 39.1 Tue 18:00 P2/EG

SURMOF ZIF-67 Thin Films for Catalytic Water Oxidation Reaction — •JIMIN SONG, ALEXEI NEFEDOV, STEFAN HEISSLER, CHRISTOF WÖLL, and YUEMIN WANG — Institute of Functional Interfaces, Karlsruhe Institute of Technology, 76344, Eggenstein-Leopoldshafen, Germany

Metal-organic frameworks emerged as promising electrocatalysts to tackle urgent energy and environmental problems. Surface-coordinated MOF thin films (SURMOFs) were grown via a liquid phase epitaxial layer-by-layer method, endowed with precisely controlled thickness, preferred growth orientation and highly-ordered surface. For the first time, high-quality crystalline ZIF-67 SURMOF thin films were fabricated and employed in water oxidation reaction (OER). The transformation from ZIF-67 to CoOOH was observed after the water oxidation reaction by applying IRRAS, Raman and XPS measurements. Mean-time, the thickness of the thin film decreased from 100 nm to 20 nm. The overpotential was reduced from 468 to 375 mA/cm² by doping with boron and nickel.

O 39.2 Tue 18:00 P2/EG

SFG microscopy of ferroelectric domains in Barium Titanate — •DOROTHEE MADER¹, DANIEL LOURENS², MAARTEN KWAAITAAL², RICHARDA NIEMANN¹, SÖREN WASSEROTH¹, SANDY GEWINNER¹, MARCO DE PAS¹, WIELAND SCHÖLLKOPF¹, MARTIN WOLF¹, ANDREI KIRILYUK², SEBASTIAN MAEHRLEIN¹, and ALEXANDER PAARMANN¹ — ¹Fritz Haber Institute of the Max Planck Society, Berlin, Germany — ²Radboud Universiteit, Nijmegen, The Netherlands

Phonons exhibit a mostly unexplored leverage on ferroic order and its dynamics. Exploring the possibility of phonon-driven changes to the ferroelectric order provides an attractive route for potential applications of ferroelectric devices. Here, infrared-visible (IR-VIS) sumfrequency generation (SFG) microscopy with IR-sub-wavelength resolution [1] is employed combining resonant phonon excitation and ferroelectric domain imaging of barium titanate [BTO]. BTO is a non-centrosymmetric perovskite oxide with a strong ferroelectric polarization in its tetragonal phase at room temperature. Typically, BTO samples exhibit a multi-domain structure. Using the FHI Infrared (IR) free electron laser (FEL) in the range of 400-800 cm⁻¹ different phonon modes of BTO are accessible. After characterization of the samples using linear optical techniques like polarization microscopy and infrared spectroscopy, the nonlinear optical properties of the ferroelectric domains are investigated using SFG-microscopy. By mapping phonon resonances in domains and domain walls, this approach may enable in-depth understanding of the underlying physics of domain formation. [1] R. Niemann et al., Appl. Phys. Lett. 120, 131102 (2022).

O 39.3 Tue 18:00 P2/EG

Investigating Heterogeneous Catalysts by Design of Experiments — •CHRISTIAN KUNKEL, FREDERIC FELSEN, SINA STOCKER, CHRISTOPH SCHEURER, and KARSTEN REUTER — Fritz-Haber-Institut der MPG, Berlin, Germany

Bringing new and improved heterogeneous catalysts to market can be economically and ecologically rewarding. Yet, catalyst development is tedious, as a plethora of experimental factors in synthesis, formation and operation potentially influence achievable educt conversion and/or product selectivity. In the planning phase of an investigation, such influences can often only inadequately be assessed based on literature knowledge, individual experience and chemical intuition, resulting in a too narrow scope of experimentation. Data-driven approaches are less biased, potentially offering a way out. Still, the amount of recordable experimental data remains to be a limiting factor even with modern (automated) multi-reactor setups, where only a few dozen data points are acquired in reasonable time. In this contribution we therefore illustrate the practical application of highly-efficient optimally designed experiments. Leveraging simultaneous factor-changes, these jointly extract a maximum of information from each experimental run. Using examples from our ongoing investigation of thin-film and powder catalysts, we illustrate how this approach leads to significant insights on catalytic behavior over a larger number of factors. With additional information coming from multiple characterization techniques, we also demonstrate how catalyst development can strongly benefit from jointly coordinated data-driven experimental efforts.

O 39.4 Tue 18:00 P2/EG

Operando sXRD study of copper-zinc-alumina (CZA) model systems under methanol synthesis conditions — •ERIK BECK^{1,2}, VEDRAN VONK^{1,2}, HESHMAT NOEI^{1,2}, and ANDREAS STIERLE^{1,2} — ¹Centre for X-ray and Nano Science, Hamburg, Germany — ²German Electron Synchrotron DESY, Hamburg, Germany

Methanol synthesis from gas mixtures of H₂, CO and CO₂ is an important industrial process in which copper-zinc-alumina (CZA) has been identified as a high performing catalyst. Typically, the products and reactants are gases used at pressures of >30 bar and a temperature of 250-300 degree C. Because of the dynamic nature of the catalyst under such industrial conditions, the underlying mechanisms and reaction paths are still under debate, since the traditional surface science techniques cannot be used at such high pressures. In order to bridge this pressure gap and gather structural information of the system in real operando conditions, we designed a special experimental setup for synchrotron-based high pressure sXRD. By using dedicated Cu and Zn UHV MBE growth chambers, we were able to prepare epitaxial model systems of the CZA catalysts composed of epitaxial Cu nanoparticles on Al₂O₃ single crystal surfaces. We performed

operando high energy x-ray diffraction experiments on such model catalysts at up to 30 bar and 300degC at the High Energy Materials Science Beamline at DESY and we were able to follow the structural changes of the Cu nanoparticles during oxidation and reduction in different gas compositions.

O 39.5 Tue 18:00 P2/EG

Surface phase transitions in doped manganite thin films — •LEONARD SCHÜLER, TIM TITZE, STEFAN MATHIAS, DANIEL STEIL, and VASILY MOSHNYAGA — I. Physikalisches Institut, Georg-August-Universität Göttingen

The symmetry breaking at the surface of strongly correlated $\text{La}_{1-x}\text{Sr}_x\text{MnO}_3$ (LSMO) thin films leads to a modification of orbital occupation compared to the bulk resulting in the formation of intrinsic magnetic and electric surface phases. To obtain a phase diagram of possible surface states, LSMO films with Sr doping over the complete range $x = 0-1$ were prepared by metalorganic aerosol deposition and have been investigated by both surface-enhanced Raman spectroscopy (SERS) and pump-probe optical (SE-PPR) reflectivity. Temperature-dependent SERS reveals magnetic phase transitions by anomalous frequency shifts of the MnO_6 octahedra's stretching mode resulting from spin-phonon coupling, as well as changes in Mn orbital occupation inferred by enhanced Raman activity of vibrational Jahn-Teller modes at the surface. Furthermore, ultrafast dynamics studied by SE-PPR reveals a surface phase transition, which is not present in the bulk LSMO.

O 39.6 Tue 18:00 P2/EG

Laser pump X-ray probe investigations of the dynamics at the liquid-vapour interface of alkali halogenide salt solutions — •LUKAS PETERSDORF¹, SVENJA HÖVELMANN^{1,2}, RAJENDRA GIRI¹, NICOLAS HAYEN¹, KARIN HANSEN¹, PHILIPP JORDT¹, ANDREA SARTORI¹, MATTHIAS GREVE¹, FLORIAN BERTRAM², OLAF MAGNUSSEN¹, and BRIDGET MURPHY^{1,3} — ¹University of Kiel (IEAP), Kiel — ²DESY, Hamburg — ³RHL, Kiel

Detailed knowledge of the surface of alkali halogenide solutions is fundamental for understanding atmospheric effects and developing technological applications such as solar thermal cells. Surface dynamics of such systems ranging from fs to s, can be studied in detail by pump-probe techniques. Our Laser pump-X-ray probe studies are based on photoionization processes at the interface induced by a 258 nm laser pulse and pumping electron solvation dynamics and ion rearrangements. With auspicious quantum yield and surface structure, the pump-probe studies were performed on salt solutions (NaI, RbBr, ErCl₃). We apply the surface sensitive techniques time resolved XRR and GIXRF to investigate the responding structural changes. A sensor monitored sample environment allows us to distinguish between laser induced and solution dependent dynamics. Upon laser excitation, changes in the specular reflectivity occur on the ms to s scale. Electron density and surface roughness change near the interface indicate a rearrangement of the ion concentration. Within the framework of the DAPHNE4NFDI project, the analysis will be supported by artificial neural networks in order to allow in-operando experimental decisions.

O 40: Poster: Semiconductor Substrates

Time: Tuesday 18:00–20:00

Location: P2/EG

O 40.1 Tue 18:00 P2/EG

Si(553)-Au and Si(775)-Au surface reconstructions with a genetic algorithm approach — •LEONARD M. VERHOFF and SIMONE SANNA — Institute for theoretical physics, Giessen, Germany

It was found by simulations and experiments, that Au atoms on a Si(553)- and Si(775)-surface form metallic nanowires. However, their precise atomic structure is still under discussion.

In this work, the respective surface reconstructions with N adatoms are searched, using a genetic algorithm implemented in the program CALYPSO. Genetic algorithms are reported to be efficient methods for structure predictions.

In the first generation, all Au atoms are distributed randomly on the surface, meaning every adatom introduces 3 degrees of freedom. For each generated structure, the fitness, i.e. the configuration's free energy, is then calculated from first principles with density functional theory implemented in VASP.

The next generation's individuals are created by moving every structure in the $3N$ -dimensional space towards the structure that minimizes the fitness so far. To avoid getting stuck in a local energy minimum, 20% of the structured are created randomly in each generation.

The last step is repeated, until a certain convergence criterion is reached.

O 40.2 Tue 18:00 P2/EG

Assessing and processing the surface quality of free-standing wurtzite GaN in ultra-high vacuum — •MOHAMMADREZA ROSTAMI¹, BIAO YANG¹, FELIX HAAG¹, FRANCESCO ALLEGRETTI¹, LIFENG CHI², MARTIN STUTZMANN³, and JOHANNES V. BARTH¹ — ¹Physics Department E20, Technical University of Munich, Garching, 85748, Germany — ²Institute of Functional Nano & Soft Materials, Collaborative Innovation Center of Suzhou Nano Science and Technology, Soochow University, Suzhou 215123, P. R. China — ³Walter Schottky Institute and Physics Department, Technical University of Munich, 85748 Garching, Germany

Gallium nitride (GaN) is proposed as an alternative candidate to metallic substrates for assembling organic molecular structures. However, the formation of a persistent surface oxide layer in air considerably limits the use of GaN for well-defined interfaces. We have investigated n-type free-standing c-plane wurtzite GaN crystals. The effect of electron bombardment on the surface quality of free-standing GaN during ammonia annealing was studied. Surface cleaning and full removal of the oxide layer on GaN surfaces could be reproducibly achieved via sputtering and annealing cycles, leading to substantial roughening of the GaN surface. Although ammonia annealing with electron bombardment increased the N/Ga atoms ratio, the surface morphology remained rough. In addition, the on-surface chemistry of 1,3,5-Tris(4-bromophenyl) benzene (TBB) 2 was studied on the cleaned GaN surface. [1] V. Bermudez, Surf. Sci. Rep. 72 (4), 147-315 (2017) [2] M. Fritton et al. J. Am. Chem. Soc 141 (12), 4824-4832 (2019)

O 40.3 Tue 18:00 P2/EG

A super-cycle approach to atomic layer deposition of indium-gallium-zinc oxide at low temperature — ALI MAHMOODINEZHAD¹, CARLOS MORALES¹, MALGORZATA KOT¹, FRANZISKA NAUMANN², PAUL PLATE², •KARSTEN HENKEL¹, and JAN INGO FLEGE¹ — ¹Applied Physics and Semiconductor Spectroscopy, Brandenburg University of Technology Cottbus-Senftenberg, Germany — ²SENTECH Instruments GmbH, Berlin, Germany

The continuing development of multifunctional devices needs novel multicomponent oxide layers, demanding a high control of both composition and thickness during their preparation. To this end, single metal oxides exhibiting high structural quality and conformity have successfully been grown by atomic layer deposition (ALD). However, the deposition of more complex compounds with specific optical and electrical properties is still challenging. In this work, we follow a bottom-up approach to design an ALD super-cycle to grow mixed indium-gallium-zinc oxide (IGZO) films with a controllable composition. For the formation of the individual indium, gallium, and zinc oxides, we found the use of plasma-enhanced ALD (PEALD) at 150 °C to be favorable when using the organometallic precursors trimethylindium, trimethylgallium, and diethylzinc together with oxygen plasma. The PEALD approach of IGZO films can particularly overcome a nucleation delay within the ZnO sub-cycle known from thermal ALD, achieving a higher growth per cycle and improving the quality and composition homogeneity of the films as shown by in-situ spectroscopic ellipsometry and ex-situ X-ray photoelectron spectroscopy.

O 40.4 Tue 18:00 P2/EG

Adsorption of spike amino acids, asparagine and cysteine, on the surface of model catalyst TiO₂ — •MIGUEL BLANCO GARCIA¹, MONA KOHANTORABI¹, MICHAEL WAGSTAFFE¹, MOHAMMAD TEHRANI¹, SILVAN DOLLING¹, ANDREAS STIERLE^{1,2}, and HESHMAT NOEI¹ — ¹Deutsches Elektronen-Synchrotron DESY, Notkestraße 85, 22607 Hamburg, Germany — ²Mathematics, Informatics, and Natural Sciences (MIN) Faculty, University of Hamburg, 20354 Hamburg, Germany

Titanium oxides are excellent candidates for the inactivation of viruses using light due to their photocatalytic properties [1]. In this study we are aiming to determine the mechanism of inactivation of SARS-CoV-2 on TiO₂ under ultraviolet treatment [2]. The two most abundant amino acids in the spike protein of the SARS-CoV-2 virus (cysteine and asparagine) [3] are adsorb under UHV and aqueous solution on TiO₂ surfaces. Surface sensitive techniques such as X-ray photoelectron spectroscopy shows changes in the amino acids upon UV treatment. Furthermore, scanning tunneling microscopy demonstrates the disposition of the amino acid molecules on the surface and the changes upon UV irradiation. GISAXS data was obtain at DESY P03 for the adsorption in aqueous solution, to understand the adsorption geometry and self-assembly of the cysteine amino acids on the rutile and anatase TiO₂ surfaces.

References: [1] Diebold, U. Surface science reports 48.5 (2003): 53-229. [2] Kohantorabi, et al., ACS Appl. Mater. Interface., Under Review. [3] Wang D, et al., Nano today 40 (2021): 101243.

O 41: Poster: Supported Nanoclusters

Time: Tuesday 18:00–20:00

Location: P2/EG

O 41.1 Tue 18:00 P2/EG

Nano-SMSI - FePt clusters on graphene/Rh(111) — •NATALIE J. WALESKA¹, EVA MARIE FREIBERGER¹, FELIX HEMAUER¹, VALENTIN SCHWAAB¹, and CHRISTIAN PAPP^{1,2} — ¹Friedrich-Alexander-Universität Erlangen-Nürnberg, Germany — ²Freie Universität Berlin, Germany

Strong metal-support interaction is found for particles supported on particular metal oxide surfaces leading, inter alia, to the encapsulation of the particle by a thin layer of the metal oxide support. As a result the adsorption ability is decreased strongly but also specific site blocking is found, offering new opportunities for site selective reactions.

In this work, we investigated graphene-supported FePt clusters on the Rh(111) single crystal surface by in situ high-resolution XPS and the utilization of CO as a probe molecule. The FePt clusters were prepared by successively depositing Fe (1.27 ML) and Pt (0.14 ML) on the graphene/Rh(111) substrate. Oxidation of Fe was achieved by beam induced CO dissociation. Heating of the FePt/graphene/Rh(111) sample to 550 K results in cluster ripening and the encapsulation of Pt by a thin FeO layer due to SMSI. Further increase of the temperature to 900 K, leads to the decomposition of the Fe oxide layer and the intercalation of Fe. Additionally the formation of a FePt alloy was observed at elevated temperature.

We thank Helmholtz-Zentrum Berlin for allocation of synchrotron-radiation beamtime and BESSY II staff for support during beamtime. This work was funded by the DFG within SFB 953 "Synthetic Carbon Allotropes" (Project #182849149).

O 41.2 Tue 18:00 P2/EG

Beyond Amorphous Carbon as an Embedding Material for Cluster Superlattice Membranes — •STEFAN SCHULTE^{1,2}, TOBIAS HARTL¹, ALEXEI PREOBRAJENSKI³, JAN KNUDSEN³, and THOMAS MICHELY¹ — ¹II. Physikalisches Institut, Universität zu Köln, Germany — ²Peter Grünberg Institut (PGI-3), Forschungszentrum Jülich, Germany — ³MAX IV Laboratory, Lund University, Sweden

Cluster super lattice membranes constitute a novel 2D template material that has recently been described (T. Hartl et al., ACS Nano, 2020). So far, metal nano clusters on a graphene or hexagonal boron nitride support were embedded in an amorphous C matrix. This provides mechanical and thermal stability to the clusters, but a non-conductive embedding material, that allows for selective removal of the support structure is sought after. Here, embedding of cluster superlattices in B is presented and embedded clusters are characterized by STM and XPS. Embedding in B exhibit mechanical and thermal stability similar to amorphous C, e.g., Ir clusters on a graphene support embedded by a few monolayers of B remain in excellent order up to 750 K. This opens the pathway to electronic characterization of the nano clusters as well as removal of the support layer to expose stable clusters to ambient conditions. Further, preliminary results on CeO₂ embedding will be presented. CeO₂ embedded metal clusters are a promising material in few-atom catalysis processes.

O 41.3 Tue 18:00 P2/EG

H₂ Evolution from Methane Activated by Ta₈ Clusters on Pt(111) — •MATTHIAS KNECHTGES, TOBIAS HINKE, KEVIN BERTRANG, SEBASTIAN KAISER, NIKITA LEVIN, MARTIN TSCHURL, and UELI HEIZ — TU Munich, School of Natural Sciences & Catalysis Research Center, Chair of Physical Chemistry

Methane as the main component of natural gas contains the highest energy density of all hydrocarbons but the activation poses great challenges, due to the high activation barrier of the C-H bonds.

Pathways to convert methane into valuable products at mild conditions are investigated in the UHV. Gas phase studies revealed that Ta₈O₂⁺ catalytically converts methane to ethane and hydrogen at room temperature. The charge and oxygen density of the clusters appear to have great impact on their activity towards methane[1].

By employing a substrate manipulating the electronic and geometric structure of the clusters, the model system approaches to industrial heterogeneous catalysis. Therefore, metallic Ta₈ clusters were deposited on different surfaces known for their electron drawing properties in analogy to the oxygen atoms in the Ta₈O₂⁺. While no activity towards methane was observed Ta₈/SiO₂, hydrogen evolution was found after methane exposition on Ta₈/Pt(111) in temperature programmed desorption(TPD) experiments.

Characterization by scanning tunnel microscopy showed randomly monodispersed flat arrangements and XPS to observe oxidation states.

[1] N.Levin et al *J.Am.Chem.Soc.* **2020**, 142, 12, 5862-5869

O 41.4 Tue 18:00 P2/EG

Influence of Strong Metal-Support Interactions on the Photoactivity of Pt-loaded TiO₂(110) — •LUCIA MENGEL, PHILIP PETZOLDT, MORITZ EDER, MARTIN TSCHURL, and UELI HEIZ — Chair of Physical Chemistry, School of Natural Sciences & Catalysis Research Center, Technische Universität München, Lichtenbergstr. 4, 85748 Garching, Germany

Pt-loaded TiO₂(110) is well-known for its capability of alcohol photoreforming. The hole-mediated photooxidation reaction yields hydrogen next to valuable organic compounds such as formaldehyde. The concept of encapsulation of clusters or nanoparticles by a metal oxide overlayer under reductive conditions is well established and has been extensively studied using a variety of techniques. Such encapsulations caused by strong metal-support interactions (SMSI) are a promising tool in photo-/electrocatalysis to improve catalyst selectivity and high-temperature stability. However, there is a lack of mechanistic understanding on the influence of an SMSI overlayer on the photocatalytic hydrogen evolution reaction.

In this poster, we discuss the influence of SMSI on the photoactivity of Pt-loaded TiO₂(110). As model reaction, methanol photoreforming is studied by catalytic measurements. We focus in particular on effects with relevance to the evolution of hydrogen, as TiO_x layers may impede the back reaction in full water splitting and thus have potential to replace currently predominant chromium oxide compounds.

O 42: Poster: Nanostructures at Surfaces

Time: Tuesday 18:00–20:00

Location: P2/EG

O 42.1 Tue 18:00 P2/EG

Nanostructuring of surfaces by slow highly charged ions — •AYMAN EL-SAID¹, RENE HELLER², and STEFAN FACSKO² — ¹Physics Department and Interdisciplinary Research Center for Advanced Materials, King Fahd University of Petroleum and Minerals, Dhahran 31261, Saudi Arabia — ²Institute of Ion Beam Physics and Materials Research, Helmholtz-Zentrum Dresden-Rossendorf, 01328 Dresden, Germany

Recently, considerable research efforts were devoted to the fabrication of extremely small nanostructures of significant potential in nanophotonics and nanoelectronics applications. Slow highly charged ions (HCI), as a promising nanotechnological tool, were successfully utilized for the creation of surface nanostructures in various solids [1]. Based on both the type of the material and ion beam parameters, nanostructures of different shapes (pits, caldera-like, hillocks) and sizes were obtained [2,3]. Here, we review the research progress on HCI-induced nanostructuring and the used theoretical approaches for understanding the creation mechanisms of the observed surface structures.

[1] A.S. El-Said, R.A. Wilhelm, R. Heller, M. Sorokin, S. Facsko, F. Aumayr, *Phys Rev Lett* **117**, 126101 (2016).

[2] F. Aumayr, S. Facsko, A. S. El-Said, C. Trautmann, and M. Schleberger, *J. Phys. Condens. Matter* **23**, 393001 (2011).

[3] S. Facsko, R. Heller, A.S. El-Said, W. Meissl, F. Aumayr, *J. Phys. condensed matter* **2**, 224012 (2009).

O 42.2 Tue 18:00 P2/EG

Quantum simulator to emulate lower dimensional physics and chemistry — •E. SIERDA, X. HUANG, D. BADRTDINOV, B. KIRALY, E. J. KNOL, A.M.H. KRIEG, N.M.M. AARTS, G. C. GROENENBOOM, M. I. KATSNELSON, M. RÖSNER, D. WEGNER, and A. A. KHAJETOORIANS — Institute for Molecules and Materials, Radboud University, Nijmegen, The Netherlands

Designing materials with tailored physical and chemical properties requires a quantitative understanding of interacting quantum systems. In order to provide predictability, a promising route is to create bottom-up platforms, where the electronic properties of individual and interacting atoms can be emulated in a tunable manner. Here, we present a quantum simulator based on patterned Cs ions embedded in a 2DEG on the surface of semiconducting InSb(110). We use this platform to emulate the structure and orbital landscape of planar organic molecules. Using STM/STS and ab initio calculations, we show that an artificial atom can be derived from localized states of patterned Cs ions. The resultant potential can be used to couple artificial atoms, leading to bonding and anti-bonding states as well as to different orbital symmetries. Based on these artificial orbitals, we emulate molecular orbitals of known organic molecules, including anti-aromatic molecules, based on various atomic structures. In a different limit where Cs atoms are much closer, this quantum simulator can also be used to probe the effect of e-e interactions. Our experimental data suggest that dense structures exhibit many-body

effects which can be extended to complex quantum states based on arbitrary lattices.

O 42.3 Tue 18:00 P2/EG

Transition Metal Nanoparticles on Graphene: Influence of Temperature — •KAI BESOCKE, MAHBOOBEH RAVANKHAH, and MATHIAS GETZLAFF — Institut für Angewandte Physik, Heinrich-Heine-Universität Düsseldorf

With its unique properties, such as high quality crystal structure, excellent electrical conductivity and high tensile strength, graphene is a promising substrate for fabricating nanocomposites.

In our research on supported transition metal nanoparticles we are investigating the influence of graphene as a substrate for the deposition of metallic nanoparticles and the influence of subsequent heating. In this contribution we present our results concerning the size distribution of $\text{Fe}_{0.5}\text{Ni}_{0.5}$ -Nanoparticles on CVD-graphene surfaces.

The graphene surfaces are prepared on a cobalt thin film on a W(110) substrate. The particles under investigation are produced by means of Ar magnetron sputtering in a Haberland source and aggregation takes place in a He atmosphere. We analyze the behaviour of particles several nm in diameter at temperatures up to 500 °C.

Particle distributions are analyzed via STM and it will be discussed, whether the nanoparticles show different behaviour upon heating on graphene compared to other surfaces.

O 42.4 Tue 18:00 P2/EG

Activity of cerium oxide thin films prepared by atomic layer deposition using custom and commercial precursors — •YULIA KOSTO¹, CARLOS MORALES¹, ANJANA DEVI², KARSTEN HENKEL¹, and JAN INGO FLEGE¹ — ¹Applied Physics and Semiconductor Spectroscopy, Brandenburg University of Technology Cottbus-Senftenberg, Konrad-Zuse-Strasse 1, Cottbus 03046, Germany — ²Inorganic Materials Chemistry, Ruhr University Bochum, Universitätsstraße 150, Bochum 44801, Germany

Atomic layer deposition (ALD) allows preparation of conformal coatings with possibility to control their thickness at the submonolayer level, making it a good tool for depositing active layers on 3D structures. Our group is working on cerium oxide-based materials for hydrogen detection, which is difficult at ambient conditions due to the low sensitivity and long response time of the sensors. The cerium oxide layers prepared by ALD contain a lot of defects and provide an opportunity to overcome these complications. Thickness and morphology of the oxide films play an important role in defining the $\text{Ce}^{3+}/\text{Ce}^{4+}$ ratio, as well as the interface with the used substrate. Here, we compare cerium oxide thin films deposited by ALD techniques on SiO_2 and Al_2O_3 substrates. The results reveal that the interface to the substrate can considerably influence the reactivity of the cerium oxide toward hydrogen and oxygen. Preparation of the oxides using two different precursors (commercial $\text{Ce}(\text{thd})_4$ and custom $\text{Ce}(\text{dpdmg})_3$) has been demonstrated to affect the redox properties of the films, their reactivity, and the reversibility.

O 42.5 Tue 18:00 P2/EG

Local work function on Graphene Nanoribbons on Au(111) — •DANIEL ROTHHARDT¹, TILMANN KLAMROTH², AMINA KIMOUCHE¹, and REGINA HOFFMANN-VOGEL¹ — ¹Institute of Physics and Astronomy, University of Potsdam, Karl-Liebknecht-Str. 24-25, 14476 Potsdam-Golm, Germany — ²Institute of Chemistry, University of Potsdam, Karl-Liebknecht-Str. 24-25, 14476 Potsdam-Golm, Germany

Graphene nanoribbons (GNRs) exhibit remarkable electronic properties due to the nature of the charge carriers and local confinements [1]. The local work function difference (LCDP) was investigated using an ultra-high-vacuum non-contact mode AFM and in addition to the topography, the local differences in the contact potential were recorded using the method of Kelvin Probe Force Microscopy. A charge transfer between the GNRs and the underlying gold substrate can be detected in the LCPD images which verifies the p-doping of the GNRs [2]. We observed a modification of the work function along the edges of the GNRs, which is due to the screening of the Au(111) of electrostatic fields from the GNR. Density functional theory (DFT) calculation supports the experimental findings.

[1] A.H. Castro, Neto et al, Rev. Mod. Phys. **81**, 109 (2009)

[2] D. Rothhardt et al, arXiv:2203.06945v1, (2022)

O 42.6 Tue 18:00 P2/EG

Spin Switching in Self-Assembled Tetramers on Ag(111) — •SVEN JOHANNSEN¹, SASCHA OSSINGER², SASCHA SCHÜDDEKOPF¹, JAN GRUNWALD³, ALEXANDER HERMANN⁴, TROELS MARKUSSEN⁵, HEIKO WENDE⁴, FELIX TUCZEK³, MANUEL GRUBER⁴, and RICHARD BERNDT¹ — ¹Institute of Experimental and Applied Physics, CAU Kiel, Germany — ²Department of Chemistry, University of Basel, Switzerland — ³Institute of Inorganic Chemistry, CAU Kiel, Germany — ⁴Faculty of Physics and CENIDE, University of Duisburg-Essen, Germany — ⁵Synsops Denmark, Fruebjergvej 3, 2100 Copenhagen, Denmark

Spin-crossover (SCO) molecules can be switched between a low spin (LS) state and a high spin (HS) state. Adsorption to a surface can lead to a drastic change

of the SCO behaviour. We present a low-temperature scanning-tunneling-microscope investigation of the switching characteristics of metal-based SCO molecules organized in tetramers on a Ag(111) surface. Via the injection of current pulses two molecules per tetramer can be reversibly switched. In addition, these molecules may be switched remotely by applying the excitation to one of the other two molecules of the tetramers. The latter molecules themselves are immutable. We induced tens of thousands of switching events using different currents and voltages and observed that the switching yields that are 2 to 3 orders of magnitude larger compared to previous results. We show that the switching is likely linked to a spin transition and also report three-state switching that involves charging of a molecule.

O 42.7 Tue 18:00 P2/EG

Simulation of electronic transport in 2D networks — •TIM GÜLDENPFENNIG, MARKUS GRUSCHWITZ, and CHRISTOPH TEGENKAMP — Institut für Physik, TU Chemnitz, Reichenhainerstr. 70, 09126 Chemnitz

Interclation of atomic hydrogen into to the interface of buffer layer systems on $\text{SiC}(0001)$ was shown to be powerful method to realize almost charge neutral quasi free monolayer graphene. This concept works also for intercalation of various metals (e.g. Pb, Sn, In) coming along with the formation of new 2D interface structures in proximity to graphene. However, defects within the buffer layer are often required for the intercalation of larger elements, thus the homogeneity of the intercalated areas depend strongly on the quality of the buffer layer and intercalation parameters. As a result, the quasi free monolayer graphene resembles a network structure rather than a homogeneous 2D phase.

In order to deduce the conductivity from our transport measurements done with a 4 point probe STM, we performed simulations. By means of COMSOL java api and the MPh library, the simulations were controlled via self-written python scripts. Next to the import of experimental data measured with high resolution SEM, own network structures were designed to study systematically the effect of anisotropy and inhomogeneities in 2D systems.

O 42.8 Tue 18:00 P2/EG

Preparation and STM study of clean Nb(111) surfaces — •JULIA GOEDECKE¹, MACIEJ BAZARNIK², and ROLAND WIESENDANGER¹ — ¹Dept. of Physics, University of Hamburg, D-20355 Hamburg, Germany — ²Institute of Physics, Poznan University of Technology, Piotrowo 3, 60-965 Poznan, Poland

Niobium with its highest transition temperature among all elemental superconductors has become a favorable substrate for realizing well-defined low-dimensional magnet-superconductor hybrid systems exhibiting novel types of exotic electronic states such as Majorana zero-energy modes. While a preparation procedure for obtaining atomically clean Nb(110) substrates has previously been reported, a suitable preparation method for clean Nb(111) surfaces is still lacking. Here, we report a recipe for cleaning Nb(111) surfaces based on an atomic hydrogen treatment followed by short flashes to elevated temperatures. The atomic surface structure of clean Nb(111) is investigated by high-resolution scanning tunneling microscopy (STM), revealing a surface reconstruction with a reduced atom density compared to the (111) plane of a bcc crystal.

O 42.9 Tue 18:00 P2/EG

Pulling single polar molecular wires by atomic force microscopy — •CHRISTOPHE NACCI and LEONHARD GRILL — Institute of Chemistry, University of Graz, Graz, Austria

The frictional properties of individual nanostructures are strongly influenced by the low dimensionality and reduced size. Probing how they respond mechanically on different surfaces is essential to understand how the static and dynamic friction depend on the interplay between chemical composition and structural commensurability. Here, we report the vertical pulling of DAD molecular wires [1] off metal surfaces by non-contact atomic force microscopy (AFM), performed under ultrahigh vacuum and at low temperatures. The chemical structure of DAD polar wires is made of a regular alternation of donor (D) and acceptor (A) units. The mechanical response of single isolated molecular wires is probed by force spectroscopy. To further explore the role of structural commensurability between polymers and surface, the polar wires are also grown on ultrathin insulating NaCl films on metal surfaces.

[1] C. Nacci et al, Nature Comm. **6**, 7397 (2015)

O 42.10 Tue 18:00 P2/EG

XRR Analysis of Al₂O₃ coated and mid-T baked niobium for future implementation in SIS-based SRF cavities — •ARTEM ZAIDMAN^{1,2}, GETNET KACHA DEYU², MARC WENSKAT², VEDRAN VONK¹, ROBERT ZIEROLD³, ROBERT BLICK^{3,4}, WOLFGANG HILLERT², and ANDREAS STIERLE^{1,2} — ¹Deutsches Elektronen-Synchrotron DESY, Germany — ²Institute of Experimental Physics, Universität Hamburg, Germany — ³Center for Hybrid Nanostructures (CHyN), Universität Hamburg, Germany — ⁴Materials Science and Engineering, University of Wisconsin-Madison, United States

Bulk niobium is currently the most used material for RF surfaces. A new approach proposed by Gurevich [1] suggests the use of a superconductor-insulator-superconductor structure (SIS) to achieve higher accelerating fields and reduced

surface resistance beyond the thermodynamic limits of Nb. As an intermediate step to pursue this model and in coordination with a similar procedure performed on a single-cell niobium cavity, a mechanically polished two-grain-Nb sample was coated with a 36 nm Al₂O₃ thin film via thermal atomic layer deposition (ALD) to create an insulating layer and baked for 3h at 300°C (mid-T bake) [2]. An XRR analysis of the sample was taken at each processing step to follow the changes in the niobium native oxide thickness and composition.

[1] A. Gurevich, Appl. Phys. Lett. 88, 012511 (2006) [2] S. Posen, et al., Phys. Rev. Applied 13, 014024 (2020)

O 42.11 Tue 18:00 P2/EG

Oxidation of α -Al₂O₃(0001)-supported Pt-Rh alloy nanoparticles — •MING-CHAO KAO, SIMON CHUNG, THOMAS F. KELLER, VEDRAN VONK, and ANDREAS STIERLE — Deutsches Elektronen-Synchrotron DESY, Center for x-ray and Nanoscience CXNS, Hamburg 22607, Germany

Metal oxide supported platinum-rhodium bimetallic alloy nanoparticles are widely deployed in the field of heterogeneous catalysis, where they often undergo oxidation-reduction cycles. To better understand the oxidation process, we monitored the nanoparticles in-situ by Grazing Incidence X-ray Diffraction (GIXRD) as a function of different alloy compositions. By heteroepitaxial growth, α -Al₂O₃(0001) substrate supported Pt, Rh, and Pt-Rh alloy nanoparticles were grown via molecular beam epitaxy. The samples were characterized by SEM, AFM, XRR, and GIXRD. The aim of this study is to uncover the oxide formation on the NPs as a function of oxygen partial pressure and temperature. The oxidation experiment is performed with an in-situ oxidation chamber, which enables experiments to be carried out up to an oxygen pressure of 1000 mbar at 450°C. From the in-situ XRD experiments performed at constant temperature

and increasing oxygen pressure, the following phenomena are deduced: particle sintering, selective oxidation, epitaxial strain, and the formation of Rh₂O₃ bulk oxide on (111)-oriented nanoparticles. Furthermore, composition-dependent changes together with selective oxidation and epitaxial strain were observed.

O 42.12 Tue 18:00 P2/EG

Structural and magnetic properties of epitaxial iron oxide nanoislands on SrTiO₃ — •STEFFEN TOBER, MAI H. HAMED, YIFAN XU, ASMAA QDEMAT, CONNIE BEDNARSKI-MEINKE, ULRICH RÜCKER, OLEG PETRACIC, EMMANUEL KENTZINGER, and THOMAS BRÜCKEL — Jülich Centre for Neutron Science (JCNS) and Peter Grünberg Institut (PGI), JARA-FIT, Forschungszentrum Jülich The chemical, electronic and magnetic properties of Fe_xO_y/oxide substrate heterostructures depend on substrate interactions and the flexible chemistry of the iron oxides, resulting in conductive or insulating, ferri- or antiferromagnetic phases. The reduced geometry of Fe_{3- δ} O₄ nanoislands grown by reactive molecular beam epitaxy enables further tuning of electronic and magnetic properties for applications in catalysts and magnetoelectric devices [1]. We present the structural and magnetic characterisation of Fe_{3- δ} O₄ nanoislands on (001) oriented SrTiO₃ with mixed SrO/TiO₂ and stepped TiO₂ surface terminations by reflection high-energy electron diffraction (RHEED), grazing incidence small angle X-ray scattering (GISAXS) and SQUID magnetometry [2,3]. Our findings indicate the growth of crystalline, evenly shaped, ferrimagnetic islands. These results form the basis for further experiments probing the local electronic and magnetic structure of the nanoislands.

[1] Y. Z. Chen et al., J. Appl. Phys. 103, 07D703 (2008), [2] G. E. Sterbinsky et al., J. Vac. Sci. Technol. B 25, 1389 (2007), [3] JCNS, JLSRF, 2, A61 (2016).

O 43: Poster: Plasmonics and Nanoptics I

Time: Tuesday 18:00–20:00

Location: P2/EG

O 43.1 Tue 18:00 P2/EG

Quantitative Modeling of Scattering-type Scanning Near-field Optical Microscope (s-SNOM) with the Finite Element Method Utilizing the Software JCMSuite — •DINGHE DAI, DARIO SIEBENKOTTEN, RICHARD CIESIELSKI, and BERND KÄSTNER — Physikalisch-Technische Bundesanstalt, Abbestr. 2-12, 10587 Berlin

Scattering-type scanning near-field optical microscopy (s-SNOM), where local field enhancement is created with an oscillating nanotip, is widely applied in the nanoscale characterization of nanostructures, surface polaritons, and biomolecular systems. s-SNOM requires quantitative evaluation schemes with analytical models or simulation methods, among which the Finite Dipole Model [1] is a sophisticated model to calculate the near-field scattering for bulk materials. Nevertheless, it cannot model the full tip size or surface nanostructures. To solve this, a numerical model, based on the finite element method (FEM) software JCMSuite, is developed. The model describes the electromagnetic field over several orders of magnitude in physical size. At various infrared incident wavelengths (μ m), the electromagnetic fields are simulated for different tip-sample gaps (nm) and demodulated at harmonics of the tapping frequency to eliminate background field effects. The agreement and deviation of amplitude and phase spectra between both models across multiple demodulation orders are discussed. The FEM by JCMSuite combined with field demodulation is a credible quantitative s-SNOM simulation method especially interesting for complex multilayer and nanooptical structures.

[1] Cvitkovic et al. Optics express 15(14) (2007): 8550-8565.

O 43.2 Tue 18:00 P2/EG

Switching nonlinear emission patterns of plasmonic nanostructures — •VALENTIN DICHTL, KILIAN WITTMAN, THORSTEN SCHUMACHER, and MARKUS LIPPITZ — Experimental Physics III, University of Bayreuth, Germany

The nonlinear third-order material response of noble metals allows to shape the third-harmonic near field around a plasmonic nanostructure [1]. The corresponding spatial emission pattern of the third harmonic hot spots changes drastically when slightly tuning the fundamental wavelength over a linear resonance of the nanorod. This raises the question of whether similar behavior can be found for other nonlinear emission processes.

Here, we demonstrate by hyperspectral imaging that not only the third- but also the second-harmonic and especially the two- (or multi-) photon excited luminescence (TPPL) emission changes spatially, when tuning over the plasmon resonance. We discuss spatial and spectral differences between these processes. The outlook is targeted towards selectively exciting single quantum emitters in the nearfield. As first step into this direction we present differences in the spatial change of luminescence of a dye film with respect to the underlying emission pattern.

[1] Wolf, D. et al. Shaping the nonlinear near field. Nat. Commun. 7:10361 (2016). doi: 10.1038/ncomms10361

O 43.3 Tue 18:00 P2/EG

Deep learning for the extraction of optical parameters of multilayer samples in scanning near-field optical microscopy — •DARIO SIEBENKOTTEN, LARA HARREN, CLEMENS ELSTER, and BERND KÄSTNER — Physikalisch-Technische Bundesanstalt, Abbestr. 2-12, 10587 Berlin

Scattering-type scanning near-field optical microscopy (s-SNOM) is a powerful method for optical material characterization at the nanoscale. However, owing to the complex interaction between tip and sample, extensive modelling is needed for the extraction of optical parameters, particularly for layered samples. The extraction of optical parameters typically requires fitting, which quickly becomes unstable [1] and can be very time intensive due to the complexity of the models. Deep Learning algorithms offer a fast alternative for the optical parameter extraction but have only been applied to bulk materials. Here, we show the extension of these approaches to systems consisting of one and two layers of polar crystals exhibiting surface phonon-polariton resonances on top of a substrate by training neural networks with model data. We present the trained neural networks and discuss the extraction accuracy for the cases of one and two layered samples. While this study is limited to polar crystals, the application to other systems, defined for example by free charge carriers or band transitions, is straight forward. [1] McArdle et al. Phys. Rev. Research 2, 023272 (2020)

O 43.4 Tue 18:00 P2/EG

Nonlinear near-field optical microscopy (NNOM) for plasmonic skyrmions — •FLORIAN MANGOLD, BETTINA FRANK, and HARALD GIESSEN — 4th Physics Institute, Research Center SCoPE, and IQST, University of Stuttgart, Pfaffenwaldring 57, 70569 Stuttgart, Germany

In recent years, plasmonic skyrmions have become a growing field of research. The state-of-the-art detection is done with PEEM (photoemission electron microscopy) or SNOM (scanning near-field optical microscopy) measurements.

An alternative to these methods is nonlinear near-field optical microscopy (NNOM) which uses an optical nonlinear process to image evanescent waves on the sub-wavelength-scale and enables real-time imaging of surface waves. By combining information from real and Fourier-space images, it is possible to calculate the phase and the amplitude of all electric field components.

The NNOM setup will be used to complement PEEM and SNOM measurements and gives us additional possibilities to investigate topological features in plasmonics such as quasicrystals, skyrmions and skyrmion bags.

O 43.5 Tue 18:00 P2/EG

Greyscale lithography with photoresist for plasmonic coupling — •JULIAN ALIN, MICHAEL SEIDEL, THORSTEN SCHUMACHER, and MARKUS LIPPITZ — Experimental Physics III, University of Bayreuth, Germany

Integrated plasmonic nanocircuits promise to play a major role for future applications of quantum optical technologies. Therefore stable, bright and narrow-band single-photon sources are required, such as self assembled epitaxially

grown GaAs quantum dots [1]. Crucial for the coupling of such a quantum dot to a waveguide is, that for a high efficiency the waveguide has to be placed close to the quantum dot. However, the spatial proximity to the surrounding semiconductor material with a high refractive index strongly attenuates the surface plasmon propagation. In order to solve this problem we try to create a structure where the waveguide will be close to the quantum dot, but far away from the semiconductor material (a few hundred nanometers). To achieve this trough-like structure the idea is to apply a photoresist on a GaAs-sample, write a trough with a focussed gaussian laser beam and place a waveguide at this position. We discuss experiments on such structures with waveguides on glass substrates and first steps on GaAs wafers.

[1] Wu et al., Nano Lett. 2017, 17, 7, 4291-4296

O 43.6 Tue 18:00 P2/EG

Resistive heating of monocrystalline plasmonic resonators — •JACOB SYNDIKUS, LUKA ZURAK, JESSICA MEIER, BERT HECHT, and THORSTEN FEICHTNER — Nanooptics & Biophotonics Group, Experimental Physics 5, RCCM, JMU Würzburg, Am Hubland, D-97074 Würzburg, Germany

Plasmonic resonators can focus light down to sub-diffraction-limited near-field intensity volumes by collective oscillations of photons and electrons. Therefore, they are hot candidates for electro-optical devices with minimal footprint, bridging the gap between fiber communication and electronics or even being optical switches by themselves. To achieve this, the plasmonic properties have to be actively tuned, the faster the better.

Here we show experimentally the modulation of the wavelength dependent scattering intensity by a gold nanorod in the MHz range by resistive heating. Application of an AC voltage heats the gold material by several tens of Kelvin, changing the electron energy density and with it the dielectric constant ϵ_{Au} . The small volume and the electrical contacts ensure fast heat dissipation. We fabricate the structures from monocrystalline goldflakes by means of Ga- and He-ion beam milling and measure the changes in the resonance curves via white light laser illumination and modelocking detection. Numerical models show that GHz modulation is feasible to be realized which makes the technique interesting for applications.

O 43.7 Tue 18:00 P2/EG

Electrochemistry of the surface of electrically contacted plasmonic resonators

— •PAUL MÖRK, LUKA ZURAK, JESSICA MEIER, BERT HECHT, and THORSTEN FEICHTNER — Nano-Optics & Biophotonics Group, Experimental Physics 5, University of Würzburg, Am Hubland, 97074 Würzburg, Germany

Catalytic processes on gold surfaces are well known to enhance electrochemical processes. When the gold is showing geometric features on the nanometer scale, plasmonic resonances in the visible wavelength range can occur. This establishes additional degrees of freedom (photon routing, heating, hot electron generation) to tailor an efficient material for photo-electrochemical processes interesting for energy applications like water splitting or CO₂ reduction.

Here we show the results of experiments with directly electrically connected plasmonic resonators made via focused ion beam milling from monocrystalline gold flakes. Under ambient conditions without any further chemical added we observe a resonance shift by several ten of nanometers on a time scale of seconds when applying a electrical potential as high as 20 Volts to the gold surface. The effect reverses when the bias voltage is switched of on the time scale of hours. We present evidence that we observe the electrochemical oxidation and reduction of gold mediated by the omnipresent waterlayer covering every surface with nanometer thickness and deliver an outlook to the application within electrochemical cells.

O 43.8 Tue 18:00 P2/EG

Exciton lifetime of decoupled phthalocyanine molecules — •AMANDEEP SAGWAL^{1,2}, JIŘÍ DOLEŽAL¹, RODRIGO CEZAR DE CAMPOS FERREIRA¹, PETR KAHAN¹, and MARTIN ŠVEC^{1,3} — ¹Institute of Physics, Czech Academy of Sciences; Praha, Czech Republic — ²Faculty of Mathematics and Physics, Charles University; Czech Republic — ³Institute of Organic Chemistry and Biochemistry, Czech Academy of Sciences; Czech Republic

A few layers of NaCl decoupling layer on metal are sufficient to prevent the non-radiative quenching of the excited state in phthalocyanine [1] and observe fluorescence in the far field from the molecule located in the junction of a scanning tunneling microscope (STM). First attempts to measure the lifetimes of exciton in the nanocavity suggested lifetimes of hundreds of picoseconds [2,3] but later studies pointed towards a transient charge state lifetime involved in the electroluminescence excitation process [4,5] and estimated the lifetime to be several orders of magnitude lower, due to the Purcell effect of the plasmonic nanocavity. Here, we use a pulsed supercontinuum laser to reveal the radiative decay of the excited state of the molecules with and without the presence of nanocavity.

[1]*F. Aguilar-Galindo et al. ACS Photonics 8, 3495 (2021) [2]*L. Zhang et al. Nat. Commun. 8, 580 (2017). [3]*J. Doležal et al. ACS Nano 15, 7694 (2021). [4] B. Yang et al. Nat. Photonics 14, 693 (2020). [5] K. Kaiser et al. arXiv:2211.01051 (2022).

O 44: Overview Talk Christian Ast

Time: Wednesday 9:30–10:15

Location: TRE Phy

Invited Talk

O 44.1 Wed 9:30 TRE Phy

Spins on Surfaces: A Gateway to the Quantum World — •CHRISTIAN R. AST — MPI for Solid State Research, Stuttgart

Many exotic phenomena that are of current interest today rely on the quantum mechanical spin. With the focus on the atomic scale, placing spins on different surfaces has been a remarkably successful platform. Over the past decades, spins as they occur in atoms and molecules have been placed not only on insulating

layers to decouple them from the environment and isolate their properties, but also on interacting normal and superconducting substrates. In this way, a plethora of different effects and concepts could be studied including, but not limited to the Kondo effect, Yu-Shiba-Rusinov states and by extension Majorana bound states, electron spin resonance as well as inelastic spin-flip spectroscopy. Here, I will present an overview of the field as well as recent developments in spins on surfaces at the atomic scale.

O 45: Focus Session: Scanning Probe Microscopy with Quartz Sensors I

Atomic Force Microscopy (AFM) was quickly adopted in science and engineering, but it took a while until the field of surface could benefit from it. 2023 marks the 25th anniversary of the introduction of the qPlus sensor. This stiff and self sensing force sensor made from quartz that often uses an etched metal tip as known from scanning tunneling microscopy (STM) replaced the silicon cantilever and allowed new types of experiments and new domains of precision. Scientists used it to resolve the structure of organic molecules with atomic resolution, to obtain sub-atomic spatial resolution, to image spin structures and spin lifetimes, to measure lateral forces, to detect tiny water molecules, to image oxides and other insulating surfaces with atomic resolution. Operation in ambient conditions, ultrahigh vacuum (UHV), low (4 K) and ultralow temperatures (10 mK) and in high magnetic fields as well as in an electrochemical cell was demonstrated.

Organizer: Franz Giessibl (U Regensburg)

Time: Wednesday 10:30–12:30

Location: CHE 89

O 45.1 Wed 10:30 CHE 89

The genesis of the qPlus sensor — •FRANZ GIESSIBL — Institute of Experimental and Applied Physics, University of Regensburg, Universitätsstraße 31, 93053 Regensburg

In 1985, Gerd Binnig found exile from the STM frenzy at IBM Rüşchlikon by a one year move to Stanford, the heart of silicon valley, and built the first atomic force microscope (AFM) together with Christoph Gerber and Calvin Quate [1]. Therefore, it is not surprising that the core of all AFMs, the cantilever, was soon

micromachined from Si. Even the first successful imaging of Si 7x7 relied on piezoresistive Si cantilevers in the frequency modulation mode, albeit at an in-sensitively large oscillation amplitude of 34 nm [2]. Benchmarking, widely used in management consulting, led to the conviction that quartz tuning forks with their utmost frequency stability would be a promising alternative. The phantastic frequency stability of the quartz forks used in Swatch watches and the realization that their stiffness allows sub-Angstrom oscillation amplitudes led to the invention of the qPlus sensor. Its stability, small amplitudes and low noise soon enabled subatomic resolution by AFM [3]. While qPlus sensors are standard in vacuum today, it is open if widespread application in ambient or liquid environments will become attractive, although atomic resolution has been demonstrated [4]. [1] G. Binnig, C.F. Quate, C. Gerber, *Phys. Rev. Lett.* 56, 930 (1986). [2] F.J. Giessibl, *Science* 267, 68 (1995). [3] F.J. Giessibl, S. Hembacher, H. Bielefeldt, J. Mannhart, *Science* 289, 422 (2000). [4] D.S. Wastl, A.J. Weymouth, F.J. Giessibl, *Phys. Rev. B* 87, 245415 (2013).

Topical Talk

O 45.2 Wed 10:45 CHE 89

Single-molecule reactions performed and characterized using atomic force microscopy — •LEO GROSS — IBM Research Europe - Zurich

Selective and reversible bond formation and dissociation can be controlled by tip-induced reduction-oxidation reactions on a surface. Molecular rearrangements leading to different constitutional isomers are selected by the polarity and magnitude of applied voltage pulses from the tip of a combined scanning tunneling microscope (STM) / atomic force microscope (AFM) [1].

Evasive molecules can be created and studied, such as cyclocarbons, i.e., molecular sp¹ hybridized carbon allotropes [2] and molecules with high-spin ground states [3,4]. Moreover, insulating substrates allow probing charge states [5] and excited states [6].

[1] F. Albrecht et al. *Science*. 377, 298-301 (2022).

[2] K. Kaiser et al. *Science*. 365, 1299-1301 (2019).

[3] N. Pavliček, et al. *Nat. Nano.* 12, 308-311 (2017).

[4] S. Mishra et al. *ACS Nano*. 16, 3264-3271 (2022).

[5] S. Fatayer et al. *Science*. 365, 142-145 (2019).

[6] S. Fatayer et al. *Phys. Rev. Lett.* 126, 176801 (2021).

O 45.3 Wed 11:15 CHE 89

On surface reaction of azaTrux molecules on Au (111) — •OUTHMANE CHAHIB¹, JUNG-CHING LIU¹, CHAO LI¹, XUNSHAN LIU², ULI ASCHAUER², SILVIO DECURTINS², SHI-XIA LIU², ERNST MEYER¹, and RÉMY PAWLAK¹ — ¹Department of Physics, University of Basel, Klingelbergstrasse 82, 4056 Basel, Switzerland — ²Department of Chemistry and Biochemistry, University of Bern, Freiestrasse 3, 3012 Bern, Switzerland

One promising way to miniaturize electronic devices is to use "bottom-up" techniques, where functional organic molecules acting as elementary nanometer-sized "building blocks" are assembled or reacted on surfaces. Here we explore the on-surface reaction of 7,12-dibromo-5H-indeno[1,2-a]indolo-[3,2-c]carbazol-15(10H)-one molecules (AzaTrux) on the Au(111) surface into graphene nanostructures. Structural and electronic properties of nanostructures are characterized by scanning tunneling microscopy (STM) and atomic force microscopy (AFM) with CO-terminated tips. Using force spectroscopy, we further probe the donor-acceptor character of these nanostructures.

O 45.4 Wed 11:30 CHE 89

A two dimensional array of radical molecules on Pb(111) — JUNG-CHING LIU¹, CHAO LI¹, H. CHEN², PING ZHOU³, XUNSHAN LIU³, ULRICH ASCHAUER³, SILVIO DECURTINS³, SHI-XIA LIU³, WULF WULFHEKEL², ERNST MEYER¹, and •RÉMY PAWLAK¹ — ¹University of Basel, Basel, Switzerland — ²Karlsruhe Institute of Technology, Karlsruhe, Germany — ³University of Bern, Bern, Switzerland

The assembly of molecules to form a quantum dot array is of interest for quantum computing with the highest areal density. In this contribution, we show the supramolecular assembly of 4,5,9,10-tetrabromo-1,3,6,8-tetraazapyrene (TB-TAP) molecules on superconducting Pb(111), self-organized in neighboring rows of radicals and neutral molecules [1]. By triggering a local field with a STM/AFM microscope at low temperature, we show that individual occupied molecules can be discharged efficiently, revealing Coulomb rings in spatial dI/dV maps. Charged molecules host spin 1/2, which is validated by dI/dV spectroscopy with μ eV resolution through the observation of a pair of in-gap Yu-Shiba-Rusinov (YSR) states in the supra-conducting gap. The unpaired electron cloud extends spatially over the entire molecule and interacts with neighbouring electrons, resulting in the formation of YSR bands along the entire molecular domain. [1] J.C. Liu et al. submitted.

O 45.5 Wed 11:45 CHE 89

Self-Assembly Study of 1,2,10,11,12,14-hexafluoropentacene on a Au(111) surface by HR-AFM — •MIGUEL WICHE¹, MAXIMILIAN DREHER², ANDRÉ SCHIRMEISEN¹, GREGOR WITTE², and DANIEL EBELING¹ — ¹Institute of Applied Physics, Justus Liebig University Giessen, Germany — ²Fachbereich Physik, Philipps-Universität Marburg, Germany

The electronic properties of 2D organic materials highly depend on the orientation of the molecules inside the molecular thin film. For designing new materials with tailored functionality, it is important to understand the self-assembly processes of the individual molecular building blocks on surfaces. For example, the role of intermolecular halogen bonds for the molecular arrangement is not well understood. A powerful tool to investigate assembly processes in a step-by-step fashion is the bond imaging AFM method, which is based on operating qPlus sensors under UHV conditions at low temperatures with CO-functionalized tips. Here, the onset of the self-assembly process of individual partially fluorinated 1,2,10,11,12,14-hexafluoropentacene molecules on Au(111) is studied. Therefore, the molecules are first evaporated onto a cold surface (around 6K) where molecular diffusion is negligible. The formation of small clusters with closely packed molecules all facing in the same direction is induced by subsequent heating steps to temperatures up to 50K. At higher temperatures (80-300K) also larger islands form. After each heating step, the sample is cooled down to 5K for determining the precise bonding angles and length of the intermolecular F...H contacts via bond imaging AFM.

O 45.6 Wed 12:00 CHE 89

On-surface synthesis of PAHs by strain and the concerted motion of adatoms.

— •BENJAMIN MALLADA^{1,2}, BRUNO DE LA TORRE^{1,2}, JESUS I. MENDIETA-MORENO², ADAM MATEJ^{1,2}, MIKULAS MATOUSEK³, JIRI BRABEC³, LIBOR VEIS³, TIMOTHEE CADART³, MARTIN KOTORA⁴, and PAVEL JELINEK^{1,2} — ¹Czech Advanced Technology and Research Institute (CATRIN), Olomouc, Czech Republic — ²Institute of Physics, Czech Academy of Sciences, Prague, Czech Republic — ³J. Heyrovsky Institute of Physical Chemistry, Prague, Czech Republic — ⁴Department of Organic Chemistry, Charles University, Prague, Czech Republic

The kinetic control of the synthesis of polycyclic aromatic hydrocarbons (PAH) is one of the most desired features in organic synthesis. In this work, we report the synthesis and characterization by STM/nc-AFM of several PAHs from one single precursor in which two different kinetic-driven mechanisms control the possible products at high temperatures. In the first mechanism, we show that the surface-induced mechanical constraints on a strained helical reactant leads to the synthesis of planar objects with non-benzenoid rings. In the second mechanism, the chemical pathway is mediated by an unusual C-C bond cleavage of the helical reactant mediated by the concerted motion of individual gold adatoms. These observations, supported by DFT and state-of-the-art QM/MM calculations, render a scenario where the molecular internal stress and the adatoms' role enable routes to the kinetic control of selected chemical reactions.

O 45.7 Wed 12:15 CHE 89

Monitoring of molecular configurations in SPM-based molecular manipulation — JOSHUA SCHEIDT¹, ALEXANDER DIENER¹, MICHAEL MAIWORM², KLAUS-ROBERT MÜLLER³, ROLF FINDEISEN², KURT DRIESSENS⁴, F. STEFAN TAUTZ¹, and •CHRISTIAN WAGNER¹ — ¹Peter Grünberg Institut (PGI-3), Forschungszentrum Jülich, Germany — ²Control and Cyber-Physical Systems Laboratory, Technische Universität Darmstadt, Germany — ³Machine Learning Group, Technische Universität Berlin, Germany — ⁴Data Science and Knowledge Engineering, Maastricht University, The Netherlands

Molecular manipulation with the SPM tip as an actuator allows creating a wide variety of molecular junction configurations. Unfortunately, the precise atomic locations in such a junction, which strongly impact its mechanical and electronic properties, cannot be observed directly. Here, we present and benchmark an approach that enables such a configuration monitoring. It overcomes the most important challenges: the need for accurate yet fast simulations, the disparity between scalar observation quantities like a force gradient and a high-dimensional unknown molecular configuration, the vast configuration space to be searched, and the need to operate on the few-minutes time scales of typical experiments. This is achieved by combining a finite state automaton to store and rapidly access the results of atomistic molecular simulations, and a particle filter to search for likely manipulation trajectories, given an input sequence of observations. We are able to assign systematic differences in generic features in force gradient data to well-defined atomic configurations for the first time.

O 46: Electron-Driven Processes at Surfaces and Interfaces

Time: Wednesday 10:30–12:15

Location: CHE 91

O 46.1 Wed 10:30 CHE 91

On the energy transfer mechanism in hyperthermal H atom scattering from surfaces — •NILS HERTL¹, CONNOR L. BOX¹, and REINHARD J. MAURER^{1,2} — ¹Department of Chemistry, University of Warwick, UK — ²Department of Physics, University of Warwick, UK

Adsorption of atomic and molecular hydrogen on surfaces is the gateway to many important chemical processes in nature. Hence, it is important to understand their adsorption mechanism if we want to understand the relevant elementary processes of these adsorbates on surfaces.

In the recent years, a series of detailed theoretical and experimental investigations of energy transfer between H atoms and a variety of material surfaces have been performed. The investigated substrates range from noble gas surfaces with a detour to semiconductors to late fcc transition metal surfaces. Transition metal surfaces with adsorbates were investigated, too. For all studies, a UHV apparatus, specifically designed for H atom scattering, has been used. The complementary theory relies on molecular dynamics simulation, where electronic excitations are described within the framework of molecular dynamics with electronic friction. The friction coefficient is treated within the local density friction approximation (LDFA).

In this talk, I will briefly revisit those studies and on the basis of them, I will formulate a couple of general concepts relevant to atom scattering from surfaces. Furthermore, I will also present first efforts to apply methods which go beyond the framework of LDFA friction for hyperthermal H atom scattering.

O 46.2 Wed 10:45 CHE 91

Simulations of H atom scattering from p(2×2) O/Pt(111) surface with orbital-dependent friction — •CONNOR L. BOX¹, NILS HERTL¹, and REINHARD J. MAURER^{1,2} — ¹Department of Chemistry, University of Warwick, United Kingdom — ²Department of Physics, University of Warwick, United Kingdom

The experimentally recorded nonadiabatic energy loss that occurs during H atom scattering from a range of clean metal surfaces is well reproduced by the molecular dynamics with electronic friction method using effective medium theory for the potential energy surface and the local-density friction approximation for the electronic friction. [1] However, it was recently reported that this method is not capable of reproducing the inelastic scattering of H atoms on the oxygen-covered Pt(111) surface. [2] We present inelastic scattering energy loss distributions for this system with an efficient ML representation of the orbital-dependent friction coefficients calculated using linear response theory based upon density functional theory. This approach additionally accounts for the anisotropy of the electronic friction tensor and the effect of the oxygen adatom on the surface electronic structure. [1] Dorenkamp et al, JCP, 2018 [2] Lecroart et al, JCP, 2021

O 46.3 Wed 11:00 CHE 91

Power discontinuity and shift of the energy onset of a molecular debromination reaction induced by hot-electron tunneling — ANA BARRAGAN¹, ROBERTO ROBLES¹, NICOLAS LORENTE^{1,3}, and •LUCIA VITALI^{1,2,3} — ¹Centro de Física de Materiales CFM/MPC (CSIC-UPV/EHU), San Sebastián, Spain — ²Ikerbasque Research Foundation for Science, Bilbao Spain — ³Donostia International Physics Center (DIPC), San Sebastian

Understanding the mechanism of molecular dissociation under applied bias is a fundamental requirement to progress in (electro)- catalysis as well as in (opto)-electronics. The working conditions of a molecular-based device and the stability of chemical bonds can be addressed in metal*organic junctions by injecting electrons in tunneling conditions. Here, we have correlated the energy of debromination of an aryl group with its density of states in a self-assembled dimeric structure of 4'-bromo-4-mercaptobiphenyl adsorbed on an Au(111) surface. We have observed that the electron-energy range where the molecule is chemically stable can be extended, shifting the bias threshold for the rupture of the -C-Br bond continuously from about 2.4 to 4.4 V by changing the electron current. Correspondingly, the power needed for the dissociation drops sharply at 3.6 V, identifying different reaction regimes and the contribution of different molecular resonance states.

A.Barragan, R.Robles, N.Lorente, L.Vitali; *Nanoscale* 13, 15215 (2021)

O 46.4 Wed 11:15 CHE 91

Quantum transport on anisotropic surfaces revealed by MONA — •MANUEL SEITZ¹, ANDREAS CHRIST¹, MARKUS LEISEGANG¹, JACEK WALUK², and MATTHIAS BODE¹ — ¹Physikalisches Institut, Experimentelle Physik II, Universität Würzburg, Am Hubland, D-97074 Würzburg, Germany — ²Institute of Physical Chemistry, Polish Academy of Sciences, ul. Kasprzaka 44/52, 01-224 Warsaw, Poland

The ability to detect how charge carriers propagate in well-defined bands is of great importance for the exploitation of novel materials, e.g., in the context of spintronics or topological insulators. We developed the molecular nanoprobe (MONA) technique [1] to investigate the details of quantum transport. It utilizes a single molecule to detect ballistic charge carriers injected by the tip of a scanning tunneling microscope (STM). In this study, we investigate charge carrier transport in the structurally anisotropic Cu(110) surface which exhibits a surface state at the Y-point of the surface Brillouin zone [2]. We performed directional-, distance-, and energy-dependent measurements that reveal an unexpectedly rich anisotropic behavior. The results can be explained by the combined influence of the band structure-dependent transport path and the molecular excitation.

[1] Leisegang, M. et. al., *Nano Lett.* 18, 2165 (2018).

[2] Jiang, J., et. al., *Phys. Rev. B* 89, 085404 (2014).

O 46.5 Wed 11:30 CHE 91

Understanding triplet-exciton transfer dynamics at the Si-tetracene interface — •MARVIN KRENZ — Universität Paderborn

Singlet-exciton fission in a tetracene overlayer and the subsequent triplet-exciton transfer into a silicon solar cell appears as promising approach to harvest high-energy photons [1]. However, the details of the exciton transfer and its dependence on the interface atomic structure are not understood. In the present contribution we employ ab initio non-adiabatic molecular dynamics to study the exciton transfer in atomistic detail. It is found that interface defects as well as thermal activation are instrumental for the exciton transfer from the organic overlayer into the Si bulk material.

[1] J.M. Luther, J.C. Johnson, *Nature* 571, 38 (2019)

O 46.6 Wed 11:45 CHE 91

Uni-directional translation of a novel adsorbate motor — •GRANT J. SIMPSON¹, MATS PERSSON², and LEONHARD GRILL¹ — ¹University of Graz, Graz, Austria — ²University of Liverpool, Liverpool, UK

Molecular motors are fascinating objects that can undergo uni-directional motion on the nanoscale. In order to independently perform meaningful work, they typically must switch between two potential energy surfaces to achieve directed motion. However, their rather complex structures often mean that their function on a surface is hindered. Here, we present a novel 'adsorbate motor' which performs strictly uni-directional translational upon excitation from the tip of a scanning tunneling microscope - in contrast to thermally induced motion of the same molecules that follows the principle of microscopic reversibility, resulting in random movement. The resulting 100% uni-directionality is then harnessed in order to perform meaningful work exemplified by the transport of single molecules across a metal surface.

O 46.7 Wed 12:00 CHE 91

Extreme magnetoresistance in high-mobility Al₂O₃/SrTiO₃ heterostructures — •DENNIS CHRISTENSEN — Technical University of Denmark, Department of Energy Conversion and Storage, 2800 Kgs Lyngby, Denmark

The heterostructure formed by depositing spinel γ -Al₂O₃ on perovskite SrTiO₃ exhibits a range of exciting properties including room temperature epitaxial growth [1,2], high electron mobility [3,4], a strain-tunable magnetic order [5] and a reordering of the t_{2g} bands due to the broken symmetry at the spinel/perovskite interface [6]. Here, I explore the magnetotransport properties of γ -Al₂O₃/SrTiO₃ and show that it exhibits a very large magnetoresistance exceeding 80,000% at 16 T and 2 K. When increasing the magnetic field, the field dependence of the magnetoresistance transitions from quadratic to linear with no saturation observed up to 16 T. I discuss the origin of this behaviour in relation to mechanisms known to produce large, unsaturated magnetoresistance.

[1] M. von Soosten, D. V. Christensen et al. *Scientific Reports* 9, 18005 (2019).

[2] Y. Z. Chen et al. *Advanced Materials* 26, 1462 (2014).

[3] Y. Z. Chen, N. Bovet, F. Trier, D. V. Christensen, et al. *Nature Communications* 4, 1371 (2013).

[4] D. V. Christensen, et al. *Physical Review Applied* 9, 054004 (2018).

[5] D. V. Christensen, et al. *Nature Physics* 15, 269 (2019).

[6] A. Chikina, D. V. Christensen et al. *ACS Nano* 15, 4347 (2021).

O 47: 2D Materials II: Growth, Structure and Substrate Interaction I

Time: Wednesday 10:30–13:00

Location: GER 37

O 47.1 Wed 10:30 GER 37

Two-Dimensional Non-van der Waals Materials from Data-Driven Research — TOM BARNOWSKY^{1,2}, MAHDI GHORBANI-ASL¹, STEFANO CURTAROLO³, ARKADY V. KRASHENINNIKOV^{1,4}, and •RICO FRIEDRICH^{1,2,3} — ¹Helmholtz-Zentrum Dresden-Rossendorf, Dresden — ²TU Dresden — ³Duke University, Durham, USA — ⁴Aalto University, Aalto, Finland

While two-dimensional (2D) materials are traditionally derived from bulk layered compounds bonded by weak van der Waals (vdW) forces, the recent surprising experimental realization of non-vdW 2D compounds obtained from non-layered crystals [1] foreshadows a new direction in 2D systems research.

Here, we present several dozens of candidates of this novel materials class derived from applying data-driven research methodologies in conjunction with autonomous *ab initio* calculations [2,3]. We find that the oxidation state of the surface cations of the 2D sheets is an enabling descriptor regarding the manufacturing of these systems as it determines their exfoliation energy: small oxidation states promote easy peel off [2]. When extending the set from oxides to sulfides and chlorides, the exfoliation energy becomes ultra low due to strong surface relaxations [3]. The candidates exhibit a wide range of appealing electronic, optical and magnetic properties making these systems an attractive platform for fundamental and applied nanoscience.

[1] A. Puthirath Balan *et al.*, Nat. Nanotechnol. **13**, 602 (2018).

[2] R. Friedrich *et al.*, Nano Lett. **22**, 989 (2022).

[3] T. Barnowsky *et al.*, submitted (2022).

O 47.2 Wed 10:45 GER 37

Phase Transitions of the BlueP-Au-network on Au(111) by Intercalation of Potassium — PHILIP GRIMM, •FELIX OTTO, MAXIMILIAN SCHAAL, FLORENTINE FRIEDRICH, ROMAN FORKER, and TORSTEN FRITZ — Institute of Solid State Physics, Friedrich Schiller University Jena, Helmholtzweg 5, 07743 Jena, Germany

In 2014, a new elemental semiconductor was postulated: Blue Phosphorene (BlueP). This monolayer of P atoms offers a layer thickness-dependent band gap and high charge carrier mobility. However, the synthesis of a highly ordered and stable monolayer of BlueP is still a challenge and could only be achieved on gold substrates by constructing a Au-P network. This undesirable coupling, which leads to a change in electronic properties, could be mitigated by the intercalation of potassium. The goal is to synthesize a free-standing monolayer of BlueP. The effects of substrate temperature during K deposition and the order of deposition of phosphorus and potassium on Au(111) were investigated. Structural properties were characterized by LEED and RHEED, chemical properties by XPS, and electronic properties by photoelectron spectroscopy methods ((AR)UPS and PMM). In the end, a (2×2) superstructure is obtained. This superstructure exhibited the most promising electronic properties, which were very close to those of the free-standing BlueP. It is assumed that K and P together form the basis of the (2×2) superstructure, since the reactive bonds of potassium could be saturated and stabilized by phosphorus. At temperatures of 250 °C, the BlueP-Au network dissolves under the influence of potassium deposition and various intermediates are formed.

O 47.3 Wed 11:00 GER 37

Structural and chemical characterization of epitaxially grown FeBr₂ on Au(111) — •S. E. HADJADI¹, C. GONZALEZ-ORELLANA², J. LAWRENCE³, D. BIKALJEVIC^{4,5}, M. PENA-DIAZ², P. GARGIANI⁶, L. ABALLE⁶, J. NAUMANN⁷, M. A. NINO⁶, M. FOERSTER⁶, S. RUIZ-GOMEZ⁸, S. THAKUR¹, I. KUMBERG¹, J. TAYLOR⁹, J. HAYES¹, J. TORRES¹, C. LUO⁹, F. RADU⁹, D. G. DE OTEYZA³, W. KUCH¹, J. I. PASCUAL⁴, C. ROGERO^{2,3}, and M. ILYN² — ¹Freie Universität Berlin, Institut für Experimentalphysik, Germany — ²Centro de Física de Materiales, Donostia, Spain — ³Donostia International Physics Center, Spain — ⁴CIC nanoGUNE-BRTA, Donostia, Spain — ⁵Institute of Physical Chemistry, University of Innsbruck, Austria — ⁶ALBA Synchrotron Light Source, Spain — ⁷Freie Universität Berlin, Dahlem Center for Complex Quantum Systems, Germany — ⁸Max Planck Institute for Chemical Physics of Solids, Dresden, Germany — ⁹Helmholtz-Zentrum Berlin, Germany

We present structural, chemical and magnetic properties of the van-der-Waals material FeBr₂ on Au(111) with thicknesses from submonolayer to multilayer. We observe that the first layer on Au(111) shows a dominant superstructure. The chemical characterization by XPS and XAS shows that the material is growing in the same composition for different thicknesses. The magnetic characterization by XMCD reveals that the magnetic moment increases with increasing thickness.

O 47.4 Wed 11:15 GER 37

Formation of Europium transition metal surface compounds and its protection below hBN — •ALAA MOHAMMED IDRIS BAKHIT^{1,2}, KHADIZA ALI^{3,4}, ANNA A. MAKAROVA^{4,5}, IGOR PIŠ⁶, FEDERICA BONDINO⁶, and FREDERIK SCHILLER^{1,4} — ¹MPC, San Sebastián, Spain — ²Universidad del País Vasco, San Sebastián, Spain — ³Chalmers University of Technology, Göteborg, Sweden — ⁴DIPC, San Sebastián, Spain — ⁵FU Berlin, Germany — ⁶IOM-CNR, Trieste, Italy

We present a comparative study of the electronic and structural properties of hBN on curved transition metal (TM) substrates, namely, Ni, Rh and Pt crystals and their modifications after Eu intercalation. hBN was grown by CVD processes. The growth quality depends strongly on the lattice mismatch and the overlayer-substrate interaction. The interface properties could be influenced by tuning the substrate material and its step density. That was shown by hBN growth on curved crystals that feature strong (Ni), medium (Rh) or weak (Pt) substrate interaction. The structural properties were investigated by Low-energy electron diffraction (LEED) and scanning tunnelling microscopy (STM). Stable facets are formed upon hBN growth on the substrates, which are changed after Eu intercalation. A formation of Eu-TM alloy is detected. The electronic structure was characterized by X-ray photoelectron spectroscopy (XPS) and angle-resolved photoemission measurements (ARPES). We studied the possible protection of Eu by the hBN layer. We observe that Eu protection was incomplete due to defects and hBN growth boundaries which resulted in Eu oxidation.

O 47.5 Wed 11:30 GER 37

Interaction of Au and Rh metals with h-BN on Rh(111) from theoretical calculations — •KRISZTIÁN PALOTÁS — Wigner Research Center for Physics, Budapest, Hungary — ELKH-SZTE Reaction Kinetics and Surface Chemistry Research Group, Szeged, Hungary

Based on density functional theory calculations, the interaction of Au and Rh metal deposits with hexagonal boron nitride (h-BN) monolayer on a Rh(111) substrate in different model systems is studied. Significant differences in the metals' adsorption, growth and intercalation mechanisms are identified [1]. As an example, the formation of a 19-atoms Rh island in the pore of the nanomesh exhibits 3D growth, in contrast to a 2D island formation of Au [2]. We found that nitrogen vacancies and Rh show systematically lower energy barrier for atomic intercalation than boron vacancies and Au. Intercalation through the middle of a BN-divacancy provided the smallest energy barriers in our considered model systems. Our theoretical results provide a microscopic understanding of related experimental results [1].

Financial support from NKFI OTKA 124100 & 138714, the János Bolyai Research Grant of the Hungarian Academy of Sciences (BO/292/21/11) and the New National Excellence Program of the Ministry for Culture and Innovation from NKFI Fund (ÚNKP-22-5-BME-282) is gratefully acknowledged.

[1] G. Vári *et al.* submitted (2022). [2] A. P. Farkas *et al.* Appl. Catal. A Gen. **592**, 117440 (2020).

O 47.6 Wed 11:45 GER 37

Local Electronic Structure of h-BN on Pt(110) — •MARCO THALER¹, FLORIAN MITTENDORFER², ERMINDAL BERTEL¹, and LAERTE PATERA¹ — ¹Institute of Physical Chemistry, University of Innsbruck, Austria — ²Institute of Applied Physics and Center for Computational Materials Science, Vienna University of Technology, Austria

The growth of large-scale single-orientation hexagonal boron nitride (h-BN) monolayer has been recently achieved on the Pt(110) surface, exploiting the inversion of the normal substrate-adsorbate relation [1]. Here we performed Scanning Tunneling Spectroscopy to locally probe the electronic structure of h-BN and investigate the bonding configuration in detail. The moiré pattern arising from the mismatch with the substrate is observed to induce a modulation of the conduction band onset of h-BN and a shift of the Pt-related state, implying varying interaction energies. In agreement with density functional theory, the local density of states near the Fermi energy indicates a localized covalent bonding between h-BN and Pt, causing a $(1 \times n)$ -missing row reconstruction of the Pt(110) surface. [1] D. Steiner, *et al.*, ACS Nano, **13**, 7083-7090 (2019).

O 47.7 Wed 12:00 GER 37

Chemical vapor deposition of high optical quality large area monolayer Janus transition metal dichalcogenides — •A. GEORGE¹, Z. GAN¹, I. PARADISANOS², A. ESTRADA-REAL², J. PICKER¹, E. NAJAFIDEHAGHANI¹, F. DAVIES³, C. NEUMANN¹, C. ROBERT², K. WATANABE⁴, T. TANIGUCHI⁴, X. MARIE², J. BISKUPEK⁵, M. MUNDSZINGER⁵, R. LEITER⁵, U. KAISER⁵, A. KRASHENINNIKOV³, B. URBASZEK², and A. TURCHANIN¹ — ¹Friedrich Schiller University Jena, Jena, Germany — ²Université de Toulouse, Toulouse, France — ³Helmholtz-Centre Dresden Rossendorf, Dresden, Germany — ⁴National Institute for Materials Science, Tsukuba, Japan — ⁵University of Ulm, Ulm, Germany

Large scale chemical vapor deposition growth of Janus SeMoS monolayers is reported, with the asymmetric top (Se) and bottom (S) chalcogen atomic planes with respect to the central transition metal (Mo) atoms. The formation of these 2D semiconductor monolayers takes place upon the thermodynamically driven exchange of the bottom Se atoms of the initially grown MoSe₂ single crystals on gold foils with S atoms. The growth process is characterized by complementary experimental techniques including Raman and X-ray photoelectron spectroscopy, transmission electron microscopy, and the growth mechanisms are rationalized by first-principles calculations. The remarkably high optical quality of the synthesized Janus monolayers is demonstrated by optical and magneto-optical measurements which reveal the strong exciton-phonon coupling and enable to obtain an exciton g-factor of -3.3. (Adv. Mater. 34, 2022, 2205226)

O 47.8 Wed 12:15 GER 37

Preparation and characterization of carborane based nanomembranes — •MARTHA FREY¹, JULIAN PICKER¹, JAKUB VIŠŇÁK², CHRISTOF NEUMANN¹, TOMÁŠ BAŠE², and ANDREY TURCHANIN¹ — ¹Friedrich Schiller University Jena, Institute of Physical Chemistry, Lessingstraße 10, 07743 Jena, Germany — ²The Czech Academy of Sciences, Institute of Inorganic Chemistry, 250 68 Husinec-Rez, c.p. 1001, Czech Republic

Carboranes are electron-delocalized molecular clusters containing boron, carbon, and hydrogen. Because of their high chemical and thermal stability as well as their structural variability, they are interesting for a wide range of applications including nanoscale engineering, catalysis, and boron neutron capture therapy. Here, we present the fabrication of a novel boron-based two-dimensional (2D) material *via* electron irradiation induced cross-linking of carborane self-assembled monolayers (SAMs) on silver substrates. Using the double-cage molecule 1,2-dicarba-*closo*-dodecaborane-9,12-dithiol, the fabrication of a mechanically stable and continuous ~1 nm thin membrane was achieved. The self-assembly, cross-linking and transfer of the resulting nanomembranes onto grids have been characterized with different complementary surface-sensitive techniques including X-ray photoelectron spectroscopy (XPS), low-energy electron diffraction (LEED), ultraviolet photoelectron spectroscopy (UPS) and scanning electron microscopy (SEM).

O 47.9 Wed 12:30 GER 37

A Metastable Pentagonal 2D Material Synthesized by Symmetry-Driven Epitaxy — •LINA LIU^{1,2} and YONG CHEN^{1,2} — ¹Department of Physics and Astronomy, Purdue University, West Lafayette, Indiana, 47907, USA — ²Institute of Physics and Astronomy and Villum Centers for Dirac Materials and for Hybrid Quantum Materials and Devices, Aarhus University, 8000 Aarhus-C, Denmark

Most two-dimensional (2D) materials experimentally studied so far have hexagons as their building blocks. Only a few exceptions, such as PdSe₂, are lower in energy in pentagonal phases and exhibit pentagons as the building blocks. Such pentagonal 2D materials demonstrate unprecedented properties and unique applications originated from low-symmetry lattice geometries. While theory has predicted a large number of pentagonal 2D materials, many of them are metastable and their experimental realization is difficult. Here, we report the first synthesis of a metastable pentagonal 2D material, the pentagonal PdTe₂ monolayer, by symmetry-driven epitaxy. Scanning tunneling microscopy is used to characterize the monolayer pentagonal PdTe₂, which demonstrates well-ordered low-symmetry atomic arrangements. Theoretical calculations, along with angle-resolved photoemission spectroscopy, reveal the band structures of monolayer pentagonal PdTe₂. In contrast to the narrow bandgap of monolayer hexagonal PdTe₂, monolayer pentagonal PdTe₂ is a semiconductor with a much bigger indirect bandgap of 1.08 eV. Our work opens an avenue for the synthesis of new, pentagon-based 2D materials and gives great opportunities to explore their applications such as multifunctional electronics.

O 47.10 Wed 12:45 GER 37

The transformation of 2D honeycombs into dodecagonal quasicrystals — •STEFAN FÖRSTER, LOI VINH TRAN, MARTIN HALLER, SEBASTIAN SCHENK, and WOLF WIDDRA — Institute of Physics, Martin-Luther-Universität Halle-Wittenberg, 06120 Halle, Germany

Oxide quasicrystals are 2D materials with an aperiodic dodecagonal symmetry [1]. Starting from a binary oxide Ti₂O₃ honeycomb structure on Pt(111), the Ti_nO_n ring structure with n=6 is transformed into a network of rings with ring sizes of n= 4, 5, 7 and 10 in the presence of Ba atoms. In these networks, n=7 rings host one Ba atom and n=10 rings host two [23].

In this contribution, the basic mechanisms for the network transformation are discussed. Stone-Wales transformations are the key mechanism to realize n=4...7 rings. In addition, by incorporating an additional oxygen atom, two neighboring n=6 rings convert into a n=10 ring [3]. The amount of Ba controls this conversion process and leads to a sequence of long-range ordered structures including a well-defined quasicrystal.

[1] S. Förster, K. Meinel, R. Hammer, M. Trautmann, and W. Widdra, Nature **502**, 215 (2013)

[2] E. Cockayne et. al, Phys. Rev. B **93**, 020101(R) (2016)

[3] S. Schenk, O. Krahn, E. Cockayne, H. L. Meyerheim, M. DeBoissieu, S. Förster, and W. Widdra, Nat. Commun, accepted (2022)

O 48: Focus Session: Semiconductor Surface Chemistry – from Reaction Mechanisms to Well-Ordered Interfaces I

The interest in the properties of semiconductor surfaces and chemical reactions on these surfaces is driven by a large range of current and future applications. They are spanning from conventional microelectronics over molecular electronics, atomic scale and quantum devices to photo(-electro)-chemical processes for large-scale synthesis of chemicals such as hydrogen and ammonia. In this focus session, the wide variety of topics in semiconductor surface chemistry is illustrated in the same way as the common aspects of the field are emphasized. In particular, the question how to control the reactivity on semiconductor surfaces, which is typically governed by the high localization of charge at the surface dangling bonds, will be addressed for the different systems. A larger part of the session will be dedicated to the reaction of organic molecules on semiconductor surfaces and how the control of these reactions can lead to the synthesis of ordered organic architectures with well-controlled properties on semiconductor surfaces.

Organizer: Michael Dürr (U Giessen)

Time: Wednesday 10:30–12:15

Location: GER 38

Topical Talk

O 48.1 Wed 10:30 GER 38

Surface functionalization of semiconductors: Introducing spectroscopic labels, monolayer control for ultra-shallow doping, and providing surface passivation for atomically-precise processes — •ANDREW TEPLYAKOV — 112 Lamont DuPont Laboratory, Department of Chemistry and Biochemistry, University of Delaware, Newark, DE 19716, USA

Over the last several decades, chemistry for surface functionalization of semiconductors went through a number of directional changes that were largely dictated by the technology development. Some of the recent work in our group has been targeting modification of both flat surfaces and the surfaces of nanoparticulate semiconductor materials to introduce spectroscopic labels, provide monolayer control for ultra-shallow doping, and also to control the passivation of surfaces for atomically-precise processes. This presentation will start with applying the basic principles of surface chemical design to silicon surfaces. Specifically, I will cover the solution reactions of boron- and nitrogen-containing compounds with hydrogen- and chlorine-terminated silicon surfaces. Parallels and major

differences between the chemistry of (100) and (111) crystal faces of silicon will be examined. The reactions of the same surfaces with metalorganic precursor molecules will be presented to evaluate the role of minority sites (defects) in atomically-precise processing. Finally, the parallels between surface chemical modification of flat silicon surfaces and metal oxide nanomaterials will be examined and the challenges in connecting physical and chemical properties of these materials will be evaluated.

O 48.2 Wed 11:00 GER 38

Theoretical studies on surface stabilities of FeCuO₂ and CuBi₂O₄ — •JULIAN BESSNER, STEFANIE BOGENRIEDER, BJÖRN KIRCHHOFF, and TIMO JACOB — Ulm University, Institute of Electrochemistry, D-89081 Ulm

Ammonia is the most important component in fertilizers, as 80% of the worldwide production goes into fertilizers.[1] Currently, the energetically expensive Haber-Bosch process is used to break the triple bond of N₂. In the last years, the photoelectrochemical (PEC) reduction of nitrogen has gained attention, pro-

viding a more affordable and sustainable ammonia production. To this end, CuFeO_2 and CuBi_2O_4 are investigated as materials for photocathodes as promising alternatives for the conversion of solar energy into chemical fuels.[2, 3] So far, most theoretical and experimental studies on these materials had focused on bulk properties. Here, we perform Density Functional Theory calculations (DFT+U) to analyze their electronic properties, thermodynamic stability of different surfaces and adsorption energy trends for the nitrogen reduction reaction (NRR) intermediates. Additionally, the influence of an aqueous surrounding on the stability of the surfaces and reaction intermediates thereon will be investigated using the hybrid QMMM simulation approach (SAFIRES) implemented in ASE and GPAW, which to this end will be extended to be compatible with periodic surface models.

[1] Smil, V. *Nature* 400, 1999, 415.

[2] Jiang, C.-M. et al. *Chem. Mater.*, 31, 7, 2019, 2524-2534

[3] Ferri, M. et al. *ACS Catalysis* 11 (4), 2021, 1897-1910.

Topical Talk

O 48.3 Wed 11:15 GER 38

Growth of organic monolayers on Si(111) — •MARTIN FRANZ — Technische Universität Berlin, Institut für Festkörperphysik, Berlin, Germany

The ever-growing number of semiconductor based applications leads to an increasing demand for a modification or functionalization of surfaces with organic molecules. However, while the formation of self-assembled monolayers of organic molecules is well established on metal surfaces, the high density of dangling bonds present on most clean semiconductor surfaces typically reduces the mobility of molecules preventing an ordered growth. A route to overcome this constraint is the modification of the surface, allowing to precisely adjust the substrate-molecule interaction enabling a controlled growth.

In this talk, examples of organic films on modified Si(111) surfaces are given, which were investigated using scanning tunneling microscopy as well as tunneling and photoelectron spectroscopy. A prominent example in this regard is the boron-modified Si(111) $\sqrt{3} \times \sqrt{3}R30^\circ$ -B surface. Here, results for N-heterocyclic carbenes, which form highly ordered monolayers with promising properties [1], and for cobalt phthalocyanine [2-3] are discussed. Further examples given include the influence of surface defects on the molecular adsorption process and the use of indium-modified Si(111) as substrate [4].

[1] M. Franz et al., *Nat. Chem.* 13, 828 (2021).

[2] S. Lindner et al., *Phys. Rev. B* 100, 245301 (2019).

[3] H. Aldahhak et al., *Phys. Rev. B* 103, 035303 (2021).

[4] M. Kubicki et al., *Appl. Phys. Lett.* 119, 133105 (2021).

O 48.4 Wed 11:45 GER 38

Organic molecular architectures synthesized by means of solution-based click chemistry on functionalized silicon surfaces — •TIMO GLASER¹, JAN-NICK ALEXANDER PETERS¹, CHRISTIAN LÄNGER¹, DOMINIK SCHARF², JANNICK MEINECKE², ULRICH KOERT², and MICHAEL DÜRR¹ — ¹Institut für Angewandte Physik und Zentrum für Materialforschung, Justus-Liebig-Universität Giessen, Germany — ²Fachbereich Chemie, Philipps-Universität Marburg, Germany

The application of organic click chemistry to selectively functionalized silicon surfaces may open the route to synthesizing new organic molecular architectures on silicon. However, this scheme seems to be an experimental contradiction since click reactions are performed in the presence of a catalyst dissolved in a solvent whereas the highly reactive Si(001) surface is prepared and stored under UHV conditions. Here we show how to combine surface functionalization performed under UHV conditions with solution-based alkyne-azide click reactions. The UHV-based functionalization of Si(001) was realized via chemoselective adsorption of ethynyl cyclopropyl cyclooctyne (ECCO) from the gas phase. The samples were then directly transferred from UHV into the reaction solution where alternating layers of bisazide and bisalkyne were coupled subsequently step by step without exposure to ambient conditions. Each reaction step was monitored by means of XPS in UHV and the selectivity of the reaction schemes in use was demonstrated. Using optimized copper(I) catalysts, reaction yields of up to 75 % were obtained.

O 48.5 Wed 12:00 GER 38

Towards Ab Initio Design of Internal Interfaces - The Adsorption of Cyclooctyne on Semiconductor Surfaces — •HENDRIK WEISKE and RALF TONNER-ZECH — Universität Leipzig, Germany

Modern Society is massively influenced by technological progress, specifically the development of the electronics industry. The controlled functionalization of semiconductor interfaces with organic molecules offers new possibilities to advance the application range of classical semiconductors. The chemoselective attachment of multifunctional organic molecules is the first step in forming well-defined organic/semiconductor interfaces.

Previously, we investigated the functionalization of Si(001) surfaces extensively [1,2]. This research focussed on bifunctional cyclooctyne, which attaches to Si(001) via its strained triple bond. This work is extended here to various semiconducting substrates, such as Ge(001), to predict new and promising interfaces. The reactivity and fundamental bonding interactions are studied using various computational methods, such as the pEDA, AIMD, and NEB.

We acknowledge funding from the DFG via SFB1083.

[1] F. Pieck, R. Tonner-Zech, *Molecules* 2021, 26, 6653

[2] L. Pecher, S. Schmidt, R. Tonner, *J. Phys. Chem. C*, 2017, 121, 26840-26850

O 49: Plasmonics and Nanooptics I: Fabrication and Application

Time: Wednesday 10:30–12:45

Location: WIL A317

O 49.1 Wed 10:30 WIL A317

Towards dynamic holograms with electrically switchable polymer metasurfaces: materials aspects — •DOMINIK LUDESCHER, JULIAN KARST, MARIO HENTSCHEL, and HARALD GIESSEN — 4th Physics Institute and Research Center SCoPE, University of Stuttgart, Germany

Holography is considered as an innovative technology that is predicted to have a significant impact on numerous fields of application such as virtual, mixed, augmented reality, medical technology, and future displays. Overlaying digital information with the real world is the general concept of augmented reality. Yet, for concepts such as 3D holographic video conferencing or surgery planning, high-resolution and high-performance dynamic holograms are inevitable. To achieve this goal, nanophotonic plasmonic approaches are considered as a very promising platform. Here, we introduce active plasmonic metasurfaces for dynamic holography based on electrically switchable metallic polymer nanoantennas. The used polymer material incorporates a metal-to-insulator phase transition in the infrared spectral range which is driven by CMOS compatible voltages of only +/-1 V. In combination with possible pixel sizes below 1 micron, this makes the polymer metasurface ideally suited for holographic display applications. Additionally, using variable angle spectroscopic ellipsometry, we investigate the optical properties of such metallic polymers. In particular, we analyze their complex dielectric function and the associated zero epsilon region around the plasma wavelength. This will lay the foundation to shift the plasmonic metasurface operation to the visible spectral range.

O 49.2 Wed 10:45 WIL A317

Sampling polar THz nearfields using nonpolar Stark-effect — •MORITZ B. HEINDL¹, NICHOLAS KIRKWOOD², TOBIAS LAUSTER³, MARKUS RETSCH³, PAUL MULVANEY², and GEORG HERINK¹ — ¹Experimental Physics VIII, University of Bayreuth, Germany — ²ARC Centre of Excellence in Exciton Science, School of

Chemistry, University of Melbourne, Australia — ³Physical Chemistry I, University of Bayreuth, Germany

Quantum-Probe Field Microscopy (QFIM) enables the imaging of ultrafast THz nearfield waveforms with a conventional fluorescence microscope at optical resolution [1]. Although the underlying quantum-confined Stark-effect scales quadratically in typical configurations, we are able to resolve the full polarity of the THz nearfields utilizing alternative approaches. Specifically, we employ a carrier-envelope phase shift of the driving THz waveform or external biasing of the THz nearfield, as we discuss in this contribution.

[1] Heindl, M. B. et al. *Light Sci. Appl.* 11, 5 (2022)

O 49.3 Wed 11:00 WIL A317

Double resonant, monocrystalline plasmonic gratings evolutionary optimized for enhanced SERS sensing — •THORSTEN FEICHTNER¹, KATJA HÖFLICH², ENNO SCHATZ¹, AMRO SWEDAN³, PAUL MÖRK¹, and MUHAMMAD BASHOUTI^{3,4} — ¹Nanooptics & Biophotonics Group, Experimental Physics 5, RCCM, JMU Würzburg, Am Hubland, D-97074 Würzburg, Germany — ²Photonic Quantum Technologies, FBH gGmbH Leibniz-Institut für Höchstfrequenztechnik, Gustav-Kirchhoff-Str. 4, D-12489 Berlin, Germany — ³IKI for Nanoscale Science & Technology, BGU of the Negev, Beer-Sheva 8410501, Israel — ⁴Department of Solar Energy and Environmental Physics, SIDEER, J. Blaustein Institutes for Desert Research, BGU of the Negev, Midreshet Ben-Gurion, 8499000, Israel

Surface enhanced Raman spectroscopy (SERS) is an extremely sensitive non-linear method to detect vibrational energy levels of molecules using visible light. However, most SERS substrates available today are quite inhomogeneous.

Here we provide experimental evidence of an efficient and homogeneous SERS substrate consisting of numerically evolutionary optimized two-dimensional gratings made from straight monocrystalline metal wires. The combination of

grating resonance and plasmonic gap resonance allows to enhance both excitation of the molecules and emission of the Raman signal, which have to be treated separately to unlock the full potential of SERS. Many experiments comparing gratings, materials and analytes will be presented to illustrate the underlying physical mechanisms and the huge potential for applications.

O 49.4 Wed 11:15 WIL A317

Topological insulating phase in non-Hermitian plasmonic waveguide arrays — •HELENE WETTER¹, STEFAN LINDEN¹, and JULIAN SCHMITT² — ¹Physikalisches Institut, Universität Bonn, Kreuzbergweg 24, 53115-Bonn, Germany — ²Institut für Angewandte Physik, Universität Bonn, Wegelerstr. 8, 53115-Bonn, Germany

Arrays of evanescently coupled plasmonic waveguides are a powerful platform to investigate topological properties of one-dimensional lattices. The underlying principle is the mathematical equivalence between the single-particle tight-binding Schrödinger equation and the coupled mode equation. By tailoring the loss distribution, we utilize non-Hermiticity as a new approach to induce topological phases in otherwise trivial systems. We employ dielectric loaded surface plasmon polariton waveguides fabricated on a thin gold film. Additional losses are introduced to specific waveguides by deposition of a thin layer of chromium below the respective waveguides. Considering a unit cell of four waveguides, a topologically nontrivial lattice can be created by adding an equal amount of losses to the two central waveguides of the unit cell. In contrast, losses on either the first or the last two waveguides of a unit cell correspond to a trivial lattice. Using leakage radiation microscopy, we observe localized states at the edge of the nontrivial lattice (edge mode) as well as at the interface between the nontrivial and the trivial lattice (interface mode). Conversely, the trivial lattice does not provide a localized edge mode. Thus, the topological properties can solely be controlled by the design of the unit cell.

O 49.5 Wed 11:30 WIL A317

Plasmonics of Silica Encapsulated Au@Ag Nanoparticles — •JOHANNES SCHULTZ¹, FELIZITAS KIRNER², PAVEL POTAPOV¹, BERND BÜCHNER^{1,3}, AXEL LUBK^{1,3}, and ELENA STURM² — ¹Leibniz-Institut für Festkörper- und Werkstoffforschung Dresden e. V., Helmholtzstraße 20, 01069 Dresden — ²Department of Chemistry, University of Konstanz, Universitätsstraße 10, 78457 Konstanz — ³Institute of Solid State and Materials Physics, Haeckelstraße 3, 01069 Dresden

Localized Surface Plasmons (LSPs) are collective charge oscillations arising at interfaces between media of opposite sign of the corresponding dielectric functions. Here, spatial confinement of the LSPs, e.g. in nanoparticles (NPs), may lead to resonant amplification of the corresponding electromagnetic (e.m.) fields. This effect is exploited in several application, e.g., surface enhanced Raman spectroscopy or plasmonic solar cells. Depending on the application, this requires specific control of the spectral positions of the LSPs. Since the latter depend on both, the dielectric function of the NP and the surrounding, tuning of the LSPs can be realized by varying the dielectric environment of the NP. Here, a novel synthesis method was used to encapsulate silver nanocubes with silica layers of uniform and adjustable thickness in the range between 8 and 22 nm to tune the dielectric environment and hence the excitation energies of the LSPs with high precision over a broad spectral range between 2.55 and 3.25 eV. Furthermore, resonant coupling between Mie-type resonances at the silica-vacuum interface and the LSPs was found which leads to an e.m. field enhancement in the range of 100 %.

O 49.6 Wed 11:45 WIL A317

Strain-driven thermal and optical instability in Ag/a-Si hyperbolic metamaterials — •LEA FORSTER^{1,2}, JOSE L. OCANA-PUJOL¹, RALPH SPOLENAK¹, and HENNING GALINSKI¹ — ¹Laboratory of Nanometallurgy, ETH Zurich, Switzerland — ²Laboratory for Multifunctional Ferroc Materials, ETH Zurich, Switzerland

In a hyperbolic metamaterial system of silver/amorphous-silicon multilayers we investigated the thermal instability which arises upon heating. Our analysis demonstrates that this instability is governed by the minimization of interfacial energy and anisotropic elastic strain energy caused by the mismatch of thermal expansion coefficients. Interestingly, the stacking order of the multilayer influences which of these two energy contributions dominates. We observed this behavior by a combination of FIB-SEM tomography, finite element simulations, and optical spectroscopy. Our results show that the thermal instability initiates at 300 °C, while the hyperbolic dispersion despite increased structural

disorder persists up to 500 °C. These findings can lead to a better understanding of thermal instabilities in multilayers and may assist in the design of hyperbolic metamaterials for high-temperature applications.

O 49.7 Wed 12:00 WIL A317

Optical grating couplers for the excitation of Bloch surface waves — •SEBASTIAN HENN, MARIUS GRUNDMANN, and CHRIS STURM — Universität Leipzig, Faculty of Physics and Earth Sciences, Felix Bloch Institute for Solid State Physics, Linnéstr. 5, 04103 Leipzig, Germany

In this contribution we demonstrate experimentally the control of the propagation of Bloch Surface Waves (BSW) in the transparent spectral range. BSW exist along the interface of a distributed Bragg reflector (DBR) with a thin top layer of a specified thickness to the ambient. Using shallow optical diffraction gratings with a sub-micron lattice constant, incident light is coupled into and out of the Bloch modes, which propagate along the surface between the gratings. The low-loss nature of evanescent BSW leads to long-range lateral propagation, on the order of micrometers, making this an interesting candidate for on-chip devices, for example by coupling to excitons, i.e. exciton-polariton applications. We give an overview of the fabrication processes as well as the results regarding the optical excitation of BSW by means of imaging ellipsometry, which is supported by rigorous coupled-wave analysis modelling.

O 49.8 Wed 12:15 WIL A317

Reconfigurable and polarization-dependent perfect absorber for large-area emissivity control based on the plasmonic phase-change material In₃SbTe₂ — •LUKAS CONRADS¹, NATALIE HONNÉ¹, ANDREAS ULM², ANDREAS HESSLER¹, MATTHIAS WUTTIG¹, ROBERT SCHMITT², and THOMAS TAUBNER¹ — ¹Institute of Physics (IA), RWTH Aachen University — ²Fraunhofer IPT

Metasurfaces with perfect infrared absorption promise integrated filters and compact, tailorable detector elements for thermal radiation. Phase-change materials (PCMs) are prime candidates for active, non-volatile absorption tuning [1]. In this work, we show flexible encoding of different absorption/emission properties within a metasurface. We employ the plasmonic PCM In₃SbTe₂ (IST) [2] to obtain control over the emissivity by patterning an adaptable perfect absorber metasurface. Using a commercial direct laser writing setup, we locally switch the IST from an amorphous dielectric into a crystalline metallic state and write nanoscale stripe gratings of cm-size above a reflecting mirror. We demonstrate modification of already written patterns by changing the laser power and thus the IST stripe width to encode different polarization-sensitive patterns with nearly perfect absorption into the same metasurface. Finally, we measure an apparent local temperature pattern due to our large-area emissivity shaping metasurface with a conventional thermal camera [3]. Our results pave the way towards low-cost, large-area and adaptable patterning of metasurfaces.

[1] Wuttig et al. *Nat. Photon.* **11**, 465 (2017) [2] Heßler et al. *Nat. Commu.* **12**, 924 (2021) [3] Conrads et al. *Adv. Opt. Mat.* submitted

O 49.9 Wed 12:30 WIL A317

Sensing at the ultimate volume limit: Refractive index sensing in attoliter volumes using Mie voids — •SERKAN ARSLAN¹, HUONG TRAN¹, JULIAN KARST¹, LIDA SHAMSAFAR¹, THOMAS WEISS², HARALD GIESSEN¹, and MARIO HENTSCHEL¹ — ¹4th Physics Institute and Research Center SCoPE, University of Stuttgart, Stuttgart, Germany — ²Institute of Physics, University of Graz, and NAWI Graz, 8010 Graz, Austria

Traditional nanophotonic sensing schemes utilize dielectric or metallic nanoparticles, which confine far-field radiation in dispersive and lossy media. Apart from ill-defined sensing volumes and moderate sensitivities, these structures suffer from the generally limited access to the modal field, which is key for sensing performance. Recently, a novel strategy for dielectric nanophotonics has been demonstrated, namely, the resonant confinement of light in air. Voids created in high-index dielectric host materials support localized resonant modes with exceptional properties. In particular, due to the confinement in air, these structures benefit from the full access to the modal field inside the void. We utilize these so-called Mie voids for refractive index sensing on the single void level with unprecedented small sensing volumes in the range of 100 attoliter and sensitivities on the order of 500 nm per refractive index unit. Strikingly, the sensitivity as well as the scattering cross sections of the voids are large enough to even identify different analytes with bare eye in an optical microscope. The combination of our Mie void sensor platform with appropriate surface functionalization will even enable specificity to biological or other analytes of interest.

O 50: Spins on Surfaces at the Atomic Scale IV

Time: Wednesday 10:30–11:30

Location: REC C 213

O 50.1 Wed 10:30 REC C 213

Growth and magnetism of ultrathin Fe films on Ta(110) — •REINER BRÜNING, ROBERTO LO CONTE, KIRSTEN VON BERGMANN, and ROLAND WIESENDANGER — Institut für Nanostruktur- und Festkörperphysik, Universität Hamburg

The field of hybrid systems, where magnetism and superconductivity are interacting with each other, is a field which is attracting more and more attention in recent years. Spin-polarized scanning tunneling microscopy (SP-STM) is an ideal tool to study the magnetic as well as the superconducting properties and investigate the interplay between each other.

Here, we investigate ultrathin Fe films on the anisotropic (110) surface of the elemental superconductor Ta by SP-STM. For the pseudomorphic Fe monolayer, theory has predicted [1] interesting magnetic ground states depending on the interlayer distance [1], e. g. a magnetic spin spiral with a period of 6 nm.

We observe pseudomorphic growth for sub-monolayer coverage, however, for higher coverage we find several different structures. Two of these three different reconstructions have been observed previously also for Fe on Nb(110) [2]. For the pseudomorphic Fe monolayer on Ta(110), we indeed find a spin spiral with a period of roughly 6 nm as the magnetic ground state at zero field.

[1] L. Rózsa *et al.*, Phys. Rev. B, **91**, 144424 (2015) [2] J. Goedecke *et al.*, ACS Nano, **16**, 14066-14074 (2022)

O 50.2 Wed 10:45 REC C 213

Spin polarization in polyaniline molecules: the role of coupling, chirality and coordination — •T. N. HA NGUYEN¹, L. L.T. BACZEWSKI², and C. TEGENKAMP¹ — ¹Solid Surface Analysis, Technische Universität Chemnitz, Germany — ²Institute of Physics, Polish Academy of Sciences, Al. Lotnikow, Warszawa, Poland

Propagation of electrons along helical polyaniline-based backbone structures comes along with a robust spin polarization effect. However, studies on a molecular scale are still rare, although this length scale provides direct insight into the role of molecular properties. The self-assembly process and electronic transmission properties of race-mats of right and left handed π -helix polyaniline (DL-PA) molecules from solution on atomically smooth and magnetically switchable Al₂O₃/Pt/Au/Co/Au substrates was investigated by ambient scanning tunneling microscopy and spectroscopy. For various lengths of molecules with and without a cysteine termination, we studied the spin polarization in detail. The phase separation into well-ordered enantiopure hexagonal phases and hetero-dimer structures (DL-PA) allow for the analysis of the spin polarization of PA molecules in different environments. The spin polarization reaches up to 70% for chemisorbed molecules arranged in an hexagonal phase. Our results clearly demonstrate that both the coupling as well as the ordering and coordination are important in order to achieve a high spin-polarization in chiral systems.

O 50.3 Wed 11:00 REC C 213

Robust Monolayers of Endohedral Fullerenes: Towards Highly Ordered Arrays of Single Molecule Magnets and Spin Qubits — •LUKAS SPREE¹, LUCIANO COLAZZO¹, CAROLINE HOMMEL¹, ANDREAS HEINRICH¹, and ALEXEY POPOV² — ¹IBS Center for Quantum Nanoscience, Seoul, South Korea — ²Leibniz Institute for Solid State and Materials Research

In 2012 DySc₂N@C₈₀ was the first endohedral fullerene proven to be a single molecule magnet. Ten years and many fullerene based single molecule magnets later, lanthanide dimetal fullerenes show high blocking temperatures of magnetization approaching 30 K and suppression of quantum tunnelling of magnetization at zero magnetic field due to coupling of two magnetic moments via an electron in a singly occupied molecular orbital. The isostructural non-magnetic versions of these molecules with Y or Sc dimers show long T₂ times and might be promising candidates for spin qubits. A great advantage of fullerene based molecules is their exceptional chemical stability.

For future research the deposition of fullerene based single molecule magnets in ordered layers is desirable to control intermolecular interactions and ease measurements with scanning probe techniques. Several causes for disorder can be identified and one approach to counteract them is chemical functionalization of the fullerene cage to promote self-assembly of monolayers. A challenge with the direct deposition of functionalized fullerenes on a substrate is a mismatch of the distance between potential binding sites and the size of the fullerenes. Therefore, templating with tetrapyrrole complexes is investigated.

O 50.4 Wed 11:15 REC C 213

Tuning the magnetic properties of self-assembled molecular networks on Au(111) and graphene — •ADAM J. WATSON, KOEN HOUTSMA, MIHAELA ENACHE, ANTONIJA GRUBIŠIĆ ČABO, and MEIKE STÖHR — Zernike Institute for Advanced Materials, University of Groningen, 9747 AG, Groningen, The Netherlands

The ability to manipulate the spin state of low dimensional magnetic networks is of emerging interest and forms the basis of prospective technologies in the atomic limit. These include molecule-based quantum computers and spintronic devices, which require addressable spin architectures. Recently, two-dimensional (2D) networks have been prepared using the methods of on-surface supramolecular self-assembly, exhibiting a variety of different magnetic exchange interactions which are experimentally accessible. [1]

In this work, we performed scanning tunnelling spectroscopy (STS) and x-ray magnetic circular dichroism (XMCD) measurements to characterize the magnetic properties of self-assembled networks of a cyano-functionalized cobalt-porphyrin derivative (CoTCPP) on Au(111) [2] and graphene. Kondo and XMCD measurements indicate a variation in spin-substrate coupling with bonding motif, and variations in magnetic moment and spin distribution. These results highlight the importance of the bonding motif within supramolecular architectures, and the role of the substrate, in tuning molecular magnetism.

[1] Girovsky, J. *et al.*, Nat. Comm. **8** (2017) 15388

[2] B. D. Baker Cortes *et al.*, J. Phys. Chem. C **123** (2019) 19681

O 51: Surface Magnetism

Time: Wednesday 11:30–13:00

Location: REC C 213

O 51.1 Wed 11:30 REC C 213

Turning by hydrogen adsorption an exchange frustrated spin-spiral into elliptical magnetic skyrmions — TIMO KNISPEL¹, VASILY TSEPLYAEV², MARKUS HOFFMANN², GUSTAV BIHLMAYER², STEFAN BLÜGEL², THOMAS MICHELY¹, and •JEISON FISCHER¹ — ¹II Physikalisches Institut, Universität zu Köln, Zülpicher Str. 77, 50937 Cologne, Germany — ²Peter Grünberg Institut and Institute for Advanced Simulation, Forschungszentrum Jülich GmbH, 52425 Jülich, Germany

Spin-spiral states may emerge either from the frustration of Heisenberg-type exchange interactions or from the competition of exchange and the relativistic Dzyaloshinskii-Moriya interaction resulting in atomic scale and mesoscale textures, respectively. However, to turn frustration-stabilized spin-spirals into skyrmions, high magnetic fields are required, hardly achievable in the lab. We report on a new principle using hydrogen adsorption to unwind an exchange-stabilized spin-spiral into skyrmions at accessible fields. With spin-polarized scanning tunneling microscopy we identify an atomic scale right-handed Néel-type spin spiral on the double layer Fe on Ir(110). Density functional theory calculations confirm the spin spiral is mainly frustration-stabilized with a formation energy of -12 meV/Fe with respect to ferromagnetic state. A field of the order of 80 T would be required to unwind the spin spiral. After adsorption of hydrogen, we observe that the nature of the spin spiral becomes of Dzyaloshinskii-type

with a seven times longer period. Elliptical skyrmions can be formed at moderate magnetic fields.

O 51.2 Wed 11:45 REC C 213

Aging in the self-induced spin glass Nd(0001) — •LORENA NIGGLI, JULIAN H. STRIK, ANAND KAMLAPURE, MIKHAIL I. KATSNELSON, DANIEL WEGNER, and ALEXANDER A. KHAJETOORIANS — Institute for Molecules and Materials, Radboud University, Nijmegen, the Netherlands

Elemental neodymium has been shown to be a self-induced spin glass, where glassy behaviour stems solely from the frustrated nature of the magnetic interactions [1]. This is in contrast to traditional spin glasses, where the presence of disorder is essential toward realizing glassy behaviour. The magnetic state of Nd(0001) is characterized by a lack of long range order, but exhibits local non-collinear order (Q-states). Upon increasing the temperature, neodymium displays an unusual magnetic phase transition from a self-induced spin glass to a long-range ordered multi-Q phase [2]. Here, we explore the aging behaviour of Nd(0001) in its self-induced spin glass state using spin-polarized scanning tunneling microscopy in varying magnetic fields and variable temperature. We explore how the favourability of the Q-states evolves as we age the system and relate these changes to the preferred structure of the ordered phase. These observations indicate that neodymium may be a multi-well system, which deviates

from the traditional energy landscape expected of prototypical spin glass systems, thus providing a new platform to study aging dynamics as well as dynamic heterogeneity.

[1] U. Kamber et al., *Science* **368** (2020).

[2] B. Verlhac et al., *Nat. Phys.* **18** (2022).

O 51.3 Wed 12:00 REC C 213

Magnetic Phase Transition in MoS₂ detected with AFM — ALEXINA OLLIER^{1,2}, AKASH GUPTA¹, MARCIN KISIEL¹, MEHDI RAMEZANI^{1,2}, ANDREAS BAUMGARTNER^{1,2}, CHRISTIAN SCHÖNENBERGER^{1,2}, and ERNST MEYER² — ¹Department of Physics, University of Basel, Klingelbergstrasse 82, CH-4056 Basel — ²Swiss Nanoscience Institute, Klingelbergstrasse 82, CH-4056 Basel

Low doping electron-electron interactions in monolayer MoS₂ lead to a ferromagnetic spin order, whereas larger occupation of spin-polarized energy bands results in paramagnetism. The electron density of MoS₂ might be tuned with gate voltage, thus providing the switch ability of the ferromagnetic to paramagnetic first-order phase transition. Spontaneous phase transition in two-dimensional semiconductor gated MoS₂ monolayer is detected by magnetic force spectroscopy.

An abrupt and reproducible changes of the magnetic force were observed at doping concentration equal to $n_c = 3.0 \times 10^{12} \text{ cm}^{-2}$ and are attributed to ferromagnetic to paramagnetic phase change. Linear dependence of force versus external magnetic field was noted in the paramagnetic state, whereas no such dependence was found in already polarised ferromagnetic state. The extracted spin susceptibility confirms the correlated electron system and the observed hysteresis of the measured magnetic force is a strong hint for first-order type of transition.

O 51.4 Wed 12:15 REC C 213

Electron Spin-Polarizing Mechanisms in Chiral CuO and CoO_x Catalyst Surfaces — PAUL VALERIAN MÖLLERS¹, JIMENG WEI², SUPRIYA GHOSH², SOMA SALAMON³, MANFRED BARTSCH¹, HEIKO WENDE³, DAVID WALDECK², and HELMUT ZACHARIAS¹ — ¹Center for Soft Nanoscience, WWU Münster, Germany — ²Department of Chemistry, University of Pittsburgh, Pittsburgh, USA — ³Faculty of Physics and Center for Nanointegration Duisburg-Essen (CENIDE), Universität Duisburg-Essen, Germany

Spin-polarized catalytic surfaces can greatly enhance the selectivity of chemical reactions, e.g., in a photoinduced water splitting process. Here, we present new insights into the mechanisms that give rise to the spin polarization in chiral cupric oxide¹ (CuO) and cobalt oxide² (CoO_x) layers deposited using a method pioneered by Switzer et al.³ Photoelectrons were excited with deep-UV laser pulses and their average spin polarization (SP) was measured. For CuO layers, the energy dependence of the spin polarization reveals that the measured SP values can be rationalized assuming an intrinsic SP in the chiral oxide layer and a chirality-induced spin selectivity (CISS)-related spin filtering of the electrons.⁴ On chiral CoO_x layers, the SP was found to depend on the Co oxidation state, which allows for reversible switching of the preferred spin orientation. The results support efforts towards a rational design of further spin-selective catalytic oxide materials. ¹K.B. Ghosh et al., *J. Phys. Chem. C* **123**, 3024 (2019) ²S. Ghosh

et al., *J. Phys. Chem. C* **124**, 22610 (2020) ³Kothari et al., *Chem. Mater.* **16**, 4232 (2004) ⁴Möllers et al., *ACS Nano* **16**, 12145 (2022)

O 51.5 Wed 12:30 REC C 213

Magnetic circular dichroism of oxygen-passivated and bare Fe(100) in threshold PEEM — DAVID HUBER¹, FRIEDERIKE WÜHRL¹, MAXIMILIAN PALESCHKE^{1,2}, FRANK SCHUMANN³, STEFAN FÖRSTER¹, and WOLF WIDDRA¹ — ¹Institute of Physics, Martin-Luther-Universität Halle-Wittenberg, Halle (Saale), Germany — ²Institute of Atomic and Molecular Sciences (IAMS), Academia Sinica, Taipei, Taiwan — ³Max Planck Institute of Microstructure Physics, Halle (Saale), Germany

Magnetic circular dichroism (MCD) in threshold PEEM enables imaging of in-plane and out-of-plane oriented ferromagnetic domains in real and momentum space [1, 2]. Here, we compare PEEM and ARPES data for Fe(100) and the oxygen-passivated Fe(100)-(1×1)-O. Imaging the in-plane domains we observe four different asymmetry levels, which we assign to the four magnetization vectors pointing in the high symmetry directions. The observed asymmetry values vary from 3% up to 5,5% comparing Fe(100)-(1×1)-O and Fe(100). The domain-specific momentum space measurements on Fe(100) are thereby in good agreement with relativistic photoemission calculations [2]. Through off-normal photoemission we increase the sensitivity of the method by one order of magnitude in comparison to previous reports [1].

[1] Marx et al., *PRL* **84**, 5888 (2000).

[2] Henk and Johansson, *J. Electr. Spectr. Relat. Phenom.* **94**, 259 (1998).

O 51.6 Wed 12:45 REC C 213

Utilizing symmetry for magnetic domain imaging via PEEM — FRANK O. SCHUMANN¹, JÜRGEN HENK², MAXIMILIAN PALESCHKE², CHENG-TIEN CHIANG³, and WOLF WIDDRA² — ¹Max-Planck Institut für Mikrostrukturphysik, Halle, Germany — ²Institut für Physik, Martin-Luther-Universität Halle-Wittenberg, Germany — ³Institute of Atomic and Molecular Sciences, Academia Sinica, Taiwan

It is a well-established fact that the photoemission intensity depends on the polarization state of the light and magnetization direction. For a microscopic description it is vital to include both the spin-orbit and exchange interaction on an equal footing. A photoelectron emission microscope (PEEM) allows the detection of all emitted electrons in the hemisphere. The magnetic contrast is achieved by collecting intensity images with circular polarized light of different helicities. Computing the difference images reveals magnetic domains in the real space imaging mode. In the momentum imaging the angle-resolved photoemission intensity becomes accessible. Symmetry considerations dictate a relation in momentum space of the asymmetry signal from opposite domains. We illustrate these insights by photoemission calculations on an Fe(100) surface for photon energies in the threshold region. These we compare with recent experiments on an Fe(100) surface employing a PEEM in this photon energy range. We discuss the benefit of selecting a window of the momentum of electrons which reach the detector. A careful choice of the allowed momentum range of the detected electrons leads to a selectivity of the magnetization direction of domains.

O 52: Heterogeneous Catalysis and Surface Dynamics I

Time: Wednesday 10:30–12:45

Location: TRE Phy

O 52.1 Wed 10:30 TRE Phy

In-situ spectro-microscopy of single PtRh nanoparticles during oxidation — JAGRATI DWIVEDI¹, LYDIA BACHMANN^{1,2}, ARNO JEROMIN¹, LIVIU C. TĂNASE³, AARTI TIWARI³, LUCAS CALDAS³, THOMAS SCHMIDT³, THOMAS F. KELLER^{1,2}, BEATRIZ ROLDÁN CUENYA³, and ANDREAS STIERLE^{1,2} — ¹CXNS, Deutsches Elektronen-Synchrotron DESY, D-22607 Hamburg, Germany — ²Physics Department, University of Hamburg, D-20355 Hamburg, Germany — ³Department of Interface Science, Fritz-Haber-Institut der Max-Planck Gesellschaft, D-14195 Berlin, Germany

Heterogeneous catalysts are an integral part of industrial scale energy production, conversion and storage. However, a detailed understanding of how their shape, size, structural arrangement and chemical composition affect catalytic activity, selectivity and lifetime remains far from understood. The characterization under catalytic conditions remains challenging, therefore, a spectroscopic analysis of individual PtRh nanoparticles can provide direct evidence of the adsorbed species and their oxidation state. Here, we examined core-shell arranged PtRh nanoparticles on niobium-doped STO single crystals that were achieved by dewetting a homogeneous Pt film and subsequent overgrowth with Rh. Ex situ Scanning Auger Microscopy before and after the oxidation showed that the overgrown Rh is sintering. Spatially resolved in situ X-ray photoemission at BESSY II indicates the formation of Rh₂O₃ at partial oxygen pressure. While the nanoparticles surface composition reflects the oxidation and H₂ reduction, the shape of the nanoparticles remains rather unchanged under the applied conditions.

O 52.2 Wed 10:45 TRE Phy

Probing Au(111) Surface Reconstruction by Electrocatalytic Reactions — JOHANNES M. HERMANN¹, AREEG ABDELRAHMAN¹, LUDWIG A. KIBLER¹, and TIMO JACOB^{1,2,3} — ¹Institute of Electrochemistry, Ulm University, Ulm, Germany. — ²Helmholtz-Institute-Ulm (HIU), Ulm, Germany. — ³Karlsruhe Institute of Technology, Karlsruhe, Germany.

Au(111) is an extensively studied single crystal and its thermodynamically most stable surface is reconstructed under UHV conditions. Besides the thermally reconstructed and the unreconstructed Au(111) surfaces, in addition, there is also a potential-induced reconstruction in electrochemical environments. The phase transition between the reconstructed and unreconstructed Au(111) electrode surfaces has mostly been investigated by means of *in situ* scanning tunneling microscopy. Kinetic studies are sparse and in the case of potential-induced reconstruction limited to *in situ* surface X-ray scattering. Since the electrocatalytic hydrogen evolution reaction (HER) on gold electrodes is strongly structure-sensitive, here we show how it can be used to monitor structural changes of the Au(111) surface [1]. The electrocatalytic activity is highest directly after the surface reconstruction had been lifted, and decreases while the potential-induced reconstruction proceeds, following a simple first-order rate law. In contrast to expectations from conventional electrode kinetics, the rate of the reconstruction process decreases with more negative potential, as the reconstructed surface is stabilized by increasing negative excess charge. [1] J.M. Hermann, et al. *Electrochim. Acta.* **2020**, 347 136287.

O 52.3 Wed 11:00 TRE Phy

Transition metal carbides vs platinum as catalysts for H₂ dissociation and hydrogenation of ethylene and acetylene — •CARLOS JIMENEZ-OROZCO¹, ELIZABETH FLOREZ¹, and JOSE RODRIGUEZ² — ¹Faculty of Basic Sciences, University of Medellin, Medellin, Colombia — ²Chemistry Division, Brookhaven National Laboratory, USA

Hydrogenation reactions are key in the chemical industry, many of them use the scarce Pt-group metals as catalysts, limiting their usage in the long term. Transition metal carbides (TMC) emerge as an alternative material. Among TMC, tungsten carbide (WC) stands out as the active phase or as support of metals. There is still a lack in the understanding of the WC performance, limiting their modulation and applications. Here, density functional theory was used to study the performance of WC in hydrogenation of acetylene (C₂H₂) and ethylene (C₂H₄) as probe molecules, together with the H₂ dissociation capability of WC. Hence, Pt, Pt/WC (Pt monolayer) and WC were compared. Hydrogen surface coverage and atomistic thermodynamics were used to achieve more realistic models. The H₂ dissociation on Pt/WC has a Pt-like behavior at high coverage. The pristine WC surface becomes as a machine for H₂ dissociation in a wide range of T and P, achieving high surface coverages. The Pt/WC has the capability to hydrogenate selectively C₂H₂ into C₂H₄, avoiding surface poisoning. The results put WC and Pt/WC under the spotlight as a promising systems alternative to Pt for hydrogenation reactions at several T and P conditions and for the selective transformation of C₂H₂ into C₂H₄.

Topical Talk

O 52.4 Wed 11:15 TRE Phy

Modeling and Design of Single-Atom Alloy Catalysts — RAFFAELE CHEULA and •MIE ANDERSEN — Department of Physics and Astronomy, Aarhus University, Denmark

In this contribution we apply molecular simulations and machine learning (ML) to study CO₂ hydrogenation (reverse water-gas shift) on single-atom alloy (SAA) catalysts, i.e., diluted bimetallic materials. SAAs have been shown to be able to break the scaling relationships that limit conventional catalysts [1]. We target a wide combinatorial space of elements of the periodic table, which makes a direct study with density-functional theory (DFT) computationally prohibitive. Therefore, we produce a database of DFT-calculated energies on a limited number of SAAs and apply physics-inspired ML techniques for the extrapolation to a wide range of materials. We use a graph-based Gaussian Process Regression ML model (WWL-GPR [2]) to calculate adsorption energies, and simpler models (e.g., multivariate regressions) to estimate the activation energies of the new materials. We employ microkinetic modeling to simulate the reaction kinetics; then, we apply sensitivity analysis and uncertainty quantification to identify the parameters that can improve the model predictions, and we refine them with additional DFT calculations. The application of the framework to CO₂ hydrogenation allows us to rationalize how reaction mechanisms and catalytic activity change with the catalyst composition, paving the way toward the design and nano-engineering of SAA catalysts.

[1] RT. Hannagan *et al.*, *Chem. Rev.* **120**, 12044 (2020)[2] W. Xu *et al.*, *Nat. Comp. Sci.* **2**, 443 (2022)

O 52.5 Wed 11:45 TRE Phy

Data-centric approach for uncovering rules to describe the CO₂ activation at metal catalysts — •HERZAIN I. RIVERA-ARRIETA, LUCAS FOPPA, and MATTHIAS SCHEFFLER — The NOMAD Laboratory at the Fritz-Haber-Institut der Max-Planck-Gesellschaft and IRIS-Adlershof of the Humboldt-Universität zu Berlin, Germany

Using CO₂ as a building block in the production of chemicals and fuels requires, in a first step, the activation of this molecule [1]. The materials space is practically infinite, but only a handful of them may enable an effective CO₂ activation. Therefore, this work focuses on the use of artificial intelligence to speed up finding new catalysts for this process. Single-atom alloys (SAA) of transition metals not only provide good model systems, but also show potential as heterogeneous catalysts [2]. Using the mBEEF functional to perform the DFT modeling of the interaction between CO₂ and different surface terminations in Cu-, Zn-, and Pd-based SAA, we generated a dataset including 50 physicochemical parameters characterizing the geometry, and electronic properties of the adsorption sites where the molecule is activated in each material. Then, we applied the subgroup-discovery (SGD) approach [3] to uncover rules correlating key parameters in the SAA with indicators of the CO₂ activation, e.g., a large C–O bond elongation. Having access to these SGD-rules, which only depend on the material, allows a fast screening and prediction of potentially effective catalysts.

[1] H. J. Freund and M. W. Roberts, *Surf. Sci. Rep.*, **25**, 225 (1996).[2] J. Schumann, *et al.*, *J. Phys. Chem. Lett.*, **12**, 10060 (2021).[3] B. R. Goldsmith, *et al.*, *New J. Phys.*, **19**, 013031 (2017).

O 52.6 Wed 12:00 TRE Phy

Machine learning interatomic potential for metallic and oxidized copper surfaces — •FELIX RICCIUS, NICOLAS BERGMANN, NICOLAS G. HÖRMANN, HENDRIK H. HEENEN, and KARSTEN REUTER — Fritz-Haber-Institut der MPG, Berlin, Germany

Copper (Cu) is a promising catalyst for the electrochemical reduction of CO₂ to chemicals and fuels since it yields many possible reduction products. The selectivity between these products is hypothesized to be altered by partial oxidation of the catalysts* surface. The extent of Cu surface oxidation, as well as accompanying morphological transformations are, however, unclear. Predictive atomistic simulations could potentially uncover this surface chemistry but time and length scales necessary for the required sampling are intractable by first-principles methods. Machine learning interatomic potentials (MLIP) trained to first principle data can overcome this limitation by retaining predictive accuracy at a fraction of the computational cost. In this work, we use Gaussian Approximation Potentials to train a MLIP for metallic Cu and Cu oxides. We design a workflow tailored to the problem at hand. Via iterative parallel tempering simulations, we sample the relevant phase space for Cu oxidation at various oxidation states during training. We demonstrate the viability of our approach, which results in a reliable potential capable of describing the chemically important regions of the configuration space. The potential gives access to (surface)phase diagrams and surface reconstruction phenomena following surface reduction and oxidation. The atomic insight may shine light on the role of (surface)oxidation in Cu electrocatalysts.

O 52.7 Wed 12:15 TRE Phy

Selectivity Trends and Role of Adsorbate-Adsorbate Interactions in CO Hydrogenation on Rhodium Catalysts — •MARTIN DEIMEL^{1,2}, HECTOR PRATS³, MICHAEL SEIBT², KARSTEN REUTER¹, and MIE ANDERSEN⁴ — ¹Fritz-Haber-Institut der MPG, Berlin, Germany — ²Chair for Theoretical Chemistry, Technical University of Munich, Germany — ³Department of Chemical Engineering, University College London, UK — ⁴Aarhus Institute of Advanced Studies and Department of Physics and Astronomy, Aarhus University, Denmark

Rh is one of the most promising elemental catalysts for the conversion of syngas (CO and H₂) into hydrocarbons and oxygenates, especially toward valuable higher oxygenates. Experimentally, an inverse relationship between activity and selectivity of the main products methane and acetaldehyde was identified with conflicting explanations for this trend.^[1,2] Here, we revisit the question of the role played by step and terrace sites, represented by the Rh(211) and Rh(111) facets, on activity and selectivity trends.^[3] We use an accelerated kinetic Monte Carlo (KMC) approach including a cluster expansion to treat lateral interactions. By comparing our results to corresponding mean-field models and experiment,^[1,2] we find that only the KMC models can correctly capture the experimental selectivity trends and that quantitatively correct activity predictions require correction for well-known errors in the density functional theory parametrization of our models.

[1] N. Yang *et al.*, *J. Am. Chem. Soc.* **138**, 3705 (2016)[2] M. Schumann *et al.*, *ACS Catal.* **11**, 5189 (2021)[3] M. Deimel *et al.*, *ACS Catal.* **12**, 7907 (2022)

O 52.8 Wed 12:30 TRE Phy

Estimating Free Energy Barriers for Heterogeneous Catalytic Reactions with Machine Learning Potentials and Umbrella Sampling — •SINA STOCKER¹, GÁBOR CSÁNYI², KARSTEN REUTER¹, and JOHANNES T. MARGRAF¹ — ¹Fritz-Haber-Institut der MPG, Berlin, Germany — ²University of Cambridge, United Kingdom

Predictive-quality first-principles based microkinetic models are increasingly used to analyze (and subsequently optimize) reaction mechanisms in heterogeneous catalysis. In full rigor, such models require the knowledge of all possible elementary reaction steps and their corresponding reaction barriers. Unfortunately, for complex catalytic processes (such as the generation of ethanol from syngas) the number of possible steps is so large that an exhaustive first-principles calculation of all barriers becomes prohibitively expensive.

To overcome this limitation, we develop machine learned (ML) interatomic potentials to model the early steps of syngas conversion on Rhodium. These ML potentials can be used to determine free energy reaction barriers at a fraction of the computational cost of the underlying first-principles method. Specifically, we use here the Gaussian Approximation Potential (GAP) framework and explore iterative training in combination with umbrella sampling for the CHO decomposition as an example.

O 53: Focus Session: Frontiers of Electronic-Structure Theory IV (joint session O/HL)

Time: Wednesday 10:30–13:00

Location: TRE Ma

O 53.1 Wed 10:30 TRE Ma

A systematic DFT+U and Quantum Monte Carlo benchmark of magnetic two-dimensional (2D) CrX₃ (X = I, Br, Cl, F) — •DANIEL WINES, KAMAL CHOUDHARY, and FRANCESCA TAVAZZA — Materials Science and Engineering Division, National Institute of Standards and Technology (NIST), Gaithersburg, MD 20899, USA

The search for two-dimensional (2D) magnetic materials has attracted a great deal of attention because of the experimental synthesis of 2D CrI₃, which has a measured Curie temperature of 45 K. Often times, these monolayers have a higher degree of electron correlation and require more sophisticated methods beyond density functional theory (DFT). Diffusion Monte Carlo (DMC) is a correlated electronic structure method that has been demonstrated successful for a wide variety of systems, since it has a weaker dependence on the Hubbard parameter (U) and density functional. In this study we designed a workflow that combines DFT+U and DMC in order to treat 2D correlated magnetic systems. We chose monolayer CrX₃ (X = I, Br, Cl, F), with a stronger focus on CrI₃ and CrBr₃, as a case study due to the fact that they have been experimentally realized and have a finite critical temperature. With this DFT+U and DMC workflow and the analytical method of Torelli and Olsen, we estimated an upper bound of 43.56 K for the T_c of CrI₃ and 20.78 K for the T_c of CrBr₃, in addition to analyzing the spin densities and magnetic properties with DMC and DFT+U. We expect that running this workflow for a well-known material class will aid in the future discovery and characterization of lesser known and more complex correlated 2D magnetic materials.

Topical Talk

O 53.2 Wed 10:45 TRE Ma

TREX: an integrated HPC software platform for quantum Monte Carlo calculations — •CLAUDIA FILIPPI — University of Twente, Enschede, The Netherlands

I will present the software development strategy and current achievements of the European Center of Excellence TREX “Targeting Real chemical accuracy at the EXascale” [1]. TREX focuses on methods at the high-end in the accuracy ladder of electronic structure approaches and, in particular, on quantum Monte Carlo methods which are uniquely positioned to fully exploit the massive parallelism of upcoming architectures. The main objective of TREX is the development of a user-friendly and open-source software suite, which integrates quantum Monte Carlo codes within an interoperable, high-performance platform. Core of our software efforts is the creation of the following two libraries:

TREXIO: A common I/O library and file format for easily exchanging data between applications, facilitating high-throughput computing workflows [2];

QMCKL: A library of computational kernels, written together by quantum Monte Carlo and HPC experts, to perform common CPU-intensive quantum Monte Carlo tasks [3].

[1] <https://trex-coe.eu>[2] <https://github.com/trex-coe/trexio>[3] <https://trex-coe.github.io/qmckl>

O 53.3 Wed 11:15 TRE Ma

Exciton-phonon coupling in luminescence of indirect band-gap materials — MATTEO ZANFROGNINI^{1,2}, FULVIO PALEARI¹, DANIELE VARSANO¹, and •LUDGER WIRTZ³ — ¹Centro S3, CNR-Istituto Nanoscienze, Modena, Italy — ²Università di Modena e Reggio Emilia, Modena, Italy — ³Department of Physics and Materials Science, University of Luxembourg, Luxembourg

Layered, quasi-2D materials, such as hexagonal boron nitride (hBN) are known to display very strong excitonic effects due to the concentration of excitons in two dimensions and due to the relatively weak dielectric screening. If the band-gap of the material is indirect, the dispersion of the lowest lying exciton can have a minimum at a finite wave vector q . Upon absorption of a photon and excitation to a vertical ($q=0$) exciton, the system will relax to the finite- q exciton. Luminescence then entails the absorption/emission of a phonon with wave vector q . We present a computational approach for phonon-assisted luminescence in the presence of strong excitonic effects using two approaches: (i) a finite-displacement approach for the exciton-phonon coupling and (ii) a diagrammatic approach, calculating the q -dependent exciton-phonon coupling from the exciton eigenvectors and electron/hole-phonon scattering matrix elements. We show that the methodology quantitatively explains recent measurements of different stackings of BN layers. [1]

[1] A. Plaud, I. Stenger, F. Fossard, L. Sponza, L. Schué, F. Ducastelle, A. Loiseau, J. Barjon, to be published.

O 53.4 Wed 11:30 TRE Ma

A combined G₀W₀/BSE scheme of characterizing photoexcitations in hydroxylated rutile TiO₂ (110) — •SAVIO LARICCHIA, ANDREA FERRETTI, DANIELE VARSANO, and CLAUDIA CARDOSO — Centro S3, CNR-Istituto Nanoscienze, 41125 Modena, Italy

In reduced TiO₂, electronic transitions originating from polaronic excess electrons in surface-localized band-gap states (BGS) are known to contribute to the photoabsorption and to the photocatalytic response of TiO₂ in the visible region. Recent state-selective studies using two-photon photoemission (2PPE) spectroscopy have also identified an alternative photoexcitation mechanism contributing to the photoabsorption of the reduced surface (110) of rutile TiO₂. This process involves $d-d$ excitations from BGS arising from surface and subsurface defects, including bridging hydroxyls and oxygen vacancies. Density Functional Theory (DFT) has been used to determine the character of the electronic excited states involved in a $d_{12g}-d_{12g}$ transitions, but its accuracy is questioned by its theoretical framework: DFT is in principle exact for ground state systems and does not describe interacting photogenerated electron-hole pairs, i.e. the excitons. This has highlighted the need to move beyond the DFT formalism, by working within a many-body perturbation theory (MBPT) framework. It will be shown how a G₀W₀ method, combined with the solution of the Bethe-Salpeter equation (BSE), provides a powerful tool for characterizing from first principles the optical excitations from BGS identified by 2PPE experiments on hydroxylated TiO₂(110).

15 min. break

O 53.5 Wed 12:00 TRE Ma

Scaling the Way for All-Electron XPS Simulations to Calculate Absolute Binding Energies of Surface Superstructures — •DYLAN MORGAN¹, SAM HALL¹, BENEDIKT KLEIN^{1,2}, MATTHEW STOODLEY^{1,2}, and REINHARD MAURER¹ — ¹Department of Chemistry, University of Warwick, United Kingdom — ²Diamond Light Source, Harwell Science and Innovation Campus, United Kingdom

First principles simulations of x-ray photoemission spectroscopy (XPS) and near-edge x-ray absorption fine-structure (NEXAFS) crucially support the assignment of surface spectra composed of many overlapping signatures. Core-level constrained Density Functional Theory calculations based on the Δ -SCF method are commonly used to predict relative XPS binding energy (BE) shifts but often fail to predict absolute BEs. The all-electron numeric atomic orbital code FHI-aims enables an accurate prediction of absolute BEs, but the legacy code lacked computational scalability to address large systems and robustness with respect to localisation of the core hole. We present a redesign of the core-hole constrained code in FHI-aims that delivers improvements to the scalability and robustness of core-hole constrained calculations in FHI-aims. We demonstrate the improved scaling behaviour and employ the new code to simulate core-level spectroscopic fingerprints of graphene moire superstructures. The code refactorisation forms the basis to expand the code towards improved core hole localisation methods and the rigorous treatment of relativistic effects for core-level spectra beyond the 1s shell.

O 53.6 Wed 12:15 TRE Ma

Efficient diagonalization of BSE electron-hole Hamiltonian using group theory — •JÖRN STÖHLER^{1,2}, DMITRII NABOK¹, STEFAN BLÜGEL¹, and CHRISTOPH FRIEDRICH¹ — ¹Peter Grünberg Institut and Institute for Advanced Simulation, Forschungszentrum Jülich, Germany — ²RWTH Aachen University, Germany

The Bethe-Salpeter equation (BSE) is the state-of-the-art method for the calculation of optical absorption and electron-energy loss spectra including excitonic effects. We solve the BSE by diagonalizing an effective electron-hole Hamiltonian. Often, a high number of k -points is needed to converge the BSE spectra, which leads to a large size of the Hamiltonian matrix and makes its diagonalization very expensive. In this work [1], we use the full spatial symmetry group to transform the electron-hole product basis into a symmetry-adapted product basis, which brings the Hamiltonian into a block-diagonal form and speeds up the subsequent diagonalization. The basis transformation is sparse and causes little overhead. We provide an implementation of our method in the FLAPW code *SpeX* and demonstrate speedups of 36, 52, 12 for Si, BN, and monolayer MoS₂, respectively.

We acknowledge financial support by MaX CoE funded by the EU through H2020-INFRAEDI-2018 (project: GA 824143).

[1] J. Stöhrler, C. Friedrich, *Unpublished*

O 53.7 Wed 12:30 TRE Ma

Excitonic effects on quadratic optical photoresponse of semiconductors — •PEIO GARCIA-GORICELAYA¹ and JULEN IBAÑEZ-AZPIROZ^{1,2} — ¹Centro de Física de Materiales, University of the Basque Country UPV/EHU, Spain — ²IKERBASQUE Basque Foundation for Science, Spain

We present a general ab initio scheme for including many-body excitonic effects in the non-linear optical photoresponse up to second order. Our practical implementation starts from the length-gauge formulation of the single-particle non-interacting optical photoresponse tensors [1] that are efficiently calculated

using Wannier interpolation [2]. Subsequently, excitonic corrections are included in the many-body interacting current-density response tensors by means of Dyson-like equations derived within TD-CDFT. These equations allow a natural connection with the formalism of the single-particle picture and the Wannier-interpolation scheme respecting the tensorial character of the response. We employ this scheme to assess the impact of excitonic effects on several quadratic optical processes as the second-harmonic generation and the shift-current bulk photovoltaic effect in technologically appealing semiconductors.

Funding provided by the European Union's Horizon 2020 research and innovation programme under the European Research Council (ERC) grant agreement No 946629.

[1] J. E. Sipe and A. I. Shkrebtii, *Phys. Rev. B* 61, 5337 (2000).

[2] G. Pizzi et al., *J. Phys. Cond. Matt.* 32, 165902 (2020)

O 53.8 Wed 12:45 TRE Ma

Electronic and optical properties of CoFe_2O_4 from density functional theory calculations, including many-body effects — •SHOHREH RAFIEZADEH¹, VIJAYA BEGUM-HUDE^{1,2}, and ROSSITZA PENTCHEVA¹ — ¹Department of Physics University of Duisburg-Essen, Germany — ²University of Illinois at Urbana-Champaign, USA

CoFe_2O_4 is a ferrimagnetic semiconductor that finds application as an anode material in photocatalytic water splitting. We present a comprehensive study of the electronic and optical properties of bulk CoFe_2O_4 using density functional theory calculations and many-body perturbation theory to clarify the broad range of reported band gaps both experimentally (0.55-4.1 eV)[1] and theoretically (0.9-1.90 eV). Starting with different exchange-correlation functionals, we obtain a direct band gap of 1.38 [PBE+($U=4$ eV)], 1.69 eV [SCAN+($U=3$ eV)], and an indirect gap of 2.02 eV (HSE06). Including quasiparticle corrections within G_0W_0 enhances and renders indirect band gaps for all functionals of 1.78, 1.95 and 2.17 eV, respectively. Excitonic effects are accounted for by solving the Bethe Salpeter equation and result in the lowest threshold for optical transitions at 1.50 eV (SCAN) and 1.61 eV (HSE06), followed by peaks at ~ 2.0, 3.5 and 5.0 eV, in agreement with experiment highlighting the importance of electron-hole interactions. Support by DFG- within CRC/TRR 247, project B04, and computational time at MagnitUDE is gratefully acknowledged. [1] S. Singh and N. Khare, *Sci. Rep.* 8, 6522 (2018).

O 54: Focus Session: Scanning Probe Microscopy with Quartz Sensors II

Time: Wednesday 15:00–17:30

Location: CHE 89

Topical Talk O 54.1 Wed 15:00 CHE 89

Peering into interfacial water by qPlus-based atomic force microscopy — •YING JIANG — International Center for Quantum Materials, School of Physics, Peking University, Beijing 100871, P. R. China

Water/solid interfaces are a central theme across an incredibly broad range of scientific and technological processes. Scanning probe microscopy (SPM) has been extensively applied to probe interfacial water, but there exist two longstanding limitations in the past decades, which makes SPM fall short compared with conventional spectroscopic methods. First, it is very difficult to image H atoms of water molecule directly; Second, it is highly possible to disturb the fragile H-bonding water structure during the imaging process. To this end, we have developed a new imaging method based on qPlus-type atomic force microscopy (AFM), which is sensitive to H and non-invasive to water structure. The key lies in probing the high-order electrostatic force between the quadrupole-like CO-terminated tip and the polar water molecules at large tip-water distances. In this talk, I will showcase the application of this technique to probe water clusters, ion hydrates, 2D ice and even bulk ice surface [1-4]. The possibility of combining qPlus-AFM with quantum sensing technology to perform nanoscale NMR measurement of interfacial water will be also briefly discussed [5-6].

[1] *Nature Commun.* 9, 122 (2018) [2] *Nature* 557, 701 (2018) [3] *Nature* 577, 60 (2020) [4] *Science* 377, 315 (2022) [5] *Nature Commun.* 12, 2457 (2021) [6] *Nature Physics* 18, 1317 (2022)

O 54.2 Wed 15:30 CHE 89

Does surface adsorption change the reactivity of an organic molecule? — JACK HENRY, PHILIP BLOWEY, and •ADAM SWEETMAN — University of Leeds, United Kingdom

Adsorption onto metal surfaces is known to alter the electronic [1], and geometric [2] structure of small organic molecules. However, the change in reactivity of a single molecule induced by the presence of a surface is less well studied. We investigated the influence of molecule-substrate bonding on the interactions experienced by a scanning probe microscope (SPM) tip by studying C60 molecules adsorbed in different configurations [3-5] on the Cu(111) surface, using qPlus NC-AFM/STM at 5K. We compare the minima in collected force spectra to complementary ab initio (DFT) simulations, and discuss the substantial differences in our results compared to the existing literature [3]. 1. Repp, J., et al. (2005). *Physical Review Letters*, 94(2), 026803. 2. L. Gross, et al. *Science* 325, 1110 (2009). 3. Jonathan Brand et al. *Nano Letters* 2019 19 (11), 7845-7851 4. W. W. Pai, et al. *Physical Review Letters* 104, (2010). 5. L. Forcier, et al. *Physical Review B* 104, (2021).

O 54.3 Wed 15:45 CHE 89

Water Dimer-Driven DNA Base Superstructure with Mismatched Hydrogen Bonding — SHUNING CAI¹, LAURI KURKI¹, •CHEN XU¹, ADAM S. ADAM^{1,2}, and PETER LILJEROTH¹ — ¹Department of Applied Physics, Aalto University, 00076 Aalto, Espoo, Finland — ²WPI Nano Life Science Institute (WPI-NanoLSI), Kanazawa University, Kakuma-machi, Kanazawa 920-1192, Japan

The existence of water dimers in equilibrium water vapor at room temperature and their anomalous properties revealed by recent studies suggest the benchmark role of water dimers in both experiments and theory. However, there have been limited observations of individual water dimers due to the challenge of water separation and generation at the single-molecule level. Here, we achieve real-space

imaging of individual confined water dimers embedded inside a self-assembled layer of a DNA base, adenine, on Ag(111). The hydration of the adenine layers by these water dimers causes a local surface chiral inversion in such a way that the neighboring homochiral adenine molecules become heterochiral after hydration, resulting in a mismatched hydrogen-bond pattern between neighboring adenine molecules. Furthermore, theoretical simulation and calculations corroborate the mutual influence between the adenine superstructure and these dynamic confined water dimers. The observation of single confined water dimers offers an unprecedented approach to studying the fundamental forms of water clusters and their interaction with the local chemical environment.

O 54.4 Wed 16:00 CHE 89

Nanoscale 3D printing technique by using the nanopipette-combined quartz tuning fork-atomic force microscope — •SANGMIN AN — Department of Physics, Institute of Photonics and Information Technology, Jeonbuk National University, Jeonju 54896, South Korea

Materials can be classified by hardness, such as gold represented by hard materials having elasticity and water represented by soft materials having viscosity. However, at the nanoscale, even solid gold exhibits viscosity [1], while liquid water also exhibits elasticity [2] revealed by a quartz tuning fork-atomic force microscope (QTF-AFM), which has the intrinsic properties of high stiffness and high sensitivity. In this presentation, I discuss how this QTF-AFM can be applied as the nanoscale 3D printing technique combined with nanopipette [3,4], which are typically used in biotechnology, along with showing the results of the elasticity and viscosity of water. In addition, I share the results of nanoscratching [5] and nanosensor [6] schemes which can be realized with the nanorod-combined QTF-AFM instead of nanopipette.

[1] *Nature* 569, 393-397 (2019).

[2] *Phys. Rev. X* 8, 041046 (2018).

[3] *Nano-Micro Lett.* 14, 13 (2022).

[4] *Nanoscale Adv.* in press (2022).

[5] *Appl. Nanosci.* 9, 67-76 (2019).

[6] *Proc. Natl. Acad. Sci. USA* 115(12), 2884-2889 (2018).

Topical Talk O 54.5 Wed 16:15 CHE 89

AFM with the qPlus sensor: An ideal tool for oxide surface science — •ULRIKE DIEBOLD — Institute of Applied Physics, TU Wien, Vienna, Austria

The past decades have seen a sustained interest in the atomic-scale properties of metal oxide surfaces. Local probes are well suited to study surface reconstructions, (point) defects, trapped local charges, and the adsorption of small molecules. Much of the work has focused on semiconducting or (ultra-)thin film samples, as these have sufficient conductivity for STM investigations. The superior resolution afforded by the qPlus sensor allows for extending such studies to highly insulating oxides, such as silicates or other minerals. In the talk, I will give an overview of recent progress, fascinating opportunities, and challenges of atomically-resolved AFM on oxides.

O 54.6 Wed 16:45 CHE 89

Atomic-scale imaging of muscovite mica and its interaction with water — •GIADA FRANCESCHI¹, PAVEL KOCAN², ANDREA CONTI¹, SEBASTIAN BRANDSTETTER¹, JAN BALAJKA¹, IGOR SOKOLOVIC¹, JIRI PAVELEC¹, MARKUS VALTNER¹, MARTIN SETVIN², FLORIAN MITTENDORFER¹, MICHAEL SCHMID¹, and ULRIKE DIEBOLD¹ — ¹Inst. Appl. Phys., TU Wien, Wiedner Hauptstr. 8-

10/E134, 1040 Vienna, Austria — ²Dept. Surface and Plasma Phys., Charles University in Prague, V Holesovickach 2, 180 00 Prague, Czech Republic

Muscovite mica is an abundant potassium aluminosilicate enjoying wide popularity in surface and interfacial science. Its prevalence is partly due to its extraordinary cleaving properties: The easily obtained atomically flat terraces are ideal for fundamental studies. To date, it is established that the cleaved surface is decorated by K^+ ions,¹ but their intrinsic ordering and their precise hydration mechanisms are not known. Here, we use non-contact atomic force microscopy to image the K^+ distribution of cleaved mica and investigate their interaction with water under ultra-high vacuum conditions. After cleaving, the ions are arranged with short-range order, which we interpret with support from theory.² Dosing water vapor at 100 K causes various hydration arrangements, consistent with previous theoretical studies, and clustering at increasing water coverage. Exposure to ultra-clean liquid water³ induces ion mobility and substitution by protons. [1] Christenson et al., *Surf. Sci. Reports* 71, 367 (2016). [2] Franceschi et al., *submitted*. [3] Balajka et al., *Rev. Sci. Instrum.* 89, 083906 (2018)

O 54.7 Wed 17:00 CHE 89

Surface structure of dry and hydrated α - Al_2O_3 (0001) — JOHANNA HÜTNER¹, DAVID KÜGLER^{1,2}, MICHAEL SCHMID¹, ULRIKE DIEBOLD¹, and •JAN BALAJKA¹ — ¹Institute of Applied Physics, TU Wien, Vienna, Austria — ²CEITEC, Brno, Czech Republic

Corundum α - Al_2O_3 is an important ceramic also widely used as a support for heterogeneous catalysis. Due to similar Al coordination, α - Al_2O_3 is an important model system for naturally occurring minerals, such as aluminosilicate clays. Detailed studies of alumina surfaces have been stymied by its insulating nature but successfully performed with atomic force microscopy [1]. We used noncontact AFM to investigate the $(\sqrt{31} \times \sqrt{31})R9^\circ$ -reconstructed Al_2O_3 (0001)

surface formed upon high-temperature annealing. The reactivity of surface sites is strongly affected by hydroxylation. However, complete surface hydroxylation requires high pressures of water vapor (1 Torr) [2] that cannot be easily achieved in a conventional ultrahigh vacuum system. We explored the interaction of the Al_2O_3 (0001) surface with varying pressures of water vapor as well as ultrapure liquid water dosed with a UHV-compatible dispenser [3]. The results will provide new insights into the hydration of environmental substrates. [1] J. V. Lauritsen, et al., *Phys. Rev. Lett.* 103, 076103 (2009) [2] P. J. Eng, et al., *Science* 288, 1029 (2000) [3] J. Balajka, et al., *Rev. Sci. Instrum.* 89, 8, 083906 (2018)

O 54.8 Wed 17:15 CHE 89

Atomic-scale imaging of the cleaved feldspar microcline (001) surface and its interaction with water — •LUCA LEZUO, ANDREA CONTI, JAN BALAJKA, IGOR SOKOLOVIĆ, FLORIAN MITTENDORFER, MICHAEL SCHMID, ULRIKE DIEBOLD, and GIADA FRANCESCHI — Institute of Applied Physics, TU Wien, Wiedner Hauptstrasse 8-10/E134, 1040 Wien, Austria

Feldspar microcline ($KAlSi_3O_8$), abundant in the Earth's crust and present as dust particles in the atmosphere, is known to be one of the best ice nucleators. The exact processes driving the interaction of microcline with water have been studied intensively [1], but atomic-scale investigations remain elusive.

We present experimental, atomic-scale studies of the microcline-water interaction. The surfaces were prepared by UHV cleaving and analysed with non-contact atomic force microscopy (nc-AFM) and x-ray photoelectron spectroscopy (XPS). The cleaved surface consists of a honeycomb array that we assign to differently back-bonded O atoms. Dosing water vapour at 100 K causes the appearance of a hexagonal lattice and the gradual formation of a connected water network. DFT calculations help us to rationalize our experimental results.

[1] A. Kumar, et al., *Atmos. Chem. Phys.* 18, 7057 (2018)

O 55: Organic Molecules on Inorganic Substrates IV: Adsorption and Growth II

Time: Wednesday 15:00–17:45

Location: CHE 91

O 55.1 Wed 15:00 CHE 91

Bias-dependent conductivity switching and rectification in metallocene-based molecular junctions — YANGBIAO LIU¹, ANDIKA ASYUDA¹, HEINRICH LANG², EGBERT ZOJER³, and •MICHAEL ZHARNIKOV¹ — ¹Angewandte Physikalische Chemie, Universität Heidelberg, 69120 Heidelberg, Germany — ²Fakultät für Naturwissenschaften, Anorganische Chemie, Technische Universität Chemnitz, D-09107 Chemnitz, Germany — ³Institute of Solid State Physics, NAWI Graz, Graz University of Technology, 8010 Graz, Austria

Self-assembled monolayers (SAMs) of ferrocenyl/ruthenocenyl-substituted biphenylthiolates and fluorenylthiolates on Au(111) exhibit two distinct conductance states (CS) in two-terminal junctions featuring a sharp tip of eutectic GaIn as top electrode. When only negatively biasing the junction, the original, high CS is preserved, while the junction is switched to a low CS when applying only positive biases. Comparing the current values for these two states, one gets an effective rectification ratio of more than 1000 - a value comparable to the best performing molecular diodes but attained already at particularly low voltages. Significantly, the switching between the conduction states is reversible and the initial, high CS can be recovered by the application of a negative bias. Moreover, as shown by the example of one of the SAMs studied, when sweeping the junction alternatingly to the maximum positive and negative bias voltages (as usually done in literature), fully symmetric J-V curves are observed. This means that for a symmetric sweeping of the junction, the effective rectification disappears.

O 55.2 Wed 15:15 CHE 91

Sensing properties of cerium oxide as an electrode material for the detection of glucose — •ANASTASIA DEINEKO¹, VIACHESLAV KALINOVYCH¹, SASCHA L. MEHL², YEVHENIIA LOBKO¹, YURII YAKOVLEV¹, TOMÁŠ SKÁLA¹, KEVIN C. PRINCE², VLADIMÍR MATOLÍN¹, IVA MATOLÍNOVÁ¹, and NATALIYA TSUD¹ — ¹Charles University, Faculty of Mathematics and Physics, Department of Surface and Plasma Science, Prague, Czech Republic — ²Elettra-Sincrotrone Trieste S.C.p.A., Basovizza, Trieste, Italy

Detection of glucose level in biological liquids is of great importance nowadays because of the growing number of people with diabetes. A variety of oxides is used as electrode material for biosensors and cerium oxide is among them due to its unique properties. In this study characterization of the cerium oxide was performed by surface analysis techniques using photoelectron and absorption spectroscopies (XPS, SRPES, RPES, NEXAFS) in combination with electrochemical measurements. Photoemission based analysis provided information on changes in the oxidation state of cerium cations on the surface and in the subsurface layers of the oxide film, and whether glucose chemically bonds to the oxide. While electrochemical testing, namely cyclic voltammetry and chronoamperometry, was used to explore the sensing properties of polycrystalline cerium oxide films in reaction with glucose in the PBS working solution. The CeO_2 working elec-

trode sensitivity and pH range of sensor stability were determined and discussed in view of the enzymatic properties of cerium oxide. Keywords: cerium oxide, glucose, photoelectron spectroscopy, electrochemistry, biosensor.

O 55.3 Wed 15:30 CHE 91

Exploiting Cooperative Catalysis for the On-Surface Synthesis of Linear Heteroaromatic Polymers via Selective C-H Activation — XUNSHAN LIU¹, ADAM MATEJ^{2,3}, TIM KRATKY⁴, JESÚS I. MENDIETA-MORENO², SEBASTIAN GÜNTHER⁴, PINGO MUTOMBO², SILVIO DECURTINS¹, ULRICH ASCHAUER¹, JASCHA REPP⁵, PAVEL JELINEK^{2,3}, SHI-XIA LIU¹, and •LAERTE L. PATERA^{4,5,6} — ¹Department of Chemistry, Biochemistry and Pharmaceutical Sciences, University of Bern, Bern, Switzerland — ²Institute of Physics of Czech Academy of Sciences, Prague, Czech Republic — ³Regional Centre of Advanced Technologies and Materials, Palacký University Olomouc, Olomouc, Czech Republic — ⁴Department of Chemistry, Technical University of Munich, Garching, Germany — ⁵Institute of Experimental and Applied Physics, University of Regensburg, Regensburg, Germany — ⁶Institute of Physical Chemistry, University of Innsbruck, Austria

Regiospecific C-H activation is a promising approach to achieve extended polymers. Herein, selective C-H activation for dehydrogenative C-C couplings of hexaazatriphenylene by Scholl reaction on Ag(111) is reported. By means of low-temperature scanning probe microscopy, we revealed the formation of one-dimensional polymers with a double-chain structure [1]. The growth process is rationalized by density functional theory calculations, pointing out a cooperative catalytic action of Na and Ag adatoms in steering the selective polymerization.

[1] X. Liu, et al., *Angew. Chem. Int. Ed.* 2013 61.5 (2022): e202112798.

O 55.4 Wed 15:45 CHE 91

PTCDA mediated Ag(111) step reconstruction as precursor to pinwheel phase — •DANYANG LIU¹, ALEŠ CAHLÍK¹, CAROLINA A. MARQUES¹, JENS OPPLIGER¹, RUSLAN TEMIROV^{2,3}, and FABIAN D. NATTERER¹ — ¹Department of Physics, University of Zurich, Winterthurerstrasse 190, CH-8057 Zurich, Switzerland — ²Peter Grünberg Institut (PGI-3), Forschungszentrum Jülich, 52425 Jülich, Germany — ³University of Cologne, Faculty of Mathematics and Natural Sciences, Institute of Physics II, 50937 Cologne, Germany

PTCDA (3,4,9,10-Perylenetetracarboxylic dianhydride) forming herringbone islands on Ag(111) is the most striking phase and the prototypical metal-supported organic semiconductor. When we co-deposit PTCDA and Ag on Ag(111) at room temperature, we find that prior to their self-assembly into PTCDA herringbone islands, the molecules implant themselves into and reshape the Ag step edges. The PTCDA-decorated-Ag steps are curved and, depending on whether the Ag steps originate from screw dislocations or a terrace, cause steps reconstruction into multilayer high spirals or isolated Ag islands that both exhibit quantum confinement. At higher coverages, the PTCDA decorated steps may nucleate a distinct pinwheel phase that occasionally proceeds to form

a metal-organic framework. Annealing to higher temperatures straightens the PTCDA/Ag steps and may grow more pinwheel phase PTCDA patches, showing yet another tuning knob for organometallic surface science.

O 55.5 Wed 16:00 CHE 91

Growth of ordered two-dimensional cobalt phthalocyanine films on a one-dimensional substrate — •MILAN KUBICKI, SUSI LINDNER-FRANZ, MARIO DÄHNE, and MARTIN FRANZ — Technische Universität Berlin, Institut für Festkörperphysik, Berlin, Germany

The formation of self-assembled layers of organic materials on solid surfaces is an important subject because of their possible application in advanced (opto-) electronic devices. While such a formation of self-assembled monolayers is well established on metal surfaces, the growth on silicon surfaces is much less studied.

Using scanning tunneling microscopy (STM) the molecular arrangement of cobalt phthalocyanine (CoPc) molecules on the In-Si(111)(4×1) surface is studied [1]. CoPc belongs to the transition metal phthalocyanines being a class of organic semiconductors, which has been already employed e.g. in organic light emitting diodes, in organic photovoltaic cells, and in organic field-effect transistors.

Our data demonstrate that for low CoPc coverages the molecules are highly mobile along the In-Si nanowires. By approaching the saturation coverage, the CoPc molecules stabilize each other by forming a highly ordered two-dimensional monolayer. Based on STM observations a structure model with a (4×4) periodicity could be developed, which precisely explains the experimental observations.

[1] M. Kubicki, S. Lindner-Franz, M. Dähne, and M. Franz, Appl. Phys. Lett. **119**, 133105 (2021).

Topical Talk

O 55.6 Wed 16:15 CHE 91

Towards Understanding and Controlling On-Surface Reactions and Self-Assembly Mechanisms — •DANIEL EBELING — Institute of Applied Physics, Justus Liebig University Giessen, Heinrich-Buff-Ring 16, 35392 Giessen, Germany

The ability to construct organic nanomaterials with atomic precision is the key for applications in molecular electronics as the (opto-)electronic properties of such quantum materials depend on their atomic structure and size. To develop new strategies for synthesizing organic nanomaterials on surfaces, in-depth knowledge about the reaction processes and self-assembly mechanisms is needed. This can be revealed by visualizing the chemical structure and orientation of individual reaction intermediates using bond imaging atomic force microscopy (AFM).

In this presentation, recent results will be discussed that offer an approach for tuning the self-assembly process of halogenated compounds via reversing the binding selectivity of intermolecular halogen bonds. [1] A strategy for building covalent nanostructures one molecule at a time on an inert sodium chloride surface via scanning probe manipulation is also presented. This enables synthesizing elusive covalent nanoarchitectures, studying structural modifications and revealing pathways of intermolecular reactions. [2] Moreover, possibilities for tweaking the bond imaging technique using torsional and flexural higher eigenmodes of qPlus sensors will be illustrated. [3]

[1] J. Tschakert et al. Nature Communications **11**, 5630 (2020)

[2] Q. Zhong et al. Nature Chemistry **13**, 1133 (2021)

[3] D. Martin-Jimenez et al. Nanoscale **14**, 5329 (2022)

O 55.7 Wed 16:45 CHE 91

Molecular orientation of DHTAP on the nanostructured Cu-CuO stripe phase — •CLAUDIA LÓPEZ-POSADAS¹, ANTONY THOMAS², THOMAS LEONI², OLIVIER SIRI², CONRAD BECKER², and PETER ZEPPEFELD¹ — ¹Institute of Experimental Physics, Johannes Kepler University Linz, Altenberger Str. 69, 4040 Linz, Austria — ²Aix-Marseille University, CNRS, CINaM, UMR 7325, F-13288 Marseille, France

We have studied the preferential adsorption, structure and molecular orientation of 5,14-dihydro-5,7,12,14-tetraazapentacene (DHTAP) layers on the regularly patterned Cu-CuO stripe phase obtained by sub-monolayer oxygen adsorption on the Cu(110) surface. Using Reflectance Difference Spectroscopy (RDS) and Scanning Tunneling Microscopy (STM) we find that the DHTAP molecules preferentially adsorb on the Cu(110) stripes, where they are always lying flat with their long molecular axis aligned parallel to the [-110]-direction. In contrast, on the subsequently covered Cu(110)-(2x1)O stripes, the DHTAP molecules are aligned with their long molecular axis parallel to the [001]-direction. The evolution of the RDS signal allows to monitor the sequential adsorption and orientation of DHTAP during monolayer formation and the subsequent multilayer growth for different oxygen pre-coverages and, hence, different Cu and CuO stripe widths. Interestingly, beyond the first monolayer, the DHTAP molecules

adopt a preferential orientation which critically depends on the initial oxygen coverage, revealing the influence of the Cu-CuO stripe width and the possibility to tune the overall optical anisotropy of these films.

O 55.8 Wed 17:00 CHE 91

Oxygen-induced reorientation of organometallic chains on Cu(110) — •ILIAS GAZIZULLIN, CHRISTOPHE NACCI, and LEONHARD GRILL — Physical Chemistry Department, University of Graz, Heinrichstraße 28, Graz, Austria

The deposition of molecules onto crystalline surfaces allows their investigation at the single-molecule level by scanning tunneling microscopy (STM). It furthermore gives access to the controllable on-surface synthesis of covalent polymers [1]. Here, we have studied dibromo-p-terphenyl molecules on Cu(110) and on the Cu(110)-(2x1)O striped phase under ultra-high vacuum conditions with low-temperature STM.

Previously, the Cu(110)-(2x1)O striped phase was used as a template for the synthesis of organometallic structures having different sizes and shapes depending on the width of copper stripes [2]. The focus of our study is how pre- or post-adsorbed oxygen and annealing, which is necessary for covalent polymerization, affect the molecular adsorption on the surface. It turns out that on the striped phase the molecules form organometallic chains on the copper areas, oriented in at least three surface directions. Increasing the sample temperature from 300 K to 450 K induces a reorientation of the organometallic chains, which occurs due to stabilization of the reoriented OM chains by embedding in the Cu-O phase.

References

[1] L. Grill, S. Hecht, Nature Chemistry **12**, 115-130 (2020)

[2] Q. Fan, J. Dai, T. Wang, J. Kuttner, G. Hilt, J. M. Gottfried, and J. Zhu, ACS Nano **3**, 3747 (2016)

O 55.9 Wed 17:15 CHE 91

Simulations of 1D Supramolecular Chains on Gold with Explicit Surface-Substrate Interactions — •KRYSZTOF BREZINA^{1,2}, HUBERT BECK¹, MARIANA ROSSI², and ONDREJ MARSALEK¹ — ¹Charles University, Faculty of Mathematics and Physics, Prague, Czech Republic — ²Max-Planck-Institut für Struktur und Dynamik der Materie, Hamburg, Germany

2,5-diaminobenzoquinone-1,4-dimine molecules deposited on Au(111) have been observed in AFM experiments to assemble into 1D hydrogen-bonded chains, which exhibit different geometries and mechanical properties depending on the conditions at the deposition [1]. While a complete explanation of this behavior remains elusive, it is clear that nuclear quantum effects on the hydrogen bonding play an important role. To clarify this effect, we aim at performing path integral molecular dynamics with *ab initio*-quality potentials, in a system that explicitly takes into account molecules and the surface. Here, we discuss the methodological advances needed to generate meaningful training sets for the neural network potentials that substitute the reference *ab initio* method, in particular when a reaction needs to be well described [2]. We show the nature of the relevant proton-transfer *ab initio* potential energy surfaces as well as initial results focusing on the specific effects of the surface on the geometry of the molecules and on the character of the nuclear quantum effects in the chains.

[1] Cahlik A. et al. ACS Nano **2021**, *15*, 6, 10357-10365

[2] Brezina K., Beck H. and Marsalek O. *In preparation* 2022

O 55.10 Wed 17:30 CHE 91

Controlled Formation of Porous 2D Lattices from C₃ Symmetric Ph₆-Me-Tribenzotriquinacene-OAc₃ — •MARKUS LEISEGANG¹, SINEM TOKSABAY¹, ANDREAS CHRIST¹, PATRICK HÄRTL¹, JOHANNES KREBS¹, TODD B. MARDER¹, SOUMYAJYOTI HALDAR², STEFAN HEINZE², MATTHIAS BODE¹, and ANKE KRUEGER^{1,3} — ¹Universität Würzburg, Germany — ²Universität Kiel, Germany — ³Universität Stuttgart, Germany

The on-surface self-assembly of molecules is a promising approach to control the properties of resulting 2D lattices. Usually, planar molecules are utilized to prepare flat, structurally confined molecular layers, with only a few recent examples of warped precursors [1,2]. However, detailed control of the superstructures is limited thus far. Herein, we report the temperature-controlled self-assembly of a bowl-shaped, acetylated C₃-symmetric hexaphenyltribenzotriquinacene derivative on Cu(111). Combining scanning tunneling microscopy (STM) and density functional theory (DFT) confirms the formation of highly differing arrangements starting with π -stacked bowl-to-bowl dimers at low coverage at room temperature via chiral honeycomb structures, an intermediate trigonal superstructure, followed by a fully carbon-based, flattened hexagonal superstructure formed by on-surface deacetylation, which is proposed as a precursor for holey graphene networks with unique defect structures [3].

[1] T. Lohr et al., J. Am. Chem. Soc. **142**, 13565 (2020)

[2] J. Urgel et al., J. Am. Chem. Soc. **141**, 13158 (2019)

[3] S. Toksabay et al., Chem. Eur. J. **2022**, e202203187 (2022)

O 56: 2D Materials III: Growth, Structure and Substrate Interaction II (joint session O/CPP)

Time: Wednesday 15:00–17:30

Location: GER 37

O 56.1 Wed 15:00 GER 37

Te on Pt(111): Structure and Growth of Surface Tellurides and Pt_xTe_y Films — TILMAN KISSLINGER, ALEXANDRA SCHEWSKI, ANDREAS RAABGRUND, HANNAH LOH, LUTZ HAMMER, and M. ALEXANDER SCHNEIDER — Lehrstuhl für Festkörperphysik, FAU Erlangen-Nürnberg, Staudtstr. 7, 91058 Erlangen

By LEED-IV, STM and DFT we investigated the tellurization of Pt(111) in UHV. For Te coverages $\Theta < 0.5$ ML surface tellurides are formed. In this coverage regime and after thermal annealing, we find only two well ordered surface telluride structures with (3×3) and (10×10) periodicity, the former was mistaken for a defective $PtTe_2$ film [1]. Our LEED-IV structure analyses determine the atomic structure and show that the Pt(111) surface undergoes massive reconstructions upon reaction with Te.

For $\Theta > 0.5$ ML, compact islands develop which eventually coalesce to a complete platinum telluride layer. Again by LEED-IV analyses we find that the first layer is a Pt_2Te_2 layer on which as second layer a $PtTe_2$ film can be grown. Both form an overlayer where 7×7 film unit cells lie on 10×10 Pt(111) unit cells. Furthermore, we find that the interface to the Pt(111) bulk still contains the ≈ 0.5 ML Te originally bound in the (10×10) superstructure. Electronic properties of the films determined by STS and implications for the MBE growth of transition metal dichalcogenides by surface tellurization will be discussed.

[1] L. Liu, D. Zemlyanov, and Y.P. Chen, *2D Mater.* **8**, 045033 (2021)

O 56.2 Wed 15:15 GER 37

Electronic, chemical and structural properties of ultrathin Ta_2NiSe_5 flakes — KATHRIN KÜSTER¹, YUANSHAN ZHANG¹, DENNIS HUANG¹, ULRICH STARKE¹, and HIDENORI TAKAGI^{1,2,3} — ¹Max-Planck-Institut für Festkörperforschung, Heisenbergstraße 1, 70569 Stuttgart, Germany — ²Institute for Functional Matter and Quantum Technologies, University of Stuttgart, 70569 Stuttgart, Germany — ³Department of Physics, University of Tokyo, 113-0033 Tokyo, Japan

The excitonic insulator is a theoretically proposed state of matter wherein a macroscopic condensate of electron-hole pairs, i.e., excitons, spontaneously forms below a transition temperature. The 2D-layered chalcogenide Ta_2NiSe_5 has arisen as a leading candidate of an excitonic insulator in a bulk crystal. Here we prepared ultrathin films (down to 2 nm) of Ta_2NiSe_5 and analyzed their structural, electronic and chemical properties with a NanoESCA (Scienta Omicron) on a local scale. Angle-resolved photoelectron spectroscopy (ARPES), X-ray photoelectron spectroscopy (XPS), together with photoelectron emission microscopy (PEEM) and imaging XPS give detailed insight into the thickness dependent properties of the flakes. By exposure to UV-light we observe a contrast change in the PEEM images which is caused by a strong modification of the work function of the flakes, which we tentatively relate to a phase transition of the Ta_2NiSe_5 flakes.

O 56.3 Wed 15:30 GER 37

Transition from fractal-dendritic to compact islands for the 2D-ferroelectric SnSe on graphene/Ir(111) — PAULUS ALEKSA, SAMMER IQBAL, MUHAMMAD ALI MARTUZA, JIAQI CAI, THAIS CHAGAS, ROBIN OHMANN, and CARSTEN BUSSE — Universität Siegen, Germany

Monolayer islands of the 2D-ferroelectric SnSe have been grown by MBE under UHV conditions using inert and weakly interacting graphene on Ir(111) as the substrate. After deposition at room temperature, fractal-dendritic islands are observed in STM. The preferential growth directions are aligned with high-symmetry directions of the substrate. Upon annealing the islands become more compact. At 560 K they exhibit their equilibrium shape, higher temperatures lead to desorption. The equilibrium shape cannot be simply explained by minimization of the number of unsaturated bonds around the perimeter of an island with given area. The model has to be extended to incorporate the polar character of SnSe, leading to island edges that are charged in dependence of their orientation.

O 56.4 Wed 15:45 GER 37

Reaction of submonolayer amounts of Ti and Te on Au(111) — ANDREAS RAABGRUND, TILMAN KISSLINGER, LUTZ HAMMER, and M. ALEXANDER SCHNEIDER — Universität Erlangen-Nürnberg, 91058 Erlangen, Germany

Titanium ditelluride ($TiTe_2$) belongs to the family of layered 2D transition metal dichalcogenides. It achieved a lot of attention due to the emergence of a charge density wave in the single layer limit. Thicker films, however, do not show this transition [1]. Aiming the MBE growth of $TiTe_2$ we investigated the initial growth of titanium telluride structures on Au(111) both structurally and electronically by STM, STS, LEED-IV structural analysis, and DFT. For a Te coverage of 0.4 ML and a Ti coverage of 0.2 ML on Au(111) a chain-like $(5 \times \sqrt{3})_{\text{rect}}$ superstructure is formed. Our LEED-IV best-fit structure with a Pendry R factor of 0.11 (redundancy $\rho = 9.6$) reveals incorporated Ti atoms each of which forms bonds to two Te atoms residing in approximately hollow positions. Our findings regarding the $(5 \times \sqrt{3})_{\text{rect}}$ superstructure disprove the proposed $TiTe_2$ monolayer on Au(111) [2]. STS shows an approximately 0.5 eV (FWHM) wide peak at +1 V

which we can correlate to the density of Ti d-states as obtained from DFT.

[1] P. Chen et al., *Nat. Commun.* **8**, 516 (2017)

[2] Z. Song et al., *Chin. Phys. B* **102**, 056801 (2019)

O 56.5 Wed 16:00 GER 37

Monolayers of $CoCl_2$ and $CoBr_2$ on Au(111) - Chemical, magnetic and structural investigation — SAMUEL KERSCHBAUMER¹, SEBASTIEN HADJADJ², ANDREA AGUIRRE BAÑOS³, DANILO LONGO³, WOLFGANG KUCH², JOSÉ IGNACIO PASCUAL³, CELIA ROGERO¹, and MAXIM ILYN¹ — ¹Centro de Física de Materiales (CSIC/UPV-EHU), 20018 Donostia-San Sebastian, Spain — ²Institut für Experimentalphysik, Freie Universität Berlin, 14195 Berlin, Germany — ³CIC nanoGUNE-BRTA, 20018 Donostia-San Sebastian, Spain

Magnetic 2D materials have gained increasing interest, due to their potential applications. But while many theoretical calculations predict magnetic order in various 2D materials [1], only few have been experimentally measured [2]. A very promising classes of materials are transition metal halides (TMHs), as many of them crystallise in Van der Waals layered structures, making them easily cleavable, while their partially filled d orbitals generate the perfect foundation for magnetic order, further increasing their attractiveness for future nanotechnologies. In this talk chemical, magnetic and structural properties of single-layer $CoCl_2$ and $CoBr_2$ on Au(111) by scanning tunnelling microscopy (STM), X-ray photoelectron spectroscopy (XPS), low energy electron diffraction (LEED) and X-ray absorption spectroscopy (XAS/XMCD) will be presented.

[1] Michael A. McGuire, *Crystals*, **7**(5), 121, (2017)

[2] Djuro Bikaljevic et al., *ACS Nano*, **15**, 14985 (2021)

O 56.6 Wed 16:15 GER 37

Structure determination of mono- and few-layers of the 2D-ferroelectric SnSe on graphene on Ir(111) — DINA WILKS¹, PAULUS ALEKSA¹, SIMON CHUNG², PETER MODREGGER¹, DMITRI V. NOVIKOV³, VEDRAN VONK², ANDREAS STIERLE^{2,4}, and CARSTEN BUSSE¹ — ¹Physics Department, University of Siegen, Germany — ²Nanolabor Centre for X-ray and Nano Science CXNS, Germany — ³Deutsches Elektronen-Synchrotron DESY, Germany — ⁴Physics Department, University of Hamburg, Germany

For conventional ferroelectrics the critical temperature T_c quickly falls below technically feasible values for very thin films. This is not the case for two-dimensional materials. Theory predicts strong ferroelectricity for group-IV monochalcogenides, where individual layers are puckered sheets with a phosphorene-like structure. For SnSe, stable ferroelectricity of monolayers at room temperature has been shown by controlled microscopic manipulation. Here, we provide the missing structure determination of these monolayers.

We use surface X-ray diffraction to determine the structure of SnSe mono- and few-layers, the influence of the substrate, and the difference in stacking between a few-layered system and the bulk. SnSe films are prepared by MBE using graphene on Ir(111) as an inert and weakly interacting substrate. We observe one phase with three different orientations of monolayer SnSe islands with respect to graphene, while for the few-layered system two phases are found, each with three different orientations. A change in structure with rising temperature for both systems is seen, which hints towards T_c .

O 56.7 Wed 16:30 GER 37

Electronic properties of epitaxially grown monolayer and bilayer VS_2 on Au(111) — MIKHAIL FONIN¹, SABINA SIMON¹, FELIX FÖRSCHNER¹, JANNIK DORNSEIFF¹, JULIA TESCH¹, ELENA VOLOSHINA², and YURIY S. DEDKOV² — ¹Department of Physics, University of Konstanz, 78457 Konstanz, Germany — ²Department of Physics, Shanghai University, 99 Shangda Road, 200444 Shanghai, China

Electronic properties of metallic two-dimensional materials can be strongly influenced by the supporting substrates, upon charge transfer or hybridization effects. In this context, suppression of many-body states in metallic transition metal dichalcogenides epitaxially grown on metallic substrates was recently reported [1]. By combination of scanning tunneling microscopy and first principle calculations we study monolayers and bilayers of VS_2 epitaxially grown on Au(111). We investigate the electronic properties of the monolayer and observe a metallic state with the presence of the incommensurate charge density wave state. Going from monolayer to bilayer VS_2 , we observe an evolution from the metallic state to an insulating state.

[1] C. E. Enders et al., *Phys. Rev. B* **94**, 081404(R) 2016.

O 56.8 Wed 16:45 GER 37

Vanadium sulphides on graphene on Ir(111): polymorphs, charge density waves, layer dependency — CAMIEL VAN EFFEREN¹, JOSHUA HALL¹, VIRGÍNIA BOIX², TOBIAS WEKKING¹, NIKOLAY VINOGRADOV³, ALEXEI PREOBRJENSKI³, JAN KNUDSEN², JEISON FISCHER¹, WOUTER JOLIE¹, and THOMAS MICHELY¹ — ¹Universität zu Köln — ²Lund University — ³MAX IV Laboratory

Among 2D materials, vanadium based compounds like VS_2 have attracted substantial research interest due to their predicted electronically correlated and magnetic ground states. However, the charge density wave (CDW) in monolayer (ML) VS_2 and VSe_2 competes with predicted magnetic ground states. This has led to new research directions attempting to unlock the magnetic moment of the V atoms, e.g. via defect creation, alloying or the intercalation of atoms between VS_2 layers.

Here, we present a comprehensive X-ray photoemission spectroscopy and scanning tunneling microscopy study of few-layer, quasi-freestanding V_4S_7 and V_5S_8 on Gr/Ir(111), which are created via annealing of stoichiometric VS_2 . Annealing ML VS_2 without background S pressure removes S atoms from the top layer of VS_2 , creating the striped compound V_4S_7 . In contrast, annealing ML VS_2 in a S atmosphere forms V_5S_8 , where V atoms have self-intercalated between the VS_2 layers in a 2×2 pattern. Surprisingly, we find that V_5S_8 has a layer-dependent CDW at low temperature, with bilayer V_5S_8 exhibiting a $\sqrt{3} \times \sqrt{3}$ CDW, while the trilayer hosts a striped CDW phase akin to that of ML VS_2 .

O 56.9 Wed 17:00 GER 37

Nucleation stage for the oriented growth of tantalum sulfide monolayers on Au(111) — •THAIS CHAGAS¹, KAI MEHLICH¹, ABDUS SAMAD², CATHERINE GROVER¹, DANIELA DOMBROWSKI^{1,3}, JIAQI CAI¹, UDO SCHWINGENSCHLÖGL², and CARSTEN BUSSE¹ — ¹Department Physik, Universität Siegen, Siegen, Germany — ²Physical Science and Engineering Division, King Abdullah University of Science and Technology, Thuwal, Saudi Arabia — ³Institut für Materialphysik, Westfälische Wilhelms-Universität Münster, Münster, Germany

We study the nucleation stage in the epitaxial growth of monolayer TaS_2 as a model system for monolayer transition metal sulfides. The growth was done under ultra-high vacuum conditions with Au(111) as a substrate on which the

metal atoms are evaporated, and the sulfur is provided from a background of H_2S . Using scanning tunneling microscopy (STM), we find small trimers with a well-defined triangular shape that act as nuclei for the further growth of extended tantalum sulfide monolayers. We identify these trimers as TaS_3 using density functional theory (DFT). We propose that the unique orientation of the trimers is the cause of the well-defined orientation of a complete TaS_2 layer found under favorable growth conditions.

O 56.10 Wed 17:15 GER 37

Growth and structure of two-dimensional single-layer HfS_2 on Au(111) — •MONIKA SCHIED, PAOLO LACOVIG, and SILVANO LIZZIT — Elettra-Sincrotrone Trieste

HfS_2 is a promising 2D material for low-power semiconductor devices due to its predicted high electron mobility and low contact resistance for n-type carrier transport. For actual applications, layers with excellent structural and electronic properties are needed. However, films with the necessary quality are only available from exfoliation, which is neither scalable nor very reproducible and only few experimental studies on a single-layer (SL) of HfS_2 have been performed so far. In analogy to the growth of high-quality SL transition metal dichalcogenides (TMDCs) such as MoS_2 and WS_2 [1,2] we have epitaxially grown an ordered layer of HfS_2 on Au(111) by chemical vapour deposition (CVD). Monitoring the S 2p and Hf 4f core levels in real time by fast X-ray photoelectron spectroscopy (XPS) allows the fine-tuning of the relevant parameters – such as the dosing rate and temperature – during the growth. The characterization by X-ray photoelectron diffraction (XPD) and low-energy electron diffraction (LEED) gives insight into the crystal structure of the film grown in this way.

[1] Bana, H., et al., 2D Mater. 5 035012 (2018)

[2] Bignardi, L. et al., Phys. Rev. Mat. 3, 014003, (2019)

O 57: Focus Session: Semiconductor Surface Chemistry – from Reaction Mechanisms to Well-Ordered Interfaces II

Time: Wednesday 15:00–17:00

Location: GER 38

Topical Talk

O 57.1 Wed 15:00 GER 38

Incorporation of arsenic into silicon (001) and germanium (001) for atomic-scale device fabrication. — •STEVEN R. SCHOFIELD — London Centre for Nanotechnology, University College London, 17-19 Gordon St, WC1H 0AH, United Kingdom

Atomic-scale electronic devices can be fabricated via the deterministic placement of individual donor atoms in semiconductors. The commonly-used technique involves the thermal decomposition of phosphine on the Si(001) surface and the patterning of a hydrogen resist layer for spatial control. However, it is now established that the desorption of phosphorus from the surface during the thermal incorporation anneal limits the scale-up of this method, e.g., for the fabrication of large numbers of qubits. In this talk, I will present exciting new work in our group demonstrating the excellent characteristics of arsine adsorption to both Si(001) and Ge(001) for the creation of atomic-scale devices. I will present combined scanning tunnelling microscopy and density functional theory work demonstrating that arsenic incorporates into the Ge(001) surface at room temperature when exposed to arsine, thus eliminating the need for the thermal anneal that is so problematic for phosphine on Si(001). Furthermore, I will present soft x-ray angle-resolved photoelectron spectroscopy (SX-ARPES) measurements of delta-doped layers in silicon that demonstrate higher confinement for arsenic layers compared to phosphorus layers. Our new results offer exciting opportunities for the fabrication of donor-based devices and their scale-up to the large numbers of qubits required for the fabrication of technological quantum devices.

O 57.2 Wed 15:30 GER 38

Controlling tip-induced reaction products of surface-adsorbed organic species on Si(001) — •ALEXA ADAMKIEWICZ¹, TAMAM BOHAMUD^{1,2}, MARCEL REUTZEL¹, GERSON METTE¹, ULRICH HÖFER¹, and MICHAEL DÜRR^{1,2} — ¹Department of Physics, Philipps University Marburg, Germany — ²Institute of Applied Physics, Justus Liebig University Giessen, Germany

Tip-induced electronic excitation via STM can give access to alternative reaction channels beyond thermal activation. We showed for the cleavage of tetrahydrofuran (THF) on Si(001) that excitation by the tunneling electrons leads to new final products, which can be selectively addressed by the type of excitation [1]. Here, we present the influence of the detailed configuration of the organic adsorbates on tip-induced ether cleavage. Due to the linear molecular structure of diethyl ether (Et_2O), the adsorbates undergo fragmentation when cleaved, thus leading to a higher degree of freedom compared to the ring-shaped THF. The final products differ significantly for both species. Furthermore, we show that upon high voltage scans, covalently bound Et_2O fragments can be further re-acted into more complex configurations which are thermally not accessible [2].

[1] Mette *et al.*, Angew. Chem. Int. Edit. 58, 3417 (2019).

[2] Adamkiewicz *et al.*, J. Phys.: Condens. Matter 33, 344004 (2021).

Topical Talk

O 57.3 Wed 15:45 GER 38

Semiconductor surface chemistry towards hybrid interfaces with ab initio approaches — •RALF TONNER-ZECH — Universität Leipzig, Leipzig, Germany

Exploiting concepts from molecular chemistry helps to improve our understanding of organic molecules reacting with semiconductor surfaces like silicon or germanium. Electronic structure analysis reveals concepts like Pauli repulsion or nucleophilic substitution reactions. Starting from this, hybrid interfaces can step by step be designed and analysed. The talk will focus on the associated challenges for theory encompassing model building, accuracy, adsorption kinetics and conceptual understanding. Finally, interface design from theory will be outlined.

[1] Pecher, Tonner, WIREs Comput. Mol. Sci. 2019, 9, e1401. [2] Luy, Molla, Pecher, Tonner, J. Comput. Chem. 2021, 42, 827. [3] Glaser, Meinecke, Freund, Langer, Luy, Tonner, Koert, Dürr, Chem.-Eur. J. 2021, 27, 8082.

O 57.4 Wed 16:15 GER 38

Oxygen vacancy occupancy influences oxygen evolution on $BiVO_4$ — •NICKLAS ÖSTERBACKA, HASSAN OUHBI, and JULIA WIKTOR — Chalmers University of Technology, Gothenburg, Sweden

Bismuth vanadate, $BiVO_4$, is one of the best semiconductor photoanode materials for photoelectrochemical water splitting. Oxygen vacancies are abundant in the material and greatly affect its photoelectrochemical properties. If present at the surface, these defects could additionally directly influence the oxygen evolution reaction. The electronic occupancy of the defect states may also play a role, but are seldom considered in mechanistic studies.

In this work, we use hybrid density functional theory to show that the surface oxygen vacancy in bismuth vanadate is most stable in its fully ionized state. We investigate how this affects the mechanics of the oxygen evolution reaction and compare the pathway with those involving the unionized surface vacancy and the defect-free surface. To quantify whether or not vacancy ionization is beneficial, the thermodynamic overpotentials required to drive the reaction are also computed and compared.

O 57.5 Wed 16:30 GER 38

Adsorption and photocatalytic inactivation of SARS-CoV-2 and virus like particles on the surface of anatase $TiO_2(101)$ — •MONA KOHANTORABI¹,

MICHAEL WAGSTAFFE¹, MARCUS CREUTZBURG¹, ESKO ERICK BECK¹, JOHANNES ROESSLER², REINHARD ZEIDLER², ALEXANDER HERRMANN³, MARTIN FEUERHERD³, GREGOR EBERT³, GABRIELA GUÉDEZ⁴, CHRISTIAN LÖW⁴, ROLAND THUENAUER⁴, THOMAS F. KELLER^{1,5}, BENEDIKT SOCHOR⁶, MATTHIAS

SCHWARTZKOPF⁶, ANDREI CHUMAKOV⁶, STEPHAN V. ROTH⁶, ULRIKE PROTZER³, WOLFGANG HAMMERSCHMIDT², ANDREAS STIERLE^{1,5}, and HESHMAT NOEI¹ — ¹Centre for X-ray and Nano Science, DESY — ²Helmholtz Zentrum München — ³Technical University of Munich — ⁴Centre for Structural Systems Biology, DESY — ⁵Department of Physics, University of Hamburg — ⁶Deutsches Elektronen-Synchrotron

In this contribution, adsorption of SARS-CoV-2 and SARS-CoV-2 like particles (VLPs) were investigated on the surface of the model photocatalyst TiO₂(101). The samples were analyzed by grazing-incidence small-angle X-ray scattering (GISAXS), atomic force microscopy (AFM), transmission electron microscopy and X-ray photoelectron spectroscopy to obtain insight into the interaction of the SARS-CoV-2 and VLPs with the surface of TiO₂(101). Furthermore, the UV induced photo inactivation of adsorbed species was investigated. AFM and GISAXS results on the UV-treated sample suggested that adsorbed viral particles undergo damage and photocatalytic oxidation on the surface of TiO₂ which can affect the structural proteins.

O 57.6 Wed 16:45 GER 38

Ab initio description of surface restructuring and phase boundaries under realistic conditions — •YUANYUAN ZHOU^{1,3}, CHUNYE ZHU^{1,2}, MATTHIAS SCHEFFLER¹, and LUCA M GHIRINGHELLI¹ — ¹The NOMAD Laboratory at the FHI of the Max-Planck-Gesellschaft and IRIS-Adlershof of the Humboldt-Universität zu Berlin — ²School of Advanced Manufacturing, Guangdong University of Technology, Jieyang 515200, China — ³Department of Physics, Technical University of Denmark, Kongens Lyngby, 2800, Denmark

A reliable description of surfaces equilibria in a reactive gas is a prerequisite for understanding mechanism of heterogeneous catalysis. However, studying phase equilibria at *ab initio* level, is a formidable challenge, especially for systems with sluggish barriers. In this work [Zhou *et al.* Phys. Rev. Lett. 128, 246101(2022)], we introduce a fully *ab initio* approach to determine temperature-pressure ($T-p$) surface phase diagram and to evaluate phase equilibria of surfaces in a gas phase. For this purpose, our replica-exchange grand-canonical (REGC) method [Zhou *et al.* Phys. Rev. B. 100, 174106(2019)], is extended by evaluating the heat capacity, $C_v(T, p)$, as function of T and p , thus locating phase boundaries where $C_v(T, p)$ shows ridges. The approach is demonstrated by addressing open questions for the Si(100) surface in a H₂ gas phase. 25 distinct stable surface phases are identified, most of which have not been observed experimentally, so far. The results also show that Si-Si-bonds forming/breaking is the driving force behind the experimentally 3×1 and 2×1 phase transition.

O 58: Plasmonics and Nanooptics II: Light-Matter Interaction and Spectroscopy I

Time: Wednesday 15:00–17:30

Location: WIL A317

O 58.1 Wed 15:00 WIL A317

Simultaneous Strong Coupling of the H- and J-Bands of Molecular Aggregates in Microcavities — •ROLAND SCHÄFER¹, LUKAS BÖHNER¹, MANUELA SCHIEK^{2,3}, KLAUS MEERHOLZ¹, and KLAS LINDFORS¹ — ¹Department für Chemie, Universität zu Köln, 50939 Köln, Germany — ²LIOS & ZONA, Johannes Kepler Universität, 4040 Linz, Austria — ³Institut für Physik, Carl von Ossietzky Universität Oldenburg, 26129 Oldenburg, Germany

We simultaneously strongly couple the H- and J-bands of aggregates of a merocyanine dye (HB238 [1]) to cavity photons. This is achieved by tuning the $3\lambda/2$ - and 1λ mode of a planar microcavity to the spectral positions of the H- and J-bands, respectively. Strong coupling behavior is confirmed via the observation of Rabi-splitting of both bands in angle-resolved reflectivity spectra.

Due to the orientation of the aggregates J-polaritons can be observed with s- and p-polarized light, while the H-polaritons can only be accessed with p-polarized light and a non-normal angle of incidence. Therefore, our system supports two or four polaritons, depending on the polarization, making it an interesting platform to study strong light-matter coupling.

[1] Bürckstümmer, H., *et al.*, *Angew. Chem. Int. Ed.* **2011**, 50: 11628-11632.

Acknowledgment: This project is funded with support from the RTG-2591 "TIDE - Template-designed Organic Electronics" (Deutsche Forschungsgemeinschaft).

O 58.2 Wed 15:15 WIL A317

Two-Dimensional Electronic Spectroscopy of Strong Exciton-Surface Plasmon Polariton Coupling — •DANIEL TIMMER¹, MORITZ GITTINGER¹, THOMAS QUENZEL¹, SVEN STEPHAN¹, JENNIFER ZABLOCKI², ARNE LÜTZEN², JIN-HUI ZHONG¹, MARTIN SILIES¹, ANTONIETTA DE SIO¹, and CHRISTOPH LIENAU¹ — ¹University of Oldenburg, Germany — ²University of Bonn, Germany

The creation of hybrid light-matter systems due to strong coupling is of major current interest for material science. Of special interest are dipolar interactions between molecular excitons (X) and plasmonic resonators, such as surface plasmon polaritons (SPP). Sufficiently strong coupling to vacuum field fluctuations allows for the coherent flow of energy between X and SPP, i.e. Rabi oscillations, forming new hybridized upper (UP) and lower (LP) polariton states [1]. We explore these strong coupling phenomena and especially their dynamics using two-dimensional electronic spectroscopy (2DES). Here, strong coupling predicts notorious "oscillating cross-peaks" between diagonal UP and LP peaks in a 2DES map. We investigate the polariton dynamics of a prototypical system for X-SPP coupling, a J-aggregate coated periodic gold slit array. In our measurements, the strongly coupled system indeed shows these hallmarks: Rabi oscillations of 2DES cross-peaks. Surprisingly, however, spatial modulations of the plasmon field seem to result in both strongly and weakly coupled excitons, which can then undergo coherent population transfer via the SPP. This conclusion is further supported by FDTD and Frenkel exciton model simulations. [1]: Vasa, Parinda, *et al.*, *Nat. Photon* **7.2**, 128-132 (2013).

Topical Talk

O 58.3 Wed 15:30 WIL A317

Phase-locked photon-electron interaction without a laser — •NAHID TALEBI — Institute for Experimental and Applied Physics, Kiel University, 24107 Kiel, Germany

Ultrafast electron-photon spectroscopy in electron microscopes commonly requires ultrafast laser setups. Photoemission from an engineered electron source is used to generate pulsed electrons, interacting with a sample that is excited by the ultrafast laser pulse at a specified time delay. Thus, developing an ultrafast electron microscope demands the exploitation of extrinsic laser excitations and complex synchronization schemes. Here, we present an inverse approach based on cathodoluminescence spectroscopy to introduce internal radiation sources in an electron microscope. Our method is based on a sequential interaction of the electron beam with an electron-driven photon source (EDPHS) and the investigated sample. An electron-driven photon source in an electron microscope generates phase-locked photons that are mutually coherent with the near-field distribution of the swift electron. Due to their different velocities, one can readily change the delay between the photons and electrons arriving at the sample by changing the distance between the EDPHS and the sample. We demonstrate the mutual coherence between the radiations from the EDPHS and the sample by performing interferometry with a combined system of an EDPHS and a WSe₂ flake. We assert the mutual frequency and momentum-dependent correlation of the EDPHS and sample radiation, and determine experimentally the degree of mutual coherence of up to 27%.

O 58.4 Wed 16:00 WIL A317

Layer-resolved resonance intensity of evanescent polariton modes — NIKOLAI C. PASSLER¹, GIULIA CARINI¹, DMITRY N. CHIGRIN^{2,3}, and •ALEXANDER PAARMANN¹ — ¹Fritz-Haber-Institut der Max-Planck-Gesellschaft, Berlin — ²DWI - Leibniz-Institut für Interaktive Materialien, Aachen — ³Institute of Physics (1A), RWTH Aachen University, Aachen

Most nanophotonic approaches rely on polaritons to confine light to the nanoscale. In particular heterostructures of strongly anisotropic polar crystals have been of key interest recently, where the twist angles between different anisotropic layers key be leveraged to create and control exotic polaritonic states [1]. To guide the designs of such multi-parameter systems, low-cost simulation tools are invaluable. Common approaches like employing the reflection coefficient under evanescent excitation enable analysis of the polariton resonances without the need to specify the exact experimental arrangement, but lack layer-specific information. Here [2], we introduce a formalism based on a 4×4 transfer matrix algorithm [3] and energy flow analysis using the Poynting vector [4], that provides full depth-resolved information even for evanescent wave excitation. We illustrate the power of the approach by analysing a state-of-the-art example of twisted bilayer molybdenum trioxide [1].

[1] G. Hu, *et al.*, *Nature* **582**, 209 (2020).

[2] N.C. Passler, *et al.*, arXiv preprint, arXiv:2209.00877 (2022).

[3] N.C. Passler & A. Paarmann, *JOSA B* **34**, 2128 (2017).

[4] N.C. Passler, *et al.*, *PRB* **101**, 165425 (2020).

O 58.5 Wed 16:15 WIL A317

Observation of multi-quantum phenomena in molecular films strongly coupled to surface plasmons using ultrafast laser spectroscopy — •SIMON BÜTTNER¹, MATTHIAS HENSEN¹, KATJA MAYERSHOFER¹, MAXIMILIAN RÖDEL², JENS PFLAUM², and TOBIAS BRIXNER¹ — ¹Institut für Physikalische und Theoretische Chemie, Universität Würzburg, Am Hubland, 97074 Würzburg, Ger-

many — ²Experimental Physics VI, University of Würzburg, Am Hubland, 97074 Würzburg, Germany

Multi-quantum phenomena such as exciton–exciton annihilation can be used to study exciton diffusion [1], which is a key process in optoelectronic devices like solar cells. Recently, our group has developed a method to isolate different multi-quantum signals using transient absorption (TA) spectroscopy. This novel method makes it possible to filter out the interaction of a distinct number of quasiparticles and their time evolution. Here, we use this method together with a new ultrafast laser setup that allows us to shape and detect femtosecond laser pulses at a repetition rate of 100 kHz. As a model system we investigate a thin Zinc phthalocyanine (ZnPc) film on a surface-plasmon-supporting gold substrate. Strong coupling between ZnPc excitons and surface plasmons leads to the formation of plexcitons [2], and thus to a delocalization of charge carriers, which is of particular interest for increasing charge carrier mobilities. In this work we focus on the influence of the strong coupling on the quasiparticle diffusion.

[1] P. Malý et al., *Chem. Sci.* 11, 456 (2020)

[2] M. Rödel et al., *J. Phys. Chem. C* 126, 4163–4171 (2022)

O 58.6 Wed 16:30 WIL A317

Resonant imaging of infrared light confinement using phonon polaritons in sub-diffractive 4H-SiC nanostructures — •RICHARDA NIEMANN¹, SÖREN WASSERROTH¹, GUANYU LU², CHRISTOPHER R. GUBBIN³, MARTIN WOLF¹, SIMONE DE LIBERATO³, JOSHUA D. CALDWELL², and ALEXANDER PAARMANN¹ — ¹Fritz Haber Institute of the Max Planck Society, Berlin, Germany — ²Vanderbilt University, Nashville, USA — ³University of Southampton, UK

Confinement of light to deeply sub-wavelength scales can be achieved using polaritons spatially confined to sub-diffractive nanostructures. Next to well-established plasmon polariton approaches, phonon polaritons supported in nanostructures made from polar dielectric crystals are a promising tool for the infrared spectral range [1].

Here, we study localized phonon polariton resonances in sub-diffractive 4H-SiC nanostructures using infrared super-resolution sum-frequency generation (SFG) microscopy [2], employing our institute's infrared free-electron laser [3]. With this technique we achieve high sensitivity to optical field enhancement associated with the spatial confinement of light. Simultaneously it is providing sub-diffractive imaging resolution, naturally enabling to study polaritons on their intrinsic length scales.

[1] Gubbin et al., *Journal of Appl. Phys.* 131, 030901 (2022)

[2] Niemann et al., *Appl. Phys. Lett.* 120, 131102 (2022)

[3] Schöllkopf et al., *Proc. SPIE* 9512, 95121L (2015)

O 58.7 Wed 16:45 WIL A317

Nano-scale Plasmonic Su-Schrieffer-Heeger Chains — •BENEDIKT SCHURR^{1,4}, PHILIPP GRIMM¹, TOBIAS HELBIG², TOBIAS HOFMANN², LUKAS WEHMEIER³, FELIX G. KAPS³, THORSTEN FEICHTNER^{1,4}, MONIKA EMMERLING¹, SUSANNE C. KEHR³, LUKAS ENG^{3,4}, RONNY THOMALE^{2,4}, and BERT HECHT^{1,4} — ¹NanoOptics & Biophotonics Group, Experimental Physics 5, University of Würzburg, Am Hubland, 97074 Würzburg, Germany — ²Institute for Theoretical Physics and Astrophysics, University of Würzburg, Am Hubland, 97074 Würzburg, Germany — ³Institut für Angewandte Physik, Technische Universität Dresden, 01062 Dresden, Germany — ⁴Würzburg-Dresden Cluster of Excellence ct.qmat, University of Würzburg, Am Hubland, 97074 Würzburg, Germany

The tight-binding Su-Schrieffer-Heeger (SSH) model describes 1D periodic chains of resonators with alternating coupling strengths. For certain configura-

tions, topologically protected collective states occur at the edges. Here, we propose a plasmonic chain SSH-system with alternating few-nanometer gaps, fabricated from mono-crystalline Au-microplatelets by means of He-ion beam milling. Full FDTD simulations show the occurrence of edge modes for such geometries in real space. The frequency at which edge states occur can be fully controlled via particle size and the next-neighbour coupling via the gaps. Scattering scanning near-field optical microscopy (sSNOM) experiments provide first evidence for the presence of topologically protected edge states.

O 58.8 Wed 17:00 WIL A317

Directional leaky polaritons in anisotropic crystals — XIANG NI¹, •GIULIA CARINI², WEILIANG MA³, ENRICO M. RENZI¹, EMANUELE GALIFFI¹, SÖREN T. WASSERROTH², MARTIN WOLF², PEINING LI³, ALEXANDER PAARMANN², and ANDREA ALÙ¹ — ¹CUNY, New York, USA — ²FHI, Berlin, Germany — ³HUST, Wuhan, China

For quite a few years now, natural hyperbolic materials have been attracting significant attention due to their ability of engaging strong interactions between light and their IR active phonon resonances. The hybridized light-matter quasiparticles arising in their bulk, known as hyperbolic phonon polaritons, display large momenta and highly directional propagation stemming from their open topology.

In our contribution, we demonstrate a new class of directional polaritons supported in the lower reststrahlen band of calcite, that feature lenticular isofrequency contours. These novel polaritons, dubbed Leaky Polaritons (LPs), arise in the type-I in-plane hyperbolic region as hybridized states between extraordinary surface-bound and ordinary propagating bulk modes. Despite their closed topology, they support highly directional, long-range, sub-diffractive propagation at the interface. Their dispersion curve also crosses the free-space light cone, providing radiative far-field coupling to both sides of the interface.

To observe the features of LPs experimentally, we employed polariton spectroscopy, far-field probing and near-field imaging, revealing their lenticular dispersion curve, their high directionality, their long lifetime and real-space propagation.

O 58.9 Wed 17:15 WIL A317

Anticrossing of a plasmonic nanoresonator mode and a single quantum dot at room temperature — •DANIEL FRIEDRICH¹, JIN QIN¹, BENEDIKT SCHURR¹, TOMMASO TUFARELLI², HEIKO GROSS¹, and BERT HECHT¹ — ¹NanoOptics & Biophotonics Group, Experimental Physics 5, University of Würzburg, Germany — ²School of Mathematical Sciences and Centre for the Mathematics and Theoretical Physics of Quantum Non-Equilibrium Systems, University of Nottingham, United Kingdom

At ambient conditions strong coupling (SC) is achieved due to the extremely small mode volume of plasmonic nanoresonators and the broadband spectral overlap between emitter and nanocavity. This results in ultrafast energy transfer which overcomes dephasing. Normal mode splittings in luminescence spectra of single quantum systems coupled to plasmonic nanoresonators have been reported and exploited to estimate the light-matter coupling strength g . However, there is only sketchy evidence for the hallmark of single-emitter strong coupling, the anticrossing of emitter and cavity resonances. Here, we exploit the light-induced oxygen-dependent blue-shift of individual CdSe/ZnS semiconductor quantum dots to tune their transition energy across the weakly radiative resonance of a scanning plasmonic slit resonator. The observed anticrossing in photoluminescence spectra recorded as a function of time provide clear proof of SC as well as a solid measure for the single-emitter coupling strength consistent with classical field simulations and a quantum model including dissipation.

O 59: Electronic Structure of Surfaces I

Time: Wednesday 15:00–17:45

Location: REC C 213

Topical Talk

O 59.1 Wed 15:00 REC C 213

Interplay of Inversion Symmetry Breaking and Spin-Orbit Coupling — •MAXIMILIAN ÜNZELMANN — Experimentelle Physik 7, Universität Würzburg and Würzburg-Dresden Cluster of Excellence ct.qmat

Inversion symmetry breaking (ISB) in crystalline solids provides an essential way of modifying electronic structures. For example, in combination with spin-orbit coupling (SOC), ISB allows for a lifting of spin degeneracy without the need for magnetism. Moreover, it is a source of Berry curvature, which is of fundamental importance in topological quantum matter. In this talk, two scenarios will be discussed, in which the interplay of ISB with SOC plays an important role: (i) At surfaces or interfaces, where inversion symmetry is inherently broken and the Rashba effect [1] enforces a locking of the electrons spin perpendicular to its momentum and (ii) in Weyl semimetals whose three-dimensional crystal structure has no inversion center, leading to the formation of Berry curvature monopoles, i.e., quantized topological charges [2].

As will be highlighted in this presentation, we find that ISB-induced unquenching of the so-called (atomic) orbital angular momentum (OAM) in the Bloch wave functions constitutes a key mechanism underlying the physics of both the Rashba effect and Weyl semimetals. Angle-resolved photoemission with variable light polarization provides detailed experimental access to the respective momentum-space orbital textures.

[1] M. Ünzelmann et al., *Phys. Rev. Lett.* 124, 176401 (2020)

[2] M. Ünzelmann et al., *Nat. Commun.* 12, 3650 (2021)

O 59.2 Wed 15:30 REC C 213

Unoccupied surface electronic structure of Re(0001) — •FABIAN SCHÖTTKE, SVEN SCHEMMELMANN, PETER KRÜGER, and MARKUS DONATH — Westfälische-Wilhelms-Universität Münster, Germany

The influence of spin-orbit interaction on the unoccupied electronic structure of the Re(0001) surface is investigated by spin- and angle-resolved inverse photoemission and density-functional theory calculations. In the two high-symmetry

azimuths $\bar{\Gamma}\bar{K}$ and $\bar{\Gamma}\bar{M}$, we identify transitions into d -derived bulk states as well as different types of surface states. The Rashba-type spin-split hole pocket around $\bar{\Gamma}$ finds continuation in empty spin-split surface states for higher k_{\parallel} , thereby forming W-shaped states whose lower parts are partially occupied.

Schöttke *et al.*, Phys. Rev. B **105**, 155419 (2022).

O 59.3 Wed 15:45 REC C 213

Establishing fundamentals of ARPES spin textures with the model material PtTe₂ — •MOHAMMED QAHOSE¹, GUSTAV BIHLMAYER², JAKUB SCHUSSER³, MUTHU MASILAMANI³, FRIEDRICH REINERT³, CLAUD M. SCHNEIDER¹, and LUKASZ PLUCINSKI¹ — ¹PGI-6 Forschungszentrum-Jülich — ²PGI-1/IAS-1 Forschungszentrum-Jülich — ³Experimentelle Physik VII and Würzburg-Dresden Cluster of Excellence ct.qmat, Universität Würzburg

A novel quantum material PtTe₂ is used to establish the connection between spin textures of angle-resolved photoemission spectroscopy (ARPES) and initial state spin textures. The crystal structure of 1T-PtTe₂ is trigonal, belongs to the space group 164 (P $\bar{3}$ m1), that contains mirror planes and inversion symmetry. Since bulk 1T-PtTe₂ is both inversion-symmetric and non-magnetic, no bulk spin-polarized bands are allowed due to the Kramers degeneracy. At the surface, a non-zero spin polarization is expected due to the broken inversion symmetry, however, it must obey the mirror and time-reversal symmetries. We measured the dependence of the spin-polarization on the symmetries of the ARPES setup. This is performed in two geometries, with the reaction plane parallel to $\bar{K}\bar{\Gamma}\bar{K}$ and $\bar{M}\bar{\Gamma}\bar{M}$ reciprocal directions, i.e. either along or orthogonal to the crystal mirror plane. The measured spin texture is symmetric when the reaction plane is parallel to $\bar{K}\bar{\Gamma}\bar{K}$. However, we see asymmetries in the spin texture when the reaction plane is parallel to $\bar{M}\bar{\Gamma}\bar{M}$. For surface states, the asymmetries are due to the geometry-induced spin filtering in ARPES [1]. For bulk states, the effect might be additionally related to the asymmetric initial state dispersions.

[1] T. Heider *et al.*, arXiv:2210.10870 (2022)

O 59.4 Wed 16:00 REC C 213

Surface electronic structure of Re(0001): A spin-resolved photoemission study — •MARCEL HOLTSMANN¹, PETER KRÜGER², KOJI MIYAMOTO³, TAICHI OKUDA³, SHIV KUMAR³, KENYA SHIMADA³, and MARKUS DONATH¹ — ¹Physikalisches Institut, WWU Münster, Germany — ²Institut für Festkörpertheorie, WWU Münster, Germany — ³HiSOR, Hiroshima University, Japan

The surface electronic structure of Re(0001) has been investigated in a combined experimental and theoretical study. (Spin- and) angle-resolved photoemission was employed to unravel the spin-dependent $E(k_{\parallel})$ dispersion along the $\bar{\Gamma}\bar{M}$ and $\bar{\Gamma}\bar{K}$ directions. The results are compared with band structures from density-functional theory. Moreover, transitions into final states have been considered by inclusion of the corresponding matrix elements. A spin-orbit-induced mixing of Shockley- and Tamm-type surface states around $\bar{\Gamma}$ and close to E_F was reported recently [1]. Here, we extend the analysis to a wider $E(k_{\parallel})$ range showcasing a multitude of electronic states along the $\bar{\Gamma}\bar{M}$ and $\bar{\Gamma}\bar{K}$ directions. In particular, Rashba-type spin splittings are observed around the high-symmetry $\bar{\Gamma}$ and \bar{M} points. At variance with theoretical predictions [2], which describe a perfect hcp(0001) surface, we do not find any out-of-plane spin polarization. This is caused by monoatomic steps of a real Re(0001) surface with alternating terminations, which lead on average to an effective sixfold surface symmetry and vanishing net out-of-plane spin polarization.

[1] M. Holtmann *et al.*, Phys. Rev. B **105**, L241412 (2022)

[2] A. Urru and A. Dal Corso, Surf. Sci. **686**, 22 (2019)

O 59.5 Wed 16:15 REC C 213

Spectroscopic evidence for a new type of surface resonance at noble-metal surfaces — •TOBIAS EUL¹, JÜRGEN BRAUN², BENJAMIN STADTMÜLLER^{1,3}, HUBERT EBERT², and MARTIN AESCHLIMANN¹ — ¹Technische Universität Kaiserslautern and Research Center OPTIMAS, 67663 Kaiserslautern, Germany — ²Department Chemie, Ludwig-Maximilians-Universität München, 81377 München, Germany — ³Institute of Physics, Johannes Gutenberg University Mainz, 55128 Mainz, Germany

We investigated the surface and bulk properties of the pristine (110) surface of silver using threshold photoemission by excitation with light of 5.9 eV. Using a momentum microscope, we identified two distinct transitions along the $\bar{\Gamma}\bar{Y}$ -direction of the crystal. The first one is a so far unknown surface resonance of the (110) noble-metal surface, exhibiting an exceptionally large bulk character that has so far been elusive in surface sensitive experiments. The second one stems from the well-known bulklike Mahan cone oriented along the $\bar{\Gamma}\bar{L}$ -direction inside the crystal but projected onto the (110)-surface cut. The existence of the new state is confirmed by photocurrent calculations, and its character is analyzed.

O 59.6 Wed 16:30 REC C 213

One monolayer of Tl on Ag(111): Hybridization of image-potential states with Tl states — •SVEN SCHEMMELMANN¹, PATRICK HÄRTL², PETER KRÜGER³, MATTHIAS BODE², and MARKUS DONATH¹ — ¹Physikalisches Institut, Westfälische Wilhelms-Universität, Münster — ²Physikalisches Institut, Experimentelle Physik II, Universität Würzburg — ³Institut für Festkörpertheorie, Westfälische Wilhelms-Universität, Münster

For one atomic layer of Tl on Ag(111) a moiré superstructure is observed. The unoccupied electronic structure of this superstructure is investigated by spin- and angle-resolved inverse photoemission. The experimental results are interpreted on the basis of DFT calculations. We observe several Tl-induced surface states and an image-potential state mainly located several Å in front of the surface. Surprisingly, we find a hybridization of this image state with a downward dispersing Tl band. This leads to spin-dependent spectral intensities that vary rapidly close to the hybridization point. The calculations show an expeditious change of the charge density from a resonant image-potential state towards a Tl-induced surface state in dependence of k_{\parallel} .

O 59.7 Wed 16:45 REC C 213

Bulk and surface electronic structure of tunnel barrier Nb₃Br₈ in the field-free Josephson diode — •MIHIR DATE^{1,2}, JONAS.A. KRIEGER¹, EMILY.C. MCFARLANE¹, VICKY HASSE³, CLAUDIA FELSER³, STUART.S.P PARKIN¹, MATTHEW WATSON², and NIELS.B.M SCHRÖTER¹ — ¹MPI-Halle, Weinberg 2, 06120 Halle (Saale), Germany — ²Diamond Light Source Ltd. Didcot, OX11 0DE, United Kingdom — ³MPI-CPFS, Nöthnitzer Straße 40, 01187 Dresden, Germany

In this work, we report the bulk and surface electronic structure of Nb₃Br₈ probed using angle resolved photoemission spectroscopy (ARPES). Nb₃Br₈ is predicted to host trivial metallic surface states (obstructed surface states (OSS)) when cleaved between specific layers [1]. Although our in-plane electronic structure is consistent with the calculated orbital resolved bandstructure, we do not observe any signatures of the OSS. Nevertheless, the doubling of periodicity of the ARPES signal along the out-of-plane momentum direction, as compared to the Brillouin zone dimension, hints towards dimerization between alternate layers through the OSS. We discuss our results in connection with the recent discovery of the field-free Josephson diode effect in the $NbSe_2/Nb_3Br_8/NbSe_2$ heterostructures [2].

[1] Xu, Y. *et al.* arXiv:2106.10276 (2021).

[2]. Wu, H. *et al.* Nature **604** (2022).

O 59.8 Wed 17:00 REC C 213

Termination dependent many-body interactions of the surface states of PdCoO₂ revealed by ARPES-based microscopy — •GESA-ROXANNE SIEMANN¹, EDGAR ABARCA MORALES^{1,2}, PHILIP A. E. MURGATROYD¹, TOMMASO ANTONELLI¹, SEUNGHYUN KHM², MATTHEW WATSON³, CEPHISE CACHO³, ANDREW P. MACKENZIE^{1,2}, and PHIL D. C. KING¹ — ¹University of St Andrews, UK — ²MPI for Chemical Physics of Solids, Dresden, Germany — ³Diamond Light Source, UK

The layered ABO₂ structure of the delafossite oxides yields markedly different electronic structures at their A- and BO₂-terminated surfaces which are either electron- (A-termination) or hole-doped (BO₂-termination) with respect to the bulk¹. A prominent example is PdCoO₂ where a giant Rashba effect can be observed on the CoO₂ terminated surface², while the Pd terminated surface hosts ferromagnetic states which are absent in the bulk^{3,4}. However, the study of these states has often been hampered by the size of domains of each distinct surface termination. Here we show how these problems can be circumvented using micro-ARPES performed in a spatially-resolved mode. Our measurements further reveal strong signatures of self-energy modulations on both surfaces due to coupling to bosonic modes, making them the ideal playground to study varying coupling mechanisms and their tunability in the same sample. ¹A. P. Mackenzie, Rep. Prog. Phys. **80**, 032501 (2017), ²V. Sunko *et al.*, Nature **549**, 492-496 (2017), ³F. Mazzola *et al.*, PNAS **115**(51)12956-12960 (2018), ⁴F. Mazzola *et al.*, npj Quantum Materials **7**, 20 (2022)

O 59.9 Wed 17:15 REC C 213

The Meservey-Tedrow-Fulde vortex in epitaxial aluminum near the monolayer limit — •WERNER M.J. VAN WEERDENBURG¹, ANAND KAMLAPURE¹, EIRIK FYHN HOLM², NIELS P.E. VAN MULLEKOM¹, XIAOCHUN HUANG², MANUEL STEINBRECHER¹, PETER KROGSTROP³, JACOB LINDER², and ALEXANDER A. KHAJETOORIANS¹ — ¹Institute for Molecules and Materials, Radboud University Nijmegen, the Netherlands — ²Center for Quantum Spintronics, Norwegian University of Science and Technology, NO-7491 Trondheim, Norway — ³NNF Quantum Computing Programme, Niels Bohr Institute, University of Copenhagen, Denmark

The critical magnetic field of 2D superconductors is greatly enhanced for fields parallel to the 2D plane. In the case of aluminum, this gives rise to a spin-splitting of the coherence peaks, referred to as the Meservey-Tedrow-Fulde (MTF) effect. In the MTF regime, it has been proposed that unconventional odd-frequency (ω_o) spin-triplet pairing is promoted [1], but their presence is experimentally hard to detect.

Here, we study vortices in thin epitaxial Al films on Si(111) in the MTF regime by applying a vector magnetic field with a large in-plane component, and find experimental evidence of odd-frequency pairing [2]. Strikingly, we find that the shape of the vortex structure is strongly modified and exhibits a gapless region. Numerical simulations confirm a connection between this vortex shape and the presence of ω_o pairing, highlighted by a paramagnetic Meissner effect.

- [1] J. Linder & J. Robinson, Scientific Reports 5, 15483 (2015)
 [2] W. van Weerdenburg et al., arXiv:2210.10645 (2022)

O 59.10 Wed 17:30 REC C 213

Exploring polaron stability and defect structures in $\text{Li}_4\text{Ti}_5\text{O}_{12}$ (LTO): A combined theoretical and experimental approach — •YU-TE CHAN¹, MATTHIAS KICK², CRISTINA GROSU², CHRISTOPH SCHEURER¹, and HARALD OBERHOFER³ — ¹Fritz-Haber-Institut der MPG, Berlin, Germany — ²Massachusetts Institute of Technology, Cambridge, USA — ³University of Bayreuth, Bayreuth, Germany
 Spinel $\text{Li}_4\text{Ti}_5\text{O}_{12}$ (LTO) is a promising anode material for next-generation all-solid-state Li-ion batteries (ASSB) due to its "zero strain" charge/discharge behavior. Pristine LTO suffers from poor ionic and electronic conductivity. Oxygen vacancies, produced by tailored sintering protocols, yield a performant, blue

LTO material. Vacancy induced polarons have been proposed as one of the origins of increased electronic conductivity. However, detailed knowledge about polaron stability, distribution, and dynamics in LTO bulk and surface have been lacking. By performing *Hubbard corrected density functional theory* (DFT+U) calculations we are able to show that in fact polaron formation and a possible polaron hopping mechanism can not only play a significant role in enhancing electronic conductivity but boost Li^+ diffusion nearby, in line with the experimentally observed improved conductivities.[1,2] In combination with positron lifetime spectroscopy data and machine learning models, we arrive at a rather complete picture of the bulk vs. surface defect chemistry in LTO particles and the resulting mixed ionic electronic conductivity. [1] M. Kick et al., J. Phys. Chem. Lett. 11 (2020), 2535 [2] M. Kick et al., ACS Appl. Energy Mater 4 (2021), 8583

O 60: Solid-Liquid Interfaces I: Structure and Spectroscopy

Time: Wednesday 15:00–18:00

Location: TRE Phy

O 60.1 Wed 15:00 TRE Phy

Investigation of the water structure at the (001) and (010) orthoclase surfaces with three-dimensional atomic force microscopy — •FRANZISKA SABATH, RALF BECHSTEIN, and ANGELIKA KÜHNLE — Physical Chemistry I, Bielefeld University, Universitätsstraße 25, 33615 Bielefeld

Feldspars are the most abundant minerals in the Earth's crust and belong to the most effective group of mineral ice nucleating particles (INP) in the atmosphere. In the crystal structure, potassium, sodium or calcium, among others, are incorporated as counterions in varying ratios. Potassium-rich feldspars are more effective INPs than the other feldspars. A representative of a potassium-rich feldspar is orthoclase. Unlike other INPs, such as silver iodide, the surfaces of feldspar do not have an ice-like structure. Therefore, it is interesting to know what other factors, such as hydroxyl groups on the surfaces or defect sites, are responsible for the high ice nucleating efficiency of K-feldspars. In particular, the water structure at the interface of K-feldspars is of interest. Here, we show the three-dimensional water structure at the two natural cleavage planes of orthoclase, the (001) and the (010) surfaces, using three-dimensional atomic force microscopy (AFM).

O 60.2 Wed 15:15 TRE Phy

Influence of substrate on supramolecular nanostructures at the solid-liquid interface — •BAOXIN JIA¹, MIHAELA ENACHE¹, SANDRA MIGUEZ-LAGO², MILAN KIVALA², and MEIKE STÖHR¹ — ¹Zernike Institute for Advanced Materials, University of Groningen, Netherlands — ²Institute of Organic Chemistry, University of Heidelberg, Germany

Self-assembly of supramolecular nanostructures at the solid-liquid interface has gained increasing academic interest in past recent years. Substrates can influence molecule-substrate interactions, which plays an important role in determining supramolecular nanostructures. In this study, we used scanning tunneling microscopy (STM) to investigate the self-assembly of two carboxylic acids at the nonanoic acid-solid interface. We performed the experiments on four substrates: HOPG, MoS₂, Au(111), and graphene/Cu foil. We also measured the water contact angle of these four substrates to obtain some information on the molecule-substrate interaction. The STM measurements showed that, on HOPG and graphene/Cu foil, both carboxylic acids can form porous and close-packed structures, which depends on the bias voltage polarity during STM measurements. On MoS₂, both carboxylic acids did not form stable self-assembled structures. On Au(111), both carboxylic acids only formed short range-ordered structures in very diluted solutions. The results reveal that the interplay between molecule-substrate, solvent-substrate and molecule-molecule interactions is important to the formation of supramolecular nanostructures at the solid-liquid interface.

O 60.3 Wed 15:30 TRE Phy

Hydrophobic pockets on the hydrophilic In_2O_3 (111) surface — CHRISTIAN RITTERHOFF¹, •BERND MEYER¹, ULRIKE DIEBOLD², and MARGARETA WAGNER² — ¹Interdisciplinary Center for Molecular Materials and Computer Chemistry Center, FAU Erlangen-Nürnberg, Germany — ²Institute of Applied Physics, TU Wien, Austria

Clean oxide surfaces are generally hydrophilic. Water molecules anchor at undercoordinated surface cations that act as Lewis acid sites, and they are stabilized by H bonds to surface oxygens. However, for In_2O_3 (111), DFT calculations predict a deviation from this general rule, which has been confirmed by TPD, XPS, STM and AFM experiments. In UHV, the first nine water molecules cover only a part of the unit cell. Within the H-bonded network three out of the nine water dissociate. Additional molecules pile up above the OH groups. The rest of the unit cell is unfavorable for adsorption and remains water-free, despite offering undercoordinated In and O sites. The first water layer thus shows ordering into nanoscopic 3D water clusters separated by hydrophobic pockets. Beyond UHV,

our *ab initio* MD simulations of a liquid water layer demonstrate the robustness of the strongly hydrophobic behavior of this region in the unit cell.

- [1] H. Chen, M.A. Blatnik, C.L. Ritterhoff, I. Sokolović, F. Mirabella, G. Franceschi, M. Riva, M. Schmid, J. Čechal, B. Meyer, U. Diebold, M. Wagner, ACS Nano, accepted, DOI: 10.1021/acsnano.2c09115

O 60.4 Wed 15:45 TRE Phy

Facet-dependent surface charge and hydration of SrTiO_3 nanoparticles at variable pH — •IGOR SIRETANU, SU SHAOQIANG, BASTIAN MEI, DIRK VAN DEN ENDE, GUIDO MUL, and FRIEDER MUGELE — Physics of Complex Fluids and Photocatalytic Synthesis Groups, MESA+ Institute, Faculty of Science and Technology, University of Twente, PO Box 217, 7500 AE Enschede, The Netherlands
 Anisotropy of shape and surface properties determine the functionality of faceted nanoparticles in various contexts including facet selective colloidal self-assembly, biosensing, improved photo/electrocatalytic activity and ions uptake. The characteristic surface properties and function of solid-liquid interfaces of crystalline faceted nanoparticles are believed to be essential for their performance but remains poorly understood and difficult to characterize and quantify. We use dual scale Atomic Force Microscopy to measure electrostatic and hydration forces of faceted SrTiO_3 nanoparticles in aqueous electrolyte at variable pH. We demonstrate (i) the ability to quantify strongly facet-dependent surface charges yielding isoelectric points of the dominant {100} and {110} facets that differ by as much as 2 pH units, ii) fluids composition controlled facet-dependent accumulation of oppositely charged (SiO_2) particles, and iii) that atomic scale defects can be resolved but are in fact rare for the samples investigated. Atomically resolved images and facet-dependent hydration structure suggest a microscopic hydration and charge generation mechanism.

O 60.5 Wed 16:00 TRE Phy

Watching Redox Activation of Gold for Water Electrolysis live: An in-situ Experiment at Home — CHRISTOPH GRIESSER, DANIEL WINKLER, TONI MOSER, ENGELBERT PORTENKIRCHNER, and •JULIA KUNZE-LIEBHÄUSER — Institute of Physical Chemistry, University of Innsbruck, Innrain 52c, Innsbruck, 6020 Austria

A fundamental understanding of processes that take place at the solid/liquid interface is of utmost importance for a rational design of (electro-)catalysts, and key for advancing energy conversion and storage technologies. We could show with in-situ electrochemical near ambient pressure X-ray photoelectron spectroscopy (NAP-XPS) that metallic Au, in alkaline media, reversibly oxidizes to Au^+ at potentials prior to and during the early oxygen evolution reaction (OER), while it reversibly oxidizes to Au^{3+} at potentials where the OER takes place at high rates. This has previously not been clearly demonstrated in-situ, so that the redox chemistry of Au in alkaline media remains a highly debated topic in the electrochemical community to date. We demonstrate the implementation of a simple, affordable and in-situ/operando- method to track dynamic processes taking place at the electrified solid/liquid interface, utilizing a lab-based NAP-XPS system with a conventional Al K α X-ray source. The method has the potential to become a gamechanger in applied (electro-)catalysis research, which makes our contribution appealing for scientists following either fundamental or applied research interests.

O 60.6 Wed 16:15 TRE Phy

Structure and Reactivity of an Ionic Liquid on Cu(111) investigated by Scanning Probe Microscopy, Photoelectron Spectroscopy and Simulations — RAJAN ADHIKARI¹, STEPHEN MASSICOT¹, LUKAS FROMM², •SIMON JAEKEL¹, TIMO TALWAR¹, AFRA GEZMIS¹, MANUEL MEUSEL¹, ANDREAS BAYER¹, FLORIAN MAIER¹, ANDREAS GÖRLING², and HANS-PETER STEINRÜCK¹ — ¹Chair of Physical Chemistry II, Friedrich-Alexander-Universität Erlangen-Nürnberg, Egerlandstraße 3, 91058 Erlangen, Germany — ²Chair of Theoretical Chemistry,

Friedrich-Alexander-Universität Erlangen-Nürnberg, Egerlandstraße 3, 91058 Erlangen, Germany

We studied the adsorption and reaction behaviour of the ionic liquid (IL) 1,3-dimethylimidazolium bis[(trifluoromethyl)sulfonyl]imide ($[(C_1C_1Im)[(TF_2N)]]$) on Cu(111) in UHV. Our nc-AFM and STM results show that the IL transitions from an ordered structure observed after annealing at 200 K into a different ordered structure and disordered islands after extended annealing at 300 K. Complementary, ARXPS reveals that the IL initially adsorbs intact and that no IL desorption occurs until 300 K but that a significant fraction of the IL is converted to a new species. We correlate the remaining unshifted peaks to the ordered phases observed in AFM and the shifted peaks to decomposition products, which appear as disordered islands. From DFT, we obtain additional information on the structure of the ordered phases and the interaction of the IL with the substrate.

O 60.7 Wed 16:30 TRE Phy

Influence of Interfacial Water and Cations on the Oxidation of CO at the Platinum/Ionic Liquid Interface — •BJÖRN RATSCHMEIER, GINA ROSS, ANDRE KEMNA, and Björn Braunschweig — University Münster, Institute of Physical Chemistry, Münster, Germany

CO oxidation is fundamental key for complete oxidation of small alcohols on Pt catalysts in fuel cells. So far, room-temperature ionic liquids (RTIL) have been used to modify the selectivity in electrocatalysis. In order to understand the mechanism of CO oxidation in RTIL we have investigated this reaction at the Pt(111)/1-butyl-3-methylimidazolium trifluorosulfonylimide [BMIM][NTf₂] electrode/electrolyte interface as a function of H₂O concentration and electrode potential using *in situ* sum-frequency generation (SFG) spectroscopy and infrared absorption spectroscopy (IRAS). Using SFG spectroscopy, we address the changes of CO molecules on Pt(111), while we monitor bulk electrolyte changes with IRAS using vibrational bands from H₂O, CO₂ and CO. The presence of water in [BMIM][NTf₂] shifts the CO onset potential by more than 200 mV with increased H₂O concentration from 0.01 to 1.5 M, which we relate to the incorporation and availability of water at the electrode/electrolyte interface. The nature of the RTIL cation has also a large effect on the surface excess of H₂O since RTILs which are prone to form closed-packed structures like [BMMIM][NTf₂] can block the incorporation of H₂O and lead to more sluggish CO oxidation with larger overpotentials and oxidation in a much broader potential.

O 60.8 Wed 16:45 TRE Phy

Resolving the structure of Cu(100) in iodine containing solutions — •NICOLAS G. HÖRMANN, NICOLAS BERGMANN, KARSTEN REUTER, BEATRIZ ROLDÁN CUENYA, GEORG H. SIMON, and CHRISTOPHER S. KLEY — Fritz-Haber-Institut der Max-Planck-Gesellschaft, Berlin, Germany

We present results from our joint experimental and theoretical effort to identify the structure of iodine adlayers on Cu(100) in electrochemical environment – a first step towards understanding the origin of the influence of iodine on the electrocatalytic carbon dioxide reduction (CO₂RR) on Cu. In particular, we resolve stable interface structures as a function of the potential by a detailed analysis of theoretical predictions from density functional theory calculations and *in-situ* EC-AFM measurements. These results are complemented by the comparison of experimental and theoretically simulated Cyclic Voltammograms [1,2], which provide additional information on electroadsorption reactions and thereby the interface composition as a function of the potential.

[1] N.G. Hörmann et al., *J. Chem. Theory Comput.* **17**(3), 1782-1794 (2021).
[2] N.G. Hörmann et al., *J. Phys. Condens. Matter.* **33**, 264004 (2021).

O 60.9 Wed 17:00 TRE Phy

Non-Random Island Nucleation in the Electrochemical Roughening on Pt(111) — •MARCEL ROST¹, LEON JACOBSE², and MARC KOPER³ — ¹Huygens-Kamerlingh Onnes Laboratory, Leiden University, Niels Bohrweg 2, 2333 CA Leiden, The Netherlands — ²Centre for X-ray and Nano Science CXNS, Deutsches Elektronen-Synchrotron DESY, Notkestrasse 85, D-22607 Hamburg, Germany — ³Leiden Institute of Chemistry, Leiden University, Einsteinweg 55, 2333 CC Leiden, The Netherlands

Many chemical surface systems develop ordered nano-islands during repeated reaction and restoration. Platinum is used in electrochemical energy applications, like fuel cells and electrolyzers, although it is scarce, expensive, and degrades.

During oxidation-reduction cycles, simulating device operation, nucleation and growth of nano-islands occurs that eventually enhances the dissolution. Preventing nucleation would be the most effective solution. However, little is known about the atomic details of the nucleation; a process almost impossible to observe.

Here, we analyze the nuclei-distance distribution mapping out the underlying atomic mechanism: a rarely observed, non-random nucleation takes place. Special, preferential nucleation sites that a priori do not exist, develop initially via a precursor and eventually form a semi-ordered Pt-oxide structure.

This precursor mechanism seems to be general, possibly explaining also the nano-island formation on other surfaces/reactions.

O 60.10 Wed 17:15 TRE Phy

Electrochemical re-structuring of the InP(100)-HCl interface monitored by operando reflection anisotropy spectroscopy — •MARGOT GUIDAT^{1,2}, MARIO LÖW², DANIEL LÖRCH¹, VIBHAV YADAV¹, JONGMIN KIM^{1,2}, and MATTHIAS M. MAY^{1,2} — ¹Institute of Physical and Theoretical Chemistry, Universität Tübingen, Germany — ²Institute of Theoretical Chemistry, Universität Ulm, Germany
A possible way to achieve a low-carbon energy system consists of hydrogen production by photoelectrochemical water splitting. Here, III-V semiconductors play an important role due to their high solar-to-hydrogen efficiencies. However, surface corrosion limits the overall performance of photoelectrochemical devices. Studies have reported that interface functionalization is a way to protect the surface. In this work, we monitor the potential-dependent restructuring of the electrochemical InP(100) interface in HCl by operando reflection anisotropy spectroscopy (RAS) [1]. We investigate the effect of electrolyte concentration on the ordering and stabilization of the surface film formed at cathodic potentials. Computational RAS qualitatively supports the formation of an InCl_x layer. The latter is further investigated quantitatively with other characterization techniques. Fitting RA-transients measured under applied potentials with adsorption isotherm models gives insight into the lifetime of the involved processes and their adsorption energies. [1] Löw, M.; Guidat, M.; Kim, J.; May, M. M. *RSC Adv.* **2022**, *12* (50), 32756-32764.

O 60.11 Wed 17:30 TRE Phy

A femtosecond resolved view of vibrationally assisted electron transfer across the metal/aqueous interface — •ZHIPENG HUANG, MANUEL BRIDGER, OSCAR ANDRES NARANJO-MONTOYA, ALEXANDER TARASEVITCH, UWE BOVENSIEPEN, YUJIN TONG, and R. KRAMER CAMPEN — Faculty of Physics, University of Duisburg-Essen

Understanding heterogeneous charge transfer is crucial if we are to build the best electrolyzers, fuel cells and photoelectrochemical water splitting devices that chemistry allows. Since the elementary processes involved have characteristic timescales ranging from femto- to milliseconds, direct simulation of all relevant processes is not generally possible.

Here we demonstrate experimentally, using a novel two photon photovoltage approach, that for a prototypical system, a ferrocene terminate alkane thiol self-assembled monolayer (SAM) on gold in contact with aqueous electrolyte, charge transfer from the Au to the ferrocene can be induced by vibrational excitation of the ferrocene aromatic CH. Intriguingly the energy of the aromatic CH vibration, 0.38 eV, is a large fraction of the effective solvent interaction strength inferred for the ferrocene/ferrocenium system in prior electrochemical studies: 0.85 eV. Our results thus imply that, solvent may effect reduction/oxidation rates in electrocatalysis by coupling to a few, perhaps widely different in energy, vibrations. If shown to be generally true such a picture would suggest the necessity of moving beyond a single effective solvent interaction in theoretical descriptions of heterogeneous electron transfer.

O 60.12 Wed 17:45 TRE Phy

Dynamic Polymorph Formation of a Trimesic Acid Derivative at Solid-Liquid Interface — •RICHAR ARJARIYA¹, VIPIN MISHRA¹, GAGANDEEP KAUR¹, SANDEEP VERMA¹, MARKUS LACKINGER², and THIRUVANCHERIL G GOPAKUMAR¹ — ¹Department of Chemistry, Indian Institute of Technology Kanpur, Kanpur, UP-208016, India — ²Department of Physics, Technical University of Munich, James-Franck-Strasse 1, Garching 85748 and Deutsches Museum, Museumsinsel 1, Munich 80538, Germany

In this work we show the self-assembly of a tricarboxylic acid derivative of trimesic acid (BTA) at heptanoic acid-, nonanoic acid-graphite interface. At both interfaces BTA forms a trimer based-self-assembly, super-flower (SF) pattern. The spontaneously formed SF pattern is observed to be dynamically converting to a dimer-based assembly, chicken-wire pattern (CW), at heptanoic acid-graphite interface while scanning. Interestingly, at nonanoic acid-graphite interface, SF pattern remains stable and not converted to CW pattern. We attribute that the formation energy of both SF and CW patterns is comparable. The difference in the stability of different patterns in heptanoic acid and nonanoic acid is most likely related to the solubility of BTA in these solvents.[1,2] 1) T. N. Ha, T. G. Gopakumar, M. Hietschold, *J. Phys. Chem. C*, **2011**, *115*, 21743. 2) M. Lackinger, S. Griessl, W. M. Heckl, M. Hietschold and G. W. Flynn, *Langmuir*, **2005**, *21*, *11*, 4984-4988

O 61: Focus Session: Frontiers of Electronic-Structure Theory V (joint session O/HL)

Time: Wednesday 15:00–17:30

Location: TRE Ma

O 61.1 Wed 15:00 TRE Ma

Phase transitions in the two-dimensional Su-Schrieffer-Heeger model — •CHANGAN LI¹, SONGBO ZHANG², SANGJUN CHOI¹, JAN BUDICH³, and BJÖRN TRAUZETTEL¹ — ¹Institute for theoretical physics and astrophysics, University of Würzburg, Würzburg, Germany — ²Department of Physics, University of Zürich, Winterthurerstrasse 190 8057, Zürich, Switzerland — ³Institute of Theoretical Physics, Technische Universität Dresden, 01062 Dresden, Germany

The 2D Su-Schrieffer-Heeger (SSH) model is endowed with rich topological physics. First we show that the random flux can induce a metal-band insulator transition in the 2D SSH, thus reporting the first example of such a transition. Remarkably, we find that the resulting insulating phase can even be a higher-order topological insulator with zero-energy corner modes and fractional corner charges. Employing both level statistics and finite-size scaling analysis, we characterize the metal-band insulator transition and numerically extract its critical exponent. By proposing another inclined 2D SSH model, a deformed one, we show that a pair of Dirac points protected by space-time inversion symmetry appear in the semimetallic phase. Interestingly, the locations of these Dirac points are not pinned to any high-symmetry points of the Brillouin zone but highly tunable through parameter modulations. Moreover, the merging of two Dirac points undergoes a topological phase transition, which leads to either an anisotropic topological insulating phase or a nodal-line metallic phase.

O 61.2 Wed 15:15 TRE Ma

Ab initio embedding approach for carbon defects in hexagonal boron nitride: A new platform to probe environmental screening — •DANIS BADRTDINOV¹, MAGDALENA GRZESZCZYK², ALEXANDER HAMPEL³, CYRUS DREYER^{3,4}, MACIEJ KOPERSKI², and MALTE RÖSNER¹ — ¹Radboud University, Nijmegen, The Netherlands — ²National University of Singapore, Singapore — ³Flatiron Institute, USA — ⁴Stony Brook University, USA

Correlated defects in layered van der Waals hosts hold high promises for realizing quantum technologies, as they allow for various possibilities to control defect properties, e.g., via altering the host thickness or by changing the substrate material. A quantitative description of the defect ground and excited states taking the details of the impurity environment into account is, however, a considerable challenge for conventional density-functional theory (DFT) based methods as the impurities might be correlated and dielectric environmental screening is not fully accounted for in DFT. To tackle these challenges we apply and extend an embedding approach that treat the defect states within exact many-body theory, while DFT is used as a starting point to describe the bulk host material. We study various carbon defects embedded in hexagonal boron nitride (hBN), allowing us to disentangle all mechanisms responsible for the alteration of defect properties including modifications to the impurity structure and changes in the environmental screening upon thinning down the hBN host. Our new embedding approach paves the way for improved identification of defects in layered materials and to tailor their properties.

O 61.3 Wed 15:30 TRE Ma

Nonequilibrium electron dynamics in a two-sites Hubbard model — •JAKUB WRONOWICZ and YAROSLAV PAVLYUKH — Department of Theoretical Physics, Wrocław University of Science and Technology

Electron dynamics in a two-sites Hubbard model is studied using the nonequilibrium Green's function approach using formalism developed in [1]. We focus on the electron dynamics arising in the adiabatic switching scenario. Many-body approximations are classified according to the channel of the Bethe-Salpeter equation in which electronic correlations are explicitly treated. They give rise to the so-called second Born, T -matrix and GW approximations. In each of these cases, the model is reduced to a system of ordinary differential equations, which resemble equations of motion for a driven harmonic oscillator with time-dependent frequencies. We discuss transient solutions for the off-diagonal density matrix. Analytical result for the steady state in second Born approximation is compared with the exact solution. It is further shown numerically that in the large Hubbard- U limit the T -matrix in the particle-hole channel and spin-adapted GW approximations converge to the same solution.

[1] Y. Pavlyukh, E. Perfetto, and G. Stefanucci, *Photoinduced dynamics of organic molecules using nonequilibrium Green's functions with second-Born, GW , T -matrix, and three-particle correlations*, Phys. Rev. B **104**, 035124 (2021).

O 61.4 Wed 15:45 TRE Ma

Time-linear quantum transport simulations with correlated nonequilibrium Green's functions — •RIKU TUOVINEN¹, YAROSLAV PAVLYUKH², ENRICO PERFETTO³, and GIANLUCA STEFANUCCI³ — ¹Department of Physics, Nanoscience Center, University of Jyväskylä, Finland — ²Department of Theoretical Physics, Wrocław University of Science and Technology, Poland — ³Dipartimento di Fisica, Università di Roma Tor Vergata, Italy

We present a time-linear scaling method for open and correlated quantum systems. The method inherits from many-body theory [1] the possibility of selecting the most relevant scattering processes, thereby paving the way for real-time characterizations of correlated ultrafast phenomena in quantum transport. The open system dynamics is described in terms of an embedding correlator from which the transient current can be calculated via the Meir-Wingreen formula [2]. We efficiently implement the method through a combination with recent time-linear schemes for closed systems [3]. Electron-electron and electron-phonon interactions can be treated on equal footing while preserving all fundamental conservation laws. We employ the method by studying transport of correlated electron-hole pairs in semiconductors [4].

[1] G. Stefanucci and R. van Leeuwen, *Nonequilibrium Many-Body Theory of Quantum Systems* (CUP 2013).

[2] Y. Meir and N. S. Wingreen, PRL **68**, 2512 (1992).

[3] N. Schlünzen, J.-P. Joost, and M. Bonitz, PRL **124** (2020) 076601.

[4] R. Tuovinen, Y. Pavlyukh, E. Perfetto, and G. Stefanucci, arXiv:2211.15635 (2022).

15 min. break

Topical Talk

O 61.5 Wed 16:15 TRE Ma

Challenges in modelling correlated electronic matter — •ROSER VALENTI — Institute of Theoretical Physics, Goethe University Frankfurt, Frankfurt, Germany

The microscopic modelling of correlated electronic matter from first principles poses a fundamental theoretical challenge due to the many-body character of the systems. In recent years there have been a few internationally coordinated efforts in theoretical method development to generate a common platform of benchmarked software tools including dynamical mean field theory and extensions.

In this talk I will present some of the challenges we face in such an endeavour and illustrate them with some examples on models and materials.

Funding from the DFG through QUAST FOR 5249-449872909 is acknowledged.

O 61.6 Wed 16:45 TRE Ma

Electron-Phonon Interactions from DFPT within an All-Electron Framework — •SEBASTIAN TILLACK, PASQUALE PAVONE, and CLAUDIA DRAXL — Humboldt-Universität zu Berlin and IRIS Adlershof, 12489 Berlin, Germany

The interplay between electrons and the motions of nuclei in solids, described in terms of phonons, play a crucial role in the modeling of functional materials, particularly for understanding temperature dependent effects. We present an implementation of density-functional perturbation theory (DFPT) within a full-potential all-electron framework as implemented in the code `exciting` [1]. Our implementation allows one to compute phonons as well as the linear response to external electric fields. We use DFPT calculations to study lattice vibrations and electron-phonon interactions (EPIs) by means of many-body perturbation theory in β -Ga₂O₃. The electron self-energy contribution is computed as a function of temperature from which various properties such as quasi-particle energies, electron linewidths, and spectral functions are derived. We further incorporate many-body electron-electron interactions described by the GW method. Beyond that, our work creates the foundation for a fully *ab initio* study of the effect of EPIs on optical excitations.

[1] A. Gulans, et al. J. Phys.: Condens. Matter **26**, 363202 (2014).

O 61.7 Wed 17:00 TRE Ma

Calculation of phonon spectra with the FLAPW method using Density Function Perturbation Theory — •ALEXANDER NEUKIRCHEN, CHRISTIAN-ROMAN GERHORST, GREGOR MICHALICEK, DANIEL WORTMANN, GUSTAV BIHLMAYER, and STEFAN BLÜGEL — Peter Grünberg Institute and Institute for Advanced Simulation, Forschungszentrum Jülich and JARA, 52425 Jülich, Germany

Computing phonons applying density functional perturbation theory (DFPT) within all-electron DFT methods is a well-known challenge due to the displacement of muffin-tin spheres and sphere-centered basis functions. In this talk, we present our current results of the phonon dispersion based on our implementation of the DFPT approach in the FLEUR code [1] (www.flapw.de), an implementation of the full-potential linearized augmented plane wave (FLAPW) method. We highlight the good agreement of our preliminary results with phonon dispersions obtained with the finite displacement method for which the FLEUR code has been combined with the phonopy tool (www.phonopy.github.io/phonopy/). We discuss the numerical challenges involved in calculating meV quantities on top of large ground state energies typical for all-electron methods and how we addressed them.

This work has been supported by the Helmholtz Postdoc Programme (VHPD-022) and by the MaX Center of Excellence funded by the EU through the H2020-

INFRAEDI-2018-1 767 (Grant No. 824143).

[1] A. Neukirchen, C.-R. Gerhorst, D. A. Klüppelberg, M. Betzinger, D. Wortmann, G. Michalick, G. Bihlmayer, S. Blügel, to be published.

O 61.8 Wed 17:15 TRE Ma

Electron-phonon interaction using a localized Gaussian basis set — •GERRIT JOHANNES MANN, THORSTEN DEILMANN, and MICHAEL ROHLFING — Institute of Solid State Theory, University of Münster, Germany

Electron-phonon interaction is a crucial mechanism in solid state physics that is responsible for a multitude of phenomena. However, in electronic structure

calculations it is usually neglected. We developed an ab-initio implementation on top of density functional theory that combines finite differences calculations with the perturbative Allen-Heine-Cardona framework in order to calculate the temperature-dependent renormalization of the electronic bandstructure due to electron-phonon interaction using a basis set of localized Gaussian orbitals.

This implementation circumvents the limiting problems of previous implementations while maintaining a good agreement with the literature. The calculated Fan-Migdal zero-point renormalization of the direct band gap of silicon amounts to about 15 meV compared to 20 meV in the literature. Also the temperature-dependence of the renormalization agrees similarly well.

O 62: Focus Session: Wissenschaftskommunikation / Outreach (joint session HL/O/TT)

Im wissenschaftlichen Umfeld wird Maßnahmen der Öffentlichkeitsarbeit eine zunehmend größere Bedeutung zugemessen, - aus der Gesellschaft heraus und auch durch die großen Fördereinrichtungen und die DPG. Dabei geht es nicht nur um die Ergebnisse der Forschung, sondern auch darum, Prozesse und Methoden von wissenschaftlicher Arbeit transparent abzubilden – eine Aufgabe, die prinzipiell alle Forschenden übernehmen können. In diesem Symposium sollen erfolgreiche Projekte der Wissenschaftskommunikation, insbesondere aus dem Bereich der Festkörperphysik, vorgestellt werden. In ihrer Gesamtheit sollen sie das Spektrum der Wissenschaftskommunikation hinsichtlich des finanziellen und zeitlichen Aufwands aufzeigen und Methoden für unterschiedliche Zielgruppen vorstellen.

So dient diese Session sowohl als Ideengeber und Inspiration als auch als eine Art Netzwerk-Treffen zum Austausch über die Wissenschaftskommunikation in unterschiedlichen Kontexten.

Time: Wednesday 15:00–18:30

Location: POT 81

Invited Talk

O 62.1 Wed 15:00 POT 81

experimentamus! Forschendes Lernen von Physik und Chemie in der Grundschule — •SEBASTIAN SCHLÜCKER — Universität Duisburg-Essen, Campus Essen

Der Sachunterricht in der Primarstufe ist ein Konglomerat aus allen Natur- und Gesellschaftswissenschaften, erst in der Sekundarstufe findet eine Aufspaltung in die einzelnen Fächer statt. Zudem unterrichten viele Grundschul-Lehrkräfte fachfremd. Auch der Zeitaufwand für die Vorbereitung von Experimenten ist nicht unerheblich. Wie also kann man trotz dieser Hürden kindgerechte physikalische und chemische Experimente bereits in der Grundschule einführen?

Ich berichte aus 10 Jahren Erfahrung mit dem Projekt experimentamus!. Dabei handelt es sich um einen Kanon aus ca. 40 Experimenten für die Klassen 2 bis 4, welcher die Themen Licht, Wärme, Magnetismus, Wasser, Luft, Feuer und Elektrizität mit einem kindgerechten Alltagsbezug abdeckt. Anstelle des darlegenden Lernens wird auf das Forschende Lernen gesetzt: Frage - Hypothese - Experiment - Beobachtung - Erklärung; diese fünf Stationen des wissenschaftlichen Erkenntnisprozesses werden immer wieder durchlaufen. Ganz im Sinne Martin Wagenscheins wird dabei nach der exemplarischen und sokratischen Methode vorgegangen. Die praktische Implementierung umfasst 1. Materialkisten für alle Themen, 2. kompakte und leicht verständliche Informationshefter für die Lehrkräfte, sowie 3. Lernheftchen für alle SuS. Am Ende möchte ich über Erfahrungen und Herausforderungen im Rahmen dieses Projektes berichten und Ideen für eine mögliche weitere Verbreitung vorstellen.

O 62.2 Wed 15:30 POT 81

Internal interfaces - goals and realisation of a scientific image film — •ULRICH HÖFER^{1,2} and MICHAEL DÜRR^{2,3} — ¹Fachbereich Physik, Philipps-Universität Marburg — ²SFB 1083, www.internal-interfaces.de — ³Institut für Angewandte Physik, Justus-Liebig-Universität Giessen, Germany

Funded by the German Science Foundation (DFG), a professional film maker has produced an image film about the research conducted in the Collaborative Research Center SFB 1083 "Structure and Dynamics of Internal Interfaces". The six-minute video clip takes the non-specialist on a journey down to atomic scale to show the progress at the forefront of research at solid/solid interfaces. It is not a demanding educational film. Rather, it is a visually stunning piece that looks like science fiction taken straight out of a movie, with tracking shots that take the viewer down to the nanometer scale, with flights through luminous molecules, exotic excitons, and space-filling laser labs. The film also has a very impressive soundtrack. Gustav Holst's (1874-1934) composition "The Planets" was re-orchestrated especially for this film. It is available on the youtube channel of the DFG (<https://www.youtube.com/watch?v=-mDt0NzHrc>). Visitors of Chemikum Marburg can watch the German version on a 4K OLED screen, a device actually based on microscopic processes at interfaces investigated by SFB 1083.

The idea behind the creation of a professional film, its conceptual design and the necessary steps towards its realization will be outlined.

O 62.3 Wed 15:45 POT 81

Outreach activities of SFB 1083 @ Chemikum Marburg — •CHRISTOF WEGSCHEID-GERLACH, LUISE CLERES, INA BUDDÉ, KARL-HEINZ MUTH, and MARION ENSSLE — Chemikum Marburg / SFB1083

The diffusion of concepts, methods, and visions of the SFB 1083 on Structure and Dynamics of Internal Interfaces into the general public is our general goal. To this end project Ö makes use of the institution Chemikum Marburg e.V., whose basic idea is to fascinate the public excited about natural sciences. The experiments offered here, stand for chemical, biological, pharmaceutical, and physical subjects related with daily phenomena or beyond. We will give an overview about the introduction of basic ideas and methods of SFB 1083 to the public as well as the institution Chemikum Marburg. The contents of the individual offers, such as experiments within the regular workspace, the workshops for the Girls' Day and the compilation of special workshops that are offered to give high-school students an understanding of the research content of the SFB 1083 are presented. An additional topic is the linking of basic research to applications for regenerative energy resources. Hydrogen fuel cells are well-known to the general public and rely on functional internal interfaces. An additional workshop which was prepared in cooperation with the district Marburg-Biedenkopf gives an overview about production, storage, and application of hydrogen as a new energy resource. We will also share various occasions at Chemikum Marburg where further outreach activities represent SFB 1083.

Invited Talk

O 62.4 Wed 16:00 POT 81

Under the Microscope - spotlighting materials and nano science — •SVENJA LOHMANN and PRANOTI KSHIRSAGAR — The Science Talk, Germany

Real Scientists Nano is a science communication project dedicated to materials and nano science. Despite the widespread relevance of materials science to everyday life, we feel that dedicated science communication in this area is much rarer than in other fields. Our aim is to provide a platform for active materials and nano scientists to directly communicate their science and life as a scientist to the public. The use of social media thereby provides a very low threshold to science communication as basically the only requirement is to have an account. We have the goal to showcase the scientific community in all its diversity, and so far (12/2022) had guest scientists from more than 30 countries of origin as well as various fields and career stages. The two main pillars of the Real Scientists Nano project are the @RealSci_Nano Twitter account and the Under the Microscope podcast. Our guest scientists are interviewed for one podcast episode, and subsequently get to tweet from the account for one week following the rotation curation concept. We let curating scientist decide for themselves what they would like to tweet about. The form and content therefore vary greatly. Many of our scientists report from their everyday life, and are for example live-tweeting from a conference, uploading videos or photos from the lab or sending the occasional "stuck in meetings, will return later" tweet. Science communication on social media thus gives the opportunity to open a direct and real-time window into the scientist's life.

30 min. break

Invited Talk

O 62.5 Wed 17:00 POT 81
Phyphox – A pocketful of physics — •CHRISTOPH STAMPFER — JARA-FIT and 2nd Institute of Physics, RWTH Aachen University, 52074 Aachen, Germany — Peter Grünberg Institute (PGI-9), Forschungszentrum Jülich, 52425 Jülich, Germany

Most smartphones are used to make phone calls, to write short messages, surf the Internet or check e-mails. However, they can do much more: With the help of the integrated sensors and the free app "phyphox" (abbreviation for Physical Phone Experiments), pupils, students, and teachers and interested others can independently perform and develop physics experiments. For example, the app can use the accelerometer to record pendulum movements and determine the rotational acceleration in a salad spinner, or the air pressure sensor to determine time-resolved differences in altitude and thus the speed of an elevator. The didactic potential of the app is great, as the students are picked up on ground that is very familiar and attractive to them (smartphones) and are introduced to experimental natural sciences in a playful way and with an extremely low barrier (zero cost, i.e. only one click away). The app helps to get students excited about scientific and technical questions and contexts at an early age. The app is available free of charge for Android and iOS (more information can be found at www.phyphox.org). In my presentation, I will go into the concept of phyphox, introduce the range of functions and show a number of application examples.

O 62.6 Wed 17:30 POT 81
Chair PR representative as a doctoral student's secondary task: A field report — •PAULA M. WEBER, FELIX FRIEDRICH, and MANUEL SEITZ — Physikalisches Institut, Experimentelle Physik II, Universität Würzburg, Am Hubland, D-97074 Würzburg, Germany

Especially in recent years, it has become more important to communicate one's scientific work and methods to the public in order to show that in the scientific world, knowledge can only be created through research and the scientific process. Yet, extra time besides research is often limited and it is thus difficult to get into science communication. In this talk, I would like to present how PhD students can use their interest in science communication to benefit their own research group as a part-time PR representative.

In the first part of my talk, I will report on our efforts to attract new bachelor and master students. This advertising is focused on an audience with a scientific background, such that lab tours and advertising posters may contain scientific

language and references. The second part is about communication with the general public, who usually know physics from their school days. Here, I will report on how we presented our research activities at the Night of Science in Physics and at the "Highlights der Physik" in Würzburg.

Working part-time as a PR representative could encourage doctoral students to try their hand at science communication and develop the associated communication skills.

O 62.7 Wed 17:45 POT 81
Real or Fake - A format in science communication that encourages critical thinking — •TOBIAS LÖFFLER — Institut für Angewandte Physik Düsseldorf
 The outreach format "Real or Fake" aims to train the audience in an critical approach to credible-sounding facts.

It is aimed at the general public and specifically at young people. At the same time, it offers an easy introduction for scientists to audience-oriented communication of science on stage. The format can be performed in front of a live audience or as an interactive online event. It has been proven to work as implemented into science festivals, nights of sciences, as a public individual event and also as part of events with constrained settings - such as outreach events at schools or as part of conferences.

"Real or Fake" was developed in 2017 by scientists around the Berlin March for Science who later founded Besserwissen e.V. with the goal to promote the format and support new organisers. I do cooperate with them since 2019 and have organized more than ten "Real or Fake" events since then.

In my talk, I will present the concept and its origins, give an overview of successful events and show what to do and what support one can get, if one wants to organize a "Real or Fake" event.

Invited Talk

O 62.8 Wed 18:00 POT 81
Physics for school and the public at the LMU — •DR. CECILIA SCORZA-LESCH — Fakultät für Physik der LMU, München

Germany lives from research and technology. Physics, as the basis of all empirical sciences and technologies, has a very special, fundamental role to play. The Faculty of Physics at LMU, the largest in Germany, comprises nine research areas, three centres and two excellence clusters. In this talk we will present the approach we use to successfully communicate our various topics of modern research, the role of physics in our daily lives and in the fight against global warming to the schools and the public in a participatory way.

O 63: Poster: Data Management

Time: Wednesday 18:00–20:00

Location: P2/EG

O 63.1 Wed 18:00 P2/EG
SciCat - a meta data catalog and research data management system — •LINUS PITHAN¹, MASSIMILIANO NOVELLI², DYLAN McREYNOLDS³, LAURA SHELMLIT⁴, CARLO MINOTTI⁵, ANASTASHIA PYLYPENKO¹, ALEXANDER GERLACH¹, ALEXANDER HINDERHOFER¹, STEPHAN EGLI⁵, TOBIAS RICHTER², and FRANK SCHREIBER¹ — ¹Uni Tübingen, DAPHNE (DE) — ²European Spallation Source (DK/SE) — ³Lawrence Berkeley National Laboratory (USA) (US) — ⁴The Rosalind Franklin Institute (UK) — ⁵Paul Scherrer Institut (CH)

SciCat is a modern and flexible data catalogue that facilitates research data management on multiple scales and thereby suits the needs of large scale research facilities, individual research groups (e.g. at universities) as well as scientific communities. SciCat [1] was initially built to serve Photon- and Neutron sources (in the beginning developed at PSI and ESS, later supported by ExPaNDS & PaNOSC and further institutions). Through the engagement of DAPHNE4NFDI (Data from PHoton and Neutron Experiments) in the SciCat project there are new use cases emerging especially - but not exclusively - for small scale installations. The use of an homogenized interface (API) to create and search datasets SciCat can e.g. also be used as infrastructure backbone for machine learning (ML) projects in communities by serving datasets for validation, testing and training of ML models. On this poster we aim to give an overview on specific use-cases of SciCat within DAPHNE, which may serve as blueprints to use SciCat also in other scientific communities.

[1] <http://scicatproject.github.io>, <http://github.com/SciCatProject>

O 63.2 Wed 18:00 P2/EG
A local solution for automated data acquisition and storage in catalysis — •ABDULRHMAN MOSHANTAF¹, MIKE WESEMANN¹, PATRICK OPPERMANN¹, HEINZ JUNKES¹, ROBERT SCHLÖGL^{1,2}, and ANNETTE TRUNTSCHKE¹ — ¹Fritz-Haber-Institut der Max-Planck-Gesellschaft, Berlin (Germany) — ²Max Planck Institute for Chemical Energy Conversion, Mühlheim 45470 (Germany)

In order to solve the current challenge in catalysis research in the development of new, scalable catalysts for hydrogen-based future technologies, a better integration of theory and experiment is required. The necessary data exchange demands extensive digitalization in catalysis. Experimental data must be generated reproducibly and with sufficient diversity, and must be available in machine-readable form. Artificial intelligence can then contribute to the discovery of correlations. We have developed a concept for a local data infrastructure and implemented it in a catalysis laboratory. In research projects, handbooks are written (preferably in machine-readable form) detailing how experimental data are obtained, including the definition of benchmark catalysts. To implement the concept of handbooks, automated systems for data acquisition and storage have been designed. Such a system consists of (i) EPICS for communication with devices and data acquisition, (ii) a database (archive), (iii) an archiving appliance for storing time series, (iv) Phoebus for creating graphical user interfaces, (v) Python/Bluesky/Jupyter notebooks for creating automations and evaluations, and (vi) S3 storage for long-term storage.

O 64: Poster: Graphene

Time: Wednesday 18:00–20:00

Location: P2/EG

O 64.1 Wed 18:00 P2/EG

An STM and XPS study of graphene on Rh (111) as a substrate for on-surface assembly of Pt-complexes — •MAJID SHAKER, NATALIE J. WALESKA, SIMON JAEKEL, EVA MARIE FREIBERGER, VALENTIN SCHWAAB, FELIX HEMAUER, RAJAN ADHIKARI, CHRISTIAN PAPP, and HANS-PETER STEINRÜCK — Lehrstuhl für Physikalische Chemie II, Friedrich-Alexander-Universität Erlangen-Nürnberg, Egerlandstr. 3, Erlangen 91058, Germany

Single platinum atoms have interesting properties and can play an important role in on-surface catalysis. One route to prepare small Pt nanoclusters or even single isolated Pt atoms is to deposit small amounts of Pt on the Moiré structure of 2D materials on lattice-mismatched transition metal surfaces. Such Moiré patterns e.g. of graphene can act as template for the formation of NCs with a narrow size distribution. In this study, a monolayer of graphene was successfully grown on the surface of a Rh(111) single crystal from ethylene (C₂H₄) as precursor under ultra-high vacuum (UHV). Very small Pt NCs (down to individual atoms) were formed in the valleys of graphene to further act as a transition metal center for the formation of metal complexes by providing appropriate ligands. Scanning tunneling microscopy and synchrotron radiation-based X-ray photoelectron spectroscopy were employed to evaluate the formed inorganic complexes.

We thank Helmholtz-Zentrum Berlin for allocation of synchrotron-radiation beamtime and the BESSY II staff for support during beamtime. This work was funded by the DFG through SFB 953.

O 64.2 Wed 18:00 P2/EG

Graphene on Ru(0001): Layer-Specific and Moiré-Site- Dependent Phonon Excitations — JOHANNES HALLE, NICOLAS NÉEL, •REBECCA CIZEK, and JÖRG KRÖGER — Technische Universität Ilmenau

Graphene phonons are excited by the local injection of electrons and holes from the tip of a scanning tunneling microscope. Despite the strong graphene-Ru(0001) hybridization, monolayer graphene unexpectedly exhibits pronounced phonon signatures in inelastic electron tunneling spectroscopy. Spatially resolved spectroscopy reveals that the strength of the phonon signal depends on the site of the moiré lattice with a substantial red-shift of phonon energies compared to those of free graphene. Bilayer graphene gives rise to more pronounced spectral signatures of vibrational quanta with energies nearly matching the free graphene phonon energies. Spectroscopy data of bilayer graphene indicate more-over the presence of a Dirac cone plasmon excitation.

O 64.3 Wed 18:00 P2/EG

DFT study on the ORR mechanism on carbon nitride materials — •JANA KOENIGSDORFF, CHANGBIN IM, BJÖRN KIRCHHOFF, and TIMO JACOB — Ulm University, Institute of Electrochemistry, D-89081 Ulm

Polymeric carbon nitrides (PCNs) have rapidly gained attention over the last years due to their promising physicochemical properties.^[1] With their adjustable narrow bandgap and high visible light responsivity, PCNs are considered as promising potential photo-(electro)-catalysts for various industrial processes such as H₂O₂ formation or CO₂ reduction.^{[2][3]} However, numerous structural and photophysical properties of this material class are not completely understood and hinder in-depth comprehension of the reaction pathways.^[2] Most simulation studies that attempted to gain a deeper insight into the reaction mechanisms were based on simple, highly ordered PCN models.^[1] However, PCNs obtained by thermal processes often exhibit inhomogeneity and a variety of microstructural motifs.^[2] In this study, we therefore perform DFT calculations to investigate the mechanism of H₂O₂ formation with various PCN models of different degrees of condensation and structural composition in order to screen a wide range of adsorption sites. We are convinced that with this approach, we can establish structure-reactivity relationships that can be used to derive understanding-driven material optimization strategies.

[1] Wei, Z. et. al., *Energy Environ. Sci.* **11** (2018) 2581 - 2589. [2] Lau, V. Lotsch, B., *Advanced Energy Materials* **12** (2022) 2101078. [3] Xia, Y. et. al., *ChemSusChem* **13** (2020) 1730 - 1734.

O 64.4 Wed 18:00 P2/EG

Electronic magneto-transport in epitaxial graphene covered with Bi(110) islands — •SERGI SOLOGUB^{1,2}, JULIAN KOCH², CHITRAN GHOSAL², and CHRISTOPH TEGENKAMP² — ¹Institute of Physics, NAS of Ukraine, Nauki avenue 46, 03028 Kyiv — ²Institut für Physik, TU Chemnitz, Reichenhainerstr. 70, 09126 Chemnitz

Magneto-conductance and Hall voltage of epitaxial graphene formed on SiC and covered with ultrathin Bi islands were measured within the range of ± 4 T. The structure and morphology of Bi coverages of average thickness up to 4 bilayers, MBE-grown at RT as well as after-annealed, were determined by SPA-LEED and STM techniques. The coverage was found to consist of needle-like (110) islands with "magic" widths and thicknesses.

The analysis of the low-field part of the magneto-conductance reveals a transition from weak-localization (WL) to weak antilocalization (WAL) with increas-

ing Bi coverage and allows to characterize the scattering of conduction electrons by determining electron scattering lengths, namely inelastic-dephasing, intervalley and intervalley symmetry breaking ones. The correlation of the average sizes of and distance between Bi(110) islands for different coverages with the characteristic lengths demonstrate the role of electron scattering on edges and within the islands in the WL-WAL transition. Calculated dependencies of Hall and magneto-resistance allow determining changes of the electron density induced by Bi adsorption and reveal the contribution of electron-electron interaction in electronic transport.

O 64.5 Wed 18:00 P2/EG

Organic Molecules on Graphene grown on a Pt(111) surface — •SHILPA PANCHAMI RAJ, CHRISTOPHE NACCI, and LEONHARD GRILL — University of Graz

Graphene, a flat monolayer of carbon atoms with two-dimensional honeycomb lattice, exhibits unique properties. If grown on a Pt(111) surface, only weak interaction is found between the substrate and the graphene sheet. This renders it an interesting system to decouple organic molecules on the graphene layer from the metal underneath as they might preserve their electronic structure. In this work, we present a scanning tunneling microscopy (STM) study under ultrahigh vacuum (UHV) with the deposition of different organic molecules on graphene that was epitaxially grown on a Pt(111) substrate. Experiments were done at cryogenic temperatures of 5 K, which allows to image single molecules in a stable fashion and also to manipulate them with the tip of the STM in a controlled way. Adsorption properties of the molecules are studied in view of the characteristic Moiré pattern of the graphene/Pt(111) system. Moreover, first attempts will be presented how chemical reactions can be induced on this system.

O 64.6 Wed 18:00 P2/EG

Electronic band structure of Pb intercalated graphene on SiC and the influence of electron doping — •BHARTI MATTA¹, PHILIPP ROSENZWEIG¹, KATHRIN KÜSTER¹, CRAIG POLLEY², and ULRICH STARKE¹ — ¹Max-Planck-Institut für Festkörperforschung, Heisenbergstraße 1, 70569 Stuttgart, Germany — ²MAX IV Laboratory, Lund University, Fotogatan 2, Lund 22484, Sweden

Intercalation is a powerful way of modifying the properties of epitaxial graphene and stabilizing two-dimensional (2D) intercalant layers at the graphene/SiC interface. In this work, we show that the charge neutrality of Pb intercalated quasi-freestanding monolayer graphene on SiC involves charge transfer from both the intercalant and the substrate. Synchrotron based angle resolved photoelectron spectroscopy measurements demonstrate the (1×1) order of the Pb layer with respect to SiC. The interlayer bands cross the Fermi level, confirming the metallic nature of intercalated Pb. Furthermore, constant initial state mapping shows no dispersion of the Pb bands with photon energy, proving the 2D nature of the intercalant layer. Polarization dependent measurements retrieve a mainly in-plane orbital character for the Pb band branches closer to the Fermi energy. Potassium deposition induces strong n-doping in the graphene layer ($E_D \approx 1.1$ eV). However, the Pb bands do not show any noticeable change, which suggests that the charge transfer from the potassium layer occurs predominantly into the graphene. Supported by DFG through FOR 5242.

O 64.7 Wed 18:00 P2/EG

Terahertz harmonic generation from graphite pencil drawings — •ATIQA ARSHAD, SEGEY KOVALEV, and JAN CHRISTOPH — Helmholtz Zentrum Dresden (HZDR)

Harmonic generation is a general characteristic of driven nonlinear systems. It can serve as an efficient tool for investigating the fundamental principles that govern the underlying ultrafast nonlinear dynamics. Here we report on terahertz third harmonic generation (THG) from graphite pencil drawings on paper. We demonstrate that the terahertz (THz)-THG efficiency at an excitation frequency of 0.5 THz in graphite is comparable to that of single-layer graphene pump field strengths on the order of 100 kV/cm-1. The THG efficiency in graphite exhibits a significantly less pronounced saturation behavior at high incident fields and thus may even surpass that of graphene at extreme pump field strengths. The less pronounced saturation can be attributed to more efficient heat dissipation in multilayer graphite flakes compared to single-layer graphene. The feasibility of using easy-to-produce graphite-based structures opens up new possibilities for highly accessible, modifiable, and nearly cost-free THz frequency multipliers. Besides the implementation of graphite-based THz frequency converters, the developed technique could be used for nonlinear THz imaging, offering the possibility to image graphite drawings covered by other materials.

O 64.8 Wed 18:00 P2/EG

In-situ monolayer graphene growth on Ru(10 $\bar{1}$ 0): an electron microscopy study — •CATHY SULAIMAN, LUKAS SCHEWE, LARS BUSS, MORITZ EWERT, and JAN INGO FLEGE — Applied Physics and Semiconductor Spectroscopy, Brandenburg University of Technology Cottbus-Senftenberg, Germany

During the last decade, the controlled growth of monolayer (MLG) and bilayer graphene has extensively been studied on the hexagonal Ru(0001) surface, which is a system that is known to form strong chemical bonds at the metal-graphene interface. Yet, little attention was paid to the influence of the substrate orientation that was demonstrated to have a significant impact for graphene growth on the Ir(001) and Ir(111) surfaces, the latter exhibiting a weak coupling between the graphene and the support. Therefore, in this study we have grown graphene on the rectangular Ru(10 $\bar{1}$ 0) surface by segregation and ethylene-supported chemical vapor deposition. A photoemission and low-energy electron microscope (PEEM & LEEM) has been utilized to directly characterize the MLG growth process with respect to variations in substrate temperature and step orientation. The expansion of the MLG islands is compared to the well-established carpet-growth mode on the Ru(0001) surface. These results have been complemented by probing of the occupied and unoccupied electronic structure of the islands using PEEM and intensity-voltage LEEM. Furthermore, the existence of two preferential surface reconstructions is identified via micro-illumination low-energy electron diffraction (LEED), whose spatial distribution is revealed by employing dark-field LEEM imaging.

O 64.9 Wed 18:00 P2/EG

Band structure and charge carrier dynamics of a Pb-intercalated graphene sheet on Ni(111) — •EVA SOPHIA WALTHER¹, KATHARINA HILGERT¹, CHRISTINA SCHOTT¹, SEBASTIAN HEDWIG¹, KA MAN YU¹, MARTIN AESCHLIMANN¹, and BENJAMIN STADTMÜLLER^{1,2} — ¹Department of Physics and Research Center OPTIMAS, RPTU Kaiserslautern, Germany — ²Institute of Physics, Material Science in Mainz, JGU Mainz, Germany

The discovery of graphene acted as a starting point for the vast research field of 2D materials. However, on metal surfaces, most of the enthusiasm for exploring graphene's unique properties has been tempered by the strong interaction with its substrate, which results in severe changes in its electronic properties. One way to reduce the graphene-surface interactions is the intercalation of heavy metal atoms between the graphene and the underlying substrate. In our work, we use the highly reactive Ni(111) surface as a graphene substrate. On this surface, the linear dispersion of the Dirac cone is severely distorted and the K-point is located far below the Fermi energy. Here, we will show that Pb intercalation recovers the linear dispersion of the free-standing graphene. Using time- and momentum-resolved photoemission, we will further determine the influence of the Pb intercalation for the ultrafast charge carriers dynamics at the K-point of the Gr/Ni(111) interface.

O 64.10 Wed 18:00 P2/EG

Controlled fabrication of the graphene/Mn₅Ge₃ interface via Mn intercalation — •VIVIEN ENENKEL¹, YURIY DEDKOV², ELENA VOLOSHINA², and MIKHAIL FONIN¹ — ¹Fachbereich Physik, Universität Konstanz, Universitätsstraße 10, 78457 Konstanz, Germany — ²Department of Physics, Shanghai University, 99 Shangda Road, 200444 Shanghai, China

Mn-based intermetallic compounds have recently been in focus of intensive research owing to their outstanding magnetic properties. In particular, epitaxial Mn₅Ge₃/Ge interfaces [1] are regarded to have the potential for the realization of efficient spin injection and manipulation in semiconductor structures compatible with the existing Si technology. Furthermore, for graphene on Mn₅Ge₃

an exchange splitting of the π states is predicted, with the two spin channels exhibiting a large difference in charge carrier mobility [2]. Here, we report on the fabrication of epitaxial graphene/Mn₅Ge₃ by Mn-intercalation at the graphene/Ge(110) interface, initially prepared by atomic carbon deposition on Ge(110) [3]. Depending on the sample temperature different phases can be generated, including Mn₅Ge₃, whose structure and electronic properties are studied by low-temperature scanning tunneling microscopy and spectroscopy.

[1] Y. Dedkov *et al.*, J. Appl. Phys. 105, 073909 (2009).

[2] E. Voloshina and Y. Dedkov, J. Phys. Chem. Lett. 10, 3212 (2019).

[3] J. Tesch *et al.*, Carbon 122, 428-433 (2017).

O 64.11 Wed 18:00 P2/EG

Force-Field Development for Graphene-Graphite Water Systems — •OTTO SCHULLIAN and ROLAND NETZ — Fachbereich Physik, Freie Universität Berlin, 14195 Berlin, Germany

The wetting behavior of water on graphene/graphite surfaces is strongly dependent on the force fields chosen for the water-carbon interaction. Previously developed force fields were optimized to reproduce a specific contact angle for water on graphite (in the range of 85° to 95°). However, experiments show that the contact angle for water on graphite depends strongly on the preparation of the surface; they suggest that freshly exfoliated graphite has a surprisingly hydrophilic contact angle of 60° ± 13°, whereas old and potentially contaminated graphite surfaces are much more hydrophobic. For graphene the variance in contact angle is even more dramatic, ranging from 10° to 127°.

Here, we simulate contact angles for a range of water-carbon interaction strengths for one to five layers of graphene to provide the necessary parameters for a whole range of contact angles (30°-115°). In this way, one can tune the wetting behavior in simulation. From our results, we see that the graphene with no underlying support has a contact angle 2°-20° higher than the corresponding graphite system depending on the interaction strength. In addition, we investigate the frequency-dependent friction on flat graphene and graphite as a function of the interaction strength and the number of graphene layers via the Green-Kubo relation including a hydrodynamic correction.

O 64.12 Wed 18:00 P2/EG

Raman features of graphene and Weyl semimetals beyond the standard nonadiabatic theory — •NINA GIOTTO and DINO NOVKO — Institute of Physics, Zagreb, Croatia

Although graphene has already been thoroughly studied with Raman spectroscopy, there still exists a disagreement about the broadening mechanisms of the E_{2g} mode and its actual temperature dependence [Nano Lett. 10, 466 (2010)]. Along with the importance of the nonadiabatic effects in graphene, higher order electron-phonon scattering processes also significantly impact the phonon spectrum. Specifically, the electron-phonon-induced lifetime and energy renormalization of the electron-hole pair excitations bring additional temperature dependence in the electron-coupled phonon modes and their corresponding linewidths. The nonadiabatic theory relying on first principles calculations, developed in [Phys. Rev. B 98, 041112(R) (2018)], is here successfully applied to graphene in various doping regimes and to Weyl semimetals, which contain a 3-dimensional analog of Dirac points in the electron band structure and are, therefore, excellent candidates for achieving a nonadiabatic regime.

O 65: Poster: Topology and Symmetry-Protected Materials

Time: Wednesday 18:00–20:00

Location: P2/EG

O 65.1 Wed 18:00 P2/EG

Topological insulator Bi₂Se₃: the effect of doping with Fe, Ru, Os, and Mo — •FRANTISEK MACA¹, STANISLAV CICHON¹, VACLAV DRCHAL¹, KATERINA HORAKOVA¹, IRENA KRATOCHVILLOVA¹, JAN LANCOK¹, VLADIMIR CHAB¹, PATRIK CERMAK², CESTMÍR DRASAR², and JIRI NAVRATIL² — ¹Institute of Physics CAS, Praha, Czech Republic — ²University of Pardubice, Pardubice, Czech Republic

Doping is one of the most suitable ways of tuning the electronic properties of topological insulators (TI) and a promising means of a band gap opening. We report a reliable method for preparation of high-quality single crystal substrates Bi₂Se₃ containing anti-site defects and vacancies and doped with VIIIIB and VIB columns elements.

We combine experimental (XPS, ARPES) and theoretical (ab initio) methods to analyze the electronic properties and chemical states of atoms and defects in the substitutional position in TI that can be achieved using the free melt crystallization method of the sample growth. Doping introduced change in the position of Dirac cone is shown and discussed.

O 65.2 Wed 18:00 P2/EG

Green's functions formulation of Floquet topological invariants — •MARCUS MESCHÉDE, HELENA DRÜEKE, and DIETER BAUER — University of Rostock

Floquet topological insulators (FTIs) allow for topological protection through their time evolution as opposed to static topological insulators, which are only protected by their band topology. FTIs have become ubiquitous in the pursuit of realizing new phases of matter. In general, the momentum-dependent quasi-energy spectrum of single-particle time evolution operators or, equivalently, Floquet Hamiltonians is used to classify the band topology. In the presence of many-particle interactions, this single-particle picture breaks down. In order to overcome this issue, topological invariants of static systems have been formulated through their single-particle Green's functions. [1,2] We expand on this work by calculating Floquet topological invariants through their Floquet Green's function. As there is much experimental work on realizing FTIs, we hope to provide another tool to determine the topological properties of these systems through their bulk spectral function.

[1] Gurarie, V. "Single-Particle Green's Functions and Interacting Topological Insulators." Physical Review B 83, 085426 (2011).

[2] He, Yuan-Yao, Han-Qing Wu, Zi Yang Meng, and Zhong-Yi Lu. "Topological Invariants for Interacting Topological Insulators. I. Efficient Numerical Evaluation Scheme and Implementations." Physical Review B 93, 195163 (2016).

O 65.3 Wed 18:00 P2/EG

Interaction-Induced Directional Transport on Driven Coupled Chains — •HELENA DRÜEKE and DIETER BAUER — Universität Rostock

We examine whether interaction between particles may introduce (topologically protected) directional transport in a driven two-particle quantum system. As a simple example, we consider two one-dimensional chains of equal length, each with one particle. The two particles interact but stay on their respective chain. The particles move alternatingly and without a preferred direction.

Without interaction between the particles, they each diffuse along their chains. Interaction between them suppresses this diffusion. With the proper timing of their alternating movement, the particles form a bound doublon state. Depending on their starting positions, this doublon either remains stationary or moves along the chain. The motion of the doublon consists of alternating, leapfrogging motion of the two particles.

O 65.4 Wed 18:00 P2/EG

Near-field investigation of topologically protected edge states in plasmonic waveguide arrays — •HANS-JOACHIM SCHILL, ANNA SIDORENKO, and STEFAN LINDEN — Department of Physics, University of Bonn, Germany

Light propagation along evanescently coupled waveguide arrays resembles mathematically the dynamics of a lattice Schrödinger equation and is, therefore, ideally suited for simulating condensed matter lattice systems. Here, we report on near-field measurements with scattering-type scanning near-field optical microscopy (s-SNOM) in transmission mode combined with leakage radiation microscopy to investigate topological effects in coupled arrays of dielectric loaded surface plasmon polariton waveguides (DLSPWs). Specifically, we implement the Su-Schrieffer-Heeger (SSH) model by fabricating arrays of DLLSPWs with alternating weak and strong couplings. The interface between two topologically distinct domains of the SSH model is known to host a topologically protected edge state. The combination of far- and near-field imaging allows us to investigate the global intensity evolution of the lattice as well as the local amplitude and phase distribution of the edge state.

O 65.5 Wed 18:00 P2/EG

Orbital Protection of a Weyl Nodal line — •TIM FIGGEMEIER^{1,3}, MAXIMILIAN ÜNZELMANN^{1,3}, PHILIPP ECK^{2,3}, JAKUB SCHUSSER^{1,3}, JENNIFER NEU^{4,5}, THEO SIEGRIST^{4,6}, DOMENICO DI SANTE⁷, GIORGIO SANGIOVANNI^{2,3}, HENDRIK

BENTMANN^{1,3,8}, and FRIEDRICH REINERT^{1,3} — ¹EP VII, Universität Würzburg, Germany — ²ITPA, Universität Würzburg, Germany — ³Würzburg-Dresden Cluster of Excellence, ct.qmat — ⁴NHMFL, Tallahassee, FL, US — ⁵Nuclear Nonproliferation Division, ORNL, Oak Ridge, Tennessee, US — ⁶FAMU-FSU, Tallahassee, FL, US — ⁷Center for Computational Quantum Physics, Flatiron Institute, New York, US — ⁸NTNU, Trondheim, Norway

We present a combined soft X-ray angle-resolved photoelectron spectroscopy (SX-ARPES) and density functional theory study on TaAs and NbP. The two compounds are usually known as paradigmatic non-magnetic Weyl semimetals. Here, however, we show that they further host twofold spin-degenerate nodal lines located at the center of a one-dimensional vortex line of Orbital Angular Momentum (OAM). These momentum space vortices can be tracked experimentally by using k_z -resolved dichroic SX-ARPES. The OAM vortex line protects the spin degeneracy against spin-orbit coupling and imparts high topological robustness to the nodal line. In order to investigate the impact of SOC on the degeneracy experimentally, we compare TaAs with NbP, which differ from each other by having a different magnitude of atomic SOC strength.

O 65.6 Wed 18:00 P2/EG

Towards higher-order topological corner states in quantum spin Hall insulating heterostructures — •MARKUS FELD^{1,2}, PHILIPP ECK^{1,2}, and GIORGIO SANGIOVANNI^{1,2} — ¹ITPA, Universität Würzburg, Germany — ²Würzburg-Dresden Cluster of Excellence, ct.qmat

Real-space obstruction in \mathbb{Z}_2 trivial systems is under current investigation as it promotes quantized electronic bulk multipoles. In two dimensions it can stabilize a higher-order topological insulator (HOTI) with insulating edges and zero energy in-gap corner states. However the recent analysis for the triangular quantum spin Hall insulator (QSHI) indenene has extended the concept of real-space obstruction to $\nu = 1$ phases [1].

We show that this is in contrast to the well established large-gap QSHI bismuthene [2], where the Wannier functions center on the atomic lattice sites. Here we present an *ab initio* based study, where we address the edges and corners of obstructed and non-obstructed interfaces by considering heterostructures of indenene and bismuthene.

[1] P. Eck et al., Phys. Rev. B **106**, 195143 (2022)[2] F. Reis et al., Science **357**, 287 (2017),**O 66: Poster: Scanning Probe Microscopy with Quartz Sensors**

Time: Wednesday 18:00–20:00

Location: P2/EG

O 66.1 Wed 18:00 P2/EG

Atomically Precise Synthesis and Characterization of Heptaurene with Triplet Ground State — XUELEI SU¹, CAN LI², •QINGYANG DU¹, KUN TAO³, SHIYONG WANG², and PING YU¹ — ¹School of Physical Science and Technology, ShanghaiTech University, 201210 Shanghai, China — ²Key Laboratory of Artificial Structures and Quantum Control (Ministry of Education), Shenyang National Laboratory for Materials Science, School of Physics and Astronomy and Tsung-Dao Lee Institute, Shanghai Jiao Tong University, Shanghai 200240, China — ³Key Lab for Magnetism and Magnetic Materials of Ministry of Education, Lanzhou University, 730000 Lanzhou, China

Heptaurene, one of the most well-known structures, is a benzene-fused bisphenalenyls in mirror symmetry with triplet ground state. However, it is difficult to synthesize heptaurene without any substituents due to its high activity. Owing to the development of on-surface synthesis, it is possible to obtain highly active species with properly-designed precursors. Here, we combined in-solution and on-surface synthesis to achieve unsubstituted heptaurene, whose chemical structure can be characterized with bond-resolved atomic force microscopy. Its triplet ground state is clearly confirmed by the Kondo resonance around zero bias in dI/dV spectra. The response of this Kondo peak to external magnetic field is also detected to verify the high-spin state. We also engineered its spin-state through hydrogen atom addition or dissociation by tip manipulation. Our work provides access to phenalenyl-based structures with high-spin ground states, potentially useful in constructing spin networks.

O 66.2 Wed 18:00 P2/EG

Novel image interpretation methods for high-resolution STM — •LAURI KURKI¹, NIKO OINONEN¹, ONDREJ KREJCI¹, and ADAM S. FOSTER^{1,2} — ¹Department of Applied Physics, Aalto University, 00076, Espoo, Finland — ²WPI Nano Life Science Institute, Kanazawa University, Kakuma-machi, Kanazawa 920-1192, Japan

Scanning tunnelling microscopy (STM) functionalized with a CO molecule on the probe apex is a method capable of capturing sub-molecular level detail of the electronic and physical structure of a sample[1]. However, the produced images are often difficult to interpret due to the convoluted nature of the signal. We

propose image interpretation tools to extract physical and electronic information directly from STM images using machine learning.

In recent years, there has been rapid development in image analysis methods using machine learning, with particular impact in medical imaging. These concepts have been proven effective also in SPM in general and in particular for extracting physical features from atomic force microscopy (AFM) images[2]. We build upon these models and show that we can extract atomic positions and electrostatics directly from STM images. We further explore how the accuracy of these predictions varies with the use of a simultaneous AFM signal and ultimately establish the limits of the approach in an experimental context.

[1] Shuning Cai, Lauri Kurki, Chen Xu, Adam S. Foster, and Peter Liljeroth. JACS **144** (44), 20227–20231 (2022)[2] Niko Oinonen, Lauri Kurki, Alexander Ilin, and Adam S. Foster. MRS Bulletin **47**, 895-905 (2022)

O 66.3 Wed 18:00 P2/EG

Distance dependence of s- and p-wave contributions in CO-tip STM — •LEONARD-ALEXANDER LIESKE, FABIAN PASCHKE, FLORIAN ALBRECHT, and LEO GROSS — IBM Research Europe - Zürich, Säumerstrasse 4, 8803 Rüschlikon, Switzerland

Functionalized tips are frequently used in high-resolution AFM, particularly CO terminated tips, to facilitate atomic resolution [1]. CO functionalized tips can also enhance contrast in STM measurements of ionic resonances, mapping orbital densities [2,3]. For CO tips both *s*- and *p*-wave character of the tip contribute to the contrast [3,4,5]. Here, we study the contributions of *s*- and *p*-wave character of CO tips as a function of tip height, bias voltage and tunneling current.

[1] L. Gross, F. Mohn, N. Moll, P. Liljeroth and G. Meyer, Science, **325**(5944), 1110-1114 (2009).[2] J. Repp, G. Meyer, S. M. Stojković, A. Gourdon and C. Joachim, Physical Review Letters, **94**(2) 026803 (2005).[3] L. Gross, N. Moll, F. Mohn, A. Curioni, G. Meyer, F. Hanke and M. Persson, Physical Review Letters, **107**(8), 086101 (2011).[4] N. Pavliček, I. Swart, J. Niedenführ, G. Meyer and J. Repp, Phys. Rev. Lett. **110**, 136101 (2013).[5] A. Gustafsson and M. Paulsson, Phys. Rev. B, **93**, 115434 (2016).

O 66.4 Wed 18:00 P2/EG

Atomic-scale imaging of individual cyclic oligosaccharides with non-contact atomic force microscopy — •MÁRKÓ GRABARICS^{1,3}, BENJAMIN MALLADA FAES^{2,3}, ALEJANDRO JIMÉNEZ-MARTÍN², PAVEL JELÍNEK², BRUNO DE LA TORRE², and STEPHAN RAUSCHENBACH¹ — ¹University of Oxford, Department of Chemistry, United Kingdom — ²Institute of Physics of Czech Academy of Sciences, Czech Republic — ³These authors contributed equally.

Carbohydrates, also referred to as saccharides, are a major class of biopolymers that are essential to all known living organisms. While important in a range of biological processes, the structural complexity of carbohydrates poses a challenge to conventional analytical techniques, which often fail to provide unambiguous structural assignment.

We aim to overcome this challenge by imaging single, surface-adsorbed carbohydrate molecules using high-resolution SPM. For these proof-of-concept experiments, β -cyclodextrin was chosen as model compound, a cyclic oligosaccharide consisting of seven glucose units linked together *via* α -1,4-glycosidic linkages. Incompatible with thermal evaporation, the molecules were deposited in ultrahigh vacuum onto close-packed noble metal surfaces using electrospray deposition. STM and non-contact AFM with CO-functionalized tips revealed two distinct adsorption geometries, with the individual glucose units clearly resolved within the macrocycles.

Our results demonstrate the potential of high-resolution SPM for the structural characterization of carbohydrates, opening up novel ways for the analysis of this important class of biomolecules.

O 66.5 Wed 18:00 P2/EG

observation and definition of lipid raft in live MCF-7 cell by AFM — •HSIANG-LING CHUANG¹, YU-CHEN FA², CHUN-HSIEN CHEN¹, LLI-CHEN WU³, and JAN AN HO^{1,2} — ¹department of chemistry, National Taiwan University, Taiwan 10617. — ²department of biochemical science and technology, National Taiwan University, Taiwan 10617. — ³department of applied chemistry, National Chi Nan University, Nantou, Taiwan 54561.

Lipid rafts are composed of cholesterol, sphingolipid, and proteins. Previous studies indicated that resveratrol and fibrinogen can bind to the receptor on α -v beta-3 integrin. Through the protein-lipid or protein-protein interactions, drug-bound integrins will aggregate into larger raft blocks with unbound integrins. Due to the limitation of optical microscopy and complicated sample preparation, the techniques on lipid rafts observation have shortages of real-time and original state information. In this study, we explore the application of in-situ atomic force microscope (AFM) for the observation of lipid rafts on the cell surface and the response upon the administration of chemicals in real time. We obtained AFM images of morphology and stiffness of live breast cancer cells (MCF-7) in phosphate buffered saline (PBS), resveratrol and fibrinogen solutions to identify the location, drifting and aggregation of lipid rafts. Via cross-comparison of AFM images, the regions are higher and stiffer than the surrounding cell membranes resemble the characteristics of lipid rafts. The developed method may be applicable to identify the location of lipid rafts in real-time and allow us to elucidate complex biological systems at the molecular level.

O 66.6 Wed 18:00 P2/EG

Balanced trolling quartz-based sensor with high quality factor used for atomic force microscopy in the liquid — RUI LIN, •YINGZI LI, JIANQIANG QIAN, and PENG CHENG — School of Physics, Beihang University, Beijing, China
Quartz tuning fork (QTF) has been widely used in atomic force microscopy (AFM) due to its self-sensing property, high quality factor, and high frequency stability. However, owing to the bulky structure and exposed surface electrode arrangement of QTF, the application of quartz-based AFM sensor in the liquid imaging is limited. One way to solve this problem is to coat the QTF with an insulating layer and immerse it into the liquid. However, it would result in a sharp drop of the quality factor and lead to reduction of force detection sensitivity. Here, a high quality factor AFM sensor based on balanced trolling QTF is proposed. Both prongs of the QTF are glued with same tips to make sure high symmetry of QTF, while only one tip is immersed in the liquid. In this configuration, the hydrodynamic interaction can be reduced so that the quartz-based sensor can maintain a high quality factor, which will improve the sensitivity of force detection in the liquid. A theoretical model is presented to analyze the sensing performance of the balanced trolling quartz-based sensor in the liquid. Then, the sensing performance of the sensor is estimated through experimental tests. Finally, the proposed sensor is applied in AFM imaging on different samples in the liquid. The results validate the high quality of the proposed balanced trolling quartz-based sensor and its feasibility of liquid imaging of AFM.

O 66.7 Wed 18:00 P2/EG

AFM characterization of surface metal oxides with an O-terminated copper tip — •PHILIPP WIESENER, BERTRAM SCHULZE-LAMMERS, HARALD FUCHS, and HARRY MÖNIG — Westfälische Wilhelms-Universität, Münster, Germany
Previously we investigated the performance of various tip terminations, namely Cu-, Xe-, CO-, and O-terminated Cu-tips (CuOx-tips), on the Cu(110)O(2x1) surface with non contact AFM. A direct comparison of the imaging and force-

spectroscopy capabilities by these different tip terminations shows, that only for the CuOx-tip a significantly selective force interaction between metal and oxygen atoms can be observed.

In this work we want to generalize the idea of chemical selective imaging by analyzing a broad spectrum of metal oxide systems with CuOx-tips. We perform constant height measurements over an extended range of tip sample distances and analyze surfaces that possess varying relative heights of metal and oxygen atoms to probe possible effects on the chemical selectivity. For an additional contrast analysis we investigate various defects of the metal oxide surfaces and complement our site-selective microscopy with force-spectroscopy measurements on the observed metal and oxygen atoms.

The performed measurements can be seen as a first step of developing CuOx-tip AFM imaging as an efficient tool for the surface characterization of metal oxide materials. Subsequently, we want to extend our methodology to more complex surface- and bulk metal oxide systems and relate them with complementary DFT calculations and AFM simulations.

O 66.8 Wed 18:00 P2/EG

On-Surface Synthesis of C144 Hexagonal Coronoid with Zigzag Edges — •XUJIE ZHU, YANAN LIU, WEIWEN PU, FANG-ZI LIU, ZHIJIE XUE, ZHAORU SUN, KAKING YAN, and PING YU — School of Physical Science and Technology, ShanghaiTech University, 201210 Shanghai, China

Coronoids as polycyclic aromatic macrocycles enclosing a cavity and they can be also regarded as nanoporous graphene molecules whose electronic properties are critically dependent on the size and topology of their outer and inner peripheries. However, because of their synthetic and characteristic challenges, the extended hexagonal coronoids with zigzag outer edges have not been reported yet. Here, we report the on-surface synthesis of C144 hexagonal coronoid with outer zigzag edges on a designed precursor undergoing hierarchical Ullmann coupling and cyclodehydrogenation on the Au(111) surface. The chemical and electronic structure is unambiguously characterized by bond-resolved non-contact atomic force microscopy and scanning tunneling spectroscopy measurements. In combination with the density functional theory calculations, the result is shown that the HOMO-LUMO energy gap oscillates with the size of the central cavity. Moreover, the values of the harmonic oscillator model of aromaticity suggest that the molecular structure is ideally represented by Clar's model. Our results provide approaches toward realizing a hexagonal coronoid with zigzag edges, potentially inspiring fabrication of hexagonal zigzag coronoids with multiple radical characters in the future.

O 66.9 Wed 18:00 P2/EG

Setup of a quartz needle sensor-based nc-AFM/STM operating at millikelvin temperatures — •SVEN JUST^{1,2}, TANER ESAT^{1,2}, DENIS KRYLOV^{1,2}, PETER COENEN^{1,2,3}, VASILY CHEREPANOV^{1,2,3}, BERT VOIGTLÄNDER^{1,2,3}, STEFAN TAUTZ^{1,2}, and RUSLAN TEMIROV^{1,2,4} — ¹Peter Grünberg Institut (PGI-3), Forschungszentrum Jülich, Jülich, Germany — ²Jülich Aachen Research Alliance (JARA), Fundamentals of Future Information Technology — ³mProbes GmbH, 52428 Jülich, Germany — ⁴Institute of Physics II, University of Cologne, 50937 Cologne, Germany

A non-contact (nc) atomic force microscope (AFM) is developed for operation in ultra-high vacuum at a base temperature of 300 mK. The AFM is based on an ultra-compact quartz needle sensor oscillating at 1 MHz with a 7.5 μ m thick tungsten tip glued to one end of the needle allowing for simultaneous operation of AFM and STM [1]. Nanopositioners with resistive readout and a scanner with a large low-temperature scan range of 30 \times 30 μ m² are used. Additionally, HF wiring for an antenna and a capillary for supply of gases, both close to the junction, are provided. The AFM setup is mounted on a removable insert (mK-stick) for usage in an existing millikelvin system based on adiabatic demagnetization refrigeration (ADR) [2]. Due to the modularity of the mK-sticks a quick exchange is possible without any need for warming up the LHe cryostat.

[1] I. Morawski et al., Rev. Sci. Instrum. **81**, 033703 (2010)[2] T. Esat et al., Rev. Sci. Instrum. **92**, 063701 (2021)

O 66.10 Wed 18:00 P2/EG

Electrostatic Discovery Atomic Force Microscopy — NIKO OINONEN¹, •CHEN XU¹, BENJAMIN ALLDRITT¹, PROKOP HAPALA², FILIPPO FEDERICI CANOVA^{1,3}, FEDOR URTEV^{1,4}, SHUNING CAI¹, ONDŘEJ KREJČÍ¹, JUHO KANNALA^{1,2,3}, PETER LILJEROTH¹, and ADAM S. FOSTER^{1,5} — ¹Department of Applied Physics, Aalto University, 00076 Aalto, Espoo, Finland — ²FZU - Institute of Physics of the Czech Academy of Sciences, 182 21 Prague 8, Czechia — ³Nanolayers Research Computing Ltd., London N12 0HL, United Kingdom — ⁴Department of Computer Science, Aalto University, 00076 Aalto, Espoo, Finland — ⁵WPI Nano Life Science Institute (WPI-NanoLSI), Kanazawa University, Kakuma-machi, Kanazawa 920-1192, Japan

While offering high resolution atomic and electronic structure, scanning probe microscopy techniques have found greater challenges in providing reliable electrostatic characterization on the same scale. In this work, we offer electrostatic discovery atomic force microscopy, a machine learning based method which provides immediate maps of the electrostatic potential directly from atomic force

microscopy images with functionalized tips. We apply this to characterize the electrostatic properties of a variety of molecular systems and compare directly to reference simulations, demonstrating good agreement. This approach offers reliable atomic scale electrostatic maps on any system with minimal computational overhead.

O 66.11 Wed 18:00 P2/EG

Building up atomically-precise topological heterostructures in one-dimensional conjugated polymers — •ALEJANDRO JIMÉNEZ-MARTÍN^{1,2,3}, SHAYAN EDALATMANESH^{1,2}, BENJAMIN MALLADA^{1,2}, HÉCTOR GONZÁLEZ-HERRERO⁴, DAVID ECÍJA⁵, PAVEL JELÍNEK^{1,2}, and BRUNO DE LA TORRE^{1,2} — ¹Czech Advanced Technology and Research Institute (CATRIN), Palacký University, Olomouc, Czech Republic — ²Czech Academy of Sciences, Prague, Czech Republic — ³Czech Technical University, Prague, Czech Republic — ⁴Universidad Autónoma, Madrid, Spain — ⁵IMDEA Nanoscience, Madrid, Spain

The discovery of topological phases in acene-based π -conjugated polymers has been one of the most exciting developments in the field of on-surface synthesis [1]. We recently demonstrated that the topological phase transition can be precisely controlled by the length of the polymer [2], where topologically protected zero-mode states forms at the boundary between two interfaces.

In this contribution, we use such new design criteria for engineering the quantum phase to place edge-gap states at specific sites within a single polymer. We investigate the electronic properties and level of hybridization in close enough topological states depending on their separation by Scanning Tunneling Microscopy and non-contact Atomic Force Microscopy. The results presented here could serve as a blueprint for creating topologically protected quantum spin chains.

[1] B. Cirera, et al., Nano letters 14, (2014).

[2] H. González-Herrero, et al., Advanced Materials 33, (2021)

O 67: Poster: Electronic Structure of Surfaces

Time: Wednesday 18:00–20:00

Location: P2/EG

O 67.1 Wed 18:00 P2/EG

Fermi-level pinning at InP(001):H surfaces — •RACHELE SCIOTTO, ISAAC AZAHEL RUIZ ALVARADO, and WOLF GERO SCHMIDT — Lehrstuhl für Theoretische Materialphysik, Universität Paderborn, 33095 Paderborn, Germany
Stable InP(001):H surfaces are characterized by fully occupied and empty surface states close to the bulk valence and conduction band edges, respectively [1]. However, photoemission shows a surface Fermi level pinning at midgap energy [2]. In order to resolve that apparent discrepancy, we perform density-functional calculations. *Ab initio* thermodynamics is used to determine the density of surface defects as a function of temperature and hydrogen pressure. The influence of spin polarization and charging on the electronic properties of the surface defects is studied in detail. It is found that in particular P dangling bonds resulting from H desorption give rise partially filled midgap electronic states that are suitable to explain the experimental findings.

[1] WG Schmidt, et al. Phys. Rev. Lett. 90, 126101 (2003); PH Hahn, WG Schmidt, Surf. Rev. Lett. 10, 163 (2003).

[2] DC Moritz, et al. ACS Appl. Mater. Interfaces 14, 47255 (2022).

O 67.2 Wed 18:00 P2/EG

Dielectric anisotropy of heteroepitaxial GaP/AlP films grown on Si(001) from first-principles calculations — •MAX GROSSMANN and ERICH RUNGE — Technische Universität Ilmenau, Ilmenau, Deutschland
Low-defect III-V semiconductor films grown on Si(001) create new opportunities for cost-effective high-performance photovoltaic and optoelectronic devices. The recent work of Nandy et al. [1] shows a route how to drastically reduce the defect concentration of such structures through a thin GaP/AlP buffer layer. The growth of the latter is best monitored via reflection anisotropy spectroscopy (RAS). The theoretical characterization of RAS spectra is therefore vital for the monitoring of semiconductor growth processes as well as the understanding and improvement thereof. For these reasons we analyse the dielectric anisotropy for the case of a GaP/AlP/Si(001) heterostructure through first-principles calculations and compare them to the RAS measurements of Ref. [1]. [1] M. Nandy, A. Paszuk, M. Feifel, C. Koppka, P. Kleinschmidt, F. Dimroth, and T. Hannappel, A Route to Obtaining Low-Defect III/V Epilayers on Si(100) Utilizing MOCVD, Crystal Growth & Design 21, 5603-5613 (2021), 10.1021/acs.cgd.1c00410

O 67.3 Wed 18:00 P2/EG

Photoemission study of a Te Kagome adatom lattice on Pt(111) — •NICOLAI TAUFERTSHÖFER^{1,2}, BEGMUHAMMET GELDIYEV^{1,2}, MAXIMILIAN ÜNZELMANN^{1,2}, ANDREAS RAABGRUND³, TILMAN KISSLINGER³, LUTZ HAMMER³, M. ALEXANDER SCHNEIDER³, HENDRIK BENTMANN⁴, and FRIEDRICH REINERT^{1,2} — ¹Experimentelle Physik VII, JMU Würzburg — ²Würzburg-Dresden Cluster of Excellence ct.qmat — ³Lehrstuhl für Festkörperphysik, FAU Erlangen-Nürnberg — ⁴Center for Quantum Spintronics (QuSpin), NTNU Trondheim
Kagome lattices can host a variety of exotic phenomena such as flat bands, topological Dirac physics, or unconventional superconductivity [1]. In this contribution, we investigate the electronic structure of a Pt(111)-(3x3)-Te structure. This phase corresponds to a Kagome adlayer on a strongly reconstructed Pt(111) surface as determined by quantitative LEED-IV and STM. Utilizing angle-resolved photoemission spectroscopy, we find a Fermi surface with a rich structure stemming from a complex manifold of bulk and surface electronic states. Intending to unravel the influence of the Kagome lattice on the surface electronic band structure, we will carefully analyse and discuss our photoemission data. Particular attention will be on the nature of a band located in the close vicinity of the Fermi level at the center of the surface Brillouin zone.

[1] T. Neupert et al., Nature Physics 18, 137-143 (2022)

O 67.4 Wed 18:00 P2/EG

Spin asymmetries in photoemission from PtTe₂ — •MUTHU PRASATH THIRUGNANASAMBANDAM MASILAMANI¹, JAKUB SCHUSSER¹, MOHAMMED QAHOSEH², GUSTAV BHLMAYER³, LUKASZ PLUCINSKI², and FRIEDRICH REINERT¹ — ¹Experimentelle Physik VII and Würzburg-Dresden Cluster of Excellence ct.qmat, Universität Würzburg, Würzburg, Germany — ²Peter Grünberg Institut (PGI-6), Forschungszentrum Jülich GmbH, Jülich, Germany — ³Peter Grünberg Institut (PGI-1) and Institute for Advanced Simulation (IAS-1), Forschungszentrum Jülich and JARA, Jülich, Germany

In our recent work [1], we addressed the occurrence of spin-resolved photoemission signal asymmetries in the Weyl type-II semimetal candidate WTe₂. Here, we aim to understand the asymmetric spin texture of electrons photoemitted from surface and bulk states and its relation to the initial state of type-II Dirac semimetal PtTe₂ with photon energy of $h\nu = 21.22$ eV at room temperature and at 50K. Our spin- and angle-resolved photoemission data were augmented by the one-step model of the photoemission within the spin-polarized relativistic Korringa-Kohn-Rostoker (SPR-KKR) Green's function method of the Munich band structure software package. In order to extract information about the different contributions to the resulting spectral weight and spin polarization, the matrix-element used in our one-step model of photoemission calculations includes all experimental parameters such as photon energy, light polarization and geometry configurations.

[1] T. Heider et al., arXiv:2210.10870 (2022).

O 67.5 Wed 18:00 P2/EG

Quasiparticle lifetime and formation of electronic states at Tellurium-metal interfaces — •BEGMUHAMMET GELDIYEV^{1,3}, MAXIMILIAN ÜNZELMANN^{1,3}, PHILIPP ECK^{2,3}, DOMENICO DI SANTE^{2,3}, GIORGIO SANGIOVANNI^{2,3}, THOMAS FAUSTER⁴, HENDRIK BENTMANN^{1,3}, and FRIEDRICH REINERT^{1,3} — ¹Experimentelle Physik 7, Universität Würzburg — ²Theoretische Physik 1, Universität Würzburg — ³Würzburg-Dresden Cluster of Excellence ct.qmat — ⁴Lst. f. Festkörperphysik, Universität Erlangen-Nürnberg

Properties of interfaces between a device material and metallic contacts can decisively influence the resulting device performance. In particular, the formation of electronic interface states (IS) with short lifetimes could speed up the charge carrier injection [1]. In this contribution, we will discuss the formation of IS at Te - noble metal interfaces, i.e., particularly in a suitable model system AgTe / Ag(111) [2]. Utilizing one- and two-photon photoemission, we find that hybridizations between Te- p_z orbitals with substrate bulk and surface states determine the interface electronic structure. Whilst the AgTe valence band states are located almost completely within the AgTe layer, the wave function of the unoccupied state γ , lying 530 meV above E_F within the projected bulk band gap, has a sizable overlap with the substrate states. Evidence is provided by a rather short lifetime $\tau = 31 \pm 3$ fs of γ as well as by light-polarization-dependent measurements revealing the orbital character of the occupied and unoccupied states.

[1] C. H. Schwalb et al., Phys. Rev. Lett. 101, 146801 (2008)

[2] M. Ünzelmann et al., Phys. Rev. Lett. 124, 176401 (2020)

O 67.6 Wed 18:00 P2/EG

Accelerating plane-wave-based *ab initio* molecular dynamics by optimization of Fast-Fourier transforms for modern HPC architectures — •CHRISTIAN RIT-TERHOFF, TOBIAS KLÖFFEL, SAGARMOY MANDAL, and BERND MEYER — Interdisciplinary Center for Molecular Materials and Computer Chemistry Center, FAU Erlangen-Nürnberg, Germany

The most important advantage of plane-wave basis sets is that wave functions can be transformed efficiently from reciprocal to real space and back by using the Fast-Fourier transform (FFT) algorithm. This allows to evaluate the kinetic

and potential energy in reciprocal and real space, respectively, where both operators are diagonal. This reduces the computational cost for applying the Hamiltonian operator from N^2 to $N \log N$. However, the scalability of current FFT libraries is rather limited on today's HPC systems, which offer large numbers of compute nodes, each of them with many cores. Here we present our optimization of the FFTX library of the Quantum Espresso software package. Data distribution and communication patterns have been revised to make optimal use of combined MPI and OpenMP parallelization. Scalability is further increased by combining FFTs into batches and by introducing overlapping computation and communication. We implemented the revised FFTX library in our optimized version of the CPMD code [1], and we demonstrate the achieved acceleration by a series of benchmark simulations.

[1] T. Klöffel, G. Mathias, B. Meyer, *Comput. Phys. Commun.* **260** (2021) 107745

O 67.7 Wed 18:00 P2/EG

Comparison of machine learning strategies in the high-throughput exploration of ABO_2 delafossites — •ARMIN SAHINOVIC, BENJAMIN GEISLER, and ROSSITZA PENTCHEVA — Fakultät für Physik, Universität Duisburg-Essen

The advent of machine learning introduced new techniques to considerably expedite materials discovery. This raises a fundamental question about how they balance interpretability versus accuracy. We address this aspect by comparing ensemble-based active learning (AL) of neural networks (NN) [1] and the sure independence screening and sparsifying operator (SISSO) [2] for the prediction of formation energies and lattice parameters in ABO_2 delafossite oxides. To this end, we generate a consistent dataset from first principles. Element embedding is found to be superior to scalar input strategies, e.g., atomic properties. In conjunction with AL, the NNs reach DFT accuracy, allowing for a significant acceleration of high-throughput materials screening. In contrast, the precision of the physically interpretable SISSO descriptors is limited by the high data complexity. We combine ABO_2 infinite-layer, ABO_3 perovskite [1] and the delafossite data to extend the unsupervised AL into the structural space, thereby enhancing the sample efficiency in the spirit of transfer learning. Finally, we compile a phase diagram that compares the relative stability of the three distinct oxide materials classes.

[1] A. Sahinovic and B. Geisler, *Phys. Rev. Research* **3**, L042022 (2021); *J. Phys.: Condens. Matter* **34**, 214003 (2022)

[2] R. Ouyang *et al.*, *Phys. Rev. Materials* **2**, 083802 (2018)

O 67.8 Wed 18:00 P2/EG

Spin-polarized very-low-energy electron diffraction from spin-orbit- and/or exchange-influenced targets — •CHRISTOPH ANGRICK¹, CHRISTIAN THIEDE¹, ANDRE REIMANN¹, ANNIKA HENRIKSEN¹, NICOLE MUTZKE¹, MORITZ EWERT^{2,3}, LARS BUSS^{2,3}, JENS FALTA³, JAN INGO FLEGE², and MARKUS DONATH¹ — ¹University of Münster, Germany — ²BTU Cottbus-Senftenberg, Germany — ³University of Bremen, Germany

Exchange (XC) or spin-orbit (SOC) interaction cause electron scattering from surfaces to be spin dependent. The resulting spin filtering of the scattered electron beam can be used in spin-polarization analyzers. These analyzers are implemented in, for instance, photoemission setups to obtain spin resolution. Therefore, for promising targets, electron reflectivity and resulting spin asymmetry of very-low-energy electrons are measured for a wide range of incident electron energies and angles. By this, the investigated target is put to a test regarding the usability as a scattering target in a spin-polarization analyzer.

Here, several results of SOC- as well as XC-influenced targets are presented.

The results of the SOC-influenced targets Au(111), single-layer $MoS_2/Au(111)$ and W(110) [1] are compared with the results of the XC-influenced target Fe(001)- $p(1 \times 1)O$ [2]. Additionally, the influence of SOC interaction in the case of the XC-influenced target is investigated. The spin asymmetry caused by SOC is found to be one order of magnitude smaller than the spin asymmetry caused by XC.

[1] Angrick *et al.*, *J. Phys.: Condens. Matter* **33**, 115001 (2020).

[2] Thiede *et al.*, *Phys. Rev. Applied* **1**, 054003 (2014).

O 67.9 Wed 18:00 P2/EG

Exploring electronic structural properties of Copper(Cu) via Auger Photoelectron Coincidence Spectroscopy — •SWARNSHIKHA SINHA^{1,2}, DANILO KÜHN¹, and ALEXANDER FÖHLISCH^{1,2} — ¹Helmholtz-Zentrum Berlin für Materialien und Energie GmbH, Albert-Einstein-Strasse 15, 12489 Berlin, Germany — ²Universität Potsdam, Institut für Physik und Astronomie

The electronic structure of the 3d transition metals are immensely influenced by many electron effects. Photoemission spectroscopy (PES) and Auger electron spectroscopy (AES) can help to learn about screening processes in core excited states and electron correlations in two-hole final states, respectively.

However, in Cu 3p photoemission and MVV Auger decay, the final state holes are located in the same main shell as the initial vacancy, leading to strong lifetime broadening in the spectra. APECS, can help in reducing lifetime broadening and revealing overlapping spectral features. [1] A comparative study of three different copper surfaces (111,110 and 100) was conducted using APECS, at the CO-ESCA station, UE52 PGM beamline at BESSYII [2]. Our results confirm a strong energy sharing between the Photo and Auger electrons [3] and substantial differences in the screening of the final states, leading to different asymmetry of the atomic multiplet peaks in the two-hole spectra of the three Cu surfaces.

[1] H.W. Haak, *et al.*, *Phys. Rev. Lett.* **41**, 1825 (1978) [2] T. Leitner, *et al.*, *J. El. Spec.* **250**, 147075 (2021) [3] E. Jensen, *et al.*, *Phys. Rev. Lett.* **62**, 71 (1989)

O 67.10 Wed 18:00 P2/EG

Improved convergence of the density response function by an incomplete-basis correction — •JÖRN STÖHLER^{1,2}, MARKUS BETZINGER¹, STEFAN BLÜGEL¹, and CHRISTOPH FRIEDRICH¹ — ¹Peter Grünberg Institut and Institute for Advanced Simulation, Forschungszentrum Jülich, Germany — ²RWTH Aachen University, Germany

The polarizability (or density response function) is a central quantity in many electronic structure methods, e.g., the GW approach, the random-phase-approximation (RPA) total-energy method, the optimized effective potential method, the Bethe-Salpeter approach, Coulomb-hole screened-exchange (COHSEX). In time-dependent perturbation theory, the polarizability can be expressed as a sum over unoccupied states. However, the resulting sum-over-states expression converges very slowly with respect to the number of bands or the basis-set size, in particular, in systems containing localized d - and f -states. Here, we discuss a method, called incomplete-basis-set correction [1,2], which augments the sum-over-states expression with a numerical solution of the radial Sternheimer equation in the atomic (muffin-tin) spheres. The method is implemented in the Spex code within the FLAPW approach. The resulting polarizability shows a considerably improved convergence behavior with respect to the basis set and the number of unoccupied states.

[1] M. Betzinger, C. Friedrich, A. Görling, S. Blügel, *Phys. Rev. B* **85**, 245124 (2012), *ibid.* *Phys. Rev. B* **92**, 245101 (2015).

[2] M. Betzinger, C. Friedrich, S. Blügel, *PRB* **88**, 075130 (2013).

O 68: Poster: Oxide and Insulator Surfaces

Time: Wednesday 18:00–20:00

Location: P2/EG

O 68.1 Wed 18:00 P2/EG

Sub-nanometer depth profiling of native transition metal oxide layers within single XPS spectra — •MARTIN WORTMANN, DOMINIK GRAULICH, NATALIE FRESE, and TIMO KUSCHEL — Bielefeld University, Bielefeld, Germany

Many transition metals form a thin oxide layer of only few nanometers upon exposure to the atmosphere, which affects their interfacial properties. Such native oxide layers are commonly analyzed using photoemission spectroscopy (PES) and X-ray photoelectron spectroscopy (XPS) in particular. The most common method to obtain compositional depth profiles in PES is based on gradual surface ablation by ion sputtering. However, it is known to affect the microstructure of the surface, compromising depth-resolution and compositional accuracy. Other methods such as angular-resolved, energy-resolved, or hard X-ray PES are associated with considerable experimental effort or demands on sample texture. Here we propose a simple and accessible approach for sub-nanometer depth profiling of native metal oxide layers within single lab-XPS spectra. Heavy transition metals usually have multiple orbital energies within the energy range of a lab-XPS giving rise to peak regions at various binding energies. The signal contributions

of oxidized and elemental metals can be distinguished by peak deconvolution. The kinetic energy of the photoelectron determines its inelastic mean free path (IMFP) length, which is a measure for the depth from which information is obtained. Different binding energies can thus be assigned to different values for IMFP, so that an oxide concentration profile can be inferred from a single XPS spectrum.

O 68.2 Wed 18:00 P2/EG

Ab-initio investigations of the order of K^+ ions on cleaved muscovite mica — •ANDREA CONTI, GIADA FRANCESCHI, MICHAEL SCHMID, ULRIKE DIEBOLD, and FLORIAN MITTENDORFER — Institute of Applied Physics, TU Wien, Wiedner Hauptstrasse 8-10/134, 1040 Vienna, Austria

Model systems based on single crystals can help to provide a better understanding of the chemistry and the catalytic activity of a given oxide surface. In this work, we present DFT calculations on the surface of muscovite mica, a common phyllosilicate whose structure consists of alternating layers of aluminosilicates and K^+ ions. This material easily splits into thin K -terminated sheets, yet the atomistic order of the surface K^+ ions has been, until recently, unknown

[Franceschi *et al.*, *submitted* (2022)]. Calculations, using the “Vienna Ab-initio Simulation Package” (VASP) and the metaGGA (r^2 SCAN) exchange-correlation functional, indicate a close correlation between the distribution of the surface K^+ ions and the arrangements of the subsurface Al^{3+} ions: the K^+ ions preferentially occupy the Al-rich rings. In addition, the calculated diffusion barriers suggest that the K^+ ions are mobile enough at room temperature to jump to more favorable sites. AFM simulations, using the Probe Particle Model, are in good agreement with the experimental images.

O 68.3 Wed 18:00 P2/EG

Vanadium and iron intermixing in honeycomb oxides on Pt(111) and Ru(0001) — •PIOTR WEMHOFF¹, CLAUDINE NOGUERA², JACEK GONIAKOWSKI², and NIKLAS NILIUS¹ — ¹Carl von Ossietzky University, Institute of Physics, D-26111 Oldenburg, Germany — ²CNRS-Sorbonne University, UMR 7588, INSP, F-75005 Paris, France

Whereas V and Fe are immiscible in bulk-type perovskite oxides, mixed oxide honeycomb layers can be prepared on Pt(111) and Ru(0001) surfaces. Their atomic composition is accessible from bias-dependent STM topographic images, as the Fe ions develop a protruding contrast with respect to V when tunneling into their 3d(z²) orbitals at elevated bias. On Pt(111), up to 50% iron can be incorporated into a V₂O₃ host oxide, whereby the Fe runs through a series of distinct configurations evolving from isolated ions to pairs in 3rd neighbor positions, short chains of 2nd neighbor Fe and finally ordered (2x2) V/Fe islands separated by domain boundaries. The observed phase behavior can be traced back to attractive Fe-V and repulsive Fe-Fe pair interactions, which have been identified by DFT calculations and enable perfect reproduction of the experimental patterns by means of Monte-Carlo simulations. In contrast, a V/Fe self-organization scheme becomes active on Ru(0001) that only allows for one unique cation arrangement in the honeycomb oxide. DFT finds a layer of interfacial oxygen between Ru(0001) and the oxide film to be responsible for this rigid structural composition.

O 68.4 Wed 18:00 P2/EG

Atomic View on the (111) Surface of a Cu₂O Single Crystal: Reconstruction, Electronic Properties and Band Bending Effects — ALEXANDER GLOYSTEIN, JACK CREED, and •NIKLAS NILIUS — Carl von Ossietzky University, Institute of Physics, D-26111 Oldenburg, Germany

The nature of the $(\sqrt{3}\times\sqrt{3})R30^\circ$ reconstruction of the Cu₂O(111) surface has been heavily debated for almost 30 years. This work demonstrates that the nano-pyramidal reconstruction model that was recently developed for Cu₂O(111) thin films is valid also for bulk samples. Well-prepared crystals develop a robust $(\sqrt{3}\times\sqrt{3})R30^\circ$ superstructure in electron diffraction, while atomically resolved STM images display extended arrays of trifold symmetric protrusions with 10.5 Å periodicity. Both findings are in perfect agreement with the nano-pyramidal model, in which Cu₄O units attach to every third Cu-O six-ring of a Cu-depleted (111) surface. STM conductance spectra reveal the p-type character of the oxide with the valence-band top pinned to the Fermi level. From band-bending effects in the tip electric field, an induced carrier concentration of 6×10^{17} cm⁻³ is determined for the $(\sqrt{3}\times\sqrt{3})R30^\circ$ phase, increasing to 4×10^{18} cm⁻³ on the few (1x1) patches covered with a Cu-poor minority phase. This difference reflects the close interplay between atomic structure, electronic properties and local screening response for a given surface termination.

O 68.5 Wed 18:00 P2/EG

The Surface Chemistry of Hydrated Lime - Wave Optics tested on a Model System — •NILS SCHEWE¹, THOMAS MAYERHÖFER², HICHAM IDRIS¹, and CHRISTOPH WÖLL¹ — ¹Institute of Functional Interfaces (IFG), Karlsruhe Institute of Technology (KIT), Hermann-von-Helmholtz-Platz 1, Eggenstein-Leopoldshafen, 76344, Germany — ²Institut für Physikalische Chemie, Friedrich-Schiller-Universität Jena, Jena, 07745, Germany

We report on the results of a combined experimental and theoretical study of the interaction of sulfur dioxide with a calcium hydroxide single crystal surface. Our investigation of this model system for flue gas desulfurization and concrete corrosion was carried out on the Ca(OH)₂ (001) surface under ultra-high-vacuum conditions. Combining polarization resolved UHV infrared reflection absorption spectroscopy (IRRAS) with calculations based on wave optical considerations, we were able to demonstrate the adsorption behavior and mode of SO₂ on this surface. We show, that the preferred angle of adsorption is 23 ° below 65 K. Heating does not lead to reaction, but fully desorbs the formed adsorbate after crystallization between 80 - 100 K. Additionally, we were able to obtain the first low energy electron diffraction (LEED) pattern of an alkaline earth metal hydroxide by using UHV exfoliation for cleaning.

O 69: Poster: Solid-Liquid Interfaces

Time: Wednesday 18:00–20:00

Location: P2/EG

O 69.1 Wed 18:00 P2/EG

Understanding the mechanism of Li-mediated nitrogen reduction reaction — •YUANYUAN ZHOU and JENS K. NØRSKOV — Department of Physics, Technical University of Denmark, Kongens Lyngby, Denmark

Green ammonia production is a key environmental goal. As a crucial step towards this goal, a direct electrocatalytic N₂ reduction (eNRR) by protons and electrons emerges as a highly desirable alternative. However, all pragmatic attempts to develop such an electrochemical route have so far been hindered by invariably low selectivities and large overpotentials. The most reliable method presently is the lithium-mediated eNRR (LiNR) in non-aqueous electrolytes. [J. Choi *et al.* Nat. Commun. 11, 1-10 (2020)] Despite significant progress made to achieve high FE and current density [K. Li *et al.* Science 374, 1593-1597 (2021), S. Li *et al.* Joule, 6, 2083-2101 (2022)], the mechanism of LiNR is yet not fully understood due to so many intricate processes involved ranging from the atomic scale to the macroscopic scale. Moreover, most Li-NRR studies have the limitations of using a sacrificial solvent as proton donors and difficulties in scaling up production in batch reactors. The talk will, address the long-term stability and high activity of PtAu in the HOR process by suppressing the unwanted THF oxidation and improving the tolerance towards CO-poison. Furthermore, the crucial step for achieving an improved understanding the dynamic change of the solid-electrolyte interphase in different LiNR reaction conditions and the effect on the performance.

O 69.2 Wed 18:00 P2/EG

When qualitative do not imply quantitative differences: Analyzing the oxygen reduction reaction using first-principles kinetic Monte Carlo simulations. — •ELIA ZONTA¹, YOUNES HASSANI ABDOLLAHI^{1,2}, KARSTEN REUTER¹, and SEBASTIAN MATERA^{1,2} — ¹Fritz Haber Institute of the Max Planck Society, Berlin, Germany — ²Institute for Mathematics, Freie Universitaet Berlin, Germany, Germany

The oxygen reduction reaction (ORR) is one of the major bottlenecks for the efficiency of fuel cell devices. We implemented a first-principles kinetic Monte Carlo model for this reaction on Pt(111) using a mechanism from literature [1]. This model possesses two reaction pathways contributing to the electrochemical current density. Disabling one of these pathways results in an identical simulated Tafel plot for this reduced model, as compared to the original model with

both pathways being active. One might conclude that the turned off pathway is effectively inactive also in the original model and, especially, has no impact on the qualitative kinetics. However, a detailed analysis reveals that both models lead to very different surface coverages and, particularly, exhibit different rate-determining steps. Thus, these qualitative microkinetic differences do not lead to any quantitative differences in the macrokinetic behavior.

[1] R.F. de Morais, P. Sautet, D. Loffreda, and A.A. Franco, *Electrochim. Acta* 56, 10842 (2011).

O 69.3 Wed 18:00 P2/EG

Electric Double Layer effect on outer-sphere benzyl halides electro-reduction mechanism — •ALEKSANDR KRAMARENKO¹, FELIX STUDDT¹, and EVGENY PIDKO² — ¹Karlsruhe Institute of Technology, Karlsruhe, Germany — ²TU Delft, Delft, The Netherlands

Electrocatalytic CO₂ fixation is one of the most efficient methods of carbon dioxide conversion, which can be carried out at room temperature and pressure. Thus, the fixation of carbon dioxide with electrochemically activated benzyl halides is an environmentally friendly and ambitious method for the synthesis of the most important carboxylic acid derivatives, which are invaluable for pharmaceuticals and fuel production. For these types of processes, electrocatalysis is a key technology, where electrified interfaces are the main object of study and where the electrochemical potential determines the stability of adsorbed particles and the structure of the electric double layer (EDL) on the electrode surface. Therefore, it is important to gain insight into the electrode-electrolyte interface and the rate-determining reaction steps in order to improve electrode material selectivity and product yields. The combination of first principles and molecular dynamics simulations gives us a good understanding at the molecular level of charged interface phenomena and allows us to study elementary chemical processes in detail, which sheds light on how to improve electrocatalytic reactivity.

O 69.4 Wed 18:00 P2/EG

Atomistic electric double layer modeling of water/metal interfaces from AIMD and continuum approaches — •SUNG SAKONG and AXEL GROSS — Ulm University, Ulm, Germany

Electrochemical interfaces are typically associated with forming an electric double layer (EDL) whose theoretical modeling requires an appropriate description

of the polarization of the electrode and the electrolyte. In principle, *ab initio* molecular dynamics (AIMD) simulations are the natural choice as they reliably treat the competing water-water and water-metal interactions and explicitly consider the electronic degrees of freedom [1]. However, this approach is computationally still very demanding and only allows simulations of relatively small canonical ensembles for limited simulation times. Thus, there is a need for computationally less demanding but still reliable approaches to model the EDL. By comparing EDL properties calculated from a continuum method based on a grand canonical scheme [2] with *ab initio* atomistic approaches [3], we will provide an outlook on possible future directions in the EDL modeling [4].

- [1] A. Groß and S. Sakong, *Chem. Rev.* **122**, 10746 (2022).
 [2] S. Sakong *et al.*, *Curr. Opinion Electrochem.* **33**, 100953 (2022).
 [3] S. Sakong, A. Groß, *Phys. Chem. Chem. Phys.* **22**, 10431 (2020).
 [4] A. Groß and S. Sakong, *Curr. Opinion Electrochem.* **14**, 1 (2019).

O 69.5 Wed 18:00 P2/EG

Water/InP(001) from Density Functional Theory — ISAAC AZAHEL RUIZ ALVARADO and WOLF GERO SCHMIDT — Lehrstuhl für Theoretische Materialphysik, Universität Paderborn, Paderborn, Germany

Water adsorption on the In-rich and P-rich InP(001) surface is studied by density functional theory [1]. Single water molecules attach to three-fold coordinated surface In atoms on In-rich surfaces. Dissociative water adsorption is energetically favorable, but hindered by an energy barrier that decreases with increasing water coverage. The oxygen and hydrogen evolution reactions on InP are characterized by overpotentials of the order of 1.7-1.8 and 0.2-0.3 eV, respectively. The In-rich InP surface band edges lie above the redox potential for oxygen and favors hydrogen evolution. Water adsorption is less favorable on P-rich surfaces and characterized by weak physisorption due to charge accumulation between the water O atom and second-layer In surface atoms.

- [1] IA Ruiz Alvarado, WG Schmidt, *ACS Omega* **7**, 19355 (2022).

O 69.6 Wed 18:00 P2/EG

CO₂ Electroreduction Reactions at Gold and Copper Electrodes in Ionic Liquids — BJÖRN RATSCHMEIER, GINA ROSS, and BJÖRN BRAUNSCHEWIG — University Münster, Institute of Physical Chemistry, Münster, Germany

Room-temperature ionic liquids (RTIL) can play a major role in CO₂ reduction reactions in mitigation of existing problems of aqueous electrolytes, such as high overpotentials and product selectivity. In this context, we have studied the influence of Au(111), Cu(111) single crystals, as well as Cu enriched Au(111) electrodes prepared by Cu underpotential deposition with Cu coverages of 1/3, 2/3 and 3/3, in 1-butyl-3-methylimidazolium trifluorosulfonylimide [BMIM][NTf₂] for CO₂RR. For Au and Cu enriched Au electrodes we observed high selectivity for H₂ and CO formation, with onset potentials at around -1.0 V vs SHE and a H₂/CO syngas ratio between 0.2-0.4, whereas for Cu only H₂ and traces of CO were detected until 1.5 V. By increasing the degrees of coverage of Cu on Au, we were able to modulate the syngas ratio to an optimum ratio of about 1.8 for a monolayer of Cu on Au(111), which approaches the ideal ratio of 2 for Fischer-Tropsch synthesis of hydrocarbons.

O 69.7 Wed 18:00 P2/EG

Exploring charge transfer at electrified interfaces via *ab initio* thermopotentiostat molecular dynamics — FLORIAN DEISSENBECK¹, MIRA TODOROVA¹, CHRISTOPH FREYSOLDT¹, JÖRG NEUGEBAUER¹, and STEFAN WIPPERMANN^{1,2} — ¹Max-Planck-Institut für Eisenforschung, Düsseldorf — ²Philipps-Universität Marburg

Developing accurate simulation techniques to explore and predict structural properties and chemical reactions at electrified liquid/solid interfaces will be critical to surmount materials-related challenges in the context of energy conversion and storage. Exciting progress in recent years allows us now to realistically describe electric fields at charged surfaces from first principles. Building on these techniques, we recently introduced a “thermopotentiostat”: a novel approach to control the electrode potential in molecular dynamics (MD) simulations [1]. We demonstrate how to implement the thermopotentiostat into density-functional codes [2]. Using *ab initio* thermopotentiostat MD simulations, we explore the splitting of liquid water and charge transfer reactions at electrified Si and Ge surfaces.

- [1] F. Deissenbeck, C. Freysoldt, M. Todorova, J. Neugebauer, S. Wippermann, *Phys. Rev. Lett* **126**, 136803 (2021)
 [2] F. Deissenbeck, S. Wippermann, arXiv:2209.04363

O 69.8 Wed 18:00 P2/EG

Density functional calculations of diffusion paths of methyl thiolate on c(2x2)Cl- and Br-covered Cu(100) surfaces — FALK WENDORFF and ECKHARD PEHLKE — Institut für Theoretische Physik und Astrophysik, Christian-Albrechts-Universität zu Kiel, 24098 Kiel, Germany

The surface dynamics of methyl thiolate on Cu(100) surfaces has been studied with video-STM in an electrochemical environment by Yang *et al.* [1]. Here we present density functional calculations for the diffusion paths and diffusion energy barriers using PWscf and PWneb from the Quantum ESPRESSO package

[2]. The diffusion path of CH₃S_{ad} substitutionally adsorbed on the c(2x2)Cl- or Br-Cu(100) surface without further halogen vacancies has been inspired by the ‘rotation’ diffusion path of S_{ad} on these surfaces [3]. Additional vacancies in the halogen adlayer enable further diffusion paths of CH₃S_{ad} with significantly lower energy barriers. In case of the Cl coadsorbate the barrier decreases from 1.2 eV to 0.7 eV and in case of Br from 1.6 eV to 0.8 eV. The dipole moment change between the adsorption position and the transition state is negative, which is consistent with the experimental observations by Yang *et al.* that a more positive sample potential leads to a higher energy barrier [1,4].

- [1] Y.-C. Yang *et al.*, *Langmuir*. **28**, 40, 14143–14154 (2012).
 [2] P. Giannozzi *et al.*, *J. Phys. Condens. Matter* **21**, 395502 (2009), *ibid.* **29**, 465901 (2017).
 [3] B. Rahn *et al.*, *Angew. Chem. Int. Ed.* **57**, 6065 (2018).
 [4] M. Giesen *et al.*, *Surface Science*. **595**, 127–137 (2005).

O 69.9 Wed 18:00 P2/EG

Growth and structure formation of [EMIm][OTf] on Au(111) — JONAS HAUNER¹, HANNA BÜHLMAYER¹, SIMON TRZECIAK², JULIEN STEFFEN³, DIRK ZAHN², ANDREAS GÖRLING³, and JÖRG LIBUDA¹ — ¹Interface Research and Catalysis, Friedrich-Alexander-Universität Erlangen-Nürnberg, Egerlandstraße 3, 91058 Erlangen, Germany — ²Computer Chemistry Center, Department of Chemistry and Pharmacy, Friedrich-Alexander-Universität Erlangen-Nürnberg, Nägelsbachstraße 25, 91052 Erlangen, Germany — ³Chair of Theoretical Chemistry, Friedrich-Alexander-Universität Erlangen-Nürnberg, Egerlandstraße 3, 91058 Erlangen, Germany

The growth mechanisms of ultrathin ionic liquid (IL) films have recently received considerable attention. We report on *in situ* studies of 1-ethyl-3-methylimidazolium trifluoromethanesulfonate ([EMIm][OTf]) on Au(111). The IL thin films were prepared by physical vapor deposition and investigated by scanning tunneling microscopy (STM). We carried out measurements at various sample temperatures and coverages, and identified three different surface structures. At low coverage, [EMIm][OTf] tends to exhibit a 2D-glass structure growing close to gold terraces and the elbows of the well-known herringbone structure of Au(111). Oblique and hexagonal structures of the IL are visible at higher coverage. With temperature-dependent measurements, possible phase transitions and melting points of [EMIm][OTf] were investigated. Small glass-like islands of IL melt at 190 - 200 K resulting in a mobile phase of 2D liquid/gas. Islands with highly ordered structures are stable up to 300 K.

O 69.10 Wed 18:00 P2/EG

In situ surface X-ray diffraction studies of Pt(110) — FINN SCHRÖTER¹, JAN OLE FEHRS¹, TIMO FUCHS¹, JAKUB DRNEC², MARTA MIROLO², DAVID HARRINGTON³, and OLAF MAGNUSSEN¹ — ¹Christian-Albrechts Universität zu Kiel — ²European Synchrotron Radiation Facility — ³University of Victoria

The surface oxidation of platinum is an important process in the degradation of platinum electrocatalysts in PEM fuel cells, limiting their lifetime. Its atomic-scale mechanism has been addressed in extensive studies by structure-sensitive *in situ* techniques. However, these studies up to now have been restricted to room temperature, whereas real fuel cells operate at elevated temperatures of 60°C or higher. We here present first temperature-dependent of the surface oxidation of Pt(111) electrodes in perchlorate solution by *in situ* high-energy surface X-ray diffraction (HESXRD). The measurements were performed at the ID31 beamline of the European Synchrotron Radiation Facility using photon energies of 70 keV. The kinetics of oxidation-induced extraction of Pt atoms out of the surface was quantitatively determined and correlated with the electrochemical charge transfer measured simultaneously in the experiments. The work was funded by the Deutsche Forschungsgemeinschaft via grant 418603497 and the BMBF via project 05K19FK3.

O 69.11 Wed 18:00 P2/EG

The self-assembly process of helical molecules — THI N. HA NGUYEN¹, F. GÜNTHER², K. PREIS¹, J. KELLING¹, C. TEGENKAMP¹, and S. GEMMING¹ — ¹Institut für Physik, TU Chemnitz, Chemnitz — ²Instituto de Física de Sao Carlos, Universidade de São Paulo, Sao Carlos, Brazil; Instituto de Geociências e Ciências Exatas, Universidade Estadual Paulista, Rio Claro, Brazil

Helical polyalanine (PA) molecules gathered a lot of interest as the propagation of electrons along the helical backbone structure comes along with spin polarization. Via liquid and solid scanning tunneling microscopy (STM) we studied the ordering of physisorbed and chemisorbed PA molecules on HOPG and Au surfaces. While enantiopure PA molecules adsorb in a hexagonally close-packed structure, we found heterochiral dimers with a rectangular unit cell for DL-PA. Despite the steric hindrance, the packing density of the DL-PA heterophase is increased by 25% compared to the enantiopure PA structure. Apparently, this is achieved by shifting D- and L-PA along their helical axis. Moreover, the alpha-helix structure of the PA molecules seems to be preserved; thus, electrostatic forces indeed play an important role for the formation and stabilization of the helical structure. In parallel, the interactions between PA homo- and heterochiral pairs were analyzed by van-der-Waals-corrected DFT-based tight binding calculations. Denser packing geometries can be reached by heterochiral PA pairs.

Second, coarse-grained classical potentials were derived from the DFTB data, and the different PA phases seen in STM were also successfully obtained from Monte-Carlo simulations.

O 69.12 Wed 18:00 P2/EG

DFT calculation of the S_{ad} diffusion energy barriers on Ag(100) in the presence of Br coadsorbates — •SÖNKE BUTTENSCHÖN and ECKHARD PEHLKE — Institut für Theoretische Physik und Astrophysik, Christian-Albrechts-Universität zu Kiel, 24098 Kiel, Germany

Coadsorbed halides are known to affect the adatom diffusion on metal surfaces [1]. As a prerequisite for theoretical modelling of the S_{ad} diffusion on Ag(100) as a function of Br coverage, we have calculated the effect of single and multiple Br coadsorbates on the S_{ad} adsorption energy as well as on the energy at the transition geometry along the S_{ad} diffusion path for various Br coadsorbate configurations with Br coverages up to 0.25. The density functional total-energy calculations have been carried through with PWscf and PWneb from the Quantum ESPRESSO package [2]. The dipole moment of S_{ad} is negative. It is larger in magnitude at the transition state (TS) than at the adsorption position. Averaged over the considered S-Br configurations the absolute value of the S_{ad} dipole moment has a tendency to decrease with Br coverage in qualitative agreement with a depolarization model. After similar averaging, for the TS configurations the superposition of individual S_{TS} -Br pair interaction energies tends to overestimate the actual S_{TS} -Br interaction. Funded by the Deutsche Forschungsgemeinschaft (DFG, German Research Foundation), project 504552981.

[1] B. Rahn, O. M. Magnussen, *ChemElectroChem* **5**, 3073 (2018).

[2] P. Giannozzi *et al.*, *J. Phys. Condens. Matter* **21**, 395502 (2009), *ibid.* **29**, 465901 (2017).

O 69.13 Wed 18:00 P2/EG

Correlation between electrostatic and hydration forces on silica and gibbsite surfaces: An Atomic Force Microscopy Study — •IGOR SIRETANU, ARAM KLAASSEN, and FRIEDER MUGELE — Physics of Complex Fluids Group, MESA+ Institute, Faculty of Science and Technology, University of Twente, PO Box 217, 7500 AE Enschede, The Netherlands

The balance between hydration and Derjaguin Landau Verwey Overbeek forces at solid-liquid interfaces controls many processes, such as colloidal stability, elec-

trochemistry and ion adsorption. Yet, the hydration forces origin and their relation to the surface charge density controlling the continuum scale electrostatic forces are poorly understood. We argue that these two types of forces are largely independent of each other. Here we performed AFM using intermediate-sized tips that enable the simultaneous detection of DLVO and oscillatory hydration forces at the interface between gibbsite:silica-aqueous electrolyte interfaces. We extract surface charge densities from forces using DLVO theory in combination with a charge regulation boundary conditions for variable pHs and salt concentrations. We simultaneously observe both DLVO and oscillatory hydration forces for an individual crystalline gibbsite particle and the amorphous silica for all fluid compositions. While the diffuse layer charge varies with pH as expected, the oscillatory hydration forces are largely independent of pH and salt concentration, supporting our hypothesis that both forces indeed have a very different origin. We rationalize this based on the distribution of OH groups available for H-bonding on the two distinct surfaces.

O 69.14 Wed 18:00 P2/EG

The interfacial (electronic) structure of InP(001) in contact with electrolytes studied via computational Reflection Anisotropy Spectroscopy — •VIBHAV YADAV¹, MARGOT GUIDAT^{1,2}, MARIO LÖW², JONGMIN KIM^{1,2}, HOLGER EUCHNER¹, and MATTHIAS M. MAY^{1,2} — ¹Institute of Physical and Theoretical Chemistry, University of Tübingen — ²Institute of Theoretical Chemistry, University of Ulm, Germany

Controlling the electrochemical interface of III-V semiconductors is of great relevance for hydrogen production in Photoelectrochemical water splitting devices. Under operating conditions InP surfaces in contact with the electrolyte can undergo polymerization or dissolution, with the possible formation of In-O-In as charge recombination centers [1,2]. In this work, we vary the oxygen adatom coverage on In-rich and P-rich InP(001) surfaces using Density-functional Theory. Furthermore, we show that combining computational and experimental Reflection Anisotropy Spectroscopy has the potential to provide a better understanding of InP surfaces and their (electronic) structure under applied potentials. [1] May MM, Lewerenz HJ, Lackner D, Dimroth F, Hannappel T. *Nat Commun* **15**, 2015, 9 (15), 8286. [2] Löw M, Guidat M, Kim J, May MM, *RSC Adv.* **2022**, **12** (50), 32756.

O 70: Poster: Plasmonics and Nanooptics II

Time: Wednesday 18:00–20:00

Location: P2/EG

O 70.1 Wed 18:00 P2/EG

Phase correction and stability of a Mach-Zehnder interferometer for 2D electronic spectroscopy — •SIMON DURST, SANCHAYEETA JANA, CHRISTOPH SCHNUPFHAGN, and MARKUS LIPPITZ — University of Bayreuth

Fluorescence detected 2D electronic spectroscopy (F-2DES) allows the measurement of ultrafast electron dynamics in complex systems, while disentangling this spectral information from energetically similar phenomena, such as molecular vibration.

The technique requires an excitation signal of four time-delayed laser pulses, which we create via a four-arm Mach-Zehnder interferometer. This interferometer receives a single pulse as an input, and, through the use of delay stages and acousto-optical modulators, outputs a desired pulse train with frequency-modulated phase profiles, used for lock-in detection.

When exciting a sample with this pulse train, special attention must be given to the phase relation between the individual pulses. A mismatch or instability in their spectral phase leads to an excitation with pulses of different lengths or unknown delays and will overall worsen the performance of the setup.

Therefore, this poster highlights the techniques and instruments we use to characterize and compensate the relative phase between the different interferometer arms: GVD correction using a spatial light modulator, a prism compressor setup and interferometric delay scans.

O 70.2 Wed 18:00 P2/EG

In-Situ TEM Study of Structural and Optical Changes by Laser-Induced Grain-Growth — •JAKOB HAGEN, MURAT SIVIS, and CLAUDIUS ROPERS — Max-Planck-Institute for Multidisciplinary Sciences, Göttingen, Germany

Resonantly excited surface-plasmons (SP) can be exploited in various scientific fields [1] and have thus sparked widespread attention. One major characteristic of these collective free-electron oscillations is the ability to localize and enhance electromagnetic fields beyond the diffraction limit [2]. Here, we created Aluminum nanodiscs by electron beam lithography (EBL), which are polycrystalline in nature. In general, single-crystalline structures are preferred because high optical quality can be obtained due to the absence of propagation-damping grain boundaries [3]. Using annealing in an ultrafast transmission electron microscope (TEM) with a pulsed laser source, a grain-growth process could be driven where the boundary migration was observed frame by frame. Upon

illumination, the number of grains reduced drastically, leading to almost perfect mono-crystals while preserving the shape. In addition, optical characterization of SPs by photon-induced near-field electron microscopy (PINEM) [4] was carried out before and after annealing. Our approach fuses the precise, nanometric positioning from EBL with the benefits of mono-crystalline plasmonics [5].

[1] S. Lal *et al.*, *Nat. Photonics* **1**, 641-648 (2007), [2] K. B. Crozier *et al.*, *J. Appl. Phys.*, **94**, 4632 (2003), [3] M. Bosman *et al.*, *Sci. Rep.* **4**, 5537 (2014), [4] L. Piazza *et al.*, *Nat. Commun.* **6**, 6407 (2015), [5] J.-S. Huang, *Nat. Commun.*, **1**:150 (2010)

O 70.3 Wed 18:00 P2/EG

Gold nanoparticles as scannable plasmonic light source for STM enabled electroluminescence — •CINJA S. MÜLLER, BERK ZENGİN, ALEŠ CAHLÍK, and FABIAN D. NATTERER — Department of Physics, University of Zurich, Winterthurerstrasse 190, CH-8057, Switzerland

The preparation of high quantum yield tips for electroluminescence includes the use of plasmonic metals, by either making tips from wires of coinage metals or coating of tungsten (or Pt/Ir) tips by violent indentation into Au or Ag crystals. While the former appears as the most logical choice, tips made from ductile coinage metals tend to be mechanically unstable. The plunging of tungsten tips into metal substrates, on the other hand, is rather crude and irreproducible. Here, we attempt to use concepts from both extremes by attaching gold nanoparticles (AuNP) onto the apex of tungsten or Pt/Ir tips. We drop-cast commercially available colloidal AuNP onto a graphite substrate from which the AuNP may be transferred to the STM tip by gentle contact. We describe our setup and characterize the electroluminescence using a fiber-coupled single photon counter.

O 70.4 Wed 18:00 P2/EG

Neuromorphic plasmonic computing - Surface plasmon polariton neurons — •MARIO F. PFEIFFER¹, TOBIAS EUL¹, EVA PRINZ¹, BENJAMIN STADTMÜLLER^{1,2}, and MARTIN AESCHLIMANN¹ — ¹Department of Physics and Research Center OPTIMAS, University of Kaiserslautern, Germany — ²Institute of Physics, Johannes Gutenberg University Mainz, Germany

Today, the classical electronic computer architecture is the limiting factor for faster, and energy efficient data processing. In combination with the rapidly increasing use of artificial intelligence in science and industry, additional ap-

proaches for a suitable hardware architecture are necessary. For this reason, neuromorphic photonics emerged as a novel research field for new classes of information processing devices that incorporate photonically integrated neural networks [1].

The hybrid nature of surface plasmon polaritons (SPPs) combines photonic advantages such as high bandwidth and speed with strong electronic interactions. These properties have the potential to further advance the development of new hardware. Here we present a concept for building an artificial neuron based on SPP interactions. We have designed initial building blocks of the neuron based on finite-difference time-domain simulations of the plasmonic response. Finally, we imaged this response using a photoemission electron microscope.

[1] Shastri, B.J., Tait, A.N., Ferreira de Lima, T. et al., *Nat. Photonics* 15, 102-114 (2021)

O 70.5 Wed 18:00 P2/EG

Optical writing of switchable mid-infrared surface phonon polariton resonators with the plasmonic phase-change material In_3SbTe_2 — •LUI SCHÜLER, LUKAS CONRADS, KONSTANTIN GEORG WIRTH, MATTHIAS WUTTIG, and THOMAS TAUBNER — I. Institute of Physics (IA), RWTH Aachen University
Chalcogenide-based phase-change materials (PCMs) are prime candidates for active nanophotonics. They can be reversibly switched between an amorphous and a crystalline state, which exhibit a strong contrast in optical and electrical properties [1]. Therefore, PCMs can be used, for example, to tune surface phonon polariton (SPhP) resonances in the infrared [2]. The recently introduced PCM In_3SbTe_2 (IST) possesses a crystalline phase which is metallic in the entire infrared range. It allows for direct writing of arbitrary resonant structures in a dielectric surrounding [3], which could also confine SPhPs in cavities of subwavelength size. However, an investigation of different confined modes in those cavities with IST has not been performed yet. Here, we investigate IST on a SiC substrate. By laser-induced phase switching, we define various SPhP resonator structures, such as circular cavities, and measure their resonant behavior with optical near- and far-field methods. This study is a first step towards rapid prototyping of switchable SPhP resonators of arbitrary shape that could be employed, for example, in chemical sensing and active metasurfaces.

[1] Wuttig, M. et al. *Nature Photonics* 11, 465-476 (2017).

[2] Sumikura, H. et al. *Nano Letters* 19, 2549-2554 (2019).

[3] Heßler et al. *Nature Communications* 12, 924 (2021).

O 70.6 Wed 18:00 P2/EG

Enhanced Second Harmonic Generation from Silver Nanoantennas — •FABIAN SCHEIDLER, JOHANNA KLOS, JESSICA MEIER, LUKA ZURAK, and BERT HECHT — Nano-Optics and Biophotonics Group, Experimental Physics 5, University of Würzburg, Am Hubland, 97074 Würzburg, Germany

Plasmonic gold nanostructures allow to achieve large field enhancement in nanoscale volumes and are therefore appealing to boost nonlinear processes such as second harmonic generation (SHG). Especially intense near-field hot spots emerge in the gaps of symmetric dimer antennas, yet strong SH sources created in the gap region oscillate out-of-phase and thus destructively interfere in the farfield [1]. Introducing local asymmetry by careful design of the antenna gap geometry allows to mitigate the so-called silencing effect and leads to enhanced SHG [2].

In the ultraviolet-visible spectral range, however, the SH efficiency for gold nanoantennas is limited due to high damping below 500 nm. Here we present silver nanoantennas fabricated from epitaxial grown single-crystalline microplatelets to boost SHG below 500 nm, where silver shows significantly less absorption losses compared to gold. The antenna design is optimised for SHG taking into account the linear scattering response with a resonance at the SH.

[1] J. Berthelot et al., *Optics express*, 20(10), 10498-10508 (2012).

[2] J. Meier et al., arXiv:221014105 (2022).

O 70.7 Wed 18:00 P2/EG

A room temperature tunable scanning fiber Fabry-Pérot cavity microscope — •LARS DENZER, PAUL STEINMANN, and STEFAN LINDEN — Physikalisches Institut, Universität Bonn, Nussallee 12, 53115 Bonn, Germany

Since the technological advancements in the fabrication of ultra-smooth concave fiber surfaces, fiber-based Fabry-Pérot cavities (FFPCs) are a field of ongoing research. Many applications emerged, ranging from light-matter coupling utilizing very small mode volumes over cavity-enhanced sensing, to cavity mi-

croscopy. Here, we report on the construction and test of a tunable scanning fiber Fabry-Pérot cavity microscope operating at room temperature. To this end, we fabricated a concave metallic mirror on the facet of an optical fiber. Using a focused CO₂ laser beam, we achieve an ultra-smooth Gaussian depression at the fiber facet. Afterwards, the fiber is gold-coated in an evaporation chamber. Coarse tuning of the cavity is possible by the use of a 3D-piezo stage and the cavity length is fine-tuned by a shear piezo. Laterally scanning the cavity enables a mapping of the sample surface. As a first test, we investigate the coupling of a MoSe₂ monolayer to the cavity field.

O 70.8 Wed 18:00 P2/EG

Near-field scanning optical microscopy of topologically protected excitons in molecular aggregates — SIDHARTHA NAYAK, CHRISTOPHER W. WÄCHTLER, and •ALEXANDER EISFELD — MPIPKS, Dresden, Germany

Delocalized excitonic eigenstates of molecular aggregates are responsible for the energy transfer from an incoming radiation into the aggregate. Static disorder, which can arise from an imperfect environment of each molecule, reduces the exciton transport and large disorders can even localize the exciton. It has been shown theoretically that a two-dimensional periodic array of tilted and interacting molecules in a homogeneous magnetic field shows topologically protected edge states [1]. With a scattering scanning near-field optical microscope setup, one can not only record position dependent absorption spectra [2] but also reconstruct the wavefunctions from these spectra [3]. We study theoretically the near field spectra of the aforementioned 2D aggregates in which the molecules experience a disordered environment because of the probing metallic tip. Due to the topological protection, the edge states are robust even in the presence of the metallic nanoparticle, such that the spectrum shows clear signatures of these states.

[1] J. Y. Zhou, S. K. Saikin, N. Y. Yao and A. Aspuru-Guzik, *Nature materials* 13, 1026-1032 (2014)

[2] S. Nayak, F. Zheng and A. Eisfeld, *J. Chem. Phys.* 155, 134701 (2021)

[3] F. Zheng, X. Gao and A. Eisfeld, *Phys. Rev. Lett.* 123, 163202 (2019)

O 70.9 Wed 18:00 P2/EG

Nanoantenna Conjugated Graphene Photodetectors — •ABHINAV RAINA, MO LU, MAX REIMER, VASILII OSIPOV, KLAUS MEERHOLZ, and KLAS LINDFORS — Department für Chemie, Universität zu Köln, 50939, Köln, Germany

Optical communications is a technology that utilizes light for the wireless transduction of signals. Over the past few decades, the rapid development of nanoscale fabrication techniques has allowed for a significant improvement in the control over the transduction of optical signals. For example, optical nanoantennas have been used in steerable wireless links.[1] In an effort to detect the signals in optical nanoantenna links as an electrical signal, we couple nanoantenna arrays with a graphene photodetector. Such a device would act as a demonstration of tunable, on-chip, wireless transmission and detection of optical signals.

[1] Dregely, D., Lindfors, K., Lippitz, M., Engheta, N., Totzeck, M., Giessen, H., *Nat. Commun.*, 2014, 5, 4354.

O 70.10 Wed 18:00 P2/EG

Fabrication of STM+AFM+TERS tips — •PETR KAHAN, JIŘÍ DOLEŽAL, AMANDEEP SAGWAL, RODRIGO FERREIRA, and MARTIN ŠVEC — Institute of Physics, Czech Academy of Sciences; Cukrovarnická 10/112, CZ16200 Praha 6, Czech Republic

Although many highly reproducible techniques[1,2,3] exist for scanning tunneling microscopy (STM) tip preparation suitable for Tip-enhanced Raman spectroscopy (TERS), none of them was employed in non-contact atomic force microscopy (nc-AFM) relying on a lightweight tip glued to the tuning fork. Here we investigate the effects of commercially available and safe metallurgy etchants[3] on STM/nc-AFM tip fabrication from plasmonic metals[4]. We devised a simple optical apparatus for quick tip quality assessment. This allows us to see the Raman and plasmon scattering of the tip surface in various stages of preparation and determine its suitability for TERS. This might pave the way towards the first demonstration of combined STM/nc-AFM and TERS with submolecular resolution with the same tip [5].

[1] Sasaki, S. S. et al. *Rev. Sci. Instrum* 84, 096109 (2013) [2] Yang, B. et al. *JPCA* 122, 16950-16955 (2018) [3] Walker, P. & Tarn, W. H. *CRC handbook of metal etchants* (CRC press, 1990) [4] Murray, W. A. & Barnes, W. L. *Adv. Mater.* 19, 3771-3782 (2007) [5] Xu, J. et al. *Science* 371 818-822 (2021)

O 71: Overview Talk Edvin Lundgren

Time: Thursday 9:30–10:15

Location: TRE Phy

Invited Talk

Surface dynamics under reaction conditions — •EDVIN LUNDGREN — Department of Synchrotron Radiation Research, Institute of Physics, Lund university, Box 118, SE-221 00 Lund, Sweden

O 71.1 Thu 9:30 TRE Phy

Catalysis is an important process and is widely applied on an industrial scale for many applications in either gas or in liquid phase. Industrial catalysts are complex materials, and consequently the gas/liquid-surface interaction between simplified single crystal surfaces and molecules in controlled environments has

been studied for decades. We have in recent years explored the possibilities to perform experiments at conditions closer to those of a technical catalyst, at elevated pressures and in an electrolyte. In this contribution, recent results using in situ/operando techniques [1-5] will be presented. Armed with structural knowledge from ultra-high vacuum experiments, the dynamics of the gas or electrolyte induced structures and phases can be observed in real time. The strength and

weaknesses of the experimental techniques will be discussed.

- [1] S. Blomberg et al; Phys. Rev. Lett. 110 (2013) 117601.
- [2] J. Gustafson et al; Science 343 (2014) 758.
- [3] J. Zetterberg et al; Nat. Comm. 6 (2015) 7076.
- [4] S. Pfaff et al; ACS Appl. Mater. Interfaces 13 (2021) 19530.
- [5] L. Rämisch et al, Appl. Surf. Sci. 578 (2022) 152048.

O 72: Gerhard Ertl Young Investigator Award Competition

Time: Thursday 10:30–13:00

Location: CHE 89

O 72.1 Thu 10:30 CHE 89

Imaging electrons in 1D: correlated states within MoS₂ mirror twin boundaries — •WOUTER JOLIE — II. Physikalisches Institut, Universität zu Köln, Germany

Electrons are prone to strong correlations when confined into one-dimensional (1D) cavities. An ideal experimental testbed for the observation of correlated electronic behavior is found in mirror twin boundaries (MTBs) of the two-dimensional material MoS₂. These MTBs function as structurally perfect 1D cavities, are only weakly coupled to the environment and accessible to spatially resolved spectroscopic investigations using scanning tunneling microscopy.

In my talk I will show that the confined quasiparticles within finite MoS₂ MTBs transform into spin and charge modes as described by the Tomonaga-Luttinger theory of strongly interacting 1D electrons [1]. In addition, a Kondo resonance, delocalized over the entire length of the MTB, emerges when the highest occupied mode is half filled [2]. The unique construction of our Kondo system enables us to directly measure the energies of both the Kondo resonance and the half filled confined level, as well as their correlated beating along the boundary. Lastly, I will outline how to alter the electronic system in MTBs through giant Fermi level shifts [3] and atomic manipulation.

- [1] W. Jolie et al., Phys. Rev. X 9, 011055 (2019)
- [2] C. van Efferen et al., arXiv:2210.09675 (2022)
- [3] C. van Efferen et al., 2D Mater. 9, 025026 (2022)

O 72.2 Thu 11:00 CHE 89

Interface-engineered quantum states in van der Waals heterostructures — •FELIX LÜPKE — Peter Grünberg Institut (PGI-3), Forschungszentrum Jülich, 52425 Jülich, Germany — Jülich Aachen Research Alliance (JARA), Fundamentals of Future Information Technology, 52425 Jülich, Germany

The assembly of van der Waals (vdW) materials into heterostructures enables the engineering of exotic quantum states by interface effects such as moiré and proximity. Scanning tunneling microscopy (STM) has become an important tool to study the properties of such heterostructure, because it gives direct access to the resulting structural and electronic properties. While the possibilities to combine different vdW materials in Lego-like fashion are virtually infinite, the fabrication of samples with atomically clean surfaces, as required for STM, was typically limited to air-stable or epitaxially grown samples, which drastically diminishes the engineering capabilities. To address this problem, we have developed a novel dry-transfer flip fabrication technique, which allows the preparation and STM study of heterostructures with atomically clean surfaces and interfaces and without exposure to air. In my talk, I will summarize our developments in heterostructure fabrication and will show results of proximity-induced superconductivity in topological insulator WTe₂, interlayer interactions in twisted bilayer WTe₂, phonon gap supported tunneling and interfacial electric fields in Fe₃GeTe₂ heterostructures, and quantum dot lattices in NbSe₂ heterostructures.

O 72.3 Thu 11:30 CHE 89

Electronic States and Polarons on Polar Surfaces — •MICHELE RETICCIOLI¹, FLORIAN ELLINGER¹, MARTIN SETVIN², and CESARE FRANCHINI^{1,3} — ¹University of Vienna (Austria) — ²Charles University, Prague (Czech Republic) — ³University of Bologna (Italy)

Polar surfaces of oxides exhibit an internal electric field and intrinsic excess charge that might be exploited for a wide range of applications, such as catalysis or electron-hole separation for solar light harvesting. However, there is very limited fundamental understanding of the processes induced by the surface polarity. In our study we attempt to shed some light on the nature of the electric

field and the interplay with surface charge. Our density functional theory calculations and scanning-probe microscopy measurements on KTaO₃(001) show spontaneous localization of the excess charge in the form of electron and hole polarons. In the absence of external perturbations, the internal electrostatic potential keeps the electron-hole polaron pairs spatially separated. We also show that the electronic properties of the surface can be tuned by adsorbing molecules and metal atoms. Finally, we apply these concepts to more debated cases, such as the SrTiO₃(001) surface, where the polarity is too weak to produce a large charge separation. We believe that our findings contribute to deepen the interpretation of polar surfaces of oxides and ionic compounds in general.

O 72.4 Thu 12:00 CHE 89

Submolecular-scale control of phototautomerization — •ANNA ROSŁAWSKA¹, KATHARINA KAISER¹, MICHELANGELO ROMEO¹, FABRICE SCHEURER¹, STÉPHANE BERCIAUD¹, TOMÁŠ NEUMAN², and GUILLAUME SCHULL¹ — ¹Université de Strasbourg, CNRS, IPCMS, UMR 7504, 67000 Strasbourg, France — ²Institut des Sciences Moléculaires d'Orsay (ISMO), UMR 8214, CNRS, Université Paris-Saclay, 91405 Orsay Cedex, France.

Photochemistry plays a central role in fundamental natural and artificial reactions such as photosynthesis, photocatalysis, or phototautomerization. Here, we demonstrate that using a tunable light source focused on a scanning tunneling microscope (STM) tip we drive and control the rate of a free-base phthalocyanine (H₂Pc) phototautomerization with sub-molecular precision, providing a path to pilot the intrinsic reactivity of the molecule with an external controllable stimulus. In addition, we probe the excited state of the molecule, which drives the tautomerization, by recording tip-enhanced photoluminescence (TEPL) spectra and maps where varying patterns for non-resonant and resonant excitation conditions are observed. These TEPL maps reflect different atomic-scale coupling between the localized plasmonic fields and the transition dipole moment of the molecule influenced by the hydrogen switching process.

O 72.5 Thu 12:30 CHE 89

Single-molecule synthesis by scanning probe manipulation of intra- and inter-molecular reactions — •QIGANG ZHONG^{1,2}, ARTUR MARDYUKOV^{2,3}, EPHRATH SOLE^{2,3}, ALEXANDER IHLE^{1,2}, DANIEL EBELING^{1,2}, PETER R. SCHREINER^{2,3}, and ANDRÉ SCHIRMEISEN^{1,2} — ¹Institute of Applied Physics, Justus Liebig University Giessen (JLU), Germany — ²Center for Materials Research, JLU, Germany — ³Institute of Organic Chemistry, JLU, Germany

Single-molecule synthesis by scanning probe manipulation has emerged as a powerful tool not only to visualize, but also to generate and couple highly reactive molecules, which often are not accessible by traditional synthetic methods. As an example of precise "intra-molecular surgery", we demonstrate the on-surface synthesis of the structurally elusive cyclotriphosphazene (P₃N₃) based on STM tip-induced sextuple dechlorination of a sub-nanometer P₃N₃Cl₆ precursor molecule on a Cu(111) surface [1]. Real-space atomic-level imaging of P₃N₃ reveals its planar D_{3h}-symmetric ring structure. This method is further expanded to the inter-molecular level to construct covalent organic nanostructures molecule-by-molecule [2]. We have achieved unprecedented control over the whole reaction process including activation, lateral transfer and inter-molecular coupling of halogenated precursors on an inert NaCl surface. Our work presents strategies for synthesizing elusive molecules as well as covalent nanoarchitectures, studying structural modifications and revealing pathways of on-surface reactions.

- [1] Preprint [<https://doi.org/10.21203/rs.3.rs-2169632/v1>]
- [2] *Nature Chemistry* 13, 1133-1139 (2021)

O 73: Metal Substrates: Adsorption and Reaction of Small Molecules II

Time: Thursday 10:30–12:30

Location: CHE 91

O 73.1 Thu 10:30 CHE 91

Benchmarking machine-learned interatomic potentials for reactive surface dynamics at metal surfaces: accuracy vs speed — •WOJCIECH STARK¹, JULIA WESTERMAYER¹, CAS VAN DER OORD², LINGJUN ZHU³, BIN JIANG³, GABOR CSANYI², and REINHARD MAURER¹ — ¹University of Warwick, UK — ²University of Cambridge, UK — ³University of Science and Technology of China, China

Machine-learned interatomic potentials (MLIP) have become widely used tools to accelerate *ab initio* molecular dynamics simulations in materials science. Many promising MLIPs emerged recently, ranging from simple linear models to deep neural networks (DNN), differing in stability, accuracy, and inference time. Reactive scattering dynamics are highly sensitive to potential corrugation and low reaction probabilities require extensive ensemble averaging. Therefore, MLIPs need to combine smooth and accurate landscapes with extremely efficient inference. In this study, we compare different families of MLIPs, from atomic cluster expansion (ACE), message-passing based Neural Network SchNet and embedded atom neural networks (EANN), to equivariant neural networks such as PaiNN and MACE on the example of reactive molecular hydrogen scattering on copper. We compare these diverse methods by measuring accuracy and inference performance directly on dynamical observables. This provides a detailed picture of MLIP accuracy, speed, and learning rate that goes beyond simple train/test error analysis.

O 73.2 Thu 10:45 CHE 91

Electrooxidation of 1-cyclohexyl ethanol on Pt single crystal electrodes — •LUKÁŠ FUSEK^{1,2}, MARÍA MINICHOVÁ³, VALENTÍN BRIEGA-MARTOS³, LUKAS FROMM¹, EVANIE FRANZ¹, JUNTAO YANG¹, ANDREAS GÖRLING¹, SERHIY CHEREVKO³, PETER WASSERCHIED^{1,3}, OLAF BRUMMEL¹, and JÖRG LIBUDA¹ — ¹Friedrich-Alexander-Universität Erlangen-Nürnberg, Germany — ²Charles University, Prague, Czech Republic — ³Helmholtz-Institut Erlangen-Nürnberg, Germany

Isopropanol can be used as a liquid organic hydrogen carrier (LOHC), which is compatible with direct alcohol fuel cells. However, it has a limited hydrogen storage capacity. 1-Cyclohexyl-ethanol is a potential LOHC with an increased hydrogen storage capacity with two different functionalities, the alcohol (2 H+) and the cyclohexyl functionality (6 H+). In this study, we investigated the electrooxidation of 0.02 M 1-cyclohexyl ethanol on Pt(hkl) electrodes in 0.1 M HClO₄ using cyclic voltammetry and electrochemical infrared reflection absorption spectroscopy. We demonstrate that it is possible to oxidize electrochemically 1-cyclohexyl-ethanol to acetophenone. Additionally, we observed 1-cyclohexyl-ethanol and decomposition products. The latter poison the Pt surface, limiting the electrocatalytic activity. The possibility to dehydrogenate electrochemically not only the alcohol but also the cyclohexyl functionality may enable us to increase the hydrogen storage capacity of fuel cell compatible LOHCs substantially, reaching values that are comparable to conventional LOHCs.

1.Sievi, G. et al. *Energy Environ Sci* 12, 2305-2314 (2019).

O 73.3 Thu 11:00 CHE 91

Ab initio-based chemisorption and thermodynamic stability of atomic H and O on Pt-Ir alloy surfaces — •TOBIAS WITTEMANN, THORSTEN KLÜNER, and HALIL IBRAHIM SÖZEN — Institute of Chemistry, Carl-von-Ossietzky University of Oldenburg, 26129 Oldenburg, Germany

Electric vehicles powered by proton-exchange membrane (PEM) fuel cells are a CO₂ emission-free alternative to conventional fossil fuel vehicles. In this study, we report density functional theory (DFT) investigations of binary Pt-Ir surfaces, which are a promising candidate for bifunctional anode catalysts in PEM fuel cells that could enable higher long-term durability of the anode catalyst. The chemisorption behaviour of atomic H and O on bimetallic Pt₃Ir(111) and PtIr(111) surfaces was investigated for different coverages and compared with the monometallic Pt(111) and Ir(111) surfaces. We found that in both cases the chemisorption on the alloys becomes more stable with increasing number of Ir atoms at the adsorption site. Using the *ab initio* thermodynamics approach, we calculated phase diagrams for the chemisorption of atomic H and O species on these metal surfaces in order to transfer our findings to finite temperature and pressure conditions prevailing in real PEMFCs. Our theoretical results can provide a fundamental understanding for subsequent studies of the hydrogen oxidation reaction (HOR) and oxygen evolution reaction (OER) on Pt-Ir alloy surfaces and are thus crucial for the rational development of new anode catalyst materials.

O 73.4 Thu 11:15 CHE 91

Approaching electrochemical interfaces by computational spectroscopy — •HOLGER EUCHNER¹, JONGMIN KIM^{1,2}, MARGOT GUIDAT¹, MARIO LÖW², and MATTHIAS M. MAY^{1,2} — ¹Institute of Physical and Theoretical Chemistry, Universität Tübingen, 72076 Tübingen, Germany — ²Institute of Theoretical Chemistry, Universität Ulm, 89081 Ulm, Germany

Understanding interfacial processes on the atomistic scale is essential for improving and tailoring the performance of electrochemical devices. Unfortunately, due to limited experimental access to the electrochemical interface such understanding is difficult to obtain. Applying reflection anisotropy spectroscopy (RAS), an operando optical high resolution technique, to electrochemical interfaces can help to overcome this issue. However, the information contained in experimental RAS spectra needs to be interpreted by comparison with those of computational model systems. In this work, we present computationally determined spectra for different metal electrode surfaces and analyze the impact of adsorbants on the resulting RAS signal. For this purpose, the surface dielectric function is determined by applying the random phase approximation. Finally, the obtained spectra are compared to available experimental data, showing the potential power of this approach.

O 73.5 Thu 11:30 CHE 91

Atomistic Insights at Au(111) / Deep Eutectic Solvents Interface using in situ STM — •YANNICK MATTAUSCH¹, AREEG ABDELRAHMAN¹, MAREN-KATHRIN HEUBACH¹, LUDWIG A. KIBLER¹, and TIMO JACOB^{1,2,3} — ¹Institute of Electrochemistry, Ulm University, Ulm, Germany. — ²Helmholtz-Institute-Ulm (HIU), Ulm, Germany. — ³Karlsruhe Institute of Technology (KIT), Karlsruhe, Germany.

Deep eutectic solvents (DESS) have outstanding electrochemical characteristics such as high electrochemical stability and conductivity.[1][2] Nonetheless, the interactions between the metal electrode surface and DESS besides their electrochemical behavior, like the electrolyte / Au(111) interface structure are still poorly understood. Recently, the electrochemical behavior and adsorption structures of Au(111) in Ethylenglycole / Cholinchloride (2:1) have been studied, including an ordered chloride structure at 0.1 V vs. Pt and the potential induced surface reconstruction of Au(111).[3] Here, we go a step further by changing the electrolyte composition and studying its influence on the electrochemical behavior as well as the dynamics at the electrode-electrolyte interface at an atomistic level. To reach this aim, *in situ* scanning tunneling microscopy (STM) is employed to observe morphological changes at the electrode surface in real time and space.

[1] Smith, E. L., Abbott, A. P. Ryder, K. S., *Chem. Rev.* **114**, 11060–11082 (2014). [2] Abbott, A. P., D'Agostino, C., Davis, S. J., Gladden, L. F. Mantle, M. D. *Chem. Chem. Phys.* **18**, 25528–25537 (2016). [3] Tan, Z. et al., *ChemElectroChem* **7**, 4601–4605 (2020).

O 73.6 Thu 11:45 CHE 91

2D chiral crystallization and thermally-induced on-surface polymerization of 2,3-dicarbonitrile-tetrahelixene on Ag(111) surface — •ALEKSANDRA CEBRAT^{1,3}, CHRISTIAN WÄCKERLIN¹, KEVIN MARTIN², MANFRED PARSCHAU¹, NARCIS AVARVARI², and KARL-HEINZ ERNST^{1,3} — ¹Empa, Swiss Federal Laboratories for Materials Science and Technology, Überlandstrasse 129, 8600 Dübendorf, Switzerland — ²Laboratoire Moltech-Anjou, CNRS-Université d'Angers, 49045 Angers, France — ³Department of Chemistry, University of Zurich, 8057 Zurich, Switzerland

The controlled on-surface polymerization using templates like metal surface and non-planar molecules can lead to synthesis of variable phthalocyanines and organic semiconducting polycyanine open-chains. Here, we report the initial results on the 2D chiral crystallization of racemic mixture of 2,3-dicarbonitrile-tetrahelixene on Ag(111) and its thermally-induced surface polymerization. Deposition of racemic diCN[4]H up to 0.9ML coverage on Ag(111) kept at 300 K leads to formation of islands of honeycomb domains built of M- and P-enantiomers. Deposition of rac-diCN[4]H on 330K up to 0.9ML leads to aggregation of molecules into long molecular lines and denser phase of unbalanced domains with either enantiomers present in excess. Subsequent annealing to 420 K leads to partial desorption of molecular lines and formation of single tetramers built from different stereoisomeric subunits. The formation of polymerized species was confirmed ToF-SIMS. Finally, we performed LT-STM lateral manipulation of the tetramers units to affirm the nature of bonds as covalent.

O 73.7 Thu 12:00 CHE 91

Interaction of chlorine with lithium and magnesium anodes in Cl-ion batteries — •KANCHAN SARKAR¹ and AXEL GROSS^{1,2} — ¹Institute of Theoretical Chemistry, Ulm University, 89069 Ulm, Germany — ²Helmholtz Institute Ulm (HIU), Electrochemical Energy Storage, 89069 Ulm, Germany

We present the results of first-principles electronic structure calculations based on density functional theory addressing the adsorption of chlorine and the formation of a surface chloride on Li(001) and Mg(0001). This process is relevant for chloride-ion batteries in which lithium and magnesium are used as anode materials, but it is also of fundamental interest, as halide adsorption on metal electrodes is an important process in electrochemistry. We discuss the adsorption properties and determine the stable adsorption structures, both with respect

to the free chlorine molecule but also as a function of the electrode potential. We will also address the process of chloride formation on the surface.

O 73.8 Thu 12:15 CHE 91

Bromine on Rh(111) - A combined XPS and LEED study — •EVA MARIE FREIBERGER¹, NATALIE J. WALESKA¹, ANTON HARRER¹, FELIX HEMAUER¹, VALENTIN SCHWAAB¹, HANS-PETER STEINRÜCK¹, and CHRISTIAN PAPP^{1,2} — ¹Friedrich-Alexander-Universität Erlangen-Nürnberg, Erlangen, Germany — ²Freie Universität Berlin, Berlin, Germany

The adsorption of halogens on metals is a fundamental question in surface science. Detailed knowledge in this regard is of interest for any processes on surfaces, in which halogens are involved as a reactant or by-product. This plays a role, for example, in electrochemistry, when the electrolyte adsorbs at the elec-

trodes, or in on-surface synthesis, which often relies on coupling reactions with halogens as the leaving group, leading to their accumulation on the surface.

We investigated the adsorption and thermal evolution of elemental bromine on the Rh(111) single-crystal surface by synchrotron radiation-based high-resolution X-ray photoelectron spectroscopy (XPS), temperature-programmed XPS, and low energy electron diffraction (LEED). The adsorption of bromine on Rh(111) held at 170 K was followed in situ by XPS, revealing a coverage-dependent shift in the Br 3d spectra. Using LEED as a complementary method, we propose that the observed shift is caused by different bromine superstructures on Rh(111): a $(\sqrt{3} \times \sqrt{3})R30^\circ$ structure for lower coverages and a compression structure for saturation coverage. Subsequent heating shows a quite high temperature stability of bromine on Rh(111) up to 925 K, indicating covalent bonding.

O 74: 2D Materials IV: Heterostructures (joint session O/CPP)

Time: Thursday 10:30–12:45

Location: GER 37

O 74.1 Thu 10:30 GER 37

In-situ growth characterization of 2D heterostructures: MoSe₂ on intercalated graphene/Ru(0001) — •LARS BUSS¹, NICOLAS BRAUD², MORITZ EWERT¹, MATTEO JUGOVAC², TEVFIK ONUR MENTES³, ANDREA LOCATELLI³, JENS FALTA², and JAN INGO FLEGE¹ — ¹Applied Physics and Semiconductor Spectroscopy, BTU Cottbus-Senftenberg, Cottbus, Germany — ²Institute for Solid State Physics, University of Bremen, Bremen, Germany — ³Eletra-Sincrotrone Trieste S.C.p.A, Bazovizza, Trieste, Italy

Despite the great fundamental interest in 2D heterostructures, most of the investigated 2D heterostructures were realized by mechanical exfoliation or chemical vapor deposition in the millibar range, preventing true in-situ characterization of the growth process. Here, we have investigated the growth of MoSe₂ on single-layer graphene on Ru(0001) via real-time in-situ low-energy electron microscopy and micro-diffraction. After preparation of the graphene by standard procedures from an ethylene precursor, MoSe₂ has been prepared via co-deposition of Mo and Se. Prior Se intercalation of the graphene appears to enhance the subsequent growth of MoSe₂ on the graphene. At elevated temperatures, rotational ordering of the MoSe₂ is facilitated by the strongly enhanced mobility of single-domain MoSe₂ islands that align with the high symmetry orientations of the underlying graphene, indicating a non-negligible interaction between the two van-der-Waals materials. Micro-spot angle-resolved photoemission proves the monolayer nature of the as-grown MoSe₂ as well as the free-standing character of the Se-intercalated graphene underneath.

O 74.2 Thu 10:45 GER 37

Designer quantum states in metal-organic frameworks — •ORLANDO J SILVEIRA¹, LINGHAO YAN¹, SHAWULIENU KEZILEBIEKE², BENJAMIN ALLDRITT¹, VILIAM VANO¹, ONDŘEJ KREJČÍ¹, JOSE LADO¹, ADAM S FOSTER^{1,3}, and PETER LILJEROTH¹ — ¹Department of Applied Physics, Aalto University, Espoo, Finland — ²University of Jyväskylä, FI-40014 University of Jyväskylä, Finland — ³Kanazawa University, Kakuma-machi, Kanazawa 920-1192, Japan

Vertical heterostructures have emerged as a promising path to the design of quantum materials with exotic properties. Here, we show that this concept can be also extended to a family of 2D kagome metal-organic frameworks (MOFs) of the family M₂DCA₃, with M= Cu and Ni. The two MOFs have been fabricated either on a graphene/Ir(111) surface or the superconducting substrate NbSe₂, and the structural and electronic properties of different phases of both 2D MOFs + substrates were studied through density functional theory (DFT) calculations. Results show that the Cu₂DCA₃ MOF is effectively decoupled from the Ir(111) metallic substrate by the graphene layer, which is important to reveal the topological properties of this family of MOF. Moreover, this study extends the synthesis and electronic tunability of 2D MOFs beyond the metal surfaces to superconducting substrates, which are needed for the development of emerging quantum materials. We show that the Ni₃DCA₂ MOF has a spin density around the Ni atom when synthesized on the NbSe₂ substrate due to charge transfer, and this makes a perfect platform to realize topological superconductivity.

O 74.3 Thu 11:00 GER 37

Phonon gap supported tunneling and Faraday screening through graphene — •TOBIAS WICHMANN^{1,2,3}, KEDA JIN^{1,2,4}, JOSE MARTINEZ CASTRO^{1,4}, HONEY BOBAN⁵, LUKASZ PLUCINSKI⁵, MARKUS TERNES^{1,2,4}, F. STEFAN TAUTZ^{1,2,3}, and FELIX LÜPKE^{1,2} — ¹Peter-Grünberg-Institut (PGI-3), Forschungszentrum Jülich, 52425 Jülich, Germany — ²Jülich Aachen Research Alliance (JARA) - 52425 Jülich, Fundamentals of Future Information Technology, Germany — ³Institut für Experimentalphysik IV A, RWTH Aachen, 52074 Aachen, Germany — ⁴Institut für Experimentalphysik II B, RWTH Aachen, 52074 Aachen, Germany — ⁵Peter-Grünberg-Institut (PGI-6), Forschungszentrum Jülich, 52425 Jülich, Germany

Encapsulation of van der Waals materials has proven a vital technique to protect them from degradation and contamination. Usually, metallic encapsulation

layers mask the properties of the underlying material when studied in scanning tunneling microscopy. Utilizing the inelastic tunneling phonon gap of graphene, however, enables the unfettered investigation of low energy phenomena (e.g. Kondo effect, Majoranas, etc.) by scanning tunneling spectroscopy, while maintaining the advantages of encapsulated samples. Furthermore, we find that the conductive nature of the graphene encapsulation layer screens the sample from tip-induced electric fields, exemplified by our low-temperature STM examination of encapsulated Fe₃GeTe₂.

O 74.4 Thu 11:15 GER 37

Fermi level tuning of a MnBi₂Te₄ monolayer — •MARCO DITTMAR¹, PHILIPP KAGERER¹, CELSO I. FORNARI¹, SIMON MÜLLER¹, SERGIO L. MORELHÃO², HENDRIK BENTMANN¹, and FRIEDRICH REINERT¹ — ¹Exp. Physik VII and Würzburg-Dresden Cluster of Excellence ct.qmat, Universität Würzburg, Germany — ²Instituto de Física, Universidade de São Paulo, Brazil

By breaking time reversal symmetry, introducing magnetic order to topological insulators leads to the opening of a 2D surface state gap at the Dirac point. As a second crucial parameter, tuning the position of the Fermi level inside this gap, enables the observation of exciting new phenomena, such as the quantum anomalous Hall effect (QAHE).

Here, we focus on the intrinsic ferromagnetic monolayer of MnBi₂Te₄, acting as a magnetic extension of the topological insulator Bi₂Te₃ [1]. We tune the Fermi level position in this compound by preparing a single layer of MnBi₂Te₄ on top of the topologically non-trivial p-n-junction of Sb₂Te₃ and Bi₂Te₃ grown by molecular beam epitaxy (MBE) [2]. We will present a study containing structural characterization of the heterostructures by X-ray diffraction and atomic force microscopy, while the electronic structure is assessed by X-ray and angle resolved photoemission spectroscopy.

[1] M. M. Otrokov *et al.*, 2D Mater 4, 025082 (2017)

[2] P. Kagerer *et al.*, arXiv 2207.14421 (2022)

O 74.5 Thu 11:30 GER 37

1D Topological superconductivity in a van der Waals heterostructure probed by Abrikosov vortices — •JOSE MARTINEZ-CASTRO^{1,2}, TOBIAS WICHMANN^{1,3}, TOMÁŠ SAMUELY⁴, KEDA JIN^{1,2}, OLEKSANDER ONUFRIENKO⁴, F. STEFAN TAUTZ^{1,3,5}, MARKUS TERNES^{1,2,3}, and FELIX LÜPKE¹ — ¹Peter Grünberg Institut (PGI-3), Forschungszentrum Jülich, 52425 Jülich, Germany — ²Institut für Experimentalphysik II B, RWTH Aachen, 52074 Aachen, Germany. — ³Jülich Aachen Research Alliance, Fundamentals of Future Information Technology, 52425 Jülich, Germany — ⁴Centre of Low Temperature Physics, Faculty of Science, P. J. Safarik University & Institute of Experimental Physics, Slovak Academy of Sciences, Kosice, Slovakia — ⁵Institut für Experimentalphysik IV A, RWTH Aachen, 52074 Aachen, Germany

The 2D topological insulator monolayer (ML) WTe₂ is characterized by an insulating interior surrounded by helical 1D edge states. When this material is brought into proximity to the s-wave superconductor NbSe₂, the spectroscopic features of the helical edge state remain intact while showing a proximity-induced superconducting gap [1]. However, so far there has been no direct evidence that the observed edge superconductivity is of different nature than that observed away from the edge. Here, by inducing Abrikosov vortices at the boundary between ML WTe₂ and NbSe₂, we show that the induced superconductivity in the helical edge is robust against magnetic fields, a strong indication of 1D topological superconductivity.

[1] Lüpke *et al.*, Nat. Phys. 16, 526 (2020)

O 74.6 Thu 11:45 GER 37

Density functional theory studies of Anthracene on MoS₂ — •GÉRALD KÄMMERER and PETER KRATZER — Faculty of Physics, University of Duisburg-Essen Thin layers of MoS₂ are attractive as transparent contacts on organic semiconductors, e.g., oligoacene. As a model for molecules with a delocalized system of

π -bonds, we investigate the physisorption of a monolayer of anthracene ($C_{14}H_{10}$) on a MoS_2 single layer using density functional theory. The calculations were carried out with the FHI-Aims code with different functionals. Van der Waals interactions are described by a pairwise potential of the Tkatchenko-Scheffler type or by a many-body dispersion technique. We determine structural properties and can identify the relative position of the molecular HOMO and LUMO (Π and Π^*) orbital concerning the band edges of MoS_2 . These results can help find the type of band alignment between MoS_2 and an anthracene molecular crystal, as well as the binding energy of the molecule on the surface. The financial support by DFG within CRC 1242 (*Project B 02*) and computation time on the MagnitUDE supercomputer system are gratefully acknowledged.

O 74.7 Thu 12:00 GER 37

Lateral heterostructures of graphene and h-BN with atomic lattice coherence and tunable rotational order — •HAOJIE GUO¹, ANE GARRO-HERNANDORENA¹, ANTONIO J. MARTÍNEZ-GALERA^{2,3}, and JOSÉ M. GÓMEZ-RODRÍGUEZ^{1,3,4} — ¹Departamento de Física de la Materia Condensada, Universidad Autónoma de Madrid, E-28049 Madrid, Spain — ²Departamento de Física de Materiales, Universidad Autónoma de Madrid, E-28049 Madrid, Spain — ³Instituto Nicolás Cabrera, Universidad Autónoma de Madrid, E-28049 Madrid, Spain — ⁴Condensed Matter Physics Center (IFIMAC), Universidad Autónoma de Madrid, E-28049 Madrid, Spain

In-plane heterostructures of graphene and h-BN exhibit exceptional properties, which are sensitive to the structure of the alternating domains. However, achieving accurate control over their structural properties, while keeping a high perfection of the graphene-h-BN boundaries, still remains a challenge. Here, the growth of lateral heterostructures of graphene and h-BN on Rh(110) surfaces is reported. The choice of the 2D material, grown firstly, determines the structural properties of the whole heterostructure layer, allowing to have control over the rotational order of the domains. The atomic-scale observation of the boundaries demonstrates a perfect lateral matching. Lateral heterostructures floating over an oxygen layer have been successfully obtained, enabling to observe intervalley scattering processes in graphene regions. The high tuning capabilities of these heterostructures suggests their usage as testbeds for fundamental studies.

O 74.8 Thu 12:15 GER 37
Relaxation mechanisms for in-plane heterostructures of transition metal dichalcogenide monolayers — •KAI MEHLICH¹, FRANCIS H. DAVIS³, THAIS CHAGAS¹, DANIELA DOMBROWSKI², DANIEL WEBER¹, CATHERINE GROVER¹, ARKADY KRASHENINNIKOV³, and CARSTEN BUSSE¹ — ¹Department Physik, Universität Siegen, Walter-Flex-Str. 3, 57072 Siegen — ²Institut für Materialphysik, WWU Münster, Wilhelm-Klemm-Str. 10, 48149 Münster — ³Ion Beam Centre, Helmholtz-Zentrum Dresden Rossendorf, Bautzner Landstraße 400, 01328 Dresden

We use sequential epitaxial growth to synthesise in-plane heterostructures of MoS_2 and TaS_2 monolayers on Au(111). Even though the two materials have significantly different lattice constants, STM-measurements show that coherent interconnection of the two materials can be achieved. Defects at the interface such as dislocations are absent. We find this for all interfaces, independent of orientation or the widths of the joined materials. This is at variance with DFT-calculations where we find that the formation of dislocations is energetically favoured, at least until a critical width of the heterostructures. Our growth process can thus lead to a metastable, defect-free interface.

O 74.9 Thu 12:30 GER 37

Predicting the Gas Sensing Performance of 2D Materials — •UDO SCHWINGENSCHLÖGL, VASUDEO BABAR, HAKKIM VOVUSHA, and ALTYNBEK MURAT — King Abdullah University of Science and Technology (KAUST), Physical Science and Engineering Division (PSE), Thuwal 23955-6900, Saudi Arabia

We study the potential of material simulations based on first-principles methods to predict gas sensing properties of 2D materials. This emerging class of materials is of particular interest to gas sensing applications due to high surface-to-volume ratios and chemical stability. We discuss results of electron transport calculations within the Landauer-Büttiker formalism and compare the conclusions to analyses in terms of the adsorption energy. Journal References: ACS Appl. Nano Mater. 2, 6076 (2019); J. Phys. Condens. Matter 32, 355602 (2020)

O 75: Focus Session: Ultrafast Dynamics in Nanostructures I

In nanostructures, the response of electrons and atoms to external stimuli often differs significantly from that of their bulk counterparts due to spatial confinement and greatly increased surface-to-volume ratios. Whereas pump-probe techniques provide real time access to the dynamics of nanostructures in excited states, investigating the response of single nanostructures and probing their dynamics locally requires ultrafast imaging techniques that provide simultaneously a high spatial and temporal resolution.

Several ultrafast nanoscale imaging methodologies have made a tremendous progress in recent years. Crucial instrumental developments have enabled time-resolved variants of scanning probe techniques, such as ultrafast scanning near-field optical microscopy and ultrafast scanning tunneling microscopy. Furthermore, bright sources for femtosecond electron as well as extreme ultraviolet and x-ray pulses now allow for the ultrafast far-field probing with nanometer resolution.

To highlight these recent developments, this focus session brings together researchers interested in ultrafast nanoscale science and in the development of ultrafast high-resolution imaging approaches.

Organizers: Melanie Müller (FHI Berlin) and Sascha Schäfer (U Regensburg)

Time: Thursday 10:30–13:15

Location: GER 38

Topical Talk

O 75.1 Thu 10:30 GER 38

Ultrafast nano-imaging: probing quantum dynamics in space and time — •MARKUS RASCHKE — Department of Physics and JILA, University of Colorado, Boulder, USA

Understanding and ultimately controlling the properties of matter, from molecular to quantum systems, requires imaging the elementary excitations on their natural time and length scales. To achieve this goal, we developed scanning probe microscopy with ultrafast and shaped laser pulse excitation for multiscale spatio-temporal optical nano-imaging. In corresponding ultrafast movies we resolve the fundamental quantum dynamics from the few-femtosecond coherent to the thermal transport regime. I will discuss specific examples visualizing in space and time the nanoscale heterogeneity in competing structural and electronic dynamic processes that define the performance in perovskite photovoltaics or energy dissipation in 2D heterostructures. I will extend the discussion to new forms of photon-matter hybrid states that emerge from confining light on the nano- to atomic scale, with imaging in tip-enhanced strong coupling of single emitters, to new regimes of nonlocal and quantum nonlinear nano-optics.

O 75.2 Thu 11:00 GER 38

Towards a nanoscale ultrafast optical oscilloscope — •ABBAS CHIMEH, SAM NOCHOWITZ, TOM JEHL, JUANMEI DUAN, SVEN STEPHAN, and CHRISTOPH LIENAU — Universität Oldenburg

Measuring the ultrafast time response on the nanoscale gives insights into the complex structure and dynamics of nanomaterials. A variety of all-optical and electron-based spectroscopy techniques are currently under development to probe such ultrafast dynamics [1].

Here, we propose and demonstrate a broadband, interferometric scattering-type scanning near-field optical spectroscopy technique to measure ultrafast response function on the nanoscale. The idea is to mix the weak optical near field that is scattered out from the gap of a laser-illuminated tip-sample junction with a broadband reference pulse in a single spatial mode. From the resulting phase-stable spectral interferogram, we can directly retrieve the linear optical response function of the coupled tip-sample system and, thus, the time structure of re-emitted electric field with sub-cycle precision. By recording scattering spectra at a rate much higher than typical tip-sample modulation frequencies, we can separate the near-field response from unmodulated signal backgrounds and directly probe the time structure of optical near-fields on the nanoscale. We demonstrate the technique by probing local light scattering from single TMDC monolayers.

Our technique provides a general approach for measuring the response functions of nanostructures in the visible and near-infrared spectral range with femtosecond temporal and nanometer spatial resolution.

[1] P. Dombi et al., *Rev. Mod. Phys.*, 92, 025003 (2020).

O 75.3 Thu 11:15 GER 38

Ultrafast electron dynamics in semiconductor nanowires — •JAN VOGELSANG^{1,2}, LUKAS WITTENBECHER¹, CORD L. ARNOLD¹, ANNE L'HUILLIER¹, and ANDERS MIKKELSEN¹ — ¹Department of Physics, Lund University, 221 00 Lund, Sweden — ²present address: Institut für Physik, Universität Oldenburg, 26129 Oldenburg, Germany

The dynamics and, in particular, the transport of charge carriers in semiconductor nanostructures after optical excitation are influenced by different processes whose interaction is not yet fully understood. Here, we employ ultrashort laser pulses in combination with a photoemission electron microscope (PEEM) to spatiotemporally resolve these processes. We observe the radial transport of charge carriers in semiconductor nanowires after impulsive optical excitation and investigate the influence of electron-hole scattering on the relaxation times of hot electrons. We conclude with a glimpse on an attosecond streaking experiment in a PEEM promising an even higher temporal resolution.

O 75.4 Thu 11:30 GER 38

SPP induced coherent electronic excitations investigated by Time- and Angle-Resolved Photoemission-Spectroscopy on Cs/Au(111) — •ALEXANDER NEUHAUS, PASCAL DREHER, DAVID JANOSCHKA, MICHAEL HORN-VON HOEGEN, and FRANK-J. MEYER ZU HERINGDORF — Faculty of Physics, University of Duisburg-Essen, 47048 Duisburg, Germany

Non-perturbative interactions of intense light fields with the electronic band structure in a solid can result in transient electronic properties. The experimental conditions required to realize the necessary field strength can be realized in nano-optical systems, as these can be designed to provide tremendous enhancements of the local field amplitude. Ultimately, observing the non-equilibrium electron dynamics in such systems requires a combination of precise control over the local driving field, state resolution, and spatial selectivity. Here, we explore electron emission from nano-focused femtosecond surface plasmon polariton (SPP) pulses, providing us with deep-subwavelength spatial selectivity. Two-dimensional time- and angle-resolved photoelectron spectroscopy using a birefringent delay line provides us with direct access to the coherent and incoherent dynamics of the electronic excitations with attosecond precision. The technique is applied to the system Cs/Au(111), where we observe SPP induced coherent electronic excitations of the first image potential state.

Topical Talk

O 75.5 Thu 11:45 GER 38

Lightwave-driven scanning tunneling microscopy and spectroscopy at the atomic scale — •VEDRAN JELIC¹, SPENCER E. AMMERMAN¹, YAJING WEI¹, VIVIAN N. BRESLIN¹, MOHAMMED HASSAN¹, NATHAN EVERETT¹, SHENG LEE¹, STEPHANIE ADAMS¹, TREVOR HICKLE¹, KAEDON CLELAND-HOST¹, QIANG SUN², CARLO A. PIGNEDOL², PASCAL RUFFIEUX², ROMAN FASEL^{2,3}, and TYLER L. COCKER¹ — ¹Department of Physics and Astronomy, Michigan State University, East Lansing, MI 48824, USA — ²Empa Swiss Federal Laboratories for Materials Science and Technology, 8600 Dübendorf, Switzerland — ³Department of Chemistry, Biochemistry and Pharmaceutical Sciences, University of Bern, 3012 Bern, Switzerland

Lightwave-driven scanning tunneling microscopy is a new technique for studying atomic-scale surfaces that exhibit sub-picosecond dynamics. By coupling free-space-propagating single-cycle terahertz pulses to an atomically sharp metal tip, lightwave-driven microscopy can achieve simultaneous sub-angstrom and sub-picosecond spatio-temporal resolution. We utilize terahertz scanning tunneling microscopy (THz-STM) to investigate seven-atom-wide graphene nanoribbons on an Au(111) surface and unveil highly localized wavefunctions that are inaccessible with conventional STM. Three-dimensional tomographic THz-STM imaging of the electron densities reveals a faster spatial decay of the valance band compared to the conduction band. Additionally, an algorithm is introduced for extracting the underlying differential conductance from THz-STS measurements in both steady-state and pump-probe scenarios.

O 75.6 Thu 12:15 GER 38

Probing hot electron dynamics in a metal nanotip with THz-STM — •VIVIAN SLEZIONA¹, FARUK KRECINIC¹, NATALIA MARTÍN SABANÉS^{1,2}, FABIAN SCHULZ^{1,3}, TAKASHI KUMAGAI^{1,4}, MARTIN WOLF¹, and MELANIE MÜLLER¹ — ¹Fritz-Haber Institute, Berlin — ²IMDEA Nanoscience, 28049 Madrid, Spain — ³CIC NanoGUNE, San Sebastian, Spain — ⁴Institute of Molecular Science, 444-8585 Okazaki, Japan

In metal nanostructures, such as the tip of a scanning tunneling microscope (STM), the excitation and dynamics of hot electrons can differ significantly from their behavior in bulk solids. However, how exactly the electrons in an STM tip respond to femtosecond (fs) laser excitation is still poorly understood, although this is important for optimizing and understanding fs-laser-excited STM oper-

ation. Here we use a THz-gated STM to study the ultrafast dynamics of photoexcited electrons in a tungsten STM tip [1]. Specifically, we investigate the role of thermalized hot electrons for the generation of ultrafast photocurrents and tunneling in STM. Knowledge of the THz voltage transient combined with simulation of the electron dynamics inside the confined volume of the STM tip allows us to extract the electronic temperature and its ultrafast decay. We evaluate the relevance for fs laser-excited STM and discuss how the tip geometry affects electronic heating on ultrafast time scales. [1] N. Martín Sabanés et al., *ACS Nano* 16, 9, 14479-14489 (2022)

O 75.7 Thu 12:30 GER 38

Spin current control by hybrid pulses — •JYOTI KRISHNA¹, SANGEETA SHARMA², JULEN IBAÑEZ-AZPIROZ^{1,3}, and SAM SHALLCROSS² — ¹Centro de Física de Materiales (CSIC-UPV/EHU), 20018, San Sebastian, Spain — ²Max-Born-Institut für Nichtlineare Optik und Kurzzeitspektroskopie, Max-Born-Straße 2A, 12489 Berlin — ³Ikerbasque Foundation, 48013 Bilbao, Spain

Spin and valley indices represent the key quantum labels of quasiparticles in a wide class of two dimensional materials, and control over these degrees of freedom, the creation of valley and spin states as well as the generation of pure spin and valley currents, remains a central challenge in these fields. Here we show that hybrid femtosecond laser pulses combining optical frequency circularly polarized pulse and a terahertz frequency linearly polarized pulse, a so-called "hencomb" pulse, can generate currents, whose magnitude and direction can be precisely controlled by the THz envelope. We explore this effect both in bilayer graphene and the dichalcogenide WSe₂, finding control over substantial currents that are nearly 100% pure valley and spin currents respectively. Employing a Wannier tight-binding method we then explore the creation of coherent photocurrents in the 2d magnets CrI₃ and FGTe, generalizing the role of the THz and optical pulses to "momentum guiding" and "excitation" components of hybrid laser pulses.

Funding was provided by the European Union's Horizon 2020 research and innovation programme under the European Research Council (ERC) grant agreement No 946629.

O 75.8 Thu 12:45 GER 38

Mode-selective ballistic pathway to a metastable electronic phase — •HANNES BÖCKMANN^{1,2}, JAN GERRIT HORSTMANN³, FELIX KURTZ^{1,2}, ABDUS SAMAD RAZZAQ⁴, STEFAN WIPPERMANN⁴, and CLAUS ROPERS^{1,2} — ¹Max Planck Institute for Multidisciplinary Sciences, Göttingen 37077, Germany — ²4th Physical Institute, Solids and Nanostructures, University of Göttingen — ³Department of Materials, ETH Zurich, Zurich — ⁴Max-Planck-Institut für Eisenforschung GmbH, Düsseldorf

Exploiting vibrational excitation for the dynamic control of material properties is an attractive goal with wide-ranging technological potential. Most metal-to-insulator transitions are mediated by few structural modes and are, thus, ideal candidates for selective driving toward a desired electronic phase. Such targeted navigation within a generally multi-dimensional potential energy landscape requires microscopic insight into the non-equilibrium pathway. However, the exact role of coherent inertial motion across the transition state has remained elusive. Here, we demonstrate mode-selective control over the metal-to-insulator phase transition of atomic indium wires on the Si(111) surface, monitored by ultrafast low-energy electron diffraction. We use tailored pulse sequences and spectrally selective excitation to individually enhance or suppress key phonon modes and thereby steer the collective atomic motion within the potential energy surface underlying the structural transformation. Our work illustrates that coherent excitation of collective modes via exciton-phonon interactions evades entropic barriers and enables the dynamic control of functionality.

O 75.9 Thu 13:00 GER 38

Nanoscale coherent phonon excitation via plasmon-matter interaction in ultrathin ZnO films — •H. WIEDENHAUPT¹, S. LIU^{1,2}, L. PARRA LÓPEZ¹, A. HAMMUD¹, I. HAMADA³, F. SCHULZ^{1,4}, M. WOLF¹, T. KUMAGAI^{1,2}, and M. MÜLLER¹ — ¹Fritz Haber Institute, Berlin, Germany — ²Institute for Molecular Science, Okazaki 444-8585, Japan — ³Hunan University, Hunan 410082, P. R. China — ⁴CIC NanoGUNE, San Sebastian, Spain

In crystalline nanostructures, nanoscale variations of the lattice and/or electronic structure can alter their microscopic response and its interaction with light. Using light-coupled scanning tunneling microscopy (STM) with plasmonic junctions, we demonstrated recently that the local electronic structure of ultrathin ZnO on Ag(111) can strongly affect light-matter interaction on the nanoscale. Specifically, resonant laser excitation of these films seems crucial for tip-enhanced Raman spectroscopy (TERS) [1] and for the nanoscale excitation and observation of coherent phonon dynamics [2]. CPs are excited by femtosecond excitation of localized surface plasmons (LSP), and modulate the femtosecond photocurrent in the STM on ultrafast time scales. To better understand the optical excitation mechanism in these films, we measure plasmon-enhanced STM-induced luminescence, which allows us to correlate the local electronic structure of the films with their light coupling efficiency on the nanoscale. [1] S. Liu, *Nano Lett.* 19, 5725 (2019), [2] S. Liu et al., *Sci. Adv.* 8, eabq5682 (2022)

O 76: Plasmonics and Nanooptics III: Light-Matter Interaction and Spectroscopy II

Time: Thursday 10:30–12:45

Location: WIL A317

O 76.1 Thu 10:30 WIL A317

Continuous-wave multiphoton-induced electron transfer in a biased tunnel junction driven by intense plasmonic fields — CHENFANG LIN¹, MELANIE MÜLLER^{1,2}, FARUK KRECINIC¹, HIROKO YOSHINO¹, ADNAN HAMMUD¹, ANLIAN PAN², MARTIN WOLF¹, and TAKASHI KUMAGAI³ — ¹Fritz Haber Institute, Faradayweg 4-6, Berlin — ²Hunan University, Hunan 410082, China — ³Institute for Molecular Science, Okazaki 444-8585, Japan

Understanding photoinduced tunneling processes in the presence of intense plasmonic fields is of crucial importance for the design of plasmon-induced hot carrier technology and optical rectennas. However, in contrast to femtosecond laser excitation, the observation of multiphoton-induced electron transfer and the understanding of the role of hot carriers under intense continuous-wave (cw) illumination remains scarce. Here we exploit the strong spatial confinement of light inside the plasmonic gap of a scanning tunneling microscope (STM) to drive photocurrents with cw optical fields at local peak intensities up to 10^9 W/cm² at low incident power. We find that the photoinduced tunneling current scales nonlinear (linear) with laser intensity at low (high) STM bias. To yield insight into the photoinduced tunneling process we analyze the photocurrent-voltage dependence for different laser wavelength and powers. We discuss two possible origins of the multiphoton-induced electron transfer, namely transport of photoexcited hot electrons and photon-assisted quantum tunneling into light-dressed states.

O 76.2 Thu 10:45 WIL A317

Atomically resolved optical spectroscopy and microscopy in a scanning-tunneling microscope: Theory and experiment — TOMAS NEUMAN^{1,2}, ANNA ROSLAWSKA¹, BENJAMIN DOPPAGNE¹, ANDREI G. BORISSOV², MICHELANGELO ROMEO¹, FABRICE SCHEURER¹, JAVIER AIZPURUA³, and GUILLAUME SCHULL¹ — ¹Universite de Strasbourg, CNRS, IPCMS, UMR 7504, F-67000, Strasbourg, France — ²Institut des sciences Moléculaires d'Orsay (ISMO), UMR 8214, CNRS, Université Paris-Saclay, 91405 Orsay Cedex, France — ³Center for Materials Physics and DIPIC, Paseo Manuel de Lardizabal 5, Donostia-San Sebastian 20018, Spain

We present a joint theoretical and experimental study of the optical properties of individual small organic molecules excited electrically by the plasmonic tip of a STM. We investigate how these properties vary as a function of the tip position with atomic-scale resolution. We show that the variation of the spectral position and width of the electroluminescence emission line of the molecular exciton can be linked with the DC Stark effect (induced by the static voltage across the tip-substrate gap) and the plasmonic Purcell effect due to the plasmonic response of the tip, respectively. We interpret the spectral line shift map as an image of the difference between the excited- and ground-state electron densities of the molecule, and the tip-position-dependent map of the excitonic line-width variation as an image of the transition electron density. In contrast, the map of light intensity emitted by the molecule reveals the information about the electronic mechanism leading to the tip-mediated generation of the exciton.

O 76.3 Thu 11:00 WIL A317

Modeling of molecular systems probed by near-field spectroscopy — SOFIA CANOLA, JIŘÍ DOLEŽAL, RODRIGO FERREIRA, and MARTIN ŠVEC — Institute of Physics, Czech Academy of Sciences, Praha, Czech Republic

Spectroscopy coupled to scanning-probe microscopy is a powerful tool to analyze molecular properties at a single molecule level with submolecular resolution. In this technique, some intrinsic limitations and selection rules of conventional spectroscopy are overcome. This aspect, together with the high resolution of the signal and the precise control over the sample, allow to obtain information otherwise not accessible, such as for example the structural arrangement of the molecule, the electronic structure of its ground or excited molecular electronic state, its charging state or its response to stimuli. To fully unpack and rationalize the information, a theoretical interpretative framework must accompany the experimental findings. A crucial aspect is the ability to describe the molecular spectroscopic response in the near-field while including all the relevant aspects of the setup. High-level quantum-chemical calculations are needed, capable of reliably modeling the molecular system in its complexity and providing the appropriate response function. In this contribution, we present the results from the application of this technique to small conjugated molecules, with particular focus on the modeling aspects and the interesting molecular properties that become accessible when experiments and theory complement.

O 76.4 Thu 11:15 WIL A317

Plasmon-Induced Molecular Switching of PTCDA on Si(111) Studied by STM-TERS — YOUNGWOOK PARK¹, ADNAN HAMMUD¹, MARTIN WOLF¹, TAKASHI KUMAGAI², and AKITOSHI SHIOTARI¹ — ¹Fritz Haber Institute of the Max Planck Society, Berlin, Germany — ²Institute for Molecular Science, Okazaki, Japan

We studied a unique plasmon-induced molecular motion of perylenetetracarboxylic dianhydride (PTCDA) single molecules on the Si(111)-7x7 surface by means of the atomic point contact (APC) tip-enhanced Raman spectroscopy (TERS) with a low temperature scanning tunneling microscope (STM) under an ultrahigh vacuum condition. In our APC-TERS scheme, a silver tip approaches close to the surface until the tip makes an atomic point contact with its counterpart. It was reported by our previous study that at the point contact with Si(111) the TERS signal was significantly enhanced. The PTCDA on the Si(111), fixed on the surface by four oxygen-silicon bonds, showed a distinctive APC-TERS pattern where the Raman intensity was dramatically enhanced at a certain gap distance during the tip approach, and then was attenuated at shorter tip-molecule distances. At the TERS "sweet spot", the STM current rapidly switched between two states, implying a fluctuating motion of PTCDA molecule between the tip and the surface. On the contrary to PTCDA, perylenetetracarboxylic diimide (PTCDI) did not show such TERS "sweet spot" nor STM current switching. We believe this unique system could provide a better understanding on the plasmon-molecule interaction, as well as their implication on the enhancement mechanism in TERS.

O 76.5 Thu 11:30 WIL A317

Photoluminescence mapping of an anionic molecule — JIŘÍ DOLEŽAL, RODRIGO FERREIRA, AMANDEEP SAGWAL, PETR KAHAN, and MARTIN ŠVEC — Institute of Physics, Czech Academy of Sciences; Cukrovarnická 10/112, CZ16200 Praha 6, Czech Republic

Only recently, the photoluminescence (PL) of a single molecule has been attained [1,2] with sub-nm resolution in a scanning tunneling microscope (STM). However, only a fluorescent peak from a neutral phthalocyanine has been observed. The observation of fluorescence from a charged molecule is still elusive, likely due to the plasmon-mediated excitation mechanism which is fundamentally different from the electroluminescence (EL) process where a charged exciton can be created via electron/hole tunneling into dication/dianion [3,4].

Here, we present STM-PL maps of PTCDA anion adsorbed on 3ML/NaCl. The anionic charge state of the adsorbed molecule [5] enables its direct excitation by a laser-induced gap plasmon. We show STM-PL photon maps of an individual molecule and small molecular clusters qualitatively comparable to STM-EL maps [5], but independent of the tunneling current. This brings a major advantage over electroluminescence as the current is a scaling factor in the photon map intensity and its elimination [5-7] creates unwanted artefacts.

[1] B. Yang et al. Nat. Photonics 14, 693 (2020). [2] H. Imada et al. Science 373, 95 (2021). [3] K. Kaiser et al. arXiv:2211.01051 (2022). [4] B. Doppagne et al. Science 361, 251 (2018). [5] J. Doležal et al. ACS Nano 16, 1082 (2022). [6] B. Doppagne et al. PRL 118, 127401 (2017). [7] Y. Zhang et al. Nature 531, 623 (2016).

O 76.6 Thu 11:45 WIL A317

A Setup for Fluorescence-Detected Two-Dimensional Electronic Spectroscopy of Single Molecules — SANCHAYEETA JANA, SIMON DURST, LUCAS LUDWIG, and MARKUS LIPPITZ — Chair for Experimental Physics III, University of Bayreuth, Bayreuth, Germany

Fluorescence-Detected Two-Dimensional Electronic Spectroscopy is a recent ultrafast technique that yields information about the coupling between the states of a system. At the same time, fluorescence-detected single molecule spectroscopy is a well-established technique since more than 30 years. By combining these two techniques one should be able to measure 2d spectra of single molecules to get new insight in molecular dynamics on ultrashort time scales.

Here we present our work towards this goal. We use four phase-modulated ultrafast pulses to excite the molecule with the help of a high NA objective. The fluorescence is registered by single-photon detectors and demodulated at several mixing frequencies to get the rephasing and non-rephasing signals. The novelty of our technique is that we can measure Fluorescence Correlation Spectroscopy (FCS) and Time-Correlated Single Photon Counting (TCSPC) simultaneously to monitor the number of molecules in our excitation focus and the fluorescence lifetime.

In this work we illustrate our experimental technique and discuss 2d spectra measured on a molecular sample at low concentration.

O 76.7 Thu 12:00 WIL A317

Luminescence from Cu₂O films and bulk crystals in the STM — ALEXANDER GLOYSTEIN, MINA SOLTANMOHAMMADI, and NIKLAS NILIUS — Carl von Ossietzky Universität, Institut für Physik, D-26111 Oldenburg, Germany

STM luminescence spectroscopy is employed to compare the optical response of bulk Cu₂O(111) and 1-10 nm thick Cu₂O/Au(111) films. Although both systems share similar structural and electronic properties and expose the same thermodynamically preferred ($\sqrt{3} \times \sqrt{3}$)R30° reconstruction, their luminescence exhibits pronounced differences. The spectra of bulk Cu₂O are dominated by the

recombination of free and defect-bound excitons, whereas a unique plasmonic response is detected for the oxide films. The latter arises from the electromagnetic coupling between STM tip and gold support, while the Cu_2O ad-layer exclusively controls the inelastic tunneling rates, i.e., the intensity, but not the spectral signature of the emission. Only upon tunneling into the Cu_2O band gap, a luminescence channel mediated by O vacancies is identified in the oxide film. The talk addresses the question why the unique exciton response of Cu_2O is covered by plasmon excitations even in films as thick as 10 nm.

O 76.8 Thu 12:15 WIL A317

Hot-carrier transfer across a nanoparticle-molecule junction: The importance of orbital hybridization and level alignment — •JAKUB FOJT¹, TUOMAS ROSSI², MIKAEL KUISMA³, and PAUL ERHART¹ — ¹Department of Physics, Chalmers University of Technology, Gothenburg, Sweden — ²Department of Applied Physics, Aalto University, Aalto, Finland — ³Department of Physics, Technical University of Denmark, Kongens Lyngby, Denmark

While direct hot-carrier transfer can increase photocatalytic activity, it is difficult to discern experimentally and competes with several other mechanisms. To shed light on these aspects, here, we model from first-principles hot-carrier generation across the interface between plasmonic nanoparticles and a CO molecule. The hot-electron transfer probability depends nonmonotonically on the nanoparticle-molecule distance and can be effective at long distances, even before a strong chemical bond can form; hot-hole transfer on the other hand is limited to shorter distances. These observations can be explained by the energetic alignment between molecular and nanoparticle states as well as the excitation frequency. The hybridization of the molecular orbitals is the key predictor

for hot-carrier transfer in these systems, emphasizing the necessity of ground state hybridization for accurate predictions. Finally, we show a nontrivial dependence of the hot-carrier distribution on the excitation energy, which could be exploited when optimizing photocatalytic systems.

O 76.9 Thu 12:30 WIL A317

Disentangling the Orientations of Spectrally Overlapping Transition Dipoles in Dense Dye Layers — •CHRISTOPH SCHNUPFHAGN¹, THORSTEN SCHUMACHER¹, PAUL MARKUS², GEORG PAPASTAVROU², OLHA AFTENIEVA³, TOBIAS A. F. KÖNIG³, VOLODYMYR DUDKO⁴, MARIAN MATEJDES⁴, JOSEF BREU⁴, and MARKUS LIPPITZ¹ — ¹Experimental Physics III, University of Bayreuth — ²Physical Chemistry II, University of Bayreuth — ³Leibniz-Institut für Polymerforschung Dresden e.V. — ⁴Inorganic Chemistry I, University of Bayreuth

The transition dipole orientations of dye assemblies in heterostructures have a crucial impact on the efficiency of novel optoelectronic devices such as organic thin-film transistors and light-emitting diodes. These devices are frequently based on heterojunctions and tandem structures featuring multiple optical transitions. Precise knowledge of preferred orientations, spatial order, and spatial variations is highly relevant. We present a fast and universal large-area screening method to determine the transition dipole orientations in dye assemblies with diffraction-limited spatial resolution. Moreover, our hyperspectral imaging approach disentangles the orientations of different chromophores. As a demonstration, we apply our technique to dye monolayers with two optical transitions sandwiched between two ultrathin silicate nanosheets. A comprehensive model for dipole orientation distributions in monolayers reveals a long-range orientational order and a strong correlation between the two transitions.

O 77: Scanning Probe Techniques: Method Development II

Time: Thursday 10:30–12:45

Location: REC C 213

O 77.1 Thu 10:30 REC C 213

How cold is the junction of a millikelvin scanning tunnelling microscope? — TANER ESAT^{1,2}, XIAOSHENG YANG^{1,2}, FARHAD MUSTAFAYEV^{1,2}, HELMUT SOLTNER³, STEFAN TAUTZ^{1,2,4}, and •RUSLAN TEMIROV^{1,5} — ¹Peter Grünberg Institut (PGI-3), Forschungszentrum Jülich, Germany — ²Jülich Aachen Research Alliance (JARA), Jülich, Germany — ³Zentralinstitut für Engineering, Elektronik und Analytik (ZEA-1), Forschungszentrum Jülich, Germany — ⁴Experimentalphysik IV A, RWTH Aachen University, Aachen, Germany — ⁵University of Cologne, Institute of Physics II, Cologne, Germany

We employ a millikelvin scanning tunnelling microscope (STM) cooled to millikelvin temperatures by an adiabatic demagnetization refrigerator (ADR) to perform scanning tunnelling spectroscopy (STS) on an atomically clean surface of Al(100) in a superconducting state using normal-metal and superconducting STM tips. Varying the ADR temperatures between 30 mK and 1.2 K, we show that the temperature of the STM junction T is decoupled from the temperature of the surrounding environment T_{env} . Simulating the Josephson current with the $P(E)$ theory, we determine that $T_{\text{env}} \approx 1.5$ K, while fitting of the superconducting gap yields the lowest $T \approx 77$ mK.

O 77.2 Thu 10:45 REC C 213

Ultrahigh Vacuum Scanning Tunneling Microscopy with z Resolution of 2 pm at 1.3 K using Combined Pulse Tube and Joule-Thomson Cooling — •MARCUS ESSER¹, MARC FRÖMMING¹, MARCO PRATZER¹, MICHAEL KRZYZOWSKI², and MARKUS MORGENSTERN¹ — ¹2.Physikalische Institut B, RWTH Aachen University, Aachen, Germany — ²CryoVac GmbH & Co KG, Troisdorf, Germany

The cooling of scanning tunneling microscopes with liquid helium by bath or flux cryostats suffers from He losses that get increasingly expensive. However, alternative closed cycle systems based on pulse tube refrigerators can induce additional mechanical noise into the tunneling contact due to mechanical vibrations in the μm range and acoustic emissions. We will present an STM system that reaches temperatures of 1.3 K and a z resolution of 2 pm (feedback loop off) with the help of a pulse tube cooler and a Joule-Thomson stage. The challenge is to provide a good thermal coupling as well as an good vibration damping. For this purpose, a new concept with multiple decoupling stages including negative stiffness isolation, detached coaxially guided shields for the different temperature stages and an optimized conical microscope design made out of Shapal Hi M-soft has been realized. Numerical calculations of transfer functions are compared with measurements on test setups using accelerometers as well as the tunneling contact of the STM. Eventual measurements on Au(111) showed atomic resolution and mechanical vibrations below 2 pm. The ongoing work to optimize spectroscopic resolution will be reported.

O 77.3 Thu 11:00 REC C 213

Development of a closed-cycle dilution refrigerator scanning tunneling microscope — •MATE STARK¹, DARIA SOSTINA², WANTONG HUANG¹, PAUL GREULE¹, CHRISTOPH SÜRGER¹, PHILIP WILLKE¹, and WOLFGANG WERNSDORFER¹ — ¹Physikalisches Institut (PHI), Karlsruhe Institute of Technology, Karlsruhe, Germany — ²Institute of Quantum Materials and Technologies (IQMT), Karlsruhe Institute of Technology, Karlsruhe, Germany

Throughout the last decades, scanning probe techniques, such as scanning tunneling microscopy (STM), have been successfully paving the way to discover and understand physics on the atomic scale. However, recent developments in studying single atoms' electronic and magnetic properties have shown experimental limitations. For instance, the combination of electron spin resonance (ESR) with STM has shown short spin relaxation time T_1 and phase coherence time T_2 on single atoms, among others limited by thermally excited electrons [Willke et al., *Sci. Adv.* 4(2), 1543 (2018)].

Here, we present the implementation of a compact closed-cycle dilution refrigerator (DR) reaching milli-Kelvin temperatures, which we combine with a commercial STM under ultra-high vacuum (UHV) conditions. This combination enables a fast cool down, shows a low vibrational level, and requires a minimum of everyday maintenance. We demonstrate the functionality of the DR-STM by performing ESR measurements on individual magnetic molecules.

O 77.4 Thu 11:15 REC C 213

Machine learning: radical technique or plus ça change? The case for automated scanning probe microscopy — •DYLAN BARKER, ADAM SWEETMAN, and PHIL BLOWEY — University of Leeds

Atomic resolution scanning probe microscopy (SPM) provides a critical tool for studying the chemical and electronic structure of surfaces at the single atom scale, however, practically these techniques require a large amount of experimental time to manually prepare the scanning probe tip in-situ, usually via controlled indents into the surface. This apparently simple, but time-consuming process, is potentially an ideal candidate for automation using machine learning and computer vision techniques. Previous attempts to automate the classification of probe tips from topographical images have been made using machine learning methods [1-2], however using prior knowledge of the system in question we find it is also possible to classify the tip state using computationally simple image analysis methods such as Fourier ring correlation and cross-correlation. In this work I will present a comparison between "deterministic" image analysis methods and machine learning approaches for tip state classification. I will also address the known issue of small sample sizes for training ML techniques for SPM image classification, via an automated (scripted) data generation approach.

[1] Rashidi, M & Wolkow, R. A. *ACS Nano* 12, 5185-5189 (2018).

[2] Gordon, O. et al. *Review of Scientific Instruments* 90, 103704 (2019).

O 77.5 Thu 11:30 REC C 213

Artificial Intelligence finds the optimal STM manipulation parameters of unknown molecules — •BERNHARD RAMSAUER¹, GRANT J. SIMPSON², LEONHARD GRILL², and OLIVER T. HOFMANN¹ — ¹Institute of Solid State Physics, NAWI Graz, Graz University of Technology, Petersgasse 16, 8010 Graz, Austria — ²Department of Physical Chemistry, Institute of Chemistry, NAWI Graz, University Graz, Heinrichstraße 28, 8010 Graz, Austria

Scanning probe microscopy gives us the possibility to precisely control the position and orientation of single molecules and unlocks the possibility of nanofabrication of novel structures with enhanced properties. However, interaction processes at the nanoscale are stochastic processes, and because their motion itself is often unintuitive and hard to predict, inducing controlled movements is not trivial at all.

In this study we present how a reinforcement learning algorithm identifies optimal manipulation parameters (i.e., the bias voltage, height, and lateral position of the STM tip relative to the molecule) for any unknown molecule to allow for precise control of its movement.

Leaving all the manipulation parameters open for investigation requires a method to exclude manipulation parameter that pick-up or destroy the molecule. Furthermore, already learned information is used to infer prior knowledge to similar manipulation parameters (e.g.: to infer knowledge at the same bias voltage to adjacent tip positions).

This allows for autonomous control of initially unknown molecules with high sub-nanometer precision that set the basis to construct molecular nanostructures from the bottom up.

O 77.6 Thu 11:45 REC C 213

Field-emission resonances at exceptional large voltages: Consequences for determining work functions — •ANIKA SCHLENHOFF¹, GERASSIMOS C. KOKKORAKIS², and JOHN P. XANTHAKIS² — ¹Institute of Physics, University of Münster, Germany — ²Electrical and Computer Engineering Department, National Technical University of Athens, Greece

In a scanning tunneling microscopy (STM) setup, a series of unoccupied electronic states evolve in the vacuum gap between the probe tip and the surface. Due to limited bias voltage ranges, so far only a small number (typically 4 - 8) of these so-called field-emission resonances (FERs) have been detected. Here, we report a combined experimental and theoretical study of FERs over an exceptional range of energy and number, typically tens of an eV and over thirty in order n [1]. Unlike commonly assumed, the triangular potential well is not found to be a good approximation for the high- n states. Although the spectroscopy mode assures a constant electric field at the tip apex, this leads only for the intermediate FERs (approx. $2 < n < 6$) to reside in a linear potential between the tip and the surface. At higher tip-sample distances d and bias voltages $U(d)$, the quantum well is no longer triangular but attains a curvature, which is d -dependent. Each high- n state resides in its own well that can be well-approximated by a polynomial of second order. Hence, the range of U_n to be analyzed in terms of spectroscopic positions needs to be chosen with great care when deducing surface work functions.

[1] A. Schlenhoff *et al.*, Appl. Phys. Lett. **120**, 261601 (2022).

O 77.7 Thu 12:00 REC C 213

Phase compensation for ultrafast dynamic measurements of atomic spins — •NICOLAJ BETZ¹, MAX HÄNZE^{1,2}, GREGORY MCMURTRIE¹, SUSANNE BAUMANN¹, and SEBASTIAN LOTH^{1,2} — ¹University of Stuttgart, Institute for Functional Matter and Quantum Technologies, Stuttgart, Germany — ²Max Planck Institute for Solid State Research, Stuttgart, Germany

O 78: Heterogeneous Catalysis and Surface Dynamics II

Time: Thursday 10:30–12:45

Location: TRE Phy

O 78.1 Thu 10:30 TRE Phy

Data-centric heterogeneous catalysis: identifying rules and materials genes of alkane selective oxidation — •LUCAS FOPPA¹, FREDERIK RÜTHER², MICHAEL GESKE², GREGOR KOCH³, FRANK GIRGSDIES³, PIERRE KUBE³, SPENCER J. CAREY³, MICHAEL HÄVECKER⁴, OLAF TIMPE³, ANDREY TARASOV³, MATTHIAS SCHEFFLER¹, FRANK ROSOWSKI², ROBERT SCHLÖGL^{3,4}, and ANNETTE TRUNTSCHKE³ — ¹The NOMAD Lab. at the FHI of the MPG and IRIS-Adlershof of HU Berlin — ²BasCat Lab. at TU Berlin — ³FHI of the MPG — ⁴Max Planck Institute for Chemical Energy Conversion

Artificial Intelligence (AI) can accelerate materials design by identifying the key parameters correlated with the performance. However, widely used AI methods require big data, and only the smallest part of catalysis-research data meets the quality requirement for data-efficient AI. We use rigorous experimental procedures [1] to measure 55 physicochemical parameters as well as the reactivity of 12 catalysts towards ethane, propane, and n -butane oxidation. By applying the sure-independence-screening-and-sparsifying-operator approach to the so-

Understanding spin dynamics is vital for a wide range of applications, such as qubit manipulation. However, in many cases, especially for single atoms on surfaces, even stroboscopic measurement techniques, like pump-probe or pulsed electron spin resonance, do not provide enough time resolution to resolve the dynamics of the individual (atomic) spins. Such measurements are generally limited by the attenuation and distortion of the sharp pulses, that inevitably occurs due to imperfections in the instrumental setup. The attenuation in the frequency domain can be measured and compensated for [M. Herve, *et al.* Appl. Phys. Lett. **107**, 093101, 2015]. However, such a compensation only has limited impact on the distortion. Here, we introduce a new technique, that enables the measurement of the phase shift between individual frequencies directly in the tunnel junction of a scanning tunneling microscope (STM). Using these phase shifts it is now possible to fully compensate arbitrary pulses and manipulate atomic spins with picosecond time resolution. Phase information also provides additional insights into stochastic resonance, an effect we recently utilized as an alternative way to measure spin dynamics [M. Hänzle, *et al.* Sci. Adv. **7**, 33, 2021], even of multiple spin states.

O 77.8 Thu 12:15 REC C 213

Simultaneous Measurement of Quasiparticle Interference and Decay Length Using Parallel Spectroscopy with the Scanning Tunneling Microscope — •BERK ZENGIN, DANYANG LIU, ALEŠ CAHLÍK, KEVIN HAUSER, and FABIAN D. NATTERER — University of Zurich, Department of Physics, Winterthurerstrasse 190, 8057 Zurich, Switzerland

Developments in signal processing unlock the possibility to perform significantly faster spectroscopic measurements with a Scanning Tunneling Microscope by utilizing the harmonics created by non-linearities in the current-voltage characteristics. Having the capability to perform spectroscopy on the order of few milliseconds to measure the local density states (LDOS), we can afford to additionally vary the tip sample distance during QPI mapping, providing spatially and energy resolved decay length information. Our work shows how LDOS and decay length mapping can yield valuable insight into the electronic structure and dispersion relation of surface electrons.

O 77.9 Thu 12:30 REC C 213

Unveiling interference of Yu-Shiba-Rusinov states with novel multi-functionalized STM probe — •ARTEM ODOBESKO, FELIX FRIEDRICH, and MATHIAS BODE — Physikalisches Institut, Universität Würzburg, 97074, Würzburg, Germany

Scattering of superconducting pairs by magnetic impurities on superconducting surface results into pairs of sharp in-gap resonances, known as Yu-Shiba-Rusinov states. By analogue with interference of quasiparticles scattered by defects in normal metals, these excitations form periodic charge density texture around magnetic impurity. Typically, STM is equipped with a superconducting (SC) probe to increase the energy resolution bypassing thermal broadening to detect these states. However, with such STM probe it almost unattainable to observe the spatial oscillatory behavior of YSR wave function due to a very fast spatial attenuation away from the impurity (with decay $\sim 1/r$). In this work, we attach a CO molecule to a SC-probe to maximize simultaneously both spatial and energy resolution. We examine the LDOS distribution of YSR states around the magnetic Fe dimer on Nb(110). The last leads to hybridization of YSR states, which can be interpreted as symmetric and antisymmetric combinations of YSR excitation of an individual Fe impurity. Using such CO-SC-probe we are able to map both symmetric and antisymmetric oscillatory interference patterns of hybridized YSR states in vicinity of Fe dimer. Compared to measurements made with CO-free probe, we demonstrate an exceptional spatial sensitivity combined with high energy resolution with a new multi-functionalized probe.

obtained data set, we identify nonlinear property-function relationships depending on several key parameters and reflecting the intricate interplay of processes governing selective oxidation. [2,3]

[1] A. Truntschke, *et al.*, *Top. Catal.* **63**, 1683-1699 (2020).

[2] L. Foppa, *et al.*, *MRS Bull.* **46**, 1 (2021).

[3] L. Foppa, *et al.*, *ChemRxiv*, 10.26434/chemrxiv-2022-xmg75 (2022).

O 78.2 Thu 10:45 TRE Phy

Adaptive Experimental Designs for the Unsupervised Exploration of Reaction Kinetic Phase Diagrams — •FREDERIC FELSEN, KARSTEN REUTER, and CHRISTOPH SCHEURER — Fritz-Haber-Institut der MPG, Berlin, Germany

In heterogeneous catalysis the interplay of various elementary processes taking place at the catalytic interface gives rise to complex kinetic phase diagrams [1]. Characteristic for such phase diagrams are regimes of smooth kinetic behavior separated by phase transitions going along with drastic changes in effective kinetics. Generally it is difficult to reconstruct the kinetic regime topology of a given

process without a detailed understanding of the underlying reaction mechanism. Here, we tackle this issue by approximating the reaction kinetics using statistically robust effective rate laws [2]. Locally fingerprinting the apparent behavior of a chemical reaction, we can generate point-wise regime labels as a basis for estimates of the position of the phase transitions. In order to achieve this in a data efficient way, we propose an iterative adaptive design algorithm, bridging between the classical theory of experimental design [3] and modern statistical learning and optimization. Using a microkinetic model, we illustrate the potential of this approach by investigating the kinetic phase diagram of CO oxidation over RuO₂.

[1] V. Zhdanov et al., *Surf. Sci. Rep.* **20**, 113, (1994).

[2] F. Felsen et al., *Chem. Eng. J.* **433**, 134121, (2022).

[3] V. Fedorov, *Theory of Optimal Experiments* (1972).

O 78.3 Thu 11:00 TRE Phy

Machine-learning Gaussian Approximation Potentials to discover RuO₂ surface reconstructions — •YONGHYUK LEE, JAKOB TIMMERMANN, CHRISTOPH SCHEURER, and KARSTEN REUTER — Fritz-Haber-Institut der MPG, Berlin, Germany

Machine-learning Gaussian Approximation Potentials (GAPs) have recently evolved into a powerful class of surrogate models for computationally demanding first-principles calculations. Combined with structure exploration techniques, they enable us to examine the potential energy surface of interest with a hitherto unforeseen combination of physical accuracy and computational efficiency and to achieve global surface structure determination (SSD) for increasingly complex systems. This can be exploited, e.g., to discover novel surface motifs, which are critical in understanding the dynamics of heterogeneous catalysts under operating conditions. In our preceding study on IrO₂, this methodology was extended by a general and data-efficient active-learning framework that allows for the on-the-fly generation of GAPs via the actual surface exploration process. During the iterative GAP refinement for RuO₂, we have now identified plenty of unknown low-energy reconstructions of RuO₂ low index facets. Intriguingly, by extending the searching space to larger surface unit cells, we discovered $c(2 \times 2)$ reconstructions of RuO₂(100), which provide solutions to longstanding questions in heterogeneous catalysis and experiments.

[1] J. Timmermann et al., *Phys. Rev. Lett.* **125**, 206101 (2020)

[2] J. Timmermann et al., *J. Chem. Phys.*, **155**, 244107 (2021)

O 78.4 Thu 11:15 TRE Phy

Exploration of IrO₂ electrocatalyst deactivation via machine learning potentials — •HAO WAN, HENDRIK HEENEN, SIMON WENGERT, CHRISTOPH SCHEURER, and KARSTEN REUTER — Fritz-Haber-Institut der Max-Planck-Gesellschaft, Berlin, Germany

IrO₂ catalysts are one of the best performing oxygen evolution reaction (OER) catalysts in terms of both catalytic activity and stability under harsh acidic conditions. Yet, they still suffer from deactivation under long term OER conditions due to possible changes in surface compositions and morphology. To shed light into these deactivation processes, characterization of the microscopic structure and composition of IrO₂ interfaces is necessary. The involved phase space, however, is vast and its exploration requires extensive sampling and automatic (surface) structure searches which are unfeasible via Density Functional Theory (DFT) calculations. Enabling the intensive computations, machine learning interatomic potentials (MLIP) retain DFT accuracy to within a few meV per atom while reducing the computational cost by up to three orders of magnitude.

In this contribution, we present a reliable MLIP based on Gaussian approximation potentials to investigate IrO₂ deactivation. Stable and metastable IrO₂ surfaces at various surface oxidation states have been extensively sampled using parallel tempering. Relevant surfaces are suggested by evaluating their relative stability compared to rutile-IrO₂(110), while considering electrochemical conditions. OER activity from these surfaces can be estimated using established reaction descriptors which will help unravel likely deactivation mechanisms.

O 78.5 Thu 11:30 TRE Phy

Machine Learning Driven Molecular Dynamics Simulation of the M1 Selective Oxidation Catalysts — •KYEONGHYEON NAM¹, YONGHYUK LEE¹, LIUDMYLA MASLIUK², THOMAS LUNKENBEIN², ANNETTE TRUNSCHKE², CHRISTOPH SCHEURER¹, and KARSTEN REUTER¹ — ¹Theory, Fritz-Haber-Institut der MPG — ²Inorganic Chem. Dept., Fritz-Haber-Institut der MPG, Berlin, Germany

The activity and selectivity of realistic heterogeneous catalysts can be altered noticeably by small changes in a multitude of factors such as bulk composition, dopants, defects, reaction conditions, etc. Their effects are furthermore interrelated in non-trivial ways. As an important first step to rationally disentangle them, we here aim to understand their influences on the evolution of local atomic-scale structural motifs presented by the catalyst. Specifically, we do this for the M1 structural modification of (Mo,V)O_x and (Mo,V,Te,Nb)O_x as an active catalyst for oxidative dehydrogenation of ethane to ethylene. The large primitive cell of the M1 catalyst challenges a detailed study of all surface terminations by means of predictive-quality first-principles calculations. To this end, we deconstruct the primitive cell into 'rod-like structures' of surface motifs with

various oxygen content. A machine-learned Gaussian Approximation Potential (GAP), trained against this structural library, faithfully reproduces experimental data from electron microscopy [1]. MD simulations of M1 catalyst hk0 prismatic faces with the iteratively improved GAP help to rationalize the influence of vanadium and niobium doping on the active surface structure.

[1] L. Masliuk et al., *J. Phys. Chem. C* **121**, 24093 (2017).

O 78.6 Thu 11:45 TRE Phy

Studying of rate-limiting steps on CO₂ reduction on ZnO/Cu(111) — •SINA DORTAJ^{1,2} and SEBASTIAN MATERA^{1,2} — ¹Fritz Haber Institute of the Max Planck Society, Berlin, Germany — ²Institute for Mathematics, Freie Universität, Berlin, Germany

To simulate the chemical kinetics of heterogeneous catalysts, the kinetic Monte Carlo (kMC) method is a common choice as it allows estimating turnover frequencies and coverages with a tunable accuracy. This advantage comes at much higher computational costs compared to classical kinetic approaches, in addition to stochastic noise on the simulation results. Thus, local sensitivity analysis to determine the rate-limiting step becomes cumbersome. Additionally, rate constants often carry some sizeable uncertainty due to the intrinsic approximations in quantum chemical methods or the noise in experimental data used to determine reaction barriers that make the use of just local methods obscure. We address both problems, high costs, and parameter uncertainties, by a novel global sensitivity analysis based on the Cramér von Mises distance and a Quasi-Monte Carlo sampling of the space of rate constants. While applicable to any model, our approach is particularly suited for the use of kMC and other Monte Carlo models. We demonstrate the approach on the CO₂ reduction on ZnO/Cu(111) catalysts identifying the key atomic scale factors controlling activity and selectivity.

O 78.7 Thu 12:00 TRE Phy

Identifying materials genes describing selectivity of catalytic CO₂ hydrogenation: an AI approach with theoretical and experimental data — •RAY MIYAZAKI¹, KENDRA BELTHLE², HARUN TÜYSÜZ², LUCAS FOPPA¹, and MATTHIAS SCHEFFLER¹ — ¹The NOMAD Laboratory at the FHI of the Max-Planck-Gesellschaft and IRIS-Adlershof of the Humboldt-Universität zu Berlin, Germany — ²Max-Planck-Institut für Kohlenforschung, Germany

Investigating CO₂ hydrogenation by heterogeneous catalysis that mimics hydrothermal vents leads to a deeper understanding of the origin of organic molecules at the early earth [1]. We focus on cobalt nanoparticles supported on M-SiO₂ where hetero atoms (e.g., Ti or Al) are incorporated into SiO₂. However, heterogeneous catalysis is governed by an intricate interplay among multi-scale processes. Thus, it is rather difficult, if not impossible, to identify the key physical parameters correlated with the catalytic performance (*materials genes*) directly by theoretical or experimental approaches. In this study, materials properties obtained from density functional theory calculations and experiments, such as adsorption energy of CO₂ and measured pore volume, are used to model the experimental selectivity of each organic molecule (e.g., CH₃OH, CH₄) by the sure-independence screening and sparsifying operator (SISSO) AI approach [2]. In order to accelerate catalyst design, we also investigate the accuracy of the models using input parameter sets with the different acquisition cost.

[1] K. S. Belthle et al., *J. Am. Chem. Soc.*, in press (2022).

[2] R. Ouyang et al., *Phys. Rev. Mater.*, **2**, 083802 (2018).

O 78.8 Thu 12:15 TRE Phy

Structural and Electronic Properties of Iron Nanoparticles onto Well-Defined Ceria Thin Films — •LESLIA PILIAI¹, MYKHAILO VOROKHTA¹, PETER MATVIJA¹, TOMÁŠ SKÁLA^{1,2}, IVAN KHALAKHAN¹, and IVA MATOLÍNOVÁ¹ — ¹Charles University, Prague, Czech Republic — ²Elettra-Sincrotrone, Elettra-Sincrotrone, Italy

The interaction of iron with ceria using model Fe/ceria systems consisting of Fe nanoparticles vapor deposited on well-ordered CeO_x(x=1,5;2) thin films grown on Cu(111) has been investigated by X-ray photoelectron spectroscopy (XPS), synchrotron radiation photoemission spectroscopy (SRPES), and scanning tunneling microscopy (STM). The Fe atoms are oxidized to Fe³⁺ and Fe²⁺ species upon deposition on CeO₂ at 300 K at the cost of the reduction of Ce⁴⁺ to Ce³⁺. With increasing the Fe coverage, the concentration of Ce³⁺ increases monotonically. The notable growth of Fe²⁺ species was observed upon deposition on CeO₂ at 300 K, but Fe³⁺ species remain predominant in Fe/CeO_x systems. Our studies demonstrate that in comparison with other transition metals, Fe remains oxidized on ceria even at higher coverage and exhibits a small particle size, likely arising from strong metal*support interactions. Combining the SRPES and STM data suggests that annealing to higher temperatures leads to the formation of an iron-ceria solid solution. These results illustrate that Fe modifies both the electronic and structural properties of ceria depending on external conditions.

O 78.9 Thu 12:30 TRE Phy

In situ characterization of cerium oxide on Au(111) under reducing and oxidizing conditions by low-energy electron microscopy — •RUDI TSCHAMMER¹, LARS BUSS^{1,2}, CARLOS MORALES¹, SANJAYA SENANAYAKE³, JENS FALTA^{2,4}, and JAN INGO FLEGE¹ — ¹Applied Physics and Semiconductor Spectroscopy, BTU Cottbus-Senftenberg, Cottbus, Germany — ²Institute of Solid State Physics, University of Bremen, Bremen, Germany — ³Chemistry Division, Brookhaven National Laboratory, Upton, NY 11973, USA — ⁴MAPEX Center for Materials and Processes, University of Bremen, Bremen, Germany

The development of novel catalysts for a variety of applications is a key challenge for modern catalysis. Inverse metal oxide catalysts consisting of oxide

nanoparticles dispersed on a metal support have recently attracted much attention, showing higher activity and selectivity compared to traditional catalytic systems, harnessing synergistic effects attributed to the so-called metal-support interaction. To gain further insights, we deposited cerium oxide nanoparticles on Au(111) and studied this system by low-energy electron microscopy (LEEM) and low-energy electron diffraction (LEED). The prepared samples demonstrate a distinct correlation between the deposition temperature and the structural order of the nanoparticles. This has been expanded upon by exploring the changes induced by reduction with H₂ and reoxidation with O₂ or CO₂, again exhibiting a connection between structural order and activity, while also showing the influence of the oxide-metal interaction on the stability of cerium oxide under reducing conditions.

O 79: Focus Session: Frontiers of Electronic-Structure Theory VI (joint session O/HL)

Time: Thursday 10:30–12:45

Location: TRE Ma

O 79.1 Thu 10:30 TRE Ma

Nailing down charge-density-wave phase-transition temperatures with downfolding approaches — •ARNE SCHOBERT¹, JAN BERGES², MICHAEL SENTEF³, ERIK VAN LOON⁴, SERGEY BRENER¹, MARIANA ROSSI³, and TIM WEHLING¹ — ¹University of Hamburg, Germany — ²University of Bremen, Germany — ³MPSD, Hamburg, Germany — ⁴Lund University, Sweden

The coupled dynamics of electrons and nuclei is an extremely complex problem of relevance to multiple branches of sciences. *Ab initio* molecular dynamics (AIMD) simulations are often challenging — especially in large systems, on long time scales, in non-equilibrium or in presence of strong correlation. We can overcome these problems by mapping the full *ab initio* density functional theory (DFT) Hamiltonian onto a low-energy lattice model through downfolding. Three different downfolding strategies based on constraining, unscreening and combinations thereof are compared. The best performing model, which properly accounts for anharmonicity, is combined with path integral molecular dynamics (PIMD). This allows us to nail down the transition temperatures of charge-density waves — for instance in 1H-TaS₂.

O 79.2 Thu 10:45 TRE Ma

Structural and electronic properties of the Ba₈Au_xGe_{46-x} clathrate: an *ab initio* study with cluster expansion — •PETER WEBER, SANTIAGO RIGAMONTI, and CLAUDIA DRAXL — Humboldt-Universität zu Berlin, Berlin, Germany

Intermetallic clathrate materials are promising candidates for high-efficiency thermoelectric applications as they can reach very low thermal conductivity. These materials possess a cage-like structure containing guest atoms. Their electronic properties can be tailored by exploiting the idea of the phonon-glass-electron-crystal which allows for reaching a large figure of merit. We study the compound Ba₈Au_xGe_{46-x} (0 ≤ x ≤ 8), which has raised interest due to its glass-like thermal conductivity [1]. Using the Zintl concept, a semiconducting state is expected to occur at the charge-balanced composition corresponding to x=5.33. This composition requires a supercell of at least 3 unit cells (162 atoms) which makes a direct *ab initio* study challenging. We tackle this problem by using the cluster expansion method combined with density-functional theory calculations. In this way, we are able to find the atomic ground-state configurations, together with various properties at different temperatures and gold content. These include lattice constants, bond lengths, site occupancies, as well as band gaps and band structures which are compared with available experimental data.

[1] P.-F. Lory, *et al.* Nature Communications **8**, 491 (2017).

Topical Talk

O 79.3 Thu 11:00 TRE Ma

New Opportunities for First Principles Simulations of Thousands of Atoms Using Linear Scaling Density Functional Theory — •LAURA RATCLIFF — University of Bristol, Bristol, United Kingdom

Density-functional theory (DFT) is routinely used to simulate a wide variety of materials and properties, however, standard implementations are cubic scaling with the number of atoms, limiting the system sizes which can be treated. This motivated the development of alternative implementations of DFT, which exploit the nearsightedness principle by using a localised description of the system, leading to algorithms with linear scaling (LS) cost which can treat large systems containing tens of thousands of atoms. One approach, which is implemented in the wavelet-based BigDFT code, uses localised orbitals, also known as support functions, which are optimised to reflect their local chemical environment, and thus constitute an accurate minimal basis set. Beyond reduced computational cost, the localised support function description also facilitates additional developments, such as the ability to automate a fragment-based description. In this talk we will present the formalism behind LS-BigDFT, including some examples of the new types of systems and analyses which are opened up by the ability to treat such large systems. We will also describe recent developments in PyBigDFT, a python-based interface which aims to simplify the usage of LS-BigDFT for complex systems and workflows.

15 min. break

O 79.4 Thu 11:45 TRE Ma

Fully Anharmonic Electronic Transport Coefficients from Temperature-dependent Spectral Functions — •JINGKAI QUAN, MATTHIAS SCHEFFLER, and CHRISTIAN CARBOGNO — The NOMAD Laboratory at the FHI of the Max-Planck-Gesellschaft and IRIS-Adlershof of the Humboldt-Universität zu Berlin The combination of *ab initio* molecular dynamics (aiMD) and band-structure unfolding techniques provides a non-perturbative route to obtain temperature-dependent spectral functions. [1] In contrast to commonly employed perturbative approaches [2], this technique accounts for all orders of anharmonic and vibronic couplings. Building on this non-perturbative formalisms, we here present an approach to obtain electronic transport coefficient such as the electrical conductivity using Kubo's formulation of the fluctuation-dissipation theorem. By this means, all relevant quantities, including electron lifetimes, are obtained from the unfolded, self-consistent wave functions computed during the aiMD runs. We critically benchmark the approach against existing perturbative data for harmonic systems, carefully analyzing to which extent short- and long-range couplings are captured with increasing supercell size. Furthermore, we demonstrate the advantages of the proposed approach for strongly anharmonic systems, for which perturbative approaches become unreliable.

[1] M. Zacharias, M. Scheffler, and C. Carbogno, *Phys. Rev. B* **102**, 045126 (2020).

[2] F. Giustino, *Rev. Mod. Phys.* **89**, 015003 (2017).

O 79.5 Thu 12:00 TRE Ma

Accurate prediction of vibrational spectra for solid state systems from *ab initio* molecular dynamics — •EKIN ESME BAS, THOMAS HEINE, and DOROTHEA GOLZE — Chair of Theoretical Chemistry, Technische Universität Dresden, 01062 Dresden, Germany

We present a highly accurate computational method to calculate vibrational spectra for solid state materials, primarily for covalent-organic frameworks (COFs). IR and Raman spectra are important tools that are frequently used for material characterization. However, the experimental spectra are often difficult to interpret without aid from theory. The computation of IR and Raman spectra is usually based on the harmonic approximation where molecular vibrations can be determined as normal modes from the second derivatives of the electronic energy with respect to the coordinates. Although this method is more straightforward and computationally less expensive, anharmonic modes cannot be captured. Thus, we employ an AIMD (*ab initio* molecular dynamics) based approach to include vibrational anharmonicities. Power, IR and Raman spectra can then be calculated via a Fourier transformation of the time correlation functions of velocities, dipole moments and polarizability tensors, respectively [1]. We discuss different approaches to compute dipole moments and polarizabilities. We present the power, IR and Raman spectra we calculated for COF-1, and we compare our AIMD based approach to the spectra obtained via harmonic approximation and experiment.

[1] M. Thomas, M. Brehm, R. Fligg, P. Vöhringer, B. Kirchner. *Phys. Chem. Chem. Phys.*, 6608-6622, 5, 2013.

O 79.6 Thu 12:15 TRE Ma

Anharmonic Fingerprints from THz Modes of Polyacene Crystals — •PAOLO LAZZARONI, SHUBHAM SHARMA, and MARIANA ROSSI — Max Planck Institute for the Structure and Dynamics of Matter, Hamburg, Germany

Organic molecular crystals exhibit strong lattice anharmonicity, especially in the collective motions that are governed by intermolecular interactions and lie in the low-frequency THz range [1]. Inspired by recent observations that the polarization-orientation (PO) Raman spectra can give exquisite insight into the anharmonic couplings between modes [2], we devise a first-principles framework that can reproduce, explain and give quantitative insight into the type and

strengths of mode coupling. This framework is based on machine-learned potentials and polarizability tensors trained on *ab initio* molecular dynamics trajectories [3]. We obtain results through the time-correlation formalism for PO Raman signals, retaining the full anharmonic nature of the potential, and perform a novel analysis of effective temperature-dependent mode couplings from our trajectories. [1] M. Asher *et al.*, *Adv. Mater.* **32**, 1908028 (2020) [2] N. Benshalom *et al.*, arXiv:2204.12528 (2022) [3] N. Raimbault *et al.*, *New J. Phys.* **21** 105001 (2019)

O 79.7 Thu 12:30 TRE Ma

A first-principles Newns-Anderson chemisorption function applied to ultrafast electron transfer — •SIMIAM GHAN¹, ELIAS DIESEN¹, CHRISTIAN KUNKEL¹, KARSTEN REUTER¹, and HARALD OBERHOFER² — ¹Fritz-Haber-Institut der MPG, Berlin, Germany. — ²University of Bayreuth, Bayreuth, Germany

We offer a method to calculate the electronic couplings H_{ad} between an adsorbate and substrate in an *ab-initio* fashion. The couplings are acquired by projec-

tion of the Kohn-Sham Hamiltonian onto a diabatic basis[1]. By averaging over the Brillouin Zone, it becomes possible to calculate a convergent chemisorption function of Newns and Anderson[2], which gives the energetic broadening of an adsorbate frontier orbital upon adsorption. This broadening corresponds to the experimentally-observable lifetime of an electron in the state, which we confirm for the case of core-excited $Ar^*(2p_{3/2}^{-1}4s)$ atoms on a number of transition metal surfaces[3].

We find that the (tunneling) model captures and elucidates aspects of energy-dependence, spin, phase cancellation and k-space in the electron transfer process, in particular suggesting a significant role played by the surface d-bands. Given the prevalence of electronic couplings - and the chemisorption function - in theoretical models, we discuss potential for further applications.

[1] S. Ghan *et al.*, *J. Chem. Theory Comput.* **16**, 7431 (2020).

[2] D. Newns, *Phys. Rev.* **178**, 3, 1123 (1969).

[3] F. Blobner *et al.*, *Phys. Rev. Lett.* **112**, 086801 (2014).

O 80: Plasmonics and Nanooptics IV: Light-Matter Interaction and Spectroscopy III

Time: Thursday 15:00–17:15

Location: CHE 89

O 80.1 Thu 15:00 CHE 89

Energy and momentum distribution of surface plasmon-induced hot carriers — •CHRISTOPHER WEISS¹, MICHAEL HARTELT¹, PAVEL N. TEREKHIN¹, TOBIAS EUL¹, ANNA-KATHARINA MAHRO¹, BENJAMIN FRISCH¹, EVA PRINZ¹, BAERBEL RETHFELD¹, BENJAMIN STADTMÜLLER^{1,2}, and MARTIN AESCHLIMANN¹ — ¹Department of Physics and Research Center OPTIMAS, TU Kaiserslautern, Germany — ²Institute of Physics, Johannes Gutenberg University Mainz, Germany

Are the spectroscopic properties of plasmon- and photon-induced hot carriers fundamentally different? Electrons excited at the bulk plasmon resonance, for example, exhibit a distinct spectroscopic signature [1]. However, bulk plasmons are rather unsuited for technological applications compared to surface plasmons.

To answer the initial question for surface plasmons, we separate the energy and momentum distributions of surface plasmon polariton (SPP)-induced hot electrons from those of photoexcited electrons in a two-color time-resolved photoemission electron microscopy experiment.

In our experiment, these SPP-induced hot electrons show only small momenta parallel to the surface and a narrow energy distribution close to the Fermi energy [2]. This result clearly distinguishes them spectroscopically from their photoinduced counterparts.

[1] Reutzel *et al.*, *Phys. Rev. Lett.* **123** (2019), 017404

[2] Hartelt *et al.*, *ACS Nano* **15**, 12 (2021), 19559–19569

O 80.2 Thu 15:15 CHE 89

Lorentz Microscopy of Optical Fields — •JOHN H. GAIDA^{1,2}, HUGO LOURENÇO-MARTINS^{1,2}, SERGEY V. YALUNIN^{1,2}, ARMIN FEIST^{1,2}, MURAT SIVIS^{1,2}, THORSTEN HOHAGE³, F. JAVIER GARCÍA DE ABAJO^{4,5}, and CLAUDIUS ROPERS^{1,2} — ¹MPI for Multidisciplinary Sciences, Göttingen, Germany — ²4th Physical Institute, University of Göttingen, Germany — ³Institute of Numerical and Applied Mathematics, University of Göttingen, Germany — ⁴ICFO-Institut de Ciències Fotòniques, Castelldefels (Barcelona), Spain — ⁵ICREA-Institució Catalana de Recerca i Estudis Avançats, Barcelona, Spain

In electron microscopy, detailed insights into nanoscale optical properties of materials are gained by spontaneous inelastic scattering leading to electron-energy loss and cathodoluminescence. Photon-induced near-field electron microscopy (PINEM) allows for mode- and polarization-selective imaging based on stimulated scattering in the presence of external sample excitation. Through this process a spatial phase profile inherited from the optical fields is imprinted onto the wave function of the probing electrons. Here, we introduce Lorentz-PINEM for the full-field, non-invasive imaging of complex optical near fields at high spatial resolution. We use energy-filtered defocus phase-contrast imaging and iterative phase retrieval to reconstruct the phase distribution of interfering surface-bound modes on a plasmonic nanotip. Our approach is universally applicable to retrieve the spatial phase of nanoscale fields and topological modes.

[1] John H. Gaida, *et al.*, 2022, Preprint at Research Square doi.org/10.21203/rs.3.rs-2150760/v1.

Topical Talk

O 80.3 Thu 15:30 CHE 89

Topological Plasmonics and Plasmonic Twistronics: Skyrmions, Merons, Quasicrystals, and Skyrmion Bags — •HARALD GIESSEN¹, BETTINA FRANK¹, PASCAL DREHER², DAVID JANOSCHKA², FRANK MEYER ZU HERINGDORF², JULIAN SCHWAB¹, TIM DAVIS^{1,4}, KOBİ COHEN³, SHAI TSESSES³, and GUY BARTAL³ — ¹4. Physikalisches Institut, Universität Stuttgart, Germany — ²CENIDE, University of Duisburg-Essen, Germany — ³Technion, Haifa, Israel — ⁴University of Melbourne, Australia

We present ultrafast vectorial electric field measurements of plasmonic skyrmions, merons, quasicrystalline structures, and skyrmion bags. 10 nm spa-

tial resolution, sub-fs temporal resolution, and vectorial properties of the surface plasmon field on single crystalline, atomically flat gold surfaces are presented. Our techniques combine ultrafast vector PEEM and interferometric s-SNOM. Our tailored model systems reveal a rich set of topological phenomena, reaching even into 4-dimensional topology.

O 80.4 Thu 16:00 CHE 89

Direct imaging of photonic band-edge states in golden-angle Vogel spirals using photoemission electron microscopy — MARTIN AESCHLIMANN¹, FELIX FENNER², TOBIAS BRIXNER³, BENJAMIN FRISCH¹, PATRICK FOLGE⁴, MICHAEL HARTELT¹, •MATTHIAS HENSEN³, THOMAS H. LOEBER⁵, WALTER PFEIFFER², SEBASTIAN PRES³, and BERND STANNOWSKI⁶ — ¹Fachbereich Physik and Research Center OPTIMAS, TU Kaiserslautern, 67663 Kaiserslautern, Germany — ²Fakultät für Physik, Universität Bielefeld, 33615 Bielefeld, Germany — ³Institut für Physikalische und Theoretische Chemie, Universität Würzburg, 97074 Würzburg, Germany — ⁴Angewandte Physik, Universität Paderborn, 33098 Paderborn, Germany — ⁵Nano-Structuring-Center, 67663 Kaiserslautern, Germany — ⁶5PVcomB, Helmholtz-Zentrum Berlin für Materialien und Energie GmbH, 12489 Berlin, Germany

Golden-angle Vogel spirals, as deterministic aperiodic structures, support isotropic photonic band gaps and have interesting applications. Especially localized modes, such as band-edge states, are essential for tailored light-matter interaction. Here we report imaging of such modes using photoemission electron microscopy (PEEM). Tunable ultrashort light pulses excite them in golden-angle Vogel spirals that were fabricated by focused-ion-beam (FIB) milling of an a-Si:H layer. The local near-field leads to electron emission which is detected spatially resolved. The demonstration of FIB-textured a-Si:H as photonic material and the ability of PEEM mode imaging offers means to spatiotemporally resolve mode dynamics and to perform nanospectroscopy.

O 80.5 Thu 16:15 CHE 89

Short-range plasmonic skyrmions — •BETTINA FRANK¹, SIMON MANGOLD¹, HARALD GIESSEN¹, PASCAL DREHER², FRANK MEYER ZU HERINGDORF², and STEFAN KAISER¹ — ¹4. Physikalisches Institut, Universität Stuttgart, Germany — ²CENIDE, University of Duisburg-Essen

We utilize ultrathin, atomically flat, single crystalline gold flakes which compress the plasmon wavelength to $\lambda_{air}/7$. Using hexagonal boundaries that are carved with focused gold ions, we demonstrate plasmonic skyrmions, both using PEEM as well as s-SNOM. The electromagnetic field is structured on a 140 nm scale, which offers opportunities for topological light-matter interaction on a deep subwavelength scale.

O 80.6 Thu 16:30 CHE 89

Phase-resolved mapping of plasmonic resonances at nanostructures — •TIM DAUWE^{1,2}, HUGO LOURENÇO-MARTINS^{1,2}, MURAT SIVIS^{1,2}, JAKOB HAGEN^{1,2}, and CLAUDIUS ROPERS^{1,2} — ¹Max Planck Institute for Multidisciplinary Sciences, 37077 Göttingen, Germany — ²IV. Physical Institute, University of Göttingen, 37077 Göttingen, Germany

In this contribution, we study resonant plasmonic nanostructures by a combination of inelastic electron-light scattering techniques. We investigate metallic nanorods using electron-energy loss spectroscopy (EELS) and photon-induced near-field electron microscopy (PINEM), elucidating spectrally-dependent mode profiles and symmetries using spontaneous and stimulated interactions. We explore multicolor excitation and nonlinear wave mixing as contrast mechanisms accessing spatial phase profiles and local nonlinear response.

O 80.7 Thu 16:45 CHE 89

Shortcut to Self-Consistent Light-Matter Interaction and Realistic Spectra from First Principles — •CHRISTIAN SCHÄFER^{1,2} and GÖRAN JOHANSSON¹ —¹Department of Microtechnology and Nanoscience, MC2, Chalmers University of Technology, 412 96 Göteborg, Sweden — ²Department of Physics, Chalmers University of Technology, 412 96 Göteborg, Sweden

Nanoplasmonic and optical cavity environments provide a novel handle to non-intrusively control materials and chemistry. We introduce here a simple approach to how an electromagnetic environment can be efficiently embedded into state-of-the-art electronic structure methods, taking the form of radiation-reaction forces [1]. We demonstrate that this self-consistently provides access to various optical effects and provides an efficient path to connect vastly different system scales [2]. As an example, we illustrate its seamless integration into time-dependent density-functional theory and its application to polaritonic chemistry with virtually no additional cost, presenting a convenient shortcut to self-consistent light-matter interactions.

[1] C. Schäfer and G. Johansson, PRL 128, 156402 (2022).

[2] C. Schäfer, J. Phys. Chem. Lett. 2022, 13, 6905–6911.

O 80.8 Thu 17:00 CHE 89

Microscopic description of the optical response in metal nanoparticles —

•JONAS GRUMM, ROBERT SALZWEDEL, MALTE SELIG, and ANDREAS KNORR — Institut für Theoretische Physik, Nichtlineare Optik und Quantenelektronik, Technische Universität Berlin, Berlin, Germany

The optical response of metal nanoparticles is dominated by the formation of collective electronic resonances, so-called localized plasmons.

Here, we present a microscopic approach to their temporal dynamics based on the self-consistent treatment of the microscopic Boltzmann transport equations and the macroscopic Maxwell's equations for the electromagnetic fields. The corresponding numerical simulations describe the formation, propagation and thermalization dynamics of plasmons via the coupled electron-phonon dynamics in the self-consistent solved optical field. The formalism allows nonlinear optical processes to be included in the description.

O 81: Oxide and Insulator Surfaces I: Adsorption and Reaction of Small Molecules

Time: Thursday 15:00–18:00

Location: CHE 91

O 81.1 Thu 15:00 CHE 91

Adsorption of phosphonic acids on Fe₃O₄ (001) surfaces - a DFT study — WERNFRIED MAYR-SCHMÖLZER, JOHANN FLEISCHHAKER, SOMAK BANERJEE, KAI SELLSCHOPP, and •GREGOR VONBUN-FELDBAUER — Institute of Advanced Ceramics, TU Hamburg, Germany

The usage of magnetite nanoparticles is interesting for diverse applications from catalysis to hybrid materials. In organic-inorganic hybrids, organic linker molecules are used to allow for the self-assembly of functionalized nanoparticles. The impact of linkers with different functional groups on the, e.g., mechanical properties of assembled materials is not fully clear yet. Here, we present results from investigating the adsorption of small phosphonic acids on the magnetite (001) surface using density functional theory calculations to shed light on this essential interface. For the surface a distorted bulk truncated termination and the sub-surface cation vacancy reconstruction model are used. The adsorption configuration space is sampled and configurations as input for DFT calculations are selected using unsupervised machine learning approaches. Structural, energetic, electronic, and vibrational results are presented and compared to carboxylic acids. Potentials for multi-scale modeling approaches are sketched.

results demonstrate different types of adsorption and dissociation of formic acid. The results of this study can be applied as a paradigm in order to provide insight into the fundamental surface science of the next generation of the hierarchical organic-linked magnetite.

O 81.4 Thu 15:45 CHE 91

Fe₃O₄(111): surface structure and CO adsorption — •JOHANNA HÜTNER¹, FLORIAN KRAUSHOFER¹, MATTHIAS MEIER^{1,2}, ZDENEK JAKUB³, CESARE FRANCHINI^{2,4}, MICHAEL SCHMID¹, ÜLRIKE DIEBOLD¹, GARETH S. PARKINSON¹, and JAN BALAJKA¹ — ¹Institute of Applied Physics, TU Wien, Austria — ²Computational Materials Physics, University of Vienna, Austria — ³CEITEC, Brno University of Technology, Czech Republic — ⁴Department of Physics and Astronomy, Università di Bologna, Italy

The surface structure of Fe₃O₄(111) has been the subject of an ongoing debate. The most stable termination, over a wide range of oxygen chemical potentials, has a layer of tetrahedrally coordinated iron atoms (Fe_{tet}). We present AFM data that show an almost perfect grid of Fe_{tet} atoms. In filled states STM images, iron atoms exhibit varying contrast, suggesting electronic structure variations among the cation sites. We study the adsorption of CO as a probe molecule on the Fe₃O₄(111) surface with noncontact AFM. The data show that CO adsorbs on top of Fe_{tet} atoms at all coverages. We identify coverage-dependent adsorption structures with varying CO–CO spacings. We propose that the apparent CO–CO repulsion is a substrate-mediated effect that could be explained by charge redistribution in the surface. The CO ordering on a defect-free Fe₃O₄(111) surface is consistent with previously measured temperature programmed desorption data. Our findings contribute to the understanding of the electronic structure of the Fe₃O₄(111) surface and will be a requisite for modeling the adsorption of more complex molecules.

O 81.5 Thu 16:00 CHE 91

Reactivity and Influence of Catalytic Support Materials - a combined in situ and operando Infrared Study of CeO₂ — •ERIC SAUTER¹, LACHLAN CAULFIELD¹, ALEXEI NEFEDOV¹, FLORIAN MAURER², DARIA GASHNIKOVINA², JAN-DIRK GRUNWALDT², and CHRISTOPH WÖLL¹ — ¹Institute of Functional Interfaces (IFG), Karlsruhe Institute of Technology (KIT), Hermann-von-Helmholtz-Platz 1, 76344 Eggenstein-Leopoldshafen, Germany — ²Institute for Chemical Technology and Polymer Chemistry (ITCP), Karlsruhe Institute of Technology (KIT), Engesserstraße 20, 76131 Karlsruhe, Germany

For most catalytic reactions the morphology, oxidation state and support were found to have a strong influence on the catalytic activity. Investigation of the most active sites, the support material and its behavior under model as well as realistic conditions is a prerequisite for a comprehensive understanding of catalytic processes. With Infrared Spectroscopy the surface composition and interaction with water, as well as carbon monoxide, can be investigated. The combination of low temperature, UHV gas adsorption as well as operando DRIFTS was used to characterize CeO₂ as catalytic support material. The adsorption of CO on single crystals was used as reference for the interpretation of more complicated spectra like powders or nanoparticles. The interactions with water have shown the high reactivity of the cerium oxide surface, which at the end leads to hydroxyl termination. With the use of in situ and operando Infrared spectroscopy the behavior of catalysts and their support material can be investigated, under realistic reaction conditions, into more detail.

O 81.3 Thu 15:30 CHE 91

Growth and adsorption studies of magnetite nanoparticles on Al₂O₃ — •MOHAMMAD EBRAHIM HAJI NAGHI TEHRANI^{1,2}, MARCUS CREUTZBURG¹, HESHMAT NOEI¹, and ANDREAS STIERLE^{1,2} — ¹Deutsches Elektronen-Synchrotron (DESY), D-22603 Hamburg, Germany — ²Fachbereich Physik Universität Hamburg, Jungiusstrasse 9, 20355 Hamburg, Germany

Magnetite (Fe₃O₄) is an important transition metal oxide with diverse applications in catalysis, data storage and biomedical imaging. In this study, we grow model catalyst magnetite nanoparticles on Al₂O₃(0001) surface under UHV conditions and at different temperatures: 150, 300, 500, and 700 °C. Grazing incidence X-ray diffraction (GIXRD) and microscopy techniques were assisted in defining the facet and morphology of the developed nanoparticles, respectively. GIXRD outcomes indicated the formation of 111 oriented nanoparticles. Fourier transmission infrared reflection-absorption spectroscopy (FTIRRAS) was performed to study the adsorption of formic acid on magnetite/Al₂O₃ samples. The

O 81.6 Thu 16:15 CHE 91

Reduction of ceria with carbon monoxide - A high resolution, operando DRIFTS study — •LACHLAN CAULFIELD, ERIC SAUTER, and CHRISTOPH WÖLL — Institute of Functional Interfaces (IFG), Karlsruhe Institute of Technology (KIT), Hermann-von-Helmholtz-Platz 1, Eggenstein-Leopoldshafen, 76344, Germany

In the last decades, ceria-based systems have seen an increase in popularity, due to its unique redox behavior and catalytic characteristics. Ceria powders are widely used in exhaust catalysts as well as other catalytic cycles, in particular due to the cheap and simple preparation methods. To gain a better understanding of the chemical and structural behavior of ceria nanoparticles and their interaction with gaseous molecules, an operando DRIFTS study was carried out. Following the complete oxidation of the powder samples, they were introduced in a carbon monoxide atmosphere at room temperature. By tuning the pressure of carbon monoxide gas as well as the reaction temperature inside the catalytic cell it was possible to observe the reduction and structural changes of ceria, induced by the presence of carbon monoxide. Using operando DRIFTS with carbon monoxide as a reducing agent as well as a probe molecule, the chemical and structural changes of ceria can be easily investigated.

O 81.7 Thu 16:30 CHE 91

Tailoring photolytic reaction products by application of a low interacting rare gas decoupling layer — •INGA LANGGUTH¹, JULIEN ROWEN², WOLFRAM SANDER², and KARINA MORGENSTERN¹ — ¹Chair of Physical Chemistry I, Ruhr-Universität Bochum, Germany — ²Chair of Organic Chemistry II, Ruhr-Universität Bochum, Germany

While carbene molecules are known to be highly reactive and short living reactants in gas phase, they are passivated on metal surfaces upon chemisorption. Thin solid rare gas films on coinage metal surfaces are a novel type of decoupling layer applicable for STM investigations. Thus, it is taken advantage of the low interacting chemical environment of xenon (Xe) monolayer on Ag(110) in order to investigate the photolytic reactions of classical carbenes. The reaction products of the carbene coupling formed on the Xe layer adsorbed on the metal are straightforwardly accessed by subsequent Xe desorption. Vast structural differences reveal that the reaction products formed on the Xe substantially differ from the species formed under the same conditions on the metal surface. Both reaction products are compared, revealing the tool function of the non-ionic, low interacting rare gas decoupling layer for tailoring reaction pathways.

O 81.8 Thu 16:45 CHE 91

Methanol and water compete for the same adsorption sites on In₂O₃(111) — CHIARA WAGNER¹, ANDREAS ZIEGLER², MICHAEL SCHMID¹, BERND MEYER², ULRIKE DIEBOLD¹, and •MARGARETA WAGNER¹ — ¹Institute of Applied Physics, TU Wien, Austria — ²Interdisciplinary Center for Molecular Materials and Computer Chemistry Center, FAU Erlangen-Nürnberg, Germany

Indium oxide, a transparent conductive oxide, has been discovered to be a highly selective catalyst for methanol synthesis by CO₂ hydrogenation. The large surface unit cell of In₂O₃(111) exhibits a variety of Lewis acid and base sites for methanol and water adsorption. We compare the adsorption of both molecules under UHV conditions by employing AFM, STM, XPS, and TPD, together with DFT calculations. For medium coverages up to 9 molecules per surface unit cell we find a similar behavior: Initially, at room temperature, both molecules dissociate and protonate the most reactive O sites of the unit cell. When both molecules are dosed consecutively, methanol readily replaces water, while water is less efficient to substitute methanol. Below 300 K, both methanol and water adsorb molecularly in less-favored regions of the unit cell, still occupying the same sites and thus forming the same structural motifs. However, at coverages beyond 9 molecules per unit cell significant difference are found due to the ability of water to form and receive two hydrogen bonds instead of only one in the case of methanol.

O 81.9 Thu 17:00 CHE 91

How the (2x1) Reconstruction of Calcite (10.4) dominates the Desorption Kinetics of Water and Ethanol — •TOBIAS DICKBREDER¹, DIRK LAUTNER², ANTONIA KÖHLER¹, LEA KLAUSFERING¹, RALF BECHSTEIN¹, and ANGELIKA KÜHNLE¹ — ¹Physical Chemistry I, Bielefeld University, 33615 Bielefeld, Germany. — ²Institute of Physical Chemistry, Johannes Gutenberg University Mainz, Duesbergweg 10-14, 55099 Mainz, Germany.

Calcite, the most abundant carbonate mineral in the Earth's crust, plays a dominant role in a variety of environmental processes. Upon cleavage, calcite exposes the (10.4) cleavage plane with a rectangular unit cell. Interestingly, several experiments have been presented that suggest a (2x1) surface reconstruction. However, clear experimental evidence and a theoretical confirmation were long missing. Recently, an atomic force microscopy study provided convincing experimental indication for a (2x1) reconstruction at 5 K. Nevertheless, it remained unclear how the (2x1) reconstruction affects the surface properties of calcite.

Here, we present temperature-programmed desorption (TPD) curves of water and ethanol desorbing from calcite (10.4) around room temperature. Our experiments can be excellently described by a kinetic model considering two different adsorption positions, as would be present in case of a (2x1) reconstruction. This finding applies to the desorption of water and ethanol, suggesting that the effect is not molecule specific, but characteristic for the calcite cleavage plane. Our results, thus, demonstrate that the (2x1) reconstruction has significant impact on the interfacial properties of calcite.

O 81.10 Thu 17:15 CHE 91

Identification of Intermediates in the Reaction Pathway of SO₂ on the CaO surface: From Physisorption to Sulfite to Sulfate — •NILS SCHEWE¹, FARAHNAZ MALEKI², GIOVANNI DI LIBERTO², HICHAM IDRIS¹, GIANFRANCO PACCHIONI², and CHRISTOPH WÖLL¹ — ¹Institute of Functional Interfaces (IFG), Karlsruhe Institute of Technology (KIT), Hermann-von-Helmholtz-Platz 1, Eggenstein-Leopoldshafen, 76344, Germany — ²Department of Materials Science, University of Milano-Bicocca, 20125 Milano, Italy

We report on the results of a combined experimental and theoretical study of the interaction of sulfur dioxide with a calcium oxide single crystal surface. Our investigation of this model system for flue gas desulfurization was carried out on the CaO (001) surface under ultra-high-vacuum conditions. Combining UHV infrared reflection absorption spectroscopy (IRRAS) with x-ray photo electron spectroscopy (XPS) and ab initio density functional theory (DFT) calculations, we were able to identify a three-step reaction path way. After the physisorption of SO₂ at temperatures below 70 K on the ubiquitously hydroxylated surface, increasing the temperature leads to insertion of the SO₂ into surface hydroxyl groups. Around 110 K the first insertion leads to a surface hydrogen-sulfite, which evolves into a surface hydrogen-sulfate with the second insertion into another OH-group above 160 K. The surface state was confirmed by DFT, where the predicted IR vibrational frequencies align with the experimentally observed ones.

O 81.11 Thu 17:30 CHE 91

Interaction and structural behavior of thymidine on polycrystalline cerium oxide films — •SASCHA MEHL¹, ANASTASIA DEINEKO², VIACHESLAV KALINOVYCH², TOMÁŠ SKÁLA², IVA MATOLINOVÁ², VLADIMÍR MATOLÍN², KEVIN C. PRINCE¹, and NATALIYA TSUD² — ¹Elettra-Sincrotrone Trieste S.C.p.A., in Area Science Park, Strada Statale 14, km 163.5, Basovizza (Trieste), 34149, Italy — ²Charles University, Faculty of Mathematics and Physics, Department of Surface and Plasma Science, V Holešovičkách 2, Prague, 18000, Czech Republic

Thymidine (dT) is a nucleoside and therefore important for the contribution to in-depth studies of cerium oxide as a potential sensing material applicable for analyses such as DNA. This topic contributes to a survey which embraces from simple nucleobases to more complex DNA components as probe molecules on a wide array of different CeO₂ films. Consequently, bridging the material gap and deposition of dT from aqueous solution on compact CeO₂ allows us to get closer towards more realistic conditions. The goals of the present study were the elucidation of the electronic structure of the biomolecule-cerium oxide interface, as well as the adsorption geometry and thermal stability of the nucleoside. Adsorption studies were carried out by using SRPES, RPES and NEXAFS techniques. A noteworthy result was the successful deposition of dT from solution and in gas phase without decomposition, which was never previously reported in the literature. The analysis of the experimental data revealed that dT molecules anchor on CeO₂ film via two carbonyl oxygen atoms and an amino group.

O 81.12 Thu 17:45 CHE 91

Modeling Bio-MOFs for Anesthetic Xenon Recovery: The Role of Noncovalent Host-Guest Interactions — •YELIZ GURDAL — Lehrstuhl für Theoretische Chemie II, Ruhr-Universität Bochum, 44780 Bochum, Germany — Research Center Chemical Sciences and Sustainability, Research Alliance Ruhr, 44780 Bochum, Germany — Department of Bioengineering, Adana Alparslan Türkeş Science and Technology University, 01250 Adana, Türkiye

Taking advantage of metal organic frameworks (MOFs) for anesthetic Xe recovery has been a recent topic studied rarely in the literature. In this work, Xe recovery performances of 43 biological MOFs (Bio-MOFs) consisting of biocompatible cations and linkers have been studied by means of Grand Canonical Monte Carlo, Density Functional Theory, and Molecular Dynamics simulations. Results reveal that Xe-host interactions are maximized mainly due to noncovalent interactions of Xe, such as charge-induced dipole and aerogen- π interactions. Polarized Xe atoms in the vicinity of cations/anions as well as π systems suggest enhanced guest-host interactions. The results of this work depict examples of superficially studied aerogen interactions playing an important role in selective adsorption of Xe in porous materials. This study has received funding from the TUBITAK under the 1002 Short Term R&D Funding Program (grant agreement No: 120Z160).

O 82: Graphene I: Adsorption, Intercalation and Doping

Time: Thursday 15:00–17:15

Location: GER 37

O 82.1 Thu 15:00 GER 37

Graphene quantum dot nanoarray in a van der Waals heterostructure — •KEDA JIN^{1,2,3}, JUNTING ZHAO^{1,2,3}, TOBIAS WICHMANN^{1,3,4}, F. STEFAN TAUTZ^{1,3,4}, JOSE MARTINEZ-CASTRO^{1,3}, MARKUS TERNES^{1,2,3}, and FELIX LÜPKE^{1,3} — ¹Peter Grünberg Institut (PGI-3), Forschungszentrum Jülich, 52425 Jülich, Germany. — ²Institut für Experimentalphysik II B, RWTH Aachen, 52074 Aachen, Germany. — ³Jülich Aachen Research Alliance (JARA), Fundamentals of Future Information Technology, 52425 Jülich, Germany. — ⁴Institut für Experimentalphysik IV A, RWTH Aachen, 52074 Aachen, Germany.

Graphene quantum dots (GQDs) are promising candidates for spin qubits because of their long spin coherence and short switching time. Although isolated GQDs have been created in van der Waals (vdW) heterostructures, the fabrication of GQD nanoarrays is still an ongoing challenge. Here, we realize a regular two-dimensional array of GQDs in a vdW heterostructure composed of graphene on a single layer of 1T-NbSe₂ on top of 2H-NbSe₂ (Gr/1T/2H-NbSe₂) by combining mechanically assembled vdW heterostructures and nanoscale phase engineering. Using scanning tunneling microscopy (STM) and non-contact atomic force microscopy (nc-AFM), we demonstrate that the 1T-NbSe₂ phase periodically dopes the graphene layer, which in response exhibits quantized charge states that can be manipulated by the local electric field of the tip. Our findings show a possible route for the creation of a highly dense GQD nanoarray with a potential application in the quantum technologies.

O 82.2 Thu 15:15 GER 37

Sn-induced superstructures at the EG/SiC(0001) interface and their influence on EG — •ZAMIN MAMIYEV, CHITRAN GHOSAL, and CHRISTOPH TEGENKAMP — Institut für Physik, Technische Universität Chemnitz

Intercalating chemical elements into the buffer layer/SiC(0001) interface is a promising approach to delaminate a single carbon layer forming extended epitaxial graphene (EG) layers with new properties. In this regard, Sn is an interesting candidate because the triangular monolayer structure on SiC(0001) was shown to exhibit a Mott state [1].

By means of low energy electron diffraction we studied recently in detail the intercalation of Sn below the buffer layer grown before on SiC(0001) and found 1×1 and ($\sqrt{3}\times\sqrt{3}$) Sn induced phases depending on details of the annealing procedure [2]. As deduced from transport but also local spectroscopy, the former is metallic while the latter reveals a band gap opening. In addition, we found a ($\sqrt{3}\times\sqrt{3}$)R30° interference pattern with respect to the EG lattice. This so-called broken Kekulé order forms due to the breaking of the bond order in EG and often found in the vicinity of buckled Sn(1×1) subsurface clusters opening the channel for K,K' scattering in EG. The electronic structure and, in particular, the formation of a Mott gap will be investigated by electron energy loss spectroscopy.

[1] S. Glass et al., PRL 114, 247602 (2015). [2] Z. Mamiyev and C. Tegenkamp, Surf. & Int. 34, 102304 (2022).

O 82.3 Thu 15:30 GER 37

Stabilizing high-overlap organic crystals by n-doped graphene — •FABIO CALCINELLI and OLIVER HOFMANN — Graz University of Technology, Graz, Austria

Organic thin-films are known for their tuneable properties, which are strongly dependent on the polymorph the films assume. Traditional ab-initio studies of thin films geometries remain computationally prohibitive, due to the immense number of possible configurations, and this results in the need for structure-property relationships to help in the design of materials with certain target properties.

In this contribution, we examine the correlation between the energy of polymorphs and their interlayer LUMO-LUMO overlap for benzoquinone on n-doped graphene. Employing smart-data machine learning, we use a small number of DFT calculations to predict the energy and the LUMO-LUMO overlap for a large sample of polymorphs. We assess the impact of the n-doping of the substrate on this overlap/stability relationship by performing the energy and overlap evaluation for different intensities of n-doping.

We find that, for low dopant concentrations, there exists no relationship between interlayer overlap and stability, while for high dopant concentrations, it appears that polymorphs with high LUMO-LUMO overlap are predominant in the stability ranking. We explain this different behavior as the consequence of charge transfer from the substrate to the first molecular layer producing different LUMO occupations for different dopant concentrations, resulting in a stabilizing effect of high LUMO-LUMO overlap for high concentrations only.

O 82.4 Thu 15:45 GER 37

Theoretical studies of nitrogen-doped corrugated graphene on metal supports — •IVAN ABILIO¹ and KRISZTIÁN PALOTÁS^{1,2} — ¹Wigner Research Center for Physics, Budapest, Hungary — ²ELKH-SZTE Reaction Kinetics and Surface Chemistry Research Group, Szeged, Hungary

For maximizing the usability of N-doped graphene materials, the microscopic understanding of their structures (graphitic, pyridinic, pyrrolic, etc) and electronic properties at the atomic scale is crucial. Motivated by this, density functional theory calculations of N-doping configurations in corrugated graphene single layers on Ir(111) and Ru(0001) substrates were performed. Taking systematically selected N-doped graphene defect configurations, their energetic preference is found to be correlated with their atomic structure. Scanning tunneling microscopy simulations with different tip models [1] were performed, and a great variety of STM image contrasts showed a good agreement with experimental STM images. The negatively charged N atoms embedded into the corrugated graphene layer suggest single atom catalytic potential for these structures.

Financial support from NKFI OTKA 124100 & 138714, the János Bolyai Research Grant of the Hungarian Academy of Sciences (BO/292/21/11), the New National Excellence Program of the Ministry for Culture and Innovation from NKFI Fund (ÚNKP-22-5-BME-282) and the Stipendium Hungaricum Scholarship is gratefully acknowledged.

[1] G. Mándi and K. Palotás, Phys. Rev. B 91, 165406 (2015).

O 82.5 Thu 16:00 GER 37

Rechargeable model of AlF₃ intercalated aggregates on HOPG surfaces for rechargeable battery applications — •SINDY RODRÍGUEZ SOTELO^{1,2}, ADRIANA CANDIA¹, IGOR STANKOVIĆ³, MARIO PASSEGGI JR.^{1,2}, and GUSTAVO RUANO⁴ — ¹IFIS, CONICET-UNL, Santa Fe, Argentina — ²FIQ, UNL, Santa Fe, Argentina — ³Scientific Computing Laboratory, Center for the Study of Complex Systems, IPB, Belgrade, Serbia — ⁴CAB, CNEA, Bariloche, Argentina

Rechargeable batteries based on ion intercalation are currently of great interest, with lithium being the most studied and with the best performance. However, the limited reserves of this material and its scarce distribution in the world have led to the research for new alternatives. In our recent work, we studied the intercalation of AlF₃ in HOPG as a new possibility to use this molecule in rechargeable batteries and to understand its role when used as a solvent component [1,2]. Based on our recent reports, in this work we theoretically and experimentally characterize the dynamics of the AlF₃ interlayers, to discuss the possibility of decoupling the first graphene layers from the HOPG under ultra-high vacuum conditions. We show experimental measurements performed by STM, XPS and AES, also proposing a model to glimpse the growth and behavior of AlF₃ in the surface layers of the HOPG substrate, to provide clarity regarding the formation of the AlF₃/HOPG interface. We complement the analysis with calculations in the formalism of DFT and molecular dynamics (MD). **References** [1] A.E. Candia *et al.* Carbon, 186 (2022) 724. [2] Rodríguez *et al.* Phys. Chem. Chem. Phys., 23 (2021), 19579.

O 82.6 Thu 16:15 GER 37

Atomic and electronic structure of intercalated Pb layers in proximity to epitaxial graphene — •CHITRAN GHOSAL, MARKUS GRUSCHWITZ, JULIAN KOCH, and CHRISTOPH TEGENKAMP — Institut für Physik, TU Chemnitz, Chemnitz, Germany

Selective intercalation into the buffer layer/SiC(0001) interface can realize atomically sharp interface layers near epitaxial graphene that resemble novel 2D heterosystems. High-Z elements are interesting candidates, not only because they are expected to host Dirac fermions, but also because spin effects are expected in graphene.

Intercalation of Pb leads to the formation of different phases, which we have studied in detail using scanning tunneling microscopy. As recently shown, intercalated Pb bilayers form nanostripes under graphene and show fingerprints of plumbene. These Pb layers are rotated with respect to graphene, which breaks the sublattice symmetry and is associated with an electronic gap in graphene [1]. Hexagonally arranged bubble-like structures with an average size of 2.3 nm were also found. Scanning tunneling spectroscopy (STS) again revealed the formation of mini-gaps in the 2D heterosystem. Spatially resolved mapping of the electronic structure also clearly showed the existence of a network of edge states around the edges of the bubbles.

[1] C. Ghosal et al., PRL 129, 116802 (2022)

O 82.7 Thu 16:30 GER 37

Tailoring permanent carrier density in epitaxial graphene by F4-TCNQ molecular doping for quantum Hall resistance standards — •YEFEI YIN, ATASI CHATTERJEE, DAVOOD MOMENI, MATTIAS KRUSKOPF, MARTIN GÖTZ, STEFAN WUNDRACK, FRANK HOHLS, KLAUS PIERZ, and HANS WERNER SCHUMACHER — Physikalisch-Technische Bundesanstalt, Bundesallee 100, 38116 Braunschweig, Germany

A prerequisite for the development of graphene electronics is the reliable control of its carrier density. Since epi-graphene on SiC already exhibits a high electron density of up to 10^{13} cm⁻², the goal is a controlled reduction towards the charge-neutrality point. This was achieved by molecular doping with the ac-

ceptor F4-TCNQ doping stacks deposited on graphene. By precise adjustment of the dopant concentration and controlling the initial carrier density of the undoped graphene, we can tune the carrier density in a wide range from intrinsic n- to the p-type. Precision measurements of the quantum Hall resistance show a quantization accuracy of 10^{-9} which underlines the high quality and suitability of this doping method for electronic device application in metrology. [1] Our data show a correlation between the electron density and the onset of the $i = 2$ quantum Hall plateau which gives a valuable criterion for evaluating graphene-based resistance standards since the *classical* relation ($n = ieB/h$) to determine the centre of the quantum Hall plateau is not valid in epi-graphene. The results are discussed in the charge transfer model. [1] Y.Yin et al., Adv. Physics Res. 2022, DOI: 10.1002/apxr.202200015.

O 82.8 Thu 16:45 GER 37

Transport properties of intercalated epitaxial graphene — •MARKUS GRUSCHWITZ, ZAMIN MAMIYEV, CHITRAN GHOSAL, SUSANNE WOLFF, THOMAS SEYLLER, and CHRISTOPH TEGENKAMP — Institut für Physik, TU Chemnitz, Chemnitz, Germany

Large-scale growth and electronic manipulation of graphene are of great interest for nanoelectronics applications. The former is already realized by epitaxial growth and intercalation of buffer layers on SiC(0001). Electronic properties such as doping level and gap opening of the decoupled graphene layer strongly depend on the element and the structure of the interface. In this study we investigated Sn, Bi and In intercalated graphene by means of nanoscopic transport, supplemented by STM, LEED and PES. Depending on the film thickness and temperature, (1x1) phases can be formed with all three elements, accompanied by the formation of free-standing graphene. The fully intercalated phases show metallic conductivity behavior ($\sigma_{\text{Sn}}=0.63 \text{ mS}/\square$, $\sigma_{\text{Bi}}=0.74 \text{ mS}/\square$). The slightly lower conductivity of 10% compared to clean MLG is most likely due to interface scattering rather than different doping levels of the EG. Further heating allows the forma-

tion of $\sqrt{3}$ -structures for all intercalants. Thereby, the conductivities drop by 2-3 orders of magnitude, accompanied by an increase of the anisotropy with respect to SiC step structure. This is indicative of inhomogeneous desorption especially around the step edges. The detailed analysis with the variable range hopping model yield localization lengths that correlate with the size of intercalated areas.

O 82.9 Thu 17:00 GER 37

Magnetotransport and structural properties of Bi(110) islands on epitaxial graphene — •JULIAN KOCH¹, SERGI SOLOGUB^{1,2}, CHITRAN GHOSAL¹, and CHRISTOPH TEGENKAMP¹ — ¹Institut für Physik, TU Chemnitz, Reichenhainerstr. 70, 09126 Chemnitz — ²Institute of Physics, NAS of Ukraine, Nauki avenue 46, 03028 Kyiv

Magnetotransport measurements at 10 K using a 4 T magnet were performed on Bi islands on monolayer graphene/SiC with average thickness up to 3.6 bilayers (BL). They are supported by structural investigations using SPA-LEED and STM, which reveal that Bi predominately grows as needle-like islands with a (110) termination.

The analysis of the magneto and Hall conductivity gives the electron concentration and the mobility. The electron concentration slightly decreases with $4 \cdot 10^{11} \text{ cm}^{-2} \text{ BL}^{-1}$ from an initial value of $1.4 \cdot 10^{13} \text{ cm}^{-2}$ for the clean surface. The mobility decreases from $2100 \text{ cm}^2 \text{ V}^{-1} \text{ s}^{-1}$ to a minimal value of $1630 \text{ cm}^2 \text{ V}^{-1} \text{ s}^{-1}$ at 2.4 BL. Moreover, the electron electron interaction contribution to the magneto conductivity, which is almost negligible for the clean surface, strongly increases linearly with approximately $0.44 \text{ mS}/\text{BL}$. At 3.6 BL it is equal to approximately half the Drude conductivity at zero field.

The weak localization (WL) of the clean surface gradually transitions to weak anti-localization (WAL) with increasing Bi coverage. This is associated with a decrease of the dephasing length of the scattered electrons, which is correlated with the average distance of the islands obtained from STM measurements.

O 83: Focus Session: Ultrafast Dynamics in Nanostructures II

Time: Thursday 15:00–17:30

Location: GER 38

Topical Talk

O 83.1 Thu 15:00 GER 38

Imaging ultrafast electron dynamics in isolated nanoparticles — •DANIELA RUPP — LFKE, ETH Zurich, Switzerland

Atomic clusters and nanodroplets are used as ideal model systems over all wavelength regimes for exploring the ultrafast physical processes underlying the formation and evolution of highly excited matter. Via single-pulse single-particle coherent diffractive imaging (CDI) with the intense femtosecond pulses from short-wavelength free electron lasers (X-FELs), it became possible to study single specimen in free flight.

In CDI, the elastically scattered light forms an interference pattern that encodes the particle's structure, allowing to investigate the morphology of fragile and short-lived specimen. Also light-induced dynamics after pulsed laser excitation can be visualized by time-resolved CDI. Even changes in the electronic properties were found to be imprinted in the CDI patterns, but their time-evolution could not be investigated with typical pulse durations of 100 femtoseconds.

We recently showed that, under favorable conditions, single helium nanodroplets can be also imaged with an intense HHG source, providing much shorter pulses. In time-resolved experiments, a moderately intense near-infrared (NIR) laser pulse, too weak to ionize helium nanodroplets, dramatically changed their scattering response in the extreme ultraviolet (XUV) regime. The ability to switch the optical properties of nanoscale matter within less than a femtosecond, and observe this temporally and spatially resolved, promise to impact a broad field of science from non-linear XUV optics to ultrafast material science.

O 83.2 Thu 15:30 GER 38

Sub-picosecond Elastic Response of a supported Pd Nanoparticle Ensemble studied by Time-resolved X-ray Diffraction — SIMON CHUNG¹, THORBEN EGGERT², •VEDRAN VONK¹, NASTASIA MUKHAROMOVA¹, SEBASTIAN MATERA², ROMAN SHAYDUK³, JOHANNES MOELLER³, NILS SCHEWE⁴, ERIC SAUTER², CHRISTOPH SCHREUER², ANDERS MADSEN³, KARSTEN REUTER², and ANDREAS STIERLE¹ — ¹CXNS - Centre for X-ray and Nanoscience, Deutsches Elektronen-Synchrotron DESY, Hamburg, Germany — ²Theory Department, Fritz-Haber-Institut der Max-Planck-Gesellschaft, Faradayweg 4-6t, Berlin, 10587, Germany. — ³European X-Ray Free-Electron Laser Facility GmbH, Holzkoppel 4, Schenefeld, 22869, Germany. — ⁴Institute of Functional Interfaces (IFG), Karlsruher Institut für Technologie (KIT), Hermann-von-Helmholtz-Platz 1, Eggenstein-Leopoldshafen, 76344, Germany.

We report on the results of a combined experimental and theoretical study of the structural response of a Pd nanoparticle ensemble upon fs-laser excitation. Time-resolved X-ray diffraction experiments, having a time resolution of approx. 100 fs, were performed at end-station MID of the European X-ray Free Electron Laser (XFEL). Molecular dynamics simulations were done taking explicitly into

account the particle size distribution, as determined from SEM. The results are interpreted in terms of the dephasing of size-dependent elastic modes and picosecond energy dissipation of the nanoparticle ensemble towards the MgO single crystal support. An overview will be given about the experimental details, data analysis and molecular dynamics simulations.

O 83.3 Thu 15:45 GER 38

Description of High Harmonic Generation in Quantum Dots using a Tight-Binding approach — •MARTIN THÜMMER¹, ALEXANDER CROY¹, STEFANIE GRÄFE¹, and ULF PESCHEL² — ¹Institute of Physical Chemistry, University of Jena — ²Institute of Condensed Matter Theory and Optics, University of Jena

Recently, high harmonic generation (HHG) was experimentally observed in quantum dots showing striking differences compared to HHG in molecules and bulk materials. At the same time, the available theoretical tools (like semiconductor Bloch-equations and real-time density-functional theory (DFT)) have proven to be insufficient to describe the size dependence of the nonlinear response of these nanostructures. Here, we present a computationally feasible, real-space tight-binding method to account for the description of inter- and intraband harmonics, and ionization effects, while all model parameters are derived from DFT calculations. Inspired by recent experiments, we present first simulation results of HHG in 3D CdSe quantum dots for linear and elliptic polarization of the driving laser.

O 83.4 Thu 16:00 GER 38

Imaging of femtosecond spin dynamics at the nanoscale — •SERGEY ZAYKO^{1,4}, HUNG-TZU CHANG¹, OFER KEIR², TIMO SCHMIDT³, JAKOB HAGEN¹, MICHAEL HEIGL³, MURAT SIVIS^{1,4}, MANFRED ALBRECHT³, and CLAUS ROPERS^{1,4} — ¹Max Planck Institute for Multidisciplinary Sciences, Göttingen, Germany — ²School of Electrical Engineering, Tel Aviv University, Tel Aviv, Israel — ³Experimental Physics IV, Institute for Physics, University of Augsburg, Germany — ⁴IV Physical Institute, Solids and Nanostructures, Georg-August University

Femtosecond pulse durations combined with broad extreme-UV spectrum inherent to high harmonic generation (HHG) grant spectroscopic access to various material properties and phenomena including charge, spin and lattice dynamics. Here, we extend the applicability of HHG sources to direct real-space imaging of ultrafast processes. Specifically, we map femtosecond spin dynamics induced by optical excitations ferro- and ferrimagnetic materials. Our results demonstrate the first implementation of HHG radiation for element specific imaging as well as the first real-space imaging of femtosecond dynamics. Moreover, the achieved spatio-temporal resolution (down to 13.5 nm spatial and 15 fs temporal) is more than an order of magnitude higher than any magneto-optical imaging scheme reported so far, which would facilitate deeper fundamental understanding and, in

particular, support application-oriented studies. Notably, the developed imaging scheme is directly applicable to a broad range of phenomena including transient absorption and structural phase transitions.

Topical Talk

O 83.5 Thu 16:15 GER 38

Ultrafast coherent manipulation of free electrons via quantum interaction with shaped optical fields — •GIOVANNI MARIA VANACORE — Department of Materials Science, University of Milano-Bicocca, Via Cozzi 55, 20126 Milano

The interaction between light and electrons can be exploited for generating radiation, or for controlling electron beams for dynamical investigation of materials, enabling new applications in quantum technologies and microscopy. In this contribution, I will describe an innovative method for coherent and versatile longitudinal/transverse manipulation of a free-electron wave function. Using appropriately shaped light fields in space and time, I will demonstrate how to modulate the energy, linear and orbital angular momenta, as well as spatial and temporal distributions of the electron wave function. The experiments have been performed in an ultrafast-TEM, where a pulsed electron beam was made to interact with shaped optical field generated via a spatial light modulator. The energy-momentum exchange resulting from such interaction was directly mapped via momentum-resolved ultrafast electron energy-loss spectroscopy. Our approach for arbitrary longitudinal/transverse electron modulation at the sub-fs timescale would pave the way to achieve unprecedented insights into non-equilibrium phenomena in advanced quantum materials, playing a decisive role in the rational design and engineering of future photonics and electronics application.

Funding source: SMART-electron project that has received funding from the EU Horizon 2020 Programme under GA No 964591.

O 83.6 Thu 16:45 GER 38

Structural Dynamics in Nanostructured Systems Probed by Ultrafast Transmission Electron Microscopy — •NORA BACH¹, ARMIN FEIST², MARCEL MÖLLER², CLAUS ROPERS², and SASCHA SCHÄFER¹ — ¹Institute of Physics, University of Oldenburg, Germany — ²Max Planck Institute for Multidisciplinary Sciences, Göttingen, Germany

One successful approach to investigate ultrafast nanoscale structural dynamics and to disentangle different excitation mechanisms in spatially inhomogeneous systems is based on local diffractive probing with nano-focused femtosecond electron pulses in an ultrafast transmission electron microscope (UTEM). Employing the Göttingen UTEM [1,2] in ultrafast convergent electron beam diffraction (U-CBED) mode [3], we study local dynamics in a multi-component model system consisting of a metal/semiconductor hybrid structure. Ultrashort optical excitation of a platinum stripe on a silicon membrane results in the generation of a multi-modal distortion wave propagating through the membrane. Pronounced lattice distortions are quantitatively tracked by U-CBED, and experimental results are reproduced by numerical simulations demonstrating that a superposition of Lamb waves at resonance frequencies of the bilayer structure [4] governs the evolution of the displacement inhomogeneity within the depth of the membrane.

[1] A. Feist, N. Bach, et al., *Ultramicroscopy* 176, 63 (2017).

[2] N. Bach et al., *Struct. Dynamics* 6, 014301 (2019).

[3] A. Feist et al., *Struct. Dynamics* 5, 014302 (2018).

[4] N. Bach et al., *Struct. Dynamics* 8, 035101 (2021).

O 83.7 Thu 17:00 GER 38

Controlling and shaping the electron recoil and energy transfer via nearfield geometry — •FATEMEH CHAHSHOURI¹ and NAHID TALEBI^{1,2} — ¹Institute of Experimental and Applied Physics, Kiel University, 24098 Kiel, Germany — ²Kiel, Nano, Surface, and Interface Science, KiNSIS, Kiel University, 24098 Kiel, Germany

Inelastic interaction of free-electrons with optical near fields has recently attracted attention for manipulating and shaping free-electron wave packets. Understanding the nature and the dependence of the inelastic cross section on the polarization of the optical near-field modes of the nanostructures is important for both fundamental studies and the development of new applications in this field. Here, we investigate the effect of the laser-field polarization and nanostructures asymmetric geometry on shaping free-electrons and controlling the energy transfer mechanisms, but also tailoring the electron recoil. We show that, an oblique incident electric field improves the coupling efficiency for coherent control of the longitudinal and transversal phase modulation of an electron wave packet. We also demonstrate the possibility of tailoring the shape of the localized plasmons by incorporating specific arrangements of nanorods to enhance or hamper the transversal and longitudinal recoils of free-electrons. Our findings open up a route towards the spatial characterization of plasmonic near-fields for the coherent manipulation and control of slow electron beams for creating desired shapes of electron wave packets.

O 83.8 Thu 17:15 GER 38

Light-induced hexatic state in a layered quantum material — •TILL DOMRÖSE¹, THOMAS DANZ¹, SOPHIE F. SCHAIBLE², KAI ROSSNAGEL^{3,4}, SERGEY V. YALUNIN¹, and CLAUS ROPERS^{1,2} — ¹Max Planck Institute for Multidisciplinary Sciences, Göttingen, Germany — ²4th Physical Institute, University of Göttingen, Germany — ³Institute of Experimental and Applied Physics, Kiel University, Germany — ⁴Ruprecht Haensel Laboratory, DESY, Hamburg, Germany

Ultrafast transmission electron microscopy (UTEM) is a powerful technique for resolving non-equilibrium dynamics on the nanoscale, employing a stroboscopic laser pump/electron probe approach [1]. Here, we harness the high-coherence electron source of the Göttingen UTEM [2] in the investigation of a structural phase transition between two charge-density wave (CDW) phases in a layered material [3]. A three-dimensional reconstruction of the nascent CDW order by means of ultrafast tilt-series nanobeam diffraction allows us to identify a transient hexatic state in the early stages of the phase formation. As the optical excitation induces a loss of interlayer correlations, this two-dimensional intermediate is characterized by a high density of topological defects suppressing the translational symmetry, while the orientational order is weakly preserved. On longer timescales, defect recombination and the establishment of the equilibrium stacking sequence lead to the formation of the long-range ordered high-temperature CDW phase.

[1] A. H. Zewail, *Science* 328, 187-193 (2010).

[2] A. Feist et al., *Ultramicroscopy* 176, 63-73 (2017).

[3] T. Domröse et al., in Review, arXiv:2207.05571 [cond-mat.mtrl-sci]

O 84: Focus Session: Making Experimental Data F.A.I.R. – New Concepts for Research Data Management I (joint session O/TT)

Data have been identified as major resource of the 21st century, unlocking great potential if refined and processed in the right way. In scientific research, particularly modern data science concepts like machine learning or neural networks enable novel types of data analysis with often strong predictive power. This Focus Session aims at providing a framework for presenting and discussing novel concepts, tools and platforms for managing experimental research data related to surface science and solid-state physics. In particular, in light of the German NFDI initiative, where several consortia are actively working on tackling the imminent challenges of research data management in experimental solid-state physics, this Focus Session will offer an ideal environment for exchange among researchers, and bringing these novel developments into the labs. The intended topics include the description of experimental data and meta data generation workflows, meta data schemas and file formats, electronic lab notebooks, novel tools for handling and analyzing scientific research data, as well as sharing and searching platforms according to F.A.I.R. principles.

Organizers: Martin Aeschlimann (TU Kaiserslautern), Laurenz Rettig (FHI Berlin) and Heiko Weber (U Erlangen)

Time: Thursday 15:00–18:30

Location: WIL A317

Topical Talk

O 84.1 Thu 15:00 WIL A317

Introducing a FAIR research data management infrastructure for experimental condensed matter physics data — •CHRISTOPH KOCH — Humboldt-Universität zu Berlin, Department of Physics & IRIS Adlershof, Berlin, Germany

Digitization and an increase in complexity and price of experimental materials characterization techniques, an increase in accuracy and system size of computational solid state physics (or computational materials science), and the maturation of machine learning tools to extract patterns from large amounts of very

diverse (annotated) data promise an acceleration of materials development by synergistically combining research data from many sources. While some labs start to upload their (raw) research data to data repositories, this is only a first but not sufficient step in leveraging the above-mentioned potential, since such repositories are typically either specific to a very particular technique or agnostic to the content of the data being uploaded. In both cases the research data cannot easily, and definitely not without significant human effort, be compared to and integrated with experimental data from other sources, or numerical predictions. In this talk I will report on recent progress of the FAIRmat NFDI consortium in extending the novel materials discovery laboratory (NOMAD), the world's largest data base for ab-initio computational materials data, to ingest experimental research data on the synthesis and characterization of materials in a machine-accessible manner, i.e. annotated with well-defined and interoperable metadata, achieved by establishing links between related (experimental and computational) quantities.

O 84.2 Thu 15:30 WIL A317

Introducing an electronic laboratory notebook in a collaborative research center — •SEBASTIAN T. WEBER¹, ANETA DAXINGER¹, PHILIPP PIRRO¹, MAREK SMAGA¹, CHRISTIANE ZIEGLER¹, MATHIAS KLÄUI², GEORG VON FREYMAN¹, BAERBEL RETHFELD¹, and MARTIN AESCHLIMANN¹ — ¹Department of Physics and Research Center OPTIMAS, RPTU Kaiserslautern-Landau — ²Institute of Physics, Johannes Gutenberg University Mainz

The basis of a FAIR data management is a well-described and detailed documentation of every single step of the experiment and data analysis. In recent decades, however, the focus has shifted from analog measuring instruments and analytical calculations to computer-based experiments and simulations. This has led to a large increase in the numbers of measurements and observed quantities and therefore in the amount of data generated. Consequently, traditional paper lab notebooks have reached their limits. Electronic lab notebooks (ELNs) are better suited for storing, indexing, searching and retrieving a large amount of entries. In particular, the automated filling-in of meta data can lead to a reduction in the workload of the scientists in the long term.

We present the lessons learned on challenges and advantages with the introduction of a joint electronic lab notebook within our collaborative research center CRC/TRR173 *Spin+X*. We report on our experiences in the daily work of the scientists and in education in student labs.

O 84.3 Thu 15:45 WIL A317

An efficient workflow for processing single event dataframes. — •STEINN ÝMIR ÁGÚSTSSON¹, M. ZAIN SOHAIL^{2,3}, DAVID DOBLAS JIMÉNEZ⁴, DMYTRO KUTNYAKHOV³, and LAURENZ RETTIG⁵ — ¹Aarhus University, DK — ²RWTH, Aachen — ³DESY, Hamburg — ⁴Eu-XFEL, Schenefeld — ⁵FHI, Berlin

Single event resolved data streams measured by delay-line-detectors allow to correlate each measured photoelectron with the state of the experimental apparatus. This allows corrections and calibrations to be applied on a shot-to-shot basis and a flexible investigation of correlations between various measurement parameters.

We are developing an open-source python package[1], where highly optimized dataframe management and binning methods enable leveraging the full potential of event-resolved data structures. The flexible design of the pipeline allows processing any event-resolved data stream.

With momentum microscopy as the primary target application, we developed axis calibration and artifact correction methods designed to be agnostic to the experimental apparatus. These methods are tested on data generated by microscopes at FELs (HEXTOF@FLASH) as well as at HHG sources (FHI), but are easily extended to other end-stations using similar detection techniques.

Our aim is to provide tools for the community which will reduce the development time for each end station, as well as an open and accessible data processing pipeline, built around the FAIR data principles.

[1] github.com/openCOMPES/sed

O 84.4 Thu 16:00 WIL A317

FAIR Data Infrastructure for Computation: Advanced many-body methods. — •JOSÉ M. PIZARRO¹, NATHAN DAELMAN¹, JOSEPH F. RUDZINSKI^{1,2}, LUCA M. GHIRINGHELLI¹, ROSER VALENTI³, SILVANA BOTTI⁴, and CLAUDIA DRAXL¹ — ¹Institut für Physik und IRIS-Adlershof, Humboldt-Universität zu Berlin — ²Max-Planck-Institut für Polymer Forschung, Mainz — ³Institut für Theoretische Physik, Goethe University Frankfurt am Main — ⁴Institut für Festkörpertheorie und Optik, Friedrich-Schiller-Universität Jena

Big-data analyses and machine-learning approaches have recently emerged as a new paradigm to study and predict properties of materials. In order to perform these analyses, materials data have to be structured in a FAIR (findable, accessible, interoperable, and reusable) format [1]. While most of the current databases deal with density-functional-theory (DFT) calculations, there is a clear need for developing FAIR-data schema for methodologies going beyond DFT. Methods such as the GW approximation, dynamical mean-field theory, and time-dependent DFT allow to calculate excited- and many-body-states properties beyond DFT, thus having a direct quantitative comparison with experiments. In this talk, we will introduce the achievements and challenges undertaken within

the FAIRmat consortium towards fully structuring the (meta)data of all these techniques. We demonstrate how users can analyze the data and compare with angle-resolved photoemission spectroscopy.

[1] M. Scheffler et al., *Nature* **604**, 635 (2022).

O 84.5 Thu 16:15 WIL A317

Electronic Laboratory Notebooks for FAIR Data Management; Evaluation and Recommendations for Solutions at Research Infrastructures — •PHILIPP JORDT¹, WIEBKE LOHSTROH², and BRIDGET MURPHY¹ — ¹IEAP, Kiel University, Germany — ²MLZ, Technische Universität München, Germany

Electronic Laboratory Notebooks (ELN) are the digital counterpart to the classical handwritten paper notebook and play a vital role in the implementation of FAIR data standards. Modern ELN solutions range from simple note taking applications to integrated tools, combining documentation, inventory management, progress tracking and more. Nowadays, ELNs are becoming more prominent in research laboratories around the world, replacing paper notebooks. This evaluation of basic needs was carried out in the context of the DAPHNE4NFDI consortia. Of special interest is the view on ELNs for combined use at large scale facilities and in the home laboratory. Thus, the requirements regarding implementation, deployment, authentication, etc., may differ from those for single or laboratory use at universities. An overview of different concepts and existing solutions is given. Multiple ELNs have been evaluated during test runs at large scale facilities and a survey on existing solutions was held. From these results, a list of ELN specifications is presented, ranging from useful to necessary. These insights may serve as a guideline for evaluating or implementing ELNs in the future.

O 84.6 Thu 16:30 WIL A317

Ontology for Experimental Data — •SANDOR BROCKHAUSER — Center for Materials Science Data, Humboldt-Universität zu Berlin, Germany

Ontology is the scientific field of formal knowledge representation. This field contributes to Data Science and helps Experimentalist to properly annotate their data and metadata on a FAIR way. During the last decades several different ways have been developed in the field of Ontology for describing knowledge as a set of information and their relationships. These include Information mapping, Concept maps, Topic maps, Mind maps, Knowledge graphs, BORO (Business Objects Reference Ontology), RDF (Resource Description Framework), OWL (Web Ontology Language), ORO (Object-Role Modeling), UML (Unified Modeling Language), ISO 15926 (standard for data sharing), OLOG (mathematical framework for knowledge representation), GELLISH (ontology language for data storage and communication), etc. For describing experimental facts, we suggest using an ontology in OWL which is derived from the NeXus community standard. It represents all the concepts developed for explaining experiments and experimental data, just like the relationships between them. Such representation allows connecting the concepts defined in NeXus also to other ontologies. Additionally, any data management systems, like NOMAD which accepts experiment data provided in the NeXus standard, can immediately link the data and metadata to the ontology and make them interoperable.

15 min. break

Topical Talk

O 84.7 Thu 17:00 WIL A317

Open Research Data for Photons and Neutrons: Applications in surface scattering and machine learning — •LINUS PITHAN — Universität Tübingen, Institut für Angewandte Physik - DAPHNE4NFDI

Open (F.A.I.R.) research data is becoming a key ingredient for data driven machine learning (ML) applications that requires access to existing data of preceding experiments - which goes well beyond data collected in the context of one's own experiments which one might keep in a secret drawer. We will discuss current possibilities as well as future opportunities and challenges with special emphasis on surface scattering. Embedded in the DAPHNE4NFDI (Data from Photon and Neutron Experiments) consortium we present efforts on how data catalogs may serve as backbone for F.A.I.R. datasets provided by synchrotron and neutron sources or through community efforts. Besides suitable metadata collection also the harmonization of data- and metadata formats are issues still to be tackled especially for systematic access to fully analyzed, experimental datasets (e.g. by adopting NeXus community conventions). After a broader overview and shining light on the SciCat meta-data catalog system,[1] we discuss as application examples efforts in the field of reflectometry (XRR, NR) [2,3] and X-Ray scattering and diffraction (WAXS, GIWAXS and XPCS).[1,4]

[1] V. Starostin, L. Pithan et al. 2022, SRN, Vol. 35, No. 4

[2] A. Greco et al. 2022, J. Appl. Cryst. 55 362

[3] L. Pithan et al., Refl. dataset, 10.5281/zenodo.6497438

[4] V. Starostin et al. 2022, npj Comp. Mat. 8, 101

O 84.8 Thu 17:30 WIL A317

NOMAD OASIS as a Tool for Electron and Atom Probe Microscopists — •MARKUS KÜHBACH — Department of Physics, Humboldt-Universität zu Berlin, Germany

Embracing the FAIR principles for sharing data and knowing how to work with different tools in research data management systems is becoming an invaluable skill in a scientist's daily life. Embracing such systems of tools, one of which is offered with NOMAD OASIS, allows you to start organizing your research data locally. Learning such tools will train you to understand what schemes and electronic lab notebooks are and how the data and metadata are processed by these tools. Example implementations of specific workflows can give you ideas where to start from and how to customize these tools for the needs of your own research and colleagues. Thereby, you can provide feedback which supports the evolution and improvement of the research data management system.

NOMAD OASIS offers you many examples which show now also how data and metadata of specific experiments can be parsed into a standardized representation. These examples teach users through detailing how data can be entered, viewed, and organized with customizable schemes in NOMAD. Furthermore, the examples suggest strategies for how the information in NOMAD can be accessed for generic or domain-specific data analytics tools.

In my talk, I will go through one or two of these examples specific to electron microscopy (orientation imaging microscopy or spectroscopy).

O 84.9 Thu 17:45 WIL A317

FAIR Data Infrastructure for Computation: Introducing the parsers for Quantum Monte Carlo and ALF — •JONAS SCHWAB¹, JOSÉ M. PIZARRO², JEFFERSON STAFUSA E. PORTELA¹, LUCA M. GHIRINGHELLI², and FAKHER F. ASSAAD¹ — ¹Institut für Theoretische Physik und Astrophysik und Würzburg-Dresden Cluster of Excellence ct.qmat, Universität Würzburg, 97074 Würzburg, Germany — ²Institut für Physik und IRIS-Adlershof, Humboldt-Universität zu Berlin

DFT calculations lead to low-energy effective models. A modern example would be Kitaev types spin Hamiltonians for RuCl_3 . Once the model is specified, many different many-body calculations can be carried out. Here, we will concentrate on the ALF [1] implementation of the auxiliary field quantum Monte Carlo algorithm that can deal with general models that includes the ones produced by DFT calculations. Being a Monte Carlo method, the ALF library produces stochastic time series. We will discuss how to implement this workflow in the NOMAD Repository & Archive (<https://nomad-lab.eu>) and concentrate on a FAIR metadata scheme. The first challenges are to define the models in a searchable way as well as standards for the Monte Carlo time series. In this talk we will discuss the present state of this project for the special case of the ALF-library and how users can exploit the benefits of the NOMAD repository to find, compare and reuse our QMC data.

[1] F. F. Assaad et al., SciPost Phys. Codebases 1 (2022).

O 84.10 Thu 18:00 WIL A317

CAMELS - A Configurable Instrument Control Software for FAIR Data — •ALEXANDER FUCHS^{1,3}, JOHANNES LEHMEYER^{1,3}, MICHAEL KRIEGER^{1,3}, HEIKO B. WEBER^{1,3}, PATRICK OPPERMAN^{2,3}, and HEINZ JUNKES^{2,3} — ¹Lehrstuhl für Angewandte Physik, Friedrich-Alexander-Universität Erlangen-Nürnberg, — ²Fritz-Haber-Institut der Max-Planck-Gesellschaft (FHI), Berlin — ³FAIRmat, Humboldt-Universität zu Berlin, Berlin, Germany

We are developing a configurable measurement software (CAMELS), targeted towards the requirements of experimental solid-state physics. Here many experiments utilize a multitude of measurement devices used in dynamically changing setups. CAMELS [1] will allow to define instrument control and measurement protocols using a graphical user interface (GUI). This provides a low entry threshold enabling the creation of new measurement protocols without programming knowledge or a deeper understanding of device communication. The GUI generates python code that interfaces with instruments and allows users to modify the code for specific applications and implementations of arbitrary devices if necessary. Even large-scale, distributed systems can be implemented. CAMELS is well suited to generate FAIR-compliant output data. Nexus standards, immediate NOMAD integration and hence a FAIRmat compliant data pipeline can be readily implemented. [1] <https://github.com/FAU-LAP/CAMELS>

O 84.11 Thu 18:15 WIL A317

OpenSemanticLab: Usecase Device Repository — •MATTHIAS A. POPP and SIMON STIER — Fraunhofer ISC, Neunerplatz 2, 97082 Würzburg, Germany

Fully automated experiments provide benefits regarding precision, repeatability, as well as data quality and therefore gain more and more popularity. However, setting them up can be time consuming, especially when computer interface information has to be manually transferred from device manuals to software.

In order to implement FAIR principles precise descriptions of measurement setups and instrumentation are necessary. Currently, this results in extra workload for experimental scientists.

With our framework OpenSemanticLab, we address this shortcoming by providing a central metadata repository for scientific instruments. The ontology-based repository meets both human (GUI) and machine requirements (APIs). A device ontology helps finding and classifying devices. In an associated Python package, abstract device drivers and concrete device metadata can be combined into executable workflows. Overall, this approach not only strengthens the transparency of research according to FAIR principles, but also significantly reduces the implementation effort for complex setups.

O 85: Electronic Structure of Surfaces II

Time: Thursday 15:00–17:45

Location: REC C 213

O 85.1 Thu 15:00 REC C 213

Electronic structure of transition metal oxide surfaces from coincident electron spectroscopy — •DANILO KÜHN¹, SWARNSHIKHA SINHA^{1,2}, ARTUR BORN^{1,2}, FREDRIK O. L. JOHANSSON³, RUSLAN OVSYANNIKOV¹, NILS MÅRTENSSON³, and ALEXANDER FÖHLISCH^{1,2} — ¹Helmholtz-Zentrum Berlin für Materialien und Energie GmbH, Albert-Einstein-Strasse 15, 12489 Berlin, Germany — ²Institut für Physik und Astronomie, Universität Potsdam, Karl-Liebknecht-Strasse 24-25, 14476 Potsdam, Germany — ³Department of Physics and Astronomy, Uppsala University, P.O. Box 256, 751 05, Uppsala, Sweden

Transition metal oxides are a much studied class of materials with a wide range of applications, e.g. solar cells, batteries, magnetic storage devices, sensors or pigments. Varying charge localizations in the s,p and d valence shells and coupling between subsystems invoke complex electronic, magnetic and optical phases as high Tc superconductivity. Here, results from the new COESCA station for coincident electron spectroscopy at the BESSY II synchrotron will be presented [Leitner, T. et al. J. El. Spec. 250, 147075 (2021)]. Combining the high transmission and energy resolution of ARTOF time-of-flight spectrometers with the tailored time structure of BESSY II, Auger- Photoelectron coincidence spectroscopy (APECS) is possible with unprecedented information rate in the soft x-ray regime. Exploiting enhanced chemical selectivity and surface sensitivity, we gain insight into the excitation-decay dynamics and electron correlation effects in Ni, Cu and their oxides [Born, A. et al. Sci Rep 11, 16596 (2021)]

O 85.2 Thu 15:15 REC C 213

Black Phosphorus and the Free-Electron Final-State Assumption in Photoemission Spectroscopy — •CHARLOTTE SANDERS¹, KLARA VOLCKAERT², DEEPNARAYAN BISWAS³, MARCO BIANCHI², PHILIP HOFMANN², and IRENE AGUILERA⁴ — ¹Central Laser Facility, STFC Rutherford Appleton Lab, Research Complex @ Harwell, OX11 0QX, UK — ²Dept. of Physics and Astronomy, Interdisciplinary Nanoscience Center, Aarhus University, 8000 Aarhus-C, DK — ³Diamond Light Source, Division of Science, Didcot, OX11 0DE, UK —

⁴Institute for Theoretical Physics, University of Amsterdam, Science Park 904, 1098 XH, Amsterdam, NL

In the photoemission process, the in-plane component (k_x, k_y) of the electron wave vector is conserved; but the k_z component is not, due to breaking of out-of-plane symmetry at the surface. This fact complicates analysis of photoemission spectra from k_z -dispersing states.

Bulk black phosphorus has a k_z -dispersing state that has been the subject of several studies wherein photoemission intensity close to the Fermi level resists interpretation on the basis of simple free-electron-like final-state assumptions. Experimental spectra have been interpreted in terms of surface resonances, or of complexities in the final state that go beyond the free-electron assumption. Here we present experimental and theoretical results concerning the latter interpretation; and, we consider the fundamental meaning of the free-electron-like final-state.

O 85.3 Thu 15:30 REC C 213

Direct observation of antiferromagnetic parity violation in the electronic structure of Mn_2Au — •YARYNA LYTUVYENKO^{1,2}, OLENA FEDCHENKO¹, LIBOR ŠMEJKAL^{1,3}, MICHAEL KALLMAYER⁴, KATERINA MEDJANIK¹, SERGEY BABENKOV¹, DMITRY VASILYEV¹, MATHIAS KLÄUI¹, JURE DEMSAR¹, GERD SCHÖNHENSE¹, MARTIN JOURDAN¹, JAIRO SINOVA^{1,3}, and HANS-JOACHIM ELMERS¹ — ¹Institute of Physics, JGU Mainz — ²Institute of Magnetism of the NAS and MES of Ukraine — ³Institute of Physics Academy of Sciences of the Czech Republic — ⁴Surface Concept GmbH

Using time-of-flight momentum microscopy with a sub- μm spatial resolution (sub- μ -ToFMM), allowing for momentum-resolved photoemission on individual antiferromagnetic domains, we observe an asymmetry in the electronic band structure, $E(\mathbf{k}) \neq E(-\mathbf{k})$, in Mn_2Au . This broken band structure parity originates from the combined time and parity symmetry, PT, of the antiferromagnetic order of the Mn moments, in connection with spin-orbit coupling [1,2]. The spin-orbit interaction couples the broken parity to the Néel order parameter direction. We

demonstrate a novel tool to image the Néel vector direction by combining spatially resolved momentum microscopy with ab-initio calculations that correlate the broken parity with the Néel vector [3].

1. L. Smejkal et al., *Phys. Rev. Lett.* **118**, 106402 (2017)
2. H.-J. Elmers et al., *ACS Nano* **14**, 17554-64 (2020)
3. O. Fedchenko et al., *J. Phys.: Condens. Matter* **34**, 425501 (2022)

O 85.4 Thu 15:45 REC C 213

Impact of atomic defects in the electronic states of $\text{FeSe}_{1-x}\text{S}_x$ superconducting crystals — •YANINA FASANO^{1,2}, JAZMIN ARAGON SANCHEZ¹, MARIA LOURDES AMIGO¹, ESTEBAN GAYONE¹, and GLADYS NIEVA¹ — ¹Instituto Balseiro and Centro Atómico Bariloche, UnCuyo-CNEA, Argentina — ²Leibniz Institute for Solid State and Materials Research, Dresden, Germany

The electronic properties of Fe-based superconductors are drastically affected by deformations on their crystal structure introduced by doping and pressure. Here we study single crystals of $\text{FeSe}_{1-x}\text{S}_x$ and reveal that local crystal deformations such as atomic-scale defects impact the spectral shape of the electronic core level states of the material. By means of scanning tunneling microscopy we image S-doping induced defects as well as diluted dumbbell defects associated with Fe vacancies. We have access to the electronic structure of the samples by means of x-ray photoemission spectroscopy (XPS) and show that the spectral shape of the Se core levels can only be adequately described by considering a principal plus a minor component of the electronic states. We find this result for both pure and S-doped samples, irrespective that in the latter case the material presents extra crystal defects associated to doping with S atoms. We argue that the second component in our XPS spectra is associated with the ubiquitous dumbbell defects in FeSe that are known to entail a significant modification of the electronic clouds of surrounding atoms.

O 85.5 Thu 16:00 REC C 213

Double Photoemission Spectroscopy of C_{60} on $\text{SrTiO}_3(001)$ with Laser VUV radiation — •KATHRIN PLASS¹, ROBIN KAMRLA¹, FRANK O. SCHUMANN², and WOLF WIDRA¹ — ¹Institute of Physics, Martin-Luther-Universität Halle-Wittenberg, Halle (Saale), Germany — ²Max Planck Institute of Microstructure Physics, Halle (Saale), Germany

Via photoelectron spectroscopy, important insights into the electronic structure of solids were obtained. However, correlation effects can only be addressed indirectly. With double photoemission spectroscopy (DPE), such phenomena can be observed directly by detecting pairs of correlated photoelectrons emitted upon absorption of a single photon [1]. C_{60} is classified as a strongly correlated material with a highly structured valence band spectrum. Moreover, theory predicts the possibility of plasmon-mediated pair emission in C_{60} [2]. In this contribution we present DPE data for C_{60} thin films on $\text{SrTiO}_3(001)$, obtained by a laboratory high-order harmonic (HHG) light source, operating at an energy range from 14 to 40 eV and MHz repetition rates [3]. We analyze the 2D energy maps and compare the data to the SPE spectrum. In addition, we discuss plasmon-mediated DPE in fullerenes.

- [1] J. Berakdar et al., *Phys. Rev. Lett.* **81**, 3535 (1998)
- [2] Y. Pavlyukh et al., *Phys. Rev. B* **91**, 155116 (2015)
- [3] A. Trützscher et al., *Phys. Rev. Lett.* **118**, 136401 (2017)

O 85.6 Thu 16:15 REC C 213

Electronic structure at the "interface" of spin-orbit and exchange interaction: Ultrathin ferromagnetic films on $\text{W}(110)$ — •PASCAL JONA GRENZ¹, PETER KRÜGER¹, MARCEL HOLTSMANN¹, KOJI MIYAMOTO², SHIV KUMAR², TAICHI OKUDA², and MARKUS DONATH¹ — ¹WWU, Münster, Germany — ²HISOR, Hiroshima, Japan

Ultrathin ferromagnetic layers on $\text{W}(110)$ provide a suitable platform for investigating spin phenomena originating from the interplay of spin-orbit coupling (SOC) and exchange interaction (XC). First, we focus on the influence of ferromagnetic adlayers on the SOC-induced topologically non-trivial surface state (TSS) hosted by the $\text{W}(110)$ surface [1,2]. Our systematic angle-resolved photoemission study of thin Ni, Co, and Fe films and their influence on the TSS will be presented and discussed in view of conflicting literature results [3]. Second, the unoccupied electronic structure of thin Ni films on $\text{W}(110)$ is surveyed by spin- and angle-resolved inverse photoemission. By carefully choosing the Ni film's thickness, we tune the relative strength of SOC and XC. In such a way, SOC induces a degeneracy of Ni-related exchange-split states. Based on density functional theory, the strong interplay of SOC and XC is traced back to the hybridization of W and Ni states.

- [1] K. Miyamoto et al., *Phys. Rev. Lett.* **108**, 066808 (2012)
- [2] P.J. Grenz et al., *J. Phys.: Condens. Matter* **33**, 285504 (2021)
- [3] K. Honma et al., *Phys. Rev. Lett.* **115**, 266401 (2015)

O 85.7 Thu 16:30 REC C 213

Circular dichroism in angle-resolved photoemission from core-level emission of $\text{W}(110)$ — •TRUNG PHUC VO¹, OLENA TKACH^{2,3}, KATERINA MEDJANIK², OLENA FEDCHENKO², HANS-JOACHIM ELMERS², GERD SCHÖNHENSE², and JÁN MINÁR¹ — ¹New Technologies - Research Centre, University of West Bohemia,

301 00 Pilsen, Czech Republic — ²Institut für Physik, Johannes Gutenberg-Universität Mainz, Staudingerweg 7, D-55128 Mainz, Germany — ³Sumy State University, Rymyski-Korsakov 2, 40007 Sumy, Ukraine

Angle-resolved photoemission spectroscopy (ARPES) is a driving experimental technique for examining the electronic structure of quantum materials. There is another technique called X-ray photoelectron diffraction (XPD) which is considered to be the same thing as ARPES from an elementary point of view, specifically the angular distribution of photoelectrons emitted from a crystal surface. Nevertheless, the angular distribution of emitted electrons represents the momentum of initial states in ARPES meanwhile it reveals the interference of photoelectron waves from final states in XPD. At high photon energies, photoelectron diffraction (PED) effects are found in ARPES measurements beside other obstacles (e.g. non-negligible phonon scattering). Here, to disentangle these diffraction influences, we present a PED implement for SPRKKR package which makes use of multiple scattering theory and one-step model in photoemission process. For the sake of applications, we have calculated the circular dichroism in angular distributions (CDAD) associated with 4f and 3d states from $\text{W}(110)$. Photoelectrons are excited by hard X-rays (6000 eV).

O 85.8 Thu 16:45 REC C 213

Automatic Quantification of Transitional Metal X-ray Photoelectron Spectra using Convolutional Neural Networks — •LUKAS PIELSTICKER, WALID HETABA, and MARK GREINER — Max Planck Institute for Chemical Energy Conversion, Mülheim an der Ruhr, Germany

In X-ray photoelectron spectroscopy (XPS), quantitative analysis of the nature and composition of surface chemical species is typically performed manually through empirical curve fitting by expert spectroscopists. However, recent advancements in the ease-of-use and reliability of XPS instruments have led to ever more (novice) users creating increasingly large data sets that are becoming harder to analyze by hand. Reflecting this development, more automated analysis techniques are desirable to aid these users with the analysis of big XPS datasets. Here we show that by training convolutional neural networks (CNN) on artificially generated XP spectra with known quantifications (i.e., for each spectrum, the concentration of each chemical species is known), it is possible to obtain models for auto-quantification of transition metal XP spectra. CNNs are shown to be capable of quantitatively determining the presence of metallic and oxide phases, achieving competitive accuracy as more conventional data analysis methods. The proposed networks are flexible enough to accommodate spectra containing multiple chemical elements and measured with different experimental settings. The use of dropout variational inference for the determination of quantification uncertainty is discussed.

O 85.9 Thu 17:00 REC C 213

Revisiting the Strongly Correlated Si-terminated $3\text{C-SiC}(100)\text{-p}(2\times 1)$ Surface with Density- and Wave Function-Based Methods — •NIKLAS THOBEN and THORSTEN KLÜNER — Carl von Ossietzky Universität, Oldenburg, Germany Silicon carbide is an environmentally friendly, abundant and chemically stable wide band gap semiconductor. From the numerous known polytypes, cubic silicon carbide (3C-SiC) shows the lowest band gap with 2.36 eV, which straddles the water redox potentials and thus making this material a possible candidate for photoelectrochemical water splitting [1]. 3C-SiC is generally obtained as thin films on $\text{Si}(100)$ substrates [2], resulting in the 3C-SiC(100) surface being the most common surface. In the Si-terminated case, this surface can exhibit a $\text{p}(2\times 1)$ reconstruction with symmetric Si-dimers [3]. In literature, this system has almost exclusively been described by periodic closed shell density functional theory (DFT) even though the symmetric dimers should be strongly correlated and thus show open shell and multi-configurational character to a certain extent. Consequentially, in this contribution we apply spin-polarized periodic hybrid DFT and multi-configurational wave function-based methods on the 3C-SiC(100)- $\text{p}(2\times 1)$ surface.

- [1] J. Jian, J. Sun, *Sol. RRL* **2020**, 4, 2000111.
- [2] V. Jokubavicius et al., *Cryst. Growth Des.* **2014**, 14, 6514.
- [3] J. Pollmann, J. Krüger, *J. Phys.: Condens. Matter* **2004**, 16, 1659.

O 85.10 Thu 17:15 REC C 213

Coulomb potential truncation in hybrid calculations — •KRISTIAN KACARS and ANDRIS GULANS — University of Latvia

Solving Poisson's equation is a fundamentally important part of electronic structure calculations. The long-range character of the Coulomb potential makes this task non-trivial in a range of applications. It leads to diverging Fock exchange and spurious interactions of periodic images of low-dimensional systems in supercell calculations. We address this problem in the context of linearized augmented plane waves (LAPW), considering two different approaches to extending Weinert's method. In the first of them, we employ a wavelet-based Poisson equation solver from the *psolver* library. In the second one, we use Coulomb potential truncation schemes. Both approaches are implemented and tested in the LAPW code *exciting*. We apply and compare these methods for bulk materials and low-dimensional systems in calculations with local and hybrid functionals.

O 85.11 Thu 17:30 REC C 213

Ultra-fast machine learning potentials for hydrogen under pressure — •THOMAS BISCHOFF¹, BASTIAN JÄCKL¹, and MATTHIAS RUPP^{1,2} — ¹Department of Computer and Information Science, University of Konstanz, Germany — ²Materials Research and Technology Department, Luxembourg Institute of Science and Technology (LIST), Luxembourg

Hydrogen exhibits remarkably complex behavior at high pressures. Its rich phase space with multiple solid and liquid polymorphs is the subject of controversial scientific debate [1,2].

We apply ultra-fast potentials (UFPs) to model hydrogen under pressure. UFPs are recent robust interpretable machine-learning potentials that enable ac-

curate simulations of large atomistic systems over long time scales [3].

We examine the accuracy of UFPs for training data from density functional theory and quantum Monte Carlo calculations. We also demonstrate the physical interpretability of UFPs for reference configurations composed of atomic and molecular hydrogen. With the obtained machine-learning potential, we investigate solid-liquid and liquid-liquid phase transitions for an extensive part of the phase diagram of dense hydrogen.

[1] (a) B. Cheng et al., *Nature* 585: 217, 2020; (b) V.V. Karasiev et al., *Nature* 600: E12, 2021; (c) B. Cheng et al., *Nature* 600: E15, 2021.

[2] A. Tirelli et al., *Physical Review B* 106(4): L041105, 2022.

[3] S. R. Xie et al., *arXiv 2110.00624*, 2021.

O 86: Solid-Liquid Interfaces II: Reactions and Electrochemistry I

Time: Thursday 15:00–17:45

Location: TRE Phy

O 86.1 Thu 15:00 TRE Phy

Enter the Void: Cavity Formation at Metal-Water Interfaces — •THORBEN EGGERT^{1,2}, NICOLAS G. HÖRMANN¹, and KARSTEN REUTER¹ — ¹Fritz-Haber-Institut der MPG, Berlin, Germany — ²Technical University of Munich, Munich, Germany

Cavity formation is an important concept when rationalizing the solvation of ions. However, most studies only analyze cavities in bulk liquids, omitting that their properties may change dramatically at solid-liquid interfaces.

Here, we study cavities at interfaces, particularly their free energy of formation based on classical molecular dynamics simulations. Specifically, we use a particle insertion approach, as well as thermodynamical integration via the Multistate Bennett Acceptance Ratio. We demonstrate that cavity formation at interfaces depends on the substrate material, which can be rationalized by the strength of the substrate-water interaction. Furthermore, we observe deviations from the bulk behavior in the second solvation layer, which underlines the importance of the substrate-specific interfacial water structure. Finally, we validate our findings with *ab initio* molecular dynamics simulations.

These results allow a quantification of the competitive nature of adsorption processes at solid-liquid interfaces. Ultimately, they could improve implicit solvation models, which typically neglect substrate-specificity.

O 86.2 Thu 15:15 TRE Phy

first-principles molecular dynamics simulations of electrified Pt(111)/H₂O interfaces — •LANG LI^{1,2}, NICOLAS HÖRMANN¹, and KARSTEN REUTER¹ — ¹Fritz-Haber-Institut of Max-Planck Society — ²Humboldt-Universität zu Berlin

Metal-water interfaces play a fundamental role in electrochemistry. An accurate understanding of their properties is required in any attempt to describe electrochemical phenomena such as electrocatalytic reactions or charge transfer processes.

In this work, we benchmark the description of electrified Pt(111)/water interfaces based on first-principles molecular dynamics simulations at applied potential conditions using density functional theory. We apply the potential by introducing excess electrons that are counterbalanced by partially charged hydrogen atoms. This method is tested with a variety of slab setups and cell sizes.

We analyze in detail the structure of the interface as well as the obtained capacitance vs. potential curves and compare these with published theoretical and experimental results [1]. Our results highlight the response of interfacial water to an applied potential and its importance for understanding the hump in the capacitance, observed at high electrolyte concentrations [2].

[1] L. Li, J.-B. Le, J. Cheng, *Cell Rep. Phys. Sci.*, 3, 100759 (2022). [2] J.B. Le, Q.Y. Fan, J.Q. Li, J. Cheng, *Sci. Adv.*, 6, eabb1219 (2020).

Topical Talk

O 86.3 Thu 15:30 TRE Phy

Novel concepts to simulate electrified liquid/solid interfaces from first principles — FLORIAN DEISSENBECK¹, CHRISTOPH FREYSOLDT¹, MIRA TODOROVA¹, JÖRG NEUGEBAUER¹, and •STEFAN WIPPERMANN^{1,2} — ¹Max-Planck-Institut für Eisenforschung — ²Philipps-Universität Marburg

Ab initio techniques have revolutionized the way how theory can help practitioners to discover and design new materials, and explore critical mechanisms. Achieving an atomistic understanding of electrochemical processes is imperative to realize disruptive innovations, e.g. power-to-X devices, supercapacitors, metal-air batteries, new concepts in sustainable metallurgy. A well known example, how novel concepts can impact our ability to perform such studies is the introduction of temperature control into *ab initio* simulations. The analogous technique to model electrochemical systems - potential control - is just emerging.

We recently introduced a “thermopotentiostat”: a novel approach to control the electrode potential in molecular dynamics (MD) simulations [1], that can be straightforwardly implemented into any density-functional code [2]. Here, we provide a perspective on the key concepts of simulating electrified liquid/solid interfaces via *ab initio* MD at controlled electrode potential. To highlight the op-

portunities provided by these developments we discuss the dielectric response and splitting of liquid water in contact with electrified semiconductor surfaces.

[1] F. Deißbeck, C. Freysoldt, M. Todorova, J. Neugebauer, S. Wippermann, *Phys. Rev. Lett* 126, 136803 (2021)

[2] F. Deißbeck, S. Wippermann, *arXiv:2209.04363*

O 86.4 Thu 16:00 TRE Phy

Entropic contributions to the stability of electrochemically adsorbed anion layers on Au(111), a microcalorimetric study — •MARCO SCHÖNIG and ROLF SCHUSTER — Karlsruhe Institute of Technology, Germany

The understanding of the solid/electrolyte interface is detrimental for rationalizing of electrochemical processes. In this contribution we use electrochemical microcalorimetry to study the entropy of formation of the interface for anion (Cl⁻, Br⁻, I⁻, SO₄²⁻) adsorption on Au(111) [1]. The entropy of formation of the interface provides information on the structure, order and composition of this interface, which are often used as descriptors in electrochemical processes. The specific adsorption of anions on Au(111) is an important model system, since the nearly ideal polarizability of the gold surface over a large potential window allows to study the formation of surface adlayers up to high surface coverages. We found a negative reaction entropy during the adsorption process, with a distinct minimum around two thirds of the maximum coverage. Additionally, we observed that the course of the reaction entropy vs. potential changes with the employed cation (Li⁺, K⁺, Cs⁺) in solution. We will discuss contributions of the solvent and the electrolyte to the entropy of formation of the interface and provide statistical mechanics models to describe the measured data. We found that it was imperative to include repulsive interactions between the adsorbates to account for the experimental results. [1] M. Schoenig and R. Schuster *Phys. Chem. Chem. Phys.*, 2022, Accepted Manuscript

O 86.5 Thu 16:15 TRE Phy

Impact of confined water on solvation and adsorption/desorption energetics of charged ions at the electrified interface — •ZHENYU WANG, MIRA TODOROVA, and JÖRG NEUGEBAUER — Department of Computational Materials Design, Max-Planck-Institut für Eisenforschung, Max-Planck-Str.-1, D-40237, Düsseldorf, Germany

Understanding processes at electrified solid/liquid interfaces is crucial for many systems and a wide range of applications in the electrochemical industry, catalytic sciences and biological engineering. Using a prototypical model system of a single ion in water confined between two charged electrodes, we perform nanosecond-scale atomistic molecular dynamics simulations to study the dielectric behavior of chemically pure water as well as the solvation of ions in the presence of an electric field. For weak electric fields, we find that the screening charge density of water is proportional to the external electric intensity, in agreement with classical polarization theory. Probing the interface structure by the single Na⁺/Cl⁻ ion we investigate the formation and evolution of the ion's solvation shell as a function of the electrode-ion distance. Comparing potential profiles from Na⁺/Cl⁻ calculations for different charge states and positions, we elucidate the role of screening and solvation shell size on reorganization energies and the transmission barrier of the ions close to the interface.

O 86.6 Thu 16:30 TRE Phy

Dynamics of the Iridium-Oxide/Water Interface from Machine Learning Potential Simulations — •NIKHIL BAPAT, SIMON WENGERT, HENDRIK H. HEENEN, and KARSTEN REUTER — Fritz-Haber-Institut der MPG, Berlin, Germany

The interaction of liquid water with a solid substrate at an electrified solid/liquid interface plays a crucial role in the activity and stability for electrocatalysts such as IrO₂. It is therefore important to obtain detailed insights about the underlying processes on these interfaces. Here, resolving the dynamical evolution at the atomic scale requires highly accurate yet efficient models that overcome the length and time scale restrictions imposed by traditional *ab initio* molecular dynamics simulations. To that end, we use the Gaussian approximation potential framework to construct a machine-learned model trained on density-functional

theory data for the $\text{IrO}_2(110)/\text{water}$ interface. The established training protocol uses an automated and iterative procedure to ensure that the training data covers the *a priori* unknown geometric and compositional motifs of the evolving working interface.

The model is then used to run reactive molecular dynamics simulations with varying surface compositions. Crucial for electrolysis, the reduced computational cost allows to efficiently explore the diverse configuration space of adsorbed intermediates in the oxygen evolution reaction. Furthermore, we investigate the mobility of water in dependence of the underlying surface composition in which, long-range effects are reflected in a strong variation of water mobility as a function of distance to the surface.

O 86.7 Thu 16:45 TRE Phy

First-principles study of electrochemical effects in Si/SiO_x-water interfaces — •KAMILA SAVVIDI¹ and ROBERT H. MEISSNER^{1,2} — ¹Institute of Polymer and Composites, Hamburg University of Technology, Hamburg, Germany — ²Institute of Surface Science, Helmholtz-Zentrum Hereon, Geesthacht, Germany

Nanoporous silicon is a prominent candidate for application in energy storage devices as silicon can be conductive under certain conditions. Computer simulations offer an understanding of the electrified semiconductor/water interfaces on the atomistic level; essential for the efficient design and optimization of these devices. We use *ab-initio* molecular dynamics (AIMD) to study the capacitive properties of Si/water interface in the presence of an electrostatic potential. A doped Ne crystal is used as counter electrode to a SiO_x slab and to a hydrogenated Si(100) slab to apply a constant bias potential while explicit water molecules constitute the electrolyte solution.[1] Differential capacitance is estimated by the time-averaged atomic charge fluctuations for each system. To obtain more information about the influence of individual electrode atoms to the differential capacitance, the charge fluctuations of each atom are used to calculate a charge-charge covariance matrix \mathbf{K}_{qq} . [2] Results are compared to the simulation of a single electrode with water on either side in an electric field.

[1] S. Surendralal *et al.*, Phys. Rev. Lett. 120, 246801 (2018)

[2] J. Seebeck, C. Merlet, R. H. Meißner, Phys. Rev. Lett. 128, 086001 (2022)

O 86.8 Thu 17:00 TRE Phy

Thermodynamic Cyclic Voltammograms from First Principles — •NICOLAS BERGMANN, NICOLAS G. HÖRMANN, and KARSTEN REUTER — Fritz-Haber-Institut der Max-Planck-Gesellschaft, Berlin, Germany

Cyclic voltammograms (CVs) are a central experimental tool for assessing the structure and activity of electrochemical interfaces. Computationally, a predictive-quality modeling of CVs is challenging due to the entangled need to accurately account for the interactions and reactive chemistry at the liquid electrolyte/solid electrode interface as well as for the applied potential [1]. For sufficiently small scan rates, thermodynamic approaches help to meet these challenges.

Here, we compare different options to derive thermodynamic CVs consistently and at low computational cost, using the well-studied model system of Ag(100) in a Br-containing electrolyte as a test case. We present our generalized ansatz to derive continuous expressions within a mean-field (MF) model, using non-parametric Gaussian process regression. We also shine light on the inherent

accuracy limitations of MF theory, by comparing it to CVs from grand-canonical lattice Monte Carlo simulations. Finally, we show how augmenting traditional zero-field calculations (computational hydrogen electrode, CHE) with capacitive double layer energetics (CHE+DL) [1] within an implicit solvent model influences the theoretical results.

[1] N.G. Hörmann *et al.*, J. Chem. Theory Comput. 2021, 17, 1782

O 86.9 Thu 17:15 TRE Phy

Electrodeposition and Electrochemical Characterization of Thin Nickel Overlayers on Au(111) — •MARKUS WITTMANN, LUDWIG A. KIBLER, and TIMO JACOB — Ulm University, Institute of Electrochemistry, 89069 Ulm, Germany
Nickel is widely used in energy storage and conversion, *e.g.* nickel-iron, nickel-cadmium, and nickel-metal hydride batteries. The behavior of nickel electrodes has been investigated extensively. However, a detailed understanding of adsorption and absorption processes on the atomic level is still missing. In particular, the distinction between surface and bulk atoms, as well as adsorbed hydrogen during electrooxidation is difficult.[1,2] Here we report on the electrochemical fabrication of thin nickel overlayers on Au(111) and their electrochemical characterization. Stable nickel overlayers have been electrochemically deposited onto Au(111) from a 1 mM NiSO_4 solution and subsequently characterized by cyclic voltammetry in a 10 mM KOH solution. The current density-potential curves of nickel overlayers on an Au(111) single crystal in comparison with the behavior of Au(111) and Ni(111) in 10 mM KOH help separating surface and bulk contributions of nickel electrooxidation. This is especially relevant for small deposits with a high surface-to-bulk ratio. In addition, relations between the structure of the nickel electrodeposit and its electrochemical behavior are addressed.

[1] D. S. Hall *et al.*, J. Electrochem. Soc. 160 (2003) 235–243.

[2] L. F. Huang *et al.*, J. Phys. Chem. C 121 (2017) 782–9789.

O 86.10 Thu 17:30 TRE Phy

Cu Underpotential Deposition on Au(111) in Presence of Carboxylic Acids — •SEBASTIAN FACKLER, MARKUS WITTMANN, LUDWIG A. KIBLER, and TIMO JACOB — Ulm University, Institute of Electrochemistry, 89069 Ulm, Germany
The underpotential deposition (UPD) of foreign metals on different host metals has been extensively studied, especially for Cu on Au(111).[1] Apart from the nature of the metals, the nature and concentration of anions in the solution govern the initial stages of the deposition process. The influence is usually explained with respect to non-specific and specific adsorbing anions, with the ability of the latter to stabilize sub-monolayers of the deposited metal on the host metal by co-adsorption on top of well-ordered superstructures.[1]

Similarities and differences of the Cu UPD on Au(111) with short-chained carboxylic acids in comparison with known inorganic anions were systematically investigated by cyclic voltammetry and current transients. Despite the non-specifically adsorbing nature of perchlorate ions, the present study demonstrates that perchlorate can influence the Cu deposition in presence of specifically adsorbing acetate ions. Similarly, it has been found by in-situ STM studies that the presence of perchlorate influences the adsorption structure of strongly adsorbing formate on Au(111).[2]

[1] E. Herrero, *et al.*, Chem. Rev. 2001, 101, 187–1930.

[2] A. Abdelrahman, Dissertation, Ulm University, 2019.

O 87: Focus Session: Scanning Probe Microscopy with Quartz Sensors III

Time: Thursday 15:00–17:30

Location: TRE Ma

Topical Talk

O 87.1 Thu 15:00 TRE Ma

Quartz-sensor detection for single-electron tunneling spectroscopy — •JASCHA REPP — Department of Physics, University of Regensburg, 93040 Regensburg, Germany

We exploit the high sensitivity of qPlus-based [1] atomic force microscopy (AFM) to perform scanning tunneling microscopy (STM) and spectroscopy on molecules in absence of any conductance of the underlying substrate. Thereby, we gain access to out-of-equilibrium charge states that are out of reach for conventional STM [2]. Extending this technique by electronic pump-probe spectroscopy [3], we measured the triplet lifetime of an individual pentacene molecule on an insulating surface [4] and lifetime quenching by nearby oxygen molecules. Combined with radio-frequency magnetic-field driving we introduce AFM-based electron spin resonance and spin manipulation showing long spin coherence in single molecules.

References: [1] F. J. Giessibl, Appl. Phys. Lett. 73, 3956 (1998). [2] L. L. Patara *et al.*, Nature 566, 245 (2019). [3] S. Loth *et al.*, Science 329, 1628 (2010). [4] J. Peng *et al.*, Science 373, 452 (2021).

O 87.2 Thu 15:30 TRE Ma

molecular diffusion studied by multidimensional cantilever-based UHV AFM — •ZUNED AHMED^{1,2}, HAO LIU^{1,2}, MANFRED PARSCHAU¹, and HANS JOSEF HUG^{1,2} — ¹Empa (Swiss Federal Laboratories for Materials Science and Technology), Dübendorf, Switzerland — ²University of Basel, Switzerland

Scanning probe microscopy permits a characterization of the diffusion of atoms or molecules on surfaces, which is governed by diffusion energy barrier and entropy difference between ground and excited states. With our home-built, cantilever based UHV, low temperature scanning force microscope [1], we studied the diffusion of benzene-based molecules with flexible and rigid hydrocarbon chains, namely, 1,3,5-Triethylbenzene (TEB) and 1,3,5-Trimethylbenzene (TMB), respectively, measured at temperatures between 6.38 and 10.68 K on Cu (111). An Arrhenius analysis revealed that the molecule with the flexible hydrocarbon arms (TEB) showed an enhanced diffusion rate which we can attribute to its higher configurational entropy of its ethyl chains. Moreover, we used multidimensional AFM to map the vertical and lateral forces required to manipulate both molecules. Compatible with the lower diffusion energy barrier of the TEB molecule, the force required to manipulate the TEB was much smaller than that of the TMB molecule. In addition, the measured flexural and torsional frequency shift data permitted a detailed analysis of the manipulation process.

[1] Liu *et al.* Beilstein J. Nanotechnol. 2022, 13, 1120-1140

O 87.3 Thu 15:45 TRE Ma

Flexible Superlubricity Unveiled in Snake-Like motion of Individual Chains — •GUILHERME VILHENA^{1,2}, RÉMY PAWLAK¹, PHILIPP D'ASTOLFO¹, XUNSHAN LIU³, ENRICO GNECCO⁴, MARCIN KISIEL¹, THILO GLATZEL¹, RÚBEN PÉREZ², ROBERT HÄNER³, SILVIO DECURTINS³, ALEXIS BARATOFF¹, GIACOMO PRAMPOLINI⁵, SHI-XIA LIU³, and ERNST MEYER¹ — ¹University of Basel, Switzerland — ²Universidad Autónoma de Madrid, Spain — ³University of Bern, Switzerland — ⁴Jagiellonian University, Poland — ⁵Consiglio Nazionale delle Ricerche, Italy

A combination of low-temperature atomic force microscopy and molecular dynamic simulations demonstrates that soft designer molecules realize a sidewinding motion when dragged over a gold surface. Exploiting their longitudinal flexibility, pyrenylene chains are indeed able to lower diffusion energy barriers via on-surface directional locking and molecular strain. The resulting ultralow friction reaches values on the order of tens of pN reported so far only for rigid chains sliding on an incommensurate surface. Therefore, we demonstrate how molecular flexibility can be harnessed to realize complex nanomotion while retaining a superlubric character. This is in contrast with the paradigm guiding the design of most superlubric nanocontacts (mismatched rigid contacting surfaces).

O 87.4 Thu 16:00 TRE Ma

Machine learning for high-resolution AFM image interpretation — •NIKO OINONEN¹, LAURI KURKI¹, CHEN XU¹, SHUNING CAI¹, MARKUS AAPRO¹, ALEXANDER ILIN², PETER LILJEROTH¹, and ADAM FOSTER^{1,3} — ¹Department of Applied Physics, Aalto University, Finland — ²Department of Computer Science, Aalto University, Finland — ³WPI Nano Life Science Institute (WPI-NanoLSI), Kanazawa University, Japan

State-of-the-art non-contact atomic force microscopy (AFM) setups operating in vacuum at low temperatures are able to resolve features on the scale of individual atoms in molecules [1]. However, the process of interpreting the resulting AFM images is often a very challenging task even for highly trained experts in the field. We are working towards greater interpretability and greater automation of the processing of AFM images using machine learning methods. We have introduced an approach based on convolutional neural networks for discovering the atomic structure and electrostatic properties of samples directly from AFM images via image descriptors that characterize the sample [2]. Our recent work refines the geometry prediction task by predicting the molecule graph of the sample using a model based on graph neural networks [3]. The current challenge is in generalizing from simulated training data to experimental test data, where we find that the choice of the training data becomes very important.

[1] L. Gross et al., *Science*, vol. 325, no. 5944, pp. 1110–1114, 2009.[2] N. Oinonen et al., *ACS Nano*, 16, 1, 89–97, 2022.[3] N. Oinonen et al., *MRS Bulletin* 47, 895–905, 2022.**Topical Talk**

O 87.5 Thu 16:15 TRE Ma

Application of atomic force microscopy with quartz sensors to quantum states in graphene and related twisted heterostructures — •JOSEPH STROSCIO — National Institute of Standards and Technology, Gaithersburg, MD, USA.

Atomic force microscopy (AFM) with quartz sensors pioneered by Franz Giessibl has opened many applications in quantum nanoscience where AFM measurements can be made simultaneously and conveniently with scanning tunneling microscopy measurements (STM). In this presentation I will review our work using combined AFM/STM measurements to give a microscopic view of the quantum states in single layer graphene and in twisted graphene heterostructures. In single layer graphene, electrostatic pn junction boundaries provide a convenient geometry for the examination of quantum Hall edge states with microscopic probes. For a graphene Hall bar device defined and tunable by dual gates, we carry out simultaneous AFM, STM, and electrical transport measurements in the system which we developed for detailed measurements of two-dimensional devices in-operando at mK temperatures and in magnetic fields up to 15 T. The AFM, operated in the Kelvin probe force microscopy (KPFM) mode, detects the chemical potential transitions when Landau levels are being filled or emptied as a function of back gate potential with the same fidelity as the scanning tunneling spectroscopy measurements. With KPFM we can map the dispersion of the Landau levels across the quantum Hall edge boundary as a function of density and spatial position.

O 87.6 Thu 16:45 TRE Ma

On the origin and elimination of cross coupling between excitation and tunneling current in scanning probe experiments that utilize the qPlus sensor — •MICHAEL SCHELCHSHORN — Institute of Experimental and Applied Physics, University of Regensburg, Universitätsstraße 31, 93053 Regensburg

The qPlus sensor is a stiff quartz cantilever that facilitates high-resolution combined STM/AFM [1]. Both a tunneling current and the deflection signal resulting from the forces at the tip are measured simultaneously; however, unwanted cross coupling between the tunneling current signal and the excitation of the sensor oscillation can occur. At one bias polarity, this cross coupling acts as an excitation of the oscillation, in the opposite bias it appears as a damping.

This unwanted effect has been observed since the early years of combined STM/AFM experiments using qPlus sensors, but was difficult to explain. Here, we present a new theory that explains this phenomenon, supported by experiments and supplemented by verified measures on how to prevent or at least minimize cross talk. [2]

[1] E.J. Giessibl, *The qPlus sensor: a powerful core for the atomic force microscope*, *Rev. Sci. Instrum.* 90, 011101 (2019).[2] M. Schelchshorn, *On the origin of cross coupling between excitation and tunneling current in combined STM/AFM qPlus experiments*, University of Regensburg, B.Sc. thesis (2022)

O 87.7 Thu 17:00 TRE Ma

Fe adsorbates and their effect on the surfaces of topological insulators TlBiSe₂ and Bi₂Se₃ — •ADRIAN WEINDL, CHRISTOPH SETESCAK, EMMA GRASSER, ALEXANDER LIEBIG, and FRANZ J. GIESSIBL — University of Regensburg, Regensburg, Germany

Can one tailor the properties of the topological surface state (TSS) of topological insulators (TIs) by magnetic doping of the TI material? Here, we study the effect of magnetic adatoms on TI surfaces by combined scanning tunneling microscopy (STM) and atomic force microscopy (AFM). Two archetypical TIs, Bi₂Se₃ and TlBiSe₂, are analyzed, which both have relatively large band gaps with their Dirac points well isolated and far from bulk states. Magnetic impurities, in this case single Fe adatoms, and their influence on the local density of states (LDOS) of the two TIs are investigated by scanning tunneling spectroscopy. We detect resonances in the LDOS for both surfaces that arise due to the scattering of electrons in the TSS at these impurities. The position and shape of these resonances are a function of the exact adsorption position of the adatoms, which can be determined by atomically-resolved AFM measurements. In addition, we detect a relaxation of surface atoms due to the presence of Fe adatoms on Bi₂Se₃. The charge state of the Fe adatoms is determined by Kelvin probe force spectroscopy.

O 87.8 Thu 17:15 TRE Ma

The (2x1) reconstruction of calcite(104) — JONAS HEGGEMANN¹, YASHASVI RANAWAT², ONDŘEJ KREJČÍ², ADAM S. FOSTER², and •PHILIPP RAHE¹ — ¹Fachbereich Physik, Universität Osnabrück, Barbarastraße 7, 49076 Osnabrück, Germany — ²Department of Applied Physics, Aalto University, Helsinki FI-00076, Finland

Calcite is an abundant material in the Earth's crust, a central constituent of biominerals in living organisms [1], and currently investigated as a capture material for CO₂ [2]. Despite intensive studies, however, there is still serious ambiguity regarding the properties of this surface due to conflictive conclusions for the so-called row-pairing [3] and (2x1) reconstruction [4].

Here, we use a combination of non-contact atomic force microscopy (NC-AFM) with CO-functionalized tips at 5K, density functional theory with state-of-the-art dispersion corrections, and NC-AFM image simulations to clarify the microscopic geometry of calcite(104). A (2x1) reconstruction and a glide plane symmetry is consistently found in the NC-AFM data and DFT results. Most importantly, we identify two different adsorption positions for CO molecules within the (2x1) unit cell. These findings are most critical for future studies where processes on calcite(104)-(2x1) are influenced by the surface geometry.

[1] L. Addadi, S. Weiner, *Angew. Chem. Int. Ed. Engl.* 31, 153 (1992). [2] P. A. E. Pogge von Strandmann, et al., *Nat. Commun.* 10, 1983 (2019). [3] A. L. Rachlin, et al., *Am. Mineral.* 77, 904 (1992). [4] S. L. S. Stipp, et al., *Geochim. Cosmochim. Acta* 58, 3023 (1994).**O 88: Members' Assembly**

Topics: Report of the Chairman, Presentation of the Gerhard Ertl Young Investigator Award, Miscellaneous

Time: Thursday 19:00–19:30

Location: HSZ 01

All members of the Surface Science Division are invited to participate.

O 89: Post-Deadline Session

Time: Thursday 19:30–20:30

Location: HSZ 01

Contributed Post-Deadline Talks

O 90: Overview Talk Karl-Heinz Ernst

Time: Friday 9:30–10:15

Location: TRE Phy

Invited Talk

O 90.1 Fri 9:30 TRE Phy

Molecular Surfaces With a Twist: Magnetochiral Asymmetries and Topological Self-Assembly — •KARL-HEINZ ERNST — Empa, Swiss Federal Laboratories for Materials Science and Technology, Dübendorf (Switzerland) — Nanosurf Laboratory, Institute of Physics, The Czech Academy of Sciences, Prague (Czech Republic) — Department of Chemistry University of Zurich, Zurich (Switzerland)

Surfaces functionalized with helically shaped aromatic hydrocarbons, so-called helicenes, are of interest for chiroptical electronic devices or for electron spin filtering. After a general introduction into the topic we will report a unique transmission of chirality from single polyaromatic hydrocarbons into two-

dimensional self-assembled monolayers on a silver surface. A helicene with relatively high molecular flexibility allows adaptation of handedness during crystal growth which is governed rather by entropy than by enthalpy. The layer is dominated by motifs, such as nodes of different topology, i.e., two-armed and three-armed spirals, and by enantiospecific lateral offset of oligomeric triangles. To our knowledge such chiral self-assembly phenomenon has been neither reported previously nor has such aperiodic tiling of the plane been previously described by geometers. Moreover, we will report spin-selective electron transport phenomena and enantioselective magnetochiral interactions of helicenes with ferromagnetic surfaces by means of photoelectron spectroscopy, spin-polarized low-energy electron microscopy and spin-polarized scanning tunneling microscopy.

O 91: Plasmonics and Nanooptics V: Waveguides and Antennas

Time: Friday 10:30–12:45

Location: CHE 89

O 91.1 Fri 10:30 CHE 89

Intermediate-field coupling of single epitaxial quantum dots to plasmonic nanowires — •MICHAEL SEIDEL¹, YUHUI YANG², SAIMON COVRE DA SILVA³, THORSTEN SCHUMACHER¹, ARMANDO RASTELLI³, STEPHAN REITZENSTEIN², and MARKUS LIPPITZ¹ — ¹Experimental Physics III, University of Bayreuth, Germany — ²Institute of Solid State Physics, TU Berlin, Germany — ³Institute of Semiconductor and Solid State Physics, Johannes Kepler University Linz, Austria

Integrated plasmonic nanocircuits are highly promising building blocks for future quantum optical applications. In combination with self-assembled epitaxially grown GaAs quantum dots as stable, bright and narrow-band single-photon sources, ultra-compact nanocircuits operating below the diffraction limit can be designed [1]. A crucial aspect is the coupling of the quantum dot emission into plasmonic waveguide modes. Typically, quantum emitters are placed in the optical near-field of a waveguide, imposing high demands on controlled nanofabrication. Furthermore, plasmonic waveguiding is drastically attenuated near high-index dielectrics due to radiative losses. We overcome these challenges by introducing a 100nm thick dielectric spacer layer, which effectively increases the propagation length and preserves acceptable coupling efficiency, resulting in a robust coupling scheme which is difficult to achieve in the near-field. We characterize the nanostructure by low-temperature photoluminescence and cathodoluminescence imaging and find good agreement to numerical simulations.

[1] Wu et al., Nano Lett. 2017, 17, 7, 4291-4296

O 91.2 Fri 10:45 CHE 89

How to obtain modes in optical fibers — •SERGEI GLADYSHEV, ADRIA CANOS VALERO, and THOMAS WEISS — Institute of Physics, University of Graz, Universitätsplatz 5, 8010 Graz, Austria

Nowadays, new and complex types of optical fibers such as bandgap photonic crystal fibers and antiresonant fibers are actively studied. To understand the physical mechanisms in such fibers, numerical modeling is of great importance. However, numerical calculations for these fibers are extremely challenging. We present an efficient numerical method for obtaining fiber modes in these systems. More specifically, we adapt the contour integral method, a method for solving nonlinear eigenvalue problems, to derive the propagation constant and the electromagnetic near fields of several modes simultaneously.

O 91.3 Fri 11:00 CHE 89

Directional transport in plasmonic waveguide arrays in the presence of disorder — •ANNA SIDORENKO and STEFAN LINDEN — Physikalisches Institut, Friedrich-Wilhelms-Universität Bonn, Kreuzbergweg 24, 53115-Bonn, Germany

Evanescently coupled waveguides provide a convenient platform for the simulation of various quantum phenomena whose experimental realization in analogous condensed matter systems is otherwise difficult. The basis for this is the mathematical equivalence of the coupled mode theory equations and the discrete Schrödinger equation in the tight-binding approximation. Here we present a comparative study of the robustness of directional transport in presence of disorder in two periodically driven waveguides systems - ratchets [1] and fast Thouless pumps [2]. Directional transport in a ratchet requires fine-tuning of

the driving parameters. In contrast, directional transport in Thouless pumping is a topological effect that exists for a range of driving frequencies considering the closed cycle in parameter space. We analyze the effect of topological protection on directional transport by introducing identical disorder distributions to both systems.

References:

[1] Z. Fedorova, C. Dauer, A. Sidorenko, S. Eggert, J. Kroha, S. Linden, "Dissipation engineered directional filter for quantum ratchets". *Physical Review Research* 3(1), 013260 (2021).

[2] Z. Fedorova, H. Qiu, S. Linden, J. Kroha, "Observation of topological transport quantization by dissipation in fast Thouless pumps," *Nature communications* 11, 3758 (2020).

O 91.4 Fri 11:15 CHE 89

Spatially resolved nonlinear plasmonics — •JOHANNES SCHUST, FLORIAN MANGOLD, NIKLAS METZ, MARIO HENTSCHEL, BETTINA FRANK, and HARALD GIessen — 4th Physics Institute, Research Center SCoPE, and IQST, University of Stuttgart, Pfaffenwaldring 57, 70569 Stuttgart, Germany

Nonlinear optical plasmonics investigates plasmonic nanoantenna fields with the help of nonlinear spectroscopy. Here we introduce nonlinear spatially resolved spectroscopy (NSRS) which is capable of imaging the k-space as well as spatially resolved single antennas while it is still possible to carry out spectroscopy.

These additional abilities give us the possibility to spatially resolve the THG signal of gold nanoantenna arrays and investigate the homogeneity of the antenna field. Furthermore, we are able to spatially resolve the THG emission centers of the third-order mode and observe their response to tuning the wavelength over the resonance.

In addition, we discovered that by increasing the laser intensity, certain antennas in our array became exceptionally bright. By correlating our spatially resolved nonlinear image with structural SEM data, we can prove that these bright antennas have deformed into a peanut shape. Thus our NSRS setup enables the investigation of the nonlinear self-enhancement process of nanoantennas under intense laser heating.

O 91.5 Fri 11:30 CHE 89

Spatio-spectral metrics in electron energy loss spectroscopy as a tool to resolve nearly degenerate plasmon modes — MICHAL HORÁK, ANDREA KONEČNÁ, TOMÁŠ ŠIKOLA, and •VLASTIMIL KRÁPEK — Brno University of Technology, Czechia

Electron energy loss spectroscopy (EELS) is utilized to characterize localized surface plasmon modes supported by plasmonic antennas (PAs) with excellent spatial resolution, including studies of hybridized modes in dimer PAs [1,2,3]. However, the spectral resolution of EELS is often insufficient to resolve the hybridized modes for weakly coupled dimers.

Here we address this issue for a case study of the dimer PA composed of two gold discs. We analyze four nearly degenerate hybridized dipole modes. With a traditional approach, the modes cannot be experimentally identified with EELS. Therefore, we propose several metrics that employ the spatial and spectral sensitivity of EELS simultaneously. We apply the metrics to experimental EELS data, demonstrating their ability to resolve three of the above-mentioned modes (with

transverse bonding and antibonding modes still unresolved), identify them unequivocally, and determine their energies. In this respect, the spatio-spectral metrics increase the information extracted from EELS applied to PAs.

- [1] V. Křápek *et al.*, *Nanophotonics* **9**, 623 (2020).
 [2] O. Bitton *et al.*, *Nat. Commun.* **11**, 487 (2020).
 [3] J.-H. Song *et al.*, *Nat. Commun.* **12**, 48 (2021).

O 91.6 Fri 11:45 CHE 89

From Static to Dynamic Modulation of Second Harmonic Generation from Plasmonic Hotspots — •JESSICA MEIER¹, LUKA ZURAK¹, ANDREA LOCATELLI², THORSTEN FEICHTNER¹, RENÉ KULLOCK¹, and BERT HECHT¹ — ¹Nano-Optics and Biophotonics Group, Experimental Physics 5, University of Würzburg, Am Hubland, 97074 Würzburg, Germany — ²Department of Information Engineering, University of Brescia, Italy

Plasmonic dimer antennas feature strong intensity enhancement squeezed into nanoscale gaps, which makes them highly attractive for boosting nonlinear processes, such as multiphoton excitation and harmonic generation [1]. Such phenomena, alongside large field enhancement, often require control over the field symmetry in the gap, which is challenging considering the nanometer length scales. Here, by means of strongly enhanced second harmonic (SH) generation, we demonstrate unprecedented control over the field distribution by systematically introducing geometrical asymmetry. We use focused helium ion beam milling of mono-crystalline gold to realize asymmetric-gap dimer antennas in which an ultra sharp tip with 3 nm apex faces a flat counterpart [2]. By tuning the tip opening angle, we systematically vary the field asymmetry, which in turn modulates the release of SH radiation to the far-field. We further extend the concept of inducing local field asymmetry to reversible tuning of the SH signal from a single antenna by applying an external voltage.

- [1] P. Dombi *et al.*, *Reviews of Modern Physics* **92**, 025003 (2020).
 [2] J. Meier *et al.*, arXiv:2210.14105 (2022).

O 91.7 Fri 12:00 CHE 89

Laser Printing of Plasmonic Dimers on Optical Fiber Tips for Fiber-based SERS — •PAUL VOSSHAGE, FRANCIS SCHUKNECHT, and THEOBALD LOHMÜLLER — Chair for Photonics and Optoelectronics, Nano-Institute Munich, Department of Physics, LMU Munich, Königinstraße 10, 80539 Munich, Germany

Raman Spectroscopy through optical fibers offers great flexibility for conducting measurements both in situ and in vivo, but shows limitations due to the weak Raman scattering cross-sections of most molecules and a considerable background introduced by the fiber material itself. However, a strong signal amplification can be obtained via surface enhanced Raman scattering (SERS) by introducing plasmonic hot-spots on the optical fiber tip.

Here, we demonstrate a single-step approach to pattern plasmonic dimer antennas directly onto glass fibers by optical means. A focused laser beam is used to transform a gold nanorod into two nanospheres of equal size via heating. Simultaneously, optical forces are harnessed to print the two spheres onto the fiber tip as a strongly coupled dimer. The resulting plasmonic dimers feature nm-sized gaps, which provide a strong electromagnetic field enhancement required for fiber-based SERS.

O 91.8 Fri 12:15 CHE 89

Reconfiguring magnetic resonances with plasmonic and dielectric phase-change materials — LUKAS CONRADS, ANDREAS HESSLER, SEBASTIAN MEYER, KONSTANTIN WIRTH, MATTHIAS WUTTIG, DIMITRY CHIGRIN, and •THOMAS TAUBNER — I. Institute of Physics (IA), RWTH Aachen University

For miniaturized active nanophotonic components, resonance tuning of nanoantennas is a key ingredient. Phase-change materials (PCMs) have been established as prime candidates for non-volatile resonance tuning based on a change in refractive index [1]. Currently, a novel material class of switchable infrared plasmonic PCMs, like In₃SbTe₂ (IST), is emerging. Since IST can be locally optically switched between dielectric (amorphous phase) and metallic (crystalline phase) states in the whole infrared range, it becomes possible to directly change the geometry and size of nanoantennas to tune their infrared resonances [2]. Here, crystalline IST split-ring resonators (SRRs) are directly optically written and reconfigured in their arm size to continuously tune their magnetic dipole resonances over a range of 2.4 μm without changing their electric dipole resonances. Furthermore, electric and magnetic dipole resonances of aluminum SRRs covered by the conventional PCM Ge₃Sb₂Te₆ can be individually tuned by addressing the hotspots locally [3]. Our concepts are well-suited for rapid prototyping, speeding up workflows for engineering ultrathin, tunable, plasmonic devices for infrared nanophotonics, telecommunications or (bio)sensing.

- [1] Wuttig *et al.*, *Nat. Photon.* **11**, 465 (2017) [2] Hessler *et al.*, *Nat. Commun.* **12**, 924 (2021) [3] Conrads *et al.* *Adv. Mat.* submitted

O 91.9 Fri 12:30 CHE 89

Nanoantenna Electro-Optical-Transducer Utilizing Monolayer WSe₂ — •PATRICK PERTSCH, RENÉ KULLOCK, MONIKA EMMERLING, ROMANA GANSER, and BERT HECHT — NanoOptics & Biophotonics Group, Experimental Physics 5, University of Würzburg, Am Hubland, 97074 Würzburg, Germany

Using light for the communication on computer chips could decrease the power consumption and increase the data bandwidth [1]. To this end, transition-metal-dichalcogenides (TMD), and especially monolayers thereof, are a very promising material class, because they can be used in electronic computing [2] as well as in optical applications [3].

To achieve high integration densities of logical elements, the transducers between electronic and optical signals should be of the same size as the nanoscale transistors used in modern electronics. But so far the photodetectors and emitters based on TMDs are usually much larger.

By combining TMDs with plasmonic nanostructures, the size of the optical elements can be decreased due to the large absorption cross section afforded by the plasmonic nanoantennas. In this work, we demonstrate single plasmonic nanoantennas on monolayer WSe₂ acting as optically-active material. This combination allows to emit and detect light by using only one single nanoscale device.

- [1] C. Sun, *et al.*, *Nature* **528**, 534-538 (2015).
 [2] C. Liu, *et al.*, *Nat. Nanotechnol.* **15**, 545-557 (2020).
 [3] Q. Wang, *et al.*, *Nat. Nanotechnol.* **7**, 699-712 (2012).

O 92: Oxide and Insulator Surfaces II: Structure, Epitaxy and Growth

Time: Friday 10:30–13:00

Location: CHE 91

O 92.1 Fri 10:30 CHE 91

Growth of ultrathin silica films on Pt(111) and Rh(111): Influence of intermixing with the support — •FLORIAN KRAUSHOFER¹, MATTHIAS KRINNINGER¹, NILS REFKVİK², FRIEDRICH ESCH¹, and BARBARA LECHNER¹ — ¹TU Munich, Germany — ²University of Alberta, Canada

Silica is a widely used catalyst support material for clusters and nanoparticles. Understanding the relationship between these clusters and the support is challenging, however, because SiO₂ is insulating, and in most applications not crystalline, which limits the use of diffraction-based experimental techniques. Several previous studies have investigated ultrathin, quasi-2D silica films on a variety of metal supports [1], which can then be measured by scanning tunneling microscopy (STM). Previous work on Pt(111) did not result in closed films, which was attributed to lattice mismatch [2]. We show that closed films can in fact be grown on Pt(111) when silica is deposited in excess, likely due to formation of a platinum silicide layer with a slightly expanded lattice constant at the interface. We also report results of film growth on Rh(111), which is a near-perfect match to the lattice constant of freestanding SiO₂ films as calculated by theory. However, no high-quality films were achieved, which we attribute to a different balance of the formation energies for silicide and oxide.

- [1] C. Büchner, M. Heyde, Two-dimensional silica opens new perspectives, *Prog. Surf. Sci.*, **92** (2017) 341-374.
 [2] X. Yu, B. Yang, J. A. Boscosoinik, S. Shaikhutdinov, and H.-J. Freund, *Appl. Phys. Lett.* **100** (2012), 151608.

O 92.2 Fri 10:45 CHE 91

Growth of single-phase honeycomb Ti₂O₃ on Pd(111) — •RAJESH CHIRALA, STEFAN FÖRSTER, and WOLF WIDDRA — Institute of Physics, Martin-Luther-Universität Halle-Wittenberg, 06120 Halle, Germany

Transition metal oxides are known to form honeycomb (HC) structures when grown on metal substrates. The oxide-substrate interaction strength defines the substrate-dependent HC lattice parameter. On Au(111), the Ti₂O₃ HC forms a (2×2) superstructure corresponding to lattice parameter of 5.77 Å [1]. On the contrary, Pt(111) has HC relaxing to a lattice parameter of 5.95 Å [2].

Here we study the growth of a Ti₂O₃ HC structure on Pd(111) from the initial stages up to monolayer coverages. The HC is grown by consecutive steps of room-temperature Ti deposition and annealing at 875 K in 7×10⁻⁹ mbar of O₂. Whilst the smallest HC patches grow with a lattice parameter of 5.8 Å with a rotation of 26° against the < 11̄2 > direction of Pd(111), they relax to a lattice parameter of 5.95 Å at higher coverage. Due to this relaxation, the HC lattice coincides with the Pd(111) at a rotation of 30°. The implications of this HC structure as template for the growth of dodecagonal oxide quasicrystal will be discussed [3].

- [1] F. Sedona *et al.*, *J. Phys. Chem. B* **109**, 24411 (2005)
 [2] C. Wu *et al.*, *J. Phys. Chem. C* **115**, 8643 (2011)
 [3] S. Schenk *et al.*, *Nat. Commun.*, accepted (2022)

O 92.3 Fri 11:00 CHE 91

Magnetite homoepitaxy observed by X-ray intensity growth oscillations — •STEFFEN TOBER^{1,2,3}, MARCUS CREUTZBURG¹, BJÖRN ARNDT¹, SIMON CHUNG¹, LEON JACOBSE¹, ARNO JEROMIN¹, VEDRAN VONK¹, and ANDREAS STIERLE^{1,2} — ¹Deutsches Elektronen-Synchrotron DESY, Centre for X-ray and Nanoscience, Hamburg — ²Universität Hamburg, Fachbereich Physik — ³Jülich Centre for Neutron Science (JCNS) and Peter Grünberg Institut (PGI), JARA-FIT, Forschungszentrum Jülich

Processes on the magnetite ($\text{Fe}_{3-\delta}\text{O}_4$) (001) surface like oxidative regrowth, (partial) lifting of the subsurface cation vacancy reconstruction and the element-specific incorporation of adatoms demonstrate the sensitive relation of oxygen pressure, cation transport and structure in the near-surface region of $\text{Fe}_{3-\delta}\text{O}_4$ influencing the performance of catalysts and devices [1,2,3]. We exemplarily studied the homoepitaxial growth of $\text{Fe}_{3-\delta}\text{O}_4$ (001) surface in dependence of the O_2 pressure and iron flux. X-ray intensity growth oscillations proved ordered growth of $\text{Fe}_{3-\delta}\text{O}_4$ for all probed conditions while atomic force microscopy revealed newly formed micrometre-sized surface structures exceeding the amount of deposited material [4]. Our results indicate the presence of multiple parallel processes during reactive $\text{Fe}_{3-\delta}\text{O}_4$ homoepitaxy suggesting similar processes to occur also in other applications of $\text{Fe}_{3-\delta}\text{O}_4$. [1] Nie et al., J. Am. Chem. Soc. 135, 10091 (2013), [2] Arndt, B. et al. PCCP 22, 8336 (2020), [3] Mirabella et al., Electrochimica Acta, 389, 138638 (2021), [4] van der Vegt et al., Phys. Rev. Lett. 68, 3335 (1992)

O 92.4 Fri 11:15 CHE 91

The dependence of structure on thickness of NiO(100) films on Ag(100) studied by IV-LEED — •JAN LACHNITT¹, SHUVANKAR DAS², KRISHNAKUMAR S. R. MENON², SUMAN MANDAL³, and JAN I. FLEGE¹ — ¹Applied Physics and Semiconductor Spectroscopy, Brandenburg University of Technology Cottbus-Senftenberg, Cottbus, Germany — ²Surface Physics & Material Science Division, Saha Institute of Nuclear Physics, Kolkata, India — ³Department of Physics, Sankaraj Mahavidyalaya, Paschim Medinipur, India

Ultrathin NiO films have prospective applications especially in heterogeneous catalysis, microelectronics, and spintronics and are thus an object of active research. The Ag(100) surface is the usual support for these films, as its cubic lattice parameter is only 2.2 % smaller than that of NiO, which enables pseudomorphic growth at very low thicknesses. We have studied the NiO(100) surface for three thicknesses of the oxide: 2 ML on Ag(100), 20 ML on the same substrate, and a bulk single crystal. We have used intensity-voltage low-energy electron diffraction (IV-LEED) in combination with X-ray photoelectron spectroscopy (XPS) and density-functional theory (DFT) calculations. We focus on differences among the three thicknesses, mainly in terms of lattice parameters and surface defects, and our study deepens existing knowledge of the growth of ultrathin NiO films. The IV-LEED calculations have been carried out using the AquaLEED package, which will also be briefly presented.

O 92.5 Fri 11:30 CHE 91

LEED I(V) with ViPerLEED: Overview and Applications — •ALEXANDER M. IMRE¹, FLORIAN KRAUSHOFER^{1,2}, FLORIAN DOERR¹, TILMAN KISSLINGER³, MICHAEL SCHMID¹, ULRIKE DIEBOLD¹, LUTZ HAMMER³, and MICHELE RIVA¹ — ¹TU Wien, Vienna, Austria — ²TU Munich, Munich, Germany — ³FAU Erlangen-Nürnberg, Erlangen, Germany

LEED $I(V)$ is an extension to qualitative Low Energy Electron Diffraction (LEED) pattern analysis in which diffraction intensities are quantitatively studied as a function of incident electron energy. This yields structural information about the surface that can be difficult to obtain otherwise. Regrettably, LEED $I(V)$ has been underutilized by the surface science community over the last decades.

Our group has developed the Vienna Package for TensErLEED (ViPerLEED); a suite of hardware and software aiming to drastically reduce the barrier of entry for the technique. The three core parts of ViPerLEED are: (1) electronics that enable upgrading existing LEED setups for LEED $I(V)$, (2) a spot tracker for easy $I(V)$ curve extraction, and (3) a Python package for LEED $I(V)$ analysis based on the TensErLEED package.

We present a quick overview of ViPerLEED and give insight into current developments. We then show LEED $I(V)$ results obtained and analyzed using ViPerLEED for the $\alpha\text{-Fe}_2\text{O}_3(012)-(1 \times 1)$ and (2×1) surfaces. While a bulk-truncation is confirmed for $\alpha\text{-Fe}_2\text{O}_3(012)-(1 \times 1)$, current structural models cannot explain the (2×1) termination.

O 92.6 Fri 11:45 CHE 91

Reduction by H₂ exposure at room temperature of ceria ultrathin films grown by atomic layer deposition — •CARLOS MORALES, YULIYA KOSTO, RUDI TSCHAMMER, KARSTEN HENKEL, and JAN INGO FLEGE — Applied Physics and Semiconductor Spectroscopy, Brandenburg University of Technology Cottbus-Senftenberg, Konrad-Zuse-Strasse 1, D-03046 Cottbus, Germany

Atomic layer deposition (ALD) exhibits a high potential for integration as a scalable process in microelectronics, allowing well-controlled layer-by-layer deposition and conformal growth on 3D structures. Yet, the ALD technique is also well

known to lead to amorphous and defective, non-stoichiometric films, potentially resulting in modified materials properties that, in the case of ultra-thin deposits, can also be affected by film/substrate interaction. Interestingly, initial in situ X-ray photoemission spectroscopy (XPS) measurements of ceria ALD-deposits on $\text{Al}_2\text{O}_3/\text{Si}$, sapphire, and SiO_2 substrates confirm a $\text{Ce}^{3+}/\text{Ce}^{4+}$ mixture dependent on the substrate interaction, deposit thickness, and morphology. Using near-ambient pressure XPS, we have significantly reduced ultrathin (< 10 nm) ceria films grown by ALD by exposing them to different O_2/H_2 partial pressures at moderate temperatures ($< 525\text{K}$). Notably, the total amount of reduction to Ce^{3+} is found to depend on the deposit thickness and initial ceria/substrate interaction. Furthermore, the intrinsic defects related to the ALD method seem to play a critical role in the reversible reduction at room temperature.

O 92.7 Fri 12:00 CHE 91

Role of orientation and oxyhydroxide formation on the OER activity of LaNiO_3 surfaces — •ACHIM FÜNGERLINGS¹, MARCUS WOHLGEMUTH², MARCEL RISCH³, FELIX GUNKEL², CHRISTOPH BÄUMER^{2,4}, and ROSSITZA PENTCHEVA¹ — ¹Department of Physics and Center for Nanointegration Duisburg-Essen (CENIDE), University of Duisburg-Essen, Duisburg, Germany — ²Peter Gruenberg Institute and JARA-FIT, Forschungszentrum Juelich GmbH, Juelich, Germany — ³Nachwuchsgruppe Gestaltung des Sauerstoffentwicklungsmechanismus, Helmholtz-Zentrum Berlin für Materialien und Energie GmbH, Berlin, Germany — ⁴MESA+ Institute for Nanotechnology, Faculty of Science and Technology, University of Twente, Enschede, Netherlands

We present a combined experimental and theoretical study of the influence of surface orientation and transformation on the OER activity of Ni-terminated (001), (110) and (111) oriented LaNiO_3 films, epitaxially grown on SrTiO_3 substrates via pulsed laser deposition and characterized by AFM and XRD, as well as Hall measurements of the electrical conductivity. Cyclic voltammetry shows the lowest overpotential for (111) and the highest for (001), and gives indication for the formation of a surface oxyhydroxide(-like) skin layer, supported by EXAFS measurements. Based on density functional theory calculations with an on site Hubbard U , we explored different models for the transformed surfaces and find a strong sensitivity of the OER activity on interlayer H concentration and number of oxyhydroxide layers with distinct behavior of the two surface orientations.

O 92.8 Fri 12:15 CHE 91

Electron-phonon coupling for the 2D electron gas at $\text{EuO}/\text{KTaO}_3(001)$ studied by HREELS — •HANNES HERRMANN, ANNE OELSCHÄGER, and WOLF WIDDRA — Martin-Luther-Universität Halle-Wittenberg, Institute of Physics, 06120 Halle, Germany

Recent studies at the $\text{KTaO}_3(111)$ surface revealed a 2D electron gas (2DEG) with much higher charge carrier density than in SrTiO_3 -based heterostructures [1]. Similar 2DEGs with lower charge carrier densities could be obtained on the (011) and (001) surfaces [2].

In this work, we study surface plasmon polaritons (SPP) and their coupling to a 2DEG with high-resolution electron energy loss spectroscopy (HREELS). By evaporating Eu on top of $\text{KTaO}_3(001)$, a 2DEG is initiated resulting in a pronounced asymmetric SPP line shape and extreme broadening compared to the phonons of the clean surface. The line shape will be analysed in terms of a strong coupling of the SPP with the 2DEG. The response can be described by a two-layer model with a 2D Drude-like response with frequency-dependent electronic mobility on top of a bulk-like KTaO_3 .

[1] A. F. Santander-Syro, C. Bareille, F. Fortuna and M. J. Rozenberg, Phys. Rev. B 86, 121107 (2012)

[2] P. D. C. King, R. H. He, T. Eknapakul and W. Meevasana, Phys. Rev. Lett. 108.117602 (2012)

O 92.9 Fri 12:30 CHE 91

2D electron gas and interdiffusion processes at the $\text{EuO}/\text{SrTiO}_3(001)$ interface — •ANNE OELSCHÄGER, HANNES HERRMANN, STEFAN FÖRSTER, and WOLF WIDDRA — Martin-Luther-Universität Halle-Wittenberg, Institute of Physics, 06120 Halle, Germany

The deposition of metallic europium (Eu) on $\text{SrTiO}_3(001)$ (STO) creates a two-dimensional electron gas (2DEG) and concomitant $\text{Ti}^{3+}\text{-O}_2$ -vacancy complexes [1]. Here we study this interface by HREELS, XPS and LEED. The phonon spectra are dominated by the dipole-active surface phonon polaritons of STO. They show a prominent broadening in the presence of the 2DEG due to strong electron-phonon coupling.

Upon annealing to 1020 K, the Ti^{3+} related photoemission lines as well as the phonon broadening vanish. We assign these changes to diffusion of oxygen from the bulk to the EuO/STO interface. Finally, the intensity ratio of $\text{Sr}3p$ and $\text{Ti}2p$ core levels indicates a diffusion of Ti to the europium oxide (EuO) layer, i.e. formation of EuTiO_3 .

[1] P. Lömker et al. Phys. Rev. Mater. 1, 062001(R), 2017

O 92.10 Fri 12:45 CHE 91

Surface Structures of $\text{La}_{0.8}\text{Sr}_{0.2}\text{MnO}_3(001)$: from Commensurate to Quasicrystal Phases — •ERIK RHEINFRAK¹, MICHAEL BRUNTHALER¹, GIADA FRANCESCHI¹, PETER MATVIJA², MICHAEL SCHMID¹, ULRIKE DIEBOLD¹, and MICHELE RIVA¹ — ¹Institute of Applied Physics, TU Wien, Austria — ²Faculty of Mathematics and Physics, Department of Surface and Plasma Science, Charles University, Prague, Czech Republic

Lanthanum-strontium manganese ($\text{La}_{0.8}\text{Sr}_{0.2}\text{MnO}_3$, LSMO) is a perovskite oxide used as a cathode material in solid oxide fuel cells, which convert chemical energy to electrical energy. To gain deeper insights into the reaction mechanisms,

it is important to understand the structure of the surface at the atomic scale. To this end, we grow atomically flat single-crystalline LSMO(001) thin films on Nb-doped SrTiO_3 (STO) substrates via pulsed laser deposition (PLD). The as-grown films have a B-site (Mn) rich surface that can be transformed into an A-site (La/Sr) rich structure by Ar^+ sputtering and subsequent annealing. The B-site rich surface is recovered by depositing Mn from a MnO target. In low-energy electron diffraction (LEED), the Mn-rich surface shows a 4-fold symmetric structure that is best explained by a set of four basis vectors. This is reminiscent of quasicrystals. Scanning tunneling microscopy reveals a non-periodic structure with a Fourier transform consistent with the LEED pattern.

O 93: Graphene II: Electronic Structure and Growth

Time: Friday 10:30–12:30

Location: GER 37

O 93.1 Fri 10:30 GER 37

Energy dissipation on magic angle twisted bilayer graphene — •MARCIN KISIEL, ALEXINA OLLIER, URS GYSIN, and ERNST MEYER — Department of Physics, University of Basel, Klingelbergstrasse 82, CH-4056 Basel, Switzerland

Understanding nanoscale energy dissipation is nowadays among few priorities particularly in quantum systems. While traditional Joule dissipation omnipresent in today's electronic devices is well understood, the energy loss of the strongly interacting electron systems remains largely unexplored. Twisted bilayer graphene (tBLG) is a host of interaction-driven correlated insulating phases, when the relative rotation is close to the magic angle (1.08deg). Here, we report on low temperature (5K) nanomechanical energy dissipation of tBLG measured by sharp tip of the pendulum atomic force microscope (pAFM). Ultrasensitive cantilever tip acting as an oscillating gate over the quantum device shows dissipation peaks attributed to different fractional filling of the flat energy bands. pAFM provides exquisite spatial resolution and thus allows to determine the twist angle distribution of tBLG. Strikingly it does it without literally touching the sample surface. Application of magnetic fields provoked strong oscillations of the dissipation signal at $3/4$ band filling, which we identified as graphene to Aharonov-Bohm oscillations. The work demonstrates that nano-mechanical energy dissipation provides a rich source of information on the dissipative nature of the correlated electronic system of tBLG, with implications for coupling a mechanical oscillator to the quantum devices.

O 93.2 Fri 10:45 GER 37

Raman features of graphene and weyl semimetals beyond the standard nonadiabatic theory — •NINA GIROTTO and DINO NOVKO — Institute of Physics, Zagreb, Croatia

Although graphene has already been thoroughly studied with Raman spectroscopy, there still exists a disagreement about the broadening mechanisms of the E_{2g} mode and its actual temperature dependence [Nano Lett. 10, 466 (2010)]. Along with the importance of the nonadiabatic effects in graphene, higher order electron-phonon scattering processes also significantly impact the phonon spectrum. Specifically, the electron-phonon-induced lifetime and energy renormalization of the electron-hole pair excitations bring additional temperature dependence in the electron-coupled phonon modes and their corresponding linewidths. The nonadiabatic theory relying on first principles calculations, developed in [Phys. Rev. B 98, 041112(R) (2018)], is here successfully applied to graphene in various doping regimes and to Weyl semimetals, which contain a 3-dimensional analog of Dirac points in the electron band structure and are, therefore, excellent candidates for achieving a nonadiabatic regime.

O 93.3 Fri 11:00 GER 37

Near-field optical investigation of tetralayer graphene reveals ABCB stacking — •KONSTANTIN G. WIRTH¹, JONAS B. HAUCK³, ALEXANDER ROTHSTEIN³, CHRISTOPH STAMPFER³, DANTE M. KENNES², LUTZ WALDECKER³, and THOMAS TAUBNER¹ — ¹I. Institute of Physics (IA), RWTH Aachen University — ²Institute for Theory of Statistical Physics, RWTH Aachen University — ³2nd Institute of Physics, RWTH Aachen University

The crystallographic structure of few-layer graphene (FLG) greatly influences its electronic and optical properties. Local probing of the stacking order is usually done by optical measurements, such as infrared absorption [1] or Raman spectroscopy, which work for non-contacted and encapsulated samples but are limited in lateral resolution by diffraction to a few micrometer. Here, we directly probe the electronic properties of tetralayer graphene (4LG) with amplitude and phase-resolved near-field spectroscopy with a broadly tunable laser source over the energy range from 0.28 to 0.56 eV. We differentiate between rhombohedral and Bernal stacking sequences and reveal domains of the previously elusive third stacking order of 4LG, namely ABCB[2], by addressing distinctive interband contributions in optical conductivity. These results establish near-field spectroscopy at the interband transitions as a semi-quantitative tool, enabling the recognition and characterization of FLG domains.

[1] Mak et al., PNAS, 2010 107, 14999-15004 [2] Wirth et al., ACS Nano 2022, 16, 16617-16623

O 93.4 Fri 11:15 GER 37

Image potential states as local probes for graphene magnetism — •MACIEJ BAZARNIK^{1,2,3}, ROLAND WIESENDANGER³, and ANIKA SCHLENHOFF¹ — ¹Institute of Physics, University of Münster, Germany — ²Institute of Physics, Poznan University of Technology, Poland — ³Department of Physics, University of Hamburg, Germany

Image-potential states (IPs) evolving in front of polarizable surfaces are known to serve as quantum sensors for various properties, including surface magnetization and interfacial coupling at buried interfaces. Using a spin-polarized scanning tunneling microscopy (SP-STM) setup, the spin-polarized IPS can be probed locally. In hybrid systems such as iron (Fe) -intercalated graphene (Gr) on Ir(111), Fe is known to grow pseudomorphically on the Ir substrate in a monolayer thickness limit. In contrast, the Gr overlayer exhibits a substantial buckling within the moiré unit cell, resulting in a laterally varying hybridization to the Fe. As a result, the monolayer Gr exhibits a laterally varying spin-polarization within the moiré unit cell.

Here, we present resonant tunneling studies on Fe-intercalated Gr, showing a much stronger contrast between the fcc and hcp parts of the moiré unit cell compared to conventional STM images on this system. Moreover, our SP-STM studies show that the IPs are sensitive to the interlayer coupling of Gr to the underlying ferromagnet. The resulting local IPS spin-polarization can be used to probe the atomic-scale magnetism within the moiré unit cell of the ferromagnet graphene hybrid system.

O 93.5 Fri 11:30 GER 37

Quantitative measurement and first principle prediction of the adsorption structure of graphene on Cu(111) — •MATTHEW A. STOODLEY^{1,2}, BENEDIKT P. KLEIN^{1,2}, LUKE A. ROCHFORD², TIEN-LIN LEE², DAVID A. DUNCAN², and REINHARD J. MAURER¹ — ¹University of Warwick, Coventry, United Kingdom — ²Diamond Light Source, Didcot, United Kingdom

Copper is the dominant substrate for the industrial scale growth of graphene, and graphene-functionalised copper foils are regularly employed as electrodes and heterogeneous catalysts. Yet, little is known about the structure of the graphene-copper interface. We report a quantitative measurement of the adsorption height of graphene on Cu(111) using the x-ray standing waves technique. Using state-of-the-art dispersion-corrected density functional theory, we tested different structural models of graphene on copper. Quantitative agreement with experiment could only be achieved by accounting for the moiré superstructure of the graphene layer on the copper surface. We further investigate how lattice strain affects long-range dispersion interactions and therefore the adsorption height of graphene on Cu(111) as well as graphene bilayer interlayer distances. We use these results to assess the predictive capabilities of common dispersion-corrected density functional approximations. Exploration of the adsorption energy of aromatic molecules of varying size, from benzene to graphene enables us to explore size effects between the substrate and organic overlayer.

O 93.6 Fri 11:45 GER 37

Determining the stability and catalytic formation of graphene on liquid Cu using machine-learning potentials — •HAO GAO¹, VALENTINA BELOVA², MACIEJ JANKOWSKI², HENDRIK H. HEENEN¹, GILLES RENAUD², and KARSTEN REUTER¹ — ¹Fritz-Haber-Institut der MPG, Berlin, Germany — ²ESRF, Grenoble, France

The rapid, high-quality synthesis of graphene (Gr) on liquid Cu catalysts is microscopically still poorly understood. This is due to the difficult characterization of the Cu liquid surface. Especially in atomistic simulations, the large length and time scales necessary to reliably emulate the temporal evolution of the liquid are a major challenge. Corresponding molecular dynamics simulations require large simulation cells and need to span well into the nanosecond regime – an endeavor presently intractable via first-principles methods. In this work we use computationally efficient machine-learning potentials (MLPs) trained to density-functional theory (DFT) data in order to extrapolate the first-principles predictive power to the required scales. Detailed benchmarking confirms that

our MLP captures the involved physics well, accurately reproducing the experimentally determined Gr adsorption height. We apply the MLP to further obtain free energy barriers of possible rate-limiting steps which can be compared to the distinct reaction kinetics found experimentally. Our work draws a path for the use of reliably trained MLPs as a multiscale modeling technique to explore previously uncharted computational problems. In that we provide new insight into the domain of liquid metal catalysts which generally lack atomic-scale understanding.

O 93.7 Fri 12:00 GER 37

In-situ photoemission electron microscopy investigation of mono- and bilayer graphene growth on Ru(10 $\bar{1}$ 0) — •LUKAS SCHEWE, CATHY SULAIMAN, LARS BUSS, MORITZ EWERT, and JAN INGO FLEGE — Applied Physics and Semiconductor Spectroscopy, Brandenburg University of Technology Cottbus-Senftenberg

Epitaxial graphene growth has often been studied on close-packed transition metal substrates, e. g., the Ru(0001) surface, which is a well-studied model system for strong graphene-support interaction. Here, we focus on a Ru surface with different symmetry, i. e., the Ru(10 $\bar{1}$ 0) surface, to investigate the influence of the presumably modified graphene-substrate interaction on the growth of epitaxial monolayer and bilayer graphene (MLG, BLG) islands. The structural and chemical differences of the graphene on the two different surfaces are investigated by photoemission electron microscopy (PEEM), delivering information on both morphology and electronic structure. In-situ PEEM observation of graphene growth on the Ru(10 $\bar{1}$ 0) substrate by ethylene decomposition reveals the growth characteristics of MLG and BLG, the latter showing second layer nucleation via surface segregation of carbon. Furthermore, depending on growth temperature and relative orientation of the growing islands and surface steps, different growth characteristics are observed, in contrast to previous studies of the

graphene/Ru(0001) system whereas similar electronic properties seem to prevail. Yet, when the MLG is decoupled from the Ru(10 $\bar{1}$ 0) substrate via intercalation of oxygen a distinct shift in work function is identified, slightly different from the resulting shift on Ru(0001).

O 93.8 Fri 12:15 GER 37

Defective graphene by topological design — BENEDIKT P KLEIN^{1,2}, MATTHEW A STOODLEY^{1,2}, JOEL DEYERLING³, MICHAEL CLARKE⁴, LUKE A ROCHFORD¹, MARC WALKER², RAYMUNDO MARCIAL HERNANDEZ⁵, CHRISTIAN B NIELSEN⁵, LARS SATTLER⁶, SEBASTIAN M WEBER⁶, GERHARD HILT⁶, ALEXANDER GENERALOV⁷, ALEXEI PREOBRAJENSKI⁷, LEON BS WILLIAMS^{1,8}, TIEN-LIN LEE¹, ALEX SAYWELL⁴, WILLI AUWÄRTER³, REINHARD J MAURER², and •DAVID A DUNCAN¹ — ¹Diamond Light Source, UK — ²University of Warwick, UK — ³Technische Universität München, Germany — ⁴University of Nottingham, UK — ⁵Queen Mary University of London, UK — ⁶Carl von Ossietzky Universität Oldenburg, Germany — ⁷MAX IV, Lund, Sweden — ⁸University of Glasgow, UK

Defective graphene is a promising material for both applications in electronic devices and as substrates for modern catalysts. However, generating deliberate imperfection in graphene often relies on brute force methods, like ion sputtering. Herein, we demonstrate one-step bottom-up synthesis of defective graphene with incorporated 5- and 7-membered ring defects by using a polyaromatic feedstock that contains the same topology as the desired defect. Furthermore, the ratio of ideal to defective graphene could be controlled by the temperature used to grow the film. By a combination of X-ray standing waves, non-contact atomic force microscopy, X-ray photoelectron spectroscopy, near-edge X-ray absorption fine structure and density functional theory, we thoroughly characterise these networks and propose this method as a novel method of functionalising graphene.

O 94: Topology and Symmetry-Protected Materials

Time: Friday 10:30–13:00

Location: GER 38

O 94.1 Fri 10:30 GER 38

Multigap topology and non-Abelian braiding of phonons from first principles — •BO PENG¹, ADRIEN BOUHON^{1,2}, BARTOMEU MONSERRAT^{1,3}, and ROBERT-JAN SLAGER¹ — ¹TCM Group, Cavendish Laboratory, University of Cambridge, J. J. Thomson Avenue, Cambridge CB3 0HE, United Kingdom — ²Nordic Institute for Theoretical Physics (Nordita), Stockholm University and KTH Royal Institute of Technology, Hannes Alfvéns väg 12, Stockholm SE-106 91, Sweden — ³Department of Materials Science and Metallurgy, University of Cambridge, 27 Charles Babbage Road, Cambridge CB3 0FS, United Kingdom

Non-Abelian braiding of quasiparticles can encode information immune from environmental noise with the potential to realize topological quantum computation. Here we propose that phonons, a bosonic excitation of lattice vibrations, can carry non-Abelian charges in their band structures that can be braided using external stimuli. Taking some earthly abundant materials such as silicates [1] and aluminium oxide [2] as representative examples, we demonstrate that an external electric field or electrostatic doping can give rise to phonon band inversions that induce the redistribution of non-Abelian charges, leading to non-Abelian braiding of phonons. We show that phonons can be a primary platform to study non-Abelian braiding in the reciprocal space, and we expand the toolset to study such braiding processes.

References: [1] Nature Communications 13, 423 (2022). [2] Physical Review B 105, 085115 (2022).

O 94.2 Fri 10:45 GER 38

Electronic Structure of the Weak 3D Topological Insulator Bi₁₂Rh₃Ag₆I₉ — •JOHANNES HESSDÖRFER^{1,2}, EDUARDO CARILLO-ARAVENA^{2,3}, ARMANDO CONSIGLIO^{2,4}, MAXIMILIAN ÜNZELMANN¹, MICHAEL RUCK^{2,3}, DOMENICO DI SANTE⁵, and FRIEDRICH REINERT^{1,2} — ¹Experimentelle Physik VII, Universität Würzburg, Germany — ²Würzburg-Dresden Cluster of Excellence ct.qmat, Germany — ³Anorganische Chemie II, Technische Universität Dresden, Germany — ⁴Theoretische Physik I, Universität Würzburg, Germany — ⁵University of Bologna, Italy

Weak three-dimensional (3D) topological insulators (TI) can be considered as a stack of 2D TI separated by insulating spacer layers. The first experimentally observed weak TI is Bi₁₄Rh₃I₉ [1], in which the TI layers are Kagome nets formed by rhodium centered bismuth cubes. Importantly, a modification of the [Bi₂I₈]²⁻ spacer layer, like e.g. by Ag-substitution, can change the coupling between the 2D-TI and with that decisively influences the topological properties. Here, we investigate Bi₁₂Rh₃Ag₆I₉ by means of angle-resolved photoemission experiments and density functional theory band structure calculations. In particular, we will discuss the influence of the modified spacer layer on the electronic structure and compare the results with Bi₁₄Rh₃I₉ and other compounds of this family.

[1] Rasche et al., Nat. Mater, 12, 422-425 (2013)

O 94.3 Fri 11:00 GER 38

Doping of coupled 1D topologically protected edge states on the (001) surface of the topological crystalline insulator (Pb,Sn)Se — •FLORIAN KELLER, ARTEM ODOBESKO, and MATTHIAS BODE — Physikalisches Institut, Lehrstuhl für Experimentelle Physik II, Julius-Maximilians-Universität Würzburg, Würzburg, Germany

Topological crystalline insulators (TCI) are a class of materials with topological protected surface states protected by crystalline symmetry. One representative of this material class is (Pb,Sn)Se which exhibits Dirac fermions at the surface and topologically protected one-dimensional edge state at the step edges with a height equivalent to an odd number of atomic layers [1]. It was shown that the 1D edge states hybridize when two or more odd step edges are in close proximity [2]. The nature of this hybridization indicates that the quasiparticle edge mode is not an infinite quantum 1D state, but is either strongly localized or has a very short coherence length along the edge. One way to check this hypothesis is to increase the coherence length by shifting the Dirac energy close to the Fermi energy [3]. Here we present experiments where Fe adatoms are deposited onto p-doped PbSnSe, resulting in a downwards-bending of the surface band structure. The dependence of the correlation length of Dirac fermions is investigated by determining the edge state hybridization for pristine and doped (Pb,Sn)Se.

[1] P. Sessi et al., Science 354, 6317 (2016)

[2] J. Jung et al., Phys. Rev. Lett. 126, 236402 (2021)

[3] P. M. Echenique et al., Surf. Sci. Rep. 52, 219 (2004)

O 94.4 Fri 11:15 GER 38

Pressure-driven tunable properties of the small-gap chalcopyrite topological quantum material ZnGeSb₂: A first-principles study — •SURASREE SADHUKHAN¹, BANASREE SADHUKHAN², and SUDIPTA KANUNGO¹ — ¹Indian Institute of Technology Goa, 403401 Ponda, India — ²KTH Royal Institute of Technology, Stockholm

Search for new topological quantum materials is the demand to achieve substantial growth topological phase of matter. In this search process, theoretical prediction is crucial besides the obvious experimental verification. The divination of topological properties in already well-known narrow gap semiconductors are flourishing in quantum material science. We revisited the semiconductor compound in the chalcopyrite series, some of which were potential topological materials. Using this density functional theory-based first-principles calculations, we report a strong topologically nontrivial phase in chalcopyrite ZnGeSb₂, which can act as a model system of strained HgTe. The estimates reveal the non-zero topological invariant (Z_2), Dirac cone crossing in the surface spectral functions with spin-momentum locked spin texture. We also report the tunable topological properties from nontrivial to trivial phases under moderate hydrostatic pressure within *7 GPa. A minor modification of a lattice parameter is enough to

achieve this topological phase transition easily accomplished in an experimental lab. We have incorporated the discontinuity in the tetragonal distortion of non-centrosymmetric ZnGeSb₂ to drive the topological quantum phase transition.

O 94.5 Fri 11:30 GER 38

Shift current in the Haldane model: analytic and numerical evaluation — •JAVIER SIVIANES CASTAÑO and JULEN IBAÑEZ AZPIROZ — Centro de Física de Materiales, Universidad del País Vasco, 20018 San Sebastián, Spain

The shift current is a second order optical response which takes place in non-centrosymmetric crystals and is characterized by a DC photocurrent. As realized recently, the shift current is sensitive to the topology of materials [1]. In particular, DFT calculations have predicted a sign change when going through a topological phase transition (TPT) in the bulk crystals BiTeI and CsPbI₃ [2]. Here we analyse the shift current in the Haldane model, as a toy model that describes inversion symmetry breaking and features non-trivial topological phases. We derive a simple analytical expression that accounts for the sign change across the TPT by relating it to the inversion of the mass term, in agreement with Ref [3]. We complement our study by a numerical evaluation on a continuum version on the Haldane model [4]. In this description we study the quantitative importance of the off-diagonal matrix elements of the position operator that are commonly discarded in the tight-binding description.

Funding provided by the European Union's Horizon 2020 research and innovation programme under the European Research Council (ERC) grant agreement No 946629.

[1] T. Morimoto and N. Nagaosa, *Sci. Adv.* **2**, 5 (2016) [2] L. Z. Tan and A. M. Rappe, *PRL* **116**, 237402 (2016) [3] Z. Yan, arXiv:1812.02191 [4] J. Ibañez-Azpiroz et al., *PRB* **92**, 195132 (2015)

O 94.6 Fri 11:45 GER 38

The 2D Ferromagnetic Extension of a Topological Insulator — •PHILIPP KAGERER^{1,2}, CELSO I. FORNARI^{1,2}, SEBASTIAN BUCHBERGER^{1,2}, BEG MUHAMMETH GELDIYEV^{1,2}, TERESA TSCHIRNER^{2,3}, LOUIS VEYRAT^{2,3,4}, ABDUL V. TCAKAEV^{2,4}, MARTIN KAMP⁵, SERGIO L. MORELHAO⁶, VLADIMIR HINKOV^{2,4}, HENDRIK BENTMANN^{1,2}, and FRIEDRICH REINERT^{1,2} — ¹Exp. Physik VII, Universität Würzburg — ²Würzburg-Dresden Cluster of Excellence ct.qmat — ³Leibniz IFW Dresden — ⁴Exp. Physik IV, Universität Würzburg — ⁵Physikalisches Institut and RCCM, Universität Würzburg — ⁶Instituto de Física, Universidade de São Paulo

3D topological insulators (TI) are known to have a topological non-trivial band structure protected by time reversal symmetry, which also guarantees the metallicity of the surface. Consequently, it is sufficient to break this symmetry only locally at the surface of the sample to gap out the topological surface state (TSS), leading to a variety of novel topological effects, e.g. an axion term in the electromagnetic response and quantized spin-selective edge channels. While most experimental approaches to date have aimed to introduce magnetism globally, we present the first experimental realisation of the *ferromagnetic extension* (1), a design directly interfacing a 3D TI with a two-dimensional non-trivial magnet. Utilizing a single septuple layer MnBi₂Te₄ on the prototypical TI Bi₂Te₃, we establish a stable 2D ferromagnetic ground state and introduce a sizeable magnetic exchange gap in the TSS (2).

(1) M.M. Otrokov et al., *2D Mater.* **4**, 025082 (2017)

(2) P. Kagerer et al., arXiv 2207.14421 (2022)

O 94.7 Fri 12:00 GER 38

Orbital angular momentum in indenene measured by circular dichroism in ARPES — •JONAS ERHARDT, CEDRIC SCHMITT, SIMON MOSER, and RALPH CLAESSEN — Physikalisches Institut und Würzburg-Dresden Cluster of Excellence ct.qmat, Universität Würzburg, Würzburg D- 97074, Germany

Indenene, a monolayer of In atoms arranged in a triangular lattice on SiC(0001), has recently been identified as a quantum spin Hall insulator (QSHI) [1]. Its topological character is encoded in a characteristic energy staggering of its orbital angular momentum (OAM) polarized Dirac states [1]. This makes indenene an ideal test case for recent claims that circular dichroism in angle-resolved photoelectron spectroscopy (CD-ARPES) gives access to local Berry curvature signatures via the OAM [2]. However, a particular challenge of such experiments is the extraction of the intrinsic OAM-related CD signal, requiring

its distinction from final state effects and extrinsic contributions induced by experimental geometry.

In this talk, I will present a systematic photon energy dependent CD-ARPES study of indenene's Dirac states and use simple geometric considerations to disentangle experimental from OAM induced CD. The resulting OAM sequence confirms indenene to be a QSHI and thus establishes a new approach to experimentally identify the topological character of a 2D quantum material directly from its bulk states.

[1] M. Bauernfeind et al., *Nat. Commun.*, **12**, 5396 (2021)

[2] M. Schüler et al., *Sci. Adv.*, **6**, 2730 (2020)

O 94.8 Fri 12:15 GER 38

Transfer matrix analysis of non-Hermitian interfaces — •JACOB FAUMAN — Max Planck Institute for the Science of Light, Erlangen, Germany

Non-Hermitian systems exhibit unique features not present in Hermitian systems, including the so-called non-Hermitian skin effect in which the modes accumulate at the surface of the system. We analyze the interface between a non-Hermitian system and a Weyl semimetal analytically using the transfer matrix method. This approach is especially well-suited to the study of spatially inhomogeneous systems, and allows for analysis of the Fermi arcs at the interface. We also consider the effect of Hermitian and non-Hermitian spectral degeneracies on the interface modes.

O 94.9 Fri 12:30 GER 38

Spectroscopic signatures of non-trivial topology in Weyl semimetals —

•JAKUB SCHUSSER¹, HENDRIK BENTMANN², MAXIMILIAN ÜNZELMANN¹, TIM FIGGEMEIER¹, CHUL-HEE MIN³, SIMON K. MOSER⁴, JENNIFER N. NEU⁵, THEO SIEGRIST⁶, and FRIEDRICH REINERT¹ — ¹Exp. Physik VII and Würzburg-Dresden Cluster of Excellence ct.qmat, JMU Würzburg — ²Center for Quantum Spintronics, NTNU Trondheim — ³Department of Physics, CAU zu Kiel — ⁴Exp. Physik IV and Würzburg-Dresden Cluster of Excellence ct.qmat, JMU Würzburg — ⁵National High Magnetic Field Laboratory, Tallahassee, Florida — ⁶Department of Chemical and Biomedical Engineering, FAMU-FSU College of Engineering, Tallahassee, Florida

By performing angle-resolved photoemission spectroscopy (ARPES) on bulk samples we show the spectroscopic manifestation of topological features and Weyl physics beyond the simple photointensity over a broad range of excitation energies from the vacuum ultraviolet to the soft X-Ray regime and compare the surface to the bulk band structure. Our experimental observations were complemented by state-of-the-art first principle photoemission calculations based on one-step model of photoemission. The determinant criterion confirms the arc character of the spoon features in the constant energy contour close to Fermi level in non-centrosymmetric TaP. We further show the drawbacks of the existing spectroscopic techniques used to determine whether the given material has non-zero Chern number and discuss an improved approach for identifying Fermi arcs by the means of differential ARPES measurements as well as the proper final state description.

O 94.10 Fri 12:45 GER 38

Extended Hatano-Nelson model, exceptional points and spectral symmetry —

•JULIUS GOHRICH^{1,2}, SHARAREH SAYYAD¹, and FLORE K. KUNST¹ — ¹Max Planck Institute for the Science of Light, Staudtstraße 2, 91058 Erlangen, Germany — ²Department of Physics, Friedrich-Alexander Universität Erlangen-Nürnberg, Staudtstraße 7, 91058 Erlangen, Germany

Non-Hermitian systems attract a lot of attention in recent years as effective description of open quantum systems. A prominent example in this context is the Hatano-Nelson model. While historically the model has short-range non-reciprocal hoppings, long-range hopping has not been systematically studied. In this talk, I will present our results on the extended Hatano-Nelson model. Using analytical techniques, we demonstrate how the underlying physics of the original Hatano-Nelson model is enriched when longer-range hoppings are also included. I will discuss how the crucial elements of the Hatano-Nelson model, namely, the non-Hermitian skin effect and the exceptional points, are modified for the generalized model.

O 95: Focus Session: Making Experimental Data F.A.I.R. – New Concepts for Research Data Management II (joint session O/TT)

Time: Friday 9:30–12:45

Location: WIL A317

Topical Talk

O 95.1 Fri 9:30 WIL A317

FAIRifying ARPES: a Route to Open Data & Data Analytics — •RALPH ERNSTORFER^{1,2}, TOMMASO PINCELLI^{1,2}, PATRICK R. XIAN², ABEER ARORA², FLORIAN DOBENER³, SANDOR BROCKHAUSER³, and LAURENZ RETTIG² — ¹TU Berlin, Germany — ²FHI Berlin, Germany — ³HU Berlin, Germany

While angle-resolved photoemission spectroscopy (ARPES) is the most direct probe of crystals' electronic structure, the globally collected ARPES data have not been merged into an open experimental electronic structure database in equivalence to well-established atomic structure databases. We discuss a data format based on NeXus [1] as a concept for unifying the data structure for all

types of photoemission experiments including time-, spin-, and time-resolved ARPES [2]. The aim is to immediately enable preprocessed data and metadata shareability according to FAIR data principles, employing existing public storage and archiving research data infrastructures such as Zenodo, OpenAIRE, and Nomad/FAIRmat. Ultimately, the multidimensional photoemission spectroscopy (MPES) format is designed to allow high-performance automated access, providing experimental databases for high-throughput material search [3]. References: [1] <https://www.nexusformat.org/> [2] <https://mpes.science/>; <https://fairmat-experimental.github.io/nexus-fairmat-proposal/> [3] R. P. Xian et al., *Scientific Data* 7, 442 (2020); R.P. Xian et al., *Nat. Comp. Sci*, in print, arXiv:2005.10210

O 95.2 Fri 10:00 WIL A317

A FAIR data infrastructure for photoemission experiments — •MARTEN WIEHN¹, TOBIAS EUL¹, BENJAMIN STADTMÜLLER^{1,2}, and MARTIN AESCHLIMANN¹ — ¹Department of Physics and Research Center OPTIMAS, TU Kaiserslautern, Germany — ²Institute of Physics, Johannes Gutenberg University Mainz, 55128 Mainz, Germany

Recent trends toward data-driven, high-tech experimental research and the growing volumes of data associated with it show the increasing importance of comprehensive data acquisition and management. We present an automated workflow for well-described photoemission data from experiment to archive and publication. Utilizing a powerful experiment control software to capture essential metadata for each measurement enables the collection of FAIR-ready data (Findable, Accessible, Interoperable, Reusable). In addition, using an electronic lab notebook pushes our lab further toward a FAIR data infrastructure that supports researchers in their daily work.

O 95.3 Fri 10:15 WIL A317

Multi-Dimensional Photoemission Spectroscopy: a concept for FAIR photoemission data — •FLORIAN DOBENER¹, TOMMASO PINCELLI^{2,3}, ABEER ARORA^{2,4}, STEINN YMR AUGUSTSSON⁵, DMYTRO KUTNYAKHOV⁶, MICHAEL HARTELT⁷, LAURENZ RETTIG¹, MARTIN AESCHLIMANN², RALPH ERNSTORFER⁷, and SANDOR BROCKHAUSER^{2,3} — ¹Department of Physics, HU Berlin, Germany — ²Fritz-Haber-Institut der Max-Planck-Gesellschaft, Berlin, Germany — ³Institut für Optik und Atomare Physik, TU Berlin, Germany — ⁴FU Berlin, Fachbereich Physik, Berlin, Germany — ⁵Institut für Physik, Johannes Gutenberg-Universität Mainz, Germany — ⁶DESY, Hamburg, Germany — ⁷Department of Physics and OPTIMAS, University of Kaiserslautern, Germany

The complexity and size of photoemission data is rapidly increasing as new technological breakthroughs have enabled multidimensional parallel acquisition. However, most of the community is currently using heterogeneous data formats and workflows. We propose a new data format based on NeXus, a hierarchically organized hdf5 structure. This multidimensional photoemission spectroscopy format is designed to allow high-performance automated access, enabling experimental databases for high-throughput material search. Our approach involves reaching out to the community using a website with extensive documentation of our proposed standard. As a demonstrator of the potential of our approach we present a workflow and data pipeline integrated into the NOMAD research data management solution, which provides powerful analysis and search functionalities.

O 95.4 Fri 10:30 WIL A317

Towards an Infrastructure for FAIR Synthesis Data — •SEBASTIAN BRÜCKNER^{1,2}, ANDREA ALBINO¹, JOSE MARQUEZ¹, FLORIAN DOBENER¹, HAMPUS NÄSSTRÖM¹, MARKUS SCHEIDGEN¹, CLAUDIA DRAXL¹, and MARTIN ALBRECHT² — ¹HU Berlin, Zum Großen Windkanal 2, 12489 Berlin — ²IKZ Berlin, Max-Born-Straße 2, 12489 Berlin

A data infrastructure based on the FAIR (findable, accessible, interoperable and reusable) principles promises a new way of sharing and exploring data by using highly efficient data analysis and artificial intelligence tools. This also applies to data related to sample synthesis. At present, most synthesis data are not structured comprehensively or not even stored digitally but in handwritten lab books. There hardly exists any data standards in synthesis, which is in contrast to data from characterization techniques. The FAIRmat project (<https://FAIRmat-NFDI.eu>) is building a FAIR data infrastructure for condensed-matter physics and the chemical physics of solids. In FAIRmat's Area A, we focus on synthesis data to make sample synthesis reproducible, accelerate the development of novel materials, and make characterization data of synthesized materials assessable. Here we summarize our ongoing work and progress including: providing a general data model for synthesis which is harmonized with data from measurements and theory (ontologies); implementation of our data model in use cases and electronic laboratory notebooks; developing tools for data acquisition and analysis; data governance guidelines to enable a sustainable change of research data management at the institute/university level.

O 95.5 Fri 10:45 WIL A317

FAIRifying Material Synthesis with the NOMAD Electronic Laboratory Notebook (ELN) — •ANDREA ALBINO¹, HAMPUS NÄSSTRÖM¹, FLORIAN DOBENER¹, JOSE MARQUEZ PRIETO¹, LAURI HIMANEN¹, DAVID SIKTER¹, MOHAMMAD NAKHAEI¹, AMIR GOLPARVAR¹, SEBASTIAN BRÜCKNER¹, MARTIN ALBRECHT², MARKUS SCHEIDGEN¹, and CLAUDIA DRAXL^{1,3} — ¹Physics Department and IRIS Adlershof, Humboldt-Universität zu Berlin, Berlin, Germany. — ²Leibniz-Institut für Kristallzüchtung, Berlin, Germany. — ³The NOMAD Laboratory at the Fritz Haber Institute of the Max Planck Society, Berlin, Germany.

Approaching the era of big data-driven materials science, one crucial step to collecting, describing, and sharing experimental data is the adoption of ELNs. The project FAIRmat (fairmat-nfdi.eu) is offering such tools by developing and operating the open-source software NOMAD. The NOMAD ELN aims at offering a secure environment to protect the integrity of both data and metadata, whilst also affording the flexibility to adopt new synthetic processes or changes to existing ones without recourse to further software development.

We find that to promote an early adoption, it is important to adapt to a single user's needs and workflows. An inductive approach, going from a particular set of experiments to a general description of the similarities recurring in each of them, led us to adopt a common data structure as a standard. The state-of-the-art ELN features for a synthetic process will be shown in the talk, highlighting the development of both data modeling and specific implementation solutions.

O 95.6 Fri 11:00 WIL A317

FAIR Data Infrastructure for Computation: Classical Simulations and Multiscale Modeling — •JOSEPH F. RUDZINSKI^{1,2}, JOSÉ M. PIZARRO¹, NATHAN DAELMAN¹, LUCA M. GHIRINGHELLI¹, KARSTEN REUTER³, KURT KREMER², SILVANA BOTTI⁴, and CLAUDIA DRAXL¹ — ¹Institut für Physik, Humboldt-Universität zu Berlin — ²Max-Planck-Institut für Polymer Forschung, Mainz — ³Fritz-Haber-Institut der Max-Planck-Gesellschaft, Berlin — ⁴Institut für Festkörpertheorie und Optik, Friedrich-Schiller-Universität Jena

The emergence of the (big-)data-centric techniques as a fundamental paradigm of science calls for the development of infrastructure for ensuring FAIR—findable, accessible, interoperable, reusable—data management. The FAIRmat consortium aims to build extensive infrastructure for a wide variety of materials-science data, including soft matter simulations [1], by expanding upon the success of the NOMAD Laboratory—a repository for atomistic calculations in materials science [2]. Both the large volume and heterogeneous nature of classical molecular-dynamics simulation data presents a number of distinct challenges. In this talk, we present FAIRmat's progress in developing infrastructure for molecular-dynamics simulations, including metadata for molecular topologies and tools for workflow management. We will also discuss the need for standardization of metadata schemas and ontologies within the community, and planned collaborations with other open science initiatives and software developers.

[1] Scheffler, M. et al. *Nature* 2022, 604, 635-642.

[2] Draxl, C.; Scheffler, M. *JPhys Materials* 2019, 2, 036001.

Topical Talk

O 95.7 Fri 11:15 WIL A317

Electronic Lab Notebooks in Teaching and Implications on Science — •MICHAEL KRIEGER — Lehrstuhl für Angewandte Physik, Department Physik, Friedrich-Alexander-Universität Erlangen-Nürnberg (FAU)

In our department, we have recently introduced Electronic Lab Notebooks (ELN) in the obligatory electronic lab course in the 4th semester of the physics curriculum. Immediate advantages for the students are obvious: all data, raw data and metadata including experiment description and experimental observations, are digitally stored at the same place. Moreover, student teams share and actively work in their group ELN with access at the university as well as at home, and script-based evaluations can be performed directly in the ELN.

The introduction of ELNs in teaching has also implications on science. Students carry their ELN experience and data competences into all research groups. There, however, modern research data management is much more complex. According to the FAIR principles, it requires structured, machine-readable data using open formats and vocabularies that meet community standards. The development of such standards is in many cases still to be done and is the core of the Nationale Forschungsdateninfrastruktur (NFDI). Here, ELNs in teaching provide a sandbox with short learning and innovation cycles for testing structured schemas. The experience helps to develop and establish sustainable and FAIR documentation of research workflows in science.

O 95.8 Fri 11:45 WIL A317

A step towards predicting synthesis conditions of metal-organic frameworks — •DINGA WONANKE¹, THOMAS HEINE², and CHRISTOF WÖLL¹ — ¹Institut für Funktionelle Grenzflächen (IFG), Karlsruhe, Germany — ²Faculty of Chemistry and Food Chemistry, Dresden, Germany

The process of synthesising metal-organic frameworks (MOFs) falls under a branch of chemistry known as reticular chemistry. Here, well defined crystalline compounds are synthesised from a well thought out design principle by linking predefined building blocks under specific conditions. Although, this approach appears to be intuitive, the synthesis of any novel MOF still follows

the conventional approach that begins with a thorough literature survey to explore reagents, calculations of aliquots and finally a series of time consuming and stressful trial-and-error syntheses. Consequently, although millions of stable hypothetical MOFs with interesting properties have been predicted, only approximately 100 thousand crystal structures of MOFs currently exist in the Cambridge Structural Database (CSD). Indicating a significant bottleneck in the intelligent design of novel stable MOFs with targeted properties.

In this talk, we will present an overview of our journey to design a new machine learning algorithm for predicting the synthesis condition of existing and hypothetical MOFs. We will discuss our experiences and challenges in mining and curating the MOF subset in the CSD. Finally, we will present our new MOF database that maps every MOF to its experimental synthetic conditions.

O 95.9 Fri 12:00 WIL A317

Deep learning surface scattering data analysis for processing large synchrotron datasets — •VLADIMIR STAROSTIN, VALENTIN MUNTEANU, LINUS PITHAN, ALEXANDER GERLACH, ALEXANDER HINDERHOFER, and FRANK SCHREIBER — Institute of Applied Physics, University of Tübingen, Germany

In situ real-time surface scattering experiments such as grazing-incidence wide-angle X-ray scattering (GIWAXS) produce large amounts of data, frequently exceeding the capabilities of traditional data processing methods. Here we demonstrate an automated pipeline for the analysis of GIWAXS images, based on a machine learning architecture for object detection, designed to conform to the specifics of the scattering data [1]. Our pipeline enables real-time GIWAXS analysis and is designed to be employed at synchrotron facilities. We also present FAIR data strategies and traceable data resources from the raw data to the corresponding scientific publication and vice versa [2] including intermediate processing steps.

We demonstrate our method on real-time tracking of lead halide perovskite structure crystallization processes, which are relevant for hybrid solar cell applications. However, our approach is equally suitable for other crystalline thin-film materials by design. In general, the solution substantially accelerates the analysis process of GIWAXS images, potentially boosting the speed of scientific discoveries in material science.

[1] V. Starostin et al. *npj Comput Mater* **8**, 101 (2022)

[2] V. Starostin et al. *Synch Rad News* **13**, 31–37 (2022)

O 95.10 Fri 12:15 WIL A317

FAIR Data Infrastructure for Computation: Mapping out the Space of Density Functionals — •NATHAN DAELMAN¹, JOSEPH F. RUDZINSKI^{1,2}, JOSÉ M. PIZARRO¹, LUCA M. GHIRINGHELLI¹, MIGUEL A. L. MARQUES³, SILVANA

BOTTI⁴, and CLAUDIA DRAXL¹ — ¹Institut für Physik und IRIS-Adlershof, Humboldt-Universität zu Berlin, Berlin — ²Max-Planck-Institut für Polymer Forschung, Mainz — ³Institut für Physik, Martin-Luther-University Halle-Wittenberg, Halle — ⁴Friedrich Schiller Universität Jena, Jena

The NOMAD Laboratory [1] holds over 135 million computational results, the vast majority of which stem from density-functional theory (DFT). The platform provides adequate querying and data analytics tools (e.g., machine-learning modelling) for processing such Big Data. However, the exchange-correlation (xc) functional with which the data was generated, limits the analysis scope of most thermodynamic and kinetic properties. Here, we present a strategy rooted in semantics for extending method interoperability. We will showcase our map of the entire xc-functional space that, in the context of the FAIRmat consortium [2], is built to be widely accessible and facilitate findability. Lastly, we will discuss the integration of this xc-functionals map into the NOMAD data platform, as well as its publication in ontology format as an effort towards a community-wide vocabulary standard.

[1] C. Draxl and M. Scheffler, *MRS Bulletin* **43**, 676–682 (2018).

[2] M. Scheffler, M. et al., *Nature* **604**, 635–642 (2022).

O 95.11 Fri 12:30 WIL A317

OpenSemanticLab: Towards Open Semantic Research — •SIMON STIER and MATTHIAS A. POPP — Fraunhofer ISC, Neunerplatz 2, 97082 Würzburg, Germany

In materials science, complex relationships exist between the properties of materials and their composition and processing. Therefore, digital transformation and acceleration in this domain represents a particularly important challenge. Although it is generally agreed that data must be linked by means of semantics and ontologies to form holistic data spaces, there is still a lack of suitable tools for integrating the necessary structures into the everyday work of scientists.

Fraunhofer ISC addresses this challenge with a broad-based strategy that closely links activities at all relevant levels. The goal hereby is the development towards Lab 4.0, the machine-readable documentation of scientific processes and the harmonization of data structures in accordance with international standards.

Core of the resulting OpenSource solution architecture is the central web data platform OpenSemanticLab [1] that links people (knowledge), machines (data) and algorithms (AI) equally. As an open system, this platform is easily adaptable even without programming knowledge and without losing the uniform structure. In this way, OpenSemanticLab enables us as scientists to contribute individually and yet in a standardized fashion to future digital materials research.

[1] <https://github.com/OpenSemanticLab>

O 96: Solid-Liquid Interfaces III: Reactions and Electrochemistry II

Time: Friday 10:30–13:00

Location: TRE Phy

O 96.1 Fri 10:30 TRE Phy

First step of the oxygen reduction reaction on Au(111): A computational study of the electrified metal/water interface — •ELIAS DIESEN, ALEXANDRA M. DUDZINSKI, HENDRIK H. HEENEN, VANESSA J. BUKAS, and KARSTEN REUTER — Fritz-Haber-Institut der MPG, Berlin, Germany

While significant insight has been gained in recent years by first-principles simulations of electrochemical processes, crucial methodological challenges remain, especially for accurate determination of reaction energies under operando conditions. One open question is how to represent the constant electrode potential in simulations of an electrified water/metal interface, where the periodic simulation setup requires a constant charge in the simulation cell throughout the reaction. Here we compare different levels of treatment of the electrochemical interface: explicit *ab initio* molecular dynamics, an implicit solvent model, and a sawtooth-potential electric field in vacuum, for the case of O₂ adsorption on Au(111). We find that all methods agree qualitatively in predicting significantly enhanced O₂ binding at more reducing conditions. Important quantitative differences, however, are also presented and discussed. Umbrella sampling simulations shed light on the underlying free-energy landscape at varying potentials, while assessing the level of detail required in first-principles models of the electric double layer.

O 96.2 Fri 10:45 TRE Phy

Multiscale simulation of nanostructured electrocatalytic systems by coupling neural network surrogates and continuum models — •YOUNES HASSANI ABDOLLAHI^{1,2}, JÜRGEN FUHRMANN³, and SEBASTIAN MATERA^{1,2} — ¹Institut f. Mathematik, Freie Universität Berlin, Berlin, Germany — ²Fritz Haber Institute of the Max Planck Society, Berlin, Germany — ³Weierstraß-Institut f. Angewandte Analysis u. Stochastik, Berlin, Germany

The kinetic Monte Carlo method (kMC) is the physically most sound approach for addressing the kinetic interplay of elementary processes at electrocatalytic surfaces but also comes at high computational costs. Therefore, computation-

ally efficient surrogate models are highly desirable which allow the utilization of kMC simulation results in coarser scale simulations.

Using the oxygen reduction reaction on Pt(111) as a prototypical example, we investigate regression neural networks as surrogates to reproduce the stationary TOF as a function of all reaction conditions, i.e. electrostatic potential, concentrations, and temperature. We found that a relatively shallow network serves as an appropriate choice. This surrogate is then coupled to a conservative and thermodynamically consistent Finite Volume discretization of a nanofluidic model. The resulting hybrid mesoscale model will be employed to discuss the interplay of the nanostructure, transport, and kinetics.

O 96.3 Fri 11:00 TRE Phy

Modeling Transport Effects on Selectivity in Electrochemical CO₂ Reduction — •HENDRIK H. HEENEN^{1,2}, GEORG KASTLUNGER², VANESSA J. BUKAS¹, KARSTEN REUTER¹, and KAREN CHAN² — ¹Fritz-Haber-Institut der MPG, Berlin, Germany — ²Technical University of Denmark, Lyngby, Denmark

Product selectivity in the electrochemical CO₂ reduction reaction (eCO₂RR) is known to change considerably with non-obvious parameters such as catalyst morphology or reactor design. In this work we explore the proposition that these parameters are related to selectivity through transport mediated desorption and adsorption of key intermediates. The mesoscopic morphology of a catalyst can be characterized by a measurable loading or roughness which determines the so-called active surface area. This area may in turn determine the selectivity by controlling the fate of desorbing (closed shell) intermediates along the reaction path: either to re-adsorb and further react on the surface, or to entirely leave the catalyst surface and form an early not fully-reduced product. We specifically show this competition in the reaction toward acetate which we propose to be governed by a solution reaction. Combining *ab initio* energetics, microkinetic and transport modeling in a multi-scale approach, we predict complex selectivity toward acetate with almost quantitative agreement to experiment. Finally, we demonstrate that the same principle applies to other important intermediates in

the eCO₂RR. Mesoscopic transport thus provides an alternative or, at least, complementary explanation to changes in selectivity that are otherwise attributed to active sites changes, to doping, or to alloying.

O 96.4 Fri 11:15 TRE Phy

Kinetics of the initial step in Pt electrochemical oxidation — JAN OLE FEHRS¹, TIMO FUCHS¹, •OLAF MAGNUSSEN¹, CHENTIAN YUAN², DAVID HARRINGTON², VALENTIN BRIEGA MARTOS³, SERHIY CHEREVKO³, and JAKUB DRNEC⁴ — ¹Christian-Albrechts Universität zu Kiel — ²University of Victoria — ³Helmholtz Institute Erlangen-Nürnberg for Renewable Energy — ⁴European Synchrotron Radiation Facility

A key event in electrochemical metal oxidation is extraction of a metal atom from its lattice site to a location in a growing oxide. The direct observation of this fundamental step is difficult for base metals that actively corrode, because of the difficulty of producing clean surfaces and the speed of the oxidation. However, use of noble metals allows preparation of clean surfaces that are well-defined on the atomic scale, and for which *in situ* methods can directly observe this extraction. Here we show by fast simultaneous electrochemical and high-energy surface X-ray diffraction measurements, performed at the ID31 beamline of the European Synchrotron Radiation Facility with a photon energy of 70 keV, that the initial extraction of Pt atoms from Pt(111) is a fast, potential-driven process whereas charge transfer for the related formation of adsorbed oxygen occurs on a slower time scale. Electrochemical oxidation is therefore inherently different from gas-phase thermal oxidation, where the extraction must be driven by the chemisorption of oxygen species on the surface.

The work was funded by the Deutsche Forschungsgemeinschaft via grant 418603497 and the BMBF via project 05K19FK3.

O 96.5 Fri 11:30 TRE Phy

CO oxidation on Pt layers on Ru(0001): A UHV-STM, DEMS, and SXRD study — •ALBERT K. ENGSTFELD¹, LUKAS FORSCHNER¹, MARIO LÖW², ZENONAS JUSYS², JOACHIM BANSMANN², R. JÜRGEN BEHM², and JAKUB DRNEC³ — ¹Ulm University, Institute of Electrochemistry, D-89069 Ulm — ²Ulm University, Institute of Surface Chemistry and Catalysis, D-89069 Ulm — ³ESRF, F-38000 Grenoble

According to the Sabatier principle, the performance of an (electro)catalyst material is determined by the fine balance between the binding strength of the reactants, reaction intermediates, and products to the catalyst surface. By changing the structural properties of the substrate, the electronic structure and in turn, also the binding of the species can be modified to tune the performance of the catalyst material. However, also the electrode's stability plays a crucial role in assessing the catalyst's performance.

Here we present results on the CO (and MeOH) electrooxidation on Pt layers with different thicknesses deposited on Ru(0001) under UHV conditions. The structural properties are studied by means of STM under UHV conditions before and after the electrochemical measurements. The electrocatalytic properties are studied in a flow cell (in a DEMS configuration) attached to the UHV chamber. This approach allows for disentangling surface redox processes from catalytic processes. Additional SXRD measurements provide additional insights into the stability of the electrodes. In combination, we discuss the fine balance between surface reactivity and electrode stability.

O 96.6 Fri 11:45 TRE Phy

Electrochemical Roughening of Stepped Platinum Surfaces — •FRANCESCO VALLS MASCARÓ¹, MARC KOPER¹, and MARCEL ROST² — ¹Leiden Institute of Chemistry, Leiden University — ²Huygens-Kamerlingh Onnes Laboratory, Leiden Institute of Physics, Leiden University

Platinum is the model catalyst to be used in electrochemical energy conversion devices due to its high activity. Nevertheless, its industrial applicability is limited, as it degrades during fuel cell operation. This has been extensively studied by Cyclic Voltammetry and Inductively Coupled Plasma Mass Spectrometry (ICP-MS) [1, 2]. It is well known that this degradation is linked to the nucleation and growth of platinum nanoislands on initially atomically flat terraces [3, 4, 5, 6]. However, there is no insight yet on the role of steps on this roughening process. In this work, we combine Cyclic Voltammetry and Electrochemical Scanning Tunneling Microscopy to study the stability of different stepped platinum surfaces upon oxidation-reduction cycling. Surprisingly, the electrochemical results indicate that neither 2D nor 3D (for Pt(533)) and no 3D (for Pt(553)) roughness develops, although we clearly observe island formation in the STM, and thus an increase in the step lengths and roughness.

[1] Topalov, A. et al., Chem. Sci., 5, 631 (2014) [2] Sandbeck D. J. S. et al., ACS Appl. Mater. Interfaces, 12, 25718 (2020) [3] Jacobse, L. et al., Nat. Mater. 17, 277 (2018) [4] Jacobse, L. et al., ACS Cent. Sci. 5 (12), 1920 (2019) [5] Rost, M. J. et al., Nat. Commun. 10, 5233 (2019) [6] Ruge, M. et al., J. Am. Chem. Soc., 139, 4532 (2017)

O 96.7 Fri 12:00 TRE Phy

Shaping the electrochemical interfaces of high-performance photoelectrodes by dedicated corrosion — •MATTHIAS M. MAY^{1,2}, ERICA A. SCHMITT^{1,2}, MARGOT GUIDAT^{1,2}, MARIO LÖW², ANNA-LENA RENZ¹, MARCO FLIEG¹, MAX NÜSSHÖR¹, VIBHAV YADAV¹, JONGMIN KIM¹, and MORITZ KÖLBACH¹ — ¹Universität Tübingen, Institute of Physical and Theoretical Chemistry, Tübingen, Germany — ²Universität Ulm, Institute of Theoretical Chemistry, Ulm, Germany

Photoelectrodes for highly efficient solar water splitting often involve III-V semiconductors, which exhibit only a limited stability under operating conditions due to (electro)chemical corrosion. Yet photoelectrochemical *in situ* functionalisation, which also involves dedicated corrosion, can effectively create an interphase that passivates the solid-liquid interface in a similar manner as solid-electrolyte interphases in batteries [1].

We show how this approach can be used to also electronically passivate III-V/Si dual junction photoelectrodes. A full understanding of the underlying photoelectrochemistry is, however, not yet achieved. To improve this understanding, we study the structural evolution of the interface in the electrolyte, using *operando* reflection anisotropy [2], improving the control of functionalisation and catalyst photoelectrodeposition.

[1] May and Jaegermann, Curr. Opin. Electrochem. 34 (2022) DOI:10.1016/j.coelec.2022.100968. [2] Löw et al., RSC Adv. 12 (2022) DOI:10.1039/D2RA05159A.

O 96.8 Fri 12:15 TRE Phy

Understanding the Interfacial Capacitance of 2D Materials in an Implicit Water Environment — •HEDDA OSCHINSKI^{1,2}, KARSTEN REUTER¹, and NICOLAS G. HÖRMANN¹ — ¹Fritz-Haber-Institut der Max-Planck-Gesellschaft, Berlin, Germany — ²Technical University of Munich, Munich, Germany

The interfacial capacitance (*C*) is a central quantity in electrochemistry. For metal electrodes, *C* is dominated by the double layer capacitance that derives from the potential drop in the solvent. However, the finite density of states (DOS) in semiconducting 2D electrodes alters the picture and leads to a vanishing *C* around the point of zero charge. This entails a challenge in describing the energy-potential relation and the connected field effects when considering adsorbates. To explore this challenge, we study the interfacial capacitance for 2D metal halides MX₂, using density-functional theory in a continuum solvent environment. We break down *C* into a DOS-filling-related quantum capacitance and the double layer capacitance. Our analysis demonstrates that such a separation into individual components is not straightforward. Nevertheless, the qualitative behavior of *C* can be rationalized, making this study a first step towards better understanding of 2D, in particular semiconducting, electrodes.

O 96.9 Fri 12:30 TRE Phy

Initial Stages of Cathodic Corrosion of Au(111) in an Ionic Liquid — •MAREN-KATHRIN HEUBACH¹, FABIAN M. SCHUETT¹, AREEG ABDELRAHMAN¹, LUDWIG A. KIBLER¹, and TIMO JACOB^{1,2,3} — ¹Institute of Electrochemistry, Ulm University, Ulm, Germany. — ²Helmholtz-Institute-Ulm (HIU), Ulm, Germany. — ³Karlsruhe Institute of Technology, Karlsruhe, Germany.

At potentials negative of 0 V vs. SHE, noble metal surfaces can be etched by a phenomenon called 'cathodic corrosion'.¹ For this process, absence of protons and presence of stabilising cations and adsorbed hydrogen at the electrode-electrolyte interface are required.² Even if the presence of water plays an important role,³ in non-aqueous electrolytes such as ionic liquids, cathodic corrosion can take place as well.⁴

In this study, the cathodic corrosion of Au(111) in the hydrophobic ionic liquid *N*-methyl-*N*-propylpiperidinium bis(trifluoromethane-sulfonyl)imide ([MPPip][TFSI]) was studied by *in situ* scanning tunnelling microscopy. Hereby, the formation of equidistant holes at the so-called 'elbows' of the Au(111) herringbone reconstruction was observed. Additionally, it was found that the water content plays a crucial role in the corrosion potential and extent. The higher the water content, the less negative is the onset potential of the cathodic corrosion and the more pits are formed at this potential.

[1] T. J. P. Hersbach, et al. Curr. Opin. Electrochem. 2021, 26, 100653. [2] A. I. Yanson, et al. Angew. Chemie Int. Ed. 2011, 50, 6346-6350. [3] M. M. Elnagar, et al. Electrochem. Sci. Adv. 2021, e2100175. [4] F. Lu, et al. RSC Adv. 2013, 3, 18791.

O 96.10 Fri 12:45 TRE Phy

Parameters Determining Electrode Modification by High Voltage Electrolysis — •LUKAS FORSCHNER, EVELYN ARTMANN, TIMO JACOB, and ALBERT K. ENGSTFELD — Institute of Electrochemistry, Ulm University, Ulm, Germany

Applying a sufficiently high voltage between two gas-evolving electrodes of different sizes in an aqueous electrolyte can lead to transition from normal electrolysis (NE) to Contact Glow Discharge Electrolysis (CGDE). Due to Joule heating, the electrolyte temperature increases significantly until enough solvent evaporates to form a stable gas sheath around the smaller electrode in which a plasma is ignited. Both in the NE and the CGDE region, the electrode surface can be altered significantly, e.g., by the formation of a Au oxide film[1] or nanoparticles.[2]

During high voltage electrolysis, there are several factors which could influence the restructuring of an electrode surface. First, to disentangle these processes, we measured the distribution of the electric potential in the electrolyte during NE using reversible hydrogen reference electrodes.[3] We found, supported by a COMSOL[®] model, that the potential distribution mainly depends on the electrolyte conductivity and the cell geometry. Furthermore, we show that

the amount of Au oxide formed on a Au electrode during NE is more closely correlated to the current (density) than the voltage (usually provided in the literature).

[1] Artmann et al., *ChemPhysChem* **22** (2021) 2429. [2] Allagui et al., *Electrochim. Acta* **93** (2013) 137. [3] Forschner et al., (2022, submitted).

O 97: Focus Session: Scanning Probe Microscopy with Quartz Sensors IV

Time: Friday 10:30–12:45

Location: TRE Ma

O 97.1 Fri 10:30 TRE Ma

qPlus-based Lateral Force Microscopy — •ALFRED J. WEYMOUTH — Universität Regensburg, Regensburg, Deutschland

Lateral force microscopy (LFM) is a branch of AFM in which a component of force perpendicular to the surface normal is measured. Long-range forces have no lateral component over a flat terrace, making LFM ideal to study short-range forces. We have established methods to extract force and potential energy from our observations, and applied these methods to study a number of systems including molecular bending. We have also studied the interaction at the side of a molecular adsorbate, and more recently shown that we can measure the energy dissipation as we pull a molecule at the tip over the surface.

Giessibl et al., *Proc. Nat. Acad. Sci.* **99**, 12006 (2002); Weymouth et al., *Science* **343**, 1120 (2014); Weymouth, *J Phys.: Condens. Matter* **29**, 323001 (2017); Weymouth et al., *Phys. Rev. Lett.* **124**, 196101(2020); Weymouth et al., *J. Jap. Appl. Phys.* **61**, SL0801 (2022)

O 97.2 Fri 10:45 TRE Ma

Exploring in-plane interactions beside an adsorbed molecule — •SHINJAE NAM¹, ELISABETH RIEGEL¹, LUKAS HÖRMANN², OLIVER T. HOFMANN², OLIVER GRETZ¹, ALFRED J. WEYMOUTH¹, and FRANZ J. GIESSIBL¹ — ¹Institute of Experimental and Applied Physics, University of Regensburg, Germany — ²Institute of Solid State Physics, Graz University of Technology, Austria

In-plane interactions between two molecules on a surface can be used to guide on-surface chemical reactions. Our implementation to study in-plane interactions is Lateral Force Microscopy (LFM), where the tip of an AFM is oscillated laterally to directly measure the lateral forces. We investigate the short-range interactions by approaching the side of an adsorbate with a CO-terminated tip. By obtaining 3D data sets at the sides of PTCDA and CO, we demonstrated the large influence of the metal dipole at the tip apex. While previous work has noted this for strongly polarized materials, including defects in ionic crystals [1] and hBN [2], we showed that the metal tip dipole above CO must be also accounted for when measuring closer to single molecules.

1. M. Ellner et al., *Nano Lett.* **16**, 1974 (2016). 2. F. Schulz et al., *ACS Nano* **12**, 5274 (2018)

O 97.3 Fri 11:00 TRE Ma

Real-space imaging σ -holes and π -holes: a source of electrostatically driven non-covalent interactions — BENJAMIN MALLADA^{1,2}, MARTIN ONDRACEK¹, AURELIO GALLARDO¹, •BRUNO DE LA TORRE^{1,2}, and PAVEL JELINEK^{1,2} — ¹Institute of Physics, Academy of Sciences of the Czech Republic, Prague, Czech Republic. — ²Regional Centre of Advanced Technologies and Materials, Palacký University, Olomouc, Czech Republic

Noncovalent interactions between molecules play an important role in supramolecular chemistry, molecular biology, and materials science. For the rational design/tweaking of supramolecular systems, it is helpful to understand the forces that make these systems stick to one another.

In this contribution, I will focus on the real-space visualization of the σ -hole (1) and π -hole (2). By a set of Atomic Force Microscopy (AFM), Kelvin Probe Force Microscopy (KPFM), and Scanning Tunneling Microscopy experiments we discriminate the emergence of both σ -hole and π -hole on a single molecule with unprecedented submolecular resolution. Our findings are fully supported by an atomistic model obtained from DFT calculations which allow us to simulate both AFM and KPFM images. These results may potentially open a new way to characterize biological and chemical systems in which anisotropic charges play a decisive role.

(1) B. Mallada et al. *Science* **2021**, 374, 863 (2) B. Mallada et al. In preparation

Topical Talk

O 97.4 Fri 11:15 TRE Ma

Heteroatom-substituted and three-dimensional nanocarbon materials studied with low temperature STM and qPlus AFM — •SHIGEKI KAWAI — National Institute for Materials Science, Tsukuba, Japan

Since the first systematic on-surface covalent coupling of bromo-substituted porphyrins,[1] on-surface chemical synthesis has attracted tremendous interest of researchers. Combining with bond-resolved scanning probe microscopy (SPM) with the qPlus sensor, [2] this field has been rapidly developed. In this contribution, I will present our recent studies on on-surface chemistry with high-

resolution SPM operating at low temperature under ultra-high vacuum. We synthesized heteroatom doped [3] and three-dimensional graphene nanoribbons (GNRs) by coupling bromo substituted-propellane molecules on Au(111).[4] In the 3D-GNR, the C-Br bonds distant from the surface remained intact even after the reaction. The radical species were formed by tip-induced debromination and were also stabilized by either Br atom or fullerene molecule. We also developed new on-surface reaction, which can synthesize graphene nanoribbon and covalent organic frameworks with silabenzene units by coupling Si atom and Br-substituted molecule.[5]

Reference: [1] L. Grill, et al., *Nat. Nanotechnol.* **2**, 687. (2007). [2] L. Gross, F. Mohn, N. Moll, P. Liljeroth, G. Meyer, *Science* **325**, 1110 (2009). [3] S. Kawai, et al *Nat. Commun.* **6**, 8098 (2015) and *Sci. Adv.* **4**, eaar7181 (2018). [4] S. Kawai, et al *Sci. Adv.* **6**, eaay8913 (2020). [5] K. Sun et al, *Nat. Chem.* (2022) doi:10.1038/s41557-022-01071-3.

O 97.5 Fri 11:45 TRE Ma

Interaction between an artificial and a natural atom — •FABIAN STILP, MARCO WEISS, and FRANZ GIESSIBL — Institute of Experimental and Applied Physics, University of Regensburg, Universitätsstraße 31, 93053 Regensburg

The surface state of Cu (111), a quasi-2-dimensional electron gas, is trapped to a small surface area of about 15 x 15 nm² by placing 48 CO-molecules in a circular shape on the surface via atomic manipulation. By doing so, one creates a quantum corral with discrete electronic states forming an artificial atom. This structure can be described reasonably well by an infinitely high circular potential well leading to corral states with Bessel-type radial functions and an angular momentum normal to the surface. To investigate the interaction between this artificial atom and a natural atom we bring Fe atoms and CO molecules inside the corral and measure the response of the corral states.

Thanks to the large corral diameter, one can study the structure of the wave functions within that artificial atom by AFM and STM showing an angular dependence of the corral states after placing the perturbations inside the corral. This change of the wave functions leads to an energy shift of a few meV. By investigating the change of the corral states due to the perturbation, one can draw conclusion about the interaction between this artificial atom and a natural atom. Here we expand the interpretation of the adatom acting repulsively on the corral states as stated by Stilp et al. [1].

[1] F. Stilp, A. Berezuk, J. Berwanger, N. Mundigl, K. Richter, F.J. Giessibl, *Science* **372**, 1196-1200 (2021).

O 97.6 Fri 12:00 TRE Ma

Revelation of an inhomogeneous broadening effect in artificial quantum structures caused by electron-adsorbate scattering — •MARCO WEISS, FABIAN STILP, and FRANZ GIESSIBL — Institute of Experimental and Applied Physics, University of Regensburg, Universitätsstraße 31, 93053 Regensburg

In 1993 Crommie et al. [1] arranged 48 Fe adatoms on a Cu(111) surface in a circle with a diameter of 14.26 nm. This quantum corral confines surface electrons in a circular potential well. Past investigations with scanning tunneling microscopy revealed energetically discrete eigenstates with radial Bessel functions. These studies on the Fe quantum corral showed unwanted movement of the corral walls during spectroscopic measurements because of the weak bonding of Fe on Cu(111) [1].

We used CO molecules to provide the corral with more stable walls. This permitted us to access a larger voltage window and allowed for a detailed line shape analysis of the corrals eigenenergy levels. Surprisingly, we discovered a dominant Gaussian broadening of the eigenstates.

We find that the spectral width is dependent on the size of the quantum structure. The introduction of a simple model linking the energy dependence of this inhomogeneous broadening with the single particle movement of surface state electrons has shown that the observed behaviour is compatible with an electronic lifetime limitation by interaction with the corral wall.

[1] M. F. Crommie et al., *Science* **262**, 218-220 (1993).

O 97.7 Fri 12:15 TRE Ma

Benchmarking atomically defined probe tips for NC-AFM experiments — DAMLA YESILPINAR¹, BERTRAM SCHULZE LAMMERS¹, ALEXANDER TIMMER¹, ZHIXIN HU², WEI JI³, SAEED AMIRJALAYER¹, HARALD FUCHS¹, and HARRY MÖNIG¹ — ¹Westfälische Wilhelms-Universität, Münster, Germany — ²Tianjin University, Tianjin, China — ³Renmin University of China, Beijing, China

Controlling the identity of the tip-terminating atom or molecule in NC-AFM constitutes a milestone in surface science. We consolidate the interpretation of such studies by directly comparing the performance of four atomically defined tips: Cu-, Xe-, CO-, and O-terminated copper (CuOx-) tips. Besides their imaging performances on a metal oxide, we directly compared their capabilities in force mapping during the lateral manipulation of single adsorbed atoms. Expectedly, Cu-tips strongly react with the surface inhibiting stable imaging and picking up the atoms to be manipulated. The chemically inert Xe- and CO-tips, allow entering the repulsive force regime. However, their flexibility leads to dynamic tip bending and pronounced artefacts due to the strongly varying potential above the oxide. Furthermore, tip deflection prevents reaching sufficient threshold forces along manipulation trajectories with high energy barriers. In contrast, the combination of moderate chemical passivation and high stiffness of CuOx-tips turned out decisive for a distinct chemical-specific contrast. Moreover, this results also in a superior performance in the manipulation experiments where their high mechanical stability allows quantitative force measurements also along the trajectories with high energy barriers.

O 97.8 Fri 12:30 TRE Ma

Visualizing electrochemical interfaces with a qPlus sensor-based AFM/STM — •ANDREA AUER, BERNHARD EDER, and FRANZ GIESSIBL — Institute of Experimental and Applied Physics, University of Regensburg, Germany

Atomic force microscopy (AFM) that can be simultaneously performed with scanning tunneling microscopy (STM) modes using metallic tips attached to self-sensing quartz cantilevers (qPlus sensors) has advanced the field of surface science by allowing for unprecedented high spatial resolution under ultra-high vacuum conditions. Applying a qPlus sensor, which offers simultaneous STM/AFM and seamless transitions in between, to the field of electrochemistry creates new possibilities to locally image both the 3D layering of the interfacial water and the lateral structure of the electrochemical double layer. In this work, a home-built AFM/STM instrument equipped with a qPlus sensor for operation under precise potential control in an electrochemical liquid cell is presented. The potential-dependent structural interface organization of the electrochemical double layer on both highly oriented pyrolytic graphite (HOPG) and Au(111) electrodes in acidic media is investigated by means of (simultaneous) AFM/STM imaging and force spectroscopy. We observe frequency shift oscillations as a function of the z-piezo distance, which correspond to the layering of the interfacial solvent molecules, where both the number of layers as well as their strength is highly dependent on the applied potential.

O 98: Overview Talk Ralph Claessen

Time: Friday 13:15–14:00

Location: HSZ 03

Invited Talk

O 98.1 Fri 13:15 HSZ 03

Surfaces go topological – third generation 2D quantum materials — •RALPH CLAESSEN — Physikalisches Institut and Würzburg-Dresden Cluster of Excellence ct.qmat, Universität Würzburg, Germany

Metal atom-decorated semiconductor surfaces have long been studied as model systems for the formation of electrical contacts to semiconductor devices. More recently, atomic monolayers on semiconductors have come into focus as two-dimensional designer quantum materials. A case in point are two-dimensional topological insulators (2D-TIs) which host 1D metallic and spin-polarized edge

states, giving rise to the quantum spin Hall (QSH) effect. Starting from the notion that a 2D honeycomb lattice favors a topologically non-trivial band structure, I will discuss several examples of such synthetic 2D-TIs, ranging from bismuthene (Bi/SiC(0001)) [1-3], whose large gap even allows the optical generation of excitons in a topological band structure [4], to indenene (In/SiC(0001)), a triangular 2D lattice of In atoms with emerging honeycomb physics and first example of a real-space obstructed QSH insulator [5, 6].

[1] Science 357, 287 (2017) [2] Nat. Phys. 16, 47 (2020) [3] Nat. Commun. 13, 3480 (2022) [4] Nat. Commun., 13, 6313 (2022) [5] Nat. Commun. 12, 5936 (2021) [6] Phys. Rev. B 106, 195143 (2022)

Physics of Socio-economic Systems Division Fachverband Physik sozio-ökonomischer Systeme (SOE)

Fakhteh Ghanbarnejad
Robert Koch Institute
Ludwig-Witthöft-Straße
15745 Wildau
GhanbarnejadF@rki.de

Philipp Hövel
Christian-Albrechts-Universität
zu Kiel
Kaiserstraße 2
24143 Kiel
philipp.hoewel@gmail.com

Eckehard Olbrich
Max Planck Institute for Mathematics in
the Sciences
Inselstraße 22
04103 Leipzig
olbrich@mis.mpg.de

Overview of Invited Talks and Sessions

(HSZ 03 and ZEU 260; Poster HSZ 02)

Invited Talks

SOE 5.1	Tue	9:30–10:00	ZEU 260	Digital Pandemology – Is that physics? — •DIRK BROCKMANN
SOE 14.1	Thu	9:30–10:00	ZEU 260	Networks in space and time – Exploring the physics in graph learning — •INGO SCHOLTES
SOE 21.1	Fri	9:30–10:00	ZEU 260	Marginal Stability and Excess volatility in firm networks — •JEAN-PHILIPPE BOUCHAUD

Invited Talks of the joint Symposium Dynamics of Opinion Formation – From Quorum Sensing to Polarization (SYOF)

See SYOF for the full program of the symposium.

SYOF 1.1	Mon	9:30–10:00	HSZ 01	Towards understanding of the social hysteresis – insights from statistical physics — •KATARZYNA SZNAJD-WERON
SYOF 1.2	Mon	10:00–10:30	HSZ 01	Polarization in attitude distributions from surveys and models of continuous opinion dynamics — •JAN LORENZ, MARTIN GESTEFELD
SYOF 1.3	Mon	10:30–11:00	HSZ 01	Collective patterns and stable misunderstandings in networks striving for consensus without a common value system — •JOHANNES FALK, EDWIN EICHLER, KATJA WINDT, MARC-THORSTEN HÜTT
SYOF 1.4	Mon	11:15–11:45	HSZ 01	A yet undetected cognitive bias, revealed by opinion dynamics simulations — •GUILLAUME DEFFUANT
SYOF 1.5	Mon	11:45–12:15	HSZ 01	Extreme switches in kinetic exchange models of opinion. — •PARONGAMA SEN, KATHAKALI BISWAS

Invited Talks of the joint Symposium SKM Dissertation Prize 2023 (SYSD)

See SYSD for the full program of the symposium.

SYSD 1.1	Mon	9:30–10:00	HSZ 04	Diffusion of antibodies in solution: from individual proteins to phase separation domains — •ANITA GIRELLI
SYSD 1.2	Mon	10:00–10:30	HSZ 04	Intermediate Filament Mechanics Across Scales — •ANNA V. SCHEPERS
SYSD 1.3	Mon	10:30–11:00	HSZ 04	Ultrafast Probing and Coherent Vibrational Control of a Surface Structural Phase Transition — •JAN GERRIT HORSTMANN
SYSD 1.4	Mon	11:00–11:30	HSZ 04	Electro-active metasurfaces employing metal-to-insulator phase transitions — •JULIAN KARST
SYSD 1.5	Mon	11:30–12:00	HSZ 04	The role of unconventional symmetries in the dynamics of many-body systems — •PABLO SALA

Sessions

SOE 1.1–1.3	Sun	16:00–18:15	HSZ 02	Tutorial: Stochastic Processes of Opinion Formation (joint session SOE/TUT)
SOE 2.1–2.1	Mon	12:30–13:00	ZEU 250	Invited Talk: Dynamics of Networks (joint session DY/SOE)
SOE 3.1–3.2	Mon	15:00–17:00	HSZ 03	Award Session: Young Scientist Award for Socio- and Econophysics (YSA)
SOE 4.1–4.14	Mon	17:00–19:00	P2/OG2	Poster
SOE 5.1–5.1	Tue	9:30–10:00	ZEU 260	Physics of Contagion Processes I (joint session SOE/DY)
SOE 6.1–6.3	Tue	10:00–10:45	ZEU 260	Physics of Contagion Processes II (joint session SOE/DY)
SOE 7.1–7.5	Tue	11:00–12:15	ZEU 260	Networks: From Topology to Dynamics I (joint session SOE/DY)
SOE 8.1–8.4	Tue	14:00–15:00	ZEU 260	Semantic Networks, Language and Culture
SOE 9.1–9.5	Wed	9:30–11:45	ZEU 260	Focus Session: Critical Transitions in Society, Economy, and Nature (joint session SOE/DY)
SOE 10.1–10.6	Wed	15:00–16:30	ZEU 260	Traffic Dynamics, Urban and Regional Systems I
SOE 11.1–11.6	Wed	16:45–18:15	ZEU 260	Traffic Dynamics, Urban and Regional Systems II
SOE 12	Wed	18:30–19:30	ZEU 260	Members' Assembly
SOE 13.1–13.8	Thu	9:30–12:00	MOL 213	Data Analytics of Complex Dynamical Systems (joint session DY/SOE)
SOE 14.1–14.1	Thu	9:30–10:00	ZEU 260	Networks: From Topology to Dynamics II (joint session SOE/DY)
SOE 15.1–15.3	Thu	10:00–10:45	ZEU 260	Networks: From Topology to Dynamics III (joint session SOE/DY)
SOE 16.1–16.5	Thu	11:00–12:15	ZEU 260	Collective Dynamics in Animal and Human Societies
SOE 17.1–17.2	Thu	15:00–15:30	ZEU 260	Evolutionary Game Theory (joint session SOE/DY)
SOE 18.1–18.4	Thu	15:30–16:30	ZEU 260	Social Systems, Opinion and Group Dynamics I
SOE 19.1–19.5	Thu	16:45–18:00	ZEU 260	Social Systems, Opinion and Group Dynamics II
SOE 20.1–20.8	Fri	9:30–11:45	ZEU 250	Networks: From Topology to Dynamics IV (joint session DY/SOE)
SOE 21.1–21.1	Fri	9:30–10:00	ZEU 260	Financial Markets and Risk Management I
SOE 22.1–22.3	Fri	10:00–10:45	ZEU 260	Financial Markets and Risk Management II
SOE 23.1–23.4	Fri	11:00–12:00	ZEU 260	Economic Models

Members' Assembly of the Physics of Socio-economic Systems Division

Wednesday 18:30–19:30 ZEU 260

- Bericht
- Verschiedenes

Sessions

– Invited Talks, Prize Talks, Topical Talks, Tutorials, Contributed Talks, and Posters –

SOE 1: Tutorial: Stochastic Processes of Opinion Formation (joint session SOE/TUT)

Time: Sunday 16:00–18:15

Location: HSZ 02

Tutorial SOE 1.1 Sun 16:00 HSZ 02

Bounded Confidence Revisited: What We Overlooked, Underestimated, and Got Wrong — •RAINER HEGSELMANN — Frankfurt School of Finance & Management, 60322 Frankfurt, Adickesallee 32-34

The talk will discuss the so called bounded confidence model (BC-model, for short). The model is very simple: Period by period, all agents average over all opinions that are not further away from their actual opinion than a given distance ϵ , their ϵ -bound of confidence*.

The simplicity of the model is deceptive. Two decades ago, Ulrich Krause and me published an analysis of the model in which we overlooked completely a decisive feature of our model: For increasing values of ϵ , our analysis back then suggests smooth transitions in the model's behavior. But in fact, the transitions are wild, chaotic, and non-monotonic.

In my talk I will present a new type of approach in which everything we overlooked at the time becomes directly obvious and, in a sense, unmissable. Key component of the new approach is an algorithm that identifies, exactly and exhaustively, all bounds of confidence, that make a difference. We get a list that, then, allows direct checks for wild behavior exhaustive of all possible cases. That is a good news. But it is accompanied by a bad one: The algorithm that does the work, requires an absolutely exact fractional arithmetic with integers of arbitrary length. As a consequence, we have to pay a price in terms of computational speed.

Tutorial SOE 1.2 Sun 16:45 HSZ 02

When intuition fails: the complex effects of assimilative and repulsive influence on opinion polarization — •MICHAEL MAES¹, ANDREAS FLACHE², SHUO LIU³, and HAOXIANG XIA³ — ¹Karlsruhe Institute of Technology, Karlsruhe, Germany — ²University of Groningen, Groningen, The Netherlands — ³Dalian University of Technology, Dalian, China

There is a debate about whether personalized services of social-media platforms contribute to the rise of bipolarization of political opinions. On the one hand, it is argued that personalized services of online social networks generate filter bubbles limiting contact between users who disagree. This reduces opportuni-

ties for assimilative social influence between users from different camps and prevents opinion convergence. On the other hand, empirical research also indicated that exposing users to content from the opposite political spectrum can activate the counter-part of assimilative influence, repulsive influence. Fostering contact that leads to opinion assimilation and limiting contacts likely to induce repulsive interactions, it has been concluded, may therefore prevent bipolarization. We demonstrate that these conclusions fail to capture the complexity that assimilative and repulsive influence generate in social networks. Sometimes, more assimilative influence can actually lead to more and not less opinion bipolarization. Likewise, increasing the exposure of users to like-minded individuals sometimes intensifies opinion polarization.

Tutorial SOE 1.3 Sun 17:30 HSZ 02

How growing connectivity and self-organization changes opinion dynamics — •PHILIPP LORENZ-SPREEN — Center for Adaptive Rationality, Max Planck Institute for Human Development, Berlin, Germany

Information technology has made various aspects of our lives more dynamic and self-organized. Connections with others can be made across spatial and socio-demographic boundaries and undone with the click of a button. Since the famous six degrees of separation, networks seem much more connected; Facebook reports 3.5 degrees of separation on its friendship graph. Yet there have been repeated reports of segregated, homophilic network structures and related trends of increasing polarization on most online platforms. The mechanism that could resolve this apparent paradox may lie behind the question of whether we change our opinions according to our friends or whether we change our friends according to our opinions. We have recently proposed that an agent's opinion changes as a process of mutual reinforcement within clusters of shared attitudes and a coevolution of the associated network structure that dynamically adapts to changing opinions and follows a probability distribution governed by homophily. This combination helps explain the potential emergence of increasing polarization even as connectivity increases. Moreover, extending this model to multiple dimensions of topics can explain the empirical observation of increasing alignment of issues, where opinions become increasingly correlated within ideological clusters.

SOE 2: Invited Talk: Dynamics of Networks (joint session DY/SOE)

Time: Monday 12:30–13:00

Location: ZEU 250

See DY 8 for details of this session.

SOE 3: Award Session: Young Scientist Award for Socio- and Econophysics (YSA)

Time: Monday 15:00–17:00

Location: HSZ 03

Presentation of the Award to the Awardee

Prize Talk SOE 3.1 Mon 15:10 HSZ 03

Initial Progress on the Science of Science — •DASHUN WANG — Northwestern University

The increasing availability of large-scale datasets that trace the entirety of the scientific enterprise, have created an unprecedented opportunity to explore scientific production and reward. Parallel developments in data science, network science, and artificial intelligence offer us powerful tools and techniques to make sense of these millions of data points. Together, they tell a complex yet insightful story about how scientific careers unfold, how collaborations contribute to discovery, and how scientific progress emerges through a combination of multiple interconnected factors. These opportunities—and challenges that come with them—have fueled the emergence of a multidisciplinary community of scientists that are united by their goals of understanding science and innovation. These practitioners of the science of science use the scientific methods to study themselves, examine projects that work as well as those that fail, quantify the patterns that characterize discovery and invention, and offer lessons to improve science as a whole. In this talk, I will highlight some examples of research in this area, hoping to illustrate the promise of science of science as well as its limitations.

Presentation of the Award to the Awardee

Prize Talk SOE 3.2 Mon 16:00 HSZ 03

Complexity science can address marginalization in society and algorithms — •FARIBA KARIMI — Technical university of Vienna — Complexity Science Hub Vienna

Structural marginality refers to structural conditions that push certain groups towards a network's margins, limiting their access to resources. Despite its importance, there are minimal quantitative understanding of its manifestation in networks and are thus we are unequipped to answer several urgent societal questions. For example, what underlying structural mechanisms drive marginalization? How can marginalized groups improve their social positions? How do AI systems reinforce these effects? Do hard (mathematical) limits exist on actions that would alleviate structural inequalities? In this talk, I argue that tools in complexity science are instrumental in measuring structural marginalities that emerge in society and algorithms.

After the Award Session, there will be an informal get-together with beer and pretzels at the poster session

SOE 4: Poster

Time: Monday 17:00–19:00

Location: P2/OG2

SOE 4.1 Mon 17:00 P2/OG2

Identifying subdominant collective effects in a large motorway network — •SHANSHAN WANG, MICHAEL SCHRECKENBERG, and THOMAS GUHR — Faculty of Physics, University of Duisburg-Essen, Duisburg, Germany

In a motorway network, correlations between parts or, more precisely, between the sections of (different) motorways, are of considerable interest. Knowledge of flows and velocities on individual motorways is not sufficient, rather, their correlations determine or reflect, respectively, the functionality of and the dynamics on the network. These correlations are time-dependent as the dynamics on the network is highly non-stationary. Apart from the conceptual importance, correlations are also indispensable to detect risks of failure in a traffic network. Here, we proceed with revealing a certain hierarchy of correlations in traffic networks that is due to the presence and to the extent of collectivity. In a previous study, we focused on the collectivity motion present in the entire traffic network, i.e. the collectivity of the system as a whole. Here, we manage to subtract this dominant effect from the data and identify the subdominant collectivities which affect different, large parts of the traffic network. To this end, we employ a spectral analysis of the correlation matrix for the whole system. We thereby extract information from the virtual network induced by the correlations and map it on the true topology, i.e. on the real motorway network. The uncovered subdominant collectivities provide a new characterization of the traffic network. We carry out our study for the large motorway network of North Rhine-Westphalia (NRW), Germany.

SOE 4.2 Mon 17:00 P2/OG2

Feasibility and goodness of bimodal on-demand public transportation. — •PUNEET SHARMA, KNUT HEIDEMANN, HELGE HEUER, STEFFEN MUEHLE, and STEPHAN HERMINGHAUS — Max Planck Institute for Dynamics and Self Organization, Goettingen

Decarbonization of passenger transport is essential for fighting climate emergency. While modern cities offer various modes of transportation, considered separately, none of them is both, sustainable and convenient. A taxi service is convenient, in a sense, due to door-to-door service, but is inefficient since it usually serves one customer only. Demand-responsive ridepooling (DRRP) with minibuses is more efficient, but leads to undue competition with line services (LS), which provide even better pooling but are less convenient due to fixed routes and stops. A combination of both modes, DRRP and LS, may provide an ideal solution but is challenging to organize. Here we introduce a model for such bimodal on-demand transportation based on a square-grid geometry. Our model quantifies under what circumstances bimodal public transportation is feasible, both in terms of convenience and ecological footprint. Moreover, the model yields estimates for how to operate (LS frequency, modal split) a bimodal transportation system optimally. Perhaps surprisingly, we find that operating LS at maximum capacity is not necessarily optimal. We also consider the intricate interplay between LS operations and DRRP performance, i.e., detours, waiting times, and occupancy, via simulations.

SOE 4.3 Mon 17:00 P2/OG2

Just in time vs. all in sync: an analysis of two types of synchronization in a minimal model of machine activity in industrial production based on excitable dynamics on graphs — •SANGHITA BOSE¹, ANNICK LESNE^{2,3}, JULIA ARLINGHAUS⁴, and MARC-THORSTEN HÜTT¹ — ¹Department of Life Sciences and Chemistry, Jacobs University Bremen, Germany — ²Institut de Génétique Moléculaire de Montpellier, University of Montpellier, CNRS, F-34293, Montpellier, France — ³Sorbonne Université, CNRS, Laboratoire de Physique Théorique de la Matière Condensée, LPTMC, F-75252, Paris, France — ⁴Otto-von-Guericke University Magdeburg, Universitätsplatz 2, 31904, Magdeburg, Germany.

The notion of synchronization in logistics is distinct from that encountered in the natural sciences, and in particular, in physics. In logistics, synchronization is often associated with a 'just in time' paradigm in supply and production systems. A perfect synchronization therefore is that the arrival (of goods at a warehouse or parts at a machine) is a cue for a subsequent transportation or manufacturing event. Globally, this type of synchronization can be envisioned as a wave of activity running through a distribution network or a production network. Here our goal is a deeper theoretical understanding of these two types of synchronization, the one from logistics and the one from physics, as well as their interplay in the context of production systems. We employ a minimal model of propagating excitations (representing machine activity) in a graph (representing a production network).

SOE 4.4 Mon 17:00 P2/OG2

Impact of interactions between layers on source localization in multilayer networks — ROBERT PALUCH, ŁUKASZ GAJEWSKI, •KRZYSZTOF SUCHECKI, and JANUSZ HOŁYST — Faculty of Physics, Warsaw University of Technology, Koszykowa 75, Warsaw, 00-662, Poland

Nowadays, it is not uncommon to have to deal with dissemination on multilayered networks, and often finding the source of said propagation can be a crucial task. We examine the issue of locating the source of Susceptible-Infected spreading process in a multilayer network using the Bayesian inference and the maximum likelihood method established for general networks and adapted here to cover multilayer topology. We show how its accuracy depends on the network and spreading parameters and find the existence of two parameter ranges with different behavior. If the inter-network spreading rate is low, observations in different layers interfere, lowering accuracy below that of relying on single-layer observers only. If it is high, on the other hand, observations synergize, raising accuracy above the level of a single-layer network of the same size and observer density. We also show a heuristic method to determine the case in a system and potentially improve accuracy by rejecting interfering observations.

SOE 4.5 Mon 17:00 P2/OG2

Mean field approach for link coupling in Heider dynamics in bilayer network — •KRISHNADAS MOHANDAS and JANUSZ HOŁYST — Warsaw University of Technology, Poland

Structural balance was observed in many social groups with simultaneous friendly and hostile relations. Frequently these interactions need to be described by multicomponent attributes and different components can be coupled together. In this study we consider a bilayer topology of Heider balance in a link multiplex, a unique multiplex in which coupling not only exists between different agents but also between corresponding links of the same agent. In social networks, for instance, agents can belong to the family, professional and friends group, where links in each layer could address either sports or politics. The dynamics of agents differs inside and between the layers and the coupling coefficients between the layers govern the strength of influence of one link-layer on another. Numerical simulations and analytical calculations using heat-bath approach and mean-field approximation demonstrate that the link polarization for both layers of a complete signed network of N agents tends towards Heider balance below critical temperature. The effect of such inter-layer coupling results in the increase of critical temperature with the strength of positive coupling. Periodical and chaotic trajectories of mean polarisations of both components are observed for a range of temperatures in the case of negative interlayer coupling.

SOE 4.6 Mon 17:00 P2/OG2

Counting Graphs and Molecules — •RANA SHOJAEI^{1,2,3} and THILO GROSS^{1,2,3} — ¹Helmholtz Institute for Functional Marine Biodiversity at the University of Oldenburg (HIFMB), Oldenburg, Germany — ²Alfred Wegener Institute-Helmholtz Centre for Marine and Polar Research, Bremerhaven, Germany — ³Carl von Ossietzky University- Institute for Chemistry and Biology of the Marine Environment (ICBM), Oldenburg, Germany

Counting the number of simple graphs that can be constructed between a given number of unlabeled (indistinguishable) nodes is a long-standing challenge. We consider this problem using Polya's counting theory. For illustration, we first consider a related problem that has historically received much attention: counting the number of chemical molecules with a given number of atoms. Indeed, it was in the context of this problem that the term 'graph' was first coined. Application of the same principles and procedure leads to a simple closed-form formula for the number of simple graphs, however, the efficient evaluation of the formula for large graphs remains an open problem.

SOE 4.7 Mon 17:00 P2/OG2

How random are team sports leagues? — MACIEJ PAWLIK¹, MICHAŁ BORUTA², ROBERT PALUCH¹, and •JANUSZ HOŁYST¹ — ¹Faculty of Physics, Warsaw University of Technology, Warsaw, 00-662, Poland — ²Faculty of Mathematics and Information Science, Warsaw University of Technology, Warsaw, 00-662, Poland

To answer the title question, the historical ranking tables of four team sports leagues (Premier League, Bundesliga, La Liga, Svenska Hockeyligan) are analyzed. We investigate the predictability level of a given league by calculating the average absolute rank change $\bar{\rho}$ between two subsequent seasons of every team. The data are applied to calibrate an agent-based model of team sports leagues where every team possesses a certain strength equal to the sum of strengths of all players that have been selected to the team from a draft list. The sign of the difference between the strengths of two teams indicates the favorite of a given game, and there is a determinism parameter $\beta \in (0, \infty)$ that controls the game predictability. We use the model to simulate many seasons of various leagues and to compute the average absolute rank change $\bar{\rho}$ of a given team between two consecutive seasons. Plotting $\bar{\rho}$ as a function of β reveals a continuous transi-

tion between phases of luck- and skill-based sports. Comparing the results of our model with the ranking tables of selected professional leagues, we show that they operate close to the transition line but in the deterministic phase. This finding suggests that random factors and abilities of team players are of comparable importance, with an advantage of the latter.

SOE 4.8 Mon 17:00 P2/OG2

Simulating neutral biodiversity in large-scale networks — •JEFFREY KELLING^{1,2}, RICHA TRIPATHI³, and JUSTIN M. CALABRESE³ — ¹Helmholtz-Zentrum Dresden-Rossendorf, Dresden, Germany — ²Chemnitz University of Technology, Chemnitz, Germany — ³Center for Advanced Systems Understanding (CASUS), Helmholtz-Zentrum Dresden-Rossendorf, Görlitz, Germany

The neutral model of biodiversity describes a Markov process of death and replacement of neutral individuals constituting the species occupying an ecosystem. It predicts a number macroscopic ecosystem observables, including local and global abundances, and can serve as advanced null-hypothesis for more complex models. We present a massively parallel approach to simulating the neutral model which both enables simulations on large networks, to, e.g., capture fine details of real river networks, and efficiently produces averages results to enable comparisons with empirical data or other models at high statistical significance or accurately compute correlations or responses.

SOE 4.9 Mon 17:00 P2/OG2

A toy model for the rise and collapse of societies — •ALEXANDER JOCHIM and STEFAN BORNHOLDT — Institute for Theoretical Physics, University of Bremen
Societal collapse as in ancient Rome is rather common than an exception along history. Similar patterns can be observed along time and space, and modern societies are potentially as vulnerable. Relying on empirical data, recent work has introduced mathematical models for long term processes in society. Here we report on a simple, physics-inspired model that exhibits metastable states and phases of collapse or sustained prosperity

SOE 4.10 Mon 17:00 P2/OG2

The Verification Dilemma in computer security: a game-theoretic perspective — •JENS CHRISTIAN CLAUSSEN and AAD VAN MOORSEL — School of Computer Science, University of Birmingham, UK

Verification protocols, as the Proof-of-Work (PoW) in blockchains, are essential mechanisms to ensure security in distributed networks. The computational costs of verification can also be organized in a shared way through special users, called miners. It has been pointed out that a Verifier's Dilemma arises between verifying and non-verifying miners [1]. Here we analyze the verification problem from game theory, identifying it as a strategic dilemma similar to a public goods game.

[1] D. Smuseva, I. Malakhov, A. Marin, A. van Moorsel and S. Rossi, Verifier's Dilemma in Ethereum Blockchain: A Quantitative Analysis, LNCS 13479, 317 (2022)

SOE 4.11 Mon 17:00 P2/OG2

Investigating the Impacts of Regulatory Changes in Energy Systems with Explainable Artificial Intelligence — •SEBASTIAN PÜTZ¹, DIRK WITTHAUT^{2,3}, and BENJAMIN SCHÄFER¹ — ¹Institute for Automation and Applied Informatics, Karlsruhe Institute of Technology, Eggenstein-Leopoldshafen, Germany — ²IEK-STE Research Centre Jülich, Jülich, Germany — ³University of Cologne, Cologne, Germany

The stable supply of electrical energy is essential for the functioning of our society. Therefore, the operation of the electrical power grid and its related markets is subject to strict regulations. As the external technical, economic or social influences on the power grid change permanently, e.g. due to the energy transition, these regulations must also be constantly adapted. It is important to find out

whether the regulatory changes lead to the intended results or whether they entail undesired side effects. We investigate regulatory changes using a data-driven approach based on publicly available techno-economic data on European power grids and electricity markets. We employ explainable machine learning models to identify important dependencies and disentangle the interaction of individual features. Using additive Shapley explanations, we identify changes due to the introduction of the 'Mischpreisverfahren' in the German balancing energy market or the splitting of the German-Austrian bidding zone.

SOE 4.12 Mon 17:00 P2/OG2

Delay Dynamics in a Nonlinear Economic Model — •SÁNDOR KOVÁCS¹, SZILVIA GYÖRGY¹, JÚLIA TOMPA², and NOÉMI GYÚRÓ² — ¹Department of Numerical Analysis, Eötvös Loránd University, Pázmány Péter sétány 1/C, H-1117 Budapest, Hungary \ E-mail: alex@ludens.elte.hu — ²Eötvös Loránd University, Pázmány Péter sétány 1/C, H-1117 Budapest, Hungary

This talk is about the qualitative behavior of an economic model proposed by D. Meyer (cf. [1]). It is shown that under certain conditions on the parameters the system has uniformly bounded and no non-trivial periodic solutions. Subsequently, a possible equilibrium on the boundary of the positive phase space not discussed in [1] was founded and showed that if there is no interior equilibrium, then the equilibrium at the boundary will become unstable, whereas the equilibrium at the boundary will be stable. In order to have more realism, two types of delay will be introduced: an infinite distributed delay and a discrete delay. It is shown that contrary to the result in [1] the distributed delay does not change the stability of the equilibrium points. Finally, by introducing a discrete delay, it was showed that at a certain parameter value Hopf bifurcation takes place: periodic solutions arise. [1] Meyer, D. Equity and Efficiency in Regional Policy. Periodica Mathematica Hungarica Vol. 56 (1), 2008, 105*119.

SOE 4.13 Mon 17:00 P2/OG2

A model of public opinion with time-dependent media influence, audience attention and social influence. — •MICHAEL SCHNABEL¹ and DANIEL DIERMEIER^{1,2} — ¹Vanderbilt University, Department of Political Sciences, Nashville, TN, USA — ²Vanderbilt University, Owen School of Management, Nashville, TN, USA

We consider a simple model of binary opinions. Individuals form their opinions based on individual preferences, time-dependent media influence and the overall opinions in the population. In addition, we also incorporate a mechanism that is responsive to the salience of the media influence and can be used to account for variations in public attention. We explore how attention affects the opinion dynamics in the population as well as the equilibrium properties in a hypothetical quasi-static environment. Our model can account for populations with heterogeneous preferences and can also be used to examine the dynamics of opinion polarization within a population.

SOE 4.14 Mon 17:00 P2/OG2

Analysis of changes of opinions and social network structure of NetSense experiment participants — •BARTŁOMIEJ ZWOLIŃSKI and PIOTR GÓRSKI — Faculty of Physics, Warsaw University of Technology, Warsaw, 00-662 Poland

We study the interrelation between interactions and opinions by using data on Bluetooth contacts between college freshmen. We research evolution of social network structure and their opinions on eight topics within two-year period.

We find weak but significant correlation between students' vectors of opinions and their further interactions. Higher number of interactions had different impact on students' opinions depending on the period of the study, polarising them or leading to opinion alignment.

Throughout the experiment, we observed change of the students' contact network from overall community to smaller groups worse interconnected with each other.

SOE 5: Physics of Contagion Processes I (joint session SOE/DY)

Time: Tuesday 9:30–10:00

Location: ZEU 260

Invited Talk

SOE 5.1 Tue 9:30 ZEU 260

Digital Pandemiology – Is that physics? — •DIRK BROCKMANN — Humboldt University of Berlin, Berlin, Germany

Three years of COVID-19 lie behind us. Experts from various fields worked constantly on understanding, mitigating and making sense of the pandemic. Novel digital tools became an essential part and complemented traditional, epidemiological methods. I will report on research activities and digital projects we

launched during the past years that delivered important insights and were helpful as real-time assessment tools during the pandemic. These include the Covid-19-mobility monitor and the Corona Data Donation Project in which more than 500,000 participants donated daily data collected by their smartwatch or wearable device. I will summarize the results we obtained from these technologies and discuss why physics, as a mindset, is helpful for understanding phenomena that unfold across the borders of traditional scientific disciplines.

SOE 6: Physics of Contagion Processes II (joint session SOE/DY)

Time: Tuesday 10:00–10:45

Location: ZEU 260

SOE 6.1 Tue 10:00 ZEU 260

Explosive Epidemics — •GEORG BÖRNER¹, MALTE SCHRÖDER¹, DAVIDE SCARSELLI², NAZMI BURAK BUDANUR^{2,3}, BJÖRN HOF², and MARC TIMME^{1,4,5} — ¹Chair for Network Dynamics, Center for Advancing Electronics Dresden (cfaed) and Institute of Theoretical Physics, Technische Universität Dresden, Dresden 01062, Germany — ²Institute of Science and Technology Austria, Klosterneuburg, Austria — ³Max Planck Institute for the Physics of Complex Systems, Dresden, Germany — ⁴Cluster of Excellence Physics of Life, Technische Universität Dresden, Dresden 01062 Germany — ⁵Lakeside Labs, Lakeside B04b, 9020 Klagenfurt, Austria

Standard epidemic models exhibit one continuous, second order phase transition to macroscopic outbreaks. However, interventions to control outbreaks may fundamentally alter epidemic dynamics. We reveal how such interventions modify the type of phase transition. In particular, we uncover three distinct types of explosive phase transitions for epidemic dynamics with capacity-limited interventions. Depending on the capacity limit, interventions may (i) leave the standard second-order phase transition unchanged but exponentially suppress the probability of large outbreaks, (ii) induce a first-order discontinuous transition to macroscopic outbreaks, or (iii) cause a secondary explosive yet continuous third-order transition. These insights highlight inherent limitations in predicting and containing epidemic outbreaks. More generally our study offers a cornerstone example of a third-order explosive phase transition in complex systems.

SOE 6.2 Tue 10:15 ZEU 260

Large-deviations of the SIR model under the influence of Lockdowns — LEO PATRICK MULHOLLAND¹, •YANNICK FELD², and ALEXANDER K. HARTMANN² — ¹Queen's University Belfast, United Kingdom — ²Institute of Physics, Carl von Ossietzky University, Oldenburg, Germany

Due to the high real-world impact of diseases, the modelling of its dynamics has long since become an important aspect of various disciplines. Statistical physics

is one of them as it gives us the tools investigate the fundamental processes through which a disease spreads throughout a population.

The transmission of a disease is affected by a lot of different factors. For example in response to the SARS-CoV 2 pandemic many governmental bodies imposed interventions to impede the spread of disease. One of the earliest non-pharmaceutical interventions (NPIs) that most countries used were lockdowns.

Motivated by that, we numerically [1] study the dynamics of the susceptible-infected-recovered (SIR) model with lockdowns on small-world networks by using a large-deviation approach, which was previously used to study the case of an unimpeded spread [2]. This allows us to obtain the probability density function of the cumulative fraction of infected nodes down to very small probabilities like 10^{-55} . The density exhibits remarkable discontinuities of the first derivative.

[1] A.K. Hartmann, *Big Practical Guide to Computer Simulations* (World Scientific, 2015)

[2] Y. Feld, A. K. Hartmann, *Phys. Rev. E* **105** 17 (2022)

SOE 6.3 Tue 10:30 ZEU 260

Short messages spread wider in online social networks — PATRYK A. BOJARSKI, •KRZYSZTOF SUCHECKI, and JANUSZ A. HOLYST — Faculty of Physics, Warsaw University of Technology, Warsaw, 00-662 Poland

We explore the behavior of an online message spreading model, that includes mutable message content, user opinions and limited processing capacities. The model shows robust power-law distribution of the number of shares for different messages and that the tail of the distribution is composed almost entirely of very short messages. The possibility to modify message content by spreaders makes already popular, short messages even more popular if the users are selective about what content they spread, but not too much. The distribution of message variants is also a power-law, in agreement with real message spreading in Facebook. The behavior of the model is robust against model parameters and network topology variations and offers an explanation as to why services focused on short messages, such as Twitter, are popular.

SOE 7: Networks: From Topology to Dynamics I (joint session SOE/DY)

Time: Tuesday 11:00–12:15

Location: ZEU 260

SOE 7.1 Tue 11:00 ZEU 260

Modelling the perception of music in brain network dynamics — •JAKUB SAWICKI^{1,2,3,4}, LENZ HARTMANN⁵, ROLF BADER⁵, and ECKEHARD SCHÖLL^{1,4,6} — ¹Potsdam Institute for Climate Impact Research — ²Institut für Musikpädagogik, Universität der Künste Berlin — ³Fachhochschule Nordwestschweiz FHNW, Basel, Switzerland — ⁴Institut für Theoretische Physik, TU Berlin — ⁵Institute of Systematic Musicology, University of Hamburg — ⁶Bernstein Center for Computational Neuroscience Berlin

We analyze the influence of music in a network of FitzHugh-Nagumo oscillators with empirical structural connectivity measured in healthy human subjects [1]. We report an increase of coherence between the global dynamics in our network and the input signal induced by a specific music song. We show that the level of coherence depends crucially on the frequency band. We compare our results with experimental data, which also describe global neural synchronization between different brain regions in the gamma-band range and its increase just before transitions between different parts of the musical form (musical high-level events). The results also suggest a separation in musical form-related brain synchronization between high brain frequencies, associated with neocortical activity, and low frequencies in the range of dance movements, associated with interactivity between cortical and subcortical regions. [1] Sawicki, J., Hartmann, L., Bader, R., Schöll, E., *Front. Netw. Physiol.* **2**, 910920 (2022).

SOE 7.2 Tue 11:15 ZEU 260

Order-disorder transition in the zero-temperature Ising model on random graphs — ARMIN POURNAKI^{1,2}, ECKEHARD OLBRICH², SVEN BANISCH³, and •KONSTANTIN KLEMM⁴ — ¹Laboratoire Lattice, CNRS & ENS-PSL, Paris — ²Max Planck Institute for Mathematics in the Sciences, Leipzig — ³Karlsruhe Institute for Technology — ⁴IFISC (UIB-CSIC), Palma de Mallorca, Spain

The zero-temperature Ising model is known to reach a fully ordered ground state in sufficiently dense graphs. In sparse random graphs, the dynamics gets absorbed in disordered local minima at magnetization close to zero. Here we find that the non-equilibrium transition between the ordered and the disordered regime occurs at an average degree that slowly grows with the system size. The system shows bistability: the distribution of the absolute magnetization in the absorbing state reached is bimodal with peaks only at zero and unity. For fixed system size, the average time to absorption behaves non-monotonically as a function of average degree. The peak value of the average absorption time grows as

a power law of system size. These findings have relevance for community detection, opinion dynamics and games on networks. Full manuscript available at <https://arxiv.org/abs/2209.09325>

SOE 7.3 Tue 11:30 ZEU 260

Analytical methods to stochastic binary-state dynamics on networks. — •ANTONIO FERNANDEZ PERALTA¹ and RAUL TORAL² — ¹Central European University, Vienna, Austria — ²IFISC (Instituto de Física Interdisciplinar y Sistemas Complejos), Palma de Mallorca, Spain

Recently, there has been a lot of effort in the development of highly accurate mathematical descriptions of the dynamics of binary-state models defined on complex networks. There are two main approaches: (i) individual based-approaches where the variables are the state of each node, and (ii) compartmental approaches where nodes are aggregated based on some topological property such as, for example, the number of neighbors in the network. Except in a few cases where stochastic effects are taken into account at some extent, the approaches are usually followed by a deterministic description, neglecting the stochastic nature of the models defined by the individual transitions rates. Stochastic effects may become relevant even for extremely large system sizes, specially if the system is close to a critical point, or the network has high degree heterogeneity. Besides, there are some models where the deterministic approach does not provide the relevant information sought. For instance, the noisy-voter (Kirman) model, the contact process or the Threshold model, are examples of relevance in which the stochastic effects greatly dominate the dynamics. The main aim of this work is to give a general theoretical approach to binary-state models on complex networks that takes into account stochastic effects, going beyond incomplete deterministic approaches.

SOE 7.4 Tue 11:45 ZEU 260

Infinite sequence of explosive transitions in network robustness — •LAURA BARTH^{1,2,3} and THILO GROSS^{1,2,3} — ¹Helmholtz Institute for Functional Marine Biodiversity (HIFMB), Oldenburg, Germany — ²Alfred-Wegener Institute (AWI), Helmholtz Center for Polar and Marine Research, Bremerhaven, Germany — ³Institute for Chemistry and Biology of the Marine Environment (ICBM), Carl-von-Ossietzky University, Oldenburg, Germany

Explosive transitions in networks have recently received much attention. Here we show that such transitions also appear in one of the most fundamental problems in network science if it is considered from a certain angle. This problem

is the fragmentation of networks under node or link removal, which has been studied extensively in the context of social networks. One key property in this context is v , the probability that a random link of a random node does not connect to the giant component. Now suppose we are constructing a random graph with a prescribed mean degree. How would we choose the degree distribution such that v is minimal after the attack? We show that the optimal degree distributions undergo an infinite sequence of discontinuous transitions as the size of the attack is changed.

SOE 7.5 Tue 12:00 ZEU 260

Information parity to measure the consonance of influence in complex networks — ALINE VIOL¹ and PHILIPP HÖVEL² — ¹Scuola Internazionale Superiore di Studi Avanzati, Italy — ²Christians-Albrechts-Universität zu Kiel, Germany

We discuss a new analytical tool to quantify the consonance of influence between nodes with respect to the whole network architecture: information par-

ity. Unlike traditional approaches to quantitative network analysis that consider only local or global scales, information parity instead quantifies pairwise statistical similarities over the entire network structure. Based on information theory and using the statistics of geodesic distances, information parity assesses how similarly a pair of nodes can influence and be influenced by the network. This allows us to quantify the access of information gathered by the nodes. To demonstrate the method's potential, we evaluate a social network and human brain networks. Our results indicate that emerging phenomena like an ideological orientation of nodes in social networks can be shaped by their information parities. We also show the potential of information parity to identify central network regions in structural brain networks placed near the mid-sagittal plane. We find that functional networks have, on average, greater information parity for inter-hemispheric homologous regions in comparison to the whole network. Finally, we explore functional brain networks under influence of a psychedelic substance.

SOE 8: Semantic Networks, Language and Culture

Time: Tuesday 14:00–15:00

Location: ZEU 260

SOE 8.1 Tue 14:00 ZEU 260

Evolution of Socio- and Econophysics in the German Physical Society (DPG) — ARMIN POURNAKI^{1,2}, SVEN BANISCH³, PHILIPP HÖVEL⁴, and ECKEHARD OLBRICH¹ — ¹Max Planck Institute for Mathematics in the Sciences, Germany — ²Laboratoire Lattice, CNRS & ENS-PSL, France — ³Karlsruhe Institute for Technology, Germany — ⁴Christians-Albrechts-Universität zu Kiel, Germany

We present an interactive visualization (<https://pournaki.com/soe/>) that allows to explore the evolution of the semantic network of all abstracts that were submitted to the division *socio-economic systems (SOE)* of the DPG spring meetings from 2002 until 2022. The online interface allows to search for semantically related work in the *DPG-Verhandlungen* (book of abstracts) by also providing a textual interface that links the abstracts back to the actual website of the *Verhandlungen*. Employing a topic model on the data one can follow the evolution of central topics over time.

Moreover, we use the semantic network to study the role of the network paradigm as an integrative concept and its interaction within and across the different subfields of the SOE division.

SOE 8.2 Tue 14:15 ZEU 260

Network analysis of the Kyiv Bylyny cycle - East Slavic epic narratives — PETRO SARKANYCH^{1,2}, NAZAR FEDORAK^{3,4}, YURIJ HOLOVATCH^{1,2,5}, PÁDRAIG MACCARRON⁶, JOSEPH YOSE^{5,2}, and RALPH KENNA^{5,2} — ¹ICMP, NAS of Ukraine, Lviv, Ukraine — ²L4 Collaboration Leipzig-Lorraine-Lviv-Coventry, Europe — ³Ivan Franko National University of Lviv, Lviv, Ukraine — ⁴Ukrainian Catholic University, Lviv, Ukraine — ⁵Coventry University, Coventry, UK — ⁶University of Limerick, Limerick, Ireland

In recent times, the advent of network science permitted new quantitative approaches to literary studies [see e.g. *Maths Meets Myths: Complexity-science approaches to folktales, myths, sagas, and histories*. R. Kenna, M. Mac Carron, P. Mac Carron (Editors), Springer, 2016]. Here, we bring the Kyiv bylyny cycle into the field - East Slavic epic narratives originating in modern-day Ukraine. By comparing them to other prominent European epics, we identify universal and distinguishing properties of the social networks in bylyny. We analyze community structures and rank most important characters. The method allows to bolster hypotheses from humanities literature - such as the position of Prince Volodymyr - and to generate new ones. We show how the Kyiv cycle of bylyny fits very well with narrative networks from other nations - especially heroic ones. We anticipate that, besides delivering new narratological insights, this study will aid future scholars and interested public to navigate their way through Ukraine's

epic story and identify its heroes [P. Sarkanych et al., *Adv. Complex Syst.* 25(4) (2022) 2240007].

SOE 8.3 Tue 14:30 ZEU 260

Dynamics of language features on complex networks: statistical physics analysis, and the introduction of linguistic temperature — CHRISTOPHER KITCHING¹, JORDAN ABBOTT¹, TOBIAS GALLA^{1,2}, HENRI KAUMANEN³, DEEPTI GOPAL⁴, and RICARDO BERMÚDEZ-OTERO¹ — ¹The University of Manchester, UK — ²Instituto de Física Interdisciplinar y Sistemas Complejos (CSIC-UIB) — ³University of Konstanz, Germany — ⁴University of Cambridge, UK

Statistical physics has made important contributions to the study of language dynamics. Here, we focus on a stochastic individual-based model of the spatio-temporal evolution of language features. Features evolve through a combination of descent across generations, and the influence of geographically neighbouring languages.

The dynamics are a variation of the two-state voter model, with spontaneous changes of state and transmission errors in the imitation process. Previous work is restricted to lattices, here we focus on complex networks. We establish a parabolic relation between the feature frequency and the density of active interfaces, modulated by the network, and 'linguistic temperature' - a measure of a feature's stability.

Results are obtained by combining the voter model, pair approximation and a new approach to networks, based on random walks. While the theoretical work has applications in other areas (e.g. opinion dynamics), our main focus is in linguistics: the frequency and isogloss density of real-world language features can be obtained from WALs and from this we calculate their temperatures.

SOE 8.4 Tue 14:45 ZEU 260

The Characteristic Time Scale of Cultural Evolution — TOBIAS WAND — Westfälische Wilhelms-Universität Münster, Institut für Theoretische Physik — Center for Nonlinear Sciences Münster

Clidynamics is a field of research that models human societies as dynamical systems, treating the study of history as a scientific discipline. Previous research on the Seshat databank has revealed one dominant principle component as an indicator of social complexity across diverse geographies and time periods. Our research expands on these findings, showing that there is a typical growth phase in social complexity that can be modelled with a universal functional form for all geographic areas included in the databank. Our findings reveal a characteristic time scale of rapid growth and can serve as a baseline to detect outliers.

SOE 9: Focus Session: Critical Transitions in Society, Economy, and Nature (joint session SOE/DY)

Organizers: Fakhteh Ghanbarnejad (Robert Koch-Institut), Diego Rybski (Potsdam Institute for Climate Impact Research)

Time: Wednesday 9:30–11:45

Location: ZEU 260

Topical Talk

SOE 9.1 Wed 9:30 ZEU 260

Many universality classes in an interface model restricted to non-negative heights — PETER GRASSBERGER¹, DEEPAK DHAR², and PRADEEP MOHANTY³ — ¹JSC, Forschungszentrum Jülich, D-52425 Jülich, Germany — ²Indian Institute of Science Education and Research, Pune, 411 008, India — ³Indian Institute of Science Education and Research - Kolkata Mohanpur, 741 246, India

We present a simple 1-d stochastic model with two control parameters and a rich zoo of phase transitions. At each (discrete) site x and time t , there is an integer $n(x, t)$ that satisfies a linear interface equation with added random noise. Depending on the control parameters, this noise may or may not satisfy detailed balance, so that the model is - for suitable initial conditions - in the Edwards-Wilkinson (EW) or in the Kardar-Parisi-Zhang (KPZ) universality class. But in

contrast to these, there is also a constraint $n(x, t) \geq 0$. Points x where $n > 0$ on one side and $n = 0$ on the other are called “fronts”. These fronts can be “pushed” or “pulled”, depending on the control parameters. For pulled fronts, the lateral spreading is in the directed percolation (DP) universality class, while it is of a novel type for pushed fronts, with yet another novel behavior in between. In the DP case, the activity at each active site can in general be arbitrarily large, in contrast to previous realizations of DP. Finally, we find two different types of transitions when the interface detaches from the line $n = 0$ (with $\langle n(x, t) \rangle \rightarrow const$ on one side, and $\rightarrow \infty$ on the other), again with new universality classes. We also discuss a mapping of this model onto a directed Oslo rice pile model in specially prepared backgrounds.

Topical Talk SOE 9.2 Wed 10:00 ZEU 260
Nonequilibrium phase transitions and critical behavior in networks — •ECKEHARD SCHÖLL — Institut für Theoretische Physik, TU Berlin — Potsdam Institute for Climate Impact Research — Bernstein Center for Computational Neuroscience Berlin

Phase transitions in nonlinear dynamical systems far from thermodynamic equilibrium have been investigated since the 1970s and 1980s, and concepts from thermodynamics and statistical physics have been applied to describe self-organization, spatio-temporal pattern formation, phase coexistence, critical phenomena, and first and second order nonequilibrium phase transitions. Much more recently, phase transitions and critical phenomena have been studied in dynamical networks, where synchronization transitions may arise, giving birth to a plethora of partial synchronization patterns and complex collective behavior, with applications to many natural, socioeconomic, and technological systems. We review these developments, and draw some connections of tipping transitions, explosive synchronization, nucleation, critical slowing down, critical exponents, etc. with nonequilibrium thermodynamics. [1] Tumash, L., Olmi, S. and Schöll, E., Effect of disorder and noise in shaping the dynamics of power grids, *Europhys. Lett.* 123, 20001 (2018). [2] Berner, R., Sawicki, J., Thiele, M., Löser, T. and Schöll, E., Critical parameters in dynamic network modeling of sepsis, *Front. Netw. Physiol.* 2, 904480 (2022). [3] Fialkowski, J., Yanchuk, S., Sokolov, I. M., Schöll, E., Gottwald, G. A. and Berner, R., Heterogeneous nucleation in finite size adaptive dynamical networks, *arXiv:2207.02939* (2022).

15 min. break

Topical Talk SOE 9.3 Wed 10:45 ZEU 260
Critical transition to monsoon: statistical physics principles of monsoon forecasting — •ELENA SUROVYATKINA — Potsdam Institute for Climate Impact Research (PIK), Potsdam, Germany — Space Research Institute of the Russian Academy of Sciences (IKI), Moscow, Russia

Numerical weather models are limited to forecasting the weather for up to 5 days in the future. A fundamental problem lies in the chaotic nature of the spatial differential equations used to simulate the atmosphere. The limitations of current prediction models prevent further progress.

I present a recently developed approach fundamentally different from the numerical weather and climate models. It is based on statistical physics principles and recently discovered spatial-temporal regularities (or teleconnections between Tipping Elements) in a monsoon system.

First, I begin with evidence in observational data that the transition from pre-monsoon to monsoon is a critical transition. Second, I show how to detect the

Tipping elements in the spatial organization of monsoon using the phenomenon of critical growth of fluctuations. Third, I explain how the regularities between the Tipping Elements allow predicting the upcoming monsoon onset and withdrawal for 40 and 70 days in advance, respectively.

Furthermore, I present the results of retrospective tests from 1951 to 2015, which show 73 % success for monsoon onset and 84 % for a withdrawal date. Remarkably, that forecasts of future monsoons showed to be successful already seven years in a row, 2016-2022.

SOE 9.4 Wed 11:15 ZEU 260

Synchronization-desynchronization transitions in neural networks — •ANNA ZAKHAROVA — BCCN Berlin, Germany

Synchronization of neurons is believed to play a crucial role in the brain under normal conditions, for instance, in the context of cognition and learning, and under pathological conditions such as Parkinson's disease or epileptic seizures. In the latter case, when synchronization represents an undesired state, understanding the mechanisms of desynchronization is of particular importance. In other words, the possible transitions from synchronized to desynchronized regimes and vice versa should be investigated. It is known that such dynamical transitions involve the formation of partial synchronization patterns, where only one part of the network is synchronized. The most prominent example is given by chimera states [1]. In the present talk, we discuss an alternative scenario. We show how the so-called solitary states in networks of coupled FitzHugh-Nagumo neurons can lead to the emergence of chimera states. By performing bifurcation analysis of a suitable reduced system in the thermodynamic limit we demonstrate how solitary states, after emerging from the synchronous state, become chaotic in a classical period-doubling cascade [2].

[1] A. Zakharova, *Chimera Patterns in Networks: Interplay between Dynamics, Structure, Noise, and Delay, Understanding Complex Systems* (Springer, Cham, 2020) doi: 10.1007/978-3-030-21714-3

[2] L. Schülen, A. Gerdes, M. Wolfrum, A. Zakharova, *Solitary routes to chimera states*, *Phys. Rev. E Letter* 106, L042203 (2022) doi: 10.1103/phys-reve.106.l042203

SOE 9.5 Wed 11:30 ZEU 260

The war in Ukraine, a statistical analysis — •JUERGEN MIMKES — Physics Department, Paderborn University

War is a serious disruption of normal social order and may be analyzed by statistics. In homogeneous systems the Lagrange function depends on two Lagrange factors: $L(\lambda, p)$. In physics, they are mean energy or temperature (λ) and pressure (p). In politics, they are mean capital or standard of living (λ) and military pressure (p). The factors $(\lambda), (p)$ determine the state or phases of a system. In materials we have solid, liquid, gas, in politics autocratic, democratic, global. Different phases can only coexist at equilibrium in the phase diagram. Outside of equilibrium water and ice cannot coexist in close contact, water is melting ice (climate crisis). Outside of equilibrium democracy and autocracy cannot coexist in close contact, democracy is *melting* autocracy since the Marshall plan in 1947. Accordingly, there has been an aggressive reaction by the autocracy: DDR 1953, Hungary 1956, CSR 1968, Ukraine 2014. There is no chance for peace, unless one party vanishes. The only solution to keep hot and cold together is a thermos, and to keep democracy and autocracy side by side is a new iron curtain like in Korea or Europe (1961 to 1989).

SOE 10: Traffic Dynamics, Urban and Regional Systems I

Time: Wednesday 15:00–16:30

Location: ZEU 260

SOE 10.1 Wed 15:00 ZEU 260
The random walks of ridepooling — •BENJAMIN KÖHLER¹, PHILIP MARSZAL¹, MARC TIMME^{1,2}, and MALTE SCHRÖDER¹ — ¹Chair for Network Dynamics, Institute of Theoretical Physics & Center for Advancing Electronics Dresden (cfaed), TU Dresden — ²Lakeside Labs, Klagenfurt, Austria

Ridepooling services have become an increasingly attractive mobility option in urban areas. As users issue requests for transport, ridepooling vehicles drive through the road network, continually adjusting their routes to pick up and deliver users with similar trips in shared rides. The quality of such services strongly depends on the dynamics of evolving vehicle routes, which collectively emerge from the interactions of the vehicles and requests. So far, theories of ridepooling services have focused on macroscopic and mean-field dynamics, neglecting the underlying microscopic route evolution. Here we analyze the structure and dynamics of these random routes in the limit of high service efficiency. We find an emerging random walk of a route that is specified not only by the current location of the vehicle, but also by the route planned ahead to pick up or drop off passengers who are currently transported in the vehicle or have already requested a ride. We map this process to an ordinary Markov random walk on an abstract graph whose nodes represent the shortest paths of the original street network.

We thereby identify emerging routing patterns and evaluate their implications for the ridepooling service. Understanding these random route processes may help to further advance service quality, for instance by designing stop networks and routing algorithms to maximize flexibility.

SOE 10.2 Wed 15:15 ZEU 260

Scaling laws of ridepooling random routes — PHILIP MARSZAL, MARC TIMME, and •MALTE SCHRÖDER — Chair for Network Dynamics, Institute of Theoretical Physics & Center for Advancing Electronics Dresden (cfaed), TU Dresden

On-demand ridepooling services are emerging as a new form of urban mobility across the globe. Users request a trip, are assigned to one of the available ridepooling vehicles, and then transported in a shared ride. Despite the complex dynamics of these systems, their efficiency and service quality is characterized by universal macroscopic scaling laws. However, the scaling laws are typically derived from mean-field calculations neglecting the details of the microscopic dynamics of individual vehicles. Here, we analyze these microscopic dynamics in terms of the *ridepooling random routes* of the vehicles as a new type of random walk process. In contrast to standard random walks, random routes are characterized by a pre-planned route of scheduled stops evolving as new requests are

added to the route and users are picked up and delivered. We identify multiple timescales emerging in the routing dynamics and quantify the resulting structure of the random routes in terms of their persistence and diffusion properties. Importantly, microscopic scaling laws of the random route properties directly give rise to macroscopic scaling laws of the overall system efficiency. This perspective of microscopic random routes in ridepooling services may help to better understand their complex dynamics and scaling laws and optimize these services by identifying recurrent route patterns or adjusting allowed stop locations to guide the self-organized routing dynamics.

SOE 10.3 Wed 15:30 ZEU 260

Bi-modal transport: united against the private car — PUNEET SHARMA, •KNUT HEIDEMANN, HELGE HEUER, STEFFEN MÜHLE, and STEPHAN HERMINGHAUS — Max-Planck-Institut für Dynamik und Selbstorganisation, Göttingen, Germany
Motorized individual traffic leads to a prohibitive waste of energy and other resources. We show that combining a line service with a fleet of ride-pooling shuttles may provide on-demand door-to-door service with a service quality superior to customary public transportation, while at the same time consuming only about 20% of the energy a corresponding fleet of private cars would require, and with a road traffic volume reduced by orders of magnitude. We find favorable performance not only in urban, but also in rural settings. While the first part relies on a mean-field model and a simple model geometry, in part two, we test our results by simulations of real-world scenarios.

SOE 10.4 Wed 15:45 ZEU 260

Demand-driven design of bike path networks — •CHRISTOPH STEINACKER¹, DAVID-MAXIMILIAN STROCH¹, MARC TIMME^{1,2}, and MALTE SCHRÖDER¹ — ¹Chair for Network Dynamics, Institute of Theoretical Physics & Center for Advancing Electronics Dresden (cfaed), TU Dresden — ²Lakeside Labs, Klagenfurt, Austria

Cycling is crucial for sustainable urban transportation. Promoting cycling critically relies on a sufficiently developed bicycle infrastructure. In general, designing efficient infrastructure networks constitutes a highly complex problem that requires balancing multiple, often opposing, constraints. In particular, bike path networks need to enable both safe and direct travel for all cyclists with an often strongly limited budget and strong competition for limited road space.

Here, we present a framework to create families of efficient bike path networks [1]. We reverse the network formation process and iteratively remove bike paths from an initially complete bike path network. In addition, we continually update cyclists' route choices, explicitly taking into account the cyclists' demand and their safety and convenience preferences. In this way, we create a sequence of networks that is always adapted to the current cycling demand.

We illustrate the applicability of this demand-driven planning scheme with empirical infrastructure and demand data. The framework may thus enable us to study properties of the structure of efficient bike path networks across cities and quantify the impact of different demand distributions.

[1] Steinacker *et al.*, Nat. Comput. Sci. 2, 655-664 (2022).

SOE 10.5 Wed 16:00 ZEU 260

Does unorganized outperform organized public transport? — •KUSH MOHAN MITTAL¹, MALTE SCHRÖDER¹, and MARC TIMME^{1,2} — ¹Chair for Network Dynamics, Institute of Theoretical Physics & Center for Advancing Electronics Dresden (cfaed), TU Dresden — ²Lakeside Labs, Klagenfurt, Austria

Organized public transport is commonly assumed to be more efficient compared to unorganized or self-organized mobility services that often prevail in the Global South. Here, we analyze OpenStreetMap route data from a total of 4500 routes of both organized and unorganized public transport services in more than 40 cities across the globe. Dividing bus routes into smaller segments and comparing their length to the shortest path distance between the segments endpoints, we find that segments more central in a route consistently exhibit substantially less detour than those towards the ends of the route. This non-homogeneous detour distribution occurs universally, irrespective of whether a city is dominated by organized or unorganized transport. These structural properties of the routes have significant implications for the attractiveness of public transport, as people living in the outskirts at the end of the routes typically both have overall longer trips and experience more (relative) detours than people living in the city center. Intriguingly, we provide quantitative evidence that decentrally self-organized transport routes typically exhibit less heterogeneity and at the same time achieve smaller overall detours. Moreover, they may also outperform organized transport in terms of social accessibility and route interconnectivity.

SOE 10.6 Wed 16:15 ZEU 260

Fix or flex? How ridepooling complements public transport — •VERENA KRALL¹, MARC TIMME^{1,2}, and MALTE SCHRÖDER¹ — ¹Chair for Network Dynamics, Institute of Theoretical Physics & Center for Advancing Electronics Dresden (cfaed), TU Dresden, Germany — ²Lakeside Labs, Klagenfurt, Austria

Urban mobility is changing rapidly, not least due to the global rise of on-demand ridepooling services. In contrast to classic public transport with fixed lines and schedules, these new services offer a flexible shared transport with stops and routes determined by demand. This flexibility might attract new users to shared transport and offer higher accessibility to mobility in districts with poor public transport infrastructure. However, a complete shift from fixed line-based to flexible on-demand services would be detrimental, increasing congestion and wasting existing infrastructure. How can the two different service types complement each other to improve public transport? We find that the service quality is optimal if both line-based and on-demand transport are available. Additionally, we investigate adaptations of public transport networks and find that replacing inefficient lines step-by-step with on-demand vehicles may strongly reduce the overall costs. Applying our approach to empirical public transport networks, we identify lines that should be replaced with on-demand service. Our study shows how the combination of classic line-based with on-demand mobility may contribute to a public transport system that is both sustainable and user-friendly.

SOE 11: Traffic Dynamics, Urban and Regional Systems II

Time: Wednesday 16:45–18:15

Location: ZEU 260

SOE 11.1 Wed 16:45 ZEU 260

Response functions as a new concept to study local dynamics in traffic networks — •SHANSHAN WANG, MICHAEL SCHRECKENBERG, and THOMAS GUHR — Faculty of Physics, University of Duisburg-Essen, Duisburg, Germany

Vehicle velocities in neighbouring road sections are correlated with memory effects. We explore the response of the velocities in the sequence of sections to a congestion in a given section and its dynamic characteristics. To this end, we transfer the concept of response functions from previous applications in finance to traffic systems. The dynamical characteristics are of particular interest. We identify two phases, a phase of transient response and a phase of long-term response. The transient response is pronounced when considering the backward propagation of heavy congestions but almost vanishes for forward propagation. For each response phase, we find a linear relation between the velocity response and the congestion correlator, implying that the correlation of congestion is most likely the cause for the velocity response. We also construct a susceptible-decelerated-withdrawing model mathematically inspired by the susceptible-infectious-recovered (SIR) model in epidemiology to describe the transient response. We find that the heavy congestion on a section propagates forward and backward at a similar rate, but the forward sections are more likely to recover from the effect of heavy congestion than the backward sections.

SOE 11.2 Wed 17:00 ZEU 260

A Fast and Modular Framework for Simulating Ridepooling Systems — •FELIX JUNG¹, DEBSANKHA MANIK¹, and MARC TIMME^{1,2} — ¹Chair for Network Dynamics, Institute of Theoretical Physics & Center for Advancing Electronics Dresden (cfaed), TU Dresden, 01062 Dresden, Germany — ²Lakeside Labs, Klagenfurt, Austria

Climate change and congested cities urgently call for a transformation of passenger road transport that today still largely relies on flexible but inefficient private cars. Ridepooling services may reduce the environmental impact while maintaining a high level of flexibility. They move passengers between arbitrary locations, ideally on-demand and on short notice, while dynamically combining trips of several passengers into the same vehicle. However, under which conditions these services are simultaneously efficient, sustainable, and performant is not well understood to date.

Most research into such questions primarily relies on extensive computer simulations, because real-world experiments are extremely expensive and may negatively influence user adoption. Existing simulation tools have a much broader scope but are hard to evaluate with respect to fundamental physical observables, are not sufficiently performant, or hard to use. Here we present a new simulation framework that overcomes these challenges and is easy to use, modular and fast. The framework is released under an Open Source license in the hope that it will benefit the research community and further collaborative development.

SOE 11.3 Wed 17:15 ZEU 260

Service Quality Paradox – Guaranteeing early deliveries causes overall delays in ride pooling services — •PHILIP MARSZAL^{1,2}, MARC TIMME^{1,2,3}, and MALTE SCHRÖDER^{1,2} — ¹Center for Advancing Electronics Dresden (cfaed), Technical University of Dresden, 01062, Dresden, Germany — ²Institute for Theoretical Physics, Technical University of Dresden, 01062, Dresden, Germany — ³Lakeside Labs, Lakeside B04b, Klagenfurt, 9020, Austria

On-demand ride pooling services become increasingly important for modern human mobility and rely on advanced forms of dispatching and coordination algorithms [1,2]. A central algorithm matches the vehicles of service providers to the trip requests of customers, aiming to efficiently combine passenger trips in order to reduce service time and distance traveled [3]. Here we reveal a service quality (SQ) paradox emerging from how such services self-organize given a dispatching strategy: enforcing a maximum delay an individual passenger can experience may increase the average delay of all passengers. We quantitatively evaluate the SQ paradox in terms of the vehicle route flexibility, a measure of how many possible passengers may be served by a single vehicle. Our results theoretically revealed conditions underlying the novel paradox and may inform future designs of ridepooling algorithms to improve the service quality of the shared mobility ecosystem.

References: [1] Schröder et al., Nature Comm. 11:4831 (2020). [2] Storch et al., Nature Comm. 12:3003 (2021). [3] Alonso-Mora et al., PNAS 114:426 (2017).

SOE 11.4 Wed 17:30 ZEU 260

Short walks enable fast and sustainable ride sharing — •CHARLOTTE LOTZE¹, PHILIP MARSZAL¹, MALTE SCHRÖDER¹, and MARC TIMME^{1,2} — ¹Chair for Network Dynamics, Institute for Theoretical Physics & Center for Advancing Electronics Dresden (cfaed), Technical University of Dresden, 01069 Dresden — ²Lakeside Labs, Klagenfurt, Austria

Ride sharing - the bundling of simultaneous trips of several people in the same on-demand vehicle - may help to reduce the carbon footprint of human mobility. Yet, predicting the efficiency and sustainability of ride-sharing systems is hard due to their complex collective dynamics. Compared to individual motorized vehicle transportation, standard door-to-door ride sharing services reduce the total distance driven per user. However, they also increase the average travel times due to several additional stops and thus detours to pick up or drop off users. Here we show that requiring some users to walk to nearby shared stops reduces detours for the buses and thus the time users wait for their bus and drive in the bus. These time savings might overcompensate the additional walk time for the users. In this way, dynamic stop pooling reduces the average travel time and may break the trade-off between distance driven and travel time prevailing in door-to-door ride sharing. For example, ride sharing providers may reduce the fleet

size to save distance driven without longer travel times when users walk a short part of their trip. Dynamic stop pooling may thus enable more sustainable ride sharing services without compromising service quality.

SOE 11.5 Wed 17:45 ZEU 260

Long-range correlations in city systems — YUNFEI LI¹, JAN W. KANTELHARDT², CELINE ROZENBLAT³, and •DIEGO RYBSKI^{1,4} — ¹Potsdam Institute for Climate Impact Research - PIK, Member of Leibniz Association, P.O. Box 601203, 14412 Potsdam, Germany — ²Institute of Physics, Martin-Luther-University, Halle (Saale), Germany — ³Institute of Geography and Sustainability, Faculty of Geoscience, University of Lausanne; — ⁴Complexity Science Hub Vienna, Josefstädterstrasse 39, A-1090 Vienna, Austria

City systems are characterized by the functional organization of cities on a regional or country scale. While there is relatively good empirical and theoretical understanding of city size distributions, insights about their spatial organization remain on a conceptual level. Here we analyze empirically the correlations between the sizes of cities (in terms of area) across long distances. Therefore, we (i) define city clusters, (ii) obtain the neighborhood network from Voronoi cells, and (iii) apply a fluctuation analysis along all shortest paths. We find that most European countries exhibit long-range correlations but in several cases these are anti-correlations. In an analogous way we study a model inspired by Central Places Theory and find that depending on the level of disorder, both positive and negative long-range correlations can be simulated. We conclude that the interactions between cities of different sizes extend over distances reaching country scale.

SOE 11.6 Wed 18:00 ZEU 260

Mapping the social structure of cities with Diffusion Maps — •THILO GROSS — Helmholtz Institute for Functional Marine Biodiversity, Oldenburg, Germany — Carl-von-Ossietzky University, Oldenburg, Germany — Alfred-Wegener Institute, Helmholtz Center for Marine and Polar Research, Bremerhaven, Germany

Human society is aggregating and accelerating, leading to a rapid growth of cities. It is well known that the social structure of cities is important for a long list of reasons, including livability, security, sustainability, and disaster resilience. Analysis of the social structure can profit from two complementary data sources: Census datasets provide a wealth of high quality, highly structured information, but are typically only available once per decade. By contrast novel sources of mobility data (e.g. from phone traces) offer an unstructured and indirect, but rich and near-real-time glimpse of human social behavior. In this talk I illustrate how diffusion maps, a network-driven analysis method, reveal important patterns in both of these types of data.

SOE 12: Members' Assembly

Time: Wednesday 18:30–19:30

Location: ZEU 260

All members of the Physics of Socio-economic Systems Division are invited to participate.

SOE 13: Data Analytics of Complex Dynamical Systems (joint session DY/SOE)

Time: Thursday 9:30–12:00

Location: MOL 213

See DY 37 for details of this session.

SOE 14: Networks: From Topology to Dynamics II (joint session SOE/DY)

Time: Thursday 9:30–10:00

Location: ZEU 260

Invited Talk

SOE 14.1 Thu 9:30 ZEU 260

Networks in space and time – Exploring the physics in graph learning — •INGO SCHOLTES — Julius-Maximilians-Universität Würzburg, Chair of Machine Learning for Complex Networks, Center for Artificial Intelligence and Data Science, D-97074 Würzburg, Germany

Network Analysis and Graph Neural Networks have become cornerstones for the application of data science and machine learning to complex systems. Addressing geometric machine learning in non-Euclidean data, I will introduce key concepts that help to apply deep learning to graphs. We cover message passing algorithms, convolutional filters, discrete Laplacians and neural representation

learning and highlight relationships between graph learning and physics.

We finally explore how time-resolved data on dynamic networks helps us to better understand complex systems and how we can incorporate the time dimension into deep graph learning. We introduce De Bruijn Graph Neural Networks (DBGNNs), a novel time-aware graph neural network architecture. Our approach accounts for temporal-topological patterns that unfold via causal walks, i.e. temporally ordered sequences of links by which nodes can influence each other over time. We develop a graph neural network architecture that utilizes De Bruijn graphs of multiple higher orders to implement a message passing scheme that follows a non-Markovian dynamics, which enables us to learn patterns in the causal topology of complex networks.

SOE 15: Networks: From Topology to Dynamics III (joint session SOE/DY)

Time: Thursday 10:00–10:45

Location: ZEU 260

SOE 15.1 Thu 10:00 ZEU 260

Understanding Braess' Paradox in power grids — •BENJAMIN SCHÄFER¹, THIEMO PESCH², DEBSANKHA MANIK³, JULIAN GOLLENSTEDT⁴, GUOSONG LIN⁴, HANS-PETER BECK⁴, DIRK WITTHAUT², and MARC TIMME^{5,3} — ¹Karlsruhe Institute of Technology — ²Forschungszentrum Jülich — ³Max Planck Institute for Dynamics and Self-Organization — ⁴Clausthal University of Technology — ⁵Technical University of Dresden

The ongoing energy transition requires power grid extensions to connect renewable generators to consumers and to transfer power among distant areas. The process of grid extension requires a large investment of resources and is supposed to make grid operation more robust. Yet, counter-intuitively, increasing the capacity of existing lines or adding new lines may also reduce the overall system performance and even promote blackouts due to Braess' paradox. Braess' paradox was theoretically modeled but not yet proven in realistically scaled power grids. Here, we present an experimental setup demonstrating Braess' paradox in an AC power grid and show how it constrains ongoing large-scale grid extension projects. We present a topological theory that reveals the key mechanism and predicts Braessian grid extensions from the network structure. These results offer a theoretical method to understand and practical guidelines in support of preventing unsuitable infrastructures and the systemic planning of grid extensions.

SOE 15.2 Thu 10:15 ZEU 260

Evolutionary Optimization of networks towards complexity: role of link distribution and cross-consistency of network complexity measures — ARCHAN MUKHOPADHYAY and •JENS CHRISTIAN CLAUSSEN — University of Birmingham, UK

In a framework utilizing complexity measures for optimizing graphs and networks towards complexity, we use one complexity measure as fitness function of an evolutionary algorithm, and evaluate the resulting graphs through other complexity measures and network properties. We consider both evolution of graphs

where the total number of links can evolve, as well as the case of constrained number of links. We find that in a certain range MA_G optimizes towards degree-regular graphs, which is not observed for other complexity measures. We also investigate the consistency among the complexity measures on artificial and real-world datasets.

SOE 15.3 Thu 10:30 ZEU 260

On the role of deleterious mutant regime in steering long-term evolution — NIKHIL SHARMA¹, •JOACHIM KRUG², and ARNE TRAUlsen¹ — ¹Department of Evolutionary Theory, Max Planck Institute for Evolutionary Biology, 24306 Plön, Germany — ²Institute for Biological Physics, University of Cologne, Köln, Germany

Evolutionary Graph Theory aims to understand the interplay of natural selection and genetic drift on spatial structures. A spatial structure is modeled as a graph with nodes representing asexually reproducing individuals, and edges dictate the interaction among these individuals. Based on the fixation probabilities of mutants on graphs, graphs are mainly categorised as amplifiers of selection and suppressors of selection. We study Moran Birth-death origin fixation dynamics on graphs, see <https://doi.org/10.1073/pnas.2205424119>. As expected, amplifiers of selection attain higher steady-state average fitness than the complete graph. However, we found that a suppressor of fixation, having a lower probability of fixing mutants regardless of their fitness values compared to the complete graph, beats the complete graph in the long term by attaining higher average fitness. It happens because of the suppressor's ability to reject deleterious mutants more efficiently. Similarly, an amplifier of fixation, a structure with a higher probability of fixing mutants regardless of their fitness values, attains lower steady-state average fitness. It happens because of the amplifier's poor ability to reject deleterious mutants. These two examples illustrate the importance of the deleterious mutant regime in steering long-term evolution, which, to our knowledge, has been overlooked in the literature.

SOE 16: Collective Dynamics in Animal and Human Societies

Time: Thursday 11:00–12:15

Location: ZEU 260

SOE 16.1 Thu 11:00 ZEU 260

Individual bias and fluctuations in collective decision making: from algorithms to Hamiltonians — •MARIANA KRASNITSKA^{1,2,3}, PETRO SARKANYCH^{1,2}, LUIS GÓMEZ-NAVA^{4,5}, ABEL JONEN⁴, PAWEŁ ROMANCZUK^{4,5}, and YURIJ HOLOVATCH^{1,2,6} — ¹ICMP, NAS of Ukraine, Lviv, Ukraine — ²L4 Collaboration Leipzig-Lorraine-Lviv-Coventry — ³Université de Lorraine, Nancy, France — ⁴Humboldt Universität zu Berlin, Germany — ⁵Research Cluster of Excellence "Science of Intelligence", Berlin, Germany — ⁶Coventry University, UK

We reconsider the spin model suggested recently to understand some features of collective decision making among higher organisms [A.T. Hartnett et al., Phys. Rev. Lett. 116 (2016) 038701]. Within the model, the state of an agent is described by the pair of variables corresponding to its opinion and a bias towards any of the opposing opinions. Collective decision making is interpreted within the non-linear voter model subject to social pressure. Here, we push such physical analogy further and give the statistical physics interpretation of the model via explicit calculation of its partition function. In such interpretation, the temperature serves as a measure of fluctuations that were not taken into account within the original formulation. We find exact solutions for the thermodynamics and dynamics of the model on the complete graph. We discuss the advantages and flaws of such an approach as well as its utility in understanding the impact of population heterogeneity, type of local interaction and fluctuations in collective decision making.

SOE 16.2 Thu 11:15 ZEU 260

Following the information footprint of firms — •EDWARD LEE¹, ALAN KWAN², RUDOLF HANEL¹, ANJALI BHATT³, and FRANK NEFFKE¹ — ¹Complexity Science Hub Vienna, Austria — ²Hong Kong University, China — ³Harvard Business School, Boston, USA

What a firm does is more revealing than how much it makes, but firms are often described with metrics for economic size. Instead, we characterize what firms know in terms of what they read, the information footprint, using a data set of hundreds of millions of records of news articles accessed by employees in millions of firms. We discover that the reading habits of firms are of limited diversity. This observation suggests that information constraints act on firms. To understand how, we relate a firm's information footprint with economic variables, showing that the former grows superlinearly with the latter. This exaggerates the classic Zipf's law inequality in the economic size of firms and reveals an

economy of scale with respect to information. Second, we reconstruct the topic space firms inhabit, finding that the space resembles a tangled "hairball" with a few dense knots of topics and many specialized strands sticking out. Some of the topics are ubiquitous, indicating inescapable demand regardless of firm size. Finally, we connect these pieces in a model of how firms grow in the space of topics. We show that diversity in firm reading habits can be explained by a mixed strategy of local exploration and recurrent exploitation on the topic graph. This shows that the constraints that the space of ideas imposes on firm growth provide a useful and new perspective on firm development.

SOE 16.3 Thu 11:30 ZEU 260

Influence of confirmation biases on collective decision-making in fluctuating environments — •CLÉMENTINE BERGEROT^{1,2}, WOLFRAM BARFUSS³, and PAWEŁ ROMANCZUK^{2,4} — ¹Charité - Universitätsmedizin Berlin, Einstein Center for Neurosciences Berlin, Germany — ²Humboldt Universität zu Berlin, Germany — ³Tübingen AI Center, University of Tübingen, Germany — ⁴Research Cluster of Excellence "Science of Intelligence", Berlin, Germany

In experimental studies of decision-making, it is now established that human agents tend to update confirmatory information with a higher weight than disconfirmatory information. This confirmation bias has been modeled within a reinforcement learning framework, using asymmetric updating of prediction errors. Interestingly, such a bias has been suggested to enhance individual performance in a wide range of multi-armed bandit tasks. However, little is known about the impact of the confirmation bias on collective performance. In order to characterize the circumstances that make this bias beneficial or detrimental to collective decision-making, we develop a multiagent model in which reinforcement learning agents can observe others' actions and rewards, and update this information asymmetrically. With agent-based simulations, we seek to understand how the confirmation bias affects collective performance in changing environments, and how network topology modulates this effect. We also study our multiagent system in the deterministic limit [W. Barfuss et al., Phys. Rev. E, 99(4) (2016) 043305], which allows us to gain an analytical understanding of the biased learning dynamics.

SOE 16.4 Thu 11:45 ZEU 260

Population waves in sessile organisms — •NIRAJ KUSHWAHA and EDWARD LEE — Complexity Science Hub Vienna, Josefstädter Straße 39, 1080 Vienna, Austria
The mathematical laws of life manifest scaling regularities such as the relationship between mass and metabolism for the smallest to the largest organisms on Earth. These laws lack essential components representing interaction between organisms while sharing limited resources. Once accounted for, these components can bring significant variation to the predicted demographic laws using just metabolic scaling theory and can give mathematical descriptions for observed ecological phenomena. The oscillations in population number, where spikes in the number of organisms of a specific size propagate from small to large organisms is an example of such a phenomena. Here, we incorporate spatial competition and resource variation in a differential equation model for the population dynamics of sessile organisms. We use analytic and numerical tools to solve the corresponding equations and to characterize the form of instabilities that generate the oscillations, which we use to identify hidden mechanisms that may drive instabilities in ecological systems such as forests. As a result, we may be able to identify the most significant factors that affect the stability of an ecosystem corresponding to resource fluctuations that may become more prominent with climate change.

SOE 16.5 Thu 12:00 ZEU 260

The role of escape angle in predator-prey interactions: the emergence of fountain effect — •PALINA BARTASHEVICH^{1,2} and PAWEŁ ROMANCZUK^{1,2} — ¹Institute for Theoretical Biology, Humboldt-Universität zu Berlin, 10115 Berlin, Germany — ²Excellence Cluster Science of Intelligence, Technische Universität Berlin, 10587 Berlin, Germany

Empirical studies of fish schooling widely described the variety of ways in which fish escape to reduce the chances of being caught by a predator while trying at the same time to stay in a group. The “fountain effect” is one such evasion maneuver that allows small fish to out-manuever the fast-moving predator by swimming away at a constant angle determined by the rear limit of the visual cone [1]. Our spatially-explicit agent-based numerical simulations recover the same optimal prey-fleeing angle as confirmed by empirical studies. Moreover, our results show that the fleeing angle not only minimizes the distance to the predator but creates a sequence of information flows that best facilitates the information propagation throughout the collective. This finding highlights the direct role of social interaction in the emergence of the fountain effect which was not addressed before. We also address the questions of how the stimulus characteristics such as the initial predator angle of attack and distance to the first responders affect the response as a whole, allowing us to make biological predictions.

[1] Hall SJ, Wardle CS and MacLennan DN 1986. Predator evasion in a fish school: test of a model for the fountain effect. *Mar. Biol.* 91: 143-148.

SOE 17: Evolutionary Game Theory (joint session SOE/DY)

Time: Thursday 15:00–15:30

Location: ZEU 260

SOE 17.1 Thu 15:00 ZEU 260

Bet hedging in populations evolving in fluctuating environments — RUBÉN CALVO¹ and •TOBIAS GALLA² — ¹Instituto Carlos I de Física Teórica y Computacional, and Departamento de Electromagnetismo y Física de la Materia, Facultad de Ciencias, Universidad de Granada, 18071 Granada, Spain — ²Instituto de Física Interdisciplinar y Sistemas Complejos IFISC (CSIC-UIB), Campus Universitat de les Illes Balears, E-07122 Palma de Mallorca, Spain

Bet-hedging strategies are strategies aimed at reducing risk in the face of uncertainty. For example, biological organisms face uncertain time-varying environmental conditions, such as dry years versus wet years. Similarly, future conditions in financial markets or other social systems are often unknown. Traditional bet-hedging theory shows that a reduction of the variance of an agent's payoff may increase their success even when their mean payoff is also reduced. Bet-hedging strategies are often built on maximum growth. Here instead, we ask how a mutant invading a resident wildtype population can maximise its chances of taking over the population (i.e., the fixation probability of the mutant). We consider a birth-death dynamics in fluctuating environments, and show that, depending on the distribution of payoffs across environmental states, a reduction in variance can either be beneficial or detrimental to the mutant. We establish conditions for either scenario to be realised, and show how this is related to the skewness of the payoff distribution.

SOE 17.2 Thu 15:15 ZEU 260

Hawk Dove Game on Networks with Continuous Populations — •LENNART GEVERS^{1,2}, TOBIAS WAND^{1,2}, and SVETLANA V. GUREVICH^{1,2} — ¹Institute for Theoretical Physics, University of Münster, Wilhelm-Klemm-Straße 9, D-48149 Münster, Germany — ²Center for Nonlinear Science (CeNoS), University of Münster, Corrensstrasse 2, D-48149 Münster, Germany

Evolutionary game theory is a population-based approach to game theoretical scenarios by analyzing the evolution of populations resembling competing strategies.

We expand the classical model analysed by (1), which assumes that no spatial or social segregation of populations occurs, with a network-based approach to the hawk-dove game which models the ability of contestants to migrate between neighboring realizations of the game by adapting different migratory behaviors. Our model reveals that competitive and cooperative populations can show preferred strategies on how to spatially organize on such territories.

Furthermore, we find that the resulting outcomes of the participating species diverge from the original model with increasing mobility of species.

(1) F. Stollmeier and J. Nagler, *Phys. Rev. Lett.* 120, 058101, 2018.

SOE 18: Social Systems, Opinion and Group Dynamics I

Time: Thursday 15:30–16:30

Location: ZEU 260

SOE 18.1 Thu 15:30 ZEU 260

Homophily-based social group formation in a spin-glass self-assembly framework — •JAN KORBEL^{1,2}, SIMON LINDNER^{1,2}, TUAN PHAM^{1,2,3}, RUDOLF HANEL^{1,2}, and STEFAN THURNER^{1,2,4} — ¹Section for the Science of Complex Systems, CeMSIIS, Medical University of Vienna, Spitalgasse 23, A-1090, Vienna, Austria — ²Complexity Science Hub Vienna, Josefstädterstrasse 39, A-1080, Vienna, Austria — ³Niels Bohr Institute, Blegdamsvej 17, 2100 Copenhagen, Denmark — ⁴Santa Fe Institute, 1399 Hyde Park Road, Santa Fe, NM, 87501, USA
Homophily, the tendency of humans to attract each other when sharing similar features, traits, or opinions, has been identified as one of the main driving forces behind the formation of structured societies. Here we ask to what extent homophily can explain the formation of social groups, particularly their size distribution. We propose a spin glass-inspired framework of self-assembly, where opinions are represented as multidimensional spins that dynamically self-assemble into groups; individuals within a group tend to share similar opinions (intra-group homophily), and opinions between individuals belonging to different groups tend to be different (inter-group heterophily). We compute the associated non-trivial phase diagram by solving a self-consistency equation for magnetization (combined average opinion). Below a critical temperature are two stable phases: one ordered with non-zero magnetization and large clusters, the other disordered with zero magnetization and no clusters. The system exhibits a first-order transition to the disordered phase.

SOE 18.2 Thu 15:45 ZEU 260

Heider balance observed for multidimensional attributes — JOANNA LINCZUK¹, PIOTR J GÓRSKI¹, BOLESŁAW K SZYMANSKI^{2,3}, and •JANUSZ A HOŁYST¹ — ¹Faculty of Physics, Warsaw University of Technology, Warsaw, Poland — ²Social Cognitive Networks Academic Research Center, Rensselaer Polytechnic Institute, Troy, USA — ³Spółeczna Akademia Nauk, Łódź, Poland

The majority of measured and studied social interactions arise from dyadic relations. An exception is the Heider Balance Theory (HBT) that postulates the existence of a social triad dynamics. Most of the past literature on HBT focuses on opinions about a single topic in such triads. In contrast, we study opinions of university students on a multidimensional set of topics. We discover limits of HBT observability by considering a novel agent-based model that accounts for: (i) multiple topics on opinions of individual students, (ii) influence of such opinions on dyadic relations (social link polarization), and (iii) influence of triadic relations on individual's sets of opinions on all topics. Using longitudinal records of university student behavior, we create a coevolving social network on which we introduce models of student interactions. We validate the model by showing that the triadic influence is empirically measurable for static and dynamic observables in this network. However, when we consider opinions on each topic separately from the others, the influence of triadic interactions is indistinguishable from the noise.

SOE 18.3 Thu 16:00 ZEU 260

Evolution of signed relations due to principles of structural balance and status theories — •ADAM SULIK¹, PIOTR J. GÓRSKI¹, GEORGES ANDRES², GIACOMO VACCARIO², and JANUSZ HOŁYST¹ — ¹Faculty of Physics, Warsaw University of Technology — ²Chair of System Design, ETH Zürich

One of the issues of social science is the analysis of why and how human relationships are formed. The causes of these phenomena are explained by structural balance theory and status theory, among others. Although the structural balance model by Antal et al. is a breakthrough in modeling the formation of social relationship structures, but by the diverse nature of positive and negative relationships in real-world social networks, it is unable to capture a complete picture of the relationships between users of different online communities. In addition to stability as understood by Heider's hypothesis, which is contained in structural balance theory, dynamics based on social status should also be taken into account.

We present two new models: an extended model of structural balance on directed networks and a model combining dynamics of structural balance and status theories. Presented numerical simulation results are consistent with analytical expectations. The theoretical observations have been verified on real networks, where the effect of status on the relationship between users of the studied websites has been noticed.

SOE 18.4 Thu 16:15 ZEU 260

Analysing the structure of opinion spaces — •ECKEHARD OLBRICH¹ and SVEN BANSICH² — ¹Max Planck Institute for Mathematics in the Sciences — ²Karlsruhe Institute for Technology

Data for understanding opinion dynamics arise in a variety of contexts: from voting patterns and multi-item surveys to hashtags use and users participation in different online groups. Despite their different origins they have a similar mathematical structure: a matrix with rows representing members of a population and columns representing e.g. items of a survey or political issues. Recently various novel methods have been proposed to make sense of correlational patterns in such data in order to identify them with cultural schemata [3] or dimensions of an underlying political space [1]. In this contribution we will compare different such methods including (1) issue bundles [1], (2) latent space models [2] and (3) correlational class analysis [3]. We will discuss their advantages and disadvantages using data sets from a survey on attitudes towards Corona measures and from Swiss public votes.

[1] E. Olbrich, and S. Bansich, The rise of populism and the reconfiguration of the German political space, *Frontiers in Big Data* 4, 731349 (2021).

[2] F. Gaisbauer, A. Pournaki, S. Bansich, and E. Olbrich, Grounding force-directed network layouts with latent space models. *arXiv:2110.11772* (2021).

[3] A. Boutyline, Improving the measurement of shared cultural schemas with correlational class analysis: Theory and method. *Sociological Science* 4.15 (2017): 353-393.

SOE 19: Social Systems, Opinion and Group Dynamics II

Time: Thursday 16:45–18:00

Location: ZEU 260

SOE 19.1 Thu 16:45 ZEU 260

Evidence-based policy-making in sports funding using a data-driven optimization approach — •JAN HURT¹, LIUHUAYING YANG¹, JOHANNES SORGER¹, THOMAS J. LAMPOLTSHAMMER², NIKE PULDA⁵, URSULA ROSENPICHLER⁵, STEFAN THURNER^{3,4}, and PETER KLIMEK^{3,1} — ¹Complexity Science Hub, Vienna, Austria — ²University for Continuing Education Krems, Krems, Austria — ³Section for Science of Complex Systems, CeMSIIS, Medical University of Vienna, Vienna, Austria — ⁴Santa Fe Institute, Santa Fe, NM, USA — ⁵Austria

Many European countries face rising obesity rates among children. Access to sports facilities depends on multiple factors, such as geographic location, proximity to population centers, budgetary constraints, and other socio-economic covariates. Here we show how an optimal allocation of government funds towards sports facilitators (e.g. sports clubs) can be achieved in a data-driven simulation model that maximizes children's access to sports facilities. We find a characteristic sub-linear relationship between the number of active club members and the budget, which depends on the socio-economic conditions of the clubs' districts. In the model, we evaluate different funding strategies. We show that an optimization strategy outperforms a naive approach by up to 115% for 5 million Euros of additional funding to attract children to sports clubs. Our results suggest that the impact of public funding strategies can be substantially increased by tailoring them to regional socio-economic characteristics in an evidence-based and individualized way.

SOE 19.2 Thu 17:00 ZEU 260

Fitting Polling Data with a Minimal Voter Model — •PHILIPP G. MEYER and RALF METZLER — Institute for Physics and Astronomy, University of Potsdam, Potsdam-Golm, Germany

The numerous versions of the voter model have various applications in opinion dynamics. We consider a two-state voter model for approval rates measured by political polls. We find that three features are essential for a realistic model.

Firstly, adding zealots (that never change their state) on both sides, prevents consensus. This behavior corresponds to the observations in the polling of parties. Such a voter model can be regarded as a stochastic process in a confining potential. Secondly, the measurement uncertainty of the polls has to be taken into account. It can be modeled by additive noise. Finally, we identify short-time autocorrelations between the steps, which lead to a higher variance than expected from the naive model.

We use techniques developed for voter models along with methods from stochastic processes for fitting data from political polls to the adapted voter model.

SOE 19.3 Thu 17:15 ZEU 260

Reddit Revisited — JOÃO PINHEIRO NETO and •RICCARDO CARLUCCI — Max Planck Institute for Dynamics and Self-Organization, Am Faßberg 17, 37077 Göttingen

Social media research using Reddit as a data source has greatly increased in recent years. Researchers have used Reddit to study a wide variety of issues such as political polarization, depression, astroturfing, and market manipulation to name a few.

This is primarily made possible by the Pushshift project, which offers an almost-complete dataset of Reddit. Such a degree of completeness is unique among major social media platforms, and bypasses sampling issues that may otherwise make large-scale analysis challenging.

However, a considerable fraction of Reddit research uses data which is now already a few years old. At the same time Reddit has been steadily growing, both in terms of content and userbase. For example: half of all threads and comments ever created date back to the last 2 years, despite Reddit being more than 15 years old. In addition, the global COVID-19 pandemic is known to have affected users' social media consumption.

Here we present an updated overview of Reddit as seen through the Pushshift dataset, using data up to August 2022. First we discuss the evolution over time of various statistical observables from a large-scale perspective. Next, we study the life cycle of subreddits, users, and submissions. Finally, we study the response of individual subreddits to external events.

SOE 19.4 Thu 17:30 ZEU 260

Topological insulators and enhancers in complex systems under generic problem-solving dynamics — •JOHANNES FALK¹, EDWIN EICHLER^{2,3}, KATJA WINDT^{3,1}, and MARC-THORSTEN HÜTT¹ — ¹Constructor University, Bremen, Germany — ²EICHLER Consulting AG, Weggis, Switzerland — ³SMS Group GmbH, Düsseldorf, Germany

The collective coordination of distributed tasks in a complex system can be represented as decision dynamics on a graph. For the case of social differentiation tasks, experimental studies on human subject networks demonstrated that shortcuts in small-world networks can speed up the finding of global solutions. Using a computational model, we illustrate that this is not always true: Depending on the actors' reasoning and the length of the added links, shortcuts can serve as topological enhancers that speed up the finding of a solution, but also as topological insulators that make the network more difficult to solve. Our findings have implications for situations where in distributed decision systems regional solutions emerge which are globally incompatible such as e.g. known from the emergence of standards.

SOE 19.5 Thu 17:45 ZEU 260

The emergence of echo-chambers in spatial collective estimation with limited connectivity — •MOHSEN RAOUFI¹, HEIKO HAMANN², and PAWEŁ ROMANCZUK¹ — ¹Department of Biology, Humboldt Universität zu Berlin, Berlin, Germany — ²Department of Computer and Information Science, University of Konstanz, Konstanz, Germany

Using a method inspired by the wisdom-of-crowds effect [1] we study the speed-vs-accuracy tradeoffs (SAT) in a spatial collective estimation scenario. In this work, we highlight the link between the speed-vs-accuracy and exploration-vs-exploitation tradeoffs. Here we elaborate upon the role of network connectivity in the tradeoffs. On one hand, the network structure influences the dynamics of consensus-making in collectives. On the other, agents modify the network based on their opinion. We model this behaviour of agents based on homophily—the tendency of nodes to establish links with other like-minded nodes. This co-evolution of the network structure and opinion of agents shows rich dynamics,

even for spatial networks. In particular, we demonstrate that in systems with limited connectivity, homophily can lead to the emergence of echo-chambers, which prevents consensus. Our focus for future work is to provide solutions within the capability of agents to bring global connectivity and thus the consensus back to

the collective. [1] Raoufi, M., et. al. Speed-vs-Accuracy Tradeoff in Collective Estimation: An Adaptive Exploration-Exploitation Case. In 2021 International Symposium on Multi-Robot and Multi-Agent Systems (MRS) (pp. 47-55). IEEE.

SOE 20: Networks: From Topology to Dynamics IV (joint session DY/SOE)

Time: Friday 9:30–11:45

Location: ZEU 250

See DY 57 for details of this session.

SOE 21: Financial Markets and Risk Management I

Time: Friday 9:30–10:00

Location: ZEU 260

Invited Talk

SOE 21.1 Fri 9:30 ZEU 260

Marginal Stability and Excess volatility in firm networks — •JEAN-PHILIPPE BOUCHAUD — CFM — Academie des Sciences

Will a large economy be stable? Building on Robert May's original argument for large ecosystems, we conjecture that evolutionary and behavioural forces conspire to drive the economy towards marginal stability. We study networks of firms in which inputs for production are not easily substitutable, as in several real-world supply chains. We argue that such networks generically become dys-

functional when their size increases, when the heterogeneity between firms becomes too strong, or when substitutability of their production inputs is reduced. At marginal stability and for large heterogeneities, we find that the distribution of firm sizes develops a power-law tail, as observed empirically. Crises can be triggered by small idiosyncratic shocks, which lead to avalanches of defaults characterized by a power-law distribution of total output losses. This scenario would naturally explain the well-known small shocks, large business cycles puzzle, as anticipated long ago by Bak, Chen, Scheinkman, and Woodford.

SOE 22: Financial Markets and Risk Management II

Time: Friday 10:00–10:45

Location: ZEU 260

SOE 22.1 Fri 10:00 ZEU 260

Microscopic origin of the persistent order flows: microscopic data analysis — YUKI SATO¹ and KIYOSHI KANAZAWA² — ¹University of Tsukuba, Tsukuba, Japan — ²Kyoto University, Kyoto, Japan

In financial markets, it is a stylised fact that the order flow exhibits persistence (or called the long-range correlation, LRC): if you observe a buy (sell) order, you will likely observe a buy (sell) order even in future. This character can be quantified as the power-law decay of the order-sign autocorrelation function $C(\tau) \propto \tau^{-\gamma}$. In explaining the origin of the LRC, the order-splitting hypothesis was proposed as a promising theory. Further, Lillo, Mike, and Farmer proposed a minimal stochastic model of order-splitting traders in 2005, showing a quantitative prediction connecting the relationship between the microscopic and macroscopic behaviour. However, the LMF quantitative prediction has not yet been verified in the lack of appropriate microscopic datasets. In this talk, we solve this long-standing econophysics problem by analysing a huge microscopic dataset in the Tokyo Stock Exchange market. We apply a strategy clustering to identify the set of splitting traders and then measure the power-law exponent α in the metaorder-length distribution for splitting traders. We finally verify the quantitative prediction of the LMF model ($\gamma = \alpha - 1$) by providing the scatterplot between α and γ .

SOE 22.2 Fri 10:15 ZEU 260

Collective Effects Relative to the Collective Market Motion in Financial Markets — •ANTON J. HECKENS and THOMAS GUHR — Universität Duisburg-Essen, Lotharstr. 1, 47048 Duisburg

Financial markets are usually non-stationary and their dynamics is dominated by strong collective effects. We introduce new measures for collectivity derived from covariance and correlation matrices [1]. The largest eigenvalue of covariance and correlation matrices corresponds to the collective motion of the whole system. By removing the collective motion of the system as a whole, we detect a remaining collectivity which corresponds to the industrial sectors. We use risk-phase diagrams to compare the remaining collectivity with the market collectiv-

ity. The time evolution of the remaining collectivity shows a remarkable property as a potential precursor for the Lehman crash in 2008. As of 2015/2016 the collectivity in the US stock markets changed fundamentally. It is connected to trend shifts from smaller mean covariances or correlations to larger ones, especially in recent years. Hence, this new kind of collectivity is connected to systemic instabilities which appear more often in recent years according to our new measures.

[1] A. J. Heckens and T. Guhr, New Collectivity Measures for Financial Covariances and Correlations, *Physica A: Statistical Mechanics and its Applications* 604, 127704 (2022), arXiv:2202.00297.

SOE 22.3 Fri 10:30 ZEU 260

Quantifying the exposure of banking system to the propagation of supply chain shocks in large scale firm-level production networks — •ZLATA TABACHOVÁ¹, CHRISTIAN DIEM¹, ANDRÁS BORSOS^{1,2}, and STEFAN THURNER¹

— ¹Complexity Science Hub Vienna, Josefstädter Strasse 39, A-1080 Vienna, Austria — ²Central Bank of Hungary, Szabadság tér 9, 1054 Budapest, Hungary

The credit risk assessment is core to sound banking business and financial stability. Traditional credit risk and macro-prudential stress testing models using solely node-level financial information can not take the risk of supply chain (SC) contagion into account, leading to potential underestimation of risks. Recent crises such as pandemic or natural disasters have drastically revealed that the propagation of shocks along SCs can potentially lead to large financial losses of firms. Based on a unique country wide dataset, we simulate how an initial failure of firms spread along the SC leading to additional firm defaults and losses to banks. We first define a financial systemic risk index (FSRI) of a firm that measures financial losses due to the SC disruptions caused by failure of that firm. We show that a small fraction of firms pose sizeable risks to the financial system, affecting up to 16% of overall bank equity. Second, we calculate expected losses, value at risk and expected shortfall of banks with and without supply network contagion. Our simulations show that these risk measures can be underestimated by a factor of 4. This indicates that it is crucial for regulators financial systemic risk assessment to monitor SC shock propagation.

SOE 23: Economic Models

Time: Friday 11:00–12:00

Location: ZEU 260

SOE 23.1 Fri 11:00 ZEU 260

Stochastics in action: how to generate profit by exploiting the inefficiencies of the soccer betting market — •RALPH STÖMMER — Private researcher, Ottonbrunn, Germany

In economy, markets are denoted as efficient when it is impossible to systematically generate profits which outperform the average. In the past years, the con-

cept has been tested in other domains such as the growing sports betting market. Surprisingly, despite its large size and its level of maturity, sports betting shows traits of inefficiency. The anomalies indicate the existence of strategies which slightly shift betting from a game of chance towards a game of skill.

This presentation shows an example for an inefficiency detected in the German soccer betting TOTO 13er Wette, which is operated by state-run lottery agen-

cies. Gamblers have to guess the outcome (win, draw, loss) of 13 soccer matches listed on a lottery tip. Applying stochastic methods, a recipe is presented to determine tendencies for single match outcomes, currently resulting in hit rates > 47,7%. More important, the recipe provides the number of lottery tips required to achieve a specific number of strikes (number of correct match forecasts per lottery tip) for a given level of safety (for instance 99,9%). As additional benefit, a useful approximation is derived with Stirling's formula to cope with large numbers in hypergeometric distributions, valid under certain constraints.

Overall, the strategy does lead to price expectations exceeding the aggregated lottery fees, resulting in consistent profits.

SOE 23.2 Fri 11:15 ZEU 260

Assessing the impact of extreme weather events on the global market for staple food — •NKONGHO AYUKETANG ARREYNDIP¹ and EBOBENOW JOSEPH² — ¹Institute of Applied Geosciences, Technical University of Darmstadt, Darmstadt, Germany — ²Physics Department, University of Buea, Cameroon.

The impacts of increasing extreme weather events under future warming may exacerbate global food insecurity. Assessing the economic impact of these disasters in the agricultural sector is critical for early mitigation planning. We model the impacts of extreme weather events by perturbing the agricultural sectors of some breadbasket regions (USA, EU, and China) with a uniform forcing for both single and concurrent extreme weather event scenarios. We consider forcing data from the 2018 Summer European heatwave. This heatwave simultaneously affected multiple Northern-hemisphere mid-latitude locations. We compute and compare the production and consumption value losses in the corn, rice, wheat, soybean, and other agricultural sectors using the FAO data and an agent-based economic model Acclimate. We show that simultaneous extreme weather events can exacerbate the loss of value of agricultural production relative to single extreme weather events. The highest global repercussion is felt in the rice sector compared to other sectors under study for concurrent extreme events scenarios involving China. Moreover, the global commodity market is hardest hit when regions that are major producers of that commodity are affected by extreme weather events such as corn for the USA, wheat for Europe, rice for Southeast Asia, and soybean for Brazil.

SOE 23.3 Fri 11:30 ZEU 260

Forecasting power grid frequency using transformers — •HADEER EL ASHHAB and BENJAMIN SCHÄFER — Institute for Automation and Applied Informatics, Karlsruhe Institute of Technology, Eggenstein-Leopoldshafen, Germany

The power grid frequency is the central observable in power system control, as it measures the balance of electrical supply and demand. A reliable frequency forecast can facilitate rapid control actions and may thus greatly improve power system stability. Here, we develop a forecasting model based on transformers and investigate its performance on data recorded in different power grids.

SOE 23.4 Fri 11:45 ZEU 260

Measuring the Robustness of Production Networks — •TOBIAS REISCH¹, GEORG HEILER^{1,2}, CHRISTIAN DIEM¹, PETER KLIMEK^{1,3}, and STEFAN THURNER^{1,3,4} — ¹Complexity Science Hub Vienna, Vienna, Austria — ²Institute of Information Systems Engineering, TU Wien, Vienna, Austria — ³Section for Science of Complex Systems, CEMSIS, Medical University of Vienna, Vienna, Austria — ⁴Santa Fe Institute, Santa Fe, NM, USA

In modern economies manufacturing happens typically along supply chains. These supply chains intersect and overlap, forming complex networks of production. The failure of single firms in production networks can cause large disruptions. To assess the robustness of economic networks, we develop a firm-level shock spreading model that takes node-specific production functions into account. We define the Economic Systemic Risk Index (ESRI) of a firm as the size of the production interruptions the firm's initial failure causes. First, we apply the new index to the empirical production network of Hungary based on VAT data. Second, we use mobile phone data to reconstruct the production network of a second country that cannot be disclosed. For both countries we find a core of less than 100 high-systemic risk firms that can affect more than 20% of the respective economy. The high-systemic risk core cannot be identified by firm-size. We discuss the network properties that give rise to the observed patterns of systemic risk. Our results contribute to the broader field of network resilience with the introduction of node specific shock spreading dynamics.

Low Temperature Physics Division Fachverband Tiefe Temperaturen (TT)

Elke Scheer
Universität Konstanz
Fachbereich Physik
78457 Konstanz
dpg-fvtiefetemperaturen@uni-konstanz.de

Overview of Invited Talks and Sessions

(Lecture halls HSZ 101, HSZ 103, HSZ 201, HSZ 204, and HSZ 304; Poster P2/2OG, P2/3OG, and P2/4OG)

Tutorial “Physics Meets Machine Learning (joint session DY/TT)”

TT 1.1	Sun	16:00–16:45	HSZ 01	Machine Learning for Quantum Technologies — •FLORIAN MARQUARDT
TT 1.2	Sun	16:45–17:30	HSZ 01	The Unreasonable Effectiveness of Gaussians in the Theory of Deep Neural Networks — •ZOHAR RINGEL
TT 1.3	Sun	17:30–18:15	HSZ 01	Computing learning curves for large machine learning models using the replica approach — •MANFRED OPPER

Plenary Talk

PLV X	Thu	14:00–14:45	HSZ 02	Single-electron-spin-resonance detection by microwave photon counting — •PATRICE BERTET
-------	-----	-------------	--------	--

Invited Talks of the joint Symposium SKM Dissertation Prize 2023 (SYSD)

See SYSD for the full program of the symposium.

SYSD 1.1	Mon	9:30–10:00	HSZ 04	Diffusion of antibodies in solution: from individual proteins to phase separation domains — •ANITA GIRELLI
SYSD 1.2	Mon	10:00–10:30	HSZ 04	Intermediate Filament Mechanics Across Scales — •ANNA V. SCHEPERS
SYSD 1.3	Mon	10:30–11:00	HSZ 04	Ultrafast Probing and Coherent Vibrational Control of a Surface Structural Phase Transition — •JAN GERRIT HORSTMANN
SYSD 1.4	Mon	11:00–11:30	HSZ 04	Electro-active metasurfaces employing metal-to-insulator phase transitions — •JULIAN KARST
SYSD 1.5	Mon	11:30–12:00	HSZ 04	The role of unconventional symmetries in the dynamics of many-body systems — •PABLO SALA

Invited Talks of the joint Symposium Ultrafast Excitation Pathways of Quantum Materials (SYUE)

See SYUE for the full program of the symposium.

SYUE 1.1	Wed	9:30–10:00	HSZ 01	Dynamics and control in quantum materials using multi-terahertz spectroscopy — •RICHARD AVERITT
SYUE 1.2	Wed	10:00–10:30	HSZ 01	Accessing the nonthermal phonon populations in 2D materials with femtosecond electron diffuse scattering — •HÉLÈNE SEILER
SYUE 1.3	Wed	10:30–11:00	HSZ 01	Exciting potentials – Exploring the realms of ultrafast phase transitions — •LAURENZ RETTIG
SYUE 1.4	Wed	11:15–11:45	HSZ 01	Sub-cycle multidimensional spectroscopy of strongly correlated materials — •OLGA SMIRNOVA
SYUE 1.5	Wed	11:45–12:15	HSZ 01	Witnessing many-body entanglement in light-driven quantum materials — •MATTEO MITRANO
SYUE 1.6	Wed	12:15–12:45	HSZ 01	Optical responses of photoexcited materials: from parametric amplification to photoinduced superconductivity — •EUGENE DEMLER

Invited Talks of the joint Symposium Topology in Quantum and Classical Physics – From Topological Insulators to Active Matter (SYQC)

See SYQC for the full program of the symposium.

SYQC 1.1	Wed	15:00–15:30	HSZ 01	Topological magnetic whirls for computing — •KARIN EVERSCHOR-SITTE
SYQC 1.2	Wed	15:30–16:00	HSZ 01	Topological waves from solids to geo/astrophysical flows — •PIERRE DELPLACE
SYQC 1.3	Wed	16:00–16:30	HSZ 01	Topological Phase Transitions in Population Dynamics — •ERWIN FREY
SYQC 1.4	Wed	16:45–17:15	HSZ 01	Topological invariants protect robust chiral currents in active matter — •EVELYN TANG
SYQC 1.5	Wed	17:15–17:45	HSZ 01	Topological defects in biological active matter — •AMIN DOOSTMOHAMMADI

Invited Talks of the joint Symposium Real-Time Measurements of Quantum Dynamics (SYQD)

See SYQD for the full program of the symposium.

SYQD 1.1	Thu	9:30–10:00	HSZ 01	Real-time measurement and control of spin dynamics in quantum dots — •SEIGO TARUCHA
SYQD 1.2	Thu	10:00–10:30	HSZ 01	Quantum Dot arrays for Quantum Information Transfer — •GLORIA PLATERO
SYQD 1.3	Thu	10:30–11:00	HSZ 01	Optical Detection of Real-Time Quantum Dynamics in Quantum Dots — •MARTIN GELLER
SYQD 1.4	Thu	11:30–12:00	HSZ 01	Cooper Pair Splitting in Real-Time — •CHRISTIAN FLINDT
SYQD 1.5	Thu	12:00–12:30	HSZ 01	Trajectory-based detection in stochastic and quantum thermodynamics — •JUKKA PEKOLA

Invited Talks of the joint Symposium Topological Superconductor-Magnet Heterostructures (SYTS)

See SYTS for the full program of the symposium.

SYTS 1.1	Thu	15:00–15:30	HSZ 01	Blending of superconductivity and magnetism via topological solitons — •CHRISTOS PANAGOPOULOS
SYTS 1.2	Thu	15:30–16:00	HSZ 01	Topological landscaping in magnet-superconductor heterostructures — •SEBASTIÁN A. DÍAZ
SYTS 1.3	Thu	16:00–16:30	HSZ 01	Experimental study of minigaps and end states in bottom-up designed multi-orbital Shiba chains — •JENS WIEBE
SYTS 1.4	Thu	16:45–17:15	HSZ 01	Quantum spins and hybridization in artificially-constructed chains of magnetic adatoms on superconducting 2H-NbSe₂ — •KATHARINA J. FRANKE
SYTS 1.5	Thu	17:15–17:45	HSZ 01	Braiding of Majorana zero modes — •STEPHAN RACHEL

Invited Talks of the joint Symposium Physics of van der Waals 2D Heterostructures (SYHS)

See SYHS for the full program of the symposium.

SYHS 1.1	Fri	9:30–10:00	HSZ 01	Novel moiré excitons and ultrafast optical dynamics in van der Waals 2D heterostructures — •STEVEN G. LOUIE
SYHS 1.2	Fri	10:00–10:30	HSZ 01	Interaction induced magnetism in 2D semiconductor moiré superlattices — •XIAODONG XU
SYHS 1.3	Fri	10:30–11:00	HSZ 01	Ions in tight places: intercalation and transport of ions in van der Waals heterostructures — •IRINA GRIGORIEVA
SYHS 1.4	Fri	11:15–11:45	HSZ 01	Spin-orbit proximity in van der Waals heterostructures — •FELIX CASANOVA
SYHS 1.5	Fri	11:45–12:15	HSZ 01	Plethora of many-body ground states in magic angle twisted bilayer graphene — •DMITRI EFETOV

Invited Talks of the Focus Session “Physics Meets ML I - Machine Learning for Complex Quantum Systems (joint session DY/TT)”

TT 2.1	Mon	9:30–10:00	HSZ 03	Enhanced variational Monte Carlo for Rydberg atom arrays — •STEFANIE CZISCHEK
TT 2.2	Mon	10:00–10:30	HSZ 03	Data mining the output of quantum simulators – from critical behavior to algorithmic complexity — •MARCELLO DALMONTE
TT 2.3	Mon	10:30–11:00	HSZ 03	Reinforcement learning for quantum technologies — •FLORIAN MARQUARDT
TT 2.4	Mon	11:00–11:30	HSZ 03	Machine learning of phase transition — •CHRISTOF WEITENBERG

Invited Talks of the Focus Session “Physics Meets ML II - Understanding Machine Learning as Complex Interacting Systems (joint session DY/TT)”

TT 13.1	Mon	15:00–15:30	ZEU 250	The challenge of structured disorder in statistical physics — •MARC MEZARD
TT 13.2	Mon	15:30–16:00	ZEU 250	The emergence of concepts in shallow neural-networks — •ELENA AGLIARI
TT 13.3	Mon	16:00–16:30	ZEU 250	Adaptive Kernel Approaches to Feature Learning in Deep Neural Networks — •ZOHAR RINGEL
TT 13.5	Mon	17:00–17:30	ZEU 250	Analysing the dynamics of message passing algorithms — •MANFRED OPPER
TT 13.6	Mon	17:30–18:00	ZEU 250	Deep Learning Theory Beyond the Kernel Limit — •CENGIZ PEHLEVAN

Invited Talks of the Focus Session “New Perspectives for Adiabatic Demagnetization Refrigeration in the Kelvin and sub-Kelvin Range (joint session TT/MA)”

TT 19.1	Tue	9:30–10:00	HSZ 03	Self-cooling molecular spin quantum processors — •MARCO EVANGELISTI
TT 19.2	Tue	10:00–10:30	HSZ 03	Triangular rare-earth borates for milli-Kelvin adiabatic demagnetization refrigeration — •PHILIPP GEGENWART
TT 19.3	Tue	10:30–11:00	HSZ 03	A millikelvin scanning tunnelling microscope in ultra-high vacuum with adiabatic demagnetisation refrigeration — •RUSLAN TEMIROV
TT 19.4	Tue	11:15–11:45	HSZ 03	ADR cryostats in low temperature physics and their applications — •DOREEN WERNICKE
TT 19.5	Tue	11:45–12:15	HSZ 03	Frustrated dipolar materials for low-temperature magnetic refrigeration — •MIKE ZHITOMIRSKY

Invited Talks of the Focus Session “Unconventional Transport Phenomena in Low-Dimensional Superconducting Heterostructures”

TT 27.1	Wed	9:30–10:00	HSZ 03	Superconducting diode effect in Rashba superlattice — •TERUO ONO
TT 27.2	Wed	10:00–10:30	HSZ 03	Quasiparticle-based and Cooper-pair based superconducting diodes — •MARIA SPIES
TT 27.3	Wed	10:30–11:00	HSZ 03	Non-reciprocal superconductivity and the field free Josephson diode — •MAZHAR ALI

Invited Talks of the Focus Session “Correlations in Moiré Quantum Matter”

TT 35.1	Wed	15:00–15:30	HSZ 03	Strongly correlated excitons in atomic double layers — •PHUONG NGUYEN
TT 35.2	Wed	15:30–16:00	HSZ 03	The Quantum Twisting Microscope — •SHAHAL ILANI
TT 35.3	Wed	16:00–16:30	HSZ 03	Light-driven phenomena in two-dimensional and correlated quantum materials — •ANGEL RUBIO
TT 35.4	Wed	16:45–17:15	HSZ 03	Cascade of transitions in twisted and non-twisted graphene layers within the van Hove scenario — •LAURA CLASSEN
TT 35.5	Wed	17:15–17:45	HSZ 03	Topology and strong correlation: From twisted bilayer graphene to the boundary zeros of Mott insulators — •GIORGIO SANGIOVANNI

Invited Talks of the Focus Session “Superconducting Nickelates”

TT 44.1	Thu	9:30–10:00	HSZ 03	Atomic-scale insights to lattice and electronic structure in superconducting nickelates — •BERIT GOODGE
TT 44.2	Thu	10:00–10:30	HSZ 03	Nickelate and cuprate superconductors: Similar yet different — •VAMSHI MOHAN KATUKURI
TT 44.3	Thu	10:30–11:00	HSZ 03	Superconducting instabilities in strongly-correlated infinite-layer nickelates — •ANDREAS KREISEL
TT 44.5	Thu	11:45–12:15	HSZ 03	Superconducting layered square-planar nickelates: Synthesis, properties, and progress — •GRACE PAN
TT 44.4	Thu	11:15–11:45	HSZ 03	Infinite-layer nickelate thin films: From synthesis to spectroscopy — •DANIELE PREZIOSI

Invited Talks not included in Focus Sessions

TT 8.1	Mon	15:00–15:30	HSZ 103	Molecules on a superconductor: Inducing magnetism and resonance-enhanced vibrational spectroscopy — •RICHARD BERNDT
TT 17.3	Mon	17:15–17:45	HSZ 304	Noise signatures of anyon statistics and Andreev scattering in the $\nu = 1/3$ fractional quantum Hall regime — •ANNE ANTHORE
TT 22.6	Tue	11:00–11:30	HSZ 204	Higgs spectroscopy of superconductors in nonequilibrium — •DIRK MANSKE
TT 28.6	Wed	10:45–11:15	HSZ 103	Studying the Fulde-Ferrell-Larkin-Ovchinnikov order parameter in quasi-2D organic superconductors — •TOMMY KOTTE
TT 39.1	Wed	15:00–15:30	HSZ 304	Sensing and control of MHz photons with microwave photon-pressure — •DANIEL BOTHNER
TT 66.1	Fri	9:30–10:00	HSZ 304	Towards ultrasensitive calorimetric detection in superconducting quantum circuits — •BAYAN KARIMI

Sessions

TT 1.1–1.3	Sun	16:00–18:15	HSZ 01	Tutorial: Physics Meets Machine Learning (joint session DY/TUT/TT)
TT 2.1–2.9	Mon	9:30–13:00	HSZ 03	Focus Session: Physics Meets ML I – Machine Learning for Complex Quantum Systems (joint session TT/DY)
TT 3.1–3.13	Mon	9:30–13:00	HSZ 103	Superconductivity: Properties and Electronic Structure
TT 4.1–4.13	Mon	9:30–13:00	HSZ 201	f-Electron Systems and Heavy Fermions I
TT 5.1–5.14	Mon	9:30–13:15	HSZ 204	Correlated Electrons: Method Development
TT 6.1–6.13	Mon	9:30–13:00	HSZ 304	Topological Semimetals
TT 7.1–7.14	Mon	9:30–13:00	HSZ 403	Spin Transport and Orbitronics, Spin-Hall Effects (joint session MA/TT)
TT 8.1–8.8	Mon	15:00–17:15	HSZ 103	Yu-Shiba-Rusinov Systems
TT 9.1–9.8	Mon	15:00–17:00	HSZ 201	f-Electron Systems and Heavy Fermions II
TT 10.1–10.12	Mon	15:00–18:15	HSZ 204	Correlated Electrons: Other Materials
TT 11.1–11.6	Mon	15:00–16:30	HSZ 304	Spintronics, Spincalorics and Magnetotransport
TT 12.1–12.8	Mon	15:00–17:15	HSZ 403	Topological Insulators (joint session MA/TT)
TT 13.1–13.8	Mon	15:00–18:30	ZEU 250	Focus Session: Physics Meets ML II – Understanding Machine Learning as Complex Interacting Systems (joint session DY/TT)
TT 14.1–14.5	Mon	15:00–17:45	POT 361	Focus Session: Graphene Quantum Dots (joint session HL/TT)
TT 15.1–15.7	Mon	15:00–17:15	POT 251	Quantum Transport and Quantum Hall Effects I (joint session HL/TT)
TT 16.1–16.18	Mon	15:00–18:00	P2/OG4	Poster: Transport
TT 17.1–17.7	Mon	16:45–18:45	HSZ 304	Topology: Quantum Hall Systems
TT 18.1–18.5	Mon	17:15–18:30	HSZ 201	Nano- and Optomechanics
TT 19.1–19.9	Tue	9:30–13:15	HSZ 03	Focus Session: New Perspectives for Adiabatic Demagnetization Refrigeration in the Kelvin and sub-Kelvin Range (joint session TT/MA)
TT 20.1–20.13	Tue	9:30–13:00	HSZ 103	Superconductivity: Tunnelling and Josephson Junctions
TT 21.1–21.9	Tue	9:30–11:45	HSZ 201	Correlated Electrons: Electronic Structure Calculations
TT 22.1–22.13	Tue	9:30–13:15	HSZ 204	Nonequilibrium Quantum Many-Body Systems I (joint session TT/DY)
TT 23.1–23.13	Tue	9:30–13:00	HSZ 304	Kagome Systems
TT 24.1–24.9	Tue	9:30–12:15	POT 151	Quantum Dots: Transport (joint session HL/TT)
TT 25.1–25.4	Tue	12:00–13:00	HSZ 201	Molecular Electronics and Photonics (joint session TT/PPP)
TT 26	Tue	14:00–15:30	HSZ 304	Members' Assembly
TT 27.1–27.10	Wed	9:30–13:00	HSZ 03	Focus Session: Unconventional Transport Phenomena in Low-Dimensional Superconducting Heterostructures
TT 28.1–28.6	Wed	9:30–11:15	HSZ 103	Unconventional Superconductors
TT 29.1–29.14	Wed	9:30–13:15	HSZ 201	Frustrated Magnets: General
TT 30.1–30.13	Wed	9:30–13:00	HSZ 204	Complex Oxides
TT 31.1–31.12	Wed	9:30–12:45	HSZ 304	Topology: Majorana Physics
TT 32.1–32.11	Wed	9:30–12:30	GÖR 226	Molecular Electronics and Excited State Properties (joint session CPP/TT)
TT 33.1–33.12	Wed	9:30–13:00	MOL 213	Many-Body Quantum Dynamics (joint session DY/TT)
TT 34.1–34.6	Wed	11:30–13:00	HSZ 103	Fe-based Superconductors
TT 35.1–35.7	Wed	15:00–18:15	HSZ 03	Focus Session: Correlations in Moiré Quantum Matter I
TT 36.1–36.10	Wed	15:00–17:45	HSZ 103	Topological Insulators
TT 37.1–37.13	Wed	15:00–18:30	HSZ 201	Ruthenates
TT 38.1–38.13	Wed	15:00–18:30	HSZ 204	Nonequilibrium Quantum Many-Body Systems II (joint session TT/DY)
TT 39.1–39.11	Wed	15:00–18:15	HSZ 304	Superconducting Electronics
TT 40.1–40.8	Wed	15:00–18:30	POT 81	Focus Session: Wissenschaftskommunikation / Outreach (joint session HL/O/TT)
TT 41.1–41.6	Wed	15:00–17:00	POT 251	Quantum Transport and Quantum Hall Effects II (joint session HL/TT)

TT 42.1–42.22	Wed	15:00–18:00	P2/OG2	Poster: Correlated Electrons I
TT 43.1–43.33	Wed	15:00–18:00	P2/OG3	Poster: Correlated Electrons II
TT 44.1–44.8	Thu	9:30–13:00	HSZ 03	Focus Session: Superconducting Nickelates I
TT 45.1–45.10	Thu	9:30–12:15	HSZ 103	Correlated Electrons: 1D Theory
TT 46.1–46.13	Thu	9:30–13:00	HSZ 201	Frustrated Magnets: Spin Liquids
TT 47.1–47.13	Thu	9:30–13:00	HSZ 204	Quantum-Critical Phenomena
TT 48.1–48.7	Thu	9:30–11:15	HSZ 304	Topological Superconductors
TT 49.1–49.6	Thu	11:30–13:00	HSZ 304	Quantum Coherence and Quantum Information Systems I
TT 50.1–50.8	Thu	15:00–17:00	HSZ 03	Focus Session: Superconducting Nickelates II
TT 51.1–51.9	Thu	15:00–17:30	HSZ 103	Correlated Electrons: Charge Order
TT 52.1–52.9	Thu	15:00–17:30	HSZ 201	Frustrated Magnets: Strong Spin-Orbit Coupling
TT 53.1–53.10	Thu	15:00–17:45	HSZ 204	Graphene
TT 54.1–54.10	Thu	15:00–17:45	HSZ 304	Quantum Coherence and Quantum Information Systems II
TT 55.1–55.9	Thu	15:00–17:30	MOL 213	Dynamics and Chaos in Many-Body Systems I (joint session DY/TT)
TT 56.1–56.11	Thu	15:00–18:30	WIL A317	Focus Session: Making Experimental Data F.A.I.R. – New Concepts for Research Data Management I (joint session O/TT)
TT 57.1–57.28	Thu	15:00–18:00	P2/OG2	Poster: Superconductivity I
TT 58.1–58.31	Thu	15:00–18:00	P2/OG3	Poster: Superconductivity II
TT 59.1–59.18	Thu	15:00–18:00	P2/OG4	Poster Session: Topology
TT 60.1–60.7	Thu	17:15–19:00	HSZ 03	Quantum Dots, Quantum Wires, Point Contacts
TT 61.1–61.5	Thu	17:45–19:00	HSZ 201	Focus Session: Correlations in Moiré Quantum Matter II
TT 62.1–62.8	Fri	9:30–11:45	HSZ 03	Ultrafast Dynamics of Light-Driven Systems
TT 63.1–63.14	Fri	9:30–13:15	HSZ 103	Superconductivity: Theory
TT 64.1–64.8	Fri	9:30–11:30	HSZ 201	Topology: Other Topics
TT 65.1–65.10	Fri	9:30–12:15	HSZ 204	Correlated Electrons: Other Theoretical Topics
TT 66.1–66.7	Fri	9:30–11:30	HSZ 304	Cryogenic Detectors
TT 67.1–67.11	Fri	9:30–12:30	MOL 213	Dynamics and Chaos in Many-Body Systems II (joint session DY/TT)
TT 68.1–68.11	Fri	9:30–12:45	WIL A317	Focus Session: Making Experimental Data F.A.I.R. – New Concepts for Research Data Management II (joint session O/TT)

Annual Meeting of the Low Temperature Physics Division

Tuesday 14:00–15:30 HSZ 304

All members of the Low Temperature Physics Division are welcome to attend!

- Report
- Elections
- Miscellaneous

Sessions

– Invited Talks, Topical Talks, Tutorials, Contributed Talks, and Posters –

TT 1: Tutorial: Physics Meets Machine Learning (joint session DY/TUT/TT)

Machine learning has revolutionized many application fields such as computer vision and natural language processing. In physics there is a growing interest in using machine learning to enhance the analysis of experimental data and to devise and optimize experiments or numerical simulations. On the other hand physicists use their intuition and methods from statistical physics and complex systems theory to better understand the working principles of modern machine learning methods. This tutorial session introduces some subfields within this area and the basic methods involved.

Organized by Sabine Andergassen (Tübingen), Martin Gärtner (Heidelberg), Moritz Helias (Jülich), and Markus Schmitt (Cologne)

Time: Sunday 16:00–18:15

Location: HSZ 01

Tutorial TT 1.1 Sun 16:00 HSZ 01

Machine Learning for Quantum Technologies — •FLORIAN MARQUARDT — Max Planck Institute for the Science of Light and Friedrich-Alexander Universität Erlangen-Nürnberg, Erlangen, Germany

Machine learning is revolutionizing science and technology. In the past few years, it has become clear that it promises significant benefits as well for the development of quantum technologies. In this tutorial I will first give a brief introduction to neural networks. I will then discuss a number of areas and examples in which machine learning is being successfully applied in this context. These include measurement data analysis and quantum state representation, approximate quantum dynamics, parameter estimation, discovering strategies for hardware-level quantum control, the optimization of quantum circuits, and the discovery of quantum experiments, discrete quantum feedback strategies, and quantum error correction protocols.

Reference: "Artificial intelligence and machine learning for quantum technologies", M. Krenn, J. Landgraf, T. Foesel, and F. Marquardt, Phys. Rev. A 107, 010101 (2023).

Tutorial TT 1.2 Sun 16:45 HSZ 01

The Unreasonable Effectiveness of Gaussians in the Theory of Deep Neural Networks — •ZOHAR RINGEL — Racah Institute of Physics, Hebrew University in Jerusalem

Physical Sciences are in many ways the success story of explaining fundamental phenomena using simple math [1]. The fact that physical phenomena could be arranged in that manner is remarkable. Yet this simplicity does not necessarily carry over to life sciences or data sciences. Indeed prominent authors have argued against our desire to rely on neat mathematical structures when analyzing big data [2].

In the past half-decade several results have emerged which balance mathematical simplicity with data-induced complexity. These could be seen as a middle ground between the above juxtaposing views. The common divider here is the use of Gaussian distributions as approximants of various different quanti-

ties in deep neural networks (DNNs). Specifically these Gaussians emerge when describing outputs of DNNs with random weights, outputs of trained DNNs at random times, outputs of fixed DNNs over random input data, and fluctuations of hidden DNN pre-activations. In this tutorial I will present these quantities, provide arguments supporting their Gaussianity, and outline several theoretical implications.

[1] The Unreasonable Effectiveness of Mathematics in the Natural Sciences. Wigner (1960)

[2] The Unreasonable Effectiveness of Data. Halevy, Norvig, Pereira (2009)

Tutorial TT 1.3 Sun 17:30 HSZ 01

Computing learning curves for large machine learning models using the replica approach — •MANFRED OPPER — Inst. für Softwaretechnik und Theor. Informatik, TU Berlin — Centre for Systems Modelling and Quantitative Biomedicine, University of Birmingham, UK

Methods of statistical physics have been used for a long time to mathematically analyse the typical performance of machine learning models in the limit where both the number of data and the number of parameters (such as network weights) is large. By defining Boltzmann-Gibbs probability distributions over parameters where the cost function of the machine learning problem plays the role of a hamiltonian, one can derive analytical expressions for training errors and generalisation errors using the corresponding partition functions and free energies in terms of a usually small number of order parameters.

Since the models depend on a set of random data to be learnt, additional appropriate statistical (so-called quenched) averages of free energies over this 'disorder' have to be performed. The replica approach is a prominent analytical tool from the statistical physics of disordered systems to solve this nontrivial technical challenge.

In this tutorial I will give an introduction to this approach. Starting with an explicit calculation for simple single layer perceptrons, I will then argue how the method can be applied to more complex problems such as kernel machines (support vector machines and Gaussian processes) and multilayer networks.

TT 2: Focus Session: Physics Meets ML I – Machine Learning for Complex Quantum Systems (joint session TT/DY)

Modern machine learning methods open new perspectives on the high-dimensional data arising naturally in complex quantum systems. The applications range from the analysis of experimental observations over optimal control to the enhancement of numerical simulations in and out of equilibrium. This focus session brings together experts in the field to discuss recent progress and promising directions for future research.

Organizers: Markus Schmitt (University of Cologne), Martin Gärtner (University of Heidelberg)

Time: Monday 9:30–13:00

Location: HSZ 03

Invited Talk TT 2.1 Mon 9:30 HSZ 03

Enhanced variational Monte Carlo for Rydberg atom arrays — •STEFANIE CZISZEK — Department of Physics, University of Ottawa, Ottawa, Canada, K1N 6N6

Rydberg atom arrays are promising candidates for high-quality quantum computation and quantum simulation. However, long state preparation times limit the amount of measurement data that can be generated at reasonable timescales. This restriction directly affects the estimation of operator expectation values, as well as the reconstruction and characterization of quantum states.

Over the last years, neural networks have been explored as a powerful and systematically tuneable ansatz to represent quantum wave functions. Via tomographical state reconstruction, such numerical models can significantly reduce the amount of necessary measurements to accurately reconstruct operator expectation values. At the same time, neural networks can find ground state wave functions of given Hamiltonians via variational energy minimization.

While both approaches experience individual limitations, a combination of the two leads to a significant enhancement in the variational ground state search by naturally finding an improved network initialization from a limited amount

of measurement data. Additional specific modifications of the neural network model and its implementation can further optimize the performance of variational Monte Carlo simulations for Rydberg atom arrays and provide significant insights into their behaviour.

Invited Talk

TT 2.2 Mon 10:00 HSZ 03

Data mining the output of quantum simulators – from critical behavior to algorithmic complexity — •MARCELLO DALMONTE — Abdus Salam International Centre for Theoretical Physics, Trieste (I)

Recent experiments with quantum simulators and noisy intermediate-scale quantum devices have demonstrated unparalleled capabilities of probing many-body wave functions, via directly probing them at the single quantum level via projective measurements. However, very little is known about to interpret and analyse such huge datasets. In this talk, I will show how it is possible to provide such characterisation of many-body quantum hardware via a direct and assumption-free data mining. The core idea of this programme is the fact that the output of quantum simulators and computers can be construed as a very high-dimensional manifold. Such manifold can be characterised via basic topological concepts, in particular, by their intrinsic dimension. Exploiting state of the art tools in non-parametric learning, I will discuss theoretical results for both classical and quantum many-body spin systems that illustrate how data structures undergo structural transitions whenever the underlying physical system does, and display universal (critical) behavior in both classical and quantum mechanical cases. I will conclude with remarks on the applicability of our theoretical framework to synthetic quantum systems (quantum simulators and quantum computers), and emphasize its potential to provide a direct, scalable measure of Kolmogorov complexity of output states.

Invited Talk

TT 2.3 Mon 10:30 HSZ 03

Reinforcement learning for quantum technologies — •FLORIAN MARQUARDT — Max Planck Institute for the Science of Light and Friedrich-Alexander Universität Erlangen-Nürnberg, Erlangen, Germany

Complex quantum devices require sophisticated control. Discovering such control strategies from scratch with the help of machine learning will enable us to keep pace with the ever-increasing demands encountered when scaling up quantum computers. In this talk, I will describe how the field of reinforcement learning can deliver on this promise. I will present examples ranging from the optimization of quantum circuits to the model-based discovery of better quantum feedback strategies. Moreover, in a recent collaboration with our experimental colleagues, we could show how to train a novel latency-optimized neural network by reinforcement learning in an experiment, acting on a superconducting qubit in cycles of less than one microsecond.

Invited Talk

TT 2.4 Mon 11:00 HSZ 03

Machine learning of phase transition — •CHRISTOF WEITENBERG — Universität Hamburg, Institut für Laserphysik, Hamburg, Germany

Machine learning is emerging as vital tool in many sciences. In quantum physics, notable examples are neural networks for the efficient representation of quantum many-body states and reinforcement learning of preparation and read-out routines. In this talk, I will present our results on machine learning of quantum phase transitions using classification techniques. This approach works very well even on noisy experimental data both with supervised and unsupervised machine learning, as we demonstrate for quantum simulators based on ultracold atoms. Next to the practical advantages, such techniques might in the future reveal phase transitions, for which conventional order parameters are not known.

15 min. break

TT 2.5 Mon 11:45 HSZ 03

Machine learning optimization of Majorana hybrid nanowires — •MATTHIAS THAMM and BERND ROSENOW — Institut für Theoretische Physik, Universität Leipzig

As the complexity of quantum systems such as quantum bit arrays increases, efforts to automate expensive tuning are increasingly worthwhile. We investigate machine learning based tuning of gate arrays using the CMA-ES algorithm for the case study of Majorana wires with strong disorder. We find that the algorithm is able to efficiently improve the topological signatures, learn intrinsic disorder profiles, and completely eliminate disorder effects. For example, with only 20 gates, it is possible to fully recover Majorana zero modes destroyed by disorder by optimizing gate voltages.

TT 2.6 Mon 12:00 HSZ 03

Model-independent learning of quantum phases of matter with quantum convolutional neural networks — •YU-JIE LIU¹, ADAM SMITH², MICHAEL KNAP¹, and FRANK POLLMANN¹ — ¹Technical University of Munich, 85748 Garching, Germany — ²University of Nottingham, Nottingham, NG7 2RD, UK

Quantum convolutional neural networks (QCNNs) have been introduced as classifiers for gapped quantum phases of matter. Here, we propose a model-independent protocol for training QCNNs to discover order parameters that are unchanged under phase-preserving perturbations. We initiate the training sequence with the fixed-point wavefunctions of the quantum phase and then add translation-invariant noise that respects the symmetries of the system to mask the fixed-point structure on short length scales. Without the translational invariance or other additional symmetries, we prove that a phase-classifying QCNN cannot exist. We illustrate this approach by training the QCNN on phases protected by time-reversal symmetry in one dimension, and test it on several time-reversal symmetric models exhibiting trivial, symmetry-breaking, and symmetry-protected topological order. The QCNN discovers a set of order parameters that identifies all three phases and accurately predicts the location of the phase boundary. The proposed protocol paves the way towards hardware-efficient training of quantum phase classifiers on a programmable quantum processor.

TT 2.7 Mon 12:15 HSZ 03

Simulating spectral functions of two-dimensional systems with neural quantum states — •TIAGO MENDES SANTOS¹, MARKUS SCHMITT², and MARKUS HEYL¹ — ¹University of Augsburg, Augsburg, Germany — ²Forschungszentrum Jülich, Jülich, Germany

Spectral functions are key tools to characterize and probe condensed matter systems. Simulating such quantities in interacting two-dimensional quantum matter is, however, still an outstanding challenge. This work presents a numerical approach to simulate spectral functions using Neural Quantum States. As the key aspect, our scheme leverages the flexibility of artificial-neural-network wave functions to access spectral properties by simulating the dynamics of localized excitations with the time-dependent variational Monte Carlo. For demonstration, we study the dynamical structure factor (DSF) of models describing two-dimensional quantum phase transitions, namely, the quantum Ising and a square-lattice Rydberg Atom Arrays model in a regime of parameters relevant to quantum simulators. When combined with deep network architectures whose number of variational parameters increase at a mild polynomial expense with the number of spins, we showcase that our approach reliably describes the DSF for unprecedented system sizes and time scales.

TT 2.8 Mon 12:30 HSZ 03

Efficient optimization of deep neural quantum states toward machine precision — •AO CHEN and MARKUS HEYL — Center for Electronic Correlations and Magnetism, University of Augsburg, 86135 Augsburg, Germany

Neural quantum states (NQSs) have emerged as a novel promising numerical method to solve the quantum many-body problem. However, it has remained a central challenge to train modern large-scale deep network architectures, which would be key to utilize the full power of NQSs and to make them competitive or superior to conventional numerical approaches. Here, we propose a minimum-step stochastic reconfiguration (MinSR) method that reduces the optimization complexity by orders of magnitude while keeping similar accuracy as compared to conventional stochastic reconfiguration. In this talk, I will show MinSR allows for an accurate training on unprecedentedly deep NQS with up to 64 layers and more than 10^5 parameters in the spin-1/2 Heisenberg J_1 - J_2 models on the square lattice. With limited numerical resources, partly obtained on single workstations, we find that this approach yields better variational energies as compared to existing NQS results and we further observe that the accuracy of our ground state calculations approaches different levels of machine precision on modern GPU and TPU hardware.

TT 2.9 Mon 12:45 HSZ 03

Time-dependent variational principle for quantum and classical dynamics — •MORITZ REH¹, MARKUS SCHMITT², and MARTIN GÄRTNER^{1,3,4} — ¹Kirchhoff-Institut für Physik, Universität Heidelberg, Im Neuenheimer Feld 227, 69120 Heidelberg, Germany — ²Institut für Theoretische Physik, Universität zu Köln, 50937 Köln, Germany — ³Physikalisches Institut, Universität Heidelberg, Im Neuenheimer Feld 226, 69120 Heidelberg, Germany — ⁴Institut für Theoretische Physik, Universität Heidelberg, Philosophenweg 16, 69120 Heidelberg, Germany

The solution of many-body quantum dynamics is a challenging feat due to the curse of dimensionality, hindering the exploration of dynamics beyond a mediocre number of qubits. Neural Networks can variationally approximate the state of interest and therefore present a promising tool as they allow to efficiently represent the quantum state at the expense of truncating the Hilbert space.

We present such a scheme that is aimed at solving dissipative quantum dynamics using a probabilistic framework, i.e. the so-called POVM-formalism and demonstrate it for spin chains of up to 40 spins. We then show that the generality of the approach allows us to translate this formalism directly to the case of partial differential equations in high dimensions, defeating the exponential growth of grid cells when adding dimensions.

TT 3: Superconductivity: Properties and Electronic Structure

Time: Monday 9:30–13:00

Location: HSZ 103

TT 3.1 Mon 9:30 HSZ 103

Band-selective quasiparticle scatterers in a two-band superconductor — •THOMAS GOZLINSKI¹, QILI LI¹, NOLA WARWICK¹, JANIC BECK¹, and WULF WULFHEKEL^{1,2} — ¹Physikalisches Institut (PHI), Karlsruher Institut für Technologie (KIT) — ²Institute for Quantum Materials and Technologies (IQMT), Karlsruher Institut für Technologie (KIT)

We study stacking fault tetrahedra (SFTs) in a bulk Pb crystal by mK scanning tunnelling microscopy and spectroscopy and find that the Bogoliubons of the two superconducting bands produce different quasiparticle interference patterns owed to the respective Fermi surface anisotropy. We believe that such extended crystal defects provide a platform to experimentally study interband couplings and scattering rates in a multiband superconductor.

TT 3.2 Mon 9:45 HSZ 103

Symmetry breaking and emergent phases in a noncentrosymmetric superconductor — •FEIFAN WANG¹, XIANGHAN XU², SANG-WOOK CHEONG², and MANFRED FIEBIG¹ — ¹Dept. of Materials, ETH Zurich, Switzerland — ²Dept. of Physics and Astronomy, Rutgers University, USA

Symmetry breaking raises rich physics in condensed matters, such as Rashba splitting, Weyl fermions, unconventional superconducting, multiferroic ordering, etc. Nonlinear optical processes, being extremely sensitive to material symmetries, offer a direct access to the observation of subtly broken or even hidden symmetries. Here we discover emergent phases in a noncentrosymmetric superconductor, Mo₃Al₂C, and resolve the symmetry lowering using second harmonic generation measurements. Together with temperature-dependent electronic conductivity measurements, the phase transition from a normal metal at high temperatures to a charge-density-wave state is proposed. In the former, all mirror symmetries are broken bringing in the structural chirality. The correlation between superconductivity/charge-density-wave transition and non-centrosymmetry/chirality will then be discussed. Exotic properties in a low-symmetry system such as Mo₃Al₂C may add new ingredients to the strong-correlation physics.

TT 3.3 Mon 10:00 HSZ 103

Hunt for FFLO superconductivity in transition metal dichalcogenides — •JIawei ZHANG¹, DENNIS HUANG¹, YOSUKE MATSUMOTO¹, MASAAHIKO ISOBE¹, THOMAS PALSTRA^{1,2}, and HIDENORI TAKAGI^{1,3,4} — ¹Max Planck Institute for Solid State Research, Heisenbergstr. 1, 70569 Stuttgart, Germany — ²University of Twente, Drienerloaan 5, 7522 NB Enschede, The Netherlands — ³Institute for Functional Matter and Quantum Technologies, University of Stuttgart, 70569 Stuttgart, Germany — ⁴Department of Physics, University of Tokyo, 113-0033 Tokyo, Japan

The Fulde-Ferrell-Larkin-Ovchinnikov (FFLO) state was proposed almost half a century ago. In contrast to the Bardeen-Cooper-Schrieffer state, the FFLO state hosts Cooper pairs with finite center-of-mass momentum, giving rise to a modulation of the superconducting gap in real space. Two-dimensionality plays an essential role in the materialization of the FFLO state. With 1T buffer layers that reduce the interlayer coupling between successive 1H superconducting layers, 4H_b-TaS₂ is a promising FFLO candidate. I will talk about the two-dimensional nature of superconductivity in this system as revealed by the Berezinskii-Kosterlitz-Thouless transition. Electrical transport measurements with in-plane magnetic field show that the superconductivity survives above the Pauli limit, providing a high-field regime in the phase diagram to host a possible FFLO state.

TT 3.4 Mon 10:15 HSZ 103

Tuning metal/superconductor to insulator/superconductor coupling via control of proximity enhancement between NbSe₂ monolayers — •O. CHIATTI¹, K. MIHOV¹, T. GRIFFIN¹, C. GROSSE¹, L. GROTE¹, K. HITE², D. HAMANN², M. B. ALEMAYEHU², A. MOGLATENKO³, D. C. JOHNSON², and S. F. FISCHER¹ — ¹Novel Materials Group, Humboldt-Universität zu Berlin, 10099 Berlin, Germany — ²Solid State Chemistry, University of Oregon, Eugene OR 97403-1253, U.S.A. — ³Ferdinand-Braun-Institut, Leibniz-Institut für Höchstfrequenztechnik, 12489 Berlin, Germany

The interplay between charge transfer and electronic disorder in transition-metal dichalcogenide multilayers [1] gives rise to superconductive coupling driven by proximity enhancement, tunneling and superconducting fluctuations. Artificial spacer layers introduced with atomic precision change the density of states by charge transfer. Here, we tune the superconductive coupling between NbSe₂ monolayers from proximity-enhanced to tunneling-dominated and correlate normal and superconducting properties in [(SnSe)_{1+δ}]_m[NbSe₂]₁ tailored multilayers with varying SnSe layer thickness (m=1-15). We show cross-overs between three regimes: metallic with proximity-enhanced coupling, disordered-metallic with intermediate coupling and insulating with Josephson tunneling. [1] A. Devarakonda *et al.*, Science **370**, 231 (2020) [2] M. Trahms *et al.*, Supercond. Sci. Technol. **31**, 065006 (2018)

TT 3.5 Mon 10:30 HSZ 103

Higgs-CDW hybrid mode in coherently-driven 2H-NbSe₂ and La_{2-x}Sr_xCuO₄ — •LIWEN FENG^{1,2,3,4}, JIAYUAN CAO², TIM PRIESSNITZ¹, GENNADY LOGVENOV¹, BERNHARD KEIMER¹, YUAN HUANG⁷, JAN-CHRISTOPH DEINERT⁵, SERGEY KOVALEV⁵, TAO DONG⁶, STEFAN KAISER^{1,3,4}, and HAO CHU^{1,2} — ¹Max Planck Institute for Solid State Research, Stuttgart, Germany — ²Shanghai Jiaotong University, Shanghai, China — ³University of Stuttgart, Stuttgart, Germany — ⁴Technical University Dresden, Dresden, Germany — ⁵Helmholtz-Zentrum Dresden-Rossendorf, Dresden, Germany — ⁶Peking University, Beijing, China — ⁷Beijing Institute of Technology, Beijing, China

Superconductivity and a charge-density-wave (CDW) are often found as close neighbors in the thermodynamic phase diagram of many materials at low temperatures. A prototypical system showing the co-existence of the two orders is 2H-NbSe₂. Here, we coherently drive collective oscillations by terahertz radiation and report on third harmonic generation (THG) from both CDW amplitude oscillations and Higgs oscillations. We find the interaction between two orders leads to a Fano interference of THG signals, which displays as an out-of-phase interference in the time-domain. This we characterize as Higgs-CDW hybrid that can be controlled by the THz driving field. Additionally, a similar phenomenon manifests in the underdoped cuprate La_{2-x}Sr_xCuO₄ (x ~ 0.12) under non-perturbative drive. As such non-linear THz drives of order parameter oscillations opening up possibilities of investigating intertwined orders in the future.

TT 3.6 Mon 10:45 HSZ 103

Clean-limit superconductivity at 197 K in high-pressure sulfur hydride — •SAM CROSS¹, ISRAEL OSMOND¹, OWEN MOULDING¹, TAKAKI MURAMATSU¹, ANNABELLE BROOKS¹, OLIVER LORD², TIMOFEY FEDOTENKO³, JONATHAN BUHOT¹, and SVEN FRIEDEMANN¹ — ¹HH Wills Physics Laboratory, University of Bristol, UK — ²School of Earth Sciences, University of Bristol, UK — ³Photon Science, DESY, Germany

The search for room temperature superconductivity in hydrogen rich compounds has accelerated since the discovery of superconductivity in sulfur hydride, H₃S, in 2015 [1]. Controlled synthesis of hydrides remains a challenge, and further work on the formation pathways will prove vital in the search for room temperature superconductivity in such compounds. Here we confirm the synthesis of cubic Im3m H₃S by laser heating elemental sulfur and hydrogen donor ammonia borane, NH₃BH₃. Superconductivity is characterised using electrical transport measurements in a diamond anvil cell, confirming a transition temperature T_c = 197 K at 153 GPa, in agreement with previous studies. The coherence length extracted from measurements of the critical field H_{c2} together with estimations of the carrier mean free path from the normal state resistance suggest that H₃S follows clean-limit behaviour. The work further highlights the potential for in-situ synthesis of clean hydrides using ammonia borane, a more accessible synthesis alternative to pure hydrogen.

[1] A.P. Drozdov *et al.*, Nature **525**, 73 (2015)

TT 3.7 Mon 11:00 HSZ 103

Unraveling charge transfer to understand superconductivity in MgB₂ — •SIMON MAROTZKE^{1,2}, JAN OLIVER SCHUNCK^{1,3}, AMINA ALIC⁴, OCTAVE DUROS⁴, MORITZ HOESCH¹, ALESSANDRO NICOLAOU⁵, GHEORGHE SORIN CHIUZBAIAN⁴, and MARTIN BEYE¹ — ¹Deutsches Elektronen-Synchrotron DESY, Hamburg, Germany — ²Christian-Albrechts-Universität zu Kiel, Kiel, Germany — ³Universität Hamburg, Hamburg, Germany — ⁴Sorbonne Université, Paris, France — ⁵Synchrotron SOLEIL, Saint-Aubin, France

Magnesium diboride (MgB₂) holds the world-record for the highest transition temperature (T_C = 39 K) in a conventional Bardeen-Cooper-Schrieffer (BCS)-type, i.e., phonon-mediated, superconductor. The undoped electron configuration of MgB₂ is still disputed as contradicting results on the appearance of charge transfer upon crossing T_C have been reported. To settle this question, we conducted high-resolution resonant X-ray emission spectroscopy (XES) as well as X-ray absorption spectroscopy (XAS) measurements around the boron K-edge at the SEXTANTS beamline at the synchrotron SOLEIL. In order to investigate the charge transfer between in-plane and out-of-plane states, we varied the polarization of the incoming photons as well as the incidence and emission angle. We report on differences in the spectral intensity for both the absorption and emission spectra upon crossing T_C to be first indications of changes in the density of the boron 2p states. Complementary density of states calculations showing good agreement with the experimental data were performed.

15 min. break

TT 3.8 Mon 11:30 HSZ 103

Emergence of incipient superconductivity in CrB₂ under anisotropic strain — ALEXANDER REGNAT¹, •ANDRÉ DEYERLING¹, CHRISTOPH RESCH¹, JAN SPALLEK¹, ALFONSO CHACON¹, PHILIPP G. NIKLOWITZ^{1,2}, ANDREAS BAUER¹, MARC A. WILDE¹, and CHRISTIAN PFLEIDERER¹ — ¹Physik-Department, Technical University of Munich, D-85748 Garching, Germany — ²Department of Physics, Royal Holloway, University of London, Egham TW20 0EX, UK

Resistivity studies of the hexagonal C32 diborides MoB₂[1], WB₂[2], and CrB₂[3,4] under ultra-high pressures of the order 100 GPa have recently revealed superconducting transitions, where the precise pressure conditions are unknown. We report a study of the electrical resistivity of the itinerant-electron antiferromagnet CrB₂ [5,6] under uniaxial, hydrostatic, and quasi-hydrostatic pressures up to 0.5 GPa, 2.2 GPa and 8 GPa, respectively. Tracking the magnetic transition temperature and the onset of incipient superconductivity we derive a phase diagram as a function of the ratio of lattice constants c/a . Supported by detailed electronic structure calculations, we suggest that the reduction of lattice constant c controls the suppression of magnetic order and concomitant emergence of superconductivity in CrB₂.

[1] C. Pei et al., arXiv:2105.13250 (2021)

[2] J. Lim et al., arXiv:2109.11521 (2021)

[3] C. Pei et al., arXiv:2109.15213 (2021)

[4] S. Biswas et al. arXiv:2211.01054 (2022)

[5] M. Brasse et al., PRB **88**, 155138 (2013)[6] A. Bauer et al., PRB **90**, 064414 (2014)

TT 3.9 Mon 11:45 HSZ 103

Annealing microstructured crystals of cuprate superconductor Tl₂Ba₂CuO_{6-x} — •AYANESH MAITI^{1,2,3}, SEUNGHYUN KHIM¹, CARSTEN PUTZKE², and ANDREW P MACKENZIE^{1,3} — ¹Max Planck Institute for Chemical Physics of Solids, Dresden — ²Max Planck Institute for Structure and Dynamics of Matter, Hamburg — ³University of St Andrews, Scotland

Cuprates exhibit a variety of interesting physics that is not well understood, ranging from unconventional superconductivity to strange metal behaviour. Past experiments have mostly focused on underdoped cuprates that have complex phases due to competing orders. Studies with overdoped samples were limited by the rarity of candidate materials and the difficulty to probe crystals with surface reconstructions. Tl₂Ba₂CuO_{6-x} is a naturally overdoped cuprate that can be grown with high enough purity to show quantum oscillations, and we can suppress the effects of surface reconstructions by using focused ion beam (FIB) microstructuring techniques. However, FIB procedures remove oxygen from the crystal surface and introduces inhomogeneities in samples, making it hard to study their intrinsic behavior. We are developing annealing techniques to re-homogenize our microstructures, using measurements of the doping-dependent high-temperature resistivity to monitor their oxygen content. This will allow us to study the overdoped part of the cuprate phase diagram and hence improve our understanding of unconventional superconductivity. Our techniques will also enable studies with the full range of doping on a single specimen, eliminating sample-to-sample variations from future experiments.

TT 3.10 Mon 12:00 HSZ 103

Vortex matching at 6 T in YBa₂Cu₃O_{7-δ} by imprinting an ultradense hexagonal pinning array with focused helium ion irradiation — •BERND AICHNER¹, LUCAS BACKMEISTER¹, MAX KARRER², KATJA WÜRSTER², CHRISTOPH SCHMID², REINHOLD KLEINER², EDWARD GOLDOBIN², DIETER KOELLE², and WOLFGANG LANG¹ — ¹Fakultät für Physik, Universität Wien, Wien, Österreich — ²Physikalisches Institut, Center for Quantum Science (CQ) and LISA⁺, Universität Tübingen, Tübingen, Deutschland

The focused beam of a helium ion microscope (HIM) is used to locally suppress superconductivity in thin films of the prototypical copper-oxide superconductor YBa₂Cu₃O_{7-δ} (YBCO). In these pillar-shaped regions, the critical temperature T_c is reduced or entirely suppressed due to pair-breaking by point defects.

The narrow spacing of these nanopillars leads to vortex commensurability effects at high magnetic fields, which appear as pronounced maxima of the critical current and corresponding resistance minima. In accordance with the calculation, these effects appear at an unprecedented high magnetic field of 6 T in a hexagonal nanopillar lattice with 20 nm spacing. In contrast to previous observations, matching phenomena persist in the whole accessible temperature range, from the onset of superconductivity down to a temperature of 2 K. At the matching field, we observe a novel behavior in voltage-current isotherms, which we

attribute to an ordered Bose glass phase. These results establish the HIM as a versatile platform for creating ultradense vortex pinning landscapes with complex designs in copper-oxide superconductors.

TT 3.11 Mon 12:15 HSZ 103

Quantum interference in a finite-width mesoscopic ring with superconducting vortices — GIAN PAOLO PAPARI^{1,2,3} and •VLADIMIR M. FOMIN^{4,5} — ¹Dipartimento di Fisica, Università di Napoli “Federico II”, I-80126 Napoli, Italy — ²CNR-SPIN, UOS Napoli, I-80126 Napoli, Italy — ³Istituto Nazionale di Fisica Nucleare (INFN), Naples Unit, I-80126 Napoli, Italy — ⁴Institute for Integrative Nanosciences (IIN), Leibniz IFW Dresden, D-01069 Dresden, Germany — ⁵Moldova State University, MD-2009, Chişinău, Republic of Moldova

We analyze the origin of the parabolic background of magnetoresistance oscillations measured in finite-width superconducting mesoscopic rings with input and output stubs and in patterned films. The transmission model [1] explaining the sinusoidal oscillation of magnetoresistance is extended to address the background as a function of the magnetic field. Apart from the interference mechanism activated by the ring, pinned superconducting vortices as topological defects introduce a further interference-based distribution of supercurrents that affects, in turn, the voltmeter-sensed quasiparticles. The onset of vortices changes the topology of the superconducting state in a mesoscopic ring in a such a way that the full magnetoresistance dynamics can be interpreted owing to the interference of the constituents of the order parameter induced by both the ring itself and the vortex lattice in it.

[1] G. P. Papari and V. M. Fomin, Phys. Rev. B **105**, 144511 (2022)

TT 3.12 Mon 12:30 HSZ 103

Frequency-locking effect in Nb open nanotubes — IGOR BOGUSH^{1,2}, OLEKSANDR V. DOBROVOLSKIY³, and •VLADIMIR M. FOMIN^{1,2} — ¹Institute for Integrative Nanosciences (IIN), Leibniz IFW Dresden, D-01069 Dresden, Germany — ²Department of Theoretical Physics, Moldova State University, MD-2009 Chişinău, Republic of Moldova — ³University of Vienna, Faculty of Physics, Nanomagnetism and Magnonics, Superconductivity and Spintronics Laboratory, 1090 Vienna, Austria

We study alternating voltage generation in Nb open nanotubes under weakly modulated transport current and magnetic field by numerically solving the time-dependent Ginzburg-Landau equation [1]. Under stationary currents and fields, as a rule, an alternating voltage with a fixed frequency is generated in the nanotube. The frequency is associated with the period of the vortex nucleation at the nanotube edges. If the transport current is modulated by a weak ac component with a frequency close to the nucleation frequency, we reveal the effect of frequency-locking of the vortex nucleation, i.e., the nucleation frequency becomes equal to the external frequency of the modulated transport current. The frequency-locking width is discussed as a function of the modulation depth. Its sensitivity to the magnetic field variation opens up opportunities for the experimental examination of the effect.

[1] I. Bogush and V. M. Fomin, Phys. Rev. B **105**, 094511 (2022)

TT 3.13 Mon 12:45 HSZ 103

Superconductivity in curved 3D nanoarchitectures — •VLADIMIR M. FOMIN^{1,2} and OLEKSANDR V. DOBROVOLSKIY³ — ¹Institute for Integrative Nanosciences (IIN), Leibniz IFW Dresden, D-01069 Dresden, Germany — ²Laboratory of Physics and Engineering of Nanomaterials, Department of Theoretical Physics, Moldova State University, MD-2009 Chişinău, Republic of Moldova — ³University of Vienna, Faculty of Physics, Nanomagnetism and Magnonics, Superconductivity and Spintronics Laboratory, 1090 Vienna, Austria

In recent years, superconductivity and vortex matter in curved 3D nanoarchitectures have turned into a vibrant research avenue because of the rich physics of the emerging geometry- and topology-induced phenomena and their prospects for applications in (electro)magnetic field sensing and information technology. We outline the experimental techniques capable of the fabrication of curved 3D nanostructures and present a selection of own results on the intertwined dynamics of screening superconducting currents, Abrikosov vortices and slips of the phase of the superconducting order parameter therein. We share our vision regarding the prospect directions and current challenges in this research domain, arguing that curved 3D nanoarchitectures open a new dimension in superconductors research and possess great potential for magnetic field sensing, bolometry, and fluxonic devices [1].

[1] V. M. Fomin, O. V. Dobrovolskiy, Appl. Phys. Lett. **120**, 090501 (2022)

TT 4: f-Electron Systems and Heavy Fermions I

Time: Monday 9:30–13:00

Location: HSZ 201

TT 4.1 Mon 9:30 HSZ 201

The potential of resonant x-ray scattering for the study of Kondo lattices — •MAREIN RAHN — Institute for Solid State and Materials Physics, Technical University of Dresden, 01062 Dresden, Germany

Kondo lattices represent a pivotal point of quantum matter - where local-itinerant correlations start being shaped by a material's lattice character and their consequences can no longer be reduced to local/mean-field models. Many traditional experimental probes cannot provide insights "beyond the mean field" because they themselves average this phenomenon over time and space. In this talk, I will showcase recent advances in momentum-resolved spectroscopies that can reveal the fine structure and dynamics of Kondo quasiparticles in unprecedented detail. Synchrotron-based techniques like resonant inelastic x-ray scattering provide a particularly interesting new perspective. Their experimental possibilities in f-electron systems have been hardly exploited, which should also be a strong motivation for progress in computational approaches.

TT 4.2 Mon 9:45 HSZ 201

Kondo screening and coherence on the Kagome lattice: Energy scales of the Kondo effect in the presence of at bands — •CHRISTOS KOURRIS and MATTHIAS VOJTA — Institut für Theoretische Physik, TU Dresden, Dresden, Germany

The formation of a heavy Fermi liquid in metals with local moments is characterized by multiple energy and temperature scales, most prominently the Kondo temperature and the coherence temperature, characterizing the onset of Kondo screening and the emergence of Fermi-liquid coherence, respectively. In the standard setting of a wide conduction band, both scales depend exponentially on the Kondo coupling. Here we discuss how the presence of flat, i.e., dispersionless, conduction bands modifies this situation. The Kagome Kondo-lattice model, due to its rich band structure, leads to a plethora of non-conventional Kondo behaviour emerging at different fillings. We utilize a parton mean-field approach to determine both the Kondo temperature and the coherence temperature as function of the conduction-band filling n_c , both numerically and analytically. For n_c values corresponding to the flat conduction band, we show that the exponential is replaced by linear and quadratic dependences for the Kondo and coherence temperature respectively, while a cubic power law emerges in the coherence temperature at n_c corresponding to the band edge between the flat and dispersive bands. We discuss implications of our results for pertinent experimental data.

TT 4.3 Mon 10:00 HSZ 201

Uniaxial strain tuning the signature of Kondo effect in the electrical resistance of heavy-fermion metals — •SOUMENDRA PANJA, ANTON JESCHE, BIN SHEN, and PHILIPP GEGENWART — Experimental Physics VI, Center for Electronic Correlations and Magnetism, University of Augsburg, 86159 Augsburg, Germany

Physical properties of Kondo lattices are determined by the interplay of the Kondo effect and the RKKY interaction, which both depend sensitively on the antiferromagnetic exchange J between f- and conduction electrons. This competition is extremely sensitive to pressure, as evidenced by very large Grüneisen parameters found in these materials. We intend to tune the Kondo-maximum signature in the electrical resistance of such materials with tensile and compressive strain by utilizing a commercial piezo-strain device. In this talk, first results will be discussed under experimentally accessible strains.

TT 4.4 Mon 10:15 HSZ 201

Kondo breakdown transitions and phase-separation tendencies in valence-fluctuating heavy-fermion materials — •PEDRO MONTEIRO CÔNSOLI and MATTHIAS VOJTA — Institut für Theoretische Physik, TU Dresden

The breakdown of the lattice Kondo effect in local-moment metals can lead to nontrivial forms of quantum criticality and a variety of non-Fermi-liquid phases. Given indications that Kondo-breakdown transitions involve criticality not only in the spin but also in the charge sector, we investigate the interplay of Kondo breakdown and strong valence fluctuations in generalized Anderson lattice models. We employ a parton mean-field theory to describe the transitions between deconfined fractionalized Fermi liquids and various confined phases. As a result, we find that rapid valence changes near Kondo breakdown can render the quantum transition first order. This leads to phase-separation tendencies which, upon inclusion of longer-range Coulomb interactions, will produce intrinsically inhomogeneous states near Kondo-breakdown transitions. We connect our findings to unsolved aspects of experimental data.

TT 4.5 Mon 10:30 HSZ 201

Quantum spin liquid in an RKKY-coupled two-impurity Kondo system — •KRZYSZTOF P. WÓJCIK^{1,2,3} and JOHANN KROHA³ — ¹M. Curie-Skłodowska University, 20-031 Lublin, Poland — ²Institute of Molecular Physics, PAS, 60-179 Poznań, Poland — ³Physikalisches Institut, Universität Bonn, 53115 Bonn, Germany

We consider a 2-impurity Anderson model with spin-exchange coupling within the conduction-band sector of the Hamiltonian. Our numerical renormalization group calculations show that for strong intraband spin correlations their competition with the Kondo spin screening stabilizes a metallic spin-liquid phase of the localized spins, even without geometric frustration. It is characterized by nonuniversal impurity spectral density, fractionalization of the phase shift between the local and conduction-band parts, and large but not complete spin-spin correlations. For weak Kondo coupling the spin liquid and the Kondo singlet phase are separated by two quantum phase transitions and an intermediate RKKY spin-dimer phase, while beyond a critical coupling they are connected by a crossover. The results suggest how a quantum spin liquid may be realized in heavy-fermion systems near a spin-density wave instability.

TT 4.6 Mon 10:45 HSZ 201

Epitaxial EuPd₂ and EuPd₃ thin films — •SEBASTIAN KÖLSCH and MICHAEL HUTH — Goethe Universität, Frankfurt (Main)

Europium-based binary compounds reveal a variety of interesting phenomena, which are attributed to strong electronic correlations and a competition between two different valence states of the europium ion, which lie close in energy [1]. As a result Eu forms intermetallic compounds usually either in a divalent (e.g. EuPd₂) or trivalent (e.g. EuPd₃) state, depending on the surrounding environment, whereas most other rare earth elements are always trivalent. Some ternary compounds even exhibit a change between both valence states, which may be tuned by temperature, pressure or high magnetic fields. As one of these rare candidates, EuPd₂Si₂ gained much interest due to a temperature driven valence transition from nearly Eu²⁺ above 200 K to Eu³⁺ below 50 K [2]. Recently we achieved for the first time the growth of epitaxial EuPd₂Si₂ thin films, where the valence transition was completely suppressed due to biaxial strain [3]. Epitaxial thin films thus offer the possibility to manipulate the strongly correlated Eu-based systems. Here we present the successful growth of EuPd₂ and EuPd₃ as epitaxial thin films and report on first results regarding their properties.

[1] Y. Onuki et al., *Phil. Mag.* 97, 36 (2017)[2] K. Kliemt et al., *Crys. Grow. & Des.*, 2022[3] S. Kölsch et al., *PRM* 6, 2022

TT 4.7 Mon 11:00 HSZ 201

Single crystal growth of EuPd₂Si₂ under enhanced gas pressure — •ALEXEJ KRAIKER, MARIUS PETERS, KRISTIN KLIEMT, and CORNELIUS KRELLNER — Physikalisches Institut, Goethe Universität Frankfurt, 60438 Frankfurt am Main, Germany

The study of collective phenomena arising from enhanced coupling between electrons and phonons is focussed on materials exhibiting phase transitions involving both, electronic and lattice-degrees of freedom. One system providing such a strongly coupled phase transition is EuPd₂Si₂ crystallizing in the ThCr₂Si₂ structure type. Because of the high vapor pressure of Eu, high-quality single crystals of EuT₂X₂-compounds are very challenging to grow in larger size. One way to prevent Eu from evaporating out of the melt, is growing the crystals in argon overpressure. In this contribution, we present the crystal growth of EuPd₂Si₂ single crystals with a 20 bar and a 150 bar Czochralski-furnace. We show that the argon overpressure slows down the evaporation process of the Eu and leads to crystals with higher quality compared to Bridgman grown samples [1].

[1] K. Kliemt et al. *Cryst. Growth Des.* 2022, 9, 5399**15 min. break**

TT 4.8 Mon 11:30 HSZ 201

Tuning the ground state of EuPd₂(Si_{1-x}Ge_x)₂ using He-gas pressure — •BERND WOLF, THERESA LUNDBECK, MARIUS PETERS, KRISTIN KLIEMT, CORNELIUS KRELLNER, and MICHAEL LANG — Physikalisches Institut, Goethe University, 60438 Frankfurt/Main, Germany

The strongly correlated intermetallic compound EuPd₂Si₂ shows a strong valence-change crossover in a small temperature range. This valence change is accompanied by pronounced lattice effects together with significant changes in the magnetic properties. The material is located on the high-pressure side (crossover range) of the second-order critical endpoint (CEP) where novel collective phenomena which originate from a particularly strong coupling between electronic-, magnetic- and lattice degrees of freedom can be expected. We present magnetic susceptibility measurements data taken on high-quality sin-

gle crystals of $\text{EuPd}_2(\text{Si}_{1-x}\text{Ge}_x)_2$ for nominal Ge-concentrations $0 \leq x_{\text{nom}} \leq 0.2$ in the temperature range $2 \text{ K} \leq T \leq 300 \text{ K}$ and He-gas pressure up to 0.5 GPa. For $x = 0$ at ambient pressure we observe a pronounced valence crossover centered around $T_V \sim 160 \text{ K}$. As expected, T_V shifts to lower temperatures with increasing Ge-concentration, reaching $T_V \sim 90 \text{ K}$ for $x_{\text{nom}} = 0.1$, while still showing a non-magnetic ground state. For $x_{\text{nom}} = 0.2$ we observe long-range antiferromagnetic order setting in below $T_N = 47.3 \text{ K}$. The important finding is that the application of a weak pressure as low as 0.2 GPa the long-range magnetic order can be suppressed giving way to a non-magnetic ground state with pronounced valence fluctuations.

TT 4.9 Mon 11:45 HSZ 201

Search for a critical endpoint in $\text{Eu}(\text{Pd}_{1-x}\text{Au}_x)_2\text{Si}_2$ single crystals — •ROBERT MÖLLER, MARIUS PETERS, KRISTIN KLIEMT, and CORNELIUS KRELLNER — Physikalisches Institut, Goethe-Universität Frankfurt, Germany

In a general phase diagram for Eu compounds [1], the intermediate valent EuPd_2Si_2 , $T_V \sim 150 \text{ K}$, is located very close, but slightly at the high-pressure side of a second order critical endpoint [2]. The analysis of polycrystalline samples of $\text{Eu}(\text{Pd}_{1-x}\text{Au}_x)_2\text{Si}_2$ revealed that in this series a critical endpoint can be found which separates the region of continuous from first order transitions. It was shown that the valence state of the material can be tuned via Au substitution and that for x between 0.04 and 0.2 the transition becomes a first order phase transition [3]. Using single crystals grown with the Czochralski method, several characterisations were done to understand the main factors affecting the valence transition of $\text{Eu}(\text{Pd}_{1-x}\text{Au}_x)_2\text{Si}_2$.

[1] Y. Onuki et al., *Phil. Mag.* 97, 3399 (2017)

[2] B. Batlogg et al., in: Wachter, Boppart (eds.): *Valence Instabilities*, North-Holland publishing company (1982)

[3] C. U. Segre et al., *Phys. Rev. Lett.* 49, 1947 (1982)

TT 4.10 Mon 12:00 HSZ 201

Orbital selective coupling in CeRh_3B_2 : co-existence of high Curie and high Kondo temperature — ANDREA AMORESE^{1,2}, PHILIPP HANSMANN³, ANDREA MARINO², PETER KÖRNER¹, THOMAS WILLERS¹, ANDREW WALTERS⁴, KEJIN ZHOU⁴, KURT KUMMER⁵, NICKOLAS B. BROOKS⁵, HONG-JI LIN⁶, CHIEN-TE CHEN⁶, PASCAL LEJAY⁷, MAURITS W. HAVERKORT⁸, LIU HAO TJENG², and •ANDREA SEVERING¹ — ¹Institute of Physics II, University of Cologne, Germany — ²MPI-CPS, Dresden, Germany — ³Department of Physics, University of Erlangen-Nürnberg, Germany — ⁴Diamond Light Source, Didcot, UK — ⁵ESRF, Grenoble, France — ⁶NSRRC, Hsinchu, Taiwan — ⁷Institut Neel, CNRS, Grenoble, France — ⁸Institute for Theoretical Physics, Heidelberg University, Germany

CeRh_3B_2 combines seemingly exclusive properties of strong intermediate valence and high temperature ferromagnetism below 116K with strongly reduced magnetic moments. Utilizing recent advances in synchrotron techniques (XAS & RIXS) in combination with ab-initio density functional calculations, we find that the Rh states are irrelevant for the high temperature ferromagnetism and the Kondo effect, and that the crystal-field strength is not sufficiently strong to account for the Ce moment reduction. Instead our investigation reveals that different Ce 4f orbitals contribute differently to the magnetic coupling and the Kondo-type hybridization in CeRh_3B_2 . The manifestation of such selective orbital coupling is a new aspect in the world of the strongly correlated 4f intermetallics.

TT 4.11 Mon 12:15 HSZ 201

Superconductivity beyond the Pauli limit in high-pressure CeSb_2 — •OLIVER SQUIRE, STEPHEN HODGSON, JIASHENG CHEN, VITALY FEDOSEEV, CHRISTIAN DE PODESTA, THEODORE WEINBERGER, PATRICIA ALIREZA, and MALTE GROSCHE — Cavendish Laboratory, University of Cambridge, Cambridge CB3 0HE, UK

The Kondo lattice system CeSb_2 has been recently found to undergo a structural transition under applied pressure. Here, we focus on the low-temperature properties in the new high-pressure structure which hosts an ultra-heavy fermion electronic state and antiferromagnetic order.

We have accessed the high-pressure structure of CeSb_2 using both piston-cylinder and anvil pressure cells at mK temperatures, and suppressed the magnetic order to a quantum critical point. In the vicinity of the quantum critical point, we have discovered a superconducting dome with $T_c = 250 \text{ mK}$. The upper critical field exceeds the conventional Pauli limit by almost an order of magnitude and displays an unusual S-shaped temperature dependence. We will discuss the relationship between the upper critical field, the locally non-centrosymmetric crystal structure and the strong electronic mass enhancement in CeSb_2 .

TT 4.12 Mon 12:30 HSZ 201

Structural and electronic instabilities in high pressure CeSb_2 — •CHRISTIAN K. DE PODESTA¹, THEODORE I. WEINBERGER¹, OLIVER P. SQUIRE¹, STEPHEN A. HODGSON¹, JIASHENG CHEN¹, RUSTEM KHASANOV², CHRISTINE BEAVERS³, PATRICIA L. ALIREZA¹, and F. MALTE GROSCHE¹ — ¹University of Cambridge, UK — ²Paul Scherrer Institut, Switzerland — ³Diamond Light Source, UK

The Kondo-lattice material CeSb_2 undergoes a cascade of at least three magnetic transitions below 16 K and - unusually for a Ce system - settles on a ferromagnetic ground state. Whereas these transitions are initially hardly affected by applied pressure, they disappear abruptly above 18 kbar. We find that this disappearance is caused by a pressure induced structural change. The high pressure structure of CeSb_2 is profoundly different. It hosts a highly renormalised heavy fermion state which itself undergoes further magnetic transitions at very low temperature. Magnetic order within the high pressure structure extrapolates to zero at a pressure tuned quantum critical point, inducing a new superconducting phase with an anomalous field dependence[1].

We present the first detailed account of the high pressure crystal structure of CeSb_2 from X-ray diffraction, alongside a comprehensive study of the associated magnetic order, using μSR , AC-heat capacity and resistivity measurements. This provides the foundation on which to understand the anomalous superconducting properties which are thought to emerge from the quantum critical point.

[1] O. P. Squire et al., arXiv:2211.00975 (2022)

TT 4.13 Mon 12:45 HSZ 201

Observation of anomalous magneto-transport properties in CeAl_2 — •CHRISTIAN OBERLEITNER, CHRISTIAN FRANZ, ALEXANDER REGNAT, JAN SPALLEK, MICHAEL PETROV, GEORG BENKA, ANDREAS BAUER, MARC WILDE, and CHRISTIAN PFLEIDERER — Physik-Department, Technische Universität München, D-85748 Garching, Germany

Rare-earth compounds historically have attracted great interest due to their diverse low-temperature properties comprising complex magnetic order, superconductivity, and heavy fermion behaviour. We report a study of the electrical transport properties of non-centrosymmetric CeAl_2 at low temperatures and large magnetic fields. For our study single crystals were grown by means of optical float-zoning, where Laue and powder x-ray diffraction as well as low residual resistivities confirm excellent sample quality. Measurements of the magnetization, specific heat, and torque magnetization were used to map out the magnetic phase diagram for different crystallographic orientations. In the regime of the antiferromagnetic order, which supports multi-k antiferromagnetic structures, the magnetoresistance and Hall effect are highly anomalously suggestive of an intricate interplay of anomalous and topological contributions.

TT 5: Correlated Electrons: Method Development

Time: Monday 9:30–13:15

Location: HSZ 204

TT 5.1 Mon 9:30 HSZ 204

Generalized Bogoliubov-Hartree-Fock theory for the Hubbard model — •CHRIS KOSCHENZ¹ and CARSTEN TIMM^{1,2} — ¹Institute of Theoretical Physics, TU Dresden, 01062 Dresden, Germany — ²Würzburg-Dresden Cluster of Excellence ct.qmat, TU Dresden, 01062 Dresden, Germany

We present the phase diagram of the Hubbard model on the square lattice up to a four-site unit cell derived via a generalized Bogoliubov-Hartree-Fock theory. Our approach allows to study magnetic ordering, charge ordering, and superconductivity on the same footing and gives additional information about the so-called mixed phases [1]. These phases emerge in parameter ranges where the system is potentially strongly affected by fluctuations and cannot be described by any set of usual Hartree-Fock states (Slater determinants) [1,2]. Furthermore, we show how to obtain the self-consistent set of order parameters by straightforward

unrestricted global minimization of the appropriate Landau functional [3]. This method allows us to study the coexistence and competition of various magnetic orders and can be used to study the possibility of additional phase transitions in the coexistence regime. [1] E. Langmann and M. Wallin, *J. Stat. Phys.* **127**, 825 (2007) [2] V. Bach *et al.*, *J. Stat. Phys.* **76**, 3 (1994) [3] R. Agra *et al.*, *Eur. J. Phys.* **27**, 407 (2006)

TT 5.2 Mon 9:45 HSZ 204

Competing instabilities with fRG in highly symmetric triangular lattice Hubbard models — •HANNES BRAUN — Max Planck Institute for Solid State Research

Motivated by, e.g., simulations via cold atomic gases and twisted multi-layer transition metal dichalcogenides, we consider Hubbard models with $\text{SU}(N) \times \text{SU}(M)$ symmetry. Such highly symmetric systems with additional degrees of freedom

offer possibilities for novel types of symmetry-broken phases and their competition. To analyse the competing correlated phases of the resulting Hubbard models, we generalise the functional Renormalization Group (fRG) approach for correlated fermionic systems to efficiently incorporate the high symmetries. The truncated unity fRG provides us with unbiased fluctuation diagnostics and allows us to analyse the interplay between charge, spin, and pairing instabilities on equal footing. We present the new set of $SU(N) \times SU(M)$ -symmetric fRG equations and first results for the two-dimensional Hubbard model on the triangular lattice.

TT 5.3 Mon 10:00 HSZ 204

Functional renormalization group without functional integrals — PETER KOPIETZ, RÜDIGER KRÄMER, and ANDREAS RÜCKRIEGEL — Institut für Theoretische Physik, Universität Frankfurt, Max-von-Laue Str. 1, 60438 Frankfurt
We show that exact functional renormalization group (fRG) flow equations for quantum systems can be derived directly within a Hamiltonian operator formalism without using functional integrals. This can be useful for teaching fRG methods to students unfamiliar with functional integrals and also opens new possibilities for applying fRG methods to quantum systems with projected Hilbert spaces such as quantum spin models or strongly interacting fermionic lattice models. In particular, by representing the Hubbard model and the $t - J$ -model in terms of so-called Hubbard X-operators we construct a new strong-coupling fRG approach to these models.

TT 5.4 Mon 10:15 HSZ 204

Reduced basis modeling of quantum spin systems based on DMRG — PAUL BREHMER¹, MICHAEL HERBST², MATTEO RIZZI^{3,4}, BENJAMIN STAMM⁵, and STEFAN WESSEL¹ — ¹Institute for Theoretical Solid State Physics, RWTH Aachen University, 52074 Aachen, Germany — ²Applied and Computational Mathematics, RWTH Aachen University, 52062 Aachen, Germany — ³FZ Jülich GmbH, Institute of Quantum Control, Peter Grünberg Institut (PGI-8), 52425 Jülich, Germany — ⁴Institute for Theoretical Physics, University of Cologne, 50937 Köln, Germany — ⁵Institute of Applied Analysis and Numerical Simulation, University of Stuttgart, 70569 Stuttgart, Germany

Within the reduced basis modeling approach, an effective low-dimensional subspace of a quantum many-body Hilbert space is constructed in order to investigate, e.g., the ground-state phase diagram. The basis of this subspace is built from solutions of snapshots, i.e., ground states corresponding to particular and well-chosen parameter values. Here, we show how a greedy strategy to assemble the reduced basis and thus to select the parameter points can be implemented based on density-matrix-renormalization-group (DMRG) calculations. Once the reduced basis is computed, observables required for the computation of phase diagrams can be computed with a computational complexity independent of the underlying Hilbert space for any parameter value. We illustrate the efficiency and accuracy of this approach for different one-dimensional quantum spin- S models with both $S = 1/2$ and $S = 1$, including anisotropic as well as biquadratic exchange interactions, leading to rich quantum phase diagrams.

TT 5.5 Mon 10:30 HSZ 204

Novel degrees of freedom in cluster Mott insulators — VAISHNAVI JAYAKUMAR and CIARÁN HICKEY — Institute for Theoretical Physics, University of Cologne, Germany

The Hubbard model provides a playground for investigating the physics of a wide range of strongly correlated systems. An important feature of these systems is the Mott insulating phase, where at half-filling, an electron gets localised on a single lattice site. In this work, we study cluster Mott insulators – where electrons are now localised on clusters of sites. To that end, we study an extended Hubbard-Kanamori model on a plethora of clusters with multiple orbitals per site, at different electron fillings. We then explore different regimes of interplay between strong correlations and hopping within these clusters, and the effective degrees of freedom that emerge. It is seen, for example, that high ground-state degeneracies are possible that are due to a combination of both spatial and orbital symmetries. We further include crystal field splitting and spin-orbit coupling to bring our model closer to real materials. Once a blueprint for these building blocks has been established, the clusters can be connected through inter-cluster terms, giving rise to potentially novel Hamiltonians.

TT 5.6 Mon 10:45 HSZ 204

Numerical linked cluster expansions for the ordered low-field phase of the transverse-field Ising model — MATTHIAS MÜHLHAUSER, MAX HÖRMANN, and KAI PHILLIP SCHMIDT — Institute for Theoretical Physics I, Friedrich-Alexander-Universität Erlangen-Nürnberg, Germany

We present a hypergraph approach to numerical linked cluster expansions (NLCEs) in the low-field limit of the transverse-field Ising model (TFIM) where the Z_2 -Symmetry of the TFIM is spontaneously broken and the ground state is magnetically ordered.

Conventional NLCEs in this limit are performed as site expansions where the magnetic order of the ground state is taken into account by longitudinal boundary fields on the graphs.

Here, using an isospectral dual description of the TFIM where the ordered phase is mapped to an effective (symmetry unbroken) polarized phase in the dual description, we demonstrate that a straightforward hypergraph expansion can be executed so that no boundary fields are necessary. This allows us to obtain competitive results for the ground-state energy of the ordered low-field phase of the TFIM.

TT 5.7 Mon 11:00 HSZ 204

Projective cluster-additive block-diagonalisation method — MAX HÖRMANN and KAI PHILLIP SCHMIDT — Institut für Theoretische Physik I, Universität Erlangen-Nürnberg, Staudtstraße 7, 91058 Erlangen

We present an efficient block-diagonalisation method that only relies on the lowest eigenvectors and eigenvalues and allows for a linked-cluster expansion. The method is applied to a low-field expansion of the transverse-field Ising model on the square lattice. Both the single spin-flip and bound-state dispersion is calculated perturbatively and non-perturbatively. The origin of the breakdown of the non-perturbative linked-cluster expansion for the bound-state dispersion at a critical field value is discussed and potential solutions to overcome this problem are examined.

15 min. break

TT 5.8 Mon 11:30 HSZ 204

Series expansions with multiple quasi-particle types for the dual Dicke-Ising model — ANDREAS SCHELLENBERGER, LEA LENKE, and KAI PHILLIP SCHMIDT — FAU Erlangen-Nürnberg, Erlangen, Deutschland

The established approach of perturbative continuous unitary transformations (pCUT) constructs effective quantum many-body Hamiltonians in a perturbative series that conserve the number of one quasi-particle type. We extend the pCUT method to similarity transformations – dubbed $pcst^{++}$ – allowing for multiple quasi-particle-types with complex-valued energies. This enlarges the field of application to closed and open quantum many-body systems with unperturbed operators corresponding to arbitrary superimposed ladder spectra. To illustrate the new possibility of the $pcst^{++}$ method to specifically tackle interacting light-matter systems, we discuss the dual Dicke-Ising model. We determine low-energy spectral properties and investigate potential conversion processes between different quasi-particle types.

TT 5.9 Mon 11:45 HSZ 204

Series expansions in open and non-Hermitian quantum many-body systems with multiple quasi-particle types — LEA LENKE, ANDREAS SCHELLENBERGER, and KAI PHILLIP SCHMIDT — FAU Erlangen-Nürnberg

The established approach of perturbative continuous unitary transformations (pCUT) constructs effective quantum many-body Hamiltonians in a perturbative series that conserve the number of one quasi-particle type. We extend the pCUT method to similarity transformations – dubbed $pcut^{++}$ – allowing for multiple quasi-particle-types with complex-valued energies. This enlarges the field of application to closed and open quantum many-body systems with unperturbed operators corresponding to arbitrary superimposed ladder spectra. To this end a generalized counting operator is combined with the quasi-particle generator for open quantum systems recently introduced by Schmiedinghoff and Uhrig [1]. The $pcut^{++}$ then yields model-independent quasi-particle conserving effective Hamiltonians and Lindbladians allowing a linked-cluster expansion similar to the conventional pCUT method. We illustrate the application of the $pcut^{++}$ method by discussing representative open and non-Hermitian quantum systems. [1] G. Schmiedinghoff and G. S. Uhrig, arXiv:2203.15532 [cond-mat.quant-ph].

TT 5.10 Mon 12:00 HSZ 204

Multi-scale space-time ansatz for correlation functions of quantum systems

— HIROSHI SHINAOKA¹, MARKUS WALLERBERGER², YUTA MURAKAMI³, KOSUKE NOGAKI⁴, RIHITO SAKURAI¹, PHILIPP WERNER⁵, and ANNA KAUCH² — ¹Department of Physics, Saitama University, Saitama 338-8570, Japan — ²Institute of Solid State Physics, TU Wien, 1040 Vienna, Austria — ³Center for Emergent Matter Science, RIKEN, Wako, Saitama 351-0198, Japan — ⁴Department of Physics, Kyoto University, Kyoto 606-8502, Japan — ⁵Department of Physics, University of Fribourg, 1700 Fribourg, Switzerland

Correlation functions of quantum systems are central objects in quantum field theories, which may be defined in high-dimensional space-time domains. The numerical treatment of these objects suffers from the curse of dimensionality, which hinders the application of sophisticated many-body theories to interesting problems.

In this talk, we propose a quantum-algorithms-inspired Multi-Scale Space-Time Ansatz (MSSTA) for correlation functions of quantum systems [1]. The space-time dependence is mapped to auxiliary qubit ($S = 1/2$ spin) degrees of freedom describing exponentially different length scales, and the ansatz assumes a separation of length scales. We numerically verify the ansatz for various equilibrium and nonequilibrium systems and show essential building blocks of diagrammatic equations, such as convolutions or Fourier transforms are formulated in the compressed form using tensor networks.

[1] H. Shinaoka et al., arXiv:2210.12984v2

TT 5.11 Mon 12:15 HSZ 204

Efficient flow equations for dissipative systems — •GARY SCHMIEDINGHOFF and GÖTZ S. UHRIG — Condensed Matter Theory, Technische Universität Dortmund, Otto-Hahn-Straße 4, 44227 Dortmund, Germany

Open quantum systems provide an essential theoretical basis for the development of novel quantum technologies, since any real quantum system inevitably interacts with its environment. Lindblad master equations capture the effect of Markovian environments. Closed quantum systems can be treated using flow equations with the particle conserving generator. We generalize this generator to non-Hermitian matrices and open quantum systems governed by Lindbladians, comparing our results with recently proposed generators by Rosso et al. In comparison, we find that our advocated generator provides an efficient flow with good accuracy in spite of truncations.

TT 5.12 Mon 12:30 HSZ 204

Dynamical mean-field study of a photon-mediated ferroelectric phase transition — •KATHARINA LENK¹, JIAJUN LI^{2,3}, PHILIPP WERNER², and MARTIN ECKSTEIN¹ — ¹I. Institut für Theoretische Physik, Universität Hamburg, 22607 Hamburg — ²Department of Physics, University of Fribourg, 1700 Fribourg Switzerland — ³Paul Scherrer Institute, Condensed Matter Theory, PSI Villigen, Switzerland

The interplay of light and matter gives rise to intriguing cooperative effects in quantum many-body systems. This is even true in thermal equilibrium, where the electromagnetic field can hybridize with collective modes of matter, and virtual photons can induce interactions in the solid. Here, we treat these light-mediated interactions using dynamical mean-field theory. We consider a minimal model of a two-dimensional material that couples to a surface plasmon polariton mode of a metal-dielectric interface. Within the mean-field approximation, the system exhibits a ferroelectric phase transition that is unaffected by the light-matter coupling. Bosonic dynamical mean-field theory provides a more accurate description and reveals that the photon-mediated interactions enhance the ferroelectric order and stabilize the ferroelectric phase.

TT 5.13 Mon 12:45 HSZ 204

Energy correlations of excited states in localization landscape theory — •TORSTEN WEBER, JOHANNES DIEPLINGER, CHRISTOPH FORSTER, LUCAS RESCH, FERDINAND EVERS, and KLAUS RICHTER — Universität Regensburg, Regensburg, Deutschland

The localization landscape method, first described in [1], is a method that enables the prediction of the localization regions of eigenfunctions of a localized

system. Additionally, the method gives a prediction of the energy of low-lying localized eigenfunctions by defining an effective potential from the landscape function [2]. This energy prediction, although providing good results for low energy eigenfunctions, ceases to work for higher energy states. Studying the method for a one-dimensional disordered system we observe a characteristic form of the ratio of the predicted eigenvalue by the landscape method and the actual eigenvalue for this region of the spectrum. We provide a possible explanation for this behaviour by extending the method leading to the energy prediction by including excited states of the effective potential. By harnessing the universal technique of quantifying excited states by counting nodes we observe a correspondence of the n -th excited states with the n -th repetition of a substructure of the characteristic behaviour described above. We go further to also find an analytic estimate for the structures.

[1] M. Filoche and S. Mayboroda, PNAS 109, 14761 (2012)

[2] D. N. Arnold et al., SIAM Journal on Scientific Computing, 41(1) (2019)

TT 5.14 Mon 13:00 HSZ 204

Extended quasiparticle Padé approximation for non-Fermi liquids — •KLAUS MORAWETZ — Münster University of Applied Sciences, Stegerwaldstrasse 39, 48565 Steinfurt, Germany — International Institute of Physics- UFRN, Campus Universitário Lagoa nova, 59078-970 Natal, Brazil

The extended quasiparticle picture is adapted to non-Fermi systems by suggesting a Padé approximation which interpolates between the known small scattering-rate expansion and the deviation from the Fermi energy. The first two energy-weighted sum rules are shown to be fulfilled independent of the interpolating function. For various models of one-dimensional Fermions scattering with impurities the quality of the Padé approximation for the spectral function is demonstrated and the reduced density matrix or momentum distribution is shown to be reproduced not possessing a jump at the Fermi energy. Though the two-fold expansion is necessary to reproduce the spectral function and reduced density it is shown that for the description of transport properties the extended quasiparticle approximation is sufficient. The T-matrix approximation leads to the delay time as the time two particles spend in a correlated state. This contributes to the reduced density matrix and to an additional part in the conductivity which is presented at zero and finite temperatures. Besides a localization at certain impurity concentrations, the conductivity shows a maximum at small temperatures interpreted as onset of superconducting behaviour triggered by impurities. The Tan contact reveals the same universal behaviour as known from electron-electron scattering.

[1] arXiv:2208.11971

TT 6: Topological Semimetals

Time: Monday 9:30–13:00

Location: HSZ 304

TT 6.1 Mon 9:30 HSZ 304

Anomalous Hall and Nernst effects in Kane fermions — •KARUN GADGE^{1,3}, SUMANTA TEWARI², and GIRISH SHARMA³ — ¹Institute for Theoretical Physics University of Göttingen, Friedrich-Hund-Platz 1, 37077 Göttingen — ²Department of Physics and Astronomy, Clemson University, Clemson, South Carolina, 29634, USA — ³School of Basic Sciences, Indian Institute of Technology, Mandi, Mandi 175005, India

Kane fermions are characterized by a linear Dirac cone intersecting with a flat band, resembling a pseudo-spin-1 Dirac semimetal. Similar to relativistic Dirac fermions, Kane fermions satisfy a linear energy-momentum relation and can be classified as being pseudorelativistic. Unlike Dirac fermions, they are not protected by symmetry or by topology, but respect time-reversal symmetry, and can emerge by suitable band engineering, for example, in mercury-telluride compounds. Here we discuss the reminiscences of Berry-phase physics in Kane fermions that emerge in the presence of broken time-reversal symmetry. We discuss anomalous transport in Kane fermions and show its similarity to transport in a Dirac semimetal. Furthermore, we study anisotropy in their response that can be probed in current experiments.

[1] PRB 105, 235420 (2022)

TT 6.2 Mon 9:45 HSZ 304

Automatic generation and topological classification of low-energy Hamiltonians at multi-fold degeneracies — •KIRILL ALPIN — Max Planck Institute for Solid State Research, Stuttgart, Germany

In this talk, we show a method of generating general high-symmetry Hamiltonian with the goal of topologically classifying all possible multi-fold crossings in bandstructures of condensed matter systems. To do so, we found all higher-dimensional irreducible representations at all high-symmetry points in all space groups. The topological phase diagrams of the automatically generated low-energy Hamiltonian at these k -points were mapped out. During this process, we identified a prevalent topological phase with an unusually high Chern number of 5 in multi-fold point crossings. A material was found featuring this

topological phase. Further ab-initio calculations of this materials surface DOS showed a high number of Fermi arcs.

TT 6.3 Mon 10:00 HSZ 304

Finite-size effects in a two-dimensional non-symmorphic wallpaper group lattice — •MIGUEL ÁNGEL JIMÉNEZ HERRERA¹ and DARIO BERCIoux^{1,2} — ¹Donostia International Physics Center, 20018 San Sebastian, Spain — ²IKERBASQUE, Basque Foundation for Science, Euskadi Plaza, 5, 48009 Bilbao, Spain

We investigate the spectral properties of a two-dimensional electronic lattice belonging to the non-symmorphic wallpaper group: the herringbone lattice. Specifically, we focus on the cases of ribbons and flakes geometry. Within a tight-binding description, we study how the different states localize inside the system both for ribbons and flakes. We apply different perturbations and symmetry breaking distortions to the lattice and investigate the robustness of the spectral features. Similarly to the bulk case, where we can gap the band structure or merge the Dirac cones into semi-Dirac cones [1], we recover the same properties along the two main directions that ribbons can be constructed. Finally, we study the finite size effects on this lattice, both on ribbon and flake geometries, and report a spectral flow of states across the bulk-like bands.

[1] Herrera & Bercioux, arXiv:2209.11653.

TT 6.4 Mon 10:15 HSZ 304

Landau quantization in the topological semimetal WTe_2 — •R. SANCHEZ-BARQUILLA¹, F. MARTIN-VEGA¹, J. J. BALDOVI², M. OCHI³, R. ARITA⁴, N. H. JO⁵, S. L. BUD'KO⁵, P. C. CANFIELD⁵, H. SUDEROW¹, and I. GUILLAMON¹ — ¹Laboratorio de Bajas Temperaturas y Altos Campos Magnéticos, UAM, E-28049, Spain — ²ICMol, UV, 46980 Paterna, Spain. — ³Department of Physics, Osaka University, Osaka 560-0043, Japan — ⁴RIKEN Center, Saitama 351-0198, Japan — ⁵Department of Physics and Astronomy, Ames, IA 50011

WTe_2 is a layered semimetal which has sparked much interest due to the non-saturating linear MR and possible non-trivial band structure properties, such as

Weyl type-II fermions. Quantum oscillations under magnetic fields signal the passage of Landau levels (LL) through the Fermi level and are easily observed in macroscopic measurements, providing a rather complete view of the FS. However, the Landau quantization of the band structure above and below the Fermi energy has not yet been resolved in detail. We present mK STM measurements up to 14T. We have obtained the band structure close to the Fermi level and identified the main electron and hole pockets thanks to QPI experiments at 0T. When applying magnetic field, the spatially averaged tunneling conductance is devoid of LL and shows no field dependence. Atomically resolved measurements present however Landau quantization. We show that the contribution from the electron and hole pockets to the tunneling density of states (DOS) compensates LL peaks in the spatially averaged DOS. We describe Landau quantization at atomic scale and show a non-trivial energy shift of the LL structure.

TT 6.5 Mon 10:30 HSZ 304

Landau levels in NbAs as seen in magneto-optics: experiment versus modeling — S. POLATKAN¹, M. ORLITA², C. SHEKHAR³, C. FELSER³, M. DRESSEL¹, and A. V. PRONIN¹ — ¹Physikalisches Institut, Universität Stuttgart, 70569 Stuttgart, Germany — ²LNCMI, CNRS-UGA-UPS-INSA-EMFL, 38042 Grenoble, France — ³Max-Planck-Institut für Chemische Physik fester Stoffe, 01187 Dresden, Germany

We measured the inter-Landau-level transitions the Weyl semimetal NbAs in magneto-optical experiments and found that the fits with pure Weyl bands do not lead to a satisfactory agreement between theory and experiment. We thus propose a coupled hyperbolic band model, supplemented by detailed 2D band structure cuts, attributing a secondary role to the presence of Weyl points. We argue that this minimalist model is sufficient to describe the measured magneto-optical spectra.

TT 6.6 Mon 10:45 HSZ 304

Static and dynamic magnetic properties of RAlSi Weyl semimetals — •TILLMANN WEINHOLD¹, HANK WU^{2,3}, RAJIB SARKAR¹, GEORGE GILL², VADIM GRINENKO⁴, FAZEL TAFTI⁵, STEPHEN BLUNDELL², and HANS-HENNING KLAUSS¹ — ¹TU Dresden, Germany — ²University of Oxford — ³MPI for Solid State Research, Stuttgart, Germany — ⁴Shanghai JiaoTong University, China — ⁵Boston College, MA, USA

Weyl semimetals show interesting electronic transport behavior like anomalous Hall effect and negative magnetoresistance. In the magnetic semimetal NdAlSi spin-density wave order was found below 7.2 K. It is proposed that the magnetic order is driven by RKKY interaction of Weyl fermions on narrow Fermi pockets.

We used NMR and μ SR experiments to gain information about local static and dynamic magnetic properties of NdAlSi and discuss the results in comparison with diamagnetic LaAlSi and canted ferromagnetic CeAlSi.

TT 6.7 Mon 11:00 HSZ 304

Optically enhanced terahertz harmonic generation in the Dirac semimetal Cd₃As₂ — •PATRICK PILCH¹, CHANGQING ZHU¹, RENATO M. A. DANTAS², ANNEKE REINOLD¹, YUNKUN YANG³, FAXIAN XIU³, and ZHE WANG¹ — ¹TU Dortmund University, Germany — ²University of Basel, Switzerland — ³Fudan University, Shanghai, China

High harmonic generation provides an efficient tool to investigate nonequilibrium dynamics of a driven system, and is also very interesting for applications. Cd₃As₂ is a well-established three-dimensional Dirac semimetal with a topologically protected crossing of linear bands at the Fermi level. Terahertz harmonic generation is observed in Cd₃As₂ due to field-driven intraband kinetics [1]. By optically pumping the electron-doped Cd₃As₂, we observe a strong enhancement of the terahertz third harmonic generation. By investigating the dependence of the terahertz third harmonic generation on the pump fluence and time delay, we can ascribe this enhancement to the kinetics of a long-lived nonequilibrium state which corresponds to a population inversion of electrons and holes in the Dirac cone with a characteristic relaxation time $\tau \leq 10$ ps.

[1] Kovalev, S. et al. Nature Commun. 11, 2451 (2020).

15 min. break

TT 6.8 Mon 11:30 HSZ 304

Signatures of a magnetic-field-induced Lifshitz transition in the ultra-quantum limit of the topological semimetal ZrTe₅ — •STANISLAW GALESKI^{1,2} and HENRY LEGG³ — ¹Max Planck Institute for Chemical Physics of Solids, Dresden, Germany — ²Physics Institute, Universität Bonn, Bonn, Germany — ³Department of Physics, University of Basel, Basel, Switzerland

The quantum limit (QL) of an electron liquid, realised at strong magnetic fields, has long been proposed to host a wealth of strongly correlated states of matter. Electronic states in the QL are, for example, quasi-one dimensional (1D), which implies perfectly nested Fermi surfaces prone to instabilities. Whereas the QL typically requires unreachably strong magnetic fields, the topological semimetal ZrTe₅ has been shown to reach the QL at fields of only a few Tesla. Here, we characterize the QL of ZrTe₅ at fields up to 64 T by a combination of electrical-transport and ultrasound measurements. We find that the Zeeman effect in

ZrTe₅ enables an efficient tuning of the 1D Landau band structure with magnetic field. This results in a Lifshitz transition to a 1D Weyl regime in which perfect charge neutrality can be achieved. Since no instability-driven phase transitions destabilise the 1D electron liquid for the investigated field strengths and temperatures, our analysis establishes ZrTe₅ as a thoroughly understood platform for potentially inducing more exotic interaction-driven phases at lower temperatures.

TT 6.9 Mon 11:45 HSZ 304

The anomalous photo-Nernst effect in a Dirac semimetal — •MAANWINDER PARTAP SINGH^{1,2}, JONAS KIEMLE^{1,2}, WALDEMAR SCHMUNK^{1,2}, ALEXANDER HOLLEITNER^{1,2}, and CHRISTOPH KASTL^{1,2} — ¹Walter Schottky Institut, Technical University of Munich, Am Coulombwall 4a, 85748 Garching, Germany. — ²Munich Center of Quantum Science and Technology (MCQST), Schellingstr. 4, 80799 Munich, Germany.

The 3D Dirac semimetal HfTe₅ is a model system to study unconventional Hall transport phenomena, such as quasi quantized and anomalous Hall effects, in the limit of very low charge carrier densities. Here, we report on anomalous photocurrents in HfTe₅, which are intimately linked to the anomalous Hall and the related Nernst conductivities. As the dominant mechanism of photocurrent generation, we establish a, hitherto hidden, anomalous photo-Nernst effect of 3D Dirac electrons. The anomalous photo-Nernst effect manifests itself as a long-range, photoresponse along the crystal edge arising from a Shockley-Ramo type response and the local symmetry breaking at the edge. The observed temperature and density dependences of the anomalous photo-Nernst currents are consistent with a dominating intrinsic Berry curvature mechanism.

TT 6.10 Mon 12:00 HSZ 304

Field-tunable inverted band gap in GdPtBi: A magneto-optical study — •S. POLATKAN¹, E. UYKUR¹, A. V. PRONIN¹, M. ORLITA², I. MOHELSKY², J. WYZULA², C. SHEKHAR³, C. FELSER³, and M. DRESSEL¹ — ¹Physikalisches Institut, Universität Stuttgart, 70569 Stuttgart, Germany — ²LNCMI, CNRS-UGA-UPS-INSA-EMFL, 38042 Grenoble, France — ³Max-Planck-Institut für Chemische Physik fester Stoffe, 01187 Dresden, Germany

GdPtBi is a half-Heusler compound that was suggested to host triple-point fermions. Such fermions may be transformed into Weyl fermions in magnetic fields. We present magneto-optical data alongside a $\mathbf{k} \cdot \mathbf{p}$ model, evidencing the exchange-interaction mediated pseudo-Zeeman splitting of the parabolic band touching at the Γ point predicted by DFT, and thus prove the existence of highly tunable Weyl cones.

TT 6.11 Mon 12:15 HSZ 304

Anisotropic optics and gravitational lensing of tilted Weyl fermions — •VIKTOR KÖNYE¹, LOTTE MERTENS^{1,2}, CORENTIN MORICE³, DMITRY CHERNYAVSKY¹, ALI G. MOGHADDAM^{4,5}, JASPER VAN WEZEL², and JEROEN VAN DEN BRINK^{1,6} — ¹Institute for Theoretical Solid State Physics, IFW Dresden and Würzburg-Dresden Cluster of Excellence ct.qmat, Helmholtzstr. 20, 01069 Dresden, Germany — ²Institute for Theoretical Physics, University of Amsterdam, Science Park 904, 1098 XH Amsterdam, The Netherlands — ³Laboratoire de Physique des Solides, CNRS UMR 8502, Université Paris-Saclay, F-91405 Orsay Cedex, France — ⁴Department of Physics, Institute for Advanced Studies in Basic Sciences (IASBS), Zanjan 45137-66731, Iran — ⁵Computational Physics Laboratory, Physics Unit, Faculty of Engineering and Natural Sciences, Tampere University, FI-33014 Tampere, Finland — ⁶Institute for Theoretical Physics, TU Dresden, 01069 Dresden, Germany

We show that tilted Weyl semimetals with a spatially varying tilt provide a platform for studying analogues to problems in anisotropic optics as well as curved spacetime. Considering particular tilting profiles, we numerically evaluate the time evolution of wave packets. We demonstrate that electron trajectories in such systems can be obtained from Fermat's principle in the presence of an inhomogeneous, anisotropic effective refractive index. On the other hand, we show how the electrons dynamics reveal gravitational features and use them to simulate gravitational lensing around a synthetic black hole.

TT 6.12 Mon 12:30 HSZ 304

Black hole mirages: Electron lensing and Berry curvature effects in inhomogeneously tilted Weyl semimetals — •ANDREAS HALLER¹, SURAJ HEDGE², CHEN XU², CHRISTOPHE DE BEULE^{1,3}, THOMAS L. SCHMIDT¹, and TOBIAS MENG² — ¹Department of Physics and Materials Science, University of Luxembourg, L-1511 Luxembourg, Luxembourg — ²Institute of Theoretical Physics and Würzburg-Dresden Cluster of Excellence ct.qmat, Technische Universität Dresden, 01069 Dresden, Germany — ³Department of Physics and Astronomy, University of Pennsylvania, Philadelphia PA 19104, USA

In this talk, I present our recent study about electronic transport in Weyl semimetals with spatially varying nodal tilt profiles. We discuss two complementary approaches that characterise the electron flow: solutions of the semiclassical equations of motion, in analogy to those encountered in black hole spacetimes, and large-scale microscopic simulations of a scattering region surrounded by semi-infinite leads. We show that the two approaches lead to equivalent results

when the wave packet is sufficiently far from the center of the tilt. The two methods are arguably a powerful toolset in the pursuit of tiltronic devices such as e.g. electronic lenses.

TT 6.13 Mon 12:45 HSZ 304

Weyl-type parallel spin-momentum locking in a chiral topological semimetal — •NIELS B. M. SCHRÖTER — Max Planck Institute of Microstructure Physics, Weinberg 2, 06120 Halle (Saale), Germany

Orthogonal Rashba-type spin-momentum locking is well-known from semiconductors and topological insulator surface states and has inspired many theoretical proposals for technological applications. In contrast, Weyl-type purely parallel spin-momentum locking – which can be considered the natural counterpart of the Rashba-type – has remained elusive in experiments because all experimentally confirmed Weyl-fermion are described by Pauli matrices that act on an

orbital pseudospin rather than the proper electron spin. Recently, chiral topological semimetals (CTS) that host single- and multifold band crossings [1,2] have been predicted to realize parallel spin-momentum locking. Here, we use spin-resolved photoemission to probe the spin-texture Fermi-arc surface states in the CTS PtGa. We find that the electron spin points orthogonal to the Fermi surface contour for momenta close to the projection of a bulk multifold fermion, which is consistent with parallel spin-momentum locking of the latter [3]. We anticipate that our discovery of parallel spin-momentum locking of multifold fermions will lead to the integration of chiral topological semimetals in novel spintronic devices that can be used for field-free switching of magnets with perpendicular magnetic anisotropy, and other novel phenomena.

[1] Schröter et al., Nat. Phys 8 759-65 (2019)

[2] Schröter et al., Science 369, 179-83 (2020)

[3] Krieger et al., arXiv:2210.08221 (2022)

TT 7: Spin Transport and Orbitronics, Spin-Hall Effects (joint session MA/TT)

Time: Monday 9:30–13:00

Location: HSZ 403

TT 7.1 Mon 9:30 HSZ 403

Topological information device operating at the Landauer limit — •AHMET MERT BOZKURT^{1,2,3}, ALEXANDER BRINKMAN⁴, and İNANC ADAGIDELI^{3,4} — ¹QuTech, Delft University of Technology, 2600 GA Delft, The Netherlands — ²Kavli Institute of Nanoscience, Delft University of Technology, 2600 GA Delft, The Netherlands — ³Faculty of Engineering and Natural Sciences, Sabanci University, Orhanli-Tuzla, Istanbul, Turkey — ⁴MESA+ Institute for Nanotechnology, University of Twente, The Netherlands

We propose and theoretically investigate a novel Maxwell's demon implementation based on the spin-momentum locking property of topological matter. We use nuclear spins as a memory resource which provides the advantage of scalability. We show that this topological information device can ideally operate at the Landauer limit; the heat dissipation required to erase one bit of information stored in the demon's memory approaches $k_B T \ln 2$. Furthermore, we demonstrate that all available energy, $k_B T \ln 2$ per one bit of information, can be extracted in the form of electrical work. Finally, we find that the current-voltage characteristics of the topological information device satisfy the conditions of an ideal memristor.

TT 7.2 Mon 9:45 HSZ 403

Controlling 3D spin textures by manipulating sign and amplitude of interlayer DMI with electrical current — •FABIAN KAMMERBAUER¹, WON-YOUNG CHOI¹, FREIMUTH FRANK^{1,2}, ROBERT FRÖMTER¹, YURIY MOKROUSOV^{1,2}, and MATHIAS KLÄUI¹ — ¹Institute of Physics, Johannes Gutenberg University, Staudingerweg 7, 55128 Mainz, Germany — ²Peter Grünberg Institut and Institute for Advanced Simulation, Forschungszentrum Jülich and JARA, 52425 Jülich, Germany

The recently discovered interlayer Dzyaloshinskii-Moriya interaction (IL-DMI) in multilayers with perpendicular magnetic anisotropy favors a canting of spins in the in-plane direction [1]. It could thus stabilize exciting spin textures such as Hopfions. A key requirement for nucleation is to control the IL-DMI and so, we investigate the influence of an electric current on the strength of the IL-DMI, as previously found for FMI. The IL-DMI is quantified using out-of-plane hysteresis loops while applying a static in-plane magnetic field at varied azimuthal angles. We observe a shift in the azimuthal dependence with increasing current, which is concluded to originate from the additional in-plane symmetry breaking introduced by the current flow. Fitting the angular dependence we demonstrate the presence of an additive current-induced term [3]. With this, an easily accessible possibility to manipulate 3D spin textures by current is realized.

[1] Han et al., Nat. Mater. 18, 703-708 (2019)

[2] Karnad et al., Phys. Rev. Lett. 121, 147203 (2018)

[3] Kammerbauer et al., arXiv:2209.01450 (2022)

TT 7.3 Mon 10:00 HSZ 403

Nonequilibrium dynamics in a spin valve with noncollinear magnetization — •RUDOLF SMORKA¹, PAVEL BALÁŽ², MICHAEL THOSS¹, and MARTIN ŽONDA^{3,1} — ¹University of Freiburg, Germany — ²Institute of Physics of the Czech Academy of Sciences Prague, Czech Republic — ³Charles University Prague, Czech Republic

Manipulation of magnetization by electric currents enables novel functions for spin-transfer torque devices. We study the nonequilibrium spin dynamics and spin-transfer torques in noncollinear spin-valve heterojunctions using a mixed quantum-classical Ehrenfest approach.

In an isolated valve for short spacer layers and weak spin-electron couplings, magnetization dynamics of the ferromagnetic layers is in agreement with the macrospin approximation. For large spacer layers, our quantum-classical approach predicts electron-induced spin relaxation. For intermediate electron-spin couplings, a change in the localization character of the electronic eigenstates

from metallic-like to insulator-like leads to a reduced indirect exchange interaction between spins mediated by the conduction electrons. In a spin valve coupled to leads, spin relaxation times differ by several orders of magnitude depending on whether the DC bias is introduced by shifting the electrochemical potentials of both leads symmetrically about the equilibrium Fermi level of the spin valve (reminiscent of a gate-tunable junction) or by shifting the chemical potential of only one lead (as realized in a scanning tunneling microscope geometry).

[1] R. Smorka, P. Baláž, M. Thoss, M. Žonda, Phys. Rev. B 2022, 106, 144435.

TT 7.4 Mon 10:15 HSZ 403

Nonrelativistic spin currents in altermagnets — •RODRIGO JAESCHKE-UBIERGO, JAIRO SINOVA, and LIBOR ŠMEJKAL — Institut für Physik, Johannes Gutenberg Universität Mainz, D-55099 Mainz, Germany

Altermagnetism has emerged recently as a third basic collinear magnetic phase [1], in addition to ferromagnets and antiferromagnets. Conventional antiferromagnets exhibit two sublattices with opposite magnetic moment related by translation or inversion. In altermagnets the magnetic sublattices are connected by a rotation or a mirror operation. The particular symmetry causes that altermagnets display time-reversal (T) symmetry breaking and spin split band structure even in absence of spin-orbit coupling [2]. In this work, we study the spin conductivity tensor in altermagnets by using spin group theory formalism [1]. We also use Kubo's linear response to calculate the spin conductivity tensor in all the altermagnetic spin point groups models. Additionally, we identify and sort 200 altermagnetic candidates into spin conductivity tensor classes. We will discuss some spin point groups that allow for a transverse spin current in detail. This is the case of spin splitter current in RuO₂ [3,4], which is a nonrelativistic effect that conserves spin unlike in general magnetic spin Hall effect in noncollinear magnets. Moreover, the spin conductivity tensor is symmetric and T-odd, which makes it different from the conventional spin Hall effect. [1] Šmejkal et al., PRX, 12, 031042 (2022). [2] Šmejkal, et al. Sci. Adv. 2020. [3] Gonzalez- Hernandez, et al. PRL 2021. [4] Šmejkal, et al. PRX 12, 011028 (2022).

TT 7.5 Mon 10:30 HSZ 403

Quantification and modulation of intrinsic spin transport in 5d transition metals — •AKASH BAJAJ, REENA GUPTA, ANDREA DROGHETTI, and STEFANO SANVITO — School of Physics and CRANN, Trinity College Dublin, Dublin 2, Ireland

Spin-Hall effect (SHE) enables charge-to-spin conversion in heavy transition metals, such as Ta and Pt, with strong spin-orbit coupling (SOC) strengths. It has been extensively studied as a viable mechanism for the development of next-generation spintronics-based non-volatile memory devices. Numerous experimental and first-principles approaches have been devised to quantify the charge-to-spin conversion efficiency i.e., the spin-Hall angle (SHA), for the SHE. However, such approaches unavoidably involve interface contributions and, in general, extrinsic effects such as disorder and impurities, which are known to be less dominant than the bandstructure-only intrinsic contribution in such heavy metals. In this work, we use density functional theory combined with a bond-current-based non-equilibrium Green's functions approach to quantify the intrinsic SHAs of bulk elemental and thin-film models of 5d transition metals. We then computationally demonstrate a strategy for modulating the SHA within the same device, using Pt and Au as contrasting examples. Our computational work not only provides a quantitative estimation of the intrinsic SHAs for these materials, but also enables its theoretical understanding aimed towards the development of higher performance and power-efficient spintronics-based non-volatile memory devices.

TT 7.6 Mon 10:45 HSZ 403

Influence of Disorder at Insulator-Metal Interface on Spin Transport — MAHSA ALSADAT SEYED HEYDARI, WOLFGANG BELZIG, and •NIKLAS ROHLING — Department of Physics, University of Konstanz

Motivated by experimental work showing enhancement of spin transport between yttrium iron garnet and platinum by the thin antiferromagnetic insulator NiO [1] between them, we consider spin transport through the interface of a non-magnetic metal and a ferro- or antiferromagnetically ordered insulator. The spin transport is carried by spin-polarized electrons in the metal and by magnons in the insulator. Spin current can be generated by a spin accumulation in the metal due to the inverse spin Hall effect, a microwave field exciting magnons in the insulator, or by a thermal gradient (spin Seebeck effect). The spin current can be computed using Fermi's Golden Rule [2]. For a perfectly clean interface, the in-plane momentum is conserved for the electron-magnon scattering events which govern the spin transport through the interface. We calculate how disorder-induced broadening of the scattering matrix elements with respect to the in-plane momentum influences the spin current. As a general result, we observe that for many experimental setups, one should expect a rather small effect of interface disorder on the measured spin current.

[1] Wang et al., Phys. Rev. Lett. 113, 097202 (2014), Phys. Rev. B 91, 220410(R) (2015); Lin et al. Phys. Rev. Lett. 116, 186601 (2016)

[2] Bender et al., Phys. Rev. Lett. 108, 246601 (2012)

TT 7.7 Mon 11:00 HSZ 403

Long-range orbital-Hall torques in Nb(or Ru)/Ni Heterostructures — ARNAB BOSE¹, FABIAN KAMMERBAUER¹, •RAHUL GUPTA¹, DONGWOOK GO², YURIY MOKROUSOV^{1,2}, GERHARD JAKOB¹, and MATHIAS KLÄUI^{1,3} — ¹Institute of Physics, Johannes Gutenberg University Mainz, Staudingerweg 7, 55128 Mainz, Germany — ²Peter Grünberg Institut and Institute for Advanced Simulation, Forschungszentrum Jülich and JARA, 52425 Jülich, Germany — ³Center for Quantum Spintronics, Department of Physics, Norwegian University of Science and Technology, NO-7491 Trondheim, Norway

We report a large orbital Hall torque (OHT) generated by Nb and Ru via strong dependence of torques on the ferromagnets, Ni, in Nb(Ru)/Ni heterostructures. We found the sign reversal of the damping-like torque in Nb/Ni. Moreover, the long-range orbital transport in the ferromagnet was revealed by the thickness dependences of Ni in Ni/Nb(or Ru) heterostructure, which are markedly different from the regular spin absorption in the ferromagnet that takes place within a few angstroms and thus it uniquely distinguishes OHT from the spin Hall torque. The experimentally measured effective orbital-Hall conductivities are found to be $6.1 \times 10^4 \frac{h}{2e} (\Omega\text{m})^{-1}$ and $5.86 \times 10^4 \frac{h}{2e} (\Omega\text{m})^{-1}$ for Nb and Ru, respectively, which is an order of magnitude higher than their measured spin Hall conductivities, as also confirmed by the density functional theory. This study opens a plethora of possibilities to further engineering the torques, utilizing the orbital degree of freedom.

TT 7.8 Mon 11:15 HSZ 403

Layer-resolved spin-orbit torque assisted magnetization dynamics in Pt/Co heterostructure — •HARSHITA DEVDA¹, ANDRÁS DEÁK², LEANDRO SALEM³, LEVENTE RÓZSA¹, LÁSZLÓ SZUNYOGH², PETER M. OPPENEER³, and ULRICH NOWAK¹ — ¹Universität Konstanz, Konstanz, Germany — ²Budapest University of Technology and Economics, Budapest, Hungary — ³Uppsala University, Uppsala, Sweden

It is well known that the spin-orbit torque (SOT) mechanism is more reliable for current induced magnetization dynamics than the spin-transfer torque. The key phenomenon behind the SOT in heavy metal/ferromagnet (HM/FM) bilayers is attributed to the spin Hall effect (SHE) and the spin Rashba-Edelstein effect (SREE). However, the exact mechanism is still under debate. So far various works have studied the SOT-driven magnetic behavior in different magnetic systems, but the layer-resolved understanding of the SOT effect in the HM/FM bilayer due to spin-orbit coupling (SOC) in heavy metal is still lacking. We focus on current-induced magnetization dynamics in a Pt/Co bilayer assisted by the SOC in Pt. We use a multiscale model which links ab initio calculations with atomistic spin dynamics simulations. We implement a linear-response formalism to compute the electrically induced magnetic moments, caused by SHE in bulk and SREE at the interface, and utilize these in atomistic spin dynamics simulations. We analyse the layer-resolved behavior of both field-like and damping-like torques in FM and determine how they affect magnetization dynamics in ferromagnets.

TT 7.9 Mon 11:30 HSZ 403

Spin and orbital Edelstein effect in a bi- and trilayer system with Rashba interaction — •SERGIO LEIVA¹, JÜRGEN HENK¹, INGRID MERTIG¹, and ANNIKA JOHANSSON² — ¹Martin Luther University Halle-Wittenberg, Halle, Germany — ²Max Planck Institute of Microstructure Physics, Halle, Germany

The spin Edelstein effect has proved to be a promising phenomenon to generate spin polarization from a charge current in systems without inversion symmetry. In recent years, current-induced orbital magnetization, also called the orbital Edelstein effect, has also been predicted for several systems with broken inversion symmetry [1-6].

In the present work, we calculate the current-induced spin and orbital magnetization for a bilayer and a trilayer system with Rashba interaction for the interface and the free-standing slab configurations. We use the modern theory of orbital magnetization [7] and the Boltzmann transport theory. We found a significantly larger orbital than spin effect, with a strong dependence on the model parameters, such as effective mass and spin-orbit coupling per layer. This dependence allows us to enhance and even revert the sign of the orbital effect.

[1] T. Yoda et al., Sci. Rep., 5, 12024 (2015).

[2] D. Go et al., Sci. Rep. 7, 46742 (2017)

[3] T. Yoda et al., Nano Lett., 18, 916 (2018).

[4] L. Salemi et al., Nat. Commun. 10, 5381 (2019)

[5] D. Hara et al., Phys. Rev. B, 102, 184404 (2020).

[6] A. Johansson et al., Phys. Rev. Research, 3, 013275 (2021).

[7] T. Thonhauser et al. Phys. Rev Lett. 95, 137205 (2005).

TT 7.10 Mon 11:45 HSZ 403

Optical detection of the orbital Hall effect in a light metal Ti — •YOUNG-GWAN CHOI^{1,2}, DAEGEUN JO³, KYUNG-HUN KO¹, DONGWOOK GO^{4,5}, KYUNG-HAN KIM³, HEE GYUM PARK⁶, CHANGYOUNG KIM^{7,8}, BYOUNG-CHUL MIN⁶, URI VOOL², GYUNG-MIN CHOI^{1,9}, and HYUN-WOO LEE^{3,10} — ¹DOES, SKKU, Suwon, Korea — ²MPI-CPFS, Dresden, Germany — ³Physics, POSTECH, Pohang, Korea — ⁴PGI and IAS, FZJ and JARA, Jülich, Germany — ⁵GSE Mainz, Mainz, Germany — ⁶Center for Spintronics, KIST, Seoul, Korea — ⁷Physics, SNU, Seoul, Korea — ⁸CCES, IBS, Seoul, Korea — ⁹CINAP, IBS, Suwon, Korea — ¹⁰APCTP, Pohang, Korea

Electrical generation of the angular momentum current enables the development of novel memory devices, similar to spin current generation. Recently, it has been theoretically proposed that the orbital angular momentum (OAM) current can be driven by a charge current, called as the orbital Hall effect (OHE). Here we report evidence of the OHE, measured by magneto-optical Kerr effect microscopy. We detect large Kerr signals in one of the 3d transition metals, Ti, in which the high orbital Hall conductivity is predicted. We also find that the large OAM is accumulated by the OHE with a relaxation length ~ 70 nm. Moreover, we present the torque results in Ti/Ni. The high torque efficiency shows that the OAM injection allows for the electrical control of the magnetization. We also propose magnetic imaging using a nitrogen-vacancy scanning probe to measure OAM accumulation directly. Our results can pave the way for a deep understanding and provide techniques for generating and detecting orbital transport.

TT 7.11 Mon 12:00 HSZ 403

Spin and orbital Edelstein effects at oxide interfaces — •ANNIKA JOHANSSON¹, BÖRGE GÖBEL², SARA VAROTTO³, SRIJANI MALLIK³, INGRID MERTIG², and MANUEL BIBES³ — ¹Max Planck Institute of Microstructure Physics, Halle, Germany — ²Martin Luther University Halle-Wittenberg, Halle, Germany — ³Unité Mixte de Physique, CNRS, Thales, Université Paris-Saclay, Palaiseau, France

The spin Edelstein effect (SEE) provides charge-spin interconversion in nonmagnetic systems with broken inversion symmetry [1,2]: An external electric field generates a charge current as well as a homogeneous spin density. Further, a finite current-induced magnetization originating from the electrons' orbital moments can be generated, which is called orbital Edelstein effect (OEE) [3-5]. In this talk, the SEE and OEE at SrTiO₃- and KTaO₃-based two-dimensional electron gases are discussed within a semiclassical Boltzmann approach [6-8]. The OEE is predicted to exceed its spin counterpart by one order of magnitude, which can be understood by a band-resolved analysis of the SEE and OEE. Further, we suggest design rules for Rashba-like systems to enhance spin-charge interconversion efficiencies.

[1] A. G. Aronov, Y. B. Lyanda-Geller, JETP Lett. 50, 431 (1989) [2] V. M. Edelstein, Solid State Commun. 73, 233 (1990) [3] T. Yoda et al., Sci. Rep. 5, 12024 (2015). [4] T. Yoda et al., Nano Lett. 18, 916 (2018). [5] L. Salemi et al., Nat. Commun. 10, 5381 (2019) [6] D. Vaz et al., Nat. Materials 18, 1187 (2019) [7] A. Johansson et al., Phys. Rev. Research 3, 013275 (2021) [8] S. Varotto et al., Nat. Commun. 13, 6165 (2022)

TT 7.12 Mon 12:15 HSZ 403

Anisotropic anomalous Hall effect in altermagnetic Mn₅Si₃ — •MIINA LEIVISKÄ¹, RAFAEL LOPES SEEGER¹, HELENA REICHOVÁ^{2,3}, ISMAÏLA KOUNTA⁴, LIBOR ŠMEJKAL^{5,3}, JAVIER RIAL¹, SEBASTIAN BECKERT², ANTONÍN BADURA^{6,7}, ISABELLE JOURMARD¹, DOMINIK KRIEGNER^{2,3}, EVA SCHMORANZEROVÁ⁶, JAIRO SINOVA⁵, TOMÁŠ JUNGWIRTH³, SEBASTIAN GOENNENWEIN⁷, LISA MICHEZ⁴, and VINCENT BALTZ¹ — ¹Univ. Grenoble Alpes, CNRS, CEA, Grenoble INP, IRIG-SPINTEC, F-38000 Grenoble — ²Institute of Solid State and Materials Physics, TU Dresden, Dresden, Germany — ³Institute of Physics, Czech Academy of Sciences, Prague, Czechia — ⁴Aix-Marseille University, CNRS, CINaM, Marseille, France — ⁵Institute for Physics, Johannes Gutenberg University Mainz, Mainz, Germany — ⁶Department of Chemical Physics and Optics, Faculty of Mathematics and Physics, Charles University, Prague, Czechia — ⁷Department of Physics, University of Konstanz, Konstanz, Germany

The altermagnetic epitaxial films of Mn₅Si₃ exhibit anomalous Hall effect (AHE) despite the vanishing net magnetization [1]. This can be explained by non-

relativistic time-reversal symmetry breaking, which allows for momentum-locked alternating spin-splitting of the bands [2]. Here, we investigate the anisotropy of the AHE by varying both the external field and the current channel orientations. In both cases, we observe unconventional, anisotropic behaviour that deviates from the typical behaviour of ferromagnets.

[1] H. Reichlova et al. arXiv:2012.15651, (2020)

[2] L. Šmejkal et al. Phys Rev X 12, 031042 (2022)

TT 7.13 Mon 12:30 HSZ 403

Observation of nonreciprocal magnon Hanle effect — •JANINE GÜCKELHORN^{1,2}, SEBASTIÁN DE-LA-PEÑA³, MATTHIAS GRAMMER^{1,2}, MONIKA SCHEUFELE^{1,2}, MATTHIAS OPEL¹, STEPHAN GEPRÄGS¹, JUAN CARLOS CUEVAS³, RUDOLF GROSS^{1,2,4}, HANS HUEBL^{1,2,4}, AKASHDEEP KAMRA³, and MATTHIAS ALTHAMMER^{1,2} — ¹Walther-Meißner-Institut, BAdW, Garching, Germany — ²Physik-Department, School of Natural Sciences, TUM, Garching, Germany — ³IFIMAC and Departamento de Física Teórica de la Materia Condensada, Universidad Autónoma de Madrid, Madrid, Spain — ⁴Munich Center for Quantum Science and Technology, München, Germany

The realization of the magnon Hanle effect, which is based on the precession of magnon pseudospin about the equilibrium pseudofield, via electrically injected and detected spin transport in an antiferromagnetic insulator demonstrates its high potential for devices and as a convenient probe for the underlying spin interactions in antiferromagnets. Here, we observe a nonreciprocity in the magnon Hanle signal measured in hematite (α -Fe₂O₃) using two spatially separated platinum electrodes as spin injector/detector [1]. Interchanging their roles was found to alter the detected magnon spin signal. The recorded difference depends on the applied magnetic field and reverses sign when the signal passes its

nominal maximum at the so-called compensation field. We explain these observations in terms of a spin transport direction-dependent pseudofield. The latter leads to a nonreciprocity, which is found to be controllable via the applied magnetic field.

[1] J. Gückelhorn et al., arXiv:2209.09040 (2022).

TT 7.14 Mon 12:45 HSZ 403

Spontaneous anomalous Hall effect arising from an unconventional compensated magnetic phase in a semiconductor — •DOMINIK KRIEGNER^{1,2}, RUBEN DARIO GONZALEZ BETANCOURT^{1,2,3,4}, JAN ZUBÁČ^{1,3}, RAFAEL JULIAN GONZALEZ HERNANDEZ⁵, KEVIN GEISHENDORF⁴, GUNTHER SPRINGHOLZ⁶, KAMIL OLEJNÍK¹, JAKUB ŽELEZNÝ¹, LIBOR ŠMEJKAL⁷, ANDY THOMAS^{2,4}, HELENA REICHLÓVÁ^{1,2}, SEBASTIAN TOBIAS BENEDIKT GOENNENWEIN⁸, and TOMAS JUNGWIRTH^{1,9} — ¹Institute of Physics, AV ČR, Prague, Czech Republic — ²IFMP, TU Dresden — ³Charles University, Prague — ⁴IFW Dresden — ⁵Universidad del Norte, Barranquilla, Colombia — ⁶JKU Linz, Austria — ⁷JGU, Mainz — ⁸University of Konstanz — ⁹University of Nottingham, United Kingdom

The anomalous Hall effect, commonly observed in metallic magnets, has been established to originate from the time-reversal symmetry breaking by an internal macroscopic magnetization in ferromagnets or by a non-collinear magnetic order. Here we observe a spontaneous anomalous Hall signal in the absence of an external magnetic field in an epitaxial film of MnTe, which is a semiconductor with a collinear antiparallel magnetic ordering of Mn moments and a vanishing net magnetization. The anomalous Hall effect arises from an unconventional phase with strong time-reversal symmetry breaking and alternating spin polarization in real-space crystal structure and momentum-space electronic structure.

R. D. Gonzalez Betancourt et al., arXiv:2112.06805

TT 8: Yu-Shiba-Rusinov Systems

Time: Monday 15:00–17:15

Location: HSZ 103

Invited Talk

TT 8.1 Mon 15:00 HSZ 103

Molecules on a superconductor: Inducing magnetism and resonance-enhanced vibrational spectroscopy — •RICHARD BERNDT¹, JAN HOMBERG¹, ALEXANDER WEISMANN¹, MANUEL GRUBER², and TROELS MARKUSSEN³ — ¹Institut für Experimentelle und Angewandte Physik, Christian-Albrechts-Universität zu Kiel, Germany — ²Fakultät für Physik, Universität Duisburg-Essen, Germany — ³Synopsys Denmark, Copenhagen, Denmark

Magnetic impurities can induce so-called Yu-Shiba-Rusinov (YSR) resonances in the energy gap of a superconductor. We use these resonances for spin detection in a scanning tunneling microscope and demonstrate that diamagnetic phthalocyanine molecules acquire a spin when they are arranged into supramolecular arrays on superconducting Pb(100). Spectroscopy and modeling reveal that the electrostatic fields of its neighbors render a molecule paramagnetic.

Inelastic tunneling spectroscopy of vibrational excitations usually suffers from low sensitivity and limited spectral resolution. We harness YSR resonances to enhance the inelastic signal by more than an order of magnitude and to improve the energy resolution beyond the thermal broadening limit. As a result, 46 vibrational peaks are resolved from Pb-phthalocyanine enabling a comparison with calculated modes. The method may help to further probe the interaction of molecules with their environment and to better understand selection rules for vibrational excitations.

TT 8.2 Mon 15:30 HSZ 103

Yu-Shiba-Rusinov impurity bound states in superconductors from first principles — •DAVID ANTOGNINI SILVA¹, PHILIPP RÜSSMANN^{1,2}, and STEFAN BLÜGEL¹ — ¹Peter Grünberg Institut and Institute for Advanced Simulation, Forschungszentrum Jülich and JARA, Jülich, Germany — ²Würzburg Universität, Germany

Materials that combine magnetism, spin-orbit interaction and conventional s-wave superconductivity are a suitable platform to study Majorana zero modes (MZM) [1], that can be used as building blocks of fault-tolerant topological qubits. In general, magnetic impurities in superconductors leads to localized Yu-Shiba-Rusinov (YSR) states at the impurity [2]. Understanding their interplay with MZMs is crucial to achieve topological quantum computers in the future.

In our work, we implemented the Bogoliubov-de Gennes (BdG) formalism in the juKKR Korrington-Kohn-Rostoker Green function impurity code (<https://iffgit.fz-juelich.de/kkr/jukkr>) to allow the material-specific description of defects perfectly embedded in superconductors from first principles. We apply it to an Fe impurity embedded in bulk Pb in the normal and superconducting state, then analyse the YSR states of different magnetic transition-metal adatoms placed on a superconducting Nb(110) surface where the influence of the impurity-substrate distance on the energy of the YSR states is discussed.

[1] Nadj-Perge et al., Science 346, 6209 (2014)

[2] L. Yu, Acta Physica Sinica 21, 75 (1965)

H. Shiba, Prog. Theor. Phys. 40, 435 (1968) A. I. Rusinov, Sov. J. Exp. Theor. Phys. 29, 1101 (1969)

TT 8.3 Mon 15:45 HSZ 103

Yu-Shiba-Rusinov states of quantum impurities in spin-split superconductors — •ANASTASIA SKURATIVSKA¹, JON ORTUZAR², SEBASTIAN BERGERET^{1,3}, DARIO BERCIOUX^{1,4}, and MIGUEL ANGEL CAZALILLA^{1,4} — ¹DIPC, 20018 San Sebastian, Spain — ²CIC nanoGUNE-BRTA, 20018 San Sebastian, Spain — ³CFM-MPC Centro Mixto CSIC-UPV/EHU, 20018 San Sebastian, Spain — ⁴IKERBASQUE, Basque Foundation for Science, 48009 Bilbao, Spain

Yu-Shiba-Rusinov (YSR) states arise as a sub-gap excitations in a system of magnetic impurity coupled to a superconducting host. Despite the quantum nature of their spin degree of freedom, magnetic impurities in such systems are often described by a classical spin. Taking into account quantum nature of the impurity-spin has proven to give useful insights into the ground-state and excitation properties of the magnetic impurity-superconductor system.

Here, we report on the spectral properties of the YSR states of a magnetic impurity on a spin-split superconductor. Using the zero-bandwidth approximation we obtain the spectral function of the YSR states. Unlike the classical model which predicts full spin polarization for the YSR peaks, we find the quantum model predicts partial polarization. The parity-changing phase transition switches the spin polarization of the YSR peaks after crossing at the center of the superconducting gap. We discuss the possibility of using this effect as a tunable spin-filter in a quantum dot or a molecule in proximity to a spin-split superconductor.

TT 8.4 Mon 16:00 HSZ 103

Building crystalline topological superconductors from Shiba lattices — •MARTINA ONDINA SOLDINI¹, FELIX KÜSTER², GLENN WAGNER¹, SOUVIK DAS², AMAL ALDARAWSHEH^{3,5}, RONNY THOMALE^{4,6}, SAMIR LOUNIS^{3,5}, STUART S. P. PARKIN², PAOLO SESSI², and TITUS NEUPERT¹ — ¹University of Zurich, Winterthurerstrasse 190, 8057 Zurich, Switzerland — ²Max Planck Institute of Microstructure Physics, Halle, Germany — ³Peter Grünberg Institut and Institute for Advanced Simulation, Forschungszentrum Jülich & JARA, Jülich, Germany — ⁴Institut für Theoretische Physik und Astrophysik, Universität Würzburg, Würzburg, Germany — ⁵Faculty of Physics, University of Duisburg-Essen and CENIDE, Duisburg, Germany — ⁶Department of Physics and Quantum Centers in Diamond and Emerging Materials (QuCenDiEM) Group, Indian Institute of Technology Madras, Chennai, India

Majorana boundary modes are the key feature of topological superconductors. Lattices of Shiba bound states, arising from magnetic adatoms placed on the surface of a conventional superconductor, may host these topological excitations. With scanning tunneling microscopy we create and probe adatom lattices to create topological crystalline superconductors. We combine theoretical modeling

and experimental analysis to reveal signatures consistent with mirror-symmetry protected topological superconductors, hosting edge and higher-order corner states. Our results show the immense versatility of Shiba lattices to design the topology of 2D superconductors.

TT 8.5 Mon 16:15 HSZ 103

Mn clusters on superconducting Ta(110) surface — •ANDRÁS LÁSZLÓFFY¹, BENEDEGÚZ NYÁRI^{2,3}, LÁSZLÓ SZUNYOGH², and BALÁZS ÚJFALUSSY¹ — ¹Wigner Research Centre for Physics, Budapest, Hungary — ²Budapest University of Technology and Economics, Budapest, Hungary — ³ELKH-BME Condensed Matter Physics Research Group, Hungary

Over the past decade, the formation of Yu-Shiba-Rusinov (YSR) states around magnetic impurities proximity coupled to superconducting materials raised considerable interest. The hybridization between these states leads to bands in magnetic chains being potential candidates for hosting Majorana edge states. In this work we solve the Bogoliubov-de Gennes equation as implemented in the first-principles Korringa-Kohn-Rostoker Green's function method. First, we provide an in-depth analysis of the YSR states of a single Mn adatom on Ta(110), and the hybridization between them in Mn dimers. We then study the formation of a minigap and zero energy states in chains with various directions and nearest-neighbor distances, making a strong implication that Majorana zero modes can emerge in these systems.

TT 8.6 Mon 16:30 HSZ 103

Effect of Fe impurities on the superconducting state of Ir/Nb overlayer — •BENEDEGÚZ NYÁRI^{1,2}, ANDRÁS LÁSZLÓFFY³, KRISZTIÁN PALOTÁS³, LÁSZLÓ SZUNYOGH^{1,2}, LEVENTE RÓZSA⁴, and BALÁZS ÚJFALUSSY³ — ¹Department of Theoretical Physics, Budapest University of Technology and Economics, Hungary — ²ELKH-BME Condensed Matter Physics Research Group, Hungary — ³Wigner Research Centre for Physics, Institute for Solid State Physics and Optics, Hungary — ⁴Department of Physics, University of Konstanz, Germany

Artificial magnetic chains on top of superconducting surfaces, where in the presence of large spin-orbit coupling or non-collinear magnetic states a topological gap can appear, are potential candidates to host Majorana edge states. Iridium as an overlayer on various metallic substrates appeared to be a good platform for the formation of spin-spiral states in magnetic overlayers and chains.

By solving the relativistic Bogoliubov-de Gennes equations, first we investigate the superconducting properties of 10 monolayers of Ir on top of Nb(110) surface. In the Ir layer we observe a strong reduction of the superconducting or-

der parameter, but the gap just slightly decreases as compared to bulk Nb. Then the effect of Fe impurities on the superconducting state is studied in different setups. For a single Fe impurity we find a huge spatial extension of the Yu-Shiba-Rusinov states. Disordered Fe impurities modelled within the coherent-potential approximation in the dilute concentration limit seem to rapidly destroy the superconducting state of the Ir overlayer.

TT 8.7 Mon 16:45 HSZ 103

Yu-Shiba-Rusinov states in small Fe clusters on Pb(111) — •NORA KUCSKA, KRISZTIÁN PALOTÁS, ANDRÁS LASZLOFFY, and BALÁZS ÚJFALUSSY — Wigner Research Centre for Physics, Budapest, Hungary

By solving the fully relativistic Bogoliubov-de Gennes equations by band-theoretical methods, we investigate the Yu-Shiba-Rusinov (YSR) states of single, double and triple magnetic Fe adatoms on the top of Pb(111) surface. First, we show that the local density of states in the normal state plays a key role in the formation of the YSR states that appear in the interior of the superconducting gap. We discuss the effects of different atomic arrangements, the role of lattice relaxations and various spin configurations on the YSR states, and we compare our results to recent experiments.

TT 8.8 Mon 17:00 HSZ 103

Yu-Shiba-Rusinov band dispersion of an infinite chain on a semi-infinite surface — •RIK BROEKHOVEN, ARTEM PULKIN, ANTONIO MANESCO, SANDER OTTE, ANTON AHKMEROV, and MICHAEL WIMMER — Delft University of Technology, Delft, the Netherlands

Chains of magnetic atoms on s-wave superconductors have been proposed to become topological superconductors, when their in-gap Yu-Shiba-Rusinov (YSR) band is p-wave gapped by for example spin-orbit coupling. As recently shown through STM experiment, however, realistic systems have many YSR bands and relatively small spin-orbit coupling limiting the topological phase. Ab initio models can help to increase our understanding and find regions of material and parameter space where the system is still predicted to be topological. These finite-size simulations must however overestimate the superconducting gap to ensure the system is smaller than the superconductor coherence length.

We combine ab initio calculation with multi-dimensional Green's functions formalism to extend the model beyond this limit. This allows us to do calculations with realistic gap size. We compute the dispersion of an infinite chain on top of a semi-infinite surface. We focus on Mn atoms on Nb(110) and show how our model compares with the dispersion measured by Schneider et al. in 2021.

TT 9: f-Electron Systems and Heavy Fermions II

Time: Monday 15:00–17:00

Location: HSZ 201

TT 9.1 Mon 15:00 HSZ 201

Quantum oscillations in heavy-fermion ferromagnet YbNi₄P₂ over many Zeeman induced Lifshitz transitions — •WILLIAM BROAD¹, SVEN FRIEDEMANN¹, OWEN MOULDING¹, TAKAKI MURAMATSU¹, KRISTIN KLIEMT², and CORNELIUS KRELLNER² — ¹University of Bristol, Bristol, United Kingdom — ²Goethe-Universität, Frankfurt am Main, Germany

YbNi₄P₂ is a heavy-fermion metal situated near a very rare ferromagnetic quantum critical point (FM QCP). Understanding the nature of this ferromagnetism requires knowledge of the Fermi surface; it has been speculated that this FM QCP is enabled by a quasi-1D Fermi surface. At the same time, the strongly renormalised band structure is readily modified by relatively small magnetic fields, with nine Lifshitz transitions below 20 T due to Zeeman splitting. Here, we present Shubnikov-de Haas oscillations up to 35T, including detailed rotation and mass studies. We present analysis over several of these Lifshitz transitions, observing frequency changes and appearances/disappearances. We model the band structure with DFT calculations of the local 4f reference compound LuNi₄P₂ and use rigid-band shifts to approximate the effect of the Kondo hybridisation. At highest fields, the Fermi surface is well modelled with a small shift to increase the Fermi volume. As the field is reduced, we find better agreement with a larger shift corresponding to stronger hybridisation of 4f electrons. Finally, we present models for the topology of the Lifshitz transitions.

TT 9.2 Mon 15:15 HSZ 201

Exploring the effect of different substitutions on the valence transition in YbInCu₄ single crystals — •MICHELLE OCKER, BEREKET GHEBRETINSAE, BERND WOLF, KRISTIN KLIEMT, MICHAEL LANG, and CORNELIUS KRELLNER — Physikalisches Institut, Goethe-Universität Frankfurt, 60438 Frankfurt/Main, Germany

At ambient pressure the compound YbInCu₄ undergoes a 1st order valence transition at T_v = 42 K by changing the temperature [1]. Thus, ytterbium in the compound is present in the Yb^{2.9+} state at high temperatures and as Yb^{2.7+} at low temperatures [2]. In analogy to Eu compounds, the line of first order valence transitions might end in a second order critical endpoint [3]. In order to

study the nature of the phase transition in more detail, single crystal samples can be prepared in In-Cu flux which are substituted with silver and gold [4]. With increasing substitution level, negative chemical pressure within the crystal is increased and the characteristics of the valence transition changes significantly. Here, we report on the single crystal growth with different substitution levels and the results of our structural, chemical and physical characterization.

- [1] I. Felner et al., Phys. Rev. B 35, (1987) 6956
- [2] H. Sato et al., Physica B 351, (2004) 298
- [3] Y. Ōnuki et al., J. Phys. Soc. Jap. 89, (2020) 102001
- [4] J. L. Sarrao et al., Phys. Rev. B 54, (1996) 12207.

TT 9.3 Mon 15:30 HSZ 201

Impact of Fe substitution on the electronic structure of URu₂Si₂ — •ANDREA MARINO¹, DENISE S. CHRISTOVAM¹, CHUN-FU CHANG¹, JOHANNES FALKE¹, CHANG-YANG KUO², CHI-NAN WU², MARTIN SUNDERMANN^{1,3}, ANDREA AMORESE^{1,3}, HLYNUR GRETARSSON^{4,5}, CAMILLA MOIR⁶, M. BRIAN MAPLE⁶, PETER THALMEIER¹, LIU HAO TJENG¹, and ANDREA SEVERING³ — ¹Max Planck Institute for Chemical Physics of Solids, Dresden, Germany — ²National Synchrotron Radiation Research Center, Hsinchu, Taiwan — ³University of Cologne, Cologne, Germany — ⁴Max Planck Institute for Solid State Research, Stuttgart, Germany — ⁵PETRA III, DESY, Hamburg, Germany — ⁶University of California, San Diego, USA

The application of pressure as well as the substitution of Ru with Fe in the hidden order (HO) compound URu₂Si₂ lead to the formation of the large moment antiferromagnetic phase (LMAFM), with the respective phase diagrams bearing similarities for low Fe content (<0.3). For higher Fe content (>1) URu_(2-x)Fe_(x)Si₂ adopts the Pauli paramagnetic ground state of UFe₂Si₂. However, the question remains open what causes the suppression of the HO in favour of the LMAFM phase. We investigate the URu_(2-x)Fe_(x)Si₂ series with 4f core-level photoelectron spectroscopy. The 4f satellite features are enhanced at low Fe content (x<0.4) and suppressed as x increases, following the trend shown by the ordered moment. We discuss this in terms of the variation of the filling of the 5f shell. Implications for the exchange interaction in a Doniach phase diagram picture are then also considered.

TT 9.4 Mon 15:45 HSZ 201

High-resolution tender x-ray RIXS at the example of UGa_2 — •MARTIN SUNDERMANN^{1,2}, ANDREA MARINO¹, DENISE CHRISTOVAM¹, ANDREA AMORESE^{1,3}, LADISLAV HAVELA⁴, BERNHARD KEIMER⁵, HLYNUR GREYARSSON^{1,2,5}, PETER THALMEIER¹, LIU HAO TJENG¹, and ANDREA SEVERING^{1,3} — ¹MPI-CPFS, Dresden, Germany — ²DESY/PETRA-III, Hamburg, Germany — ³Institute of Physics II, University of Cologne, Germany — ⁴Condensed Matter Physics, Karls-Universität, Prag, Czech — ⁵MPI-FKF, Stuttgart, Germany

The nature of the $5f$ electrons in U intermetallic compounds, usually thought to be on the verge between localization and itinerant states, still challenges the reach of well-established condensed matter physics' techniques. Yet, it is not uncommon that U-based compounds show no inelastic neutron scattering excitations, and the question remains, if these compounds are fully delocalized or if multiplet states are present but not observable. Cutting-edge instrumental developments enables us to perform tender x-ray high-resolution (150 meV) resonant inelastic X-ray scattering (RIXS) experiments at the strong U $M_{4,5}$ absorption edges. We demonstrate the potential of this technique at the example of the intermetallic high T_C ferromagnet UGa_2 . We observe multiplet excitations that are well reproduced with a full multiplet calculation that includes the crystal-electron field splitting and is based on an U $5f^2$ configuration. Further we show that, although crystal-field splittings are too small to be resolved, the directional dependence of the scattering cross-section gives access to the ground-state symmetry.

TT 9.5 Mon 16:00 HSZ 201

Electronic structure of UO_2 studied by high-resolution tender-x-ray RIXS — •DENISE S. CHRISTOVAM¹, MARTIN SUNDERMANN^{1,2}, ANDREA MARINO¹, DAISUKE TAKEGAMI¹, ANDREA AMORESE^{1,3}, HLYNUR GREYARSSON^{2,4}, BERNHARD KEIMER⁴, PHILIPP RAISON⁵, ROBERTO CACIUFFO⁵, ANDREA SEVERING^{1,3}, and LIU HAO TJENG¹ — ¹MPI-CPFS, Dresden, Germany — ²DESY/PETRA-III, Hamburg, Germany — ³Institute of Physics II, University of Cologne, Germany — ⁴MPI-FKF, Stuttgart, Germany — ⁵Joint Research Centre, European Commission, Karlsruhe, Germany

The investigation of the $5f$ electronic states in uranium-based compounds is a great challenge for x-ray instrumentation. Recent instrumental developments in the tender x-ray regime enable us to carry out resonant inelastic x-ray scattering (RIXS) experiments at the strong U $M_{4,5}$ absorption edge with an experimental resolution of 150 meV. In this work, we studied the electronic structure of UO_2 . We observe the excitations the $U^{4+} 5f^2$ ionic multiplet states as well as the excitations involving the O $2p$ to U $5f$ charge transfer satellites. Detailed insight in the many-body nature of the ground state and excited states of UO_2 is obtained by analysing the data with full-multiplet cluster calculations which also take into account crystal field and hybridization effects.

TT 9.6 Mon 16:15 HSZ 201

Strain-tuning of charge frustration in the heavy $3d$ fermion oxide LiV_2O_4 — •RYOSUKE OKA^{1,2}, DENNIS HUANG¹, MINU KIM¹, PETER WOCHNER¹, and HIDENORI TAKAGI^{1,2,3} — ¹Max Planck Institute for Solid State Research, Stuttgart, Germany — ²Department of Physics, University of Tokyo, Tokyo, Japan — ³Institute for Functional Matter and Quantum Technologies, University of Stuttgart, Stuttgart, Germany

The mixed-valent spinel LiV_2O_4 is the first discovered $3d$ electron system showing heavy fermion behavior without localized f moments, but its origin has remained a decades-old mystery. Amongst numerous scenarios proposed so far, including an analogy with a dense Kondo system, one of the leading scenarios

is charge frustration inherent in the pyrochlore sublattice of the spinel. In this scenario, the ground state is composed of a macroscopic number of degenerate charge orderings (COs), and the frustration prevents the system from undergoing a metal-to-insulator transition, thereby enhancing the effective mass. By applying external perturbations that lift the degeneracy in different ways, various insulating COs can be selected out of the frustrated metallic ground state. For example, hydrostatic pressure and biaxial tensile strain in the (001) plane stabilize distinct [111]- and [001]-oriented COs, respectively. We have grown LiV_2O_4 thin films on various substrates, in order to apply uniaxial strain in different directions. We used synchrotron x-ray diffraction to characterize the applied strain and transport measurements to probe how the heavy fermion phase in LiV_2O_4 moves toward possible distinct charge-ordered states.

TT 9.7 Mon 16:30 HSZ 201

Evolution of the $4f$ states in $\text{TmSe}_{1-x}\text{Te}_x$ from semimetals to semiconductors — •CHUL HEE MIN¹, SIMON MÜLLER², MICHAEL HEBER³, LENART DUDY⁴, HENDRIK BENTMANN³, MATTHIAS KALLÄNE¹, MARKUS SCHOLZ³, WOOJAE CHOI⁵, YONG SEUNG KWON⁵, FRIEDRICH REINERT², and KAI ROSSNAGEL^{1,3} — ¹IEAP, CAU Kiel, Germany — ²EP7 and ct.qmat, University of Würzburg, Germany — ³DESY, Hamburg, Germany — ⁴Synchrotron SOLEIL, Saint-Aubin, France — ⁵Dep. of EMS, DGIST, South Korea

Localized $4f$ states are often considered to become coherent states at low temperatures by hybridizing with itinerant conduction $5d$ states. In the standard Anderson model, only one type of interaction between the two states is taken into account, which is sufficient to describe Kondo physics. However, additional interaction has been suggested for the mixed valence regime to satisfy the Friedel sum rule when two charge states exist on a short time scale [1]. Here we present photoemission results of mixed-valent Thulium monochalcogenide $\text{TmSe}_{1-x}\text{Te}_x$. This system allows us to study the evolution of the localized $4f$ states between semimetallic and semiconducting phases without applying external pressure and disturbing the periodicity of Tm ions. Our results show two different interactions between $4f$ and $5d$ states across the phase transition.

[1] F. Haldane, Phys. Rev. B 15, 2477 (1976)

C. Varma, Phys. Rev. B 102, 155145 (2022)

TT 9.8 Mon 16:45 HSZ 201

Orbital-selective Mott transition and heavy-fermion physics in the van der Waals ferromagnet $\text{Fe}_{3-x}\text{GeTe}_2$ — •FRANK LECHERMANN¹, XIAOJIAN BAI², YAOHUA LIU², YONGQIANG CHENG², ALEXANDER I. KOLESNIKOV², FENG YE², TRAVIS J. WILLIAMS², SONGXUE CHI², TAO HONG², GARRETT E. GRANROTH², ANDREW F. MAY³, and STUART CALDER² — ¹Institut für Theoretische Physik III, Ruhr-Universität Bochum, D-44780 Bochum, Germany — ²Neutron Scattering Division, Oak Ridge National Laboratory, Oak Ridge, TN 37831, USA — ³Materials Science and Technology Division, Oak Ridge National Laboratory, Oak Ridge, TN 37831, USA

The van der Waals ferromagnet $\text{Fe}_{3-x}\text{GeTe}_2$ is a fascinating material that attracts combined strong interest from magnetoelectronics as well as from strong correlation physics. While near room temperature, the possibilities to exfoliate conducting ferromagnetic layers is investigated, at temperatures below $T \sim 100$ K the system displays surprising signatures of heavy-fermion physics. By means of first-principles many-body calculations, we here show that the latter temperature regime is governed by a rare orbital-selective Mott phase. This leads to emergent Kondo(-lattice) behavior in a unique transition-metal $3d$ compound, accompanied by antiferromagnetic fluctuations within the ferromagnetic phase. These fluctuations are experimentally revealed by neutron scattering.

TT 10: Correlated Electrons: Other Materials

Time: Monday 15:00–18:15

Location: HSZ 204

TT 10.1 Mon 15:00 HSZ 204

Towards a complete quantum oscillatory assessment of the Fermi surface of CoSi — •NICO HUBER¹, SIMON RÖDER¹, GEORG BENKA¹, ANDREAS BAUER¹, SANU MISHRA^{2,3}, ILYA SHEIKIN², CHRISTIAN PFLEIDERER¹, and MARC A. WILDE¹ — ¹Physik-Department, TU Munich, D-85748 Garching, Germany — ²LNCMI-CNRS, Grenoble, France — ³Los Alamos National Laboratory, Los Alamos, USA

The B20 compound CoSi has recently attracted great interest due to its electronic structure hosting multifold fermions at the Γ - and R-point [1] and topologically non-trivial nodal planes on the Brillouin zone boundary [2,3]. While quantum oscillations (QOs) arising from the Fermi surface (FS) around the R-point have been studied in great detail and are well understood [3,4], only limited information has been presented on QOs related to the FS around the Γ -point [5]. Here, we report the experimental identification of previously unobserved QOs arising from heavy FS sheets around Γ in the Shubnikov-de Haas and de Haas-van Alphen spectra of CoSi. The oscillation frequencies, their angular dispersion, and the associated effective masses are in good agreement with first principle cal-

culations. Our observations confirm the calculated bandstructure of CoSi, thus completing the experimental verification of the Fermi surface based on quantum oscillations.

[1] Rao *et al.*, Nature 567, 496 (2019)Sanchez *et al.*, Nature 567, 500 (2019)[2] Wilde *et al.*, Nature 594, 374 (2021)[3] Huber *et al.*, PRL 129, 026401 (2022)[4] Guo *et al.*, Nat. Phys. 18, 813 (2022)[5] Wang *et al.*, PRB 102, 115129 (2020)Sasmal *et al.*, J. Phys.: Condens. Matter 34, 425702 (2022)

TT 10.2 Mon 15:15 HSZ 204

Miniaturized setup for quantum oscillatory studies under temperature modulation — •MICHELLE HOLLRICHER, CHRISTIAN PFLEIDERER, and MARC A. WILDE — Physik-Department, Technical University of Munich, D-85748 Garching, Germany

Measurements of the magnetization and its derivatives provide fundamental insights into the magnetic properties of metals. In particular this is true for magnetic quantum oscillations. We report the development of a miniaturized setup for direct measurements of the temperature derivative of the magnetization as a function of magnetic field and temperature, using a modular setup comprising AC heating with inductive signal pick-up. The dimensions of our setup have been optimized to permit use in combination with standard mechanical rotators, this way enabling measurements of the magnetization as a function of magnetic field orientation down to ultra-low temperatures. Following thorough characterization of the frequency response of our miniaturized setup, we revisited the de Haas-van Alphen effect in bismuth, focusing on the electronic structure of the electron pockets.

TT 10.3 Mon 15:30 HSZ 204

Torque magnetometry of FeSi at low temperatures — •CAROLINA BURGER, VIVEK KUMAR, ANDREAS BAUER, and CHRISTIAN PFLEIDERER — Physik-Departement, Technical University of Munich, D-85748 Garching, Germany

We report a study of the torque magnetization of the correlated small-band-gap semiconductor FeSi in the regime of the saturation of the resistivity at temperatures below a few Kelvin. The magnetic field dependence of the electrical transport properties provides strong circumstantial evidence of a high-mobility surface conduction channel, that is insensitive to the additional presence of an impurity band in the bulk [1, 2]. The surface conduction channel shares great similarities with properties reported for topological insulators, but displays a striking lack of sensitivity to the presence of ferromagnetic impurities as studied by means of a series of single crystals with slightly different starting compositions. We discuss the torque magnetization observed in FeSi with respect to key characteristics observed in the field-polarized state of isostructural magnetic B20 compounds such as MnSi or $\text{Fe}_{1-x}\text{Co}_x\text{Si}$.

[1] Y. Fang, et al., Proc. Natl. Acad. Sci. 115, 8558 (2018)

[2] B. Yang, et al., Proc. Natl. Acad. Sci. 118, e2021203118 (2021)

TT 10.4 Mon 15:45 HSZ 204

Metal-insulator transition and onset of magnetic order in $\text{Fe}_{1-x}\text{Co}_x\text{Si}$ — •JULIUS GREFF¹, PHILIPP HERRE¹, YANNIS HILGERS¹, FELIX LABBUS¹, NINA LÜER¹, MAURICIO DE MELO^{1,2}, JOCHEN LITTE¹, STEFAN SÜLLOW¹, and DIRK MENZEL¹ — ¹Inst. für Physik der Kondensierten Materie, Technische Universität Braunschweig, Germany — ²Departamento de Física, Universidade Estadual de Maringá, Brazil

The B20 transition metal silicides (Fe,Co,Mn)Si have been under investigation for many decades. Although the general observations regarding the electronic and magnetic properties are similar, various details of the phase diagram of $\text{Fe}_{1-x}\text{Co}_x\text{Si}$ are not yet well-established. We have prepared a series of $\text{Fe}_{1-x}\text{Co}_x\text{Si}$ single crystals and investigated the metal-insulator transition as well as the onset of magnetic order in the low Co percentage range by means of transport and susceptibility measurements. In addition, we present for the first time single-crystal Mössbauer spectroscopy experiments in order to complement our study using a microscopic probe. Our investigation sheds light on the physics of quantum criticality and metal-insulator transition and their interplay in the regime of small Co concentrations.

TT 10.5 Mon 16:00 HSZ 204

Temperatur dependence of the lattice constants of $\text{Mn}_{1-x}\text{Fe}_x\text{Si}$ and $\text{Mn}_{1-x}\text{Co}_x\text{Si}$ — •TOBIAS KONRAD, ALEXANDER ENGELHARDT, CHRISTOPH RESCH, ANDREAS BAUER, and CHRISTIAN PFLEIDERER — Physik Department, Technical University Munich, D-85748 Garching, Germany

When magnetic order in the chiral magnet MnSi is suppressed under hydrostatic pressure, topological non-Fermi-liquid behavior emerges, where neutron Larmor diffraction of the lattice constants establishes the absence of quantum criticality [1-3]. Magnetic order in MnSi may also be suppressed by substitutional replacement of iron or cobalt on the manganese sites [4,5]. Using powder x-ray diffraction, we have studied the temperature dependence of the lattice constants of $\text{Mn}_{1-x}\text{Fe}_x\text{Si}$ ($0 \leq x \leq 0.22$) and $\text{Mn}_{1-x}\text{Co}_x\text{Si}$ ($0 \leq x \leq 0.04$) between room temperature and ~ 12 K. The evolution of the lattice constants as a function of iron and cobalt concentration is discussed in comparison to changes of the lattice constants of MnSi under hydrostatic pressure.

[1] C. Pfleiderer et al., Nature **414**, 427 (2001)

[2] C. Pfleiderer et al., Science **316**, 1871 (2007)

[3] R. Ritz et al., Nature **497**, 231 (2013)

[4] A. Bauer et al., Phys. Rev. B **82**, 064404 (2010)

[5] J. Kindervater et al., Phys. Rev. B **101**, 104406 (2020)

TT 10.6 Mon 16:15 HSZ 204

Effect of anion substitution on the Mott insulating instability in the organic conductors κ -(BEDT-TTF)₂X studied by magnetic quantum oscillations — •SHAMIL ERKENOV^{1,2}, FLORIAN KOLLMANNBERGER^{1,2}, WERNER BIBERACHER¹, ILYA SHEIKIN³, TONI HELM⁴, NATALIA KUSHCH¹, RUDOLF GROSS^{1,2}, and MARK KARTSOVNIK¹ — ¹Walther-Meißner-Institut, Garching, Germany — ²Technische Universität München, Garching, Germany — ³Laboratoire National

des Champs Magnétiques Intenses, Grenoble, France — ⁴Hochfeld-Magnetlabor Dresden, HZDR, Dresden, Germany

The layered organic charge-transfer salts κ -(BEDT-TTF)₂X have been extensively employed as model systems for studying the Mott metal-insulator transition. The insulating instability in these materials is very sensitive to external pressure and to minor chemical changes, e.g., variation of the insulating anion. The anion substitution is broadly believed to act similarly to pressure, leading to a modification of the correlation strength ratio U/t . However, recent first-principles band-structure calculations [1] suggest that anion substitution in κ salts influences the ground state chiefly through the spin-frustration effect by changing the transfer-integral anisotropy ratio t'/t rather than through U/t . Here we report on comparative studies of magnetic quantum oscillations in the salts with X = NCS, Cl, and Br, aiming at disentangling the roles of the electronic correlations and spin frustration in the insulating instability within this family. [1] T. Koretsune and C. Hotta, Phys. Rev. B **89**, 045102 (2014).

15 min. break

TT 10.7 Mon 16:45 HSZ 204

Mott criticality in the deuterated variant of κ -(BEDT-TTF)₂ Cu[N(CN)₂]Br studied by thermal expansion under He-gas pressure — •YASSINE AGARMANI, HARALD SCHUBERT, BERND WOLF, and MICHAEL LANG — PI, GU Frankfurt, CRC/TRR288, DE

The understanding of the nature of the critical behavior at the Mott transition has recently been given a new twist by thermodynamic measurements on the Mott insulator κ -(ET)₂Cu[N(CN)₂]Cl (κ -Cl). While so far mainly electronic scenarios have been considered to describe the Mott transition, the observations of strong non-linearities in the strain-stress relation around the Mott critical endpoint in κ -Cl showed that the lattice degrees of freedom play a crucial role [1]. This behavior has been found to be consistent with the proposed scenario of critical elasticity [2], which considers a non-perturbatively strong coupling of the elastic- to the electronic degrees of freedom, causing a softening of the lattice. These observations raise the question of the implication of critical elasticity for our understanding of the general phase diagram of the κ -(ET)₂X family. To address this question, we have chosen a system related to κ -Cl, namely the fully deuterated κ -(ET)₂Cu[N(CN)₂]Br, which is known to be near the Mott critical endpoint at ambient pressure. By using an extension [3] of the setup used in [1], which enables us to fine-tune the He-gas pressure while performing high-resolution measurements of length changes, we aim to compare our results with those on κ -Cl in terms of the extension of the range of critical elasticity.

[1] Gati et al., Sci. Adv. 2, e1601646 (2016)

[2] Zacharias et al., PRL 109, 176401 (2012)

[3] Agarmani et al., RSI 93, 113902 (2022)

TT 10.8 Mon 17:00 HSZ 204

Effect of uniaxial strain on the phononic and electronic excitations of Ta₂NiS₅ — •MAI YE, AMIR-ABBAS HAGHIGHIRAD, and LE TACON MATTHIEU — Institute for Quantum Materials and Technologies, Karlsruhe Institute of Technology, 76021 Karlsruhe, Germany

Semiconductor Ta₂NiS₅ exhibits a structural transition from orthorhombic phase to monoclinic phase at 120 K, driven by acoustic instability [1]. Two Raman-active phonon modes, which have the same symmetry as the order parameter (B_{2g} symmetry), show continuous frequency softening on cooling from 300 K to 20 K. Moreover, a sharp exciton mode in the B_{2g} symmetry channel has been observed at 0.3 eV. We study the phonon modes and interband excitations of Ta₂NiS₅ under uniaxial strain at low temperature. With increasing tensile strain along crystallographic a axis, the frequency of the two B_{2g} -symmetry phonon modes and the band gap of this semiconductor both increase, with a 6.5% frequency increase of the lowest-energy B_{2g} phonon mode corresponding to a 4.1% increase of the gap size. On the contrary, the frequency change of the non-softening phonons is less than 1%. By analyzing the phonon intensity, we further find that the magnitude of the order parameter, and in turn the phase transition temperature, increases with the tensile strain. These experimental results demonstrate Ta₂NiS₅ as a suitable platform to explore the manipulation of lattice dynamics and electronic structure by applying uniaxial strain.

[1] Phys. Rev. B 104, 045102 (2021)

TT 10.9 Mon 17:15 HSZ 204

Magnetic anisotropy and low-energy spin dynamics in magnetic van der Waals compounds Mn₂P₂S₆ and MnNiP₂S₆ — •JOYAL JOHN ABRAHAM^{1,2}, YURII SENYK¹, YULIA SHEMERLIUK¹, SEBASTIAN SELTER¹, SAICHARAN ASWARTHAM¹, BERND BÜCHNER^{1,3}, VLADISLAV KATAEV¹, and ALEXEY ALFONSOV¹ — ¹Leibniz IFW Dresden, D-01069 — ²Institute for Solid State and Materials Physics, TU Dresden, D-01069 — ³Institute for Solid State and Materials Physics and Würzburg-Dresden Cluster of Excellence ct.qmat, TU Dresden, D-01062

We report a comprehensive high-field electron spin resonance (ESR) study performed on single crystals of Mn₂P₂S₆ and MnNiP₂S₆ in the broad ranges of temperatures, frequencies and magnetic fields. Analysing the antiferromagnetic

modes well below the ordering temperature T_N , we have found that the ground state, the order type and magnetic anisotropy (MA) change with increasing x in $(\text{Mn}_{1-x}\text{Ni}_x)_2\text{P}_2\text{S}_6$. In the case of $\text{Mn}_2\text{P}_2\text{S}_6$, an application of the linear spin wave theory enabled us to determine the anisotropy and exchange constants, important for a quantitative description of the ground state. A systematic increase of the g -factor and its anisotropy, measured at $T \gg T_N$, is observed with increasing Ni content, which, in turn, sheds light on the nature of MA in the ordered state. The investigation of the T -dependence of line shifts from the paramagnetic resonance position reveals already well above T_N the presence of the short range spin-spin correlations static on ESR time scale, which are more pronounced in MnNiP_2S_6 .

TT 10.10 Mon 17:30 HSZ 204

Switching of magnetic anisotropy from out-of-plane to in-plane in quasi-2D van der Waals $(\text{Mn}_{1-x}\text{Ni}_x)_2\text{P}_2\text{S}_6$ single crystals — •YULIYA SHEMERLIUK, ANJA U. B. WOLTER, BERND BÜCHNER, and SAICHARAN ASWARTHAM — Institut für Festkörperforschung, Leibniz IFW Dresden, Helmholtzstraße 20, 01069 Dresden, Germany

In the recent years magnetic two-dimensional van der Waals materials are at the forefront of the research. Magnetism has been extensively investigated in the family of $\text{TM}_2\text{P}_2\text{S}_6$ (TM= Ni, Co, Fe, Mn & V). Transition metal TM substitution has been used as a technique to control magnetism in this family of compounds [1-3]. In this talk, we will present crystal growth by chemical vapor transport together with a thorough structural and magnetic characterization of the quasi-2D magnets $(\text{Mn}_{1-x}\text{Ni}_x)_2\text{P}_2\text{S}_6$ with $x = 0, 0.3, 0.5, 0.7$ & 1 . As-grown crystals exhibit a layered morphology with weak van der Waals interlayer interactions parallel to the crystallographic ab plane of the monoclinic symmetry in the space group $C2/m$ (No. 12). In this series, the two neighboring members $\text{Mn}_2\text{P}_2\text{S}_6$ and $\text{Ni}_2\text{P}_2\text{S}_6$ differ in magnetic atoms, magnetic easy axes, spin anisotropy, and nearest neighbor magnetic interactions. The magnetization measurements show an antiferromagnetic ground state for all grown crystals. The magnetic ordering temperature T_N shows nonmonotonic behavior. The magnetic anisotropy switches from out-of-plane to in-plane as a function of composition.

TT 10.11 Mon 17:45 HSZ 204

Single crystal growth, structural and transport properties of the Mott insulator BaCoS_2 — •HANEEN ABUSHAMMALA, TESLIN THOMAS, ANDREAS KREYSSIG, and ANNA BÖHMER — Institute for Experimentalphysik IV, Ruhr-Universität Bochum, Universitätsstrasse 150, 44801 Bochum, Germany.

The quasi-2D BaCoS_2 is a Mott insulator with a stripe-like antiferromagnetic ordering at $T_N=290$ K. Both chemical doping or hydrostatic pressure drive the

system into a paramagnetic metallic phase. Interestingly, there is no structural transition at the metal-insulator transition of this phase, which offers ideal conditions to investigate the Mott transition in a model multiband system [1].

Nevertheless, BaCoS_2 remains little studied, and the interplay of electronic and structural features is still unclear. High-quality single crystals are needed to elucidate this issue. The synthesis of single-crystalline BaCoS_2 is challenging owing to its metastability, with a decomposition into Ba_2CoS_3 , CoS and S below 850°C . The BaCoS_2 phase can only be obtained via quenching from high temperature. Moreover, BaCoS_2 melts incongruently, which calls for a flux growth method necessitating separation of the crystals from the flux by the end of the growth. We have successfully grown single crystals of pure and the hole-doped BaCoS_2 using a self-flux method with high-temperature flux separation and quench. The structural and anisotropic electrical transport properties are determined and discussed.

[1] H. Abushammala, B. Lenz, B. Baptiste, M. Casula, Y. Klein and A. Gauzzi, in preparation (2022).

TT 10.12 Mon 18:00 HSZ 204

Spin-orbit entangled crystal-field excitations in $5d^4$ $j = 0$ osmates — •PHILIPP WARZANOWSKI¹, MARCO MAGNATERRA¹, PHILIPP STEIN¹, QUENTIN FAURE², CHRISTOPH SAHLE², HOLGER SCHWAB¹, THOMAS LORENZ¹, PETRA BECKER³, LADISLAV BOHATÝ³, PAUL H. M. VAN LOOSDRECHT¹, and MARKUS GRÜNINGER¹ — ¹Institute of Physics II, University of Cologne — ²European Synchrotron Radiation Facility, Grenoble Cedex, France — ³Sect. Crystallography, Institute of Geology and Mineralogy, University of Cologne

For strong spin-orbit coupling, the d^4 electron configuration may show a non-magnetic $j = 0$ ground state. In $5d^4$ iridates, magnetic behavior has been discussed controversially and finally it has been attributed to defects, while excitonic magnetism has been proposed for $4d^4$ ruthenates. We show that the $j = 0$ state is very well realized in the cubic antiferroite-type $5d^4$ osmates K_2OsCl_6 and K_2OsBr_6 . The magnetic susceptibility exhibits van-Vleck type magnetism without a sizeable Curie-Weiss contribution. Employing resonant inelastic x-ray scattering (RIXS) and infrared spectroscopy as complementary techniques, we investigate the electronic excitations and determine the electronic parameters by comparison with local multiplet calculations. The cubic crystal-field splitting $10 Dq$ and the charge transfer energy are 15% smaller for the chlorine compound than for its bromide sister, whereas the intra- t_{2g} excitation energies are reduced by 4%. This allows us to quantify the influence of the e_g orbitals on the effective spin-orbit coupling for the t_{2g} orbitals.

TT 11: Spintronics, Spincalorics and Magnetotransport

Time: Monday 15:00–16:30

Location: HSZ 304

TT 11.1 Mon 15:00 HSZ 304

Van der Waals/non-van der Waals hybrids for superconducting spintronics — ROMAN HARTMANN, ALFREDO SPURI, DANILO NIKOLIC, WOLFGANG BELZIG, ELKE SCHEER, and •ANGELO DI BERNARDO — Universität Konstanz, Konstanz, Germany

The realization of Cooper pairs of electrons with parallel-aligned spins (i.e., spin-triplet pairs) has been demonstrated for a variety of three-dimensional (3D) superconductor/ferromagnet (S/F) heterostructures. Several studies have shown that using S/F system with a magnetically inhomogeneous F [1-2] it is possible to convert the spin-singlet pairs of a conventional S into fully-polarized spin triplets - this has paved the way for superconducting spintronics. Van-der-Waals (vdW) heterostructures host a variety of unconventional phases, both superconducting and magnetic, which can be explored to realize two-dimensional (2D) superspintronic devices with novel functionalities and types of control compared to devices based on 3D S/F hybrids. The conversion of spin singlets into spin triplets across a 2D S/F vdW interface represents, however, the first step towards superconducting spintronics based on vdW hybrids. In this talk, I will show recent magnetotransport experiments obtained on F nanoflakes that are cleaved from 3D ionic F single crystals through a new approach. The unique properties of these nanoflakes are used for the fabrication of novel superspintronic devices, where the nanoflakes are coupled to conventional 2D vdW S materials.

[1] J. W. A. Robinson et al., Science 329, 59 (2010)

[2] A. Di Bernardo et al., Nat. Commun. 6, 8053 (2015)

TT 11.2 Mon 15:15 HSZ 304

Thermal transport in weakly coupled spin- $\frac{1}{2}$ Heisenberg ladders — •ANJA WENGER, CHRISTIAN NORTHE, and EWELINA HANKIEWICZ — Institut für Theoretische Physik und Astrophysik, Universität Würzburg, 97074 Würzburg, Germany

We investigate the weakly coupled spin- $\frac{1}{2}$ Heisenberg ladder in the low energy limit. As magnetic excitations significantly contribute to the thermal transport,

we expose the ladder to a magnetic field and analyze the thermal conductivity and the specific heat capacity depending on the magnetization. Starting point is the spin- $\frac{1}{2}$ Heisenberg chain and its fermionic and bosonic description by conformal field theory. From coupling two spin chains and applying the (rescaled) bosonisation technique, a free theory for spin-ladders and its spectrum is obtained. Special interest lies on the conformal anomaly and the Tomonaga-Luttinger Liquid parameters. Introducing temperature to the theory gives access to the thermal transport properties.

TT 11.3 Mon 15:30 HSZ 304

Critical current control in ferromagnetic proximity junctions by magnetization and spin injection — •LUKAS KAMMERMEIER and ELKE SCHEER — Universität Konstanz, Konstanz, Germany

We exploit the inverse proximity effect of a ferromagnet on a superconductor to locally suppress the superconductivity in a thin wire and thereby create a Josephson junction.

We show that we can control the critical current I_c over a wider range by manipulating the magnetization state of the ferromagnet, possibly sensitive to single magnetic domains in proximity to the constriction. Additionally, the efficiency of spin injection by running a current from the spin-polarized ferromagnet into the junctions constriction will be presented.

TT 11.4 Mon 15:45 HSZ 304

On the connection between the chiral-induced spin selectivity effect and the chiro-optical activity: The case of an electron in a helix — •SOLMAR VARELA¹, GIANAURELIO CUNIBERTI¹, RAFAEL GUTIERREZ¹, ERNESTO MEDINA², VLADIMIRO MUJICA³, and JESUS UGALDE⁴ — ¹Chair of Materials Science and Nanotechnology, TU Dresden, Dresden — ²Departamento de Física, Colegio de Ciencias e Ingeniería, Universidad San Francisco de Quito, Ecuador — ³School of Molecular Sciences, Arizona State University, USA — ⁴Kimika Fakultatea, Euskal Herriko Unibertsitatea (UPV/EHU), Spain

We have obtained a connection between the chiro-optical activity and the spin-orbit interaction for a model system of an electron constrained to a helix, taking explicitly spin into account, in the presence of an electromagnetic field as a perturbation. Because of the chiral nature of the system, spatial inversion symmetry is broken, which in turn induces a connection between the electric and the magnetic responses of the system to the external electromagnetic field, that is absent in achiral systems. Despite the apparent simplicity of the model, it contains most of the relevant physics involved in this problem, and we have established a relationship between the optical activity response, via the Rosenfeld tensor and the spin polarization, defined as the average value of the Pauli spin-1/2 matrices. This relationship between the optical response and the CISS responses, can guide new efforts in the fields of reticular chemistry and material design for spintronics, and spin-selective chemistry.

TT 11.5 Mon 16:00 HSZ 304

Electron and spin-phonon interaction in DNA: A minimum analytical model — •MAYRA PERALTA¹, SOLMAR VARELA¹, VLADIMIRO MUJICA², RAFAEL GUTIÉRREZ¹, ERNESTO MEDINA³, and GIANAURELIO CUNIBERTI¹ — ¹Institute of Materials Science and Nanotechnology, Technische Universität Dresden, Dresden 01062, Germany — ²School of Molecular Sciences, Arizona State University, TEMPE, AZ 85287 — ³Departamento de Física, Colegio de Ciencias e Ingeniería, Universidad San Francisco de Quito, Diego de Robles y Vía Interoceánica, Quito, 170901, Ecuador

We analyze the influence of electron-phonon and spin-phonon interaction in a model for electron transfer(ET) in DNA in terms of the envelope function approach. We are specifically concerned with the effect of these interactions on the coherence of the ET process and how to model the interaction of DNA with phonon reservoirs of biological relevance. We assume that the electron bearing orbitals are half filled and derive the physics of the electron- and spin-phonon

coupling in the vicinity in reciprocal space. In a first model for spinless electrons we find that at half filling, the acoustical modes are decoupled to ET at first order, while optical modes are predominant. The latter are associated with inter-strand vibrational modes in consistency with previous studies involving polaron models of ET. Coupling to acoustic modes depends on electron doping of DNA, while optical modes are always coupled within our model. When the spin is included, through the Spin-orbit coupling whose intensity is geometry dependent, we find that acoustical phonons become coupled independently of the doping.

TT 11.6 Mon 16:15 HSZ 304

Gate-tunable insulator-metal transition and weak antilocalization in two-dimensional tellurium — •DORSA FARTAB¹, JOSÉ GUIMARÃES^{1,2}, MARCUS SCHMIDT¹, and HAIJING ZHANG¹ — ¹Max Planck Institute for Chemical Physics of Solids, 01187 Dresden, Germany — ²School of Physics and Astronomy, University of St Andrews, St Andrews KY16 9SS, UK

Charge carrier density control is a key factor to modify the electronic functionality of materials. The ability to induce high charge carrier concentration into various two-dimensional materials has led to exotic phenomena such as insulator-metal transition and superconductivity. So far, different techniques have been used to achieve this. Meanwhile, electric double layer transistor (EDLT) is a highly promising platform as it can provide high charge carrier density of up to 10^{15} cm^{-2} in its channel material. This is two orders of magnitude larger than that in the conventional transistors as a result of using ionic liquids instead of common solid dielectrics. First, I will give a short overview on the EDLTs, then I will present our experimental results of ionic liquid gated two-dimensional tellurium (Te). Our results show the possibility of gate tuning insulator-metal phase transition and the gate and temperature-dependent weak antilocalization in p-type Te films. More interestingly, we have shown the ability of controlling the spin-orbit interaction in the material by changing the applied gate voltage.

TT 12: Topological Insulators (joint session MA/TT)

Time: Monday 15:00–17:15

Location: HSZ 403

TT 12.1 Mon 15:00 HSZ 403

Benchmark study of symmetry-adapted ML-DFT models for magnetically doped topological insulators — •JOHANNES WASMER¹, RUBEL MOZUMDER¹, PHILIPP RÜSSMANN^{1,2}, IRA ASSENT^{1,3}, and STEFAN BLÜGEL¹ — ¹Forschungszentrum Jülich, Germany — ²University of Würzburg, Germany — ³Aarhus University, Denmark

We present a benchmark study of surrogate models for impurities embedded into crystalline solids. Using the Korringa-Kohn-Rostoker Green Function method [1], we have built databases of several thousand calculations of single impurities (monomers) embedded into different elemental crystals, as well as magnetic transition metal impurity dimers embedded in the topological insulator Bi_2Te_3 . We predict the converged monomer impurity electron potential and the isotropic exchange interaction of the impurity dimer in the classical Heisenberg model. From these surrogates, we intend to build transferable models for larger systems in the future, which will accelerate the convergence of our DFT codes. The study compares various recent E(3)-equivariant models such as ACE and MACE [2] in terms of performance and reproducible end-to-end workflows.

[1] P. Rüßmann et al., *npj Comput Mater* 7, 13 (2021)

[2] I. Batatia et al., arXiv:2206.07697 (2022)

TT 12.2 Mon 15:15 HSZ 403

High throughput magnetic topological materials search II — •IÑIGO ROBREDO^{1,2}, YUANFENG XU^{3,4}, ANDREI BERNEVIG^{2,3}, CLAUDIA FELSER¹, NICOLAS REGNAULT^{3,6}, LUIS ELCORO⁵, and MAIA G. VERGNIORY^{1,2} — ¹MPI CPFS Dresden — ²DIPC — ³Princeton University — ⁴Zhejiang University — ⁵Basque Country University — ⁶Sorbonne Université

The development of topological quantum chemistry has proven to be a game changing tool for predicting topological phases in realistic materials, both non-magnetic and magnetic. Building on the work of previous studies, in this work we expand the family of magnetic insulators and semimetals with non-trivial topological properties. We analyzed 408 magnetic structures from the Bilbao Crystallographic Server magnetic database, whose crystal and magnetic structures have been experimentally reported. To take into account the localized nature of magnetic elements, we perform electronic structure calculations and topological diagnosis as a function of the Hubbard U parameter. This results in a topological phase diagram for each material as a function of the Hubbard interaction potential. We provide full details of the materials, which can be readily grown to explore their new topological phenomena.

TT 12.3 Mon 15:30 HSZ 403

Manipulating topological feature of massive Dirac particle with scalar potential — •SUMIT GHOSH^{1,2}, YURIY MOKROUSOV^{1,2}, and STEFAN BLÜGEL¹ — ¹PGI-1, Forschungszentrum Jülich, Germany — ²Institute of Physics, Johannes Gutenberg University Mainz, Germany

Topology is one of the central aspect of modern spintronics. Different physical observables as well as transport properties that originates from the nontrivial topology of the system shows significant robustness against different external perturbation. Manipulating the topology of a system on the other hand is a highly non-trivial task since it requires tuning the internal degrees of freedom. In this presentation we are going to present an intrinsic mechanism to manipulate the topological feature and associated transport properties by using scalar potential. We systematically demonstrate how a scalar potential can invert the mass term of a massive Dirac particle which subsequently leads to the change of the topological index. We further demonstrate how this mechanism can be exploited to control the formation of edge states which can control the transport properties. This study thus provides a better understanding of the origin of the topological properties as well as a simple way to manipulate them. [<https://arxiv.org/abs/2204.06412>]

TT 12.4 Mon 15:45 HSZ 403

Mapping out the topological phase diagram of FeSn — SOUMYA SANKAR¹, RUIZI LIU², XUEJIAN GAO¹, QIFANG LI^{3,4}, JIACHANG ZHENG¹, CAIYUN CHEN¹, CHENGPING ZHANG¹, KUN QIANG², ZI YANG MENG^{3,4}, KAM TUEN LAW¹, QIMING SHAO^{1,2}, and •BERTHOLD JÄCK¹ — ¹HKUST, Clear Water Bay, Kowloon, Hong Kong SAR — ²HKUST, Department of Computer Science and Electrical Engineering, Clear Water Bay, Kowloon, Hong Kong SAR — ³Hong Kong University, Department of Physics, Pokfulam Road, Hong Kong SAR — ⁴University of Tokyo, Department of Physics, Hongo, Bunkyo City, Tokyo

Metallic kagome magnets exhibit a flat band and a Dirac point in their electronic structure and long-range magnetic order. The combination of these properties creates favourable conditions to search for strongly correlated and topological electronic states. The near-ideal kagome band structure of the inter metallic kagome series X1Y1 offers opportunities to study the interplay between strong electronic correlations, topology, and magnetism.

We have used molecular beam epitaxy and electronic transport measurements to study the interplay of magnetism and band topology in thin films of antiferromagnetic FeSn. We will present results from a magnetic field and temperature dependent study of the anomalous Hall effect. Combining these measurements with magnetic Monte-Carlo simulations and theoretical model calculations, we map out the topological phase diagram of FeSn over a large temperature range.

We acknowledge support by the GRC, and the Croucher Foundation.

15 min. break

TT 12.5 Mon 16:15 HSZ 403

Investigation of the magnetic topological insulator family (MnPn₂Te₄) (Pn=Bi, Sb) by μ SR and NMR — •MANASWINI SAHOO^{1,2}, ANNA ISAEVA¹, BERND BÜCHNER¹, and ROBERTO DE RENZI² — ¹Leibniz IFW Dresden, Dresden, Germany — ²University of Parma, Parma, Italy

Time-reversal symmetry breaking in a topological insulator (TI) opens a surface gap and distinguishes chiral quantum states that could eventually be exploited in electrically controlled spintronic devices. The recent discovery of layered van der Waals materials opens a new approach to achieve this. (MnBi₂Te₄) (Bi₂Te₃) n is one of the first such examples, where the increasing number n of TI layers controls the magnetic dimensionality of the material. These compounds do display the quantum anomalous Hall effect, where spontaneous magnetization and spin-orbit coupling lead to a topologically non-trivial electronic structure. In the case of (MnBi₂Te₄) (Bi₂Te₃) n, Zero Field μ SR shows more than one internal field at the muon site with the majority one decreasing in value when n is increased. The muon spin precessions display very fast relaxations of static inhomogeneous nature. Whereas in the sister compound MnSb₂Te₄, Zero Field μ SR shows a broader distribution of magnetic field at the muon due to larger intermixing between Mn/Sb in the sample. Importantly, the weak Transverse Field shows a sharp magnetic transition at the same T_c, with a clear relaxation peak due to critical fluctuations, taking place in the whole volume of the material. This local information from μ SR together with NMR is crucial to correctly interpret macroscopic magnetization data.

TT 12.6 Mon 16:30 HSZ 403

Magnetic dilution effect and topological phase transitions in antiferromagnet Mn_{1-x}Pb_xBi₂Te₄ — •YUEH-TING YAO¹, TIEMA QIAN², TAY-RONG CHANG^{1,3,4}, and NI NI² — ¹Department of Physics, National Cheng Kung University, Tainan 70101, Taiwan — ²Department of Physics and Astronomy and California NanoSystems Institute, University of California, Los Angeles, California 90095, USA — ³Center for Quantum Frontiers of Research and Technology (QFort), Tainan 701, Taiwan — ⁴Physics Division, National Center for Theoretical Sciences, Taipei 10617, Taiwan

The interplay between magnetism and topology have taken the central stage of modern condensed matter physics in the past three years. The fine control of magnetism and topology in a magnetic topological insulator is crucial for realizing various novel magnetic topological phases, such as axion insulator, magnetic Weyl semimetals, etc. In this work, we investigate the evolution of magnetism and band topology in Mn_{1-x}Pb_xBi₂Te₄ via angle resolved photoemission spectroscopy (ARPES), first-principles calculations, and electronic transports. We present the comprehensive phase diagram by controlling Pb content and magnetism in this alloy system. Moreover, we provide the first topological crystalline insulator with non-trivial glide mirror Chern number in MnBi₂Te₄-family materials, which is protected by non-symmorphic symmetry arise from antiferromagnetic (AFM) configuration. Our work provides a fruitful platform with continuously tunable magnetism and topology for investigating emergent phenomena and pave a way towards potential new applications of nanoelectronics.

TT 12.7 Mon 16:45 HSZ 403

Thermal Hall Effect of Magnon-Phonon Hybrid Quasiparticles in a Fluctuating Heisenberg-Kitaev Antiferromagnet — •ROBIN R. NEUMANN¹, ALEXANDER MOOK², JÜRGEN HENK¹, and INGRID MERTIG¹ — ¹Martin Luther University Halle-Wittenberg, Halle (Saale), Germany — ²Johannes Gutenberg University, Mainz, Germany

Magnons, the quantized excitations of localized spins, and phonons, the quantized excitations of the lattice, are two types of quasiparticles that are responsible for heat transport in magnetic insulators. However, phonons by themselves do not contribute to the *transverse* heat current induced by a temperature gradient, i.e., the thermal Hall effect (THE). Magnons, on the other hand, may exhibit a Berry curvature, a magnetic field in reciprocal space, that leads to an intrinsic THE.

In this talk, I address the THE in a Heisenberg-Kitaev antiferromagnet subjected to a magnetic field. The applied field drives the system from a zigzag antiferromagnetic to a spin-flop state. The magnon-driven THE indicates the magnetic phase transition by a sign change at the critical field. Furthermore, when the magnetoelastic interaction is considered, the phonon and magnon bands hybridize and additional Berry curvature at the avoided crossings emerge. Depending on the strength of the spin-phonon coupling, this may lead to an overall reversal of the THE while the field-induced sign change at the critical field remains mostly robust. These results showcase that magnon-phonon hybridization can be pivotal for the interpretation of transport experiments.

TT 12.8 Mon 17:00 HSZ 403

Limitations of the Bulk-Boundary Correspondence in Topological Magnon Insulators due to Magnon-Magnon Interactions — •JONAS HABEL¹, JOHANNES KNOLLE¹, ALEXANDER MOOK², and JOSEF WILLISHER¹ — ¹Technical University of Munich, Germany (Theory of Quantum Matter and Nanophysics) — ²Johannes Gutenberg University Mainz, Germany

Magnon excitations in ordered quantum magnets can exhibit topological band structures characterized by non-zero Chern numbers. Such magnonic Chern insulators are widely believed to host protected chiral edge modes due to the bulk-boundary correspondence, in analogy to electronic Chern insulators. However, in contrast to electrons, magnons are bosons and can thus be subject to exotic number-non-conserving many-body interactions, enabling potentially strong spontaneous decays at zero temperature.

To assess their effect on the chiral edge magnons, we study a topological honeycomb-lattice ferromagnet with Dzyaloshinskii-Moriya interactions using many-body perturbation theory. We discover that non-harmonic terms of the spin-wave expansion may lead to severe lifetime reduction of edge modes and their delocalisation into the bulk. For sufficiently strong interactions, the spectral weight of the chiral edge magnons vanishes entirely. These findings indicate that topological magnon bands within the harmonic framework do not necessarily give rise to protected edge modes in the full spin theory, suggesting limitations of the bulk-boundary correspondence in this case.

TT 13: Focus Session: Physics Meets ML II – Understanding Machine Learning as Complex Interacting Systems (joint session DY/TT)

Machine-learning has recently entered and is now transforming many fields of science, enabling discoveries in a data-driven manner. As a scientific method, however, ML often lacks one defining feature: Explainability. We here seek discussions with pioneers in understanding, explaining, and improving machine learning methods from the point of view as a physical system of interacting elements. In fact, the history of approaching neuronal networks and problems of inference and learning as a problem of statistical physics has a long history, with a number of important discoveries early on. The close relation between spin glasses and neuronal networks are being currently exploited to address pressing questions, such as the remarkable generalization properties of neuronal networks despite their massive overparameterization and their behavior reminiscent of renormalization group transformations.

Organized by Sabine Andergassen (Tübingen) and Moritz Helias (Jülich)

Time: Monday 15:00–18:30

Location: ZEU 250

Invited Talk

TT 13.1 Mon 15:00 ZEU 250

The challenge of structured disorder in statistical physics — •MARC MEZARD — Bocconi University, Milan

Statistical physics offers many interesting tools to study machine learning. In most cases it needs to use a statistical ensemble of data. Most of the theoretical work has relied on unstructured data. Yet, the highly structured character of data used in training deep networks is a crucial ingredient of their performance. Modelling structured data, analyzing the learning and the generalization of deep networks trained on this data, are major challenges. This talk will describe several recent developments in this direction.

Invited Talk

TT 13.2 Mon 15:30 ZEU 250

The emergence of concepts in shallow neural-networks — •ELENA AGLIARI — Piazzale A. Moro 5, 00185 Roma

In the first part of the seminar I will introduce shallow neural-networks from a statistical-mechanics perspective, focusing on simple cases and on a naive scenario where information to be learnt is structureless. Then, inspired by biological information-processing, I will enrich the framework and make the network able to successfully and cheaply handle structured datasets. Results presented are both analytical and numerical.

Invited Talk

TT 13.3 Mon 16:00 ZEU 250

Adaptive Kernel Approaches to Feature Learning in Deep Neural Networks —

•ZOHAR RINGEL — Racah Institute of Physics, Hebrew University in Jerusalem

Following the ever-increasing role of deep neural networks (DNNs) in our world, a better theoretical understanding of these complex artificial objects is desirable. Some progress in this direction has been seen lately in the realm of infinitely overparameterized DNNs. The outputs of such trained DNNs behave essentially as multivariate Gaussians governed by a certain covariance matrix called the kernel. While such infinite DNNs share many similarities with the finite ones used in practice, various important discrepancies exist. Most notably the fixed kernels of such DNNs stand in contrast to feature learning effects observed in finite DNNs. Such effects are crucial as they are the key to understanding how DNNs process data. To accommodate such effects within the Gaussian/kernel viewpoint, various ideas have been put forward. Here I will provide a short overview of those efforts and then discuss in some detail a general set of equations we developed for feature learning in fully trained/equilibrated DNNs. Interestingly, our approach shows that DNNs accommodate strong feature learning via mean-field effects while having decoupled layers and decoupled neurons within a layer. Furthermore, learning is achieved not by compression of information but rather by increasing neuron variance along label-relevant directions in function space.

TT 13.4 Mon 16:30 ZEU 250

Interpreting black-box ML with the help of physics — •MIRIAM KLOPOTEK — University of Stuttgart, SimTech Cluster of Excellence EXC 2075, Stuttgart, Germany

Complexity is an unavoidable part of systems with emergent or even so-called intelligent capabilities. Ultimately, it stems from the many microscopic constituents with multiple possible states, which introduces a vast space of degrees of freedom. This is true both for many-body systems as well as modern machine learning (ML) systems. Today, the latter suffer notoriously from the 'black-box problem', i.e. they are inherently opaque. We argue that an engagement with physics can offer deep insights ultimately for a theory of operation and thus an interpretation, as well as powerful ways to assess their reliability and shortcomings. We show some results for a case study with beta-variational autoencoders (β -VAEs) [1], which we trained on data from a well-characterized model system of hard rods confined to 2D lattices [2].

[1] D. P. Kingma and M. Welling, ICLR 2014. D. J. Rezende, S. Mohamed, and D. Wierstra, ICML 2014, p. 1278-1286.

[2] P. Quiring, M. Klopotek and M. Oettel, Phys. Rev. E 100, 012707 (2019).

15 min. break**Invited Talk**

TT 13.5 Mon 17:00 ZEU 250

Analysing the dynamics of message passing algorithms — •MANFRED OPPER^{1,2} and BURAK ÇAKMAK¹ — ¹Institut für Softwaretechnik und Theoretische Informatik, Technische Universität Berlin, 10587, Germany — ²Centre for Systems Modelling and Quantitative Biomedicine, University of Birmingham, B15 2TT, United Kingdom

Message passing algorithms are deterministic methods which are designed for efficiently computing marginal statistics for probabilistic, Bayesian data models used in machine learning and statistics. Such algorithms have been developed in parallel within the machine learning and the statistical physics communities. They often provide highly accurate approximations at a much higher speed compared to exact Monte Carlo sampling. The fixed points of such algorithms can be analysed for high dimensional models (under the assumption of specific data distributions) using the replica method of statistical physics. In this talk we will focus on the dynamical properties of the algorithms. Applying dynamical func-

tional techniques to the nonlinear dynamics, the degrees of freedom which interact via a random matrix can be decoupled in the limit of large systems resulting in exact stochastic single node dynamics. For general dynamical models, it is hard to further analyse this effective dynamics due to the occurrence of memory terms. Surprisingly, for message passing algorithms memory terms are absent and exact results for convergence rates and stability can be derived for specific data distributions.

Invited Talk

TT 13.6 Mon 17:30 ZEU 250

Deep Learning Theory Beyond the Kernel Limit — •CENGİZ PEHLEVAN — Harvard University, USA

Deep learning has emerged as a successful paradigm for solving challenging machine learning and computational problems across a variety of domains. However, theoretical understanding of the training and generalization of modern deep learning methods lags behind current practice. I will give an overview of our recent results in this domain, including a new theory that we derived by applying dynamical field theory to deep learning dynamics. This theory gives insight into internal representations learned by the network under different learning rules.

TT 13.7 Mon 18:00 ZEU 250

Solving the Bethe-Salpeter equation with exponential convergence — •MARKUS WALLERBERGER¹, HIROSHI SHINAOKA², and ANNA KAUCH¹ — ¹TU Wien, Vienna, Austria — ²Saitama University, Japan

The Bethe-Salpeter equation plays a crucial role in understanding the physics of correlated fermions, relating to optical excitations in solids as well as resonances in high-energy physics. Yet, it is notoriously difficult to control numerically, typically requiring an effort that scales polynomially with energy scales and accuracy. This puts many interesting systems out of computational reach.

Using the intermediate representation and sparse modeling for two-particle objects on the Matsubara axis, we develop an algorithm that solves the Bethe-Salpeter equation in $O(L^8)$ time with $O(L^4)$ memory, where L grows only logarithmically with inverse temperature, bandwidth, and desired accuracy. This opens the door for computations in hitherto inaccessible regimes. We benchmark the method on the Hubbard atom and on the multiorbital weak-coupling limit, where we observe the expected exponential convergence to the analytical results. We then showcase the method for a realistic impurity problem.

[1] M. Wallerberger et al., Phys. Rev. Research 3, 033168 (2021)

TT 13.8 Mon 18:15 ZEU 250

Making machines untangle the parquet equations — •SAMUEL BADR¹, ANNA KAUCH¹, HIROSHI SHINAOKA², KARSTEN HELD¹, and MARKUS WALLERBERGER¹ — ¹TU Wien, Vienna, Austria — ²Saitama University, Saitama, Japan

Diagrammatic theories at the two-particle level are increasingly important in understanding the subtle interplay of phenomena occurring in strongly correlated electron systems. The parquet equations are a centerpiece of many such theories, since they are the simplest unbiased topological classification of two-particle diagrams. However, due to their eponymous interlocking structure, the parquet equations are vexingly difficult to solve, requiring prohibitive amounts of memory.

We tackle this problem using the recently developed, machine learning inspired, techniques: firstly, the overcomplete intermediate representation, a highly compressed model for two-particle objects which is guaranteed to converge exponentially; secondly, a sparse set of Matsubara frequencies tailored to the structure of the parquet equations. This allows us to perform convolutions and frequency shifts at no loss of accuracy.

We benchmark our solver for the Hubbard atom, where we reproduce analytic results, and then showcase the solver for more extended systems.

TT 14: Focus Session: Graphene Quantum Dots (joint session HL/TT)

Quantum dots have emerged as one of the contenders for a future quantum information processor. Bilayer graphene is now established as a material that allows high quality bi-polar Coulomb blockade measurement, time-dependent transport measurements and first relaxation time measurements. In contrast to the more conventional GaAs and Si-based systems, several exiting and unexpected observations in graphene have been explained by the peculiar graphene bandstructure, which is gate-tunable, the additional valley degree of freedom, and spin-valley coupling.

Organized by Klaus Ensslin

Time: Monday 15:00–17:45

Location: POT 361

Invited Talk

TT 14.1 Mon 15:00 POT 361

Spin and valley lifetime in graphene quantum dots — •GUIDO BURKARD — University of Konstanz, Germany

Graphene with its low nuclear spin density and weak spin-orbit coupling allows for long electron spin relaxation and coherence times. The spin and valley de-

grees of freedom of localized electrons can therefore be seen as potential embodiments of classical or quantum bits for computation. However, the formation of localized states in quantum dots requires some form of badgap engineering, and the mechanisms for spin and valley relaxation have not been completely understood so far. Bilayer graphene has an electrically controllable bandgap that

allows for the formation of quantum dots. We present general theoretical considerations regarding the formation of quantum dots in graphene and report on recent progress in understanding the relevant physical mechanisms of spin and valley relaxation in electrostatically gated bilayer graphene quantum dots.

Invited Talk TT 14.2 Mon 15:30 POT 361
Microscopic modelling of electrostatically induced bilayer graphene quantum dots — •ANGELIKA KNOTHE — Institut für Theoretische Physik, Universität Regensburg, D-93040 Regensburg, Germany

Quantum nanostructures, e.g., quantum wires and quantum dots, are needed for applications in quantum information processing devices, such as transistors or qubits. In gapped bilayer graphene, one can confine charge carriers purely electrostatically, inducing smooth confinement potentials and thereby limiting edge-induced perturbances while allowing gate-defined control of the confined structure. In this talk, I will give an overview of our recent contributions toward the theoretical modelling of gate-defined bilayer graphene quantum dots, taking into account microscopic details of the material properties and the confinement. As an outlook, I will point towards current and future challenges in describing coupled bilayer graphene nanostructures, e.g., setups with multiple bilayer graphene quantum dots.

TT 14.3 Mon 16:00 POT 361
Valley relaxation in a single-electron bilayer graphene quantum dot — •LIN WANG and GUIDO BURKARD — Department of Physics, University of Konstanz, D-78457, Germany

Bernal-stacked bilayer graphene (BLG) has a tunable gap controlled by an out-of-plane electric field. This makes BLG a possible candidate to form quantum dots (QDs) via quantum confinement. Spin-based qubits in BLG QDs have received great attention due to outstanding spin-coherence properties. Very recently, long spin relaxation times of a single-electron state in BLG QDs was reported [1,2]. In addition to spin, valley pseudospin is another degree of freedom in BLG. The two valleys experience opposite Berry curvatures and associated magnetic moments via an out-of-plane electric field. This provides a promising way to control valleys and further establish valley qubits. To assess the potential of valley qubits, the valley relaxation time is a crucial parameter since it directly limits the lifetime of encoded information. Here, we investigate the valley relaxation in a single-electron BLG QD due to intervalley coupling assisted by (i) $1/f$ charge noise and (ii) electron-phonon couplings arising from the deformation potential and bond-length change. Our calculation shows that valley relaxation time decreases with a power law dependence as a function of magnetic field, which is in a good agreement with very recent experiment.

References: [1] L. Banszerus, K. Hecker, S. Möller, E. Icking, K. Watanabe, T. Taniguchi, C. Volk and C. Stampfer, *Nat. Commun.* 13, 3637 (2022). [2] Lisa Maria Gächter et al., *PRX Quantum* 3, 020343 (2022).

30 min. break

TT 15: Quantum Transport and Quantum Hall Effects I (joint session HL/TT)

Time: Monday 15:00–17:15

Location: POT 251

TT 15.1 Mon 15:00 POT 251
Local Chern patches and networks of chiral modes in quantum Hall phases with spatial magnetic field profiles. — •SURAJ HEGDE and TOBIAS MENG — Institute of Theoretical Physics and Würzburg-Dresden Cluster of Excellence ct.qmat, Technische Universität Dresden, 01069 Dresden, Germany.

Transport experiments on curved Hall bars show a variety of non-trivial transport signatures. Motivated by these experiments, we develop a model that accounts for various features in multi-terminal Hall bar measurements and perform numerical simulations using KWANT. We model the effect of curvature of the sample through spatial variation of the magnetic field profile and find that it results in patches of quantum Hall phases characterised by different local Chern markers. We find that most of the transverse and longitudinal transport can be understood in terms of local Chern patches and an intricate interplay of chiral modes at the interface of different patches. We also show that the spatial magnetic field textures could provide a novel platform to engineer lattices formed by networks of chiral modes.

TT 15.2 Mon 15:15 POT 251
Effect of the external fields in high Chern number quantum anomalous Hall insulators — •YURIKO BABA^{1,2}, FRANCISCO DOMÍNGUEZ-ADAME¹, and RAFAEL A. MOLINA-FERÁNDEZ² — ¹GISC, Departamento de Física de Materiales, Universidad Complutense, E-28040 Madrid, Spain — ²Instituto de Estructura de la Materia, IEM-CSIC, E-28006 Madrid, Spain
Multilayer structures consisting of alternating magnetic and undoped topologi-

Invited Talk TT 14.4 Mon 16:45 POT 361
Single-shot spin and valley Pauli blockade read-out in bilayer graphene quantum dots — •CHUYAO TONG¹, REBEKKA GARREIS¹, WISTER WEI HUANG¹, ANNIKA KURZMANN^{1,2}, JOCELYN TERLE¹, SAMUEL JELE¹, KENJI WATANABE³, TAKASHI TANIGUCHI³, THOMAS IHN¹, and KLAUS ENSSLIN¹ — ¹ETH Zurich, CH-8093 Zurich, Switzerland — ²RWTH Aachen University, Aachen, 52074, Germany — ³National Institute for Materials Science, 1-1 Namiki, Tsukuba 305-0044, Japan

In bilayer graphene quantum dots, apart from spins up and down, the additional valley degree of freedom K- and K+ gives rise to an unconventional single-dot two-carrier ground state: spin-triplet valley-singlet, altering the canonical even-odd double dot Pauli spin blockade picture. This ground state can be switched to a spin-singlet valley-triplet by a perpendicular magnetic field, allowing us to switch between valley-blockade at low, and spin-blockade at higher magnetic field for the two-carrier Pauli blockade (1,1) to (0,2). We employ charge sensing technology and perform single-shot Pauli blockade read-out at the two field regimes, probing characteristic relaxation times T1 between spin or valley -triplet and -singlet. The spin-T1 is measured to be up to 60ms, drastically decreasing with increasing inter-dot tunnel coupling and corroborating with recent experiments performed with single-dot Elzerman read-out. Moreover, we observe exceedingly long valley T1 longer than 500ms, robust with inter-dot tunnel coupling. These promisingly long spin- and valley T1 herald for long-living spin and valley bilayer graphene quantum dot qubits.

Invited Talk TT 14.5 Mon 17:15 POT 361
Particle-hole symmetry protects spin-valley blockade in graphene quantum dots — •CHRISTIAN VOLK^{1,2}, LUCA BANSZERUS^{1,2}, SAMUEL MÖLLER^{1,2}, KATRIN HECKER^{1,2}, EIKE ICKING^{1,2}, KENJI WATANABE³, TAKASHI TANIGUCHI⁴, FABIAN HASSLER⁵, and CHRISTOPH STAMPFER^{1,2} — ¹JARA-FIT and 2nd Institute of Physics, RWTH Aachen University — ²Peter Grünberg Institute (PGI-9), Forschungszentrum Jülich — ³Research Center for Functional Materials, NIMS, Tsukuba, Japan — ⁴International Center for Materials Nanoarchitectonics, NIMS, Tsukuba, Japan — ⁵JARA-Institute for Quantum Information, RWTH Aachen University

Particle-hole symmetry plays an important role for the characterization of topological phases in solid-state systems. Graphene is a prime example of a gapless particle-hole symmetric system. The intrinsic Kane-Mele spin-orbit coupling in graphene leads to a lifting of the spin-valley degeneracy and renders graphene a topological insulator in a quantum spin-Hall phase while preserving particle-hole symmetry.

Here, we show that the Kane-Mele spin-orbit gap leads to a lifting of the spin-valley degeneracy in bilayer graphene quantum dots, resulting in Kramer's doublets with different ordering for electron and hole states preserving particle-hole symmetry. We observe the creation of single electron-hole pairs with opposite quantum numbers and use the electron-hole symmetry to achieve a protected spin-valley blockade in electron-hole double quantum dots. The latter will allow spin-to-charge and valley-to-charge conversion, which is essential for the operation of spin and valley qubits.

cal insulator layers have been proved so far to be a convenient platform for creating a quantum Anomalous Hall state with a high Chern number [1]. However, in previous proposals, the Chern number can only be tuned by varying the doping concentration or the width of the magnetic topological insulator TI layers. This restricts the applications of the dissipationless chiral edge currents in electronics, since the number of conducting channels remains fixed. In this work, we propose a way of varying the Chern number at will by means of an external electric field applied along the stacking direction. The electric field generates the hybridization of the inverted bands, generating new topological channels. In this way, the number of Chern states can be tuned externally in the sample, without the need of modifying the number and width of the layers or the doping level. We showed that this effect can be uncovered by the variation of the transverse conductance as a function of the electric field at constant injection energy at the Fermi level. [2]

[1] Zhao, Y. F. et al., *Nature*, 588 (2020) 419

[2] arXiv:2208.03585

TT 15.3 Mon 15:30 POT 251
Novel thermo-electric transport channel in the conformal limit of tilted Weyl semimetals — THORVALD BALLESTAD¹, ALBERTO CORTIJO², MARIA VOZMEDIANO³, and •ALIREZA QAIUMZADEH¹ — ¹Center for Quantum Spintronics, Norwegian University of Science and Technology, Trondheim, Norway — ²Universidad Autonoma de Madrid, Madrid, Spain — ³Instituto de Ciencia de Materiales de Madrid, CSIC, Madrid, Spain

Recently, a new contribution to the Nernst current was proposed in 3D Dirac and Weyl semimetals, originated from quantum conformal anomaly [1,2]. In the present study, we analyze the effect of the tilt on the transverse thermo-electric coefficient of Weyl semimetals in the conformal limit, i.e., zero temperature and zero chemical potential. Using the Kubo formalism, we find a non-monotonic behavior of the thermoelectric conductivity as a function of the tilt perpendicular to the magnetic field, and a linear behavior when the tilt is aligned to the magnetic field. An "axial Nernst" current is generated in inversion symmetric materials when the tilt vector has a projection in the direction of the magnetic field. This analysis will help in the design and interpretation of thermo-electric transport experiments in recently discovered topological quantum materials [3].

[1] M. N. Chernodub et al, Phys. Rev. Lett. 120, 206601 (2018). [2] V. Arjona et al, Phys. Rev. B 99, 235123 (2019). [3] T. M. Ballestad, A. Cortijo, M. A. H. Vozmediano, A. Qaiumzadeh, arXiv:2209.14331 (2022).

TT 15.4 Mon 15:45 POT 251

Selective scattering between counter-propagating edge states in a topological insulator — •MENG HAO^{1,2}, LI-XIAN WANG^{1,2}, FABIAN SCHMITT^{1,2}, HARTMUT BUHMANN^{1,2}, and LAURENS W. MOLENKAMP^{1,2} — ¹Institute for Topological Insulators, Würzburg, Germany — ²Physikalisches Institut (EP III) Würzburg University, Würzburg, Germany

The quantum Hall state, known by its dissipationless nature, comprises chiral edge states in a two-dimensional electron gas (2DEG). In the ordinary quantum Hall effect, all edge states propagate in the same direction, populated equally. Thus, they are immune to inter-edge-state scattering. In contrast, counter-propagating edge states, populated unequally, are naturally sensitive to the scattering process. However, a realization of this scenario so far was only possible by stacked layers of high-mobility 2DEGs, e.g., quantum wells or graphene. Here we realize the counter-propagating edge states in a three-dimensional topological insulator controlled by top and bottom gates. Surprisingly, the counter-propagating edge states prove to scatter into each other selectively. Our first attempt shows that this inter-edge-state scattering occurs exclusively between Landau levels with the same Landau index. We further propose a cross bar equipped with split-gates to determine the selection rule of scattering and scattering parameters unambiguously. Following this proposal, we will show some preliminary results and report our experimental advances.

30 min. break

TT 15.5 Mon 16:30 POT 251

Edge modes, Hall conductivity and topological features of a dice lattice: Fate of flat bands under strain — •SAYAN MONDAL and SAURABH BASU — Indian Institute of Technology Guwahati

We study the topological properties of a dice lattice, which has three atoms per unit cell (A, B, and C). In addition, the bands are systematically deformed via the introduction of anisotropy among the nearest neighbour (NN) hoppings in two distinct ways. In the first case, we apply the uniaxial strain, which alters the NN hoppings (between the sublattices A-B and B-C) along the direction of applied strain. While in the second case, we selectively tune the NN hopping between A and B sublattices which may be achieved by a controlled chemical pressure. The first case yields the Chern insulating lobes in the phase diagram with $C = \pm 2$ till a certain critical anisotropy, where the spectral gap vanishes. The quantized plateau in the anomalous Hall conductivity and the pair of chiral

edge modes at each edge of a ribbon support the obtained values of the Chern numbers. Whereas, the second case (selective strain) shows distorted flat band in the dispersion spectrum, which alters the gap-closing condition as compared to the case of uniaxial strain. Also, the Chern insulating lobes in the phase diagram and the Hall conductivity have distinct features compared to the case above. However, in both cases, topological phase transitions take place which is demonstrated via the Chern number changing discontinuously from ± 2 to zero across the gap-closing transitions.

TT 15.6 Mon 16:45 POT 251

Structure-imposed electronic topology in graphene nanoribbons — •FLORIAN ARNOLD¹, TSAI-JUNG LIU¹, AGNIESZKA KUC², and THOMAS HEINE^{1,2,3} — ¹Technische Universität Dresden, Dresden, Germany — ²HZDR, Leipzig, Germany — ³Yonsei University, Seoul, Republic of Korea

Zigzag graphene nanoribbons (ZGNR) can be transformed into new structure types by removing terminal carbon atoms in a regular pattern. When a single atom is removed on each zigzag edge so-called cove-edged ZGNR (ZGNR-C) are created, while removing multiple atoms results in gulf-edged ZGNR (ZGNR-G). In our seminal work, we demonstrated the direct structure-electronic structure relation based on the structural parameters that unambiguously characterize ZGNR-C. This allowed to create a scheme that classifies their electronic state, i.e., if they are metallic, topological insulators or trivial semiconductors, and to find an empirical formula for the band gap of the semiconducting ribbons. Since then, we were able to expand this description to ZGNR-G systems where the chemical space of possible structures increases further due to the variable size of the gulf edges. With this, we give guidance to realize new graphene nanoribbon heterojunctions hosting topological states and investigate the transport properties of exemplary systems.

TT 15.7 Mon 17:00 POT 251

Massive and topological surface states in strained HgTe and evidence for parity anomaly — •WOUTER BEUGELING^{1,2}, LIXIAN WANG^{1,2}, DAVID M. MAHLER^{1,2}, VALENTIN L. MÜLLER^{1,2}, EWELINA M. HANKIEWICZ³, HARTMUT BUHMANN^{1,2}, and LAURENS W. MOLENKAMP^{1,2} — ¹Institute for Topological Insulators, Würzburg, Germany — ²Physikalisches Institut (EP III), Würzburg University, Würzburg, Germany — ³Institute for Theoretical Physics and Astrophysics (TP IV), Würzburg University, Würzburg, Germany

The idea that band inversion in a narrow-gap material can lead to Dirac-type surface states was noted by Volkov and Pankratov in the 1980's. Only about two decades later, it was realized that the surface states of topological insulators are the gapless Dirac states predicted by them. The massive Volkov-Pankratov states received much less attention. They are pulled from the bulk in a sufficiently large electric field and are topologically trivial. Until recently, direct evidence in the form of transport measurements was elusive.

From our magneto-transport experiments on a three-dimensional topological insulator heterostructure (strained HgTe), we demonstrate the coexistence of massless and massive Volkov-Pankratov states. The well-developed Hall quantization in the n- and the p-type regime is due to the topological surface state and the massive Volkov-Pankratov states, respectively, as confirmed by k-p theory. In a second series of experiments, we find a remarkable re-entrant quantum Hall effect in the p-type regime, which we can trace to spectral asymmetry, a salient manifestation of parity anomaly in a solid-state system.

TT 16: Poster: Transport

Time: Monday 15:00–18:00

Location: P2/OG4

TT 16.1 Mon 15:00 P2/OG4

Asymmetric and spatially resolved power dissipation in quantum transport — •NICO LEUMER — Université de Strasbourg, CNRS, IPCMS, UMR 7504, F-67000 Strasbourg, France

Dissipation is a natural byproduct of quantum transport caused by various inelastic scattering events of electrons and their lost energy stimulates in turn the temperature profile of the underlying bulk material. Importantly though, electronic current may run only through a narrow part of the sample as, for instance, happens in the quantum Hall regime of graphene due to chiral edge channels (1); thus, dissipation has to be seen as a local quantity. The still rather recent invention of the Squid-on-tip technique in 2016 (2), paved the way to experimental access this challenge, where the temperature increases by merely a few hundred micro Kelvin on length scales of the order of nanometers.

Quantum point contacts (QPC's) are of particular interest in nanoscale transport, as electrons experience now a -perhaps energy dependent- transmission probability. On a hand waving level, QPC's increase the resistance electrons face from the sample locally, which is accompanied by areas of higher dissipation. In our recent project, we predict where and how much power is dissipated.

[1] A. Marguerite et al., Nature 575, 628 (2019)

[2] D. Halbertal et al., Nature 539, 407 (2016)

TT 16.2 Mon 15:00 P2/OG4

Resistive switching and peculiarities of conductivity of TiTe₂ point contacts — •OKSANA KVITNITSKAYA¹, LUMINITA HARNAGEA², DMITRI EFREMOV³, BERND BÜCHNER^{3,4}, and YURI N. NAIDYUK¹ — ¹B.Verkin Institute for Low Temperature Physics and Engineering, NASU, Kharkiv, Ukraine — ²Dep. of Physics, Indian Institute of Science Education and Research, Pune, Maharashtra, India — ³Institute for Solid State Research, IFW Dresden, Dresden, Germany — ⁴Institut für Festkörper- und Materialphysik und Würzburg-Dresden Cluster of Excellence ct.qmat, TU Dresden, Dresden, Germany

Ti-based dichalcogenides TiX₂ (X = S, Se, Te), display a variety of physical properties, depending on their lattice distortions, native defects, self-doping effects, intercalation, external pressure. They can exhibit semiconducting, semimetallic, CDW, and superconducting behavior, which together with their layered structure and unique properties upon exfoliation to monolayer limit, make them particularly interesting. Recently, we observed the resistive switching effect in TiTe₂ point-contacts (PCs). We attributed the effect to Se vacancy drift due to a high electric field in the PC core. Here we report the resistive switching in PCs with isoelectronic TiTe₂, where the ratio of the high resistance state to the low resistance state was so far up to several times, contrary to up to two orders of magnitude for TiSe₂. Additionally, we observed "camel-like" $dV/dI(V)$ spec-

tra of TiTe_2 at helium temperature with two symmetric $v_s V=0$ humps around $\pm(200-300)$ mV, which vanished near 200 K.

TT 16.3 Mon 15:00 P2/OG4

Nonmonotonous Temperature Dependence of the Thermopower of Gold Atomic Contacts — THOMAS MÖLLER¹, MARCEL STROHMEIER¹, RUBEN ZERFASS¹, KIM NIKOLAI KIRCHBERGER¹, DANIAL MAJIDI², JUAN CARLOS CUEVAS³, JOHANNES BONEBERG¹, PAUL LEIDERER¹, WOLFGANG BELZIG¹, and ELKE SCHEER¹ — ¹University of Konstanz, 78457 Konstanz, Germany — ²Université Grenoble Alpes, CNRS, Grenoble INP, Institut Néel, 38042 Grenoble, France — ³Universidad Autónoma de Madrid, E-28049 Madrid, Spain

We present measurements of the thermopower of atomic-size gold contacts realized by the mechanically controllable break junction (MCBJ) technique over a temperature range from 10 K to 295 K. While the conductance histograms confirm the quantum nature of the transport, we observe a non-monotonous temperature dependence of the ensemble-averaged thermopower (taking into account contacts between 1 and $20 G_0 = 2e^2/h$) with a minimum of $-2 \mu\text{V/K}$ at about 150 K. Our observations at low and high temperature are compatible with values reported in the literature [1-5], but the non-monotonous behavior in between disagrees with the expected linear increase of the thermopower for quantum coherent conductors described by the Landauer formula. We discuss several possible mechanisms, that may be at the origin of the deviation, such as phonon contributions or an energy-dependent transmission function. Both aspects can be addressed experimentally by analyzing current-voltage characteristics. We present here results obtained for Au and for Cu atomic contacts.

TT 16.4 Mon 15:00 P2/OG4

Analyzing vibrational instabilities arising from non-conservative current-induced forces in nanosystems with a semi-classical approach — ROBIN L. GREYER, SAMUEL RUDGE, and MICHAEL THOSS — Physikalisches Institut, Albert-Ludwigs-Universität Freiburg, Deutschland

Understanding the electric properties of nanosystems such as molecular junctions is a crucial task for modern physics. For molecular junctions, these properties are often governed by an electronic-vibrational coupling, which can lead to an instability of the junction in some cases.

We provide an in-depth analysis of the vibrational instabilities caused by non-conservative current-induced forces in a molecular junction using a semi-classical approach that exploits the time-scale separation between the fast electronic dynamics and the much slower vibrational dynamics. In particular, we use a Born-Markov master equation for the electronic degrees of freedom in combination with a semi-classical Langevin equation for the vibrational dynamics [1]. Within this framework, we study the dynamics of a junction composed of two electronic levels and two harmonic vibrational modes [2] for various parameters.

- [1] W. Dou *et al.*, J. Chem. Phys. **145**, 054102 (2016)
[2] J.-T. Lü *et al.*, Phys. Rev. B **85**, 245444 (2012)

TT 16.5 Mon 15:00 P2/OG4

Full counting statistics of electron transport through periodically driven quantum dots analysed with factorial cumulants — JOHANN ZÖLLNER, ERIC KLEINHERBERS, and JÜRGEN KÖNIG — Theoretische Physik, Universität Duisburg-Essen, Lotharstr. 1, 47048 Duisburg

The electron transport through quantum dots is a stochastic process. Factorial cumulants of full counting statistics can be used to analyse current and current fluctuations of electrons [1]. We present methods to calculate factorial cumulants for periodically driven systems. This makes it possible to investigate effects in which a periodic drive and noise both take part. An example for such an effect is stochastic resonance, which has already been observed in quantum dots [2]. We will explain the meaning of factorial cumulants for stochastic resonance.

- [1] P. Stegmann, B. Sothmann, A. Hucht, J. König, Phys. Rev. B **92**, 155413 (2015)
[2] T. Wagner, P. Talkner, J. C. Bayer, E. P. Rugeramigabo, P. Hänggi, R. J. Haug, Nat. Phys. **15**, 330(2019)

TT 16.6 Mon 15:00 P2/OG4

Rational design of halide perovskite-based quantum dots using ab-initio many body techniques — MANASWITA KAR, BENJAMIN LENZ, and MICHELE CASULA — IMPMC, Sorbonne Université-CNRS, Jussieu, 75005 Paris, France
Quantum dots (QDs) have attracted increasing attention as next generation functional materials, because of their unique size dependent colour tunability, due to quantum-confinement effect. However, the cost of production of these QDs is very high, thereby limiting their large scale industrial applications. Halide perovskite-based QDs provide single photon emission at room temperature and can be manufactured comparatively easily. These perovskites have a complex structural form and bears a large compositional space. As a result of this, only a limited number of these perovskite QDs have been tested so far. Here, we aim to identify the most promising perovskite based QDs for coherent photon emission applications by characterising their optical properties from theoretical simulations. Towards this aim, we employ the many body Green's function (GW) and Bethe-Salpeter equation (BSE) techniques to study the excited state properties of the QDs, which are known to be not well captured by standard ground state methods, such as Density Functional Theory (DFT). From this study, we finally

envision find the best halide perovskite based quantum dot, that is both structurally and thermodynamically stable and can be manufactured for large scale commercial applications.

TT 16.7 Mon 15:00 P2/OG4

Device and contact engineering of MoS_2 nanotubes and nanoribbons — KONSTANTIN D. SCHNEIDER¹, ROBIN T. K. SCHOCK¹, JONATHAN NEUWALD¹, MATTHIAS KRONSEDER¹, LUKA PIRKER², MAJA REMŠKAR², and ANDREAS K. HÜTTEL¹ — ¹Institute for Experimental and Applied Physics, University of Regensburg, 93040 Regensburg, Germany — ²Solid State Physics Department, Institute Jožef Stefan, 1000 Ljubljana, Slovenia

Even though low-temperature transport measurements of a MoS_2 nanotube have already demonstrated Coulomb blockade at 300 mK,¹ Fermi level pinning near the conduction band at the metal- MoS_2 interface requires reactive low-work function metals, which then damage the MoS_2 . Recently, bismuth² was shown to drastically reduce contact resistances in planar MoS_2 .

Here, we present millikelvin transport measurements on MoS_2 nanotubes and nanoribbons with bismuth contacts.³ Our nanotubes are grown via a chemical transport reaction, yielding diameters down to 7 nm and lengths up to several millimeters. Nanotubes were either suspended or placed on hexagonal boron nitride (hBN) in order to reduce disorder from the SiO_2 substrate. The resulting devices show Coulomb blockade, with a rich set of features. Contacts are transparent, and the temperature dependence hints at single level transport.

- [1] S. Reinhardt *et al.*, Phys. Stat. Sol. RRL **13**, 1900251 (2019)
[2] P. C. Shen *et al.*, Nature **593**, 211 (2021)
[3] R. T. K. Schock *et al.* arXiv:2209.15515

TT 16.8 Mon 15:00 P2/OG4

Weak localization in semiconductor heterostructures with strong spin orbit interaction — SIMON FEYERER, JAYDEAN SCHMIDT, MICHAEL PRAGER, DOMINIQUE BOUGEARD, and CHRISTOPH STRUNK — Institute of Experimental and Applied Physics, University of Regensburg, Germany

We present measurements of weak localization (WL) and weak anti-localization (WAL) performed on quasi-1D wires patterned into an InAs based quantum well. Due to the confinement of the electrons along the wires, the D'yakonov-Perel spin relaxation is expected to be suppressed resulting in WL instead of WAL. As consequence of the spin orbit interaction anisotropy, the amplitude of the WL is sensitive to the direction of an applied in-plane magnetic field and provides an estimate of the ratio between the Rashba and Dresselhaus spin orbit coefficient [1,2].

By fitting the measured WAL and WL-curves, the highest spin relaxation rate was extracted for the wires orientated along the [011] crystal axis. A clear suppression of spin relaxation was observed along the [001] wire direction.

- [1] T. Nishimura *et al.*, Phys. Rev. B **103**, 094412 (2021)
[2] A. Sasaki *et al.*, Nat. Nanotechnol. **9**, 703 (2014)

TT 16.9 Mon 15:00 P2/OG4

Revealing the role of Klein tunneling in Aharanov-Bohm graphene rings — CHING-HUNG CHIU and MING-HAO LIU — Department of Physics, National Cheng Kung University, Tainan City, Taiwan

Graphene, the ideal testbed of relativistic quantum mechanics, have been widely used to explore not only the exotic transport properties of Dirac fermions but also to confirm classic quantum-mechanical phenomena such as the Aharanov-Bohm effect. Motivated by a recent experiment [1], here we perform quantum transport simulations in the ballistic limit at zero temperature, considering an Aharanov-Bohm ring made of graphene with the same sample and gate geometry as the experiment. Preliminary properties from our simulations such as the gate and magnetic field dependence of the two-terminal conductance are rather consistent with the experiment, confirming their claim of the observed Aharanov-Bohm effect. To probe the effect of Klein tunneling, however, we propose a modified design using a local gate that makes pn interfaces perpendicular to the arm of the ring, different from the experiment. Based on our new design, we show that Klein tunneling may sharpen the Aharanov-Bohm oscillation frequency due to the screening of the transverse modes.

- [1] J. Dauber *et al.*, arXiv:2008.02556v3

TT 16.10 Mon 15:00 P2/OG4

Transport properties of pn junctions in 2D materials: Graphene vs MoS_2 — YU-TING XIAO and MING-HAO LIU — Department of Physics, National Cheng Kung University, Tainan 70101, Taiwan

Graphene and monolayer MoS_2 both belong to the family of 2D materials. The former is known as a Dirac semimetal where electrons behave like relativistic Dirac fermions due to the gapless energy band linear in momentum, while the latter shows typical semiconducting behaviors due to the gapped energy band quadratic in momentum, with which electrons behave as standard Schrödinger fermions. In terms of transport, Dirac and Schrödinger electrons exhibit distinct behaviors, among which the so-called Klein tunneling [1] is perhaps one of the best known. To further identify their difference in transport properties, here we perform quantum transport simulations for pn junctions in various 2D systems, including graphene, MoS_2 , and other toy models for 2D semiconductors. Our

results identify transport properties that are unique to Dirac fermions as well as those that do not significantly differ from the two.

[1] M. Katsnelson, K. Novoselov, and A. Geim, *Nat. Phys.* 2, 620 (2006)

TT 16.11 Mon 15:00 P2/OG4

Quantum transport simulation for graphene devices with sawtooth-shaped n-p-n junctions — •ZHE-BIN HSU and MING-HAO LIU — Department of Physics, National Cheng Kung University, Tainan 70101, Taiwan

Graphene, a gapless two-dimensional semimetal made of carbon atoms arranged in a honeycomb lattice, is an ideal platform for studying electron optics both experimentally and theoretically. Because of its lack of energy gap, n- and p-type carriers in graphene can be easily tuned simply by electrical gating. Typical graphene n-p-n junctions are created by local gates of rectangular shapes that exhibit Fabry-Pérot interference of electron waves in the clean limit. A recent experiment [1] realized a Dirac fermion reflector of graphene using sawtooth-shaped npn junctions, reporting not only the suppressed Fabry-Pérot interference but also resistance enhancement. Motivated by this experiment, we perform quantum transport simulations for graphene considering similar gate and sample geometries. Good consistency between our simulation and the experiment [1] will be shown. Further tests on other shaped top gates are performed in order to find the optimal gate geometry for best enhanced resistance. Our work shows that sawtooth-shaped graphene n-p-n junctions cannot work as a field-effect transistor (FET), even though the transmission can be reduced by a certain amount.

[1] S. Morikawa et al., *Semicond. Sci. Technol.* 32, 045010 (2017)

TT 16.12 Mon 15:00 P2/OG4

Electron correlation and confinement effects in quasi-one-dimensional quantum wires at high-density — ANKUSH GIRDHAR¹, VINOD ASHOKAN¹, NEIL DRUMMOND², •KLAUS MORAWETZ^{3,4}, and KARE NARAIN PATHAK⁵ — ¹Department of Physics, Dr. B.R. Ambedkar National Institute of Technology, Jalandhar (Punjab), 144 011, India — ²Department of Physics, Lancaster University, Lancaster LA1 4YB, United Kingdom — ³Münster University of Applied Sciences, Stegerwaldstrasse 39, 48565 Steinfurt, Germany — ⁴International Institute of Physics- UFRN, Campus Universitário Lagoa nova, 59078-970 Natal, Brazil — ⁵Centre for Advanced Study in Physics, Panjab University, 160014 Chandigarh, India

The correlation energy, pair-correlation function, static structure factor, and momentum density of ferromagnetic quasi-one-dimensional quantum wires are calculated using the quantum Monte Carlo (QMC) method for various wire widths b and density parameters r_s . The peak in the static structure factor at $k = 2k_F$ grows as the wire width decreases. The Tomonaga-Luttinger liquid parameter K_ρ is found to increase by about 10% between wire widths $b = 0.01$ and $b = 0.5$. The ground-state properties of finite thickness wires is compared to the first-order random phase approximation (RPA), which is exact in the high-density limit. Analytical expressions for the static structure factor and correlation energy are derived.

[1] *Eur. Phys. J. B* 91 (2018) 29

[2] *Phys. Rev. B* 97 (2018) 155147

[3] *Phys. Rev. B* 101 (2020) 075130

[4] *Phys. Rev. B* 104 (2021) 035149

[5] *Phys. Rev. B* 105 (2022) 115140

TT 16.13 Mon 15:00 P2/OG4

Ground state properties of electron-electron biwire systems — RAJESH O. SHARMA¹, NEIL DRUMMOND², VINOD ASHOKAN¹, KARE NARAIN PATHAK³, and •KLAUS MORAWETZ^{4,5} — ¹Department of Physics, Dr. B.R. Ambedkar National Institute of Technology, Jalandhar (Punjab), 144 011, India — ²Department of Physics, Lancaster University, Lancaster LA1 4YB, United Kingdom — ³Centre for Advanced Study in Physics, Panjab University, 160014 Chandigarh, India — ⁴Münster University of Applied Sciences, Stegerwaldstrasse 39, 48565 Steinfurt, Germany — ⁵International Institute of Physics- UFRN, Campus Universitário Lagoa nova, 59078-970 Natal, Brazil

Variational Monte Carlo (VMC) method is used to study the ground-state properties of a parallel infinitely-thin electron-electron quantum biwire system. The ground-state energy, the correlation energy, the interaction energy, the pair-correlation function (PCF), the static structure factor (SSF), and the momentum distribution (MD) function is calculated. As two parallel wires approach each other, inter-wire correlations increase while intra-wire correlations decrease. The SSF shows a peak at $2k_F$ at higher densities. A second peak starts to appear at $4k_F$ when $r_s = 2$ and $d = 0.2$ a.u. For lower densities, the first peak completely disappears and the height of the second peak keeps increasing with r_s and d . The behaviour of the PCF and SSF show that the electron-electron biwire system under goes into a quasi-Wigner crystalline state at densities higher compared to the case of a single wire.

[1] *Eur. Phys. J. B* 91 (2018) 29

[2] *Phys. Rev. B* 97 (2018) 155147

[3] *Phys. Rev. B* 101 (2020) 075130

[4] *Phys. Rev. B* 104 (2021) 035149

TT 16.14 Mon 15:00 P2/OG4

Integrating coplanar resonators and carbon nanotubes for microwave optomechanics — AKONG LOH, FABIAN STADLER, •FURKAN ÖZYGIT, NICOLE KELLNER, NIKLAS HÜTTNER, and ANDREAS K. HÜTTEL — Institute for Experimental and Applied Physics, University of Regensburg, 93040 Regensburg, Germany

The optomechanical coupling of a carbon nanotube and a superconducting coplanar microwave resonator has been achieved [1,2] in our previous work. The carbon nanotube acts as a quantum dot, responding to gate voltages in a highly nonlinear way. This can be used to enhance the optomechanical coupling strength by several orders of magnitude. Recent work has focused on improving the electronic properties of the microwave resonators, to maximize quality factors in presence of the nanotube coupling electrodes. Currently, we redevelop insertion of carbon nanotubes as the mechanical counterpart. Here, we give an overview of recent improvements and ongoing measurements on this fascinating optomechanical system: at proper optimization, it can have figures of merit close to several interesting parameter regimes, as, e.g., strong optomechanical coupling (with hybridization of vibrons and photons) and the quantum coherent limit (where manipulation is faster than thermal decoherence).

[1] S. Blien *et al.*, *Nat. Comm.* 11, 1636 (2020)

[2] N. Hüttner *et al.*, in preparation.

TT 16.15 Mon 15:00 P2/OG4

Description of defective graphene by means of the Dirac equation coupled to curvature and torsion — •ENKELETA BERISHA and NIKODEM SZPAK — Fakultät für Physik, Universität Duisburg-Essen, Duisburg, Germany

The continuum theory of lattice defects (dislocations and disclinations) offers a practical description of the electron transport at the mesoscale at which the microscopic (ab initio) models become too complex. It can be linked to the geometrical concepts of curvature and torsion within the Riemann-Cartan geometry. In General Relativity there is an ongoing discussion about the equivalence of these two objects. In solid state physics both objects have concrete interpretations in terms of disclinations and dislocations. The application to a two-dimensional system can shed new light on this problem. We focus on graphene whose electron dynamics is described by the Dirac equation which exhibits such defects. This leads to the coupling of the effective Dirac equation to curvature and torsion, thus opening the possibility of mapping these objects onto each other. We study particular lattice configurations and interpret them in terms of curvature or torsion. Moreover, we compare the quantum current flows with the semiclassical trajectories in the effective Riemann-Cartan geometry.

TT 16.16 Mon 15:00 P2/OG4

Strain-induced pseudo-Landau levels in semimetals from dimensional reduction — •FABIAN KÖHLER and MATTHIAS VOJTA — Würzburg-Dresden Cluster of Excellence ct.qmat, Technische Universität Dresden, Germany

Non-uniform strain applied to graphene's honeycomb lattice can induce pseudo-Landau levels in the single-particle spectrum. We generalize this procedure to d-dimensional hyperdiamond-lattices and solve the corresponding continuum theory. The unstrained tight-binding Hamiltonian has semimetallic bandstructure with a (d-2)-dimensional nodal manifold, which transforms into a series of relativistic Landau levels under suitable strain. We show that a mechanism of dimensional reduction is at play here that goes beyond the conventional minimal coupling framework. This mechanism generates two-dimensional Landau-level problems with identical level spacing at each point of the nodal manifold.

TT 16.17 Mon 15:00 P2/OG4

Semi-classical vibrational dynamics in molecular junctions: Anharmonic potentials and non-linear couplings — •MARTIN MÄCK, SAMUEL RUDGE, and MICHAEL THOSS — Physikalisches Institut, Universität Freiburg

Non-conservative current-induced forces can lead to vibrational instabilities in molecular junctions, even at low bias voltages [1]. A common approach is to treat the vibrational dynamics semi-classically as influenced by quantum mechanical electronic degrees of freedom. Within these treatments, the vibrational modes are often assumed to be harmonic and linearly coupled to the electronic degrees of freedom. However, at the onset of vibrational instabilities, such harmonic potentials might no longer realistically describe the dynamics.

In this contribution, we use a recently developed hierarchical equations of motion (HEOM) approach [2] to semi-classical Langevin dynamics [3] to study systems for which the introduction of anharmonic potentials and non-linear electron-vibrational coupling might play an important role for the vibrational dynamics of the system.

[1] J.T. Lü, M. Brandbyge, and P. Hedegård, *Nano Lett.* 2010, 10, 5, 1657

[2] C. Schinabeck, A. Erpenbeck, R. Härtle, and M. Thoss, *Phys. Rev. B* 94, 201407

[3] S. L. Rudge, Y. Ke, and M. Thoss, arXiv: 2211.14215

TT 16.18 Mon 15:00 P2/OG4

Solving non-interacting open bosonic systems — •STEVEN KIM and FABIAN HASSLER — JARA Institute for Quantum Information, RWTH Aachen University

Open quantum systems that interact with their Markovian environment are described by a Lindblad master equation. We study non-interacting bosonic systems that are subject to single photon loss. The corresponding Liouvillian superoperator is at most of quadratic order in ladder operators. An analysis of the eigenvalues can give insight into possible instabilities as well as phase transitions. Especially the latter has gained growing interest for PT-symmetric systems. The

difficulty in solving such systems for its eigenmodes lies in preserving the canonical commutation relation, which is why the standard way of diagonalization is not possible. In this work, we propose a new method to obtain the diagonalized form of any non-interacting bosonic system using symplectic transformations. We are able to diagonalize a general complex matrix, while maintaining the symplectic form that encodes the commutation relations of the bosonic ladder operators. We show that non-Hermitian Hamiltonians naturally appear while solving the Lindblad master equation and that the eigenmodes can be obtained by solving a reduced system. Including counting fields into the Lindbladian makes the efficient calculation of the cumulant generating functions of arbitrary observables possible.

TT 17: Topology: Quantum Hall Systems

Time: Monday 16:45–18:45

Location: HSZ 304

TT 17.1 Mon 16:45 HSZ 304

Quantum Hall effect in the 2d topological insulator HgTe in pulsed magnetic fields of up to 65 T — •CHRISTOPHER FUCHS^{1,2}, TOBIAS KIESSLING^{1,2}, SAQUIB SHAMIM^{1,2}, LENA FÜRST^{1,2}, HARTMUT BUHMANN^{1,2}, and LAURENS W. MOLENKAMP^{1,2} — ¹Physikalisches Institut, Universität Würzburg, Germany — ²Institute for Topological Insulators, Würzburg, Germany

HgTe quantum wells are a two-dimensional topological insulator with highest electron mobilities as large as $1 \cdot 10^6 \text{ cm}^2/\text{Vs}$. As a result of this outstanding sample quality, the material shows a well-resolved electron-type as well as hole-type quantum Hall effect, which has been studied extensively at lowest temperatures and in fields of up to 16 T. Here, we present an extension of this parameter space all the way to 65 T using pulsed magnetic fields. The high field behavior of the electron-type quantum Hall effect is studied, revealing that it forms a smooth continuation of the low field ($< 20 \text{ T}$) behavior. For example, a characteristic breakdown of the quantum Hall effect, which occurs at the filling factor $\nu = 1/2$, is observed at $> 50 \text{ T}$ for corresponding carrier densities. In addition, a general circuit, wiring and analysis scheme for measurements of the quantum Hall effect within a few milliseconds (a magnetic field pulse lasts only around 100 ms) is presented, along with design rules for gated samples. The presented method is universal and can be applied to any other gated semiconductor/2d sample for transport studies in pulsed magnetic fields.

TT 17.2 Mon 17:00 HSZ 304

Robustness of the topological quantization of the Hall conductivity for correlated lattice electrons at finite temperatures — ANTON MARKOV¹, •GEORG ROHRINGER², and ALEXEY RUBTSOV¹ — ¹Moscow, Russia — ²Institute of Theoretical Physics, University of Hamburg, 20355 Hamburg, Germany

Electrons on a two-dimensional lattice which is exposed to a strong uniform magnetic field show intriguing physical phenomena. The spectrum of such systems exhibits a complex (multi)band structure known as Hofstadter's butterfly. For fillings at which the system is a band insulator, one observes a quantized integer-valued Hall conductivity σ_{xy} corresponding to a topological invariant, the first Chern number C_1 . This is robust against many-body interactions as long as no changes in the gap structure occur. Strictly speaking, this stability holds only at zero temperatures T , while for $T > 0$ correlation effects have to be taken into account. In our paper, we address this question by presenting a dynamical mean-field theory (DMFT) study of the Hubbard model in a uniform magnetic field. The inclusion of local correlations at finite temperature leads to (i) a shrinking of the integer plateaus of σ_{xy} as a function of the chemical potential and (ii) eventually to a deviation from these integer values. We demonstrate that these effects can be related to a correlation-driven narrowing and filling of the band gap, respectively.

Invited Talk

TT 17.3 Mon 17:15 HSZ 304

Noise signatures of anyon statistics and Andreev scattering in the $\nu = 1/3$ fractional quantum Hall regime — •ANNE ANTHORE, PIERRE GLIDIC, OLIVIER MAILLET, COLIN PIQUARD, ABDEL AASSIME, and FRÉDÉRIC PIERRE — U Paris Cité, U Paris-Saclay, CNRS, C2N, Palaiseau (France)

Anyons are exotic quasiparticles which can carry a fractional charge of an electron and with an exchange statistics inbetween that of fermions and bosons. These properties were revealed using quantum point contacts (QPC) in the fractional quantum Hall regime[1,2].

In this talk, I will report further noise investigation of anyon physics. Sourcing $e/3$ anyons at a first QPC, noise measured on a downstream "analyzer" QPC reveals different mechanisms. Setting the analyser to allow $e/3$ tunneling charges, we reproduce the negative cross-correlations previously observed², indicative of a non-trivial anyon exchange phase[3]. When $1 e$ charges tunnel across the analyser, the braid phase is predicted to be trivial. Our observation of negative cross-correlations points on a scattering mechanism akin to Andreev reflection at Normal/Superconductor interfaces, as suggested in[4].

Remarkably, in both cases, electrical conduction across the analyzer conserves neither the nature nor the number of quasiparticles, rendering the beam-splitter analogy of a QPC lapsed.

[1] L. Saminadayar et al., PRL 79, 2526 (1997)

[2] H. Bartolomei et al., Science 368, 173 (2020)

[3] B. Rosenow et al., PRL 116, 156802 (2016)

[4] C. L. Kane and M. P. A. Fisher, PRB 67, 045307 (2003)

TT 17.4 Mon 17:45 HSZ 304

Topological properties of a two-dimensional non-symmorphic wallpaper group lattice — •MIGUEL ÁNGEL JIMÉNEZ HERRERA¹ and DARIO BERCIoux^{1,2} — ¹Donostia International Physics Center, 20018 San Sebastian, Spain — ²IKERBASQUE, Basque Foundation for Science, Euskadi Plaza, 5, 48009 Bilbao, Spain

We investigate the topological spectral properties of a two-dimensional electronic lattice belonging to a non-symmorphic wallpaper group: the herringbone lattice. We induce the topological phase either by applying an external magnetic field perpendicular to the plane of the lattice, and by enabling spin-orbit coupling of Kane-Mele type. On the one hand, when applying a magnetic field, the bands of the lattice rearrange into Landau levels. The phase diagram of the system shows a fractal disposition of the band gaps, known as the Hofstadter butterfly. Each gap is characterized by a non-zero Chern number whose distribution follows the Diophantine equation. On the other hand, we study the effects of enabling spin-orbit coupling in the lattice. We study both bulk and ribbon geometry, to reveal the helical states appearing at the edges of the ribbon, arising from the topological properties of the bulk.

TT 17.5 Mon 18:00 HSZ 304

Hofstadter butterflies in hyperbolic space — •ALEXANDER STEGMAIER¹, LAVI UPRETI⁴, RONNY THOMALE¹, and IGOR BOETTCHER^{2,3} — ¹Institut für Theoretische Physik und Astrophysik, Universität Würzburg, 97074 Würzburg, Germany — ²Department of Physics, University of Alberta, Edmonton, Alberta T6G 2E1, Canada — ³Theoretical Physics Institute, University of Alberta, Edmonton, Alberta T6G 2E1, Canada — ⁴Department of Physics, University of Konstanz, 78464 Konstanz, Germany

Hofstadter's Butterfly is the spectrum of a charged particle moving in a tight binding lattice under a constant magnetic field. Beyond its well-known fractal-shaped spectrum, this model is also relevant as a prototypical topological Chern insulator.

In light of recent interest in the physics of lattices in hyperbolic space, we reconsider the problem of Hofstadter's butterfly in $\{p,q\}$ lattices. They tile the hyperbolic plane, a 2D space with constant negative curvature, with regular p -gons, q of which meet at each vertex. We develop methods to calculate the bulk spectra of a hyperbolic tight-binding system and apply them to uncover the features of Hofstadter's Butterflies in hyperbolic space. We find that the move to negatively curved space destroys the spectra's fractality, but preserves features of the spectral gaps, depending on the type of tiling $\{p,q\}$.

TT 17.6 Mon 18:15 HSZ 304

Observation and applications of non-Hermitian topology in a multi-terminal quantum Hall device — •KYRYLO OCHKAN¹, VIKTOR KÖNYE¹, ANASTASIA CHYZHYKOVA^{1,2}, JAN BUDICH³, JEROEN VAN DEN BRINK¹, COSMA FULGA¹, and JOSEPH KYRYLO¹ — ¹IFW Dresden, Deutschland — ²Taras Shevchenko National University of Kyiv, Ukraine — ³TU Dresden, Deutschland

One of the simplest examples of non-Hermitian topology is encountered in the Hatano-Nelson (HN) model, a one-dimensional chain where the hopping in one direction is larger than in the opposite direction. We present here the first experimental observation of non-Hermitian topology in a quantum condensed-matter system. The measurements are done in a multi-terminal quantum Hall device etched in a high mobility GaAs/AlGaAs two-dimensional electron gas ring. The conductance matrix that connects the currents flowing from the active contacts

to the ground with the voltage of the active contacts is topologically equivalent to the HN Hamiltonian.

In our device, we directly measure and evidence the non-Hermitian skin effect. We also compute for our experimental device two topological invariants that are found to be more robust than the Chern number. We finally use the unique properties of our system and continuously tune the system configuration between open and periodic boundary conditions.

In this talk, we present the latest developments with regard to the application of the devices with these topological properties.

TT 17.7 Mon 18:30 HSZ 304

Dirac Landau levels on a pseudosphere — •MAXIMILIAN FÜRST¹, DENIS KOCHAN^{1,2}, COSIMO GORINI³, and KLAUS RICHTER¹ — ¹Universität Regensburg, 93053 Regensburg, Deutschland — ²Slovak Academy of Sciences, 84511 Bratislava, Slovakia — ³Université Paris-Saclay, 91191 Gif-sur-Yvette, France
Topological insulator nanowires host Dirac-like surface states with strongly suppressed backscattering [1]. As suggested in Ref. [2], surfaces with conical sin-

gularity could host Quantum Hall states which lead to an intrinsic angular momentum quantization of an electronic fluid which is put on the tip of the singularity. Topological insulators might be a good platform to examine this experimentally. However, they host surface states with Dirac-like dispersion instead of Schrödinger-like which is assumed in Ref. [2]. This raises the question if such effect may also be observed in those systems. A first step towards the answer is to choose an appropriate surface and calculate the Dirac Landau levels on it. We choose the pseudosphere which has a conical singularity and allows for analytical solution of the emerging eigenvalue equations. The spectrum and the eigenstates are computed for a constant magnetic field which is aligned perpendicularly to the surface. We further use the tight-binding package *Kwant* [3] to verify our analytically gained results numerically (see Ref. [4]).

[1] X.-L. Qi and S.-C. Zhang, *Rev. Mod. Phys.* **83**, 1057 (2011)

[2] T. Can *et al.*, *Phys. Rev. Lett.* **117**, 266803 (2016)

[3] C. W. Groth *et al.*, *New J. Phys.* **16**, 063065 (2014)

[4] R. Kozlovsky *et al.*, *Phys. Rev. Lett.* **124**, 126804 (2020)

TT 18: Nano- and Optomechanics

Time: Monday 17:15–18:30

Location: HSZ 201

TT 18.1 Mon 17:15 HSZ 201

Microwave optomechanics of the transversal carbon nanotube vibration — •AKONG LOH, FABIAN STADLER, FURKAN ÖZYIGIT, NICOLE KELLNER, NIKLAS HÜTTNER, and ANDREAS K. HÜTTEL — Institute for Experimental and Applied Physics, University of Regensburg, 93040 Regensburg, Germany

Recently, optomechanical coupling of a carbon nanotube and a coplanar microwave resonator has been achieved [1,2]. In this case, the nanotube acts as a mechanical resonator as well as a quantum dot. The coupling is enhanced by several order of magnitude by via the nonlinearity of Coulomb blockade. This novel optomechanical system presents several interesting features. For optimized parameters, e.g., strong optomechanical coupling (with hybridization of vibrons and photons) and the quantum coherent limit (where manipulation is faster than thermal decoherence) could be reached. Significant improvements of our microwave resonators have recently been achieved. Ongoing work aims to optimize the mechanical resonator, via improving the nanotube growth and the transfer of the nanotubes onto the resonator chip, as well as the cryogenic millikelvin setup for the measurements.

[1] S. Blien *et al.*, *Nat. Comm.* **11**, 1636 (2020)

[2] N. Hüttner *et al.*, in preparation.

TT 18.2 Mon 17:30 HSZ 201

Squeezed mechanical states in nano-electromechanical systems — •KORBINIAN RUBENBAUER^{1,2,3}, THOMAS LUSCHMANN^{1,2,3}, RÜDOLF GROSS^{1,2,3}, and HANS HUEBL^{1,2,3} — ¹Walther-Meißner-Institut, Bayerische Akademie der Wissenschaften, Garching, Germany — ²Technical University of Munich, TUM School of Natural Sciences, Physics Department, 85748 Garching, Germany — ³Munich Center for Quantum Science and Technologies, Munich, Germany

The generation of nonclassical quantum states in a mechanical system such as squeezed states is not only an essential milestone for quantum-enhanced sensing of ultra-small forces and accelerations, but will also enhance our understanding of the foundations of quantum theory. Optomechanical systems coupling a mechanical displacement to a microwave resonator represent one way to implement protocols resulting in squeezed mechanical states and their readout. Here, we experimentally explore a scheme for the generation and detection of squeezed mechanical states using microwave control and spectroscopy of a nano-electromechanical system. In detail, we investigate a system based on a nanomechanical string resonator inductively coupled via a SQUID to a superconducting microwave resonator. Within this presentation, we discuss the challenges regarding the experimental implementation and the required parameter regime, and present preliminary experimental data.

TT 18.3 Mon 17:45 HSZ 201

Nanowire deflection detection based on a coupled mechanical oscillator — MANEESHA SHARMA, ANIRUDDHA SATYADHARMA PRASAD, NORBERT H. FREITAG, BERND BÜCHNER, and •THOMAS MÜHL — Leibniz Institute for Solid State and Materials Research IFW Dresden, 01069 Dresden, Germany

The field of nanowire (NW) technology represents an exciting and steadily growing research area with applications in ultra-sensitive mass and force sensing. Ex-

isting detection methods for NW deflection and oscillation include optical and field emission approaches. However, they are challenging for detecting small diameter NWs because of heating produced by the laser beam and the impact of the high electric field. Alternatively, the deflection of a NW can be detected indirectly by co-resonantly coupling the NW to a cantilever and measuring it using a scanning probe microscope. Here, we prove experimentally that co-resonantly coupled devices are sensitive to small force derivatives in a similar way as standalone NWs do. We detect force derivatives as small as 10^{-9} N/m with a bandwidth of 1 Hz at room temperature. The detection technique presented in this work verifies a major step in boosting NW-based force and mass sensing.

TT 18.4 Mon 18:00 HSZ 201

Symmetry breaking in a parametrically modulated quantum oscillator — •DANIEL BONESS¹, MARK DYKMAN², and WOLFGANG BELZIG¹ — ¹Department of Physics, University of Konstanz, 78457 Konstanz, Germany — ²Department of Physics and Astronomy, Michigan State University, East Lansing, Michigan 48824, USA

A weakly damped nonlinear oscillator modulated close to twice its eigenfrequency has two stable states, which have the same vibration amplitudes but opposite phases. The states are equally populated due to classical or quantum fluctuations.

An extra force at half the modulation frequency lifts the symmetry of the states, generally. We study how the symmetry breaking occurs in the quantum regime.

As we show, a significant change of the state populations can take place already for a weak extra force. The mechanism is the force-induced change of the rates of interstate switching. The change is exponential in the ratio of the force amplitude to the appropriately scaled quantum length. It is large even where the effect of the force on the mean-field oscillator dynamics is small.

TT 18.5 Mon 18:15 HSZ 201

Quantum friction between metals in the hydrodynamic — •KUNMIN WU, THOMAS SCHMIDT, and MARIA BELÉN FARIAS — Faculty of Science, Technology and Medicine, 162 A, avenue de la Faiencerie, L-1511 Luxembourg

In this work, we study the phenomenon of quantum friction in a system consisting on a moving atom at a constant speed parallel to a metallic slab. We use a hydrodynamic model to describe the degrees of freedom of a clean metal without internal dissipation. The moving and polarizable atom is modeled as a two-level system with a unique ($l = 0$) ground state and a three-fold degenerate ($l = 1$) excited state. We show that a quantum frictional force is present even in the absence of intrinsic damping in the metal, but that there is a velocity threshold giving rise to such a force. In particular, to have non-vanishing friction demands that the atom must move at a velocity larger than the effective speed of sound in the material. We provide analytical arguments to show that this result holds at all orders in perturbation theory. Besides, we also explore how the spatial dispersion, which is determined by the sound speed in the hydrodynamic regime, affects the friction. Our numerical results show that the spatial dispersion has less effect on the friction when the speed of atom is much higher than the sound speed.

TT 19: Focus Session: New Perspectives for Adiabatic Demagnetization Refrigeration in the Kelvin and sub-Kelvin Range (joint session TT/MA)

Efficient cooling into the Kelvin and sub-Kelvin range is a long-standing challenge relevant to both fundamental research and future quantum technologies. The standard cooling cycle based on vapor compression exploits expensive and rare helium. Low-temperature physicists world-wide are presently looking for cheaper and accessible alternatives, not to mention the need of compact cooling technology for desktop quantum technology, or special requirements for applications such as space missions and scanning tunneling microscopes. One of the key candidates is adiabatic demagnetization refrigeration (ADR). ADR is based on magnetic solids with a huge magnetocaloric effect and requires no helium. Even if paramagnetic salts are known and used for ADR applications for almost a century, there is an ongoing quest for materials with better magnetocaloric and mechanical properties, thermal conductivity, and vacuum compatibility. In this symposium, new fundamental ideas and the recent successful design and characterization of quantum materials for improved ADR will be highlighted. These materials exploit collective phenomena in correlated electron systems, such as the concept of geometrically frustrated magnetism to push the entropy to low temperatures, as well as heavy-fermion, and quantum-critical states.

Organizers: Andreas Honecker (CY Cergy Paris Université) and Jürgen Schnack (Universität Bielefeld)

Time: Tuesday 9:30–13:15

Location: HSZ 03

Invited Talk

TT 19.1 Tue 9:30 HSZ 03

Self-cooling molecular spin quantum processors — •MARCO EVANGELISTI¹, FERNANDO LUIS¹, ELIAS PALACIOS¹, DAVID AGUILA², and GUILLEM AROMÍ² — ¹INMA, CSIC & Universidad de Zaragoza, Spain — ²Dept. Química Inorgánica, Universidad de Barcelona, Spain

Cryogenic refrigeration is crucial for a wide range of emerging applications in the field of quantum technologies. Indeed, thermal energy must be minimized to avoid the excitation of vibrational motions that could disturb quantum operations. Synthetic chemistry provides a sophisticated methodology for the design and synthesis of materials displaying a wide variety of properties. Molecular materials are capable of excellent and unique characteristics that can be exploited either for caloric cooling[1] or spin-based quantum computing[2]. However, these features are not yet being implemented as such to act together within the same material, that is, at the molecular scale. Here, we show that a spin qubit (or qudit) can be brought into proximity with a spin centre that acts as a cooler. To this end, we make use of rare-earth-based asymmetric molecular dimers. A chemically engineered structural asymmetry introduces different coordination environments for each metal ion, operating similarly as for molecular quantum gates reported by some of us[3]. This strategy allows selecting individually both constituent ions, leading to e.g. the direct observation of the cooling of a single Er(III) ion qubit, or a Tm(III) electronuclear spin qudit, driven chiefly by the demagnetization of a single Gd(III) ion located within the same molecule.

[1] Dalton Trans. 39, 4672 (2010)

[2] Nat. Chem. 11, 301 (2019)

[3] Phys. Rev. Lett. 107, 117203 (2011)

Invited Talk

TT 19.2 Tue 10:00 HSZ 03

Triangular rare-earth borates for milli-Kelvin adiabatic demagnetization refrigeration — •PHILIPP GEGENWART — Experimental Physics VI, Center for Electronic Correlations and Magnetism, University of Augsburg

Adiabatic demagnetization refrigeration (ADR) is a classical cooling technique with renewed recent attention as alternative to costly and elaborate ³He/⁴He dilution refrigeration. Established water containing ADR salts suffer from chemical instability which requires delicate treatment to avoid degradation and ensure good thermal contact. Water-free KBaYb(BO₃)₂ is an excellent alternative with high entropy density that allows ADR to below 20 mK [1]. Sintered pellets with silver powder admixture to ensure good thermal coupling are easy to manufacture, inexpensive and long-term stable even upon heating up to 700°C, enabling also ultra-high vacuum applications. KBaYb(BO₃)₂ belongs to a family of rare-earth-based borates with triangular arrangement of magnetic moments. We discuss the impact of geometrical frustration and structural randomness on its low-temperature properties and demonstrate the enormous tunability of cooling power and operating temperature by chemical substitution.

[1] Y. Tokiwa, S. Bachus, K. Kavita, A. Jesche, A.A. Tsirlin, and P. Gegenwart, Commun. Mater. 2 (2021) 42.

Invited Talk

TT 19.3 Tue 10:30 HSZ 03

A millikelvin scanning tunnelling microscope in ultra-high vacuum with adiabatic demagnetisation refrigeration — •RUSLAN TEMIROV — Peter Grünberg Institut (PGI-3), Forschungszentrum Jülich, Germany — University of Cologne, Institute of Physics II, Cologne, Germany

Scanning tunnelling microscopes (STMs) operating in ultra-high vacuum (UHV) and low-temperature conditions are used widely for imaging and precise manipulation of surface nanostructures. A growing interest in studies of quantum-coherent phenomena in such nanostructures stimulates the develop-

ment of STMs that operate at very low millikelvin temperatures. This contribution presents the design of a first-ever UHV STM cooled by adiabatic demagnetisation refrigeration (ADR) to below 30 mK. The use of ADR makes the STM design modular and helps it to reach a remarkable degree of mechanical stability. Tunnelling spectra collected on an atomically clean superconducting Al(100) surface reveal that the electronic temperature of the tunnelling junction is less than 80 mK. The inelastic electron tunnelling spectroscopy of an individual electron spin performed in magnetic fields of up to 8 Tesla validates the STM capabilities for quantum nanoscience research.

15 min. break

Invited Talk

TT 19.4 Tue 11:15 HSZ 03

ADR cryostats in low temperature physics and their applications — •DOREEN WERNICKE — Entropy GmbH, Gmunder Str. 37a, 81379 München

Entropy GmbH is a company founded in 2010 in Munich, Germany, specializing in the development and manufacture of low temperature cryostats. All Entropy cryostats are based on closed-cycle pre-cooling to temperatures below 3K. Further cooling stages such as ADR units, Joule-Thomson stages, and dilution refrigerators including electronics and software are proprietary developments. The modular design of all cryostats offers the possibility of adaptation to many different experiments and applications. One of Entropy's most common products are the ADR cryostats. The presentation will explain the principle of ADR cooling and features such as base temperature and holding time at operating temperature. Applications for low temperature device operation such as various types of superconducting detectors (TES, MKIDs, SQUIDS, SNSPDs) and Qubit characterization will be presented to demonstrate the performance and limitations of adiabatic demagnetization refrigeration.

Invited Talk

TT 19.5 Tue 11:45 HSZ 03

Frustrated dipolar materials for low-temperature magnetic refrigeration — •MIKE ZHITOMIRSKY — Institute of Interdisciplinary Research, CEA-Grenoble, France

Low-temperature refrigeration is crucial for emergent quantum-information technologies and other scientific applications that outstretch from space telescopes to medicine. This growing demand fuels an interest in alternative low-temperature techniques including the adiabatic demagnetization refrigeration. The existing ADR technologies for the sub-Kelvin range utilize dilute paramagnetic salts of Cr and Fe magnetic ions, which have limited efficiency at higher temperatures. I shall discuss general directions of the ongoing search of prospective refrigerant materials by exploring collective effects in systems of interacting magnetic moments as opposed to noninteracting moments in paramagnetic salts. Specifically, I focus on geometrically frustrated magnets with a residual ground-state degeneracy as well as on dipolar magnets. I present new experimental and theoretical results obtained recently in Grenoble for two dipolar materials: Yb₃Ga₅O₁₂, which is a spin-1/2 dipolar ferromagnet on a hyper-Kagome lattice, and GdLiF₄, which exhibits a hidden magnetic frustration. The striking properties of the latter material including a fractional magnetization plateau demonstrate importance of new magnetocaloric materials not only for applied but also for basic research in magnetism.

TT 19.6 Tue 12:15 HSZ 03

ADR based sub-Kelvin cryostats for applied quantum technologies — •PAU JORBA¹, FELIX RUCKER¹, STEFFEN SÄUBERT¹, ALEXANDER REGNAT¹, JAN SPALLEK¹, and CHRISTIAN PFLEIDERER² — ¹kiutra GmbH, Flößergasse 2, D-81369 München, Germany — ²Physik-Department, Technische Universität München, D-85748 Garching, Germany

In view of the increasing demand for the cooling of quantum electronic devices, the development of scalable cooling solutions that provide low temperatures independent of rare helium-3 will be mandatory for the adoption and commercial use of next-generation quantum technologies. We present novel ADR based sub-Kelvin cryostats¹ specifically developed for the characterization and operation of quantum devices. We address how known challenges of ADR systems such as limited hold time and magnetic stray fields can be overcome. Specifically, we describe how continuous sub-Kelvin cooling and wide-range temperature control can be achieved by combining multiple ADR units and mechanical thermal switches. We also present a novel sample loader mechanism² that allows taking advantage of the solid-state nature of ADR and to cool samples from room temperature to 100 mK in less than 3 hours.

[1] Regnat et al. (2018) Cryogen-free cooling apparatus (EP 3163222). European Patent Office.

[2] Spallek et al. (2022) System and method for inserting a sample into a chamber (EP 3632560). European Patent Office.

TT 19.7 Tue 12:30 HSZ 03

ADR below the ordering temperature in triangular K₂BaGd(BO₃)₂ — •NOAH WINTERHALTER-STOCKER¹, ALEXANDER BELLON¹, FABIAN HIRSCHBERGER¹, SEBASTIAN BACHUS¹, SEBASTIAN ERDMANN¹, ALEXANDER TSIRLIN^{1,2}, YOSHIFUMI TOKIWA^{1,3}, ANTON JESCHE¹, and PHILIPP GEGENWART¹ — ¹Experimental Physics VI, Center for Electronic Correlations and Magnetism, University of Augsburg, D-86159 Augsburg, Germany — ²Felix Bloch Institute for Solid-State Physics, Leipzig University, D-04103 Leipzig, Germany — ³Advanced Science Research Center, Japan Atomic Energy Agency, Tokai, Ibaraki 319-1195, Japan

Compared to the triangular ADR magnet K₂BaYb(BO₃)₂ [1] the isostructural sister compound K₂BaGd(BO₃)₂ with spin 7/2 moments has a three times enhanced magnetic entropy density of 192 mJ⁻¹K⁻¹cm⁻³. We report a low-temperature magnetic and thermodynamic investigation of polycrystalline K₂BaGd(BO₃)₂ down to 50 mK. Specific heat indicates an antiferromagnetic phase transition at 263 mK, strongly broadened due to randomness and frustration, that becomes suppressed beyond 0.5 T. Further increase of magnetic field shifts the available entropy of R log 8 towards high temperatures. Interestingly, ADR of a pellet utilizing the same setup as used in [1] reveals a minimal temperature if $T_{\min} = 122$ mK that is more than twice below T_N along with a hold time of more than 8 hours. The combination of minimal temperature and entropy density in K₂BaGd(BO₃)₂ is outstanding among known ADR materials.

[1] Y. Tokiwa et al., Communications Materials 2.1, 1-6 (2021)

TT 19.8 Tue 12:45 HSZ 03

Magnetocaloric properties of (RE)₃Ga₅O₁₂ (RE=Tb, Gd, Nd, Dy) — MARKUS KLEINHANS¹, KLAUS EIBENSTEINER^{1,2}, JON LEINER¹, •CHRISTOPH RESCH¹, LUKAS WORCH¹, MARC WILDE¹, JAN SPALLEK^{1,2}, ALEXANDER REGNAT^{1,2}, and CHRISTIAN PFLEIDERER¹ — ¹Physik Department, Technical University Munich, D-85748 Garching, Germany — ²kiutra GmbH, Rupert-Mayer-Str. 44, D-81379 Munich, Germany

We report the characteristic magnetic properties of several members of the rare earth garnet family, Gd₃Ga₅O₁₂ (GGG), Dy₃Ga₅O₁₂ (DGG), Tb₃Ga₅O₁₂ (TGG), and Nd₃Ga₅O₁₂ (NGG), and compare their relative potential utility for magnetocaloric cooling, including their minimal adiabatic demagnetization refrigeration (ADR) temperatures and relative cooling parameters. A main objective of this work was to find potential improvements over the magnetocaloric properties of GGG for use in low temperature ADR cryostats. Using Tb⁺³ and Dy⁺³ in the RE-site offers, in principle, a higher saturation magnetization and Nd⁺³ gives a lower de Gennes factor and therefore potentially low transition temperature. Our results show that Dy₃Ga₅O₁₂ yields an optimal relative cooling parameter (RCP) at low applied fields and a low transition temperature, which would allow for the design of more efficient ADR cryostats.

[1] M. Kleinhans et al., arXiv/2204.01752; Phys. Rev. Appl. in press (2022).

TT 19.9 Tue 13:00 HSZ 03

Study of the large rotational magnetocaloric effect in Ni(en)(H₂O)₄SO₄·2H₂O — •RÓBERT TARASENKO, PETRO DANYLCHENKO, ERİK ČIŽMÁR, VLADIMÍR TKÁČ, ALEXANDER FEHER, ALŽBETA ORENDÁČOVÁ, and MARTIN ORENDÁČ — Institute of Physics, Faculty of Science, Pavol Jozef Šafárik University, Park Angelinum 9, 041 54 Košice, Slovakia

The title compound Ni(en)(H₂O)₄SO₄·2H₂O (en = ethylenediamine) has been identified as a spin-1 paramagnet with the nonmagnetic ground state introduced by the easy-plane anisotropy $D/k_B = 11.6$ K with $E/D = 0.1$ and negligible exchange interactions $J \approx 0$. We present an experimental study of the rotational magnetocaloric effect (MCE) in single crystals at temperatures above 2 K, associated with adiabatic crystal rotation between the easy plane and hard axis in magnetic fields up to 7 T. The experimental observations are completed with *ab initio* calculations of the anisotropy parameters. Theoretical simulations of the rotational MCE in the $S = 1$ paramagnet were performed and the simulations were compared with experimental data. A large rotational magnetic entropy change ≈ 16.9 Jkg⁻¹K⁻¹ has been achieved in 7 T. The adiabatic rotation of the crystal in 7 T starting at the initial temperature of 4.2 K leads to the cooling of the sample down to 0.34 K, which suggests the application of this material in low-temperatures cooling. Our simulations show that $S = 1$ Ni(II)-based systems with easy-plane anisotropy can have better rotational magnetocaloric properties than costly materials containing rare-earth elements.

Supported by project No. APVV-18-0197.

TT 20: Superconductivity: Tunneling and Josephson Junctions

Time: Tuesday 9:30–13:00

Location: HSZ 103

TT 20.1 Tue 9:30 HSZ 103

Calorimetry of a phase slip in a Josephson junction — EFE GÜMÜS¹, DANIAL MAJIDI¹, DANILO NIKOLIC², PATRICK RAIF², BAYAN KARIMI³, JOONAS PELTONEN³, ELKE SCHEER², JUKKA PEKOLA³, HERVÉ COURTOIS¹, WOLFGANG BELZIG², and •CLEMENS WINKELMANN¹ — ¹Univ. Grenoble Alpes, CNRS, Grenoble INP, Institut Néel, Grenoble, France — ²Fachbereich Physik, Universität Konstanz, Konstanz, Germany — ³Centre of Excellence, Department of Applied Physics, Aalto University School of Science, Aalto, Finland

Josephson junctions are a central element in superconducting quantum technology; in these devices, irreversibility arises from abrupt slips of the quantum phase difference across the junction. This phase slip is often visualized as the tunnelling of a flux quantum in the transverse direction to the superconducting weak link, which produces dissipation. Here we detect the instantaneous heat release caused by a phase slip in a Josephson junction, signalled by an abrupt increase in the local electronic temperature in the weak link and subsequent relaxation back to equilibrium. Beyond the advance in experimental quantum thermodynamics of observing heat in an elementary quantum process, our approach could allow experimentally investigating the ubiquity of dissipation in quantum devices, particularly in superconducting quantum sensors and qubits.

TT 20.2 Tue 9:45 HSZ 103

Measurement of two coupled Bloch oscillators based on Al/AlO_x/Al-Josephson junctions — •FABIAN KAAP and SERGEY LOTKHOV — Physikalisch-Technische Bundesanstalt, Bundesallee 100, 38116 Deutschland Braunschweig

We investigate a system of two coupled Bloch oscillators based on $\sim 50 \times 50$ nm² Josephson junctions, where one oscillator is a flux tunable SQUID and one is

a single junction, respectively. To suppress the quantum oscillations of charge and enable the occurrence of coherent Bloch oscillations, the leads include high ohmic microstrips made from oxidized titanium. Between the resistors and junctions, we design the connection via a capacitively coupled pair of high-kinetic-inductance meanders of granular aluminum. When only the single junction is actively driven by an external bias current I_{B1} the Coulomb blockade of this junction can be tuned by the flux through the passive, non-driven SQUID. If additionally a current I_{B2} is applied through the SQUID we observe synchronisation effects in the IV-curves of both Bloch oscillators when the currents coincide, $I_{B1} \approx I_{B2}$. We address experimental issues, such as electron overheating in the leads, the presence of higher harmonics at low bias currents and the onset of Zener tunneling.

TT 20.3 Tue 10:00 HSZ 103

Phase-dependent transport in thermally driven superconducting single-electron transistors — ALEXANDER G. BAUER and •BJÖRN SOTHMANN — Theoretische Physik, Universität Duisburg-Essen and CENIDE, D-47048 Duisburg, Germany

We investigate thermally driven transport of heat and charge in a superconducting single-electron transistor by means of a real-time diagrammatic transport theory. Our theoretical approach allows us to account for strong Coulomb interactions and arbitrary nonequilibrium conditions while performing a systematic expansion in the tunnel coupling. We find that a temperature bias across the system gives rise to finite heat and charge currents close to the particle-hole symmetric point which depend both on the gate voltage as well as on the phase difference between the superconducting reservoirs. The finite thermoelectric effect arises due to level renormalization from virtual tunneling processes. Fur-

thermore, we find that the phase bias can give rise to finite charge currents even in the presence of an inversion-symmetric temperature bias.

TT 20.4 Tue 10:15 HSZ 103

Josephson nanojunctions fabricated by He focused ion beam irradiation — •EDWARD GOLDOBIN¹, MAX KARRER¹, CHRISTOPH SCHMID¹, KATJA WURSTER¹, RAMÓN MANZORRO^{2,3}, JAVIER PABLO-NAVARRO^{2,3}, CESAR MAGEN^{2,3}, REINHOLD KLEINER¹, and DIETER KOELLE¹ — ¹Physikalisches Institut, Center for Quantum Science (CQ) and LISA⁺, Universität Tübingen, Germany — ²Instituto de Nanociencia y Materiales de Aragón (INMA), CSIC-Universidad de Zaragoza, Spain — ³Laboratorio de Microscopías Avanzadas (LMA), Universidad de Zaragoza, Spain

We use a focused He ion beam (He-FIB) for the nanofabrication of Josephson junctions (JJs) and more complex devices based on YBa₂Cu₃O_{7-δ} (YBCO) thin films [1]. Using an optimum He-FIB irradiation dose, we “write” Josephson barriers across YBCO microbridges. Such JJs have RCSJ-like I - V characteristics, and the dependence of the critical current vs. magnetic field resembles a Fraunhofer pattern. Using higher irradiation doses, we induce insulating regions that can be used for nanopatterning of various circuits, i.e., patterning of SQUID loops, constriction JJs (cJJs), etc.

Investigations of the irradiated regions by scanning transmission electron microscopy (STEM) provide information on the modification of the crystalline structure of YBCO on the atomic scale. STEM analysis reveals the amorphization thresholds for irradiation of 1D and 2D patterns (depending on the beam size), and provides insights into the current resolution limits for the fabrication of YBCO cJJs.

[1] B. Müller et al., Phys. Rev. Applied **11**, 044082 (2019)

TT 20.5 Tue 10:30 HSZ 103

Theory of scanned Josephson tunneling spectroscopy in cuprates — •PEAYUSH CHOUBEY¹ and PETER HIRSCHFELD² — ¹Department of Physics, Indian Institute of Technology Roorkee, Roorkee 247667, India — ²Department of Physics, University of Florida, Gainesville, Florida 32611, USA

The scanned Josephson tunneling spectroscopy (SJTS) is a direct local probe of superconducting gap order parameter. To the best of our knowledge, SJTS studies have been limited to the cases where superconducting sample and superconducting tip, both, have the same gap symmetry- either s-wave or d-wave. One might assume that in an s-to-d SJTS study of cuprates the critical current would vanish everywhere, as naively expected for planar junctions. We show here that this is not the case. Employing first-principles Wannier functions for Bi₂Sr₂CaCu₂O₈, we develop a scheme to compute Josephson critical current and quasiparticle tunneling current measured by SJTS with sub-angstrom resolution. We demonstrate that the critical current due to tunneling between an s-wave tip and a superconducting cuprate sample has largest magnitude above O sites and it vanishes above Cu sites as a direct consequence of the d-wave gap symmetry in cuprates. Moreover, we predict various signatures of pair density waves in underdoped cuprates that can be tested in future SJTS studies.

TT 20.6 Tue 10:45 HSZ 103

Critical temperature of superconductor-ferromagnetic bilayers with helimagnetic metals — •DANILO NIKOLIC, SUBRATA CHAKRABORTY, ALFREDO SPURI, ELKE SCHEER, ANGELO DI BERNARDO, and WOLFGANG BELZIG — Fachbereich Physik, Universität Konstanz, D-78457 Konstanz, Germany

Motivated by recent experiments on the proximity effect in superconductor-ferromagnet structures with the helimagnetic ordering of magnetization in the latter, we present a systematic theoretical study of the critical temperature of such systems. By employing the quasiclassical Usadel approach [1], we account for two different configurations of magnetization in the ferromagnet and investigate their impact on the critical temperature (T_c) of the superconductor. Besides recovering the known results for the case of uniform magnetization [2], we find a nontrivial behavior of T_c in the case of spiral magnetization. Our theory suggests that this can be attributed to the emergence of long-range spin-triplet correlations generated in the ferromagnet [3]. Finally, our model predicts that the presence of spiral magnetization can reduce the critical temperature in the experimentally relevant range of parameters. This effect is the subject of ongoing experiments.

[1] A. I. Buzdin, Rev. Mod. Phys. **77**, 935 (2005)

[2] Z. Radović et al., Phys. Rev. B **44**, 759 (1991);

Ya. V. Fominov et al., Phys. Rev B **66**, 014507 (2002)

[3] A. F. Volkov et al., Phys. Rev. B **73**, 104412 (2006)

TT 20.7 Tue 11:00 HSZ 103

Equal-spin Cooper pair injection in superconducting spintronics devices — •MATTHIAS ESCHRIG¹ and XAVIER MONTIEL² — ¹Institute of Physics, University of Greifswald, Germany — ²Department of Materials Science & Metallurgy, University of Cambridge, UK

In a number of recent experiments unusual behavior was observed in ferromagnet/ferromagnet/superconductor devices when a precession of the magnetization was induced by ferromagnetic resonance. By using a non-equilibrium Us-

adel Green function formalism, we solve for spin-resolved distribution functions and demonstrate that the spin injection process in superconductors is governed by the inverse proximity effect in the superconducting layer. We find that equal-spin Cooper pairs, which are produced by the two misaligned ferromagnetic layers, transport spin inside the S layer. This then results in an increase of the injected spin current below the superconducting critical temperature. Our calculations provide the first evidence of the essential role of equal-spin Cooper pairs on spin-transport properties of S/F devices and pave new avenues for the design of superconducting spintronics devices.

15 min. break

TT 20.8 Tue 11:30 HSZ 103

Vortex phase transitions in frustrated two-dimensional semiconductor-superconductor Josephson junction arrays — •SIMON REINHARDT¹, CHRISTIAN BAUMGARTNER¹, SERGEI GRONIN², GEOFFREY C. GARDNER², TYLER LINDEMANN², MICHAEL J. MANFRA², TATYANA I. BATURINA¹, NICOLA PARADISO¹, and CHRISTOPH STRUNK¹ — ¹Institute for Experimental and Applied Physics, University of Regensburg, 93040 Regensburg, Germany — ²Purdue University, West Lafayette, Indiana 47907, USA

We study two-dimensional Josephson junction arrays in hybrid aluminum/InGaAs/InAs semiconductor-superconductor heterostructures. Using a cold resonator technique, we measure both the inductive response as well as the DC transport properties of the array. A perpendicular magnetic field induces highly ordered vortex configurations for integer and fractional values of the frustration parameter. In the vicinity of the matching fields we observe pronounced dip-to-peak transitions of the differential resistance as a function of current bias, which have previously been interpreted as signatures of a non-equilibrium vortex Mott transition [1]. The scaling behaviour of the differential conductance in our array of ballistic SNS junctions is compared with previous results on diffusive Josephson junction arrays.

[1] N. Poccia et al., Science **349**, 1202 (2015)

TT 20.9 Tue 11:45 HSZ 103

Engineering the speedup of quantum tunneling in Josephson systems via dissipation — •DOMINIK MAILE¹, JOACHIM ANKERHOLD¹, SABINE ANDERGASSEN², WOLFGANG BELZIG³, and GIANLUCA RASTELLI⁴ — ¹Institut für Komplexe Quantensysteme, Universität Ulm — ²Institut für Theoretische Physik and Center for Quantum Science, Universität Tübingen — ³Fachbereich Physik, Universität Konstanz — ⁴INO-CNR BEC Center and Dipartimento di Fisica, Università di Trento

We theoretically investigate the escape rate occurring via quantum tunneling in a system affected by tailored dissipation [1]. Specifically, we study the environmental assisted quantum tunneling of the superconducting phase in a current-biased Josephson junction. We consider Ohmic resistors inducing dissipation both in the phase and in the charge of the quantum circuit. We find that the charge dissipation leads to an enhancement of the quantum escape rate. This effect appears already in the low Ohmic regime and also occurs in the presence of phase dissipation that favors localization. Inserting realistic circuit parameters, we address the question of its experimental observability and discuss suitable parameter spaces for the observation of the enhanced rate.

[1] D.Maile et al., PRB **106**, 045408 (2022)

TT 20.10 Tue 12:00 HSZ 103

Complete magnetic control over the superconducting thermoelectric effect — •JABIR ALI OUASSOU¹, CÉSAR GONZÁLEZ-RUANO², DIEGO CASO², FARKHAD G. ALIEV², and JACOB LINDER¹ — ¹Center for Quantum Spintronics, Department of Physics, Norwegian University of Science and Technology, NO-7491 Trondheim, Norway — ²Departamento Física de la Materia Condensada C-III, INC and IFIMAC, Universidad Autónoma de Madrid, Madrid 28049, Spain

Giant thermoelectric effects are known to arise at the interface between a superconductor and strongly polarized ferromagnet, and this enables the construction of efficient thermoelectric generators. We predict that the thermopower of such generators can be completely controlled by a magnetic input signal: not only can the thermopower be toggled on and off by rotating a magnet, but even the sign of the thermopower can be reversed. This *in situ* control diverges from conventional thermoelectrics, where the thermopower is usually fixed by the device design.

TT 20.11 Tue 12:15 HSZ 103

Quantum phases in a frustrated sawtooth chain of Josephson junctions — •BENEDIKT J.P. PERNACK, MIKHAIL V. FISTUL, and ILYA M. EREMIN — Ruhr-Universität Bochum, Bochum Germany

We present a theoretical study of quantum phases occurring in a frustrated sawtooth chain of small Josephson junctions. In the model the frustration f arises due to the Josephson couplings having alternating signs (0 and π Josephson junctions) in a single lattice cell. At the critical value of $f = 3/4$ such a system displays a phase transition from the ordered state into the frustrated one with a highly degenerate ground state characterized by penetration of topological (anti)vortices

[1]. Introducing additional capacitances to the ground, we derive an effective Ising quantum spins model with a long-range interaction between well separated vortices/antivortices, and obtain various collective quantum phases and quantum phase transitions between them.

[1] A. Andreanov and M. V. Fistul, *J. Phys. A: Math. Theor.* **52**, 105101 (2019)

TT 20.12 Tue 12:30 HSZ 103

Low-energy model for superconducting quantum dot systems — •VLADISLAV POKORNÝ¹ and MARTIN ŽONDA² — ¹FZU - Institute of Physics, Czech Academy of Sciences, Na Slovance 2, 182 21 Prague, Czech Republic — ²Faculty of Mathematics and Physics, Charles University, Ke Karlovu 5, 121 16 Prague, Czech Republic

We present a method to extract the Andreev bound state energies of a single-level quantum dot connected to superconducting leads from the imaginary-time results of quantum Monte-Carlo method without the use of analytic continuation techniques like maximum entropy method. We describe the system using the superconducting impurity Anderson model and show that for low energies it maps on an atomic-like model. The parameters of this model can be extracted from the self-energy calculated in imaginary-frequency domain using the hybridization-expansion quantum Monte Carlo method. We compare the results to zero-temperature numerical renormalization group data to show the limits of usability of the low-energy model.

TT 20.13 Tue 12:45 HSZ 103

Tracking current path in multi-terminal graphene Josephson junctions — •DEVANG PARMAR — Institute for Quantum Materials and Technologies (IQMT), Karlsruhe Institute of Technology, 76021 Karlsruhe, Germany.

Multiterminal Josephson junctions have been predicted to be platforms to observe various exotic phenomena such as new topological phases of matter [1], correlated states [2-5] or the so-called Andreev molecules [6,7]. In order to control the electronic properties of these complex devices, it is important to comprehend and track the supercurrent flow with respect to their geometries and superconducting lead peculiarities.

Here, we investigated the supercurrent in multi-terminal superconductor-graphene-superconductor (SGS) junctions. Together with magnetic interferometry experiments in these multiterminal graphene devices, we clearly observe that the contact transparencies can be very different from one lead to the other which mainly drives the entire transport properties in SGS. Our work provides insights of the supercurrent flow in multiterminal Josephson junctions and paves the way for further investigations in more complex multiterminal devices.

- [1] R. P. Riwar et al., *Nat Commun* **7**, 11167 (2016)
 [2] A. Freyn et al., *Phys. Rev. Lett.* **106**, 257005 (2011)
 [3] A. H. Pfeffer et al., *Phys. Rev. B* **90**, 075401 (2014)
 [4] R. Mélin et al., *Phys. Rev. B* **100**, 035450 (2019)
 [5] K.-F. Huang et al., arXiv preprint arXiv:2008.03419 (2020)
 [6] Z. Su et al., *Nat. Commun.* **8**, 585 (2017)
 [7] J.-D. Pillet et al., *Nano Lett.* **19**, 7138 (2019)

TT 21: Correlated Electrons: Electronic Structure Calculations

Time: Tuesday 9:30–11:45

Location: HSZ 201

TT 21.1 Tue 9:30 HSZ 201

Revealing electronic correlations in YNi₂B₂C using photoemission spectroscopy — •AKI PULKKINEN¹, GEOFFROY KREMER², VLADIMIR STROCOV³, FRANK WEBER⁴, JÁN MINÁR¹, and CLAUDE MONNEY⁵ — ¹New Technologies-Research Center, University of West Bohemia, Pilsen, Czech Republic — ²Département Physique de la Matière et des Matériaux, Institut Jean Lamour, Université de Lorraine/CNRS, France — ³Paul Scherrer Institut, Swiss Light Source, Villigen, Switzerland — ⁴Institute for Quantum Materials and Technologies, Karlsruhe Institute of Technology, Karlsruhe, Germany — ⁵Département de Physique and Fribourg Center for Nanomaterials, Université de Fribourg, Fribourg, Switzerland

YNi₂B₂C is an intermetallic borocarbide superconductor with a complex electronic band structure that has a very strong Ni character near the Fermi energy. We present density functional theory (DFT) and one-step model of photoemission results for YNi₂B₂C and compare them to experimental soft x-ray angle resolved photoemission spectroscopy (SX-ARPES) measurements. We show that moderate electron correlations have to be included, using dynamical mean field theory (DFT+DMFT) applied to the Ni d-states, to reach the best agreement between the experimental and theoretical SX-ARPES spectra. The one-step model calculations allow us to identify the effect of DFT+DMFT on the energy bands observed in the SX-ARPES measurements.

TT 21.2 Tue 9:45 HSZ 201

Distortion and pressure induced phase transitions in double perovskite La₂CoTiO₆ — •SROMONA NANDI¹, ASHIS K. NANDY², and RUDRA SEKHAR MANNA¹ — ¹Department of Physics, Indian Institute of Technology Tirupati, Tirupati 517619, AP, India — ²School of Physical Sciences, National Institute of Science Education and Research, An OCC of Homi Bhabha National Institute, Jatni-752050, India

We study the density-functional theory spin-polarized electronic structure calculations for a double perovskite La₂CoTiO₆ where the magnetic moment comes from the Co²⁺ as Ti is in 4⁺ state. Due to the rotation and volume mismatch between the TiO₆ and CoO₆ octahedra (∠Co-O-Ti is 151–153°), the system is distorted at ambient pressure. The Co-moments align antiferromagnetically at low temperature and show an insulating transport property with a band gap of 1 eV, consistent with the experiment [1]. With the removal of distortion, i.e., ideal undistorted structure (∠Co-O-Ti is 180°) shows a metallic behavior. Such metallic state can also be achieved with the application of hydrostatic pressure on the distorted structure accompanied by the quenching of Co-moment in the metallic phase which can be understood by the shifting of the exchange splitting of the Co 3d orbitals at the Fermi level. In addition, atomic projected density of states analysis of the Co sublattices shows an interesting half-metallic like intermediate state which could be interesting for spintronics applications.

[1] K. L. Holman et al., *J. Solid State Chem.* **180**, 75 (2007)

TT 21.3 Tue 10:00 HSZ 201

Oxygen vacancies at the origin of pinned moments in oxide interfaces: the example of tetragonal CuO/SrTiO₃ — •BENJAMIN BACQ-LABREUIL¹, BENJAMIN LENZ², and SILKE BIERMANN³ — ¹Institut Quantique, Université de Sherbrooke, Sherbrooke, Canada — ²Institut de Minéralogie, de Physique des Matériaux et de Cosmochimie, Sorbonne Université, Paris, France — ³Centre de Physique Théorique, Ecole Polytechnique, Palaiseau, France

Obtaining an accurate theoretical description of the emergent phenomena in oxide heterostructures is a major challenge. Recently, intriguing paramagnetic spin and pinned orbital moments have been discovered by x-ray magnetic circular dichroism measurements at the Cu L_{2,3}-edge of a tetragonal CuO/SrTiO₃ heterostructure. Using first principles calculations, we propose a scenario that explains both types of moments [1], based on the formation of oxygen vacancies in the TiO₂ interface layer. We show the emergence of a paramagnetic 2D electron gas hosted in the interface CuO layer. It is invisible at the Ti L_{2,3}-edge since the valence of the Ti atoms remains unchanged. Strong structural distortions breaking both the local and global fourfold rotation C₄ symmetries at the interface lead to the in-plane pinning of the Cu orbital moment close to the vacancy. Our results, and in particular the pinning of the orbital moment, may have implications for other systems, especially monoxide/dioxide interfaces with similar metal-oxygen bond length and weak spin-orbit coupling.

[1] B. Bacq-Labreuil, et al, arXiv:2210.15084 (2022).

TT 21.4 Tue 10:15 HSZ 201

New superexchange paths due to synergetic breathing and hopping in corner-sharing cuprates — •NIKOLAY A. BOGDANOV¹, GIOVANNI LI MANNI¹, SANDEEP SHARMA^{1,2}, OLLE GUNNARSSON¹, and ALI ALAVI^{1,3} — ¹Max Planck Institute for Solid State Research, Stuttgart, Germany — ²Department of Chemistry, University of Colorado Boulder, Boulder, CO, USA — ³University Chemical Laboratory, Cambridge, UK

We present *ab initio* quantum chemistry calculations of the nearest-neighbour superexchange antiferromagnetic spin coupling *J* for two cuprates, Sr₂CuO₃ and La₂CuO₄. Good agreement with experimental estimates is obtained for both systems. We also find that *J* increases substantially as the distance between Cu and apical O is increased.

Analysis of the correlated wavefunctions together with extended superexchange models shows that there is an important synergetic effect of the Coulomb interaction and the O–Cu hopping. When an extra electron hops into Cu 3d orbital, Coulomb interaction leads to the orbital breathing (expansion), which on its turn reinforces electron hopping. This correlated breathing-enhanced hopping mechanism is a new ingredient in superexchange models. Our analysis shows that suppression of the described mechanism leads to a drastic reduction in the antiferromagnetic coupling, indicating that it is of primary importance in generating the strong interactions.

TT 21.5 Tue 10:30 HSZ 201

DFT with corrections for an efficient and accurate description of strong electron correlations in NiO — •JULIAN GEBHARDT^{1,2} and CHRISTIAN ELSÄSSER^{1,2,3} — ¹Fraunhofer IWM, 79108 Freiburg — ²Cluster of Excellence livMatS, University of Freiburg — ³Freiburg Materials Research Center, University of Freiburg

An efficient and accurate description of the electronic structure of a strongly correlated oxide like NiO has been notoriously difficult. Here, we study the capabilities and limitations of two frequently employed correction schemes, a DFT+*U* on-site correction and a DFT+1/2 self-energy correction. While both methods individually are unable to provide satisfactory results, in combination they provide a very good description of all relevant physical quantities. Since both methods cope with different shortcomings of common DFT methods (using local-density or generalized-gradient approximations), their combination is not mutually dependent and remains broadly applicable. The combined approach retains the computational efficiency of DFT calculations while providing significantly improved predictive power.

TT 21.6 Tue 10:45 HSZ 201

LaVO₃: A true Kugel-Khomskii system — •XUEJING ZHANG¹, ERIK KOCH^{1,2}, and EVA PAVARINI^{1,2} — ¹Institute for Advanced Simulation, Forschungszentrum Jülich, 52425 Jülich, Germany — ²JARA High-Performance Computing, 52062 Aachen, Germany

Almost 50 years ago, Kugel' and Khomskii (KK) showed in a classic paper that, in strongly correlated materials, orbital ordering can arise from pure superexchange interactions [1]. It can, however, also result from the crystal-field splitting via a lattice distortion, i.e., from electron-lattice coupling. Despite the intensive search, it has been hard to find an undisputed realization of a KK system. We identify that the t_{2g}^2 perovskite LaVO₃, in its orthorhombic phase, is a rare case of a system hosting an orbital-ordering KK phase transition rather than being controlled by the Coulomb-enhanced crystal-field splitting [2]. We find that, as a consequence of this, the magnetic transition is close to (and even above) the superexchange driven orbital-ordering transition, whereas typically magnetism arises at much lower temperatures than orbital ordering. To explore the effects of crystal-field splitting and filling, we compare to YVO₃ and t_{2g}^1 titanates. In all these materials the crystal field is sufficiently large to suppress the KK phase transition [3].

[1] K. I. Kugel' and D. I. Khomskii, Zh. Eksp. Teor. Fiz. **64**, 1429 (1973) [Sov. Phys. JETP **37**, 725 (1973)]

[2] X. J. Zhang, E. Koch, E. Pavarini, Phys. Rev. B **106**, 115110 (2022)

[3] X. J. Zhang, E. Koch, E. Pavarini, Phys. Rev. B **102**, 035113 (2020)

TT 21.7 Tue 11:00 HSZ 201

Orbital-selective metal-insulator transitions in the presence of strong magnetic fluctuations — •EVGENY STEPANOV — CPHT, CNRS, École polytechnique, Institut Polytechnique de Paris, 91120 Palaiseau, France

Orbital-selective phenomena that can be realised in materials attract enormous interest. A prominent example is an orbital-selective Mott phase, where itinerant and localised electrons live in different orbitals of the same material. Since its theoretical prediction, the orbital-selective Mott transition has been intensively studied by the state-of-the-art theoretical methods that are based on local approximations to electronic correlations, namely the dynamical mean-field

theory and the slave-spin approach. Nevertheless, the existence of the orbital-selective Mott phase in realistic materials is still heavily debated and has not yet been realised experimentally.

In this talk, I will show that consistently taking into account non-local magnetic fluctuations completely changes the physical picture in the Hubbard-Kanamori model, where the orbital-selective Mott transition was predicted in the framework of the local theories. I will show that upon lowering temperature the considered system undergoes the Néel transition to an ordered antiferromagnetic phase before it experiences the orbital-selective Mott transition. Importantly, the former occurs simultaneously for all orbitals, which eliminates the orbital selectivity from the metal-insulator transition. The possibility to realise an orbital selective Néel transition will also be discussed.

TT 21.8 Tue 11:15 HSZ 201

Quantum chemical study on cobalt(II) in honeycomb lattices based on multi-configurational approaches — •THORBEN PETERSEN and LIVIU HOZOI — Leibniz IFW Dresden, 01069 Dresden, Germany

Quantum Spin Liquids (QSLs) are fascinating materials that display quantum entanglement and host unconventional fractionated excitations. While QSL behavior was found in Cu(II) $3d^9$ cuprates, $4d^5$ RuCl₃, $5d^5$ iridates and triangular-lattice $4f^{13}$ oxides, we here explore $3d^7$ Co(II) compounds such as Na₂Co₂TeO₆, which form spin-orbit-entangled $J_{\text{eff}} = 1/2$ pseudo-spin moments at Co(II) sites that potentially realize Kitaev-magnetism. In this study, we apply multi-configurational quantum-chemistry methods like CASSCF and beyond to model the $t_{2g}^5 e_g^2$ magnetic sites in these honeycomb oxides by carefully designing an embedded cluster model to represent the extended bulk lattice. With this, we quantify the extent of the $3d$ -site multiplet structure and spin-orbit coupling associated with the $^4T_{2g}$ ground state term. Moreover, our model will be validated against experimental magnetization data and first impressions on the $3d^7$ - $3d^7$ intersite couplings will be given.

TT 21.9 Tue 11:30 HSZ 201

Calculation of atomic forces for correlated materials, preliminary results — •DOROTA GOTFRYD¹, ROBINSON OUTEROVITCH¹, MARC TORRENT¹, AMBROISE VAN ROEKEGHEM², and BERNARD AMADON¹ — ¹CEA, DAM, DIF 91297 Arpajon CEDEX, France — ²CEA, LITEN 38054 Grenoble, France

Atomic forces are crucial ingredients for phonon spectra or molecular dynamics calculations. Within Abinit package, one can currently perform such calculations for weakly or strongly correlated systems, obtaining forces via density functional theory (DFT) or DFT + *U* methods, correspondingly.

We are working on extending the existing implementation of atomic forces in Abinit to DFT+DMFT (dynamical mean-field theory). Such application would allow for the calculation of forces close to metal/Mott insulator transition where the details of electronic correlations matter and DFT + *U* approximation is often insufficient for capturing the physics.

We derive the atomic forces for DFT + DMFT as functional derivatives of the free energy functional over the atomic positions and transform them to the projector-augmented wave (PAW) approximation of DFT using Wannier functions as correlated orbitals. We show that the DFT and DFT + DMFT versions of the forces differ by just two terms in the PAW language and we discuss the details of the implementation.

TT 22: Nonequilibrium Quantum Many-Body Systems I (joint session TT/DY)

Time: Tuesday 9:30–13:15

Location: HSZ 204

TT 22.1 Tue 9:30 HSZ 204

Ultrafast dynamics of quantum many-body systems including dynamical screening and strong coupling — •MICHAEL BONITZ¹, JAN-PHILIP JOOST¹, HANNES OHLDA¹, ERIK SCHROEDTER¹, and IVA BREZINOVA² — ¹CAU Kiel, Institute for Theoretical Physics and Astrophysics — ²TU Wien, Institute of Applied Physics, Vienna, Austria

Dynamical screening is a key property of charged many-particle systems. Its theoretical description is based on the GW approximation that is extensively applied for ground-state and equilibrium situations. The main limitation of the GW approximation is the neglect of strong electronic correlation effects. Here we derive the nonequilibrium dynamically screened ladder (DSL) approximation that self-consistently includes, in addition to the GW diagrams, also particle-particle and particle-hole T-matrix diagrams. Our DSL approach is formulated within the G1-G2 scheme [1,2] that is linear in time, in contrast to the cubic scaling of standard Nonequilibrium Green functions simulations. The price to pay for this speedup is the need to store the two-particle Green function. This can be avoided with a recently developed quantum fluctuations approach [3].

[1] N. Schluenzen et al., Phys. Rev. Lett. **124**, 076601 (2020)

[2] J.-P. Joost et al., Phys. Rev. B **105**, 165155 (2022)

[3] E. Schroedter et al., Cond. Mat. Phys. **25**, 23401 (2022)

TT 22.2 Tue 9:45 HSZ 204

Spectral response of a charge density wave insulator to periodic driving —

•ALEXANDER OSTERKORN, CONSTANTIN MEYER, and SALVATORE MANMANA — Institut für Theoretische Physik, Georg-August-Universität Göttingen, Germany Periodically driven quantum many-body systems host unconventional behavior not realized at equilibrium. Here we address in detail the emergence of a cosine-like band in the gap region of the non-equilibrium single-particle spectral function of strongly interacting spinless fermions on a chain in the charge density wave phase [1]. We compare the dynamics of the periodically driven system to the quench dynamics with an effective Floquet Hamiltonian and discuss the role of doublon excitations in both cases. This is investigated using both matrix product state based time evolution techniques as well as time-dependent Hartree-Fock. [1] arXiv:2205.09557

TT 22.3 Tue 10:00 HSZ 204

Floquet engineering in tilted lattices — •MELISSA WILL¹, PABLO SALA^{2,3}, and FRANK POLLMANN¹ — ¹Department of Physics, T42, Technische Universität München, James-Frank-Straße 1, D-85748 Garching, Germany — ²Department of Physics and Institute for Quantum Information and Matter, California Institute of Technology, Pasadena, California 91125, USA —

³Walter Burke Institute for Theoretical Physics, California Institute of Technology, Pasadena, California 91125, USA

Quantum many-body systems out of equilibrium can exhibit very rich and exciting phenomena. A particularly important question is whether and how a quantum system thermalizes under unitary evolution. In this context three classes of systems have been identified: ergodic, localized and an intermediate regime exhibiting so called quantum many-body scars. In this talk we discuss whether a time-periodic, local drive can induce thermalization of a localized system. We consider interacting hard-core bosons in an one dimensional, tilted system with periodic driving. We find that the system becomes ergodic for resonant driving frequencies. In contrast, if the tilt is not close to a multiple of driving frequency, the system stays localized. This observation can theoretically be understood by deriving an effective Hamiltonian using a Magnus expansion. Using large scale numerical methods, we explore entanglement entropy and imbalance over time. Our theoretical predictions are in good agreement with numerics.

TT 22.4 Tue 10:15 HSZ 204

Photoinduced spinful excitons in Hubbard systems with magnetic superstructures — CONSTANTIN MEYER and •SALVATORE R. MANMANA — Institute for Theoretical Physics, Göttingen University, Friedrich-Hund-Platz 1, 37077 Göttingen

The possibility to form excitons in photo-illuminated correlated materials is central from fundamental and application oriented perspectives. We show how the interplay of electron-electron interactions and a magnetic superstructure leads to the formation of a peculiar spinful exciton, which can be detected in the nonequilibrium spectral function and the time-dependent optical conductivity. We study these quantities by using matrix product states (MPS) following an electron-hole excitation in a class of one-dimensional Hubbard models with on-site interactions and alternating local magnetic fields, which realize correlated band insulators. An excitation in only one specific spin direction leads to an additional band in the gap region of the spectral function only in the opposite spin direction, and to an additional peak in the optical conductivity. We discuss implications for experimental studies in correlated insulator systems.

TT 22.5 Tue 10:30 HSZ 204

Photoinduced pairing states of excitonic insulators — •SATOSHI EJIMA — DLR Quantencomputing-Initiative, Hamburg, Germany

Applying the time-dependent density-matrix renormalization group technique, we explore photoinduced pairing states in the half-filled extended Falicov-Kimball model (EFKM) in one dimension, both with and without internal SU(2) symmetry. In the time-dependent photoemission spectra simulated with the optimal pump pulse parameters, an extra band appears above the Fermi energy after pulse irradiation, implying a photoinduced metallization. Even in the absence of the SU(2) structure, the electron-electron pair correlations can also be enhanced during the pump, while they decrease over time after pulse irradiation. This suggests a possible photoexcited metallization of Ta₂NiSe₅, a strong candidate for an excitonic insulator material, for which the EFKM is considered to be the minimal theoretical model. Computing the time-dependent photoemission spectra with the parameter set for this material, i.e., in the EFKM without SU(2) symmetry, we demonstrate the photoinduced insulator-to-metal transition, in accord with recent findings in time- and angle-resolved photoemission spectroscopy experiments on Ta₂NiSe₅.

[1] S. Ejima, F. Lange, H. Fehske, Phys. Rev. B **105**, 245126 (2022)

15 min. break

Invited Talk

TT 22.6 Tue 11:00 HSZ 204

Higgs spectroscopy of superconductors in nonequilibrium — •DIRK MANSKE — Max-Planck-Institut für Festkörperforschung

Higgs spectroscopy is a new and emergent field [1-3] that allows to classify and determine the superconducting order parameter by means of ultra-fast optical spectroscopy. There are two important ways to activate the Higgs mode in superconductors, namely a single-cycle *quench* or an adiabatic, multicycle *drive* pulse, which I will discuss in detail. Furthermore, I will review and report on the latest progress on Higgs spectroscopy, in particular on the role of the third-harmonic-generation (THG) [4-6] and the possible IR-activation of the Higgs mode by impurities or external dc current [7,8]. I also provide new predictions for time-resolved ARPES experiments in which, after a quench, a continuum of Higgs mode is observable and a phase information of the superconducting gap function would be possible to extract [9]. Finally, I show that the Higgs mode may shed some light on the 25-years-old A1g-puzzle in equilibrium Raman scattering on high-T_c cuprates [10].

[1] Nat. Commun. **11**, 287 (2020)

[2] Phys. Rev. B **101**, 184519 (2020)

[3] Nat. Commun. **11**, 1793 (2020)

[4] Phys. Rev. B **104**, 174508 (2021)

[5] Nature Commun., accepted (2022)

[6] Nature Commun., submitted (2022)

[7] Phys. Rev. B **101**, 220507 (2020)

[8] Phys. Rev. B **104**, 134504 (2021)

[9] Phys. Rev. B **101**, 224510 (2020)

[10] Phys. Rev. Lett. **127**, 197001 (2021)

TT 22.7 Tue 11:30 HSZ 204

Periodically driven spin-1/2 XXZ antiferromagnetic chains — •ASLAM PARVEJ, IMKE SCHNEIDER, and SEBASTIAN EGGERT — Technische Universität Kaiserslautern, Kaiserslautern, Germany

Time-periodically driven quantum systems are of great interest due to the possibility of unconventional states of matter and Floquet engineering. The interplay of many-body interactions and time-periodic manipulations facilitate new phenomena in the steady state. We analyze the Floquet steady states of finite spin-1/2 XXZ antiferromagnetic chains with periodically driven anisotropy parameter at frequencies below the band width, so that resonances are in principle possible. We use a numerical real-time approach with an adiabatic time evolution protocol by ramping up the driving amplitude of the external periodic drive to prepare a non-equilibrium Floquet steady state. Parametric resonances are expected when the driving frequencies are equal to twice the energy gaps in a finite system. However, the observed resonance absorption of energy and heating is surprisingly weak in our system even for large driving amplitude. This changes if a square wave is used for driving.

TT 22.8 Tue 11:45 HSZ 204

Controllable effects of the mass term in time-periodic driven sine-Gordon models. — •DIMO CLAUDE¹, SIMON JÄGER¹, CHRISTOPH DAUER¹, PIOTR CHUDZINSKI², IMKE SCHNEIDER¹, and SEBASTIAN EGGERT¹ — ¹Physics Department and Research Center OPTIMAS, Technische Universität Kaiserslautern, 67663 Kaiserslautern, Germany. — ²Institute of Fundamental Technological Research, Polish Academy of Science, 02-106 Warszawa, Poland.

Recently, the full Floquet solution of a Luttinger Liquid with periodically modulated interactions has been derived and resonant wave-vectors have been identified. There, the quantum state can only be stabilized when damping mechanisms of the one-dimensional systems are included. In our work, we investigate the time-periodic Luttinger Liquid under a non-linear perturbation which originates from the Sine-Gordon potential. This term provides interactions among the different modes of the Luttinger Liquid and can potentially confine the parametrically amplified modes. We investigate this model up to fourth order of the phase field using a mean-field approach. The resulting effective model is quadratic in the field operators while the non-linearity remains, due to the explicit dependence of the frequencies on the time-dependent quantum state. Using a self-consistency relation between the number of density wave excitations and the systems' energy, we discuss the formation of a non-equilibrium steady state and study its stability.

TT 22.9 Tue 12:00 HSZ 204

Influence of phononic dissipation on impact ionization processes in a photo-driven Mott insulator — •PAOLO GAZZANEO, TOMMASO MARIA MAZZOCCHI, JAN LOTZE, and ENRICO ARRIGONI — Institute of Theoretical and Computational Physics, Graz University of Technology, 8010 Graz, Austria

It has been suggested that in strongly correlated materials, highly photoexcited charge carriers could use their extra energy to excite additional carriers across the Mott gap via impact ionization [1,2]. However, the influence of electron-phonon scattering on photocurrent and impact ionization in Mott photovoltaic setups is still an open question.

We address this issue in a nonequilibrium steady state study on the occurrence of impact ionization in a simplified model of a Mott photovoltaic device in presence of acoustic phonons [3], consisting of a Mott-insulating layer coupled to two wide-band fermion leads.

For a small hybridization to the leads, we obtain a peak in the photocurrent as a function of the driving frequency which can be associated with impact ionization processes, while for larger hybridizations we find a suppression of impact ionization with respect to direct photovoltaic excitations. The effect of acoustic phonons produces a slight enhancement of the photocurrent for small driving frequencies and a suppression at frequencies around the main peak at all considered hybridization strengths.

[1] E. Manousakis, Phys. Rev. B **82**, 125109 (2010)

[2] J. E. Coulter et al., Phys. Rev. B **90**, 165142 (2014)

[3] Gazzaneo et al., Phys. Rev. B **106**, 195140 (2022)

TT 22.10 Tue 12:15 HSZ 204

Correlated Mott insulators in strong electric fields: Role of phonons in heat dissipation — •TOMMASO MARIA MAZZOCCHI, PAOLO GAZZANEO, JAN LOTZE, and ENRICO ARRIGONI — Institute of Theoretical and Computational Physics, Graz University of Technology, 8010 Graz, Austria

Mott-insulating models can undergo an insulator-to-metal transition when subject to a constant bias voltage [1], which makes them suitable to describe the resistive switch observed in correlated insulators [2]. Nonequilibrium state-of-the-art techniques rely on the coupling to fermion baths to dissipate the field-induced excess energy [1,3]. However, a realistic description of heat-exchange requires the inclusion of phonons. In [4] we study a single-band Hubbard model in a

static electric field coupled to electron and acoustic phonon baths. The nonequilibrium steady-state is addressed via the dynamical mean-field theory using the auxiliary master equation approach as impurity solver. Phonons are included via the Migdal approximation. Using both the electron and phonon baths the steady-state current is slightly enhanced by phonons for field strengths close to half of the gap and suppressed at the gap resonance. With phonons alone, dissipation can occur only at the resonances and the current at the metallic phase is suppressed by almost one order of magnitude.

- [1] C. Aron, Phys. Rev. B 86, 085127 (2012)
 [2] E. Janod et al., Adv. Funct. Mater. 25, 6277 (2015)
 [3] Y. Murakami et al., Phys. Rev. B 98, 075102 (2018)
 [4] T.M. Mazzocchi et al., Phys. Rev. B 106, 125123 (2022)

TT 22.11 Tue 12:30 HSZ 204

Correlated Mott insulators and photovoltaics out of equilibrium: phonons and heat dissipation — ENRICO ARRIGONI, TOMMASO MAZZOCCHI, PAOLO GAZZANE, DANIEL WERNER, and JAN LOTZE — Institute of Theoretical and Computational Physics, Graz University of Technology, 8010 Graz Austria

I will present recent results for correlated Mott systems in a nonequilibrium driven steady state. Results are obtained via nonequilibrium Dynamical Mean Field Theory with an impurity solver based upon a combination of Keldysh Green's functions and Lindblad formalism for open quantum systems [1]. Recent improvements based upon a Configuration Interaction treatment of the many body Lindblad equation allow for an efficient solution of the impurity problem deep in the Kondo regime [2].

In particular, I will discuss the interplay of strong correlation and Joule dissipation by phonons near the Mott dielectric breakdown [3] and in photoexcitation induced transport across a Mott insulating gap [4].

- [1] E. Arrigoni et al., Phys. Rev. Lett. 110, 086403 (2013)
 A. Dorda et al., Phys. Rev. B 89 165105 (2014)
 A. Dorda et al., Phys. Rev. B 92, 125145 (2015)
 [2] D. Werner et al., arXiv:2210.09623 (2022)
 [3] T. Mazzocchi et al., Phys. Rev. B 106, 125123 (2022)
 [4] M. Sorantin et al., Phys. Rev. B 97, 115113 (2018)
 P. Gazzaneo et al. Phys. Rev. B 106, 195140 (2022)

TT 22.12 Tue 12:45 HSZ 204

Photoinduced prethermal order parameter dynamics in the two-dimensional large-N Hubbard-Heisenberg model — ALEXANDER OSTERKORN and STEFAN KEHREIN — Institut für Theoretische Physik, Georg-August-Universität Göttingen, Germany

We study the microscopic dynamics of competing ordered phases in a two-dimensional correlated electron model [1], which is driven with a pulsed electric field of finite duration. In order to go beyond a mean-field treatment of the electronic interactions we adopt a large- N generalization of the Hubbard model and combine it with the semiclassical fermionic truncated Wigner approximation as a time evolution method. This allows us to calculate dephasing corrections to the mean-field dynamics and to obtain stationary states, which we interpret as prethermal order. We use this framework to simulate the light-induced transition between two competing phases (bond density wave and staggered flux) and find that the post-pulse stationary state order parameter values are not determined alone by the amount of absorbed energy but depend explicitly on the driving frequency and field direction. While the transition between the two prethermal phases takes place at similar total energies in the low- and high-frequency regimes, we identify an intermediate frequency regime for which it occurs with minimal heating [2].

- [1] Phys. Rev. B 39, 11538 (1989)
 [2] arXiv:2205.06620

TT 22.13 Tue 13:00 HSZ 204

Observation of magnon bound states in the long-range, anisotropic Heisenberg model — FLORIAN KRANZL¹, STEFAN BIRNKAMMER², MANOJ JOSHI¹, ALVISE BASTIANELLO², RAINER BLATT¹, MICHAEL KNAP², and CHRISTIAN ROOS¹ — ¹Universität Innsbruck, Innsbruck, Austria — ²Technische Universität München, Garching, Germany

Over the recent years coherent, time-periodic modulation has been established as a versatile tool for realizing novel Hamiltonians. Using this approach, known as Floquet engineering, we experimentally realize a long-ranged, anisotropic Heisenberg model with tunable interactions in a trapped ion quantum simulator. We demonstrate that the spectrum of the model contains not only single magnon excitations but also composite magnon bound states. For the experimentally realized long-range interactions, the group velocity of magnons is unbounded. Nonetheless, for sufficiently strong interactions we observe bound states of these unconventional magnons which possess a non-diverging group velocity. By measuring the configurational mutual information between two disjoint intervals, we demonstrate the implications of the bound state formation on the entanglement dynamics of the system. Our observations provide key insights into the peculiar role of composite excitations in the non-equilibrium dynamics of quantum many-body systems.

TT 23: Kagome Systems

Time: Tuesday 9:30–13:00

Location: HSZ 304

TT 23.1 Tue 9:30 HSZ 304

Broadband optical investigations of the CDW state in Kagome metals AV_3Sb_5 ($A = K, Rb, Cs$) — E. UYKUR^{1,2}, M. WENZEL¹, B.R. ORTIZ^{3,4}, S.D. WILSON⁴, S. WINNERL², M. DRESSEL¹, and A. A. TSIRLIN⁵ — ¹Physikalisches Institut, Universität Stuttgart, 70569, Stuttgart, Germany — ²Helmholtz-Zentrum Dresden-Rossendorf, Inst. Ion Beam Phys. & Mat. Res., 01328 Dresden, Germany — ³Materials Department and California Nanosystems Institute, University of California Santa Barbara, Santa Barbara, CA, 93106, United States — ⁴Materials Department, University of California Santa Barbara, Santa Barbara, CA, 93106, United States — ⁵Felix Bloch Institute for Solid-State Physics, Leipzig University, 04103 Leipzig, Germany

We present a broadband optical study of non-magnetic Kagome metals AV_3Sb_5 ($A = K, Rb, Cs$) down to 10 K. Different contributions to the optical spectra have been discussed and compared with the DFT calculations in normal and charge density wave (CDW) states. Spectra reflect the response of the 2D Dirac fermions and are frequency-independent in a broad energy range. Low energies are governed by the itinerant and localized charge carriers that show a spectral weight redistribution below the CDW transition. Our results show that the CDW gaps evolve systematically between the siblings ($K < Cs < Rb$) in line with their transition temperatures. We further use the experimental spectral weight to gauge the effect of electronic correlations and find it increasing with reducing the size of A .

TT 23.2 Tue 9:45 HSZ 304

Complex charge order in the AV_3Sb_5 kagome metals — MORTEN CHRISTENSEN¹, TURAN BIROL², BRIAN ANDERSEN¹, and RAFAEL FERNANDES³ — ¹Niels Bohr Institute, University of Copenhagen — ²Department of Chemical Engineering and Materials Science, University of Minnesota — ³School of Physics and Astronomy, University of Minnesota

The kagome lattice, consisting of an array of corner-sharing triangles, offers a rich platform to study the behavior of correlated electrons. In kagome metals,

the electronic band structure exhibits Dirac points, flat bands, and van Hove singularities - features which promote the role of electronic correlations. A family of recently discovered kagome metals, AV_3Sb_5 ($A=K, Rb, Cs$), provides a realization of these features. These materials exhibit an enigmatic superconducting order, which emerges from a three-dimensional charge-density wave (CDW) phase. While the precise nature of the CDW phase is still unknown, there are indications of both time-reversal symmetry breaking and nematicity inside the charge-ordered phase. Starting from the low-energy electronic states near the van Hove singularities, we construct a phenomenological model to describe the CDW phase. The order parameters of this model are either real, corresponding to bond distortions, or imaginary, corresponding to loop-currents. These CDW orders can coexist or compete which results in a rich landscape of subsidiary orders, including various types of multipolar magnetic orders. These have unique experimental signatures which can aid in pinpointing the precise nature of the CDW phase observed in experiments.

TT 23.3 Tue 10:00 HSZ 304

Investigation of the charge density wave in single crystal CsV_3Sb_5 under hydrostatic pressure — FABIAN STIER¹, TOBIAS RITSCHL¹, MAREIN RAHN¹, CHANDRA SHEKHAR², CLAUDIA FELSER², and JOCHEN GECK¹ — ¹IFMP, TU Dresden, Germany — ²MPI CPFS, Dresden, Germany

The topological Z_2 kagome materials AV_3Sb_5 ($A = K, Rb, Cs$) show a nontrivial electronic topology, exhibit superconductivity (SC) and a charge-density-wave (CDW) order. CsV_3Sb_5 shows a CDW below 90K with a $2 \times 2 \times 4$ superstructure, which changes around 60K to a $2 \times 2 \times 2$ superstructure. To investigate the interplay of CDW-order and SC we performed single crystal x-ray diffraction under hydrostatic pressure, with Argon as a pressure medium, up to 2 GPa and 20K. In this pressure range the SC shows two distinct domes, where T_c is enhanced and shows two maxima. The $2 \times 2 \times 2$ CDW at low temperatures persists under pressure up to the first extremum of $T_c \sim 0.7$ GPa, where for a short pressure range both, the CDW and a new emerging incommensurate CDW coexists. While the

first CDW quickly vanishes, the incommensurate CDW persists up to pressures where the SC shows another extremum in T_c . Above this pressure, ~ 1.5 GPa, no CDW could be detected. An accurate knowledge of these structural modifications will be essential to explain the relationship of topology and superconductivity in this class of materials.

TT 23.4 Tue 10:15 HSZ 304

Indication of a strong coupling charge density wave in CsV₃Sb₅ — •LEANDER PEIS^{1,2,3}, GE HE^{1,4}, and RUDOLF HACKL^{1,2,3} — ¹Walther Meissner Institut, Bayerische Akademie der Wissenschaften, Garching 85748, Germany — ²Technische Universität München, Garching 85748, Germany — ³IFW Dresden, Dresden 01062, Germany — ⁴University College Cork, Cork, Ireland

A prominent example for studying the interplay of electronic correlations and non-trivial topology is the material class of AV₃Sb₅ (A=K,Rb,Cs), displaying unconventional charge order in the range of 100 K and superconductivity at temperatures below 2.5 K. Here, we present a polarization-dependent Raman scattering study of the Kagome metal CsV₃Sb₅, focusing on the charge density wave (CDW). We resolve several signatures of strong-coupling between the lattice and the electronic system. First, the energy of the A_{1g} Γ -point phonon exhibits a discontinuity at the phase transition temperature $T_{CDW} = 95$ K. Second, the magnitude and symmetry dependence of the observed CDW energy gap 2Δ suggest strong coupling and a substantial anisotropy. Third, the observed A_{1g} amplitude mode depends weaker on temperature than expected and displays an asymmetric Fano-type line shape, particularly around 70 K. We interpret this deviation in terms of strong coupling between the phonon-like amplitude mode and the electronic continuum. To the best of our knowledge such an asymmetry of an amplitude mode has not been observed before.

TT 23.5 Tue 10:30 HSZ 304

X-ray diffraction on the charge-density wave in the Kagome superconductor RbV₃Sb₅ — •SABREEN HAMMOUDA¹, YU-HUI LIANG², PO-CHUN CHANG², CARSTEN PAULMANN³, YISHUI ZHOU¹, ADRIAN MERRITT¹, PIKESH PAL¹, RAHAF YASEEN¹, HONGXIONG LIU⁴, YOUGUO SHI⁴, CHAO-HUNG DU², and YIXI SU¹ — ¹JCNS-MLZ, Forschungszentrum Jülich, 85748 Garching, Germany — ²Dept. of Phys., Tamkang University, Tamsui 251, Taiwan — ³DESY, 22607 Hamburg, Germany — ⁴IOP, CAS, Beijing 100190, China

The newly discovered Kagome superconductors AV₃Sb₅ (A=K, Rb or Cs), in which non-trivial band topology, charge-density wave (CDW), and superconductivity are intertwined, have attracted tremendous interests. Despite extensive recent investigations via X-ray diffraction (XRD) and other complementary local probe techniques, it remains a major challenge to gain a consistent picture of the CDW modulation across different AV₃Sb₅ samples. In this talk, we will present our recent single-crystal XRD investigations (in-house and synchrotron) of the CDW modulations over a wide temperature range in the less-studied RbV₃Sb₅. A unique CDW modulation of the 2x2x2 type can be confirmed for RbV₃Sb₅ below $T_{CDW} = 102$ K, and no evidence for CDW fluctuations above T_{CDW} could be found. Our detailed temperature dependence measurements of the CDW superstructure reflections indicate a second-order phase transition with a 2D Ising character. A comparison to other AV₃Sb₅ compounds and possible implications on the understanding of the nature of the CDW in these Kagome superconductors will be given.

TT 23.6 Tue 10:45 HSZ 304

Z₂ topological insulator and Hubbard interactions on the Kagome lattice — IRAKLI TITVINIDZE¹, •JULIAN LEGENDRE^{2,3}, MAARTEN GROTHUS¹, BERNHARD IRSIGLER¹, KARYN LE HUR², and WALTER HOFSTETTER¹ — ¹Institut für Theoretische Physik, Goethe-Universität, 60438 Frankfurt am Main, Germany — ²CPHT, CNRS, Institut Polytechnique de Paris, Route de Saclay, 91128 Palaiseau, France — ³Department of Physics and Materials Science, University of Luxembourg, 1511 Luxembourg, Luxembourg

The study of topological phase transitions has been a very active field of research since the 80's; in recent decades topological insulators have been one of the major foci in this field. Understanding the role of the interactions in such systems is also currently a major challenge for the scientific community. In this talk, I will present a study of a time-reversal invariant topological model, with Hubbard interactions, on the Kagome lattice. The topological model contains intrinsic and Rashba spin-orbit coupling terms and position-dependent onsite energies. Relying on several analytical methods, I will show how the Z₂ topological phase, resulting from the flux term, is tuned by varying the amplitude(s) of on-site energy terms and/or of the Rashba spin-orbit coupling term, at filling $n = 2/3$. Then, we will study the effect of Hubbard interactions on the topological properties for a specific on-site energy configuration and at vanishing Rashba spin-orbit coupling. We will use perturbation theory in the large Hubbard amplitude U limit and a mean-field method for smaller U . I will compare these analytical results with numerical results obtained by our collaborators.

TT 23.7 Tue 11:00 HSZ 304

Temperature-dependent pump-probe spectroscopy of the magnetic Kagome metal Fe₃Sn₂ — •M. G. FARIA¹, Q. WANG², H. C. LEI², A. PASHKIN¹, S. WINNERL¹, M. HELM^{1,3}, and E. UYKUR¹ — ¹Helmholtz-Zentrum Dresden-Rossendorf, 01328 Dresden, Germany — ²Department of Physics and Beijing Key Laboratory of Opto-electronic Functional Materials & Micro-nano Devices, Renmin University of China, 100872 Beijing, China — ³Institute for Applied Physics, Technische Universität Dresden, 01069 Dresden, Germany

In this study, we present optical pump-probe measurements on a magnetic Kagome metal, Fe₃Sn₂, under different temperatures down to 10 K. The obtained spectra can be fitted with a double exponential decay, indicating that the system has two distinct relaxation processes. Additionally, some unexpected and pronounced oscillations are dominating the spectra, giving evidence of a strong electron-phonon coupling in Fe₃Sn₂, at least in this ultra-fast regime. The frequency of this coupled phonon is determined to be around 2.5 THz. Finally, we will discuss the temperature and pump fluence dependence of the observed phonon coupling and the distinct relaxation dynamics in this material.

15 min. break

TT 23.8 Tue 11:30 HSZ 304

Complex magnetic orders and the emergent topological Hall effect in the Kagome metal ErMn₆Sn₆ — •YISHUI ZHOU¹, CHANGJIANG YI², DMITRY KHALYAVIN³, FABIO ORLANDI³, PASCAL MANUEL³, SABREEN HAMMOUDA¹, ADRIAN MERRITT¹, CLAUDIA FELSER², THOMAS BRÜCKEL⁴, and YIXI SU¹ — ¹JCNS-MLZ, Forschungszentrum Jülich GmbH, Garching, Germany — ²Max Planck Institute for Chemical Physics of Solids, Dresden, Germany — ³ISIS Neutron & Muon Facility, STFC, Rutherford Appleton Laboratory, Didcot, UK — ⁴JCNS-2 & PGI-4, Forschungszentrum Jülich GmbH, Jülich, Germany

Following the discovery of a quantum-limit magnetic Chern phase in TbMn₆Sn₆, the magnetic topological metal series RMn₆Sn₆ (R=Gd-Yb, and Y, Lu, etc.), that possesses an ideal Kagome lattice of Mn, has emerged as a new platform to explore exotic states and novel functionalities. We have recently carried out the growth of high-quality single crystals of the magnetic Kagome metal ErMn₆Sn₆, and the physical properties characterizations via the magnetic susceptibility, heat capacity, and Hall conductivity measurements. We have also undertaken comprehensive neutron diffraction experiments on both single-crystal and powder samples at the WISH diffractometer at ISIS. Our study has clearly hinted a fascinating interplay between topologically non-trivial electronic band structures, magnetism and electronic correlations in ErMn₆Sn₆.

TT 23.9 Tue 11:45 HSZ 304

Thermodynamics of the spin-half square Kagome lattice antiferromagnet — •JÜRGEN SCHNACK¹, OLEG DERZHKO², and JOHANNES RICHTER³ — ¹Fakultät für Physik, Universität Bielefeld, Germany — ²Institute for Condensed Matter Physics, National Academy of Sciences of Ukraine, 79011 Lviv, Ukraine — ³Institut für Physik, Universität Magdeburg & Max-Planck-Institut für Physik Komplexer Systeme, Dresden, Germany

Over the last decade, the interest in the spin-1/2 Heisenberg antiferromagnet (HAF) on the square Kagome lattice has been growing as a model system of quantum magnetism with a quantum paramagnetic ground state, flat-band physics near the saturation field, and quantum scars. Here, we present large-scale numerical investigations of the specific heat, the entropy, as well as the susceptibility by means of the finite-temperature Lanczos method for system sizes of $N = 18, \dots, 54$. We find that the specific heat exhibits a low-temperature shoulder below the major maximum which can be attributed to low-lying singlet excitations filling the singlet-triplet gap, which is significantly larger than the singlet-singlet gap. For the susceptibility the singlet-triplet gap leads to an exponentially activated low-temperature behavior. The maximum of the susceptibility is found at a pretty low temperature $T/J = 0.146$ (for $N = 42$). We find a striking similarity of our data with the corresponding ones for the Kagome HAF down to very low temperatures.

TT 23.10 Tue 12:00 HSZ 304

Asymmetric melting of the 1/3-plateau for the Kagome lattice antiferromagnet — •HENRIK SCHLÜTER¹, JÜRGEN SCHNACK¹, and JOHANNES RICHTER² — ¹Bielefeld University, Bielefeld, Germany — ²University of Magdeburg and MPIPKS Dresden, Germany

The Kagome lattice Heisenberg antiferromagnet (KHAF) is a rich source of unconventional physics not only regarding its spin-liquid ground state but also with respect to its behavior at non-zero field and temperature.

Here we investigate the phenomenon of the asymmetric melting of the magnetization plateau at 1/3 of the saturation magnetization, see Refs. [1, 2]. We explain the effect by discussing the energy diagram and the density of states constructed from finite-temperature Lanczos data for KHAF with up to 48 sites [3].

- [1] J. Schnack, J. Schulenburg, J. Richter, Phys. Rev. B 98, 094423 (2018)
- [2] Takahiro Misawa, Yuichi Motoyama, and Youhei Yamaji, Phys. Rev. B 102, 094419 (2020)
- [3] H. Schlüter, F. Gayk, H.-J. Schmidt, A. Honecker, J. Schnack, Z. Naturforsch. A 76, 823 (2021)

TT 23.11 Tue 12:15 HSZ 304

Classical and quantum frustrated models of planar X-Y spins on the Kagome lattice: anisotropic magnetic patterns — •OLIVER NEYENHUYS, MIKHAIL FIS-TUL, and ILYA EREMIN — Ruhr Universität Bochum

We present a theoretical study of various highly anisotropic magnetic patterns occurring in the geometrically frustrated model of planar X-Y spins on the Kagome two-dimensional lattice. Frustration is introduced by a specific spatial arrangement of both ferromagnetic and anti-ferromagnetic bonds between adjacent magnetic moments on the lattice vertices. At the critical value of frustration $f = 3/4$ such a system displays the phase transition from an ordered ferromagnetic state to frustrated regime featuring a highly degenerate ground state in which topological (anti)vortices penetrate each cell. Taking into account a generous amount of topological constraints, the thermal fluctuations and the quantum tunneling induced transitions between these vortices/anti-vortices, we derive an effective Ising spin Hamiltonian on the corresponding hexagonal lattice, in which a strong long-range interaction between a well separated (anti)vortices occurs. By making use of the mean field analysis and direct numerical diagonalization of the Hamiltonian we characterize various classical and quantum phases and phase transitions between them for large and small Kagome lattices. Experimental observation of such magnetic patterns with coherent networks of superconducting qubits will be discussed.

TT 23.12 Tue 12:30 HSZ 304

Magnon-phonon coupling in the Kagome-lattice antiferromagnet Mn_3Ge — •ALEKSANDR SUKHANOV, NIKITA ANDRIUSHIN, ANTON KULBAKOV, and DMYTRO INOSOV — Institut für Festkörper- und Materialphysik, Technische Universität Dresden, D-01069 Dresden

Magnons and phonons, which are quanta of spin excitations and crystal-lattice vibrations in ordered materials, respectively, can be strongly coupled together when their dispersion relations intersect in reciprocal space. This results in hybridised collective spin-lattice excitations, also known as magnetoelastic (ME) modes.

The metallic hexagonal compound Mn_3Ge is characterized by a noncollinear spin order due to the geometric frustration of the Kagome lattice formed by Mn ions. Our earlier studies showed that Mn_3Ge belongs to a rare class of materials

that possess very strong ME coupling. The ME effect is manifested in the large negative thermal expansion of the material and high-pressure tuning of its remarkable anomalous Hall effect. Most intriguing is a previous observation that the noncollinear spin structure of Mn_3Ge can be driven into a collinear ferromagnetic state under a hydrostatic pressure of ~ 5 GPa. This, in turn, provides hints on how the magnetic structure is linked to the unconventional electron transport phenomena in this material.

In this talk, we will discuss the results of our recent single-crystal inelastic neutron and x-ray scattering spectroscopy measurements of Mn_3Ge . We were able to clearly resolve momenta and energy of the ME hybridization. The experimental results are supported with the first-principle lattice dynamics calculations.

TT 23.13 Tue 12:45 HSZ 304

Raman scattering study of magnetism in the Kagome materials Fe_3Sn_2 and $Co_3Sn_2S_2$ — •RUDI HACKL^{1,2,3}, GE HE⁴, and LEANDER PEIS^{1,2,3} — ¹Walther-Meißner-Institut, 85748 Garching, Germany — ²Technische Universität München, 85748 Garching, Germany — ³IFW Dresden, Dresden 01062, Germany — ⁴University College Cork, Cork, Ireland

Fe_3Sn_2 and $Co_3Sn_2S_2$ have triangularly coordinated layers of $3d$ transition metal ions sitting on a Kagome network. Both compounds have Dirac and Weyl nodes in the band structure. Fe_3Sn_2 is ferromagnetic below 670 K, and the spins start to reorient from perpendicular to parallel to the Kagome layer below 150 K. This reorientation was first observed by Mössbauer spectroscopy but has in general little influence on other observables such as thermal expansion or magnetization. In our Raman study we find an anomaly of the line width and the energy of the lowest A_{1g} phonon where the Sn atoms vibrate perpendicular to the Fe plane. We interpret the anomaly in terms of an enhanced spin-phonon coupling below approximately 150 K. $Co_3Sn_2S_2$ starts ordering antiferromagnetically below 175 K and turns into a ferromagnet in the low-temperature limit. Here, the spins are first in plane and the order is nearly frustrated. Below 100 K the spins point along the c -axis and are parallel. The A_{1g} phonon couples strongly to a continuum as highlighted by the asymmetric Fano-type line shape. The asymmetry is maximal close to the magnetic transition. We argue that small changes of the lattice have an effect on the magnetism.

TT 24: Quantum Dots: Transport (joint session HL/TT)

Time: Tuesday 9:30–12:15

Location: POT 151

TT 24.1 Tue 9:30 POT 151

Contact formation analysis of nickel to SiGeOI to form Nickel-Germanosilicide using Flash lamp annealing — •MUHAMMAD MOAZZAM KHAN¹, SŁAWOMIR PRUCNAL¹, and YORDAN M. GEORGIEV^{1,2} — ¹Institute of Ion Beam Physics and Materials Research, Helmholtz-Zentrum Dresden-Rossendorf, Bautzner Landstraße 400, D-01328 Dresden, Germany — ²Institute of Electronics at the Bulgarian Academy of Sciences, 72, Tzarigradsko chaussee blvd, 1784-Sofia, Bulgaria

In CMOS technology, parasitic source/drain (S/D) resistance becomes more crucial in determining the overall device performance as the device dimensions get smaller. The contact resistance dominates this parasitic S/D resistance to a great extent, which limits the drive current. In order to have minimal impact on electrical performance, the contact should have linear Current-Voltage characteristics and negligible resistance in comparison to the device resistance. When replacing silicon with silicon-germanium as a channel material in future devices, it is necessary to investigate the contact formation mechanism in order to develop suitable contacts for energy-efficient devices. In this work, we are investigating metal semiconductor contact formation on SiGeOI using flash lamp annealing and studying their properties using structural and electrical characterization.

TT 24.2 Tue 9:45 POT 151

Predicting charge density maps in 2D nanostructures with machine learning techniques — •AMANDA TEODORA PREDA^{1,2,3}, CALIN ANDREI PANTIS-SIMUT^{1,2,3}, NICOLAE FILIPOIU^{2,3}, LUCIAN ION², ANDREI MANOLESCU⁴, and GEORGE ALEXANDRU NEMNES^{1,2,3} — ¹Research Institute of the University of Bucharest (ICUB), Sos. Panduri 90, Bucharest, Romania — ²University of Bucharest, Faculty of Physics, 077125 Magurele-Ilfov, Romania — ³Horia Hulubei National Institute for Physics and Nuclear Engineering, 077126 Magurele-Ilfov, Romania — ⁴Department of Engineering, Reykjavik University, Menntavegur 1, IS-102 Reykjavik, Iceland

Machine learning (ML) models have the potential to significantly improve and assist the design process of nanodevices that require precise control of the quantum states.

For 2D nanoelectronic structures, charge and spin densities are relevant observables and are also suited for ML techniques which employ image processing. The model systems that we considered are two dimensional quantum dots with multiple electrons and random confinement potentials. With convolutional neu-

ral networks, we built a ML model to predict whether a configuration displays singlet-triplet transitions in the ground state. For image translation problems, we used models based on conditional generative adversarial networks in order to predict the charge density distribution for arbitrary interacting systems taking as input either the non-interacting cases or just the shape of the confining potential.

TT 24.3 Tue 10:00 POT 151

Mesoscopic transport properties of individually prepared GaN-nanowire field-effect transistors — •HANNES HERGERT^{1,2}, MATTHIAS T. ELM^{1,2,3}, and PETER J. KLAR¹ — ¹Institute of Experimental Physics I, Giessen, Germany — ²Center for Materials Research, Giessen, Germany — ³Institute of Physical Chemistry, Giessen, Germany

In order to keep the optimization of transistors within Moore's law new material systems as well as new transistor concepts such as GaN-nanowire field effect transistors (NW-FET) are needed. In this work we characterize the electrical transport properties of single NW-FET. Furthermore, we are able to obtain a deeper understanding of the mesoscopic transport processes. Unintentionally doped GaN-nanowires were fabricated using molecular-beam-epitaxy and device fabrication was performed by a combination of different lithographic methods and atomic layer deposition. After an annealing process the nanowire's resistance shows an ohmic behaviour. Electrical transport measurements were performed between 2 and 280 K. The investigated NW-FET exhibits a transfer characteristic identical to those of classical field-effect transistors. We show that the electrical transport is dominated by two transport processes: a transport within a metal-like impurity band at low temperatures and a hopping process at higher temperatures. Furthermore we were able to identify universal conductance fluctuations at temperatures below 140 K, which arise from the shift of the Fermi level when applying a topgate voltage.

TT 24.4 Tue 10:15 POT 151

Multi-Channel Kondo Effect in Few-Electron Quantum Dots — •OLFA DANI¹, JOHANNES C. BAYER¹, TIMO WAGNER¹, GERTRUD ZWICKNAGL², and ROLF J. HAUG¹ — ¹Institut für Festkörperphysik, Leibniz Universität Hannover, Germany — ²Institut für Mathematische Physik, Technische Universität Braunschweig, Germany

The Kondo effect is a many particle entangled system, that involves the interaction between a localized spin in the quantum dot and free electrons in the

electron reservoirs. This entanglement can be calculated using simplifying assumptions concerning the electronic structure of the quantum dot.

In this work we investigate a quantum dot device formed electrostatically in a two-dimensional electron gas using top-gates. A quantum point contact is used as a sensitive charge detector to detect single-electrons tunneling through the system. This enables us to know the exact number of electrons in the quantum dot (Ne). By changing the applied gate voltage, we are able to control Ne.

A Zero-bias anomaly is observed for a strong coupling to the leads and possible symmetrical tunnel barriers. This Kondo resonance appears for successive Ne showing a deviation from the conjectured odd-even behavior. The Kondo resonance is strongest for Ne=9 and displays a particle-hole symmetry for Ne =7,...,11. It is absent for Ne =6 and Ne = 12. These observations indicate the influence of the shell structure [1] of the electronic states in the quantum dot where orbital degeneracy is present.

[1] L. P. Kouwenhoven, et. al., Rep. Prog. Phys. 64, 701-736 (2001).

TT 24.5 Tue 10:30 POT 151

Highly Conductive Silicon Nanowires by Modulation-Doping via Aluminum-Induced Acceptor States in a SiO₂-shell — •DANIEL HILLER¹, INGMAR RATSCHINSKI¹, SOUNDARYA NAGARAJAN², JENS TROMMER², THOMAS MIKOLAJICK^{2,3}, and DIRK KÖNIG⁴ — ¹Institute of Applied Physics, TU Bergakademie Freiberg, Germany — ²Nanoelectronic Materials Laboratory gGmbH, Dresden, Germany — ³Institute of Semiconductors and Microsystems, TU Dresden, Germany — ⁴Integrated Materials Design Lab, ANU, Canberra, Australia

Silicon nanowires (Si NWs) enable maximum gate control over the source-drain current when configured in a gate-all-around FET-architecture. However, Si NWs with few nm in diameter suffer from severe difficulties with efficient impurity doping due to a multitude of physical and technological problems (diffusion, dielectric and quantum confinement, statistics of small numbers, etc.). Here, we present a novel doping concept for Si NWs comparable to the modulation doping approach of III-V semiconductors. Based on results from density functional theory (DFT) calculations, we use Al-doped SiO₂ shells around the Si NWs, which contain unoccupied Al-induced acceptor states that are energetically located below the Si valence band edge. These states can capture electrons from the Si, creating free holes as majority charge carriers [1-5]. In this presentation, recent results from the experimental realization of this concept on Si NWs are shown. We demonstrate that modulation doping using SiO₂:Al-shells allows for several orders of magnitude lower resistances when compared to undoped SiO₂-shells. [1] D. König et al., Sci. Rep. 7, 46703 (2017)

30 min. break

TT 24.6 Tue 11:15 POT 151

Carrier dynamics in quantum-dot tunnel-injection structures: microscopic theory and experiment — •MICHAEL LORKE¹, IGOR KHANONKIN², STEPHAN MICHAEL¹, JOHANN PETER REITHMAIER³, GADI EISENSTEIN², and FRANK JAHNKE¹ — ¹Institute for Theoretical Physics, University of Bremen, Otto-Hahn-Allee 1, Bremen, 28359, Germany — ²Electrical Engineering Department and Rus- sel Berrie Nanotechnology Institute, Technion, Haifa, 32000, Israel — ³Technische Physik, Institute of Nanostructure Technologies and Analytics, Center of Interdisciplinary Nanostructure Science and Technology (CINSA^T), University of Kassel, Kassel, 34132, Germany

Among the challenges for the next generation of semiconductor lasers is the enhancement of their modulation speed to satisfy the need for higher data transfer rates. For this purpose, tunnel injection lasers are an appealing concept, as they promise improved modulation rates and better temperature stability. Moreover, they eliminate a major detrimental effect of quantum dot lasers, which is the gain nonlinearity caused by hot carriers. It is shown in this work how the aforementioned improvements depend on the design of tunnel-injection devices. We perform a theory-experiment comparison on scattering times in tunnel injection devices to highlight the importance of alignment between the injector well and the quantum dot ensemble. It is shown how differences in the coupling to the injector quantum well caused by the alignment lead to scattering times into the quantum dot ensemble that vary by an order of magnitude.

TT 24.7 Tue 11:30 POT 151

Electron transport through a quantum dot in controlled heat bath environment — •HATEF GHANNADI MARAGHEH, JOHANNES C. BAYER, and ROLF J. HAUG — Institute for Solid State Physics, Leibniz Universität Hannover, Appelstraße 2, 30167 Hannover, Germany

For optimizing any device, amongst them semiconductor-based qubit, one has to understand the effects of the environment on them. In this sort of devices, not just quantum states of the channel but also the state of the particles is affected [1-3]. The device consists of split-gate quantum dot in a GaAs/AlGaAs heterostructure. The temperature of the measurement ranged from 49.9 mK to 800 mK.

There have been several works on explaining how electron transport through the quantum dot system would behave for different temperatures [4-5]. As the temperature changes, the Fermi distribution of the lead*s changes. This influenced the conductivity of the dot since in the presence of the bias voltage the transport window gets altered. Besides, depending on the presence of energy levels in the transfer window, the conductivity is manipulated by changing the temperature. For low temperatures, due to the local density of states and coupling of the barrier gates to the leads, fluctuations start to emerge.

[1]*K. C. Nowack et al, Science 318, 1430-1433 (2007)

[2]*Pioro-Ladrière, et al, Nature Physics 4, 776*779 (2008)

[3]*Jan K Kühne, et al, physica status solidi (b) 256(6) (2019)

[4]*E. B. Foxman, et al, Phys. Rev. B 47, 10020(R) (1993)

[5]*O. Dani, et al, Communications Physics 5 (1), 1-7 (2022)

TT 24.8 Tue 11:45 POT 151

Manipulation of temporal correlations in single-electron tunneling — •JOHANNES C. BAYER, ADRIAN SCHMIDT, TIMO WAGNER, and ROLF J. HAUG — Institut für Festkörperphysik, Leibniz Universität Hannover

Precisely timed single-particle operations are of critical importance for quantum technologies operating at fixed clock cycles. A detailed understanding of the interplay between an external drive and the response of the single-particle source is essential for achieving and improving the accuracy in the time domain. We here demonstrate a high level of control over the time domain of a driven single electron transistor (SET). Using a gate defined quantum dot connected to a highly sensitive charge detector [1] allows detecting electrons tunneling into and out of the SET in real-time [2, 3]. The tunneling rates of such devices are controllable by gate voltages. We drive the SET by modulating gate voltages periodically in time and use time-dependent tunneling rates [2] and waiting time distributions [4] to analyze the impact of the driving parameters on temporal correlations in the tunneling times.

[1] J. C. Bayer, T. Wagner, E. P. Rugeramigabo and R. J. Haug, Ann. Phys. 531, 1800393 (2019)

[2] T. Wagner, P. Talkner, J. C. Bayer, E. P. Rugeramigabo, P. Hänggi and R. J. Haug, Nat. Phys. 15, 330-334 (2019)

[3] R. Hussein, S. Kohler, J. C. Bayer, T. Wagner and R. J. Haug, Phys. Rev. Lett. 125, 206801 (2020)

[4] F. Brange, A. Schmidt, J. C. Bayer, T. Wagner, C. Flindt and R. J. Haug, Sci. Adv. 7, eabe0793 (2021)

TT 24.9 Tue 12:00 POT 151

Scalable integrated readout electronics for semiconductor quantum dots — •JONAS BÜHLER¹, ARUN ASHOK¹, LAMMERT DUIMPANS¹, PATRICK VLIEX¹, CHRISTIAN GREWING¹, ANDRÉ ZAMBANINI¹, and STEFAN VAN WAASEN^{1,2} — ¹Central Institute of Engineering, Electronics and Analytics, Electronics Systems (ZEA-2) Forschungszentrum Jülich GmbH, 52428 Jülich, Germany — ²Faculty of Engineering, Communication Systems, University Duisburg-Essen, 47057 Duisburg, Germany

Quantum computing is one of the promising candidates to overcome the limitations of *classical* computing, e.g. von Neumann architecture. Nowadays much progress has been made on the implementation of scalable qubits. This work focuses on semiconductor qubits, which need operating temperatures near 0 K. Room temperature electronics for control and readout, which are limiting the bandwidth and the scalability due to parasitic elements and heat conduction, are still widely used. Some progress has been made to integrate the qubit control and readout in the direct vicinity of the qubit at cryogenic temperatures. Especially readout electronics still have a limited scalability because of circuit size and power consumption. This work tries to overcome those limitations by comparing different readout architectures and implement a multiplexed and integrated readout circuit with lower area and power consumption. This integrated circuit in a 22nm FD-SOI technology will be placed on top of scalable quantum computing architectures and therefore might be a crucial step on the way to a multi-million qubit quantum computer.

TT 25: Molecular Electronics and Photonics (joint session TT/CPP)

Time: Tuesday 12:00–13:00

Location: HSZ 201

TT 25.1 Tue 12:00 HSZ 201

Single photon emitters in hBN via ultra-low energy helium ion implantation — •RENU RANI¹, MIHN BUI^{1,2}, CHENFENG LU^{1,2}, BILAL MALIK^{1,2}, FELIX JUNGE³, THORSTEN BRAZDA¹, DETLEV GRÜTZMACHER^{1,2}, HANS HÖFSÄSS³, and BEATA KARDYNAŁ^{1,2} — ¹Peter Grünberg Institut-9, Forschungszentrum Jülich, Jülich — ²Department of Physics, RWTH Aachen, Aachen — ³II. Institute of Physics, University of Göttingen, 37077 Göttingen

A discovery of quantum emitters in hexagonal boron nitride (hBN) has recently incited immense interest for quantum technologies. It offers a platform for fundamental science but is also of interest for applications in quantum photonics owing to its robust single photon emission at room temperature. Recent studies have suggested that these SPEs are associated with intrinsic defects, which led to efforts to engineer the SPE in hBN by various methods such as plasma treatment, annealing, laser, e-beam and ion irradiation methods. Despite these efforts, the origin of single photon emission and the correlation of emission with particular defects still need to be scrutinized. Here we use ultra-low energy ion implantation to introduce defects in hBN. We show that helium ions with energies as low as 50 eV are extremely efficient in introducing single photon emitters in hBN. We also show that low temperature annealing increases the density of the emitters. We consider the possible defects that helium ions at the implantation energy can generate in hBN and use statistical data on single photon emitters to discuss the possible origin of the emission. Finally, we discuss the viability of creating emitters in pre-selected locations.

TT 25.2 Tue 12:15 HSZ 201

Mechanosensitive single-molecule junctions — •FABIAN PAULY — University of Augsburg, Augsburg, Germany

Quantum interference of electron waves passing through a single-molecule junction provides a powerful way to influence its electrical properties. By distorting a molecule, showing a destructive quantum interference, small changes of electrode distance can lead to huge changes of electrical conductance. This mechanosensitivity is a desirable feature for highly sensitive stress sensors. Here, I will discuss recent combined experimental and theoretical studies of mechanosensitive molecular wires based on paracyclophanes and porphyrins [1-4]. Experimental findings are interpreted in terms of quantum interference effects between molecular frontier orbitals by theoretical calculations based on density functional theory and the Landauer scattering formalism.

- [1] D. Stefani et al., Nano Lett. 18, 5981 (2018)
- [2] K. Reznikova et al., J. Am. Chem. Soc. 143, 13944 (2021)
- [3] W. M. Schosser et al., Nanoscale 14, 984 (2022)
- [4] C. Hsu et al., Chem. Sci. 13, 8017 (2022)

TT 25.3 Tue 12:30 HSZ 201

Designing mechanosensitive molecules: A genetic algorithm-based approach — •MATTHIAS BLASCHKE and FABIAN PAULY — Institute of Physics, University of Augsburg, D-86159 Augsburg, Germany

Single molecules can be used as miniaturized functional electronic components, when connected to metallic electrodes. Mechanosensitivity describes a change of conductance for a certain change of electrode separation and is a desirable feature for applications such as ultrasensitive stress sensors [1-4]. We combine methods of artificial intelligence with high-level simulations based on electronic structure theory to design optimized mechanosensitive molecules from predefined building blocks. In this way we overcome time-consuming, inefficient trial and error cycles in molecular design. We unveil the black-box machinery usually connected to methods of artificial intelligence by presenting all important evolutionary processes. In addition, we identify general features that characterize well-performing molecules. Our genetic algorithm provides a systematic and powerful way to search chemical space and to identify the most promising molecular candidates.

- [1] D. Stefani et al., Nano Lett. 18, 5981 (2018)
- [2] K. Reznikova et al., J. Am. Chem. Soc. 143, 13944 (2021)
- [3] W. M. Schosser et al., Nanoscale 14, 984 (2022)
- [4] C. Hsu et al., Chem. Sci. 13, 8017 (2022)

TT 25.4 Tue 12:45 HSZ 201

Towards cavity-mediated molecule-molecule coupling — •ANDRÉ PSCHERER¹, JAHANGIR NOBAKHT¹, TOBIAS UTIKAL¹, STEPHAN GÖTZINGER^{2,1,3}, and VAHID SANDOGHDAR^{1,2} — ¹Max Planck Institute for the Science of Light, Erlangen, Germany — ²Department of Physics, Friedrich-Alexander University Erlangen-Nürnberg (FAU), Erlangen, Germany — ³Graduate School in Advanced Optical Technologies (SAOT), Friedrich-Alexander University Erlangen-Nürnberg, Erlangen, Germany

We recently demonstrated that a single molecule coupled to a Fabry-Pérot cavity reacts nonlinearly to light at the single-photon level. This was shown in four-wave mixing, optical switching and photon number sorting experiments [1]. We aim to exploit this level of control to couple two molecules to each other via the cavity mode and to explore two-photon transitions that become possible in such a system. We gain access to the excited state population through spectrally tailored cavity mirrors which transmit red-shifted fluorescence. In this contribution, we will report on our progress, challenges, and intermediate results.

- [1] A. Pscherer et al., Phys. Rev. Lett. 127, 133603 (2021)

TT 26: Members' Assembly

Topics: Status report on current meeting, Elections, Miscellaneous, Outlook 2024

Time: Tuesday 14:00–15:30

Location: HSZ 304

All members of the Low Temperature Physics Division are invited to participate.

TT 27: Focus Session: Unconventional Transport Phenomena in Low-Dimensional Superconducting Heterostructures

The investigation of new superconducting systems and effects is key to the development of superconducting electronics and quantum technologies. Recent studies have demonstrated that systems of low dimensionality in particular offer enormous possibilities for the realization of unconventional superconducting phases and quantum states. An effect hosted by low-dimensional superconducting systems is the supercurrent diode effect. The supercurrent diode effect was experimentally observed in 2020 and has since then been intensively investigated worldwide. The effect has been seen in a variety of low-dimensionality hybrid systems, such as two-dimensional van der Waals heterostructures, in magnetic proximity systems as well superlattices. The origin of the effect, however, is still under debate and several explanations have been proposed for its underlying mechanism including lack of inversion symmetry, spin-orbit coupling and screening effects. This Focus session will bring together the most recent developments in the field of superconducting effects in low-dimensionality systems and update the community on their physics and perspective applications, with particular attention to recent results related to the supercurrent diode effect.

Organizers: Wolfgang Belzig and Angelo Di Bernardo (Universität Konstanz)

Time: Wednesday 9:30–13:00

Location: HSZ 03

Invited Talk

TT 27.1 Wed 9:30 HSZ 03

Superconducting diode effect in Rashba superlattice — •TERUO ONO — Kyoto University, Japan

The diode effect is fundamental to electronic devices and is widely used in rectifiers and AC-DC converters. However, conventional diodes have an energy loss due to finite resistance. We found the superconducting diode effect (SDE) in Nb/V/Ta superlattices with a polar structure, which is the ultimate diode effect exhibiting a superconducting state in one direction and a normal state in the other [1-3]. SDE can be considered as the nonreciprocity of the critical current for the metal-superconductor transition. We also found the reverse effect, i.e., the nonreciprocal critical magnetic field under the application of the supercurrent [4]. We also found that the polarity of the superconducting diode shows a sign reversal as a magnetic field is increased, which can be considered as the crossover and phase transitions of the finite-momentum pairing states predicted theoretically [5]. SDE in Nb/V/Ta superlattices needs an application of an external magnetic field to break the time reversal symmetry, which is a disadvantage in applications. We recently succeeded in demonstrating SDE in a zero-field by introducing ferromagnetic layers in superlattices [6]. The polarity of the SDE is controlled by the magnetization direction of the ferromagnetic layer, leading to development of novel non-volatile memories and logic circuits with ultralow power consumption.

[1] J. Magn. Soc. Japan 43, 17 (2019)

[2] Nature 584, 373 (2020)

[3] Jpn. J. Appl. Phys. 60, 060902 (2021)

[4] Appl. Phys. Express 14, 073003 (2021)

[5] Phys. Rev. Lett. 128, 037001 (2022)

[6] Nat. Nanotechnol. 17, 823 (2022)

Invited Talk

TT 27.2 Wed 10:00 HSZ 03

Quasiparticle-based and Cooper-pair based superconducting diodes — •MARIA SPIES¹, STEFAN ILIĆ², SEBASTIÁN BERGERET², FRANCESCO GIAZZOTTO¹, and ELIA STRAMBINI¹ — ¹NEST, Istituto Nanoscienze-CNR and Scuola Normale Superiore, I-56127 Pisa, Italy — ²Centro de Física de Materiales (CFM-MPC) Centro Mixto CSICUPV/EHU, E-20018 Donostia-San Sebastián, Spain

Diodes are key elements for electronics, optics, and detection. Their evolution towards low dissipation electronics has led to the hybridization with superconductors (S) and the realization of non-reciprocal transport of both quasiparticles and Cooper pairs. That occurs when both spatial inversion and time-reversal symmetries are broken.

Here, we review both effects comparing their efficiencies and basic principles. The quasi-particle diode is a superconducting tunnel junction with zero conductance in only one direction. The directionselective propagation of the charge has been obtained through the broken electron-hole symmetry induced by the spin selection of a ferromagnetic tunnel barrier made of a EuS thin film separating a superconducting Al and a normal metal Cu layer. It achieves a large rectification of up to 40%.

On the other hand, supercurrent diodes made with hybrid S/spinorbit/ S Josephson Junctions or with two-dimensional Rashba superconductors have been demonstrated to show zero resistance in only one direction. We describe the equation of the supercurrent diode effect in a generic formalism that may inspire novel devices based on helical magnetism induced in conventional superconductors.

Invited Talk

TT 27.3 Wed 10:30 HSZ 03

Non-reciprocal superconductivity and the field free Josephson diode — •MAZHAR ALI — TU Delft, Delft, Netherlands

Nonreciprocal transport is incredibly important in technology; for example, asymmetry in the current-voltage response in semiconductor junctions has been the cornerstone of computing technology for half a century. The diode effect is a very basic demonstration of nonreciprocity. Nonreciprocal superconductivity, however, proved elusive, and only in 2020 was the superconducting diode effect (superconducting in one direction while normal conducting in the other) discovered for the first time in a bulk alloy of V/Nb/Ta. By breaking both inversion and time reversal symmetry (using an applied magnetic field), a difference in the critical superconducting current (I) for positive vs negative voltages (V) was seen. Recently, we demonstrated a Josephson diode (JD), created in a quantum material Josephson junction (QMJJ), a junction made up of two superconductors separated by a barrier comprised of a quantum material). A diodic effect was seen without an applied magnetic field; a puzzling result for theoretical physicists but an important advance for potential technological application. Using an inversion symmetry breaking heterostructure of NbSe₂/Nb₃Br₂/NbSe₂, half-wave rectification of a square-wave excitation was achieved with low switching current density, high rectification ratio, and high robustness. Future directions for optimizations and novel explorations, as well as a broader impact of using other quantum materials will be discussed.

15 min. break

TT 27.4 Wed 11:15 HSZ 03

Investigating the mechanism behind the Josephson Diode Effect in NiTe₂/superconductor Devices — •EMILY C. MCFARLANE¹, JONAS A. KRIEGER¹, MIHIR DATE¹, BANABIR PAL¹, PROCOPIOS C. CONSTANTINOU², VLADIMIR N. STROCOV², STUART S. P. PARKIN¹, and NIELS B. M. SCHRÖTER¹ — ¹Max Planck Institute of Microstructure Physics, Halle, Germany — ²Swiss Light Source, Paul Scherrer Institute, Villigen, Switzerland

The Josephson diode - recently realized in NiTe₂/superconductor devices in the presence of an external magnetic field [1] - has many potential uses in new superconducting memory and logic devices. These NiTe₂/Ti/Nb devices are the first Josephson diodes where the Josephson diode effect (JDE) was concluded to arise from finite momentum Cooper pairing. However, the role of the Ti layer directly at the NiTe₂ interface is not yet fully understood. Ti-doped NiTe₂ is seen to be superconducting [2], so here we investigate the possibility of intrinsic superconductivity at the NiTe₂/Ti interface by investigating its electronic structure with angle-resolved photoelectron spectroscopy. In isostructural PdTe₂, a van Hove singularity (vHS) near the Fermi level was linked to intrinsic superconductivity [3]. We find a similar vHS in the vicinity of the Fermi level in the electronic structure of NiTe₂, which can be shifted in energy at the interface due to a doping effect by aluminium.

[1] B. Pal *et al.*, Nat. Phys. 18, 1228 (2022)[2] B. S. de Lima *et al.*, Solid State Commun. 283, 27 (2018)[3] Kyoo Kim *et al.*, Phys. Rev. B 97, 165102 (2018)

TT 27.5 Wed 11:30 HSZ 03

Reversal of the AC and DC supercurrent diode effect in ballistic Josephson junctions — ANDREAS COSTA¹, CHRISTIAN BAUMGARTNER¹, SIMON REINHARDT¹, SERGEI GRONIN², GEOFFREY C. GARDNER², TYLER LINDEMANN², MICHAEL J. MANFRA², DENIS KOCHAN¹, JAROSLAV FABIAN¹, •NICOLA PARADISO¹, and CHRISTOPH STRUNK¹ — ¹University of Regensburg — ²Purdue University

Recent experiments [1,2] have demonstrated that the supercurrent diode effect (SDE), -i.e., a nonreciprocal supercurrent- can be obtained by applying a Zeeman field in the presence of spin-orbit coupling. The effect consists in a finite difference ΔI_c between positive I_c^+ and negative $|I_c^-|$ critical current (DC SDE), and an asymmetry in the Josephson inductance as a function of current (AC SDE). In this work, we show that, at high in-plane fields, the AC and DC SDE both change sign. Based on a minimal and analytical model, we clearly identify the origin of this sign change in terms of a $0-\pi$ -like transition -an effect predicted in the literature [3] but so far never experimentally observed. Thanks to our inductance measurements we can directly link the AC SDE reversal to the modification of the CPR induced by the Zeeman field. Our results illustrate the power of the Josephson inductance as a probe of phase transitions in unconventional superconductors.

[1] Ando *et al.*, Nature 584, 373 (2020)[2] Baumgartner *et al.*, Nature Nano. 17, 39, (2022)[3] Yokoyama *et al.*, Phys. Rev. B 89, 195407 (2014)

TT 27.6 Wed 11:45 HSZ 03

Theoretical study of the supercurrent diode effect in 2DEG Josephson junctions — •ANDREAS COSTA¹, DENIS KOCHAN^{1,2}, and JAROSLAV FABIAN¹ — ¹University of Regensburg, Germany — ²Slovak Academy of Sciences, Slovakia

Superconducting junctions exhibit fascinating physical phenomena, making them promising building blocks for quantum computing. The competition between the two fundamental spin interactions—ferromagnetic exchange and spin-orbit interaction (SOI)—and superconductivity has already been demonstrated to substantially modify the spectroscopic and transport signatures of these junctions, and potentially results in topological superconductivity.

In this talk, we will focus on 2DEG-based S-N-S Josephson junctions that combine intrinsic SOI with proximity-induced superconductivity originating, e.g., from top Al islands. We will demonstrate that turning the nonsuperconducting (N) weak link additionally ferromagnetic—e.g., through a magnetic field—can imprint a strong direction dependence on the current-phase relation, which finally rises a substantial difference between positive and negative critical currents, and thereby a pronounced supercurrent diode effect. Motivated by pioneering experimental studies [1-3], we will elaborate on powerful theoretical approaches—such as numerical tight-binding simulations [2, 3] and analytical studies of the Andreev spectrum—to characterize and understand the features of this Josephson supercurrent diode effect.

[1] Phys. Rev. Lett. 126, 037001 (2021)

[2] Nat. Nanotechnol. 17, 39 (2022)

[3] J. Phys. Condens. Matter 34, 154005 (2022)

TT 27.7 Wed 12:00 HSZ 03

Plasmons and dynamical screening in layered superconducting heterostructures — •YANN IN 'T VELD¹, MIKHAIL KATSNELSON¹, ANDREW MILLIS^{2,3}, and MALTE RÖSNER¹ — ¹Radboud University, Nijmegen, the Netherlands — ²Flatiron Institute, New York, USA — ³Columbia University, New York, USA

Layered metals host low-energetic plasmonic and phononic excitations, which both strongly couple to electrons. At the same time these excitations hybridize with each other, which can be tuned by the surrounding material, resulting in a complex interplay of different bosons. Here we investigate how this interplay affects superconductivity in layered materials and how it is affected by the substrate material. To this end we use a one-loop theory which consistently treats phonons, plasmons, their mutual interaction and environmental screening on the same footing. We find two regimes with large transition temperatures, controlled by the substrate screening. One is mediated by conventional phonon pairing, which shows a significantly reduced transition temperature due to consistent screening. The other regime is dominated by the unconventional electron-plasmon interaction, where we find strong effects of normal-state renormalization on the superconducting state. These results show how crucial a consistent treatment of all pairing and screening channels is for low-dimensional superconductivity.

TT 27.8 Wed 12:15 HSZ 03

Investigation of Nb gate-controlled superconducting nanoscale devices. — •LEON RUF, ELKE SCHEER, and ANGELO DI BERNARDO — 78464 Konstanz, Konstanz Germany

The electrical conductance in nanoscale devices can be modulated by an applied electric field (EF). In semiconductors the charge density is low, and the EF can penetrate deeply. However, in superconductors the charge carrier density is high and the external EF decays exponentially over a short distance. In 2018, it was reported [1] that the superconducting state can be partially and fully suppressed in gated nano constrictions by a strong applied EF which they attribute to an EF induced perturbation of the superconducting state. Since then, the observations were controversially discussed attributing them to an EF effect [1], high-energy quasiparticle injection [2], low-energy-mediated phonon excitation [3] or hot-spot generation [4]. Here, we are studying Nb gated Dayem bridges. Our observations show reversible full suppression of the supercurrent for Nb devices made by lift off, not for geometrically comparable etched devices. We discuss our observations in the light of the suggested mechanisms [1-4].

[1] G. De Simoni *et al.*, Nat. Nanotechnol. 13, 802 (2018)[2] L. D. Alegria *et al.*, Nat. Nanotechnol. 16, 404 (2021)[3] M. F. Ritter *et al.*, Nat. Electron. 5, 71 (2022)[4] J. Basset *et al.*, Phys. Rev. Res. 3, 043169 (2021)

TT 27.9 Wed 12:30 HSZ 03

Gate-controlled switching in non-centrosymmetric superconducting devices

— •JENNIFER KOCH, LEON RUF, ELKE SCHEER, and ANGELO DI BERNARDO — Universität Konstanz, Konstanz, Germany

Gate-controlled superconducting devices have become of great interest for the development of energy-efficient hybrid superconductor/semiconductor computing architectures. The idea behind this technology stems from the recent discovery that superconducting devices can be controlled electrically with the application of a gate voltage [1-3].

We investigate gate-controlled switching devices made of the non-centrosymmetric superconductor Nb_{0.18}Re_{0.82} for different gate-to-wire distances. This material promises a low switching voltage due to its disordered structure and should therefore be more suitable for the realization of devices compatible with CMOS transistors.

[1] G. De Simoni *et al.*, Nature Nanotech. 13, 802 (2018)[2] F. Paolucci *et al.*, Nano Lett. 18, 4195 (2018)[3] F. Paolucci *et al.*, Phys. Rev. Applied 11, 024061 (2019)

TT 27.10 Wed 12:45 HSZ 03

Microscopic theory of gate-voltage mediated surface pair breaking and its impact on a superconducting wire — •SUBRATA CHAKRABORTY, DANILO NIKOLIC, and WOLFGANG BELZIG — Fachbereich Physik, Universität Konstanz, D-78457 Konstanz, Germany

Gate-induced supercurrent suppression in a superconducting nano-bridge is a hot topic for research in present days. Recent experiments find supercurrent suppression in this nano-bridge for high gate electric fields [1-3]. The microscopic understanding of this effect is not clear till now. According to many experimental findings, there are three distinct tentative mechanisms, which could be responsible for this event, at high gate fields. In our work, we theoretically investigate the role of gate-mediated surface pair breaking on the supercurrent suppression. We show that in presence of a small concentration of magnetic impurities on the surface of the bridge, large gate-fields result in strong spin-flip scattering at the surface. Using microscopic modelling based on the quasiclassical Usadel equation we present the full phase diagram of the wire, that shows a supercurrent suppression very similar to some experiment. We speculate, that our generic theoretical predictions based on this microscopic effect can be tested experimentally by modifying the surface.

[1] G. De Simoni *et al.*, Nat. Nanotechnol. 13, 802 (2018)[2] I. Golokolenov *et al.*, Nat. Commun. 12, 2747 (2021)[3] L. D. Alegria *et al.*, Nat. Nanotechnol. 16, 404 (2021)

TT 28: Unconventional Superconductors

Time: Wednesday 9:30–11:15

Location: HSZ 103

TT 28.1 Wed 9:30 HSZ 103

Fermi surface study of the putative spin-triplet superconductor UTe₂ — •ALEXANDER EATON¹, THEODORE WEINBERGER¹, ZHEYU WU¹, ALEXANDER HICKEY¹, NICHOLAS POPIEL¹, and MICHAL VALISKA² — ¹Cavendish Laboratory, University of Cambridge, UK — ²MGML, Charles University, Prague

The unconventional superconductor UTe₂ exhibits numerous properties indicative of spin-triplet pairing, including an upper critical field far in excess of the Pauli paramagnetic limit, and re-entrant superconductivity at high magnetic fields > 40 T. However, a detailed understanding of the material's Fermi surface remains a key open question hampering efforts to attain a more detailed theoretical picture of the microscopic pairing mechanism(s) at play.

Here, we report a detailed de Haas-van Alphen study of the Fermi surface of UTe₂. We measured quantum oscillations in the magnetic torque and contactless resistivity of several high quality samples (RRR ~ 900, T_c = 2.1 K) in a dilution refrigerator at temperatures down to 19 mK and magnetic fields up to 28 T, through two orthogonal rotation planes. Importantly, access to field strengths this high allowed us to measure directly along the [001] direction, which has previously been proposed to run parallel to the axis of cylindrical Fermi surface sections.

We present a summary of our angle- and temperature-dependent results performed to date, and compare to DFT and DMFT calculations that we find to capture the majority of the observed behaviour.

TT 28.2 Wed 9:45 HSZ 103

High pressure study of the unconventional superconductor CeRh₂As₂ — •MEIKE PFEIFFER¹, KONSTANTIN SEMENIUK², SEUNGHYUN KHM², and ELENA HASSINGER¹ — ¹Technische Universität Dresden Institut für Festkörper- und Materialphysik, 01069 Dresden — ²Max Planck Institute for Chemical Physics of Solids, 01187 Dresden

The heavy-fermion superconductor CeRh₂As₂ hosts two distinct superconducting states which are currently understood as even- and odd-parity states. The compound crystallizes in a layered lattice that is globally centrosymmetric but

lacks local inversion symmetry at the Ce sites. This results in a strong spin-orbit coupling, believed to lead to a very high ratio of upper critical field (> 15 T) to critical temperature (T_c = 0.26 K). The normal state of the compound hosts an additional phase below 0.4 K, believed to be a quadrupole-density wave (QDW) order. We present a high-pressure electrical resistivity study of CeRh₂As₂ across different generations of samples. The QDW order is highly sensitive to lattice compression and gets fully suppressed at P_c ≈ 0.6 GPa. The superconducting transition temperature T_c decreases at a significantly lower rate, and both superconducting phases persist well above 2 GPa. Thus, we confirm that the QDW is not responsible for the phase switching from even- to odd-parity state. At the same time, the in-plane magnetic field peaks at P_c, suggesting a different kind of interplay between the two orders.

TT 28.3 Wed 10:00 HSZ 103

Superconductivity versus quadrupole density wave in CeRh₂As₂ —

•KONSTANTIN SEMENIUK¹, DANIEL HAFNER¹, PAVLO KHANENKO¹, JAVIER LANDAETA¹, THOMAS LÜHMANN¹, CHRISTOPH GEIBEL¹, SEUNGHYUN KHM¹, ELENA HASSINGER², and MANUEL BRANDO¹ — ¹MPI-CPS, Dresden, Germany — ²TU Dresden, Dresden, Germany

A heavy-fermion superconductor CeRh₂As₂ (T_c ≈ 0.3 K) undergoes a phase transition at the temperature T₀ ≈ 0.5 K, proposed to be a quadrupole density wave (QDW) instability. The compound hosts two distinct superconducting (SC) phases, presumably of different parity. These are separated by a first order phase boundary at magnetic field μ₀H* = 4 T, applied along the c axis of the tetragonal lattice. Recent studies suggest that the QDW phase boundary could meet the T_c(H) line at exactly at H*. This would imply that the SC phase switching is driven by the field-induced suppression of the QDW order coexisting with the superconductivity. Inability to reliably track T₀ near 4 T has left the question standing.

We present a study of a new generation of CeRh₂As₂ crystals, showing sharper signatures of phase transitions. From our measurements of heat capacity and electrical resistivity in c-axis magnetic field, we produce a more detailed phase

diagram which shows that the QDW and SC phase boundaries meet at 6 T. We conclude that the QDW state is not responsible for the SC phase switching at H^* and discuss the possible interplay between the two orders with reference to the Fermiology of CeRh_2As_2 as well as thermodynamic considerations.

TT 28.4 Wed 10:15 HSZ 103

Exploring the unconventional superconducting state in $\text{Ce}_3\text{PtIn}_{11}$ — JAN FIKÁČEK¹, SARAH R. DUNSIGER², SÉBASTIEN LAUGHREA³, ANDREA D. BIANCHI³, SHINSAKU KAMBE⁴, HIRONORI SAKAI⁴, YO TOKUNAGA⁴, MANUEL BRANDO⁵, and •JEROEN CUSTERS¹ — ¹Charles University, Faculty of Mathematics and Physics, Department of Condensed Matter Physics, Ke Karlovu 5, 121 16 Prague 2, Czech Republic — ²Centre for Molecular and Materials Science, TRIUMF, Vancouver, British Columbia, Canada V6T 2A3 — ³Département de Physique, Université de Montréal, Montréal, Canada — ⁴Advanced Science Research Center, Japan Atomic Energy Agency, Tokai-mura, Ibaraki 319-1195, Japan — ⁵Max Planck Institute for Chemical Physics of Solids, Nöthnitzer Strasse 40, D-01187, Dresden, Germany

The properties of the heavy fermion compound $\text{Ce}_3\text{PtIn}_{11}$ are certainly enigmatic. At ambient pressure, the compound displays two consecutive magnetic transitions into antiferromagnetic (AFM) states at $T_{\text{N}1} = 2.2\text{K}$ and $T_{\text{N}} = 2.0\text{K}$, respectively. Below $T_c = 0.32\text{K}$ superconductivity (SC) is found. It has been speculated that AFM and SC coexist because the compound harbors two inequivalent Ce sites each having a specific environment favoring either a magnetic or superconducting state. We focus on the SC state and present specific heat, ¹¹⁵In NQR and recent μSR experiments at ambient pressure and down to 20mK. The results sketch a picture of an unusual unconventional SC state.

TT 28.5 Wed 10:30 HSZ 103

Surface-acoustic-wave-induced unconventional superconducting pairing — •VIKTORIA KORNIKH — Julius-Maximilians-Universität Würzburg

Exotic materials, topological states, and quantum collective phenomena are of high interest for fundamental science and technology, because they provide complex and stable performance even at a very small scale. The field of unconventional superconductivity investigates new features and phenomena occurring in superconducting materials and setups. However, the exact processes, which lead

to unconventional superconducting states are usually not clear and subject to numerous hypotheses and attempts to experimentally verify them. Here, I will discuss how to use externally applied acoustic waves in order to induce unconventional superconducting pairing of different types in solid state matter, primarily in thin films and 2D materials. I will consider a simple setup consisting of a solid state material with conduction electrons and an applied surface acoustic wave, that breaks spatial translation symmetry. I will show that the symmetries of the possible surface-acoustic-wave-induced order parameters depend on the shape of the applied wave. As an example, I will show that even-frequency spin-triplet odd-parity order parameter can occur due to Rayleigh surface acoustic wave.

Invited Talk

TT 28.6 Wed 10:45 HSZ 103

Studying the Fulde-Ferrell-Larkin-Ovchinnikov order parameter in quasi-2D organic superconductors — •TOMMY KOTTE¹, S. MOLATTA¹, D. OPPERDEN¹, G. KOUTROULAKIS², S. E. BROWN³, J. A. SCHLUETER^{4,5}, H. KÜHNE¹, G. ZWICKNAGL⁶, and J. WOSNITZA^{1,7} — ¹Hochfeld-Magnetlabor Dresden, HZDR — ²UC Santa Barbara, USA — ³UC Los Angeles, USA — ⁴NSF, Alexandria, USA — ⁵ANL, Argonne, USA — ⁶IMP, TU Braunschweig — ⁷IFMP, TU Dresden

The Fulde-Ferrell-Larkin-Ovchinnikov (FFLO) state can emerge in superconductors for which the orbital critical field exceeds the Pauli limit. This unconventional superconducting state is characterized by a spatial modulation of the superconducting order parameter. Although evidence of the formation of an FFLO state has been found in various classes of materials, it is still theoretically debated and experimentally unexplored how the superconducting order parameter evolves within the FFLO phase. Here, we present two fundamental studies concerning this question in quasi-2D organic superconductors, which are well established to host an FFLO state: (i) By means of ¹³C NMR spectroscopy on $\beta''\text{-(ET)}_2\text{SF}_5\text{CH}_2\text{CF}_2\text{SO}_3$, we were able to quantify the modulation amplitude of the spin polarization throughout the FFLO state. This quantity is related to the modulated superconducting gap, hence representing the order parameter. (ii) By means of angular-resolved specific-heat measurements on $\kappa\text{-(ET)}_2\text{Cu(NCS)}_2$, we furthermore show how the FFLO order parameter becomes unstable against orbital interactions, leading to a crossover from the FFLO into Abrikosov-like states of higher-order Landau levels.

TT 29: Frustrated Magnets: General

Time: Wednesday 9:30–13:15

Location: HSZ 201

TT 29.1 Wed 9:30 HSZ 201

Possible stress-driven spiral-to-Néel transition in the triangular antiferromagnet PdCrO_2 — •NINA STILKERICH^{1,2}, SEUNGHYUN KHMIM², ANDREW MACKENZIE^{2,3}, JOCHEN GECK¹, and CLIFFORD HICKS^{2,4} — ¹Institut für Festkörper- und Materialphysik, Technische Universität Dresden, 01062 Dresden, Germany — ²Max Planck Institute for Chemical Physics of Solids, Nöthnitzer Str. 40, 01187 Dresden, Germany — ³Scottish Universities Physics Alliance (SUPA), School of Physics and Astronomy, University of St. Andrews, St. Andrews KY16 9SS, United Kingdom — ⁴School of Physics and Astronomy, University of Birmingham, Birmingham B15 2TT, United Kingdom

PdCrO_2 is a triangular antiferromagnet that undergoes a transition from a double-q to single-q magnetic structure under moderate uniaxial stress [1]. Due to a high sensitivity of the magnetic anisotropy to uniaxial stress, another transition from spiral order to a linear antiferromagnetic structure is predicted for higher stress of about 1 GPa [1].

We performed stress-strain measurements on PdCrO_2 and were able to identify the double- to single-q transition as a jump in strain. We report the discovery of an additional transition under higher stress, which might be the spin spiral to Néel transition suggested previously. [1] D. Sun et al., New J. Phys. 23, 123050 (2021)

TT 29.2 Wed 9:45 HSZ 201

Thermodynamic study of the partially polarized state of the sawtooth chain atacamite, $\text{Cu}_2\text{Cl(OH)}_3$ — LEONIE HEINZE¹, TOMMY KOTTE², ALBIN DE MUER³, SVEN LUTHER^{2,4}, ANDREW AMMERLAAN⁵, ÜLI ZEITLER⁵, ANJA U.B. WOLTER⁶, BERND BÜCHNER⁶, KIRRILY C. RULE⁷, HANNES KÜHNE², and •STEFAN SÜLLOW¹ — ¹TU Braunschweig, Braunschweig, Germany — ²HLD, HZ Dresden-Rossendorf, Germany — ³LNCMI, CNRS, Grenoble, France — ⁴TU Dresden, Dresden, Germany — ⁵HFML, Radboud University, Nijmegen, The Netherlands — ⁶ANSTO, Lucas Heights, Australia — ⁷IFW Dresden, Dresden, Germany

Recently, the natural mineral atacamite, $\text{Cu}_2\text{Cl(OH)}_3$, has been established as a unique model compound of the $S = 1/2$ quantum sawtooth chain with a dominant magnetic exchange $J \sim 360\text{K}$ along the chain spine and $J' \sim 102\text{K}$ within the sawtooth [1]. Residual interchain couplings of a few Kelvin drive atacamite into an antiferromagnetic (AFM) ground state below $T_N = 8.4\text{K}$. The AFM phase is suppressed in magnetic fields of $\sim 30\text{T}$. Upon suppression of AFM order,

the magnetization becomes plateau-like close to $M_{\text{sat}}/2$.

By now, we have been able to study the magnetic phase diagram up into the unusual partially polarized state by means of specific heat. Here, we present a corresponding study and present evidence for quantum critical behavior occurring upon suppression of AFM order.

[1] L. Heinze et al., Phys. Rev. Lett. 126, 207201 (2021).

TT 29.3 Wed 10:00 HSZ 201

Weakly coupled triangles forming a star lattice in an organic-inorganic copper sulfate — •OLEG JANSON¹, ULRICH K. RÖSSLER¹, and HAJIME ISHIKAWA² — ¹Leibniz IFW Dresden, Germany — ²ISSP, University of Tokyo, Japan

The recently synthesized organic-inorganic copper sulfate $[(\text{CH}_3)_2(\text{NH}_2)]_3[\text{Cu}_3(\text{OH})(\text{SO}_4)_4] \cdot 0.24\text{H}_2\text{O}$ has been proposed as a material realization of the $S = \frac{1}{2}$ star lattice model [1]. We report high-field magnetization measured on powder samples showing a broad plateau at $\frac{1}{3}$ of the saturation magnetization. Full saturation was reached at about 105 T in a destructive pulsed-field experiment. Low-field and low-temperature measurements on single crystals show no indications of magnetic ordering and reveal a sizable anisotropy of magnetization. Density-functional-theory (DFT) calculations indicate the relevance of two inequivalent exchanges J_T and J_D with $J_T \gg J_D$, placing this material in the limit of weakly coupled triangles. Anisotropic components of J_T were estimated by noncollinear DFT+ U calculations. We demonstrate that a simple model of isolated triangles accounts for the thermodynamic behavior of this compound.

[1] M. Sorolla et al., J. Am. Chem. Soc. 142, 5013 (2020)

TT 29.4 Wed 10:15 HSZ 201

Temperature-dependent transitions of the rare-earth delafossite NaGdS_2 — •JUSTUS GRUMBACH¹, MATHIAS DOERR¹, ELLEN HAEUSSLER², and SERGEY GRANOVSKY¹ — ¹Institut für Festkörper- und Materialphysik, Technische Universität Dresden, 01062 Dresden, Germany — ²Fakultät für Chemie und Lebensmittelchemie, Technische Universität Dresden, 01062 Dresden, Germany

Rare-earth delafossites are materials containing ideal triangular magnetic planes, which are frustrated. Due to their properties, rare-earth delafossites are promising candidates for a QSL ground state. In recent years this state occurred in some $S = \frac{1}{2}$ -delafossites with transitions in the mK range.

Now a number of own new measurements were made on NaGdS_2 single crystals. This delafossite with magnetic Gd^{3+} ions, which has been extensively in-

investigated for the first time, is of special interest due to the pure spin moment $J=S=\frac{7}{2}$. Measurements of several different thermodynamic and magnetic properties were performed on very small samples (size $\sim \mu\text{m}$) down to lowest temperatures (40 mK).

Essential physical data could be extracted, which show correspondingly a AFM-groundstate below ~ 250 mK, which is kind of expected. An additionally investigated modification at 60 K, indicating an anisotropy in the system, is still under theoretical debate and will form a main part of the talk.

TT 29.5 Wed 10:30 HSZ 201

Study of CoNb_2O_6 magnetic properties from first principles — •AMANDA KONIECZNA¹, KIRA RIEDL¹, ROSER VALENTI¹, and RADU COLDEA² — ¹Goethe-Universität, Frankfurt am Main, Germany — ²University of Oxford, Oxford, England

The quasi-one-dimensional ferromagnet CoNb_2O_6 offers an interesting playground to investigate the interplay of anisotropic magnetic interactions in real materials. A variety of magnetic models was proposed for this material, including longer-range Heisenberg exchange, dominant anisotropic Ising and bond-dependent Kitaev-type magnetic interactions.

In this talk, we discuss our theoretical approach to extract the magnetic exchange in CoNb_2O_6 . We first obtain material-specific hoppings from ab-initio methods and proceed by moving from a description in terms of the Hubbard model to the Spin Hamiltonian using exact diagonalization and perturbation theory. Finally, we will discuss how our results fit into the picture of available results for this system, both on the theoretical and experimental side.

We gratefully acknowledge funding by the DFG (German Research Foundation): QUAST-FOR5249 - 449872909 (Project TP4).

TT 29.6 Wed 10:45 HSZ 201

Valence bond solid state in explicitly dimerized chain with magnetic frustration — •JĘDRZEJ WARDYN¹, SATOSHI NISHIMOTO^{1,2}, and CLIÖ EFTHIMIA AGRAPIDIS³ — ¹IFW Dresden, 01069 Dresden, Germany — ²TU Dresden, 01062 Dresden, Germany — ³Faculty of Physics, University of Warsaw, Pasteura 5, 02093 Warsaw, Poland;

We consider the spin-1/2 dimerized frustrated ferromagnetic (FM) $J_1-J_1'-J_2$ model, with $J_1, J_1' < 0$ FM first neighbours coupling and $J_2 > 0$ antiferromagnetic second neighbors coupling. This model serves as a minimal model for LiCuSbO_4 and $\text{Rb}_2\text{Cu}_2\text{Mo}_3\text{O}_{12}$. We introduce the frustration parameter $J_2/|J_1| = \alpha$ and the dimerization parameter $J_1'/J_1 = \beta$. There are two special limits of dimerization: fully dimerized at $\beta=0$ and the undimerized J_1-J_2 model at $\beta=1$. Earlier studies have identified phases featured in the special limits as valence bond solid with a finite spin gap for $\beta=1$ and a Haldane-like state for $\beta=0$. For our model, the spin gap and phase diagram was investigated in a 2017 study by Agrapidis *et al.* [1]. Thanks to new insight, we revisit these results with applying new boundary conditions, which allow us to correctly estimate the spin gap which was previously underestimated. We compute the spin gap, the string order parameter (SOP), and dimer-dimer correlations using the density matrix renormalization group method (DMRG). We prove that the model features a VBS state. Our results allow us to determine this state as \mathcal{O}_3 -VBS state adiabatically connected to the Haldane-like state in the limit of $\beta=0$.

[1] C. E. Agrapidis *et al.*, Phys. Rev. B, 95, 220404 (2017).

TT 29.7 Wed 11:00 HSZ 201

The effect of nonlocal electronic correlations on different lattice geometries - A dynamical vertex approximation study — •MARVIN LEUSCH¹, ANDREAS HAUSOEL², ALESSANDRO TOSCHI³, GIORGIO SANGIOVANNI⁴, and GEORG ROHRINGER¹ — ¹Universität Hamburg, Hamburg, Germany — ²IFW Dresden, Germany — ³Julius-Maximilians-Universität Würzburg, Würzburg, Germany — ⁴TU Wien, Vienna, Austria

In the last decades, dynamical mean-field theory (DMFT) has become a standard tool for describing strongly correlated electron systems. It captures all purely local correlations effects and, hence, provides exact results in the limit of infinite coordination number and thus spacial dimensions. For finite dimensional systems, it neglects nonlocal correlation effects which are captured by diagrammatic extensions of DMFT such as the dynamical vertex approximation (DVA). In our work, we analyze the three dimensional Hubbard model on various lattice types to investigate the effect of different coordination numbers on local and nonlocal correlations. In particular, we study the magnetic phase diagram of the Hubbard model on a simple cubic (sc), body-centered cubic (bcc) and face-centered cubic (fcc) lattice within DVA and compare their transition temperatures to magnetically ordered states to corresponding DMFT results. Our numerical findings demonstrate, that the nonlocal correlations of DVA generally reduce the size of the ordered region with respect to DMFT while the actual magnitude of this reduction depends on the specific lattice type and, in particular, on the coordination number.

15 min. break

TT 29.8 Wed 11:30 HSZ 201

Systematic analysis of diagonal ordering patterns in bosonic lattice models with algebraically decaying density-density interactions — •JAN ALEXANDER KOZIOL¹, ANTONIA DUFT¹, GIOVANNA MORIGI², and KAI PHILLIP SCHMIDT¹ — ¹Department of Physics, Staudtstraße 7, Friedrich-Alexander-Universität Erlangen-Nürnberg, Germany — ²Theoretical Physics, Saarland University, Campus E2.6, D-66123 Saarbrücken, Germany

We propose a general approach to analyse diagonal ordering patterns in bosonic lattice models with algebraically decaying density-density interactions on arbitrary lattices. The key idea is a systematic search for the energetically best order on all unit cells of the lattice up to a given extent. Using resummed couplings we evaluate the energy of the ordering pattern in the thermodynamic limit using finite unit cells. We apply the proposed approach to the atomic limit of the extended Bose-Hubbard on a triangular lattice at fillings $f = 1/2$ and $f = 1$. We investigate the ground-state properties of the antiferromagnetic long-range Ising model on the triangular lattice and determine a six-fold degenerate plain-stripe phase to be the ground state for finite decay exponents. We also probe the classical limit of the Hamiltonian describing Rydberg atom arrangements on the sites and links of the Kagome lattice.

TT 29.9 Wed 11:45 HSZ 201

Phases of the spin-1/2 Heisenberg antiferromagnet on the diamond-decorated square lattice in a magnetic field — •NILS CACI¹, KATARÍNA KARL'OVÁ², TARAS VERKHOLYAK³, JOZEF STREČKA², STEFAN WESSEL¹, and ANDREAS HONECKER⁴ — ¹Institute for Theoretical Solid State Physics, RWTH Aachen University, Germany — ²Department of Theoretical Physics and Astrophysics, P.J. Šafárik University, Košice, Slovakia — ³Institute for Condensed Matter Physics, National Academy of Sciences of Ukraine, Lviv, Ukraine — ⁴Laboratoire de Physique Théorique et Modélisation, CNRS UMR 8089, CY Cergy Paris Université, France

The spin-1/2 Heisenberg antiferromagnet on the highly frustrated diamond-decorated square lattice is a spin system of orthogonal spin dimers that features various ground-state phases, consisting of extended monomer-dimer and dimer-tetramer ground states as well as a ferrimagnetic regime. By using a combination of density matrix renormalization group (DMRG), exact diagonalization, as well as unbiased sign-problem free quantum Monte Carlo (QMC) methods, we investigate this system in the presence of a finite magnetic field. We find at high magnetic fields the emergence of a spin-canted phase, with continuously rising magnetization, as well as the fully polarized paramagnetic phase. At intermediate field strength, we identify the presence of a first-order quantum phase transition line between a ferrimagnetic phase and the monomer-dimer regime, which extends to finite temperatures and terminates in a line of critical points belonging to the Ising universality class.

TT 29.10 Wed 12:00 HSZ 201

Ground-state degeneracy and magneto-thermodynamics of the spin-1/2 Heisenberg antiferromagnet on the diamond-decorated square lattice — •ANDREAS HONECKER¹, NILS CACI², TARAS VERKHOLYAK³, KATARÍNA KARL'OVÁ⁴, STEFAN WESSEL², and JOZEF STREČKA⁴ — ¹Laboratoire de Physique Théorique et Modélisation, CNRS UMR 8089, CY Cergy Paris Université, France — ²Institute for Theoretical Solid State Physics, RWTH Aachen University, Germany — ³Institute for Condensed Matter Physics, National Academy of Sciences of Ukraine, Lviv, Ukraine — ⁴Department of Theoretical Physics and Astrophysics, P.J. Šafárik University, Košice, Slovakia

The spin-1/2 Heisenberg antiferromagnet on the diamond-decorated square lattice exhibits a rich ground-state phase diagram in a magnetic field [1]. We investigate the thermodynamic properties of this model using a combination of analytical and numerical methods, including full diagonalization up to effectively $N = 30$ sites. We focus in particular on the vicinity of a "dimer-tetramer" phase at low magnetic fields that maps to a classical dimer model on the square lattice and retains a macroscopic ground-state degeneracy in a magnetic field. We discuss the consequences of this degeneracy for the thermodynamic and magnetocaloric properties of the system.

[1] N. Caci, K. Karlova, T. Verkholyak, J. Strečka, S. Wessel, A. Honecker, preprint arXiv:2210.15330

TT 29.11 Wed 12:15 HSZ 201

Thermodynamics of the frustrated Heisenberg model on the truncated hexagonal lattice — •ADRIEN REINGRUBER¹, NILS CACI², and STEFAN WESSEL² — ¹Institut für Theoretische Physik und Astrophysik, Universität Würzburg, Germany — ²Institut für Theoretische Festkörperphysik, RWTH Aachen University, Aachen, Germany

The thermodynamical properties of the spin-1/2 Heisenberg antiferromagnet on the truncated hexagonal lattice are studied using trimer-based cluster quantum Monte Carlo simulations. The system consists of an arrangement of spin-trimers on a honeycomb lattice with dimer couplings interconnecting neighboring trimers. The physics of this frustrated quantum spin system is investigated for different spin-coupling strengths. The severeness of the quantum Monte Carlo sign problem with respect to the single-site, dimer and trimer basis is exam-

ined. In the parameter regime of weakly coupled trimers an effective spin-1/2 Hamiltonian can be derived to describe the low-temperature physics. This effective model yields antiferromagnetic effective spin-1/2 trimer-spin interactions with bond-dependent coupling strengths. Unbiased quantum Monte Carlo simulations confirm the validity of the effective model within the low-temperature regime.

TT 29.12 Wed 12:30 HSZ 201

Another exact ground state of a 2D quantum antiferromagnet — PRATYAY GHOSH, •TOBIAS MÜLLER, JANNIS SEUFERT, and RONNY THOMALE — Julius-Maximilians-Universität, Würzburg, Germany

We present the exact dimer ground state of a quantum antiferromagnet on the maple-leaf lattice. A coupling anisotropy for one of the three inequivalent nearest-neighbor bonds is sufficient to stabilize the dimer state. Together with the Shastry-Sutherland Hamiltonian, we show that this is the only other model with an exact dimer ground state for all two-dimensional lattices with uniform tilings. We furthermore discuss the stability of this ground state from the perspective of perturbation theory.

TT 29.13 Wed 12:45 HSZ 201

Bound states and plateaus: Magnetization behavior of the maple leaf lattice — •JANNIS SEUFERT, PRATYAY GHOSH, TOBIAS MÜLLER, and RONNY THOMALE — Julius-Maximilians-Universität, Würzburg, Germany

Recently, the maple leaf lattice equipped with a Heisenberg-Hamiltonian was shown to exhibit an analytically exact antiferromagnetic dimer ground state analogous to the better known Shastry-Sutherland model. Anticipating that its even stronger frustration will lead to both familiar and exotic magnetic behav-

ior, we present the calculation of magnetization plateaus in the maple leaf model with Ising- and Heisenberg-spins. For the latter, this is achieved within a perturbation theory of magnetic excitations incorporating triplet-triplet interactions and correlated hopping, which promotes the emergence of bound states.

TT 29.14 Wed 13:00 HSZ 201

Exact analytical solutions of a distorted spin-1/2 tetrahedron with ring exchange — ROLF SCHUMANN¹ and •STEFAN-LUDWIG DRECHSLER² — ¹TU-Dresden, D-1169 Dresden, Germany — ²IFW-Dresden, D-1169 Dresden, Germany

We present exact analytical solutions for the eigenvalues of a general spin-1/2 Hamiltonian with 6 bilinear (Heisenberg) J_i and 3 ring exchange K_i couplings. Focusing on the experimentally interesting orthorhombically, tetragonally, trigonally and non-distorted ideal tetrahedra (ITH) we consider their thermodynamic properties as the magnetization M , susceptibility, entropy, and specific heat at any temperature T and external magnetic field H and derive from the magnetization steps $M(H)$ at high-fields and low- T the saturation field H_s , the critical ferrimagnetic field H_{c1} , and the width of the corresponding plateau as a function of the cyclicity. As a result we find enhanced H_s and lowered H_{c1} values with increasing ring exchange $K > 0$ due to the reduced frustration. We present exact mapping equations to extract the relevant exchange integrals J_i and K_i from experimentally observed transition energies and provide an analytical mapping of the single-band Hubbard model on the ITH valid at any coupling strength U/t , where U is the onsite Coulomb repulsion and t the NN-hopping integral. The experimental situations with respect to the magnitude and sign of $\kappa = J/K$ for $\text{Cu}_2\text{Te}_2\text{OBr}_2$, Cu_2OSeO_3 , and $\text{Cu}_4\text{X}_6\text{L}_4$ with $\text{X}=\text{Cl,Br}$ and L being various ligands are briefly discussed.

TT 30: Complex Oxides

Time: Wednesday 9:30–13:00

Location: HSZ 204

TT 30.1 Wed 9:30 HSZ 204

Planar superconducting resonators on SrTiO₃ and KTaO₃: GHz properties of quantum paraelectrics — VINCENT T. ENGL, NIKOLAJ G. EBENSPERGER, LARS WENDEL, MARIUS TOCHTERMANN, ILENIA NEUREUTHER, ISHAN SARVAIYA, CENK BEYDEDA, and •MARC SCHEFFLER — 1. Physikalisches Institut, Universität Stuttgart, Stuttgart, Germany

SrTiO₃ is a common substrate for perovskite thin films, and it hosts a superconducting interface when covered with LaAlO₃. Recently, similar superconducting interfaces based on KTaO₃ were realized. Any cryogenic electronics application using SrTiO₃ or KTaO₃ faces the quantum-paraelectric nature of both materials: upon cooling to temperatures of a few K, their very large real part ϵ_1 of the dielectric function complicates high-frequency device design, while the imaginary part ϵ_2 indicates rather high losses for SrTiO₃ at GHz frequencies.

Overcoming the challenges of the high ϵ_1 , we present coplanar superconducting Nb microwave resonators on SrTiO₃ and KTaO₃ substrates, which we operate at temperatures down to 25 mK. For SrTiO₃ with $\epsilon_1 \approx 20000$ at low temperatures, we couple the coplanar resonator to a conventional 50 Ω feedline using a distant-flip-chip geometry.[1,2] With loaded quality factors exceeding 800 for SrTiO₃ and 8000 for KTaO₃ we advance the prospects of these quantum paraelectrics towards applications in oxide-based superconducting quantum circuitry.

[1] L. Wendel *et al.*, Rev. Sci. Instrum. **91**, 054702 (2020)

[2] V. T. Engl *et al.*, arXiv:1911.11456 [cond-mat.supr-con]

TT 30.2 Wed 9:45 HSZ 204

Revisiting magnetic and orbital ordering in V₂O₃ — LOUIS-VICTOR SCHÄFER and •MARIA DAGHOFER — Institut für funktionelle Materie und Quantentechnologien, Universität Stuttgart

We revisit the correlated bands of V₂O₃ using the variational cluster approximation. Starting from various sets of one-particle parameters discussed in the literature, double counting of correlations turns out to be relevant here, as also reported in the literature. Settling onto consistent parameters, we then find that a careful treatment of inter-layer dimers is crucial to reproduce the experimentally observed magnetic ordering. Additionally, bonds in the planes orthogonal to the dimers affects orbital densities. Antiferromagnetic ordering is the found to go in hand with orbital symmetry breaking within the e_g sector. We find any models that reproduce the measured a_{1g} orbital densities also leads to active orbital degrees of freedom above the Neel transition.

TT 30.3 Wed 10:00 HSZ 204

Direct imaging of valence orbitals using hard x-ray photoelectron spectroscopy — •DAISUKE TAKEGAMI¹, LAURENT NICOLAÏ², YUKI UTSUMI¹, ANNA MELÉNDEZ-SANS¹, DARIA A. BALATSKY¹, CARIAD-A. KNIGHT¹, CONNOR DALTON¹, SHAO-LUN HUANG¹, CHI-SHENG CHEN¹, LI ZHAO¹, ALEXANDER C. KOMAREK¹, YEN-FA LIAO³, KU-DING TSUEI¹, JÁN MINÁR², and LIU HAO TJENG¹ — ¹Max Planck Institute for Chemical Physics of Solids, Dresden, Germany —

²University of West Bohemia, Pilsen, Czech Republic — ³National Synchrotron Radiation Research Center, Hsinchu, Taiwan

It was hypothesized already more than 40 years ago that photoelectron spectroscopy should in principle be able to image atomic orbitals. If this can be made to work for orbitals in crystalline solids, one would have literally a different view on the electronic structure of a wide range of quantum materials. Here, we demonstrate how hard x-ray photoelectron spectroscopy can make direct images of the orbitals making up the band structure of our model system, ReO₃ [1]. The images are energy specific and enable us to unveil the role of each of those orbitals for the chemical bonding and the Fermi surface topology. The orbital image information is complementary to that from angle-resolved photoemission and thus completes the determination of the electronic structure of materials.

[1] D. Takegami *et al.*, Phys. Rev. Res. **4**, 033108 (2022)

TT 30.4 Wed 10:15 HSZ 204

Orbital imaging of the spin state transition in LaCoO₃ — BRETT LEEDAHL¹, DAISUKE TAKEGAMI¹, MARTIN SUNDERMANN^{1,2}, HLYNUR GRETARSSON^{1,2}, ALEXANDER KOMAREK¹, ARATA TANAKA³, MAURITS HAVERKORT⁴, and •LIU HAO TJENG¹ — ¹MPI-CPS, Dresden, Germany — ²DESY/PETRA-III, Hamburg, Germany — ³Department of Quantum Matter, Hiroshima University, Japan — ⁴Institute for Theoretical Physics, Heidelberg University, Germany

Here we have investigated the Co $3d$ orbital occupation in LaCoO₃ across the spin state transition using the recently developed x-ray-based orbital-imaging method. The images collected allow for a direct determination of the amount of the Co t_{2g} and e_g holes. We find that, at the lowest temperatures, the low-spin state with the nominally $t_{2g}^6 e_g^0$ electron configuration *does* have holes in the t_{2g} subshell which we attribute to the presence of spin-orbit interaction. The hole amount, however, sets limits to the minimum energy gap between the lattice-frozen low-spin and high-spin states. At high temperatures, we find that the high-spin state occupation is about *half* (!) of the value reported in the most recent literature. Implications for the ab-initio modeling of the spin-state transition process are discussed.

TT 30.5 Wed 10:30 HSZ 204

Directional ballistics in ultra-pure delafossite metals — •MICHAL MORAVEC^{1,2}, GRAHAM BAKER³, MAJA D. BACHMANN^{1,2}, PHILIPPA H. MCGUINNESS^{1,2}, MARKUS KÖNIG¹, SEUNGHYUN KHM¹, and ANDREW P. MACKENZIE^{1,2} — ¹Max Planck Institute for Chemical Physics of Solids, Dresden, Germany — ²School of Physics and Astronomy, University of St Andrews, St Andrews, United Kingdom — ³University of British Columbia, Vancouver, Canada

Studying electrical transport in extremely pure materials has led to the discovery of novel phenomena. The delafossite metals, with their two-dimensional electronic structure and mean free paths in excess of 20 μm , are a recent addition to

the ultra-pure materials class. Here we study electrical transport in bars of varied width in delafossite metals PdCoO₂ and PtCoO₂. The bar-like structures are sculpted in two crystal orientations using the focused ion beam and sequentially narrowed across the width corresponding to the mean free path. We observe a cross-over from Ohmic to ballistic transport and gradual increase in resistivity anisotropy between the two orientations, as the channel is narrowed. This anisotropy is not allowed by the symmetry of the bulk crystal lattice; it is an example of symmetry lowering due to the imposition of shapes of finite size and the Fermi surface anisotropy [1]. We also complement our measurements with numerical solutions to the Boltzmann equation including the ARPES Fermi surface parametrisation. We obtain a good qualitative agreement with resistivity the data.

[1] M.D. Bachmann et al. Nat. Phys. 18, 819 (2022)

TT 30.6 Wed 10:45 HSZ 204

Electronic structure of the Fe²⁺ compound FeWO₄: a combined experimental and theoretical X-ray photoelectron spectroscopy study — •SIMONE G. ALTENDORF¹, DAISUKE TAKEGAMI¹, ANNA MELÉNDEZ-SANS¹, VANDA M. PEREIRA¹, CHANG-YANG KUO^{1,2,3}, CHUN-FU CHANG¹, CHIEN-TE CHEN², MASATO YOSHIMURA², KU-DING TSUEI², ANTOINE MAIGNAN⁴, MARCUS SCHMIDT¹, ARATA TANAKA⁵, and LIU-HAO TJENG¹ — ¹Max Planck Institute for Chemical Physics of Solids, 01187 Dresden, Germany — ²National Synchrotron Radiation Research Center, Hsinchu 30076, Taiwan — ³Department of Electrophysics, National Yang Ming Chiao Tung University, Hsinchu 30010, Taiwan — ⁴CRISMAT, Normandie Univ, ENSICAEN, UNICAEN, CNRS, Caen 14000, France — ⁵Quantum Matter Program, Hiroshima University, Higashi-Hiroshima 739-8530, Japan

Iron tungstate (FeWO₄) is one of the rare oxide compounds with a nearly pure divalent iron valence state. We investigate the electronic structure of FeWO₄ experimentally by X-ray photoelectron spectroscopy. Using various photon energies, cross-section effects allow to identify the individual contributions of the Fe and W states to the valence band. A comparison with band structure and full atomic multiplet configuration interaction calculations yields important insights into the correlations in the material.

The research in Dresden is partially supported by the DFG through SFB 1143.

TT 30.7 Wed 11:00 HSZ 204

Imaging the orbital-switching in Ti₂O₃ across the metal-insulator transition — •PAULIUS DOLMANTAS¹, CHUN-FU CHANG¹, MARTIN SUNDERMANN^{1,2}, BRETT LEEDAHL¹, ANDREA AMORESE¹, HLYNUR GRETARSSON^{1,2}, ALEXANDER KOMAREK¹, ARATA TANAKA³, MAURITS W. HAVERKORT⁴, and LIU HAO TJENG¹ — ¹MPI-CPFS, Dresden, Germany — ²DESY/PETRA-III, Hamburg, Germany — ³Department of Quantum Matter, Hiroshima University, Japan — ⁴Institute for Theoretical Physics, Heidelberg University, Germany

Using the recently developed x-ray-based *orbital-imaging* method, we have been able to observe a switching of the Ti 3d orbital occupation across the metal-insulator transition in Ti₂O₃. We find that in the insulating state only the a_{1g} of the t_{2g} subshell is occupied, while in the metallic state also the e_g^π gets filled at the expense of the a_{1g}. The insulator-metal transition may then be viewed as a transition from a solid of isolated Ti-Ti c-axis singlet dimers into a solid of electronically partially broken dimers, where the Ti ions acquire additional hopping in the a-b plane via the e_g^π channel. These findings have implications for the ab-initio modeling of the metal-insulator transition.

15 min. break

TT 30.8 Wed 11:30 HSZ 204

Effect of cation dynamics on polar instabilities of perovskite derived structures — •RINIS FERIZAJ¹, FLORIAN BÜSCHER¹, PETER LEMMENS¹, HIROSHI KAGEYAMA², and TONG ZHU² — ¹IPKM, TU Braunschweig — ²Energy Chemistry, Univ. Kyoto, Japan

Perovskite derived structures have a huge variability in structural, electronic and magnetic properties. This makes them leading candidates for todays search for novel energy materials. Using Raman scattering we probe phonon dynamics in such material and focus to the cation dynamics to better understand transitions into different polar/nonpolar low temperature phases.

We acknowledge support by DFG GrK 1952/2, Metrology for Complex Nanosystems-NanoMet, and DFG EXC-2123 QuantumFrontiers - 390837967.

TT 30.9 Wed 11:45 HSZ 204

Anomalous magnetotransport in SrIrO₃ (111) films — •JI SOO LIM¹, MERIT SPRING¹, MARTIN KAMP¹, LOUIS VEYRAT^{1,2}, AXEL LUBK², BERND BÜCHNER², MICHAEL SING¹, and RALPH CLAESSEN¹ — ¹Physikalisches Institut und Würzburg-Dresden Cluster of Excellence ct.qmat, Universität Würzburg, Würzburg, Germany — ²Leibniz Institute for Solid State and Materials Research and Würzburg-Dresden Cluster of Excellence ct.qmat, Dresden, Germany

Complex oxides provides an inexhaustible playground for the study of interactions between charge, spin, orbital, and lattice degrees of freedom. In particular, spin-orbit coupling can be of comparable magnitude to electron correlations in

5d iridates, leading to exotic quantum phases such as spin liquids and correlated topological semimetals [1]. Perovskite SrIrO₃ (SIO) films grown along the <111> direction exhibit a buckled honeycomb lattice, and are predicted to be topological crystalline insulators with a relatively large band gap [2].

Here we report on the epitaxial growth of ultrathin SIO films on SrTiO₃ (111) that display a twinned perovskite-like superlattice structure with a periodicity of 3 unit cells and the observation of unusual magnetotransport properties, namely the anomalous Hall effect. We observe a sign change of the magnetoresistance and hysteresis loops with increasing coercive fields below 10 K. By comparing with theoretical results, we discuss the origin of the unusual transport behavior.

[1] J. Chakhalian et al., APL Mater. 8, 050904 (2020)

[2] P. M. Gunnink et al., J. Phys.: Condens. Matter 33, 085601 (2021)

TT 30.10 Wed 12:00 HSZ 204

Magnetoelectric coupling of terbium orthotantalates — •XIAOTIAN ZHANG¹, NICOLA KELLY², CHENG LIU¹, SIÂN DUTTON¹, and SIDDHARTH SAXENA¹ — ¹Cavendish Laboratory, University of Cambridge, Cambridge, United Kingdom — ²Department of Chemistry, University of Oxford, Oxford, United Kingdom

Quantum multiferroic materials form a new and emerging area of physics where one expects to find emergence of novel quantum phases induced by subtle coupling between spin and charge degrees of freedom at low temperatures. Experimental study of such phenomena is limited by the lack of model materials where magnetism and dielectric properties can be tuned using magnetic fields at low temperatures.

In a recent breakthrough, we found that TbTaO₄ exhibits enhancement in dielectric response below 2 K on application of magnetic field, indicating magnetoelectric coupling. Previously, using susceptibility and heat capacity measurements we showed that TbTaO₄ orders at T_N = 2.25 K; powder neutron diffraction (PND) was used to solve the magnetic structure, which is A-type antiferromagnetic.

These rare-earth tantalates LnTaO₄ (Ln = Y, La-Lu) are of wide interest as a result of their luminescent, proton-conducting, oxide-ion-conducting and dielectric properties. In addition, in the monoclinic M polymorph of the tantalates with Ln = Nd-Er, the magnetic Ln³⁺ ions are arranged on an elongated diamond lattice. Materials with such a magnetic lattice have the potential for unusual magnetic behaviour owing to the interplay of the crystal electric field with the (possibly competing) J1 and J2 interactions.

TT 30.11 Wed 12:15 HSZ 204

S = 1 dimer system K₂Ni(MoO₄)₂: A candidate for magnon Bose-Einstein condensation — •BENJAMIN LENZ¹, BOMMISSETTI KOTESWARARAO², SILKE BIERMANN^{3,4,5}, PANCHANAN KHUNTIA^{6,7}, MICHAEL BAENITZ⁷, and SWARUP K. PANDA⁸ — ¹IMPMC, Sorbonne Université, Paris, France — ²IIT Tirupati, Tirupati, India — ³CPHT, Ecole Polytechnique, Palaiseau, France — ⁴Collège de France, Paris, France — ⁵Lund University, Lund, Sweden — ⁶IIT Madras, Chennai, India — ⁷MPI for Chemical Physics of Solids, Dresden, Germany — ⁸Bennett University, Greater Noida, India

Dimerized quantum magnets provide a unique possibility to investigate the Bose-Einstein condensation of magnetic excitations in crystalline systems at low temperature. Here, we model the low-temperature magnetic properties of the recently synthesized spin S = 1 dimer system K₂Ni(MoO₄)₂ and propose it as a candidate material for triplon and quintuplon condensation. Based on a first-principles analysis of its electronic structure, we derive an effective spin dimer model that we first solve within a mean-field approximation to refine its parameters in comparison to experiment. Finally, the model is solved by employing a numerically exact quantum Monte Carlo technique which leads to magnetic properties in good agreement with experimental magnetization and thermodynamic results. We discuss the emergent spin model of K₂Ni(MoO₄)₂ in view of the condensation of magnetic excitations in a broad parameter regime. Finally, we comment on a geometrical peculiarity of the proposed model and discuss how it could host a supersolid phase upon structural distortions.

TT 30.12 Wed 12:30 HSZ 204

The crucial influence of side groups on magnetic superexchange - a modification of the Goodenough-Kanamori-rules — DIJANA MILOSAVLJEVIC¹, OLEG JANSON², STEFAN-LUDWIG DRECHSLER², and •HELGE ROSNER³ — ¹Max-Planck-Institut für Mikrostrukturphysik, 06120 Halle, Germany — ²IFW Dresden, 01069 Dresden, Germany — ³Max-Planck-Institut für Chemische Physik fester Stoffe, 01187 Dresden, Germany

According to the famous Goodenough-Kanamori-Anderson rules, the key structural feature that determines the magnetic exchange coupling constant for superexchange in magnetic insulators is the magnetic ion-ligand-magnetic ion bond angle. Here, we demonstrate that this angle is not the only determining factor. An at least equally important influence on the exchange coupling has the presence of side groups attached to the ligands. Applying density functional calculations and subsequently derived realistic parameters for a multiband tight-binding model, we provide a quantitative analysis for the example case of edge-sharing Cu-O chains with bond angles near 90 degrees. We find that a single parameter, the difference in onsite-energies of the ligand orbitals parallel and

perpendicular to the Cu-O chain, is at least as important as the bond angle for sign and size of the superexchange. This parameter strongly depends on the position of side groups outside the superexchange pathway. For a fixed bond angle, changes of a side group position, only, can cause changes in the superexchange of several hundred Kelvin and thus dramatic changes in the magnetic properties.

TT 30.13 Wed 12:45 HSZ 204

A consistent microscopic magnetic model of the edge-sharing chain cuprate CuSiO_3 — •DIJANA MILOSAVLJEVIC^{1,2}, ANDREI GIPPIUS³, OLEG JANSON⁴, MICHAEL BAENITZ¹, YURI PROTS¹, JOHANNES RICHTER⁵, and HELGE ROSNER¹ — ¹MPI for Chemical Physics of Solids, Dresden — ²MPI of Microstructure Physics, Halle — ³Moscow, Russia — ⁴IFW, Dresden — ⁵MPI Physics of Complex Systems, Dresden

A unique place in the family of low-dimensional magnets occupies the Cu^{2+} compounds featuring a series of square-planar CuO_4 plaquettes connected via their edges, forming in this way a chain. The edge-shared plaquettes in Li_2CuO_2 show ferromagnetic ordering [1], whereas similar chains with increased Cu-O-Cu bond angle bridging neighboring Cu atoms in CuGeO_3 , undergo a spin-Peierls transition [2]. A compound with a Cu-O-Cu angle essentially identical to the one in Li_2CuO_2 and isostructural to the famous Spin-Peierls system CuGeO_3 is spin-1/2 cuprate CuSiO_3 [3]. In a combined experimental-theoretical approach, we derive a new magnetic model of CuSiO_3 , consistent with all reported experimental results.

[1] E.L.M Chung et al., Phys. Rev. B **68**, 144410 (2003)

[2] M. Hase et al., Phys. Rev. Lett. **70**, 3651 (1993)

[3] H. H. Otto et al., Z. Kristallogr. **214**, 558 (1999)

TT 31: Topology: Majorana Physics

Time: Wednesday 9:30–12:45

Location: HSZ 304

TT 31.1 Wed 9:30 HSZ 304

Photonic noise as a probe of Majorana bound states — •LENA BITTERMANN¹, FERNANDO DOMINGUEZ¹, and PATRIK RECHER^{1,2} — ¹Institut für Mathematische Physik, Technische Universität Braunschweig, D-38106 Braunschweig, Germany — ²Laboratory for Emerging Nanometrology Braunschweig, D-38106 Braunschweig, Germany

We propose a route to detect Majorana bound states (MBSs) by coupling a topological superconductor to a quantum dot (QD) in a pn-junction. Here, two MBSs are coherently coupled to electrons on the QD, which recombine with holes in situ to photons. Importantly, the polarization of the emitted photons provides direct information on the spin structure [1,2] and nonlocality [2,3] of the MBSs. Here, we focus on the shot noise of the emitted photons which allows to clearly distinguish the cases of well separated MBSs at zero energy from overlapping MBSs. In addition, we show that quasiparticle poisoning changes the shot noise from super-Poissonian to sub-Poissonian [4]. Furthermore, this setup can be extended by coupling a second QD close to the second MBS which gives rise to nonlocal shot noise correlations leading to additional signatures of MBSs.

[1] D. Sticlet, C. Bena, and P. Simon, PRL **108**, 096802 (2012)

[2] E. Prada, R. Aguado, and P. San-Jose, PRB **96**, 085418 (2017)

[3] A. Schuray, L. Weithofer, and P. Recher, PRB **96**, 085417 (2017)

[4] L. Bittermann, C. De Beule, D. Frombach, and P. Recher, PRB **106**, 075305 (2022)

TT 31.2 Wed 9:45 HSZ 304

Statistical Majorana bound state spectroscopy — •ALEXANDER ZIESEN¹, ALEXANDER ALTLAND², REINHOLD EGGER³, and FABIAN HASSLER¹ — ¹JARA Institute for Quantum Information, RWTH Aachen University, Aachen, Germany — ²Institut für Theoretische Physik, Universität zu Köln, Köln, Germany — ³Institut für Theoretische Physik, Heinrich-Heine-Universität, Düsseldorf, Germany

Tunnel spectroscopy data for the detection of Majorana bound states (MBS) is often criticized for its proneness to misinterpretation of genuine MBS with low-lying Andreev bound states. Here, we suggest a protocol removing this ambiguity by extending single shot measurements to sequences performed at varying system parameters. We demonstrate how such sampling, which we argue requires only moderate effort for current experimental platforms, resolves the statistics of Andreev side lobes, thus providing compelling evidence for the presence or absence of a Majorana center peak.

TT 31.3 Wed 10:00 HSZ 304

Disentanglement, disorder lines, and Majorana edge states in a solvable quantum chain — GENNADY Y. CHITOV¹, •KARUN GADGE^{2,3}, and PAVEL N. TIMONIN⁴ — ¹Département de Physique, Institut Quantique, Université de Sherbrooke, Sherbrooke, Québec J1K 2R1, Canada — ²Institute for Theoretical Physics, Georg-August-University Göttingen, Friedrich-Hund-Platz 1, D-37077 Göttingen, Germany — ³School of Basic Sciences, Indian Institute of Technology Mandi, Mandi 175005, India — ⁴Rostov-on-Don, Russia

We study the exactly solvable one-dimensional model: the dimerized XY chain with uniform and staggered transverse fields, equivalent upon fermionization to the noninteracting dimerized Kitaev-Majorana chain with modulation. The criticality is controlled by the properties of zeros of model's partition function, analytically continued onto the complex wave numbers. In the ground state they become complex zeros of the spectrum of the Hamiltonian. The analysis of those roots yields the phase diagram which contains continuous quantum phase transitions and weaker singularities known as disorder lines (DLs) or modulation transitions. The salient property of zeros of the spectrum is that the ground state is shown to be separable (factorized), and the model is disentangled on a subset of the DLs. From analysis of those zeros we also find the Majorana edge states and their wave functions. Reference: PRB **106**, 125146 (2022)

TT 31.4 Wed 10:15 HSZ 304

Unifying the theoretical description of Andreev, Majorana, quasi-Majorana bound states — •PASQUALE MARRA^{1,2} and ANGELA NIGRO³ — ¹Graduate School of Mathematical Sciences, The University of Tokyo, 3-8-1 Komaba, Meguro, Tokyo 153-8914, Japan — ²Department of Physics, and Research and Education Center for Natural Sciences, Keio University, 4-1-1 Hiyoshi, Yokohama, Kanagawa 223-8521, Japan — ³Dipartimento di Fisica 'E. R. Caianiello', Università degli Studi di Salerno, 84084 Fisciano (Salerno), Italy

In one-dimensional topological superconductors systems, zero-energy Majorana edge modes localize at the domain walls between topologically distinct phases, similar to the case of Jackiw-Rebbi solitons, which are solutions of the Majorana-Dirac equation on an inhomogeneous background. On the other hand, topologically trivial Andreev states below the particle-hole gap can originate from disorder or spatial inhomogeneities. Distinguishing between Majorana and Andreev states is an ongoing challenge that generated intense debate in the scientific community. Indeed, there is a continuous crossover between topologically nontrivial Majorana and trivial Andreev states induced by smooth inhomogeneities, which can occur without closing the bulk gap. Here, we describe nontrivial Majorana and Andreev bound states induced by spatial inhomogeneities and disorder, Shockley states, and Jackiw-Rebbi solitons in a unifying framework, introducing a characteristic length scale that can unambiguously distinguish between different regimes.

TT 31.5 Wed 10:30 HSZ 304

Majorana zero modes in fermionic wires coupled by Aharonov-Bohm cages — •NIKLAS TAUSENDPFUND^{1,2}, SEBASTIAN DIEHL², and MATTEO RIZZI^{1,2} — ¹Peter Grünberg Institut 8, Forschungszentrum Jülich, Germany — ²Institute for Theoretical Physics, University of Cologne, Germany

We devise a number-conserving scheme for the realization of Majorana Zero Modes in an interacting fermionic ladder coupled by Aharonov-Bohm cages. The latter provide an efficient mechanism to cancel single-particle hopping by destructive interference. The crucial parity symmetry in each wire is thus encoded in the geometry of the setup, in particular, its translation invariance. A generic nearest-neighbor interaction generates the desired correlated hopping of pairs. We exhibit the presence of an extended topological region in parameter space, first in a simplified effective model via bosonization techniques, and subsequently in a larger parameter regime with matrix-product-states numerical simulations. We demonstrate the adiabatic connection to previous models, including exactly-solvable ones, and we briefly comment on possible experimental realizations in synthetic quantum platforms, like cold atomic samples.

TT 31.6 Wed 10:45 HSZ 304

Tunable coupling of quantum dots via Andreev bound states - towards a Kitaev chain — CHUN-XIAO LIU, GUANZHONG WANG, TOM DVIR, and •MICHAEL WIMMER — Qutech and Kavli Institute for nanophysics, TU Delft, Niederlande

We show that the coupling between two quantum dots can be effectively mediated via Andreev bound states in a central superconducting segment. This gives rise to an effective superconducting and normal coupling between quantum dot states. Both coupling strengths can be independently controlled by changing the properties of the Andreev bound states, e.g. by a gate voltage. This allows to implement a Kitaev chain that can easily be tuned to a topological phase [1]. We will also discuss first experimental results implementing a two-site Kitaev chain [2, 3].

[1] arXiv:2203.00107

[2] arXiv:2205.03458

[3] arXiv:2206.08045

TT 31.7 Wed 11:00 HSZ 304

Odd-frequency pairing in Floquet topological superconductors — •ESLAM S. AHMED, SHUN TAMURA, and YUKIO TANAKA — Department of Applied Physics, Nagoya University, Japan

Time-periodic (Floquet) Hamiltonians offer a unique and tunable way to engineer topological systems with intriguing edge modes. In particular, Floquet superconductors can possess multi-Majorana edge modes at energies $E = 0$ and $E = \pi$.

It is well-established that there is a direct relationship between odd-frequency Cooper pairing amplitudes and the topological invariants in the static superconductors. In our study, we discuss this relationship in the time-periodic regime.

We consider a Kitaev chain alternating in time between two different values for chemical potential. By tuning the time-periodicity of the alternating chemical potential, we show that the chain admits multiple zero and π energy Majorana modes at the edge of the chain. Furthermore, we show that odd-frequency Cooper pairing amplitude at the edge of the chain is correlated to the presence of Zero and π Majorana modes.

15 min. break

TT 31.8 Wed 11:30 HSZ 304

Phase diagram of an extended parafermion chain — JURRIAN WOUTERS¹, FABIAN HASSLER², HOSHO KATSURA³, and •DIRK SCHURICHT¹ — ¹Institute for Theoretical Physics, Center for Extreme Matter and Emergent Phenomena, Utrecht University — ²JARA-Institute for Quantum Information, RWTH Aachen University — ³Department of Physics, Graduate School of Science, The University of Tokyo

We study the phase diagram of an extended parafermion chain, which, in addition to terms coupling parafermions on neighbouring sites, also possesses terms involving four sites. Via a Fradkin–Kadanoff transformation the parafermion chain is shown to be equivalent to the non-chiral \mathbb{Z}_3 axial next-nearest neighbour Potts model. We discuss a possible experimental realisation using heteronanostructures. The phase diagram contains several gapped phases, including a topological phase where the system possesses three (nearly) degenerate ground states, and a gapless Luttinger-liquid phase.

TT 31.9 Wed 11:45 HSZ 304

Interacting Majorana fermions — •LUKAS JANSSEN¹ and URBAN F. P. SEIFERT² — ¹Technische Universität Dresden, Dresden, Germany — ²University of California, Santa Barbara, USA

I will present our study of models of interacting Majorana fermions with global $SO(N)$ symmetry. The models can be understood as real counterparts of the $SU(N)$ Hubbard–Heisenberg models and may be realized in Abrikosov vortex phases of topological superconductors, or in fractionalized phases of strongly frustrated spin-orbital magnets. I will describe the zero-temperature phase diagrams and discuss the nature of the occurring quantum phase transitions, with the help of mean-field, renormalization group, and quantum Monte Carlo approaches.

[1] L. Janssen and U. F. P. Seifert, Phys. Rev. B 105, 045120 (2022)

TT 31.10 Wed 12:00 HSZ 304

Multiplicative Majorana zero modes — •ADIPTA PAL — Max Planck Institute for the Physics of Complex Systems, Dresden, Germany

Topological qubits composed of unpaired Majorana zero-modes are under in-

tense experimental and theoretical scrutiny in efforts to realize practical quantum computation schemes. In this work, we show the minimum four ‘unpaired’ Majorana zero-modes required for a topological qubit according to braiding schemes and control of entanglement for gate operations are inherent to multiplicative topological phases, which realize symmetry-protected tensor products—and maximally-entangled Bell states—of unpaired Majorana zero-modes known as multiplicative Majorana zero-modes. We introduce multiplicative Majorana zero-modes as topologically-protected boundary states of both one and two-dimensional multiplicative topological phases, using methods reliant on multiplicative topology to construct relevant Hamiltonians from the Kitaev chain model. We furthermore characterize topology in the bulk and on the boundary with established methods while also introducing techniques to overcome challenges in characterizing multiplicative topology. In the process, we explore the potential of these multiplicative topological phases for an alternative to braiding-based topological quantum computation schemes, in which gate operations are performed through topological phase transitions.

TT 31.11 Wed 12:15 HSZ 304

Controlling Majorana modes via Fulde-Ferrell-Larkin-Ovchinnikov phases in topological superconductors and superfluids — •PASQUALE MARRA^{1,2}, DAISUKE INOTANI², TAKESHI MIZUSHIMA³, and MUNETO NITTA² — ¹Graduate School of Mathematical Sciences, The University of Tokyo, 3-8-1 Komaba, Meguro, Tokyo 153-8914, Japan — ²Department of Physics, and Research and Education Center for Natural Sciences, Keio University, 4-1-1 Hiyoshi, Yokohama, Kanagawa 223-8521, Japan — ³Department of Materials Engineering Science, Osaka University, Toyonaka, Osaka 560-8531, Japan

The next milestones in the route to topological quantum computation with Majorana modes are demonstrating their nonabelian braiding statistics and realizing Majorana-based topological qubits. To achieve this, most proposals require the manipulation of electric gates or magnetic fields in networks of proximitized semiconducting nanowires. Here, we focus on an alternative platform to obtain Majorana modes by employing inhomogeneous Fulde-Ferrell-Larkin-Ovchinnikov (FFLO) phases in topological superconductors and superfluids. The FFLO state spontaneously breaks translational symmetry, inducing a periodic and spatial modulation of the superconducting pairing. We explore the interplay between FFLO order, nontrivial topology, and emergent quantum-mechanical supersymmetry and consider possible routes to realize nonabelian braiding in these platforms.

TT 31.12 Wed 12:30 HSZ 304

Time-reversal invariant topological superconductor in the Coulomb blockade regime — •STEFFEN BOLLMANN¹, ELIO KÖNIG¹, and JUKKA VÄYRYNEN² — ¹Max Planck Institute for Solid State Research, Stuttgart — ²Purdue University, West Lafayette, Indiana USA

Floating topological superconductors coupled to conduction electrons can realize unconventional $O(N)$, $Sp(2N)$, or multi-channel Kondo effects. Here, we introduce a new topological superconducting mesoscopic device, a time-reversal invariant version of the Majorana Cooper pair box in the Coulomb blockade regime. In this setup of Cartan–Altland–Zirnbauer class DIII, spinful Majorana zero modes appear at the edges of a topological triplet superconductor with fluctuating Cooper pair spin and charge. We study the Kondo effect in the limit of dominating charging energy and in the limit of both small and large spin fluctuations. Beyond its value in the context of exotic mesoscopic Kondo effects, our study sheds light on the intricate interplay of band topology and strong quantum fluctuations of non-Abelian order parameter fields.

TT 32: Molecular Electronics and Excited State Properties (joint session CPP/TT)

Time: Wednesday 9:30–12:30

Location: GÖR 226

TT 32.1 Wed 9:30 GÖR 226

Strong Solvatochromism in a Two Metal Center Photocatalyst Molecule — •MIFTAHOSSURUR HAMIDI PUTRA¹ and AXEL GROSS^{1,2} — ¹Universität Ulm Institut für Theoretische Chemie Mez-Starck-Haus Oberberghof 7 89081 Ulm Deutschland — ²Helmholtz Institute Ulm (HIU) Electrochemical Energy Storage, 89069 Ulm, Deutschland

In the theoretical study presented here, we show that the electronic and optical properties of a molecular photocatalyst can strongly depend on the solvent it is dissolved in [1]. Ground-state density functional theory and linear response time dependent density functional theory calculations are applied in order to investigate the influence of implicit solvents on the structural, electronic and optical properties of a two metal center molecular photocatalyst $[(\text{tbbpy})_2\text{Ru}(\text{tpphz})\text{PtI}_2]^{2+}$ (RuPtI_2) [2]. These calculations predict a significant dependence of the HOMO-LUMO gap of the photocatalyst on the dielectric constant of the solvent. We elucidate the electronic origins of this strong solvatochromic effect and sketch the consequences of these insights for the use of photocatalysts in different environments.

[1] M. K. Nazeeruddin, S. M. Zakeeruddin, R. Humphry-Baker, M. Jirousek, P. Liska, N. Vlachopoulos, V. Shklover, C.-H. Fischer, M. Grätzel, Inorg. Chem. **38**, 6298–6305 (1999).

[2] M. G. Pfeffer, T. Kowacs, M. Wächtler, J. Guthmüller, B. Dietzek, J. G. Vos, S. Rau, Angew. Chem. **54**, 6627–6631 (2015).

TT 32.2 Wed 9:45 GÖR 226

Dynamic Charge-Transport and Charge-Transfer Regimes for Electron-Phonon-Coupled Molecular Systems — •MICHEL PANHANS, SEBASTIAN HUTSCH, and FRANK ORTMANN — Department of Chemistry, TU München

Different approaches for charge transport in organic solids exist but they differ significantly in the described physics of the electron-phonon coupling. In our recent work, we investigate the charge-transfer dynamics, the fading of transient localization (TL) and the formation of polarons for a large range of vibration frequencies and temperatures in the phase space of the two-site Holstein model. The combined numerical and analytical method is based on the time-domain Kubo formula of electrical conductivity to describe the highly correlated

electron-phonon dynamics from femtoseconds to very large time scales, reaching nanoseconds. We identify three charge-transport regimes, which are TL, soft gating, and polaron transport. Of particular interest is the built up of correlations between the electronic motion and the nuclei manifesting in the crossover between TL and polaron transport. We find, that the transition between these two limiting cases is seamless at all temperatures and all adiabatic ratios even for the low-frequency vibrational modes that were often considered to be frozen.

TT 32.3 Wed 10:00 GÖR 226

Multichromophore Macrocycles of Perylene Bisimide Dyes as Fluorescent OLED Emitters — •BJÖRN EWALD¹, ULRICH MÜLLER¹, PETER SPENST², PHILIPP KAGERER¹, THEODOR KAISER¹, MATTHIAS STOLTE², FRANK WÜRTHNER², and JENS PFLAUM¹ — ¹Experimental Physics VI, University of Würzburg, 97074 Würzburg — ²Institut für Organische Chemie and Center for Nanosystems Chemistry, University of Würzburg, 97074 Würzburg

Highly efficient electroluminescence from Organic Light Emitting Diodes (OLEDs) is limited by the non-radiative character of triplet states for conventional fluorophores. While fluorescent emitters benefit from high radiative recombination rates on the order of 10^9 s^{-1} , they lack from dark triplet states with lifetimes up to several μs or ms. Here we elucidate the potential of perylene bisimide macrocycles as a novel class of fluorescent OLED emitters by applying photon-correlation studies. The correlation experiments unfold additional excitonic relaxation pathways shortening the dark state lifetime for the covalently linked perylene bisimide chromophores. A trimeric chemical design leads to efficient single-photon emission from optically excited thin film samples and even under electrical operation in OLEDs. To the best of our knowledge this is the first indication of electrically-driven single-photon emission from a fluorescent molecule [1]. Therefor we consider our work to constitute an important step towards the design of state-of-the art fluorescent OLED emitters that might also feature a high potential for application in non-classical single-photon sources.

[1] Ulrich Müller et al., *Adv. Optical Mater.* 2022, 10, 2200234.

TT 32.4 Wed 10:15 GÖR 226

A Tool Kit for Analyzing Emission Spectra of Multi-Molecular States — •SEBASTIAN HAMMER^{1,4}, THERESA LINDERL², KRISTOFER TVINGSTEDT¹, WOLFGANG BRUETTING², and JENS PFLAUM^{1,3} — ¹Experimental Physics VI, University of Würzburg, 97074 Würzburg — ²Institute of Physics, University of Augsburg, 86135 Augsburg, Germany — ³Bayerisches Zentrum für Angewandte Energieforschung (ZAE Bayern), 97074 Würzburg — ⁴Departments for Physics and Chemistry, McGill University, Montreal, Canada

The performance of opto-electronic devices is often crucially impacted by multi-molecular excited states such as charge-transfer (CT) states or excimers. Hence, the spectroscopic analysis of these states is a common tool in the characterization of such systems. Due to the many parameters at play full quantum mechanical interpretations are tedious and therefore the analysis is often performed on a phenomenological level only. Here we present a tool kit to analyze temperature dependent emission spectra using a Franck-Condon based approach with a single effective inter-molecular vibrational mode and discuss the implications of considering different potentials for the ground and excited state harmonic oscillators [1]. Finally, we show that fundamental parameters of the potential energy landscape can be extracted from temperature dependent steady state emission spectra using the example of a tetraphenylidibenzoperiflanthene: C_{60} CT heterostructure [2]. Funding from the DFG (Project 490894053) is gratefully acknowledged.

[1] Hammer et al., *Mater. Horiz.* (2022). doi: 10.1039/D2MH00829G

[2] Linderl et al., *Phys. Rev. Appl.* 13 024061 (2020)

TT 32.5 Wed 10:30 GÖR 226

Singlet Fission search in polyacene molecules in gas-phase and on rare-gas clusters using ab initio methods — •SELMANE FERCHANE and MICHAEL WALTER — Institute of Physics, University of Freiburg, Germany

Singlet fission (SF), is a spontaneous photo-excited splitting phenomenon. Where an organic chromophore dimer, converts its singlet exciton into a pair of triplet excitons. A great promise for future photon-to-current conversion of solar energy using organic materials with high efficiency. To get more insight into these processes of SF, we employed different ab initio theories and approaches in our investigation, namely, density functional theory (DFT), TD-DFT, MCTDH, and CASPT2/CASSCF. Since the spatial orientation is crucial to whether the molecule will go SF and the rate of it due to the orbital coupling of both molecules, based on recent studies. We calculate the most favorable orientation of the chromophores with the binding energies in the gas phase and adsorbed on Argon and Neon surfaces. Then we calculate the lowest-lying excited states that contribute to the singlet and triple transition plus the search for the possible conical intersection that crosses the surface potential energies.

TT 32.6 Wed 10:45 GÖR 226

Template-Designed Organic Electronics — •KLAUS MEERHOLZ — Chemistry Department, University of Cologne, Greinstr. 4-6, 50939 Cologne, Germany
Worldwide, organic electronic devices such as OLEDs and solar cells have rev-

olutionized the field of electronics; however, technological progress has been largely made by empirical research and development, while fundamental knowledge is often still incomplete.

This presentation will report results from the DFG-funded Research Training Group Template-Designed Organic Electronics addressing the question, how structural order influences the optoelectronic properties of pi-conjugated materials, and how these properties can be improved via the use of templates for the optimization of devices. Our approach spans all the way from the design of appropriate pi-conjugated molecular building blocks and surface-active templates, investigation of surfaces and interfaces by different spectroscopies, fabrication of optoelectronic devices, and finally theoretically modelling.

TT 32.7 Wed 11:00 GÖR 226

Optically detected magnetic resonance of TADF OLED emitters — •PASCAL SCHADY, MONA LÖTHER, FABIAN BINDER, VLADIMIR DYAKONOV, and ANDREAS SPERLICH — Experimental Physics VI, Julius Maximilian University of Würzburg, 97074 Würzburg

Thermally activated delayed fluorescence (TADF) is an efficient triplet harvesting mechanism for organic light-emitting diodes (OLED). Molecular TADF Donor-Acceptor type emitters are limited by low reverse intersystem crossing (rISC) rates and broad spectra, making them less suitable for potential OLED devices. In contrast, so-called multiple resonance (MR) effect emitters, are very promising as they show narrowband emission, even for deep blue wavelengths. MR-TADF emitters consist mostly of planar and rigidly bound benzyl groups with boron and nitrogen substituents for HOMO and LUMO pinning. As a result, the exchange integral is small, therefore the energy gap between singlet and triplet states is low enough to efficiently populate emissive singlet states by up-converting long-lived triplet states via thermal excitation, even at room temperature. However, many MR-TADF materials, like the DABNA-series behave differently in solution or as a solid. We therefore are investigating the spin system of those emitters by optically detected magnetic resonance (ODMR) in order to shed light on spin-dependent efficiency limiting pathways and how to address them to improve future OLED devices.

15 min. break

TT 32.8 Wed 11:30 GÖR 226

Influence of Fluorination on the Temperature Dependent Optical Transition in β -Phase ZnPc Single Crystals — •LISA SCHRAUT-MAY¹, KILIAN STRAUSS¹, SEBASTIAN HAMMER², KILIAN FRANK³, BERT NICKEL³, and JENS PFLAUM¹ — ¹Experimental Physics VI, University of Würzburg — ²Departments of Physics and Chemistry, McGill University, Montreal, Canada — ³Department of Physics, LMU Munich

The possibility of fluorination renders zinc phthalocyanine (ZnPc) an excellent model system to study the interplay between molecular packing and optoelectronic properties [1]. Here, we conduct temperature as well as polarisation dependent photoluminescence (PL) studies on β -phase ZnPc single crystals with different degrees of fluorination to modify the microscopic packing and, thus, the interaction between the molecules. For plain ZnPc an exceptionally sharp PL peak can be observed at temperatures below 100 K, which can be attributed to a superradiant enhancement [2]. Since this coherent coupling between several molecules strongly depends on the intermolecular spacing, we show, that this phenomenon can be steered by the fluorination of the molecules involved. We interpret the resulting PL signal and its temperature dependence in combination with X-ray studies by a model based on coupled excitons whose coupling is affected by the spatial anisotropy of the thermal contraction of the crystal lattice.

We thank the Bavarian research network SolTech for financial support. [1] Rödel et al., *J. Phys. Chem. C* (2022) [2] Hestand et al., *Chem. Rev.* (2018)

TT 32.9 Wed 11:45 GÖR 226

Charge Delocalization and Vibronic Couplings in Quadrupolar Squaraine Dyes — DANIEL TIMMER¹, FULU ZHENG², MORITZ GITTINGER¹, THOMAS QUENZEL¹, •DANIEL C. LÜNEMANN¹, KATRIN WINTE¹, YU ZHANG³, MOHAMED E. MADJET², JENNIFER ZABLOCKI⁴, ARNE LÜTZEN⁴, JIN-HUI ZHONG¹, ANTONIETTA DE SIO¹, THOMAS FRAUENHEIM², SERGEI TRETIAK³, and CHRISTOPH LIENAU¹ — ¹University of Oldenburg, Germany — ²University of Bremen, Germany — ³Los Alamos National Laboratory, USA — ⁴University of Bonn, Germany

Squaraines are prototypical quadrupolar charge-transfer chromophores. Their optical properties are often rationalized using an essential state model, predicting that optical transitions to the lowest excited state (S1) are one-photon allowed and to the next higher state (S2) are only two-photon-allowed and that vibronic coupling to high-frequency modes is greatly reduced. Here, we combine time-resolved spectroscopy techniques and quantum-chemical simulations to test and rationalize these predictions. We find the one-photon-allowed S1 and two-photon-allowed S2 states to be energetically well-separated. Also, we find small Huang-Rhys factors, especially for the high-frequency modes. The resulting concentration of the oscillator strength in a narrow spectral region around the S1 transition makes squaraines almost perfect optical two-level. Thus, these

molecules and their aggregates are exceptionally interesting for e.g. strong coupling applications. [1]: Timmer, Daniel, et al., *J. Am. Chem. Soc.*, 144, 41, 19150-19162 (2022)

TT 32.10 Wed 12:00 GÖR 226

In-operando observation of polaron formation in SAMFETs using NEXAFS spectroscopy — MANUEL JOHNSON, ANDREAS SPÄTH, BAOLIN ZHAO, MARCUS HALIK, and RAINER H. FINK — FAU Erlangen-Nürnberg, Erlangen, Germany

We present an in-operando near-edge x-ray absorption fine structure (NEXAFS) study on p-type BTBT-based self-assembled monolayer (BTBT-SAM) films. As a 2D-model system, the BTBT-SAM offers direct electron spectroscopic insight into the active organic semiconductor layer without interfering bulk contributions. This optimized geometry allows for the first time the observation of polaronic states caused by charged species at the dielectric/organic interface using a core-level spectroscopic tool. Linear NEXAFS dichroism is employed to derive the molecular orientation of the BTBT subunit. In addition to the conventional C K-edge NEXAFS resonances, we observe modifications in the density of unoccupied states. The spectral changes are affected by the strength and polarity of the applied gate voltage. Furthermore, the related energies match the energy levels of polaronic states. Thus, we have clear indications to interpret the data in the context of polaron formation due to charge accumulation induced by the applied electric field in our ultrathin device.[1] The study has been funded by the

DFG within GRK 1896 and the SolTECH initiative. [1] M. Johnson et al., *Appl. Phys. Lett.* 121 (2022) 183503.

TT 32.11 Wed 12:15 GÖR 226

Machine learning for molecular design of organic molecules and reaction optimization — JULIA WESTERMAYR¹, REINHARD J. MAURER², and DETLEV BELDER³ — ¹Artificial Intelligence in Theoretical Chemistry Group, Leipzig University, Germany — ²Computational Surface Chemistry Group, University of Warwick, UK — ³Analytical Chemistry, Leipzig University, Germany

High-throughput screening of reaction conditions and electronic properties of molecules plays a crucial role in chemical industry and can be facilitated by automated workflows and machine learning. However, the high combinatorial complexity of the various parameters affecting molecular properties leaves unguided searches in chemical space highly inefficient and the optimization of reactions to synthesize these molecules often fails as theoretical protocols are usually decoupled from experiments. In this talk, we will show how predictive and generative deep learning models can be combined to theoretically design new molecules with potential relevance to organic electronics [1]. Further, we will present how these tools can be coupled with experiments to enable automated micro-laboratories [2] for targeted chemical synthesis. [1] JW et al. *Nat. Comp. Sci.*, in press (2023). [2] R. J. Beulig et al., *Lab Chip* 17, 1996 (2017).

TT 33: Many-Body Quantum Dynamics (joint session DY/TT)

Time: Wednesday 9:30–13:00

Location: MOL 213

Invited Talk

TT 33.1 Wed 9:30 MOL 213

Many-body localization from Hilbert- and real-space points of view — IVAN KHAYMOVICH¹, GIUSEPPE DE TOMASI², FRANK POLLMANN³, and SIMONE WARZEL³ — ¹Nordic Institute for Theoretical Physics, Stockholm, Sweden — ²University of Illinois Urbana-Champaign, USA — ³Technical University Munich, Germany

Many-body localization (MBL), known as a generic mechanism to break quantum ergodicity, has been recently shown to be not the Hilbert-space Anderson localization. Instead, the MBL eigenstate occupies a fractal support [1-2], with extensive number of configurations. On the other hand, the well-established and accepted by the community picture of an emergent set of local integrals of motion [3] provides the structure of the MBL in the real space.

In this talk, I will provide the observable (later measured in the experiment [4]) which combines the fractality in the Hilbert space with the presence of local integrals of motion [2]. This observable, being the radial profile of the eigenstate over the Hamming distance, keeps the information about both the Hilbert-space fractal dimensions and the real-space localization lengths and uncovers the structure of these measures across the MBL transition. Phenomenological picture behind this behavior is consistent with the Kosterlitz-Thouless scenario of the MBL transition, suggested in the literature.

Literature: [1] N. Macé et al., *PRL* 123, 180601 (2019). [2] G. De Tomasi, I. M. Khaymovich et al. *PRB* 104, 024202 (2021). [3] Abanin et al., *RMP* 91, 021001 (2019). [4] Y. Yao et al *arXiv*:2211.05803.

TT 33.2 Wed 10:00 MOL 213

Bridging classical and quantum many-body information dynamics — ANDREA PIZZI^{1,2}, DANIEL MALZ^{3,4}, ANDREAS NUNNENKAMP⁵, and JOHANNES KNOLLE^{6,4,7} — ¹Department of Physics, Harvard University, Cambridge 02138, Massachusetts, USA — ²Cavendish Laboratory, University of Cambridge, Cambridge CB3 0HE, United Kingdom — ³Max-Planck-Institute of Quantum Optics, Hans-Kopfermann-Str. 1, 85748 Garching, Germany — ⁴Munich Center for Quantum Science and Technology (MCQST), 80799 Munich, Germany — ⁵Faculty of Physics, University of Vienna, Boltzmanngasse 5, 1190 Vienna, Austria — ⁶Department of Physics, Technische Universität München, James-Frank-Str. 1, 85748 Garching, Germany — ⁷Blackett Laboratory, Imperial College London, London SW7 2AZ, United Kingdom

The fundamental question of how information spreads in closed quantum many-body systems is often addressed through the lens of the bipartite entanglement entropy. Among its most striking features are unbounded linear growth in the thermodynamic limit, asymptotic extensivity in finite-size systems, and measurement-induced phase transitions. Here, we show that these key qualitative features emerge naturally also for the classical bipartite mutual information, the natural classical analogue of the quantum entanglement entropy. Key for this observation is treating the classical many-body problem on par with the quantum one, that is, explicitly accounting for the exponentially large probability distribution. Our analysis is supported by extensive numerics on prototypical cellular automata and Hamiltonian systems.

TT 33.3 Wed 10:15 MOL 213

Performance boost of a collective qutrit refrigerator — DMYTRO KOLISNYK¹ and GERNOT SCHALLER² — ¹Jacobs University Bremen, Campus Ring 1, 28759 Bremen, Germany — ²Helmholtz-Zentrum Dresden-Rossendorf, Bautzner Landstraße 400, 01328 Dresden, Germany

A single qutrit with transitions selectively driven by weakly-coupled reservoirs can implement one of the world's smallest refrigerators. We analyze the performance of N such fridges that are collectively coupled to the reservoirs. We observe a quantum boost, manifest in a quadratic scaling of the steady-state cooling current with N . As N grows further, the scaling reduces to linear, since the transitions responsible for the quantum boost become energetically unfavorable. Fine-tuned inter-qutrit interactions may be used to maintain the quantum boost for all N and also for not-perfectly collective scenarios.

[1] D. Kolisnyk and G. Schaller, Performance boost of a collective qutrit refrigerator, *arXiv*:2210.07844.

[2] M. Kloc, K. Meier, K. Hadjikyriakos, and G. Schaller, Superradiant Many-Qubit Absorption Refrigerator, *Phys. Rev. Applied* 16, 044061 (2021).

[3] N. Linden, S. Popescu, and P. Skrzypczyk. How small can thermal machines be? The smallest possible refrigerator. *Phys. Rev. Lett.* 105:130401, 2010.

TT 33.4 Wed 10:30 MOL 213

Hidden Phase of the Spin-Boson Model — FLORIAN OTTERPOHL^{1,2}, PETER NALBACH³, and MICHAEL THORWART^{2,4} — ¹Center for Computational Quantum Physics, Flatiron Institute, New York, New York 10010, USA — ²I. Institut für Theoretische Physik, Universität Hamburg, Notkestraße 9, 22607 Hamburg, Germany — ³Fachbereich Wirtschaft und Informationstechnik, Westfälische Hochschule, Münsterstraße 265 46397 Bocholt, Germany — ⁴The Hamburg Centre for Ultrafast Imaging, Luruper Chaussee 149, 22761 Hamburg, Germany

A quantum two-level system immersed in a sub-Ohmic bath experiences enhanced low-frequency quantum statistical fluctuations which render the nonequilibrium quantum dynamics highly non-Markovian. Upon using the numerically exact time-evolving matrix product operator approach, we investigate the phase diagram of the polarization dynamics. In addition to the known phases of damped coherent oscillatory dynamics and overdamped decay, we identify a new third region in the phase diagram for strong coupling showing an aperiodic behavior. We determine the corresponding phase boundaries. The dynamics of the quantum two-state system herein is not coherent by itself but slaved to the oscillatory bath dynamics.

TT 33.5 Wed 10:45 MOL 213

Exploring anomalies by many-body correlations — KLAUS MORAWETZ — Münster University of Applied Sciences, Stegerwaldstrasse 39, 48565 Steinfurt, Germany — International Institute of Physics- UFRN, Campus Universitário Lagoa nova, 59078-970 Natal, Brazil

The quantum anomaly can be written alternatively into a form violating conservation laws or as non-gauge invariant currents seen explicitly on the example of chiral anomaly. By reinterpreting the many-body averaging, the connection to Pauli-Villars regularization is established which gives the anomalous term a new interpretation as arising from quantum fluctuations by many-body correlations at short distances. This is exemplified by using an effective many-body quan-

tum potential which realizes quantum Slater sums by classical calculations. It is shown that these quantum potentials avoid the quantum anomaly but approaches the same anomalous result by many-body correlations. A measure for the quality of quantum potentials is suggested to describe these quantum fluctuations in the mean energy. Consequently quantum anomalies might be a short-cut way of single-particle field theory to account for many-body effects. This conjecture is also supported since the chiral anomaly can be derived by a completely conserving quantum kinetic theory. [Eur. Phys. J. B 92 (2019) 176, Phys. Lett. A 383 (2019) 1362, Phys. Status Solidi B (2021) 2100316]

TT 33.6 Wed 11:00 MOL 213

Non-Markovian Stochastic Schrödinger Equation: Matrix Product State Approach to the Hierarchy of Pure States — XING GAO¹, JIAJUN REN², ZHIGANG SHUAI², and ALEXANDER EISFELD³ — ¹Sun Yat-sen University, Shenzhen, Guangdong, China — ²Tsinghua University, Beijing, China — ³MPI-PKS, Dresden

We derive a stochastic hierarchy of matrix product states (HOMPS) for non-Markovian dynamics in open quantum system at finite temperature, which is numerically exact and efficient. HOMPS is obtained from the stochastic hierarchy of pure states (HOPS) by expressing HOPS in terms of formal creation and annihilation operators. The resulting stochastic first order differential equation is then formulated in terms of matrix product states and matrix product operators. In this way the exponential complexity of HOPS can be reduced to scale polynomial with the number of particles. The validity and efficiency of HOMPS is demonstrated for the spin-boson model and long chains where each site is coupled to a structured, strongly non-Markovian environment.

[1] X. Gao, J. Ren, A. Eisfeld, Z. Shuai, *Phys. Rev. A* 105, L030202 (2022)

TT 33.7 Wed 11:15 MOL 213

ultrafast gap dynamics near the zone boundary in a cuprate superconductor — QINDA GUO, MACIEJ DENDZIK, MAGNUS BERNTSEN, CONG LI, WANYU CHEN, YANG WANG, DIBYA PHUYAL, and OSCAR TJERNBERG — Department of Applied Physics, KTH Royal Institute of Technology, Hannes Alfvéns väg 12, 114 19 Stockholm, Sweden

The time- and angle- resolved photoemission spectroscopy (tr-ARPES) is a powerful technique to directly probe the ultrafast electron dynamics in the momentum space. Our recently developed narrow-bandwidth tr-ARPES setup enabled us to access the ultrafast dynamics of the quasiparticle population as well as the superconducting gap, in the whole surface Brillouin zone of the photoexcited cuprate superconductor (Bi2212). The results show non-trivial dynamics at the d-wave antinode and provide new insights into the enigma of the Cooper-pair formation process and condensation that takes place in the high-temperature cuprate superconductor.

15 min. break

TT 33.8 Wed 11:45 MOL 213

Controlling Many-Body Quantum Chaos — LUKAS BERINGER¹, STEVEN TOMSOVIC^{1,2}, JUAN DIEGO URBINA¹, and KLAUS RICHTER¹ — ¹Institut für Theoretische Physik, Universität Regensburg, D-93040 Regensburg, Germany — ²Department of Physics and Astronomy, Washington State University, Pullman, WA USA

Targeting in classical chaos control problems makes optimal use of the system's exponential instabilities to direct a given initial state to a predetermined final target state. A generalization to chaotic quantum systems in the semiclassical regime is possible [1], but also requires controlling an initially localized evolving quantum state's spreading. A coherent procedure of this kind enables directing highly excited, far-out-of-equilibrium states from an initial to some final target quantum state. Such methods have been successfully developed and applied to initially minimum uncertainty wave packets in a quantum kicked rotor system. The aim of our work is to extend those procedures to bosonic many-body systems. More specifically, we demonstrate how to make a localized quantum initial state follow special chaotic mean-field solutions of a Bose-Hubbard system toward an arbitrary localized target final state.

[1] S. Tomsovic, J. D. Urbina, and Klaus Richter, Controlling Quantum Chaos: Optimal Coherent Targeting, arXiv:2211.07408

TT 33.9 Wed 12:00 MOL 213

Environment-induced decay dynamics of antiferromagnetic order in Mott-Hubbard systems — GERNOT SCHALLER¹, FRIEDEMANN QUEISSER^{1,2}, NIKODEM SZPAK³, JÜRGEN KÖNIG³, and RALF SCHÜTZHOLD^{1,2} — ¹Helmholtz-Zentrum Dresden-Rossendorf, Bautzner Landstraße 400, 01328 Dresden, Germany — ²Institut für Theoretische Physik, Technische Universität Dresden, 01062 Dresden, Germany — ³Fakultät für Physik und CENIDE, Universität Duisburg-Essen, Lotharstraße 1, 47057 Duisburg, Germany

We study the dissipative Fermi-Hubbard model in the limit of weak tunneling and strong repulsive interactions, where each lattice site is tunnel-coupled to a Markovian fermionic bath. For cold baths at intermediate chemical potentials, the Mott insulator property remains stable and we find a fast relaxation of the particle number towards half filling. On longer time scales, we find that the antiferromagnetic order of the Mott-Néel ground state on bipartite lattices decays, even at zero temperature. For zero and nonzero temperatures, we quantify the different relaxation time scales by means of waiting time distributions, which can be derived from an effective (non-Hermitian) Hamiltonian and obtain fully analytic expressions for the Fermi-Hubbard model on a tetramer ring.

[1] G. Schaller *et al.*, *Phys. Rev. B* 105, 115139 (2022).

TT 33.10 Wed 12:15 MOL 213

Arrow of time concept based on properties of Lanczos coefficients — CHRISTIAN BARTSCH, MATS H. LAMANN, ROBIN HEVELING, LARS KNIPSCHILD, JIAOZI WANG, ROBIN STEINIGEWEG, and JOCHEN GEMMER — Fachbereich Physik, Universität Osnabrück, Barbarastr. 7, DE-49076 Osnabrück

We introduce an arrow of time concept based on a specifically defined class of arrow of time functions (ATF) consisting of a limited number of Krylov space generating observables. These ATF's are found to be essentially monotonously decaying in time which is measured by some quantifying parameter. The ATF's are constructed to be upper bounds for pertinent autocorrelation functions. Employing certain features of the Lanczos coefficients and the wave package-like excitation moving on the Krylov chain, we find reasonable agreement with corresponding numerics.

TT 33.11 Wed 12:30 MOL 213

Fast Time-Evolution of Matrix-Product States using the QR decomposition — JAKOB UNFRIED^{1,2}, JOHANNES HAUSCHILD¹, and FRANK POLLMANN^{1,2} — ¹Department of Physics, TFK, Technische Universität München, James-Frank-Straße 1, D-85748 Garching, Germany — ²Munich Center for Quantum Science and Technology (MCQST), Schellingstr. 4, 80799 München, Germany

Numerical simulations of quantum many-body dynamics in and out of equilibrium is essential for the understanding of a wide range of physical phenomena. Efficient matrix product state simulation techniques, such as time evolution block decimation (TEBD), are widely successful in extracting experimentally relevant signatures, such as dynamical correlation functions. We propose and benchmark a modified TEBD algorithm that uses a truncation scheme based on the QR decomposition instead of the singular value decomposition (SVD). The modification reduces the scaling with the dimension of the physical Hilbert space d from d^3 down to d^2 . Unlike the SVD, the QR decomposition allows for highly efficient implementations on GPU hardware. In a benchmark simulation of a global quench in a quantum clock model, we observe a speedup of orders of magnitude comparing the QR based scheme on a GPU to the SVD based TEBD on CPU.

TT 33.12 Wed 12:45 MOL 213

Simulating infinite temperature spin dynamics by a dynamic mean-field theory — TIMO GRÄSSER¹, KRISTINE REZAI², ALEXANDER O. SUSHKOV², and GÖTZ S. UHRIG¹ — ¹Condensed Matter Theory, TU Dortmund University, Otto-Hahn Straße 4, 44221 Dortmund, Germany — ²Department of Physics, Boston University, Boston, MA 02215, USA

We develop a dynamic mean-field theory for spin systems at infinite temperature (spinDMFT) [1]. The idea is to replace the large environment of a spin by a dynamic mean-field which displays a random Gaussian temporal evolution. Its autocorrelations are self-consistently linked to the quantum mechanic expectation values of spin-spin correlations. This approach becomes exact in the limit of large lattice coordination numbers. We improve the approach by considering spin clusters quantum-mechanically (cluster spinDMFT). The extended model is able to describe dynamic spin correlations measured in recent experiments [2] where an inhomogeneous spin- $\frac{1}{2}$ ensemble on a diamond surface is probed using nitrogen-vacancy centers as sensors.

[1] T. Gräßer *et al.*, *Phys. Rev. Research* 3, 043168 (2021).

[2] K. Rezaei *et al.*, arXiv:2207.10688 (2022).

TT 34: Fe-based Superconductors

Time: Wednesday 11:30–13:00

Location: HSZ 103

TT 34.1 Wed 11:30 HSZ 103

Efficient tuning of the superconductor BaNi_2As_2 by Calcium substitution - Single crystal Growth and Characterization — •FABIAN HENSSLER, KRISTIN WILLA, MEHDI FRACHET, TOM LACMANN, CHRISTOPH MEINGAST, MICHAEL MERZ, AMIR-ABBAS HAGHIGHIRAD, and MATTHIEU LE TACON — Institut für Quantenmaterialien und Technologien, KIT Karlsruhe, Deutschland

BaNi_2As_2 is a highly tunable superconductor, which is non-magnetic and isostructural to the Fe-based parent compound BaFe_2As_2 . Beyond superconductivity, recent publications reinforce the strong interplay between nematicity, charge density waves (CDW), and structural distortions [1,2,3]. At about 145 K, an incommensurate CDW forms, which coincides with a small lattice distortion ($\delta \sim 10^{-4}$) [4]. At slightly lower temperatures (T_c), the system undergoes a first-order transition, which can be suppressed e.g. by P- or Sr-substitution. Thereby, the superconducting transition temperature T_c can be enhanced by a factor of six [5]. In the case of Sr substitutions, however, a concentration as large as $x_{\text{Sr}} \sim 0.7$ is required. As an alternative, we report on the growth of Ca-substituted single crystals with Ca content up to $x_{\text{Ca}} \sim 0.1$. Specific heat and electrical transport measurements indicate that Ca is about eight times more efficient than Sr to suppress T_c .

[1] M. Frachet et al., arXiv:2207.02462 (2022)

[2] C. Meingast et al., Phys. Rev. B 106, 144507 (2022)

[3] S. M. Souliou et al., arXiv:2207.07191 (2022)

[4] M. Merz et al., Phys. Rev. B 104, 184509 (2021)

[5] C. Eckberg et al., Nat. Phys. 16, 346-350 (2020)

TT 34.2 Wed 11:45 HSZ 103

Electronic theory for FFLO state in KFe_2As_2 superconductor — •LUKA JIBUTI and ILYA EREMIN — Ruhr Universität Bochum, Bochum, Germany

Following the experimental observation of the Frude-Ferrel-Larnik-Ovchinnikov (FFLO) state in heavily hole-doped KFe_2As_2 , we develop a microscopic theory of multi-orbital FFLO phase in this system, based on the microscopic low-energy model consisting of two Γ -centered hole pockets created by xz and yz orbitals and the sizeable spin-orbit coupling between them. We use the leading angular harmonics approximation (LAHA) to write down the general form of the interaction, that involves both s -wave and d -wave channels. By decomposing the interaction into s - and d -wave channels, employing the mean-field approximation and solving the self-consistent equations for the order parameters, we analyse the creation of the FFLO phase, with the appearance of the non-zero, symmetry preserving q vector for the nodal d -wave state and s -wave with accidental nodes. We also discuss the role of spin-orbit coupling and possible orbital FFLO state, discussed recently in the context of Ising superconductors.

TT 34.3 Wed 12:00 HSZ 103

Superconductivity of $\text{CaKFe}_4\text{As}_4$ under anisotropic strains — B. ZÚÑIGA CÉSPEDÉS¹, A. VALADKHANI², S. MANDLOI¹, M. XU^{3,4}, J. SCHMIDT^{3,4}, S. L. BUD'KO^{3,4}, P. C. CANFIELD^{3,4}, A. P. MACKENZIE^{1,5}, R. VALENTÍ², and •E. GATI¹ — ¹MPI CPFS, 01187 Dresden, DE — ²Inst. for Theor. Physics, Goethe University, 60438 FFM, DE — ³Ames Lab, US DOE, Ames, IA 50011, USA — ⁴Dept. of Physics and Astronomy, Iowa State Uni, Ames, IA 50011, USA — ⁵Scottish Universities Physics Alliance, School of Physics and Astronomy, Uni of St Andrews, UK

$\text{CaKFe}_4\text{As}_4$ is an exceptional member of the family of Fe-based superconductors. First, it is a stoichiometric superconductor at ambient pressure with high critical temperature $T_c \sim 35$ K. Second, this superconducting phase can be found in close proximity to a so-called hedgehog vortex magnetic order (SVC), which does preserve tetragonal symmetry. This is in contrast to the ubiquitous stripe-type magnetic order (SSDW) in the Fe-based superconductors that is accompanied by a vestigial nematic phase. Thus, $\text{CaKFe}_4\text{As}_4$ is an important testbed to

investigate the interplay of superconductivity with different magnetic orders and nematicity. Here, we will discuss the impact of anisotropic strains, which couple directly to the nematic order parameter, on superconductivity. To this end, we present measurements of T_c as well as results of DFT calculations of the stability of SVC vs. SSDW order under large strains. Our results support the notion that nematic fluctuations contribute to superconducting pairing in this high- T_c superconductor. *Funded through the SFB/TRR288 (Elasto-Q-mat).*

TT 34.4 Wed 12:15 HSZ 103

The resistive anisotropy of FeSe in the nematic state — •CLIFFORD HICKS^{1,2}, JACK BARTLETT², ALEXANDER STEPPKE², SUGURU HOSOI³, TAKASADA SHIBAUCHI⁴, and ANDREW MACKENZIE² — ¹University of Birmingham, U.K. — ²Max Planck Institute for Chemical Physics of Solids, Dresden — ³Osaka University, Japan — ⁴University of Tokyo, Japan

We employed strain tuning to adjust the degree of twinning of samples of FeSe. By doing so, we were able to measure the resistive anisotropy in the nematic state. The resistive anisotropy of the nematic state, along with the dependence of the resistivity and the superconducting critical temperature on biaxial strain suggest a strong role for the yz orbital in electronic scattering in FeSe.

TT 34.5 Wed 12:30 HSZ 103

The low-temperature specific heat and thermal expansion of YFe_2Ge_2 — •PAVLO KHANENKO^{1,2}, JIASHENG CHEN², JACINTHA BANDA¹, THOMAS LUEHMANN¹, F. MALTE GROSCHKE², and MANUEL BRANDO¹ — ¹Max Planck Institute for Chemical Physics of Solids, Germany — ²Cavendish Laboratory, University of Cambridge, Cambridge, UK

We present specific heat and thermal expansion coefficient measurements of the layered iron-based superconductor YFe_2Ge_2 down to 40 mK and in magnetic field. A new generation of crystals [1] with residual resistivity ratios larger than 500 and $T_c = 1.2$ K have been investigated. These crystals display a sharp superconducting anomaly in both specific heat and thermal expansion. From the jump magnitudes and using the Ehrenfest relation we derive a small positive pressure dependence of T_c , $dT_c/dp = 24.4$ mK/GPa. Despite the high purity of the crystals, the residual Sommerfeld coefficient is relatively large $\gamma_0 \approx 40$ mJ/K²mol, i.e., less than about half of the value in the normal state (100 mJ/K²mol). The field dependences of $\gamma_0(B)$ and its respective coefficient in thermal expansion $\alpha_0(B)$ are analyzed within the frame of two gap scenario.

[1] J. Chen et al., Phys. Rev. Lett. 125, 237002 (2020)

TT 34.6 Wed 12:45 HSZ 103

Spin-density-wave order and evidence for superconductivity in single-crystal LuFe_2Ge_2 — •JIASHENG CHEN and F. MALTE GROSCHKE — Cavendish Laboratory, Cambridge, UK

The discovery of unconventional superconductivity in YFe_2Ge_2 [1, 2] has encouraged the search for more iron-based superconductors in the germanide family. The isostructural and isoelectronic compound, LuFe_2Ge_2 , exhibits physical properties that closely resemble those of YFe_2Ge_2 . Despite the additional spin-density-wave order observed below 9 K in LuFe_2Ge_2 , the overall shape and magnitude of the resistivity and susceptibility above 10 K, and the similarly enhanced Sommerfeld coefficient $C/T > 70$ mJ/molK² suggest a similar underlying physics in the two systems [3]. Using the liquid transport flux growth method [2], we investigated the effect of changing growth conditions on the crystal quality and on the spin-density-wave order in LuFe_2Ge_2 . In the best samples with RRR reaching 170, we observe evidence of superconductivity, making it the second iron-germanide superconductor discovered to date.

[1] J. Chen et al., PRL 116, 127001 (2016)

[2] J. Chen et al., PRL 125, 237002 (2020)

[3] M. Avila et al., J. Magn. Magn. Mater. 270, 51 (2004)

TT 35: Focus Session: Correlations in Moiré Quantum Matter I

Topological quantum phenomena and breakthroughs in time-resolved spectroscopy pose new challenges for many-body theory: Spatio-temporal electronic correlations often strongly impact topological and dynamical material properties but at the same time hinder an unambiguous interpretation of experiments, let alone a reliable quantitative prediction of material properties. Moiré quantum matter, i.e. systems where fundamental electronic properties and correlation phenomena emerge beyond the atomic scale exemplify these challenges. This Focus Session brings together the most recent developments in the field.

Organizers: Roser Valentí (Goethe-Universität Frankfurt) and Tim Wehling (Universität Hamburg)

Time: Wednesday 15:00–18:15

Location: HSZ 03

Invited Talk TT 35.1 Wed 15:00 HSZ 03
Strongly correlated excitons in atomic double layers — •PHUONG NGUYEN¹, LIGUO MA¹, RAGHAV CHATURVEDI¹, KENJI WATANABE², TAKASHI TANIGUCHI², KIN FAI MAK^{1,3,4}, and JIE SHAN^{1,3,4} — ¹School of Applied and Engineering Physics, Cornell University, Ithaca, NY, USA — ²National Institute for Materials Science, Tsukuba, Japan — ³Laboratory of Atomic and Solid State Physics, Cornell University, Ithaca, NY, USA — ⁴Kavli Institute at Cornell for Nanoscale Science, Ithaca, NY, USA

Excitons (bound electron-hole pairs) in solids have been proposed as a platform to achieve high temperature Bose-Einstein condensation. The small exciton binding energy in conventional semiconductors has limited the condensation temperature to about 1 K. In the past several years, a new class of two-dimensional semiconductors with much larger exciton binding energy has emerged. In this talk, we discuss the development of transition metal dichalcogenide double layer structures and electrical injection of interlayer excitons up to 10^{12} cm^{-2} . We establish electrical control of the chemical potential of interlayer excitons and probe their thermodynamic properties by capacitance measurements. We present experimental evidence for an excitonic insulating state and discuss the possibility of probing exciton superfluidity in the atomic double layer system.

Invited Talk TT 35.2 Wed 15:30 HSZ 03
The Quantum Twisting Microscope — •SHAHAL ILANI — Weizmann Institute
 In this talk I will present a fundamentally new type of scanning probe microscope, the Quantum Twisting Microscope (QTM), capable of performing local quantum interference measurements at a twistable interface between two quantum materials. Its working principle is based on a unique tip, made of an atomically-thin two-dimensional material. This tip allows electrons to coherently tunnel into a sample at many locations at once, with quantum interference between these tunneling events, making it a scanning electronic interferometer. With an extra twist degree of freedom, our microscope becomes a momentum-resolving local probe, providing powerful new ways to study the energy dispersions of interacting electrons. I will present various experiments performed with this microscope, demonstrating quantum interference at room temperature, probing the conductance of in-situ twisting interfaces, and imaging local energy dispersions in a variety of quantum materials.

Invited Talk TT 35.3 Wed 16:00 HSZ 03
Light-driven phenomena in two-dimensional and correlated quantum materials — •ANGEL RUBIO — Max Planck Institute for the Structure and Dynamics of Matter, Luruper Chaussee 149, 22761 Hamburg, Germany — Center for Computational Quantum Physics Flatiron Institute, Simons Foundation, 10010 NY, USA
 We will introduce our newly developed quantum electrodynamics density-functional formalism (QEDFT) as a first principles framework to predict, characterize and control the appearance of ordered phases of strongly interacting light-matter hybrid. We will pursue whether it is possible to create these new states of materials as ground-states of the system. To this end we will show how the emerging (vacuum) dressed states resembles Floquet states in driven systems. Strong light-matter coupling in cavities provides a pathway to break fundamental materials symmetries, like time-reversal symmetry in chiral cavities. We will discuss how to realize non-equilibrium states of matter that have so far been only accessible in ultrafast and ultrastrong laser-driven materials. We illustrate the realization of those ideas in molecules and 2D materials and show that the combination of cavity-QED and 2D twisted vdW heterostructures provides a novel and unique platform for the seamless realization of a plethora of interacting quantum phenomena, including exotic and elusive correlated and topological phases of matter.

15 min. break

Invited Talk TT 35.4 Wed 16:45 HSZ 03
Cascade of transitions in twisted and non-twisted graphene layers within the van Hove scenario — •LAURA CLASSEN¹, DMITRY CHICHINADZE², YUXUAN WANG³, and ANDREY CHUBUKOV² — ¹Max Planck Institute for Solid State Research, Stuttgart, Germany — ²University of Minnesota, Minneapolis, USA — ³University of Florida, Gainesville, USA

Fermions in layered graphene structures are described by both spin and valley degrees of freedom. Due to weak coupling between valleys, this can lead to an approximate SU(4) symmetry made from combined spin and valley transformations, which plays out differently depending on filling and interactions. Motivated by measurements of compressibility and STM spectra in twisted bilayer graphene, we analyze the pattern of symmetry breaking for itinerant fermions near a van Hove singularity. Making use of the approximate SU(4) symmetry of the Landau functional, we show that the structure of the order parameter changes with increasing filling via a cascade of transitions. We compute the feedback from different spin/valley orders on fermions and argue that each order splits

the initially 4-fold degenerate van Hove peak in a particular fashion, consistent with the STM data and compressibility measurements, providing a unified interpretation of the cascade of transitions in twisted bilayer graphene. Our results follow from a generic analysis of an SU(4)-symmetric Landau functional and are valid beyond a specific underlying fermionic model. We argue that an analogous van Hove scenario explains the cascade of phase transitions in non-twisted Bernal bilayer and rhombohedral trilayer graphene.

Invited Talk TT 35.5 Wed 17:15 HSZ 03
Topology and strong correlation: From twisted bilayer graphene to the boundary zeros of Mott insulators — •GIORGIO SANGIOVANNI¹, NIKLAS WAGNER¹, GAUTAM RAI², LORENZO CRIPPA¹, TIM WEHLING², and ROSER VALENTI³ — ¹Institut für Theoretische Physik und Astrophysik and Würzburg-Dresden Cluster of Excellence ct.qmat, Universität Würzburg — ²I. Institut für Theoretische Physik, Universität Hamburg — ³Institut für Theoretische Physik, Goethe-Universität Frankfurt am Main
 Strong electronic correlations drive materials towards atomic-like Mott phases. How to topologically classify these many-body insulators is an open and highly debated question. In this talk I am going to start from twisted bilayer graphene, an example of the interplay between low-energy protection of single-particle eigenvalues and non-perturbative effects of electron-electron interactions. From this, I plan to move to a broader concept which has been spelled out in rather different ways in the recent literature: topological Mott insulators. Most of the proposed realizations rely either on Hartree-Fock approximations or on appropriately defined auxiliary degrees of freedom. I am going to present a novel, remarkably simple way of describing a topological Mott insulator without long-range order, based on the topological properties of their Green's function zeros in momentum space. After discussing the fate of the bulk-boundary correspondence in these systems, I will show how the zeros can be seen as a form of "topological antimatter" with distinctive features associated to the annihilation with conventional topologically protected edge modes.

TT 35.6 Wed 17:45 HSZ 03
Transport and electron correlations in magic-angle twisted bilayer graphene: A dynamical mean field theory study — •GAUTAM RAI¹, LORENZO CRIPPA², GIORGIO SANGIOVANNI², ROSER VALENTI³, and TIM WEHLING¹ — ¹I. Institut für Theoretische Physik, Universität Hamburg, Hamburg, Germany — ²Institute for Theoretical Physics and Astrophysics, Julius-Maximilians-Universität Würzburg, Würzburg, Germany — ³Institut für Theoretische Physik, Goethe-Universität Frankfurt am Main, Frankfurt am Main, Germany
 Fully characterising the low-temperature phase diagram of magic-angle twisted bilayer graphene (MATBG) has proven to be one of the most compelling challenges in recent condensed matter physics. Correlation effects dominate due to the flatness of the low-energy bands. By varying doping and temperature, one can tune between superconductor, correlated-insulator, and strange metal phases. It has been difficult to apply standard strong-correlation computational techniques because of a topological obstruction, which precludes the existence of exponentially localized, symmetry-preserving Wannier functions for the flat bands. Recently, a heavy Fermion model has been proposed that successfully treats the hybrid localised-delocalised nature of MATBG [1]. We apply dynamical mean field theory (DMFT) to the heavy Fermion model to describe electron correlation effects in MATBG. In particular, we demonstrate how filling commensurability affects transport at low temperatures.
 [1] Z. D. Song and B. A. Bernevig, PRL 129, 047601 (2022)

TT 35.7 Wed 18:00 HSZ 03
Moiré minibands of twisted MoS₂ heterostructures — •CHITHRA H. SHARMA^{1,2}, MARTA PRADA¹, JAN-HENDRICK SCHMIDT¹, LARS TIEMANN¹, TOBIAS STAUBER³, TAKASHI TANIGUCHI⁴, KENJI WATANABE⁴, ROBERT ZIEROLD¹, KAI ROSSNAGEL², and ROBERT H. BLICK^{1,5} — ¹Universität Hamburg, Luruper Chaussee 149, 22761 Hamburg — ²CAU Kiel, Leibnitzstrasse 19, 24118 Kiel — ³ICMM-CSIC, Sor Juana Inés de la Cruz 3, Madrid 28049 Spain — ⁴Research Center for Functional Materials, National Institute for Materials Science, Namiki 1-1, Tsukuba, 305-0044, Ibaraki, Japan — ⁵Material Science and Engineering, University of Wisconsin-Madison, University Ave. 1550, Madison, 53706, Wisconsin, USA
 In the last decade, the evolution of van der Waals material systems has provided a multitude of options to manipulate, control, and engineer materials properties to various needs by combination, proximity, and twisting. Moiré superlattices formed as a result of lattice mismatch or twist angle modify the electronic structure to create flat bands and host exotic correlated electron phases. Here we observe the existence of low-dispersing mini-bands near the conduction band edge of MoS₂ twisted devices. We employ transport measurements and resolve discrete states within the band gap at low temperatures, in agreement with first-principles density functional theory calculations. We could also infer that the mini-bands correspond to iso-spin flavors as a result of interaction in the system coherent with our temperature dependence.

TT 36: Topological Insulators

Time: Wednesday 15:00–17:45

Location: HSZ 103

TT 36.1 Wed 15:00 HSZ 103

In-plane magnetic field induced asymmetric magnetoconductance in topological insulator kinks — •GERRIT BEHNER^{1,2}, ABDUR REHMAN JALIL^{1,2}, KRISTOF MOORS^{1,2}, ERIK ZIMMERMANN^{1,2}, PETER SCHÜFFELGEN^{1,2}, DETLEV GRÜTZMACHER^{1,2}, and THOMAS SCHÄPERS^{1,2} — ¹Peter Grünberg Institut (PGI-9), Forschungszentrum Jülich, 52425 Jülich, Germany — ²JARA-Fundamentals of Future Information Technology, Jülich-Aachen Research Alliance, Forschungszentrum Jülich and RWTH Aachen University, Germany

The study of the transport properties of quasi one-dimensional topological insulator (TI) nanostructures under the application of an in-plane magnetic field is crucial for the later realization of topological quantum computation building blocks. We present low temperature measurements of selectively grown TI-kinks under the application of an in-plane magnetic field. A dependence of the TI-kink resistance on the in-plane magnetic field angle is visible in the magnetotransport data resulting in a π -periodic change of the conductance. This phenomenon originates from an orbital effect, leading to a periodic alignment of the phase-coherent states on the bottom and top surface of the topological insulator. Respectively, once the states are aligned an increased conductance in the device is observed. The measurement results are supported theoretically by an analysis of a surface Rashba-Dirac model and tight-binding calculations of an effective three-dimensional model.

TT 36.2 Wed 15:15 HSZ 103

Topological quantum chemistry with a twist — •AXEL FÜNFHAUS, MARIUS MÖLLER, and ROSER VALENTÍ — Goethe Uni Frankfurt, Frankfurt am Main, Germany

It is well known that many topological phases can be indicated by the symmetry behavior of their band structure at high symmetry points, which culminated in the development of topological quantum chemistry. This approach becomes problematic once interactions are added, as this does not permit conserved particle occupation numbers in reciprocal space. We face this challenge by generalizing the Brillouin zone for translation invariant many-body wave functions via a torus of twisted boundary conditions. This allows for a symmetry analysis of the ground state wave function in twisted boundary space. We apply this ansatz to detect topological phases in interacting Chern insulators and fractional Chern insulators as well as Mott insulating systems that cannot adiabatically be connected to atomic limits.

TT 36.3 Wed 15:30 HSZ 103

Phonon-induced breakdown of Thouless pumping in the Rice-Mele-Holstein model — •SUMAN MONDAL, ERIC BERTOK, and FABIAN HEIDRICH-MEISNER — Institut für Theoretische Physik, Georg-August-Universität Göttingen, D-37077 Göttingen, Germany

Adiabatic and periodic variations of the lattice parameters can make it possible to transport charge through a system even without net external electric or magnetic fields, known as Thouless charge pumping. The amount of charge pumped in a cycle is quantized and entirely determined by the system's topology, which is robust against perturbations such as disorder and interactions. However, coupling to the environment may play a vital role in topological transport in many-body systems. In this talk, we will discuss the topological Thouless pumping, where the charge carriers interact with local optical phonons. The semi-classical multi-trajectory Ehrenfest method is employed to treat the phonon trajectories classically and charge carriers quantum mechanically. We find a breakdown of the quantized charge transport in the presence of phonons. It happens for any finite electron-phonon coupling strength at the resonance condition when the pumping frequency matches the phonon frequency, and it takes finite phonon coupling strength away from the resonance. Moreover, there exist parameter regimes with non-quantized negative and positive charge transport. The modified effective pumping path due to electron-phonon coupling accurately explains the underlying physics.

Supported by DFG (Deutsche Forschungsgemeinschaft) via FOR 2414.

TT 36.4 Wed 15:45 HSZ 103

Large thermal Hall effect in a disordered topological insulator — •ROHIT SHARMA, MAHASWETA BAGCHI, OLIVER BREUNIG, YOICHI ANDO, and THOMAS LORENZ — II. Physikalisches Institut, Universität zu Köln, Zùlpicher Straße 77, D-50937 Köln, Germany

Topological insulators mother compounds ($\text{Bi}_2\text{Se}_3, \text{Bi}_2\text{Te}_3$) are notorious for their high thermoelectric figure of merit and to quantify that, they have been under scrutiny in the past for their longitudinal thermal transport. Surprisingly no attention has been paid on the transverse part of heat transport. Motivated by the recent findings of thermal Hall effect in some oxide and magnetic insulators[1], we have experimentally observed a large thermal Hall effect in disordered topological insulator $\text{TlBi}_{0.15}\text{Sb}_{0.85}\text{Te}_2$ [2]. By comparing thermal conductivity κ_{xx} and thermal Hall effect κ_{xy} data with the electrical counterparts (σ_{xx} & σ_{xy}), we

study a possible influence of phonon drag on thermal transport. Electrical hall conductivity (σ_{xy}) shows multi-band behaviour in the whole temperature range (4-300K). Electronic contribution to thermal transport κ_e was calculated by using Wiedemann-Franz law and then compared with the measured thermal transport data, where it was found that both κ_{xx} and κ_{xy} shows phonon dominated behaviour. When compared κ_{xy} and κ_e , former shows an order of magnitude higher signal than the latter one. Possible reasons for large thermal Hall effect in $\text{TlBi}_{0.15}\text{Sb}_{0.85}\text{Te}_2$ will be discussed.

Funded by the DFG via CRC 1238 Projects A04 and B01

[1] M. Boulanger et al., Nat. Commun. 11, 5325 (2020)

[2] O. Breuning et al., Nat. Commun. 8, 15545 (2017)

TT 36.5 Wed 16:00 HSZ 103

Mixed higher-order topology: boundary non-Hermitian skin effect induced by a Floquet bulk — •HUI LIU and ION COSMA FULGA — Leibniz Institute for Solid State and Materials Research, Dresden

We show that anomalous Floquet topological insulators generate intrinsic, non-Hermitian topology on their boundary. As a consequence, removing a boundary hopping from the time-evolution operator stops the propagation of chiral edge modes, leading to a non-Hermitian skin effect. This does not occur in Floquet Chern insulators, however, in which boundary modes continue propagating. By evaluating the local density of states, we found that the resulting non-Hermitian skin effect is critical, i.e. scale-invariant, due to the nonzero coupling between the bulk and the edge. Further, it is a consequence of the nontrivial topology of the bulk Floquet operator, which we show by designing a real-space topological invariant. Our work introduces a form of 'mixed' higher-order topology, where a bulk system characterized by Floquet topology produces a boundary system characterized by non-Hermitian topology, without the need for any added perturbations. This opens an alternate direction in the study of topological classifications, and provides a route towards generating non-Hermitian skin effects by means of periodic driving.

15 min. break

TT 36.6 Wed 16:30 HSZ 103

PT-symmetric photonic topological insulator — •ALEXANDER FRITZSCHE^{1,2}, TOBIAS BIESENTHAL², LUKAS MACZEWSKY², KAROLIN BECKER², MAX ERHARDT², MATTHIAS HEINRICH², RONNY THOMALE¹, YOGESH JOGLEKAR³, and ALEXANDER SZAMEIT² — ¹Fakultät für Physik und Astronomie, Julius-Maximilians-Universität Würzburg, Würzburg, Germany — ²Institut für Physik, University of Rostock, Rostock, Germany — ³Department of Physics, Indiana University-Purdue University Indianapolis (IUPUI), Indianapolis, Indiana, USA

Gain and loss are characteristic features of open or non-Hermitian systems and lead, in general, to unstable, exponentially increasing and decreasing states. However, these instabilities can be avoided when parity-time (PT) symmetry is added to such arrangements. Because of its unique properties it has been tried to combine PT symmetry with the unrivalled robustness of transport in topological insulators. In this work we propose and experimentally realize a periodically driven topological insulator with two counterpropagating boundary states where gain and loss are distributed not only spatially but also temporally using photonic waveguides as the experimental platform. Here, the periodic driving allows us to circumvent the problems that have so far hindered the combination of PT symmetry and topological insulators thereby providing the missing link between these two realms.

TT 36.7 Wed 16:45 HSZ 103

Time-reversal invariant finite-size topology — •RAFAEL ALVARO FLORES CALDERON, RODERICH MOESSNER, and ASHLEY COOK — Max Planck Institut für die Physik of Complex Systems, Dresden, Germany

We report finite-size topology in the quintessential time-reversal (TR) invariant systems, the quantum spin Hall insulator (QSHI) and the three-dimensional, strong topological insulator (STI): previously-identified helical or Dirac cone boundary states of these phases hybridize in wire or slab geometries with one open boundary condition for finite system size, and additional, topologically-protected, lower-dimensional boundary modes appear for open boundary conditions in two or more directions. For the quasi-one-dimensional (q(2-1)D) QSHI, we find topologically-protected, quasi-zero-dimensional (q(2-2)D) boundary states within the hybridization gap of the helical edge states, determined from q(2-1)D bulk topology characterized by topologically non-trivial Wilson loop spectra. We show this finite-size topology furthermore occurs in 1T'-WTe₂ in ribbon geometries with sawtooth edges, based on analysis of a tight-binding model derived from density-functional theory calculations, motivating experimental investigation of our results. In addition, we find quasi-two-dimensional (q(3-1)D) finite-size topological phases occur for the STI, yielding helical boundary modes distinguished from those of the QSHI by a non-trivial magneto-electric polarizability linked to the original 3D bulk STI.

TT 36.8 Wed 17:00 HSZ 103

Spectral functions of a topological Fermi-Hubbard model in one dimension — •DAVID MIKHAIL and STEPHAN RACHEL — School of Physics, University of Melbourne, Parkville, VIC 3010, Australia

We study the effects of electron-electron interactions on the charge excitation spectrum of the spinful Su-Schrieffer-Heeger model, a prototype of a one-dimensional bulk obstructed topological insulator. In light of recent progress in the fabrication of dopant-based quantum simulators we focus on experimentally detectable signatures of interacting topology in finite lattices. Importantly, these semiconductor platforms allow for local high-precision measurements using scanning tunnelling spectroscopy (STS). To this end we use Lanczos-based exact diagonalization to calculate the single-particle spectral function in real space which generalizes the local density of states to interacting systems. Its spatial and spectral resolution allows for the direct investigation and identification of edge states. While the non-trivial topology is manifested in zero-energy spin-like edge excitations for any finite interaction strength, our analysis of the spectral function shows that the single-particle charge excitations are gapped out on the boundary. Despite the loss of topological protection, we find that these edge excitations are quasiparticle-like as long as they remain within the bulk gap and as such serve as an indicating signature of the correlated topological phase measurable in single-particle measurement techniques such as STS. Our results are available at Phys. Rev. B 106, 195408 (2022).

TT 36.9 Wed 17:15 HSZ 103

Topological phases of one and two Su-Schrieffer-Heeger wires on a semiconducting substrate — •KESHAB SONY¹, ANAS ABDELWAHAB², and ERIC JECKELMANN³ — ¹Leibniz universität, Hannover, Germany — ²Leibniz universität, Hannover, Germany — ³Leibniz universität, Hannover, Germany

Atomic wires deposited on semiconducting substrates attracted lots of attention in the last two decades as a platform of quasi one-dimension (1D) properties. The

Su-Schrieffer-Heeger (SSH) model is one of the simplest models that manifests the typical features of topological phases in quasi 1D characterized by topological invariant (winding number) and corresponding number of zero edge states. In this study, we consider models of one and two SSH wires coupled to semiconducting three-dimensional (3D) substrates and investigate the topological phases of these models with respect to the model parameters, eg. dimerization, wire-wire coupling, wire-substrate hybridization. The phase diagram of single wire coupled to the substrate shows stability of the existing phases without substrate but with changing effectively the wire parameters. We also address the issue of how the presence of the substrate change or preserve the phase diagrams of the two-leg ladders without substrate. We discuss the local density of states for different cases we consider.

TT 36.10 Wed 17:30 HSZ 103

Thermal diode effect in Dirac hybrid junctions — •PHILLIP MERCEBACH and PABLO BURSET — Autonomous University of Madrid, Madrid, Spain

Thermo-electric devices are utilized for nano-scale refrigeration or to harness waste heat to produce electric power in electronic circuits. These devices usually require semiconductor materials or complex geometries to induce thermo-electric effects which may suffer from a narrow range of operation or poor efficiency. To counteract these shortcomings, we propose a simple device consisting of a ferromagnet (F) in proximity to a Dirac semi-metal (N) creating a ballistic NFN junction with a large operating window. We theoretically study the heat and electric currents through the junction and show strong Seebeck and Peltier effects arising from the Dirac physics and Klein tunneling in the ballistic junction. We use the device's high tunability to create a thermal diode allowing for refrigeration of a hot reservoir or for power production induced by a temperature gradient. Finally, we discuss refrigeration efficiency and the effective electron cooling temperature taking into account the phonon contribution in quasi-two-dimensional materials, like graphene or topological insulators.

TT 37: Ruthenates

Time: Wednesday 15:00–18:30

Location: HSZ 201

TT 37.1 Wed 15:00 HSZ 201

Elastocaloric determination of the phase diagram of Sr_2RuO_4 — •YOU-SHENG LI¹, MARKUS GARST^{2,3}, JÖRG SCHMALLIAN^{3,4}, SAYAK GHOSH⁵, NAOKI KIKUGAWA⁶, DMITRY SOKOLOV¹, CLIFFORD HICKS^{1,7}, FABIAN JERZEMBECK¹, MATTHIAS IKEDA⁸, ZHENHAI HU¹, BRAD RAMSHAW⁵, ANDREAS ROST⁹, MICHAEL NICKLAS¹, and ANDREW MACKENZIE^{1,9} — ¹Max Planck Institute for Chemical Physics of Solids — ²Institut für Theoretische Festkörperphysik, Karlsruher Institut für Technologie — ³Institut für Quantenmaterialien und -technologien, Karlsruher Institut für Technologie — ⁴Institut für Theorie der Kondensierten Materie, Karlsruher Institut für Technologie — ⁵Laboratory of Atomic and Solid State Physics, Cornell University — ⁶National Institute for Materials Science — ⁷School of Physics and Astronomy, University of Birmingham — ⁸Department of Applied Physics, Stanford University — ⁹School of Physics and Astronomy, University of St Andrews

Uniaxial pressure has shown the capabilities of tuning the electronic structures of Sr_2RuO_4 across a Van Hove singularity (VHS). By performing high precision ac-elastocaloric effect (ECE) measurements under uniaxial strain along $\langle 100 \rangle$ direction, we mapped out the phase diagram of Sr_2RuO_4 in detail. Similar to many unconventional superconductors, Sr_2RuO_4 has a SC dome in proximity to a magnetic phase. Besides, we observe a strong reversal of the ECE around the VHS upon entering the SC state. Together with a model calculation, these results strongly suggest a node-less gap opening at the VHS and, thus, put a strong constraint on possible SC order parameters.

TT 37.2 Wed 15:15 HSZ 201

High-resolution elastocaloric effect measurement of $110\text{-Sr}_2\text{RuO}_4$ — •ZHENHAI HU^{1,2}, YOU-SHENG LI¹, FABIAN JERZEMBECK¹, MICHAEL NICKLAS¹, ANDREW P. MACKENZIE^{1,2}, and CLIFFORD W. HICKS^{1,3} — ¹Max Planck Institute for Chemical Physics of Solids, Dresden, Germany — ²Scottish Universities Physics Alliance, School of Physics and Astronomy, University of St Andrews, St Andrews, UK — ³School of Physics and Astronomy, University of Birmingham, Birmingham, UK

The symmetry of the order parameter of superconducting Sr_2RuO_4 remains an undetermined question. Whether the order parameter has more than one component is still under debate. If the superconducting order parameter is degenerate and protected by lattice symmetry, the degeneracy will be lifted when the lattice symmetry is broken. Uniaxial pressure, which can continuously break the lattice symmetry, is thus a powerful tool to distinguish whether there is a degeneracy. However, the second transition was not observed in the previous heat capacity and elastocaloric effect measurements with strain applied along $\langle 100 \rangle$. Although stringent constraints on the nature of superconducting states at zero strain were placed by the absence of the second transition with $\langle 100 \rangle$ strain,

there remains a possibility that a second transition exists under $\langle 110 \rangle$ strain. Here we report the latest progress on elastocaloric measurement of Sr_2RuO_4 crystal with strain applied along $\langle 110 \rangle$. Within our experimental precision, no signal indicating a second phase transition below T_c is observed.

TT 37.3 Wed 15:30 HSZ 201

Strain dependence of the superconducting state of Sr_2RuO_4 under $\langle 110 \rangle$ uniaxial pressure: No evidence for multi-component order parameter — •FABIAN JERZEMBECK¹, YOU-SHENG LI¹, ZHENHAI HU¹, NAOKI KIKUGAWA², DMITRY SOKOLOV¹, YOSHITERU MAENO³, MICHAEL NIKLAS¹, ANDREW MACKENZIE¹, and CLIFFORD HICKS⁴ — ¹Max Planck Institute for Chemical Physics of Solids, D-01187 Dresden, Germany — ²National Institute for Materials Science, Tsukuba 305-0003, Japan — ³Department of Physics, Kyoto University, Kyoto 606-8502, Japan — ⁴School of Physics and Astronomy, University of Birmingham, Birmingham B15 2TT, United Kingdom

After more than 25 years of intense research, the order parameter of the unconventional superconductor Sr_2RuO_4 is still unknown. Recent experiments suggest that the order parameter is even-parity and multi-component [1,2], which would result in distinct features in the strain dependence of the superconducting state, such as a kink in the strain dependence of T_c around zero strain [3]. Here, we present uniaxial pressure results along the crystallographic $\langle 110 \rangle$ -axis and find no evidence for a discontinuity in T_c , predicted for a multi-component order parameter. However, we can place tight constraints on the thermodynamics of several discussed two-component order parameters.

[1] Pustogov et al., Nature 574, 72 (2019)

[2] Ghosh et al., Nat. Phys. 17, 199 (2021)

[3] Kivelson et al., npj Quantum Materials 5, 43 (2020)

TT 37.4 Wed 15:45 HSZ 201

Giant lattice softening at a Lifshitz transition in the normal state of Sr_2RuO_4 — •HILARY M. L. NOAD¹, KOUSUKE ISHIDA¹, YOU-SHENG LI¹, VERONIKA STANGIER², NAOKI KIKUGAWA³, DMITRY A. SOKOLOV¹, BONGJAE KIM⁴, IGOR I. MAZIN⁵, MARKUS GARST², JÖRG SCHMALLIAN², ANDREW P. MACKENZIE^{1,6}, and CLIFFORD W. HICKS^{1,7} — ¹Max Planck Institute for Chemical Physics of Solids, Dresden, Germany — ²Karlsruhe Institute of Technology, Karlsruhe, Germany — ³National Institute for Materials Science, Tsukuba, Japan — ⁴Kunsan National University, Gunsan, Korea — ⁵George Mason University, Fairfax, USA — ⁶University of St Andrews, St Andrews, UK — ⁷University of Birmingham, Birmingham, UK

The interplay between lattice and electronic degrees of freedom is a central theme in condensed matter physics. In Sr_2RuO_4 , the quasi-two-dimensional Fermi surface can be tuned through a Lifshitz transition—a change in its topology—with

uniaxial pressure along the (100) direction. We investigated the influence of this electronic transition on the lattice by using a piezo-based uniaxial pressure cell to measure the stress-strain relation of Sr_2RuO_4 across the Lifshitz transition. We find a large and strongly temperature-dependent softening of the [100] Young's modulus at the Lifshitz transition. From thermodynamic arguments and comparison to a tight-binding model, we establish that the softening is indeed driven by conduction electrons.

TT 37.5 Wed 16:00 HSZ 201

Effect of superconductivity on the stress-strain relationships of Sr_2RuO_4 — •KOUSUKE ISHIDA¹, HILARY NOAD¹, YOU-SHENG LI¹, VERONIKA STANGIER², NAOKI KIKUGAWA³, DMITRY SOKOLOV¹, MICHAEL NICKLAS¹, MARKUS GARST², JÖRG SCHMALIAN², ANDREW MACKENZIE^{1,4}, and CLIFFORD HICKS^{1,5} — ¹Max Planck Institute for Chemical Physics of Solids, Dresden, Germany — ²Karlsruhe Institute of Technology, Karlsruhe, Germany — ³National Institute for Materials Science, Tsukuba, Japan — ⁴University of St. Andrews, St. Andrews, United Kingdom — ⁵University of Birmingham, Birmingham, United Kingdom

In the unconventional superconductor Sr_2RuO_4 , applying uniaxial stress along a (100) crystalline direction induces a Lifshitz transition. Here we report on measurement of the stress-strain relationships across this transition down to temperatures below the superconducting transition. In the normal state, the Young's modulus softens by $\approx 10\%$ in the vicinity of the Lifshitz transition, indicating that this is a local maximum in the electronic free energy. We find that the onset of superconductivity causes a slight hardening of the lattice, though the electronic free energy remains a local maximum at the Lifshitz transition.

TT 37.6 Wed 16:15 HSZ 201

Effect of strain and momentum dependent spin-orbit coupling on the superconducting phase of Sr_2RuO_4 — •JONAS HAUCK^{1,2}, SOPHIE BECK¹, DANTE KENNES^{2,3}, ANTOINE GEORGES^{1,4,5,6}, and OLIVIER GINGRAS¹ — ¹Center for Computational Quantum Physics, Flatiron Institute, NY 10010, USA — ²Institut für Theorie der Statistischen Physik, RWTH Aachen, 52056 Aachen, Germany and JARA - Fundamentals of Future Information Technology — ³Max Planck Institute for the Structure and Dynamics of Matter, Center for Free Electron Laser Science, 22761 Hamburg, Germany — ⁴Collège de France, 75005 Paris, France — ⁵CPHT, CNRS, École Polytechnique, Institut Polytechnique de Paris, 91128 Palaiseau, France — ⁶DQMP, Université de Genève, CH-1211 Genève, Switzerland

The nature of Sr_2RuO_4 's superconducting order parameter is a long-standing puzzle. First proposed to be a triplet superconductor, the current preferred picture is that of a degenerate singlet order parameter. The main driving force behind this development is the unification of experimental measurements and theoretical predictions. In this talk, we will employ a functional renormalization group approach to first-principles derived tight binding models to study the behavior of the leading order parameter under strain. Additionally, we examine the influence of momentum dependent spin-orbit coupling. Our results suggest the possible pairing candidates should be restricted to combinations of a d-wave pseudospin singlet with another order parameter whose critical temperature is not influenced by strain.

15 min. break

TT 37.7 Wed 16:45 HSZ 201

Gate-controlled superconductivity in Sr_2RuO_4 — •PRIYANA PULIYAPPARA BABU¹, ROMAN HARTMANN¹, ROSALBA FITTIPALDI², ANTONIO VECCHIONE², ELKE SCHEER¹, and ANGELO DI BERNARDO¹ — ¹University of Konstanz, 78457 Konstanz, Germany — ²University of Salerno, I-84084 Fisciano, Italy

The electrical field effect was believed to be inapplicable for superconductors until 2018 when it was found that the supercurrent I_c in nanowires can be controlled by the application of strong enough voltages to gate electrodes, which has been interpreted as field effect. This discovery has great potential in the future to build hybrid superconductor/semiconductor architectures which might serve reducing the increasing energy demands of modern supercomputers. The majority of observations of such gate effects have been made for BCS superconductors like Ti, Va, Nb, Al etc. Here we report gate control of I_c in transistors made of Sr_2RuO_4 flakes. Sr_2RuO_4 is an unconventional superconductor found in 1994 which has been intensively studied to understand the nature of its superconducting order parameter. Single crystals of Sr_2RuO_4 were mechanically exfoliated to produce flakes which were then patterned into gated nanodevices using a gallium focused ion beam. Total suppression of I_c was observed for gate voltages V_G above 8.3 V. The V_G dependence of I_c at different temperatures and different fields were also investigated. We will also discuss the role of leakage currents between wire and gate and possibilities to further minimize them.

TT 37.8 Wed 17:00 HSZ 201

Non-local electrodynamics and field angle dependence of the superfluid density in Sr_2RuO_4 — •JAVIER LANDAETA¹, KONSTANTIN SEMENIUK¹, JOOST ARETZ¹, ISMARDO BONALDE², and ELENA HASSINGER¹ — ¹Max Planck Institute

for Chemical Physics of Solids, 01187 Dresden, Germany — ²Centro de Física, Instituto Venezolano de Investigaciones Científicas, Caracas 1020-A, Venezuela

Although being extensively studied for more than 25 years, the nature of the superconducting order parameter (SOP) of the weak type II superconductor Sr_2RuO_4 is still strongly debated. To get insight into the nodal structure of the SOP, we carried out a comprehensive study of the temperature dependence of the superfluid density n_s at various field orientations. By measuring the superconducting lower critical field $H_{c1}(T)$ in a spherical sample with ac-susceptibility, we obtained the temperature dependence of $n_s = H_{c1}(T)/H_{c1}(0)$ down to $0.03 T_c$. Our results show that follows a low-temperature power law of T^2 up to $0.7T_c$ irrespective of the field angle. The observed behavior is in excellent agreement with what is expected of a type II superconductor with vertical nodes, with a strong influence of non-local electrodynamics. The discussed mechanisms are highly relevant for all weak type II superconductors.

TT 37.9 Wed 17:15 HSZ 201

Propagating charge carrier plasmon in Sr_2RuO_4 — MARTIN KNUPFER¹, FABIAN JERZEMBECK², NAOKI KIKUGAWA³, FRIEDRICH ROTH⁴, and JÖRG FINK¹ — ¹Leibniz Institute of Solid State and Materials Research, Dresden — ²MPI for Chemical Physics of Solids, Dresden — ³National Institute for Material Science, Tsukuba, Japan — ⁴Institute of Exp. Physics, TU Bergakademie Freiberg

We report on studies of charge carrier plasmon excitations in Sr_2RuO_4 by transmission Electron Energy-Loss Spectroscopy. In particular, we present results on the plasmon dispersion and its width as a function of momentum transfer. The dispersion can be qualitatively explained in the framework of RPA calculations, using an unrenormalized tight-binding band structure. The constant long-wavelength width of the plasmon indicates, that it is caused by a decay into inter-band transition and not by quantum critical fluctuations. The results from these studies on a prototypical highly correlated metal system show that the long-wavelength plasmon excitations near 1 eV are caused by resilient quasiparticles and are not influenced by correlation effects.

TT 37.10 Wed 17:30 HSZ 201

Transport and structural characterisation of the metal to insulator transition in Ca_2RuO_4 nanoflakes — •ROMAN HARTMANN¹, ANITA GUARINO², ROSALBA FITTIPALDI³, MARIO CUOCO², ELKE SCHEER¹, ANTONIO VECCHIONE², GERARDINA CARBONE³, and ANGELO DI BERNARDO¹ — ¹Department of Physics, Universität Konstanz, Konstanz, Germany — ²CNR-Spin, Salerno, Italy — ³Max IV Laboratory, Lund, Sweden

The Mott-insulator Ca_2RuO_4 (CRO) has attracted considerable attention due to its insulator to metal transition (IMT) with a transition temperature of 357 K (insulating below, metallic above) and the ability to trigger the IMT using pressure, current or an electric field of just 40 V/cm [1,2]. Unfortunately, stress from a structural transition (orthorhombic to tetragonal) during the IMT with an increase in unit cell volume [1] generally breaks bulk crystals. To overcome this limitation we have developed a method to fabricate CRO nanoflakes (despite it not being a layered material) that we can contact using standard lithographic methods. In these nanoflakes we can reversibly trigger the IMT thousands of times by passing current without breaking the sample. The robustness of the devices also enabled us to perform spatially resolved nano-diffraction measurements showing the current-dependent local formation of the metallic phase, confirming the reversibility and giving first insights in the timescale of the IMT.

[1] F. Nakamura et al. *Sci. Rep.* 3, 2536 (2013)

[2] R. Okazaki et al., *JPSJ* 82, 103702 (2013)

TT 37.11 Wed 17:45 HSZ 201

Tuning van Hove singularities in strontium ruthenate with isovalent Barium doping — •CAITLIN I O'NEIL^{1,2}, MAXIMILLIAN T PELLY^{1,2}, BEN GADE¹, ALEXANDRA S GIBBS^{1,3,4}, and ANDREAS W ROST^{1,2} — ¹SUPA, School of Physics and Astronomy, University of St Andrews, St Andrews, UK — ²MPI for Chemical Physics of Solids, Dresden, Germany — ³MPI for Solid State Research, Stuttgart, Germany — ⁴ISIS Neutron and Muon Source, STFC Rutherford Appleton Laboratory, Harwell Campus, Didcot, OX11 0QX, UK

Controlling a van Hove singularity (VHS) close the Fermi energy (E_F) of a compound allows control of the low temperature phases as shown for example in recent experiments in single layer ruthenates [1,2]. This study pursues a new direction of structural doping of $\text{Sr}_3\text{Ru}_2\text{O}_7$ by the substitution of barium onto the strontium site. Powder samples of $(\text{Sr}_{1-x}\text{Ba}_x)_3\text{Ru}_2\text{O}_7$ were synthesised from $x=0.0 - 0.12$. The samples were analysed with X-ray and neutron diffraction, magnetic susceptibility and heat capacity measurements. The unit cell volume changes linearly with doping with the primary structural change being an adjustment of the RuO_6 octahedral rotation mode magnitude. Using heat capacity we map the evolution of the VHS towards the E_F , crossing it at $x=0.08$. Intriguingly, heat capacity shows that the strength of the singularity is decreased, contrary to standard scenarios. In combination with DFT calculations we trace this back to the primary role of the rotation mode in controlling the VHS in ruthenates.

[1] Y.-S. Lie et al., *Nature* 607, 276 (2022)

[2] C. A. Marques et al., *Adv. Mater.* 33, e21005

TT 37.12 Wed 18:00 HSZ 201

Imaging of compass-like control of the electronic structure in $\text{Sr}_3\text{Ru}_2\text{O}_7$ — MASAHIRO NARITSUKA¹, IZIDOR BENEDIČIĆ¹, LUKE RHODES¹, CAROLINA MARQUES¹, CHRISTOPHER TRAINER¹, ZHIWEI LI², ALEXANDER KOMAREK², and •PETER WAHL¹ — ¹SUPA, School of Physics and Astronomy, University of St Andrews, North Haugh, St Andrews, Fife, KY16 9SS, United Kingdom — ²Max Planck Institute for Chemical Physics of Solids, Nöthnitzer Straße 40, 01178 Dresden, Germany

Electronic nematicity results in a surprisingly strong symmetry-breaking reconstruction of electronic states without a significant lattice distortion. An enigmatic example of a nematic state is found in $\text{Sr}_3\text{Ru}_2\text{O}_7$, where a large resistivity anisotropy is stabilized by external magnetic field. The direction of the anisotropy can be controlled by the in-plane component of the magnetic field. Recently, STM measurements have revealed symmetry breaking of the electronic structure at the surface of $\text{Sr}_3\text{Ru}_2\text{O}_7$ even in zero magnetic field. Here, we use low-temperature scanning tunnelling microscopy to study the electronic structure in $\text{Sr}_3\text{Ru}_2\text{O}_7$ in vector magnetic fields. We find that the electronic structure is strongly affected even by relatively small external field when applied in the crystallographic a-b-plane, and is evolving continuously as a function of in-plane field direction. Our result establishes compass-like control over the electronic structure in the surface layer of $\text{Sr}_3\text{Ru}_2\text{O}_7$. We can rationalise the continuous

evolution of the electronic structure with field direction through the interplay of magnetism and spin-orbit coupling.

TT 37.13 Wed 18:15 HSZ 201

Optical study of domains and domain walls in $\text{Ca}_3\text{Ru}_2\text{O}_7$ as a function of temperature and uniaxial pressure tuning — •SIMLI MISHRA¹, FEI SUN¹, ELENA GATI¹, HILARY NOAD¹, ANDREW P MACKENZIE^{1,2}, and VERONIKA SUNKO^{1,3} — ¹Max Planck Institute, Chemical Physics of Solids, 01187, Dresden, Germany — ²School of Physics and Astronomy, University of St. Andrews, St. Andrews, KY16 9SS, UK — ³Department of Physics, University of California, Berkeley, California, 94720, USA

Using optical methods to investigate a material is a powerful non-contact method to explore fundamental physics. In our experiment, we use optics as a versatile microscope to investigate birefringence as well as thermal transport with micron-scale spatial resolution. It can be combined with an in-situ controllable uniaxial pressure device, which has recently been shown to be a powerful tuning parameter to control lattice symmetries in quantum materials. In this contribution, we present the birefringence of an anisotropic material, $\text{Ca}_3\text{Ru}_2\text{O}_7$, which has structural domains at room temperature and can be tuned through a structural phase transition by lowering the temperature at ambient pressure. We will discuss the spatial evolution of its domains as a function of temperature and uniaxial pressure.

TT 38: Nonequilibrium Quantum Many-Body Systems II (joint session TT/DY)

Time: Wednesday 15:00–18:30

Location: HSZ 204

TT 38.1 Wed 15:00 HSZ 204

Hilbert space fragmentation in open quantum systems — •YAHUI LI, PABLO SALA, and FRANK POLLMANN — Department of Physics, TFK, Technische Universität München, James-Frank-Straße 1, D-85748 Garching, Germany

Several mechanisms have been identified that can lead to a breakdown of thermalization in closed quantum systems-including integrability and many-body localization. Recently, a novel mechanism for ergodicity breaking has been discovered in systems with certain dynamical constraints, where the Hilbert space fragments into exponentially many disconnected subspaces. An open question is how such systems evolve when they are coupled to a dissipative bath.

We find that the Hilbert space fragmentation can be utilized to preserve coherence in the presence of dissipation. We study a quantum fragmented model, which fragments in an entangled basis due to unconventional non-Abelian symmetries. We investigate the Lindblad dynamics under two different couplings, which either preserves or destroys the quantum fragmentation structure. At sufficiently large couplings, the operator space entanglement is suppressed, which allows for an efficient numerical simulation using tensor networks. Surprisingly, under the structure-preserving noise, we observe finite Renyi negativity, indicating non-vanishing quantum correlations. Using an analytic approach, we derive the stationary states under both couplings, which explains the long-time behaviors observed in numerical simulations.

TT 38.2 Wed 15:15 HSZ 204

Hilbert space fragmentation and interaction-induced localization in the extended Fermi-Hubbard model — •PHILIPP FREY, LUCAS HACKL, and STEPHAN RACHEL — University of Melbourne

We study Hilbert space fragmentation in the extended Fermi-Hubbard model with nearest and next-nearest neighbor interactions. Using a generalized spin/mover picture and saddle point methods, we derive lower bounds for the scaling of the number of frozen states and for the size of the largest block preserved under the dynamics. We find fragmentation for strong nearest and next-nearest neighbor repulsions as well as for the combined case. Our results suggest that the involvement of next-nearest neighbor repulsions leads to an increased tendency for localization. We then model the dynamics for larger systems using Markov simulations to test these findings and unveil in which interaction regimes the dynamics becomes spatially localized. In particular, we show that for strong nearest and next-nearest neighbor interactions random initial states will localize provided that the density of initial movers is sufficiently low.

[1] arXiv:2209.11777 (accepted for publication in PRB Letter)

TT 38.3 Wed 15:30 HSZ 204

Rate functions and the approach to adiabaticity in quantum many body systems — •VIBHU MISHRA, SALVATORE MANMANA, and STEFAN KEHREIN — Institute for Theoretical Physics, Georg-August-Universität Göttingen, Friedrich-Hund-Platz 1, 37077 Göttingen

The quantum adiabatic theorem is a fundamental result in quantum mechanics with applications ranging from quantum adiabatic computation to topological systems, while also serving as a theoretical foundation to many body perturbation theory via the Gell-Mann Low theorem.

We establish an inherent competition between ramp times T for an adiabatic process vs the system size N , in the behavior of relevant many body overlaps. We study this interplay between T and N by analyzing the properties of rate functions which are defined to be intensive quantities that give us a quantitative measure of the deviation from adiabaticity in the thermodynamic limit.

We analyze the Transverse Field Ising Model and the XXZ chain in 1D using exact diagonalization. We find that the rate functions show algebraic decay with increasing ramp time T . The decay exponent of the rate function for ramps within the gapped phase is 2, for ramps across Ising critical point it is 0.5 and within the Luttinger Liquid phase it is 1. The immediate implication is that the many body adiabatic time scales grow unavoidably with system size, namely as the \sqrt{N} for ramps within the gapped phase, and with N within the Luttinger Liquid phase.

TT 38.4 Wed 15:45 HSZ 204

Classical route to ergodicity and scarring phenomena in a two-component Bose-Josephson junction — DEBABRATA MONDAL¹, SUDIP SINHA¹, •SAYAK RAY², JOHANN KROHA², and SUBHASIS SINHA¹ — ¹Indian Institute of Science Education and Research Kolkata, Mohanpur, Nadia 741246, India — ²Physikalisches Institut, Rheinische Friedrich-Wilhelms-Universität Bonn, Nußallee 12, 53115 Bonn, Germany

We consider a Bose-Josephson junction (BJJ) formed by the binary mixture of ultracold atoms to investigate the manifestation of coherent collective dynamics on ergodicity and quantum scars, unfolding the connection between them. By tuning the inter and intra-species interaction, we demonstrate a rich variety of Josephson dynamics and transitions between them, which plays a crucial role in controlling the overall ergodic behaviour. The signature of underlying classicality is revealed from the entanglement spectrum, which also elucidates the formation of quantum scars of unstable steady states and of periodic orbits leading to athermal behaviour in a reduced Hilbert space. We show how the degree of ergodicity across the energy band and the scarring phenomena can be probed from the auto-correlation function as well from the phase fluctuation of the condensates, which has relevance in cold atom experiments. The model can also be realized in spin systems with application to information processing and lattice-gauge simulation.

[1] D. Mondal, S. Sinha, S. Ray, J. Kroha, and S. Sinha, Phys. Rev. A **106**, 043321 (2022)

TT 38.5 Wed 16:00 HSZ 204

Ultrafast dynamics of cold Fermi gas after a local quench — NIKOLAY GNEZDILOV¹, •ANDREI PAVLOV^{2,3}, VLADIMIR OHANESJAN⁴, YEVHENIIA CHEPESH⁴, and KOENRAAD SCHALM⁴ — ¹Department of Physics, University of Florida, Gainesville, USA — ²The Abdus Salam International Centre for Theoretical Physics (ICTP) Strada Costiera 11, Trieste, Italy — ³Institut für QuantenMaterialien und Technologien, Karlsruhe Institute of Technology, Hermann-von-Helmholtz-Platz 1, Eggenstein-Leopoldshafen, Germany — ⁴Instituut-Lorentz, Universiteit Leiden, Leiden, The Netherlands

We consider energy dynamics of two initially independent reservoirs A and B filled with a cold Fermi gas coupled and decoupled by two quantum quenches following one another. The energy change in the system adds up the heat trans-

ferred between A and B and the work done by the quench to uncouple the reservoirs. In case when A and B interact for a short time, we find an energy increase in both reservoirs upon decoupling. This energy gain results from the quenches' work and does not depend on the initial temperature imbalance between the reservoirs. We relate the quenches' work to the mutual correlations of A and B expressed through their von Neumann entropies. Utilizing this relation, we show that once A and B become coupled, their von Neumann entropies grow (on a timescale of the Fermi time) faster than thermal transport within the system. For a metallic setup, this implies the characteristic timescale of correlations' growth to be in the femtosecond range, while for the ultracold atoms, we expect it to be in the millisecond range.

TT 38.6 Wed 16:15 HSZ 204

A conjecture regarding the overlap of different ground states within the same phase — •SARAH DAMEROW and STEFAN KEHREIN — Georg-August Universität Göttingen

An extension of the adiabatic theorem to quantum quenches, i.e. non-adiabatic changes, is presented. Using exact diagonalisation, we numerically study the Transverse Field Ising Model (TFIM) and the Axial Next Nearest Neighbour Ising Model (ANNNI). We numerically test the following conjecture: Within the same phase, the overlap between the initial ground state and the ground state of the quenched Hamiltonian is the largest possible eigenstate overlap. In the TFIM, this conjecture is confirmed for both the paramagnetic (PM) and the ferromagnetic (FM) phases. In the ANNNI model results are ambiguous in some phases, due to both numerical errors and finite size effects.

15 min. break

TT 38.7 Wed 16:45 HSZ 204

Charge, spin, and heat shot noises in the absence of average currents — •LUDOVICO TESSER, MATTEO ACCIAI, CHRISTIAN SPÄNSLÄTT, JULIETTE MONSEL, and JANINE SPLETTSTOESSER — Chalmers University of Technology, Gothenburg, Sweden

Shot noise in electronic conductors occurs when the system is brought out of equilibrium, e.g., by a stationary bias. However, nonequilibrium does not imply that an average current flows. Indeed, the situation where selected currents are suppressed is of interest in fields like thermoelectrics and spintronics, raising the question of how the related noises behave.

I will present results on zero-current charge, spin, and heat noises in two-terminal mesoscopic conductors induced by voltage, spin and temperature biases. The nonequilibrium shot noises can be arbitrarily large, even if the respective average currents vanish. However, as soon as a temperature bias is present, additional equilibrium (thermal-like) noise necessarily occurs. This equilibrium noise sets an upper bound on the zero-current nonequilibrium charge and spin shot noise [1,2]. We have shown that the bound on the charge noise for strictly two-terminal conductors even extends into the finite-frequency regime. By contrast, these bounds can be overcome for heat transport by breaking the spin and electron-hole symmetries, respectively.

[1] J. Eriksson, M. Acciai, L. Tesser, J. Splettstoesser, Phys. Rev. Lett. 127, 136801 (2021)

[2] L. Tesser, M. Acciai, C. Spänslätt, J. Monsel, J. Splettstoesser, arXiv:2210.06051 [cond-mat.mes-hall] (2022)

TT 38.8 Wed 17:00 HSZ 204

Maximally chaotic to Fermi liquid crossover in a generalized SYK model — •NICK VON SELZAM and STEFAN KEHREIN — Institute for Theoretical Physics, University of Göttingen, Germany

We consider a generalized Sachdev-Ye-Kitaev (SYK) model: Majorana fermions on \mathcal{N} sites with random $\frac{q}{2}$ -body all to all interactions plus a kinetic energy term.

The SYK model can be seen as a toy model for quantum chaos and does not allow for a quasiparticle description. We discuss the continuous crossover between the Fermi liquid regime, dominated by the kinetic term, and the maximally chaotic regime, dominated by the SYK interaction, by studying the quantum Lyapunov exponents.

For fixed interaction strength there exists a crossover temperature for which the Lyapunov exponent becomes maximal. For lower temperatures the Lyapunov exponent is exponentially small. For larger temperatures the behaviour is close to indistinguishable from the pure SYK term.

TT 38.9 Wed 17:15 HSZ 204

Vibrationally-coupled electron transport in a quantum shuttle: A study using the hierarchical equations of motion approach — •SALVATORE GATTO, CHRISTOPH KASPAR, and MICHAEL THOSS — Institute of Physics, Albert-Ludwigs-Universität Freiburg

A quantum shuttle is an archetypical nanoelectromechanical device, in which the coupling of electronic and mechanical degrees of freedom is crucial [1]. In this contribution, we investigate transport properties of quantum shuttles, with a particular focus to the so-called shuttling regime, in which the transport of electrons is synchronized with the mechanical motion. The transport characteristics

are strongly influenced by the interplay of electronic and vibrational degrees of freedom, which manifests itself in step structures of the current-voltage characteristics. An effective molecule-lead coupling results in an increase of the current with respect to the tunneling regime. The study uses the hierarchical equations of motion approach, which allows a numerically exact simulation of nonequilibrium transport in general open quantum systems involving multiple bosonic and fermionic environments [2].

[1] Novotný et al., Phys. Rev. Lett. 92, 248302 (2004)

[2] J. Bätge, Y. Ke, C. Kaspar, and M. Thoss, Phys. Rev. B 103, 235413 (2021)

TT 38.10 Wed 17:30 HSZ 204

Effective form factors for finite temperature correlation functions — •OLEKSANDR GAMAYUN — University of Warsaw, ul. Pasteura 5, 02-093 Warsaw, Poland

The behavior of dynamical correlation functions in one-dimensional quantum systems at zero temperature is now very well understood in terms of linear and non-linear Luttinger models. The "microscopic" justification of these models consists in exactly accounting for the soft-mode excitations around the vacuum state and at most few high-energy excitations. At finite temperature, or more generically for finite entropy states, this direct approach is not strictly applicable due to the different structure of soft excitations. To address these issues we study the asymptotic behavior of correlation functions in one-dimensional free fermion models. On the one hand, we obtain exact answers in terms of Fredholm determinants. On the other hand, based on "microscopic" resummations, we develop a phenomenological approach that introduces the effective form factors and reduces the problem to the zero temperature case. The information about the initial state is transferred into the scattering phase of the effective fermions. I will demonstrate how this works for correlation functions in the XY model, mobile impurity, and the sine-kernel Fredholm determinants.

TT 38.11 Wed 17:45 HSZ 204

Transfer-matrix summation of path integrals for transport through nanostructures — SIMON MUNDINAR, •ALEXANDER HAHN, JÜRGEN KÖNIG, and ALFRED HUCHT — Theoretische Physik, Universität Duisburg-Essen and CENIDE, 47048 Duisburg, Germany

On the basis of the method of iterative summation of path integrals (ISPI), we develop a numerically exact transfer-matrix method to describe the nonequilibrium properties of interacting quantum-dot systems. For this, we map the ISPI scheme to a transfer-matrix approach [1], which is more accessible to physical interpretation, allows for a more transparent formulation of the theory, and substantially improves the efficiency. In particular, the stationary limit is directly implemented, without the need of extrapolation. The resulting new method, referred to as "Transfer-matrix Summation of Path Integrals" (TraSPI), is then applied to resonant electronic transport through a single-level quantum dot [2].

[1] S. Mundinar, P. Stegmann, J. König, and S. Weiss, Phys. Rev. B 99, 195457 (2019)

[2] S. Mundinar, A. Hahn, J. König, and A. Hucht, Phys. Rev. B 106, 165427 (2022)

TT 38.12 Wed 18:00 HSZ 204

Quasi-particle excitations at Mott-metal interfaces — •JAN VERLAGE¹, FRIEDEMANN QUEISSER^{2,3}, PETER KRATZER¹, and RALF SCHÜTZOLD^{2,3} — ¹Fakultät für Physik, Universität Duisburg-Essen — ²Institut für Theoretische Physik, Helmholtz-Zentrum Dresden-Rossendorf — ³Institut für Theoretische Physik, Technische Universität Dresden

We investigate excitations at the interface between a metallic bulk and a strongly correlated Mott insulator. Employing a hierarchy of correlations we identify effective quasi-particle and hole excitations in the heterostructure. To leading order in the hierarchy, the modes satisfy an effective two-component evolution equation. This allows the investigation of evanescent modes at the interface and tunneling through a Mott insulating layer.

The project is funded by the DFG, grant # 278162697 (CRC 1242).

TT 38.13 Wed 18:15 HSZ 204

Configuration interaction based nonequilibrium steady state impurity solver — •DANIEL WERNER, JAN LOTZE, and ENRICO ARRIGONI — ITPCP, Graz, Austria

We present a solver for correlated impurity problems out of equilibrium based on a combination of the so-called auxiliary master equation approach (AMEA) and the configuration interaction (CI) expansion. Within AMEA one maps the original impurity model onto an auxiliary open quantum system with a restricted number of bath sites which can be addressed by numerical many-body approaches such as ED or MPS. While the mapping becomes exponentially more accurate with increasing number of bath sites, ED implementations are severely limited due to the fast increase of the Hilbert space dimension for open systems, and the MPS solver typically requires rather long runtimes. Here, we propose to adopt a CI approach to solve numerically the correlated auxiliary open quantum system. This allows access to a larger number of bath sites at lower computational costs than for ED. We benchmark the approach with NRG results in equilibrium and with MPS out of equilibrium. We evaluate the current, the con-

ductance as well as the Kondo peak and its splitting. We obtain a rather accurate scaling of the conductance as a function of the bias voltage and temperature rescaled by TK for moderate to strong interactions in a wide range of param-

eters. The approach combines the fast runtime of ED with an accuracy close to the one achieved by MPS making it an attractive solver for nonequilibrium DMFT. (arXiv: 2210.09623)

TT 39: Superconducting Electronics

Time: Wednesday 15:00–18:15

Location: HSZ 304

Invited Talk

TT 39.1 Wed 15:00 HSZ 304

Sensing and control of MHz photons with microwave photon-pressure — INES C. RODRIGUES^{1,2}, GARY A. STEELE¹, and DANIEL BOTHNER^{1,3} — ¹Kavli Institute of Nanoscience, Delft University of Technology, The Netherlands — ²Department of Physics, ETH Zürich, Switzerland — ³Physikalisches Institut, Center for Quantum Science (CQ) and LISA+, Universität Tübingen, Germany
Superconducting microwave circuits have emerged as one of the leading platforms for quantum information science and quantum sensing in the recent decade. In 2018, a new type of interaction between a superconducting microwave circuit and a low frequency (LF) circuit has been realized, so called photon-pressure coupling, which is the all-circuit analogue of the radiation-pressure interaction between a mechanical oscillator and an optical cavity in optomechanics. Since 2020, several milestone experiments with photon-pressure circuits have been reported, such as the interferometric thermometry of an LF circuit, the observation of parametric strong-coupling or sideband-cooling of an LF mode into its quantum groundstate. Quite recently, we have realized a series of experiments in these circuits, for which we add a strong parametric drive to the Kerr-nonlinear high-frequency mode. This approach allows for parametrically enhanced interaction strengths, for the observation of nonreciprocal heat flow and for the implementation of photon-pressure with a "negative mass" microwave mode that inverts dynamical backaction and sideband-cooling effects. In our presentation, we will give an overview of photon-pressure circuits, discuss the most recent developments and possible future directions.

TT 39.2 Wed 15:30 HSZ 304

Waveguide quantum electrodynamics in high impedance networks — MIRIAM RESCH¹, CIPRIAN PADURARIU¹, BJÖRN KUBALA^{1,2}, FRANK GROSSMANN³, and JOACHIM ANKERHOLD¹ — ¹ICQ and IQST, Ulm University, Ulm, Germany — ²Institute of Quantum Technologies, German Aerospace Center (DLR), Ulm, Germany — ³Institut für Theoretische Physik, Technische Universität Dresden, Dresden, Germany

The emerging field of high impedance quantum circuits aims to exploit the extraordinary properties of high kinetic inductance materials, such as granular superconductors. The low propagation speed of electromagnetic excitations in such devices enables to strongly couple various types of qubits or resonators and waveguides. Theoretical description of such strongly coupled systems is challenging as the localized modes of the sub-unit couple to many waveguide modes simultaneously so that many common approximation schemes break down. Furthermore for a more realistic description of the system, Kerr nonlinearities are included in the model of the granular superconductor. To tackle this challenging regime in a numerically efficient way, we use the multi Davydov-Ansatz [1], where the wave function of the full system is described by a superposition of coherent states. As a first step we investigate how Kerr nonlinearities modify properties of qubit decay or readout, with the ultimate goal of identifying strong-coupling signatures in those observables, which are accessible to our experimental collaborators.

[1] M. Werther and F. Großmann, Phys. Rev. B **101**, 174315 (2020).

TT 39.3 Wed 15:45 HSZ 304

High-impedance resonators based on granular aluminum — MAHYA KHORRAMSHAHI, MARTIN SPIECKER, PATRICK PALUCH, NICOLAS ZAPATA, RITIKA DHUNDHWAL, IOAN M. POP, and THOMAS REISINGER — Karlsruhe Institute of Technology, Germany

Superconductors with characteristic impedance larger than the resistance quantum are a valuable resource in superconducting circuits. They enable the design of protected qubits such as Fluxoniums or 0- π qubits and can improve the coupling to small-dipole-moment objects, which may be useful for interfacing to spin-qubits, donor spins, etc. Here we present compact resonators in the lower GHz regime with a high characteristic impedance given by a high-kinetic-inductance material, namely granular aluminum, with spurious modes above 10GHz. We fabricated the resonators with an electron-beam lithography lift-off process, and we coupled them using a 50 Ohm coplanar waveguide architecture. Measurements performed in a dilution cryostat reveal that the resonators maintain high-quality factors in the single photon regime, a valuable resource for future quantum hardware implementations.

TT 39.4 Wed 16:00 HSZ 304

Surface acoustic wave resonators on thin film piezoelectric substrates for quantum acoustics — THOMAS LUSCHMANN^{1,2,3}, ALEXANDER JUNG^{1,2}, STEPHAN GEPRÄGS^{1,2}, RUDOLF GROSS^{1,2,3}, and HANS HUEBL^{1,2,3} — ¹Walther-Meißner-Institut, Bayerische Akademie der Wissenschaften, Garching, Germany — ²Technische Universität München, TUM School of Natural Sciences, Physics Department, Garching, Germany — ³Munich Center for Quantum Science and Technology, Munich, Germany

Lithium Niobate (LNO) is a well established material for Surface Acoustic Wave (SAW) devices including resonators, delay lines and filters. Recently, multi-layer substrates based on LNO thin films have become commercially available. Here, we present a systematic study of the performance of SAW devices fabricated on LNO-on-Insulator (LNOI) and LNO-on-Silicon substrates and compare them to bulk LNO devices. Our study aims at applications of these substrates for quantum acoustics, i.e. the integration with superconducting circuits operating in the quantum regime. To this end, we design SAW resonators with a target frequency of 5 GHz and perform our experiments at millikelvin temperatures and microwave power levels corresponding to single photons or phonons. We investigate the device quality factors as a function of the excitation power and temperature and model the observed losses by the coupling of the resonator to a bath of two-level-systems (TLS). Our results suggest that SAW devices on thin film LNO on Silicon have sufficient performance to be used in future SAW based quantum acoustic devices.

TT 39.5 Wed 16:15 HSZ 304

Towards hybrid quantum systems coupling superconducting qubits to cold atoms — BENEDIKT WILDE, NICOLAS ALBENGE, MANUEL KAISER, CONNY GLASER, MALTE REINSCHMIDT, ANDREAS GÜNTHER, JÓZSEF FORTÁGH, DIETER KOELLE, REINHOLD KLEINER, and DANIEL BOTHNER — Physikalisches Institut, Center for Quantum Science (CQ) and LISA+, Universität Tübingen

Coupling superconducting quantum circuits to ultracold atom clouds promises the possibility of exploiting the advantages of both systems, enabling new advances in both fundamental research and potential technological applications. One can realize such a hybrid quantum system by using a superconducting microwave resonator that is simultaneously coupled to both sub-systems. While coupling superconducting resonators to superconducting qubits is state-of-the-art, several challenges arise when trying to couple cold atoms to the integrated circuit. These challenges include achieving the required microwave field homogeneity, engineering a sufficiently large interaction strength and keeping a high resonator quality factor despite environmental factors suitable to deteriorate the performance of superconducting circuits, such as laser beams or magnetic atom traps. We present our recent developments and advances, discussing design considerations, simulations and intermediate results.

15 min. break

TT 39.6 Wed 16:45 HSZ 304

Parameter spread in Josephson traveling-wave parametric amplifiers: Vulnerabilities and tolerances — CHRISTOPH KISSLING, VICTOR GAY-DAMACHENKO, FABIAN KAAP, MARAT KHABIPOV, RALF DOLATA, ALEXANDER B. ZORIN, and LUKAS GRÜNHaupt — Physikalisches-Technische Bundesanstalt, Bundesallee 100, 38116 Braunschweig, Germany

Josephson traveling-wave parametric amplifiers (JTWPAs) hold great promise for wideband amplification of few-photon-level signals at microwave frequencies. These devices typically consist of thousands of nominally identical circuit elements, which are subject to fabrication variations. We analyse the effect of circuit parameter variation on the performance of a JTWPA using transient circuit simulations. Using this tool, we analyze two dispersion engineering concepts, resonant phase matching and periodic capacitance modulation, and compare their parameter spread tolerances. We identify circuit elements, which are critical concerning parameter spread, and explore ways to mitigate the impact of spread. Furthermore, we present the status of our practical implementation of rf-SQUID based JTWPAs and show experimental results.

TT 39.7 Wed 17:00 HSZ 304

Fabrication of low-loss Josephson parametric circuits — •KEDAR E. HONASOGE^{1,2}, YUKI NOJIRI^{1,2}, DANIL E. BAZULIN^{1,2}, LEON KOCH^{1,2}, THOMAS LUSCHMANN^{1,2}, NIKLAS BRUCKMOSER^{1,2}, MARIA-TERESA HANDSCHUH¹, FLORIAN FESQUET^{1,2}, MICHAEL RENGER^{1,2}, FABIAN KRONOWETTER^{1,2,4}, ACHIM MARX¹, RUDOLF GROSS^{1,2,3}, and KIRILL G. FEDOROV^{1,2} — ¹Walther-Meißner-Institut, 85748 Garching, Germany — ²Physik- Department, Technische Universität München, 85748 Garching, Germany — ³Munich Center for Quantum Science and Technology (MCQST), 80799 München, Germany — ⁴Rohde & Schwarz GmbH, 81671 München, Germany

The emergence of quantum information processing with superconducting circuits has stimulated the development of various interest in Josephson parametric devices. The latter offer a wide range of applications ranging from quantum-limited amplification to the generation of entangled squeezed states of light. We fabricate low-loss devices by employing careful cleaning steps during the fabrication of the superconducting circuits. Upon optimization, we fabricate Josephson parametric devices with internal quality factors in excess of 10^5 . We characterize bandwidth, gain, noise, dynamic range, and other properties of the realized devices. Based on these investigations, we derive useful criteria for the development of more intricate devices incorporating Josephson parametric circuits.

TT 39.8 Wed 17:15 HSZ 304

Nb SQUIDs patterned by He and Ne focused ion beams — •SIMON KOCH¹, TIMUR GRIENER¹, SIMON PFANDER¹, JULIAN LINEK¹, THOMAS WEIMANN², REINHOLD KLEINER¹, OLIVER KIELER², and DIETER KOELLE¹ — ¹Physikalisches Institut, Center for Quantum Science (CQ) and LISA⁺, Universität Tübingen, Germany — ²Department Quantum Electronics, Physikalisch-Technische Bundesanstalt (PTB), Braunschweig, Germany

Nanopatterning of superconducting thin film structures with focused He or Ne ion beams (He/Ne-FIB) offers a flexible tool for creating constriction-type Josephson junctions (cJJs) which can be integrated into strongly miniaturized superconducting quantum interference devices (nanoSQUIDs) for magnetic sensing on the nanoscale. We present our attempts to use He/Ne-FIB for fabricating Nb cJJs and nanoSQUIDs which shall provide ultra-low noise and high spatial resolution for their application in scanning SQUID microscopy (SSM). Moreover, we address the possibility to implement multiterminal, multi-JJ SQUIDs that provide flexibility in SQUID readout. The nanoSQUIDs are designed as sensors for magnetic flux and dissipation. They shall be integrated on custom-made Si cantilevers, which will provide the possibility of simultaneous conventional topographic imaging by atomic force microscopy (AFM). We will discuss the status of this project and challenges that have to be met on the way to combine SSM and AFM on the nanoscale.

We acknowledge the European Commission under H2020 FET Open grant FIB-superProbes (number 892427).

TT 39.9 Wed 17:30 HSZ 304

Synchronization in Josephson photonics devices in the presence of shot noise — FLORIAN HÖHE[†], CIPRIAN PADURARIU¹, BRECHT DONVIL¹, LUKAS DANNER^{1,2}, JOACHIM ANKERHOLD¹, and •BJÖRN KUBALA^{1,2} — ¹ICQ and IQST, Ulm University, Ulm, Germany — ²Institute of Quantum Technologies, German Aerospace Center (DLR), Ulm, Germany

For many quantum sources the exploitation and characterization of their quantum properties, such as entanglement and squeezing, is hampered by phase instability. Josephson photonics devices, where microwave radiation is created by inelastic Cooper pair tunneling across a *dc-biased* Josephson junction in-series

with a microwave resonator are particularly vulnerable lacking the reference phase provided by an ac-drive. To counter this issue, sophisticated measurement schemes have been used in [1] to prove entanglement, while in [2] a weak ac-signal was put in to lock phase and frequency of the emission. Intrinsic shot noise of the Josephson-photonics device inevitably diffuses the oscillators phase and requires an extension of classical synchronization theories to the quantum regime.

Performing multi-time scale perturbation theory we derive an effective Fokker-Planck equation for the phase to analyze quantum locking and synchronization in an Adler-type equation. Injection locking and synchronization lead to a narrowing of the photon emission statistics, while the shot noise induces phase slips.

[1] A. Peugeot et al., Phys. Rev. X 11, 031008 (2021).

[2] M. C. Cassidy et al., Science 355, 939 (2017).

TT 39.10 Wed 17:45 HSZ 304

Mitigating losses in NbTiN superconducting circuits under magnetic fields. — •ARNE BAHR, MATTEO BOSELLI, BENJAMIN HUARD, and AUDREY BIENFAIT — Laboratoire de Physique - École normale supérieure de Lyon, France

Quantum superconducting circuits enable quantum information processing as well as quantum sensing at microwave frequencies. One predominant factor limiting their performance is the presence of impurities creating microwave losses, triggering intense research effort for their identification and mitigation[1]. Here we probe these impurities in the context of using superconducting circuits under magnetic fields, which has application for coupling to other spin systems[2] and also detecting electron spin resonance (ESR) at the few spin levels[3].

We report continuous wave ESR measurements on spin impurities in resonators fabricated in NbTiN on a sapphire substrate. A simple etch through a resist layer process results in the presence of many spin impurities, preventing any ESR measurement near the spin 1/2 line. Following the characterization and identification of these spin signals, we improve our fabrication process to remove these spurious spin signals so that the resonators exhibit internal quality factors above $5 \cdot 10^5$ that remain constant up to 350 mT.

[1] N. P. de Leon et al., Science (2021)

[2] A. J. Landig et al., Nat. Com. (2019)

[3] V. Ranjan et al., Appl. Phys. Lett. (2020)

TT 39.11 Wed 18:00 HSZ 304

Pressure drop measurements and flow simulations of different regenerator fillings in a single stage GM-type pulse tube cryocooler — •BERND SCHMIDT^{†,2}, ELIAS EISENSCHMIDT^{1,3}, JACK-ANDRÉ SCHMIDT^{1,2}, JENS FALTER¹, HARDY WEISWEILER³, and ANDRÉ SCHIRMEISEN^{1,2} — ¹TransMIT-Center for Adaptive Cryotechnology and Sensors, Giessen, Germany — ²Institute of Applied Physics, Justus-Liebig-University Giessen, Germany — ³Technische Hochschule Mittelhessen, Friedberg, Germany

Although pulse tube cryocoolers (PTCs) reaching liquid Helium temperature were already presented in the 1990s[1], they are still subject to vivid development in many directions. Much of this development is done with the help of simulations and empirical values. A crucial part of a PTC is the regenerator, which is usually filled with multiple layers of porous materials with high heat capacity. These porous materials come in different shapes, mainly packed spheres and wire meshes.

In this talk we present measurements and simulations of pressure drop and gas flow through different regenerator fillings. We show the differences between the different kinds of fillings from the fluid mechanics point of view.

[1] C. Wang et al., Cryogenics, 37, 159 (1997)

TT 40: Focus Session: Wissenschaftskommunikation / Outreach (joint session HL/O/TT)

Im wissenschaftlichen Umfeld wird Maßnahmen der Öffentlichkeitsarbeit eine zunehmend größere Bedeutung zugemessen. - aus der Gesellschaft heraus und auch durch die großen Fördereinrichtungen und die DPG. Dabei geht es nicht nur um die Ergebnisse der Forschung, sondern auch darum, Prozesse und Methoden von wissenschaftlicher Arbeit transparent abzubilden – eine Aufgabe, die prinzipiell alle Forschenden übernehmen können. In diesem Symposium sollen erfolgreiche Projekte der Wissenschaftskommunikation, insbesondere aus dem Bereich der Festkörperphysik, vorgestellt werden. In ihrer Gesamtheit sollen sie das Spektrum der Wissenschaftskommunikation hinsichtlich des finanziellen und zeitlichen Aufwands aufzeigen und Methoden für unterschiedliche Zielgruppen vorstellen.

So dient diese Session sowohl als Ideengeber und Inspiration als auch als eine Art Netzwerk-Treffen zum Austausch über die Wissenschaftskommunikation in unterschiedlichen Kontexten.

Time: Wednesday 15:00–18:30

Location: POT 81

Invited Talk

TT 40.1 Wed 15:00 POT 81

experimentamus! Forschendes Lernen von Physik und Chemie in der Grundschule — •SEBASTIAN SCHLÜCKER — Universität Duisburg-Essen, Campus Essen

Der Sachunterricht in der Primarstufe ist ein Konglomerat aus allen Natur- und Gesellschaftswissenschaften, erst in der Sekundarstufe findet eine Aufspaltung in die einzelnen Fächer statt. Zudem unterrichten viele Grundschul-Lehrkräfte fachfremd. Auch der Zeitaufwand für die Vorbereitung von Experimenten ist

nicht unerheblich. Wie also kann man trotz dieser Hürden kindgerechte physikalische und chemische Experimente bereits in der Grundschule einführen?

Ich berichte aus 10 Jahren Erfahrung mit dem Projekt experimentamus!. Dabei handelt es sich um einen Kanon aus ca. 40 Experimenten für die Klassen 2 bis 4, welcher die Themen Licht, Wärme, Magnetismus, Wasser, Luft, Feuer und Elektrizität mit einem kindgerechten Alltagsbezug abdeckt. Anstelle des darlegenden Lernens wird auf das Forschende Lernen gesetzt: Frage - Hypothese - Experiment - Beobachtung - Erklärung; diese fünf Stationen des wissenschaftlichen Erkenntnisprozesses werden immer wieder durchlaufen. Ganz im Sinne Martin Wagenscheins wird dabei nach der exemplarischen und sokratischen Methode vorgegangen. Die praktische Implementierung umfasst 1. Materialkisten für alle Themen, 2. kompakte und leicht verständliche Informationshefter für die Lehrkräfte, sowie 3. Lernheftchen für alle SuS. Am Ende möchte ich über Erfahrungen und Herausforderungen im Rahmen dieses Projektes berichten und Ideen für eine mögliche weitere Verbreitung vorstellen.

TT 40.2 Wed 15:30 POT 81

Internal interfaces - goals and realisation of a scientific image film — •ULRICH HÖFER^{1,2} and MICHAEL DÜRR^{2,3} — ¹Fachbereich Physik, Philipps-Universität Marburg — ²SFB 1083, www.internal-interfaces.de — ³Institut für Angewandte Physik, Justus-Liebig-Universität Giessen, Germany

Funded by the German Science Foundation (DFG), a professional film maker has produced an image film about the research conducted in the Collaborative Research Center SFB 1083 "Structure and Dynamics of Internal Interfaces". The six-minute video clip takes the non-specialist on a journey down to atomic scale to show the progress at the forefront of research at solid/solid interfaces. It is not a demanding educational film. Rather, it is a visually stunning piece that looks like science fiction taken straight out of a movie, with tracking shots that take the viewer down to the nanometer scale, with flights through luminous molecules, exotic excitons, and space-filling laser labs. The film also has a very impressive soundtrack. Gustav Holst's (1874-1934) composition "The Planets" was re-orchestrated especially for this film. It is available on the youtube channel of the DFG (https://www.youtube.com/watch?v=-_mDt0NzHrc). Visitors of Chemikum Marburg can watch the German version on a 4K OLED screen, a device actually based on microscopic processes at interfaces investigated by SFB 1083.

The idea behind the creation of a professional film, its conceptional design and the necessary steps towards its realization will be outlined.

TT 40.3 Wed 15:45 POT 81

Outreach activities of SFB 1083 @ Chemikum Marburg — •CHRISTOP WEGSCHEID-GERLACH, LUISE CLERES, INA BUDDER, KARL-HEINZ MUTH, and MARION ENSSLE — Chemikum Marburg / SFB1083

The diffusion of concepts, methods, and visions of the SFB 1083 on Structure and Dynamics of Internal Interfaces into the general public is our general goal. To this end project Ö makes use of the institution Chemikum Marburg e.V., whose basic idea is to fascinate the public excited about natural sciences. The experiments offered here, stand for chemical, biological, pharmaceutical, and physical subjects related with daily phenomena or beyond. We will give an overview about the introduction of basic ideas and methods of SFB 1083 to the public as well as the institution Chemikum Marburg. The contents of the individual offers, such as experiments within the regular workspace, the workshops for the Girls' Day and the compilation of special workshops that are offered to give high-school students an understanding of the research content of the SFB 1083 are presented. An additional topic is the linking of basic research to applications for regenerative energy resources. Hydrogen fuel cells are well-known to the general public and rely on functional internal interfaces. An additional workshop which was prepared in cooperation with the district Marburg-Biedenkopf gives an overview about production, storage, and application of hydrogen as a new energy resource. We will also share various occasions at Chemikum Marburg where further outreach activities represent SFB 1083.

Invited Talk

TT 40.4 Wed 16:00 POT 81

Under the Microscope - spotlighting materials and nano science — •SVENJA LOHMANN and PRANOTI KSHIRSAGAR — The Science Talk, Germany

Real Scientists Nano is a science communication project dedicated to materials and nano science. Despite the widespread relevance of materials science to everyday life, we feel that dedicated science communication in this area is much rarer than in other fields. Our aim is to provide a platform for active materials and nano scientists to directly communicate their science and life as a scientist to the public. The use of social media thereby provides a very low threshold to science communication as basically the only requirement is to have an account. We have the goal to showcase the scientific community in all its diversity, and so far (12/2022) had guest scientists from more than 30 countries of origin as well as various fields and career stages. The two main pillars of the Real Scientists Nano project are the @RealSci_Nano Twitter account and the Under the Microscope podcast. Our guest scientists are interviewed for one podcast episode, and subsequently get to tweet from the account for one week following the rotation curation concept. We let curating scientist decide for themselves what they would like to tweet about. The form and content therefore vary greatly. Many of

our scientists report from their everyday life, and are for example live-tweeting from a conference, uploading videos or photos from the lab or sending the occasional "stuck in meetings, will return later" tweet. Science communication on social media thus gives the opportunity to open a direct and real-time window into the scientist's life.

30 min. break

Invited Talk

TT 40.5 Wed 17:00 POT 81

Phyphox - A pocketful of physics — •CHRISTOPH STAMPFER — JARA-FIT and 2nd Institute of Physics, RWTH Aachen University, 52074 Aachen, Germany — Peter Grünberg Institute (PGI-9), Forschungszentrum Jülich, 52425 Jülich, Germany

Most smartphones are used to make phone calls, to write short messages, surf the Internet or check e-mails. However, they can do much more: With the help of the integrated sensors and the free app "phyphox" (abbreviation for Physical Phone Experiments), pupils, students, and teachers and interested others can independently perform and develop physics experiments. For example, the app can use the accelerometer to record pendulum movements and determine the rotational acceleration in a salad spinner, or the air pressure sensor to determine time-resolved differences in altitude and thus the speed of an elevator. The didactic potential of the app is great, as the students are picked up on ground that is very familiar and attractive to them (smartphones) and are introduced to experimental natural sciences in a playful way and with an extremely low barrier (zero cost, i.e. only one click away). The app helps to get students excited about scientific and technical questions and contexts at an early age. The app is available free of charge for Android and iOS (more information can be found at www.phyphox.org). In my presentation, I will go into the concept of phyphox, introduce the range of functions and show a number of application examples.

TT 40.6 Wed 17:30 POT 81

Chair PR representative as a doctoral student's secondary task: A field report

— •PAULA M. WEBER, FELIX FRIEDRICH, and MANUEL SEITZ — Physikalisches Institut, Experimentelle Physik II, Universität Würzburg, Am Hubland, D-97074 Würzburg, Germany

Especially in recent years, it has become more important to communicate one's scientific work and methods to the public in order to show that in the scientific world, knowledge can only be created through research and the scientific process. Yet, extra time besides research is often limited and it is thus difficult to get into science communication. In this talk, I would like to present how PhD students can use their interest in science communication to benefit their own research group as a part-time PR representative.

In the first part of my talk, I will report on our efforts to attract new bachelor and master students. This advertising is focused on an audience with a scientific background, such that lab tours and advertising posters may contain scientific language and references. The second part is about communication with the general public, who usually know physics from their school days. Here, I will report on how we presented our research activities at the Night of Science in Physics and at the "Highlights der Physik" in Würzburg.

Working part-time as a PR representative could encourage doctoral students to try their hand at science communication and develop the associated communication skills.

TT 40.7 Wed 17:45 POT 81

Real or Fake - A format in science communication that encourages critical thinking — •TOBIAS LÖFFLER — Institut für Angewandte Physik Düsseldorf

The outreach format "Real or Fake" aims to train the audience in an critical approach to credible-sounding facts.

It is aimed at the general public and specifically at young people. At the same time, it offers an easy introduction for scientists to audience-oriented communication of science on stage. The format can be performed in front of a live audience or as an interactive online event. It has been proven to work as implemented into science festivals, nights of sciences, as a public individual event and also as part of events with constrained settings - such as outreach events at schools or as part of conferences.

"Real or Fake" was developed in 2017 by scientists around the Berlin March for Science who later founded Besserwissen e.V. with the goal to promote the format and support new organisers. I do cooperate with them since 2019 and have organized more than ten "Real or Fake" events since then.

In my talk, I will present the concept and its origins, give an overview of successful events and show what to do and what support one can get, if one wants to organize a "Real or Fake" event.

Invited Talk

TT 40.8 Wed 18:00 POT 81

Physics for school and the public at the LMU — •DR. CECILIA SCORZA-LESCH — Fakultät für Physik der LMU, München

Germany lives from research and technology. Physics, as the basis of all empirical sciences and technologies, has a very special, fundamental role to play. The Faculty of Physics at LMU, the largest in Germany, comprises nine research areas,

three centres and two excellence clusters. In this talk we will present the approach we use to successfully communicate our various topics of modern research, the

role of physics in our daily lives and in the fight against global warming to the schools and the public in a participatory way.

TT 41: Quantum Transport and Quantum Hall Effects II (joint session HL/TT)

Time: Wednesday 15:00–17:00

Location: POT 251

TT 41.1 Wed 15:00 POT 251

Aharonov-Bohm-type oscillations in phase-pure core/shell GaAs/InAs nanowires — •FARAH BASARIC^{1,2}, ANTON FAUSTMANN^{1,2}, ERIK ZIMMERMANN^{1,2}, GERRIT BEHNER^{1,2}, ALEXANDER PAWLIS^{1,2}, CHRISTOPH KRAUSE^{1,2}, HANS LÜTH^{1,2}, DETLEV GRÜTZMACHER^{1,2}, and THOMAS SCHÄPERS^{1,2} — ¹Peter Grünberg Institut (PGL-9), Forschungszentrum Jülich, 52425 Jülich, Germany — ²JARA-Fundamentals of Future Information Technology, Jülich-Aachen Research Alliance, Forschungszentrum Jülich and RWTH Aachen University, Germany

Epitaxially grown phase-pure GaAs/InAs core/shell nanowires offer uniformity in their electrical, mechanical and optical properties due to the absence of a crystallographic disorder. Magnetotransport measurements were carried out at variable temperatures and for different gate voltages, under an applied in-plane magnetic field. Pronounced Aharonov-Bohm-type oscillations in the conductance are observed for this nanowire type. In measurements at different gate voltages, significantly higher oscillation amplitudes are observed in comparison to the corresponding measurements on polymorphic core/shell nanowires. Furthermore, measurements at different temperatures show robustness of these oscillations against high temperatures as a result of reduced disorder. Finally, strong indications of a quasi-ballistic transport regime could be recognized for the phase-pure nanowire type. Obtained results indicate a strong effect of disorder reduction in GaAs/InAs nanowire transport properties, manifested in superior transport properties.

TT 41.2 Wed 15:15 POT 251

Spin valves based on bilayer graphene quantum point contacts — •EIKE ICKING^{1,2}, CHRISTIAN VOLK^{1,2}, CHRISTOPHER SCHATTAUER³, LUCA BANSZERUS^{1,2}, KENJI WATANABE⁴, TAKASHI TANIGUCHI⁵, FLORIAN LIBISCH³, BERND BESCHOTEN¹, and CHRISTOPH STAMPFER^{1,2} — ¹RWTH Aachen University, Germany — ²Forschungszentrum Jülich, Germany — ³TU Vienna, Austria — ⁴Research Center for Functional Material, Japan — ⁵International Center for Materials Nanoarchitectonics, Japan

Bernal bilayer graphene (BLG) is a unique material as it allows opening and electrostatically tuning a sizeable band gap by applying a perpendicular electric field. Recently, charge carriers have been confined successfully in one dimension to form quantum point contacts (QPC) based on split gates separated by a channel of a few hundred nanometers. Moreover, spin-polarized quantum transport through such structures has been demonstrated up to $6 e^2/h$ using a high in-plane magnetic field. The threshold magnetic field at which the lowest modes become spin-polarized depends on the subband spacing and thus on the width of the split gate channel. In this work, we combine two QPCs of different geometric widths, resulting in different threshold magnetic fields, to spin-polarize the first QPC and use it as a filter for the second QPC. In particular, we report on a spin-valve achieving spin-polarized channels with a total conductance of up to $10 e^2/h$.

TT 41.3 Wed 15:30 POT 251

Optical and electrical tuning between the normal insulating and topological insulating phase of InAs/GaSb bilayer quantum wells — •MANUEL MEYER¹, TOBIAS FÄHNDRICH¹, SEBASTIAN SCHMID¹, SEBASTIAN GEBERT¹, GERALD BASTARD^{1,2}, FABIAN HARTMANN¹, and SVEN HÖFLING¹ — ¹Technische Physik, Physikalisches Institut und Würzburg-Dresden Cluster of Excellence ct.qmat, Am Hubland, D-97074 Würzburg, Germany — ²Physics Department, École Normale Supérieure, PSL 24 rue Lhomond, 75005 Paris, France

Topological insulators (TI) based on InAs/GaSb bilayer quantum wells (BQW) are appealing due to their rich phase diagram with a TI and normal insulating (NI) phase[1]. The switching between both phases can be achieved by external electric fields using a top and back gate (TG and BG)[2]. However, especially a fully functional BG is difficult to realize in antimonides due to leakage issues. To overcome this bottleneck we present another tuning knob using optical excitation to switch from the NI to the TI phase over the TI gap[3]. By monitoring the charge carrier densities we can identify the hybridized band structure and in-plane magnetic field measurements evidence the TI gap. Furthermore, a top-gate sample is investigated. Without a back gate we find properties from both phases for magnetotransport measurements which points to a mixing of NI and TI states. This is further indicated by the resistance peak evolutions with temperature for both samples.

[1] C. Liu et al., PRL 100, 236601 (2008)

[2] F. Qu et al., PRL 115, 036803 (2015)

[3] G. Knebl et al., PRB 98, 041301(R) (2018)

30 min. break

TT 41.4 Wed 16:15 POT 251

Transport in high mobility HgTe heterostructures — •MICHAEL KICK, LENA FÜRST, JOHANNES KLEINLEIN, SAQUIB SHAMIM, HARTMUT BUHMANN, and LAURENS W. MOLENKAMP — Experimentelle Physik III, Physikalisches Institut, Universität Würzburg, Am Hubland, 97074 Würzburg, Germany

The Fractional Quantum Hall Effect (FQHE) has not yet been observed in the material system of HgTe. Due to recent progress in MBE growth, routinely charge carrier mobilities of HgTe heterostructures of over $\mu > 1 \cdot 10^6 \text{ cm}^2/\text{Vs}$ are obtained which is in the same order of magnitude as in the first reported experimental observation of the FQHE in GaAs/GaAlAs heterostructures. This opens up new prospects for transport investigations into the long time still open question of fractional states in this material system.

In 2-dimensional HgTe quantum wells, transport measurements show well pronounced quantum Hall plateaus for all filling factors, but no indication of any fractional state. High magnetic field measurements show a prolonged $\nu = 1$ plateau and a transition to an insulating state. Intriguingly, the $\nu = 1$ plateau exhibits a transition to an insulating state for filling factor $\nu = 1/2$.

Another possibility to observe the FQHE in HgTe is provided by the 2D surface states of a 3D topological insulator. High mobility layers, $\mu > 1 \cdot 10^6 \text{ cm}^2/\text{Vs}$, of tensile strained HgTe are subject of extensive magneto-transport investigations. First results reveal a good and detailed correspondence to recent k.p band structure calculations for non-interacting electron systems.

TT 41.5 Wed 16:30 POT 251

Electron Density Depended Giant Negative Magnetoresistance — •LINA BOCKHORN and ROLF J. HAUG — Institut für Festkörperphysik, Leibniz Universität Hannover, 30167 Hannover, Germany

Ultra-high mobility two-dimensional electron gases not only show an increasing number of new fractional filling factors, but also an astonishing robust negative magnetoresistance at zero magnetic field [1 -5]. The theoretical description of this negative magnetoresistance is still an open issue due to its complex dependencies on several parameters.

The behavior of the giant negative magnetoresistance is affected by different scattering events, e. g. interface roughness, oval defects, background impurities and remote ionized impurities, which leads to a strong dependence on different parameters. Here, we take a closer look on the temperature dependence of the giant negative magnetoresistance for different electron densities. At low temperatures we observe the predicted temperature dependence of $T^{1/2}$ [6].

[1] L. Bockhorn et al., Phys. Rev. B 83, 113301 (2011).

[2] A. T. Hatke et al., Phys. Rev. B 85, 081304 (2012).

[3] R. G. Mani et al., Scientific Reports 3, 2747 (2013).

[4] L. Bockhorn et al., Phys. Rev. B 90, 165434 (2014).

[5] L. Bockhorn et al., Appl. Phys. Lett. 108, 092103 (2016).

[6] I. V. Gornyi et al., Phys. Rev. B. 69, 045313 (2004).

TT 41.6 Wed 16:45 POT 251

Massless Dirac fermions on a space-time lattice with a topologically protected Dirac cone — •MICHAŁ PACHOLSKI¹, ALVARO DONÍS VELA³, GAL LEMUT³, JAKUB TWORZYDŁO², and CARLO BEENAKKER³ — ¹Max Planck Institute for the Physics of Complex Systems, Dresden, Germany — ²Warsaw University, Warsaw, Poland — ³Lorentz Institute, Leiden, The Netherlands

The symmetries that protect massless Dirac fermions from a gap opening may become ineffective if the Dirac equation is discretized in space and time, either because of scattering between multiple Dirac cones in the Brillouin zone (fermion doubling) or because of singularities at zone boundaries. Here we introduce an implementation of Dirac fermions on a space-time lattice that removes both obstructions. The quasi-energy band structure has a tangent dispersion with a single Dirac cone that cannot be gapped without breaking both time-reversal and chiral symmetries. We show that this topological protection is absent in the familiar single-cone discretization with a linear sawtooth dispersion, as a consequence of the fact that there the time-evolution operator is discontinuous at Brillouin zone boundaries.

TT 42: Poster: Correlated Electrons I

Time: Wednesday 15:00–18:00

Location: P2/OG2

TT 42.1 Wed 15:00 P2/OG2

Single crystal growth and characterization of CeCoIn₅ and Ce₂IrIn₈ — •ANJA PHILIPP, KRISTIN KLIEMT, and CORNELIUS KRELLNER — Max-von-Laue-Straße 1

The heavy-fermion series Ce_nT_mIn_{3n+2} (n=1,2; T = Co, Rh, Ir) with the unique tetragonal crystal structure, leading to a quasi-two dimensional Fermi surface, received growing attention over the past decades [1],[2],[3]. In these compounds, there are strong electronic interactions between conduction electrons and localized 4f-electrons of the Ce ions, which lead to a variety of interesting phenomena like spin and valence fluctuations, Kondo effect, magnetic order, non Fermi-liquid behaviour and unconventional superconductivity [3].

In this contribution, the results of the self-flux growth of CeCoIn₅ and Ce₂IrIn₈ single crystals are shown. The crystallographic orientation of the single crystals was determined using microscopy and Laue X-ray diffraction. The physical properties like resistivity, heat capacity and magnetic susceptibility down to 2K were measured for both compounds and were analyzed in this work.

[1] R.T. Maculso et al., Chem Mater. 15, 1394 (2003)

[2] G.D. Morris et al., Phys. Rev. B 69, 214415 (2004)

[3] A. Ikeda et al., Phys. Soc. Jap. 70, 2248 (2001)

TT 42.2 Wed 15:00 P2/OG2

Search for superconductivity in CeSb₂ under chemical pressure — •JAN WEBER, KRISTIN KLIEMT, and CORNELIUS KRELLNER — Max-von-Laue Straße 1, 60438 Frankfurt am Main, Physikalisches Institut

Recently, an unconventional superconducting state was discovered at a pressure-induced magnetic quantum critical point in the Kondo-lattice system CeSb₂ [1]. Under normal pressure CeSb₂ crystallizes in the orthorhombic SmSb₂ structure (Space group 64) [2]. At high pressures, the crystal structure changes and CeSb₂ adopts the ZrSi₂ - structure (Space group 63)[1]. This change in structure precedes the superconductivity around the magnetic quantum critical point. In this contribution, we present first attempts to replace the physical pressure using adequate substituents to reproduce the high-pressure structure at ambient pressure.

[1] O.P. Squire et al., arXiv:2211.00975 [cond-mat.str-el] (2022)

[2] R. Wang et al., Inorg. Chem. 6, 1685 (1967)

TT 42.3 Wed 15:00 P2/OG2

Searching for the critical endpoint in cobalt-doped EuRh₂Si₂ — •FRANZISKA WALTHER, ALEXEJ KRAIKER, KRISTIN KLIEMT, and CORNELIUS KRELLNER — Physikalisches Institut, Goethe-Universität Frankfurt, 60438 Frankfurt/Main, Germany

The rare europium-based intermetallic compounds with the ThCr₂Si₂-type structure show a variety of intriguing physical properties due to the coupling between lattice and electronic degrees of freedom. Eu ions can be present in a magnetic divalent or non-magnetic trivalent state. Under variation of temperature and pressure, it's possible to enforce a valence transition associated with a change of the unit cell volume [1]. At ambient pressure, EuRh₂Si₂ orders antiferromagnetically below T_N = 24 K in a stable divalent state [2], whereas the isoelectronic related compound EuCo₂Si₂ is nearly trivalent and indicates no magnetic ordering [1]. EuRh₂Si₂ undergoes a pressure-induced first order valence transition [3]. We expect the second order critical endpoint in the pressure range from 1.7 to 2.1 GPa, where the first-order phase transition terminates and critical elasticity may occur. We want to approach the critical endpoint by applying chemical pressure through substituting Rh in EuRh₂Si₂ with Co. We report on the growth of samples of the Eu(Rh_{1-x}Co_x)₂Si₂ -system and the characterization of their physical and chemical properties.

[1] Y. Onuki et al., J. Phys. Soc. Japan 89, 102001 (2020)

[2] S. Seiro, C. Geibel, J. Phys.: Condens. Matter 26, 046002, (2014)

[3] F. Honda et al., J. Phys. Soc. Japan 85, 063701 (2016)

TT 42.4 Wed 15:00 P2/OG2

Symmetry-broken low-temperature state in the Kondo system Ce₂Rh₂Ga — •SAJAL NADUVILE THADATHIL^{1,2}, J STIRNAT^{1,2}, P DEVI¹, M BAENITZ³, A STRYDOM⁴, D SOHOLOV⁴, J WOSNITZA^{1,2}, and T HELM¹ — ¹Dresden High Magnetic Field Laboratory (HLD-EMFL), HZDR, Germany — ²Institute of Solid State and Materials Physics, TU Dresden, Germany — ³Max Planck Institute for Chemical Physics of Solid, Dresden, Germany — ⁴University of Johannesburg, South Africa

Cerium-based heavy-fermion conductors often exhibit unconventional transport and thermodynamic properties related to 4f-electron physics. Ce₂Rh₂Ga exhibits a structural phase transition around T_p ≈ 130 K from an orthorhombic to monoclinic crystal structure accompanied by an extreme anisotropy in its electrical conduction. Recent nuclear quadrupole resonance studies on polycrystals found evidence for the emergence of two inequivalent Ce ions below 2 K with different electronic environments that may provide grounds for multi-ion Kondo physics [1]. Here, we present results from magnetotransport studies on

micron-sized devices cut from single crystals. We investigated the anisotropy between 0.3 and 300 K in fields up to 16 T. Below 5 K, the angular dependence of the magnetoresistance exhibits a significant change in its rotational anisotropy, indicating a broken symmetry. These findings may provide further evidence for multi-ion Kondo physics in Ce₂Rh₂Ga.

[1] Sh. Yamamoto et al., Phys. Rev. B 106, 115125 (2022)

TT 42.5 Wed 15:00 P2/OG2

Spin excitations in the field-induced phase of Ce₂Bi — •NIKOLAI PAVLOVSKII¹, ANTON KULBAKOV¹, ALEKSANDR SUKHANOV¹, MICHAEL SMIDMAN², FEDERICO MAZZA³, and DMYTRO INOSOV¹ — ¹TU Dresden, Dresden, Germany — ²Zhejiang University, Hangzhou, China — ³Vienna University of Technology, Austria

The compound Ce₂Bi represents a rare example of the heavy fermion materials that exhibit the coexistence of an antiferromagnetic magnetic (AFM) order and a tricritical point (TCP) in their temperature-magnetic field phase diagram. This combination is unusual because the TCP typically occurs in the ferromagnetic (FM) heavy fermion materials. In AFMs, the magnetic order can in many cases be continuously suppressed to zero temperature at a quantum critical point (QCP) by tuning pressure, magnetic fields, or chemical substitution. In the case of FMs, the situation is usually different. There, a QCP is generally avoided by changing the character of the magnetic phase transition from the second order to the first order, which induces a TCP. Using neutron time-of-flight spectroscopy, we observed two weakly-dispersed magnetic excitations modes in Ce₂Bi below Neel temperature that seem to show a nontrivial response to the applied magnetic field.

TT 42.6 Wed 15:00 P2/OG2

Transverse-field susceptibility of spin freezing at the mesoscale quantum phase transitions in LiHoF₄ — •MICHAEL LAMPL, ANDREAS WENDL, FELIX RUCKER, and CHRISTIAN PFLIEDERER — Physik-Department, Technical University of Munich, 85748 Garching, Germany

The perhaps best understood example of a quantum critical point is the response of the dipolar Ising ferromagnet LiHoF₄ under a transverse field [1-3]. When tilting the magnetic field away from the hard axis such that the Ising symmetry is always broken, a line of well-defined phase transitions emerges from the transverse-field quantum critical point, characteristic of further symmetry breaking, and in stark contrast to a crossover expected microscopically [4]. Detailed theoretical modelling in excellent agreement with experiment identifies this line of phase transitions as mesoscale quantum criticality. We report an experimental study of the transverse-field susceptibility of this mesoscale quantum criticality into a regime of spin freezing under large field tilting angles. Our observations will be compared with the characteristics of spin freezing, kinetic arrest, and quantum annealing observed in heavily diluted LiHo_xY_{1-x}F₄.

[1] D. Bitko et al., Phys. Rev. Lett. 77, 940 (1996)

[2] H. M. Ronnow et al., Science 308, 389 (2005)

[3] P. B. Chakraborty et al., Phys. Rev. B 70, 144411 (2004)

[4] A. Wendl et al., Nature 609, 65 (2022)

TT 42.7 Wed 15:00 P2/OG2

Phase diagram study of the Falicov-Kimball model on the two-dimensional Kagome lattice — YOUNES JAVANMARD¹ and •AMMAR NEJATI² — ¹Leibniz Universität Hannover, Hannover, Germany — ²Jülich Centre for Neutron Science (JCNS), Forschungszentrum Jülich

The Falicov-Kimball Model (FKM) is a relatively simple model of coupled quantum and classic degrees of freedom, in the middle of the spectrum between the Hubbard and the Anderson models. A number of studies have revealed its rich phase diagram in two-dimensional lattices, e.g. square and triangular lattices [1,2]. In a square lattice with half-filling, depending on the interaction strength and temperature, FKM exhibits a rich variety of phases: At sufficiently low temperatures, there is a charge density wave (CDW) phase; at high temperatures and weak interactions, a weakly localized phase appears which becomes an Anderson-localized phase in the thermodynamic limit; at high temperatures and strong interactions, a Mott insulating phase emerges [1]. In addition, there are two other phases called "quantum liquid" and "classical liquid" in triangular lattices and away from half-filling at sufficiently low temperatures and weak interactions [2].

We set up a Monte Carlo algorithm for the two-dimensional FKM away from the half-filling regime on a Kagome lattice to study this model's rich phase diagram, and to extend the previous studies regarding the consequences of geometry on the emergent quantum phases and the corresponding phase transitions.

[1] Phys. Rev. Lett. 117, 146601

[2] Phys. Rev. Lett. 122, 197601

TT 42.8 Wed 15:00 P2/OG2

Quantum-critical properties of random transverse-field Ising models extracted by quantum Monte Carlo methods — •CALVIN KRÄMER, ANJA LANGHELD, JAN KOZIOL, MAX HÖRMANN, and KAI PHILLIP SCHMIDT — Lehrstuhl für Theoretische Physik I, Staudtstraße 7, Universität Erlangen-Nürnberg, D-91058 Erlangen, Germany

The transverse-field Ising model with quenched disorder is studied in one and two dimensions at zero temperature by stochastic series expansion quantum Monte Carlo simulations. Using a sample-replication method we are able to determine distributions of pseudo-critical points, from which critical shift and width exponents $\nu_{s/w}$ are extracted by finite-size scaling. The scaling of the averaged magnetisation at the critical points is used further to determine the order-parameter critical exponent β . The dynamical scaling in the Griffiths phase is investigated by measuring the local susceptibility in the disordered phase and the critical exponent z' is extracted.

TT 42.9 Wed 15:00 P2/OG2

Numerical investigation of the Ising model in a light-induced quantized transverse field — •ANJA LANGHELD and KAI PHILLIP SCHMIDT — Lehrstuhl für Theoretische Physik I, Staudtstraße 7, Friedrich-Alexander Universität Erlangen-Nürnberg, D-91058 Erlangen, Germany

We investigate the Ising model in a light-induced quantized transverse field [1] with a particular focus on antiferromagnetic, potentially frustrated Ising interactions. Using exact diagonalization, we provide data for the antiferromagnetic chain in a longitudinal field that is inconsistent with earlier results coming from mean-field considerations [2]. In order to study the model on frustrated, two-dimensional lattice geometries, we extend the mean-field calculation and develop a quantum Monte Carlo update based on the recently introduced worm-hole update [3], for which the photons are integrated out. By this means, the photons induce a retarded spin-spin interaction in imaginary time that is also non-local in space in contrast to the Ising interaction inherent to the model.

[1] J. Rohn et al., Phys. Rev. Research 2, 023131 (2020)

[2] Y. Zhang et al., Sci. Rep. 4, 4083 (2014)

[3] M. Weber et al., Phys. Rev. Lett. 119, 097401 (2017)

TT 42.10 Wed 15:00 P2/OG2

High-order series expansions and crystalline structures for Rydberg atom arrays — •ANTONIA DUFT, JAN KOZIOL, MATTHIAS MÜHLHAUSER, PATICK ADELHARDT, and KAI PHILLIP SCHMIDT — Friedrich-Alexander-Universität Erlangen-Nürnberg

We investigate a model of hardcore bosons on the links of a Kagome lattice subject to a long-range decaying van-der-Waals interaction. This model is known to be the relevant microscopic description of Rydberg atom arrays excited by a detuned laser field which has been realized in experiments recently. Particular interest lies on this system as it is an engineerable quantum platform which has been predicted to host a topological phase. We investigate the quantum phase diagram for different limiting cases with a main focus on the low interaction-strength limit where we apply high-order linked cluster expansions.

TT 42.11 Wed 15:00 P2/OG2

Superexchange and spin-orbit coupling in the half-filled t_{2g} shell — •MARCO SCHÖNLEBER, DANIEL PRANJIC, and MARIA DAGHOFER — Institut für Funktionelle Materie und Quantentechnologien, Universität Stuttgart

Strongly correlated and spin-orbit coupled t_{2g} systems have been extensively investigated. By coupling orbital and spin angular momentum into one quantity, spin-orbit coupling (SOC) tends to reduce orbital degeneracy, e.g. for the widely studied case of one hole in the t_{2g} shell. However, the opposite has to be expected at half filling. Without spin-orbit coupling, all orbitals are half filled, no orbital degree of freedom is left and coupling to the lattice can be expected to be small. At dominant spin-orbit coupling, in contrast, one of the $j = 3/2$ states is empty and the system couples to the lattice. We investigate this issue. One finding is that the low-energy manifold evolves smoothly from the four $S = 3/2$ states in the absence of SOC to the four $j = 3/2$ states with dominant SOC. These four states are always separated from other states by a robust gap. We then discuss relevant superexchange models.

TT 42.12 Wed 15:00 P2/OG2

From linear to circular polarized light - Floquet engineering in Kitaev-Heisenberg materials with Lissajous figures — •PASCAL STROBEL¹ and MARIA DAGHOFER^{1,2} — ¹Institute for Functional Matter and Quantum Technologies, University of Stuttgart, 70550 Stuttgart, Germany — ²Center for Integrated Quantum Science and Technology, University of Stuttgart, Pfaffenwaldring 57, 70550 Stuttgart, Germany

Floquet engineering is a promising tool for tuning magnetic interactions in the candidate Kitaev material α -RuCl₃. Amplitude and frequency of the time periodic light field are able to modulate both sign and strength of Kitaev-, Heisenberg-, and Γ -interactions present in α -RuCl₃. This paves the way of possibly driving α -RuCl₃ into the sought after Kitaev spin-liquid phase.

We want to discuss possibilities of Floquet engineering with arbitrary polar-

ized light in α -RuCl₃. In order to do so, we describe the influence of arbitrary polarization via an effective model including Lissajous figures. This model is derived via perturbation theory up to fourth order. Starting from linear and circular polarized light we bridge the gap between those two limiting cases. Moreover we study more complex Lissajous figures and general trends arising for them.

TT 42.13 Wed 15:00 P2/OG2

Complete field-induced spectral response of the spin-1/2 triangular-lattice antiferromagnet CsYbSe₂ — •STANISLAV NIKITIN¹, T. XIE², A. A. EBERHARTER⁷, J. XING², S. NISHIMOTO^{3,4}, M. BRANDO⁵, P. KHANENKO⁵, J. SIGHELSCHMIDT⁵, A. A. TURRINI¹, D. G. MAZZONE¹, P. G. NAUMOV¹, L. D. SANJEEWA², A. S. SEFAT², B. NORMAND^{1,6}, A. M. LAUCHLI^{1,6}, and A. PODLESNYAK² — ¹Paul Scherrer Institut, Switzerland — ²Oak Ridge National Laboratory, USA — ³TU Dresden, Germany — ⁴IFW, Germany — ⁵MPI CPFS, Germany — ⁶EPFL, Switzerland — ⁷Universität Innsbruck, Austria

The spin 1/2 triangular lattice Heisenberg antiferromagnet remains on of the most attractive models to explore highly entangled quantum spin states in proximity to magnetic order. In my presentation I will discuss our recent results on CsYbSe₂. This material exhibits strong two-dimensional magnetic behavior in absence of exchange and structural disorder and its spin Hamiltonian is well described by J_1 - J_2 AFM Heisenberg model. We performed comprehensive INS measurements over the whole field scale starting from zero field up to the saturation and observed that corresponding excitation spectra evolve from continuum-like to relatively sharp spin-wave modes in the up-up-down phase, then back to continua and back to spin waves. We further support our observation by cylinder MPS calculation, which reproduce all observed features with semi-quantitative accuracy. Thus our comprehensive experimental and theoretical analysis of the field-induced spin excitations in the CsYbSe₂ provides valuable insight into the dynamics of a broad class of quantum many-body systems.

TT 42.14 Wed 15:00 P2/OG2

Low energy, mobile excitations in herbertsmithite revealed by magnetothermal conductivity — •RALF CLAUD, JAN BRUIN, YOSUKE MATSUMOTO, JÜRGEN NUSS, MASAHIKO ISOBE, and HIDENORI TAKAGI — Max Planck Institute for Solid State Research, Stuttgart, Germany

We report the magnetothermal conductivity $k(B)$ of the Kagome quantum spin liquid candidate herbertsmithite ($ZnCu_3(OH)_6Cl_2$) in the temperature range from 100 mK to 70 K with applied magnetic fields up to 12 T for heat flow parallel and perpendicular to the Kagome planes. We identify both phonon and magnetic contributions to k and find that the latter is only present for heat flow within the Kagome planes. These 2D magnetic contributions persist down to at least 200 mK, consistent with the presence of low-lying quantum spin liquid excitations with a gapless excitation spectrum.

TT 42.15 Wed 15:00 P2/OG2

Field-tuned critical fluctuations in the triangular-lattice delafossite NaYbO₂ probed by ²³Na NMR — •S. LUTHER^{1,2}, K. M. RANJITH^{3,4}, D. OPHERDEN¹, S. KHM³, H. YASUOKA³, J. WOSNITZA^{1,2}, M. BAENITZ³, and H. KÜHNE¹ — ¹Hochfeld-Magnetlabor Dresden, HZDR — ²Institut für Festkörper- und Materialphysik, TU Dresden — ³MPI-CPFS, Dresden — ⁴IFW Dresden

The frustrated triangular-lattice delafossite NaYbO₂ is a promising candidate for realizing a quantum spin liquid (QSL) ground state. The combination of a strong spin-orbit coupling and crystalline-electric-field effects leads to a magnetic anisotropy and a pseudospin-1/2 state of the Yb³⁺ ions at low temperatures. The absence of magnetic order and emergence of pronounced low-energy spin fluctuations have been shown by several experimental techniques, such as specific heat, inelastic neutron scattering, and muon spin relaxation. We present ²³Na NMR investigations of the low-temperature spin correlations by means of spectroscopy and $1/T_1$ measurements of polycrystalline NaYbO₂. At small magnetic fields and low temperatures, a strongly increased $1/T_1$ rate, as well as the absence of significant spectral line broadening suggest the presence of a QSL ground state with critical fluctuations at the verge of a magnetic instability. Above about 1 T, a crossover regime with persistent strong spin fluctuations and an onset of static magnetic ordering is observed. For fields above about 2 T, the formation of field-induced long-range magnetic order yields a strongly suppressed $1/T_1$ rate and an inhomogeneously broadened spectral lineshape.

TT 42.16 Wed 15:00 P2/OG2

Disorder effects in spiral spin liquids — •PEDRO MONTEIRO CÔNSOLI and MATTHIAS VOJTA — Institut für Theoretische Physik, TU Dresden

Spiral spin liquids are a special kind of paramagnetic state that features a sub-extensive classical ground-state degeneracy related to a family of spin spirals whose ordering wave vectors form a submanifold of momentum space. As the number of their theoretical and experimental realizations grows, there is cumulative evidence that, under additional perturbations, spiral spin liquids constitute a promising platform for the emergence of exotic phases of matter and excitations, including quantum spin liquids, multiple- q states, and skyrmions. However, little is known about their response to quenched disorder. In this poster, we investigate how various types of defects affect the classical ground-state manifold

of a spiral spin liquid on the honeycomb lattice. Among our results, we describe how different order-by-disorder mechanisms can arise, compete among themselves, and lead to spin-glass physics in these systems.

TT 42.17 Wed 15:00 P2/OG2

Second-harmonic generation in the Kitaev model — •OLEŚIA KRUPNITSKA^{1,2} and WOLFRAM BRENIG¹ — ¹Institute for Theoretical Physics, Technical University Braunschweig, D-38106 Braunschweig, Germany — ²Institute for Condensed Matter Physics, National Academy of Sciences of Ukraine, 1 Svientsitskii Street, Lviv, 79011, Ukraine

Optical spectroscopies are important probes for elementary excitations of quantum magnets. In the present study, we investigate second-harmonic generation in the hexagonal Kitaev model induced by external electric fields. The prime interest is to identify fingerprints of fractionalization as has been shown to exist in this model in terms of Majorana particles and gauge excitations. For that purpose second order response functions are calculated within the equation of motion approach. Analytical results for the spectrum will be presented in the homogeneous gauge sector and exchange anisotropy and temperatures of Majorana fermions will be analyzed. The impact of gauge flux excitation will be speculated upon.

TT 42.18 Wed 15:00 P2/OG2

Magnetostriction in frustrated planar quantum magnets — •ALEXANDER SCHWENKE and WOLFRAM BRENIG — Institute for Theoretical Physics, Technical University Braunschweig, D-38106 Braunschweig, Germany

Using the numerical linked cluster expansion (NLCE) focussing on the single-site representation, we study the field-induced thermodynamic and magnetoelastic properties of paradigmatic frustrated planar spin models. Results are presented for the energy, the specific heat and the magnetization. Employing simple magnetoelastic modelling we calculate the linear magnetostriction coefficient versus temperature and external magnetic field. In particular we consider magnetostriction at field-induced quantum phase transitions. Results obtained for the generalized Kitaev honeycomb model are extended to include findings on the anisotropic triangular Heisenberg antiferromagnet.

TT 42.19 Wed 15:00 P2/OG2

Continuous similarity transformation for critical phenomena: bilayer antiferromagnetic Heisenberg-model and $J_1 - J_2$ -model — •MATTHIAS R. WALTHER¹, DAG-BJÖRN HERING², GÖTZ S. UHRIG², and KAI P. SCHMIDT¹ — ¹Friedrich-Alexander-Universität Erlangen-Nürnberg, Institut für Theoretische Physik I, Staudtstraße 7, 91058 Erlangen — ²Technische Universität Dortmund, Department of Physics, Condensed Matter Theory, Otto-Hahn-Str. 4, 44227 Dortmund

We apply continuous similarity transformations (CSTs) to the bilayer antiferromagnetic Heisenberg model and the antiferromagnetic $J_1 - J_2$ model on the square lattice. The bilayer Heisenberg model features a well studied, continuous phase transition in the $O(3)$ universality class between a gapless Néel phase and a gapped paramagnetic dimer phase (valence bond solid). The $J_1 - J_2$ features a gapless Néel phase for $J_1 \gg J_2$, a gapless columnar phase for $J_2 \gg J_1$ and an intermediate phase whose nature is still under debate. We start in both models from the magnetically ordered, collinear phases and approach the quantum phase transitions indicating the breakdown of these long-range ordered phases. The CST flow equations are truncated in momentum space by the scaling dimension d so that all contributions with $d \leq 2$ are taken into account. We determine critical points by studying the breakdown of the ordered phases and try to determine critical exponents from the flow of the couplings, the ground-state magnetization and the ground-state energy.

TT 42.20 Wed 15:00 P2/OG2

Continuous similarity transformation for critical phenomena: easy-axis antiferromagnetic XXZ model — •DAG-BJÖRN HERING¹, MATTHIAS R. WALTHER², KAI P. SCHMIDT², and GÖTZ S. UHRIG¹ — ¹Technische Universität Dortmund, Department of Physics, Condensed Matter Theory, Otto-Hahn-Str. 4, 44227 Dortmund — ²Friedrich-Alexander-Universität Erlangen-Nürnberg, Institut für Theoretische Physik I, Staudtstraße 7, 91058 Erlangen

We apply continuous similarity transformations (CSTs) to the easy-axis antiferromagnetic XXZ-model on the square lattice. The CST flow equations are truncated in momentum space by the scaling dimension d so that all contributions with $d \leq 2$ are taken into account. The resulting quartic magnon-conserving effective Hamiltonian is analyzed in the zero-, one-, and two-magnon sector. In this way, a quantitative description of the ground-state energy, the one-magnon dispersion and its gap as well as of two-magnon bound states is gained for anisotropies ranging from the gapped Ising model to the gapless Heisenberg model. We discuss the critical properties of the gap closing as well as the evolution of the one-magnon roton minimum. The excitation energies of two-magnon bound states are calculated and their decay into the two-magnon continuum is determined via the inverse participation ratio.

TT 42.21 Wed 15:00 P2/OG2

Quantum criticality of the frustrated transverse-field Ising model on a triangular lattice using enhanced perturbative continuous unitary transformations — •LUKAS SCHAMRISS¹, MATTHIAS R. WALTHER¹, DAG-BJÖRN HERING², and KAI P. SCHMIDT¹ — ¹Department of Physics, Friedrich-Alexander-Universität Erlangen-Nürnberg, Staudtstraße 7, 91058 Erlangen, Germany — ²Condensed Matter Theory, Technische Universität Dortmund, Otto-Hahn-Straße 4, 44221 Dortmund, Germany

Ising models in a transverse field are paradigmatic models for quantum phase transitions of various universality classes which occur depending on the lattice geometry and the choice of antiferromagnetic or ferromagnetic coupling. We investigate the quantum phase diagram of the bilayer antiferromagnetic transverse field Ising model on a triangular lattice with an Ising-type interlayer coupling. Without a field, the model is known to host a classically disordered ground state, and in the limit of decoupled layers it exhibits the 3dXY transition of the corresponding single layer model. Our starting point for the unknown parts of the phase diagram is a high-order perturbative calculation from the limit of isolated dimers. Enhanced perturbative continuous unitary transformations (epCUTs) are used to derive series expansions for the ground state and the energy gap. These are refined by directly evaluated epCUTs (deepCUTs) which provide estimates which coincide with the perturbative series up to its respective order and add a non-perturbative correction. These allow to draw conclusions about the nature of occurring phase transitions.

TT 42.22 Wed 15:00 P2/OG2

Quantum simulation of transverse field Ising model using numerical linked cluster expansions with variational quantum eigensolver — •SUMEET SUMEET, MAX HÖRMANN, and KAI P. SCHMIDT — Institut für Theoretische Physik I Friedrich-Alexander-Universität Erlangen-Nürnberg

With the advancements in quantum technologies it has become inevitable to investigate the potential existence of quantum advantage for the paradigmatic models of quantum-many body physics. One of the very basic models is the transverse field Ising model that can be simulated on a quantum computer to compute properties such as the ground-state energy of a spin system. This problem, when tackled on a classical computer, leads to an exponential surge in the cost of computation with increasing system size. The advent of classical-quantum hybrid algorithms has shifted the focus to investigate the solution to this problem with algorithms such as the variational quantum eigensolver (VQE) which is considered reasonably good for obtaining the ground-state energies of quantum many-body systems in the NISQ era. In this work, we exploit the Hamiltonian variational ansatz for calculating the ground-state energy and fidelity of the transverse-field Ising model on one- and two-dimensional geometries. We devise strategies to compute the ground-state energy in the thermodynamic limit on quantum computers. In that regard, we apply numerical linked cluster expansions (NLCE) to VQE in order to simulate infinite spin systems using calculations on finite graphs. Further, we extend this approach to geometrically frustrated systems.

TT 43: Poster: Correlated Electrons II

Time: Wednesday 15:00–18:00

Location: P2/OG3

TT 43.1 Wed 15:00 P2/OG3

Interplay between order-by-disorder and long-range interactions — •JAN ALEXANDER KOZIOL and KAI PHILLIP SCHMIDT — Department of Physics, Staudtstraße 7, Friedrich-Alexander-Universität Erlangen-Nürnberg, Germany
We study the ground-state properties of the antiferromagnetic long-range transverse-field Ising model in the limit of small transverse fields. We present degenerate perturbation theory calculations on the extensively degenerate nearest-neighbour ground-state space for finite systems, treating the long-range inter-

action and the transverse field perturbatively. The long-range interaction breaks the degeneracy and stabilises a gapped six-fold degenerate plain stripe phase in the absence of a transverse field. An infinitesimal transverse-field leads to an order-by-disorder emergent six-fold degenerate gapped clock-ordered phase in the nearest-neighbour case. We demonstrate a level crossing transition between the plain stripe phase and clock ordered phase for finite transverse fields and long-range interactions.

TT 43.2 Wed 15:00 P2/OG3

Magnetic dilution of a frustrated triangular-lattice spin system — FLORIAN BÄRTL^{1,2}, ELLEN HÄUSSLER³, THOMAS DOERT³, JÖRG SICHELSCHEIDT⁴, SVEN LUTHER^{1,2}, TOMMY KOTTE¹, JOCHEN WOSNITZA^{1,2}, MICHAEL BAENITZ⁴, and HANNES KÜHNE¹ — ¹Hochfeld-Magnetlabor Dresden (HLD-EMFL), HZDR, Dresden — ²Institut für Festkörper- und Materialphysik, TU Dresden — ³Fakultät für Chemie und Lebensmittelchemie, TU Dresden — ⁴Max-Planck-Institut für Chemische Physik fester Stoffe, Dresden

Among the Yb-based triangular-lattice magnets, the delafossite NaYbS₂ is one of the promising candidates for realizing a quantum-spin-liquid (QSL) ground state. The magnetic phase diagram was probed by several experimental methods, such as specific-heat, magnetization, and NMR measurements. The proposed QSL ground state of NaYbS₂ is suppressed at fields of several tesla, and long-range order with various spin configurations is manifested. As a next step, we investigated possible changes to this phenomenology by diluting the magnetic lattice of NaYbS₂ by means of Lu substitution. A series of NaYb_{1-x}Lu_xS₂ single crystals, with $0 \leq x \leq 1$, were synthesized and characterized by various probes, including ESR spectroscopy. The ESR data reveal a systematic reduction of the Weiss temperature as x is increased. Further, we present recent specific-heat measurements for samples with $x \leq 0.5$, which reveal a systematic suppression of the transition temperatures to long-range order in magnetic fields with increasing Lu substitution.

We acknowledge the support of the SFB 1143.

TT 43.3 Wed 15:00 P2/OG3

Dynamic flash method for probing heat transport of quantum magnets — MAXIMILIAN SCHIFFER¹, XIAOCHEN HONG¹, MARTIN VALLDOR², CHRISTIAN HESS^{1,3}, and BERND BÜCHNER³ — ¹Fakultät für Mathematik und Naturwissenschaften, Bergische Universität Wuppertal, 42097 Wuppertal, Germany — ²Centre for Materials Science and Nanotechnology (SMN), Department of Chemistry, University of Oslo, P.O. Box 1033 Blindern, N-0315 Oslo, Norway — ³Leibniz-Institute for Solid State and Materials Research (IFW-Dresden), 01069 Dresden, Germany

Transport experiments in principle provide access to the investigation of exotic entropy carrying quasiparticles in quantum magnets, such as spinons in spin chains, triplons in spin ladders and Majorana fermions and visons in spin liquids. Generally, the thermal conductivity of an insulating, magnetic compound consists of phononic and magnetic contributions: $\kappa_{xx} = \kappa_{xx,ph} + \kappa_{xx,mag}$. Thus, measurement of κ_{xx} can offer a fine grasp of the above mentioned quasiparticles, which are currently under hot debate in the field of solid state physics.

Here we address heat transport experiments at elevated temperature which becomes important in materials with sizeable exchange interactions $J/k_B \geq 100$ K. It is well known that standard steady state heat transport measurements are difficult for $T \geq 200$ K due to inevitable radiation losses. We present Laser Flash Analysis as a method for avoiding this problem. The method will be introduced, and initial results on various quantum materials will be discussed.

TT 43.4 Wed 15:00 P2/OG3

Modified nanoparticles of Prussian Blue metal organic frameworks — SASCHA A. BRÄUNINGER and HERMANN SEIFERT — Institute of General Radiology and Medical Physics, University of Veterinary Medicine Foundation, Hannover, Germany

Prussian Blue compounds (PBC), e.g. soluble $AFe^{3+}[Fe^{2+}(CN)_6] \cdot xH_2O$ ($A = K, Na, NH_4$), have shown a huge potential of applications in physics, chemistry, medicine and radioecology, e.g., PBC acting as efficient ion exchanger extracting the radioisotope ¹³⁷Cs in solutions. For potassium, proposed ferromagnetism by superexchange is discussed between Fe(III) with $S = 5/2$ and an effective magnetic moment of $\mu_{eff} \approx 5.98\mu_B$ consistent with a spin-only value of Fe(III) high-spin. Powder neutron diffraction studies showed a Curie temperature $T_C \approx 5.6$ K consistent with susceptibility measurements. Here, we are presenting the synthesis and low-energy investigation of modified magnetic Prussian-blue nanoparticles protected by PVP (polyvinylpyrrolidene).

TT 43.5 Wed 15:00 P2/OG3

Experimental studies of phase diagram of compound $Ni(2aepy)_2Cl(H_2O)Cl \cdot H_2O$ - a spin-1 antiferromagnetic chain — MARIA HOLUB¹, SLAVOMÍRA ŠTERBINSKÁ², MARC UHLARZ³, JURAJ ČERNÁK², and ERIK ČIŽMÁR¹ — ¹Institute of Physics, Faculty of Science, P.J. Šafárik University, Park Angelinum 9, Košice, Slovakia — ²Institute of Chemistry, Faculty of Science, P.J. Šafárik University, Moyzsova 11, Košice, Slovakia — ³Dresden High Magnetic Field Laboratory (HLD-EMFL), Helmholtz-Zentrum Dresden-Rossendorf, Bautzner Landstraße, Dresden, Germany

We present the study of compound $Ni(2aepy)_2Cl(H_2O)Cl \cdot H_2O$ ($2aepy = 2$ -aminoethylpyridine) identified as a spin-1 antiferromagnetic chain with ratio of $D/J=1.14$ (D is the single-ion anisotropy, J is the intrachain exchange interaction). It represents a unique experimental example of a system close to the quantum critical point (QCP), which is a topological phase transition that separates Haldane and Large-D gapped phases for spin-1 chains. In this work, we observed the presence of field-induced crossover into the gapless Tomonaga-Luttinger liq-

uid phase using low-temperature specific heat measurements. A very low first critical field is in good agreement with the small energy gap predicted close to QCP. Estimation of saturation field (second critical field) using D and J parameters was confirmed by high-field magnetic measurements at ≈ 12.5 T.

This work was supported by APVV-18-0016, APVV-18-0197, and HLD-HZDR, member of the European Magnetic Field Laboratory (EMFL).

TT 43.6 Wed 15:00 P2/OG3

Electrical and thermal transport properties of delafossite oxide $CuCr_{1-x}Fe_xO_2$ — MITHUN KUMAR MAJEE¹, RATNAMALA CHATTERJEE¹, and PREETI BHOBE² — ¹Department of Physics, Indian Institute of Technology Delhi, Hauz Khas, New Delhi 110016, India — ²Department of Physics, Indian Institute of Technology Indore, Khandwa Road, Simrol, Indore-453552, India

In order to improve the thermoelectric property of a material the effect of phonon/magnon drag, and spin fluctuations are other central parameters apart from carrier concentration, and lower thermal conductivity. It is known from the literature that $CuCrO_2$ has a large Seebeck value of around $350 \mu V/K$ at room temperature, but its electronic concentration is low, hence the thermoelectric figure-of-merit (ZT) turns out to be quite poor. Hence to better its ZT, we attempt to replace some Cr ions with Fe in the series, $CuCr_{1-x}Fe_xO_2$ ($0 < x < 1$) and study its electrical and thermal conductivity, heat capacity, and Seebeck coefficient. Our results exhibit a large and complex Seebeck coefficient in $20 K < T < 380$ K. The low-temperature electrical conduction is observed to obey 3D variable range hopping mechanism. Unlike, nonmagnetic Cu-based Delafossites, we show that the thermal conductivity is strongly affected by spin-phonon scattering in $CuCr_{1-x}Fe_xO_2$ compositions. The heat capacity measurements identify the Debye temperature and effects due to magnetic ordering temperatures. Out of the different contributed processes, the role of the phonon drag effect and complexity in temperature dependence is observed in the Cr-rich compositions.

TT 43.7 Wed 15:00 P2/OG3

Influence of lattice strain on the electronic and magnetic properties of $SrRuO_3/SrTiO_3$ heterostructures — ROBIN HEUMANN, ROBERT GRUHL, and PHILIPP GEGENWART — Experimentalphysik VI, Universität Augsburg, 86159 Augsburg, Germany

Layered ruthenate Sr_2RuO_4 , consisting of strontium- and ruthenium-oxide stacks along the c-axis, is a prototype unconventional superconductor and continues to attract strong interest. Artificial heterostructures composed of layers of $SrRuO_3$ (SRO) and $SrTiO_3$ (STO) were recently considered by band-structure calculations [1,2]. It is predicted that SRO_n/STO_1 bilayers show a variety of emergent quantum states tunable by lattice strain, including ferro- and checkerboard-type antiferromagnetism, spin-density waves [1] and even unconventional superconductivity [2].

Utilizing metal-organic aerosol deposition [SRO_n/STO_n]_m epitaxial heterostructures were grown. The superlattices show sharp interfaces and an atomically smooth surface morphology. Different substrates were used to study the effect of tensile and compressive lattice strain. Besides structural studies by x-ray diffraction, reciprocal space mapping and TEM imaging we utilized Hall- and magnetoresistance as well as magnetization measurements to investigate the electronic and magnetic properties.

[1] M. Kim *et al.*, Phys. Rev. B **106** (2022) L201103.

[2] B. Kim *et al.*, Phys. Rev. B **101** (2020) 220502(R).

TT 43.8 Wed 15:00 P2/OG3

Manipulating the metal-insulator transition in ultrathin oxide films by strain engineering — SIZHAO HUANG, PHILIPP SCHEIDERER, JUDITH GABEL, MICHAEL SING, and RALPH CLAESSEN — Physikalisches Institut and Würzburg-Dresden Cluster of Excellence ct.qmat, Universität Würzburg, 97074 Würzburg, Germany

The relationship between metal-insulator transition (MIT) and strain relaxation in films of strongly correlated perovskite oxides has been intensively studied. The oxide films can emerge numerous phenomena when the film thickness is reduced towards the 2D limit, such as $SrVO_3$ (SVO). In our previous studies on $SrTiO_3$ (STO) capped SVO films, a transition from the Mott insulating state at 6 u.c. to metallic behaviour at 10 u.c. film thickness has been found. In order to further explore the relationship between MIT transition and orbital occupation, we have grown coherently strained SVO thin films on various substrates with different lattice constants by pulsed laser deposition (PLD) in an Ar gas background. Using x-ray photoelectron spectroscopy and transport measurements, we have found that the MIT in SVO thin films can be fine-tuned by both film thickness and strain.

TT 43.9 Wed 15:00 P2/OG3

Towards noise spectroscopy at the Mott critical endpoint — TIM THYZEL¹, HARALD SCHUBERT¹, MICHAEL LANG¹, TAKAHIKO SASAKI², and JENS MÜLLER¹ — ¹Institute of Physics, Goethe-Universität Frankfurt, Frankfurt (Main), Germany — ²Institute of Materials Research, Tohoku University, Sendai, Japan

Quasi-two-dimensional organic charge-transfer salts are ideal model systems for studying strongly correlated electrons due to their chemical variability, good physical tunability and rich phase diagrams.

Of special interest has been the family of Mott-Insulators κ -(ET)₂Cu[N(CN)₂]Z where Z is Br or Cl, which exhibit superconductivity and an insulator-to-metal transition in an easily accessible temperature-pressure window. In particular, we focus on the critical endpoint of the Mott transition, where a breakdown of Hooke's law of elasticity has been observed [1], as well as indications of ergodicity breaking [2].

We employ resistance noise spectroscopy as a powerful method to detect slow dynamics in charge transport near the Mott endpoint, which we access in a cryogenic hydrostatic gas pressure setup. Using this technique, we search for a slowing-down of carrier dynamics, as well as the appearance of non-stationary fluctuations hinting at critical behaviour. Details on the experimental setup will be presented, as well as initial spectroscopy scans of the phase diagram.

[1] E. Gati, *Sci. Adv.* **2**, e1601646 (2016)

[2] B. Hartmann, *Phys. Rev. Lett.* **114**, 216403 (2015)

TT 43.10 Wed 15:00 P2/OG3

Thermal-history-dependent electronic properties of κ -(BEDT-TTF)₂Cu[N(CN)₂]Br close to the Mott metal-insulator transition — •FLORIAN KOLLMANNBERGER^{1,2}, SHAMIL ERKNOV^{1,2}, NATALIA KUSHCH¹, TONI HELM³, WERNER BIBERACHER¹, and MARK KARTSOVNIK¹ — ¹Walther-Meißner-Institut, 85748 Garching, Germany — ²Technische Universität München Fakultät Physik, 85748 Garching, Germany — ³Hochfeld-Magnetlabor Dresden, HZDR, 01328 Dresden, Germany

The partially deuterated organic charge-transfer salt κ -(BEDT-TTF)₂Cu[N(CN)₂]Br (shortly, κ -Br) can be tuned over the Mott-metal-insulator transition (MIT) by rapid cooling through the temperature interval around $T_g \approx 75$ K where a glassy ordering of the BEDT-TTF ethylene endgroups occurs. It was suggested [1,2] that this tuning happens due to a change of the conduction bandwidth, an effect similar to that induced by hydrostatic pressure. We investigated the influence of the ethylene group ordering in purely hydrogenated κ -Br. To this end, we have studied the resistance as a function of temperature and magnetic field for samples cooled through the glass transition at different rates. In particular, we have studied the variation in the behavior of magnetoresistance quantum oscillations. This allows us to trace the change in the Hubbard model parameter U/t extracted from the renormalized effective cyclotron mass.

[1] B. Hartmann et al., *Phys. Rev. B* **90**, 195150(2014).

[2] D. Guterding et al., *Phys. Rev. B* **92**, 081109(R) (2015).

TT 43.11 Wed 15:00 P2/OG3

Tetragonal CuO : Suppression of nearest-neighbour correlations in a strongly correlated material — •BENJAMIN BACQ-LABREUIL¹, MAX BRAMBERGER², MARTIN GRUNDNER², SILKE BIERMANN³, ULRICH SCHOLLWÖCK², SEBASTIAN PAECKEL², and BENJAMIN LENZ⁴ — ¹Institut Quantique, Université de Sherbrooke, Sherbrooke, Canada — ²Arnold Sommerfeld Center of Theoretical Physics, University of Munich, Munich, Germany — ³CPHT, Ecole Polytechnique, Palaiseau, France — ⁴IMPMC, Sorbonne Université, Paris, France

Since tetragonal CuO (t-CuO) is composed of well separated 2D CuO planes, it appears as an ideal candidate to connect model calculations with real materials in the quest of understanding the nature of high-temperature superconductivity. In this work [1], we investigate the low-energy electronic properties of t-CuO by means of Cellular Dynamical Mean Field Theory (CDMFT) using a 2D Hubbard model. From experiment it was proposed that single layers of t-CuO can be viewed as two weakly interconnected sublattices. Our calculations support this assumption: we find a suppression of the nearest-neighbour (NN) correlations for the benefit of the next-nearest neighbour (NNN) ones. The calculated spectral function is in remarkable agreement with photoemission experiments, showing that a one-band model is sufficient to capture the low-energy physics of t-CuO. Finally, we study the transition from the paramagnetic to antiferromagnetic phase at finite temperature and elucidate the nature of the insulating regime in both phases.

[1] M. Bramberger et al., arXiv:2203.07880 (2022)

TT 43.12 Wed 15:00 P2/OG3

Thermal expansion measurements at low temperatures of a valence fluctuating system close to a critical endpoint. — •ARIF ATA, BERND WOLF, JAN ZIMMERMANN, MARIUS PETERS, KRISTIN KLIEMT, CORNELIUS KRELLNER, and MICHAEL LANG — PI, SFB/TRR288, Goethe Univ., Frankfurt/M., Germany

Thermodynamic investigations of highly correlated electron systems at low-temperatures are of general interest. Especially strong-coupling effects between lattice- and electronic degrees of freedom, which are expected around second-order critical endpoints [1], have become topics of current interest. These include phenomena such as critical softening and deviations from Hooke's law of elasticity [1]. The intermetallic compound EuPd₂Si₂ and its Ge-doped variants, which show different kinds of phase transitions such as valence- and magnetic- transitions, are promising target materials for such investigations [2]. Of particular interest is the possibility to approach the critical regime by the combination of chemical pressure (Ge-doping) and He-gas pressure. In this work we present results of thermal expansion measurements on single crystalline EuPd₂(Si_{1-x}Ge_x) as a function of temperature for $4.2 \text{ K} \leq T \leq 300 \text{ K}$ and He-gas pressure $P \leq 12$

kbar. The data have been obtained by using a strain gauge, enabling measurements of thermal expansion and compressibility to be performed at high pressure, i.e., in P-T parameter ranges where He is in its solid phase.

[1] E. Gati et al., *Sci. Adv.* **2**, e1601646 (2016).

[2] Y. Onuki et al., *Philosophical Magazine* **97**, 3399 (2017).

TT 43.13 Wed 15:00 P2/OG3

Probing the electron-lattice coupling near the valence transition in YbLn_{1-x}Ag_xCu₄ — •JAN ZIMMERMANN, BERND WOLF, MICHELLE OCKER, KRISTIN KLIEMT, CORNELIUS KRELLNER, and MICHAEL LANG — PI, SFB/TR288, Goethe Univ., Frankfurt/M., Deutschland

The recently proposed phenomenon of *critical elasticity* is linked to a non-perturbatively strong coupling between lattice- and critical electronic degrees of freedom [1]. Intermetallic compounds that show various types of phase transitions such as valence- or structural instabilities that make it possible to study such collective phenomena, are currently a field of high interest. It has been shown that doping can be used in EuPd₂(Si_{1-x}Ge_x)₂ to generate chemical pressure which may open up the possibility to experimentally access directly the area around the critical endpoint [2]. It is expected to find similar effects for the valence transition in the doped intermetallic compound YbLn_{1-x}Ag_xCu₄ [3]. We are investigating the elasticity of YbLn_{1-x}Ag_xCu₄ using ultrasound-wave-propagation. In addition to measurements performed under variable temperature, we have developed a new setup that allows ultrasonic measurements to be performed under variable He-gas pressure. We will discuss first results on the elasticity, in comparison with data on the magnetic susceptibility, and highlight the additional experimental possibilities the new setup offers.

[1] E. Gati et al., *Sci. Adv.* **2**, e1601646 (2016)

[2] B. Wolf et al., arXiv:2210.12227, (2022)

[3] S. Zherlitsyn et al., *Phys. Rev. B*, **60**, 5, (1999)

TT 43.14 Wed 15:00 P2/OG3

Order from disorder phenomena in BaCoS₂ — •BENJAMIN LENZ¹, MICHELE FABRIZIO², and MICHELE CASULA¹ — ¹IMPMC, Sorbonne Université, CNRS, MNHN, 4 Place Jussieu, 75005 Paris, France — ²International School for Advanced Studies (SISSA), Via Bonomea 265, I-34136 Trieste, Italy

We investigate different nematic and orbital ordered instabilities in the antiferromagnetic insulating phase of BaCoS₂, which shows a Néel transition at a surprisingly high temperature of $T_N \sim 300$ K. Based on *ab initio* simulations, we discuss several competing orders in terms of magnetic order, orbital composition and structural distortions to identify a set of nematic and orbital ordered states as possible candidates for the ground state. From these considerations we derive an effective spin model of $J_1 - J_2 - J_3$ type and discuss the consequences of the most probable, orbital ordered ground state for its parametrization. We finally identify a driving mechanism which allows to explain the high Néel temperature by C₄-symmetry breaking through orbital order and draw parallels to other quasi-2D materials such as pnictides.

TT 43.15 Wed 15:00 P2/OG3

Basis dependence of the Mott transition in Ba₂IrO₄ within Dynamical Mean Field Theory — •FRANCESCO CASSOL¹, LÉO GASPARD², CYRIL MARTINS², MICHELE CASULA¹, and BENJAMIN LENZ¹ — ¹L'Institut de Minéralogie, de Physique des Matériaux et de Cosmochimie (IMPMC), Sorbonne Université, Paris, France — ²Laboratoire de Chimie et Physique Quantiques, Université Toulouse III Paul Sabatier, Toulouse, France

Among strongly correlated materials Sr₂IrO₄ is often presented as a paradigmatic system for the complex competition that takes place between ligand field, spin-orbit coupling (SOC), Coulomb correlation and structural distortion. Ba₂IrO₄ has recently attracted some interest being simpler in view of the absence of structural distortion and being isostructural to La₂CuO₄. Normally, the physics of iridates has been described within a $j_{eff} = \frac{1}{2}$ basis representation solved by means of Dynamical Mean Field Theory (DMFT). This picture however, while it partially alleviates the sign problem of Quantum Monte Carlo solver, often goes in hands with some approximation that prevent the application of a fully *Ab initio* DFT+DMFT scheme. In this work, we will go beyond standard approximation comparing the usual schemes to the orbital picture.

TT 43.16 Wed 15:00 P2/OG3

Calculating moments for many-electrons systems — •ELAHEH ADIBI and ERIK KOCH — Institute for Advanced Simulation, Forschungszentrum Jülich, 52425 Jülich, Germany

We present a technique for computing the moments $\langle E^M \rangle = \text{Tr } H^M$ of the many-electron spectrum. Taking the trace over a basis of Slater determinants $|I\rangle$ and expressing the Hamiltonian in the same orbital basis, matrix elements $\langle I|H^M|I\rangle$ can only be non-zero when the orbital indices of the creation operators are a permutation of those of the annihilation operators. Writing the permutations in cycle notation and realizing that the trace over a cycle with different orbital indices only depends on the number of descends, we can write the trace as a sum over products of Eulerian numbers times binomial factors involving the number of orbitals and electrons.

TT 43.17 Wed 15:00 P2/OG3

Exact diagonalization with twisted boundary conditions — •BENJAMIN HEINRICH — Institut für funktionelle Materie und Quantentechnologie, Universität Stuttgart

When using exact diagonalization, using twisted instead of periodic boundary conditions gives access to additional momentum points. We investigate here in detail flavour-specific twisted boundary conditions, where each spin and/or orbital can have different boundary conditions. One goal is to assess whether and to which extent this improves estimates of observables (e.g. the ground-state energy). As increased momentum resolution is of particular interest in excitation spectra, a second aim is to estimate the quality of these additional data. We investigate the method for one- and two-dimensional one- and two-band Hubbard models. First results suggest that the additional momenta work well where the relevant physics is to a large extent captured by one quasiparticle (e.g. the magnon in case of magnetic spectra), but are less reliable in more complex scenarios (e.g. two spinons).

TT 43.18 Wed 15:00 P2/OG3

Symmetries and independent parameters of Coulomb matrix elements — •CORALINE LETOUZÉ, GUILLAUME RADTKE, BENJAMIN LENZ, and CHRISTIAN BROUDER — Sorbonne Université, Muséum National d'Histoire Naturelle, UMR CNRS 7590, IRD, Institut de Minéralogie, de Physique des Matériaux et de Cosmochimie, IMPMC, 75005 Paris, France

In realistic (DFT+DMFT) calculations of correlated materials, the matrix of the partially-screened electron-electron Coulomb interaction is usually approximated in spherical symmetry and parameterized by Slater integrals (or, equivalently, Racah parameters). Few works have considered the real point-group symmetry of the Coulomb matrix. We suggest parameterizing the Coulomb matrix by its eigenvalues on the irreducible representations of the point group: this respects the point-group symmetry of the system and, compared to other approaches, is completely basis-independent. The permutation symmetry of the 1-electron states in the Coulomb matrix is also taken into account in the two cases of real and complex wavefunctions, to further reduce the number of independent parameters. Finally we apply this method to 3d-transition-metal monoxides.

TT 43.19 Wed 15:00 P2/OG3

Phase diagram of the SU(3) Fermi-Hubbard model with next-neighbor interactions — •ARTURO PÉREZ ROMERO^{1,2}, JERESON SILVA VALENCIA², and ROBERTO FRANCO PEÑALOZA² — ¹Institut für Theoretical Physics, Georg-August-Universität Göttingen, D-37077 Göttingen, Germany — ²Departamento de Física, Universidad Nacional de Colombia, A. A. 5997 Bogotá, Colombia.

We explore the zero-temperature phase diagram of a one-dimensional gas composed of three-color fermions, which interact locally and with their next neighbors. Using the density matrix renormalization group method and considering one-third filling, we characterize the ground state for several values of the parameters, finding diverse phases, namely: phase separation, spin density wave, pairing phase, a metallic phase, two different charge-density waves, and a non-separable state with modulation of charge. We show that the von Neumann block entropy and the fidelity susceptibility are useful for estimating the borders between the phases.

TT 43.20 Wed 15:00 P2/OG3

Spatiotemporal dynamics of classical and quantum density profiles in low-dimensional spin systems — TJARK HEITMANN¹, JONAS RICHTER², FENGPING JIN³, KRISTEL MICHELSEN³, HANS DE RAEDT⁴, and •ROBIN STEINIGEWEG¹ — ¹University of Osnabrück, DE — ²University College London, UK — ³FZ Jülich, DE — ⁴University of Groningen, NL

We provide a detailed comparison between the dynamics of high-temperature spatiotemporal correlation functions in quantum and classical spin models. In the quantum case, our large-scale numerics are based on the concept of quantum typicality, which exploits the fact that random pure quantum states can faithfully approximate ensemble averages, allowing the simulation of up to 40 spin-1/2 spins. Due to the exponentially growing Hilbert space, we find that for such system sizes even a single random state is sufficient to yield results with extremely low noise. In contrast, a classical analog of typicality is missing. In particular, in order to obtain data with a similar level of noise in the classical case, extensive averaging over classical trajectories is required, no matter how large the system size. Focusing on (quasi)-one-dimensional spin chains and ladders, we find a remarkably good agreement between quantum and classical dynamics. Comparing space-time profiles of the spin and energy correlation functions, the agreement is found to hold not only in the bulk but also in the tails of the resulting density distribution. The mean-squared displacement of the density profiles is found to exhibit similar scaling for quantum and classical models.

TT 43.21 Wed 15:00 P2/OG3

Probing real-time broadening of nonequilibrium density profiles via a local coupling to a Lindblad bath — •TJARK HEITMANN¹, JONAS RICHTER², JACEK HERBRYCH³, JOCHEN GEMMER¹, and ROBIN STEINIGEWEG¹ — ¹University of Osnabrück, Germany — ²University College London, UK — ³Wroclaw University of Science and Technology, Poland

The Lindblad master equation is one of the main approaches to open quantum systems. While it has been widely applied in the context of condensed matter systems to study properties of steady states in the limit of long times, the actual route to such steady states has attracted less attention yet. Here, we investigate the nonequilibrium dynamics of spin chains with a local coupling to a single Lindblad bath and analyze the transport properties of the induced magnetization. Combining typicality and equilibration arguments with stochastic unraveling, we unveil for the case of weak driving that the dynamics in the open system can be constructed on the basis of correlation functions in the closed system, which establishes a connection between the Lindblad approach and linear response theory at finite times. In this way, we provide a particular example where closed and open approaches to quantum transport have to agree strictly. We demonstrate this fact numerically for the spin-1/2 XXZ chain at the isotropic point and in the easy-axis regime, where superdiffusive and diffusive scaling is observed, respectively.

TT 43.22 Wed 15:00 P2/OG3

Configuration interaction based nonequilibrium steady state impurity solver for the Anderson-Holstein model — •DANIEL WERNER and ENRICO ARRIGONI — ITPCP, Graz, Austria

Recently we developed a non-equilibrium impurity solver based on the Auxiliary Master Equation Approach using Configuration Interaction (CI). This allowed us to treat a larger auxiliary system, which can more accurately model physical environments with more challenging hybridization functions, as compared to ED. Due to the promising results we obtained, we extended the solver to include phonons, since this gives access to interesting physical phenomena. In particular we are investigating the vibrational steps in the differential conductance in the Kondo regime. We limited ourselves to a single phonon mode, i.e. Holstein phonons, which we again treated with CI to keep the increase of the state space low. Preliminary results, as well as possible extensions for a more complicated treatment of phonons are being discussed.

TT 43.23 Wed 15:00 P2/OG3

Hilbert space fragmentation in open quantum systems — •YAHUI LI, PABLO SALA, and FRANK POLLMANN — Department of Physics, TFK, Technische Universität München, James-Franck-Straße 1, D-85748 Garching, Germany

Several mechanisms have been identified that can lead to a breakdown of thermalization in closed quantum systems-including integrability and many-body localization. Recently, a novel mechanism for ergodicity breaking has been discovered in systems with certain dynamical constraints, where the Hilbert space fragments into exponentially many disconnected subspaces. An open question is how such systems evolve when they are coupled to a dissipative bath.

We find that the Hilbert space fragmentation can be utilized to preserve coherence in the presence of dissipation. We study a quantum fragmented model, which fragments in an entangled basis due to unconventional non-Abelian symmetries. We investigate the Lindblad dynamics under two different couplings, which either preserves or destroys the quantum fragmentation structure. At sufficiently large couplings, the operator space entanglement is suppressed, which allows for an efficient numerical simulation using tensor networks. Surprisingly, under the structure-preserving noise, we observe finite Renyi negativity, indicating non-vanishing quantum correlations. Using an analytic approach, we derive the stationary states under both couplings, which explains the long-time behaviors observed in numerical simulations.

TT 43.24 Wed 15:00 P2/OG3

Floquet engineering in tilted lattices — •MELISSA WILL¹, PABLO SALA^{2,3}, and FRANK POLLMANN¹ — ¹Department of Physics, T42, Technische Universität München, James-Franck-Straße 1, D-85748 Garching, Germany — ²Department of Physics and Institute for Quantum Information and Matter, California Institute of Technology, Pasadena, California 91125, USA — ³Walter Burke Institute for Theoretical Physics, California Institute of Technology, Pasadena, California 91125, USA

Quantum many-body systems out of equilibrium can exhibit very rich and exciting phenomena. A particularly important question is whether and how a quantum system thermalizes under unitary evolution. In this context three classes of systems have been identified: ergodic, localized and an intermediate regime exhibiting so called quantum many-body scars. In this talk we discuss whether a time-periodic, local drive can induce thermalization of a localized system. We consider interacting hard-core bosons in an one dimensional, tilted system with periodic driving. We find that the system becomes ergodic for resonant driving frequencies. In contrast, if the tilt is not close to a multiple of driving frequency, the system stays localized. This observation can theoretically be understood by deriving an effective Hamiltonian using a Magnus expansion. Using large scale

numerical methods, we explore entanglement entropy and imbalance over time. Our theoretical predictions are in good agreement with numerics.

TT 43.25 Wed 15:00 P2/OG3

Impact of decoherence on the route to equilibrium — •JIAOZI WANG and JOCHEN GEMMER — University of Osnabrück, Osnabrück, Germany

We study the time evolution of a small quantum system when coupling to a quantum chaotic bath, within the framework of projection operator techniques. We study this problem by employing a different approach which also take the so called pure-dephasing term as a part of the unperturbed Hamiltonian. With this method, a new formula of the relaxation rate is derived analytically in a random matrix model, which is also confirmed by numerical results. We find that, the relaxation process is slowed down by decoherence, which is in consistent with the quantum zeno effect.

TT 43.26 Wed 15:00 P2/OG3

Nonequilibrium steady-states in photodoped Mott insulators — •FABIAN KÜNZEL — Universität Hamburg, Hamburg, Germany

Photodoped states in Mott insulators are peculiar states which simultaneously host strongly correlated electron and hole-like carriers, and can show instabilities into various non-thermal orders. Here we stabilize a stationary photodoped state in a Mott insulator using Dynamical-Mean-Field-Theory (DMFT) in the nonequilibrium steady-state formalism. This formalism provides a description of the longtime dynamics of microscopic models with well separated timescales. The photodoping can be established by coupling the Hubbard model with external baths that pump holon and doublon excitations in the Hubbard bands. In particular, we develop an algorithm to stabilize DMFT solutions with a prescribed nonthermal distribution function in the local Green's functions. This formulation may allow for a nonperturbative solution of the DMFT impurity model, using methods like Quantum Monte Carlo, and it opens the possibility to study the dynamics of photodoped states using a Quantum Boltzmann equation.

TT 43.27 Wed 15:00 P2/OG3

Quantum oscillations beyond the Onsager relation in a doped Mott insulator — •VALENTIN LEEB^{1,2} and JOHANNES KNOLLE^{1,2,3} — ¹Technical University of Munich, Germany; TUM School of Natural Sciences, Department of Physics, TQM — ²Munich Center for Quantum Science and Technology (MC-QST), 80799 Munich, Germany — ³Blackett Laboratory, Imperial College London, London SW7 2AZ, United Kingdom

The kinetic energy of electrons in a magnetic field is quenched resulting in a discrete set of highly degenerate Landau levels (LL). This gives rise to fascinating phenomena like quantum oscillations or the integer and fractional quantum Hall effect. The latter is a result of interactions partially lifting the degeneracy within a given LL while inter-LL interactions are usually assumed to be unimportant. Here, we study the LL spectrum of the Hatsugai-Kohmoto model, a Hubbard-like model which is exactly soluble on account of infinite range interactions. For the doped Mott insulator phase in a magnetic field we find that the degeneracy of LLs is preserved but inter-LL interactions are important leading to a non-monotonous reconstruction of the spectrum. As a result, strong interactions lead to aperiodic quantum oscillations of the metallic phase in contrast to Onsager's famous relation connecting oscillation frequencies with the Fermi surface areas at zero field. In addition, we find unconventional temperature dependencies of quantum oscillations and effective mass renormalizations. We discuss the general importance of inter-LL interactions for understanding doped Mott insulators in magnetic fields.

TT 43.28 Wed 15:00 P2/OG3

Magnetism of graphene beyond half filling using a mean-field approach — •MAXIME LUCAS, ANDREAS HONECKER, and GUY TRAMBLÉ DE LAISSARDIÈRE — Laboratoire de Physique Théorique et Modélisation, CY Cergy Paris Université / CNRS, France

The discovery of correlations between electronic flat-band states due to a Moiré pattern in twisted bilayers of graphene [1] or other 2D materials has recently stimulated studies of their magnetic properties. It is shown experimentally and theoretically that the filling of the flat bands is an essential parameter for understanding their properties. However, the behavior of a simple graphene layer is still unclear. Indeed, its half-filled case is well known and it has been studied by various theoretical approaches (mean-field theories (MFT), Monte Carlo) [2], but beyond half filling its magnetic properties are still unknown. Here, we present a detailed study of graphene magnetism using a combination of the Hubbard model and MFT. We focus on non half-filling cases, taking into account non-collinear magnetic moments.

[1] Y. Cao *et al.*, *Nature* **556**, 43 (2018); *Nature* **556**, 80 (2018)

[2] M. Raczkowski, R. Peters, T.T. Phung, N. Takemori, F. F. Assaad, A. Honecker, J. Vahedi, *Phys. Rev. B* **101**, 125103 (2020), and references therein

TT 43.29 Wed 15:00 P2/OG3

Spectral densities of quantum magnets with quenched disorder using the coherent potential approximation and perturbative continuous unitary transformations — •MAX HÖRMANN and KAI PHILLIP SCHMIDT — Institut für Theoretische Physik I, Universität Erlangen-Nürnberg, Staudtstraße 7, 91058 Erlangen

We combine perturbation theory by means of perturbative continuous transformations together with the coherent potential approximation to derive approximations for the averaged spectral density of the antiferromagnetic dimer-diluted Heisenberg bilayer model and the spin-diluted transverse-field Ising model on the square lattice. To this end, we calculate a dilution dependent series for the real and imaginary part of the one quasi-particle self-energy. While the real part shifts the extremal energy of the spectral density for fixed momentum the imaginary part reflects the finite-lifetime of momentum modes. Using extrapolations we study the applicability of this approach to critical behaviour and derive approximations for averaged spectral densities in non-perturbative regimes.

TT 43.30 Wed 15:00 P2/OG3

The influence of continuous electric bias fields on the dielectric loss of atomic tunneling systems — •JAN BLICKBERNDT, CHRISTIAN STÄNDER, LUKAS MÜNCH, MARCEL HAAS, ANDREAS REISER, ANDREAS FLEISCHMANN, and CHRISTIAN ENSS — Kirchhoff-Institute for Physics, Heidelberg, Germany

The low temperature properties of amorphous solids are dominated by atomic tunneling systems (TSs), which are known to act as a major source of noise and decoherence in superconducting quantum devices. We investigate the non-equilibrium dielectric loss of atomic tunneling systems under the influence of continuous electric bias fields at very low temperatures. The dielectric loss of an amorphous sample is obtained by measuring the quality factor of a micro-fabricated superconducting resonator. Simultaneously, an electric bias field can be applied via a cover electrode, which allows us to sweep TSs through the resonance frequency by modulating their energy splitting. Experimentally, we found that for slow changing bias fields, TSs are saturated by the driving field leading to a constant loss. For faster bias rates, more and more TSs are swept through resonance and therefore contribute to an increasing loss. In the limit of fast continuous bias sweeps, relaxation in between consecutive crossings diminishes and multiple coherent Landau-Zener transitions are possible, reducing the loss back to the saturation limit. We are able to verify these experimental results with a Monte Carlo based numerical simulation that shows good qualitative agreement.

TT 43.31 Wed 15:00 P2/OG3

Electrically and acoustically biased resonators for investigations of dielectric low temperature properties of amorphous solids — •CHRISTIAN STÄNDER, JAN BLICKBERNDT, JOYCE GLASS, BENEDIKT FREY, ANDREAS REIFENBERGER, ANDREAS FLEISCHMANN, ANDREAS REISER, and CHRISTIAN ENSS — Kirchhoff-Institute for Physics, Heidelberg University, D-69120 Heidelberg

The low temperature properties of amorphous solids are governed by atomic tunnelling systems, which can be described as two-level systems (TLS) with a distribution of their energy splitting E , as assumed by the phenomenological standard tunnelling model. Recent interest in these systems due to their deteriorative effects on the performance of superconducting quantum devices lead to novel experimental investigations of atomic tunnelling systems driven by novel measurement techniques.

We use newly designed microfabricated superconducting LC-resonators to study the dielectric rf-response of the amorphous sample in the presence of an electric bias field. A novel method of applying this electrical bias field was introduced to the resonators. Compared to previous experiments, the bias field is applied via an electrode placed above the resonator chip. We present first results of this new way of introducing a bias, which modifies the energy splitting E of a TLS.

In addition we tried to achieve a similar effect as with the electrical bias field with a mechanical strain field. To induce such a strain field, the amorphous substrate of the resonator chip was flexed by a piezo-actuator.

TT 43.32 Wed 15:00 P2/OG3

Investigating the Non-Equilibrium Dynamics of Two-Level Systems at Low Temperatures — •MARCEL HAAS, MAREIKE DINGER, LUKAS MÜNCH, JAN BLICKBERNDT, ANDREAS REISER, ANDREAS FLEISCHMANN, and CHRISTIAN ENSS — Kirchhoff-Institute for Physics, Heidelberg, Germany

The dielectric loss of amorphous materials along with noise and decoherence is the major limiting factor in many applications like superconducting circuits, Josephson junctions and quantum computing. It is mainly determined by atomic tunneling systems described by quantum mechanical two-level systems (TLS), which are broadly distributed low-energy excitations in the sample. The spontaneous phonon emission of an excited TLS gives rise to a relaxation time T_1 and the interaction between TLSs with their thermally excited surrounding induces a decoherence time T_2 . These effects mainly determine the measurable dielectric loss in the observed material, which we ascertain by measuring the quality factor of a bridge type superconducting LC-resonator. The dielectric medium in between the capacitor plates is a sputter deposited a-SiO₂ film. The setup shows a unique property when two off-resonant pump tones are applied symmetrically.

In this limit, the resonator is emitting at the intermediate frequency of the driving fields. The underlying mechanism can therefore be explained by a nonlinear interaction of the rf-field with the TLSs and the resonator which is creating additional lines in the frequency spectrum. We present measurements and a phenomenological description of the effect for a frequency of 1 GHz.

TT 43.33 Wed 15:00 P2/OG3

Machine learning stochastic dynamics of order parameters — FRANCESCO CARNAZZA¹, FEDERICO CAROLLO¹, IGOR LESANOVSKY¹, GEORG MARTIUS², SABINE ANDERGASSEN¹, and MIRIAM KLOPOTEK³ — ¹University of Tuebingen — ²Max Planck Institute for Intelligent Systems — ³University of Stuttgart

The dynamics of coarse-grained observables, or of order-parameters, in many-body systems is usually rather intricate due to emergent nonlinearities and collective effects. In fact, except for few exactly solvable models, it is typically not

possible to find the form of the differential equation describing the dynamics of these observables. Here, we address this problem exploiting a machine learning approach. We consider single trajectories of the thermal dynamics of a two-dimensional Ising model and feed these to a neural network. These trajectories, simulated by Monte Carlo methods, are intrinsically stochastic. Their dynamics can be approximated by a stochastic differential equation parametrised by a smooth term, the drift, and one multiplied by the differential of a Wiener process, that is, the diffusion.

In [1] a neural solver for stochastic differential equation was introduced, by means of which the drift and diffusion terms are approximated by neural networks. A classical integration method, e.g., Euler-Maruyama, is then adopted to recover full trajectories. We adopt this method to learn the drift and diffusion terms and infer the properties of the Ising model.

[1] Li et al., PMLR 108:3870-3882,2020.

TT 44: Focus Session: Superconducting Nickelates I

The discovery of superconductivity in hole-doped infinite-layer nickelates in 2019 has brought a breath of fresh air to the research on unconventional superconducting materials. These nickel oxides structurally closely resemble high- T_c cuprates and show a formally analogous nickel $d^{9-\delta}$ electronic configuration. Other striking similarities with cuprates have been recently reported, such as a dome-like doping dependence of the superconducting phase, sizeable antiferromagnetic exchange couplings, and a charge order instability in the underdoped region of the phase diagram. Likewise, a number of studies identified clear differences, e.g. concerning selected transport behavior as well as magnetic properties, and with regard to the relevance of oxygen- $2p$ states. It is precisely this combination of strong similarities and specific differences that promises new, game-changing insights into the origin of high-temperature superconductivity. The goal of this focus session is to bring together the latest results for low-valence nickelates from studies of structure, electronic structure, magnetism, charge density waves and superconductivity, and thus setting the stage for a coherent picture of these complex quantum materials.

Organizers: Eva Benckiser (Max-Planck-Institute for Solid State Research, Stuttgart) and Frank Lechermann (Ruhr-Universität Bochum)

Time: Thursday 9:30–13:00

Location: HSZ 03

Invited Talk

TT 44.1 Thu 9:30 HSZ 03

Atomic-scale insights to lattice and electronic structure in superconducting nickelates — BERIT GOODGE — School of Applied and Engineering Physics, Cornell University — Kavli Institute at Cornell for Nanoscale Science, Cornell University — Max Planck Institute for Chemical Physics of Solids

Although the synthesis of superconducting nickelates [1,2] remains notoriously challenging [3,4], many materials realities including epitaxial strain, extended defects, impurities, and secondary phases are largely undiscussed in the context of understanding their measured properties. As direct probes of lattice and electronic structure down to the atomic scale, scanning transmission electron microscopy (STEM) and electron energy loss spectroscopy (EELS) offer unique insights to build a holistic understanding of both the intrinsic physical properties in these materials as well as more extrinsic features and their consequences, many of which arise from their multistep synthesis. Here, we discuss how quantitative lattice-scale measurements can disentangle many of these effects, revealing, for example, multi-band hole interactions [5], nontrivial interface reconstruction [6], and the impact of epitaxial strain [2, 7].

[1] Li et al., Nature 572, 624 (2019)

[2] Lee et al., arXiv:2203.02580 (2022)

[3] Lee et al., APL Mat. 8:4, 041107 (2020)

[4] Pan et al., Nat. Mat. 21, 160 (2022)

[5] Goodge et al., PNAS 118:2, (2021)

[6] Goodge et al., arXiv:2201.03613 (2022)

[7] Segedin et al., under review (2022)

Invited Talk

TT 44.2 Thu 10:00 HSZ 03

Nickelate and cuprate superconductors: Similar yet different — VAMSHI MOHAN KATUKURI — Max Planck Institute for Solid State Research, Stuttgart, Germany

The discovery of superconductivity in hole-doped infinite-layer NdNiO_2 – a transition metal oxide that is both isostructural and isoelectronic to cuprate superconductors – has led to renewed enthusiasm in the hope of understanding the origin of unconventional superconductivity. In this talk, I will present and discuss the similarities and differences in the electronic structure of nickelates and cuprates from the perspective of *ab initio* many body wavefunction analysis derived from state-of-the-art quantum chemistry calculations. After highlighting the main differences in the parent (undoped) infinite-layered NdNiO_2 and CaCuO_2 compounds, I will discuss the character of the doped hole by analyzing the electron-removal (which mimics hole-doping) states in the two compounds. In the end, I will discuss the evolution of the electronic structure of nickelates under pressure.

Invited Talk

TT 44.3 Thu 10:30 HSZ 03

Superconducting instabilities in strongly-correlated infinite-layer nickelates — ANDREAS KREISEL — Niels Bohr Institute, University of Copenhagen, Denmark

Unconventional superconductivity is often referred to as originating from a pairing mechanism different from electron-phonon interactions and connected to an anisotropic superconducting order parameter with sign change of the Cooper pair wavefunction. In this talk, I will start from a discussion of the mechanism of spin-fluctuation mediated pairing that can lead to d -wave states as evidenced in the cuprate superconductors, but also the sign-changing s_{\pm} state that seems to be realized in Fe-based superconductors. The discovery of superconductivity in infinite-layer nickelates has immediately posed the question about the pairing mechanism and the pairing symmetry in this system and sparked proposals of analogs towards well studied families of materials in the class of unconventional superconductors. To connect to this open question, the leading superconducting instability is computed from magnetic fluctuations relevant for infinite-layer nickelates incorporating the strongly correlated multi-orbital nature of the low-energy electronic degrees of freedom. Observing the interplay between the $\text{Ni } d_{x^2-y^2}$ and d_{z^2} orbitals as well as the self-doping band, a transition from d -wave pairing symmetry to nodal s_{\pm} superconductivity is uncovered. This is driven by strong fluctuations in the d_{z^2} -dominated orbital states. As probe of the detailed superconducting gap structure, we discuss the properties of the resulting superconducting condensate in light of tunneling and penetration depth experiments.

15 min. break

Invited Talk

TT 44.4 Thu 11:15 HSZ 03

Infinite-layer nickelate thin films: From synthesis to spectroscopy — DANIELE PREZIOSI — Université de Strasbourg, CNRS, IPCMS UMR 7504, F-67034 Strasbourg, France

In the last three decades, special efforts were devoted to the realization of nickelates mimicking the electronic structure of cuprates. These efforts led to the realization of infinite-layer nickelates characterized by a stable $\text{Ni-}3d^9$ configuration and reduced dimensionality. A superconducting state below 15 K was reported for $\text{Nd}_{0.8}\text{Sr}_{0.2}\text{NiO}_2$ thin films deposited onto (001) SrTiO_3 (STO). Soon after this discovery, x-ray absorption spectroscopy (XAS) and resonant inelastic x-ray scattering (RIXS) experiments on undoped (LaNiO_2 , NdNiO_2) and doped ($\text{Nd}_{1-x}\text{Sr}_x\text{NiO}_2$) samples showed that infinite-layer nickelates show some important differences compared to layered cuprates, in particular a larger charge transfer energy and an important Nd 5d-Ni 3d hybridization. In this talk, after introducing our efforts to stabilize the infinite-layer phase, I will show that some

of those aforementioned differences depend also on the presence/absence of a STO-capping-layer. A robust charge order is observed in undoped capping-free thin films, while strong magnetic excitations around 200 meV energy-loss characterize capped samples. Polarization-resolved RIXS measurements unambiguously demonstrated that also the low-energy excitations for uncapped samples are magnetic in nature, but largely damped. The 'altered' doping effect as observed from the enlarging of the XAS feature at the NiL_3 -edge combined to a strong $Ni3d - Nd5d$ hybridization for uncapped samples, may speak in favor of this extra softening.

Invited Talk

TT 44.5 Thu 11:45 HSZ 03

Superconducting layered square-planar nickelates: Synthesis, properties, and progress — •GRACE PAN¹, DAN FERENC SEGEDIN¹, HARRISON LABOLLITA², QI SONG¹, BERIT GOODGE³, LENA KOURKOUTIS³, CHARLES BROOKS¹, ANTIA BOTANA², and JULIA MUNDY¹ — ¹Harvard University, Cambridge, MA, USA — ²Arizona State University, Tempe, AZ, USA — ³Cornell University, Ithaca, NY, USA

Since the discovery of high- T_c superconductivity in the cuprates, there have been sustained efforts to both understand the origins of this phase and discover new cuprate-like superconductors. One prime materials platform has been the rare-earth nickelates; indeed, superconductivity was discovered in the doped compound $Nd_{0.8}Sr_{0.2}NiO_2$ in 2019. Undoped $NdNiO_2$ belongs to a series of layered square-planar nickelates with chemical formula $Nd_{n+1}Ni_nO_{2n+2}$ and is known as the infinite-layer ($n=\infty$) nickelate. Here, we describe the synthesis of the quintuple-layer ($n=5$) member, $Nd_6Ni_5O_{12}$, in which optimal cuprate-like electron filling ($d^{8.8}$) is achieved without chemical doping. We observe a superconducting transition beginning at ~ 13 K. Electronic structure calculations fortified with experiments suggest that $Nd_6Ni_5O_{12}$ interpolates between cuprate-like and infinite-layer nickelate-like behaviour. By engineering a distinct superconducting nickelate, we identify the square-planar nickelates as a new family of superconductors that can be tuned via both doping and dimensionality. In this talk, I will further discuss ongoing experimental progress on the synthesis and characterization of these layered nickelates.

TT 44.6 Thu 12:15 HSZ 03

Nickelate superconductors: One-band Hubbard model plus decoupled A pocket picture — •KARSTEN HELD¹, MOTOHARU KITATANI², LIANG SI^{1,3}, and PAUL WORM¹ — ¹Institute for Solid State Physics, TU Wien, Austria — ²University of Hyogo, Japan — ³Northwest University, Xi'an, China

At first glance, nickelate superconductors appear to be more complicated than their cuprate peers. Based on density functional theory (DFT) plus dynamical mean-field theory (DMFT) we however arrived at a picture that the physics of nickelate superconductors is dominated by the $Ni d_{x^2-y^2}$ -band and the pockets are, in many respects, merely passive bystanders [1]. Other groups have argued instead for the importance of the $Ni d_{z^2}$ -band based, e.g., on self-interaction corrected (sic)DFT+DMFT [2].

Taken the premise of a $d_{x^2-y^2}$ -band Hubbard model description, we have predicted the phase diagram, superconducting critical temperature T_c vs. doping x

[1]. Later experiments synthesizing high-quality films are in excellent qualitative and even quantitative agreement [3], as is the resonant inelastic x-ray (RIXS) spectrum. Also the pentalayer nickelate superconductor which has no pockets in DFT+DMFT and the increase T_c with pressure nicely match this picture [4].

[1] M. Kitatani *et al.*, npj Quantum Materials 5, 59 (2020)

[2] F. Lechermann, Phys. Rev. B 101, 081110 (2020);

A. Kreisel *et al.*, Phys. Rev. Lett. 129, 077002 (2022)[3] K. Lee *et al.*, arXiv:2203.02580[4] P. Worm *et al.*, Phys. Rev. Mater. 6, L091801 (2022)

TT 44.7 Thu 12:30 HSZ 03

Single-layer T' nickelates — KERSTIN WISSEL¹, FABIO BERNARDINI², HEESU OH², SAMI VASALA³, BJÖRN BLASCHKOWSKI², PIETER GLATZEL³, MATTHIAS BAUER⁴, OLIVIER CLEMENS¹, and •ANDRÉS CANO⁵ — ¹University of Stuttgart, Stuttgart, Germany — ²University of Cagliari, Cagliari, Italy — ³ESRF, Grenoble, France — ⁴Padeborn University, Padeborn, Germany — ⁵Institut NEEL, CNRS, Grenoble, France

The discovery of superconductivity in the infinite-layer nickelates has renewed the interest in these potential analogs of the high- T_c cuprates motivating the search for additional materials in this class [1]. In the talk, I will introduce the recently synthesised single-layer T' nickelates [2,3] and discuss their structural and electronic properties in relation to previous nickelates and cuprates.

[1] See e.g. A. Botana, F. Bernardini and A. Cano, JETP 159, 711 (2021) for a review.

[2] K. Wissel *et al.*, Chem. Mater. 32, 3160 (2020)[3] K. Wissel *et al.*, Chem. Mater. 34, 7201 (2022)

TT 44.8 Thu 12:45 HSZ 03

Synthesis and physical properties of perovskite and infinite-layer nickelate crystals — •PASCAL PUPHAL¹, VIGNESH SUNDARAMURTHY¹, VALENTIN ZIMMERMANN¹, BJÖRN WEHINGER², GASTON GARBARINO², KATHRIN KÜSTER¹, ULRICH STARKE¹, JÜRGEN NUSS¹, BERNHARD KEIMER¹, MASAHIKO ISOBE¹, and MATTHIAS HEPTING¹ — ¹Max Planck Institute for Solid State Research — ²European Synchrotron Radiation Facility

Infinite-layer (IL) nickelates are an emerging family of superconductors whose synthesis in thin film form is an established process by now, whereas the growth of their bulk counterparts remains a formidable challenge. In a previous study, we achieved the reduction of perovskite $La_{1-x}Ca_xNiO_3$ single-crystals grown by a flux method under high external pressure to the IL phase $La_{1-x}Ca_xNiO_2$ [1]. The typical lateral dimension of these crystals was $150 \mu m$. As an advanced approach, we recently accomplished the reduction of millimeter-sized $LaNiO_3$ crystals obtained by optical floating zone growth under high oxygen gas pressure to the IL phase $LaNiO_2$ [2]. We will present our characterization of the crystalline, magnetic, and electronic properties of the $LaNiO_2$ crystals, and give an outlook on the synthesis of millimeter-sized crystals of pure $LaNiO_3$ and $PrNiO_3$ as well as ones with hole- and electron doping.

[1] P. Puphal *et al.*, Sci. Adv. 7, eabl8091 (2021)[2] P. Puphal *et al.*, arXiv:2209.12787 (2022)**TT 45: Correlated Electrons: 1D Theory**

Time: Thursday 9:30–12:15

Location: HSZ 103

TT 45.1 Thu 9:30 HSZ 103

On the alternating spin chain with continuous spectrum of scaling dimensions — MOUHCINE AZHARI and •ANDREAS KLÜMPER — Universität Wuppertal We investigate the low-lying spectrum of an integrable staggered Heisenberg spin-1/2 chain possessing in the large length (L) limit a CFT structure with logarithmic corrections ($1/(\log L)^2$). This realizes a continuous spectrum of conformal weights similar to that of for instance the $SL(2, R)/U(1)$ black hole sigma model.

The quantum spin chain is exactly "solvable" by Bethe ansatz and other techniques from the theory of integrability. However, the analysis of the resulting Bethe Ansatz equations is challenging and manageable by numerical techniques only for relatively small sizes L . Integral equations for the distribution functions of the Bethe roots suffer from singularities of the kernel functions.

Due these phenomena and challenges the model attracted interest by several groups of authors (Ikhlef, Jacobsen, Saleur 08, 12; Frahm, Martins 12; Candu, Ikhlef 13; Frahm, Seel 14; Bazhanov, Kotousov, Koval, Lukyanov 20).

In our contribution we report on recent progress allowing us to rewrite already existing non-linear integral equations (NLIE) with a singular, i.e. long-ranged kernel in a novel form without such problems. We present results for the lowest lying excitations for system sizes $L = 10, 10^2, 10^3, \dots, 10^9, \dots$

TT 45.2 Thu 9:45 HSZ 103

Electron spin resonance as a direct probe of spinon interactions in a $S = 1/2$ chain — •KIRILL POVAROV^{1,2}, TIMOFEI SOLDATOV³, REN-BO WANG⁴, ANDREY ZHELUDEV¹, ALEXANDER SMIRNOV³, and OLEG STARYKH⁴ — ¹Laboratory for Solid State Physics, ETH Zürich — ²Dresden High Magnetic Field Laboratory (HLD), Helmholtz-Zentrum Dresden-Rossendorf (HZDR) — ³P.L. Kapitza Institute for Physical Problems RAS — ⁴Department of Physics and Astronomy, University of Utah

The presence of well-hidden backscattering between the fractionalized spinon excitations was known to be a somewhat exotic part of the $S = 1/2$ chain physics. However, its dramatic consequences for the dynamics were realized recently [1]. They are challenging for observation, as applied field and nonzero momenta are simultaneously required. We have succeeded in the experimental verification of these effects using electron spin resonance as probe [2]. Our observations are enabled by the specific pattern of Dzyaloshinskii–Moriya interactions in our target material $K_2CuSO_4Br_2$. Description of the observed spectrum requires accounting for the backscattering on a qualitative level. Quantitative analysis allows us to estimate the backscattering constant as $2.4J$ (intra-chain exchange), in agreement with the renormalization group predictions. This work has been supported by SNSF Division II (ETHZ), the NSF CMMT grant DMR-1928919 (U. Utah), and the RSF Grant 17-12-01505 (IPP).

[1] A. Keselman *et al.*, PRL 125, 187201 (2020)[2] K. Povarov *et al.*, PRL 128, 187202 (2022) *Editor's Suggestion*

TT 45.3 Thu 10:00 HSZ 103

Dominant superconducting correlations in a Luttinger liquid induced by spin fluctuations — •NIELS HENRIK AASE and ASLE SUDBØ — Center for Quantum Spintronics, Department of Physics, Norwegian University of Science and Technology, NO-7491 Trondheim, Norway

In the last decades, heterostructures of magnetic materials and various conductors have received much attention. Several studies have focused on the emergent interfacial phenomena and their possible application in spintronic devices. Motivated by this, we study the simplest equivalent heterostructure in one dimension: an interacting metallic chain coupled to a spin chain. Confining interacting electrons to one dimension causes the breakdown of Fermi liquid theory, so our study provides insight into how spin fluctuations can induce superconductivity in a strongly correlated non-Fermi liquid with repulsive electronic interactions only.

Treating the system using bosonization, we calculate the correlation functions of the electrons in the metal. Based on the non-universal power-law decay of different order parameters, we outline the electron phase diagram as a function of the interchain coupling and the interactions in the metal. The coupling favors triplet pairing, suggesting that the metal chain can sustain a spin-polarized supercurrent. In some parameter regimes, the superconducting triplet correlations persist in the case of repulsive interactions in the metal. The spin chain is thus an essential ingredient for overcoming electron repulsion in a Luttinger liquid.

TT 45.4 Thu 10:15 HSZ 103

The role of electron-electron interactions in electron emission from arrays of nanotubes — •NAIRA GRIGORYAN¹ and PIOTR CHUDZINSKI^{1,2} — ¹Institute of Fundamental Technological Research, Polish Academy of Sciences, Adolfa Pawlinskiego 5b, 02-106 Warsaw, Poland — ²School of Mathematics and Physics, Queen's University Belfast, University Road, Belfast, NI BT7 1NN, United Kingdom

Nanotubes and nanorods have been recently established as very good materials to build electron sources in the cold emission process. These are 1D materials where electron-electron interactions are known to play a crucial role in their physics. The interactions in 1D systems lead to a collective modes' physics that is usually described using Tomonaga-Luttinger liquid (TLL) formalism. The advantage is that within this method all correlation functions are known and can be expressed in terms of power laws with non-universal, interaction dependent, exponents. To capture this situation we generalize a canonical Fowler-Norheim theory of field emission to solve the case of a barrier described by any power-law potential. With this generalization, expressed in terms of a confluent hypergeometric function, we are able to compute currents from arrays of carbon nanotubes. We shall present results showing an influence of various interaction terms, as encoded in varying TLL parameters, as well as effects of a finite temperature.

TT 45.5 Thu 10:30 HSZ 103

Delta-T noise for weak tunneling in one-dimensional systems: interactions versus quantum statistics — GU ZHANG¹, IGOR V. GORNYI², and •CHRISTIAN SPANSLÄTT³ — ¹Beijing Academy of Quantum Information Sciences, 100193 Beijing, China — ²Institute for Quantum Materials and Technologies, Karlsruhe Institute of Technology, 76021 Karlsruhe, Germany — ³Department of Microtechnology and Nanoscience (MC2), Chalmers University of Technology, S-412 96 Göteborg, Sweden

Delta-T noise - excess charge noise at zero charge current but due to a finite temperature bias - has recently emerged as a novel transport spectroscopy tool for mesoscopic systems. In this talk, I present recent work [1] on delta-T noise for weak tunneling in one-dimensional, interacting systems. We show that the sign of the delta-T noise is generically determined by the scaling dimensions of the dominating tunneling process. Importantly, we clarify how this sign can be related to the quantum exchange statistics of the tunneling quasiparticles.

In systems with interacting and chiral channels, we find that when the delta-T noise is negative, the tunneling particles are boson-like, revealing their tendency towards bunching. Thus, one might expect that negative delta-T noise is a smoking gun for detecting "intrinsic anyons". Here, we find that this is not the case, since boson-like particles do not necessarily produce negative delta-T noise. Our findings clarify how delta-T noise can be used to probe the nature of collective excitations in interacting one-dimensional systems.

[1] G. Zhang, I. V. Gornyi, C. Spänslätt, PRB 105, 195423 (2022)

TT 45.6 Thu 10:45 HSZ 103

Terminable transitions in a topological fermion ladder — YUCHI HE^{1,2}, DANTE KENNES^{2,3}, CHRISTOPH KARRASCH⁴, and •ROMAN RAUSCH⁴ — ¹Rudolf Peierls Centre for Theoretical Physics, Clarendon Laboratory, Parks Road, Oxford OX1 3PU, United Kingdom — ²Institut für Theorie der Statistischen Physik, RWTH Aachen University and JARA - Fundamentals of Future Information Technology, 52056 Aachen, Germany — ³Max Planck Institute for the Structure and Dynamics of Matter, Center for Free Electron Laser Science, 22761 Hamburg, Germany — ⁴Technische Universität Braunschweig, Institut für Mathematische Physik, Mendelssohnstraße 3, 38106 Braunschweig, Germany

Interacting fermion ladders are important platforms to study quantum phases of matter including various Mott-insulators with different symmetry properties, such as the D-Mott and S-Mott phase. The latter hold pre-formed electron pairs and become paired liquids (d-wave and s-wave) upon doping. We show that the D-Mott and S-Mott phases are in fact two facets of the same topological phase and that the transition between them is terminable. With this, we provide a quantum analog of the well-known terminable liquid-gas transition. However, the phenomenology we uncover is even richer, as in contrast to the liquid-gas transition, the order of the transition can be tuned by the interaction and bears relevance for the topological properties of the system. The numerical results are obtained using the variational uniform matrix-product state (VUMPS) formalism, and are complemented by analytical field-theoretical explanations.

15 min. break

TT 45.7 Thu 11:15 HSZ 103

Critical and topological phases of a dimerized Kitaev chain in the presence of a quasiperiodic potential — •SAURABH BASU¹, SK NOOR NABI², and SHILPI ROY¹ — ¹Department of Physics, Indian Institute of Technology Guwahati-Guwahati, 781039 Assam, India — ²Department of Physics, Indian Institute of Technology Kharagpur, Kharagpur - 721302, West Bengal, India

We investigate the localization and topological properties of a dimerized Kitaev chain with p-wave superconducting correlations and a quasiperiodically modulated chemical potential. In the localization studies, we illustrate the existence of distinct phases, such as, the extended phase, the critical (intermediate) phase, and the localized phase that arise due to the competition between the dimerization and the onsite quasiperiodic potential. Most interestingly, the critical phase comprises of two distinct phase transitions that are found to exist between the extended to the localized phase, and between the critical (multifractal) and localized phases. Furthermore, we study the topological properties of the zero-energy edge modes via computing the real-space winding number and number of the Majorana zero modes present in the system. We specifically demonstrate that our model undergoes a phase transition from a topologically trivial to a non-trivial phase (topological Anderson phase) beyond a critical dimerization strength under the influence of the quasiperiodic potential strength. Finally, in presence of a large potential, we demonstrate that the system undergoes yet another transition from the topologically non-trivial to an Anderson localized phase.

TT 45.8 Thu 11:30 HSZ 103

Statistics induced phase transitions in the extended bosonic anyon Hubbard model — •IMKE SCHNEIDER¹, KEVIN JÄGERING¹, MARTIN BONKHOF¹, SHIJIE HU², AXEL PELSTER¹, and SEBASTIAN EGGERT¹ — ¹Department of Physics and Research Center Optimas, Technical University of Kaiserslautern, 67663 Kaiserslautern, Germany — ²Beijing Computational Science Research Center, Beijing 100193, China

We study a 1D extended Hubbard model of anyons with statistical exchange phases ranging from bosons to pseudo-fermions. The model can be realized in optical lattice experiments implementing occupation-dependent hopping amplitudes. We enforce a two-body hard-core constraint and numerically determine the full phase diagram including attractive on-site interactions. Surprisingly, the symmetry protected topological Haldane phase remains robust up to large statistical angles close to the pseudo-fermionic limit. However, for a critical angle the phase diagram qualitatively changes involving a dimer phase while the Haldane phase disappears. This behavior is analytically described by an adapted bosonization approach.

TT 45.9 Thu 11:45 HSZ 103

Fractonic Luttinger liquids and supersolids in a constrained Bose-Hubbard model — •PHILIP ZECHMANN^{1,2}, EHUD ALTMAN³, MICHAEL KNAP^{1,2}, and JOHANNES FELDMEIER^{1,2,4} — ¹Department of Physics, Technical University of Munich, 85748 Garching, Germany — ²Munich Center for Quantum Science and Technology (MCQST), Schellingstr. 4, 80799 München, Germany — ³Department of Physics, University of California, Berkeley, CA 94720 — ⁴Department of Physics, Harvard University, Cambridge, MA 02138, USA

Quantum many-body systems with fracton constraints are widely conjectured to exhibit unconventional low-energy phases of matter. In this work, we demonstrate the existence of a variety of such exotic quantum phases in the ground states of a dipole-moment conserving Bose-Hubbard model in one dimension. For integer boson fillings, we perform a mapping of the system to a model of microscopic local dipoles, which are composites of fractons. We apply a combination of low-energy field theory and large-scale tensor network simulations to demonstrate the emergence of a novel dipole Luttinger liquid phase. At non-integer fillings our numerical approach shows an intriguing compressible state described by a quantum Lifshitz model in which charge density-wave order coexists with dipole long-range order and superfluidity - a 'dipole supersolid'. While this supersolid state may eventually be unstable against lattice effects in the thermodynamic limit, its numerical robustness is remarkable. We discuss potential experimental implications of our results.

TT 45.10 Thu 12:00 HSZ 103

Phase diagram detection via Gaussian fitting of number probability distribution — DANIELE CONTESSI^{1,2,3}, ALESSIO RECATI¹, and MATTEO RIZZI^{2,3} — ¹Università di Trento & INO-CNR Pitaevskii BEC Center, Povo, Italy — ²Peter-Grünberg-Institut 8, FZ Jülich, Germany — ³Institute for Theoretical Physics, University of Cologne, Germany

In recent years, methods for automatic recognition of phase diagrams of quantum systems have gained large interest in the community: Among others, machine learning analysis of the entanglement spectrum has proven to be a promis-

ing route. Here, we discuss the possibility of using an experimentally readily accessible proxy, namely the number probability distribution that characterizes sub-portions of a quantum many-body system with globally conserved number of particles. We put forward a linear fitting protocol capable of mapping out the ground-state phase diagram of the rich one-dimensional extended Bose-Hubbard model: The results are quantitatively comparable with more sophisticated traditional numerical and machine learning techniques. We argue that the studied quantity should be considered among the most informative and accessible bipartite properties.

[1] D. Contessi, A. Recati, M. Rizzi, arXiv:2207.01478

TT 46: Frustrated Magnets: Spin Liquids

Time: Thursday 9:30–13:00

Location: HSZ 201

TT 46.1 Thu 9:30 HSZ 201

Magnetic and elastic properties of spin ice materials in high magnetic fields — NAN TANG^{1,2}, MASAKI GEN³, MINGXUAN FU², HUIYUAN MAN⁴, AKIRA MATSUO⁵, KOICHI KINDO⁵, AKIHIKO IKEDA^{5,6}, YASUHIRO H. MATSUDA⁵, KAZUYUKI MATSUHIRA⁷, YOSHIMITSU KOHAMA⁵, and SATORU NAKATSUJI^{2,5} — ¹Experimental Physics VI, Center for Electronic Correlations and Magnetism, University of Augsburg, Augsburg, Germany — ²Department of Physics, University of Tokyo, Tokyo, Japan — ³Riken Center for Emergent Matter Science, Saitama, Japan — ⁴Geballe Laboratory for Advanced Materials, Stanford University, California, U.S.A. — ⁵ISSP, University of Tokyo, Chiba, Japan — ⁶Department of Engineering Science, University of Electro-Communications, Tokyo, Japan — ⁷Department of Engineering, Kyushu Institute of Technology, Fukuoka, Japan

Spin ice is a prototypical state of frustrated magnets, in which Ising spins form a short-range "2-in, 2-out" correlation instead of a long-range order due to geometrical frustrations of pyrochlore lattice. Local Ising anisotropy induced by the competition between crystal electric field (CEF) effect and magnetic interactions play important roles to stabilize such spin-ice correlations. Generally, frustrated magnets show characteristic magnetostrictive responses and in this study, we measured both magnetization and magnetostriction of classical spin ice $\text{Ho}_2\text{Ti}_2\text{O}_7$ and quantum spin ice $\text{Pr}_2\text{Zr}_2\text{O}_7$ under high magnetic fields to explore the regime beyond the Ising limit. In the talk, we will discuss the influences of CEF splitting and exchange-striction on the magnetostrictive responses in the two spin ice materials.

TT 46.2 Thu 9:45 HSZ 201

XMCD studies of honeycomb lattice compound RuBr_3 — SAHANA ROESSLER¹, X. WANG¹, S. AGRESTINI², Z. HU¹, C. GUILLEMARD³, J. HERRERO-MARTIN³, U. SCHWARZ¹, M. W. HAVERKORT⁴, and L. H. TJENG¹ — ¹Max-Planck Institute for Chemical Physics of Solids, Dresden Germany — ²Diamond Light Source, Oxfordshire, United Kingdom — ³ALBA Synchrotron Light source, Barcelona, Spain — ⁴Institute of theoretical physics, Heidelberg University, Germany.

The high-pressure phase of RuBr_3 consisting of a honeycomb lattice [1] is structurally essentially isotopic to the Kitaev quantum spin liquid candidate $\alpha\text{-RuCl}_3$. As in $\alpha\text{-RuCl}_3$, Ru^{3+} ion in RuBr_3 is in $4d^5$ electronic configuration and expected to be in a spin-orbit coupled $J_{\text{eff}} = 1/2$ doublet ground state. Here, we will present the results of X-ray magnetic circular dichroism (XMCD) measurements on RuBr_3 performed at the Ru $L_{2,3}$ absorption edges. The spin and orbital moments were determined using the sum rule analysis. In addition, the XMCD spectra were simulated using the full atomic-multiplet cluster calculations within the configuration interaction approach. By comparing the experimental spectra with the theoretical simulations, we determined the ratio of spin to orbital moments along with the values of the crystal field splitting and the spin-orbit coupling in RuBr_3 . Our results indicated the $J_{\text{eff}} = 1/2$ ground state for RuBr_3 , which is one of the requisites for the Kitaev quantum spin-liquid behavior. [1] Imai et al., Phys. Rev. B 105, L041112 (2022).

TT 46.3 Thu 10:00 HSZ 201

Structural transition in single crystals of Kagome compound $\text{Y}_3\text{Cu}_9(\text{OH})_{19}\text{Cl}_8$ — KATHARINA M. ZOCH¹, PASCAL PUPHAL², and CORNELIUS KRELLNER¹ — ¹Physikalisches Institut, Goethe-Universität Frankfurt, 60438 Frankfurt am Main, Germany — ²Max-Planck-Institute for Solid State Research, 70569 Stuttgart, Germany

Kagome systems serve as the ideal candidates to obtain an experimental realization of a quantum spin liquid, a class of matter where the spins strongly fluctuate down to lowest temperatures, thus preventing order. $\text{Y}_3\text{Cu}_9(\text{OH})_{19}\text{Cl}_8$ presents a distorted Kagome lattice with a rich magnetic phase diagram [1]. The improved synthesis of phase-pure single crystals crystals via an external gradient method lead to the evidence of subtle structural instabilities at 33 K and 13 K in thermodynamic measurements while preserving the magnetic model of the system. The compound shows a magnetic phase transition at 2.2 K with persistent spin

dynamics below the ordered state in powder samples [2]. We present the single crystal growth as well as thermodynamic and magnetic measurements of this compound.

[1] M. Hering et al., npj Comput. Mater. 8, 10 (2022)

[2] Q. Barthelemy et al., Phys. Rev. Mater. 3, 074401 (2019)

TT 46.4 Thu 10:15 HSZ 201

Thermodynamics of the spin liquid candidate KYbS_2 — FRANZISKA GRUSSLER¹, SEBASTIAN BACHUS¹, NOAH WINTERHALTER-STOCKER¹, MAMOUN HEMMIDA², HANS-ALBRECHT KRUG VON NIDDA², YURI SKOURSKI³, PHILIPP GEGENWART¹, and ALEXANDER TSIRLIN⁴ — ¹Experimental Physics VI, Center for Electronic Correlations and Magnetism, University of Augsburg — ²Experimental Physics V, Center for Electronic Correlations and Magnetism, University of Augsburg — ³High Magnetic Field Laboratory, Helmholtz-Zentrum Dresden-Rossendorf — ⁴Felix Bloch Institute for Solid-State Physics, University of Leipzig

Triangular antiferromagnets with competing nearest-neighbor and next-nearest-neighbor interactions offer a promising playground for realizing quantum spin liquid behavior. However, detailed nature of this state and its manifestations in real materials remain heavily debated. Here, we show that a quantum disordered, potentially spin liquid state can be realized in the disorder-free triangular antiferromagnet KYbS_2 and report its temperature-field phase diagram using heat capacity, dilatometry, magnetocaloric and magnetization measurements down to below 0.1 K. The phase diagram reveals an additional phase between the up-up-down and putative spin liquid phases, so far not observed in other members of the same structural family. Following a systematic analysis of the nuclear contribution and its evolution in the applied field, we conclude that at zero field the magnetic specific heat shows quadratic behavior in the low-T limit in accordance with the expectations for a gapless Dirac spin liquid.

TT 46.5 Thu 10:30 HSZ 201

Anisotropic phonon-spin scattering in the quantum spin liquid candidate NaYbS_2 — MATTHIAS GILLIG^{1,2}, XIAOCHEN HONG^{1,3}, ELLEN HÄUSSLER², PHILIPP SCHLENDER², THOMAS DOERT², BERND BÜCHNER^{1,2}, and CHRISTIAN HESS^{1,3} — ¹IFW Dresden — ²TU Dresden — ³Bergische Universität Wuppertal

A perfect triangular spin lattice and absence of long-range magnetic order down to $T = 260$ mK make the delafossite material NaYbS_2 a prime candidate to host a quantum spin liquid ground state. We present the results of heat transport experiments on NaYbS_2 in the low-temperature limit ($T < 1$ K), where the in-plane thermal conductivity κ_{ab} shows a peculiar temperature dependence mimicking a potential residual linear term that decays below 500 mK. Application of in-plane magnetic field drastically enhances the thermal conductivity until it saturates in the field polarized limit. This behavior hints at phonon dominated heat transport with very strong magnetic phonon scattering where magnetic field suppresses the phonon scattering off spin fluctuations and the phonon thermal conductivity recovers at high field. In the field-dependence of κ broad features appear that indicate possible field-induced phase transitions in the magnetic system. Within this framework no clear evidence for magnetic heat transport due to spin excitations is observed. The investigation of the anisotropy of κ reveals that the phonon-spin scattering is strongly anisotropic and the out-of-plane coupling of phonons to spin excitations is weakened.

TT 46.6 Thu 10:45 HSZ 201

Thermodynamics studies on RE_3BWO_9 (RE = Nd and Pr) spin-liquid candidate systems — AHMED ELGHANDOUR¹, P KHUNTIA², and RÜDIGER KLINGELER¹ — ¹Kirchhoff Institute for Physics, Heidelberg University, Heidelberg, Germany — ²Department of Physics, IIT Madras, Chennai 600036, India

Boratungstates exhibit a distorted Kagome structure of rare-earth ions (RE), thereby providing a platform to unveil the pure Kagome physics fully dominated by magnetic frustration of RE moments while avoiding the influence of conduction electrons. We report the thermodynamic properties of poly crystals of RE_3BWO_9 (RE = Nd and Pr) by means of means of DC magnetometry (0.4 - 350

K) and heat capacity studies (0.4 - 270 K). In Nd_3BWO_9 , our dc magnetization and c_p data indicate a possible transition at $T = 1$ K while there is no evidence of long-range order at higher temperatures. This yields $\frac{\theta}{T_N} = 45$. Isotherm magnetization measured at $T = 400$ mK, demonstrates saturation up to 7 T at half of the expected saturation magnetization, which we attribute to crystal-field effects. In addition, there are two low field anomalies at $\frac{1}{4}$ and $\frac{1}{8}$ of the theoretical saturation field. In contrast, Pr_3BWO_9 does not signal long-range order down to $T = 90$ mK [5] (i.e., $\frac{\theta}{T_N} > 300$) and M vs B only shows smooth right bending at $T = 400$ mK again with reduced saturation moment ($0.8 \mu_B/\text{Pr}$ at $B = 7$ T). The data are discussed in terms of an unconventional persistent fluctuating paramagnetic ground state as suggested by recent NMR data [1].

[1] Zeng et al., PRB 104, 155150 (2021)

TT 46.7 Thu 11:00 HSZ 201

Low temperature phase diagram of $\text{PbCuTe}_2\text{O}_6$ for magnetic fields $B \parallel (110)$ — •PAUL EIBISCH¹, CHRISTIAN THURN¹, ULRICH TUTSCH¹, ARIF ATA¹, ABANOUB R. N. HANNA², A. T. M. NAZMUL ISLAM², SHRAVANI CHILLAL², BELLA LAKE², BERND WOLF¹, and MICHAEL LANG¹ — ¹PI Goethe-University Frankfurt — ²HZ Berlin

The quantum-spin-liquid (QSL) state shows interesting phenomena such as fractional spin excitations and spin entanglement. Here we investigate the spin-liquid-candidate system $\text{PbCuTe}_2\text{O}_6$ where antiferromagnetic interactions among $s = 1/2$ spins lead to a 3D network of triangles similar to the hyper-Kagome lattice. While first experiments on polycrystalline samples, were found to be consistent with the QSL state [1], a recent study on single crystals showed a far more complex scenario including a ferroelectric transition at $T = 1$ K with strong lattice distortions and a quantum critical behaviour close to $B = 0$ T [2]. For the present study we combine thermodynamic, dielectric and magnetic experiments to investigate the field- and temperature phase diagram of $\text{PbCuTe}_2\text{O}_6$ for fields up to $B = 14.5$ T parallel to the [110] direction. In addition to the ferroelectric state we find a structurally distorted phase which coincides with the ferroelectric state at low fields but splits above $B = 6$ T as well as a long-range magnetically ordered phase for fields $B > 11$ T. Based on our experimental results we discuss how the elastic, dielectric and magnetic degrees of freedom are coupled.

[1] S. Chillal et al., Nat. Commun. 11, 2348 (2020)

[2] C. Thurn et al., npj Quantum Materials 6:95 (2021)

15 min. break

TT 46.8 Thu 11:30 HSZ 201

Delafossite magnet AgCrSe_2 : frustration, short range correlations, and field-tuned anisotropic order — •MICHAEL BAENITZ¹, S. LUTHER^{2,3}, M. PIVA¹, J. SICHELSCHMIDT¹, M. NICKLAS¹, H. ZHANG¹, B. SCHMIDT¹, H. ROSNER¹, D. KHALYAVIN⁴, P. MANUEL⁴, J. WOSNITZA^{2,3}, H. KUEHNE², and M. SCHMIDT¹ — ¹MPI for Chemical Physics of Solids, D-01187 Dresden, Germany — ²Hochfeld-Magnetlabor Dresden (HLD-EMFL), Helmholtz-Zentrum Dresden-Rossendorf, 01328 Dresden, Germany — ³Institut für Festkörper- und Materialphysik, TU Dresden, 01062 Dresden Germany — ⁴ISIS Neutron and Muon Source, Rutherford Appelton Laboratory, Chilton, Didcot OX11 0QX, United Kingdom

In contrast to Cr based oxy delafossites (DFs) with predominant antiferromagnetic (afm) nearest neighbor (nn) interaction in the Heisenberg triangular lattice, AgCrSe_2 as a non oxy DFs member is characterized by competing interactions (ferromagnetic nn- vs afm third neighbor interaction). Due to this, the magnetism, can be tuned by relatively small magnetic fields, allowing us to probe the H-T phase diagram in great detail. Large single crystals are grown by chemical vapor transport and studied by magnetization, specific heat, and thermal expansion and Cr-electron spin resonance and neutron diffraction as local probes. An anisotropic cycloidal ordering with unusual extended two-dimensional fluctuations is found [1]. The impact of antisymmetric interactions (Dzyaloshinskii-Moriya) due to the noncentrosymmetric polar space group (R3m) is discussed. [1] M. Baenitz et al. PRB 104, 134410 (2021)

TT 46.9 Thu 11:45 HSZ 201

Dynamical signatures of symmetry broken and liquid phases in an $S = 1/2$ Heisenberg antiferromagnet on the triangular lattice — •MARKUS DRESCHER¹, LAURENS VANDERSTRAETEN², RODERIC MOESSNER³, and FRANK POLLMANN^{1,4} — ¹TU München, 85748 Garching, Germany — ²University of Ghent, 9000 Ghent, Belgium — ³Max-Planck-Institut für Physik komplexer Systeme, 01187 Dresden, Germany — ⁴Munich Center for Quantum Science and Technology, 80799 Munich, Germany

We present the dynamical spin structure factor of the antiferromagnetic spin- $\frac{1}{2}$ $J_1 - J_2$ Heisenberg model on a triangular lattice obtained from large-scale matrix-product state simulations. The high frustration due to the combination of antiferromagnetic nearest and next-to-nearest neighbour interactions yields a rich phase diagram. We resolve the low-energy excitations both in the 120° -ordered phase and in the putative spin liquid phase at $J_2/J_1 = 0.125$. In the ordered phase, we observe an avoided decay of the lowest magnon-branch, demonstrating the

robustness of this phenomenon in the presence of gapless excitations. Our findings in the spin-liquid phase chime with the field-theoretical predictions for a gapless Dirac spin liquid, in particular the picture of low-lying monopole excitations at the corners of the Brillouin zone. We comment on possible practical difficulties of distinguishing proximate liquid and solid phases based on the dynamical structure factor.

TT 46.10 Thu 12:00 HSZ 201

Generic interplay of magnetism and structural dimerization in pressured Kitaev materials — •BIN SHEN¹, FRANZISKA BREITNER¹, ANGEL M. AREVALO-LOPEZ², DANIL PRISHCHENKO³, MAXIMILIAN SEIDLER¹, FRIEDRICH FREUND¹, ANTON JESCHE¹, PHILIPP GEGENWART¹, and ALEXANDER A. TSIRLIN^{1,4} — ¹EP VI, EKM, University of Augsburg, Germany — ²University of Lille, France — ³Yekaterinburg, Russia — ⁴Felix Bloch Institute, University of Leipzig, Germany

Quantum spin liquids in the Kitaev honeycomb model feature quantum entanglement and exotic fractionalized spin excitations, thus attracting tremendous attention. However, experimental realization of Kitaev quantum spin liquid phases in real materials has been proven difficult due to the presence of competing interactions beyond Kitaev exchange. Almost all known structurally ordered Kitaev candidate materials host a magnetically ordered ground state. Suppression of the order by various tuning parameters is currently subject of extensive investigations. We explore the possibility of suppressing magnetic order by high-pressure magnetization measurements on several Kitaev materials under hydrostatic pressure and reveal a generic interplay of magnetism and structural dimerization: Upon applying hydrostatic pressure, structural dimerization emerges and becomes visible as step in the temperature dependence of the magnetic susceptibility that shifts to higher temperatures upon further compression. We also investigate how magnetic order disappears once dimerization emerges.

TT 46.11 Thu 12:15 HSZ 201

Variational States for the $S=3/2$ Kitaev spin liquids — •WILLIAM MAS-SASHI HISANO NATORI^{1,2}, HUI-KE JIN³, FRANK POLLMANN^{3,4}, and JOHANNES KNOLLE^{2,3,4} — ¹Institut Laue-Langevin — ²Imperial College London — ³Technische Universität München — ⁴Munich Center for Quantum Technology and Science

The lack of a mapping to free fermion models has for a long time prevented the analytical characterization of Kitaev spin liquids (KSLs) for general values of S . The most complicated of these spin liquids was the $S=3/2$ KSL, which defied both the analytical and numerical techniques. This problem importance increased thanks to recent studies pointing out the relevance of Kitaev interactions on chromium-based van der Waals magnets.

We recently uncovered the ground state of the $S=3/2$ KHM perturbed by a single-ion anisotropy (SIA) using an $\text{SO}(6)$ parton mean-field theory that displayed a remarkable quantitative agreement with DMRG simulations (Nat. Comm. 13, 3813). In this follow-up work, we uncover similarities between the $S=3/2$ KSL and the Majorana quantum spin-orbital liquids that emerge as ground states of exactly solvable Kugel-Khomskii models. We show that expectation values of several observables can be exactly calculated over a set of parton wavefunctions without Gutzwiller-projection, including the own KHM, quadrupolar parameters and correlation functions. The $S=3/2$ KSLs are then identified to the Gutzwiller projection of the state in this set minimizing the energy.

TT 46.12 Thu 12:30 HSZ 201

Linked-cluster expansions of perturbed topological phases — •VIKTOR KOTT, MATTHIAS MÜHLHAUSER, and KAI PHILLIP SCHMIDT — FAU, Erlangen-Nürnberg, Deutschland

We investigate the robustness of Kitaev's toric code in a uniform magnetic field on the square and honeycomb lattice by perturbative linked cluster expansions using a full graph decomposition. In particular, the full graph decomposition allows to correctly take into account the non-trivial mutual exchange statistics of the elementary anyonic excitations. This allows us to calculate the ground-state energy and excitation energies of the topological phase which are then used to study the quantum phase transitions out of the topologically ordered phase as a function of the field direction.

TT 46.13 Thu 12:45 HSZ 201

Spin-Peierls instability of the $U(1)$ Dirac spin liquid — •JOSEF WILLISHER¹, URBAN SEIFERT², and JOHANNES KNOLLE^{1,3,4} — ¹TU Munich, Germany — ²Kavli Institute, University of California, Santa Barbara, USA — ³MCQST, Munich, Germany — ⁴Imperial College London, UK

Quantum spin liquids are tantalising phases of quantum matter, but experimental evidence of their existence has remained elusive. Recent theoretical and numerical studies have provided evidence that triangular-lattice Heisenberg magnets may host a $U(1)$ Dirac spin liquid (DSL): a state of matter whose low-energy description is given by compact quantum electrodynamics in $2+1$ dimensions coupled to four Dirac fermions, which is believed to flow to a strongly interacting conformal fixed point. Monopole operators constitute a strongly relevant perturbation to this fixed point, driving the spin liquid into magnetically ordered or VBS states, but are forbidden by the microscopic (UV) symmetries on the tri-

angular lattice. However, in this work we show that a coupling between certain monopoles and phonons is symmetry-allowed and produces a 2+1-dimensional analog of the spin-Peierls instability for a spin liquid. We study monopole-phonon interactions within a conformal field theory framework and show that the DSL state is generically unstable to a static deformation, precipitating VBS

ordering. Finally, we discuss implications for experimental realisations and signatures of the DSL in real 2D materials by addressing a full dynamical quantum model of phonons; here we predict a weak-coupling regime within which the spin-liquid phase remains stable.

TT 47: Quantum-Critical Phenomena

Time: Thursday 9:30–13:00

Location: HSZ 204

TT 47.1 Thu 9:30 HSZ 204

The mystery of the missing heavy-fermion weight — •CHIA-JUNG YANG¹, OLIVER STOCKERT², HILBERT V. LÖHNEYSSEN³, SHOYON PAL^{1,4}, JOHANN KROHA⁵, and MANFRED FIEBIG¹ — ¹Department of Materials, ETH Zurich, Switzerland — ²MPI for Chemical Physics of Solids, Dresden, Germany — ³KIT Karlsruhe, Germany — ⁴School of Physical Science, NISER Bhubaneswar, India — ⁵University of Bonn, Germany

The fermionic quasiparticle weight is one of the keys to understanding the quantum critical scenarios across a quantum phase transition (QPT). In heavy-fermion compounds, CeCu_{6-x}Au_x (CCA), Cu substitution by Au expands the lattice, thereby inducing a QPT at $x = 0.1$ from a paramagnetic Fermi-liquid state to an antiferromagnetically-ordered ground state. Recently, the evolution of spectral weight has been revealed in CCA at $x = 0, 0.1$, and 1.0 via terahertz (THz) time-domain spectroscopy [1,2]. Here, we further investigate the spectral weight within the RKKY-dominated region where $x = 0.2$ and 0.3 . In both samples, we find that the spectral weight increases slightly with decreasing temperature (T), but settles at a strongly suppressed, T -independent value already at and below 100 K, about two orders of magnitude above the Néel temperature [3]. This indicates that across QPT in CCA, the Kondo singlet formation is suppressed by the T -independent RKKY interaction, not by the critical magnetic fluctuations, in agreement with theoretical predictions [4].

[1] Nat. Phys. **14**, 1103 (2018)

[2] PRR **2**, 033296 (2020)

[3] Eur. Phys. J. B **5**, 447 (1998)

[4] PRL **118**, 117204 (2017)

TT 47.2 Thu 9:45 HSZ 204

Phonon softening close to a structural instability at zero temperature — T. GRUNER^{1,2}, S. LUCAS¹, C. GEIBEL¹, K. KANEKO³, S. TSUTSUI^{4,5}, K. SCHMALZL⁶, and •O. STOCKERT¹ — ¹Max-Planck-Institut für Chemische Physik fester Stoffe, 01187 Dresden, Germany — ²Cavendish Laboratory, University of Cambridge, Cambridge CB3 0HE, United Kingdom — ³Materials Sciences Research Center, Japan Atomic Energy Agency, Tokai, Naka, Ibaraki 319-1195, Japan — ⁴Japan Synchrotron Radiation Research Institute, SPring-8, Sayo, Hyogo 679-5198, Japan — ⁵Institute of Quantum Beam Science, Graduate School of Science and Engineering, Ibaraki University, Hitachi, Ibaraki 316-8511, Japan — ⁶Jülich Centre for Neutron Science JCNS, Forschungszentrum Jülich GmbH, Outstation at ILL, 38042 Grenoble, France

The structural transition in LuPt₂In is interesting since it can be tuned to zero temperature upon substituting Pd for Pt in Lu(Pt_{1-x}Pd_x)₂In. Of particular interest is the appearance of a superconducting dome around the structural quantum criticality. We combined inelastic neutron and x-ray scattering measurements and studied in detail this structural transition in Lu(Pt_{1-x}Pd_x)₂In. As a result we determined the low-energy phonon dispersions and clearly identified the relevant phonon branch becoming soft at the transition. In general, the theoretical calculations broadly agree with the measured dispersion. However, large tails of the superstructure intensity above the structural transition clearly point to a non-mean-field behavior, which might be related to quantum criticality and/or the superconducting dome.

TT 47.3 Thu 10:00 HSZ 204

Search for ferromagnetic quantum phase transitions in CePt — MARC SEIFERT¹, •FLORIAN KÜBELBÄCK¹, PAU JORBA¹, MICHAEL SCHULZ², GEORG BENKA¹, ANDREAS BAUER¹, and CHRISTIAN PFLEIDERER¹ — ¹Physik-Department, Technical University of Munich, D-85748 Garching, Germany — ²MLZ, Technical University of Munich, D-85748 Garching, Germany

We report an investigation of the ferromagnetic properties and the putative existence of quantum phase transitions in CePt. Tracking the neutron depolarization of polycrystalline samples under pressure by means of bespoke diamond anvil cell and focussing neutron guides [1], we confirm the presence of a ferromagnetic to paramagnetic quantum phase transition at 13 GPa as inferred previously from the resistivity [2]. An additional drop in the depolarization deep in the ferromagnetic state for pressures up to 5 GPa suggests an additional small moment to large moment transition. We explore the nature and possible existence of a second quantum phase transition in the ferromagnetic state of single-crystal CePt grown under ultra-high vacuum compatible conditions. The pressure versus temperature phase diagram of CePt and its magnetic properties will

be compared with the emergence of a Kondo cluster glass in the isostructural sibling CePd of CePt when suppressing ferromagnetic order by substitutional Rh doping [3].

[1] P. Jorba et al., Phys. Stat. Solidi b, 2100623 (2022)

[2] J. Larrea et al., Phys. Rev. B, **72**, 035129 (2005)

[3] M. Seifert et al., Phys. Rev. Res. **4**, 043029 (2022)

TT 47.4 Thu 10:15 HSZ 204

Quantum criticality on a compressible lattice — SAHELI SARKAR, •LARS FRANKE, NIKOLAS GRIVAS, and MARKUS GARST — Institut für Theoretische Festkörperphysik, Karlsruhe, Germany

It is a long standing result in the theory of classical criticality that a second order phase transition when coupled to a compressible lattice will become first order if the Larkin-Pikin criterion[1] is satisfied. More recently the extension of these results to quantum criticality has sparked the interest of the community[2,3]. However, until now a detailed analysis of a microscopic theory describing a quantum phase transition on a compressible lattice and its implications for the nature of the phase transition as well as the consequences for the lattice has been missing. Here we provide this calculation for a Lorentz-invariant ϕ^4 -theory with quadratic coupling to strain and analyse it using renormalization group (RG) methods to one-loop order. We find that both critical and phonon velocity flow with RG leading to an additional fixed point where the phonons have a renormalized dynamical exponent. Furthermore, our results show that the quantum version of the Larkin-Pikin criterion[2] holds, but even when the criterion is not satisfied a structural instability can still occur, if the coupling is large enough.

[1] A. Larkin and S. Pikin, Sov. Phys. JETP **29**, 891 (1969)

[2] P. Chandra, P. Coleman, M. A. Continentino, and G. G. Lonzarich, Phys. Rev. Res. **2**, 043440 (2020)

[3] A. Samanta, E. Shimshoni, and D. Podolsky, Phys. Rev. B **106**, 035154 (2022)

TT 47.5 Thu 10:30 HSZ 204

Marginal Fermi liquid at a magnetic quantum critical point from dimensional confinement — •BERNHARD FRANK¹, ZI HONG LIU², FAKHER F. ASSAAD², MATTHIAS VOJTA¹, and LUKAS JANSSEN¹ — ¹Institut für Theoretische Physik und Würzburg-Dresden Cluster of Excellence ct.qmat, Technische Universität Dresden, 01062 Dresden, Germany — ²Institut für Theoretische Physik und Astrophysik und Würzburg-Dresden Cluster of Excellence ct.qmat, Universität Würzburg, 97074 Würzburg, Germany

Metallic quantum criticality is frequently discussed as a source for non-Fermi liquid behavior, but controlled theoretical treatments are scarce. Here, we identify and study a novel magnetic quantum critical point in a two-dimensional antiferromagnet coupled to a three-dimensional environment of conduction electrons. By combining an effective field theory analysis and sign-problem-free quantum Monte Carlo simulations, we demonstrate that the quantum critical point exhibits marginal Fermi liquid behavior. In particular, we compute the electrical resistivity for transport across the magnetic layer, which is shown to display a linear temperature dependence at criticality. Experimental realizations in Kondo heterostructures are discussed.

TT 47.6 Thu 10:45 HSZ 204

Transverse-field quantum phase transitions in CoNb₂O₆ — •ALEXANDER ENGELHARDT¹, ANDREAS WENDL¹, ANDREAS BAUER¹, ANDREAS ERB², MATTHIAS VOJTA³, and CHRISTIAN PFLEIDERER¹ — ¹Physik-Department, Technical University of Munich, D-85748 Garching, Germany — ²Walther-Meißner-Institut, D-85748 Garching, Germany — ³Institut für Theoretische Physik, Technical University of Dresden, D-85748 Garching, Germany

The ferromagnetic Ising chain in a transverse magnetic field displays the perhaps best understood theoretical example of a quantum phase transition. One of the closest realizations has been reported in the columbite compound CoNb₂O₆ [1,2,3], in which, however, weak interchain couplings result in incommensurate antiferromagnetism as a function of decreasing temperature, followed by a transition to commensurate antiferromagnetic order. We have grown high-quality single-crystal CoNb₂O₆ by means of optical float-zoning. Measuring the transverse magnetic ac susceptibility of a spherical sample down to 90 mK under arbitrary field orientations, we have mapped out the emergence of the quantum phase transitions associated with the incommensurate and commensurate antiferromagnetic order under transverse field, as well as the evolution of the mag-

netic phase diagram when systematically tilting the magnetic field away from the hard magnetic axis.

[1] R. Coldea et al., *Science* **327**, 177 (2010)

[2] M. Fava et al., *PNAS* **117**, 25219 (2020)

[3] C. M. Morris et al., *Nat. Phys.* **17**, 852 (2021)

TT 47.7 Thu 11:00 HSZ 204

Non-Fermi liquid behavior at flat hot spots at the onset of density wave order in two-dimensional metals — •LUKAS DEBBELER and WALTER METZNER — Max Planck Institute for Solid State Research, Stuttgart, Germany

We analyze the quantum critical point (QCP) at the transition towards incommensurate charge or spin density wave order with a $2k_F$ wave vector that connects a single pair of hot spots on the Fermi surface. From a theoretical point of view the fate of this QCP is debated. Strong fluctuations might lead to a discontinuously opening gap and therefore a first order transition [1]. On the other hand a fluctuation driven flattening at the hot spots of the Fermi surface has been found [2,3], which could protect the QCP. Hence, we investigate the effect of quantum critical fluctuations for a flat Fermi surface at the nesting points. We report non-Fermi liquid properties and provide numerical values for anomalous exponents.

[1] B. L. Altshuler et al., *Phys. Rev. B* **52**, 5563 (1995)

[2] J. Sýkora et al., *Phys. Rev. B* **97**, 155159 (2018)

[3] J. Halbinger et al., *Phys. Rev. B* **99**, 195102 (2019)

15 min. break

TT 47.8 Thu 11:30 HSZ 204

Frozen deconfined quantum criticality — •VIRA SHYTA^{1,2}, JEROEN VAN DEN BRINK^{1,3}, and FLAVIO NOGUEIRA¹ — ¹Institute for Theoretical Solid State Physics, IFW Dresden, Helmholtzstr. 20, 01069 Dresden, Germany — ²Kyiv Academic University, 36 Vernadsky blvd., Kyiv 03142, Ukraine — ³Institute for Theoretical Physics and Würzburg-Dresden Cluster of Excellence ct.qmat, TU Dresden, 01069 Dresden, Germany

There is a number of contradictory findings with regard to whether the theory describing easy-plane quantum antiferromagnets undergoes a second-order phase transition. The traditional Landau-Ginzburg-Wilson approach suggests a first-order phase transition, as there are two different competing order parameters. On the other hand, it is known that the theory has the property of self-duality which has been connected to the existence of a deconfined quantum critical point (DQCP). The latter regime suggests that order parameters are not the elementary building blocks of the theory, but rather consist of fractionalized particles that are confined in both phases of the transition and only appear at the critical point. Here we establish from exact lattice duality transformations and renormalization group analysis that the easy-plane CP1 antiferromagnet does feature a DQCP. We uncover the criticality starting from a regime analogous to the zero temperature limit of a certain classical statistical mechanics system which we therefore dub frozen. At criticality our bosonic theory is dual to a fermionic one with two massless Dirac fermions, which thus undergoes a second-order phase transition as well.

TT 47.9 Thu 11:45 HSZ 204

Finite temperature entanglement negativity of fermionic topological phases and quantum critical points — •WONJUNE CHOI^{1,2}, FRANK POLLMANN^{1,2}, and MICHAEL KNAP^{1,2} — ¹Department of Physics, Technical University of Munich, 85748 Garching, Germany — ²Munich Center for Quantum Science and Technology (MCQST), Schellingstr. 4, 80799 München, Germany

In condensed matter physics, topology is vital in describing quantum phases of matter beyond the Ginzburg-Landau paradigm. Two symmetry-preserving quantum states may not be adiabatically connected if the topological structure encoded in the many-body entanglements is distinct. Hence, this talk presents how quantum entanglements can be quantified to unveil the underlying topological nature of the gapped topological phases and the quantum critical points. We demonstrate that the logarithmic negativity between spatially separated disjoint intervals can sharply count the topologically protected edge modes. Notably, the quantized values of the negativity could reveal the topological indices of the gapless quantum states described by the conformal field theories having the same central charge. At finite temperatures, the entanglement negativity for the disjoint intervals is no longer quantized. However, the negativity for the two adjacent intervals leaves the structure similar to the quantum critical fan, which

signals the highly entangled ground state even at a finite temperature window.

TT 47.10 Thu 12:00 HSZ 204

Symmetry enriched topological quantum phase transition in projected entangled pair states — •LUKAS HALLER, YU-JIE LIU, WEN-TAO XU, and FRANK POLLMANN — Department of Physics, Technical University of Munich, 85748 Garching, Germany

Phase transitions between topologically ordered phases can exhibit a rich structure and are generically challenging to study. In this context, we consider the 2D toric code decorated with 1D symmetry protected topological states and construct a family of parametrized projected entangled pair states (PEPS), which describes the ground states of time-reversal (TR) symmetric Hamiltonians. The system can exhibit three distinct phases of matter: (i) A trivial phase; (ii) the toric code phase, where TR symmetry is not fractionalized; (iii) a symmetry enriched topological (SET) phase, where TR symmetry can be fractionalized on anyons. We characterize different phases using topological entanglement entropy and membrane order parameters. By mapping the PEPS to the partition functions of 2D classical models, we show that the trivial phase is separated from the toric code and the SET phases by critical points described by an Ising conformal field theory (CFT) with central charge $c = 1/2$, while the phase transition between the toric code and the SET phase is described by a compactified free-boson CFT with $c = 1$. The model realizes a direct phase transition between the toric code and the SET phases at a microscopic level.

TT 47.11 Thu 12:15 HSZ 204

Antiferromagnetic Weyl quantum criticality in three-dimensional Luttinger semimetals — •DAVID JONAS MOSER and LUKAS JANSSSEN — Technische Universität Dresden, Dresden, Deutschland

Luttinger semimetals are three-dimensional strongly-spin-orbit-coupled systems, in which valence and conduction bands touch quadratically at the Fermi level. They provide a rich playground for highly unconventional physics and serve as a parent state to a number of exotic states of matter, such as Weyl semimetals, topological insulators, or spin ice. Here, we discuss a quantum critical point between Luttinger and antiferromagnetic Weyl semimetals using a renormalization group approach. Our results are relevant for the low-temperature behavior of rare-earth pyrochlore iridates, such as $\text{Pr}_2\text{Ir}_2\text{O}_7$ or $\text{Nd}_2\text{Ir}_2\text{O}_7$.

TT 47.12 Thu 12:30 HSZ 204

Renormalization group flow of the Yukawa-SYK model — •NIKLAS CICHUTEK and PETER KOPIETZ — Goethe University Frankfurt

We use the functional renormalization group to calculate the global renormalization group flow of the Yukawa-SYK model describing N fermions on a quantum dot which are coupled to M phonons by a disorder-induced Yukawa coupling in the large N and M limit for an arbitrary ratio $\frac{N}{M}$. By determining the fixed-point structure we identify the different phases as well as the quantum critical point and their corresponding anomalous dimensions. The stability analysis of the fixed points sheds light on the self-tuning to criticality of the Yukawa-SYK model.

TT 47.13 Thu 12:45 HSZ 204

Quantum criticality of Heisenberg systems with long-range interactions — •PATRICK ADELHARDT and KAI PHILLIP SCHMIDT — Friedrich-Alexander-Universität Erlangen-Nürnberg (FAU)

The majority of numerical approaches investigating long-range quantum systems is restricted to one-dimensional systems and systems in two dimensions with quickly decaying long-range interactions. While models with discrete symmetries like the long-range transverse-field Ising model have been studied thoroughly, much less is known about long-range models with continuous symmetries where long-range interactions can circumvent the Hohenberg-Mermin-Wagner theorem in one dimension allowing the spontaneous breaking of continuous symmetries or can give rise to massive excitations violating Goldstone's theorem. We study the breakdown of the rung-singlet phase in the quasi one-dimensional Heisenberg ladders as well as two-dimensional Heisenberg bilayer systems with algebraically decaying long-range interactions. To this end we use the method of perturbative continuous unitary transformations (pCUT) as a white graph expansion with classical Monte Carlo simulations yielding high-order series in the thermodynamic limit about the limit of isolated dimers. This allows us to determine the critical point as well as critical exponents as a function of the decay exponent.

TT 48: Topological Superconductors

Time: Thursday 9:30–11:15

Location: HSZ 304

TT 48.1 Thu 9:30 HSZ 304

Superconductivity mediated by topological phonons — •ALESSIO ZACCONE — Department of Physics, University of Milan, 20133 Milano, Italy

Topological phononic insulators are the counterpart of three-dimensional quantum spin Hall insulators in phononic systems and, as such, their phononic topological surfaces are characterized by Dirac cone-shaped gapless edge states arising as a consequence of a bulk-boundary correspondence. We proposed [1] a theoretical framework for the possible superconductivity in these materials, where the attractive interaction between electrons is mediated by topological phonons in nontrivial boundary modes. Within the BCS limit, we developed a self-consistent two-band gap equation, whose solutions show that the superconducting T_c has a nonmonotonic behavior with respect to the phononic frequency in the Kramers-like point. This remarkable behavior is produced by a resonance that occurs when electrons and phonons on the topological surfaces have the same energy: this effectively increases the electron-phonon interaction and hence the Cooper pair binding energy, thus establishing an optimal condition for the superconducting phase. With this mechanism, the T_c can be increased by well over a factor 2, and the maximum enhancement occurs in the degenerate phononic flat-band limit.

[1] D. Di Miceli, C. Setty, A. Zaccane, Phys. Rev. B 106, 054502 (2022)

TT 48.2 Thu 9:45 HSZ 304

Topological superconductivity on the honeycomb lattice: Effect of normal state topology and disorder — •STEPHAN RACHEL — School of Physics, University of Melbourne, Australia

The search for topological superconductors is one of the most pressing and challenging questions in condensed-matter and material research. Despite some early suggestions that doping a topological insulator might be a successful recipe to find topological superconductors, to date there is no general understanding of the relationship of the topology of the superconductor and the topology of its underlying normal state system. Here we present an analysis of doped insulators - topological and trivial. Our approach allows us to study and compare superconducting instabilities of different normal state systems and present rigorous results about the influence of the normal state system's topology. If time permits we will also discuss the influence of disorder on topological superconductivity on the honeycomb lattice.

TT 48.3 Thu 10:00 HSZ 304

Ground state topology of a multiterminal superconducting double quantum dot — •LEV TESHLEHER, HANNES WEISBRICH, and WOLFGANG BELZIG — Universität Konstanz, Konstanz, Germany

Multiterminal Josephson junctions can provide topological Andreev bound states in the space of the superconducting phases [1]. The topology of the Andreev bound states manifests itself in a quantized transconductance when applying voltages to two terminals. Such systems are candidates to realise higher-dimensional topology and non-Abelian Berry phases using their synthetic dimensions [2]. For practical purposes a linear arrangement of quantum dots coupled to superconductors might be beneficial and was shown to exhibit nontrivial topology [3]. In this work, we study a double quantum dot in which each dot is coupled to two superconductors. This system that depends on three superconducting phase differences already displays non-trivial topology in terms of the first Chern number and is an example that allows to study the fundamental properties of this class of systems. We will study the ground state and the respective topological phase diagram for different sets of parameters of the double quantum dot. Furthermore, we will also discuss the influence of Coulomb interaction and Zeeman splitting on the topological properties of the ground state.

[1] R.-P. Riwar et al., Nat. Commun. 7, 1 (2016)

[2] H. Weisbrich et al., PRX Quantum 2, 010310 (2021)

[3] R. Klees et al., Phys Rev B 103, 014516 (2021)

TT 48.4 Thu 10:15 HSZ 304

Fractional transconductance via non-adiabatic topological Cooper pair pumping — •HANNES WEISBRICH¹, RAFFAEL L. KLEES², ODED ZILBERBERG¹, and WOLFGANG BELZIG¹ — ¹Universität Konstanz — ²Universität Würzburg

Many robust physical phenomena in quantum physics are based on topological invariants, which are intriguing geometrical properties of quantum states. A prime example is the 2D quantum Hall effect with its quantized quantum Hall conductance in units of $\frac{e^2}{h}$ protected by the respective 2D topology. A comparable effect in superconducting systems is the appearance of a quantized transconductance in units of $\frac{4e^2}{h}$ for topological Andreev bound states in multiterminal Josephson junctions.

In this work, we theoretically demonstrate how fractional quantized plateaus in the transconductance can be observed as a result of topological Cooper pair pumping in a chain of Josephson junctions. The fractional plateaus in the transconductance are stabilized by non-adiabatic Landau-Zener transitions which even allow for a robustness to disorder in the chain.

TT 48.5 Thu 10:30 HSZ 304

Magnetic-domain mediated topological superconductivity in a Josephson Junction — •IGNACIO SARDINERO¹, RUBÉN SEOANE SOUTO^{2,3}, and PABLO BURSET¹ — ¹Department of Theoretical Condensed Matter Physics, Condensed Matter Physics Center (IFIMAC) and Instituto Nicolás Cabrera, Universidad Autónoma de Madrid, 28049 Madrid, Spain — ²Division of Solid State Physics and NanoLund, Lund University, S-221 00 Lund, Sweden — ³Center for Quantum Devices, Niels Bohr Institute, University of Copenhagen, DK-2100 Copenhagen, Denmark

Topological superconductors are appealing building blocks for robust and reliable quantum information processing. Most platforms for engineering topological superconductivity rely on a combination of materials with intrinsic spin-orbit coupling and external magnetic fields, which are usually challenging to manipulate. We propose and describe a setup without spin-orbit or magnetic fields where a conventional Josephson junction is linked by a narrow ferromagnetic insulator with multi-domain structure along the interface. Our calculations show that sequences of magnetic domains preserving the net magnetization's rotation direction are sufficient for generating topological superconductivity in a wide range of parameters and degrees of disorder. We find that the topological phase transition strongly depends on the magnitude and period of the net magnetization. Interestingly, a phase bias across the junction can control and tune the formation and localization of a pair of Majorana zero-energy modes along the junction interface, with an observable effect on the current-phase relation.

TT 48.6 Thu 10:45 HSZ 304

Symmetry enriched entanglement properties of chiral Skyrme insulators —

•JOE WINTER^{1,2,3}, BERND BRAUNECKER³, and ASHLEY COOK^{1,2} — ¹Max Planck Institute for Chemical Physics of Solids, Nothnitzer Straße 40, 01187 Dresden, Germany — ²Max Planck Institute for the Physics of Complex Systems, Nothnitzer Straße 38, 01187 Dresden, Germany — ³SUPA, School of Physics and Astronomy, University of St. Andrews, North Haugh, St. Andrews KY16 9SS, UK

The expectation value of an observable \mathcal{O} may be computed with a density matrix ρ as $\text{Tr}(\rho\mathcal{O})$. In this work, we introduce the symmetry-enriched partial trace operation for density matrices, $\tilde{\rho}_{\mathcal{T}} = \tilde{\text{Tr}}_{\mathcal{T}}(\rho)$, a partial trace performed over \mathcal{T} degrees of freedom on a density matrix as part of partial computation of an expectation value for an observable \mathcal{O} . That is, for representation of observable \mathcal{O} after tracing out \mathcal{T} being $\mathcal{O}_{\mathcal{T}}$, $\tilde{\rho}_{\mathcal{T}}$ satisfies $\text{Tr}(\rho\mathcal{O}) = \langle \mathcal{O} \rangle = \langle \mathcal{O}_{\mathcal{T}} \rangle = \text{Tr}(\tilde{\rho}_{\mathcal{T}}\mathcal{O}_{\mathcal{T}})$, with symmetry-enrichment deriving from differences in symmetry between \mathcal{O} and $\mathcal{O}_{\mathcal{T}}$. We use this to characterize bulk-boundary correspondence of topological skyrmion phases, by computing the symmetry-enriched reduced density matrix in the 2D bulk of a topological skyrmion phase, and for slab geometries with open boundary conditions in one direction. We show winding of this reduced density matrix matches winding of the spin expectation value vector in the bulk, and the entanglement spectrum of the reduced density matrix for the slab geometry reveals \mathcal{Q} topologically-protected, chiral edge modes for skyrmion number \mathcal{Q} characterizing the bulk topological skyrmion phase.

TT 48.7 Thu 11:00 HSZ 304

Non-Hermitian dimerized interacting Kitaev chain — •SHARAREH SAYYAD¹ and JOSE LADO² — ¹MPI for the science of light, Erlangen, Germany — ²Aalto University, Espoo, Finland

Non-Hermitian models have risen as a new paradigm to manipulate and interpret various emergent quantum phenomena. While numerous studies have been focused on exploring (effective) non-Hermitian non-interacting models. The role of interactions in modifying the non-interacting non-Hermitian physics still needs to be well-explored. In this talk, I will present how incorporating many-body interactions can enrich non-interacting physics. To be more precise, combining our exact analytical results and tensor-network numerical calculations, I will discuss the phase diagram of the non-Hermitian dimerized interacting Kitaev chain. Here, the non-Hermiticity is due to the complex-valued nearest-neighbor density-density interaction strength. I will show that the ground state degeneracy of this system may be fourfold, twofold, or nondegenerate, depending on the parameter regimes. I will further discuss how these degeneracies are lifted in the presence of non-Hermiticity. Elaborating on this behavior clarifies the role of non-Hermiticity in washing out multiple phases in the phase diagram of the Hermitian interacting model.

TT 49: Quantum Coherence and Quantum Information Systems I

Time: Thursday 11:30–13:00

Location: HSZ 304

TT 49.1 Thu 11:30 HSZ 304

Inter-lab quantum microwave teleportation — •MICHAEL RENGER^{1,2}, SIMON GANDORFER^{1,2}, WUN KWAN YAM^{1,2}, FLORIAN FESQUET^{1,2}, KEDAR HONASOGE^{1,2}, FABIAN KRONWETTER^{1,2,3}, YUKI NOJIRI^{1,2}, ACHIM MARX¹, RUDOLF GROSS^{1,2,4}, and KIRILL G. FEDOROV^{1,2} — ¹Walther-Meißner-Institut, BadW, 85748 Garching, Germany — ²TUM School of Natural Sciences, Technische Universität München, Garching, Germany — ³Rohde & Schwarz GmbH & Co. KG, 81671 Munich, Germany — ⁴Munich Center for Quantum Science and Technology, 80799 Munich, Germany

Quantum communication enables secure and efficient information exchange among different quantum nodes. To avoid inefficient frequency conversion for data transfer between superconducting quantum processors, we implement our quantum communication protocols with propagating quantum microwave states, directly in the microwave frequency regime which relies on ambient temperatures below 100 mK. To realize such a microwave quantum channel, we connect two dilution refrigerators over a distance of 6.5 m via a cryogenic link, operating at a base temperature of 52 mK. We employ our system to demonstrate inter-lab quantum teleportation of coherent microwave states, where we achieve the teleportation fidelity of 55%, exceeding the classical threshold. We discuss quantum advantage and security of this protocol and provide an outlook into the future of microwave quantum communication.

TT 49.2 Thu 11:45 HSZ 304

A co-design superconducting quantum circuit for quantum simulations — •DARIA GUSENKOVA, JAYSHANKAR NATH, HSIANG-SHENG KU, JULIA LAMPRICH, NICOLA WURZ, STEFAN POGORZALEK, FLORIAN VIGNEAU, PING YANG, FRANK DEPPE, ANTTI VEPSÄLÄINEN, ALESSANDRO LANDRA, VLADIMIR MILCHAKOV, CASPAR OCKELOEN- KORPI, WEI LIU, LAN-HSUAN LEE, SEUNG-GOO KIM, HERMANNI HEIMONEN, MANISH THAPA, and INÉS DE VEGA — IQM Germany GmbH, Nymphenburger Str. 86, 80335 Munich

The co-design concept of building application-specific quantum processors is a viable strategy for reaching quantum advantage with noisy intermediate-scale quantum computers. We consider many-body problems which map onto a Hamiltonian with all-to-all interacting qubits. Here, a prototypical example is the simulation of a nanoscale NMR system consisting of an NV center coupled to multiple nuclear spins. We discuss the implementation on a star-topology circuit developed in IQM. Compared to the general-purpose square-grid topology, the star reduces the number of SWAP gates in the algorithm implementation, and thus tolerates higher gate errors for a given computational precision [1]. In order to allow for hardware scaling, we use a distributed-element resonator as a center component in the circuit. To use this resonator as a computational element, we develop qubit-resonator SWAP and CZ gates. In this talk, we present the experimental progress towards digitally simulating the nanoscale NMR problem.

[1] M. G. Algaba et. al., Phys. Rev. Research 4, 043089 (2022)

TT 49.3 Thu 12:00 HSZ 304

Showcasing the effective direct interaction between a readout resonator and a strongly coupled junction defect mediated by a transmon qubit — •ALEXANDER K. HÄNDEL, ALEXANDER BILMES, ALEXEY V. USTINOV, and JÜRGEN LISENFELD — Physikalisches Institut, Karlsruhe Institute of Technology, 76131 Karlsruhe, Germany

Decoherence from material defects constitutes a principal problem on the way to improve superconducting quantum bits. Strongly coupled defects residing in the Josephson junction pose a particular challenge, demonstrating coupling strengths of multiple MHz. This strong coupling leads to avoided level crossings when qubit and defect come into resonance, and spoils qubit performance. In this work, we reveal an additional decoherence channel that occurs due to the resonant interaction between defects in the qubit's Josephson junction with the qubit's readout resonator, through an interaction mediated by the qubit. We investigate this effect using multi-photon spectroscopy and QuTiP simulations of the tripartite energy level spectrum.

TT 49.4 Thu 12:15 HSZ 304

Modular flip-chip architecture for generalized flux qubits — •SOEREN HESSEN¹, SIMON GEISERT¹, MARTIN SPIECKER², PATRICK WINKEL², WOLFGANG WERNSDORFER^{1,2}, and IOAN M. POP^{1,2} — ¹Institute for Quantum Materials and Technologies, Karlsruhe Institute of Technology, Germany — ²Physikalisches Institut, Karlsruhe Institute of Technology, Germany

Superconducting circuits are a promising and widely-used platform to implement quantum information processing hardware. However, scaling up to more sophisticated devices requires major engineering efforts due to the complexity of the mandatory coupling, readout and control circuitry. To investigate innovative coupling and scaling strategies, we developed a modular flip-chip architecture, in which the various circuit elements reside on dedicated chips that are capacitively coupled. A unit cell of our architecture consists of a qubit chip that is flipped above a control chip. The qubit chip contains a single generalized flux qubit (GFQ) and a harmonic readout mode, through which dispersive readout is possible. The control chip is used to excite, read out and flux bias the qubit. We tested our architecture by characterizing the GFQs in all conventional flux qubit regimes by modifying the qubit loop inductance as well as the shunt capacitance and the Josephson energy of the alpha junction. This resulted in qubit frequencies between 150 MHz and 7.5 GHz, and dispersive shifts of 60 kHz to 6 MHz. Coupling between unit cells may be achieved through coupler chips, so that our unit cell can be used as a basic building block of a scalable qubit array.

TT 49.5 Thu 12:30 HSZ 304

Improving Fabrication Methods for Highly Coherent Superconducting Qubits — •NIKLAS BRUCKMOSER^{1,2,3}, LEON KOCH^{1,2,3}, DAVID BUNCH^{1,2,3}, TAMMO SIEVERS^{1,2,3}, KEDAR E. HONASOGE^{1,2,3}, THOMAS LUSCHMANN^{1,2,3}, and STEFAN FILIPP^{1,2,3} — ¹Walther-Meißner-Institut, Bayerische Akademie der Wissenschaften, Garching, Germany — ²Technical University of Munich, TUM School of Natural Sciences, Physics Department, Garching, Germany — ³Munich Center for Quantum Science and Technology (MCQST), Munich, Germany

Superconducting qubits and resonators with long coherence times pave the way towards useful quantum processors. Significant improvements in coherence time have already been made over the last years. However, the fidelity is still limited by decoherence due to noise and losses arising in the local environment of the qubit. It is thus an integral endeavor of fabrication efforts to mitigate these effects. Here, we demonstrate that qubit lifetimes well beyond 0.1 ms can be achieved by a combination of substrate cleaning, etching optimization and post-process sample cleaning. By improving on these processes we reach quality factors above 4×10^6 for thin-film niobium coplanar waveguide resonators in the single photon regime and qubit lifetimes of more than 0.2 ms for niobium based transmons.

TT 49.6 Thu 12:45 HSZ 304

Dynamics of superconducting qubit coherence times due to fluctuations of two-level systems — •IVAN TSITSILIN^{1,2} and STEFAN FILIPP^{1,2} — ¹Technical University of Munich, TUM School of Natural Sciences, Physics Department, 85748 Garching, Germany — ²Walther-Meißner-Institut, Bayerische Akademie der Wissenschaften, 85748 Garching, Germany

Recent studies have shown that the stability of coherence times is strongly affected by two-level systems (TLSs). This is caused by chaotic frequency fluctuations of TLSs, which, when in proximity to the qubit resonance, significantly reduce its T_1 times. Understanding and mitigating this behavior is crucial to realize functional quantum processing devices based on superconducting qubits. In this work, we perform a long-time stability analysis of the qubit T_1 times as a function of qubit frequency utilizing the AC-Stark shifting technique[1]. We present an extensive analysis of the TLS distributions and their impact on T_1 times for different qubit sample materials and RF line configurations. Furthermore, our results provide insight into the effect of the noise spectrum on the behavior and density of TLSs.

[1] Carroll et al., arXiv:2105.15201

TT 50: Focus Session: Superconducting Nickelates II

Time: Thursday 15:00–17:00

Location: HSZ 03

TT 50.1 Thu 15:00 HSZ 03

Fermi liquid on the verge of antiferromagnetism: Non-local correlations in bulk LaNiO₃ as seen by SX-ARPES — •JOHANNES FALKE¹, CHENG-EN LIU^{1,2,3}, KENG-YUNG LIN^{1,4}, CHANG-YANG KUO^{1,2,3}, HANJIE GUO¹, ALEXANDER KOMAREK¹, CHUN-FU CHANG¹, PHILIPP HANSMANN⁵, and LIU HAO TJENG¹ — ¹MPI CPFS, Dresden, Germany — ²NYCU, Hsinchu, Taiwan — ³NSRRC, Hsinchu, Taiwan — ⁴NTU, Taipei, Taiwan — ⁵FAU, Erlangen, Germany

Soft X-ray ARPES measurements were performed on large single crystals of the metallic oxide LaNiO₃ along high symmetry directions, revealing the bulk electronic structure of the full valence band. The experimental Fermi surface is accurately reproduced by conventional band theories, whereas the nonzero frequency part of the spectra shows k -dependent renormalizations that cannot be explained by DFT even accounting for octahedral rotations and require true many-body methods to accurately explain.

TT 50.2 Thu 15:15 HSZ 03

Insights into the electronic structure of oxygen reduced and doped nickelates from core-level spectroscopy — •REBECCA PONS — Max-Planck Institut für Festkörperforschung, Stuttgart, Germany — Stewart Blusson Quantum Matter Institute, UBC Vancouver, Canada

With the observation of superconductivity in Sr-doped infinite-layer nickelate $\text{Nd}_{0.8}\text{Sr}_{0.2}\text{NiO}_2$ research interest in this material class intensified. We used ozone assisted molecular beam epitaxy to grow RNiO_3 thin films ($R=\text{La,Pr}$) and investigated the subsequent topotactic soft-chemistry reaction, needed to synthesize the square-planar phase, at different stages of reduction by x-ray absorption spectroscopy. We observe the evolution of the Ni oxidation state and that the process is laterally homogeneous down to length scales of 50 nm. To reach the superconducting phase hole doping of the infinite-layer nickelates is required with an optimal doping level around $x=0.2$. This can be achieved by self-doping in quintuple-layer Ruddlesden-Popper nickelates or alkaline-earth doping, Ca or Sr, in infinite-layer films. Using angle-resolved photoemission spectroscopy (ARPES) we studied changes in the Fermi surface upon alkaline-earth doping in $(\text{La,Ca})\text{NiO}_3$.

TT 50.3 Thu 15:30 HSZ 03

Thickness-dependent interface polarity in infinite-layer nickelate superlattices — •CHAO YANG¹, ROBERTO A. ORTIZ¹, YI WANG², WILFRIED SIGLE¹, HONGGUANG WANG¹, EVA BENCKISER¹, BERNHARD KEIMER¹, and PETER A. VAN AKEN¹ — ¹Max Planck Institute for Solid State Research, Stuttgart, 70569, Germany — ²Center for Microscopy and Analysis, Nanjing University of Aeronautics and Astronautics, Nanjing, 210016, P.R. China

The interface polarity plays a vital role in the physical properties of oxide hetero-interfaces, since it can enforce a reconstruction of the electronic and atomic structure. In the recently discovered superconducting nickelate thin films, interfacial effects could play an important role. This motivated our investigation of the electronic and atomic structure at the atomic scale at interfaces of infinite-layer nickelate thin films. Using four-dimensional scanning transmission electron microscopy (4D-STEM) and electron energy-loss spectroscopy (EELS), we systematically studied the effects of oxygen distribution and site occupancy, polyhedral distortion, elemental intermixing, as well as dimensionality on interface properties of infinite-layer $\text{NdNiO}_2/\text{SrTiO}_3$ superlattices. The oxygen intensity and distribution maps show the local symmetry change from octahedral to square planar induced by the reduction process and a gradual change of the oxygen content in the nickelate layers. Remarkably, we demonstrate spatially controlled interface polarity with accompanying interface reconstructions. Our results provide insights to understand the effects of polarity and dimensionality on the interface properties of infinite-layer nickelates.

TT 50.4 Thu 15:45 HSZ 03

GW+EDMFT investigation of $\text{Pr}_{1-x}\text{Sr}_x\text{NiO}_2$ under pressure — •VIKTOR CHRISTIANSSON, FRANCESCO PETOCCHI, and PHILIPP WERNER — University of Fribourg, Fribourg, Switzerland

The recent experimental observation of a large pressure effect on T_c in $\text{Pr}_{1-x}\text{Sr}_x\text{NiO}_2$ opens up an interesting prospect for reaching even higher values of T_c in the nickelates. On the theoretical side, systematic changes with pressure also provides a new possibility for probing the single- versus multi-orbital nature of these systems. In this talk, we discuss the electronic structure of this system as a function of pressure and doping, based on numerical calculations using self-consistent GW+EDMFT. We show that the normal state properties demonstrate a non-trivial interplay between physical pressure and chemical doping, and we find small but systematic changes with increasing pressure. The proper treatment of correlation effects, beyond density functional theory, is shown to play an important role in revealing these trends. While the pressure dependent changes of the undoped compound suggest a more single-orbital-like behavior towards the high-pressure regime, a qualitatively different behavior is observed for the doped system with a multi-orbital nature manifesting itself also at high pressures.

TT 50.5 Thu 16:00 HSZ 03

Nature of magnetic coupling in bulk infinite-layer nickelates versus cuprates — •ARMIN SAHINOVIC, BENJAMIN GEISLER, and ROSSITZA PENTCHEVA — Fakultät für Physik, Universität Duisburg-Essen

In contrast to cuprates, where the proximity of antiferromagnetism (AFM) and superconductivity is well established, first indications for AFM interactions in superconducting infinite-layer nickelates [1] were only recently obtained [2,3]. Here, we explore, based on first-principles simulations, the nature of the magnetic coupling in NdNiO_2 as a function of the on-site Coulomb and exchange interaction, varying the explicit hole doping and the treatment of the Nd 4f

electrons. The U - J phase diagrams for undoped nickelates and cuprates indicate G-type ordering, yet show different U dependency. By either Sr hole doping or explicit treatment of the Nd 4f electrons, we find a transition to a Ni C-type AFM ground state. We trace this back to a distinct response of the Ni vs. Cu e_g orbitals to the hole doping. The interaction between Nd 4f and Ni 3d spin stabilizes C-type AFM order on both sublattices. Though spin-orbit interactions induce a band splitting near the Fermi energy, the bad-metal state is retained under epitaxial strain. The magnetocrystalline anisotropy features an in-plane easy axis, related to the planar NiO_2 coordination. These results establish the nickelates as a unique platform to study unconventional superconductivity.

[1] D. Li et al., Nature 572, 624 (2019)

[2] J. Fowlie et al., Nature Physics 18, 1043 (2022)

[3] H. Lu et al., Science 373, 213 (2021)

TT 50.6 Thu 16:15 HSZ 03

Magnetic interactions in InNiO_3 compared to RNiO_3 — •ALEXANDER YARESKO, GRAHAM MCNALLY, MINU KIM, and HIDENORI TAKAGI — Max-Planck-Institut für Festkörperforschung, Stuttgart, Germany

RNiO_3 nickelates undergo with lowering temperature a metal-to-insulator (MIT) transition, accompanied by orthorhombic-to-monoclinic distortion of their crystal structure, and another transition at T_N to a magnetically ordered state with the ordering vector $\mathbf{q}=(1/2, 0, 1/2)$. Two Ni sites in the monoclinic unit cell are nonequivalent, with the average Ni_1 -O distance being significantly larger than Ni_2 -O. In compounds with the large radius of a R^{3+} ion the two transitions occur simultaneously. As the R size decreases, the crystal structure becomes more distorted. As a consequence, the MIT temperature increases while T_N decreases. Recently, a new InNiO_3 compound, in which an In^{3+} ion is even smaller than the smallest rare-earth Lu^{3+} , has been synthesized. We performed DFT(+ U) calculations for InNiO_3 and compare the results to other nickelates. In order to quantify the effect of structural distortions on the magnetic properties we estimated exchange interactions between magnetic Ni_i ions by mapping the energies of spin-spirals with different wave vectors \mathbf{q} to an effective Heisenberg model. We found that the strongest interactions are those along Ni_1 -O- Ni_2 -O- Ni_1 bonds but their strength decreases with increasing lattice distortions. The experimental $\mathbf{q}=(1/2, 0, 1/2)$ order can only be reproduced if a sufficiently small value of Coulomb repulsion U is used for more covalent Ni_2 ion.

TT 50.7 Thu 16:30 HSZ 03

Transport properties of $\text{Nd}_{1-x}\text{Sr}_x\text{NiO}_2$ based on a realistic 3-band model — •STEFFEN BÖTZEL, ILYA EREMIN, and FRANK LECHERMANN — Institut für theoretische Physik III, Ruhr-Universität Bochum, Bochum, Germany

Here, we consider theoretically the quasiparticle transport in the superconducting nickelate $\text{Nd}_{1-x}\text{Sr}_x\text{NiO}_2$ based on a realistic 3-band low-energy model derived from a first-principle approach [1]. The transport properties are obtained from the standard Kubo formalism. They depend on the band structure near the Fermi surface and are consequently a probe of the hitherto poorly understood low-energy electronic structure. We find significant contributions from different orbitals and bands depending on temperature and doping. Their interplay gives rise to multi-band characteristics, which are in accordance to available experimental data. This observation is important for the ongoing debate whether the low-energy physics is single- or multi-band like and points towards multi-band physics in these compounds.

[1] F. Lechermann, Phys. Rev. X 10, 041002 (2020)

TT 50.8 Thu 16:45 HSZ 03

High-pressure crystal growth and physical properties of Ruddlesden-Popper trilayer nickelates $\text{La}_4\text{Ni}_3\text{O}_{10}$ — •NING YUAN, KAUSTAV DEY, JAN ARNETH, AHMED ELGHANDOUR, and RÜDIGER KLINGELER — Kirchhoff Institute for Physics, Heidelberg University, Germany

Single crystals of $\text{La}_4\text{Ni}_3\text{O}_{10}$ were successfully grown by the high-pressure optical floating-zone method under 20 bar oxygen pressure. We investigate the different growth and post-annealing processes leading to two different polymorphs, namely $P2_1/a$ (No.14) and $Bmab$ (No.64), respectively, and report high-resolution thermal expansion, specific heat and magnetometry data on both of them. Our thermodynamic studies show sharp anomalies associated with the reported Metal-to-Metal Transition (MMT) in $\text{La}_4\text{Ni}_3\text{O}_{10}$ and distinct anisotropy. For the $P2_1/a$ phase, the MMT transition is found at 134 K while it appears at 152 K for $Bmab$. Our thermal expansion data in particular confirm that the MMT transition is associated with strong lattice changes (cf. [1]) but is also reveals clear contradictions to the published XRD data [2].

[1] D. Rout et al., Phys. Rev. B 102, 195144 (2020)

[2] J. Zhang et al., Phys. Rev. M 4, 083402 (2020)

TT 51: Correlated Electrons: Charge Order

Time: Thursday 15:00–17:30

Location: HSZ 103

TT 51.1 Thu 15:00 HSZ 103

The zoo of magnetic states in the 2D Hubbard model — •ROBIN SCHOLLE, PIETRO BONETTI, DEMETRIO VILARDI, and WALTER METZNER — MPI FKF Stuttgart

We use real-space Hartree-Fock theory to construct a magnetic phase diagram of the two-dimensional Hubbard model as a function of temperature and doping. We are able to detect various spin- and charge order patterns including Néel, stripe and spiral order without biasing the system towards one of them. For an intermediate interaction strength we predominantly find Néel order close to half-filling, stripe order for low temperatures or large doping, and an intermediate region of spiral order.

I will give a short summary of the method followed by a presentation of our current results and an outlook for possible further applications.

TT 51.2 Thu 15:15 HSZ 103

Effect of higher-order van Hove singularity on the formation of spin density waves — ALKISTIS ZERVOU¹, GARRY GOLDSTEIN², JOSEPH BETOURAS¹, and •DMITRY EFREMOV³ — ¹Department of Physics and Centre for the Science of Materials, Loughborough University, Loughborough LE11 3TU, UK. — ²Physics Department, Boston University, Boston MA 02215, USA — ³Leibniz Institute for Solid State and Materials Research Dresden, Helmholtzstrasse 20, D-01069 Dresden, Germany.

Van-Hove singularities in the density of states, which occur due to Lifshitz transitions in electronic band structures, affect different types of ordering in quantum materials. In addition to the usual Van Hove singularities, there are higher-order Van Hove singularities (HOVHS) with DOS divergence according to the power law. We find that the spin wave density and charge density of the phase formation can be enhanced by the presence of a singularity depending on the strength of certain interactions, with the critical temperature increasing by orders of magnitude. We discuss the application of our findings to various experimental systems such as Sr₃Ru₂O₇.

15 min. break

TT 51.3 Thu 15:45 HSZ 103

Kinetic theory of charge-density waves — •VIKTOR HAHN and PETER KOPIETZ — Institut für Theoretische Physik, Universität Frankfurt, Max-von-Laue Strasse 1, 60438 Frankfurt, Germany

We present a theoretical study of the dynamics of the collective amplitude and phase modes in the charge-density wave (CDW) state of the electronically quasi one-dimensional material K_{0.3}MoO₃ (blue bronze). For this purpose we formulate a kinetic theory using the method of expansion in connected equal-time correlations. Our kinetic equations for the CDW order parameter has the same form as the phenomenological equation of motion obtained within a time-dependent Ginzburg-Landau approach. From the numerical solution of our kinetic equations we extract the frequencies and the damping of the collective amplitude and phase modes in the CDW state. We find that the damping is strongly enhanced when the temperature approaches the critical temperature from below, in agreement with recent experiments.

TT 51.4 Thu 16:00 HSZ 103

Collective modes in the quasi one-dimensional charge-density wave material blue bronze — •MAX OBERON HANSEN — Goethe University, Frankfurt am Main, Germany

We calculate the spectrum of collective modes (amplitude, phase, phonon, and plasmon) in the charge-density wave state of the quasi-one dimensional metal K_{0.3}MoO₃, named blue bronze. Using a functional integral approach we derive effective actions for the different types of collective modes in Gaussian approximation and compare our results with experiments. Our approach emphasizes the role of acoustic phonons to guarantee that the phase mode remains gapless in the presence of long-range Coulomb interactions.

TT 51.5 Thu 16:15 HSZ 103

Lattice instability in charge-frustrated CsW₂O₆ — •PASCAL REISS¹, PETER WOCHNER¹, ARMIN SCHULZ¹, JÜRGEN NUSS¹, MASAHIKO ISOBE¹, and HIDE-NORI TAKAGI^{1,2,3} — ¹Max Planck Institute for Solid State Research, 70569 Stuttgart, Germany — ²Institute for Functional Matter and Quantum Technologies, University of Stuttgart, Germany — ³Department of Physics, The University of Tokyo, Bunkyo, Tokyo, Japan

The transition metal compound CsW₂O₆ represents an intriguing example of a pyrochlore structure at quarter filling. Starting from a bad metal with a nominal W^{5.5+} oxidation state, the system suffers a metal-to-insulator transition around $T_c \approx 215$ K. Here, a breathing distortion leads to the formation of regular molecular W₃ trimers with 2 localised electrons each, and a remaining W⁶⁺ site devoid

of 5d electrons [1]. However, the origin of the transition as well as the electronic nature of the low-temperature phase remain unclear [2].

To elucidate the origin of the 215 K transition, we will present our recent structural investigations and transport measurements on CsW₂O₆ conducted under high pressures, where we uncover another structural instability, distinct from the ambient pressure one.

[1] Y. Okamoto et al., Nat. Commun. 11 (2020)

[2] N. Nakai and C. Hotta, Nat. Commun. 13 (2022)

TT 51.6 Thu 16:30 HSZ 103

Pressure-induced stabilization mechanism of molecular orbital crystals in IrTe₂ — •TOBIAS RITSCHHEL¹, QUIRIN STAHL¹, MAXIMILIAN KUSCH¹, GASTON GARBARINO², VOLODYMYR SVITLYK², MOHAMED MEZOUAR², JUNJIE YANG³, SANG-WOOK CHEONG⁴, and JOCHEN GECK¹ — ¹Institute of Solid State and Materials Physics, TU Dresden, 01069 Dresden, Germany — ²ESRF, Grenoble, France — ³New Jersey Institute of Technology, Newark, New Jersey 01702, USA — ⁴Rutgers, New Jersey, USA

Doped IrTe₂ is considered a platform for topological superconductivity and therefore receives currently a lot of interest. In addition, the superconductivity in these materials exists in close vicinity to electronic order and the formation of molecular orbital crystals, which we explore here by means of high-pressure single crystal x-ray diffraction in combination with density functional theory. Our crystallographic refinements provide detailed information about the structural evolution as a function of applied pressure up to 42 GPa. Using this structural information for density functional theory calculations, we show that the local multicenter bonding in IrTe₂ is driven by changes in the Ir-Te-Ir bond angle. When the electronic order sets in, this bond angle decreases drastically, leading to a stabilization of a multicenter molecular orbital bond. This unusual local mechanism of bond formation in an itinerant material provides a natural explanation for the different electronic orders in IrTe₂. It further illustrates the strong coupling of the electrons with the lattice and is most likely relevant for the superconductivity in this material.

TT 51.7 Thu 16:45 HSZ 103

Lifshitz transition at the onset of superconductivity from mismatched nesting in TiSe₂ — •ROEMER HINLOPEN¹, OWEN MOULDING^{1,2}, FELIX FLICKER³, CHARLES SAYERS⁴, ENRICO DA COMO⁴, JASPER VAN WEZEL⁵, and SVEN FRIEDEMANN¹ — ¹University of Bristol, UK — ²Institut Néel, Grenoble, France — ³Cardiff University, UK — ⁴University of Bath, UK — ⁵University of Amsterdam, The Netherlands

Fermi surface reconstructions and topological (Lifshitz) transitions can have a profound effect on the electronic ground state of a metal. For example, re-entrant superconductivity (SC) in URhGe may be due to the appearance of a small pocket [1], whereas in Bechgaard salts [2] and doped BaFe₂As₂ [3] the appearance of large pockets from mismatched nesting may give rise to SC within the magnetic phase.

Here, we report quantum oscillation measurements and DFT calculations under pressure in the prototypical charge density wave (CDW) compound TiSe₂. We observe the emergence of new Fermi surface pockets at 2 GPa within the CDW arising as a result of mismatched nesting. This Lifshitz transition coincides with the emergence of superconductivity [4], suggesting an intimate link between SC and the presence of these Fermi pockets similar to BaFe₂As₂. This suggests that SC in TiSe₂ might be of extended s[±]-wave character - the first such case in a CDW system.

[1] Yelland, Nat. Phys. 7, 890 (2011)

[2] Bourbonnais, C. R. Physique 12, 532 (2011)

[3] Liu, Nat. Phys. 6, 419 (2010)

[4] Kusmartseva, PRL 103, 236401 (2009)

TT 51.8 Thu 17:00 HSZ 103

Spin stripe fluctuations in antiferromagnetic Pr_{2-x}Sr_xNiO_{4+δ} — •AVISHEK MAITY¹, RAJESH DUTTA^{2,3}, and WERNER PAULUS⁴ — ¹Heinz Maier-Leibnitz Zentrum (MLZ), Technische Universität München, 85747 Garching, Germany — ²Institut für Kristallographie, RWTH Aachen Universität, 52066 Aachen, Germany — ³Jülich Centre for Neutron Science (JCNS) at Heinz Maier-Leibnitz Zentrum (MLZ), 85747 Garching, Germany — ⁴ICGM, Univ. Montpellier, CNRS, ENSCM, Montpellier, France

Spin and charge stripe correlations and their dynamics have been well explored in the ordered state of RE-based 214-nickelates for last 3 decades. In this regards, what remains less explored is the fluctuating state of the spin stripes from which the long-range spin stripes develop on cooling. In this talk, we present our recent inelastic neutron scattering study of the low energy spin stripe fluctuations in Pr_{2-x}Sr_xNiO_{4+δ} with magnetic incommensurability $\epsilon = 0.33$ above the spin stripe ordering temperature $T_{so} = 190$ K [1]. The spin stripe fluctuations measured at the at the incommensurate wave vector show a non-

dispersive character with no detectable anisotropy persisting up to a maximum energy 10 meV, and strongly suppressed already below the charge stripe ordering temperature $T_{co} = 255$ K. Our results clearly indicate the presence of static charge stripe order is essential for the spin stripe fluctuations in 214-type nickelates.

[1] A. Maity *et al.*, Phys. Rev. B 106, 024414 (2022)

TT 51.9 Thu 17:15 HSZ 103

Glass-like transitions in the frustrated charge system θ -(BEDT-TTF) $_2$ MM'(SCN) $_4$ ($MM' = \text{CsZn, CsCo, and RbZn}$) revealed by thermal expansion measurements — •YOHEI SAITO¹, TATJANA THOMAS¹, YASSINE AGARMANI¹, TIM THYZEL¹, KENICHIRO HASHIMOTO², TAKAHIKO SASAKI^{2,3}, JENS MÜLLER¹, and MICHAEL LANG¹ — ¹Goethe University Frankfurt, Frankfurt (M), Germany — ²University of Tokyo, Chiba, Japan — ³Tohoku University, Sendai, Japan

Geometrical frustration causes degenerate states and a frustrated charge system is proposed in organic conductors. It is expected that charge order (CO) is suppressed and is possibly replaced by a charge glass state. In organic conductors, the CO transition accompanies a structural transition. Therefore, investigating their elastic properties is of fundamental interest. We performed thermal expansion measurements on θ -(BEDT-TTF) $_2$ MM'(SCN) $_4$ ($MM' = \text{CsZn, CsCo, and RbZn}$): whereas the CsZn and CsCo salts exhibit no CO transition, slowly-cooled RbZn salt shows the transition. The thermal expansion coefficient of no-CO salts exhibited a glassy transition at 90-100 K. This behavior is reminiscent of the freezing of the terminal ethylene end-groups on the BEDT-TTF molecules. For the RbZn salt we observe a CO transition at 210 K and also an ethylene-group related glass-like transition at 80-100 K. Therefore, the glass-like anomaly around 90 K appears as a common feature in θ -type salts regardless of whether long-range CO exists. These results point to the importance of the lattice degrees of freedom in the frustrated charge system.

TT 52: Frustrated Magnets: Strong Spin-Orbit Coupling

Time: Thursday 15:00–17:30

Location: HSZ 201

TT 52.1 Thu 15:00 HSZ 201

Finite temperature nonlinear optical response of the Kitaev magnet — •WOLFRAM BREINIG¹ and OLESIA KRUPNITSKA^{1,2} — ¹Institute for Theoretical Physics, Technical University Braunschweig, D-38106 Braunschweig, Germany — ²Institute for Condensed Matter Physics, NASU, Svientsitskii Str. 1, 79011 Lviv, Ukraine

One of the key properties of a quantum spin liquid is fractionalization. In the spin liquid hosted by the Kitaev model, this occurs in terms of two types of quasiparticles, i.e., itinerant Majorana fermions and localized gapped Z_2 fluxes. A multitude of probes have been suggested to provide evidence for the response and spectral continua related to such fractionalization. Here we report results on the nonlinear optical response of a Kitaev magnet at finite temperature. Our analysis is based on complementary calculations in the low-temperature homogeneous gauge and a mean-field treatment of thermal gauge fluctuations, valid at intermediate and high temperatures.

TT 52.2 Thu 15:15 HSZ 201

Thermal decomposition of the Kitaev material α -RuCl $_3$ and its influence on the low-temperature properties — •FRANZISKA BREITNER¹, ANTON JESCHE¹, VLADIMIR TSURKAN², and PHILIPP GEGENWART¹ — ¹Experimental Physics VI, Center for Electronic Correlations and Magnetism, University of Augsburg, 86159 Augsburg, Germany — ²Experimental Physics V, Center for Electronic Correlations and Magnetism, University of Augsburg, 86159 Augsburg, Germany

Thermally driven decomposition and reduction of honeycomb ruthenium-trichloride has been known long before the material attracted considerable interest as a Kitaev system [1,2]. We systematically explore the effect of heat treatment in argon atmosphere under various temperatures up to 500°C on single crystals by study of the mass loss, microprobe energy dispersive x-ray spectroscopy, powder x-ray diffraction, as well as low-temperature magnetic susceptibility and specific heat experiments. For annealing temperatures beyond 300°C we detect clear signatures of dechlorination and oxidation of Ru. The specific heat is consistently described by the sum of a major α -RuCl $_3$ and minor RuO $_2$ volume fraction, whose latter C~T contribution dominates the total specific heat below 1 K. Comparison with measurements on unannealed crystals suggests that even therein a tiny RuO $_2$ metal fraction cannot be excluded, which could be relevant also for other physical properties.

[1] A.E. Newkirk and D.W. McKee, J. Catal. 11, 370 (1968)

[2] J.A. Sears *et al.*, Phys. Rev. B 91, 144420 (2015)

TT 52.3 Thu 15:30 HSZ 201

Spin-phonon dynamics in α -RuCl $_3$ probed by ultrasound — •ANDREAS HAUSPURG^{1,2}, S. ZHERLITSYN¹, T. HELM¹, V. TSURKAN³, K. Y. CHOI⁴, S. H. DO⁵, W. BREINIG⁶, N. PERKINS⁷, and J. WOSNITZA^{1,2} — ¹Hochfeld-Magnetlabor Dresden, HZDR, Germany — ²Institut für Festkörper- und Materialphysik, TU Dresden, Germany — ³Institute of Physics, University of Augsburg, Germany — ⁴Department of Physics, Sungkyunkwan University, Republic of Korea — ⁵Oak Ridge National Lab, USA — ⁶Institute for Theoretical Physics, TU Braunschweig, Germany — ⁷School of Physics and Astronomy, University of Minnesota, USA

Among the most studied honeycomb-lattice materials predicted to host Kitaev interactions is the spin-orbit-coupled Mott insulator α -RuCl $_3$. Despite antiferromagnetic ordering at 7 K, α -RuCl $_3$ is considered proximate to the Kitaev quantum spin liquid (QSL) state, which features fractionalized quasiparticle excitations. A promising approach to study such excitations is to investigate the spin-phonon interaction in this material. Our studies of the elastic properties of α -RuCl $_3$ by means of ultrasound pulse-echo technique indicate unconventional physics of the debated QSL phase. Here, we present low-temperature results of

the sound velocity and attenuation in external magnetic fields and discuss their behavior with respect to the quasiparticle excitations in α -RuCl $_3$. In our studies we observed a linear temperature dependence of the attenuation beyond the ordered state at 8 T that follows a characteristic C_6 symmetry. Anomalies in the acoustic properties shed new light on the H - T phase diagram.

TT 52.4 Thu 15:45 HSZ 201

Rethinking α -RuCl $_3$ again — •MARIUS MÖLLER¹, ROSER VALENTÍ¹, and ALEXANDER L. CHERNYSHEV² — ¹Institute for Theoretical Physics, Goethe University Frankfurt, Max-von-Laue-Strasse 1, 60438 Frankfurt am Main, Germany — ²Department of Physics and Astronomy, University of California, Irvine, California 92697, USA

The honeycomb Kitaev material α -RuCl $_3$ is widely investigated due to its originally suspected proximity to a spin liquid state suggested by unusual neutron scattering results. The magnetic Hamiltonian was initially formulated as a generalized Kitaev model K_1 - J_1 - Γ_1 - Γ_1 - J_3 in a cubic spin reference orientated along the Ru-Cl bonds. Recent studies, however, suggest that a crystallographic parametrization of the Hamiltonian in a spin-ice-like language $J(XY)$ - Δ - $J_{\pm\pm}$ - $J_{z\pm}$ - J_3 could lead to significant reduction of the parameter space, hinting towards a potential minimal model of α -RuCl $_3$. We present the classical and quantum phase diagram of this $J(XY)$ - $J_{z\pm}$ - J_3 minimal model candidate obtained by Luttinger-Tisza method (LT), Exact Diagonalization (ED) and Density Matrix Renormalization Group (DMRG). Further, we present the phase diagrams of three interesting parameter regions with constrained anisotropic exchanges K_1 , Γ_1 , Γ_1' leading to effective J_1 - J_3 models which possibly capture the relevant region to describe the essential physics of α -RuCl $_3$.

M.M. and R.V. gratefully acknowledge funding by the DFG(German Research Foundation): TRR 288 - 422213477; M.M. gratefully acknowledges funding by Studienwerk Villigst.

TT 52.5 Thu 16:00 HSZ 201

Evolution of electronic and magnetic properties of the Kitaev-type compound Ru(Br $_{1-x}$ I $_x$) $_3$ — •JIHUAN GU¹, TOMOHIRO TAKAYAMA^{1,2}, ALEXANDER YARESKO¹, and HIDENORI TAKAGI^{1,2} — ¹Max-Planck Institute for Solid State Research, 70569 Stuttgart, Germany — ²Institut für Funktionelle Materie und Quantentechnologien, University of Stuttgart, 70550 Stuttgart, Germany

Kitaev magnets like α -RuCl $_3$ have attracted great attention in the field of solid-state physics as a potential realization of exotic quantum spin-liquid state. If such Kitaev materials are turned into a metallic state, exotic electronic properties may be realized near the critical phase boundary, such as unconventional superconductivity. So far, carrier doping via intercalation or application of pressure has been attempted to induce a metal-insulator transition (MIT), but no metallic state has been obtained. Recently, the two honeycomb compounds RuBr $_3$ and RuI $_3$, which are isostructural to α -RuCl $_3$, have been reported. While RuBr $_3$ is a Mott insulator with a zigzag magnetic order, RuI $_3$ was reported to be a correlated semimetal, likely induced by the enhanced d-p hybridization. Hence, the MIT phase boundary should be expected between RuBr $_3$ and RuI $_3$. We thus synthesized Ru(Br $_{1-x}$ I $_x$) $_3$ with various doping levels x . The successful substitution of Br with I was confirmed by the systematic change of lattice parameters. The MIT phase boundary seems to be at x around 0.7. We will discuss the evolution of electronic and magnetic properties in the series of Ru(Br $_{1-x}$ I $_x$) $_3$ and a marginal metallic state near MIT.

15 min. break

TT 52.6 Thu 16:30 HSZ 201

Milli-Kelvin thermal conductivity of YbAlO₃, a quasi-one-dimensional quantum magnet — •PARISA MOKHTARI^{1,2,3}, ULRIKE STOCKERT¹, STANISLAV NIKITIN⁴, LEONID VASYLECHKO⁵, MANUEL BRANDO², and ELENA HASSINGER¹ — ¹Institute of Solid State and Materials, Dresden, Germany — ²Max-Planck-Institute for Chemical Physics of Solids, Dresden, Germany — ³Physics Department, Technical University of Munich, Garching, Germany — ⁴Paul Scherrer Institute, Villigen, Switzerland — ⁵Lviv Polytechnic National University, Lviv, Ukraine

In 2019, Wu *et al.* found the typical excitation spectrum of the fractionalised magnetic excitations, so-called spinons, in the Q-1D material YbAlO₃ via neutron scattering at 1 K. YbAlO₃ exhibits AFM ($J_c=2.3$ K) and FM ($J_{ab}=0.8$ K) exchange interaction along and perpendicular to the chain direction, respectively [1, 2]. In zero field (B), a 3D AFM order is established at 0.88 K. For $B \parallel a$, this order is suppressed and replaced by an incommensurate-AFM state, until the field-polarised state occurs for $B > 1.5$ T.

In this work, we investigate the thermal conductivity (κ) of YbAlO₃ down to 30 mK in B up to 4 T, with a focus on the magnetic excitations' contribution in thermal transport within different phases and their interactions with lattice vibrations. Notably, our results are in agreement with the previous reports, as well as providing new anomalies compared to thermodynamics' probes and theoretical predictions.

[1] L. S. Wu *et al.*, Nat. Commun. 10, 698 (2019).

[2] L. S. Wu *et al.*, Phys. Rev. B 99, 195117 (2019).

TT 52.7 Thu 16:45 HSZ 201

Thermal expansion and magnetostriction as the probe of exotic magnetism in honeycomb BaCo₂(AsO₄)₂ — •PRASHANTA K. MUKHARJEE¹, BIN SHEN¹, ANTON JESCHE¹, JULIAN KAISER¹, PHILIPP GEGENWART¹, and ALEXANDER TSIRLIN² — ¹Experimental Physics VI, Center for Electronic Correlations and Magnetism, University of Augsburg, 86159 Augsburg, Germany — ²Felix Bloch Institute for Solid-State Physics, University of Leipzig, 04103 Leipzig, Germany

The 3d⁷ Co-based honeycomb materials have received wide attention as a possible platform for the experimental realization of the celebrated Kitaev model. Here, we elucidate the thermodynamic properties of the candidate material BaCo₂(AsO₄)₂ using high-resolution thermal expansion and magnetostriction measurements. At 2 K, with an increase in field, the linear magnetostriction coefficient shows two well-separated anomalies around critical field $H_{c1} \sim 0.2$ T and $H_{c2} \sim 0.5$ T transition around H_{c1} is hysteretic, pointing towards a first-order type transition, whereas the transition at H_{c2} lacks hysteresis, reflecting the second-order nature. The linear thermal expansion coefficient shows a sharp positive peak in 0 T, which decreases, then changes its sign with the rise in the field and smears out entirely above H_{c2} . Below T_N , for $H_{c1} \ll H \ll H_{c2}$, our angle-dependent magnetization shows an apparent six-fold symmetry, whereas significant deviations have been observed below H_{c1} and above H_{c2} . We draw the in-plane phase diagram from the above experiments and other complementary techniques and discuss the interplay of first and second-order transitions in this material.

TT 52.8 Thu 17:00 HSZ 201

Phononic-magnetic dichotomy of the thermal Hall effect in the Kitaev-Heisenberg candidate material Na₂Co₂TeO₆ — MATTHIAS GILLIG¹, XIAOCHEN HONG^{2,1}, CHRISTOPH WELLM¹, VLADISLAV KATAEV¹, WEILIANG YAO³, YUAN LI³, BERND BÜCHNER¹, and •CHRISTIAN HESS^{2,1} — ¹Leibniz Institute for Solid State and Materials Research, 01069 Dresden, Germany — ²Fakultät für Mathematik und Naturwissenschaften, Bergische Universität Wuppertal, 42097 Wuppertal, Germany — ³International Center for Quantum Materials, School of Physics, Peking University, 100871 Beijing, China

We investigate the thermal Hall effect of the Kitaev quantum spin liquid candidate material Na₂Co₂TeO₆ in both the magnetically ordered and the paramagnetic phase, with a magnetic field perpendicular to the honeycomb layers of this material. The transversal heat conductivity κ_{xy} is sizeable, but remains at all temperatures investigated significantly smaller than one half of the thermal conductance quantum which has been predicted as fingerprint of topologically protected Majorana edge modes in a Kitaev quantum spin liquid. κ_{xy} is negative in the paramagnetic phase but becomes positive deep in the antiferromagnetically ordered phase suggesting a non-phononic origin. However, distinct similarities are present in κ_{xy} and the longitudinal thermal conductivity κ_{xx} concerning both their temperature and field dependences. Thus our findings imply an at least two-component, i.e. magnetic and phononic origin of the thermal Hall effect in Na₂Co₂TeO₆.

TT 52.9 Thu 17:15 HSZ 201

Triple-Q order in Na₂Co₂TeO₆ from proximity to hidden-SU(2)-symmetric point — •WILHELM KRÜGER¹, WENJIE CHEN², XIANGHONG JIN², YUAN LI^{2,3}, and LUKAS JANSSEN¹ — ¹Institut für Theoretische Physik und Würzburg-Dresden Cluster of Excellence ct.qmat, TU Dresden, 01062 Dresden, Germany — ²International Center for Quantum Materials, School of Physics, Peking University, Beijing 100871, China — ³Collaborative Innovation Center of Quantum Matter, Beijing 100871, China

In extended Heisenberg-Kitaev-Gamma-type spin models, hidden-SU(2)-symmetric points are isolated points in parameter space that can be mapped to pure Heisenberg models via nontrivial duality transformations. Such points generically feature quantum degeneracy between conventional single-Q and exotic multi-Q states. We argue that recent single-crystal inelastic neutron scattering data place the honeycomb magnet Na₂Co₂TeO₆ in proximity to such a hidden-SU(2)-symmetric point. The low-temperature order is identified as a triple-Q state arising from the Néel antiferromagnet with staggered magnetization in the out-of-plane direction via a 4-sublattice duality transformation. This state naturally explains various distinctive features of the magnetic excitation spectrum, including its surprisingly high symmetry and the dispersive low-energy and flat high-energy bands. Our result demonstrates the importance of bond-dependent exchange interactions in cobaltates, and illustrates the intriguing magnetic behavior resulting from them.

TT 53: Graphene

Time: Thursday 15:00–17:45

Location: HSZ 204

TT 53.1 Thu 15:00 HSZ 204

Andreev and normal reflections processes in gated bilayer graphene — •PANCH RAM¹, DETLEF BECKMANN², ROMAIN DANNEAU², and WOLFGANG BELZIG¹ — ¹Fachbereich Physik, Universität Konstanz, D-78457 Konstanz, Germany — ²Institute for Quantum Materials and Technologies, Karlsruhe Institute of Technology, D-76021 Karlsruhe, Germany

We present our theoretical study of the Andreev and normal reflections processes in a bilayer graphene normal-superconductor junction where gate fields are applied (equal and opposite). Gating can induce a gap in the dispersion of the graphene layer. We employ the Dirac-Bogoliubov-de Gennes equation for the low-energy gated bilayer graphene Hamiltonian and calculate the Andreev and normal reflections probabilities using the scattering theory, and also obtain the differential conductance within the Blonder-Tinkham-Klapwijk formalism [1, 2]. We observe the Andreev retro-reflection (specular-reflection) below (above) the Fermi energy when the bias voltage is within the superconducting gap [3]. Interestingly, both retro-reflection as well as specular reflection are strongly modified in the presence of the gate field. For small gate field, they can be tuned to either specular or retro Andreev reflection by changing the Fermi energy. Moreover, we find double Andreev reflections and double normal reflections (specular and retro) when the gate field becomes comparable to the interlayer coupling strength.

[1] A. F. Andreev, Sov. Phys. JETP 19, 1228 (1964)

[2] G. E. Blonder *et al.*, Phys. Rev. B 25, 4515 (1984)

[3] C. W. J. Beenakker, Phys. Rev. Lett. 97, 067007 (2006)

TT 53.2 Thu 15:15 HSZ 204

Graphene superlattice due to twisted hexagonal boron nitride monolayers — •MING-HAO LIU — Department of Physics, National Cheng Kung University, Tainan 70101, Taiwan

Stacking of two-dimensional (2D) materials of similar lattice structures on top of each other with a small twist angle leads to the so-called Moiré pattern due to the large-scale lattice interference. When one of them is a conducting material such as graphene, the Moiré pattern serves as a large-scale periodic potential, turning the host conducting lattice into a superlattice, whose modified electronic properties can be seen in transport experiments and simulations. Graphene placed on a hexagonal boron nitride (hBN) layer is one of the best known graphene superlattices, while twisted bilayer graphene made of two monolayers of graphene is another example under intensive investigations during the past years. Twisted monolayers of hBN also form the Moiré pattern, yet its effect on transport properties of neighboring graphene is less known. Here, we consider graphene put on monolayers of twisted hBN (thBN), and perform quantum transport simulations considering the effect of the charge-polarized superlattice potential [1]. Due to the exceptionally long Moiré wavelength of the twisted hBN, multiple satellite Dirac points emerge in the transmission spectrum within the experimentally accessible range of the carrier density. Possible experiments confirming the model of graphene on thBN as well as further exploring novel transport behaviors due to the thBN will be discussed.

[1] C. R. Woods *et al.*, Nat. Commun. 12, 347 (2021)

TT 53.3 Thu 15:30 HSZ 204

Transport signatures of Van Hove singularities in mesoscopic twisted bilayer graphene — •ALEKSANDER SANJUAN CIEPIELEWSKI¹, JAKUB TWORZYDŁO², TIMO HYART^{1,3}, and ALEXANDER LAU¹ — ¹MagTop, IF PAN, Warsaw, Poland — ²University of Warsaw, Poland — ³Aalto University, Finland

Magic-angle twisted bilayer graphene (TBG) exhibits quasiflat low-energy bands with Van Hove singularities (VHS) close to the Fermi level. These singularities play an important role in the exotic phenomena observed in this material, such as superconductivity and magnetism, by amplifying electronic correlation effects. In this work [1], we study the correspondence of four-terminal conductance and the Fermi surface topology as a function of the twist angle, pressure, and energy in mesoscopic, ballistic samples of small-angle TBG. We establish a correspondence between features in the wide-junction conductance and the presence of VHS in the density of states. Moreover, we identify additional transport features, such as a large, pressure-tunable minimal conductance, conductance peaks coinciding with nonsingular band crossings, and unusually large conductance oscillations as a function of the system size. Our results suggest that TBG close the magic angle is a unique system featuring simultaneously large conductance due to the quasiflat bands, strong quantum nonlinearity due to the VHS, and high sensitivity to external parameters, which could be utilized in high-frequency device applications and sensitive detectors.

[1] A. Sanjuan Ciepielewski, J. Tworzydło, T. Hyart, and A. Lau, Phys. Rev. Research 4, 043145 (2022)

TT 53.4 Thu 15:45 HSZ 204

Coulomb blockade effects in minimally twisted bilayer graphene — •PATRICK WITTIG¹, FERNANDO DOMINGUEZ¹, CHRISTOPHE DE BEULE^{2,3}, and PATRIK RECHER^{1,4} — ¹Institute for Mathematical Physics, TU Braunschweig, 38106 Braunschweig, Germany — ²Department of Physics and Materials Science, University of Luxembourg, L-1511 Luxembourg — ³Department of Physics and Astronomy, University of Pennsylvania, Philadelphia PA19104 — ⁴Laboratory of Emerging Nanometrology, 38106 Braunschweig, Germany

In the presence of a finite interlayer electric field, minimally twisted bilayer graphene displays a triangular network of chiral valley Hall states that propagate along the AB/BA interfaces and scatter at the metallic AA regions. Previous studies model the chiral network using a phenomenological scattering matrix approach based entirely on the symmetries of the system [1,3]. So far, the physics of the metallic AA scattering regions has been disregarded, although in the chiral network regime are also flat bands corresponding to a finite density of states in the AA region [2]. Therefore, we include in the phenomenological scattering matrix the AA regions in form of quantum dots: A set of discrete energy levels with Coulomb interaction, which we treat in mean field theory. We study the resulting network through the energy spectrum and magneto-conductance calculations.

[1] D. Efimkin, A. MacDonald, PRB 98, 035404 (2018)

[2] A. Ramires, J. Lado, PRL 121, 146801 (2018)

[3] C. De Beule, F. Dominguez, P. Recher, PRL 125, 096402, (2020)

TT 53.5 Thu 16:00 HSZ 204

Twisted bilayer graphene at charge neutrality: Spontaneous symmetry breaking of SU(4) Dirac electrons — •NIKOLAOS PARTHENIOS and LAURA CLASSEN — Max-Planck Institute for Solid State Research, Stuttgart, Germany

We study possible patterns for spontaneous symmetry breaking in twisted bilayer graphene at charge neutrality. Starting from an effective Dirac Hamiltonian, we show how an SU(4) symmetry emerges that is composed of combined spin, valley and sublattice transformations. We construct the corresponding low-energy model that includes all symmetry-allowed four-fermion interactions and employ a renormalization group treatment to identify the critical points that describe transitions into the different ordered phases. The resulting phase diagram depends on the number of fermion flavours and we argue that for twisted bilayer graphene it is governed by a quantum Hall state or SU(4) manifolds of spin-valley orders with emergent Lorentz symmetry. Due to the large symmetry, small perturbations will determine the final symmetry breaking mechanism.

TT 53.6 Thu 16:15 HSZ 204

Analog gravity in twisted bilayer graphene — •MIREIA TOLOSA-SIMEÓN¹, STEFAN FLOERCHINGER², and MICHAEL SCHERER¹ — ¹Institut für Theoretische Physik III, Ruhr-Universität Bochum — ²Theoretisch-Physikalisches Institut, Friedrich-Schiller-Universität Jena

Condensed-matter systems can sometimes be used to emulate and study phenomena from a completely different field of physics, for example, from elementary particle physics or gravity. Such analog condensed-matter models may provide a novel perspective to approach difficult problems in the original systems, and can potentially be realized experimentally in a well-controlled environment.

In this contribution, we will address the problem of cosmological fermion production in expanding universes using twisted bilayer graphene as an analog model. In particular, we study twisted bilayer graphene's Dirac electrons near charge neutrality, which acquire a mass gap through a symmetry-breaking phase transition. Introducing a time-dependent Fermi velocity, we show the emergence

of an analog of cosmological pair production. Our scenario could be scrutinized experimentally in the future.

15 min. break

TT 53.7 Thu 16:45 HSZ 204

Quantum transport simulation for graphene on transition-metal dichalcogenides — •WUN-HAO KANG and MING-HAO LIU — Department of Physics, National Cheng Kung University, Tainan, Taiwan

The strength of spin-orbit coupling (SOC) in pristine graphene was found from first-principles calculations to be in the order of μeV [1], which gives nearly no effects in transport experiments. Subsequent studies showed that the SOC can be significantly enhanced to the order of meV by putting graphene on transition-metal dichalcogenides (TMDC) [2]. Very recently, Tiwari P. et al. reported that the enhanced SOC can be experimentally observed in graphene/WSe₂ systems [3]. Here we perform quantum transport simulations for graphene on TMDCs based on real-space tight-binding models [4], considering the Fabry-Pérot interferometer by using a gate-induced potential barrier as the cavity.

[1] M. Gmitra et al., Phys. Rev. B 80, 235431 (2009)

[2] M. Gmitra et al., Phys. Rev. B 93, 155104 (2016)

[3] P. Tiwari et al., npj 2D Mater Appl. 6, 68 (2022)

[4] M. Zubair et al., Phys. Rev. B 101, 165436 (2020)

TT 53.8 Thu 17:00 HSZ 204

Theory of broken symmetry quantum Hall states in the $N = 1$ Landau level of Graphene — •NIKOLAOS STEFANIDIS¹ and INTI SODEMANN^{2,1} — ¹Max-Planck-Institut für Physik komplexer Systeme, Dresden 01187, Germany — ²Institut für Theoretische Physik, Universität Leipzig, D-04103, Leipzig, Germany

We study many-body ground states for the partial integer fillings of the $N = 1$ Landau level in graphene, by constructing a model that accounts for the lattice scale corrections to the Coulomb interactions. Interestingly, in contrast to the $N = 0$ Landau level, this model contains not only pure delta function interactions but also some of its derivatives. Due to this we find several important differences with respect to the $N = 0$ Landau level. For example at quarter filling when only a single component is filled, there is a degeneracy lifting of the quantum hall ferromagnets and ground states with entangled spin and valley degrees of freedom can become favourable. Moreover at half-filling of the $N = 1$ Landau level, we have found a new phase that is absent in the $N = 0$ Landau level, that combines characteristics of the Kekulé state and an antiferromagnet. We also find that according to the parameters extracted in a recent experiment, at half-filling of the $N = 1$ Landau level graphene is expected to be in a delicate competition between an AF and a CDW state, but we also discuss why the models for these recent experiments might be missing some important terms.

TT 53.9 Thu 17:15 HSZ 204

Multi-layered atomic relaxation in van der Waals heterostructures — DORRI HALBERTAL¹, •LENNART KLEBL², VALERIE HSIEH¹, JACOB COOK³, STEPHEN CARR⁴, GUANG BIAN³, CORY DEAN¹, DANTE M. KENNES^{5,6}, and DMITRI N. BASOV¹ — ¹Department of Physics, Columbia University, United States — ²1st Institute of Theoretical Physics, University of Hamburg, Germany — ³Department of Physics and Astronomy, University of Missouri, United States — ⁴Physics Department, Brown University, United States — ⁵Institut für Theorie der Statistischen Physik, RWTH Aachen University, Germany — ⁶Max Planck Institute for the Structure and Dynamics of Matter, Hamburg, Germany

When two-dimensional van der Waals materials are stacked to build heterostructures, Moiré patterns emerge from twisted interfaces or from mismatch in lattice constant of individual layers. Relaxation of the atomic positions is a direct, generic consequence of the Moiré pattern, with many implications for the physical properties. Motivated by experimental findings in multi-layered van der Waals heterostructures, we develop a generic continuum approach to model (multi-layered) relaxation processes based on the generalized stacking fault energy functional. The continuum property of the approach enables us to access large scale regimes and achieve agreement with experimental findings. Furthermore, we study the impact of multi-layered relaxation on the local density of states of a twisted graphitic system. We identify measurable implications for the system, experimentally accessible by scanning tunneling microscopy.

TT 53.10 Thu 17:30 HSZ 204

Non-destructive low-temperature contacts to MoS₂ nanoribbon and nanotube quantum dots — •ROBIN T. K. SCHOCK¹, JONATHAN NEUWALD¹, KONSTANTIN D. SCHNEIDER¹, MATTHIAS KRONSEDER¹, LUKA PIRKER², MAJA REMŠKAR², and ANDREAS K. HÜTTEL¹ — ¹Institute for Experimental and Applied Physics, University of Regensburg, 93040 Regensburg, Germany — ²Solid State Physics Department, Institute Jožef Stefan, 1000 Ljubljana, Slovenia

Planar TMDCs are at the center of manifold research efforts due to their intrinsic two dimensional nature. Despite detailed studies of their optical parameters, worldwide efforts to reach single level transport in lithographically designed quantum dots at low temperatures have so far been largely unsuccessful. This is due to the requirement for very small confinement potentials as well as disorder

from dangling bonds at the edges of nanoflakes. Both issues can be circumvented by using as-grown MoS₂ nanotubes and nanoribbons. First Coulomb blockade measurements were recently performed on a MoS₂ nanotube[1], so far limited by disorder below the metallic scandium contacts.

Here, we present low temperature measurements on MoS₂ nanotubes and nanoribbons contacted with bismuth[2]. Our data clearly shows the non-

destructive and transparent nature of these contacts to our quantum dots and indicates quantum confinement[3].

[1] S. Reinhardt *et al.*, pssRRL **13**, 1900251 (2019)

[2] P. C. Shen *et al.*, Nature **593**, 211 (2021)

[3] R. T. K. Schock *et al.*, arXiv:2209.15515 (2022).

TT 54: Quantum Coherence and Quantum Information Systems II

Time: Thursday 15:00–17:45

Location: HSZ 304

TT 54.1 Thu 15:00 HSZ 304

Dominant materials losses in superconducting circuits based on tantalum thin films — •RITIKA DHUNDHWAL¹, HAORAN DUAN², DIRK FUCHS¹, ALEXANDER WELLE³, MAHYA KHORRAMSHAHI¹, JASMIN AGHASSI-HAGMANN², IOAN M. POP¹, and THOMAS REISINGER¹ — ¹Institut für Quantenmaterialien und Technologien — ²Institut für Nanotechnologie — ³Institut für Funktionelle Grenzflächen, Karlsruher Institut für Technologie

Superconducting quantum circuits are a promising hardware platform in the fields of quantum computing and detection. To improve their performance, exploring new materials is highly relevant. One promising candidate material is tantalum (Ta), which was recently shown to improve transmon qubit lifetimes[1]. However, the understanding of the dominant loss mechanisms related to Ta is limited. Here, we present a study of losses in epitaxial Ta films deposited using magnetron sputtering, with the aim of relating basic material properties to loss mechanisms. A variation in the deposition parameters (mainly substrate temperature) leads to structurally different films. We characterized these using high-resolution X-ray diffraction, Time-of-Flight secondary-ion mass spectrometry, scanning electron microscopy and superconducting transition temperature measurements. We fabricated lumped element resonators from the films and measured their quality factors as a function of photon number and temperature. In addition, we vary the energy participation ratio of Ta metal-substrate interface to find the dominant loss mechanism.

[1] A. P. M. Place *et al.*, Nat. Commun. **12**, 1779 (2021)

TT 54.2 Thu 15:15 HSZ 304

Many body localization of 2D transmon arrays with a quasi-periodic potential and perturbative Walsh-Hadamard coefficients — •EVANGELOS VARVELIS and DAVID DIVINCENZO — JARA, Aachen, Germany

Recently it has been shown that transmon qubit architectures experience a phase transition between many body localized and quantum chaotic. It is crucial for quantum computation that the system remains in the localized regime, yet the most common way to achieve this relies on random disorder. Here we propose a quasi-periodic potential as a substitute for random disorder, with the purpose of localizing a 2D transmon array. We demonstrate, using the Walsh-Hadamard diagnostic, that the quasiperiodic potential is more effective at achieving localization. In order to study the localizing properties of our new potential for experimentally relevant system sizes, we develop a many-body perturbation theory whose computational cost scales only with the non-interacting system dimensions.

TT 54.3 Thu 15:30 HSZ 304

Linear response for pseudo-Hermitian Hamiltonian systems: Application to PT -symmetric qubits — •MIKHAIL V. FISTUL, LEANDER TETLING, and ILYA M. EREMIN — Ruhr-Universität Bochum, Bochum Germany

We develop the linear response theory formulation suitable for application to various *pseudo-Hermitian Hamiltonian* systems. The analytical expressions for the generalized temporal quantum-mechanical correlation function and the time-dependent dynamic susceptibility, $\chi(t)$, are derived [1].

We apply our results to two PT -symmetric non-Hermitian quantum systems: a single qubit and two unbiased/biased qubits coupled by the exchange interaction. For both systems we identify PT -symmetry unbroken and broken quantum phases and quantum phase transitions between them. The temporal oscillations of the dynamic susceptibility of the qubits polarization, $\chi(t)$, relate to *ac* induced transitions between different eigenstates, and we analyze the dependencies of the oscillations frequency and the amplitude on the gain/loss parameter γ and the interaction strength g .

Studying the time dependence of $\chi(t)$ we observe different types of oscillations, i.e., undamped, heavily damped and amplified ones, related to the transitions between eigenstates with broken (unbroken) PT -symmetry. These predictions can be verified in the microwave transmission experiments.

[1] L. Tetling, M. V. Fistul, and I. M. Eremin, Phys. Rev. B **106**, 134511 (2022).

TT 54.4 Thu 15:45 HSZ 304

High kinetic inductance microstrip networks for integrated quantum information devices — •NIKLAS GAISER¹, CIPRIAN PADURARIU¹, BJÖRN KUBALA^{1,2}, NADAV KATZ³, and JOACHIM ANKERHOLD¹ — ¹ICQ and IQST, University of Ulm, Ulm, Germany — ²Institute of Quantum Technologies, German Aerospace Center (DLR), Ulm, Germany — ³The Racah Institute of Physics, The Hebrew University of Jerusalem, Israel

Modern superconducting quantum information devices integrate qubits and readout resonators into complex microwave circuits. Efficient qubit operation and fast readout require relatively strong coupling. This, however, can compromise the qubit lifetime due to spontaneous emission through the resonator. An elegant solution is provided by a Purcell filter, an added circuit element that suppresses transmission at the qubit frequency.

Here, we present a theoretical proposal for circuit architectures that realize qubit readout with Purcell filters, utilizing the highly versatile platform of high-kinetic inductance microstrip networks experimentally realized in [1]. The strongly reduced phase velocities in such materials allow compact filter designs that can be integrated on-chip. We describe band-structure design techniques to build an efficient Purcell filter and provide quantitative estimations for the suppression of unwanted relaxation channels.

[1] S. Goldstein, G. Pardo, N. Kirsh, N. Gaiser, C. Padurariu, B. Kubala, J. Ankerhold, and N. Katz, New J. Phys. **24** 023022 (2022)

TT 54.5 Thu 16:00 HSZ 304

Microwave radiation emitted by a phase qubit — •SURANGANA SENGUPTA¹, CIPRIAN PADURARIU¹, BJOERN KUBALA^{1,2}, and JOACHIM ANKERHOLD¹ — ¹ICQ and IQST, Ulm University, Germany — ²German Aerospace Center (DLR), Ulm, Germany

Josephson photonics devices consist of a DC-biased Josephson junction in series with a superconducting microwave cavity and are promising sources of bright quantum states of microwave radiation. Such devices realize the regime of strong-coupling circuit quantum electrodynamics, when the effective fine structure constant of the circuit approaches unity. In this case, multi-photon down-conversion processes, where one tunnelling Cooper pair emits k photons in the cavity ($k \leq 6$), have been observed [1].

Here, we propose a new regime for Josephson photonics devices, where both the inductive as well as the capacitive behavior of the Josephson junction is taken into account [2]. Thereby, the Josephson phase is treated as an electronic degree of freedom, characterized by the plasma frequency of the junction, that is independent of the photonic degree of freedom, described by the phase of the cavity. We present a preliminary study of the coupled photonic and electronic dynamics, discuss the nature of the coupling and present a detailed comparison to conventional Josephson photonics dynamics. As an example, we focus on the case when the Josephson junction is operated as a phase qubit and study the resulting statistics of radiation emitted in the cavity.

[1] G. C. Ménard *et al.*, Phys. Rev. X **12**, 021006 (2022)

[2] C. Yan *et al.*, Nat. Electron. **4**, 885-892 (2021)

15 min. break

TT 54.6 Thu 16:30 HSZ 304

Heat transport and rectification in an ultrastrongly-coupled qubit-resonator system — •LUCA MAGAZZU¹, MILENA GRIFONI¹, and ELISABETTA PALADINO² — ¹Regensburg University — ²University of Catania

Inspired by the recent experimental developments in the field of heat transport in the quantum regime, we consider a flux qubit coupled to a superconducting resonator as a composite open quantum system.

The two elements of this open quantum Rabi system interact with two heat baths held at different temperatures. At the steady state, a heat current is established which is the result of photon exchanges between the system and the baths. Due to the geometry of the setup, the coupling to the heat baths is asymmetric. In turn this entails the presence of a preferred direction for the heat current, to a degree quantified by the heat rectification.

We calculate the heat current and rectification in different coupling regimes and considering a periodic driving applied to the qubit. The rectification displays

the signatures of multi-photon processes that occur when the qubit-resonator coupling enters the nonperturbative regime.

[1] A. Ronzani *et al.*, Nat. Phys. 14, 991 (2018)

[2] J. Senior, A. Gubaydullin, B. Karimi, J. T. Peltonen, J. Ankerhold, and J. P. Pekola, Commun. Phys. 3, 40 (2020)

[3] B. Bhandari, P. Andrea Erdman, R. Fazio, E. Paladino, and F. Taddei, Phys. Rev. B 103, 155434 (2021)

[4] L. Tesser, B. Bhandari, P. A. Erdman, R. Fazio, E. Paladino, and F. Taddei, New J. Phys. 24, 035001 (2022)

TT 54.7 Thu 16:45 HSZ 304

Qubit reset using frequency modulation by AC Stark effect — •JAMI RÖNKKÖ, VASILII SEVRIUK, ANTTI VEPSÄLÄINEN, and FABIAN MARXER — IQM Quantum Computers, Espoo, Finland

We present a theory for an unconditional reset scheme utilizing qubit's frequency modulation by AC Stark effect and a coupled lossy resonator. In AC Stark effect, off-resonant microwave drive shifts the frequency of a qubit without causing strong Rabi oscillations. Modulating the frequency of this drive creates sidebands around the qubit frequency. By setting the modulation frequency equal to the difference between the qubit and resonator frequencies, one of the sidebands becomes resonant with the resonator frequency. This leads to the transfer of the qubit excitation to the lossy resonator, resulting in a qubit reset. With typical parameters, the reset is achieved in only tens of nanoseconds

TT 54.8 Thu 17:00 HSZ 304

Fabrication of a superconducting transmission line in a planar design on a spin-doped crystalline membrane — •GEORG MAIR^{1,2}, ANA STRINIC^{1,2,3}, NIKLAS BRUCKMOSER^{1,2}, MICHAEL STANGER¹, ANDREAS ERB^{1,2}, RUDOLF GROSS^{1,2,3}, and NADEZHDA KUKHARCHYK^{1,2,3} — ¹Technical University of Munich, TUM School of Natural Sciences, Physics Department, 85747 Garching, Germany — ²Walther-Meißner-Institut, Bayerische Akademie der Wissenschaften, 85748 Garching, Germany — ³Munich Center for Quantum Science and Technology, 80799 Munich, Germany

Scaling up the density of superconducting qubits on a chip is reaching its limits, and a supplementing microwave quantum memory is a promising way to enhance the computing power [1]. Rare-earth doped crystals are potential candidates to realize such microwave quantum memories, due to the long coherence times of their spin states [2]. For efficient operation, one needs to have precise control over the distribution of strength and orientation of the oscillating magnetic field inside the sample. Here, we introduce a novel, planar superconducting transmission line design based on a thin crystalline CaWO₄ membrane. The transmission line is designed to exhibit high transmission in the range of 1 – 8 GHz, i.e. the frequency range of the hyperfine transitions of the rare-earth ions in near-zero external magnetic field. Fabrication techniques are explained and transmission spectra recorded at cryogenic temperatures are discussed.

[1] É. Gouzien and N. Sangouard, Phys. Rev. Lett. 127, 140503 (2021)

[2] N. Kukharchyk *et al.* New J. Phys. 20, 023044 (2018)

TT 54.9 Thu 17:15 HSZ 304

Quantum state storage in spin ensembles — •PATRICIA OEHL^{1,2}, JULIAN FRANZ^{1,2}, MANUEL MÜLLER^{1,2}, NADEZHDA KUKHARCHYK^{1,2,3}, KIRILL G. FEDOROV^{1,2}, RUDOLF GROSS^{1,2,3}, and HANS HUEBL^{1,2,3} — ¹Walther-Meißner-Institut, Bayerische Akademie der Wissenschaften, Garching, Germany — ²Technical University of Munich, TUM School of Natural Sciences, Physics Department, Garching, Germany — ³Munich Center for Quantum Science and Technologies (MCQST), Munich, Germany

The storage of quantum states is considered as a key element for successful realization of a multimode quantum network, enabling various applications, such as secure communication and distributed quantum computing [1]. In order to allow for connection of multiple quantum nodes without frequency conversion, several requirements have to be met, such as frequency compatibility and connectivity between chosen quantum systems. As superconducting quantum circuits operate in the microwave regime, solid-state spin ensembles with their exceptional coherence times are promising candidates [2]. Here, we present a hybrid system consisting of a superconducting lumped-element microwave resonator coupled to a phosphorus donor electron spin ensemble hosted in isotopically engineered silicon. We show experimental results toward the storage of quantum states and their retrieval based on Hahn-echo type pulse sequences.

We acknowledge financial support from the Federal Ministry of Education and Research of Germany (project number 16KISQ036).

[1] M. Pompili *et al.*, Science 372, 6539 (2021)

[2] M. Steger *et al.*, Science 336, 1280 (2012)

TT 54.10 Thu 17:30 HSZ 304

Broadband electron spin resonance spectroscopy of rare earth spin ensembles at mK temperatures — •ANA STRINIC^{1,2,3}, HANS HUEBL^{1,2,3}, RUDOLF GROSS^{1,2,3}, and NADEZHDA KUKHARCHYK^{2,1,3} — ¹Technical University of Munich, TUM School of Natural Sciences, Physics Department, Garching, Germany — ²Walther-Meißner-Institut, Bavarian Academy of Sciences, Garching, Germany — ³Munich Center for Quantum Science and Technologies, Munich, Germany

Rare earth spin ensembles exhibit spin coherence times in the millisecond range and possess transitions at microwave frequencies [1,2]. These properties make them attractive candidates for realizing microwave quantum memories, which can be directly interfaced with superconducting quantum processors. In principle, there are two options for the implementation of spin-based quantum memories: (i) coupling them to resonators, or (ii) interfacing them with an open transmission line. In particular, the latter is considered for multi-modal concepts or the storage of information based on atomic frequency comb protocols. In this work we characterize the electron spin resonance Hamiltonian of an ¹⁶⁷Er spin ensemble in a ⁷LiYF₄ host crystal at mK temperatures using a broadband microwave spectroscopy approach. We find good agreement with published g and hyperfine tensors, which is key for the implementation of microwave quantum memory schemes at low magnetic fields.

[1] P.-Y. Li *et al.*, Phys. Rev. Appl. 13, 024080 (2020)

[2] A. Ortu *et al.*, Nat. Mater. 17, 671 (2018)

TT 55: Dynamics and Chaos in Many-Body Systems I (joint session DY/TT)

Time: Thursday 15:00–17:30

Location: MOL 213

TT 55.1 Thu 15:00 MOL 213

Imperfect Many-Body Localization in Exchange-Disordered Isotropic Spin Chains — •JULIAN SIEGL and JOHN SCHLIEMANN — University of Regensburg
We study many-body localization in isotropic Heisenberg spin chains with the local exchange parameters being subject to quenched disorder. The Hamiltonian is invariant under global SU(2)-rotations and incorporates therefore a non-abelian symmetry. Systems of common spin length 1/2 and 1 are studied numerically using random matrix techniques. In both cases we find a transition from an ergodic phase at small disorder strength to an incompletely localized phase at stronger disorder. The transition is signaled by a maximum of the sample-to-sample variance of the averaged consecutive-gap ratio. The incompletely localized phase found here is distinguished from a fully localized system by the scaling behavior of the sample-to-sample variance.

TT 55.2 Thu 15:15 MOL 213

Magnetic Dipole Clusters - Resurrection of Catastrophe Machines — •INGO REHBERG and SIMEON VÖLKELEL — Experimental Physics, University of Bayreuth
Hysteretic transitions between stable configurations of a hexagonal magnetic dipole cluster [1] are set in a broader context by revealing the nature of the corresponding instabilities [2]. Following the animation of this bifurcation scenario [3], we present an experimental setup where the height of the centre dipole serves as the bifurcation parameter. This catastrophe machine demonstrates the two instabilities forming the hysteresis loop, and it might provide a hint to the unresolved puzzle of the slowing down of one of the eigenmodes [4].

[1] Andrew D.P. Smith *et al.*, JMMM 549, 168991 (2022).

[2] Simeon Völkel *et al.*, JMMM 559, 169520 (2022).

[3] <https://doi.org/10.5281/zenodo.6380539> (18.5.2022).

[4] Peter T. Haugen *et al.*, Chaos 32, 063108 (2022).

TT 55.3 Thu 15:30 MOL 213

Signatures of the interplay between chaos and local criticality on the dynamics of scrambling in many-body systems — FELIX MEIER¹, •MATHIAS STEINHUBER², JUAN DIEGO URBINA², DANIEL WALTNER¹, and THOMAS GUHR¹ — ¹University of Duisburg-Essen, Lotharstr. 1, 47048 Duisburg, Germany — ²University of Regensburg, Universitätsstr. 31, 93040 Regensburg, Germany

Fast scrambling, quantified by the exponential initial growth of Out-of-Time-Ordered-Correlators (OTOCs), is the ability to efficiently spread quantum correlations among the degrees of freedom of interacting systems, and constitutes a characteristic signature of local unstable dynamics. As such, it may equally manifest both in systems displaying chaos or even in integrable systems around criticality. We discuss the results from our recent publication [1], where we go beyond these two well-studied regimes with an exhaustive study of the interplay between local criticality and chaos. We address many-body systems with a well-defined classical (mean-field) limit, as coupled large spins and Bose-Hubbard chains, thus allowing for semiclassical analysis. Our aim is to investigate the dependence of the exponential growth of the OTOCs, defining the quantum Lyapunov exponent λ_q on quantities derived from the classical system with mixed

phase space, specifically the local stability exponent of a fixed point λ_{loc} as well as the maximal Lyapunov exponent λ_L of the chaotic region around it.

[1] Meier, F., Steinhuber, M., Urbina, J. D., Waltner, D. & Guhr, T. arxiv:2211.12147

TT 55.4 Thu 15:45 MOL 213

Characterizing quantum chaoticity of kicked spin chains — •TABEA HERMANN, MAXIMILIAN F. I. KIELER, and ARND BÄCKER — TU Dresden, Institut für Theoretische Physik, Dresden, Germany

Quantum many body systems are commonly considered as quantum chaotic if their spectral statistics, such as the level spacing distribution, agree with those of random matrix theory. Using the example of the kicked Ising chain we demonstrate that even if both level spacing distribution and eigenvector statistics agree well with random matrix predictions, the entanglement entropy deviates from the expected Page curve. We propose a new measure of the effective spin interactions and obtain the corresponding random matrix result. By this the deviations of the entanglement entropy can be understood.

TT 55.5 Thu 16:00 MOL 213

Entanglement Characterization of Measurement-Induced Phase Transition in Fermionic Chains — •JIANGTIAN YAO^{1,2}, SEBASTIAN DIEHL¹, and MICHAEL BUCHHOLD¹ — ¹Institute for Theoretical Physics, University of Cologne, D-50937 Cologne, Germany — ²Max Planck Institute for the Physics of Complex Systems, 01187 Dresden, Germany

We report characterization of measurement-induced phase transition in Gaussian fermionic chains. We use various entanglement measures to characterize the two phases as well as the nature of the transition. Through a numerical study on the entanglement spectra, we observe closure of the entanglement gap in the critical phase and relate the scaling of the closure to the effective central charge of the system. In addition, we numerically extract the effective Luttinger liquid parameter of the system and use it to characterize the critical phase. Lastly, we use the scaling behavior of the effective Luttinger liquid parameter as well as the Schmidt gap to estimate the critical point for the phase transition.

15 min. break

TT 55.6 Thu 16:30 MOL 213

Dynamical characterization of the chaotic phase in the Bose-Hubbard model — DAVID PEÑA MURILLO and •ALBERTO RODRÍGUEZ — Departamento de Física Fundamental, Universidad de Salamanca, E-37008 Salamanca, Spain

We study the dynamical manifestation of the Bose-Hubbard model's chaotic phase [1] by analysing the temporal behaviour of connected two-point density correlations on experimentally accessible time scales up to a few hundred tunneling times. The time evolution of initial Mott states with unit density in systems including up to 17 bosons (Hilbert space dimension $\approx 10^9$) reveals that the chaotic phase can be unambiguously identified from the early time fluctuations of the considered observable around its equilibrium value [2]. The emergence of the chaotic phase is also seen to leave an imprint in the initial growth of the time signals. The possibility to discern specific features of this many-body chaotic phase, on top of the universal prediction of random-matrix theory, from these experimentally accessible measures is explored.

[1] L. Pausch *et al.*, Phys. Rev. Lett. 126, 150601 (2021)

[2] D. Peña Murillo, MSc Thesis, Universidad de Salamanca (2022)

TT 55.7 Thu 16:45 MOL 213

Universal Eigenvalue Distribution for Locally Interacting Quantum Systems — •TOBIAS HELBIG, TOBIAS HOFMANN, RONNY THOMALE, and MARTIN GREITER — Institut für Theoretische Physik und Astrophysik, Universität Würzburg, D-97074 Würzburg, Germany

Wigner has shown [1] that the eigenvalue distribution of a Gaussian orthogonal or unitary ensemble of random matrices approaches a semicircle in the thermodynamic limit. Here, we show that the joint eigenvalue distribution of locally interacting quantum systems, that is, ensembles of finite dimensional subsystems with local interactions between them, approaches a Gaussian distribution as the number of subsystems is taken to infinity [2]. In the talk, we present our analytical results supported by numerical data and discuss possible implications of a Gaussian density of states for physical problems.

[1] E. P. Wigner. On the statistical distribution of the widths and spacings of nuclear resonance levels. *Mathematical Proceedings of the Cambridge Philosophical Society*, 47(4): 790-798 (1951).

[2] T. Hofmann, T. Helbig, R. Thomale, and M. Greiter. In preparation.

TT 55.8 Thu 17:00 MOL 213

Power-law decay of correlations after a global quench in the massive XXZ chain — •FLÁVIA BRAGA RAMOS¹, ANDREW URICHUK^{2,3}, IMKE SCHNEIDER¹, and JESKO SIRKER³ — ¹Fachbereich Physik und Research Center OPTIMAS, Technische Universität Kaiserslautern, Kaiserslautern, Germany — ²University of Manitoba, Winnipeg, Canada — ³Bergische Universität Wuppertal, Wuppertal, Germany

While there have been great advances in understanding the final equilibration of integrable systems after a quantum quench, relatively little is known about their precise relaxation towards the steady state. In this context, the XXZ chain provides a playground for the investigation of interaction effects in out-of-equilibrium properties of quantum many-body systems. We investigate the relaxation dynamics of equal-time correlations in the antiferromagnetic phase of the XXZ spin-1/2 chain following a global quantum quench of the anisotropy parameter. In particular, we focus on the relaxation dynamics starting from an initial Néel state. Using the exact solution of an effective free-fermion model, state-of-art density matrix renormalization group simulations, and the quench-action approach, we show that the late-time relaxation is characterized by a power-law decay $\sim t^{-3/2}$ independent of anisotropy. Overall, we find remarkable agreement in the results obtained from the distinct approaches.

TT 55.9 Thu 17:15 MOL 213

Universal correlations in chaotic many-body quantum states: lifting Berry's Random Wave Model into Fock space — RÉMY DUBERTRAND¹, JUAN-DIEGO URBINA², KLAUS RICHTER², and •FLORIAN SCHÖPPL² — ¹Department of Mathematics, Physics and Electrical Engineering, Northumbria University, NE1 8ST Newcastle upon Tyne, United Kingdom — ²Institut für Theoretische Physik, Universität Regensburg, 93040 Regensburg, Germany

Using a semiclassical analysis based on Berry's ansatz [1] we investigate the universal statistical features of eigenstate correlations in chaotic mesoscopic many-body quantum systems, focusing on Bose-Hubbard lattices, where the existence of a classical (mean-field) limit allows for the use of many-body semiclassical methods [2]

For this, we first have to lift Berry's ansatz into the many-body space by expanding the microscopic correlations and the conjectured multivariate Gaussian distribution of expansion coefficients into the Fock space of quantum fields. Together with numerical evidence, which supports the extension to multi-point correlations of the known Gaussian distribution for a single expansion coefficient, the universality of eigenstate correlations can be extended well beyond random matrix theory, where these correlations are absent. Our results bring the correlation backbone of eigenfunctions into a precise signature of quantum chaos in many-body mesoscopic systems.

[1] M. V. Berry, *Journal of Physics A: Mathematical and General* **10**, 2083 (1977)

[2] K. Richter, J.D. Urbina, and S. Tomsovic. "Semiclassical roots of universality in many-body quantum chaos," (2022)

TT 56: Focus Session: Making Experimental Data F.A.I.R. – New Concepts for Research Data Management I (joint session O/TT)

Data have been identified as major resource of the 21st century, unlocking great potential if refined and processed in the right way. In scientific research, particularly modern data science concepts like machine learning or neural networks enable novel types of data analysis with often strong predictive power. This Focus Session aims at providing a framework for presenting and discussing novel concepts, tools and platforms for managing experimental research data related to surface science and solid-state physics. In particular, in light of the German NFDI initiative, where several consortia are actively working on tackling the imminent challenges of research data management in experimental solid-state physics, this Focus Session will offer an ideal environment for exchange among researchers, and bringing these novel developments into the labs. The intended topics include the description of experimental data and meta data generation workflows, meta data schemas and file formats, electronic lab notebooks, novel tools for handling and analyzing scientific research data, as well as sharing and searching platforms according to F.A.I.R. principles.

Organizers: Martin Aeschlimann (TU Kaiserslautern), Laurenz Rettig (FHI Berlin) and Heiko Weber (U Erlangen)

Time: Thursday 15:00–18:30

Location: WIL A317

Topical Talk

TT 56.1 Thu 15:00 WIL A317

Introducing a FAIR research data management infrastructure for experimental condensed matter physics data — •CHRISTOPH KOCH — Humboldt-Universität zu Berlin, Department of Physics & IRIS Adlershof, Berlin, Germany
Digitization and an increase in complexity and price of experimental materials characterization techniques, an increase in accuracy and system size of computational solid state physics (or computational materials science), and the maturation of machine learning tools to extract patterns from large amounts of very diverse (annotated) data promise an acceleration of materials development by synergistically combining research data from many sources. While some labs start to upload their (raw) research data to data repositories, this is only a first but not sufficient step in leveraging the above-mentioned potential, since such repositories are typically either specific to a very particular technique or agnostic to the content of the data being uploaded. In both cases the research data cannot easily, and definitely not without significant human effort, be compared to and integrated with experimental data from other sources, or numerical predictions. In this talk I will report on recent progress of the FAIRmat NFDI consortium in extending the novel materials discovery laboratory (NOMAD), the world's largest data base for ab-initio computational materials data, to ingest experimental research data on the synthesis and characterization of materials in a machine-accessible manner, i.e. annotated with well-defined and interoperable metadata, achieved by establishing links between related (experimental and computational) quantities.

TT 56.2 Thu 15:30 WIL A317

Introducing an electronic laboratory notebook in a collaborative research center — •SEBASTIAN T. WEBER¹, ANETA DAXINGER¹, PHILIPP PIRRO¹, MAREK SMAGA¹, CHRISTIANE ZIEGLER¹, MATHIAS KLÄUT², GEORG VON FREYMAN¹, BAERBEL RETHFELD¹, and MARTIN AESCHLIMANN¹ — ¹Department of Physics and Research Center OPTIMAS, RPTU Kaiserslautern-Landau — ²Institute of Physics, Johannes Gutenberg University Mainz

The basis of a FAIR data management is a well-described and detailed documentation of every single step of the experiment and data analysis. In recent decades, however, the focus has shifted from analog measuring instruments and analytical calculations to computer-based experiments and simulations. This has led to a large increase in the numbers of measurements and observed quantities and therefore in the amount of data generated. Consequently, traditional paper lab notebooks have reached their limits. Electronic lab notebooks (ELNs) are better suited for storing, indexing, searching and retrieving a large amount of entries. In particular, the automated filling-in of meta data can lead to a reduction in the workload of the scientists in the long term.

We present the lessons learned on challenges and advantages with the introduction of a joint electronic lab notebook within our collaborative research center CRC/TRR173 *Spin+X*. We report on our experiences in the daily work of the scientists and in education in student labs.

TT 56.3 Thu 15:45 WIL A317

An efficient workflow for processing single event dataframes. — •STEINN ÝMIR ÁGÚSTSSON¹, M. ZAIN SOHAIL^{2,3}, DAVID DOBLAS JIMÉNEZ⁴, DMYTRO KUTNYAKHOV³, and LAURENZ RETTIG⁵ — ¹Aarhus University, DK — ²RWTH, Aachen — ³DESY, Hamburg — ⁴Eu-XFEL, Schenefeld — ⁵FHI, Berlin

Single event resolved data streams measured by delay-line-detectors allow to correlate each measured photoelectron with the state of the experimental apparatus. This allows corrections and calibrations to be applied on a shot-to-shot basis and a flexible investigation of correlations between various measurement parameters.

We are developing an open-source python package[1], where highly optimized dataframe management and binning methods enable leveraging the full

potential of event-resolved data structures. The flexible design of the pipeline allows processing any event-resolved data stream.

With momentum microscopy as the primary target application, we developed axis calibration and artifact correction methods designed to be agnostic to the experimental apparatus. These methods are tested on data generated by microscopes at FELs (HEXTOF@FLASH) as well as at HHG sources (FHI), but are easily extended to other end-stations using similar detection techniques.

Our aim is to provide tools for the community which will reduce the development time for each end station, as well as an open and accessible data processing pipeline, built around the FAIR data principles.

[1] github.com/openCOMPES/seed

TT 56.4 Thu 16:00 WIL A317

FAIR Data Infrastructure for Computation: Advanced many-body methods.

— •JOSÉ M. PIZARRO¹, NATHAN DAELMAN¹, JOSEPH F. RUDZINSKI^{1,2}, LUCA M. GHIRINGHELLI¹, ROSER VALENTI³, SILVANA BOTTI⁴, and CLAUDIA DRAXL¹ — ¹Institut für Physik und IRIS-Adlershof, Humboldt-Universität zu Berlin — ²Max-Planck-Institut für Polymer Forschung, Mainz — ³Institut für Theoretische Physik, Goethe University Frankfurt am Main — ⁴Institut für Festkörpertheorie und Optik, Friedrich-Schiller-Universität Jena

Big-data analyses and machine-learning approaches have recently emerged as a new paradigm to study and predict properties of materials. In order to perform these analyses, materials data have to be structured in a FAIR (findable, accessible, interoperable, and reusable) format [1]. While most of the current databases deal with density-functional-theory (DFT) calculations, there is a clear need for developing FAIR-data schema for methodologies going beyond DFT. Methods such as the *GW* approximation, dynamical mean-field theory, and time-dependent DFT allow to calculate excited- and many-body-states properties beyond DFT, thus having a direct quantitative comparison with experiments. In this talk, we will introduce the achievements and challenges undertaken within the FAIRmat consortium towards fully structuring the (meta)data of all these techniques. We demonstrate how users can analyze the data and compare with angle-resolved photoemission spectroscopy.

[1] M. Scheffler et al., *Nature* **604**, 635 (2022).

TT 56.5 Thu 16:15 WIL A317

Electronic Laboratory Notebooks for FAIR Data Management; Evaluation and Recommendations for Solutions at Research Infrastructures — •PHILIPP JORDT¹, WIEBKE LOHSTROH², and BRIDGET MURPHY¹ — ¹IEAP, Kiel University, Germany — ²MLZ, Technische Universität München, Germany

Electronic Laboratory Notebooks (ELN) are the digital counterpart to the classical handwritten paper notebook and play a vital role in the implementation of FAIR data standards. Modern ELN solutions range from simple note taking applications to integrated tools, combining documentation, inventory management, progress tracking and more. Nowadays, ELNs are becoming more prominent in research laboratories around the world, replacing paper notebooks. This evaluation of basic needs was carried out in the context of the DAPHNE4NFDI consortia. Of special interest is the view on ELNs for combined use at large scale facilities and in the home laboratory. Thus, the requirements regarding implementation, deployment, authentication, etc., may differ from those for single or laboratory use at universities. An overview of different concepts and existing solutions is given. Multiple ELNs have been evaluated during test runs at large scale facilities and a survey on existing solutions was held. From these results, a list of ELN specifications is presented, ranging from useful to necessary. These insights may serve as a guideline for evaluating or implementing ELNs in the future.

TT 56.6 Thu 16:30 WIL A317

Ontology for Experimental Data — •SANDOR BROCKHAUSER — Center for Materials Science Data, Humboldt-Universität zu Berlin, Germany

Ontology is the scientific field of formal knowledge representation. This field contributes to Data Science and helps Experimentalist to properly annotate their data and metadata on a FAIR way. During the last decades several different ways have been developed in the field of Ontology for describing knowledge as a set of information and their relationships. These include Information mapping, Concept maps, Topic maps, Mind maps, Knowledge graphs, BORO (Business Objects Reference Ontology), RDF (Resource Description Framework), OWL (Web Ontology Language), ORO (Object-Role Modeling), UML (Unified Modeling Language), ISO 15926 (standard for data sharing), OLOG (mathematical framework for knowledge representation), GELLISH (ontology language for data storage and communication), etc. For describing experimental facts, we suggest using an ontology in OWL which is derived from the NeXus community standard. It represents all the concepts developed for explaining experiments and experimental data, just like the relationships between them. Such representation allows connecting the concepts defined in NeXus also to other ontologies. Additionally, any data management systems, like NOMAD which accepts experiment data provided in the NeXus standard, can immediately link the data and metadata to the ontology and make them interoperable.

15 min. break

Topical Talk

TT 56.7 Thu 17:00 WIL A317

Open Research Data for Photons and Neutrons: Applications in surface scattering and machine learning — •LINUS PITHAN — Universität Tübingen, Institut für Angewandte Physik - DAPHNE4NFDI

Open (F.A.I.R.) research data is becoming a key ingredient for data driven machine learning (ML) applications that requires access to existing data of preceding experiments - which goes well beyond data collected in the context of one's own experiments which one might keep in a secret drawer. We will discuss current possibilities as well as future opportunities and challenges with special emphasis on surface scattering. Embedded in the DAPHNE4NFDI (DAta from PHoton and Neutron Experiments) consortium we present efforts on how data catalogs may serve as backbone for F.A.I.R. datasets provided by synchrotron and neutron sources or through community efforts. Besides suitable metadata collection also the harmonization of data- and metadata formats are issues still to be tackled especially for systematic access to fully analyzed, experimental datasets (e.g. by adopting NeXus community conventions). After a broader overview and shining light on the SciCat meta-data catalog system,[1] we discuss as application examples efforts in the field of reflectometry (XRR, NR) [2,3] and X-Ray scattering and diffraction (WAXS, GIWAXS and XPCS).[1,4]

- [1] V. Starostin, L. Pithan et al. 2022, SRN, Vol. 35, No. 4
- [2] A. Greco et al. 2022, J. Appl. Cryst. 55 362
- [3] L. Pithan et al., Refl. dataset, 10.5281/zenodo.6497438
- [4] V. Starostin et al. 2022, npj Comp. Mat. 8, 101

TT 56.8 Thu 17:30 WIL A317

NOMAD OASIS as a Tool for Electron and Atom Probe Microscopists — •MARKUS KÜHBACH — Department of Physics, Humboldt-Universität zu Berlin, Germany

Embracing the FAIR principles for sharing data and knowing how to work with different tools in research data management systems is becoming an invaluable skill in a scientist's daily life. Embracing such systems of tools, one of which is offered with NOMAD OASIS, allows you to start organizing your research data locally. Learning such tools will train you to understand what schemes and electronic lab notebooks are and how the data and metadata are processed by these tools. Example implementations of specific workflows can give you ideas where to start from and how to customize these tools for the needs of your own research and colleagues. Thereby, you can provide feedback which supports the evolution and improvement of the research data management system.

NOMAD OASIS offers you many examples which show now also how data and metadata of specific experiments can be parsed into a standardized representation. These examples teach users through detailing how data can be entered, viewed, and organized with customizable schemes in NOMAD. Furthermore,

the examples suggest strategies for how the information in NOMAD can be accessed for generic or domain-specific data analytics tools.

In my talk, I will go through one or two of these examples specific to electron microscopy (orientation imaging microscopy or spectroscopy).

TT 56.9 Thu 17:45 WIL A317

FAIR Data Infrastructure for Computation: Introducing the parsers for Quantum Monte Carlo and ALF — •JONAS SCHWAB¹, JOSÉ M. PIZARRO², JEFFERSON STAFUSA E. PORTELA¹, LUCA M. GHIRINGHELLI², and FAKHER F. ASSAAD¹ — ¹Institut für Theoretische Physik und Astrophysik und Würzburg-Dresden Cluster of Excellence ct.qmat, Universität Würzburg, 97074 Würzburg, Germany — ²Institut für Physik und IRIS-Adlershof, Humboldt-Universität zu Berlin

DFT calculations lead to low-energy effective models. A modern example would be Kitaev types spin Hamiltonians for RuCl_3 . Once the model is specified, many different many-body calculations can be carried out. Here, we will concentrate on the ALF [1] implementation of the auxiliary field quantum Monte Carlo algorithm that can deal with general models that includes the ones produced by DFT calculations. Being a Monte Carlo method, the ALF library produces stochastic time series. We will discuss how to implement this workflow in the NOMAD Repository & Archive (<https://nomad-lab.eu>) and concentrate on a FAIR metadata scheme. The first challenges are to define the models in a searchable way as well as standards for the Monte Carlo time series. In this talk we will discuss the present state of this project for the special case of the ALF-library and how users can exploit the benefits of the NOMAD repository to find, compare and reuse our QMC data.

[1] F. F. Assaad et al., SciPost Phys. Codebases 1 (2022).

TT 56.10 Thu 18:00 WIL A317

CAMELS - A Configurable Instrument Control Software for FAIR Data — •ALEXANDER FUCHS^{1,3}, JOHANNES LEHMEYER^{1,3}, MICHAEL KRIEGER^{1,3}, HEIKO B. WEBER^{1,3}, PATRICK OPPERMANN^{2,3}, and HEINZ JUNKES^{2,3} — ¹Lehrstuhl für Angewandte Physik, Friedrich-Alexander-Universität Erlangen-Nürnberg, — ²Fritz-Haber-Institut der Max-Planck-Gesellschaft (FHI), Berlin — ³FAIRmat, Humboldt-Universität zu Berlin, Berlin, Germany

We are developing a configurable measurement software (CAMELS), targeted towards the requirements of experimental solid-state physics. Here many experiments utilize a multitude of measurement devices used in dynamically changing setups. CAMELS [1] will allow to define instrument control and measurement protocols using a graphical user interface (GUI). This provides a low entry threshold enabling the creation of new measurement protocols without programming knowledge or a deeper understanding of device communication. The GUI generates python code that interfaces with instruments and allows users to modify the code for specific applications and implementations of arbitrary devices if necessary. Even large-scale, distributed systems can be implemented. CAMELS is well suited to generate FAIR-compliant output data. Nexus standards, immediate NOMAD integration and hence a FAIRmat compliant data pipeline can be readily implemented. [1] <https://github.com/FAU-LAP/CAMELS>

TT 56.11 Thu 18:15 WIL A317

OpenSemanticLab: Usecase Device Repository — •MATTHIAS A. POPP and SIMON STIER — Fraunhofer ISC, Neunerplatz 2, 97082 Würzburg, Germany

Fully automated experiments provide benefits regarding precision, repeatability, as well as data quality and therefore gain more and more popularity. However, setting them up can be time consuming, especially when computer interface information has to be manually transferred from device manuals to software.

In order to implement FAIR principles precise descriptions of measurement setups and instrumentation are necessary. Currently, this results in extra workload for experimental scientists.

With our framework OpenSemanticLab, we address this shortcoming by providing a central metadata repository for scientific instruments. The ontology-based repository meets both human (GUI) and machine requirements (APIs). A device ontology helps finding and classifying devices. In an associated Python package, abstract device drivers and concrete device metadata can be combined into executable workflows. Overall, this approach not only strengthens the transparency of research according to FAIR principles, but also significantly reduces the implementation effort for complex setups.

TT 57: Poster: Superconductivity I

Time: Thursday 15:00–18:00

Location: P2/OG2

TT 57.1 Thu 15:00 P2/OG2

Influence of reduced dimensionality on the superconducting properties of ultrathin aluminum films — WERNER M.J. VAN WEERDENBURG¹, ANAND KAMLAPURE¹, EIRIK HOLM FYHN², XIAOCHUN HUANG¹, NIELS P.E. VAN MULLEKOM¹, MANUEL STEINBRECHER¹, PETER KROGSTRUP³, JACOB LINDER², and ALEXANDER A. KHAJETOORIANS¹ — ¹Institute for Molecules and Materials, Radboud University, 6525 AJ Nijmegen, the Netherlands — ²Center for Quantum Spintronics, Department of Physics, Norwegian University of Science and Technology, NO-7491 Trondheim, Norway — ³NNF Quantum Computing Programme, Niels Bohr Institute, University of Copenhagen, 2100 Copenhagen, Denmark

Study of superconductivity (SC) in lower dimensional systems is vital to devices involving multilayers and heterostructures for future quantum information applications. In this work, using scanning tunneling microscopy/spectroscopy, we study SC in ultrathin epitaxial Al films on Si(111) as we approach the 2D limit. With reducing thickness, we observe enhancement of SC where critical temperature and gap size shows threefold enhancement. In addition, we characterize the vortex structure in presence of strong Zeeman fields and find evidence for extended vortices showing paramagnetic Meissner effect originating from triplet pairing contributions. These results illustrate two striking influences of reduced dimensionality and present a new platform to study SC in presence of large magnetic fields. Reference: arXiv:2210.10645(2022).

TT 57.2 Thu 15:00 P2/OG2

Demonstration of 300 mm CMOS-compatible superconducting HfN and ZrN thin films — ROMAN POTJAN^{1,3}, RAIK HOFFMANN¹, MARCUS WISLICENUS¹, BENJAMIN LILIENTHAL-UHLIG¹, and J. WOSNITZA^{2,3} — ¹Fraunhofer Institute for Photonic Microsystems (IPMS), Center Nanoelectronic Technologies (CNT), Dresden, Germany — ²Hochfeld-Magnetlabor Dresden (HLD-EMFL), HZDR, Dresden, Germany — ³Institut für Festkörper- und Materialphysik, TU Dresden, Germany

The increasing interest in quantum computing is pushing the development of new superconducting materials for semiconductor fab process technology. However, these are often facing CMOS process incompatibility. In contrast to common CMOS materials such as TiN and TaN, reports on the superconductivity of other suitable transition-metal nitrides are scarce, despite potential superiority. Hence, we demonstrate fully CMOS-compatible fabrication of HfN and ZrN thin films on state-of-the-art 300 mm semiconductor process technology, employing reactive DC magnetron sputtering on silicon wafers. Mechanical stress, thickness, and roughness measurements of the thin films imply process compatibility. Material phase and stoichiometry in bulk and interfaces are investigated by structural analysis. HfN and ZrN exhibit transitions into the superconducting state with critical temperature up to 5.1 and 6.1 K, respectively. A decrease in critical temperature with decreasing film thickness indicates geometric limitations and proximity effects of the interfaces. The results prepare a scalable application of HfN and ZrN in quantum computing and related applications.

TT 57.3 Thu 15:00 P2/OG2

Unraveling Charge Transfer to Understand Superconductivity in MgB₂ — SIMON MAROTZKE^{1,2}, JAN OLIVER SCHUNCK^{1,3}, AMINA ALIC⁴, OCTAVE DUROS⁴, MORITZ HOESCH¹, ALESSANDRO NICOLAOU⁵, GHEORGHE SORIN CHIUZBAIAN⁴, and MARTIN BEYE¹ — ¹Deutsches Elektronen-Synchrotron DESY, Hamburg, Germany — ²Christian-Albrechts-Universität zu Kiel, Kiel, Germany — ³Universität Hamburg, Hamburg, Germany — ⁴Sorbonne Université, Paris, France — ⁵Synchrotron SOLEIL, Saint-Aubin, France

Magnesium diboride (MgB₂) holds the world-record for the highest transition temperature ($T_C = 39$ K) in a conventional Bardeen-Cooper-Schrieffer (BCS)-type, i.e., phonon-mediated, superconductor. The undoped electron configuration of MgB₂ is still disputed as contradicting results on the appearance of charge transfer upon crossing T_C have been reported. To settle this question, we conducted high-resolution resonant X-ray emission spectroscopy (XES) as well as X-ray absorption spectroscopy (XAS) measurements around the boron K-edge at the SEXTANTS beamline at the synchrotron SOLEIL. In order to investigate the charge transfer between in-plane and out-of-plane states, we varied the polarization of the incoming photons as well as the incidence and emission angle. We report on differences in the spectral intensity for both the absorption and emission spectra upon crossing T_C to be first indications of changes in the density of the boron 2p states. Complementary density of states calculations showing good agreement with the experimental data were performed.

TT 57.4 Thu 15:00 P2/OG2

Strain device for in-situ uniaxial strain measurements of strongly correlated electron materials in scanning tunneling microscopy — CAROLINA A. MARQUES¹, DANYANG LIU¹, ALEXANDER STEPPKE^{1,2}, and FABIAN D. NATTERER¹ — ¹University of Zurich, Winterthurerstrasse 190, CH-8057 Zurich,

Switzerland — ²Paul Scherrer Institut Forschungsstrasse 111 5232 Villigen PSI Switzerland

Uniaxial strain is an effective way to tune the properties of strongly correlated electron systems without introducing disorder. One seminal example is the doubling of the critical temperature of Sr₂RuO₄.

Strain devices for the *in-situ* application of strain have been used in several different measurement techniques: transport, specific heat, angle-resolved photoemission spectroscopy, muon spin relaxation, and neutron scattering measurements. Here, we describe the design and construction of a strain device compatible with a scanning tunneling microscope. Our piezo-element based strain-cell is temperature compensated and enables the continuous tuning of strain, allowing to monitor local strain response. It opens up the possibility to locally track changes to the low-energy electronic states as a function of strain, giving insight into the underlying physical mechanisms.

TT 57.5 Thu 15:00 P2/OG2

Magnon dispersion of SrRuO₃ studied by inelastic neutron scattering experiments — KEVIN JENNI¹, AKSHAY TEWARI¹, STEFAN KUNKEMÖLLER¹, AGUSTINUS AGUNG NUGROHO², RUSSELL EWINGS³, YVAN SIDIS⁴, ASTRID SCHNEIDEWIND⁵, PAUL STEFFENS⁶, and MARKUS BRADEN¹ — ¹II. Phys. Institut, Universität zu Köln — ²Institut Teknologi Bandung, Bandung 40132, Indonesia — ³ISIS Brillouin Neutron and Muon Source, United Kingdom — ⁴Laboratoire Léon Brillouin, Gif-sur-Yvette CEDEX, France — ⁵Jülich Centre for Neutron Science (JCNS), Garching, Germany — ⁶Institut Laue Langevin, Grenoble, France

Weyl points in the ferromagnetic state in SrRuO₃ not only determine anomalous magnetotransport properties but also modify the spin dynamics leading to a peculiar temperature dependence of both the spin gap and of the stiffness in the ferromagnetic state [1]. In contrast the magnon chirality in SrRuO₃ remains normal, i.e. right handed [2]. To extend the analysis of the magnon dispersion we performed inelastic neutron scattering experiments with the time-of-flight technique as well as with polarization analysis. The magnon dispersion can be followed to about 30 meV and there is no indication for a crossover into a Stoner continuum. There is evidence for additional coupling beyond just the nearest neighbors. In addition magnon excitations exhibit pronounced broadening that further increases upon heating possibly related to the strong coupling between ferromagnetism and conductivity in SrRuO₃.

[1] K. Jenni et al. Phys. Rev. Lett. **123**, 17202 (2019). [2] K. Jenni et al. Phys. Rev. B. **105**, L180408 (2022).

TT 57.6 Thu 15:00 P2/OG2

Screening in a two-band model for infinite-layer nickelate — THARATHEP PLENUMRUNG^{1,2}, MARIA DAGHOFER^{1,2}, MICHAEL SCHMID³, and ANDRZEJ M. OLES^{4,5} — ¹Institute for Functional Matter and Quantum Technologies, University of Stuttgart, Stuttgart, Germany — ²Center for Integrated Quantum Science and Technology, University of Stuttgart, Stuttgart, Germany — ³Waseda Research Institute for Science and Engineering, Waseda University, Tokyo, Japan — ⁴Max Planck Institute for Solid State Research, Stuttgart, Germany — ⁵Institute of Theoretical Physics, Jagiellonian University, Kraków, Poland

Considering two-band model for infinite-layered nickelates, containing *d*- and *s*-like orbitals, on two-dimensional lattice. The extended nature of the *s*-like orbital leads to less electronic correlation. We thus parameterize the electronic correlations of the *s*-like orbital by introducing *screening parameter*. With exact diagonalization, we calculate the pairing symmetries and other electronic properties of the two-band model on two-dimensional lattice. We find that the screening strength of the *s*-like band plays an important role in the electronic properties of the two-band model. Interestingly, depending on the screening strength of *s*-like band, we find both *d*- and *s*-wave pairing symmetries within the two-band model. In strong screening, the *d*-wave pairing is found while the *s*-wave pairing is formed in the weak screening regime. The phase diagram of the two-band model for different ratio of J/U is also presented.

TT 57.7 Thu 15:00 P2/OG2

Magnetic and thermoelectric properties of Bi-substituted La_{0.95-x}Bi_xSr_{0.05}CoO₃ — DIVYA PRAKASH DUBEY and RATNAMALA CHATTERJEE — IIT Delhi Hauz Khas New Delhi 110016 India

We present the results of a comprehensive investigation of electric and thermal transport properties of polycrystalline Bi substituted La_{0.95-x}Bi_xSr_{0.05}CoO₃ for $x=0, 0.1$ and 0.2 (LBSCO-0, 1 & 2). The electrical resistivity reflects the semiconducting nature with interesting n-type to p-type transition 52K for LBSCO-1 and LBSCO-2 samples. The substitution of higher atomic weight elements Bi at La site drastically affects overall thermal conductivity by reducing the lattice contribution ($\kappa \approx 0.12$ W/m-K at T= 50K) and also enhance the Seebeck coefficient ($S \approx 354 \mu\text{V/K}$). The increase in the resistivity and Seebeck coefficient for Bi-substituted system is related to the decrease in the available charge carrier concentration ($\approx 5.12 \cdot 10^{20} \text{ cm}^{-3}$). The phonon mediated charge transport via phonon

drag effect below 50K and a large increment in ZT 0.17 at RT for LBSCO-2 composition has been observed that is 1-order larger to pristine undoped LBSCO-0 and even higher to the other existing cobaltite*s-based thermoelectric choice.

TT 57.8 Thu 15:00 P2/OG2

High pressure T-P phase diagram of 2H-TaSe₂ — •YULIIA TYMOSHENKO¹, XINGCHEN SHEN¹, AMIR-ABBAS HAGHIGHIRAD¹, TOM LACMANN¹, GASTON GARBARINO², and FRANK WEBER¹ — ¹Institute for Quantum Materials and Technologies, Karlsruhe Institute of Technology, 76021 Karlsruhe, Germany — ²European Synchrotron Radiation Facility, 71 avenue des Martyrs, CS 40220, Grenoble 38043, France

Many layered materials featuring charge-density waves (CDW), a modulation of the electronic density of states, acquire a superconducting ground state often associated with a quantum critical point (QCP) of the CDW order. Although 2H polymorph of tantalum diselenide (2H-TaSe₂) with a layered hexagonal crystal structure is one of the most studied CDW systems, to the best of our knowledge, previous studies of the phase diagram have not been carried out at pressures sufficient to suppress the CDW order at low temperatures. We investigated the CDW phase diagram in its most crucial but still unexplored area and determined the CDW quantum critical point in 2H-TaSe₂ under pressure via high-resolution synchrotron x-ray diffraction (XRD). Its position together with previously published resistivity measurements and our recent ambient-pressure study of the soft phonon mode at the CDW transition enable us to argue that this compound likely has a CDW quantum critical point closely connected to the emergent superconducting phase. This can serve as a textbook example where both phases are mediated by the same mechanism, electron-phonon coupling of the CDW soft phonon mode.

TT 57.9 Thu 15:00 P2/OG2

Clarifying the origin of CDW and finding the routes to superconductivity in 1T-TiSe₂ — •ANDRII KUIBAROV¹, ALEXANDER FEDOROV^{1,2}, RUI LOU^{1,2}, YULIIA SHEMERLIUK¹, OLEKSANDR SUVOROV¹, SAICHARAN ASWARTHAM¹, BASTIAN RUBRECHT¹, DMITRY EFREMOV¹, HELMUTH BERGER³, BERND BÜCHNER¹, and SERGEY BORISENKO¹ — ¹Leibniz-Institut für Festkörper- und Werkstofforschung Dresden — ²Helmholtz-Zentrum Berlin für Materialien und Energie, BESSY II — ³Institute of Condensed Matter Physics, Ecole Polytechnique Fédérale de Lausanne

The relationship between charge density waves (CDW) and superconductivity was always one of the important questions of solid-state physics. Even though they are often observed on the phase diagram next to each other, it is still unknown whether CDW competes or cooperates with superconductivity. Utilizing the photon energy-dependent ARPES we investigate the 3D electronic structure of well-known CDW-bearing material TiSe₂, superconductor Cu_xTiSe₂, and TiSeS. Our results suggest that neither Mott nor the excitonic insulator model is applicable to the electronic structure of TiSe₂. In contrast to the generally accepted model, we find a crucial agreement with the conventional band structure calculations, which predict the absence of the energy gap in this material.

Additionally, we perform temperature-dependent ARPES studies and show that the CDW phase remains in doped superconducting samples Cu_xTiSe₂. On the basis of the obtained results, we propose a mechanism for both CDW and superconductivity TiSe₂ family.

TT 57.10 Thu 15:00 P2/OG2

Nematic susceptibility in heavily hole-doped iron based superconductors — •FRANZ ECKELT¹, XIAOCHEN HONG¹, VILMOS KOCSIS², VADIM GRINENKO², CHUL-HO LEE³, BERND BÜCHNER², and CHRISTIAN HESS¹ — ¹Bergische Universität Wuppertal, 42097 Wuppertal, Germany — ²Leibniz-Institute for Solide State and Materials Research (IFW-Dresden), 01069 Dresden, Germany — ³National Institute of Advanced Industrial Science and Technology (AIST), Tsukuba, Ibaraki 305-8568, Japan

We investigate the elastoresistivity of the heavily hole doped iron-based superconductor Ba_{1-x}K_xFe₂As₂ in the range x= 0.68 - 0.98 using a piezoelectric measurement technique. We observe a divergent increase in elastoresistance along the [100] direction during cooling for all samples studied so far. We discuss our findings in terms of nematic fluctuations and Fermi surface effects in the vicinity of a Lifshitz transition.

TT 57.11 Thu 15:00 P2/OG2

Towards topological superconductivity on the surface of LiFeAs — •LUISE MERKWITZ¹, ANDRII KUIBAROV¹, RUI LOU^{1,2}, ALEXANDER FEDOROV^{1,2}, SABINE WÜRMEHL¹, SAICHARAN ASWARTHAM¹, IGOR MOROZOV¹, BERND BÜCHNER¹, and SERGEY BORISENKO¹ — ¹Leibniz-Institute for Solid State Research, IFW-Dresden, D-01171 Dresden, Germany — ²Helmholtz-Zentrum Berlin, BESSY, D-12489 Berlin, Germany

Realisation of topological superconductivity is theoretically possible in iron-based superconductors, where the s-wave pairing in the bulk can induce superconductivity of the topological surface states. The detection of the latter by angle-resolved photoemission spectroscopy (ARPES) in LiFeAs and FeSeTe systems is questionable since the bulk-originated dispersions can mimic the Dirac crossing and inverted gap is expected to be very small (of the order of 5 meV). The only

feasible possibility to detect topological surface states in such a small gap is to bring it to the Fermi level where the scattering is minimal. We have synthesized differently doped LiFe_{1-x}Y_xAs (Y=Co, V) crystals and performed synchrotron-based ARPES studies to map k_z-dispersion in detail. Our results demonstrate the principal possibility of tuning the binding energy of the inverted gap in these systems and point to the optimal composition where this binding energy is close to zero. In addition, our results reveal considerable renormalization anisotropy of the Fe d-states never detected earlier.

TT 57.12 Thu 15:00 P2/OG2

The superconducting symmetries of CeRh₂As₂ — •FABIAN JAKUBCZYK^{1,2}, JULIA M. LINK^{1,2}, and CARSTEN TIMM^{1,2} — ¹Institute of Theoretical Physics, Technische Universität Dresden, 01062 Dresden, Germany — ²Würzburg-Dresden Cluster of Excellence ct.qmat, Technische Universität Dresden, 01062 Dresden, Germany

Multiphase unconventional superconductivity is a rare phenomenon, which has recently been discovered in the tetragonal but locally noncentrosymmetric heavy-fermion compound CeRh₂As₂. Here, the transition between two distinct superconducting phases occurs as a function of magnetic field applied along the c axis and the formation of superconductivity takes place around T_{SC1} = 0.26 K. At μ₀H* ≈ 4 T the superconductor changes from a low-field to a high-field state with a large critical field of μ₀H_{c2} = 14 T. However, for in-plane fields only the low-field phase appears, with μ₀H_{c2} = 2 T. Recent As-NQR experiments further increased the variety of intriguing phenomena in this material, for they detected the onset of antiferromagnetism within the superconducting low-field phase, i.e. at T_N < T_{SC1}. In order to study the coexistence and interplay of the potential superconducting and magnetic phases, as well as the effect of an external magnetic field, we conduct a symmetry analysis followed by the construction of a Landau-type energy functional. Thereby we can give a statement about the probable symmetries of the superconducting states.

TT 57.13 Thu 15:00 P2/OG2

Flat bands of surface states in chiral symmetric superconductors — •CLARA JOHANNA LAPP^{1,2}, JULIA M. LINK^{1,2}, and CARSTEN TIMM^{1,2} — ¹Institute of Theoretical Physics, Technische Universität Dresden, 01069 Dresden, Germany — ²Würzburg-Dresden Cluster of Excellence ct.qmat, Technische Universität Dresden, 01062 Dresden, Germany

Nodal noncentrosymmetric superconductors can support flat bands of zero-energy surface states in part of their surface Brillouin zone if they obey time-reversal symmetry. These bands are protected by a winding number that relies on chiral symmetry, which in these systems is realized as the product of time-reversal and particle-hole symmetry. We examine which symmetry conditions a model must obey such that a winding number is well defined and can be nonzero. In particular, time-reversal symmetric Bogoliubov-de Gennes Hamiltonians which conserve one spin component can be interpreted as chiral symmetric in each of the spin-blocks and exhibit a nonzero winding number that protects zero energy surface modes. Moreover, we classify which types of sublattice symmetry lead to nonzero winding numbers.

TT 57.14 Thu 15:00 P2/OG2

Eliashberg theory calculations for magnetically mediated superconductivity — •RAN TAO and MALTE GROSCHE — Department of Physics, Cavendish Laboratory, University of Cambridge, Cambridge CB3 0HE, United Kingdom

Computational modelling for realistic material parameters can speed up the search for new unconventional superconductors.

We have implemented calculations of the superconducting transition temperature in Eliashberg theory for spin fluctuation mediated superconductivity and validated them by reproducing previously published results in simple systems (e.g. [1]). Next, our code has been extended to a minimal model for iron-based superconductors, namely a 2D compensated metal with varying Fermi surface volume and interaction strength. Developing this approach further in the spirit of the UppSC code (e.g. [2]), numerical calculations are used to investigate the effects of applied field and to assist the discovery of new unconventional superconductors by surveying large numbers of candidate materials.

[1] P. Monthoux and G. G. Lonzarich, Phys. Rev. B 59, 14598 (1999)

[2] A. Aperis, P. Maldonado, and P. M. Oppeneer, Phys. Rev. B 92, 054516 (2015)

TT 57.15 Thu 15:00 P2/OG2

Yu-Shiba-Rusinov states in unconventional superconductors — •MICHAEL HEIN¹, WOLFGANG BELZIG¹, and JUAN CARLOS CUEVAS² — ¹Universität Konstanz, Konstanz, Germany — ²Universidad Autónoma de Madrid, Madrid, Spain Recently there has been a huge effort to investigate individual magnetic impurities on superconducting surfaces in the context of scanning tunneling microscopy (STM) [1]. These STM-based experiments have enabled to elucidate the properties of the in-gap superconducting bound states known as Yu-Shiba-Rusinov states. These bound states are a key signature of the interplay between magnetism and superconductivity at the atomic scale and, in turn, they lead to a strong local modification of the superconducting state. In this regard, we present here our theoretical efforts to understand the physics of YSR states in the con-

text of unconventional superconductivity, with special attention to the so-called Ising superconductors. We show that the study of YSR states can provide a very valuable way to reveal the underlying properties of unconventional superconductors.

[1] B. W. Heinrich, J. I. Pascual, and K. J. Franke, *Prog. Surf. Sci.* **93**, 1 (2018)

TT 57.16 Thu 15:00 P2/OG2

RKKY interaction in non-centrosymmetric superconductors — •FINJA TIETJEN and JACOB LINDER — Department of Physics, Center for Quantum Spintronics, Norwegian University of Science and Technology, 7491, Trondheim, Norway Recent advances in experimental studies have raised interest in how spin interactions are manifested in unconventional superconductors, which can potentially be used for spintronic devices. In particular, superconducting triplet states featuring spin-polarized Cooper pairs are expected to qualitatively alter spin interaction compared to non-superconducting materials.

We consider the RKKY-interaction between two impurity spins in a non-centrosymmetric superconductor. Such superconductors feature antisymmetric spin-orbit coupling and, generally, coexisting singlet and triplet Cooper pairs. The RKKY-interaction is treated perturbatively with a Schrieffer-Wolff transformation within the Bogoliubov-de Gennes framework. Exact numerical studies complement the analytical approach and show local decreases in the total superconducting gap as well as a change in local density of states at impurity sites. The RKKY interaction is affected by the superconductor and the corresponding change in the ground-state spin configuration is also clearly visible. We expect that the spin configuration can thus be externally controlled by entering or leaving the superconducting state.

Ongoing studies on the exact dependencies as well as advances in the analytical approach promise further insights closer to the conference date.

TT 57.17 Thu 15:00 P2/OG2

Analytical parquet renormalization group for multipocket systems — •NORA TAUFERTSHÖFER, MATTEO DÜRRNAGEL, and RONNY THOMALE — Theoretische Physik I, Universität Würzburg

Materials with multi-pocket fermiology may exhibit unconventional superconductivity which arises from inter-pocket scattering. Studying this problem in the weak coupling regime by renormalization group (RG) methods requires a perturbative expansion in each flow step.

As electronically driven instabilities are predominantly governed by states close to the Fermi surface, the RG analysis can be restricted to a few distinct momentum channels between the Fermi pockets. The parquet RG [1] embeds the truncation of the flow equations into a rigorous analytical scheme to investigate superconductivity and its interplay with various competing phases. Within this framework we discuss the relevance of nematic fluctuations in a 2D model for GaAs/AlAs heterostructures, which may host the possibility for gate-tunable unconventional superconductivity [2].

[1] S. Maiti and A. V. Chubukov, *Phys. Rev. B* **82**, 214515 (2010)

[2] A. V. Chubukov and S. A. Kivelson, *Phys. Rev. B* **96**, 174514 (2017)

TT 57.18 Thu 15:00 P2/OG2

Higgs mode in superconductors with Rashba spin-orbit coupling — •TOBIAS KUHN and BJÖRN SOTHMANN — Fakultät für Physi, Universität Duisburg-Essen, Lotharstraße 1, 47057 Duisburg, Germany

When a superconductor is periodically driven by electromagnetic radiation, the superconducting order parameter shows radial oscillation with twice the driving frequency. This so called Higgs mode can be excited resonantly when the driving frequency equals the absolute value of the order parameter. Here, we study Higgs modes for superconductors with Rashba spin-orbit coupling using two methods. We discuss the resonance condition by analyzing the dynamics of Anderson pseudospins. In addition, we use Floquet Green's functions to generalize the pseudospin approach and discuss the impact of spin-orbit coupling on the order parameter dynamics.

TT 57.19 Thu 15:00 P2/OG2

Order-parameter evolution in the FFLO phase — •H. KÜHNE¹, S. MOLATTA¹, T. KOTTE¹, D. OPPERDEN¹, G. KOUTROULAKIS², J.A. SCHLUETER^{3,4}, G. ZWICKNAGL⁵, S.E. BROWN⁶, and J. WOSNITZA^{1,7} — ¹Hochfeld-Magnetlabor Dresden, HZDR — ²UC Santa Barbara, USA — ³ANL, Argonne, USA — ⁴NSF, Alexandria, USA — ⁵IMP, TU Braunschweig — ⁶UC Los Angeles, USA — ⁷IFMP, TU Dresden

The Fulde-Ferrell-Larkin-Ovchinnikov (FFLO) state represents a general concept of pairing in multi-component Fermi liquids with strong population imbalance. In the superconducting FFLO state, the spin polarization varies as the modulus of the spatially modulated superconducting gap amplitude, and, thus, its modulation amplitude represents the order parameter. Indeed, NMR experiments of the organic superconductors β'' -(ET)₂SF₅CH₂CF₂SO₃ and κ -(ET)₂Cu(NCS)₂ showed the emergence of inhomogeneous line broadening, stemming from the spatially modulated spin polarization. We report on our studies of the temperature-dependent order parameter of the superconducting FFLO state. For that, we utilize ¹³C NMR spectroscopy of β'' -

(ET)₂SF₅CH₂CF₂SO₃. From a comparison of the NMR spectra to a comprehensive modeling, we determine the evolution of the local spin-polarization modulation amplitude upon condensation of the FFLO state. Further, the modeling allows to quantify the decrease of the average spin polarization, stemming from the spin-singlet coupling of the superconducting electron pairs.

TT 57.20 Thu 15:00 P2/OG2

Comparison of window-type and cross-type Nb/Al-AIO_x/Nb Josephson tunnel junctions — •FABIENNE BAUER¹, MARTIN NEIDIG¹, CHRISTIAN ENSS², and SEBASTIAN KEMPF¹ — ¹Institute of Micro- and Nanoelectronic Systems, Karlsruhe Institute of Technology — ²Kirchhoff Institute of Physics, Heidelberg University

Josephson tunnel junctions (JJs) are the heart of numerous superconducting electronic devices such as SQUIDS, qubits or parametric amplifiers. Out of the multitude of junction variants, Nb/Al-AIO_x/Nb junctions have somehow become the state of the art as they are resilient to thermal cycling and additionally show a very high junction quality and reproducibility of characteristic junction properties. Against this background, we present two anodization-free fabrication processes for Nb/Al-AIO_x/Nb Josephson junctions. One is a variant of the selective niobium etching process (SNEP) for fabricating window-type junctions. The second is a process for producing self-aligning, low-capacitance cross-type Josephson junctions. For comparing both processes, we comprehensively characterized fabricated junctions by studying resonance phenomena in unshunted dc-SQUIDS to determine the intrinsic junction capacitance and determined characteristic junction figures of merit. We show that both of our processes yield very high quality JJs. However, our cross-type Josephson junctions turn out not only to greatly simplify the fabrication process and to provide much lower junction capacitance, but also to show a greatly improved homogeneity of critical current density distribution as determined by analysing the magnetic field dependence of the critical current.

TT 57.21 Thu 15:00 P2/OG2

Process optimisation for the fabrication of cross-type Nb/Al-AIO_x/Nb Josephson junctions — •A. STOLL, F. BAUER, L. MÜNCH, D. HENGSTLER, A. FERRING-SIEBERT, F. KRÄMER, N. KAHNE, D. MAZIBRADA, A. FLEISCHMANN, and C. ENSS — Kirchhoff-Institute for Physics, Heidelberg University, Germany. Josephson tunnel junctions (JJs) are the basic element of many superconducting electronic devices such as qubits or superconducting quantum interference devices (SQUIDS). Since many applications demand a large number of Josephson junctions, a reliable wafer-scale fabrication process yielding JJs with a reproducible and uniform high quality is required. Very often window-type JJs are used, in which the JJ area is defined by openings in an insulating layer. The size of the JJ is thus limited by the alignment accuracy, therefore causing the need for low critical current densities j_c and in turn long oxidation times. The transition to cross-type JJs is motivated by reducing the junction area as well as parasitic capacities, and in turn suppressing or completely removing parasitic effects, e.g. LC-resonances, with the additional benefit of simplistic and time efficient fabrication steps. We present how we optimised and retained the quality of our cross-type Nb/Al-AIO_x/Nb junctions, for which quality checks of our in-house sputter-deposited niobium films and oxidized aluminium layers were carried out, including the measurement of the critical temperature T_c , stress of the niobium film and junction specific quality features. The parameters for the magnetron sputtering, like the Ar-pressure and power of the sputtering source, were optimised accordingly.

TT 57.22 Thu 15:00 P2/OG2

Realization of He-FIB induced Josephson junction THz detectors in YBCO thin films — •KENNY FOHMANN, CHRISTOPH SCHMID, ERIC DORSCH, EDWARD GOLDOBIN, DIETER KOELLE, and REINHOLD KLEINER — Physikalisches Institut, Center for Quantum Science (CQ) and LISA⁺, Universität Tübingen, Germany We designed and fabricated ultrawideband thin-film antennas from the high-temperature superconductor YBa₂Cu₃O_{7- δ} (YBCO) partially covered with Au. By using a focused He ion beam (He-FIB) we “draw” a Josephson Junction (JJ) [1] into the microbridge footpoint of the spiral antenna. Under microwave irradiation the JJ exhibits Shapiro steps in the $I - V$ characteristic.

We report on design optimization. This includes improved matching of the impedances of the antenna and the JJ in an ultrawide frequency band by using a logarithmic periodic antenna. Moreover, we performed simulations using CST STUDIO-SUITE to improve the coupling of a plane-wave signal to the antenna.

To characterize the antennas, we compare the excitation of the JJ embedded in a simple linear YBCO bridge (~ 1 mm) with the one embedded in the footpoint of the antenna, for frequencies up to 40 GHz. The ultimate goal of such an antenna with a YBCO JJ is to detect the radiation from a BSCCO-mesa (placed on another chip nearby) in the frequency range ≥ 0.5 THz. The latest measurements will be presented.

[1] B. Müller et al., *Phys. Rev. Appl.* **11**, 044082 (2019)

TT 57.23 Thu 15:00 P2/OG2

Investigation and optimization of $\text{YBa}_2\text{Cu}_3\text{O}_{7-\delta}$ Josephson junctions written with a focused He ion beam — •CHRISTOPH SCHMID¹, MAX KARRER¹, KATJA WURSTER¹, MORITZ MEICHSNER¹, ISABELLE VANDERMOETEN¹, NOOR HASAN¹, RAMÓN MANZORRO^{2,3}, JAVIER PABLO-NAVARRO^{2,3}, CESAR MAGEN^{2,3}, DIETER KOELLE¹, REINHOLD KLEINER¹, and EDWARD GOLDOBIN¹ — ¹Physikalisches Institut, Center for Quantum Science and LISA⁺, Universität Tübingen, Germany — ²Instituto de Nanociencia y Materiales de Aragón (INMA), CSIC-Universidad de Zaragoza, Spain — ³Laboratorio de Microscopías Avanzadas (LMA), Universidad de Zaragoza, Spain

We use a focused He Ion Beam (He-FIB) to “write” Josephson barriers across $\text{YBa}_2\text{Cu}_3\text{O}_{7-\delta}$ (YBCO) thin-film bridges. Such Josephson junctions (JJs) exhibit RCSJ-like I - V characteristics, and the dependence of critical current vs. magnetic field resembles a Fraunhofer pattern [1]. Scanning transmission electron microscopy (STEM) shows that He-FIB irradiation modifies locally (~ 10 nm) the YBCO crystal structure that can partially heal with time. Electric transport measurements provide the evolution of the JJ parameters with time or thermal annealing. Those reveal barrier recovery processes and show how to stabilize the JJ parameters on short time scales. Furthermore, we investigated the interaction of two and more JJs placed close to each other and biased in series. Using a multi-terminal arrangement we found some unexpected behavior that will be discussed. Several approaches to synchronize arrays of He-FIB written JJs are investigated.

[1] B. Müller et al., Phys. Rev. Applied **11**, 044082 (2019)

TT 57.24 Thu 15:00 P2/OG2

On-chip driving of a phase-slip junction for dual Shapiro steps — •DAVID SCHEER and FABIAN HASSLER — JARA Institute for Quantum Information, RWTH Aachen University, 52056 Aachen, Germany

A single Josephson junction in the phase-slip regime exhibits Bloch oscillations that relate current to frequency if supplied with a DC voltage-bias. If additionally an AC-drive is applied to the junction, the Bloch oscillations can synchronize with the driving frequency. This leads to the emergence of dual Shapiro steps with constant current in the IV-curve of the junction with the current determined by the driving frequency. An AC-drive in the required frequency regime of > 10 GHz is challenging to implement experimentally without detrimental effects due to stray capacitances. We investigate the use of a Josephson junction with a DC-bias as an on-chip AC-voltage source. We discuss the relevant coupling parameters between the oscillations caused by the DC-Josephson effect and the Bloch oscillations as well as the back action of the Bloch oscillations on the Josephson oscillations. We identify the regime in which the back action is minimized in order to obtain a steady voltage source to create dual Shapiro steps.

TT 57.25 Thu 15:00 P2/OG2

MOCCA: A 4k-pixel molecule camera for the position and energy resolved detection of neutral molecule fragments — •DANIEL KREUZBERGER¹, CHRISTIAN ENSS¹, ANDREAS FLEISCHMANN¹, LISA GAMER², LOREDANA GASTALDO¹, CHRISTOPHER JAKOB², ANSGAR LOWACK¹, OLDŘICH NOVOTNY², ANDREAS REIFENBERGER¹, DENNIS SCHULZ¹, and ANDREAS WOLF² — ¹Heidelberg University — ²Max Planck Institute for Nuclear Physics, Heidelberg

The MOCCA detector is a 4k-pixel high-resolution molecule camera based on metallic magnetic calorimeters and read out with SQUIDS that is able to detect neutral molecule fragments with keV kinetic energies. It will be deployed at the Cryogenic Storage Ring CSR at the Max Planck Institute for Nuclear Physics in Heidelberg, a storage ring built to prepare and store molecular ions in their rotational and vibrational ground states, enabling studies on electron-ion interactions. To reconstruct the reaction kinematics, MOCCA measures the energy and position of incident particles on the detector, even with multiple particles hitting the detector simultaneously.

We present a new read-out scheme which uses only 32 SQUID channels for the 4096 pixels of the detector as well as some new fabrication details including copper-filled through-wafer vias to heat-sink the detector to the wafer backside. In addition we present the results of first characterization measurements.

TT 57.26 Thu 15:00 P2/OG2

Towards large-area 256-pixel MMC arrays for high resolution X-ray spectroscopy — •ANDREAS ABELN, STEFFEN ALLGEIER, AXEL BRUNOLD, LARS EISENMANN, DANIEL HENGSTLER, LUKAS MÜNCH, ALEXANDER ORLOW, ANDREAS FLEISCHMANN, and CHRISTIAN ENSS — Kirchhoff-Institute for Physics, Heidelberg University

Metallic Magnetic Calorimeters (MMCs) are energy-dispersive cryogenic particle detectors. Operated temperatures below 50 mK, they provide very good energy resolution, high quantum efficiency as well as linearity over a large energy range. In many precision experiments on X-ray spectroscopy the photon flux is small, thus a large active detection area is desirable. Therefore, we develop arrays with increasing number of pixels. For a cost-effective read-out of a growing number of detector channels we investigate different multiplexing techniques. In this contribution we present the design of a novel 16×16 pixel MMC array. The pixels provide a total active area of $4 \text{ mm} \times 4 \text{ mm}$ and are equipped with $5 \mu\text{m}$ thick absorbers made of gold. This ensures a stopping power of at least 50 % for photon energies up to 20 keV. The expected energy resolution is $\Delta E = 1.4 \text{ eV}$ (FWHM) at an operating temperature of 20 mK. We give an overview about the microfabrication process and focus on the challenging task of producing through wafer vias to heat sink the MMC pixels to the wafer backside. These vias are realized by holes etched through the silicon substrate and subsequently lined with gold to achieve high thermal coupling between detector pixels and the cryostat.

TT 57.27 Thu 15:00 P2/OG2

A dedicated 2-dimensional array of metallic magnetic microcalorimeters to resolve the 29.18 keV doublet of ^{229}Th — •A. BRUNOLD, A. ABELN, S. ALLGEIER, J. GEIST, D. HENGSTLER, A. ORLOW, L. GASTALDO, A. FLEISCHMANN, and C. ENSS — Heidelberg University

The isotope ^{229}Th has the nuclear isomer state with the lowest presently known excitation energy, which possibly allows to connect the fields of nuclear and atomic physics with the potential application as a nuclear clock. In order to excite this very narrow transition with a laser a precise knowledge of the transition energy is needed. Recently the isomer energy (8.338 ± 0.024 eV [Kraemer et al., arXiv:2209.10276, 2022]) could be precisely determined. To get additional valuable insights, we will improve our recent high-resolution measurement [Sikorsky et al., PRL 125, 2020] of the γ -spectrum following the α -decay of ^{233}U . This decay results in excited ^{229}Th with a nuclear state at 29.18 keV. Resolving the doublet, that results from subsequent de-excitation to the ground and isomer state, respectively, would allow an independent measurement of the isomer energy and the branching ratio of these transitions. To resolve this doublet, we develop a 2D detector array consisting of 8×8 metallic magnetic calorimeters (MMCs). MMCs are operated at millikelvin temperatures and convert the energy of a single incident γ -ray photon into a temperature pulse which is measured by a paramagnetic temperature sensor. The detector array features an active detection area of 4 mm^2 , a stopping power of 63.2% for 30 keV photons and an energy resolution below 3 eV (FWHM).

TT 57.28 Thu 15:00 P2/OG2

X-ray spectroscopy of U^{90+} ions with a 64-pixel metallic magnetic calorimeter array — •A. ORLOW¹, S. ALLGEIER¹, A. ABELN¹, A. BRUNOLD¹, M. FRIEDRICH¹, A. GUMBERIDZE², D. HENGSTLER¹, F. M. KRÖGER^{2,3,4}, P. KUNTZ¹, A. FLEISCHMANN¹, M. LESTINSKY², E. B. MENZ^{2,3,4}, PH. PFÄFFLEIN^{2,3,4}, U. SPILLMANN², B. ZHU⁴, G. WEBER^{2,3,4}, TH. STÖHLKER^{2,3,4}, and C. ENSS¹ — ¹KIP, Heidelberg University — ²GSI/FAIR, Darmstadt — ³IOQ, Jena University — ⁴HI Jena

Metallic magnetic calorimeters (MMCs) are energy-dispersive X-ray detectors which provide an excellent energy resolution over a large dynamic range combined with a very good linearity. MMCs convert the energy of each incident photon into a temperature pulse which is measured by a paramagnetic temperature sensor. The resulting change of magnetisation is read out by a SQUID magnetometer.

To investigate electron transitions in U^{90+} at CRYRING@FAIR within the framework of the SPARC collaboration, we developed the 2-dimensional maXS-100 detector array. It features 8×8 pixels with a detection area of 1 cm^2 and a stopping power of 40 % at 100 keV. Four on-chip thermometers allow to correct for temperature drifts and to achieve an energy resolution of 40 eV at 60 keV. We show preliminary X-ray spectra of the recent U^{90+} beamtime. Due to the small rate of emitted X-rays, a good suppression of background radiation is mandatory, which was ensured by a coincidence measurement with a particle detector. To increase the stopping power to above 60 % at 100 keV we develop a new maXS-100 detector with $100 \mu\text{m}$ thick absorbers.

TT 58: Poster: Superconductivity II

Time: Thursday 15:00–18:00

Location: P2/OG3

TT 58.1 Thu 15:00 P2/OG3

Low temperature MMC-based muon veto for IAXO — •DANIEL UNGER, CHRISTIAN ENSS, ANDREAS FLEISCHMANN, DANIEL HENGSTLER, ASHISH JADHAV, and LOREDANA GASTALDO — Kirchhoff Institute for Physics, Heidelberg University, Im Neuenheimer Feld 227, 69120 Heidelberg, Germany.

An array of Metallic Magnetic Calorimeter (MMC) operated at a few mK in a dilution refrigerator is considered as a possible focal plane detector for the IAXO helioscope. For such an experiment, the background rate must be smaller than $10^{-6} \text{ keV}^{-1} \text{ cm}^{-2} \text{ s}^{-1}$. However, we expect the rate of events related to cosmic muons to be two orders of magnitude larger. A traditional muon veto composed by scintillating panels would have to cover the full cryostat, a volume of about 3 m^3 . A cryogenic muon veto surrounding the 150 cm^3 volume of the detector module could veto muon related events more efficiently. We present the development of a large-area MMC-based muon veto. Muons will be detected through their energy deposition while traversing a silicon wafer with thickness of 0.4 mm and an area of 30 cm^2 . We discuss the design and the fabrication challenges of the muon veto in addition to the prototype setup for testing purposes. We aim to characterize the performance of the large silicon detector and at the same time study the spectrum of muon related events detected by the MMC array as well as of the residual background due to natural radioactivity. Finally, we evaluate the suitability of MMC arrays for low background measurements.

TT 58.2 Thu 15:00 P2/OG3

Dc-SQUID readout with high dynamic range and intrinsic frequency-domain multiplexing capability — •L. MÜNCH, A. ABELN, N. KAHNE, F. KRÄMER, D. HENGSTLER, L. HOIBL, D. MAZIBRADA, D. RICHTER, A. STOLL, A. FLEISCHMANN, and C. ENSS — Kirchhoff-Institute for Physics, Heidelberg University, Im Neuenheimer Feld 227, 69120 Heidelberg, Germany.

Dc superconducting quantum interference devices (dc-SQUIDs) are periodic flux-to-voltage converters whose linear flux range is rather small. For this reason, a flux locked loop (FLL) circuit is typically used to linearize the output signal and increase the dynamic range. However, the measurement of large signals while maintaining the excellent noise performance of SQUIDs sets high demands on the digitizer sampling the SQUID signal in terms of voltage resolution. Furthermore, FLL operation often sets a practical limit for the realization of massive multi-channel SQUID systems since feedback wires have to be routed to every SQUID.

In this contribution, we discuss a SQUID readout approach which relaxes the hardware requirements of a SQUID system while maintaining a linearized output signal and a large dynamic range. At the same time, it allows for reducing the number of wires within multi-channel SQUID systems due to its intrinsic frequency-domain multiplexing (FDM) capability. We introduce the basic concept of our readout approach and demonstrate its intrinsic FDM-capability using a custom-made four channel multiplexer device. We also present a new chip design optimized for the read-out of a novel 16×16 pixel MMC array.

TT 58.3 Thu 15:00 P2/OG3

Integrated two-stage SQUID-chip with 6 nH input impedance — •DAVID MAZIBRADA, FABIAN KRÄMER, ALEXANDER STOLL, NICOLAS KAHNE, LUKAS MÜNCH, DANIEL HENGSTLER, ANDREAS FLEISCHMANN, and CHRISTIAN ENSS — Kirchhoff-Institute for Physics, Im Neuenheimer Feld 227, 69120 Heidelberg, Germany.

SQUIDs are sensitive superconducting magnetic flux to voltage converters, whose operation is based on the Josephson effects. To increase the signal-to-noise ratio of a SQUID-based readout system one can amplify the signal with an N -SQUID series array. We present our first integrated two-stage chip design which combines a single current sensing dc-SQUID as front-end and a 18-dcSQUID series array as amplifier stage, in one compact, well thermalized chip. This not only eliminates the need for two separate chips, but also achieves low signal propagation delay and larger bandwidth. Compared to our most recent single-stage current sensing SQUIDs, the first stage SQUID features a 2-turn input coil with increased inductance of 6 nH increasing the input current sensitivity by a factor of about 2. To counteract the resistive heating of the two-stage setup, large thermalization pads made of gold are implemented to thermalize the resistive elements and in addition the chip can be thermally anchored to the sample holder by means of gold bonds. In future designs lossy striplines will be used in order to provide delocalized broad-band damping and suppress effects of parasitic resonances without introducing new noticeable sources of noise.

TT 58.4 Thu 15:00 P2/OG3

Identification of noise sources in superconducting microstructures — •R. YANG, A. FLEISCHMANN, D. HENGSTLER, M. HERBST, D. MAZIBRADA, L. MÜNCH, A. REIFENBERGER, C. STÄNDER, and C. ENSS — Kirchhoff-Institute for Physics, Heidelberg University, Im Neuenheimer Feld 227, 69120 Heidelberg, Germany.

Improving the performance of a superconducting device often means identifying and eliminating noise. Many potential noise sources are independent of the specific experimental set-up and transferable across many device categories such as qubits, SQUIDs, and superconducting detectors. We have constructed a stand-alone device able to representably probe specific noise sources. The set-up consists of a Wheatstone-like bridge of microfabricated superconducting inductors and a pair of two-stage dc-SQUID read-out chains. Cross-correlation removes noise contributions from the read-out electronics giving us the sum total of all noise in the superconducting circuit. If, in comparison, the Wheatstone bridge is AC-driven, we can measure a sample material's magnetic noise via the material's complex AC susceptibility using the fluctuation-dissipation theorem. The experiment is performed at temperatures between $T = 10 \text{ mK}$ and 1000 mK in the frequency range from $f = 100 \text{ mHz}$ to 100 kHz on an experimental holder with excellent thermal coupling and shielding. We present first results of measurements on SiO_2 and Ag:Er thin films and compare these results with previous measurements on Au:Er . In addition, we demonstrate our device's ability to probe the dynamics of magnetic moments in a sample material.

TT 58.5 Thu 15:00 P2/OG3

Recent insights into low frequency excess flux noise in superconducting quantum devices — •ANNA FERRING-SIEBERT, FABIAN KAAP, DAVID MAZIBRADA, LUKAS MÜNCH, MATTHEW HERBST, ANDREAS FLEISCHMANN, CHRISTIAN ENSS, and SEBASTIAN KEMPF — Kirchhoff-Institute for Physics, Im Neuenheimer Feld 227, 69120 Heidelberg, Germany.

In many applications low frequency excess flux noise (EFN), with a frequency dependence of $1/f^\alpha$, limits the performance of superconducting quantum devices such as SQUIDs and Qubits. Although it was long believed that its magnitude expressed in units of magnetic flux $S_\Phi(1 \text{ Hz})$ and exponent α are fairly independent of the device material and inductance, there meanwhile exist hints for the contrary. It is also known that EFN can depend on the equipment used for device fabrication, the reason for that however remained unknown up to now.

In this contribution, we discuss origins of fabrication induced EFN as well as means to minimize it. In particular, we show that material layers deposited with commercial deposition equipment can contain magnetic impurities causing EFN. In this context, we present how we have modified commercial sputtering sources to reduce EFN and provide evidence for a relationship between EFN amplitude and the DC magnetization of the deposited material layers. Finally, recent measurements investigating the dependence of EFN on device inductance are discussed, suggesting that energy sensitivity $\epsilon(1 \text{ Hz}) = S_\Phi(1 \text{ Hz})/(2L)$, rather than magnetic flux noise, is the more appropriate metric to describe EFN.

TT 58.6 Thu 15:00 P2/OG3

Impedance engineering of flux-pumped Josephson traveling wave parametric amplifier — •DANIIL E. BAZULIN^{1,2}, KEDAR E. HONASOGE^{1,2}, LEON KOCH^{1,2}, NIKLAS BRUCKMOSER^{1,2}, YUKI NOJIRI^{1,2}, THOMAS LUSCHMANN^{1,2}, ACHIM MARX¹, STEFAN FILIPP^{1,2,3}, and KIRILL G. FEDOROV^{1,2} — ¹Walther-Meißner-Institut, Bayerische Akademie der Wissenschaften, 85748 Garching, Germany — ²Technical University of Munich, TUM School of Natural Sciences, Physics Department, 85748 Garching, Germany — ³Munich Center for Quantum Science and Technology (MCQST), 80799 Munich, Germany

Scalable quantum computing with superconducting qubits relies on efficient and fast readout of multiple qubits. This goal can be achieved by exploiting broadband Josephson Traveling Wave Parametric Amplifiers (JTWPAs). Here, we investigate fabrication and characterization of a specific type of the JTWPA based on aluminium Superconducting Nonlinear Asymmetric Inductive elements (SNAILs) exploiting the 3-wave mixing down-conversion process. This approach allows for separating signal and pump paths, which is expected to enhance the overall JTWPA performance by mitigating back action amplification processes and avoiding the pump depletion. Additionally, we implement a single-layer 50Ω impedance matching approach by exploiting fish-bone capacitors fabricated simultaneously with the Josephson junctions. This technique avoids using extra dielectric layers, which are typical sources of losses and noise in JTWPAs.

TT 58.7 Thu 15:00 P2/OG3

Large-scale fabrication of Josephson parametric devices — •MARIATERESA HANDSCHUH^{1,2}, KEDAR E. HONASOGE^{1,2}, YUKI NOJIRI^{1,2}, NIKLAS BRUCKMOSER^{1,2}, LEON KOCH^{1,2}, DANIIL BAZULIN^{1,2}, FLORIAN FESQUET^{1,2}, FABIAN KRONOWETTER^{1,2,4}, MICHAEL RENGER^{1,2}, WUN K. YAM^{1,2}, ACHIM MARX¹, RUDOLF GROSS^{1,2,3}, and KIRILL G. FEDOROV^{1,2} — ¹Walther-Meißner-Institut, 85748 Garching, Germany — ²Technical University of Munich, TUM School of Natural Sciences, Physics Department, 85748 Garching, Germany — ³Munich Center for Quantum Science and Technology, 80799 Munich, Germany — ⁴Rohde & Schwarz GmbH & Co. KG, 81671 Munich, Germany

The rapid progress in the field of quantum information processing with superconducting circuits requires the development of large-scale fabrication to in-

crease fabrication efficiency, reproducibility as well as to reduce costs. Moreover, many advanced quantum applications and experiments rely on using multiple nominally identical chips, such as flux-driven Josephson parametric amplifiers (JPAs) [1]. To this end, the goal is to establish good control over various fabrication parameters, such as critical current density and microwave losses, in JPAs with Nb/Al-AlO_x/Nb Josephson junctions on 4-inch high-resistivity silicon wafers. We provide a detailed analysis of the related parameter distribution across the wafer and make proposals for future improvements.

[1] K. G. Fedorov et al., *Sci. Adv.* 7, eabk0891 (2021)

TT 58.8 Thu 15:00 P2/OG3

Microwave quantum memory based on rare earth doped crystal — •JIANPENG CHEN^{3,1,2}, ANA STRINIC^{3,1,2}, ACHIM MARX^{1,3}, KIRILL G. FEDOROV^{1,3}, HANS HUEBL^{1,2,3}, RUDOLF GROSS^{1,2,3}, and NADEZHDA KUKHARCHYK^{3,1,2} — ¹Walther-Meißner-Institut, Bayerische Akademie der Wissenschaften, 85748 Garching, Germany — ²Munich Center for Quantum Science and Technology, 80799 Munich, Germany — ³Technical University of Munich, TUM School of Natural Sciences, Physics Department, 85748 Garching, Germany

Quantum memory is an essential element in the development of future quantum technologies, such as quantum computing circuits and quantum communication links. Specifically, crystals doped with rare earth ions are promising competitive candidates due to their long coherence times [1] and potential multiplexing capability [2]. Here, we aim to couple coherent microwave signals to rare earth ion dopants in yttrium orthosilicate crystals (Y₂SiO₅) at 10 mK. We will discuss the impact of the transmission line design on the efficiency of quantum information storage and its multimodality potential.

We acknowledge financial support from the Federal Ministry of Education and Research of Germany (project number 16KISQ036).

[1] M. Zhong, *Nature* 517, 177 (2015)

[2] A. Ortu et al., *Quantum Sci. Technol.* 7, 035024 (2022)

TT 58.9 Thu 15:00 P2/OG3

Non-Markovian effects in Er:YSO — •OWEN THOMAS HUISMAN^{1,2,4}, ANA STRINIC^{1,2,3}, RUDOLF GROSS^{1,2,3}, and NADEZHDA KUKHARCHYK^{1,2,3} — ¹Walther-Meißner-Institut, Bayerische Akademie der Wissenschaften, Garching, Germany — ²Physik-Department, Technische Universität München, Garching, Germany — ³Munich Center for Quantum Science and Technologies, München, Germany — ⁴Delft University of Technology, Delft, Netherlands

Erbium doped Y₂SiO₅ (Er:YSO) has proven to be a suitable platform to realise quantum memory protocols based on microwave ESR techniques [1]. The successful storage and retrieval of a microwave quantum state depends on the coherence and relaxation of spectral holes burned in inhomogeneously broadened spin transitions. Recent work has shown that relaxation and decoherence processes in Er:YSO at sub-Kelvin temperature may be affected by the phonon bottleneck process [2]. Several attempts have been made to develop a microscopic theory of the phonon bottleneck [3,4]. In this work, we attempt to connect the phonon bottleneck to more recent investigations of non-Markovian open quantum systems [5]. We propose an experiment to confirm the presence of non-Markovian effects in Er:YSO and justify the connection with a phonon bottleneck.

[1] S. Probst et al., *Phys. Rev. B* 92, 014421 (2015)

[2] R. P. Budoyo et al., *Appl. Phys. Express* 11, 043002 (2018)

[3] D. A. Garanin, *Phys. Rev. B* 75, 094409 (2007)

[4] D. A. Garanin, *Phys. Rev. B* 77, 024429 (2008)

[5] C.-F. Li et al., *EPL* 127, 50001 (2019)

TT 58.10 Thu 15:00 P2/OG3

Microwave single-shot quantum key distribution — •FLORIAN FESQUET^{1,2}, FABIAN KRONOWETTER^{1,2,4}, MICHAEL RENGER^{1,2}, NADEZHDA KUKHARCHYK^{1,2}, HANS HUEBL^{1,2,3}, ACHIM MARX¹, RUDOLF GROSS^{1,2,3}, and KIRILL G. FEDOROV^{1,2} — ¹Walther-Meißner-Institut, 85748 Garching, Germany — ²Technical University of Munich, TUM School of Natural Sciences, Physics Department, 85748 Garching, Germany — ³Munich Center for Quantum Science and Technology (MCQST), 80799 Munich, Germany — ⁴Rohde & Schwarz GmbH, 81671 Munich, Germany

Security of modern classical data encryption often relies on computationally hard-to-solve problems. A potential remedy for this challenge is quantum communication (QC) which takes advantage of the laws of quantum physics to provide secure exchange of information. Here, quantum key distribution (QKD) represents a powerful tool, allowing unconditionally secure QC between remote parties. A demand for QC at microwave frequencies has emerged due to the tremendous progress in quantum information processing with superconducting circuits. To this end, we present a realization of a continuous-variable QKD protocol based on displaced squeezed microwave states. We use a Josephson parametric amplifier (JPA) to generate squeezed microwave states at cryogenic temperatures. By implementing a single-shot quadrature readout with a second JPA in the phase-sensitive regime with quantum efficiency of 38 %, we demonstrate the unconditional security of this microwave QKD protocol. We analyze these results in terms of losses and noise in order to map them on possible real-world scenarios.

TT 58.11 Thu 15:00 P2/OG3

3D-Integration of superconducting qubits using flip-chip bump bonding technology — •FRANZISKA WILFINGER^{1,2}, IVAN TSITSILIN^{1,3}, and STEFAN FILIPP^{1,2,3} — ¹Walther-Meißner-Institut, Bayerische Akademie der Wissenschaften, Garching, Germany — ²Physik Department, Technische Universität München, Garching, Germany — ³Munich Center for Quantum Science and Technologies (MCQST), Munich, Germany

Superconducting quantum circuits are typically realized in a planar architecture. This approach is, however limited to dozens of qubits due to the complexity of routing signal lines when scaling beyond. 3D-integration can overcome these limitations by separating circuit components on different layers and on different chips. One promising 3D-integration strategy is to assemble two chips, patterned on one side, through flip-chip bonding using indium bumps. Quantum components such as qubits and couplers containing Josephson junctions can then be separated from the control- and readout-lines on different faces. Here, we discuss design concepts and test-structures in a flip-chip architecture and their simulated performances with respect to quality factors, decay rates and gate times. Finite-element simulation is applied to extract design parameters such as the qubit coupling to readout- and control lines and to other qubits. These parameters are optimized in order to achieve a performance comparable with planar structures. Moreover, the influence of inaccuracies in fabrication is investigated by simulating varying distance parameters and analyzing their impact on relevant quantities.

TT 58.12 Thu 15:00 P2/OG3

Probing the density of states of defects in superconducting flux qubits — •BENEDIKT BERLITZ, ALEXANDER KONSTANTIN HÄNDEL, ALEXEY V. USTINOV, and JÜRGEN LISENFELD — Physikalisches Institut, Karlsruhe Institute of Technology (KIT), Karlsruhe, Germany

Material defects forming two-level systems (TLS) present a source of decoherence and unwanted degrees of freedom in superconducting quantum circuits. Current theoretical models make different assumptions about the frequency dependence of the TLS' density of states (DOS). To measure the TLS' DOS in a wide frequency range, spanning from about 0.1 to 20 GHz, we fabricated flux qubits as TLS detectors. Measuring the DOS will enhance our understanding of the underlying physics of TLS in amorphous materials.

TT 58.13 Thu 15:00 P2/OG3

Fast quantum state tomography with superconducting qubits — •ANDRAS DI GIOVANNI¹, ADRIAN AASEN³, MORITZ REH³, MARTIN GÄRTNER³, MARKUS GRIEDEL², HANNES ROTZINGER^{1,2}, and ALEXEY USTINOV^{1,2} — ¹Physikalisches Institut, Karlsruher Institut für Technologie, Karlsruhe — ²Institut für Quantenmaterialien und Technologien, Karlsruher Institut für Technologie, Karlsruhe — ³Kirchhoff-Institut für Physik, Heidelberg

Quantum simulators promise insights into quantum many-body problems in regimes where classical simulation methods hit a complexity wall. One challenge towards this goal is to develop well characterized building blocks that allow to scale system sizes up while conserving reliability in terms of errors. A promising platform for building such quantum simulators are superconducting quantum circuits. We characterize small-scale quantum processors in the time domain with single-shot accuracy and minimal hardware and post-processing overhead. For this purpose we use reactive basis rotations based on greedy algorithms and adaptive Bayesian tomography. We present experimental results measured on a transmon qubit and compare the data with theoretical predictions.

TT 58.14 Thu 15:00 P2/OG3

Infrared filters for superconducting qubit applications — •MARKUS GRIEDEL^{1,2}, SEBASTIAN KOCH², ALEX STEHLI², HANNES ROTZINGER^{1,2}, and ALEXEY V. USTINOV^{1,2} — ¹Institut für Quantum Materials and Technologies (IQMT), Karlsruhe Institut für Technologie (KIT) — ²Physikalisches Institut (PHI), Karlsruhe Institut für Technologie (KIT)

Superconducting qubits are manipulated and read out using microwave signals which are generated at room temperature and guided through coaxial cables to the millikelvin temperature stage. One common problem of coax cables is their high transparency to infrared radiation originating from a rather high photon flux sources at elevated temperatures of cryostat stages. Filtering out the infrared radiation requires a low-pass filter with a sharp cutoff in the micro- or low mm-wave frequency range. We present simulations as well as experimental data on a new generation of powder based filters. The samples are investigated over the full band of infrared radiation using conventional detectors as well as superconducting qubits directly.

TT 58.15 Thu 15:00 P2/OG3

Superconducting flux qubits with stacked Josephson junctions — •ALEX KREUZER¹, HOSSAM TOHAMY¹, THILO KRUMREY¹, MARKUS GRIEDEL^{1,2}, HANNES ROTZINGER^{1,2}, and ALEXEY V. USTINOV^{1,2} — ¹Physikalisches Institut (PHI), Karlsruher Institut für Technologie (KIT) — ²Institut für Quantenmaterialien und -technologien (IQMT), Karlsruher Institut für Technologie (KIT)

Josephson junctions are often employed as nonlinear inductive elements in superconducting qubits as they allow to tailor specific circuit properties. The

promising flux qubit types as fluxonium or qurton qubits require compact inductances which are often implemented as arrays of Josephson junctions. Here, the stray capacitance originating, for instance, from the capacitive coupling of an array island to ground, introduces the major limitation of this approach, since it introduces parasitic resonances at GHz frequencies which may degrade the overall qubit performance. We explore the possibility of implementing the qubit inductances by stacking Josephson junctions vertically and thus reducing the capacitance to ground. We present transport as well as microwave measurement data of stacked Josephson junctions and flux qubits made from them. Furthermore, we present a comparison of our experimental data with a detailed numerical simulation.

TT 58.16 Thu 15:00 P2/OG3

Flux escape mitigation in gradiometric fluxonium qubits — •DENIS BÉNÂTRE¹, MATHIEU FÉCHANT¹, MARTIN SPIECKER^{1,2}, and IOAN POP^{1,2} — ¹IQMT, Karlsruhe Institute of Technology, 76344 Eggenstein-Leopoldshafen, Germany — ²PHI, Karlsruhe Institute of Technology, 76131 Karlsruhe, Germany Superconducting fluxonium qubits have grown in the past decade as an interesting alternative to the now standard transmons. In 2022, Gusenkova et al. proposed a new design, the gradiometric fluxonium qubit, whose two loops have been shown to suppress sensitivity to homogeneous magnetic field and open the door for its use in hybrid quantum systems. However, these devices undergo flux escape triggered by radioactive and cosmic impacts, and thus require shielding from ionizing radiation, e.g. in deep-underground facilities [Gusenikova et al., 2022]. We present new designs of gradiometric fluxoniums aimed at intrinsically mitigating the rate of trapped flux escape.

TT 58.17 Thu 15:00 P2/OG3

Towards millimeter-wave superconducting qubits — •PHILIPP LENHARD, JÜRGEN LISENFELD, and ALEXEY V. USTINOV — Physikalisches Institut, Karlsruhe Institute of Technology (KIT), Karlsruhe, Germany

Superconducting circuits are a promising platform to realize a solid-state quantum computer. However, scaling up to larger multi-qubit circuits is severely hindered by decoherence of various origins. While contemporary qubits are typically operated between 3 and 6 GHz resonance frequencies, here we investigate qubit designs for millimeter-wave operation frequencies between 80 and 110 GHz. We present first spectroscopic measurements of resonant energy level transitions in a current-biased Josephson junction in the millimeter-wave regime. In addition, we show simulations of designs for integrating qubits and readout resonators in 3D-waveguides.

TT 58.18 Thu 15:00 P2/OG3

Towards dissipatively coupled photon-pressure circuits — •JANIS PETER, MOHAMAD ADNAN EL KAZOUNI, EMILY GUO, KEVIN UHL, and DANIEL BOTHNER — Physikalisches Institut, Center for Quantum Science (CQ) and LISA⁺, Universität Tübingen, Germany

Photon-pressure circuits are a superconducting all-circuit equivalent of cavity optomechanics. They recently gained a lot of attention since they are providing a new toolbox for sensing and controlling radiofrequency (rf) photons by high-frequency (hf) circuits. In contrast to optomechanical systems, this platform only consists of LC circuits without any mechanical resonators. As a result they offer a larger flexibility regarding device parameters and a simplified fabrication process. Until now, photon-pressure circuits have been realized using the so-called dispersive interaction: the rf-resonator modulates the resonance frequency ω_0 of the hf-circuit. To reach the quantum regime by ground state cooling, dispersively coupled devices need to be in the so-called sideband-resolved regime, that is, the resonance frequency Ω_0 of the rf-resonator is much larger than the decay rate of the hf-circuit κ (typically several 100 kHz). Extending the quantum regime to even lower frequency photons (≤ 1 MHz) requires a different interaction: dissipative photon-pressure coupling, where κ is modulated instead of ω_0 . We present our progress on implementing a dissipative photonpressure interaction between two superconducting circuits and discuss in this context simulation, fabrication, device design and intermediate experimental milestones.

TT 58.19 Thu 15:00 P2/OG3

Towards non-classical state preparation in photon-pressure circuits — •MOHAMAD ADNAN EL KAZOUNI, JANIS PETER, EMILY GUO, KEVIN UHL, and DANIEL BOTHNER — Physikalisches Institut, Center for Quantum Sciences (CQ) and LISA⁺, Universität Tübingen, Germany

Photon-Pressure is a non-linear interaction between two electromagnetic modes in LC circuits, which gained considerable attention in the past years due to its unique possibilities to sense and control radio-frequency photons. To date, several milestone experiments have been performed such as interferometric radio-frequency thermometry, the observation of parametric strong-coupling, and the realization of resolved-sideband cooling of a low-frequency LC circuit (~ 100 MHz) into its quantum ground state. Although photon-pressure is in principle providing the possibilities, non-classical states like quantum squeezed and entangled states of MHz photonic modes have not been realized yet in these systems. Those states, however, have the potential to enhance quantum-limited sensing of

bosonic modes in the radio-frequency regime, an application of photon-pressure systems that have been discussed for instance in the context of the search for dark-matter axions. In our poster, we will present our progress in developing photon-pressure devices that are being engineered toward the preparation of non-classical radio-frequency photon states and we will discuss the next steps and our future plans.

TT 58.20 Thu 15:00 P2/OG3

Towards room temperature microwave quantum teleportation — •WUN KWAN YAM^{1,2}, MICHAEL RENGER^{1,2}, SIMON GANDORFER^{1,2}, FLORIAN FESQUET^{1,2}, KEDAR HONASOGE^{1,2}, FABIAN KRONOWETTER^{1,2,3}, YUKI NOJIRI^{1,2}, ACHIM MARX¹, RUDOLF GROSS^{1,2,4}, and KIRILL G. FEDOROV^{1,2} — ¹Walther-Meißner-Institut, BAdW, 85748 Garching, Germany — ²Physik-Department, TUM, 85748 Garching, Germany — ³Rohde & Schwarz GmbH & Co. KG, 81671 Munich, Germany — ⁴Munich Center for Quantum Science and Technology, 80799 Munich, Germany

Microwave quantum communication enables efficient and unconditionally secure exchange of quantum states. This paves the way towards distributed quantum computing and open-air quantum key distribution. One of the relevant quantum communication protocols is quantum teleportation. In the microwave regime, quantum teleportation has been successfully demonstrated by using superconducting Josephson circuits in a cryogenic setup. To investigate the limits of microwave quantum teleportation under more realistic application scenarios, we study the influence of thermal noise and losses in microwave communication channels. We show that the teleportation protocol is robust against noise in the feedforward channel and analyze experimental limits of distributing entanglement via thermal channels. Furthermore, we describe the experimental implementation of microwave quantum teleportation with the room temperature feedforward and consider microwave quantum teleportation in the open air.

TT 58.21 Thu 15:00 P2/OG3

Experimental investigations and flow simulation of regenerator configurations of a single stage GM-type pulse tube cooler — •ELIAS EISENSCHMIDT^{1,3}, JACK-ANDRÉ SCHMIDT^{2,3}, BERND SCHMIDT^{2,3}, JENS FALTER³, and ANDRÉ SCHIRMEISEN^{2,3} — ¹Technische Hochschule Mittelhessen, Friedberg, Germany — ²Justus-Liebig-university, Giessen, Germany — ³TransMIT-Center for Adaptive Cryotechnology and Sensors, Giessen, Germany

Pulse tube coolers are increasingly used in industry and research due to their low vibrations and long service intervals. The regenerator and especially the filling of the regenerator has a great influence on the cooling capacity as well as the achievable, minimum temperatures. The temperature-dependent heat storage capacity of the materials used in the regenerator is usually the main focus of attention when selecting regenerator fillings. [1, 2]

This poster deals with the pressure drop of two regenerator fillings of stainless steel spheres and sieves. Steady-state and transient measurements of the two regenerator fillings will be discussed. In comparison of the two fillings used, the meshes show lower pressure drops, resulting in a higher cooling efficiency as regenerator filling, while spheres are more cost efficient in time and acquisition.

[1] N. Almtire et al., J. Low Temp. Phys. 199, 1179 (2020)

[2] P. P. Steijaert, Thermodynamical aspects of pulse-tube refrigerators, Technische Universiteit Eindhoven (1999)

TT 58.22 Thu 15:00 P2/OG3

Characterization of the cooling power on a two stage 4 K pulse tube cooler operated with solenoid valves — •XAVIER HERRMANN¹, JACK-ANDRÉ SCHMIDT^{1,2}, BERND SCHMIDT^{1,2}, JENS FALTER², and ANDRÉ SCHIRMEISEN^{1,2} — ¹Institute of Applied Physics, Justus-Liebig-University Giessen, Germany — ²TansMIT-Center for Adaptive Cryotechnology and Sensors, Giessen, Germany

Closed-cycle cryocoolers have become an important tool for low temperature scientific research [1]. Here we focus on Gifford-McMahon (GM) type pulse tube coolers (PTC), which offer low maintenance and long measurement periods. In order to create a temperature difference between the cold and hot end of the cooler, Helium is periodically compressed and expanded within the cooler. In order to do so a valve - commonly a rotary valve - allows high pressure Helium to enter the cooler or to relieve the pressure within. The high and low pressure levels are supplied by a Helium compressor [2]. In order to reduce complexity and improve flexibility of the system [3], this poster will look into the operation of a two stage 4 K PTC with solenoid valves. This removes the rotary valve from the system and therefore allows for easy access and change of parameters like high- and low-pressure duration, quiet times after high- and low-pressure pulse or frequency.

[1] R. Güsten et al., Nature 568, 357 (2019)

[2] R. Radebaugh, J. Phys.: Condens. Matter 21, 164219 (2009)

[3] S. Wild, Fortschr.-Ber. VDI Reihe 19 Nr. 105, Düsseldorf 1997

TT 58.23 Thu 15:00 P2/OG3

Development of a miniaturized, modular, nuclear demagnetization stage — •LEO MAXIMOV¹, NICO HUBER¹, ANDREAS BAUER¹, KEIYA SHIRAHAMA², and CHRISTIAN PFLEIDERER¹ — ¹Physik-Department, Technical University of Munich, D-85748 Garching, Germany — ²Keio University, Hiyoshi 3-14-1, Kohoku-ku, Yokohama, Japan

Experimental studies of condensed matter systems at sub-milli Kelvin temperatures are effectively only possible by virtue of nuclear adiabatic demagnetization refrigeration (NADR). While copper is the most commonly used refrigerant for NADR, both the development and operation of copper based NADR-stages are technically demanding and limited due to the very low starting temperatures needed for demagnetization. To overcome these limitations, hyperfine-enhanced refrigerants may be used. Here, we present the design and implementation of a compact, miniaturized, modular nuclear demagnetization stage for optional use with a conventional dilution refrigerator. Comprising a superconducting aluminum heat switch, a demagnetization stage using PrNi₅ with a bespoke superconducting coil, and a CMN thermometer, the setup is conceived for exploratory studies in the milli-Kelvin regime and below.

TT 58.24 Thu 15:00 P2/OG3

Study of the magnetocaloric effect in [Ni(C₄H₃O₄)₂(H₂O)₄] - A Potential Realization of a Spin-1 Spatially Anisotropic Square Lattice with Ferromagnetic Interactions — •PETRO DANYLCHENKO, RÓBERT TARASENKO, ERİK ČIŽMÁR, VLADIMÍR TKÁČ, ALŽBETA ORENDÁČOVÁ, and MARTIN ORENDÁČ — Institute of Physics, Faculty of Science, Pavol Jozef Šafárik University, Park Angelinum 9, 04154 Košice, Slovakia

The magnetocaloric effect in [Ni(C₄H₃O₄)₂(H₂O)₄] was investigated using specific heat and magnetization measurements in the temperature range from 0.4 K to 50 K in magnetic fields up to 7 T. A magnetic entropy change $-11.2 \text{ JK}^{-1} \text{ kg}^{-1}$ at a temperature of about 3.5 K is achieved for magnetic field of 7 T. The temperature dependence of the magnetic specific heat in a zero magnetic field was compared with an $S = 1$ model with single-ion anisotropy parameters D and E (axial and rhombic). The best agreement was found for the parameters $D/k_B = 7.82 \text{ K}$ and $E/k_B = 2.15 \text{ K}$. The divergence which appears between experimental and theoretical data at non-zero magnetic fields indicates the presence of additional factors in the system such as exchange interaction between magnetic ions. Broken-symmetry DFT calculations provided the values of ferromagnetic exchange interactions, $J_1/k_B = 1.50 \text{ K}$ and $J_2/k_B = 1.44 \text{ K}$. The presence of such ferromagnetic correlations may explain the enhanced magnetocaloric effect. *Supported by project No. APVV-18-0197.*

TT 58.25 Thu 15:00 P2/OG3

Noise thermometers for mK- and μ K-temperatures in high magnetic fields — •PASCAL WILLER, CHRISTIAN STÄNDER, NATHALIE PROBST, ANDREAS REISER, ANDREAS FLEISCHMANN, and CHRISTIAN ENSS — Kirchhoff-Institute for Physics, Heidelberg University, Im Neuenheimer Feld 227, 69120 Heidelberg, Germany.

To measure the temperature in the presence of high magnetic fields is one of the big challenges in solid state physics labs. We developed a prototype of a cross-correlated, current sensing noise thermometer for mK-temperatures for application in high magnetic fields. The basic concept relies on the thermal motion of charge carriers in a bulk metal resistor. Two DC-SQUIDS detect the corresponding noise signal which is then recorded via two identical but independent amplifier chains. The method of cross correlation is used to eliminate uncorrelated noise contributions from the amplifier chains. As resistor materials we use the alloys Ag₆₀Cu₄₀ as well as Pt₉₂W₈, the latter being characterized by an extremely small temperature dependence of the electrical resistivity as well as the smallest magneto-resistance known to date. We show that this approach towards a relative primary thermometer for high magnetic fields is able to cover the complete temperature range below 4 K. We discuss the design and the necessary considerations of both thermometers and present first experimental results at mK temperatures.

TT 58.26 Thu 15:00 P2/OG3

Variable temperature probe stick with 2D coil system — •CLAUDIA KÖHN¹, SYLKE BECHSTEIN², and DOREEN WERNICKE³ — ¹Entropy GmbH, Abbestr. 2-12, 10587 Berlin — ²PTB, Abbestr. 2-12, 10587 Berlin — ³Entropy GmbH, Gmunder Str. 37a, 81379 München

Within a technology transfer cooperation with PTB, Entropy made a probe stick for characterization of superconducting devices commercially available. It is an easy to use dip stick that can be cooled down directly in the liquid helium transport vessel while providing the possibility to vary temperature and apply magnetic fields.

The stick has two temperature stages. A 4.2 K stage and one with variable temperature (\sqrt{T}) stage, that can be heated up to 10 K with a temperature stability of 1 mK.

The device under test at the \sqrt{T} stage is placed inside a 2D coil system providing up to 500 mT parallel and 100 mT perpendicular to the chip. Homogeneity is 5% within a 1.5 mm radius around the center in the chip plane. At the moment

we are optimizing the fabrication process of the coil bodies to provide better homogeneity of the magnetic field perpendicular to the chip.

TT 58.27 Thu 15:00 P2/OG3

Cryogenic scanning tunneling microscope — •JULIA BESPROSWANNY¹, SEBASTIAN SCHIMMEL¹, RONNY SCHLEGEL², DANNY BAUMANN², BERND BÜCHNER², RALF VOIGTLÄNDER², DIRK LINDACKERS², and CHRISTIAN HESS¹ — ¹University of Wuppertal, 42119 Wuppertal, Germany — ²IFW Dresden, 01069 Dresden, Germany

We report the construction of a compact cryogenic scanning tunneling microscope. The design will allow to study local electronic structures at temperatures down to 2.5 K and magnetic fields of up to 15 T with atomic resolution in real space and a high energy resolution of 2 meV at 6 K. The microscope has a scanning range of $1 \mu\text{m} \times 1 \mu\text{m}$ and a built-in cleaving mechanism that renders it possible to cleave the samples at a cryogenic temperature. Samples can be exchanged within a day while the measurement time can reach up to 6 weeks. These qualities combined with its compact and portable design make this STM a comfortable tool to study low temperature phenomena, e.g. superconductivity.

TT 58.28 Thu 15:00 P2/OG3

Cyclotron resonance on germanium probed by coplanar microwave resonators — •ANASTASIA BAUERNFEIND, FREDERIK BOLLE, MARTIN DRESSEL, and MARC SCHEFFLER — 1. Physikalisches Institut, University of Stuttgart, Stuttgart, Germany

Cyclotron resonance is a powerful way to investigate the Fermi surface of various materials. In our research we performed cyclotron resonance experiments on the semiconductor germanium by using metallic coplanar waveguides (CPW). In comparison to conventional three-dimensional cavity resonators, CPW resonators have the advantage of multiple well-accessible resonances. Furthermore, CPWs open the possibility of implementation in a dilution refrigerator, which makes the performance down to the mK regime possible, which is also interesting for Kondo insulators. By using a superconducting magnet (up to 8T) and the access to a broad frequency range in the microwave regime (up to 25 GHz), we were able to investigate the cyclotron resonance in germanium in detail. Here we analysed the frequency-, temperature- (2-40K) and power dependence of the cyclotron resonance signal. Beside the investigation of the electronic bands, we present interesting phenomena like the generation of charge carriers by the power of the microwave electric field and the process of impact ionization in p-doped germanium.

TT 58.29 Thu 15:00 P2/OG3

Sample environment communication protocol (SECoP) — •KLAUS KIEFER¹, GEORG BRANDL², NIKLAS EKSTRÖM³, ENRICO FAULHABER⁴, THOMAS HERRMANNSDÖRFER⁵, BASTIAN KLEMKE¹, THORSTEN KRACHT⁶, ANDERS PETTERSSON³, LUTZ ROSSA¹, and MARKUS ZOLLIKER⁷ — ¹HZB, Berlin — ²FZJ, Garching — ³ESS, Lund — ⁴TUM, Garching — ⁵HZDR, Dresden — ⁶DESY, Hamburg — ⁷PSI, Villigen

We would like to present the Sample Environment Communication Protocol (SECoP), a software and initiative that addresses the standardization of communication between instrument-control software, sample-environment equipment (SE), and acquisition of metadata. The International Society for Sample Environment (ISSE) has developed SECoP in order to support a wide research community by tackling the challenges of data acquisition in daily laboratory routine, ([1] and references therein). Using SECoP as a common standard for controlling SE equipment will save resources and intrinsically give the opportunity to supply standardized and FAIR-data compliant SE metadata. It will also supply a well-defined interface for user-provided SE equipment, e.g. shared by different research facilities and of industry. In this poster presentation we will give an overview of the present status of SECoP and the developments within the SECoP@HMC project supported by the Helmholtz Metadata Collaboration. We would also like to advertise the SECoP booth at the exhibition of this conference, a possibility to get a first practical experience with SECoP.

[1] K. Kiefer et al., J. Neutron Res. 21, 181 (2020)

TT 58.30 Thu 15:00 P2/OG3

Lab::Measurement - measurement control with Perl 5 — MIA SCHAMBECK, ERIK FABRIZZI, SIMON REINHARDT, and •ANDREAS K. HÜTTEL — Institute for Experimental and Applied Physics, Universität Regensburg, Regensburg, Germany

Lab : :Measurement is a collection of object-oriented Perl 5 modules for control of test and measurement devices. It allows for quickly setting up complex tasks with diverse hardware. Instruments can be connected via GPIB (IEEE 488.2), USB, or VXI-11 / raw network sockets on Ethernet. Internally, third-party backends as, e.g., Linux-GPIB, the NI-VISA library, or Zurich Instruments' LabOne API are used, in addition to lightweight drivers for USB and TCP/IP-based protocols. This enables cross-platform portability of measurement scripts between Linux and Windows machines. Based on roles within Moose that provide communication standards such as SCPI, dedicated instrument driver classes take care of internal details. A high-level sweep layer allows for fast and flexible creation

of nested measurement loops, where, e.g., several input variables are varied and data is logged into a customizable folder structure. Sweeps can also be retrieved directly from an instrument as, e.g., a spectrum or network analyzer. Further features include live plotting and obtaining attested timestamps for measurement data. Recent enhancements focus on support for the Nanonis Tramea quantum measurement system and for fast measurements using arbitrary waveform generators as voltage sources. Lab : :Measurement is free software and available at <https://www.labmeasurement.de/>

[1] S. Reinhardt *et al.*, *Comp. Phys. Comm.* **234**, 216 (2019)

TT 58.31 Thu 15:00 P2/OG3

Modeling a vibrating carbon nanotube Josephson junction — •ANDREAS K. HÜTTEL^{1,2}, KEIJO KORHONEN², and PERTTI HAKONEN² — ¹Institute for Experimental and Applied Physics, University of Regensburg, 93040 Regensburg, Germany — ²Low Temperature Laboratory, Department of Applied Physics, Aalto University, P.O. Box 15100, 00076 Aalto, Finland

A carbon nanotube suspended between superconducting electrodes acts simultaneously as a nanomechanical resonator and as a Josephson junction. Its energy-dependent density of states and with that position-dependent critical current further adds to the complexity of the system, as does both mechanical and electronic nonlinearity.

Using parallelized Julia code [1], we numerically solve the coupled differential equation system of the driven (via an ac gate voltage and/or ac current or voltage bias) system for realistic device parameters and characterize the evolving steady state. Specific attention is given to the impact of the Josephson junction behaviour on the mechanical resonance frequency and the vibration amplitude, and on the impact of the carbon nanotube motion on the phase evolution of the junction. [1] <https://julialang.org/>

TT 59: Poster Session: Topology

Time: Thursday 15:00–18:00

Location: P2/OG4

TT 59.1 Thu 15:00 P2/OG4

Density-dependence of surface transport in tellurium-enriched nanograined bulk Bi₂Te₃ — •SEPIDEH IZADI¹, AHANA BHATTACHARYA², SARAH SALLOUM³, STEPHAN SCHULZ³, MARTIN MITTENDORFF², and GABI SCHIERNING¹ — ¹Bielefeld University, Department of Physics, 33615 Bielefeld, Germany — ²University of Duisburg-Essen, Department of Physics, 47057 Duisburg, Germany — ³University of Duisburg-Essen, Department of Chemistry, 45141 Essen, Germany

Three-dimensional topological insulators (3D TI) demonstrate conventional parabolic bulk bands together with protected Dirac surface states. Bi₂Te₃ material is considered as a well-known 3D TI model, however, due to its complicated defect chemistry, high number of charge carriers in the bulk dominate transport signal, even as nanograined structures. Herein we introduce Te-enriched Bi₂Te₃ nanoparticles synthesis as a method to control the bulk charge carrier density. Therewith, defects-free and stoichiometric Bi₂Te₃ nanoparticles with sizes between 4 and 40 nm are synthesized using ionic-liquid based approach. Grain boundaries along Bi₂Te₃ facets are investigated using high resolution transmission electron microscopy (HRTEM). The resulting nanoparticles were compacted into nanograined pellets of varying porosity, thereby emphasizing the surface transport contribution. The nanograined pellets were characterized by a combination of electrical transport together with THz time-domain reflectivity measurements. Using the Hikami-Larkin-Nagaoka (HLN) model, a characteristic coherence length of ~200 nm that is considerably larger than nanograins diameter is reported.

TT 59.2 Thu 15:00 P2/OG4

Topological phases in TaRhTe₄: from monolayer to bulk — •XIAO ZHANG — Leibniz Institute for Solid State and Material Research, Dresden, Germany

Topological phases are studied in different dimensional TaRhTe₄ using the method of density functional theory (DFT). We find that bulk TaRhTe₄ is a Weyl semimetal, whereas both monolayer and bilayer TaRhTe₄ display features of quantum spin Hall (QSH) insulator. A complete phase diagram linking monolayer, bilayer, and bulk TaRhTe₄ is obtained by varying intra- and inter-bilayer distance of the three-dimensional structure. It contains phases of Weyl semimetal, weak topological insulator, and normal insulator.

TT 59.3 Thu 15:00 P2/OG4

Quantum transport through resonant Dirac states in topological insulator nanowire constrictions — •MICHAEL BARTH¹, MAXIMILIAN FÜRST¹, COSIMO GORINI², and KLAUS RICHTER¹ — ¹Institute of Theoretical Physics, University of Regensburg, D-93040 Regensburg, Germany — ²Université Paris-Saclay, CEA, CNRS, SPEC, 91191, Gif-sur-Yvette, France

Quantum transport in topological insulator (TI) nanowires is expected to be mediated by surface states which wrap phase coherently around the circumference [1]. The spectrum corresponds to a quantized and gapped Dirac cone, where the gap is present because of a Berry phase of π which arises due to spin-momentum locking. In this work, we numerically study transport in TI constrictions which are subjected to an axial magnetic field. More specifically, we consider a realistic junction of a narrow TI wire which is smoothly connected at its two ends to broad TI leads and calculate the transmission through the setup with respect to the Fermi energy and the magnetic field. The latter is tuned to close the Berry gap [2]. It turns out, that perpendicular field components in the constriction lead to the formation of magnetic barriers which result in resonant Dirac states. The proposed system can be used to spectroscopically study the Dirac spectrum with respect to its gate and flux dependence. Moreover, different transport regimes are identified, which depend on the length of the central wire segment.

[1] J. H. Bardarson, P. W. Brouwer, and J. E. Moore *Phys. Rev. Lett.* **105**, 156803 (2010)

[2] J. Ziegler *et al.*, *Phys. Rev. B* **97**, 035157 (2018)

TT 59.4 Thu 15:00 P2/OG4

Topological insulator as barrier in Josephson junction — •ANTON MONTAG, ALEXANDER ZIESEN, and FABIAN HASSLER — RWTH Aachen University, Aachen, Germany

We numerically study the behavior of a long Josephson junction in a superconductor-topological insulator-superconductor setup. An *s*-wave superconductor is deposited on the disordered surface of a three-dimensional topological insulator proximitizing the surface states on both sides of the junction. The normal region is probed by a local tunnelling contact. We simulate the tunnel spectrum at energies below the bulk gap of the topological insulator as a function of the phase difference of the superconducting order parameter across the junction. The low-energy spectrum can be divided into trivial Andreev bound states usually appearing at higher energies and chiral edge modes which become gapless at a phase difference of π . Since the latter are topologically protected, they are essentially not affected by symmetry preserving onsite potential disorder on the topological insulator surface. We show the simulated tunnel spectra for various disorder configurations and compare it to analytical calculations.

TT 59.5 Thu 15:00 P2/OG4

Towards the quantum anomalous Hall effect in magnetic topological insulator structures — •JUSTUS TELLER^{1,2}, ERIK ZIMMERMANN^{1,2}, MICHAEL SCHLEENVOIGT^{1,2}, GERRIT BEHNER^{1,2}, KRISTOF MOORS^{1,2}, PETER SCHÜFFELGEN^{1,2}, GREGOR MUSSLER^{1,2}, DETLEV GRÜTZMACHER^{1,2}, and THOMAS SCHÄPERS^{1,2} — ¹Peter Grünberg Institut (PGI-9), Forschungszentrum Jülich, D-52425 Jülich, Germany — ²JARA-Fundamentals of Future Information Technology, Jülich-Aachen Research Alliance, Forschungszentrum Jülich and RWTH Aachen University, Germany

Three-dimensional topological insulators (TIs) are a material class which may enable robust topological quantum computing by using so-called Majorana zero modes. Published theoretical work predicts the Majorana state to exist in hybrid structures of superconductors and magnetic topological insulators which exhibit the quantum anomalous Hall effect (QAHE). We present magnetotransport measurements of Cr-doped magnetic (Bi_{0.27}Sb_{0.73})₂Te₃ layers. At 1.2 K, the uniformly Cr-doped samples exhibit a magnetic signature whose behaviour is probed under gate influence. Based on these measurements, an existing QAHE is ruled out. The results are compared to a magnetic TI heterostructure which is comprised of a plain TI layer embedded into two layers of magnetic TI. This structure reveals the QAHE. The temperature dependence of the effect is measured. In addition, the magnetic energy gap is probed by a gate dependent measurement. The QAHE is improved by current adjustment.

TT 59.6 Thu 15:00 P2/OG4

Axial topological insulator based DC SQUID in external SQUID layout — •JAN KARTHEIN^{1,3}, ERIK ZIMMERMANN^{1,3}, MAX VASSEN CARL^{1,3}, GERRIT BEHNER^{1,3}, ABDUR REHMAN JALIL^{1,3}, GREGOR MUSSLER^{1,3}, PETER SCHÜFFELGEN^{1,3}, HANS LÜTH^{1,3}, DETLEV GRÜTZMACHER^{1,2,3}, and THOMAS SCHÄPERS^{1,3} — ¹Peter Grünberg Institut (PGI-9), Forschungszentrum Jülich, 52425 Jülich, Germany — ²Peter Grünberg Institut (PGI-10), Forschungszentrum Jülich, 52425 Jülich, Germany — ³JARA-Fundamentals of Future Information Technology, Jülich-Aachen Research Alliance, Forschungszentrum Jülich and RWTH Aachen University, 52425 Jülich, Germany

A three-dimensional topological insulator (TI) nanowire proximitized with a superconductor is predicted to be host to Majorana bound states that provide a platform for fault-tolerant quantum computation. Recently, axial TI-nanowire based DC SQUIDs showed coherent oscillations originating from the interference of topological surface states. We fabricate an axial TI-nanowire based DC SQUID with a neighboring Josephson junction completely in-situ, using selective-area growth and shadow mask fabrication techniques. An out-of-plane magnetic field is able to tune the flux inside the so formed external SQUID loop, while being decoupled from the in-plane magnetic field that tunes the flux inside the TI-nanowire. Coherent SQUID oscillations are visible when sweeping both the out-of-plane and in-plane magnetic field, proving that the axial TI-nanowire based DC SQUID and the external DC SQUID are experiencing phase-coherent transport.

TT 59.7 Thu 15:00 P2/OG4

Controlling the real-time dynamics of a spin coupled to the helical edge states of the Kane-Mele model — •ROBIN QUADE¹ and MICHAEL POTTHOFF^{1,2} — ¹I. Institute of Theoretical Physics, Department of Physics, University of Hamburg, Notkestraße 9-11, 22607 Hamburg, Germany — ²The Hamburg Centre for Ultrafast Imaging, Luruper Chaussee 149, 22761 Hamburg, Germany

The time-dependent state of a classical spin locally exchange coupled to an edge site of a Kane-Mele model in the topologically non-trivial phase is studied numerically by solving the full set of coupled microscopic equations of motion for the spin and the electron system. Dynamics in the long-time limit is accessible thanks to dissipative boundary conditions, applied to all but the zigzag edge of interest. We study means to control the state of the spin via transport of a spin-polarization cloud through the helical edge states. The cloud is formed at a distant edge site using a local magnetic field to inject an electron spin density and released by suddenly switching off the injection field. This basic process, consisting of spin injection, propagation of the spin-polarization cloud, and scattering of the cloud from the classical spin, can be used to steer the spin state in a controlled way. We find that the effect of a single basic process can be reverted to a high degree with a subsequent process. Furthermore, we show that by concatenating several basic injection-propagation-scattering processes, the spin state can be switched completely and that a full reversal can be achieved.

TT 59.8 Thu 15:00 P2/OG4

Fermi-surface investigation of CaCdGe and CaCdSn — •B.V. SCHWARZE^{1,2}, F. HUSTEDT^{1,2}, M. UHLARZ¹, D. KACZOROWSKI³, and J. WOSNITZA^{1,2} — ¹Hochfeld-Magnetlabor Dresden (HLD-EMFL) and Würzburg-Dresden Cluster of Excellence-ct.qmat, HZDR, Germany — ²Institut für Festkörper- und Materialphysik, TU Dresden, Germany — ³Institute of Low Temperature and Structure Research, Polish Academy of Sciences, Poland

CaCdSn and CaCdGe are nodal-line semimetal candidate materials. These materials have one-dimensional lines or loops of topologically protected band-touching nodes. They sparked interest, due to their unique response to high magnetic or electric fields, including giant linear magnetoresistance and high charge-carrier mobility. These properties make them candidates for future technological applications. Band-structure calculations [1, 2] show for both systems non-topological and topological valence bands with the nodal band crossings above the Fermi level. Previous measurements of the magnetoresistance provide some support for the topological nature of the materials. Here, we present our investigation of the Fermi surfaces of CaCdSn and CaCdGe by use of de Haas-van Alphen measurements and band-structure calculations. Our measurements reveal many quantum-oscillation frequencies, which are not predicted by calculations. This discrepancy calls the calculated band structures [1, 2] and, thus, the precise nature of the topology of these systems into question.

[1] A. Laha et al., Phys. Rev. B 102, 035164 (2020).

[2] E. Emmanouilidou et al., Phys. Rev. B 95, 245113 (2017).

TT 59.9 Thu 15:00 P2/OG4

Ultrasound propagation in candidate material for electron hydrodynamics, Weyl semimetal WTe₂ — •RAFAL WAWRZYŃCZAK¹, STANISŁAW GALESKI^{1,2}, and JOHANNES GOOTH^{1,2} — ¹Max Planck Institute for Chemical Physics of Solids, Nöthnitzer Straße 40, 01187 Dresden, Germany — ²Physikalisches Institut, Universität Bonn, Nussallee 12, D-53115 Bonn, Germany

Interactions between electrons might lead to the appearance of a regime where the dominating time-scale is defined by momentum-conserving processes. This is manifested by electron liquid exhibiting features characteristic for classical liquids, like Poiseuille flow, resulting in non-Ohmic, sample-width-dependent resistivity. This was recently observed in a two-dimensional metal PdCoO₂ and two Weyl semimetals. Neither of the observations was accounted for with complete microscopic description. For WTe₂ there was proposed a mechanism based on the electron-electron scattering process involving a virtual phonon.

Here we report results of ultrasound propagation study performed on WTe₂ Weyl semimetal. We have analyzed temperature and field dependence of propagation of longitudinal and two transverse modes of different polarization propagating along the a crystallographic directions. The data shows anomalous decrease in speed of the longitudinal mode below 10 K and non-monotonous T-

dependence of its attenuation. Moreover, quantum oscillations observed in all six measured quantities reveal the details of coupling between measured phonon modes and different parts of systems Fermi surface.

TT 59.10 Thu 15:00 P2/OG4

Photo-thermal imaging of ZrTe₅ in the quasi-quantized Hall regime — •ERICA WARTH PÉREZ ARIAS¹, RAFAL WAWRZYŃCZAK¹, STANISŁAW GALESKI¹, JOHANNES GOOTH², CLAUDIA FELSER¹, and FABIAN MENGES¹ — ¹Max Planck Institute for Chemical Physics of Solids, Germany — ²University of Bonn, Germany

ZrTe₅ has recently gained attention due to various intriguing experimental observations including the chiral magnetic effect [1] and the quasi-quantized 3D quantum Hall effect [2]. However, it remains challenging to probe the characteristic features of gapless surface and edge states experimentally. Addressing this challenge, we devised an optoelectronic detection scheme based on cryogenic magneto-optical laser scanning microscopy. The technique relies on a global electrical read-out of locally-induced currents, and contrasts previous all-optical studies of photogalvanic effects. We characterized ZrTe₅ single crystals with this approach and visualized rich spatial patterns of photo-induced transport as function of temperature and magnetic field. Remarkably, current maps obtained in the quasi-quantized Hall regime display long-range photoresponse over mm-distances and oscillations in magnetic field, hinting towards charge movement of ambient carriers in the system [3] driven by the photo-thermal effect [4] and the external magnetic field.

[1] Q. Li et al., Nat. Phys. 12, 550-554 (2016)

[2] S. Galeski et al., Nat. Commun. 12, 3197 (2021)

[3] J. C. W. Song et al., Phys. Rev. B 90, 075415 (2014)

[4] Y. Wang et al., arXiv:2203.17176 [cond-mat.mtrl-sci] (2022)

TT 59.11 Thu 15:00 P2/OG4

Anomalous transverse transport and phase transitions in Weyl semimetals RAlSi (R = La, Ce) — •ERJIAN CHENG — Leibniz Institute for Solid State and Materials Research (IFW-Dresden), 01069 Dresden, Germany

The noncentrosymmetric RAlPn (R = rare earth elements, Pn = Si or Ge) with the space-inversion (SI) symmetry breaking and/or the time-reversal (TR) symmetry breaking host multiple types of Weyl fermions, providing a fertile platform for the exploration of novel topological matter states. In particular, when magnetic configuration couples with the electronic wavefunctions, exotic anomalous transverse transport phenomena emerge. Here, by resorting to electrical and thermoelectrical transport, we systematically studied the ferromagnetic CeAlSi and its nonmagnetic analog LaAlSi, revealing the anomalous Hall effect (AHE) and/or anomalous Nernst effect (ANE). In addition, for LaAlSi, quantum oscillations reveal five frequencies. Moreover, a temperature-induced Lifshitz transition is unveiled in LaAlSi. For CeAlSi, magnetism enhances the anomalous transverse transport, implying that magnetism tunes the positions of Weyl nodes. Besides, high-pressure electrical transport and X-ray diffraction (XRD) measurements were also implemented, demonstrating multiple phase transitions. These results indicate that LaAlSi and CeAlSi provide unique and tunable systems to explore exotic topological physics, and a potential paradise for an array of promising applications for spintronics.

TT 59.12 Thu 15:00 P2/OG4

Electronic structure of topological superconductor candidate Li₂Pd₃B — •GABRIELE DOMAINE¹, JONAS A. KRIEGER¹, WEI YAO¹, CHANGJIANG YI², CLAUDIA FELSER², STUART S. P. PARKIN¹, and NIELS B. M. SCHRÖTER¹ — ¹Max Planck Institute for Microstructure Physics, Halle, Germany — ²Max Planck Institute for Chemical Physics of Solids, Dresden, Germany

Chiral crystals are known to host a number of exotic quasiparticles which carry large Chern numbers and, as they are unconstrained from the celebrated spin statistics connection, can exhibit a range of unconventional (effective) spins [1]. These include, for instance, spin 3/2 Rarita-Schwinger, Kramers-Weyl, spin-1 and multifold fermions, which can be considered a generalization of conventional Weyl-fermions [2]. Here we present our preliminary results for the first Angle-Resolved Photoemission Spectroscopy (ARPES) measurements of the chiral crystal Li₂Pd₃B which is expected to host an as-yet unobserved multifold topological superconducting phase of class DIII, which is time reversal invariant), even without odd parity pairing [3]. The superconducting gap is expected to arise from the intraband coupling at time-reversal invariant momentum points leading to an unconventional multiband gap function and nodal rings [4].

[1] N. B. M. Schröter et al. Nat. Phys. 15, 759 (2019)

[2] B. Bradlyn et al., Science 353, 6299 (2016)

[3] Z. S. Gao et al., Quantum Front 1, 3 (2022)

[4] C. Lee et al., Phys. Rev. B 104, L241115 (2021)

TT 59.13 Thu 15:00 P2/OG4

Implementing superconductor/skymrion-host heterostructures using exfoliated Fe_3GeTe_2 on NbN — •MAXIMILIAN DASCHNER^{1,2}, THOMAS REINDL², MARION HAGEL², JÜRGEN WEIS², and MALTE GROSCHE¹ — ¹Cavendish Laboratory, University of Cambridge, UK — ²Max-Planck Institute for Solid State Research, Stuttgart, Germany

Experimental coupling of chiral magnetism and superconductivity through the proximity effect is a challenging and unexplored field that can lead to novel physics. Chiral magnets host topological excitations known as skyrmions that, when coupled to the vortices in a superconductor, are predicted to form Majorana fermions at its boundaries and vortex cores. The van-der-Waals material Fe_3GeTe_2 is known to host a skyrmion state over temperature and field ranges that depend on the sample thickness. We have exfoliated flakes of Fe_3GeTe_2 from a high quality crystal grown by vapour transport, deposited them on a NbN film and patterned electrical contacts using standard e-beam lithography techniques. The resulting Hall bar shaped nanodevices provide a convenient system for investigating skyrmion/superconductor interactions: Hall measurements above the superconducting transition temperature T_c in combination with magnetic force measurements survey the skyrmion state as a function of applied field, and measurements of the critical current density below T_c probe skyrmion-assisted vortex nucleation and pinning.

TT 59.14 Thu 15:00 P2/OG4

Pressure-dependent structural instabilities and transport phenomena in candidate topological semimetal LaSb_2 — •THEODORE WEINBERGER, CHRISTIAN DE PODESTA, JIASHENG CHEN, STEPHEN HODGSON, and MALTE GROSCHE — Cavendish Laboratory, University of Cambridge, Cambridge CB3 0HE, United Kingdom

At low temperatures, and in the presence of large magnetic fields, LaSb_2 exhibits large, linear, non-saturating magnetoresistance, defying Fermi liquid behaviour. This phenomenon is thought to be caused by the onset of charge density wave order (CDW) below a sharp, hysteretic anomaly seen in resistivity data at ~ 355 K. This anomaly is rapidly pushed to lower temperatures under applied hydrostatic pressure, where above 6 kbar, it is fully suppressed. Surprisingly, the anomalous magnetoresistance persists to pressures beyond 20 kbar even after the suppression of the resistive anomaly. Hence, we suggest that the magnetoresistance is not driven by the onset of CDW order. Instead, we propose that the high temperature anomaly corresponds to a structural transition, similar to that seen in CeSb_2 , which is supported by *ab initio* density functional theory calculations. Further, these calculations indicate that the Fermi surface of LaSb_2 contains small pockets in both its high and low pressure structures. Small Fermi surface pockets suggest that LaSb_2 's band structure might feature topological, Dirac-like, cones which may explain the observed large, linear magnetoresistance.

TT 59.15 Thu 15:00 P2/OG4

2π domain walls for tunable Majorana devices — •DANIEL HAUCK¹, STEFAN REX^{2,3}, and MARKUS GARST¹ — ¹Karlsruhe Institute of Technology, Institute for Theoretical Solid State Physics, Wolfgang-Gaede-Str. 1, 76131 Karlsruhe — ²Institute for Quantum Materials and Technologies, Karlsruhe Institute of Technology, 76021 Karlsruhe, Germany — ³Institute for Theoretical Condensed Matter Physics, Karlsruhe Institute of Technology, 76131 Karlsruhe

Superconductor-magnet hybrid structures provide a platform for investigating topological phases with localized Majorana states. Such states have previously been predicted for elongated Skyrmions in the magnetic layer. Here we consider 2π domain walls that can be easily controlled experimentally. Depending on the boundary conditions, we demonstrate that localized Majorana states can be found at both ends of such walls. This establishes 2π domain walls as tunable elements for the realization of Majorana devices.

TT 60: Quantum Dots, Quantum Wires, Point Contacts

Time: Thursday 17:15–19:00

Location: HSZ 03

TT 60.1 Thu 17:15 HSZ 03

Spin-texture topology in curved circuits driven by spin-orbit interactions — ALBERTO HIJANO^{1,2}, EUSEBIO J. RODRÍGUEZ³, •DARIO BERCIoux^{4,5}, and DIEGO FRUSTAGLIA³ — ¹Centro de Física de Materiales (CFM-MPC) Centro Mixto CSIC-UPV/EHU, E-20018 Donostia-San Sebastián, Spain — ²Department of Condensed Matter Physics, University of the Basque Country UPV/EHU, 48080 Bilbao, Spain — ³Departamento de Física Aplicada II, Universidad de Sevilla, E-41012 Sevilla, Spain — ⁴Donostia International Physics Center (DIPC), 20018 Donostia-San Sebastián, Spain — ⁵IKERBASQUE, Basque Foundation for Science, Plaza Euskadi 548009 Bilbao, Spain

We study the response of spin carriers to the effective field textures developed in curved one-dimensional circuits subject to the joint action of Rashba and Dresselhaus spin-orbit interactions. By using a quantum network technique, we establish that the interplay between these two non-Abelian fields and the circuit's

TT 59.16 Thu 15:00 P2/OG4

DMRG simulations of the one-dimensional anyon Hubbard model — •YANNICK WERNER, MAXIMILIAN KIEFER-EMMANOULIDIS, PASCAL JUNG, and SEBASTIAN EGGERT — Department of Physics, Technical University of Kaiserslautern, 67663 Kaiserslautern, Germany

The recent detection of anyons in setups of ultra-cold gases has further encouraged the in-depth studies of anyonic systems. Although the existence of conventional anyons is limited to two dimensions, a realization of fractional exchange statistics in a 1D system is possible which leads to a continuous interpolation between bosons and (pseudo-)fermions. In this poster we present the effects of perturbations i.e. local impurities, in a one-dimensional anyonic Hubbard model with onsite and nearest neighbor interactions on local densities, correlation functions and density transport. Here anyonic statistics are fulfilled by mapping bosonic operators via Jordan-Wigner-transformation, leading to a density dependent Peierl's phase in the hopping term. Additionally, in the case of small filling rates, we compute and analyze numerically the Luttinger parameter via Density Matrix Renormalization Group methods and compare it with analytical results.

TT 59.17 Thu 15:00 P2/OG4

Dynamical structure factor of an anyonic Luttinger liquid — •PASCAL JUNG, MARTIN BONKHOFF, YANNICK WERNER, and SEBASTIAN EGGERT — Department of Physics and Research Center Optimas, Technical University of Kaiserslautern, 67663 Kaiserslautern, Germany

Luttinger liquids are a powerful tool to describe the low-energy excitations of bosonic and fermionic systems in one spatial dimension. Anyonic systems, which allow a continuous transition between those two fundamental types of statistics, can be included in this framework by an additional coupling of the current and density excitations. This results into different velocities for the left and right movers, breaking the spatio-temporal symmetries.

To study the effects of this symmetry breaking on experimentally verifiable quantities, characteristic correlation functions are calculated. Using these, the dynamical structure factor for a finite system is determined. The broken symmetry leads here to a characteristic imbalance between left and right movers with typical power laws. Furthermore, the impact of local impurities is investigated using the perturbative renormalization group. These results are compared to numerical simulations obtained by the DMRG algorithm.

TT 59.18 Thu 15:00 P2/OG4

Quantum spin dynamics in the spin-chain compound $\text{Cu}_2\text{OH}_3\text{Br}$ — •ANNEKE REINOLD¹, KIRILL AMELIN², ZHIYING ZHAO³, CHANGQING ZHU¹, PATRICK PILCH¹, HANS ENGELKAMP⁴, TOOMAS RÖÖM², URMAS NAGEL², and ZHE WANG¹ — ¹TU Dortmund University, Germany — ²National Institute of Chemical Physics and Biophysics, Tallinn, Estonia — ³Fujian Institute of Research on the Structure of Matter, Chinese Academy of Sciences, Fuzhou, China — ⁴Radboud University, Nijmegen, The Netherlands

In low-dimensional quantum magnets, exotic spin phenomena can emerge due to strong spin fluctuations. Here we investigate spin dynamics of the quantum spin-chain compound $\text{Cu}_2\text{OH}_3\text{Br}$ by high-resolution terahertz spectroscopy as a function of temperature and in high magnetic fields. Below the Néel temperature $T_N=9.3$ K, this compound exhibits a unique magnetic structure consisting of alternating ferromagnetic and antiferromagnetic spin-1/2-chains of Cu^{2+} -ions [1,2]. In this ordered phase we observed magnetic excitations, which are characteristic for this unique spin structure and consistent with results of inelastic neutron scattering [2]. Moreover, we are able to track these spin excitations in applied magnetic fields crossing field-induced phase transitions [1].

[1] Z. Y. Zhao *et al.*, J. Phys.: Condens. Matter **31**, 275801 (2019)[2] H. Zhang *et al.*, Phys. Rev. Lett. **125**, 037204 (2020)

geometry modify the geometrical characteristics of the spinors, particularly on square circuits, leading to the localisation of the electronic wave function and the suppression of the quantum conductance. We propose a topological interpretation by classifying the corresponding spin textures in terms of winding numbers. [1] A. Hijano *et al.*, arXiv:2209.11653 [cond-mat.mes-hall]

TT 60.2 Thu 17:30 HSZ 03

Stochastic resonance of electron tunneling in a quantum dot in spite of a periodically blind eye — •ERIC KLEINHERBERS, HENDRIK MANNEL, JOHANN ZÖLLNER, MARCEL ZÖLLNER, MARTIN GELLER, AXEL LORKE, and JÜRGEN KÖNIG — Faculty of Physics and CENIDE, University Duisburg-Essen, 47057 Duisburg, Germany

The key idea of stochastic resonance is to amplify a signal by adding noise. For electron tunneling in a quantum dot, this can be used to facilitate a periodic elec-

tron transfer, where during each period a single electron enters and leaves the quantum dot. In stochastic resonance, the noise (tunneling) rate must be well adjusted to the frequency of the periodic drive that is applied to the quantum dot. The Fano factor is a possible indicator of this effect [1]. Here, we study the full counting statistics and, in particular, factorial cumulants as higher-order indicators of stochastic resonance. We discuss experimental data of electron tunneling into and out of a self-assembled InAs quantum dot, where the full counting statistics is measured using a resonance fluorescence readout scheme. We find that even if the detector is blind during half of each period, a stochastic resonance is visible in the full counting statistics.

[1] T. Wagner *et al.*, Nat. Phys. 15, 330 (2019)

TT 60.3 Thu 17:45 HSZ 03

Modifications of the local dissipation profile imposed by quantum point contacts — •NICO LEUMER — Université de Strasbourg, CNRS, IPCMS, UMR 7504, F-67000 Strasbourg, France

Recent experimental progress provides access to local temperature changes on the nanoscale, three orders of magnitude lower than the sample temperature itself [1]. Since electric current is accompanied by an energy loss of the charge carriers, this advance implies that the dissipated power became in fact a local observable. The key role is adopted by electron-phonon interactions transferring the electronic energy loss to the bulk material and thus; stimulating the sample temperature profile.

Quantum point contacts (QPC) have been reported to modify the dissipation and, especially, the energy loss of charge carriers may be distributed asymmetrically around the QPC. Inspired by this feature, we develop a theory to determine why, where and how much dissipation occurs in experimental relevant geometries.

[1] D. Halbertal *et al.*, Nature 539, 407 (2016)

[2] C. Blaas-Anselmi *et al.*, SciPost Phys. 12, 105 (2022)

TT 60.4 Thu 18:00 HSZ 03

Resonant tunneling energy harvesters: Improving performance via quantum interference. — •JOSÉ BALDUQUE¹ and RAFAEL SÁNCHEZ^{1,2} — ¹Departamento de Física Teórica de la Materia Condensada, Universidad Autónoma de Madrid, Madrid, Spain. — ²Condensed Matter Physics Center (IFIMAC), and Instituto Nicolás Cabrera, Universidad Autónoma de Madrid, Madrid, Spain.

The spectral filtering of quantum dots can be used for heat to power conversion in electronic conductors. A proposal based on resonant-tunneling three-terminal devices [1] has been recently verified experimentally [2]. Two quantum dots connect the two terminals of a conductor to a hot electronic cavity where carriers exchange heat via thermalization. We propose the heat source to be separated from the conductor via a beam-splitter (e.g., the tip of a scanning microscope) that mediates the system-bath coupling. The resulting ballistic electron propagation gives rise to interferences [3] able to improve the engine performance, both in the extracted power and efficiency [4].

[1] A.N. Jordan *et al.*, Phys. Rev. B 87, 075312 (2013)

[2] G. Jaliel *et al.*, Phys. Rev. Lett. 123, 117701 (2019)

[3] R. Sánchez *et al.*, Phys. Rev. B 104, 115430 (2021)

[4] J. Balduque and R. Sánchez, in preparation.

TT 60.5 Thu 18:15 HSZ 03

Vibrational instabilities arising from non-conservative current-induced forces in nanosystems: A comparison of quantum and semi-classical approaches — •SAMUEL RUDGE, CHRISTOPH KASPAR, and MICHAEL THOSS — Institute of Physics, University of Freiburg, Germany

Understanding the vibrational dynamics of molecular junctions is of paramount importance to creating junctions that are mechanically stable. In systems with

more than one vibrational degree of freedom, instabilities can arise due to non-conservative current-induced forces, an effect that can occur at lower voltages than the well-understood mechanism of current-induced heating [1].

In recent years, such non-conservative forces have been largely explored with semi-classical Langevin-type equations for the vibrational degrees of freedom, where the electronic friction tensor and average electronic force can be analyzed directly [1]. In this work, however, we employ both a semi-classical Langevin equation as well as a quantum master equation approach to explore instabilities in a model system with two electronic levels and two vibrational modes. Both approaches derive from the numerically exact hierarchical equations of motion (HEOM) method [2], and the resulting analysis is able to show in which regimes such semi-classical treatments can be used.

[1] J. T. Lü *et al.*, Phys. Rev. B 85, 245444 (2012)

[2] S.L. Rudge, Y. Ke, and M. Thoss, arXiv:2211.14215 (2022)

TT 60.6 Thu 18:30 HSZ 03

Asymmetric couplings of quantum dot systems to environments — •LUKAS LITZBA, NIKODEM SZPAK, ERIC KLEINHERBERS, and JÜRGEN KÖNIG — Fakultät für Physik, Universität Duisburg-Essen, Lotharstraße 1, 47057 Duisburg, Germany

We study systems with a few quantum dots, represented by the Fermi-Hubbard model, coupled to several Markovian baths with different coupling strengths. On the one hand, we compare different approximations (such as Redfield equation, coherent Lindblad approximation [1]) for a Master equation in first order of the quantum dot-bath coupling for strongly interacting electrons. On the other hand, we find exact solutions for non-interacting electrons. We compare the results for different coupling strength regimes and discuss the qualitative changes in the system behavior. Thereby we observe significant effects of the coupling asymmetry on energy coherences, which is linked to local versus global coupling. We look closer at systems from two to ten dots and study the non-equilibrium dynamics based on dressed excitation energies of the system as well as the associated damping rates. In this context we find transitions from global to local coupling behavior with increasing coupling strength asymmetry.

[1] E. Kleinherbers, N. Szpak, J. König, R. Schützhold, PRB 101, 125131 (2020)

TT 60.7 Thu 18:45 HSZ 03

Relaxation dynamics in Fermi-Hubbard systems coupled to environment — •NIKODEM SZPAK¹, GERNOT SCHALLER², RALF SCHÜTZHOLD^{2,3}, and JÜRGEN KÖNIG¹ — ¹Theoretische Physik und CENIDE, Universität Duisburg-Essen, Lotharstr. 21, 47048 Duisburg — ²Helmholtz-Zentrum Dresden-Rossendorf, Bautzner Landstraße 400, 01328 Dresden — ³Institut für Theoretische Physik, Technische Universität Dresden, 01062 Dresden

We study a chain of quantum dots coupled to environment and describe it with the Fermi-Hubbard model coupled to fermionic baths. For different coupling regimes (interdot vs bath-dot) we derive separate Lindblad master equations and compare their properties. It is shown that for strong repulsive onsite (Coulomb) interactions and low bath temperatures the system quickly reaches a low-energy sector described effectively by the Heisenberg model. Within this sector the further dynamics depends strongly on the relative coupling strengths. For weak bath-dot coupling, the system relaxes globally to the unique anti-ferromagnetic ground state with zero total spin. For strong bath-dot coupling, the system increases its total spin to the maximal possible value and ends up in (degenerate) states exhibiting ferromagnetic order. We provide rigorous derivations as well as numerical examples.

[1] E. Kleinherbers, N. Szpak, J. König, and R. Schützhold, Phys. Rev. B 101, 125131 (2020)

[2] G. Schaller, F. Queisser, N. Szpak, J. König, and R. Schützhold, Phys. Rev. B 105, 115139 (2022)

TT 61: Focus Session: Correlations in Moiré Quantum Matter II

Time: Thursday 17:45–19:00

Location: HSZ 201

TT 61.1 Thu 17:45 HSZ 201

Magnetism and metallicity in Moiré transition metal dichalcogenides — •PATRICK TSCHEPPE¹, JIAWEI ZANG², MARCEL KLETT¹, SEHER KARAKUZU³, THOMAS MAIER⁴, MICHEL FERRERO^{5,6}, ANDREW MILLIS^{2,3}, and THOMAS SCHÄFER¹ — ¹Max-Planck-Institut für Festkörperforschung, Heisenbergstraße 1, 70569 Stuttgart, Germany — ²Department of Physics, Columbia University, 538 West 120th Street, New York, New York 10027, USA — ³Center for Computational Quantum Physics, Flatiron Institute, 162 5th Avenue, New York, New York 10010, USA — ⁴Computational Sciences and Engineering Division, Oak Ridge National Laboratory, Oak Ridge, Tennessee 37831-6164, USA — ⁵CPHT, CNRS, Ecole Polytechnique, Institut Polytechnique de Paris, Route de Saclay, 91128 Palaiseau, France — ⁶Collège de France, 11 place Marcelin Berthelot, 75005 Paris, France

The Moiré transition metal dichalcogenide homobilayer WSe₂ has recently been observed both to undergo continuous Mott transitions and to display quantum

critical behavior, while also allowing for high tunability of its electronic parameters. At the same time, the effective low-energy physics of WSe₂ is believed to be adequately described by a simple one-band Hubbard model. We study the rich interplay between perfect nesting and dynamical as well as non-local correlations in this model using the cellular dynamical mean-field theory (CDMFT) in conjunction with the dynamical cluster approximation (DCA). In this way we elucidate the nature of both interaction and magnetic field-driven metal-insulator crossovers, previously observed in experiments.

TT 61.2 Thu 18:00 HSZ 201

Switching between Mott-Hubbard and Hund physics in Moiré quantum simulators — •SIHEON RYEE and TIM WEHLING — I. Institute of Theoretical Physics, University of Hamburg, Hamburg, Germany

Mott-Hubbard and Hund electron correlations have been realized thus far in separate classes of materials. In this talk, we show that a single Moiré homobi-

layer encompasses both kinds of physics in a controllable manner. We develop a microscopic multiband model which we solve by dynamical mean-field theory to nonperturbatively address the local many-body correlations. We demonstrate how tuning with twist angle, dielectric screening, and hole density allows to switch between Mott-Hubbard and Hund correlated states in twisted WSe₂ bilayer. The underlying mechanism bases on controlling Coulomb-interaction-driven orbital polarization and energetics of concomitant local singlet and triplet spin configurations. From comparison to recent experimental transport data, we find signatures of a filling-controlled transition from a triplet charge-transfer insulator to a Hund-Mott metal. Our finding establishes twisted transition metal dichalcogenides as a tunable platform for exotic phases of quantum matter emerging from large local spin moments.

TT 61.3 Thu 18:15 HSZ 201

Tunable topological order of pseudo spins in semiconductor heterostructures — CLEMENS KUHLENKAMP^{1,2,3}, •WILHELM KADOW^{1,2}, ATAC IMAMOGLU³, and MICHAEL KNAP^{1,2} — ¹Department of Physics, Technical University of Munich, 85748 Garching, Germany — ²Munich Center for Quantum Science and Technology (MCQST), Schellingstr. 4, D-80799 München, Germany — ³Institute for Quantum Electronics, ETH Zürich, CH-8093 Zürich, Switzerland

We propose a novel platform to realize highly-tunable, frustrated Hubbard physics with topological order in multi-layer Moiré structures. Identifying a layer degree of freedom as a pseudo spin, allows us to retain SU(2) symmetry, while controlling ring exchange processes and concurrently quenching the kinetic energy by large external magnetic fields. This way, a broad class of interacting Hofstadter states and their transitions can be studied. Remarkably, in the limit of strong interactions the system becomes Mott insulating and we find exceptionally stable spin liquid phases which are induced by the magnetic field. As the magnetic flux can be easily tuned in Moiré systems, our approach provides a promising route towards the experimental realization and control of topologically ordered phases of matter. We also discuss how layer pseudo-spin can be probed in near-term experiments.

TT 61.4 Thu 18:30 HSZ 201

Nontrivial quantum geometry of multiband systems and implications for flat bands — •JOHANNES MITSCHERLING — Department of Physics, University of California, Berkeley, California 94720, USA

Studying the geometry of wave function manifolds helps us to identify and un-

derstand phenomena whose descriptions are not captured by the sole knowledge of the energy dispersion. A prominent example of recent interest is the distance between wave functions captured by the quantum metric. Flat-band systems are promising candidates for novel fascinating quantum metric effects since well-known contributions to observables that depend on the slope or curvature of the dispersion vanish. For instance, the dominant contribution to the superfluid stiffness and the dc electrical conductivity is proportional to the integrated quantum metric for flat bands. In this talk, I will address the role of band degeneracy in these quantum metric effects. I will use the developed framework for dc electrical conductivity [PRB 105, 085154 (2022), PRB 106, 165133 (2022)] to contrast nondegenerate and degenerate band manifolds. We will explore the common mathematical description in terms of Grassmannian manifolds and its concrete implications, such as lower bounds and the nonadditivity of the quantum metric. I close by illustrating how these concepts can be directly extended to other observables.

J.M. acknowledges support by the German National Academy of Sciences Leopoldina through grant LPDS 2022-06.

TT 61.5 Thu 18:45 HSZ 201

Magnetism in twisted bilayer graphene with heterostrain — AHMED MISSAOUI¹, FLORIE MESPLE², JAVAD VAHEDI³, ANDREAS HONECKER¹, VINCENT RENARD², and •GUY TRAMBLÉ DE LAISSARDIÈRE¹ — ¹Laboratoire de Physique Théorique et Modélisation, CY Cergy Paris Université / CNRS, Cergy-Pontoise, France — ²Université Grenoble Alpes, CEA, Grenoble INP, IRIG, PHELIQS, Grenoble, France — ³Jacobs University, School of Engineering and Science, Bremen, Germany

The discovery of correlated insulators and superconductivity due to flat bands in twisted bilayer graphene (TBG) at so-called “magic angles” has stimulated the study of their magnetic properties [1]. Furthermore, it is now well established that heterostrain, which is generally present in the samples, is a key parameter in understanding the actual shape of the flat bands [2]. Here, we present a theoretical study of magnetism in magic-angle TBG combining a Hubbard model and the mean-field approach including non-collinear magnetic terms. We show how heterostrain strongly modifies the magnetization and the local order of magnetic state for realistic Coulomb interaction values.

[1] J. Vahedi *et al.*, *SciPost Phys.* **11**, 083 (2021) and references therein

[2] L. Huder *et al.*, *Phys. Rev. Lett.* **120**, 156405 (2018);

F. Mesples *et al.*, *Phys. Rev. Lett.* **127**, 126405 (2021)

TT 62: Ultrafast Dynamics of Light-Driven Systems

Time: Friday 9:30–11:45

Location: HSZ 03

TT 62.1 Fri 9:30 HSZ 03

Ultrafast dynamics of spin-density wave order in BaFe₂As₂ under high pressures — IVAN FOTEV^{1,2}, STEPHAN WINNERL¹, SAICHARAN ASWARTHAM², SABINE WÜRMEHL^{3,4}, BERND BÜCHNER^{3,4}, HARALD SCHNEIDER¹, MANFRED HELM^{1,2}, and •ALEXEJ PASHKIN¹ — ¹Helmholtz-Zentrum Dresden-Rossendorf, Germany — ²Technische Universität Dresden, Germany — ³IFW Dresden, Germany — ⁴Würzburg-Dresden Cluster of Excellence ct.qmat, Germany

We utilize pump-probe spectroscopy to measure the quasiparticle relaxation dynamics of BaFe₂As₂ in a diamond anvil cell at pressures up to 4.4 GPa and temperatures down to 8 K. Tracing the amplitude of the relaxation process results in an electronic phase diagram that illustrates the variation of the spin-density wave (SDW) order across the whole range of the applied pressures and temperatures. We observe a slowing down of the SDW relaxation dynamics in the vicinity of the phase transition boundary. However, its character depends on the trajectory in the phase diagram: the slowing down occurs gradually for the pressure-induced transition at low temperatures and abruptly for the thermally-driven transition. Our results suggest that the pressure-induced quantum phase transition in BaFe₂As₂ is related to the gradual worsening of the Fermi-surface nesting conditions.

TT 62.2 Fri 9:45 HSZ 03

Probing the superconducting transition in a cuprate superconductor by multi-dimensional terahertz spectroscopy — •ALBERT LIU¹, DANICA PAVICEVIC¹, MICHAEL FECHNER¹, PEDRO LOZANO², GENDA GU², and ANDREA CAVALLERI^{1,3} — ¹Max Planck Institute for the Structure and Dynamics of Matter, Hamburg, Germany — ²Brookhaven National Laboratory, New York, USA — ³Oxford University, Oxford, UK

We develop two-dimensional terahertz spectroscopy in both a non-collinear and reflection geometry. We demonstrate the technique by distilling the terahertz optical response of a superconducting plasma into its constituent nonlinearities, up to fifth-order. Subsequent measurements at temperatures approaching and crossing the phase transition reveal a phase-disordering transition in lieu of a BCS transition. An outlook for probing light-induced superconducting states will be provided.

TT 62.3 Fri 10:00 HSZ 03

Tracing the dynamics of the superconducting order via transient THG — •MINJAE KIM^{1,2,3}, GENNADY LOGVENOV², BERNHARD KEIMER², DIRK MANSKE², LARA BENFATTO⁴, and STEFAN KAISER^{1,2,3} — ¹Institute of Solid State and Materials Physics, Technical University Dresden, 01062 Dresden, Germany — ²Max Planck Institute for Solid State Research, 70569 Stuttgart, Germany — ³4th Physics Institute and Research Center SCoPE, University of Stuttgart, 70569 Stuttgart, Germany — ⁴Department of Physics and ISC-CNR, Sapienza University of Rome, 00185 Rome, Italy

Nonlinear THz third harmonic generation (THG) was shown to directly probe internal degrees of freedoms of the superconducting condensate and its exposure to external collective modes in the framework of driven Higgs modes [1-3]. Here we extend this idea to light-driven nonequilibrium states in superconducting La_{2-x}Sr_xCuO₄ establishing a transient Higgs spectroscopy. We perform an optical pump-THz-THG drive experiment and using 2D-spectroscopy we disentangle the driven TH response into the excited quasiparticles and condensates response. As such the light induced changes of the THG signals probe the ultrafast pair breaking dynamics and transient pairing amplitude of the condensate.

[1] *Nat. Comm.* **11**, 1 (2020)

[2] *Nat. Comm.* **11**, 287 (2020)

[3] arXiv:2109.09971

TT 62.4 Fri 10:15 HSZ 03

Influence of impurities on the Higgs mode in non-centrosymmetric superconductors — •SIMON KLEIN and DIRK MANSKE — Max-Planck Institut für Festkörperforschung, Stuttgart, Deutschland

Recent interest for collective amplitude (Higgs) excitations focused on third harmonic generation (THG) experiments in single- and multi-band superconductors, both for singlet *s*- and *d*-wave gap structure. A resonance in the THG intensity appears, when matching the driving frequency to the energy of the corresponding investigated mode, leading to a phase jump at the resonance frequency. We extend these studies to superconductors without an inversion symmetry, which can be effectively described by a two-band model with an order parameter, consisting of spin singlet (even parity) and spin triplet (odd parity)

components. We calculate the THG response, showing that it contains contributions from three distinguishable sources, namely the Higgs mode, the Leggett mode and quasiparticles. In the clean limit the quasiparticle contributions dominate the collective modes for all singlet-triplet ratios of the gap structure. By including already a small amount of impurities in the system, we find a significant enhancement of the Higgs mode contributions to the THG signal. Furthermore, we notice a significant change in the phase jump, which helps to differentiate between clean and dirty superconductors.

15 min. break

TT 62.5 Fri 10:45 HSZ 03

Non-equilibrium phenomena in a two-band superconductor MgB_2 driven by narrow-band THz pulses — •SERGEI SOBOLEV¹, AMON LANZ¹, TAO DONG², ALEXEJ PASHKIN³, AMRIT POKHAREL¹, ZI ZHAO GAN², LI YU SHI², NAN LIN WANG², STEPHAN WINNERL³, MANFRED HELM³, and JURE DEMSAR¹ — ¹Uni-Mainz, Mainz — ²Peking Uni., Beijing — ³HZDR, Dresden

Excitation of a superconductor (SC) with a low energy electromagnetic pulse leads to a non-equilibrium state, which may profoundly differ from a quasi-thermal one, driven by optical excitation. Such a non-equilibrium may be especially pronounced in a multi-band SC. Here, we report on systematic time-resolved studies of the dynamics of the SC order following resonant excitation with intense narrow-band THz pulses in thin films of MgB_2 , the prototype two-band SC with two distinct superconducting gaps. We demonstrate that the temperature and excitation density dependent dynamics qualitatively follows the behavior predicted by the phenomenological Rothwarf-Taylor model for dynamics in a single gap BCS superconductor implying strong coupling between the two condensates on the ps timescale. Tracking the dependence of the amplitude of the THz driven gap suppression, however, displays a pronounced minimum near $0.6T_c$, that cannot be accounted by the phenomenological model. Comparison of the results to those obtained by excitation with NIR pulses suggests that resonant THz excitation results in long-lived (100 ps timescale) non-thermal quasiparticle distribution, which gives rise to Eliashberg-type enhancement of superconductivity, competing with pair-breaking.

TT 62.6 Fri 11:00 HSZ 03

Semi-classical analysis of high harmonic spectra in Dirac materials — •WOLFGANG HOGGER¹, VANESSA JUNK¹, ALEXANDER RIEDEL¹, COSIMO GORINI², JUAN-DIEGO URBINA¹, and KLAUS RICHTER¹ — ¹Institute for theoretical physics, University of Regensburg, Germany — ²Université Paris-Saclay, CEA, CNRS, SPEC, 91191, Gif-sur-Yvette, France

The study of high-order harmonic generation (HHG) in solids by virtue of intense laser pulses provides a fascinating platform to study ultrafast electron dynamics as well as material properties. We theoretically investigate HHG on the basis of massive Dirac Fermions, serving as a prototypical model for topologically non-trivial matter. The high harmonic spectra resulting from a numerical solution of the equations of motion for the density-matrix are supplemented and compared to a semiclassical saddle-point analysis known as the Lewenstein or simple-man model[1,2]. We demonstrate that HHG can be interpreted as a result of interfering classical trajectories generated at different half-cycles of the laser pulse. A transparent and compact analytical formula for the high harmonic spectrum in the limit of long pulses is provided and discussed regarding

the range of its validity as well as corrections arising from short waveforms.

[1] M. Lewenstein, P. Balcou, M. Y. Ivanov, A. L'Huillier, and P. B. Corkum, Phys. Rev. A 49, 2117 (1994)

[2] G. Vampa, C. R. McDonald, G. Orlando, D. D. Klug, P. B. Corkum, and T. Brabec, Phys. Rev. Lett. 113, 073901 (2014)

TT 62.7 Fri 11:15 HSZ 03

Driven lattice fluctuations in quantum paraelectric SrTiO_3 — •MICHAEL FECHNER¹, MICHAEL FÖRST¹, ANKIT DISA¹, MICHELE BUZZI¹, ALEX VON HOEGEN¹, GAL ORENSTEIN², VIKTOR KRAPIVIN², QUYNH LE NGUYEN², ROMAN MANKOWSKY³, MATHIAS SANDER³, HENRIK LEMKE³, YUNPEI DENG³, MARIANO TRIGO², and ANDREA CAVALLERI¹ — ¹Max Planck Institute for the Structure and Dynamics of Matter, Hamburg, Germany — ²Stanford Linear Accelerator Center, Menlo Park, United States of America — ³Paul Scherrer Institute, Villigen, Switzerland

Enhanced fluctuations are the precursors of quantum phase transition. In the case of ferro- and antiferrodistortive structural transitions, these fluctuations arise at specific points in reciprocal space. Here we use time-resolved x-ray diffuse scattering to show how a resonantly driven zone center optical phonon in cubic SrTiO_3 selectively modulates lattice fluctuations on the Brillouin zone boundary. On short time scales, enhanced and oscillating lattice fluctuations are found at the R-point, which reduce to below the equilibrium value on the picosecond time scale. We attribute the fast dynamics to a finite-momentum fourth-order phonon-phonon interaction between the driven infrared-active Ti-O stretch mode and the antiferrodistortive zone-boundary soft mode. The long-term reduction indicates nonlinear coupling of the antiferrodistortive distortions to strain. We discuss the implications of these findings for the recently observed light-induced ferroelectric state of SrTiO_3 [1].

[1] T.F. Nova et al., Science 364, 1075 (2019)

TT 62.8 Fri 11:30 HSZ 03

Decay of photoinduced orbital excitations in the spin-Peierls system TiOCl : a study from first principle — •PAUL FADLER¹, PHILIPP HANSMANN¹, KAI PHILLIP SCHMIDT¹, ANGELA MONTANARO², DANIELE FAUSTI^{1,2}, and MARTIN ECKSTEIN³ — ¹Friedrich-Alexander-Universität Erlangen-Nürnberg — ²University of Trieste — ³Universität Hamburg

In spin-Peierls materials, the magnetic interactions caused by the electronic correlations drive a phase transition in which the unit cell is distorted. TiOCl is a quasi one-dimensional transition metal oxide with well-defined orbital (d-d) excitations that transitions to a spin-Peierls state below 67K, by doubling the unit cell along the 1-D chain. Recently, optical transmissivity measurements after a double pump excitation into the orbital excitations revealed a dependence of the decay time on the excitation sequence, which may indicate different lifetimes of various orbital excitations. To unveil the microscopic origins of this observation, we study a material-realistic multi-orbital Hubbard Hamiltonian derived from ab initio density-functional theory. The localized strong-coupling native of TiOCl then allows for perturbative elimination of charge-excitations, leading to a spin-orbital model of Kugel-Khomskii type. We compute its spin dispersion in the absence of orbital excitations. Based on this, and the computed intra and inter-orbital matrix elements, we then estimate the decay time of orbital excitations via (multi) spinon emission, and compare to the experimental findings.

TT 63: Superconductivity: Theory

Time: Friday 9:30–13:15

Location: HSZ 103

TT 63.1 Fri 9:30 HSZ 103

Sharp Kohn-like phonon anomalies due to charge order can strongly enhance the superconducting T_c — •ALESSIO ZACCONE — Department of Physics, University of Milan, 20133 Milano, Italy

Phonon softening is a ubiquitous phenomenon in condensed matter systems which is usually associated with charge density wave (CDW) instabilities and anharmonicity. The interplay between phonon softening, CDW and superconductivity is a topic of intense debate. In this work, the effects of anomalous soft phonon instabilities on superconductivity are studied based on a recently developed theoretical framework that accounts for phonon damping and softening within the Migdal-Eliashberg theory [1]. Model calculations [2] show that the phonon softening in the form of a dip in the phonon dispersion relation, either acoustic or optical (including the case of Kohn-type anomalies typically associated with CDW), can cause a manifold increase of the electron-phonon coupling constant λ . This, under certain conditions, which are consistent with the concept of optimal frequency introduced by Bergmann and Rainer, can produce a large increase of the superconducting transition temperature T_c . These results suggest the possibility of reaching high-temperature superconductivity by exploiting soft phonon anomalies restricted in momentum space.

[1] M. Baggioli, C. Setty, A. Zaccane, Phys. Rev. B 101, 214502 (2020)

[2] arXiv:2211.12015v2

TT 63.2 Fri 9:45 HSZ 103

Universal suppression of superfluid weight by non-magnetic disorder in s-wave superconductors independent of quantum geometry and band dispersion — •ALEXANDER LAU¹, SEBASTIANO PEOTTA², DMITRY I. PIKULIN³, ENRICO ROSSI⁴, and TIMO HYART^{1,2} — ¹MagTop, IF PAN, Warsaw, Poland — ²Aalto University, Finland — ³Microsoft Quantum, Redmond, USA — ⁴William & Mary, Williamsburg, USA

Motivated by the experimental progress in controlling the properties of the energy bands in superconductors, significant theoretical efforts have been devoted to study the effect of the quantum geometry and the flatness of the dispersion on the superfluid weight. In conventional superconductors, where the energy bands are wide and the Fermi energy is large, the contribution due to the quantum geometry is negligible, but in the opposite limit of flat-band superconductors the superfluid weight originates purely from the quantum geometry of Bloch wave functions. Here, we study how the energy band dispersion and the quantum geometry affect the disorder-induced suppression of the superfluid weight [1]. In particular, we consider non-magnetic disorder and s-wave superconductivity. Surprisingly, we find that the disorder-dependence of the superfluid weight is universal across a variety of models, and independent of the quantum geometry and the flatness of the dispersion. Our results suggest that a flat-band superconductor is as resilient to disorder as a conventional superconductor.

[1] SciPost Phys. 13, 086 (2022)

TT 63.3 Fri 10:00 HSZ 103

Correction to Morel-Anderson-Tolmachev pseudopotential for nonlocal Coulomb interaction in 2D superconductors — •MANUEL SIMONATO, MALTE RÖSNER, and MIKHAIL I. KATSNELSON — Radboud University, Nijmegen, NL
The repulsive Coulomb interaction between electrons is detrimental to conventional superconductivity. The widely accepted model to account for this is to describe this repulsion with a purely local interaction of strength μ_C . Morel, Anderson, and Tolmachev then showed that the superconducting quantities are effectively described by a renormalized parameter μ_C^* , as a direct consequence of the energy scale separation between phonons and electrons. In 2D the screening properties are less efficient and modeling the Coulomb repulsion with a strictly local interaction can result in inaccurate description. We therefore study how superconducting properties are affected by nonlocal Coulomb repulsions. We find that the superconducting state can still be accurately described when a revised Coulomb pseudopotential $\tilde{\mu}_C^*$ is used. We show that the revised parameter, which accounts for nonlocal interactions, is always larger than the conventional μ_C^* . The non-local Coulomb interaction thus suppresses superconductivity and the critical temperature even further. Analyzing the Bethe-Salpeter equation describing the screening of Coulomb interaction in 2D, we obtain an analytical expression for $\tilde{\mu}_C^*$, and show that the structure of the nonlocal Coulomb interaction weakens the screening effects from high-energy pair fluctuations and therefore yields larger values of the pseudopotential.

TT 63.4 Fri 10:15 HSZ 103

Coherence and pairing fluctuations in strongly correlated superconductors — •NIKLAS WITT^{1,2}, SERGEY BRENER¹, YUSUKE NOMURA³, RYOTARO ARITA^{4,5}, ALEXANDER LICHTENSTEIN^{1,2}, and TIM WEHLING^{1,2} — ¹University of Hamburg, Germany — ²The Hamburg Centre for Ultrafast Imaging, Germany — ³Keio University Japan — ⁴University of Tokyo, Japan — ⁵RIKEN CEMS, Japan
The fundamental properties of superfluids and superconductors are determined by the spatial coherence of the macroscopic condensate. Central to this characterization is the knowledge of the coherence length ξ , as it specifies the relevant length scales for fluctuations pertinent to, e.g., the formation of vortex lattices or magneto-thermal transport. While the description of ξ is well established in weak-coupling BCS theory and Eliashberg-theory, it is a generally unknown quantity in strongly correlated superconductors, where spatiotemporal fluctuations influence the critical temperature [1] and might underlie light-induced enhancement of superconductivity [2].

In this work, we establish a link to directly calculate the coherence length for superconductors with strong electron correlations from microscopic theories and first principles. We illustrate with the example of Alkali-doped fullerides (A_3C_{60}) how proximity of superconducting and Mott-localized states impact superconducting coherence, pairing fluctuations, and critical temperature. Our analysis shows Eliashberg-type behavior of strongly correlated superconductors. [1] Emery & Kivelson, *Nature* **374** (1995) [2] Fausti et al., *Science* **331** (2011) Mitrano et al., *Nature* **530** (2016)

TT 63.5 Fri 10:30 HSZ 103

Superconductivity from repulsive interactions due to strong-coupling to a Mott-insulating layer — •CLARA S. WEBER^{1,2}, DANTE M. KENNES¹, and MARTIN CLAASSEN² — ¹RWTH Aachen, Aachen, Germany — ²University of Pennsylvania, Philadelphia, USA

While superconductors in their conventional form are established by effective attractive interactions, mechanisms for emergent electronic pairing from strong repulsive electron-electron interactions remain under considerable debate. Here, we establish a strong-coupling mechanism that realizes intertwined superconductivity and magnetic order in a Kondo-like bilayer system with purely repulsive interactions, composed of a two-dimensional Mott insulator with strong Hubbard interactions coupled to a layer of weakly-interacting itinerant electrons. Remarkably, this model allows for a rigorous strong-coupling analysis, where we find that itinerant electrons in the nearly-metallic layer are subject to an effective attractive electron-electron interaction as a function of magnetic ordering in the Mott-insulating layer. We carefully study this behavior numerically using large scale DMRG calculations and find that the superconducting behavior persists in a wide parameter range beyond the strong-coupling regime. Additionally, we classify the rich magnetic phase diagram and find a 2-site antiferromagnetic and a 4-site antiferromagnetic phase, along with a phase separation regime. Finally, we discuss possible applications and realizations of the proposed mechanism.

TT 63.6 Fri 10:45 HSZ 103

Simulating superconducting properties of overdoped cuprates: The role of inhomogeneity — MAINAK PAL², •ANDREAS KREISEL¹, WILLIAM A. ATKINSON³, and PETER J. HIRSCHFELD² — ¹Niels Bohr Institute, University of Copenhagen, Denmark — ²Department of Physics, University of Florida, USA — ³Department of Physics and Astronomy, Trent University, Canada

Theoretical studies of disordered d -wave superconductors have focused, with a few exceptions, on optimally doped models with strong scatterers. Addressing recent controversies about the nature of the overdoped cuprates, however,

requires studies of the weaker scattering associated with dopant atoms. Here we study simple models of such systems in the self-consistent Bogoliubov-de Gennes (BdG) framework, and compare to disorder-averaged results using the self-consistent-T-matrix-approximation (SCTMA). Despite surprisingly linear in energy behavior of the low-energy density of states even for quite disordered systems, the superfluid density in such cases retains a quadratic low-temperature variation of the penetration depth, unlike other BdG results reported recently. We trace the discrepancy to smaller effective system size employed in that work. Overall, the SCTMA performs remarkably well, with the exception of highly disordered systems with strongly suppressed superfluid density. We explore this interesting region where gap inhomogeneity dominates measured superconducting properties, and compare with overdoped cuprates.

[1] M. Pal, A. Kreisel, W.A. Atkinson, P.J. Hirschfeld arXiv:2211.13338 (2022)

TT 63.7 Fri 11:00 HSZ 103

Finite energy Cooper pairing in multiband superconductors — •MASOUD BAHARI¹, SONG-BO ZHANG², CHANG-AN LI¹, SANG-JUN CHOI¹, CARSTEN TIMM³, and BJÖRN TRAUZETTEL¹ — ¹University of Würzburg, Würzburg, Germany — ²University of Zürich, Zürich, Switzerland — ³Technische Universität Dresden, Dresden, Germany

Extensive efforts have been carried out to understand the superconducting pairing symmetry since the birth of Bardeen-Cooper-Schrieffer theory. In weakly interacting systems, the essential ingredient is a weak effective electron-electron interaction at the Fermi energy resulting in particular bulk properties including superconducting gaps possibly with nodes.

We demonstrate and discuss the bulk and surface spectral properties of a novel pairing mechanism that occurs at finite excitation energies in multiband superconductors. In the bulk, it is manifested by the appearance of superconducting coherence peaks in the density of states at finite energies. Interestingly, on the surface, we predict the emergence of a pair of helical topological Dirac surface cones when the finite energy pairing is odd-parity.

Finally, we propose aluminum in proximity with (111) surface of gold to realize the bulk properties of finite energy pairing. We discuss the pairing symmetry of the system by employing the density-functional theory, and an analytical model based on the Bogoliubov-de Gennes formalism. The signature of such a pairing gives important information about the correct pairing symmetry of a superconductor.

15 min. break

TT 63.8 Fri 11:30 HSZ 103

Fragmented Cooper pair condensation in striped superconductors — •ALEXANDER WIETEK — Max Planck Institute for the Physics of Complex Systems, Nöthnitzer Strasse 38, Dresden 01187, Germany

Condensation of bosons in Bose-Einstein condensates or Cooper pairs in superconductors refers to a macroscopic occupation of a few single- or two-particle states. A condensate is called *fragmented* if not a single, but multiple states are macroscopically occupied. While fragmentation is known to occur in particular Bose-Einstein condensates, we propose that fragmentation naturally takes place in striped superconductors. To this end, we investigate the nature of the superconducting ground state realized in the two-dimensional t^*t^*J model. In the presence of charge density modulations, the condensate is shown to be fragmented and composed of partial condensates located on the stripes. The fragments of the condensates hybridize to form an extended macroscopic wave function across the system. The results are obtained from evaluating the singlet-pairing two-particle density matrix of the ground state on finite cylinders computed via the density matrix renormalization group method. Our results shed light on the intricate relation between stripe order and superconductivity in systems of strongly correlated electrons.

TT 63.9 Fri 11:45 HSZ 103

Superconductivity on the honeycomb lattice: A truncated unity perspective — •MATTHEW BUNNEY^{1,2}, JACOB BEYER^{1,2}, CARSTEN HONERKAMP², and STEPHAN RACHEL¹ — ¹School of Physics, University of Melbourne, Melbourne, Australia — ²Theoretical Solid State Physics, RWTH Aachen University, Aachen, Germany

The honeycomb lattice provides one of the simplest scenarios with sublattice degrees of freedom. For Cooper pairing of electrons on this lattice, this opens extensive and intricate opportunities of interplay between the momentum space wavefunction, the electron spins and the orbital (sublattice) dependencies. Recent advances and improvements in truncated unity versions of the functional renormalization group allows us to fully capture these phenomena. We thus revisit the honeycomb Hubbard model and its electron pairing and density wave instabilities. A particular emphasis is placed on the formation of sublattice singlets and the resulting exotic pairing states.

TT 63.10 Fri 12:00 HSZ 103

A low-dimensional ML Surrogate Model for Critical Temperature Prediction of Superconductors — •ANGEL DIAZ CARRAL¹, MARTIN ROITEGUI ALONSO¹, and MARIA FYTA² — ¹Institute for Computational Physics, Universität Stuttgart, Allmandring 3, 70569, Stuttgart, Germany — ²Computational Biotechnology, RWTH-Aachen University, Worringerweg 3, 52074, Aachen, Germany

A general theory of superconductivity has been the focus of research over the last decades. Machine learning (ML) approaches based on chemical and structural features have been developed in order to predict both the critical temperature (T_c) and potential novel superconducting structures. Nevertheless, the applied ML models lack interpretability; either the feature matrix is reduced via SVD/PCA transformations or augmented with statistical feature generation. Here, we introduce a ML model based only on electronic descriptors derived from the composition formula and the individual elements. We reach a very high accuracy (R^2 over 91%) using a considerably reduced descriptor dimensionality, while retaining the physical meaning of the feature space. Our active learning model is efficiently tested in predicting critical temperatures and links to the discovery of new superconducting structures.

TT 63.11 Fri 12:15 HSZ 103

Ab initio study of magnetic doping in an Ising superconductor — •MOHAMMAD HEMMATI¹, PHILIPP RÜSSMANN^{1,2}, and STEFAN BLÜGEL¹ — ¹Peter Grünberg Institut and Institute for Advanced Simulation, Forschungszentrum Jülich and JARA, Jülich, Germany — ²University of Würzburg, Germany

The transition-metal dichalcogenide $NbSe_2$ is a layered superconducting material that exhibits unconventional Ising superconductivity that is particularly robust to certain directions of external magnetic fields [1]. We combined the Bogoliubov-de-Gennes formalism in the Korringa-Kohn-Rostoker Green function method with the Coherent Potential Approximation [2,3], to study superconducting $NbSe_2$ in the presence of dilute concentrations of magnetic transition-metal impurities. The ab initio results show a suppression of superconductivity at higher magnetic impurity concentration, which is in agreement with the Abrikosov-Gorkov theory.

*This work was funded by the Deutsche Forschungsgemeinschaft (DFG, German Research Foundation) under Germany's Excellence Strategy * Cluster of Excellence Matter and Light for Quantum Computing (ML4Q) EXC 2004/1 * 390534769.*

[1] K. S. Novoselov *et al.*, *Science* **353**, aac9439 (2016)[2] <https://julkkr.fz-juelich.de>[3] P. Rüßmann and S. Blügel, *PRB* **105**, 125143 (2022)

TT 63.12 Fri 12:30 HSZ 103

Chiral surface superconductivity in half-Heusler semimetals — •TILMAN SCHWEMMER¹, DOMENICO DI SANTE^{2,3}, JÖRG SCHMALIAN⁴, and RONNY THOMALE¹ — ¹Institute for Theoretical Physics, University of Wuerzburg — ²Department of Physics and Astronomy, University of Bologna, Italy — ³CCQ, Flatiron Institute, New York, USA — ⁴Institute for Theory of Condensed Matter and Institute for Quantum Materials and Technologies, KIT Karlsruhe

We propose the metallic and weakly dispersive surface states of half-Heusler semimetals as a possible domain for the onset of unconventional surface super-

conductivity ahead of the bulk transition. Using density functional theory (DFT) calculations and the random phase approximation (RPA), we analyse the surface band structure of LuPtBi and its propensity towards Cooper pair formation induced by screened electron-electron interactions in the presence of strong spin-orbit coupling. Over a wide range of model parameters we find a chiral superconducting condensate featuring Majorana edge modes to be favoured energetically, while low-dimensional order parameter fluctuations trigger time-reversal symmetry breaking preceding the superconducting transition.

TT 63.13 Fri 12:45 HSZ 103

Transport in superconducting heterostructures: Quasiclassical theory and finite element method — •KEVIN MARC SEJA and TOMAS LÖFWANDER — Department of Microtechnology and Nanoscience - MC2, Chalmers University of Technology, Gothenburg, Sweden

We present results on steady-state transport in mesoscopic conventional and unconventional superconductors coupled to either normal-metal or superconducting reservoirs. Our self-consistent simulations are using nonequilibrium quasiclassical theory in the Eilenberger formulation which allows different order parameter symmetries at arbitrary mean free path. Previously we investigated the thermoelectric effect[1] and spectral rearrangements due to a voltage bias[2] in d-wave superconductors. These studies on nonequilibrium effects assumed translational invariance normal to the transport direction.

This talk will address the question of how to go beyond such quasi one-dimensional models and study superconducting hybrid structures in realistic device geometries. To this end we present a finite element method[3] for the self-consistent solution of the underlying quasiclassical transport equations in dimensions larger than one, and give examples of its application.

[1] Seja & Löfwander, *Phys. Rev. B* **105**, 104506 (2022)[2] Seja & Löfwander, *J. Phys.: Condens. Matter* **34**, 425301 (2022)[3] Seja & Löfwander, *Phys. Rev. B* **106**, 144511 (2022)

TT 63.14 Fri 13:00 HSZ 103

Nonlinear response of diffusive superconductors to ac electromagnetic Fields — •PASCAL DERENDORF, ANATOLY VOLKOV, and ILYA EREMIN — Institut für Theoretische Physik III, Ruhr-Universität Bochum, Bochum, Germany

Using the generalized Usadel equation, we theoretically study the nonlinear response of a diffusive BCS superconductor to the action of electromagnetic fields. The response is found in the second order of the perturbation in the amplitude of the field E for the superconducting order parameter Δ and in the third order for the current j . We represent the matrix Keldysh function \hat{g}^K as the sum of a regular function \hat{g}^{reg} and an anomalous function \hat{g}^{an} . On the basis of this approach, general formulas for deviations of the retarded (advanced) Green's functions, as well as the Keldysh function for an arbitrary number of harmonics of the incident field are explicitly obtained. The frequency and temperature dependencies of zero harmonic $\delta\Delta_0$ (Eliashberg effect) and the second harmonic $\delta\Delta_{2\Omega}$ under action of a monochromatic irradiation are analyzed. We also study the third harmonic $j_{3\Omega}$ and the possibility of parametric amplification of a signal with a frequency Ω_x in the presence of a pumping with a frequency Ω which excites the Higgs (amplitude) mode.

TT 64: Topology: Other Topics

Time: Friday 9:30–11:30

Location: HSZ 201

TT 64.1 Fri 9:30 HSZ 201

Fermi arc reconstruction in synthetic photonic lattice — •DUY HOANG MINH NGUYEN¹, CHIARA DEVESCOVI¹, DUNG XUAN NGUYEN², HAI SON NGUYEN^{3,4}, and DARIO BERCILOUX^{1,5} — ¹Donostia International Physics Center, Donostia-San Sebastian, Spain — ²Center for Theoretical Physics of Complex Systems, Institute for Basic Science (IBS), Daejeon, Republic of Korea — ³Univ Lyon, Ecole Centrale de Lyon, CNRS, INSA Lyon, Université Claude Bernard Lyon 1, CPE Lyon, CNRS, INL, UMR5270, Ecully, France — ⁴Institut Universitaire de France (IUF), Paris, France — ⁵IKERBASQUE, Basque Foundation for Science, Euskadi Plaza, 5, Bilbao, Spain

The chiral surface states of Weyl semimetals are known for having an open Fermi surface called Fermi arc. At the interface between two Weyl semimetals, these Fermi arcs are predicted to potentially deform into unique interface states. In this work, we numerically study a one-dimensional (1D) dielectric trilayer grating where the relative displacements between adjacent layers play the role of two synthetic momenta. The lattice is described by an effective Hamiltonian whose spectral properties coincide closely with rigorous electromagnetic simulations. Our trilayer system is a simple but versatile platform that emulates 3D crystals without time-reversal symmetry, including Weyl semimetal, nodal line semimetal, and 3D Chern insulator. It allows us to not only observe phenomena such as the phase transition between Weyl semimetal and Chern insulator but also confirm the Fermi arc reconstruction between two Weyl semimetals.

[1] arXiv:2211.07230

TT 64.2 Fri 9:45 HSZ 201

Electronic correlations and pseudo Fermi arcs due to geometry of the Fermi surface in semimetals — •ELENA DERUNOVA — IFW, Helmholtz str.20, Dresden

Moving forward from topological theory I present a geometrical approach to analyze the bandstructures and Fermi surfaces. Particularly, the effect of hyperbolic geometry of the Fermi surface on the Fermi liquid breakdown and correlated transport effects will be presented. As a mechanism for realizing these correlations, I introduce pseudo Fermi arcs connecting separate pockets of hyperbolic Fermi surface. A breakdown of time-reversal symmetry via tunneling through those pseudo arcs is referred as Fermi Surface Geometry Effect (FS-GE). The predictable power of FS-GE is tested on the spin and anomalous Hall effects, traditionally associated with intrinsic time-reversal symmetry breaking. An index, H_F , quantifying FS-GE in a particular direction, shows a universal correlation ($R^2 = 0.97$) with the experimentally measured intrinsic anomalous Hall conductivity in that direction, of 16 different compounds spanning a wide variety of crystal, chemical, and electronic structure families, where the topological methods give just $R^2 = 0.52$. This raises a question about the principal limits of topological physics, dominating now the predictions of non-trivial electron transport, and its transformation into a wider study of bandstructures' and Fermi surfaces' geometries, opening a horizon for the prediction of phenomena beyond topological understanding.

TT 64.3 Fri 10:00 HSZ 201

Markers in Landau levels for topological transitions in Bernal bilayer graphene — •NILS JACOBSEN¹, ANNA SEILER¹, ZHIYU DONG², THOMAS WEITZ¹, and LEONID LEVITOV² — ¹1st Physical Institute, Faculty of Physics, University of Göttingen, Göttingen, Germany — ²Department of Physics, Massachusetts Institute of Technology, Cambridge, USA

This talk will discuss Landau levels in an electron band that exhibits the topological Lifshitz transition. We focus on Bernal-stacked bilayer graphene, a system that has drawn a lot of attention recently. A dual gated experimental setup allows to tune the out-of-plane displacement field and the charge carrier density independently, giving insights in exotic correlation effects [1]. Depending on the charge carrier density its Fermi surface changes its topology, that is, four disconnected pockets merge together to form one connected Fermi sea [2].

This topological transition results in a complex series of Landau levels which are not valley-symmetric and, as a result, change their order and degeneracy when the magnetic field is varied. These effects are added to the degeneracies that are already present due to valley and spin degrees of freedom. By virtue of numerical diagonalization methods based on a realistic tight binding model, we extract this Landau level sequence and directly relate it to transport measurements. Our model allows us to access the range of parameters of interest where the topological Lifshitz transition can occur.

[1] A. M. Seiler et al., Nature 608, 298 (2022)

[2] E. McCann et al. Rep. Prog. Phys. 76, 056503 (2013)

TT 64.4 Fri 10:15 HSZ 201

Topological classification of single-particle Green functions and effective Hamiltonians for interacting systems — MAXIMILIAN KOTZ¹ and •CARSTEN TIMM^{1,2} — ¹Institute of Theoretical Physics, TU Dresden, 01062 Dresden, Germany — ²Würzburg-Dresden Cluster of Excellence ct.qmat, TU Dresden, 01062 Dresden, Germany

The single-particle Green function for any interacting-electron system can be written as the resolvent of a generally frequency-dependent and non-Hermitian effective Hamiltonian. Both these properties together allow for 54 instead of ten global-symmetry classes. The absence of Hermiticity also requires to reconsider the concept of a spectral gap. If the limits of the effective Hamiltonian for frequency $\omega \rightarrow \pm\infty$ coincide one can compactify the frequency axis and consider winding in $(d+1)$ -dimensional momentum-frequency space. We derive a complete list of the homotopy groups for the 54 classes and spatial dimensions d , for the cases without and with frequency dependence.

TT 64.5 Fri 10:30 HSZ 201

Solitons and topology: Observation of cnoidal wave localization in non-linear topoelectric circuits — •HENDRIK HOHMANN¹, TOBIAS HOFMANN¹, TOBIAS HELBIG¹, HAUKE BRAND², LAVI K. UPRETI¹, ALEXANDER STEGMAIER¹, ALEXANDER FRITZSCHE¹, TOBIAS MÜLLER¹, CHING HUA LEE³, MARTIN GREITER¹, LAURENS W. MOLENKAMP², TOBIAS KIESSLING², and RONNY THOMALE¹ — ¹Institute for Theoretical Physics and Astrophysics, University of Würzburg, D-97074 Würzburg, Germany — ²Physikalisches Institut, Universität Würzburg, 97074 Würzburg, Germany — ³Department of Physics, National University of Singapore, Singapore, 117542

Topological phases have been realized in a variety of classical metamaterials. They provide easily accessible platforms to study topology in regimes beyond experimental limitations of real materials.

While most implementations are limited to the linear regime, investigating non-linear effects promises to reveal a plethora of new phenomena, such as solitons and chaos.

To study the intertwining of topology and non-linearity we engineered a topoelectric circuit reminiscent of the Su-Schrieffer-Heeger (SSH) model with

added tunable onsite non-linearity. We observe the localized cnoidal (LCn) state which maintains the spatial exponential localization of the SSH edge mode while distorting a sinusoidal input into eccentric waves in time domain.

In this talk, we complement the non-linear differential equations with the theory of topological localization and develop an analytic description of the LCn state.

TT 64.6 Fri 10:45 HSZ 201

Non-Hermitian diamond chain — •CAROLINA MARTINEZ STRASSER¹, MIGUEL ÁNGEL JIMENEZ HERRERA¹, and DARIO BERCIoux² — ¹Donostia International Physics Center (DIPC), 20018 Donostia-San Sebastián, Spain — ²Ikerbasque, Basque Foundation for Science, Plaza Euskadi 5 48009 Bilbao, Spain

We investigate the spectral properties of a non-Hermitian quasi-one-dimensional lattice in several possible dimerization configurations. Specifically, we focus on a non-Hermitian diamond chain that presents a zero-energy flat band. In the Hermitian case, this flat band originates from wave interference and results in a wave function localized only on a subset of sites on the unit cell [1]. We transform the system into a non-Hermitian one by considering asymmetric hopping terms between some of the lattice sites of the chain. This leads to the accumulation of eigenstates, known as the skin effect. Despite this accumulation of eigenstates, we can characterize the presence of non-trivial edge states at zero energy by a real-space topological invariant known as biorthogonal polarization. We show that this invariant, evaluated using the destructive interference method, can also characterize the non-trivial phase of the non-Hermitian diamond chain [2].

[1] D. Bercioux, O. Dutta, and E. Rico, Ann. Phys. (Berl.) 529, 1600262 (2017)

[2] F. K. Kunst et al., Phys. Rev. Lett. 121, 026808 (2018)

TT 64.7 Fri 11:00 HSZ 201

Direct optical probe of magnon topology in two-dimensional quantum magnets — •MICHAEL SENTEF¹, EMIL BOSTRÖM¹, TAHEREH PARVINI², JAMES McIVER¹, ANGEL RUBIO¹, and SILVIA VIOLA KUSMINSKIY³ — ¹Max Planck Institute for the Structure and Dynamics of Matter, Hamburg — ²University of Greifswald — ³RWTH Aachen

Controlling edge states of topological magnon insulators is a promising route to stable spintronics devices. However, to experimentally ascertain the topology of magnon bands is a challenging task. Here we derive a fundamental relation between the light-matter coupling and the quantum geometry of magnon states. This allows to establish the two-magnon Raman circular dichroism as an optical probe of magnon topology in honeycomb magnets, in particular of the Chern number and the topological gap. Our results pave the way for interfacing light and topological magnons in functional quantum devices.

arXiv:2207.04745

TT 64.8 Fri 11:15 HSZ 201

Inelastic topological light scattering in chiral liquids — SILVIA MÜLLNER¹, FLORIAN BÜSCHER¹, ANGELA MÖLLER², and •PETER LEMMENS¹ — ¹IPKM, TU Braunschweig — ²Anorg. Chemie, JGU Mainz

Vortex beams of light contain spin (SAM, helicity) and angular momentum (OAM, chirality). However, there is a long debate whether OAM can couple to a topological system. In a recent experimental study of chiral liquid crystals we demonstrate the effect of vortex light with different topological charge. We give evidence for roton like quasiparticles with a dispersion that dominates the scattering at small and intermediate scattering vectors [1].

Work supported by DFG LE967/16-1, GrK 1952/2, Metrology for Complex Nanosystems**NanoMet*, and DFG EXC-2123 *QuantumFrontiers* - 390837967.

[1] S. Müllner, F. Büscher, A. Möller, and P. Lemmens, Phys. Rev. Lett. 129, 207801 (2022)

TT 65: Correlated Electrons: Other Theoretical Topics

Time: Friday 9:30–12:15

Location: HSZ 204

TT 65.1 Fri 9:30 HSZ 204

Quantum oscillations beyond the Onsager relation in a doped Mott insulator — •VALENTIN LEEB^{1,2} and JOHANNES KNOLLE^{1,2,3} — ¹Technical University of Munich, Germany; TUM School of Natural Sciences, Department of Physics, TQM — ²Munich Center for Quantum Science and Technology (MC-QST), 80799 Munich, Germany — ³Blackett Laboratory, Imperial College London, London SW7 2AZ, United Kingdom

The kinetic energy of electrons in a magnetic field is quenched resulting in a discrete set of highly degenerate Landau levels (LL). This gives rise to fascinating phenomena like quantum oscillations or the integer and fractional quantum Hall effect. The latter is a result of interactions partially lifting the degeneracy within a given LL while inter-LL interactions are usually assumed to be unimportant. Here, we study the LL spectrum of the Hatsugai-Kohmoto model, a Hubbard-like model which is exactly soluble on account of infinite range inter-

actions. For the doped Mott insulator phase in a magnetic field we find that the degeneracy of LLs is preserved but inter-LL interactions are important leading to a non-monotonous reconstruction of the spectrum. As a result, strong interactions lead to aperiodic quantum oscillations of the metallic phase in contrast to Onsager's famous relation connecting oscillation frequencies with the Fermi surface areas at zero field. In addition, we find unconventional temperature dependencies of quantum oscillations and effective mass renormalizations. We discuss the general importance of inter-LL interactions for understanding doped Mott insulators in magnetic fields.

TT 65.2 Fri 9:45 HSZ 204

Non-Fermi-liquid behavior from critical electromagnetic vacuum fluctuations — •PENG RAO and FRANCESCO PIAZZA — Max Planck Institute for the Physics of Complex Systems, Dresden, Germany

We study two-dimensional materials where electrons are coupled to the vacuum electromagnetic field of a cavity. We show that, at the onset of the superradiant phase transition towards a macroscopic photon occupation of the cavity, the critical electromagnetic fluctuations, consisting of photons strongly overdamped by their interaction with electrons, can in turn lead to the absence of electronic quasiparticles. Since transverse photons couple to the electronic current, the appearance of non-Fermi-Liquid behavior strongly depends on the lattice. In particular, we find that in a square lattice the phase space for electron-photon scattering is reduced in such a way to preserve the quasiparticles, while in a honeycomb lattice the latter are removed due to a non-analytical frequency dependence of the damping $\propto |\omega|^{2/3}$. Standard cavity probes could allow to measure the characteristic frequency spectrum of the overdamped critical electromagnetic modes responsible for the non-Fermi-liquid behavior.

TT 65.3 Fri 10:00 HSZ 204

Collapse of fermionic quasiparticles upon coupling to local bosons — ADAM KŁOSIŃSKI, PIOTR WRZOSEK, KRZYSZTOF WOHLFELD, and •CLIO EFTHIMIA AGRAPIDIS — Institute of Theoretical Physics, Faculty of Physics, University of Warsaw, Poland

We study the stability of the fermionic quasiparticle in a fermion-boson model on a Bethe lattice, with fermions interacting with local bosons through a Peierls coupling. We solve the model by mapping it onto a non-interacting chain with a site-dependent potential. We show that the model does not support a quasiparticle solution – provided that a finite number of local bosonic excitations cost zero energy. The quasiparticle disappearance becomes easier with an increase in: (i) the total number of bosons with zero energy, and (ii) the relative strength of the coupling between bosons and fermions. The postulated model can be applied to study systems in which fermions are coupled to condensed bosons or magnons in spin stripes embedded in hole-doped 2D antiferromagnets or Ising-like magnetic interfaces (ferromagnetic-antiferromagnetic). Finally, we show how this model leads to an in-depth understanding of the onset of quasiparticles in the 1D and 2D t - J^z model.

TT 65.4 Fri 10:15 HSZ 204

Breakdown of the many-electron perturbation expansion beyond particle-hole symmetry — •HERBERT ESSL, MATTHIAS REITNER, and ALESSANDRO TOSCHI — Institute of Solid State Physics, TU Wien

The breakdown of the self-consistent perturbation theory for many-electron systems has several physical and formal manifestations. Among the latter, one of the most studied is the divergence of two-particle irreducible vertex functions. Hitherto most investigations of the divergences appearing in the irreducible vertex functions of many-electron systems have been restricted to the particle hole symmetric cases and the calculations were performed at finite temperatures. This work is a first step beyond such restrictions. To this aim we investigate the two particle properties of the Hubbard Atom, both for positive (repulsive) and negative (attractive) on-site interaction. As a main result a *universal phase diagram* of vertex divergences, valid for arbitrary (finite) temperatures, has been determined. Using this result as a "compass", the $T=0$ limit has been investigated, in order to unveil possible connections between the vertex divergences and the validity or the violation of the Luttinger Theorem. We also study the convergence of the self-consistent perturbation series beyond the particle-hole symmetry condition, determining specific constraints for the convergence of the series to the physical solution at arbitrary electronic densities.

TT 65.5 Fri 10:30 HSZ 204

Cooling and heating in the Bose-Hubbard model by parameter tuning — •SEBASTIAN EGGERT, SVEN STAWINSKI, and AXEL PELSTER — University of Kaiserslautern

We investigate short-range interacting Bosons in an optical lattice at finite temperature. It is well known that the system shows a Mott-Superfluid transition when changing the repulsion U , the hopping t and/or the filling. However, it is much less clear how the temperature is affected by those changes, assuming the parameters U and/or t are tuned adiabatically. We now present higher order calculations for the full Free energy and derive the temperature and entropy in a large parameter space. We discuss where significant heating or cooling effects can be expected in the superfluid phase, in the Mott region and near the phase transition lines.

15 min. break

TT 65.6 Fri 11:00 HSZ 204

Fixed-point annihilation and duality in the SU(2)-symmetric spin-boson model — •MANUEL WEBER^{1,2} and MATTHIAS VOJTA² — ¹Max-Planck-Institut für Physik komplexer Systeme, Dresden, Germany — ²Institut für Theoretische Physik und Würzburg-Dresden Cluster of Excellence ct.qmat, Technische Universität Dresden, Germany

The annihilation of two intermediate-coupling renormalization-group (RG) fixed points is of interest in diverse fields from statistical mechanics to high-energy physics, but has so far only been studied using perturbative techniques. Using the recently developed wormhole quantum Monte Carlo method, we

present high-accuracy results for the SU(2)-symmetric $S = 1/2$ spin-boson (or Bose-Kondo) model. We study the model with a power-law bath spectrum $\propto \omega^s$ where, in addition to a critical phase predicted by perturbative RG, a stable strong-coupling phase is present. Using a detailed scaling analysis, we provide direct numerical evidence for the collision and annihilation of two RG fixed points at $s^* = 0.6540(2)$, causing the critical phase to disappear for $s < s^*$. In particular, we uncover a surprising duality between the two fixed points, corresponding to a reflection symmetry of the RG beta function, which we utilize to make analytical predictions at strong coupling which are in excellent agreement with numerics. Our work makes phenomena of fixed-point annihilation accessible to large-scale simulations, and we comment on the consequences for impurity moments in critical magnets.

TT 65.7 Fri 11:15 HSZ 204

Thermodynamics properties of interacting Dirac fermion with SO(3) symmetry — •ZHONG LIU¹, MATTHIAS VOJTA², FAKHER F. ASSAAD¹, and LUKAS JANSSEN² — ¹Institut für Theoretische Physik und Astrophysik und Würzburg-Dresden Cluster of Excellence ct.qmat, Universität Würzburg, 97074 Würzburg, Germany — ²Institut für Theoretische Physik und Würzburg-Dresden Cluster of Excellence ct.qmat, Technische Universität Dresden, 01062 Dresden, Germany

In the previous work [Physical Review Letters, 128(8):087201, 2022], we figure out the zero temperature phasediagram of an interacting Dirac fermion model processed explicit SO(3) symmetry with unbiased quantum Monte Carlo (QMC) method. By threading size dependent magnetic flux ($B \sim 1/L^2$) across two dimensional honeycomb lattice, we reduce the finite size effect in the QMC simulation and suppress the superconductivity in the strong coupling region. In this scenario, the ground state phase diagram of the model is splitted by two phase transitions. In this talk, we implement the QMC simulation by turning off the magnetic flux. Without the external magnetic field, the model recover to a higher symmetry and the superconductivity emergence in the strong coupling region on the ground state. In addition, we investigate the thermodynamics properties near the second transition point, where the finite temperature phase boundary are determined by the Ising type particle-hole order parameter and the Kosterlitz-Thouless transition governed by the U(1) symmetry breaking.

TT 65.8 Fri 11:30 HSZ 204

Long-term memory magnetic correlations driven by local electronic repulsion — •EMIN MOGHADAS¹, MATTHIAS REITNER¹, CLEMENS WATZENBÖCK¹, GIORGIO SANGIOVANNI², and ALESSANDRO TOSCHI¹ — ¹TU Wien — ²University of Würzburg

We investigate the onset of non-decaying temporal magnetic correlations in simple electronic models with on-site (Hubbard) electrostatic repulsion U . This effect [1] corresponds to the existence of a finite difference between the static/isothermal and the zero-frequency limit of the dynamical Kubo (magnetic) susceptibility. The long-term behavior is studied, on the one hand, analytically for the non-interacting Bethe lattice case in infinite dimensions and, on the other hand, for finite-size Hubbard ring-molecules by means of exact diagonalization. This way, we can directly observe and investigate the link between the emergence of infinitely long-lived temporal correlations and the degeneracies of the exact many-body eigenspectrum, possibly inferring underlying relations with the entropic properties of the system. Our findings also pave the way to study the enhancement of the static/isothermal density response in the proximity of metal-insulator transitions [2] and, in particular, of its possible impact on the renormalization of electron-phonon coupling.

[1] C. Watzenböck et al., Sci. Post Phys. (2022)

[2] M. Reitner et al., PRL (2020) and references therein.

TT 65.9 Fri 11:45 HSZ 204

Simulation of anyonic tight-binding Hamiltonians — •NICO KIRCHNER¹, ADAM SMITH^{2,3}, BABATUNDE AYENI⁵, FRANK POLLMANN^{1,4}, and JOOST SLINGERLAND^{5,6} — ¹Department of Physics, TFK, Technische Universität München, James-Frank-Straße 1, D-85748 Garching, Germany — ²School of Physics and Astronomy, University of Nottingham, Nottingham, NG7 2RD, UK — ³Centre for the Mathematics and Theoretical Physics of Quantum Non-Equilibrium Systems, University of Nottingham, Nottingham, NG7 2RD, UK — ⁴Munich Center for Quantum Science and Technology (MCQST), Schellingstr. 4, 80799 München, Germany — ⁵Department of Mathematical Physics, National University of Ireland, Maynooth, Ireland — ⁶Dublin Institute for Advanced Studies, School of Theoretical Physics, 10 Burlington Rd, Dublin, Ireland

Anyons are quasiparticles with exotic exchange statistics that can be supported in two-dimensional systems such as quantum spin liquids and fractional quantum Hall systems. In general, even effective models for such systems are not exactly solvable, which leads to numerical approaches to study the properties of anyons. In this talk, I will discuss how to numerically simulate anyonic tight-binding Hamiltonians for general abelian and non-abelian anyon models using the formalism of fusion diagrams. The presented results for such tight-binding Hamiltonians include energy level spacing statistics, which reveal level repulsion for all considered anyons. Further, it is observed that the density distribution following a quench becomes homogeneous at large times for these systems, which indicates thermalization.

TT 65.10 Fri 12:00 HSZ 204

Absence of fractal quantum criticality in the quantum Newman-Moore model — •RAYMOND WIEDMANN^{1,2}, LEA LENKE¹, MATTHIAS MÜHLHAUSER¹, and KAI PHILLIP SCHMIDT¹ — ¹Friedrich-Alexander-Universität, Erlangen-Nürnberg, Germany — ²MPI-FKE, Stuttgart, Germany

The quantum phase transition between the high-field polarized phase and the low-field fracton phase with type-II fracton excitations is investigated in the two-

dimensional self-dual quantum Newman-Moore model. We apply perturbative and numerical linked cluster expansions to calculate the ground-state energy per site in the thermodynamic limit revealing a level crossing at the self-dual point. In addition, high-order series expansions of the relevant low-energy gaps are determined using perturbative continuous unitary transformations indicating no gap-closing. Our results therefore predict a first-order phase transition between the low-field fracton and the high-field polarized phase at the self-dual point.

TT 66: Cryogenic Detectors

Time: Friday 9:30–11:30

Location: HSZ 304

Invited Talk

TT 66.1 Fri 9:30 HSZ 304

Towards ultrasensitive calorimetric detection in superconducting quantum circuits — •BAYAN KARIMI^{1,2}, KUAN-HSUN CHIANG², YU-CHENG CHANG², DANILO NIKOLIC³, JOONAS T. PELTONEN², WOLFGANG BELZIG³, and JUKKA P. PEKOLA² — ¹QTF Centre of Excellence, Department of Physics, Faculty of Science, University of Helsinki, Finland — ²Pico group, QTF Centre of Excellence, Department of Applied Physics, Aalto University, Finland — ³Fachbereich Physik, Universität Konstanz, D-78467, Germany

We demonstrate experimentally an ultra-sensitive thermal detector formed of an electronic absorber coupled to a phonon bath, which reaches the ultimate noise level dictated by the fundamental thermal fluctuations [1]. A scheme of coupling a superconducting qubit to this calorimeter is presented and we conclude positively about sufficient signal-to-noise ratio (SNR) in detecting a microwave photon emitted by it [2,3,4]. Recently this scheme was applied to the thermal detection of quantum phase slips in a Josephson junction [5], and currently we are performing experiments on the proposed qubit calorimetry.

[1] J. P. Pekola and B. Karimi, *Rev. Mod. Phys.* 93, 041001 (2021)

[2] B. Karimi and J. P. Pekola, *Phys. Rev. Lett.* 124, 170601 (2020)

[3] B. Karimi, D. Nikolic, T. Tuukkanen, J. T. Peltonen, W. Belzig, and J. P. Pekola, *Phys. Rev. Applied* 13, 054001 (2020)

[4] J. P. Pekola and B. Karimi, *Phys. Rev. X* 12, 011026 (2022)

[5] E. Gumus, D. Majidi, D. Nikolic, P. Raif, B. Karimi, J. T. Peltonen, E. Scheer, J. P. Pekola, H. Courtois, W. Belzig, and C. B. Winkelmann, arXiv:2202.08726 [cond-mat.mes-hall]

TT 66.2 Fri 10:00 HSZ 304

Novel concept for a superconducting microcalorimeter with tunable gain — •CONSTANTIN SCHUSTER, GABRIEL JÜLG, and SEBASTIAN KEMPF — Institute of Micro- and Nanoelectronic Systems, Karlsruhe Institute of Technology, Karlsruhe, Germany

Cryogenic microcalorimeters such as metallic magnetic calorimeters (MMC) or transition edge sensors (TES) are becoming a mature technology and are hence presently used in various applications requiring an excellent energy resolution. They rely on transducing the temperature rise upon the absorption of an energetic particle into a change of magnetic flux (MMC) or electrical current (TES) which is measured using a SQUID. Despite the overall great success, it turns out that the resolving power still lacks behind the fundamental limit set by fluctuations of thermal energy among different degrees of freedom of the detector. Against this background, we present a novel detector concept which may help to improve the energy resolution. It is based on the strong temperature dependence of the magnetic penetration depth of a superconductor close to its critical temperature. By embedding a properly chosen superconductor directly into the SQUID loop and using a special input circuit configuration, a change in temperature is transduced into a change in magnetic flux threading the SQUID loop. Moreover, it turns out that the temperature to flux transfer coefficient can be tuned in-situ. We present our detector concept and gauge the possible performance and energy resolution of this novel detector concept by discussing simulation results and first experimental data.

TT 66.3 Fri 10:15 HSZ 304

Advances in microwave SQUID multiplexing of magnetic microcalorimeters — •MARTIN NEIDIG, ALEXANDER MAATZ, FELIX SCHUDERER, MARVIN VÖLLINGER, MATHIAS WEGNER, STEFAN WÜNSCH, and SEBASTIAN KEMPF — Institute of Micro- and Nanoelectronic Systems, Karlsruhe Institute of Technology, Karlsruhe, Germany.

The excellent energy resolution, very fast signal rise time and almost ideal linear detector response over a wide energy range makes magnetic microcalorimeters (MMCs) an exceedingly attractive detector technology for applications in various fields of science. The increasing necessity to operate large-scale detector arrays consisting of thousands to millions of individual detectors inherently poses the challenge of developing a suitable multiplexing technique. The presently most promising one is microwave SQUID multiplexing. Here, each individual detector is inductively coupled to a non-hysteretic, unshunted rf-SQUID that, in turn, is inductively coupled to a superconducting microwave resonator having a unique resonance frequency. In this configuration, an actual detector event

results in a change of the effective SQUID inductance and hence in the resonance frequency of the related resonator. Moreover, capacitively coupling many of such readout channels to a single transmission line ultimately allows to read out hundreds to thousands of detectors simultaneously. In this contribution, we summarize our latest developments regarding the implementation of a microwave SQUID multiplexer for MMC readout. This includes aspects regarding to microfabrication as well as device characterization using software defined radio based readout electronics.

TT 66.4 Fri 10:30 HSZ 304

Design, fabrication and characterization of magnetic microcalorimeters for radionuclide metrology within the EMPIR project Prima-LTD — •MICHAEL MÜLLER, FABIENNE BAUER, RIA-HELEN ZÜHLKE, TRUNG DUC TRAN, ALEX MOCANU, and SEBASTIAN KEMPF — Institute of Micro- and Nanoelectronic Systems, Karlsruhe Institute of Technology, Karlsruhe.

The EMPIR project “Prima-LTD” aims to provide ultra-precise measurements of the decay spectra of several radionuclides to enable activity standardization for medicine and industry. As the measurements require an outstanding energy resolution and great linearity over a wide energy range, magnetic microcalorimeters (MMCs) are used as detector technology. The latter are cryogenic particle detectors that make use of a paramagnetic temperature sensor linked to a particle absorber in which the radionuclide is embedded. The sensor is biased by a magnetic field to create a temperature dependent sensor magnetization which is altered by the temperature rise upon a radioactive decay within the absorber and measured using a SQUID. To provide a flexible detector platform, we designed three optimized MMC layouts allowing for different methods of source preparation. For in-house microfabrication of the detectors, we established deposition processes for the various materials needed. This particularly includes an electroplating process for thick, highly conductive absorbers made of gold that are free-standing on stems having a diameter of only 5 μm . We summarize the detector layouts as well as the fabrication status of the detectors and discuss characterization measurements of detector prototypes.

TT 66.5 Fri 10:45 HSZ 304

Fluxon counters and velocimeters at superconducting strips — •OLEKSANDR DOBROVOLSKIY — University of Vienna, Faculty of Physics, Nanomagnetism and Magnonics, SuperSpin Laboratory

Thin strips with large critical current I_c are required for superconducting microstrip single-photon detectors (SMSPDs) [1] and Cherenkov generators/detectors of spin waves by ultra-fast moving fluxons [2]. In this regard, high I_c implies blocking of the penetration of vortices via the strip edges and their control via material and edge-barrier engineering [3]. Thus, at sufficiently large transport currents I_{tr} , a slit at the edge of a superconducting strip acts as a gate for the vortices entering into it. These vortices form a jet, which is narrow near the slit and expands due to the repulsion of vortices as they move to the opposite edge of the strip, giving rise to a transverse voltage V_p . In my talk, I will present our experimental results on voltage kinks in the I-V curves which occur each time the number of fluxons crossing the strip is increased by one [4]. I will also dwell on the appearance of the non-monotonic V_p in MoSi strips with slits milled by FIB at various distances from the transverse voltage leads [5]. Our findings are relevant for the performance of SMSPDs and superconducting devices operated in the single-fluxon regime.

[1] Korneeva et al., *PRAppl.* 13, 024011 (2020)

[2] Dobrovolskiy et al., arXiv:2103.10156

[3] Budinska et al., *PRAppl.* 17, 034072 (2021)

[4] Bezv et al., submitted

[5] Bezuglyj et al., *PRB* 105, 214507 (2022)

TT 66.6 Fri 11:00 HSZ 304

Superconducting 3D-cavity architecture for microwave single-photon detection — •YUKI NOJIRI^{1,2}, KEDAR E. HONASOGE^{1,2}, DANIIL BAZULIN^{1,2}, FLORIAN FESQUET^{1,2}, MARIA-TERESA HANDSCHUH^{1,2}, FABIAN KRONOWETTER^{1,4}, MICHAEL RENGER^{1,2}, ACHIM MARX¹, KIRILL G. FEDOROV^{1,2}, and RUDOLF GROSS^{1,2,3} — ¹Walther-Meißner-Institute, Bavarian Academy of Sciences and Humanities, Germany — ²Technical University of Munich, TUM School of Nat-

ural Sciences, Physics Department, 85748 Garching, Germany — ³Munich Center for Quantum Science and Technology (MCQST), Schellingstr. 4, 80799 Munich, Germany — ⁴Rohde & Schwarz GmbH & Co. KG, Mühldorfstraße 15, 81671 München

Microwave single-photon detectors (SPDs) are essential quantum devices required in a large variety of quantum communication and quantum computation protocols. First microwave SPDs have been realized with the help of superconducting qubits and resonators. Here, we experimentally study an SPD design compatible with the superconducting 3D cavity architecture. We exploit the multimode nature of horseshoe aluminum cavities in combination with transmon qubits to experimentally realize efficient detection of single microwave photons. We analyze the performance of such devices and discuss possible ways to improve it.

TT 66.7 Fri 11:15 HSZ 304

Novel susceptibility thermometer for mK-temperatures based on Au:Er micro-fabricated on a copper substrate — •NATHALIE PROBST, ANDREAS FLEISCHMANN, ANDREAS REIFENBERGER, ANDREAS REISER, and CHRISTIAN ENSS — Kirchhoff-Institute for Physics, Heidelberg University

There are not too many options for fast, highly sensitive and reliable thermometers for use at low and ultra-low temperatures. Here, we present a novel concept of a susceptibility thermometer based on the paramagnetic alloy Au:Er that has the potential to meet these requirements. To ensure very good thermal contact, the superconducting readout coils and the paramagnetic materials are micro fabricated on a polished copper wafer. In this concept, four planar meander-shaped niobium coils each with a width of $5\mu\text{m}$ and a total length of 20m, are arranged as a Wheatstone bridge. Two opposite coils are covered with sensor material. The inductances of the covered and uncovered coils were chosen so that the bridge is balanced at a certain temperature, as indicated by the zero detector. This temperature can be conveniently set by the erbium concentration and the design of the coils. For certain applications, this can serve as an individual fixed point for precise temperature stabilization. The imbalance due to the paramagnetic contribution of the Au:Er at different temperatures is used to establish a temperature scale by calibration with another thermometer. We will discuss the design, fabrication, function and readout of this novel susceptibility thermometer.

TT 67: Dynamics and Chaos in Many-Body Systems II (joint session DY/TT)

Time: Friday 9:30–12:30

Location: MOL 213

TT 67.1 Fri 9:30 MOL 213

Towards a more fundamental understanding of eigenstate thermalization — •TOBIAS HOFMANN, TOBIAS HELBIG, RONNY THOMALE, and MARTIN GREITER — Institut für Theoretische Physik und Astrophysik, Universität Würzburg, 97074 Würzburg, Germany

We explore several venues how eigenstate thermalization may be understood on a more fundamental level. In particular, we report on extensive numerical work in spin systems with random interactions, where a small subsystem is subject to thermalization. We discuss possible directions towards an understanding of our numerical results.

TT 67.2 Fri 9:45 MOL 213

Spectral Response of Disorder-Free Localized Lattice Gauge Theories — •NILOTPAL CHAKRABORTY¹, MARKUS HEYL^{1,2}, PETR KARPOV¹, and RODERICH MOESSNER¹ — ¹Max Planck Institute for Physics of Complex Systems, Dresden — ²University of Augsburg

We show that certain lattice gauge theories exhibiting disorder-free localization have a characteristic response in spatially averaged spectral functions: a few sharp peaks combined with vanishing response in the zero frequency limit. This reflects the discrete spectra of small clusters of kinetically active regions formed in such gauge theories when they fragment into spatially finite clusters in the localized phase due to the presence of static charges. We obtain the transverse component of the dynamic structure factor, which is probed by neutron scattering experiments, deep in this phase from a combination of analytical estimates and a numerical cluster expansion. We also show that local spectral functions of large finite clusters host discrete peaks whose positions agree with our analytical estimates. Further, information spreading, diagnosed by an unequal time commutator, halts due to real space fragmentation. Our results can be used to distinguish the disorder-free localized phase from conventional paramagnetic counterparts in those frustrated magnets which might realize such an emergent gauge theory.

TT 67.3 Fri 10:00 MOL 213

Chaos in the three-site Bose-Hubbard model - classical vs quantum — •GORAN NAKERST¹ and MASUDUL HAQUE^{1,2} — ¹Institut für Theoretische Physik, Technische Universität Dresden, D-01062 Dresden, Germany — ²Max-Planck-Institut für Physik komplexer Systeme, D-01187 Dresden, Germany

We consider a quantum many-body system - the Bose-Hubbard system on three sites - which has a classical limit, and which is neither strongly chaotic nor integrable but rather shows a mixture of the two types of behavior. We compare quantum measures of chaos (eigenvalue statistics and eigenvector structure) in the quantum system, with classical measures of chaos (Lyapunov exponents) in the corresponding classical system. As a function of energy and interaction strength, we demonstrate a strong overall correspondence between the two cases. In contrast to both strongly chaotic and integrable systems, the largest Lyapunov exponent is shown to be a multi-valued function of energy.

TT 67.4 Fri 10:15 MOL 213

Many-Body Dwell-time and Density of States — •GEORG MAIER, CAROLYN ECHTER, JUAN-DIEGO URBINA, and KLAUS RICHTER — Universität Regensburg, Regensburg, Germany

Many body systems with a large number of degrees of freedom are usually described by statistical physics on the theoretical side while experiments usually

relay on scattering (e.g. particle physics). Is it possible to relate scattering and statistical physics, or to measure scattering-related observables which directly relate to quantities of statistical physics? At least for single particle systems a close relation exists between the well known Wigner-Smith delay time in scattering theory and the density of states of the scattering system.

I will present a novel ansatz relating a many-body version of dwell-/Wigner-Smith delay time and many body density of states based on the famous Birman-Krein-Friedel-Lloyd formula connecting scattering theory and statistical observables in the many-body context. This formalism could provide answers to a wide variety of interesting questions, e.g. can we observe the effect of interactions (or even the emergence of chaos) through the lens of the dwell-time? Another interesting point is the roll of particle statistics on dwell-time meaning e.g. does it take longer for a particle to leave a fermionic or bosonic system?. I will present our analytical and numerical results on these questions.

TT 67.5 Fri 10:30 MOL 213

Dynamical correlations and domain wall relocalisation in transverse field Ising chains — •PHILIPPE SUCHSLAND¹, BENOÎT DOUÇOT², VEDIKA KHEMANI³, and RODERICH MOESSNER¹ — ¹Max Planck Institute for the Physics of Complex Systems, Nöthnitzer Str. 38, 01187 Dresden, Germany — ²LPTHE, UMR 7589, CNRS and Sorbonne Université, 75252 Paris Cedex 05, France — ³Department of Physics, Stanford University, Stanford, California 94305, USA

We study order parameters and out-of-time-ordered correlators (OTOCs) for a wide variety of transverse field Ising chains: classical and quantum, clean and disordered, integrable and generic. The setting we consider is that of a quantum quench. We find a remarkably rich phenomenology, ranging from stable periodic to signals decaying with varying rates. This variety is due to a complex interplay of dynamical constraints (imposed by integrability and symmetry) which thermalisation is subject to. In particular, a process we term dynamical domain wall relocalisation provides a long-lived signal in the clean, integrable case, which can be degraded by the addition of disorder even without interactions. Our results shed light on a proposal to use an OTOC specifically as a local dynamical diagnostic of a quantum phase transition even when evaluated in a state with an energy density corresponding to the paramagnetic phase.

15 min. break

TT 67.6 Fri 11:00 MOL 213

Time evolution at the quantum-critical point of the sawtooth chain — •JANNIS ECKSELER, FLORIAN JOHANNESMANN, and JÜRGEN SCHNACK — Fakultät für Physik, Universität Bielefeld, Postfach 100131, D-33501 Bielefeld, Germany

It is known for the antiferromagnetic sawtooth chain with Heisenberg interactions to develop a flat band at the quantum-critical point of $J_1 = 2J_2$, where J_1 is the exchange interaction between nearest neighbors and J_2 the interaction at the base of the triangles [1]. We investigate the time evolution of several observables of the sawtooth chain, especially near that point and in particular in view of their equilibration properties. [1] J. Schulenburg, A. Honecker, J. Schnack, J. Richter, H.-J. Schmidt, Phys. Rev. Lett. 88 (2002) 167207

TT 67.7 Fri 11:15 MOL 213

Quantum Noise as a Symmetry-Breaking Field — •PAUL McCLARTY¹, BEATRIZ DIAS², DOMAGOJ PERKOVIC³, MASUDUL HAQUE⁴, and PEDRO RIBEIRO⁵ — ¹MPI PKS, Dresden, Germany — ²TU Munich, Garching, Germany — ³Cavendish Lab, University of Cambridge, UK — ⁴TU Dresden, Germany — ⁵IST, Lisbon, Portugal

We investigate the effect of quantum noise on the measurement-induced quantum phase transition in monitored random quantum circuits. Using the efficient simulability of random Clifford circuits, we find that the transition is broadened into a crossover and that the phase diagram as a function of projective measurements and noise exhibits several distinct regimes. We show that a mapping to a classical statistical mechanics problem accounts for the main features of the random circuit phase diagram. The bulk noise maps to an explicit permutation symmetry breaking coupling; this symmetry is spontaneously broken when the noise is switched off. These results have implications for the realization of entanglement transitions in noisy quantum circuits.

TT 67.8 Fri 11:30 MOL 213

Finite-size prethermal behavior at the chaos-to-integrable transition — •JOHANNES DIEPLINGER¹ and SOUMYA BERA² — ¹Institute of Theoretical Physics, University of Regensburg, D-93040 Germany — ²Department of Physics, Indian Institute of Technology Bombay, Mumbai 400076, India

We investigate the dynamics of the complex Sachdev-Ye-Kitaev model complemented with a single particle hopping term, leading to a chaos-to-integrable transition of the eigenstates. We determine the dynamics close to the transition via the density-density correlator, where we observe a prethermal plateau in the ergodic phase. This indicates a finite time localised behavior up to an interaction-dependent thermalization time scale. This time scale is quantified as $t_{th} \propto 2^{\alpha/\sqrt{\lambda}}$ as a function of the relative interaction strength λ . The results are validated by investigating the time-dependent structure of the time-evolved wave functions in the Fock space.

TT 67.9 Fri 11:45 MOL 213

Quasiparticle Description of Entanglement Growth — •MOLLY GIBBINS, BRUNO BERTINI, and ADAM SMITH — University of Nottingham

The quasiparticle picture of entanglement is a novel way to describe a feature unique to quantum many-body systems. Recent research has found excellent agreement of this description with numeric results: a description that had been shown to hold for the general family of Rényi entanglement entropies, for different classes of quench and different geometries of the boundary across which entanglement develops.

The aim of this project is to develop a quasiparticle description of the entanglement growth in free-fermionic systems with translational invariance in both 1D and 2D. The propagation of quasiparticles across this cut will respect this translational invariance and it is expected that the entanglement generated between these particles will be in very good agreement with the exact solution for these systems.

TT 67.10 Fri 12:00 MOL 213

Excitation Transport in Molecular Aggregates with Thermal Motion — •RITESH PANT and SEBASTIAN WÜSTER — Indian institute of science education and research, Bhopal, India

Molecular aggregates can under certain conditions transport electronic excitation energy over large distances due to the long range dipole-dipole interactions. These interactions are also the characteristics of Rydberg aggregates which have been proved as the quantum simulators for molecular aggregates. An idea that naturally arises in Rydberg aggregates, is adiabatic excitation transport through atomic motion, where slow motion of the atoms combined with excitation transport can result in efficient and guided transport of the excitation from one end of an atomic chain to the other. Based on the analogy between Rydberg and Molecular aggregates, in ref. [1] we explore whether the adiabatic excitation transport can play a functional role in molecular aggregates in the absence of intra-molecular vibrations. But because the transport is partially adiabatic and because it involves transitions between non-eigenstates, it is challenging to estimate the adiabaticity of transport in molecular aggregates. Hence, in ref [2] we established a measure to quantify the adiabatic character of quantum transitions in general. Next, the effect of intramolecular vibrations is included by extending our calculation for excitation transport to an open-quantum- system technique [3].

[1] R. Pant and S. Wüster, Physical Chemistry Chemical Physics 22, 21169 (2020). [2] R. Pant, et al., <https://arxiv.org/abs/2007.10707>. [3] R. Pant, et al., (Manuscript in preparation)

TT 67.11 Fri 12:15 MOL 213

Tailoring the Phonon Environment of Embedded Rydberg Aggregates — •SIDHARTH RAMMOHAN¹, SEBASTIAN WÜSTER¹, and ALEXANDER EISFELD² — ¹IISER Bhopal, Madhya Pradesh, India — ²MPIPKS, Dresden, Germany

State-of-the-art experiments can controllably create Rydberg atoms inside a Bose-Einstein condensate (BEC) such that the Rydberg electron orbital volume contains many neutral atoms, which can be tuned, resulting in electron-atom scattering events [1]. In my talk, I will discuss the physics of the interaction and corresponding dynamics of a single or multiple Rydberg atoms in two internal electronic states embedded inside a BEC, to assess their utility for controlled studies of decoherence and quantum simulations of excitation transport similar to photosynthetic light-harvesting. We initially developed a theoretical framework to calculate the open quantum system input parameters for a single Rydberg atom, possibly in two internal states, in BEC and then for a chain of Rydberg atoms, forming an aggregate [2]. The electron-atom interactions lead to Rydberg-BEC coupling, creating phonons in the BEC. Using the spin-boson model with the calculated parameters, we then examine the decoherence and the Non-Markovian features of a Rydberg atom in a superposition, resulting from the interaction with the environment [3]. The scenario with a single Rydberg atom is then extended to the aggregate case, allowing us to set up dynamics similar to those found in light-harvesting complexes. Ref:1. J. B. Balewski, et al; Nature 502 664 (2013).2. S. Rammohan, et al; PRA 103, 063307 (2021).3. S. Rammohan, et al; PRA 104, L060202 (2021).

TT 68: Focus Session: Making Experimental Data F.A.I.R. – New Concepts for Research Data Management II (joint session O/TT)

Time: Friday 9:30–12:45

Location: WIL A317

Topical Talk

TT 68.1 Fri 9:30 WIL A317

FAIRifying ARPES: a Route to Open Data & Data Analytics — •RALPH ERNSTORFER^{1,2}, TOMMASO PINCELLI^{1,2}, PATRICK R. XIAN², ABEER ARORA², FLORIAN DOBENER³, SANDOR BROCKHAUSER³, and LAURENZ RETTIG² — ¹TU Berlin, Germany — ²Fritz-Haber-Institut Berlin, Germany — ³HU Berlin, Germany

While angle-resolved photoemission spectroscopy (ARPES) is the most direct probe of crystals' electronic structure, the globally collected ARPES data have not been merged into an open experimental electronic structure database in equivalence to well-established atomic structure databases. We discuss a data format based on NeXus [1] as a concept for unifying the data structure for all types of photoemission experiments including time-, spin-, and time-resolved ARPES [2]. The aim is to immediately enable preprocessed data and metadata shareability according to FAIR data principles, employing existing public storage and archiving research data infrastructures such as Zenodo, OpenAIRE, and Nomad/FAIRmat. Ultimately, the multidimensional photoemission spectroscopy (MPES) format is designed to allow high-performance automated access, providing experimental databases for high-throughput material search [3]. References: [1] <https://www.nexusformat.org/> [2] <https://mpes.science/>; <https://fairmat-experimental.github.io/nexus-fairmat-proposal/> [3] R. P. Xian et al., Scientific Data 7, 442 (2020); R.P. Xian et al., Nat. Comp. Sci, in print, arXiv:2005.10210

TT 68.2 Fri 10:00 WIL A317

A FAIR data infrastructure for photoemission experiments — •MARTEN WIEHN¹, TOBIAS EUL¹, BENJAMIN STADTMÜLLER^{1,2}, and MARTIN AESCHLIMANN¹ — ¹Department of Physics and Research Center OPTIMAS, TU Kaiserslautern, Germany — ²Institute of Physics, Johannes Gutenberg University Mainz, 55128 Mainz, Germany

Recent trends toward data-driven, high-tech experimental research and the growing volumes of data associated with it show the increasing importance of comprehensive data acquisition and management. We present an automated workflow for well-described photoemission data from experiment to archive and publication. Utilizing a powerful experiment control software to capture essential metadata for each measurement enables the collection of FAIR-ready data (Findable, Accessible, Interoperable, Reusable). In addition, using an electronic lab notebook pushes our lab further toward a FAIR data infrastructure that supports researchers in their daily work.

TT 68.3 Fri 10:15 WIL A317

Multi-Dimensional Photoemission Spectroscopy: a concept for FAIR photoemission data — •FLORIAN DOBENER¹, TOMMASO PINCELLI^{2,3}, ABEER ARORA^{2,4}, STEINN YMR AUGUSTSSON⁵, DMYTRO KUTNYAKHOV⁶, MICHAEL HARTELT⁷, LAURENZ RETTIG¹, MARTIN AESCHLIMANN², RALPH ERNSTORFER⁷, and SANDOR BROCKHAUSER^{2,3} — ¹Department of Physics, HU Berlin, Germany —

²Fritz-Haber-Institut der Max-Planck-Gesellschaft, Berlin, Germany — ³Institut für Optik und Atomare Physik, TU Berlin, Germany — ⁴FU Berlin, Fachbereich Physik, Berlin, Germany — ⁵Institut für Physik, Johannes Gutenberg-Universität Mainz, Germany — ⁶DESY, Hamburg, Germany — ⁷Department of Physics and OPTIMAS, University of Kaiserslautern, Germany

The complexity and size of photoemission data is rapidly increasing as new technological breakthroughs have enabled multidimensional parallel acquisition. However, most of the community is currently using heterogeneous data formats and workflows. We propose a new data format based on NeXus, a hierarchically organized hdf5 structure. This multidimensional photoemission spectroscopy format is designed to allow high-performance automated access, enabling experimental databases for high-throughput material search. Our approach involves reaching out to the community using a website with extensive documentation of our proposed standard. As a demonstrator of the potential of our approach we present a workflow and data pipeline integrated into the NOMAD research data management solution, which provides powerful analysis and search functionalities.

TT 68.4 Fri 10:30 WIL A317

Towards an Infrastructure for FAIR Synthesis Data — •SEBASTIAN BRÜCKNER^{1,2}, ANDREA ALBINO¹, JOSE MARQUEZ¹, FLORIAN DOBENER¹, HAMPUS NÄSSTRÖM¹, MARKUS SCHEIDGEN¹, CLAUDIA DRAXL¹, and MARTIN ALBRECHT² — ¹HU Berlin, Zum Großen Windkanal 2, 12489 Berlin — ²IKZ Berlin, Max-Born-Straße 2, 12489 Berlin

A data infrastructure based on the FAIR (findable, accessible, interoperable and reusable) principles promises a new way of sharing and exploring data by using highly efficient data analysis and artificial intelligence tools. This also applies to data related to sample synthesis. At present, most synthesis data are not structured comprehensively or not even stored digitally but in handwritten lab books. There hardly exists any data standards in synthesis, which is in contrast to data from characterization techniques. The FAIRmat project (<https://FAIRmat-NFDI.eu>) is building a FAIR data infrastructure for condensed-matter physics and the chemical physics of solids. In FAIRmat's Area A, we focus on synthesis data to make sample synthesis reproducible, accelerate the development of novel materials, and make characterization data of synthesized materials assessable. Here we summarize our ongoing work and progress including: providing a general data model for synthesis which is harmonized with data from measurements and theory (ontologies); implementation of our data model in use cases and electronic laboratory notebooks; developing tools for data acquisition and analysis; data governance guidelines to enable a sustainable change of research data management at the institute/university level.

TT 68.5 Fri 10:45 WIL A317

FAIRifying Material Synthesis with the NOMAD Electronic Laboratory Notebook (ELN) — •ANDREA ALBINO¹, HAMPUS NÄSSTRÖM¹, FLORIAN DOBENER¹, JOSE MARQUEZ PRIETO¹, LAURI HIMANEN¹, DAVID SIKTER¹, MOHAMMAD NAKHAE¹, AMIR GOLPARVAR¹, SEBASTIAN BRÜCKNER¹, MARTIN ALBRECHT², MARKUS SCHEIDGEN¹, and CLAUDIA DRAXL^{1,3} — ¹Physics Department and IRIS Adlershof, Humboldt-Universität zu Berlin, Berlin, Germany. — ²Leibniz-Institut für Kristallzüchtung, Berlin, Germany. — ³The NOMAD Laboratory at the Fritz Haber Institute of the Max Planck Society, Berlin, Germany.

Approaching the era of big data-driven materials science, one crucial step to collecting, describing, and sharing experimental data is the adoption of ELNs. The project FAIRmat (fairmat-nfdi.eu) is offering such tools by developing and operating the open-source software NOMAD. The NOMAD ELN aims at offering a secure environment to protect the integrity of both data and metadata, whilst also affording the flexibility to adopt new synthetic processes or changes to existing ones without recourse to further software development.

We find that to promote an early adoption, it is important to adapt to a single user's needs and workflows. An inductive approach, going from a particular set of experiments to a general description of the similarities recurring in each of them, led us to adopt a common data structure as a standard. The state-of-the-art ELN features for a synthetic process will be shown in the talk, highlighting the development of both data modeling and specific implementation solutions.

TT 68.6 Fri 11:00 WIL A317

FAIR Data Infrastructure for Computation: Classical Simulations and Multiscale Modeling — •JOSEPH F. RUDZINSKI^{1,2}, JOSÉ M. PIZARRO¹, NATHAN DAELMAN¹, LUCA M. GHIRINGHELLI¹, KARSTEN REUTER³, KURT KREMER², SILVANA BOTTI⁴, and CLAUDIA DRAXL¹ — ¹Institut für Physik, Humboldt-Universität zu Berlin — ²Max-Planck-Institut für Polymer Forschung, Mainz — ³Fritz-Haber-Institut der Max-Planck-Gesellschaft, Berlin — ⁴Institut für Festkörpertheorie und Optik, Friedrich-Schiller-Universität Jena

The emergence of the (big-)data-centric techniques as a fundamental paradigm of science calls for the development of infrastructure for ensuring FAIR—findable, accessible, interoperable, reusable—data management. The FAIRmat consortium aims to build extensive infrastructure for a wide variety of materials-science data, including soft matter simulations [1], by expanding upon the success of the NOMAD Laboratory—a repository for atomistic calculations in ma-

terials science [2]. Both the large volume and heterogeneous nature of classical molecular-dynamics simulation data presents a number of distinct challenges. In this talk, we present FAIRmat's progress in developing infrastructure for molecular-dynamics simulations, including metadata for molecular topologies and tools for workflow management. We will also discuss the need for standardization of metadata schemas and ontologies within the community, and planned collaborations with other open science initiatives and software developers.

[1] Scheffler, M. et al. *Nature* 2022, 604, 635–642.

[2] Draxl, C.; Scheffler, M. *JPhys Materials* 2019, 2, 036001.

Topical Talk

TT 68.7 Fri 11:15 WIL A317

Electronic Lab Notebooks in Teaching and Implications on Science — •MICHAEL KRIEGER — Lehrstuhl für Angewandte Physik, Department Physik, Friedrich-Alexander-Universität Erlangen-Nürnberg (FAU)

In our department, we have recently introduced Electronic Lab Notebooks (ELN) in the obligatory electronic lab course in the 4th semester of the physics curriculum. Immediate advantages for the students are obvious: all data, raw data and metadata including experiment description and experimental observations, are digitally stored at the same place. Moreover, student teams share and actively work in their group ELN with access at the university as well as at home, and script-based evaluations can be performed directly in the ELN.

The introduction of ELNs in teaching has also implications on science. Students carry their ELN experience and data competences into all research groups. There, however, modern research data management is much more complex. According to the FAIR principles, it requires structured, machine-readable data using open formats and vocabularies that meet community standards. The development of such standards is in many cases still to be done and is the core of the Nationale Forschungsdateninfrastruktur (NFDI). Here, ELNs in teaching provide a sandbox with short learning and innovation cycles for testing structured schemas. The experience helps to develop and establish sustainable and FAIR documentation of research workflows in science.

TT 68.8 Fri 11:45 WIL A317

A step towards predicting synthesis conditions of metal-organic frameworks — •DINGA WONANKE¹, THOMAS HEINE², and CHRISTOF WÖLL¹ — ¹Institut für Funktionelle Grenzflächen (IFG), Karlsruhe, Germany — ²Faculty of Chemistry and Food Chemistry, Dresden, Germany

The process of synthesising metal-organic frameworks (MOFs) falls under a branch of chemistry known as reticular chemistry. Here, well defined crystalline compounds are synthesised from a well thought out design principle by linking predefined building blocks under specific conditions. Although, this approach appears to be intuitive, the synthesis of any novel MOF still follows the conventional approach that begins with a thorough literature survey to explore reagents, calculations of aliquots and finally a series of time consuming and stressful trial-and-error syntheses. Consequently, although millions of stable hypothetical MOFs with interesting properties have been predicted, only approximately 100 thousand crystal structures of MOFs currently exist in the Cambridge Structural Database (CSD). Indicating a significant bottleneck in the intelligent design of novel stable MOFs with targeted properties.

In this talk, we will present an overview of our journey to design a new machine learning algorithm for predicting the synthesis condition of existing and hypothetical MOFs. We will discuss our experiences and challenges in mining and curating the MOF subset in the CSD. Finally, we will present our new MOF database that maps every MOF to its experimental synthetic conditions.

TT 68.9 Fri 12:00 WIL A317

Deep learning surface scattering data analysis for processing large synchrotron datasets — •VLADIMIR STAROSTIN, VALENTIN MUNTEANU, LINUS PITHAN, ALEXANDER GERLACH, ALEXANDER HINDERHOFER, and FRANK SCHREIBER — Institute of Applied Physics, University of Tübingen, Germany

In situ real-time surface scattering experiments such as grazing-incidence wide-angle X-ray scattering (GIWAXS) produce large amounts of data, frequently exceeding the capabilities of traditional data processing methods. Here we demonstrate an automated pipeline for the analysis of GIWAXS images, based on a machine learning architecture for object detection, designed to conform to the specifics of the scattering data [1]. Our pipeline enables real-time GIWAXS analysis and is designed to be employed at synchrotron facilities. We also present FAIR data strategies and traceable data resources from the raw data to the corresponding scientific publication and vice versa [2] including intermediate processing steps.

We demonstrate our method on real-time tracking of lead halide perovskite structure crystallization processes, which are relevant for hybrid solar cell applications. However, our approach is equally suitable for other crystalline thin-film materials by design. In general, the solution substantially accelerates the analysis process of GIWAXS images, potentially boosting the speed of scientific discoveries in material science.

[1] V. Starostin et al. *npj Comput Mater* 8, 101 (2022)

[2] V. Starostin et al. *Synch Rad News* 13, 31–37 (2022)

TT 68.10 Fri 12:15 WIL A317

FAIR Data Infrastructure for Computation: Mapping out the Space of Density Functionals — •NATHAN DAELMAN¹, JOSEPH F. RUDZINSKI^{1,2}, JOSÉ M. PIZARRO¹, LUCA M. GHIRINGHELLI¹, MIGUEL A. L. MARQUES³, SILVANA BOTTI⁴, and CLAUDIA DRAXL¹ — ¹Institut für Physik und IRIS-Adlershof, Humboldt-Universität zu Berlin, Berlin — ²Max-Planck-Institut für Polymer Forschung, Mainz — ³Institut für Physik, Martin-Luther-University Halle-Wittenberg, Halle — ⁴Friedrich Schiller Universität Jena, Jena

The NOMAD Laboratory [1] holds over 135 million computational results, the vast majority of which stem from density-functional theory (DFT). The platform provides adequate querying and data analytics tools (e.g., machine-learning modelling) for processing such Big Data. However, the exchange-correlation (xc) functional with which the data was generated, limits the analysis scope of most thermodynamic and kinetic properties. Here, we present a strategy rooted in semantics for extending method interoperability. We will showcase our map of the entire xc-functional space that, in the context of the FAIRmat consortium [2], is built to be widely accessible and facilitate findability. Lastly, we will discuss the integration of this xc-functionals map into the NOMAD data platform, as well as its publication in ontology format as an effort towards a community-wide vocabulary standard.

[1] C. Draxl and M. Scheffler, MRS Bulletin 43, 676-682 (2018).

[2] M. Scheffler, M. et al., Nature 604, 635-642 (2022).

TT 68.11 Fri 12:30 WIL A317

OpenSemanticLab: Towards Open Semantic Research — •SIMON STIER and MATTHIAS A. POPP — Fraunhofer ISC, Neunerplatz 2, 97082 Würzburg, Germany

In materials science, complex relationships exist between the properties of materials and their composition and processing. Therefore, digital transformation and acceleration in this domain represents a particularly important challenge. Although it is generally agreed that data must be linked by means of semantics and ontologies to form holistic data spaces, there is still a lack of suitable tools for integrating the necessary structures into the everyday work of scientists.

Fraunhofer ISC addresses this challenge with a broad-based strategy that closely links activities at all relevant levels. The goal hereby is the development towards Lab 4.0, the machine-readable documentation of scientific processes and the harmonization of data structures in accordance with international standards.

Core of the resulting OpenSource solution architecture is the central web data platform OpenSemanticLab [1] that links people (knowledge), machines (data) and algorithms (AI) equally. As an open system, this platform is easily adaptable even without programming knowledge and without losing the uniform structure. In this way, OpenSemanticLab enables us as scientists to contribute individually and yet in a standardized fashion to future digital materials research.

[1] <https://github.com/OpenSemanticLab>

Vacuum Science and Technology Division Fachverband Vakuumphysik und Vakuumtechnik (VA)

Stylios Varoutis
Karlsruhe Institute of Technology
Institute for Technical Physics (ITEP)
Hermann-von-Helmholtz-Platz 1
76344 Eggenstein-Leopoldshafen
stylios.varoutis@kit.edu

Overview of Invited Talks and Sessions

(Lecture hall HSZ 301; Poster P2/OG2)

Invited Talks of the joint Symposium SKM Dissertation Prize 2023 (SYSD)

See SYSD for the full program of the symposium.

SYSD 1.1	Mon	9:30–10:00	HSZ 04	Diffusion of antibodies in solution: from individual proteins to phase separation domains — •ANITA GIRELLI
SYSD 1.2	Mon	10:00–10:30	HSZ 04	Intermediate Filament Mechanics Across Scales — •ANNA V. SCHEPERS
SYSD 1.3	Mon	10:30–11:00	HSZ 04	Ultrafast Probing and Coherent Vibrational Control of a Surface Structural Phase Transition — •JAN GERRIT HORSTMANN
SYSD 1.4	Mon	11:00–11:30	HSZ 04	Electro-active metasurfaces employing metal-to-insulator phase transitions — •JULIAN KARST
SYSD 1.5	Mon	11:30–12:00	HSZ 04	The role of unconventional symmetries in the dynamics of many-body systems — •PABLO SALA

Sessions

VA 1.1–1.5	Mon	9:30–12:00	HSZ 301	Vacuum Technology: New Developments and Applications
VA 2.1–2.2	Mon	14:00–16:00	P2/OG2	Vacuum Technology: New Developments and Applications – Poster

Sessions

– Contributed Talks and Posters –

VA 1: Vacuum Technology: New Developments and Applications

Time: Monday 9:30–12:00

Location: HSZ 301

VA 1.1 Mon 9:30 HSZ 301

Ultra-high-quality-factor membrane oscillators for gas pressure sensing — •HOSSEIN MASALEHDAN¹, CHRISTOPH REINHARDT², AXEL LINDNER², and ROMAN SCHNABEL¹ — ¹Institut für Laserphysik und Zentrum für Optische Quantentechnologien der Universität Hamburg, 22761 Hamburg, Germany — ²Deutsches Elektronen Synchrotron (DESY), 22607 Hamburg, Germany

Recent years have seen a rapid development of nanomechanical resonators with ultra-high mechanical quality factors Q . As a result, these devices become increasingly sensitive to smallest changes in certain environmental parameters, such as the pressure of the surrounding gas. In this work, we demonstrate the practical use of a mm-scale nanomechanical trampoline resonator with intrinsically-limited $Q \sim 10^7$ for gas pressure sensing. To this end, we place the trampoline inside an ultra-high-vacuum chamber and investigate the pressure-dependency of its resonance frequency and Q from high-vacuum to ambient pressure. We present a combined model, including molecular and viscous loss, which matches measured values within $\pm 15\%$, for air and helium gas. Finally, we discuss potential applications and possible next steps towards improved sensing capabilities.

*This work was supported and partly financed (HM) by the DFG under Germany's Excellence Strategy EXC 2121 'Quantum Universe'-390833306 and via a PIER Seed Project.

VA 1.2 Mon 10:00 HSZ 301

Transient modeling of neutral gas flow in particle exhaust system of fusion reactors — •CHRISTOS TANTOS, STYLIANOS VAROUTIS, and CHRISTIAN DAY — Karlsruhe Institute of Technology, Karlsruhe, Germany

In the present work the transient response of the neutral gas flows inside the geometrical complex particle exhaust systems of fusion reactors is studied. In this study the particle exhaust system of DEMO fusion reactor is investigated in a wide range of the operating conditions. The transient flow behavior is analyzed by solving the Boltzmann equation by applying kinetic models supplemented with the Discrete Velocity Method (DVM). The time of the neutral gas flow establishment is studied as a function of the initial divertor conditions as well as the pumping capability of the vacuum pumps. In addition, the effect of the intermolecular interaction law on the transient distributions of the neutrals gas flow quantities is also investigated. The analysis shows that the applied deterministic methodology allows a computationally efficient transient study of the neutral gas dynamics in the particle exhaust of the future fusion reactors.

VA 1.3 Mon 10:30 HSZ 301

Advanced simulation methodologies for optimizing aerosol injectors used for single-particle diffractive imaging — •SURYA KIRAN PERAVALI^{1,4}, LENA WORBS^{1,2}, AMIT K SAMANTA^{1,3}, MUHAMED AMIN¹, JOCHEN KÜPPER^{1,2,3}, PHILIPP NEUMANN⁴, and MICHAEL BREUER⁴ — ¹Center for Free-Electron Laser Science, Deutsches Elektronen-Synchrotron DESY, Hamburg, Germany — ²Department of Physics, Universität Hamburg, Germany — ³Center for Ultrafast Imaging, Universität Hamburg, Germany — ⁴Fakultät für Maschinenbau, Helmut-Schmidt-Universität, Germany

Single particle diffractive imaging (SPI) is a technique used for imaging atomic-scale structures and dynamics of nano-particles or bio-molecules. These experiments require the collection of thousands of diffraction patterns from identical particles. The particles are transferred into the gas phase and the collimated par-

ticle stream is then extracted in vacuum. The sample injection methods used for SPI must be optimized to produce high-quality particle beams, i.e., a high particle density and sample purity. We present a novel simulation framework which provides a quick and efficient way to search the experimental parameter space for optimizing the process. The framework requires simulating the gas flow inside the particle injectors and the expansion into the experimental vacuum chamber. Since the flow is at least partially in the rarefied regime i.e., high Knudsen number, a multi-scale approach combining simulation tools for continuum and free-molecular flow is applied. Subsequently, particle trajectories are computed using the forces obtained from interpolated force fields.

VA 1.4 Mon 11:00 HSZ 301

Novel Ionization Vacuum Gauge Suitable as Reference Standard — •MATTHIAS BERNIEN¹, FRÉDÉRIC BOINEAU², NENAD BUNDALESKI³, CLAUS ILLGEN¹, BERTHOLD JENNINGER⁴, JANEZ ŠETINA⁵, RICARDO A.S. SILVA³, ANKE STÖLTZEL⁴, ORLANDO M.N.D. TEODORO³, MARTIN WÜEST⁶, and KARL JOUSTEN¹ — ¹PTB, Abbestr. 2-12, 10587 Berlin, Germany — ²LNE, 1 rue Gaston Boissier, 75724 Paris Cedex 15, France — ³CEFITEC, Nova University of Lisbon 2829-515 Caparica, Portugal — ⁴CERN, 1211 Geneva 23 Switzerland — ⁵IMT, Lepi pot 11, 1000 Ljubljana, Slovenia — ⁶INFICON AG, Alte Landstrasse 6, LI-9496 Balzers, Liechtenstein

Within the EURAMET project 16NRM05 (www.ptb.de/empir/16nrm05-home.html) a new type of ionization vacuum gauge was developed for the pressure range from 10^{-6} Pa to 10^{-2} Pa. Unlike conventional Bayard-Alpert and extractor gauges, the new gauge features well-defined electron trajectories and mechanically robust electrodes. It exhibits excellent stability and linearity resulting in a measurement uncertainty of 1%, a reduction by one order of magnitude compared to the conventional gauges. The gauge revealed excellent metrological properties and is suitable as accurate reference and transfer standard.

At the moment the ISO standard 6737 is written standardizing the essential parameters of the gauge geometry and electrode voltages. By adhering to the standard manufactures can produce gauges with predictable gauge sensitivity and relative gas sensitivity factors without the need of characterizing them metrologically.

VA 1.5 Mon 11:30 HSZ 301

Inelastic electron scattering at a single-beam structured light wave — •SVEN EBEL¹ and NAHID TALEBI^{1,2} — ¹Institute of Experimental and Applied Physics, Kiel University, 24098 Kiel, Germany — ²Kiel Nano, Surface and Interface Science KiNSIS, Kiel University, 24118 Kiel, Germany

In this work we demonstrate the inelastic scattering of slow-electron wave packets at a propagating Hermite-Gaussian light beam. The pulsed Hermite-Gaussian beam thereby forms a pondermotive potential for the electron with large enough momentum components, leading to the inelastic scattering of electrons and their bunching along the longitudinal direction. We show that the resulting energy-gain spectra after the interaction is strongly influenced by the self-interference of the electron in this pondermotive potential. It is shown that this effect is observable for various optical wavelengths and intensities and further discuss how the variation of the electron velocity and the light intensity allow to control the energy modulation of the electron wave packet. This effect opens up a new platform for manipulating the electron wave packet by utilizing the vast landscape of structured electromagnetic fields.

VA 2: Vacuum Technology: New Developments and Applications – Poster

Time: Monday 14:00–16:00

Location: P2/OG2

VA 2.1 Mon 14:00 P2/OG2

A Novel Multilayer Barrier Coatings For Improved Cold-Field Electron Emitters — •DANIEL BURDA — Institute of Scientific Instruments of the CAS, v. v. i., Královopolská 147, 612 64 Brno, Czech Republic

By fabricating ultrathin, hard multilayer barrier coatings on top of the cold-field tungsten emitter, the parameters of the electron emission can be tuned. A multilayer structure of semiconducting and dielectric layers, i.e. Al₂O₃, HfO₂, on top of the electropolished tungsten tip is fabricated using Atomic Layer Deposition. The introduction of multilayered barriers enables modification of macroscopically observable electron emission parameters. The optimized material properties of the multilayer structure such as number of layers, thickness of single layers, and crystallinity lead to improvements in the emitted electron beam parameters, mainly in lowering the threshold emission voltage, increasing the spatial and temporal electron beam stability.

VA 2.2 Mon 14:00 P2/OG2

Repairing the seal faces of an MBE main flange — •TIMO A. KURSCHAT^{1,2}, SASCHA R. VALENTIN², FINN KRAGE¹, and ANDREAS D. WIECK¹ — ¹Angewandte Festkörperphysik, Ruhr-Universität Bochum, Universitätsstraße 150, D-44780 Bochum — ²Gesellschaft für Gerätebau mbH, Klönnestraße 99, D-44143 Dortmund

During the refurbishment of an MBE the surface of the main flange was attacked by an etching solution used for cleaning. This also affected the seal faces of the 500 mm main flange, a 250 mm CF flange and five 40 mm CF flanges. The surface was very rough and therefore not UHV compatible any more.

In the absence of a sufficiently large lathe and because the 40 mm flanges are not arranged concentrically, we designed manual tools with specialized geometry to sand and polish the flanges. The grid size of the sandpaper used was between 1000 and 3000. The seal faces were polished until the surfaces were smooth and specular again. After cleaning and assembly, we performed a leak test and did not find any leaks after the procedure.

The details of the individual work steps, the geometry of the tools, and also the tools themselves will be shown.

Working Group on Industry and Business Arbeitskreis Industrie und Wirtschaft (AIW)

Udo Weigelt
Grünecker Patent- und Rechtsanwälte PartG mbB
Leopoldstr. 4
80802 München

Overview of Invited Talks and Sessions

(Lecture hall KRO 1.11)

Invited Talks

AIW 1.1	Wed	13:45–14:15	KRO 1.11	Als Physiker*in Krankenhäuser digitalisieren? Klar doch! — •CHARLES LUDWIG MAJER
AIW 1.2	Wed	14:15–14:45	KRO 1.11	From the Lab to Customer Engineering at Google – the Unconventional Career Path of an Experimental Physicist — •DIANA NANOVA
AIW 1.3	Wed	14:45–15:15	KRO 1.11	Von der Promotion zur eigenen Firma — •OLIVER DE HAAS
AIW 2.1	Wed	15:30–16:00	KRO 1.11	How start-ups and alumni networks enrich young scientist's career options — •JOACHIM RÄDLER
AIW 2.2	Wed	16:00–16:30	KRO 1.11	Karrieremöglichkeiten für Physikerinnen und Physiker auf dem Gebiet des Gewerblichen Rechtsschutzes — •UDO WEIGELT

Sessions

AIW 1.1–1.3	Wed	13:45–15:15	KRO 1.11	AIW Industrietag I
AIW 2.1–2.2	Wed	15:30–16:30	KRO 1.11	AIW Industrietag II
AIW 3	Wed	16:45–17:30	KRO 1.11	Podiumsdiskussion
AIW 4	Wed	17:30–18:30	KRO 1.11	Gemütlicher Ausklang mit Networking bei Bier & Brezn

Sessions

– Invited Talks –

AIW 1: AIW Industrietag I

Time: Wednesday 13:45–15:15

Location: KRO 1.11

Invited Talk AIW 1.1 Wed 13:45 KRO 1.11

Als Physiker*in Krankenhäuser digitalisieren? Klar doch! — •CHARLES LUDWIG MAJER — Siemens Healthcare GmbH, Weissacher Str. 11, 70499 Stuttgart
Als Physiker*in ist man bestens vorbereitet neue, komplexe und vielfältige Themenfelder zu erfassen und sich diese zu Eigen zu machen. In diesem Sinne sind auch der Gesundheitssektor und im Besonderen Krankenhäuser ein spannendes Entwicklungsfeld für Physiker*innen – und das nicht nur als Medizinphysiker*in. Als Digital Portfolio Expert bin ich vertrieblich verantwortlich für das gesamte digitale Portfolio von Siemens Healthineers. Zu meinen Aufgaben gehört es, dieses bei Kund*innen vorzustellen und vor allem zu erklären.

Da digitale Systeme hochspezialisiert sind und individuell an jeden Einzelfall und die bereits vorhandene IT-Infrastruktur angepasst werden müssen, ist ein konzeptionelles Arbeiten ein Muss. Aber nicht nur die IT-technischen Voraussetzungen müssen Berücksichtigung finden, sondern auch die individuellen Bedürfnisse der Anwender*innen und gegebenenfalls der Patient*innen. Bereits aus diesen beiden Anforderungen können sehr komplexe Projekte entstehen.

Zudem ergibt sich durch sich immer schneller entwickelnde Trends und Änderungen im Gesundheitswesen, der Geschäftsmodelle unserer Kund*innen und der gesetzlichen Rahmenbedingungen ein hoch spannendes klinisches Ökosystem. Sich in diesem komplexen System tagtäglich zu bewegen ist eine meiner vielen spannenden Aufgaben als Physiker bei Siemens Healthineers.

Invited Talk AIW 1.2 Wed 14:15 KRO 1.11

From the Lab to Customer Engineering at Google – the Unconventional Career Path of an Experimental Physicist — •DIANA NANOVA — Google, Tucholskystr. 2, 10117 Berlin

Current takes the path of least resistance – so did I as a physics student, and went straight after my Diploma degree into a Ph.D. without having a wider career plan. Only after finishing the Ph.D program, I realized that I lack the imagination of possible career paths if I don't want to stay in Academia. By coincidence, I found my way into the IT industry, which later helped me to land my dream job as a Customer Engineer at Google Cloud. Learn in this session how you can prepare your career steps and what value and skills you bring as a physicist at a company like Google.

Invited Talk AIW 1.3 Wed 14:45 KRO 1.11

Von der Promotion zur eigenen Firma — •OLIVER DE HAAS — evico GmbH, Großenhainer Str. 101, 01127 Dresden

An guten Ideen und neuen technischen Lösungen mangelt es nicht. Als Doktorand oder wissenschaftlicher Mitarbeiter läuft man ihnen regelmäßig über den Weg. Aber wenige wollen das Wagnis eingehen, eigene Ideen am Markt umzusetzen. Wer es dennoch versucht, hat gute Chancen auf Erfolg – ein Erfahrungsbericht.

AIW 2: AIW Industrietag II

Time: Wednesday 15:30–16:30

Location: KRO 1.11

Invited Talk AIW 2.1 Wed 15:30 KRO 1.11

How start-ups and alumni networks enrich young scientist's career options — •JOACHIM RÄDLER — Ludwig-Maximilians-Universität, Geschwister-Scholl-Platz 1, München

The Center for NanoScience (CeNS) at LMU Munich has fostered relations with alumni and start-ups that emerged from the center. In my talk I will share our experience how institutionalized relations between industry and university enrich the academic landscape, improve career options of young scientists and leverage excellence in research.

Invited Talk AIW 2.2 Wed 16:00 KRO 1.11

Karrieremöglichkeiten für Physikerinnen und Physiker auf dem Gebiet des Gewerblichen Rechtsschutzes — •UDO WEIGELT — Partner Grünecker Patent- und Rechtsanwälte, Leopoldstr. 4, 80802 München

In dem Vortrag werden das Gebiet des gewerblichen Rechtsschutzes und die Karrierechancen, die Physikerinnen und Physikern auf diesem Gebiet offenste-

hen, vorgestellt. Dem Studium der Physik und/oder der Promotion in Physik schließt sich ein Training on the Job an, in dem die erforderlichen juristischen Kenntnisse erlernt werden. Neben und gleichzeitig zu diesem Training on the Job können weitere Zusatzqualifikationen in Form einer Ausbildung zum Europäischen Patentanwalt und/oder zum deutschen Patentanwalt und/oder in Form eines Studiums zum Master of Laws und/oder eines Jurastudiums als Doppelstudium erworben werden. In Abhängigkeit von den erworbenen Zusatzqualifikationen lassen sich verschiedenste Karrieren auf dem Gebiet des gewerblichen Rechtsschutzes einschlagen, im öffentlichen Dienst als einfacher Prüfer in Patentämtern bis zur leitenden Stellung in denselben oder als einfacher Richter in Patentgerichten und Zivilgerichten bis zur leitenden Stellung in denselben, oder in der Privatwirtschaft als einfacher Mitarbeiter in einer Patentabteilung in kleinen und großen Unternehmen bis zur Leitung einer Patentabteilung, als angestellter Patentanwalt, als freiberuflicher Patentanwalt in eigener Kanzlei oder als Gesellschafter einer Anwaltskanzlei.

AIW 3: Podiumsdiskussion

Time: Wednesday 16:45–17:30

Location: KRO 1.11

Podiumsdiskussion

AIW 4: Gemütlicher Ausklang mit Networking bei Bier & Brezn

Time: Wednesday 17:30–18:30

Location: KRO 1.11

Im Anschluss an die Sitzungen lädt der Arbeitskreis Industrie und Wirtschaft zu Bier und Brezn ein. In diesem Rahmen kann die Diskussion mit den Referenten und weiteren anwesenden Mitgliedern des AIW im persönlichen Gespräch vertieft werden.

Working Group on Equal Opportunities Arbeitskreis Chancengleichheit (AKC)

Agnes Sandner
Sprecherin des AKC
sandner@akc.dpg-physik.de

Overview of Invited Talks and Sessions (Lecture hall ZEU 250)

Invited Talks

AKC 1.1	Tue	10:30–11:30	ZEU 250	The tragic destiny of Mileva Marić Einstein — •PAULINE GAGNON
AKC 1.2	Tue	11:30–12:00	ZEU 250	Physik-Projekt-Tage – Ein Workshop für Schülerinnen der Oberstufe — ANNA ALBRECHT, •ANNA BENECKE, DIETMAR BLOCK, FRANKO GREINER, ANDREAS HINZMANN, ROMAN KOGLER
AKC 1.3	Tue	12:00–12:30	ZEU 250	Belonging – a key to success in STEM?! — LENNART BRADEMANN, DENISE DÖRFEL, •BARBARA M. GORDALLA, ANIKA IHMELS

Sessions

AKC 1.1–1.3	Tue	10:30–12:30	ZEU 250	AKC
AKC 2	Tue	12:30–13:30	ZEU 250 Foyer	Women in Physics Lunch

Sessions

– Invited Talks –

AKC 1: AKC

Time: Tuesday 10:30–12:30

Location: ZEU 250

Invited Talk AKC 1.1 Tue 10:30 ZEU 250

The tragic destiny of Mileva Marić Einstein — •PAULINE GAGNON — CERN, Geneva

What were Albert Einstein's first wife's contributions to his extraordinary productivity in the first years of his career? A first biography of Mileva Marić Einstein was published in Serbian in 1969 but remained largely unknown despite being translated first in German, then in French in the 1990's. The publication of Mileva and Albert's love letters in 1987 revealed how they lived together while two recent publications shed more light on Mileva Marić's life and work. I will review this evidence in its social and historical context to give a better idea of her contributions. In this presentation, I avoid all type of speculation and do not attack Albert Einstein personally, but rather strictly stick to facts. The audience will be able to appreciate why such a talented physicist has been so unkindly treated by history.

Invited Talk AKC 1.2 Tue 11:30 ZEU 250

Physik-Projekt-Tage – Ein Workshop für Schülerinnen der Oberstufe — ANNA ALBRECHT², •ANNA BENECKE¹, DIETMAR BLOCK³, FRANKO GREINER³, ANDREAS HINZMANN² und ROMAN KOGLER⁴ — ¹Université catholique de Louvain, CP3 — ²Universität Hamburg, Inst. f. Exp. Physik — ³CAU Kiel, Sektion Ohysik, IEAP — ⁴DESY, CMS, Hamburg

Gleichstellungsarbeit ist gerade auch in der Physik ein wichtiges Thema. Dies zeigen nicht zuletzt die Einschreibezahlen von Studentinnen in den Physikstudiengängen. In Kiel z.B. liegt der Prozentsatz von der Frauen hier bei etwa 15%. Die Gleichstellungsarbeit erst an der Universität zu beginnen genügt daher nicht. Statt dessen müssen bereits die Schulen einbezogen werden. Mit den Physik-Projekt-Tagen (PPT) wurde ein viertägiger Workshop nur für Schülerinnen ins Leben gerufen. Die Teilnehmerinnen haben die Möglichkeit, zu Schuljahresbeginn vier Tage lang in einem Projekt ihrer Wahl zu experimentieren, ihr Interesse an Physik zu steigern und Netzwerke über Schulgrenzen hinweg aufzubauen. *Die Projekte umspannen verschiedene Forschungsfelder der Physik und reichen von Teilchenphysik, über Laserphysik und Plasmaphysik bis hin zu Nanowissenschaften. Zur Qualitätssicherung und Weiterentwicklung dieser Veranstaltung werden die PPT von einer kritischen Evaluation begleitet. Das Konzept

der PPT, Inhalte und ausgesuchte Ergebnisse der Evaluation werden vorgestellt. Seit 2015 ist das Projekt im Instrumentenkasten für Gleichstellungsarbeit der DFG.

Invited Talk AKC 1.3 Tue 12:00 ZEU 250

Belonging – a key to success in STEM?! — LENNART BRADEMANN, DENISE DÖRFEL, •BARBARA M. GORDALLA, and ANIKA IHMELS — TU Dresden, Faculty of Psychology, WOP

Women continue to be underrepresented in science, technology, engineering or mathematics (STEM) fields as students and also in professional roles. What factors influence women's choice, persistence, and success? In the US, studies evidenced that women do not feel like they belong in STEM community: they experience an impeding study climate (also called *chilly climate*) or suffer from stereotypical views on possible careers. This results in a decreased desire to choose a STEM carrier (for an overview see Shapiro & Sax, 2011). The probability to drop out of the program (Höhne & Zander, 2019b; Peters et al., 2015) is increased in the case of high *belonging uncertainty*, or when there is a conflict between an occupational stereotype and one's self-description.

The talk presents results from an online survey conducted among students, focusing on the field of physics. 122 physics students (40% female) completed it regarding success in studying physics (GPA, number of last attempts for an exam), turnover intention, chilly climate (e.g. exclusion, hostility), expectation of success (e.g. perceived potential, sense of belonging (e.g. belonging uncertainty), identification with physics, enjoyment, interest, a list of adjectives to describe oneself and to describe a *successful physicist*, and sociodemographic variables.

Results revealed lower social belonging and higher belonging uncertainty as well as a worse stereotype fit for women as compared to non-female students. Especially, social belonging turned out to be the most important predictor for GPA, identification, turnover intention, interest, enjoyment, perceived potential and self-efficacy. Social belonging hence was identified as an important influencing factor to enhance women's interest, persistence, and success in STEM. Therefore, this factor demands for more attention in the future, both in research and in actual working environments - for a continued success of Germany in STEM fields.

AKC 2: Women in Physics Lunch

Time: Tuesday 12:30–13:30

Location: ZEU 250 Foyer

Female physicists of all career stages are cordially invited to join our meet-and-greet networking lunch. Diverse and all kinds of interested colleagues are also welcome!

Author Index

- A.C. Apfelbeck, Fabian CPP 17.46
A. Haas, Pierre BP 15.2
A. Ivanov, Boris MA 17.1
A. Lombardi, Gustavo MA 39.3
A. Nimmi Das DY 56.7
A. Ortiz, Roberto TT 50.3
A. Reus, Manuel CPP 17.20
A.S. Silva, Ricardo VA 1.4
A. van Aken, Peter TT 50.3
A. Veettil, Radhakrishnan BP 28.34
A. Yastremsky, Ivan MA 17.1
Aapro, Markus O 87.4
Aarts, N.M.M. O 42.2
Aase, Niels Henrik TT 45.3
Aasen, Adrian TT 58.13
Aassime, Abdel TT 17.3
Aballe, L. O 47.3
Aballe, Lucia MA 38.1
Abarca Morales, Edgar O 59.8
Abbasi, Amir DY 44.18
Abbasi, Fatemeh BP 8.2
Abbaspour, Leila BP 30.2
Abbott, Jordan SOE 8.4
Abd El-Fattah, Zakaria M. O 14.2
Abdalla, Hassan DS 16.6
Abdel, Dilara DS 11.5
Abdeldayem, Mohamed DS 12.50
Abdel-Hafiez, Mahmoud MA 40.56
Abdelkawy, Ahmed MM 27.4
Abdelrahman, Areeg O 52.2, O 73.5, O 96.9
Abdelsamie, Maged DS 11.3
Abdelwahab, Anas TT 36.9
Abdi, Fatwa F. HL 47.7
Abdoli, Iman DY 27.7, DY 56.1
Abdollahi, Younes Hassani O 69.2
Abdou Ahmed, Marwan HL 12.5
Abdullah, Hasan MA 31.5
Abele, Tobias BP 11.37
Abeln, A. TT 57.27, TT 57.28, TT 58.2
Abeln, Andreas TT 57.26
Abert, Claas MA 17.1, MA 40.3, MA 50.3
Abilio, Ivan O 82.4
Abo El Fadl, E. DS 12.48
Abou-ras, Daniel HL 4.6, HL 7.37
Abou-Shewarib, Asmaa HL 23.2
Abraham, Joyal John TT 10.9
Abrosimov, N. V. HL 7.17
Abrosimov, Nikolay HL 50.3
AbuAwwad, Nihad MA 21.1
Abusaa, Muayyad MA 35.7
Abushammala, Haneen KFM 11.5, TT 10.11
Acciai, Matteo TT 38.7
Achinuq, B. MA 12.5
Achtermann, Anthony HL 33.12
Ackermann, Kevin MA 23.25
Acosta, Matias KFM 1.6
Adabifiroozjaei, Esmail MA 3.4
Adagideli, Inanc MA 4.1, TT 7.1
Adak, Abhishek K. O 11.3
Adam, Adam S. O 54.3
Adam, Roman MA 22.4
Adamkiewicz, Alexa O 19.7, O 57.2
Adams, Ellen BP 17.2, BP 27.1
Adams, Ellen M. BP 11.43
Adams, Stephanie O 75.5
Adelhardt, Patick TT 42.10
Adelhardt, Patrick TT 47.13
Adelhelm, Philipp TUT 4.1, MA 1.1
Adelmann, Christoph MA 34.7
Adelung, Rainer KFM 9.9
Adessi, Christophe KFM 4.6
Adhikari, Rajan O 60.6, O 64.1
Adhikari, Ronojoy DY 32.11
Adibi, Elaheh TT 43.16
Adiyodi Veettil, Radhakrishnan BP 28.39
Adlung, Robin DS 12.27
Adnan el Kazouini, Mohamad TT 58.18, TT 58.19
Adriano, Cris MA 39.3
Adrien, Wafflard DY 7.1
Aeschlimann, Martin PSV X, MA 31.3, MA 40.7, MA 40.8, MA 40.9, MA 46.7, O 10.2, O 14.5, O 19.5, O 19.8, O 22.4, O 37.10, O 38.1, O 59.5, O 64.9, O 70.4, O 80.1, O 80.4, O 84.2, O 95.2, O 95.3, TT 56.2, TT 68.2, TT 68.3
Afanasyev, Dmytro O 8.7
Afteniya, Olha CPP 56.6, O 76.9
Agar, Joshua KFM 1.8
Agarmani, Yassine TT 10.7, TT 51.9
Agarwal, Seema CPP 35.11
Aggoune, Wahib HL 47.1
Aggrawal, Neha DS 12.22
Aghassi-Hagmann, Jasmin TT 54.1
Aghelmaleki, Atiyeh DY 18.7
Agió, Mario HL 29.10
Agliari, Elena DY 11.2, TT 13.2
Agradidis, Clió Efthimia TT 29.6, TT 65.3
Agrestini, S. TT 46.2
Agudo-Canalejo, Jaime BP 24.11, DY 38.11
Aguir Teixeira, Camila MM 40.6
Aguilá, David MA 13.1, TT 19.1
Aguilera, Irene HL 7.38, O 85.2
Aguirre Banos, Andrea O 36.5, O 56.5
Ágústsson, Steinn Ymir O 84.3, TT 56.3
Aharonovich, Igor HL 3.8, HL 22.10
Ahkmerov, Anton TT 8.8
Ahlers, Jonas BP 17.2
Ahmad, Ather HL 7.21
Ahmadiniaz, Naser DY 9.6, DY 43.13
Ahmadirahmat, Abolfazl DY 42.13
Ahmed, Eslam S. TT 31.7
Ahmed, Safa L. O 15.12
Ahmed, Zuned O 87.2
Ahnfeldt, Jan Philipp HL 33.29
Ahrens, Heiko BP 11.0
Aiboudi, Oumaima O 3.1, O 3.3
Aichner, Bernd TT 8.10
Aiello, Gaetano KFM 6.23, KFM 8.6, KFM 8.8, KFM 8.9
Aif, Serhii BP 10.5
Aikkila, Paula BP 10.2, BP 10.6, BP 11.29
Ait Yahia, Mehdi BP 28.54
Aizpurua, Javier O 76.2
Ajanovic, Benjamin BP 11.36
Ajdari, Mohsen O 10.7
Ajmail, Karim BP 28.20
Akberian, Maryam DY 27.4
Akashdeep, Akashdeep MA 5.5, MA 23.66
Akbarian, Ziba O 12.4
Akhmadaliev, Shavkat DS 10.5
Ahkmerov, Anton R. KFM 11.8
Akhmetshina, Tatiana MM 25.2
Akhtar, Arub DS 8.5
Akhundova, Fatima HL 25.10, HL 25.11
Akhundzada, Sapida KFM 6.34, MA 5.2, MA 23.36, MA 38.4, MA 40.28
Akimov, Ilya A. HL 35.4, HL 35.8
Akinsinde, Lewis O. O. MA 38.5
Akisheva, Anna CPP 35.13
Akkerman, Quinten HL 25.7
Akkerman, Quinten A. CPP 51.1, HL 25.2
Akmaz, Necmettin E. HL 42.7
Ako Khajetoorians, Alexander O 30.2
Akopyan, A. MA 33.6
Akrítidis, Michail DY 49.10
Aktas, Cenk CPP 13.1
Al Beattie, Bakr BP 11.74, BP 11.75, DY 18.5, DY 37.7
Al Mamoori, Mohamad MA 40.37
Alaasar, Mohamed HL 2.3
Alam, Aftab MA 37.2
Alam, Shahidul CPP 1.4, CPP 1.9, CPP 17.17, CPP 17.29, CPP 36.7, CPP 43.2
Alameh, Kafa BP 11.66
Aland, Sebastian BP 8.1, CPP 8.8, CPP 52.3, DY 29.3
Alarслан, Fatih KFM 14.4
Alavi, Ali TT 21.4
Alavizargar, Azadeh BP 3.1, BP 11.34
Albaladejo-Siguan, Miguel DS 10.2
Albe, Karsten HL 25.4, MM 5.3, MM 29.5
Albenge, Nicolas TT 39.5
Albers, Tony DY 45.5
Alberti, Gabriele O 24.2
Alberti, Simon BP 12.8
Albertini, Franca SYGM 1.3
Albino, Andrea HL 25.11, O 95.4, O 95.5, TT 68.4, TT 68.5
Albohn, Lena CPP 35.39, CPP 35.40, CPP 35.46
Albrecht, Anna AKC 1.2
Albrecht, Florian O 66.3
Albrecht, Jan DY 26.6
Albrecht, Manfred DS 14.1, MA 15.3, MA 23.72, MA 40.55, O 83.4
Albrecht, Martin HL 47.1, O 95.4, O 95.5, TT 68.4, TT 68.5
Albus, Marie Irene O 23.5
Aldahhak, Hazem O 28.4
Aldarawsheh, Amal MA 35.7, TT 8.4
Aldosary, Haya CPP 17.17
Aleksa, Paulus O 56.3, O 56.6
Alemayehu, M. B. TT 3.4
Alemayehu, Rekikua Sahilu DS 12.56
Alert, Ricard BP 11.3, BP 15.2, BP 30.4
Alet, Fabien DY 27.2
Aletsee, Clara O 29.8
Alex, Ben HL 20.2, O 35.2
Alexakis, Alexandros BP 19.2, CPP 41.2
Alexakis, Alexandros E. CPP 52.5, DS 12.34
Alexander, Gareth P. BP 2.7
Alexandre, Arthur DY 32.4
Alexe, Marin KFM 2.5, MA 32.1
Alexeeva, Elena MM 16.1
Alexiou, Christoph HL 29.4
Alff, Lambert DS 9.2, DS 9.3, DS 11.4, DS 12.36, MA 17.5
Alfken, Jette BP 29.3
Alfonsov, Alexey TT 10.9
Alfreider, Markus MM 9.1
Alhafez, Iyad DY 29.4
Al-Hamdo, Hassan MA 18.1, MA 18.2
Al-Hilfi, Samir H. O 32.8
Ali, Khadiza MM 14.7, O 47.4
Ali, Mazhar TT 27.3
Ali, Syed Yunus DY 44.16
Ali, Zayan Ahsan MA 19.2
Alic, Amna TT 3.7, TT 57.3
Aliev, Farkhad G. TT 20.10
Aliqia, Armando A. O 33.1
Alikhah, Sanaz MA 23.52
Alim, Karen BP 9.4, BP 9.5, BP 10.9, BP 11.52, BP 28.19, BP 28.20, BP 28.31, BP 28.40, BP 28.44, DY 31.1, DY 42.7, DY 45.6, DY 45.13
Alin, Julian O 43.5
Alireza, Patricia TT 4.11
Alireza, Patricia L. TT 4.12
Alirezaeizanjani, Zahra BP 26.5
Aljasem, Farouk HL 33.41
Alkemade, Rinske DY 14.1
Alkofer, Moritz DY 57.3
Alldritt, Benjamin O 66.10, O 74.2
Allegretti, Francesco O 14.6, O 14.8, O 32.2, O 36.6, O 40.2
Allen, Rosalind BP 16.1
Allen, Thomas BP 28.15
Allende, Sebastian MM 22.1
Allgeier, S. TT 57.27, TT 57.28
Allgeier, Steffen TT 57.26
Alling, Björn MM 22.6
AlMutairi, AbdulAziz O 34.4
Al-Nuaimi, Nedhal HL 7.41
Alok, Amar HL 33.54
Alonso-González, Pablo DS 7.1
Alp, Esen E. MA 42.2
Alpin, Kirill TT 6.2
Alqahtani, Obaid CPP 11.4
Alqurashi, Maryam CPP 11.2
Al-Samman, Talal MM 20.3
Alshaikh, Ahmed DS 16.4, HL 42.1
Al-Shakran, Mohammad O 14.10
Alsfuyani, Wejdan CPP 11.2, CPP 17.17
Altaner, Bernhard BP 10.6
Altendorf, Simone G. HL 51.3, HL 51.6, TT 30.6
Althammer, Matthias MA 4.13, MA 23.50, MA 23.76, MA 23.80, MA 34.6, MA 40.15, MA 40.65, TT 7.13
Althobaiti, Wejdan CPP 1.4, CPP 1.9, CPP 17.17
Altland, Alexander TT 31.2
Altman, Ehud TT 45.9
Alü, Andrea O 58.8
Alvarez Herrera, Pablo A. CPP 35.61
Alvarez, Nayra MA 40.60, MA 40.61
Álvarez-Pérez, Gonzalo DS 7.1
Alvaro, Laura MA 38.1
Amadon, Bernard TT 21.9
Amann, Peter O 11.4, O 29.6
Amaro, Mariana Manuela O 26.7
Amati, Graziano DY 9.12
Ambacher, Oliver MM 11.2
Amber, Zeeshan KFM 6.8
Amber, Zeeshan H. KFM 14.2
Amber, Zeeshan Hussain KFM 6.18, KFM 6.35
Ambrosetti, Alberto HL 13.6, O 4.7, O 17.6
Amelin, Kirill TT 59.18
Amenitsch, Heinz CPP 17.54
Amigo, Maria Lourdes O 85.4
Amin, Muhamed VA 1.3
Amir, Ariel BP 6.4
Amirabbasi, Mohammad MA 21.5
Amiri, Behnam BP 28.49
Amirjalayer, Saeed O 97.7
Ammerlaan, Andrew TT 29.2
Ammerman, Spencer E. O 75.5
Amorese, Andrea TT 4.10, TT 9.3, TT 9.4, TT 9.5, TT 30.7
Amouyal, Y. DS 7.2
An, Sangmin O 54.4
Anand, Aman CPP 17.29, CPP 36.7
Anand, Ketan HL 37.6
Andergassen, Sabine TT 20.9, TT 43.33
Anders, Frithjof B. HL 15.4
Anders, Janet DY 40.3
Andersen, Brian TT 23.2
Andersen, Mie O 52.4, O 52.7
Anderson, Lennart DY 43.22
Ando, Yoichi TT 36.4
Andorfer, Fabian MM 23.32, MM 26.2
Andreas Wilde, Marc MA 9.4
Andreev, Marat CPP 19.1
Andres, Georges SOE 18.3
Andres Naranjo-Montoya, Oscar O 60.11
Andresen, Kurt BP 25.4
Andrienko, Denis CPP 1.4
Andriushin, Nikita MA 44.7, TT 23.12
Andryushin, Nikita MA 23.1
Angel Niño, Miguel MA 31.2
Angenent, Vanessa CPP 2.4
Anghel, Sergiu HL 4.10
Angrick, Christoph O 67.8
Anjard, Christophe BP 22.10
Ankerhold, Joachim DY 9.5, DY 9.8, DY 9.9, DY 10.9, DY 43.19, MA 16.7, O 7.5, TT 20.9, TT 39.2, TT 39.9, TT 54.4, TT 54.5
Annie, Simon KFM 10.6
Anooz, Saud Bin HL 4.8
Anson, Christopher E. MA 24.6
Anstett, Martin O 38.1
Antczak, Grazyna O 2.10
Anthopoulos, Thomas CPP 1.1
Anthore, Anne TT 17.3
Anthuparambil, Nimmi Das BP 11.46
Antognini Silva, David TT 8.2
Anton, Arthur Markus CPP 43.2, CPP 43.3
Anton, Christoph BP 28.38
Anton, Markus CPP 20.10
Antonelli, Tommaso O 30.1, O 59.8
Antonio, Stocco BP 1.8
Antonov, Alexander P. DY 56.6
Antón-Solanas, Carlos HL 1.2, HL 1.7
Antrack, Tobias DS 10.2
Antunes, Goncalo BP 2.9
Anwander, Emanuel CPP 17.30
Anwar, Shadab MA 9.10
Anyfantis, Dimitrios MA 23.55
Anzivino, Carmine DY 16.2, DY 23.1
Aoki, Hideo SYUE 1.4
Apfelbeck, Fabian A.C. CPP 53.6
Appavou, Marie-Sousai CPP 8.3
Appel, Stephan KFM 10.1
Appold, Nico BP 10.5
Apsite, Indra CPP 8.8, DY 29.3
Apuzzo, Eugenia DY 16.11
Aqeel, Aisha MA 23.11
Arabi, Soroush MA 21.7, O 33.2
Aradi, Bálint KFM 6.5
Aragon Sanchez, Jazmin O 85.4
arai, noriyoshi CPP 2.5
Arapan, Sergiu MA 28.5
Araya Day, Isidora KFM 11.8
Arend, Germaine HL 10.9
Aretz, Jonas BP 1.2
Aretz, Joost TT 37.8
Ariaee, Sina CPP 17.54
Arican, Bariscan MM 33.6
Ariel, Gil DY 26.2, DY 31.2
Arima, Taka-hisa MA 2.6
Arita, R. TT 6.4
Arita, Rytaro TT 63.4
Arita, Bose BP 24.12, DY 38.12
Arjariya, Richa O 60.12
Arjun, A BP 3.9
Arlinghaus, Julia SOE 4.3
Armbruster, Leon BP 18.2, DY 33.2
Armengol-Collado, Josep-Maria BP 4.9
Armenta, Carlos HL 18.2

Armin, Ardalan CPP 1.10
 Arndt, Björn O 92.3
 Arneht, Jan •MA 24.5, MA 40.23,
 TT 50.8
 Arnhold, Lukas •O 15.5, O 15.11,
 O 20.7
 Arnold, Cord L. O 75.3
 Arnold, Florian •HL 11.6, •TT 15.6
 Arnold, Jonas •MA 9.1
 Arnold, Zdeněk MA 37.6
 Arnoldi, Benito O 19.5, O 19.8, O 22.4
 Aromi, Guillem MA 13.1, TT 19.1
 Aronson, Igor •BP 7.6, •DY 10.6
 Arora, Abeer •MA 46.4, O 95.1, O 95.3,
 TT 68.1, TT 68.3
 Arora, Himani HL 33.10
 Arregi, Jon Ander MA 40.10
 Arreyndip, Nkongho Ayuketang
 •SOE 23.2
 Arrigoni, Enrico TT 22.9, TT 22.10,
 •TT 22.11, TT 38.13, TT 43.22
 Arroyo, Marino BP 4.5, BP 4.8
 Arshad, Atiqah BP 11.43, MM 23.35,
 •O 64.7
 Arslan, Serkan •O 49.9
 Artmann, Evelyn •O 14.10, O 96.10
 Artzyukhin, Sergey MA 12.7, •MA 50.6
 Aruga, Tetsuya O 32.4
 Arzumanov, Alexey DS 9.2, DS 11.4,
 DS 12.36
 As, Donat J. HL 51.10
 Asano, Hidefumi MA 31.5
 Aschauer, Uli O 45.3
 Aschauer, Ulrich O 38.4, O 45.4,
 O 55.3
 Aschwanden, Rebecca •HL 33.30
 Asfia, Shima •BP 11.35
 Asghar, Umm-e-hani DS 2.1
 Ashok, Arun HL 16.9, HL 50.11,
 TT 24.9
 Ashok, Sanjay MA 8.4, •MA 46.7
 Ashokan, Vinod TT 16.12, TT 16.13
 Ashour, Ahmed DY 7.6
 Ashoush, Mostafa O 14.5
 Ashoush, Mustafa A. O 14.2
 Asl-Gohrbani, Mahdi DS 12.19
 Aßmann, Marc HL 33.26
 Assaad, Fakher F. O 84.9, TT 47.5,
 TT 56.9
 Assent, Ira MA 10.1, TT 12.1
 Ast, Christian R. O 21.7
 Ast, Christian O 20.5
 Ast, Christian R. O 7.5, •O 44.1
 Ast, Johannes MM 4.4
 Astakhov, Georgy HL 3.9, HL 10.8,
 HL 50.3
 Aswartham, Saicharan MA 40.57,
 MA 40.59, TT 10.9, TT 10.10, TT 57.9,
 TT 57.11, TT 62.1
 Asyuda, Andika O 55.1
 Ata, Arif •TT 43.12, TT 46.7
 Atature, Mete •PLV 1
 Atilla, Achraf MM 41.5
 Atkinson, William A. TT 63.6
 Atodirese, Nicolae O 36.11
 Attallah, Ahmed DS 6.1
 Attallah, Ahmed Gamal •CPP 35.17,
 KFM 6.30, KFM 9.5
 Attou, Aymen •BP 27.6
 Atxitia, Unai MA 8.2, MA 46.13
 Atzen, Madlen MM 23.30
 Aubert, A. •MA 48.3
 Aubert, Alex MA 3.2, MA 3.3
 Aue, Leonard •MM 23.7
 Auer, Andrea •O 97.8
 Auerbach, Paul CPP 8.8, DY 29.3
 Auernhammer, Günter K. CPP 44.1,
 CPP 44.6, DY 7.10
 Aufinger, Lukas BP 11.72, BP 11.73
 Auge, Manuel O 24.1, O 31.1
 Auger, Thierry MM 33.2
 August, Sophie-Charlotte BP 28.2
 Augustsson, Steinn Ymir O 95.3,
 TT 68.3
 Auler, Normen HL 7.52, HL 7.53,
 •HL 42.6
 Aumayr, F. O 5.2
 Aumayr, Friedrich O 13.2, O 24.2,
 O 31.4, O 31.7
 Auwärter, Willi O 3.7, O 14.2, O 36.6,
 O 93.8
 Au-Yeung, Kwan Ho •O 3.1, O 3.3
 Auzele, Thomas HL 7.40
 Avanzini, Francesco DY 40.7
 Avarvari, Narcis O 73.6
 Avdeev, Maxim MA 40.25, MA 44.8
 Avdoshenko, Stanislav MA 31.7

Avdoshenko, Stanislav M. O 2.7
 Averitt, Richard •SYUE 1.1
 Avila, J. DS 7.2
 Avilov, Ivan BP 25.1
 Awsaf, Chowdhury MA 40.12,
 MA 40.55
 Axmann, Peter KFM 10.3
 Axt, Marleen •O 19.9
 Axt, Vollrath Martin HL 7.39
 Ayni, Babatunde TT 65.9
 Azhari, Mouhcine TT 45.1
 Azinfar, Amir BP 11.38
 Azizi, Jafar •MM 16.3, MM 16.6
 Azizmalayeri, Reza •CPP 44.1
 Azzouzi, Mohammed CPP 11.6
 B, Grabowski MM 40.8
 Baba, Yuriko •HL 11.2, •TT 15.2
 Babar, Vasudeo CPP 54.3, O 74.9
 Babenko, Iaroslav •BP 12.10
 Babenkov, S. MM 26.8, O 30.4
 Babenkov, Sergey HL 36.2, O 85.3
 Babin, Hans-Georg HL 7.42, HL 7.57,
 •HL 42.4
 Bacaksiz, Cihan •BP 11.53
 Bach, Nora •O 83.6
 Bachmann, Lydia O 52.1
 Bachmann, Maja D. TT 30.5
 Bachus, Sebastian MA 13.7, TT 19.7,
 TT 46.4
 Back, Christian H. MA 20.10, MA 48.4
 Bäckler, Arnd DY 21.1, DY 43.7,
 DY 43.15, DY 48.4, TT 55.4
 Backholm, Matilda BP 28.37
 Backmann, Pia BP 11.58
 Backmeister, Lucas TT 3.10
 Backofen, Rainer •MM 14.8,
 MM 23.33
 Bacq-Labreuil, Benjamin •TT 21.3,
 •TT 43.11
 Baczewski, L. L. T. O 50.2
 Badala Viswanatha, Chetana •O 22.4
 Bader, Andreas •HL 17.5
 Bader, Rolf SOE 7.1
 Bader, Verian BP 17.2
 Badr, Samuel •DY 11.8, •TT 13.8
 Badrtidinov, D. O 42.2
 Badrtidinov, Danis •HL 31.2, •O 61.2
 Badura, A. MA 41.2
 Badura, Antonin MA 4.12, MA 40.63,
 TT 7.12
 Bae, Yujeong O 15.6
 Baenitz, M TT 42.4, TT 42.15
 Baenitz, Michael MA 27.1, MA 31.4,
 TT 30.11, TT 30.13, TT 43.2, •TT 46.8
 Bag, Soumen DS 12.28
 Bagchi, Mahasweta TT 36.4
 Bagrheer, Matias DS 12.56
 Bagrov, Andrey MA 35.4
 Bahadorian, Mohammadreza
 •BP 18.6, •DY 33.6
 Bahari, Masoud •TT 63.7
 Bahnmüller, Ulrich J. CPP 51.7
 Bahr, Arne •TT 39.10
 Bai, Xiaojian TT 9.8
 Baidakova, Marina O 14.11
 Baidukova, Olga BP 25.16
 Baiesi, Marco BP 23.8
 Bailey, Joe MA 48.5
 Bajaj, Akash •MA 4.5, •TT 7.5
 Baje Shankarakrishna Bhat, Swasthik
 •HL 50.11
 Bajpai, Ashna MA 43.3
 Baker, Graham •MM 6.7, TT 30.5
 Baki, Aykut DS 12.50
 Baklanov, Aleksandr O 3.7, O 36.6
 Balajka, Jan O 26.4, O 54.6, •O 54.7,
 O 54.8, O 81.4
 Balakrishnan, Geetha MA 9.8,
 MA 11.6, MA 33.7
 Balakrishnan, Harishankar HL 38.2
 Balan, Aravind P. MA 23.57
 Balashov, Timofey MA 2.5
 Balasubramanian, Priyadarshini
 DS 12.35
 Balatsky, Daria A. TT 30.3
 Baláz, Pavel MA 4.3, TT 7.3
 Baldovi, J. J. TT 6.4
 Baldrati, Lorenzo MA 31.3
 Balduque, José •TT 60.4
 Balembois, Leo PLV X
 Balguri, Sudhama MA 9.5
 Bali, Rantej MA 9.10
 Balland, Martial BP 31.2
 Ballestad, Thorvald HL 11.3, MA 39.5,
 TT 15.3
 Baltazar, Samuel MM 22.1, MM 26.5
 Baltes, Carsten Alexander •BP 28.52

Baltusch, Simone BP 28.13
 Baltz, V. MA 41.2
 Baltz, Vincent MA 4.12, MA 22.2,
 MA 40.63, TT 7.12
 Balzer, Bizan N BP 23.2
 Balzer, Karsten O 31.5, O 31.7
 Bampoulis, Pantelis O 29.9
 Banda, Jacintha TT 34.5
 Bandarenka, Aliaksandr CPP 17.16
 Banerjee, Atreyee •CPP 50.1
 Banerjee, Somay O 81.1
 Banerji, Natalie CPP 43.6
 Banetta, Luca DY 23.1
 Bang, Joohee •KFM 1.4
 Bange, Jan Philipp O 34.4
 Bange, Lukas •BP 1.3
 Bangert, Ursel O 31.1
 Banifarsi, Sanaz MM 23.16
 Banisch, Sven SOE 7.2, SOE 8.1
 Banks, Hadra •CPP 19.12
 Bansal, Namrata •MA 16.9
 Bansich, Sven SOE 18.4
 Bamsmann, Joachim O 96.5
 Bansenzer, L. HL 33.17
 Bansenzer, Luca HL 9.5, HL 30.2,
 TT 14.5, TT 41.2
 Banterle, Niccolò BP 17.6
 Baouche, Yanis •DY 42.6
 Bapat, Nikhil •O 86.6
 Baptista, Luis A. CPP 12.1
 Baquero, Eduard BP 23.1
 Bar, M. DS 12.48
 Bär, Marcus HL 25.10
 Bär, Markus •DY 31.2, DY 31.5, DY 42.1
 Bar, Michael DS 12.10
 Baraldi, Alessandro O 29.5
 Baran, Derya CPP 11.2
 Baranczuk, Lilla DY 57.1
 Baranowski, D. DS 7.2, MA 40.53
 Baranski, Maciej HL 10.2
 Baranwal, Prince MM 24.1
 Baratoff, Alexis O 87.3
 Barbeau, Marion MA 8.11
 Barbosa, Matheus •MA 23.20
 Barbour, Andi MA 43.6
 Barcikowski, Stefan MA 3.2
 Bardolaza, Hannah HL 17.6
 Barfuss, Wolfram SOE 16.3
 Bargheer, Matias HL 33.61, MA 23.70,
 MA 40.10, MA 40.34, MA 40.66,
 MM 12.3, O 37.7
 Bari, Sadia BP 3.11
 Barke, Ingo BP 28.13, O 28.3
 Barker, Dylan •O 77.4
 Barla, Alessandro O 15.12
 Barlow, Stephen CPP 17.24, CPP 18.1
 Barner, Joerg •BP 31.7
 Barnes, M. HL 33.62
 Barnoush, Afrooz •MM 24.1
 Barnowsky, Tom •O 36.4, O 47.1
 Baron, Elias HL 51.10
 Baron, Michael •HL 33.21
 Barragan, Ana O 46.3
 Barreteau, Cyrille •MA 30.2
 Barrett, Rhyann •MM 12.13
 Barsacchi, Rico BP 21.4, BP 28.12
 Bärschneider, Toni •CPP 43.10
 Barsoum, Michel MA 42.9
 Bart, Nikolai HL 7.44, •HL 42.5
 Bartal, Guy O 80.3
 Bartashevich, Palina BP 22.4,
 •SOE 16.5
 Bartell, Jason M. MA 43.6
 Bartels, Nina •BP 21.8
 Barth, Johannes O 14.8
 Barth, Johannes V. O 11.3, O 11.6,
 O 11.9, O 14.4, O 14.5, O 14.6, O 32.2,
 O 36.6, O 40.2
 Barth, Laura •SOE 7.4
 Barth, Michael •TT 59.3
 Barth, Stephan DS 12.4
 Barthel, Etienne MM 28.9
 Barthelmi, Katja HL 37.8
 Bärtl, Florian •TT 43.2
 Bartlett, Jack TT 34.4
 Bartlett, Philip CPP 45.3
 Bartlett, Tim HL 33.30, KFM 6.1
 Bartok-Partay, Albert MM 15.2
 Bartölke, Rabea BP 11.42
 Bartolucci, Giacomo BP 10.8
 Bartosik, Matthias MM 4.6
 Bartsch, Christian •DY 25.10,
 •TT 33.10
 Bartsch, Manfred O 51.4
 Bartsch, Hagen DS 12.4
 Barua, Avijit •HL 24.3
 Bas, Ekin Esme •HL 40.5, •O 79.5

Basaric, Farah •HL 30.1, •TT 41.1
 Baschnagel, Jörg CPP 19.3
 Baše, Tomáš O 47.8
 Basermann, Achim BP 11.76
 Basharova, Dinar •HL 7.52
 Bashouti, Muhammad O 49.3
 Basov, Dmitri N. TT 53.9
 Bassi, Nicolò •O 20.10
 Bastard, Gerald HL 30.3, TT 41.3
 Bastianello, Alvise TT 22.13
 Bastmeyer, Martin BP 11.37
 Bastonero, Lorenzo HL 21.1
 Basu, Saurabh HL 11.5, TT 15.5,
 •TT 45.7
 Basu, Swarnavo •DY 45.13
 Batista Pessoa, Walter HL 14.9
 Battagliani, Fernando DY 16.11
 Battistelli, Riccardo MA 43.6
 Baturina, Tatyana I. TT 20.8
 Bauch, David HL 7.50, HL 7.64,
 •HL 24.6
 Bauer, Alexander G. TT 20.3
 Bauer, Andreas MA 9.4, MA 26.2,
 TT 3.8, TT 4.13, TT 10.1, TT 10.3,
 TT 10.5, TT 47.3, TT 47.6, TT 58.23
 Bauer, Dieter O 65.2, O 65.3
 Bauer, F. TT 57.21
 Bauer, Fabienne •TT 57.20, TT 66.4
 Bauer, Hans G. MA 23.68, MA 23.73
 Bauer, Janka •BP 17.5
 Bauer, John B. DS 12.8, O 2.4, O 22.5
 Bauer, Karl MA 8.9, MA 20.3
 Bauer, Lisa S. CPP 44.10
 Bauer, Matthias TT 44.7
 Bauer, Nicolas P. •DY 44.11
 Bauer, Stephanie HL 7.43, HL 7.62
 Bauer, Tobias HL 7.48
 Bauerhenne, Bernd DS 4.1, DS 12.6,
 KFM 6.37, •O 6.6
 Bäuerle, Peter HL 48.8
 Bauermann, Jonathan BP 22.9,
 BP 22.12
 Bauernfeind, Anastasia •TT 58.28
 Baum, Peter DY 49.5, •MA 34.1,
 MM 3.4, MM 39.2
 Baumann, Aljoscha Felix •MM 5.2
 Baumann, Danny TT 58.27
 Baumann, Elisabeth •BP 28.15
 Baumann, Maximilian HL 2.3
 Baumann, Susanne O 12.1, O 15.5,
 O 15.11, O 20.7, O 36.8, O 77.7
 Bäumchen, O. BP 11.7
 Bäumchen, Oliver BP 9.1, BP 25.6,
 BP 28.37
 Bäumer, Christoph O 92.7
 Baumgarten, Lutz DS 12.5
 Baumgartner, Andreas O 51.3
 Baumgartner, Benedikt BP 11.36
 Baumgartner, Christian TT 20.8,
 TT 27.5
 Baumgärtner, Kiana O 22.7
 Baunack, Stefan MA 23.35
 Bausch, Andreas BP 1.2
 Baxter, Olivia KFM 4.1
 Bayer, Andreas O 60.6
 Bayer, Johannes C. HL 16.4, HL 16.7,
 •HL 16.8, TT 24.4, TT 24.7, •TT 24.8
 Bayer, Manfred HL 4.10, HL 15.2,
 HL 15.3, HL 35.4, HL 35.8, HL 35.9,
 HL 47.2
 Baykusheva, Denitsa SYUE 1.5
 Bayo, Djénabou •DY 17.3
 Bayrak, Turkan HL 42.2, HL 42.3
 Bazarnik, Maciej MA 14.1, O 42.8,
 •O 93.4
 Bazarova, Alina BP 11.76
 Bazulin, Daniil TT 58.7, TT 66.6
 Bazulin, Daniil E. TT 39.7, •TT 58.6
 Beach, G S D MA 31.1
 Beach, Geoffrey MA 40.5
 Beach, Geoffrey S.D. MA 43.6
 Beanland, Richard CPP 45.3
 Beaulieu, Samuel O 16.5, O 16.7
 Beauvois, Ketty MA 37.4
 Beavers, Christine TT 4.12
 Bebbo, Pascal HL 25.11
 Bebon, Rick •DY 56.2
 Bebon, Robin •DY 42.8
 Beccard, Henrik KFM 14.2, KFM 14.3
 Bechberger, Moritz MA 16.5,
 •MA 23.74
 Becher, Christoph HL 7.48
 Bechinger, Clemens BP 24.2, DY 16.1,
 DY 16.4, DY 16.6, DY 16.7, DY 31.7,
 DY 31.10, DY 38.2
 Bechler, Nicolai Timon •MA 26.3
 Bechstedt, Friedhelm HL 18.1

Author Index

- Bechstein, Ralf O 60.1, O 81.9
 Bechstein, Sylke TT 58.26
 Becht, Conny HL 23.3, HL 23.6
 Bechtel, Tim HL 6.8, •MM 29.1, O 9.8
 Beck, Claudio MA 38.4
 Beck, Erik •O 39.4
 Beck, Esko Erik O 29.6
 Beck, Hans-Peter SOE 15.1
 Beck, Hubert O 55.9
 Beck, Janic TT 3.1
 Beck, Philip O 32.9
 Beck, Sophie TT 37.6
 Beck, Timon •BP 12.8
 Becker, Christian MA 23.34
 Becker, Conrad O 55.7
 Becker, Hanka MM 12.16
 Becker, K.-D. KFM 6.46
 Becker, Karolin TT 36.6
 Becker, Klaus-Dieter KFM 13.5, •KFM 13.6
 Becker, Martin DS 8.4
 Becker, Maximilian R •CPP 44.9
 Becker, Michael A. •HL 50.6
 Becker, Nils B. BP 11.18
 Becker, Petra MA 44.5, TT 10.12
 Becker, Sebastian O 22.4
 Becker, Simon •CPP 57.4
 Becker, Sven MA 5.5, MA 23.66
 Beckert, Sebastian MA 4.12, •MA 40.63, TT 7.12
 Beckmann, Benedikt KFM 6.31, MA 3.8, MA 3.9, MA 42.2, •MA 42.9
 Beckmann, Detlef TT 53.1
 Beddrich, Lukas MA 40.42
 Bednar, Hynek DY 37.6
 Bednarski-Meinke, Connie DS 12.25, DS 14.6, MA 5.6, O 42.12
 Bednarz, Beatrice •MA 40.30
 Bednyakov, Petr KFM 14.3
 Beenakker, Carlo HL 30.6, TT 41.6
 Beenken, Wichard J.D. HL 38.1
 Beer, Avraham DY 31.2
 Beer, Max •HL 29.5, HL 37.1
 Beg, Marijan MA 23.14, MA 26.4
 Begam, Nafisa BP 11.46, DY 37.1
 Begum-Hudde, Vijaya O 53.8
 Behle, Eric •BP 3.3, BP 27.5
 Behler, Jörg CPP 45.6, MM 12.18, MM 16.6, MM 25.4, O 26.6
 Behm, R. Jürgen O 96.5
 Behner, Gerrit HL 29.9, HL 30.1, •TT 36.1, TT 41.1, TT 59.5, TT 59.6
 Behrends, Jan MM 16.1
 Behrens, Malte MA 36.1
 Behrens, Peter HL 34.4, HL 42.7
 Beida, Wejdan •MA 27.4
 Beier, Sönke DY 31.3
 Beierlein, Johannes HL 24.13
 Beigang, René MA 22.5
 Bein, Thomas HL 45.2
 Beiner, Mario CPP 35.31
 Bejarano, Mauricio MA 23.78
 Bekemeier, Simon •MM 12.28, MM 12.30
 Bektas, Umutcan •HL 41.2
 Belabbes, Abderrezak HL 18.1
 Belayeva, Tatyana CPP 35.13
 Belder, Detlev CPP 28.11, TT 32.11
 Belke, Christopher HL 34.4
 Bellaiche, Laurent MA 18.7
 Bellon, Alexander MA 13.7, TT 19.7
 Belova, Valentina O 93.6
 Belfthle, Kendra O 78.7
 Belyaeva, Tatyna CPP 35.41
 Belykh, Vasily V. HL 15.2
 Belzig, Wolfgang MA 4.6, MA 23.62, TT 7.6, TT 11.1, TT 16.3, TT 18.4, TT 20.1, TT 20.6, TT 20.9, TT 27.10, TT 48.3, TT 48.4, TT 53.1, TT 57.15, TT 66.1
 Ben, Shuai HL 48.1
 Bénâtre, Denis •TT 58.16
 Benchabane, Sarah •HL 10.2
 Benckiser, Eva TT 50.3
 Bendaoud, Mohammed BP 8.3
 Benduhn, Johannes CPP 17.14, CPP 17.15, CPP 43.4, CPP 43.5, CPP 43.6, CPP 43.8, •CPP 43.9, DS 10.2, HL 7.12
 Benecke, Anna •AKC 1.2
 Benedičič, Izidor TT 37.12
 Beneke, Grischa •MA 23.3, MA 29.1, MA 31.2
 Benestad, Jacob •HL 33.27
 Benetatos, Panayotis •BP 19.4, CPP 35.3, •CPP 41.4
 Benetti, Edmondo Maria CPP 8.4
 Benfatto, Lara TT 62.3
 Bengone, Olivier O 7.9
 Benhayoun, Othmane •DS 4.1, •DS 12.6
 Benitez, Maria J. HL 7.32
 Benitez, Maria Jose HL 41.5
 Benka, Georg MA 26.2, TT 4.13, TT 10.1, TT 47.3
 Benndorf, G. DS 12.48
 Bennecke, Wiebke O 34.4
 Bennemann, Benjamin HL 29.9
 Bennenhei, Christoph •HL 2.5, •HL 2.6
 Benner, Dominik HL 8.10
 Bennewitz, Roland O 4.3
 Benoit, Mahault BP 24.12, DY 38.12
 Benoit-Maréchal, Lucas •DY 4.6
 Bentkamp, Lukas DY 5.7
 Bentmann, Hendrik O 65.5, O 67.3, O 67.5, O 74.4, O 94.6, O 94.9, TT 9.7
 Benyagoub, Abdenacer O 5.6
 Benyoucef, Mohamed CPP 35.52, HL 49.6
 Bera, Soumya DY 55.8, TT 67.8
 Berakdar, Jamal MA 23.68, MA 40.34
 Beran, Premysl KFM 10.3
 Berche, Bertrand BP 29.9, •DY 45.15, MA 23.47
 Berciaud, Stéphane O 72.4
 Bercieux, Dario TT 6.3, TT 8.3, TT 17.4, •TT 60.1, TT 64.1, TT 64.6
 Berek, Franz P. DY 46.2
 Berencen, Yonder HL 18.8, HL 50.3
 Beret, Dorian O 18.3
 Berger, Andreas MA 46.9
 Berger, Bernd HL 33.26
 Berger, Christoph •HL 44.1
 Berger, Esmée •O 38.6
 Berger, Helmuth MA 12.6, TT 57.9
 Berger, Richard K. O 28.10
 Berger, Rüdiger CPP 35.62, CPP 44.2
 Berger, Stefan A. •MM 22.2
 Bergeret, Sebastian TT 8.3, TT 27.2
 Bergerot, Clémence •SOE 16.3
 Berges, Jan HL 40.1, O 79.1
 Berggren, Magnus DS 16.6
 Berghold, Michael KFM 3.2
 Bergler, Thomas •MM 6.5
 Bergman, Anders MA 47.6
 Bergmann, Annika •DS 12.16, HL 33.7
 Bergmann, M. A. HL 23.5
 Bergmann, Michael A. HL 23.1
 Bergmann, Nicolas O 52.6, O 60.8, •O 86.8
 Bergmeier, Tim •O 37.11
 Bergschneider, Andrea HL 33.16
 Beringer, Lukas •DY 25.8, •TT 33.8
 Berisha, Enkeleta •TT 16.15
 Berja, Alba MA 38.1
 Berkelbach, Timothy C. DS 1.6
 Berlin, Johannes MM 18.4, MM 23.3, MM 23.31, •MM 40.4
 Berlitz, Benedikt •TT 58.12
 Bermes, Pit •MA 23.33
 Bermúdez-Otero, Ricardo SOE 8.3
 Bernabeu, Miguel o. BP 8.3
 Bernacki, Marc MM 23.30
 Bernardi, Davide •BP 9.3, •BP 13.3
 Bernardini, Fabio TT 44.7
 Berndt, Jasper MM 18.2
 Berndt, Richard O 7.8, O 20.9, O 33.5, O 33.7, O 42.6, •TT 8.1
 Berner, Rico DY 57.3
 Berners, Lukas MM 37.1, •MM 41.3
 Bernevig, Andrei MA 10.2, TT 12.2
 Bernhard, Nils HL 41.7
 Bernhardt, Felix KFM 6.2, •KFM 6.4
 Bernhardt, Moritz MA 19.1
 Bernhardt, Nils •HL 22.3, HL 41.3
 Bernien, Matthias •VA 1.4
 Berning, Lena BP 5.3
 Bernöcker, Simon HL 33.13
 Bernstorff, Sigrid CPP 35.18, CPP 35.43
 berntsen, magnus DY 25.7, •O 8.8, TT 33.7
 Berntsen, Magnus H. O 6.3, O 37.12
 Berritta, Fabrizio HL 33.27
 Berritta, Marco MA 23.52
 Berrod, Quentin MA 24.6
 Bertacco, Riccardo MA 11.2
 Bertaina, Sylvain PLV X
 Bertel, Erminald O 47.6
 Bertet, Patrice •PLV X
 Berth, Gerhard HL 22.1
 Bertin, Alexandre •MA 44.5
 Bertinetti, Daniela KFM 8.5
 Bertini, Bruno DY 55.9, TT 67.9
 Bertok, Eric TT 36.3
 Bertram, Florian O 39.6
 Bertram, Frank HL 7.6
 Bertrang, Kevin O 29.4, •O 29.5, O 41.3
 Berwan, Patrick HL 29.3, HL 37.3
 Beryani Nezaifat, Negin •DS 12.11, DS 12.55
 Beschoten, Bernd HL 14.5, HL 14.8, HL 22.5, HL 30.2, HL 33.9, HL 33.12, TT 41.2
 Besenius, Pol BP 11.14, CPP 12.2
 Beßner, Julian •O 48.2
 Besocke, Kai •O 42.3
 Besproswanny, Julia •TT 58.27
 Bessarab, Pavel F. MA 35.9
 Best, James MM 26.1
 Best, James P. MM 9.7, MM 33.3
 Bestha, Kranthi Kumar •MA 40.57
 Beta, Carsten DY 31.3, DY 56.11
 Bethkenhagen, Mandy MM 12.11
 Betker, Marie CPP 17.26, CPP 36.6, CPP 52.5, CPP 58.2, •DS 12.34
 Betouras, Joseph TT 51.2
 Bett, Andreas HL 4.7
 Bett, Andreas W. HL 4.3
 Bette, Henrik •DY 37.2
 Bettinger, Holger O 22.5
 Bettinger, Holger F. DS 12.8, O 2.4
 Betz, Fridtjof HL 37.5, KFM 6.34
 Betz, Markus HL 4.10
 Betz, Nicolaj O 15.5, O 15.11, O 20.7, •O 77.7
 Betz, Timo BP 4.4, BP 8.2, BP 8.4, BP 11.19, •BP 11.55, BP 25.1, BP 28.11, BP 28.18, BP 28.21, BP 28.23, BP 28.51, DY 32.2
 Betzinger, Markus O 67.10
 Betzold, Simon HL 5.1, HL 18.4
 Beugeling, Wouter •HL 11.7, •TT 15.7
 Beutier, Guillaume MA 43.1
 Beyazit, Yasin O 8.3
 Beydeda, Cenk TT 30.1
 Beye, Martin TT 3.7, TT 57.3
 Beyer, Franziska HL 17.4
 Beyer, Jacob TT 63.9
 Beyer, Jan HL 17.4
 Beyer, Jörn MA 18.8
 Beyer, Lukas •MA 3.5, MA 42.1
 Beyreuther, E. KFM 6.9
 Beyreuther, Elke KFM 6.19, KFM 6.20, KFM 14.3
 Bhandary, Sumanta MA 7.3, MA 20.7
 Bharadwaj, Venkata MA 40.60, MA 40.61
 Bharadwaj, Venkata Krishna •MA 47.9
 Bhardwaj, Atmika •CPP 19.4
 Bhaskaran, L. MA 44.3
 Bhat, Mohammed Kamran MM 26.1
 Bhat, Pooja CPP 8.6
 Bhatt, Anjali SOE 16.2
 Bhatt, Shalini •MM 3.6
 Bhattacharya, Ahana TT 59.1
 Bhattacharyya, Semonti •HL 14.4
 Bhoobe, Preeti TT 43.6
 Bhuiyan, A F M Anhar Uddin HL 41.4
 Bhukta, Mona •MA 12.4, MA 40.29
 Bi, Wenli MA 39.2
 Bian, Baixue •MM 41.2
 Bian, Guang TT 53.9
 Bianchi, Andrea D. TT 28.4
 Bianchi, Marco O 6.3, O 85.2
 Biben, Thierry MM 33.5
 Biber, Herbert O 13.2
 Biberacher, Werner TT 10.6, TT 43.10
 Biberger, Simon CPP 17.42
 Bibes, Manuel MA 4.11, TT 7.11
 Biboy, Jacob BP 16.1
 Bickmann, Jens BP 24.4, DY 38.4
 Bidan, Cécile M. •BP 12.4
 Bidoggia, Davide O 19.4, O 34.10
 Biedenweg, Doreen BP 8.11, MA 23.54
 Bieder, Steffen DS 13.2
 Biedinger, Jan •DS 12.47
 Bieganowska, Antonina HL 18.4
 Bieler, Mark HL 17.1
 Bienfait, Audrey TT 39.10
 Bierbach, David BP 11.64
 Biermann, Klaus HL 3.4, HL 10.4
 Biermann, Silke TT 21.3, TT 30.11, TT 43.11
 Biersack, Matthias DY 7.2, DY 57.7, DY 57.8
 Bierwagen, Oliver DS 12.50, HL 47.3
 Biesenthal, Tobias TT 36.6
 Biesner, Tobias HL 17.2
 Biewald, Alexander CPP 51.1
 Bigi, Chiara MA 27.1, O 30.1
 Bihlmayer, Gustav HL 31.7, KFM 2.1, MA 14.4, •MA 14.5, MA 21.3, MA 39.1, O 30.5, O 51.1, O 59.3, O 61.7, O 67.4
 Bijani, Shanti CPP 43.7
 Bikaljevic, D. O 47.3
 Biktajirov, Timur •HL 33.28, •HL 33.52
 Bild, Marius HL 3.1
 Bilgrim Otto Seibertz, Bertwin CPP 29.10
 Bilk, Johannes O 22.2
 Billaud, Eric PLV X
 Bilmes, Alexander TT 49.3
 Bilous, Oksana DY 7.2, •DY 57.7, •DY 57.8
 Bin Anuar, Mohd Afiq •CPP 35.26
 Bin-Anooz, Saud DS 8.5
 Binder, Fabian •CPP 18.9, CPP 28.7, TT 32.7
 Binder, Patrick •BP 11.18
 Binkowski, Felix HL 33.48
 Birch, Max T. MA 11.6
 Birge, N O MA 31.1
 Birge, Norman MA 40.5
 Birk Hellenes, Anna •MA 41.4
 Birk, Tobias •O 2.7
 Birkhöhd, Moritz HL 43.4
 Birla, Hariom O 3.2
 Birnkammer, Stefan •TT 22.13
 Birol, Turan TT 23.2
 Birowska, M. DS 7.2
 Bischoff, Lothar HL 50.3
 Bischoff, Thomas •O 85.11
 Bisht, Onima •CPP 17.3
 Biskupek, J. O 47.7
 Biskupek, Johannes O 18.3
 Bisquerra, Andre HL 7.48
 Bissolo, Michele HL 33.13, •HL 34.5, MA 32.5
 Bista, Pravash •CPP 35.65, CPP 44.10
 Biswas, Abin BP 11.67, BP 25.7
 Biswas, Deepnarayan O 85.2
 Biswas, Kathakali SYOF 1.5
 Biswas, Mahitosh •HL 5.3
 Biswas, Naireeta CPP 36.8
 Biswas, Subham BP 8.5
 Bitsch, Martin CPP 13.8
 Bittencourt, Victor A. S. V. MA 34.6
 Bitter, Daniel MM 14.3
 Bittermann, Lena •TT 31.1
 Bittihn, Philip •BP 6.2, BP 30.2
 Bittrich, Eva CPP 43.8
 Bitzek, Erik MM 4.1, MM 4.3, MM 12.35, MM 15.4, MM 15.7, MM 15.8, MM 32.2, MM 41.5
 Björk, Jonas O 11.6, O 11.9
 Black, Maximilian MM 26.7
 Blagojevic, Niklas •CPP 12.4
 Blaha, Peter MM 14.10
 Blanchard, Nicholas MM 23.11
 Blanch-Mercader, Carles BP 15.4
 Blanco Garcia, Miguel •O 40.4
 Blank, Kerstin BP 19.5, CPP 41.5
 Blank, Kerstin G. BP 23.3
 Blaschke, Matthias •TT 25.3
 Blaschkowski, Björn TT 44.7
 Blasing, Jürgen HL 7.6, HL 51.7, O 32.1
 Blatt, Rainer TT 22.13
 Blaurock, S. DS 12.48, HL 7.16, HL 7.19
 Blaurock, Steffen HL 7.22
 Bleibel, Johannes DY 27.3
 Blesio, German G. O 33.1
 Blevins, Brianna DS 13.4
 Bleyer, Ulrich •PSV VIII
 Blick, Robert DS 16.4, HL 42.1, MM 23.19, O 42.10
 Blick, Robert H. HL 3.3, HL 14.1, TT 35.7
 Blickberndt, Jan •TT 43.30, TT 43.31, TT 43.32
 Blinder, Rémi DS 12.35
 Blob, Anna •BP 28.24
 Block, Dietmar AKC 1.2
 Blom, Kristian •DY 49.6
 Blowey, Phil O 77.4
 Blowey, Philip O 54.2
 Blugel, Stefan MA 14.4
 Blügel, Stefan HL 7.38, HL 8.8, HL 26.6, HL 31.7, MA 2.4, MA 10.1, MA 10.3, MA 14.5, MA 21.3, MA 23.4, MA 23.32, MA 26.5, MA 27.4,

- MA 35.8, MA 39.1, MA 47.7,
MM 12.27, O 30.5, O 36.11, O 51.1,
O 53.6, O 61.7, O 67.10, TT 8.2,
TT 12.1, TT 12.3, TT 63.11
- Bluhm, Hendrik HL 29.5, HL 37.1,
HL 37.4, HL 37.7, HL 50.7
- Bluhm, Moritz MM 12.29
- Blum, Michaela DS 12.57
- Blum, Moritz MM 12.30
- Blum, Volker HL 13.3, O 17.3
- Blumberg, Johannes BP 8.6, •BP 8.9
- Blundell, Stephen TT 6.6
- Boban, H. DS 7.2, MA 40.53
- Boban, Honey •O 30.3, O 74.3
- Bobowski, Jake MM 6.6
- Bocchini, Adriana •KFM 6.1, KFM 6.17
- Bochkarev, Anton MM 29.4
- Bochud, Nicolas MM 23.21
- Bock, Karlheinz HL 33.10
- Bockhorn, Lina •HL 30.5, •TT 41.5
- Böckmann, Hannes •O 75.8
- Böckmann-Clemens, Hannes O 34.5
- Bockstedte, Michel HL 18.11
- Bocquet, Francois C. O 19.7
- Bocquet, Lydéric BP 22.3
- Bocquet, Marie-Laure O 7.9
- Bode, Mathias O 77.9
- Bode, Matthias MA 14.2, MA 14.4,
MA 14.5, MA 14.6, O 2.2, O 20.11,
O 28.8, O 46.4, O 55.10, O 59.6,
O 94.3
- Boden, Dajo O 36.2
- Bodenschatz, Eberhard DY 4.1, DY 5.6
- Bodenschatz, Jonathan BP 28.28
- Boderius, Mathis MM 42.6
- Bodesheim, David •MM 3.10
- Bodlos, Rishi MM 37.4
- Bodnar, Stanislav •HL 15.1, MA 18.3
- Bodziony, Francisco CPP 44.2
- Boeglin, Alex O 2.6
- Boehm, M. MA 33.6
- Boehmer, Anna KFM 11.5
- Boekhoff, Cornelius MM 11.4
- Boesenberg, Ulrike MM 12.3
- Boettcher, Igor TT 17.5
- Bogdan, Mikhail MA 40.1
- Bogdanoff, Nils O 7.2, O 20.6, O 33.4
- Bogdanov, Nikolay A. •TT 21.4
- Boggenrieder, Stefanie O 48.2
- Bogush, Igor TT 3.12
- Bohamud, Tamam O 57.2
- Bohatý, Ladislav MA 44.5, TT 10.12
- Bohlemann, Chris Yannic •HL 7.8
- Bohm, Sebastian •DY 29.7
- Böhme, Frank CPP 35.42, CPP 58.5
- Böhme, Lisa DS 12.23, •HL 7.35
- Böhmer, Anna TT 10.11
- Böhmer, Jan •HL 7.54
- Böhmer, Michael CPP 17.30, CPP 51.4
- Bohnen, Tim CPP 17.54
- Böhner, Lukas CPP 18.8, CPP 35.30,
O 58.1
- Böhning, Martin CPP 20.4
- Bohomolov, Danylo •HL 44.6
- Bohorquez, Laura MA 44.8
- Bohorquez, Laura Teresa Corredor
MA 40.57
- Boineau, Frédéric VA 1.4
- Boix, Virginia O 56.8
- Bojarski, Patryk A. SOE 6.3
- Bojer, Mareike DY 45.8
- Boldt, Regine CPP 19.7, CPP 35.28
- Bolhuis, Peter G BP 3.9
- Boliasova, Olha •MA 23.79
- Boll, Torben HL 7.7, MM 23.32
- Bolle, Frederik TT 58.28
- Bollmann, Steffen •TT 31.12
- Bolsmann, Katrin •MA 15.2
- Boltynjuk, Evgeniy •MM 28.7
- Boltz, Horst-Holger BP 24.6, DY 38.6
- Bomers, Mario PSV 10
- Bommert, Max •O 10.4
- Bonafé, Franco P. O 6.7
- Bonalde, Ismarco TT 37.8
- Bonanni, Alberta HL 22.1
- Bondan, Erdem BP 11.5
- Bondino, Federica O 47.4
- Bondzio, Laila MA 37.3, •MA 40.45
- Boneberg, Johannes TT 16.3
- Boneß, Daniel •TT 18.4
- Bonetti, Pietro TT 51.1
- Bonfanti, Silvia •MM 33.7
- Bonitz, Michael •O 31.5, O 31.7,
•TT 22.1
- Bonkhoff, Martin TT 45.8, TT 59.17
- Bonn, Daniel BP 30.1
- Bonn, Doug MM 6.7
- Boorman, Tobias •DY 21.5
- Bootz, Philipp •HL 45.4
- Boras, Dominik •KFM 9.4, •KFM 11.3,
KFM 11.6
- Borchers, Andre MA 23.13
- Borchert, Anna Juliane HL 4.3
- Borchert, Juliane HL 4.7
- Borchert, Martin MA 40.39
- Bordacs, Sandor MA 23.13, MA 40.51
- Borgens, Peter O 21.2
- Borgmann, Ralf •HL 7.6, HL 51.1,
HL 51.7
- Borie, Benjamin MA 17.2
- Borisenko, Sergey TT 57.9, TT 57.11
- Boriskovsky, Dima DY 27.1
- Borisov, Vladislav •MA 47.3, •MA 47.6
- Borissov, Andrei G. O 76.2
- Borlido, Pedro MM 31.7
- Born, Artur MA 8.9, O 85.1
- Born, Philip •DY 7.3
- Borne, Vincent •BP 28.4
- Bornemann, Steffen HL 33.44
- Börner, Georg •SOE 4.9
- Bornholdt, Stefan DY 45.16, SOE 6.1
- Borrmann, Horst MM 6.10
- Börsch, Michael BP 21.2
- Borsos, Andrés SOE 22.3
- Bort, Lara DY 56.11
- Bortis, Amadé KFM 1.7
- Boruta, Michał SOE 4.7
- Borynskiy, V. MA 16.6
- Börzsenko, Yelyzaveta A. MA 18.6
- Börzsönyi, Tamás DY 7.7
- Bosche, Jonas BP 12.6
- Bose, Arnab MA 4.7, •MA 41.5, TT 7.7
- Bose, Sanghita •SOE 4.3
- Boselli, Matteo TT 39.10
- Bosi, Marco DY 42.17
- Bosoni, Emanuele HL 6.1, O 9.1
- Bossak, Alexei MM 23.34
- Bosse, Harald O 12.4
- Bossert, Marine •CPP 52.2,
•MM 23.27
- Bostelmann, Marc •HL 50.8
- Boström, Emil TT 64.7
- Botana, Antia TT 44.5
- Bothner, Daniel •TT 39.1, TT 39.5,
TT 58.18, TT 58.19
- Botti, S. HL 18.5
- Botti, Silvana HL 5.4, HL 18.1,
MM 31.7, O 84.4, O 95.6, O 95.10,
TT 56.4, TT 68.6, TT 68.10
- Bötzel, Steffen •TT 50.7
- Bouaziz, Juba MA 27.4, •MA 39.1
- Boucaud, P. HL 43.6
- Bouchaud, Jean-Philippe •SOE 21.1
- Bouchet, Freddy DY 32.9
- Boudalis, AK MA 23.21
- Bougeard, Dominique TT 16.8
- Bouhon, Adrien O 94.1
- Bounds, Christopher HL 14.4
- Bourdarot, Frédéric MM 23.34
- Bourdon, Bjoern KFM 6.44
- Bourgon, Julie MM 33.2
- Bourret, Edith KFM 1.2, KFM 1.8,
KFM 4.5
- Bovensiepen, Uwe MA 8.7, MA 19.3,
O 8.3, O 16.2, O 16.9, O 19.1, O 19.6,
O 37.2, O 37.3, O 60.11
- Box, Connor L. O 46.1, •O 46.2
- Boy, Johannes HL 41.6
- Bozkurt, Ahmet Mert •MA 4.1, •TT 7.1
- Bozkurt, Mert HL 49.4
- Braatz, Thomas HL 48.2
- Brabec, Christoph CPP 11.5, CPP 36.1,
CPP 36.5, HL 25.3
- Brabec, Christoph J. CPP 1.11
- Brabec, Jiri O 45.6
- Bracht, Thomas •HL 7.39, HL 24.2,
HL 24.4, HL 24.5
- Brademann, Lennart AKC 1.3
- Braden, Markus MA 40.17, MA 40.19,
MA 44.5, TT 57.5
- Brader, Joseph DY 27.7
- Bradley, R Mark O 13.3
- Braga Ramos, Flávia •DY 48.8,
•TT 55.8
- Bramberger, Max TT 43.11
- Branch, Timothy W MM 6.7
- Brand, Hauke TT 64.5
- Brand, Izabella BP 1.6, BP 11.28
- Brandhoff, Jonas •O 22.3, O 22.9
- Brandl, Georg TT 58.29
- Brandner, Kay DY 6.5
- Brando, M. TT 42.13
- Brando, Manuel TT 28.3, TT 28.4,
TT 34.5, TT 52.6
- Brandstätter, Tom •BP 11.3, BP 28.29
- Brandstetter, Sebastian O 54.6
- Brandt, Martin S. HL 7.4, HL 33.38
- Brandt, Matthias BP 8.2
- Brandt, Oliver HL 7.40
- Braniste, Tudor HL 7.30
- Brant, William R. KFM 11.3
- Bräse, Stefan CPP 26.3
- Bratek, Dominik •HL 7.1, HL 7.2
- Bratschitsch, Rudolf HL 18.10
- Brauburger, Simon BP 8.9
- Brauch, Uwe HL 12.5
- Braud, Nicolas O 74.1
- Braun, Dieter BP 10.2, BP 10.6,
BP 10.9, BP 11.29, •BP 26.3
- Braun, Fiona HL 49.2
- Braun, Franziska •BP 11.4, CPP 3.4
- Braun, Frederic O 26.8
- Braun, Hannes •TT 5.2
- Braun, Jürgen O 59.5
- Braun, Nils DS 12.44, •DS 12.46
- Braunbeck, Georg HL 50.1
- Braunecker, Bernd DY 21.5, TT 48.6
- Bräuninger, Sascha A. •TT 43.4
- Braunschweig, Björn CPP 35.51,
CPP 35.59, CPP 53.5, O 60.7, O 69.6
- Bray, Simon BP 3.8
- Brazda, Thorsten HL 22.2, TT 25.1
- Bredas, Jean-Luc CPP 17.5
- Brede, Thomas •MM 18.3, MM 23.7,
MM 23.14, MM 23.15, •MM 23.33
- Bredol, Philipp HL 3.9, HL 10.6,
•HL 10.8
- Bredow, J. HL 7.20
- Bredow, Jorrit DS 10.4, DS 12.12,
•DS 12.54
- Bredow, Thomas DS 12.41
- Breer, Fiete •KFM 6.41, KFM 14.5
- Brehm, Lucas BP 28.5
- Brehm, Simon •MM 12.19
- Brehm, Verena •MA 29.3
- Brehmer, Paul •TT 5.4
- Breitbach, David •MA 16.5, MA 23.44,
MA 23.74, MA 40.33
- Breitfelder, Sebastian KFM 11.6
- Breitner, Franziska TT 46.10, •TT 52.2
- Brem, Samuel O 34.2, O 34.4
- Bremer, Lucas HL 49.6
- Bremerich, Alice O 18.8
- Bremers, Heiko HL 33.41, HL 33.43,
HL 51.2, HL 51.8
- Brems, Maarten BP 17.7, MA 12.8
- Brems, Maarten A. MA 2.2, MA 23.2,
MA 23.3, MA 23.6, •MA 29.1,
MA 47.2
- Brener, Sergey HL 40.1, O 79.1,
TT 63.4
- Brenig, W. TT 52.3
- Brenig, Wolfram TT 42.17, TT 42.18,
•TT 52.1
- Brenneis, Luisa •HL 33.60
- Brenner, Günter O 16.1
- Brenner, Maxwell J. MM 36.9
- Breoni, Davide •DY 26.8
- Breslavets, Oleksiy MM 12.9
- Breslin, Vivian N. O 75.5
- Brett, Calvin J. BP 19.1, BP 19.2,
CPP 41.1, CPP 41.2, MA 38.5
- Breu, Josef O 76.9
- Breuer, Lars O 5.7, •O 13.4, O 13.5,
O 13.7, O 24.4, O 31.6
- Breuer, Michael VA 1.3
- Breunig, Oliver TT 36.4
- Brezina, Krystof •O 55.9
- Brezinova, Iva TT 22.1
- Bridger, Manuel O 60.11
- Briega Martos, Valentin O 96.4
- Briega-Martos, Valentin O 73.2
- Brieger, Emily •BP 28.29
- Brill, Lorenz O 36.9
- Brill, Wolfgang BP 26.7
- Brinckmann, Steffen MM 4.6, MM 9.6
- Bringa, Eduardo DY 29.4, MM 22.1,
MM 26.5
- Brink, Tobias •MM 26.1
- Brinker, Manuel MM 23.21, •MM 42.3
- Brinker, Sascha O 33.5
- Brinkman, Alexander MA 4.1, TT 7.1
- Brinkmann, Kai-Thomas HL 7.21
- Brinkop, Achim BP 13.4, BP 21.1
- Brisch, Jonathan DY 37.6
- Britt, Tristan CPP 17.8
- Brixner, Tobias HL 33.60, O 58.5,
O 80.4
- Broad, William •TT 9.1
- Brocker, Kathrin •CPP 36.2
- Brockhauser, Sandor DS 13.3,
•O 84.6, O 95.1, O 95.3, •TT 56.6,
TT 68.1, TT 68.3
- Brockmann, Dirk •SOE 5.1
- Broedersz, Chase BP 11.3, DY 27.10
- Broedersz, Chase P. BP 28.29,
BP 31.5
- Broekhoven, Rik •TT 8.8
- Bröker, Stephan BP 24.4, DY 38.4
- Brommer, Peter MM 40.1
- Bronsch, Wibke O 16.3, •O 19.2,
O 19.4, •O 34.8, O 34.10
- Bronstein, Hugo CPP 1.5
- Brooks, Annabelle TT 3.6
- Brooks, Charles TT 44.5
- Brooks, Nickolas B. TT 4.10
- Brosco, Valentina DS 5.2
- Brötzner, Johannes •O 13.2
- Brouder, Christian TT 43.18
- Brouwers, Rebecca BP 16.1
- Brown, S. E. TT 28.6, TT 57.19
- Brox, Olaf HL 23.2
- Brücher, Eva DS 5.4, HL 21.2
- Bruchmann-Bamberg, Vitaly DS 14.3
- Brückel, Thomas DS 12.25, DS 14.6,
MA 5.6, MA 40.16, O 42.12, TT 23.8
- Bruckhoff, Mike Jos •MA 46.6
- Bruckmann, Christian •O 32.1
- Bruckmoser, Niklas TT 39.7, •TT 49.5,
TT 54.8, TT 58.6, TT 58.7
- Brückner, David •BP 2.4, BP 11.3
- Brückner, Sebastian HL 25.11,
•O 95.4, O 95.5, •TT 68.4, TT 68.5
- Bruder, Enrico KFM 2.3, KFM 2.5,
MM 9.7
- Bruetting, Wolfgang CPP 28.4,
TT 32.4
- Brugués, Jan BP 30.8
- Bruin, Jan TT 42.14
- Brumme, Thomas HL 1.5, HL 34.7,
MA 7.7
- Brummel, Olaf O 29.2, O 73.2
- Brune, Harald O 15.12
- Brune, Yannik •HL 33.26
- Brunhuber, Christoph •HL 7.31
- Brünig, Florian •BP 27.1, •CPP 2.11
- Brüning, Daniel MA 44.5
- Brüning, Reiner •O 50.1
- Brunner, Daniel DY 17.7, HL 12.7,
HL 43.5
- Bruno, Alessandro HL 3.1
- Brunold, A. •TT 57.27, TT 57.28
- Brunold, Axel TT 57.26
- Bruns, Sebastian MA 28.1
- Brunst, Daniel MA 33.7
- Brunthaler, Michael O 92.10
- Brütting, Fabian •HL 7.59
- Brütting, Wolfgang CPP 17.12,
CPP 18.10, HL 7.25
- Bryja, Hagen DS 12.46
- Buca, Dan HL 18.3, HL 18.9
- Buccheri, Alexander HL 6.2,
MM 12.25, O 9.2
- Buch, Marcel DS 12.45
- Buchberger, Sebastian •O 34.9,
O 94.6
- Bucher, Dominik BP 10.2
- Buchhold, Michael DY 48.5, TT 55.5
- Buchholz, Cara CPP 19.12
- Buchholz, Christopher •HL 7.60
- Buchholz, Christopher Henrik HL 37.2
- Buchinger, Quirin HL 24.13
- Büchl, Adrian •BP 11.52
- Buchleitner, Andreas DY 43.5
- Büchner, B. KFM 11.9
- Büchner, Bernd MA 10.5, MA 23.35,
MA 32.2, MA 38.2, MA 40.59,
MA 48.6, O 49.5, TT 10.9, TT 10.10,
TT 12.5, TT 16.2, TT 18.3, TT 29.2,
TT 30.9, TT 43.3, TT 46.5, TT 52.8,
TT 57.9, TT 57.10, TT 57.11, TT 58.27,
TT 62.1
- Buchner, Florian O 6.10, •O 81.2
- Büchner, Robby MA 8.9
- Buckel, Alexander KFM 11.3
- Buczek, Pawel DS 12.26, MA 23.12,
MA 23.31, MA 27.6, MA 40.62
- Budanur, Burak DY 37.6
- Budanur, Nazmi Burak DY 5.2,
•DY 29.1, SOE 6.1
- Budde, Ina HL 27.3, O 62.3, TT 40.3
- Budich, Jan HL 31.1, O 61.1, TT 17.6
- Budich, Jan Carl DY 44.1
- Bud'ko, S. L. TT 6.4, TT 34.13
- Budniak, A. K. DS 7.2, MA 40.53
- Buechner, Bernd MA 40.57
- Buettner, Felix MA 43.6
- Bugiel, Michael BP 23.5

Author Index

- Buhl, Janek MM 26.7
 Bühler, Dominik D. HL 10.3
 Bühler, Jonas +HL 16.9, HL 50.12,
 •TT 24.9
 Bühlmeier, Hanna •O 69.9
 Buhmann, Hartmut HL 5.3, HL 11.4,
 HL 11.7, HL 30.4, HL 33.61, TT 15.4,
 TT 15.7, TT 17.1, TT 41.4
 Buhot, Jonathan TT 3.6
 Bui, Hong •O 15.3
 Bui, Mihn TT 25.1
 Bui, Minh HL 22.2
 Bui, Thanh Quynh BP 21.9
 Bui Thi, Hong •O 15.6
 Bui-Le, Quangminh •DY 46.3
 Bukas, Vanessa J O 3.4, O 96.1,
 O 96.3
 Bükér, Björn MA 23.42
 Bulai, Georgiana DS 12.9
 Bullerjahn, Jakob Tómas •BP 27.9
 Bulut, Nebahat HL 33.8, •MM 12.16,
 •MM 23.2
 Bulut, Yusuf CPP 13.9, CPP 17.4,
 CPP 17.26, CPP 17.35, •CPP 29.8,
 CPP 36.6, CPP 52.5
 Bunch, David TT 49.5
 Bundaleski, Nenad VA 1.4
 Bunk, Benito HL 7.13
 Bunk, Carolin CPP 35.42, CPP 58.5
 Bunney, Matthew •TT 63.9
 Bünnte, Judith •MA 23.42
 Bunz, Uwe DS 15.2
 Bunz, Uwe H. F. O 10.7
 Burchert, Jan-Philipp •BP 28.1
 Burda, Daniel •VA 2.1
 Bureković, Sumeja •DY 46.9
 Burger, Carolina •TT 10.3
 Bürger, Friedrich •DS 12.29
 Bürger, Ludwig •BP 10.4
 Bürger, Sabine CPP 29.3
 Bürger, Sven HL 33.48, HL 33.50,
 HL 37.5, KFM 6.34
 Bürgerhammer, Manfred BP 28.2
 Burghard, Marko DS 10.3
 Burgholzer, Katharina HL 22.1
 Bürgler, D.E. O 2.8
 Bürgler, Daniel MA 22.4
 Burkard, Guido •HL 9.1, HL 9.3,
 HL 29.8, HL 37.9, •TT 14.1, TT 14.3
 Burkart, Tom •BP 22.8
 Burkert, Oliver BP 17.8
 Burkhardt, Ulrich MA 32.2
 Burkhart, Ines BP 11.21, BP 26.4
 Burset, Pablo TT 36.10, TT 48.5
 Burwitz, Vassily CPP 35.4, KFM 6.24
 Burwitz, Vassily Vadimovitch
 •DS 14.5, KFM 9.10
 Buß, Lars O 64.8, •O 74.1, O 78.9,
 O 93.7
 Buscema, M. HL 33.62
 Busch, Ingo O 12.4
 Busch, Kurt DY 22.4
 Busch, Mark MM 42.6
 Busch, Oliver •MA 8.6, MA 8.8
 Busch, Ralf MM 28.2
 Busch, Sebastian MM 27.10, MM 36.6
 Buschbeck, Robin •KFM 6.35
 Büscher, Florian TT 30.8, TT 64.8
 Büscher, Markus MA 22.4
 Busiello, Daniel Maria •BP 16.6
 Buss, Florenz O 11.5
 Buss, Jan-Heide HL 48.2
 Buss, Lars O 67.8
 Busse, Carsten O 18.8, O 36.11,
 •O 56.3, O 56.6, O 56.9, O 74.8
 Busse, Madleen BP 28.1
 Butcher, Tim A. •MA 43.3
 Butkevich, Andrey •CPP 18.4,
 CPP 35.35
 Butsic, Van DY 49.4
 Butt, Hans Jürgen CPP 52.1
 Butt, Hans-Jürgen CPP 19.10,
 CPP 35.9, CPP 35.62, CPP 35.65,
 •CPP 44.2, CPP 44.10, O 12.2
 Buttenschön, Sönke •O 69.12
 Butterling, Maik CPP 35.17, DS 6.1,
 DS 14.5, HL 5.5, KFM 6.30, •KFM 9.5,
 KFM 9.8, KFM 9.10, MA 31.7
 Büttner, F MA 31.1
 Büttner, Simon •O 58.5
 Buyan-Arivjikh, Altantulga •CPP 17.43
 Buzzi, Michele TT 62.7
 Bykov, E. •MA 23.19
 Bykov, Eduard MA 23.18, MA 42.3
 C. A. Taylor, Victoria MA 46.11
 C. Peets, Darren MA 44.7
 C. Souza, Jean MA 39.3
 Cabrera Galicia, Alfonso Rafael
 •HL 50.9, HL 50.11
 Cacho, Cephise O 59.8
 Caci, Nils DY 49.7, •TT 29.9, TT 29.10,
 TT 29.11
 Caciuc, Vasile O 36.11
 Caciuffo, Roberto TT 9.5
 Cadart, Timothee O 45.6
 Cadenbach, Thomas HL 7.32,
 •HL 41.5
 Cadore, Alisson HL 22.4
 Cagnon, Laurent CPP 52.2, MM 23.27
 Cahen, David HL 25.8
 Cahlik, Ales MA 19.7, •O 28.7, O 55.4,
 O 70.3, O 77.8
 Cai, Jiaqi O 18.8, O 36.11, O 56.3,
 O 56.9
 Cai, Shuning O 6.8, O 54.3, O 66.10,
 O 87.4
 Cakaj, Albin •HL 7.25
 Cakmak, Burak DY 11.5, TT 13.5
 Calabrese, Justin M. SOE 4.8
 Calarco, Tommaso HL 37.7, HL 50.7
 Calati, Stefano O 34.3
 Calcinelli, Fabio •O 82.3
 Caldas, Lucas O 52.1
 Calder, Stuart TT 9.8
 Caldwell, Joshua D. O 58.6
 Callsen, Gordon HL 36.6, HL 51.5
 Caltzidis, Ioannis HL 22.1, HL 33.31,
 HL 33.35
 Calvi, V. •HL 33.62
 Calvo, Rubén SOE 17.1
 Calzona, Alessio DY 44.11
 Camacho Ibarra, Oscar HL 7.47,
 •HL 33.31, HL 33.35
 Camp, Philip J. CPP 57.12
 Campen, R. Kramer O 25.2, O 60.11
 Campen, Richard Kramer O 30.10
 Campi, Filippo HL 48.2
 Canavan, Mark O 15.2
 Candia, Adriana O 82.5
 Canfield, P. C. TT 6.4, TT 34.3
 Cangil, Attila •HL 6.4, HL 6.5,
 MM 12.11, MM 12.26, MM 31.8,
 •O 9.4, O 9.5
 Cano, Andrés •TT 44.7
 Canola, Sofia O 10.3, •O 76.3
 Cañón Bermúdez, Gilbert Santiago
 MA 40.47, MA 49.6, MA 49.7,
 MA 49.8
 Canos Valero, Adria O 91.2
 Canova, Filippo Federici O 66.10
 Cantin, Jean-Louis HL 33.28
 Cao, Jiayuan TT 3.5
 cao, lei MA 40.16
 Cao, Nan O 11.6, •O 11.9
 Cao, Qi-Tao DY 21.3
 Cao, S. X. MA 18.4
 Cao, Wei CPP 17.38, MA 38.5
 Cao, Xin DY 16.6
 Capellini, Giovanni HL 18.3, HL 18.9,
 HL 37.6, KFM 9.6
 Caprini, Lorenzo •DY 32.6
 Caraglio, Michele BP 11.1, DY 42.4,
 DY 42.13
 Carbogno, Christian SYUE 1.2, HL 4.8,
 HL 13.3, HL 36.3, HL 40.4, HL 41.1,
 HL 47.1, MM 31.2, MM 31.6, MM 36.7,
 O 17.3, O 79.4
 Carbone, Gerardina TT 37.10
 Carbone, Maurizio DY 5.7
 Cardenas-Gamboa, Jorge •MM 12.5
 Cardias, Ramon MA 20.7
 Cardinali, G. HL 23.1
 Cardinali, Giulia •HL 23.5, HL 44.5
 Cardoso, Claudia •HL 20.3, HL 26.4,
 •O 35.3, O 53.4
 Cardozo, Edson HL 10.10
 Carenza, Livio BP 4.9
 Carey, Spencer J. O 78.1
 Carrillo-Aravena, Eduardo O 94.2
 Carini, Giulia O 58.4, •O 58.8
 Carl, Max Vaßen TT 59.6
 Carlin, Jean-François HL 36.6,
 HL 51.5
 Carlos, Marques BP 1.8
 Carlson, Chelsea HL 1.4
 Carlucci, Riccardo •SOE 19.3
 Carnazza, Francesco •TT 43.33
 Carnio, Edoardo DY 43.5
 Carollo, Federico TT 43.33
 Caron, Luana MA 23.16, MA 23.17,
 MM 12.30
 Carpenter, Michael MA 32.1
 Carr, Stephen TT 53.9
 Carrasco, Carolina •BP 23.11
 Carrascoso, Felix HL 33.4
 Carrère, Adrien BP 22.10
 Carrete, Jesús O 6.10, O 81.2
 Carrez, Philippe •KFM 2.4
 Carrico, Pedro MM 31.7
 Carrillo-Cabrera, Wilder MM 26.9
 Carstens, Niko CPP 56.2
 Cartus, Johannes MM 31.5, O 28.10
 Cartus, Johannes J. O 4.6, O 28.1
 Caruso, Fabio SYUE 1.2
 Carva, Karel •MA 21.4
 Casademunt, Jaume BP 30.4
 Casanova, Felix •SYHS 1.4
 Casari, Carlo S. O 15.12
 Casilius, Mathias DY 16.2
 Caso, Diego TT 20.10
 Caspari, Verena •O 21.1
 Caspers, Juliana •DY 16.1, DY 16.4,
 DY 16.7
 Cassabois, Guillaume MA 32.6
 Cassol, Francesco •TT 43.15
 Castellanos-Gomez, Andres HL 33.4
 Castro, Catherine CPP 43.1
 Casu, Maria Benedetta DS 3.3, DS 3.4
 Casula, Michele DY 43.20, TT 16.6,
 TT 43.14, TT 43.15
 Catalan, Gustau DS 6.3, •KFM 4.7
 Catalan, Rodrigo •BP 25.6
 Catalano, Rachele •BP 11.48
 Cates, Michael E. BP 24.4, DY 38.4
 Catindig, Gerald Angelo HL 17.6
 Cats, Peter CPP 29.4
 Caulfield, Lachlan O 81.5, •O 81.6
 Causer, Grace MA 40.41
 Cavalleri, Andrea TT 62.2, TT 62.7
 Caviglia, Andrea •MA 34.5
 Cavina, Vasco DY 23.4
 Cazailia, Miguel Angel TT 8.3
 Cebrat, Aleksandra •O 73.6
 Cedervall, Johan MA 47.6
 Ceolin, Marcelo DY 16.11
 Ceratti, Davide HL 25.8
 Cerda-Donate, Elisa BP 6.3
 Čermák, Jan CPP 36.9
 Čermak, Patrik O 65.1
 Černák, Juraj TT 43.5
 Černý, Miroslav MM 32.7
 Cerqueira, Tiago MM 31.7
 Cerreta, Andrea MA 40.40
 Cerullo, G. HL 48.4
 Cerullo, Giulio HL 34.8, KFM 3.1
 Chab, Vladimir O 65.1
 Chacon, Alfonso TT 3.8
 Chagas, Thais O 36.11, O 56.3,
 •O 56.9, O 74.8
 Chahare, Nimesh BP 4.8
 Chahare, Nimesh Ramesh •BP 4.5
 Chahib, Outhmane O 38.4, •O 45.3
 Chahshouri, Fatemeh O 83.7
 Chakraborti, Subhadip •BP 9.9
 Chakraborty, A. KFM 11.9
 Chakraborty, Nilotpal •DY 55.2,
 •MA 23.10, •TT 67.2
 Chakraborty, Poulami MM 37.7
 Chakraborty, Ritam O 11.3
 Chakraborty, Shauri DY 42.10
 Chakraborty, Snigdha CPP 35.24
 Chakraborty, Subrata TT 20.6,
 •TT 27.10
 Champion, Yannick •MM 35.1
 Chan, Karen O 96.3
 Chan, Yu-Te •O 59.10
 Chandrabose, Sreelakshmi HL 2.4
 Chaneliere, Thierry PLV X
 Chang, Chun-Fu HL 51.3, HL 51.6,
 TT 9.3, TT 30.6, TT 30.7, TT 50.1
 Chang, Hung-Tzu •HL 48.5, O 83.4
 Chang, Johan KFM 9.7
 Chang, Po-Chun TT 23.5
 Chang, Tay-Rong MA 10.6, TT 12.6
 Chang, Yoohyun BP 11.40
 Chang, Yu-Cheng TT 66.1
 Changiarath Sivasadan, Arya BP 3.4
 Chao, Youchuang •CPP 35.63
 Chao, Yu-Chen BP 2.2
 Charabarty, Poulami MM 15.9
 Chardès, Claire BP 15.6
 Charitart, Thierry BP 1.12
 Charkina, Oksana •MA 40.1
 Charsooghi, Mohammad BP 6.3
 Chassé, Thomas DS 12.8
 Chatterjee, Anasua HL 33.27
 Chatterjee, Atasi O 82.7
 Chatterjee, Rakesh •BP 11.59,
 BP 12.11
 Chatterjee, Ratnamala MA 23.21,
 MA 37.2, MA 40.18, TT 43.6, TT 57.7
 Chatterjee, Swarnajit BP 7.2,
 •BP 9.10, DY 10.2
 Chattopadhyay, S. MA 40.58
 Chattopadhyay, Sumanta MA 44.6
 Chaturvedi, Raghav TT 35.1
 Chaudhary, Abdullah R. BP 25.8
 Chaudhary, Swati DS 7.5
 Chaudhuri, Joydip •CPP 12.7
 Chaudhuri, Shayantan •O 29.7
 Chauhan, Balwant Singh •MA 23.21
 Chauleau, Jean-Yves MA 11.1
 Chauraud, Dimitri MM 41.5
 Chaves, Andrey DS 2.1
 Chavez Rojas, Daniel BP 17.3
 Che, Ping MA 12.6
 Chechkin, Aleksei DY 44.10
 Chechkin, Aleksei V. DY 56.4
 Checkelsky, Joseph G. O 16.3
 Chepesh, Yevheniia TT 38.5
 Chekhonin, Paul HL 41.2
 Chekhova, Maria •HL 35.7
 Chellali, Reda MA 3.1
 Chellu, Abhiroop HL 49.7
 Chemelli, Angela CPP 57.7
 Chen, Ao •DY 2.8, •TT 2.8
 Chen, Bingjie •HL 29.1
 Chen, Caiyun MA 10.4, TT 12.4
 Chen, Chien-Te HL 51.3, HL 51.6,
 TT 4.10, TT 30.6
 Chen, Chi-Sheng TT 30.3
 Chen, Chun-Hsien O 66.5
 Chen, H. O 45.4
 chen, hongyan •MA 19.5
 Chen, Jianjun DY 21.3
 Chen, Jianpeng •TT 58.8
 Chen, Jiasheng TT 4.11, TT 4.12,
 TT 34.5, •TT 34.6, TT 59.14
 Chen, Jie •MM 22.4
 Chen, Jinghao O 37.2, O 37.3
 Chen, Kai MA 19.6
 Chen, Ke •MM 8.6
 Chen, Pin-Chuan •DY 4.9
 Chen, Qing DS 12.34
 Chen, Shouzheng •CPP 29.5,
 CPP 35.1
 Chen, Si •CPP 1.8
 Chen, Siyu BP 10.9, BP 28.40
 chen, wanyu DY 25.7, O 8.8, •O 37.12,
 TT 33.7
 Chen, Wei BP 19.1, CPP 17.38,
 CPP 29.2, CPP 41.1
 Chen, Weimin DS 16.6
 Chen, Wenjie TT 52.9
 Chen, Xi •BP 29.5
 Chen, Xu MM 37.2
 Chen, Yi O 15.6
 Chen, Yong O 47.9
 Chen, Yuchao BP 2.2, BP 30.3
 Chen, Yunfei O 4.5
 Chen, Zhi O 11.9
 chen, ziang HL 47.5
 Cheng, Bingqing MM 8.6
 cheng, erjian •TT 59.11
 Cheng, Peng O 66.6
 Cheng, Ya-jun CPP 17.50, CPP 29.2,
 CPP 35.15, CPP 35.16
 Cheng, Yongqiang TT 9.8
 Cheng, Yu DS 14.2
 Chennur, Madhuri HL 42.2, •HL 42.3
 Cheong, Sang-Wook TT 3.2, TT 51.6
 Cherasse, Marie HL 17.9
 Cherepanov, Vasily O 21.2, O 66.9
 Cherevko, Serhiy O 73.2, O 96.4
 Chernikov, Alexey DS 1.6, DS 2.4,
 HL 34.3
 Chernov, S. MM 12.1
 Chernyavsky, Dmitry MM 12.37,
 TT 6.11
 Chernyshev, Alexander L. TT 52.4
 Cherstvy, Andrey G. DY 44.6
 Chervanyov, Alexander •CPP 13.4
 Cheula, Raffaele O 52.4
 Chi, Lifeng O 32.2, O 40.2
 Chi, Songxue TT 9.8
 Chiang, Cheng-Tien O 51.6
 Chiang, Kuan-Hsun TT 66.1
 Chiang, Kuo-Yang O 6.5
 Chiappini, Leonardo CPP 35.61
 Chiari, Luca KFM 9.5
 Chiatti, O. •TT 3.4
 Chichinadze, Dmitry TT 35.4
 Chigrin, Dmitry O 91.8
 Chigrin, Dmitry N. O 58.4
 Chillal, Shravani TT 46.7
 Chimeh, Abbas •O 75.2
 Chinnakanna Muruga, Lokesh
 •CPP 35.24

Author Index

- Chioncel, Liviu MA 27.3
 Chirala, Rajesh •O 92.2
 Chirita Mihaila, Marius Constantin
 O 13.8
 Chirkova, Alisa MA 3.4, MM 12.28
 Chirkova, Alisa M. MA 42.6
 Chitov, Gennady Y. TT 31.3
 Chiu, Ching-Hung •TT 16.9
 Chiuzbajan, Gheorghe Sorin TT 3.7,
 TT 57.3
 Cho, Changsoon DS 10.2
 Cho, Eunkyung CPP 17.5
 Cho, Yeongsu DS 1.6
 Chochos, Christos L. CPP 43.2
 Choi, Dasom O 20.8
 Choi, Eun Sang MA 9.7
 Choi, Gyung-Min MA 4.10, TT 7.10
 Choi, K. Y. TT 52.3
 Choi, Kwang-Yong MA 40.23
 Choi, Luka HL 22.3
 Choi, Nuri •MM 41.4
 Choi, Sangjun HL 31.1, O 61.1, TT 63.7
 Choi, Wonjune •TT 47.9
 Choi, Won-Young MA 4.2, TT 7.2
 Choi, Woojae TT 9.7
 Choi, Young-Gwan •MA 4.10, •TT 7.10
 Cholsuk, Chanaprom DS 2.5
 Chotorlishvili, Levan MA 23.12
 Chou, Ta-Shun DS 8.5
 Choubey, Peayush •TT 20.5
 Choudhary, Akash •DY 31.12
 Choudhary, Ankita HL 7.48, •HL 7.63,
 HL 24.9
 Choudhary, Kamal HL 26.1, O 53.1
 Choueikani, Fadi O 36.5
 Choueiri, George DY 29.1
 Christ, Andreas •O 2.2, O 46.4,
 O 55.10
 Christ, Simon •BP 11.22, BP 26.2
 Christen, Jürgen HL 7.6
 Christensen, Dennis •O 46.7
 Christensen, Morten •TT 23.2
 Christiansen, Ruben O 20.2, O 33.9
 Christiansen, Dominik DS 12.30,
 HL 35.6
 Christiansson, Viktor •TT 50.4
 Christoph, Jan O 64.7
 Christovam, Denise TT 9.4
 Christovam, Denise S. •TT 9.5
 Chrostowski, Lukas HL 49.5
 Chryssos, Leon •KFM 6.24
 Chu, Hao TT 3.5
 Chu, Yiwen •HL 3.1
 Chuang, Hsiang-Ling •O 66.5
 Chubukov, Andrey TT 35.4
 Chudzinski, Piotr TT 22.8, TT 45.4
 Chulanova, Elena CPP 17.53,
 •CPP 29.7
 Chulliparambil Shaju, Sandra
 •MA 23.15
 Chumakov, Andrei CPP 17.56,
 CPP 51.1, DS 12.34, •MA 38.5, O 57.5
 Chung, Simon O 16.1, O 29.6, O 42.11,
 O 56.6, O 83.2, O 92.3
 Churikova, A MA 31.1
 Chushkin, Yuriy BP 29.3
 Chyzyhkova, Anastasiia TT 17.6
 Ciandrini, Luca BP 11.70
 Ciarchi, Matteo BP 29.7
 Cibotaru, Sandu DS 12.9
 Cichetto Jr., Leonèlio MA 11.2
 Cichon, Stanislav O 65.1
 Cichos, Frank CPP 43.3, DY 4.9
 Cichutek, Niklas •TT 47.12
 Cicuta, Pietro BP 16.1
 Ciers, J. HL 23.1
 Ciers, Joachim HL 23.5, HL 51.5
 Ciesielski, Richard O 43.1
 Cilentò, Federico O 16.3, O 19.2,
 O 19.4, O 34.8, O 34.10
 Cimalla, Volker HL 50.4
 Cimiano, Philipp MM 12.30
 Cimpoesu, Nicanor DS 12.9
 Cimurs, Janis MM 8.1
 Cinchetti, Mirko HL 17.10
 Ciobanu, Anca HL 36.2
 Ciobanu, Vladimir •HL 7.30
 Ciola, Riccardo •MA 12.6
 Cisternas, M. BP 11.10, BP 11.11,
 BP 11.12
 Ciubotariu, Oana T. DS 14.1
 Ciubotaru, Florin MA 34.7
 Ciuculkaitė, Agnė MA 22.5
 Civita, Donato •O 25.4
 Çivitioğlu, Burak •DY 22.2
 Cizek, Rebecca •O 64.2
 Čizmár, Erik MA 13.9, TT 19.9,
 TT 43.5, TT 58.24
 Claassen, Martin SYUE 1.5, TT 63.5
 Claessen, Ralph DS 1.3, O 36.12,
 O 94.7, •O 98.1, TT 30.9, TT 43.8
 Claeys, Pieter W. DY 9.1, DY 43.3
 Clark, Jenny CPP 43.3
 Clarke, Michael O 93.8
 Claro Rodriguez, Juan Nicolas
 •BP 28.16
 Classen, Laura •TT 35.4, TT 53.5
 Claude, Dimo DY 43.16, •TT 22.8
 Claudia, Kofahl •KFM 13.3
 Claus Michael Schneider, Claus
 DS 12.1
 Claus, Ralf •TT 42.14
 Claussen, Jens Christian •DY 4.11,
 •SOE 4.10, •SOE 15.2
 Cleland-Host, Kaedon O 75.5
 Clemens, Olivier TT 44.7
 Clement, Antoine MM 33.2
 Clement, Eric CPP 57.1
 Clement, J. H. BP 11.7
 Cleres, Luise HL 27.3, O 62.3, TT 40.3
 Clua-Provost, Tristan MA 32.6
 Clulow, Rebecca MA 47.6
 Cobet, Christoph •DS 15.1
 Cobet, M. HL 23.1
 Cobet, Munise HL 23.5
 Cocchi, Caterina CPP 17.34,
 CPP 18.3, HL 25.8, MM 16.8
 Cocco, Caterina O 16.8
 Cocco-Magnard, Pierre MM 22.1
 Cocconi, Luca •DY 34.4
 Cocean, Alexandru DS 12.9
 Cocean, Georgiana DS 12.9
 Cocean, Iuliana DS 12.9
 Cochet-Escartin, Olivier BP 22.10
 Cocker, Tyler L. O 75.5
 Codutti, Agnese BP 6.3, •DY 31.1
 Coenen, Peter O 21.2, O 66.9
 Cohen, Kobi O 80.3
 Cohen, R. E. KFM 1.3
 Cohn, J. L. MA 33.6
 Cohn, Ryan MM 26.2
 Cojocariu, I. DS 7.2
 Colazzo, Luciano O 15.12, O 20.8,
 O 50.3
 Coldea, Radu TT 29.5
 Cölfen, Helmut MM 23.12
 Collard, Ylona DY 31.8, DY 31.9
 Colling, Maurice •MA 40.21
 Collins, Brian CPP 11.4
 Collomb, David O 15.10, O 20.3
 Colom, Rémi KFM 6.34
 Colson, Dorothee MA 11.1
 Comin, Riccardo O 16.3
 Concepción, Omar HL 18.3, HL 18.9
 Confalone, Tommaso DS 5.2,
 DS 12.20
 Connolley, Lara •BP 12.12
 Conrads, Lukas •O 49.8, O 70.5,
 O 91.8
 Conroy, Shelly MM 4.7
 Consejo, C. HL 17.8
 Consiglio, Armando O 94.2
 Constance köst, Victoria HL 33.20
 Constante, Gissela •CPP 8.8,
 •DY 29.3
 Constantinou, Anna P. CPP 8.2
 Constantinou, Procopios C. TT 27.4
 Contessi, Daniele TT 45.10
 Conti, Andrea O 54.6, O 54.8, •O 68.2
 Cook, Ashley MA 31.4, TT 36.7,
 TT 48.6
 Cook, Ashley M. MM 41.6
 Cook, Jacob TT 53.9
 Copéret, Christophe MA 19.1
 Coquelin, Daniel BP 11.76
 Coraux, Johann MA 32.6
 Cordero-Edwards, Kumara •KFM 4.9
 Coria-Oriundo, Lucy DY 16.11
 Corley-Wiciak, Agnieszka A. HL 18.9,
 HL 37.6
 Corley-Wiciak, Agnieszka Anna
 •HL 18.3
 Corley-Wiciak, Cedric •HL 37.6
 Cornelius, Steffen •DS 13.2
 Corni, Stefano MM 3.8
 Coronado Mirales, Eugenio DS 4.6
 Coronas, Luis Enrique BP 22.11
 Corral-Rascon, Eduardo O 11.9
 Corte, Héctor CPP 36.7
 Cortes-Huerto, Robinson •CPP 12.1,
 DY 6.9
 Cortijo, Alberto HL 11.3, MA 39.5,
 TT 15.3
 Cosco, Francesco MA 22.1
 Cossio, Pilar CPP 2.8
 Costa, Andreas TT 27.5, •TT 27.6
 Costa, António •MA 20.4
 Costa Guedes, Beatriz •MA 7.7
 Coto, Pedro B. CPP 17.25
 Cottenier, Stefaan •HL 6.1, •O 9.1
 Courtois, Carla O 29.8
 Courtois, Hervé TT 20.1
 Covino, Roberto BP 3.9, •CPP 2.8
 Covre da Silva, Saimon HL 24.2,
 HL 24.4, HL 24.5, O 91.1
 Covre da Silva, Saimon F. HL 7.65
 Covre da Silva, Saimon Filipe HL 7.66
 Coy, Emerson O 16.7
 Cramer, Pierre-Louis BP 11.5
 Crawford, Janice BP 4.7
 Creed, Jack O 68.4
 Cremer, Jonas DY 31.1
 Cremer, Paul S. CPP 53.2
 Cremer, Sonja •DS 12.44, DS 12.46
 Crespo-Poveda, Antonio HL 3.4,
 HL 10.3
 Creutzburg, Marcus O 57.5, O 81.3,
 O 92.3
 Creutzburg, Nelson HL 7.51
 Crippa, Lorenzo TT 35.5, TT 35.6
 Cristea, Ligia Loreta DY 45.11
 Croitor, D. MA 40.14
 Cross, Sam •TT 3.6
 Croy, Alexander CPP 2.6, HL 36.1,
 •MM 3.9, MM 3.10, O 83.3
 Cruz Hidalgo, Raúl DY 7.7
 Csanyi, Gabor MM 15.3, MM 31.10,
 O 52.8, O 73.1
 Csizsár, Gábor MM 23.16
 Cubitt, Robert CPP 8.4, CPP 53.4
 Cuccu, Marzia •HL 34.3
 Cuenya, Beatriz Roldán O 52.1
 Cuevas, Juan Carlos MA 4.13,
 TT 7.13, TT 16.3, TT 57.15
 Cugini, Francesco MA 3.8
 Cui, Mengnan •MM 3.7
 Cui, Yin •MM 4.2
 Cuniberti, Gianuario CPP 2.6,
 HL 36.1, MM 3.9, MM 3.10, TT 11.4,
 TT 11.5
 Cuoco, Mario TT 37.10
 Cupak, Christian O 24.2
 Curcio, Davide O 6.3
 Curtarolo, Stefano MM 36.9, O 47.1
 Custers, Jeroen •TT 28.4
 Čutuk, Ana •HL 12.4, HL 12.5
 Cuvelier, Damien BP 31.2
 Cyganik, Piotr CPP 54.4
 Czajka, Titus •BP 29.3
 Czerner, Michael HL 51.4, MA 23.45
 Czernik, Stefanie •DY 2.1, •TT 2.1
 Czystanowski, Tomasz HL 33.49
 D. Sheka, Denis MA 17.1, MA 38.2
 Da Como, Enrico TT 51.7
 da Silva Pinto, Manoel Wilker
 •MM 28.1
 Dabrowski, Jarek HL 14.9
 Daddi-Moussa-Ider, Abdallah DY 31.4
 Dadgar, Armin HL 7.6, HL 44.1,
 •HL 51.1, HL 51.7, HL 51.9, O 32.1,
 O 32.6
 Dadhichi, Lokrshi Prawar •DY 34.2
 Daelman, Nathan O 84.4, O 95.6,
 •O 95.10, TT 56.4, TT 68.6, •TT 68.10
 Daeneke, Torben HL 14.4
 Daffé, Niéli MA 19.1, MA 40.32
 Daghofer, Maria •TT 30.2, TT 42.11,
 TT 42.12, TT 57.6
 Dahl, Margarethe •CPP 57.10
 Dahle, Sebastian O 11.7
 Dahlenburg, Marcus •DY 6.7
 Dähne, Mario O 28.4, O 28.6, O 55.5
 Dai, Dinghe •O 43.1
 Dake, Jules M. MM 23.30, MM 23.32,
 MM 26.2
 Dal Conte, Stefano HL 34.8
 Daldrop, Jan CPP 2.11
 Daldrop, Jan O. DY 44.20
 d'Alessandro, Joseph BP 22.10
 Dalmonte, Marcello •DY 2.2, •TT 2.2
 Dalton, Benjamin DY 23.5
 Dalton, Connor TT 30.3
 Damerau, Florian •HL 7.15
 Damerow, Sarah •TT 38.6
 D'Amico, Pino •MM 3.8
 Dammann, Lars •MM 23.28
 Dan, Minjiang •HL 33.3
 dan, yaping HL 34.2
 Dangel, Christian HL 7.44, HL 42.5
 D'Angelo, Olfa DY 7.9
 Dani, Olfa •HL 16.4, •TT 24.4
 Daniel, Leon •O 24.5
 Danielli, Carlo DY 43.10
 Danke, Varun CPP 35.31
 Danneau, Romain TT 53.1
 Danegger, Tobias MA 46.5
 Dannenberg, Simon •BP 13.2
 Danner, Lukas TT 39.9
 Danon, Jeroen HL 33.27
 Dantas, Renato M. A. TT 6.7
 Danylchenko, Petro MA 13.9, TT 19.9,
 •TT 58.24
 Danz, Thomas O 83.8
 Daoulas, Kostas •CPP 12.2
 Daqiqshirazi, Mohammadreza
 •HL 1.5
 Dargasz, Michelle BP 11.46
 Darras, Alexis BP 8.3, BP 11.60,
 •BP 22.7, DY 4.2
 Darvishi Kamachali, Reza •MM 37.5
 Das, Debankur •DY 16.6
 Das, Dibyendu BP 18.2, DY 33.2
 Das, Mandira •MM 16.7
 Das, Mowpriya O 28.4, O 28.6
 Das, S. MA 18.4
 Das, Saunak O 37.1
 Das, Shuvankar O 92.4
 Das, Souvik TT 8.4
 Das, Sukanya CPP 18.11
 Das, Suman •BP 10.3, DY 27.1
 Dasanna, Anil Kumar BP 2.10
 Dasari, Durga HL 29.7, HL 37.3
 Daschner, Maximilian •TT 59.13
 Dasgupta, Moumita BP 18.2, DY 33.2
 Dash, Aditya •HL 33.56, •HL 36.5
 Dash, Saroj p. MM 14.7
 Dašić, Milijan •CPP 20.3, •CPP 35.55
 D'Astolfo, Philipp O 87.3
 Date, Mihir DS 12.15, •O 59.7, TT 27.4
 Datta, Agniva •DY 31.3
 Datta, Sawani •MM 14.7
 Dauer, Christoph MA 16.1, TT 22.8
 Daum, Lydia •MM 26.3
 Daum, Winfried O 38.5
 Daumann, Florian CPP 17.9
 Daurer, Benedikt MA 43.2
 Dauwe, Tim O 34.5, •O 80.6
 David, Alessandro •HL 37.7, HL 50.7
 David, Felix •HL 3.9, •HL 10.6, HL 10.8
 David, Robert BP 28.55
 Davies, Annabel L. DY 57.6
 Davies, F. O 47.7
 Dávila, María E O 14.11
 Davis, Francis H. O 74.8
 Davis, Tim O 80.3
 Davoodi, Fatemeh MM 26.7
 Davoudiniya, Masoumeh MA 23.58
 Davydko, Anton KFM 9.9
 Dax, Ingrid •CPP 29.9
 Daxinger, Aneta O 84.2, TT 56.2
 Day, Christian •VA 1.2
 Day, James MM 6.7
 De, Anulekha MA 40.7
 de Beer, Sissi CPP 8.1
 De Beule, Christophe TT 6.12, TT 53.4
 de Campos Ferreira, Rodrigo Cezar
 •O 10.3, O 43.8
 De Donno, Marcello •MM 25.3
 De Gregorio, Marco HL 24.13,
 •HL 49.5
 de Haas, Oliver •AIW 1.3
 de Kinkelder, Eloy •BP 8.1
 de la Fuente, Jesus BP 30.4
 de la Torre, Bruno O 45.6, O 66.4,
 O 66.11, •O 97.3
 de Liberato, Simone O 58.6
 de Lima Jr., Mauricio M. HL 10.3
 De Los Reyes, Alexander HL 17.6
 de los Santos Pereira, Andres
 CPP 35.62
 de Loubens, G. MA 16.6
 de Loubens, Gregoire MA 23.61
 de Luca, Guillaume •MM 33.8
 de Melo, Mauricio TT 10.4
 de Muer, Albin TT 29.2
 de Oliveira Lima, Vitor •DS 12.25
 de Oliveira, Thales BP 11.43, HL 48.9
 de Oliveira, Thales V.A.G. DS 7.1,
 HL 17.3
 de Oteyza, D. G. O 47.3
 De Padova, Paola O 14.11
 De Pas, Marco O 39.2
 de Podesta, Christian TT 4.11,
 TT 59.14
 de Podesta, Christian K. •TT 4.12
 De Raedt, Hans TT 43.20
 De Sio, Antonietta BP 11.42, CPP 28.9,
 HL 25.8, HL 48.8, O 58.2, TT 32.9

- De Teresa, J.M MA 23.39
De Tomasi, Giuseppe DY 25.1, TT 33.1
de Vasconcellos Lourenço, Rodrigo
•HL 33.43, HL 51.8
de Vega, Inés TT 49.2
Deák, András MA 4.8, MA 46.5, TT 7.8
Deak, Peter HL 13.4, O 17.4
Dean, Cory TT 53.9
Dean, David DY 32.4
Deb, Marwan MA 40.34
Deb, Swarup •HL 8.9, HL 33.6
Debais, Gabriel DY 16.11
Debbeler, Lukas •TT 47.7
Deblais, Antoine •BP 30.1
Debnath, Bharati HL 45.4, HL 45.6
Debnath, Jayashrita •BP 3.6
Debnath, Tushar HL 25.7
Debus, Charlotte BP 11.76
Debut, Alexis HL 7.32
Decker, Régis •MA 8.9, MA 20.3
Decurtins, Silvio O 38.4, O 45.3,
O 45.4, O 55.3, O 87.3
Dedenon, Mathieu •BP 15.4
Dedé, Philipp •PSV 14
Dedkov, Yuriy KFM 9.1, KFM 11.1,
O 64.10
Dedkov, Yuriy S. O 56.7
Defuant, Guillaume •SYOF 1.4
Degünther, Julius DY 40.4, •DY 40.5
Dehm, Gerhard MM 26.1, MM 27.3,
MM 33.3
Deibel, Carsten CPP 1.4, •CPP 1.7,
CPP 1.11, CPP 36.3
Deilmann, Thorsten •HL 1.6, HL 22.8,
HL 31.8, O 30.8, O 61.8
Deimel, Martin •O 52.7
Deineko, Anastasiia •O 55.2, O 81.11
Deinert, Jan-Christoph BP 11.43,
MM 23.35, TT 3.5
Deißenbeck, Florian •O 69.7, O 86.3
Deka, Antaran BP 6.6
del Castillo, Yelko •O 15.4
del Ser, Nina •MA 15.4
del Valle, Elena HL 7.65
del Valle, Javier DS 12.28
de-la-Peña, Sebastián MA 4.13,
TT 7.13
Delatowski, Felix-Florian DS 12.10
Delens, Megan DY 31.8, •DY 31.9
Deleporte, Emmanuelle HL 17.9
Delesma, Francisco •HL 20.7, •O 35.7
Delin, Anna MA 47.3, MA 47.6
Delis, Wassilios •MM 32.3
Dellago, Christoph BP 3.9, MM 25.4
Dellasega, David O 24.2
Delle Site, Luigi DY 23.2
Delley, Bernard MA 19.1
Delplace, Pierre •SYQC 1.2
Deltenre, Kira •HL 15.4
Deluca, Marco KFM 6.39
Deluigi, Orlando DY 29.4
Demarina, Nataliya HL 29.9
Dembecki, Marco N. •HL 33.13
Dementyev, Petr CPP 54.5
Demir, Johannes •MA 40.49
Demir, Merve •HL 4.5
Demler, Eugene •SYUE 1.6
Demming, Maximilian •MM 28.2
Demming, Maximilian MM 28.6
Dempewolf, Anja HL 7.6
Dempsey, Nora •SYGM 1.4
Demsar, Jure MA 18.3, O 85.3,
TT 62.5
dendzik, maciej DY 25.7, O 6.3, O 8.8,
•O 16.5, O 16.7, O 37.12, TT 33.7
Deneke, Kristian HL 42.1
Deng, Shengfeng DY 57.1
Deng, Yunpei TT 62.7
Denisenko, Andrej MA 32.4
Denker, Christian MA 23.7
Denner, Michael Marco KFM 9.7
Denneulin, Thibaud MA 23.4
Denuault, Guy CPP 45.3
Denz, Cornelia BP 24.3, DY 38.3
Denzer, Lars •O 70.7
Deppe, Frank TT 49.2
Deppe, Michael HL 51.10
Derendorf, Pascal •TT 63.14
Derevjanko, Dennis •CPP 18.13
Dergianlis, Vasilis HL 1.10
Deringer, Volker L. MM 29.5
Dernbach, Daniel •DY 29.11
Derunova, Elena •TT 64.2
Derzhko, Oleg TT 23.9
Deschler, Felix DS 11.3, HL 15.1,
MA 23.40
Deslys, Alexandre BP 31.2
Desplat, Louise MA 2.5
Detcheverry, François •BP 22.10
Dethloff, C. HL 7.20
Dethloff, Christiane DS 10.4, DS 12.12,
DS 12.54, •DS 16.3
Dette, Holger MM 12.24
Deußen, Tobias •HL 33.17
Deussen, Andreas DY 26.9
Deutsch, Dennis •HL 37.2
Devda, Harshita •MA 4.8, •TT 7.8
Devescovi, Chiara TT 64.1
Devi, Anjana O 42.4
Devi, P TT 42.4
Devi, Parul MA 32.2, •MA 42.5,
•MA 42.10
Devishvili, Anton MA 37.4
Dey, Amrita HL 25.2
Dey, Bashab •HL 7.49
Dey, Kaustav TT 50.8
Dey, Pou lumi •MM 27.2
Dey, Tusharkanti MA 44.5
Deyerling, André •TT 3.8
Deyerling, Joel •O 14.2, O 93.8
Dhar, Deepak SOE 9.1
Dhawan, Prerak HL 7.15
Dhundhwal, Ritika TT 39.3, •TT 54.1
Di Bartolomeo, Antonio O 5.8
Di Bernardo, Angelo •TT 11.1, TT 20.6,
TT 27.8, TT 27.9, TT 37.7, TT 37.10
Di Giovanni, Andras •TT 58.13
Di Liberto, Giovanni O 81.10
Di Pietro Martínez, Marisel •MA 43.1,
MA 43.2
Di Sante, Domenico O 65.5, O 67.5,
O 94.2, TT 63.12
Di Santo, Giovanni O 34.10
Di Terlizzi, Ivan •BP 23.8
Dianat, Arezoo •CPP 2.6, HL 36.1,
MM 3.10
Dias, Beatriz DY 55.7, TT 67.7
Diaz Carral, Angel •TT 63.10
Diaz Maier, Joel •CPP 57.6
Díaz, Sebastián A. •SYTS 1.2, MA 35.6
Díaz-García, Álvaro SYGM 1.5
Dichtl, Valentin •O 43.2
Dick, Daniel DY 45.11, •HL 33.58
Dickbreder, Tobias •O 81.9
Diddens, Christian CPP 44.7
Diddens, Diddo CPP 2.2, CPP 35.53,
CPP 53.8, MM 16.5, O 25.3
Didier, Loriane BP 29.9
Dieball, Cai •DY 32.3
Diebold, Ulrike O 6.1, O 6.4, O 26.4,
•O 54.5, O 54.6, O 54.7, O 54.8,
O 60.3, O 68.2, O 81.4, O 81.8, O 92.5,
O 92.10
Diehl, Sebastian DY 48.5, TT 31.5,
TT 55.5
Diekmann, F. O 30.4
Diekmann, Florian K. O 19.6
Diekmann, Jan •CPP 44.12
Dielmann, Fabian O 11.5
Diem, Christian SOE 22.3, SOE 23.4
Diener, Alexander O 45.7
Dieplinger, Johannes •DY 55.8,
TT 5.13, •TT 67.8
Diercks, Alexander HL 4.1
Diermeier, Daniel SOE 4.13
Diesen, Elias HL 40.7, O 79.7, •O 96.1
Diesing, Detlef O 8.3, O 19.1
Diestelhorst, Elise CPP 35.20
Dieterich, Peter DY 26.9
Dietrich, Paul M. BP 11.8, BP 11.9,
BP 17.9
Dietrich, Siegfried BP 2.9, DY 31.11
Dietzel, Dirk •O 4.2, O 4.4, O 21.3
Diez, Néstor O 10.4
Diez, Stefan BP 5.2, BP 8.5, BP 11.48,
BP 12.6, BP 23.9, BP 30.5
Dil, J. Hugo O 8.9
Dillenz, Manuel •MM 16.1
Dimakis, Emmanouil HL 17.4
Dimitropoulos, Andrea BP 25.4
Dimou, Aris •KFM 1.3
Dinescu, Adrian MA 34.7
Ding, Fei HL 24.8
Ding, Kuan •MM 9.7
Ding, L. L. •KFM 6.9
Ding, Lili •KFM 13.7
Ding, Pan CPP 17.46
Ding, Yong CPP 17.32, CPP 51.6
Dingel, Kristina MA 36.3
Dingeldein, Lars CPP 2.8
Dinger, Mareike TT 43.32
Dingreville, Remi •MM 9.4
Dinter, Julius Konstantin DS 12.13
Diop, L. V. B. MA 28.4
Dippel, Ann-Christin DS 12.7, KFM 9.7,
O 29.6
Dirin, Dmitry N. HL 4.10, HL 35.8
Disa, Ankit TT 62.7
Dittmar, Marco •O 74.4
Dittrich, Lars DY 29.7
Ditz, Nikolas DY 16.1
DiVincenzo, David TT 54.2
Divinski, Sergiy MM 18.1, MM 18.6,
MM 28.6
Divinski, Sergiy V. MM 18.2, MM 40.8
Divinskiy, Sergiy V. MM 12.4
Diz-Muñoz, Alba BP 31.2
Djurabekova, Flyura HL 44.2
Do, S. H. TT 52.3
Dobener, Florian •DS 13.3, O 95.1,
•O 95.3, O 95.4, O 95.5, TT 68.1,
•TT 68.3, TT 68.4, TT 68.5
Doblas-Jimenez, David O 37.9
Döblinger, Markus HL 25.2, HL 45.4
Dobroserdova, Alla CPP 3.3, DY 42.16
Dobrovolskiy, Oleksandr •TT 66.5
Dobrovolskiy, Oleksandr V. TT 3.12,
TT 3.13
Dobson, John HL 13.6, O 17.6
Dockhorn, Ron •CPP 20.9,
•CPP 35.47, CPP 35.57
Doctor, Louis Philip •HL 2.2
Doerr, Florian O 92.5
Doerr, M. MA 33.6
Doerr, Mathias •MA 23.1, TT 29.4
Doerries, Timo J. •DY 56.4
Doert, T. KFM 11.9, MA 40.58
Doert, Thomas MA 40.22, MA 44.6,
TT 43.2, TT 46.5
Dogadov, Oleg HL 34.8
Dohi, Takaaki MA 12.4, MA 23.5,
MA 40.29
Döhn, Johannes •KFM 10.4
Dolai, Pritha •DY 27.12
Dolata, Ralf TT 39.6
Doležal, Jiří O 10.3, O 43.8, O 70.10,
O 76.3, •O 76.5
Doll, Larissa CPP 57.10
Doll, Sven •HL 7.4
Dolleman, Robin HL 33.12
Dolling, Silvan O 29.3, O 40.4
Dolmantis, Paulius •TT 30.7
Doltsinis, Nikos DY 43.17
Doltsinis, Nikos L. O 2.5
Dolynchuk, Oleksandr CPP 17.18
Domaine, Gabriele •TT 59.12
Dombrowski, Daniela O 56.9, O 74.8
Dömer, Niklas •KFM 6.42, KFM 14.5
Dominguez, Adriel O 37.8
Dominguez, Alvaro •DY 27.3,
•DY 31.11
Dominguez, Claribel DS 12.28
Dominguez, Fernando TT 31.1,
TT 53.4
Dominguez Vázquez, Eduardo J. O 20.2, O 33.9
Dominguez-Adame, Francisco
HL 11.2, TT 15.2
Dominguez-Castro, Adrian MM 10.2,
O 37.8
Domke, Katrin F. •O 27.1
Domke, Sören •KFM 6.44, KFM 14.5
Domröse, Till O 8.1, •O 83.8
Donarini, Andrea HL 22.7
Donat, Clara BP 10.9
Donath, Markus O 18.5, O 59.2,
O 59.4, O 59.6, O 67.8, O 85.6
Donati, Fabio •O 15.12
Dong, Bowen •CPP 35.37
Dong, Huifang •DY 22.1
Dong, Iris BP 7.3, DY 10.3
Dong, Shuo O 16.5, O 16.7
Dong, Tao TT 3.5, TT 62.5
Dong, Yulian •KFM 10.8, MM 5.5,
•MM 23.9
Dong, Zhiyu TT 64.3
Dongare, Srishti •MA 23.51, MA 23.64
Donges, Jan •HL 33.24, HL 49.6
Donis Vela, Alvaro HL 30.6, TT 41.6
Donnelly, Claire MA 40.3, MA 43.1,
MA 43.2, MA 50.1, MM 26.9
Donner, Wolfgang KFM 6.31
Donvil, Brecht DY 9.8, •DY 9.10,
TT 39.9
Doostmohammadi, Amin •SYQC 1.5,
DY 26.4
Doppagne, Benjamin O 76.2
Dörfel, Denise AKC 1.3
Dörflinger, Patrick •CPP 17.32,
•CPP 51.6
Dorfner, Maximilian Franz Xaver
•CPP 17.7
Dormann, Dorothee BP 3.4, BP 17.5
Dormann, Kay-Robert •DY 42.3
Dornbusch, Daniel BP 11.43
Dornseifer, Jan L. •MM 26.10
Dornseiff, Jannik O 56.7
Dörr, Kathrin MA 17.4, MA 23.63
Dorsch, Eric TT 57.22
Dörschel, Björn DY 44.12
Dortaj, Sina DY 17.1, •O 78.6
dos Santos Dias, Manuel MA 14.7,
MA 21.1, O 15.9
Dösinger, Christoph MM 9.1, MM 9.5,
•MM 37.6
Dotan, Michael KFM 6.36
Dotter, Marius •CPP 17.27
Doucot, Benoît DY 55.5, MA 23.10,
TT 67.5
Drasar, Cestmir O 65.1
Drauschke, Fenja DY 57.3
Drautz, Ralf TUT 3.1, MM 1.1,
MM 26.6, MM 29.4, MM 36.2,
MM 36.5, MM 40.2
Drawer, Jens-Christian HL 1.2
Draxl, Claudia SYUE 1.2, HL 6.2,
HL 6.8, HL 13.5, HL 20.2, HL 20.6,
HL 25.3, HL 25.11, HL 31.6, HL 40.2,
MM 8.5, MM 12.25, MM 29.1, O 9.2,
O 9.8, O 17.5, O 35.2, O 35.6, O 61.6,
O 79.2, O 84.4, O 95.4, O 95.5, O 95.6,
O 95.10, TT 56.4, TT 68.4, TT 68.5,
TT 68.6, TT 68.10
Drchal, Vaclav MA 23.29, O 65.1
Drechsler, Hauke BP 5.2
Drechsler, M. L. •HL 43.6
Drechsler, Stefan-Ludwig •TT 29.14,
TT 30.12
Dreher, Maximilian O 45.5
Dreher, Pascal O 75.4, O 80.3, O 80.5
Dreher, Yannik BP 11.59
Dreiser, Jan MA 19.1, MA 40.32, O 2.7
Dreißigacker, Christoph CPP 51.4
Dreißigacker, Christoph CPP 17.30
Drescher, Jörg CPP 51.4
Drescher, Markus •TT 46.9
Drescher, Sophie •MM 40.9
Dreßler, Christian •DY 6.10
Dressel, M. TT 6.5, TT 6.10, TT 23.1
Dressel, Martin HL 17.2, MA 9.9,
TT 58.28
Dreuw, Andreas O 10.7
Drevelow, Tim •MA 14.6, MA 21.2,
MA 40.52
Drewes, Jonas CPP 17.4, CPP 29.2,
CPP 29.8
Drewniok, Jan HL 14.6
Dreyer, Cyrus HL 31.2, O 61.2
Dreyer, Rouven MA 23.51, •MA 23.68,
MA 23.73, MA 43.7
Driessens, Kurt O 45.7
Drnec, Jakub O 69.10, O 96.4, O 96.5
Droghetti, Andrea MA 4.5, MA 7.3,
•MA 27.3, MM 6.8, TT 7.5
Drozowski, Oliver M. •BP 28.43
Drozella, Johannes HL 50.2
Druëke, Helena O 65.2, •O 65.3
Drummond, Neil TT 16.12, TT 16.13
Dsouza, Raynol •MM 25.5
DSouza, Sunil Wilfred •MA 47.5,
O 18.7
Du, Chao-Hung TT 23.5
du, nan HL 47.5
Du, Qingyang •O 66.1
du Roure, Olivia CPP 57.1
Du, Yixuan CPP 44.6
Duan, Haoran TT 54.1
Duan, Hong-Guang MM 10.4
Duan, Juanmei HL 5.5, O 75.2
Duan, Yu •HL 14.10
Duarte Correa, Maria Jazmin
•MM 27.3
Duberland, Rémy DY 48.9, TT 55.9
Dubey, Divya Prakash •TT 57.7
Dubey, Garav MM 23.69
Dubs, Carsten MA 16.5, MA 23.35,
MA 23.74, MA 40.33
Duc, Huynh Thanh HL 17.1
Duchamp, Baptiste BP 31.2
duchon, tomas MA 40.16
Dück, Gerald KFM 10.9
Duclut, Charlie •BP 4.1, BP 28.22
Dudin, P. DS 7.2
Dudka, Maxym DY 49.2
Dudko, Volodymyr O 76.9
Dudy, Lenart TT 9.7
Dudziak, Mateusz CPP 17.1
Dudzinski, Alexandra M. O 96.1

Author Index

- Duenweg, Burkhard .BP 18.3, DY 33.3
Dues, Christof .CPP 35.46
Dufouleur, Joseph .MA 40.64
Dufour, Pauline .MA 11.1
Dufresne, Eric R. .BP 11.5
Duft, Antonia .TT 29.8, •TT 42.10
Duine, Rembert A. .MA 20.9
Duipmans, Lammert .HL 16.9, TT 24.9
Duits, Michel .CPP 50.2
Dulle, Martin .•CPP 19.9
Dumesnil, Karine .MA 40.66
Duncan, David .O 14.8, O 36.11
Duncan, David A .•O 36.6, O 93.5, •O 93.8
Dunin-Borkowski, Rafal .MA 23.4, MA 47.7
Dunin-Borkowski, Rafal E. .•PLV II
Dunkel, Jorn .BP 30.3
Dunsiger, Sarah R. .TT 28.4
Dunsing, Valentin .•BP 15.6
Dünweg, Burkhard .CPP 12.7
Duong, Dinh Loc .DS 10.3
Dupé, Bertrand .MA 2.5, MA 18.7
Duran, Stefan .HL 17.4
Durand, Alrik .MA 32.6
Durdyyev, Rustam .•DS 12.42
Düreth, Johannes .•HL 18.4
Düring, Pia Maria .•O 32.5
Durmaz, Ali Riza .•MM 20.1
Duros, Octave .TT 3.7, TT 57.3
Dürr, Michael .HL 27.2, O 48.4, O 57.2, O 62.2, TT 40.2
Dürnagel, Matteo .TT 57.17
Durst, Karsten .MM 9.7
Durst, Simon .•O 70.1, O 76.6
Dusabirane, Felix .•MA 8.10
Dutta, Rajesh .TT 51.8
Dutton, Sian .TT 30.10
Dvir, Tom .TT 31.6
Dwivedi, Jagrati .•O 52.1
Dyakonov, Vladimir .CPP 11.7, CPP 17.32, CPP 18.9, CPP 28.7, CPP 51.6, HL 22.10, TT 32.7
Dykman, Mark .TT 18.4
Dziarzhyski, Sjarhei .O 16.1
Dziarzhyski, Sirhei .O 37.8
Dzinnik, Marvin J. .•HL 42.7
Dzubiella, Joachim .•CPP 53.1
E. Böhrner, Anna .DS 6.4
Eaton, Alexander .•TT 28.1
Ebel, Jasper .•CPP 17.37
Ebel, Sven .•VA 1.5
Ebeling, Daniel .O 45.5, •O 55.6, O 72.5
Ebensperger, Nikolaj G. .TT 30.1
Eberharder, A. A. .TT 42.13
Eberheim, Kevin .CPP 35.39, CPP 35.40, •CPP 35.46
Eberl, Chris .MM 20.1
Ebersbach, Clara .MA 23.1
Ebert, Gregor .O 57.5
Ebert, H. .MA 8.3, MA 34.8
Ebert, Hubert .HL 34.5, HL 45.2, MA 16.8, MA 20.1, MA 27.5, O 59.5
Ebert, Jan .CPP 2.7
Ebling, Fabien .•MM 27.9
Ebrahimi Viand, Roya .•MM 14.5
Echter, Carolyn .•DY 6.8, DY 55.4, TT 67.4
Ecija, David .O 66.11
Eck, Philipp .O 18.9, O 36.12, O 65.5, O 65.6, O 67.5
Eckelt, Franz .O 26.8, •TT 57.10
Eckert, Jürgen .MM 28.4, MM 28.5, MM 42.9
Eckhoff, Marco .O 26.6
Eckner, Stefanie .HL 4.9
Eckselser, Jannis .•DY 55.6, •TT 67.6
Eckstein, Martin .SYUE 1.4, TT 5.12, TT 62.8
Edalati, Kaveh .MM 27.7
Edalatanesh, Shayan .O 66.11
Eder, Bernhard .O 97.8
Eder, Moritz .O 29.8, O 41.4
Ederth, Thomas .DS 16.6
Edgar, James H. .MA 32.6
Edman, Ludvig .CPP 17.13
Edte, Moritz .•BP 21.1
Edwards, Brendan .O 30.1
Edwards, Thomas E. J. .•MM 4.4
Edzards, Joshua .•MM 16.8
Efe, Ipek .•KFM 4.2
Eftetov, Dmitri .•SYHS 1.5
Efremov, Dmitri .TT 16.2
Efremov, Dmitri .•TT 51.2, TT 57.9
Eggeler, Gunther .MM 23.5
Eggeling, Christian .BP 21.2, BP 21.6, BP 28.9, HL 18.12
Eggeling, Nico .•HL 7.17
Egger, David .•CPP 44.11
Egger, Reinhold .TT 31.2
Eggert, Benedikt .MA 3.3, MA 3.8, MA 9.10, MA 42.2, •MA 42.7
Eggert, Sebastian .DY 43.16, MA 16.1, TT 22.7, TT 22.8, TT 45.8, TT 59.16, TT 59.17, •TT 65.5
Eggert, Thorben .O 83.2, •O 86.1
Eggle-Sievers, Benedikt .MM 4.3, •MM 15.7
Egli, Stephan .O 63.1
Eglington, Joshua .•DY 6.5
Egorov, Oleg .HL 24.13
Ehgartner, Caroline .CPP 17.51
Ehm, Alexander .•HL 7.11
Ehresmann, Arno .DS 4.6, DS 12.2, KFM 6.34, MA 5.2, MA 5.4, MA 23.36, MA 36.3, MA 36.4, MA 38.4, MA 40.28, MA 40.31, MA 40.43
Ehrhardt, Martin .KFM 7.4
Ehrig, Carina .•PSV II
Eibensteiner, Klaus .MA 13.8, TT 19.8
Eibisch, Paul .•TT 46.7
Eich, Sebastian .•MM 14.3, MM 14.4
Eichberger, Rainer .HL 47.2
Eichel, Rüdiger-A. .DY 46.2, MM 16.7
Eichhorn, Johanna .•HL 38.2, HL 45.1
Eichler, Edwin .SYOF 1.3, SOE 19.4
Eickhoff, Martin .HL 14.7
Eidel, Bernhard .•MM 36.10
Eiguren, Asier .O 15.9
Eilenberger, Falk .HL 1.2, HL 2.5, HL 2.6
Eilmsteiner, David .•MA 23.12, MA 40.62
Einfeldt, Sven .•HL 23.2
Eisebitt, Stefan .MA 8.2, MA 40.39, MA 43.6
Eisenmann, Lars .TT 57.26
Eisenschmidt, Elias .TT 39.11, •TT 58.21
Eisenstein, Gadi .HL 16.6, TT 24.6
Eisert, Jens .MA 40.26
Eisfeld, Alexander .DY 18.8, •DY 25.6, •DY 43.18, DY 55.11, •O 70.8, •TT 33.6, TT 67.11
Eisner, Flurin .•CPP 11.6
Eivazi, Faranak .•MA 23.28
Ejima, Satoshi .•TT 22.5
Ekaterina, Ekaterina .DY 42.16
Ekström, Niklas .TT 58.29
El Ashhab, Hadeer .•SOE 23.3
El Azzouzi, Fatima .KFM 13.5
Elbracht, Michael .•MA 40.13
Elcoro, Luis .MA 10.2, TT 12.2
El-Fattah, Zakaria M. Abd .O 14.5
Elgeti, Jens .BP 28.48
Elghandour, Ahmed .MA 23.25, •TT 46.6, TT 50.8
Elhajhasan, Mahmoud .•HL 36.6, HL 51.5
Eli, Basil .MM 12.29, MM 12.30
Ellenbroek, Wouter .BP 19.5, CPP 41.5
Ellinger, Florian .O 72.3
Elm, Matthias .•DS 12.13, MA 36.5
Elm, Matthias T. .HL 16.3, TT 24.3
El-Melegy, Tarek .MA 42.9
Elmers, H.-J. .HL 36.2, MM 12.1, MM 26.8, O 30.4
Elmers, Hans-Joachim .MA 18.3, O 85.3, O 85.7
El-Said, Ayman .•O 42.1
Elsässer, Christian .HL 4.4, MM 5.2, MM 5.6, MM 9.3, MM 11.1, MM 11.2, MM 32.6, TT 21.5
Elsässer, Philipp .•DY 16.9
Elsherif, Ahmed Gamal .KFM 9.8
Elster, Clemens .O 43.3
Emamverdi, Farnaz .•CPP 20.4
Embid, Ismael dP. .•HL 10.4
Embs, J.P. .MA 44.3
Emmerich, David Alexander Darek .•HL 14.5
Emmerling, Monika .HL 5.1, HL 18.4, HL 24.13, O 58.7, O 91.9
Emminger, Carola .DS 13.3, HL 18.2
Enache, Mihaela .O 50.4, O 60.2
Ender, Milan .MA 23.44, MA 23.67, MA 34.7
Endesfelder, Ulrike .•BP 21.7
Endres, Frank .•DS 9.1
Eneklit, Vivien .O 2.7, •O 64.10
Ener, S. .MA 28.4
Eng, L. M. .KFM 6.9, KFM 14.1
Eng, Lukas .HL 17.11, KFM 6.6, KFM 6.8, KFM 6.35, MA 32.1, O 58.7
Eng, Lukas M. .DS 7.1, DS 12.14, DS 12.17, HL 17.3, KFM 6.15, KFM 6.18, KFM 6.19, KFM 6.20, KFM 13.7, KFM 14.2, KFM 14.3, MA 23.60, MA 44.1, O 12.8
Eng, Lukas Matthias .KFM 3.1
Engbers, Michael .•DY 46.4
Engbring, Kirsten .DY 27.11
Engel, Dieter .MA 8.2
Engel, Gregory .O 34.1
Engel, Lena .•HL 12.6
Engel, Michael .CPP 2.10, DY 16.5, O 14.7
Engelhardt, Alexander .TT 10.5, •TT 47.6
Engelhardt, Fabian .MA 34.6
Engelkamp, Hans .TT 59.18
Engl, Vincent T. .TT 30.1
Engler, Thea .•KFM 9.12
Engster, Katharina .O 28.3
Engstfeld, Albert K. .O 14.10, •O 96.5, O 96.10
Ennen, Inga .MA 23.42, MA 23.46, •MA 37.3, MM 12.30
Enniful, Henry R. N. B. .•MM 23.22, •MM 42.8
Enns, Sven .KFM 7.9
Enslin, J. .HL 23.1
Enslin, Johannes .HL 23.2, HL 23.5
Enss, C. .TT 57.21, TT 57.27, TT 57.28, TT 58.2, TT 58.4
Enss, Christian .TT 43.30, TT 43.31, TT 43.32, TT 57.20, TT 57.25, TT 57.26, TT 58.1, TT 58.3, TT 58.5, TT 58.25, TT 66.7
Enssle, Marion .HL 27.3, O 62.3, TT 40.3
Ensslin, Klaus .HL 9.4, TT 14.4
Enzner, Stefan .•O 36.12
Epp, Dennis .•O 8.5
Erb, Andreas .TT 47.6, TT 54.8
Erb, Denise .MA 5.3, MA 50.3, •O 24.3
Erb, Denise Jennifer .O 31.2
Erbe, Artur .HL 3.9, HL 10.8, HL 33.10, HL 42.2, HL 42.3, HL 50.3, •KFM 7.1
Erben, Elena .•BP 5.8, CPP 20.2, DY 29.6
Erbes, Elisabeth .•CPP 36.8, DS 12.34
Erdmann, Sebastian .MA 13.7, TT 19.7
Erdmann, Stephan .•MA 28.2
Eremenko, Zoya .•MM 12.9
Eremin, Alexey .CPP 53.9, HL 2.3, MA 36.2
Eremin, Ilya .DY 49.3, TT 23.11, TT 34.2, TT 50.7, TT 63.14
Eremin, Ilya M. .TT 20.11, TT 54.3
Erhard, Linus C. .•MM 29.5
Erhardt, Jonas .DS 1.3, •O 94.7
Erhardt, Max .TT 36.6
Erhardt, Sylvia .BP 29.4
Erhart, Paul .O 38.6, O 76.8
Eric, Opsomer .DY 7.1
Erick Beck, Esko .O 57.5
Ericsson, Tore .KFM 11.3
Eriksson, Lukas .BP 21.3, •O 26.1
Eriksson, O. .MA 28.4
Eriksson, olle .•SYGM 1.1, MA 7.1, MA 20.7, MA 47.3, MA 47.6
Erkenov, Shamil .•TT 10.6, TT 43.10
Ernst, Arthur .MA 23.12, MA 23.31, MA 27.6, MA 40.62
Ernst, Karl-Heinz .DS 4.3, O 28.7, O 73.6, •O 90.1
Ernst, K-H. .O 2.8
Ernst, Marcel .•BP 11.51
Ernst, Stefan .MA 23.41
Ernstorfer, Ralph .SYUE 1.2, MA 46.11, MA 46.13, O 8.9, O 16.5, O 16.7, O 34.7, •O 95.1, O 95.3, •TT 68.1, TT 68.3
Eroğlu-Kayıkçı, Süheyla .BP 29.4
Er-Rajji, Oussama .HL 4.3
Ersfeld, Klaus .BP 28.5
Ershadrad, Soheil .MA 7.5, •MA 23.49
Ertel, Benjamin .•BP 23.6
Esakkiraja, Neelamegan .MM 18.6
Esat, Taner .MA 21.7, O 21.2, O 33.2, O 66.9, O 77.1
Escalante-Quiceno, A.T. .•MA 23.39
Esch, Friedrich .O 25.4, O 92.1
Eschenlohr, Andrea .MA 8.7, O 16.2, •O 16.4, •O 37.2, O 37.3
Eschrig, Matthias .•TT 20.7
Esguerra, Luisa .DY 22.4, DY 46.7
Eshaghi, Ghazaleh .DS 1.2
Eskandari, Mohammad Amin .BP 11.19
Eßl, Herbert .•TT 65.4
Esmann, Martin .HL 1.2, HL 2.5, HL 2.6, •HL 10.10
Esposito, Massimiliano .DY 23.4, DY 34.3, DY 40.7, DY 40.9
Esser, Marcus .•O 77.2
Esser, Norbert .O 28.4, O 28.6
Esser, Tim .•BP 21.3, BP 28.14, O 26.1, O 26.5
Esser, Tim K. .BP 11.41, BP 11.45
Estacio, Elmer .HL 17.6
Estebnez, Pablo .KFM 8.8
Esters, Marco .MM 36.9
Esteve, Daniel .PLV X
Estrada-Real, A. .O 47.7
Etzkorn, Markus .KFM 6.16
Euchler, Eric .CPP 19.7, •CPP 35.28
Euchner, Holger .CPP 29.11, MM 16.3, MM 16.4, MM 16.6, O 69.14, •O 73.4
Eul, Tobias .O 14.5, O 37.10, •O 59.5, O 70.4, O 80.1, O 95.2, TT 68.2
Evangelisti, Marco .•MA 13.1, •TT 19.1
Evans, Benjamin A. .MA 40.47
Evans-Lutherodt, Kenneth .O 24.3
Everett, Christopher R. .•CPP 13.8, CPP 17.31, CPP 29.2, CPP 29.10, CPP 36.6
Everett, Nathan .O 75.5
Evers, Ferdinand .DY 9.3, DY 43.9, O 2.3, O 7.7, TT 5.13
Evers, Martin .MA 46.1
Everschor-Sitte, Karin .•SYQC 1.1, DY 44.12, MA 23.15, MA 35.6, MA 40.4, MA 47.9, MA 47.11
Ewald, Björn .•CPP 17.10, •CPP 28.3, •TT 32.3
Ewald, Johannes .•DY 44.22
Ewald, Norman Vincenz .DY 46.7, HL 24.3
Ewert, Moritz .O 64.8, O 67.8, O 74.1, O 93.7
Ewings, Russell .TT 57.5
Eyre, Lissa .DS 11.3
Ezequiel, Marco .MM 33.2
F. Assaad, Fakher .TT 65.7
F. Huber, Linus .CPP 17.51
F. Morgado, Felipe .MM 3.6
Fa, Yu-Chen .O 66.5
Fabbri, Gilberto .MA 39.2
Faber, Christian .BP 11.16, BP 11.76, •BP 11.77
Faber, Lea .O 32.7
Fabian, Jaroslav .DS 1.5, HL 1.1, HL 8.1, TT 27.5, TT 27.6
Fabiano, Simone .DS 16.6
Fabre, Florentin .MA 32.6
Fabrice, Thalmann .BP 1.8
Fabris, Stefano .O 29.2
Fabrizio, Michele .MM 14.9, TT 43.14
Fabrizzi, Erik .TT 58.30
Fabry, Ben .DY 26.5
Facio, Jorge I. .MA 41.3
Fackler, Sebastian .•O 86.10
Facsko, Stefan .O 24.3, O 31.2, O 42.1
Fadel, Matteo .HL 3.1
Fadler, Paul .•TT 62.8
Faella, Enver .O 5.8
faham, mohamed amine .•MM 20.2
Fähler, Sebastian .MA 3.10, •MM 17.1, MM 17.2, MM 21.1
Fähnrich, Tobias .HL 30.3, TT 41.3
Faisst, Jared .•CPP 1.6
Faivre, Damien .BP 6.3
Fajman, Christian E. .CPP 37.2
Fakharuddin, Azhar .CPP 43.7
Fakhri, Nikta .BP 2.2, BP 30.3
Falcke, Martin .BP 11.62, BP 28.49
Faley, Michael .DS 12.25
Falk, Hans H. .•HL 4.9
Falk, Johannes .•SYOF 1.3, •SOE 19.4
Falke, Johannes .TT 9.3, •TT 50.1
Fall, William .CPP 19.3
Falta, Jens .O 67.8, O 74.1, O 78.9
Falter, Jens .TT 39.11, TT 58.21, TT 58.22
Fan, Bo .DY 7.7
Fan, Yuzhu .O 8.8
Fang, Shiang .O 16.3
Fang, Xufei .•KFM 2.2, KFM 2.3, MM 9.7
Fangohr, Hans .MA 2.3, MA 23.14, MA 26.4, MA 47.2
Farag, Ahmed .HL 4.1
Farenbruch, Andreas .HL 35.9, •HL 47.2
Fares, Nicolas .BP 9.1
Farhat, Hanan .MM 24.1

Author Index

- Faria Junior, Paulo DS 2.1
 Faria Junior, Paulo E.•HL 1.1, HL 8.1
 Faria, M. G.•TT 23.7
 Farias, Maria Belén TT 18.5
 Farinacci, Laetitia•O 7.2, O 15.2
 Farle, Michael BP 5.7, DS 10.1,
 MA 38.3, MA 42.9, MM 40.10
 Farlorsti, Francesca HL 14.3
 Farnesi Camellone, Matteo O 29.2
 farooqui, osama•HL 7.27
 Farrell, Patricio DS 11.5, HL 5.2
 Fartab, Dorsa HL 34.6, MA 31.4,
 •TT 11.6
 Fasano, Yanina•O 85.4
 Fasel, Roman O 20.10, O 33.3, O 75.5
 Faßl, Paul HL 4.1
 Fassbender, Alexander DS 12.37
 Fassbender, Jürgen MA 5.3
 Fassbender, Jürgen BP 11.69, DS 6.1,
 MA 11.4, MA 16.3, MA 17.1, MA 18.6,
 MA 23.78, MA 31.7, MA 38.2,
 MA 43.5, MA 49.5, MA 49.6,
 MA 49.7, MA 49.8, MA 50.3
 Fässler, Reinhard BP 1.2
 Fässler, Thomas F. CPP 37.2
 Faulhaber, Enrico TT 58.29
 Fauman, Jacob•O 94.8
 Faupel, Franz•CPP 13.1, CPP 29.2,
 CPP 29.8, CPP 56.2
 Faupel, Franz Faupel CPP 17.4
 Faure, Quentin TT 10.12
 Fauser, Thomas O 67.5
 Fausti, Daniele TT 62.8
 Faustmann, Anton HL 29.9, HL 30.1,
 TT 41.1
 Fazzi, Daniele DS 16.6
 Féchant, Mathieu TT 58.16
 Fechner, Michael MA 18.8, MA 48.7,
 TT 62.2, •TT 62.7
 Fedchenko, O. MM 12.1, MM 26.8,
 •O 30.4
 Fedchenko, Olena HL 36.2, O 85.3,
 O 85.7
 Fedorak, Nazar SOE 8.2
 Fedorov, Alexander TT 57.9, TT 57.11
 Fedorov, Kirill G. TT 39.7, TT 49.1,
 TT 54.9, TT 58.6, TT 58.7, TT 58.8,
 TT 58.10, TT 58.20, TT 66.6
 Fedoseev, Vitaly TT 4.11
 Fedotenko, Timofey TT 3.6
 Fedyanin, Dmitry Yu. HL 29.10
 Feher, Alexander MA 13.9, TT 19.9
 Fehn, Natalie DS 11.3
 Fehrs, Jan Ole O 69.10, O 96.4
 Feichtner, Thorsten O 43.6, O 43.7,
 •O 49.3, O 58.7, O 91.6
 Feig, M. MA 44.3
 Feig, Manuel MA 44.8
 Feige, Michael MA 23.48, MM 12.29,
 MM 12.30
 Feist, Armin•HL 10.9, O 8.1, O 80.2,
 O 83.6
 Fekri, Zahra•HL 33.10
 Feld, Markus•O 65.6
 Feld, Yannick•SOE 6.2
 Feldmann, Jochen CPP 51.1, HL 25.2,
 HL 25.7, HL 45.4, HL 45.6
 Feldmeier, Johannes TT 45.9
 Felea, V. MA 33.6
 Felea, Viorel MA 18.5, MA 44.2
 Fellinger, Martina•O 24.2
 Fellner, Korbinian•MA 40.42
 Fellner, Simon MM 28.4
 Felsen, Frederic O 39.3, •O 78.2
 Felser, C. MA 12.5, TT 6.5, TT 6.10
 Felser, Claudia MA 3.6, MA 10.2,
 MA 12.3, MA 32.2, MA 37.4, MA 44.1,
 MM 6.10, O 59.7, TT 12.2, TT 23.3,
 TT 23.8, TT 59.10, TT 59.12
 Feneberg, Martin HL 2.3, HL 33.42,
 HL 41.4, HL 51.9, HL 51.10
 Feng, Liwen HL 48.9, •TT 3.5
 Feng, Wanxiang•MA 41.6
 Feng, Xinliang CPP 54.1, DS 12.15,
 O 33.3
 Fennel, Franziska DS 12.23
 Fenner, Felix O 80.4
 Fenzl, Florian CPP 18.10
 Ferchane, Selmane•CPP 28.5,
 •TT 32.5
 Ferenc Segedin, Dan TT 44.5
 Ferizaj, Rinis•TT 30.8
 Fernandez, Ignacio BP 23.1
 Fernandes, Rafael TT 23.2
 Fernandez, Claudia•MA 38.1
 Fernández, Cynthia O 38.2
 Fernández, Cynthia Carolina O 11.2
 Fernandez, Edgar O 15.12
 Fernandez Peralta, Antonio•SOE 7.3
 Fernández, V.V. MA 23.39
 Fernandez-Fernandez, David
 SYQD 1.2
 Fernandez-Gonzalez, Claudia
 MA 50.1
 Fernandez-Pacheco, Amalio
 MA 40.3, MA 50.1, MM 26.9
 Fernandez-Roldan, Jose A. •MA 43.5,
 •MA 50.3
 Fernández-Rossier, Joaquin MA 20.4,
 O 15.4
 Fernengel, Bernd Michael•DY 43.14
 Ferrai, Carmelo BP 29.4
 Ferrari, Ulisse BP 11.24
 Ferreira, Rodrigo O 70.10, O 76.3,
 O 76.5
 Ferreira, Tiago BP 3.10
 Ferrer, Jaime MA 24.2
 Ferrero, Michel TT 61.1
 Ferretti, Andrea HL 20.3, HL 26.4,
 MM 3.8, O 35.3, O 53.4
 Ferrier, Alban PLV X
 Ferrin, Max BP 11.33
 Ferring-Siebert, A. TT 57.21
 Ferring-Siebert, Anna•TT 58.5
 Fery, Andreas DS 13.5
 Fesquet, Florian TT 39.7, TT 49.1,
 TT 58.7, •TT 58.10, TT 58.20, TT 66.6
 Fessler, Florent CPP 57.2
 Fetai, Omer•MA 40.4
 Fétida, Alex•O 7.9
 Fettar, Farid MA 43.1
 Feuerbacher, Michael MM 37.8
 Feuerherd, Martin O 57.5
 Feulner, Peter O 14.8, O 36.6
 Feyer, V. DS 7.2, MA 40.53
 Feyerherm, Ralf MA 18.8
 Feyer, Simon•TT 16.8
 Fichtler, Julius BP 11.59
 Fichtner, Simon•KFM 1.5
 Fickentscher, Rolf BP 11.5
 Fiebig, Florian•HL 36.3
 Fiebig, Manfred•PRV I, DS 15.3,
 KFM 1.7, KFM 4.2, KFM 6.27,
 MA 48.2, MA 50.7, TT 3.2, TT 47.1
 Fiedler, Andreas DS 12.50
 Fiedler, Lenz•HL 6.5, •O 9.5
 Fielden, Brent BP 23.5
 Fiete, Gregory DS 7.5
 Figgemeier, Tim•O 65.5, O 94.9
 Figueiredo, Johannes HL 8.4
 Figueroa, José Silvestre Mendoza
 DS 16.6
 Fihey, Arnaud MM 21.5
 Fikáček, Jan TT 28.4
 Filianina, Mariia MA 18.3
 Filimonova, Evgenia•CPP 35.32
 Filion, Laura•DY 14.1
 Filipiak, Zuzanna MM 6.6
 Filipoiu, Nicolae DS 12.43, HL 16.2,
 TT 24.2
 Filipp, Stefan TT 49.5, TT 49.6,
 TT 58.6, TT 58.11
 Filippetti, Alessio MA 20.5
 Filippi, Claudia•HL 26.2, •O 53.2
 Filippova, I. MA 40.14
 Filippova, Irina MA 23.65
 Filser, Jakob•CPP 2.9
 Finco, Aurore•MA 11.1, •MA 32.6
 Findeisen, Rolf O 45.7
 Findler, Christoph•DS 12.35,
 KFM 6.40
 Fineberg, Jay•MM 38.1, MM 38.3
 Finizio, Simone MA 40.3, MA 43.3,
 •MA 48.5
 Fink, Christa•KFM 6.2
 Fink, Jörg•TT 37.9
 Fink, Lukas•MA 3.10
 Fink, Rainer H. CPP 17.52, CPP 28.10,
 TT 32.10
 Finkler, Jonas MM 25.4
 Finkler, Jonas A. CPP 45.6, O 26.6
 Finley, Jonathan HL 7.44, HL 37.8,
 HL 42.5
 Finley, Jonathan J. HL 10.3, HL 33.13,
 HL 34.5, MA 32.5
 Finocchio, G. MA 16.6
 Finsterbusch, Martin KFM 10.9
 Finzel, Kati MA 44.6
 Firlus, Alexander•MM 28.3
 Firme, Philipp HL 7.31
 Fischer, Andreas HL 15.4
 Fischer, Axel CPP 17.13
 Fischer, Jan•BP 11.60, •KFM 6.11
 Fischer, Jeison•O 51.1, O 56.8
 Fischer, Lukas•CPP 13.7, MA 33.7,
 O 31.8
 Fischer, Mark Hannes KFM 9.7
 Fischer, Mirko•CPP 35.53
 Fischer, Peter CPP 17.29
 Fischer, Quinn Emilia•DY 42.17
 Fischer, S. F. TT 3.4
 Fischer, Saskia•HL 36.4, •HL 41.6
 Fischer, Utz HL 2.6, HL 18.4
 Fischer-Friedrich, Elisabeth BP 8.1,
 BP 15.1, BP 25.2
 Fisher, Adam•MM 40.1
 Fistul, Mikhail DY 49.3, TT 23.11
 Fistul, Mikhail V. TT 20.11, •TT 54.3
 Fitch, Samuel CPP 45.3
 Fittipaldi, Rosalba TT 37.7, TT 37.10
 Fivel, Marc•MM 4.1
 Fix, Mrio MA 40.55
 Flache, Andreas TUT 2.2, SOE 1.2
 Flamm, Alexander CPP 11.3
 Flashar, Katarina-Sophie•HL 45.1
 Flatae, Assegid M. HL 29.10
 Flathmann, Christoph HL 33.57
 Flege, Jan I. O 92.4
 Flege, Jan Ingo HL 4.2, O 40.3,
 O 42.4, O 64.8, O 67.8, O 74.1, O 78.9,
 O 92.6, O 93.7
 Fleischhaker, Johann O 81.1
 Fleischmann, A. TT 57.21, TT 57.27,
 TT 57.28, TT 58.2, TT 58.4
 Fleischmann, Andreas TT 43.30,
 TT 43.31, TT 43.32, TT 57.25,
 TT 57.26, TT 58.1, TT 58.3, TT 58.5,
 TT 58.25, TT 66.7
 Flenner, Silja MM 42.6
 Fleury, Jean-Baptiste BP 11.35
 Flick, Johannes CPP 45.5
 Flicker, Felix TT 51.7
 Flieg, Marco HL 38.7, O 96.7
 Flindt, Christian•SYQD 1.4
 Flipon, Baptiste MM 23.30
 Floerchinger, Stefan TT 53.6
 Floess, Moritz•BP 12.7
 Flommersfeld, Johannes BP 31.5
 Florent, Fessler•BP 1.8
 Flores Calderon, Rafael Alvaro
 •TT 36.7
 Florez, Elizabeth O 52.3
 Florian, Hilsber HL 7.41
 Florian, Matthias DS 2.4, HL 8.5
 Flöß, Moritz BP 12.2
 Flötto, Aaron HL 7.1, HL 7.2, HL 7.8,
 •HL 38.1, HL 38.3
 Flurin, Emmanuel PLV X
 Fodor, Étienne BP 2.12, BP 24.5,
 BP 24.10, DY 38.5, DY 38.10
 Foerster, M. O 47.3
 Foerster, Michael MA 38.1, MA 50.1
 Foggetti, Francesco•MA 22.1,
 MA 22.3, MA 50.6
 Föhlich, Alexander MA 8.9, MA 20.3,
 O 67.9, O 85.1
 Fohmann, Kenny•TT 57.22
 Fojt, Jakob•O 76.8
 Fokina, Vladislava CPP 19.9
 Folge, Patrick O 80.4
 Fomin, Vladimir M.•DS 7.4, •TT 3.11,
 •TT 3.12, •TT 3.13
 Fonin, Mikhail O 2.7, •O 56.7, O 64.10
 Font-Clos, Francesc MM 33.7
 Foppa, Lucas MM 21.3, O 52.5,
 •O 78.1, O 78.7
 Förg, Michael HL 33.34
 Forget, Anne MA 11.1
 Forker, Roman O 18.4, O 22.3, O 22.9,
 O 47.2
 Fornari, Celso I. O 74.4, O 94.6
 Förner, Andreas MM 40.2
 Förschner, Felix O 56.7
 Förschner, Lukas O 14.10, O 96.5,
 •O 96.10
 Forslund, Axel•MM 36.8
 Först, Michael TT 62.7
 Forster, Christoph TT 15.3
 Forster, Lea MA 48.2, •O 49.6
 Förster, Michael MA 31.2
 Förster, Stefan O 14.1, •O 47.10,
 O 51.5, O 92.2, O 92.9
 Förster, Stephan CPP 19.9, CPP 57.5
 Förster, Tobias MA 44.2
 Forsting, Johanna BP 23.10
 Förstner, Jens HL 7.64, HL 24.6
 Fort, Kyle L. BP 11.41
 Fortágh, József TT 39.5
 Forti, Mariano•MM 36.2
 Fortmann, Jill DS 6.4
 Förtsch, Andre DY 4.4
 Fortunato, Isabela Corina BP 30.4
 Föslleitner, Elias•MM 31.5
 Foster, Adam O 6.8, O 87.4
 Foster, Adam S MM 12.14, O 66.2,
 O 66.10, O 74.2, O 87.8
 Foster, Peter BP 30.3
 Foster, Sarah BP 25.4
 Fotev, Ivan TT 62.1
 Fowley, Ciaran HL 50.3
 Fowlie, Jennifer DS 12.28
 Frachet, M. O 30.4
 Frachet, Mehdi TT 34.1
 Fraenheim, Thomas O 6.7
 Fragkopoulos, Alexandros•BP 9.1,
 BP 25.6, BP 28.37
 França, Hugo•BP 28.42, CPP 44.3
 Franceschi, Giada O 33.8, •O 54.6,
 O 54.8, O 68.2, O 92.10
 Franchi, Stefano O 29.1
 Franchini, Cesare O 72.3, O 81.4
 Franch, Max•HL 14.9
 Franco Peñaloza, Roberto TT 43.19
 Franco, Victorino•SYGM 1.5
 Frang Christiansen, Emil KFM 1.8
 Frank, Bernhard•TT 47.5
 Frank, Bettina O 43.4, O 80.3, •O 80.5,
 O 91.4
 Frank, Carolin•O 5.7
 Frank, Freimuth MA 4.2, TT 7.2
 Frank, J. Thorben MM 36.7
 Frank, Jonathan DS 15.4, KFM 6.14
 Frank, Kilian CPP 17.6, •CPP 19.11,
 CPP 28.8, HL 45.4, HL 45.6, TT 32.8
 Frank, Marcus BP 28.13
 Frank, Maximilian CPP 17.11,
 CPP 17.48, •CPP 53.7
 Franke, Katharina O 7.4
 Franke, Katharina J.•SYTS 1.4, O 7.2,
 O 7.6, O 20.4, O 20.6, O 21.1, O 22.6,
 O 33.4, O 33.8
 Franke, Lars•TT 47.4
 Franke, Oliver•MA 33.4
 Frosch, Thomas BP 11.1,
 CPP 17.55, DY 42.4, DY 42.13,
 DY 44.8, DY 46.10
 Fransson, Erik MM 23.34
 Franz, Christian MA 40.42, TT 4.13
 Franz, Evanie O 73.2
 Franz, Julian TT 54.9
 Franz, Martin O 28.4, O 28.6, •O 48.3,
 O 55.5
 Franz, Ronald KFM 7.4
 Franze, Kristian BP 25.4, •BP 32.1
 Franzén, Daniel MA 2.3
 Franzese, Giancarlo•BP 22.11
 Franzke, Katharina Lorena•HL 33.51
 Fratino, Lorenzo DS 12.28
 Frauenheim, Thomas CPP 28.9,
 HL 13.4, KFM 6.5, MM 10.2, MM 10.3,
 MM 21.5, O 17.4, O 37.8, TT 32.9
 frauhammer, timo MA 19.5
 Frederic, Laquai CPP 1.8
 Frederiksen, Anders BP 11.42
 Fregin, Bob BP 8.8, BP 8.11
 Freiburger, Eva Marie O 23.1, O 23.3,
 O 41.1, O 64.1, •O 73.8
 Freier, Erik HL 23.2
 Freindl, Kinga MA 41.7
 Freitag, Norbert H. MA 32.2, TT 18.3
 Freitas, Nahuel DY 40.9
 Fremdling, Paul•BP 11.41, BP 21.3,
 O 26.1
 Frenzel, Jan•BP 12.1, MM 23.5
 Frenzel, Maximilian HL 17.7
 Frenzel, Maximilian HL 17.9,
 •HL 33.53
 Frenzke, Susann CPP 36.8
 Frese, Natalie CPP 35.20, O 68.1
 Freudenberger, Jens MA 3.5,
 MM 40.9
 Freudenstein, Josef O 8.7
 Freund, Friedrich TT 46.10
 Freund, Martina MM 37.1, •MM 37.8
 Frey, Benedikt TT 43.31
 Frey, Erwin•SYQC 1.3, BP 7.6,
 BP 16.3, BP 22.8, DY 4.5, DY 10.6
 Frey, Felix•BP 1.5
 Frey, Marthia DS 1.2, •O 47.8
 Frey, Pascal MA 23.67
 Frey, Philipp•TT 38.2
 Freysoldt, Christoph MM 3.1, MM 3.6,
 MM 36.4, •O 30.7, O 69.7, O 86.3
 Friák, Martin MA 3.8, MA 37.1,
 •MA 37.6, •MM 19.1, •MM 32.7
 Fricbezer, Nora CPP 58.5
 Fricke, Jörg HL 23.2
 Friebe, Christian CPP 1.4

Author Index

- Friedemann, Sven TT 3.6, TT 9.1, TT 51.7
- Friederich, Pascal MM 31.1
- Friedrich, Benjamin M. BP 8.7, BP 12.10, BP 30.5
- Friedrich, Bernhard HL 29.4
- Friedrich, Christoph HL 7.38, HL 26.6, O 53.6, O 67.10
- Friedrich, Daniel O 58.9
- Friedrich, Dennis HL 47.7
- Friedrich, Felix HL 27.6, O 20.11, O 62.6, O 77.9, TT 40.6
- Friedrich, Florentine O 47.2
- Friedrich, Jochen HL 37.3
- Friedrich, M. TT 57.28
- Friedrich, Markus S. MM 26.10
- Friedrich, Rico MM 36.9, O 36.4, O 47.1
- Fries, Max MA 25.1
- Friesen, Cody MA 20.8
- Frisch, Benjamin O 80.1, O 80.4
- Frischknecht, Friedrich BP 28.47
- Frischmann, Michael BP 15.3, BP 21.11
- Fritsch, Daniel HL 5.2, HL 13.2, O 17.2
- Fritsch, Marco MA 49.7
- Fritz, Jonas DY 32.12
- Fritz, Torsten CPP 36.9, O 18.4, O 22.3, O 22.9, O 36.9, O 47.2
- Fritze, H. KFM 14.1
- Fritze, Holger KFM 6.20, KFM 13.4, KFM 13.5, KFM 13.6
- Fritzsche, Alexander TT 36.6, TT 64.5
- Fröhlich, Dietmar HL 35.9, HL 47.2
- Frohloff, Lennart CPP 17.40
- Frohoff-Hülsmann, Tobias BP 24.4, DY 4.3, DY 38.4
- Frolov, Timofey MM 31.4
- Frömling, Till KFM 2.5, KFM 2.6
- Fromm, Lukas O 60.6, O 73.2
- Frömming, Marc O 77.2
- Frömter, Robert MA 4.2, MA 12.4, TT 7.2
- Frost, Jarvist Moore CPP 1.5
- Frühauf, Dietmar DS 12.4
- Frustaglia, Diego TT 60.1
- Fu, Mingxuan TT 46.1
- Fu, Yonghuan KFM 10.5
- Fuchs, Alexander O 84.10, TT 56.10
- Fuchs, André DY 5.1, DY 32.9
- Fuchs, Carmen MM 18.5
- Fuchs, Christopher TT 17.1
- Fuchs, Dirk TT 54.1
- Fuchs, Florian DS 1.1, HL 33.58
- Fuchs, Harald O 66.7, O 97.7
- Fuchs, Laura CPP 17.58
- Fuchs, Matthias DY 11.6
- Fuchs, Phillippe BP 16.10
- Fuchs, Sophia HL 24.11
- Fuchs, Timo O 69.10, O 96.4
- Fuhrer, Michael S. HL 14.4
- Fuhrmann, Felix MA 5.5
- Fuhrmann, Jürgen CPP 17.13, O 96.2
- Fujinami, Masanori KFM 9.5
- Fukushima, Takanori O 37.1
- Fulga, Cosma TT 17.6
- Fulga, Ion Cosma MA 41.3, TT 36.5
- Fumeron, Sébastien BP 29.9
- Funato, Mitsuru HL 23.3, HL 23.6
- Fünfhaus, Axel TT 36.2
- Fünferlings, Achim O 92.7
- Furat, Orkun MM 23.30
- Furchner, Andreas DS 13.1, DS 13.4
- Fürst, Lena HL 30.4, TT 41.4
- Fürst, Lena TT 17.1
- Fürst, Maximilian TT 17.7, TT 59.3
- Furthmüller, Jürgen HL 18.1
- Fusek, Lukáš O 29.2, O 73.2
- Fusil, Stéphane MA 11.1
- Fyhn, Eirik Holm TT 57.1
- Fyhn Holm, Eirik O 59.9
- Fyta, Maria BP 11.53, TT 63.10
- Fytas, Nikolaos G. DY 49.10
- G. Pagliuso, Pascoal MA 39.3
- G. Ramachandran, Rahul BP 15.2
- G. Vergniory, Maia MM 6.10
- Gaal, Peter DS 6.2, HL 33.33, MM 17.1
- Gabel, Judith TT 43.8
- Gabel, Stefan MM 4.3
- Gabriel, Jan CPP 50.3
- Gabriel, Philipp MA 3.2
- Gaczynski, Piotr KFM 13.6
- Gade, Ben TT 37.11
- Gade, Vamshidhar R. BP 28.17
- Gadge, Karun TT 6.1, TT 31.3
- Gadzekpo, Aaron BP 11.59, BP 12.11
- Gaerner, Maik MA 15.1
- Gaertner, Daniel MM 18.2
- Gagel, Philipp HL 5.1
- Gagnon, Pauline AKC 1.1
- Gaida, John H. O 80.2
- Gaiffe, Olivier HL 10.2
- Gaimnon, Mario U. DY 17.2
- Gaisner, Niklas TT 54.4
- Gajewski, Lukasz DY 57.2, SOE 4.4
- Galante, Mario CPP 45.1
- Galazka, Zbigniew HL 21.3, HL 41.6, HL 41.7
- Galeski, Stanislaw TT 6.8, TT 59.9
- Galeski, Stansilaw TT 59.10
- Gali, Adám MA 32.4
- Galiffi, Emanuele O 58.8
- Galindez-Ruales, E.F. MA 18.4
- Galinski, Henning O 49.6
- Galla, Tobias BP 18.4, DY 33.4, DY 57.6, SOE 8.3, SOE 17.1
- Gallardo, Aurelio O 97.3
- Gallardo Domínguez, Laura MM 42.6
- Gallardo, Laura CPP 35.64
- Gallei, Markus CPP 13.8
- Galli, André O 13.2
- Galstian, Iryna MM 12.31
- Gamayun, Oleksandr TT 38.10
- Gambassi, Andrea DY 32.1
- Gambino, Davide MM 22.6
- Gamer, Lisa TT 57.25
- Gámez, Francisco MA 36.6
- Gammer, Christoph MM 28.4
- Gan, Z. O 47.7
- Gan, Zi Zhao TT 62.5
- Gan, Ziyang DS 12.14, DS 12.16, HL 14.6, O 4.3, O 5.3, O 18.1, O 18.3, O 18.4
- Gandhi, Poshika DY 16.8
- Gandorfer, Simon TT 49.1, TT 58.20
- Gandy, Amy S. MM 40.7
- Gangal, Chenmay CPP 19.1
- Ganguli, Nirmal MA 20.6
- Ganie, Umar Bashir KFM 13.2
- Ganschow, S. KFM 6.46
- Ganschow, Steffen KFM 6.42, KFM 6.44, KFM 13.4, KFM 13.5, KFM 13.6, KFM 14.6
- Ganser, Romana O 91.9
- Ganss, Fabian DS 6.1, MA 31.7
- Gant, Patricia HL 33.4
- Ganter, Markus BP 11.18
- Gao, Feng HL 10.2
- Gao, Hao O 93.6
- Gao, Shang MA 2.6
- Gao, Timm HL 1.7
- Gao, Xing DY 25.6, TT 33.6
- Gao, Xuejian MA 10.4, TT 12.4
- Gao, Yilun DY 43.8
- Gaponenko, Iaroslav KFM 4.9
- Garai-Marin, Haritz O 15.9
- Garbarino, Gaston TT 44.8, TT 51.6, TT 57.8
- García, Alejandra MM 26.5
- García Arcos, J. M. BP 31.2
- García, Carlos DY 42.14
- García de Abajo, F. Javier O 80.2
- García, José MM 12.5
- García Jr., Ailton HL 7.65, HL 7.66
- García, Martin E. BP 13.5, DS 4.1, DS 12.6, KFM 6.37, O 6.6
- García, Vincent MA 11.1
- García-Fuente, Amador MA 24.2
- García-Goricelaya, Peio HL 26.7, O 53.7
- García-Lekue, Aran O 7.8
- García-Page, Ana MM 6.10
- García-Vergniory, Maia MA 9.3
- Gardner, Geoffrey C. TT 20.8, TT 27.5
- Garg, Charu MA 9.5, MA 9.6, MA 39.4, MA 40.37
- Gargiani, P. O 47.3
- Gariglio, Stefano DS 12.28
- Garlapati, Mohan Muralikrishna MM 40.8
- Garnica, Manuela O 3.7
- Garnweitner, Georg KFM 6.16
- Garofide, Silvia DS 12.9
- Garreis, Rebekka HL 9.4, TT 14.4
- Garro-Hernandorena, Ane O 74.7
- Garst, Markus MA 2.5, MA 12.6, MA 35.5, MA 47.8, TT 37.1, TT 37.4, TT 37.5, TT 47.4, TT 59.15
- Gärttner, Martin DY 2.9, TT 2.9, TT 58.13
- Gaß, Sebastian MA 44.8
- Gasenzer, Thomas DY 27.9
- Gashnikovina, Daria O 81.5
- gaspar, ana belén MA 19.5
- Gaspard, Léo TT 43.15
- Gastaldo, L. TT 57.27
- Gastaldo, Loredana TT 57.25, TT 58.1
- Gat, Omri DY 9.7
- Gati, E. TT 34.3
- Gati, Elena TT 37.13
- Gatsios, Christos CPP 17.24
- Gatto, Salvatore TT 38.9
- Gauckler, Cornelius MM 16.4
- Gaudig, Maria HL 7.15
- Gault, Baptiste MM 15.9, MM 27.8, MM 36.4, MM 37.7
- Gault, Joseph BP 11.41
- Gaur, Kartik HL 12.2, HL 33.47
- Gaurav, Kumar BP 3.4
- Gavalda-Diaz, Oriol MM 4.7
- Gavara Edo, Miguel DS 4.6
- Gaydamachenko, Victor TT 39.6
- Gayles, Jacob MA 37.4
- Gayone, Esteban O 85.4
- Gazizulina, Alsu MA 40.38
- Gazizullin, Ilias O 55.8
- Gazzaneo, Paolo TT 22.9, TT 22.10, TT 22.11
- Ge, Yuqing MA 2.2
- Gebel, Steven MA 2.7
- Gebel, Matthew HL 14.4
- Gebert, S. HL 17.8
- Gebert, Sebastian HL 30.3, TT 41.3
- Gebhardt, Julian HL 4.4, MM 5.6, MM 27.5, TT 21.5
- Gebremichael, Zekarias Teklu CPP 51.8
- Geck, J. MA 44.3
- Geck, Jochen MA 2.7, MA 40.20, MA 44.8, TT 23.3, TT 29.1, TT 51.6
- Geelhaar, Lutz HL 7.40
- Geers, Patrick O 18.5
- Gegenwart, Philipp MA 13.2, MA 13.7, MA 23.9, TT 4.3, TT 19.2, TT 19.7, TT 43.7, TT 46.4, TT 46.10, TT 52.2, TT 52.7
- Gehrer, Simone BP 15.5
- Geibel, C. TT 47.2
- Geibel, Christoph TT 28.3
- Geiger, Christina CPP 8.4, CPP 53.4
- Geilen, Moritz MA 15.3, MA 34.7
- Geilenkeuser, Julian BP 11.71
- Geirhos, Korbinian MA 44.2
- Geisel, Theo DY 46.1
- Geisert, Simon TT 49.4
- Geishendorf, Kevin MA 4.14, MA 23.60, MA 40.64, TT 7.14
- Geisler, Benjamin O 67.7, TT 50.5
- Geißler, Nicole MM 12.31
- Geist, J. TT 57.27
- Geldiyev, Begmuhammet O 67.3, O 67.5, O 94.6
- Geller, M. HL 7.56, HL 29.2
- Geller, Martin SYQD 1.3, HL 1.10, HL 7.46, HL 7.51, HL 24.10, HL 24.12, TT 60.2
- Geller, Martin Paul DY 9.6
- Gellert, Florian BP 1.10
- Gembé, Martin MA 40.24
- Gemmer, Jochen DY 25.10, TT 33.10, TT 43.21, TT 43.25
- Gemming, S. O 69.11
- Gemming, Sibylle CPP 36.3, DS 14.1, DY 57.1, HL 33.58, MA 40.44, O 36.1, O 36.7
- Gen, Masaki TT 46.1
- Generalov, Alexander O 93.8
- Gensch, Marc CPP 29.2, MA 38.5
- Genthon, Arthur BP 16.2
- Gentle, Angus HL 22.3
- George, A. O 47.7
- George, Ann Rosna BP 2.6
- George, Antony DS 12.14, DS 12.16, HL 14.6, O 4.3, O 5.3, O 18.1, O 18.3, O 18.4
- George, Janine MM 12.36
- Georges, Antoine TT 37.6
- Georgiev, Yordan M. HL 16.1, TT 24.1
- Georgiou, K. HL 48.4
- Georgiou, Theoni K. CPP 8.2
- Geprägs, Stephan MA 4.13, MA 23.50, MA 23.77, MA 23.80, MA 34.6, MA 40.15, MA 40.65, TT 7.13, TT 39.4
- Gerasimenko, Yaroslav O 34.2
- Gerber, Dennis MM 11.5
- Gerber, Simon O 21.4
- Gerdes, Olga CPP 1.11
- Gerhards, Luca BP 1.6
- Gerhardt, Holger BP 28.15, BP 28.57
- Gerhorst, Christian-Roman HL 31.7, O 61.7
- Gericke, Dirk O. O 16.6
- Gerken, Martina MM 26.7
- Gerlach, Alexander CPP 19.12, CPP 29.7, O 63.1, O 95.9, TT 68.9
- Gerland, Ulrich BP 10.4, BP 10.6, BP 22.5, DY 45.8, DY 45.9, DY 45.12
- Gernhäuser, Roman CPP 51.4
- Gerold, Marcel DS 10.5
- Gerstel, Miriam CPP 35.52
- Gerstmann, Uwe HL 7.14, HL 33.28, HL 33.51, HL 33.52, KFM 6.1, KFM 6.17, O 28.4, O 36.10
- Geske, Michael O 78.1
- Geßler, Philipp MA 26.6
- Gessert, Denis DY 6.11
- Gessner, Julia Anthea MA 23.40
- Gestefeld, Martin SYOF 1.2
- Geßwein, Holger MA 3.1
- Getzlaff, Matthias BP 28.26, BP 28.27, MA 23.26, MA 23.27, O 42.3
- Gevers, Lennart SOE 17.2
- Gewinner, Sandy O 39.2
- Geyer, Veikko F. BP 2.11, BP 30.5
- Gezmiş, Afra O 6.2, O 11.2, O 38.2, O 60.6
- Ghafariollahi, Alireza MM 15.8
- Ghan, Simiam HL 40.7, O 79.7
- Ghannadi maragheh, Hatfeh HL 16.7, TT 24.7
- Gharabeiki, Sevan HL 45.5
- Gharat, Soham KFM 6.15
- Ghassemizadeh, Reyhaneh MM 9.3, MM 11.1
- Ghaziz, Nasser BP 22.10
- Ghazinezhad, Zahrasadat MA 40.17
- Ghebretinsae, Bereket MA 40.37, TT 9.2
- Ghim, Minsu MM 19.5
- Ghiringhelli, Luca M. MM 31.4, MM 31.6, O 57.6, O 84.4, O 84.9, O 95.6, O 95.10, TT 56.4, TT 56.9, TT 68.6, TT 68.10
- Gholami, Abbas DY 23.2
- Gholinia, Ali HL 4.6
- Ghorbani-Asl, Mahdi O 47.1
- Ghosal, Chitran O 36.7, O 64.4, O 82.2, O 82.6, O 82.8, O 82.9
- Ghosh, Pratyay TT 29.12, TT 29.13
- Ghosh, Sayak TT 37.1
- Ghosh, Sheuly MM 29.3
- Ghosh, Subhradip MM 16.7
- Ghosh, Sukanya MA 7.5, MA 23.49
- Ghosh, Sumit MA 10.3, TT 12.3
- Ghosh, Supriya O 51.4
- Ghosh, Tanmoy KFM 6.25
- Giammarino, Alessandro O 34.8
- Giazotto, Francesco TT 27.2
- Gibbins, Molly DY 55.9, TT 67.9
- Gibbs, Alexandra S TT 37.11
- Giberti, Claudio DY 56.10
- Giebler, Lars MM 23.5
- Giers, Peter HL 12.5
- Gierster, Lukas MA 30.3, O 34.3, O 37.4
- Gieß, Aaron DS 8.1, HL 7.8
- Gies, Christopher DY 9.2, HL 8.7, HL 43.1, HL 49.1, HL 50.8
- Giese, Christian MA 23.41
- Giese, Wolfgang BP 28.57
- Giesen, Jan Mathis MA 16.1
- Giessen, Harald BP 12.2, BP 12.7, CPP 37.3, DS 2.2, HL 50.2, HL 50.5, KFM 7.2, KFM 7.3, MM 8.2, O 43.4, O 49.1, O 49.9, O 80.3, O 80.5, O 91.4
- Giessibl, Franz O 45.1, O 97.5, O 97.6, O 97.8
- Giessibl, Franz J. O 87.7, O 97.2
- Gigan, Sylvain DY 26.8
- Gil, Bernard MA 32.6
- Gilbert, Jennifer BP 27.4
- Gildemeister, Nora CPP 18.8, CPP 35.30
- Gilkes, Joe DY 57.4
- Gill, George TT 6.6
- Gilles, Ralph CPP 17.47, CPP 45.3, KFM 10.3, KFM 10.9
- Gillett, Alexander J. CPP 11.7
- Gillig, Matthias TT 46.5, TT 52.8
- Gimperlein, Matthias DY 17.6
- Ginga, Victoria MA 7.9
- Gingras, Olivier TT 37.6
- Ginot, Felix DY 16.1, DY 16.4, DY 16.6,

DY 16.7
 Ginzel, Florian•HL 29.8
 Giomi, Luca BP 4.9, BP 30.7
 Giorgianni, Flavio MA 46.10
 Gippius, Andrei TT 30.13
 Girard, Martin•BP 11.39, BP 17.3,
 BP 18.3, CPP 2.12, DY 33.3
 Girdhar, Ankush TT 16.12
 Girelli, Anita•SYSD 1.1, BP 11.46,
 DY 37.1
 Girschies, Frank O 78.1
 Giri, Amal Kanta•MM 6.1
 Giri, Rajendra O 39.6
 Giri, Rajendra P. BP 1.11
 Gironella, Marta BP 23.8
 Girones Paya, Paula BP 1.4, •BP 28.8
 Giroto, Antoine BP 25.6, •BP 28.37
 Giroto, Nina•O 64.12, •O 93.2
 Gitschier, David E. BP 25.8
 Gittinger, Moritz CPP 28.9, HL 2.5,
 O 58.2, TT 32.9
 Giuliani, Finn•MM 4.7
 Gizer, Gökhan O 29.6
 Gjana, Erbara•BP 28.36
 Gkouzia, Georgia•MA 17.5
 Glaab, Johannes HL 23.2
 Gladrow, Jannes DY 32.11
 Gladyshev, Sergei•O 91.2
 Glaser, Conny TT 39.5
 Glaser, Timo•O 48.4
 Glass, Joyce TT 43.31
 Glatzer, Otto CPP 57.7
 Glatzel, Pieter TT 44.7
 Glatzel, Thilo O 4.5, •O 12.6, O 32.8,
 O 38.3, O 87.3
 Glaum, Julia•KFM 1.6
 Glazman, Leonid I. O 33.8
 Glazov, Mikhail M. DS 2.4, HL 15.2,
 HL 34.3
 Gleißner, Helena•O 16.1, O 37.8
 Gleißner, Robert O 11.4, •O 29.6
 Glidic, Pierre TT 17.3
 Glitzyk, Annegret CPP 17.13
 Gloaguen, Richard O 26.2
 Globisch, Christoph BP 11.45
 Glorius, Frank O 28.4, O 28.6
 Glöß, Daniel DS 12.4
 Gloskovskii, A.•MA 5.1, MM 12.1,
 MM 26.8
 Gloystein, Alexander ... O 68.4, O 76.7
 Gmitra, Martin DS 1.5, HL 1.1
 Gnavarro, Gema O 4.5
 Gnecco, Enrico O 87.3
 Gnezdilov, Nikolay TT 38.5
 Go, Dongwook MA 4.7, MA 4.10,
 MA 16.9, MA 31.5, TT 7.7, TT 7.10
 Göbel, Børge•MA 4.11, •MA 12.1,
 MA 35.1, TT 7.11
 Gobert, Christian•HL 29.3, HL 33.19,
 HL 33.22, HL 33.23
 Godec, Aljaz DY 32.3, DY 49.6,
 DY 56.2
 Godwin, Jonathan HL 6.8, O 9.8
 Goedecke, Julia•O 42.8
 Goedecker, Stefan CPP 45.6, MM 14.1
 Goedeke, Sven•BP 22.1
 Goennenwein, S.T.B. MA 41.2
 Goennenwein, Sebastian ... MA 4.12,
 TT 7.12
 Goennenwein, Sebastian T. B.
 MA 23.60, MA 23.62, MA 40.63
 Goennenwein, Sebastian Tobias
 Benedikt MA 4.14, MA 40.64,
 TT 7.14
 Goerzen, Moritz A.•MA 35.9,
 MA 40.52
 Gögelein, Christoph•CPP 58.3
 Gohar, Yomna BP 29.4
 Göhler, Clemens CPP 1.11, •CPP 11.3,
 CPP 36.2
 Gohsrich, Julius•O 94.10
 Goirand, Florian BP 9.5
 Göken, Mathias•MM 4.3
 Gokhale, Shreyas BP 30.3
 Goldberg, Joshua E. MA 3.6
 Golde, Tom BP 4.5, •BP 4.8
 Goldhahn, Rüdiger HL 33.42, HL 41.4,
 HL 51.9, HL 51.10
 Goldner, Philippe PLV X
 Goldobin, Edward TT 3.10, •TT 20.4,
 TT 57.22, TT 57.23
 Goldstein, Garry TT 51.2
 Gofek, Franciszek O 2.10
 Golestanian, Ramin BP 6.2, BP 9.2,
 BP 24.11, BP 30.2, DY 23.3, DY 31.4,
 DY 38.11
 Golias, Evangelos MA 19.4, MA 19.6

Golitsyn, Yury CPP 35.22
 Goll, David CPP 26.3
 Goll, Raphael MA 9.1
 Gollenstede, Julian SOE 15.1
 Golombek, Alexander O 13.7
 Golparvar, Amir O 95.5, TT 68.5
 Golze, Dorothea HL 20.1, HL 20.5,
 HL 20.7, HL 40.5, O 35.1, O 35.5,
 O 35.7, O 79.5
 Gölzhäuser, Armin CPP 54.5, O 28.9,
 O 36.3
 Goman, Denis O 12.5
 Gomez, G. MA 48.3
 Gomez Melo, Santiago•BP 17.6
 Gomez-Eslava, Gabriel MA 3.3
 Gómez-González, Manuel BP 30.4
 Gómez-Nava, Luis BP 11.64, SOE 16.1
 Gómez-Rodríguez, José M O 29.1,
 O 74.7
 Gomez-Vierling, N. BP 11.10, BP 11.11,
 BP 11.12
 Gomonay, O MA 31.1
 Gomonay, Olena MA 18.1, MA 18.2,
 MA 31.3, MA 40.5, MA 50.4
 Gompfer, Gerhard BP 28.48
 Gönczy, Pierre BP 17.6
 Gong, Qihuang DY 21.3
 Goniakowski, Jacek O 68.3
 Gonnella, Giuseppe•DY 27.8
 Gönheimer, Nils•MM 19.2
 Gonzalez Betancourt, Ruben Dario
 MA 4.14, •MA 40.64, TT 7.14
 Gonzalez Hernandez, Rafael Julian
 MA 4.14, MA 40.64, TT 7.14
 Gonzalez Oliva, Mariana Azevedo
 BP 28.35
 Gonzalez, Rafael MM 22.1
 Gonzalez-Cuixart, Marc O 14.8
 González-Hernández, R. MA 41.2
 González-Hernández, Rafael MA 41.4
 González-Herrero, Héctor O 66.11
 Gonzalez-Julian, Jesus MM 22.4,
 MM 22.5
 Gonzalez-Orellana, C. O 47.3
 González-Ruano, César TT 20.10
 Goodall, Russell MM 40.7
 Goodge, Berit•TT 44.1, TT 44.5
 Goodwin, Christopher O 11.4, O 29.6
 Goordevaya, Korneliya CPP 52.5
 Gooth, Johannes TT 59.9, TT 59.10
 Gopakumar, Thiruvancheril G. •O 3.2,
 O 60.12
 Gopal, Ashwin•DY 40.9
 Gopal, Deepti SOE 8.3
 Göpprich, Kerstin BP 5.2, BP 11.37,
 BP 11.59, BP 12.11
 Gorbunov, D. MA 33.6, MA 40.58
 Gorbunov, Denis MA 44.2, MA 44.6
 Gordalla, Barbara M.•AKC 1.3
 Gordeev, Ivan HL 7.8
 Gördes, Jendrik MA 19.4, •MA 40.12,
 MA 40.55
 Gordeyeva, Korneliya MA 38.5
 Gorelik, Tatiana DS 12.19
 Gorelov, Evgeny SYUE 1.4
 Gorenflot, Julien CPP 1.8, CPP 1.9,
 •CPP 11.2, CPP 43.1
 Gorgis, Azad MM 8.3, MM 12.33
 Gorini, Cosimo O 8.6, O 37.6, TT 17.7,
 TT 59.3, TT 62.6
 Gorkov, Dmitry MA 44.5
 Görling, Andreas O 60.6, O 69.9,
 O 73.2
 Gornyi, Igor V. TT 45.5
 Goronczy, Marvin•MA 40.11
 Górski, Piotr SOE 4.14
 Górski, Piotr J SOE 18.2, SOE 18.3
 Goss, Christina BP 28.33
 Gosse, Charlie BP 23.1
 Gössel, J. KFM 14.1
 Goswami, Jayesh CPP 35.24
 Gotfryd, Dorota•TT 21.9
 Götsch, Thomas MM 5.10
 Gottfried, J. Michael O 2.4, O 10.5,
 O 22.8, O 23.5
 Göttling, Niclas•DY 9.2, HL 8.7
 Gottschalch, V. DS 12.48, HL 7.20,
 HL 18.5
 Gottschalk, Kay-Eberhard .. BP 28.35
 Gottschall, T. MA 23.19, MA 42.4,
 MA 42.8
 Gottschall, Tino MA 3.9, •MA 23.18,
 MA 42.1, MA 42.3, MA 42.6
 Gottscholl, Andreas HL 22.10
 Götz, Alicia O 32.8
 Götz, Markus BP 11.76
 Götz, Martin O 82.7

Götzinger, Stephan HL 50.6, TT 25.4
 Gozłinski, Thomas•TT 3.1
 Graalmann, Jan-Hauke•HL 18.10
 Grabarics, Márkó BP 28.14, O 26.1,
 O 26.5, •O 66.4
 Grabowski, Blazej MM 5.8, MM 12.12,
 MM 14.2, MM 18.1, MM 27.7,
 MM 36.8, MM 39.3, MM 40.3
 Gracias, Josef MA 37.1
 Graczykowski, Bartłomiej HL 21.3
 Gradauskaitė, Elzbieta KFM 4.2,
 KFM 6.27
 Gradhand, Martin MA 23.4
 Gradl, Christian•CPP 35.21
 Gradziuk, Grzegorz DY 27.10
 Graf, Thomas HL 12.5
 Gräfe, Stefanie O 83.3
 Gräfensteiner, Phillip CPP 45.4
 Gräff, Kevin•CPP 29.3
 Grafke, Tobias DY 5.3
 Grammel, Jonas HL 49.3
 Grammer, Matthias MA 4.13, TT 7.13
 Granberg Cauchi, Sabastian
 •MA 23.32
 Grandjean, Nicolas HL 36.6, HL 51.5
 Grandy, Carolin BP 28.35
 Granovsky, Sergey MA 23.1, TT 29.4
 Granroth, Garrett E. TT 9.8
 Granwehr, Josef DY 46.2, MM 16.2
 Gräßler, Timo•DY 25.12, •TT 33.12
 Gräßler, Nico CPP 35.37
 Grassberger, Peter•SOE 9.1
 Grasser, Emma O 87.7
 Gratz, Sebastian•DS 12.45
 Grauer, Rainer DY 5.3, DY 46.9
 Graulich, Dominik O 68.1
 Graupeter, S. HL 23.1
 Graupeter, Sarina HL 28.5, HL 44.5
 Grava, Miriam•BP 26.8
 Gravouil, Anthony MM 33.5
 grawitter, josua BP 9.6, •MA 44.13
 Grazu, Valeria BP 30.4
 Greb, Christian•MA 22.4
 Greenhalgh, Ryan BP 25.4
 Greer, J A MA 31.1
 Grefe, Julius•TT 10.4
 Gregg, John MA 23.69
 Gregg, Marty KFM 4.1
 Greif, Julian•MM 12.12
 Greilich, Alex HL 15.2
 Greiner, Franko AKC 1.2
 Greiner, Mark O 85.8
 Greiter, Martin DY 48.7, DY 55.1,
 TT 55.7, TT 64.5, TT 67.1
 Grenz, Pascal Jona•O 85.6
 Gresista, Lasse•MA 7.10
 Gretarsson, Hlynur TT 9.3, TT 9.4,
 TT 9.5, TT 30.4, TT 30.7
 Greten, David•MM 8.4
 Greten, Lara HL 1.4, •HL 1.9
 Grether, Robin L.•TT 16.4
 Gretz, Oliver O 97.2
 Greule, Paul O 15.10, •O 20.3, O 77.3
 Greve, Daniel•CPP 44.4
 Greve, Matthias O 39.6
 Greving, Imke MM 42.6
 Grewing, Christian HL 16.9, HL 50.11,
 HL 50.12, TT 24.9
 Grieb, Tim HL 14.7
 Griedel, Markus TT 58.13, •TT 58.14,
 TT 58.15
 Griener, Timur TT 39.8
 Grieppe, Theodor MA 46.13
 Gries, Lukas•MA 9.8
 Gries, Stella•MM 42.6
 Griesinger, Andreas CPP 13.2,
 MM 12.6
 Griesser, Christoph O 60.5
 Griffin, T. TT 3.4
 Grifoni, Milena TT 54.6
 Grigoletto, M. HL 23.1
 Grigoletto, Massimo•HL 28.5
 Grigorev, Petr MA 18.3
 Grigorev, Vladimir MA 18.3
 Grigorieva, Irina•SYHS 1.3
 Grigoryan, Naira•TT 45.4
 Grill, Leonhard BP 31.1, O 23.4,
 O 25.4, O 25.5, O 38.7, O 42.9, O 46.6,
 O 55.8, O 64.5, O 77.5
 Grimm, Fabian CPP 35.36
 Grimm, Philip O 47.2
 Grimm, Philipp O 58.7
 Grinenko, Vadim TT 6.6, TT 57.10
 Grinenkov, Vadim MA 44.6
 Grisdard, Stefan HL 35.4, •HL 35.8
 Grivas, Nikolas TT 47.4
 Gröbmeyer, Johannes DS 1.4

Grochot, Krzysztof MA 41.7
 Groenenboom, G. C. O 42.2
 Groll, Daniel•HL 10.5
 Gronenberg, Ole DS 12.57
 Gronin, Sergei TT 20.8, TT 27.5
 Gröning, Oliver O 10.4
 Groot, I.M.N. HL 33.62
 Groot, Irene O 36.2
 Groß, Axel CPP 28.1, KFM 10.4,
 MM 16.4, MM 16.6, O 3.6, O 69.4,
 TT 32.1
 Gros, Claudius DY 45.1
 Groß, Hendrik DS 12.57
 Grosche, F. Malte TT 4.12, TT 34.5,
 TT 34.6
 Grosche, Malte TT 4.11, TT 57.14,
 TT 59.13, TT 59.14
 Großenbach, Sebastian MA 46.3
 Großmann, Max•O 67.2
 Großmann, Robert•BP 24.9, DY 26.6,
 DY 31.3, •DY 38.9, •DY 56.11
 Gross, Axel CPP 35.49, MM 16.3,
 O 73.7
 Gross, Heiko O 58.9
 Gross, Leo O 22.1, •O 45.2, O 66.3
 Gross, Rudolf MA 4.13, MA 23.50,
 MA 23.76, MA 23.77, MA 23.80,
 MA 34.6, MA 40.15, MA 40.35,
 MA 40.65, TT 7.13, TT 10.6, TT 18.2,
 TT 39.4, TT 39.7, TT 49.1, TT 54.8,
 TT 54.9, TT 54.10, TT 58.7, TT 58.8,
 TT 58.9, TT 58.10, TT 58.20, TT 66.6
 Gross, Thilo SOE 4.6, SOE 7.4,
 •SOE 11.6
 Gross, Wolfgang BP 25.8
 Grosse, C. TT 3.4
 Grosseck, A. S.•O 5.2
 Grosseck, Alexander Sagar O 13.8
 Grossman, Frank DY 43.1
 Grossmann, Frank TT 39.2
 Grossmann, Marius HL 12.1, HL 12.4
 Grosu, Cristina MM 16.2, O 59.10
 Grote, L. TT 3.4
 Grothe, Timo•CPP 35.20
 Grothuis, Maarten TT 23.6
 Grott, Sebastian CPP 51.4
 Gröttrup, Jorit KFM 9.9
 Grötzer, Gabriel HL 45.1
 Grover, Catherine O 56.9, O 74.8
 Grover, Rahul BP 8.5, BP 11.48,
 BP 23.9
 Gruber, Florian DS 13.2
 Gruber, Manuel•O 33.7, O 42.6, TT 8.1
 Gruber, Raphael MA 2.2, •MA 12.8,
 MA 23.6, MA 23.8, MA 23.11
 Grubišić Cabo, Antonija O 50.4
 Grubišić-Cabo, Antonija •O 6.3, O 8.8,
 O 37.12
 Gruenewald, Marco O 18.4
 Gruhl, Robert•MA 23.9, TT 43.7
 Gruhn, Thomas CPP 19.9
 Grumbach, Justus•TT 29.4
 Grümbel, Jona HL 33.42, •HL 51.9
 Grumm, Jonas•O 80.8
 Grundler, Dirk MA 12.6
 Grundmann, M. DS 12.48, HL 7.16,
 HL 7.19, HL 7.20, HL 18.5
 Grundmann, Marius DS 8.3, DS 10.4,
 DS 12.10, DS 12.12, DS 12.54, DS 13.3,
 DS 16.2, DS 16.3, HL 7.22, HL 7.29,
 HL 7.31, HL 47.4, HL 47.6, O 49.7
 Grundner, Martin TT 43.11
 Grüne, Jeannine CPP 11.7
 Grüneberg, Raimund DS 8.5
 Grünebohm, Anna PSV III, KFM 1.3,
 KFM 4.4, MM 12.8
 Grüneis, Andreas•HL 13.1, •O 17.1
 Gruner, Markus MA 8.7, O 8.3
 Gruner, Markus E. MA 3.8, MA 42.7
 Gruner, Markus Ernst MA 46.6, O 8.2
 Gruner, T. TT 47.2
 Grunert, Malte•MM 23.25
 Grünwald, Mona BP 8.5
 Grünhaupt, Lukas TT 39.6
 Grüninger, Markus TT 10.12
 Grunwald, Jan MA 19.4, O 42.6
 Grünwald, Marco O 36.9
 Grunwaldt, Jan-Dirk O 81.5
 Gruschwitz, Markus O 42.7, O 82.6,
 •O 82.8
 Grußler, Franziska•TT 46.4
 Grützmacher, Detlev DS 12.1, HL 18.3,
 HL 29.9, HL 30.1, TT 25.1, TT 36.1,
 TT 41.1, TT 59.5, TT 59.6
 Grychtol, Patrik O 37.9
 Grygiel, Clara HL 44.2, O 5.6
 Grzanka, Szymon HL 23.3, HL 23.6,

Author Index

- HL 28.3
Grzeszczyk, Magdalena HL 31.2,
O 61.2
Gu, Genda DS 5.2, DS 12.20, TT 62.2
Gu, Jihuan TT 52.5
Guan, Dong O 6.8
Guan, Tianfu CPP 17.4, CPP 17.46,
CPP 29.2, CPP 29.8, CPP 53.6
Guardado Calvo, Pablo BP 23.1
Guardi, Giorgia MM 12.7
Guarino, Anita TT 37.10
Guatieri, Francesco KFM 3.2
Gubaev, Konstantin MM 12.12,
MM 14.2
Gubbin, Christopher R. O 58.6
Guck, Jochen BP 11.67, BP 12.8,
BP 25.7, BP 28.17, BP 31.3
Guckeisen, Tobias BP 19.3,
CPP 41.3
Gückelhorn, Janine MA 4.13,
MA 23.50, MA 23.76, TT 7.13
Güdde, Jens O 8.7, O 34.2, O 37.11
Gueckstock, Oliver MA 22.2
Guédez, Gabriela O 57.5
Guennou, Mael MM 23.34
Guénolé, Julien MM 41.5
Guénon, Stefan DS 12.28
Guenther, Christian M. MA 43.6
Guérin, Thomas DY 32.4, DY 32.8
Guerra, Roberto MM 33.7
Guerra Santillan, Karla Yanin BP 15.1
Guerrini, Michele O 16.8
Guha, Sougata BP 18.2, BP 29.8,
DY 33.2
Gühr, Thomas DY 9.7, DY 37.2,
DY 48.3, SOE 4.1, SOE 11.1, SOE 22.2,
TT 55.3
Guidat, Margot HL 38.7, O 60.10,
O 69.14, O 73.4, O 96.7
Guignard, Léo BP 15.6
Guillamon, I. TT 6.4
Guillemond, C. TT 46.2
Guillonnet, Gaylord MM 28.9
Guimaraes, Filipe S. M. O 33.5
Guimaraes, Jose HL 34.6, TT 11.6
Guimaraes, Luiz R. MM 20.3
Guin, Satya N. MA 3.6
Guina, Mircea HL 12.3, HL 49.7
Guizzardi, M. HL 48.4
Gulans, Andris HL 13.5, MM 8.1,
MM 12.25, MM 14.1, O 17.5, O 85.10
Güldenpfennig, Tim O 42.7
Guldi, Dirk CPP 36.1
Güler, Seçil DS 11.2
Gülker, Gerd DY 5.8
Gumberidze, A. TT 57.28
Gumbsch, Peter MM 20.1
Gumeniuk, R. MA 44.3
Gumeniuk, Roman KFM 6.10,
MA 40.25, MA 44.8
Gümüs, Efe TT 20.1
Günay, Bensu O 25.5
Gunkel, Felix O 92.7
Gunnarsson, Olle TT 21.4
Günther, Andreas TT 39.5
Günther, F. O 69.11
Günther, Florian CPP 17.21
Gunther, Florian Steffen CPP 18.6,
O 36.1
Günther, Sebastian O 55.3
Günzing, Damian MA 3.3, MA 9.10,
MA 17.5
Guo, Cong O 22.8
Guo, Emily TT 58.18, TT 58.19
Guo, Hanjie TT 50.1
Guo, Haojie O 29.1, O 74.7
Guo, Ming BP 11.3
guo, qinda DY 25.7, O 6.3, O 8.8,
O 37.12, TT 33.7
Guo, Renjun CPP 17.44, CPP 51.4
Guo, Yaqian MA 41.3
Gupalo, Marina CPP 35.13, CPP 35.41
Gupta, A. MA 5.1
Gupta, Akash O 51.3
Gupta, M. MA 5.1
Gupta, Rahul MA 4.7, TT 7.7
Gupta, Reena MA 4.5, MM 6.8,
TT 7.5
Gurbuz, Emel MM 23.17
Gurdal, Yeliz O 81.12
Gurevich, Svetlana V. DY 45.4,
SOE 17.2
Gurlek, Burak HL 50.6
Gurlui, Silviu DS 12.9
gürsoy, emre MM 3.5
Gusenkova, Daria TT 49.2
Guskova, Olga CPP 8.5, CPP 17.22,
CPP 35.45, CPP 56.3, HL 7.28
Gustavsson, J. HL 23.1
Gustavsson, Johan HL 23.5
Gustmann, Tobias MM 12.31
Gustus, René MM 11.4
Gutfleisch, O. MA 23.19, MA 28.4,
MA 48.3
Gutfleisch, Oliver TUT 4.4, KFM 6.31,
MA 1.4, MA 3.1, MA 3.2, MA 3.3,
MA 3.4, MA 3.7, MA 3.8, MA 3.9,
MA 3.11, MA 28.1, MA 42.2, MA 42.3,
MA 42.7, MA 42.9, MA 48.8
Gutierrez, Rafael HL 36.1, TT 11.4,
TT 11.5
Gutowski, Olof DS 12.7, O 29.6
Gutsch, Sebastian CPP 35.23
Gutt, Christian BP 11.46, DY 37.1
Guttman, M. HL 23.2
Guttman, Martin HL 23.2
Gutzeit, Florian O 20.9
Gutzeit, Mara MA 40.52
Guzzinati, Giulio O 21.5
György, Szilvia SOE 4.12
Györök, Michael O 2.10
Gypens, Pieter MA 29.4
Gysin, Urs O 12.6, O 93.1
Gyürö, Noémi SOE 4.12
H. Gröschel, André CPP 12.6
H Panhwar, Muzaffar BP 8.8
Ha, Minjeong MA 40.47, MA 49.6
Haag, Felix O 14.6, O 36.6, O 40.2
Haas, Heinrich BP 26.7
Haas, Heinrich BP 26.8
Haas, Marcel TT 43.30, TT 43.32
Haas, Pierre A. BP 4.6
Haas, Rainer BP 5.4
Haase, Nadin BP 26.2
Habel, Jonas MA 10.8, TT 12.8
Habenschaden, Christopher
MA 40.40
Habermann, Ludwig BP 5.6
Habershon, Scott DY 57.4
Hache, Toni MA 32.4
Hackl, Lucas TT 38.2
Hackl, Rudi TT 23.13
Hackl, Rudolf TT 23.4
Hadaeghi, Niloofar DS 12.36
Hader, Tristan HL 24.13
Hadjab, Moufdi CPP 35.45, HL 7.28
Hadjadi, S. E. O 47.3
Hadjadi, Sebastien MA 40.55, O 56.5
Hadjadi, Sebastien Elie O 36.5
Hadjaj, Sebastien MA 19.4
Hadlich, Christoph HL 42.3
Haeger, Sarah BP 6.6
Haenen, Ken HL 29.10
Haertl, Patrick MA 14.4
Haeussler, Ellen TT 29.4
Hafeez, Asad BP 28.6
Hafermann, Martin DS 12.45
Hafner, Daniel TT 28.3
Hagedorn, Sylvia HL 44.3
Hagel, Marion TT 59.13
Hägele, D. HL 29.2
Hägele, Daniel HL 33.25, KFM 6.11
Hagemann, Johannes DY 18.7,
KFM 9.12
Hagemann, Ulrich O 5.7
Hagen, Jakob HL 48.5, O 70.2,
O 80.6, O 83.4
Hager, Mareike CPP 35.12
Hager, Martin CPP 1.4
Häggrström, Lennart KFM 11.3
Haghighirad, Amir-Abbas MA 16.9,
TT 10.8, TT 34.1, TT 57.8
Haglund, Å. HL 23.1
Haglund, Åsa HL 23.5, HL 51.5
Hagmann, Kevin CPP 58.5
Hahn, Alexander TT 38.11
Hahn, Christian PSV V
Hahn, Christopher O 24.2
Hahn, Horst MA 3.1, MM 28.7
Hahn, Marc Benjamin BP 11.8,
BP 11.9, BP 11.44, BP 11.78, BP 17.9
Hahn, Nico DY 9.7
Hahn, Thilo HL 3.7, HL 10.5, HL 33.18
Hahn, Viktor TT 51.3
Haider, Ferdinand MM 3.2, MM 12.2,
MM 18.4, MM 23.3, MM 23.31,
MM 40.4
Haindl, Rudolf O 8.1
Haines, Charles MA 32.1
Haisch, Christoph CPP 29.2
Hajdel, Mateusz HL 23.4
Haji Naghi Tehrani, Mohammad
Ebrahim O 81.3
Hajiri, Tetsuya MA 31.5
Hajzadeh, Nima HL 41.3
Hakkarainen, Teemu HL 49.7
Hakonen, Pertti TT 58.31
Halbauer, Max O 2.1
Halbental, Dorri TT 53.9
Halbritter, Thomas O 3.2
Haldar, Ritesh CPP 26.3
Haldar, Soumyajyoti MA 14.3,
MA 21.2, MA 40.52, O 55.10
Halder, Anita MA 7.3
Halik, Marcus CPP 17.52, CPP 28.10,
TT 32.10
Hall, Joshua O 56.8
Hall, Sam HL 26.5, O 53.5
Hallatschek, Oskar BP 10.5
Halle, Johannes O 64.2
Haller, Andreas TT 6.12
Haller, Lukas TT 47.10
Haller, Martin O 14.1, O 47.10
Hallier, Dorothea C. BP 11.9, BP 11.44,
BP 17.9
Hamada, I. O 75.9
Hamadeh, A. MA 16.6
Hamadeh, Abbass MA 23.8,
MA 23.61
Hamadeh, Alexandre Abbass MA 16.1
Hamann, D. TT 3.4
Hamann, Heiko SOE 19.5
Hamed, Mai H. O 42.12
Hamed, Mai Hussein DS 12.25,
DS 14.6, MA 5.6
Hammer, Lutz MA 14.2, O 56.1,
O 56.4, O 67.3, O 92.5
Hammer, Sebastian CPP 17.6,
CPP 17.8, CPP 17.24, CPP 28.4,
CPP 28.8, TT 32.4, TT 32.8
Hammer, Sina HL 50.2
Hammerschmidt, Thomas MM 36.2,
MM 40.2
Hammerschmidt, Wolfgang O 57.5
Hammouda, Sabreen TT 23.5,
TT 23.8
Hammud, A. O 75.9
Hammud, Adnan O 12.7, O 76.1,
O 76.4
Hamouche, Zehoua MM 33.2
Hampel, Alexander HL 31.2, O 61.2
Hampel, Silke CPP 35.37
Hamrle, Jaroslav MA 15.1
Han, Dan HL 45.2
Han, Jeong Woo MM 23.5
Han, Jian MM 26.4
Han, Seung Heon O 18.1
Han, Yisung CPP 45.3
Han, YuLong BP 11.3
Händel, Alexander K. TT 49.3
Händel, Alexander Konstantin
TT 58.12
Handschuh, Maria-Teresa TT 39.7,
TT 58.7, TT 66.6
Hanel, Rudolf SOE 16.2, SOE 18.1
Häner, Robert O 38.4, O 87.3
Hang, Hung-Hsiang MA 2.5
Hangleiter, Andreas HL 33.41,
HL 33.43, HL 51.2, HL 51.8
Hangleiter, Tobias HL 37.1
Hanic, Maja BP 11.28
Hanke, Kai Daniel HL 7.10
Hanke, Michael DS 8.2, DS 12.22
Hänke, Torben MA 40.36, MA 49.3
Hankiewicz, Ewelina TT 11.2
Hankiewicz, Ewelina M. HL 11.7,
TT 15.7
Hanna, Abanoub R. N. TT 46.7
Hannappel, Thomas HL 7.8, HL 7.9,
HL 7.10, HL 7.58
Hannebauer, Adrian HL 42.7
Hannezo, Edouard BP 2.3
Hans, Marcus MM 32.3, MM 37.8
Hanschke, Lukas HL 7.65, HL 7.66,
HL 33.34
Hansemann, Moritz DS 8.2
Hansen, Karin BP 1.11, O 39.6
Hansen, Lina MA 23.56, O 30.6
Hansen, Max Oberon TT 51.4
Hansen, Thomas MM 40.5
Hansmann, Philipp TT 4.10, TT 50.1,
TT 62.8
Hänze, Max O 77.7
Hao, Meng HL 11.4, TT 15.4
Hapala, Prokop O 66.10
Haque, Masudul DY 55.3, DY 55.7,
TT 67.3, TT 67.7
Harald, Schmidt KFM 13.3
Haraszti, Tamás DS 13.3
Harbig, Jana MA 3.2
Harbola, Varun DS 14.4
Harder, Constantin CPP 13.9,
CPP 17.26, CPP 26.1, CPP 29.5,
CPP 35.1, CPP 36.6, CPP 36.8,
CPP 37.2, CPP 52.5, DS 11.3,
DS 12.34
Harder, Ross KFM 9.9
Harder, Tristan H. HL 5.1
Hardt, Michael CPP 35.59,
CPP 53.5
Hardt, Steffen CPP 44.10
Haring Bolivar, Peter HL 29.10
Harris, Dimitrios HL 4.6
Harkort, Carolin HL 15.3
Harmon, Tyler BP 11.33, BP 29.5
Harmon, Tyler S. BP 22.9
Harms, Christina HL 33.42
Harnagea, Luminita TT 16.2
Harouri, Abdelmounaim HL 10.10
Harper, Angela F. DY 44.2
Harren, Lara O 43.3
Harrer, Anton O 73.8
Harriman, Katie MA 19.1
Harrington, David O 69.10, O 96.4
Harrison, George CPP 1.9
Hartel, Jan-Gabriel HL 7.47
Hartelt, Michael O 80.1, O 80.4,
O 95.3, TT 68.3
Harth, Kirsten DY 7.8, DY 29.10
Harting, Jens BP 2.9, CPP 18.2,
CPP 51.5, CPP 52.4
Härtl, Patrick MA 14.5, O 2.2, O 55.10,
O 59.6
Hartl, Tobias O 29.9, O 41.2
Hartmann, Alexander K. BP 11.58,
DY 40.1, DY 44.5, DY 44.7, DY 46.4,
DY 49.1, SOE 6.2
Hartmann, Andreas BP 23.4
Hartmann, Bálint DY 57.1
Hartmann, Claas MA 28.1
Hartmann, Dorit CPP 35.22
Hartmann, Fabian HL 17.5, HL 30.3,
TT 41.3
Hartmann, Felix DY 40.3
Hartmann, Frank CPP 13.8
Hartmann, Jana HL 44.3
Hartmann, Lenz SOE 7.1
Hartmann, Roman MM 3.4, TT 11.1,
TT 37.7, TT 37.10
Hartmann, Simon CPP 8.1, CPP 44.4,
CPP 44.7
Hartmann, Vincent MM 5.5
Hartnoll, Sean MM 6.6
Hartschuh, Achim CPP 51.1, HL 38.2
Härtter, Daniel BP 4.7, BP 28.30
Hartung, Conrad V. HL 41.7
Hartung, Conrad Valentin HL 41.3
Hasan, Noor TT 57.23
Haschke, Heiko BP 31.7
Häser, Maria DS 12.38
Hashimoto, Kenichiro TT 51.9
Haskel, Daniel MA 39.2
Haslbeck, Franz MA 40.35
Hassan, Alaa CPP 35.29, CPP 53.3
Hassan, Mohammed O 75.5
Hassan, Syed Ali CPP 17.8
Hassani Abdollahi, Younes O 96.2
Hassanpour, Ehsan MA 50.7
Hasse, Vicky O 59.7
Hasselbrink, Eckart DS 12.31,
DS 12.32
Hassing, Elena TT 28.2, TT 28.3,
TT 37.8, TT 52.6
Hassler, Fabian HL 9.5, TT 14.5,
TT 16.18, TT 31.2, TT 31.8, TT 57.24,
TT 59.4
Hastenteufel, Luca David BP 11.54
Hatami, Fariba HL 33.33
Hatem, Osama HL 17.3
Hatta, Shinichiro O 32.4
Hättig, Christof CPP 2.4
Hatton, Peter D. MA 11.6
Hatzoglou, Constantinos KFM 4.3
Hauch, Jens HL 25.3
Hauck, Daniel TT 59.15
Hauck, Jonas TT 37.6
Hauck, Jonas B. O 93.3
Hauseis, Vincent MA 23.80
Haug, Rolf J. HL 16.4, HL 16.7,
HL 16.8, HL 30.5, HL 34.4, HL 42.7,
TT 24.4, TT 24.7, TT 24.8, TT 41.5
Haugerud, Ivar BP 11.31
Haugerud, Ivar Svalheim BP 10.8
Hauke, Lara BP 28.30, BP 28.41
Hauner, Jonas O 69.9
Häupl, Daniel HL 33.22
Hauptmann, Nadine O 30.2
Hauschild, Johannes DY 25.11,

TT 33.11
 Hauser, Kevin O 77.8
 Häußler, Ellen MA 40.22, TT 43.2, TT 46.5
 Häusler, I. HL 23.1
 Häusler, Wolfgang MA 35.2
 Häußler-Möhring, Adrian DY 29.11
 Hausoel, Andreas TT 29.7
 Hauspurg, Andreas TT 52.3
 Hautier, Geoffroy MA 47.1
 Hävecker, Michael O 78.1
 Havela, Ladislav TT 9.4
 Havenith, Martina BP 17.2, BP 27.1
 Haverkamp, René CPP 57.10
 Haverkamp, Robert MA 8.9
 Haverkort, M. W. TT 46.2
 Haverkort, Maurits TT 30.4
 Haverkort, Maurits W. MA 23.25, TT 4.10, TT 30.7
 Hawkins, Rhoda Joy BP 28.54
 Hawly, Tim CPP 17.52
 Hayen, Nicolas BP 1.11, DS 12.7, O 39.6
 Hayes, J. O 47.3
 Hayes, Patrick MA 40.48
 Haykal, Angela MA 11.1
 Haze, Masahiro O 15.6
 Hazra, Binoy K. MA 23.51, MA 23.64, MA 31.6, MA 43.7
 He, Fei HL 25.2, HL 25.7
 He, Ge TT 23.4, TT 23.13
 He, Jiali KFM 1.8, KFM 4.5
 He, Lu HL 45.7
 he, suqin MA 40.16
 He, Yakun CPP 36.1, CPP 36.5
 He, Yuchi TT 45.6
 Heber, M. MM 12.1
 Heber, Michael O 16.1, O 37.8, TT 9.7
 Hecht, Bert O 43.6, O 43.7, O 58.7, O 58.9, O 70.6, O 91.6, O 91.9
 Hecht, Lukas BP 7.3, DY 10.3, DY 42.3
 Hecht, Stefan CPP 26.3, O 23.4
 Heckel, Alexander O 3.2
 Heckens, Anton J. SOE 22.2
 Hecker, Daniel HL 7.51
 Hecker, K. HL 33.17
 Hecker, Katrin HL 9.5, TT 14.5
 Heckhoff, Tobias O 13.4
 Heckschen, Markus O 8.3
 Hector, Andrew CPP 45.3
 Heczko, Martin MA 37.5
 Hedge, Suraj TT 6.12
 Hedrich, Natascha DS 6.1, MA 11.4, MA 31.7
 Hedwig, Sebastian O 19.5, O 19.8, O 37.10, O 64.9
 Heenen, Hendrik O 78.4
 Heenen, Hendrik H. O 52.6, O 86.6, O 93.6, O 96.1, O 96.3
 Heermeier, Niels HL 33.49
 Heerwig, A. CPP 17.2
 Hegarty, Peter KFM 6.8
 Hegarty, Peter Andrew KFM 6.35
 Hegde, Suraj HL 11.1, TT 15.1
 Hegemann, Peter BP 25.6
 Heger, Julian CPP 17.16, DS 12.34
 Heger, Julian E. BP 19.1, CPP 41.1, CPP 53.6
 Heggemann, Jonas O 87.8
 Hegselmann, Rainer TUT 2.1, SOE 1.1
 Hehemann, T. KFM 6.46
 Hehemann, Tobias KFM 14.5
 Hehn, Michel MA 23.70, MA 40.34, MA 12.3
 Heidemann, Knut SOE 4.2, SOE 10.3
 Heidenreich, Sebastian DY 31.2, DY 42.1
 Heider, Tristan O 30.5
 Heidkamp, Jan-Niklas HL 33.6, HL 33.7
 Heidrich-Meisner, Fabian TT 36.3
 Heidtfeld, Sarah MA 22.4
 Heifetz, Eyal BP 24.4, DY 38.4
 Heigl, Michael O 83.4
 Heijnen, Sandrine DY 26.8
 Heiler, Georg SOE 23.4
 Heiliger, Christian HL 51.4, MA 23.45, MA 36.5
 Heilmaier, Martin MM 40.9
 Heimonen, Hermann TT 49.2
 Hein, Michael TT 57.15
 Heindel, Tobias HL 1.7, HL 37.5
 Heindl, Markus DS 11.3
 Heindl, Moritz HL 7.59
 Heindl, Moritz B. O 49.2

Heine, Thomas CPP 17.60, HL 11.6, HL 34.7, HL 40.5, MA 7.7, O 3.3, O 79.5, O 95.8, TT 15.6, TT 68.8
 Heinen, Philipp DY 27.9
 Heinis, Nils HL 7.50
 Heinke, Lars MA 19.6
 Heinrich, Andreas O 15.3, O 15.6, O 20.8, O 50.3
 Heinrich, Benjamin TT 43.17
 Heinrich, Benjamin W. O 7.2
 Heinrich, Martin MA 19.1
 Heinrich, Matthias TT 36.6
 Heins, Christopher MA 23.78
 Heintzmann, Rainer BP 21.2, BP 28.6
 Heinz, Björn MA 16.5, MA 23.74
 Heinz, Marcel BP 27.4
 Heinze, Leonie TT 29.2
 Heinze, Stefan MA 14.3, MA 14.6, MA 21.2, MA 35.9, MA 40.52, O 55.10
 Heinzl, Thomas BP 5.3, BP 5.4
 Heißenbüttel, Marie-Christin HL 22.8
 Heissler, Stefan O 39.1
 Heitmann, Johannes O 26.2
 Heitmann, Tjark TT 43.20, TT 43.21
 Heiz, Ueli O 29.4, O 29.5, O 29.8, O 41.3, O 41.4
 Helbig, Tobias DY 48.7, DY 55.1, O 58.7, TT 55.7, TT 64.5, TT 67.1
 Helbig, Tom MA 9.10
 Held, Karsten DY 11.8, TT 13.8, TT 44.6
 Held, Tobias MA 8.4, O 16.6
 Heller, Lars MA 43.3
 Heller, René O 31.2, O 42.1
 Hellweg, Thomas CPP 57.10
 Helm, Christiane A. BP 1.10, BP 11.38, CPP 17.57
 Helm, M. TT 23.7
 Helm, Manfred HL 3.9, HL 5.5, HL 10.8, HL 17.11, HL 33.10, HL 34.2, HL 50.3, TT 62.1, TT 62.5
 Helm, T. MA 12.5, TT 42.4, TT 52.3
 Helm, Toni MA 44.2, TT 10.6, TT 43.10
 Helstroffer, Swen BP 1.12
 Helvoort, Antonius KFM 4.3
 Hemaid, Mustafa DS 12.16
 Hemauer, Felix O 23.1, O 23.3, O 41.1, O 64.1, O 73.8
 hemke, torben HL 47.5
 Hemm, Ralf O 10.2
 Hemmati, Mohammad TT 63.11
 Hemmida, Mamoun TT 46.4
 Hemond, Olivia DY 49.4
 Hempel, Alexander DY 43.7, MA 16.3
 Hempel, Franz KFM 3.1, KFM 6.35
 Hempel, Hannes HL 7.37, HL 25.9, HL 25.10, HL 25.11, HL 47.7
 Hemsel, Tobias BP 28.26, BP 28.27
 Hemstede - van Urk, Marjan CPP 58.3
 Hendricks, Adam G. BP 25.8
 Hengstler, D. TT 57.21, TT 57.27, TT 57.28, TT 58.2, TT 58.4
 Hengstler, Daniel TT 57.26, TT 58.1, TT 58.3
 Hénin, Jérôme BP 27.9
 Henk, Jürgen MA 4.9, MA 8.6, MA 8.8, MA 10.7, O 51.6, TT 7.9, TT 12.7
 Henke, Jan-Wilke HL 10.9
 Henkel, Gerald KFM 6.1
 Henkel, Karsten HL 4.2, O 40.3, O 42.4, O 92.6
 Henkelmann, Gideon MM 42.5
 Henn, Sebastian HL 7.22, O 49.7
 Hennig, Joshua HL 17.4
 Hennig, Richard G. O 30.7
 Henning, Alex HL 45.1
 Henning, Philipp HL 51.8
 Henning, Pia DS 14.3, MA 46.8
 Henrard, Luc HL 14.9
 Henriksen, Annika O 67.8
 Henry, Jack O 54.2
 Hens, Zeger HL 24.1
 Henschel, Cristiane CPP 35.43, CPP 35.61
 Hensel, Daniel DS 6.2, HL 33.33
 Hensen, Matthias HL 33.60, O 58.5, O 80.4
 Henßler, Fabian TT 34.1
 Henrich, Andreas DS 11.1
 Hentschel, Mario CPP 37.3, DS 2.2, O 49.1, O 49.9, O 91.4
 Hentschel, Martina DY 43.2, DY 43.11
 Hentschke, Reinhard CPP 19.6
 Heo, Tae Wook MM 27.6
 Heo, Youun KFM 1.6, KFM 6.27
 Hepting, Matthias TT 44.8

Herberg, Friedrich W. KFM 8.5
 Herbert, Corentin DY 32.9
 Herbych, Jacek TT 43.21
 Herbst, M. TT 58.4
 Herbst, Matthew TT 58.5
 Herbst, Michael TT 5.4
 Herfort, Jens DS 8.2
 Hergert, Hannes HL 16.3, TT 24.3
 Herges, Rainer O 7.8, O 20.9
 Hering, Dag-Björn TT 42.19, TT 42.20, TT 42.21
 Hering-Stratemeier, Julian KFM 7.3
 Herink, Georg HL 7.59, O 49.2
 Héripré, Eva MM 33.2
 Herkommer, Alois HL 50.2, KFM 7.3
 Hermann, Alexander O 42.6
 Hermann, Johannes M. O 52.2
 Hermann, Sophie DY 6.1
 Herrminghaus, Stephan SOE 4.2, SOE 10.3
 Hernandez, Julio DS 13.2
 Hernández-Mínguez, Alberto HL 3.4, HL 3.5, HL 3.8
 Hernangómez-Pérez, Daniel HL 22.7
 Herold, Julian BP 3.3, BP 27.5
 Herper, H. C. MA 28.4
 Herre, Philipp TT 10.4
 Herrera, Santiago DY 16.11
 Herrera-Diez, Liza MA 40.30
 Herrero Martínez, Carlos MA 43.1
 Herrero-Martin, J. TT 46.2
 Herrgen, Paul MA 31.3, MA 40.9
 Herritsch, Jan O 10.5, O 22.8, O 23.5
 Herrmann, Alexander O 57.5
 Herrmann, Anna HL 37.8
 Herrmann, Erik O 26.2
 Herrmann, Felix BP 18.3, DY 33.3
 Herrmann, Hannes O 92.8, O 92.9
 Herrmann, Niklas DS 15.5
 Herrmann, Paul HL 33.3
 Herrmann, Tabea DY 48.4, TT 55.4
 Herrmann, Xaver TT 58.22
 Herrmannsdorfer, T. MA 40.58
 Herrmannsdorfer, Thomas MA 44.6, TT 58.29
 Herrmeier, Niels HL 43.3
 Hertäg, Kathrin BP 11.61
 Hertel, Dirk CPP 18.8, CPP 35.30
 Hertel, Riccardo MA 23.15
 Hertl, Nils O 46.1, O 46.2
 Hertwig, Andreas CPP 29.6
 Hertzsch, Benjamin DY 43.15
 Hervé, Marie MA 2.5
 Herz, Laura PLV IX
 Herzog, Marc HL 33.61, MM 12.3, O 37.7
 Herzog, Max CPP 43.8
 Herzog, Thomas HL 49.3
 Heßdörfer, Johannes O 94.2
 Hesjedal, T. MA 12.5
 Heßler, Andreas O 49.8, O 91.8
 Heßler, Martin DY 37.5
 Hesnard, Julie BP 22.10
 Hess, Christian TT 43.3, TT 46.5, TT 52.8, TT 57.10, TT 58.27
 Hess, Ortwin HL 3.7, HL 10.5
 Hessmo, Björn O 37.12
 Hetaba, Walid KFM 3.3, MM 10.1, O 85.8
 Heubach, Maren-Kathrin O 73.5, O 96.9
 Heuer, Andreas BP 3.1, BP 11.34, CPP 2.2, CPP 35.53, CPP 53.8, DY 24.2, DY 45.10, MM 16.5, O 25.3
 Heuer, Helge SOE 4.2, SOE 10.3
 Heuer-Jungemann, Amelie PSV III, BP 5.5
 Heumann, Robin TT 43.7
 Heumüller, Thomas CPP 1.11, CPP 36.5
 Heupel, Julia KFM 6.12, KFM 6.34, KFM 8.4
 Heuplick, Lukas O 2.4
 Heuthe, Veit-Lorenz DY 31.10
 Heveling, Robin DY 25.10, TT 33.10
 Heyda, Jan CPP 12.5, CPP 35.50, CPP 53.2
 Heydarian, Maryamsadat HL 4.7
 Heyden, Stefanie BP 11.5
 Heydenreich, Lina BP 8.10, BP 28.46
 Heyen, Hauke Lars MA 23.7
 Heyl, Christoph M. O 37.9
 Heyl, Markus DY 2.7, DY 2.8, DY 27.2, DY 55.2, TT 2.7, TT 2.8, TT 67.2
 Heymann, Michael BP 12.2
 Heyn, Christian DS 16.4, HL 42.1

Heyn, Johannes Clemens Julius BP 28.49
 Hezcko, Martin MM 36.11
 Hicke, Tilmann TUT 3.1, MA 28.3, MM 1.1, MM 15.9, MM 18.6, MM 32.1, MM 32.4, MM 32.5, MM 37.7, MM 41.7
 Hickey, Alexander TT 28.1
 Hickey, Ciarán MA 33.8, MA 40.24, TT 5.5
 Hickle, Trevor O 75.5
 Hicks, Clifford TT 29.1, TT 34.4, TT 37.1, TT 37.3, TT 37.5
 Hicks, Clifford W. KFM 14.2, TT 37.2, TT 37.4
 Hicks, David MM 36.9
 Hiemer, Stefan MM 33.7
 Hierro-Rodríguez, A. MA 23.39
 Hierro-Rodríguez, Aurelio MA 40.3
 Hierzenberger, Anke O 24.5
 Higgins, Jacob O 34.1
 Higgins, Paul BP 6.1
 Higinbotham, Hugh BP 30.3
 Hijano, Alberto TT 60.1
 Hilbert, Lennart BP 11.59, BP 12.11, BP 29.4
 Hilbig, Thomas MM 12.30
 Hildebrand, Viet CPP 53.4
 Hildebrandt, Patrick-Nigel SYUE 1.2
 Hildebrandt, R. DS 12.48, HL 7.16, HL 7.19, HL 7.20
 Hilger, Andre CPP 45.4
 Hilgers, Yannis TT 10.4
 Hilgert, Katharina O 64.9
 Hill, Nicolas HL 22.9
 Hillebrands, Burkard MA 16.4, MA 16.5, MA 23.44, MA 23.71, MA 23.74, MA 34.7, MA 40.7, MA 40.33
 Hiller, Daniel HL 16.5, TT 24.5
 Hillert, Wolfgang O 42.10
 Hilska, Joonas HL 49.7
 Hilt, Gerhard O 93.8
 Himanen, Lauri HL 25.3, O 95.5, TT 68.5
 Himcinschi, Cameliu KFM 6.10, MM 12.19
 Hinaut, Antoine O 4.5, O 32.8, O 38.3
 Hinderhofer, Alexander CPP 51.2, DS 10.2, O 63.1, O 95.9, TT 68.9
 Hinke, Tobias O 29.4, O 29.5, O 41.3
 Hinkov, Vladimir O 94.6
 Hinlopen, Roemer TT 51.7
 Hinrichs, Karsten DS 13.1, DS 13.4
 Hinterstein, Manuel KFM 1.6
 Hinzke, Denise MA 40.6
 Hinzmann, Andreas AKC 1.2
 Hippler, Marc BP 11.37
 Hirmath, Praveenkumar MM 9.2
 Hirn, Ulrich CPP 45.4
 Hirose, Tomoki MA 47.10
 Hirsch, Antje HL 17.4
 Hirschberger, Fabian MA 13.7, TT 19.7
 Hirschberger, Max MA 2.6
 Hirschfeld, Peter TT 20.5
 Hirschfeld, Peter J. TT 63.6
 Hirschmann, Eric CPP 35.17, DS 6.1, DS 14.5, HL 5.5, KFM 6.30, KFM 9.5, KFM 9.8, KFM 9.10
 Hirschmann, Frank BP 27.8
 Hirschmann, Julian HL 45.6
 Hisano Natori, Willian Massashi TT 46.11
 Hite, K. TT 3.4
 Hjort, F. HL 23.1
 Hjort, Filip HL 23.5
 Hlawacek, Gregor HL 41.2, HL 50.3, MM 40.7, O 31.3
 Hlinka, Jiří HL 5.4, KFM 14.3
 Ho, Ja-An O 66.5
 Hoang, Le Phuong DS 6.3
 Hobe, Stephan BP 17.1
 Hobler, Gerhard O 13.3
 Hodgson, Stephen TT 4.11, TT 59.14
 Hodgson, Stephen A. TT 4.12
 Hodžić, Melvin O 19.3, O 34.6
 Hoefler, Jonas MA 46.7
 Hoek, Harmen CPP 8.1
 Hoepfl, Raphael MA 40.15
 Hoeppe, Hannes Paul DY 18.7
 Hoesch, M. MM 12.1, MM 26.8
 Hoesch, Moritz HL 36.2, TT 3.7, TT 57.3
 Hof, Björn DY 29.1, SOE 6.1
 Hof, Martin O 26.7
 Hofemeier, Arne BP 4.4, BP 28.11, BP 28.23

Author Index

- Höfer, Thomas BP 11.18
Höfer, Ulrich HL 27.2, O 8.7, O 19.7,
O 19.9, O 34.2, O 37.11, O 57.2,
•O 62.2, •TT 40.2
Hoff, Felix DS 15.4, •DS 16.5,
KFM 6.14
Hoffman, Noah MM 31.7
Hoffmann, Cedric CPP 43.6
Hoffmann, Christian BP 29.3
Hoffmann, Felix HL 50.4
Hoffmann, Georg HL 47.3
Hoffmann, Ingo BP 1.3
Hoffmann, Ludwig A. •BP 30.7
Hoffmann, Markus MA 27.4,
MA 35.8, O 51.1
Hoffmann, Marvin O 10.7
Hoffmann, Raik TT 57.2
Hoffmann, Veit HL 23.2
Hoffmann-Vogel, Regina O 32.7,
O 42.5
Höfft, Oliver DS 3.5
Höfler, Mathias •BP 28.19
Höflich, Katja O 49.3
Höfling, Felix •BP 24.9, DY 4.10,
DY 38.9
Höfling, Sven HL 5.1, HL 17.5, HL 18.4,
HL 24.13, HL 30.3, HL 35.4, HL 49.5,
HL 49.7, TT 41.3
Hofmaier, Mirjam DS 13.5
Hofmann, Alexander HL 7.25
Hofmann, Anna I. CPP 18.13
Hofmann, Anna-Lena •CPP 43.8
Hofmann, Damian SYUE 1.5
Hofmann, Dennis CPP 26.3
Hofmann, Gregor HL 28.4
Hofmann, Jan P. HL 7.10
Hofmann, Kay DY 34.1
Hofmann, Marvin MA 42.1
Hofmann, Oliver O 82.3
Hofmann, Oliver T. MM 31.5, O 4.6,
•O 28.1, O 28.10, O 77.5, O 97.2
Hofmann, Philip O 34.9, O 85.2
Hofmann, Stephan O 34.4
Hofmann, Tobias •DY 21.4, DY 48.7,
•DY 55.1, O 58.7, TT 55.7, TT 64.5,
•TT 67.1
Hofsäss, Hans MM 23.10, O 24.1,
•O 31.1, TT 25.1
Hofstetter, Walter TT 23.6
Hogan, Conor O 28.4
Hogger, Wolfgang O 8.6, O 37.6,
•TT 62.6
Hohage, Thorsten O 80.2
Höhe, Florian TT 39.9
Hohls, Frank O 82.7
Hohlstamm, Anselm •DY 26.9
Hohmann, Hendrik •TT 64.5
Hoibl, L. TT 58.2
Holder, Jacob •DY 49.5
Hölderle, Tobias •KFM 10.2
Holger, Fritze KFM 13.3
Holíková, Karolína •MM 23.30,
MM 26.2
Holl, Max Philipp DY 26.7
Holleitner, Alexander DS 1.4, HL 8.4,
HL 37.8, TT 6.9
Holleitner, Alexander W. DS 10.3
Hollenbach, Michael HL 50.3
Hollendonner, Maximilian •HL 29.7,
HL 33.19, HL 33.21, •HL 33.23,
HL 33.29
Holler, Mirko MA 43.3
Hölling, Michael DY 5.9
Höllmer, Philipp •DY 6.3
Hollricher, Michelle •TT 10.2
Höllring, Kevin BP 15.5
Hollweger, Simon •O 28.10
Holm, Elizabeth A. MM 26.2
Holovatch, Yuriy DY 45.15, •DY 49.2,
MA 23.47, •SOE 8.2, SOE 16.1
Hölscher, Hendrik O 4.8
Hölscher, Thorsten HL 4.5, HL 25.4
Holters, Johannes MM 12.23
Holtgrewe, Kris •O 32.3
Holtmann, Marcel O 18.5, •O 59.4,
O 85.6
Holub, Mariia •TT 43.5
Holubec, Viktor DY 4.9, DY 42.11
Holyst, Janusz DY 57.2, SOE 4.4,
SOE 4.5, •SOE 4.7, SOE 18.3
Holyst, Janusz A. SOE 6.3, •SOE 18.2
Holzer, Marco •MM 12.36
Holzwarth, Moritz •MM 12.21
Homann, Simon •O 3.5
Homberg, Jan O 20.9, TT 8.1
Hommel, Caroline •O 20.8, O 50.3
Hommelhoff, Peter O 37.5
Honasoge, Kedar TT 49.1, TT 58.20
Honasoge, Kedar E. •TT 39.7,
TT 49.5, TT 58.6, TT 58.7, TT 66.6
Honchar, Yulian •MA 23.47
Honecker, Andreas DY 17.3, DY 22.5,
TT 29.9, •TT 29.10, TT 43.28, TT 61.5
Honerkamp, Carsten TT 63.9
Hong, Seung-Ju •MA 7.2, •MA 7.12
Hong, Tao TT 9.8
Hong, Xiaochen TT 43.3, TT 46.5,
TT 52.8, TT 57.10
Hong, Yuanjian MM 27.1
Honig, Hauke •DS 12.4
Hönig, Markus CPP 13.3
Honné, Natalie O 49.8
Hono, Kazuhiro SYGM 1.2
Hoock, Benedikt BP 11.25
Hoormann, Matthias •HL 44.3
Hoffmann, Caspar HL 7.48, HL 7.52,
HL 7.63, •HL 24.8, HL 24.9
Höpfner, Jakob •HL 28.4, HL 28.5
Hoppe, Harald •CPP 1.3, CPP 1.4,
CPP 17.17, CPP 17.19, CPP 17.29,
CPP 36.7, CPP 36.9, CPP 43.2,
CPP 51.8
Hoppe, Wolfgang MA 23.63
Horák, Michal O 14.9, O 91.5
Horakova, Katerina O 65.1
Hordiichuk, Oleh HL 15.3
Horenburg, Philipp HL 33.43
Hörich, Florian HL 7.6, •HL 51.7
Hörmann, Lukas MM 31.5, •O 4.6,
O 28.1, O 28.10, O 97.2
Hörmann, Max TT 5.6, •TT 5.7,
TT 42.8, TT 42.22, •TT 43.29
Hörmann, Nicolas O 86.2
Hörmann, Nicolas G. O 52.6, •O 60.8,
O 86.1, O 86.8, O 96.8
Hormozi, Mohammad O 12.2
hormozi, mohammadali •DY 29.9
Hörner, Gerald CPP 17.9
Hornung, Florian HL 7.62
Horn-von Hoegen, Michael HL 48.3,
O 75.4
Horstmann, Jan Gerrit •SYSD 1.3,
•MA 48.2, O 34.5, O 75.8
Horstmann, Julia •HL 25.4
Horvath, Raphael DS 13.4
hosdez, jérôme MM 20.2
Hosoi, Suguru TT 34.4
Hossain, Manoar •MM 12.25
Hosseinfar, Rahil MA 19.4, MA 40.15,
•MA 40.55
Hou, Shujin CPP 17.16
Hou, Xiao •DS 12.1, O 30.3
Hou, Youmin CPP 52.1
Houdkova, Jana HL 7.8
Hourahine, Benjamin KFM 6.5
Houston, Alexander J. H. •BP 2.7
Houtsma, Koen O 50.4
Hövel, Philipp DY 18.4, •SOE 7.5,
SOE 8.1
Hövelmann, Svenja O 39.6
Hövelmann, Svenja C. •BP 1.11
Hovořáková, Kristýna MA 23.37
Hovorka, Ondrej MA 23.14
Hovovřáková, Kristýna MA 40.6
Howarth, James HL 33.18
Hoyer, Rhea •MA 16.2
Hozoi, Liviu TT 21.8
Hppel, Lea BP 30.6
Hrabec, Ales MA 43.2
Hreb, V. KFM 14.7
Hribar Boštjančič, Patricija MA 36.2
Hricovini, Karol O 18.7
Hrkac, Stjepan KFM 9.9
Hruski, Fedor HL 29.3, •HL 33.19,
HL 33.21, HL 33.23, HL 33.29
Hsieh, Valerie TT 53.9
Hsieh, Ya-Chu O 28.7
Hsu, Chiao-Peng •BP 1.2
Hsu, Hsiao-Ping •CPP 20.6,
CPP 35.54, CPP 50.1
Hsu, Kuei-Shen HL 17.4
Hsu, Zhe-Bin •TT 16.11
Hu, Chun •DS 4.5
Hu, Michael MA 42.2
Hu, Shijie TT 42.8
Hu, Wen MA 43.6
Hu, Xiao CPP 44.8
Hu, Yunbin O 32.8
Hu, Z. TT 46.2
Hu, Zhenhai TT 37.1, •TT 37.2,
TT 37.3
Hu, Zhixin O 97.7
Hua, Qin •HL 14.1
Huang, Dennis O 56.2, TT 3.3, TT 9.6
Huang, Di HL 35.1
Huang, Guanhao HL 10.9
Huang, Haonan O 7.5, O 20.5, O 21.7
Huang, Lingling HL 33.30
Huang, Mantao MA 43.6
Huang, Ruomeng CPP 45.3
Huang, Shao-Lun TT 30.3
Huang, Shuyu •O 4.5, O 38.3
Huang, Sizhao •TT 43.8
Huang, Tzu-Yen CPP 36.6
Huang, Wantong •O 15.10, O 20.3,
O 77.3
Huang, Wister Wei HL 9.4, TT 14.4
Huang, X. O 42.2
Huang, Xiaochun O 59.9, TT 57.1
Huang, You HL 50.1
Huang, Yuan TT 3.5
Huang, Zipeng •O 25.2, •O 60.11
Huard, Benjamin TT 39.10
Huber, David •O 51.5
Huber, Felix •O 12.1
Huber, Liam MM 25.5
Huber, Linus F. CPP 17.44, •CPP 35.2
Huber, Max •CPP 44.8
Huber, Nico •TT 10.1, TT 58.23
Huber, Norbert MM 42.7
Huber, Patrick CPP 35.64, DY 24.4,
MM 23.19, MM 23.21, MM 23.28,
MM 42.3, MM 42.6
Huber, Rupert O 8.7, O 34.2
Huber-Loyola, Tobias HL 24.13,
HL 49.5, HL 49.7
Hubert, Hubert MA 46.12
Hubert, Maxime •BP 15.5
Hübner, René DS 6.1, MA 11.4,
MA 31.7, MA 43.5, MM 40.7
Hübner, Ruven •HL 8.5
Hübner, Uwe HL 14.6, O 18.1
Hübner, Wolfgang O 37.2
Hübschmann, Henry Volker •HL 22.1
Hucht, Alfred TT 38.11
Huck, Christian DS 15.5
Hudson, Thomas MM 40.1
Huebl, Hans MA 4.13, MA 23.50,
MA 23.62, MA 23.76, MA 23.80,
•MA 34.3, MA 34.6, MA 40.15,
MA 40.65, TT 7.13, TT 18.2, TT 39.4,
TT 54.9, TT 54.10, TT 58.8, TT 58.10
Huebner, Jens HL 7.17
Huesmann, Moritz •KFM 6.45
Huettig, Annette O 14.4
Hufenbach, Julia Kristin MA 3.5
Hug, Hans Josef O 87.2
Hugel, Thorsten •SYFP 1.2
Hugenschmidt, Christoph CPP 35.4,
DS 14.5, KFM 6.24, •KFM 9.3,
KFM 9.10
Hüger, Daniel CPP 54.4
Hughes, Stephen HL 1.4, HL 1.9
Huh, Joonsuk DY 43.1
Hühne, Ruben DS 12.27
Huhnstock, Rico MA 5.4, MA 36.3,
•MA 36.4, MA 40.31, MA 40.43
Huijen, Nora O 30.2
Huisken, Jan BP 28.11
Huisman, Owen Thomas •TT 58.9
Hula, Tobias MA 23.78
Hüllen, Isabell HL 36.6, HL 51.5
Hülser, Tobias •DY 17.1
Hultman, Lars MM 15.5
Hultzsck, Thomas CPP 11.5
Hummer, Gerhard BP 3.6, BP 3.9,
BP 27.9
Hümmer, Thomas HL 33.34
Humpohl, Simon HL 37.1
Hung, Tzu-Chao •O 2.5
Hunger, David HL 49.3, KFM 8.4
Hungerland, Jonathan •BP 6.7
Hunnestad, Kasper •KFM 4.3
Hupe, Lukas BP 6.2
Hurskyj, Stepan KFM 13.4, KFM 13.5
Hurt, Jan •SOE 19.1
Hüsam, Elif HL 25.10
Hüsling, Nicola CPP 17.51
Huss, Tabea MM 6.2, •MM 6.3
Hussain, Muhammad HL 35.5
Husstedt, F. TT 59.8
Huth, Michael MA 40.37, TT 4.6
Hüttner, Johanna O 54.7, •O 81.4
Hutsch, Sebastian CPP 28.2,
CPP 36.4, TT 32.2
Hütt, Marc-Thorsten SYOF 1.3,
BP 16.5, SOE 4.3, SOE 19.4
Hüttel, Andreas K. TT 16.7, TT 16.14,
TT 18.1, TT 53.10, •TT 58.30,
•TT 58.31
Hütten, Andreas MA 23.42,
MA 23.46, MA 23.48, MA 37.3,
MA 40.45, MM 12.29, MM 12.30
Hutter, Mark O 19.7
Hüttner, Niklas TT 16.14, TT 18.1
Hyart, Timo TT 53.3, TT 63.2
I. Madeira, Teresa HL 45.7
I. Vasyuchka, Vitaliy MA 18.1
Iakovlev, Zakhar A. HL 34.3
Ibañez Azpiroz, Julien O 94.5
Ibañez-Azpiroz, Julien HL 26.7, O 15.9,
O 53.7, O 75.7
Ibarra, Rebeca MA 37.4
Ibrahim, Eslam •MM 36.5
Icking, E. HL 33.17
Icking, Eike HL 9.5, •HL 30.2, TT 14.5,
•TT 41.2
Icking, Eike Thomas HL 14.5
Ide, Niklas O 33.5
Idema, Timon BP 1.5
Iden, Sandra BP 28.38
Idri, Mohammed MM 33.8
Idriss, Hicham O 68.5, O 81.10
Ihle, Alexander O 72.5
Ihle, Friederike MM 42.1
Ihle, Thomas BP 24.6, DY 38.6
Ihmels, Anika AKC 1.3
Ihn, Thomas HL 9.4, TT 14.4
Ihssen, Soeren •TT 49.4
Ikeda, Akihiko TT 46.1
Ikeda, Matthias TT 37.1
Ikeda, Yuji MM 5.8, •MM 27.7
Ilani, Shahal •TT 35.2
Ilhan, Beybin CPP 50.2
Ilić, Stefan TT 27.2
Ilin, Alexander O 87.4
Illgen, Claus VA 1.4
Illig, Maja •BP 5.2
Illing, Rico MA 49.6, MA 49.7,
MA 49.8
Ilyakov, Igor BP 11.43
Ilyn, M. O 47.3
Ilyn, Maxim O 36.5, O 56.5
Im, Changbin •O 30.11, O 64.3
Imamoglu, Atac TT 61.3
Imbrasas, Paulius DS 10.2
Imloczyk, Claudia •BP 12.2
Imlau, M. KFM 6.46, KFM 14.7
Imlau, Mirco KFM 6.41, KFM 6.42,
KFM 6.43, KFM 6.44, KFM 6.45,
KFM 14.4, •KFM 14.5
Imre, Alexander M. •O 92.5
in 't Veld, Yann •TT 27.7
Inamdar, Mandar M. BP 4.1
Incardona, Pietro BP 28.22
Ingo Flege, Jan DS 12.50
Ingold, Gert-Ludwig CPP 57.3
Inosov, D. S. •MA 33.6, MA 44.3
Inosov, Dmitro MA 23.1
Inosov, Dmytro MA 37.4, MA 40.22,
MA 40.25, MA 44.7, MA 44.8,
TT 23.12, TT 42.5
Inosov, Dmytro S. MA 9.7
Inotani, Daisuke TT 31.11
Iñurrieta, Mikel I. MA 9.3
Ioannidis, Ioannis O 7.1
Ioann, Alexander DY 44.15, DY 44.19
Ion, Lucian HL 16.2, TT 24.2
Ionov, Leonid CPP 8.8, DY 29.3,
MA 49.8
Iqbal, Sammer O 56.3
Iqbal, Yasir MA 40.24
Irländer, Kilian MA 24.1
Irsen, Stephan HL 1.3
Irsigler, Bernhard TT 23.6
Isaeva, Anna MA 10.5, TT 12.5
Isele, Marc •DY 34.1
Isensee, Jonas BP 6.2
Ishida, Kousuke TT 37.4, •TT 37.5
Ishii, Ryota HL 23.3, HL 23.6
Ishikawa, Hajime TT 29.3
Islam, A. T. M. Nazmul TT 46.7
Islam, Md Moidul CPP 1.4, •CPP 43.2
Ismail, Maneesha •O 21.7
Isobe, Masahiko TT 3.3, TT 42.14,
TT 44.8, TT 51.5
Isufi Nezir, Egzona •DS 4.3
Ito, Suguru •O 8.7, O 37.11
Ivankovic, Goran Ivkovic CPP 51.4
Ivanisenko, Julia MM 12.7
Ivanov, Alexandre MA 44.7
Ivanov, Alexey DY 42.16
Ivanov, Dmitry S. DS 4.1, DS 12.6
Ivanov, Misha SYUE 1.4
Ivanov, Tzvetan DS 12.57
Ivanov, Viktor CPP 35.32
Ivanova, Daniela •MM 12.27
Ivashko, Oleh KFM 9.7

Author Index

- Iwaya, Motoaki HL 28.1
Iwayama, Sho HL 28.1
Izadi, Sepideh DS 12.11, DS 12.55,
•TT 59.1
Izquierdo, Manuel O 14.11, O 37.9
J. Schupp, David MM 23.12
Jabeen, Faudia HL 5.1, HL 17.5
Jabri, slaheddine •KFM 6.16
Jachowski, Tobias BP 23.11
Jäck, Berthold •MA 10.4, •TT 12.4
Jäckl, Bastian O 85.11
Jacob, Timo BP 27.7, CPP 43.11,
MM 18.5, O 3.5, O 12.3, O 14.10,
O 30.11, O 48.2, O 52.2, O 64.3,
O 73.5, O 86.9, O 86.10, O 96.9,
O 96.10
Jacobse, Leon O 29.6, O 60.9, O 92.3
Jacobsen, Nils •TT 64.3
Jacques, Vincent MA 11.1, MA 32.6
Jacucci, Gianni DY 26.8
Jadhav, Ashish TT 58.1
Jaegermann, Wolfram HL 7.10
Jaekel, Simon •O 60.6, O 64.1
Jaeschke, Rodrigo MA 40.60,
MA 40.61
Jaeschke-Ubiergo, Rodrigo •MA 4.4,
•TT 7.4
Jafari, Majid •CPP 35.36
Jafarian, Hanieh O 26.7
Jäger, Gustav J. L. CPP 13.7
Jäger, Lukas HL 7.54
Jäger, Miriam BP 3.8
Jäger, Simon TT 22.8
Jäger, Simon B. DY 43.16
Jägering, Kevin TT 45.8
Jäggi, Noah O 13.2
Jagirdar, Gayatri BP 8.8
Jagtap, Nagesh HL 50.3
Jagtap, Nagesh Shamrao •HL 3.9
Jagus, Rommel HL 17.6
Jahn, Reinhard BP 17.4
Jahnel, Marcus BP 11.43
Jahnke, Frank HL 16.6, HL 25.8,
HL 43.6, TT 24.6
Jahnke, Kevin •BP 1.1, BP 5.2,
BP 11.37, BP 11.59
Jain, Archa HL 42.2, HL 42.3
Jain, Mitisha •O 5.5
Jaiswal, Pranay •BP 11.31
Jäkel, Anna C. •BP 11.72, •BP 11.73
Jakes, Peter MM 16.2
Jakob, Christopher TT 57.25
Jakob, G. MA 18.4
Jakob, Gerhard MA 4.7, MA 5.5,
MA 17.2, MA 22.2, MA 23.5,
MA 23.66, MA 29.2, MA 40.29,
MA 40.30, TT 7.7
Jakob, Konstantin •MM 31.3
Jakob, Peter O 28.2
Jakoby, Rolf DS 11.4
Jaksch, Dieter MA 9.2
Jakub, Zdenek •O 81.4
Jakubczyk, Fabian •TT 57.12
Jal, Emmanuelle •MA 30.4
Jalaal, Maziyar BP 7.7, BP 28.42,
•CPP 44.3, CPP 44.7, DY 10.7
Jalarvo, Niina KFM 10.9
Jalil, Abdur Rehman DS 12.1, TT 36.1,
TT 59.6
Jambor, Michal MA 43.3
Jamebozorgi, Vahid •O 11.8, •O 23.2
Jana, Sanchayeeta O 70.1, •O 76.6
Janas, Arkadiusz O 5.3
Janczak, Mikolaj HL 33.49
Janik, Alexander •BP 28.58
Janisch, Rebecca MM 12.24,
MM 12.34, •MM 15.6
Janke, Wolfgang DY 6.1
Jankowski, Maciej O 93.6
Jannasch, Anita •BP 23.5
Janoschka, David O 75.4, O 80.3
Jansen, G. S. Mathijs O 34.4
Jansen, Marvin Marco HL 29.9
Janshoff, Andreas BP 28.28
Janson, O. MA 44.3
Janson, Oleg MA 27.7, MA 41.3,
•TT 29.3, TT 30.12, TT 30.13
Janssen, Jacqueline •BP 29.2
Janssen, Lukas •TT 31.9, TT 47.5,
TT 47.11, TT 52.9, TT 65.7
Janssen, Mathijs MM 21.2
Jany, Benedykt R. O 5.3
Janzen, Benjamin M. HL 21.3, HL 41.7
Janzen, Benjamin Moritz •HL 41.3
Janzen, Christian DS 12.2, MA 5.2,
•MA 38.4, MA 40.28
Jaouen, Nicolas MA 11.1, MA 11.6,
MA 43.1
Japtap, Nagesh S. HL 10.8
Jarecki, Jasmin •MA 23.70,
MA 40.10, MM 12.3
Jarosik, Alexander •CPP 53.9
Järsvall, Emmy CPP 18.13
Jaurigue, Lina DY 22.1, DY 46.5
Jayaloyes, Julien DY 4.8, DY 45.4
Javanmard, Younes TT 42.7
Jawerth, Louise BP 11.56
Jayabalan, Jesumony O 19.1, •O 19.6
Jayakumar, Vaishnavi •TT 5.5
Jayaprakash, R. HL 48.4
Jayaram, Ashreya •BP 24.2, •DY 38.2
Jayaram, Sreehari •MA 23.38
Jazvandi-Ghamsari, Shima HL 23.2
Jeckelmann, Eric TT 36.9
Jeggle, Julian •BP 24.3, •DY 38.3
Jehle, Tom O 75.2
Jele, Samuel HL 9.4, TT 14.4
Jelezko, Fedor DS 12.35, KFM 6.40,
MA 32.3
Jelic, Vedran •O 75.5
Jelínek, Pavel MA 19.7, O 45.6,
O 55.3, O 66.4, O 66.11, O 97.3
Jena, Jagannath MA 12.1
Jena, Suchit Kumar •MA 44.9
Jenderny, Sebastian BP 11.74,
BP 11.75, DY 18.4
Jenekhe, Samson DS 16.6
Jenni, Kevin MA 40.17, MA 44.5,
TT 57.5
Jenninger, Berthold VA 1.4
Jentgens, Henrik MA 50.5
Jeon, Hansol CPP 35.63, •MM 22.3
Jeong, T.K. CPP 17.2
Jerabek, Paul MM 27.6, MM 31.9
Jeremic, Ivana •BP 28.7
Jeromin, Arno O 52.1, O 92.3
Jerzembeck, Fabian TT 37.1, TT 37.2,
•TT 37.3, TT 37.9
Jesche, Anton MA 13.7, •MA 24.3,
TT 4.3, TT 19.7, TT 46.10, TT 52.2,
TT 52.7
Jessewitsch, T. HL 48.4
Jetter, Michael HL 7.43, HL 7.48,
HL 7.62, HL 12.1, HL 12.4, HL 12.5,
HL 12.6, HL 43.2, HL 43.4, HL 49.2,
HL 49.3
Jha, Ajay •MM 10.4
Ji, Karen O 34.1
Ji, Wei O 97.7
Jia, Baoxin •O 60.2
Jian, Jianfei BP 28.45
Jiang, Bin O 73.1
Jiang, Jianfei •BP 28.50
Jiang, Song •O 2.6
Jiang, Tianshu MA 3.4
Jiang, Xin HL 29.10
Jiang, Xinyu CPP 17.17, CPP 29.10
Jiang, Xiongzhuo •CPP 17.35
Jiang, Ying O 6.8, •O 54.1
Jibuti, Luka TT 34.2
Jimenez, Carlos HL 50.2
Jiménez, David Doblaz O 84.3,
TT 56.3
Jiménez Herrera, Miguel Ángel
•TT 6.3, •TT 17.4, TT 64.6
Jiménez-Martín, Alejandro O 66.4,
•O 66.11
Jimenez-Orozco, Carlos •O 52.3
Jiménez-Sánchez, Mariano D O 29.1
Jin, Fengping TT 43.20
jin, haolin •DS 12.18
Jin, Hui-Ke TT 46.11
Jin, Keda O 18.2, O 28.2, O 74.3,
O 74.5, •O 82.1
Jin, Limei •DY 46.2
Jin, Lin HL 33.22
Jin, Xianghong TT 52.9
Jing, Guangying CPP 57.1
Jinnouchi, Ryosuke MM 12.10
Jo, Daeyeun MA 4.10, TT 7.10
Jo, N. H. TT 6.4
Jo, Wonhiuk MM 12.3
Joachim, Christian O 3.1
Joanny, J.-F. •BP 31.2
Jobst, Nicola KFM 10.3
Jochim, Alexander •SOE 4.9
Jochum, Johanna MA 48.1
Jochum, Johanna K. MA 40.42
Jochym, Paweł T. HL 21.2
Jocic, Angelina CPP 35.14
Joglekar, Yogesh TT 36.6
Johánek, Viktor O 29.2
Johannesmann, Florian DY 55.6,
TT 67.6
Johannsen, Sven •O 42.6
Johansson, Annika MA 4.9, •MA 4.11,
TT 7.9, •TT 7.11
Johansson, Fredrik O. L. O 85.1
Johansson, Göran O 80.7
Johansson, Mats CPP 29.5,
CPP 35.1, •CPP 58.1, CPP 58.2
John, Robin MA 40.6
John, Thomas BP 8.3, BP 11.60,
BP 18.1, BP 22.7, •BP 29.6, DY 4.2,
DY 33.1
Johnson, D. C. TT 3.4
Johnson, Manuel CPP 17.52,
CPP 28.10, TT 32.10
Johnson, Steven O 19.4
Johnson, T N MA 31.1
Jolakoski, Petar •DY 44.15, DY 44.19
Jolie, Wouter O 36.11, O 56.8, •O 72.1
Joly, Nicolas HL 33.22
Jonak, Martin MA 40.56
Jonas, Bex BP 24.12, DY 38.12
Jonas, Björn HL 7.45
Jonen, Abel SOE 16.1
Jonigk, Danny BP 21.9
Jöns, Klaus HL 37.2
Jöns, Klaus D. HL 7.45, HL 7.47,
HL 7.64, HL 7.65, HL 7.66, HL 22.1,
HL 24.6, HL 33.30, HL 33.31,
HL 33.34, HL 33.35
Jónsson, Hannes MA 26.5
Joos, Raphael •HL 7.43
Joost, Jan-Philip O 31.5, TT 22.1
Jorba, Pau •MA 13.6, •TT 19.6,
TT 47.3
Jordt, Philipp BP 1.11, DS 12.7,
•KFM 9.9, O 39.6, •O 84.5, •TT 56.5
Jörke, C. BP 11.7
Jörns, Arne •HL 7.29
Jose, Rose Mary •HL 7.40
Joseph, Dijo Moonnukandathil
BP 21.2
Joseph, Ebobenow SOE 23.2
Joseph, Jesvin BP 21.2, •BP 28.3
Joseph, Yvonne HL 33.8
Joshi, Manoj TT 22.13
Joshi, Nidhi CPP 19.8
Joshi, Yug •MM 16.9, •MM 23.8,
•MM 23.16
Jouault, B. HL 17.8
Journard, Isabelle MA 4.12, TT 7.12
Jourdan, Martin MA 18.1, MA 18.3,
O 85.3
Jousten, Karl VA 1.4
Jover-Carrasco, Elena MM 4.1
Juffmann, Thomas O 26.7
Jugovac, Matteo O 74.1
Jukam, Nathan HL 33.54
Jülg, Gabriel TT 66.2
Jüllicher, Frank BP 4.1, BP 11.33,
BP 11.56, BP 11.65, BP 22.9,
BP 22.12, BP 28.22, BP 29.2, BP 29.5,
BP 31.6, DY 29.2, DY 42.15
Julien, Jean-Daniel DY 45.6
Jun, Suckjoon BP 16.3
Jung, Alexander TT 39.4
Jung, Christoph BP 27.7, •CPP 43.11
Jung, Felix •SOE 11.2
Jung, Florian A. CPP 17.54
Jung, Gerhard CPP 17.55, DY 44.8
Jung, Hendrik •BP 3.9
Jung, Hyein •MA 46.11, MA 46.13,
O 34.7
Jung, Hyunwook •O 11.1
Jung, Jong Hyun MM 36.8
Jung, Michael •CPP 35.7, •CPP 35.8
Jung, Pascal TT 59.16, •TT 59.17
Junge, Felix •O 24.1, O 31.1, TT 25.1
Junghans, Kira •O 20.2, O 33.9
Junghöfer, Tobias DS 3.3, •DS 3.4
Jungwirth, Nicolas HL 18.11
Jungwirth, T. MA 41.2
Jungwirth, Tomáš MA 4.12, MA 4.14,
MA 16.8, MA 40.63, MA 40.64,
MA 41.4, TT 7.12, TT 7.14
Junk, Vanessa •O 8.6, O 37.6, TT 62.6
Junkes, Heinz O 63.2, O 84.10,
TT 56.10
Jurado, Alejandro BP 28.21
Jurado Jiménez, Alejandro •BP 28.18
Jürgens, Kevin •HL 33.2
Juricek, Michal O 33.3
Jurkat, Jonathan HL 24.13
Just, Sven •O 66.9
Jusys, Zenonas O 96.5
Jyoti, Jyoti •BP 16.5
K. Chandran, Anoop •HL 7.38
K. Georgiou, Theoni CPP 35.58
K Vayalil, S. MA 5.1
Kaap, Fabian •TT 20.2, TT 39.6,
TT 58.5
Kabbinahithlu, Mahendra •O 16.2,
O 37.3
Kacars, Kristians MM 8.1, •O 85.10
Kacha Deyu, Getnet O 42.10
Kaczmarek, A MA 31.1
Kaczorowski, D. TT 59.8
Kadjani, Sadeq S. •DY 23.4
Kador, Lothar CPP 17.33
Kadow, Wilhelm •TT 61.3
Kadzielawa, Andrzej MA 28.5
Kaestner, Lars BP 8.3, BP 11.60,
BP 22.7
Kafar, Anna •HL 23.3, •HL 23.6,
HL 28.3
Käferstein, L. HL 7.16
Kagerer, Philipp CPP 28.3, O 74.4,
•O 94.6, TT 32.3
Kageyama, Hiroshi TT 30.8
Kahan, Petr O 43.8, •O 70.10, O 76.5
Kahl, Robert CPP 17.18
Kahle, Hermann •HL 12.3
Kahmen, Gerhard DY 37.7
Kahne, N. TT 57.21, TT 58.2
Kahne, Nicolas TT 58.3
Kainbacher, Nina •O 22.5
Kainka, Lucina •BP 25.9, BP 28.38
Kaiser, Benjamin HL 34.8
Kaiser, David DS 1.2
Kaiser, Florian HL 37.3
Kaiser, Julian TT 52.7
Kaiser, Katharina •O 22.1, O 72.4
Kaiser, Kathi BP 25.9
Kaiser, Manuel TT 39.5
Kaiser, Marius M. BP 25.8
Kaiser, Nico DS 9.2, DS 9.3
Kaiser, Sebastian O 29.4, O 29.5,
O 41.3
Kaiser, Stefan HL 48.9, O 80.5,
TT 3.5, TT 62.3
Kaiser, Theodor •CPP 17.10,
CPP 28.3, TT 32.3
Kaiser, U. O 47.7
Kaiser, Ute DS 3.1, DS 4.4, DS 12.19,
DS 12.21, O 18.3
Kákay, Attila MA 16.3, MA 23.78,
MA 35.3, MA 38.2
Kalácska, Szilvia MM 4.4
Kalajyan, Mane •HL 29.9
Kalbac, Martin O 26.7
Kale, Sahana CPP 19.8, CPP 57.9
Kaliman, Sara BP 15.5
Kalinovych, Viacheslav •O 28.5,
O 55.2, O 81.11
Kalkan, Sirri Batuhan HL 14.6
Kaikhoff, Lukas O 5.7, •O 13.7
Kalläne, Matthias TT 9.7
Kalle Kossio, Yaroslav Felipe BP 22.1
Kallert, Patricia •HL 7.45, HL 7.66
Kallinger, Birgit HL 37.3
Kallmayer, M. O 30.4
Kallmayer, Michael O 85.3
Kalpazidou, Sofia BP 15.3
Kalthoff, Mona SYUE 1.5
Kalz, Erik •DY 56.1
Kamarád, Jiří MA 37.6
Kambe, Shinsaku TT 28.4
Kamber, Umot O 30.2
Kamiński, Bartosz HL 33.49
Kamiyama, Satoshi HL 28.1
Kamlapure, Anand O 20.1, O 51.2,
O 59.9, •TT 57.1
Kämmer, Elisa BP 29.4
Kammerbauer, Fabian •MA 4.2,
MA 4.7, MA 12.8, MA 23.2, MA 23.3,
MA 23.5, MA 23.6, MA 23.22,
MA 23.23, MA 23.53, •TT 7.2, TT 7.7
Kämmerer, Gérald MA 19.3, •O 74.6
Kammermeier, Lukas •TT 11.3
Kamp, Christel BP 11.22
Kamp, Jan-Christopher BP 21.9
Kamp, Martin HL 35.4, O 36.12,
O 94.6, TT 30.9
Kampfrath, Tobias MA 22.2
Kampmann, Lucas BP 10.5
Kampmann, Rebecca •BP 28.26,
BP 28.27
Kampmann, Steffen CPP 2.6
Kampmann, Tobias BP 24.8, DY 38.8
Kampmann, Tobias Alexander
BP 11.13
Kamps, Oliver DY 37.3, DY 37.5,
DY 37.8
Kampshoff, Christoph BP 21.12
Kamra, Akashdeep MA 4.13,

Author Index

- MA 23.62, *MA 34.2, MA 46.12, TT 7.13
- Kamrla, Robin O 85.5
- Kanak, Jaroslav MA 41.7
- Kanazawa, Kiyoshi *SOE 22.1
- Kaneko, K. TT 47.2
- Kang, Chae Yeon BP 11.40
- Kang, Ji-Hye HL 23.2
- Kang, Jingxuan HL 7.40
- Kang, Kisung *HL 4.8
- Kang, Ming O 16.3
- Kang, Tong H. MA 23.34
- Kang, Wun-Hao *TT 53.7
- Kani, Nagaarjhuna MA 3.4
- Kanistras, Nikos *MA 23.55
- Kanj, Anemar Bruno MA 19.6
- Kanjilal, Anwasha *MM 33.3
- Kannala, Juho O 66.10
- Kantelhardt, Jan W. SOE 11.5
- Kantelhardt, Jannik *CPP 35.10, CPP 57.11
- Kantorovich, Sofia CPP 3.3, CPP 35.13, CPP 35.41, CPP 45.2, DY 57.7, DY 57.8
- Kantorovich, Sofia S. CPP 57.12, DY 7.2
- Kantz, Holger DY 32.7, *DY 37.6
- Kanungo, Sudipta MM 14.6, O 94.4
- Kao, Ming-Chao *O 42.11
- Kap, Özlem *CPP 8.1
- Kapaklis, Vassilios MA 22.5
- Kapil, Venkat O 6.5
- Kappe, Florian HL 7.39, *HL 24.2, HL 24.4, *HL 24.5, HL 24.5
- Kappen, Hilbert J. O 20.2, O 33.9
- Kappert, F. Jasmin HL 10.9
- Kappl, Michael CPP 19.10, CPP 35.9, CPP 52.1, O 12.2
- Kappler, Julian *DY 32.11
- Kaps, Felix G. *O 12.8, O 58.7
- Kar, Manaswita *TT 16.6
- Karadimitriou, Nikolaos CPP 35.66
- Karakuzu, Seher TT 61.1
- Karalis, Orestis HL 7.37
- Karan, Sujoy O 7.5, O 20.5
- Kärcher, Annemarie DS 14.5
- Kardynal, Beata O 31.1, TT 25.1
- Kardynał, Beata E. HL 22.2
- Karetta, Bennet MA 40.60, MA 40.61, *MA 50.4
- Karimi, Bayan TT 20.1, *TT 66.1
- Karimi, Fariba *SOE 3.2
- Karimnia, Martin *O 12.3
- Karla Yanín, Christian BP 15.1
- Karlı, Yusuf HL 7.39, HL 24.2, *HL 24.4, HL 24.5
- Karlová, Katarína TT 29.9, TT 29.10
- Karnaushenko, Daniil *KFM 7.6
- Karnaushenko, Daniil MA 23.34, MA 43.4
- Karnaushenko, Dmitriy D. MA 23.34
- Karouzian, Aras DS 11.3
- Karpenkov, A. MA 23.19
- Karpenkov, Alexey MA 3.3
- Karpitschka, Stefan BP 6.6, BP 30.2, CPP 35.63
- Karpov, Petr DY 55.2, TT 67.2
- Karr, Leonie *DY 42.7
- Karrasch, Christoph TT 45.6
- Karrer, Max TT 3.10, TT 20.4, TT 57.23
- Karsai, Ferenc *MM 12.10
- Karst, Julian *SYSYD 1.4, CPP 37.3, O 49.1, O 49.9
- Karthein, Jan HL 29.9, *TT 59.6
- Kartik, Vijay DY 56.7
- Kartsovnik, Mark TT 10.6, TT 43.10
- Karuthedath, Safakath CPP 43.1
- Karzel, Ulrich HL 15.3
- Käß, Hanno KFM 10.1
- Kaspar, Christoph TT 38.9, TT 60.5
- Kaspari, Jan *HL 7.61
- Kasprzak, Jacek HL 3.7, HL 33.18
- Kassa, Atekelte *DS 12.22
- Kassel, Johannes A. *DY 32.7
- Kassen, Alexander HL 48.3
- Kastenmeier, Maximilian O 29.2
- Kaštil, Jiří MA 37.6
- Kastl, Christoph PSV III, DS 10.3, HL 37.8, TT 6.9
- Kastlunger, Georg O 96.3
- Kästner, Bernd O 43.1, O 43.3
- Kataev, Vladislav TT 10.9, TT 52.8
- Kataria, Meenal *CPP 18.12
- Katnagalli, Shyam *MM 3.1, MM 3.6, MM 36.4
- Katoorani, Seyede Parya *DY 43.13
- Katsch, Florian HL 35.6
- Katsnelson, M. I. O 42.2
- Katsnelson, Mikhail SYUE 1.4, MA 8.11, MA 23.31, MA 27.6, O 30.9, TT 27.7
- Katsnelson, Mikhail I. MA 7.1, MA 35.4, O 20.1, O 51.2, TT 63.3
- Katsura, Hoshio TT 31.8
- Katukuri, Vamshi Mohan *TT 44.2
- Katz, Nadav TT 54.4
- Katzer, Manuel *HL 1.8, HL 8.4, HL 34.8, HL 35.6
- Katzmeier, Florian *BP 2.5
- Kauch, Anna DY 11.7, DY 11.8, TT 5.10, TT 13.7, TT 13.8
- Kauffmann, Alexander MM 40.9
- Kauhanen, Henri SOE 8.3
- Kaulich, Burkhard MA 43.2
- Kaur, Gagandeep O 60.12
- Kaur, Harpreet *BP 11.1
- Kaur, Ranbir HL 49.6
- Kawa, Karol *HL 24.7
- Kawai, Shigeki *O 97.4
- Kawakami, Roland K. MA 23.52
- Kawakami, Yoichi HL 23.3, HL 23.6
- Kaxiras, Efthimios O 16.3
- Kayser, Jona *BP 10.5
- Kazemian, Majid MA 43.2
- Kazenwadel, Daniel DY 49.5, MM 3.4, *MM 39.2
- Kazmaier, Stefan HL 7.48
- Kedia, Mayank HL 4.2
- Keeney, Lynette *KFM 1.1
- Kehlberger, Andreas MA 17.2
- Kehr, Susanne HL 17.11, KFM 6.15
- Kehr, Susanne C. DS 7.1, DS 12.14, DS 12.17, HL 17.3, O 12.8, O 58.7
- Kehrein, Stefan TT 22.12, TT 38.3, TT 38.6, TT 38.8
- Keil, Robert HL 24.4, HL 24.8
- Keim, Peter *DY 16.3
- Keimer, Bernhard HL 48.9, MA 44.7, TT 3.5, TT 9.4, TT 9.5, TT 44.8, TT 50.3, TT 62.3
- Keisers, Johannes *BP 11.70
- Keller, Bettina *SYFP 1.3
- Keller, Elisabeth *MM 19.3
- Keller, Florian *O 94.3
- Keller, Martin *HL 18.1
- Keller, Nils MA 40.34
- Keller, Thomas F. CPP 35.25, O 29.3, O 42.11, O 52.1, O 57.5
- Kelling, J. *O 69.11
- Kelling, Jeffrey *DY 57.1, *SOE 4.8
- Kellner, Nicole TT 16.14, TT 18.1
- Kellner, Philipp BP 21.6, *HL 18.12
- Kelly, Nicola TT 30.10
- Kelly, Rebecca KFM 4.1
- Kelterborn, Simon BP 25.6
- Kemerink, Martijn CPP 1.2, CPP 11.3, CPP 18.4, CPP 18.7, CPP 18.13, CPP 35.35, CPP 36.2, DS 16.6, HL 2.1, HL 33.56, HL 36.5
- Kemna, Andre O 60.7
- Kempa, Heiko HL 4.5, HL 4.6, HL 25.4
- Kemper, Ulrich HL 42.3
- Kempf, K. *KFM 6.9
- Kempf, Michael HL 8.9, HL 33.4
- Kempf, Sebastian TT 57.20, TT 58.5, TT 66.2, TT 66.3, TT 66.4
- Kempkes, Marie BP 13.5
- Kendzo, Gutenberg MA 18.1
- Kenna, Ralph DY 45.15, MA 23.47, SOE 8.2
- Kennes, Dante SYUE 1.5, HL 33.12, TT 37.6, TT 45.6
- Kennes, Dante M. O 93.3, TT 53.9, TT 63.5
- Kentsch, Ulrich HL 50.3, O 31.2
- Kentzinger, Emmanuel DS 12.25, DS 14.6, MA 5.6, O 42.12
- Kepić, Peter O 14.9
- Keppeler, Daniel BP 21.12
- Kerber, Nico MA 23.5
- Kerfoot, James CPP 17.59
- Kermode, James *MM 15.1, MM 15.2
- Kermouche, Guillaume MM 28.9
- Kern, Christian S. O 19.3, O 34.6
- Kern, Klaus BP 21.1, MA 21.7, MA 32.4, O 20.5
- Kernbach, Martin *HL 24.11
- Kerres, Peter DS 12.38
- Kerschbaumer, Samuel O 36.5, *O 56.5
- Kerski, J. *HL 29.2
- Kerski, Jens SYQD 1.3, HL 7.51
- Kerstingskötter, Maik *MA 46.5
- Kerz, Sabrina *CPP 17.49, CPP 58.4
- Kerzel, Ulrich MM 20.4
- Kesici, Merve-Zeynep BP 5.5
- Kesselheim, Stefan BP 11.76, *CPP 2.7
- Kessler, Raphael DY 7.3
- Kestler, Matthias HL 45.6
- Ketting, René BP 3.4
- Ketzmerick, Roland DY 21.2, DY 43.6, DY 43.15
- Keupert, Savio MA 33.2
- Keyser, Ulrich *PLV XI, BP 25.4
- Keyser, Ulrich F. DY 32.11
- Kezilebieke, Shawulienu O 74.2
- Kézmárkai, István KFM 4.5, MA 18.5, MA 23.65, MA 40.51, MA 44.2
- Kézmárkai, István MA 23.13
- Kfir, Ofer HL 10.9, O 83.4
- Khabipov, Marat TT 39.6
- Khademorezaian, Saba *MM 28.6, MM 41.4
- Khajetoorians, A. A. O 42.2
- Khajetoorians, Alexander *MA 26.1
- Khajetoorians, Alexander A. O 2.5, O 7.6, O 20.1, O 20.2, O 20.4, O 33.9, O 51.2, O 59.9, TT 57.1
- Khalakhan, Ivan O 78.8
- Khalili Hezarjaribi, Mahdi *HL 51.2
- Khalayavin, D. TT 46.8
- Khalayavin, Dmitry TT 23.8
- Khamseh, Farnaz HL 12.6
- Khan, Aun N. SYGM 1.5
- Khan, Jafar CPP 1.9
- Khan, Jafar I. CPP 1.4
- Khan, Muhammad *MA 48.8
- Khan, Muhammad Bilal MA 28.1
- Khan, Muhammad Moazzam *HL 16.1, *TT 24.1
- Khan, Muhammad Zubair *DS 5.3, O 31.3
- Khan, Nabeel HL 17.5
- Khanchandani, Heena MM 27.8
- Khanenko, P. TT 42.13
- Khanenko, Pavlo TT 28.3, *TT 34.5
- Khanonkin, Igor HL 16.6, TT 24.6
- Kharbanda, Vansh *BP 11.50
- Kharsah, Osamah *HL 33.15, O 5.8
- Khasanov, Rustem TT 4.12
- Khavasi, Amin *MA 47.11
- Khaymovich, Ivan *DY 25.1, *TT 33.1
- Khayya, Neita CPP 54.5
- Khelif, Abdelkrim HL 10.2
- Khemani, Vedika DY 55.5, TT 67.5
- Kher-Elden, Mohammad A. O 14.2
- Khim, S. TT 42.15
- Khim, Seunghyun MM 6.7, O 59.8, TT 3.9, TT 28.2, TT 28.3, TT 29.1, TT 30.5
- Kholina, Yevheniia *KFM 11.4
- Khomskii, Daniel MA 44.5
- Khorramshahi, Mahya *TT 39.3, TT 54.1
- Khosla, Mallika *DS 6.2
- Khosravian, Narjes O 38.6
- Khrantsov, Igor A. HL 29.10
- Khuntia, P. TT 46.6
- Khuntia, Panchanan TT 30.11
- Khurram, Muhammad *CPP 17.57
- Ki, Stuart MM 36.9
- Kibler, Ludwig A. O 52.2, O 73.5, O 86.9, O 86.10, O 96.9
- Kick, Matthias O 59.10
- Kick, Michael *HL 30.4, *TT 41.4
- Kieburg, Mario DY 9.7
- Kiechl, Thomas *DY 42.4
- Kiefer, Henrik *DY 23.5
- Kiefer, Klaus MA 18.8, *TT 58.29
- Kiefer-Emmanouilidis, Maximilian TT 59.16
- Kiehart, Daniel P. BP 4.7
- Kiel, Lorenz *HL 7.33
- Kieler, Maximilian F. I. *DY 21.1, DY 48.4, TT 55.4
- Kieler, Oliver TT 39.8
- Kiemle, Jonas DS 10.3, TT 6.9
- Kiener, Daniel MM 9.1
- Kienitz, Paul HL 29.10
- Kienle, Lorenz DS 12.7, DS 12.44, DS 12.46, DS 12.57, KFM 1.5, KFM 9.9, MA 17.2
- Kierfeld, Jan BP 3.7, BP 8.10, BP 11.13, BP 24.8, BP 28.46, DY 38.8
- Kiese, Dominik MA 7.10
- Kießling, Tobias TT 17.1, TT 64.5
- Kiessler, Filippo BP 21.11
- Kiessler, Filippo D. BP 13.4
- Kihm, Alexander BP 8.3
- Kiiamov, A. MA 40.14
- Kikugawa, Naoki TT 37.1, TT 37.3, TT 37.4, TT 37.5, TT 37.9
- Kim, Bongjae TT 37.4
- Kim, Changyoung MA 4.10, TT 7.10
- Kim, Hongwon *CPP 18.10
- Kim, Hyun-Jung HL 8.8
- Kim, Hyuntae *BP 11.17
- Kim, Jinhong DS 3.2
- Kim, Jongmin HL 36.4, O 60.10, O 69.14, O 73.4, O 96.7
- Kim, Kyoohyun BP 11.67, BP 12.8, BP 25.7, *BP 28.17
- Kim, Kyung-Han MA 4.10, TT 7.10
- Kim, Min-Jae HL 48.9, *TT 62.3
- Kim, Minu TT 9.6, TT 50.6
- Kim, Ryon CPP 1.10
- Kim, Se-Ho MM 37.7
- Kim, Seo-Jin *MA 27.1, MA 31.4
- Kim, Seung-Goo TT 49.2
- Kim, Steven *TT 16.18
- Kim, Tae Yun MA 7.4, *MA 7.6, MA 7.12
- Kim, Taewook *DS 9.2, DS 9.3
- Kim, Timur DS 1.3
- Kimmus, Len *MM 16.5
- Kimouche, Amina O 42.5
- Kimura, Akatsuki BP 21.10
- Kimura, Tsuyoshi MA 18.8
- Kindo, Koichi TT 46.1
- King, Phil O 30.1
- King, Phil D. C. MA 27.1, O 34.9, O 59.8
- Kinyanjui, Michael K. DS 12.19, DS 12.21
- Kipgen, Lalminthang MA 19.4
- Kipnusu, Wycliffe CPP 20.10, *KFM 11.11
- Kipp, Jonathan *MA 21.6
- Kippenberg, Tobias J. HL 10.9
- Kiraly, B. O 42.2
- Kiraly, Brian O 2.5
- Kirbus, Benjamin KFM 14.3
- Kirch, Anton *CPP 17.13
- Kirchartz, Thomas DS 11.2, HL 7.38
- Kirchberger, Kim Nikolai TT 16.3
- Kirchheim, Reiner MM 18.3
- Kirchhoff, Alexander *O 30.8
- Kirchhoff, Björn BP 27.7, O 3.5, O 30.11, O 48.2, O 64.3
- Kirchlechner, Christoph MM 4.6, MM 9.6, MM 40.6
- Kirchner, Nico *TT 65.9
- Kirchner, Robert KFM 7.4
- Kirilyuk, Andrei O 39.2
- Kirkwood, Nicholas O 49.2
- Kirner, Felizitas O 49.5
- Kirsan, Azad *DY 46.8
- Kirsch, Johann CPP 17.12
- Kirscht, Patrick *MM 23.10
- Kirstein, Erik *HL 15.2, HL 15.3
- Kischel, Florian *DY 49.7
- Kiselev, Nikolai *MA 2.1, MA 47.7
- Kiseleva, I. KFM 14.1
- Kiseleva, Iuliia KFM 6.8, KFM 6.19, *KFM 6.20
- Kisiel, Marcin O 51.3, O 87.3, *O 93.1
- Kißlinger, Tilman O 56.1, O 67.3, O 92.5
- Kissling, Christoph *TT 39.6
- Kisslinger, Ryan HL 7.3
- Kisslinger, Tilman MA 14.2, O 56.4
- Kitahara, Yuki BP 6.4
- Kitatani, Motoharu TT 44.6
- Kitching, Christopher *SOE 8.3
- Kivala, Milan CPP 35.14, O 10.6, O 60.2
- Klaassen, Aram O 69.13
- Klaui, Mathias MA 31.5
- Klamroth, Tilmann O 42.5
- Clapp, Sabine H. L. BP 7.4, BP 7.8, DY 10.4, DY 10.8, DY 42.1, DY 42.5
- Klar, Peter MA 36.5
- Klar, Peter J. DS 8.4, HL 16.3, MM 26.10, TT 24.3
- Klaß, Yannick HL 3.9, HL 10.6, HL 10.8
- Klasen, Alexander *CPP 17.59
- Klaßen, Philipp MA 9.10
- Kläui, M. MA 18.4
- Kläui, Mathias MA 2.2, MA 2.3, MA 4.2, MA 4.7, MA 5.5, MA 12.4, MA 12.8, MA 17.2, MA 18.1, MA 18.3, MA 22.2, MA 23.2, MA 23.3, MA 23.4, MA 23.5, MA 23.6, MA 23.8, MA 23.11, MA 23.57, MA 23.66, MA 26.4, MA 29.1, MA 29.2, MA 31.2, MA 31.3, MA 40.29, MA 40.30,

Author Index

- MA 47.2, O 30.3, O 84.2, O 85.3,
TT 7.2, TT 7.7, TT 56.2
- Klauß, Hans-Henning TT 6.6
- Klaus, Kern O 33.2
- Klaus, Severina BP 11.18
- Klausfering, Lea O 81.9
- Klauss, Hans-Henning MA 44.6,
MM 6.10
- Klebl, Lennart TT 53.9
- Kleemann, Hans CPP 45.9
- Kleenen, Jan KFM 14.5
- Klees, Raffael L. TT 48.4
- Kleibert, Armin MA 18.3, MA 40.30,
MA 43.3
- Kleimeier, Nils Fabian O 37.13
- Klein, Benedikt HL 26.5, O 14.8,
O 53.5
- Klein, Benedikt P. O 93.5, O 93.8
- Klein, Dominic MM 8.3
- Klein, Dominik MM 12.22, MM 12.32,
MM 12.33
- Klein, Eugen HL 7.35
- Klein, Julian HL 33.3
- Klein, Maren DS 12.8, O 22.5
- Klein, O. MA 16.6
- Klein, Olivier MA 23.61
- Klein, Rupert DY 23.2
- Klein, Sebastian MM 8.2
- Klein, Simon TT 62.4
- Kleinbek, Timo MA 40.56
- Kleine, Hannah HL 13.5, O 17.5
- Kleiner, Amir HL 22.7
- Kleiner, Reinhold DS 12.28, TT 3.10,
TT 20.4, TT 39.5, TT 39.8, TT 57.22,
TT 57.23
- Kleinhaus, Markus MA 13.8, TT 19.8
- Kleinherbers, Eric SYQD 1.3, TT 16.5,
TT 60.2, TT 60.6
- Kleinlein, Johannes HL 30.4, TT 41.4
- Kleinschmidt, Peter HL 7.8, HL 7.58
- Klembt, Sebastian HL 5.1, HL 18.4,
HL 24.13
- Klemke, Bastian MA 18.8, TT 58.29
- Klemm, Konstantin DY 57.5,
SOE 7.2
- Klemme, Stephan MM 18.2
- Klempahn, Sophie BP 9.11
- Klennen, J. KFM 14.7
- Klennen, Jan KFM 6.41, KFM 14.4
- Klett, Marcel TT 61.1
- Kley, Christopher S. O 60.8
- Kliemt, Kristin MA 9.5, MA 39.4,
MA 46.4, TT 4.7, TT 4.8, TT 4.9,
TT 9.1, TT 9.2, TT 42.1, TT 42.2,
TT 42.3, TT 43.12, TT 43.2
- Klier, Jens HL 17.4
- Klimek, Anton BP 28.56
- Klimek, Peter SOE 19.1, SOE 23.4
- Klimm, Detlef DS 12.50
- Klimmer, Sebastian HL 35.5
- Klingbeil, Finn MA 40.46
- Klingberg, Tim BP 29.4
- Klingeler, Rüdiger CPP 35.14,
CPP 35.37, MA 9.8, MA 20.25,
MA 24.5, MA 33.7, MA 40.23,
MA 40.56, MA 44.4, TT 46.6, TT 50.8
- Klingner, Nico HL 50.3, O 31.3
- Klinke, Christian HL 7.35
- Klinovaja, Jelena MA 16.2, MA 47.10
- Klitzing, Regine von CPP 35.5
- Klöffel, Tobias O 67.6
- Klokkers, Thomas HL 37.8
- Klopf, J. Michael DS 7.1
- Klopotek, Miriam DY 11.4, DY 17.2,
DY 34.5, TT 13.4, TT 43.33
- Klopp, Christoph DY 29.8
- Klos, Christian BP 22.1
- Klos, Johanna O 70.6
- Klose, Christopher MA 43.6
- Kłosiński, Adam TT 65.3
- Kluibenschedl, Florian HL 7.34
- Klümper, Andreas DY 44.4, TT 45.1
- Klumpp, Stefan BP 6.3, BP 13.2,
BP 23.10
- Klüner, Thorsten MA 28.2, MA 28.3,
O 25.1, O 73.3, O 85.9
- Kluth, Elias HL 41.4
- Knaak, Moritz HL 14.3, HL 33.14
- Knap, Michael DY 2.6, TT 2.6,
TT 22.13, TT 45.9, TT 47.9, TT 61.3
- Knapman, Ross MA 23.15, MA 35.6
- Knappe-Grüneberg, Silvia MA 48.7
- Knauer, Daniel MA 44.4
- Knauff, Manuel O 37.5
- Knechtges, Matthias O 29.4, O 29.5,
O 41.3
- Knechtges, Philipp BP 11.76
- Kneer, Simon DY 5.2
- Kneiß, Max DS 16.2
- Kneisl, M. HL 23.1
- Kneissl, Michael HL 23.2, HL 23.5,
HL 28.4, HL 28.5, HL 44.5
- Knight, Cariad-A. TT 30.3
- Knight, Jacob DY 34.4
- Knippenberg, Timo DY 31.7
- Knipschild, Lars DY 25.10, TT 33.10
- Knispel, Timo O 51.1
- Knittel, Peter HL 50.4
- Knoch, Joachim HL 29.1
- Knol, E. J. O 42.2
- Knoll, Alexander L. M. MM 16.6,
O 26.6
- Knolle, Johannes DY 25.2, MA 10.8,
TT 12.8, TT 33.2, TT 43.27, TT 46.11,
TT 46.13, TT 65.1
- Knoop, Florian MM 36.7
- Knoop, Franz Niklas O 38.5
- Knopf, Heiko HL 2.5, HL 2.6
- Knop-Gericke, Axel MM 5.10
- Knorr, Andreas DS 12.30, HL 1.4,
HL 1.8, HL 1.9, HL 8.4, HL 34.8,
HL 35.6, O 80.8
- Knorr, Gergely HL 8.3
- Knothe, Angelika DY 43.11, HL 9.2,
TT 14.2
- Knotz, Gabriel BP 11.55, DY 32.2
- Knuksen, Jan O 29.9, O 41.2, O 56.8
- Knupfer, Martin HL 2.2, HL 7.23,
TT 37.9
- Kny, Anna DS 12.41
- Ko, Kyung-Hun MA 4.10, TT 10.7
- Ko, Tsz Wai MM 25.4, O 26.6
- Kobayashi, Takuma HL 18.11
- Kobl Müller, Gregor HL 34.5
- Köbrich, Manuel MM 4.3, MM 40.2
- Kocan, Pavel O 54.6
- Kocarev, Ljupco DY 44.10, DY 44.13,
DY 44.15, DY 44.19
- Kocer, Emir MM 25.4, O 26.6
- Koch, Alexander HL 7.54
- Koch, Aron DY 26.7
- Koch, Christoph O 84.1, TT 56.1
- Koch, David KFM 6.31, MA 3.7,
MA 3.8, MA 42.9
- Koch, Elias R. DY 45.4
- Koch, Erik TT 21.6, TT 43.16
- Koch, Frieder O 13.4, O 13.5
- Koch, Gregor O 78.1
- Koch, Jennifer TT 27.9
- Koch, Julian O 64.4, O 82.6, O 82.9
- Koch, Juliane HL 7.58
- Koch, Leon TT 39.7, TT 49.5, TT 58.6,
TT 58.7
- Koch, Martin M. MA 17.4
- Koch, Norbert CPP 17.5, CPP 17.24,
CPP 17.40, CPP 18.1
- Koch, Robert DS 10.5
- Koch, Sebastian TT 58.14
- Koch, Simon TT 39.8
- Kochan, Denis TT 17.7, TT 27.5,
TT 27.6
- Köcher, Nikolas HL 7.50
- Kockert, Maximilian HL 36.4
- Kocsis, Vilmos MA 40.51, MA 40.57,
TT 57.10
- Kodalle, Tim DS 11.3
- Kodde, F. KFM 14.7
- Kodde, Felix KFM 6.41, KFM 14.5
- Koelle, Dieter DS 12.28, TT 3.10,
TT 20.4, TT 39.5, TT 39.8, TT 57.22,
TT 57.23
- Koempe, K. KFM 14.7
- Koenigsdorff, Jana O 64.3
- Koerner, Chris MA 23.73, MA 43.7
- Koert, Ulrich O 48.4
- Koeth, Johannes HL 17.5
- Kofahl, Claudia KFM 13.4, KFM 13.5
- Kogler, Roman AKC 1.2
- Kohama, Yoshimitsu TT 46.1
- Kohantorabi, Mona O 40.4, O 57.5
- Köhl, Michael HL 33.16
- Kohl, Peter PSV 10.1
- Köhler, Anna CPP 17.9, CPP 17.33,
CPP 17.42, HL 7.26, HL 7.33
- Köhler, Antonia O 81.9
- Köhler, Benjamin SOE 10.1
- Köhler, Fabian TT 16.16
- Köhler, Werner CPP 35.10, CPP 35.11,
CPP 35.12, CPP 57.11
- Kohlmann, Marcel MA 23.37,
MA 40.6
- Kohlstedt, Hermann DY 18.5, KFM 1.5
- Kohlstedt, Raphael HL 33.40
- Köhn, Claudia TT 58.26
- Köhne, Ingo CPP 35.52
- Kokalj, David KFM 6.29
- Kokkorakis, Gerassimos C. O 77.6
- Kokott, Sebastian HL 13.3, O 17.3
- Kolar, Ken O 38.7
- Kolár, Martin DY 42.11
- Kolatschek, Sascha HL 7.43
- Kölbach, Moritz HL 38.7, HL 47.7,
O 96.7
- Kolbe, T. HL 23.1
- Kolbe, Thomas BP 11.15
- Kolbe, Tim HL 23.5
- Kolesnichenko, Pavel DS 15.2
- Kolesnikov, Alexander I. TT 9.8
- Kolhe, Nagesh DS 16.6
- Koliogiorgos, Athanasios HL 7.55
- Kolisnyk, Dmytro DY 25.3, TT 33.3
- Kolley, Francine BP 8.7
- Kollmannsberger, Florian TT 10.6,
TT 43.10
- Kolmangadi, Mohamed Aejaz
CPP 37.4, DY 24.4
- Kolobkova, Elena V. HL 15.2
- Kolorenc, Jindrich MA 19.7, O 33.6
- Kölpin, Nadja CPP 35.1
- Kölsch, Sebastian TT 4.6
- Komaragiri, Yesaswini BP 8.8
- Komarek, Alexander TT 30.4, TT 30.7,
TT 37.12, TT 50.1
- Komarek, Alexander C. TT 30.3
- Komissinskiy, Philipp DS 11.4,
DS 12.36
- Kompatscher, Anton HL 2.1
- Kondovych, Svitlana MM 23.20
- Kondratenko, Serhiy HL 7.11
- Konečná, Andrea O 14.9, O 91.5
- Konieczna, Amanda TT 29.5
- König, Dirk HL 16.5, TT 24.5
- König, Elio TT 31.12
- König, Jürgen SYQD 1.3, DY 9.6,
DY 25.9, TT 16.5, TT 33.9, TT 38.11,
TT 60.2, TT 60.6, TT 60.7
- König, Lukas KFM 3.1, KFM 6.35
- König, Markus MA 40.3, MM 26.9,
TT 30.5
- König, Patricia MM 3.3
- König, Tobias CPP 17.3
- König, Tobias A. F. CPP 56.4,
CPP 56.5, CPP 56.6, O 76.9
- Kononenko, D.Y. MA 44.3
- Kononenko, Denys MM 12.37
- Kononenko, Denys Y. MA 18.6,
MA 27.7
- Kononenko, Iryna MA 12.8
- Konrad, Jennifer O 4.4
- Konrad, Paul HL 18.12, HL 22.10
- Konrad, Tobias TT 10.5
- Könye, Viktor TT 6.11, TT 17.6
- Koo, Changhyun MA 23.25, MA 44.4
- Koo, Changyun MA 24.5
- Koper, Marc O 60.9, O 96.6
- Koperski, Maciej HL 31.2, O 61.2
- Kopietz, Peter MA 9.1, MA 33.2,
TT 5.3, TT 47.12, TT 51.3
- Kopnarski, Michael KFM 8.5
- Kopp, Juri MA 36.2
- Kopp, Marvin MA 9.5, MA 39.4
- Kopp, Robin A. BP 7.4, DY 10.4
- Koppe, Nicklas BP 4.3
- Koppitz, Boris KFM 6.18
- Köppel, Tobias BP 11.25
- Kopteva, Natalia E. HL 15.3
- Kopteva, Natalia E. HL 15.2
- Korbel, Jan SOE 18.1
- Körbel, Sabine KFM 4.6
- Körper, Lukas MA 16.3, MA 23.78
- Körper, Rainer MA 48.7
- Korecki, József MA 41.7
- Korhonen, Keijo TT 58.31
- Kori, Hiroshi DY 8.1
- Körmann, Fritz MM 29.3
- Kormányos, Andor HL 14.2
- Korn, Annika MM 23.14
- Korn, Tobias DS 12.16, DS 12.23,
DS 12.40, HL 7.35, HL 8.9, HL 33.4,
HL 33.6, HL 33.7, HL 33.11
- Körner, Peter TT 4.10
- Körner, Wolfgang MM 11.1
- Korneychuk, Svetlana MM 23.13
- Kornich, Viktoriia TT 28.5
- Körnig, André BP 31.7
- Körstgens, Volker BP 19.1, CPP 36.8,
CPP 41.1, CPP 56.2
- Korte, Carsten KFM 2.1
- Korte-Kerzel, Sandra MM 20.3,
MM 20.4, MM 32.3, MM 37.1,
MM 37.8, MM 41.5
- Kortmann, Joscha MM 20.4
- Kortus, Jens CPP 35.33, CPP 35.34,
HL 33.8, KFM 6.10, MM 12.16,
MM 12.19, MM 23.2
- Korytár, Richard O 2.3, O 7.7
- Korzyński, Maciej MA 19.1
- Kosbab, Canan O 28.6
- Kosbahn, David CPP 13.8
- Kosbahn, David P. CPP 17.31,
CPP 51.1
- Koschensch, Chris TT 5.1
- Köser, Rebecca MM 23.12
- Kosina, Vit KFM 4.8
- Koskamp, Tjacco O 30.9
- Koske, Daniel CPP 35.20
- Kosma, Adamantia MA 2.4
- Kosov, Dmitry MM 20.5
- Kossacki, Piotr HL 33.18
- Kossak, A. MA 31.1
- Kostarev, Aleksandr BP 11.47
- Köster, Janis DS 12.19, DS 12.21
- Koster, Malte MA 23.75
- Köster, Sarah PSV V, BP 8.6, BP 23.10,
BP 28.1, BP 28.2, BP 28.24, BP 28.25,
BP 28.28, BP 28.32, BP 28.33
- Köstler, Mike Gerd Georg HL 33.19
- Kosto, Yulia O 28.5, O 42.4, O 92.6
- Kostrz, Dorota BP 23.1
- Kosub, Tobias DS 6.1, MA 11.4,
MA 31.7
- Kot, Małgorzata HL 4.2, O 40.3
- Kot, Piotr O 21.7
- Kotakoski, Jani O 5.6, O 29.9
- Koteswararao, Bommisetti TT 30.11
- Kotora, Martin O 45.6
- Kott, Viktor TT 46.12
- Kotte, T. TT 57.19
- Kotte, Tommy TT 28.6, TT 29.2,
TT 43.2
- Kottke, Malena BP 3.2
- Kottlarz, Inga DY 37.4
- Kotz, Maximilian TT 64.4
- Koujouk, Abbas MA 23.61
- Koula-Simos, Aris HL 22.4
- Koula-Simos, Aris HL 12.7,
HL 33.48, HL 33.50, HL 43.3
- Kounta, Ismaila MA 4.12, MA 40.63,
TT 7.12
- Kour, Sadra O 13.5
- Kourkoutis, Lena TT 44.5
- Kourris, Christos TT 4.2
- Kouta, I. MA 41.2
- Koutentakis, Georgios HL 7.34
- Koutná, Nikola DS 4.5, MM 15.5
- Koutroulakis, G. TT 28.6, TT 57.19
- Kouyate, Maryke CPP 54.1
- Kovacs, Andras MA 17.5, MA 23.4
- Kovács, Péter MM 14.10
- Kovács, Sándor SOE 4.12
- Kovalenko, Maksym V. HL 4.10,
HL 15.3, HL 35.8
- Kovalenko, Sergey O 16.2, O 16.8
- Kovalev, Segey O 64.7
- Kovalev, Sergey BP 11.43, HL 48.9,
MM 23.35, TT 3.5
- Kovalev, Vadim M. HL 3.3
- Kowalska, Joanna PSV V
- Kowalski, Marvin BP 11.46
- Kozioł, Jan TT 42.8, TT 42.10
- Kozioł, Jan Alexander TT 29.8,
TT 43.1
- Kozioł-Rachwał, Anna MA 41.7
- Kozub, Agnieszka HL 7.14
- Krach, Thorsten TT 58.29
- Krafft, Christoph BP 21.2
- Kraft, Florian MA 23.72
- Krage, Finn VA 2.2
- Kraiker, Alexej TT 4.7, TT 42.3
- Krakoviack, Vincent DY 42.13
- Kralj, Marko O 18.8
- Krall, Verena SOE 10.6
- Kramar, Mirna BP 9.4
- Kramarenko, Aleksandr O 69.3
- Krämer, Calvin TT 42.8
- Krämer, F. TT 57.21, TT 58.2
- Krämer, Fabian TT 58.3
- Krämer, Johannes C. BP 28.48
- Krämer, Rüdiger TT 5.3
- Krane, Nils O 33.3
- Kranz, Florian TT 22.13
- Křápek, Vlastimil O 14.9, O 91.5
- Krapivin, Viktor TT 62.7
- Krashennnikov, A. O 47.7
- Krashennnikov, Arkady DS 12.19,
O 5.5, O 74.8
- Krashennnikov, Arkady V. DS 12.21,
O 31.6, O 31.8, O 36.4, O 47.1

Krasnytska, Mariana•DY 44.3, DY 45.15, DY 49.2, •SOE 16.1
 Krass, Hendrik•MM 28.8
 Kratky, TimO 55.3
 Kratochvilova, IrenaO 65.1
 Kratz, Felix S.•BP 3.7
 Kratzer, MarkusKFM 6.39
 Kratzer, PeterDY 9.6, HL 22.9, MA 19.3, •MA 21.5, O 30.10, O 74.6, TT 38.12
 Kraus, Jakob •CPP 35.33, CPP 35.34, HL 33.8, MM 12.19
 Kraus, MirkoBP 17.4
 Kraus, TeresaHL 48.8
 Krause, AstinMA 44.5
 Krause, Christoph ..HL 29.9, HL 30.1, TT 41.1
 Krause, ConstantinHL 24.13
 Krause, Hans-Joachim ..MA 23.28
 Krause, JensBP 11.64
 Krause, Johannes ..HL 33.6, •HL 33.7
 Krause, VeitBP 3.12
 Krause-Rehberg, Reinhard ..KFM 9.8
 Kraushofer, Florian ...O 81.4, •O 92.1, O 92.5
 Kraus-Römer, SebastianBP 6.1
 Krauss, PatrickDY 26.5
 Krauss, SebastianBP 28.5
 Krauss, Sebastian W.•BP 1.4, BP 28.34, BP 28.39
 Krauth, WernerDY 6.3
 Krautscheid, H.DS 12.48, HL 7.16, HL 7.19, HL 7.20, HL 18.5
 Krautscheid, HaraldHL 7.22
 Kravchuk, VolodymyrMA 2.5, MA 12.6, •MA 35.5
 Kravchuk, Volodymyr P.MA 35.3
 Kraxner, Julia•BP 28.57
 Krebber, SarahMA 9.5, •MA 39.4
 Krebs, JohannesO 55.10
 Krecinic, FarukO 75.6, O 76.1
 Krefl, Maximilian M.BP 31.5
 Krehl, JonasO 21.5
 Krehse, SebastianHL 7.60
 Kreie, Jakob•CPP 54.8
 Kreienkamp, Kim L.•BP 7.8, •DY 10.5
 Kreil, Alexander J.E.MA 16.4
 Kreis, ChristianBP 28.37
 Kreisel, Andreas•TT 44.3, •TT 63.6
 Krejci, Ondrej O 66.2, O 66.10, O 74.2, O 87.8
 Krellner, Cornelius ..MA 9.5, MA 39.4, MA 46.4, TT 4.7, TT 4.8, TT 4.9, TT 9.1, TT 9.2, TT 42.1, TT 42.2, TT 42.3, TT 43.12, TT 43.13, TT 46.3
 Kremer, Friedrich•CPP 20.10, CPP 43.3, CPP 50.3, KFM 11.11
 Kremer, GeoffroyO 8.9, TT 21.1
 Kremer, KurtCPP 12.1, CPP 20.6, CPP 35.54, CPP 50.1, O 95.6, O 68.6
 Kremer, MarkusHL 51.4
 Kremer, NelliDS 12.31
 Kremer, Reinhard K.•DS 5.4, •HL 21.2
 Kremeyer, LaurenzCPP 17.8
 Krempaský, JurajO 8.9
 Kremser, Stephan ..DY 45.8, DY 45.9
 Krenner, HubertHL 10.7
 Krenner, Hubert J.HL 10.3
 Krenz, Marvin•O 46.5
 Kress, HolgerBP 25.8
 Kresse, GeorgMM 12.10
 Kretschmer, Fred•CPP 17.15
 Kretschmer, Katarina•BP 3.2
 Kretschmer, SilvanDS 12.19, DS 12.21, O 5.5, O 31.6, •O 31.8
 Kreutzer, Tom-NiklasKFM 1.5
 Kreuzberger, Daniel•TT 57.25
 Kreuzer, Alex•TT 58.15
 Kreuzer, Lucas•MM 40.5
 Kreuzer, Lucas P. ..BP 19.2, CPP 41.2
 Kreuzer, Lucas Philipp ..CPP 8.4
 Kreysing, Eva•BP 25.4
 Kreysing, MoritzBP 5.8, BP 21.4, BP 28.12, CPP 20.2, DY 29.6
 Kreyszig, AndreasDS 6.4, TT 10.11
 Krieg, A.M.H.O 42.2
 Krieg, Elisha•BP 12.3
 Krieg, TimoO 32.5
 Krieger, DominikMA 12.3
 Krieger, Jonas A.DS 12.15, •MA 9.3, O 59.7, TT 27.4, TT 59.12
 Krieger, Michael ..HL 18.11, O 84.10, •O 95.7, TT 56.10, •TT 68.7
 Kriegner, D.MA 41.2
 Kriegner, Dominik MA 4.12, •MA 4.14, MA 40.63, MA 40.64, TT 7.12, •TT 7.14

Krifa, Ahmed ... CPP 17.30, CPP 51.1
 Krill III, Carl E. ... MM 23.30, MM 23.32, •MM 26.2
 Krinitsin, Wladislaw•DY 43.12
 Krinninger, MatthiasO 92.1
 Krischok, StefanDS 8.1, DS 12.4, DS 12.33, HL 7.1, HL 7.2, HL 38.3, HL 38.6
 Krishna, Jyoti•O 75.7
 Krishna Kumar, Karthika ..DY 16.1, •DY 16.7
 Krishnamoorthy, Anand Narayanan CPP 2.2
 Krishnaswamy, VenkatBP 21.4, CPP 20.2
 Krishnaswamy, Venkat Raghavan •BP 28.12
 Kristin Gupta, VerenaO 37.8
 Krivoruchko, VladimirMA 23.79
 Kröger, F. M.TT 57.28
 Kröger, JörgO 64.2
 Kröger, NilsBP 12.10
 Krogstrup, PeterO 59.9, TT 57.1
 Kroh, Matthias ..MM 3.2, •MM 12.2
 Kroha, JohannTT 4.5, TT 38.4, TT 47.1
 Krohn, SonjaHL 24.1
 Krois, EvaCPP 29.2
 Krok, FranciszekO 5.3
 Kroll, MartinDS 10.2, MM 12.24
 Kroll, TimDY 37.3, •DY 37.8
 Kromin, RaphaelMA 40.4
 Kronast, F.MA 31.1
 Kronast, Florian ..DS 5.3, MA 17.1, MA 40.55, MA 50.3
 Kronowetter, Fabian TT 39.7, TT 49.1, TT 58.7, TT 58.10, TT 58.20, TT 66.6
 Kronseder, Matthias TT 16.7, TT 53.10
 Krooß, PhilippMA 3.7
 Kroy, Klaus ..DY 4.9, DY 34.2, DY 40.8, DY 42.9, DY 42.11
 Krpenský, JanO 14.9
 Krstić, MarjanCPP 26.3
 Kruck, Timo•HL 7.57, HL 42.4
 Krueger, AnkeO 55.10
 Krueger, TimmBP 8.3
 Krug, Joachim ..BP 10.3, BP 11.30, •DY 27.1, •SOE 15.3
 Krug, MalteDY 43.19
 Krug von Nidda, H.-A.MA 40.14
 Krug von Nidda, Hans-Albrecht TT 46.4
 Krüger, David Alan•MA 27.2
 Krüger, E.•DS 12.48, •HL 7.16, •HL 18.5
 Krüger, EvgenyHL 7.22
 Krüger, Matthias ..BP 11.55, DY 16.1, DY 16.4, DY 16.6, DY 16.7, DY 27.4, DY 32.2, MM 12.20
 Krüger, Peter ..O 59.2, O 59.4, O 59.6, O 85.6
 Krüger, SebastianHL 12.7
 Krüger, Severin•HL 33.45
 Krüger, Wilhelm•TT 52.9
 Kruk, MonikaCPP 54.4
 Kruk, RobertMA 3.1
 Krumrey, ThiloTT 58.15
 Krupkov, GeorgMM 12.2
 Krupnitska, Olesia •TT 42.17, TT 52.1
 Kruse, KarstenBP 15.4
 Kruskopf, MattiasO 82.7
 Krylov, Denis ..O 15.12, •O 21.2, O 66.9
 Kryssig, AndreasKFM 11.5
 Krywka, ChristinaKFM 9.9
 Krzywda, JanHL 33.27
 Krzywowski, MichaelO 77.2
 Kshirsagar, Aseem Rajan ..HL 27.4, O 62.4, TT 40.4
 Ku, Hsiang-ShengTT 49.2
 Kubala, BjoernTT 54.5
 Kubala, BjörnO 7.5, TT 39.2, •TT 39.9, TT 54.4
 Kubar, TomasBP 11.42
 Kube, PierreO 78.1
 Kübel, ChristianKFM 9.9
 Kübelbäck, Florian•TT 47.3
 Kubetzka, AndréMA 14.1
 Kubicki, Milan•O 55.5
 Kublitski, Jonas .CPP 43.4, CPP 43.9
 Kuc, AgnieszkaDS 2.1, HL 11.6, TT 15.6
 Kuch, W.O 47.3
 Kuch, Wolfgang ..MA 19.4, MA 19.6, MA 40.12, MA 40.55, O 36.5, O 56.5
 Kühle, Johannes TO 36.6
 Kucska, Nora•TT 8.7

Kudlacik, DennisHL 15.3
 Kudrnovsky, JosefMA 23.29
 Kuechle, Theresa•HL 8.3
 Kuehne, H.TT 46.8
 Kuehne, TimO 3.3
 Kuemmeth, Ferdinand ..HL 33.27
 Kuerten, LukasKFM 6.27
 Kufner, CorinnaBP 10.2
 Kugler, DavidO 54.7
 Kühbach, Markus ...•O 84.8, •TT 56.8
 Kühl, FlorianHL 28.4
 Kuhl, MatthiasHL 45.1
 Kuhl, UlrichDY 21.4
 Kuhlenskamp, Clemens ..TT 61.3
 Kuhn, C.HL 23.1
 Kühn, DaniloO 67.9, •O 85.1
 Kühn, Franziska•MA 23.71
 Kuhn, JuleBP 1.11
 Kühn, OliverHL 7.5
 Kuhn, Tilmann ..HL 3.7, HL 10.5, HL 33.2
 Kühn, Tobias ..•BP 11.24, •BP 18.5, •DY 33.5, •TT 57.18
 Kuhn, Valentina•BP 28.33
 Kühne, Florian ..O 8.3, •O 16.9, •O 19.1
 Kühne, H.TT 28.6, TT 42.15, •TT 57.19
 Kühne, Hannes ..TT 29.2, TT 43.2
 Kühne, TimO 3.1
 Kühnel, MarkBP 21.9
 Kuhnén, Raphael ..DS 12.4
 Kühner, HannesCPP 26.3
 Kuhnhold, AnjaDY 16.8
 Kühnle, Angelika•CPP 29.1, O 60.1, O 81.9
 Kuibarov, Andrii ...•TT 57.9, TT 57.11
 Kuisma, MikaelO 76.8
 Kukharichy, Nadezhda ...MA 40.35, TT 54.8, TT 54.9, TT 54.10, TT 58.8, TT 58.9, TT 58.10
 Kukhareno, Oleksandra ..CPP 50.1
 Kulbakov, A.A.MA 44.3
 Kulbakov, Anton MA 40.22, •MA 44.8, TT 23.12, TT 42.5
 Kulikov, Ilija•MM 16.1
 Kulkarni, Shruti G.•BP 31.4
 Kullig, Julius•DY 21.3
 Kullock, RenéO 91.6, O 91.9
 Kulossa, Markus•DY 6.4
 Kumagai, T.O 75.9
 Kumagai, TakashiO 2.1, O 12.7, O 75.6, O 76.1, O 76.4
 Kumar, Aditya•MA 23.57, MA 31.2
 Kumar, Aman•MA 33.3
 Kumar, AmitKFM 4.1
 Kumar, AnandDS 2.5
 Kumar, AnkitDS 14.7
 Kumar, Karthika Krishna ..DY 16.4
 Kumar Kuppasamy, Senthil .MA 19.3
 Kumar Parthasarathy, Shravan HL 33.21
 Kumar, PawanMA 11.1, MA 32.6
 Kumar, PriyaBP 29.4
 Kumar, RandhirHL 50.6
 Kumar, SaravanaCPP 29.4
 Kumar, ShivO 59.4, O 85.6
 Kumar, Vivek •MA 9.4, •MA 20.6, TT 10.3
 Kumberg, I.O 47.3
 Kumberg, IvarMA 19.4, MA 40.12, MA 40.55
 Kümmel, Simon•MM 12.22
 Kummer, KurtMA 39.4, TT 4.10
 Kumpf, Christian ..O 10.2, O 19.7
 Kundu, Avijit•BP 28.10
 Kundu, Moumita•MA 8.7
 Kunkel, Christian CPP 35.38, HL 40.7, MM 8.6, O 6.9, •O 39.3, O 79.7
 Kunkemöller, StefanTT 57.5
 Kunst, Flore K.O 94.10
 Künstle, Kevin•MA 23.69
 Künstler, LisaDY 7.3
 Kunte, NilsHL 2.6
 Kuntz, P.TT 57.28
 Kunz, Yannik•MA 15.3, MA 23.69, MA 23.72
 Kunze, PhilippHL 29.4
 Kunze, UlrichHL 33.45
 Künzel, Fabian•TT 43.26
 Kunze-Liebhäuser, Julia•O 60.5
 Kunzelmann, Viktoria F.HL 7.4
 Kunzfeld, Nicolas•KFM 7.5
 Kunzmann, Alexander•MM 23.5
 Kunzmann, Dominic J.HL 28.3, •HL 33.40
 Kunzmann, Susanne•MM 12.8
 Kunzmer, M.KFM 14.1

Kuo, Chang-Yang ... HL 51.3, HL 51.6, TT 9.3, TT 30.6, TT 50.1
 Kupferer, AstridBP 12.1
 Küpper, JochenVA 1.3
 Kurjahn, Maximilian BP 6.6, •BP 30.2
 Kurki, Lauri ...O 54.3, •O 66.2, O 87.4
 Kurnia, FranKFM 4.1
 Kurpas, MarcinHL 1.1
 Kurschat, Timo A.•VA 2.2
 Kürsten, Rüdiger ...•BP 7.11, BP 24.6, •DY 10.11, DY 38.6
 Kurth, Jutta G.•DY 45.3
 Kurtz, Felix•O 34.5, O 75.8
 Kurzchalia, Teymuraz V.BP 28.17
 Kurzmann, A.HL 29.2
 Kurzmann, Annika .SYQD 1.3, HL 9.4, TT 14.4
 Kurzthaler, ChristinaDY 42.6
 Küß, MatthiasMA 15.3
 Kusampudi, NavyanthMM 36.4
 Kusber, Anncharlott•HL 7.23
 Kusch, MaximilianTT 51.6
 Kuschel, TimoMA 15.1, O 68.1
 Kuschch, Natalia ..TT 10.6, TT 43.10
 Kushimoto, Maki•HL 28.2
 Kushwaha, Niraj•SOE 16.4
 Kusminkiy, Silvia Viola ..MA 34.6
 Kusnezoff, MihailsMA 49.7
 Küspert, JuliaKFM 9.7
 Küss, MatthiasMA 23.72
 Kussauer, SophieBP 28.54
 Küster, FelixTT 8.5
 Küster, Kathrin•O 56.2, O 64.6, TT 44.8
 Kuswik, PiotrMA 36.4, MA 38.4
 Kutelak, Leonardo•MA 39.2
 Kutnyakhov, D.MM 26.8
 Kutnyakhov, Dmytro ...O 16.1, O 37.8, O 84.3, O 95.3, TT 56.3, TT 68.3
 Kuznetsov, Alexander•HL 3.4
 Kuznetsov, Alexander S.HL 10.4
 Kuznetsov, AndreyCPP 35.41
 Kuznetsov, M.MA 40.14
 Kuznetsova, Maria S.HL 15.2
 Kвашnin, Yaroslav MA 7.1, MA 20.7
 Kvintitskaya, Oksana•TT 16.2
 Kwaaitaal, MaartenO 39.2
 Kwan, AlanSOE 16.2
 Kwiatek, NataliaMA 41.7
 Kwon, Yong SeungTT 9.7
 Kyosev, YordanMM 11.5
 Kyrylo, JosephTT 17.6
 Kyvala, DariaO 33.6
 L. Panadés-Barrueta, Ramón HL 20.1, O 35.1
 L. Portalupi, SimoneHL 7.62
 L. Ravensburg, AnnaMA 22.5
 L. Weindl, ChristianCPP 35.19
 Laan, LiedewijBP 29.1
 Laarmann, Tim ..CPP 26.1, CPP 36.6
 Labbus, FelixTT 10.4
 LaBollita, HarrisonTT 44.5
 Laborie, EmelineBP 22.11
 Labrie-Boulay, IsaacMA 2.3
 Lach, PhilippBP 11.5
 Lachnitt, Jan•O 92.4
 Lackinger, MarkusO 60.12
 Lackner, LukasHL 2.5
 Lacmann, TomTT 34.1, TT 57.8
 Lacovig, PaoloO 14.8, O 56.10
 Lado, JoseO 74.2, TT 48.7
 Ladurner, GeorgBP 28.29
 Lafon, SusanneDY 45.6
 Laforsch, ChristianBP 25.8
 Lägel, BertMA 16.5, MA 23.74
 Lagomarsino, StefanoHL 29.10
 Lagoudakis, P.G.•HL 48.4
 Laha, Sudarshana•BP 22.9
 Lahiri, Abhiroop•DY 43.20
 Lahnsteiner, Jonathan ..MM 12.10
 Lai, King Chun ...MM 19.2, •MM 36.3
 Lai, Yi-Chieh•DY 26.3
 Laibe, GuillaumeSYQC 1.2
 Lake, B.MA 40.58
 Lake, BellaTT 46.7
 Lakkis, Ali•DY 7.2, DY 57.7, DY 57.8
 Lakkome, Nils-Alexander ..•BP 17.4
 Lakshminpathy, Tarakeshwar MM 12.35, •MM 15.4
 Lalkens, BirkaO 12.4
 Lallemand, MaxBP 23.2
 Lamann, Mats H.DY 25.10, TT 33.10
 Lambai, AlosiousMM 4.5
 Lambert, Kim•MM 12.20
 Lammel, M.MA 41.2
 Lammel, MichaelaMA 20.2, •MA 23.60, MA 23.62

- Lämmerzahl, TimDS 12.31
 Lampe, Carola CPP 19.11
 Lamperti, Alessio MA 17.2
 Lampl, MichaelTT 42.6
 Lampoltshammer, Thomas J.
 SOE 19.1
 Lamprich, Julia TT 49.2
 Lamsaadi, Hassan O 18.3
 Lan, Jinggang O 6.5
 Lan, Qianqian MA 47.7
 Lance, Romain DY 17.7
 Lanco, Loic HL 10.10
 Lancock, Jan O 65.1
 Landaeta, Javier TT 28.3, TT 37.8
 Landers, Joachim MA 36.1, MA 36.2
 Landra, Alessandro TT 49.2
 Landwehr, Felix O 10.7
 Lang, Heinrich O 55.1
 Lang, Johannes DS 12.35, KFM 6.40
 Lang, MartinMA 23.14, MA 26.4
 Lang, MichaelCPP 3.2, CPP 35.57,
 CPP 58.6, TT 4.8, TT 9.2, TT 10.7,
 TT 43.9, TT 43.12, TT 43.13, TT 46.7,
 TT 51.9
 Lang, Nicola HL 50.4
 Lang, Nicolas KFM 7.9
 Lang, Wolfgang TT 3.10
 Lange, H. MA 34.8
 Lange, Hannah MA 46.12
 Lange, Holger HL 24.1
 Lange, Michael KFM 6.6, KFM 14.2
 Lange, Regina BP 28.13, O 28.3
 Langeheine, Ch. Schüssler- MA 46.4
 Langen, Tim HL 50.2
 Länger, Christian O 48.4
 Langer, Jurgen MA 17.2, MA 40.29
 Langer, Manuel MA 43.3
 Langer, Marcel F. MM 36.7
 Langer, Moritz HL 7.63, HL 24.9
 Langer, Tim HL 7.45
 Langguth, Inga O 81.7
 Langheinrich, Wolfram HL 37.6
 Langheld, Anja TT 42.8, TT 42.9
 Langrehr, Adrian CPP 35.4, KFM 9.10
 Langrock, Veit HL 37.7
 Lanz, Amon TT 62.5
 Lanz, Amon P. MA 18.3
 Lanzillotti-Kimura, Daniel HL 10.10
 Lapp, Clara Johanna TT 57.13
 Laqua, Heinrich Peter KFM 8.6
 Laquai, Frédéric CPP 1.4, CPP 1.9,
 CPP 11.2, CPP 17.17, CPP 43.1
 Laricchia, Savio HL 26.4, O 53.4
 Lars, Dörner KFM 13.3
 Larsen, Jes HL 4.9
 Laschewsky, André CPP 35.60,
 CPP 35.61, CPP 53.4
 Laschke, Matthias w. BP 8.3
 Laschewsky, André CPP 35.43
 Lass, Jakob MA 9.7
 Lászlóffy, András TT 8.5, TT 8.6,
 TT 8.7
 Lau, Alexander TT 53.3, TT 63.2
 Lau, Michael MA 35.2
 Laube, Mandy BP 4.3
 Lauchli, A. M. TT 42.13
 Laudani, Floriana HL 33.49
 Lauer, Christian CPP 35.48
 Lauer, Kevin HL 7.1, HL 7.2, HL 38.1,
 HL 38.3, HL 38.6
 Laufer, Jan BP 28.15
 Lauga, Eric BP 5.8
 Laughrea, Sébastien TT 28.4
 Lauhoff, Christian MA 3.7
 Lausch, K. Nikolas O 26.6
 Laussy, Fabrice P. HL 7.65
 Lauster, Tobias O 49.2
 Lautenschläger, Franziska BP 12.5,
 BP 25.3, BP 25.9, BP 28.36,
 BP 28.38, BP 28.52
 Lauth, Jannika CPP 29.7
 Lautner, Dirk O 81.9
 Laux, Paul-Friedmar O 13.6
 Lavina, Barbara MA 42.2
 Law, Jia Yan SYGM 1.5
 Law, Kam Tuen MA 10.4, TT 12.4
 Lawitzki, Robert MM 16.9, MM 23.16
 Lawoko, Martin CPP 58.2
 Lawrence, J. O 47.3
 Lawrence, Joseph E. DY 32.10
 Laxhuber, Kathrin BP 22.12
 Lazewski, Jan HL 21.2
 Lazzaroni, Paolo HL 40.6, O 79.6
 Le Brun, Anton CPP 36.6
 le Coutre, Nils DS 12.23
 Le Dantec, Marianne PLY X
 Le Dü, Morgan CPP 17.20, CPP 35.43
 Le Hur, Karyn TT 23.6
 Le Lay, Gay O 14.11
 Le Nguyen, Quynh TT 62.7
 Le Tacon, M. O 30.4
 Le Tacon, Matthieu TT 34.1
 Le Vay, Kristian BP 10.6
 Le Verge Serandour, Mathieu BP 4.2,
 BP 28.31
 Lebius, Henning O 5.6
 Lebrun, R. MA 18.4
 Lebs, Sarina MA 35.8
 Lechermann, Frank TT 9.8, TT 50.7
 Lechner, Barbara O 92.1
 Leckron, Kai MA 8.10, MA 46.2
 Leclerc, Armand SYQC 1.2
 Lecrivain, Gregory KFM 7.4
 Ledingham, Patrick HL 3.6
 Lee, Ching Hua TT 64.5
 Lee, Chul-Ho TT 57.10
 Lee, Edward SOE 16.2, SOE 16.4
 Lee, Hovan MA 21.7, O 33.2
 Lee, Hyun-Woo MA 4.10, TT 7.10
 Lee, Jai Sung MM 41.4
 Lee, Lan-Hsuan TT 49.2
 Lee, Po-Heng BP 6.7
 Lee, Sang-Eun MA 46.4, MA 46.13,
 O 16.7
 Lee, Sheng O 75.5
 Lee, Subin MM 4.6, MM 9.6, MM 40.6
 Lee, Tien-Lin DS 1.3, DS 6.3, O 36.6,
 O 36.11, O 93.5, O 93.8
 Lee, Wanhee MM 29.2
 Lee, Wooyoung HL 36.4
 Lee, Yang-Jun MA 7.4
 Lee, Yejin DS 5.2, DS 12.18, DS 12.20,
 MA 12.3
 Lee, Yohan CPP 37.3
 Lee, Yonghyuk MM 3.3, O 78.3,
 O 78.5
 Leeb, Valentin TT 43.27, TT 65.1
 Leedah, Brett TT 30.4, TT 30.7
 Lefkidis, Georg O 37.2
 Legendre, Julian TT 23.6
 Legg, Henry TT 6.8
 Legge, Isabelle BP 28.14, O 26.5
 Leguay, Lucie HL 44.7
 Legut, Dominik MA 28.5
 Lehl, Nikolaj HL 33.54
 Lehmann, Jannis DS 15.3, MA 48.2
 Lehmann, Louis DY 44.21
 Lehmann, Matthias DS 3.2, HL 2.3
 Lehmann, Michael DS 12.3
 Lehmann, Paul MA 31.7
 Lehmeier, Johannes O 84.10,
 TT 56.10
 Lehmeier, Johannes A. F. HL 18.11
 Lehnen, Jonas BP 11.6
 Lehner, Markus O 5.3
 Lehnert, Tibor O 18.3
 Lehnertz, Klaus DY 45.3
 Lehniger, Kevin KFM 6.33
 Lehr, Fabrice BP 11.76
 Lehr, Matthias U. PSV IX
 Lei, H. C. TT 23.7
 Lei, Yong DS 12.51, HL 7.58, HL 14.10,
 HL 38.4, HL 45.3, KFM 6.7, KFM 6.13,
 KFM 6.26, KFM 10.5, KFM 10.8,
 KFM 10.10, MM 5.4, MM 5.5, MM 5.7,
 MM 11.3, MM 23.9, MM 23.25,
 MM 23.26, MM 37.2, MM 42.10
 Leibauer, Benjamin CPP 35.62
 Leiderer, Paul TT 16.3
 Leiner, Jon MA 13.8, TT 19.8
 Leiner, Jonathan MA 40.42, MA 48.1
 Leineweber, Andreas MM 12.16
 Leipnitz, Steen BP 18.1, DY 33.1
 Leisegang, Markus MA 14.4, MA 14.5,
 O 2.2, O 46.4, O 55.10
 Leist, Christopher DS 4.4
 Leitenstorfer, Alfred HL 35.3
 Leiter, R. O 47.7
 Leitherer, Andreas MM 31.4
 Leitold, Christian BP 3.9
 Leiva, Sergio MA 4.9, TT 7.9
 Leiviska, M. MA 41.2
 Leiviskä, Miina MA 4.12, MA 40.63,
 TT 7.12
 Lejay, Pascal TT 4.10
 Lejcek, Pavel MM 41.1
 Lekka, Malgorzata BP 31.4
 Leliaert, Jonathan MA 29.4
 Lemaître, Aristide HL 10.10
 Lembo, Sergio BP 31.2
 Lemcke, Heiko BP 28.55
 Lemell, C. O 5.2
 Lemesh, Ivan MA 43.6
 Lemeshko, Mikhail HL 7.34
 Lemke, Edward BP 26.1
 Lemke, Henrik TT 62.7
 Lemmens, Peter TT 30.8, TT 64.8
 Lemut, Gal HL 30.6, TT 41.6
 Len, Evgen MM 12.31
 Lenart, Peter BP 25.1
 Leng, Andreas O 23.1
 Lenger, Malik MA 23.38
 Lenhard, Philipp TT 58.17
 Lenk, Katharina TT 5.12
 Lenke, Lea TT 5.8, TT 5.9, TT 65.10
 Lenne, Pierre-François BP 15.6
 Lenser, Christian CPP 35.36
 Lensker, Eric KFM 6.21
 Lensker, Eric N. DS 16.5
 Lentfert, Akira MA 40.7
 Lentsch, Tammo DY 44.5
 Lentz, Florian HL 33.12
 Lentz, Sarah DS 13.5
 Lenz, Benjamin TT 16.6, TT 21.3,
 TT 30.11, TT 43.11, TT 43.14,
 TT 43.15, TT 43.18
 Lenz, Thomas BP 5.3
 Lenzing, Nicolas MA 23.30, MA 27.2
 Leo, Karl CPP 17.14, CPP 17.15,
 CPP 43.4, CPP 43.5, CPP 43.6,
 CPP 43.8, CPP 43.9, CPP 45.9,
 DS 10.2, HL 7.12
 Leo, Naëmi MA 29.4, MA 40.3
 Leon, Andrea MA 7.7
 Leon, Dario A. HL 20.3, O 35.3
 Leone, Francesco DY 23.1
 Leonetti, Marco DY 46.10
 Leoni, Thomas O 55.7
 Lerner, Sören HL 7.18
 Leroy, Eric MM 33.2
 Lesanovsky, Igor TT 43.33
 Leßmeister, Jannis O 37.10
 Lesne, Annick SOE 4.3
 Lesne, Edouard MA 37.4
 Lestinsky, M. TT 57.28
 Letouze, Coraline TT 43.18
 Lettermann, Leon BP 28.18, BP 28.21,
 BP 28.47
 Leumer, Nico TT 16.1, TT 60.3
 Leupold, Nico HL 7.33
 Leusch, Marvin TT 29.7
 Leuth, N. DS 7.2, MA 40.53
 Leuth, Niklas MA 40.54
 Leutner, Kilian MA 2.3
 Levchenko, Sergiu HL 4.9
 Levin, Nikita O 41.3
 Levin, Oleg MM 16.1
 Levis, Demian BP 7.11, DY 10.11,
 DY 42.9
 Levitov, Leonid TT 64.3
 Lewis, Alan HL 6.7, O 9.7
 Leyzner, Maxim HL 12.5
 Lezu, Luca O 54.8
 Lhost, Olivier CPP 19.3
 L'Huillier, Anne O 75.3
 Li, Can O 66.1
 Li, Changan HL 31.1, O 61.1, TT 63.7
 Li, Chao O 7.8, O 33.7, O 38.4, O 45.3,
 O 45.4
 Li, Cheng-Wu CPP 20.7
 Li, Chun MA 19.6
 li, cong DY 25.7, O 8.8, O 37.12,
 TT 33.7
 Li, Dongqi DS 12.15
 Li, Dongzhe MA 21.2
 Li, Hong CPP 17.5
 Li, Hongshuai DS 4.2
 Li, Jiahua MA 32.6
 Li, Jiajun TT 5.12
 Li, Jiang MA 31.7
 Li, Jianjun MM 9.7
 Li, Jiejie MM 9.7
 Li, Jingwen DS 15.3
 Li, Junang BP 30.3
 Li, Lang O 86.2
 Li Manni, Giovanni TT 21.4
 Li, Maxwell MA 23.36
 Li, Nian BP 19.1, CPP 13.9, CPP 41.1
 Li, Ning CPP 1.11, CPP 36.1, CPP 36.5
 Li, Peining O 58.8
 Li, Qifang MA 10.4, TT 12.4
 Li, Qili MA 16.9, TT 3.1
 Li, Quiyang O 34.3
 Li, Rongxin HL 34.5
 Li, Shuai O 12.2
 Li, Shulun HL 33.36, HL 33.37
 Li, Tang KFM 6.22
 Li, Wei HL 34.7
 Li, Xiangfeng MA 24.5
 Li, Xiaomei CPP 44.2
 Li, Xiaoqin Elaine HL 35.1
 Li, Yahui TT 38.1, TT 43.23
 Li, Yanan CPP 13.9
 Li, Yi DS 14.2, HL 34.2
 Li, Yingzi O 66.6
 Li, Yong MM 42.5
 Li, You-Sheng TT 37.1, TT 37.2,
 TT 37.3, TT 37.4, TT 37.5
 Li, Yuan TT 52.8, TT 52.9
 Li, Yunfei SOE 11.5
 Li, YuTao MM 6.2
 Li, Zerui CPP 17.20, CPP 17.30,
 CPP 35.43
 Li, Zhangtao MM 4.2
 Li, Zhijie MM 4.2
 Li, Zhilin MA 9.6
 Li, Zhiwei TT 37.12
 Li, Zhongyang MM 17.4, MM 23.29
 Li, Zhuoqing MM 23.19
 Liang, Suzhe CPP 17.4, CPP 29.2,
 CPP 29.8, CPP 35.19
 Liang, Xian-Ting MM 10.4
 Liang, Yanyan MM 26.6
 Liang, Yingjie DY 44.6
 Liang, Yu-Hui TT 23.5
 Liang, Yuxin CPP 17.46
 Liao, Weida BP 5.8
 Liao, Yen-Fa TT 30.3
 Libisch, Florian HL 30.2, HL 33.12,
 TT 41.2
 Libuda, Jörg O 29.2, O 69.9, O 73.2
 Lichtenegger, Michael F. HL 14.6
 Lichtenstein, Alexander SYUE 1.4,
 TT 63.4
 Lichtenstein, Alexander I. MA 7.1,
 O 33.5
 Lidzey, D.G. HL 48.4
 Liebchen, Benno BP 7.3, BP 7.5,
 BP 7.9, DY 10.3, DY 10.5, DY 10.9,
 DY 26.10, DY 42.3
 Lieberwirth, Eric BP 28.13
 Liebhauer, Eva O 7.4
 Liebig, Alexander O 87.7
 Liebing, Niklas MA 23.68, MA 23.73
 Liebmann, M. MA 40.53
 Liebsch, Yossarian O 5.6, O 5.8
 Liebscher, Christian MM 30.1
 Liebscher, Christian H. MM 31.4
 Liedke, Maciej Oskar CPP 35.17,
 DS 14.5, HL 5.5, KFM 6.30, KFM 9.5,
 KFM 9.8, KFM 9.10, MA 31.7
 Liedke, Oskar DS 6.1
 Liedtke, Fabian HL 33.45
 Lienau, Christoph BP 11.42, CPP 28.9,
 HL 2.5, HL 25.8, HL 48.8, O 58.2,
 O 75.2, TT 32.9
 Lien-Medrano, Carlos R. MM 21.5,
 O 6.7
 Liero, Matthias CPP 17.13
 Liese, Susanne DY 29.2
 Lieske, Leonard-Alexander O 22.1,
 O 66.3
 Lifshitz, E. DS 7.2, MA 40.53
 Ligmajer, Filip O 14.9
 Lihm, Jae-Mo MM 19.5, MM 29.2
 Lillenthal-Uhlig, Benjamin TT 57.2
 Liljeroth, Peter O 6.8, O 54.3, O 66.10,
 O 74.2, O 87.4
 Lill, Johanna MA 3.3, MA 3.8,
 MA 42.2, MA 42.7
 Lilleodden, Erica MM 2.1
 Lim, Ji Soo TT 30.9
 Lima Fernandes, Imara MA 47.4
 Lima, Jonas R F HL 37.9
 Limame, Imad HL 8.2, HL 12.2,
 HL 12.7, HL 33.24, HL 33.47,
 HL 33.50, HL 43.3, HL 43.5
 Limbeck, Andreas DS 4.5
 limodin, nathalie MM 20.2
 Limot, Laurent O 7.9
 Lin, Becky HL 49.5
 Lin, Binbin MM 20.4
 Lin, Chenfang O 76.1
 Lin, Guosong SOE 15.1
 Lin, Hong-Ji TT 4.10
 Lin, Kaiman DS 14.2, HL 34.2
 Lin, Kai-Qiang PRV III
 Lin, Keng-Yung TT 50.1
 Lin, Lisa BP 2.2
 Lin, Nan KFM 6.25
 Lin, Rui O 66.6
 Lin, Shuyao DS 4.5, MM 15.5
 Linczuk, Joanna SOE 18.2
 Lindackers, Dirk TT 58.27
 Lindahl, Erik BP 3.5
 Lindemann, Tyler TT 20.8, TT 27.5
 Linden, Stefan CPP 56.7, DS 12.37,
 HL 1.3, HL 29.6, HL 33.1, O 49.4,

O 65.4, O 70.7, O 91.3
 Lindenthal, Jakob •HL 7.12
 Linder, Jacob O 59.9, TT 20.10,
 TT 57.1, TT 57.16
 Linderl, Theresa CPP 28.4, TT 32.4
 lindfors, klas HL 7.27, O 58.1, O 70.9
 Lindfors-Vrejoiu, Ionela MA 12.2
 Lindhorst, Thisbe K. BP 1.11
 Lindner, Anke •CPP 57.1
 Lindner, Axel VA 1.1
 Lindner, Benjamin BP 9.3, BP 11.62,
 BP 13.3, •BP 22.2, •DY 27.11
 Lindner, Julian MA 18.8
 Lindner, Jürgen MA 23.78
 Lindner, Simon SOE 18.1
 Lindner-Franz, Susi O 55.5
 Linek, Julian TT 39.8
 Link, Julia M. TT 57.12, TT 57.13
 Linke, Matthias •DS 12.32
 Linkenheil, Anna •DS 12.57
 Linnartz, Jasper MA 33.7
 Lino, Yuki MA 18.8
 Linß, Franziska HL 14.1
 Linscott, Edward MM 16.10, MM 21.4
 Linsmeier, Christian MM 22.4,
 MM 22.5
 Lippitz, Markus O 43.2, O 43.5, O 70.1,
 O 76.6, O 76.9, O 91.1
 Lips, Klaus KFM 6.38
 Liseanski, Mariia MM 42.6
 Lisenfeld, Jürgen TT 49.3, TT 58.12,
 TT 58.17
 Lisjak, Darja MA 36.2
 Lissel, Franziska O 3.1, O 3.3
 List, Mathias CPP 1.6
 Litman, Yair •O 6.5
 Litnovsky, Andrey MM 22.4, MM 22.5
 Litterst, Jochen MA 23.13, MA 40.20,
 MA 44.8, TT 10.4
 Litterst, Maximilian •CPP 35.35
 Littlehales, Matthew T. MA 11.6
 Litzba, Lukas •TT 60.6
 Litzius, K MA 31.1
 Litzius, Kai MA 40.5, MA 43.6
 Liu, Albert •TT 62.2
 Liu, Betty S. BP 12.7
 Liu, Bing O 36.12
 Liu, Chao CPP 1.11
 Liu, Cheng TT 30.10
 Liu, Cheng-En TT 50.1
 Liu, Chun-Xiao TT 31.6
 Liu, Chun-Yu •MA 20.3
 Liu, Danyang O 28.7, •O 55.4, O 77.8,
 TT 57.4
 Liu, Fang-Zi O 66.8
 Liu, Fupin MA 23.20, O 2.7
 Liu, Hanqing HL 33.36, HL 33.37
 Liu, Hao O 87.2
 Liu, Hongxiong TT 23.5
 Liu, Hsuan-Wei HL 50.6
 Liu, Hui DY 21.3, MA 41.3, •TT 36.5
 Liu, Jessica A.-C. MA 40.47
 Liu, Jianhong KFM 10.5
 Liu, Jianing •MA 3.2
 Liu, Jie •DY 43.10
 Liu, Jinghui •BP 2.2
 Liu, Jung-Ching •O 38.4, O 45.3,
 O 45.4
 Liu, Junqiu HL 10.9
 Liu, Lina •O 47.9
 Liu, Maowen MM 42.5
 Liu, Ming-Hao TT 16.9, TT 16.10,
 TT 16.11, •TT 53.2, TT 53.7
 Liu, Pin-Chi MA 19.4
 Liu, Qinglong •HL 20.1, •O 35.1
 Liu, Ruizhi MA 10.4, TT 12.4
 Liu, S. O 75.9
 Liu, Shangpu DS 11.3, HL 15.1,
 MA 23.40
 Liu, Shi-Xia O 38.4, O 45.3, O 45.4,
 O 55.3, O 87.3
 Liu, Shuo TUT 2.2, SOE 1.2
 Liu, Shuwei •MM 41.6
 Liu, Tonghua •CPP 35.27
 Liu, Tsai-Jung HL 11.6, TT 15.6
 Liu, W. MA 23.19
 Liu, Wei •MA 42.3, TT 49.2
 Liu, Xiaoyu •HL 8.8
 Liu, Xunshan O 45.3, O 45.4, O 55.3,
 O 87.3
 Liu, Yan MA 32.3
 Liu, Yanan O 66.8
 Liu, Yangbiao O 55.1
 Liu, Yaohua TT 9.8
 Liu, Ying KFM 4.7
 Liu, Yufei DS 14.2
 Liu, Yu-Jie •DY 2.6, •TT 2.6, TT 47.10

Liu, Yuxiang •MM 10.3
 Liu, Zhao O 4.3
 Liu, Zi Hong TT 47.5
 Liu, Zihao •HL 33.5
 Liu, Zihong •TT 65.7
 Liu, Zihui MM 10.4
 Liu, Zitong O 37.13
 Liutkute, Aiste BP 28.33
 Livraghi, Mattia MM 33.6
 Lizee, Mathieu BP 22.3
 Lizzit, Silvano O 14.8, O 56.10
 Lloyd, Lawson •O 34.1
 Lo Conte, Roberto •MA 14.1, O 50.1
 Lo Gerfo M., Giulia HL 2.4
 Lobanova, Evgeniya O 14.11
 Lobko, Yevheniia O 55.2
 Lobo Ploch, N. HL 23.1
 Locatelli, Andrea O 74.1, O 91.6
 Lochbrunner, Stefan DS 12.23,
 DS 12.40
 Lochbrunner, Stephan HL 33.11
 Lochner, P. HL 7.56
 Lochner, Pia SYQD 1.3
 Locmelis, Sonja HL 34.4
 Loeber, Thomas H. O 80.4
 Löffler, Jörg F. MM 25.2, MM 28.3,
 MM 39.1
 Löffler, Tobias •HL 27.7, •O 62.7,
 •TT 40.7
 Löfgren, Joakim O 38.6
 Lofink, Fabian KFM 1.5
 Löfwander, Tomas TT 63.13
 Logsdail, Andrew J. O 29.7
 Logvenov, Gennady TT 3.5, TT 62.3
 Loh, Akong TT 16.14, •TT 18.1
 Loh, Hannah O 56.1
 Lohmann, Svenja •HL 27.4, •MM 40.7,
 •O 62.4, •TT 40.4
 Lohmüller, Theobald BP 5.6, O 91.7
 Lohof, Frederik DY 9.2, HL 8.7,
 •HL 43.1, HL 49.1, HL 50.8
 Löhner, Franziska C. CPP 56.2
 Lohrey, Nicole MM 20.3
 Lohss, Friedemann O 33.8
 Lohstroh, Wiebke CPP 8.3, O 84.5,
 TT 56.5
 Loi, Federico O 29.5
 Loidl, A. MA 33.6
 Loidl, Alois MA 23.13
 Lojewski, Tobias •MA 8.5, MA 8.7,
 O 16.2
 Lokamani, Mani MM 12.11, •MM 31.8
 Lomadze, Nino CPP 8.5
 Lomakin, V. MA 16.6
 Lomakin, Vitaliy MA 23.61
 Lombardi, Gustavo MA 39.2
 Lombez, Laurent O 18.3
 Lömker, Patrick O 11.4, O 29.6
 Londi, Giacomo CPP 11.7
 London, Tyler MM 40.1
 Long, Yuxi BP 4.7
 Longo, Danilo O 36.5, O 56.5
 Lonsky, Martin MA 40.37
 Loos, Sarah •DY 34.6, DY 40.8
 Loos, Sarah A.M. •DY 32.1
 Lopes Dias, Nelson Filipe KFM 6.29
 Lopes, Joao Marcelo J. O 4.3
 Lopes, Marcelo DS 12.22
 Lopes Marques, Miguel Alexandre
 •HL 6.3, •O 9.3
 Lopes Seeger, R. MA 41.2
 Lopes Seeger, Rafael MA 4.12,
 TT 7.12
 Lopez Freixes, Marti MM 15.9
 Lopez Galan, Oscar Alberto •HL 7.7
 Lopez, Hender BP 27.8
 Lopez Mora, Nestor Fabian O 26.7
 Lopez, Sandra P. Gonzalez CPP 17.17
 López-Posadas, Claudia •O 55.7
 Loran, Edwin DY 26.10
 Lörch, Daniel O 60.10
 Lord, Oliver TT 3.6
 Lorente, Nicolas O 3.1, O 7.9, O 15.7,
 O 15.8, O 33.7, O 46.3
 Lorenz, Charlotta •BP 11.5, •BP 23.10
 Lorenz, Erik E. •DS 16.1
 Lorenz, Florian •DY 43.6
 Lorenz, Jan •SYOF 1.2
 Lorenz, Katharina HL 44.2
 Lorenz, Pierre •KFM 7.4
 Lorenz, Sandra O 26.2
 Lorenz, Thomas MA 40.19, MA 44.5,
 TT 10.12, TT 36.4
 Lorenz-Spreen, Philipp •TUT 2.3,
 •SOE 1.3
 Lorke, A. HL 7.56, HL 29.2
 Lorke, Axel SYQD 1.3, DY 9.6, HL 1.10,

HL 7.46, HL 7.51, HL 24.10, HL 24.12,
 O 8.3, O 29.10, TT 60.2
 Lorke, Michael •HL 13.4, •HL 16.6,
 HL 25.8, •O 17.4, •TT 24.6
 Lösche, Matthias •BP 11.36
 Löser, Lucas •CPP 35.42
 Löser, Thomas DY 57.3
 Loss, Daniel MA 16.2, MA 47.10
 Lotfy, Ahmed S. KFM 6.19
 Lotfy, Ahmed Samir •KFM 6.27
 Loth, Sebastian O 12.1, O 15.5,
 O 15.11, O 20.7, O 36.8, O 77.7
 Löther, Mona CPP 18.9, CPP 28.7,
 TT 32.7
 Lotkhov, Sergey TT 20.2
 Lotnyk, Andriy DS 12.44, DS 12.46,
 MA 17.2
 Lotsch, Bettina MA 23.4
 Lott, James HL 43.3
 Lott, Tyler HL 48.3
 Lottemoser, Thomas KFM 1.7,
 MA 48.2, MA 50.7
 Lotze, Charlotte •SOE 11.4
 Lotze, Christian O 21.1, O 22.6,
 •O 33.4, O 33.8
 Lotze, Jan TT 22.9, TT 22.10,
 TT 22.11, TT 38.13
 Lou, Rui TT 57.9, TT 57.11
 Louie, Steven G. •SYHS 1.1
 Lounasvuori, Mailis •DS 5.1
 Lounis, Samir MA 11.5, MA 14.7,
 MA 21.1, MA 35.7, •MA 47.4, O 15.9,
 O 33.5, TT 8.4
 Lourenço-Martins, Hugo HL 10.9,
 O 80.2, O 80.6
 Lourens, Daniel O 39.2
 Lovas, Izabella DY 9.11
 Love, Jaden HL 18.2
 Lovric, Petar •CPP 17.39
 Löw, Christian O 57.5
 Löw, Mario •CPP 29.11, O 60.10,
 O 69.14, O 73.4, O 96.5, O 96.7
 Lowack, Ansgar TT 57.25
 Löwen, Hartmut DY 26.8, DY 27.7,
 DY 32.6, DY 56.1
 Loyola, Yokari Godinez O 2.5
 Lozano, Celia DY 31.7
 Lozano, Pedro TT 62.2
 Lu, Chenfeng TT 25.1
 Lu, Guanyu O 58.6
 Lu, Hao •DS 8.4
 Lu, Jiong MA 19.7
 Lu, Junjie DY 21.4
 Lu, Junqi •CPP 35.66
 Lu, Mo O 70.9
 Lu, Shuaihua •MM 31.2
 Lu, Wei MM 12.3
 Lu, Zhiyi MM 37.2
 Lubeck, Sven HL 13.5, HL 20.2,
 O 17.5, O 35.2
 Lubber, Matthias •BP 11.19
 Lubk, A. KFM 11.9, MA 31.1
 Lubk, Axel MA 12.2, MA 31.7,
 MA 32.2, MA 38.2, O 21.5, O 49.5,
 TT 30.9
 Lucas, Maxime •TT 43.28
 Lucas, S. TT 47.2
 Ludacka, Ursula •KFM 1.8, KFM 4.5
 Lüdemann, Kevin •DY 5.4
 Lüder, Hannes MM 26.7
 Lüders, Anton •BP 7.10, •DY 10.10,
 DY 31.7
 Ludescher, Dominik KFM 7.2, •O 49.1
 Lüdge, Kathy DY 22.1, DY 46.5
 Luding, Stefan •CPP 20.1
 Ludwig, A. HL 7.56, HL 29.2
 Ludwig, Alfred DS 6.4
 Ludwig, Arne SYQD 1.3, HL 7.42,
 HL 7.44, HL 7.46, HL 7.51, HL 7.57,
 HL 24.10, HL 24.12, HL 33.45,
 HL 42.4, HL 42.5
 Ludwig, Karl O 24.3
 Ludwig, Lucas O 76.6
 Ludwig, Philipp DS 15.2
 Ludwig, Tim •MA 20.9
 Ludwigs, Sabine •CPP 8.7, CPP 18.12,
 CPP 35.66
 Lueer, Larry CPP 36.1
 Luehmann, Thomas TT 34.5
 Lüer, Larry CPP 11.5
 Lüer, Nina TT 10.4
 Luetkens, Hubertus MA 44.6
 Luferau, Andrei •HL 17.11
 Lühmann, Thomas TT 28.3
 Lührs, Lukas MM 17.4, MM 23.23,
 MM 23.29, •MM 42.1, MM 42.5
 Lui, Ming Hong •BP 28.21

Luibrand, Theodor DS 12.28
 Lüth, Fernando MA 13.1, TT 19.1
 Lukianov, Daniil MM 16.1
 Lukosius, Mindaugas HL 14.9
 Luksch, Jutta •MM 4.5
 Lukyanchuk, Igor MM 23.20
 Luley, Peter BP 28.2, BP 28.28
 Lunzer, Lukas HL 33.61
 Lundbeck, Theresa TT 4.8
 Lundgren, Edvin •O 71.1
 Lünemann, Daniel C. BP 11.42,
 •CPP 28.9, •TT 32.9
 Lungwitz, Dominique CPP 18.1
 Lunin, Leonid •MA 40.39
 Lunkenhein, Thomas MA 36.1,
 MM 5.10, O 78.5
 Lünser, Klara MM 17.1, •MM 17.2
 Luo, C. O 47.3
 Luo, Chen MA 19.4, MA 19.6, MA 48.4
 Luo, Sijun DS 8.3
 Lüpke, Felix O 18.2, •O 72.2, O 74.3,
 O 74.5, O 82.1
 Luschmann, Thomas MA 34.6,
 TT 18.2, •TT 39.4, TT 39.7, TT 49.5,
 TT 58.6
 Lüßmann, Frederik HL 44.3
 Lütth, Hans HL 30.1, TT 41.1, TT 59.6
 Luther, S. •TT 42.15, TT 46.8
 Luther, Stefan DY 37.4
 Luther, Sven TT 29.2, TT 43.2
 Lüttich, Christopher HL 51.7, HL 51.9
 Lüttig, Julian HL 33.60
 Lutz, Tyler CPP 13.7
 Lützen, Arne CPP 28.9, HL 2.5,
 O 58.2, TT 32.9
 Lützenkirchen-Hecht, Dirk O 26.8
 Lutzi, Matthias •MA 28.1
 Lux, Cassia •CPP 58.4
 Lux, Fabian MA 31.5
 Lux, Fabian R. MA 21.6
 Luy, Jan-Niclas O 10.5
 Luzzietti, Nicholas BP 23.12
 Lv, Hua DS 12.22
 Lyalin, Igor MA 23.52
 Lykhach, Yaroslava •O 29.2
 Lykov, Vladimir •O 11.5
 Lysogorskiy, Yury MM 26.6, MM 29.4,
 MM 36.5
 Lytyvnenko, Y. MM 12.1, MM 26.8
 Lytyvnenko, Yaryna MA 18.1, MA 18.3,
 •O 85.3
 Lyu, Lu •O 14.5, O 38.1
 Lyubomirskiy, Mikhail KFM 6.22
 M. Arevalo-Lopez, Angel TT 46.10
 M. Friedrich, Benjamin BP 2.11
 M. Ghiringhelli, Luca MM 31.2
 M. Kulić, Igor BP 2.6
 M.N.D. Teodoro, Orlando VA 1.4
 M. Oppeneer, Peter MA 4.8, TT 7.8
 M. Papadakis, Christine CPP 35.58,
 CPP 53.4
 M. Piva, Mario •MA 39.3
 M. Pop, Ioan TT 54.1
 M. Schupp, Stefan •MM 23.12
 M. Volkov, Oleksii MA 5.3, •MA 17.1,
 •MA 38.2
 M. Zirdehi, Elias •CPP 12.6
 Ma, Le MM 40.7
 Ma, Liguó TT 35.1
 Ma, Weiliang O 58.8
 Ma, X. X. MA 18.4
 Maas, André MA 19.3, O 5.8, O 13.5,
 •O 24.4
 Maaß, Robert MM 12.36
 Maass, Benjamin HL 24.3
 Maass, Corinna C. •BP 7.7, •DY 10.7
 Maass, Philipp DY 5.5, DY 42.17,
 DY 56.6
 Maatz, Alexander TT 66.3
 Mabrouk, Youssef CPP 2.2
 Maca, Frantisek •O 65.1
 Maccari, Fernando MA 42.9,
 MM 23.33
 MacCarron, Pádraig SOE 8.2
 Mach, Marek KFM 4.10
 Machado Charry, Eduardo CPP 45.4
 Machnikowski, Paweł HL 10.5,
 HL 24.7
 Maciołek, Anna BP 11.63
 Mäck, Martin •TT 16.17
 Mackenzie, A. P. TT 34.3
 Mackenzie, Andrew MA 31.4, MM 6.6,
 MM 6.7, TT 29.1, TT 34.4, TT 37.1,
 TT 37.3, TT 37.5
 Mackenzie, Andrew P. O 59.8, TT 3.9,
 TT 30.5, TT 37.2, TT 37.4, TT 37.13
 MacKintosh, Fred BP 19.6, CPP 41.6

Author Index

- MacQueen, Rowan W. KFM 6.34
Maczewsky, Lukas TT 36.6
Madalaimuthu, Jose Prince
•CPP 17.19, CPP 17.29, CPP 36.7
Madauf, Lukas O 5.6
Madej, Ewa MA 41.7, MA 50.1
Mader, Dorothee •O 39.2
Madhual, Sudeshna •MM 6.4
Madjet, Mohamed HL 48.8
Madjet, Mohamed E. CPP 28.9,
•MM 10.2, TT 32.9
Mädler, Christin •DS 10.3
Madriz Diaz, Yuleika Carolina . . . O 26.2
Madsen, Anders DY 18.7, MM 12.3,
O 83.2
Madsen, Georg K. H. MM 14.10,
O 6.10, O 81.2
Maeder, Xavier MM 4.4
Maehrlein, Sebastian HL 17.7,
HL 33.55, O 39.2
Maehrlein, Sebastian F. HL 17.9,
HL 33.53
Maeno, Yoshiteru MM 6.7, TT 37.3
Maes, Christian DY 27.12
Maes, Michael •TUT 2.2, •SOE 1.2
Maftuhin, Wafa CPP 8.6
Magazzu, Luca •TT 54.6
Magén, C. MA 23.39
Magen, Cesar TT 20.4, TT 57.23
Mager, Heiko •CPP 18.5
Maggs, A. C. DY 6.3
Maghelli, Nicola BP 5.8, CPP 20.2
Magnaterra, Marco TT 10.12
Magnussen, Olaf KFM 9.9, O 39.6,
O 69.10, •O 96.4
Magnussen, Olaf M. BP 1.11
Magrez, Arnaud MA 12.6
Mahatha, Sanjoy HL 36.2
Mahault, Benoit BP 9.2, BP 30.2,
DY 23.3
Mahendru, Bharti •O 20.6
Maheu, Clément HL 7.10
Mahler, David M. HL 11.7, TT 15.7
Mahmoodinezhad, Ali O 40.3
Mahmoud, Mohamed •HL 4.3
Mahro, Anna-Katharina O 80.1
Mai, Han Lin •MM 32.4
Mai, Oliver •DY 37.3
Maia Neto, Paulo A. CPP 57.3
Maib, B. •HL 7.56
Maiberg, Matthias HL 4.6
Maier, Berenike BP 6.1, •BP 6.5
Maier, Christian KFM 6.39
Maier, Florian O 6.2, O 11.2, O 38.2,
O 60.6
Maier, Georg DY 6.8, •DY 55.4,
•TT 67.4
Maier, Hans Jürgen MM 11.4
Maier, Paul BP 28.11
Maier, Rouven •MA 23.43
Maier, Thomas TT 61.1
Maignan, Antoine TT 30.6
Maile, Dominik •DY 9.5, DY 9.8,
DY 9.10, MA 16.7, •TT 20.9
Maillet, Olivier TT 17.3
Mainz, Roland HL 25.4
Mair, Georg •TT 54.8
Maisch, Julian HL 49.3
Maischberger, Anna CPP 19.12
Maiti, Ayanesh •TT 3.9
Maiti, Kalobaran MM 14.7
Maiti, Moumita •CPP 2.2
Maity, Avishek MA 40.38, •TT 51.8
Maiworm, Michael O 45.7
Majchrzak, Paulina O 34.9
Majee, Arghya •BP 11.65
Majee, Mithun Kumar •TT 43.6
Majer, Charles Ludwig •AIW 1.1
Majewska, Marta BP 11.28
Majewski, Martin •CPP 51.5
Majidi, Daniel TT 16.3, TT 20.1
Major, Marton MA 17.5
Majstorovic, Nikola CPP 35.11
Majumdar, Arnab •MM 27.10
Majumdar, Satya •SYFP 1.1
Maķ, Kin Fai TT 35.1
Makarov, Alexander A. BP 11.41
Makarov, Denys BP 11.69, DS 6.1,
MA 5.3, MA 11.4, MA 17.1, MA 18.6,
MA 31.7, MA 38.2, MA 40.47,
MA 43.5, MA 49.2, MA 49.5,
MA 49.6, MA 49.7, MA 49.8,
MA 50.3, MM 11.3
Makarova, Anna A. O 47.4
Makhladi, Saad HL 23.2
Maklar, Julian O 8.9, O 16.5, O 16.7
Makowski, Marcin BP 28.37
Makushko, Pavlo DS 6.1, MA 5.3,
MA 17.1, •MA 31.7, MA 49.8
Malavolti, Luigi BP 21.1
Malchou, Marvin CPP 17.33
Maleki, Farahnaz O 81.10
Maletinsky, Patrick DS 6.1, MA 11.4,
MA 31.7
Malgarretti, Paolo BP 2.9
Malgeretti, Paolo CPP 52.4
Malic, Ermin O 34.2, O 34.4
Malik, Bilal TT 25.1
Malinowski, Gregory MA 40.34,
MM 12.3
Mallada, Benjamin •O 45.6, O 66.11,
O 97.3
Mallada Faes, Benjamin O 66.4
Mallik, Srijani MA 4.11, TT 7.11
Malmström, Eva BP 19.2, CPP 41.2,
CPP 52.5
Maltitz, Jeremy •DS 12.24
Malz, Daniel DY 25.2, TT 33.2
Mameka, Nadiia MM 42.2
Mamiyev, Zamin •O 82.2, O 82.8
Mampe, Tim •HL 44.5
Man, Huiyuan TT 46.1
Manacorda, Alessandro •BP 2.12,
BP 24.10, DY 38.10
Manapany, Andy •BP 29.9
Manca, Nicola MA 11.2
Mancini, Leonardo BP 16.1
Mancini, Marilena KFM 10.3
Mandal, Sagarmoy DY 46.8, O 67.6
Mandal, Souraj •CPP 35.5, CPP 35.44
Mandal, Suman O 92.4
Mandloi, S. TT 34.3
Mandziak, Anna MA 50.1
Manesco, Antonio TT 8.8
Manfra, Michael J. TT 20.8, TT 27.5
Mang, Christian MA 23.80
Manganelli, Costanza L. HL 5.2,
HL 18.9, HL 37.6
Mangeat, Matthieu •BP 7.2, BP 9.10,
•DY 10.2, DY 32.4, •DY 42.10
Mangold, Florian •O 43.4, O 91.4
Mangold, Markus DS 13.4
Mangold, Simon KFM 7.3, O 80.5
Manik, Debsankha SOE 11.2, SOE 15.1
Manish Wani, Yashraj CPP 35.9
Manke, Ingo CPP 45.9
Mankovsky, S. MA 8.3, •MA 34.8
Mankovsky, Sergiy MA 16.8, MA 46.12
Mankowsky, Roman TT 62.7
Manmana, Salvatore TT 22.2, TT 38.3
Manmana, Salvatore R. •TT 22.4
Mann, Gerrit Johannes •HL 31.8,
•O 61.8
Mann, Julian Georg •HL 25.7
Manna, Rudra Sekhar TT 21.2
Manna, Santanu HL 7.65, HL 7.66
Mannathanath Chakkingal, A.
MA 44.3
Mannathanath Chakkingal, Aswathi
•MA 40.25
Mannel, H. HL 7.56
Mannel, Hendrik SYQD 1.3, HL 7.46,
•HL 24.10, HL 24.12, TT 60.2
Mannhart, Jochen DS 14.4
Mannix, Dan MA 23.77
Mannsfeld, Stefan C.B. CPP 43.6
Mannstadt, Wolfgang MM 28.8
Manolescu, Andrei HL 16.2, TT 24.2
Manschwetius, Bastian •HL 48.2
Manske, Dirk •TT 22.6, TT 62.3,
TT 62.4
Mansour, Ahmed E. CPP 18.1
Mansouri, Masoud O 7.8
Mansson, Martin BP 19.2, CPP 41.2
Manuel, Luis O. O 33.1
Manuel, P. TT 46.8
Manuel, Pascal TT 23.8
Manzoni, Anna Maria CPP 17.1
Manzorro, Ramón TT 20.4, TT 57.23
Maple, M. Brian TT 9.3
Marchetti, M Cristina •PLV VI
Marcial Hernandez, Raymundo
O 93.8
Marder, Seth R. CPP 17.24, CPP 18.1
Marder, Todd B. O 55.10
Mardyukov, Artur O 72.5
Marehalli Srinivas, Shesha Gopal
•DY 40.7
Marek, Andreas HL 13.3, O 17.3
Marek, Štěpán •O 2.3
Maresca, Francesco •MM 15.3
Marrgraf, Marcella Naomi HL 41.3
Marrgraf, Johannes CPP 35.38
Marrgraf, Johannes T. •HL 6.6,
MM 3.7, MM 8.4, MM 8.6, MM 8.7,
MM 19.2, MM 19.3, MM 31.3, •O 9.6,
O 11.1, O 52.8
Marrgraf, Johannes Theo MM 31.10
Marie, X. O 47.7
Marie, Xavier MA 32.6
Marinero, Mario MM 16.4
Marini, Andrea O 16.5
Marini Bettolo Marconi, Umberto
DY 32.6
Marino, Andrea TT 4.10, •TT 9.3,
TT 9.4, TT 9.5
Mark, Christoph DY 26.5
Markert, S. BP 11.7
Markmann, Jürgen MM 22.2,
MM 22.3, MM 42.4, MM 42.7
Markou, Anastasios MA 37.4
Markov, Anton TT 17.2
Markovic, Igor MM 6.6
Markus, Paul O 76.9
Markus, Philipp MA 2.5
Markussen, Troels O 42.6, TT 8.1
Marmodoro, Alberto •MA 16.8,
•MA 20.1
Marotzke, S. MM 26.8
Marotzke, Simon •TT 3.7, •TT 57.3
Marquardt, Florian •TUT 1.1, •DY 1.1,
•DY 2.3, •TT 1.1, •TT 2.3
Marque, Clément •BP 11.32
Marques, Carlos CPP 57.2
Marques, Carolina TT 37.12
Marques, Carolina A. O 28.7, O 55.4,
•TT 57.4
Marques, Miguel MM 31.7
Marques, Miguel A. L. O 95.10,
TT 68.10
Marquez, Jose •HL 25.3, O 95.4,
TT 68.4
Marquez, Jose A. •HL 25.11
Marquez Prieto, Jose O 95.5, TT 68.5
Marra, Pasquale •TT 31.4, •TT 31.11
Marsalek, Ondrej O 55.9
Marschner, Felix O 2.10
Marshall, Holger CPP 44.2
Marsili, Margherita MM 3.8, •O 4.1
Marston, Brad SYQC 1.2
Marszal, Philip SOE 10.1, SOE 10.2,
•SOE 11.3, SOE 11.4
Marszalek, Tomasz MA 23.22,
MA 23.23, MA 23.53
Mårtensson, Nils O 85.1
Marth, Ludwig HL 4.2
Marti, Othmar BP 28.58, CPP 13.2,
MM 12.6
Martin Axt, Vollrath HL 24.2
Martin, Carolina MA 38.1
Martin, J.I. MA 23.39
Martin, Jens DS 12.24
Martin, Kevin O 73.6
Martin, Lane KFM 4.9
Martin, Phillip HL 3.1
Martin, Pierre •BP 11.2
Martín Sabanés, Natalia O 75.6
Martinez Castro, Jose O 74.3
Martinez Strasser, Carolina •TT 64.6
Martínez-Carracedo, Gabriel MA 24.2
Martínez-Castro, Jose •O 18.2,
•O 74.5, O 82.1
Martínez-Galera, Antonio J. •O 29.1,
O 74.7
Martini, Mickey DS 5.2, DS 12.18,
DS 12.20
Martiniani, Stefano DY 16.2
Martins, Cyril TT 43.15
Martin-Vega, F. TT 6.4
Martius, Georg TT 43.33
Marton, Pavel HL 5.4
Martuza, Muhammad Ali O 56.3
Marx, Achim TT 39.7, TT 49.1,
TT 58.6, TT 58.7, TT 58.8, TT 58.10,
TT 58.20, TT 66.6
Marx, Dorian •BP 28.51
Marx, Konrad BP 6.3
Marxer, Fabian TT 54.7
Maryshev, Ivan BP 7.6, DY 10.6
Marzari, Nicola HL 21.1, •KFM 10.7,
MM 16.10, MM 19.4, MM 21.4
Masalehdan, Hossein •VA 1.1
Mascaraque, Arantzazu MA 38.1
Masciocchi, Giovanni •MA 17.2
Mascot, Eric MA 14.1
Maseim Bassis, Kenmoe •DY 43.4
Masell, Jan MA 26.3, MA 26.6,
MA 40.21
Masilamani, Muthu O 59.3
Maskill, Jan MA 16.5, •MA 23.44
Masliuk, Liudmyla O 78.5
Masničák, Nikolas MM 19.1
Maspero, Federico MA 11.2
Massicot, Stephen O 11.2, O 38.2,
O 60.6
Mast, Christof •BP 10.2, BP 11.29
Mast, Christof B. BP 10.6
Mastalerz, Michael CPP 35.14
Matala, Mathias HL 23.2
Matczak, Michał MA 38.4
Matej, Adam O 45.6, O 55.3
Matejdes, Marian O 76.9
Matera, Sebastian DY 17.1, MM 14.5,
MM 16.2, MM 36.3, O 69.2, O 78.6,
O 83.2, O 96.2
Materne, Anne •BP 28.22
Materzanini, Giuliana KFM 10.7
Mathes, Lucian CPP 35.4, DS 14.5,
•KFM 9.10
Mathew, Anagha •MA 23.64
Mathew Roy, Renjith •MA 9.9
Mathews, Prince MM 32.1, •MM 41.7
Mathias, Stefan MA 46.8, O 34.4,
O 39.5
Mathisen, Anders KFM 4.3
Matic, Stipo DS 11.4
Matković, Aleksandar DS 5.3, O 31.3
Matolin, Vladimír O 28.5, O 55.2,
O 81.11
Matolinová, Iva O 28.5, O 55.2, O 78.8,
O 81.11
Matousek, Mikulas O 45.6
Matreux, Thomas BP 10.2, •BP 10.6,
BP 11.29
Matsuda, Yasuhiro H. TT 46.1
Matsuhira, Kazuyuki TT 46.1
Matsumoto, Yosuke TT 3.3, TT 42.14
Matsuo, Akira TT 46.1
Matsuzaki, Korenobi HL 50.6
Matta, Bharti O 37.12, •O 64.6
Mattausch, Yannick •O 73.5
Mattern, Max MM 12.3
Mattern, Maximilian HL 33.61,
MA 23.70, •MA 40.10, MA 40.66,
O 37.7
Matthes, F. O 2.8
Matthes, Tjorben •DS 2.5
Matthieu, Le Tacon TT 10.8
Matts, Olga •MM 42.2
Matveyev, Yury DS 12.5
Matvija, Peter O 78.8, O 92.10
Maultzsch, Janina HL 24.1
Maurer, Felix •DY 4.2
Maurer, Felix Milan BP 11.54
Maurer, Florian O 81.5
Maurer, Reinhard HL 26.5, O 53.5,
O 73.1
Maurer, Reinhard J. CPP 28.11,
DY 57.4, O 29.7, O 46.1, O 46.2,
O 93.5, O 93.8, TT 32.11
Maurya, Manoj Kumar •CPP 58.7
Maus-Friedrichs, Wolfgang DS 3.5,
DS 12.29, DS 12.39, MM 11.4, O 11.7
Mavropoulos, Phivos MA 2.4,
MA 23.4
Mawass, M A MA 31.1
Mawass, Mohamad-Assaad MA 17.1,
MA 50.3
Maximov, Ivan CPP 35.25
Maximov, Leo •TT 58.23
May, Andrew F. TT 9.8
May, Matthias HL 38.7
May, Matthias M. CPP 29.11, O 60.10,
O 69.14, O 73.4, •O 96.7
May, Sandra DY 5.3
Mayer, Benjamin HL 10.7
Mayer, Christian G. •HL 5.1
Mayer Martins, Jonas •DY 4.8
Mayer, Thomas •BP 27.3, HL 7.10
Mayerhöfer, Thomas O 68.5
Mayerhofer, Katja O 58.5
Mayoh, Daniel MA 9.8
Mayr, F. MA 40.14
Mayr, Stefan BP 12.1
Mayrhofer, Leonhard MM 5.1
Mayrhofer, Paul H. DS 4.5
Mayr-Schmölzer, Wernfried O 81.1
Mazhjuo, Donya •MA 21.3
Mazibrada, D. TT 57.21, TT 58.2,
TT 58.4
Mazibrada, David •TT 58.3, TT 58.5
Mazin, Igor I. TT 37.4
Maznichenko, Igor •DS 12.26,
MA 40.62
Mazza, Federico •MA 9.7, TT 42.5
Mazzocchi, Francesco •KFM 8.7
Mazzocchi, Tommaso TT 22.11
Mazzocchi, Tommaso Maria TT 22.9,

Author Index

- TT 22.10
Mazzoli, Claudio MA 43.6
Mazzone, D. G. TT 42.13
Mazzone, Daniel MA 9.7
Mc Mullin, Kaitlyn HL 4.7
McCann, Edward •KFM 11.10
McClarty, Paul •DY 55.7, •TT 67.7
McCord, Jeffrey MA 23.7
McCord, Jeffrey MA 40.46, MA 40.48,
MA 49.4
McCulloch, Iain CPP 11.4
McEniry, Eunan MM 15.9
McFarlane, Emily C. DS 12.15, O 59.7,
•TT 27.4
McGhee, K.E. •HL 48.4
McGlinchey, Amy •DS 12.49
McGuinness, Philippa MM 6.6,
MM 6.7
McGuinness, Philippa H. TT 30.5
McHugh, Jeffrey BP 25.4
McIver, James TT 64.7
McMurtrie, Gregory O 77.7
McNally, Graham TT 50.6
McQuaid, Raymond •KFM 4.1
McReynolds, Dylan O 63.1
Medghalchi, Setareh MM 20.3,
•MM 20.4
Medina, Ernesto TT 11.4, TT 11.5
Medjanik, K. MM 26.8, O 30.4
Medjanik, Katerina O 85.3, O 85.7
Medjanik, Katya HL 36.2
Medlin, Rostislav O 18.7
Meer, Hendrik MA 31.2, •MA 31.3
Meerholz, Klaus CPP 18.8, •CPP 28.6,
CPP 35.30, O 58.1, O 70.9, •TT 32.6
Mehl, Michael J. MM 36.9
Mehl, Sascha O 29.2, •O 81.11
Mehl, Sascha L. O 28.5, O 55.2
Mehlich, Kai O 36.11, O 56.9, •O 74.8
Mehta, Bijal •MM 23.1
Mei, Bastian O 60.4
Mei, Yunhao •BP 28.6
Meichsner, Florian CPP 17.18
Meichsner, Moritz TT 57.23
Meier, Andreas •KFM 6.23, KFM 8.6,
KFM 8.8, KFM 8.9
Meier, Dennis •PLV VII, KFM 1.2,
KFM 1.8, KFM 4.3, KFM 4.5, MA 18.8,
MA 48.7, •O 14.4, O 14.8
Meier, Felix •DY 48.3, TT 55.3
Meier, Jessica O 43.6, O 43.7, O 70.6,
•O 91.6
Meier, Matthias O 81.4
Meier, Michael A. R. CPP 58.2
Meier, Quintin •MM 39.4
Meier, Stefan O 37.5
Meier, Torsten HL 17.1, HL 35.4,
HL 48.1
Meierhofer, Florian HL 44.3
Meierhofer, Manuel O 8.7
Meigel, Felix J. •BP 11.57
Meinecke, Jannick O 48.4
Meinecke, Moritz •HL 24.13
Meinel, Jonas MA 23.43
Meingast, Christoph TT 34.1
Meinhardt, Alexander •CPP 35.25
Meißner, Laura •BP 12.6
Meißner, Moritz HL 41.3, •HL 41.7
Meißner, Robert MM 21.2
meißner, robert h. MM 3.5, O 86.7
Meißner, Robert Horst MM 23.28
Meissner, Robert BP 3.11
Meltzner, Rico CPP 36.7, CPP 43.2
Mejia-Monasterio, Carlos DY 56.10
Mejuto-Zaera, Carlos •MM 14.9
Melampianaki, Eirini CPP 8.2,
CPP 35.58
Melčák, Martin •CPP 35.50
Meledam, Geethu P. CPP 35.61
Melendez-Sans, Anna •HL 51.3,
HL 51.6, TT 30.3, TT 30.6
Melin, Solveig MM 9.2
Melinte, Georgian MM 23.13
Melischek, Larissa O 20.6
Melkov, G. MA 16.6
Memmesheimer, Raoul-Martin
BP 22.1
Menahem, Matan DS 1.6
Mena-Osteritz, Elena HL 48.8
Mendes Santos, Tiago •DY 2.7,
•TT 2.7
Méndez-Córdoba, Fabio Pablo Miguel
•MA 9.2
Mendieta-Moreno, Jesus I. ... O 45.6,
O 55.3
Mendoza Delgado, Miriam •KFM 6.12
Meneghini, Giuseppe O 34.4
Meng, Lingyu HL 41.4
Meng, Tobias HL 11.1, TT 6.12, TT 15.1
Meng, Xiangzhi •O 7.8
Meng, Zi Yang MA 10.4, TT 12.4
Mengel, Lucia •O 41.4
Menger, Michael d. BP 8.3
Menges, Fabian TT 59.10
Menniti, Matteo MA 29.4
Menon, Krishnakumar S. R. ... O 92.4
Mensing, Jonas •DY 45.10
Menten, Julia KFM 3.3, •MM 10.1
Mentes, Tevfik Onur O 74.1
Mentik, Johan H. MA 29.1
Mentink, Johan H. MA 23.3
Mentzer, Steven J. BP 12.7
Menz, E. B. TT 57.28
Menzel, Andreas M. •BP 7.1,
CPP 13.7, •DY 10.1, DY 31.6
Menzel, Dirk MA 38.5, TT 10.4
Menzel, Ferdinand MA 32.5
Menzler, Norbert CPP 35.36
Meola, Annalisa BP 23.1
Mercebach, Phillip •TT 36.10
Mercurio, Giuseppe DS 6.3
Merdon, Christian HL 5.2
Meredith, Paul CPP 1.10
Merkel, Konrad CPP 17.58, CPP 54.1,
•CPP 54.2
Merkel, Maximilian •MA 5.4, MA 36.4,
•MA 40.31
Merker, Daniel •KFM 8.5
Merker, S. DS 12.48, HL 7.16
Merkert née Gunkelmann, Nina
DY 29.4
Merkert, Nina •MM 7.1
Merkwitz, Luise •TT 57.11
Merle, Benoit MM 4.3
Merlitz, Holger CPP 56.3
Merrin, Jack DY 29.1
Merritt, Adrian TT 23.5
Merritt, Adrian TT 23.8
Merschroth, Holger MA 3.2
Mertelj, Alenka MA 36.2
Merten, Lena DS 10.2
Mertens, Julian DS 15.4, KFM 6.14
Mertens, Lotte TT 6.11
Mertig, Ingrid DS 12.26, HL 34.1,
MA 4.9, MA 4.11, MA 8.6, MA 8.8,
MA 10.7, MA 12.1, MA 35.1, TT 7.9,
TT 7.11, TT 12.7
Mertig, M. CPP 17.2
Mertin, Paul CPP 35.52
Merz, Florian HL 13.3, O 17.3
Merz, Michael TT 34.1
Merz, Rolf KFM 8.5
Merz, Steffen MM 16.2
Meschede, Marcus •O 65.2
Meßner, Christoph HL 4.7
Meßner, Leon DY 46.7
Mespel, Florie TT 61.5
Messer, Tobias BP 11.37
Metlitski, Max A. DY 49.9
Mette, Gerson O 19.9, O 57.2
Mettin, Robert DY 18.7
Mettus, Denis •MA 48.1
Metz, Niklas O 91.4
Metzger, Christian O 22.7
Metzler, Ralf DY 17.4, DY 44.6,
DY 44.10, DY 44.13, DY 56.1, DY 56.4,
SOE 19.2
Metzner, Claus •DY 26.5
Metzner, Walter TT 47.7, TT 51.1
Meusel, Manuel O 60.6
Mewes, Claudia MA 20.10
Mewes, Mathis DS 12.7
Mewes, Tim MA 20.10, MA 23.36
Meyer, Andreas CPP 51.4, MM 40.5
Meyer, Bernd DY 46.8, •O 60.3,
O 67.6, O 81.8
Meyer, Constantin TT 22.2, TT 22.4
Meyer, Ernst O 4.5, O 12.6, O 32.8,
O 38.3, O 38.4, O 45.3, O 45.4, O 51.3,
O 87.3, O 93.1
Meyer, Hendrik •CPP 19.3
Meyer, Jörg O 36.2
Meyer, Julia •BP 11.58
Meyer, Manuel •HL 30.3, •TT 41.3
Meyer, Michael O 21.4
Meyer, Philipp G. •SOE 19.2
Meyer, Ruth •BP 28.28
Meyer, Sebastian •MA 18.7, MA 35.9,
O 91.8
Meyer, Tobias HL 33.57
Meyer zu Heringdorf, Frank .. O 80.3,
O 80.5
Meyer zu Heringdorf, Frank-J. O 75.4
Meyerbröcker, Nikolaus O 36.3
Meyerheim, Holger L. MA 31.6
Meyers, Marc DY 29.4
Meyners, Dirk MA 40.48
Mezard, Marc •DY 11.1, •TT 13.1
Mezger, Markus BP 11.14
Mezouer, Mohamed TT 51.6
Michael, Stephan HL 16.6, TT 24.6
Michaelis de Vasconcellos, Steffen
HL 18.10
Michaelis, Dennis BP 11.74
Michaels, Thomas C.T. BP 22.9
Michalčová, Alena MM 19.1
Michalíček, Gregor HL 31.7,
MA 23.32, O 61.7
Michalik, Stefan MM 28.3
Michalsky, Ina O 10.6
Michel, Simon MA 23.30
Michelitsch, Georg S. O 3.7
Michely, Thomas O 29.9, O 36.11,
O 41.2, O 51.1, O 56.8
Michez, L. MA 41.2
Michez, Lisa MA 4.12, MA 40.63,
TT 7.12
Michiardi, Matteo O 6.3
Michielsen, Kristel TT 43.20
Michl, Johannes •HL 49.7
Michler, Johann MM 4.4
Michler, Peter HL 3.6, HL 7.43,
HL 7.48, HL 7.62, HL 12.1, HL 12.4,
HL 12.5, HL 12.6, HL 43.2, HL 43.4,
HL 49.2, HL 49.3
Mickeloff, F. BP 11.7
Midtvedt, Daniel •BP 21.5
Mietke, Alexander BP 30.3
Miguez-Lago, Sandra O 60.2
Mihatsch, Jakob •BP 24.6, •DY 38.6
Mihov, K. TT 3.4
Mikhail, David •TT 36.8
Mikheev, Aleksandr N. DY 27.9
Mikkelsen, Anders O 75.3
Mikolajick, Thomas DS 12.5, HL 16.5,
TT 24.5
Milchakov, Vladimir TT 49.2
Milde, Peter MA 32.1, MA 44.1
Miles, Sebastian •HL 49.4
Milesi-Brault, Cosme MM 23.34
Miliaieva, Daria CPP 36.9
Milkin, Pavel CPP 8.8, DY 29.3,
MA 49.8
Mill, Agnes DS 12.46
Miller, Fabian •MM 23.31
Miller, Nina •HL 7.3
Miller, R. J. Dwayne MM 10.4
Millis, Andrew TT 27.7, TT 61.1
Milosavljevic, Dijana TT 30.12,
•TT 30.13
Miloudi, Mohammed El Amine
•HL 7.5
Milovanovic, Dragomir BP 29.3
Mimkes, Juergen •SOE 9.5
Mimoso, Tiago •BP 28.25
Min, Byoung-Chul MA 4.10, TT 7.10
Min, Chul Hee •TT 9.7
Min, Chul-Hee O 94.9
Minar, J. MM 26.8
Minár, Jan MA 47.5, O 8.9, O 18.7,
O 30.5, O 85.7, TT 21.1, TT 30.3
Mingo, Natalio MM 39.4
Minichová, Maria O 73.2
Minko, Sergiy DS 13.4
Minnert, Christian KFM 2.3
Minopoli, Antonio BP 5.8, CPP 20.2,
•DY 29.6
Minotti, Carlo O 63.1
Mir, Showkat H. O 3.2
Mirau, Luca CPP 3.4, CPP 29.3,
CPP 35.44
Mirolo, Marta O 69.10
Miroshkina, Olga N. •MA 3.8
Mirzapour, Fatemeh BP 28.20
Mirzapour-Shafiyi, Fatemeh DY 42.7
Míšek, Martin MA 37.6
Mishra, Aritra DY 43.18
Mishra, Sanu TT 10.1
Mishra, Simli MM 6.6, •TT 37.13
Mishra, Vibhu •TT 38.3
Mishra, Vipin O 60.12
Misof, Philipp MM 25.4
Missaoui, Ahmed TT 61.5
Misselwitz, Adrian •DY 45.6
Misselwitz, Erik CPP 35.14
Mitchell, Matthew HL 49.5
Mittand, Rüdiger HL 36.4, HL 41.6
Mitra, Mithun K. BP 18.2, BP 29.8,
DY 33.2
Mitra, Souvik •CPP 53.8
Mitrano, Matteo •SYUE 1.5
Mitric, Roland DS 3.2
Mityrakhin, Victor •HL 1.2
Mitscherling, Johannes •TT 61.4
Mitsioannou, Vasilios MA 33.2
Mittal, Kush Mohan •SOE 10.5
Mittendorf, Martin MM 23.5
Mittendorfer, Florian O 47.6, O 54.6,
O 54.8, O 68.2
Mittendorff, Martin TT 59.1
Mittenzwey, Henry •HL 34.8
Miwa, Jill O 34.9
miwake, hideki CPP 2.5
Miyake, Hideto HL 28.1
Miyamoto, Koji O 59.4, O 85.6
Miyata, Atsuhiko MA 44.2
Miyazaki, Ray •O 78.7
Mizaikoff, Boris BP 17.8
Mizushima, Takeshi TT 31.11
Mocanu, Alex TT 66.4
Möckel, Conrad •BP 11.67
Mockute, Aurelija •DS 6.4
Modes, Carl D. BP 4.1, BP 18.6,
DY 33.6
Modes, Johanna •HL 4.7
Modregger, Peter O 56.6
Moeckel, Michael •DY 22.3
Moeller, Johannes O 83.2
Moerman, Evgeny MM 21.3
Moessner, Roderich DY 9.1, DY 43.3,
DY 55.2, DY 55.5, MA 23.10, MM 6.7,
TT 36.7, TT 46.9, TT 67.2, TT 67.5
Moghadas, Emin •TT 65.8
Moghaddam, Ali G. TT 6.11
Mogilatenko, A. TT 3.4
Mogilatenko, Anna HL 23.2
Mohamed, Mohamed Abdullah
Abdullah CPP 35.37
Mohammadi, Mahdad •DS 12.36
Mohammadi, Mahdieh •DY 7.6
Mohammadinejad, Sarah BP 13.2
Mohammadzadeh, Hossein MA 16.7
Mohammed Idris Bakhit, Alaa O 47.4
Mohanad, Alkaales HL 49.6
Mohandas, Krishnadas •SOE 4.5
Mohanraj, John •HL 25.5
Mohanty, Gaurav MM 4.5
Mohanty, Pradeep SOE 9.1
Mohapatra, Subhadra •O 34.3
Moharana, Ashish •MA 23.22,
•MA 23.23, MA 23.53
Mohd, Ibrahim •BP 23.2, BP 23.2,
BP 26.8, •BP 27.4
Mohd Yusoff, Abd. Rashid bin
CPP 43.7
Mohelsky, I. TT 6.10
Möhl, Gilles •CPP 45.3
Mohseni, M. MA 16.6
Mohseni, Morteza MA 34.7
Möhwald, Kai MM 11.4
Moir, Camilla TT 9.3
Mokbel, Marcel •CPP 52.3
Mokhtari, Parisa •TT 52.6
Mokhtari, Zahra BP 24.9, DY 38.9
Mokrousov, Yuriy MA 4.2, MA 4.7,
MA 10.3, MA 16.9, MA 21.6, MA 23.4,
MA 31.5, O 30.3, TT 7.2, TT 7.7,
TT 12.3
Mokry, Pavel •KFM 4.8, •KFM 4.10
Molatta, S. TT 28.6, TT 57.19
Molenkamp, Laurens W. •HL 5.3,
HL 11.4, HL 11.7, HL 30.4, TT 15.4,
TT 15.7, TT 17.1, TT 41.4, TT 64.5
Molenkamp, Laurenz HL 33.61
Molina Luna, Leopoldo MA 3.4
Molina-Ferández, Rafael A. ... HL 11.2,
TT 15.2
Molina-Luna, Leopoldo DS 9.2, DS 9.3
Molinari, Alan MA 3.1
Molinari, Elisa HL 20.3, O 35.3
Mölleken, Andre •O 26.3
Möller, Angela TT 64.8
Möller, Jenny O 7.8
Möller, Marcel •MA 15.5, O 8.1, O 8.5,
O 83.6
Möller, Marius TT 36.2, •TT 52.4
Möller, Robert •TT 4.9
Möller, Rolf O 26.3
Möller, S. HL 33.17
Möller, Samuel HL 9.5, TT 14.5
Möller, Thomas TT 16.3
Möllerherm, Lars BP 3.7
Möllers, Paul Valerian •O 51.4
Molnar, Gergely •MM 28.9
Molter, Daniel HL 17.4
Momeni, Davood O 82.7
Monaco, Eduard HL 7.30
Monasson, Rémi BP 18.5, DY 33.5

Mönch, Ingolf MA 49.6
 Mondal, Badal HL 18.7
 Mondal, Chandana DY 26.4
 Mondal, Debabrata TT 38.4
 Mondal, Debashish DY 44.16
 Mondal, Debasmita BP 28.56
 Mondal, Ritwik MA 46.3
 Mondal, Sayan HL 11.5, TT 15.5
 Mondal, Suman TT 36.3
 Mönig, Harry O 66.7, O 97.7
 Monnet, Isabelle HL 44.2
 Monney, Claude O 8.9, TT 21.1
 Monsel, Juliette TT 38.7
 Monserrat, Bartomeu DY 44.2, O 94.1
 Montag, Anton TT 59.4
 Montag, Verena HL 28.5
 Montalvo, Galia BP 25.3
 Montanaro, Angela TT 62.8
 Monteiro Cônsoli, Pedro TT 4.4, TT 42.16
 Montemurro, Domenico DS 5.2, DS 12.20
 Montero, Ana M. O 33.5
 Montiel, Xavier TT 20.7
 Monzel, Cornelia BP 5.5, BP 5.7, BP 21.8
 Monzon, Gina A. Monzon BP 11.48
 Moody, Galan HL 10.1
 Mook, Alexander MA 10.7, MA 10.8, MA 16.2, MA 47.10, TT 12.7, TT 12.8
 Moon, Hongjae HL 36.4
 Moors, Kristof TT 36.1, TT 59.5
 Moos, Ralf HL 7.33
 Moradi, Amin O 26.7
 Moraga, N. BP 11.10, BP 11.11, BP 11.12
 Morais Smith, Cristiane MA 20.9
 Morales, Carlos O 40.3, O 42.4, O 78.9, O 92.6
 Morales Fernandez, Imelda Pamela MA 40.3
 Morales, Pamela MA 50.1
 Morales Sánchez, Carlos DS 12.50
 Morari, Vadim DS 12.53
 Morassi, Martina HL 10.10
 Moravec, Michal TT 30.5
 Morawetz, Klaus DY 25.5, TT 5.14, TT 16.12, TT 16.13, TT 33.5
 Morelhão, Sergio L. O 74.4, O 94.6
 Moreno, Juan DY 18.8
 Moreno-Ramírez, Luis M. SYGM 1.5
 Moresco, Francesca O 3.1, O 3.3
 Morgan, Dylan HL 26.5, O 53.5
 Morgenstern, Karina O 11.5, O 16.9, O 81.7
 Morgenstern, M. DS 7.2, MA 40.53
 Morgenstern, Markus O 77.2
 Morice, Corentin TT 6.11
 Morigi, Giovanna TT 29.8
 Moritz, Dominik C. HL 7.10
 Moritz, Philipp DS 3.5, DS 12.39
 Mörk, Paul O 43.7, O 49.3
 Morozov, Igor TT 57.11
 Morr, Dirk K. MA 14.1
 Morral, Raúl DY 9.11
 Morris, Andrew J. DY 44.2
 Mortazavi, Armina BP 28.45, BP 28.50
 Moruzzi, Floriana CPP 11.4
 Mosch, Sindy MA 49.5, MA 49.7
 Moser, David Jonas TT 47.11
 Moser, Simon DS 1.3, MA 40.64, O 18.9, O 94.7
 Moser, Simon K. O 94.9
 Moser, Tobias BP 21.12
 Moser, Toni O 60.5
 Moshantaf, Abdulrhman O 63.2
 Moshnyaga, Vasily DS 14.3, MA 46.8, O 39.5
 Mößle, Michael PSV V
 Mostarac, Deniz CPP 45.2
 Motte, Jean-François MA 43.1
 Motz, Christian MM 4.5
 Motzoi, Felix HL 37.7, HL 50.7
 Moueddenne, Leila DY 49.8
 Moueddenne, Leila BP 29.9
 Moukhader, R. MA 16.6
 Moulding, Owen TT 3.6, TT 9.1, TT 51.7
 Mouritsen, Henrik BP 11.42
 Mourkh, Lev HL 3.3
 Moussa, Amgad DY 16.2
 Moya, Jaime MA 2.7
 Mozara, Roberto O 33.5
 Mozumder, Rubel MA 10.1, TT 12.1
 Mrovec, Matous MM 26.6, MM 29.4, MM 36.5

Msallamová, Šárka MM 19.1
 Msiska, Robin MA 40.4
 Much, Alexander CPP 17.18
 Mücke, David DS 3.1
 Muckenhuber, Helmut O 5.3
 Muehle, Steffen SOE 4.2
 Mueller, Kai HL 42.5
 Mueller, Niclas S. O 16.7
 Muenker, Till BP 4.4, BP 11.55
 Muenker, Till M. BP 8.4, DY 32.2
 Mugele, Frider CPP 8.1
 Mugele, Frieder CPP 29.4, CPP 50.2, O 60.4, O 69.13
 Muhammad, M DY 29.11
 Muhammad, Qaisar KFM 2.6
 Muhiin, Anton HL 28.4
 Mühl, Thomas MA 23.35, MA 32.2, MA 48.6, TT 18.3
 Mühle, Steffen SOE 10.3
 Mühlhauer, Matthias TT 5.6, TT 42.10, TT 46.12, TT 65.10
 Mühlnickel, Lukas DY 46.5
 Muigg, Luca CPP 17.55
 Mujica, Vladimiro TT 11.4, TT 11.5
 Mujid, Fauzia O 34.1
 Mukhamadiarov, Ruslan BP 29.7
 Mukharamova, Nastasia O 83.2
 Mukharjee, Prashanta K. TT 52.7
 Mukherjee, Tania MA 21.8
 Mukherji, Debashish CPP 58.7
 Mukhopadhyay, Archan SOE 15.2
 Mukhopadhyay, Aritra K. BP 7.9, DY 10.9
 Mukhopadhyay, Soham BP 11.20
 Mul, Guido O 60.4
 Mulholland, Leo Patrick SOE 6.2
 Müllen, Klaus O 32.8
 Müller, Aaron Merlin KFM 1.7
 Müller, Alexandru MA 34.7
 Müller, Andreas HL 7.22
 Müller, Christian CPP 18.13
 Müller, Cinja S. O 70.3
 Müller, Diana BP 11.21, BP 26.4
 Müller, Elisabeth MA 43.3
 Müller, Jan-Hendrik BP 21.9
 Müller, Jens MA 9.5, MA 9.6, MA 39.4, MA 40.37, TT 43.9, TT 51.9
 Müller, Judith BP 26.5
 Müller, Judith A. BP 11.23
 Müller, Kai HL 7.44, HL 7.65, HL 10.3, MA 19.6
 Müller, Klaus-Robert O 45.7
 Müller, M. O 75.9
 Müller, Mahni HL 36.4
 Müller, Manuel MA 23.76, MA 23.80, MA 34.6, MA 40.15, MA 40.65, TT 54.9
 Müller, Marcus BP 1.9, CPP 12.3, CPP 12.4
 Müller, Maren O 12.2
 Müller, Marius DS 13.3
 Müller, Martin DS 13.5, MM 27.10, MM 36.6
 Müller, Martina DS 12.5, MA 17.6, MA 50.5, O 32.5
 Müller, Matthias KFM 8.1
 Müller, Maximilian KFM 6.21, KFM 11.2
 Müller, Maximilian J. DS 16.5
 Müller, Melanie O 12.7, O 75.6, O 76.1
 Müller, Michael TT 66.4
 Muller, Pierre BP 1.12
 Müller, Ralf MM 12.36
 Müller, Robin HL 7.1
 Müller, Robin Lars Benedikt HL 7.2
 Müller, Sarah MM 8.3
 Müller, Simon O 74.4, TT 9.7
 Müller, Tobias MA 33.1, TT 29.12, TT 29.13, TT 64.5
 Müller, Ulrich CPP 17.10, CPP 28.3, TT 32.3
 Müller, Valentin L. HL 11.7, TT 15.7
 Müller-Bender, David DY 4.7, DY 18.3, DY 45.5
 Müller-Buschbaum, Peter BP 19.1, BP 19.2, CPP 8.4, CPP 13.8, CPP 13.9, CPP 17.4, CPP 17.6, CPP 17.17, CPP 17.20, CPP 17.26, CPP 17.28, CPP 17.30, CPP 17.31, CPP 17.35, CPP 17.36, CPP 17.37, CPP 17.38, CPP 17.39, CPP 17.41, CPP 17.43, CPP 17.44, CPP 17.45, CPP 17.46, CPP 17.47, CPP 17.50, CPP 17.51, CPP 26.1, CPP 29.2, CPP 29.8, CPP 29.10, CPP 35.1, CPP 35.2, CPP 35.15, CPP 35.16, CPP 35.18, CPP 35.19, CPP 35.43,

CPP 35.60, CPP 36.6, CPP 36.8, CPP 37.2, CPP 41.1, CPP 41.2, CPP 45.8, CPP 51.1, CPP 51.4, CPP 52.5, CPP 53.4, CPP 53.6, CPP 56.2, DS 11.3, DS 12.34, KFM 10.2, KFM 10.9, MA 38.5
 Müllner, Julia BP 11.49
 Müllner, Silvia TT 64.8
 Mulvaney, Paul O 49.2
 Münch, L. TT 57.21, TT 58.2, TT 58.4
 Münch, Lukas TT 43.30, TT 43.32, TT 57.26, TT 58.3, TT 58.5
 Müncker, Till BP 25.1
 Mundinar, Simon TT 38.11
 Mundsinger, M. O 47.7
 Mundy, Julia TT 44.5
 Mungan, Muhittin DY 27.1, DY 27.6
 Mungpara, Dhavalkumar MA 11.2, MA 40.36, MA 49.3, O 12.5
 Munk, Axel BP 28.24
 Munkhbat, Battulga HL 33.48
 Munoz, Omar BP 6.3, BP 25.7
 Münster, Florian O 23.5
 Münster, Lambert DY 44.7
 Münster, Lasse O 34.2
 Munteanu, Bogdan Silvestru DS 12.9
 Munteanu, Valentin O 95.9, TT 68.9
 Muntwiler, Matthias MA 19.1, O 29.6, O 36.6
 Munuera, Carmen HL 33.4
 Munzberg, Julian HL 24.4
 Münzenberg, Markus MA 23.7, MA 23.37, MA 23.54, MA 40.6
 Münzer, Philipp KFM 6.39
 Murad, Ahmad HL 2.3
 Murakami, Yuta TT 5.10
 Muralikrishna Garlapati, Mohan MM 41.2
 Muramatsu, Takaki TT 3.6, TT 9.1
 Muras, Laura BP 23.11
 Murat, Altynbek O 74.9
 Murgatroyd, Philip A. E. O 59.8
 Murillo, Michael S. DY 23.1
 Murphy, Bridget DS 12.7, KFM 9.9, O 39.6, O 84.5, TT 56.5
 Murphy, Bridget M. BP 1.11
 Murray, Sean BP 12.12
 Murugesu, Murallee MA 19.1
 Musiał, Anna HL 33.49
 Musienko, Artem HL 2.4
 mussenbrock, thomas HL 47.5
 Mussler, Gregor TT 59.5, TT 59.6
 Mustafa, Luqman DS 6.4
 Mustafayev, Farhad O 77.1
 Musytschuk, Vladislav HL 22.9
 Muth, Karl-Heinz HL 27.3, O 62.3, TT 40.3
 Mutombo, Pingo O 55.3
 Mutschler, Hannes BP 10.6
 Mutschler, Julius MA 19.2, MA 24.6
 Muttathukattil, Aswathy CPP 2.10
 Mutter, Daniel MM 5.1, MM 5.2, MM 32.6
 Mützel, Carina O 28.8
 Mutzke, Nicole O 67.8
 Muzevic, Matko O 18.8
 Muziol, Grzegorz HL 23.4
 Muzychko, Herman MA 23.77
 Myint, Peco O 24.3
 Mysliveček, Josef O 29.2
 n. saggau, christian DS 12.18
 Nabi, Sk Noor TT 45.7
 Nabok, Dmitrii HL 26.6, O 53.6
 Nacci, Christophe O 25.5, O 38.7, O 42.9, O 55.8, O 64.5
 Nádas, Hajnalka MA 36.2
 Nádaždy, Vojtech CPP 1.4, CPP 17.17, CPP 36.9
 Nadiia, Mameka MM 23.24
 Nadville Thadathil, Sajal TT 42.4
 Naeimi, Moha O 28.3
 Nagarajan, Soundarya HL 16.5, TT 24.5
 Nagata, Yuki O 6.5
 nagel, peter MA 19.5
 Nagel, Urmas TT 59.18
 Nagy, Roland HL 29.3, HL 29.4, HL 29.7, HL 33.20, HL 33.21, HL 33.22, HL 33.23, HL 33.29, HL 37.3
 Naidyuk, Yurii TT 16.2
 Naimer, Thomas DS 1.5
 Nair, Rakesh CPP 45.9
 Najafidehaghani, E. O 47.7
 Najafidehaghani, Emad HL 14.6, O 18.1, O 18.3

Naji, Ali DY 44.18
 Nakajima, Taro MA 2.6
 nakatake, ryouichi CPP 2.5
 Nakatsuji, Satoru TT 46.1
 Nakerst, Goran DY 55.3, TT 67.3
 Nakhhae, Mohammad O 95.5, TT 68.5
 Nalabothula, Muralidhar HL 34.9
 Nalbach, Peter DY 25.4, TT 33.4
 Nalini Radhakrishnan, Byjesh BP 24.5, DY 38.5
 Nallathambi, Varatharaja MM 40.10
 Nalupurackal, Gokul CPP 35.24
 Nam, Kyeonghyeon O 78.5
 Nam, Shinjae O 97.2
 Nambiar, Sankalp DY 31.12
 Nandi, Sromona TT 21.2
 Nandi, Ashis K. TT 21.2
 Nandy, Manali HL 7.8
 Nanova, Diana AIW 1.2
 Narag, Dean Von Johari HL 17.6
 Narang, Prineha CPP 45.5
 Narasimhan, Shobhana O 11.3
 Narayan, K.S. CPP 18.11
 Narducci, Daniele MA 34.7
 Narinder, N BP 24.2, DY 38.2
 Narita, Akimitsu O 32.8, O 38.3
 Naritsuka, Masahiro TT 37.12
 Nasio, Despina DS 9.2
 Nasio, Despoina DS 9.3
 Nasir, Tauqir CPP 45.3
 Nasiri, Mahdi DY 26.10
 Nasouri, Babak DY 31.4
 Näsström, Hampus HL 25.11, O 95.4, O 95.5, TT 68.4, TT 68.5
 Nath, Jayshankar TT 49.2
 Natsch, Nelly KFM 1.7
 Natterer, Fabian D. O 28.7, O 55.4, O 70.3, O 77.8, TT 57.4
 Natterer, Fabian Donat KFM 9.7
 Naumann, Franziska O 40.3
 Naumann, J. O 47.3
 Naumann, Jan MA 40.26
 Naumann, Jonas BP 4.3
 Naumann, Tim O 2.4
 Naumov, P. G. TT 42.13
 Navarro, Gema O 38.3
 Navarro, Julien CPP 29.5
 Navas, Salman Fariz DY 42.5
 Navratil, Jiri O 65.1
 Nawrath, Cornelius HL 3.6, HL 7.43, HL 7.48
 Nayak, Pabitra MM 10.4
 Nayak, Sidhartha O 70.8
 Naydenov, Boris KFM 6.34, KFM 6.36, KFM 6.38
 Nazeeruddin, Mohammad Khaja CPP 17.32, CPP 51.6
 Ndione, Pascal D. O 16.6
 Neathery, Noel MM 39.2
 Neckernuß, Tobias BP 28.58
 Nedelea, Vitalie HL 33.32
 Nedvěďová, Lucie O 18.7
 Néel, Nicolas O 64.2
 Neelamegan, Esakkiraja MM 18.2
 Neethirajan, Jeffrey N. MA 32.4, MA 43.2
 Nefedov, Alexei CPP 26.3, MA 19.6, O 39.1, O 81.5
 Neffke, Frank SOE 16.2
 Neher, Dieter CPP 11.4, CPP 11.5, HL 2.4
 Nehring, Mike Thomas O 28.4, O 28.6
 Neidig, Martin TT 57.20, TT 66.3
 Neipel, Jonas BP 31.6
 Neitzert, Heinz-Christoph HL 33.39
 Nejadi, Ammar TT 42.7
 Nelias, Corentin DY 46.1
 Nell, Declan MA 27.3
 Nelson, Andrew CPP 8.4
 Nelson, Jenny CPP 1.5, CPP 11.1, CPP 11.6
 Nemeck, Paul DY 45.12
 Nemnes, George Alexandru DS 12.43, HL 16.2, TT 24.2
 Neogi, Anupam MM 15.6
 Nest, Leona HL 33.55
 Nestmann, Konstantin DY 9.4
 Netrvalová, Marie O 18.7
 Netz, Roland BP 27.1, BP 28.56, CPP 2.11, DY 23.5, DY 44.21, O 64.11
 Netz, Roland R. CPP 44.9, DY 44.18, DY 44.20, DY 56.8
 Neu, Jennifer O 65.5
 Neu, Jennifer N. O 94.9
 Neu, Volker MA 23.34, MA 23.35,

MA 32.2, MA 43.4, MA 48.6
 Neubauer, AnnikaHL 50.5
 Neuber, NicoMM 28.2
 Neuber, SvenCPP 17.57
 Neubert, LaviniaBP 21.9
 Neugebauer, Joerg MM 3.1, MM 32.2
 Neugebauer, JörgTUT 3.1, MM 1.1,
 MM 3.6, MM 15.9, MM 25.5,
 MM 27.4, MM 29.3, MM 32.1,
 MM 32.4, MM 32.5, MM 37.3,
 MM 37.7, MM 41.7, O 30.7, O 69.7,
 O 86.3, O 86.5
 Neugebauer, Nils MA 23.45, MA 36.5
 Neuhaus, AlexanderO 75.4
 Neuhaus, CharlotteBP 29.3
 Neuhaus, LarsDY 5.9
 Neuhaus, LeonardO 23.5
 Neuhaus-Steinmetz, JannisO 7.1
 Neukirchen, AlexanderHL 31.7,
 O 61.7
 Neuman, TomášO 2.6, O 72.4,
 O 76.2
 Neumann, BrunoMM 21.1
 Neumann, C.O 47.7
 Neumann, ChristofCPP 54.4, DS 1.2,
 O 18.1, O 18.3, O 18.4, O 47.8
 Neumann, JoanneCPP 17.56
 Neumann, Laura CPP 19.7, CPP 35.28
 Neumann, MatthiasCPP 45.4
 Neumann, MaximilianMA 40.44
 Neumann, PaulaO 29.8
 Neumann, PhilippVA 13.1
 Neumann, Robin R.MA 10.7,
 TT 12.7
 Neumann, TanjaBP 31.7
 Neumeier, SteffenMM 40.2
 Neupert, TitusKFM 9.7, TT 8.4
 Neureuther, IleniaTT 30.1
 Neuß, DeborahMM 32.3, MM 37.8
 Neusch, AndreasBP 5.7
 Neuwald, Jonathan TT 16.7, TT 53.10
 Nevermann, Daniel HenrikDY 45.3
 Neves, PaulO 16.1
 Newhouse-Ilige, TMA 31.1
 Neyenhuys, OliverTT 23.11
 Ngo, CongHL 17.1
 Nguyen, Binh-MinhCPP 17.12
 Nguyen, DucDS 12.24
 Nguyen, Dung XuanTT 64.1
 Nguyen, Duy Hoang MinhTT 64.1
 Nguyen, Hai ChauO 36.11
 Nguyen, Hai SonTT 64.1
 Nguyen, MyMM 23.15
 Nguyen, PhuongTT 35.5
 Nguyen, Q.L.MM 12.1, MM 26.8
 Nguyen, QuynhHL 36.2
 Nguyen, T. N. HaO 50.2
 Nguyen, T.T. NhungO 36.10
 Nguyen, Thi N. HaO 69.11
 Nguyen, Tuan DungDS 10.3
 Nguyen, Xuan TrungHL 25.8
 Ni, HaiqiaoHL 33.36, HL 33.37
 Ni, NiMA 10.6, TT 12.6
 Ni, XiangO 58.8
 Nicholson, Chris W.O 8.9
 Nicholson, DavidCPP 19.1
 Nickel, BertBP 11.36, CPP 17.6,
 CPP 19.11, CPP 28.8, HL 14.6,
 HL 45.4, HL 45.6, TT 32.8
 Nickel, FelixMA 14.3
 Nickel, OleMM 21.2
 Nicklas, M.TT 46.8
 Nicklas, MichaelMA 31.4, MA 39.3,
 TT 37.1, TT 37.2, TT 37.5
 Nicley, Shannon S.HL 29.10
 Nicolai, Laurent O 8.9, O 18.7, TT 30.3
 Nicolaou, Alessandro TT 3.7, TT 57.3
 Nicolas, VandewalleDY 7.1
 Nicoletti, GiorgioBP 16.6
 Nicolini, PaoloCPP 35.55
 Nicolou, AlexandraMA 34.7
 Nie, WeijieHL 24.8
 Niebuur, Bart-JanCPP 8.3
 Niehaus, Jan SteffenHL 24.1
 Niehaus, ThomasKFM 6.5
 Niehoff, T.MA 42.4
 Niehoff, TimoMA 23.18
 Nielaba, PeterBP 7.10, DY 10.10,
 DY 31.7, DY 34.1, DY 49.5
 Nielsch, KorneliusTUT 4.2, DS 5.2,
 DS 12.20, DS 12.27, DS 12.52,
 MA 1.2, MA 3.10, MA 23.60,
 MM 17.1, MM 17.2, MM 23.5
 Nielsen, Christian BO 93.8
 Nielsen, IdaKFM 11.3
 Niemann, AdrianDY 7.8
 Niemann, RichardaO 39.2, O 58.6

Niendorf, ThomasMA 3.7
 Nienhaus, HermannO 23.6, O 26.3
 Niermann, LauraDS 12.3
 Niermann, ToreDS 12.3
 Nies, Thomas GiacomoBP 28.24
 Nieva, GladysO 85.4
 Nieves, PabloMA 28.5
 Niewegowski, KrzysztofHL 33.10
 Niggas, A.O 5.2
 Niggas, AnnaO 5.3, O 31.4, O 31.5,
 O 31.7, O 31.8
 Niggli, LorenaO 20.1, O 51.2
 Nigro, AngelaTT 31.4
 Nikipar, SeddighehDY 46.6
 Nikitin, AlexeyDS 7.1
 Nikitin, StanislavTT 42.13, TT 52.6
 Niklas, MichaelTT 37.3
 Niklowitz, Philipp G.TT 3.8
 Nikolic, DaniloTT 11.1, TT 20.1,
 TT 20.6, TT 27.10, TT 66.1
 Nikolo, MartinMA 9.7
 Nikolov, SvetoslavMM 31.8
 Nikonova, ViktoriiaMM 12.37
 Nikoubashman, ArashBP 12.9,
 BP 17.1, BP 17.5, CPP 2.5, CPP 12.6,
 CPP 19.10, CPP 35.9
 Nilius, Niklas O 68.3, O 76.7
 Nina, TverdokhlebovCPP 20.5
 Ninkovic, JovicaBP 15.3
 Nino, M. A.O 47.3
 Nino, Miguel AngelMA 50.1
 Nippert, F.HL 23.1, HL 43.6
 Nippert, FelixHL 22.3, HL 23.5,
 HL 41.3, HL 41.7
 Nishida, JunO 12.7
 Nishimoto, S.MA 44.3, TT 42.13
 Nishimoto, Satoshi MA 33.5, TT 29.6
 Nisi, KatharinaDS 10.3
 Nitsche, AnnaCPP 35.22
 Nitschke, IngoDY 4.6
 Nitta, MunetoTT 31.11
 Niu, ZhichuanHL 33.36, HL 33.37
 Noack, PhilippHL 43.2
 Noad, HilaryTT 37.5, TT 37.13
 Noad, Hilary M. L.TT 37.4
 Nobakht, JahangirTT 25.4
 Nochowicz, SamO 75.2
 Noe, JonathanHL 33.34
 Noei, Heshmat O 11.4, O 16.1, O 29.6,
 O 37.8, O 39.4, O 40.4, O 57.5, O 81.3
 Noei, NedaO 33.5
 Noethel, TabataCPP 54.4
 Nogaki, KosukeTT 5.10
 Nogueira, FlavioTT 47.8
 Noguera, ClaudineO 68.3
 Noh, GeunhoCPP 35.3
 Noh, Jae DongBP 10.0
 Nojiri, H.MA 40.58
 Nojiri, YukiTT 39.7, TT 49.1, TT 58.6,
 TT 58.7, TT 58.20, TT 66.6
 Noky, Jonathan MA 3.6, MM 6.10
 Noll, MaximilianeDY 18.5
 Nollmann, CathrinBP 5.4
 Nollmann, CathrinBP 5.3
 Nolte, LennartHL 33.57
 Nomura, ToshihiroMA 44.2
 Nomura, YusukeTT 63.4
 Noori, YasirCPP 45.3
 Nordlund, KaiHL 44.2
 Nordström, LarsMA 7.1
 Nörenberg, TobiasDS 7.1, DS 12.14
 Normand, B.TT 42.13
 Normand, BruceMA 46.10
 Norman-Reiner, MariaHL 23.2
 Nørskov, Jens K.O 69.1
 Northe, ChristianTT 11.2
 Novak, Ekaterina CPP 3.3, CPP 35.41
 Novelli, MassimilianoO 63.1
 Novikau, IvanCPP 3.3
 Novikov, Dmitri V.O 56.6
 Novko, DinoO 18.8, O 64.12, O 93.2
 Novoselova, IuliiaBP 5.7
 Novotny, OldřichTT 57.25
 Nowak, UlrichMA 4.8, MA 8.7,
 MA 23.5, MA 23.57, MA 40.6,
 MA 46.1, MA 46.3, MA 46.5,
 MA 46.12, TT 7.8
 Nowakowski, PiotrBP 11.63,
 DY 44.17
 Nowik-Boltyk, EwaDS 3.3
 Ntallis, NikolaosMA 47.6
 Nufer, PaulMA 16.9
 Nugroho, Agustinus Agung MA 40.17,
 TT 57.5
 Nuić, LovroBP 15.5
 Nunnenkamp, AndreasDY 25.2,
 TT 33.2

Nürnberg, ElinaBP 11.26
 Nuss, JürgenTT 42.14, TT 44.8,
 TT 51.5
 Nussbör, MaxHL 38.7, O 96.7
 Nutz, ManuelHL 33.34
 Nuzhina, DariaMA 26.2
 Nyári, BendegúzTT 8.5, TT 8.6
 Nyenhuus, MarvinDY 43.17
 Nylander, TommyBP 27.4
 Nysten, EmelineHL 10.7
 Nysten, Emeline D. S.HL 10.3
 O. Balayeva, NarminaHL 45.7
 Oberhofer, HaraldCPP 2.9, HL 40.7,
 MM 6.1, MM 6.5, O 6.9, O 59.10,
 O 79.7
 Oberleitner, ChristianTT 4.13
 Oberthuer, MarkusCPP 29.5
 Oberthür, MarkusCPP 35.1
 Obst, MaximilianDS 7.1, DS 12.17,
 HL 17.11
 Ócal, BarisHL 7.24
 Ocana-Pujol, Jose L.O 49.6
 Ochi, M.TT 6.4
 Ochkan, KyrlyoTT 17.6
 Ochner, HannahBP 21.1
 Ochoa-Martinez, EfrainCPP 43.7
 Ochs, Andrew M.MA 3.6
 Ochs, KarlheinzBP 11.74, BP 11.75,
 DY 18.4, DY 18.5, DY 37.7
 Ockeloen-Korppi, CasparTT 49.2
 Ocker, MichelleTT 9.2, TT 43.13
 Odobesko, ArtemO 20.11, O 77.9,
 O 94.3
 Ódor, GézaDY 57.1
 Oechsle, Anna LenaCPP 36.6
 Oechsle, Anna-LenaCPP 35.18
 Oehri, PatriciaTT 54.9
 Oelschläger, AnneO 92.8
 Oelschläger, AnneO 92.9
 Oelschläger, FabioMM 8.3
 Oesinghaus, LukasBP 27.3
 Oesterlin, HeinerMM 27.9
 Oestreich, MichaelHL 7.17
 Oettel, MartinBP 27.8, CPP 57.9,
 DY 17.5, DY 27.3, DY 34.5
 Oezaslan, MehtapO 25.1
 Offermann, TobiasHL 37.4
 Ogrin, FeodorMA 43.1
 Ogunmoye, KehindeCPP 51.8
 Ogura, MasakoHL 34.5
 Oh, HeesuTT 44.7
 Ohanesjan, VladimirTT 38.5
 Ohkubo, TadakatsuSYGM 1.2
 Ohlbad, HannesO 31.5, TT 22.1
 Ohlendorf, RahelMA 33.7, MA 44.4
 Ohm, WiebkeBP 19.1, CPP 41.1
 Ohmann, RobinO 18.8, O 36.11,
 O 56.3
 Ohmer, JürgenHL 2.6, HL 18.4
 Oinonen, NikoO 6.8, O 66.2, O 66.10,
 O 87.4
 Oishi, CassioCPP 44.3
 Oka, RyosukeTT 9.6
 Okamoto, Junichi DY 43.21, MA 17.3
 Okamura, YuO 16.7
 Okotete, ElohoMM 9.6
 Okuda, TaichiO 59.4, O 85.6
 Okur, Halil I.CPP 53.2
 Okuyama, HiroshiO 32.4
 Olbrich, EckehardSOE 7.2, SOE 8.1,
 SOE 18.4
 Oldenburg, KevinBP 28.13
 Olejník, KamilMA 4.14, MA 40.64,
 TT 7.14
 Olés, Andrzej M.HL 21.2, TT 57.6
 Olga, MattsMM 23.24
 Olha, BezsmeretnaMA 49.5
 Oliva, MiriamHL 7.40
 Oliveros Mata, Eduardo Sergio
 MA 5.3, MA 17.1, MA 49.6, MA 49.8
 Oliveros-Mata, Eduardo Sergio
 MA 40.47, MA 49.5, MA 49.7,
 MA 50.3
 Olivier, YoannCPP 11.7
 Ollefs, K.MA 48.3
 Ollefs, KatharinaMA 3.3, MA 3.8,
 MA 8.7, MA 17.5, MA 42.2, MA 42.7
 Ollier, AlexinaO 51.3, O 93.1
 Ollivier, AntoineMM 23.11
 Ollivier, J.MA 33.6
 Ollivier, JacquesMA 24.6, MA 44.7
 Olmeda, FabrizioBP 22.6, BP 29.7
 Olsen, Nicholas MichaelO 34.3
 Olsson, Pär A. T.MM 9.2
 Olsthoorn, BartMA 48.5
 Olthof, SelinaHL 7.24, HL 7.36,
 HL 25.1, HL 25.5

Omar, HassanCPP 29.6
 Onat, EgeHL 50.12
 Ondo, DanielCPP 12.5
 Ondracek, MartinO 97.3
 O'Neil, Caitlin ITT 37.11
 Ong, A.CPP 17.2
 Ono, TeruoTT 27.1
 Ontrup, FinnKFM 6.29
 Onufriienko, OleksanderO 18.2,
 O 74.5
 Önür, AlpcanBP 11.45
 Onyikiienko, Y. O.MA 33.6
 Opel, MatthiasCPP 13.8, MA 4.13,
 MA 23.50, MA 40.15, TT 7.13
 Opherden, D.TT 28.6, TT 42.15,
 TT 57.19
 Opitz, AndreasCPP 17.24, CPP 18.1,
 CPP 18.10
 Oppen, Felix vonO 20.6
 Oppeneer, PeterMA 22.3, MA 40.6
 Oppeneer, Peter M.MA 22.1,
 MA 23.52
 Opper, ManfredTUT 1.3, DY 1.3,
 DY 11.5, DY 26.6, TT 1.3, TT 13.5
 Oppermann, PatrickO 63.2, O 84.10,
 TT 56.10
 Oppliger, JensKFM 9.7, O 55.4
 Or, Wing KitCPP 35.29, CPP 53.3
 Orazov, SabinaDY 45.8
 O'Regan, DavidMA 7.3
 Orendáč, MartinMA 13.9, TT 19.9,
 TT 58.24
 Orendáčová, AlžbetaMA 13.9,
 TT 19.9, TT 58.24
 Orenstein, GalTT 62.7
 Orghici, RozaliaBP 19.3, CPP 41.3
 Orio, HibikiO 22.7
 Orlandi, FabioMA 9.3, TT 23.8
 Orlita, M.TT 6.5, TT 6.10
 Orlow, A.TT 57.27, TT 57.28
 Orlow, AlexanderTT 57.26
 Oroszlany, LászlóMA 24.2
 Ortiz, B.R.TT 23.1
 Ortiz-Mahecha, CarlosBP 3.11
 Ortmann, FrankCPP 17.7, CPP 17.58,
 CPP 28.2, CPP 36.4, CPP 43.6,
 CPP 54.1, CPP 54.2, TT 32.2
 Ortzuar, JonTT 8.3
 Oschinski, HeddaO 96.8
 Oses, CoreyMM 36.9
 Oshima, YuichiHL 51.9
 Oshipov, VasiliiO 70.9
 Osmond, IsraelTT 3.6
 Ossinger, SaschaMA 19.4, O 42.6
 Ostanian, SergeyDS 12.26
 Ostapovets, AndriyMM 17.3
 Ostendorf, StefanMM 26.3
 Österbacka, NicklasO 57.4
 Osterhage, HermannO 7.6, O 20.2,
 O 20.4, O 33.9
 Osterhoff, MarkusDY 18.7
 Osterkamp, ChristianDS 12.35
 Osterkorn, AlexanderPSV III,
 TT 22.2, TT 22.12
 Ostheimer, DavidHL 7.9, HL 7.10
 Otañora, Jorge A. MA 23.34, MA 43.4
 Ott, FlorianDS 12.2, MA 23.36
 Otte, MagdalenaBP 28.13
 Otte, SanderO 15.2, TT 8.8
 Otten, RenéHL 50.10
 Otterpohl, FlorianDY 25.4, TT 33.4
 Otto, AndreasMA 16.3
 Otto, FelixCPP 36.9, O 18.4, O 22.3,
 O 22.9, O 36.9, O 47.2
 Otto, FrederikDS 12.3
 Otto, Oliver BP 8.8, BP 8.11, MA 23.54
 Ou, YongliangMM 5.8
 Ouaj, TaoufikHL 14.8
 Ouassou, Jabir AliTT 20.10
 Ouazan-Reboul, VincentBP 24.11,
 DY 38.11
 Oudah, MohamedMM 6.7
 Ouhbi, HassanO 57.4
 Ouladidif, BachirMA 37.4
 Outerovitch, RobinsonTT 21.9
 Ouzeri, AdamBP 4.5
 Ovsyannikov, RuslanO 85.1
 Öz, Seren DilaraHL 7.36
 Ozawa, TomokoBP 21.10
 Özcan, Basak CigdemHL 33.38
 Özden, AyberkKFM 6.10
 Özer, BurakMA 40.59, MA 40.59
 Özmen, EgeO 32.6
 Özyigit, FurkanTT 16.14, TT 18.1
 P. Constantinou, AnnaCPP 35.58
 P. Kravchuk, VolodymyrMA 17.1
 P. Schmidt, KaiTT 42.22

Author Index

- P. Tran, Mai BP 11.59
 Paap, Ulrike O 6.2
 Paarmann, Alexander O 39.2, O 58.4,
 O 58.6, O 58.8
 Pablo-Navarro, Javier TT 20.4,
 TT 57.23
 Pabst, F. MA 40.58
 Pabst, Falk MA 40.25, MA 44.6
 Pacchioni, Gianfranco O 81.10
 Pachat, Rohit MA 40.30
 Pacholski, Michal HL 30.6, TT 41.6
 Padmanabhan, Padma Kumar
 MM 6.4
 Padurariu, Ciprian O 7.5, TT 39.2,
 TT 39.9, TT 54.4, TT 54.5
 Paeckel, Sebastian TT 43.11
 Paetzold, Lukas MA 5.2, MA 36.4,
 MA 40.28
 Paetzold, Ulrich W. HL 4.1
 Pérez Larios, Francisco BP 28.9
 Pagnini, Gianni DY 6.7
 Pahi, Sampannah MM 33.6
 Pahujani, Sakshi BP 11.30
 Pajimans, Joris BP 4.1
 Paischer, Sebastian MA 23.31,
 MA 27.6, MA 40.62
 Pal, Adipta TT 31.10
 Pal, Banabir TT 27.4
 Pal, Mainak TT 63.6
 Pal, Pikeshe TT 23.5
 Pal, Shovon DS 15.3, TT 47.1
 Palacios, Elias MA 13.1, TT 19.1
 Paladino, Elisabetta TT 54.6
 Palato, Samuel O 16.8
 Palazzese, S. MA 40.58
 Palazzese, Sabrina MA 44.6
 Paleari, Fulvio HL 26.3, O 53.3
 Palekar, Chirag HL 8.2, HL 12.2,
 HL 12.7, HL 22.4, HL 33.36, HL 33.37,
 HL 33.48
 Palermo, Giorgio O 4.7
 Paleschke, Maximilian O 51.5, O 51.6
 Paleti, Sri Harish Kumar CPP 11.2
 Pallares, Macià-Esteve BP 30.4
 Pallmann, Maximilian KFM 8.4
 Palotás, Krisztián MA 14.1, O 47.5,
 O 82.4, TT 8.6, TT 8.7
 Palstra, Thomas TT 3.3
 Paluch, Ewa BP 16.4
 Paluch, Patrick TT 39.3
 Paluch, Robert SOE 4.4, SOE 4.7
 Palutke, Steffen O 16.1, O 37.8
 Pan, Anlian O 76.1
 Pan, Grace TT 44.5
 Pan, Guangjiu CPP 13.8, CPP 17.16,
 CPP 17.31, CPP 17.51, CPP 52.5
 Pan, Wun-Chang O 28.8
 Pan, Yang HL 8.6, HL 33.5
 Panadés Barrueta, Ramón L.
 HL 20.5, O 35.5
 Panagopoulos, Christos SYTS 1.5
 Panchami Raj, Shilpa O 64.5
 Pancholi, Agnieszka BP 29.4
 Panda, Swarup K. TT 30.11
 Pandey, Atul MA 23.64, MA 43.7
 Panhans, Michel CPP 28.2,
 CPP 36.4, CPP 43.6, TT 32.2
 Panizon, Emanuell DY 31.10
 Panja, Soumendra TT 4.3
 Panjwani, Naitik MM 16.1
 Panosetti, Chiara KFM 10.6, MM 3.3,
 MM 16.2
 Pant, Ritesh DY 55.10, TT 67.10
 Pantis-Simut, Calin Andrei HL 16.2,
 TT 24.2
 Pantis-Simut, Calin-Andrei DS 12.43
 Panzer, Fabian CPP 17.42, HL 7.33
 Paoluzzi, Matteo DY 42.12
 Paone, Domenico MA 32.4
 Papadakis, Christine M. CPP 8.2,
 CPP 8.3, CPP 17.54, CPP 35.43,
 CPP 35.60, CPP 35.61
 Papageorgiou, Anthoula C. O 11.3,
 O 14.4
 Papaioannou, Evangelos Th.
 MA 22.5, MA 23.55, MA 40.50
 Papanikolaou, Nikos DY 27.5
 Papari, Gian Paolo TT 3.11
 Papastavrou, Georg O 76.9
 Papeňu, Franziska BP 6.6
 Papp, Christian O 23.1, O 23.3, O 41.1,
 O 64.1, O 73.8
 Pappenberger, Ronja HL 4.1
 Paradisanos, I. O 47.7
 Paradisanos, Ioannis O 18.3
 Paradiso, Nicola TT 20.8, TT 27.5
 Pardo, Luis Carlos MM 36.6
 Pargmann, Max CPP 2.7
 Paris, Eugenio MA 46.10
 Parisen Toldin, Francesco DY 49.9
 Park, Cheol-Hwan MA 7.2, MA 7.4,
 MA 7.6, MA 7.12, MM 19.5, MM 29.2
 Park, Hee Gyum MA 4.10, TT 7.10
 Park, Jitae MA 40.38
 Park, Jiwoong O 34.1
 Park, Suk-in HL 24.3
 Park, Sung-yul HL 24.3
 Park, Youngwook O 76.4
 Parkin, S.S.P. KFM 11.9
 Parkin, Stuart MA 12.1, MA 43.7,
 O 32.4
 Parkin, Stuart S. P. MA 9.3, MA 23.51,
 MA 31.6, O 59.7, TT 8.4, TT 27.4,
 TT 59.12
 Parkin, Stuart SP MA 23.64
 Parkinson, Gareth S. O 6.1, O 6.4,
 O 81.4
 Parks, Sarah C. DS 14.4
 Parley, Jack T. DY 6.2
 Parlitz, Ulrich DY 37.4
 Parmar, Anshul Deep Singh DY 24.2
 Parmar, Devang TT 20.13
 Parmigiani, Fulvio O 16.3, O 19.2,
 O 19.4, O 34.8, O 34.10
 Parodi, Margherita MA 12.7
 Parra López, L. O 75.9
 Parschau, Manfred O 73.6, O 87.2
 Parthasarathy, Shrawan Kumar
 HL 29.3, HL 33.19, HL 33.23,
 HL 33.29, HL 37.3
 Parthenios, Nikolaos TT 53.5
 partovifard, arghavan BP 9.6
 Partyka-Jankowska, Ewa O 30.3
 Paruch, Patrycja KFM 4.9
 Parui, Kaushick MA 40.22
 Parvej, Aslam TT 22.7
 Parvini, Tahereh TT 64.7
 Paschen, Silke MA 9.7
 Paschke, Fabian O 2.7, O 66.3
 Pascual, J. I. O 47.3
 Pascual, Jose Ignacio O 36.5, O 56.5
 Paseggi Jr., Mario C.G. DY 42.7
 Pashkin, A. TT 22.14
 Pashkin, Alexej HL 17.11, MA 31.7,
 TT 62.1, TT 62.5
 Pashkin, Oleksiy MA 40.51
 Pasko, Grigori O 22.8
 Paspalides, Christos HL 8.4
 Passeggi Jr., Mario O 82.5
 Passler, Nikolai C. O 58.4
 Passoni, Matteo O 24.2
 Passos, Ingrid DY 44.4
 Pastier, Florian HL 10.10
 Pastoetter, Dominik CPP 54.1
 Pastryk, Kai-Florian CPP 19.12
 Paszúk, Agnieszka HL 7.8, HL 7.9,
 HL 7.10
 Patel, Himanshu P DY 7.10
 Patel, Kuntal DY 29.5
 Patel, Tarun MA 17.3
 Patera, Laerte O 47.6
 Patera, Laerte L. O 55.3
 Path, Michael P. MA 40.46
 Pathak, Kare Narain TT 16.12,
 TT 16.13
 Patil, Pranay DY 27.2
 Patterson, Robert I.A. BP 24.9,
 DY 38.9
 Patthey, Francois O 15.12
 Pattis, Alexander BP 5.6
 Patwari, Jayita O 16.9
 Paul, Alope MM 18.2, MM 18.6
 Paul, Neelima KFM 10.3
 Paul, Shuvojit BP 24.2, DY 38.2
 Paul, Wolfgang CPP 19.2, CPP 35.48,
 CPP 37.1
 Paulmann, Carsten TT 23.5
 Paulsen, Michael MA 18.8, MA 48.7
 Paulus, Fabian CPP 51.2
 Paulus, Jonas BP 11.27
 Paulus, Michael KFM 6.29, KFM 6.33
 Paulus, Werner TT 51.8
 Pauly, Fabian TT 25.2, TT 25.3
 Pausch, Lukas DY 43.5
 Pavarini, Eva TT 21.6
 Pavelec, Jiri O 6.1, O 26.4, O 54.6
 Pavicevic, Danica TT 62.2
 Pavlov, Andrei TT 38.5
 Pavlovskii, Nikolai MA 44.7, TT 42.5
 Pavlí, Jana MA 37.1
 Pavlyukh, Yaroslav HL 13.7, HL 31.3,
 HL 31.4, O 17.7, O 61.3, O 61.4
 Pavone, Pasquale HL 31.6, O 61.6
 Pawlak, Rémy O 38.4, O 45.3, O 45.4,
 O 87.3
 Pawlik, Maciej SOE 4.7
 Pawlis, Alexander HL 29.9, HL 30.1,
 TT 41.1
 Paysen, Ekaterina KFM 9.6
 Pazhedath, Akshay Menon HL 50.7
 Pazhedath, Anees HL 21.1
 Pazniak, Hanna MA 38.3
 Pearce, Daniel BP 9.7
 Pecchia, Alessandro HL 36.1, MM 3.9
 Pedersen, Jonas DS 16.6
 Pedroni, Matteo O 24.2
 Peets, D.C. MA 44.3
 Peets, Darren MA 23.1, MA 40.22,
 MA 40.25, MA 44.8
 Peh, Katharina HL 7.1, HL 7.2,
 HL 38.3, HL 38.6
 Pehlevan, Cengiz DY 11.6, TT 13.6
 Pehlke, Eckhard O 69.8, O 69.12
 Pei, Jian CPP 18.1
 Peil, Oleg MM 9.1, MM 9.5, MM 37.6
 Peil, Oleg E. DS 5.3
 Peinke, Joachim DY 5.1, DY 5.5,
 DY 5.8, DY 5.9, DY 32.9
 Peis, Leander TT 23.4, TT 23.13
 Peiser, Heiko DS 12.8, O 22.5
 Peixoto, T.R.F. MM 12.1, MM 26.8
 Pejov, Ljupco DY 44.13
 Pekola, Jukka SYQD 1.5, TT 20.1
 Pekola, Jukka P. TT 66.1
 Pelella, Aniello O 5.8
 Pellegrino, Luca MA 11.2
 Pelly, Maximilian T TT 37.11
 Pelster, Axel TT 45.8, TT 65.5
 Peltonen, Joonas TT 20.1
 Peltonen, Joonas T. TT 66.1
 Pelz, Philipp KFM 9.2
 Peña Murillo, David DY 48.6, TT 55.6
 Peña Unigarro, Andres David
 CPP 18.6, O 36.1, O 36.7
 Pena-Diaz, M. O 47.3
 Pendem, Prashanth O 36.6
 Peneva, Kalina HL 8.3
 Peng, Bo O 94.1
 Peng, Yan MA 24.6
 Pengerla, Monica HL 49.6
 Peniakov, Giora HL 49.7
 Penner, Patrick O 28.9
 Pensalfini, Marco BP 4.8
 Pentcheva, Rossitza HL 26.8, MA 8.7,
 MA 46.6, O 8.2, O 8.3, O 53.8, O 67.7,
 O 92.7, TT 50.5
 Pentz, Sebastian MM 3.2, MM 12.2
 Peotta, Sebastiano TT 63.2
 Pepic, Jovana BP 28.14
 Peralta, Mayra TT 11.5
 Peravali, Surya Kiran VA 1.3
 Perea-Causin, Raul O 34.2
 Pereira, A.L. DS 12.48, HL 7.16,
 HL 7.20
 Pereira, Antonio MM 23.11
 Pereira, Lino O 31.1
 Pereira, Lino M.C. O 24.1
 Pereira, Vanda M. HL 51.3, HL 51.6,
 TT 30.6
 Pereiro, Manuel MA 47.6
 Peres, Nuno MA 20.4
 Peressi, Maria O 19.4, O 34.10
 Perez, Lucas MA 38.1
 Perez, Nicolas SYQC 1.2, MM 23.5
 Pérez Romero, Arturo TT 43.19
 Pérez, Rúben O 87.3
 Perez Tirado, Amaury BP 28.28
 Perez-Lara, Angel BP 17.4
 Perfetti, Luca HL 17.9
 Peretto, Enrico HL 31.4, HL 48.6,
 HL 48.7, O 16.5, O 61.4
 Perkins, N. TT 52.3
 Perkovic, Domagoj DY 55.7, TT 67.7
 Perlin, Piotr HL 23.3, HL 23.6, HL 28.3
 Perna, Salvatore MA 23.61
 Pernack, Benedikt J.P. TT 20.11
 Pernice, Wolfram HL 33.22
 Perrot, Manolis SYQC 1.2
 Pershin, Anton MA 32.4
 Persson, L. HL 23.1
 Persson, Mats O 46.6
 Pertsch, Patrick O 91.9
 Pesch, Thiemo SOE 15.1
 Peschel, Fabian HL 6.2, O 9.2
 Peschel, Ulf O 83.3
 Peschka, Dirk CPP 44.5
 Pesquera, David DS 6.3
 Pestka, B. DS 7.2, MA 40.53
 Petaccia, Luca O 34.10
 Peter, Christine BP 11.45
 Peter, Janis TT 58.18, TT 58.19
 Peter, Melina HL 7.65, HL 7.66
 Peterlechner, Martin DS 4.2,
 MM 23.18, MM 26.3, MM 28.2
 Peters, A. HL 33.17
 Peters, Jannick Alexander O 48.4
 Peters, Marius TT 4.7, TT 4.8, TT 4.9,
 TT 43.12
 Peters, Olof O 20.6
 Peters, Tobias MA 15.1, MA 23.59
 Petersdorf, Lukas BP 1.11, O 39.6
 Petersen, Carolin MM 12.15
 Petersen, Clemens HL 47.4, HL 47.6
 Petersen, Nanning CPP 2.12
 Petersen, Nina MM 17.4, MM 23.29
 Petersen, Thorben TT 21.8
 Petit, Erick MA 25.3
 Petocchi, Francesco TT 50.4
 Petoukhoff, Christopher E. CPP 17.17
 Petracic, Oleg DS 14.6, MA 5.6,
 MA 40.16, O 42.12
 Petraru, Adrian KFM 1.5
 Petrenko, Oleg MA 33.7
 Petreska, Irina DY 44.13
 Petricek, V. MA 41.2
 Petrich, Lukas MM 23.30
 Petrich, Rebecca DS 12.4
 Petrow, Michael TT 4.13
 Petrova, Anastasiia BP 22.8
 Petrova, Vera MM 33.4
 Petry, Winfried MM 40.5
 Pettersson, Anders TT 58.29
 Pettersson, Love MM 31.7
 Pettinger, Nina DS 1.4
 Petz, Dominik CPP 45.8
 Petzak, Tobias HL 10.7
 Petzold, Albrecht CPP 19.5,
 CPP 35.27
 Petzold, Heike BP 21.4
 Petzold, Stefan DS 9.2
 Petzoldt, Philip O 29.8, O 41.4
 Pezzotti, Simone BP 17.2
 Pfäfflein, Ph. TT 57.28
 Pfalzgraf, Daniel MM 5.1
 Pfander, Simon TT 39.8
 Pfannstiel, A. KFM 6.46
 Pfannstiel, Anton KFM 6.42,
 KFM 14.5, KFM 14.6
 Pfauf, Bastian MA 40.39, MA 43.6
 Pfeifer, Hannes DS 12.37
 Pfeifer, Veronika DY 31.3
 Pfeiffelmann, Timo HL 4.9
 Pfeiffer, Florian KFM 6.4
 Pfeiffer, Florian Alexander O 22.2
 Pfeiffer, Mario F. O 70.4
 Pfeiffer, Martin CPP 1.11
 Pfeiffer, Meike TT 28.2
 Pfeiffer, Ramon KFM 6.21
 Pfeiffer, Walter O 80.4
 Pfeil, Jonas BP 28.35
 Pfenning, Andreas HL 49.5, HL 49.7
 Pfeuffer, Lukas MA 3.9, MA 3.11
 Pfister, Ulrich HL 7.62
 Pflaum, Jens CPP 13.3, CPP 17.6,
 CPP 17.8, CPP 17.10, CPP 17.11,
 CPP 17.24, CPP 17.48, CPP 28.3,
 CPP 28.4, CPP 28.8, CPP 35.21,
 CPP 53.7, DS 3.2, O 58.5, TT 32.3,
 TT 32.4, TT 32.8
 Pfleiderer, Christian MA 2.6, MA 9.4,
 MA 13.6, MA 13.8, MA 25.5, MA 26.2,
 MA 40.41, MA 40.42, MA 48.1,
 TT 3.8, TT 4.13, TT 10.1, TT 10.2,
 TT 10.3, TT 10.5, TT 19.6, TT 19.8,
 TT 42.6, TT 47.3, TT 47.6, TT 58.23
 Pham, Thien An CPP 17.47
 Pham, Tuan SOE 18.1
 Phanse, Pradny O 37.13
 Phark, Soo-Hyon O 15.3, O 15.6
 Phi, Hai Binh DY 29.7
 Philipp, Anja TT 42.1
 Philipp, Julian BP 26.6, BP 26.8
 Philipp, Luca Nils DS 3.2
 Phillips, Nicholas W. MM 25.2
 phuyal, dibya DY 25.7, O 8.8, TT 33.7
 Phuyal, Dibya O 6.3
 Piazza, Francesco TT 65.2
 Piccinin, Simone O 29.2
 Pichler, Cornelia F. O 4.8
 Picker, J. O 47.7
 Picker, Julian O 18.1, O 18.4, O 47.8
 Pidko, Evgeny O 69.3
 Pieluch, Timo CPP 17.36
 Piekarz, Przemyslaw HL 21.2
 Piel, Matthieu BP 31.2
 Pielich, Borna O 18.8
 Pielstickler, Lukas O 85.8
 Pierre, Frédéric TT 17.3

- Pierre, Muller BP 1.8
Pierz, Klaus O 82.7
Pietka, Isabel •MM 40.2
Pietschnig, Rudolf CPP 35.52
Pietzonka, Patrick •SYFP 1.5,
DY 42.15
Pietzsch, Annette MA 8.9, MA 20.3
Pignedoli, Alessandro •DY 44.12
Pignedoli, Carlo A. O 75.5
Pi-Jaumà, Irina BP 30.4
Pikulin, Dmitry I. TT 63.2
Pilch, Patrick HL 17.10, •TT 6.7,
TT 59.18
Pillai, Lesia O 28.5, •O 78.8
Pillai, Eva BP 25.4
Pillich, Cynthia MA 42.7
Pinar Sole, Andres •MA 19.7
Pincelli, Tommaso MA 46.13, O 16.5,
•O 16.7, O 95.1, O 95.3, TT 68.1,
TT 68.3
Pinchasik, Bat-El ... BP 24.7, DY 38.7
Ping, Xiaofei BP 3.4
Pinheiro Neto, João SOE 19.3
Pinnock, Samuel W. •HL 17.2
Pinto, Dinesh MA 32.4
Pionteck, Mike •KFM 6.6
Piorunek, David MM 23.5
Piovano, Andrea MM 23.34
Piquard, Colin TT 17.3
Piquero-Zulaica, Ignacio O 14.2,
O 14.5, O 14.6
Pirker, Luka TT 16.7, TT 53.10
Piro, Lorenzo •BP 9.2
Piros, Eszter DS 9.2, DS 9.3
Pirro, P. MA 16.6
Pirro, Philipp MA 15.3, MA 16.1,
MA 16.5, MA 18.1, MA 23.44,
MA 23.61, MA 23.67, MA 23.74,
MA 23.75, MA 34.7, MA 40.7,
MA 40.33, O 84.2, TT 56.2
Piš, Igor O 47.4
Pistidda, Claudio MM 27.6, MM 31.9
Pithan, Linus CPP 51.2, •O 63.1,
•O 84.7, O 95.9, •TT 56.7, TT 68.9
Piva, M. TT 46.8
Piva, Mario MA 31.4
Pivarníková, Ivana •KFM 10.9
Pivetta, Marina O 15.12
Pizarro, José M. •O 84.4, O 84.9,
O 95.6, O 95.10, •TT 56.4, TT 56.9,
TT 68.6, TT 68.10
Pizzi, Andrea •DY 25.2, •TT 33.2
Pizzi, Giovanni HL 6.1, MM 19.4, O 9.1
Plass, Kathrin •O 85.5
Plaszko, Noel HL 14.2
Plate, Paul HL 4.2, O 40.3
Platero, Gloria •SYQD 1.2
Platzer, Barbara O 26.7
Plettenberg, Pascal O 6.6
Plienbumrung, Tharathep •TT 57.6
Plock, Matthias HL 37.9
Ploss, Lydia •CPP 17.5
Plucinski, L. DS 7.2
Plucinski, Lukasz DS 12.1, O 18.9,
O 30.3, •O 30.5, O 59.3, O 67.4,
O 74.3
Pluntke, Luciana CPP 29.5, •CPP 35.1
Pobedinskias, Paulius HL 29.10
Poccia, Nicola DS 5.2, •DS 7.3,
DS 12.18, DS 12.20, DS 12.52
Poddig, Hagen MA 44.8
Podlesnyak, A. TT 42.13
Podsednik, Maximilian DS 4.5
Poggemann, Hanna-Friederike •BP 27.7
Poggiali, Francesco HL 50.1
Pogorzalek, Stefan TT 49.2
Pohl, Benjamin •HL 33.20
Pohl, D. CPP 17.2
Pohl, Darius •MA 12.3, MA 23.60
Pohle, Ulrike BP 28.15
Pohlitz, Merlin MA 22.5
Pöhls, Jonas HL 14.3
Pointner, Andre •HL 29.4, HL 33.19,
HL 33.20, HL 33.21, HL 33.23,
HL 33.29
Pokart, Tim HL 7.63
Pokharel, Amrit TT 62.5
Pokharel, Amrit Raj MA 18.3
Pokhrel, Krishna K. MA 21.4
Pokorný, Vladislav •TT 20.12
Polák, Jakub CPP 12.5
Polarz, Sebastian CPP 51.7
Polatkan, S. TT 6.5, •TT 6.10
Polcar, Tomáš CPP 35.55, HL 7.55
Polesya, S. •MA 8.3, MA 34.38
Polesya, Svitlana HL 34.5, MA 46.12
Polewczyk, Vincent MA 27.1
Poley, Lyle •BP 18.4, •DY 33.4
Policht, Veronica HL 34.8
Politti, Yael BP 23.3
Polley, Craig O 64.6
Polli, Dario KFM 3.1
Pollmann, Erik HL 22.9, O 30.10
Pollmann, Frank DY 2.6, DY 9.11,
DY 25.1, DY 25.11, TT 2.6, TT 22.3,
TT 33.1, TT 33.11, TT 38.1, TT 43.23,
TT 43.24, TT 46.9, TT 46.11, TT 47.9,
TT 47.10, TT 65.9
Pollock, Jonathan BP 11.20
Položij, Miroslav CPP 17.60
Poltavsky, Igor MA 40.1
Pomjakushin, Vladimir MA 40.22,
MA 40.25
Pongó, Tivadar DY 7.7
Pongsangangan, Kitinan •MM 6.9
Pönsch, Wolfram •BP 16.4
Ponomarev, Ilija CPP 35.55
Ponomaryov, Alexey BP 11.43,
MM 23.35
Pons, Rebecca •TT 50.2
Ponson, Laurent MM 33.8
Pontius, Niko MA 40.12, MA 46.4,
MA 46.13
Pontoni, Diego BP 29.3
Pop, Ioan TT 58.16
Pop, Ioan M. TT 39.3, TT 49.4
Popescu, H. MA 12.5
Popescu, Horia MA 11.6, MA 43.1
Popescu, Mihail DY 31.11
Pop-Georgievski, Ognen CPP 35.62
Popiel, Nicholas TT 28.1
Popov, Alexey MA 23.20, O 50.3
Popov, Alexey A. O 2.7
Popov, Cyril KFM 6.12, KFM 6.34,
KFM 8.4, KFM 8.5
Popova, Elena MA 40.34
Popovic, Marko BP 11.56
Popp, Andreas DS 8.5
Popp, Matthias A. •O 84.11, O 95.11,
•TT 56.11, TT 68.11
Port, Fabian BP 28.35
Portalupi, Simone L. HL 7.48, HL 49.3
Portalupi, Simone Luca HL 3.6,
HL 7.43
Porte, Xavier DY 17.7
Portenkirchner, Engelbert O 60.5
Portman, James R BP 23.1
Porz, Lukas KFM 2.5
Pöschel, Thorsten DY 7.4, DY 7.9
Posselt, Dorte CPP 17.54
Posske, Thore O 7.1
Post, Matthias BP 3.8
Postolachi, Cristina •DS 12.9
Potapov, Pavel O 49.5
Potemski, Marek HL 33.2
Potjan, Roman •TT 57.8
Potorochin, Dmitrii HL 36.2
Potten, Janik •MA 33.1
Potthoff, Michael MA 23.30, MA 27.2,
MA 40.13, TT 59.7
Poudel, Bhuwan •CPP 35.54
Poudel, Manisha MM 5.1
Poul, Marvin MM 14.3, MM 14.4,
MM 32.1, •MM 32.2
Poulopoulos, Panagiotis MA 23.55
Poumirol, Jean-Marie O 18.3
Pounot, Kevin BP 11.46
Pournaki, Armin SOE 7.2, •SOE 8.1
Povarov, Kirill •TT 45.2
Povstugar, Ivan MM 22.5
Powalla, Lukas DS 10.3
Powell, Annie K. MA 24.5, MA 24.6
Pozo, Óscar •HL 18.6
Prabhu, Mahesh O 36.2
Prada, Claire MM 23.21
Prada, Marta TT 35.7
Prager, Michael TT 16.8
Prajapati, Gulloo Lal •MM 23.35
Prakash, Arun •MM 36.1
Pramanik, Krishnanjan MM 6.4
Prampolini, Giacomo O 87.3
Pranav, Manasi •CPP 11.5
Pranjic, Daniel TT 42.1
Prasai, N. MA 33.6
Pratap Singh, Sunil •BP 2.8
Prats, Hector O 52.7
Pratzer, Marco O 77.2
Preda, Amanda Teodora DS 12.43,
•HL 16.2, •TT 24.2
Predeschly, Benjamin CPP 51.4
Prehl, Janett •DY 45.1
Preis, K. •MA 8.3, MA 34.38
Preobrajenski, Alexei O 41.2, O 56.8,
O 93.8
Pres, Sebastian O 80.4
Pressacco, Federico O 37.8
Pretsch, Thorsten CPP 8.8, DY 29.3
Preuß, Oliver •KFM 2.3
Preziosi, Daniele •TT 44.4
Priante, Fabio MM 12.14, •O 6.8
Pries, Julian DS 16.5
Priessnitz, Tim •HL 48.9, TT 3.5
Primešnič, Andreas BP 28.41
Primetzhofer, Daniel O 13.2
Prince, Kevin C. O 28.5, O 29.1,
O 55.2, O 81.11
Princippi, Emiliano DS 4.1, DS 12.6
Prinz, Eva O 37.10, O 70.4, O 80.1
Prinz, Günther HL 1.10
Prishchenko, Danil TT 46.10
Pritzl, Stefanie BP 5.6
Priya, Priya HL 10.10
Priya, Ravi •O 28.2
Priyadarshi, Shekhar HL 17.1
Prizak, Roshan BP 29.4
Probst, Nathalie TT 58.25, •TT 66.7
Procházka, Michal O 18.7
Prodan, Lilian •MA 18.5, •MA 23.65,
MA 44.2
Prokhenko, O. MA 40.58
Prokofiev, Andrey MA 9.7
Prokop, N. HL 23.1
Pronin, A. V. •TT 6.5, TT 6.10
Pronin, Artem V. HL 17.2
Prost, Tobias •O 23.6
Protik, Nakib HL 20.6, •MM 8.5,
O 35.6
Prots, Yurii TT 30.13
Protzer, Ulrike O 57.5
Prucnal, Sławomir DS 14.2, HL 5.5,
HL 16.1, HL 18.8, HL 34.2, HL 36.2,
TT 24.1
Pscherer, André •TT 25.4
Psota, Pavel KFM 4.10
Ptaszyński, Krzysztof •DY 34.3
Ptok, Andrzej HL 21.2
Pu, Weiwen O 66.8
Pudell, Jan-Etienne HL 33.61,
MA 23.70, MA 40.66, •MM 12.3,
O 37.7
Puente-Orench, I. MA 44.3
Puente-Orench, Ines MA 44.8
Puglisi, Andrea DY 32.6
Pulcinski, L. MA 40.53
Pulda, Nike SOE 19.1
Puliappara Babu, Priyana •TT 37.7
Pulkin, Artem TT 8.8
Pulkkinen, Aki •TT 21.1
Pundt, Astrid MM 12.7, MM 23.13,
MM 23.32, MM 27.1, MM 27.9
Punke, Maik •MM 25.1
Puntel, Denny •O 16.3, O 19.2, O 19.4,
O 34.8, O 34.10
Puphal, Pascal •TT 44.8, TT 46.3
Purcell, Thomas A. R. •MM 31.6
Puschig, Peter O 19.3, O 22.5,
•O 34.6
Pusterla, Julio BP 26.8
Putra, Miftahussurur Hamidi •CPP 28.1, •TT 32.1
Puttison, Yuttapoom DS 16.6
Pütz, Sebastian •SOE 4.11
Putzke, Carsten TT 3.9
Putzke, Mischa •BP 11.68
Puy, Andreu •BP 22.4
Puy, Johannes MA 3.7
Puzyrev, Dmitry DY 7.6, •DY 7.8,
DY 17.10, DY 46.6
Pyanzina, Elena •CPP 35.13,
CPP 35.41, DY 42.16
Pyka, Leon •MM 12.35
Pylypenko, Anastasiia O 63.1
Pylypenko, Anton •CPP 17.53,
CPP 29.7
Pylypovskiy, Oleksandr DS 6.1,
MA 31.7, MA 43.5, MA 50.3
Pylypovskiy, Oleksandr V. •MA 11.4,
•MA 18.6, MA 49.8
Qahosh, Mohammed O 30.3, •O 59.3,
O 67.4
Qaiumzadeh, Alireza •HL 11.3,
•MA 8.11, MA 29.3, •MA 39.5,
•TT 15.3
Qamar, Minaam •MM 39.5
Qdemat, Asmaa DS 14.6, MA 5.6,
O 42.12
Qi, Haoyuan DS 3.1, DS 4.4
Qi, Jing •MA 14.2, MA 14.6, O 28.8
Qi, Peng CPP 35.25
Qi, Ruoxuan •CPP 35.16
Qi, Yingpeng SYUE 1.2
Qi, Yinpeng O 16.7
Qi, Yubo O 36.3
Qian, Jianqiang O 66.6
Qian, Tiama MA 10.6, TT 12.6
Qian, Yan-Jun DY 21.3
Qiang, Yu MA 10.4, TT 12.4
Qiang, Yun CPP 35.26
Qiao, Junfeng •MM 19.4
qiao, yulong •DY 43.1
Qin, Jin O 58.9
Qin, Shuyu KFM 1.8
Qiu, Cheng-Wei DY 21.3
Qiu, Jiajia •DS 12.51, HL 7.58,
•MM 42.10
Qiu, Zijie MA 23.53, O 32.8
Qu, Bin BP 25.3
Quade, Robin •TT 59.7
Quan, Jingkai •HL 40.4, •O 79.4
Quandt, Eckhard MA 40.48
Quasebarth, Gwendolyn •DY 18.2,
MA 16.3
Queißer, Friedemann DY 43.13
Queisser, Friedemann DY 25.9,
TT 33.9, TT 38.12
Quellmalz, Patricia MA 23.41
Quenzel, Thomas CPP 28.9, O 58.2,
TT 32.9
Qui, Caihao MM 26.4
Quintana, Mikel •MA 46.9, MA 50.3
Quintana-Cataño, César Augusto •BP 23.4
Qun, Jin HL 29.10
R. Pakuszewski, Kevin MA 39.3
R. T. Zahn, Dietrich HL 45.7
Raab, Klaus •MA 23.2, MA 23.3,
MA 29.1
Raabe, Dierk MM 32.3, MM 36.4
Raabe, Jörg MA 43.3, MA 48.5
Raabgrund, Andreas O 56.1, •O 56.4,
O 67.3
Raake, Niklas DY 44.17
Rabe, Anna •MA 36.1
Rabe, Martin •DS 17.1
Rabl, Peter •HL 3.2
Raccanelli, Andrea O 21.2
Rachel, Stephan •SYTS 1.5, TT 36.8,
TT 38.2, •TT 48.2, TT 63.9
Radetinac, Aldin DS 12.36
Radić, Dražen MM 28.1
Rädler, Joachim BP 11.71, BP 26.5,
BP 26.6, BP 26.8, •AIW 2.1
Rädler, Joachim O. BP 11.23,
BP 28.29, BP 31.5
Rädler, Joachim Oskar BP 28.49
Radmacher, Manfred BP 31.4
Radnik, Jörg BP 11.8, BP 11.9, BP 17.9
Radonjić, Miloš MA 27.3
Radons, Günter DY 4.7, DY 18.3,
DY 45.5
Radtke, Guillaume TT 43.18
Radu, F. O 47.3
Radu, Florin MA 19.4, MA 19.6,
MA 48.4
Raeliarjaona, Aldo KFM 1.3
Rafeek, Rafna DY 44.16
Rafiezadeh, Shohreh •HL 26.8,
•O 53.8
Ragulskaya, Anastasia BP 11.46,
•DY 37.1
Rahali, Radia O 5.6
Rahe, Philipp •O 87.8
Rahimzadeh, Amin •CPP 3.1,
CPP 35.56
Rahmann, Hendrik DY 37.1
Rahn, M. MA 12.5
Rahn, Marein MA 2.7, •TT 4.1, TT 23.3
Rai, Gautam TT 35.5, •TT 35.6
Raif, Patrick TT 20.1
Raina, Abhinav •O 70.9
Raison, Philipp TT 9.5
Raith, Johannes BP 10.6
Raj, Manthan BP 11.43
Rajala, Patrick HL 12.3
Rajan, Adithya MA 31.2, •MA 31.5
Rajan, Akhil O 30.1
Rakholiya, Bhavadip Bharatbhai MA 38.4
Rakytá, Péter •HL 14.2
Ram, Panch •TT 53.1
Ramakrishna, Kushal MM 12.11,
MM 31.8
Ramchandani, Sagar •MA 33.8
Ramermann, Daniela •KFM 3.3,
MA 23.42
Ramesh, Prashanth BP 7.7, DY 10.7
Ramezani, Mehdi O 51.3

Author Index

- Ramin, Golestanian BP 24.12, DY 38.12
- Ramirez Alarcon, Roberto .. BP 28.16
- Ramirez, Ivan CPP 1.11
- Ramirez, Omar HL 38.5
- Ramlow, Lukas •BP 11.62
- Ramming, Philipp •CPP 17.33
- Rammler, Manuel BP 27.1
- Rammohan, Sidharth •DY 55.11, •TT 67.11
- Ramos, Manuel HL 7.7
- Ramos, Osyvanny MM 33.5
- Ramos, Rafael MA 31.2, MA 31.3
- Rampp, Markus HL 13.3, O 17.3
- Rampp, Michael A. •DY 9.1, •DY 43.3
- Ramsauer, Bernhard •O 77.5
- Ramshaw, Brad TT 37.1
- Ramsteiner, Manfred DS 12.22
- Ran, Yan •KFM 10.10
- Rana, D.S. DS 14.7
- Rana, Dhanvir Singh MM 23.35
- Ranawat, Yashasvi O 87.8
- Rancic, Milos PLV X
- Rani, Deepika •MA 37.2
- Rani, Renu HL 22.2, •TT 25.1
- Ranjith, K. M. TT 42.15
- Rao, Jing MM 27.3
- Rao, Peng •TT 65.2
- Raoufi, Mohsen •SOE 19.5
- Raptakis, Antonios MM 3.10
- Rasch, Florian MA 44.8
- Raschke, Markus •O 75.1
- Rashidi, Yazdan •BP 8.3
- Rasim, Karsten O 11.8, O 23.2
- Rasmussen, Torbjørn HL 33.27
- Rasouli, Hamid Reza •DS 1.2
- Rasper, Fabian DS 12.21
- Rastelli, Armando HL 7.65, HL 7.66, HL 24.2, HL 24.4, HL 24.5, O 91.1
- Rastelli, Gianluca TT 20.9
- Rata, Aurora Diana MA 23.63
- Rata, Diana A. MA 17.4
- Ratcliff, Laura •HL 40.3, •O 79.3
- Rath, David •O 6.1
- Rathgeber, Silke BP 19.3, CPP 41.3
- Rathje, Christopher MA 23.56
- Raths, Miriam O 19.7
- Ratschinski, Ingmar HL 16.5, TT 24.2.5
- Ratschmeier, Björn •O 60.7, •O 69.6
- Ratschow, Aaron D. •CPP 44.10
- Ratzenberger, J. KFM 14.1
- Ratzenberger, Julius •KFM 6.8, KFM 6.20, KFM 6.35, KFM 14.2
- Rau, Uwe DS 11.2, HL 7.38
- Rauch, Darius BP 25.6
- Rauch, Philipp BP 23.12
- Rauch, Tomáš •HL 5.4
- Rauland, Emma CPP 17.33
- Rauls, Eva O 36.10
- Rauls, Simon •MA 9.10
- Rausch, Konstantin •HL 7.26
- Rausch, Roman •TT 45.6
- Rauschenbach, Stephan BP 11.41, BP 11.45, BP 21.3, BP 28.14, O 26.1, O 26.5, O 66.4
- Ravankhah, Mahboobeh O 42.3
- Ravelosona, Dafine MA 17.2, •MA 25.2
- Ravishankar, Rachappa •MA 23.35, MA 43.4, MA 48.6
- Rawle, Jonathan CPP 45.3
- Ray, Avijeet •MA 7.11, •MA 31.8
- Ray, Sayak •TT 38.4
- Ray, Soumya Jyoti MA 21.8
- Razavi, Atieh CPP 3.1, •CPP 35.56
- Razumovskiy, Vsevolod MM 9.5, MM 37.6
- Razzaq, Abdus Samad O 75.8
- real, José Antonio MA 19.5
- Reale, Stefano O 15.12
- Reb, Lennart DS 11.3
- Reb, Lennart K. CPP 17.30, CPP 51.1
- Reb, Lennart Klaus •CPP 51.4
- Reber, Simone BP 11.67, BP 25.7
- Recalde, Oscar MA 3.4
- Recati, Alessio TT 45.10
- Recher, Patrik TT 31.1, TT 53.4
- Reck, Kristian CPP 17.4, CPP 29.8
- Reddy, V. R. MA 5.1
- Redlin, Harald O 16.1
- Reecht, Gael O 7.2, O 7.4, O 20.6, O 22.6
- Reehuis, Manfred MA 44.9
- Refaely-Abramson, Sivan HL 22.7, •O 1.1
- Refvik, Nils O 92.1
- Reginka, Meike KFM 6.34, MA 5.4, MA 40.31
- Reglinski, Katharina BP 21.2, BP 28.9
- Regnat, Alexander MA 13.6, MA 13.8, •MA 25.5, TT 3.8, TT 4.13, TT 19.6, TT 19.8
- Regnault, Nicolas MA 10.2, TT 12.2
- Reh, Moritz •DY 2.9, •TT 2.9, TT 58.13
- Reh, Roman •CPP 35.11, CPP 35.12
- Rehberg, I. BP 11.7
- Rehberg, Ingo •DY 48.2, •TT 55.2
- Rehfeldt, Florian BP 15.5, BP 28.8, BP 28.34, BP 28.39, BP 28.41
- Rehm, Jana •DS 8.5
- Rehm, Oliver •DS 12.5
- Rehman, Uzair MM 33.3
- Reich, Stephanie O 16.7
- Reich, Veronika •MM 36.6
- Reichardt, Sven HL 25.6, •HL 34.9
- Reiche, Christopher F. MA 32.2
- Reichel, Felix •BP 31.3
- Reichelt, Matthias HL 35.4
- Reichenberger, Sven MM 40.10
- Reichert, Joachim O 11.3, O 14.4
- Reichhardt, Rilana •HL 35.3
- Reichlova, H. •MA 41.2
- Reichlová, Helena MA 4.12, MA 4.14, MA 23.60, MA 40.63, MA 40.64, TT 7.12, TT 7.14
- Reichmann, Alexander MM 9.1, •MM 9.5
- Reichmann, Felix HL 37.6
- Reichmann, Jakob •BP 21.9
- Reichmann, Klaus KFM 6.39
- Reifenberger, A. TT 58.4
- Reifenberger, Andreas TT 43.31, TT 57.25, TT 66.7
- Reinhardt-Szyba, Maria BP 11.41
- Reijnders, Koen O 30.9
- Reiker, Tobias •O 37.13
- Reimann, Andre O 67.8
- Reimer, Max •O 70.9
- Reimers, Sonka MA 18.1
- Rein, Constantijn •DY 42.11
- Reina Gálvez, Jose O 15.7
- Reina-Galvez, Jose •O 15.8
- Reinalter, Luis Frieder DY 16.4
- Reindl, Thomas TT 59.13
- Reineke, Bernhard HL 33.30
- Reineke, Sebastian CPP 17.13, CPP 26.2, CPP 43.10, DS 10.2
- Reinert, Friedrich O 22.7, O 59.3, O 65.5, O 67.3, O 67.4, O 67.5, O 74.4, O 94.2, O 94.6, O 94.9, TT 9.7
- Reinert, Frierich O 30.5
- Reingruber, Adrien •TT 29.11
- Reinhard, Friedemann BP 28.55, DS 12.23, HL 50.1, MA 23.41
- Reinhardt, Christoph VA 1.1
- Reinhardt, Simon •TT 20.8, TT 27.5, TT 58.30
- Reinig, Peter KFM 7.7
- Reinke, Philipp HL 50.4
- Reinken, Henning •DY 42.1
- Reinold, Anneke HL 17.10, TT 6.7, •TT 59.18
- Reinschmidt, Malte TT 39.5
- Reis, Ricardo MA 39.2
- Reisch, Tobias •SOE 23.4
- Reise, Franziska BP 1.11
- Reiser, Andreas TT 43.30, TT 43.31, TT 43.32, TT 58.25, TT 66.7
- Reiser, Anita BP 26.5
- Reiser, Mario DY 37.1
- Reiser, Patrick MM 31.3
- Reisinger, Thomas TT 39.3, TT 54.1
- Reiss, Günter DS 12.47, MA 23.59, MA 40.49, MM 12.30
- Reiss, Pascal •TT 51.5
- Reitenbach, Julija CPP 8.4, CPP 35.43, CPP 53.4
- Reiter, Doris HL 24.2, HL 24.4, HL 24.5
- Reiter, Doris E. HL 7.39, HL 7.61, •HL 35.2, HL 35.4
- Reith, Heiko MM 23.5
- Reithmaier, Johann P. KFM 8.4, KFM 8.5
- Reithmaier, Johann Peter CPP 35.52, HL 16.6, KFM 6.12, KFM 6.34, TT 24.6
- Reitner, Matthias TT 65.4, TT 65.8
- Reitzenstein, S. HL 43.6
- Reitzenstein, Stephan HL 7.52, HL 7.53, HL 8.2, HL 12.2, HL 12.7, HL 22.4, HL 24.3, HL 33.24, HL 33.47, HL 33.48, HL 33.49, HL 33.50, HL 43.3, HL 43.5, HL 49.6, O 91.1
- Reitzenstein, Stephen HL 33.36,
- HL 33.37
- Reitzig, Sven KFM 6.6, KFM 6.35, KFM 14.2, MA 23.60
- Rellinghaus, B. CPP 17.2, MA 12.5
- Rellinghaus, Bernd MA 12.3, MA 23.60
- Remesh, Vikas HL 7.39, HL 24.2, HL 24.4, HL 24.5
- Remini, Khalil •CPP 44.5
- Remlein, Benedikt •DY 40.2
- Remškar, Maja TT 16.7, TT 53.10
- Ren, Jiajun DY 25.6, TT 33.6
- Ren, Zengyao MA 5.5
- Ren, Zhe DY 56.7
- Ren, Ziyuan BP 16.3
- Renard, Vincent TT 61.5
- Renaud, Gilles O 93.6
- Renger, Michael TT 39.7, •TT 49.1, TT 58.7, TT 58.10, TT 58.20, TT 66.6
- Renger, Roman •BP 23.12
- Renner, Lars •BP 6.4
- Renucci, Pierre MA 32.6
- Renz, Anna-Lena HL 38.7, O 96.7
- Renzi, Enrico M. O 58.8
- Renzi, Roberto De MA 10.5, TT 12.5
- Reparaz, Juan Sebastian HL 21.3
- Repp, Jascha O 15.1, O 22.1, O 55.3, •O 87.1
- Resch, Christoph •MA 13.8, •MA 26.2, TT 3.8, TT 10.5, •TT 19.8
- Resch, Lucas TT 5.13
- Resch, Miriam •TT 39.2
- Restuccia, Paolo O 4.1
- Retamal, B.J. BP 11.12
- Rethfeld, Barbel MA 8.4, MA 31.3, MA 46.2, O 8.4, O 16.6, O 80.1, O 84.2, TT 56.2
- Rethfeld, Bärbel MA 8.10, MA 40.8, MA 46.7
- Reticioli, Michele •O 72.3
- Retsch, Markus O 49.2
- Rettig, Laurenz PSV X, •SYUE 1.3, MA 8.7, MA 46.4, MA 46.13, O 8.9, O 16.5, O 16.7, O 84.3, O 95.1, O 95.3, TT 56.3, TT 68.1, TT 68.3
- Retzbach, Sebastian •BP 11.46
- Reuban, Anicha •MM 22.5
- Reus, Manuel CPP 52.5
- Reus, Manuel A. CPP 13.8, CPP 17.31, CPP 17.44, CPP 35.43, •CPP 51.1, MA 38.5
- Reuss, Andreas •DS 12.37
- Reuter, Dirk HL 7.45, HL 7.52, HL 7.53, HL 33.35, HL 37.2, HL 42.6
- Reuter, Karsten CPP 2.9, CPP 35.38, CPP 44.11, DY 46.2, HL 40.7, MM 3.3, MM 3.7, MM 5.9, MM 5.10, MM 6.2, MM 6.3, MM 8.4, MM 8.6, MM 8.7, MM 19.2, MM 19.3, MM 31.3, MM 31.10, MM 36.3, MM 39.6, O 3.4, O 3.7, O 6.9, O 11.1, O 39.3, O 52.6, O 52.7, O 52.8, O 60.8, O 69.2, O 78.2, O 78.3, O 78.4, O 78.5, O 79.7, O 83.2, O 86.1, O 86.2, O 86.6, O 86.8, O 93.6, O 95.6, O 96.1, O 96.3, O 96.8, TT 68.6
- Reuther, Cordula BP 8.5, •BP 23.9
- Reutter, Eric HL 7.62
- Reutzel, Marcel •O 34.4, O 57.2
- Revuelta-Losada, Jorge SYGM 1.5
- Rex, Stefan TT 59.15
- Rey, Felix BP 23.1
- Reynaud, Serge CPP 57.3
- Rezaei, Majid •CPP 35.49
- Rezai, Kristine DY 25.12, TT 33.12
- Rezek, Bohuslav CPP 36.9
- Rhein, Benoît MA 36.2
- Rheinfrank, Erik •O 92.10
- Rhodes, Luke TT 37.12
- Rial, Javier MA 4.12, TT 7.12
- Ribca, Iuliana CPP 29.5, CPP 35.1, •CPP 58.2
- Ribeiro de Assis, Ismael •MA 35.1
- Ribeiro, Pedro DY 55.7, TT 67.7
- Ribelles Pérez, Valèria •DY 45.8
- Rica, Raul A. •SYFP 1.4
- Ricci, Matteo HL 13.6, O 17.6
- Riccus, Felix •O 52.6
- Rich, Andrea M. MM 25.2
- Richardson, Jerem DY 9.12
- Richardson, Jeremy O. DY 32.10
- Richarz, Leonie •KFM 1.2, KFM 4.5
- Richert, Claudia MM 42.7
- Richter, Carsten HL 37.6
- Richter, Christine O 18.7
- Richter, Claudia DS 12.5
- Richter, D. TT 58.2
- Richter, Johannes MA 40.24, TT 23.9, TT 23.10, TT 30.13
- Richter, Jonas TT 43.20, TT 43.21
- Richter, Julia •O 26.2
- Richter, Klaus DY 6.8, DY 25.8, DY 43.11, DY 48.9, DY 55.4, O 8.6, O 37.6, TT 5.13, TT 17.7, TT 33.8, TT 55.9, TT 59.3, TT 62.6, TT 67.4
- Richter, Kornel MA 23.7
- Richter, Martin •DS 15.2
- Richter, R. •BP 11.7
- Richter, Reinhard DY 7.2, DY 57.7, DY 57.8
- Richter, Tilman •CPP 52.4
- Richter, Tobias O 63.1
- Rickert, Lucas •HL 37.5
- Rickhoff, Clara •BP 11.34
- Rico, Felix •BP 23.1
- Rieche, Antonia MA 17.4, •MA 23.63
- Riedel, Alexander O 8.6, •O 37.6, TT 62.6
- Riedel, Lukas •MM 42.4
- Riedel, Robert HL 48.2
- Riedinger, Andreas CPP 2.12
- Riedl, Kira TT 29.5
- Riedmiller, Nikolai MM 23.31
- Riegel, Elisabeth O 97.2
- Rieger, Heiko BP 2.10, BP 7.2, BP 9.10, DY 10.2, DY 42.10
- Rieth, Tim HL 7.4
- Rietz, Frank •DY 7.5
- Rieu, Jean-Paul BP 22.10
- Rigamonti, Santiago HL 40.2, O 79.2
- Righi, Maria Clelia O 4.1
- Rignanese, Gian-Marco KFM 10.7
- Rigoni, Aaron MM 28.7
- Riley, Drew B. •CPP 1.10
- Rimek, F. HL 7.56
- Rimek, Fabio •HL 7.46, HL 24.10, HL 24.12
- Rimmbach, Christian BP 28.55
- Rimmler, Berthold H. •MA 31.6
- Rinaldi, Matteo •MM 29.4
- Rinaldin, Melissa •BP 30.8
- Ringel, Zohar •TUT 1.2, •DY 1.2, •DY 11.3, •TT 1.2, •TT 13.3
- Rings, Thorsten DY 45.3
- Rinke, Patrick HL 20.7, O 35.7
- Risch, Marcel O 92.7
- Rishabh, Rishabh CPP 17.14
- Riss, Alexander O 11.6, O 11.9, •O 21.6
- Ristau, Mariam BP 4.4, •BP 28.23
- Ritort, Felix BP 23.8
- Ritschar, Jana BP 25.8, BP 28.5
- Ritschel, Tobias MA 40.20, TT 23.3, •TT 51.6
- Ritter, Clemens MA 44.6
- Ritter, Konrad HL 4.9
- Ritterhoff, Christian O 60.3, •O 67.6
- Ritzert, Philipp •CPP 13.10
- Ritzinger, P. MA 41.2
- Ritzinger, Philipp MA 40.64
- Riva, Michele O 92.5, O 92.10
- Rivera-Arrieta, Herzain I. •O 52.5
- Rivero Arias, Melissa HL 18.2
- Rivetti, Marco BP 28.37
- Rivière, Charlotte BP 22.10
- Rivoirard, Sophie •MA 25.3
- Rizzi, Matteo DY 43.12, MA 40.26, TT 5.4, TT 31.5, •TT 45.10
- Robert, C. O 47.7
- Robert, Cédric MA 32.6
- Robert-Philip, Isabelle MA 32.6
- Roberts, Connor DY 34.4
- Robertson, Elizabeth •DY 17.7, DY 22.4, DY 46.7
- Robin, Paul •BP 22.3
- Robinson, Joshua BP 11.61
- Robinson, Tom BP 6.3
- Robles, Roberto O 3.1, O 33.7, O 46.3
- Robredo, Iñigo MA 9.3, •MA 10.2, •TT 12.2
- Rocabert, Ulysse •MA 3.11
- Roca-Cusachs, Pere BP 4.5, BP 30.4
- Rocco, Rodolfo DS 12.28
- Roche, Léo HL 33.36, HL 33.37, HL 33.48, •HL 33.50
- Rochford, Luke A. O 93.5, O 93.8
- Rockstuhl, Carsten CPP 26.3, HL 7.15
- Roddatis, Vladimir DS 12.46
- Rodek, Aleksander HL 33.18
- Rödel, Jürgen KFM 2.3, KFM 2.5, KFM 2.6
- Rödel, Maximilian CPP 17.8, •DS 3.2, O 58.5
- Rodemund, Tom •DY 43.2
- Roden, Stephanie •MA 40.8

Rodenbücher, Christian *KFM 2.1
 Röder, Christian HL 17.4, O 26.2
 Röder, Simon TT 10.1
 Rodrigues, Davi MA 40.4
 Rodrigues, Ines C. TT 39.1
 Rodríguez, Alberto *DY 43.5,
 *DY 48.6, *TT 55.6
 Rodríguez, Anne HL 10.10
 Rodríguez Diaz, Manuel MM 11.4
 Rodríguez, Eusebio J. TT 60.1
 Rodríguez, Jose O 52.3
 Rodríguez, R. BP 11.10
 Rodríguez Sotelo, Sindy *O 82.5
 Rodríguez Sotelo, Sindy J. *DY 42.14
 Rodríguez-Barea, Borja *HL 42.2,
 HL 42.3
 Rodríguez-Fernandez, Angel MM 12.3
 Rodríguez-Hierro, Aurelio ... MA 50.1
 Rodt, Sven HL 7.52, HL 7.53, HL 12.2,
 HL 33.24, HL 33.36, HL 33.37,
 HL 33.47, HL 33.49, HL 43.5, HL 49.6
 Roede, Erik D. KFM 4.5
 Roeper, Matthias *KFM 13.7
 Roessler, Johannes O 57.5
 Roessler, Sahana *TT 46.2
 Roessler, Ulrich K. MA 18.6
 Rogal, Lukasz MM 40.8
 Rogalev, A. MA 48.3
 Rogalev, Andrei DS 10.1, MA 3.3,
 MA 42.7
 Rogero, C. O 47.3
 Rogero, Celia O 36.5, O 56.5
 Rogers, Bradley A. CPP 53.2
 Rogers, Sarah BP 19.2, CPP 41.2
 Roghani, Mehran *CPP 13.5
 Rogić, Luka BP 15.5
 Roh, Seulki HL 17.2, MA 9.9
 Rohleder, Darius MM 23.13
 Rohlfing, Michael HL 18.10, HL 22.8,
 HL 31.8, O 18.6, O 30.8, O 61.8
 Rohling, Niklas *MA 4.6, *TT 7.6
 Rohrbeck, Pascal *CPP 51.3
 Rohrer, Jochen MM 29.5
 Rohringer, Georg *TT 17.2, TT 29.7
 Roichman, Yael DY 27.10, DY 27.11
 Roitgeui Alonso, Martin TT 63.10
 Rojas, Javier MM 22.1
 Rojas, Pablo *BP 13.5
 Rojas, S. BP 11.10
 Rojas-Nunez, Javier *MM 26.5
 Rojer, Markus KFM 6.16
 Roland, Nagy HL 33.19
 Roldán Cuenya, Beatriz O 60.8
 Roldan, Edgar DY 32.1
 Roleder, Krystian KFM 4.7
 Rolf, Daniela O 21.1
 Rolland, Joran DY 32.9
 Rolley, Étienne CPP 52.2, MM 23.27
 Romanczuk, Pawel BP 11.64, BP 22.4,
 SOE 16.1, SOE 16.3, SOE 16.5,
 SOE 19.5
 Romaner, Lorenz *MM 9.1, MM 9.5,
 MM 37.4, MM 37.6
 Romankov, Vladyslav *MA 19.1,
 MA 40.32, O 2.7
 Romano, Jacopo *DY 23.3
 Romanova, Alena MA 2.3
 Romanyuk, Oleksandr HL 7.8, HL 7.10
 Romeis, Dirk CPP 13.5, *CPP 13.6
 Romeo, Michelangelo O 7.9, O 72.4,
 O 76.2
 Romer, Felix BP 11.26
 Römer, Friedhard HL 28.4
 Römer, Rudolf DY 46.3
 Römer, Rudolf A. DY 17.3, DY 22.5,
 DY 43.8, DY 43.10, HL 33.46
 Römer-Stumm, Malte MA 23.7
 Ronca, Enrico CPP 45.5
 Ronceray, Pierre *DY 32.5
 Rondoni, Lamberto DY 56.10
 Rong, Kexiu DY 21.3
 Rönkkö, Jami *TT 54.7
 Ronning, Carsten DS 12.45, HL 7.18,
 HL 7.54
 Rønnow, Henrik M. MA 12.6
 Ronsin, Olivier CPP 18.2, CPP 51.5
 Rontani, Massimo *HL 22.6
 Rööm, Toomas TT 59.18
 Roondhe, Vaishali O 14.3
 Roos, Christian TT 22.13
 Roos, Tobias O 25.2
 Roosen-Runge, Felix BP 27.8
 Ropers, Claus *PLV V, HL 10.9,
 HL 48.5, O 8.1, O 8.5, O 34.5, O 70.2,
 O 75.8, O 80.2, O 80.6, O 83.4, O 83.6,
 O 83.8
 Roß, Gina *CPP 35.51

Rosa, Bárbara HL 8.2, *HL 22.4,
 HL 33.48
 Rosa, Priscila MA 39.2, MA 40.37
 Rosado, Eric Kramer MM 12.14
 Rosander, Petter *MM 23.34
 Rösch, Roland CPP 17.29
 Rose, Hendrik *HL 35.4
 Rose, Jonas *HL 51.1
 Roseker, Wojciech *DY 56.7
 Rosen, Johanna O 11.6
 Rosenauer, Andreas HL 14.7
 Rosenberg, Margaret *CPP 57.12
 Rosenberger, Paul *MA 17.6, MA 50.5
 Rosenfeldt, S. BP 11.7
 Rosenow, Bernd DY 2.5, TT 2.5
 Rosenpichler, Ursula SOE 19.1
 Rosenzweig, Philipp O 64.6
 Roser, Oliver *CPP 13.2, *MM 12.6
 Rosławska, Anna *O 72.4, O 76.2
 Rößler, Ulrich K. MA 27.7, TT 29.3
 Roßnagel, K. O 30.4
 Roßnagel, Kai O 19.5, O 19.6
 Rosner, H. TT 46.8
 Rösner, Harald MM 28.1, MM 28.7
 Rosner, Helge MA 27.1, MA 31.4,
 *TT 30.12, TT 30.13
 Rösner, M. O 42.2
 Rösner, Malte HL 31.2, O 61.2,
 TT 27.7, TT 63.3
 Rosowski, Frank O 78.1
 Ross, Gina O 60.7, O 69.6
 Ross, Stewart MA 9.7
 Ross, Ulrich DS 14.3
 Rossa, Lutz TT 58.29
 Rossell, Marta D. KFM 4.2
 Rosselló, Juan Manuel DY 18.7
 Rossi, Enrico TT 63.2
 Rossi, Mariana DY 17.9, HL 6.7,
 HL 13.3, HL 40.1, HL 40.6, O 9.7,
 O 17.3, O 55.9, O 79.1, O 79.6
 Rossi, Tuomas O 76.8
 Rossini, Mirko *DY 9.8, DY 9.10
 Rössle, Matthias DS 12.56, HL 33.61
 Rossnagel, K. MM 12.1, MM 26.8
 Rossnagel, Kai DS 2.2, DS 6.3, O 7.4,
 O 22.7, O 83.8, TT 9.7, TT 35.7
 Rossow, Uwe HL 33.41, HL 33.43,
 HL 51.2, HL 51.8
 Rost, Andreas TT 37.1
 Rost, Andreas W TT 37.11
 Rost, Marcel *O 36.2, *O 60.9, O 96.6
 Rostami, Habib HL 35.5
 Rostami, Mohammadreza *O 32.2,
 *O 40.2
 Rostami, Peyman CPP 44.1
 Roth, Friedrich TT 37.9
 Roth, Johannes *MM 8.3, MM 12.21,
 MM 12.22, MM 12.32, MM 12.33
 Roth, Stephan CPP 17.16, CPP 19.7,
 CPP 35.28, DS 11.3
 Roth, Stephan V. BP 19.1, *BP 19.2,
 CPP 17.26, CPP 17.31, CPP 17.35,
 CPP 17.44, CPP 29.2, CPP 29.5,
 CPP 29.8, CPP 29.10, CPP 35.1,
 CPP 35.2, CPP 36.6, CPP 36.8,
 CPP 37.2, CPP 41.1, *CPP 41.2,
 CPP 51.1, CPP 52.5, CPP 53.6,
 CPP 56.2, CPP 58.2, DS 12.34,
 MA 38.5, O 57.5
 Roth, Stephan Volkher CPP 26.1
 Roth, Tobias Alexander *DY 4.5
 Rothenbach, Nico MA 8.7
 Rothenberg, Steffen-Rambert O 10.2
 Rothhardt, Daniel *O 42.5
 Rothkirch, André CPP 56.2
 Rothmayr, Florian HL 17.5
 Rothörl, Jan CPP 12.2, *MA 2.2,
 MA 12.8, MA 23.2, MA 23.6, MA 29.1,
 MA 47.2
 Rothstein, Alexander HL 33.12, O 4.3,
 O 93.3
 Rott, Karsten MA 40.49
 Röttger, Adriana *HL 7.37
 Rottler, Jörg MM 13.1
 Rottler, Jörg CPP 12.3
 Rotzinger, Hannes TT 58.13, TT 58.14,
 TT 58.15
 Rougemaille, Nicolas MA 32.6
 Roupcová, Pavla MM 19.1
 Rousseau, Ian HL 36.6
 Rout, Pares C. MA 7.11, MA 31.8
 Rouzbahani, Rozita HL 29.10
 Rouzegar, Reza MA 22.2
 Rovenská, Katarína O 14.9
 Rovazzi, Mauro MA 42.7
 Rowen, Julien O 81.7
 Roy, Basudev CPP 35.24

Roy, Debesh MM 23.1
 Roy, Shilpi TT 45.7
 Roy, Sresta CPP 35.24
 Roychowdhury, Subhajt *MA 3.6,
 MA 44.1, MM 6.10
 Rozek, Piotr HL 49.4
 Rozenberg, Marcelo DS 12.28
 Rozenblat, Celine SOE 11.5
 Rózsa, Levente MA 4.8, MA 14.1,
 *MA 46.3, TT 7.8, TT 8.6
 Ruan, Yating *DS 11.4
 Ruan, Zilin *O 2.4
 Ruano, Gustavo O 82.5
 Rüb, Matthias O 19.5
 Rüb, Michael DS 10.5
 Ruban, Andrei MM 40.3
 Rubeck, Jan CPP 17.56, CPP 29.2
 Rubek, Jan CPP 36.8
 Ruben, Mario MA 19.3, O 11.9, O 14.4
 Rubenbauer, Korbinian MA 23.76,
 *TT 18.2
 Rübhausen, Michael A. MA 38.5
 Rubio, Angel CPP 45.5, O 37.8,
 *TT 35.3, TT 64.7
 Rubrecht, Bastian TT 57.9
 Rubtsov, Alexey TT 17.2
 Rüdhardt, Baltasar DY 37.4
 Ruchka, Pavel *HL 50.2, MM 8.2
 Ruck, M. KFM 11.9, MA 40.58
 Ruck, Michael MA 44.6, O 94.2
 Rucker, Felix MA 13.6, TT 19.6,
 TT 42.6
 Rucker, Ulrich MA 5.6, O 42.12
 Rückriegel, Andreas MA 9.1,
 *MA 33.2, *TT 5.3
 Rudel, Stefan S HL 45.2
 Rudenko, Alexander *MA 7.8
 Rudge, Samuel TT 16.4, TT 16.17,
 *TT 60.5
 Rudolf, Rüdiger BP 11.26
 Rudolph, Jörg KFM 6.11
 Rudolf, Sophia BP 11.22, BP 26.2,
 *BP 26.5
 Rudzinski, Axel KFM 7.5
 Rudzinski, Joseph *BP 17.3
 Rudzinski, Joseph F. O 84.4, *O 95.6,
 O 95.10, TT 56.4, *TT 68.6, TT 68.10
 Rüegg, Christian MA 46.10
 Ruesing, Michael KFM 6.41
 Ruf, Leon *TT 27.8, TT 27.9
 Ruffenach, S. HL 17.8
 Ruffieux, Pascal O 20.10, O 33.3,
 O 75.5
 Ruffine, Valentin *BP 25.2
 Rühle, Rebecca *HL 12.1
 Ruhwedel, Moritz MA 18.1
 Ruiz Alvarado, Isaac Azahel ... O 67.1,
 *O 69.5
 Ruiz, Sandra MA 38.1
 Ruiz-Gomez, S. O 47.3
 Ruiz-Gómez, Sandra MA 40.3,
 *MA 50.1
 Ruiz-Lorenzo, Juan DY 49.2
 Rulands, Steffen BP 11.57, *BP 13.1,
 BP 22.6, BP 29.7
 Rule, Kirilly C. TT 29.2
 Runeson, Johan DY 9.12
 Runge, Erich DY 29.7, HL 7.8, HL 38.1,
 O 67.2
 Rungger, Ivan MA 27.3
 Runkel, Robert BP 17.7
 Ruocco, Giancarlo DY 42.12, DY 46.10
 Ruoko, Tero-Petri DS 16.6
 Ruotsalainen, Kari MA 8.9, MA 20.3
 Rupp, Christian HL 7.43
 Rupp, Daniela *O 83.1
 Rupp, Matthias MM 28.8, MM 36.7,
 O 85.11
 Ruppel, Artur BP 31.2
 Ruppert, Thomas MA 24.6
 Rurali, Ricardo HL 21.3
 Rusch, Regina *DY 44.8
 Rüschenbaum, Matthias BP 24.3,
 DY 38.3
 Ruseska, Ivana BP 31.1
 Rusing, M. KFM 6.9, KFM 14.1
 Rusing, Michael *KFM 3.1, KFM 6.6,
 KFM 6.8, KFM 6.15, KFM 6.18,
 KFM 6.19, KFM 6.20, KFM 6.35,
 KFM 13.7, *KFM 14.2, KFM 14.3
 Rübmann, Philipp MA 2.4, MA 10.1,
 MA 23.4, TT 8.2, TT 12.1, TT 63.11
 Rusponi, Stefano O 15.12
 Rusu, Marin HL 7.37, HL 25.10
 Rütter, Frederik O 78.1
 Rutledge, Gregory *CPP 19.1
 Rütten, Lisa *O 7.4

Ryabov, Artem DY 56.6
 Ryan, Paul T. P. *O 26.4
 Ryan, Paul TP O 36.6
 Ryazanov, Vasily *DY 44.9
 Rybak, M. DS 7.2
 Rybakov, Philipp MA 47.7
 Rybski, Diego *DY 49.4, *SOE 11.5
 Ryburn, Finlay MA 23.69
 Rye, Siheon *TT 61.2
 Ryndyk, Dmitry A. O 3.1, O 3.3
 Rysov, Rustam CPP 51.2, DY 56.7
 S. Christovam, Denise TT 9.3
 S. Nair, Akhil *MM 21.3
 S. Sankaran MM 40.8
 S. Wienhold, Kerstin CPP 35.19
 Saalwächter, Kay CPP 19.5,
 CPP 35.22, CPP 35.26, CPP 35.42
 Saavedra, D. *BP 11.10, *BP 11.11,
 BP 11.12
 Saba, Kiran HL 23.3, HL 23.6
 Sabass, Benedikt BP 11.49, BP 11.50,
 *BP 25.5, BP 28.45, BP 28.50
 Sabath, Franziska *O 60.1
 Sabik, Agata O 2.10
 Sabir, Bushra MA 37.4
 Sabitova, Aizhan MA 21.7, O 33.2
 Sächl, Radek O 26.7
 Sack, Achim DY 7.4, DY 7.9
 Sadanandan, Adithya *O 20.7
 Sadhukhan, Banasree MM 14.6,
 O 94.4
 Sadhukhan, Surasree *MM 14.6,
 *O 94.4
 Sadiq, Sarah BP 5.7
 Sadowski, Marcel *MM 5.3
 Sadrollahi, Elaheh *MA 23.13,
 *MA 40.20, MA 44.8
 Saedifard, Farzaneh CPP 18.1
 Saerbeck, Thomas CPP 8.4, MA 5.2
 Safari, M.R. *O 2.8
 Sagar, Saurbh MM 27.2
 Saggau, Christian DS 12.20
 Saggau, Christian N. *DS 5.2,
 DS 12.52
 Saglamkaya, Elifnaz *HL 2.4
 Sagnes, Isabelle HL 10.10
 Sagwal, Amandeep O 10.3, *O 43.8,
 O 70.10, O 76.5
 Saha, Bodhisattwa BP 11.41
 Saha, Prithwidip BP 23.1
 Sahebmoammadi, Leila *BP 11.14
 Sahinovic, Armin *O 67.7, *TT 50.5
 Sahlberg, Martin MA 47.6
 Sahle, Christoph TT 10.12
 Sahoo, Jaya Prakash DS 14.7
 Sahoo, Manaswini *MA 10.5, *TT 12.5
 Sailer, Sebastian *MA 20.2
 Saito, Yohei *TT 51.9
 Saitoh, Eiji MA 31.2, MA 31.3
 Saiz, Eduardo MM 4.7
 Sajid Raja, Arslan HL 10.9
 Sakai, Hironori TT 28.4
 Sakaki, Atsushi HL 23.3, HL 23.6
 Sakar, Baha *MA 32.3
 Sakong, Sung CPP 35.49, *O 3.6,
 *O 69.4
 Saksena, Aparna *MM 27.8
 Sakurai, Rihito TT 5.10
 Sala, Pablo *SYSD 1.5, TT 22.3,
 TT 38.1, TT 43.23, TT 43.24
 Saladina, Maria *CPP 1.11
 Salaita, Khalid *BP 5.1
 Salamon, Soma MA 19.3, MA 36.1,
 MA 36.2, O 51.4
 Salang, Cyril *HL 17.6
 Salazar Mejia, C. MA 42.4, MA 42.8
 Salazar-Mejia, C. MA 42.5, MA 42.10
 Salazar-Mejia, Catalina MA 23.18,
 *MA 42.6
 Salbreux, Guillaume BP 16.4
 Salditt, Tim BP 21.9, BP 21.12,
 BP 28.1, BP 29.3, DY 18.7
 Salemi, Leandro MA 4.8, TT 7.8
 Sall, Mamour HL 44.2
 Sallermann, Moritz *MA 26.5,
 MA 35.7, MA 35.8
 Salloum, Sarah TT 59.1
 Salman, Zaher MA 9.3
 Salusti, Francesco HL 7.66, *HL 33.34
 Salut, Roland HL 10.10
 Salvador, Arnel HL 17.6
 Salvalaglio, Marco DY 4.6, MM 14.8,
 MM 25.1, MM 25.3, *MM 26.4
 Salvan, Georgeta DS 5.3, DS 14.1
 Salvati, Fabio *MA 35.4
 Salzmann, Tim *MA 38.3
 Salzwedel, Robert *HL 1.4, HL 1.9,

- O 80.8
 Samad, Abdus O 56.9
 Samadi, Mohsen •MM 26.7
 Samanta, Amit K VA 1.3
 Samanta, Bipasa HL 25.5
 Samanta, Kartik MA 3.6
 Samanta, Tapas •MA 23.16,
 MA 23.17, MM 12.30
 Sambale, Anna Katharina •CPP 19.7,
 CPP 35.28
 Samtsevich, Artem •MM 39.6
 Samuely, Tomás O 18.2, O 74.5
 Sánchez Calzado, Juan MM 42.6
 Sánchez, Cristián G. O 6.7
 Sánchez, Juan CPP 35.64
 Sánchez, Pedro DY 57.7, DY 57.8
 Sanchez, Pedro A. DY 7.2
 Sánchez, Rafael TT 60.4
 Sanchez, Valeria •HL 7.32
 Sanchez-Barquilla, R. •TT 6.4
 Sanchez-Barriga, Jaime O 14.11
 Sánchez-Portal, Daniel O 7.8
 Sandberg, Oskar J. CPP 1.10
 Sander, Mathias TT 62.7
 Sander, Nicole •MA 23.26, MA 23.27
 Sander, Wolfram O 81.7
 Sanders, Charlotte O 34.9, •O 85.2
 Sanders, Charlotte E. O 6.3
 Sandev, Trifce •DY 44.10, DY 44.13,
 DY 44.15, DY 44.19
 Sandlöbes-Haut, Stefanie .. MM 32.3,
 MM 37.1
 Sandoghdar, Vahid .. HL 50.6, TT 25.4
 Sandra, Korte-Kerzel MM 41.3
 Sangiovanni, Davide MM 15.5
 Sangiovanni, Giorgio .. O 18.9, O 36.12,
 O 65.5, O 65.6, O 67.5, TT 29.7,
 •TT 35.5, TT 35.6, TT 65.8
 Sanjeeva, L. D. TT 42.13
 Sanjuan Ciepielowski, Aleksander
 •TT 53.3
 Sankar, Soumya MA 10.4, TT 12.4
 Sanna, S. •KFM 6.46
 Sanna, Simone CPP 35.39,
 CPP 35.40, CPP 35.46, KFM 6.2,
 KFM 6.3, KFM 6.4, KFM 6.6,
 KFM 13.1, KFM 14.6, O 22.2, O 32.3,
 O 40.1
 Santarossa, Angel •DY 7.9
 Santen, Ludger BP 11.48, BP 12.6,
 BP 25.9
 Santer, Svetlana CPP 8.5
 Santiago-Pérez, Darío G. DS 7.4
 Santin, Gabriele BP 11.25
 Santos Franca, Aldilene .. CPP 35.66
 Santos, Paulo HL 3.4
 Santos, Paulo V. HL 3.8, HL 10.3,
 HL 10.4
 Santos-Otte, Paula BP 23.9
 Santucci, Stéphane MM 33.5
 Sanvito, Stefano MA 4.5, MA 7.3,
 MM 6.8, TT 7.5
 Sanyal, Biplob MA 7.5, MA 23.49,
 •MA 23.58, MM 23.17
 Sanz, Ruy MA 38.1
 Saphianikova, Marina CPP 13.5,
 CPP 13.6, •CPP 20.5
 Sapotta, Benedikt CPP 26.3
 Sapozhnik, Alexey MA 18.3
 Sarah, Loebner CPP 20.5
 Sardar, Suman DS 14.7
 Sardinero, Ignacio •TT 48.5
 Saremi, Sahar KFM 4.9
 Sarkanych, Petro DY 44.3, SOE 8.2,
 SOE 16.1
 Sarkar, Jit MA 46.4
 Sarkar, Kanchan •O 73.7
 Sarkar, Rajib TT 6.6
 Sarkar, Saheli TT 47.4
 Sarkar, Suchetana O 3.1, •O 3.3
 Sarkar, Swagato •CPP 56.5
 Sarott, Martin KFM 1.4
 Sartison, Marc HL 33.31, •HL 33.35
 Sartori, Andrea BP 1.11, O 39.6
 Sarvaiya, Ishan TT 30.1
 Sasaki, Takahiko TT 43.9, TT 51.9
 Sasi, Sarath •O 18.7
 Sasioglu, Ersoy •HL 34.1
 Sassnick, Holger-Dietrich .. MM 16.8
 Sastry, Srikanth DY 27.6
 Sata, Sai Preetham •DY 17.10
 Sathiyanesan, Thevashangar
 BP 24.8, DY 38.8
 Sathyadhama Prasad, Aniruddha
 MA 23.35, •MA 48.6
 Sato, Yuki SOE 22.1
 Sattler, Lars O 93.8
 Sattler, Rene •CPP 35.31
 Satyadhama Prasad, Aniruddha
 TT 18.3
 Säubert, Marius •MA 40.23
 Säubert, Steffen MA 13.6, TT 19.6
 Sauer, Simeon BP 11.26
 Sauerland, Lena O 11.1
 Saunderson, Tom MA 23.4, MA 31.5
 Saunderson, Tom G O 30.3
 Saur, Michael •MA 46.12
 Sauter, Eduard HL 7.17
 Sauter, Eric •O 81.5, O 81.6, O 83.2
 Savan, Alan DS 6.4
 Savchenko, Andrii •MA 47.7
 Savchenko, Vladyslav CPP 8.5,
 CPP 17.22, CPP 35.45, CPP 56.3
 Savelkoul, Jacqueline KFM 6.33
 Savvidi, Kamila •O 86.7
 Sawar, Awais CPP 43.9
 Sawicki, Jakob DY 57.3, •SOE 7.1
 Saxena, Alaukik •MM 36.4
 Saxena, Rishabh HL 7.26
 Saxena, Siddharth TT 30.7
 Sayers, Charles TT 51.7
 Saywell, Alex O 93.8
 Sayyad, Sharareh O 94.10, •TT 48.7
 Sbalzarini, Ivo F. BP 28.22
 Scaffi, Laura DY 23.5, •DY 56.8
 Scanlon, David O. HL 45.2
 Scarselli, Davide SOE 6.1
 Scavuzzo, Alessio DS 10.3
 Schaaf, Peter DS 12.57
 Schaal, Maximilian CPP 36.9, O 18.4,
 O 22.3, •O 22.9, O 36.9, O 47.2
 Schady, Pascal CPP 18.9, •CPP 28.7,
 •TT 32.7
 Schaedel, Laura •BP 8.5, BP 28.24
 Schaefer, Florian MM 4.5
 Schaeper, Anja BP 28.13
 Schaeper, Jannis Justus •BP 21.12
 Schäfer, Benjamin SOE 4.11,
 •SOE 15.1, SOE 23.3
 Schäfer, Christian •CPP 45.5, •O 80.7
 Schäfer, Kilian •MA 28.1, MA 48.8
 Schäfer, Louis-Victor TT 30.2
 Schäfer, Lukas MA 3.2
 Schäfer, Marlon HL 7.48
 Schäfer, Moritz R. •CPP 45.6, O 26.6
 Schäfer, Nils Andre •KFM 13.1
 Schäfer, Roland •O 58.1
 Schäfer, Rudolf MA 23.34, MA 23.35,
 MA 40.59, MA 43.4, MA 43.5,
 MA 48.6
 Schäfer, Sascha MA 23.56, O 30.6,
 O 83.6
 Schäfer, Thomas TT 61.1
 Schäfer, Timo •CPP 2.3
 Schäfer, Tobias DY 46.9
 Schäfer, Alexander F. MA 23.68
 Schäffer, Erik BP 11.47, BP 23.5,
 BP 23.11
 Schäffler, Nathalie •BP 11.71
 Schaffrath, Nico •BP 24.8, •DY 38.8
 Schaible, Sophie F. O 83.8
 Schalk, Martin MA 32.5
 Schall, Johannes HL 33.24, HL 33.36,
 HL 33.37, HL 49.6
 Schaller, Gernot •DY 9.6, DY 25.3,
 •DY 25.9, DY 43.13, TT 33.3,
 •TT 33.9, TT 60.7
 Schaller, Mareen CPP 19.5
 Schalm, Koenraad TT 38.5
 Schambeck, Mia TT 58.30
 Schamriß, Lukas •TT 42.21
 Schäpers, A. HL 33.17
 Schäpers, Thomas HL 29.9, HL 30.1,
 TT 36.1, TT 41.1, TT 59.5, TT 59.6
 Scharf, Dominik O 48.4
 Scharfstadt, Moritz •HL 33.16
 Schattauer, Christoph HL 33.12
 Schattauer, Christopher HL 30.2,
 TT 41.2
 Schatz, Enno O 49.3
 Schäublin, Robin E. MM 25.2,
 MM 28.3
 Schaumburg, Felix •HL 1.10
 Schawe, Jürgen E.K. MM 39.1
 Scheel, Manuel E. CPP 35.2
 Scheer, David •TT 57.24
 Scheer, Elke TT 11.1, TT 11.3, TT 16.3,
 TT 20.1, TT 20.6, TT 27.8, TT 27.9,
 TT 37.7, TT 37.10
 Scheer, Roland HL 4.5, HL 4.6,
 HL 25.4
 Scheffler, Daniel MA 23.60
 Scheffler, Marc •TT 30.1, TT 58.28
 Scheffler, Matthias HL 4.8, HL 13.3,
 HL 36.3, HL 40.4, HL 41.1, HL 47.1,
 MM 21.3, MM 31.2, MM 31.6,
 MM 36.7, O 17.3, O 52.5, O 57.6,
 O 78.1, O 78.7, O 79.4
 Scheffold, Marlene BP 5.2
 Scheibel, F. MA 23.19
 Scheibel, Franziska •MA 3.7, MA 3.9,
 MA 42.3
 Scheibel, Thomas DS 13.5
 Scheiber, Daniel MM 9.1, MM 9.5,
 MM 37.4, MM 37.6
 Scheidemann, Claus BP 28.26,
 BP 28.27
 Scheiderer, Philipp TT 43.8
 Scheidgen, Markus HL 25.3, O 95.4,
 O 95.5, TT 68.4, TT 68.5
 Scheidler, Fabian •O 70.6
 Scheidt, Joshua O 45.7
 Scheiter, Juliane MM 23.5
 Schelchshorn, Michael •O 87.6
 Scheler, Theresa DS 12.57
 Scheler, Ulrich •CPP 20.8
 Schell, Andreas W. HL 24.11
 Schell, Juliana MM 40.8
 Schellenberger, Andreas •TT 5.8,
 TT 5.9
 Scheller, Daniel HL 33.19, HL 33.21,
 •HL 33.22, HL 33.23, HL 33.29
 Schellhammer, Sebastian CPP 26.2
 Schemmelmann, Sevast O 59.2,
 •O 59.6
 Schenk, A. S. BP 11.7
 Schenk, Harald KFM 7.7
 Schenk, Sebastian O 47.10
 Schepers, Anna V. •SYSD 1.2,
 BP 28.28, BP 28.32
 Scherb, Sebastian O 4.5, •O 32.8
 Scherer, Michael MA 7.10, TT 53.6
 Scherer, Theo KFM 6.23, •KFM 8.2,
 KFM 8.6, KFM 8.7, KFM 8.8, KFM 8.9
 Scherf, U. HL 48.4
 Scherz, Andreas DS 6.3
 Scheu, Bettina BP 10.6
 Scheu, Christina MM 41.7
 Scheuchenpflug, Ludwig MA 23.9
 Scheuer, Laura •MA 22.5, MA 23.55,
 MA 40.7, MA 40.50
 Scheuerer, Philipp O 15.1
 Scheufele, Monika MA 4.13,
 MA 23.50, MA 23.77, •MA 23.80,
 TT 7.13
 Scheunemann, Dorothea .. CPP 18.7,
 CPP 18.13, CPP 36.2, DS 16.6,
 HL 33.56, HL 36.5
 Scheurer, Christoph CPP 2.9,
 CPP 44.11, DY 46.2, KFM 10.6,
 MM 3.3, MM 5.9, MM 5.10, MM 6.2,
 MM 6.3, MM 16.2, MM 36.3,
 MM 39.6, O 39.3, O 59.10, O 78.2,
 O 78.3, O 78.4, O 78.5
 Scheurer, Fabrice O 2.6, O 72.4,
 O 76.2
 Schewe, Lukas O 64.8, •O 93.7
 Schewe, Nils •O 68.5, •O 81.10, O 83.2
 Schweski, Alexandra O 56.1
 Schick, Christoph KFM 11.11
 Schick, Daniel MA 8.2, MA 40.39
 Schick, Lisa •BP 9.4, BP 11.52
 Schied, Monika •O 56.10
 Schiek, Manuela O 58.1
 Schieming, Gabi DS 12.11, DS 12.55,
 MM 12.8, MM 23.4, MM 23.5, TT 59.1
 Schießel, Helmut BP 9.11
 Schiffer, Maximilian •TT 43.3
 Schill, Hans-Joachim HL 1.3, HL 29.6,
 •O 65.4
 Schiller, Frederik O 47.4
 Schilling, Achim DY 26.5
 Schilling, Jörg HL 7.13, HL 44.4
 Schilling, Julian-Steven •CPP 17.48,
 CPP 53.7
 Schilling, Marcel HL 28.4
 Schilling, Rolf CPP 17.55
 Schilling, Tanja DY 16.9
 Schimmel, Sebastian TT 58.27
 Schirmacher, Walter •DY 42.12,
 •DY 46.10
 Schirmreisen, André O 4.2, O 4.4,
 O 21.3, O 45.5, O 72.5, TT 39.11,
 TT 58.21, TT 58.22
 Schlabach, Sabine MM 12.7, MM 27.1
 Schlachter, Paul •CPP 17.11
 Schlawin, Frank •MA 9.2
 Schleberger, Marika HL 1.10, HL 22.9,
 HL 33.15, MA 19.3, •O 5.1, O 5.6,
 O 5.7, O 5.8, O 13.5, O 13.7, O 19.1,
 O 24.4, O 24.5, O 30.10, O 31.6
 Schlenvoigt, Micheal TT 59.5
 Schlegel, Julius •MA 46.1
 Schlegel, Ronny TT 58.27
 Schlemmer, Alexander •DY 37.4
 Schlerer, Philipp TT 46.5
 Schlenhoff, Anika •O 77.6, O 93.4
 Schlenz, Patrick DS 13.2
 Schleuning, Markus HL 47.7
 Schlichting, Hartmut O 14.4
 Schlickum, Uta KFM 6.16, O 12.4
 Schliemann, John DY 48.1, HL 7.49,
 TT 55.1
 Schlierf, Michael BP 23.4
 Schlipf, Simon KFM 7.7
 Schlitz, R. MA 41.2
 Schlitz, Richard MA 23.60
 Schliwa, Andrei HL 44.7
 Schlögl, Robert MM 5.10, MM 10.1,
 O 63.2, O 78.1
 Schlörb, Heike MA 20.2
 Schlücker, Sebastian •HL 27.1,
 •O 62.1, •TT 40.1
 Schlueter, C. MA 5.1, MM 12.1,
 MM 26.8
 Schlueter, Christoph DS 12.5, O 11.4,
 O 29.6, O 36.11
 Schlueter, J. A. TT 28.6, TT 57.19
 Schlupp, Peter HL 7.31
 Schlußler, Raimund BP 12.8
 Schlüter, Christoph HL 36.2
 Schlüter, Henrik •TT 23.47
 Schmalhorst, Jan-Michael DS 12.10
 Schmalian, Jörg MM 6.7, TT 37.1,
 TT 37.4, TT 37.5, TT 63.12
 Schmalofski, Timo •MM 12.24
 Schmalzl, K. TT 47.2
 Schmauder, Siegfried MM 33.4,
 MM 40.3
 Schmeink, Jennifer •HL 22.9, O 5.7,
 O 24.5
 Schmelcher, Peter BP 7.9, DY 10.9
 Schmeller, Leonie CPP 44.5
 Schmid, Almut BP 10.2, BP 10.6
 Schmid, Christoph TT 3.10, TT 20.4,
 TT 57.22, •TT 57.23
 Schmid, Friederike BP 11.6, BP 11.15,
 BP 17.1, BP 26.7
 Schmid, Harald O 7.4
 Schmid, Jonas •MM 12.32
 Schmid, Markus CPP 17.12, HL 7.25
 Schmid, Michael •KFM 7.2, •KFM 7.3,
 O 6.1, •O 6.4, O 26.4, O 54.6, O 54.7,
 O 54.8, O 68.2, O 81.4, O 81.8, O 92.5,
 O 92.10, TT 57.6
 Schmid, Rochus CPP 2.4
 Schmid, Sebastian HL 30.3, TT 41.3
 Schmid, Valentin CPP 51.6
 Schmid-Gund, Rüdiger DS 12.33
 Schmidt, Adrian HL 16.8, TT 24.8
 Schmidt, Annette MA 36.2
 Schmidt, B. TT 46.8
 Schmidt, Bernd •TT 39.11, TT 58.21,
 TT 58.22
 Schmidt, Christoph F. BP 4.7,
 BP 28.30
 Schmidt, Daniel DS 6.2, HL 33.33,
 MM 17.1
 Schmidt, Franz-Philipp MA 36.1,
 MM 5.10
 Schmidt, Georg MA 22.5
 Schmidt, Gordon HL 7.6
 Schmidt, Harald KFM 13.4, KFM 13.5
 Schmidt, Heinz-Jürgen MA 40.24
 Schmidt, J. TT 34.3
 Schmidt, Jack-André TT 39.11,
 TT 58.21, TT 58.22
 Schmidt, Jan Robert •DY 21.2
 Schmidt, Jan-Hendrick TT 35.7
 Schmidt, Jaydean TT 16.8
 Schmidt, Jessica BP 11.42
 Schmidt, Jonathan •MM 31.7
 Schmidt, Kai P. TT 42.19, TT 42.20,
 TT 42.21
 Schmidt, Kai Phillip TT 5.6, TT 5.7,
 TT 5.8, TT 5.9, TT 29.8, TT 42.8,
 TT 42.9, TT 42.10, TT 43.1, TT 43.29,
 TT 46.12, TT 47.13, TT 62.8, TT 65.10
 Schmidt, M. TT 46.8
 Schmidt, Marcel HL 42.5
 Schmidt, Marco •DY 45.16
 Schmidt, Marcus HL 34.6, MA 27.1,
 MA 31.4, TT 11.6, TT 30.6
 Schmidt, Matthias DY 6.1
 Schmidt, Maurice MA 23.2
 Schmidt, Mike O 13.6
 Schmidt, Oliver G. HL 24.8, HL 24.9,
 MA 23.34, MA 43.4

Author Index

- Schmidt, Paul Philip •O 32.7
 Schmidt, Philipp HL 14.5
 Schmidt, Robert HL 18.10
 Schmidt, Stefan HL 1.4
 Schmidt, Thomas BP 24.5, DY 38.5,
 O 52.1, TT 18.5
 Schmidt, Thomas L. DY 23.4, TT 6.12
 Schmidt, Timo O 83.4
 Schmidt, Tizian BP 28.25
 Schmidt, Volker CPP 45.4, MM 23.30
 Schmidt, Wolf Gero HL 7.14,
 HL 33.28, HL 33.51, HL 33.52,
 KFM 6.1, KFM 6.17, O 28.4, O 67.1,
 O 69.5
 Schmidt-Mende, Lukas CPP 43.7,
 CPP 51.7, MM 23.12
 Schmidtpeter, Jan •MA 49.2
 Schmied, Christian-Marcel DY 27.9
 Schmiedeberg, Michael •DY 16.5,
 DY 17.6
 Schmiedinghoff, Gary •TT 5.11
 Schmitt, Cedric •DS 1.3, O 94.7
 Schmitt, Christin •MA 31.2, MA 31.3
 Schmitt, David O 34.4
 Schmitt, Erica •HL 38.7
 Schmitt, Erica A. O 96.7
 Schmitt, Fabian HL 11.4, TT 15.4
 Schmitt, Julian O 49.4
 Schmitt, Markus DY 2.7, DY 2.9,
 DY 43.12, TT 2.7, TT 2.9
 Schmitt, Maurice •MA 23.4
 Schmitt, Robert O 49.8
 Schmitt, Thorsten MA 46.10
 Schmitz, Guido MM 14.3, MM 16.9,
 MM 23.8, MM 23.16
 Schmitz, Gunnar •CPP 2.4, O 26.6
 Schmitz-Antoniak, Carolin MA 8.7
 Schmoll, Philipp MA 40.26
 Schmoranzero, E. MA 41.2
 Schmoranzero, Eva MA 4.12,
 MA 23.37, MA 40.6, MA 40.63,
 TT 7.12
 Schmunk, Waldemar TT 6.9
 Schnabel, Allard MA 48.7
 Schnabel, Lucas BP 12.12
 Schnabel, Michael •SOE 4.13
 Schnabel, Roman VA 1.1
 Schnack, Jürgen DY 55.6, •MA 24.1,
 MA 24.4, •TT 23.9, TT 23.10, TT 67.6
 Schnatmann, Lauritz •MM 23.4
 Schneck, Emanuel BP 1.3, BP 26.8
 Schneeweiss, Oldřich MA 37.6,
 MM 19.1
 Schneider, C.M. O 2.8
 Schneider, Carina CPP 3.4, CPP 35.44
 Schneider, Christian HL 1.2, HL 1.7,
 HL 2.5, HL 2.6, HL 24.13, HL 35.4
 Schneider, Claus M. MA 22.4, O 30.5,
 O 59.3
 Schneider, Claus Michael O 30.3
 Schneider, Eckhardt DY 57.3
 Schneider, Eric DS 13.2, •KFM 6.29,
 KFM 6.33
 Schneider, Hans Christian MA 8.4,
 MA 8.10, MA 23.24, MA 40.8,
 MA 40.11, MA 46.2, MA 46.7
 Schneider, Harald TT 62.1
 Schneider, Horst CPP 35.22
 Schneider, Imke DY 43.16, DY 48.8,
 MA 16.1, TT 22.7, TT 22.8, •TT 45.8,
 TT 55.8
 Schneider, Konrad CPP 19.7,
 CPP 35.28, DS 12.34
 Schneider, Konstantin D. •TT 16.7,
 TT 53.10
 Schneider, Lucas •O 7.1, O 7.3, O 32.9
 Schneider, M. Alexander MA 14.2,
 •O 56.1, O 56.4, O 67.3
 Schneider, Michael MA 15.3,
 MA 23.69, MA 23.72, MA 43.6
 Schneider, Robin BP 28.3
 Schneider, S. MA 12.5
 Schneider, Sebastian CPP 18.1,
 MA 12.3
 Schneider, Thomas HL 4.5
 Schneider-Stock, Regine HL 29.4
 Schneidewind, Astrid TT 57.5
 Schnelle, Walter MA 37.4
 Schnick, Wolfgang HL 45.2
 Schnitzlerlein, Miriam •BP 28.53
 Schnitzspan, Leo •MA 29.2
 Schnohr, C.S. HL 18.5
 Schnohr, Claudia S. HL 4.9
 Schnorrer, Frank BP 8.7
 Schnupfhnag, Christoph O 70.1,
 O 76.9
 Schober, Jan-Christian •O 29.3
 Schober, Maximilian •HL 18.11
 Schöberl, Claudia •KFM 10.1
 Schobert, Arne •HL 40.1, •O 79.1
 Schock, Robin T. K. TT 16.7, •TT 53.10
 Schofield, Steven R. •O 57.1
 Schoger, Tanja •CPP 57.3
 Schöll, Eckehard •DY 57.3, SOE 7.1,
 •SOE 9.2
 Schöll, Eva HL 7.45, HL 7.65,
 •HL 7.66, HL 33.34
 Scholle, Robin •TT 51.1
 Schöllkopf, Wieland O 39.2
 Schollwöck, Ulrich TT 43.11
 Scholtes, Ingo •SOE 14.1
 Scholz, M. MM 12.1, MM 26.8
 Scholz, Markus HL 36.2, O 22.7,
 TT 9.7
 Scholz, Reinhard •CPP 3.2
 Scholz, Tanja MA 23.4
 Schön, Carl-Friedrich DS 12.38,
 MM 12.27
 Schöne, Philip •CPP 35.34
 Schönenberger, Christian O 51.3
 Schönenberger, Norbert O 37.5
 Schönenberger, Thomas MA 12.6
 Schönfeld, Dennis •CPP 8.8, DY 29.3
 Schönhals, Andreas CPP 20.4,
 CPP 29.6, CPP 37.4, DY 24.4
 Schönhense, G. •MM 12.1, MM 26.8,
 O 30.4
 Schönhense, Gerd HL 36.2, O 85.3,
 O 85.7
 Schöning, Marco •O 86.4
 Schöning, Sonja MA 23.48,
 MM 12.29, MM 12.30
 Schönleber, Marco •TT 42.11
 Schönweger, Georg KFM 1.5
 Shoof, Benedikt O 14.4
 Schoop, Leslie MA 9.3
 Schöpe, Hans Joachim •CPP 19.8,
 •CPP 57.9, •DY 16.10, DY 34.5
 Schöpf, Jörg MA 12.2
 Schopmans, Henrik •MM 31.1
 Schöppach, Fabian •HL 47.6
 Schöppel, Florian •DY 48.9, •TT 55.9
 Schorlepp, Timo •DY 5.3
 Schott, Christina O 64.9
 Schott, R. HL 29.9
 Schöttke, Fabian •O 59.2
 Schötz, Konstantin CPP 17.9,
 CPP 17.42, HL 7.33
 Schraad, Simon •CPP 26.1, CPP 36.6
 Schramm, Jakob •O 10.9
 Schramm, Miriam •BP 23.4
 Schramma, Nico BP 28.40,
 •BP 28.42, BP 28.44
 Schraut-May, Lisa CPP 17.6,
 •CPP 28.8, •TT 32.8
 Schreck, Sabine KFM 6.23, KFM 8.6,
 •KFM 8.8, KFM 8.9
 Schreckenberger, Lea-Marie •HL 50.10
 Schreckenberger, Michael SOE 4.1,
 SOE 11.1
 Schreiber, Christoph BP 28.49
 Schreiber, Frank BP 11.46, CPP 17.53,
 CPP 19.12, CPP 29.7, CPP 29.9,
 CPP 35.6, CPP 51.2, DS 10.2, DY 37.1,
 O 63.1, O 95.9, TT 68.9
 Schreiber, Lars HL 37.6
 Schreiber, Lars R. HL 29.1, HL 29.5,
 HL 37.1, HL 37.4, HL 37.7, HL 50.7
 Schreier, Paul •MA 23.67
 Schreiner, Peter R. O 72.5
 Schreuer, Christoph O 83.2
 Schreyer, Philipp DS 9.2, •DS 9.3
 Schröder, Alexander •O 30.6
 Schröder, Arne DS 12.2
 Schröder, Benjamin O 8.5
 Schröder, Christian MA 40.37,
 MM 12.28, MM 12.30, O 11.8, O 23.2
 Schröder, Malte DY 18.1, SOE 6.1,
 SOE 10.1, •SOE 10.2, SOE 10.4,
 SOE 10.5, SOE 10.6, SOE 11.3,
 SOE 11.4
 Schröder, Stefan CPP 13.1
 Schroeder, Jonas •CPP 17.14
 Schroeder, Uwe DS 12.5
 Schroedter, Erik TT 22.1
 Schroer, Christian G. KFM 9.12
 Schröder, Julian DS 12.40, •HL 33.11
 Schröter, Finn •O 69.10
 Schröter, Matthias DY 7.5
 Schröter, Niels O 32.4
 Schröter, Niels B.M. DS 12.15, MA 9.3,
 O 59.7, •TT 6.13, TT 27.4, TT 59.12
 Schuba, Stefanie •BP 11.69
 Schubert, Alina DS 12.40, •HL 33.4,
 HL 33.11
 Schubert, Harald TT 10.7, TT 43.9
 Schubert, Juri DY 42.5
 Schubert, Markus Andreas HL 14.9
 Schubert, Mathias •DS 17.2
 Schubert, Ulrich S. CPP 1.4,
 CPP 17.19, CPP 17.29, CPP 36.7,
 CPP 36.9, CPP 43.2, CPP 51.8
 Schüddokopf, Sascha O 42.6
 Schuderer, Felix TT 66.3
 Schuett, Fabian M. O 96.9
 Schüffelgen, Peter TT 36.1, TT 59.5,
 TT 59.6
 Schug, Alexander BP 3.3, BP 11.16,
 BP 11.76, BP 11.77, BP 27.5
 Schug, Felix •MA 23.45
 Schuh, Christopher •MM 32.8
 Schuknecht, Francis •BP 5.6, O 91.7
 Schüle, Karolina DS 12.35, •KFM 6.40
 Schuler, Bruno O 10.4
 Schüller, D. BP 11.7
 Schüller, Leonard •O 39.5
 Schüller, Luis •O 70.5
 Schüller, Michael O 8.7
 Schull, Guillaume O 2.6, O 72.4,
 O 76.2
 Schullian, Otto •O 64.11
 Schulte, Alfons CPP 8.3
 Schulte, Stefan O 29.9, •O 41.2
 Schultheiß, Jan KFM 1.2
 Schultheiss, Helmut MA 23.78
 Schultheiss, Jan KFM 4.3
 Schultheiss, Katrin MA 23.78
 Schultz, Johannes •O 21.5, •O 49.5
 Schulz, Armin TT 51.5
 Schulz, Benjamin •DY 46.1
 Schulz, Dennis TT 57.25
 Schulz, F. O 75.9
 Schulz, Fabian O 75.6
 Schulz, Michael HL 48.2, TT 47.3
 Schulz, Stephan TT 59.1
 Schulz, Tomek MA 25.5
 Schulze, Dirk HL 7.1, HL 7.2, HL 38.3,
 HL 38.6
 Schulze, Holger DY 26.5
 Schulze, Jörg HL 33.22
 Schulze Lammers, Bertram O 97.7
 Schulze, Patricia HL 4.3
 Schulze, Patricia S. C. HL 4.7
 Schulze, Tim KFM 7.7
 Schulze-Lammers, Bertram O 66.7
 Schumacher, Claus HL 33.61
 Schumacher, Hans W. MA 32.3
 Schumacher, Hans Werner O 82.7
 Schumacher, Stefan HL 7.50, HL 7.64,
 HL 24.6
 Schumacher, Thorsten O 43.2,
 O 43.5, O 76.9, O 91.1
 Schumann, Frank O 51.5
 Schumann, Frank O. •O 51.6, O 85.5
 Schumann, Rolf TT 29.14
 Schummer, Bernhard •CPP 37.5
 Schunck, Jan Oliver TT 3.7, TT 57.3
 schuppler, stefan MA 19.5
 Schuricht, Dirk •TT 31.8
 Schurr, Benedikt •O 58.7, O 58.9
 Schuß, Andreas MM 23.3
 Schüßler-Langeheine, Christian MA 40.12, MA 46.13
 Schusser, Jakob O 30.5, O 59.3,
 O 65.5, O 67.4, •O 94.9
 Schust, Johannes •O 91.4
 Schuster, Constantin •TT 66.2
 Schuster, Jörg CPP 44.8, DS 1.1,
 DS 16.1, HL 33.58
 Schuster, Rolf O 86.4
 Schütt, Freerk •CPP 17.34
 Schütt, Julian BP 11.69
 Schütte, Marc HL 22.5, •HL 33.9
 Schütte, Nils-Erik •HL 8.7
 Schüttler, Konstantin M. O 14.10
 Schütz, Emilia Rosa •CPP 43.7
 Schütz, G. MA 31.1
 Schützhold, Ralf DY 9.6, DY 25.9,
 DY 43.13, TT 33.9, TT 38.12, TT 60.7
 Schwaab, Valentin O 23.1, •O 23.3,
 O 41.1, O 64.1, O 73.8
 Schwab, Holger TT 10.12
 Schwab, Jonas •O 84.9, •TT 56.9
 Schwab, Julian O 80.3
 Schwabe, Stefan MM 17.1
 Schwake, Gerlinde BP 26.5
 Schwalbe, Harald BP 11.21, BP 26.4
 Schwan, Lennart •MA 23.48,
 •MM 12.29, MM 12.30
 Schwarberg, Jannik HL 33.22
 Schwartz, Rico DS 12.16, DS 12.40,
 HL 7.35, HL 8.9, HL 33.4, HL 33.6,
 HL 33.7, HL 33.11
 Schwartzkopf, Matthias CPP 13.8,
 CPP 17.4, CPP 17.16, CPP 17.31,
 CPP 17.44, CPP 17.46, CPP 17.51,
 CPP 17.56, CPP 19.7, CPP 29.2,
 CPP 29.10, CPP 35.19, CPP 35.28,
 CPP 36.8, CPP 37.2, CPP 51.1,
 CPP 53.6, •CPP 56.2, DS 12.34,
 MA 38.5, O 57.5
 Schwarz, Alexander •MA 11.2,
 MA 40.36, •MA 49.3, •O 12.5
 Schwarz, Daniel DY 18.7
 Schwarz, Emil MM 23.12
 Schwarz, Larissa •DY 43.16
 Schwarz, Martin O 3.7, O 36.6
 Schwarz, U. TT 46.2
 Schwarz, Ulrich BP 8.9, BP 17.6,
 HL 23.3, HL 23.6
 Schwarz, Ulrich S. BP 8.6, BP 11.18,
 BP 28.33, BP 28.43, BP 28.47
 Schwarz, Ulrich T. HL 23.2, HL 28.3,
 HL 33.40, HL 44.6
 Schwarz, Ulrich Theodor HL 23.4
 Schwarzburg, Klaus HL 47.7
 Schwarze, B.V. •TT 59.8
 Schwarzhuber, Felix MA 20.10
 Schwarzkopf, Jutta DS 6.2, DS 12.24,
 DS 12.50, HL 4.8
 Schwarz-Selinger, Thomas DS 14.5
 Schweiger, Severin •KFM 7.7
 Schweizer, Matthias R. •MA 16.4,
 MA 23.71
 Schwemmer, Tilman •TT 63.12
 Schwenke, Alexander •TT 42.18
 Schwenke, Philipp MA 23.8,
 •MA 23.11
 Schwierz, Frank DS 12.57
 Schwierz, Nadine BP 11.21, BP 26.4,
 BP 26.8, BP 27.4
 Schwieter, Felix BP 28.46
 Schwingenschloegl, Udo MA 31.5
 Schwingenschlögl, Udo •CPP 54.3,
 MA 7.11, MA 31.8, O 56.9, •O 74.9
 Schwob, Lucas BP 3.11
 Schwuchow, Maik •CPP 36.3
 Sciaini, Germán HL 48.3
 Sciotto, Rachele •O 67.1
 Scipioni, L MA 31.1
 Scorza-Lesch, Dr. Cecilia •HL 27.8,
 •O 62.8, •TT 40.8
 Sebastian, Thomas •MA 25.4
 Sebastiani, Daniel DY 6.10
 Seçkin, Sezer CPP 17.3, •CPP 56.4
 Seckler, Henrik •DY 17.4
 Seddon, Samuel •KFM 14.3, •MA 32.1
 Seddon, Samuel D. KFM 13.7, MA 44.1
 Seehaus, Mattis MM 41.3
 Seega Sivakumar, Nikhil •O 30.2
 Seelbinder, Benjamin BP 21.4,
 CPP 20.2
 Seema, Seema •MA 50.5
 Seemann, Lukas •DY 43.11
 Seemann, Ralf BP 11.35, CPP 35.7,
 CPP 35.8, CPP 44.5
 Seemann, Wilken HL 36.6, •HL 51.5
 Seewald, Felix •MA 44.6
 Seewald, Tobias CPP 43.7, •CPP 51.7
 Sefat, A. S. TT 42.13
 Segets, Doris O 29.10
 Sehlmeier, Birte BP 28.26, •BP 28.27
 Seibel, Christopher •MA 8.4, MA 40.8
 Seibt, Michael HL 33.57, O 52.7
 Seidel, Claus AM BP 21.8
 Seidel, Jan KFM 1.6
 Seidel, Marcus O 37.9
 Seidel, Michael O 43.5, •O 91.1
 Seidel, Ralf HL 42.2, HL 42.3
 Seidel, Thomas •HL 45.4
 Seidelmann, Tim HL 7.39, HL 24.2
 Seidler, Dennis •MA 40.48
 Seidler, Inga HL 29.1, HL 29.5, HL 37.1
 Seidler, Maximilian TT 46.10
 Seidlmayer, Stefan KFM 10.9
 Seidow, Z. •MA 40.14
 Seifert, Hermann TT 43.4
 Seifert, M. HL 18.5
 Seifert, Marc TT 47.3
 seifert, sebastian DS 12.18, MM 26.9
 Seifert, Tim Johannes O 12.4
 Seifert, Tom S. MA 22.2
 Seifert, Udo •PLV IV, BP 23.6,
 DY 32.12, DY 40.2, DY 40.4, DY 40.5
 Seifert, Urban TT 46.13
 Seifert, Urban F. P. TT 31.9
 Seiffert, Sebastian CPP 58.5
 Seiler, Anna HL 14.3, TT 64.3

Author Index

- Seiler, Hélène•SYUE 1.2, O 16.7
 Seiler, JanaCPP 36.2
 Seils, SaschaMM 40.9
 Seith, Adrian•DY 9.3
 Seitsonen, Ari PO 36.6
 Seitz, HaraldBP 11.9, BP 11.44,
 BP 17.9
 Seitz, ManuelHL 27.6, •O 46.4,
 O 62.6, TT 40.6
 Seja, Kevin Marc•TT 63.13
 Sek, GrzegorzHL 33.49
 Selbmann, FranzHL 33.8
 Seleznev, MikhailMM 12.37
 Selig, MalteDS 12.30, HL 1.4, HL 1.8,
 HL 1.9, HL 8.4, HL 34.8, HL 35.6,
 O 8.9
 Sellies, Lisanne•O 15.1
 Sellschopp, Kai•MM 31.9, O 81.1
 Selter, SebastianMA 40.57,
 MA 40.59, TT 10.9
 Selyshev, AleksandrHL 7.11
 Selzer, MichaelMM 31.9
 Semeniuk, KonstantinTT 28.2,
 •TT 28.3, TT 37.8
 Semione, Guilherme D. L.O 29.6
 Sen, Onur Can•MM 12.34
 Sen, Parongama•SYOF 1.5
 Sen, SandipanMM 40.8, MM 41.2
 Senanayake, SanjayaO 78.9
 Senft, Maximilian D.BP 11.46,
 •CPP 35.6
 Senge, Mathias O.O 11.9
 Sengupta, Surangana•TT 54.5
 Sens, PierreBP 31.2
 Sentef, MichaelSYUE 1.5, HL 40.1,
 O 8.7, O 79.1, •TT 64.7
 Senyk, YuriiTT 10.9
 Senyshyn, AnatoliyCPP 45.8,
 KFM 10.2
 Seo, We-HyoO 15.3
 Seoane Souto, RubénTT 48.5
 Sepehri-Amin, Hossein•SYGM 1.2
 Sequeira, Miguel C.•HL 44.2
 Serbyn, MaksymDY 29.1
 Serebrennikova, Alexandra•CPP 45.7
 Sereika, RaimundaMA 39.2
 Serga, Alexander A.MA 16.4,
 MA 23.71
 serpico, giuseppeDS 12.18
 Serra, AnnaMM 17.3
 Serrano Escalante, Valentina HL 45.5
 Serrano, GiuliaO 20.7
 Serre, IngridMM 33.2
 Serwane, Friedhelm BP 13.4, BP 15.3,
 •BP 21.11
 Sessi, PaoloTT 8.4
 Sessoli, RobertaO 20.7
 Šesták, PetrMA 37.5, •MM 36.11
 Setescaj, ChristophO 87.7
 Šetina, JanezVA 1.4
 Setoudeh, Maryam•BP 4.6
 Settanni, Giovanni BP 11.6, BP 11.15,
 BP 11.27, •BP 26.7, BP 27.2, •CPP 2.3
 Setvin, MartinO 54.6, O 72.3
 Seufert, JannisTT 29.12, •TT 29.13
 Seufert, KnudO 14.2
 Severing, Andrea•TT 4.10, TT 9.3,
 TT 9.4, TT 9.5
 Sevilla, MauricioCPP 12.1
 Sevilla Moreno, Jose Mauricio
 •DY 6.9
 Sevinchan, Yunus •BP 10.7, •BP 11.64
 Sevlikar, Shradha V.•MM 12.4
 Sevriuk, VasiliTT 54.7
 Seyed Heydari, Mahsa Alsatat
 MA 4.6, TT 7.6
 Seyidov, PalvanMA 43.7
 Seyller, ThomasO 82.8
 Seyrich, MartinKFM 6.22, •KFM 9.11
 Sha, Mo•HL 45.3, •KFM 6.26
 Shaban, Ateeb•HL 33.8
 Shabbir, Huzafa•DY 22.2
 Shadabroo, Mohammad Saeed
 HL 2.4
 Shaebani, RezaBP 12.5, BP 25.9
 Shafarman, William N.HL 4.9
 Shah, Karan•MM 12.26
 Shah, Prexa•CPP 52.1
 Shahee, AgaMA 23.4
 Shaikh, SaifHL 18.8
 Shakeel, Shahrukh •MA 5.3, MA 50.3
 Shaker, Majid•O 64.1
 Shakeri, PegahCPP 35.7, CPP 35.8
 Shakirov, Timur •CPP 19.2, CPP 35.32
 Shallcross, SamO 75.7
 Shamim, SaqibHL 30.4, TT 17.1,
 TT 41.4
 Shamsafar, LidaO 49.9
 Shan, HangyongHL 1.2
 Shan, JieTT 35.1
 Shao, LiCPP 45.3
 Shao, QimingMA 10.4, TT 12.4
 Shaoqiang, SuO 60.4
 Shapeev, AlexanderMM 29.3
 Shargaleva, Aleksandra HL 25.11
 Sharifi Panah, SetarehDY 56.11
 Sharma, Abhimanyu•BP 2.11
 Sharma, Abhinav •BP 19.6, •CPP 41.6,
 DY 27.7, DY 56.1
 Sharma, AnirudhCPP 11.2
 Sharma, ApoorvaDS 5.3, DS 14.1
 Sharma, C.MM 12.1
 Sharma, Chithra H.•TT 35.7
 Sharma, Chithra S.HL 14.1
 Sharma, GirishTT 6.1
 Sharma, ManeeshaTT 18.3
 Sharma, Nand Lal HL 7.48, HL 7.52,
 HL 7.63, HL 24.8, •HL 24.9
 Sharma, NikhilSOE 15.3
 Sharma, PankajKFM 1.6
 Sharma, PrernaBP 28.56
 Sharma, Priyanka•MA 40.18
 Sharma, Puneet•SOE 4.2, SOE 10.3
 Sharma, Rajesh O.TT 16.13
 Sharma, Rohit•TT 36.4
 Sharma, SancharHL 29.7
 Sharma, SandeepTT 21.4
 Sharma, Sandhya KFM 9.1, •KFM 11.1
 Sharma, Sangeeta •MA 30.1, O 75.7
 Sharma, Shubham •DY 17.9, HL 40.6,
 O 79.6
 Sharma, SitanshCPP 54.3
 Sharma, VaibhavCPP 57.2
 Sharp, Ian CPP 17.46, DS 11.3, HL 7.3,
 HL 38.2
 Sharp, Ian D.HL 7.4, HL 45.1
 Shaw, Nathan•HL 33.46
 Shayanfar, NavidMA 3.9
 Shayduk, RomanMM 12.3, O 83.2
 Shcherbakov, AndriiHL 15.1
 Sheikin, IlyaTT 10.1, TT 10.6
 Sheka, Denis D.MA 11.4, MA 18.6,
 MA 40.2, MA 50.2
 Shekar, C.MA 12.5
 Shekarabi, SaharHL 7.10
 Shekarabi, SaharHL 7.9
 Shekhar, C.TT 6.5, TT 6.10
 Shekhar, Chandra MA 3.6, MM 6.10,
 TT 23.3
 Shelton, ElijahBP 15.3, BP 21.11
 Shelton, Elijah R.BP 13.4
 Shemerliuk, Yullia TT 10.9, •TT 10.10,
 TT 57.9
 Shemilt, LauraO 63.1
 Shen, BinTT 4.3, •TT 46.10, TT 52.7
 Shen, ChenBP 1.11
 Shen, XiaoMM 9.7
 Shen, XingchenTT 57.8
 Shen, ShaoxiangO 36.8
 Shengoy, Lakshmi•MM 15.2
 Shepard, AMA 31.1
 Sherman, Dov•MM 38.2
 Shi, JianminKFM 13.6
 Shi, Li YuTT 62.5
 Shi, LikunMM 41.6
 Shi, QiangDY 9.9
 Shi, RuiO 37.2
 Shi, ShanMM 22.3, MM 23.23,
 MM 42.4, MM 42.7
 Shi, YouguoMA 9.6, TT 23.5
 Shibauchi, TakasadaTT 34.4
 Shields, Brenan J.MA 11.4
 Shields, BrendanDS 6.1, MA 31.7
 Shih, Ching-WenHL 8.2, HL 12.2,
 •HL 12.7, HL 33.24, HL 33.47,
 HL 33.50, HL 43.3, HL 43.5
 Shima, Jazavandi-Ghamsari HL 42.3
 Shimada, KenyaO 59.4
 Shin, DongguenCPP 17.40
 shin, SoohyeonMA 9.9
 Shinaoka, HiroshiDY 11.7, DY 11.8,
 •TT 5.10, TT 13.7, TT 13.8
 Shinwari, TauqirMA 40.12
 Shinwari, TauqirMA 19.4
 Shiotori, AkitoshiO 2.1, •O 12.7,
 O 76.4
 Shipilin, MikhailO 11.4, O 29.6
 Shirahama, KeiyaTT 58.23
 Shivers, JordanBP 19.6, CPP 41.6
 Shkodich, Natalia•MM 40.10
 Shlyannikov, Valery•MM 20.5
 Shoae, SafaCPP 11.4, CPP 11.5,
 HL 2.4
 Shojaei, Rana•SOE 4.6
 Shokof, YairBP 24.7, DY 27.10,
 DY 38.7
 Shokrani, Morteza•DS 16.6
 Shokri, SanazDS 5.2, DS 12.18,
 DS 12.20, •DS 12.52
 Shomali, Elaheh•O 8.2, O 8.3
 Shpyrko, OlegKFM 9.9
 Shree, SinduKFM 9.9
 Shtender, VitaliiMA 47.6
 Shuai, ZhigangDY 25.6, TT 33.6
 Shubbak, Yahya•DS 4.6, •MA 36.3,
 MA 40.43
 Shukla, AlokO 14.3
 Shukla, D.MA 33.6
 Shyta, Vira•TT 47.8
 Si, LiangTT 44.6
 Siber, Maxime•CPP 18.2
 Siboni, Henrik•BP 31.1
 Sibylle, GemmingHL 7.41
 Sichelschmidt, J.TT 42.13, TT 46.8
 Sichelschmidt, JörgTT 43.2
 Sichwardt, AnastasiaCPP 17.29,
 CPP 36.9
 Sick, BernhardMA 36.3
 Sicolo, SabrinaMM 5.3
 Sidikejiang, Shawutijiang HL 51.8
 Sidis, YvanTT 57.5
 Sidor, ClaraBP 8.7
 Sidorenko, AnnaO 65.4, •O 91.3
 Siebenkotten, DarioO 43.1, •O 43.3
 Siebentritt, Susanne•HL 38.5,
 HL 45.5
 Siebert, Dustin•HL 7.64, HL 24.6
 Siebrecht, JanisO 21.7
 Siefke, ThomasHL 7.18
 Siegel, Katherine J.DY 49.4
 Siegert, Marie•CPP 13.3, CPP 35.21
 Siegert, Tobias•CPP 17.42
 Siegl, Julian•DY 48.1, •TT 55.1
 Siegl, LuiseMA 23.60, •MA 23.62
 Siegrist, TheoO 65.5, O 94.9
 Siemann, GesaMA 27.1
 Siemann, Gesa-Roxanne•O 59.8
 Sienkiewicz, Julian•DY 57.2
 Sierda, E.•O 42.2
 Sievers, SibylleMA 32.3, MA 40.40
 Sievers, TammoTT 49.5
 Sieweke, TimonMM 23.4
 Siff, Markus•HL 29.2, •HL 33.25
 Sigel, Reinhard•CPP 17.23
 Sigl, LukasHL 8.4, HL 37.8
 Sigl, Maria•MA 23.50
 Sigle, WilfriedTT 50.3
 Siiira, OlegMA 7.9
 Sikola, TomášO 14.9, O 91.5
 Sikter, DavidO 95.5, TT 68.5
 Silber, RobinMA 15.1
 Silbernagl, Dorothee•CPP 17.1
 Silies, MartinHL 1.2, HL 2.5, O 58.2
 Sill, AnnekatrinCPP 17.57
 Siller, JulianHL 24.11
 Silligmann, RobinCPP 17.21
 Silva, AlessandroDY 40.6
 Silva, CaioO 8.9, O 36.11
 Silva Valencia, Jereson TT 43.19
 Silveira, Orlando J•O 74.2
 Silvestrelli, Pier Luigi •HL 13.6, O 4.7,
 O 17.6
 Silvioni, Riccardo•MA 32.5
 Sim, So-Kumneeth•DY 5.5
 Simionato, GretaBP 8.3
 Simmchen, JulianeBP 2.6
 Simmel, FriedrichBP 27.3
 Simmel, Friedrich C. BP 2.5, BP 11.72,
 BP 11.73
 Simon, Alessandro•DY 17.5
 Simon, Georg H.O 60.8
 Simon, J. Rika•O 22.6
 Simon, PaulMM 26.9
 Simon, RowenaBP 28.3
 Simon, SabinaO 56.7
 Simonato, Manuel•TT 63.3
 Simoncelli, MicheleHL 21.1
 Simonov, Arkadiy KFM 11.4, •KFM 11.7
 Simpson, GrantO 38.7
 Simpson, Grant J.•O 46.6, O 77.5
 Simsek, IbrahimHL 7.37
 Sinclair, Chad•MM 13.1
 Sinder, MishaKFM 13.6
 Sinenlik, ArtemHL 35.5
 Sing, MichaelTT 30.9, TT 43.8
 Singer, KilianKFM 6.12
 Singer, LennartCPP 35.37
 Singer, MirkoBP 28.47
 Singh, BahadurMM 14.7
 Singh, Balram •MA 23.34, •MA 43.4
 Singh, EktaKFM 6.6, KFM 14.2,
 KFM 14.3
 Singh, HarishMA 3.1
 Singh, Jayant K.O 3.2
 Singh, M.MA 5.1
 Singh, Maanwinder Partap ••TT 6.9
 Singh, Manjesh KumarCPP 58.7
 Singh, RajendraO 5.6, O 29.9
 Singh, S.MA 42.5, MA 42.10
 Singh, SanjayMA 47.5
 Singh, SukritiMM 6.10
 Singh Vishen, Amit•BP 31.2
 Singha, AparajitaMA 32.4, O 15.12
 Singhania, Ayushi•MA 33.5
 Singraber, AndreasMM 12.10,
 MM 25.4
 Sinha, SubhasisTT 38.4
 Sinha, SudipTT 38.4
 Sinha, Swarnshikha•O 67.9, O 85.1
 Sinova, J.MA 41.2
 Sinova, JairoMA 4.4, MA 4.12,
 MA 31.3, MA 40.60, MA 40.61,
 MA 40.63, MA 41.4, MA 46.2,
 MA 47.9, O 85.3, TT 7.4, TT 7.12
 Šipr, OndřejMA 16.8, MA 20.1,
 •MA 27.5
 Siretanu, IgorCPP 8.1, CPP 29.4,
 •O 60.4, •O 69.13
 Siri, OlivierO 55.7
 Siria, AlessandroBP 22.3
 Sirker, JeskoDY 48.8, TT 55.8
 Sischka, JanBP 30.6
 Sittig, RobertHL 7.43, HL 7.62,
 HL 49.3
 Siverin, Nikita V.•HL 35.9
 Sivanies Castaño, Javier•O 94.5
 Sivis, MuratHL 48.5, O 70.2, O 80.2,
 O 80.6, O 83.4
 Siwick, BradleyCPP 17.8
 Skála, TomášO 28.5, O 29.2, O 55.2,
 O 78.8, O 81.11
 Skalli, AnasDY 17.7
 Skobijin, GregorMA 20.2
 Skokov, K.MA 23.19, MA 48.3
 Skokov, K. P.MA 28.4
 Skokov, Konstantin MA 3.1, MA 3.2,
 MA 3.3, MA 3.4, MA 3.9, MA 42.2,
 MA 42.3, MA 42.7, MA 42.9
 Skolaut, Julian•MA 40.5
 Skopinski, LuciaO 5.7, O 5.8, O 24.4,
 O 24.5, •O 31.6
 Skourski, Y.MA 44.3
 Skourski, YuriMA 23.1
 Skourski, YuriiMA 18.3, MA 44.2,
 TT 46.4
 Skourskii, YuriiMA 18.5
 Skowroński, WitoldMA 41.7
 Skuratovska, Anastasiia•TT 8.3
 Slager, Robert-JanO 94.1
 Sledz, Florian•HL 29.10
 Sleziona, Stephan HL 1.10, HL 33.15,
 MA 19.3, O 5.7, •O 5.8, O 19.1, O 24.4,
 O 24.5, O 30.10
 Sleziona, Vivien•O 75.6
 Slimi, YounesDS 12.4, •DS 12.33
 Slingerland, JoostTT 65.9
 Slobodianiuk, D.MA 16.6
 Slowik, Josef BerndCPP 36.7
 Sluka, TomasKFM 4.8
 Smaga, MarekO 84.2, TT 56.2
 Smales, Glen J.BP 11.44
 Smales, Glen JacobCPP 20.4
 Smallenburg, FrankDY 14.1
 Šmejkal, LiborMA 4.4, TT 7.4
 Šmejkal, L.MA 41.2
 Šmejkal, LiborMA 4.12, MA 4.14,
 MA 40.60, MA 40.61, MA 40.63,
 MA 40.64, •MA 41.1, MA 41.4,
 MA 46.2, O 85.3, TT 7.12, TT 7.14
 Smiatek, JensBP 17.8, •CPP 2.1
 Smidman, MichaelTT 42.5
 Smink, SanderDS 14.4
 Smirnov, AlexanderTT 45.2
 Smirnov, DmitriiO 14.11
 Smirnova, Olga•SYUE 1.4
 Smith, Adam DY 2.6, DY 55.9, TT 2.6,
 TT 65.9, TT 67.9
 Smith, Ana-SunčanaBP 11.63,
 BP 15.5, DS 12.42, DY 44.17, MM 33.6
 Smith, David M.MM 33.6
 Smoliarova, Tatiana•HL 36.7
 Smolyarova, TatjanaMM 40.10
 Smorka, Rudolf•MA 4.3, •TT 7.3
 Smutek, JakobCPP 35.50
 Snaith, HenryMM 10.4
 Snyder, JoshuaMA 42.9
 Soavi, GiancarloHL 8.3, HL 33.3,
 HL 35.5

Šob, Mojmir MA 3.8, •MA 37.1, MA 37.6, MM 19.1, MM 32.7
 Šobaň, Zbynek MA 40.64
 Sobol, Tomasz O 30.3
 Sobolev, Sergei MA 18.3, •TT 62.5
 Sobucki, Marcel BP 29.4
 Sochiera, Simon •MA 23.53
 Sochor, Benedikt CPP 17.26, CPP 26.1, CPP 29.8, •CPP 36.6, CPP 36.8, CPP 37.2, CPP 52.5, CPP 58.2, DS 12.34, O 57.5
 Sodemann, Inti TT 53.8
 Söderberg, Daniel CPP 52.5, MA 38.5
 Söderberg, L. Daniel BP 19.2, CPP 17.26, CPP 41.2, DS 12.34
 Sofer, Zdenek HL 33.3
 Sohail, M. Zain O 84.3, TT 56.3
 Sohn, Seoyun •MM 42.7
 Soholov, D TT 42.4
 Sohoni, Siddhartha O 34.1
 Sokalski, Vincent MA 23.36
 Sokeng, Aurelien D. CPP 1.4
 Sokeng Djoumessi, Aurelien •CPP 17.29, •CPP 36.9
 Sokolov, Dmitry MM 6.6, TT 37.1, TT 37.3, TT 37.5
 Sokolov, Dmitry A. TT 37.4
 Sokolovic, Igor O 54.6, O 54.8
 Sokolowski, Moritz DS 12.41
 Sokolowski-Tinten, Klaus MA 8.7, O 13.7
 Solar, Mathieu CPP 37.1
 Soldatov, Ivan MA 23.34, MA 40.59, MA 43.4, MA 43.5
 Soldatov, Timofei TT 45.2
 Soldemo, Marcus O 29.6
 Soldemo, Markus O 11.4
 Soldini, Martina Ondina •TT 8.4
 Soleimany, Mehrzad •KFM 2.5
 Solel, Ephrath O 72.5
 Sollich, Peter DY 6.2, DY 24.1, DY 27.4, DY 42.2
 Sologub, Sergii •O 64.4, O 82.9
 Solov'ov, Ilia BP 3.2, BP 11.28
 Solov'ov, Ilia A. BP 1.6, BP 6.7, BP 11.42
 Soltani, Navid HL 29.10
 Soltani, Siavash MM 13.1
 Soltanizhad, Mohammad BP 28.6
 Soltanmohammadi, Mina O 76.7
 Soltner, Helmut O 77.1
 Softwedel, Olaf BP 26.8
 Solzi, Massimo MA 3.8
 Somintac, Armando HL 17.6
 Sommer, Jens Uwe DY 22.2
 Sommer, Jens-Uwe BP 29.5, CPP 19.4, CPP 20.9, CPP 35.47, CPP 58.6, DY 27.7, DY 56.1
 Sommer, Michael CPP 13.3
 Sommermann, Daniel •CPP 57.11
 Sondhi, Harpreet •HL 33.59
 Song, Chang-Yun •HL 4.6
 Song, Geonho •BP 19.5, •CPP 41.5
 Song, Jimin •O 39.1
 Song, Jin-Dong HL 24.3
 Song, Kaikai MM 28.5
 Song, Qi TT 44.5
 Song, Shaotang MA 19.7
 Song, Wenwen MM 9.7
 Song, Xiaohong HL 48.1
 Song, Yiming O 4.5, •O 21.3, O 32.8
 Sony, Keshab •TT 36.9
 Sood, Mohit HL 45.5
 Sophie Härtel, Marlene CPP 29.10
 Şopu, Daniel •MM 28.4, MM 28.5, MM 42.9
 Soranzio, Davide O 19.4, O 34.10
 Sorger, Johannes SOE 19.1
 Sorn, Sopheak •MA 47.8
 Sorrentino, Andrea L O 20.7
 Sosa, Raul Ian •CPP 45.1
 Sostina, Daria O 15.5, O 15.10, •O 15.11, O 20.3, O 77.3
 Sothmann, Björn O 8.3, •TT 20.3, TT 57.18
 Soto-Arriaza, M. BP 11.11
 Sotoudeh, Mohsen MM 16.4
 Sotskov, Vadim MM 29.3
 Soubatch, Sergey O 10.2, O 19.7
 Souliou, M. O 30.4
 Soumann, Valérie HL 10.2
 Souri, Somayah •HL 48.8
 Souza Neto, Narcizo MA 39.2
 Sözen, Halil Ibrahim MA 28.2, •MA 28.3, •O 25.1, O 73.3
 Spachmann, Sven MA 33.7, MA 40.56
 Spachtholz, Raffael O 15.1

Späh, Peter •KFM 8.3
 Spallek, Domenik MM 16.1
 Spallek, Jan MA 13.6, MA 13.8, MA 25.5, TT 3.8, TT 4.13, TT 19.6, TT 19.8
 Spanier, Lukas V. •CPP 17.30, CPP 29.10
 Spanier, Lukas Viktor CPP 51.4
 Spänslätt, Christian TT 38.7, •TT 45.5
 Spantzel, Lukas BP 21.2
 Sparmann, Tobias MA 12.8, •MA 23.6, MA 31.2
 Spasojevic, Irena DS 6.3
 Späth, Andreas •CPP 17.52, •CPP 28.10, •KFM 6.28, •TT 32.10
 Spathis, Panayotis CPP 52.2, MM 23.27
 Speck, Thomas BP 24.2, DY 27.5, DY 38.2, DY 42.8
 Speckhard, Daniel •HL 6.8, MM 29.1, •O 9.8
 Speidel, Moritz HL 7.62
 Speier, Stephan DY 26.9
 Speller, Sylvia BP 28.13, O 28.3
 Spencer, Michael •HL 17.7, HL 17.9
 Spencer, Michael S. HL 33.53
 Spencer, Michael Scott HL 33.55
 Spencer, Russell •BP 1.9
 Spende, Hendrik HL 33.44
 Spens, Peter CPP 28.3, TT 32.3
 Sperl, Matthias DY 7.3
 Sperlich, Andreas •CPP 11.7, CPP 18.9, CPP 28.7, HL 18.12, HL 22.10, TT 32.7
 Spest, Peter CPP 17.10
 Spetzler, Benjamin •DS 11.5, DS 12.57, MA 49.4
 Spetzler, Elizaveta •MA 49.4
 Spiecker, Erdmann CPP 17.52
 Spiecker, Martin TT 39.3, TT 49.4, TT 58.16
 Spieckermann, Florian MM 28.4
 Spiegler, Stefanie BP 8.8, BP 8.11
 Spieker, Lea •MA 19.3
 Spies, Maria •TT 27.2
 Spillmann, U. TT 57.28
 Spindler, Ephraim •MA 23.8, MA 23.11
 Spiridis, Nika MA 41.7
 Spirito, Davide HL 18.3, HL 18.9
 Spitaler, Tobias MM 9.1, •MM 37.4
 Spitz, Leonie •MA 2.6, •MA 46.10
 Spitzer, Nikolai •HL 7.42, HL 42.5
 Spletstoesser, Janine TT 38.7
 Splith, Daniel DS 16.3, HL 7.31
 Spolenak, Ralph O 49.6
 Spoltore, Donato CPP 43.6
 Spooner, Kieran B. HL 45.2
 Sposini, Vittoria •DY 56.3
 Sprafke, Alexander HL 7.15
 Spree, Lukas O 20.8, •O 50.3
 Spreng, Benjamin CPP 57.3
 Sprengel, Carla •BP 5.3
 Sprenger, Alexander R. •DY 31.6
 Spring, Merit TT 30.9
 Springate, Emma O 34.9
 Springholz, Gunther HL 17.10, MA 4.14, MA 40.64, O 8.9, TT 7.14
 Sprinkart, Nico •MM 3.4
 Sprung, Michael CPP 29.9, DY 37.1, DY 56.7
 Spuri, Alfredo TT 11.1, TT 20.6
 Spychala, Kai Jürgen KFM 6.18
 Squire, Oliver •TT 4.11
 Squire, Oliver P. TT 4.12
 Sreeparvathy, P. C. MA 37.2
 Sriniva, Shesha G.M. DY 18.1
 Srinivasan, Prashanth MM 5.8, MM 14.2, MM 36.8, •MM 39.3
 Srivastava, A.K. KFM 11.9
 Srivastava, Nishit BP 31.2
 Srolovitz, David J. MM 26.8
 Srut Rakic, Iva O 18.8
 Staab, Torsten E.M. KFM 11.3, •KFM 11.6
 Staacke, Carsten MM 6.2, MM 6.3
 Stadler, Fabian TT 16.14, TT 18.1
 Stadtmüller, Benjamin MA 31.3
 Stadtmueller, Benjamin •PRV II
 Stadtmüller, Benjamin MA 23.24, MA 40.7, MA 40.8, MA 40.9, MA 46.7, O 10.2, O 14.5, O 19.5, O 19.8, O 22.4, O 37.10, O 38.1, O 59.5, O 64.9, O 70.4, O 80.1, O 95.2, TT 68.2
 Stafusa E. Portela, Jefferson O 84.9, TT 56.9
 Stahl, Q. MA 44.3
 Stahl, Quirin TT 51.6

Stähler, Julia •MA 30.3, O 16.2, O 16.8, O 34.3, O 37.4
 Stallberg, Klaus O 38.5
 Stam, Guido O 26.7
 Stamm, Benjamin TT 5.4
 Stammer, Moritz BP 29.3
 Stamos, Dimitar R. BP 31.7
 Stampfer, C. HL 33.17
 Stampfer, Christoph HL 9.5, HL 14.5, HL 14.8, HL 22.5, •HL 27.5, HL 30.2, HL 33.9, HL 33.12, O 4.3, •O 62.5, O 93.3, TT 14.5, •TT 40.5, TT 41.2
 Stan, Camelia DY 29.4
 Ständer, C. TT 58.4
 Ständer, Christian TT 43.30, •TT 43.31, TT 58.25
 Stange, Roland BP 28.1
 Stanger, Michael TT 54.8
 Stangier, Veronika TT 37.4, TT 37.5
 Stanko, Štefan T. •MM 39.1
 Stanković, Igor CPP 20.3, DY 42.14, O 82.5
 Stannarius, Ralf DY 7.6, DY 7.7, DY 7.8, DY 17.10, DY 29.8, DY 46.6
 Stannowski, Bernd O 80.4
 stark, holger BP 9.6, BP 11.2, BP 11.68, CPP 44.13, DY 29.5, DY 31.2, DY 31.5, DY 31.12, DY 44.14
 Stark, Máté O 15.10, O 20.3, •O 77.3
 Stark, Wojciech •O 73.1
 Starke, Ulrich O 37.12, O 56.2, O 64.6, TT 44.8
 Starkov, Grigory •DY 49.3
 Starosielec, Sebastian HL 48.2
 Starostin, Vladimir DY 37.1, •O 95.9, •TT 68.9
 Starykh, Elizaveta •KFM 6.36
 Starykh, Oleg TT 45.2
 Staszewski, Luke •MA 40.27
 Statz, Martin •HL 14.3, HL 33.14
 Stauber, Tobias TT 35.7
 Staude, Isabelle HL 35.5
 Staunton, Julie B. MA 39.1
 Stawinski, Sven TT 65.5
 Steeb, Holger CPP 35.66
 Steeger, Paul HL 18.10
 Steele, Gary A. TT 39.1
 Steenbock, Liska MM 11.5
 Stefanidis, Nikolaos •TT 53.8
 Stefanucci, Gianluca HL 31.4, HL 48.6, •HL 48.7, O 16.5, O 61.4
 Steffen, David •CPP 12.3
 Steffen, Julien O 69.9
 Steffens, Paul TT 57.5
 Stegemerten, Fenna DY 45.7
 Stegmaier, Alexander •TT 17.5, TT 64.5
 Stegmann, Philipp SYQD 1.3
 Stegmüller, Tobias MM 18.4, •MM 23.3, MM 23.31, MM 40.4
 Stehli, Alex TT 58.14
 Stehlik, Štěpán CPP 36.9, CPP 37.5
 Steidl, Jakob •O 10.6
 Steil, Daniel MA 46.8, O 34.4, O 39.5
 Steil, Sabine O 34.4
 Stein, David •MM 18.4
 Stein, Philipp TT 10.12
 Steinacker, Christoph •SOE 10.4
 Steinacker, Lorenz DS 12.4
 Steinbach, Felix •MA 8.2
 Steinbrecher, Manuel O 2.5, O 7.6, O 20.4, O 59.9, TT 57.1
 Steinbrecher, René CPP 35.60
 Steiner, Jacob F. O 20.6
 Steiner, Ullrich CPP 43.7, •CPP 56.1
 Steinhart, Martin KFM 14.4
 Steinhäuser, Aaron MA 40.44
 Steinhoff, Alexander DS 2.4, HL 8.5
 Steinhuber, Mathias •DY 48.3, •TT 55.3
 Steingeweg, Robin DY 25.10, TT 33.10, •TT 43.20, TT 43.21
 Steininger, Christina BP 25.8
 Steinkühler, Jan •BP 1.7
 Steinle, Tobias BP 12.7, MM 8.2
 Steinle, Verena BP 12.7
 Steinmann, Andy BP 12.2
 Steinmann, Paul •HL 29.6, O 70.7
 Steinrück, Hans-Georg KFM 6.1
 Steinrück, Hans-Peter O 6.2, O 11.2, O 23.1, O 23.3, O 38.2, O 60.6, O 64.1, O 73.8
 Stellbrink, Jörg •CPP 57.5
 Stelzl, Lukas •BP 3.4, BP 17.5
 Stender, Frederik MM 23.7
 Stengele, Philipp BP 7.10, DY 10.10
 Stenz, Christian MM 12.15, •MM 12.23

Stepanov, Evgeny •TT 21.7
 Stepanov, Evgeny A. MA 7.1
 Stephan, Sven HL 1.2, O 58.2, O 75.2
 Stephani, Justus C. •BP 1.6
 Steppke, Alexander TT 34.4, TT 57.4
 Šterbinská, Slavomíra TT 43.5
 Stermann, Leonel MM 33.1
 Sternemann, Christian DS 13.2, KFM 6.33
 Sterneck, Fabio BP 22.11
 Stetsovych, Oleksandr MA 19.7
 Stettner, Monja O 19.7
 Stetzuhn, Nele MA 8.2
 Steuer, Oliver DS 14.2, HL 18.8
 Stewart, Francis BP 23.11
 Stief, Tobias BP 17.4
 Stiehl, Martin MA 40.8, MA 46.7
 Stier, Andreas V. MA 32.5
 Stier, Fabian •TT 23.3
 Stier, Simon O 84.11, •O 95.11, TT 56.11, •TT 68.11
 Stierl, Dario MA 37.3
 Stierle, Andreas O 11.4, O 16.1, O 29.3, O 29.6, O 37.8, O 39.4, O 40.4, O 42.10, O 42.11, O 52.1, O 56.6, O 57.5, O 81.3, O 83.2, O 92.3
 Stiewe, Finn-Frederik MA 23.54
 Stilkerich, Nina •TT 29.1
 Stilp, Fabian •O 97.5, O 97.6
 Stirnat, J TT 42.4
 Stöber, Jonas DY 43.7
 Stöberl, Stefan •BP 31.5
 Stocco, Antonio BP 2.6, BP 11.32, •CPP 57.2
 Stock, Gerhard BP 3.8
 Stock, Sebastian •CPP 3.4, CPP 35.44
 Stock, Sebastian CPP 29.3
 Stockburger, Jürgen T. •DY 9.9, DY 43.19
 Stocker, Sina O 11.1, O 39.3, •O 52.8
 Stockert, O. •TT 47.2
 Stockert, Oliver TT 47.1
 Stockert, Ulrike TT 52.6
 Stöckl, Johannes O 22.4
 Stöckmann, Hans-Jürgen DY 21.4
 Stoev, Iliya •CPP 20.2
 Stöhler, Jörn •HL 26.6, •O 53.6, •O 67.10
 Stöhlker, Th. TT 57.28
 Stöhr, Meike O 50.4, O 60.2
 Stöhr, Rainer MA 32.4
 Stoica, Mihai MM 28.3
 Stojkovic, Marija •MM 16.10, •MM 21.4
 Stolarczyk, Jacek HL 45.4
 Stoll, A. •TT 57.21, TT 58.2
 Stoll, Alexander TT 58.3
 Stölmacker, Christoph HL 23.2
 Stolte, Evert O 15.2
 Stolte, Matthias CPP 17.10
 Stolte, Matthias CPP 17.11, CPP 28.3, DS 3.2, TT 32.3
 Stalterfoht, Martin HL 25.9
 Stöltzel, Anke •VA 1.4
 Stolz, Heinrich HL 47.2
 Stommel, Markus CPP 19.7, CPP 35.28
 Stömmer, Ralph •SOE 23.1
 Stoodley, Matthew HL 26.5, O 53.5
 Stoodley, Matthew A. •O 93.5, O 93.8
 Storck, Jan Lukas CPP 35.20, •MM 11.5
 Storeck, Gero O 34.5
 Stork, Björn BP 5.3
 Storm, Alexander •DS 12.19, DS 12.21
 Storr, Mark DY 57.4
 Storz, Simon CPP 19.12
 Stötzer, Markus MA 44.8
 Stralka, Tillmann DS 10.4, DS 12.12
 Strambini, Elia TT 27.2
 Strampe, Laura •BP 28.11
 Stransky, François BP 23.1
 Strasdas, J. •DS 7.2, MA 40.53
 Straßheim, M. •MA 42.8
 Strassert, Cristian A. O 2.5
 Strassheim, Marc MA 23.18
 Straube, Arthur •DY 4.10
 Strauß, Dirk KFM 6.23, KFM 8.7
 Strauß, Kilian •CPP 17.6, CPP 28.8, TT 32.8
 Strauss, Dirk KFM 8.6, KFM 8.8, •KFM 8.9
 Strebel, Oliver •DY 45.2
 Strečka, Jozef TT 29.9, TT 29.10
 Strehle, Steffen DY 29.7
 Streib, Simon MA 20.7

Streit, Achim BP 11.76
 Strenzke, Vincent HL 14.1
 Strick, Terence BP 23.1
 Striegler, Martin BP 30.5
 Strik, Julian H. O 20.1, O 51.2
 Strinc, Ana MA 40.35
 Stringe, Mark MM 28.1
 Strinic, Ana TT 54.8, TT 54.10,
 TT 58.8, TT 58.9
 Strittmatter, André HL 7.6, HL 44.1,
 HL 51.1, HL 51.7, O 32.1, O 32.6
 Strkalj, Nives DS 15.3, KFM 1.4
 Strobel, Pascal TT 42.12
 Strobel, Tim HL 7.48
 Strobl, Clemens HL 10.7
 Strobl, Timo KFM 11.6
 Stroch, David-Maximilian SOE 10.4
 Strocov, Vladimir TT 21.1
 Strocov, Vladimir N. TT 27.4
 Stroganov, Vladislav CPP 54.4
 Stroh, Karen DS 14.3
 Stroh, Karen P. MA 46.8
 Strohmeier, Marcel TT 16.3
 Strocio, Joseph O 87.5
 Strothmann, Robert CPP 35.38
 Struck, Tom HL 29.1, HL 37.1, HL 37.4
 Strunk, Christoph TT 16.8, TT 20.8,
 TT 27.5
 Strunskus, Thomas CPP 13.1,
 CPP 17.4, CPP 29.2, CPP 29.8,
 CPP 56.2
 Struve, Marti HL 2.6
 Strydom, A TT 42.4
 Stubb, Aki BP 16.4
 Studd, Felix O 69.3
 Stumper, Sebastian DY 43.21
 Stumpf, Bernd Henning BP 11.63
 Stumpf, Steffi CPP 36.7
 Sturm, C. DS 12.48, HL 7.16, HL 7.19,
 HL 7.20, HL 18.5
 Sturm, Chris DS 13.3, HL 7.22,
 HL 7.31, O 49.7
 Sturm, Elena O 49.5
 Sturm, Heinz CPP 17.1
 Sturm, Joris DS 12.30
 Stutzer, Lars Torbjørn DY 42.2
 Stutzmann, Martin O 40.2
 Style, Robert W. BP 11.5, BP 23.10
 Su, Linfeng MM 37.2
 Su, Xuelei O 66.1
 Su, Yixi TT 23.5, TT 23.8
 Subakti, S. KFM 11.9
 Subramaniam, Sivaraman BP 23.11
 Subramanian, Kaushikaram BP 21.4
 Suchanek, Thomas DY 40.8
 Suchecki, Krzysztof SOE 4.4,
 SOE 6.3
 Suchsland, Philippe DY 55.5,
 TT 67.5
 Sudbø, Asle TT 45.3
 Suderow, H. TT 6.4
 Sudersan, Pranav O 12.2
 Sudzius, Markas DS 10.2
 Suess, Dieter MA 50.3
 Sugak, D. KFM 14.7
 Suhak, Yuriy KFM 13.4, KFM 13.5,
 KFM 13.6, KFM 14.6
 Sukhanov, Aleksandr TT 23.12,
 TT 42.5
 Sukhanov, Alexandr MA 37.4
 Sulaiman, Cathy O 64.8, O 93.7
 Sulamanidze, Aleksandr MM 20.5
 Sulik, Adam SOE 18.2
 Süllow, Stefan TT 10.4, TT 29.3
 Sulmoni, L. HL 23.1
 Sulmoni, Luca HL 23.2, HL 28.5
 Sumbul, Fidan BP 23.1
 Sumeet, Sumeet TT 42.22
 Sun, Binhan MM 27.8
 Sun, Bowen CPP 11.4, CPP 11.5,
 HL 2.4
 Sun, Fei MM 6.6, TT 37.13
 Sun, Haonan MM 23.23
 Sun, Hengda DS 16.6
 Sun, Kun CPP 17.20, CPP 17.44,
 CPP 17.46, CPP 35.43
 Sun, Pei Ling MM 37.1
 Sun, Pei-Ling MM 37.8
 Sun, Qiang O 75.5
 sun, qing MA 19.5
 Sun, Zhaoru O 66.8
 Sundaramurthy, Vignesh TT 44.8
 Sunderamann, Martin TT 30.4
 Sündermann, Eric BP 8.11
 Sundermann, Martin TT 9.3, TT 9.4,
 TT 9.5, TT 30.7
 Sung-Min Choi, L. HL 43.6

Sunko, Veronika MM 6.6, TT 37.13
 Sunyer, Raimon BP 30.4
 Surayadevara, Nithin O 14.4
 Suresh, K. Gopi MA 37.2
 Suresh Kumar, Kiran CPP 58.6
 Surfaro, Furio CPP 19.12
 Sürgers, Christoph O 15.10, O 20.3,
 O 77.3
 Suri, Balachandra DY 29.1
 Surovyatkina, Elena SOE 9.3
 Surówka, Piotr MM 6.7
 Sushkov, Alexander O. DY 25.12,
 TT 33.12
 Süß, Dieter MA 40.3
 Sutter-Fella, Carolin DS 11.3
 Sütterlin, Jana BP 28.9, HL 18.12
 Suvorov, Oleksandr TT 57.9
 Švec, Martin O 10.3, O 43.8, O 70.10,
 O 76.3, O 76.5
 Svetlana, Santer CPP 20.5
 Svitlyk, Volodymyr TT 51.6
 Swedan, Amro O 49.3
 Sweetman, Adam O 54.2, O 77.4
 Swekis, Peter MA 23.60
 Swinburne, Thomas MM 25.5
 Sydorochuk, V. KFM 14.7
 Syed, Nitu HL 14.4
 Syndikus, Jacob O 43.6
 Syskaki, M-A MA 12.4
 Syskaki, Maria-Andromachi MA 12.8,
 MA 17.2, MA 23.5, MA 23.22,
 MA 23.23, MA 23.53, MA 40.29,
 MA 40.30
 Syvorotka, N. KFM 6.46
 Syvorotka, Natalia KFM 13.6
 Szabó, Dorothee Vinga MM 23.32
 Szabo, Gabriel L. O 5.3
 Szabo, Gabriel Lukas O 13.6, O 13.8
 Szabo, Paul S. O 5.3
 Szabo, Paul Stefan O 13.2
 Szafarska, Maik MM 11.4
 Szaller, Dávid MA 44.2
 Szameit, Alexander TT 36.6
 Szczefanowicz, Bartosz O 4.3
 Szczepanik, Magdalena O 30.3
 Szelwicka, Jolanta DS 13.2
 Szilva, Attila MA 7.1
 Sznajd-Weron, Katarzyna SYOF 1.1
 Sztot, Kristof KFM 2.1
 Szpak, Nikodem DY 25.9, TT 16.15,
 TT 33.9, TT 60.6, TT 60.7
 Szunyogh, László MA 4.8, MA 14.1,
 MA 24.2, MA 46.5, TT 7.8, TT 8.5,
 TT 8.6
 Szyjka, Thomas DS 12.5
 Szymanski, Boleslaw K SOE 18.2
 Szymoniak, Paulina CPP 29.6,
 CPP 37.4
 T Amawi, Mohammad HL 50.1
 T.B. Goennenwein, Sebastian MA 20.2
 T. N Diaye, Alpha MA 17.5
 Taake, Chris MA 23.16, MA 23.17
 Tabachová, Zlata SOE 22.3
 Tafti, Fazel MA 9.5, TT 6.6
 Tagirov, L. MA 40.14
 Tagliacruzchi, Mario DY 16.11
 Taguchi, Yasujiro MA 40.51, MA 50.7
 Taheriniya, Shabnam MM 41.2
 Tahmasbi, Hossein MM 12.11,
 MM 31.8
 Tahouni-Bonab, Farnaz DS 12.28
 Tahraoui, Abbes DS 12.22, HL 3.4,
 HL 7.40
 Takagi, Hidenori O 56.2, TT 3.3,
 TT 9.6, TT 42.14, TT 50.6, TT 51.5,
 TT 52.5
 Takaki, Ryota BP 11.56
 Takayama, Tomohiro TT 52.5
 Takegami, Daisuke TT 9.5, TT 30.3,
 TT 30.4, TT 30.6
 Takeuchi, Tetsuya HL 28.1
 Taleb, Masoud DS 2.2, MM 26.7
 Talebi, Nahid DS 2.2, DS 2.3,
 MM 26.7, O 58.3, O 83.7, VA 1.5
 Talib, Ayesha BP 23.3
 Talnack, Felix CPP 43.6, CPP 43.8
 Talwar, Timo O 11.2, O 38.2, O 60.6
 Tamir, Idan O 20.6, O 21.1
 Tamura, Shun TT 31.7
 Tan, Anne Marie Z. O 30.7
 Tan, Tzer Han BP 30.3
 Tanaka, Arata TT 30.4, TT 30.6,
 TT 30.7
 Tanaka, Yukio TT 31.7
 Tănase, Liviu C. O 52.1
 Tanda Bonkano, Boubacar O 16.8

Tang, Evelyn SYQC 1.4
 Tang, Nan TT 46.1
 Tang, Xin SYGM 1.2
 Tanguy, Döme MM 23.11, MM 33.1
 Taniguchi, T. HL 33.17, O 47.7
 Taniguchi, Takashi DS 1.6, DS 2.4,
 DS 12.20, HL 9.4, HL 9.5, HL 14.5,
 HL 22.5, HL 30.2, HL 33.10, HL 33.12,
 HL 33.18, HL 34.3, TT 14.4, TT 14.5,
 TT 35.1, TT 35.7, TT 41.2
 Tanimura, Katsumi O 34.2
 Tank, Tejas DS 14.7
 Tannoury, Lama CPP 37.1
 Tantos, Christos VA 1.2
 Tänzler, Victor BP 3.6
 Tao, Cong MM 32.8
 Tao, Kun O 66.1
 Tao, Ran TT 57.14
 Tao, Yijie MM 23.8
 Tao, Yinghao KFM 6.32
 Tapias, Diego DY 24.1
 Tappe, Torben MA 23.46, MA 40.45
 Tarasenko, Róbert MA 13.9,
 TT 19.9, TT 58.24
 Tarasevitch, Alexander O 60.11
 Tarasevych, Dmytro MA 33.2
 Tarasov, Andrey O 78.1
 Tarasov, Ivan DS 10.1, HL 36.7,
 MA 38.3
 Tarrach, Lena CPP 19.6
 Tarucha, Seigo SYQD 1.1
 Tatar-Mathes, Philipp HL 12.3
 Tatham, Elizabeth BP 16.1
 Tatzelt, Jörg BP 17.2
 Taubel, Andreas MA 3.9
 Täuber, Daniela BP 21.2, BP 28.3,
 BP 28.6
 Taubert, Oskar BP 11.16, BP 11.76
 Taubner, Thomas O 49.8, O 70.5,
 O 91.8, O 93.3
 Taufertshöfer, Nicolai O 67.3
 Taufertshöfer, Nora TT 57.17
 Tausendpfund, Niklas DY 43.12,
 TT 31.5
 Tausendpfund, Timon MA 35.6
 Taute, Katja DY 26.1
 Tautz, F. S. O 10.1
 Tautz, F. Stefan MA 21.7, O 18.2,
 O 19.7, O 21.2, O 33.2, O 45.7, O 74.3,
 O 74.5, O 82.1
 Tautz, Stefan O 66.9, O 77.1
 Tavabi, Amir MA 23.4
 Tavaddod, Sharareh BP 16.1
 Tavakoli, Abolfazl MA 23.24
 Tavazza, Francesca HL 26.1, O 53.1
 Taylor, J. O 47.3
 Taylor, James M MA 23.51, MA 23.64,
 MA 48.4
 Taylor, Victoria C. A. MA 46.13,
 O 34.7
 Tayurskii, D. MA 40.14
 Tcakaev, Abdul V. O 94.6
 te Vrugt, Michael BP 24.4, DY 26.7,
 DY 38.4, DY 44.1
 Tea, Lingsam CPP 57.5
 Tebbe, David HL 22.5, HL 33.9
 Techert, Simone CPP 36.8, DS 12.34
 Tegeder, Petra DS 15.2, DS 15.5,
 O 10.6, O 10.7
 Tegenkamp, C. O 50.2, O 69.11
 Tegenkamp, Christoph O 36.7,
 O 36.10, O 42.7, O 64.4, O 82.2,
 O 82.6, O 82.8, O 82.9
 Tegerer, Petra CPP 26.3
 Tehlan, Kartikay MA 32.5
 Tehrani, Ali MM 15.9, MM 32.1,
 MM 32.5
 Tehrani, Mohammad O 40.4
 Teichert, Christian DS 5.3, KFM 6.39,
 O 31.3
 Teichert, Fabian CPP 17.21
 Telezki, Vitali BP 6.3
 Teller, Justus TT 59.5
 Temirov, Ruslan MA 13.3, MA 21.7,
 O 21.2, O 33.2, O 55.4, O 66.9,
 O 77.1, TT 19.3
 Temmen, Michael O 21.4
 Tenbrake, Lukas DS 12.37
 Teng, Sheng-Han KFM 4.4
 Tepsaß, Jannina HL 23.4
 Teplyakov, Andrew O 48.1
 Teppe, F. HL 17.8
 Terakawa, Shigemi O 32.4
 Terekhin, Pavel N. O 80.1
 Terfort, Andreas O 37.1
 Terle, Jocelyn HL 9.4, TT 14.4
 Ternes, Markus MA 21.7, O 18.2,

O 33.2, O 74.3, O 74.5, O 82.1
 Terres, Sophia DS 1.6
 Terwey, Alexandra MA 42.7
 Tesch, Julia O 56.7
 Teshler, Lev TT 48.3
 Teske, Julian D. HL 37.7
 Tessarek, Christian HL 14.7
 Tesser, Francesca CPP 57.1
 Tesser, Ludovico TT 38.7
 Tetling, Leander TT 54.3
 Tetzner, Yannick CPP 35.64
 Teuerle, Laura CPP 45.9
 Tewari, Akshay MA 40.17, TT 57.5
 Tewari, Sumanta TT 6.1
 Thai, Quang Minh BP 11.43
 Thakur, S. O 47.3
 Thakur, Sangeeta MA 19.4, MA 40.12,
 MA 40.55
 Thaler, Marco O 47.6
 Thalla, Divyendu Goud BP 28.52
 Thalmann, Karin S. CPP 17.25
 Thalmeier, Peter TT 9.3, TT 9.4
 Thamizhavel, Arumugam MM 14.7
 Thamm, Matthias DY 2.5, TT 2.5
 Thampi, Arsha MA 12.2
 Thanbichler, Martin BP 12.12
 Thapa, Manish TT 49.2
 Thapa, Samudrajit BP 24.7,
 DY 27.10, DY 38.7
 That Ton, Khai O 7.1
 Thauer, Elisa CPP 35.14
 Theilen, Marcel O 19.7
 Thelakkat, Mukundan CPP 17.18
 Thelen, Marc MM 23.21
 Thelen, Richard O 4.8
 Theuner, David O 13.4
 Thewes, Filipe DY 27.4
 Thiede, Christian O 67.8
 Thiele, Simon HL 50.2, KFM 7.3
 Thiele, Uwe BP 24.4, CPP 8.1,
 CPP 44.4, CPP 44.7, CPP 44.12,
 DY 4.3, DY 26.7, DY 37.3, DY 38.4,
 DY 45.7
 Thiemann, Fabian HL 48.3
 Thieme, Jan KFM 6.12
 Thiering, Nicola KFM 6.29
 Thima, Daniel O 13.6
 Thirugnanasambandam Masilamani,
 Muthu Prasanth O 67.4
 Thoben, Niklas O 85.9
 Thole, Lars HL 34.4
 Thomale, Ronny DY 48.7, DY 55.1,
 MA 33.1, O 58.7, TT 8.4, TT 17.5,
 TT 29.12, TT 29.13, TT 36.6, TT 55.7,
 TT 57.17, TT 63.12, TT 64.5, TT 67.1
 Thomas, A. MA 41.2
 Thomas, Akhil MM 20.1
 Thomas, Andy MA 4.14, MA 12.3,
 MA 20.2, MA 23.60, MA 40.63,
 MA 40.64, TT 7.14
 Thomas, Anitta R. BP 11.42
 Thomas, Antony O 55.7
 Thomas, Carsten MM 37.8
 Thomas, Heidi CPP 26.2
 Thomas, Nithin DY 43.9
 Thomas, Sarah HL 3.6
 Thomas, Tatjana TT 51.9
 Thomas, Teslin KFM 11.5, TT 10.11
 Thome, Ulrich BP 4.3
 Thompson, Asha O 26.5
 Thonig, Danny MA 20.7, MA 47.6
 Thormählen, Lars DS 12.7, MA 40.48
 Thorneywork, Alice DY 32.11
 Thorn-Seshold, Oliver BP 11.36
 Thorwart, Michael DY 25.4, MA 35.2,
 TT 33.4
 Thoss, Michael CPP 17.25, MA 4.3,
 TT 7.3, TT 16.4, TT 16.17, TT 38.9,
 TT 60.5
 Thota, Subhash MA 44.9
 Thränhardt, Angela CPP 17.21,
 CPP 36.3
 Thuenauer, Roland O 57.5
 Thümler, Moritz DY 18.1, DY 18.2
 Thümler, Martin O 83.3
 Thun, Tobias BP 10.4
 Thunström, P. MA 28.4
 Thunström, Patrik MA 47.3
 Thürmer, Daniel DY 29.4
 Thurn, Christian TT 46.7
 Thurn-Albrecht, Thomas CPP 17.18,
 CPP 19.5, CPP 35.26, CPP 35.27
 Thurner, Stefan SOE 18.1, SOE 19.1,
 SOE 22.3, SOE 23.4
 Thyen, Laurenz DS 16.2
 Thyzel, Tim TT 43.9, TT 51.9
 Tian, Ting CPP 17.16, CPP 35.18,

Author Index

- CPP 35.19
Tian, Ye O 6.8
Tiemann, Lars HL 3.3, HL 14.1, TT 35.7
Tietjen, Finja •TT 57.16
Tietze, Rainer HL 29.4
Tiginyanu, Ion HL 7.30
Tikhodeeva, Ekaterina •O 14.11, •O 37.9
Tilger, Thomas CPP 17.49, •CPP 57.8
Tilgner, Andreas DY 5.4
Tillack, Sebastian •HL 31.6, •O 61.6
Timm, Carsten TT 5.1, TT 57.12, TT 57.13, TT 63.7, •TT 64.4
Timm, Matthew James •O 23.4
Timme, Marc DY 17.8, DY 18.1, DY 18.2, SOE 6.1, SOE 10.1, SOE 10.2, SOE 10.4, SOE 10.5, SOE 10.6, SOE 11.2, SOE 11.3, SOE 11.4, SOE 15.1
Timmer, Alexander O 97.7
Timmer, Daniel •BP 11.42, CPP 28.9, HL 25.8, •O 58.2, TT 32.9
Timmermann, Jakob O 78.3
Timmermann, Sonja BP 11.46
Timonin, Pavel N. TT 31.3
Timpe, Olaf O 78.1
Timr, Stepan BP 22.11
Tindall, Joseph MA 9.2
Ting, Po-Chieh O 34.1
Tinnefeld, Philip •CPP 56.8
Tirpanci, Saban MA 43.7
Titov, Mikhail MA 8.11
Titvinidze, Irakli TT 23.6
Titze, Tim MA 46.8, O 39.5
Tiwari, Aarti O 52.1
Tiwari, Vandana MM 10.4
Tjeng, L. H. TT 46.2
Tjeng, Liu Hao HL 51.3, HL 51.6, TT 4.10, TT 9.3, TT 9.4, TT 9.5, TT 30.3, •TT 30.4, TT 30.7, TT 50.1
Tjeng, Liu-Hao TT 30.6
tjernberg, oscar DY 25.7, O 8.8, O 37.12, TT 33.7
Tkáč, Vladimír MA 13.9, TT 19.9, TT 58.24
Tkach, O. MM 12.1, •MM 26.8, O 30.4
Tkach, Olena O 85.7
Tkatchenko, Alexandre CPP 45.1
Tkhov, Prokhor •HL 22.2
Tlili, Sham BP 15.6
Tober, Steffen DS 14.6, MA 5.6, O 29.6, •O 42.12, •O 92.3
Tochtermann, Marius TT 30.1
Todorova, Mira MM 27.4, MM 32.1, MM 37.3, •MM 37.7, O 69.7, O 86.3, O 86.5
Toellner, Tom MA 42.2
Tohamy, Hossam TT 58.15
Toher, Cormac MM 36.9
Tokita, Alea Miako •MM 12.18, O 26.6
Tokiva, Yoshifumi MA 13.7, TT 19.7
Tokmoldin, Nurlan •CPP 11.4
Toksabay, Sinem O 55.10
Tokunaga, Yo TT 28.4
Tokunaga, Yusuke MA 50.7
Tokura, Yoshinori MA 2.6, MA 50.7
Tolan, Metin •PSV VI
Tolosa-Simeón, Mireia •TT 53.6
Tomar, Ritu •DS 12.41
Tomilo, Artem V. MA 11.4, MA 18.6
Tomba, Júlia SOE 4.12
Tomsovic, Steven DY 25.8, TT 33.8
Tomut, Marilena MM 28.6
Ton, Khai That •O 7.3
Toney, Michael F. CPP 18.1
Tong, Anh MA 26.2
Tong, Chuyao •HL 9.4, •TT 14.4
Tong, Johnny BP 28.40, •BP 28.44
Tong, Yujin O 25.2, O 30.10, O 60.11
Tongay, Sefaattin HL 22.4
Tonisch, Katja DS 12.4
Tonner-Zech, Ralf HL 18.7, O 10.5, O 10.9, O 48.5, •O 57.3
Topmøller, Jan-Phillip •O 18.6
Toral, Raul SOE 7.3
Tormann, Constantin •CPP 1.2, CPP 18.7
Torokar, Maytal Caspary HL 25.5
Toroşyan, Garik MA 22.5
Torrent, Marc TT 21.9
Torres, E. O 47.3
Torres, J. HL 17.8, O 23.1
Torres, Jorge •MA 19.4
Toschi, Alessandro TT 29.7, TT 65.4, TT 65.8
Toschke, Yannic KFM 6.45
Tosi, Ezequiel O 14.8
Toth, Milos HL 22.3
Toulouse, Andrea BP 12.2, KFM 7.3
Toulouse, Constance MM 23.34
Trabs, Mathias KFM 9.12
Tracy, Joseph B. MA 40.47
Trahms, Martina O 20.6
Trainer, Christopher TT 37.12
Trajanovski, Pece DY 44.15, •DY 44.19
Trallero-Giner, Carlos DS 7.4
Trambly de Laissardière, Guy TT 43.28, •TT 61.5
Trampert, Achim DS 8.2, KFM 9.6
Tran, Huong O 49.9
Tran, Loi Vinh O 47.10
Tran, Mai BP 12.11
Tran, Nam •HL 49.3
Tran, Trung Duc TT 66.4
Tran, Tuan •O 5.4
Tranchida, Julian MM 31.8
Trassin, Morgan DS 15.3, KFM 1.4, KFM 4.2, KFM 6.27
Traulsen, Arne DY 45.14, SOE 15.5
Trautmann, Christina O 13.3
Trautmann, Julius •BP 21.6
Trauzettel, Björn DY 44.11, HL 31.1, O 61.1, TT 63.7
Traxdorf, Maximilian DY 26.5
Trebin, Hans-Rainer MM 12.21
Trebst, Simon MA 7.10, MA 33.8, MA 40.24
Trefflich, Lukas HL 7.31
Treichel, Marten •O 20.9
Trelin, Andrii •BP 28.55, HL 50.1
Trellenkamp, Stefan HL 33.12
Tremisina, E MA 31.1
Tremisina, Elizaveta MA 40.5
Trepast, Xavier BP 4.5, BP 4.8, BP 30.4
Tress, Martin CPP 35.29
Tress, Martin •CPP 50.3, CPP 53.3
Tretiak, Sergei CPP 28.9, HL 38.7, TT 32.9
Trifonov, Artur V. HL 35.4, HL 35.8
Trigo, Mariano TT 62.7
Trimaille, Isabelle CPP 52.2, MM 23.27
Tripathi, Richa SOE 4.8
Tripathi, Sarthak HL 12.2, •HL 33.47
Tripathi, Vikram MA 33.3
Trippé-Allard, Gaelle HL 17.9
Triscone, Jean-Marc DS 12.28
Trishin, Sergey O 33.4, •O 33.8
Trittel, Torsten DY 7.6, DY 7.8
Trofimov, Sergei KFM 6.34, •KFM 6.38
Tröger, Lucas •BP 9.5
Trömer, Manuel CPP 12.6
Trommer, Clara W. A. MA 19.4
Trommer, Jens HL 16.5, TT 24.7
Tromp, Ruud O 26.7
Trösemeyer, Jan-Hendrik BP 11.22
Troupe, Mirco HL 8.4, HL 37.8
Trummer, Florian •CPP 57.7
Trunschke, Annette O 63.2, O 78.1, O 78.5
Truong, Dong-Jiunn Jeffery BP 11.71
Trzeciak, Simon O 69.9
Tschagaew, Roman O 26.2
Tschammer, Rudi •O 78.9, O 92.6
Tscheppe, Patrick •TT 61.1
Tschirner, Teresa MA 40.64, O 94.6
Tschulik, Kristina •TUT 4.3, •MA 1.3
Tschurikow, Xenia BP 11.59, BP 12.11
Tschurl, Martin •O 29.8, O 41.3, O 41.4
Tsen, Adam MA 17.3
Tseplyaev, Vasily O 51.1
Tsesses, Shai O 80.3
Tsirlin, A. A. TT 23.1
Tsirlin, Alexander MA 7.9, MA 13.7, MA 18.5, MA 23.65, TT 19.7, TT 46.4, TT 52.7
Tsirlin, Alexander A. MA 44.2, TT 46.10
Tsitsilianis, Constantinos CPP 17.54
Tsitsilin, Ivan •TT 49.6, TT 58.11
Tsud, Nataliya O 28.5, O 29.2, O 55.2, O 81.11
Tsuei, Ku-Ding TT 30.3, TT 30.6
Tsurkan, V. MA 33.6, MA 40.14, TT 52.3
Tsurkan, Vladimir MA 18.5, MA 23.13, MA 23.65, MA 44.2, TT 52.2
Tsutsui, S. TT 47.2
Tu, Jih-h-Sian HL 29.5, HL 37.1
Tu, Suo •CPP 17.16, CPP 35.18, CPP 35.19
Tückmantel, Philippe KFM 4.9
Tuczek, Felix MA 19.4, O 42.6
Tufarelli, Tommaso O 58.9
Tumanguil, Mae Agatha HL 17.6
Tümmler, Paul CPP 57.6
Tuniz, Manuel O 16.3, O 19.2, •O 19.4, O 34.8, •O 34.10
Tuovinen, Riku •HL 31.4, •O 61.4
Turchanin, A. O 47.7
Turchanin, Alexander •DS 12.14
Turchanin, Andrey CPP 54.4, DS 1.2, DS 12.14, DS 12.16, HL 14.6, O 4.3, O 5.3, O 18.1, O 18.3, O 18.4, O 47.8
Turco, Elia •O 33.3
Turek, Ilja MA 16.8, •MA 23.29, MA 37.6
Turek, P MA 23.21
Türk, Hanna MM 3.3, •MM 5.10
Turlier, Hervé BP 4.2
Turnbull, Luke MA 43.1
Turnbull, Luke A. •MA 11.6
Turriani, A. A. TT 42.13
Tutsch, Ulrich TT 46.7
Tüysüz, Harun O 78.7
Tverdokhlebo, Nina CPP 35.45, CPP 56.3
Tverskoy, Olena O 10.7
Tvingstedt, Kristofer CPP 28.4, TT 32.4
Tworzydło, Jakub HL 30.6, TT 41.6, TT 53.3
Tymoshenko, Y. V. MA 33.6
Tymoshenko, Yuliia MA 44.7, •TT 57.8
Tzschaschel, Christian •MA 8.1
U. B. Wolter, Anja MA 40.57
Uali, Aitolkyn S. BP 6.7
Ubl, Monika CPP 37.3
Ucar, Mehmet Can •BP 27.3
Uccello, Andrea O 24.2
Udachin, Viktor •O 11.7
Uderhardt, Stefan BP 28.53
Udvarhelyi, Péter MA 32.4
Ueberricke, Lucas CPP 35.14
Uehlein, Markus •O 8.4
Ugalde, Jesus TT 11.4
Ugokwe, Chikezie Williams •CPP 51.8
Ugrina, Marijana •BP 11.21, •BP 26.4
Uhl, Kevin TT 58.18, TT 58.19
Uhlarz, M. TT 59.8
Uhlarz, Marc TT 43.5
Uhlrig, Kai CPP 19.7, CPP 35.28
Uhlrig, Lukas HL 23.2, HL 23.4, •HL 28.3
Uhlir, Vojtech MA 40.10
Uhlmann, Max DY 37.7
Uhrig, Götz S. DY 25.12, TT 5.11, TT 33.12, TT 42.19, TT 42.20
Újfalussy, Balázs TT 8.5, TT 8.6, TT 8.7
Uklee, Victor MA 48.4
Uliana, Yakhnevych KFM 13.3
Ullmann, Fabian •DS 8.1
Ulm, Andreas O 49.8
Ulrich, Nils O 13.5
Ulstrup, Søren O 34.9
Undisz, Andreas MM 17.2
Unfried, Jakob •DY 25.11, •TT 33.11
Unger, Daniel •TT 58.1
Unger, Eva HL 25.11
Unold, Thomas HL 7.37, HL 25.3, HL 25.9, HL 25.10, HL 25.11
Unsal, Elif •HL 36.1, MM 3.9
Unzelmann, Maximilian O 22.7, •O 59.1, O 65.5, O 67.3, O 67.5, O 94.2, O 94.9
Upadhyay, Utkarsh •BP 11.16
Upadhyayula, Krishna Koundinya •HL 44.4
Upreti, Lavi TT 17.5
Upreti, Lavi K. TT 64.5
Upreti, Tanvi CPP 1.2
Urban, Adrian O 37.13
Urban, Alexander DS 11.3
Urban, Alexander S. CPP 19.11, HL 14.6
Urban, Daniel MM 5.2, MM 5.6, MM 27.5
Urban, Daniel F. •MM 9.3, MM 11.1, •MM 11.2, MM 32.6
Urban, Joanna HL 17.7
Urban, Joanna M. •HL 17.9
Urban, Piet MA 23.51
Urbassek, Herbert DY 29.4
Urbaszek, B. O 47.7
Urbaszek, Bernhard O 18.3
Urbina, Juan-Diego DY 25.8, DY 48.3, TT 33.8, TT 55.3
Urbina, Juan-Diego DY 6.8, DY 48.9, DY 55.4, TT 55.9, TT 62.6, TT 67.4
Ureña Marcos, José Carlos •BP 7.5, •DY 10.5
Ürgüp, Kaan •BP 28.32
Urchuk, Andrew DY 48.8, TT 55.8
Urtev, Fedor O 66.10
Uslu, Jan-Lucas •HL 14.8
Ustinov, Alexey TT 58.13
Ustinov, Alexey V. TT 49.3, TT 58.12, TT 58.14, TT 58.15, TT 58.17
Utikal, Tobias TT 25.4
Utsumi, Yuki TT 30.3
Uykur, E. TT 6.10, •TT 23.1, TT 23.7
V. Divinski, Sergiy MM 41.2, MM 41.4
V. Gurevich, Svetlana DY 4.8
v. Helversen, Martin HL 1.7
v. Klitzing, Regine CPP 13.0
v. Löhnneysen, Hilbert TT 47.1
V. Pylypovskiy, Oleksandr MA 17.1, MA 38.2
V. Roth, Stephan CPP 13.9, CPP 17.4, CPP 17.46, CPP 17.51
Vaccario, Giacomo SOE 18.3
Vaclavkova, Diana MA 19.1, •MA 40.32
Vadimov, Vasilii DY 43.19
Vagadia, Megha •DS 14.7
Vagias, Apostolos •CPP 8.4, CPP 13.9, CPP 35.18, CPP 52.5, CPP 53.4
Vagin, Sergei CPP 17.20
Vagizov, F. MA 40.14
Vagne, Quentin BP 28.22
Vahedi, Javad TT 61.5
Vahl, Alexander CPP 13.1
Vaibhav, Sharma BP 1.8
Valadkhani, A. TT 34.3
Valadkhani, Adrian MA 40.60, MA 40.61
Valani, Rahil N. DY 18.3
Valencia, Ana M. CPP 17.34
Valencia, Ana Maria •CPP 18.3
Valencia, Felipe •MM 22.1
Valencia, Sergio DS 5.3
Valenti, R. TT 34.3
Valenti, Roser •HL 31.5, MA 40.61, •O 61.5, O 84.4, TT 29.5, TT 35.5, TT 35.6, TT 36.2, TT 52.4, TT 56.4
Valentin, Sascha R. VA 2.2
Valentinis, Davide MM 6.7
Valenzuela, Javier MA 36.6
Valido, Dario A. Leon MM 3.8
Valiska, Michal TT 28.1
Valiullin, Rustem MM 23.22, MM 42.8
Valldor, Martin TT 43.3
Vallet, Maxime MM 33.2
Valls Mascaró, Francesc •O 96.6
Valmispil, Viktor SYUE 1.4
Valotteau, Claire BP 23.1
Valsson, Omar CPP 2.12
Valtiner, Markus O 54.6
Valvidares, M. MA 12.5
Van Avermaet, Hannes HL 24.1
van de Kamp, Thomas O 4.8
van de Krol, Roel HL 47.7
van den Brink, Jeroen MA 18.6, MA 27.7, MA 33.5, MA 41.3, MM 12.37, TT 6.11, TT 17.6, TT 47.8
van den Ende, Dirk O 60.4
van der Giessen, Erik MM 15.3
van der Heide, Tammo •KFM 6.5
van der Jagt, Gyan MA 17.2
Van der Laan, G. MA 12.5
van der Laan, Gerrit MA 43.1
van der Linden, Lize BP 12.8
van der Meer, Jann BP 23.6, •DY 40.4
van der Molen, Sense Jan O 26.7
van der Oord, Cas O 73.1
van der Voort, Nicolaas TM BP 21.8
van Efferen, Camiel •O 56.8
van Helvoort, Antonius •KFM 1.8
van Helvoort, Antonius T.J. •KFM 1.2
van Hulst, Niek F. HL 2.4
van Loon, Erik HL 40.1, O 79.1
van Loosdrecht, Paul H. M. TT 10.12
van Midden Mavric, Marion O 30.2
van Moorsel, Aad SOE 4.10
van Mullekom, Niels O 20.4
van Mullekom, Niels P.E. •O 7.6, O 20.2, O 33.9, O 59.9, TT 57.1
van Nieuwenburg, Evert HL 33.27
van Rijn, R. HL 33.62
Van Roekeghem, Ambroise MM 39.4, TT 21.9
van Roij, René CPP 29.4
van Ruitenbeek, Jan O 7.7

Author Index

- van Teeffelen, Sven BP 6.4
 Van Waasen, Stefan HL 16.9,
 HL 50.10, HL 50.11, HL 50.12, TT 24.9
 van Weerdenburg, Werner M.J. O 7.6,
 O 20.2, O 20.4, O 33.9, +O 59.9,
 TT 57.1
 van Wezel, Jasper TT 6.11, TT 51.7
 Vana, Phillipp MM 23.13
 Vanacore, Giovanni Maria O 83.5
 Vanberg, Jan DY 9.4
 Vandermoeten, Isabelle TT 57.23
 Vanderstraeten, Laurens TT 46.9
 Vandewalle, Nicolas +DY 31.8, DY 31.9
 Vanel, Loïc MM 23.11, MM 33.1,
 +MM 33.5
 Vano, Viliam O 74.2
 Vardanyan, Vahagn O 37.9
 Varela Rosales, Nydia Roxana +O 14.7
 Varela, Solmar MM 12.5, +TT 11.4,
 TT 11.5
 Varentcova, Anastasiia KFM 11.8
 Varjas, Dániel HL 49.4, +KFM 11.8
 Varotto, Sara MA 4.11, TT 7.11
 Varoutis, Stylianos VA 1.2
 Varsano, Daniele HL 20.3, HL 26.3,
 HL 26.4, MM 3.8, O 35.3, O 53.3,
 O 53.4
 Vartanyants, Ivan DS 6.3
 Varvelis, Evangelos +TT 54.2
 Váry, Tomáš CPP 1.4, CPP 17.17
 Vasala, Sami TT 44.7
 Vasileiadis, Thomas SYUE 1.2, O 16.7
 Vasilevskiy, Mikhail MA 20.4
 Vasilopoulos, Alexandros +DY 49.10
 Vasilopoulou, Maria CPP 43.7
 Vasilyev, D. MM 12.1, MM 26.8, O 30.4
 Vasilyev, Dmitry O 85.3
 Vassalli, Massimo BP 28.35
 Vassallo, Espedito O 24.2
 Vassholz, Malte DY 18.7
 Vassilopoulos, Stéphane BP 31.2
 Vasylechko, Leonid TT 52.6
 Vasyuchka, Vitaliy MA 23.8,
 MA 23.11, MA 23.69
 Vaughan, Gavin KFM 6.31, MM 28.3
 Vavassori, Paolo MA 29.4
 Vaynzof, Yana DS 10.2
 Väyrynen, Jukka TT 31.12
 Vaz, Carlos A. F. MA 43.3
 Vecchione, Antonio TT 37.7, TT 37.10
 Vedmedenko, Elena +MA 2.8,
 +MA 49.1
 Veigel, Claudia BP 22.8
 Veis, Libor O 45.6
 Veit, Peter HL 7.6
 Veldman, Lukas +O 15.2
 Venaille, Antoine SYQC 1.2
 Venkatesh, Varun DY 26.4
 Venkova, Larisa BP 31.2
 Venturilli, Davide DY 32.1
 Ventzke, Roman David BP 28.24
 Vepsäläinen, Antti TT 49.2, TT 54.7
 Verba, R. MA 16.6
 Verba, Roman MA 34.7
 Vercelli, Gabriel DY 45.9
 Verdozzi, Claudio MM 31.7
 Vereijken, Arne MA 5.2, +MA 23.36,
 MA 38.4
 Veremchuk, Igor MA 31.7
 Veremchuk, Ihor +DS 6.1
 Vereshchagin, Anatoliy MM 16.1
 Verezhak, Joel MA 11.6
 Vergniory, Maia G. MA 3.6, MA 10.2,
 TT 12.2
 Verhoeven, Jan MM 23.15
 Verhoff, Leonard M. +KFM 6.3,
 +O 40.1
 Verkholyak, Taras TT 29.9, TT 29.10
 Verlage, Jan +TT 38.12
 Verleden, Stijn BP 21.9
 Verlhac, Benjamin O 7.6
 Verlhac, Benjamin A. O 20.4
 Verma, Akshay Kumar HL 42.6
 Verma, Rahul MM 14.7
 Verma, Ritu +MM 17.3
 Verma, Sandeep O 60.12
 Vernuccio, Federico KFM 3.1
 Verona, Ivan Cedrick HL 17.6
 Verstraete, Matthieu J. MA 18.7
 Verstraten, Robin C. MA 20.9
 Vesalimahmoud, Newsha +O 37.3
 Veslin, Timo +DS 15.4
 Veyrat, Arthur MA 40.64, O 94.6,
 TT 30.9
 Veziroglu, Salih CPP 13.1
 Vezzoni Vicente, Pablo +O 14.8
 Vieira Mendes, Toni +DY 32.8
 Vietz, Kevin MM 12.32, +MM 12.33
 Vignale, Giovanni MA 23.31, MA 27.6
 Vignaud, Dominique HL 14.9
 Vigneau, Florian TT 49.2
 Vijayan, Ponraj HL 7.43, +HL 49.2,
 HL 49.3
 Viji, Priya +CPP 18.7
 Vilardi, Demetrio TT 51.1
 Vilfan, Andrej +DY 31.4
 Vilhena, Guilherme +O 87.3
 Vinai, Giovanni MA 27.1
 Vinayakumar, Vineetha O 29.10
 Vinnichenko, Mykola MA 49.5,
 MA 49.7
 Vinogradov, Nikolay O 56.8
 Vinogradova, Olga V +O 3.4
 Vinograd, Valerii DS 12.20
 Vinokur, Valerii M. DS 5.2
 Viol, Aline SOE 7.5
 Viola Kusminskiy, Silvia HL 29.7,
 +MA 34.4, TT 64.7
 Vion, Denis PLV X
 Vir, P. MA 12.5
 Vir, Praveen MA 12.3
 Viret, Michel MA 11.1
 Virgili, T. HL 48.4
 Virgilio, Michele HL 18.9, HL 37.6
 Virnau, Peter +BP 17.7, CPP 12.2,
 MA 2.2, MA 12.8, MA 23.2, MA 29.1
 Vishwakarma, Aditya +MM 18.6
 Višňák, Jakub O 47.8
 Visser, Lino HL 29.5, HL 37.4
 Vit, Jakob +MA 40.51
 Vitacolonna, Mario +BP 11.26
 Vitale, Francesco HL 7.18
 Vitali, Domenico DY 23.5, DY 56.8
 Vitali, Lucia +O 46.3
 Vittadello, L. KFM 14.7
 Vittadello, Laura KFM 6.41, KFM 14.4,
 KFM 14.5
 Viveros-Méndez, Perla MA 36.6
 Vizuete, Karla HL 7.32
 Vliex, Patrick HL 16.9, HL 50.10,
 HL 50.11, TT 24.9
 Vo, T.P. MM 26.8
 Vo, Trung Phuc +O 85.7
 Voehringer, David BP 11.20
 Vogel, Alexander KFM 4.2
 Vogel, Michael +MA 20.10, MA 23.36,
 MA 38.4
 Vogel, Tim +MA 40.33
 Vogel, Tobias DS 9.2, DS 9.3
 Vogelsang, Jan +O 75.3
 Vogl, David HL 7.4, HL 33.38
 Vogl, Lukas +MA 40.35, MA 40.42
 Vogl, Michael +DS 7.5
 Vogl, Tobias +DS 2.5
 Vogler, Annika A. +BP 28.34, BP 28.39
 Vogt, S. HL 7.20
 Vogt, Sofie +DS 10.4, +DS 12.12,
 DS 12.54, DS 16.3
 Voigt, Axel +BP 3.12, +BP 30.6, DY 4.6,
 MM 14.8
 Voigt, Clemens MA 49.5, MA 49.7
 Voigt, Hendrik +MM 28.7
 Voigt, Jens MA 48.7
 Voigt, Jorrit DY 22.3
 Voigt, Niels BP 28.33
 Voigtländer, Bert O 66.9
 Voigtländer, Ralf TT 58.27
 Vojta, Matthias TT 4.2, TT 4.4,
 TT 16.16, TT 42.16, TT 47.5, TT 47.6,
 TT 65.6, TT 65.7
 Vokert, Cynthia MM 12.20
 Volckaert, Klara O 85.2
 Volk, C. HL 33.17
 Volk, Christian +HL 9.5, HL 30.2,
 +TT 14.5, TT 41.2
 Völkel, Berthold O 28.9
 Völkel, Simeon DY 48.2, TT 55.2
 Volkert, Cynthia MM 23.7, MM 23.15
 Volkert, Cynthia A. MM 18.3,
 MM 23.14
 Volkher Roth, Stephan CPP 35.19
 Volkmann, U.G. BP 11.10, BP 11.11,
 BP 11.12
 Völkner, Christian BP 28.13, O 28.3
 Volkov, Anatoly TT 63.14
 Volkov, Oleksii MA 43.5, MA 50.3
 Volkov, Oleksii M. MA 49.8
 Volkova, Kseniia +KFM 6.34
 Vollhüter, Jan MM 4.3
 Völlinger, Marvin TT 66.3
 Vollmer, Jürgen DY 29.11, DY 44.22,
 +DY 56.10
 Vollmer, Sergej HL 12.6, HL 43.2
 Vollmer, Waldemar BP 16.1
 Vollroth, Lucas +MA 23.37, MA 40.6
 Volmer, Frank HL 14.5
 Volmer, Mats HL 29.1, HL 37.4
 Volokitina, Anna O 2.10
 Voloshina, Elena +KFM 9.1, KFM 11.1,
 O 56.7, O 64.10
 Volovichev, Igor MM 12.9
 Volpe, Giorgio DY 26.8
 Völzer, Tim DS 12.23, +DS 12.40,
 HL 33.11
 Vomschee, Kevin +O 13.5
 von Bardeleben, Hans Jürgen
 HL 33.28
 von Bergmann, Kirsten MA 14.1,
 MA 14.3, O 50.1
 von Bredow, Christian +O 32.9
 von Bülow, Sören BP 27.9
 von Coelln, Nadine +DS 15.5
 von den Driesch, Nils HL 29.9
 von Destinon, Richard +MM 23.18
 von Freymann, Georg HL 17.4,
 KFM 7.9, MA 16.4, MA 23.71,
 MA 23.75, MA 40.7, O 84.2, TT 56.2
 von Hansen, Yann DY 44.20
 von Hoegen, Alex TT 62.7
 von Kenne, Albert +DY 31.5
 von Klitzing, Regine +PLV III, BP 11.4,
 BP 11.14, CPP 3.1, CPP 3.4,
 CPP 17.49, CPP 29.3, CPP 35.44,
 CPP 35.56, CPP 57.4, CPP 57.8,
 CPP 58.4, CPP 58.5, DY 29.9
 von Korff Schmising, Clemens
 MA 8.2
 von Lüpke, Uwe HL 3.1
 von Malottki, Stephan MA 35.9,
 +MA 47.1
 von Oppen, Felix O 7.2, O 7.4, O 33.4,
 O 33.8
 von Reppert, Alexander MA 23.70,
 MA 40.34, +MA 40.66, MM 12.3,
 +O 37.7
 von Seggern, Rieke +MA 23.56
 von Selzam, Nick +TT 38.8
 von Wenckstern, Holger DS 10.4,
 DS 12.10, DS 12.12, DS 12.54, DS 16.2,
 DS 16.3, HL 7.29, HL 7.31, HL 47.4,
 HL 47.6
 von Zimmermann, Martin KFM 9.7
 Vona, Cecilia HL 13.5, O 17.5
 Vonbun-Feldbauer, Gregor +O 81.1
 vonbun-feldbauer, gregor b. MM 3.5
 Vondrak, Martin +MM 8.7
 Voneshen, D. J. MA 33.6
 Vönhoff, Fredrik HL 15.4
 Vonk, Vedran O 29.6, O 39.4, O 42.10,
 O 42.11, O 56.6, +O 83.2, O 92.3
 vool, uri DS 12.18, MA 4.10, TT 7.10
 Vormann, Katharina BP 17.4
 Vorobevskaia, Ekaterina BP 23.4
 Vorobyov, Vadim MA 23.43
 Vorokhta, Mykhailo O 78.8
 Vos, Bart +BP 25.1, BP 28.51
 Vos, Bart E. BP 8.4
 Voß, Florian +DY 45.7
 Voß, Lukas +O 26.8
 Voss, Lennart DS 12.44, DS 12.46
 Vossage, Paul +O 91.7
 Vovusha, Hakkim O 74.9
 Vozmadiano, Maria HL 11.3, MA 39.5,
 TT 15.3
 Vuijk, Hidde Derk DY 56.1
 Vyalikh, Denis MA 39.4
 Vyalikh, Denis V. MA 46.4
 W. Baron, Joseph BP 18.4, DY 33.4
 W. da Siva Pinto, Manoel MM 41.4
 Waack, Jan M. +HL 51.4
 Waag, Andreas HL 33.44, HL 44.3
 Wachinger, Kaspar +BP 28.40,
 BP 28.44
 Wachter, Andreas BP 17.1
 Wachter, Irina BP 29.4
 Wächter, Matthias DY 5.1, DY 32.9
 Wächtler, Christopher W DY 18.8,
 O 70.8
 Wäckerlin, Christian DS 4.3, MA 19.7,
 O 73.6
 Wackerermann, Ken MM 27.9
 Wadhwa, Payal +MA 20.5
 Waentig, Albrecht Ludwig CPP 54.1
 Wagener, Martin MA 23.73
 Wagner, Andreas CPP 35.17, DS 6.1,
 DS 14.5, HL 5.5, KFM 6.30, KFM 9.5,
 +KFM 9.8, KFM 9.10, MA 31.7
 Wagner, Barbara CPP 44.5
 Wagner, Chiara O 81.8
 Wagner, Christian BP 8.3, BP 11.54,
 BP 11.60, BP 18.1, BP 22.7, BP 29.6,
 DY 4.2, DY 33.1, +O 45.7
 Wagner, Glenn TT 8.4
 Wagner, Joachim CPP 57.6, DY 6.4
 Wagner, Kai DS 6.1, MA 11.4, MA 31.7
 Wagner, Koloman HL 34.3
 Wagner, Laura HL 45.1
 Wagner, Lukas +HL 3.6, HL 7.48
 Wagner, M. R. HL 23.1, HL 43.6
 Wagner, Margareta O 60.3, +O 81.8
 Wagner, Marie DS 12.8
 Wagner, Markus R. +HL 21.3, HL 22.3,
 HL 23.5, HL 41.7
 Wagner, Markus Raphael HL 41.3
 Wagner, Michael O 13.5
 Wagner, Nico +HL 51.8
 Wagner, Niklas TT 35.5
 Wagner, Stefan MM 12.7, MM 23.13,
 MM 23.32, +MM 27.1
 Wagner, Susan +BP 21.4, BP 28.12,
 CPP 20.2, DY 29.6
 Wagner, Thorsten +O 2.10
 Wagner, Tim O 36.12
 Wagner, Timo HL 16.4, HL 16.8,
 +O 29.10, TT 24.4, TT 24.8
 Wagner, Tobias MA 18.1, +MA 18.2
 Wagner, Willi L. +DY 31.5
 Wagstaffe, Michael O 11.4, O 16.1,
 O 29.6, O 37.8, O 40.4, O 57.5
 Wahl, Peter +TT 37.12
 Wahl, Sophia DS 12.38
 Wahenström, Göran MM 23.34
 Waldeck, David O 51.4
 Waldecker, Lutz HL 14.8, HL 22.5,
 HL 33.9, O 93.3
 Waldmann, Jannis DS 12.33
 Waldmann, Oliver MA 19.2, MA 24.6
 Waldow, Diana MM 42.5
 Waleska, Natalie J. O 23.1, O 23.3,
 +O 41.1, O 64.1, O 73.8
 Walker, Marc O 93.8
 Wallauer, Robert O 19.7, O 34.2
 Wallerberger, Markus +DY 11.7,
 DY 11.8, TT 5.10, +TT 13.7, TT 13.8
 Wallmeyer, Bernhard BP 28.18
 Walmsley, Ian HL 3.6
 Walowski, Jakob MA 23.7, MA 23.37,
 MA 40.6
 Walter, Benjamin DY 32.1, DY 32.7
 Walter, Christopher +DS 12.10
 Walter, Marcel MA 19.4, MA 40.12
 Walter, Michael +CPP 8.6, CPP 28.5,
 TT 32.5
 Walters, Andrew TT 4.10
 Walther, Eva Sophia +O 64.9
 Walther, Franziska +TT 42.3
 Walther, Matthias R. +TT 42.19,
 TT 42.20, TT 42.21
 Waltner, Daniel DY 48.3, TT 55.3
 Waluk, Jacek O 46.4
 Walz, Andreas O 14.4
 Walzer, Karsten CPP 1.11
 Wang, Hao +O 78.4
 Wand, Tobias +SOE 8.4, SOE 17.2
 Wang, Bingzhe CPP 36.1
 Wang, Boyi +DY 42.15
 Wang, Dashun +SOE 3.1
 Wang, Di KFM 9.9
 Wang, Feifan +TT 3.2
 Wang, Guanzhong TT 31.6
 Wang, Hai-Chen MM 31.7
 Wang, Hongguang TT 50.3
 Wang, Jiaozhi DY 25.10, TT 33.10,
 +TT 43.25
 Wang, Jing +DY 7.7, DY 46.6
 Wang, Lin +HL 9.3, +TT 14.3
 Wang, Li-Xian HL 11.4, HL 11.7,
 TT 15.4, TT 15.7
 Wang, Mao HL 5.5, HL 36.2
 Wang, Meng +MM 38.3
 Wang, Nan Lin TT 62.5
 Wang, Peixi CPP 8.4, +CPP 53.4
 Wang, Q. TT 23.7
 Wang, Qisi KFM 9.7
 Wang, Ren-Bo TT 45.2
 Wang, Rong CPP 11.5
 Wang, Rui Ning HL 10.9
 Wang, Shanshan +SOE 4.1, +SOE 11.1
 Wang, Shiyong O 66.1
 Wang, Shuanglong MA 23.22,
 MA 23.23, MA 23.53
 Wang, Taowen HL 45.5
 Wang, Wei DY 44.6
 Wang, Wen O 4.2
 Wang, X. TT 46.2
 Wang, Xiangzun DY 4.9
 Wang, Xiao-Ye O 32.8

Wang, Xi-guang . MA 23.12, MA 40.34
 Wang, Xing . O 38.4
 Wang, Y. . KFM 11.9
 wang, yang . DY 25.7, O 8.8, TT 33.7
 Wang, Yi . MA 36.5, TT 50.3
 Wang, You . HL 25.2
 Wang, Yu . O 15.3, O 15.6, O 20.11
 Wang, Yude . KFM 10.10
 Wang, Yumin . O 39.1
 Wang, Yunshan . BP 12.7
 Wang, Yuqi . MA 21.7, O 33.2
 Wang, Yutong . BP 28.6
 Wang, Yuxuan . TT 35.4
 Wang, Zefan . CPP 19.5
 Wang, Zhe . HL 17.10, TT 6.7, TT 59.18
 Wang, Zhen . TT 29.6
 Wang, Zhenyu . O 86.5
 Wang, Zhiren . PLV X
 Wang, Zidong . KFM 6.7, MM 5.4
 Wani, Yashraj . CPP 19.10
 Wanierke, Friedrich . O 36.9
 Wanzenböck, Ralf . O 6.10, O 81.2
 Wardenberg, Laurids . HL 7.13
 Wardyn, Jędrzej . TT 29.6
 Varias, Jonas E. . BP 1.11
 Warnatz, Tobias . MA 22.5
 Warren, Ross . CPP 17.5
 Wartelle, Alexis . MA 43.1
 Wartenberg, Ariani C. . DY 49.4
 Warth Pérez Arias, Erica . TT 59.10
 Warwick, Nola . TT 3.2
 Warzanowski, Philipp . TT 10.12
 Warzel, Simone . DY 25.1, TT 33.1
 Waseda, Osamu . MM 18.6
 Wasmer, Johannes . MA 10.1, TT 12.1
 Wasserchied, Peter . O 73.2
 Wasserroth, Sören . O 39.2, O 58.6
 Wasserroth, Sören T. . O 58.8
 Watanabe, K. . HL 33.17, O 47.7
 Watanabe, Kenji . DS 1.6, DS 2.4, DS 12.20, HL 9.4, HL 9.5, HL 14.5, HL 22.5, HL 30.2, HL 33.10, HL 33.12, HL 33.18, HL 34.3, TT 14.4, TT 14.5, TT 35.1, TT 35.7, TT 41.2
 Watson, Adam J. . O 50.4
 Watson, Matthew . O 59.7, O 59.8
 Watzenböck, Clemens . TT 65.8
 Waurischk, Tina . MM 12.36
 Wawra, Jonas . DS 12.27
 Wawrzynczak, Rafal . MA 37.4, TT 59.9, TT 59.10
 Weber, Birgit . CPP 17.9
 Weber, Cedric . MA 21.7, O 33.2
 Weber, Christoph . BP 11.31, BP 11.66, DY 29.2
 Weber, Christoph A. . BP 10.8, BP 11.65, BP 22.9, BP 29.2
 Weber, Clara S. . TT 63.5
 Weber, Daniel . O 74.8
 Weber, Frank . MA 40.38, TT 21.1, TT 57.8
 Weber, Fried . MA 23.70
 Weber, G. . TT 57.28
 Weber, Heiko B. . PSV X, HL 18.11, O 84.10, TT 56.10
 Weber, Jan . TT 42.2
 Weber, Johannes . MA 23.80, MA 34.6, MA 40.15, MA 40.65
 Weber, Jonathan . MA 23.56
 Weber, Ksenia . HL 50.2
 Weber, Mads C. . MA 50.7
 Weber, Manuel . TT 65.6
 Weber, Marius . MA 40.8, MA 46.2
 Weber, Niklas . MM 12.20
 Weber, Paula . O 28.8
 Weber, Paula M. . HL 27.6, MA 14.2, MA 14.6, O 62.6, TT 40.6
 Weber, Peter . HL 40.2, O 79.2
 Weber, Sebastian M . O 93.8
 Weber, Sebastian T. . MA 8.4, MA 40.8, O 8.4, O 16.6, O 84.2, TT 56.2
 Weber, Stefan . CPP 43.7
 Weber, Stefan A.L . CPP 35.65, CPP 44.10, CPP 51.3
 Weber, Thomas . KFM 1.4, KFM 11.4
 Weber, Torsten . TT 5.13
 Weck, Johann Moritz . BP 5.5
 Wecker, Julia . HL 49.3
 Wedemann, Gero . BP 27.6
 Weerda, Erik . MA 40.26
 Wege, Stephan . PSV VII
 Wegener, Martin . BP 11.37
 Wegerhoff, Max . HL 33.1
 Wegewijs, Maarten . DY 9.4
 Wegewitz, Lienhard . DS 3.5, DS 12.29
 Wegner, Anja . BP 28.53
 Wegner, D. . O 42.2

Wegner, Daniel . O 2.5, O 20.1, O 30.2, O 51.2
 Wegner, Mathias . TT 66.3
 Wegscheid-Gerlach, Christof . HL 27.3, O 62.3, TT 40.3
 Wehenkel, D. . HL 33.62
 Wehinger, Björn . TT 44.8
 Wehling, Tim . HL 8.10, HL 40.1, O 79.1, TT 35.5, TT 35.6, TT 61.2, TT 63.4
 Wehmeier, Lukas . O 58.7
 Wehrspohn, Ralf . HL 7.15
 Wei, Jimeng . O 51.4
 Wei, Qing . DY 56.9
 Wei, Wei . HL 4.4, MM 5.6
 Wei, Yajing . O 75.5
 Weidenhiller, Franz . MA 23.50, MA 23.76
 Weidig, Daniel . DY 6.4
 Weidt, Nikolai . MA 40.43
 Weiel, Marie . BP 11.76
 Weig, Eva . PLV VIII, HL 3.9, HL 10.6, HL 10.8
 Weigand, M . MA 31.1
 Weigand, Markus . MA 40.5
 Weigel, Martin . DY 6.11, DY 44.7, DY 49.10
 Weigelt, Udo . AIW 2.2
 Weigold, Matthias . MA 3.2
 Weigt, Martin . BP 10.1
 Weihs, Gregor . HL 7.39, HL 24.2, HL 24.4
 Weiler, Mathias . MA 5.5, MA 15.3, MA 18.1, MA 18.2, MA 23.8, MA 23.11, MA 23.69, MA 23.72, MA 34.7
 Weilert, Jan . CPP 19.6
 Weimann, Thomas . DS 1.2, TT 39.8
 Weinberger, Theodore . TT 4.11, TT 28.1, TT 59.14
 Weinberger, Theodore I. . TT 4.12
 Weinbrenner, Paul . DS 12.23, MA 23.41
 Weindl, Adrian . O 87.7
 Weindl, Christian L. . CPP 37.2
 Weindl, Christian Ludwig . CPP 51.4
 Weinert, Tom . O 31.2
 Weingart, Maximilian . BP 10.9
 Weinhold, Tillmann . TT 6.6
 Weiß, Christopher . O 80.1
 Weis, Jürgen . HL 7.62, TT 59.13
 Weiß, Marco . O 97.6
 Weiß, Matthias . HL 10.3, HL 10.7
 Weiß, Tobias . O 14.8
 Weisbrich, Hannes . TT 48.3, TT 48.4
 Weise, Bruno . MA 3.5, MA 42.1
 Weise, Lukas Paul . BP 11.13
 Weißenhofer, Markus . MA 22.3, MA 23.5, MA 46.12
 Weiske, Hendrik . O 48.5
 Weismann, Alexander . O 7.8, O 20.9, O 33.5, O 33.7, TT 8.1
 Weißmüller, Jörg . MM 42.5
 Weiss, Marco . O 97.5
 Weiss, Matthias . BP 1.4, BP 21.10, BP 28.4, BP 28.5, BP 28.7, BP 28.8, BP 28.34, BP 28.39, DY 56.5
 Weiss, Mattias . BP 28.10
 Weiss, Stephan . DY 5.6
 Weiss, Thomas . O 49.9, O 91.2
 Weiss, Tobias . O 3.7
 Weissenrieder, Jonas . O 8.8, O 37.12
 Weissmann, Volker . DY 40.2
 Weissmüller, Jörg . MM 17.4, MM 23.29, MM 42.1, MM 42.4, MM 42.7
 Weisweiler, Hardy . TT 39.11
 Weitenberg, Christof . DY 2.4, TT 2.4
 Weitkamp, Philipp . CPP 18.8, CPP 35.30
 Weitz, David A. . BP 1.1
 Weitz, R. Thomas . O 34.4
 Weitz, Thomas . HL 14.3, HL 33.14, TT 64.3
 Wekking, Tobias . O 56.8
 Welker, Till . DY 44.1
 Welle, Alexander . TT 54.1
 Wellert, Stefan . CPP 57.10
 Wellesen, Imke . MA 23.26, MA 23.27
 Wellm, Christoph . TT 52.8
 Welter, Edmund . HL 4.9
 Wemhoff, Piotr . O 68.3
 Wen, Shuyu . HL 18.8
 Wende, H. . MA 48.3
 Wende, Heiko . MA 3.3, MA 3.8, MA 8.7, MA 9.10, MA 17.5, MA 19.3, MA 36.1, MA 36.2, MA 42.2, MA 42.7, O 16.2, O 42.6, O 51.4
 Wendel, Lars . TT 30.1

Wenderoth, Martin . O 31.1
 Wendl, Andreas . TT 42.6, TT 47.6
 Wendler, Elke . DS 10.5
 Wendorff, Falk . O 69.8
 Wenger, Anja . TT 11.2
 Wenger, Christian . HL 14.9
 Wengert, Simon . MM 31.10, O 78.4, O 86.6
 Wenskat, Marc . O 42.10
 Wenthaus, L. . MM 26.8
 Wenthaus, Lukas . O 16.1, O 37.8
 Wenzel, Hans . HL 23.2
 Wenzel, M. . TT 23.1
 Wenzel, Sabine . O 19.7
 Wenzel, Wolfgang . CPP 26.3
 Werkovits, Anna . O 28.1, O 28.10
 Werl, Matthias . O 13.6, O 31.4, O 31.7
 Werner, Daniel . TT 22.11, TT 38.13, TT 43.22
 Werner, Florian . BP 12.7
 Werner, Marco . CPP 19.4, DY 22.2
 Werner, Peter . DY 40.1
 Werner, Philipp . O 8.9, TT 5.10, TT 5.12, TT 50.4
 Werner, Yannick . TT 59.16, TT 59.17
 Wernicke, Doreen . MA 13.4, TT 19.4, TT 58.26
 Wernicke, T. . HL 23.1
 Wernicke, Tim . HL 23.5, HL 28.4, HL 28.5, HL 44.5
 Wernsdorfer, Wolfgang . O 15.10, O 15.11, O 20.3, O 77.3, TT 49.4
 Weschke, Daniel . DY 56.7
 Weschke, E. . MA 40.58
 Weschke, Eugen . MA 44.8
 Wesemann, Mike . O 63.2
 Wessel, Stefan . DY 49.7, TT 5.4, TT 29.9, TT 29.10, TT 29.11
 Wessels, Teresa . MA 17.5
 Wester, Tom T. B. . DY 5.8
 Westerbeck, Dennis . MA 24.4
 Westermayr, Julia . CPP 28.11, MM 12.13, O 73.1, TT 32.11
 Westermeyer, Fabian . BP 11.46, DY 37.1, DY 56.7
 Westerhout, Tom . MA 35.4
 Westmeyer, Gil . BP 11.71
 Westphal, Michael . O 36.3
 Wetter, Helene . O 49.4
 Wetzel, Christian . HL 44.2
 Wetzel, Jakob . DS 12.17
 Weyer, Henrik . BP 16.3, DY 4.5
 Weyers, Markus . HL 23.2, HL 44.5
 Weymouth, Alfred J. . O 4.6, O 97.1, O 97.2
 Wiche, Miguel . O 45.5
 Wichmann, Tobias . O 18.2, O 74.3, O 74.5, O 82.1
 Wick, Christian R. . DS 12.42, MM 33.6
 Wickenhäuser, Tom . CPP 35.14
 Widra, Wolf . O 14.1, O 47.10, O 51.5, O 51.6, O 85.5, O 92.2, O 92.8, O 92.9
 Widmann, S. . MA 40.14
 Widmer, Roland . O 10.4
 Widulla, Anton . HL 7.12
 Wiebe, Jens . SYTS 1.3, O 7.1, O 7.3, O 32.9
 Wieck, A.D. . HL 7.56, HL 29.2
 Wieck, Andreas . SYQD 1.3, DY 43.22, HL 7.42, HL 24.10, HL 33.45, HL 33.54
 Wieck, Andreas D. . HL 7.44, HL 7.46, HL 7.51, HL 7.57, HL 24.12, HL 42.4, HL 42.5, VA 2.2
 Wiedenhaupt, H. . O 75.9
 Wiedmann, Raymond . TT 65.10
 Wiedmann, Stefan . MA 33.7
 Wiedwald, Ulf . BP 5.7, DS 10.1, HL 36.7, MA 38.3, MA 42.9
 Wiehn, Marten . O 95.2, TT 68.2
 Wieland, Simon . BP 25.8
 Wielert, Isabelle . BP 6.1
 Wiersig, Jan . DY 21.3
 Wiese, Roland . DY 42.9
 Wiesendanger, Roland . MA 14.1, MA 14.3, MA 20.8, MA 49.1, O 7.1, O 7.3, O 32.9, O 42.8, O 50.1, O 93.4
 Wiesener, Philipp . O 66.7
 Wietek, Alexander . MA 40.27, TT 63.8
 Wietek, Edith . DS 2.4
 Wigger, Daniel . HL 3.7, HL 10.5, HL 33.2, HL 33.18
 Wijitpatima, Setthanat . HL 7.53
 Wikfeldt, Kjartan Thor . MA 47.6
 Wiktor, Julia . O 57.4
 Wilczek, Michael . DY 5.7

Wild, Christoph . KFM 6.23, KFM 8.8
 Wild, Johannes . MA 20.10, MM 23.32
 Wilde, Benedikt . TT 39.5
 Wilde, Gerhard . DS 4.2, MM 12.4, MM 18.2, MM 23.18, MM 26.3, MM 28.1, MM 28.2, MM 28.6, MM 28.7, MM 40.8, MM 41.2, MM 41.4
 Wilde, Marc . MA 13.8, TT 4.13, TT 19.8
 Wilde, Marc A. . TT 3.8, TT 10.1, TT 10.2
 Wildes, A. . MA 44.3
 Wildes, Andrew . MA 44.8
 Wilfinger, Franziska . TT 58.11
 Wilgocka-Slezak, Dorota . MA 50.1
 Wilhelm, F. . MA 48.3
 Wilhelm, Fabrice . DS 10.1, MA 3.3, MA 42.7
 Wilhelm, Jan . DY 9.3, HL 20.4, O 2.3, O 20.10, O 35.4
 Wilhelm, Paul . DY 17.8
 Wilhelm, R. A. . O 5.2
 Wilhelm, Richard A. . O 5.3, O 31.4, O 31.8
 Wilhelm, Richard Arthur . O 13.6, O 13.8, O 31.5, O 31.7
 Wilhelm, Thomas . MM 23.30
 Wilhem, Jan . DY 43.9
 Wilkins, David . O 6.5
 Wilkins, Stuart B. . MA 43.6
 Wilks, Dina . O 56.6
 Wilksen, Steffen . HL 49.1, HL 50.8
 Will, Melissa . TT 22.3, TT 43.24
 Will, Moritz . O 29.9
 Willa, Kristin . TT 34.1
 Willburger, Timo . HL 43.3
 Willem Coenen, Jan . MM 22.4
 Willenberg, Sebastian . BP 13.4, BP 21.11
 Willer, Pascal . TT 58.25
 Willers, Thomas . TT 4.10
 Williams, Leon BS . O 93.8
 Williams, Travis J. . TT 9.8
 Williard, Alice . BP 31.2
 Wilke, Philip . O 15.5, O 15.10, O 15.11, O 20.3, O 77.3
 Willner, Lutz . CPP 57.5
 Willsher, Josef . MA 10.8, TT 12.8, TT 46.13
 Wilson, Murray N. . MA 11.6
 Wilson, Nathan P. . MA 32.5
 Wilson, S.D. . TT 23.1
 Wilson, Thomas . BP 4.5
 Wimmer, Michael . HL 49.4, TT 8.8, TT 31.6
 Wind, N. . MM 12.1, MM 26.8
 Windbacher, Niklas . DY 16.6
 Windischbacher, Andreas . O 19.3, O 34.6
 Windsor, William . MA 8.7
 Windsor, Yoav Will . MA 46.4
 Windsor, Yoav William . SYUE 1.2, MA 46.11, MA 46.13, O 34.7
 Windt, Katja . SYOF 1.3, SOE 19.4
 Wines, Daniel . HL 26.1, O 53.1
 Winkel, Patrick . TT 49.4
 Winkel, Tristan . MA 23.54
 Winkelmann, A. . MM 26.8, O 30.4
 Winkelmann, Aimo . HL 36.2
 Winkelmann, Clemens . TT 20.1
 Winkelmann, Clemens B. . O 20.6
 Winkelmann, Ricarda . PSV I
 Winkelmann, Stefanie . DY 4.10
 Winkhofer, Konstanze . BP 17.2
 Winkler, Andreas . KFM 7.8
 Winkler, Daniel . O 60.5
 Winkler, Louis Conrad . CPP 17.15, CPP 43.4, CPP 43.9
 Winkler, Lucy . CPP 43.8
 Winkler, Robert . DS 9.2, MA 3.4
 Winkler, Roland G. . BP 2.1
 Winkler, Thomas . MA 2.3, MA 23.3
 Winkler, Thomas Brian . MA 26.4, MA 47.2
 Winnerl, S. . TT 23.1, TT 23.7
 Winnerl, Stephan . HL 17.11, TT 62.1, TT 62.5
 Winte, Katrin . CPP 28.9, HL 25.8, HL 48.8, TT 32.9
 Winter, Joe . TT 48.6
 Winter, Leonhard . O 11.2, O 38.2
 Winter, Lucas . MA 46.3
 Winter, M. . MA 12.5
 Winter, Michael . HL 8.10
 Winter, Moritz . MA 12.3
 Winterhalter-Stockler, Noah . MA 13.7, TT 19.7, TT 46.4

Author Index

- Winterott, MoritzMA 11.5
Wintz, SMA 31.1
Wintz, SebastianMA 40.3, MA 40.5
Wippermann, StefanO 69.7, O 75.8,
•O 86.3
Wirth, Felix•MA 40.19
Wirth, KonstantinO 91.8
Wirth, Konstantin G.•O 93.3
Wirth, Konstantin GeorgO 70.5
Wirtz, Ludger•HL 26.3, HL 34.9,
•O 53.3
Wislicenus, MarcusTT 57.2
Wissel, KerstinTT 44.7
Witt, ChristinaHL 7.33
Witt, DonaldHL 49.5
Witt, Niklas•TT 63.4
Witte, GregorO 45.5
Witte, RalfMA 3.1
Witte, WolframHL 4.6
Wittmann, Tobias•O 73.3
Wittenbecher, LukasO 75.3
Witthaut, DirkSOE 4.11, SOE 15.1
Wittig, Patrick•TT 53.4
Wittkowski, Raphael•BP 24.1,
BP 24.3, BP 24.4, DY 26.7, •DY 38.1,
DY 38.3, DY 38.4
Wittman, KilianO 43.2
Wittmann, AngelaMA 23.22,
MA 23.23, MA 23.53, •MA 31.1,
MA 40.5
Wittmann, Markus•O 86.9, O 86.10
Wittmann, MartinBP 2.6
Wittmann, RenéDY 27.7
Wittröck, SteffenMA 23.61
witz, jean FrançoisMM 20.2
Witzigmann, BerndCPP 35.52,
HL 28.4
Witzky, Yannick•BP 17.1
Wochner, PeterTT 9.6, TT 51.5
Woerner, EckhardKFM 8.8
Wohlfahrt-Mehrens, Margret
KFM 10.3
Wohlfeld, KrzysztofTT 65.3
Wohlgemuth, MarcusO 92.7
Wöhrl, NicolasPSV VIII, O 29.10
Wójcik, Krzysztof P.•TT 4.5
Wolansky, JakobCPP 17.15,
•CPP 43.6, CPP 43.8
Wolf, AdrianaHL 5.1
Wolf, AndreasTT 57.25
Wolf, Bernd•TT 4.8, TT 9.2, TT 10.7,
TT 43.12, TT 43.13, TT 46.7
Wolf, BettinaBP 21.12
Wolf, ChristophO 15.6, •O 15.7,
O 15.8, O 15.12
Wolf, D.KFM 11.9, MA 12.5, MA 31.1
Wolf, DanielDS 12.20, MA 12.2,
MA 31.7, MA 32.2, MA 38.2
Wolf, Elisabeth H.KFM 3.3
Wolf, Eugen•KFM 6.43
Wolf, M.O 75.9
Wolf, MarcellCPP 8.3
Wolf, MartinHL 17.9, HL 33.55, O 2.1,
O 12.7, O 16.5, O 16.7, O 39.2, O 58.6,
O 58.8, O 75.6, O 76.1, O 76.4
Wolf, Pierre-ÉtienneCPP 52.2,
MM 23.27
Wolf, Stefaan DeCPP 1.9
Wolf, StefanDY 16.5
Wolf, Steffen•BP 3.8
Wolff, GerhardDS 12.35
Wolff, NiklasDS 12.7, KFM 1.5,
KFM 9.9, MA 17.2
Wolff, SusanneO 82.8
Wolff, UlrikeMM 23.5
Wolke, CarmenBP 8.8
Wöll, ChristofCPP 26.3, DS 15.2,
MA 19.6, O 39.1, O 95.8, TT 68.8
Wöll, ChristophO 68.5, O 81.5, O 81.6,
O 81.10
Wollenweber, Maximilian A.
•MM 20.3
Wolter, AnjaMA 44.8
Wolter, Anja U. B.TT 10.10, TT 29.2
Wolter, Stefan•HL 33.44
Wolters, JanikDY 17.7, DY 22.4,
DY 46.7, HL 24.3
Woltersdorf, GeorgMA 23.51,
MA 23.64, MA 23.68, MA 23.73,
MA 43.7
Wolz, LukasHL 38.2, HL 45.1
Wonanke, Dinga•O 95.8, •TT 68.8
Wondrak, ThomasMA 49.2
Wong, FelixBP 6.4
Woo, Chul-UngBP 9.10
Wood, Brandon•MM 27.6
Wood, GeorgeMA 9.8
Wood, MichaelMM 31.8
Wood, RyanO 34.1
Wöpke, ChristopherCPP 1.11
Worbs, AndreasMA 43.5
Worbs, LenaVA 1.3
Worch, LukasMA 13.8, TT 19.8
Worlitzer, VascoDY 31.2
Worm, PaulTT 44.6
Wörner, EckhardKFM 6.23
Wörthmüller, DennisBP 17.6
Wortmann, DanielHL 31.7, MA 23.32,
MM 12.27, O 61.7
Wortmann, JonasCPP 36.5
Wortmann, MartinCPP 35.20,
•MM 12.30, •O 68.1
Woschée, DanielBP 26.5
Wosnitza, J.MA 23.18, MA 23.19,
MA 40.58, MA 42.4, MA 42.5,
MA 42.8, MA 42.10, TT 28.6, TT 42.4,
TT 42.15, TT 46.8, TT 52.3, TT 57.2,
TT 57.19, TT 59.8
Wosnitza, JoachimMA 18.5
Wosnitza, JochenMA 42.6, MA 44.2,
MA 44.6, TT 43.2
Wouters, JurriaanTT 31.8
Woutersen, SanderBP 30.1
Woźniak, Tomasz•DS 2.1, HL 1.1
Wrachtrup, JörgMA 23.43, MA 32.4
Wright, JonMM 4.4
Wronowicz, Jakub•HL 31.3, •O 61.3
Wrzosek, PiotrTT 65.3
Wu, Chi-NanTT 9.3
Wu, FupengO 33.3
Wu, HankTT 6.6
Wu, HaoMA 23.22, MA 23.23,
MA 23.53
Wu, HuanMM 40.1
Wu, JamesCPP 58.7
Wu, KexinCPP 37.2
Wu, Kunmin•TT 18.5
Wu, Kuo-AnDY 26.3
Wu, Lili-ChenO 66.5
Wu, MingjianCPP 17.52
Wu, Nian•MM 12.14
Wu, Tsuei-Shin•MA 44.1
Wu, WeishanO 28.2
Wu, Yao-TingO 28.7
Wu, Yu-Jung•DS 14.4
Wu, YuquanCPP 35.14
Wu, ZheyuTT 28.1
Wucher, AndreasO 13.4, O 13.7
Wüest, MartinVA 1.4
Wührl, FriederikeO 51.5
Wulfhekkel, Wulf•MA 2.5, MA 16.9,
MA 19.5, O 21.4, O 45.4, TT 3.1
Wunderlich, Hannes•BP 28.7
Wundrack, StefanO 82.7
Wünsch, StefanTT 66.3
Würfel, UliCPP 1.6
Wurl, Anika•BP 3.10
Wurmehl, SabineTT 57.11, TT 62.1
Wurmshuber, MichaelMM 9.1
Wurstbauer, UrsulaHL 8.4, HL 10.7
Wurster, KatjaTT 3.10, TT 20.4,
TT 57.23
Würthner, FrankCPP 17.10, CPP 17.11,
CPP 28.3, DS 3.2, O 28.8, TT 32.3
Würthner, LaeschkirBP 16.3, BP 22.8
Wurz, NicolaTT 49.2
Wurz, Peter•O 13.1, O 13.2
Wust, StephanMA 31.3
Wüster, SebastianDY 55.10, DY 55.11,
TT 67.10, TT 67.11
Wuttig, MatthiasDS 12.38, DS 15.4,
DS 16.5, •KFM 6.14, KFM 6.21,
KFM 6.25, KFM 11.2, MM 12.15,
MM 12.23, MM 12.27, O 49.8, O 70.5,
O 91.8
Wysmolek, PaulinaBP 21.11
Wysmolek, Paulina M.BP 13.4
Wysocki, Adam•BP 2.10, DY 42.10
Wyżula, J.TT 6.10
Xanthakis, John P.O 77.6
Xia, HaoxiangTUT 2.2, SOE 1.2
Xia, SenlinCPP 56.2
Xia, YonggaoCPP 35.15
Xian, Patrick R.O 95.1, TT 68.1
Xian, R. PatrickO 16.5
Xian, Rui PatrickO 16.7
Xiang, FeifeiO 20.10
Xiao, Hongyi•DY 7.4
Xiao, TianxiaoCPP 17.16, •CPP 17.38,
CPP 35.18
Xiao, Yun-FengDY 21.3
Xiao, Yu-Ting•TT 16.10
Xibraku, Malwin•KFM 6.37
Xie, RuiwenDS 12.36, MA 3.2
Xie, T.TT 42.13
Xie, Yingjie•KFM 6.17
Xie, ZhuochengMM 41.3, •MM 41.5
Xing, J.TT 42.13
Xiong, Shuxian•CPP 17.26
Xiu, FaxianTT 6.7
Xu, Bai-XiangMM 20.4
Xu, BinMA 18.7
Xu, ChangfanDS 12.51, •KFM 6.13,
•MM 5.7, MM 42.10
Xu, ChenO 6.8, •O 54.3, •O 66.10,
O 87.4, TT 6.12
Xu, HanDY 56.7
Xu, Hongxiang•O 11.3
Xu, JingjingBP 11.42
Xu, KaiDS 16.6, HL 21.3
Xu, M.TT 34.3
Xu, MengDY 9.9, •DY 43.19
xu, qi•MM 42.9
Xu, QichenMA 47.6
Xu, RuiMA 43.5, MA 49.5, •MA 49.8,
•MM 11.3, •MM 23.6
Xu, WenqiCPP 8.2, •CPP 35.58
Xu, Wen-TaoTT 47.10
Xu, Xiang•MM 40.3
Xu, XianghanTT 3.2
Xu, Xiaodong•SYHS 1.2
Xu, Yifan•DS 14.6, •MA 5.6, O 42.12
Xu, YuanfengMA 10.2, TT 12.2
Xu, ZhiyunCPP 26.3, DS 15.2
Xu, ZhuijunCPP 17.35, CPP 17.46,
•CPP 35.15
Xu, ZhuoCPP 17.19, •CPP 36.7
Xue, NanBP 11.5
Xue, RanHL 29.1, HL 29.5, •HL 37.1,
HL 37.4
Xue, ZhijieO 66.8
Xylander, Max•O 18.9
Yadav, KhushbooO 3.2
Yadav, SonamHL 18.2
Yadav, VibhavO 60.10, •O 69.14,
O 96.7
Yadavalli, Nataraja SekharDS 13.4
Yadollahi Farsani, Fatemeh
CPP 35.36
Yaffe, OmerDS 1.6
Yagoobi, Sedigheh•DY 45.14
Yakhnevych, U.•KFM 14.1, KFM 14.7
Yakhnevych, UlianaKFM 6.20,
•KFM 13.4, KFM 13.5, KFM 13.6
Yakhou-Harris, FloraMA 43.1
Yakovlev, Dmitri R.HL 4.10, HL 15.2,
HL 15.3, HL 35.8, HL 35.9, HL 47.2
Yakovlev, YuriiO 55.2
Yalcinkaya, YenalCPP 43.7, CPP 51.3
Yalunin, SergeyO 34.5
Yalunin, Sergey V.O 8.1, O 80.2,
O 83.8
Yam, Chi-YungMM 10.3
Yam, Wun K.TT 58.7
Yam, Wun KwanTT 49.1, •TT 58.20
Yamamoto, Sh.MA 40.58
Yamamoto, ShingoMA 42.6, MA 44.6
Yamamoto, YujiHL 37.6
Yan, Chengzhan•HL 38.4, •MM 23.26
Yan, ChuanyuCPP 53.2
Yan, KakingO 66.8
Yan, LinghaoO 74.2
Yan, XinlinMA 9.7
Yan, YamingDY 9.9
Yan, Yingying•CPP 17.45
Yan, ZewuKFM 1.2, KFM 1.8, KFM 4.5
Yanagisawa, MihoBP 12.9
Yanakiyeva, IskraBP 16.4
Yang, BiaoO 11.3, •O 11.6, O 14.6,
O 32.2, O 40.2
Yang, BowenMA 17.3
Yang, Chao•TT 50.3
Yang, Chia-JungDS 15.3, •TT 47.1
Yang, Chi-YuanDS 16.6
Yang, FanMM 40.5
Yang, Hanbo•CPP 1.5
Yang, Hung-HsiangMA 16.9, MA 19.5
Yang, Ji Young•BP 17.8
Yang, JiabaoO 32.4
Yang, JingMM 32.1, •MM 37.3
Yang, JunjieTT 51.6
Yang, JuntaoO 73.2
Yang, Lin•O 2.9
Yang, LiuhuayingSOE 19.1
Yang, LuyanMA 47.7
Yang, Mingwei•DY 22.4, •DY 46.7
Yang, PingTT 49.2
yang, poyaDS 12.18
Yang, R.•TT 58.4
Yang, RunMA 9.9
Yang, SangsunMM 41.4
Yang, Tao•O 30.10
Yang, TingluCPP 53.2
Yang, WeiMA 23.20
Yang, WeifengHL 48.1
Yang, Wenchao•CPP 43.1
Yang, XiaoshengO 21.2, O 77.1
Yang, YangO 36.3
Yang, YingMA 3.2
Yang, YuHL 3.1
Yang, YuhuiHL 22.4, •HL 33.36,
•HL 33.37, HL 33.50, O 91.1
Yang, YujiaHL 10.9
Yang, YunkunTT 6.7
Yao, Jiangtian•DY 48.5, •TT 55.5
Yao, Wei•DS 12.15, O 14.5, TT 59.12
Yao, WeiliangTT 52.8
Yao, XuelinO 32.8
Yao, YiHL 13.3, O 17.3
Yao, Yueh-Ting•MA 10.6, •TT 12.6
Yao, Yuxuan•O 6.9
Yao, Zhen•O 36.3
Yaqoob, MisbahMA 18.1
Yaresko, Alexander•TT 50.6, TT 52.5
yarragolla, sahitya•HL 47.5
Yaseen, RahafTT 23.5
Yasuoka, H.TT 42.15
Yazdanshenas, BaharCPP 8.3,
•CPP 17.54
Ye, FangyuanHL 25.9
Ye, FengTT 9.8
Ye, JingjingHL 42.2, HL 42.3
Ye, Mai•TT 10.8
Ye, XingchenMA 36.5
Ye, Xinglong•MA 3.1
Yeates, ToddBP 17.7
Yershov, Kostiantyn V.MA 18.6,
•MA 35.3, •MA 40.2, •MA 50.2
Yesilpinar, DamlaO 97.7
Yetkin, MelisCPP 19.10, •CPP 35.9
Yhang, ChengzhangMM 23.25
Yi, ChangjiangTT 23.8, TT 59.12
Yik, Hiufai•DY 5.6
yin, chenyang•MA 40.16
Yin, MarianaCPP 44.2
Yin, ShanshanBP 19.1, CPP 13.9,
CPP 17.16, CPP 17.51, CPP 29.2,
CPP 29.10, CPP 35.18, CPP 35.19,
CPP 41.1, MA 38.5
Yin, Yefei•O 82.7
Yogi, Rachana•O 14.3
yokoyama, takahiro•CPP 2.5
Yöküler, ÖzlemCPP 2.4
Yoo, Su-HyunMM 37.7
Yose, JosephSOE 8.2
Yoshimura, MasatoTT 30.6
Yoshino, HirokoO 76.1
you, haoranMA 19.5
Young, A. PeterDY 49.1
Young, Jeff F.HL 49.5
Yu, Boram•BP 28.2
Yu, Ji HunMM 41.4
Yu, Jingjing•DS 8.3
Yu, Ka ManO 38.1, O 64.9
Yu, Ka-ManO 10.2
Yu, MinghaoDS 12.15
Yu, PingO 66.1, O 66.8
Yu, ShangxuanHL 49.5
Yu, YeKFM 7.4
Yu, YuanKFM 6.25
Yu, Zi-DiCPP 18.1
Yuan, ChentianO 96.4
Yuan, Mingyun•HL 3.8
Yuan, Ning•TT 50.8
Yuan, Xudong•MM 28.5, MM 42.9
Yue, ChangmingO 8.9
Yugova, Irina A.HL 15.2
Yuhui, YangHL 33.48
Yuriy, SuhakKFM 13.3
Yuvanc, AlevDS 12.24
Zabila, YevhenMA 49.2, •MA 49.6,
MA 49.8
Zabila, ZevhenMA 49.7
Zablocki, JenniferCPP 28.9, HL 2.5,
O 58.2, TT 32.9
Zaburdaev, VasilyBP 9.9, BP 11.20,
BP 11.59, BP 11.67, BP 12.11, BP 25.7,
BP 28.53, BP 29.4
Zaccone, AlessioDY 16.2, DY 23.1,
•DY 24.3, •TT 48.1, •TT 63.1
Zacharias, HelmutO 37.13, O 51.4
Zacharias, MariosSYUE 1.2
Zaharko, OksanaMA 44.7
Zahn, DanielaSYUE 1.2, MA 46.13,
O 16.7
Zahn, Dietrich R. T.HL 7.11, HL 8.6,
HL 33.5
Zahn, DirkO 69.9

- Zahn, Manuel KFM 1.8, KFM 4.5, •KFM 6.19, KFM 6.20
- Zaidman, Artem •O 42.10
- Zaiser, Michael MM 33.7
- Zaitsev, Ignatii •HL 18.9, HL 37.6
- Zajac, Peter •HL 7.44, HL 33.45, HL 42.5
- Zajadacz, Joachim KFM 7.4
- Zajusch, Sarah O 34.2
- Zakeri, Khalil MA 40.62
- Zakharova, Anna •SOE 9.4
- Zaks, Michael •DY 18.6
- Zallo, Eugenio HL 33.13, HL 34.5
- Zaluzhnyy, Ivan CPP 29.9, •CPP 51.2
- Zamarripa, Cesy HL 18.2
- Zambanini, André HL 16.9, HL 50.11, TT 24.9
- Zamponi, Michaela CPP 8.3
- Zanchi, Marco MM 33.7
- Zanfrognini, Matteo HL 26.3, O 53.3
- Zang, Jiawei TT 61.1
- Zanotti, Jean-Marc MA 24.6
- Zapata, Nicolas TT 39.3
- Zapperi, Stefano MM 33.7
- Zare Pour, Mohammad Amin HL 7.9, •HL 7.10
- Zaretsky, Daniel DY 27.10
- Zarkua, Zviadi O 24.1
- Zarotiadis, Rhiannon A. •DY 32.10
- Zarrabi, Nasim CPP 1.10
- Zarzuela, Ricardo •MA 11.3, MA 47.9
- Zasedatelev, A. HL 48.4
- Zaslansky, Paul BP 6.3
- Zatterin, Edoardo HL 37.6
- Zaumseil, Jana DS 15.5
- Zaverkin, Victor MM 14.2
- Zavickis, Davis •MM 8.1
- Zavodszky, Emese •BP 28.41
- Zayko, Sergey HL 48.5, •O 83.4
- Zech, Sandra •HL 24.1
- Zechman, Philip •TT 45.9
- Zechner, Christoph BP 18.6, DY 33.6
- Zeeshan, Hafiz Muhammad •KFM 9.1, KFM 11.1
- Zegenhagen, Jörg DS 6.3
- Zeidler, Reinhard O 57.5
- Zeitler, Uli TT 29.2
- Zeitner, Uwe HL 7.18
- Zelena, Anna •BP 8.6, BP 28.33
- Zelenkovski, Kiril DY 44.15, DY 44.19
- Zelený, Martin MA 37.5, MA 37.6, MM 36.11
- Železný, Jakub MA 4.14, MA 40.64, TT 7.14
- Zeller, Rudolf •MM 12.17
- Zemp, Yannik •MA 50.7
- Zendehroud, Sina •DY 44.20
- Zeng, Xianzhe •O 20.5
- Zengin, Berk O 70.3, •O 77.8
- Zentgraf, Thomas HL 33.30
- Zeppenfeld, Peter O 2.10, O 55.7
- Zerba, Caterina •DY 40.6
- Zerfaß, Ruben TT 16.3
- Zerhoch, Jonathan HL 15.1, MA 23.40
- Zervou, Alkistis TT 51.2
- Zett, Lukas •DY 45.9
- Zetzl, Matthias •MA 40.41
- Zeuschner, Steffen O 37.7
- Zeuschner, Steffen Peer •MA 40.34
- Zhakina, Elina •MM 26.9
- Zhang, Chengping MA 10.4, TT 12.4
- Zhang, Deqing O 37.13
- Zhang, Fajun BP 11.46, CPP 35.6, DY 37.1
- Zhang, Gu TT 45.5
- Zhang, Guoxiu •DS 14.2
- Zhang, H. TT 46.8
- Zhang, Haijing HL 34.6, MA 27.1, •MA 31.4, TT 11.6
- Zhang, Hongbin DS 12.36, MA 3.1, MA 3.2
- Zhang, Jiahuan CPP 29.10
- Zhang, Jiawei •TT 3.3
- Zhang, Jinhua •BP 5.6
- Zhang, Jinsheng •CPP 17.28
- Zhang, Lei MM 15.3
- Zhang, Lichaun MA 16.9
- Zhang, Lin MM 27.1
- Zhang, Peiran •CPP 35.60
- Zhang, Ruifeng MA 28.5
- Zhang, Sam HL 14.10
- Zhang, Shihao MA 28.5
- Zhang, Shu •MA 29.5
- Zhang, Siyuan MM 9.7, MM 41.3, MM 41.7
- Zhang, Songbo HL 31.1, O 61.1, TT 63.7
- Zhang, Tianyi •CPP 43.5
- Zhang, Xi •MM 18.1, MM 40.3, MM 40.8
- Zhang, Xiang •O 37.4
- Zhang, Xianghui O 28.9
- Zhang, Xiao •TT 59.2
- Zhang, Xiaotian •TT 30.10
- Zhang, Xuejing •TT 21.6
- Zhang, Yadong CPP 17.24
- Zhang, Yi •O 36.8
- Zhang, Yingying •CPP 17.60
- Zhang, Yinxia •MM 4.6
- Zhang, Yi-Qi O 14.6
- Zhang, Yiwei •BP 24.10, •DY 38.10
- Zhang, Yu CPP 28.9, O 34.9, TT 32.9
- Zhang, Yuanshan O 56.2
- Zhang, Yuhao •HL 1.3
- Zhang, Ziyang HL 42.6
- Zhao, Baolin CPP 28.10, TT 32.10
- Zhao, Bin •CPP 35.23
- Zhao, Binyu •CPP 44.6
- Zhao, Hongping HL 41.4
- Zhao, Huaping DS 12.51, HL 7.58, HL 14.10, HL 38.4, HL 45.3, KFM 6.7, KFM 6.13, KFM 6.26, KFM 10.5, KFM 10.8, KFM 10.10, MM 5.4, MM 5.5, MM 5.7, MM 23.9, MM 23.25, MM 23.26, MM 37.2, MM 42.10
- Zhao, Jiyong MA 42.2
- Zhao, Junting O 82.1
- Zhao, Li TT 30.3
- Zhao, Pai •HL 3.3, HL 14.1, MM 23.19
- Zhao, Shiteng DY 29.4
- Zhao, Shuo •HL 41.1
- Zhao, Weisheng MA 14.7
- Zhao, Wenchao •O 14.6
- zhao, xianyue HL 47.5
- Zhao, Xueping DY 29.2
- Zhao, Yani CPP 12.2
- Zhao, Zhiying TT 59.18
- Zhao, Zhiyong O 37.1
- Zharnikov, Michael •O 37.1, •O 55.1
- Zheludev, Andrey TT 45.2
- Zheng, Feifei •CPP 8.2, CPP 8.3, CPP 35.58
- Zheng, Fengshan MA 47.7
- Zheng, Fulu CPP 28.9, HL 48.8, MM 10.2, TT 32.9
- Zheng, JiaChang MA 10.4, TT 12.4
- Zheng, Jianshu •MM 14.4
- Zheng, Jinyang MM 27.1
- Zheng, Tianle •CPP 17.50
- Zheng, Yifan BP 12.7
- Zherlitsyn, S. MA 33.6, TT 52.3
- Zherlitsyn, Sergei MA 18.5, MA 44.2
- Zheru, Qiu HL 10.9
- Zhitomirsky, Mike •MA 13.5, •TT 19.5
- Zhong, Huaying CPP 17.36, CPP 17.37, CPP 17.39, •CPP 29.10, CPP 52.5
- Zhong, Jin-Hui CPP 28.9, O 58.2, TT 32.9
- Zhong, Qigang •O 72.5
- Zhou, Chengshuang MM 27.1
- Zhou, Guanda HL 38.2
- Zhou, Hangyu •MA 14.7
- Zhou, Jungui CPP 17.44
- Zhou, Kejin TT 4.10
- Zhou, Ping O 8.3, O 16.9, O 19.1, O 19.6, O 37.2, O 37.3, O 38.4, O 45.4
- Zhou, Qi BP 8.3
- Zhou, Shengqiang HL 5.5, HL 18.8, HL 34.2, HL 36.2, MA 5.3
- Zhou, Shengqing DS 14.2
- Zhou, Xiaoyi •DS 1.4
- Zhou, Yishui TT 23.5, •TT 23.8
- Zhou, Yuanyuan •O 57.6, •O 69.1
- zhou, yunxia MA 40.16
- Zhou, Zimo •HL 20.6, •O 35.6
- Zhou, Ziwei CPP 56.3
- Zhour, Kazem •O 25.3
- Zhu, B. TT 57.28
- Zhu, Bonan HL 45.2
- Zhu, Changqing •HL 17.10, TT 6.7, TT 59.18
- Zhu, Chunye O 57.6
- Zhu, Jihang MA 31.4
- Zhu, Lingjun O 73.1
- Zhu, Shuaifei CPP 26.2
- Zhu, Tong TT 30.8
- Zhu, Xiaoyang O 34.3
- Zhu, Xujie •O 66.8
- Zhukov, Evgeny A. HL 15.2
- Zhuo, Fangping KFM 2.3
- Zhuocheng, Xie MM 37.1
- Zhuoqing, Li DY 24.4
- Zhuravlev, Evgeny KFM 11.11
- Zidek, Karel KFM 4.10
- Ziebarth, Benedikt MM 28.8
- Ziebert, Falko BP 28.43, BP 28.47
- Ziefuß, Anna MA 3.2
- Ziegler, Andreas O 81.8
- Ziegler, Christiane O 84.2, TT 56.2
- Ziegler, Jonas D. HL 34.3
- Ziegler, Jonas David DS 1.6
- Ziegler, Martin DS 12.57
- Ziegler, Sina •MM 5.9
- Ziehmer, Markus MM 22.2
- Zielinski, Robert O 28.4, •O 28.6
- Zienert, Andreas CPP 44.8
- Ziepkke, Alexander BP 7.6, DY 10.6
- Zierold, Robert O 42.10, TT 35.7
- Ziese, Ferdinand •CPP 35.39, CPP 35.40, CPP 35.46
- Ziesen, Alexander •TT 31.2, TT 59.4
- Zieske, Katja •BP 11.40
- Ziethen, Noah •BP 9.8
- Zijie, Qiu MA 23.22, MA 23.23
- Zilberberg, Oded TT 48.4
- Ziletti, Angelo MM 31.4
- Zimmer, Andreas BP 31.1
- Zimmer, David Noel •BP 27.2
- Zimmer, Joanne •CPP 35.44
- Zimmer, Klaus KFM 7.4
- Zimmer, Michael HL 12.6, HL 43.2, •HL 43.4
- Zimmermann, Bernhard MA 20.10
- Zimmermann, Erik HL 29.9, HL 30.1, TT 36.1, TT 41.1, TT 59.5, TT 59.6
- Zimmermann, Jan TT 43.12, •TT 43.13
- Zimmermann, Jonas E. O 19.9
- Zimmermann, Michael •DY 6.6, KFM 3.2
- Zimmermann, Philipp DS 1.4
- Zimmermann, Sascha Jan •DS 12.39
- Zimmermann, Valentin TT 44.8
- Zimmermann, Walter •DY 4.4
- Zimmermann, Wolfram BP 4.4
- Zimmermann, Wolfram-Hubertus BP 28.30
- Zink, Mareike BP 4.3
- Zinke, Gregor •O 19.8
- Zinth, Wolfgang BP 10.2
- Zintler, Alexander DS 9.2, MA 3.4
- Ziolkowski, Franziska MA 8.6, •MA 8.8
- Zitko, Rok •O 33.1
- Zitzke, Liesa BP 5.7
- Zivanovic, Andela O 30.1
- Zoch, Katharina M. •TT 46.3
- Zoellner, Marvin H. HL 37.6
- Zoellner, Marvin Hartwig HL 18.3
- Zohair, Fazeel •HL 47.3
- Zojer, Egbert CPP 26.3, •O 10.8, O 55.1
- Zojer, Karin •CPP 45.4, CPP 45.7
- Zolliker, Markus TT 58.29
- Zöllner, Johann •TT 16.5, TT 60.2
- Zollner, Klaus DS 1.5, HL 1.1, •HL 8.1
- Zöllner, M. HL 7.56
- Zöllner, Marcel SYQD 1.3, HL 1.10, HL 7.46, HL 24.10, •HL 24.12, TT 60.2
- Zollner, Stefan •DS 17.3, •HL 18.2
- Zoltner, Kassandra O 23.5
- Zonda, Martin MA 4.3, TT 7.3, TT 20.12
- Zonta, Elia •O 69.2
- Zorin, Alexander B. TT 39.6
- Zorn, Reiner CPP 37.4
- Zotti, Linda Angela •BP 23.7
- Zöttl, Andreas CPP 57.1
- Zou, Yuqin •CPP 17.41
- Zouros, Grigorios MM 12.9
- Zrenner, Artur HL 7.45, HL 7.60
- Zscharschuch, Jens HL 33.10
- Zschornack, Günter O 13.6
- Zschumme, Philipp MM 31.9
- Zsurka, Eduárd HL 14.2
- Zu, Fengshuo CPP 17.40
- Zubáč, Jan MA 4.14, MA 40.64, TT 7.14
- Zubizarreta Casalengua, Eduardo HL 7.65
- Zühlke, Ria-Helen TT 66.4
- Zülske, Tilo BP 27.6
- Zúñiga Céspedes, B. TT 34.3
- Zuñiga Puelles, Esteban KFM 6.10
- Zuo, Ruixin •HL 48.1
- Zurak, Luka O 43.6, O 43.7, O 70.6, O 91.6
- Zurita, Juan SYQD 1.2
- Zutta Villate, Julian Mateo BP 11.78
- Zverev, Vladimir •DY 42.16
- Zvyagin, S.A. MA 44.3
- Zweck, Josef MA 20.10
- Zwicker, David BP 9.8, BP 11.51, •BP 29.1
- Zwicznagl, G. TT 28.6, TT 57.19
- Zwicznagl, Gertrud HL 16.4, TT 24.4
- Zwoliński, Bartłomiej •SOE 4.14
- Zykov, Ilia •O 26.7
- Zykov, Vladimir •DY 4.1

Index of Exhibitors Dresden (SKM) 2023

Exhibition venue:

Technische Universität Dresden, Campus Südvorstadt, Bergstraße 64, 01069 Dresden

- Lecture Hall Centre (HSZ)
- Tent A (A)

Opening hours exhibition:

- Tuesday, 28 March 09:00 – 18:00
- Wednesday, 29 March 09:00 – 18:00
- Thursday, 30 March 09:00 – 16:00

Company	Location	Stand-No.
ADDITIVE Soft- und Hardware für Technik und Wissenschaft GmbH Max-Planck-Straße 22 b, 61381 Friedrichsdorf <i>ADDITIVE steht für Berechnen, Visualisieren, Automatisieren für Statistik und Wissensmanagement im Qualitäts-/Ingenieurwesen mit den Produkten Minitab, Origin, Mathematica und ADDITIVE-Cloud-Services.</i>	Tent A	A 69
ADL Analoge & Digitale Leistungselektronik GmbH Bunsenstraße 30, 64293 Darmstadt <i>DC-, unipolare und bipolare Plasmastromversorgungen</i>	Tent A	A 50
Agilent Technologies Sales & Services GmbH & Co. KG Hewlett-Packard-Straße 8, 76337 Waldbronn <i>Vakuumpumpen, Vakuummessgeräte, Lecksucher</i>	Tent A	A 07
AHF analysentechnik AG Kohlplattenweg 18, 72074 Tübingen <i>AHF provides optical filters, LED/laser light sources, image splitters and quality monitoring tools for professional and challenging (fluorescence) microscopy. Customers benefit from long-term and interdisciplinary expertise.</i>	HSZ	H 20
Allectra GmbH Traubeneichenstraße 62-66, 16567 Schönfließ <i>Vakuumkomponenten, el. Durchführungen, Kabel</i>	Tent A	A 49
Amplitude Laser Group 11 avenue de Canteranne, 33600 Pessac, France <i>Diodengepumpte Femtosekunden-Festkörperlaser (Yb, TiSa), diodengepumpte Ultrakurzpuls-Faserlaser und Femtosekunden-Faserlaser (Yb), Hochenergetische Nanosekunden-Laser</i>	Tent A	A 67
AMT Andreas Mattil - Technischer Vertrieb Talstraße 33, 67737 Frankelbach <i>Flanges and fittings, viewports, electrical feedthroughs, electronics and instruments, motion and manipulation, helium leak detectors, gauges, SEM coatings, titanium sublimation pumps and much more.</i>	Tent A	A 80
ANFATEC Instruments AG Melanchthonstraße 28, 08606 Oelsnitz (V) <i>Rastersonden-Mikroskope, LockIn-Verstärker</i>	Tent A	A 93
attocube systems AG Eglfinger Weg 2, 85540 Haar <i>Piezo-based nanopositioners, low temperature microscopes, dry and liquid cryostats</i>	Tent A	A 03 / A 04
AXO Dresden GmbH Gasanstaltstraße 8 B, 01237 Dresden <i>Röntgenspiegel, Upgradelösungen, Präzisionsbeschichtung</i>	Tent A	A 79

<p>BelektroniG GmbH Hauptstraße 38, 01705 Freital <i>Temperature controller, Peltier element, frequency controller, SAW generator, acoustofluidics, electronic design</i></p>	Tent A	A 34
<p>Bluefors Arinatie 10, 003700 Helsinki, Finland <i>Cryogenfree dilution refrigerator measurement systems, which can be equipped with options like experimental wiring, optical access, magnet integration etc. We operate in a world of cold, where laws are determined by quantum mechanics.</i></p>	Tent A	A 40 / A 41
<p>Bruker Nano GmbH Am Studio 2D, 12489 Berlin <i>Bruker provides industry-leading surface analysis instruments for nanoscale materials characterization and process monitoring, addressing R&D and QA/QC questions with speed, accuracy, and ease. More information: www.Bruker.com</i></p>	HSZ	H 23
<p>Cambridge University Press Shaftesbury Road, Cambridge, CB2 2RU, United Kingdom <i>Publisher, Books, Journals</i></p>	Tent A	A 59
<p>ChemPur Feinchemikalien und Forschungsbedarf GmbH Rüppurrer Straße 92, 76137 Karlsruhe <i>Metalle, Anorganika, Aufdampfmaterialien, Sputtertargets</i></p>	Tent A	A 84
<p>CLASS 5 PHOTONICS GmbH Notkestraße 85, 22607 Hamburg <i>Ultrafast High Power Laser Systems, HHG-Sources, XUV-, EUV-, VUV-, VIS-, N/MIR-Sources, OPCPA, MPC</i></p>	HSZ	H 19
<p>CreaPhys GmbH Niedersedlitzer Straße 75 (Eingang A), 01257 Dresden <i>Vakuumbeschichtung, Komponenten und Anlagen (Beschichtungsquellen), Sublimationsanlagen, Reinste organische Substanzen/Service, Inertgasanwendung, Glovebox/Gasreinigung</i></p>	Tent A	A 16
<p>CreaTec Fischer & Co. GmbH Industriestraße 9, 74391 Erligheim <i>Manufacturer of customized LT-STM/AFM, MBE, RTA and molecular spray systems including associated electronics with software solutions as well as a wide range of equipment for use in (ultra-high) vacuum.</i></p>	Tent A	A 12
<p>CryLaS Crystal Laser Systems GmbH Ostendstraße 25, 12459 Berlin <i>UV lasers, pulsed nanosecond lasers from 213 to 1064 nm, and small linewidth cw lasers at 266 nm</i></p>	Tent A	A 54
<p>Cryoandmore Budzylek GbR Hermann-Cossmann-Straße 19, 41472 Neuss <i>4K Cryostats, Pulse Tube Cryocooler up to 2.7W@4.2K, GM Cryocooler up to 2W@4.2K Ultra Low Vibration Cryostats, Custom Cryostats</i></p>	Tent A	A 99 / A 100
<p>Cryogenic Ltd. Action Park Estate, London, W3 7QE, United Kingdom <i>Cryogen-free, superconducting, 20 Tesla, magnets, measurement, beamline, neutron, scattering, 3He, magnetism, VSM, conductivity, electrical, transport, low-temperature, UHV, SQUID, resonance, NMR, EPR, dilution refrigerator</i></p>	Tent A	A 02
<p>CryoVac GmbH & Co. KG Langbaughstraße 13, 53842 Troisdorf <i>Helium-Bad- und Verdampferkryostate, Temperaturmess- und Regelgeräte</i></p>	Tent A	A 51 / A 52

DAPHNE4NFDI <i>c/o DESY (FS-SC), Notkestrasse 85, 22607 Hamburg Daten aus PHotonen und Neutronen Experimenten</i>	HSZ	H 27
D.I.S. Germany GmbH Breite Straße 2, 01796 Pirna <i>Ion beam sources, charged particle optics and diagnostics, ion irradiation facilities, gas analytics, and custom solutions</i>	Tent A	A 53
DCA Instruments Oy Vajossuonkatu 8, 20360 Turku, Finland <i>Thin Film Deposition</i>	Tent A	A 96
Delft Circuits B.V. Lorentweg 1, 2628 CJ Delft, Niederlande <i>Flexible cryogenic RF wiring Cri/oFlex</i>	HSZ	H 26
Deutsche Forschungsgemeinschaft (DFG) 53170 Bonn <i>Information und Beratung zu den Förderprogrammen der DFG</i>	HSZ	H 03
Digital Surf 16 rue Lavoisier, 25000 Besancon, France <i>Digital Surf provides software solutions for analyzing data from a range of instruments including Scanning Probe Microscopes (SPM), Scanning Electron Microscopes (SEM), profilometers and spectroscopy.</i>	Tent A	A 46
Dr. Eberl MBE-Komponenten GmbH Josef-Beyerle-Straße 18/1, 71263 Weil der Stadt <i>MBE-Systeme, Effusionszellen, Elektronenstrahlverdampfer, kundenspezifische UHV-Lösungen</i>	Tent A	A 81
Edwards High Vacuum International Ltd. Burgess Hill, West Sussex, RH15 9TW, United Kingdom <i>Complete Vacuum Solutions: Edwards stellt seine Vakuumpumpen sowie Zubehör/Messgeräte (wie APG200) vor.</i>	HSZ	H 05
Entropy GmbH Gmunder Straße 37 a, 81379 München <i>Entropy GmbH is a cryostat manufacturer based in Munich, Germany. The product range offers various types of closed-cycle cryostats for the temperature range of Kelvin and Millikelvin.</i>	Tent A	A 94
FAIRmat c/o Humboldt-Universität zu Berlin, Zum Großen Windkanal 2, 12489 Berlin <i>FAIRe Dateninfrastruktur für die Physik der kondensierten Materie und die Chemische Physik von Stoffen</i>	HSZ	H 27
Ferrovac GmbH Thurgauerstr. 72, 8050 Zürich, Switzerland <i>Ferrovac GmbH provides world-leading Swiss UHV technology. We specialise in sample handling, transfer, and transport equipment, with our dynamic design team offering customised solutions across our range.</i>	Tent A	A 83
Focus GmbH Neukirchner Straße 2, 65510 Hünstetten-Kesselbach <i>Instruments for surface science</i>	Tent A	A 08
GVL Cryoengineering Dr. George V. Lecomte GmbH Aachener Straße 89, 52223 Stolberg <i>3He/4He Mischkryostaten, Tieftemperaturzubehör</i>	Tent A	A 68

<p>Hamamatsu Photonics Deutschland GmbH Arzbergerstraße 10, 82211 Herrsching <i>We are a manufacturer of optoelectronic components for highest demands. Small quantities, customization, or series production, whatever you need: We will find a solution. Talk to us at booth H 10 (Lecture Hall Centre).</i></p>	HSZ	H 10
<p>Heinz Maier-Leibnitz Zentrum (MLZ) Lichtenbergstraße 1, 85747 Garching <i>As a cooperation between TU München, Forschungszentrum Jülich GmbH and Helmholtz-Zentrum hereon GmbH, the MLZ is a user facility for cutting-edge research with neutrons and positrons.</i></p>	Tent A	A 85
<p>Helmholtz-Zentrum Dresden-Rossendorf e. V. (HZDR) Hochfeld-Magnetlabor Dresden (HLD) Bautzner Landstraße 400, 01328 Dresden <i>Hardware und PC für Demonstration der SECoP-Software</i></p>	Tent A	A 18
<p>Hidden Analytical Europe GmbH Kaiserswerther Straße 215, 40474 Düsseldorf <i>Quadrupol Massenspektrometer: Restgas-, Oberflächen-, Cluster-, Molekularstrahl-analyse; SIMS/SNMS/ToF-qSIMS/TPD-Workstations; Gas-Analyse-Geräte, MIMS & DEMS; Plasmadiagnostik- & Energie-Analysatoren</i></p>	Tent A	A 15
<p>HORIBA Jobin Yvon GmbH Hans-Mess-Straße 6, 61440 Oberursel <i>Ihr Partner für instrumentelle Analytik und innovative Spektroskopie</i></p>	Tent A	A 55
<p>Hositrad Deutschland Lindnergasse 2, 93047 Regensburg <i>CF, KF, ISO, UHV-Vakuumbauteile, Elektrische Durchführungen, Membranbalgen, Special Products</i></p>	Tent A	A 39
<p>Hübner Photonics Heinrich-Hertz-Straße 2, 34123 Kassel <i>HÜBNER PHOTONICS: Single-Frequenz CW DPSS-, Faser- und durchstimmbare Laser, UV bis Mid-IR, von 10 mW bis 130 W</i></p>	Tent A	A 98
<p>HZDR Innovation GmbH Bautzner Landstraße 400, 01328 Dresden <i>Messgeräte zur elektrischen Charakterisierung</i></p>	Tent A	A 35
<p>ICEoxford Avenue 4, Station Lane, Witney, Oxon, OX28 4BN, United Kingdom <i>Cryostats</i></p>	Tent A	A 20
<p>Incienta Technologie GmbH Pommernstraße 22, 63110 Rodgau-Weiskirchen <i>Cryogenics, Ferro and Piezoelectric Testing, UHV and Thin Film Technology</i></p>	Tent A	A 29 / A 30
<p>IndiScale GmbH Lotzestraße 22a, 37083 Göttingen <i>Agile open-source research data management software, seamless integration into existing workflows and infrastructure, data management workshops and support for data management plans.</i></p>	Tent A	A 45
<p>InfraTec GmbH Infrarotsensorik und Messtechnik Gostritzer Straße 61-63, 01217 Dresden <i>Infrared cameras with excellent thermal, spatial and temporal resolution for precise measurements and efficient integration into physics experiment setup.</i></p>	Tent A	A 71
<p>Institut für Luft- und Kältetechnik gemeinnützige Gesellschaft mbH Bertolt-Brecht-Allee 20, 01309 Dresden <i>Kryotechnik, Kryostate, tiefkalte Elektronik, Messdienstleistungen Exponate: Kryoflüssigkeitspumpe, Elektronik, Kryostate</i></p>	Tent A	A 75

<p>Institute of Physics Publishing Temple Circus, Temple Way, Bristol, BS1 6BE, United Kingdom <i>Publishers of journals, magazines, community websites</i></p>	Tent A	A 63
<p>ISEG Spezialelektronik GmbH Bautzner Landstraße 23, 01454 Radeberg / Rossendorf <i>Hochspannungsversorgungen, Hochspannungsnetzgeräte, HV-DC/DC- Konverter</i></p>	Tent A	A 88
<p>JCM Dr. Jürgen Christian Müller Zeilweg 19, 60439 Frankfurt / Main <i>Vakuumtechnik, Dünnschichttechnik, Tieftemperaturtechnik, supraleitende Magnete</i></p>	Tent A	A 28
<p>Jobbörse <i>Companies from industry, consulting and public authorities present themselves as attractive employers. The presentations in room HSZ 405 last one hour including a Q&A session. On the day of the respective slots, the contact persons can also be found at the booth.</i></p>	HSZ	H 16 / H 17
<p>JUST VACUUM GmbH Daimlerstraße 17, 66849 Landstuhl <i>Vakuumtechnik</i></p>	Tent A	A 57
<p>Kashiyama Europe GmbH Leopoldstraße 244, 80807 München <i>Kashiyama is a manufacturer of reliable and low-maintenance dry Multi-Stage Roots Pumps offering a wide range of pumping speed options.</i></p>	Tent A	A 97
<p>kiutra GmbH Flößergasse 2, 81369 München <i>Cryogen-free closed-cycle cryostats; ADR and cADR cryostats, Modell "L-Type Rapid" fast sub-Kelvin characterization cryostat; Model "S-Type" compact, rack-mountable sub-Kelvin operation platform</i></p>	Tent A	A 31
<p>Kleindiek Nanotechnik GmbH Aspenhaustraße 25, 72770 Reutlingen <i>Micromanipulators, nanopositioners, nanoprobing, in situ AFM, cryo TEM sample liftout, nanoassembly, manipulators for UHV, force measurement, etc. Give your microscope a hand! www.kleindiek.com</i></p>	HSZ	H 13
<p>Korvus Technology Ltd. Kings Grove Kings Grove, Maidenhead SL6 4DP, United Kingdom <i>Vacuum Deposition Equipment</i></p>	Tent A	A 95
<p>Kurt J. Lesker GmbH Fritz-Schreiter-Straße 18, 01259 Dresden <i>Chambers, valves, pumps, materials, thin film deposition systems, process equipment</i></p>	Tent A	A 66
<p>LASER 2000 GmbH Argelsrieder Feld 14, 82234 Weßling <i>Laser & Strahlquellen, Optik & Optomechanik, Optische Messtechnik, Laserschutz, LWL-/Netzwerktechnik</i></p>	HSZ	H 22
<p>Leiden Probe Microscopy B.V. J.H. Oortweg 19, 2333 CH Leiden, The Netherlands <i>High Pressure STM, Reactor STM, CVD, Graphene growth</i></p>	Tent A	A 91
<p>Leybold GmbH Bonner Straße 498, 50968 Köln <i>Vakuumpumpen</i></p>	HSZ	H 04
<p>MaTeck - Material-Technologie & Kristalle GmbH Im Langenbroich 20, 52428 Jülich <i>Einkristalle, Sputtertargets, Substrate, hochreine Materialien, Isotope, Halbleiterkristalle</i></p>	HSZ	H 06

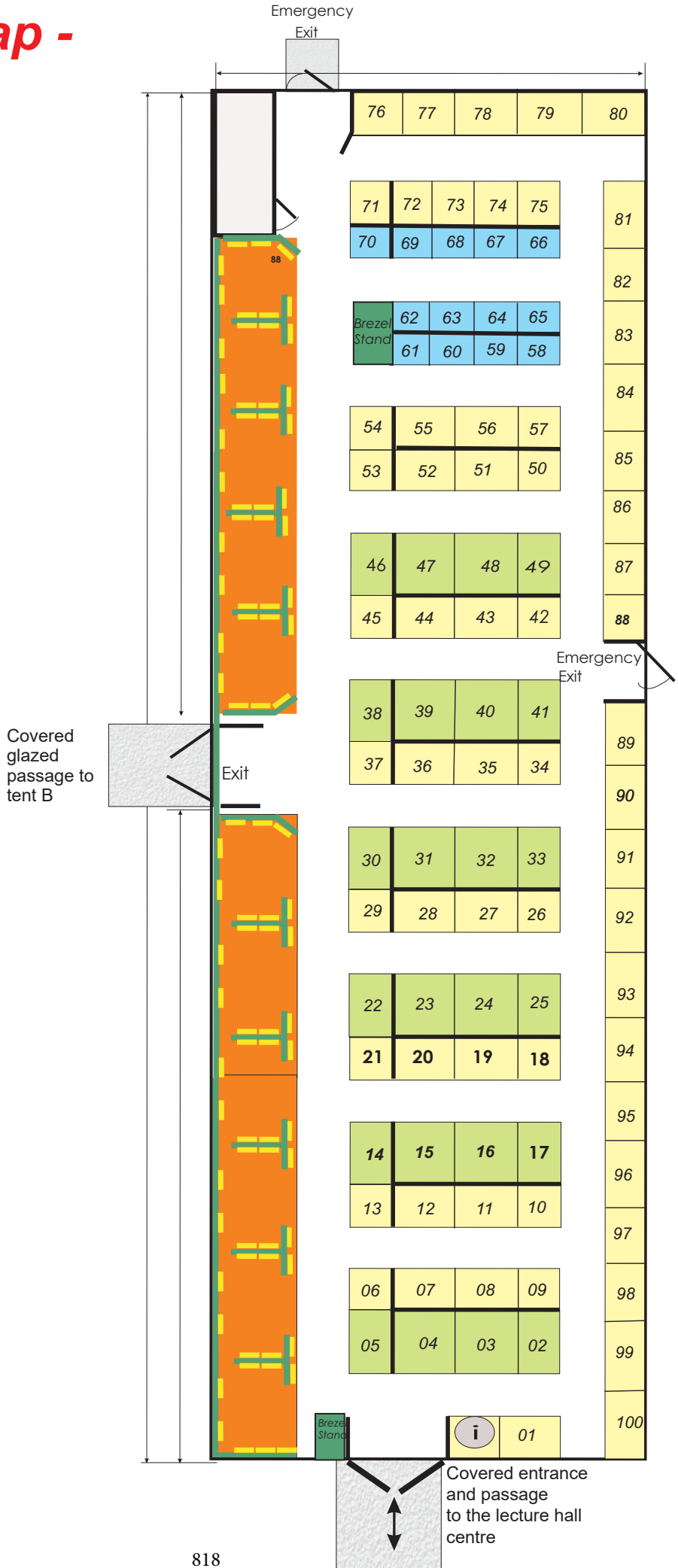
<p>Maybell Quantum Industries 7100 Broadway Building 3 / Suite D-E, Denver CO 80221, USA <i>Maybell Quantum is an American manufacturer of dilution refrigerators with innovative features and compact footprint. Maybell also supplies ultra high density ribbon cables, Flexlines, with low thermal load and superior performance.</i></p>	Tent A	A 44
<p>Menlo Systems GmbH Bunsenstraße 5, 82152 Martinsried <i>Frequency Combs, Quantum Systems, THz System, Femtosecond Lasers</i></p>	Tent A	A 36 / A 37
<p>MG Optical Solutions GmbH Industriestraße 23, 86919 Utting/Ammersee <i>Laser Servo and Controller / Spectroscopy / DBR-Laser / Wavelength Meter, Spectrum Analyzer / MIR Spectrometers, Detectors and Camera / Terahertz Imaging Systems and Laser</i></p>	Tent A	A 64
<p>Munich Quantum Valley Leopoldstraße 244, 80807 München <i>Munich Quantum Valley promotes quantum science and quantum technologies in Bavaria and offers various research positions, especially in connection to quantum computing.</i></p>	Tent A	A 33
<p>Nanosurf GmbH Rheinstraße 5, 63225 Langen <i>AFM, SPM, Atomic Force Microscopes, Scanning Probe Microscopes</i></p>	HSZ	H 11 / H 12
<p>Newport Spectra-Physics GmbH Guerickeweg 7, 64291 Darmstadt <i>Motion Control, Opto-Mechanik, Optiken, Laser, Lichtquellen, Optische Tische, Schwingungsisolierung</i></p>	Tent A	A 23
<p>Nikalyste Ltd 77 Heyford Park, OX25 5HD Upper Heyford, Bicester, United Kingdom <i>NL50 benchtop nanoparticle system</i></p>	Tent A	A 26
<p>Oxford Instruments NanoTechnology Tools Ltd Tubney Woods, Abingdon, Oxon OX13 5QX, United Kingdom <i>Oxford Instruments NanoScience designs, supplies and supports market-leading research tools that enable quantum technologies, nanotechnology research, advanced materials and nanodevice development in the physical sciences.</i></p>	Tent A	A 60 / A 61
<p>Park Systems Europe GmbH Schildkrötstraße 15, 68199 Mannheim <i>Atomic Force Microscopy + Active Vibration Isolation</i></p>	HSZ	H 07 / H 08
<p>Pfeiffer Vacuum GmbH Berliner Straße 43, 35614 Asslar <i>Vakuumpumpen, Messgeräte, Turbopumpen, Lecksucher</i></p>	Tent A	A 13 / A 14
<p>Picovac Ziegelhüttenweg 30a, 65232 Taunusstein <i>Thin Film Deposition Systems, Instruments for In-situ/Operando Research, Nanoparticle Deposition. Representing Korvus Technology, Leiden Probe Microscopy, Moorfield Nanotechnology, Nikalyste</i></p>	Tent A	A 92
<p>PIEZOCONCEPT 15 Rue du Bocage, 69008 Lyon, France <i>Piezo stage, nanopositioner, stages for microscopy, optical metrology, AFM</i></p>	Tent A	A 65
<p>PINK GmbH Vakuumtechnik Gyula-Horn-Straße 20, 97877 Wertheim <i>Vakuum- und UHV-Kammern, Beschleunigerkomponenten, vakuumtechnische Anlagen und Systeme, Manipulatoren</i></p>	Tent A	A 25

PREVAC sp.z.o.o. Raciborska Str. 61, 44362 Rogów, Poland <i>Thin Films, Surface Science, Vacuum Science and Technology</i>	Tent A	A 70
Qioptiq Photonics GmbH & Co. KG Hans-Riedl-Straße 9, 85622 Feldkirchen (München) <i>Präzisionsoptik und Mechanik, Faseroptik, Aufbausysteme, Laser</i>	Tent A	A 89
Qlibri GmbH Maistraße 67, 80337 München <i>Cavity-based microscopes for absorption microscopy, fiber-based micromirrors, and quantum optics at ambient and cryogenic temperatures</i>	HSZ	H 18
Qnami AG Hofackerstrasse 40B, 4132 Muttenz, Switzerland <i>Quantum Sensor</i>	Tent A	A 19
Quantum Design GmbH Im Tiefen See 58, 64293 Darmstadt <i>Kryostate, Optische Kryostate, Kryogene Probe-Stations, Magnetsysteme für die Materialcharakterisierung, Magnetometer, Heliumverflüssiger, Temperatur Sensoren & Controller, Elektrische Messtechnik, CCD-, ICCD-, EMCCD-Detektoren, Spektrographen</i>	Tent A	A 21 / A 22
Quantum Machines Fruebjergvej 3, 2100 Copenhagen, Denmark <i>Control systems for quantum physics experiments</i>	HSZ	H 21
Raith GmbH Konrad-Adenauer-Allee 8, 44263 Dortmund <i>Raith is a leading precision technology manufacturer for nanofabrication, electron beam lithography, FIB SEM nanofabrication, nanoengineering, process control and reverse engineering applications.</i>	Tent A	A 05 / A 06
SAES Getters S.P.A. Viale Italia 77, 20020 Lainate (Milan), Italy <i>UHV NEG-Pumpen, Alkalimetall-Dispenser, Hochvakuumpumpen, Getter</i>	Tent A	A 56
Schaefer Technologie GmbH Robert-Bosch-Straße 31, 63225 Langen <i>Rastersondenmikroskopie, Kryo-xyz-stages, Nanoprobing</i>	Tent A	A 76 / A 77 / A 78
Schäfter + Kirchhoff GmbH Kieler Straße 212, 22525 Hamburg <i>Polarization-maintaining fiber optic components including laser beam coupler, fiber collimators, fiber cables, polarization analyzers and fiber port clusters</i>	Tent A	A 38
Scienta Omicron GmbH Limburger Straße 75, 65232 Taunusstein <i>Systems and Instruments for Surface Science and Thin Film Technology</i>	Tent A	A 17
Seismion GmbH Berliner Straße 8, 30457 Hannover <i>Actively controlled vibration isolators for high-precision applications in metrology and scientific advancement. Sub-Hertz isolation of vibrations at nanometer scale and adaptive levelling.</i>	HSZ	H 09
SEKELS GmbH Dieselstraße 6, 61239 Ober-Mörlen <i>Weichmagnetische Werkstoffe, magnetische Abschirmungen, Magnetsysteme, Induktivitäten, magnetische Messtechnik</i>	Tent A	A 43

SENTECH Instruments GmbH Schwarzschildstraße 2, 12489 Berlin <i>Plasma-Prozess-Technologie und Ellipsometer</i>	Tent A	A 87
SI Scientific Instruments GmbH Römerstraße 67, 82205 Gilching <i>Spektrometer, Lock-In Verstärker</i>	Tent A	A 01
Sirah Lasertechnik GmbH Heinrich-Hertz-Straße 11, 41516 Grevenbroich <i>Laser, Laseroptik</i>	Tent A	A 09
SmarAct GmbH Schütte-Lanz-Straße 9, 26135 Oldenburg <i>SmarAct Kleingeräte</i>	Tent A	A 47
SPECS Surface Nano Analysis GmbH Voltastraße 5, 13355 Berlin <i>Photoelektronenspektroskopie, Rastersondenmikroskopie, winkelaufgelöste Photoemission, Elektronenmikroskopie</i>	HSZ	H 24 / H 25
Springer-Verlag GmbH Tiergartenstraße 17, 69121 Heidelberg <i>Wissenschaftliche Bücher und Zeitschriften</i>	Tent A	A 32
Staub Instrumente GmbH Hagenaustraße 22, 85416 Langenbach <i>In-situ Oberflächenanalyse, RHEED, Auger, AES, XPS, UPS, REELS, ELS, Elektronenquellen, Ionenquellen, Analysatoren</i>	Tent A	A 62
Surface Concept GmbH Am Sägewerk 23 a, 55124 Mainz <i>Momentum Microscop. MCP based Detectors, Time Measurement Systems, Scientific Cameras, Fast Analogue Electronics</i>	Tent A	A 86
SweepMe! GmbH Bienertstraße 18, 01187 Dresden <i>Modular test & measurement software, Instrument automation with Python, Data acquisition</i>	Tent A	A 34
tectra GmbH Reuterweg 51-53, 60323 Frankfurt/M. <i>UHV Komponenten, Dünnschichttechnik, Plasmaquellen</i>	Tent A	A 90
Tecum AG Applied Vacuum Technology Gertrudstrasse 1, 8400 Winterthur, Schweiz <i>VCM600 Thermal Vacuum Evaporator Systems</i>	Tent A	A 82
TESCAN GmbH Zum Lonnenhohl 46, 44319 Dortmund <i>Elektronenmikroskopie</i>	Tent A	A 24
THORLABS GmbH Münchner Weg 1, 85232 Bergkirchen <i>Optische & optomechanische Komponenten, Test & Measurement Systeme, optische Tische und Vibrationskontrolle, Nanopositionierungen, Lichtquellen sowie Imaging, Mikroskopie und Life Science Komponenten</i>	Tent A	A 10 / A 11
TOPTICA Photonics AG Lochhamer Schlag 19, 82166 Gräfelfing / München <i>New Tunable Diode Lasers, New Laser Frequency Stabilization, Femto Fiber Lasers, Wavelength Meters</i>	HSZ	H 01 / H 02

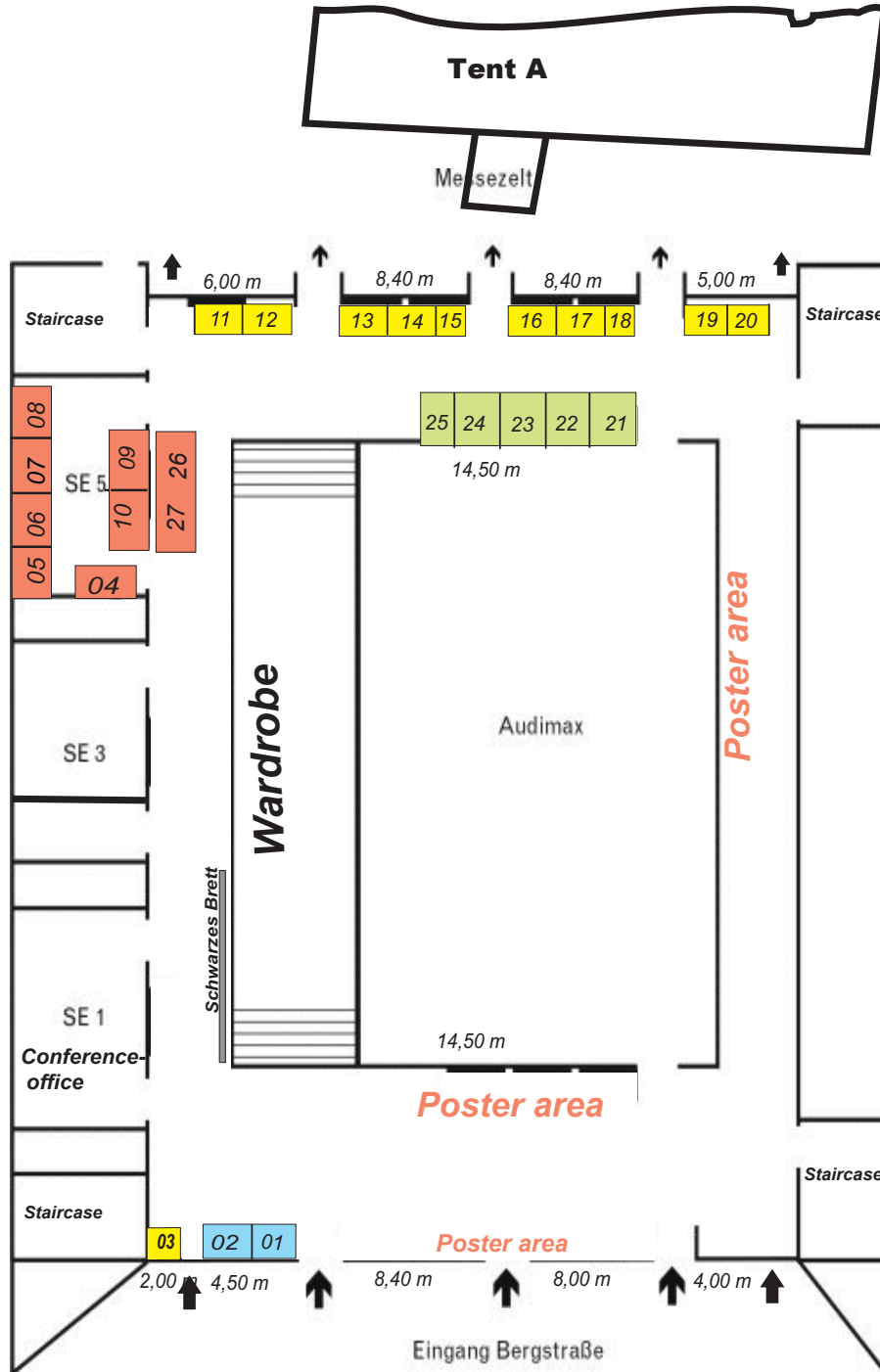
TransMIT GmbH Kerkrader Straße 3, 35394 Gießen <i>TransMIT GmbH – Center for Adaptive Cryotechnology and Sensors</i>	Tent A	A 42
UHV Design Ltd. Judge House Lewes Road, Laughton, East Sussex BN8 6BN, <i>HV and UHV motion and heating products</i>	Tent A	A 74
vakuumfinder.de c/o CompoNext GbR Freiligrathstraße 35, 07743 Jena <i>Vakuumkomponenten, Vakuumtechnik, Vakuummesstechnik</i>	Tent A	A 48
Vaqtec-scientific Mario Melzer Thulestraße 18B, 13189 Berlin <i>Komponenten der UHV- und HV-Technik: u.a. Stromdurchführungen, Schaugläser, Schichtdicken-Messgeräte</i>	Tent A	A 58
Wiley-VCH GmbH Boschstraße 12, 69469 Weinheim <i>Physik Journal – das Mitglieder-Journal der DPG, wissenschaftliche Bücher und Zeitschriften, elektronische Produkte für die Wissensvermittlung, Karriereportale</i>	HSZ	H 15
WITec Wissenschaftliche Instrumente und Technologie GmbH Lise-Meitner-Straße 6, 89081 Ulm <i>Hochauflösende Mikroskope: AFM, Raman, SNOM</i>	Tent A	A 27
World Scientific Publishing and Imperial College Press 57 Shelton Street, London WC2H 9HE, United Kingdom <i>International scientific books and journals covering all topics in Condensed Matter Physics</i>	HSZ	H 14
Zurich Instruments AG Technoparkstrasse 1, 8005 Zurich, Switzerland <i>Test & Measurement, lock-in amplifiers, high quality data</i>	HSZ	H 06

Booth map - Tent A



Lecture Hall Centre

Booths



Timetable

Start	Sunday, March 26	Monday, March 27	Tuesday, March 28	Wednesday, March 29	Thursday, March 30	Friday, March 31
08:15						
08:30		Plenary Talk (HSZ 01)	Plenary Talk (HSZ 01)	Plenary Talk (HSZ 01)	Plenary Talk (HSZ 01)	Plenary Talk (HSZ 01)
08:45						
09:00						
09:15						
09:30						
09:45						
10:00						
10:15						
10:30						
10:45						
11:00						
11:15						
11:30						
11:45						
12:00						
12:15						
12:30						
12:45						
13:00						
13:15						
13:30						
13:45						
14:00						
14:15						
14:30						
14:45						
15:00						
15:15						
15:30						
15:45						
16:00						
16:15						
16:30						
16:45						
17:00						
17:15						
17:30						
17:45						
18:00						
18:15						
18:30						
18:45						
19:00						
19:15						
19:30						
19:45						
20:00						
20:15						
20:30						
20:45						
21:00						
21:15						
21:30						
21:45						

R e g i s t r a t i o n

Tutorials
(HSZ 01-HSZ 04)

Welcome Evening
(Tent A)

Public Evening
Lecture
(HSZ 01)

EinsteinSlam
(HSZ 01)

Special Plenary Session
with Award Ceremony
and Ceremonial Talk
(HSZ 01)

SYOF
(HSZ 01)

SKM
Diss. Prize
Symp.
(SYSD)
(HSZ 02)

SYFP
(HSZ 01)

AKC (ZEU
250)

Lunch Talk
(HSZ 02)

Prize Talk
(HSZ 01)

Lunch Talk
(HSZ 02)

DFG
(HSZ 03)

Prize Talk
(HSZ 01)

Lunch Talk
(HSZ 02)

Disc. Lunch
(HSZ 03)

Plenary Talks
(HSZ 01 + HSZ 02)

Sessions
of Divisions

Plenary Talks
(HSZ 01 + HSZ 02)

Plenary Talks
(HSZ 01 + HSZ 02)

Prize Talk
(HSZ 01)

Lunch Talk
(HSZ 02)

Disc. Lunch
(HSZ 03)

SYOF
(HSZ 01)

SKM
Diss. Prize
Symp.
(SYSD)
(HSZ 02)

SYFP
(HSZ 01)

AKC (ZEU
250)

SYUE
(HSZ 01)

Plenary Talks
(HSZ 01 + HSZ 02)

Plenary Talks
(HSZ 01 + HSZ 02)

Prize Talk
(HSZ 01)

Lunch Talk
(HSZ 02)

Disc. Lunch
(HSZ 03)

Plenary Talks
(HSZ 01 + HSZ 02)

Plenary Talks
(HSZ 01)

Plenary Talks
(HSZ 01)

Plenary Talks
(HSZ 01)

Plenary Talks
(HSZ 01)

Plenary Talks
(HSZ 01)

Plenary Talks
(HSZ 01)

Plenary Talks
(HSZ 01)

Plenary Talks
(HSZ 01)

Plenary Talks
(HSZ 01)

Plenary Talks
(HSZ 01)

Plenary Talks
(HSZ 01)

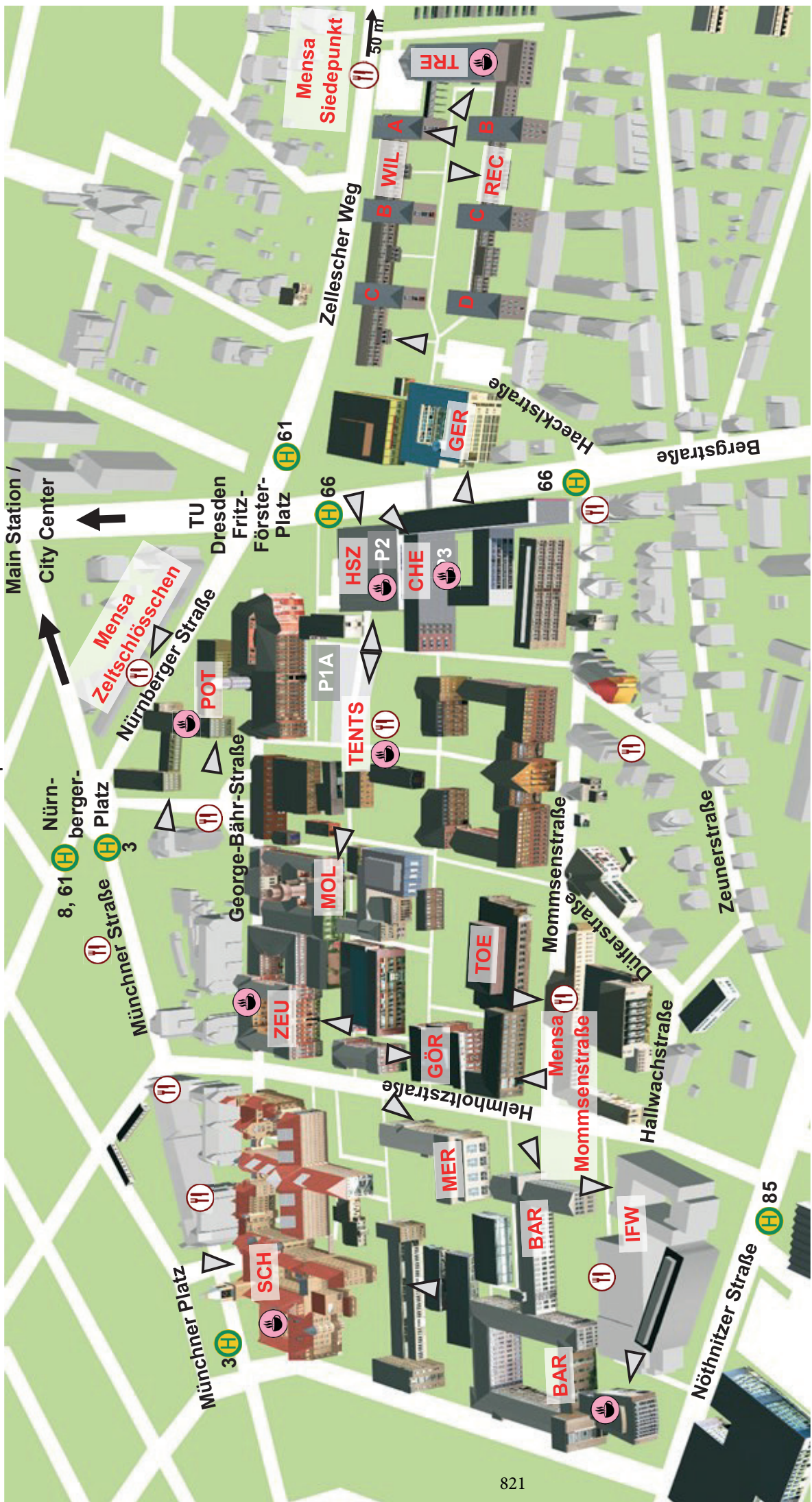
Plenary Talks
(HSZ 01)

Plenary Talks
(HSZ 01)

Plenary Talks
(HSZ 01)

Plenary Talks
(HSZ 01)

Plenary Talks
(HSZ 01)



- HSZ** Lecture hall name (abbreviation)
 - <https://navigator.tu-dresden.de>
 - Entrance
 - Coffee
 - Mensa, Snacks
 - Tram or bus stop with number
- | | | | |
|-----|--|-----------|---|
| BAR | Barkhausen-Bau | POT | Gerhard-Potthoff-Bau |
| CHE | Chemiegebäude, Poster P3 | REC | Recknagel-Bau |
| GER | von-Gerber-Bau | SCH | Georg-Schumann-Bau |
| GÖR | Görge-Bau | TOE | Toepler-Bau |
| HSZ | Hörsaalzentrum (Lecture Hall Center) | TRE | Treffz-Bau |
| | Poster P2, Conference office, Plenary talks, Symposium, Tutorials, Einstein Slam, Evening talk, Job market, Exhibition | Tent A, B | Poster P1A, Exhibition & Coffee, Snacks |
| MER | Merkel-Bau | WIL | Willers-Bau |
| MOL | Mollier-Bau | ZEU | Zeuner-Bau |